



Scientific and Technical Aerospace Reports

Annual Indexes (Section I) January-December 1971

Each entry in these indexes includes a group of identifying numbers in the following form: 07 p1002 471 18987. The first two digits (07) identify the issue in which the document was announced. The "p" and the four digits that follow (1002) refer to the page number in the designated issue on which the abstract of the document appears. The next group of numbers (471-18987) is the NASA Accession Number, a unique identification number assigned by NASA to each document that was received, indexed, and announced in STAB during the year.

TABLE OF CONTENTS

In addition to these identifying numbers, each entry in the Subject Index contains a Notation of Content, a brief description of the contents of the document. Each entry in the Personal Author and Corporate Source Indexes contains the exact title of the document.

Page

SECTION I

Introduction	iii
Subject Index (A-Mic)	A-1

SECTION II

Subject Index (Mid-Z)	A-700
---------------------------------	-------

SECTION III

Personal Author Index	B-1
---------------------------------	-----

SECTION IV

Corporate Source Index	C-1
Contract Number Index	D-1
Report/Accession Number Index	E-1
Accession/Report Number Index	F-1



TABLE OF CONTENTS

Page

SECTION I

Introduction	A-1
Subject Index (A-Misc)	

SECTION II

Subject Index (Misc)	A-700
----------------------	-------

SECTION III

Personal Author Index	B-1
-----------------------	-----

SECTION IV

Corporate Source Index	C-1
Contract Number Index	D-1
Report/Accession Number Index	E-1
Accession/Report Number Index	F-1

Introduction

WHAT STAR ANNUAL INDEXES ARE

These Annual Indexes are edited consolidations of the indexes to the individual issues of *Scientific and Technical Aerospace Reports (STAR)* for the calendar year 1971 (Volume 9, Numbers 1 through 24). For the convenience of the user, they are divided into four sections, each bound separately. Sections I and II contain the Subject Index. Section III contains the Personal Author Index. Section IV contains a Corporate Source Index, a Contract Number Index, a Report/Accession Number Index, and an Accession Number/Report Index. The Annual Indexes supersede the semimonthly and semiannual indexes previously issued during 1971.

Each entry in these indexes includes a group of identifying numbers in the following form: 07 p1002 N71-16987. The first two digits (07) identify the issue in which the document was announced. The "p" and the four digits that follow (1002) refer to the page number, in the designated issue, on which the abstract of the document appears. The next group of numbers (N71-16987) is the NASA Accession Number, a unique identification number assigned by NASA to each document that was acquired, indexed, and announced in *STAR* during the year.

In addition to these identifying numbers, each entry in the Subject Index contains a Notation of Content (a brief description of the contents of the document); each entry in the Personal Author and Corporate Source Indexes contains the exact title of the document.

At the beginning of each index in this cumulation, a typical listing is illustrated with each of its elements identified to assist the reader in using the different types of index entries.

HOW TO USE THE SUBJECT INDEX

Subject terms in this cumulative index are arranged alphabetically, and are supplemented with cross-references which are intended to serve as directions that will enable the user to modify, enlarge, or narrow his search in accordance with his specific interests. Two types of cross-references are used:

1. Use (U) references indicate that the subject term is not "postable", i.e., not a valid term, and that the following term or terms are used instead. For example,

COLUMBIUM

U NIOBIUM

ANNULAR JETS

U ANNULAR FLOW

U JET FLOW

2. Narrower Term (NT) references refer the user to more specific headings in the same subject area, under which additional material on the subject may be found.

For example:

EMISSION

NT ELECTRON EMISSION

NT NEUTRON EMISSION

NT THERMAL EMISSION

Eng'g.
2629.13
U58TA
v.9
1971
Index
sec. 1-2

Finally, a searcher should use the notations of content in the index to narrow further his quest for particular items. This is because subject terms can readily refer to more than one class of document. For example:

CATHODES

Cesium plasma cathodes as sources of high intensity electron beams.

Cathode material testing in electrochemical half cells.

illustrates a case where two references on different topics are listed under the same subject term.

HOW TO USE THE CORPORATE SOURCE INDEX

The corporate source index entries are abridged versions of the corporate sources used in the abstract-section citations in the individual issue supplements. The corporate source supplementary (organizational component) does not appear in the index. For example:

NEW MEXICO STATE UNIV. LAS CRUCES. DEPARTMENT OF BIOLOGY.

(Corporate source at citation)

NEW MEXICO STATE UNIV. LAS CRUCES.

(Corporate source index entry)

HOW TO USE THE PERSONAL AUTHOR INDEX

All personal authors identified in the abstract-section citations in the individual *STAR* issues appear in this index. Differences in transliteration schemes may require multiple searching of the index for variants of an author's name. For example:

EMELIANOV, M. D.

YEMELYANOV, M. D.

HOW TO USE THE CONTRACT NUMBER INDEX

All contract numbers that are identified in the abstract-section citations in the individual *STAR* issues appear in this index. Changes by agencies in the style in which contract numbers are presented may require multiple searching for variants.

For example:

AF 33(615)-67-C-1758

F33615-67-C-1758

A COMPREHENSIVE INFORMATION SERVICE

The National Aeronautics and Space Administration makes the results of worldwide research and development activities in aeronautics, space, and supporting disciplines promptly available to participants in its programs. NASA's scientific and technical information system now contains nearly a million documents, which are abstracted, indexed, and obtainable through retrieval and dissemination services. These services, which include the abstract journal, *Scientific and Technical Aerospace Reports (STAR)*, are described fully in a bulletin, *The NASA Scientific and Technical Information System . . . and How to Use It*, available at no charge from the NASA Scientific and Technical Information Facility, P.O. Box 33, College Park, Maryland 20740.

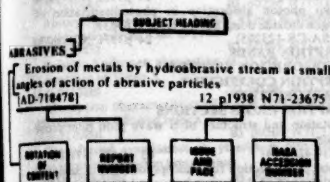
AVAILABILITY OF DOCUMENTS

Information concerning the availability of documents announced in the *STAR* issues covered in this index is found in the Introduction to the most currently issued semi-monthly issue.

SUBJECT INDEX

SCIENTIFIC AND TECHNICAL AEROSPACE REPORTS VOLUME 9 NUMBERS 1-24

TYPICAL SUBJECT INDEX LISTING



The subject heading is a key to the subject content of the document. The Notation of Content (NOC), other than the title of the document, is used to provide a more exact description of the subject matter. The report number helps to indicate the type of document cited (e.g., NASA report, translation, NASA contractor report). The issue and page identify the STAR issue in which the document was announced and the page number on which the citation appears. The NASA accession number denotes the number by which the citation is identified on that page. The NOC's are arranged under each subject heading in ascending accession number order.

A

ASTROPHYSICS
Astronomical catalog containing spectra, colors, and magnitudes of O-A stars in Milky Way galaxy [NLS-75-6050] 10 p1646 N71-21775
Abundance anomalies in A-pe stars caused by diffusion processes, and nucleosynthesis of elements between Si-28 and Co-59 14 p2339 N71-26443

AIRCRAFT
External store interference caused by rocket launcher pod positioning on aircraft wing 09 p1319 N71-19387

AIRCRAFT
Statistical analysis of gyrocompass mode of A-6A aerial navigation system 17 p2780 N71-30315

SATELLITE
U ECHO 2 SATELLITE 17 p2780 N71-30315

WIND TUNNEL
Wind tunnel techniques to obtain load relief for AATF Skybolt launch vehicles [NASA-TM-X-64604] 17 p2850 N71-30163

UNREVEALED
U SYMBOLS 17 p2850 N71-30163

FUNCTION
Numerical analysis of Abelian subgroups of p-groups 02 p0251 N71-11765

NUMERICAL
New subgroup and extension problems for Abelian groups 12 p1948 N71-23532

NUMERICAL
Numerical integration of Abelian integral equation for X-ray radiant flux density using spline functions [FOA-C-2455] 20 p3290 N71-33010

ABERRATION
Aberrations and ray tracing for double hemispherical shell mirror and ultraviolet grating spectrometers [WPL-QU-13] 06 p0902 N71-15795

MECHANICS
Mechanics and optics of Cassegrain multiplexed telescope for Jupiter planet tracking including aberration due to temperature effects 08 p1201 N71-18607

GEOMETRICAL
Geometrical aberrations and transfer matrix of multiplexed lenses in guiding devices or finite multimode beam matching systems and application to multiplexed triplet study 14 p2311 N71-26669

MAGNETIC
Magnetic lens aberration correction in electron microscopy 16 p2592 N71-28245

ABSORPTION
Absorption and reflectance in calcite filter for atmospheric photometry using Schmidt telescope 22 p3584 N71-35526

ABSORPTION
Absorption theory and computerized design of novel concave gratings for high resolution far UV

spectrometers 23 p3760 N71-36808
Alignment of optical system in astronomical telescopes 24 p3922 N71-37972

ABLATION

Analysis of charring ablation with description of associated computing program [NASA-TN-D-6083] 02 p0304 N71-11127
Determination of energy transfer in char zone of charring ablator 02 p0175 N71-11232

Ablation performance of glasslike carbons, pyrolytic graphite, and artificial graphite in stagnation pressure range 0.035 to 15 atm [NASA-TN-D-7005] 04 p0534 N71-14138
Hypersonic test facility for studying ablation in models under high pressure and high temperature [NASA-CASE-XLA-00378] 06 p0830 N71-15925
Arc chamber tests of Teflon pipe ablation in supersonic laminar and turbulent flows 09 p1484 N71-20247

Design of hypersonic test facility for ablation tests and performance tests of vehicles under conditions of high temperature and pressure [NASA-CASE-XLA-05378] 10 p1536 N71-21475
Ablation sensor for measuring char layer recession rate using electric wires [NASA-CASE-XLA-01794] 10 p1663 N71-21586

Ablation sensor for measuring surface ablation rate of material on vehicles entering earth's atmosphere on entry into planetary atmospheres [NASA-CASE-XLA-01791] 11 p1765 N71-22991

Compressible turbulent boundary layer flow past wind tunnel walls noting conductive heat transfer and ablation [VKI-TN-67] 13 p2022 N71-24499

Differential equations governing transient response of ablating axisymmetric orthotropic bodies and effect of shape change [NASA-TN-D-6220] 14 p2353 N71-26035

Thermochemical and thermophysical properties and ablation test data for three charring ablators [NASA-CR-111834] 16 p2691 N71-28795

Evaluation of interaction between reentry vehicle heat shield ablation and aerodynamic parameters [AD-724188] 20 p3351 N71-32936

Ablative response of silica phenolic to simulated liquid propellant rocket engine operating conditions [NASA-CR-72701] 23 p3776 N71-36909

Computer program for analyzing transient response of ablating axisymmetric bodies including effects of shape change [NASA-TM-X-2375] 23 p3867 N71-37569

Ablation cooling in rocket engine with combustion chamber liner and nozzle constructed of silica phenolic ablative material [NASA-CR-120798] 24 p4029 N71-38749

Analysis of reacting flow of pyrolysis products through char layer of low density, nylon phenolic resin, charring ablators and porous graphite [NASA-CR-1903] 24 p4031 N71-38765

ABLATIVE MATERIALS

CFA carbonaceous molding material development for ablative nozzles on solid rocket engines [NASA-CR-72766] 01 p0071 N71-10427

Vacuum method for molding thermosetting compounds used as ablative materials [NASA-CASE-XLA-01091] 01 p0060 N71-10672

Guidelines for designing combustion stability control devices [NASA-CR-111405] 02 p0290 N71-11884

Low cost, ablative heat shield for space shuttles [NASA-CR-111795] 02 p0306 N71-12067
Ablative resins used for retarding regression in ablative material [NASA-CASE-XLE-05913] 04 p0620 N71-14032

Numerical analysis of thermodynamics of aluminum ablative materials [AD-713095] 05 p0783 N71-15384
Design, development, and characteristics of ablation structures [NASA-CASE-XMS-01816] 05 p0785 N71-15623
Constant heating rate thermogravimetry of car-

bon/graphite cloth reinforced aromatic/heterocyclic resins to 1400 C [AD-714084] 06 p0680 N71-16486

Performance of low density silicone-phenolic and commercial ablative composites [NASA-TN-D-6130] 06 p0960 N71-16872

Evaluating effect of liquid fuel injectants on ablative performance of low cost nozzle materials [NASA-CR-72792] 07 p1011 N71-17677

Development of low cost ablative heat shields for space shuttles [NASA-CR-111814] 07 p1120 N71-17770

Ablation technology for planetary entry heat shielding [NASA-TM-X-66946] 09 p1484 N71-20246

Mathematical model for predicting erosion of charring ablator in aerodynamic environment 09 p1484 N71-20248

Crack effects in ablative heat shield on substructure heating 09 p1484 N71-20249

Method and apparatus for fabrication of heat insulating and ablative reentry structure [NASA-CASE-XMS-02009] 10 p1660 N71-20834

Planetary Atmospheric Experiments Test /PAET/ ablative afterbody thermal performance and component mechanical properties [NASA-CR-114293] 11 p1844 N71-22715

Fabrication of prototype low density ablative heat shield panels for space shuttles with production cost estimates [NASA-CR-111874] 12 p2015 N71-24333

Ablation sensors and thermocouples used to measure thermal response of phenolic-synlon material of spacecraft launched by Pacemaker vehicle system [NASA-TN-D-6293] 14 p2353 N71-26034

Production and application of sprayable fiber reinforced ablation material [NASA-CASE-XLA-4251] 14 p2278 N71-26100

High temperature measurement in rocket nozzle ablative materials 14 p2356 N71-26364

Materials and thermal protection, propulsion, environmental control, life support, and crew accommodation data for space shuttle design [NASA-CR-111847] 16 p2691 N71-28795

Artificial meteor ablation studies of natural minerals composed of magnetite and hematite [NASA-TM-X-63025] 15 p2419 N71-26911

Analysis of high temperature oxidation rate of carbon for use as reentry material [NASA-TN-D-6310] 16 p2616 N71-28012

Thermochemical and thermophysical properties and ablation test data for three charring ablators [NASA-CR-111834] 16 p2691 N71-28795

Hot isostatic compaction at 3000 F and 30,000 psi used for successfully preparing single phase bulk graphite for ablation testing [SC-CR-70-6169] 17 p2768 N71-29219

Light weight, low cost, ablative thermal protection system for space shuttles 17 p2847 N71-29456

Design of low cost ablator leading edge for space shuttle thermal protection system 17 p2847 N71-29457

Two dimensional axisymmetric transient heat conduction material ablation computer program [SC-DR-70-510] 19 p3192 N71-32342

Low cost replaceable ablative heat shield panels for space shuttles [NASA-CR-111800] 21 p3320 N71-35083

ABLATIVE NOSE CONES

Numerical method of unsteady adjustment for calculating inviscid flow fields about convex and concave shapes on atmospheric entry with ablation
[NASA-CR-121371] 20 p3203 N71-32801

ABNORMALITIES

NT GEOMAGNETIC HOLLOW

NT MAGNETIC ANOMALIES

Resonator anomalies in ocean

[AD-711979] 02 p0218 N71-12055

Anomalous upper atmospheric parameters derived from two aero-high rocket firings

[WRE-TN-HSA-175] 05 p0718 N71-15156

Anomalous damping of large-amplitude electron plasma oscillations - computer experiments

[AD-715074] 07 p1084 N71-18091

Solar geophysical relationships using radio telescope and satellite data

[AD-715938] 09 p1382 N71-19554

Abnormal glow discharge from cathode configuration for use as laboratory test bed to develop and calibrate plasma diagnostic sensors

[NASA-TN-D-6136] 11 p1813 N71-22676

Temperature anomaly of July 1968 in Romania

[NLL-M-20007-5828.4F] 12 p1956 N71-23962

Air-sea surface temperature anomalies in eastern tropical Pacific Ocean

[NASA-TM-X-65558] 15 p2404 N71-27668

Mathematical model for abnormal current in MOS transistor substrates

[LAAS-PUBL-777] 18 p2900 N71-30629

Computer editing routine for data abnormalities in multivariate statistical analysis

[NASA-TN-D-6472] 18 p2896 N71-31371

Calculation of specific heat anomalies caused by low concentration of impurities randomly distributed in Heisenberg ferromagnets

19 p3143 N71-32669

Anomalous water from cleaned and uncleaned capillary tubes, from weak H₂O₂ solutions, and from water extractions of crushed glass

[AD-726761] 23 p3720 N71-36517

Numerical analysis of persistence of degree of anomaly of fields of meteorological elements

[NLL-M-20652-5828.4F] 23 p3792 N71-37029

Turbulent heatings and anomalous diffusion in pinch plasmas related to drift instability in electron cyclotrons

[CONF-710607-66] 24 p3989 N71-38460

ABORT APPARATUS

Development of liquid propellant rocket abort fire model

[SC-RR-70-454] 07 p1098 N71-17229

LAAS DART minithruster safety evaluation tests during abort processes

[SC-RR-710012] 21 p3460 N71-34630

ABORT TRAJECTORIES

Mathematical modeling of F-8 aircraft wave off trajectories for aircraft carrier approaches

[AD-727121] 23 p3708 N71-36439

ABORTED MISSIONS

Aborted missions of Apollo 13 due to loss of cryogenic oxygen in service module

[NASA-TM-X-66409] 03 p0456 N71-13073

Success probability of manned spacecraft emergency return from low earth orbit

[AD-713106] 05 p0770 N71-14512

Development of liquid propellant rocket abort fire model

[SC-RR-70-454] 07 p1098 N71-17229

Aerodynamic forces and moments on orbiter and booster during space shuttle abort separation

[NASA-CR-103197] 21 p3520 N71-35085

Space shuttle abort stage separation wind tunnel tests of orbiter and booster vehicles - booster proximity data, Mach number 5

[NASA-CR-119973] 24 p4017 N71-38659

Space Shuttle abort stage separation wind tunnel tests of orbiter and booster vehicles - orbiter proximity data, Mach number 5

[NASA-CR-119971] 24 p4017 N71-38661

Space shuttle abort stage separation wind tunnel tests of orbiter and booster vehicles - orbiter proximity data, Mach number 3

[NASA-CR-119968] 24 p4017 N71-38662

Space shuttle abort stage separation wind tunnel tests of orbiter and booster vehicles - booster proximity data, Mach number 2

[NASA-CR-119969] 24 p4017 N71-38663

Space shuttle abort stage separation wind tunnel tests of orbiter and booster vehicles - orbiter proximity data, Mach number 2

[NASA-CR-119970] 24 p4017 N71-38664

ABRASION

Hydroabrasive wear of metals under cavitation

[PB-192268] 03 p0393 N71-13031

Particle shape effect on abrasiveness of graphite and molybdenum disulfides

[RAB-TR-69024] 04 p0534 N71-14137

Fracture mechanics and statistical failure analysis of brittle materials and erosion and abrasion machining processes

18 p2929 N71-31209

ABRASION RESISTANCE

Abrasive wear resistance of manganese cast iron insulated with cerium and studied with KH4-B machine

[AD-711156] 01 p0068 N71-10633

Erosion of metals by hydroabrasive stream at small angles of action of abrasive particles

[AD-718478] 12 p1938 N71-23675

Correspondence of hydroabrasive wear resistance and hardness of heat treated steels

[AD-721022] 15 p2423 N71-27301

Friction and abrasion properties of single gold crystals

18 p2998 N71-31445

ABRASIVES

Erosion of metals by hydroabrasive stream at small angles of action of abrasive particles

[AD-718478] 12 p1938 N71-23675

Process and apparatus for making diamond abrasives

[NASA-TM-X-64543] 12 p1927 N71-23775

ABSCISSAS

U COORDINATES

ABSOLUTE TEMPERATURE SCALES

U TEMPERATURE SCALES

ABSORBERS

Fluid flow control valve for regulating fluids in molecular quantities

[NASA-CASE-XLE-00703] 06 p0863 N71-15967

Stability of molecular sieve as regenerable carbon dioxide and water absorber in closed controlled atmospheres

[AD-716748] 10 p1503 N71-20629

Test on effects of curing temperature and relative humidity on dimensional stability of molded molecular sieve desiccant

[BDX-613-380] 18 p2884 N71-30581

ABSORBERS (MATERIALS)

NT NEUTRON ABSORBERS

NT SOLAR ENERGY ABSORBERS

Corrosion inhibitor effects on water coalescing characteristics of DOD type filter/coalescer elements

[AD-712999] 03 p0445 N71-13070

Analytical photoionization mass spectrometer with argon gas filter between light source and monochromator

[NASA-CASE-LAR-10180-1] 04 p0486 N71-13461

Procedure for extinguishing fires in activated carbon adsorbers used in air cleaning systems

[UCRL-72496] 04 p0517 N71-14499

Shaped thermal neutron flux filters for in-pile test capsule

[NASA-TM-X-2196] 07 p1066 N71-17932

Radiation shielding standards including shield materials, benchmark problems, and shield performance evaluation

[ORNL-TM-3251] 10 p1610 N71-20650

Amine absorbent for carbon dioxide concentrator in long term life support system

10 p1506 N71-20961

Elastomeric cross-linked polymers as dietary fat control and oil slick absorbing agents

11 p1697 N71-22558

Development of filter system for control of outgas contamination in vacuum conditions using absorbent beds of molecular sieve zeolite, silica gel, and charcoal

[NASA-CASE-MFS-14711] 14 p2262 N71-26185

Zero-gravity absorption refrigeration system design and performance testing for space station environmental control application

[NASA-CR-103114] 14 p2211 N71-26390

Testing of resonance absorbers for suitability as sandwich detectors for determining neutron spectra in fast reactors below 10 keV

[KFK-1233] 15 p2461 N71-27120

Development and characteristics of calorimeter with integral heat sink for maintenance of constant temperature

[NASA-CASE-XMF-04208] 16 p2693 N71-29051

Fire test facility with filter plenums and glovebox for studying effects of fire originating within glovebox system

17 p2730 N71-29874

PEARLS, FORTRAN code, for solution of neutron slowing down equations in multiregion lattices of resonance absorbers using IBM 360/50H computer

[AAEC-E-213] 24 p3981 N71-38407

ABSORPTION

Cycloel induced changes in internal structure of cotton leaves to reflectance, transmittance, and absorptance of near infrared radiation

06 p0800 N71-16151

Evaluating flight performance of 2.93 white paint in SERT 2 spacecraft thermal control system by changes in paint absorptance

[NASA-TM-X-52970] 09 p1404 N71-19681

Integrating sphere reflectometer for measuring absorptance of cavity type receivers

[NBS-TN-575] 18 p2892 N71-31518

ABSORPTION

Nonlinear absorption properties of organic dye molecules used with ruby lasers

[AD-717095] 10 p1571 N71-21787

Meson capture neutron yield in oxygen, sulfur, calcium and lead

18 p2979 N71-30701

Radar backscatter measurement to determine electron temperature dependence of F region absorption

[RSD-65] 22 p3573 N71-35464

Photoconductivity in Gallium arsenides single crystals by two photon absorption of light quanta from Nd glass laser

24 p3932 N71-38054

Two photon absorption in photodissociation of nitrogen dioxide using pulsed laser at 6943 Å

[NASA-CR-123205] 24 p3971 N71-38326

ABSORPTION BANDS

U ABSORPTION SPECTRA

ABSORPTION COEFFICIENT

U ABSORPTIVITY

ABSORPTION CROSS SECTIONS

Rotation and structure of S wave pion pion cross section

[COO-1428-174] 03 p0427 N71-12835

Total cross section for photoproduction of hadrons and hydrogen on deuterium between 1.0 and 6.4 GeV

[DESY-70/17] 03 p0430 N71-29065

Absorption model for direct transfer reactions

[UJVF-2433-F] 04 p0577 N71-13748

Oxygen molecular absorption cross sections and solar ultraviolet radiation absorption in Scheman-Runge bands

04 p0521 N71-13781

Fission cross section and resonance calculations for uranium 235 from 62 eV to 300 eV

[PB-193921] 04 p0584 N71-14202

Neutron fission and absorption cross sections of Pu 239 between 0.02 eV and 30 keV

[ORNL-TM-2598] 04 p0593 N71-14421

Investigating nuclear reactions of radionuclides, thermal neutron capture cross sections, solvent extraction, and application of radioisotopes

[NYO-3417-12] 05 p0738 N71-15009

Transferring neutron diffusion coefficient for infinite homogeneous media to general heterogeneous systems

[REP7-6-49] 06 p0912 N71-15810

Radiation source and detection system for measuring amount of liquid inside tanks independently of liquid configuration

[NASA-CASE-MSC-12280] 06 p0938 N71-16348

Resonance cross shielding in reactor analysis

[BNWL-1509] 07 p1071 N71-17268

Investigating characteristics and efficiency of fast power reactors

[JPRS-52290] 06 p1240 N71-18783

Evaluating changes in 26th group fission cross sections of U-235 and capture cross sections of U-238 from critical mass of ZPR-3 reactor

08 p1261 N71-18790

Photon density detection for determining liquid beam excess electron absorption cross sections at infrared wave lengths

10 p1612 N71-20720

Photoabsorption cross section data as function of wavelength for 24 atoms

[NASA-SP-3064] 14 p2303 N71-26087

Liquid hydrogen targets for determining total cross section of particle interactions

[JINR-PB-5212] 15 p2457 N71-26851

Radiative neutron capture cross sections of thorium up to 15 MeV

[WAPD-TM-971] 15 p2460 N71-27078

U 238 capture cross section data in 2 keV to 10 MeV neutron energy region of fast nuclear reactors

[INDC/NDS-18/N] 15 p2464 N71-27235

Exchange degeneracy with SU(3) symmetry and absorptive corrections in hypercharge and charge exchange reactions for meson baryon scattering

[PTB-36] 15 p2488 N71-27400

Absorption at rest and low energy elastic scattering of negative kaons by meson with various final state interaction data

[TID-25667] 16 p2653 N71-29007

Low and high field level crossing experiments in 2F state of atomic hydrogen and measurement of Sommerfeld fine structure constant

16 p2657 N71-29134

Differential cross section for low momentum negative kaon helium-4 elastic scattering from 115 to 160 MeV/c

17 p2806 N71-30106

Experimental device for measuring gamma absorption cross section of materials used for nuclear construction

[DEMO-70/11] 19 p3147 N71-32042

Ion trajectory and capture cross sections in quadrupole field for determining ion quadrupole effects in ion-molecule collisions

[NASA-TM-X-67888] 19 p3155 N71-32345

Photoabsorption cross sections for molecules of aeronomic and astrophysical interest at wavelengths less than 3000 Å

[NASA-CR-122098] 22 p3646 N71-34000

SUBJECT INDEX

- Calculation of effective electromagnetic absorption and scattering cross sections 23 p3390 N71-37439
- Ratio of U-235 and Pu-239 capture and fission cross sections measured with neutron spectrometer (NP-15769) 24 p3969 N71-38315
- ## ABSORPTION SPECTRA
- ### NT FRAUNHOFER LINES
- Luminescence of rocks and of natural and synthetic inorganic materials - laboratory studies 01 p0045 N71-10087
- Measuring neutral hydrogen absorption in galaxy M81 by radio telescope 02 p0294 N71-11137
- Absorption spectrum of barium vapor in region of autoionization from 2382 to 1760 (AD-711783) 02 p2669 N71-11144
- Galactic hydrogen absorption at 21 cm wavelength in direction of Virgo A 02 p0294 N71-11894
- Absorption characteristics of major components of dust clouds in infrared region (AD-712999) 03 p0366 N71-12730
- Far-infrared resonances in yttrium orthoferrite near spin reorientation temperature (N70-2391-106) 03 p0428 N71-12881
- Measurement of absorption spectra and absorptivity of solidified krypton and xenon for photon energies between 30 eV and 500 eV 03 p0419 N71-13340
- Chemical properties of superoxide ion and other alkali species in molten fluorides (TID-25480) 04 p0486 N71-13459
- Absorption spectra of gadolinium /Zr< in crystals of alkaline earth fluorides at hatched D energy levels (AD-712667) 04 p0380 N71-14010
- Electron scattering spectrum of carbon dioxide including scattering processes through formation of short lived negative molecule-ion compound states 04 p0592 N71-14393
- Spectrographic method for determining europium and cerium in rare earth mixtures (BARC-476) 05 p0639 N71-14709
- Molecular orbital, energy level diagram of soft X-ray L_{II,III} emission and absorption spectra from titanium and vanadium compounds (AD-713100) 05 p0730 N71-15387
- Potential energy barriers to internal molecular rotation from relative intensities of microwave absorption spectra lines 05 p0751 N71-15349
- Ultraviolet absorption spectra of transition metal ions in rare-gas matrices (AD-714726) 06 p0920 N71-16267
- Molecular absorption and light scattering in flame spectroscopy (IS-T-335) 06 p0812 N71-16791
- Influence of impurities on microanalysis of soil mixtures using absorption spectrophotometry (REPT-ID-51-70-05) 07 p0967 N71-16998
- Rapid atomic absorption spectrophotometric analysis of group 4B, 5B, and 6B metals in uranium alloys (LA-4329) 07 p1042 N71-17349
- Spectral coincidences between emission lines of CO laser and absorption lines of nitrogen oxides (AD-715293) 07 p1041 N71-18033
- Far ultraviolet absorption spectra of sodium vapor (REBIN-IN-101) 07 p1080 N71-18086
- Atmospheric absorption effects on spectroscopic analysis and electromagnetic radiation transmission (AD-715402) 08 p1191 N71-18835
- Zenon-modulated resonant cavity spectroscopy of gas-phase free radical microwave rotational absorption spectra (UCRL-50899) 08 p1264 N71-19103
- Visible ultraviolet and photochemical studies on silica 09 p1342 N71-19551
- Optical properties of rare earth doped germanate glasses (AD-716386) 09 p1395 N71-19573
- Analysis of crystal-field splittings, Zeeman effect, and line strengths for GdCl₃-Et₃SO magnetic dipole transitions (AD-716606) 09 p1454 N71-20094
- Infrared molecular beam absorption resonance as a high-time frequency reference for argon ion laser stabilization (NASA-CR-117528) 10 p1570 N71-21443
- Use of CO and CO₂ lasers to detect pollutants in atmospheric between laser emission lines and infrared absorption lines of NO (AD-717173) 10 p1571 N71-21788
- Infrared absorption spectra gas analysis of air pollution 11 p1761 N71-22063
- Spectral absorption and photoionization cross sections of CO₂, NH₃, O₂, CO, NO, N₂, and vinyl chloride using vacuum ultraviolet spectroscopy (AD-717771) 11 p1696 N71-22249
- Vertical temperature profile in Arctic atmosphere determined by absorption of microwave radiation by molecular oxygen 11 p1755 N71-22827

- Vibronic absorption and emission spectra of F centers in calcium oxide 11 p1818 N71-22898
- Absorption spectra and excited electronic energy levels of nitrogen dioxide in C₂H₅O₂CCl₄ and C₂H₅O₂NO₃ 12 p1949 N71-23257
- Measurement of ultrasonic absorption in high molecular weight polyethylene oxide at temperatures from room temperature to melting point (AD-718810) 12 p1942 N71-23392
- Cosmic attimeter sanitization and gamma ray background spectrum (NASA-TM-X-45517) 13 p2160 N71-24962
- Method for calculating spectra of gamma radiation in sea water with constant salt composition 14 p2248 N71-25967
- Microwave absorption and emission from magnetized afterglow plasma column in S band waveguide 14 p2332 N71-26345
- Silicon radiation detector production engineering for biological and medical applications and explanation of continuous absorption spectra using RC delay line as equivalent circuit (BMBW-FBR-70-15) 15 p2374 N71-26914
- Absorption spectra metals in soft X-ray and ultraviolet range (DESY-70/48) 15 p2420 N71-26966
- Oscilloscopes, analog and logic units, generators of visual function, and method of associated dialog for nuclear physics visualization unit adapted to C2-90-10 computer (CRA-N-1363) 15 p2467 N71-27293
- Line intensities in different spectral widths and intervals for atmospheric water vapor absorption using rigid and nonrigid rotor models 15 p2461 N71-27504
- Transmission functions in 15 micron carbon dioxide band 15 p2401 N71-27583
- Atmospheric oxygen absorption spectra and construction of growth curves for stratified atmosphere 15 p2401 N71-27587
- Absorption function of ozone 4.7 to 9.6 micron spectral bands noting their fine structure 15 p2401 N71-27589
- Doppler shifted cyclotron resonance absorption of helicon waves in indium and GaAs-AlGaAs heterostructures 15 p2477 N71-27577
- Metagalactic gamma ray spectra calculated for relativistic electron bremsstrahlung interaction (NASA-TM-X-45377) 15 p2315 N71-27646
- Numerical methods of quantitative analysis of digital gamma spectra (RT/PROT-70/21) 15 p2482 N71-27749
- Absorption region of SO₂ in neon and argon at 5.6 K 15 p2456 N71-27779
- Forbidden transition absorption spectra in cesium and rubidium atoms due to rare gas presence 16 p2648 N71-28439
- Effects of magnetic ordering on optical absorption spectrum of rubidium nickel fluoride 16 p2641 N71-29130
- Atomic absorption spectra of clouds formed by laser-induced vaporization of chromium steel (NASA-TT-F-13688) 17 p2758 N71-29225
- Neutron absorption and transmission measurements on Fe-240 from 20 eV to approximately 1 keV (RPI-328-223) 17 p2800 N71-30048
- Measurement of far infrared absorption spectrum of water by Fourier spectrometer (NASA-TT-F-13746) 17 p2717 N71-30320
- Absorption spectra of Pu(III), Pu(IV), Pu(VI), U(IV), and U(VI) in nitric acid and tri-n-butyl phosphate-n-alkane solutions and their use in automatic process control (EPK-1366) 18 p2884 N71-30601
- Reflected waves method and corresponding absorption parameters for determining sedimentary stratum from point seismic sounding 18 p2910 N71-30704
- Spectral reflectivity of solid surfaces at low temperatures (NASA-CR-119069) 18 p2965 N71-31192
- First-order correction of diffusion length for neutrons in medium with small absorption (RCN-134) 19 p3149 N71-32104
- Line absorption analysis and reaction kinetics of two metastable nitrogen atomic energy levels (NASA-CR-119685) 19 p3154 N71-32295
- Absorption spectra of gaseous n-alkanes and reflectance measurements of solid methane and ethane films in vacuum ultraviolet (DESY-78-71/1) 19 p3157 N71-32498
- Absorption in soft X-ray region of Sc K α spectrum (NASA-TT-F-13763) 19 p3177 N71-32526
- Electronic energy levels of Pr³⁺/Nd³⁺ optical absorption studies of Pr(NO₃)₃/Et₂SO on single crystals at 77 K 19 p3150 N71-32559

ABSORPTION SPECTROSCOPY

- Atmospheric models and strong-line profiles in pure absorption for late-type dwarf stars in 5200 to 3200 Å effective temperature range 19 p3102 N71-32705
- Galactic 21 cm line absorption in 97 radio source spectra using two element interferometer (AD-724162) 19 p3182 N71-32783
- Intra-cavity absorption experiment and molecular laser study (AD-724331) 20 p3281 N71-32980
- Flash lamp with ballistic piston compressor for absorption spectroscopy measurements in ultraviolet region (NASA-CR-120704) 21 p3405 N71-34226
- Optical-model search code including spin orbit terms in scattering and absorption potentials for spin-1/2 and spin-1 particles (ANU-P-508) 21 p3473 N71-34793
- Kinetics of emissions and absorptions of molecular nitrogen and carbon dioxide ions in ground states produced by pulsed radiolysis of N₂ and CO₂ (ANL-TRANS-401) 21 p3477 N71-34760
- Total absorption measurements of absolute calibration strengths for Fe I lines at lambda_{lab} 2833, 2873, 3439, 3483, and 4057 (AD-726997) 22 p3552 N71-35300
- Measurements of off-axis irradiance produced by laser beam in water (AD-726936) 22 p3591 N71-35573
- FORTRAN computer program for automatic analysis of gamma ray spectra from Ge(Li)-detectors (LUNP-7101) 22 p3634 N71-35905
- Atomic absorption spectrophotometry for rapid analysis of impurities in uranium (CRA-R-3070) 22 p3635 N71-35913
- Light absorption in molecular crystal by triplet excitation pair with singlet spin state (ITP-70-74) 22 p3645 N71-35971
- Absorption spectra of trivalent Nd in single crystal LiYF₄ and comparison of measured 1372 and 1522 quadruplet spin ground state molecular energy levels with theoretical predictions 22 p3648 N71-36012
- Free-free absorption coefficient of negative hydrogen ion and dipole adiabatic exchange wave functions of polarized orbital theory 22 p3648 N71-36015
- Spectral absorption coefficients of helium, neon, and nitric oxide mixtures with oxygen as functions of pressure, temperature, and wave number (NASA-CR-123188) 24 p3884 N71-37687
- Projects and techniques including mass spectrometry, gas chromatography, combustion carbon analysis, atomic absorption spectrophotometry, and related analytical chemistry methods (UCRL-50806-71) 24 p3885 N71-37693
- Nonlinear-optical effects in sulfur-hexafluoride at low pressure - saturation of infrared absorption 24 p3886 N71-37702
- Photoelectron emission spectroscopic absorption band calculations for bound-subband transitions in solution and interpretation of unbound electron random walk with kinetic energy loss (AD-727096) 24 p3981 N71-38412
- High resolution absorption spectra of isotopic modifications of nitrogen dioxide and other small molecules 24 p3983 N71-38425
- ## ABSORPTION SPECTROSCOPY
- Procedure for identifying silver iodide particles in ice crystals as snow crystal nuclei (PB-192754) 02 p0260 N71-12124
- Establishing detection limits for emission spectroscopic approach in determination of trace metals in biological materials (NASA-TM-X-52932) 03 p0331 N71-12339
- Measuring total precipitable water vapor and correlations between water vapor and local meteorological parameters (NASA-TM-X-44498) 03 p0482 N71-12596
- Investigating neutron and charged particle reactions and gamma and beta ray spectroscopy of radioactive sources (ANL-7630) 03 p0420 N71-12598
- Investigating band structures of crystals by studying two-photon absorption process (AD-712595) 03 p0444 N71-13234
- Polarization curves for four Gallium sulfides of Japitor (NASA-CR-115783) 04 p0809 N71-13556
- Increasing maximum energy and improving beam intensity of 85 MeV linear electron accelerator at Amsterdam 05 p0657 N71-14529
- Measuring optical spectra of triply ionized erbium in calcium tungstate using absorption and fluorescence spectroscopy (AD-715008) 07 p1079 N71-18043
- Auroral absorption measurement during absorption substorm development at geophysical observatories separated in longitude 12 p1989 N71-23561
- Comparison of atomic fluorescence fluorescence spectroscopy with atomic absorption flame spectroscopy 14 p2124 N71-26218

ABSORPTIVE INDEX

Metal ion analysis techniques including neutron activation, ion exchange, solvent extraction, spectrophotometry, and X ray, absorption, mass, and emission spectroscopy
[MLM-1801] 17 p2716 N71-30227

Study of two stage condensation polymerization reaction of polypropyleneimide by IR absorption spectroscopy
[TR-61] 18 p2887 N71-31355

Complete atomic absorption analysis of solid samples using heated graphite cell
[REF-433] 20 p3316 N71-30428

Flameless atomic absorption spectroscopy for analyzing trace elements in serum and urine
[NASA-TT-F-13983] 23 p3714 N71-36473

ABSORPTIVE INDEX U ABSORPTIVITY ABSORPTIVITY

Microwave mass absorption coefficient in granular silicates from plate measurements and effects of scattering
[NASA-CR-111023] 01 p0048 N71-10458

Measurement of absorption spectra and absorptivity of solidified krypton and xenon for photon energies between 30 eV and 300 eV
03 p0419 N71-13340

Absorption sensitive mechanical and machining properties of soda-lime glass
[AD-713594] 05 p0710 N71-15402

Reflectivity and absorptivity of cadmium crystal
[IS-T-395] 07 p1067 N71-17032

Measuring average absorption coefficients of carbon dioxide gas as function of temperature and pressure
07 p1128 N71-17041

Investigating effects of heat transfer, viscosity, and scattering on absorption coefficients of porous media saturated with water or petroleum
[NASA-TT-F-13426] 07 p1067 N71-17464

Pressure effects on high temperature vibrational absorption coefficients for atomic hydrogen collisions in hydrogen gas
[NASA-TN-D-6155] 07 p1076 N71-17514

Absorption coefficient measurements of semiconductor compounds at room temperature in 36 to 150 eV region
12 p1984 N71-23146

Absorptivity and emissivity hydrodynamic equations for suprathermal electrons gyrating in magnetized plasma including Doppler effect with solar radio emission examples
[AD-721337] 16 p2662 N71-28966

Comparison of theoretical and data analysis of Rayleigh waves generated by aerial nuclear explosions in USSR including earth absorptivity values
[AWRE-O-8870] 17 p2738 N71-29376

Optical imaging system for increasing absorbing efficiency of light or radiant energy at light sensitive face of imaging detector
[NASA-CASE-ARC-10194-1] 18 p2964 N71-31142

P-state wave function of two-electron atom and absorption coefficient of negative hydrogen ion
20 p3326 N71-33930

Transition radiation angular distributions excited by nonrelativistic particles for different indices of refraction and absorption coefficients
[JINR-P-5690] 21 p3469 N71-34698

Fast reactor control and absorber studies including radiation damage and reliability of absorbing materials
[SRAE-P-96] 23 p3800 N71-37092

ABSTRACTS

Abstract journal on stress corrosion cracking
[AD-709903] 01 p0065 N71-10168

Abstracts of research in oceanography, astronomy, and meteorology
[JPRS-51452] 01 p0136 N71-10285

ORNL decentralized Nuclear Science Abstracts preparation, and cost and time comparison with centralized preparation
[PB-190501] 02 p0275 N71-11910

Selected bibliography of abstracts on pressurized water power reactors
[NEIC-RR-39] 04 p0545 N71-13563

Plasma physics abstracts
[NASA-CR-111734] 04 p0598 N71-14129

Abstracted bibliography on meteorology, climatology, and oceanography of Caribbean region
[AD-713492] 05 p0677 N71-15504

Abstract reports for 1969 earthtremors
[NOAA-NOS-MSA-143] 05 p0682 N71-15693

Abstracts on chemical research reports
[AD-715001] 07 p0990 N71-17849

Literature review and abstracts on shock and vibration
[AD-717046] 10 p1653 N71-21062

Proceedings and abstracts of presentations at symposium on long wave propagation
[AD-716739] 10 p1526 N71-21798

Environmental engineering abstracts and bibliographical data
[SC-E-70-4211] 13 p0978 N71-25480

Abstracts of research studies performed at Swedish Research Institute for National Defense
[RAB-LIB-TRANS-1542] 13 p2193 N71-25550

Annotated bibliography of theoretical physics, magnetohydrodynamics of ionospheres and magnetospheres
[NASA-CR-118991] 16 p2661 N71-28032

Survey of management abstracts including subject categories in contract, personnel, program, and project management, research and development, tools, techniques, and philosophy of management
[NASA-SP-7300/05] 18 p3029 N71-30889

Abstracts on electrical engineering and data compression
[TR-EE-70-45] 18 p2900 N71-31479

Selected abstracts of world literature on production and industrial uses of radioisotopes
[ORNL-UC-30-PT-4] 18 p2990 N71-31545

Annotated bibliographies of reports relating to design and improvement of National Aerospace System
19 p3193 N71-31613

Cross-referenced directory of reports of Human Engineering Laboratories 1953 to 1970
19 p3047 N71-31617

Soviet Bloc research in geophysics, meteorology, oceanography, upper atmosphere, and space - abstracts
[JPRS-53605] 19 p3179 N71-32000

Error correcting codes and data compression techniques for PCM adaptive telemetry systems - abstracts
[NASA-CR-119679] 19 p3057 N71-32408

Abstracts of BOMEX related conference papers, sample products from BOMEX cloud photography and radar surveillance, and status summaries of BOMEX data processing and reduction
[NASA-CR-119761] 19 p3201 N71-32755

Abstracts of conference papers on preliminary results from BOMEX and methods and techniques used to collect data
19 p3201 N71-32756

Bibliographies and abstracts on air pollution emission sources - nitric acid manufacturing
[AP-93] 20 p3257 N71-33036

Abstracting and indexing periodicals in field of physical sciences
[ISS-70/21] 20 p3371 N71-33975

Compendium of graphs, expansions, properties, and integrals for unnormalized associated Legendre functions
[NASA-CR-121744] 21 p3445 N71-34518

Bibliography of publications and compilation of abstracts on Explorer 33 and 35 satellites
[NASA-CR-121895] 22 p3665 N71-36130

Soviet technical literature relevant to explosions, soil mechanics, laser and particle beams, and rostrum problems - bibliography
[AD-727584] 24 p0035 N71-38790

ABUNDANCE

Source abundances of cosmic ray nuclei from all-cone burning process in supernovae
[NASA-TM-X-65389] 03 p0450 N71-13033

Neutron activation analyses of lunar sample abundances
[NASA-CR-114841] 07 p1112 N71-17709

Neutron activation analysis of O, Si, Al, Mg, and Fe abundances in lunar rocks and fines from Apollo 12 mission
07 p1112 N71-17710

Neutron activation analysis of O, Si, Al, and Fe abundances in Apollo 12 lunar rock 12013
07 p1112 N71-17711

Neutron activation analysis of O, Si, and Al abundances in Apollo 12 lunar samples
07 p1112 N71-17712

Instrumental activation analyses of abundances in lunar rock chips
07 p1113 N71-17714

Calculating production of deuterium, He-3, boron, lithium, and beryllium by galactic cosmic rays in interstellar medium
[SAO-SPECIAL-REPT-330] 08 p1285 N71-18704

Uranium isotopic standard reference materials and absolute isotopic abundances determined by mass spectrometry
[NBS-SPEC-PUBL-260-27] 12 p1922 N71-23803

Flux-corrected radiative atmospheric models and metal abundances for R Cygni
13 p2167 N71-25066

Atmospheric and abundance analyses of photoelectric standard star 29 Pac
[NASA-TM-X-65347] 14 p2335 N71-25774

Abundance anomalies in A-poc stars caused by diffusion processes, and nucleosynthesis of elements between Si-28 and Co-59
14 p2339 N71-26443

AC [CURRENT]

U ALTERNATING CURRENT

AC GENERATORS
Two dimensional nonlinear numerical solution of solid rotor induction motor
[AD-71570] 02 p0195 N71-11369

Experimental operation of gas-bearing turboalternator for spacecraft power supplies
[NASA-TN-D-6956] 02 p0236 N71-12026

Nuclear Brayton turboalternator compressor with turbine inlet temperature consistent with SNAP 8 capabilities
[NASA-CR-111565] 03 p0417 N71-13064

SUBJECT INDEX

Characteristics of superconducting alternators with iron core and iron-free structures
[AD-713523] 05 p0631 N71-14046

Motoring tests of single shaft turbine compressor alternator
[NASA-TM-X-2154] 07 p0975 N71-17570

Motor-starting characteristics of modified Lundell alternator for single shaft, Brayton cycle, space power system
[NASA-TM-X-2200] 07 p0976 N71-17604

Dynamic electrical characteristics of 400 Hz Brayton cycle turbogenerator and controls for space application
[NASA-TN-D-6185] 11 p1677 N71-22564

Windage tests of cylindrical and Lundell-coiled rotors in ambient air producing Reynolds numbers up to 100,000 for high speed alternators
[NASA-TM-X-67809] 12 p1837 N71-23114

Superconducting alternator designs with cryogenic field for cooling windings below critical temperatures
[NASA-CASE-XLE-42323] 12 p1087 N71-23440

Design and application of tool-steel ball bearings in turbogenerator and mercury pump of SNAP-8 electrical generator
[NASA-CR-72825] 15 p2414 N71-30910

Turbogenerator for SNAP 8 power system subjected to expected vehicle launch vibration and shock loading
[NASA-TM-X-67851] 15 p2370 N71-27801

Control programs for optimization of nonlinear homopolar induction alternators
[AD-721315] 16 p2337 N71-28778

Numerical integration of ac generator coil equations into flux linkage equations with iterative solution for three phase machines
16 p2604 N71-28995

Inconel-steel, paddle-welded rotor slip and magnetic testing for use in 35,000 rpm Lundell alternator
[NASA-TM-X-67929] 22 p3339 N71-35344

Design and characteristics of radial inflow turbine stage for use as an alternative to stage of Brayton cycle turbo-alternator compressor unit
[NASA-CR-72808] 23 p3836 N71-37372

Evaluation of SNAP 8 turbine alternator assembly after 19,283 hours of operation
[NASA-CR-72921] 24 p3960 N71-38251

ACCELERATED LIFE TESTS

Design for space qualified helium-neon laser
[NASA-CR-1663] 01 p0062 N71-10045

Postirradiation examination of French Bottom reactor element B16-01 after exposure to 300 effective full power days
[GAMD-9911] 04 p0351 N71-12949

Durability and service life of ball bearings
[NASA-TT-F-13460] 08 p1208 N71-19889

Accelerated life tests for statistical failure prediction
09 p1400 N71-26229

Charged particle energy transfer for accelerating simulation of accelerated radiation tests
09 p1439 N71-26233

Theory, calculation, and design of centrifugal compressor machines
[AD-717878] 12 p1925 N71-23297

Dual grid electrostatic thrust vectoring system with capability of vectoring beam from 0 to 360 degrees in pitch or yaw or more
14 p2332 N71-30304

Reduced burnup characteristic and long life performance of regenerative coating material / 50 percent U-234 and 10 percent U-235 / in developing thermal neutron detectors for reactor
[WHAN-FR-37] 15 p0458 N71-20807

Sol-gel processes and remote handling equipment for coating particles, preparation of thorium, uranium, and plutonium fuels, and accelerated life testing of nuclear fuel elements
[ORNL-4629] 15 p2447 N71-27208

This film Ca2S-CaS solar cells thermally cycled for 10,850 cycles under simulated orbital conditions
[NASA-TM-X-67847] 15 p2369 N71-27806

Low density and adequate mechanical properties of surface compression strengthened glasses permitting their use in weapons and other lightweight structures for long periods
[AD-721327] 16 p2618 N71-26415

Reliability testing of aerospace problems includes sampling, distribution functions, and accelerated life tests
[NASA-TM-X-67877] 21 p3632 N71-34415

Performance testing and design parameters evaluated for UO2-Zr fuel assemblies in boiling water reactor
[RISO-M-1350] 21 p3457 N71-34884

Accelerated life test models, criteria for model selection, and extrapolation in overstress models
[NASA-CR-121645] 21 p3526 N71-35124

Correlation equation relating creep deformation of tubes to stress and temperature functions, and application to design of heat exchanger tubes
[NASA-TM-X-2372] 21 p3329 N71-33147

Teflon FEP investigated as cover for silicon solar cells including process for heat sealing
[NASA-CR-72970] 22 p3542 N71-35521

SUBJECT INDEX

Irradiation experiment for testing spherical fuel elements for high temperature reactors
[JUL-78-12W] 23 p3795 N71-37056

ACCELERATING AGENTS
Delayed action accelerating agent for curing Neoprene compounds 07 p0989 N71-17638

ACCELERATION
MED Rayleigh problem with accelerating and decelerating motion of flat wall 22 p3571 N71-35432

ACCELERATION [PHYSICS]
NT ANGULAR ACCELERATION
NT DECELERATION
NT HIGH ACCELERATION
NT IMPACT ACCELERATION
NT LUNAR GRAVITATIONAL EFFECTS
NT PARTICLE ACCELERATION
NT PLASMA ACCELERATION
NT SPIN REDUCTION
NT TRANSVERSE ACCELERATION
Table 10g and requirements of gyroscopic materials under acceleration 03 p0412 N71-13212
Linear motion of accelerometers on centrifuge 03 p0412 N71-13213
Two stream instability in Colgate supernova model of cosmic ray acceleration [UCRL-50695] 04 p0995 N71-13574
Relativistic solution and nonlinear waves as bunches for coherent acceleration [JHEP-PP-5990] 04 p0373 N71-13653
Orbit and center of gravity acceleration during launch of Boeing 707 aircraft [ARC-CP-1120] 06 p0793 N71-15721
Center of gravity vertical acceleration and wing stresses of Boeing 720-B aircraft [TD-87-1790] 07 p0970 N71-17119
Initial velocity and penetration depth of explosively accelerated metal balls [HEPT-9/09] 06 p1307 N71-18475
Molecular beam apparatus combining aerodynamic acceleration and arc heating techniques 06 p1263 N71-18083
Detection of quantized vortex lines in liquid helium 2 accelerated from rest [TD-25595] 09 p1434 N71-19992
Positive effects on flight crew tolerance to positive acceleration 09 p1335 N71-20357
Effects of positive G acceleration on blood oxygen saturation and pleural pressure relations in dogs breathing air and liquid fluorocarbons in whole body water immersion respirator [NASA-CR-117159] 09 p1336 N71-20358
Age and exercise factors influencing osteoporosis, bone strength, and acceleration tolerance investigated with chronic monkeys 09 p1336 N71-20359
Shock, vibration, and acceleration-load tests of SHAP-8 motor-driven lubricant-coolant pump [NASA-TN-X-52972] 10 p1002 N71-20947
Tests for analysis of acceleration-induced transient burning rate augmentation of aluminum solid rocket propellant 10 p1637 N71-21522
Development of method for producing artificial gravity in manned spacecraft [NASA-CASE-XNP-02595] 11 p1830 N71-21801
Comparison of operator performance limits and symptoms induced by angular accelerations about pitch and yaw axes [AD-717596] 11 p1686 N71-21913
Analysis of normal accelerations through center of gravity of aircraft due to landing impacts and ground reactions associated with taxi, takeoff, and landing [NASA-TN-D-6124] 11 p1676 N71-22620
Table of comparative equivalents using standardized terminology for use in acceleration studies 12 p1965 N71-23338
Fundamental principles and physiological effects of acceleration on human body 12 p1862 N71-23339
Annotated bibliography of worldwide biodynamics research findings [NASA-TN-X-67130] 12 p1866 N71-23344
Effects of high accelerations and heat fluxes on water boiling of water in axisymmetric rotating tubes [NASA-TN-D-6307] 12 p2012 N71-24282
Investigation of visual perception ability during acceleration and deceleration and thresholds for perceived motion changes 13 p2057 N71-24727
Physiological effects of positive acceleration on cardiovascular system based on requirements for cardiovascular stimulation [AD-719902] 14 p2203 N71-25674
Determination of acceleration limits for passenger comfort in urban transportation system 14 p2203 N71-26118
Effect of acceleration on space required to perform maneuvers with urban transportation tracked vehicle 14 p2358 N71-26119

Vibration control of flexible bodies in steady acceleration environments 15 p3415 N71-37169
Accelerator for launching hypervelocity projectile by drag force of jet produced by gaseous explosive products [NASA-CR-115067] 17 p3279 N71-39227
Electro-optical acceleration of oscillator tubes 17 p3252 N71-39269
Orbital acceleration of ellipsoidal high altitude balloons utilizing solar radiation pressure [X-550-70-92] 19 p3179 N71-31870
Numerical analysis of acceleration flight data of Mariner Mars 69, OAO 2, and ATS to determine disturbing forcing function of Centaur engines at main engine cutoffs [NASA-CR-119469] 19 p3185 N71-32570
Computer plots of acceleration flight data of Mariner Mars 69, OAO 2, and ATS showing selected global axis forcing functions and dynamic response of Centaur main engine cutoffs [NASA-CR-119493] 19 p3185 N71-32571
Method for calculating vertical derivatives of earth acceleration [AD-74498] 20 p3259 N71-33200
Digital control of beavron acceleration cycle resulting reduction of heat and noise [UCRL-20183] 20 p3248 N71-33900
Six parameter model of range-rate observable showing differentiated tracking data for improved orbit determination with constant accelerations 21 p3391 N71-34128
Gas dynamics and magnetic field effects on shock wave gradient acceleration and experimental design applications [UCRL-TRANS-10532] 21 p3412 N71-34281
Laboratory and sea tests of gyro-stabilized marine gravimeter for measuring disturbing accelerations and tilts in submarines 21 p3417 N71-34316
Instrument for synchronous photographic recording of perturbing acceleration and residual tilts of gyro-stabilized platform 21 p3418 N71-34320
Motion of test body inside system of oscillating masses in laboratory conditions [JHEP-P13-5685] 21 p3472 N71-34719
Explicit and recursive formulas for acceleration and gravity gradient derived from spherical harmonics [NASA-CR-121909] 22 p3572 N71-35442
Acceleration measurements during transportation in small delivery van [FTL-A-AL609-14] 22 p3629 N71-35862
Anomalous accelerations of Pegasus satellite and application of theory to predict perturbations in mass motion [NASA-TM-X-65683] 22 p3673 N71-36189
Analysis of design concepts for mechanical simulation of flight acceleration for testing of functional requirements of arming and safing devices used in anti-air warfare adaptation kits [AD-726926] 22 p3681 N71-36250
Effect of alcohol and disorientation responses on syntheses and vertigo during angular acceleration with and without visual fixation [FAA-AW-71-16] 23 p3714 N71-36477
Techniques for determining reliability of electronic equipment after acceleration tests 23 p3758 N71-36786
Measurements and analysis of solid propellant rocket vibrations obtained during captive flight of Nike rocket [NASA-TN-D-6517] 23 p3863 N71-37359
Acceleration of condensate drops in axial gap of turbine stage [RAE-LIB-TRANS-1602] 24 p3906 N71-37837
Structure of relativistic solutions and nonlinear waves as bunches for coherent acceleration [UCRL-TRANS-1443] 24 p3980 N71-38405

ACCELERATION PROTECTION
Conditioning suit for normal function of astronaut cardiovascular system in gravity environment [NASA-CASE-XLA-02595] 09 p1341 N71-20368

ACCELERATION STRESS (PSYCHOLOGY)
Blood pressure changes in heart cavities and large vessels in dogs during acceleration in various directions 02 p0159 N71-11477
Characteristics of adaptation processes in vestibular systems 02 p0160 N71-11490
Investigating effects of gravitational and inertial forces on cardiovascular and respiratory dynamics [NASA-CR-111686] 03 p0321 N71-12294
Examining dynamics of changes in sympathetic nucleus of hypothalamus in rats exposed to transverse accelerations 08 p1159 N71-18096
Acceleration effect on hamato-epithelium barrier permeability in rabbits 08 p1154 N71-19060
Changes in bioelectric potentials in brains of rabbits subjected to X ray irradiation and acceleration on centrifuge [FPLB-52-080] 08 p1154 N71-19064

ACCELEROMETERS

Dynamic models of human body response to acceleration environments and determination of tolerance limits [NASA-TM-X-67080] 10 p201 N71-21598
Development of method for producing artificial gravity in manned spacecraft [NASA-CASE-XNP-02595] 11 p1830 N71-21801
Acceleration and gravity effects on function and behavior of lungs [AGARDGRAPH-135] 11 p1679 N71-21981
Biodynamics, aerospace medicine, acceleration stresses, human tolerance, centrifuges, test facilities, and associated bibliography [AGARDGRAPH-150] 12 p1843 N71-23337
Table of comparative equivalents using standardized terminology for use in acceleration studies 12 p1965 N71-23338
Fundamental principles and physiological effects of acceleration on human body 12 p1862 N71-23339
Tabular and graphical summary of human tolerance to prolonged acceleration stresses 12 p1862 N71-23341
Acceleration effects on ventilator stimulation of external respiratory function and respiration center neuron activity 14 p2544 N71-28261
Vector analysis for estimating acceleration forces affecting human receptors in semicircular canals during rotation 16 p2544 N71-28263
Radial acceleration effects on spinal cord induced potentials of intact and labyrinthectomized rats 20 p3258 N71-33456
Dysrhythmic myocardial damage in rat hearts caused by prolonged acceleration 20 p3222 N71-33470
Combined effects of reduced nutrition, hypokinesia, and centrifugal acceleration on human body [JPRS-54104] 23 p3716 N71-34688

ACCELERATION TOLERANCE
Psychologic response to short duration positive G sub 3 maneuvers [AD-710596] 01 p0813 N71-10892
Four-degree-of-freedom lumped parameter model for vertical accelerations of seated human body as might be imposed by aircraft ejection systems [AD-721225] 15 p2570 N71-26944
Electronic detection system for peak acceleration limits in vibrational testing of spacecraft components [NASA-CASE-NPO-10556] 15 p2468 N71-27185
Evaluation of human vestibular tolerance by Coriolis acceleration test 16 p2544 N71-28262
Physiological effects and acceleration tolerance after weightlessness based on space environment simulation with human centrifuges and bed rest [NASA-CR-115068] 17 p2786 N71-29216
Evidence for test of dynamic motion function considered in relation to responses from patient with idiopathic progressive vestibular degeneration [AD-722318] 19 p0842 N71-31768
Pilot injuries on high speed low altitude flight noting acceleration due to gust effects 19 p0848 N71-31888
Mechanical responses of human hand subjected to acceleration loads determined for use in construction of artificial hand 19 p0845 N71-32547

ACCELERATORS
Cost analysis of accelerator magnet system [JNP-18357] 04 p0347 N71-13628
Comparison of health physics measuring procedures at accelerators [DESY-70/27] 03 p0727 N71-15889
Ventilation for radioactive materials in storage, nuclear reactors, and accelerators [AD-716265] 09 p1417 N71-19863
Accelerator studies on positron scattering, excited atomic energy levels, and resonance charge exchange reactions [CERN-1-1232] 09 p1446 N71-20587
Medium energy physics research in accelerator structure, power systems, and control and instrumentation [LA-4571] 12 p1897 N71-23727
Communication system for 3-MV Super-tilt injector using PCM telemetry [UCRL-20179] 21 p3395 N71-34167
Neutronium location for minimum accelerator cost on 30 conductor diameter flat beam transport [NASA-TM-X-67920] 22 p3662 N71-34114

ACCELEROMETERS
Light modulated accelerometer for pantograph measurements on railway vehicles [PB-195452] 01 p0057 N71-10809
Free flight measurements of aerodynamic lateral force and moment coefficients using gyroscopes and accelerometers [NASA-TN-164] 03 p0141 N71-11091
Testing methods for components of inertial guidance systems [AGARDGRAPH-130] 05 p0416 N71-13201
Review of gyro and accelerometer testing 05 p0411 N71-13203

Performance prediction and testing methods for accelerometers 03 p0411 N71-13207

Linear motion of accelerometers on centrifuge 03 p0412 N71-13213

Testing of gyros and accelerometers having hydrostatic gas bearing axes 03 p0412 N71-13214

Design optimization and production of fluidic accelerometer for angular rate measurements [NASA-CR-102931] 03 p0383 N71-13322

Superconductive accelerometer employing variable force principle to determine acceleration of bodies [NASA-CASE-XMF-01099] 06 p0850 N71-15969

Describing device for velocity control of electro-mechanical drive mechanism of scanning mirror of interferometer [NASA-CASE-XOS-03532] 07 p1031 N71-17627

Error analysis of Cactus high sensitivity accelerometer for flight performance tests [ONERA-TR-875] 06 p1209 N71-18450

Sterilization and environmental testing of solid state rate sensor with rectangular metal beam for planetary space flight [NASA-CR-111853] 08 p1202 N71-18964

Error analysis of counting accelerometer data from F-4 and RF-4 aircraft and structural fatigue analysis [AD-717151] 10 p1497 N71-20796

Accelerometer round robin measurement comparisons 12 p1897 N71-23633

Alignment and calibration of strapdown inertial measuring unit using accelerometer, gyrocompass, and optical filtering techniques [RE-67] 12 p1960 N71-24007

Velocity components and radial pressure distribution in vortex gyros for measuring angular velocity [FOA-2-C-2358-54] 14 p2256 N71-26260

Model of spatial Newtonmeter (accelerometer) set on moving object and theory of inertial navigation [AD-720381] 14 p2299 N71-26347

Elimination of pitch and yaw vibrational motions in a portable television camera using two accelerometers [TR-78-E-13] 14 p2219 N71-26375

Engineering drawings and performance test data for train time accelerometers 15 p2412 N71-27793

Mathematical model of missile inertial guidance based on accelerometer and gyroscope stabilized platform sensor data [AD-722919] 17 p2779 N71-29504

Omnidirectional liquid filled accelerometer design with liquid and housing temperature compensation [NASA-CASE-HQN-10780] 17 p2754 N71-30265

Three-axis accelerometer for determination of atmospheric density with low altitude research satellites [AD-728666] 18 p2926 N71-31470

Vertical accelerometers for observing ground motion caused by ocean tides, low frequency ocean waves, and atmospheric pressure [AD-728669] 19 p3084 N71-31726

Transportation shock and vibration monitor for recording acceleration in shipment of complex equipment [UCRL-727448] 19 p3101 N71-32311

Null balance, floated pendulum accelerometers with analog feedback servos amplifiers [NAL-TR-230] 20 p3273 N71-33241

Wide band tidal and seismic frequency studies using quartz accelerometer with simple internal geometry 20 p3262 N71-33344

Zero-shift and remanence polarization reorientations in polycrystalline ferroelectrics used in piezoelectric shear-type accelerometers [SC-RR-70-755] 21 p3429 N71-34401

Silicon photovoltaic cells for calibrating piezoelectric accelerometers [AQD/Y77] 23 p3759 N71-36796

Image shearing eyepiece for calibrating acceleration transducer [AQD/Y72] 23 p3759 N71-36799

ACCEPTABILITY
Cost and failure analyses and acceptability data from electronic equipment testing of various electronic components [NASA-CR-115981] 18 p2897 N71-30650

Standardization of structural acceptance tests conducted on flight hardware [NASA-SP-0045] 18 p3018 N71-31033

ACCEPTANCE
U ACCEPTABILITY
Simultaneous donor and acceptor concentration determination in n-type semiconductors using Hall effect measurements [ONERA-NT92/1670] 02 p0285 N71-11856

Neural effects in mercury telluride single crystals grown by Bridgman method in mercury vapors 07 p1047 N71-17125

First-order radiative transition rate electron transfer from neutral donors to neutral acceptors in silica at low temperatures 09 p1432 N71-19927

Kinetics of radiative recombination processes between donor and acceptor impurities in silicon 13 p2143 N71-25581

ACCIDENT INVESTIGATION

NT AIRCRAFT ACCIDENT INVESTIGATION
Systems approach to accident investigation in civil aviation and homes 01 p0002 N71-10115

Investigation of cryogenic oxygen tank anomaly on Apollo 13 flight [NASA-TM-X-66463] 01 p0126 N71-10614

Survey of accidents at air separation plants [NASA-TT-F-13388] 03 p0384 N71-12657

Evaluation of effect of Apollo 13 malfunction on related subsystems [NASA-TM-X-66928] 09 p1470 N71-19953

Analysis of anomalies, cause, and results of command service module oxygen tank failure on Apollo 13 flight [NASA-TM-X-66922] 09 p1470 N71-19954

Thermodynamic analysis of Apollo 13 oxygen tank to describe stratification phenomenon preceding tank failure [NASA-TM-X-66934] 09 p1470 N71-19955

Organization, activities, and recommendations of safety, reliability, and quality control panel during Apollo 13 flight investigation [NASA-TM-X-66924] 09 p1471 N71-19961

Analysis of spacecraft components and systems with potential for failures similar to Apollo 13 flight emergency [NASA-TM-X-66918] 09 p1471 N71-19963

Survey of breathing systems design and reliability conducted by accident investigation panel following Apollo 13 flight emergency [NASA-TM-X-66925] 09 p1471 N71-19964

SM-1A core 4 design and nuclear analysis, steady state thermal-hydraulic behavior, and transients of accident situations 11 p1793 N71-22226

Aviation and surface transportation safety for 1970 with related accident investigations and recommendations [AR-4] 13 p2191 N71-24925

Crash survivability and escape possibilities from motor vehicles [PB-158773] 19 p3196 N71-32198

ACCIDENT PREVENTION
Computer programs and predictor displays for solving air traffic control problems [NASA-CR-111372] 02 p0262 N71-11466

Systematic failure study of reactor protection systems [BAW-10019] 04 p0556 N71-14094

Nuclear Safety Program at ORNL with emphasis on environment pollution [ORNL-TM-5661] 04 p0558 N71-14164

Description of manual on prevention of electrical breakdowns in spacecraft 06 p0828 N71-16649

Analysis of spacecraft components and systems with potential for failures similar to Apollo 13 flight emergency [NASA-TM-X-66918] 09 p1471 N71-19963

Conference on safety problems in transportation and storage of explosives [AD-716790] 10 p1662 N71-21202

Bibliography on shipping containers, critically in handling, transport regulations, and safety practices for radioactive materials [ORNL-NSIC-84] 10 p1619 N71-21635

Test and evaluation of lap belt protection and comparison with lap belt plus air cushion restraint on human and baboon subjects 11 p1683 N71-22451

Aviation and surface transportation safety for 1970 with related accident investigations and recommendations [AR-4] 13 p2191 N71-24925

Accident prevention and safety devices for water cooled reactors compared with liquid metal cooled, fast breeder reactor safety [WHAN-SA-43] 14 p2291 N71-25684

Aerospace energy absorbing guardrail concept designed for redirecting errant vehicle parallel to normal traffic flow with minimum damage to vehicle and passengers 17 p2855 N71-30296

Accident prevention systems for liquid metal fast breeder reactor safety design [BAW-1354] 19 p3136 N71-32063

Flammable Fabrics program reporting standards for carpets and rugs, blankets, mattresses, and apparel for children [NBS-TN-596] 23 p3776 N71-36914

ACCIDENT PROMENESS
Health effects of sonic booms noting human reactions and performance, sleep deprivation and accident proneness [ISVR-TR-25] 10 p1504 N71-20699

ACCIDENTS
NT AIRCRAFT ACCIDENTS
NT AUTOMOBILE ACCIDENTS
Noble gas confinement after accidents [DUN-6653] 01 p0090 N71-10671

Theoretical treatment of conceivable serious accidents at fast breeder reactors in context of Reth-Telt method [EURPNE-748] 04 p0546 N71-13568

FREADM-1 code, fast multichannel accident analysis program, restricted to accidents within annular or cylindrical coaxial core regions [GEAP-13608] 10 p1604 N71-21218

Individual factors which produce risk in materials handling of explosives, noting safety management, incident prevention, and damping of explosions [ICT-1770] 12 p1980 N71-23438

Accidental external irradiation and accidental radioactive contamination - rules and therapeutic procedures [CEA-N-1365] 15 p2481 N71-27801

Accident analysis of light water reactor by digital computer program NURLOC-1.0 [JAERI-4194] 15 p2451 N71-27813

Use of existing data to analytically describe boiling water and pressurized water reactor accidents [BME-1904] 23 p3790 N71-37877

ACCLIMATIZATION
NT ALTITUDE ACCLIMATIZATION
NT COLD ACCLIMATIZATION
Effects of thermal stress, exposure time, and acclimatization on human performance [AD-711012] 01 p0009 N71-10393

Investigating gas preference reactions in man and animals to hypoxic, hyperoxic, or hypercapnic environments [JPRS-52332] 07 p0981 N71-17440

North Atlantic Treaty Organization conference on adaptation and acclimatization in aerospace medicine [AGARD-CP-82-71] 09 p1334 N71-28051

Annotated bibliography on human acclimation and acclimatization to heat [NASA-TM-X-62008] 13 p2083 N71-23399

Statistical analysis of effects of acclimatization on hemopoiesis of Antarctic expeditionary personnel [JPRS-55884] 21 p3382 N71-34803

ACCOMMODATION
NT VISUAL ACCOMMODATION
ACCOMMODATION COEFFICIENT
Mechanical getter technique for determining rate of thermal accommodation coefficients of helium 4 and helium 3 isotopes on bare tungsten at low and moderate temperatures 11 p1777 N71-22220

ACCRETION
U DEPOSITION
ACCUMULATORS
NT DUST COLLECTORS
NT SOLAR COLLECTORS
NT SOLAR REFLECTORS

Multistage depressed electrostatic collector for magnetically focused spaceborne klystrons [NASA-CR-72767] 01 p0630 N71-10820

Sublimed thermionic emitter and collector coatings [TEE-4125-2] 08 p1276 N71-18187

Small plasma probe using tungsten wire collector in tubular shield [NASA-CASE-XLE-02578] 10 p1627 N71-20707

Carbon monoxide accumulator cell for spacecraft mass spectrometer atmospheric sensor system [NASA-CR-111855] 11 p1764 N71-22809

Temperature effects on thermionic diode with open charge model including emitter and accumulator electrode emissions [NASA-CR-72885] 16 p2566 N71-33376

Computational method for determining performance of ten stage electrostatic depressed collector for klystrons [NASA-CR-119683] 19 p3067 N71-33410

Evaluation tests to demonstrate feasibility of increasing efficiency of linear beam microwave tubes using novel depressed collector [NASA-TM-X-2322] 19 p3067 N71-33402

Methods for analyzing multistage electron beam collector schemes, with and without transverse magnetic fields, for traveling wave tubes [NASA-CR-72950] 19 p3068 N71-33612

Superconducting inductive energy accumulator as standby electrical energy source, as energy source for load factor in power systems, or as source for high speed electric pulses [JPRS-54821] 23 p3710 N71-36468

ACCURACY
Evaluation results and accuracy improvement of two flux switching mathematical models for magnetic cores [NASA-TN-D-6032] 01 p0036 N71-10807

Device using laser interferometer for measuring translational motion with directional accuracy of 0.05 microns 02 p0239 N71-11599

Investigating various sources of attitude errors in Black Arrow third stage and effects on accuracy of velocity increment error [RAE-TR-68207] 02 p0299 N71-11900

Accuracy in range, azimuth and elevation angle measurements to determine impact area of ballistic trajectories [REFT-1-1969] 03 p0334 N71-12394

Comparison of space and simulated environments conditions using temperature inaccuracy of hollow cylinder 03 p0357 N71-12718

SUBJECT INDEX

High accuracy optical mechanical telescope - conference
[NLL-RRE-TRANS-222-0036.6251]
10 p1562 N71-21745

Improving accuracy of gyrostat using floating
integrating gyroscopes with feedback
10 p1562 N71-21747

Inherent accuracy of DSN as radio navigation
instrument for lunar and planetary missions
11 p1753 N71-22770

Procedures for qualitative evaluation of frequency
accuracy and stability of communication-electronics
equipment
[AD-71706]
12 p1878 N71-23529

Measurement of total cross sections of pions/mines
proton interaction in energy range from 4.0 to 6.0 GeV
with systematic error not more than 30 microbars
using Compton telescopes
[NBS-71-5465]
13 p2145 N71-25591

Medium density and chemical composition and mea-
surement geometry effects on accuracy of neutron
scatter measurement method
[JEP-709]
16 p2659 N71-29172

Accuracy of Doppler determinations of satellite ob-
serving station positions
[AD-72172]
17 p2846 N71-29420

Misweighing as important error source in activity
measurements to explain discrepancies between inter-
national measurement comparisons
[CNA-2-4169]
18 p2973 N71-30542

OBOS 2 satellite tracking accuracy comparisons of
SAO laser and NASA mobile ruby laser systems in-
cluding data analysis procedures
[DAO-486-92]
19 p3107 N71-31850

Cryogenic flow measurement facility performance
evaluation and accuracy statements for mass and volu-
metric flow
[NBS-TN-406]
19 p3075 N71-32730

Comparisons of accuracies of 500 mb charts made by
weather services of 8 different countries
[NLL-M-20657-5828.4F1]
21 p3452 N71-34572

Complete numerical algorithm for computing inter-
nal three-dimensional supersonic flows with second-
order accuracy
22 p3570 N71-35428

Accuracy of Cartesian and spherical coordinates of
OBOS 2 determined by synchronous observation from
Riga and Vigorod
22 p3677 N71-36221

Accuracy, adequacy, and limitations of NASTRAN
computer program static load structural analysis solu-
tions
22 p3682 N71-36258

Accuracy, usability, and economics of using NAST-
TRAN program
23 p3686 N71-36286

Effect of coefficient rounding in floating point
digital filters
[AD-727073]
24 p3898 N71-37784

Techniques for improving calibration accuracy stan-
dards from boundary layer calculations
[J71/23]
24 p3908 N71-37851

Instrument constants of astronomical cameras com-
pared with object positions obtained by other methods
[AD-727062]
24 p3926 N71-38012

ACETALDEHYDE
Paramagnetic resonance and mass spectroscopic
analysis of hydration products in aqueous acetal-
dehyde solutions
[JES-7015]
20 p3229 N71-33414

ACETALS
Synthesis of Schiff bases for heat shields by acetal
amine reactions
[NASA-CASE-XMP-00652]
22 p0176 N71-11243

ACETATES
Acetate content determination in polymeric materi-
als using gas chromatography
[AD-712512]
02 p0247 N71-11655

Chemical properties of cellulose acetate gels in both
dry and gel states
[NRC-TT-1439]
10 p1512 N71-21208

Macromolecular structure and distribution of
monomer units in ethylene-vinyl acetate copolymers
by method of infrared spectroscopy
[NLL-RTS-60231]
10 p1514 N71-21334

Kinetics of free radical initiated copolymerization
of 1-vinyl-3,5-dimethyladamantane and vinyl acetate
as function of glass transition temperatures
21 p3308 N71-34106

Peach scale model of improved cellulose acetate
membranes for reversed osmosis
[PS-199523]
21 p3444 N71-34507

Characterization, optimization, production, and
performance of cellulose acetate butyrate membranes
[PS-199504]
22 p3669 N71-35649

ACETIC ACID
NT ETHYLENEDIAMINETETRAACETIC
ACIDS
Derivation of pH CSTR dynamic equations based
on acetic acid-sodium hydroxide neutralization and
equilibrium equations for chemical reaction
13 p2040 N71-25046

Computerized simulation and time optimal control
of pH in acetic acid-sodium hydroxide CSTRs and

comparison with Ziegler-Nichols controller for chemi-
cal reaction
13 p2040 N71-25047

ACETONE
Crystallization of BSX solvents from nitromethane,
acetone, and acetone by evaporation of saturated
solutions studied by X ray diffraction
[ERDE-TM-18]
12 p1871 N71-23574

Nuclear dynamic polarization for investigating in-
termolecular dynamics in solutions of selected free
radicals and fluorocarbons in acetone
20 p3250 N71-33807

ACETYL COMPOUNDS
Decomposition of stabilized polyoxymethylene
under elevated pressure
[AD-714053]
07 p1049 N71-17956

Effect of lithium and calcium ions on
acetylcholinesterase activity of erythrocytes
[NASA-TT-F-13476]
09 p1333 N71-20179

EPR study of two anionic A liquid crystals using
vanadyl acetyl acetate as paramagnetic probe
[NASA-TN-D-6289]
14 p2270 N71-26047

Protein synthesis by catalytic polymerization of
aminoacrylates and effects of ammonium and various
catalysts
[NASA-TT-F-13713]
18 p2884 N71-30510

ACETYLENE
Nonequilibrium excitation origin in sodium atoms,
hydroxyl radicals, or water molecules occurring be-
hind hydrogen-oxygen or acetylene-oxygen com-
bustion shock waves
[NASA-TT-F-14422]
12 p1909 N71-23264

Preparation of dicyanooxyethylene and vinylidene
copolymers using organic compounds
[NASA-CASE-XMP-03250]
12 p1870 N71-23500

Gas laser and plasma tube operation and outputs in-
cluding acetylene laser design
[AD-720404]
14 p2266 N71-26051

Studying neutral oxidation of acetylene on platinum-
gold alloys at 80 C in solutions of constant pH and unit
normality
15 p3423 N71-27257

Consecutive ion-molecule reactions in acetylene in-
vestigated by charge exchange mass spectrometry as
function of energy transfer during initial ionization
[AD-722470]
18 p2884 N71-30719

Infrared molecular spectra of linear acetylene
molecule and its C13 enriched isotopic bands
18 p2988 N71-31501

Analysis of acetylene oxygen detonation spectra in
3000-6000 A
[MEIA-71-1]
20 p3364 N71-33405

Development of method for determining flow field
behind detonation wave formed by acetylene-oxygen
detonation based on wall heat transfer - Vol. 3
[MEIA-71-3]
23 p3867 N71-37571

Measurement of heat transfer from acetylene-oxy-
gen detonations in shock tube-Vol. 2
[MEIA-71-2]
23 p3868 N71-37572

ACIDOMETRIES
Comparison of aluminum 26 radioactivities of Bru-
derholm chondrites, lunar rocks, and schondrites
[NASA-TM-X-65578]
15 p2517 N71-27870

ACID BASE EQUILIBRIUM
Effects of changes in partial pressure of carbon
dioxide on acid-alkali equilibrium in human blood
16 p2546 N71-26409

Stress effects of intermittent exposure to 3 per cent
CO2 on acid-base balance and electrolyte excretion in
submarine personnel
[AD-722642]
18 p2877 N71-31238

ACIDITY
Potentiokinetic polarization, potentiostatic current-
time behavior, and electron microscopy of nickel dis-
solution surface topology in dilute acid solutions from
25 to 300 C
10 p1581 N71-21438

ACIDS
NT ACETIC ACID
NT AMINO ACIDS
NT ASPARTIC ACID
NT BENZOIC ACID
NT BUTYRIC ACID
NT CARBOXYLIC ACIDS
NT DEOXYRIBONUCLEIC ACID
NT ETHYLENEDIAMINETETRAACETIC
ACIDS
NT PATTY ACIDS
NT GLUTAMIC ACID
NT GLYCINE
NT HISTIDINE
NT HYDROCHLORIC ACID
NT HYDROFLUORIC ACID
NT LACTIC ACID
NT LEUCINE
NT NITRIC ACID
NT NUCLEIC ACIDS
NT OLEIC ACID
NT OXALIC ACID
NT PEPTIDES
NT PERCHLORIC ACID
NT PHOSPHORIC ACID
NT PYRIDINE NUCLEOTIDES
NT RIBONUCLEIC ACIDS
NT SULFURIC ACID

NT THYMINE
NT URIC ACID
Effects of acid and groups and structural anomalies
on thermal coloration of polycrystalline
[RAB-LIB-TRANS-1495]
13 p3041 N71-25138

Chemical reactions between alkyl-lead oxide silica
glasses and acid solution at low temperatures
18 p2940 N71-31264

ACOUSTIC ATTENUATION
NT SHOCK WAVE ATTENUATION
Measuring attenuation of first sound near lambda
transition point in liquid helium
[AD-713470]
05 p0734 N71-15275

Investigating deterioration in automatic power level
control due to violation of assumption of time-invari-
ance in underwater acoustic imaging
[SC-CR-70-0102]
05 p0735 N71-15646

Noise reduction of Boeing 707 during landing ap-
proach by modifying turbofan nacelle with polyamide
fiber glass acoustic sandwich materials
[NASA-CR-1713]
06 p0794 N71-15964

Acoustic attenuation determined experimentally
during engine ground tests of XB-70 airplane and com-
parison with predictions
[NASA-TM-X-2223]
07 p0974 N71-17951

Sonic boom in interaction of conical field and plane
shock wave
16 p2532 N71-28366

Suppression of acoustic modes of combustion instab-
ility in space shuttle engines by use of cavity resonators
[BC-71-28]
17 p2837 N71-29601

Attenuation and spatial coherence of underwater
acoustic signals generated by explosions in rough sea
[BMVG-PBWT-71-4]
18 p2890 N71-31174

Crystal defect effects on ultrasonic attenuation and
phase scattering in germanium
[AD-724328]
20 p3352 N71-33817

Critical velocity and attenuation changes for lon-
gitudinal and shear ultrasound in rare earth metals, in-
sulators, and Cr at magnetic transition temperatures
20 p3315 N71-33751

Multipath transmission and attenuation in deep
ocean and single range plots for interpretation of
acoustic and single-pulsed signal number and intensity
at receivers
[AD-727101]
24 p3966 N71-38294

ACOUSTIC COMBUSTION
U COMBUSTION STABILITY
ACOUSTIC DELAY LINES
Determination of delay time variations in acoustic
surface wave by measuring oscillation frequency
changes
01 p0052 N71-10220

Physical concepts in diffraction of light by ul-
trasonic waves and specific form of linear acoustic
delay lines
[AD-712975]
09 p0418 N71-13047

Performance of acoustic dispersive broadband sur-
face wave delay lines using Love and Rayleigh waves
[DASM-53-669-CLAC/PT]
10 p006 N71-28937

Design and fabrication of matched longitudinal
acoustic wave transducers with operation over 500
MHz bandwidth centered at 1.7 GHz
[AD-726028]
14 p2229 N71-26817

Broadband sound wave delay line with low insertion
losses
23 p3731 N71-36408

Delay line with acoustic transverse wave and inser-
tion loss compensation, using piezoelectric transduc-
ers
23 p3732 N71-36401

Large time bandwidth product microwave delay line
with acoustic surface wave operating at microwave
frequencies
[AD-726044]
23 p3733 N71-36410

Multipath thin film piezoelectric transducers for
sound wave generation, Rayleigh wave delay line sur-
face wave transducers, and dispersive surface wave
delay line study
23 p3734 N71-36418

Ray theory analysis of magnetoacoustic wave
propagation in ferromagnetic media with application
to delay lines
23 p3738 N71-36453

ACOUSTIC DUCTS
Mathematical model for two-dimensional, long-
wave propagation in curved acoustic ducts determin-
ing vibrational velocity distribution and variation and
phase of motion at any point in system
[NASA-TM-X-67184]
14 p2219 N71-26338

Flow-duct test facility data on acoustic behavior of
fluid ducts and duct-lining materials for turbojet en-
gines
[NASA-CR-111807]
14 p2199 N71-26417

Computer program for predicting subsonic flow of
slightly converging nozzles and acoustic liners in three
dimensional acoustic field
[NASA-CR-119941]
22 p3367 N71-35405

Long acoustic wave propagation in curved ducts
and junctions between straight and curved ducts utiliz-
ing Bessel functions for steady and decaying fields of
motion
[NASA-TM-X-67944]
23 p3601 N71-37103

ACOUSTIC EXCITATION

- Vibrational response of stiffened cylindrical shell to reverberant acoustic fields
[NASA-CR-114832] 07 p1124 N71-17562
- Low frequency excitation for inducing stress and cracking in metal samples applied to ultrasonic pulse-echo crack detection
[AD-716643] 09 p1396 N71-19634
- Acoustic resonant frequency computation of two and three dimensional cascade flow
[ESEP-100771] 11 p1734 N71-21908
- Development of electronic circuits for forming scanned acoustic holograms
[ARL/DST-73] 12 p1935 N71-24076
- Acoustically excited, incompressible, turbulent, subsonic Couette air flow around circular cylinder
13 p2066 N71-23839
- Acoustic resonance excited by vortex shedding from circular cylinders and thin plates in wind tunnels noise generation products
[AIRC-CP-1141] 15 p2365 N71-27716
- Evaluation of three methods for determining response analysis of plate and shell structures under random acoustic excitation
[NASA-CR-115903] 21 p3526 N71-35125
- Acoustic pressure distribution from forced harmonic vibrations of clamped circular plate in acoustic field
23 p3965 N71-37555

ACOUSTIC GENERATORS

U SOUND GENERATORS

ACOUSTIC IMPEDANCE

- Investigation of sound transmission into small enclosures, and induced coupling between shell modes
[AD-712452] 03 p4919 N71-13384
- Tables on mutual and self acoustic radiation impedance for pistons in plane infinite rigid baffles
[AD-718153] 12 p1967 N71-23949
- Development of nonlinear acoustic theory for rigid porous materials and concept of temporal impedance operator
[NASA-TN-D-4196] 16 p2639 N71-28777
- Inlet noise suppressors having perforated plate over honeycomb wall construction evaluated over range of passage heights and engine speeds using turbojet engine as noise source
[NASA-TN-D-4395] 18 p2872 N71-31096

ACOUSTIC INSTABILITY

- Guidelines for designing combustion stability control devices
[NASA-CR-111405] 02 p2920 N71-11884
- Stabilizing influence of acoustic cavities on acoustic modes of combustion instability in rocket engines
[NASA-CR-115067] 20 p3363 N71-32897

ACOUSTIC MEASUREMENTS

- Air and land transportation noise sources and measurement, noise level scales, and individual and community responses - conference
[PB-191117] 01 p0003 N71-10349
- Acoustic leak detection in water cooled liquid sodium steam generators
[AFDA-256] 01 p0084 N71-10483
- Determining feasibility of using transformer and common base preamplifier impedances matching to detect very low level electrical signals from accelerometers
[AD-711639] 01 p0013 N71-10690
- Measuring head velocities of elements, surface pressure, and far-field pressure of planar arrays of piston type sound sources
[AD-711567] 02 p0268 N71-11776
- Determining modulus of elasticity of bi-directional material by sound wave transmission
[AD-711799] 02 p0268 N71-11779
- Measurement of noise levels during OV-10 aircraft operations
[AD-712667] 03 p0313 N71-12230
- Maxima and pulse duration impulse acoustic measurements
[LEA-TR-265] 03 p0419 N71-13330
- Using acoustic emission techniques for flow detection in structural members of reactor pressure vessels
[IN-1398] 04 p0618 N71-14099
- Updated computer program for determining acoustic admittance to aluminum double-root solution and to fit root-mean-square data curves by statistical means
[NASA-CR-102838] 04 p0567 N71-14213
- Acoustic analysis for materials research and structural integrity evaluation
[UCRL-72505] 05 p0708 N71-15064
- Measurement of engine exhaust noise during ground operation of TB-70 aircraft
[NASA-TN-D-7043] 06 p0794 N71-15820
- Analyzing sound transmission through clamped circular plate set in infinite rigid wall exposed to dense acoustic medium and excited by obliquely incident plane wave
[AD-714381] 06 p0996 N71-16406
- Acoustic and structural path transmission through shroud enclosed spacecraft
[NASA-CR-116541] 06 p0952 N71-16882
- Measurement of variability of aircraft noise during low level flight flyovers
[NASA-CR-11752] 08 p1144 N71-18065

- Noise measurement evaluation of takeoff and approach profiles optimized for noise abatement
[NASA-TN-D-6246] 08 p1144 N71-18029
- Sources and characteristics of aircraft noise for conventional and V/STOL aircraft
09 p1320 N71-19457
- Acoustic measurements of deflected jet VTOL aircraft
[AD-719939] 09 p1320 N71-19549
- Determining types of acoustical measurements suitable for test section of NASA Langley wind tunnel
[NASA-CR-111068] 09 p1364 N71-19630
- Inlet plenum chamber noise measurement comparison of 20 inch diameter fan rotors with aspect ratios of 3.6 and 6.6
[NASA-TN-X-2191] 09 p1516 N71-19707
- Sound pressure levels produced by C-5A during ground tests
[AD-716814] 10 p1006 N71-20624
- Urban air and surface vehicle noise levels and abatement potential
[OBT-ONA-71-1-VOL-3] 10 p1607 N71-21083
- Model studies of room acoustics, sound insulation measurement, and traffic noise estimation near roadways
[AD-716950] 10 p1607 N71-21372
- Design and test evaluation of prototype one-third octave band spectrum analyzer for measurement and analysis of acoustic and vibration data onboard space vehicles
[NASA-CR-111860] 11 p1761 N71-22023
- Underwater acoustic measurements of dolphins and harbor porpoise activity under various situations and conditions
11 p1682 N71-22217
- Automatic, remotely controlled noise-level recorder for telecommunication equipment production, calibration, and maintenance
12 p1679 N71-23649
- Identification and control of aerodynamic factors associated with aircraft noise and acoustic measurements during C-141 operational missions
[AD-718097] 12 p1857 N71-23748
- Industrial foundry acoustic and vibration measurements and intensity and octave spectrum analysis
[NASA-TT-F-13604] 12 p1964 N71-23829
- Climbout and landing approach noise measurements for three engine turbofan transport aircraft
[NASA-TN-D-6137] 13 p2023 N71-24582
- Procedure for measuring ordinary threshold displacements and production of ordinary masking patterns
[FAA-AM-71-1] 13 p1214 N71-24746
- Interior sound pressure measurements in C-5A aircraft
[AD-719746] 13 p2027 N71-25060
- Analysis of noise radiated from submarines and various aspects of underwater acoustics
[AD-719736] 13 p2126 N71-25168
- Acoustic measurements on prop-fan model propulsion system - Vol. 2, appendices
[NASA-CR-111842-2] 14 p2295 N71-25784
- Acoustic measurements on prop-fan model propulsion system
[NASA-CR-111840-1] 14 p2296 N71-25785
- Numerical analysis of loudness, loudness level, and sound-pressure level of pure tones of steady noise that does not exceed critical bandwidth
[NASA-TN-X-2256] 14 p2204 N71-25789
- Industrial noise and countermeasures - research methods and measuring devices
[AD-720414] 14 p2296 N71-25787
- Familiarization of Federal Aviation Administration personnel in acoustic measurement techniques and procedures involved in noise certification of aircraft
[HEC-TR-300] 14 p2198 N71-26304
- Techniques and procedures for measuring effective perceived noise level during aircraft noise type certification
[HEC-TR-300-SUPPL-2] 14 p2198 N71-26305
- Acoustic measurements of helicopter rotor noise at hover
[AD-721312] 16 p2531 N71-28275
- Extrapolation of measured overpressure data for predicting sonic boom characteristics of different aerodynamic configurations
16 p2536 N71-28392
- Pulsed ultrasonic telemetry for determining rock properties in iron ore mine
[NASA-TT-F-13636] 16 p2509 N71-28836
- Noisierous noise of flames from co-firing jets of fuel and oxidizer and flames from impinging jets of fuel and oxidizer
17 p2787 N71-29702
- Statistical energy analysis for studying dynamic behavior of large, complex structures and acoustic spaces
[NASA-CR-110987] 17 p2789 N71-29808
- Development of noise measurement units for airport and aircraft noise reduction and psychoacoustic studies
18 p2871 N71-30786
- Feasibility of model acoustic measurements in wind tunnel for predicting total sound power
[NASA-CR-114532] 18 p2882 N71-30825

- Acoustical measurements of vortex noise for rotating blades with and without shed vane blade development - tables
[NASA-TN-D-4364] 18 p2845 N71-34028
- UH-1P helicopter acoustic measurements during profile and rocket firing including biplanar flow field
[AD-713830] 19 p3043 N71-35610
- Ultrasonic and nondestructive testing of pressure vessels for reactor safety
[PB-192774] 19 p3141 N71-32710
- Performance and acoustic near field measurements on variable camber propeller having STOL applications
[AD-724145] 20 p3308 N71-32912
- Underwater sound propagation analyzed using geometric ray acoustics
[AD-724349] 20 p3310 N71-32908
- Acoustic data obtained during launch of ESSO I-3 satellite and GRS-A satellite by Scout launch vehicle
[NASA-TN-D-43509] 20 p3354 N71-33040
- Ultrasonic measurements on electromagnetic induction near the superconducting transition temperature
20 p3312 N71-33571
- Inventory of acoustic fatigue test facilities in NATO countries
[AQARD-R-584-71] 21 p3408 N71-34228
- Acoustic back-scattering measurements from dynamic model of sea surface
[PHEL-1971-5] 21 p3463 N71-34661
- Evaluating reciprocity combining engine noise at two different places using subjective and objective measurements
[NASA-TT-F-13043] 22 p3628 N71-33860
- Measurement of sound absorption coefficient in sea water at frequencies from 6.1 to 30 kHz as function of temperature and salinity
[POA-3-C-3608-57] 22 p3639 N71-33961
- Program for tidal measurements in Pacific area
23 p3707 N71-34978
- Loudness comparisons between profiles of simulated tones having different envelope shapes and spectra
[TRANS-2713-1922.811] 23 p3885 N71-37127
- Design and performance of continuous wave ultrasonic interferometer for measuring transit time of sound waves in solids
[NFO-2504-77] 24 p3904 N71-36086

ACOUSTIC PROPAGATION

- Diffraction evidence for acoustic rays in three dimensional medium moving with arbitrary velocity
[AD-713191] 01 p0050 N71-10706
- Coupled electromagnetic and electron acoustic wave propagation in inhomogeneous plasma sheet
[AD-713910] 06 p1273 N71-10600
- Air-coupled acoustic energy loss and through rail with emphasis on shear wave propagation
[AD-716342] 09 p1424 N71-19851
- Energy transport velocity model for classification of all possible acoustic modes propagation in medium, in-vicinity, homogeneous, time independent ducted air flow
[ONERA-TR-945] 20 p3251 N71-33330
- Solution of acoustic field due to monochromatic point source located in stratified media by direct numerical integration of hydrodynamic field equations
24 p3968 N71-36080

ACOUSTIC PROPERTIES

- NT ACOUSTIC IMPEDANCE
NT ACOUSTIC INSTABILITY
NT ACOUSTIC SCATTERING
NT ACOUSTIC VELOCITY
NT REVERBERATION
NT SOUND INTENSITY
NT ZERO SOUND
- Ultrasonic holographic and light diffraction techniques applied to coherent acoustic imaging during nondestructive tests
[AD-711685] 01 p0008 N71-10097
- Research in Bragg diffraction from magnetosonic waves using acoustic surface waves
[AD-711101] 01 p0091 N71-10027
- Ultrasonic method for studying structure of wave cover
[AD-711918] 02 p0228 N71-12104
- Acoustic properties of supersonic fan with short blade span
[NASA-TN-X-52937] 03 p0311 N71-12210
- Propagation of stress pulses in stratified elastic medium
[AD-712376] 03 p0997 N71-13151
- Behavior of acoustic and acoustic waves in three dimensional acoustic fields
[NASA-CR-102908] 05 p0700 N71-14642
- Acoustic and flow characteristics of subsonic and supersonic jets from convergent nozzles
[NASA-CR-1095] 05 p0864 N71-14980
- Acoustic instability of burning in cold fuel rocket engines associated with reflections from burning surface
[AD-713753] 05 p0761 N71-15331
- Mechanism describing vibrational and acoustic properties of sonic booms
[NASA-CR-111639] 06 p0830 N71-14989
- Useful mechanical, electrical, and acoustic properties of BaTiO₃
[AD-714229] 06 p0870 N71-14982

Measuring acoustic parameters of volcanic rocks from conventional and shear wave velocities [USGS-474-49] 06 p0851 N71-16388

Shock tube procedure and tone-burst technique for evaluating sound absorption of materials at high intensities [NASA-CR-1698] 06 p0907 N71-16660

Application of acoustic-boiling-detection techniques to liquid metal cooled reactors [ANL-7449] 07 p1063 N71-17249

Sound transmission through liquids and fundamental liquid state research [AD-715165] 07 p1069 N71-17845

Ultrasonic absorption and velocity measurements in liquid alkali metals [AD-714864] 07 p1045 N71-17912

Linear velocity models and linear reverberation calculations [NASA-CR-116418] 07 p1117 N71-18119

Acoustic properties of plastic flow in magnetostrophic and metallic materials [AD-715654] 08 p1243 N71-18567

Acoustical properties of liquid base foams and application for jet noise reduction [NASA-CR-16955] 08 p1285 N71-19139

Tubulated mechanical and acoustic properties for selected foams, nonferrous, and plastic materials [AD-716033] 09 p1404 N71-19676

Investigation of generation of sound by jet of air at high subsonic velocity issuing from slot nozzle and passing over rigid flat plate of finite dimensions [RAE-LIB-TRANS-1466] 08 p1541 N71-21226

Information on parameters associated with generation of acoustic energy by boiling bubbles [AO-3911-53] 10 p1609 N71-21778

Ocean bottom acoustical properties and long range sound performance [AD-719935] 13 p2126 N71-25421

Numerical analysis of loudness, loudness level, and sound-pressure level of pure tones of steady noise that does not exceed critical bandwidth [NASA-TM-X-2298] 14 p2204 N71-25789

Measurement of acoustic output from long sparks produced during electrical discharge from laboratory equipment 14 p2296 N71-25826

Frequency distribution of acoustical and exocoustic emissions from metal fatigue [AD-723598] 14 p2347 N71-25932

Measurement of second harmonic distortion in acoustic output of transducer by Michelson laser interferometer technique [AD-721721] 16 p2592 N71-28309

Slotted blades and vanes and rotor tip design for tightly loaded, low speed fan stage applicable to low noise aircraft engines [NASA-CR-729653] 16 p2671 N71-28315

Development of wind tunnel microphone structures to minimize effects of vibrations and eliminate unwanted signals in microphone output [NASA-CASB-XNP-00250] 16 p2578 N71-28779

Acoustic emission analysis of material properties and defect structure [UCRL-72457] 17 p2786 N71-29268

Structural response and acoustic transmission characteristics of glass pane and standard wood frame construction wall panels subjected to sonic booms [NASA-CR-111925] 19 p3190 N71-32488

Physical models for measuring acoustic instabilities of high temperature gaseous uranium for use in gaseous core nuclear reactor system 20 p3304 N71-33451

Adaptation of NASTRAN program to solve acoustic mode problems of solid rocket motor cavities by finite element method 22 p3684 N71-36271

Changes in acoustic properties of perforated plates resulting from interaction of flows normal and tangential to plate surface [NASA-TM-X-2361] 23 p3804 N71-37119

Acoustoelectric surface wave amplifier with net terminal gain, low power dissipation, and stable continuous drift field operation 23 p3837 N71-37365

ACOUSTIC RADIATION
U SOUND WAVES
ACoustic SCATTERING
NT REVERBERATION
Experimental investigation of characteristics of acoustic energy reflected from rough, time-varying surfaces [AD-730468] 05 p0731 N71-14505

Design, assembly, and test of six-frequency noise array system [AD-713236] 05 p0646 N71-14933

Mathematical models for acoustic scattering by grooved elliptic cylinder with nonlinear resistance [NASA-TM-X-67019] 10 p1607 N71-21408

Approximative sound wave scattering behind sonic boom overpressure signatures 16 p2532 N71-28348

Atmospheric turbulence effects on sonic boom shock wave scattering 16 p2532 N71-28369

Anomalous rise times of acoustic sonic boom waveforms caused by atmospheric turbulence 16 p2533 N71-28374

Pressure pulse diffraction by three dimensional structural corner subjected to sonic boom 16 p2533 N71-28375

Statistical analysis including covariance functions of underwater acoustic scattering from lake surface [AD-724333] 20 p3310 N71-33042

Acoustic scattering theory and echo sounding profile used to estimate magnitude of ocean bottom roughness [AD-724321] 20 p3258 N71-33083

Measurement of hypersonic sound speeds in methane at moderate pressure and comparison with ultrasonic speed data 20 p3274 N71-33477

Temporal and spatial variations in underwater acoustic scattering layers in Pacific Ocean off Oregon coast [RL0-1750-62] 21 p3417 N71-34312

Acoustic back-scattering measurements from dynamic model of sea surface [PHL-1971-5] 21 p3465 N71-34661

Integral equation methods for calculating sound radiation and scatter from arbitrary closed surface [AD-726404] 22 p3630 N71-35863

Diffraction of plane acoustic waves by free orthogonal trihedron [three dimensional corner] 23 p3788 N71-37882

ACOUSTIC SIMULATION
Transmission of sonic booms into rooms through open windows 04 p0473 N71-13413

Acoustic signature analyses for bearing and gear failure mode identification 09 p1393 N71-20227

Prediction methods for sonic boom generation and propagation with overpressure minimization in supersonic transport design and operation [NASA-SP-253] 16 p2532 N71-28363

Wind tunnel models for sonic boom simulation at high Mach numbers 16 p2533 N71-28377

Sonic boom in near field and far field of nonlifting rectangular wing 16 p2534 N71-28379

Wind tunnel effects on experimental sonic boom signature determinations 16 p2534 N71-28383

Aircraft design and atmospheric turbulence effects on sonic boom generation and overpressure prediction methods using flight test data 16 p2536 N71-28393

Limitations of overpressure prediction methods for sonic boom configuration research 16 p2536 N71-28394

Acoustic vibration tests for noise reduction by helium and polyurethane foam in stainless steel cylinders for application as Skylab and Apollo vibration isolators 16 p2683 N71-29101

Optimal digital controller based on linear approximation of acoustical test facility, for determining effects of supersonic rocket engine noise on vehicle surface [NASA-CR-115073] 18 p2902 N71-30741

Human reactions to sleep deprivation by simulated sonic booms [ISVR-TR-41] 20 p3226 N71-32865

ACOUSTIC STABILITY
U FREQUENCY STABILITY
ACOUSTIC STREAMING
Flow acoustic problems of ventilators, sound production mechanisms, and noise reduction [NASA-TT-F-13798] 20 p3252 N71-33411

ACOUSTIC VELOCITY
Penetration of sonic boom energy into ocean in experimental simulation [AD-711963] 01 p0002 N71-10094

Measuring velocity of sound through two-component solid-gas medium as function of solid particle concentration [AD-712412] 05 p0418 N71-13048

Sound velocity in iron and iron alloys in solid and liquid state [LA-578-21] 06 p0907 N71-16756

Applying fundamental concepts of thermodynamics of irreversible processes to acoustic wave propagation in two-phase steam media 07 p1067 N71-17011

Sonic velocity and startup considerations in heat pipe design [LA-4518] 08 p1305 N71-18944

Dynamics of ocean movements in Sargasso Sea revealed in sound velocity and temperature measurements made aboard Atlantic 2 cruise 23 during June, July, and August 1966 [AD-718343] 12 p1907 N71-23523

Total analysis of processes influencing sound propagation and speed in two-phase media based on thermodynamics of irreversible processes [NASA-TT-F-13582] 13 p2064 N71-24598

Derivation of equations for coupled gas species concentration equations in chemical equilibrium using free energy and equilibrium methods for specific heat and acoustic velocity calculations [AD-728046] 14 p3213 N71-25941

High pressure shock and acoustic velocity data for calculating equation of state of aluminum 14 p3297 N71-26492

Shear acoustic velocity of ferroelectric phase transition at 122 K of K₂FeP₄ single crystals 15 p2453 N71-27509

Molecular structure, detonation, acoustic velocity, density, and pyrolysis of isomeric diazo methane and propane [AD-723483] 17 p2713 N71-27897

Electroacoustic transducer measurements of secondary sound velocity and inertial mass as function of He-3 concentration and temperature of He-3/He-4 mixture vapor pressure 17 p2789 N71-28293

Sound velocity in low temperature carbon dioxide (TRG-2078) 18 p2962 N71-30647

Velocity seismograms from underground nuclear explosion [NVO-1163-218] 19 p3092 N71-32114

Critical velocity and attenuation changes for longitudinal and shear ultrasound in rare earth metals, insulators, and Cr at magnetic transition temperatures 20 p3313 N71-33751

Penetration of ion-acoustic barrier when alternating current flows in toroidal magnetized plasma [CN-2878-10] 24 p3983 N71-38439

ACOUSTIC VIBRATIONS
U SOUND WAVES
ACOUSTICS
NT BIOACOUSTICS
NT HARMONIC GENERATIONS
NT MAGNETOACOUSTICS
NT PSYCHOACOUSTICS
NT UNDERWATER ACOUSTICS
Acousto-optic Q switch device considerations [AD-712977] 03 p0308 N71-13821

Survey on acoustics technology emphasizing noise reduction and human tolerances [NASA-SP-5093] 04 p0568 N71-14307

Acoustic emission testing and microstructure processes in solids [AD-715019] 07 p1127 N71-17953

Bibliography, and review of acoustic surface waves [AD-715674] 08 p1146 N71-18537

Physiological and psychological limits and ranges of human response to acoustic stimuli 09 p1335 N71-28352

Farfield and nearfield acoustic environments of space shuttle 13 p2171 N71-24667

Far infrared, thermal, and sound phenomena in solid-state physics [NYO-3391-126] 15 p2469 N71-27579

Low pressure turbofan rotor, stator, frame, and exhaust nozzle designs for turbofan engine noise reduction including acoustics and engine tests [NASA-CR-72967-VOL-2] 16 p2673 N71-29108

Biomedical electronics, information sciences, plasma and quantum electronics, cold state electronics, acoustics, and radio sciences [AD-722873] 17 p2727 N71-29499

Scattering of plane waves from thin rigid porous elliptic cylindrical shells and Mathieu function [NASA-TN-D-6348] 18 p2966 N71-31435

ACQUISITION
NT DATA ACQUISITION
NT TARGET ACQUISITION
ACRYLATES
Adhesive resins used for retarding regression in ablative material [NASA-CASE-XLB-63913] 04 p0620 N71-14052

Transport of noble gases in poly(methyl acrylate) [AD-712411] 14 p2341 N71-26250

ACRYLIC RESINS
Copolymerization of esters of bis allyltrimethyl phosphonic acid with methylmethacrylates [AD-713459] 05 p0780 N71-15270

Stress evaluation of prototype spherical acrylic underwater hull [AD-715772] 08 p1296 N71-16923

Flat disc acrylic windows for new-rated hyperbaric chambers for experimental diving suit [AD-716751] 10 p1651 N71-20736

Characteristics of acrylic windows for use in hydrostatic pressure vessels and underwater vehicles [AD-710812] 12 p2006 N71-23901

Developments in production of nylon fabric to improve garment comfort and thermal resistance through diffusion and copolymerization of polyacrylic acid [AD-722913] 19 p3119 N71-31731

ACRYLONITRILES
Preparation and properties of polyacrylonitrile fibers with different acrylonitrile comonomers [RAE-LIB-TRANS-1464] 05 p0789 N71-15175

Effects of acid and group and structural anomalies on thermal coloration of polyacrylonitrile [RAE-LIB-TRANS-1495] 13 p2041 N71-25138

Thermal degradation of polyacrylonitrile polymers for conversion to high modulus carbon and graphite reinforcement fibers
[AD-72205] 17 p2760 N71-29546
Stretching and heat treatment effects on microstructure of polyacrylonitrile fibers
[RAE-LIB-TRANS-1508] 17 p2771 N71-30392
Fabrication and environmental tests of circuit boards with polyimide plastic dielectrics and pyrolyzed polyacrylonitrile conductors
[NASA-CR-119994] 22 p3562 N71-35373

ACTH
ADRENOCORTICOTROPIN [ACTH]

ACTINIDE SERIES
NT AMERICIUM
NT AMERICIUM ISOTOPES
NT AMERICIUM 241
NT BERKELIUM
NT CALIFORNIUM
NT CALIFORNIUM ISOTOPES
NT CURIUM
NT CURIUM ISOTOPES
NT CURIUM 244
NT LAWRENCIUM
NT NEPTUNIUM
NT NEPTUNIUM ISOTOPES
NT NOBELIUM
NT PLUTONIUM
NT PLUTONIUM ISOTOPES
NT PLUTONIUM 238
NT PLUTONIUM 239
NT PLUTONIUM 240
NT PLUTONIUM 241
NT RADIUM
NT RADIUM ISOTOPES
NT RADIUM 226
NT THORIUM
NT THORIUM ISOTOPES
NT TRANSURANIC ELEMENTS
NT URANIUM
NT URANIUM ISOTOPES
NT URANIUM 232
NT URANIUM 233
NT URANIUM 235
NT URANIUM 238

Phase transformations in actinides
[UCRL-72557] 05 p0390 N71-12738
Complexing ability of trivalent lanthanides and actinides in chloride solution
[ORNL-TR-2342] 04 p0484 N71-13442
Periodicity of lanthanide and actinide properties
[JNRL-1212] 14 p2303 N71-26201
Revised periodic table for incorporating actinides and lanthanides
[UCRL-TRANS-10510] 15 p2376 N71-26886
Neutron cross sections at thermal, resonance, and fast energies for transactinoid isotopes
[KFK-1186] 16 p2641 N71-28020
Single particle energies, wave function potentials and odd parity levels of actinide nuclei
[JNRL-54-5470] 16 p2644 N71-28098
Crystal structure and morphology of hydrous oxides and hydroxides in lanthanide and actinide series
[ORO-3953-2] 16 p2667 N71-28797
Electronic band structure and physical properties of actinide metals and their compounds
[COO-2103-3] 21 p3439 N71-34469

ACTINIDE SERIES COMPOUNDS
NT NEPTUNIUM COMPOUNDS
NT PLUTONIUM COMPOUNDS
NT PLUTONIUM OXIDES
NT THORIUM COMPOUNDS
NT THORIUM OXIDES
NT URANIUM CARBIDES
NT URANIUM COMPOUNDS
NT URANIUM FLUORIDES
NT URANIUM OXIDES

Magnetic permeability, electrical resistivity, and specific heat measurements on actinide carbides and actinide nitrides
[CEA-R-4113] 15 p2471 N71-27415

Electronic band structure and physical properties of actinide metals and their compounds
[COO-2103-3] 21 p3439 N71-34469

ACTINOMETERS

NT INFRARED DETECTORS
NT INFRARED SCANNERS
NT INFRARED SPECTROMETERS
NT INFRARED SPECTROPHOTOMETERS
NT MICROWAVE RADIOMETERS
NT PYRANOMETERS
NT RADIOMETERS
NT SOLAR SPECTROMETERS
NT SPECTROHELIOGRAPHS
NT SPECTROPHOTOMETERS
NT SPECTROPHOTOMETERS
NT ULTRAVIOLET SPECTROMETERS
NT ULTRAVIOLET SPECTROPHOTOMETERS

Computer programs for processing actinometric data from satellite data transmissions
[NASA-TT-N-13367] 02 p0167 N71-11317

Equations for radiation heat cells, which are used for designing actinometric and radiometric devices
06 p0961 N71-16999

Corrective shadow effect calculations for sunshade recorder location
[NLL-M-20185-5828.48F] 12 p1879 N71-23670
Soviet meteorological satellite borne actinometric equipment and systems engineering
[JPRS-53137] 14 p2253 N71-23838

Actinometers for measuring atmospheric turbidity characteristics, resulting from general statistical regularities
[AD-72064] 14 p2247 N71-29599
Climatology of net radiation of earth surface atmosphere system deduced from satellite actinometric measurements
15 p2400 N71-27494

ACTIVATION

Activation of some UO₂ powders by milling and oxidation-reduction
[WHAN-FR-8] 07 p1066 N71-17684
Internal and superficial oxygen content of molybdenum samples determined by activation with 54-MeV alpha particles
[LYCEN-7076] 14 p2316 N71-26746
Activation enthalpy of carbon self diffusion in cubic carbides
[LA-TR-71-13] 16 p2667 N71-28847
Measuring spatial distribution of iodine activation in water using Cf-252 source with results compared with computer program calculations
[WAPD-TM-991] 23 p3813 N71-37187

ACTIVATION ANALYSIS

NT NEUTRON ACTIVATION ANALYSIS
Instrumental activation analysis of rare earth mixtures
[IS-T-340] 02 p0271 N71-11742
Measuring fast neutron spectra in core and thermal column of Bikkio reactor by foil activation method
[IAERU-7001] 02 p0278 N71-12180
Activation technique for absolute calibration of standard long counter in neutron energy range from 30 to 1300 keV
[AERE-R-6429] 03 p0432 N71-12935
Use of X ray detectors in activation analysis
[IRI-133-70-1] 04 p0571 N71-13616
Beryllium determination in gamma activated samples
[Y-1733] 04 p0573 N71-13650
Nondestructive activation analysis of environmental samples, and computerized data reduction
[COO-1705-6] 04 p0581 N71-14074
Investigating flux characterization and neutron cross sections in EBR-2 using foil activation techniques
[ANL-7629] 05 p0738 N71-15008
Instrumental activation analyses of abundances in lunar rock chips
07 p1113 N71-17714
Instrumental activation analysis technology for analysis of meteorites and lunar materials
07 p1113 N71-17715
Monodimensional burnup code for reactor core also radial distribution of short-lived activations
[FN-E-109] 08 p1248 N71-18196
Microdetermination of fluorine in high purity tungsten by nondestructive photoactivation analysis
[GA-10125] 08 p1256 N71-18373
Radiochemistry activation analysis feasibility using gamma photons of 18 to 27 MeV
[NLL-CE-TRANS-5208-59022.09] 10 p1616 N71-21171

Comparison of charged particle activation analysis and infrared spectroscopy for carbon and oxygen trace contaminant determination in silicon and aluminum
14 p2214 N71-26262
Determination of zirconium and hafnium in meteorites and terrestrial materials by activation analysis and chemical separation after neutron irradiation
14 p2338 N71-26351
Determination of low oxygen contents in silicon by alpha particle activation
[LYCEN-7060] 14 p2329 N71-26384
Alpha, deuteron, and helium 3 activation determination of carbon isotopes
[ORO-3972-2] 16 p2660 N71-29191
Operating characteristics of nuclear reactor for activation analysis and application to research activities
[NBS-TN-540] 17 p2731 N71-30034
Bibliography of activation analysis publications up to 31 Jan. 1971
[NBS-TN-467-PT-1] 17 p2717 N71-30266
Activation analysis bibliography up to 31 Jan. 1971 including chemical element, methodology, matrix analysis, and author indexes
[NBS-TN-467-PT-2] 17 p2717 N71-30267
Photoproduction of charged pions from nuclei measured by activation analysis
[LUNF-7007] 18 p2973 N71-30546
Effect of activation by magnesium and calcium on thermoluminescence and X ray luminescence of LiF crystals
[ANL-TRANS-874] 18 p2999 N71-31457

Pneumatic rabbit system for activation analysis with short-lived radionuclides, emphasizing oxygen analysis
[KFK-1293] 19 p3148 N71-32054

Review of nuclear methods for trace analysis including activation analysis
[BARC-529] 19 p3153 N71-32323

Application of gamma-gamma coincidence counting techniques to nondestructive activation analysis of meteoric materials
19 p3051 N71-32394

Irradiated cobalt and tantalum tracers measured by activation analysis in river and sea arm sediment transport studies
[IRI-133-70-06] 20 p3316 N71-33440

Neutron spectra determination from activation data using RP01 only for threshold detectors and RP07 codes
[KFK1-70-30-RPT] 22 p3631 N71-35075

Correlation of irradiation data using activation fluxes and irradiation temperature
[NASA-TM-X-67098] 23 p3760 N71-36839

Comparison of bubble method and end measurements of Al and Cu activities in molten Al-Cu alloy reactions with AlCl₃
[NLL-RTS-6273] 23 p3774 N71-36889

Neutron energy dependent cross section of LMFBR determined by foil activation method
[WHAN-SA-107] 23 p3816 N71-37216

ACTIVATION ENERGY

Activation energy for apparent gaseous diffusion of hydrogen in multi-run metal are welding deposits
02 p0367 N71-13315
Spin-echo technique of nuclear magnetic resonance used to determine activation energy of aluminum
[IS-T-410] 07 p1079 N71-17944
Arrhenius activation energy and reaction rate constants for polyphenylene oxide
[AD-715358] 08 p1223 N71-10825
Calculation techniques for estimating heat power levels of radioactive decay of fission and activation products
13 p2113 N71-24331

Activation energy and hole mobility in aluminum determined by nuclear magnetic relaxation including temperature effects
[COO-1198-801] 15 p2477 N71-27330

Heat activated cell with aluminum anode
[NASA-CASE-LEW-11559] 16 p2538 N71-28579
Measurement of 472 state lifetimes in ruby with fluorescent and nonfluorescent transitions and dynamic model including activation energies, Franck-Condon principle, and frequency factors
16 p2658 N71-29145

Determination of activation energy of superheated solid solution of manganese in aluminum by plasma-spraying
[SC-RR-70-356] 19 p3116 N71-33644

Nuclear magnetic resonance spin echo method used to determine self diffusion activation energy in aqueous solutions of electrolytes
20 p3230 N71-33623

ACTIVE SATELLITES

NT EARLY BIRD SATELLITES

ACTIVITY (BIOLOGY)

Psychophysiological stimulation of humans, monkeys and rats by color schemes for spacecraft cabin interiors
16 p2550 N71-28239

Design and performance of relief valve assembly for metabolic activity system of biological experiment on orbital workshop vehicle
[NASA-CR-119177] 17 p2757 N71-30152

Development of analog model of neuron adaptation and simulation of spontaneous activity of neuron network
[JPRS-53597] 19 p3043 N71-32802

Characteristics of water environment and relationship to biogeocenology
20 p3224 N71-33511

Effect of solar radiation on energy balance of biogeocenosis
20 p3224 N71-33512

Application of biogeocenology principles to land reclamation activities
20 p3224 N71-33513

ACTIVITY CYCLES (BIOLOGY)

Adaptation of human physiological functions and performance to variations in diurnal sleep and wakefulness cycles
16 p2543 N71-28238

ACTUATORS

Peristaltic action microinch actuator for primary mirror active-optics system of orbiting astronomical telescope
[NASA-CR-1658] 01 p0052 N71-10011

Design and data for selecting aerodynamic surface control and thrust vector control servomotor
[NASA-CR-106685] 02 p0149 N71-11609

Review of pneumatic piston type actuators for prosthetics
[BAE-TR-68027-REV] 05 p0094 N71-15576

Thermally-actuated explosive release mechanism for actuator device
[NASA-CASE-XGS-00624] 06 p0064 N71-16070

SUBJECT INDEX

Burst diaphragm flow initiator for installation in short duration wind tunnels
 (NASA-CASE-MPS-12913) 07 p1004 N71-17600

Mechanical and electrical design of actuator for SEKT 7 spacecraft
 (NASA-TM-X-3150) 07 p0976 N71-17865

Performance of valve operated by cartridge discharge pressure
 (UCRL-50930) 07 p1038 N71-18069

Hand controller operable about three respectively perpendicular axes and capable of actuating signal generator for attitude control devices
 (NASA-CASE-XMS-07487) 12 p1925 N71-23255

Mechanical actuator wherein linear motion changes to rotational motion
 (NASA-CASE-XGS-04548) 12 p1929 N71-24045

Actuated louvers for satellite thermal control in microenvironment
 14 p2351 N71-25697

Hydraulic actuator design for space deployment of heat radiators
 (NASA-CASE-MSC-11817-1) 14 p2264 N71-26611

Electromechanical control actuator system using deflex differential screws
 (NASA-CASE-HRC-10022) 14 p2264 N71-26635

System to control speed of hydraulically movable members by limiting energy applied to actuators with hydraulic servo loop
 (NASA-CASE-ARC-10131-1) 15 p2416 N71-27754

Bearings, lubricants, and seals for lubricated and hydraulic components for space shuttle with high temperature and vacuum operating capabilities
 17 p2755 N71-29469

Reversion pole-face windings power system with high voltage transformer actuator
 (UCRL-20191) 20 p3247 N71-33889

Development and characteristics of gas operated actuator designed to eliminate need for external supply of drive gas for operation
 (NASA-CASE-NPO-11369) 21 p3432 N71-34419

Development and characteristics of redundant hydraulic control system which operates following failure of one or two major control elements
 (NASA-CASE-MPS-20844) 21 p3433 N71-34426

History actuator design for displaying pivotally supported structure onboard spacecraft
 (NASA-CASE-NPO-10680) 21 p3520 N71-35080

Hydraulic power and actuation requirements of survivable flight control system utilizing fly by wire control for F-4 aircraft
 (AD-727763) 24 p3873 N71-37608

ACTIVITY

NT VISUAL ACUITY

Acoustic evaluation of aging pilots hearing acuity in relation to flying time
 11 p1690 N71-22320

ADAPTATION

NT ACCLIMATIZATION

NT ALTITUDE ACCLIMATIZATION

NT COLD ACCLIMATIZATION

NT LIGHT ADAPTATION

NT RETINAL ADAPTATION

Adaptation techniques for human tasks and man machine systems
 (AD-711965) 02 p0170 N71-11205

Physiological adaptation problems during long range aerial troop deployment
 (AD-714348) 06 p0802 N71-16411

North Atlantic Treaty Organization conference on adaptation and acclimatization in aerospace medicine
 (AGARD-CP-82-71) 09 p1334 N71-20351

Stress and adaptation problems associated with large scale, long range, rapid reaction time, aerial troop deployments
 09 p1336 N71-20360

Effects of education and pharmacodynamics on adaptability of human beings to degraded sensorial environments
 09 p1337 N71-20364

Computer program for converting IBM FORTRAN to CDC 6600 computer use
 (LA-4355) 10 p1530 N71-21658

Adaptation of human physiological functions and performance to variations in diurnal sleep and wakefulness cycles
 16 p2543 N71-28258

Environmental adaptation and operational performance of humans in space missions
 16 p2554 N71-28547

Physiological adaptation to unilateral otosclerotic ear impairment compared to unilateral labyrinthectomy
 (ASRU-R-67-3) 18 p2881 N71-31541

Adaptation of terrestrial microorganisms to simulated space environment
 (NASA-TT-F-15944) 23 p3714 N71-36472

ADAPTERS

NT MULTIPLE DOCKING ADAPTERS

Closed circuit television air guidance adapter for air to air intercepting vehicle
 (NASA-CASE-102896) 01 p0861 N71-10974

Camera adapter design for image magnification in display line and illuminator
 (NASA-CASE-XMP-03844-1) 14 p2256 N71-26474

Electric connectors, adapters, and cables - technology transfer

(NASA-SP-5934/01) 19 p3067 N71-32371

Electric equipment and drive adapter endurance tests for INAP 8

(NASA-CASE-72938) 24 p3960 N71-38248

ADAPTIVE CONTROL

NT SELF ADAPTIVE CONTROL SYSTEMS

NT SELF ADAPTIVE CONTROL SYSTEMS

Qualitative analysis of adaptive control systems using random search algorithm convergence in continuous time
 (RB-3963) 01 p0076 N71-10821

Evaluating use of adaptive techniques in control of tasks or stimuli
 (AD-712124) 02 p0158 N71-11120

Amorphous semiconductor switches for control elements in electroluminescent display panel
 (AD-712546) 02 p0192 N71-11349

Self organizing control system demonstrator to obtain minimum variance principles pertaining to control of flight vehicles
 (AD-712099) 02 p0262 N71-11760

Measuring time response of adaptive array antennas for communication satellites for case of strong interference in earth receiving antennas
 (NASA-CR-111617) 03 p0334 N71-12387

Adaptive and goal-seeking system formulation and simulation theory
 03 p0341 N71-12470

Design of proportional-integral-derivative controllers using optimal linear regulator theory
 (NASA-CR-111514) 03 p0353 N71-12552

Algorithm providing maximum likelihood estimates for linear dynamic systems with unknown parameters
 (AD-712804) 03 p0400 N71-13186

Computer control of phased array radar system for simultaneous multiple target tracking
 04 p0498 N71-13934

Adaptive learning computer system for raw data processing
 (AD-713449) 05 p0630 N71-14874

Exact solution to adaptive linear estimation problem
 (AD-713098) 05 p0655 N71-14926

Optimization and estimation models for automatic navigation
 (AD-714699) 06 p0894 N71-16204

Performance and nonlinear control of twin gyro attitude control system with passive compensation
 07 p1058 N71-17821

Stable adaptive control with gain constraints
 (NASA-CR-116428) 07 p1082 N71-17871

Application of conjugate gradient method for guidance and control of aerospace vehicles for Mars entry
 (AD-716767) 09 p1468 N71-20328

Asymptotic properties and simulation of adaptive stochastic control for linear systems
 (NASA-CR-117182) 09 p1411 N71-20372

Adaptive patterns in central nervous tissue learning process
 (NASA-CR-117806) 11 p1692 N71-23059

Biomechanical model for adaptive flight control system
 (NASA-CR-117807) 11 p1693 N71-23060

Social and industrial applications of learning response patterns
 11 p1721 N71-23061

Developments in engineering cybernetics and application to Latvian scientific and technical progress
 (NILL-M-20340/5828.4P) 12 p1894 N71-24133

Adaptive control technique for unstable mechanical systems
 (AD-719743) 13 p2182 N71-26430

Self testing and repairing computer comprising control and diagnostic unit and rollback points for error correction
 (NASA-CASE-NPO-10567) 13 p2049 N71-24653

Synthesis procedure for adaptive control systems for adjusting parameter vectors
 (AD-719838) 13 p2040 N71-25140

Amplifier gain control for Apollo scan television signal enhancement
 13 p2048 N71-25339

Adaptive antenna array processing technique allowing spatial signal field characterization of multiple sources in background of uncorrelated noise
 (AD-719896) 14 p2237 N71-25686

Application of dynamic programming and theory of control processes to biological phenomena including evolution of consciousness
 (TR-71-17) 14 p2284 N71-25937

Development of adaptive estimators for application to numerical analysis of automatic navigation and control
 (AD-720394) 14 p2282 N71-26007

Kalman formulation of minimum mean square linear estimation with random variables and unknown distributions producing biased results
 (NASA-CR-118665) 14 p2284 N71-26429

Analysis of control system containing two nonlinearities to determine existence, stability, and values of amplitude and limit cycles frequency
 (NASA-TM-X-64601) 14 p2283 N71-26430

Moment algorithm for suboptimal adaptive non-linear filtering and signal analysis

14 p2285 N71-26417

Synchronous dc direct-drive system comprising multiple-loop hybrid control system controlling load directly connected to actuator

(NASA-CASE-GSC-10065-1) 15 p2308 N71-27136

Synthesis of signal for adaptive control systems using Ljapunov theory

15 p2309 N71-27529

Explicit feedback control law for singular linear quadratic-Gaussian stochastic control

(AD-720541) 15 p2309 N71-27542

Predictive and adaptive processes in control of Air Force systems

(AD-721220) 15 p2375 N71-27609

Practical simulation of random functions in adaptive control systems

16 p2573 N71-28076

Control theory extended to hypothesis distributed processes with identification strategy incorporated in closed-loop adaptive controller

16 p2575 N71-28092

Automatic machine learning and control of manipulators and adaptive control based on pattern recognition and decision making

16 p2576 N71-28025

Remote temperature sensor for cutting tools and application to adaptive control systems

(Y-DA-4076) 17 p2751 N71-29277

Fuzzy dynamic programming for use in synthesis of flight control system, and computer algorithm for obtaining guaranteed cost function

(AD-722458) 18 p2947 N71-31379

Adaptive sampled data control of time varying bending modes of flexible airframe

(AD-722846) 18 p3020 N71-31582

Derivation of equations describing dynamic properties of typical nonlinear load distributed system for computerized design of control system

(AD-723232) 19 p1222 N71-32008

Development of control system for maintaining space station in close proximity to one of earth-moon libration points

(AD-724113) 20 p3350 N71-32855

Comprehensive survey of status of adaptive control as applied to machining processes

(Y-1759) 20 p3280 N71-33535

Adaptive approach to dynamic allocation and release of buffer storage within computer systems

(NASA-CR-119705) 21 p3997 N71-34171

Principles of situation control and practical application of situational control models for complex systems including airports, drydocks, and street crossroads

(JPRS-53913) 21 p3448 N71-34536

Pattern search algorithm for feedback control system parameter optimization

(AD-726465) 22 p3543 N71-35577

Application of Ljapunov method for parameter adaptive control of unknown plants

(NASA-CR-121961) 22 p3605 N71-35673

Adaptive control problem of constructing robot riding bicycle at constant velocity

(JPRS-53972) 22 p3606 N71-35684

Research and development in adaptive control systems, optimal tracking, and signal processing for navigation and guidance of space vehicles

(AD-727650) 22 p3619 N71-35784

Adaptive nonparametric approach to estimation and signal processing combining learning, decision, and optimization mathematical techniques

23 p3726 N71-36561

Optimization of systems with sensitivity constraints with emphasis on launch vehicle trajectories

(AD-727136) 24 p3901 N71-37805

ADAPTIVE CONTROL SYSTEMS

U ADAPTIVE CONTROL

ADAPTIVE FILTERS

Performance of discrete suboptimal Kalman filters and discrete optimal adaptive filters
 (NASA-CR-111414) 02 p0197 N71-11378

Four theorems characterizing optimal filtered and smoothed estimates for linear parameter systems
 (AD-712404) 03 p0269 N71-12995

Adaptive procedure for removing multimodal power spectra using cascade transversal digital filters
 (AD-716974) 10 p1532 N71-20804

Adaptive notch filter, using modulation techniques for reversed phase noise signal
 (NASA-CASE-XMP-01892) 11 p1729 N71-22985

Dual control algorithms for self adaptive filters and optimal control law for linear systems with unknown input gains
 (AD-721461) 16 p2573 N71-28052

Telecommunications at Hirt Research Center including filter design, computer aided circuit design, and systems theory
 (AD-723331) 17 p2726 N71-29731

ADAPTERS (CIRCUITS)

U ADDING CIRCUITS

ADDITION CIRCUITS

Error correction circuitry for binary signal channels
 (NASA-CASE-XNP-03263) 08 p1170 N71-10843

ADDITION RESINS

NT ACRYLIC RESINS

ADDITION RESINS

ADDITION THEOREM

NT VINYL COPOLYMERS

ADDITION THEOREM

Algorithms to find suboptimal addition chains as optimal procedure for obtaining power of associative operator
(TD-25620) 10 p1394 N71-21626

ADDITIONS

NT ANTICORROSION ADDITIVES

NT ANTIOXIDANTS

NT OIL ADDITIVES

NT PROPELLANT ADDITIVES

NT PROPELLANT BINDERS

NT SOLID ROCKET BINDERS

Synergistic effect of detergent and antioxidant additives during colloidal dissolution
(AD-71152) 01 p0072 N71-10597

Effectiveness of selected antiwear additives in synthetic esters
(AD-711667) 01 p0073 N71-10831

Reliability of testing oils with added detergents in single cylinder engines
(AD-711749) 01 p0073 N71-10970

Synthesis of oil additives, action mechanisms, and production techniques for motor and insulating oils
(AD-712830) 03 p0397 N71-13181

Ammonium perchlorate composite propellant with organic Cu(II) chelate catalytic additive
(NASA-CASE-LAR-10173-1) 04 p0604 N71-14090

Antiswear and extreme pressure additive effects during bearing spinning with synthesized hydrocarbon oils
(NASA-TM-X-52931) 05 p0691 N71-14786

Acceptance test for nickel-cadmium cells with cobalt additive
(NASA-CR-115788) 06 p0796 N71-15746

Capacitance calculation for diffused p-n junction with exponential doping gradients
(NASA-TM-X-2179) 07 p1094 N71-17806

Additions improving properties and facilitating manufacture of U-Pa-C-M fuel - conference
(CRA-CONF-1632) 08 p1235 N71-18210

Gold transport by complex metal chloride vapors
(BM-RI-7409) 08 p1219 N71-19138

Factors influencing gain in neodymium doped laser glass
(AD-716677) 09 p1395 N71-19518

Optical properties of rare earth doped germanate glasses
(AD-716386) 09 p1395 N71-19573

Additions of nickel and niobium to improve ductility of APC-77 steel for rivet material
(AD-716677) 09 p1395 N71-19573

Oxidation of cobalt-nickel-aluminum alloys at 1351 K to 1429 K
(BM-RI-7496) 09 p1401 N71-20431

Influence of additives in aluminum to improve refinement during zone melting
(AD-716677) 10 p1573 N71-20872

Effects of additives of rare earth oxides on polymorphism of zirconium dioxide
(AD-717059) 10 p1588 N71-21001

Shrinkage, density, stability, microhardness, and microstructure dependence of tungsten molybdenum on sintering temperature and ruthenium, rhodium, palladium, and cerium additives
(NLL-TRANS-746-540-79022.401/) 10 p1578 N71-21231

Stearic acid additives in lubricants for improved contact fatigue life of ball bearing steel surfaces
(AD-717824) 11 p1782 N71-22079

Preparation of additives containing phosphorus, sulfur, and chlorine from the ethers of glycerol alpha-methacrylate
(AD-718693) 12 p1943 N71-23671

Feasibility of ash-free organic compounds containing phosphorus, nitrogen, and boron as antioxidant additives for lubricating oils
(AD-717895) 12 p1946 N71-23952

Development and tests of slots and ejectors for introducing additive solutions in aqueous boundary layers to reduce turbulent frictional resistance
(AD-719375) 13 p2063 N71-24636

Quantitative analysis of motor oil additives based on dependence of surface tension on temperature and additive content
(AD-720377) 14 p2277 N71-25886

Preparation and properties of polyfunctional polymeric lubricant additives
(AD-720369) 14 p2278 N71-25895

Purification and distillation of lubricant additive alkylphenol
(AD-720927) 15 p2427 N71-26813

Additive INKBP-46 containing sulfur, chlorine, and phosphorus to improve functional properties of lubricating oils used in reduction gears with Novikov gearing
(AD-721031) 15 p2430 N71-27336

Effects of zirconium additions on mechanical and physical properties of nickel
(NLL-L-TI-746-467-79022.401/) 16 p2607 N71-28013

Impurity doping and surface treatment effects on electrokinetics of silicon carbide
(AD-721031) 17 p2770 N71-29040

Stationary and moving electric fields in silver- and gold-doped cadmium sulfides
(AD-723563) 18 p2941 N71-31468

Effects of silver addition on stress corrosion resistance of Al-Zn-Mg-Cu alloys
(AD-723563) 19 p3110 N71-31745

Structural semiconductor analysis by ion implantation and Hall and channeling effect measurements
(AD-723563) 19 p3168 N71-31821

Effect of aluminum doping on thermal stability of silicon carbide polytypes in 2000 to 2400 C range
(AD-724102) 20 p3353 N71-33046

Low temperature thermal conductivity of Sb and Ga after Te and Zn doping and electron irradiation
(NPL-18836) 22 p3658 N71-36083

Influence of fuel additives on automobile exhaust emissions and composition of exhaust hydrocarbons
(TPR-40) 22 p3661 N71-36109

Additive effects on boundary lubricant-metal surface interactions during friction process
(AD-727085) 24 p3929 N71-38037

Yield and stability of pyrolytic carbon fiber products improved by chemical modification of cellulose fibers and metal additives
(AD-727411) 24 p3943 N71-38128

ADDUCTS

Differential scanning calorimetry and analysis by thermogravimetry of some metal chelates and some adducts of these metal chelates
(ORO-2124-24) 13 p2098 N71-25520

Effect of process conditions on tensile properties of DGEBA and phenol novolac resin reacted with adduct of methylene dianiline and phthalic anhydride
(NRC-MS-132) 20 p3287 N71-33496

Dilatometric and vacuum drying techniques for adductive crystallization studies and solvent concentration, viscosity, and dielectric constant effects on nucleation
(UTCHIE-7111) 23 p3721 N71-36521

ADENOSINE

NT RIBONUCLEIC ACIDS

ADENOSINE TRIPHOSPHATE (ATP)

Measuring decrease in concentration of adenosine triphosphate in brain of rats before onset of convulsions induced by hypoxia
(AD-712242) 02 p0158 N71-11122

Detection instrument for light emitted from ATP biochemical reaction
(NASA-CASE-XGS-05534) 06 p0905 N71-16355

Describing method for hypolipidization of luciferase containing mixtures for use in life detection reactions
(NASA-CASE-XGS-05532) 07 p0990 N71-17705

Automated procedure for direct cell count of bacteria in urine by bioluminescence reaction of luciferase when mixed with ATP
(NASA-TM-X-65521) 13 p2034 N71-25035

Bioluminescent reaction of adenosine triphosphate with enzyme luciferase for quantitative analysis of bacteria in urine samples
(NASA-CASE-GSC-11092-1) 15 p2373 N71-27991

Automatic bioassay instrument for urinalysis based on adenosine triphosphate bioluminescent proportionality to urine sample bacterial content
(NASA-CASE-GSC-11169-1) 15 p2373 N71-27992

Effect of amylotriazine and adenosine triphosphate toward increasing natural body radioresistance and intensification of postirradiation recovery in dogs
(AD-72546) 16 p2546 N71-28485

Automated apparatus for analyzing bacterial ATP in urine samples
(NASA-CASE-GSC-11169-2) 21 p3385 N71-34079

ADENOGENES

NT ADENOSINE TRIPHOSPHATE (ATP)

ADENOGENY

Accuracy, adequacy, and limitations of NASTRAN computer program static load structural analysis solutions
(AD-709962) 22 p3682 N71-36258

ADHEROMETERS

U ADHESION TESTS

ADHESION

Nondestructive tests developed for bonded material evaluation
(AD-709962) 01 p0070 N71-10072

Surface free energy of polymer adhesion
(AD-709962) 04 p0619 N71-15597

Adhesion of single crystal metals to clean iron surface studied by emission spectroscopy
(NASA-TN-D-7018) 06 p0663 N71-15928

Gas exposure experiments of metal soil with microchemical, microphysical, and adhesion analysis
(NASA-CR-114916) 09 p1467 N71-20277

Interatomic (forces and adherence of plasma sprayed coatings to substrates
(NLL-TRANS-734-4553-79022.401/) 10 p1589 N71-21375

Effects of aluminum phosphate additions on thermal stability and adhesive properties of erosion resistant ZnO and Al₂O₃ coatings
(NASA-TT-P-13555) 12 p1928 N71-23813

Floating adhesion of air bubbles and droplets of apolar reagent to mineral particle surface
(NLL-RTS-6124) 17 p2786 N71-29269

Adhesion of polymers to tungsten as studied by field ion microscopy
(NASA-TN-4524) 23 p3744 N71-38024

Characterization of adhesion properties of platinum and gold in contact with tungsten and hafnium oxide field ion microscopy techniques
(NASA-TN-D-6492) 24 p3950 N71-38024

ADHESION TESTS

Activated gas plasma spraying of polymers for adhesive bonding
(AD-711011) 01 p0059 N71-10800

Apparatus for determining quality of bond between high density material and low density material
(NASA-CASE-MFS-13666) 07 p1658 N71-18812

Investigating energy concept of adhesive failure and pressurized disk test for measuring adhesive value of bonded elastomers
(NASA-CR-116834) 08 p1223 N71-19506

Substrate surface free energy, contact angle, and bondline thickness nondestructive measurement based on ultrasonic radiation and reflectometers
(AD-717663) 11 p1778 N71-22025

Adhesion tests of several solar cell adhesives after thermal exposure
(BMW-FW-71-16) 19 p3040 N71-31706

Analysis of bonded metal surfaces used in manufacture of helicopter components
(AD-724663) 20 p3283 N71-33000

High temperature cycling tests of high performance adhesives for aerospace applications
(NASA-CR-121632) 21 p3442 N71-34000

ADHESIVE BONDING

Fabrication of solar cell banks for attaching solar cells to base members or substrates
(NASA-CASE-XNP-00826) 10 p1495 N71-30800

Method for honeycomb panel bonding by the nondestructive effects with electrical heat source
(NASA-CASE-XMF-01402) 10 p1591 N71-34000

Failure prediction for stressed adhesive bonds by reaction rate analysis at high humidity
(AD-717554) 11 p1782 N71-19506

Etching aluminum alloys with aqueous solutions containing sulfuric acid, hydrofluoric acid, and an acid metal dichromate for adhesive bonding
(NASA-CASE-XMF-02303) 12 p1939 N71-23812

Adhesive spray process for attaching biomedical skin electrodes
(NASA-CASE-XFR-07658-1) 14 p2211 N71-30800

Additive effects on adhesion thermodynamics of polymer dispersions on Mylar film
(AD-722338) 14 p2357 N71-34000

Theories of adhesion and bond failure mechanisms caused by water desorption
(SC-RR-70-915) 15 p2453 N71-27119

Adhesive bond shear strength of aluminum at constant strain rate
(AD-722338) 16 p2600 N71-30800

Technique for predicting adhesive metal bond failure times under constant stress and low humidity
(AD-722251) 16 p2617 N71-30800

Developing thermally stable adhesives for bonding titanium and boron composite structures
(NASA-CR-1824) 17 p2770 N71-30700

Strength of adhesive of carbon fiber composite material bonds
(DLR-FB-71-31) 20 p3287 N71-31000

Static and fatigue tests of aluminum double riv joints bonded with nitrile epoxy adhesive
(UTIAS-160) 22 p3689 N71-36258

ADHESIVES

NT GLUES

Nondestructive tests for evaluating bonded materials
(AD-709963) 01 p0071 N71-10074

Tensile properties of flexible epoxy adhesive film (FPL-126)
(AD-709963) 02 p0248 N71-10074

Characteristics, production, and stress analysis of adhesive bonded joints
(UTIAS-28) 02 p0236 N71-10074

Polysiloxane-benzotriazines used for high temperature adhesives, laminating resins, protecting coatings, and films
(AD-712407) 03 p0330 N71-12507

Fracture mechanics and time dependent strength of adhesive joints
(NASA-CR-111761) 04 p0617 N71-15597

Sintered diamond compacts using cobalt on basis
(NASA-CR-116491) 07 p1049 N71-18812

Mechanical properties of adhesives after space environment simulation in vacuum chamber
(R-1107) 10 p1588 N71-30800

Mechanical properties of adhesives after exposure to simulated space environments
(R-1173) 10 p1588 N71-30800

Cost analysis of thermal vacuum and ultraviolet vacuum tests on adhesives, thermoplastic resins, and polymeric films
(PR-4) 10 p1512 N71-28000

Cost analysis of thermal vacuum and ultraviolet vacuum tests on adhesives, polymeric films, thermoplastic and thermosetting resins
(PR-4) 10 p1512 N71-28000

SUBJECT INDEX

AERIAL EXPLOSIONS

Thermodynamic affinity and adhesive forces for separating polymer molecules of different lengths on films
[AD-717284] 11 p1781 N71-31871

Optical aging of adhesive sealants under various environments
[NACA-TR-70-163] 11 p1769 N71-23530

Adhesion tests of several solar cell adhesives after thermal exposure
[NBS-WF-W-71-16] 19 p3040 N71-31786

Adhesive cell adhesives resistance to high temperature and to ultraviolet radiation testing transparency
[NBS-WF-W-71-15] 19 p3040 N71-31787

High temperature cycling tests of high performance adhesives for aerospace applications
[NASA-CR-121632] 21 p3442 N71-34495

Interdependence of continuum mechanics and physical chemistry in failure analysis of adhesives
[NASA-CR-121857] 21 p3527 N71-35130

Adhesive and coating material formulations and manufacturing processes for high-velocity low-permeability joints for use in high altitude balloons
[NASA-CR-111964] 22 p3539 N71-35208

Static and fatigue tests of aluminum double strap joints bonded with nitro epoxy adhesive
[UTIAS-168] 22 p3689 N71-36307

Chemical analysis of amines curing agent used in adhesive manufacturing to determine compliance with specifications
[NASA-G13-400] 23 p3777 N71-36918

ADHESIVE CONDITIONS

Adhesive perturbation theory in cellular mechanics
[NASA-TT-X-45379] 01 p0076 N71-10589

Adhesive phenomenon of particle drift shell arising by magnetosheath electric field
[AD-712844] 02 p2952 N71-11922

Proton adiabaticity in mirror-quadrupole fields of BPF device
[ORNL-TM-3121] 05 p0744 N71-15150

Equation of state for adiabatic electron plasma
[COO-2029-3] 05 p0754 N71-15225

Semi-empirical determination of adiabatic efficiency of isentropic compressor stage
[AD-715053] 07 p1104 N71-18036

Steady, adiabatic, inviscid, supersonic flow along corner formed by two intersecting wedges
08 p1183 N71-18964

Adiabatic compressional cooling of He 3 to millikelvin temperatures
[UCSD-34-F-143-27] 08 p1305 N71-19050

Developmental history of adiabatic invariance including contributions to radiation energy transfer and adiabatic mechanics concepts
[NASA-TM-X-65498] 12 p1968 N71-24056

On film cooling past nonadiabatic flat plate
12 p2014 N71-24306

Isenthalpic and adiabatic compressibility of liquid metals, particularly lead, from melting point to critical region
[DYO-4176-4] 15 p2425 N71-27482

Thermodynamics of liquid-vapor system with application to various adiabatic and nonadiabatic one dimensional flows
[AD-726574] 22 p3569 N71-35419

Low-lying states of pulex system in London-Pekar adiabatic approximation
23 p3823 N71-37267

Ultrahigh frequency heating and adiabatic compression of plasmas in Tuman-2 facility
[CONF-710607-141] 23 p3826 N71-37287

Instabilities in hot electron plasmas created by adiabatic compression in pulsed magnetic field
23 p3833 N71-37335

Ion and electron plasma confinement and kinetic instabilities in adiabatic traps
23 p3853 N71-37467

Transport theory and adiabatic model for particle capture along equator of outer radiation belt
23 p3854 N71-37468

ADHESIVE EQUATIONS

Adiabatic approximation of gas reactor critical mass during nuclear fuel density oscillations
[BAE-1964] 17 p2783 N71-29528

Adiabatic equations for charged particle trajectories in geostrophic tail null zones
20 p3314 N71-32852

ADHESIVE FLOW

Computerized calculations of adiabatic laminar boundary layer and shock wave interactions using Ekinovich method
[VKS-TN-60] 02 p0143 N71-11017

Numerical solution of Navier-Stokes equations for viscous supersonic flows adjacent to isothermal and adiabatic surfaces
09 p1574 N71-19839

Nonlinear approximation of uniform adiabatic laminar laminar gas flow around symmetric profile
11 p1738 N71-22350

Two-layer flow in supersonic nozzles with different adiabatic exponent and gas flow rate ratios
[NASA-TT-F-13524] 12 p1899 N71-23383

Liquid film dispersion in air-water eddylike channel flow with and without obstacles with wall shear stress

and film thickness measurement for reactor core design
[GEAP-10248] 15 p3394 N71-37651

ADJOINTS

Eigenvalue approximation method for non-self-adjoint operators using Galerkin method for estimating eigenvalue perturbations of self-adjoint operators
[NASA-CR-119027] 16 p3653 N71-38548

ADJUSTMENT

U MANAGEMENT

U ELECTRICAL IMPEDANCE

ADRENAL GLAND

Diurnal variation in endocrine and adrenocortical systems during prolonged bed rest
23 p3711 N71-36458

ADRENAL METABOLISM

Oxygen consumption in isolated rat intestine deprived of adrenals
[NASA-TT-F-13418] 03 p0326 N71-12325

ADRENOCORTICOTROPIN (ACTH)

Altitude effects on drug action in glucose metabolism and ACTH release in dogs
07 p0982 N71-17660

Radioimmunochemical assay for ACTH levels in human plasma hormones
23 p3712 N71-36463

ADSORBENTS

Iodine adsorption properties of metal-loaded molasses and applications to gas filtration beds in nuclear fuel processing plants
17 p2715 N71-29662

Inorganic material adsorbent air sampling system for analysis of airborne iodine isotopes and compounds in nuclear reactor containment atmospheres
17 p2743 N71-29663

Testing of fire extinguisher for activated carbon adsorbents in air cleaning systems
17 p2731 N71-29675

Inflow and heat engineering studies on MTR fuel and adsorbent elements for FRJ-1 swimming pool reactor
[JUL-695-RR] 18 p2960 N71-30822

Numerical analysis of radioactive decay heat generation and effects on charcoal adsorbents for reactor accident simulation
[ORNL-4602] 20 p3309 N71-33988

ADSORPTION

NT CHEMISORPTION

Adsorption of helium 4 on activated carbon
[CRA-CONF-1505] 08 p1221 N71-18389

Sorption equilibrium and kinetics of water vapor on modified aluminum
[AD-715914] 08 p1158 N71-18457

Silver diffusion into iron-palladium alloys and internal adsorption of palladium in iron
[TT-70-57070] 08 p2119 N71-19106

Clarifying existing mechanisms in gas-liquid chromatography by study of solute adsorption on liquid-coated adsorbents
11 p1695 N71-21856

Adsorption characteristics at zero surface coverage of solutes at gas-liquid interface of water and dilute solutions
[AD-717735] 11 p1696 N71-22256

Metallic surface interaction - ion microscope adsorption and mass spectrometry desorption analyses, and field emitted electron energy distribution measurements
[COO-1383-11] 13 p2041 N71-25191

Drug reduction and adsorption of polyethylene in aqueous solutions
[AD-719385] 13 p2067 N71-25230

Supercritical fluid chromatography system with micro adsorption detector
14 p2256 N71-26270

Anodic polarization of iron and iron alloys and adsorption of reagents on AISI 4340 steel foil
15 p2424 N71-27427

Characteristics and application of adsorption purification methods for production of superpure inorganic materials
16 p2555 N71-28294

Capillary condensation and evaporation in porous adsorbents
16 p2648 N71-28438

Infrared spectroscopic study of allyl alcohol vapor adsorption on Li, Na, Cs, and Fe specimens of Plinkar monomer/monomers
[NLL-RT-6208] 16 p2559 N71-28013

Effect of gamma radiation on adsorption of iodine and methyl iodide on activated carbon exposed to flowing mixtures of steam and air
17 p2715 N71-29636

Inorganic adsorbent materials for trapping of fission product iodine in fuel reprocessing plants and gas cleaning inside reactor containment
17 p2784 N71-29839

Adsorption properties of metal zeolites for airborne iodine species to provide support for full scale testing of air pollutants
17 p2715 N71-29860

Analysis of concurrent adsorption and chemical reactions
17 p2715 N71-29861

Flow characteristics of adsorbable gases in porous bodies and isotopic separation by gaseous diffusion
[N7-18567] 16 p2904 N71-30420

Heat capacities of sub-monolayer He-3 and He-4 adsorbed on organophosphorus copper surfaces
18 p3883 N71-31200

Substrate mediated interaction between adsorbed atoms caused by exchange of phonons
[RLO-1368-665] 18 p3883 N71-31219

Lead and Auger electron spectroscopy study of oxygen adsorption on tungsten (110)
[NASA-TN-D-5399] 18 p3890 N71-31454

Dissociation thermodynamics of vinyl azepanes for submonolayer helium films adsorbed on solids
[N7UB-2667] 18 p3827 N71-31523

Temperature relaxation of highly purified gas applied to adsorption and condensation vacuum pumps
[NASA-TT-F-15784] 19 p3192 N71-32213

Theory of intermolecular NMR relaxation of molecules adsorbed on solid surfaces, extended to processes with finite jumping lengths of molecules adsorbed surface
[ORNL-TN-3458-PT-2] 19 p3162 N71-32777

Measuring gas adsorption in electric fields by method of thermal conductivity in gaseous mixtures
[NASA-TT-F-19394] 20 p3253 N71-33700

Cryogenic porous media bed for trapping rare gases in aerostats
[DUM-7221-VOL-2] 20 p3308 N71-33743

Radioisotope procedure for investigating chlorine ion adsorption of alpha iron III oxide in sodium chloride
[AD-726412] 22 p3594 N71-35596

Polar and ionic adsorbents, chemical image force laws, electron gas dielectrics, and related surface chemistry and physics topics
[AD-726453] 23 p3720 N71-36515

Physicochemical factors affecting activated charcoal adsorption of contaminants using mathematical models - tables
[NASA-CR-115202] 24 p3809 N71-37657

Oxygen, nitrogen, hydrogen, and carbon monoxide adsorption on platinum surface
[RFP-1456] 24 p3883 N71-37692

ADSORPTIVITY

Physics of carbon adsorbents
17 p2770 N71-30135

Mathematical model for gas adsorption efficiencies of porous and solid reactor materials
18 p2607 N71-31449

ADVANCED TEST REACTORS

Predicting bearing fatigue failure and life in primary coolant check valves of advanced test reactors
[IN-1338] 04 p0357 N71-14153

ADVECTION

Micrometeorological investigations of momentum, energy, and mass transfers above vegetative surfaces with von Karman constant, diabatic profile functions and eddy-transfer coefficients
[AD-721501] 16 p2625 N71-28225

Micrometeorological data acquired during advection conditions from California
[AD-724612] 20 p3295 N71-32990

Accuracy of fine mesh 500 mb barotropic predictions
[NOAA-TM-NWS-TDL-42] 21 p3451 N71-34562

AE-B SATELLITE

U EXPLORER 32 SATELLITE

ABOLIAN TONES

Aerodynamic characteristics of new wakes produced by periodic vortex shedding from airfoils
[AD-718975] 12 p1964 N71-23245

ABSORPTION

Air intakes and flow aeratics in hydroturbines
[PB-19339PT] 01 p0044 N71-10942

AERIAL EXPLOSIONS

Investigating disturbances in ionosphere and circumterrestrial space from high altitude nuclear explosions
[RAE-LIB-TRANS-1448] 05 p0675 N71-15435

Detection of atmospheric nuclear explosion by study of extremely low frequency waves and ionospheric disturbances
[AD-716001] 09 p1383 N71-19683

Design and development of positive air shock wave attenuator
[AD-716013] 09 p1475 N71-19681

Low altitude explosive generation of ionospheric disturbances by acoustic gravity waves
11 p1710 N71-22934

Developments in automatic processing of data obtained from sensors of nuclear explosions and capabilities of nuclear detection systems
[AD-719360] 13 p2875 N71-25170

Relationship between air blast injury and impairment of pulmonary function in dogs and sheep
[AD-709972] 14 p2286 N71-28302

Comparison of theoretical and data analysis of Rayleigh waves generated by aerial nuclear explosions in US50 including earth absorption system
[AWE-O-8870] 17 p2738 N71-29376

Analysis of effects of nuclear explosions on ionosphere
[FOA-C-4415-29] 22 p3370 N71-35408

AERIAL PHOTOGRAPHY

AERIAL PHOTOGRAPHY

- Mass data storage requirements for radar image simulation of urban area from aerial photographs [AD-711385] 01 p0024 N71-10665
- Reflectometers for color aerial photography [AD-710978] 01 p0056 N71-10745
- Aerial and spaceborne photography and infrared imagery in earth hydrogeology and oceanography [NASA-TM-X-64481] 02 p0205 N71-11151
- Aerial infrared sensing for thermal mapping of power plant cooling reservoir 02 p0205 N71-11152
- Infrared and color photography for water inlet survey in Alaska 02 p0205 N71-11153
- Aerial infrared photography for remote sensing of plant transpiration 02 p0206 N71-11154
- Aerial synoptic sensing by infrared imagery and color photography of lake area in Florida 02 p0206 N71-11155
- Aerial infrared sensing of springs and sinks in Florida 02 p0206 N71-11156
- Color infrared photography for remote sensing of shallow water areas by air 02 p0206 N71-11157
- Remote aerial sensing and multippectral data processing for hydrobiological survey in Florida 02 p0206 N71-11159
- Microwave radiometry for snow and ice sensing in aerial reconnaissance 02 p0206 N71-11160
- Aerial remote sensing data for locating ground water areas 02 p0207 N71-11162
- Remote airborne measurements of ocean color 02 p0208 N71-11167
- Aerial multispectral sensing test on submerged body in ocean 02 p0208 N71-11168
- Aerial photography of water wave refraction for depth determination 02 p0208 N71-11169
- Aerial photography for studying coastal ecology 02 p0208 N71-11170
- Coder design for SECAM color television system and stereotelevision system using time parallax [JPRS-51782] 02 p0183 N71-11287
- Time parallax method for obtaining stereotelevision pictures in aerial photography 02 p0183 N71-11289
- Use of aerial photography in geocryological surveys [AD-711926] 02 p0212 N71-11539
- Interim results and progress on use of space and aircraft photography for range resource inventories 02 p0216 N71-11979
- Evaluating potential for making broad land use maps and earth resource surveys from spaceborne and airborne photography 02 p0217 N71-11980
- Research progress on multispectral data collection and infrared instrumentation for specially configured aircraft 02 p0227 N71-11984
- Color aerial photography of Douglas fir tussock moth damage [PB-193698] 02 p0221 N71-12164
- Procedures for determining photographic image quality and photointerpretation capabilities [AD-712705] 03 p0376 N71-12765
- Airborne multispectral data collection and ground based reproduction facilities [NASA-CR-106717] 04 p0516 N71-14467
- Identification, characteristics, and distribution of slope failure forms as depicted by selected remote sensor returns 05 p0667 N71-14746
- Computerized analytic triangulation for compiling topographic maps from aerial photographs 05 p0683 N71-14842
- Computer programs for analytical aerial triangulation and automatic reduction of stereocomputer measured coordinates 05 p0652 N71-15500
- Investigating measurement accuracy and automatic processing of aerial photographs [JPRS-51920] 06 p0857 N71-15772
- Investigating accuracy in sighting and identifying points on aerial photographs when measuring coordinates 06 p0857 N71-15773
- Using adjustable values for processing aerial photographs in photogrammetric instruments 06 p0857 N71-15774
- Aerial photointerpretation of surface changes in near vicinity of ground zero after underground nuclear explosion [NVO-1163-TM-23] 06 p0840 N71-15845
- Aerial multispectral sensing for determining geological and geographic aspects in Earth Resources Aircraft Program [NASA-TM-X-62564] 06 p0842 N71-16126

Multispectral aerial sensing for geological survey in southern California 06 p0842 N71-16127

Aerial multispectral sensing and ground truth observations for California earth resources study 06 p0842 N71-16128

Aerial multispectral sensing for terrain analyses and urban planning 06 p0842 N71-16129

Aerial infrared imagery for fire site detection in tropical grassland area of Florida 06 p0842 N71-16130

Aerial remote imagery for urban planning 06 p0842 N71-16131

Aerial photography and radar imagery for terrain mapping 06 p0842 N71-16132

Multispectral imagery of aerial remote sensors and television simulation for terrain analysis 06 p0838 N71-16133

Aerial infrared imagery for terrain analysis in California crater area 06 p0843 N71-16134

Airborne infrared radiometer sensing of thermal terrain properties in California lake region 06 p0843 N71-16135

Aerial infrared imagery of geological region in southern California taken during pre-dawn and post-sunrise hours 06 p0843 N71-16136

Aerial radar and infrared imagery for geodetic survey of northern Arizona 06 p0843 N71-16137

Multispectral remote aerial sensing for geological terrain analysis 06 p0843 N71-16139

Infrared aerial sensing of high temperature geothermal water sources 06 p0843 N71-16140

Aerial infrared imagery and radiometric survey of coastal areas 06 p0844 N71-16142

Photographic applications of NASA Earth Resources Survey Program 06 p0859 N71-16148

Crop and soil identification from aerial photography 06 p0845 N71-16150

Identification of western forest species by means of aerial remote sensing 06 p0800 N71-16160

Anticipating sinkhole collapse by using remote sensors to identify and delineate relic features 06 p0846 N71-16169

Using remote sensors for classification of lake hydrology 06 p0846 N71-16170

Aerial photography as technique for remote sensing of hydrobiological features in swamp and coastal regions 06 p0846 N71-16171

Investigating radar imagery for application in terrain analysis of drainage basins 06 p0847 N71-16175

Using airborne radiometers for ocean bottom surveying 06 p0846 N71-16180

Learning machine with adaptive control for aerial photograph interpretation [AD-714576] 06 p0860 N71-16580

Aerial photography of Russian geomorphology [AD-715050] 07 p1022 N71-17834

Aerial photography of coastal waters of New York and Long Island [AD-715804] 08 p1186 N71-18334

Aerial multispectral and infrared scanning of Massachusetts coastline [NASA-CR-116782] 08 p1187 N71-18402

Digital computer processing of visible and reflective infrared scanner data for automatic computer mapping of Yellowstone National Park 08 p1197 N71-19254

Geologic value of small scale aerial photographs and comparison of high altitude oblique and vertical photographs of California 08 p1197 N71-19259

Satellite and aerial thematic land use mapping 08 p1196 N71-19264

Aerial and satellite-borne photography of Imperial Valley agricultural land use characteristics 08 p1196 N71-19265

Color infrared aerial photography for acquiring and classifying data on urban housing quality 08 p1204 N71-19266

Separation of multispectral images from multiband film 08 p1245 N71-19267

Multispectral aerial photographic remote sensors for pollution determination in estuaries [PB-195976] 09 p1379 N71-19410

Microwave radiometry, spaceborne and aerial photography, and oceanographic data from ships evaluated for remote sensing of coastal oceans [NASA-CR-117316] 09 p1387 N71-20422

SUBJECT INDEX

Aerial reconnaissance of oil spill in Gulf of Mexico with photographic, infrared and radar type systems [NASA-CR-117497] 10 p1553 N71-21200

Adaptive pattern representation and recognition system for application to mechanized interpretation of pictorial data from aerial reconnaissance photography [AD-716561] 10 p1559 N71-21201

Automatic photointerpretation system for pattern recognition in image processing 11 p1767 N71-22200

Remote sensing of coastal areas by aerial and spaceborne photography [AD-717936] 12 p1906 N71-23216

Tubulation of B-57 aerial cloud photography of tropical convection systems for 11 to 28 July 1969 with flight path over Barbados Islands [ESSA-TM-ERLTM-BOMAP-1] 12 p1921 N71-23716

Aerial photomicros used to simulate spaceborne photographs in general macro and thematic agricultural land use [NASA-CR-104253] 12 p1914 N71-24005

Aerial infrared photography for water educational recreation [NASA-CR-107636] 12 p1914 N71-24007

Decidability of small topographic objects in large scale aerial photography of forests [AD-720765] 14 p2249 N71-20307

Comparison of August 1968 aerial infrared images of Surrey, Iceland with survey data of 1966 14 p2252 N71-20407

Application of Apollo space photography and sequential high altitude NASA aircraft photography for evaluating natural and cultural resources in southeastern Arizona - map [NASA-CR-115056] 17 p2750 N71-20310

Quantitative evaluation of multiband photographic techniques using combination of black and white and color photos [NASA-CR-115055] 17 p2751 N71-20311

Evaluation of high altitude balloon aerial photography for earth resources and oceanography including photographic formats and camera systems and packaging [NASA-TM-X-22008] 17 p2753 N71-20309

Research on fundamental properties required of networks for automatically extracting patterns from pictorial data such as aerial photos [AD-722697] 17 p2724 N71-20146

Aerial and ground surveillance of southern coast built in New Belt States during 1971 [NASA-NEWS-RELEASE-71-129] 17 p2709 N71-20175

Computer graphic mapping of Maryland coasts from aerial color and infrared photographic remote sensors including microdensitometer analysis [RM-5091] 17 p2749 N71-20176

Comparison of aerial and spaceborne photographic methods and photointerpretation techniques using northwest Saudi Arabia geomorphology [NASA-TM-X-65594] 17 p2749 N71-20177

Holographic imagery for aviation and space flight [JPRS-53420] 17 p2760 N71-20181

Generalized characteristics of coastal currents based on statistical analysis of aerial photographs of areas of Black Sea and Baltic Sea [NOO-TRANS-486] 18 p2918 N71-31170

Inventory of high level cloud photography mission results during oceanographic and meteorologic experiment in Barbados area [NOAA-TM-ERL-BOMAP-4] 18 p2925 N71-31180

Aerial photographs of US agricultural regions to determine status of aerial coverage 18 p2926 N71-31178

Installation and structure of aerial laser camera for photographic scanning from aircraft [AD-723820] 19 p3098 N71-31717

Development of computer program for analytical strip triangulation applied to aerial photography [PB-198922] 19 p3085 N71-31817

Interferometer for evaluation of aerial photographs [AD-723432] 19 p3103 N71-32010

Aerial photographic tracing of pulp mill waste plumes used to study waste disposal sites [PB-198232] 19 p3096 N71-31816

Photographic film sensitivity calibration for use in forestry aerial color and infrared photography [NASA-CR-121372] 20 p3270 N71-32015

Evaluation of enhancement of light intensity differences on color aerial photographs and thermal infrared imagery [NASA-CR-121430] 20 p3260 N71-32010

Utilization of remote sensor data by Virginia state agencies including aerial photography, radar detection, and infrared detectors [NASA-CR-119721] 20 p3370 N71-31809

Results of combined fully instrumented subsurface geophysical experiment including spectrophotometry of earth surface [JPRS-53895] 21 p3419 N71-34110

Photointerpretation of aerial color infrared photography for analysis of urban land use [NASA-CR-121652] 21 p3424 N71-34000

Range management in color infrared aerial photography and phenology of vegetation [PB-199226] 21 p3429 N71-34000

SUBJECT INDEX

Aerial photography for monitoring and evaluating offshore from ocean waste disposal processes
[AD-724488] 22 p3584 N71-35528
Borehole aerial sensing and automatic mapping for forest resources information system
[NASA-CR-122922] 23 p3755 N71-36770
Techniques for aerial three-lens cloud photographic analysis, Doppler navigation data analysis, and photogrammetric data acquisition
23 p3787 N71-36990
Shallow ocean depth measurements by aerial photographs of wave refraction and wavelength changes and by multispectral scanning of wave reflection
[NASA-CR-123194] 24 p3909 N71-37862
Interpretation of color infrared photography of Florida tidalwater coastline
24 p3916 N71-37924
Mathematical logic applied to aerial photograph interpretation
[AD-727459] 24 p3925 N71-38009
Quantity and quality of geodetic information transmitted by space photography compared with low altitude aerial photography
[JB-USGS-225] 24 p3926 N71-38013
AIRIAL RECONNAISSANCE
Presentations at conference on color of ocean with application to survey of earth resources by satellite observation and aerial reconnaissance
[NASA-CR-115178] 03 p3969 N71-39390
Design and development of pulse code modulation telemetry system for earth resources survey aircraft
[NASA-CR-108701] 06 p489 N71-13477
Aerial survey of Bessy Waste Dump at Nevada Test Site
[DGC-1183-1481] 04 p3992 N71-14402
Geological analysis of aerial geomagnetic survey of northeastern Alaska
[BULL-1271-F] 05 p0681 N71-15671
Investigating feasibility of locating, identifying and quantifying surface and near-surface fish stocks from aircraft and spacecraft
06 p0848 N71-16182
Aerobore remote sensing techniques applied to pollution by oil on ocean surface
[AD-716349] 09 p1382 N71-19606
Aerial reconnaissance of oil spill in Gulf of Mexico with photographic, infrared and radar type systems
[NASA-CR-117497] 10 p1553 N71-21304
Adaptive pattern representation and recognition system for application to mechanized interpretation of pictorial data from aerial reconnaissance photography
[AD-716856] 10 p1559 N71-21488
Aerial reconnaissance of Northern California and Oregon conditions to determine extent of erosion
[AD-717359] 11 p1747 N71-22152
Aerial reconnaissance and radar scanning of ice flows in Greenland waters-1963
[BBR-47-7478-005-0] 11 p1750 N71-22518
Results and analysis of combined aerial and ground strength frequency noise survey in urban area
[NASA-TM-X-2244] 11 p1702 N71-22623
Summary of findings and recommendations on airborne reconnaissance to improve forecasting and monitoring of severe storms
11 p1791 N71-22662
Feasibility of mapping variation in rock strength on basis of electrical conductivities measured by airborne equipment
[AD-718438] 12 p1907 N71-23522
Visual detection probability for moving target against static target
[AD-720000] 14 p2208 N71-25849
Operation of weather reconnaissance aircraft and analysis of data obtained during reconnaissance flights in Atlantic Ocean
17 p2778 N71-29556
Development of computer program for analytical map triangulation applied to aerial photography
[PB-198592] 19 p3083 N71-31817
Sample measurement of soil moisture content in Imperial Valley, California and Phoenix, Arizona and comparison with microwave radiation temperatures
[NASA-CR-121439] 20 p2565 N71-33088
Application of aerial reconnaissance and remote sensing techniques to development of master engineering soil plans
[PB-199422] 22 p3573 N71-35447
Research Flight Facility participation in BOMBEX program and aircraft data inventory
[NOAA-TN-ERL-198-RFF-4] 22 p3574 N71-35453
Bibliography of remote sensor applications and study of earth resources using airborne and earth satellite techniques
22 p3577 N71-35479
Characteristics of sensors for aerial observation of ice formations and comparison of effectiveness of various methods
[JPRS-54162] 23 p3759 N71-36801
AEROSPACE ROCKET VEHICLE
Aerobore-borne electron accelerators for ejecting electron beams into upper atmosphere
[NASA-CR-116087] 06 p0939 N71-15894
Pulse rail control for Aerobore rocket vehicle
[NASA-CR-73499] 08 p1294 N71-18745

Secondary electron emission measurement in aurora using Aerobore rocket vehicle
[NASA-CR-116658] 08 p1193 N71-18995
WO measurement in auroral arc by mass spectrometer onboard Aerobore rocket
[NASA-CR-116877] 08 p1194 N71-18997
Aerobore rocket-borne instruments for auroral measurements, including electron and proton counters, electron density and temperature probes, X ray counters, and light photometers
[AD-719734] 13 p2161 N71-25198
Aerobore 350 flight and instrument data including preflight tests, instrument installation and orientation, and postflight analysis information
[NASA-TM-X-45539] 14 p2253 N71-25837
Aerobore 350 recovery system comprising parachute and extended skirt parachute deceleration devices and incorporating electrical control, pyrotechnic, and pneumatic subsystems - tests
[NASA-CR-118628] 14 p2342 N71-25883
Postflight analysis of Aerobore rocket vehicle's attitude determination with solar aspect sensors and magnetometers
[NASA-TM-X-45570] 15 p3442 N71-27738
Design, development, fabrication, and acceptance test results for two fluidic proportional thrusters for use in SPARC-4
[NASA-CR-114333] 19 p3186 N71-32794
AERODONTALGIA
U TOOTH DISEASES
AERODYNAMIC BRAKES
NT BALLISTICS
NT LEADING-EDGE SLATS
NT TRAILING-EDGE FLAPS
NT WING FLAPS
Moving low cylindrical model for aerobraking tests at high speed in drop wire facility
18 p2867 N71-31109
Criteria and recommended practices for design, selection, analysis, and testing of deployable aerodynamic deceleration systems
[NASA-SP-4066] 18 p2873 N71-31303
AERODYNAMIC BUZZ
U FLUTTER
AERODYNAMIC CHARACTERISTICS
NT AERODYNAMIC DRAG
NT AERODYNAMIC STABILITY
NT INTERFERENCE DRAG
NT INTERFERENCE LIFT
NT JET LIFT
NT LIFT
NT ROTOR LIFT
NT STATIC AERODYNAMIC CHARAC-
TERISTICS
NT SUPERSONIC DRAG
NT ZERO LIFT
Low-speed wind tunnel tests of series of twin-kel all-flexible parawings
[NASA-TM-X-5936] 01 p0002 N71-10052
Pilot impressions of lifting body vehicles
01 p0125 N71-10107
Computerized aerodynamic optimization of aircraft propellers
[AD-710356] 01 p0002 N71-10122
Leading-edge effect on aerodynamic characteristics of 70 deg swept delta wing
[AD-712087] 02 p0142 N71-11007
Cold air tests on axial flow turbine with transpiration cooled discrete hole stator blades to determine coolant flow ejection effect on turbine aerodynamic performance
[NASA-TM-X-2133] 02 p0142 N71-11010
Low speed aerodynamic characteristics of airfoil profiles including effects of upper surface roughness simulating hair frost
[NPL-AERO-1308] 02 p0143 N71-11016
Subsonic wind tunnel investigation of rotary wing configurations for VTOL aircraft in cruise mode
[NASA-D-5945] 02 p0145 N71-11025
Flexible trailing wire effect on aerodynamic characteristics and radar cross sections of hypervelocity cone
[AD-712509] 03 p0309 N71-12205
Testing low reaction jet turbine stator blades in air-blade cascade cascade
[NASA-CR-1675] 03 p0312 N71-12227
Investigating effects of air permeability and porosity on performance of parachutes
[NASA-TT-F-13431] 03 p0314 N71-12245
Performance and handling qualities criteria for V/STOL aircraft
[AGARD-B-577-70] 03 p0315 N71-12248
Technology review on unmanned flight vehicles
[AD-713833] 03 p0456 N71-13861
Aerodynamic characteristics and flight dynamics of unmanned missiles and spacecraft
[AD-713032] 03 p0458 N71-13241
Aerodynamic characteristics of free flight bodies in ballistic ranges
[NASA-TM-X-46534] 04 p0472 N71-13583
Calculating flutter boundaries and estimating stresses in infinite sparrows array of panels using exact model of Zeydel
[NASA-CR-1721] 04 p0617 N71-14086

AERODYNAMIC CHARACTERISTICS

Measurement of external and internal flow fields during parachute inflation
[AD-713520] 05 p0627 N71-14539
Aerodynamic characteristics of large-scale model with lift fan mounted in 3 percent thick turbulent wing
[NASA-TM-X-7031] 05 p0636 N71-14638
Aerodynamic performance of shuttle-orbiter configuration with variable delta wing geometry in low turbulence subsonic wind tunnels
[NASA-TM-X-2206] 05 p0626 N71-14943
Longitudinal aerodynamic characteristics of hypersonic lifting body spacecraft with variable sweep wings
[NASA-TM-X-2102] 05 p0626 N71-14945
Air launch characteristics of HL-10 manned lifting reentry vehicle
[NASA-TM-X-1668] 05 p0770 N71-15002
Vertical tail loads and control surface hinge moment measurements on M2-F2 lifting body at subsonic speeds
[NASA-TM-X-1712] 05 p0775 N71-15003
Air launch characteristics of M2-F2 lifting body from B-52 aircraft
[NASA-TM-X-1713] 05 p0776 N71-15004
Computer manual for implementing digital program in space station dynamics simulation
[NASA-CR-102971] 05 p0771 N71-15159
Low subsonic aerodynamic characteristics of space shuttle-orbiter concept with blended delta wing-body
[NASA-TM-X-2209] 05 p0772 N71-15485
Free boundary value problems of heat flow around aerodynamic bodies
[AD-714621] 06 p0958 N71-15963
Designing spacecraft for flight into space, atmospheric reentry, and landing at selected sites
[NASA-CASE-XAC-62058] 06 p0794 N71-16067
Aerodynamic characteristics of flow field about axisymmetric and two dimensional bodies in supersonic flow
[AD-713917] 06 p0835 N71-16309
Subsonic aerodynamic characteristics of model of HL-10 flight research vehicle with basic and modified tip fins
[NASA-TM-X-2119] 06 p0793 N71-16358
Aerodynamic design of symmetrical blading for three stage axial flow compressor test rig
[AD-714585] 06 p0793 N71-16365
Longitudinal aerodynamic characteristics of Viking lander spacecraft at hypersonic speed
[NASA-TM-X-2205] 07 p0967 N71-17253
Acoustic and aerodynamic performance of six foot diameter fan for turbofan engines with noise suppressors
[NASA-TN-D-4178] 07 p1099 N71-17254
Pitch and yaw characteristics of supersonic transport aircraft with variable sweep wings at various Mach numbers
[NASA-TM-X-2164] 07 p0970 N71-17415
Flight characteristics of V/STOL transport model with four pod-mounted lift fans
[NASA-TN-D-4129] 07 p0971 N71-17423
Vortex-lattice FORTRAN program for estimating subsonic aerodynamic characteristics of complex planforms
[NASA-TN-D-4143] 07 p0967 N71-17424
Feasibility evaluation on optical probing of supersonic aerodynamic turbulence with statistical correlation
[NASA-TN-D-4077] 07 p1009 N71-17444
Dirichlet solutions for thin airfoil problems
[NASA-TT-F-13471] 07 p0967 N71-17468
Investigating effects of leading-edge blowing on aerodynamic characteristics of jet flap airfoil
[AD-716508] 07 p0968 N71-17702
Resonance instability of finned bodies with nonlinear aerodynamic characteristics
[AD-715101] 07 p0968 N71-17733
Helicopter application studies of variable deflection thrust jet flaps
[AD-715071] 07 p0973 N71-17907
Practical aerodynamics of Mi-6 helicopter - lift system and fuselage
[AD-714915] 07 p0973 N71-17908
Real gas effects on drag and trajectories of nonlifting conical shell during Mars atmospheric entry
[NASA-TN-D-6240] 07 p1116 N71-18013
Aerodynamic characteristics of V/STOL transport model with tandem lift fans mounted at mid-span of wing
[NASA-TN-D-6234] 08 p1141 N71-18538
Lift and drag characteristics of HL-10 lifting body during subsonic gliding flight
[NASA-TN-D-6263] 08 p1142 N71-18667
Design and characteristics of double ball dirigible airship
[JPRS-52330] 08 p1145 N71-19217
Aerodynamic characteristics of HL-10 reentry vehicle model at subsonic and supersonic speeds
[NASA-TN-D-6018] 08 p1293 N71-19270
Determining aerodynamic characteristics of chemically deformed lead bearing wing using large aspect ratio model
[AD-716509] 09 p1315 N71-19539

Determining equations of motion and aerodynamic characteristics for Magnus rotors by flight tests [AD-716345] 09 p1315 N71-19560

Calculation of profile drag of airfoils at low Mach numbers by predicting instability and transition points [NAL-TR-198] 09 p1317 N71-20181

Analytical and simulator investigations of height control system for vertical takeoff aircraft [NAL-TR-200] 09 p1323 N71-20182

Supersonic aerodynamic characteristics of rocket vehicle model with low aspect ratio wing and tail surfaces [NASA-TM-X-2159] 09 p1318 N71-20181

Feasibility of using fixed simulator to determine stall and spin characteristics of fighter aircraft [NASA-TM-D-6117] 09 p1324 N71-20192

Predicting aerodynamic characteristics of arrow, delta, and diamond wing planforms using Prandtl-Glauert transformation [NASA-TM-D-6243] 11 p1669 N71-21973

Dynamics of three dimensional motion of guided, rotating, and roll stabilized rockets [AD-717821] 11 p1830 N71-23018

Nose bluntness effect on aerodynamic characteristics of flared body in supersonic wind tunnel [NAL-TR-221] 11 p1670 N71-22160

Computer program to generate turbine aerodynamic requirements, approximate external blade geometries, and coolant flow requirements for two stage axial flow turbines [NASA-TM-X-2229] 11 p1670 N71-22568

Numerical analysis of dynamic and thermodynamic state of plenum-type air-cushion vehicle to determine heave response and control system operating characteristics [NASA-TM-D-6257] 11 p1739 N71-22589

Wind tunnel tests to determine effects of wing dihedral angle on aerodynamic characteristics of highly swept fixed-wing configuration [NASA-TM-X-2261] 11 p1671 N71-22622

Numerical analysis of influence coefficients, natural frequencies, and mode shapes of vibration of triangular inflatable wing [AD-717821] 11 p1671 N71-22666

Effect of engine position and high lift devices on aerodynamic characteristics of external flow, jet flap STOL model - graphs [NASA-TM-D-6222] 12 p1852 N71-23124

Wind tunnel investigation of hypersonic transport model aerodynamic characteristics at Mach numbers to 6 - graphs [NASA-TM-D-6191] 12 p1852 N71-23127

Low subsonic longitudinal aerodynamic characteristics of twin body space shuttle booster configuration using low turbulence pressure tunnel - graphs [NASA-TM-X-2162] 12 p1850 N71-23135

Aerodynamic characteristics affecting stability and controllability of supersonic aircraft [AD-718474] 12 p1856 N71-23538

Aerodynamic performance of sweptback-bladed centrifugal compressor in argon as function of equivalent weight flow [NASA-TM-X-2269] 12 p1851 N71-23659

Effects of flow containing dust on results of hypersonic wind tunnel experiments [NASA-TT-F-11529] 12 p1901 N71-23702

Investigation of longitudinal and lateral stability and controllability of supersonic aircraft [AD-718285] 12 p1857 N71-23818

Wind tunnel investigation of static longitudinal and lateral characteristics of full scale mockup of light twin engine aircraft [NASA-TM-D-6238] 12 p1857 N71-23860

Wind tunnel investigation of longitudinal aerodynamic characteristics of semispan wing deflected upstream configuration with double slotted flap and auxiliary wing [NASA-TM-D-6232] 12 p1851 N71-23861

Cold-air tests to determine performance characteristics of single-stage turbine with stator blades employing transpiration coolant ejection through wire mesh shell [NASA-TM-X-2176] 12 p1991 N71-23980

Aerodynamic characteristics of large angle blunt cone with and without fence-type afterbodies [NASA-TM-D-6269] 12 p2001 N71-24083

Development of mathematical model for opening behavior of parachutes noting drag and velocity as functions of time [AD-719698] 13 p2025 N71-24433

Analysis of empenage loads and aerodynamic response of T-tail transport aircraft in continuous atmospheric turbulence 13 p2024 N71-24996

Flight data analysis and electromechanical simulation of sounding rocket stability using rigid body energy techniques [AD-719730] 13 p2175 N71-25387

Investigation of flight path and longitudinal dynamic characteristics of free flight rocket model [AD-724188] 13 p2028 N71-25395

Flight evaluation of lateral handling, stability, control, and flying qualities of jet transport aircraft during

up-and-away and approach flight in landing configuration [NASA-TM-D-6339] 13 p2028 N71-25357

Wind tunnel tests to determine aerodynamic characteristics of booster and ascent shuttle configuration from Mach 0.28 to 10.4 [NASA-TM-X-2265] 14 p2341 N71-25803

Hypersonic theoretical/experimental correlations of aerodynamic characteristics for space shuttle design 14 p2195 N71-26666

Wind tunnel tests to determine low-speed aerodynamic characteristics of large-scale STOL transport model with augmented jet flap [NASA-TM-X-62017] 14 p2198 N71-26183

Analysis of aerodynamic forces on DL-4 lifting entry vehicle and comparison with theoretical methods [NASA-TM-X-1994] 14 p2196 N71-26354

Flight dynamics of rocket vehicle in powered phase [AD-720739] 14 p2340 N71-26666

Wind tunnel investigation of aerodynamic characteristics of wing-body and lifting body configurations for hypersonic cruise aircraft at hypersonic speeds [NASA-TM-X-2287] 16 p2536 N71-28861

Wind tunnel investigation of aerodynamic interference between two lifting surfaces in tandem 17 p2699 N71-29343

Conference on performance of propulsion systems for hypersonic vehicles and some aerodynamic characteristics [ONERA-NT-169] 17 p2834 N71-29568

Aerodynamic problems related to hypersonic vehicles and space shuttles 17 p2700 N71-29572

Computed aided design of wing structures and application of optimal law of material distribution [AD-722303] 17 p2704 N71-29657

Aerodynamic characteristics of thin, highly cambered airfoils in incompressible flow [NASA-CR-1767] 17 p2701 N71-29693

Design and characteristics of supersonic inlet controls for minimizing inlet unstarts [NASA-TM-D-6408] 17 p2839 N71-30072

Wind tunnel investigation of static longitudinal aerodynamic characteristics of semispan swept wing for STOL jet transport with deflected thrust and boundary layer control [NASA-TM-D-6256] 17 p2705 N71-30282

Application of Fredholm integral equations of second kind for determining pressure distribution on cascade of thick airfoils [NASA-TT-F-702] 18 p2865 N71-30488

Experimental and analytical study of subsonic longitudinal and lateral aerodynamic characteristics of slender sharp edge 74 deg swept wings [NASA-TM-D-6344] 18 p2865 N71-30530

Aerodynamic and deployment characteristics of twin keel all-flexible parawing rigged with several variations of multistage canopy and suspension line reefing system [NASA-TM-D-6306] 18 p2865 N71-30748

Aerodynamic characteristics, rocket nozzles, spacecraft propulsion, antenna design, and internal combustion engines [NASA-CR-119315] 18 p3014 N71-31106

Aerodynamic characteristics of vehicle models in aluminum tube 18 p2867 N71-31108

Static force tests of model of twin jet fighter aircraft at various angles of attack and sideslip angles to obtain data for theoretical spin studies [NASA-TM-D-6425] 18 p2873 N71-31330

Aerodynamic characteristics of wings, propeller blades, and entire aircraft at various velocities including flow viscosity and compressibility - textbook [AD-723542] 19 p3033 N71-31932

Internal aerodynamics design manual considering internal air flow system effect on aircraft performance including bibliography [AD-723623] 19 p3173 N71-32059

Aerodynamic design manual considering internal air flow system effects on aircraft performance [AD-723624] 19 p3173 N71-32060

Predicted and measured aerodynamic characteristics for blended delta-wing orbiter at hypersonic speeds [NASA-TM-X-62046] 19 p3184 N71-32106

Aerodynamic characteristics at Mach numbers 1.60 to 2.16 of blunt-nose missile model having triangular cross section and fixed triform fins [NASA-TM-X-2240] 19 p3033 N71-32211

Flight test data on geometric, aerodynamic, and kinematic characteristics of two twin keel parawings during deployment [NASA-CR-1708] 19 p3189 N71-32303

Evaluation of performance, stability, and control characteristics of XV-11 A short takeoff aircraft [AD-724124] 20 p3208 N71-32818

Evaluation of interaction between reentry vehicle heat shield ablation and aerodynamic parameters [AD-724188] 20 p3351 N71-32936

Scheme of notation and nomenclature for aircraft dynamics and aerodynamics [ARC-RM-5562-PT-1] 20 p3204 N71-33027

Mathematical and standardization data for aircraft dynamics and associated aerodynamics nomenclature and symbols system [ARC-RM-5562-PT-5] 20 p3204 N71-33027

Computer program for aerodynamic characteristics evaluation of multiple-component airfoils in subsonic viscous flow [NASA-CR-1843] 20 p3205 N71-33100

Determination of transonic aerodynamic characteristics of spherically blunted 55 and 60 degree half angle cones in ballistic range tests [NASA-TM-D-6409] 20 p3206 N71-33100

Determination of aircraft longitudinal motion during takeoff and landing after loss of lift from boundary layer control system 20 p3211 N71-33100

Calculation of mean line camber ordinates for laterally symmetrical wings with polygonal planforms [NASA-TM-X-2311] 20 p3207 N71-33100

Theoretical and experimental determination of lift and pitching moment distribution on jet flap wings of rectangular design with various aspect ratios [NASA-TT-F-13715] 20 p3207 N71-33100

Development of method for determining angle of pitch, flight path angle, and angle of attack for aircraft during steady or nonsteady flight [VTH-156] 20 p3208 N71-33100

Low speed wind tunnel measurement of induced drag characteristics of three 60 degree delta wings with different leading edge spanwise distributions [KTH-AERO-TR-57] 21 p3373 N71-33100

FA-200XS experimental aircraft for investigating operational problems of STOL type aircraft [NAL-TR-229] 21 p3373 N71-33100

Calculations of aerodynamic properties of fluidic wing grid using Reynolds number [NT-21] 21 p3373 N71-33100

Design and basic characteristics of bearings to gyroscopic devices for aerodynamic and acoustic bearings [JPRS-53883] 21 p3428 N71-33100

Low speed aerodynamic characteristics of McDonnell Douglas scale model space shuttle booster [NASA-CR-103161] 21 p3520 N71-33100

Transonic wind tunnel tests of longitudinal aerodynamic characteristics of GDC/Convair 580 space shuttle booster model [NASA-CR-103158] 21 p3521 N71-33100

Subsonic aerodynamic stability characteristics of NAR 1348 delta wing space shuttle [NASA-CR-103193] 21 p3522 N71-33100

Low speed wind tunnel test to define space shuttle model cruise and landing aerodynamic characteristics [NASA-CR-119855] 21 p3522 N71-33100

Low speed wind tunnel tests of subsonic aerodynamic properties of generic high cross ramp shuttle orbiter [NASA-CR-119859] 21 p3522 N71-33100

Low speed wind tunnel tests of subsonic aerodynamic characteristics of 0.04 scale model of space shuttle [NASA-CR-119862] 21 p3522 N71-33100

Low speed wind tunnel tests of GAC 3A earth orbiting shuttle aerodynamic characteristics [NASA-CR-103153] 21 p3523 N71-33100

Aerodynamic characteristics of GAC 518 earth orbital shuttle at Mach 170 [NASA-CR-103198] 21 p3523 N71-33100

Subsonic aerodynamic characteristics of MDAC/MMC space shuttle booster configuration at Mach 0.26 [NASA-CR-103199] 21 p3525 N71-33100

Aerodynamic characteristics of lift fan installation for direct lift V/STOL aircraft [NASA-TM-X-62006] 22 p3538 N71-33100

Aerodynamic characteristics and flutter of T-tail aircraft configurations [RAE-LIB-TRANS-1546] 22 p3540 N71-33100

Aerodynamic and flight characteristics of supersonic aircraft and spacecraft motion in planetary gravitational fields [AD-726580] 22 p3541 N71-33100

Wind tunnel study of tip vortex modification by mass flow injection [AD-726736] 23 p3706 N71-33100

Development of near-field method for determining supersonic flow properties about bodies of revolution [NASA-TM-D-6508] 23 p3705 N71-33100

Partial admission performance of single stage supersonic turbine at low Reynolds numbers [NASA-TM-X-2382] 23 p3705 N71-33100

Single degree of freedom roll response due to vertical random two dimensional vertical gusts [NASA-CR-111966] 23 p3706 N71-33100

Magnus force and moment data for standard 10 degree cone calibration model as determined in supersonic wind tunnel [BC-DC-71-5031] 23 p3743 N71-33100

Wind tunnel tests to determine static aerodynamic characteristics of space shuttle booster configuration at subsonic speeds [NASA-CR-119964] 23 p3858 N71-33100

SUBJECT INDEX

AERODYNAMIC DRAG

Development of methods for measuring and predicting behavior of rotor with stiff blades at high advance ratios and low rotor speeds
[NASA-TM-X-114362] 24 p3871 N71-37594

Te-134 aerodynamic characteristics during takeoff, climb, horizontal flight, landing stability and maneuverability, and strength under various loads
[AD-727196] 24 p3874 N71-37612

Aerodynamic characteristics of variable sweep wings under a variety of operating conditions
[AD-727210] 24 p3874 N71-37615

Aircraft takeoff, navigation, and landing aids, aerodynamic characteristics, and crew rescue equipment
[AD-727860] 24 p3874 N71-37618

Aerodynamic calculations in designing axial compressors with emphasis on compressors of stationary installations - handbook
[AD-727191] 24 p3929 N71-38032

Low speed wind tunnel tests of 1/25 scale models of aircraft orbital spaceplanes for subsonic aerodynamic data at Mach 0.17
[NASA-CR-119902] 24 p0019 N71-38674

Low speed wind tunnel tests of takeoff, landing, and cruise aerodynamic characteristics of space shuttle booster with exhaust effect simulation
[NASA-CR-119973] 24 p0019 N71-38678

Aerodynamic characteristics of scale model of space shuttle booster at cruise and landing speed of Mach 0.2
[NASA-CR-119974] 24 p0019 N71-38679

Nonlinear angular velocity aerodynamic damping coefficient effects on statically stable missile configurations and internal mass distribution effect based on wind tunnel stability tests
[AD-727113] 24 p0022 N71-38697

Aerodynamic characteristics of TEL-10 lifting body and aerodynamic loads on center fin and control surfaces at subsonic, transonic, and supersonic speeds
[NASA-TM-X-24159] 24 p0022 N71-38700

AERODYNAMIC CHORDS
U AIRFOIL PROFILES
U CHORDS (GEOMETRY)
AERODYNAMIC COEFFICIENTS

Transient pressures and aerodynamic coefficients of rectangular wings in subsonic flow using linear superposition
[NACA-TR-163] 04 p0471 N71-13402

Aerodynamic coefficients, pressure, load and force distributions on cambered delta wings
[ARC-CP-1129] 07 p0966 N71-17112

Trailing vortex systems generated by jet-flapped wing operating at high lift coefficients
[AD-725151] 07 p0973 N71-17753

Dependence of aerodynamic coefficients on maximum thickness and length of axisymmetric bodies in supersonic flow
[JPL-TR-70-54] 08 p1140 N71-18444

Numerical determination of aerodynamic coefficients for thin supersonic wings at various angles of attack
[NASA-TT-F-13521] 08 p1142 N71-18987

Numerical calculation of steady three dimensional potential flow around lifting nonsingular aerodynamic configurations based on surface distribution of quadrilateral vortex rings
[TT-7007] 09 p1317 N71-20115

Approximate solutions for heat transfer and drag coefficients in viscous interacting flow on thin three dimensional body
[NASA-TT-F-13538] 09 p1377 N71-20256

Lift coefficient for wind induced vibration of shrouded cylindrical body
[AD-717759] 11 p1735 N71-22169

Numerical integration method based on potential flow theory to evaluate aerodynamic characteristics of thin supersonic wings
[JPL-TR-71-01] 12 p1851 N71-23597

Measurements of aerodynamic drag, interference lift, and pitching moment on delta wings
[JPL-TR-71-01] 12 p0023 N71-24573

First-order theory of fluctuating lift and drag coefficients for aerodynamically induced motions of rising and falling spherical balloon wind sensors
[NASA-TN-D-6373] 16 p2624 N71-28129

Numerical analysis of aerodynamic loads and coefficients for tandem and T tail surfaces harmonically oscillating in subsonic flow
17 p2696 N71-29335

Drag coefficients of vehicle traveling coaxially with uniform velocity through solid wall tube of finite height
[P-57071] 19 p3076 N71-31763

Computation of aerodynamic basic definitions, including aerodynamic coefficients and relations, expressions, and derivatives of forces and moments
[ARC-RM-3562-PT-4] 20 p3204 N71-32975

Mathematical and standardization data for aircraft dynamics and associated aerodynamics nomenclature and symbols system
[ARC-RM-3562-PT-5] 20 p3204 N71-33028

Free-body tests of flat circular parachutes and determination of aerodynamic drag coefficients during wind tunnel tests
[NASA-TN-D-6423] 20 p3206 N71-33395

Calculation of mean line camber ordinates for laterally symmetrical wings with polygonal planforms
[NASA-TM-X-23111] 20 p3207 N71-35546

Theoretical analysis of trailing edge blowing effects on circulation around airfoils based on iterative solutions with lift coefficients
[AD-726434] 22 p3538 N71-35202

Calculations of helicopter airloads using lifting surface theory compared with experimental data
[AD-726717] 22 p3541 N71-35226

Isothermal elastohydrodynamic theory for full range of pressure-viscosity coefficient for heavily loaded rolling contacts
[NASA-CR-1929] 22 p3588 N71-35550

AGARD report on engine-airplane interference and wall corrections in transonic wind tunnel tests
[AGARD-AR-36-71] 23 p5703 N71-36400

Conclusions and recommendations concerning wind tunnel tests of interaction between engine flow and wall corrections in transonic wind tunnels
23 p5703 N71-36401

Wall corrections for airplanes with interference lift in transonic wind tunnel tests
23 p5704 N71-36403

Drag coefficient measurements in flow around rectangular cylinders
23 p5744 N71-36605

New flow field data for tube-vehicle systems and drag coefficient relationships with relative Mach numbers and relative flow velocity ratios to vehicle velocity
[OASL-TR-70-749] 24 p3908 N71-37856

AERODYNAMIC CONFIGURATIONS
Optimization techniques in aircraft configuration design
02 p0144 N71-11023

Development and characteristics of translating horizontal tail assembly for aircraft stability
[NASA-CASE-XLA-08001-1] 02 p0147 N71-11043

Experimentally determined aerodynamic noise environment analysis for three nose-cylinder configurations
[NASA-CR-102953] 03 p0310 N71-12210

History of Weerling Bf 163 aircraft and configuration modifications
03 p0314 N71-12238

Computer code for prediction of hypersonic flow over cone on high speed sphere-cone vehicles
[SC-DR-70-373] 03 p0343 N71-12489

Application of multivariable search techniques to design of low sonic boom overpressure
[NASA-CR-73496] 05 p0625 N71-14613

Characteristic coefficients technique for probability models of wind profiles in missile design and environment analysis
05 p0718 N71-15215

Variable geometry manned orbital vehicle having high aerodynamic efficiency over wide speed range and incorporating auxiliary pivot wings
[NASA-CASE-XLA-03691] 05 p0773 N71-15674

Experimental aerodynamic performance characteristics of rotor entry vehicle configuration - subsonic
[NASA-TN-D-7046] 06 p0792 N71-16533

European hypersonic wind tunnels for testing hypersonic transport aircraft, and space shuttle aerodynamic configurations
06 p1175 N71-18452

Computer program for determining low speed interference effects of flow fields about arbitrary bodies by superposition
09 p1314 N71-19377

Afterburner-equipped jet engine nacelle with slotted configuration afterbody
[NASA-CASE-XLA-10450] 10 p1639 N71-21493

Wind tunnel tests to determine effects of wing dihedral angle on aerodynamic characteristics of highly swept fixed-wing configuration
[NASA-TM-X-2261] 11 p1671 N71-22622

Steady state inflated shape and included volume of 24 and 30 gore flat circular, extended skirt, porous ring slot, and porous ribbon parachutes
[AD-718008] 12 p1853 N71-23367

Effects of aerostaticity on static longitudinal aerodynamic derivatives
13 p2024 N71-24707

Optimum lift coefficient and aspect ratio determined analytically as conditions for construction of gliders with lift drag ratio of 100
[RAE-LIB-TRANS-1363] 16 p2538 N71-28010

Computerized simulation of shock waves and flow fields behind supersonic edge delta wings and wing-body combinations
16 p2532 N71-28265

Parameter effects on consequences of nose and wing shocks in wing/body pressure signatures for sonic boom reduction
16 p2534 N71-28285

Computerized multivariate design analysis for low sonic boom overpressure supersonic transport configuration
16 p2535 N71-28306

Extrapolation of measured overpressure data for predicting sonic boom characteristics of different aerodynamic configurations
16 p2536 N71-28392

Configuration optimization and performance of air braked hypersonic cruise vehicles
[AD-721471] 16 p2529 N71-28380

Wind tunnel investigation of aerodynamic characteristics of wing-body and lifting body configurations for hypersonic cruise aircraft at hypersonic speeds
[NASA-TM-X-2287] 16 p2536 N71-28061

Symposium on unsteady aerodynamic forces, loads, and configurations for aerodynamic analysis of interior surfaces
[AGARD-CP-80-71-PT-3] 17 p3086 N71-29338

Computer program used for design criteria of stall characteristics of straight wing aircraft
[NASA-CR-16446] 18 p3867 N71-31154

Slotted wind tunnel wall configuration with minimal interference for conventional and V/STOL models
[AD-723294] 19 p3073 N71-31094

High lift aerodynamic and propulsion system configurations for short takeoff aircraft design - bibliography
[AD-724186] 20 p3200 N71-33015

Low speed longitudinal, directional, and lateral static stability characteristics of straight wing aircraft during configuration build-up
[NASA-CR-103156] 21 p3534 N71-33113

Aerodynamic characteristics and flutter of T-tail aircraft configurations
[RAE-LIB-TRANS-1546] 22 p3540 N71-35215

Draft designing of vertical takeoff and landing aircraft
[AD-726572] 22 p3540 N71-35219

Structural analysis of analytical dynamic space shuttle configuration models
22 p3604 N71-36367

Landing edge section of thin airfoil theory
[ARL/SM-NOTE-360] 23 p3703 N71-36399

Minimum drag aircraft shape solutions with respect to flow and turbulent boundary layers for given chord length and heat transfer rate
[AD-726767] 23 p3704 N71-36409

Theoretical method for calculating aerodynamic loading on wing-body combinations
[NASA-TN-D-6441] 23 p3705 N71-36411

Methods for prediction of camberline shock layer thickness and pressure distribution on delta wing body configurations
[NASA-TN-D-6530] 23 p3706 N71-36418

Prediction formulations for transonic fluctuating pressure environments including protruberance induced turbulent boundary layer flows
[NASA-CR-119947] 23 p3741 N71-36677

Aerodynamic characteristics of variable sweep wings under a variety of operating conditions
[AD-727210] 24 p3074 N71-37415

AERODYNAMIC DRAG
NT SUPERSONIC DRAG
Nose lateral spacing effect on drag and performance of twin jet airframe configurations with convergent nozzles at Mach 0.6 to 2.2
[NASA-TM-X-2099] 01 p0115 N71-10276

Geometry of directional gyroscopes mounted on swinging base and aerodynamic resistance of gyroscopes motor
[AD-727229] 02 p0263 N71-11756

Measurement of sphere drag in pressurized gas using magnetic wind tunnel balance
[AD-712741] 05 p0662 N71-14091

Lift, aerodynamic drag and pitching moment study of transport aircraft horizontal tail surfaces in low speed wind tunnels
[ARC-RM-3642] 06 p0791 N71-15702

Aerodynamic drag effects on ramjet missile booster rocket engine
[DLR-FB-70-43] 07 p1117 N71-17036

Lift and aerodynamic drag due to trailing-edge flap on sweptback wings in inviscid subsonic flow
[ARC-CP-1110] 07 p0966 N71-17114

Lift and aerodynamic drag data on slender wings with trailing edge sweepback
[ARC-CP-1130] 07 p0966 N71-17117

Aerodynamic drag measurements on VC-10 aircraft in viscous wind tunnel models
[ARC-CP-1125] 07 p0969 N71-17118

Three dimensional interactions in heat convection fields and effects on laminar momentum adjacent to aircraft fuselage
09 p1309 N71-19547

Wind tunnel evaluation of lifting body store configurations for captive flight drag and separation characteristics
09 p1314 N71-19586

Calculation of profile drag of airfoils at low Mach numbers by predicting laminar and transition points
[NAL-TR-150] 09 p1317 N71-30401

Drag in turbulent wakes behind bluff bodies measured directly and compared with measurements derived from von Karman equation
[DLR-FB-70-37] 10 p1491 N71-30685

Aerodynamic drag inclusion in Vinti missile theory and application to heavy air drag satellite San Marco 2 with increased compressed orbit equation
[NASA-TM-X-65407] 12 p1947 N71-33219

Low aerodynamic drag airfoil designing by Lightbulb method
[ARC-RM-3618] 13 p2021 N71-34090

Dray control method for space shuttle orbiter entry trajectory guidance 14 p2344 N71-26071

Wind tunnel tests to determine effects of retrorocket exhaust on drag of 120 deg cone at subsonic speeds 16 p2682 N71-28115
[NASA-TM-X-2275]

Aerodynamic drag and effects of cavity resonance within two-dimensional rectangular notches in transonic and supersonic turbulent flow with model for cavity drag predictions 17 p2734 N71-29729

Aerodynamic drag of many bodies of revolution in supersonic flow 17 p2702 N71-30325
[DLR-FB-71-04]

Drag coefficient of vehicle traveling coaxially with uniform velocity through solid wall tube of finite length 19 p3174 N71-32144
[PB-197871]

Thrust measurement system and aerodynamic drag effects of underwing J-85 engine nozzles on F-106 aircraft propulsion system performance 19 p3174 N71-32144
[NASA-TM-X-2336]

Near-free molecule drag of slender pointed cones, with reference to hypersonic reentry 19 p3034 N71-32222
[P-4521]

Theoretical analysis of aerodynamic interference induced by cruise and lift fans on transport type aircraft 19 p3034 N71-32453
[NASA-CR-1730]

Free-body tests of flat circular parachutes and determination of aerodynamic drag coefficients during partial inflation 20 p3206 N71-33395
[NASA-TN-D-6423]

AERODYNAMIC FORCES

NT AERODYNAMIC DRAG

NT AERODYNAMIC LOADS

NT GUST LOADS

NT HYPERSONIC FORCES

NT INTERFERENCE LIFT

NT JET LIFT

NT LIFT

NT ROTOR LIFT

NT SUPERSONIC DRAG

NT WING LOADING

NT ZERO LIFT

FORTRAN program for calculating aerodynamic forces from pressure or velocity distributions on blade sections 01 p0001 N71-10467
[NASA-TM-X-2123]

Flutter analysis for thin lifting surfaces by application of supersonic kernel function procedure 01 p0131 N71-10866
[NASA-TN-D-6912]

Free flight measurements of aerodynamic lateral force and moment coefficients using gyroscopes and accelerometers 02 p0141 N71-11001
[BSA-TN-164]

Aerodynamic forces on lifting bodies and delta wings in hypersonic slip flow 06 p0791 N71-15704
[BMW-FB-W-70-41]

Numerical analysis of aerodynamic forces on thin airfoil operating in unsteady potential flow 06 p0792 N71-15827
[NASA-CR-111843]

Mathematical models for aerodynamic forces of aircraft tandem wings using lifting line wing representation 08 p1139 N71-18439
[ONERA-TP-891]

Smooth double-slotted circular cylinder aerodynamic force characteristics measured for circulation control by slot suction 09 p1377 N71-20196
[NRC-11714]

Measurement of force and pressure fluctuations on airfoils during transverse and streamwise gust flows 11 p1670 N71-22374
[CUBDA-TURBO/FR-21]

Data reduction techniques for deriving aerodynamic forces and moments in absence of support interference 12 p1895 N71-23122
[NASA-CR-111844]

Assessment of disturbance torques due to interaction of spacecraft with atmosphere in long duration orbits for use in design of spacecraft attitude control systems 14 p2342 N71-25935
[NASA-SP-8058]

Aerodynamic forces produced in turbine stage by van cascade of cascade series 14 p2339 N71-25998
[NASA-TT-F-13631]

Investigation of aerodynamic forces imposed on vehicles proposed for operation in improved urban transportation system 14 p2196 N71-36129

Measurement of lift and drag forces experienced by ejector in wind tunnel and correlation with geometry and static performance of device 15 p2363 N71-36920
[AD-721192]

Aerodynamic forces and dynamic stability of high-speed, magnetically suspended rocket sled moving close to stationary wall 15 p2390 N71-36943
[SC-DR-70-967]

Computerized simulation of helicopter tactical maneuvers in three body, three dimensional environment including fixed wing and rotary wing aerodynamic forces 16 p2565 N71-38409
[AD-721527]

Unsteady flow in aerodynamic cascades of turbomachinery 16 p2583 N71-38927
[AD-721599]

Symposium on unsteady aerodynamic forces, loads, and configurations for aerostatic analysis of interfering surfaces 17 p2698 N71-29338
[AGARD-CP-80-71-PT-2]

Computer programs for calculating airforce coefficients of wing-horizontal tail and fin-horizontal tail oscillating in subsonic flow 17 p2699 N71-29342

Method for calculating flutter using interference aerodynamic forces between wing and tail 17 p2699 N71-29345

Aerodynamic characteristics of elastic swept wing of aircraft in subsonic flow with given weight, overload, and dynamic head 18 p2865 N71-30656
[NASA-TT-F-13717]

Wind tunnel free flight model trajectory control using photoelectric screen for aerodynamic force determination 19 p3072 N71-31694
[VKI-TN-72]

Compilation of aerodynamic basic definitions, including aerodynamic coefficients, and relations, expansions, and derivatives of forces and moments 20 p3204 N71-32975
[ARC-R/M-3562-PT-4]

Mathematical and standardization data for aircraft dynamics and associated aerodynamics nomenclature and symbols system 20 p3204 N71-33028
[ARC-R/M-3562-PT-5]

Aerodynamic forces and moments on orbiter and booster during space shuttle abort separation 21 p3520 N71-35085
[NASA-CR-103197]

Calculated values of air forces on oscillating thin wings obtained by linearized potential flow 22 p3537 N71-35198
[AGARD-R-583-71]

Aerodynamic force and moment coefficient data for parallel burn vehicle launch configurations tested in isonic wind tunnel for static stability 24 p4018 N71-38671
[NASA-CR-119991]

Supersonic force data for scale model of space shuttle delta wing orbiter 24 p4018 N71-38672
[NASA-CR-119990]

Aerodynamic force and moment coefficients for scale model of expendable second stage modified S-2 alone and mounted piggyback on space shuttle booster from Mach 0.6 to 4.96 24 p4019 N71-38676
[NASA-CR-119977]

Aerodynamic force and static stability data for scale model of space shuttle delta-wing orbiter from Mach 0.4 to 1.3 24 p4019 N71-38677
[NASA-CR-119976]

AERODYNAMIC HEAT TRANSFER

NT HYPERSONIC HEAT TRANSFER

NT SUPERSONIC HEAT TRANSFER

Boundary layer interactions with turbulent heated compressed flows from hypersonic inlets 09 p1376 N71-19552
[NASA-CR-119990]

Mathematical model for predicting erosion of charging ablator in aerodynamic environment 09 p1484 N71-20248
[NASA-CR-119990]

Performance of reentry nose tip facility for missile heat transfer simulations 09 p1568 N71-20251
[SC-DR-70-6162]

Numerical analysis of rare gas injection effects on aerodynamic heat transfer and wall shear stress on blunt bodies under reentry conditions 15 p2394 N71-27608
[SC-DR-70-6162]

Minimum drag airfoil shape solutions with supersonic flow and turbulent boundary layers for given chord length and heat transfer rate 23 p3704 N71-36409
[AD-726787]

AERODYNAMIC HEATING

NT SHOCK HEATING

Eddy viscosity-intermittency factor approach to numerical calculation of laminar, transitional, turbulent heating of sharp cones in hypersonic flow 06 p0835 N71-16217
[AD-714058]

Development of thermal insulation system for wing and control surfaces of hypersonic aircraft and reentry vehicles 07 p1131 N71-17897
[NASA-CASE-XLA-00892]

Aerodynamic heating and structural analyses for radiatively cooled delta wing of hypersonic aircraft 07 p1128 N71-18025
[NASA-TN-D-6138]

Interactions of atoms with space shuttle surface and methods for improving heat transfer 09 p1485 N71-20523
[NASA-TX-62016]

Heat flux sensor adapted for mounting on aircraft or spacecraft to measure aerodynamic heat flux inflow to aircraft skin 11 p1845 N71-23065
[NASA-CASE-XFE-03802]

Conductive heat transfer effect on temperature distributions in vicinity of wing leading edge in hypersonic flow 13 p2184 N71-24446
[ARC-CP-1126]

Tests to determine short-term creep of metals and alloys under conditions of aerodynamic heating with high velocity air flow 14 p2272 N71-25822
[NASA-TT-F-13633]

Heat transfer, aerodynamics, and operational flight mechanics in space shuttle technology 14 p2343 N71-26051
[NASA-TM-X-2272]

Comparison of space shuttle aerodynamic heating analyses for metallic heat shield and surface insulation concepts 14 p2354 N71-26054
[NASA-CR-1042]

Boundary layer transition thermodynamic test data for space shuttle configuration and trajectory analysis 14 p2340 N71-26050
[NASA-CR-1042]

Flow visualization, thermocouple measurements, and analyses of shock interference heating effects on straight wing space shuttle model 14 p2354 N71-26057
[NASA-CR-1042]

Hypersonic shock/density ratio effects in aerodynamic heating of space shuttle configuration 14 p2354 N71-26058
[NASA-CR-1042]

Lee surface flow and aerodynamic heating on delta wing orbiter 14 p2354 N71-26059
[NASA-CR-1042]

Leeward aerodynamic heating of lifting reentry vehicle configurations 14 p2354 N71-26060
[NASA-CR-1042]

Aerodynamic heat determination on blunt bodies in hypersonic flow with force and pressure measurements 15 p2364 N71-27616
[BMW-FB-W-71-08]

Aerodynamic heating distributions on model of space shuttle delta wing orbiter with twin wing tip vertical tails 22 p3694 N71-36841
[NASA-TM-X-62057]

Aerodynamic heating of space shuttle delta-wing booster at free Mach stream 7.4 22 p3695 N71-36842
[NASA-TM-X-62058]

Mach 8 variable-density tunnel used for determination of aerodynamic heating of attached inflatable decelerator configurations 24 p4030 N71-38720
[NASA-TM-X-2355]

Measurement of base heating characteristics of high angle, blunt cones at hypersonic speed 24 p4031 N71-38721
[NASA-CR-1920]

AERODYNAMIC LIFT

U LIFT

AERODYNAMIC LOADS

NT GUST LOADS

NT WING LOADING

Correlation of lift test loads with wind tunnel predicted loads on three lifting body vehicles 01 p0125 N71-10466
[NASA-TM-X-2123]

Low noise turbofan engine without aerodynamic blade loading 02 p0290 N71-11820
[NASA-TN-D-6000]

Fin loads and control surface hinge moments measured in full scale wind tunnel tests on X-24A flight vehicle 05 p0625 N71-16008
[NASA-TM-X-1922]

Effects of external loads on strength of flight vehicles 05 p0627 N71-16009
[AD-713461]

Vertical tail loads and control surface hinge moment measurements on M2-F2 lifting body at subsonic speeds 05 p0775 N71-15800
[NASA-TX-1712]

Stability and postcritical response of infinite wing panels on hinge supports due to aerodynamic loads in hypersonic speed 05 p0779 N71-15804
[NASA-CR-115854]

Computerized prediction of interference flow field for wing-fuselage store location on bomber aircraft 09 p1319 N71-18008
[NASA-CR-119990]

Aircraft wake turbulence with downdraft loading of wing canopy 12 p1851 N71-24446
[AD-718024]

Transonic wind tunnel tests of vertical fin loads on rudder hinge moments on M2-F3 lifting body model at Mach 0.50 to 1.30 13 p2023 N71-30001
[NASA-TM-X-2286]

Analysis of campanage loads and aerodynamic response of T-tail transport aircraft in continuous atmospheric turbulence 13 p2024 N71-30002
[NASA-CR-119990]

Numerical analysis of aerodynamic loads on wing and tail surfaces with oscillations in unsteady supersonic and subsonic flow including interference lift 17 p2697 N71-29340
[AGARD-CP-80-71-PT-1]

Aerodynamic load predicting for control surfaces in unsteady supersonic and subsonic flow 17 p2697 N71-29341
[NASA-CR-1042]

Numerical analysis of aerodynamic loads and coefficients for tandem and T tail surfaces harmonically oscillating in subsonic flow 17 p2698 N71-29342
[NASA-CR-1042]

Wing interference lift line lattice simulation and application to aerodynamic loads on tandem wings in steady flow 17 p2699 N71-29343
[NASA-CR-1042]

Box collocation method for calculating aerodynamic loads on tandem delta wings with oscillations in supersonic flow 17 p2699 N71-29344
[NASA-CR-1042]

Symposium on unsteady aerodynamic forces, loads, and configurations for aerostatic analysis of interfering surfaces 17 p2698 N71-29338
[AGARD-CP-80-71-PT-3]

Kinematics of viscous unsteady airflows on multiple lifting surfaces 17 p2699 N71-29345
[NASA-CR-1042]

Parametric turbine vector diagram calculator for design of highly loaded multistage fan driven turbine 18 p2865 N71-30656
[NASA-CR-1042]

- Calculation of aerodynamic loads acting on
 structures and subprojectiles resulting from shock
 waves [AD-721178] 20 p3383 N71-32814
 High body load relief and model suppression con-
 trol systems for space shuttle vehicles
 [NASA-CR-115165] 22 p3673 N71-36191
 Theoretical method for calculating aerodynamic
 loading on wing-body combinations
 [NASA-TN-D-6441] 23 p3705 N71-36411
 Measurements of unsteady, rotary wing air loads
 and time derivatives for rotor blade intersecting
 constantly rolled up vortex [NASA-CR-15995] 24 p3872 N71-37598
 Wind tunnel study of levels and spectra of pressure
 fluctuations acting on lowered side of straight wing
 open shuttle orbiter during reentry
 [NASA-CR-111960] 24 p4016 N71-38654
 Aerodynamic characteristics of HL-10 lifting body
 and aerodynamic loads on center fin and control sur-
 face at subsonic, transonic, and supersonic speeds
 [NASA-TM-X-3415] 24 p4022 N71-38700
- AEROELASTIC MOMENTS**
U STABILITY DERIVATIVES
AEROELASTIC NOISE
 Experimentally determined aerodynamic noise en-
 vironment analysis for three nose-cylinder configura-
 tions [NASA-CR-102933] 03 p0310 N71-12210
 Aerodynamic broadband noise mechanism applica-
 ble to axial compressors 07 p1013 N71-17958
 Investigation of generation of sound by jet of air at
 high subsonic velocity issuing from slot nozzle and
 passing over rigid, flat plate of finite dimensions
 [NAA-LIB-TRANS-1460] 10 p1541 N71-21226
 Proceedings and recommendations of conference on
 sonic booms [JPLA-71478] 11 p1672 N71-21976
 Aerodynamic sound production and method of
 unified asymptotic expansions 11 p1798 N71-22467
 Aerodynamic characteristics of near wakes
 produced by periodic vortex shedding from airfoils
 [AD-718853] 12 p1964 N71-23245
 Analytic functions and fluid mechanics for noise
 propagation in supersonic jet exhaust flow
 [NASA-CR-1846] 15 p2364 N71-27028
 Chord and rotary wing span differential pressure
 distribution effects on high frequency aerodynamic
 noise propagation from helicopters [AD-721661] 16 p2536 N71-28507
 Relation of Eulerian and Lagrangian structure of
 sound pressure and velocity fields in turbulent
 flow to aerodynamic noise generation
 [NASA-CR-119359] 18 p2906 N71-31211
 Effective source position, strength, and phase cal-
 culations using sound pressure and phase measure-
 ments in near field of choked screw jets
 [DNC-12111] 22 p3629 N71-35855
- AEROELASTIC STABILITY**
 Aerodynamic data recording for determining long-
 range static stability of US-2A aircraft
 [AD-716722] 01 p0805 N71-10563
 Investigation of engine-exhaust-airframe inter-
 ference on cruise vehicle at Mach 6
 [NASA-TN-D-6460] 05 p0625 N71-14635
 Flight test methods for determining aircraft dynamic
 stability [AGARD-R-573-70] 06 p0953 N71-16039
 Resonance instability of finned bodies with non-
 linear aerodynamic characteristics
 [AD-715110] 07 p0968 N71-17733
 Compressible circular jet instabilities with respect
 to spatially growing disturbances
 [NLR-718-51] 08 p1178 N71-18471
 Stability characteristics affecting aerodynamic
 stability over heterogeneous terrain
 [AD-716361] 09 p1382 N71-19603
 Estimated aerodynamics of all-body hypersonic air-
 craft configurations [NASA-TM-X-2891] 09 p1315 N71-19706
 Aerodynamic stability of supersonic free flight
 model from static and dynamic subsonic and super-
 sonic wind tunnel tests [NLR-71-210] 09 p1316 N71-19749
 Stability and response characteristics of diversity
 control rigid rotors at high advance ratios and con-
 tribution of mathematical model with wind tunnel test
 data [NASA-CR-114290] 09 p1325 N71-20421
 Aerodynamically stable meteorological balloon
 using carbon roughness effect [NASA-CASE-XMP-04163] 11 p1677 N71-23007
 Flaps and leading edge modifications for improved
 aerodynamic control stability of military aircraft
 12 p1850 N71-23422
 Steady ground-wind loads with models of space
 shuttle configurations to assess aerodynamic instabil-
 ity on oriented space shuttle vehicles
 13 p2171 N71-24657
 Least squares method and iterative technique for
 obtaining aerodynamic stability derivatives
 13 p3023 N71-24703
- Wind tunnel tests to determine helical engraving ef-
 fects on aerodynamic stability of standard ammunition
 and models 13 p2191 N71-24644
 Aerodynamic characteristics of delta wing space
 shuttle configurations 14 p2195 N71-26862
 Aerodynamic stability control for reentry trajectory
 of space shuttle orbiter at transition maneuver
 14 p2343 N71-26863
 Pressure sensor network for measuring liquid
 dynamic response in flight including fuel tank ac-
 celeration, liquid shock amplitude, and fuel depth
 monitoring [NASA-CASE-XLA-05341] 14 p2242 N71-26387
 Approximation method for turbulence effects on
 aircraft aerodynamic stability with B-52 examples
 15 p2367 N71-27520
 Wind tunnel investigation of control surface instabil-
 ity of lifting body reentry vehicle configurations at
 Mach 15 [NASA-TN-D-6301] 18 p0918 N71-31241
 Linear formulation of aerodynamic stability of plane
 sandwich-type structures placed in current of super-
 sonic gas [NASA-TT-F-13778] 19 p3190 N71-32452
 Dynamic stability of jet transport configuration with
 high thrust-weight ratio and externally blown jet flap
 [NASA-TN-D-6440] 22 p3539 N71-35213
 Principles of helicopter flight including flight stabil-
 ity [AD-724841] 23 p3707 N71-36429
 Satellite stability and interstellar dust grain studies
 [NASA-CR-121929] 24 p4005 N71-38558
- AEROELASTIC STALLING**
 Delayed bubble movement on airfoil during
 helicopter stall [AD-711540] 02 p0141 N71-11085
 Feasibility of using fluid simulator to determine
 stall and reattach characteristics of fighter aircraft
 [NASA-TN-D-6117] 09 p1324 N71-20292
 Unsteady airfoil stall characteristics using static
 data input for predicting stall flutter boundaries of
 space shuttle wing [NASA-CR-111906] 17 p2697 N71-29221
 Analytical investigation of effects of blade flexibili-
 ty, unsteady aerodynamics, and variable inflow on
 helicopter rotor stall characteristics [NASA-CR-1760] 23 p3704 N71-36404
- AEROELASTIC VEHICLES**
U AIRCRAFT
AEROELASTICITY
NT AEROTHERMODYNAMICS
NT HYPERSONICS
NT ROTOR AERODYNAMICS
 Measurements of hypersonic, rarefied flow field of
 disk [AD-710641] 01 p0042 N71-10461
 Basic kinematics and dynamics of human cen-
 trifuges and other aerospace simulators including
 coriolis and gyroscopic effects [AD-711635] 01 p0014 N71-10183
 Designs and data for selecting aerodynamic surface
 control and thrust vector control servomechanism
 [NASA-CR-108686] 02 p0149 N71-11059
 Aerodynamic and structural aspects of all-flexible
 parawings [NASA-CR-1674] 04 p0471 N71-13404
 Subject and author index on aerelasticity docu-
 ments [AGARD-R-578-71] 07 p0967 N71-17432
 Aerodynamics and applications of lift augmentation
 devices - AGARD lecture series [AGARD-LS-43-71] 09 p1321 N71-20051
 Aerodynamic effects of mechanical high lift devices
 on conventional airfoils 09 p1322 N71-20052
 Aerodynamics of pneumatic high lift devices
 09 p1322 N71-20053
 Aerodynamics of variable sweep aircraft design
 09 p1322 N71-20054
 Aerodynamics of two dimensional flow on high lift
 systems 09 p1323 N71-20067
 Wind tunnel investigation of helicopter directional
 control in rearward flight in ground effect [NASA-TN-D-6118] 09 p1346 N71-20191
 Annotated bibliography on engineering aspects of
 design, construction, evaluation, testing, and per-
 formance of aircraft and associated components,
 equipment, and systems [NASA-SP-7037] 10 p4091 N71-20748
 Measurement of macroscopic aerodynamic quanti-
 ties in plasma jets produced by electrothermal and
 hall current accelerators 11 p1812 N71-22639
 Influence of space shuttle configurations on wing
 aerodynamic behavior 13 p2171 N71-24658
 Aircraft development facility with wind tunnel test-
 ing capability [AD-711882] 13 p2027 N71-25043
 Annotated bibliography and indexes on aeronautical
 engineering and aerodynamics - Jan. 1971
 [NASA-SP-7037/02] 14 p2196 N71-26709
- Critique of topics discussed at AGARD meeting on
 aerodynamic interference 18 p2067 N71-31439
 Basics of high speed aerodynamic theory and
 characteristics of gas flows for rockets [NASA-TT-F-601] 18 p3036 N71-31467
 Progress in aerodynamic research and aircraft
 design in Ukraine from 1920 to 1930 [NASA-TT-F-12870] 19 p3033 N71-32185
 Annotated bibliography and indexes on aeronautical
 engineering and aerodynamics - May 1971
 [NASA-SP-7037/05] 19 p3035 N71-32511
 Annotated bibliography and indexes on aeronautical
 engineering and aerodynamics - May 1971
 [NASA-SP-7037/04] 20 p3284 N71-33034
 Annotated bibliography and indexes on aeronautical
 engineering and aerodynamics - July 1971
 [NASA-SP-7037/07] 20 p3285 N71-33174
 Annotated bibliography and indexes on aeronautical
 engineering and aerodynamics - August 1971
 [NASA-SP-7037/08] 21 p3766 N71-36430
 Aerodynamic calculations of poorly stream-
 lined surface and submerged ship structures
 [AD-722268] 24 p3771 N71-37395
 Annotated bibliography and indexes on aeronautical
 engineering and aerodynamics - September, 1971
 [NASA-SP-7037/09] 24 p3772 N71-37399
 Canadian National Science Council research in low
 speed aerodynamics, machine learning, and turbulent
 jet transport [DME/NAS-1971/12] 24 p4013 N71-38626
 National Science Council goals in low speed
 aerodynamics - Canada 24 p4013 N71-38627
 Summaries of air force research activities
 [AD-727338] 24 p4025 N71-38709
- AEROELASTICITY**
 Application of aerelastic constraints in structural
 optimization of aircraft design 03 p0463 N71-15131
 Panel flutter and divergence on structural aerelastic
 problems leading to fatigue failure [NASA-CR-111821] 04 p0471 N71-13405
 Characteristics of flutter in thin plates, shells, or
 membranes due to aerodynamic loading 04 p0415 N71-13610
 Subject and author index on aerelasticity docu-
 ments [AGARD-R-578-71] 07 p0967 N71-17432
 Deterministic aerodynamic characteristics of elasti-
 cally deformed load bearing wing using large aspect
 ratio [AD-716599] 09 p1315 N71-19559
 Optimal control of rotational and translational mo-
 tions of flight vehicles based on torsional and flexural
 deformations [AD-716517] 09 p1320 N71-19696
 Optimization of aerelastic constraints for aircraft
 design using differential equation linearization and
 the element approximation 09 p1479 N71-20139
 Hydroelasticity, aerelasticity, and dynamic stability
 of bars, plates, shells, and beams of various struc-
 tural elements [AD-716038] 10 p1452 N71-20811
 Parameters contributing to aerelastic problems in
 thermal protection of space shuttle 13 p2179 N71-24661
 Aerelasticity and unsteady flow problems of air-
 craft 13 p2023 N71-24706
 Effects of aerelasticity on static longitudinal
 aerodynamic derivatives 13 p2024 N71-24707
 Symposium on unsteady aerodynamic (force, loads,
 and configurations for aerelastic analysis of inter-
 ference surfaces [AGARD-CP-40-71-PT-2] 17 p2088 N71-29358
 Aerelastic and flutter analysis for T tail of Fokker
 F-28 17 p2093 N71-29344
 Aircraft structure elasticity effects on control lever
 deflection and control forces 18 p2172 N71-31043
 Linear formulation of aerelastic stability of plane
 sandwich-type structures placed in current of super-
 sonic gas [NASA-TT-F-13778] 19 p3190 N71-32452
 Semi-infinite flat panel with either homogeneous or
 nonuniform cross section considered for panel flutter
 problems in aerelastic optimization problem [AD-724333] 20 p3536 N71-32974
 Modifications and computational tasks required for
 aerelastic capability in NASTRAN [NASA-CR-111918] 20 p3538 N71-33383
 Examining modal theory for static and dynamic
 aerelastic phenomena 20 p3540 N71-33805
 Experimental aerelastic analysis to determine air-
 worthiness of T-tail configuration of F-38 aircraft
 21 p3573 N71-34082
 Development of method for predicting fatigue life of
 panels under flutter conditions with application to
 Saturn 5 launch vehicle structures [NASA-CR-115994] 21 p3596 N71-34082

Module design modification requirements for incorporating aerostatic capabilities into NASTRAN structural analysis program 22 p3688 N71-36303

AEROGYRO HELICOPTERS

U XH-51 HELICOPTER

AEROLOGY

Optimum interpolations of wind vectors at network grid intersections using aerological station soundings [AD-714432] 06 p0891 N71-16296

Aerological ozone sounding tables and graphs 10 p1547 N71-20854

Tables and graphs of aerological ozone soundings at Hohenpeissenberg, Germany for first half of 1969 10 p1549 N71-21095

Tables on aerological data of Japan - Jan. 1970 11 p1789 N71-22264

Tables on aerological data of Japan - Mar. 1970 11 p1789 N71-22265

Tables of upper air data of Japan for June 1970 12 p1951 N71-23142

Tables of upper air data of Japan for Feb. 1970 12 p1952 N71-23143

Tables of upper air data of Japan for Apr. 1970 12 p1952 N71-23144

Tables of upper air data of Japan for May 1970 12 p1952 N71-23145

Fallout from nuclear explosions, atmospheric turbulence, aerosol propagation, and aerological and hydrometeorological measurements 12 p1952 N71-23178

Tables of aerological and rocket sonde data of Japan - Sept. 1969 21 p3419 N71-34325

Aerological ozone soundings and total ozone measurements during first half of 1970 from West Germany 22 p3614 N71-35742

Standard methods for storage and retrieval of aerometric data [APTD-0663] 24 p3897 N71-37776

AEROMAGNETISM

U GEOMAGNETISM

AEROMAGNETO FLUTTER

U FLUTTER

AERONAUTICAL ENGINEERING

Advanced technology for production of aerospace engines - conference 02 p0289 N71-11626

Foundary precision in domain of aeronautical turbines 02 p0231 N71-11638

Introduction of electrochemical machining in aeronautical industry 02 p0233 N71-11647

Historical development, limits, and future trends in rocket technology 03 p0452 N71-12416

Panel flutter and divergence as structural aerostatic problems leading to fatigue failure [NASA-CR-111821] 04 p0471 N71-13405

Annotated bibliography on engineering aspects of design, construction, evaluation, testing, and performance of aircraft and associated components, equipment, and systems [NASA-SF-7037] 10 p1491 N71-20748

Summary of aeronautical research, and wind tunnels 12 p1852 N71-23931

Annotated reference bibliography on aeronautical engineering documents [NASA-SF-7037/II] 12 p1852 N71-24172

Scientific results from ESRO satellites and from sounding rocket campaign including aeronautical fields, management planning, satellite development, and telecommunication - 1969 report 13 p2188 N71-24447

Tropospheric and ionospheric absorption at VHF for North Atlantic aeronautical satellite system [NASA-TM-X-65507] 13 p2046 N71-24914

Annotated bibliography and indexes on aeronautical engineering and aerodynamics - Jan. 1971 [NASA-SF-7037/III] 14 p2196 N71-26709

Test facilities on structural engineering at FFA, Sweden [FFA-MEMO-61] 17 p2730 N71-29578

Problem of wind gust absorption by aircraft structures, and flight tests of prototype H-100 [NASA-TT-F-13754] 18 p2871 N71-30848

Bibliography of aeronautical engineering with abstracts [NASA-SF-7037/III] 18 p2866 N71-30861

Bibliographies of aeronautical engineering, design, production, evaluation, operation, and performance of aircraft and associated components equipment, and systems [NASA-SF-7037/IV] 18 p2872 N71-31263

Critique of topics discussed at AGARD meeting on aerodynamic interference [AGARD-AR-34-71] 18 p2867 N71-31459

Annotated bibliography and indexes on aeronautical engineering and aerodynamics - May 1971 [NASA-SF-7037/V] 19 p3035 N71-32511

Annotated bibliography and indexes on aeronautical engineering and aerodynamics - May 1971 [NASA-SF-7037/VI] 20 p3204 N71-33036

Annotated bibliography and indexes on aeronautical engineering and aerodynamics - July 1971 [NASA-SF-7037/VI] 20 p3205 N71-33174

Annotated bibliography of aeronautical and mechanical engineering and test reports - Jan. 1971 20 p3371 N71-33948

Thermally resistant polymers for fuel tank sealants of advanced high speed aircraft [NASA-CR-119466] 22 p3587 N71-35546

Annotated bibliography and indexes on aeronautical engineering and aerodynamics - August 1971 [NASA-SF-7037/VI] 23 p3706 N71-36420

Annotated bibliography and indexes on aeronautical engineering and aerodynamics - September, 1971 [NASA-SF-7037/VI] 24 p3672 N71-37599

AERONAUTICS

Proposed objectives of aeronautical and space research 06 p0948 N71-16858

Application of spacecraft technology to aircraft for improvement in systems, materials, and performance [NASA-TM-X-67073] 11 p1826 N71-22394

History of development of aviation and astronautics in USSR [NASA-TT-F-13142] 13 p2191 N71-25024

Survey of very high and ultrahigh frequency utilization in US aeronautics for communication satellite frequency assignment [NASA-TM-X-65527] 14 p2217 N71-25920

Personal and information index for proposed 1972 hearings before Committee on Science and Astronautics of United States Congress 20 p3371 N71-33961

Evaluation of air traffic control parameters and relationship to future of aeronautics [NASA-CR-1833] 21 p3376 N71-34025

AERONOMY

Investigating composition, behavior, and morphology of upper atmosphere over equatorial belt [AD-713199] 05 p0669 N71-14809

Stable aerosol red arcs [BNWL-1484] 07 p1105 N71-16966

Coordinated rocket, satellite, aircraft, and ground measurement program studying physical chemistry of ionospheric D region - PCA 69 [AD-716345] 09 p1382 N71-19575

Activities related to atmospheric physics at IFA, Italy, during 1969 including aeronomy, atmospheric radiation, and atmospheric optics [IFA-TR-29] 15 p2398 N71-27062

Bibliography of Canadian geomagnetism and aeronomy studies 20 p3255 N71-32914

Geomagnetic elements during 1968 for Spain 20 p3266 N71-33601

Photoabsorption cross sections for molecules of aeronomic and astrophysical interest at wavelengths less than 3000 Å [NASA-CR-122098] 22 p3646 N71-36003

Abstracts on solar system, cosmography, meteorology, geophysics, and aeronomy [JPRS-54029] 24 p4036 N71-38796

AEROPHYSICS

U ATMOSPHERIC PHYSICS

AEROSOLS

NT FOG

Gas dynamic stability and damping of detonation wave in aerosols [AD-711753] 01 p0044 N71-10943

Variability and scattering properties of stratospheric aerosols [AD-711682] 01 p0852 N71-10955

Feasibility and capability of electron microprobe analysis for measuring pollutant aerosol particles in atmosphere [PB-189282] 02 p0150 N71-11068

Electron microprobe X ray analysis of atmospheric aerosol particles [PB-189283] 02 p0152 N71-11079

Absorption characteristics of major components of dust clouds in infrared region [AD-712909] 03 p0346 N71-12730

Atmospheric fine structure effect on aerosol vertical distribution in mountainous regions [AD-713024] 03 p0402 N71-12759

Atmospheric haze - components and formation [PB-192102] 03 p0403 N71-13022

Fluorescent particle diffusion test for determining atmospheric motion of chemical warfare agents in forest area [AD-713009] 03 p0404 N71-13376

Aerosol filtration by electrified fibrous filter mats [REPT-1970-17] 04 p0509 N71-13519

Describing aerosol model of hypothetical LMFBR accidents [AF-AEC-12977] 04 p0550 N71-13760

Investigating aerosol transport in laminar, condensing steam boundary layer for analysis of nuclear reactor containment [BNWL-1125] 04 p0554 N71-14015

Measuring fractions of aerosol beta activity in precipitations and settled dust 05 p0720 N71-15706

Determination of atmospheric turbidity by comparing circumferential aerosols with equivalent Rayleigh scattering [AD-714582] 06 p0834 N71-16043

Developing computational procedure to predict characteristics of inertial impactor used for collection of aerosol particles [COO-1240-31] 06 p0923 N71-16744

Diffusion of aerosols in atmosphere near earth surface 07 p1052 N71-14093

Chemical aspects of reactor safety including release and transport of fission products, aerosol behavior, and chemical reactions of metal cladding [HMI-B-99] 08 p1235 N71-16211

Fast reactor program including reactor physics, fuel performance, radiation damage in cladding materials, corrosion behavior in cladding materials, and aerosol research [EURFNR-822] 08 p1235 N71-16211

Axial and radial aerosol diffusion in circular pipes [HASL-238] 08 p1177 N71-16266

Combustion of large magnesium particles during pressure change in ambient medium within range from 100 to 760 mm Hg [NASA-TT-F-13303] 09 p1485 N71-20213

Aerosol analysis during long term simulation of manned regenerative life support system 10 p1506 N71-20064

Piezoelectric disk with ultrasonic nebulization for atomic absorption spectrophotometry [AD-717189] 10 p1561 N71-21996

Equilibrium equations for small ions in region of aerosols and nonaerosol clouds, and reducing atmospheric concentration of charged particles by aerosols [JPRS-52562] 10 p1553 N71-21008

Aerosol and flame ionization techniques for air pollution sampling gas analysis 11 p1747 N71-22808

Thermal conductivity and optical properties of its aerosols [NVO-841-23] 11 p1731 N71-22819

Aerosol behavior and filtration in high pressure environments [AD-717733] 11 p1687 N71-22220

Fallout from nuclear explosions, atmospheric turbulence, aerosol propagation, and aerological and hydrometeorological measurements 12 p1952 N71-23178

Applicability of holography to optical properties of atmospheric aerosols 12 p1968 N71-24008

Characteristics and operating principles of instrument for measuring size of fog droplets and aerosol particles [NLL-M-20291-5828.4F/] 12 p1923 N71-24010

Design and flight performance of rocket-borne dust photometer system for study of aerosol particle distribution in noctilucent cloud [AD-719005] 13 p2105 N71-24010

Diffusion of ion and gas molecules to aerosol particles in nonaerosol regions 13 p2067 N71-23805

Light scattering calculations for brightness effect in Mars atmosphere caused by aerosols 13 p2168 N71-25278

Content and distribution of atmospheric aerosols over the USSR [TT-68-50637] 14 p2252 N71-26009

Atmospheric oxygen, water vapor, and carbon dioxide concentration effects on drop size and sodium compound structures in sodium fire aerosols [AERE-R-6460] 15 p2377 N71-27408

Water vapor and aerosol effects on atmospheric transparency over USSR 15 p2439 N71-27511

Vertical and size distribution of aerosols in troposphere and stratosphere 15 p2402 N71-27522

Mie scattering and absorption parameters of clouds and aerosols 15 p2402 N71-27523

Preservation of coherence in light scattering through aerosols 15 p2439 N71-27524

Tropospheric aerosol effects on light scattering 15 p2402 N71-27525

Atmospheric aerosol effect on elliptical polarization of scattered skylight 15 p2402 N71-27527

Atmospheric aerosols and light scattering 15 p2402 N71-27528

Aerosol concentration within different layers of atmosphere derived from pyrolytic and optical measurements 15 p2402 N71-27529

Relationship of atmospheric scattering coefficient and aerosols acting relative moisture content 15 p2403 N71-27537

Size distribution determination of natural atmospheric aerosols by extinction coefficient 15 p2403 N71-27538

SUBJECT INDEX

AEROSPACE ENVIRONMENTS

Atmospheric models for determining radioactive aerosol particle diffusion into troposphere (RAE-TR-6276) 15 p2403 N71-27700

Aerosol sampling devices and vertical distribution of long lived radioactive and stable elements in atmosphere (N71-16633) 15 p2403 N71-27710

Microanalysis on removal of radioactive aerosols from environment (CONF-70016-VOL-1) 15 p2406 N71-27976

Movements of Co-137 radioactivity and total beta activity from nuclear explosion fallout and aerosols in air suspension over continents, mountains, and oceans (JRA-8-3977) 17 p2738 N71-29236

New habits and abstracts of scientific articles concerning microstructure of aerosols, wind components, and measuring mechanism in thunderstorms 17 p2776 N71-29401

Meteorological and chemical aspects of air pollution and propagation and dispersal of air pollutants - survey of USSR air pollution literature (N71-16634) 17 p2743 N71-29834

Hypodermic acid generated by injection of dissolved iodine into clean air atmosphere or by purging distal aqueous solution of iodine in water with air or other gases - airborne species 17 p2743 N71-29835

Absorption properties of metal aerosols for airborne iodine species to provide support for full scale testing of air pollutants 17 p2715 N71-29860

Pushed bed interparticle porosity calculation from desorption breakthrough distribution moments 17 p2797 N71-29864

NASA specifications for high efficiency particulate aerosol filters including testing and installation (NASA-TM-X-67249) 17 p2756 N71-29879

Statistical correlation between atmospheric moisture content, aerosol particle size, and visual range (JPL-M-9767-5828-4B1) 17 p2744 N71-29889

Collection efficiency of water droplets freely falling through silver chloride aerosol determined by light scattering (N70-3647-2) 17 p2798 N71-30015

Measurement of extinction parameter of tungsten-hydrogen aerosols as function of wavelength at high pressures and temperatures (N71-16641) 18 p3023 N71-30494

Isolation time and flow velocity effects on aerosol wet deposition in pipes with turbulent air flow 18 p2905 N71-31184

Ground-based and snowflake disnometer for particle size measurement of fog and aerosols (AD-72452) 18 p2954 N71-31286

Annotated bibliography of aerosols and particle characteristics of air pollutants (AD-729008) 19 p3092 N71-32630

Aerosol measurements in Los Angeles/California area (N71-16616) 19 p3095 N71-32528

Air pollution in relation to certain atmospheric and meteorological conditions and methods employed in survey and analysis of air pollutants (N71-16527) 19 p3096 N71-32601

Atmospheric circulation and aerosol pollution transport rates of temperature inversions (JRA-82P-34) 20 p3215 N71-32863

High sensitivity and stability characteristics of light scattering photometer for measuring aerosol concentrations (LA-457) 20 p3275 N71-33520

Feasibility of condensing steam in designing aerosol scrubbers for polluted air streams (ORNL-4654) 20 p3245 N71-33533

Calculation of light scattering from aerosols for two standard particle distribution functions (LA-464) 20 p3267 N71-33540

Mathematical model for application of uniform withdrawal assumption in continuous crystallizer design equations to continuous mixing vessel operation 21 p3501 N71-34940

Fog and aerosol analysis with ultra-sensitive detector utilizing optical transmission and light scattering (AD-71766) 24 p3952 N71-38193

Isolation information due to aerosols (JPL-M-30545-9028-4F1) 24 p4004 N71-38557

AEROSPACE ENGINEERING

NT AERONAUTICAL ENGINEERING

Results of lifting body flight tests and findings from other related studies evaluated for application to space shuttle (NASA-TM-X-2101) 01 p0134 N71-10101

Lifting body application to design of space shuttle system 01 p0124 N71-10102

Summary of primary results of lifting body program for space shuttle system 01 p0125 N71-10108

Analysis of research on space shuttle systems 01 p0125 N71-10112

Modeling existing solar cells for temperature control (NASA-CASE-MPO-10109) 02 p0148 N71-11049

Investigating various classes of thermal control surfaces for satellites (RAE-TR-6276) 02 p0305 N71-11136

Thermal insulation for cryogenic applications in aerospace technology 02 p0349 N71-12091

Reviewing development of digital computer systems and components for aerospace vehicles 03 p0346 N71-12682

Investigating federated and integrated architectures to digital computer design for aerospace vehicles 03 p0346 N71-12685

Investigating data word and instruction format factors for selecting common word length in aerospace computers 03 p0347 N71-12687

Bibliography on emittance of high temperature materials including refractory materials, oxides, carbon, graphite, char, and ablative materials for use in aerospace engineering (NASA-CR-102934) 03 p0468 N71-12968

Air cushion landing systems for space shuttle vehicles (NASA-CR-111803) 03 p0457 N71-13087

Considering specific benefits and technology transfer from space research to business, industry, and individual citizens (REFR-91-1673) 04 p0622 N71-14088

Mechanical engineering research in aerospace technology, machine design and industrial processing, and weapons 05 p0636 N71-14667

History of USSR aviation industry, aircraft design, and air transportation 05 p0630 N71-14734

Congressional hearings on feasibility of establishing NASA aerospace museum 05 p0787 N71-15407

Proceedings of Sixth Agard Annual Meeting 06 p0962 N71-16093

Bibliography of technical reports on scientific and engineering studies, November 1970 (NASA-CR-116804) 06 p1288 N71-18705

Bibliography of technical reports on scientific and engineering studies, December 1970 (NASA-CR-116805) 06 p1288 N71-18706

Engineering and scientific information for Mars VII, Mariner Venus-Mercury, and Viking Mars programs (NASA-CR-116806) 06 p1288 N71-18872

Mathematical programming techniques applied to aerospace structural design - algorithmic tools, applications, and literature review (AGARD-AG-169-71) 09 p1478 N71-20128

Basic concepts of mathematical programming applied to structural design of aerospace vehicles 09 p1478 N71-20129

Design optimization of aerospace structures made of elastic/perfectly plastic materials 09 p1479 N71-20131

Analysis of solid rotors used in high speed induction motors for aerospace applications 11 p1677 N71-21898

Test facility to verify design concepts and mathematical models of chromatograph for atmospheric composition analysis of Mars (NASA-CR-117448) 11 p1760 N71-21931

Design and tests of graphite radiant heater for high heat flux sources in spacecraft thermostructural tests (NASA-CR-111841) 11 p1839 N71-21942

Aerospace science and technology transfer to air pollution control problems including mass spectrometry modifications and air pollution monitoring equipment improvements (NASA-CR-117469) 11 p1746 N71-21989

Canadian research on aerospace sciences and engineering, gas and plasma dynamics, and related topics 11 p1827 N71-22513

Structural design criteria applicable for earth-to-orbit space shuttles and independent of external vehicle configuration (NASA-SP-8057) 11 p1832 N71-22570

Review on bionics and interdisciplinary bioengineering areas in aerospace research 11 p1692 N71-23054

Metallic film diffusion for boundary lubrication in aerospace engineering (NASA-CASE-XLE-10337) 12 p1929 N71-24046

Implications of Saturn 5 systems approach to education and other programs (NASA-CR-61347) 12 p2018 N71-24080

Aerospace engineering and computer programming manual for space shuttle synthesis program to simulate spacecraft trajectory and weight analysis for performance prediction (NASA-CR-114906) 13 p2173 N71-24823

Aerospace engineering weight/volume manual for space shuttle synthesis program trajectory and performance predictions (NASA-CR-114907) 13 p2173 N71-24826

Activities in transferring aerospace technology including impact on general public (NASA-CR-118273) 13 p2191 N71-25187

Review of accomplishments in space exploration and future applications of aerospace technology (NASA-TT-X-13674) 13 p2192 N71-25219

Bibliography of technical literature resulting from aerospace research and development at Jet Propulsion Laboratories (NASA-CR-118263) 13 p2192 N71-25249

Assessment of disturbance torques due to interaction of spacecraft with atmosphere in long duration orbits for use in design of spacecraft attitude control systems (NASA-SP-8058) 14 p2342 N71-25925

Preparation and selective applications of high strength steels, titanium alloys, and titanium alloys, polymeric materials, ceramic materials, and composite materials in aerospace engineering (AGARD-LS-51-71) 15 p2429 N71-27038

Soldering device particularly suited to making high quality wiring joints for aerospace engineering utilizing capillary attraction to regulate flow of solder (NASA-CASE-XLA-08911) 15 p2416 N71-27214

Design features of Black Arrow X3 aircraft and experiments including thermal control finishing, improved lightweight solar cell assemblies, and hybrid electronic assemblies (RAE-TR-69203) 16 p2682 N71-28148

Soviet developments in upper atmosphere and space sciences 16 p2584 N71-28150

Research, development, support, and test activities in aerospace nuclear safety program with stress analysis of Pioneer heat shield and Haves Show-I program progress (SC-PR-70-882) 16 p2683 N71-28837

Space engineering, exploration, and communication, and geosynchronous observations of earth resources and astronomy (JPRS-53280) 16 p2686 N71-29148

Lubrication, friction, and wear processes analyzed for space vehicle design criteria (NASA-SP-8063) 18 p2931 N71-31471

Transfer of aerospace technology to nonaerospace problems-NASA project (NASA-CR-121638) 21 p3384 N71-34072

Data on oxygen properties commonly used for engineering calculations over wide temperature and pressure ranges (NASA-CR-121739) 21 p3386 N71-34089

Advanced aerospace systems and control including thrust modulation, optimizer research, fluidic devices, hydraulic jet valves, and related research (NASA-CR-121643) 21 p3413 N71-34256

Reliability testing of aerospace problems including sampling, distribution functions, and accelerated life tests (NASA-TM-X-47877) 21 p3432 N71-34415

Design criteria for passive gravity-gradient libration dampers (NASA-SP-8071) 21 p3453 N71-34598

Design criteria for extendable-retractable nozzles for space engines (NASA-CR-115119) 21 p3502 N71-34947

Design criteria for liquid rocket engine turbopump inducers (NASA-SP-8052) 21 p3502 N71-34950

Handbook of external refrigeration systems for long term cryogenic storage (NASA-CR-115190) 23 p3866 N71-37561

AEROSPACE ENVIRONMENTS

NT COSMOLAR SPACE

NT DEEP SPACE

NT INTERPLANETARY SPACE

NT INTERSTELLAR SPACE

High voltage insulators for direct current in acceleration system of electrostatic thruster (NASA-CASE-XLE-01902) 01 p0116 N71-10374

Metallic film diffusion into metal or ceramic surfaces for boundary lubrication in aerospace environments (NASA-CASE-XLE-01765) 01 p0073 N71-10772

Feasibility of space manufacturing processes at weightless or low gravity conditions 02 p0235 N71-11728

Production of single crystals from containerless melts in weightless space environment 02 p0283 N71-11724

Biophysical evaluation of human vestibular system for aerospace applications (NASA-CR-111607) 03 p0322 N71-12362

Comparison of space and simulated environment conditions using temperature inaccuracy of hollow cylinder 03 p0357 N71-12718

Biological investigations in space environments including circadian rhythms (NASA-CR-111608) 04 p0478 N71-13858

Procedures for employing solar furnace in aerospace environments (CONF-700330-2) 05 p0631 N71-14610

Interpretation of sequence of diffuse plasma resonance observed in space for verification of weak turbulence theory (NASA-TM-X-45435) 06 p0930 N71-16690

Detection of dc voltage breakdown and breakdown processes in space flight environments 06 p0922 N71-16645

Parametric analysis of microwave and laser systems for communication and tracking with emphasis on aspects of operational environment and system implementation [NASA-CR-1689] 07 p0992 N71-17582

Internal loads and stresses caused by space vehicle vibration resulting from induced or natural environments [NASA-SP-8050] 08 p1301 N71-19281

Power input, variation of operating properties, and lubricant consumption of oil lubricated antenna bearing system for communication satellites with force and moment calculations [RAB-LIB-TRANS-1451-PT-2] 09 p1393 N71-19632

Mirror movement analysis by holographic interferometry for application to spaceborne telescopes [NASA-TM-X-2227] 09 p1396 N71-19633

Preparation of inorganic solid film lubricants with long wear life and stability in aerospace environments [NASA-CASE-XMF-03988] 10 p1566 N71-21403

Prelaunch, launch, and inflight earth orbital environment data for HEAO spacecraft [NASA-TM-X-64576] 11 p1831 N71-22178

Natural environment support for space shuttle tests and operations - advanced design and operations concepts [NASA-CR-61346] 11 p1832 N71-22492

Momentum-velocity analyzer for measuring minute space particles [NASA-CASE-XMS-04201] 11 p1765 N71-22990

Metal alloy bearing materials for space applications [NASA-CASE-XLE-03033] 12 p1927 N71-23810

Homogeneity and anisotropy measurements of thermal radiation field surrounding planet Earth 12 p1995 N71-24323

Method and apparatus for adjusting thermal conductance in electronic components for space use [NASA-CASE-XNF-05324] 13 p2185 N71-24876

Space environment simulator for testing spacecraft components under aerospace conditions [NASA-CASE-NPO-10141] 13 p2061 N71-24964

Maneuverable electron beam welder for welding and cutting thin metal sheets in space environment 13 p2087 N71-25239

Manufacturing processes in space environment, including melting and solidification [NASA-TM-X-67178] 14 p2260 N71-26009

Manufacturing processes in space environment for Skylab orbital workshop 14 p2261 N71-26010

Zero-g melting and solidification processes in aerospace environment 14 p2261 N71-26011

Space manufacturing processes based on potential and limitations of g-environment 14 p2261 N71-26012

Chemical and biochemical space manufacturing using scaling laws and Gibbs functions 14 p2261 N71-26013

Electromechanical devices to transfer, position, and retrieve space manufacturing equipment 14 p2261 N71-26014

Environmental adaptation and operational performance of humans in space missions 16 p2554 N71-28547

Oxide and carbide metal matrix composites with thermal shock resistance for use in aerospace environments [AD-721667] 16 p2618 N71-28649

High dc switch for causing abrupt, cyclic, decreases of current to operate under zero or varying gravity conditions [NASA-CASE-LEW-10155-1] 16 p2573 N71-29035

Geophysics and space data bulletin for Oct., Nov. and Dec. 1970 [AD-722438] 17 p2745 N71-29913

Experimental data on high velocity impacts up to 20 km/sec applied to punctures in space and concentration of micrometeoritic material near earth [NASA-TT-F-13740] 18 p3022 N71-31484

Head and eye movements affected by angular velocity and linear acceleration in aerospace environments [DR-208-VOL-1] 18 p2878 N71-31526

Vestibular system associated with body movement in aerospace environments [AMRU-R-46-2] 18 p2880 N71-31536

Aerospace environments affecting flight crew fatigue [AMRU-R-47-3] 18 p2881 N71-31542

Angular velocity and linear acceleration effects on visual perception in aerospace environment [AMRU-R-48-2] 18 p2881 N71-31544

Performance tests on cadmium sulfide and cadmium telluride thin film solar cells to be used in aerospace environments [ONERA-NT/82/19/70] 20 p3213 N71-33189

Conference on aerospace environments, manned space flight, weightlessness simulation, musculoskeletal and cardiovascular systems, bone loss, mineral metabolism, and hematology [NASA-SP-269] 20 p3216 N71-33251

Space environment radiation effects on solar cell degradation [NASA-CR-121614] 21 p3378 N71-34036

Measurement and analysis of heavy cosmic rays with high altitude balloons 21 p3506 N71-34977

Requirements, quantities, location, and temperature environment limitations of sensors for space shuttles 21 p3514 N71-35038

Developing suitable solid state power controllers for space vehicles electrical power systems [NASA-CR-119961] 24 p3898 N71-37781

Van Allen belt radiation on Tiros/TOS/ITOS spacecrafts - graphs [NASA-TM-X-63717] 24 p4002 N71-38546

Space environmental conditions, solar radio emission, solar spectrum, cosmic rays and terrestrial magnetism [AD-727778] 24 p4014 N71-38636

AEROSPACE INDUSTRY

NT AIRCRAFT INDUSTRY

Manufacturing technology and production engineering methods in aerospace industry 02 p0231 N71-11627

Value engineering effects on engine design and production in aerospace industry 02 p0231 N71-11628

Electromagnetic pulse forming process for aerospace assembly manufacturing 02 p0233 N71-11649

Modern welding methods in aircraft and aerospace industry 02 p0233 N71-11650

Policies for participation of French aerospace industry in space programs 02 p0307 N71-12669

Results of 1968 survey of industrial research and development [NSF-70-29] 06 p0962 N71-16806

European aerospace industry and NASA space shuttle and space station programs 07 p1132 N71-17159

European aerospace and electronic equipment industrial cooperation for air traffic control and communication satellites 07 p1132 N71-17181

Participation of European aerospace industry in European space programs and NASA programs 07 p1133 N71-17182

European aerospace industry role in NASA space shuttle program 07 p1118 N71-17211

US and European international aerospace industry cooperation 07 p1133 N71-17215

Soviet aviation R and D structure and management [AD-716410] 09 p1320 N71-19769

Recommendations for future NASA manned and unmanned programs [RIB-A-59] 10 p1666 N71-21581

Aerospace price indexes for component and material cost changes [AD-718089] 12 p2019 N71-24108

Economic appraisal of British aerospace industry and plans for future development 18 p3029 N71-30940

Conversion of US scientific and technical resources from defense and aerospace to civilian objectives [GUPS-MON-8] 20 p3371 N71-33825

AEROSPACE MEDICINE

Annotated bibliography and indexes on Aerospace Medicine and Biology - Sept. 1970 [NASA-SP-7011/80/1] 01 p0008 N71-10125

Physiopathology and pathology of spinal affections in aerospace medicine [AGARD-AG-140-70] 01 p0008 N71-10175

Aviation medicine studies - bibliography [AM-70-11] 01 p0009 N71-10298

Peculiarities of human heat exchange under reduced atmosphere pressure and sufficient oxygen supply [NASA-TT-F-13374] 01 p0010 N71-10367

Homeostasis during weightlessness [NASA-TT-F-13373] 01 p0010 N71-10368

Research progress in technology transfer by NASA Biomedical Application Team [NASA-CR-111131] 01 p0012 N71-10541

Annotated bibliography of reports related to aerospace medicine including radiobiology and stress physiology [AD-710764] 01 p0012 N71-10594

Lectures in aerospace medicine [AD-711792] 02 p0153 N71-11085

Aerospace medicine and bioastronautics conference papers [JPRS-51660] 02 p0156 N71-11105

Legal, preventive, and clinical aspects of aerospace medicine [AGARD-CP-61-70] 02 p0161 N71-11101

Medical and legal aspects of aircraft accident fatality investigation by aviation pathologist 02 p0162 N71-11105

Utilization of potassium superoxide in regenerating expired gas 02 p0165 N71-11180

Annotated bibliography and indexes on Aerospace Medicine and Biology - Sept. 1970 [NASA-SP-7011/81/1] 03 p0322 N71-12800

Military aeromedical education, physiological training, civil aeromedical education, and survival training in various countries 04 p0477 N71-13810

Aeromedical training in Canadian facilities 04 p0477 N71-13811

Education and training of US Air Force flight engineers 04 p0477 N71-13812

Aviation medicine training in US army 04 p0477 N71-13813

Aviation medicine training in Royal Air Force 04 p0477 N71-13814

Functions of aeromedical training section of Royal Air Force 04 p0477 N71-13815

Aerospace medicine training in France 04 p0477 N71-13816

German aeromedical training for medical and paramedical personnel 04 p0477 N71-13817

Norwegian Air Force aerospace medicine training programs 04 p0477 N71-13818

Italian aerospace medicine training for military and civilian personnel 04 p0478 N71-13819

Civil aerospace medical activities in Germany 04 p0478 N71-13820

Requirements of English medical schools for diploma in aviation medicine 04 p0478 N71-13821

Training of flight surgeons for civil aviation in Great Britain 04 p0478 N71-13822

Canadian aircrew operational aeromedical training 04 p0482 N71-13823

Physiological training of flying personnel in German Armed Forces 04 p0482 N71-13824

Aerospace medical training in Royal Netherlands Air Force 04 p0478 N71-13825

Survival training in Royal Netherlands Air Force 04 p0483 N71-13826

Physiological training of military and civilian aircrews in cooperation with engineers in France 04 p0483 N71-13827

Positive pressure breathing techniques for stress survival in low pressure environments 04 p0483 N71-13828

Radiology and radiobiology instruction for aerospace medicine applications 04 p0478 N71-13829

Aerospace medical training and qualifications of medical personnel 04 p0478 N71-13830

Annotated bibliography and indexes on Aerospace Medicine and Biology - Nov. 1970 [NASA-SP-7011/82/1] 04 p0480 N71-14471

Auditory damage risk criteria applied to aerospace operations [AD-713071] 05 p0734 N71-15300

Biomedical effects of weightlessness and confinement on man and other organisms [AD-714406] 06 p0801 N71-16239

Biomedical technology applications and operational description of Application Team Program [NASA-CR-116150] 06 p0803 N71-16488

Aeromedical aspects of manned space flight [JPRS-52309] 06 p0803 N71-16489

Annotated bibliography and indexes on Aerospace Medicine and Biology - Nov. 1970 [NASA-SP-7011/83/1] 07 p0982 N71-17449

Annotated bibliography and indexes on Aerospace Medicine and Biology - Dec. 1970 [NASA-SP-7011/84/1] 07 p0982 N71-17450

Noise associated with operation of C-9A aeromedical evacuation aircraft [AD-715222] 08 p1142 N71-18310

Investigating physiological and biological effects of prolonged space flight on Soyuz 9 crew members [JPRS-52402] 08 p1149 N71-18311

Discussing basic principles and methods for evaluating health, functional capacity, and psychological peculiarities in cosmonaut selection 08 p1150 N71-18312

Transactions on space biology and medicine [JPRS-52121] 08 p1153 N71-18313

Proceedings summary for meeting on aviation and space medicine research 08 p1156 N71-18314

Summary data on aviation and space medicine research 08 p1156 N71-18315

Schedule of AGARD conferences for 1971, and summaries of 1970 AGARD publications [AGARD-BUL-71-1] 08 p1142 N71-19114

AGARD Glossary of Aerospace Medical Terms [AGARD-AG-153-71] 09 p1332 N71-20876

SUBJECT INDEX

AEROSPACE VEHICLES

- North Atlantic Treaty Organization conference on adaptation and acclimatization in aerospace medicine (AGARD-CP-42-71) 09 p1334 N71-20351
Medical observation of spacecrew during long duration space station simulation test 10 p1498 N71-20990
Physical fitness of flying personnel and aging of flight crew performance (AGARD-CP-41-71) 11 p1687 N71-23301
Space biology and medicine including selection and training of cosmonauts, flight safety, and health during long space flights (JPRS-53229) 12 p1862 N71-23241
Biodynamics, aerospace medicine, acceleration stresses, human tolerances, centrifuges, test facilities, and associated bibliography (AGARD-CP-156) 12 p1863 N71-23337
Agreement between NASA and Academy of Sciences of USSR for data exchange (NASA-NEWS-RELEASE-51-77) 12 p2016 N71-23742
Annotated bibliography indexes on Aerospace Medicine and Biology - Feb. 1971 (NASA-SP-7011/847) 12 p1864 N71-24174
Annotated bibliography of translations of foreign language articles on aviation medicine, vestibular function, body temperature, and physiological effects (PAA-AIM-71-5) 13 p2033 N71-24745
Annotated bibliography and indexes on Aerospace Medicine and Biology - March 1971 (NASA-SP-7011/877) 14 p2203 N71-25745
Metabolic effects of long duration exercise at moderate work loads including tables of heart rate, vital temperature, minute volume, water balance, and respiratory quotient (NASA-CR-113033) 15 p2372 N71-27784
Aerospace medicine, life support system, and psychophysiological problems and environmental factors in space flight (JPRS-53311) 16 p2549 N71-28094
Microbiological ecology of manned space flights, canning, sterilization, and life support systems (JPRS-53308) 16 p2542 N71-28248
Space biology and aerospace medicine research studies 16 p2696 N71-28267
Regenerative space station simulator and test procedures for 4 man, 90 day testing of life support systems (NASA-CR-111882) 16 p2559 N71-28281
Pressure sensors, blood flow transducers, pH electrodes, and photographic recording of biological data for use in aerospace medicine (NASA-CR-119024) 16 p2550 N71-28284
Effects of changes in partial pressure of carbon dioxide on acid-alkali equilibrium in human blood 16 p2546 N71-28489
Medical examination of civil aviation flight personnel to determine predisposing factors for atherosclerosis 16 p2547 N71-28491
Biotechnological problems of man machine systems required for long duration space flights (NASA-SP-285) 16 p2551 N71-28526
Nonregenerative tradeoff study for cabin atmosphere selection in manned space flight 16 p2552 N71-28531
Work environment and task factor effects on long term crew effectiveness (AD-72417) 17 p2711 N71-29482
Technology transfer and applications in medicine and biology (NASA-CR-119181) 17 p2709 N71-30290
Bibliography of Soviet literature on high altitude and aerospace medicine and biology - 1965 to 1967 (JPRS-53329) 17 p2846 N71-30367
Annotated bibliography and indexes on Aerospace Medicine and Biology - Apr. 1971 (NASA-SP-7011/887) 18 p2876 N71-30856
Cumulative index for abstracts of NASA documents on aerospace medicine and biology (NASA-SP-7011/851) 18 p2876 N71-31077
Annotated bibliography and indexes on aerospace medicine and biology - May 1971 (NASA-SP-7011/891) 18 p2876 N71-31201
Annotated bibliography and indexes on Aerospace Medicine and Biology - May 1971 (NASA-SP-7011/907) 18 p2876 N71-31230
Annotated bibliography and indexes on Aerospace Medicine and Biology - June 1971 (NASA-SP-7011/911) 18 p2877 N71-31231
Analysis of equipment, crew training, and operation involved in use of fixed wing aircraft for astronomical transportation (PAA-AIM-71-18) 19 p3038 N71-32060
Description and application of aeromedical standards to crew selection, aircraft design features, and operational guidelines for spacecraft design (PAA-AIM-71-33) 19 p3044 N71-32083
Research and development, weightlessness simulation, calcium metabolism, manned space flight, pressure suits, immobilization, and aerospace medicine 20 p3219 N71-33273

- Medical and biological problems of prolonged manned space flight (JPRS-53801) 20 p3220 N71-33451
Hardware and techniques for studying human circulatory performance in space environment (NASA-CR-121666) 21 p3580 N71-34052
Combined effects of reduced nutrition, hypokinesia, and centrifugal acceleration on human body (JPRS-54104) 23 p3716 N71-36488
Annotated bibliography and indexes on Aerospace Medicine and Biology - Aug. 1971 (NASA-SP-7011/921) 23 p3716 N71-36490
Annotated bibliography and indexes on Aerospace Medicine and Biology - Sept. 1971 (NASA-SP-7011/931) 23 p3716 N71-36491
AEROSPACE SCIENCES
Conference on new horizons in aerospace science 02 p6388 N71-12106
Organization and research projects of aerospace laboratory during 1969 03 p0469 N71-12983
Applications of aerospace technology in biology and medicine (NASA-CR-115888) 05 p0636 N71-14601
Developments in space science that led to Apollo 11 flight 05 p0766 N71-14615
Space science training materials and motivation of high school algebra students 07 p1133 N71-17778
Technological, medical, geological, and meteorological advancements produced by space program (NASA-TM-X-58055) 07 p1116 N71-18003
Bibliography of technical reports on scientific and engineering studies, November 1970 (NASA-CR-116804) 08 p1288 N71-18705
Bibliography of technical reports on scientific and engineering studies, December 1970 (NASA-CR-116803) 08 p1288 N71-18706
Application of spacecraft technology to aircraft for improvement in systems, materials, and performance (NASA-TM-X-67073) 11 p1826 N71-22394
Aerospace scientific and technological studies in 1969 for satellite systems and spacecraft missions (NASA-SP-251) 13 p2192 N71-25256
Supplement to Data Catalog of Satellite Experiments (NASA-TM-X-67181) 14 p2338 N71-26321
Congressional hearings on NASA accomplishments and future programs for space exploration, aerospace sciences, and technology utilization 14 p2361 N71-26777
Abstracts of published Soviet articles concerning research in geophysics, astronomy, and space (JPRS-52989) 15 p2396 N71-26859
Sino-Soviet block countries accomplishments in sciences of astronomy, oceanography, terrestrial geophysics, and upper air and space (JPRS-53134) 15 p2396 N71-26901
Flights to other planets, Cosmos satellites, international space law, and USSR space achievements 15 p2397 N71-26906
Effect of scientific and technical progress in controlling national economy and evaluation of effectiveness of science 16 p2695 N71-29066
Developments in scientific research, plasma physics, electronics, information theory, radio astronomy, and lasers (AD-726234) 16 p2695 N71-29067
Space research program in Finland during 1970 (S-39-1971) 17 p2861 N71-29633
Comparison of productivity of scientific work in industrial production in USSR (AD-722607) 17 p2862 N71-30277
Geology of minerals as space age earth resource possibility 18 p2911 N71-30841
Statistical mechanics for wall shear turbulence in Couette flow based on Brownian motion and comparison with stochastic theory based on Navier-Stokes equation (NASA-SP-4014) 19 p3034 N71-32246
Strain hardening and stress relaxation effects on crack propagation with problem notes on plasma physics, communication sciences, electronics, metallurgy, and ocean and space technology 20 p3360 N71-33871
Personal and information index for proposed 1972 hearings before Committee on Science and Astronautics of United States Congress 20 p3371 N71-33961
Application of aerospace technology to aerospace problems (NASA-CR-121636) 21 p3414 N71-34295
Chemical spot test for identification of titanium and titanium alloys for aerospace use (NASA-CASB-LAR-10539-1) 21 p3437 N71-34457
Application of aerospace and defense industry resources and technology to solution of environmental problems 21 p3533 N71-35180
Scientific developments in Europe involving treatment of cholera, treatment of bacterial endocarditis,

- automated system for epidemiological information, and air traffic control (JPRS-53877) 21 p3534 N71-35187
Analysis of role of research and development in furthering national welfare and allocation of scientific resources (NSF-71-18) 21 p3534 N71-35189
Proceedings of Panel on Science and Technology before Committee on Science and Astronautics of US House of Representatives, Ninety-second Congress 21 p3534 N71-35190
Curriculum supplement to assist general chemistry teachers in updating instruction materials with aerospace developments (NASA-EP-87) 24 p3083 N71-37091
AEROSPACE SYSTEMS
Concepts of Space Programming Language (AD-711708) 02 p0189 N71-11338
Research and development in aerospace nuclear safety program (SC-PR-70-435) 03 p0422 N71-12667
Design and operation of aerospace phased array radar 04 p0496 N71-13916
Mass loading effects on pyrotechnic shock environment of aerospace systems 08 p1300 N71-19250
Program and introduction for Fifth NASA Intercenter and Contractors Conference on Plasma Physics (NASA-TM-X-64953) 09 p1447 N71-19805
Program of proceedings and abstracts presented at Sixth NASA Intercenter and Contractors Conference on Plasma Physics (NASA-TM-X-64950) 09 p1448 N71-19809
Computerized simulation of aerospace systems for advanced spacecraft design 09 p1567 N71-20234
Research and development in aerospace systems including design and fabrication of 4-ft trisonic wind tunnel 11 p1731 N71-22331
Dynamic electrical characteristics of 400 Hz Brayton cycle turboalternator and controls for space application (NASA-TN-D-6183) 11 p1677 N71-22364
Cost distributions and facility and tooling cost impact on unit production costs for 2 and 20 per unit production rates in state of art, improved, and advanced manufacturing technologies (NASA-CR-114281) 12 p1931 N71-34180
Economic analysis of facilities, tooling, premanufacturing and manufacturing operations, and quality control labor in aluminum aerospace industry base on Saturn/Apollo data (NASA-CR-114282) 12 p1931 N71-34181
Manufacturing factors and technologies in aluminum aerospace industry base on Saturn/Apollo data (NASA-CR-114283) 12 p1931 N71-34182
Considerations by NATO of transonic wind tunnel requirements to support evolution of aeromedical and aerospace systems during next decade (AGARD-AR-35-71) 13 p2066 N71-25073
Microelectronic power supply circuits for aerospace applications (NASA-CR-119918) 20 p3214 N71-33595
High temperature cycling tests of high performance adhesives for aerospace applications (NASA-CR-121632) 21 p3442 N71-34495
Basic principles, development, and earth and space applications of isotopic SNAP systems 21 p3477 N71-34764
Computer controlled electric power distribution system for aerospace systems 21 p3514 N71-35040
Self adjusting numerical control of linear system and application to aerospace system (ONELA-P-134) 22 p3486 N71-33679
AEROSPACE VEHICLES
Remote data acquisition terminals for aerospace vehicles 04 p0305 N71-13817
Application of ray tracing method to computer program for estimation of sound intensity from rising space vehicle (NASA-CR-102945) 04 p0506 N71-14081
Motion of liquids enclosed in aerospace vehicle tanks under weak gravitational fields - Vol. I (NASA-CR-113117) 04 p0604 N71-14225
Selective excitation spectroscopy used in plasma diagnostics for advanced aerospace vehicles (AD-716002) 09 p1449 N71-20015
Conference papers on thermodynamics and thermophysics involved with spacecraft temperature control (AD-717822) 11 p1830 N71-22819
Development of resilient fastener for attaching skin of aerospace vehicles to permit movement of skin relative to framework (NASA-CASB-XLA-01827) 12 p3081 N71-34035
Computer program using numerical integration techniques for computation of meteoroid impact and angular distributions over complex geometric spacecraft configurations (NASA-CR-103102) 12 p3083 N71-34935

- Performance, dynamics, and design of aeronautical and space vehicles
[NASA-SP-238] 13 p2172 N71-34701
- Scheme of notation and nomenclature for aircraft dynamics and aerodynamics
[ARC-R/M-3562-PT-1] 20 p3204 N71-33027
- Pre-processor, post-processor, and multiple level restructuring routines for data management in support of NASTRAN finite element structural analysis of spacecraft
22 p3688 N71-36298
- NASTRAN post-processor routine for space-truss structural frameworks
22 p3688 N71-36300
- AEROSPACEPLANES**
- Linear multichannel control systems for supersonic aerospace vehicles orbiting in earth atmosphere
[AD-714796] 07 p1057 N71-17747
- Low speed wind tunnel tests of 1/25 scale models of reusable orbital spaceplanes for subsonic aerodynamic data at Mach 0.17
[NASA-CR-119982] 24 p4019 N71-38674
- AEROSTATS**
- U AIRSHIPS**
- AKROTHERMOCHEMISTRY**
- Mathematical model for impulsive heat releases by chemically generated waves in atmosphere
[NASA-TM-X-65560] 15 p3441 N71-27844
- AKROTHERMODYNAMICS**
- Electric and magnetic cross field effects on aerodynamics and thermal regime of gas flame cone
[AD-712336] 02 p0306 N71-12075
- Combustion chemistry and mixing in supersonic flow
[AD-714109] 06 p0961 N71-16886
- Aerothermodynamics of space shuttles
[NASA-TM-X-668977] 08 p1292 N71-18433
- Lift augmentation devices effect on STOL engine - Part 2, thermodynamic problems
09 p1323 N71-20062
- Thermal analysis of space hold performance of multilayer insulation on upper half of unshrouded liquid hydrogen tank within sun oriented vehicle
[NASA-TN-D-6255] 10 p1663 N71-21557
- Enthalpy and wall heat flux calculations for stagnation region aft of blunt axisymmetric bodies in hypersonic axial flow
[AD-717418] 11 p1735 N71-22087
- Combined free and forced laminar convective heat transfer to nonNewtonian fluids flowing in constant wall temperature vertical tubes and controlling parameter analysis
11 p1742 N71-22702
- Wind tunnel simulations of flow fields and aerothermodynamics of space shuttle orbiters
14 p2240 N71-26053
- Air flow thermodynamics for low sonic boom design of supersonic transport configurations
16 p2535 N71-28367
- French research aerothermodynamic facility at Modane-Avrioux including wind tunnels and auxiliary installations
[ONERA-NT-181] 19 p3073 N71-31814
- AEROZINE**
- Bubble-point method and gas content-method for determining helium saturation level of AeroZINE-50 and nitrogen tetroxide
[NASA-TN-D-6249] 11 p1832 N71-22612
- APC (CONTROL)**
- U AUTOMATIC FREQUENCY CONTROL**
- APCS (CONTROL SYSTEM)**
- U AUTOMATIC FLIGHT CONTROL**
- APERTURE NERVOUS SYSTEMS**
- Ischemic differentiation of striated muscle tissue
08 p1153 N71-19058
- AFFINITY**
- Affinity of metals to sulfur
[TT-70-57082] 03 p0391 N71-12830
- Electron affinity calculations for Li, B, O, F, C, and N and self consistent field equations for multiple open shells
21 p3492 N71-34878
- AFRICA**
- Nimbus 2 and 3 HIR measurements of upwelling along Somali coast
[NASA-TM-X-65387] 03 p0369 N71-13088
- Magnetic survey of iron deposits in Tanzania
[BULL-120] 05 p0671 N71-14844
- Regional significance of volcanic geochemistry in far Triple Junction, Ethiopia
[NASA-CR-117136] 09 p1383 N71-19732
- Atmospheric temperature annual variations obtained from North Africa upper atmosphere radio probe
[GEOPHYSDEW-FM/164-PT-9] 12 p1912 N71-23691
- Atmospheric density annual variations obtained from North Africa upper atmosphere radio probe
[GEOPHYSDEW-FM/165-PT-10] 12 p1912 N71-23692
- Geological examination and petrographic analysis of Rikhat and Semsiyat domes in central Mauritania
18 p2913 N71-30994
- Comparison of continental margins of eastern North America at Cape Hatteras and Africa coast at Cap Blanc
18 p2915 N71-31010
- Geophysical data and regional geology indications of existence of salt domes in Atlantic Ocean off coast of northwest Africa
18 p2915 N71-31012
- Analysis of meteorological conditions leading to hurricane formation and determination of point of origin off coast of Africa
18 p2951 N71-31015
- Analysis of structure and motion of four major wave disturbances over Africa and development of three storms into hurricanes
18 p2951 N71-31017
- Color enhancement and multispectral methods for studying dynamics of upwelling water in connection with Somali, Canary, Benguela, and Agulhas Currents - satellite data
[NASA-TM-X-65643] 19 p3092 N71-32148
- Measurement of radioisotopes and nuclides in environment near nuclear research center of South Africa
[FRL-205] 21 p3467 N71-34682
- Radiation measurements in Africa applied to evaporation-perspiration determination in tropical region climate
22 p3613 N71-35738
- AFTERBODIES**
- Nozzle lateral spacing effect on drag and performance of twin jet afterbody configurations with convergent nozzles at Mach 0.6 to 2.2
[NASA-TM-X-2099] 01 p0115 N71-10276
- Aircraft afterbody and engine nozzle interferences at subsonic, transonic, and supersonic speeds
[NASA-TM-X-66888] 09 p1313 N71-19368
- Afterburner-equipped jet engine nacelle with slotted configuration afterbody
[NASA-CASE-XLA-10450] 10 p1639 N71-31493
- Planetary Atmospheric Experiments Test (PAET) ablative afterbody thermal performance and component mechanical properties
[NASA-CR-114293] 11 p1844 N71-22715
- Aerodynamic characteristics of large angle blunt cone with and without fence-type afterbodies
[NASA-TN-D-6269] 12 p2001 N71-24083
- Measurement of convective heat transfer rates on conical nosecap and hemispherical afterbody configuration at hypersonic speed
[NASA-TN-D-64533] 16 p2691 N71-28862
- Transonic testing of double fuel engine nacelles with two separate models for air intake and afterbody
[ONERA-TP-943] 20 p3287 N71-33794
- Thrust-noise-drag forces and pressure distributions of closely spaced twin-jet afterbodies with diffusers inboard-outboard fairing and nozzle shapes
[NASA-TM-X-2329] 23 p3705 N71-36412
- AFTERBURNERS**
- U AFTERBURNING**
- Gas dynamics of fan jets at various injection angles
[AD-714796] 07 p1104 N71-18034
- Two variations of gas generator method to calculate thrust of afterburning turbofan engines installed in F-111A aircraft
[NASA-TN-D-6297] 11 p1821 N71-22614
- Gaseous fission measurements from jet engine afterburners over range of fuel-air ratios
[NASA-TM-X-2323] 17 p2859 N71-30117
- Afterburning flame stabilization in turbofan engines
[NASA-TT-P-13657] 17 p2840 N71-30350
- Exhaust emissions from reciprocating aircraft engines, and afterburning of exhaust gases on contact with ambient air - air pollution study
[PB-197627] 18 p3028 N71-31569
- Preliminary sector tests at 920 K of three afterburner concepts proposed for inlet temperature of 1260 F and comparison of results with conventional V-gutter flame holder
[NASA-TN-D-6437] 19 p3192 N71-32191
- AFTERGLOW**
- NT HELIUM AFTERGLOW**
- Enhanced transmission of strong right hand circular wave near cyclotron resonance in afterglow helium slab plasma occurring earlier than corresponding weak electromagnetic field
[AD-723293] 19 p3166 N71-32596
- AFTERIMAGES**
- Computerized simulation of lateral inhibitory networks of visual afterimages
11 p1693 N71-23067
- AGC (CONTROL)**
- U AUTOMATIC GAIN CONTROL**
- AGE DETERMINATION**
- U CHRONOLOGY**
- AGE FACTOR**
- Age and exercise factors influencing osteoporosis, bone strength, and acceleration tolerance investigated using rhesus monkeys
[AMRL-TR-70-74] 09 p1336 N71-20359
- Seasonal variations in thermoregulation of residents in hot, dry climates with respect to age and sex
11 p1679 N71-22083
- AGE HARDENING**
- U PRECIPITATION HARDENING**
- AGGREGATES**
- Uniqueness and convergence of discrete aggregate model in polycrystalline plasticity
[AD-712660] 03 p0441 N71-12810
- AGING (BIOLOGY)**
- Physical fitness of flying personnel and aging effects on flight crew performance
[AGARD-CP-81-71] 11 p1687 N71-32000
- Physical fitness assessment of older pilots in relation to flight requirements and physiological responses
11 p1687 N71-32001
- Exercise effects on physical fitness and cardiovascular system of aging pilot
11 p1689 N71-32002
- Electrocardiographic and blood pressure standards of physical fitness for aging pilots
11 p1689 N71-32003
- Coronary system diseases in aging flight crews and removal from flying status
11 p1689 N71-32004
- Aging effects on military flight crew body compositions and physical exercise performance
11 p1689 N71-32005
- Cardiovascular disease effects in aging flying personnel on physical exercise performance
11 p1689 N71-32006
- Arteriosclerosis and electrocardiographic abnormalities in aging pilots of French Air Force
11 p1689 N71-32007
- Aging effects on pilot psychophysiological abilities and flying proficiency
11 p1690 N71-32008
- Audiometric evaluation of aging pilots hearing ability in relation to flying time
11 p1690 N71-32009
- Formula for predicting physical fitness of flying personnel in Belgian Air Force during aging process from spirometric measurements
11 p1690 N71-32010
- Control of aging processes in human body composition
[NASA-TT-F-12964] 23 p3713 N71-36406
- AGING (MATERIALS)**
- NT AGING (METALLURGY)**
- Basic studies of liquid crystals related to electro-optical and other devices - thermal stability, aging, and oxidation resistance
[AD-716093] 09 p1343 N71-19728
- Mixing, firing, and aging methods for titanium and oxide ceramic materials with high dielectric constant, low loss, and thermal stability
11 p1783 N71-22320
- Outdoor aging of adhesive sealants under various environments
[SC-RR-70-163] 11 p1769 N71-22320
- Changes in mechanical properties and internal friction during aging of stainless, dispersion hardened chromium steels
[NLL-LT-746-680-19022.401] 22 p3596 N71-35800
- AGING (METALLURGY)**
- Heat aging evaluation of common coated copper conductor
[RM-4837] 02 p0340 N71-11330
- Pore weld annealing for stabilizing tungsten alloy weld structure
[NASA-CR-1610] 05 p0703 N71-13300
- Annealing or aging of aluminum alloys
[AD-713921] 06 p0871 N71-14800
- Using thin-film electron microscopy to study effects of cold working and aging on substructure and precipitation in cobalt-base alloy L-605
[NASA-TN-D-7051] 07 p1043 N71-17400
- Aging characteristics of barium titanate and lead zirconate-titanate ferroelectric ceramics
[AD-715634] 08 p1279 N71-18800
- Aging time and temperature effects on alpha precipitation from aluminum silicon alloy
[NOL-2394-40] 09 p1216 N71-18800
- Effect of aging and finishing sequence on fatigue performance of maraging steel
[TN-270] 09 p1228 N71-18800
- Characteristics of aging nickel-chromium alloys of aluminum alloys by work hardening at room temperature
[NLL-LT-746-637-19022.401] 16 p2615 N71-30810
- Room temperature tensile properties and changes in microstructures of steel XCrNiMoVNb 1615 alloy, Inconel 718 after aging at 600 to 1000 F
[EUREP80-873] 18 p2053 N71-30810
- Aging behavior of co-deposited aluminum alloy film
19 p3117 N71-32000
- Mathematical model of vacancy concentration compared with AlZnMg alloys age hardening behavior to determine Mg atom-vacancy pair concentration effect on clustering rate
[NLL-M-20407-15028.4F] 21 p3441 N71-30810
- Structural and mechanical properties of AlZnMg, AlMgSi, and AlCuMg alloys as function of aging prior to artificial aging
[NLL-M-20408-15028.4F] 22 p3596 N71-32000

SUBJECT INDEX

Metallurgical examinations of stainless steel microstructure after aging in power reactor temperatures
[AD-716353] 24 p3934 N71-38063

Electron microscopic analysis of aluminum alloy structure, intermetallic compounds, and structural hardening mechanisms
[NLL-M-20571-5828.4F] 24 p3941 N71-38113

MITATION
NT ULTRASONIC ACQUISITION
AGRICULTURAL AIRCRAFT
U UTILITY AIRCRAFT
AGRICULTURE

Remote sensing for detecting soil limitations in agricultural areas
[NASA-CR-111423] 02 p0215 N71-11974

Applying advanced remote sensing and processing techniques to agricultural resources
02 p0217 N71-11982

Reviewing research on processing data from multi-spectral band scanners for agricultural applications
02 p0191 N71-11983

Total fatigue damage estimates from ground and flight loads on fixed-wing light aircraft subjected to operational operations
[LTH-ST-422] 03 p0313 N71-12233

Evaluation of time resolution radar imagery for making operational determinations
[NASA-CR-115831] 03 p0675 N71-15001

Remote agricultural remote sensing research projects
[LAPR-132] 03 p0690 N71-15633

Conference on agriculture, forestry, and sensor status related to NASA Earth Resources Program - Vol. 2
[NASA-TM-X-62565] 06 p0844 N71-16147

Biophysical research at Laboratory for Agricultural Remote Sensing, Purdue University
06 p0806 N71-16153

Data processing program activities at Laboratory for Agricultural Remote Sensing, Purdue
06 p0845 N71-16154

Physical measurements program at Laboratory for Agricultural Remote Sensing, Purdue
06 p0845 N71-16155

Remote sensing of agriculture by radar imagery
06 p0813 N71-16156

Data processing and interpretation of remote sensed data for agricultural purposes
06 p0846 N71-16163

Multispectral discrimination technique improvement for remote sensing in agriculture and data calibration, atmospheric scattering effect, and predictive model analysis
[RPT-226-12-F] 10 p1560 N71-21445

Automatic identification and classification of wheat from airborne multispectral data in agricultural remote sensing
[RPT-279] 12 p1913 N71-23731

Development of separators using centrifugal force and load in agriculture and biochemistry
13 p2189 N71-24464

Development of separators using centrifugal force for agricultural and other uses
13 p2189 N71-24465

Introduction of efficient water use and conservation to farmers by Agricultural Extension Service
13 p2072 N71-25004

Application of Apollo space photography and sequential high altitude NASA aircraft photography for evaluating natural and cultural resources in southeastern Arizona - map
[NASA-CR-115056] 17 p2750 N71-29233

Aerial photographs of US agricultural regions to determine status of aerial coverage
18 p2926 N71-31478

Remote multispectral sensing and data processing techniques for agricultural applications
[NASA-CR-121169] 21 p3416 N71-34305

ALBINOIS
Device for controlling rotary potentiometer mounted on aircraft steering wheel or altimeter control
[NASA-CASE-XAC-10019] 12 p1927 N71-23809

AMPS
U EXPLORER 35 SATELLITE

AL
NT ALVEOLAR AIR
NT COMPRESSED AIR
NT EXPLODED AIR
NT HIGH TEMPERATURE AIR

Open cycle hydrocarbon-air fuel cell power plant
[AD-715328] 05 p0631 N71-14407

Supersonic two phase flow realized by air-water mixtures
[NIVTDG-FWWT-70-1] 06 p1140 N71-18441

Impurities for electrical conductivity of plasmas applied to equilibrium air at 3000 to 28,000 K
[NASA-TN-D-5977] 06 p1273 N71-18715

On line derating and after deflagration of spherical shell of fuel air mixture
[AD-716359] 09 p1370 N71-19555

Acoustic acoustic energy into and through soil with emphasis on shear wave propagation
[AD-716423] 09 p1424 N71-19851

Global combustion rate determination of air ignited particulate borne propellant secondary combustion in rocket engines
[AD-716350] 09 p1483 N71-20049

Transformation of form and displacement of air inclusions in ice due to molecular rearrangement of ice crystals and temperature gradients
11 p1759 N71-22862

Gas purged dry box glove reducing permeation of air or moisture into dry box or faster by diffusion through glove
[NASA-CASE-XLE-42531] 11 p1694 N71-23080

Relaxation and nonequilibrium radiation between shock waves in air
[NASA-TT-P-13528] 12 p1901 N71-23708

Air ionization and effects of positive ions in air on mass using Am-241 sources
[ORNL-TN-3427] 13 p2035 N71-25438

Behavior of cavity formed by projectile entering water vertically predicted as function of time based on size, shape, and pressure of projectile
14 p2298 N71-26630

Detection and determination of chemical characteristics of trace constituents in sea water and air
[MIT-905-162] 16 p3888 N71-31567

Cascade ionization of air by radio frequency fields and by intense laser beams
[AD-723183] 19 p3107 N71-31807

Combustion dynamics of air/methane supersonic diffusion flame in ducts
19 p3365 N71-33449

Environmental radiation measurements in air and water around atomic gaseous diffusion plant
[GAT-629] 21 p3479 N71-34776

Alpha and beta radiation measurements from air, soil, vegetation, and water samples in Ames reactor environment
[IS-2541] 22 p3644 N71-35983

Program for calculating saturation curves and condensation characteristics of gaseous mixtures of binary organic vapor and air
[BM-RF-7545] 23 p3720 N71-36519

Systems study of high power pulse transmission and nonlinear interactions in air
[AD-726638] 23 p3820 N71-37311

Eigenvalue analysis of air temperature distributions over Atlantic Ocean
[NLL-M-20364-5828.4F] 24 p3918 N71-37938

Air and precipitation beta radioactivity at Los Alamos, New Mexico, for 1970
[LA-4661] 24 p3951 N71-38190

Sensitivity of Monte Carlo calculations to neutron cross sections for neutron transport in aluminum and in air
[UCRL-51031] 24 p3977 N71-38379

Plasma-ion engines utilizing atmospheric gases to form ion jet for propulsion
[AD-727496] 24 p4001 N71-38537

Thermophysical properties of air and air components - tables and diagrams
[TT70-50095] 24 p4030 N71-38755

AIR BEARING
U GAS BEARINGS

AIR BLASTS
U AERIAL EXPLOSIONS

AIR BREATHING DEVICES
NT BRISTOL-SIDDELEY OLYMPUS 593 ENGINE

NT DUCTED FAN ENGINES
NT GAS TURBINE ENGINES
NT J-57 ENGINE
NT J-85 ENGINE
NT JET ENGINES
NT PULSEJET ENGINES
NT RAMJET ENGINES
NT SUPERSONIC COMBUSTION RAMJET ENGINES

NT TURBOFAN ENGINES
NT TURBOJET ENGINES
NT TURBOPROP ENGINES
NT TURBOPURJET ENGINES

Advanced jet engine combustor test facility
[NASA-TN-D-6036] 01 p0037 N71-10069

Effects of nonequilibrium free-radical content and composition variation of supersonic streams entering air breathing engines on ignition points and delays
[NASA-CR-111571] 02 p0280 N71-11467

Wind tunnel tests of mixed compression axisymmetric inlet system at Mach numbers 0.6 to 3.5
[NASA-TN-D-6078] 03 p0469 N71-13624

Air breathing engines for first stage of recoverable space shuttle
03 p0459 N71-13320

Fing and nacelle geometry effects on conical plug nozzle performance at subsonic and supersonic velocities
[NASA-TM-X-2086] 04 p0605 N71-14019

Development of digital system for on-line control of airbreathing propulsion systems
[NASA-TN-X-2148] 07 p1102 N71-17385

Air breathing engines for space shuttle reentry
[NASA-TM-X-64716] 08 p1284 N71-18429

Application and characteristics of cryogenic fuels for air breathing gas turbine engines
09 p1415 N71-19463

AIR COOLING

Development of bearings, seals, and lubricants for air breathing turbojet engines
09 p1392 N71-19464

Design requirements for air breathing aircraft engines
[AD-716496] 09 p1458 N71-19488

Requirements analysis of airbreathing gas turbine engines for shuttle vehicles
[NASA-TM-X-67006] 12 p1990 N71-23764

Air breathing engine principles for improved guided missiles and artillery projectiles
[FOA-2-C-2363-1246] 14 p2352 N71-26527

Experimental investigation of large scale, two dimensional, mixed compression inlet system
[NASA-TN-D-6392] 15 p2363 N71-26985

Configuration optimization and performance of air breathing hypersonic cruise vehicles
[AD-721471] 16 p2529 N71-28590

Future technology trends in air breathing propulsion systems for aircraft
[NASA-TM-X-67871] 16 p2672 N71-28947

Design and development of auxiliary power unit and air breathing propulsion system for space shuttle vehicle
17 p2838 N71-29643

Design and development of air breathing engine system for space shuttle vehicle
17 p2831 N71-29607

Air breathing, hydrogen fueled engine studies for space shuttle application
17 p2838 N71-29608

Method for predicting compressible turbulent boundary layers in adverse pressure gradients applied to hypersonic air breathing propulsion
[NASA-TM-X-2302] 19 p3078 N71-32210

Performance tests of compressor seals and stator pivot seals used with air breathing propulsion systems - Part 2
[NASA-CR-72887] 23 p3839 N71-37373

Design and characteristics of 28-inch diameter seals for air breathing propulsion systems - Part 1
[NASA-CR-72819] 23 p3839 N71-37374

AIR CARGO
NT AIR MAIL

Analysis of stresses and deflections in platforms used for airdrop operations
[AD-711556] 02 p0300 N71-11948

Aerial delivery system for dropping emergency pumping equipment to distressed boats - Phase 1
[AD-712288] 03 p0537 N71-12337

Aerial delivery system for dropping emergency pumping equipment to distressed boats - Phase 2
[AD-712289] 03 p0538 N71-12338

Airdrop impact load effect on complex structures
[AD-711555] 04 p0618 N71-14163

Control problems in airline operations particularly air cargo handling
04 p0674 N71-14430

Report of aircraft accident due to forward shift of improperly secured cargo
[NTSB-AAR-71-4] 08 p1145 N71-19041

Support systems planning for expanded passenger and cargo traffic in civil aviation
11 p1676 N71-22390

Statement by Honorable Secar D. Brown, chairman, CAB, presented to Part of Senate Air Cargo Conference, January 19, 1971
21 p3534 N71-35185

Freight, express, and mail tonnage forecasts for domestic airline operations
24 p4035 N71-38793

Growth rate of US air cargo markets - tables
24 p4036 N71-38794

AIR CONDITIONING

Effects of air conditioning on human body
[IFR-38-26] 03 p0320 N71-12226

Aircraft pilot thermal environment, thermal comfort and cockpit air conditioning
[ARCC-CP-1094] 07 p0985 N71-17096

Cabin air conditioning for passenger aircraft using air purification and recirculation, odor control, and pressurization requirements
[ARCC-CP-1136] 10 p1492 N71-20849

AIR CONDITIONING EQUIPMENT

Design and development of air conditioned protective clothing
[AD-713581] 05 p0637 N71-14741

Design and performance of thermal air conditioning equipment during long term manned space environment simulation
10 p1503 N71-30538

Portable apparatus producing high velocity ammonia air columns surrounding low velocity, ethanol, superclean air control core for industrial clean room environmental control
[NASA-CASE-XMR-03212] 11 p1770 N71-22721

Performance of aircraft environmental control systems under simulated tactical conditions
[AD-715101] 13 p2023 N71-34461

AIR COOLING

Mathematical model for calculating blade temperatures in convective cooled gas turbines
07 p1089 N71-17373

Efficiency of air cooling blade design for Olympus 593 gas turbine engine
07 p1089 N71-17376

AIR CURRENTS

Heat transfer in air cooling and sweat cooling techniques for high temperature gas turbine engine components 07 p1100 N71-17383

Temperature field measurements within convection cooled rotor blade of gas turbine engine 07 p1101 N71-17387

Air cooling systems for nozzle guide vanes of air-craft gas turbines 07 p1129 N71-17396

Operational design criteria for gas turbine engines 07 p1101 N71-17402

Performance of stator with wire mesh shell blading during cold air investigation of turbine with transpiration cooled stator blades - Vol. 3 [NASA-TM-X-2166] 07 p0968 N71-17590

Describing operating characteristics and costs of air-cooled heat exchangers and condensers for industry 08 p1304 N71-18812

Measurement of cooling air pressure changes through stationary turbine disk and airflow distribution within a blade at room temperature and pressures from 28 to 100 psia [NASA-TM-X-2171] 11 p1741 N71-22680

Racetrack microtome with modest shielding and air cooling [UCRL-20230] 16 p2654 N71-29060

Comparison of water, convective air, and reversed air flow cooled units for body temperature thermoregulation in high temperature environments [FPRC-1307] 17 p2712 N71-30127

Aerodynamic and heat transfer performance of air cooled nozzle cascade for high temperature turbine [NAL-TR-231-PT-1] 20 p3364 N71-33304

AIR CURRENTS

NT JET STREAMS [METEOROLOGY]

NT MERIDIONAL FLOW

NT VERTICAL AIR CURRENTS

AIR CUSHION VEHICLES

U GROUND EFFECT MACHINES

AIR DEFENSE

NT ANTIMISSILE DEFENSE

AIR DUCTS

Numerical solution of Fredholm equation for air duct vertices of shrouded propeller with tip clearance [DLR-FB-71-15] 19 p3033 N71-31788

AIR FILTERS

Particle bounce phenomena in mechanical air filtration theory 08 p1208 N71-19028

Internal recirculating air cleaning loop tests in containment systems [WHAN-SA-39] 13 p2121 N71-25380

Methods, instruments, and performance of air filters used to cleanse contained atmospheres - conferences [CONF-700616-VOL-2] 17 p2743 N71-29851

Inorganic adsorbent materials for trapping of fission product iodine in fuel reprocessing plants and gas cleaning inside reactor containment 17 p2743 N71-29851

Carbon bed filtration system for removing particulate matter and gaseous radioactive contaminants from radioactive wastes 17 p2770 N71-29870

Testing of fire extinguisher for activated carbon adsorbers in air cleaning systems 17 p2731 N71-29875

AIR FLOW

NT JET STREAMS [METEOROLOGY]

NT MERIDIONAL FLOW

NT VERTICAL AIR CURRENTS

Air intakes and flow aeration in hydroturbines [PB-193589T] 01 p0044 N71-10942

Investigating air flow in noisy wind tunnels using holographic flow visualization system 03 p0379 N71-12795

Correlation of criterion for air flow separation from wind waves and relationship between surface roughness and wind stress [AD-712788] 03 p0370 N71-13175

Measurement of external and internal flow fields during parachute inflation [AD-713520] 05 p0627 N71-14559

Inviscid hypersonic flow of chemically relaxing air about pointed circular cones 05 p0659 N71-14748

Water wave effects on air flow in atmospheric boundary layer above lake [AD-713694] 05 p0719 N71-15401

Air flow over roughness discontinuity [AD-712113] 05 p0665 N71-15465

Composition distribution and equivalent body shape for reacting, coaxial, supersonic hydrogen air flow [NASA-TN-D-6123] 05 p0785 N71-15639

Effect of injectant molecular weight on mixing of normal jet in Mach 4 airstream - tables and graphs [NASA-TN-D-6061] 06 p0837 N71-16595

Performance prediction for turbine blade film cooling with injection through holes [NASA-CR-116376] 07 p1101 N71-17388

Impact pooling method for turbine rotor blades 07 p1129 N71-17397

Smooth double-slotted circular cylinder aerodynamic force characteristics measured for circulation control by slot suction [NRC-11714] 09 p1377 N71-20196

Laminar airflow and airborne contamination control concepts with clean room specifications and laminar flow facility designs [NASA-CR-116185] 09 p1368 N71-20425

Cabin air conditioning for passenger aircraft noting air purification and recirculation, odor control, and pressurization requirements [ARC-CP-1136] 10 p1492 N71-20849

Experimental determination of heat transfer and friction in circular tube with laminar flow of air under conditions of large transverse temperature gradients 10 p1542 N71-21283

Theory describing hydrostatically neutral air flow adjustment in turbulent boundary layer power portion after abrupt surface roughness change perpendicular to flow direction 12 p1901 N71-23665

Air flow velocity, altitude, fuel-air ratio, fuel flow velocity, and pressure effects on fuel temperature before and after preheating in ramjet engines [NASA-TT-F-16605] 12 p1989 N71-24053

On-line mass spectrometric analysis of nonequilibrium air flows in low density wind tunnel nozzle [AD-718955] 13 p2063 N71-24477

Plant canopy effects on air flow and evapotranspiration 13 p2074 N71-25022

Acoustically excited, incompressible, turbulent, subsonic Coanda air flow around circular cylinder 13 p2066 N71-25039

Characteristics of chemically reacting air flow in large, air heated, hypersonic wind tunnel nozzle 16 p2581 N71-28721

Short-term creep properties of OT-4 alloy in high speed air flows under aerodynamic vibrations [NASA-TT-F-13658] 16 p2614 N71-28832

Method for maintaining good performance in gas turbine during air flow distortion [NASA-CASE-LEW-10286-1] 16 p2672 N71-28915

Internal aerodynamics design manual considering internal air flow system effect on aircraft performance including bibliography [AD-723823] 19 p3173 N71-32059

Aerodynamic design manual considering internal air flow system effects on aircraft performance [AD-723824] 19 p3173 N71-32060

Short term creep of nickel in vacuum and high speed air flow at high temperature [NASA-TT-F-13661] 19 p3114 N71-32234

Characteristics of air motion with respect to ground and analysis of dynamics of aircraft in turbulent air [NASA-TT-F-606] 19 p3035 N71-32719

Energy transport velocity model for classification of all possible acoustic modes propagating in uniform, inviscid, homogeneous, time independent ducted air flow [ONERA-TP-965] 20 p3251 N71-33530

Velocity and turbulence characteristics of air flow in three ratios of concentric annuli by location of zero shear position [RD-B-N-1878] 22 p3566 N71-35401

Flow pattern of two phase flow of water/air at ambient temperature and pressure [NLL-CE-TRANS-5472-19022.09] 22 p3570 N71-35427

Visualized flow patterns of airflow in centrifugal rotors with thin plate blading and with thick airfoil blades [ME-238] 23 p3705 N71-36410

High low noise control device for use with free jet circular breakers based on automatic control of air blast intensity [NLL-CE-TRANS-5365-19022.09] 23 p3733 N71-36616

Statistical analysis of pressure fluctuations in fluidized beds of copper and glass particles with air 23 p3741 N71-36676

Theoretical and experimental analyses of surges in air charging systems of supercharged diesel engines [TB-72] 23 p3841 N71-37388

Characteristics of turbulent air stream over progressive water waves [AD-728008] 24 p3917 N71-37929

AIR FREIGHT

U AIR CARGO

AIR INLETS

U AIR INTAKES

AIR INTAKES

NT ENGINE INLETS

NT HYPERSONIC INLETS

NT SUPERSONIC INLETS

Air intakes and flow aeration in hydroturbines [PB-193589T] 01 p0044 N71-10942

Jet VTOL fighter-type model inlet-air temperature rise analysis with various exhaust pressure ratios and gas temperatures and surface wind velocities for correlating parameters 09 p1324 N71-20271

Blowing effect on static efficiency of two dimensional air intakes with momentum injection in boundary layer control form [ARC-R/M-3656] 15 p2364 N71-27149

SUBJECT INDEX

Noise reduction in turbulent axisymmetric gas jet by repeated air injection method applied to supersonic transport aircraft [NASA-TT-F-13667] 16 p2531 N71-28225

Normal shock control systems for supersonic inlet compression inlet using feedback loops [NASA-TM-D-6382] 17 p2839 N71-28916

Transonic testing of double flux engine nacelles with two separate models for air intake and nozzle [ONERA-TP-943] 20 p3307 N71-33714

Modifying air intake and fuel injection parameters to reduce diesel engine nitrogen oxide emissions [BM-BI-7579] 23 p3841 N71-37929

AIR JETS

Pressure fluctuation measurements with microphones in air jet free flow [DLR-FB-70-22] 07 p1008 N71-17140

Model of peripheral air jets in air cushion vehicles bowing over water surface [NT-27-1971] 19 p3075 N71-31460

AIR LAUNCHING

Air launch characteristics of HL-10 manned lifting reentry vehicle [NASA-TM-X-1668] 05 p0770 N71-15080

Air launch characteristics of M2-F2 lifting body from B-52 aircraft [NASA-TM-X-1713] 05 p0770 N71-15080

AIR LOCKS

Spacecraft air lock system to provide ingress and egress of astronaut without subjecting vehicle environment to vacuum of space [NASA-CASE-XLA-620-50] 11 p1832 N71-22808

System for removing and repairing spacecraft control thrusters by use of portable air locks [NASA-CASE-MPS-20325] 15 p2512 N71-27805

AIR MAIL

Air mail transportation by contract operations 01 p0138 N71-10035

Freight, express, and mail tonnage forecasts for domestic airline operations 24 p4035 N71-30790

AIR MASSES

Analysis of synoptic meteorology in Europe with application to theory of fronts and air masses 03 p0402 N71-12575

Balloon sounding of radioactive air masses from nuclear test [CEA-R-4093] 09 p1461 N71-20440

Numerical methods of forecasting baric field, wind, trajectory of air particles, and movements of typhoons [AD-719813] 13 p2107 N71-25119

Vertical air mass exchange in troposphere studied by isotopic labeling [NLL-M-9265-5828.4F1] 17 p2744 N71-29807

Air mass thunderstorm forecasts at Nellis Air Force Base, Nevada using temperature curves and Yucca Flat 1200 Z ROAE [AD-724679] 20 p3295 N71-33880

Air mass exchange study using stratospheric Bu-7 and P-32 air sensors 22 p3575 N71-35466

Spectroscopic observations of planets showing absorption variations in NH3 and CH4 bands [NASA-CR-123152] 24 p4007 N71-38175

AIR NAVIGATION

NT ALL-WEATHER AIR NAVIGATION

Display relationship problems applied to prediction of aircraft attitude and guidance information [AD-713179] 05 p0637 N71-14740

Random errors in a twenty-four hour orbit satellite navigation system, air navigation and covariance matrices [DLR-FB-70-36] 07 p1056 N71-17120

Computerized solution of nonlinear differential equations for inertial navigation systems [AD-717058] 10 p1599 N71-20700

Monte Carlo general purpose shielding computer program in FORTRAN 4 for IBM 7094 computer [PNSI-TR-70-0501-1-VOL-1] 11 p1792 N71-23519

Simulation, analysis, and reconstruction of flight profile of Concord aircraft to predict and achieve improvements in aircraft operation - Vol. 2 [PNSI-TR-70-0501-2-VOL-2] 11 p1792 N71-23519

Relationship of cirrus cloud formation /maus tails and jet streams in troposphere examined for aerial navigation application [NASA-TT-F-13606] 12 p1953 N71-23519

Time synchronization of Iona C navigation system and characteristics of sky wave reception operation [NASA-TM-X-65515] 13 p2105 N71-30608

Momentum wheel stabilized, sun-oriented, synchronous equatorial satellite for astronomical satellite system NETCOS [NASA-TM-X-65509] 14 p2341 N71-25411

Bibliography on radar and radio navigation [DLR-MIT-70-21] 15 p2441 N71-30770

Evolution of flight plan position information display for ocean flying control [FAA-NA-71-31] 19 p1332 N71-33064

Operating instructions of Decca Mark 19 navigation system 20 p3299 N71-33880

SUBJECT INDEX

- Operating instructions for Decca Mark 23 navigation system 20 p3299 N71-32917
- Broadband model of digitally controlled very high frequency synthesizer for use in aviation navigation receiver [NASA-TN-D-6389] 21 p3395 N71-34164
- Navigation accuracy resulting from sidetone signals relayed by two synchronous ATIS- and ATIS-3 systems and application to aircraft navigation [NASA-CR-121977] 22 p3617 N71-35770
- Development and testing of VHF omnirange transmitter for aircraft azimuth guidance [FAA-RD-71-45] 22 p3618 N71-35779
- Automatic computation of navigation coordinates using analog and digital computers [AD-726683] 22 p3618 N71-35782
- Airline view of air navigation problems 24 p3913 N71-37896
- ## AIR PIACRY
- Analysis of US efforts for detection and prevention of air piracy with application to foreign countries 01 p0135 N71-10236
- Senate hearings on Federal anti-skyjacking program 18 p3031 N71-31511
- Recommended airline and legal procedures prior to, during, and after hijackings 18 p3031 N71-31562
- Air piracy resolutions presented to Congress and US and worldwide air piracy statistics 19 p3199 N71-32689
- Convention for suppression of unlawful aircraft seizure and article by analysis 23 p3870 N71-37390
- ## AIR POLLUTION
- Air pollution reduction by urban tri-state air transportation system around New York City [FAA-NO-76-14] 01 p0008 N71-10124
- Papers presented at conference on atmospheric composition in confined spaces 01 p0045 N71-10176
- Steady-state noninvasive Gaussian computer model for simulating air quality in region of New York City [E8-3921] 01 p0013 N71-10712
- Air pollution mixing height determinations by means of instrumented aircraft 01 p0009 N71-10095
- Development of photoelectric microbalance for continuous measurement of aerosol mass concentration [PB-195362] 01 p0057 N71-10910
- Atmospheric scavenging of radioactive isotopes [TT-69-55099] 01 p0081 N71-10923
- Feasibility and capability of electron microprobe analysis for measuring pollutant aerosol particles in atmosphere [PB-195232] 02 p0150 N71-11068
- Optical analysis of ten-year sampling of suspended particulate matter over urban and nonurban sites [PB-192233] 02 p0151 N71-11069
- Data tabulated from 274 stations in US and Canada on air pollution effects on materials 02 p0151 N71-11071
- District of Columbia air quality display model for comparing seasonal concentration estimates [PB-191941] 02 p0151 N71-11072
- Bibliography of research projects in air pollution for year 1969 [PB-192220] 02 p0152 N71-11077
- Selective bibliography of water and air pollution for business and industry [PB-192318] 02 p0152 N71-11078
- Electron microprobe X ray analysis of atmospheric aerosol particles [PB-192233] 02 p0152 N71-11079
- Studying air pollution as regional problem in Arizona 02 p0155 N71-11100
- Chattanooga interstate air quality control region 02 p0156 N71-11106
- Air pollution report of federal facilities in metropolitan Baltimore interstate air quality control region 02 p0156 N71-11108
- Proposed boundaries for metropolitan Detroit-Port Huron interstate air quality control region 02 p0156 N71-11109
- Battling refractor plate correlation spectrometer to remote sensing instrument of pollutant gases in atmosphere [NASA-CR-111373] 02 p0223 N71-11421
- Forecasting meteorological parameters for air pollution potential [NLL-M-9129-5828.4F] 02 p0253 N71-11454
- Relation between synoptic meteorological condition and hazardous air pollution in cities [NLL-M-9128-5828.4F] 02 p0258 N71-11680
- Measuring atmospheric temperature inversions for air pollution and weather forecasting [NLL-M-9143-5828.4F] 02 p0259 N71-11754
- Optical correlation methods for remote sensing of trace gases at high altitudes 02 p0228 N71-11993

- Carbon monoxide oxidation rates for automobile exhaust manifold reactor conditions [NASA-TN-D-7024] 02 p0306 N71-12066
- Environmental problems including air pollution, water pollution, radioactive wastes, smog, sewage, aircrafts, and garbage disposal [AD-712722] 03 p0321 N71-12297
- Conference on application of science and technology to problems of pollution, transportation, and employment [PB-192329] 03 p0323 N71-12306
- Cost analysis of air pollution effects on electric contacts [PB-192478] 03 p0350 N71-12525
- Wavelength-selective, repetitively pulsed CO₂ laser for nonlinear optical effects studies and atmospheric pollutant detection [NASA-TM-X-66497] 03 p0387 N71-12574
- Stratospheric photochemical and hydrophobic CO oxidation and tropospheric CO reaction with ozone as atmospheric CO sinks [PB-192168] 03 p0366 N71-12693
- Carbon dioxide content changes in atmosphere [NLL-M-9147-5828.4F] 03 p0367 N71-12864
- Atmospheric haze - components and formation [PB-192102] 03 p0403 N71-13022
- Air pollution, and condensation nuclei measurement in Rome [IITA-TR-28] 03 p0404 N71-13270
- Air pollution problems in California and methods for air quality forecasting 04 p0475 N71-13429
- Simplified slide rule for determination of downward safety limits for toxic vapors [REPT-1970-13] 04 p0476 N71-13432
- Developing molten alkali carbonate eutectic in removing lead compounds from spark ignition engine exhaust gases [PB-194132] 04 p0484 N71-13444
- Investigating infrared spectroscopic methods for monitoring concentration of sulfur dioxide in fine smog [PB-194136] 04 p0484 N71-13445
- Sampling by frontal analysis for determination of carbon monoxide in air [NASA-TT-F-13434] 04 p0485 N71-13454
- Analytical photoionization mass spectrometer with argon gas filter between light source and monochromator [NASA-CASE-LAR-10180-1] 04 p0486 N71-13461
- Air pollution of fossil and nuclear power plants [CONF-700810-20] 04 p0549 N71-13756
- Data analysis and methods improvement for Los Angeles Basin [PB-194660] 04 p0542 N71-14274
- Turbulent air and water polluting plumes in laminar cross flow [FIML-PUBL-70-8] 04 p0520 N71-14312
- Radioactive fallout program review [HASL-217] 04 p0479 N71-14470
- Annotated bibliography of technical literature related to nitrogen oxides and air pollution control [PB-194429] 04 p0480 N71-14472
- Mathematical model for environmental transport of lead from several sources and subsequent intake by man [PB-194412] 04 p0481 N71-14478
- Long term climatological and atmospheric effects of air pollution [PB-193801] 04 p0522 N71-14493
- Body exposure rate calculated for dose from Kr-85 released to earth atmosphere [BNWL-SA-3233-A] 05 p0635 N71-14706
- Program design and methodology data summary for atmospheric reaction studies in Los Angeles, California Basin - Vol. 1 [PB-194661] 05 p0678 N71-15506
- Atmospheric reaction data for commerce area of Los Angeles, California Basin - Vol. 2 [PB-194662] 05 p0678 N71-15507
- Atmospheric reaction studies in Los Angeles Basin El Monte area - Vol. 3 05 p0678 N71-15508
- Airborne data from atmospheric studies in Los Angeles, California Basin - Vol. 4 [PB-194664] 05 p0678 N71-15509
- Microchemical analyses of air pollutants and preparation of standard reference materials for gas analyses [NBS-TN-545] 05 p0641 N71-15596
- Sulfur oxides, smoke, and air pollution tables from Belgian weather stations, Mar. 1970 06 p0685 N71-15709
- Sulfur oxides, smoke, and air pollution tables from Belgian weather stations, Feb. 1970 06 p0686 N71-15710
- Contamination free separation unit eliminating combustion products from ambient surroundings generated by oil firing [NASA-CASE-XGS-01971] 06 p0663 N71-15922
- Quantitative data on air pollutant emission from Federal facilities in Michigan/Ohio interstate region 06 p0653 N71-16582

AIR POLLUTION

- Air pollution and soiling index for Saint Louis, Missouri, 1968 [PB-194762] 06 p0654 N71-16655
- Air pollution and soiling index for District of Columbia, 1968 [PB-194763] 06 p0655 N71-16656
- Air pollution and soiling index for Denver, 1968 [PB-194760] 06 p0655 N71-16657
- Air pollution and soiling index for Philadelphia, Pennsylvania, 1968 [PB-194761] 06 p0655 N71-16658
- Air pollution and soiling index for Cincinnati, 1968 [PB-194768] 06 p0655 N71-16726
- Air pollution and soiling index for Chicago, 1968 [PB-194767] 06 p0655 N71-16745
- Bibliography on urban economics and planning [AD-714500] 06 p0662 N71-16874
- Diffusion of aerosols in atmosphere near earth surface 07 p0652 N71-16923
- Air pollution sampling in vicinity of ammunition plant [PB-195145] 07 p0105 N71-16996
- Air pollution in southern Alabama [PB-194674] 07 p0106 N71-16999
- Air pollution control in Kanawha Valley, West Virginia [PB-194881] 07 p0106 N71-17000
- Air pollution, smoke, and sulfur dioxide measurements - Apr. 1970 07 p0103 N71-17077
- Computerized simulation of dispersion models for airport air pollution [RE-3982] 07 p0105 N71-17923
- Remote sensing of wind profiles in atmospheric boundary layer for air pollution monitoring [BSSA-TR-ERL-168-WPL-12] 07 p0103 N71-18061
- Environmental control methods to reduce air and water pollution in United States of America 07 p0135 N71-18071
- Multiple source urban atmospheric dispersion model for Chicago air pollution [ANL-ES-CC-7] 08 p0185 N71-18296
- Biosphere sinks for carbon monoxide emissions to atmosphere [PB-195433] 08 p0186 N71-18307
- Photoionization characteristics released in air due to thermal stress [BNWL-SA-3379] 08 p0102 N71-18313
- Feasibility study of remote monitoring of NO and SO₂ pollutant emissions by Raman spectroscopy [RR-362] 08 p0193 N71-18978
- Determining cycle in air pollution in urban environment by measuring solar radiation [REPT-27] 08 p0204 N71-19297
- Maximum allowable photoion-239 lead in humans and maximum allowable photoion-239 concentration in air at work locations [ANL-TRANS-064] 08 p0157 N71-19347
- Computer analysis of multichannel scanning electron microscopy and X ray images from fine particles [AD-716562] 09 p0425 N71-19445
- Proposal for international air pollution information analysis center 09 p0101 N71-19531
- Radiological monitoring and environmental sampling data for Phobos 2A reactor tests [SWRHL-72-R] 09 p0332 N71-19917
- Automobile exhaust manifold thermal reactor systems comparison in control of hydrocarbon and carbon monoxide emissions [NASA-TM-X-2230] 09 p0488 N71-19946
- Atmospheric pollution by plutonium in comparison with normal composition [CEA-R-7081] 09 p0305 N71-20185
- Large, giant, and sulfate containing atmospheric particle number concentration for aerosol air pollution in New Mexico [AD-716999] 10 p0153 N71-21845
- Air pollution monitoring and pollutant source surveillance system, and effective regulations and enforcement means for San Francisco Bay area [NASA-CR-114292] 10 p0352 N71-21298
- Annotated bibliography on hydrocarbons and air pollution [PB-197165] 10 p0666 N71-21697
- Photochemical aspects of air pollution data for Los Angeles [PB-194825] 10 p0355 N71-21728
- Unilateral air pollution control operations [PB-196841] 10 p0667 N71-21784
- Use of CO and CO₂ lasers to detect pollutants in atmosphere between laser emission lines and infrared absorption lines of NO [AD-717171] 10 p0171 N71-21788
- Manual of electrostatic precipitators for particulate emission control 10 p0360 N71-21811
- Bibliography of electrostatic precipitators for particulate emission control 10 p0360 N71-21813
- Aerospace science and technology transfer to air pollution control problems including mass spec

trometry modifications and air pollution monitoring equipment improvements
[NASA-CR-117469] 11 p1746 N71-21989

Sulfur oxides, smoke, and air pollution tables from Belgian weather stations, May 1970 11 p1788 N71-22015

Sulfur oxides, smoke, and air pollution tables from Belgian weather stations, Sep. 1970 11 p1789 N71-22016

Sulfur oxides, smoke, and air pollution tables from Belgian weather stations, Jul. 1970 11 p1789 N71-22017

Techniques and equipment for industrial air pollution monitoring and sampling
[JPRS-52566] 11 p1747 N71-22055

Industrial pollution properties summary including data on toxicity and control, air sampling, and gas analysis 11 p1747 N71-22056

Polarographic, coulometric, and polarographic gas analyzers for air pollution measurements 11 p1761 N71-22058

Luminescent analysis techniques and devices for air pollution measurements 11 p1802 N71-22059

Aerosol and flame ionization techniques for air pollution sampling gas analysis 11 p1747 N71-22060

Reduction oxidation reactions for colorimetric analysis of atmospheric toxicity 11 p1695 N71-22061

Infrared absorption spectra gas analysis of air pollution 11 p1761 N71-22063

Bionics modeling of enzyme analysis of toxic compounds and olfactory system simulation 11 p1686 N71-22065

Sulfur oxides, smoke, and air pollution tables from Belgian weather stations, Jun. 1970 11 p1789 N71-22083

Sulfur oxides, smoke, and air pollution tables from Belgian weather stations, Aug. 1970 11 p1789 N71-22085

Development of theoretical mechanism for producing reactions and conditions involved in air pollution 11 p1697 N71-22069

Feasibility of large-scale terrestrial plants for future generation of pollution free electrical power from solar energy
[NASA-TM-X-65497] 12 p1860 N71-23700

Sources and control of air pollution 12 p1956 N71-23854

Urban development effects on climatology of Paris [REPT-52] 12 p1958 N71-24057

Description of projects for determining effect of atmospheric pollutants on weather and climate
[ESSA-TK-ERL-185-APCL-15] 12 p1958 N71-24115

Data tables of air pollution by smoke and sulfur dioxide at Belgian weather stations for Oct. 1970 12 p1205 N71-24442

Data tables of air pollution by smoke and sulfur dioxide at Belgian weather stations for Nov. 1970 12 p1205 N71-24443

Instructions for use of National Meteorological Center Air Pollution Potential products
[AD-718966] 13 p2106 N71-24485

International scientific cooperation for environmental pollution control 13 p2189 N71-24752

Air sampling over Japanese atomic research facility [JAERI-MEMO-4175] 13 p2075 N71-25122

Atmospheric cycles analyzed to determine sources, abundance, and fate of gaseous atmospheric pollutants 13 p2075 N71-25147

Smog forming reactivities of exhaust aldehydes measured using test mixtures similar to exhaust at atmospheric dilution
[BM-R1-7537] 14 p2212 N71-25798

Atmospheric pollution as influenced by various gas ejection sources 14 p2239 N71-25908

Flight adaptability and human factors engineering of aerial radiological detection equipment
[AD-720567] 14 p2255 N71-26191

Atmospheric corrosion and air pollution effects
[FOA-I-C-1333-92] 14 p2279 N71-26259

Economic analysis of aeronautical R and D efforts in US and aeronautical contributions to noise and air pollution, including technology assessment and data analysis techniques
[NASA-CR-1809] 15 p2366 N71-27011

Analysis of Sr-90, Cs-137, and fission products in atmospheric dust and rainfall in Great Britain up to mid 1970
[AERE-R-6556] 15 p2495 N71-27966

Discussions on removal of radioactive aerosols from environment
[CONF-700816-VOL-1] 15 p2496 N71-27976

Five-year federal plan to provide air pollution control meteorological service for support of federal, state, and local pollution control agencies
[COM-71-00700] 16 p2589 N71-28853

Meteorological parameters and wind statistics for North and South Carolina and Georgia for use in air pollution investigations
[COM-71-00214] 16 p2627 N71-28977

Periodic variations of air pollution dust and sulfur dioxide particle densities for urban areas of Ohio
[NOAA-TM-NWS-ER-39] 16 p2627 N71-29001

Air pollution estimate in Germany from visibility measurements, noting influence of wind and atmospheric moisture 17 p2776 N71-29377

Factors relevant to development of fuels and energy policies compatible with environmental control
17 p2861 N71-29471

Contamination measurement of radiogenic argon with atmospheric argon by neutron activation analysis using scintillation spectrometry
[IFA-MR-33] 17 p2752 N71-29545

Instruction manual for chemiluminescent ozone meter for continuous air monitoring
[PB-198065] 17 p2752 N71-29744

Raman spectroscopy and nitrogen laser applications in remote sensing of nitrogen oxide and sulfur dioxide air pollutants from electric power plant emissions
[PB-198204] 17 p2758 N71-29748

Monitoring techniques for biological and chemical atmospheric contaminants in closed environment
[NASA-CR-1826] 17 p2711 N71-29763

Atmospheric and meteorological aspects of air pollution - survey of USSR air pollution literature
[PB-198061] 17 p2742 N71-29831

Susceptibility or resistance to gas and smoke of various arboreal species grown under diverse environmental conditions in industrial regions
[PB-198063] 17 p2742 N71-29832

Effects and symptoms of air pollutants on vegetation noting resistance and susceptibility of various plant species in various habitats and relation to plant utilization for shelter belts
[PB-198062] 17 p2742 N71-29833

Meteorological and chemical aspects of air pollution and propagation and dispersal of air pollutants - survey of USSR air pollution literature
[PB-198064] 17 p2743 N71-29834

Hypoidous acid generated by injection of elemental iodine into steam-air atmosphere or by purging dilute aqueous solution of iodine in water with air or other gases - airborne species 17 p2743 N71-29853

Air quality criteria for nitrogen oxides and their toxicological effects on animals, plants, and human beings
[PB-197333] 18 p2918 N71-31309

Control equipment and engine development for air pollution control from jet aircraft engine emissions
18 p2919 N71-31403

Electric power plant cooling tower effluent effect on urban atmospheric composition
[PB-197562] 18 p2920 N71-31487

Predictive methods for solar and atmospheric thermal energy budgets in lakes and streams
[PB-197267] 18 p2920 N71-31488

Exhaust emission from reciprocating aircraft engines, and afterburning of exhaust gases on contact with ambient air - air pollution study
[PB-197627] 18 p3028 N71-31569

Application of binormal continuous plume dispersion model to estimate concentrations of air pollutants tables and graphs 19 p3125 N71-31626

Two techniques for removal of particulate contaminants from spark ignition engine exhausts
[PB-198033] 19 p3173 N71-31762

Impact of jet aircraft emissions on air quality in vicinity of Los Angeles International Airport
[PB-198699] 19 p3036 N71-31779

Deficiencies in combustion technology, and 5 year research and development plan for air pollution control by combustion process modification
[PB-198066] 19 p3192 N71-31900

Annotated bibliography of aerosols and particle characteristics of air pollutants
[AD-723900] 19 p3092 N71-32030

Experimental measurements of spread patterns of large amounts of airborne radioactivity suddenly released in DR3-reactor shell using Ar-41
[RISO-205] 19 p3153 N71-32252

Human reactions to air pollution and responses to ecology and environmental control
[UCRL-73063] 19 p3093 N71-32258

Operational methods for control of air pollution emissions from aircraft turbine engine combustor
[NASA-TM-X-67887] 19 p3174 N71-32484

California Mulford-Carrel Air Resources Act, Model State Air Pollution Act, and summaries of all state air pollution control laws 19 p3197 N71-32524

Aerosol measurements in Los Angeles [California] smog
[PB-198816] 19 p3095 N71-32528

Procedures for estimating control costs and emission reductions for specified air pollution sources - users manual
[PB-198779] 19 p3198 N71-32589

Air pollution in relation to certain atmospheric and meteorological conditions and methods employed in survey and analysis of air pollutants
[PB-198527] 19 p3096 N71-32600

Atmospheric circulation and aerosol pollution transport noting role of temperature inversions
[IFA-RDP-36] 20 p3215 N71-32602

Sulfate ion as dominant constituent in cloud and fog condensation nuclei for nonurban areas
[AD-724610] 20 p3294 N71-32609

Annotated bibliography on emission sources in electric power plants and air pollution effects
20 p3255 N71-32601

Guidelines for developing minimally adequate air pollution surveillance network
[AP-58] 20 p3255 N71-32604

Theory of atmospheric diffusion in fog conditions and relation to air pollution
[AD-724104] 20 p3295 N71-32674

Bibliographies and abstracts on air pollution emission sources - nitric acid manufacturing
[AP-93] 20 p3257 N71-32605

Assessment of cost of air pollution corrosion damage to metal systems and structures in US, both presently and by 1980 20 p3283 N71-33112

Mathematical and diffusion models for abatement and control of air pollution over urban areas
[PB-198400] 20 p3260 N71-33120

Air pollution sources, distribution, biological effects, and mathematical models
[P-4571] 20 p3261 N71-33279

Guidelines for design and implementation of emergency action plans for avoiding air pollution episodes
[AP-76] 20 p3265 N71-33378

Guidelines for design and implementation of emergency action plans to prevent air pollution episodes in medium sized urban areas
[AP-77] 20 p3266 N71-33377

Guidelines for design and implementation of emergency action plans for avoiding air pollution episodes in small urban areas
[AP-78] 20 p3266 N71-33378

Analysis of air pollution problem, including types of pollutants, monitoring systems, and development of global air quality standards
[EGG-1183-22-02] 20 p3267 N71-33337

Bibliographies of air pollution emission sources created by municipal incineration
[AP-92] 20 p3268 N71-33377

Inventory of automatic sampler-analyzers, mechanized samplers, and static samplers used for air pollution monitoring in US and Puerto Rico
[PB-198329] 21 p3420 N71-34354

Feasibility of satellite surveillance for global air pollution monitoring
[PB-198621] 21 p3421 N71-34350

Probability graphs and statistical analysis of air pollution data
[NLL-M-20589-[5828.4F]] 21 p3422 N71-34353

Development of computer program for calculation of atmospheric pollution from many sources
[NLL-M-20634-[5828.4F]] 21 p3423 N71-34358

Effect of coherence and multiple scattering on laser radar air pollution measurements
[NASA-CR-121873] 21 p3435 N71-34441

Estimates of governmental and private expenditures for prevention and control of air pollution
[S-DOC-92-6] 21 p3532 N71-35375

Application of aerospace and defense industry resources and technology to solution of environmental problems 21 p3533 N71-35310

Manpower and training needs for air pollution control - public and private sectors
[S-DOC-91-98] 21 p3533 N71-35312

Toxicological evaluation of carbon monoxide, atmospheric contaminants, and propellants in environmental pollution
[AD-727022] 22 p3546 N71-35358

Fuel burning and refuse disposal practices, air pollutant emissions, and abatement plans for Federal facilities in counties in Kansas and Missouri 22 p3577 N71-35431

Survey of air pollution by Federal facilities in Milwaukee air control region 22 p3577 N71-35432

Types of measurement, and solutions to air pollution problems caused by transportation vehicles
[DHO-RRL-69] 22 p3578 N71-35485

Microwave radiometer for detecting air pollution
[PB-199427] 22 p3584 N71-35522

Chemical and physical properties and mass response to nitrogen oxides in atmosphere
[AP-84] 22 p3612 N71-35730

Fundamentals of calculating concentration and diffusion of air pollutants
[AD-726984] 22 p3615 N71-35730

Fast analysis by 14 MeV neutron activation of fluoride deposits on vegetation in polluted area
[CEA-CONF-1747] 22 p3641 N71-35956

Air pollution sources and control procedures and 1970 Clean Air Act summary
[PB-199479] 22 p3699 N71-36978

SUBJECT INDEX

- Air pollution by gas turbine aircraft engines 22 p3700 N71-36387
 Organization and activities of Industrial Pollution Control Council 22 p3700 N71-36389
 Radiation monitoring data for radioactive fallout in German Democratic Republic for 1969 23 p3713 N71-36471
 Primary and secondary air pollution from asphalt plants 23 p3749 N71-36733
 Developmental program for SO₂, NO_x, and particulate pollutant level lowering and control in fine gas from fossil fuel combustion using fluidized beds with limestone [ANL/BS-CHEM-1003] 23 p3750 N71-36736
 Buffer oxides, smoke, and air pollution tables from Indian weather stations, Dec. 1970 23 p3790 N71-37012
 Development of mathematical meteorological diffusion models for analysis and solution of urban air pollution problems 23 p3792 N71-37031
 Standard methods for storage and retrieval of atmospheric data 24 p3807 N71-37776
 Air pollution from plant affecting quality of commercial Christmas trees in Maryland and West Virginia [AFD-0454] 24 p3917 N71-37954
 Continuous measurement of activity concentration of radionuclides in air using NaI [d] crystal detector [EPFL-71-13] 24 p3919 N71-37948
 Design and construction of Holmium spectral analyzer to aid in research of air pollutants [NASA-CR-125170] 24 p3930 N71-37957
AIR PURIFICATION
 Secondary flow in electrostatic precipitators 24 p3957 N71-38229
 Ion exchange beads as microstandards for air purification, chromatography for lithium analysis, infrared measurements on polymer crosslinking, and filtration of contaminants [DHS-TN-549] 25 p3641 N71-35595
 High expansion foam for extinguishing air bearing leaks [DUN-SA-141] 26 p3876 N71-35869
 Developing high pressure gas purification and filtration systems for use in test operations of space vehicles [NASA-CASE-MPS-12806] 27 p1036 N71-37588
 Chlorine cultivation for purifying isolated environments of toxic gaseous contaminants 28 p1153 N71-39033
 Control of nitrogen dioxide in stack emission by reaction with ammonia [NASA-TM-X-22357] 29 p1345 N71-30367
 Cabin air conditioning for passenger aircraft noting air purification and recirculation, odor control, and pressurization requirements 30 p1492 N71-20849
 Portable apparatus producing high velocity annular air column surrounding low velocity filter, operation in central core for industrial clean room environmental control [NASA-CASE-XMP-43212] 31 p1770 N71-22721
 Methods, instruments, and performance of air filtration used to cleanse contained atmospheres - continued [CONTR-700816-VOL-2] 32 p2743 N71-29851
 Energy sources in US to achieve future electric energy needs and environmental compatibility requirements 33 p2743 N71-29852
 Hypoiodous acid generated by injection of elemental iodine into steam-air atmosphere or by purging dilute aqueous solution of iodine in water with air or other gases - airborne species 33 p2743 N71-29853
 In-place testing of charcoal adsorbent bed filters with methyl iodide as test penetrant using pyrolyzer-microcoulometer detector 34 p2743 N71-29854
 In-place test results of M reactor charcoal confinement filters using iodine tagged with iodine 131 tracer 34 p2743 N71-29855
 Effect of gamma radiation on adsorption of iodine and methyl iodide on activated carbon exposed to flowing mixtures of steam and air 34 p2715 N71-29856
 Activated carbon in reactor confinement systems to remove radioiodine from effluent gases in event of nuclear accident 35 p2715 N71-29857
 Iodine behavior and control in processing plants for fast reactor fuels and removal of radioiodine from plant effluents 35 p2784 N71-29858
 Langmuir adsorbent materials for trapping of fission product iodine in fuel reprocessing plants and gas during iodine reactor containment 36 p2784 N71-29859
 Analysis of concurrent adsorption and chemical reaction 36 p2715 N71-29861

- Environmental engineering and management for natural environment - regional plan for water, sewage, air, and refuse comparing automatic vehicle monitoring system dispatching police vehicles to conventional system [PB-190290] 19 p3083 N71-31627
 Amino silica gel adsorbents for atmospheric purification systems of spacecraft cabins 20 p3222 N71-33468
 Function of condensing steam in designing scrubbers for polluted air streams 20 p3243 N71-33533
 Estimates of governmental and private expenditures for prevention and control of air pollution 21 p3353 N71-35175
AIR SAMPLING
 Upper air sampling for radioactive contaminants using balloons flights [COO-481-162] 25 p3649 N71-34784
 Detection of atmospheric regions of disturbed index refraction [PB-192345] 25 p3672 N71-34865
 Air pollution sampling in vicinity of summation plant [PB-193145] 27 p1015 N71-36994
 Atmospheric sampling apparatus design to follow changes in natural radioactive decay products of radon in free and conditioned atmosphere [CRA-R-4048] 28 p1230 N71-18233
 Mass and infrared spectrometric and gas chromatographic analysis of air samples from space station simulator during 90 day manned test [NASA-CR-111831] 29 p1413 N71-19636
 Air sampling after nuclear entering detonation in Project Salsomero [UCRL-72534] 30 p1624 N71-21792
 Technology and equipment for industrial air pollution monitoring and sampling [DTR-52546] 31 p1747 N71-22055
 Industrial pollution properties summary including data on toxicity and control, air sampling, and gas analysis 32 p1747 N71-22056
 Photocolorimetric gas analysis methods and equipment 33 p1761 N71-22057
 Aerosol and flame ionization techniques for air pollution sampling gas analysis 33 p1747 N71-22060
 Systems analysis and cybernetics simulation of automatic air sampling systems 34 p1728 N71-22064
 Air sampling over Japanese atomic research facility [JAERI-MEMO-4175] 35 p2075 N71-25123
 Aerosol sampling devices and vertical distribution of long lived radioactive and stable elements in atmosphere [NPL-18633] 36 p2485 N71-27710
 In-place testing of charcoal adsorbent bed filters with methyl iodide as test penetrant using pyrolyzer-microcoulometer detector 37 p2743 N71-29854
 Inorganic material adsorbent air sampling system for analysis of airborne iodine isotopes and compounds in nuclear reactor containment atmospheres 37 p2743 N71-29863
 Remote air sampling and monitoring system for gas analysis of radioactive isotopes in containment atmospheres after loss of coolant tests 37 p2744 N71-29865
 Application of remote air sampling and monitoring system to nuclear power industrial safety and analysis of radioactive isotopes in containment atmospheres 37 p2744 N71-29866
 Atmospheric sampling and analysis of neon, water vapor, hydrogen, carbon dioxide, and radon radioactivity by thermal absorption and gas chromatography 37 p2744 N71-29867
 Application of bismol continuous plasma dispersion model to estimate concentrations of air pollutants - tables and graphs [PB-191482] 39 p3125 N71-31626
 Inventory of automatic sampler-analyzers, mechanized samplers, and static samplers used for air pollution monitoring in US and Puerto Rico [PB-190329] 41 p3420 N71-34334
 Off-site fallout surveillance activities of Southwestern Radiological Health Laboratory from Jan. through June 1969 [SWRHL-97-R] 41 p3478 N71-34772
 Volume, diaphragm elasticity and area, orifice area, and L/D ratio effects on pulsation dampener efficiency for smoothing personal respirable dust sampler flows [BM-R1-7545] 42 p3548 N71-35276
 Continuous measurement of activity concentration of radioiodine in air using NaI [d] crystal detector [KFEI-71-13] 44 p3919 N71-37948
AIR-SEA INTERACTIONS
 U. AIR WATER INTERACTIONS
 AIR SICKNESS
 U. MOTION SICKNESS

AIR TRAFFIC CONTROL

- AIR TRAFFIC**
 Air traffic pattern prediction for 1968 peak summer periods in London, England terminal area 21 p3082 N71-30163
 Analysis of airport travel demands at Lambert-St. Louis Municipal Airport [PB-192057] 24 p3515 N71-35895
 Survey of Hawthorne pattern of commercial air traffic [NASA-CR-115000] 25 p3708 N71-37553
 Survey of rapid transit railway impact on airport passenger traffic [PB-193045] 27 p1085 N71-16990
 Tabulations for rapid transit system effect on airport traffic [PB-193049] 27 p1085 N71-16991
 Rapid transit railway effect on airport passenger traffic [PB-193046] 27 p1085 N71-16992
 Research and development aspects of air transportation system for state of Texas [PB-190053] 30 p1404 N71-21620
 Compilation of references on various aspects of air transportation for Texas [PB-190054] 30 p1404 N71-21620
 Proceedings and recommendations of conference on state buses [DGA-174-8] 31 p1472 N71-31976
 Prediction of civilian air travel increase and airport use in United States of America for 1980 [AD-720732] 32 p3367 N71-37159
 Meteorological charts for air space over Toulouse-Bagnas 33 p3951 N71-30952
 Trends in air transportation and airline industry operations from 1970 to 1980 33 p3951 N71-31512
 Graphs and tables of aircraft traffic over North America - 1966 through 1969 [RAE-LIB-TRANS-1590] 34 p3954 N71-38210
AIR TRAFFIC CONTROL
 Experimental design of three dimensional air traffic control radar tracking system 35 p1082 N71-10164
 National Aviation Facilities Experimental Center history and programs 35 p1082 N71-10164
 Evaluation of systems, procedures, and instrumentation for air traffic control [AD-711662] 35 p1083 N71-10737
 Computer programs and predictor displays for solving air traffic control problems [NASA-CR-111572] 35 p1082 N71-11466
 Project DROCURES for global sea and air traffic control using synchronous satellites for ground-air-ground communications 36 p2563 N71-17768
 Performance ratings and personality test factors of air traffic controllers [AM-70-14] 36 p3329 N71-12350
 Feasibility of satellite navigation system for subsonic and supersonic air traffic control over North Atlantic Ocean 36 p3407 N71-12594
 Cost analysis of joint NASA-European space program involving navigation and communication satellites for civil air traffic control [ESRO-SP-41] 36 p3409 N71-12754
 Military air traffic report for calendar year 1969 in United States and overseas [REPT-70-10] 36 p4073 N71-13418
 Analysis of New York air transportation system and recommended improvements [PR-3] 36 p3515 N71-13777
 Digital radar data transmission system for use in air traffic control 36 p3505 N71-13840
 Investigating computer program functions and test procedures for failure analysis of NAS En Route Stage A Model I System [PAA-NA-70-31] 36 p3786 N71-14567
 Capacity measurement methodology for air traffic control system with long range objectives [PAA-RD-70-70] 36 p3630 N71-14635
 Optimization techniques for aircraft multiple flight paths [AD-713136] 36 p3721 N71-15392
 Investigation of transponder reply failure in vicinity of O'Hare Airport, Chicago, Illinois [PAA-RD-70-75] 36 p3648 N71-15498
 Methodology for evaluating capacity of air traffic control systems [PAA-RD-70-69] 36 p3788 N71-15358
 Description of Air Force tactical air control and communication system 36 p3693 N71-16490
 Workload and performance limiting factors of air traffic control radar operators 37 p3679 N71-16914
 Work-rest cycles in air traffic control tasks 37 p3679 N71-16915
 European aerospace and electronic equipment industrial cooperation for air traffic control and communication satellites 37 p1132 N71-17181

Proposed STOL operations in Northeast Corridor with respect to air traffic control

07 p0974 N71-17963

Systems analysis summary on New York metropolitan area air traffic capacity

07 p1134 N71-18040

Surveying air traffic controller occupation and development of performance objectives

07 p1138 N71-18105

Establishing minimum operational requirements for airborne air traffic control transponder systems

07 p0995 N71-18109

Survey of air traffic control radar beacon system operational problems

07 p0995 N71-18116

European Space Research Organization meteorological, communications and air traffic satellites program

08 p1293 N71-18640

System description of field test model of ARTS 2 modular alphanumeric nontracking ATC system

08 p1166 N71-18815

Traffic control system for supersonic transports using synchronous satellite for data relay between vehicles and ground station

[NASA-CASE-GSC-10087-1] 08 p1145 N71-19287

Design, construction, operation, and management of military airports

[AD-716603] 09 p1365 N71-19702

Cockpit display of automatic radar control systems data

[AD-716425] 09 p1415 N71-19848

Development of improved surveillance and communication subsystems for automated air traffic control system

[AD-716816] 10 p1599 N71-20774

Aircraft safety and aircraft reliability, noting pilot performance, landing approach and takeoff, and clear air turbulence

11 p1674 N71-22197

Satellite applications to aircraft communications, navigation, and surveillance over US including synthesized satellite network and aircraft equipment for air traffic control

11 p1792 N71-22339

Location/identification transmitter and equipment for use in satellite applications in aircraft communication, navigation, and surveillance for US air traffic control

[NASA-CT-117739] 11 p1792 N71-22340

Market forecasts and traffic control technologies of Boeing 747 aircraft and supersonic aircraft operations

11 p1675 N71-22383

US cooperation with ESRO UHF satellite system development for air traffic control in Europe

[NASA-TT-F-13651] 12 p1960 N71-23967

Terminal air traffic control facility for approach systems tests

[AD-719104] 13 p1209 N71-24451

Physiological and biochemical measurements of air traffic controller personnel at O'Hare Airport to determine effects of duties

[FAA-AM-71-2] 13 p2037 N71-24747

Evaluation of dual input transponder with upper and lower aircraft antennas as resolution for problems with air traffic control radar beacons system limitations

[FAA-NA-71-39] 13 p2857 N71-24082

Bibliography on aeronautical satellite system air traffic control and propagation factors

[NASA-TM-X-65511] 13 p1213 N71-24942

General aviation traffic implied densities and interaction frequencies computed with model using southern California to judge difficulty for naval air traffic

[AD-719906] 14 p2197 N71-25621

Biodynamic evaluation of air traffic control students from 1960 to 1963

[FAA-AM-71-8] 16 p2549 N71-28005

Mathematical models and optimal control for uncertain systems

[AD-721470] 16 p2628 N71-28060

Improved surveillance and communication capability of air traffic control

[AD-721463] 16 p2629 N71-28085

Analysis of aircraft accidents and establishment of rational, quantitative air traffic safety control goals

[FAA-RD-71-36] 17 p2702 N71-29309

Third order-two signal intermodulation products for 242 frequencies between 225 and 400 MHz as used in FAA frequency assignment processes

[ECAC-PR-70-018] 17 p2719 N71-29551

Third order-two signal intermodulation products for 360 frequencies between 118 and 136 MHz when 50 kHz channel spacing is used as in FAA frequency assignment processes

[ECAC-PR-70-016] 17 p2719 N71-29552

Third order-two signal intermodulation products within 118-136 MHz band with 50 kHz spacing

[ECAC-PR-70-015] 17 p2719 N71-29554

Fundamental characteristics of analog and digital modulation used in ATC communication system

[ESSA-TM-ERL-TTS-232] 17 p2719 N71-29555

Evaluation of airborne transponders used for air traffic control facilities

[AD-723028] 17 p2779 N71-30253

Holographic imagery for aviation and space flight [JPRS-53430] 17 p2760 N71-30361

Systems analysis approach to airport planning and predicting terminal facility and aircraft demands in year 2000 for air traffic control systems

[NASA-CR-119287] 18 p2871 N71-30800

Mathematical simulation and queuing models for air traffic control systems

[AD-721726] 19 p3132 N71-32065

Evaluation of flight plan position information display for ocean flying control

[FAA-NA-71-31] 19 p3132 N71-32084

Analysis of two plans for assigning identity codes to aircraft by digital computer simulation of peak IFR traffic conditions

[NBS-TN-568] 19 p3039 N71-32456

NASA balloon-aircraft ranging, data and voice experiment for determining best approach for using ATS in air traffic control

[NASA-TM-X-65649] 19 p3057 N71-32527

Coordination of traffic flow and holding patterns of aircraft landing on same runway

[NASA-CR-121466] 20 p3301 N71-33747

Operational evaluation of capability of bright radar microwave remote sensing to provide useful radar data in satellite control tower

[FAA-RD-71-48] 20 p3236 N71-33788

Evaluation of air traffic control parameters and relationship to future of aeronautics

[NASA-CR-1833] 21 p3376 N71-34025

Physiological and psychological reactions to sonic booms and effects on efficiency of air traffic control personnel

[FAA-AM-71-29] 21 p3383 N71-34068

Research of control optimization, stochastic stability, and air traffic control problems

[NASA-CR-121630] 21 p3397 N71-34173

Summary of instrument flight rule off-airway routes for commercial and military aviation in US and overseas areas

21 p3455 N71-34592

Centralized flow control concepts and applications in air traffic control

21 p3456 N71-34594

Scientific developments in Europe involving treatment of cholera, treatment of bacterial endocarditis, automated system for epidemiological information, and air traffic control

[JPRS-53877] 21 p3534 N71-35187

Biomedical evaluations of cardiovascular and overall physical fitness of air traffic control personnel

[FAA-AM-71-19] 22 p3544 N71-35243

Development of analysis techniques for determining causes for airport congestion and interaction of various causes

[FAA-RD-71-55] 22 p3565 N71-35393

Range and azimuth resolution characteristics and aircraft separation measurement capability of radar beacon-digital subsystem

[FAA-NA-71-16] 23 p3793 N71-37038

Attitudes and motivational factors in job performance of terminal area air traffic control personnel

[FAA-AM-71-30] 23 p3794 N71-37041

Airborne traffic situation display system for use with radar control terminal system

[AD-727769] 23 p3794 N71-37042

Alternate air traffic control co-channel separation criteria based on probability-of-interference considerations

[IST-101] 24 p3888 N71-37712

Automatic data processing systems for air traffic control, health services, operations research, management planning, information systems, and reading machines

24 p3892 N71-37742

Computerized real time data processing and display system for air traffic control in airspace over Belgium, Luxembourg, the Netherlands, and Germany

24 p3893 N71-37744

Evaluation of design concept and operational feasibility of 11-sided control tower cab

[FAA-NA-71-37] 24 p3904 N71-37826

Effectiveness of control towers in reducing aircraft accidents and approach time

24 p3955 N71-38213

Air traffic control, communications, navigation, frequency management, systems analysis, and aircraft SRDS program developments

24 p3955 N71-38214

Performance evaluation of automatic flight progress strip cutter and loader used in air traffic control facility

[ACTEU-330] 24 p3955 N71-38215

AIR TRANSPORTATION

Systems maintenance program evaluation of Eastern Region air transportation facilities

01 p0037 N71-10114

Traveler service problems in domestic intercity air, bus, and rail transportation

[AD-719360] 01 p0135 N71-10116

Air pollution reduction by urban tri-state air transportation system around New York City

[FAA-NO-70-14] 01 p0608 N71-10124

Demonstration plan for Western Region Short Haul Air Transportation Program

[ATR-71-7190-1-VOL-1] 01 p0003 N71-10029

Technical studies for Western Region Short Haul Air Transportation Program

[ATR-71-7190-1-VOL-2] 01 p0003 N71-10030

High speed access system evaluation for transportation from airport to Miami with cost estimates and network descriptions

[PB-192842] 01 p0038 N71-10087

Status of federal involvement in short haul air transportation

02 p0145 N71-11005

Various vertical takeoff and landing and short takeoff model configurations for air transportation

[PB-190940] 02 p0145 N71-11007

Air mode service analysis in Northeast Corridor

[PB-190935] 02 p0145 N71-11009

Legal aspects of air and surface carrier interaction in freight transportation

02 p0306 N71-12119

Possible benefits of local and trunk air carrier mergers

02 p0313 N71-12120

Conceptual framework and example analysis to determine feasibility of V/STOL air transportation system in Appalachian region

03 p0313 N71-12237

Analysis of New York air transportation system and recommended improvements

04 p0515 N71-13777

Analysis of air transportation facilities in Gulf Coast region of US - Vol. 1

[PB-194339] 04 p0516 N71-13800

Analysis of civil aviation facilities in Gulf Coast region of US - Vol. 2

[PB-194340] 04 p0516 N71-13801

Organizational structure and operational procedures of USSR civil aviation

[AD-713415] 05 p0627 N71-14255

Investigating technology and analytic techniques for solving late-airport transportation problems

[AD-702738] 05 p0657 N71-14810

Physiological adaptation problems during long range aerial troop deployment

[AD-714368] 06 p0802 N71-14611

Civil aeronautics operations review

07 p1133 N71-17779

Problems in civil air transportation and logistics

07 p1134 N71-17799

Systems analysis and mathematical model for air transportation design

[NASA-CR-116431] 07 p1134 N71-17801

Members attitudes on revisions to Warsaw Convention and The Hague Protocol amendments on liability to international air transport passengers

[REPT-1970/E-B] 07 p1138 N71-18100

Feasibility of inter-metropolitan transport system using Braguet 941 STOL aircraft

[REPT-30] 07 p0974 N71-18104

Air transport supply on scheduled services in Europe-Mediterranean and Southeast Asia regions

[REPT-1970/E-B] 07 p1138 N71-18112

Physiological effects on air transportation, including atmospheric and runway conditions

07 p0556 N71-18117

Statistical analysis of origin-destination survey at Philadelphia International Airport

08 p1308 N71-18926

Visual factors in air and surface transportation systems

[PB-190614] 09 p1487 N71-19997

Survey of passenger volume and destinations at Theodore F. Green State Airport in R.I.

[PB-193940] 09 p1365 N71-19865

Economic analysis of intercity short-haul business passenger travel

[NASA-TM-X-2228] 09 p1488 N71-20114

Stresses and adaptation problems associated with large scale, long range, rapid reaction time, aerial troop deployments

09 p1336 N71-20540

Research and development aspects of air transportation system for state of Texas

[PB-190833] 10 p1494 N71-21620

Compilation of references on various aspects of air transportation for Texas

[PB-190936] 10 p1494 N71-21620

Air transportation system noise propagation and reduction

[PB-196391] 10 p1609 N71-21610

Air transportation system and Civil Aeronautics Board decisions

12 p1857 N71-23720

Aviation and surface transportation safety in 1970 with related accident investigations and recommendations

[AR-4] 13 p2191 N71-24025

Analysis of current status and future outlook of US commuter airline industry

[AD-718871] 16 p2531 N71-28216

Analysis of medical, psychological, and environmental aspects of mass air transportation

[FAA-AM-71-10] 17 p2710 N71-29800

SUBJECT INDEX

Congressional hearings on chartered airline travel 17 p2601 N71-29707

Trends in air transportation and airline industry questions from 1970 to 1980 18 p3031 N71-31512

Investigation of air charter operations utilizing large airplanes to fulfill demands of aircraft capacity and speed, cargo type and size, as well as frequency of operation 19 p3199 N71-31624

Analysis of equipment, crew training, and operations involved in use of fixed wing aircraft for commercial transportation 19 p3203 N71-32000

(FAA-AW-71-18) 19 p3038 N71-32000

Measurement and analysis of atmospheric turbulence along Pacific Coast air routes in Japan (JNAL-TR-222) 20 p3297 N71-33583

Noise reduction laws for air, rail, and highway transportation including legal liability in US (DOT-DAA-71-1-VOL-7) 20 p3212 N71-33936

Conclusions of studies by French Committee for Air Transport to prepare proposals and recommendations in air transport field for next five years (NASA-TT-7-1947) 21 p3375 N71-34015

Development of methodology for evaluating potential benefits of alternative transportation proposals for regions - Vol. 1 (RM-6324-DOT-VOL-1) 21 p3407 N71-34245

Development of methodology for evaluating transportation services with emphasis on effectiveness of service - Vol. 2 (RM-6324-DOT-VOL-2) 21 p3408 N71-34246

Development of methodology for evaluating alternative proposed changes to mix of transportation modes in northeast corridor of US - Vol. 3 (RM-6324-DOT-VOL-3) 21 p3408 N71-34247

Travel agent guide to air travel in US 21 p3535 N71-35194

Design, development, and performance requirements for large rigid airships for freight and cargo transportation (RIS-53) 23 p3707 N71-36425

Guidelines for national aviation system planning and R and D policy (FAA-AV-71-2) 24 p4036 N71-38798

AIR WATER INTERACTIONS

Characteristics of turbulent air stream over progressive water waves (AD-720005) 24 p3917 N71-37929

AEROSPACE EQUIPMENT

NT AIRBORNE/SPACEBORNE COMPUTERS

Performance characteristics of Bendix type DRA-12 defense Doppler radar system (FAA-NA-78-50) 01 p0022 N71-10394

Failure analysis of recovery flanking axon lamp on Apollo 18 flight 02 p0227 N71-11989

Automatic pilot and associated airborne equipment developments for automatic landing systems 03 p0405 N71-12434

Flight maneuvers and airborne and ground equipment for landing VTOL aircraft in adverse conditions 03 p0406 N71-12436

Historical review of growth of guidance and control systems based on use of digital computers for manned aircraft 03 p0408 N71-12603

Investigating problems encountered in developing and maintaining airborne computer programs for guidance and control 03 p0346 N71-12606

Investigating system requirements of airborne data processors 03 p0408 N71-12608

Investigating small digital processors as interface between computer and sensor in airborne systems 03 p0347 N71-12609

Describing digital computer used in navigation and attack system of Aegaeus aircraft 03 p0408 N71-12611

Airborne electronic read fuse (NARA-RC-115791) 04 p0511 N71-13527

Data handling equipment for aerospace and ground support applications - conference (AARD-CP-47-70) 04 p0504 N71-13826

Airborne data acquisition system incorporating recycling metal tape flight data recorder 04 p0505 N71-13836

Build state power modules for airborne phased array 04 p0496 N71-13918

Surveillance radar installed on helicopter for obstacle avoidance 04 p0499 N71-13938

Measuring dynamic errors of infrared radiometers used in measure ocean and sea surface temperature (JRES-73039) 05 p0686 N71-15438

Verification of geography in Rio de Janeiro by using satellite photography (LARS-13-VOL-2) 05 p0680 N71-15546

Investigating application of airborne remote sensors to hydrology and oceanography (NARA-TT-X-62565) 06 p0846 N71-16161

Airborne tests of multiplexed scanners to determine usefulness of remote sensors in surveying river, coastal, and deep-sea phenomena
 06 p0848 N71-16184
 Design and development of broadband model of airborne radar
 [AD-715884] 06 p0859 N71-16214
 Simulation model for advanced avionics digital command
 [AD-714140] 06 p0894 N71-16295
 Stochastic process error analysis of airborne gravimetry
 [AD-715268] 07 p1021 N71-17731
 Minimum performance standards for airborne radio marker receiving equipment operating on 75 MHz
 [DO-143] 07 p0995 N71-18098
 Minimum performance standards for airborne radio receiving and direction finding equipment operating on radio frequency range of 200-450 kilohertz
 [DO-142] 07 p0995 N71-18101
 Establishing minimum operational requirements for airborne air traffic control transponder systems
 [DO-144] 07 p0995 N71-18109
 Spectrophotometric results from NASA 1968 Airborne Auralor Expedition and tentative identification of several molecular nitrogen emission bands
 [NASA-CR-116856] 08 p1196 N71-19148
 Application of airborne and satellite-borne remote sensing systems geological surveys
 08 p1196 N71-19252
 Airborne photoreactive particle counter for mapping clear air turbulence
 [NASA-CR-111864] 09 p1414 N71-20398
 Field and laboratory equipment and methods for airborne electroprospecting using rotating magnetic fields and anomalous effect calculations for conducting and irregular form bodies
 [TT-78-50059] 10 p1555 N71-21671
 Collection, reduction, and evaluation of electric field phenomena and geomagnetic field data at both low and high altitudes
 [AD-717779] 11 p1748 N71-22343
 Reference frequency generator and modulator for airborne data acquisition system
 [ARL-FI-44] 11 p1724 N71-22441
 Airborne laser-radar measurements of atmospheric clear air turbulence by optical digital processing
 11 p1776 N71-22960
 Delay circuits for pulse compression in airborne FM demodulator
 [RAE-TR-70110] 12 p1874 N71-23363
 Interference prediction model for evaluating expected interactions between avionics equipment on aircraft
 [AD-718997] 13 p2042 N71-24357
 Tests on bottles for oxygen, air, and other gases to be used as airborne equipment, noting filament winding
 [TRC-BR-22373] 13 p2030 N71-25051
 Airborne photometer instrumentation and measurement data on high latitude hydroxyl airglow emission
 [NASA-CR-118320] 13 p1262 N71-25211
 Measurement of Alaska sea ice thickness from aircraft using beamstrutter projectiles
 [SC-71-3664] 13 p0798 N71-25432
 Airborne target recognition and acquisition equipment testing
 [AD-720569] 14 p2118 N71-26175
 Communication, surveillance, and airborne electronic equipment performance testing in tropical environments
 [AD-720577] 14 p2118 N71-26176
 Evaluation of airborne laser systems for mapping, range finding, communication, and fire control
 [AD-720532] 14 p2266 N71-26188
 Test procedures to evaluate airborne rescue equipment for use in crash rescue operations
 [AD-728563] 14 p2198 N71-26195
 Airborne interferometric measurements on atmospheric airglow emission
 [AD-720873] 15 p2399 N71-27188
 Digital time code generator for airborne use comprising solid state visual display of time and synchronization with another time generator
 [ARL/F-45] 15 p2411 N71-27622
 Portable rotating gradiometer for measuring gravity gradients under dynamic conditions tested for noise-free operation
 [AD-721742] 16 p2588 N71-28451
 Optical and inspection sampling methods for sizing and counting water droplets in clouds for use in sampling from aircraft
 [AD-721677] 16 p2625 N71-28457
 Airborne electronics equipment design for indicating helicopter fuel capability using a X-ray backscatter from Kr-85, temperature sensor, and digital computer
 [SAN-805-1] 17 p2702 N71-29215
 Airborne radiometric measurement of water stored in snowpack on mountain watershed
 [RL0-2061-1] 17 p2737 N71-29217
 Compact, self contained, symmetrical antenna for airborne use at high frequencies with capability to function in two independent modes for both transmission and reception
 [AD-727361] 17 p2726 N71-29208

Low-cost pilot indicator for midair collision avoidance 18 p2869 N71-30760

Airborne infrared detector performance tests for detection of earth impacted radioactive isotope heat sources [SC-DR-710095] 18 p2903 N71-31182

Airborne sea surface temperature measurement over North Sea discussing isotherms [BRVG-FBW7-71] 19 p3083 N71-31790

Systems and equipment for civil aircraft approach and landing [REPT-52] 20 p3299 N71-32858

Airborne ocean surface temperature measurement using infrared radiometers [BMVG-FBW7-71-6] 20 p3256 N71-32997

Airborne infrared telescope for flux measurements of astronomical objects with spectral energy peaks concentrated at wavelengths of more than 25 microns [NASA-CR-121414] 20 p3272 N71-33205

Flight tests of airborne dissemination devices for chemical warfare [AD-726350] 22 p3540 N71-35218

Airborne audio-video recording system design and requirements [AD-727025] 22 p3549 N71-35280

Aerial surveys for determining plutonium concentrations using array of NaI detectors [BGG-1183-1517] 22 p3444 N71-33980

Cost ownership analysis of avionic equipment 23 p3750 N71-36784

Characteristics of sensors for aerial observation of ice formations and comparison of effectiveness of various methods [JPRS-54162] 23 p3759 N71-36801

Airborne traffic situation display system for use with radar control terminal system [AD-727769] 23 p3794 N71-37042

C band radar transmitter for airborne radar system [AD-727085] 24 p3887 N71-37767

Flight sampling of flora using atmospheric probe [NASA-CR-114378] 24 p3920 N71-37938

Design of scanning laser radar for spaceborne applications [NASA-CR-121014] 24 p3991 N71-38047

AIRBORNE TERRAIN ANALYSIS
U. TERRAIN ANALYSIS
AIRBORNE/SPACEBORNE COMPUTERS

Flight control software package for digital flight control and landing system of CH-46C helicopter [NASA-CR-110903] 01 p0827 N71-10283

Guidance software package for digital flight control and landing system of CH-46C helicopter [NASA-CR-111023] 01 p0828 N71-10284

Spacecraft crew function classification and methods for crew loading with onboard computer [NASA-CR-102993] 01 p0858 N71-10526

LSI circuitry using MOS structures for airborne computers 03 p0348 N71-12631

Main machine systems and astronaut and onboard computer communications [NASA-CR-102933] 05 p0651 N71-14999

Application of domain tip logic in designing associative networks for spaceborne use [NASA-CR-115566] 05 p0652 N71-15535

Logic circuit to ripple add and extract binary counters for spaceborne computers [NASA-CASE-XGS-04766] 08 p1164 N71-18682

Digitalized optical detectors for cloud data processing onboard satellites using Fourier analysis 13 p2126 N71-25321

Stored program computer for onboard spacecraft data processing 13 p2652 N71-25325

Vocabulary for spacecraft communication systems with spaceborne computers with graphic display devices [NASA-CR-103171] 14 p2221 N71-25922

Airborne computer architecture and organization for executing computer programs written in space programming language [AD-726798] 14 p2221 N71-25930

Airborne/in-spaceborne computer design and hardware for space shuttle data communication system [NASA-CR-115832] 15 p2384 N71-27782

Airborne FDP 15 computerized simulation for jet aircraft gunnery and navigation training including head-up display and real time computer programming [AD-716733] 16 p2365 N71-28327

Digital data processor for use with large scale integrated circuit technology and spaceborne computer application [NASA-CASE-GBC-10975-1] 16 p2365 N71-28420

Action of onboard computer to spacecraft's instrument sequential program control [D-2] 17 p2722 N71-29041

Onboard optical data processing for earth resource spacecraft and planetary spacecraft [NASA-TM-X-434093] 17 p2723 N71-29883

Airborne direction finding techniques having multiple antennas tracking capability [AD-725541] 18 p2956 N71-31418

Estimation method for real correlation coefficient of spacecraft data processing system [NASA-TT-F-13792] 19 p3061 N71-32121

- Computerized simulation of statistical onboard data analyses for long range spacecraft
[NASA-TT-F-13791] 19 p3062 N71-32346
- Bit-plane encoding and other aperture methods for data redundancy removal for onboard spacecraft data management
19 p3063 N71-32343
- Consequences of introduction of spacecraft computers on data handling in conjunction with telemetry equipment and transmitter receiver operations
[D-64] 20 p3238 N71-33039
- Design criteria for guidance and control spacecraft computer selection including physical and functional characteristics and reliability
[NASA-SF-8070] 20 p3239 N71-33679
- Feasibility of Mafli thin films for spacecraft optical mass memory applications
[NASA-CR-119897] 21 p3463 N71-34647
- Space shuttle onboard crew/computer communication utilizing remote graphic displays and technology oriented vocabulary
22 p3675 N71-36202
- Architectural design of spacecraft computer system operating in multi-element configuration
[NASA-CR-121016] 24 p3892 N71-37737
- Advanced avionics digital computer development program
[AD-727607] 24 p3895 N71-37765
- AIRCRAFT**
- Performance, dynamics, and design of aeronautical and space vehicles
[NASA-SF-358] 13 p3172 N71-34701
- Aerodynamic and unsteady flow problems of aircraft
13 p3023 N71-34706
- Random process theory method for estimating response of flexible airplanes to atmospheric turbulence
13 p3026 N71-34708
- Potential feasibility of safe, practical, and economical air-breathing nuclear propulsion system for aircraft and air cushion vehicles
[NASA-TM-X-67837] 13 p3123 N71-35524
- Calculating and testing anticing systems of aircraft and helicopters
[AD-719922] 14 p3197 N71-35622
- Effect of turbulent shear on decay of trailing vortex system behind aircraft
[AD-720852] 15 p3294 N71-37333
- Intrusion detector for parked aircraft using sensing technique to detect human touch
19 p3070 N71-31651
- Aerodynamic characteristics of wing, propeller blades, and entire aircraft at various velocities including flow viscosity and compressibility - textbook
[AD-723542] 19 p3033 N71-31932
- Algorithm for identification of system parameters from input-output data with application to air vehicles
[NASA-TN-D-6468] 19 p3124 N71-32373
- Synthesis of aircraft across track errors using mathematical models with statistical parameters
[REPT-EJC-2] 20 p3299 N71-32885
- Results of combined fully instrumented subsatellite geophysical experiment including spectrophotometry of earth surface
[JPRS-53895] 21 p3419 N71-34328
- Static electrification of aircraft when flying through clouds and precipitation
[AD-726581] 22 p3541 N71-35225
- Cost effectiveness of built in test provisions in aircraft operations
23 p3757 N71-36780
- Flight dynamics and calculation of flight trajectories of various aircraft and spacecraft
[AD-727474] 24 p3872 N71-37602
- Development of rain erosion resistant plastic coatings as high speed aircraft surface finish
[AD-727750] 24 p3944 N71-38133
- Air traffic control, communications, navigation, frequency management, systems analysis, and aircraft SRDS program developments
24 p3955 N71-38214
- Impact of air activity on environment and federal interest in environmental studies
24 p4035 N71-38792
- AIRCRAFT ACCIDENT INVESTIGATION**
- Aircraft accident report and investigation of Air France Boeing 747, St. Jean, Canada, August 17, 1970
[NTSB-AAR-70-26] 01 p0004 N71-10531
- Summary and statistical analysis of aircraft accidents
[NTSB-AAS-70-1] 01 p0005 N71-10674
- Incidence and costs of pilot disorientation Army aircraft accidents during fiscal year 1967
[AD-710987] 01 p0013 N71-10695
- Jet aircraft crash during instrument approach due to electrical systems failure
[NTSB-AAR-70-22] 01 p0005 N71-10812
- Low jet crash during instrument approach due to descent below path profile
[NTSB-AAR-70-21] 01 p0005 N71-10813
- Douglas DC 9 aircraft crash during takeoff caused by ice formation on airfoils
[NTSB-AAR-70-20] 01 p0005 N71-10815
- Aircraft accident investigation of United Air Lines, Boeing 727-22C near Los Angeles, 18 Jan. 1969
[PB-150812] 01 p0006 N71-10914
- Statistical tabulation of United States civil aircraft accident histories for 1969
[PB-190792] 01 p0006 N71-10932
- Statistical tabulation of United States civil aircraft accident histories in 1968
[PB-190811] 01 p0006 N71-10933
- Aircraft accident investigation including types of aircraft, pilot certificates, and accidents
[NTSB-BA-70-4] 02 p0145 N71-11024
- Legal, preventive, and clinical aspects of aerospace medicine
[AGARD-CP-61-70] 02 p0161 N71-11801
- Operational characteristics and pilot experience in civil aviation accidents caused by alcohol intoxication
02 p0161 N71-11802
- Post-mortem lactate analysis on pilot tissues to determine presence of technical malfunction in aircraft accident
02 p0162 N71-11803
- Medical and legal aspects of aircraft accident fatality investigation by aviation pathologist
02 p0162 N71-11805
- Aircraft accident report of Martin 404 N40412
[NTSB-AAR-70-25] 04 p0473 N71-13416
- Aircraft accident report for Douglas DC-8-43P
[NTSB-AAR-70-24] 04 p0473 N71-13417
- Preliminary report of aircraft accident of DC-8 at Anchorage, Alaska
[SB-71-5] 06 p0794 N71-14059
- Preliminary report of aircraft accident of DHC-6 at LaCrosse, Wisconsin
[SB-71-6] 06 p0794 N71-14070
- Investigating aircraft crash landing caused by engine failure and aircrew errors
[NTSB-AAR-70-17] 07 p0949 N71-17063
- Investigation of Douglas DC-9 accident at Harlingen, Texas, on 11 Jan. 1970
07 p0971 N71-17476
- Investigating statistics of aircraft accidents by region and operator
[REPT-1970/10-E] 07 p0974 N71-18115
- Tabulation data on United States commercial aircraft accidents during 1958 to 1952
[PB-196672] 10 p1493 N71-21624
- Tabulation data on United States commercial aircraft accidents during 1953 to 1957
[PB-196673] 10 p1494 N71-21663
- Tabulation data on United States commercial aircraft accidents during 1958 to 1963
[PB-196674] 10 p1494 N71-21665
- Accident investigations, flight control systems, and operational recordings for improved aircraft flight mechanics
[AGARD-CP-76-71] 12 p1853 N71-23410
- Pattern of accident distribution for V/STOL aircraft in United States of America
12 p1855 N71-23426
- Flight mechanics problems in accident investigations for V-101 aircraft
12 p1855 N71-23428
- Weather factors in fatal civil transport aircraft accidents
12 p1856 N71-23431
- Investigation of Mississippi Valley Airways De Havilland DHC-6, N956SM crash at LaCrosse, Wisconsin Nov. 9, 1970
[NTSB-AAR-71-1] 17 p2704 N71-29914
- Analysis of 56 Army midair collisions which occurred during period Jan. 1963 to Nov. 1969 with conclusions and recommendations
[AD-724682] 20 p3210 N71-33278
- Accident investigation of Alitalia Airlines Douglas DC-8-62 at J.F.K. International Airport 15 Sept. 1970
[NTSB-AAR-71-9] 21 p3377 N71-34029
- Aircraft accident report for Ecuadorian C-54 at Miami International Airport 14 April 1970
[PB-199330] 21 p3377 N71-34031
- Medico-legal examination of aircraft parts to determine cause of crash
[AD-726559] 22 p3541 N71-35222
- Aircraft accident briefs for 1969 including date, location, aircraft data, injuries, flight purpose, and pilot data
[NTSB-BA-71-2] 23 p3708 N71-36433
- Aircraft accident investigation of Alaska Airlines Flight 1866 on Sept. 4, 1971
[SB-71-57] 23 p3708 N71-36434
- AIRCRAFT ACCIDENTS**
- US general aviation and supplemental air carrier accident statistical tables for 1969
[NTSB-BA-70-6] 07 p0971 N71-17475
- Causes and results of aircraft accident of Lear jet aircraft
[NTSB-AAR-71-3] 07 p0971 N71-17511
- Causes and results of transport aircraft accident
[NTSB-AAR-70-27] 07 p0972 N71-17512
- Incidence and costs of orientation-error accidents in Army UH-1 helicopter operations
[AD-715107] 07 p0973 N71-17854
- Surveying crash fire and rescue equipment at North American and Canadian airports
07 p1005 N71-18101
- Midair collision hazards, incidents, and recommendations for safe aircraft operations
07 p0974 N71-18100
- Report of transport aircraft accident and probable causes
[NTSB-AAR-71-4] 08 p1145 N71-19808
- Report of aircraft accident due to forward shift of improperly secured cargo
[NTSB-AAR-71-6] 08 p1145 N71-19808
- Proceedings and recommendations of conference on prevention of midair collisions
[NTSB-AAS-70-2] 09 p1145 N71-19808
- Thickened freonage environmental conditions in pressurized fuel lines
[FAA-RD-71-3] 09 p1321 N71-41908
- Influence of environmental factors in aircraft carrier landings and accidents
09 p1325 N71-20809
- Investigation of midair collision between Boeing 70 and Cessna 150 at Edison, New Jersey, on January 1, 1971
[SB-71-28] 10 p1493 N71-21109
- Satellite aided aircraft collision avoidance system effective for large number of aircraft
[NASA-CASE-ERC-10090] 13 p2189 N71-34040
- Studying aircraft accidents to determine hazard angle and speed criteria for designing nuclear airplane fuselage product containment vessel
[NASA-TM-X-2245] 13 p2122 N71-35411
- Aircraft accident at Miami, Florida involving Republic of Ecuador C-54D during climb following instrument descent
[NTSB-AAR-71-2] 14 p2197 N71-36008
- Test procedures to evaluate aircraft borne equipment for use in crash rescue operations
[AD-720563] 14 p2198 N71-36015
- Survey of civil airports to determine status of crash fire and rescue equipment available for use following accidents involving scheduled or local service air carrier aircraft
14 p2327 N71-36446
- Whistling swan as potential hazard to aircraft during migration periods along Eastern flyway
[AD-720889] 15 p3267 N71-27228
- Comparison of fatal aircraft accidents with medical personnel as pilots against aircraft accident fatalities among general aviation pilots
[FAA-AM-71-9] 15 p3267 N71-27428
- Investigation and conclusions concerning noise and fatigue in aircraft components as cause of civil aircraft accidents
15 p3268 N71-27429
- Comparison of physiological characteristics of accident and nonaccident flying personnel for years 1965 - 1967
[FAA-AM-70-18A] 15 p3272 N71-27608
- Selected aircraft accident reports in brief form occurring in US civil aviation operations during 1970
[NTSB-BA-71-1] 16 p2331 N71-38110
- Analysis of aircraft accidents and establishment of rational, quantitative air traffic safety control goals
[FAA-RD-71-36] 17 p2702 N71-29910
- Performance of smoke hood for protection of human respiratory system in aircraft accidents and passenger evacuation
[FAA-AM-70-20] 17 p2711 N71-29640
- Aircraft accident report of DC-9 civilian aircraft ditching near St. Croix, Virgin Islands, May 1970 following fuel exhaustion
[NTSB-AAR-71-5] 17 p2705 N71-30829
- Annotated bibliography on bird aircraft hazards and accidents from Oct. 1967 to Jan. 1971
[TDCK-50961] 17 p2705 N71-30838
- Aircraft accident involving Federal Aviation Administration DC-3 aircraft at La Guardia airport, New York in January, 1971
[NTSB-AAR-71-11] 18 p2873 N71-31333
- Analysis of aircraft structures which cause majority of injuries in aircraft accidents and recommendations for structural improvements to reduce accident severity
[FAA-AM-71-3] 19 p3038 N71-32647
- Statistical compilation of annual aircraft accident data of US general aviation for 1969
[NTSB-ARG-71-11] 19 p3038 N71-32654
- Aircraft incident report involving DC-9 type aircraft damage incurred when aircraft contacted water surface during approach to Martha's Vineyard airport
[SB-71-64] 19 p3039 N71-32648
- Aircraft accident report on midair collision involving DC-9 commercial aircraft and Marine Corps F-4B aircraft near Duarte, California on June 6, 1971
[SB-71-62] 19 p3039 N71-32648
- Aircraft accident report on Convair 440 aircraft crash at New Haven, Connecticut on June 7, 1971
[SB-71-65] 19 p3039 N71-32650
- Analysis of general aviation during year 1969 noting growth of aircraft operation, accident data, analysis of accidents, and injuries resulting from accidents
19 p3039 N71-32654
- Collision avoidance system for detecting probable aircraft accidents - France
[ONERA-TP-938] 20 p3300 N71-33825
- Aircraft accident investigation of fatal DC-8 crash at Kennedy Airport, New York during ferry flight on September 8, 1970
[NTSB-AAR-71-12] 21 p3377 N71-34039

SUBJECT INDEX

Statistical, cause/factor and injury tables, accident rates, and briefs of accidents involving US carriers in 1969
[N75-AR-7L-1] 23 p3708 N71-36437
Aircraft hazards and accidents due to birds
[AD-727811] 24 p3874 N71-37617
Effectiveness of control towers in reducing aircraft accidents and approach time
24 p3955 N71-38213

AIRCRAFT ANTENNAS
Ultrahigh frequency directional spiral aircraft antennas for spacecraft communication
[RAE-TR-70062] 08 p1162 N71-18519
Device and method for calculating optimal fairings for aircraft antennas
[JPRS-52608] 10 p1521 N71-21258
Tests for determining spectral signatures of integrated high-frequency antenna systems for F-3 aircraft
[AD-718054] 12 p1899 N71-23609
Evaluation of dual input transponder with upper and lower aircraft antennas as resolution for problems with air traffic control radar beacon system limitations
[FAA-NA-71-39] 13 p2057 N71-24882
Impedance measurements on modified broadband metal antenna for speech communication
[FOA-3-C-3402-41] 14 p2218 N71-26150
Compact, self contained, symmetrical antenna for airborne use at high frequencies with capability to function in two independent modes for both transmission and reception
[AD-727754] 17 p2726 N71-29895

AIRCRAFT APPROACH INSTRUMENTS
U APPROACH INDICATORS
Human factors in use of terminal radar /analog/ display systems
[FAA-NA-70-55] 01 p0010 N71-10381
Mathematical simulation and queuing models for air traffic control systems
[AD-721726] 19 p3132 N71-32065
Transition, approach, and vertical landing tests for VTOL transport in terminal area
[NASA-TN-X-62083] 22 p3539 N71-35209

AIRCRAFT BASES
U MILITARY AIR FACILITIES
AIRCRAFT BRAKES
NT LEADING EDGE SLATS
NT TRAILING-EDGE FLAPS
NT WING FLAPS
Influence of gravel depth and tire inflation pressure on soft-ground arresting of civil aircraft
[RAE-TR-69001] 02 p0147 N71-11040
Chevron cutting and effects of braking on wear of aircraft tires
18 p2869 N71-30768
Evaluation of braking performance of light, twin engine airplane on grooved and ungrooved runway surfaces
[NASA-TN-D-6444] 23 p3707 N71-36431

AIRCRAFT BREATHING APPARATUS
U BREATHING APPARATUS
AIRCRAFT CARRIERS
Development of signal acquisition methods for television aided aircraft carrier landing operations
[AD-712511] 05 p0410 N71-13194
Influence of environmental factors in aircraft carrier landings and accidents
09 p1325 N71-20369
Student naval aviator anxiety in simulation of first aircraft carrier landing
[AD-718306] 12 p1846 N71-23393
Shipboard test procedures of Pressed lens optical landing system MK 6 MOD 2 for carrier landings
[AD-718333] 12 p1856 N71-23488
Development and performance testing of visibility system and aircraft runway and carrier lighting equipment
[JPRS-10-577] 19 p3071 N71-31619
Development and characteristics of aircraft, helicopters, and airships for detecting and destroying submarines
[AD-723358] 19 p3036 N71-31772
Mathematical modeling of F-8 aircraft wave off trajectories for aircraft carrier approaches
[AD-727121] 23 p3708 N71-36439

AIRCRAFT COMMUNICATION
Technical synthesis and development of advanced communication systems for aircraft landings
05 p0405 N71-12430
Measurements of urban, suburban, and rural radio frequency noise interfering with aircraft communications
[NASA-CR-72802] 05 p0643 N71-14754
Aircraft communication using ATS links
[PUB-A-57] 10 p1646 N71-21727
Multiple access digital communication system for low flying aircraft with intrapass users
11 p1690 N71-21855
Methods for predicting speech interference within windows of fixed wing and rotary wing aircraft
[AD-718996] 12 p1870 N71-23528
Validity of L band communication system between preliminary satellites and aircraft terminals
[NASA-TM-X-65508] 13 p3045 N71-34913

Bibliography on aeronautical satellite system air traffic control and propagation factors
[NASA-TM-X-65511] 13 p2173 N71-24942
Nomenclature for computing multipath effects on VHF and UHF aircraft radio communication
[RAE-TR-70097] 17 p2718 N71-29361
Calculation of divergence factor of earth surface reflected signals on aircraft radio communication, and multipath transmission between two aircraft
[RAE-TR-70210] 17 p2719 N71-29438
NASA balloon-aircraft ranging, data and voice experiment for determining best approach for using ATS in air traffic control
[NASA-TM-X-65649] 19 p3057 N71-32527
Alternate air traffic control co-channel separation criteria based on probability-of-interference considerations
[DST-101] 24 p3888 N71-37712

AIRCRAFT CONFIGURATIONS
Calculating carrying capacity and rigidity of design for flight vehicles
[AD-712822] 03 p0456 N71-13065
Wind tunnel investigation of jet transport airplane configuration with external flow jet flap and inboard pod-mounted engines - graphs
[NASA-TN-D-7004] 05 p0629 N71-14605
Finite element computer program for estimating airplane aerodynamic interference
[NASA-TM-X-66084] 09 p1311 N71-19357
Flow field interference beneath swept wing-fuselage store installation on aircraft
09 p1318 N71-19380
Television simulation for aircraft and space flight
[NASA-CASE-XFB-03107] 09 p1357 N71-19449
Estimated aerodynamics of all-body hypersonic aircraft configurations
[NASA-TM-X-2091] 09 p1315 N71-19706
Simulation of ground effect in hydrodynamic tunnel analyzed by visualizations
[NASA-TT-F-15799] 20 p3251 N71-33494
Wind tunnel investigation of external-flow jet flap transport configuration having full-span tripped-slotted flaps
[NASA-TN-D-6391] 21 p3377 N71-34028
Dynamic stability of jet transport configuration with high thrust-weight ratio and externally blown jet flap
[NASA-TN-D-6440] 22 p3539 N71-35213
Fixed wing aircraft employing free fall and circling-line techniques in rescue of personnel and retrieval of equipment
[AD-727007] 22 p3541 N71-35228

AIRCRAFT CONSTRUCTION
U AIRCRAFT STRUCTURES
AIRCRAFT CONTROL
NT HELICOPTER CONTROL
Aerodynamic data recording for determining longitudinal static stability of US-2A aircraft
[AD-710722] 01 p0005 N71-10563
Development and characteristics of control system for flexible wings
[NASA-CASE-XLA-06958] 02 p0146 N71-11038
Reliability of aircraft primary control
[NASA-TT-F-12709] 04 p0473 N71-13412
Transfer functions of pilot for determining longitudinal aircraft controllability and pilot performance prediction
[NASA-TN-D-6104] 05 p0630 N71-14944
Control power requirements of VTOL aircraft
[NASA-CR-115907] 05 p0630 N71-15090
Aircraft pilot direct lift control for aircraft landing and reducing gust load effects
[ARC-R/M-3629] 07 p0909 N71-17102
Development of attitude control system for vertical takeoff aircraft using reaction nozzles displaced from various axes of aircraft
[NASA-CASE-XAC-08972] 09 p1325 N71-20370
Accident investigations, flight control systems, and operational recordings for improved aircraft flight mechanics
[AGARD-CP-76-71] 12 p1853 N71-23410
Flight simulator and airframe test stand for evaluating operational performance of aircraft flight control system
12 p1853 N71-23413
Flaps and leading edge modifications for improved aerodynamic control stability of military aircraft
12 p1850 N71-23422
Device for controlling rotary potentiometer mounted on aircraft steering wheel or allison control
[NASA-CASE-XAC-10019] 12 p1927 N71-25809
Stability, control, and handling quality characteristics of STOL and V/STOL airplanes
13 p3025 N71-34702
Linear transfer function for describing human response to aircraft control
13 p2036 N71-24710
En route aircraft flap control during descent and holding
[ARB-TN-99] 13 p2027 N71-24920
Comparison of pilot performance using center stick, dual side stick, and single side stick configuration
[AD-720846] 14 p2197 N71-25846

AIRCRAFT DESIGN
Direct lift control system having flaps with slots adjacent to their leading edge and particularly adapted for lightweight aircraft
[NASA-CASE-LAR-10249-1] 14 p2198 N71-26110
Supersonic or hypersonic vehicle control system comprising elevons with hinge line sweep and free of adverse aerodynamic cross coupling
[NASA-CASE-XLA-08977] 13 p3466 N71-27088
Development of aircraft control system with high performance electrically controlled and mechanically operated hydraulic valves for precise flight operation
[NASA-CASE-XAC-08048] 16 p3537 N71-29128
Systems analysis of aircraft, aircraft guidance and control systems, and atmospheric turbulence for low visibility instrument landing system requirements
[AD-722773] 17 p2785 N71-34173
Evaluating analytical models of turbulence having non-Gaussian space distributions and effects of wind shear on aircraft operations
18 p2802 N71-34778
Lower atmosphere wind shear determined for aircraft approach control from observations in different American sites
18 p2950 N71-30837
Computerized simulation of aerodynamic loads and dynamic responses for aircraft control system design based on optimal and feedback control theories
[AD-722653] 19 p3037 N71-31933
Aircraft, missile, and spacecraft radio control systems analysis and network synthesis
[JPRS-53789] 19 p3058 N71-32694
Design and characteristics of control system for Tu-154 aircraft
[NASA-TT-F-15789] 19 p3039 N71-32699
Correlation studies based on wind tunnel test data and flight tests to determine performance, stability and control of XB-70-1 aircraft
[NASA-CR-114333] 21 p3373 N71-34001
Wind tunnel tests of stability and control characteristics of large scale model representative of propeller-driven STOL transport aircraft
[NASA-TN-D-6393] 23 p3708 N71-36435
Feasibility study of combined laminar and turbulent boundary layer control system using distributed suction with application to low-speed research aircraft of glass reinforced plastic
[AD-727767] 24 p3673 N71-37609
Analysis of criteria for survivable flight control system using fly-by-wire and integrated actuator package techniques
[AD-727763] 24 p3674 N71-37616
Conversion of computational algorithms for decreasing length of word format of control computers for aircraft
[AD-727917] 24 p3686 N71-37772

AIRCRAFT DESIGN
NT HELICOPTER DESIGN
Fighter aircraft design with consideration to armament, detection capability, thrust, speed, and load factor performance tradeoffs
[AD-710497] 01 p0002 N71-10183
Congressional hearing on investigation of contract for TFX aircraft
02 p0146 N71-11034
Visual approach slope indicator system for long-bodied aircraft
[FAA-ED-70-76] 02 p0199 N71-11985
Design of supersonic aircraft with novel fixed, swept wing planforms
[NASA-CASE-XLA-04451] 03 p0314 N71-12243
Feasibility study of counter inaccuracy aircraft with suction boundary layer control
[AERO-1] 04 p0473 N71-13415
Scatter factor in statistical aircraft fatigue life estimation
[ARL/SIM-350] 05 p0773 N71-15154
Human factors in aircraft simulation
[AGARD-CP-79-70] 06 p0830 N71-14000
Flight simulations for accelerated development of aircraft at reduced cost
06 p0831 N71-14002
Flight simulator mathematical modeling for aircraft design
06 p0831 N71-14003
Aerodynamics of variable sweep aircraft design
09 p1322 N71-20854
High lift applications in transport aircraft design
09 p1322 N71-20858
High lift systems design for combat aircraft
09 p1322 N71-20859
Optimizing propulsive/lift system for turboprop STOL aircraft considering cost effectiveness
09 p1459 N71-20863
Optimization of aerodynamic constraints for aircraft design using differential equation identification and finite element optimization
[NASA-CR-117196] 09 p1479 N71-20839
Computer and optimization techniques in aircraft design
09 p1479 N71-20840
Performance test of single stage turbine with low solidity tandem rotor blade assembly
[NASA-CR-11003] 12 p1809 N71-23132

- Power spectrum method for determining gust frequency response functions in dynamic aircraft design 12 p1850 N71-23211
- Accident investigations, flight control systems, and operational recordings for improved aircraft flight mechanics [AGARD-CP-76-71] 12 p1853 N71-23410
- Onboard data acquisition for improved aircraft design and operational flight safety 12 p1854 N71-23412
- Design modifications on short takeoff Brucro aircraft resulting from combat operations tests 12 p1854 N71-23416
- Human factors and safety requirements in aircraft design 12 p1855 N71-23423
- Aircraft development facility with wind tunnel testing capability [AD-719802] 13 p2027 N71-25048
- Noise data with models of both internally and externally blown jet flaps designed for STOL aircraft [NASA-TM-X-67850] 12 p2364 N71-27673
- Low sonic boom design for supersonic transport configurations 16 p2534 N71-28382
- Aircraft design and atmospheric turbulence effects on sonic boom generation and overpressure prediction methods using flight test data 16 p2536 N71-28393
- Limitations of overpressure prediction methods for sonic boom configuration research 16 p2536 N71-28394
- Computed aided design of wing structures and application of optimal law of material distribution [AD-722303] 17 p2704 N71-29657
- Applications of supercritical airfoils to transport aircraft designs 18 p2866 N71-30769
- Aircraft design, flight characteristics, and atmospheric effects on sonic boom during supersonic and hypersonic flight 18 p2871 N71-30787
- Bibliographies of aeronautical engineering, design, production, evaluation, operation, and performance of aircraft and associated components equipment, and systems [NASA-SP-703704] 18 p2872 N71-31263
- Critique of topics discussed at AGARD meeting on aerodynamic interference [AGARD-AR-34-71] 18 p2867 N71-31459
- Aircraft design concepts for prevention of structural failure including stress analysis [AD-723317] 19 p3035 N71-31683
- Computerized simulation of aerodynamic loads and dynamic responses for aircraft control system design based on optimal and feedback control theories [AD-723652] 19 p3037 N71-31933
- Progress in aerodynamic research and aircraft design in Ukraine from 1920 to 1930 [NASA-TT-B-12878] 19 p3033 N71-32185
- Development of power spectral density method for determining gust criteria for airplane structural strength based on discrete gusts [NAL-TR-233] 20 p3211 N71-33547
- Analysis of feasibility of designing transport aircraft to carry up to 1,600 passengers and methods for predicting aircraft performance [CRAFIELD-AERO-3] 21 p3375 N71-34018
- Tip-turbine lift fan design and specifications [NASA-CR-72974] 21 p3502 N71-34945
- Aerodynamic characteristics of lift fan installation for direct lift V/STOL aircraft [NASA-TM-X-62086] 22 p3538 N71-35204
- Influence of advanced technology and design philosophies on general aviation aircraft for 1985 [NASA-CR-114338] 22 p3540 N71-35217
- Draft designing of vertical takeoff and landing aircraft [AD-726572] 22 p3540 N71-35219
- Reference text on design of aviation structural elements [AD-726586] 22 p3540 N71-35220
- AIRCRAFT DETECTION**
- Aircraft echoes and clutter signals obtained by digital surveillance radar 04 p4094 N71-13906
- Digital plotting of primary radar data from aircraft echoes 04 p4098 N71-13933
- Computerized simulation of performance and probability of MTI in aircraft detection in clutter [JRE-TN-739] 12 p1878 N71-23508
- AIRCRAFT ENGINES**
- NT HELICOPTER ENGINES**
- Aircraft gas turbine engine design and construction [AD-711575] 01 p0116 N71-10833
- X ray fluorescence analysis for quality control of gas turbine aircraft engine parts during manufacture and overhaul 02 p2322 N71-11641
- Influence of Concorde powerplant operating conditions on design of Olympus 593 fuel and oil system 02 p2289 N71-11653
- Design and materials engineering for aircraft turbine engines [NASA-TT-F-13398] 04 p0606 N71-14188
- Computerized statistical analysis of engine smoke measurements [AD-713612] 05 p0762 N71-14617
- Investigation of engine-exhaust-airframe interference on cruise vehicle at Mach 6 [NASA-TN-D-4060] 05 p0625 N71-14635
- Cost reduction procedures for aircraft turbine engines used in civil aviation [NASA-TM-X-52951] 06 p0941 N71-16592
- Ingestion of debris into aircraft engine inlets during takeoff [ARC-CP-1114] 07 p0969 N71-17084
- Automation of technological processes in aircraft engine production [AD-714858] 07 p1038 N71-17832
- Aerodynamic interference caused by rear fuselage mounted power plants on BAC aircraft 09 p3114 N71-19375
- Proceedings of conference on aircraft propulsion [NASA-SP-239] 09 p1436 N71-19451
- Characteristics of fans and compressors for aircraft turbine engines 09 p1457 N71-19452
- Aerodynamic characteristics of advanced turbine engines 09 p1457 N71-19453
- Development of improved turbine cooling processes and facilities for conducting turbine cooling research 09 p1457 N71-19454
- Effects of engine design and propulsion system configurations on combustion efficiency 09 p1457 N71-19455
- Development and characteristics of low cost engines for general aviation aircraft 09 p1457 N71-19458
- Effects of engine inlet disturbances on engine stall performance 09 p1458 N71-19461
- Design requirements for air breathing aircraft engines [AD-716496] 09 p1458 N71-19468
- Protective coatings for heat resistant materials for aircraft gas turbine engines, and refractory metals for jet engine vehicles 09 p1404 N71-16677
- Lift augmentation devices effect on STOL engine - Part 1, interface problems between engine and airframe 09 p1322 N71-20061
- Lift augmentation devices effect on STOL engine - Part 2, thermodynamic problems 09 p1323 N71-20062
- Evaluation of fuel flowmeter instrumentation conducted during flight tests [AD-719280] 13 p2079 N71-24479
- Assembly methods for three types of aircraft gas turbine engines [AD-719623] 13 p2156 N71-25209
- Fundamentals of aircraft gas turbine engines [AD-719913] 14 p2331 N71-25808
- Aircraft gas turbine combustion chamber design [NAL-TR-208] 14 p2332 N71-26298
- Production and efficiency of small gas turbine engines for helicopter and surface vehicles [AGARD-LS-46-71] 15 p2511 N71-26951
- Components for low weight/small volume aircraft gas turbine engines 15 p2512 N71-26955
- Thermodynamic properties of small gas turbines for power generation in aeronautics, space, and industry 15 p2512 N71-26957
- Comparison of small gas turbine and diesel engine power plants for aircraft and ground vehicle propulsion 15 p2512 N71-26958
- Application of noise reduction technology to design of propulsion system for subsonic civil transport aircraft [NASA-TM-X-67884] 18 p3001 N71-31191
- Exhaust emission from reciprocating aircraft engines, and afterburning of exhaust gases on contact with ambient air - air pollution study [PB-197627] 18 p3028 N71-31569
- Operational methods for control of air pollution emissions from aircraft turbine engine combustor [NASA-TM-X-67887] 19 p3174 N71-32484
- Cold weather tests to determine effectiveness of resonant combustor as power source for starting aircraft engines [AD-724125] 20 p3338 N71-32804
- Performance tests of single stage, transonic compressor for advanced aircraft [NASA-CR-72806] 20 p3250 N71-33201
- Conclusions and recommendations concerning wind tunnel tests of interaction between engine flow and wall corrections in transonic wind tunnels 23 p3703 N71-36401
- Combustion characteristics of gas turbine aircraft engines [AD-727173] 23 p3841 N71-37387
- Analysis of gas turbine design and application to aircraft operation with description of components, safety factors, and vibration problems [AD-727188] 24 p4001 N71-38238
- AIRCRAFT EQUIPMENT**
- NT AIRCRAFT LIGHTS**
- NT AIRCRAFT TIRES**
- NT EJECTION SEATS**
- Formulas for determining flying weight of aircraft electric generator systems 05 p0431 N71-14640
- Annotated bibliography on engineering aspects of design, construction, evaluation, testing, and performance of aircraft and associated components, equipment, and systems [NASA-SP-7037] 10 p1491 N71-20748
- Satellite applications to aircraft communications, navigation, and surveillance over US including synthesized satellite network and aircraft equipment for air traffic control [NASA-CR-117768] 11 p1792 N71-22319
- Location/identification transmitter and equipment for use in satellite applications in aircraft communications, navigation, and surveillance for US air traffic control [NASA-CR-117739] 11 p1792 N71-22310
- Test procedures for aircraft defogger/defroster equipment [AD-719109] 13 p2025 N71-24482
- Procedures for evaluating compatibility of aviation material with related equipment [AD-719107] 13 p2025 N71-24482
- Performance of aircraft environmental control systems under simulated tactical conditions [AD-719101] 13 p2025 N71-24482
- Design, development, and test of ground support equipment for analyzing aircraft equipment condition and performance [AD-719675] 13 p2026 N71-24489
- Evaluation of dual input transponder with upper and lower aircraft altitude as resolution for problems with air traffic control radar beacon system limitations [FAA-NA-71-39] 13 p2057 N71-24882
- Aircraft survival equipment testing including maintainability, systems compatibility, human factors engineering, and reliability of rations, protective clothing, floats, and parachutes [AD-720225] 14 p2210 N71-26138
- Test procedures to determine ability of aircraft equipment and armament to withstand storage and operate effectively in tropic environment [AD-720570] 14 p2198 N71-26134
- Evaluation procedures to determine effectiveness of visible and infrared searchlights mounted on fixed and rotary wing aircraft during tactical support missions [AD-721155] 15 p2366 N71-28895
- Methods for determining reliability of aircraft equipment [AD-722721] 17 p2704 N71-29796
- Methods and techniques for training personnel in operation and test of aviation equipment, subsystems, and related accessories [AD-723032] 17 p2712 N71-30254
- Safety tests for aircraft equipment [AD-723033] 19 p3037 N71-31940
- Demonstration and evaluation of crash-resistant bladder fuel tank system in full-scale aircraft wing assembly [FAA-NA-71-34] 19 p3037 N71-32877
- Test procedures for evaluating capability of utilizing/deicing equipment aboard aircraft [AD-724082] 20 p3209 N71-33885
- Integration of photographic methods in test procedures for military aircraft, aircraft weapons, and ancillary equipment [AD-724081] 20 p3271 N71-33889
- Analytical procedures for predicting coupled fluid structural responses of aircraft hydraulic systems 22 p3665 N71-36236
- Aircraft takeoff, navigation, and landing risk aerodynamics characteristics, and crew rescue equipment [AD-727860] 24 p3874 N71-37818
- AIRCRAFT EXHAUST**
- U EXHAUST GASES**
- AIRCRAFT FUEL SYSTEMS**
- Influence of Concorde powerplant operating conditions on design of Olympus 593 fuel and oil system 02 p2289 N71-11653
- Gasoline icing inhibitors for aircraft carburetors and fuel systems 04 p0473 N71-13414
- Effectiveness of nitrogen inerting of aircraft fuel tanks under conditions of fuel sloshing [AD-721675] 16 p2670 N71-28276
- Determination and evaluation of safety parameters of jet fuels in aircraft fuel tanks when using nitrogen as inerting agent [FAA-NA-71-26] 19 p3038 N71-32385
- AIRCRAFT FUELS**
- Section and pressure head and temperature effects on cavitation flow in aircraft fuel pumps [ARC-CP-1120] 07 p1007 N71-17844

SUBJECT INDEX

Proceedings of conference on aircraft propulsion
[NASA-SP-259] 09 p1456 N71-19451
Heat flux distributions in pools of burning aircraft
fuels for design of protective clothing for firefighting
personnel [AD-722774] 18 p3030 N71-31376
Chemical and physical properties of aircraft fuels
gelled with hydrocarbon resins [FAA-NA-71-17] 19 p3172 N71-32078
Small scale impact tests of aircraft type fuels for gas
turbines to determine burning, misting, and splatter
characteristics [FAA-NA-71-12] 19 p3172 N71-32087
Development of procedures for conducting service
tests of aircraft refueling and defueling systems
[AD-726872] 22 p3541 N71-35227
Determination of physical and chemical properties
of fuels gelled with carboxyhydro resins to evaluate ef-
fectiveness in reducing aircraft fire hazards [FAA-NA-71-18] 23 p3839 N71-37369
Control and chemical composition of aircraft fuels,
lubricants, and special liquids [AD-727199] 24 p4000 N71-38331
AIRCRAFT GUIDANCE
Guidance software package for digital flight control
and landing system of CH-46C helicopter
[NASA-CR-111025] 01 p0028 N71-10284
Systems analysis of flight control and guidance of
CH-46C helicopter [NASA-CR-111024] 01 p0003 N71-10297
Visual aids for secondary airports [FAA-NA-70-51] 02 p0198 N71-11474
Guidance developments for all-weather landing
[AD-727199] 03 p0405 N71-12433
Post-1970 scanning beam guidance for approach and
landing 03 p0406 N71-12435
Investigating tasks of data processing equipment in
advanced navigation systems for aircraft 03 p0408 N71-12604
Microwave landing guidance systems initial concept
validation tests in RTCA signal format [AD-717183] 10 p1600 N71-21368
Microwave scanning guidance system for aircraft
approach and landing [DO-148-VOL-1] 15 p2365 N71-26804
Systems analysis of aircraft, aircraft guidance and
control systems, and atmospheric turbulence for low
visibility instrument landing system requirements
[AD-722773] 17 p2705 N71-30173
Vertical situation display concept for alleviating
problems of inadequate guidance and display infor-
mation for making steep approaches 18 p2869 N71-30770
Evaluation of automatic guidance modes and soft-
ware for V/STOL aircraft flight control [NASA-CR-121768] 21 p3375 N71-34016
Aircraft tracking and guidance facility using FFS-16
radar supplemented by laser tracker permanently
mounted on antenna [NASA-CR-111931] 21 p3407 N71-34240
All weather landing system design, development,
and field and flight testing 22 p3618 N71-35777
Development and testing of VHF omnirange trans-
mitter for aircraft azimuth guidance [FAA-RD-71-65] 22 p3618 N71-35779
AIRCRAFT HAZARDS
Severe thunderstorm radar tracking and related
weather events hazardous to aviation operations
[BSSA-TM-ERLTM-NSSL-46] 01 p0079 N71-10720
Synoptic meteorological conditions for clear air tur-
bulence and turbulence effects on aircraft flight
characteristics [DLR-FB-78-29] 07 p0970 N71-17145
Measurements and analysis of lightning-induced
voltages in aircraft electrical circuits [NASA-CR-1744] 06 p1170 N71-19122
Survey conducted to develop minimum requirements
for airport fire fighting and rescue services
[FAA-AS-71-1] 09 p1364 N71-19426
Fuel tank vapor space characteristics for simulated
helicopter fuel tank and evaluation of existing poten-
tial hazard from vibration environment [AD-727981] 10 p1660 N71-20702
Investigation of major collision between Boeing 707
and Conquest 150 at Edison, New Jersey, on January 9,
1971 [SB-71-30] 10 p1493 N71-21169
Safety measures to eliminate aircraft trailing vortex
hazards [NASA-TM-X-67125] 12 p1834 N71-23418
Automated bibliography on bird aircraft hazards and
incidents from Oct. 1967 to Jan. 1971 [TDCR-58861] 17 p2705 N71-30128
Synoptic meteorological conditions for clear air tur-
bulence and turbulence effects on aircraft flight
characteristics [BMWG-FB-WT-70-9] 19 p3127 N71-31781
Synoptic meteorological conditions for clear air tur-
bulence and turbulence effects on aircraft flight
characteristics 19 p3127 N71-31885

Analysis of general aviation during year 1969 noting
growth of aircraft operating, accident data, analysis of
accidents, and injuries resulting from accidents 20 p3208 N71-32854
Computer simulation of aircraft collision-hazard
warning radar techniques in terminal area 21 p3396 N71-34170
Analysis of aviation hazards produced by visual illu-
sions due to spiral aftereffect parameters of perceived
size and distance [FAA-AM-71-31] 22 p3545 N71-35254
Aircraft hazards and accidents due to birds
[AD-727881] 24 p3874 N71-37617
AIRCRAFT INDUSTRY
Modern welding methods in aircraft and aerospace
industry 02 p0233 N71-11650
History of USSR aviation industry, aircraft design,
and air transportation [NASA-TT-F-627] 03 p0630 N71-14734
US commercial aircraft export strategy and recom-
mendations for financing and expansion 07 p1136 N71-18087
Economic analysis of aeronautical R and D efforts
in US and aeronautical contributions to noise and air
pollution, including technology assessment and data
analysis techniques [NASA-CR-1809] 15 p2366 N71-27011
Airline operations, costs, effects on aircraft indus-
try, and cooperation with CAB 17 p2860 N71-29256
Test facilities on structural engineering at FFA,
Sweden [PFA-MEMO-41] 17 p2730 N71-29378
AIRCRAFT INSTRUMENTS
NT ALTIMETERS
NT ANEMOMETERS
NT APPROACH INDICATORS
NT ATTITUDE INDICATORS
NT AUTOMATIC PILOTS
NT COMPASSES
NT FLIGHT RECORDERS
NT GYRO HORIZONS
NT GYROCOMPASSES
NT HOT-WIRE ANEMOMETERS
NT MAGNETIC COMPASSES
NT POSITION INDICATORS
NT RADIO ALTIMETERS
NT RADIO DIRECTION FINDERS
NT SPACECRAFT POSITION INDICATORS
NT TACHOMETERS
Maintenance programs, evaluation, acceptance, and
monitoring procedures for transport aircraft 02 p0144 N71-11020
Aircraft altimeter containing X ray source 07 p1027 N71-16093
Development and characteristics of frequency
separated display devices for aircraft control [AD-715438] 06 p1144 N71-18739
Selection of scanning systems for aircraft thermal
viewers 06 p1204 N71-19220
Benefits and problems of using head-up displays in
commercial general aviation aircraft [NASA-CR-117135] 09 p1388 N71-19752
Human factors tests to determine effects of aircraft
controls placement on lightly clothed or pressure
suited flight crews [AD-715975] 09 p1341 N71-19911
Design and development of flight director systems
based on theory of manual control displays [NASA-CR-1748] 10 p1534 N71-21087
Optical projector system for establishing optimum
arrangement of instrument displays in aircraft,
spacecraft, other vehicles, and industrial instrument
consoles [NASA-CASE-XNP-03853] 11 p1796 N71-21082
Combined optical attitude and altitude indicating in-
strument for use in aircraft or spacecraft [NASA-CASE-XLA-01907] 12 p1917 N71-23268
Development and application of heads up aircraft
instrument display for improvement in aircraft safety
during adverse weather [FAA-NA-71-9] 17 p2702 N71-29305
Aircraft indicating instruments with digital cathode
ray tube display [DLR-FB-71-27] 19 p3064 N71-31695
Aircraft mechanical and battery operated clocks re-
sistant to high intensity magnetic fields [AD-726700] 23 p3707 N71-36430
Pilot performance in recognizing electronic display
systems under varying dazzle and color conditions in
cockpits [BAE-LIB-TRANS-1545] 24 p3875 N71-37621
AIRCRAFT LANDING
NT CRASH LANDING
NT DITCHING (LANDING)
Comparison of aircraft and surface vehicle stopping
performance under varying runway conditions
[NASA-TN-D-6098] 03 p0313 N71-12335
Advanced ILS and automatic landing systems for
conventional and V/STOL aircraft - conference
[AGARD-CP-59-70] 03 p0404 N71-12436

AIRCRAFT LANDING

All-weather automatic landing systems and problem
areas 03 p0404 N71-12427
Technical systems and development of advanced
communication systems for aircraft landings 03 p0405 N71-12430
Importance of aircraft speed control relative to lo-
calized touchdown dispersion 03 p0405 N71-12432
Guidance developments for all-weather or low
visibility landings 03 p0405 N71-12433
Automatic pilot and associated airborne equipment
developments for automatic landing systems 03 p0405 N71-12434
Post-1970 scanning beam guidance for approach and
landing 03 p0406 N71-12435
Flight maneuvers and airborne and ground equip-
ment for landing VTOL aircraft in adverse conditions 03 p0407 N71-12436
Flight tests of all-weather landing systems 03 p0406 N71-12437
All-weather automatic landing systems for use on
aircraft carriers and training carriers 03 p0406 N71-12438
Automatic pilot system for landing commercial air-
craft 03 p0406 N71-12440
All weather landing systems of Thompson/CSF 03 p0407 N71-12446
Development of signal acquisition methods for
television aided aircraft carrier landing operations
[AD-712511] 03 p0410 N71-13194
Aircraft landing characteristics during aircraft car-
rier approach [AD-715125] 03 p0427 N71-14558
Revised assessment of aircraft landing characteristics
[AD-713502] 03 p0457 N71-14902
Aircraft landing lift decay and elevator oscillation
analysis [ARC-CP-1119] 06 p0793 N71-15722
Aircraft pilot direct lift control for aircraft landing
and reducing gust load effects [ARC-RM-3629] 07 p0969 N71-17102
Establishment of take-off and landing safety mar-
gins for Boeing 941 07 p0971 N71-17441
In-flight determination of lateral-directional dynam-
ics for landing approach [AD-715317] 07 p0973 N71-17792
Noise measurement evaluation of takeoff and ap-
proach profiles optimized for noise abatement [NASA-TN-D-6366] 08 p1144 N71-18929
Developing basic methodology for predicting air-
craft stopping distance on wet runway using com-
puterized simulation [FAA-NA-70-5] 09 p1323 N71-20048
Influence of environmental factors in aircraft car-
rier landings and accidents 09 p1325 N71-20369
Design and development of flight director systems
based on theory of manual control displays [NASA-CR-1748] 10 p1534 N71-21087
A vision guided lighting, visual landing aids, dual
baseline transceiver, photometric measurements
of deck-landing projector sight, and lamp for F-4 Phantom
optical landing system [NBS-10088] 11 p1676 N71-22456
Speed and field length safety factors for approach
and landing mechanics of Bruggart aircraft 12 p1855 N71-23420
Design and characteristics of continuous wave,
microwave scanning-beam aircraft landing system
operating at C band and superhigh frequencies
[AD-710972] 13 p2189 N71-24535
Climbout and landing approach noise measurements
for three engine turbofan transport aircraft [NASA-TN-D-6137] 13 p2023 N71-24582
Experimental pulsed modulated laser system
modified for measuring dust visibility conditions for
aircraft landing operations [AD-716483] 16 p2531 N71-28217
Weighted defect densities of asphalt and cement
concrete pavement in airfield pavement condition sur-
vey, USNAA Cecil Field, Florida [AD-721325] 16 p2577 N71-30422
Weighted defect densities of asphalt and cement
concrete pavement in airfield pavement condition sur-
vey, USNAA Willow Grove, Pennsylvania [AD-721326] 16 p2577 N71-30423
Weighted defect densities of asphalt and cement
concrete pavement in airfield pavement condition sur-
vey, USNAA Charleston, Rhode Island [AD-721325] 16 p2577 N71-30424
Determination of effectiveness of clawfoot type
markings to indicate potentially deceptive, unob-
scured paved areas before runway thresholds [FAA-NA-71-27] 17 p2729 N71-29206
Mathematical perturbation models of aircraft ILS
approach and landing [VTN-159] 17 p2783 N71-29496
Flight tests and simulation for determining effects
of peripheral visual fixation on pilot performance dur-
ing commercial aircraft landing [RAB-TR-70205] 17 p2783 N71-29497

AIRCRAFT LANDING INSTRUMENTS

- Aircraft accident involving Federal Aviation Administration DC-3 aircraft at La Guardia airport, New York in January, 1971
[NTSB-AAR-71-11] 18 p2873 N71-31333
- Test and evaluation of aircraft glide slope landing system operating at ultrahigh frequency
[FAA-NA-71-15] 19 p3133 N71-32085
- Aircraft accident report involving DC-9 type aircraft damage incurred when aircraft contacted water surface during approach to Martha's Vineyard airport
[SB-71-64] 19 p3039 N71-32460
- Systems and equipment for civil aircraft approach and landing
[REPT-52] 20 p3299 N71-32830
- Determination of aircraft longitudinal motion during takeoff and landing after loss of lift from boundary layer control system
20 p3211 N71-33545
- Coordination of traffic flow and holding patterns of aircraft landing on same runway
[NASA-CR-121466] 20 p3301 N71-33747
- Performance tests and evaluation of wire cable materials for use with aircraft arresting gear
[AD-724284] 22 p3359 N71-35211
- Performance characteristics of air cushioned landing and takeoff system during aircraft lift-off operation mode
[AD-726606] 22 p3541 N71-35223
- Mathematical modeling of F-4 aircraft wave off trajectories for aircraft carrier approaches
[AD-727121] 23 p3708 N71-36439
- Airborne remote sensing of Mojave Desert playas for use as natural landing areas
[AD-727031] 23 p3751 N71-36748
- Equations of motion for elastic plate foundation system under dynamic load applied to aircraft landing
23 p3684 N71-37543
- Tu-134 aerodynamic characteristics during takeoff, climb, horizontal flight, landing stability and maneuverability, and strength under various loads
[AD-727196] 24 p3874 N71-37612
- Effect of wet, icy, and snow covered runways on aircraft stopping distance and directional control in crosswinds, effect of surface texture and contamination on runway slipperiness
[PS-160-65-68-2] 24 p3903 N71-37820
- AIRCRAFT LANDING INSTRUMENTS**
U. LANDING INSTRUMENTS
AIRCRAFT LAUNCHING DEVICES
Statistical prediction of external store separation characteristics from aircraft
09 p3130 N71-19388
- AIRCRAFT LIGHTS**
Compilation of optical properties data of xenon flash tubes for pilot warning indicator systems
[NASA-TN-D-6372] 10 p3559 N71-21098
- Functional suitability of internal/external lighting systems for military aircraft
[AD-723043] 17 p2704 N71-29797
- AIRCRAFT MAINTENANCE**
Army aircraft modification program management review and recommendations
01 p0136 N71-10287
- Maintenance programs, evaluation, acceptance, and monitoring procedures for transport aircraft
02 p0144 N71-11020
- Universal aircraft flight simulator/trainer system definition
[AD-717179] 10 p1503 N71-20604
- Evaluating adequacy of tool sets for aircraft maintenance
[AD-719103] 13 p2084 N71-24379
- Aircraft maintenance for civil aviation
[AD-720366] 14 p2197 N71-25955
- Cleanliness control effects on aircraft components and immunization vaccine productions in Sweden
[FOA-1-C-1323-76] 14 p2212 N71-26566
- Lubrication by boundary, elastohydrodynamic, and fluid films, wear due to fretting, erosion, scuffing, and pitting, and friction in aircraft
[NASA-TN-X-67872] 18 p2929 N71-31134
- Maintenance, management planning, and requirements for single seat attack/fighter aircraft
[AD-723227] 19 p3036 N71-31805
- Handbook for airframe and powerplant mechanics preparing for mechanic certification for FAA aircraft and engine mechanic examinations
[FAA-AC-65-9] 20 p3212 N71-33678
- Fabrication and field testing of lightweight, recoverable, air-transportable hangars
[AD-727051] 22 p3565 N71-35396
- Fabrication and field testing of aircraft maintenance hangars and general purpose shelters
[AD-727047] 22 p3566 N71-35397
- AIRCRAFT MODELS**
Free flight suspension system for use with aircraft models in wind tunnel tests
[NASA-CASE-XLA-00939] 06 p0830 N71-15926
- Dynamic characteristics and linear control theory for aircraft simulation
06 p0831 N71-16061
- Evacuation tests from 280-passenger SST mock-up through different type exits
[FAA-AM-70-19] 09 p1321 N71-19812

SUBJECT INDEX

- Roll-control effectiveness of spoiler configurations on aircraft model with variable sweep wings at supersonic speeds
[NASA-TM-X-2165] 09 p1317 N71-20126
- Low speed wind tunnel model assessment of porous boundary layer control by suction at civil aircraft leading edge flaps
[ARC-R/M-3640] 10 p1491 N71-20847
- Model design for vertical takeoff aircraft cockpit noting navigation aids, visual displays, and console configuration
11 p1674 N71-22196
- Steady tailplane lift effect on subcritical response of subsonic T tail flutter aircraft model in low speed wind tunnels
[ARC-R/M-3652] 15 p2366 N71-27096
- Evaluating analytical models of turbulence having non-Gaussian gust distributions and effects of wind shear on aircraft operations
18 p2902 N71-30778
- Examining model theory for static and dynamic aerodynamic phenomena
20 p3360 N71-33805
- AIRCRAFT NOISE**
NT JET AIRCRAFT NOISE
NT SONIC BOOMS
Research and developments in aircraft noise reduction
01 p0002 N71-10171
- Air and land transportation noise sources and measurement, noise level scales, and individual and community responses - conference
[PB-191117] 01 p0003 N71-10349
- Response of, and acoustic radiation from panels excited by turbulent boundary layers
[AD-710696] 01 p0004 N71-10386
- Airspeed contribution to noise level within fixed and rotary wing aircraft
[AD-711359] 01 p0090 N71-10705
- Community physical, psychological, and social reactions to aircraft noise around 7 US international airports
[NASA-CR-111316] 02 p0146 N71-11032
- Characteristics of acoustic damage found in technical military personnel
02 p0171 N71-11808
- Sound attenuation characteristics of military aircraft protective devices and helmets
02 p0171 N71-11819
- Low noise turbofan engine without aerodynamic blade loading
[NASA-TN-D-6080] 02 p0290 N71-11882
- Noise problems in air evacuation operations and effectiveness of ear protective devices
[AD-713882] 06 p0801 N71-16284
- Flight acoustical and performance evaluations of DC 8 nacelle modifications to reduce fan-compressor noise in airport communities
[NASA-CR-1708] 06 p0796 N71-16627
- Development of acoustic lining for turbofan nacelle modification to minimize fan compressor noise radiation
[NASA-CR-1712] 07 p0972 N71-17591
- Flightworthy nacelle development to minimize fan compressor noise radiation - Vol. 4
[NASA-CR-1714] 07 p0972 N71-17668
- Measurement of variability of aircraft noise during level flight flyovers
[NASA-CR-1752] 08 p1144 N71-18865
- Noise measurement evaluation of takeoff and approach profiles optimized for noise abatement
[NASA-TN-D-6246] 08 p1144 N71-18929
- Sources and characteristics of aircraft noise for conventional and V/STOL aircraft
09 p1320 N71-19457
- Noise and vibration effects on commercial helicopter pilot safety, performance, and comfort
[NASA-CR-117181] 09 p1332 N71-20113
- Sound pressure levels produced by C-5A during ground taxi
[AD-716814] 10 p1606 N71-20824
- Urban air and surface vehicle noise levels and abatement potential
[OST-ONA-71-1-VOL-2] 10 p1607 N71-21085
- Aircraft noise generation, propagation, and reduction and noise effects on environment
[PB-196392] 10 p1609 N71-21796
- Routine unprotected exposure to acoustic noise within cockpits of trainer aircraft presenting potential hazardous stress
[AD-717832] 11 p1796 N71-22426
- Interior sound pressure measurements in C-5A aircraft
[AD-719746] 13 p2027 N71-25060
- Weighting method for aircraft auditory risk limits when wearing ear protectors
[AD-719861] 13 p2038 N71-25086
- Proceedings of conference to train personnel in conducting aircraft noise certification tests
[HRC-TR-300-SUPPL-1] 14 p2198 N71-26303
- Personnelization of Federal Aviation Administration personnel in acoustic measurement techniques and procedures involved in noise certification of aircraft
[HRC-TR-300] 14 p2198 N71-26304

- Techniques and procedures for measuring effective perceived noise level during aircraft noise type evaluations
[HRC-TR-300-SUPPL-2] 14 p2198 N71-26303
- Economic analysis of aeronautical R and D efforts in US and aeronautical contributions to noise and air pollution, including technology assessment and data analysis techniques
[NASA-CR-1809] 15 p2366 N71-27861
- Noise data with models of both internally and externally blown jet flaps designed for STOL aircraft
[NASA-TM-X-67850] 15 p2364 N71-27870
- Acoustic measurements of helicopter rotor noise at hover
[AD-721312] 16 p2531 N71-28270
- Slotted blades and vanes and rotor tip design for highly loaded, low speed fan stage applicable to low noise aircraft engines
[NASA-CR-72895] 16 p2671 N71-28313
- Analysis of aircraft noise recordings to determine experimental values of atmospheric noise absorption
[NASA-CR-1751] 16 p2536 N71-28803
- Community reactions to aircraft and airport noise from physical, psychological, and social aspects
[NASA-CR-1761] 16 p2536 N71-28803
- Judgment of effects of Doppler shifts on perceived noisiness of aircraft made by subjects in anechoic chamber
[NASA-CR-1779] 17 p2709 N71-29890
- Development of noise measurement units for airports and aircraft noise reduction and psychoacoustic studies
18 p2871 N71-30706
- Comparison test to evaluate perceived noise level for STOL and other aircraft sounds
[WR-70-9] 18 p2872 N71-31875
- Inlet noise suppressors having perforated plate over honeycomb wall construction evaluated over range of passage heights and engine speeds using turbojet engine as noise source
[NASA-TN-D-6395] 18 p2872 N71-31806
- Analysis of factors creating aircraft noise problems and efforts to reduce level of aircraft noise
19 p3038 N71-32806
- Effects of aircraft system noise and signal fading on pilot performance during IFR approach based on computerized simulation of XV-5 aircraft and UH-1 helicopter
[AD-724336] 20 p3209 N71-33676
- Aircraft/aircraft system noise reduction including land use and noise forecasting
[OST-ONA-71-1-VOL-3] 20 p3212 N71-33937
- Relations between aircraft and road traffic noise and noise tolerance in communities
[TT-7102] 21 p3375 N71-34869
- Aircraft noise problems in vicinity of Kennedy International Airport, New York and recommendations for noise reduction
[PB-199723] 21 p3377 N71-34002
- Legal aspects of compulsory soundproofing for structures next to John F. Kennedy International Airport
[PB-199725] 21 p3377 N71-34893
- Noise characteristics of model STOL wing with externally blown flaps in vicinity of aircraft propellers
[NASA-CR-111956] 24 p3565 N71-35393
- AIRCRAFT PARTS**
Electron fluorography for high strength steel to determine fatigue life of military aircraft parts
[NLR-TR-69043-U] 03 p0395 N71-13364
- AIRCRAFT PERFORMANCE**
NT HELICOPTER PERFORMANCE
Fighter aircraft designs with consideration to armament, detection capability, thrust, speed, and load factor performance tradeoffs
[AD-710497] 01 p0002 N71-10183
- Application of weight and balance principles for aircraft operation
[FAA-AC-91-23] 03 p0314 N71-12241
- Performance and handling qualities criteria for V/STOL aircraft
[AGARD-R-577-70] 03 p0315 N71-12248
- Automatic pilot TAPER
03 p0407 N71-12444
- Aircraft handling characteristics during aircraft carrier approach
[AD-713125] 05 p0627 N71-14128
- Investigation of engine-exhaust-airframe interference on cruise vehicle at Mach 6
[NASA-TN-D-6060] 05 p0625 N71-14520
- Flight test methods for determining aircraft dynamic stability
[AGARD-R-577-70] 06 p0953 N71-16819
- Quadratic performance index for VTOL aircraft model reference attitude control system
[NASA-TN-D-6231] 08 p1172 N71-18838
- Optimal control of rotational and translational motions of flight vehicles based on torsional and flexural deformations
[AD-716517] 09 p1320 N71-19469
- Annotated bibliography on engineering aspects of design, construction, evaluation, testing, and performance of aircraft and associated components, equipment, and systems
[NASA-SP-7037] 10 p1491 N71-26748

SUBJECT INDEX

Investigation of longitudinal and lateral stability and controllability of supersonic aircraft
[AD-71283] 12 p1857 N71-23818

Low wing load in STOL transport ride smoothing using Boeing aircraft
[NASA-CR-111819] 13 p2026 N71-24586

Allocation of lateral and longitudinal gust effects on aircraft
13 p2024 N71-24769

For vertical takeoff aircraft pilot cockpit simulator for controlling aircraft flight performance
[ARC-R/M-3647] 13 p2027 N71-25063

Computer program for optimum flight path defined by flight test investigation of performance characteristics (excess thrust, fuel flow, and climb potential) of F-104G aircraft
[NASA-TN-D-6394] 15 p2366 N71-27002

Flight simulator evaluation of aircraft instrument display procedures
17 p2703 N71-29635

Survey and taxiway profile and airplane response measurements to determine runway roughness
18 p2902 N71-30766

Applications of supercritical airfoils to transport aircraft designs
18 p2866 N71-30769

Analysis of 79,000 hours data obtained from NASA V-ORION flight recorders installed on 734 general aircraft engaged in eight types of operations
18 p2871 N71-30782

Estimation of lateral and longitudinal rigid body responses of aircraft structures continuous and random atmospheric turbulence
[NASA-TN-D-6273] 18 p2872 N71-31242

Prediction method for performance of total pilot-vehicle system in turbulence with application to cockpit tests
[AD-72855] 18 p2873 N71-31288

Commercial aircraft performance and cost analysis data for 1968 and 1969 in US
19 p3035 N71-31611

Full scale tests on tilted propeller and tilting rotor models in transonic wind tunnel of Modane-Avivert, France, for aircraft performance prediction
[ONERA-NT-161] 19 p3073 N71-31813

Aerodynamic design manual considering internal air flow system effects on aircraft performance
[AD-72824] 19 p3173 N71-32060

Summary of flight test methods used for performance measurement of Concorde aircraft
[NASA-TT-F-13728] 19 p3039 N71-32455

Analysis of coupled roll-spiral mode, pilot induced oscillation occurring with M-2F2 lifting body
[NASA-TN-D-6496] 20 p2906 N71-33307

Effect of turbulence and aircraft performance on US approach task and longitudinal stability
[NASA-CR-1821] 20 p3210 N71-33325

Development of method for determining angle of pitch, flight path angle, and angle of attack for aircraft during steady or nonsteady flight
[VTR-156] 20 p3208 N71-33926

Correlation studies based on wind tunnel test data and flight tests to determine performance, stability and control of XE-70-1 aircraft
[NASA-CR-114355] 21 p3373 N71-34001

FA-260X experimental aircraft for investigating operational problems of STOL type aircraft
[NAL-TR-259] 21 p3373 N71-34005

Analysis of influence of wind shear on longitudinal motion of aircraft during approach and landing
[NASA-TN-D-6430] 21 p3376 N71-34022

Compilation of responses to questionnaire on engine-airframe interference in transonic tests
23 p3703 N71-36402

Wall corrections for airplanes with interference lift in transonic wind tunnel tests
23 p3704 N71-36403

Wind tunnel performance characteristics of single-engine fighter model fitted with in-flight thrust reverser
[NASA-TN-D-6460] 23 p3840 N71-37584

Computer program for analyzing and simulating attack of low flying aircraft by antiaircraft missiles and probability of aircraft survival
[RAE-LIB-TRANS-1578] 24 p3896 N71-37774

Performance and costs of nuclear aircraft used in transonic commerce
[NASA-TM-X-2386] 24 p3964 N71-38277

AVIATION PILOTS
Evaluating current and future requirements and resources for pilots and mechanics in US civil aviation
02 p0167 N71-11187

Aircraft pilot thermal environment, thermal comfort and cockpit air conditioning
[ARC-CF-1094] 07 p0965 N71-17896

Aircraft pilot direct lift control for aircraft landing and reducing gust load effects
[ARC-R/M-5629] 07 p0969 N71-17102

Noise and vibration effects on commercial helicopter pilot safety, performance, and comfort
[NASA-CR-117181] 09 p1332 N71-20113

Speech discrimination test for pilot pure-tone hearing standards
[AD-716564] 10 p1499 N71-21061

Characteristic flight effects on toothache development in aircraft pilots
11 p1688 N71-22309

Electrocardiographic and blood pressure standards of physical fitness for aging pilots
11 p1689 N71-22314

Artificially induced and electrocardiographic abnormalities in aging pilots of French Air Force
11 p1690 N71-22318

Audiometric evaluation of aging pilots hearing acuity in relation to flying time
11 p1690 N71-22320

Use of electroencephalograms in evaluation of emotional state of aircraft pilot during flight
[JPRS-53269] 16 p2548 N71-29149

Helicopter pilot visual acuity determined from flight tests
[ISVR-TR-44] 19 p3047 N71-31660

Antipropagative survey of aviation personnel with bivariate tables noting relationships between selected variables
[AD-725794] 19 p3048 N71-31942

Protective features and compatibility with airborne communication systems considered in study of aviation helmets
[AD-724000] 20 p3226 N71-33123

Fixed wing aircraft employing free fall and circling-line techniques in rescue of personnel and retrieval of equipment
[AD-727007] 22 p3541 N71-35228

Aircraft accident briefs for 1969 including date, location, aircraft data, injuries, flight purpose, and pilot data
[NTSB-BA-71-2] 23 p3708 N71-36433

AVIATION POWER SOURCES
U AVIATION ENGINES
AVIATION RELIABILITY
Tentative airworthiness standards for powered lift transport category aircraft
07 p0972 N71-17553

Aircraft safety and aircraft reliability, noting pilot performance, landing approach and takeoff, and clear air turbulence
11 p1674 N71-22197

Determination of inspection intervals and nature of inspections for safe and economical operation of aircraft structures
[FFA-128] 11 p1676 N71-22431

Actions and recommendations of Ninth Meeting of Airworthiness Committee
[DOC-8923] 21 p3375 N71-34020

AVIATION SAFETY
Possibility of using flexible rotor blades for ejection systems
[AD-711642] 02 p0144 N71-11022

Air operations safety and noise control research in aerospace medicine
02 p0171 N71-11820

Radar observations of bird migrations to reduce risk of bird-aircraft collisions
[AD-712720] 03 p0313 N71-12232

Application of weight and balance principles for aircraft operation
[FAA-AC-91-23] 03 p0314 N71-12241

Capacity measurement methodology for air traffic control system with long range objectives
[FAA-TR-70-70] 05 p0630 N71-14635

Airplane interior materials ignition and fire extinguishers
[FAA-TR-70-81] 06 p0796 N71-16818

Establishment of take-off and landing safety margins for Breguet 941
[NASA-TT-F-13453] 07 p0971 N71-17441

Aircraft safety and aircraft reliability, noting pilot performance, landing approach and takeoff, and clear air turbulence
11 p1674 N71-22197

Determination of inspection intervals and nature of inspections for safe and economical operation of aircraft structures
[FFA-128] 11 p1676 N71-22431

Proceedings of Air Line Pilots Association annual safety forum
12 p1853 N71-23234

Accident investigations, flight control systems, and operational recordings for improved aircraft flight accident
[AARAD-CP-76-71] 12 p1853 N71-23410

Operational flight data analysis for improved aviation safety levels
12 p1853 N71-23411

Onboard data acquisition for improved aircraft design and operational flight safety
12 p1853 N71-23412

High intensity zone flashback lights for increasing conspicuity of rotor helicopters during daytime and nighttime flights
[AD-718639] 13 p2026 N71-24669

Potential feasibility of safe, practical, and economical air-breathing nuclear propulsion system for aircraft and air cushion vehicles
[NASA-TM-X-67837] 13 p2123 N71-25524

Calculating and testing anticing systems of aircraft and helicopters
[AD-719922] 14 p2197 N71-25622

AIRCRAFT STABILITY

Acceptance tests of various upper torso restraints by automobile users with application to general aviation aircraft
[FAA-AM-71-12] 16 p2549 N71-28006

Development and application of loads up aircraft instrument display for improvement in aircraft safety during adverse weather
[FAA-NA-71-9] 17 p2702 N71-29985

Analysis of aircraft accidents and establishment of rational, quantitative air traffic safety control goals
[FAA-TR-71-56] 17 p2702 N71-29989

Conference on NASA research in aircraft safety and operating problems
[NASA-SF-276] 18 p2868 N71-30756

Ditching behavior of dynamic C-5A model
18 p2868 N71-30757

Magnitude of induced voltages and their relation to characteristics of lightning discharge and electrical properties of aircraft electrical systems
18 p2869 N71-30761

Safety characteristics for powered lift of commercial STOL aircraft
18 p2869 N71-30773

Safety tests for aircraft equipment
[AD-723033] 19 p3037 N71-31940

Design criteria for crashworthy aircraft fuel systems for military aircraft
[AD-723968] 20 p3269 N71-32992

Evaluation of air traffic control parameters and relationship to future of aeronomics
[NASA-CR-1833] 21 p3376 N71-34025

Development of numerical rating for correlating safety-of-flight factors with aircraft speed and visibility restrictions
[FAA-ED-70-48] 22 p3413 N71-35735

Determination of physical and chemical properties of fuels gelled with carbonylhydride resins to evaluate effectiveness in reducing aircraft fire hazards
[FAA-NA-71-18] 23 p3658 N71-37340

AVIATION STABILITY
NT HOVERING STABILITY
Application of weight and balance principles for aircraft operation
[FAA-AC-91-23] 03 p0314 N71-12241

Mechanical stabilization system for VTOL aircraft
[NASA-CASE-XLA-86339] 04 p0674 N71-13422

Vibration stability of basic airplane structures
[JPRS-51966] 04 p0618 N71-14144

Turbulence measurements in and near thunderstorms correlated with aircraft stability measurements from ground based radar
[NRC-11703] 05 p0717 N71-15152

Wind tunnel studies of external store induced flow field instability effects on longitudinal stability of arrow wing aircraft
09 p3159 N71-19382

Investigation of longitudinal and lateral stability and controllability of supersonic aircraft
[AD-718285] 12 p1857 N71-23818

Wind tunnel investigation of static longitudinal and lateral characteristics of full scale mockup of light twin engine aircraft
[NASA-TN-D-62318] 12 p1857 N71-23860

Stability, control, and handling quality characteristics of STOL and V/STOL airplanes
13 p2026 N71-24702

Investigation of stability and controllability parameters for supersonic aircraft under varying aerodynamic load conditions
[AD-719804] 13 p2027 N71-23832

Stability and controllability of supersonic swept wing aircraft
[AD-719803] 13 p2027 N71-23840

Tracking error frequency response function and human psychomotor performance under aircraft vertical and lateral vibration conditions
[AD-719754] 13 p2028 N71-23867

Equations of motion for time vector calculus for aircraft lateral stability
[ARC-R/M-36311] 15 p2367 N71-27007

Approximation method for turbulence effects on aircraft aerodynamic stability with B-52 examples
15 p2367 N71-27320

Complexity of supersonic aircraft systems for stability and controllability
[AD-712027] 15 p2367 N71-27354

Engine dynamic requirements implied by three dimensional control for VTOL aircraft
[NASA-TT-F-13755] 18 p3882 N71-31453

Conference papers on low level turbulence models to determine influence on aircraft stability and mission trajectories
[DLR-MITT-70-12] 19 p3056 N71-31882

Pilot injuries on high speed low altitude flight noted acceleration due to gust effects
19 p3048 N71-31888

Horizontal and vertical gust load frequency and power spectra influence on longitudinal aircraft stability
19 p3057 N71-31890

Atmospheric turbulence models showing gust load influence on aircraft yaw motion
19 p3057 N71-31891

Characteristics of air motion with respect to ground and analysis of dynamics of aircraft in turbulent air
[NASA-TT-F-606] 19 p3053 N71-32719

AIRCRAFT STRUCTURES

First order motion of cable towed and tethered bodies for predicting aircraft dynamic stability performance
[VKE-TN-48] 20 p3205 N71-33116

Application of least squares method for determining longitudinal aerodynamic derivatives of aircraft from flight test data
[Z-12] 20 p3206 N71-33305

Analysis of coupled roll-spiral-mode, pilot induced oscillation occurring with M-2F2 lifting body
[NASA-TN-D-6496] 20 p3206 N71-33307

Correlation studies based on wind tunnel test data and flight tests to determine performance, stability and control of XB-70-1 aircraft
[NASA-CR-114333] 21 p3373 N71-34001

Analysis of influence of wind shear on longitudinal motion of aircraft during approach and landing
[NASA-TN-D-6436] 21 p3376 N71-34022

Relation between turbulence in stratosphere causing aircraft buffeting, and vertical distribution of meteorological parameters calculated from radiosonde data
[NASA-TT-F-13981] 23 p3703 N71-36398

Horizontal temperature and wind distribution effects on aircraft buffeting in stratosphere
[NASA-TT-F-13978] 24 p3872 N71-37600

Spin tunnel tests to determine effectiveness of deployable, flexible ventral fins for spin recovery device on fighter aircraft
[NASA-TN-D-5599] 24 p3873 N71-37603

AIRCRAFT STRUCTURES

NT AIRFRAMES

NT FUSELAGES

Parametric study of natural frequencies of skin stringer structures
[AD-711383] 01 p0005 N71-10734

Penetration of metal aircraft surfaces
[AD-711950] 02 p0243 N71-11670

Application of aerodynamic constraints in structural optimization of aircraft design
03 p0463 N71-13131

Computer system for optimal design of aircraft structures
03 p0464 N71-13132

Matrix methods in computer-aided design optimization of aircraft structures
03 p0464 N71-13135

Vibration stability of basic airplane structures
[JPRS-51966] 04 p0618 N71-14144

Effects of external loads on strength of flight vehicles
[AD-713461] 05 p0627 N71-14584

Finite element analysis of structures in plastic range
[NASA-CR-1649] 08 p1301 N71-19276

Comparison of hydrogen and methane as coolants in regeneratively cooled panels
[NASA-CR-1652] 08 p1305 N71-19289

Aerodynamic interference characteristics of airframe-propulsion systems of transport and military aircraft
[AGARD-CP-71-71] 09 p1311 N71-19353

Optimization of interferences between aircraft components in supersonic flow
09 p1311 N71-19356

Swept wing body configurations for reduced drag at supersonic speed
09 p1312 N71-19358

Three dimensional interactions in half cone pressure fields and effects on intakes mounted adjacent to aircraft fuselage
09 p1369 N71-19367

Solution of problems in structural design with emphasis on interaction between materials, structures, and design requirements
[AD-717576] 11 p1673 N71-22136

Determination of inspection intervals and nature of inspections for safe and economical operation of aircraft structures
[FFA-120] 11 p1676 N71-22431

Engineering design analysis of hydrogen cooled structural panels for application to hypersonic aircraft
[NASA-CR-1650] 11 p1843 N71-22625

Heat flux sensor adapted for mounting on aircraft or spacecraft to measure aerodynamic heat flux inflow to aircraft skin
[NASA-CASE-XPR-03802] 11 p1845 N71-23085

Transfer functions in modelling human pilot and dynamic structural aircraft responses
[AGARD-R-506-71] 12 p1850 N71-23210

Mathematical modelling of aircraft structural response modes to active control system
12 p1852 N71-23212

Computation and measurements of dynamic aircraft transfer functions to atmospheric turbulence
12 p1852 N71-23213

Material specifications, flammability, safety considerations, and design criteria for materials used in construction of commercial aircraft interiors
12 p1941 N71-23232

Abstracts of papers presented at US Air Force materials symposium held at Miami Beach, Florida in May, 1970
[AD-714323] 12 p1943 N71-23625

Nondestructive testing of aircraft structures using thulium and iridium gamma sources
[JAEI-MEMO-4163] 13 p2181 N71-24849

Development and characteristics of high strength, stress corrosion resistant aluminum alloys for aircraft structures
[AD-720398] 14 p2273 N71-25876

Computer aided design of wing structures and application of optimal law of material distribution
[AD-722303] 17 p2704 N71-29657

Fatigue crack length relationship with aircraft inspection intervals and structural reinforcement, high strength materials, and aircraft usage effects
18 p3021 N71-30783

Approximate solution of nonlinear potential equation for small disturbance in transonic range and pressure distribution on aircraft
18 p2872 N71-31061

Aircraft structure elasticity effects on control lever deflection and control forces
18 p2872 N71-31065

Estimation of lateral and longitudinal rigid body responses of aircraft structures continuous and random atmospheric turbulence
[NASA-TN-D-6273] 18 p2872 N71-31242

Aircraft design concepts for prevention of structural failure including stress analysis
[AD-723317] 19 p3035 N71-31683

Numerical analysis of derivatives of flutter velocity of aircraft structures to determine optimization of complex structures
[NASA-CR-111955] 21 p3526 N71-35126

Assessment of nonlinear response of aeronautical structures with nonlinear characteristics under vibration conditions
[ARL/SM-355] 21 p3527 N71-35134

NASTRAN computer program differential stiffness and static load analysis methods compared for aircraft tandem side opening canopies
22 p3682 N71-36260

Modal analysis of response and fatigue of aluminum aircraft panels modal response
22 p3684 N71-36273

Use of NASTRAN as analysis tool in structural design optimization process applied to aircraft fuselage type structure
22 p3685 N71-36280

Chemical and structural analysis techniques for materials suitable for aircraft structures
[AD-727017] 22 p3691 N71-36323

Variability of aluminum alloy aircraft structure fatigue life under symmetric and asymmetric loads
[ARL/SM-REPORT-329] 23 p3861 N71-37524

Reduction of resonant vibrations in integrally stiffened skin-stringer panels using viscoelastic materials
[AD-727773] 23 p3863 N71-37540

Structural analysis of corrugated aircraft wing skin panels to determine effects of corrosion damage
[AD-728009] 24 p3975 N71-37619

AIRCRAFT TIRES

Stresses and deformations in multi-ply aircraft tires subject to inflation pressure loading
[AD-711073] 01 p0004 N71-10434

Influence of gravel depth and tire inflation pressure on soft-ground arresting of civil aircraft
[RAE-TR-69001] 02 p0147 N71-11040

Rate of wheel spin-up, and tire degradation at aircraft touchdown with different runway grooves
[FAA-RD-71-2] 09 p1323 N71-20069

Directional control capability of 18 x 5.5, type 7 aircraft tires on wet surfaces
[NASA-TN-D-6202] 09 p1324 N71-20158

Chevron cutting and effects of braking on wear of aircraft tires
18 p2869 N71-30768

Grooved and ungrooved runway surface effects on aircraft tire spin-up characteristics and tread damage
[NASA-TM-X-2345] 19 p3039 N71-32798

Elastic response and characteristics of bias ply aircraft tires subjected to braking forces and simple flexure
[NASA-TN-D-6426] 21 p3376 N71-34027

Stresses and deformations in multiply bias pneumatic aircraft tires subjected to inflation pressure loading
22 p3693 N71-36341

AIRCRAFT WAKES

NT HELICOPTER WAKES

NT PROPELLER SLIPSTREAMS

NT SLIPSTREAMS

Review of aircraft wake turbulence
[AD-712080] 02 p0200 N71-11129

Flow visualization of trailing vortex wakes in towing tank
[DI-82-1004] 04 p0519 N71-13800

Aircraft wake turbulence with downwash loading of wing span
[AD-718024] 12 p1851 N71-23660

Effect of wing-tip vortex wakes generated by large jet transport aircraft on smaller airplanes
18 p2866 N71-30764

Flight tests for evaluating effect of wing-tip vortex wake generated by large jet transports on smaller aircraft
18 p2866 N71-30765

AIRCRAFTS

U FLIGHT CREWS

SUBJECT INDEX

AIRFIELD SURFACE MOVEMENTS

Testing ASM/transporter for moving emergency service vehicles on airfields during poor visibility conditions
17 p2719 N71-29935

Analysis of aircraft ground flotation characteristics based on aircraft type and airfield construction
[AD-720273] 21 p3376 N71-34026

AIRFOIL CHARACTERISTICS

U AIRFOILS

AIRFOIL PROFILES

NT WING PROFILES

NT WING SPAN

Low speed aerodynamic characteristics of airfoil profiles including effects of upper surface roughness simulating hair frost
[NPL-AERO-1308] 02 p0143 N71-11044

Pressure distributions calculated with 3d method on series of quasi-elliptical symmetrical airfoils in sub-critical flow
[NRC-11693] 05 p0625 N71-14612

Two dimensional thin airfoil theory with strong late flow on upper surface
[AD-714076] 06 p0795 N71-16361

Direct and inverse application of Dornedyn techniques to incompressible transonic flow over symmetric Joukowski airfoil sections
[NAL-TR-2207] 09 p1316 N71-19729

High lift and boundary layer separation behavior of sweptback wing airfoil profile noting trailing and leading edge stall pattern
[ARC-R/M-3648] 13 p0821 N71-34488

Hodographs applied to calculation of compressible flow on turbomachine blades and use of visualization techniques
[ONERA-TN-179] 19 p0876 N71-31786

Solutions of potential flow for two dimensional compressible flow for quasi-elliptical airfoil profiles noting pressure distribution
[NLR-TR-69028-U] 19 p0777 N71-31791

Design of two dimensional airfoil profile with prescribed velocity distribution using conformal mapping
[SAAB-TN-67] 20 p3205 N71-33037

Digital computer and plotter for simulating flow about Joukowski airfoil
[TECH-71-4] 20 p3206 N71-33488

AIRFOIL SECTIONS

U AIRFOIL PROFILES

AIRFOIL THICKNESS

U AIRFOIL PROFILES

AIRFOILS

NT ALLERONS

NT ARROW WINGS

NT CAMBERED WINGS

NT CARBET WINGS

NT CRUCIFORM WINGS

NT DELTA WINGS

NT ELEVATORS [CONTROL SURFACES]

NT ELECONS

NT FIXED WINGS

NT FLAPS [CONTROL SURFACES]

NT FLEXIBLE WINGS

NT HORIZONTAL TAIL SURFACES

NT INFINITE SPAN WINGS

NT JET FLAPS

NT LEADING EDGE SLATS

NT LIFTING ROTORS

NT LOW ASPECT RATIO WINGS

NT PARAWINGS

NT PROPELLER BLADES

NT RECTANGULAR WINGS

NT RIGID ROTORS

NT RING WINGS

NT ROTARY WINGS

NT SLENDER WINGS

NT SPOILERS

NT SUPERCRITICAL WINGS

NT SUPERSONIC AIRFOILS

NT SWEEP WINGS

NT SWEEPBACK WINGS

NT THIN AIRFOILS

NT THIN WINGS

NT TILTING ROTORS

NT TIP DRIVEN ROTORS

NT TRAILING-EDGE FLAPS

NT TRAPEZOIDAL WINGS

NT UNCAMBERED WINGS

NT UNSWEPT WINGS

NT VARIABLE SWEEP WINGS

NT WING FLAPS

NT WINGS

Subcritical flows over two dimensional airfoils by multistrip method of integral relations
[RE-393] 01 p0801 N71-10881

Douglas DC 9 aircraft crash during takeoff caused by ice formation on airfoils
[NTSB-AAR-70-20] 01 p0005 N71-10815

Oscillating flow effects on pressure force normal to symmetrical airfoil chord
[AD-711830] 02 p0142 N71-11011

Three dimensional flow patterns obtained during boundary layer separation on airfoils
[NPL-AERO-1309] 02 p0143 N71-11014

SUBJECT INDEX

- Test cases for numerical analysis of airfoil two dimensional transonic flow
[AGARD-R-575-76] 03 p0362 N71-12674
- Transonic pressure distribution on airfoils
[AD-712397] 03 p0363 N71-13060
- Electric heating for measuring induced drag on non-planar airfoils
[NASA-CASB-XLA-00735] 04 p0472 N71-13410
- Electric heating for measuring induced drag on non-planar airfoils
[NASA-CASB-XLA-05828] 04 p0472 N71-13411
- Region upstream and downstream from shock waves of airfoils in uniform and transonic flow
[NASA-TT-F-13472] 08 p1177 N71-18401
- Aerodynamic effects of mechanical high lift devices on conventional airfoils
09 p1322 N71-20052
- Two dimensional wind tunnel tests on airfoils with high lift devices
09 p1316 N71-20056
- Representations of flow separation bubbles near airfoil leading edge
09 p1323 N71-20064
- Calculation of profile drag of airfoils at low Mach numbers by predicting instability and transition points
[NATL-TR-156] 09 p1317 N71-20101
- Application of integral relations to inviscid supersonic flow over symmetric airfoils at zero angle of attack
[AD-717339] 11 p1669 N71-22098
- Graphical computer simulation of incompressible flow about airfoil
[TR-71-2] 11 p1715 N71-22149
- Measurement of force and pressure fluctuations on airfoils during transverse and streamwise gust flows
[CUBANA-TURBO-TR-21] 11 p1676 N71-22374
- Procedure for predicting properties of transonic flow about thin airfoils and slender bodies
[NASA-CR-1722] 12 p1849 N71-23133
- Potential test equipment for evaluating Fockler airfoil wing
[NLR-TR-70088-L] 12 p2005 N71-23157
- Aerodynamic characteristics of rear wings produced by periodic vortex shedding from airfoils
[AD-710093] 12 p1964 N71-23245
- Low aerodynamic drag airfoil designed by Lightbulb method
[AIRC-RM-3618] 13 p2021 N71-24498
- Unsteady airfoil stall characteristics using static data input for predicting stall flow boundaries of open airfoil wing
[NASA-CR-111966] 17 p2697 N71-29221
- Use of aerodynamic lift for application to high speed ground transportation by two dimensional airfoils
[PB-197242] 17 p2700 N71-29762
- Application of Frobenius integral equations of second kind for determining pressure distribution on cambered thin airfoils
[NASA-TT-F-702] 18 p2865 N71-30488
- Computer program for aerodynamic characteristics evaluation of multiple-component airfoils in subsonic, viscous flow
[NASA-CR-1843] 20 p3285 N71-33140
- Surface pressure measurements and schlieren photographs of flow about Laysan shock flow airfoil
[AIAA-80-323] 20 p3286 N71-33482
- Numerical analysis of plane steady transonic flows past lifting airfoils with freestream Mach numbers less than unity
[D180-12936-1] 21 p3412 N71-34273
- Numerical analysis of laminar, incompressible flow along corner formed by intersection of two thin airfoils
[AD-726546] 22 p3538 N71-35201
- Theoretical analysis of trailing edge blowing effects on circulation around airfoils based on iterative solution with lift coefficients
[AD-726546] 22 p3538 N71-35202
- Leading edge suction of thin airfoil theory
[AIAA-80-323] 23 p3703 N71-36399
- Wind tunnel study of tip vortex modification by mass flow injection
[AD-726546] 23 p3704 N71-36406
- Viscous flow patterns of airfoil in centrifugal flow with thin plate blading and with thick airfoil blading
[D18-238] 23 p3785 N71-36410
- Development of procedure for scaling of experimental turbine vane airfoil temperatures from low to high gas temperatures
[NASA-TT-D-6510] 23 p3866 N71-37563
- Two dimensional flow tests of transonic airfoils
[NASA-TT-F-13988] 24 p3871 N71-37593
- Unsteady, compressible, and perfect gas flow over a thin airfoil in two dimensional testing of pitching airfoils
[D18-14134-1] 24 p3904 N71-37827
- AIRFRAME MATERIALS**
- Stiff strength, stiffness, fatigue, and damage resistance of materials in design optimization for shell structures
03 p0465 N71-13143
- Aluminum alloy stress cycles and fatigue life of airframe materials
[PB-76-1969] 07 p1124 N71-17524

- Problems in riveting and welding of high strength aluminum aircraft alloys
[AD-717033] 10 p1632 N71-20994
- Solution of problems in structural design with emphasis on interaction between materials, structures, and design requirements
[AD-717576] 11 p1673 N71-22136
- Effect of heat conduction of material on temperature distribution in vicinity of wing leading edge in hypersonic flow
[REPT-4901] 11 p1841 N71-22494
- Fatigue and fracture mechanics of airframes and materials including structural design and stress analysis techniques
[AD-719736] 13 p2028 N71-25092
- Application of photochromic coatings to provide nondestructive inspection for aerospace materials and structures
[AD-720239] 14 p2280 N71-26383
- Properties and selective applications of high strength steels, aluminum and titanium alloys, polymeric materials, ceramic materials, and composite materials in aerospace engineering
[AGARD-LS-31-71] 15 p2429 N71-27038
- Properties and selective applications of aluminum alloys in airframe construction
15 p2414 N71-27044
- Properties and selective applications of titanium alloys in airframes and jet engines
15 p2421 N71-27045
- Experimental investigation on effect of spot welded or adhesively bonded thermocouples and fatigue behavior of two titanium alloys suitable for use in high speed airplanes
[NASA-TM-X-2288] 16 p2614 N71-28891
- AIRFRAMES**
- Investigation of engine-exhaust-airframe interference on cruise vehicle at Mach 6
[NASA-TN-D-6990] 05 p0623 N71-14633
- International conference on rain erosion and associated phenomena
[AD-715108] 07 p0973 N71-17906
- High bypass turbofan powered propulsion simulator for airframe engine integration analyses at subsonic and supersonic speeds
09 p1456 N71-19369
- Construction and operation of AN-24 airplane including airframe description
[AD-716499] 09 p1320 N71-19515
- Lift augmentation devices effect on STOL engine - Part 1, interface problems between engine and airframe
09 p1322 N71-20061
- Digital computer program description with updating case data mode and extended force method matrix generation capability
[AD-715923] 09 p1356 N71-20180
- FORTRAN program for Koller-type method for finite element analysis of nonlinear structural behavior of airframes
[AD-717181] 10 p1527 N71-20695
- Koller method for asymptotic analysis of postbuckling behavior reformulated in finite element notation
[AD-717440] 11 p1837 N71-22485
- Fatigue and fracture mechanics of airframes and materials including structural design and stress analysis techniques
[AD-719736] 13 p2028 N71-25092
- Engine-airframe contribution to combat aircrew rescue simulation
[AD-720238] 14 p2211 N71-26371
- Adaptive sampled data control of time varying bending modes of flexible airframe
[AD-725466] 18 p3020 N71-31582
- General fatigue prediction method based on Newber notch stresses and strains for aluminum alloy airframes
[AD-726331] 19 p3108 N71-32023
- Analysis of bonded metal surfaces used in manufacture of helicopter components
[AD-726463] 20 p3283 N71-32953
- Analysis of feasibility of designing transport aircraft to carry up to 1,000 passengers and methods for predicting aircraft performance
[CRANFIELD-AERO-3] 21 p3375 N71-34018
- Reference text on design of aviation structural elements
[AD-726586] 22 p3540 N71-35220
- Evaluation of NASTRAN system based on large complex airframe analysis
22 p3686 N71-36282
- Technical aviation handbook covering aircraft maintenance, navigation, airframes, lubricants, piston and gas turbine engines, and checkout procedures
[AD-727153] 24 p3874 N71-37613
- AIRGLOW**
- NT NIGHTGLOW**
- Airborne filter colorimeter measurements of atmospheric diurnal glow brightness
01 p0049 N71-10587
- Filter measurements of smelt intensities for industrial components of airglow
[NASA-TT-F-13596] 02 p0308 N71-11393

AIRLINE OPERATIONS

- Linear semidirectional component of OI/5577A1 night airglow
[ULU-ENG-70-263] 03 p0480 N71-15629
- Treating large scale topographic disturbances with inhomogeneous linear integral equation and Green function
[AD-717204] 10 p1547 N71-20795
- Large aperture Fabry-Perot spectrophotometer with helium-neon laser to reduce instrumental drift
13 p2079 N71-24419
- Airborne photometer instrumentation and measurement data on high latitude hydroxyl airglow emission
[NASA-CR-118526] 13 p1462 N71-25211
- OGO-D photometric airglow measurements
13 p2076 N71-25248
- Airborne interferometric measurements on atmospheric airglow emission
[AD-726673] 15 p2599 N71-27188
- Spectral variability analysis on airborne sodium and airglow emission data
[NASA-CR-119183] 17 p2748 N71-30139
- Upper atmospheric emissions from He, O, and Na during solar eclipses of 15 Feb. 1961
[NRC-TT-1459] 21 p3416 N71-34007
- Photoelectron excitation of atomic oxygen resonance radiation in terrestrial airglow
[NASA-CR-121007] 23 p3372 N71-35440
- AIRLINE OPERATIONS**
- Pricing system for landing and takeoff slots by passenger flights for use of Washington National Airport
01 p0087 N71-10170
- Statistical data on delays and cost of delays at airline terminals
01 p0083 N71-10366
- Air mail transportation by contract operations
01 p1038 N71-10816
- Subsidies for American certificated air carriers
02 p3508 N71-12190
- International aviation and all-weather automatic landing systems
03 p0405 N71-12428
- Control problems in airline operations particularly air cargo handling
04 p0474 N71-14430
- Airline meteorological radar operational policies and procedures
[AD-713636] 05 p0716 N71-14623
- Problems of local airlines in providing service to rural communities
05 p0787 N71-15390
- Civil aeronautics operations review
07 p1133 N71-17779
- Problems in civil air transportation and logistics
07 p1134 N71-17799
- Problems facing local air transport industry, communities, and government agencies
07 p1135 N71-18078
- Market research and management planning for optimization of civilian airline operations in France
[REPT-1970-7-E] 07 p1136 N71-18093
- Cybernetic and economic international study group for civil aviation in France
07 p1136 N71-18094
- Mathematical models for optimization of airline operations
07 p1136 N71-18095
- Planning estimates in air traffic forecasting
07 p1136 N71-18096
- Investigating statistics of aircraft accidents by region and operator
[REPT-1970/10-E] 07 p0974 N71-18115
- Airline passenger survey to determine future requirements for state airport system
[PB-195939] 09 p1364 N71-19611
- Analysis and statistics of airports, air carrier fleet operation, aircraft production, and status of civilian pilot personnel for September, 1970
11 p1672 N71-21977
- Analysis of Boeing 727 aircraft impact on environment, passenger processing, passenger boarding trends, and scheduled and total operation trends
11 p1672 N71-21978
- Simulation, analysis, and recommendations for flight profile of C-130 aircraft to predict and achieve improvements in aircraft operation - Vol. 2
[PNSI-TR-70-0301-2-VOL-2] 11 p1792 N71-22380
- Planning for expected civil aviation developments caused by change-over to Boeing 747 aircraft and supersonic transport
11 p1674 N71-22381
- Planning for civil aviation operations including Boeing 747 aircraft and supersonic aircraft
11 p1675 N71-22382
- Market forecasts and traffic control technologies of Boeing 747 aircraft and supersonic aircraft operations
11 p1675 N71-22383
- Economics and operational planning for future civil air transportation
11 p1675 N71-22384
- Civilian airline operations with Boeing 747 aircraft and supersonic aircraft
11 p1675 N71-22385

Planning for Boeing 747 aircraft integration into
Israel airline operations

11 p1675 N71-22388

Support systems planning for expanded passenger
and cargo traffic in civil aviation

11 p1676 N71-22390

Integrated systems approach for developing require-
ments of increased civil aviation in Israel

11 p1676 N71-22391

Proceedings of Air Line Pilots Association annual
safety forum

12 p1853 N71-23234

Analysis of magnitude, growth, and carrier partici-
pation of passenger traffic in major short-haul mar-
kets

14 p2199 N71-26528

Contributions and effects of commercial airline ser-
vice on growth of manufacturing facilities in urban
areas below 40,000 population

14 p2199 N71-26529

Predicted civilian air travel increase and airport use
in United States of America for 1980

[AD-720732] 15 p2367 N71-27155

Analysis of current status and future outlook of US
commercial airline industry

[AD-718871] 16 p2531 N71-28216

Community reactions to aircraft and airport noise
from physical, psychological, and social aspects

[NASA-CR-1761] 16 p2536 N71-29023

Airline operations, costs, effects on aircraft indus-
try, and cooperation with CAB

17 p2860 N71-29256

Analysis of physical and economic factors pertain-
ing to effective operation of vertical takeoff and land-
ing aircraft short range commercial transportation -
Vol. 1

[AE-326/021-VOL-1] 17 p2860 N71-29285

Identification and analysis of potential sites for
vertical takeoff and landing aircraft facilities in Great
Britain - Vol. 2

[AE-326/021-VOL-2] 17 p2860 N71-29286

Aircraft accident report of DC-9 civilian aircraft
climbing near St. Croix, Virgin Islands, May 1970 fol-
lowing fuel exhaustion

[NTSB-AAR-71-8] 17 p2705 N71-30029

Review of policies affecting civil aviation, problems
confronting it, and potential for future contributions to
national benefits

[NASA-SP-265] 18 p2867 N71-30506

Remarks by chairman of Civil Aeronautics Board to
conference of airline finance managers

18 p2868 N71-30517

Conference on NASA research in aircraft safety
and operating problems

[NASA-SP-276] 18 p2868 N71-30756

Recommended airline and legal procedures prior to,
during, and after hijackings

18 p3031 N71-31562

Pros and cons of SST aircraft for civil airline opera-
tions

[BL-147] 20 p3211 N71-33438

Sonic boom carpets from operation of SST aircraft

20 p3211 N71-33440

Panel approach to solution of probable and possible
effects of sonic booms resulting from future SST
operations

[BL-139] 20 p3211 N71-33441

Civil Aeronautics Board regulatory actions taken
fiscal year 1970

21 p3534 N71-35186

Travel agent guide to air travel in US

21 p3535 N71-35194

Minimization of space shuttle maintenance costs
through application of commercial airline maintenance
concepts

22 p3674 N71-36195

Industrial relations, mediation, work stoppage, and
emergency dispute experience of airlines under Rail-
way Labor Act

22 p3699 N71-36380

Congressional hearings on airline service to small
communities and towns

22 p3700 N71-36395

Cost effectiveness of built in test provisions in air-
craft operations

23 p3757 N71-36780

Simulation of aircraft ground operations for Dallas-
Fort Worth Regional Airport

24 p3873 N71-37607

Airline view of air navigation problems

24 p3913 N71-37896

Freight, express, and mail tonnage forecasts for
domestic airline operations

24 p4035 N71-38793

AIRLINERS

U COMMERCIAL AIRCRAFT

U PASSENGER AIRCRAFT

AIRPORT LIGHTS

NT RUNWAY LIGHTS

Measuring intensity distribution of omnidirectional
semi-flush airport lights

07 p1005 N71-18113

AIRPORT PLANNING

Air traffic pattern prediction for 1980 peak summer
periods in London, England terminal area

01 p0082 N71-10163

Program effectiveness and facility criteria for ILS
investment decisions

01 p0136 N71-10355

National Aviation Facilities Experimental Center
history and programs

01 p0038 N71-10356

Statistical analysis of direct rail rapid transit system
impact on transportation to Cleveland airport

01 p0157 N71-10370

File formats and code descriptions for analysis of
direct rail rapid transit system impact on transporta-
tion to Cleveland airport

01 p0038 N71-10371

General aviation airport planning for east central
Florida

[PB-191239] 04 p0517 N71-14694

Investigating technology and analytic techniques for
solving intra-airport transportation problems

[AD-702738] 05 p0657 N71-14810

Airport master plan for Poplar Bluff, Missouri

[PB-189728] 05 p0657 N71-14895

Planning system for metropolitan airports

[FAA-AC-150/3070-5] 07 p1004 N71-17546

Systems analysis summary on New York
metropolitan area air traffic capacity

07 p1134 N71-18040

Planning for expected civil aviation developments
caused by change-over to Boeing 747 aircraft and su-
per-sonic transport

11 p1674 N71-22381

Planning parameters for high capacity international
airport system

11 p1676 N71-22389

Analysis of adequacy of access routes to Dallas In-
ternational Airport and need for additional facilities to
accommodate future expansion

[PB-194094] 14 p2237 N71-26301

Analysis of road traffic problems at Washington Na-
tional Airport and recommendations to improve air-
port access

[REPT-3] 14 p2238 N71-26526

Community values and social problems associated
with construction of air and surface transportation
facilities

15 p2525 N71-26802

Airport study for Vigo County, Indiana with data
bank of airport activity for past 10 years

[PB-197309] 17 p2730 N71-29721

Airport development recommendations for Lane
County, Oregon with projections of passenger and air-
craft operations at 5 year intervals through 1990

[PB-197860] 17 p2730 N71-29756

Systems analysis approach to airport planning and
predicting terminal facility and aircraft demands in
year 2000 for air traffic control systems

[NASA-CR-119287] 18 p3871 N71-30000

South Carolina statewide aviation and airports plan
to accommodate needs of air carrier and general avi-
ation to year 1980

[PB-197728] 19 p3073 N71-31893

Economic aspects and regional planning for inter-
national airport facility at Ontario, California

[PB-199695] 22 p3565 N71-35391

Development of analysis techniques for determining
causes for airport congestion and interaction of vari-
ous causes

[FAA-RD-71-35] 22 p3565 N71-35393

AIRPORT TOWERS

Physiological and biochemical measurements of air
traffic controller personnel at O'Hare Airport to deter-
mine effects of duties

[FAA-AM-71-2] 13 p3037 N71-34747

Wind shear vertical distribution periodic variations
at three Canadian airport towers

18 p2949 N71-30830

Evaluation of design concept and operational feasi-
bility of 11-sided control tower cab

[FAA-NA-71-37] 24 p3904 N71-37826

Effectiveness of control towers in reducing aircraft
accidents and approach time

24 p3955 N71-38213

AIRPORTS

Rapid rail transit service to airports

01 p0027 N71-10167

Pricing system for landing and takeoff slots by pas-
senger flights for use of Washington National Airport

01 p0037 N71-10170

Air carrier demand for slots particularly in area of
Washington-Baltimore

[PB-193350] 01 p0038 N71-10347

Selected tabulations from Cleveland Hopkins Air-
port user surveys before and after rail transit service

01 p0137 N71-10360

High speed access system evaluation for transporta-
tion from airport to Miami with cost estimates and net-
work descriptions

[PB-192845] 01 p0038 N71-10417

Impact of rapid rail transit service from central
business district to airport

01 p0137 N71-10440

Development study for VFR heliport standard
lighting system

[AD-710982] 01 p0039 N71-10406

Inventory of existing airport system in Rhode Island

[PB-189332] 02 p0145 N71-11888

Community physical, psychological, and social
reactions to aircraft noise around 7 US international
airports

[NASA-CR-111316] 02 p0146 N71-11890

Visual aids for secondary airports

[FAA-NA-70-51] 02 p0198 N71-11874

Analysis of airport travel demands at Lambert-
St. Louis Municipal Airport

[PB-192057] 04 p0515 N71-11889

Computerized optimization of airport roadway
design

04 p0495 N71-11891

Aeronautical climatological tables of international
commercial airports

05 p0717 N71-13140

Development model for Oklahoma airport

[PB-194957] 07 p1002 N71-10887

Data processing and impact analysis on rapid rail
access system for airport

[PB-195047] 07 p1002 N71-10888

Data recordings and computer codes for airport
rapid transit access system study

[PB-195048] 07 p1002 N71-10889

Survey of rapid transit railway impact on airport
passenger traffic

[PB-195045] 07 p1003 N71-10890

Tabulations for rapid transit system effect on air-
port traffic

[PB-195049] 07 p1003 N71-10891

Rapid transit railway effect on airport passenger
traffic

[PB-195046] 07 p1003 N71-10892

Computerized simulation of dispersion models for
airport air pollution

[RE-3983] 07 p1055 N71-11923

Economic analysis of airport construction in south
central Texas region, emphasizing employment and
dollar value of purchases

07 p1005 N71-10899

Public transportation in airport access systems

08 p1307 N71-11891

Mass transport systems for airport access

08 p1308 N71-11892

Problems in mass transportation systems for access
to Tokyo airport

08 p1308 N71-11893

Public transportation requirements for Heathrow
Airport

08 p1308 N71-11894

Providing ground access to Kansas City Airport

08 p1308 N71-11895

Existing access systems for Logan International
Airport, and plans for improvement

08 p1308 N71-11897

Survey conducted to develop minimum require-
ments for airport fire fighting and rescue services

[FAA-AE-71-1] 09 p1364 N71-11925

Feasibility of rail access to Friendship International
Airport from Wash., D.C. and Baltimore, Md.

[PB-196023] 09 p1364 N71-11924

Airline passenger survey to determine future
requirements for state airport system

[PB-195939] 09 p1364 N71-11911

Design, construction, operation, and management
of military airports

[AD-716603] 09 p1365 N71-11912

Survey of passenger volume and destinations at
Theodore F. Green State Airport in R.I.

[PB-195940] 09 p1365 N71-11913

Climatological tables of ceiling, visibility, surface
wind, and temperature for Lappeenranta Airport, Fin-
land

[REPT-25] 09 p1414 N71-30885

Climatological tables of ceiling, visibility, surface
wind, and temperature for Kuopio Airport, Finland

[REPT-24] 09 p1414 N71-30887

Aeronautical climatological conditions at Kalvi-
o Airport, Finland

[REPT-21] 09 p1414 N71-30888

Aeronautical climatological conditions at Kuus-
kylä Airport, Finland

[REPT-23] 09 p1414 N71-30889

Fog modification over airports using helicopters

[AD-716818] 10 p1596 N71-31589

Climatology at Rovaniemi Airport, Finland

[REPT-28] 10 p1598 N71-31519

Airfield tests of specially formulated marking paint
for coastal pavements

[AD-716755] 10 p1598 N71-31518

Climatology at Mairiinkangas Airport, Finland

[REPT-26] 10 p1598 N71-31519

Climatology at Vasa Airport, Finland

[REPT-30] 10 p1598 N71-31519

Climatology at Turku Airport, Finland

[REPT-29] 10 p1598 N71-31519

Climatology at Oulu Airport, Finland

[REPT-27] 10 p1598 N71-31519

Inventory of private and public airports and air
facilities in state of Texas

[PB-196935] 10 p1494 N71-31610

SUBJECT INDEX

- Year forecast for eight major traffic categories at Washington National and Dallas International airports for period 1971 through 1983
- Development and description of basic descriptors used to analyze jet engine noise, aircraft noise, and noise level of airports
- Tables and maps of selected landing airfields for shuttle orbiters with various crossranges
- Tables on mean and maximum wind velocities for Helsinki, Koopeo, and Vasa airports in Finland 1965
- Airfield climatology for European Low Countries and British Isles
- Airfield climatology for Scandinavia and northern Europe
- Survey of civil airports to determine status of crash fire and rescue equipment available for use following accidents involving scheduled or local service air carrier aircraft
- Noise data with models of both internally and externally blown jet flaps designed for STOL aircraft
- Synoptic meteorology for airports in Spain, Austria, France, Switzerland, and Alps
- Community reactions to aircraft and airport noise from physical, psychological, and social aspects
- Probable impact of future supersonic transport aircraft operations on noise environment around seven airports in US
- Extension of New York Waterfront Commission to new airports and establishment of security measures to combat air cargo theft
- Wind pressure and cross flow velocity profiles for short take-off aircraft building roof airports
- Dynamic characteristics of wind and temperature profile vertical distribution over Paris-north airport site
- Wind shear in 0-100-m layer over Koyay-on-France Airport determined from wind and temperature profiles
- Analysis of transit access to Oakland International Airport, Oakland, California, and recommendations for improved service
- Intruder detector for parked aircraft using sensing techniques to detect human touch
- Impact of jet aircraft emissions on air quality in vicinity of Los Angeles International Airport
- Systems approach in design, construction, operation, and maintenance of airport runways
- Aircraft noise reduction including had use and noise forecasting
- Legal aspects of compulsory soundproofing for structures next to John F. Kennedy International Airport
- Environmental effects of jetport near Everglades Park in southern Florida
- Applications of situational control models examined for lock sections of canals, seaports and airports, network of street crossroads, and other large systems
- Micrometeorological data for Hunter-Liggett military airfield - Nov. 1970
- Reduction of jet exhaust noise at airports
- Computing dispersal of atmospheric pollutants near airports by use of mean wind and temperature profiles
- Manual for development of needs estimates and capital improvement programs for airports and other facility terminals for 1970 to 1990
- Investigating economic and engineering aspects of wing drooping in construction
- Design and characteristics of double hull dirigible airship
- Aerodynamic characteristics of captive balloons other than lighter than air devices
- Design and basic characteristics of bearings for propionic devices for aerodynamic and aerostatic bearings
- Design, development, and performance requirements for large rigid airships for freight and cargo transportation
- Systems analysis summary on New York metropolitan area air traffic capacity
- Centralized flow control concepts and applications in air traffic control
- Airspeed contribution to noise level within fixed and rotary wing aircraft
- Mass flow, velocity, and in-flight thrust measurements by ion deflection
- Jet transport aircraft airspeed control and controllability data obtained by flight recorders
- Arcs, rotors, rotors, engine rigging, and gross weight effects on UH-1 C helicopter during autorotation
- Airworthiness
- Airworthiness requirements
- Air pollution in southern Alabama
- Warning systems
- Thermal erosion of permafrost on Beaufort Sea coast in Alaska
- Geological analysis of aerial geomagnetic survey of northeastern Alaska
- Snow cover physical properties at Fort Greely, Alaska
- Alaskan earth tilts, crustal failure, and microseisms
- Climatology for North American coastal areas from Vancouver to Alaska
- Synoptic observations for Alaskan coastal marine areas
- Geomorphology of ocean bottom structure and topography of Bering Sea and Gulf of Alaska
- Statistical analysis of population distribution, variation, and mortality among Alaskan natives
- Data tables of synoptic marine surface meteorology for Bristol Bay and St. Paul Island, Alaska
- Data tables of synoptic marine surface meteorology for Nunivik, St. Matthew, and St. Lawrence islands, Cape Lisburne, and Barrow, Alaska
- Telemetry network and borehole installations for measurements of crustal deformation release, failure, and tilts in Alaska
- Tables on seismological disturbances in Aleutian Islands
- Measurement of Alaska sea ice thickness from aircraft using penetrometer projections
- Dynamics of magneto-ionospheric disturbances in polar auroral zone
- Technical and cost factors for implementation of Alaska communication satellite system
- Measurement of vertical crustal movement of sea floor following Alaska earthquakes
- Analysis of processes maintaining seasonal heat storage in 0 to 230 meter surface layer of North Pacific Ocean
- Relictological effects of underground nuclear explosion on environment of Amchitka Island, Alaska
- Monitoring seismicity of Aleutian/Amchitka areas after nuclear detonations
- Data tables on snow survey measurements in Alaska
- Microseismic analysis of Denali fault in Alaska and under ground nuclear explosions and microseismic survey of Nevada, Utah, Idaho, Montana, and Wyoming
- Meteorological data measured at Fort Greely, Alaska - Nov. 1970

ALGAE

- Precipitation, atmospheric pressure and temperature, solar radiation, and wind velocity data for Fort Greely, Alaska - Oct. 1970
- Climatology, precipitation, atmospheric temperature, and wind direction and velocity data for Fort Wainwright, Alaska - Nov. 1970
- Climatology, geography, geology, and botany of Yukon Territory, Canada and Chukotka Peninsula, Alaska
- Aircraft accident investigation of Alaska Airlines Flight 1866 on Sept. 4, 1971
- Harmonic method of predicting shallow water tide for use at Anchorage, Alaska
- Location of Aleutian low center, and pressure at center
- Cosmic ray albedo
- Earth albedo
- Relationship between variations of radiation fluxes and albedo on subpolar ice caps in summer
- Relationship between albedo of water surface of small lakes and chrominance and transparency of water mass
- Operational characteristics and pilot experience in civil aviation accidents caused by alcohol intoxication
- Thermochromism of calcium oleate in alcohol
- Electron irradiation induced separation of Sb from SbCl₃ solution in anhydrous alcohols, ethers, ketones, acids, esters, and aromatic hydrocarbons
- Infrared spectroscopic study of allyl alcohol vapor adsorption on Li, Na, Cs, and Fe specimens of Fischer mordenites
- Physiological effects of two levels of alcohol on vertigo and synaptogram responses resulting from caloric irrigations with visual conditions and darkness of subjects controlled
- Disoriented visual tracking performance of humans during angular acceleration as result of alcohol consumption
- Physiological effects of alcohol and oxygen limitation levels on pilot performance and flying safety
- Effect of alcohol and discrimination responses on synaptogram and vertigo during angular acceleration with and without visual fixation
- Vacuum ultraviolet photoionization and photoelectron spectroscopy of associated and polymeric systems of liquid water and alcohols
- Mass spectra of alkyl carbonates derived from primary, secondary, and tertiary alcohols by use of deuterium labeling and high resolution mass spectroscopy
- Acetaldehyde
- Formaldehyde
- Direct synthesis of polymeric Schiff bases from two amines and two aldehydes
- Synthesis of rane polymers for heat shields by azine-aromatic aldehyde reaction
- Synthesis of aromatic diamines and dihydride polymers using Schiff base
- Smog forming reactivities of exhaust aldehydes measured using test mixtures similar to exhaust at atmospheric dilution
- Nutritional properties of unicellular algae compared to soy protein

- Uric acid levels in men fed algae and yeast as protein sources 03 p0526 N71-12330
- Harvesting of algae through chemical flocculation and flotation [REPT-321] 04 p0487 N71-13462
- Biochemistry of growth, gametogenesis, and fertilization in algae 05 p0635 N71-14722
- Regeneration of spacecraft cabin atmospheres utilizing photosynthesis of unicellular algae [AD-719831] 13 p2658 N71-25099
- Hydrostatic pressure effects on photosynthesis, growth, and oxygen production of algae cultures [AD-720401] 14 p2204 N71-25867
- Mechanisms of inactivation and repair in determination of effects of ultraviolet radiation on algae [COO-1793-J] 20 p3324 N71-33577
- Terrestrial organisms survive in simulated Jupiter atmosphere - studies with one-celled algae and aquatic plant [Eldred] 20 p3349 N71-33588
- Algae and plankton photosynthesis requirements for optimization of oceanographic resources 20 p3577 N71-35476
- Cloud condensation nuclei effects on rainfall during spring droughts in Florida from peat, algae, seaweeds, and leaf fire smoke [ESSA-TT-7-13905] 23 p3784 N71-36975
- ALGEBRA**
- NT ADJOINTS
- NT BANACH SPACE
- NT BINOMIAL THEOREM
- NT BINOMIALS
- NT CANONICAL FORMS
- NT CUBIC EQUATIONS
- NT CURRENT ALGEBRA
- NT DETERMINANTS
- NT EIGENVALUES
- NT EIGENVECTORS
- NT GROUP THEORY
- NT HERMITIAN POLYNOMIAL
- NT HILBERT SPACE
- NT HOMOMORPHISMS
- NT JORDAN FORM
- NT LIE GROUPS
- NT LINEAR EQUATIONS
- NT LINEAR TRANSFORMATIONS
- NT MATRICES [MATHEMATICS]
- NT NONLINEAR EQUATIONS
- NT POLYNOMIALS
- NT QUADRATIC EQUATIONS
- NT SPINOR GROUPS
- NT STATE VECTORS
- NT STOKES THEOREM [VECTOR CALCULUS]
- NT STRESS TENSORS
- NT SUBGROUPS
- NT TENSORS
- NT VECTOR SPACES
- NT VECTORS [MATHEMATICS]
- NT VORTICITY
- Controlability and observability with algebraic systems theory [NASA-CR-111112] 01 p0074 N71-10327
- Algebraic approach to theory of nuclear structure [NYO-2171-308] 01 p0094 N71-10336
- Algebraic theory for elementary particle dynamics [AD-711441] 01 p0100 N71-10736
- Algebraic topology as mathematical tool for production engineering 02 p0251 N71-11611
- Test matrices for numerical algorithms in linear algebra problems [AD-712679] 03 p0398 N71-12761
- Chiral SU(2) x SU(2) hard pion current algebra models [NUB-2039] 04 p0539 N71-14242
- Self-adjoint algebras of unbounded operators using quantum theory [NYO-2171-318] 04 p0541 N71-14484
- Structural properties of generalized automata and algebras [AD-712377] 05 p0659 N71-14737
- Algebraic systems and stochastic processes in military communication and information handling [AD-714114] 06 p0816 N71-16315
- Space science training materials and motivation of high school algebra students 07 p1153 N71-17778
- Algebraic realization of unitary symmetry with sum rules derived for well established supermultiplets providing predictions for mesons with some established members [JINR-E2-5229] 14 p2308 N71-26545
- Condition for equality of local algebras of relativistic quantum field theory [JINR-P2-5330] 15 p2460 N71-27072
- Comparison of standard Z transform and algebraic substitution synthesis methods for digital filters [AD-721571] 16 p2560 N71-28397
- Algebraic theory of superselection rules applied to problem of constructing field quantities from local observables [ITP-70-66-E] 18 p2943 N71-30567

- Asymptotic behavior of covariance matrix solution for discrete matrix Riccati equation [AD-722597] 18 p2944 N71-30880
- Application of algebraic realizations to pion-meson couplings in chiral dynamics and Yang-Mills field theory [JINR-P2-5759] 22 p3640 N71-35950
- Synthesis algorithm, Boolean algebra, and mappings for interval generalization of switching theory [COO-2118-3] 24 p3894 N71-37754
- Algebraizing integral equations for T matrix for reactions in system of heavy nucleus and two neutrons [ITP-70-97-P] 24 p3970 N71-38322
- ALGEBRA**
- Climatological tide observation in Algerian Sahara 20 p3261 N71-33336
- ALGOL**
- Semantics of elementary ALGOL like statements [AD-712460] 04 p0499 N71-13490
- Analysis of ALGOL computerized simulation statistics at NPL, Great Britain [NPL-CCU-11] 07 p0996 N71-17071
- ALGOL computer programs for linear system time dependence [ARC-CP-1124] 07 p0996 N71-17133
- Solution of partial differential equations in magnetohydrodynamics using symbolic style of ALGOL [AD-716404] 09 p1449 N71-20916
- Algorithm using ALGOL 68 type language for computerized determination of three dimensional path for numerical control of machine tools [AD-717777] 11 p1768 N71-22258
- Computer program using parts of ALGOL to be used with Univac operating system 17 p2722 N71-29440
- ALGOL computer program for estimation of maximum of analytical functions with arbitrarily small error bound 17 p2772 N71-29482
- Simulation of paging drum channel system by ALGOL and SIMULA programs on Univac 1108 [NASA-CR-121653] 21 p3397 N71-34172
- ALGOL program for determining satellite period variations and celestial equator transit time 22 p3679 N71-36233
- Algorithms for operator identification in ALGOL 68 23 p3729 N71-36581
- ALGORITHMS**
- Comparison of two quadratic programming algorithms [AD-710227] 01 p0074 N71-10009
- Algorithms for tree threading for encoder traversal [AD-709231] 01 p0026 N71-10014
- Developing models of atmospheric density to formulate algorithms for control of spacecraft motion in atmosphere [NASA-TT-7-13359] 01 p0045 N71-10046
- Deriving incomplete gamma functions for various applications and using Chebyshev polynomial approximations for solution of Lane-Emden equation 01 p0074 N71-10254
- Sensitivity algorithm for random error in Kalman filter and predictors [NASA-CR-111108] 01 p0036 N71-10384
- Quantitative analysis of adaptive control systems using random search algorithm convergence in continuous time [RE-3963] 01 p0076 N71-10821
- Research on programming algorithmic languages [AD-710643] 01 p0029 N71-10872
- PORTAN 4 computer program for calculating satellite photograph coordinates [PB-193514] 01 p0051 N71-10888
- Algorithm to sequence search tree file structure for nonuniform access frequencies [TR-6] 02 p0185 N71-11303
- Design and characteristics of matrix oriented cellular computer [AD-711305] 02 p0187 N71-11311
- Fast algorithm for minimization of Boolean functions to two level and/or form [NASA-CR-102918] 02 p0187 N71-11314
- Mutual exclusion or interlock problem applied to computer operations [NASA-CR-111401] 02 p0188 N71-11319
- Design of parallel processor for Bose Chandhuri Hocquenghem/BCH decoding [AD-711306] 02 p0190 N71-11332
- Language programming for linguistic algorithms - ALTEXT 2 [AD-711387] 02 p0190 N71-11335
- Algorithm for fault isolation of multistate electronic networks 02 p0196 N71-11377
- Performance of discrete suboptimal Kalman filters and discrete optimal adaptive filters [NASA-CR-111414] 02 p0197 N71-11378
- Algorithm for synthesis of distributed systems to solve circuit design problems [NASA-CR-111809] 02 p0197 N71-11379
- Algorithm for roving vehicle motion control 02 p0199 N71-11758
- Evaluating use of digital computers in aided navigation systems to make optimum estimates of system

- state or to perform coordinate transformation functions in strapdown systems 03 p0409 N71-12808
- Calculation of bending moments of transverse continuous rectangular plates with matrix algorithms 03 p0460 N71-12779
- Test matrices for numerical algorithms in linear algebra problems [AD-712679] 03 p0398 N71-12761
- Algorithm providing maximum likelihood estimates for linear dynamic systems with unknown parameters [AD-712894] 03 p0400 N71-12766
- Parallel tangents and steepest descent algorithm with computer implementation for application to partially linear models [AD-712401] 03 p0400 N71-12767
- Analysis of bounded limit signal transmission by means of optimum signal [NASA-CR-115816] 04 p0490 N71-13490
- Survey of resource allocation disciplines in multiprocessor systems with application of algorithms 04 p0503 N71-13480
- Heuristic optimization algorithm for arranging N page open string 04 p0503 N71-13480
- Deriving algorithms for computations involving sparse matrices [NASA-CR-115777] 04 p0536 N71-13729
- Techniques for manipulation of long Poisson series also used for SPAS3 04 p0538 N71-14009
- Equivalent algorithms for optimal planning and scheduling of project networks [DISS-4355] 05 p0713 N71-14759
- Matrix method and stiffly stable algorithms in numerical integration for computer aided network design programming [NASA-CR-111837] 05 p0651 N71-14808
- Deriving algorithm for floating point arithmetic using single length arithmetic registers for most accurate approximation 05 p0713 N71-15250
- Kalman filtering algorithm for hybrid navigation in army aircraft [AD-713553] 05 p0721 N71-15250
- Thinning algorithms on rectangular, hexagonal, and triangular arrays [NASA-CR-116131] 06 p0883 N71-15902
- Syntax algorithm for on-line pattern recognition [AD-714017] 06 p0819 N71-16080
- Algorithm for converting polar stereographic projection to stereographic horizon projection [NASA-TN-D-7095] 06 p0883 N71-16082
- Applying queuing theory, network synthesis, and signal encoding to information systems [JPRS-51962] 07 p1001 N71-16071
- Deriving algorithm for solving maximum stationary flow in network having exponential delay 07 p1001 N71-16075
- Deriving algorithms for finding limiting characteristics and carrying capacities of dynamic systems with feedback and internal noise 07 p0996 N71-16077
- Digital computer program for calculation of heat temperature and mass flux in cooling channels of fast elements [ANL-TRANS-858] 07 p1059 N71-17080
- Algorithm for linear, nonlinear and quadratic programming [NPL-MA-57] 07 p0996 N71-17072
- Control algorithm for optimization of nonlinear stochastic processes with discounted performance criteria [NASA-CR-116417] 07 p1051 N71-16085
- Algorithm for calculating electron and positron tracks in propane bubble chamber, accounting for radiative losses [JINR-P1-5357] 07 p1080 N71-18123
- Mathematical models for optimal queue with Poisson arrivals and time distribution [AD-714802] 08 p1224 N71-18126
- Algorithm for digital resolution of range for V-STOL aircraft [NASA-TN-D-62332] 08 p1144 N71-18206
- Investigating symbolic mathematical computation using PL1 FORMAC batch system and Scope FORMAC interactive system [FSC-69-0512] 08 p1227 N71-18105
- Investigating interaction between FORMAC data organization and algorithm design 08 p1227 N71-18107
- Investigating problem of formulating symbolic integration of elementary functions 08 p1228 N71-18104
- Presenting proposals for implementation of algorithm for computing and manipulating asymptotic expansions 08 p1228 N71-18105
- Deriving computing time bounds for polynomial reduced sequence algorithm for computing common divisor of two polynomials with integer coefficients 08 p1228 N71-18106

SUBJECT INDEX

ALGORITHMS

Methods for finding numerical models suitable for use in computers for computer-aided analysis and design of bipolar junction devices
[AD-716339] 09 p1358 N71-19561

Algorithm for accessing symbol tables in compiler
[NASA-CR-117123] 09 p1352 N71-19597

Definition and implementation of simple L/R/I contact free grammars
[NASA-CR-117123] 09 p1353 N71-19600

Algorithmic techniques of conjugate gradient method applied to spacecraft guidance and control
[AD-716445] 09 p1415 N71-19902

Mathematical programming techniques applied to aerospace structural design - algorithmic tools, applications, and literature review
[AD-AG-149-71] 09 p1478 N71-20128

Feasible direction algorithms for solving general nonlinear programming problems
09 p1410 N71-20135

Computer programs for optimum, least weight design of complex elastic aerospace structures
09 p1356 N71-20136

Discriminator algorithm for computer pattern recognition and texture recognition
[NASA-TN-D-5933] 09 p1390 N71-20264

Development of algorithms for parameter optimization problems including inequality constraints, noisy measurements, and locations of global optima
[REF-70-E-16] 09 p1412 N71-20537

Algorithm for numerical integration of data between points using interpolation
[NPL-MA-93] 10 p1591 N71-20785

Description of algorithm for performing automated direct form integration of formulas in elliptic motion
[NASA-CR-114963] 10 p1594 N71-21572

Algorithms to find suboptimal addition chains as optimal procedure for obtaining power of associative operator
[TID-25430] 10 p1594 N71-21626

Perfect shuffle interconnection pattern and FFT for parallel processing algorithms
[ITAN-38-78-158-APP-5] 10 p1595 N71-21681

Complex optimization techniques applied to various sensitivity coefficient determination for distributed-impedance networks
[NASA-CR-117377] 11 p1767 N71-22177

Algorithm using ALGOL 68 type language for computerized determination of three dimensional path for numerical control of machine tools
[AD-717777] 11 p1768 N71-22258

Algorithms for thin-walled axisymmetrically loaded tubes of revolution elastic stability problems including cylindrical, conical, spherical, and toroidal shells
11 p1837 N71-22495

Information preserving data compression systems with coding algorithm developed for noiseless channel
[NASA-CR-117846] 11 p1716 N71-22549

Algorithm elements for closed cycle control of complex scientific experiments
11 p1718 N71-22727

Machine algorithm statistics for processing experimental data
11 p1718 N71-22730

Data processing algorithm for real time digital modeling of dynamic systems
11 p1718 N71-22731

Verbi algorithm for decoding convolutional codes for space channel application
11 p1720 N71-22775

Block model for adaptive flight control system
[NASA-CR-117807] 11 p1693 N71-23060

Evaluation of quality of signs used in construction of pattern recognition algorithms
[AD-717887] 12 p1865 N71-23294

Edge T-matrix theory used to derive algorithms for solving basic problems of network theory
[AD-718325] 12 p1892 N71-23334

Optimal scheduling algorithm applied to problems of job sequencing type with network flow analogy
[AD-71943] 12 p1949 N71-23576

Analysis of computer requirements for linear filter structures
[AD-718416] 12 p1949 N71-23577

Optimum design of two dimensional nonreversible digital filters
[UCRL-72463] 12 p1949 N71-23711

Feasibility, design, and algorithms of integrated circuit content addressable memories
12 p1891 N71-24025

Performance sensitivity minimization for optimal control problem variations by steepest descent algorithm
12 p1951 N71-24186

Methodological and algorithmic considerations in synthesis of linear multidimensional automatic control systems
12 p1896 N71-24221

Construction of N-norm amplitude according to negative intercept and abnormal parity trajectories
[LPTRE-71/11] 12 p1979 N71-24344

Algorithmic inaccessibility of finding asymptotic behavior of Shannon function with bounded deter-

minate operators based on finite system of finite automatic devices
[JPS-5-52737] 13 p2103 N71-25201

Algorithm of self organization, artificial intelligence, and tree search applied to various practical problems
[AD-719930] 14 p2207 N71-25652

Statistical algorithms and computer programs for remote sensor multispectral data analysis
[NASA-CR-103182] 14 p2230 N71-25921

Algorithm for solving Popov stability criterion applied to sampled data systems
[NASA-TM-X-64600] 14 p2282 N71-26042

Digital computer algorithm for determining gain bandwidth properties of distributed parameter loads
14 p2230 N71-26547

Moment algorithm for suboptimal adaptive nonlinear filtering and signal analysis
14 p2283 N71-26617

Optimal quadratic Liapunov function generating algorithm for estimating domain of equilibrium attraction of nonlinear star tracker attitude control systems for OAO stability
[NASA-CR-1729] 15 p2433 N71-26816

Decoding algorithm for maximum likelihood detection of uniform convolutional codes transmitted with white random noise
15 p2301 N71-27319

Algorithmic method for optimal flight vehicle design using digital computers
[AD-720915] 15 p2519 N71-27330

Algorithms for calculation of eigenvalues and two center problem of quantum mechanics
[JINR-P4-5040] 15 p2468 N71-27344

Variants of secant method for solving nonlinear system of equations comprising algebraic and related convergence techniques
[NASA-TM-X-65453] 15 p2436 N71-27785

Dual control algorithms for self adaptive filters and optimal control law for linear systems with unknown input parameters
[AD-721461] 16 p2573 N71-28052

Algorithmic procedure for optimization of antenna arrays
[RE-409] 16 p2559 N71-28055

Decoding algorithm for data reduction and transmission through noisy space channels using sequential and hybrid computers
[NASA-CR-114277] 16 p2564 N71-28088

Algorithm proposed for approximate integration of specific boundary value problem of nonlinear system of differential equations with delayed argument and satisfying Lipschitz condition
[NASA-TT-F-13694] 16 p2622 N71-28321

Existence and extendability of continuous observer for branches and application of nonlinear programming algorithms to nonlinear heat generation and rotating string problems
[NASA-CR-119020] 16 p2623 N71-28630

Formulas and algorithms for computing portions of numbers and derivatives of composite function
[UCRL-20215] 16 p2635 N71-28760

Self-similarity and algorithms for use with digital computers
17 p2723 N71-29670

Algorithm for simultaneous minimization of multiple Boolean functions with application to telemetry systems
[NASA-CR-119630] 17 p2723 N71-30096

Machine algorithm for establishing derivability in classical calculus using inverse method
[NLL-RTS-5855] 17 p2724 N71-30163

Algorithms for labeling, counting, and composing connected objects in binary three dimensional array
[NASA-CR-119187] 17 p2774 N71-30217

Formulation of Volterra equations describing Raleigh problem, and algorithm based on Kruok equation
[TR-34] 17 p2775 N71-30372

Formulation of Volterra equations describing nonlinear piston problem, and algorithm based on Kruok equation
[TR-37] 17 p2775 N71-30373

Unconstrained optimization algorithm for nonlinear functions using quasi-Newton method
[NPL-MA-97] 18 p2942 N71-30519

Algorithm for automatic failure analysis of gates in logic circuitry
[LAAS-O-3-E-1] 18 p2892 N71-30520

Algorithms for solving set of linear inequalities expressed in binary variables
[LAAS-STI-770] 18 p2942 N71-30534

Quadrature algorithm for spline interpolation
[NASA-TM-X-65616] 18 p2943 N71-30577

Tracking algorithm for electrostatically controlled radar using phased arrays based on statistical methods
[BMVO-PB-WT-70-5] 18 p2899 N71-30616

Optimal digital controller based on linear representation of acoustical test facility, for determining effects of supersonic rocket engine noise on vehicle surface
[NASA-CR-115073] 18 p2902 N71-30741

Algorithmic pattern generation with applications to isomorphic and biological structures, and other branches of mathematics and computer science
[PB-197604] 18 p2947 N71-31314

Data processing algorithms for investigating functional organization and operational principles of visual systems
[JPRS-33644] 18 p2895 N71-31329

Boolean matrix synthesis of digital networks for construction of algorithms
18 p2900 N71-31446

Algorithms for finding M-center of graph
[AD-722589] 18 p2948 N71-31489

Optimization techniques for synthesis of cellular logic networks
19 p3070 N71-32272

Algorithm for automatic control of gauge and shape in roll forming
[PB-193648] 19 p3106 N71-32419

Derivation and evaluation of algorithms for error analysis, sensitivity of filtering, and smoothing solutions to nonlinear estimation problems
19 p3071 N71-32441

Numerical method for restoration of planar image algorithm for use on digital computers
[UCRL-75000] 19 p3062 N71-32469

Algorithm for identification of system parameters from input-output data with application to air vehicles
[NASA-TN-D-4468] 19 p3124 N71-32473

FORTRAN-based version, FORAAL, of graph algorithmic language GRAAL
[NASA-CR-119770] 19 p3062 N71-32494

Theory of logic-dynamic control systems and multi-layer theory of statistical decisions
[JPRS-53706] 20 p3280 N71-32822

Algorithm structure for multi-layer theory of statistical decisions
20 p3289 N71-32824

Algorithm for local minimum of indefinite quadratic computer programming
[NPL-DNAC-1] 20 p3230 N71-32840

Presentation of algorithm for filtration of mixing parameters for navigation
20 p3290 N71-32948

Numerical integration of Fourier integrals using spline algorithm
[FOA-2-C-3446] 20 p3290 N71-32949

Computer language for implementation of graphic theoretical algorithms
[NASA-CR-119723] 20 p3299 N71-33564

Computational algorithm to mechanize theory of optimal time-invariant output-feedback controllers - Vol. 3
[NASA-CR-119913] 20 p3294 N71-33962

Composite surface algorithm for optimum search procedure in automated design
20 p3361 N71-33971

Three algorithms for Ford sequence generation of length 2 to the nth power, a large for digital communication equipment
21 p3391 N71-34131

Blizard decoding algorithm for binary linear error correcting codes
21 p3392 N71-34134

Algorithm for cost and potential benefit assessment of TV networking on mode of disseminating information to biomedical communities
[RM-6204-NLM] 21 p3393 N71-34166

Area and closed curves in digital pictures with thinning algorithms
[NASA-CR-121715] 21 p3397 N71-34175

Branch-and-bound algorithms for cube data storage and insertion reduction
[A-4059-1] 21 p3399 N71-34193

Iterative digital computer algorithm for solving optimization problems for linear electrostatic systems
[NASA-CR-119796] 21 p3406 N71-34521

Modified equalization algorithm for solving nonlinear equations
[NASA-CR-121654] 21 p3406 N71-34522

Digital computer simulation of two strapdown system attitude algorithms by response in angular rates
[NASA-CR-121731] 21 p3447 N71-34527

Design of conventional algorithms for optimal control by Hilbert space methods, and involving cost function
[NASA-TN-D-6308] 21 p3449 N71-34531

Algorithms for determining usings of fields for long range weather forecasting
[NLL-M-20086-3028-AP] 21 p3453 N71-34579

Data compression algorithms for processing electrostatic and vectorized digital data
[NASA-CR-115177] 22 p3355 N71-33523

Digital computer fault detection procedure for combinational logic circuits with algorithm for efficient generation of minimum fault test schedules
[AD-726383] 22 p3363 N71-33575

Pattern search algorithm for feedback control system parameter optimization
[AD-724445] 22 p3363 N71-33577

Complete geometrical algorithm for computing internal three-dimensional supersonic flows with second-order accuracy
22 p3370 N71-33438

- Convergence of centers algorithm for solving non-linear programming problems
[NASA-CR-121911] 22 p3605 N71-35672
- Algorithm for p-q solution of degenerate linear system
[NASA-TM-X-58069] 22 p3605 N71-35675
- Quasi-Newtonian minimization methods extended to infinite dimensional Hilbert space with applications to optimal control problems
[NASA-CR-111975] 22 p3605 N71-35676
- Geometrical interpretations of Sandwich theorem related to geography and algorithm and program for achieving solutions
[AD-726403] 22 p3608 N71-35696
- Development of algorithm for calculating satellite positions from photographic observations
22 p3608 N71-36244
- Computer learning algorithm to improve parameter search efficiency in system modeling with man-machine interaction
23 p3718 N71-36505
- Robbins-Monro stochastic approximation algorithm for Doppler frequency estimation of radar echoes
23 p3727 N71-36570
- Algorithms for operator identification in ALGOL-68
23 p3729 N71-36581
- Algorithm and subroutine for solving Kepler equation for elliptical orbits
[NASA-CR-122933] 23 p3848 N71-37426
- Algorithm for determining artificial satellite position from magnetometric measurements
23 p3859 N71-37512
- Algorithm for solving general quadratic programming problem with linear constraints
[NASA-CR-123214] 24 p3892 N71-37739
- Synthesis algorithm, Boolean algebra, and mappings for interval generalization of switching theory
[COO-2118-5] 24 p3894 N71-37754
- Synthesizing logic circuits and boolean function circuits with not more than three variables
[AD-727972] 24 p3896 N71-37769
- Conversion of computational algorithms for decreasing length of word format of control computers for aircraft
[AD-727917] 24 p3896 N71-37772
- ALIGNMENT**
- Experimental techniques for prealigning and clamping inertial measurement sensors without major system recalibration
[NASA-CR-111365] 82 p0262 N71-11427
- Galactic rotation model for axial alignment of interstellar disturbances
06 p0947 N71-16783
- In-situ measurement of objective lens data for alignment of high resolution electron microscope
[NASA-TM-X-62018] 09 p1308 N71-17995
- ESRO 1 satellite experiment on magnetic field aligned electric field near or in ionosphere
10 p1550 N71-21154
- Electrical and electromechanical trigonometric computation assembly and space vehicle guidance system for aligning perpendicular axes of two sets of three-axis coordinate references
[NASA-CASE-XMF-00684] 10 p1600 N71-21688
- Description of device for aligning stacked sheets of paper for repetitive cutting
[NASA-CASE-XMS-04178] 11 p1771 N71-22796
- Design, operation, and alignment of single channel broadband modulator, demodulator, and phase locked loops for double sideband signals
[NASA-CR-103116] 13 p2057 N71-24883
- Spacecraft solar cell system design including electric relays, photodiodes, and switching circuits to maintain alignment during switching
[NASA-CASE-GSC-10669-1] 16 p2537 N71-28413
- Laser beam projector for continuous, precise alignment between target, laser generator, and astronomical telescope during tracking
[NASA-CASE-NFO-11087] 16 p2640 N71-29125
- Effectiveness of flame straightening mechanisms on high strength steel structures
[AD-721537] 18 p3023 N71-31595
- Centering drift tube quadrupole magnets and measuring their harmonic field components
[SNC-A-71-1] 21 p3465 N71-34668
- Optical alignment technique for missile warhead section assembly stand
[AD-726925] 22 p3565 N71-35394
- Alignment of optical system in astronomical telescopes
24 p3922 N71-37972
- ALIPHATIC COMPOUNDS**
- NT ACETALDEHYDE
- NT ACETALS
- NT ACETIC ACID
- NT ACETONE
- NT ACETYL COMPOUNDS
- NT ACETYLENE
- NT ACRYLATES
- NT ACRYLONITRILES
- NT ADENOSINE TRIPHOSPHATE (ATP)
- NT ALKANES
- NT ALKENES
- NT ALKYL COMPOUNDS
- NT ALKYNES
- NT ALLYL COMPOUNDS
- NT ANTHRACENE
- NT BUTADIENE
- NT BUTENES
- NT CARBAMATES [TRADENAME]
- NT CARBON TETRACHLORIDE
- NT CELLULOSE
- NT CHLOROETHYLENE
- NT CHLOROPROMAZINE
- NT CYCLIC HYDROCARBONS
- NT DIALLYL COMPOUNDS
- NT DICHLORODIPHENYL
- NT TRICHLOROETHANE
- NT DIHYDRAZINE
- NT DIMETHYLHYDRAZINES
- NT ETHANE
- NT ETHYL ALCOHOL
- NT ETHYLENE
- NT ETHYLENEDIAMINETETRAACETIC ACIDS
- NT GLUCOSE
- NT GLUTAMIC ACID
- NT GLYCEROLS
- NT GLYCOLS
- NT HYDRAZINES
- NT KETENES
- NT KETONES
- NT LACTATES
- NT LACTIC ACID
- NT LACTOSE
- NT METHANE
- NT METHYL ALCOHOLS
- NT METHYL COMPOUNDS
- NT METHYLHYDRAZINE
- NT MONOSACCHARIDES
- NT NITRATE ESTERS
- NT NITROAMINES
- NT NITROPROPANE
- NT OLEIC ACID
- NT OXALIC ACID
- NT PARAFFINS
- NT PENTANES
- NT PHOSGENE
- NT PROPANE
- NT STEARATES
- NT SUGARS
- NT THIOLS
- NT TRIMETHYL COMPOUNDS
- NT URETHANES
- NT VINYLIDENE
- Selecting and processing solid carriers for organophosphorus compounds using gas chromatography
[JPRS-53065] 13 p2040 N71-25137
- Thermal and solubility properties of lower ordered aliphatic imide-quinoxaline copolymers to obtain strong films and fibers
[AD-720687] 14 p2279 N71-26220
- ALKALI HALIDES**
- NT CESIUM FLUORIDES
- NT CESIUM HALIDES
- NT CESIUM IODIDES
- NT POTASSIUM IODIDES
- NT SODIUM CHLORIDES
- NT SODIUM FLUORIDES
- NT SODIUM IODIDES
- Optical absorption by excitons in alkali halides, personnel accident dosimeters, electromagnetic wave propagation in atmosphere, metallurgy, and related research
06 p0908 N71-15747
- Transient optical absorption by self-trapped excitons in alkali halide crystals
06 p0908 N71-15748
- Electric dipole interactions among substitutional polar molecules and atoms in alkali halides
[NYO-2391-117] 07 p1093 N71-17458
- Reaction kinetics of hydrogen and bromine interactions and surface generation for alkali halide dimers
[JHUX-3780-33] 07 p0990 N71-17891
- Low frequency dielectric constants of LiF, NaF, NaCl, NaBr, KCl, and KBr by substitution method
[COO-623-153] 08 p1280 N71-19032
- Crossed molecular beam for studying alkali atom alkali halide exchange reactions
08 p1265 N71-19201
- Calculation of conduction electronic energy bands and L bands in alkali halide crystals
08 p1283 N71-19309
- Ultrasonic measurements on paramagnetic impurities in alkali halides compared with predictions of tunneling model
[NYO-2471-47] 11 p1784 N71-22581
- Recombination processes observed in alkali halides from radioactive decay of optical anisotropy at fixed temperature
[NYO-2842-12] 15 p2463 N71-27194
- Exciton mobility in pure and doped alkali halides studied by detecting diffusion of photo-created excitons
15 p2481 N71-27693
- Radiation absorption and crystal defects in alkali and alkaline earth halides
[ONERA-NT-02-23] 17 p2792 N71-29369
- Effect of electric field and temperature on radiative lifetime of excited F center in KCl, KBr, and NaF
[NYO-3463-23] 18 p2990 N71-31568

- Rheological properties of alkali borate glass and influence of water on rheological properties of boric oxide glass and two sodium borate glasses
21 p3443 N71-34440
- Angular distribution and velocity analysis of alkali chloride reactions
21 p3490 N71-34900
- Microwave resonance studies in alkali halides, at transced generated by eddy currents in potassium electron-electron scattering in tungsten, and related studies
[NYO-2150-66] 21 p3497 N71-34970
- Electric field induced alignment and reorientation kinetics of paraelectric impurities in alkali halide crystals, using optical and calorimetric methods
22 p3459 N71-34590
- ALKALI METAL COMPOUNDS**
- Photo degradation of electronic transport properties in spacecraft alkaline paint interface with aluminum
[NASA-TM-X-64942] 69 p1407 N71-36000
- ALKALI METALS**
- NT BARIUM ISOTOPES
- NT CESIUM
- NT CESIUM VAPOR
- NT CESIUM 133
- NT CESIUM 134
- NT CESIUM 137
- NT CESIUM 144
- NT LIQUID POTASSIUM
- NT LIQUID SODIUM
- NT LITHIUM
- NT LITHIUM ISOTOPES
- NT POTASSIUM
- NT POTASSIUM ISOTOPES
- NT RUBIDIUM
- NT RUBIDIUM ISOTOPES
- NT RUBIDIUM 86
- NT SODIUM
- NT SODIUM ISOTOPES
- NT SODIUM VAPOR
- Electric deflection molecular beam system with mass spectrometric detector
[AD-710656] 01 p0018 N71-14000
- Low energy interactions of alkali metal atoms and molecules
[AD-711110] 01 p0097 N71-14071
- Corresponding states and glass transition for alkali metal nitrates
05 p0710 N71-12026
- Ultrasonic absorption and velocity measurements in liquid alkali metals
[AD-714866] 07 p1045 N71-17902
- Boiling of liquid alkali metals in tubes
[BNL-TR-365] 08 p1303 N71-18044
- Pseudopotential formalism used to calculate vacancy formation energy and volume for alkali metals
[NYO-4185-2] 11 p1779 N71-22008
- Hydride physico-chemical and chemical properties, reactions, purification, isolation, and analysis techniques
[AD-718179] 12 p1870 N71-23029
- Analytical test apparatus and method for determining oxygen content in alkali liquid metal
[NASA-CASE-XLE-01997] 12 p1871 N71-23027
- Composition and production method of alkali metal alloys of interest with ultraviolet reflection properties
[NASA-CASE-XGS-04799] 12 p1947 N71-24018
- Intrinsic potentials for alkali metals from combinations in electron liquids
[ANL-7761] 13 p2096 N71-25322
- Design and characteristics of heat activated elastic cell with anode made from one or more alkali metals and cathode made from oxidizing material
[NASA-CASE-LEW-11358] 14 p2200 N71-26880
- Analysis of insulating properties of alkali metal colloids and problem of charge generation by cathode ionization
[AD-721197] 15 p2368 N71-26880
- Gibbs free energy, enthalpy, and entropy of alkali metal alloys
[NPL-DCS-10] 15 p2524 N71-26880
- Evaluation of refractory metal alloy motoring and isolation valves for alkali metal service at 1900 P
[NASA-CR-18161] 16 p2687 N71-26880
- Thermophysical properties of alkali metals in liquid and vapor phases based on analysis of experimental and theoretical data from literature
[AD-721947] 16 p2556 N71-26880
- Chemical reactions between alkali-lead oxide glasses and acid solution at low temperature
18 p2940 N71-31568
- Hot atom beam in halogen and hydrogen compounds, cathode sputtering of non-metals, and hot atom reactions of alkali metals
[AD-722450] 19 p3030 N71-32008
- Nuclear magnetic resonance study of electron-electron interactions in palladium, platinum, and alloys, and alkali metals
19 p3160 N71-32008
- Computer calculation of vacancy and interstitial migration using pair-interaction potential in alkali metals
[CIRA-R-3840] 22 p3634 N71-36000
- Heating surface material, surface condition and geometry, contact duration, and coolant impurity and

SUBJECT INDEX

Heat gas coolant effects on heat transfer in boiling alkali metals
[JLL-RLSLEY-TRANS-2165-19091.9F] 34 p0633 N71-38773

ALKALES

NT LITHIUM HYDROXIDES
NT SODIUM HYDROXIDES
Thermodynamic constants of alkali metalates and metalates
[NASA-TT-F-13421] 03 p0440 N71-12670
Basic properties of alkali syntheses from October
[NASA-TT-F-13549] 09 p1386 N71-20300
Finite difference method for calculating cosmic boom
signature signatures in vicinity of caustics
[AD-718835] 12 p1949 N71-23738
Gravity wave behavior near straight caustic in deep
wave tank and in shallow water
[AD-721437] 16 p2639 N71-28746

ALKALINE BATTERIES

Method for determining state of charge of alkali bat-
teries by using tritium as tracer
[NASA-CASE-XNP-01464] 01 p0077 N71-10728
Sealed nickel-cadmium battery assembly BB-635
[AD-714343] 06 p0797 N71-16349
Alkaline-type coulometer cell for primary charge
control in secondary battery recharge circuits
[NASA-CASE-XGS-05434] 09 p1327 N71-30491

ALKALINE EARTH COMPOUNDS

Using electron paramagnetic resonance spectroscopy
to investigate Ti-2 plus and Mn-2 plus V minus/
super-hyperfine interaction in alkaline earth fluorides
at microwave frequencies 09 p1431 N71-29926

ALKALINE EARTH METALS

Thermogravimetric analysis of hydrofluoride sta-
bility of alkaline earth metals
[AD-720744] 14 p2214 N71-26082
Radiation absorption and crystal defects in alkali
and alkaline earth halides
[ONERA-NT-62-23] 17 p2792 N71-29360
Spectral line drift measurements on alkaline earth
metals in hollow cathode discharge by interferometer
[AD-726160] 19 p3166 N71-32782

ALKALINE EARTH OXIDES

NT BARIUM OXIDES
NT BERYLLIUM OXIDES
NT CALCIUM OXIDES
NT MAGNESIUM OXIDES

ALKALOIDS

NT RESERPINE
Molecular crystals structure analysis on quinelini-
um sesquibenzomalonate/VI and beta picoline-N-
oxide fumaric acid adduct
[BT-439] 15 p2509 N71-27908

ALKANES

NT ETHANE
NT METHANE
NT NITROPROPANE
NT PARAFFINS
NT PENTANES
NT PROPANE

Electron impact changes in methoxy alkane systems
using mass spectroscopy 03 p0330 N71-12354

Sensitivity properties of diastereoisomers

[AD-715474] 05 p0783 N71-15344
Radioactive hydrocarbons in tobacco tissue cultures
[NASA-CR-116887] 08 p1152 N71-19018

Loss of heavy alkalines in Apollo 11 and 12 lunar soil
samples
[NASA-CR-114919] 09 p1466 N71-30174

Absorption spectra of Pa(III), Pu(IV), Pu(VI),
U(VI), and U(VII) in nitric acid and tri-n-butyl
phosphate-alkane solutions and their use in auto-
matic process control
[EPF-1506] 18 p2884 N71-30601

Absorption spectra of gaseous n-alkanes and
substituted derivatives of solid methane and
ethane films in vacuum ultraviolet
[NBS-SR-71/1] 19 p3157 N71-32408

ALKENES

NT BUTADIENE
NT BUTENES
NT ETHYLENE
NT VINYLIDENE

Effect of structure on rate and mechanism of addi-
tion of dichloromethane to methyl acrylate
[AD-718911] 02 p0172 N71-11210

Measurement of addition of singlet oxygen to olefins
03 p0440 N71-15489

Photolysis of nitrogen oxide, nitrogen oxide/
nitrogen mixtures, and nitrogen olefin mixtures
[NASA-CR-114442] 07 p0985 N71-17091

Ultraviolet and photoionization studies on
olefins 09 p1342 N71-19351

ALKYL RESINS

Alkyl resins lacquer peeling on glass and other sub-
strates 16 p2616 N71-28324

ALKYL COMPOUNDS

NT TRIMETHYL COMPOUNDS
Acids and polymerization of beta-alkylstyrenes
[AD-718077] 02 p0173 N71-11218

Hydrogen tritium and hydrogen deuterium exchange
reaction in alkyl aromatics during catalytic hydrogena-
tion [SC-T-70-0831] 02 p0270 N71-11399

Investigating ester and alkyl compounds as lubricat-
ing oils for use with liquid oxidizers
[NASA-CR-103907] 02 p0246 N71-11419

Differential thermal analysis and autoxidant activi-
ty of nickel, zinc, lead, copper, and cadmium dialkyl-
dicarbamates [PTD-HT-23-353-70] 10 p1513 N71-21230

Mass spectra of alkyl carbanates derived from pri-
mary, secondary, and tertiary alcohols by use of deu-
terium labeling and high resolution mass spectroscopy
[NASA-CR-123194] 24 p3804 N71-37668

ALKYNES

NT ACETYLENE
Polymerization of organic superconductors diphen-
ylacetylene, diphenylacetylene, and phenyl-
acetylene [AD-721916] 16 p2557 N71-28357

ALGAE PHOTOGRAPHY

All sky photography of U-shaped polar auroras in
ionosphere 17 p2746 N71-30679

ALL-WEATHER AIR NAVIGATION

All-weather automatic landing systems and problem
areas 03 p0404 N71-12427

International aviation and all-weather automatic
landing systems 03 p0405 N71-12428

Guidance developments for all-weather landing
03 p0405 N71-12433

Flight tests of all-weather landing systems
03 p0406 N71-12437

All-weather automatic landing systems for use on
aircraft carriers and training ashore 03 p0406 N71-12438

Aided initial flight test experiments for all weather
V/STOL operations [NASA-TM-X-64490] 03 p0406 N71-12439

Autopilot for C-141 all-weather landing system
[AD-720214] 03 p0406 N71-12442

All weather landing systems of Thomson-CSF
03 p0407 N71-12446

Position accuracy estimates and man-machine rela-
tionships required in low level, all-weather navigation
system [AD-713426] 05 p0720 N71-15221

Weather outline generators for producing contours
around radar weather clutter for all weather air naviga-
tion [FAA-NA-70-62] 07 p1054 N71-17327

Tuned radio frequency receiver and phase estimator
of all weather, low level navigation system
[AD-720214] 14 p2290 N71-26401

ALLOCATIONS

NT RESOURCE ALLOCATION
Federal fund allocations for research and develop-
ment and other scientific activities for FY 1969, 1970,
and 1971 [NSF-70-38] 05 p0788 N71-15631

Computer solution of allocation problem having
3600 variables, and Dantzig algorithm for solving con-
vex function minimized over closed convex set
[AD-722584] 18 p3895 N71-31344

ALLOYS

NT ALUMINUM ALLOYS
NT AUSTENITIC STAINLESS STEELS
NT BEARING ALLOYS

NT BERYLLIUM ALLOYS
NT BINARY ALLOYS
NT COPPER ALLOYS
NT BORON ALLOYS

NT BRASSES
NT BRONZES
NT CADMIUM ALLOYS
NT CARBON STEELS

NT CHROMIUM ALLOYS
NT CHROMIUM STEELS
NT COBALT ALLOYS

NT COBALT ALLOYS
NT COPPER ALLOYS
NT ERBIUM ALLOYS

NT EUTECTIC ALLOYS
NT GALLIUM ALLOYS
NT GERMANIUM ALLOYS

NT GOLD ALLOYS
NT HAFNIUM ALLOYS
NT HASTELLOY (TRADEMARK)

NT HEAT RESISTANT ALLOYS
NT HIGH STRENGTH ALLOYS
NT HIGH STRENGTH STEELS

NT INCONEL (TRADEMARK)
NT INDIUM ALLOYS
NT IRON ALLOYS
NT KOVAR (TRADEMARK)

NT LEAD ALLOYS
NT LIGHT ALLOYS
NT LITHIUM ALLOYS
NT MAGNESIUM ALLOYS

NT MANGANESE ALLOYS
NT MANGANESE (TRADEMARK)
NT MARAGING STEELS
NT MARTENSITIC STAINLESS STEELS
NT MERCURY ALLOYS

ALLOYS

NT MERCURY AMALGAMS
NT MOLYBDENUM ALLOYS
NT MULBERRY (ALLOY)

NT NICKEL (TRADEMARK)
NT NICKEL ALLOYS
NT NICKEL STEELS

NT NIMONIC ALLOYS
NT NIOBIUM ALLOYS
NT PALLADIUM ALLOYS

NT PERMALLOY (TRADEMARK)
NT PLATINUM ALLOYS
NT PLUTONIUM ALLOYS

NT POTASSIUM ALLOYS
NT QUATERNARY ALLOYS
NT RARE EARTH ALLOYS

NT REFRACTORY METAL ALLOYS
NT RENEALLOY ALLOYS
NT RENEALLOY ALLOYS

NT RUTHERFORD ALLOYS
NT SILICON ALLOYS
NT SILVER ALLOYS

NT SODIUM ALLOYS
NT SOLDIERS
NT STAINLESS STEELS

NT STEELS
NT TANTALUM ALLOYS
NT TELLURIUM ALLOYS

NT TERNARY ALLOYS
NT THORIUM ALLOYS
NT TIN ALLOYS

NT TITANIUM ALLOYS
NT TUNGSTEN ALLOYS
NT URANIUM ALLOYS

NT VANADIUM ALLOYS
NT WASPALOY
NT YTTRIUM ALLOYS

NT ZINC ALLOYS
NT ZIRCALOY 2 (TRADEMARK)
NT ZIRCALOYS (TRADEMARK)

NT ZIRCONIUM ALLOYS
Kondo effect in dilute alloys
[AD-710297] 01 p0665 N71-10853

Low gravity manufacturing of metal alloys from in-
melt liquid phase melts in space laboratory 03 p0335 N71-11710

Screening tests on friction and wear of materials in
sodium [LMSC-70-10] 03 p0390 N71-12696

Vibratory cavitation for metal and superalloy
etching in dilute water [NASA-TM-X-52529] 03 p1392 N71-12961

Stress effects on chemical potentials of interstitial
constituents in alloys [AD-713046] 06 p0873 N71-16383

Transport properties and magnetic susceptibility of
magnetic alloys [AD-714014] 06 p0886 N71-16401

Thermotransport of oxygen and nitrogen in sodium
beta-irradiation, beta-irradiation, and beta-irradiation
[NPL-18496] 09 p1211 N71-18135

Determination of effects of heat on properties of
metals and alloys by method of elastic vibrations
[TT-70-57076] 08 p1218 N71-19099

Electron diffusion thermoelectric power in metals
and dilute alloys investigated over wide range of tem-
peratures [COO-423-152] 06 p1281 N71-19373

Behavior of various alloys, polymers and com-
posites 09 p1474 N71-19729

Bibliography on quenching alloys from liquid and
solid [CALT-422-17] 09 p1399 N71-19097

NBS data index of physical properties of metals and
alloys [NBS-SPEC-PUBL-324] 10 p1572 N71-28830

Columbium method of counterflow crystallization of al-
loys in molten state 10 p1573 N71-28808

Growth of chemically homogeneous single crystals
of alloys 10 p1633 N71-28809

Conference review on critical phenomena in alloys,
magnets, and superconductors [AD-716047] 10 p1634 N71-28807

Deformation behavior of alloys and stress-strain
relationships for ductile metals [RAE-LB-TRANS-1491] 10 p1582 N71-21519

Electrical resistivity versus temperature measure-
ments on metallic amorphous alloys [CALT-422-30] 10 p1583 N71-21582

Electron diffraction contrast effects from surface
boundaries and dislocations in ordered superlattice
alloy interfaces [ORO-3853-4] 11 p1779 N71-32481

Braking alloy adapted for braking corrosion re-
sistant steel to refractory metals, also for heating
refractory metals to other refractory metals [NASA-CASE-XNP-03063] 12 p1957 N71-23365

Effect of cooling rates on dislocation structure of
maraging 500 alloy, size and distribution of inclusions
related to tensile and fatigue properties [AD-718921] 12 p1957 N71-23389

Metal alloy bearing materials for space applications
[NASA-CASE-XLE-03633] 12 p1957 N71-23610

Microstructure of spinodal alloys determined by electron microscopes [UCRL-19629] 13 p2093 N71-24871

High thermal emittance black surface coatings and process for applying to metal and metal alloy surfaces used in radiative cooling of spacecraft [NASA-CASE-XLA-96199] 13 p2086 N71-24875

Thermal stability of eta carbides of alloys containing iron, nickel, cobalt, molybdenum, and tungsten [ORNL-TR-2425] 13 p2101 N71-25437

Tests to determine short-term creep of metals and alloys under conditions of aerodynamic heating with high velocity air flow [NASA-TT-F-13633] 14 p2272 N71-25822

Effect of hardening temperature on change in resistance to abrasive failure of alloys [AD-720379] 14 p2273 N71-25875

Mechanical properties and stress corrosion evaluation of MP 35N multiphase alloy at cryogenic temperatures [NASA-TM-X-64591] 14 p2274 N71-26043

Alloy compositions and metal working processes for roller bearing technology 15 p2413 N71-26835

Mechanical properties of polycrystalline nickel-copper and nickel-copper-cobalt alloys at temperatures from 78 to 523 K 15 p2422 N71-27222

Effects of prior plastic deformation of austenite on nucleation of martensite in Fe-Ni-C alloys 15 p2423 N71-27308

Sliding and wear behavior of steels and alloys in liquid sodium [KFK-1251] 16 p2610 N71-28449

Strength evaluation of brass alloys used for linear accelerator components [LA-4584] 16 p2613 N71-28781

Adjustable rigid mount for tribological mirror formed of alloy with small coefficient of thermal expansion supporting screws and spring-biased plates [NASA-CASE-XNP-08907] 16 p2640 N71-29123

Development of atomic absorption spectrophotometric techniques for analysis of alloying elements in stainless steels [AD-721896] 17 p2763 N71-29548

Effects of hydrostatic pressure in metals and alloys and applications to industrial processes [AD-722416] 17 p2763 N71-29548

Magnetic response of pure type I superconductors and their alloys with emphasis on metastable states [AD-727871] 17 p2787 N71-29654

Strain effects on plastic cross slip of hardening dislocations in two phase alloys 17 p2824 N71-29989

Corrosion of light metals at elevated temperatures and methods to prevent corrosion [CEA-CONF-1729] 18 p2932 N71-30428

Ion plating and radio frequency sputtering method for plating adherent alloy films on objects with complex geometries [NASA-CASE-LEW-10920-1] 18 p2935 N71-31130

Tensile, mechanical, and compression properties of metals, alloys, and steels derived from flow curves [RAE-LIB-TRANS-1523] 19 p3115 N71-32265

Description of laboratory metallurgy techniques involving mechanical properties tests, crystallography, creep, and fatigue [CEA-N-14272] 21 p3437 N71-34453

Wettability and formation of alloyed coatings on iron castings [NLL-M-21010-1828.4F] 21 p3441 N71-34485

Applying rigid band model to metal and alloy band structure determinations [NRC-TT-1475] 22 p3593 N71-35584

Analysis of rates of evaporation and erosion of silicon carbide ceramics in air at high temperatures 22 p3598 N71-35624

Fracture mechanics of plastic stress and strain fields near crack tip and computer simulation of fracture spreading in viscoelastic solid [AD-72645] 22 p3691 N71-36321

Effect of laser beam impingement on metal surface and determination of ratio of liquid and gaseous phases [NASA-TT-F-13906] 23 p3768 N71-36858

Electrical resistivity of amorphous alloys PdNi14B18 containing Cr or Fe as function of concentration and temperature 23 p3770 N71-36868

Analysis of diffusion behavior in ternary systems by method in which matrix of diffusion coefficients is replaced by relative penetration tendencies [AD-726458] 23 p3770 N71-36871

Radiation effects on structural alloys [NASA-CR-1873] 23 p3772 N71-36885

Effect of laser action and temperature gradients on thermionic emission of metal alloys [AD-727849] 24 p3932 N71-38037

Optimum excitation voltage for X ray microanalysis of pure elements, alloys, and mixtures [DIP-10887] 24 p3933 N71-38063

Developing metal alloys of ultrafine grain size with improved mechanical properties [AD-727746] 24 p3938 N71-38093

Tables of magnetic structures determined by neutron diffraction with emphasis on rhombohedral and hexagonal systems [NP-18845] 24 p3970 N71-38319

ALLYL COMPOUNDS

Synthesis of bis-/gamma-alkoxy-beta-chloropropyl sulfides and disulfides by reacting sulfur chlorides with allyl esters, and their use as oil additives [AD-720943] 15 p3431 N71-37400

Correlation of calculated and experimental product yields as functions of gas molecule residence time, power, gas pressure, and allyl alcohol in electrolysis of hydrazine from ammonia [JCR-C/N345] 23 p3719 N71-36510

ALMUCANTAR

U ELEVATION ANGLE

ALOUETTE SATELLITES

NT ALOUETTE 1 SATELLITE

NT ALOUETTE 2 SATELLITE

Space plasma experiments involving Alouette resonances and diagnostic techniques applied to electron density and temperature and local magnetic field strength measurement [NASA-CR-117844] 11 p1812 N71-22585

Time duration versus latitude, altitude, and electron plasma frequency to electron cyclotron frequency ratio for ionospheric plasma resonances observed by Alouette satellites [NASA-TM-X-65601] 17 p2750 N71-30273

ALOUETTE 1 SATELLITE

Alouette 1 ionospheric sounding synoptic data tables for Nov. 1968 01 p0046 N71-10277

Alouette 1 satellite electron density data and diurnal variation of Greenland auroras 04 p0615 N71-14298

ALOUETTE 2 SATELLITE

Tubulations of electron number density profiles from Alouette 2 ionograms 03 p0366 N71-12696

Comparison of Alouette-2 andOGO-5 observation of turbulence of magnetospheric electrostatic electron cyclotron harmonic waves [NASA-TM-X-65660] 19 p3093 N71-32442

ALPHA DECAY

Al₂O₃ decay, and chemical properties of isotopes of element 104 [UCRL-18633] 03 p0421 N71-12647

Alpha cluster structure of lithium 6 and lithium 7 with alpha/2 alpha reaction [NP-18232] 03 p0430 N71-12902

Decay of C-12 into 3 alpha [CEA-CONF-1496] 03 p0432 N71-12930

Calculating differential cross section for alpha, 2 alpha/alpha reaction using impulse approximation [LYCEN-7033] 07 p1082 N71-18146

Device for detecting alpha active nuclei of nuclear reactions induced by heavy ions [JINR-P1-5353] 13 p2129 N71-24575

Alpha and gamma decay structure of highly excited complex nuclei [JINR-E4-5155] 15 p2466 N71-27285

On-line, alpha and proton decay spectrometry for determination of second order interference effects, second class currents, and beta to neutrino correlations in weak interactions [ORO-3820-7] 15 p2497 N71-27998

Nuclear chemistry of fissions, alpha decay in osmium isotopes, alpha radioactivity in air samples, and nuclear levels, nucleic masses, and lifetimes of heavy elements [MNC-3783-9] 17 p2794 N71-29651

Alpha decay of eleven resonance states in reaction Sm-147/a.alpha./Nd-144 [JINR-P3-5553] 19 p3154 N71-32334

Test of supermultiplet model for light nuclei [LYCEN-7083] 22 p3640 N71-35945

Internal alpha decay in thorium for investigating radiation damage by conventional techniques [UCRL-51009] 23 p3769 N71-36865

ALPHA PARTICLES

Superconducting effects on alpha particle differential energy loss in tin, vanadium, and lead superconductors [NASA-TM-X-52896] 01 p0110 N71-10239

Spectrometric analyses of granites for transuranium and anomalous alpha emitters 01 p0094 N71-10307

Scattering of 42-MeV alpha particles from Sc-45 [NASA-TM-X-52912] 01 p0095 N71-10392

Microscopic analysis theoretical model for elastic scattering of deuterons and alpha particles [CTC-32] 01 p0100 N71-10744

Effects of helium on high temperature ductility of Sandvik 12X728V and Inco IN-744X [AI-AEC-12960] 02 p0244 N71-12111

Investigating differential range of reaction mechanism for alpha and He-3 reactions in Cu-65 and energy dependence of recoil properties of products from proton reactions in U-238 [COO-1505-42] 03 p0422 N71-12700

Catalog of alpha particle spectra for 35 nuclides obtained with silicon surface-barrier detectors [IN-1261] 03 p0426 N71-12846

Angular distributions for elastic and inelastic scattering of alpha particles by Mg-26 [RLO-1388-110] 03 p0428 N71-12846

Application of gridded ionization chamber for alpha spectroscopy [JINR-1182] 03 p0429 N71-12847

Alpha cluster structure of lithium 6 and lithium 7 with alpha/2 alpha reaction [NP-18232] 03 p0430 N71-12902

Elastic and inelastic scattering of 26.5 MeV alpha particles on Se-28, P-31, and S-32 nuclei [INP-699/P1.1] 03 p0432 N71-12903

Energy spectra of alpha particles induced by 1 MeV neutrons in erbium isotopes [JINR-1175] 04 p0571 N71-13017

Durable capture of 1 to 8 MeV solar alpha particles into geomagnetically trapped orbits [NASA-CR-111732] 04 p0607 N71-13017

P-18 influence on oxygen determination in alloys by alpha particle activation [LYCEN-7038] 05 p0751 N71-13208

Cross section ratio of radiative capture and alpha fission for U-235 and Po-239 in resonance region of neutron energies [JINR-P3-5113] 06 p0910 N71-13700

Extending cascade-evaporation model of nuclear interaction of particles with nuclei to light nuclei [ORNL-TR-2373] 06 p0914 N71-13700

Investigating mechanism of nitrogen luminescence from irradiation by Po-210 alpha particles at pressures between 50 and 700 torr [JINR-18425] 08 p1253 N71-14800

Mechanism of alpha, 2alpha/alpha breakup reaction in three body formulation [LYCEN-7036] 08 p1256 N71-14800

Investigating ionizing particle detection in collinear nitrate and mechanisms explaining alpha particle track formation in plastic detectors [NP-18411] 08 p1259 N71-14800

Facility and procedures for processing alpha, beta, gamma, and neutron emitters [ORNL-TM-3225] 08 p1176 N71-13906

Heavy particle transfer model of backward elastic alpha particle scattering and cluster structure of O-8 and C-12 [INVO-2171-327] 09 p1426 N71-13930

Deuteron and alpha particle acceleration in synchrophasotron [JINR-P5-5311] 09 p1441 N71-13931

Electromagnetic correction calculations for strong pion-alpha scattering 10 p1621 N71-13700

Radiation induced nucleation of bubbles caused by alpha particles in superheated water [SU-326-P-13-5] 12 p1968 N71-23236

Wave functions for N plus alpha system study using resonating group method [COO-1764-105] 12 p1974 N71-23911

Alpha particle-nucleus collision model for nuclear energy and angular distribution prediction and residual nuclei cross sections [NASA-CR-118026] 12 p1974 N71-23911

Returned Surveyor 3 camera visor examined for alpha radioactive deposit formed by decay of noble isotopes diffusing out of lunar surface 13 p2129 N71-34018

Cluster expansion applications for alpha particle nuclear matter mixture, He-3/He-4 mixture and isospin problem 13 p2137 N71-25482

Using Faddeev equations for studying model of three rigid alpha particles for nucleus of C-12 13 p2144 N71-25988

Geometrical characteristics and thermal stability of nuclear interaction tracks produced by protons and alpha particles in mica [NASA-CR-110608] 14 p2396 N71-26044

Determination of low oxygen contents in alloys by alpha particle activation [LYCEN-7060] 14 p2329 N71-26044

Using 52 MeV deuterons and 104 MeV alpha particles for investigating T equals 0 excited states of Bi-214 [KPK-1055] 14 p2312 N71-26049

Differential cross sections for elastic scattering of 104 MeV alpha particles on He-3 [KPK-1204] 14 p2312 N71-26049

Internal and superficial oxygen content of metal-ceramic composites determined by activation with 54-MeV alpha particles [LYCEN-7076] 14 p2316 N71-26046

Neoclassical separable potential formulation for elastic alpha scattering by helium [LYCEN-7041] 15 p2465 N71-27900

Oxygen and alpha beam excitation of He-134, 136, and 138 and He-150 15 p2496 N71-27970

Alpha particle acceleration and detection using collective method [ANP-P-5558] 15 p2497 N71-27970

Angular distributions and correlations of alpha and beta particles, electrons, and electromagnetic radiation from oriented nuclei [LA-4563] 16 p2645 N71-28157

SUBJECT INDEX

ALUMINUM

- Angular momentum effects on probability of composite nucleus formation and alpha particle evaporation in de-excitation of Te-120
[JBO-392-5] 16 p2646 N71-28165
- Alpha and beta particle range determination, using scintillation detectors for gamma ray spectrometry
[CEA-R-4052] 16 p2655 N71-29072
- Real part of alpha nucleus potential obtained by finite difference procedure
[BNP-720] 16 p2657 N71-29141
- Proton and alpha particle reflections from atomic and ionic chains
17 p2795 N71-29758
- Angular distributions for α particle reactions on Zn-66, Mo-92 and 96 at 41.5 MeV
[NASA-TN-D-6413] 17 p2795 N71-29745
- Comparison of integrated scattering cross sections of α particles in Mg-23/4, alpha/Ne-23 and Al-23/4, alpha/Ne-23 reactions
[NASA-TN-D-6412] 17 p2795 N71-29779
- Neutron scintillation counter design and performance tests using alpha particles and cosmic ray muons
[UNEP-70-1] 17 p2753 N71-30120
- Reactivity effects in absolute determination of alpha emitter in low geometry counters
[NP-10644] 18 p2975 N71-30573
- Coincidence methods for measuring decay of C-12
[JBO-10636] 18 p2975 N71-30574
- Alpha-particle densitometer with variable response tailored to energy distribution of alpha source
[JBO-4137] 18 p2974 N71-31124
- Long range alpha particle emission in thermal neutron induced fission of U-235
18 p2986 N71-31259
- Spectroscopic data for Zn-68 and Zn-70 by inelastic alpha scattering
[JBO-2045] 18 p2989 N71-31506
- Ionization rates due to atmospheric attenuation of alpha particles and alpha particles in upper atmosphere
[AD-723627] 19 p3175 N71-31824
- Alpha decay of element 105 isotopes, produced by American 243 irradiation with neon 22 ions
[JPE-TR-350] 19 p3150 N71-32123
- Measurement of reactivity changes in high purity alpha-plutonium due to self irradiation damage
[JBO-6-6906] 19 p3153 N71-32261
- Static scattering of Ge-70, Zn-90, Ag-107, and Ce-140 alpha particles to resolve discrete real well depth ambiguities found in optical model analysis
20 p3317 N71-33522
- Calculations of ionization-excitation source rates in gaseous media irradiated by fission fragments and alpha particles
20 p3307 N71-33667
- Coincidence spectra of alpha particles from reaction α - ^{91}In , alpha- ^{91}In -4 measured for several angular configurations at 1.55 MeV bombarding energy
20 p3326 N71-33944
- Mach meter using semiconductor detectors of alpha particles produced by americium 241 sources
[CEA-R-4107] 21 p3426 N71-34381
- Quasi-free cluster knockout reaction mechanisms of (muon, proton alpha) and (alpha, 2 alpha) in Li-6 and Li-7 at 60 MeV
21 p3488 N71-34847
- Mechanism of alpha-amino acid synthesis in UV-irradiated formaldehyde and ammonium nitrate solution and planetary evolution
[NASA-TT-P-13797] 22 p3549 N71-35282
- Comparison of excitation functions in Rb-85 by alpha particles to those induced in Sr-88 by protons
[LYCEN-7091] 22 p3631 N71-35872
- Effect of gamma and alpha ionizing radiations on mixed and degassed aqueous solutions of neptunium and americium
22 p3637 N71-35925
- Alpha and beta radiation measurements from air, soil, vegetation, and water samples in Ares reactor component
[JBO-3541] 22 p3644 N71-35985
- Alpha particle acceleration by collective method and alpha particle detection technique
[UCL-TRANS-1434] 22 p3647 N71-36010
- Two-neutron transfer reactions Fe-54(alpha, n)Ni-56 and $^{54}\text{Fe}(\alpha, t)^{54}\text{Fe}$ produced by 28 MeV deuteron
[LYCEN-7087] 23 p3806 N71-37137
- Comparison of angular distributions based on various models for elastic scattering of 25 MeV alpha particles
[BNP-723] 23 p3820 N71-37250
- Nucleation of cavitation by alpha particle irradiation of liquid helium, and existence of audible cavitation and hysteresis effect in helium I and II
23 p3822 N71-37263
- Design, development, fabrication, test, checkout, and support activities for delivery of integrated X ray and alpha particle spectrometer systems for lunar altimeter
[NASA-CR-115216] 24 p3921 N71-37959
- Strength, alpha particle transparency, chemical attack and contamination resistance, and ease of decontamination for alpha activity monitor sealing membranes used in solutions
[CEA-N-1440] 24 p3942 N71-38122
- Astrophysical ionization yield as function of proton energy, using alpha spectra measurements
[JINR-P-5530] 24 p3972 N71-38334
- ALPHA PLASMA DEVICES
Alpha particle acceleration by collective method and alpha particle detection technique
[UCL-TRANS-1434] 22 p3647 N71-36010
- ALPHA RADIATION
U ALPHA PARTICLES
ALPHANUMERIC CHARACTERS
NT BINARY DIGITS
ALSEP
U APOLLO LUNAR SURFACE EXPERIMENTS PACKAGE
ALTERATION
U REVISIONS
ALTERNATING CURRENT
Investigating problems of stability and flux jumping in superconducting materials
[NASA-CR-102919] 02 p0283 N71-11455
Alternating current field induced cholesteric and nematic liquid crystal phase transitions
[A70-20053] 03 p0325 N71-12319
Circuitry for automatic control of alternating current motors
[AD-713946] 05 p0654 N71-15482
Low cost high performance lock-in detector for balancing bridges with reactive and resistive components nulling simultaneously
[IS-2389] 07 p1000 N71-17893
Frequency control network for current feedback oscillators converting dc voltage to ac or higher dc voltages
[NASA-CASE-GSC-10041-1] 09 p1361 N71-19418
Blood pressure measuring system for separately recording dc and ac pressure signals of Korotkoff sounds
[NASA-CASE-XMS-06061] 12 p1865 N71-23317
Alternating current gated flip-flop implementation in sequential circuit design
12 p1880 N71-23787
Solid state circuit for switching alternating current input signal as function of direct current gating transistor
[NASA-CASE-XNP-06505] 13 p2059 N71-24799
Device for voltage conversion using controlled pulse widths and arrangements to generate ac output voltage
[NASA-CASE-MFS-10068] 13 p2060 N71-25139
Inverters for changing direct current to alternating current
[NASA-CASE-XGS-06226] 14 p2232 N71-25950
Maximum length of arc in altitudes up to 9500 ft in 200 volt ac and dc electric aircraft system
[RAE-TR-69259] 16 p2573 N71-28063
AC test technique for measuring high temperature specific heat of small wire or foil samples
[UCL-50962] 22 p3696 N71-36360
Designing alternating current electric wheel for military construction and cargo vehicles
[AD-726956] 23 p3763 N71-36827
Development and characteristics of electrical power supplies for converting variable frequency ac to fixed frequency ac
[AD-727748] 24 p3876 N71-37627
Development and characteristics of energy injection circuit for ac power continuity device
[AD-727581] 24 p3899 N71-37795
Penetration of ion-acoustic barrier when alternating current flows in toroidal magnetized plasma
[CN-28/B-10] 24 p3983 N71-38439
- ALTERNATING CURRENT GENERATORS
U AC GENERATORS
ALTERNATIVES
Presenting techniques for assessing utility of complex alternatives in transportation problems
[RAE-TR-69259] 16 p2573 N71-28063
- ALTERNATORS (GENERATORS)
U AC GENERATORS
ALTIMETERS
NT LASER ALTIMETERS
NT RADIO ALTIMETERS
Aircraft accident investigation of United Air Lines, Boeing 727-22C near Los Angeles, 18 Jan. 1969
[PB-190612] 01 p0006 N71-10914
Laser altimeter-range finder techniques applied to geodetic measurement and mapping
[NASA-TM-X-66409] 03 p0387 N71-12425
Verification experiment design for satellite-borne geodetic altimeter operating over seas
[NASA-CR-115897] 05 p0660 N71-14791
Aircraft altimeter containing X ray source
07 p1027 N71-16993
GEOS-3 altimeter bias recovery simulation using range and angle tracking data
[NASA-TM-X-65619] 18 p2922 N71-30592
Study of concept of inertially aided barometric altimetry system to meet vertical separation requirements of 1000 and 2000 feet for Mach 3.5 aircraft in altitudes held at 80,000 feet
[NASA-CR-1770] 18 p2898 N71-31307
- Geodetic satellite program and planning for GEOS-C altimetry
[NASA-TM-X-67200] 19 p3090 N71-31867
Error sources in GEOS-C satellite short arc orbit determination method as determined by altimeter experiment
19 p3091 N71-31877
Error correction for GEOS-C altimeter system from range and angle observations
19 p3099 N71-31878
Coherent radar system for determining radar altimeter bias from GEOS-C tracking
19 p3055 N71-31880
Design criteria for radar altimeter for GEOS-C geodetic satellite
19 p3055 N71-31881
- ALTITUDE
NT FLIGHT ALTITUDE
NT HIGH ALTITUDE
NT LOW ALTITUDE
NT SIMULATED ALTITUDE
Representation of heterospheric semiannual variation as density variation with amplitudes as functions of altitude
[NASA-CR-117137] 09 p1413 N71-19765
Stress effects of temperature and altitude on human performance
09 p1337 N71-20643
Combined optical altitude and altitude indicating instrument for use in aircraft or spacecraft
[NASA-CASE-XLA-01907] 12 p1917 N71-23248
- ALTITUDE ACCLIMATIZATION
Investigating state of brain and muscles during high altitude acclimation and effects of physical training on basal tolerance of man
[JPRS-52200] 07 p0980 N71-17066
Investigating changes in brain cortex and gastrocnemius muscle functions during adaptation to high mountainous altitudes
07 p0980 N71-17067
Human acclimatization to high altitudes, monsoons, and hot, dry weather
[JPRS-52594] 11 p679 N71-22001
Physiological adaptation to high altitudes in experienced and novice mountain climbers from northern and southern regions
11 p1680 N71-22004
Physiological responses to long term living at high altitudes
11 p1680 N71-22005
Physiological responses to long term living at medium elevations
11 p1680 N71-22006
High altitude acclimatization and physiological changes in humans
11 p1680 N71-22007
Comparison of ground level rats to rats exposed to altitude of 18,000 feet to determine cardiovascular responses
[AD-717851] 11 p1682 N71-22240
- ALTITUDE SIMULATION
Decreased diuresis in response to thiazide diuretic at simulated altitude
[AD-713069] 05 p0635 N71-14702
Preliminary study of airplane-captain responses to atmospheric turbulence while operating in altitude-hold and altitude-hold modes
18 p2870 N71-30780
- ALTITUDE TESTS
NT HIGH ALTITUDE TESTS
ALTITUDE TOLERANCE
Psychomotor performance during vacuum chamber altitude tolerance tests
[DLR-FB-70-37] 07 p0980 N71-17146
- ALU (COMPUTER COMPONENTS)
U ARITHMETIC AND LOGIC UNITS
ALUMINA
U ALUMINUM OXIDES
ALUMINATES
Determining suitability of aluminates for use in electrochemical systems
[AD-714609] 05 p0797 N71-16115
Self-radiation damage in Cu-244 oxide and aluminates including lattice swelling, metastable state formation, and phase transformations
[DP-MS-70-44] 12 p1969 N71-32340
Cochran's method for investigating yttrium orthochromite as optically pumped laser host material
[AD-718980] 13 p2088 N71-24436
Analysis of subvalent Hg ion discovered in molten chloroaluminate
[CONF-701204-1] 14 p2212 N71-25407
Adiabatic elastic moduli of vitreous calcium aluminates to 3.5 kilobars
23 p3789 N71-37004
- ALUMINIZING
U ALUMINUM COATINGS
ALUMINUM
NT ALUMINUM ISOTOPES
NT ALUMINUM 26
NT ALUMINUM 27
NT POWDERED ALUMINUM
Interaction of moving dislocations with electrons and phonons in aluminum
[AD-709940] 01 p0093 N71-10057

- Voids in neutron irradiated aluminum subjected to annealing and re-irradiation
[PB-192483] 01 p0069 N71-10996
- Nickel thin film growth on Ti/Aluminum surfaces
[RAE-TR-68266] 02 p0242 N71-11592
- Mixing of aluminum oxide into molten aluminum during weightlessness in planned space laboratory experiment
02 p0233 N71-11709
- Developing aluminum motoric simulators for hypervelocity impact test using shaped charges
[NASA-CR-108730] 03 p0353 N71-12664
- Fast neutron irradiation effects on diffusion phenomena in Al-Mg system
[CEA-CONF-1327] 03 p0429 N71-12885
- Extinction coefficient and reflectance of aluminum, magnesium fluoride, and magnesium fluoride coated aluminum mirrors for far ultraviolet radiation
[NPL-QU-12] 03 p0418 N71-13319
- Crack formation in aluminum spool cables of F84 F aircraft
[TDCK-53807] 05 p0704 N71-13267
- Numerical analysis of thermodynamics of aluminum ablative materials
[AD-713093] 05 p0783 N71-13584
- Positron annihilation and conduction electrons in aluminum, bismuth, and ytterbium
[UCRL-19647] 06 p0870 N71-15902
- Al neutron elastic and inelastic scattering cross sections from 4.19 to 8.56 MeV
[ORNL-4516] 06 p0921 N71-16306
- Impurity generation in aluminum using electron beam for high energy density heating
[AD-714538] 06 p0954 N71-16402
- Fatigue in 1-mil diameter thermocompression and ultrasonic bonding of aluminum wire
[NASA-TM-X-64366] 06 p0866 N71-16494
- Optical properties of aluminum evaporated in ultrahigh vacuum between 500 and 1400 angstroms
07 p1041 N71-16942
- Investigating electrodeposition of aluminum from aluminum chloride-lithium aluminum hydride-tetrahydrofuran baths
07 p1041 N71-17009
- Spin-echo technique of nuclear magnetic resonance used to determine activation energy of aluminum
[IS-T-410] 07 p1079 N71-17944
- Sorption equilibrium and kinetics of water vapor on modified aluminum
[AD-715914] 08 p1158 N71-18457
- Electrical resistivity and Hall effect in phosphorus doped and aluminum compensated α -type silicon explained by conduction bands
[ONERA-DETS-NT-02-17] 08 p1171 N71-18582
- Yield surfaces for aluminum 1100 at elevated temperatures
08 p1209 N71-19143
- Measured and calculated electrical resistance changes in shock compressed aluminum
[AD-716328] 09 p1399 N71-19871
- Oxidation of cobalt-nickel-aluminum alloys at 1351 K to 1429 K
[BM-R1-7496] 09 p1401 N71-20431
- Joining aluminum to stainless steel by bonding aluminum coatings onto titanium coated stainless steel and brazing aluminum to aluminum/titanium coated steel
[NASA-CASE-MPS-07369] 09 p1395 N71-20443
- Influence of additives in aluminum to improve refinement during zone melting
10 p1573 N71-20872
- Vaporization of magnesium impurities from high purity aluminum melt in vacuum apparatus reduces electrical resistance of aluminum
10 p1575 N71-20882
- High temperature crack initiation and propagation in aluminum and aluminum alloys with emphasis on grain size effects
10 p1576 N71-21013
- Void formation in high purity aluminum from neutron irradiation
[ORNL-TM-3109] 10 p1585 N71-21789
- Testing tensile strength of aluminum in cold channel of nuclear reactor under neutron irradiation
[NLL-WISLEY-TRANS-1958-79091.5F] 11 p1837 N71-22504
- Belomoment measurement of copper, aluminum, and stainless steel emittances at cryogenic temperatures
11 p1785 N71-23045
- Low concentration alkaline solution treatment of aluminum with metal phosphate surface coatings to improve chemical bonding and reduce coating weight
[NASA-CASE-XLA-01995] 11 p1786 N71-23047
- High temperature uniaxial tensile tests performed on aluminum-graphite composites
[AD-718153] 12 p1942 N71-23402
- Etching aluminum alloys with aqueous solution containing sulfuric acid, hydrofluoric acid, and an alkali metal dichromate for adhesive bonding
[NASA-CASE-XMF-02303] 12 p1939 N71-23828
- Etched and other surface waves produced by small explosions in aluminum block
[AD-717985] 12 p1939 N71-24012
- Process for producing dispersion strengthened nickel with aluminum comprising metallic matrices embedded with oxides or other hyperfine compounds
[NASA-CASE-XLE-06969] 12 p1940 N71-24142
- Impurity tracer diffusion coefficients in aluminum and dilute aluminum alloys including ion core and electrostatic effects in vacancy-impurity interactions
[ORO-3036-31] 12 p1940 N71-24299
- Lattice parameter measurements on aluminum after electron irradiation at low temperatures
[JUL-464-FN] 13 p2091 N71-24428
- Nickel plating onto etched aluminum castings
[NASA-CASE-XNP-04148] 13 p2093 N71-24830
- Quasi-stable elementary particles in aluminum and tungsten targets irradiated by 70 GeV protons
[JINR-P1-5399] 13 p2132 N71-25044
- Effects of negative NO₃ or NO₂ ions on photochemical polarization of Al in aqueous solutions of NaCl
[RAE-LIB-TRANS-1510] 13 p2095 N71-25057
- Magnesium fluoride and lithium fluoride-optical coatings for aluminum mirror in space astronomy
13 p2083 N71-25320
- Outgassing of sample material, e.g. aluminum foil, coaxial cables
[REPT-710-229/70] 14 p2267 N71-25616
- Structure and phase composition of diffusion layer formed by interdiffusion of iron and aluminum
[TT-70-58191] 14 p2268 N71-25647
- Volumetric and grain boundary effects on silver isotope diffusion into aluminum single and polycrystals during annealing
[TT-70-57845] 14 p2269 N71-25661
- Gamma ray scattering cross sections from neutron irradiation of aluminum with neutron energies between 5.3 and 9.0 MeV using time of flight spectrometers
[ORNL-TM-3284] 14 p2301 N71-25737
- Method of plating copper on aluminum to permit conventional soldering of structural aluminum bodies
[NASA-CASE-XLA-00966-1] 14 p2273 N71-25983
- Aluminum contacting technique for lead telluride thermoelectric converter module
[NASA-CR-110637] 14 p2254 N71-25926
- Electrotransport analysis of commercially pure aluminum
[TT-70-57009] 14 p2273 N71-25946
- Influence of aluminum on friction and wear of iron-aluminum alloys dry and lubricated in argon atmosphere
[NASA-TN-D-6359] 14 p2261 N71-26045
- Comparison of charged particle activation analysis and infrared spectroscopy for carbon and oxygen trace contaminant determination in silicon and aluminum
14 p2214 N71-26262
- Calculated equations of state for solid sodium and aluminum
14 p2326 N71-26489
- High pressure shock and acoustic velocity data for calculating equation of state of aluminum
14 p2297 N71-26492
- Magnetic spark spectroscopy and scattering cross sections from proton irradiation of aluminum nuclei
[IPVE-SEF/OP-70-13] 14 p2314 N71-26719
- Phase interactions and properties of Al₃Si as dispersion phase for high flux reactors
[KFK-1232] 15 p2445 N71-27024
- Static fracture behavior of surface flawed aluminum plate
[AD-720392] 15 p2424 N71-27449
- X ray determination of lattice parameters and thermal expansion coefficients of Al, Ag, and Mo powders using back reflection diffraction camera
15 p2425 N71-27483
- Activation energy and hole mobility in aluminum determined by nuclear magnetic relaxation including temperature effects
[COO-1190-001] 15 p2477 N71-27580
- Anodic oxide coating thickness effect on fracture of aluminum single crystals and polycrystals
[ORO-3401-16] 15 p2508 N71-27902
- Anodic oxide and metal coating effects on plastic deformation and mechanical properties of aluminum single crystals
[ORO-3401-15] 15 p2509 N71-27909
- Aluminum panel flutter tests at supersonic Mach numbers
[NASA-CR-1857] 16 p2685 N71-28161
- Mechanical behavior of aluminum-stainless steel composite subjected to elevated temperature under strain and wires pulled to failure after extraction from composite
[AD-721374] 16 p2610 N71-28441
- Heat activated and cells with aluminum anode
[NASA-CASE-LEW-113391] 16 p2538 N71-28579
- Mathematical models for measuring frictional behavior of bond and aluminum surfaces in ultrahigh vacuum
16 p2602 N71-28678
- Plastic deformation in microtomed thin films of copper and aluminum single crystals
16 p2666 N71-28776
- Superconductive tunneling in single and polycrystalline aluminum thin films
16 p2668 N71-28990
- Production, consumption, and utilization of aluminum during 1969
17 p2761 N71-29000
- Electroless nickel coatings on aluminum using electrically heated water-cooled specimens in out-of-slow flow
[ORNL-TM-3297] 17 p2781 N71-29000
- Electrochemical and corrosion behavior of high purity aluminum exposed to oxygen-free and oxygen-saturated saline solutions of varying pH content
[AD-722165] 17 p2783 N71-29007
- Sub-boundary corrosion in polymerized polyethylene aluminum containing iron and copper impurities and exposed to HF and HCl solutions
17 p2764 N71-29018
- Microstructure interdiffusion and temperature effects on aluminum and aluminum-magnesium alloy plate strengths
[RAE-LIB-TRANS-1512] 17 p2766 N71-29019
- Calculations of flow induced in adjoining slots of PMMA and aluminum as shock wave propagates through composite plate
[AD-723444] 17 p2771 N71-29019
- Negative pion, kaon, antiproton, and antineutron production in 10 GeV proton irradiation of aluminum and beryllium nuclei
[IPVE-SEF-70-38] 17 p2810 N71-29019
- Aerodynamic characteristics of vehicle models in aluminum tube
18 p2867 N71-31100
- Low voltage aluminum electrolyte capacitors with high capacitance
[BCR-16] 18 p2890 N71-31119
- Reversed creep tests on chemical lead, aluminum, and copper and creep deformation behavior under repeated stress reversals
[NASA-CR-72949] 20 p3357 N71-33300
- Analysis of metal combustion using isolated aluminum particles ignited by laser and burning in controlled mixture of oxygen and argon
20 p3366 N71-33700
- Correlation between substructure and stress-strain behavior in fiber reinforced aluminum stainless and composites
20 p3286 N71-33800
- Analysis of aluminum and nonmetallic buffer for use with liquid oxygen containers to prevent chocking
[NASA-CR-10888] 21 p3413 N71-34016
- Nondestructive tests to determine origin of molting problem encountered during welding of aluminum wire
[BDX-613-321] 21 p3434 N71-34016
- Crystal structure and characteristics of beryllium wire after coating with aluminum by electrolysis
[SC-T-71-3021] 21 p3439 N71-34016
- Effects of sulfur hexafluoride on tensile and yield strengths of aluminum and steel with application to thrust gas case from rocket engines
[NASA-TM-X-2333] 21 p3440 N71-34016
- Electrical resistivity of Al and Cu during rapid heating to melting point and fracture in investigation of metallic melting mechanisms
[NLL-M-21006-SE28.4F] 21 p3441 N71-34016
- Internal friction in aluminum single crystals, γ -irradiated and worked at low temperatures, determined by ultrasonic measurements
21 p3497 N71-34016
- Prediction and inhibition of radiolysis of water in sealed aluminum capsules at reactor facility
[NASA-TM-X-67099] 22 p3550 N71-35016
- Technical-economic data for copper and aluminum conductors and superconductors for high field magnets
[LNF-70/19] 22 p3437 N71-35016
- Analysis of true stress variation as function of degree of deformation based on tensile tests of aluminum, copper, and unalloyed steels with varying carbon contents
[RAE-LIB-TRANS-1587] 22 p3688 N71-35016
- Microautoradiogram of impurity distribution in aluminum foil irradiated by thermal neutrons
[NLL-WINDSCALE-448-19091.5F] 23 p3774 N71-35016
- Comparison of bubble method and end measurements of Al and Cu activities in molten Al-Cu alloys reacting with AlCl₃
[NLL-RTS-6373] 23 p3774 N71-35016
- Characteristics of aluminum composites joints and methods for analyzing contact corrosion
[NLL-OA-TRANS-637-6196.3] 23 p3775 N71-35016
- Microstructure and mechanical properties relationships and reactor materials applications of dispersoid strengthened aluminum and aluminum oxides
[RISO-233] 24 p3936 N71-35016
- Volume photomicroscopy model and photomicroscopic determination of electron attenuation lengths in molybdenum and aluminum
[ORNL-TM-2617] 24 p3980 N71-35016
- ALUMINUM ALLOYS
- Heat treatment effects on discontinuous yielding of aluminum-copper alloys
[AD-710517] 01 p0064 N71-10996
- Ti-6Al-4V-2Sn fatigue behavior
[AD-710635] 01 p0066 N71-10996

SUBJECT INDEX

Mechanical properties of cryogenically stretched
type 301 stainless steel and aluminum alloys 2021-T81
and 7007-T6 01 p0667 N71-10447
[NASA-TN-72733]

Base formability of titanium-aluminum-vanadium
alloy over temperature range 01 p0659 N71-10537
[AS-710083]

Decomposition in vapor quenched aluminum-silver
alloys 02 p0174 N71-11228

Low self diffusion parameters in Fe delta-region and
in Fe alloys with small Al additions
(TT-70-57843) 02 p0240 N71-11389

Auger electron spectroscopy study of surface
composition in copper-aluminum alloys
[NASA-TN-D-69953] 02 p0241 N71-11430

Pulse testing apparatus for measuring strain levels
at aluminum alloys with constant force or amplitude
control at 20 kHz 02 p0241 N71-11563
(MAT-3)

Wear tests of ceramic coatings for aluminum alloys
spalled by flame and plasma spraying and sherry
(AD-712503) 02 p0247 N71-11663

Isotonic deformation of aluminum alloys under
combined stress at high temperature
(AD-712497) 02 p0244 N71-12063

Heat treatment studies of aluminum alloy type 7079
including tensile strength, fatigue and crack
initiation and stress corrosion studies
(NLR-TR-69538-L) 02 p0245 N71-12126

D and s electron interactions in iron-aluminum
system diffusion
(TT-70-57046) 02 p0245 N71-12149

Mechanical, physical, technological, and corrosive
properties of welded aluminum
(AD-712348) 03 p0389 N71-12659

Effects of quench rate on distribution of
precipitates at grain boundaries in Al, Zn, Mg alloys
(AD-712095) 03 p0393 N71-13152

Residual and geometric stress concentration effects
on fatigue life of aluminum alloy clamped joints
(R77-111270) 03 p0396 N71-13263

ARPA coupling program on stress-corrosion
cracking including treating specimens types, titanium
and aluminum alloys, high strength steels, and surface
alloys
(AD-713059) 03 p0396 N71-13397

Micro- and macro-plastic behavior and stress cor-
rosion cracking of titanium-aluminum alloys
(AD-712476) 04 p0328 N71-13948

Effect of trace elements on precipitation in Al-Cu
alloys
(JCLM-19137) 04 p0329 N71-14007

Cryogenic mechanical properties of aluminum al-
loys, titanium alloys, and stainless steel - Vol. I
(AD-713519) 05 p0732 N71-14685

Investigating relationship between ultrasonic indica-
tion and actual characteristics of defects in alloys
(J28-43) 05 p0726 N71-15076

Temperature stability of lubrication layers during
fatigue of alloyed aluminum on steel
(AD-713770) 05 p0693 N71-15434

Procedure for surface alloying of refractory metals
aluminum alloys
(AD-714415) 05 p0685 N71-16083

Amalgam aging of aluminum alloys
(AD-715021) 05 p0671 N71-16255

Investigating crystal growth and dendritic character
of aluminum of transition metals in aluminum alloys
(AD-714400) 05 p0935 N71-16323

Fracture, fatigue, and crack propagation of alu-
minum alloy sheet and flat plates
(AD-714019) 05 p0872 N71-16330

Dependence of fatigue life and flow stress on
microstructure of precipitation hardened Al-Cu alloys
(AD-714085) 05 p0872 N71-16343

Alloying quenched-in vacancies in Al-Zn alloys
and kinetics of coarsening process of Guinier-Preston
zones
(NRL-TR-23753) 05 p0872 N71-16354

Tensile test strain rate effects on mechanical prop-
erties of aluminum alloys, steels, and titanium
(AD-714086) 05 p0873 N71-16382

Combined deformation and heat treatment effects
on aluminum alloys
(AD-715979) 05 p0873 N71-16436

Resonance errors in aluminum alloy fatigue tests and
basis metal
(MCC-CP-1123) 07 p1123 N71-17330

Precipitation voids in aluminum base fuel dispensers
exposed to high flux isotope reactor and advanced
reactor
(NRL-6411) 07 p1063 N71-17361

Aluminum alloy stress cycles and fatigue life of alu-
minum materials
(P-70-1900) 07 p1124 N71-17524

Evaluation of materials for use in structures sub-
jected to random low cycle vibration
(AD-715373) 07 p1123 N71-17783

Inductance measurements and bond structures of
gold aluminum silver alloys and aluminum gold al-
loys
(NRL-38004) 07 p1084 N71-17839

Fracture ductility of aluminum and titanium alloys
and steels as function of stress state
(AD-715320) 07 p1044 N71-17844

Measurement of fatigue crack propagation in alu-
minum alloys at high stress
[NASA-CR-1732] 07 p1127 N71-18002

Crack propagation in aluminum alloy sheet materi-
als under flight simulation loading
(AD-715331) 06 p1211 N71-18245

Uranium 235 content in U-Al alloy determined by
detecting fission neutrons, emitted by slow neutron ir-
radiation
[JAERI-MEMO-4106] 06 p1256 N71-18384

Refracting liquid metal embrittlement of aluminum
and zinc-cadmium alloys to electroactivity of par-
ticularly solid and liquid metal
(AD-715741) 06 p1214 N71-18532

Welded joint mechanical properties noting porosity
defects in aluminum alloys
(CRIP-MT-54) 06 p1296 N71-18590

Fatigue mechanics of aluminum alloy and steel
crack tip regions
(AD-715421) 06 p1297 N71-18645

Mechanical properties of aluminum alloy 7173 with
T736 forging
(AD-715678) 06 p1214 N71-18758

Microprobe scanning for analyses of protective
chromium aluminum layer on Inconel turbine blade
[NASA-TT-F-13497] 06 p1218 N71-19027

Magnesium addition effects on microstructure,
hardness, and tensile properties of zinc aluminum al-
loys
(BME-R1-7491) 06 p1218 N71-19030

Macroscopic fracture transition phenomena in 7075-
T651 aluminum
(AD-715678) 06 p1299 N71-19141

Discontinuous precipitation of gamma prime in
nickel-cobalt-aluminum alloys by transmission elec-
tron microscopy
(AD-715678) 06 p1230 N71-19272

Aluminum-clad glass rods affecting core midplane
power shape
[BAW-3647-19-PT-3] 09 p1419 N71-19982

Corrosion resistance of aluminum-silicon alloy in
relation to hydrogen content introduced by various
refining processes
[NASA-TT-F-13506] 09 p1408 N71-20082

Steady pit region at tips of stress corrosion cracks
in aluminum alloys associated with onset of precipi-
tation
(AD-714680) 09 p1400 N71-20091

Combustion physics and flammability of aluminum
magnesium alloy aerogels
[NASA-TT-F-13505] 09 p1484 N71-20511

High strength aluminum coating alloy for cryogenic
applications in aerospace engineering
[NASA-CASE-XMF-02706] 10 p1572 N71-20743

Problems in riveting and welding of high strength
aluminum aircraft alloys
(AD-717053) 10 p1652 N71-20924

Porosity formation and feeding for sand cast alu-
minum alloy sheets
(AD-717053) 10 p1576 N71-21012

High temperature crack initiation and propagation in
aluminum and aluminum alloys with emphasis on grain
size effects
(AD-717053) 10 p1576 N71-21013

Comparison of two drill bits and two lubricants for
aluminum alloy drilling
(AD-717053) 10 p1564 N71-21146

Copper-bearing alloy replacement with aluminum
alloys in distillation desalination plants for sea water
corrosion resistance
[ORNL-TR-2413] 10 p1581 N71-21436

Fracture toughness of precipitation hardening alu-
minum alloys with microstructure and fractography
observations
(AD-717053) 10 p1581 N71-21441

Tensile, fatigue, and creep rupture properties of ex-
tended nickel-based aluminum, titanium carbide, and
beryllium oxide alloys and aluminum-based silicon,
copper, and iron alloys
[NASA-CR-117502] 10 p1583 N71-21587

Diffusion-viscous flow contribution to high tem-
perature creep of copper aluminum alloys
[NRL-CE-TRANS-5323-7022.00V] 10 p1584 N71-21603

Impact tests on annealed small grain 1100 F alu-
minum rods using in-surface diffraction grating strain
transducers illuminated by pulsed ruby laser
(AD-717328) 11 p1776 N71-21987

Elevated temperature effects on fatigue life of ten-
sile stressed titanium alloys, aluminum alloys, and
stainless steels
[NASA-TN-D-6145] 11 p1777 N71-22076

Linear viscoelastic analysis of incremental load test
data on AU-401 aluminum alloy sheet subjected to
tensile creep at 473 deg K
[NASA-CR-117383] 11 p1780 N71-22594

Comparison between silicon-magnesium-aluminum
alloy and copper aircraft electric conductors and ter-
minals noting types of tests
[TRC-BR-17925] 12 p1089 N71-23547

Development of aluminum-graphite composite
(AD-718409) 12 p1543 N71-23619

ALUMINUM ALLOYS

Effects of material strength on transient response,
crater formation, and shock propagation in thick alu-
minum targets subjected to hypervelocity impact
[AD-718461] 12 p1938 N71-23624

Trace element influence on aluminum-copper alloy
quenching microstructure and precipitation hardening
(AD-718461) 12 p1938 N71-23713

Stress-strain behavior of aluminum alloys under en-
vironmental temperature conditions and fracture mechanics
of copper-aluminum eutectic alloys
(AD-718360) 12 p1944 N71-23765

Etching aluminum alloys with aqueous solution con-
taining sulfuric acid, hydrofluoric acid, and an alkali
metal dichromate for adhesive bonding
[NASA-CASE-XMF-02303] 12 p1939 N71-23828

Matrix and for lattice precipitation phase condition
and quality determination of Co-Al alloy coercive
force
[NRL-CE-TRANS-5323-7022.00V] 12 p1939 N71-24090

Impurity tracer diffusion coefficients in aluminum
and dilute aluminum alloys including ion core and elec-
tronostatic effects in vacancy-ion interactions
[ORO-2036-21] 12 p1940 N71-24209

Constant load amplitude tests and program tests of
lap joints and strap joints for riveted Alclad metal
under bending stress
[NLR-TR-69116U] 12 p2008 N71-24282

Fracture and crack growth for welded joints of 5A1-
2.5Sn titanium in environment of low pressure, high
purity hydrogen
[NASA-CR-114859] 13 p2091 N71-24378

Analysis of cause for concentration perturbation in
off-eutectic aluminum-beryllium alloy caused by
changes in freezing rate during progressive freezing
and zone melting
(AD-718964) 13 p2092 N71-24534

Effect of alloying additives such as manganese,
chromium, and zirconium on mechanical properties of
Al-Zn-Mg-Li alloy
(AD-719478) 13 p2092 N71-24562

Method for determination of trace amounts of hafnium
in aluminum-uranium alloys
[CNEA-276] 13 p2093 N71-24673

Specification and procurement of CP-5 cylindrical
Al-U fuel tubes
[ANL-7708] 13 p2120 N71-25207

Production of oxidation resistant aluminumized iron
and nickel alloy coatings for heat resistant alloys
[NASA-TN-D-63239] 13 p2097 N71-25446

Changes in elasticity, magnetostriction, and electric
resistance of iron-aluminum alloys during ordering
[DMDC-5793] 14 p2271 N71-25802

Development and characteristics of high strength,
stress corrosion resistant aluminum alloys for aircraft
structures
(AD-720598) 14 p2273 N71-25876

Welding thermal and residual stress analysis and
material property and weld parameter effects on ther-
mal stresses and elastoplastic deformation of alu-
minum alloys, steel, titanium, and tantalum
[NASA-CR-613531] 14 p2261 N71-26143

Development of chemical nitriding process for
applying ten-in and wear resistant coatings for
machine parts made of aluminum alloy
(AD-720742) 14 p2263 N71-26310

Characteristics of aluminum-copper alloys deter-
mined by electron microbeam probe X ray analysis of
emission spectra
(AD-720661) 14 p2275 N71-26450

Piezoresistive shock wave profile measurements for
determining aluminum alloy strength
(AD-720661) 14 p2243 N71-26491

Effects of silicon on strength and microstructure of
aluminum alloys
(AD-720661) 14 p2275 N71-26534

Method for predicting fatigue lives of 2024 T3 and
6061 T6 aluminum alloys subjected to either constant
amplitude sinusoidal or wide band random fatigue
loadings
[SCL-TR-710175] 15 p2420 N71-27017

Properties and selective applications of aluminum
alloys in aircraft construction
(AD-720661) 15 p2414 N71-27044

High quality weld of charring during hot rolling of
VAD-23 alloy sheets
(AD-721834) 15 p2416 N71-27335

Finite difference integration of dynamic Lagrangian
equations for impact shock wave profiles in aluminum
alloys
(AD-720716) 15 p2404 N71-27467

Stress corrosion and fatigue tests and fractography
analysis of high strength aluminum alloy cylinders
(AD-720857) 15 p2425 N71-27629

Feasibility of boron-matrix reinforced aluminum
alloy for horizontal tubular structure of DC 8 air-
craft and recommendations for demonstration pro-
gram
[NASA-CR-111913] 15 p2360 N71-27864

Plastic deformation in single crystals of zinc cad-
mium and copper aluminum alloy systems
(AD-720857) 15 p2360 N71-27862

Fatigue crack inhibition and propagation in alu-
minum alloy boron and beryllium matrix composites
(AD-720857) 16 p2380 N71-28181

Interface effects on off-axis and transverse tensile properties of boron-reinforced aluminum alloys [AD-722020] 16 p3608 N71-28184

Adhesive bond shear strength of aluminum at constant strain rate [AD-722238] 16 p2600 N71-28185

Determining internal energy coefficients of Al from ultrasonic measurements of longitudinal and shear wave speeds with hydrostatic pressure, uniaxial stress, and temperature variations [AD-721368] 16 p2610 N71-28443

Electron microprobe analysis of solute segregation near grain boundaries in Al-Zn-Mg alloy after different quenching /brine, water, oil, and air/ and aging heat treatments [AD-722034] 16 p2610 N71-28454

Wave propagation and crater growth characteristics in hypervelocity impact on hard and soft aluminum alloys analyzed using two dimensional Eulerian numerical code [AD-721468] 16 p2612 N71-28748

Characteristics of aging nickel-aluminum alloys and simon alloys by work hardening at room temperature [NLL-LTT-746-637/9022.401/] 16 p2615 N71-29159

Production, consumption, and utilization of aluminum during 1969 [AD-721781] 17 p2761 N71-29280

Spot welding of aluminum alloy joints using primers for corrosion prevention [D-MAT-178] 17 p2755 N71-29388

Response of linear spring-mass-damper system of aluminum alloy subjected to wide band random force input of constant spectral density [AD-721564] 17 p2851 N71-29645

Oxidation mechanism and morphology of scale formation on Ni-Cr-Al alloys at 1000 °C [AD-721781] 17 p2764 N71-29683

Variability of mechanical properties of construction materials, notched rivets, aluminum alloys, and castings [ARC-R/M-3654] 17 p2853 N71-30044

Magnetometric permeability measurements on cerium yttrium compounds and gadolinium doped nickel aluminum alloys [AD-726611] 17 p2766 N71-30151

Heat treatment and stress corrosion analyses on aluminum alloy single- and bicrystal microstructures [NASA-CR-119849] 17 p2766 N71-30151

Deformation behavior of aluminum alloy at elevated temperatures [RAE-LIB-TRANS-1489] 17 p2766 N71-30197

Microstructure interdiffusion and temperature effects on aluminum and aluminum magnesium alloy yield strength [RAE-LIB-TRANS-1512] 17 p2766 N71-30249

Analysis of crack propagation in Alclad sheet specimens under two types of random loading based on fast spectrum [NLR-TR-71014-U] 17 p2855 N71-30303

Qualitative comparison of oxidation resistance of nickel-aluminum alloys with additions of chromium, silicon, and titanium at high temperatures [NASA-TN-D-6414] 18 p2932 N71-30521

Orbital fatigue tester for Skylab program - test and design of titanium alloy and aluminum alloy specimens having various sizes [NASA-CR-111923] 18 p2925 N71-31382

Improved corrosion resistance of aluminum brass for use in sea water conversion plants [PB-190643] 19 p3110 N71-31730

Effects of silver addition on stress corrosion resistance of Al-Zn-Mg-Cu alloys [AD-723563] 19 p3110 N71-31745

Development of iron-aluminum alloy with maximum sea water corrosion resistance and minimum aluminum content [PB-190641] 19 p3110 N71-31770

Fracture mechanics for predicting fatigue crack propagation and velocity in aluminum alloy [AD-723285] 19 p3187 N71-31778

Desulfurizing of steels using aluminum, calcium, and cesium alloy vapor injection [AD-723192] 19 p3111 N71-31902

General fatigue prediction method based on Neuber notch stresses and strains for aluminum alloy airframes [AD-723631] 19 p3188 N71-32025

Dynamic plastic behavior of aluminum alloy cylindrical shells subjected to impulse loads on inner surface [AD-723831] 19 p3188 N71-32028

Low temperature effects on electrical resistivity of copper aluminum alloys with trace amounts of iron [BM-R1-7538] 19 p3116 N71-32395

Phase decomposition in liquid-quenched aluminum-silver alloys and determination of change in electrical resistance [AD-723631] 19 p3116 N71-32395

Determination of activation energy of superaturated solid solution of manganese in aluminum by plasma-spraying [SC-RR-70-356] 19 p3116 N71-32464

Aging behavior of co-deposited aluminum alloy thin films [AD-724195] 19 p3117 N71-32549

Mechanical and thermal properties of aluminum alloys 6061-T6, 2014-T6, and 2024-T3 [AD-724195] 19 p3117 N71-32549

Auger emission spectroscopy, low energy electron diffraction, sputtering studies, and adhesion and friction experiments on single crystals of Cu-Sn, Cu-Al, and Fe-Al alloys [NASA-TM-X-67900] 20 p3284 N71-33248

Crack propagation in aluminum alloys reinforced with boron and stainless steel fibers [UCRL-20524] 20 p3288 N71-33598

Equipment and procedures for determining basic mechanisms in oxide film formation of plasma anodized aluminum [AD-724195] 20 p3288 N71-33598

Thermodynamic investigation of effect of electron concentration in ternary alloys based upon aluminum-zinc binary system [NLL-M-20410-5828.4F] 21 p3441 N71-34484

Precipitation, reprecipitation, and hardening mechanisms in heat treated aluminum alloys [NLL-M-20410-5828.4F] 21 p3441 N71-34484

Mathematical model of vacancy concentrations compared with AlZnMg alloys age hardening behavior to determine Mg atom-vacancy pairs concentration effect on clustering rate [NLL-M-20407-5828.4F] 21 p3441 N71-34487

Stress analysis of aluminum alloy under torsion conditions when subjected to sharp increase in strain rate [AD-722669] 21 p3528 N71-35142

Studying fracture surface striations and crack propagation in aluminum alloy by electron microscope [NLR-MP-69014-U] 21 p3529 N71-35149

Controlled eutectic Al-Si ingots [AD-726424] 22 p3594 N71-35595

Fracture safe design of nonfrangible structural aluminum alloys [AD-726411] 22 p3594 N71-35597

Defect structure of Al-Zn alloy induced by quenching and low temperature aging [AD-726582] 22 p3595 N71-35599

Mechanical properties of as-grown aluminum alloy single crystals compared with those of similar alloys [AD-726714] 22 p3595 N71-35602

Susceptibility of aluminum alloys to stress corrosion cracking during precipitation hardening [AD-726713] 22 p3595 N71-35603

Structural and mechanical properties of AlZnMg, AlMgSi, and AlCuMg alloys as function of natural aging prior to artificial aging [NLL-M-20408-5828.4F] 22 p3596 N71-35606

Aluminum concentration effects on stress corrosion cracking of titanium alloys at ambient temperatures in aqueous solutions of salt [NASA-CR-122935] 23 p3769 N71-36862

Chemical spot tests for identifying alloying elements in aluminum alloys [BM-R1-7544] 23 p3769 N71-36863

Electron microscopy creep properties study of beta NiAl thin film specimens from deformed single crystals [COO-1489-10] 23 p3770 N71-36869

Effects of resolution treatment and overheating on fatigue properties of notched and unnotched D.T.D. 683/3 aluminum alloy bar [ARL/SM-NOTE-258] 23 p3770 N71-36870

Computer program for mixed phase equation of state for aluminum alloys to determine effects of nuclear radiation [AD-726992] 23 p3770 N71-36872

Analysis of structural state of mono and polycrystals of aluminum and copper alloys after deformation [AD-726731] 23 p3770 N71-36874

Characterization and prevention of filiform corrosion on aluminum [AD-726739] 23 p3771 N71-36877

Stable surface treatments for 301 stainless steel, copper, and aluminum alloy contact with liquids [NASA-CR-72975] 23 p3775 N71-36908

Electrochemical technique for remote measurement of instantaneous rate of uniform corrosion of aluminum alloys in nuclear reactor heavy water circuits [ZIE-96] 23 p3796 N71-37074

Variability of aluminum alloy aircraft structure fatigue life under symmetric and asymmetric loads [ARL/SM-REPORT-329] 23 p3861 N71-37524

Influence of geometric variables on K sub c values for two thin sheet aluminum alloys [AD-726684] 23 p3861 N71-37525

Manufacturing procedures for production of high quality hydraulic tubing of metastable beta titanium alloy [AD-727779] 24 p3929 N71-38033

Effects of diisobutyl-dichlorovinyl phosphine and sodium chloride solution on stress corrosion cracking of aluminum and steel [NASA-TM-X-64617] 24 p3933 N71-38060

Aluminum alloy compounds as wide band semiconductor for electroluminescent light source [NASA-CR-111976] 24 p3934 N71-38060

Vibration strength of compressor blade made of titanium alloys, and aluminum alloys at high temperatures [AD-727951] 24 p3938 N71-38060

Matrix and grain boundary influence on mechanical and stress properties of aluminum alloy [RM-522] 24 p3941 N71-38060

Electron microscopic analysis of aluminum alloy structure, intermetallic compounds, and structural hardening mechanisms [NLL-M-20371-5828.4F] 24 p3941 N71-38060

ALUMINUM ANTIMONIDES

Electronic transitions in infrared absorption spectrum of aluminum antimonide [AD-727951] 13 p2155 N71-38060

Mossbauer effect measurements of aluminum, iron, and gallium antimonides and isotopic ordering [AD-727951] 20 p3336 N71-38060

ALUMINUM CHLORIDES

Transuranium element separation using gas chromatography of aluminum chloride vapors [ANL-TRANS-643] 04 p0484 N71-38060

Experimental and computational electrochemical measurements in fused sodium aluminum chloride [NASA-CR-117056] 09 p3452 N71-38060

Aluminum chloride containing solvent systems in organic reactions media - literature survey [AD-727951] 09 p3452 N71-38060

Acid-base equilibrium in aluminum chloride salt and electrochemical measurements [AD-727951] 09 p3453 N71-38060

ALUMINUM COATINGS

Microprobe analysis of diffusion layers with application to chromic acid anodized Inconel 713 [ONERA-TR-436] 02 p0241 N71-38060

Investigating aluminum film deposition processes and effects on device performance [AD-727951] 07 p1091 N71-38060

Performance of aluminate coatings in simulated high temperature tests on gas turbine engine inlets [NASA-CR-116374] 07 p1043 N71-38060

Oxidation resistance of modified aluminum coating for stainless steel [NASA-TM-X-2201] 07 p1044 N71-38060

Testing aluminum coating for surface protection of nozzle blades [AD-719815] 13 p2096 N71-38060

Aluminate coatings for nickel-base superalloy developed for high temperature jet engine components [NASA-CR-72863] 13 p2097 N71-38060

Metallizing parameters developed for sequential deposition of molybdenum, aluminum, and titanium alloys as protective coatings for superalloys [NASA-CR-72832] 13 p2098 N71-38060

Electron and ion microprobes applied in characterizing aluminate coating on IN-100 nickel alloy in high temperature oxidation resistance [NASA-TN-D-6317] 14 p2271 N71-38060

Diffusion layer structure and aluminumizing effect on heat resistant nickel alloy [AD-728370] 14 p2273 N71-38060

Resistance of aluminumized diffusion layers on nickel-chromium alloy [AD-728365] 14 p2278 N71-38060

Evaluation of high gas velocity and static oxidation behavior of fused-salt-aluminized IN 100 tubes 1038 and 1149 C [NASA-TN-D-6400] 17 p2764 N71-38060

Aluminizing 7.61-m collimating mirror for JPL 16-m space telescope [NASA-CR-119688] 19 p3075 N71-38060

Cyclic furnace and high velocity oxidation of aluminate-coated high strength nickel alloy [B-1900] 22 p3393 N71-38060

Molten-salt fluoride volatility process for removing decontaminated uranium from aluminum clad fuel elements [ORNL-4574] 22 p3624 N71-38060

Thermal cycling, humidity, and salt spray tests of plasma-sprayed aluminum coatings for ceramic parts in space materials [BDX-613-008] 23 p3777 N71-38060

Removal of astronomical telescope mirrors for aluminizing [AD-727951] 24 p3923 N71-38060

ALUMINUM COMPOUNDS

NT ALUMINATES

NT ALUMINUM ANTIMONIDES

NT ALUMINUM CHLORIDES

NT ALUMINUM NITRIDES

NT ALUMINUM OXIDES

NT ALUMINUM SILICATES

NT BERYL

NT CORDERITE

NT FELDSPARS

NT MONTMORILLONITE

NT SAPPHIRE

Solid state diffusion growth of compounds suitable containing continuous NiAl fibers in aluminum matrices from hot-pressed aluminum embedded nickel wires [AD-711346] 02 p0246 N71-38060

SUBJECT INDEX

Time-of-flight thermal neutron spectra measurements of Al-Pu fuel 05 p0724 N71-14718
 (NA-1016-RV1)
 Production and optical properties of zinc selenide aluminum arsenide heterojunctions and platinum zinc selenide Schottky junctions 07 p1095 N71-17879
 (NARS-CT-116443)
 Effects of aluminum phosphate additions on thermal stability and adhesive properties of erosion resistant ZrO₂ and Al₂O₃ coatings 12 p1928 N71-23813
 (NARS-TT-F-13535)
 Analysis of space group symmetry, polytypism, layer twinning, and stacking for application to aluminum boride structures 14 p2326 N71-26348
 Electrochromic quantum efficiency of gallium arsenide phosphide, gallium indium phosphide, and aluminum arsenide diodes 15 p2508 N71-27901
 Reaction between chlorodimethyl mercury and aluminum yielding silicon aluminum compound 21 p3389 N71-34109

ALUMINUM ISOTOPES
 NT ALUMINUM 27
 Energy spectrum of identified protons and excited functions following decay of Al-23 20 p3322 N71-33793
 Search for high-spin states in Al-27 in range of excitation energies from 4.8 to 8.0 MeV 20 p3324 N71-33867
 (ANU-P5221)
 Revolution of nuclear structure based on sd shell model with emphasis on mass 29 nuclei of Al and Si 21 p3491 N71-34870

ALUMINUM NITRIDES
 Model for exchange of nitrogen isotopes taking into account two pellets of aluminum nitride in tandem coil 01 p0020 N71-10965
 (AD-71653)

ALUMINUM OXIDES
 NT SAPPHIRE
 Process for production of oxide fibers by melt draw technique 01 p0070 N71-10048
 (NARS-CT-72762)
 Core sheath process for production of oxide fibers 01 p0070 N71-10049
 (NARS-CT-72758)
 Optical absorption in transparent materials during 15 MeV electron irradiation 01 p0068 N71-10380
 (NARS-CT-110907)
 Inverse-time stage desaturation kinetics of alumina impregnated in vacuum 01 p0059 N71-10630
 (AD-710605)
 Thermal stress determinations in quenching treated alumina rods based on X ray diffraction 02 p0246 N71-11589
 (AD-712382)
 Mixing of aluminum oxide into molten aluminum during weightlessness in planned space laboratory experiment 02 p0255 N71-11709
 Surface tension and density of molten alumina 03 p0396 N71-12614
 (AD-711964)
 Hook's slip in aluminum oxide single and polycrystals 03 p0441 N71-12839
 (AD-711824)
 Wave functions incorporating electron correlation for magnesium oxides, lithium oxides, aluminum oxide, and titanium oxides 03 p0433 N71-12942
 (AD-711973)
 Hazards plugging mechanisms occurring in casting alumina containing steel 03 p0393 N71-13282
 (NARS-CT-72758)
 High temperature electrical resistivity of refractory alumina oxides 04 p0533 N71-13998
 (NARS-CT-72758)
 Temperature profiles and AJO resonant spectra of fluorophores 05 p0671 N71-14840
 (AD-713676)
 Diffusion kinetics and phase equilibria in alumina thin crystals 06 p0935 N71-16440
 (NARS-CT-72758)
 Performance of aluminum oxide hygrometer on aircraft meteorological observatory 07 p1028 N71-17274
 (NARS-CT-72758)
 Production of aluminum oxide fibers by floating zone fiber drawing technique 08 p1224 N71-19222
 (NARS-CT-72758)
 Deformation processes in forging polycrystalline alumina ceramics 08 p1224 N71-19225
 (NARS-CT-72758)
 Shock tube experiments to determine infrared band intensities of iron and aluminum oxides 09 p1405 N71-18803
 (AD-713676)
 Carbazole method for growing aluminum oxide single crystals in phase form for transparent armor applications 09 p1405 N71-18804
 (AD-713676)
 Process technology required for production of rose emitting lead rods of pure aluminum oxides for basic studies of laser degradation 09 p1397 N71-19948
 (AD-716421)

Production of aluminum oxide fibers by direct melt fiberization process 05 p1393 N71-20125
 (NARS-CT-72812)
 Non-basal slip in alumina at high temperatures and pressures 10 p1631 N71-20611
 (AD-716788)
 Surface and structural defects in alumina ceramic armor caused by ballistic impact 11 p1781 N71-21864
 (AD-717323)
 Effects of aluminum phosphate additions on thermal stability and adhesive properties of erosion resistant ZrO₂ and Al₂O₃ coatings 12 p1928 N71-23813
 (NARS-TT-F-13535)
 Creep properties of iron doped polycrystalline magnesium oxide and iron and chromium doped polycrystalline aluminum oxide between 1300 and 1500 C 12 p1945 N71-23951
 (COO-1591-3)
 Development of furnace designs, operating, casting, and annealing procedures to improve structural properties of fused-cast aluminum oxide articles 12 p1946 N71-24095
 Thermospheric density determined from ESRO rocket release of aluminum oxide artificial clouds 13 p2078 N71-24568
 (NARS-TM-X-2303)
 Reactor irradiation of thermionic diode insulators - two beryllia and two alumina bonded triayers 13 p2116 N71-24635
 (NARS-TM-X-2271)
 Residual gas analysis for ultraviolet degradation studies on aluminum oxide powder 13 p2041 N71-25314
 Impurity caused grain boundary sliding in alumina ceramics during compression 15 p2508 N71-27903
 (ORO-3228-17)
 Post-cured electrical test of bonded alumina triayer at 1325 K in vacuum environment 16 p2616 N71-28035
 (NARS-TM-X-2303)
 Hot-pressed alumina with molybdenum or molybdenum oxide additives characterized by metallographic and X ray diffraction analyses 16 p2611 N71-28552
 (AD-722359)
 Basalt production and consumption during 1969 17 p2768 N71-29278
 Radiative heat transfer in flames bubbled engine fueled with solid rocket propellants containing aluminum oxide particles 17 p2829 N71-29392
 (ONERA-P-133)
 Temperature effects on microwave frequency compression wave attenuation in aluminum oxide and ruby crystals 17 p2721 N71-29912
 Fracture energy and strength behavior of sodium borosilicate glass Al₂O₃ composite materials system 17 p2771 N71-30196
 (AD-722349)
 Thermal treatment, thermal equilibrium, and microstructural effects on intergranular creep in sintered and fused cast alumina 18 p3022 N71-31367
 (ORO-3228-13)
 Nickel, carbon, and aluminum oxide particle velocity measurement after injection into arc plasma jets 18 p2999 N71-31560
 (LA-TR-71-37)
 Derivation, fabrication and tests of alumina ceramic anvils for cryogenic electrically-suspended gyroscopes 19 p3165 N71-32259
 (NARS-CT-119855)
 Immersion calorimeter for measuring Wigner energy in irradiated BeO, MgO, Al₂O₃, and SiO₂ at high temperatures 19 p3102 N71-32396
 (CEA-N-1171)
 Vertical temperature thermospheric distribution determined by analysis of aluminum oxide artificial cloud spectra during ESRO rocket sounding in Italy 20 p3254 N71-32873
 Effect of aluminum doping on thermal stability of silicon carbide polytypes in 2000 to 2400 C range 20 p3333 N71-33046
 (AD-724102)
 Flexural strength of alumina ceramics increased by reduction of crystal anisotropy 20 p3287 N71-33085
 (AD-724315)
 Progress in growth of ultra-pure Al₂O₃ crystals as laser material, measurement of oxygen diffusion in oxides, and measurement of laser beam damage threshold energy in glass 20 p3287 N71-33128
 (AD-724662)
 Band structures of aluminum oxide determined using bands not having 50 line functions and 15 plane waves 21 p3445 N71-34514
 Dislocation glide, deformation twinning and grain boundary sliding in compressive creep of single and bicrystalline aluminum oxide 21 p3500 N71-34932
 Feasibility of crystal growth technique for beta alumina membrane from molybdenum, tungsten, and lithium 23 p3833 N71-37336
 (NARS-CT-72812)
 Iron doping effects on growth kinetics and electron spin resonance of aluminum oxide single crystals 23 p3834 N71-37342
 Fracture strength of polycrystalline aluminum oxide in relation to microstructure 23 p3834 N71-37343

AMERICIUM ISOTOPES

Microstructure and mechanical properties relationships and reactor materials applications of dispersible strengthened aluminum and aluminum oxides 24 p3936 N71-38079
 (RISO-223)
ALUMINUM SILICATES
 NT MONTMORILLONITE
 Mathematical model for measurement of MOX processes in Al-SiO₂-Si system used in fabrication of integrated circuits 07 p1091 N71-17807
 Chemical composition and structure of low silic sodium hydroaluminosilicates determined by IR spectroscopy 10 p1513 N71-21239
 (NLL-MRE-TRANS-286-0036.477)
 White point production by heating impure aluminum silicate clay having low color absorption 12 p1947 N71-24184
 (NARS-CASE-XNP-62139)
ALUMINUM 26
 Comparison of aluminum 26 radioactivities of Brederhorn chondrites, lunar rocks, and achondrites 15 p2517 N71-27870
 (NARS-TM-X-63578)
 Spallation cross sections for Al-26 production in Fe and Si by high energy proton irradiation 22 p3637 N71-33922
 (NARS-CT-72758)
ALUMINUM 27
 Calculation of Si-28 photodisintegration rate from Al-27 (p, gamma) Si-28 and Mg-24 (alpha, gamma) Si-28 reactions 21 p3487 N71-34844
 Spins and parities of resonances in Al-27 (proton, gamma) Si-28 reaction 21 p3492 N71-34872

ALVEOLAR AIR
 Alveolar gas exchange and cardiovascular functions during respiratory inhibition 07 p0980 N71-17097
 (PB-194823)

AMALGAMS
 U MERCURY AMALGAMS
 Statistical analysis for underwater ambient noise 24 p3967 N71-38299
 (AD-727595)

AMBIENT TEMPERATURE
 Correction formulas for effect of ambient temperature drift on hot-wire anemometer measurements in incompressible flow 02 p0225 N71-11544
 (NPL-AR-1302)
 Considering operation of infrared radiometer affected by secondary fluxes of optical system as function of ambient medium temperature 08 p1204 N71-19132
 Effects of vacuum level on solar receiver materials such as Cu-Zr alloys 09 p1407 N71-20432
 (NARS-CT-72812)
 Performance of simplex and dual orifice fuel nozzles with ambient and heated fuel in annular turbojet combustor 16 p2671 N71-28041
 (NARS-TM-D-6355)
 Pretreating corrosion of stainless steel-copper and Zircaloy 2 in water at ambient temperature 16 p2610 N71-28450
 (RTI/ENG-70/14)
 Flow pattern of two phase flow of water/air at ambient temperature and pressure 22 p3570 N71-35427
 (NLL-CE-TRANS-5472-1922.091)

AMBIGUITY
 Resolution of pulse Doppler radar using pulse compression, noting ambiguity function, and experimental design of autocorrelation 18 p2889 N71-30627
 (RFT-2-76)

AMBIOPOLAR DIFFUSION
 Deriving Fokker-Planck equation for Coulomb scattering into loss cone in presence of ambipolar potential 07 p1465 N71-18148
 (CEA-CONF-1660)
 Three dimensional analysis of ambipolar ratio frequency diffusion coefficient in semiconductor 13 p2580 N71-27915
 (NARS-CT-72758)

AMBY
 U FIELD THEORY (PHYSICS)
AMBULANCES
 Analysis of equipment, crew training, and operations involved in use of fixed wing aircraft for aeromedical transportation 19 p3838 N71-37300
 (FAA-AIM-71-18)

AMERICIUM
 NT AMERICIUM ISOTOPES
 NT AMERICIUM 241
 Ternary oxides of neptunium (IV) and americium (III) with molybdenum or tungsten 06 p0527 N71-13687
 (ORNL-TR-2363)
 Synthesis of element 105 in bombardment of Am-243 with Ne-22 ions 06 p0811 N71-15798
 (JENR-P7-5164)
 Effect of gamma and alpha ionizing radiation on sorbed and desorbed aqueous solutions of neptunium and americium 22 p3637 N71-33923
 (NARS-CT-72758)

AMERICIUM ISOTOPES
 NT AMERICIUM 241
 Cross sections of production of spontaneously fissioning isotopes of uranium, plutonium, and americium in neutron reactions 16 p2653 N71-28009
 (JENR-P5-3328)

Alpha decay of element 105 isotopes, produced by Americium 243 irradiation with neon 22 ions [KFE-TR-350] 19 p3150 N71-32123
Angular distribution of neutron and gamma emission from excited and spin states in isotopic americium 241 to americium 242 decay [RPI-3947-13] 20 p3318 N71-33566
Epicadmium integral fission cross section measurements for twelve heavy nuclides including plutonium and uranium isotopes 22 p3450 N71-36031

AMERICIUM 241

Studying capture cross sections of Np-237 and Am-241 in two reactor spectra by reactor oscillator [BNL-50242] 10 p1620 N71-21731
Air ionization and effects of positive ions in air on man using Am-241 sources [ORNL-TR-2427] 13 p2035 N71-25438
Error analysis of thickness measuring devices with Am-241 and Cs-137 sources including errors due to chemical composition of steel, temperature distribution, and statistical variation [PB-19269] 19 p19102 N71-32420
Mach meter using semiconductor detectors of alpha particles produced by americium 241 sources [CEA-R-4107] 21 p3426 N71-34381

AMIDES

NT POLYIMIDES

NT UREAS

Molecular structure of thioamides from vibrational spectra 03 p0330 N71-12355

Protective efficiency, synergism, and polarity of ferrous and nonferrous metal, oil-soluble corrosion inhibitors including sulfonates, nitrates, amines, and amides [AD-717011] 10 p1578 N71-21232

Austriation plastic based on polyamide fibers as fillers for phenol resins [AD-71927] 13 p2101 N71-25117

AMINES

NT AMPHETAMINES

NT ANILINE

NT DIAMINES

NT DIMETHYLHYDRAZINES

NT HISTIDINE

NT NITROAMINES

Direct synthesis of polymeric schiff bases from two amines and two aldehydes [NASA-CASE-XMF-08655] 02 p0176 N71-11239

Synthesis of schiff bases for heat shields by acetal amine reactions [NASA-CASE-XMF-08652] 02 p0176 N71-11243

Mechanism of adsorption of amine-type corrosion inhibitors [AD-718295] 04 p0488 N71-13472

Amine catalyst effects on compressive strength of rigid urethane foams [BDX-613-170] 07 p1047 N71-17260

Pulse radiolysis studies of aqueous solutions of aminoalcohols and compounds related to nucleic acid [GA-10208] 07 p1075 N71-17482

Amine absorbent for carbon dioxide concentrator in long term life support system 10 p1506 N71-20961

Protective efficiency, synergism, and polarity of ferrous and nonferrous metal, oil-soluble corrosion inhibitors including sulfonates, nitrates, amines, and amides [AD-717011] 10 p1578 N71-21232

Pressure effects on ferric hydroxamates and ferri-chrome A based on electromagnetic absorption and Mossbauer resonance [COO-1196-777] 11 p1784 N71-22486

Monoamine oxidase inhibitors and norepinephrine decrease by reenzyme affecting brain amines in aldehyde exposed rats 14 p2204 N71-29957

Amino silica gel absorbers for atmospheric purification systems of spacecraft cabins 20 p3222 N71-33468

Effect of process conditions on tensile properties of DOBEA and phenol novolac resin reacted with adduct of methylene dianiline and phthalic anhydride [NRC-ME-152] 20 p3287 N71-33496

Electro deposition of palladium from amine-palladium hydroxide, bromide, and sulfamate electrolytes and electrolyte preparations [NLL-LT-746-732-[9022.401]] 22 p3589 N71-35562

Ammonia chloride near order-disorder transition explained by physical model having singular and nonsingular free energy parts and verified by specific heat measurements 18 p2398 N71-31099

Phoson system model having disordered forces constants and ordered masses of ions applied to ammonium chloride and disordered magnetic system phases [MUB-2087] 20 p3317 N71-33578

Analysis of electrodeposition of palladium from alkaline ammonium chloride electrolyte using rotating disc electrode and temperature kinetic method [NLL-LT-746-739-[9022.401]] 22 p3590 N71-35563

Pressure dependence of electrolytic conductance at 30 C to pressure of 3000 kg/cm² for solutions of potassium iodide and series of tetraalkyl ammonium salts 19 p3051 N71-31720

Mechanism of alpha-amino acid synthesis in UV-A irradiated formaldehyde and ammonium nitrate solutions and planetary evolution 22 p3549 N71-35282

Photomultiplier nanoammeter design for converting current to voltage [RM-493] 07 p1033 N71-17949

Forced convection of gaseous ammonia at high wall temperature [LA-TR-70-12] 01 p0044 N71-10802

Ion and electron production in proton and hydrogen atom collisions with carbon monoxide, carbon dioxide, methane, and ammonia 03 p0436 N71-13377

Electrosynthesis of hydrazine from gaseous ammonia [ECRC/R264] 04 p0484 N71-13440

W values in mixtures of gases containing ammonia [ORO-2001-14] 05 p0750 N71-15358

Amino acid syntheses by heating formaldehyde and ammonia mixtures in molecular evolution research [NASA-CR-118031] 12 p1872 N71-24022

Cathode insulator modifications of radiation cooled MPD arc thruster tested in power range of 9.8 to 46.4 kW using ammonia as principal propellant [NASA-CR-728911] 14 p3231 N71-25770

Measuring local thermodynamic equilibrium plasma temperatures for determining characteristics of reaction between hydrogen atoms and ammonia 17 p2812 N71-30053

Differential thermal and electrical conductivity studies of phase transitions in Li₂/V2O₅, single crystals of WO₃ and WO₃ minus x, and metal-ammonia systems 18 p2887 N71-31345

One-electron and two-electron cavities in metal-ammonia solutions, electron-molecule and intermolecular reactions, and corrections for effective intermolecular pair argon potentials 21 p3389 N71-34111

Nuclear magnetic resonance analysis of molecular motion in liquid and solid ammonia between 1 to 239.8 K 21 p3489 N71-34852

Inversion barrier energies in NH₃ and PH₃ and calculations of electronic properties in TiO₆(minus x) clusters 21 p3491 N71-34866

Using photometric titration and cation exchange methods to study formation of pentavalent plutonium and neptunium chelates with alpha-amino acids [LIB/TRANS-261] 05 p0736 N71-14580

Amino acid synthesis by shock and ultraviolet photoirradiation [NASA-CR-117896] 12 p1869 N71-23209

Amino acid syntheses by heating formaldehyde and ammonia mixtures in molecular evolution research [NASA-CR-118031] 12 p1872 N71-24022

Quantitative analysis of gamma amino butyric acid in brain after locomotion and pure oxygen breathing [DLR-FB-71-03] 12 p2032 N71-24456

Amino acids produced by long UV irradiation of gas mixtures using hydrogen sulfide as initial photon acceptor, simulating prebiological earth conditions [NASA-CR-118329] 13 p2040 N71-25081

Production of aminoacetonitrile metal chains of copper, zinc, nickel, and cobalt and catalytic action of metal chains in Sorbitol and glycine oxidation [NASA-TT-F-137111] 17 p2716 N71-30212

Spin interactions between slow electrons and evaporated aromatic amino acid films [ORO-3799-7] 19 p3150 N71-32126

Automated analysis system for separating and identifying amino acids to detect extraterrestrial life [NASA-TT-F-13765] 19 p3044 N71-32232

Mechanism of alpha-amino acid synthesis in UV-irradiated formaldehyde and ammonium nitrate solutions and planetary evolution 22 p3549 N71-35282

Photomultiplier nanoammeter design for converting current to voltage [RM-493] 07 p1033 N71-17949

Forced convection of gaseous ammonia at high wall temperature [LA-TR-70-12] 01 p0044 N71-10802

Ion and electron production in proton and hydrogen atom collisions with carbon monoxide, carbon dioxide, methane, and ammonia 03 p0436 N71-13377

Electrosynthesis of hydrazine from gaseous ammonia [ECRC/R264] 04 p0484 N71-13440

W values in mixtures of gases containing ammonia [ORO-2001-14] 05 p0750 N71-15358

Amino acid syntheses by heating formaldehyde and ammonia mixtures in molecular evolution research [NASA-CR-118031] 12 p1872 N71-24022

Cathode insulator modifications of radiation cooled MPD arc thruster tested in power range of 9.8 to 46.4 kW using ammonia as principal propellant [NASA-CR-728911] 14 p3231 N71-25770

Measuring local thermodynamic equilibrium plasma temperatures for determining characteristics of reaction between hydrogen atoms and ammonia 17 p2812 N71-30053

Differential thermal and electrical conductivity studies of phase transitions in Li₂/V2O₅, single crystals of WO₃ and WO₃ minus x, and metal-ammonia systems 18 p2887 N71-31345

One-electron and two-electron cavities in metal-ammonia solutions, electron-molecule and intermolecular reactions, and corrections for effective intermolecular pair argon potentials 21 p3389 N71-34111

Nuclear magnetic resonance analysis of molecular motion in liquid and solid ammonia between 1 to 239.8 K 21 p3489 N71-34852

Inversion barrier energies in NH₃ and PH₃ and calculations of electronic properties in TiO₆(minus x) clusters 21 p3491 N71-34866

Low temperature photodetachment of carbon dioxide, ammonia, and nitrous oxide condensed gas molecules utilizing ultraviolet light 22 p3628 N71-35847

Correlation of calculated and experimental product yields as functions of gas molecule residence time, power, gas pressure, and allyl alcohol in electro-synthesis of hydrazine from ammonia [ECRC/N343] 23 p3719 N71-36310

Cathode surface temperature effects in argon and ammonia discharges [MDC-Q0450] 24 p3924 N71-38000

Rotational constants for ammonia and phosphine determined from rotational transition spectra in sub-millimeter range 24 p3983 N71-38426

Cyclool induced changes in internal structure of cotton leaves to reflectance, transmittance, and absorption of near infrared radiation 06 p0800 N71-16151

Development of theory to explain behavior of ammonium chloride near first order transition at high temperatures 18 p2995 N71-31099

Phoson system model having disordered forces constants and ordered masses of ions applied to ammonium chloride and disordered magnetic system phases [MUB-2087] 20 p3317 N71-33578

Analysis of electrodeposition of palladium from alkaline ammonium chloride electrolyte using rotating disc electrode and temperature kinetic method [NLL-LT-746-739-[9022.401]] 22 p3590 N71-35563

Pressure dependence of electrolytic conductance at 30 C to pressure of 3000 kg/cm² for solutions of potassium iodide and series of tetraalkyl ammonium salts 19 p3051 N71-31720

Mechanism of alpha-amino acid synthesis in UV-A irradiated formaldehyde and ammonium nitrate solutions and planetary evolution 22 p3549 N71-35282

ESR studies of radiation effects on ammonium monofluorocarbonate and ammonium difluorocarbonate at room temperature 22 p3644 N71-33008

Combustion efficiency of hydrocarbon fuels with ammonium nitrate propellant additive and solidified oxygen and fluorine gas oxidizers [BMW-FB-W-70-47] 07 p1098 N71-17227

Phase transformations in ammonium nitrate with stabilizing additives measured by volumetric analysis of thermal expansion [ICT-4/69] 12 p1980 N71-25911

Thermogravimetry and calorimetry experiments to study phenomenology of synergistic system for catalysis of ammonium nitrate decomposition in solid state propellants [AD-724317] 20 p3337 N71-32008

Ammonium perchlorate surfaces wetted by aqueous liquids to determine binder/oxidant interface in plastic propellants [AD-71269] 02 p0288 N71-14180

Ammonium perchlorate composite propellant with organic Cu/II chelate catalytic additive [NASA-CASE-LAR-10173-1] 04 p0604 N71-14480

Using isomorphous and phase rule concepts to obtain ammonium perchlorates and nitrates in solid crystals for propellants 05 p0761 N71-15378

Mathematical models for ammonium perchlorate combustion and composite propellant burning mechanism 07 p1080 N71-30866

Degradation of hydrocarbon polymers by exposure to 275 F for 400 hours in presence and in absence of ammonium perchlorates [NASA-CR-119003] 16 p2554 N71-30844

Surface flame spreading characteristics of KClO₄ reference composite propellant composed of ammonium perchlorate with polyurethane binder 18 p3026 N71-34017

Linear surface pyrolysis of ammonium perchlorate by convective heating [AD-727991] 24 p3806 N71-37866

Ammonium sulfate optical constant calculations based on reflectance, transmittance, and Fresnel reflection measurements in infrared region 24 p3969 N71-38949

Air pollution sampling in vicinity of ammoniac plant [PB-193143] 07 p1015 N71-14096

Wind tunnel tests to determine helical engraving effects on aerodynamic stability of standard ammonium and models [AD-719235] 13 p2191 N71-30866

Development of plating technique for electroplating plating metal rotating bands used on 155 millimeter artillery shells [BDX-613-236] 23 p3762 N71-35023

SUBJECT INDEX

AMORPHOUS MATERIALS

- Temperature dependence of initial permeability of amorphous amorphous Co-P alloy
(AD-711087) 01 p0892 N71-10918
- Characteristics of phenomena in amorphous solids and selective motion in simple liquids
(RFP-109) 02 p0206 N71-11975
- Mechanisms of structural transformation in amorphous solids studied by X ray radial distribution analysis and infrared techniques
(AD-712612) 03 p0398 N71-13390
- Investigating low-temperature transformation of amorphous alloys obtained by rapid quenching from liquid state
(CALT-822-11) 05 p0703 N71-15231
- Initial research on electrical and metallurgical properties of amorphous semiconductors
(AD-713483) 05 p0758 N71-15345
- Using amorphous and phase rule concepts to obtain correlation peroxide and nitrate in mixed oxides for propellants
(AD-713564) 05 p0761 N71-15378
- Electrical properties of noncrystalline materials
(AD-713948) 05 p0934 N71-16302
- Electronic properties of solids including atomic and band structure calculations
(AD-714099) 06 p0934 N71-16304
- Electronic properties of amorphous and crystalline materials
(CALT-822-15) 06 p0973 N71-16368
- Material and optical properties of amorphous materials
(AD-714029) 06 p0996 N71-16473
- Molecular field model for amorphous semiconductors with semiconductivity variations
(CALT-822-16) 07 p1069 N71-18068
- Resonance measurements of cleaved single crystal Ge and amorphous Ge films
(AD-715742) 08 p1579 N71-18084
- Electrical resistivity versus temperature measurements on magnetic amorphous alloys
(CALT-822-20) 10 p1583 N71-21582
- Band structure and electrical properties of amorphous semiconductors
(AD-716793) 13 p2150 N71-24082
- Investigation of structure, bonding, electronic conduction, and transport properties of amorphous semiconductors
(AD-719419) 13 p2150 N71-24440
- Theoretical aspects of semiconductivity in amorphous semiconductors from viewpoint of chemical bonding
(RFP-596) 13 p2153 N71-25491
- Polymer physics and constitutive equations for thermoelectric amorphous materials
(AD-720290) 16 p2616 N71-28182
- Determination of optical constants of amorphous thin films of selenium and arsenic trisulfide from infrared reflectivity spectra
(AD-723533) 19 p3169 N71-32155
- Physical properties of metallic layers implanted in amorphous oxide glass
(NASA-CR-111953) 21 p3405 N71-34228
- X ray diffraction analysis of amorphous samples of Fe-Si alloy irradiated with fast neutrons or fission neutrons
(NASA-CR-16993) 21 p3438 N71-34462
- Carbon and hole drift mobilities in photoconductive amorphous selenium
(NASA-TN-D-6508) 21 p3499 N71-34926
- Electrical resistivity of amorphous alloys FeNi10Al18 containing Cr or Fe as function of composition and temperature
23 p3770 N71-36668
- AMORPHOUS SEMICONDUCTORS**
Structural, electrical, and magnetic properties of transition metal oxide-phosphate glasses and glasses in Al2O3-Al2O3 system for amorphous semiconductors
(AD-727154) 24 p3996 N71-38316
- CRYSTALLINITY**
ELECTRIC CURRENT
MECHANISMS
Effects of d-amphetamine on carbohydrate metabolism at ground level and simulated high altitude
(AD-713736) 05 p0633 N71-14641
- HYDROGEN**
AMORPHOUS AIRCRAFT
HYDROGEN
This prediction for nuclear aircraft, amphibious thrust operations, and geodesic surveys
23 p3790 N71-37010
- AMORPHOUS VEHICLES**
AMORPHOUS AIRCRAFT
HYDROGEN
Using infrared spectroscopy in analysis of amorphous vehicles
(ALL-1-71-746-650-19022-401/1) 16 p2598 N71-28912

NT SOUND AMPLIFICATION

- Amplification of acoustic waves in piezoelectric semiconductors by interaction with superoxide electron drift in electric field
01 p0108 N71-10140
- Producing single-frequency lasers by quality discrimination of optical cavity modes
01 p0663 N71-10640
- Microvoltage gain mechanism in high mobility semiconductors
05 p0758 N71-15177
- Mathematical models for seismic amplification and ground motion of recording station geology
(NVO-1163-211) 06 p0946 N71-15912
- Clamped amplifier circuit for horizon scanner enabling amplification and accurate measurement of specified parameters
(NASA-CASE-X08-01704) 10 p1536 N71-20782
- Diversity receiving system with diversity phase lock
(NASA-CASE-X08-01222) 10 p1537 N71-20841
- Antenna tapering angle optimization within structural member design for improved antenna performance
11 p1703 N71-22781
- Radio amplifiers with instantaneous automatic gain control
(JPRS-52891) 13 p2043 N71-24720
- Use of instantaneous automatic gain control in tracking radar
13 p2043 N71-24721
- Digital computer algorithm for determining gain bandwidth properties of distributed parameter loads
14 p2239 N71-26547
- Characterization of spatial profile of laser beam before and after amplification
(AD-72874) 16 p2606 N71-28400
- Flow of time-varying electromagnetic energy, and wide variety of energy gain mechanisms in homogeneous media
(RFP-4117) 18 p2994 N71-31508
- Criteria of absolute, convective, and global instability and criteria of amplification and nonreciprocity of vibrations
(JTF-70-04-9) 23 p3810 N71-37162
- Formalism for describing radiation-matter nonlinear interactions in terms of quantum oscillator properties applied to single mode parametric amplifiers
23 p3821 N71-37254
- Electromagnetic field amplification in finite three-dimensional resonator
(AD-727269) 24 p3887 N71-37708
- Nanosecond pulse amplifier with continuously adjustable gain, working in both polarities
(CEA-N-1439) 24 p3897 N71-37778
- Broadband differential amplifier having gain of 16 from dc to 150 MHz
(CEA-N-1439) 24 p3897 N71-37779
- AMPLIFICATION FACTOR**
U AMPLIFICATION
AMPLIFIER DESIGN
Redesigning Protzold-Ragener balloon sounding ozonometer, noting transistor amplifier, experimental design, and Fourier analysis
02 p0212 N71-11540
- Design and performance of injected beam crossed field amplifier
(NASA-CR-72810) 06 p0623 N71-16378
- Broadband model of broadband pulse width modulated amplifier
(NASA-CR-102997) 06 p0624 N71-16398
- Tunnel diode amplifier circuit stability and background noise effects in terms of bias, temperature, and bandwidth variations
(CEA-R-3709) 09 p1360 N71-20084
- Distribution and mixer amplifiers for human voice communication
(AD-723810) 19 p3064 N71-31710
- Computerized design of integrated selective amplifier as feedback structure or as net-work topology
23 p3739 N71-36660
- Synthesis procedure for negative resistance amplifiers with the delay over finite frequency band
23 p3739 N71-36664
- AMPLIFIERS**
NT BEAM PLASMA AMPLIFIERS
NT BROADBAND AMPLIFIERS
NT CROSSED FIELD AMPLIFIERS
NT CURRENT AMPLIFIERS
NT DIFFERENTIAL AMPLIFIERS
NT DISTRIBUTED AMPLIFIERS
NT FEEDBACK AMPLIFIERS
NT FLUID AMPLIFIERS
NT FREQUENCY MODULATION PHOTOMULTIPLIERS
NT JET AMPLIFIERS
NT LIGHT AMPLIFIERS
NT LINEAR AMPLIFIERS
NT MICROWAVE AMPLIFIERS
NT PARAMETRIC AMPLIFIERS
NT PARAMULTIPLIER TUBES
NT POWER AMPLIFIERS
NT PREAMPLIFIERS
NT SERVOAMPLIFIERS
NT TRANSISTOR AMPLIFIERS
NT TRAVELING WAVE AMPLIFIERS
NT VOLTAGE AMPLIFIERS

AMPLITUDE MODULATION

- Synthetic techniques for active RC filters using operational amplifiers
(AD-712466) 03 p0350 N71-12537
- Nonlinear logarithmic amplifiers as function generators and logarithmic multipliers for nonlinear differential equations
03 p0353 N71-12530
- Classification and signal analysis of pulse width modulated amplifiers
(NASA-CR-102999) 04 p0309 N71-13517
- Trigger circuit for phase difference measurements on alternating current signals
(RFP-5-77) 04 p0311 N71-13533
- Development of stable electronic amplifier adaptable for monolithic and thin film construction
(NASA-CASE-X08-02012) 09 p1557 N71-19466
- Rat estimator for monitoring blood oxygenation and pressure, pulse rate, and pressure pulse curve, using dc and ac amplifiers
(NASA-CASE-XAC-05422) 12 p1861 N71-23185
- Preparation and synthesis of RC network with operational amplifier
(AD-716564) 12 p1890 N71-23615
- Applications for small current amplifying device including solid state sensors, Schottky junctions, and other low noise devices
(AD-719748) 13 p2054 N71-24448
- High gain and low time constant requirements of IACQ amplifiers
13 p2045 N71-24722
- Comb type traveling wave mass amplifier for improved high gain broadband output
(NASA-CASE-XPO-10540) 13 p2080 N71-24831
- Vibromechanograph compensating low weight and small volume piezoelectric microphones with amplifier having high input impedances for high sensitivity and low frequency response
(NASA-CASE-XFP-07172) 15 p2374 N71-27234
- Digital data handling circuits for pulse amplifiers
(NASA-CASE-XNP-01001) 16 p2575 N71-28739
- Design of 6-channel stereomicrophone amplifier prototype
(JLEA-292) 18 p2897 N71-30807
- Computerized design of high frequency amplifiers
(AD-726290) 20 p3361 N71-33136
- Research on avalanche type semiconductor radiation detectors using video amplifiers
(NVO-1246-TA-6) 20 p3328 N71-33775
- Performance data and specifications for amplifiers and signal analyzers for nuclear instruments
(JAEI-MEMO-4383) 22 p3584 N71-33524
- Evaluation of solid state RF amplifier for VOR applications
(FAA-NA-71-38) 23 p3732 N71-36682
- Integrated circuits designed for radio frequency output amplifier and line output stage of television receiver
23 p3736 N71-36641
- Acoustoelectric surface wave amplifier with net terminal gain, low power dissipation, and stable continuous drift field operation
23 p3857 N71-37543
- Nanosecond pulse amplifier with continuously adjustable gain, working in both polarities
(CEA-N-1439) 24 p3897 N71-37778
- Synthesis procedure for developing arbitrary rational admittance matrices using operational amplifiers and RC one ports
24 p3901 N71-37809
- AMPLIFIERS (TRADENAME)**
U PLANOTRONS
AMPLITUDE DISTRIBUTION ANALYSIS
Methods ray oscilloscope for analyzing electrical waveforms representing amplitude distribution of time function
(NASA-CASE-XNP-01383) 01 p0804 N71-10639
- Refractive index estimates for target amplitude comparison and detection by monostatic radar in cluttered environment
04 p0485 N71-13909
- Statistical spectral amplitude distribution of space measurements on atmospheric at very low frequencies during thunderstorms
(NASA-TM-X-67136) 11 p1703 N71-22905
- Antenna response patterns, Doppler spectra, and amplitude distributions of transmittal microwave scatter propagation
12 p1675 N71-23433
- Power supply effects on amplitude distribution and detection efficiency of light pulses by photomultiplier
(JFVS-587-70-11) 18 p2697 N71-36632
- AMPLITUDE MODULATION**
Feedback averaging amplitude modulated laser communication system
(AD-710954) 01 p0825 N71-10874
- Investigating autocorrelation of optical signals and phase fluctuations in diffraction waves on rough screens
(AD-712335) 03 p0357 N71-12465
- Development of demodulation system for receiving transients modulation from two quadrature displaced data bearing signals
(NASA-CASE-XAC-04036) 09 p1363 N71-19472

AMPLITUDE PROBABILITY ANALYSIS

- Equivalent circuit analysis of low frequency collector self modulation in transmitter output stage and frequency-amplitude distortion measurements [AD-716529] 09 p1358 N71-19634
- Numerical analysis of radio signal modulation by amplitude, frequency, and phase modulation 09 p1348 N71-19645
- Introduction to design and use of AM subcarrier telemetry systems, with bibliography [SC-M-70-644] 10 p1534 N71-21247
- Satellite microwave receiver systems which convert carrier frequencies and modulation formats to produce signals compatible with VHF-UHF television receivers for low-cost service [NASA-TM-X-67880] 10 p1521 N71-21299
- Development of apparatus for amplitude modulation of diode laser by periodic discharge of direct current power supply [NASA-CASE-XMS-04269] 11 p1776 N71-22895
- Diurnal phase and amplitude changes in long distance very low frequency radio transmissions over high latitudes 11 p1706 N71-22911
- Electron density changes causing amplitude and phase variations in ionospherically propagated very low frequency radio signals during solar flares 11 p1706 N71-22912
- Ionospheric electron density anomalies effects on space communication wave amplitude and phase stability [NASA-CR-117805] 11 p1711 N71-22941
- Vibrating element electrometer producing high conversion gain by input current control of elements resonant frequency displacement amplitude [NASA-CASE-XAC-02807] 11 p1727 N71-23021
- Mean square exceedance characteristics of single tuned system to amplitude modulated random noise applicable to structural design - graphs 12 p2009 N71-24305
- Radio frequency interference in telemetry systems due to crosslink transferred to phase modulated carrier from single subcarrier modulated with PCM telemetry [AD-719733] 13 p2047 N71-25166
- Scanning signal phase and amplitude electronic control device with hybrid T waveguide junction [NASA-CASE-NFO-10302] 14 p2233 N71-26142
- Meteorological radar echo amplitude modulator for continuous data recording [AD-721249] 15 p2380 N71-27178
- High efficiency transformerless amplitude modulator coupled to RF power amplifier [NASA-CASE-GSC-10668-1] 16 p2561 N71-28430
- Techniques and circuits used in designing AM highly flexible telemetry system comprising single sideband/double sideband/constant bandwidth compatible system - space application 17 p2718 N71-29323
- Recursive functions of sampled bandpass filter input amplitude for calculating output amplitude 17 p2728 N71-29769
- High-dynamic range rise time to amplitude converters [CEA-N-1430] 19 p3070 N71-32092
- Optimization of varactor frequency multiplier amplitude and phase modulations 23 p3723 N71-36535
- Amplitude and frequency modulation characteristics and applications of CW Gunn effect oscillators 23 p3734 N71-36623
- Theory and analysis of demodulating suppressed carrier AM baseband in noise and recorder flutter 24 p3890 N71-37729
- AMPLITUDE PROBABILITY ANALYSIS**
- U. AMPLITUDE DISTRIBUTION ANALYSIS**
- AMPLITUDES**
- NT PULSE AMPLITUDE**
- NT SCATTERING AMPLITUDE**
- Local geology effects on seismic wave amplitudes [NVO-1163-265-VOL-3] 02 p0221 N71-12142
- Measurement of amount of nonlinearity introduced by amplitude dependent time delay computer model [EGG-1183-333] 05 p0645 N71-14918
- K sub L and K sub S regeneration amplitude in copper at 2.5 GeV/c CP non-invariance [NEVS-184] 05 p0746 N71-15236
- Nonfactorizable expression for asymptotic multiparticle amplitude signature with Toller angle variables [RLO-1308-591] 09 p1435 N71-20037
- Transfer function and amplitude frequency characteristics of two degree of freedom gyroscope with position integral negative feedback 11 p1761 N71-22097
- Construction of N-meson amplitude according to positive intercept and abnormal parity trajectories [LPTHE-71/11] 12 p1979 N71-24344
- Circuits for amplitude limiting of random noise inputs [NASA-CASE-NFO-10169] 13 p2059 N71-24844
- Double partial wave expansion of elastic scattering amplitude and particle interactions 14 p2299 N71-25608

- Phase and amplitude scintillations of microwave signals over elevated atmospheric path for obtaining atmospheric density profiles 16 p2561 N71-28431
- [NASA-CR-111926]
- Amplitude and amplitude build up for orthotropic elastic plate subjected to oscillatory in-plane load 17 p2833 N71-29804
- Complete closed forms for amplitude and phase fluctuations in forward scattering study of electromagnetic waves transmitted through turbulent media 19 p3071 N71-32712
- Approximate analytic evaluation of tidal waves [NASA-TM-X-65658] 19 p3097 N71-32795
- Electromagnetic wave propagation in random interstellar media and amplitude fluctuations of radio sources 20 p3231 N71-32838
- Lagrangian functional integral formulation of dual resonance amplitudes [LPTHE-71/23] 20 p3291 N71-33383
- General properties and formula for multiple free dual amplitudes with Mandelstam analyticity [LPTHE-71/26] 20 p3293 N71-33903
- Approximations for predicting amplitudes of reflected and transmitted waves in inhomogeneous media [FTAS/TR-71-59] 21 p3389 N71-34114
- Quadratically divergent terms in amplitudes of weak nonequilibrium processes with photon emission studied in theory with intermediate boson [NP-18777] 21 p3487 N71-34840
- Phase distribution, amplitude, and amplitude distribution in relation to latitude for 11 year fluctuations of atmospheric pressure caused by sun [NLL-M-20631-3428.4F] 21 p3505 N71-34972
- Single mode analysis for calculating shifts in amplitude and frequency of E X B instability 22 p3656 N71-36076
- Design, operation, and calibration of signal amplitude measuring system for computer secondary standard magnetic tapes by reference tapes [NBS-SP-260-29] 23 p3730 N71-36590
- Astrological observations of free diurnal nutation amplitudes of earth 23 p3748 N71-36725
- Mathematical analysis of plane sound waves of finite amplitude in nondissipative medium [NRC-12146] 23 p3803 N71-37112
- Comparison of amplitude scintillations in S band and VHF region from ESSA 9 and ITOS 1 transmissions at high latitudes [NOAA-TR-ERL-207-OD-6] 24 p3890 N71-37725
- High precision thermostat for gravimetric recording of earth tide amplitudes 24 p3910 N71-37870
- Small frequency and amplitude variations of satellite radio signals 24 p3915 N71-37919
- Amplitude variations and longitude asymmetry with respect to sunspot activity 24 p4011 N71-38400
- Temperature drift and peak current degradation in tunnel diodes used for amplitude discrimination 24 p4013 N71-38622
- ANALOG CIRCUITS**
- Electric network for monitoring temperatures, detecting critical temperatures, and indicating critical time duration [NASA-CASE-XMF-01097] 06 p0827 N71-16058
- Automatic closed circuit television arc guidance control for welding joints [NASA-CASE-MFS-13046] 09 p1346 N71-19433
- Electronic divider and multiplier for analog electric signals [NASA-CASE-XPR-05637] 09 p1358 N71-19480
- Quantized random signal correlator output signal to noise ratio expression and comparison with output ratio of analog and polarity coincidence correlators [AD-7118803] 12 p1892 N71-23378
- Comparison of analog and digital waveform discriminators for radiation counters [JUL-640-ZE] 15 p2468 N71-27312
- Magnetic cores for analog computer storage devices 17 p2723 N71-30025
- ANALOG COMPUTERS**
- Advances in electronic and analog computers [JPRS-51522] 01 p0028 N71-10504
- Analog computer simulation of parasitically loaded rotating electrical power generating system [NASA-TN-D-6070] 01 p0088 N71-10963
- Design of analog computer with constant diagnostic monitoring [AD-711144] 02 p0186 N71-11309
- TAPECLIP data system for processing isotograms from analog magnetic tape [NASA-CR-73483] 02 p0190 N71-11334
- Digital fluorimetric compensator for analog fluid systems [AD-713026] 03 p0345 N71-13383
- Analog simulation in nuclear power engineering [AD-713273] 05 p0722 N71-14543
- On-line solid-state reactivity computer for reactor physics testing [WAPD-TM-896] 05 p0728 N71-15113

- Perturbation expansion of Coulomb potential for determining pair distribution function in plasmas [AD-717038] 10 p1527 N71-20000
- Digital and analog computer processes of artificial intelligence 11 p1721 N71-22899
- Mathematical models for analog computer representation of wheeled vehicle electric systems [AD-718075] 12 p1927 N71-24779
- Digital simulation, digital filters, PDP 9 computer, on-line programming, hybrid computers, computer graphics, plotters, analog computers, optimization and integrated circuits [REF-15-70-400] 12 p1882 N71-24880
- Monte Carlo technique using repetitive analog computer for estimating lowest eigenvalues for certain partial differential equations with Dirichlet boundary conditions 12 p1884 N71-24880
- Hybrid analog computer for magnetogram data processing 13 p2053 N71-24900
- Applicability of gradient method as optimization strategy for use with hybrid analog computers [NRP-18464] 14 p2224 N71-26000
- Analog computer for neutron-gamma discrimination in proportional counter pulse amplitudes [CEA-N-1314] 15 p2470 N71-27700
- Analog signal processing using analog computer components [DLR-MITT-71-06] 19 p3060 N71-31807
- Analog and digital techniques for computation of shock and Fourier spectra compared on basis of speed, accuracy, and ease of use [AD-723536] 19 p3061 N71-31810
- Spectral analysis of submarine perturbations using analog computers 21 p3417 N71-34066
- Automatic computation of navigation coordinates using analog and digital computers [AD-726603] 22 p3618 N71-37978
- Analog study of ship propulsion reactors [CEA-CONF-1750] 22 p3261 N71-34880
- Handbook presenting classification of electronic and analog computers and analog devices [AD-727263] 24 p3895 N71-37700
- Basic requirements for computers designed for operations with control automation systems [AD-727265] 24 p3895 N71-37700
- ANALOG DATA**
- Whistler recorder using autocorrelation and analog data - frequency and field strength variation of ionospheric whistler [BMW-FB-W-70-58] 08 p1189 N71-19088
- Data compression processor for monitoring analog signals by sampling procedure [NASA-CASE-NFO-10068] 08 p1167 N71-19088
- Wide range analog data compression system [NASA-CASE-XGS-02612] 09 p1352 N71-19428
- Solid state monolithic integrated analog multiplexers based on controlled transconductance principle [NASA-CR-118014] 12 p1884 N71-22879
- Evaluation of analog techniques for image registration of vidicon television cameras on ERTS-A 14 p2259 N71-25608
- Analog coding in nonlinear data transmission systems [AD-712228] 15 p2380 N71-27178
- Restoration of time function of radiant flux in thermal radiometer by means of analog techniques 15 p2411 N71-27394
- Analog signal processing using analog computer components [DLR-MITT-71-06] 19 p3060 N71-31807
- ANALOG SIMULATION**
- Fluorescent particle diffusion test for determining stochastic motion of chemical warfare agents in forest area [AD-713069] 03 p0404 N71-11378
- NASA program for evaluating underwater vehicle crew performance as space station operational analog [NASA-TM-X-64548] 06 p0850 N71-14010
- Stability of finite-difference analogues to formulating equations for barotropic motion in incompressible hydrostatic fluid [NOAA-TM-NWS-NMC-49] 06 p0885 N71-14077
- Analog computer simulation of design parameter effects on stability of direct acting gas pressure regulator based on Brayton cycle space power generator [NASA-TN-D-6267] 10 p1496 N71-21111
- Physical analog model for human vestibular response in guidance and control systems [NASA-CR-117008] 11 p1685 N71-22880
- Analog simulation of peripheral, ascending, and central auditory perception mechanisms and bandwidth compression relationships to speech recognition [AD-720466] 14 p2206 N71-25608
- Analog simulation of neutron flux distribution by Xe-135 poisoning in nuclear reactors [NLL-CE-TRANS-5363-9022.09] 16 p2637 N71-29840
- Analog models to measure two-dimensional and three-dimensional distribution of magnetic field density of magnet for bubble chamber [JSC-T-70-2] 18 p2960 N71-30004

SUBJECT INDEX

Development of analog model of source adaptation and simulation of spontaneous activity of neuron network
[N75-53597] 19 p3043 N71-32032

Analog flicker noise simulation using white noise processes by mathematical models
[N75-TN-494] 19 p3068 N71-32747

Theoretical analog for sonic boom indoor pressure wave effect on structural members
[N75-TN-158] 20 p3212 N71-33964

ANALOG TO DIGITAL CONVERTERS

Use of circuit codes in analog to digital conversion
[AD-711944] 62 p0189 N71-11327

Both isolation techniques for analog to digital conversion of speech signals
[N75-49023] 63 p0343 N71-12492

Computer program ADMAG for analog to digital conversion of data on XDS 990 computer
[AD-712674] 63 p0344 N71-12498

Analog to digital converter for converting pulses to frequencies
[NASA-CASE-XLA-06670] 63 p0344 N71-12501

Complexing conversion of signals into common digital form and transmission by time division multiplexing along wire or fiber optic cables
63 p0347 N71-12621

Fundamental possibilities of digital phase measurement
[BAR-LIB-TRANS-1428] 64 p0513 N71-13541

Analog/digital method for realizing matched filters for radar signal processing
64 p0508 N71-13924

Analysis of high speed analog to digital conversion system for use with MTI radar data
[N75-118] 65 p0649 N71-14029

Reliable chamber on-line film plane digitizing system using CDC 3100 computer
[N75-70-19] 65 p0685 N71-14982

Automatic system for analog to digital conversion and digital recording of seismic signals
[NASA-C-497-26] 65 p0651 N71-14989

Analog to digital converter development, including circuit diagrams
[AD-717666] 66 p0818 N71-16096

Interfacing continuous analog to digital converter with parallel digital output and nonlinear feedback
[NASA-CASE-XAC-04931] 66 p1164 N71-18594

Voltage drift compensation circuit for analog-to-digital converter
[NASA-CASE-XNP-04780] 69 p1353 N71-19487

Field experiments, using analog to digital converter
[JUL-495-PP] 69 p1450 N71-20377

Analog to digital converters using parallel voltage dividers and pulsed power supplies
11 p1719 N71-22243

Development and characteristics of fluid oscillator using a digital converter with variable frequency controlled by signal passing through conditioning circuit
[NASA-CASE-LBW-10345-1] 14 p2232 N71-25899

Data acquisition system for converting displayed analog signal to digital values
[NASA-CASE-NPO-10344] 14 p2235 N71-26544

Lighting of radar echoes for presentation of navigation rate grid maps
[N75-FB-70-32] 15 p2437 N71-26973

Apparatus for automatically testing analog to digital converters for open and short circuits
[NASA-CASE-XLA-06713] 16 p2596 N71-28991

Specifications and performance tests for digital pressure transducers designed for spacecraft application
17 p2751 N71-29321

Analog to digital and digital data processing of temperature and velocity fluctuations recorded above and below the surface power spectra
[AD-722922] 18 p2897 N71-31436

Analog to digital converters for voice signal analysis
[N75-53065] 19 p3042 N71-32609

Analog to digital converters for description and recognition of voice signals
19 p3042 N71-32611

Handbook presenting classification of electronic and analog computers and analog devices
[AD-77282] 24 p3893 N71-37758

Analog to digital converter design for residual class system operation without conversion to numerical problem operation
[AD-727976] 24 p3896 N71-37767

ANALOGS

Hydrodynamic analogy in celestial mechanics
[NASA-CR-111364] 62 p0294 N71-11414

Analogy for use of analogies in areas of decision-making and situation analysis
[AD-709042] 64 p0623 N71-14362

Computer program for solving n-dimensional transient or steady state heat flow problems by creating electrical analogy of problem and solving by finite difference method
[NASA-CR-72916] 24 p3892 N71-37754

Using automatic electron trajectory tracer for studying image properties of electrostatic image tubes
21 p3464 N71-34224

Algorithms for determining analogs of fields for long range weather forecasting
[NLL-M-20694-58284P] 21 p3453 N71-34579

He-3, J, reaction and isobaric analog state in Ti, Fe, Ni, and Zn isotopes
22 p3649 N71-36021

ANALYSES

U ANALYZING

ANALYSES [MATHEMATICS]

NT ABEL FUNCTION

NT ANALYTIC FUNCTIONS

NT ASYMPTOTES

NT ASYMPTOTIC SERIES

NT BANACH SPACE

NT BESSEL FUNCTIONS

NT BETHE-SALPETER EQUATION

NT BINARY INTEGRATION

NT BURGER EQUATION

NT CALCULUS

NT CALCULUS OF VARIATIONS

NT CHANDRASEKHAR EQUATION

NT COLLINEABILITY

NT COMBINATORIAL ANALYSIS

NT COMPLEX VARIABLES

NT COMPOSITE FUNCTIONS

NT CONFORMAL MAPPING

NT CONTINUITY [MATHEMATICS]

NT CONVOLUTION INTEGRALS

NT CUBIC EQUATIONS

NT DELTA FUNCTION

NT DEPENDENT VARIABLES

NT DIFFERENTIAL CALCULUS

NT DIFFERENTIAL EQUATIONS

NT EINSTEN EQUATIONS

NT ELLIPTIC DIFFERENTIAL EQUATIONS

NT ELLIPTIC FUNCTIONS

NT ENTIRE FUNCTIONS

NT EXISTENCE THEOREMS

NT EXPONENTIAL FUNCTIONS

NT EXTREMUM VALUES

NT FOKKER-PLANCK EQUATION

NT FOURIER ANALYSIS

NT FOURIER SERIES

NT FOURIER TRANSFORMATION

NT FOURIER-BESSEL TRANSFORMATIONS

NT FREDHOLM EQUATIONS

NT FUNCTION SPACE

NT FUNCTIONAL ANALYSIS

NT FUNCTIONAL INTEGRATION

NT GAMMA FUNCTION

NT GAUSS EQUATION

NT GREEN FUNCTION

NT HALF SPACES

NT HARMONIC ANALYSIS

NT HARMONIC FUNCTIONS

NT HELMHOLTZ VORTICITY EQUATION

NT HILBERT SPACE

NT HILBERT TRANSFORMATION

NT HYPERBOLIC FUNCTIONS

NT INTEGRAL CALCULUS

NT INTEGRAL EQUATIONS

NT INTEGRAL TRANSFORMATIONS

NT JACOBI MATRIX METHOD

NT KERNEL FUNCTIONS

NT LAGUERRE FUNCTIONS

NT LAME WAVE EQUATIONS

NT LAPLACE TRANSFORMATION

NT LEBESGUE FUNCTIONS

NT LIAPUNOV FUNCTIONS

NT LIMITS [MATHEMATICS]

NT LINEAR EQUATIONS

NT LIOUVILLE EQUATIONS

NT LIPSCHITZ CONDITION

NT LOGARITHMS

NT MATHEW FUNCTION

NT MAXIMA

NT MEASURE AND INTEGRATION

NT MEMORPHIC FUNCTIONS

NT MINIMA

NT NEUMANN PROBLEM

NT NONLINEAR EQUATIONS

NT NUMERICAL ANALYSIS

NT NUMERICAL INTEGRATION

NT ORTHOGONAL FUNCTIONS

NT PADE APPROXIMATION

NT PARABOLIC DIFFERENTIAL EQUATIONS

NT PARTIAL DIFFERENTIAL EQUATIONS

NT PERIODIC FUNCTIONS

NT PHASE-SPACE INTEGRAL

NT POISSON EQUATION

NT POWER SERIES

NT QUADRATIC EQUATIONS

NT RATIONAL FUNCTIONS

NT REAL VARIABLES

NT RUNGE-KUTTA METHOD

NT SERIES [MATHEMATICS]

NT SINGULAR INTEGRAL EQUATIONS

NT SINGULARITY [MATHEMATICS]

NT SPHERICAL HARMONICS

NT STURM-LIOUVILLE THEORY

NT TANGENTS

NT TESSELAR HARMONICS

NT TRIGONOMETRIC FUNCTIONS

NT VECTOR ANALYSIS

NT VLASOV EQUATIONS

ANALYTIC FUNCTIONS

NT VOLTERRA EQUATIONS

NT VORTICITY

NT WEIGHTING FUNCTIONS

NT WIENER HOPF EQUATIONS

NT ZONAL HARMONICS

Calculations on hot spot factor in thermal design of reactor cores
[NASA-TT-P-13390] 62 p0264 N71-11459

Analytical procedures for predicting mechanical properties of fiber reinforced composites
[AD-713675] 65 p0707 N71-14540

Mathematical analysis of geological formations of effect on seismic motions
[UCRL-50096] 65 p0667 N71-14095

Research progress in various aspects of applied mathematics, meteorology, engineering, nuclear physics, and optical measurement
65 p0679 N71-15544

Equations for radiation heat cells, which are used for designing actinometric and radiometric devices
66 p0961 N71-16099

Radiation theory and effects of interference in infinite planar arrays - MART program
[AD-714887] 66 p1161 N71-18294

Radiation theory and effects of scattering interfaces in infinite planar arrays - MART program
[AD-714888] 66 p1161 N71-18295

Mathematical representation of ion beam current density profiles
[NASA-TM-X-52992] 10 p1634 N71-30940

Mathematical procedure for Born stability determination of body centered cubic crystal lattice tensile properties
[AD-717696] 11 p1817 N71-23423

Brownian motion of interstellar grains and mean quadratic displacement calculations
11 p1824 N71-22900

Analysis and synthesis of linear feedback control systems using state vector control
13 p2035 N71-24711

Motion stability analysis of satellite with main rigid body and three pairs of flexible booms
[NASA-CR-116639] 14 p2342 N71-25933

Two methods of analysis, synthesis, and self-regulation of nonlinear units in control systems
[NLL-CE-TRANS-5486-7002.09] 17 p7773 N71-29739

Asymptotical relations for averaged oscillations and generalizations of some asymptotical equalities when violating microcausality
[ITP-70-90-E] 18 p3943 N71-36385

Formula for calculating rate of condensation growth of drops in clouds considering latent heat of condensation
[AD-724165] 20 p2394 N71-32803

Variation of Marinkina no-joint production turnpike theorem when production possibilities vary with time
[P-4493] 21 p3448 N71-34541

ANALYTIC FUNCTIONS

NT ENTIRE FUNCTIONS

Defining set of global real analytic coordinates for Teichmüller space with respect to Fréchet model
65 p0714 N71-15586

Analytical models of two phase transfer flow in pipes
[PB-194836] 67 p0005 N71-16926

Investigating interaction between FORMAC data organization and algorithm design
68 p1227 N71-19187

Analytic functions and fluid models for noise propagation in supersonic jet exhaust flow
[NASA-CR-1848] 15 p2364 N71-27028

ALGOL computer program for estimation of maximum of analytical functions with arbitrarily small error bound
17 p2772 N71-29482

Analytic solutions of reference spectrum equation for nuclear matter
[DEMO-7024] 18 p2943 N71-30419

Integral representation for functions holomorphic in tube domains over arbitrary proper cones
[ITP-70-33] 18 p2976 N71-30633

Approximate analytic evaluation of tidal waves
[NASA-TM-X-43638] 19 p3087 N71-32795

Analytic functions solving equations of motion in Newton theory for ballistic trajectory in atmospheric medium
[DLR-FB-71-16] 22 p3670 N71-36148

Structural analysis of uniform beam under various end conditions using finite element and analytic methods
22 p3683 N71-36263

Conference on analytical functions and topology of algebraic spaces
24 p3947 N71-36159

Pinkestens theorems on convex and concave spaces for holomorphic transformations
24 p3948 N71-36160

Approximation theorem of Grunert for holomorphic functions
24 p3948 N71-36161

Holomorphic fibers in sub-spaces of Stein spaces
24 p3948 N71-36164

Holonomy theory for analytic vector fields
24 p3948 N71-36166

ANALYTIC GEOMETRY

Holomorphic matrix method for linearization of analytical bundles and in series convergence
24 p3948 N71-38167
Rings of holomorphic function germs in Banach space
24 p3948 N71-38168

ANALYTIC GEOMETRY

NT CONICS
NT CYCLOIDS
NT ELLIPSES
NT HYPERBOLAS
NT LOCUS
NT MERCATOR PROJECTION
NT OBLATE SPHEROIDS
NT PARABOLAS
NT PROLATE SPHEROIDS
NT S CURVES
NT SPHEROIDS
NT TANGENTS
NT TORUSES
NT TRIANGOMETRY
Geometric stress mechanics for crystal lattice defects
17 p2823 N71-29990
Kinematic distribution of crystal lattice defects
17 p2823 N71-29992
Analytic method for interface relationships between different surface geometries
20 p3291 N71-33280
ANALYTICAL CHEMISTRY
High efficiency counting of Bi-210 by liquid scintillation technique
00 p0433 N71-12951
Construction of unique underground whole body counter - conference
07 p1061 N71-17213
[UCL-72799]
Chemical analysis techniques and equipment for nuclear chemistry
15 p3277 N71-37202
Determining micro amounts of elements contained in natural water by means of neutron-activation analysis
23 p3812 N71-37179
[RT/CIL-70133]
Projects and techniques including mass spectrometry, gas chromatography, combustion carbon analysis, atomic absorption spectrophotometry, and related analytical chemistry methods
24 p3885 N71-37693
[UCL-50066-71]

ANALYZERS
NT SIGNAL ANALYZERS
Creve electron-energy-analyzing scanning microscope design
01 p0056 N71-10762
[ANL-7656]
Design, development, and fabrication of personnel armor lead profile analyzer
02 p0166 N71-11180
[AD-71876]
Quantitative determination of structure-property relationships in nuclear fuel element materials
08 p1238 N71-18327
[SRO-552-5]
Regarding potential analyzer used with vacuum monochromator for recording photoelectron spectra of iodine and bromine
13 p2041 N71-23565
[ADP-101]
Mixed liquid and vapor phase analyzer design with thermocouples for relative heat transfer measurement
14 p2255 N71-26199
[NASA-CASE-NPO-10691]
Performance data of undersea atmospheric sensor system to monitor and display atmospheric constituents
14 p2258 N71-26607
[NASA-CR-111890]
Automated fluid chemical analyzer for microchemical analysis of small quantities of liquids by use of selected reagents and analyzer units
14 p2216 N71-26754
[NASA-CASE-XNP-49451]
Time structure analyzer for monitoring high frequency components of Manned accelerator beam structure
18 p2959 N71-30498
[REEL/R-210]
Partial pressure analyzer calibration and techniques for measuring gas mixtures and leakage
19 p3078 N71-32227
[SCL-DE-70-275]
Angular electron velocity analyzer for use with scanning electron microscope to identify low concentrations of elements on surfaces of semiconductor devices
21 p3425 N71-34371
[NASA-CR-111968]
Microchemical analyzer using arrays of interconcentrated capacitors and low detector
21 p3427 N71-34382
[NASA-CASE-ARC-10463-1]
High resolution energy analyzer with time of flight spectrometer for studying highly ionized hydrogen and helium plasmas
23 p3826 N71-37291
[UPT-DT-22]
Design and construction of Holmium spectral analyzer to aid in research of air pollutants
24 p3928 N71-37957
[NASA-CR-123170]

ANALYZING
Automated microbial metabolism life detection experiments for astrobiological studies
14 p2206 N71-26380
[NASA-CR-118499]
ANATOMY
NT ADRENAL GLAND
NT ARTERIES
NT BLOOD VESSELS
NT BOWELS
NT BRAIN

NT BRAIN STEM
NT CAPILLARIES [ANATOMY]
NT CARDIAC VENTRICLES
NT CARDIOVASCULAR SYSTEM
NT CEREBRAL CORTEX
NT CREMORECEPTORS
NT CIRCULATORY SYSTEM
NT COCHLEA
NT CRANIUM
NT EAR
NT ERYTHROCYTES
NT EYE [ANATOMY]
NT FINGERS
NT FOREARM
NT HAND [ANATOMY]
NT HEAD [ANATOMY]
NT HEART
NT HEMATOPOIESIS
NT HIPPOCAMPUS
NT HUMAN BODY
NT JOINTS [ANATOMY]
NT KIDNEYS
NT LABYRINTH
NT LEG [ANATOMY]
NT LEUKOCYTES
NT LIVER
NT LUNGS
NT LYMPHOCYTES
NT MUSCULOSKELETAL SYSTEM
NT MYOCARDIUM
NT NOSE [ANATOMY]
NT ORGANS
NT OTOLITH ORGANS
NT PHOTORECEPTORS
NT PUPILS
NT RESPIRATORY SYSTEM
NT RETINA
NT SCIATIC REGION
NT SEMICIRCULAR CANALS
NT SENSE ORGANS
NT SKULL
NT SPLEEN
NT SYSTOLE
NT TESTES
NT THYMUS GLAND
NT THYROID GLAND
NT TRACHEA
NT VASCULAR SYSTEM
NT VERTEBRAE
NT VERTEBRAL COLUMN
NT VESTIBULES
ANCHORS [FASTENERS]
Precision oceanographic free vehicle instrument system using programmed time release
21 p3417 N71-34311
[UCSD-34-F-127-4]
ANECROSC CHAMBERS
Ninety foot quasi-tapered anechoic chamber for radiation measurement from low to VHF and millimeter wavelength frequencies
02 p0198 N71-11534
[AD-711646]
Electromagnetic theory, antennas, microwave equipment, and radio anechoic chamber
10 p1517 N71-20602
[DI-121]

ANELASTICITY
Analytic study of divanancy damping in gold
03 p0440 N71-12803
[COO-1198-725]
Anelastic properties of neutron irradiated graphite and irradiation-induced interstitials
07 p0196 N71-18129
[CEA-CONF-1636]
Anelastic behavior of austenites, martensites, and bcc refractory alloys, and dislocation-solute atom interactions and interstitial hardening in bcc alloys
08 p1211 N71-18259
[COO-1676-13]
ANEMOMETERS
NT HOT-FILM ANEMOMETERS
NT HOT-WIRE ANEMOMETERS
Maximeters for peak wind speed anemometry for Saturn 5 launch umbilical tower and normal meteorological environment
02 p0259 N71-11797
[NASA-CR-61337]
Appropriate anemometer heights for Froude scaling of wind stresses
03 p0404 N71-13247
[AD-712789]
Sea surface wind stress measurements using thrust anemometer
05 p0676 N71-15439
[AD-713167]
Analysis of pulsed wire anemometer to determine errors caused by finite yaw response of probe
05 p0687 N71-15471
[REPT-70-07]
Portable thermomemometer for measuring temperature, velocity, and direction of gas stream
05 p0688 N71-15480
[AD-712646]
Cooled film anemometer for high temperature gas measurements in environments with transient phenomena and small heat transfer to sensor
11 p1763 N71-22611
[AD-713167]
Anemometer with braking mechanism to prevent rotation of wind driven elements
12 p1921 N71-23726
[NASA-CASE-XMF-65224]
Directional ion current anemometer for measuring direction and elevation angles and speed of wind to 3 centimeters per second
14 p2289 N71-26183
[AD-720573]
Design and wind tunnel tests of two-axis wind speed and angle sensor for meteorological applications
24 p3953 N71-38198
[AD-727280]

ANEMOMETRY
U VELOCITY MEASUREMENT
ANESTHESIA
Broadband testing of automated anesthesia machines
23 p3761 N71-38000
[NASA-CR-122646]
ANESTHETICS
Profound effects on anaphylax rigidity of cat gastrocnemius-colens muscles and neuromuscular responses to shock
02 p0158 N71-14157
[AD-712212]
ANGELS
Characteristics of angel cluster on radar display
04 p0494 N71-13180
ANGLE OF ATTACK
NT ZERO ANGLE OF ATTACK
Dynamic stability derivatives of twin-jet fighter model for angles of attack from -10 deg to 110 deg
05 p0629 N71-14000
[NASA-TN-D-6591]
Examining three-dimensional motion of flying vehicle entering atmosphere at low angles of attack
07 p0965 N71-18000
Measuring value of entropy on surface of body in revolution at nonzero angle of attack
07 p0965 N71-18000
Investigation of angle of attack information display for pilots to increase efficiency of general aviation aircraft operations
08 p1143 N71-18000
[NASA-TN-D-6210]
Angle of attack effects on induced rolling moments of low aspect ratio models at transonic speeds
09 p1312 N71-18000
Accelerated supersonic motion of plane of thin angle of attack
12 p1850 N71-18000
[NASA-TT-F-13525]
Measurement of oscillatory pitching moment derivatives on sharp-edged delta wing at vortex breakdown angle of attack
13 p2023 N71-18000
Jet penetration into Mach 2 aluminum using drop back injectors at angle of attack
17 p3736 N71-18000
[NASA-TN-D-2319]
Pressure distribution over 10 deg cone in hypersonic wind tunnel at Mach-14 for various angles of attack
22 p3537 N71-18000
[AD-726533]
ANGLES [GEOMETRY]
NT ANGLE OF ATTACK
NT BRAGG ANGLE
NT BREWSTER ANGLE
NT DIRECTIONAL ANGLE
NT ELEVATION ANGLE
Gage for measuring internal angle of flare on cold tube
15 p2410 N71-18000
[NASA-CASE-XMF-04415]
Optical device containing rotatable prism and reflecting mirror for generating precise angles
14 p2285 N71-18000
[NASA-CASE-XGS-04173]
Simultaneous measurement of direct solar and sky corona radiation using pyroheliometers and goniophotometers
15 p2410 N71-18000
Hybrid computer program for determination of Euler angle sequence transient response
19 p3060 N71-18000
[DLR-FB-71-19]
Root mean square slope angles of Venus surface from radar backscattering and Venus surface slope map data
19 p3183 N71-18000
[FR-49]
Method for determining solar aspect angle from satellite-borne magnetometer data
20 p3300 N71-18000
[RISA-180]
ANGULAR ACCELERATION
Helicopter gyro displacement measurements of differing flying conditions
14 p2199 N71-18000
[FOA-2-C-2356-49-772]
Disoriented visual tracking performance of humans during angular acceleration as result of alcohol consumption
19 p3064 N71-18000
[FAA-AM-71-20]
Angular acceleration effects on guinea pig vestibular nystagmus
20 p3223 N71-18000
Single cell responses within cat medulla during constant angular accelerations
21 p3383 N71-18000
[AD-724628]
ANGULAR CORRELATION
Precision measurement of He-203 beta-gamma directional correlation
01 p0095 N71-18000
[COO-1746-41]
Deriving phase-space relative velocity expressions for angular correlations of particles in final state of nuclei A B yields C D E
04 p0579 N71-18000
[LA-TR-70-15]
Method for extraction of first-forbidden beta nuclei elements from angular correlation data
05 p0749 N71-18000
[COO-1746-44]
Internal fields and relaxation effects for dysprosium in ferromagnetic TBAE studied by perturbed angle correlation
05 p0809 N71-18000
[UUD-464]
Perturbed angular correlation technique for studying effect of cubic lattice on electronic levels of gadolinium ions in HoAl₂
06 p0909 N71-18000
[UUD-465]

SUBJECT INDEX

Gamma-gamma directional correlation measurements in tellurium 124
[COO-1746-40] 06 p0919 N71-16249

Measuring alpha-gamma angular correlations from reaction $Mg-24(\alpha, \alpha')$ gamma/ $Mg-24$ at incident alpha particle energy of 16.65 MeV
[CTC-5] 06 p0920 N71-16257

Investigating angular correlation of angles and twist cross sections in nucleon reactions
[KX-1216] 08 p1230 N71-18236

Gamma-gamma angular correlation function degree of perturbation to recoilless emission probability in ^{151}Eu
08 p1283 N71-19308

Proton recoil spectrum analysis for measuring angular correlation coefficient in neutron decay
[AD-7164-6] 09 p1433 N71-19978

Comparison of Mosebauer effect to time differential perturbed angular correlations in Fe-57-Ni system
[CONF-700114-1] 09 p1454 N71-20022

Relativistic phase-space volumes for angular pion N correlations in reaction N plus N yields N plus pion
[JINR-P7-4917] 09 p1438 N71-20122

Perturbed angular correlation measurements on $Rh-101$ in metal host near Curie temperature
[JINR-25397] 09 p1462 N71-20449

Angular dependence of cyclotron resonance in single gallium crystals
11 p1800 N71-21873

Positron sensitive semiconductor detectors used in measuring angular correlations for helium induced fission of uranium 238
[JINR-7383-7] 11 p1804 N71-22275

Angular correlations of gadolinium conversion electron, vanadium isotope beta particles, and bremsstrahlung
12 p1970 N71-23445

Implication into ferromagnetic materials by Coulomb excitation, perturbed angular correlation method
[COO-585-7] 13 p2139 N71-25495

Simultaneous recording of true and random coincidences using two parameter pulse height analyzer system tested in connection with angular correlation measurements
[JN-1814] 14 p2369 N71-26573

Angular distributions and correlations of alpha and beta particles, electrons, and electromagnetic radiation from oriented nuclei
[LA-065] 16 p2645 N71-28157

Beta-gamma ICP -asymmetry coefficients in isoscalar fission mixed beta transitions
[LFX-1249] 16 p2651 N71-28938

Determination of half life and spins of Gd-155 levels by method of delayed coincidences and angular gamma-gamma correlations
[JINR-55518] 18 p2970 N71-30455

Hyperspherical interactions in research fields including perturbed angular correlation, NMR, Coulomb recoil repulsion, rotational states, and electric monopoles
[JN-18792] 19 p3157 N71-32478

Coincidence spectra of alpha particles from reaction $Be-9He-4$ alpha/ $He-4$ measured for several angular configurations at 1.55 MeV bombarding energy
20 p3326 N71-33944

Particle gamma ray angular correlation study of $Ni-57$ levels in $Ni-58$, alpha gamma $Ni-57$ reaction
21 p3492 N71-34877

Positron barrier excitation states and angular correlation of fission fragments in relation to saddle point deformation
22 p3630 N71-36026

ANGULAR DISTRIBUTION

Tables of angular functions for describing angular measure of light field scattered by spherical particles of different sizes
[AST-70-57-BULL] 01 p0091 N71-10859

Multiple formulation for calculating angular distribution of proton scattering on carbon 12 nuclei
[JN-70-18] 02 p0271 N71-11501

Life times and magnetic moments of excited proton states after proton irradiation determined from angular distribution of gamma rays to establish validity of shell model
02 p0272 N71-11748

Transient analysis of α , β , γ reactions using computer graphs
[JINR-7031] 02 p0278 N71-12171

P up 0 decay angular distribution of nuclear reaction at 4.19 GeV/c
[COO-1192-194] 03 p0422 N71-12678

Proton probe for Pioneer spectroscopy to measure ion and electron density and angular distributions in space
[NASA-CN-73486] 03 p0576 N71-12768

Measuring linear and angular displacements using dual exposure and real time holographic interferometry
03 p0579 N71-12789

Angular distributions for elastic and inelastic scattering of alpha particles by ^{20}Ne
[JN-1206-110] 03 p0428 N71-12863

Electric interaction in the isotopes of cryogenic fission, noting use of Mosebauer effect
03 p0444 N71-13362

Production and decay angular distributions of Delta+/hyperons from pion/proton reactions
[COO-1423-232] 04 p0575 N71-13978

Investigating reaction K^-/p plus N yields K^- plus N plus pion in isoscalar channel near K^-N threshold
[UCRL-19774] 05 p0748 N71-15280

Comparing intrinsic efficiencies of spherical NaI/Tl detectors with efficiencies of cylindrical NaI/Tl detectors
[NASA-TM-X-65393] 05 p0687 N71-15436

Angular distribution measurements of fragments from neutron-induced fission
[LA-4369-TR] 05 p0731 N71-15618

Angular distributions of nuclear transfer reactions between heavy ions
[NP-18448] 06 p0918 N71-16282

Measuring angular distributions and fragment yields for photofission of even-even nuclei near threshold
[LA-4385-TR] 06 p0920 N71-16258

Angular distribution shape of ^{116}Sn , ^{117}Sn and ^{118}Sn charge exchange transitions to 0/1 analog states
[NYO-2171-321] 06 p0923 N71-16724

Angular distributions and polarizations of emerging particle in three body problem using Faddeev equations
[LYCEN-7046] 06 p1248 N71-18202

Numerical calculations of small angle electron scattering cross section dependence on source displacement
[LNF-70/33] 08 p1249 N71-18225

Angular distributions of resonance decay products in reactions positive pion proton yields nucleon resonance neutral rho-meson, and nucleon resonance omega-meson at 2.34 GeV/c
[JINR-P1-5236] 08 p1252 N71-18300

Tabulating observations on angular distributions of scattered neutrons and reaction products of fast neutrons and nuclei
[BNL-400-VOL-1] 08 p1253 N71-18370

Partial cross sections and angular distributions for negative kaon P interactions
09 p1426 N71-19522

Scaling and angular distribution of cosmic ray events for proton plus proton yields pion plus anything reaction
[RLO-1388-587] 09 p1426 N71-19539

Angular energy distribution of particles produced in inelastic pion-nucleon and nucleon-nucleon collisions at superhigh energies
[JINR-P2-5331] 09 p1433 N71-19976

Angular distribution calculations of elastic and inelastic proton scattering by C-12 with allowance for wave function distortion in multiple formalism
[JINR-70-50] 09 p1440 N71-20256

ESRO 1 satellite observation of variations and fine structure in flux density and angular distribution of electrons with energies above 40 keV
10 p1530 N71-21158

Angular diversity propagation paths of space antennas in tropospheric transhorizon scatter link
12 p1876 N71-23459

Angular distribution of small-pitch-angle synchrotron radiation
[NASA-CR-117902] 12 p1973 N71-23933

Alpha particle-nucleon collision model for nucleon energy and angular distribution prediction and residual nuclei cross sections
[NASA-CR-118026] 12 p1974 N71-23994

Angular distribution shapes of ^{116}Sn , ^{117}Sn and ^{118}Sn transitions to positive 0 analog states compared to Noble data
[COO-535-625] 12 p1976 N71-24112

Reorientation effect of gamma ray angular distribution in Cd isotopes caused by Coulomb excitation
13 p2141 N71-25540

Yield and angular distribution of photoneuclear reactions of protons with N-14
13 p2143 N71-25574

Fission product angular distributions from C-12 ion impact with Ge-136 and O-16 ion impact with Sm-154 which yield 107 MeV excited Yb-170 compound nuclei
[CU-1019-76] 14 p2302 N71-25750

Phenomenologically determined isobar angular distributions for neutron-nucleon and pion-nucleon reactions below 3 GeV
[ORNL-TM-3132] 14 p2302 N71-25797

Neutron cross sections and angular distributions for Li-7/ α , n /Be-9 reactions including neutron spectra indications of atomic energy levels
[JINR-P15-5143] 14 p2313 N71-26710

High stability apparatuses for investigating angular distribution of charge particles of 10 to 13th and 14th power eV
[KPKI-70-21-HEP] 14 p2314 N71-26729

Angular distributions and total cross sections of Be-9/deuteron, alpha-0/Li-7/ α and Be-9/deuteron, alpha-1/Li-7/ α reactions in 0.9 to 2.2 MeV energy range
[JINR-1200] 14 p2316 N71-26744

Angular distribution of up final state interaction of D⁺ yields π^+ plus reaction studied with 52 MeV deuteron
[JN-1156] 14 p2319 N71-26794

Proton proton target with high polarization and large angular access - conference
[RP/PA-81] 15 p3439 N71-26982

ANGULAR DISTRIBUTION

Report of experiments including neutron polarization, elastic and inelastic scattering of neutrons on C-12, and angular distribution of fission fragments in U-238 neutron reaction
[BMEW-FBK-70-14] 15 p3459 N71-27047

Angular neutron distribution from beryllium boron reaction
[JINR-P15-5148] 15 p3470 N71-27383

Angular distributions of deuterons and protons in magnesium 24 to magnesium 25 transition
[JINR-B4-5339] 15 p3471 N71-27413

Angular reflection and dissociation of molecular silver oxide beam incident on tungsten surface
15 p3471 N71-27414

Collimation method of identifying elements 102 and 104 and measurement of integral angular distribution of nuclear reaction products for identifying atomic number of elements
[KPKI-TR-329] 15 p3473 N71-27441

Angular distribution vector analysis of polarized deuteron elastic scattering from helium 4 at energies between 3 to 11 MeV
15 p3476 N71-27575

Differential cross sections of elastic and inelastic angular distributions of neutrons scattered from C-12 and excited states of C-13 at angles from 15 deg to 135 deg
15 p3489 N71-27884

Angular distributions and excitation functions of pick up reactions with neutrons measured by bombarding nuclei with N-14 and 15 ions
[JINR-P7-5094] 16 p2643 N71-28079

Angular distributions and correlations of alpha and beta particles, electrons, and electromagnetic radiations from oriented nuclei
[LA-4365] 16 p2645 N71-28157

Measuring angular and energy distributions of electrons ejected from nitrogen using crossed molecular and electron beams
[SC-RR-710050] 17 p2791 N71-29290

Angular distributions and absolute cross sections measured for Be-9 plus t reaction below Coulomb barrier
[CEA-R-4117] 17 p2793 N71-29477

Angular distributions for α , β , γ reactions on Zr-90, Mo-92 and 96 at 41.5 MeV
[NASA-TN-D-6413] 17 p2795 N71-29745

Earth atmospheric thermal radiation spectra and angular distributions and sodium borate scintillators and temperature measuring instruments
[NASA-TT-F-626] 17 p2752 N71-29778

Negative pion-nucleon Coulomb scattering cross sections including angular distributions, transverse momentum distributions, and comparisons with nuclear models
17 p2797 N71-29882

Elastic scattering angular distributions for 13 to 27 MeV helium 3 beam from light targets
17 p2802 N71-30133

Distinct classes in magnetic quadrupole gamma transitions and development of automatic angular correlation measuring equipment
[NP-18492] 18 p2975 N71-30571

Time dependent perturbation theory for evaluating angular distribution of electrons emitted from inner atomic shells by proton impact
18 p2983 N71-31133

High resolution channel plate image intensifier, cooling electron energy and angular distribution
18 p2984 N71-31149

Long slit geometry apparatus for measuring angular distribution of gamma quanta from positron annihilation in single insulator crystals
[CEA-R-4130] 19 p3170 N71-33429

Cyclotron radiation, relativistic velocities, angular distribution, total power, electron distribution, and inverse Compton scattering
20 p3344 N71-33240

Angular distribution of neutron and gamma emission from excited and spin states in isotopic americium 241 to americium 242 decay
[RFP-3947-13] 20 p3318 N71-33566

Disk source energy and angular distribution calculations using gamma ray transport codes
20 p3337 N71-33954

Angular distributions for nuclear reaction Be-12 plus deuteron yields Be-125 plus proton
[ANU-P1511] 20 p3328 N71-33977

Neutron polarization from Be-14/ α , Be-4 reaction at low deuteron energies
[JINR-1252] 21 p3409 N71-34092

Transition radiation angular distributions excited by nonrelativistic particles for different indices of refraction and absorption coefficients
[JINR-P4-5086] 21 p3409 N71-34098

Energy and angular distributions of neutron emissions from targets for T(d, α)He-4 reactions
[JINR-45-65] 21 p3477 N71-34759

Angular and energy distributions of particles produced in inelastic pion-nucleon and N-N collisions in center of mass system at superhigh energies
[ORNL-TR-3433] 21 p3480 N71-34782

Multiplex Hadamard-transform target designed to measure angular distribution of particles in presence of large background
[JINR-P15-5099] 21 p3482 N71-34885

- Cyclotron for measuring angular distributions from 15 deg to 165 deg for transitions in B-10 states - reaction mechanism and cluster structure
- Absolute cross section and angular distribution of deuteron photodisintegration
- Spectroscopic analysis of deuteron angular distributions in titanium isotopes using [B,4] and [p,4] reactions
- Angular distribution and velocity analysis of alkali chloride reactions
- Irradiation yield curves and angular distributions for Li-6 C-12 reaction
- Angular and energy distributions of neutrons produced by bombarding thick beryllium targets with 33.8-MeV deuterons
- Angular and energy distributions during molecular dissociation due to electron bombardment
- Auroral proton spectra and angular distribution from Cosmos 261 satellite observations, and polar substorm concept
- Pitch distribution of protons precipitating in auroral zone in range of hundreds keV, as observed from Cosmos 261 satellite
- Effect of optical parameters of refractive index on yield and angular distribution of transition radiation of nonrelativistic charged particles
- Comparison of angular distributions based on various models for elastic scattering of 25 MeV alpha particles
- Hadamard transform acclimation counter for measuring angular and spatial distributions of nuclear and atomic particles in presence of noise
- Angular distributions and nuclear interactions of pions from oxygen
- ANGULAR MOMENTUM
- Large angle proton-proton elastic scattering at intermediate momenta
- High resolution neutron scattering measurements and analysis of resonance angular momentum and parity
- FORTRAN 4 subroutines for coupling coefficients and matrix elements in quantum mechanical theory of angular momentum
- Evidence for angular momentum fractionation in decay of compound nuclei
- Divergent Regge helicity sums, distributions and Toller angles
- Nonfactorizable expression for asymptotic multiparticle amplitude signature with Toller angle variables
- Angular momentum effects on nuclear fusion reactions of gold, platinum, tantalum, lead and bismuth
- Heisenberg ferromagnetism at low temperatures with boson theory of angular momentum including spin operators
- High energy total summation of perturbation series and particle spin angular momentum effects on scattering amplitudes including Regge trajectories
- Vector analysis of stripping reactions and elastic scattering from deuteron irradiation of O-16, Cr-52, Fe-54, and Zn-90 targets
- Complex angular momentum of partial wave amplitudes examined for production of three particles in collisions of two strongly interacting particles at high energy
- Polarization measured for secondary protons emitted at about 640 MeV in reactions proton proton yields pion/pion/ proton neutron and proton proton yields pion/pion/ proton proton
- Angular momentum effects on probability of compound nucleus formation and alpha particle evaporation in de-excitation of Te-120
- Negative pion-meson Coulomb scattering cross sections including angular distributions, transverse momentum distributions, and comparisons with nuclear models
- Riemann method for arbitrary angular momentum in inverse problem of scattering theory
- Angular momentum flux carried by solar wind calculated from Mariner 5 data
- Angular momentum restrictions of s-channel exchange from s-channel helicity conservation in elastic reactions
- Angular momentum decomposition of three body problem and binding energy per particle of nuclear matter
- Application of Regge pole theory to large angle positive pion photoproduction
- In Tokamak plasma, canonical angular momentum of trapped particles drifting toward magnetic axis
- ANGULAR MOTION
- ANGULAR VELOCITY
- Measuring energy and angle dependence of cross section in pion-pion scattering
- Orbital calculation and elements of Proton 4 satellite and upper atmosphere angular velocity
- Describing angular position and velocity sensing apparatus
- Gas bearing angular velocity control system
- Angular velocity evolution of solar system isolated planets, asteroids, and comets
- Velocity components and radial pressure distributions in vortex gyros for measuring angular velocity
- Head and eye movements affected by angular velocity and linear acceleration in aerospace environments
- Anticonspicuous oculomotor response during rapid head rotation at high angular velocity
- Angular velocity transduction of semicircular canals of head
- Interactions between optokinetic and vestibulo-ocular responses during head rotation of angular velocity in various planes
- Vestibular mechanics of semicircular canal function during angular velocity
- Dynamic model of semicircular canal affected by angular velocity
- Angular velocity and linear acceleration effects on visual perception in aerospace environment
- Vortex flows of second-order nonnewtonian liquids investigated using mathematical model
- Statistical nonlinear model of axisymmetric charged particle beams with nonzero angular velocities
- Control of angular motion of space vehicle during atmospheric reentry
- Nonlinear angular velocity aerodynamic damping coefficient effects on statically stable missile configurations and internal mass distribution effect based on wind tunnel stability tests
- ANGULOIDES
- NT FEROXIDES
- Electron irradiation induced separation of Sb from SnO₂ solutions in anhydrous alcohols, ethers, ketones, acids, esters, and aromatic hydrocarbons
- Effect of process conditions on tensile properties of DOEBA and phenol novolac resin reacted with adduct of methylene diamine and phthalic anhydride
- Synthesis of high purity disulfide
- Chemical analysis of sulfide and cyclohexane mixtures to determine viscosity in critical region
- ANGULOIDES
- NT BATS
- NT BEES
- NT BIRDS
- NT CATS
- NT CHICKENS
- NT DOGS
- NT DOLPHINS
- NT FISHES
- NT FROGS
- NT GUINEA PIGS
- NT HUMAN BEINGS
- NT INSECTS
- NT MAMMALS
- NT MICE
- NT MICROSPORES
- NT MONKEYS
- NT PARAMECIA
- NT PIGEONS
- NT POCKET MICE
- NT PORPOISES
- NT PRIMATES
- NT PROTOZOA
- NT RABBITS
- NT RATS
- NT RODENTS
- NT SHARES
- NT SPORES
- NT SWINE
- Biological effects on animals and plants cultured
- Zood-5, 6, and 7
- Characteristics of optokinetic eye-movement patterns and synergisms in man and animals
- Radiation hardened transmitter surgical implantation in animals for electrocardiogram biotelemetry in AD-718151
- Biomedical telemetric systems for monitoring physiological parameters of animals
- Hypoxic hypoxia effects on human and animal resistance to infectious diseases and immunobiological reactivity
- Extrapolation of animal tolerance of air contaminants to human tolerances for diver breathing under hyperbaric conditions
- Air quality criteria for nitrogen oxides and their toxicological effects on animals, plants, and human beings
- Use of nutritional markers for studies of food intake, passage, and absorption in gastrointestinal tract of humans and animals
- Radiotelemetry equipment used in investigation Recording Location System, and results in roosts ground, aircraft, and satellite tracking of elk and black bear
- ANIMATION
- U MOTION
- ANIONS
- Development of positive ion detectors to measure ion characteristics in directed pulse plasmas
- Anion exchange separation of neptunium from uranium and thorium in aqueous tetramethylammonium hydroxide
- Negative ion vacancy formation efficiency measurements of KBr as functions of temperature and lattice energy between 6K and 300K
- Resin crosslinking effects on anion exchange separation of rare earth-EDTA complexes at trace loadings
- Oxidation and reduction half wave potentials, and electron spin resonance of positive and negative radicals
- Collisional ionization between calcium atoms and NO₂, N₂O, and O₂ molecules
- Fabrication and properties of hot-pressed polycrystalline magnesium oxide containing silver impurities
- Ductile fracture in anisotropic solids studied by Dugdale model
- Calculation of growth rates of electrostatic waves in infinite homogeneous plasma
- Propagation of amplitude modulated, high RF plan electromagnetic wave through anisotropic plasmas
- Radio wave scattering from random electron density fluctuations in cold anisotropic magnetoplasmas
- Determination of dipole antenna electrical impedance in anisotropic media using charge distribution on radio frequency impedance probe surface
- Hydrodynamic equations for arbitrary anisotropic plasma allowing for Coulomb collisions among plasma particles
- Analysis of pion/minor proton yields versus pion/minor proton/minor in pion/minor equals 1,2,3 and pion/minor proton yields neutron 2 pion/minor in equals 1,2 reactions

SUBJECT INDEX

ANNIHILATION REACTIONS

Open circuit sensitivity of radially polarized ferromagnetic ceramic hollow sphere transducer ceramic to magnetic material
[AD-722611]

Continuous mechanics for nonlinear dynamic dislocation analysis on anisotropic elastic media
[AD-728221]

Validation derivation of partial differential equation for Saint Venant torsion problem of non-homogeneous anisotropic bars
[AD-728221]

ANISOTROPIC PLATES
Photo-elastic analysis of anisotropic circular disks subjected to sufficient internal pressure to cause plastic deformation
[AD-714376]

Calculation of flexure and stability of rectangular and nonrectangular anisotropic plates by differential element method
[AD-710779]

Residual stress and incompatibility problem in linear elastic distortion of infinite anisotropic body
[AD-710779]

Structural and elastic properties of zonal twin dislocations in anisotropic crystals
[AD-710779]

Magnetohydrodynamics of plasma flows in plasma with anisotropic pressure
[AD-710779]

Polynomial approximation and linear anisotropic diffusion in one-dimensional cylindrical geometry
[AD-710779]

Large velocity discontinuities in solar wind in anisotropic medium
[AD-710779]

Determination of models for collision induced anisotropic polarizability by moment method
[AD-710779]

Flexural strength of alumina ceramics increased by reduction of crystal anisotropy
[AD-710779]

Anisotropy of gamma radiation emitted by Fe-142 nuclei in polycrystalline prosoyolite
[AD-710779]

Time resolved neutron measurement of anisotropy and relaxation of deuteron velocity distribution
[AD-710779]

Determination of monochromatic emissivity of pyrographites at various temperatures and effect on anisotropy of emission properties
[AD-710779]

Fast neutron spectra analysis emphasizing resonance scattering effects and influence of anisotropic scattering on energy-spatial distribution of neutrons
[AD-710779]

Effects of anisotropy on intensity of conduction electron spin resonance in high purity silicon
[AD-710779]

Castiglione theorem validity in variable modular elasticity theory of anisotropic body subjected to plane stress state
[AD-710779]

VOIDS IN NEUTRON IRRADIATED ALUMINUM SUBJECTED TO DIFFUSION AND RE-RADIATION
[AD-710779]

Increase of chromium-1 concentration in X ray irradiated ruby during isothermal annealing measured by EPR techniques
[AD-710779]

Low temperature annealing of electron irradiated germanium
[AD-710779]

Post weld annealing for stabilizing tungsten alloy weld structure
[AD-710779]

Annealing or aging of aluminum alloys
[AD-710779]

Annealing quenched-in vacancies in Al-Zn alloys and kinetics of coarsening process of Ostwald-Freeman zones
[AD-710779]

Annealing behavior of Cu-based solid solutions and CuAl₃
[AD-710779]

Irradiation strengthening of bcc metals and solid solution annealing mechanisms in vanadium
[AD-710779]

High pressure stress annealing, pyrolytic graphite in aqueous solutions, emphasizing non-Faraday capacity
[AD-710779]

Radiation damage and recovery in phosphorus doped silicon semiconductor exposed to electron irradiation
[AD-710779]

Empirical equations to determine interdependency of swelling, void diameter, and void number density in annealed A516 type 304 stainless steel
[AD-710779]

Simulation of space radiation damage and defect annealing in semiconductors
[AD-710779]

Metal oxide semiconductor X ray and electron irradiation damage and annealing effect
[AD-710779]

Fine structure of superconducting Zr-Ni alloy during plastic deformation and annealing
[AD-710779]

Fast neutron spectra analysis of deuteron velocity distributions in deuteron plasmas
[AD-710779]

ANNEALING REACTIONS
NT POSITRON ANNIHILATION
Spectral function from electron positron annihilation
[AD-710779]

Positron electron annihilation into muons
[AD-710779]

Four pion and five pion final states in muon positron annihilation in hydrogen at 940 MeV/c
[AD-710779]

Photon photon forward scattering studied with positron electron annihilation process
[AD-710779]

Statistical analysis for estimating modification of electron-positron pairs into mesons
[AD-710779]

Plastic deformation effects on alpha to gamma conversion phase and element distribution in iron nickel alloys
[AD-710779]

Anger spectroscopy of low alloy steel, copper, brass, and alloy, and refractory metal annealing and sintering contributions due to grain boundary fracture, corrosion, and mobility
[AD-710779]

Development of furnace design, operating, casting, and annealing procedures to improve structural properties of fused-cast aluminum oxide articles
[AD-710779]

Shielded glove box apparatus for remote handling, inspecting, and annealing of coated nuclear fuel microspheres
[AD-710779]

Heat transfer calorimetry in annealing of electron irradiation induced Frankel defects in platinum below 40 K
[AD-710779]

Volcanic and grain boundary effects on silver isotope diffusion into aluminum single and polycrystals during annealing
[AD-710779]

C 14 diffusion coefficients during annealing of titanium wire between 1223 to 1923 K
[AD-710779]

C 14 diffusion coefficients during annealing of titanium wire between 1223 to 1923 K
[AD-710779]

Annealing and temperature gradients effect on plutonium distribution in fast reactor fuel elements
[AD-710779]

Co-60 gamma radiation and increased annealing temperature effects on minority carrier lifetime of Al and Li doped bulk silicon
[AD-710779]

Nickel, magnesium, and aluminum annealing effects on neutron irradiation induced crystal defects in low temperature environments
[AD-710779]

Transient measurements of field effect transistors following exposure to pulse of neutron and observation of transient annealing of drain to source resistance in n- and p-channels
[AD-710779]

Electron irradiation effects on thermal conversion of intermetallics in copper
[AD-710779]

Effect of neutronization and thermal annealing on thermoluminescence of polished silicon semiconductors
[AD-710779]

Cryostat for low heavy ion irradiation and isothermal annealing at 77 to 300 deg K to study lattice defects in metals by Moessbauer spectroscopy and other experiments
[AD-710779]

Krypton and helium bubble migration on dislocations in copper foil, and measurement of root mean square random migration distances during isothermal annealing
[AD-710779]

Effect of intermediate annealing conditions on crystallographic texture of transformer steel after high temperature annealing
[AD-710779]

Diffusion coefficient of chromium in Fe-Cr alloys annealed at 1250 C determined by evaporation in vacuum
[AD-710779]

Annealing preparation and superconducting behavior of CuNi₂ and its Gd, Mn, Co, and Ni containing mixed phases
[AD-710779]

Isothermal annealing of 0.97 eV luminescence in electron irradiated silicon semiconductors
[AD-710779]

Radiation damage and thermal annealing of defects in molybdenum and tungsten - reactor technology
[AD-710779]

Problems of high temperature annealing of PTFE/LRP discs used for heating radiation dosimetry
[AD-710779]

Lithium fluoride glow-pink growth due to annealing and analysis of half-wave rectifying circuit with theoretical efficiency of 100 percent
[AD-710779]

Analysis of lithium fluoride glow-pink growth due to annealing
[AD-710779]

ANNEALING REACTIONS
NT POSITRON ANNIHILATION
Spectral function from electron positron annihilation
[AD-710779]

Positron electron annihilation into muons
[AD-710779]

Four pion and five pion final states in muon positron annihilation in hydrogen at 940 MeV/c
[AD-710779]

Photon photon forward scattering studied with positron electron annihilation process
[AD-710779]

Statistical analysis for estimating modification of electron-positron pairs into mesons
[AD-710779]

Plastic deformation effects on alpha to gamma conversion phase and element distribution in iron nickel alloys
[AD-710779]

Anger spectroscopy of low alloy steel, copper, brass, and alloy, and refractory metal annealing and sintering contributions due to grain boundary fracture, corrosion, and mobility
[AD-710779]

Development of furnace design, operating, casting, and annealing procedures to improve structural properties of fused-cast aluminum oxide articles
[AD-710779]

Shielded glove box apparatus for remote handling, inspecting, and annealing of coated nuclear fuel microspheres
[AD-710779]

Heat transfer calorimetry in annealing of electron irradiation induced Frankel defects in platinum below 40 K
[AD-710779]

Volcanic and grain boundary effects on silver isotope diffusion into aluminum single and polycrystals during annealing
[AD-710779]

C 14 diffusion coefficients during annealing of titanium wire between 1223 to 1923 K
[AD-710779]

C 14 diffusion coefficients during annealing of titanium wire between 1223 to 1923 K
[AD-710779]

Annealing and temperature gradients effect on plutonium distribution in fast reactor fuel elements
[AD-710779]

Co-60 gamma radiation and increased annealing temperature effects on minority carrier lifetime of Al and Li doped bulk silicon
[AD-710779]

Nickel, magnesium, and aluminum annealing effects on neutron irradiation induced crystal defects in low temperature environments
[AD-710779]

Transient measurements of field effect transistors following exposure to pulse of neutron and observation of transient annealing of drain to source resistance in n- and p-channels
[AD-710779]

Electron irradiation effects on thermal conversion of intermetallics in copper
[AD-710779]

Effect of neutronization and thermal annealing on thermoluminescence of polished silicon semiconductors
[AD-710779]

Cryostat for low heavy ion irradiation and isothermal annealing at 77 to 300 deg K to study lattice defects in metals by Moessbauer spectroscopy and other experiments
[AD-710779]

Krypton and helium bubble migration on dislocations in copper foil, and measurement of root mean square random migration distances during isothermal annealing
[AD-710779]

Effect of intermediate annealing conditions on crystallographic texture of transformer steel after high temperature annealing
[AD-710779]

Diffusion coefficient of chromium in Fe-Cr alloys annealed at 1250 C determined by evaporation in vacuum
[AD-710779]

- Heavy meson resonances in antiproton proton annihilation reaction at 3.6 GeV/c
[NP-18466] 08 p1351 N71-18262
- Gamma ray production from cosmic proton antiproton annihilations, selection rules, and Matsuda statistical model
13 p2158 N71-34767
- Cosmic gamma ray spectra from extragalactic proton antiproton annihilations into mesons
13 p2159 N71-34775
- Cosmic antimatter annihilation and gamma ray background spectrum
[NASA-TM-X-65317] 13 p2160 N71-34962
- Relativistic magnetohydrodynamic equations of proton antiproton annihilation reactions and Klein-Aliu cosmology
13 p2131 N71-25829
- Antiproton annihilations at rest with bound neutrons in deuterium
13 p2141 N71-25543
- Upper limit on omega meson yields 2 pion decay rate from antiproton-neutron annihilations at rest
15 p2469 N71-27073
- Meson and hyperon production in antiproton proton, antiproton neutron, and antiproton deuteron annihilations at high energies
15 p2481 N71-27701
- Antiproton annihilations with neutrons into final pion states
15 p2467 N71-27838
- Proportion of meson resonances in antiproton proton annihilations
[JSC-P-70-1] 18 p2974 N71-30552
- Mass spectra of antiproton proton annihilations into 4 or 5 pions at 3 GeV/c
[NP-18730] 18 p2974 N71-30563
- Phenomenological effective Lagrangian for annihilation of two pions into pions
[NYO-3829-04] 21 p3483 N71-34811
- Cosmological gamma ray production calculations from matter-antimatter annihilations in universe
[NASA-TM-X-65789] 23 p3842 N71-37395
- Broken scale invariance with canonical three dimensional scale and annihilation cross sections
[NUB-3096] 24 p3982 N71-38418
- ANNOTATIONS**
- Annotated bibliography of worldwide biodynamics research studies
[NASA-TM-X-67138] 12 p1866 N71-23344
- Annotated bibliography on human acclimation and acclimatization to heat
[NASA-TM-X-62008] 13 p2035 N71-23393
- Annotated bibliography of data compression and data connection from information theory literature
[AD-723525] 21 p3395 N71-34165
- ANNUAL VARIATIONS**
- Graphical analysis of ten-year sampling of suspended particulate matter over urban and suburban sites
[PB-192223] 02 p0151 N71-11069
- District of Columbia air quality display model for computing seasonal concentration estimates
[PB-189194] 02 p0151 N71-11072
- Monocyclic winds over Ascension Island in January
[AD-711851] 02 p0257 N71-11666
- Seasonal sea surface temperature variations in Persian Gulf recorded by Nimbus 2 HIR
[NASA-TM-X-65385] 03 p0369 N71-13067
- Interannual renovation of radar stations
[JPRS-51916] 05 p0658 N71-15448
- Variations in phenological events and climatic epochs in European USSR
06 p0808 N71-15771
- Model of global circulation induced by solar radiation and aerosol heating, for determining semimonthly effect in atomic oxygen concentration
[NASA-TM-X-65443] 07 p01018 N71-17261
- Seasonal variations in antisymmetric diurnal and semidiurnal variations of cosmic rays
[NASA-TT-F-13513] 09 p1462 N71-20411
- Seasonal variations of current and salinity of Deschamps River induced by changes in wind and rain
[AD-717321] 11 p1744 N71-21858
- Hurricane analysis of seasonal variations of atmospheric circulation in Northern Hemisphere
11 p1752 N71-22206
- Long range forecasting of annual variations of ice cover in Arctic
11 p1752 N71-22807
- Possible effect of multimonth variations in tide generating forces of moon and sun on oceans and atmosphere
11 p1754 N71-22821
- Annual variations of winter hydrological characteristics in surface waters of East Siberia and Chukotka seas due to salinity and temperature anomalies
11 p1756 N71-22835
- Seasonal variations of geophysical process interaction in Northern and Southern Hemispheres in total atmospheric circulation
[AD-716777] 12 p1911 N71-23406
- Solar convective streams and atmospheric circulation influenced by seasonal variations
[NASA-TT-F-13425] 12 p1993 N71-23804

- Seasonal profiles of radiative heating and thermal cooling of earth's atmosphere.
[MIT-2341-58] 13 p2077 N71-25401
- Annual variation of mean daily and relative global solar radiation over northern Norway and Spitzbergen
15 p2482 N71-27516
- Number density profiles for oxygen and nitrogen profiles in lower thermosphere compatible with US standard atmosphere for winter, summer, and spring/fall at 15, 30, 45, and 60 degrees N
[COM-71-30004] 16 p2588 N71-24946
- Features of 500 mb height field in Northern Hemisphere during natural synoptic seasons
[NLL-M-9266-3828.4F] 16 p2591 N71-29118
- Lower atmosphere vertical distribution of boundary layer wind shear annual variations as observed in Canada
18 p2049 N71-30829
- Using numerical model to examine annual variations in motion of stratosphere and mesosphere
18 p2916 N71-31043
- Variations of atmospheric circulation in Northern Hemisphere
[AD-722846] 18 p2954 N71-31216
- Pacific Ocean influence upon seasonal precipitation patterns of western US and Baja, Calif.
[PB-198124] 19 p3126 N71-31713
- Annual variations in ice area, thickness, and position of ice edge in Black and Azov seas
[AD-724671] 20 p3259 N71-33196
- Monthly mean values of energy balance components of earth surface in Finland
20 p3267 N71-33497
- Surface layer stability parameter distribution over USSR and over time
[NLL-M-30714-5828.4F] 21 p3423 N71-34356
- Annual variation of isonephic drift in E region at Garchy, France using signal fading method
[GRI/NTT/87] 23 p3730 N71-36739
- Diurnal and semidiurnal variations of upper atmosphere density determined from Cosmos satellite drag data
[D-16] 23 p3751 N71-36744
- Hourly, diurnal, and annual data on geomagnetic declination and intensity, Hartland, England - 1962, 1963, and 1964
23 p3753 N71-36760
- Rotation of solar electron corona autocorrelation analyses establishing average yearly rotation rates
23 p3788 N71-36994
- Diurnal and annual variations of scintillation measured during Isatoh 2 and ATS 3 transmission
24 p3912 N71-37885
- Semimonthly variations of ionospheric electron content
24 p3912 N71-37891
- ANNULAR CORE PULSE REACTORS**
- Calibration factor P_{pulsed}/P_{steady} for measuring fast fission rate in annular fuel region of Mk 3 gas cooled reactor fuel elements
[AEEW-M-975] 15 p2447 N71-27258
- ANNULAR FLOW**
- Analytical models of two phase annular flow in pipes
[PB-194836] 07 p1006 N71-16926
- Numerical solution of turbulent annular swirl flows
[AD-716450] 09 p1370 N71-19607
- Fluid dynamic properties of turbulent swirl flows in annular duct
[AD-716452] 09 p1370 N71-19608
- Friction factor of cylinder rotating in high Reynolds number annular flow
10 p1541 N71-21138
- Velocity profile control tests of diffuser wall bleed to control combustor inlet airflow distribution
[NASA-TN-D-6435] 18 p3000 N71-30817
- ANNULAR JETS**
- U ANNULAR FLOW**
- U JET FLOW**
- ANNULAR NOZZLES**
- Electrostatic microthruster propulsion system with annular slit orifice thruster
[NASA-CASE-GSC-10709-1] 13 p2156 N71-25213
- ANNULAR PLATES**
- Parametric study of uniformly loaded annular plates supported between edges with equally spaced columns
[REPT-292] 02 p0301 N71-12012
- Bending solutions of uniformly loaded annular plates supported by columns on one boundary with other boundary simply supported
[REPT-287] 02 p0301 N71-12014
- Annular disk supported on columns along inner boundary and fixed at outer boundary
[REPT-293] 02 p0303 N71-12094
- Elastic-plastic analysis of anisotropic annular disks subjected to sufficient internal pressure to cause plastic deformation
[AD-714370] 06 p0954 N71-16113
- Analyzing polyimide plates using modified Ritz variational process
07 p1122 N71-17038
- ANNULI**
- Liquid film flow and critical heat flux measurements in concentric, internally heated annuli
[ABCL-3456] 05 p0460 N71-14757

- Transient film growth during initial 10 milliseconds of transient film boiling in horizontal annulus filled with saturated liquid
18 p3025 N71-30829
- Prediction of heat transfer to gas flowing in counter-past annular reactor channels
[AERE-R-6564] 19 p3192 N71-32208
- ANODES**
- NT CHILL ANODES**
- NT TUBE ANODES**
- Anode potential fluctuations observed in copper electrode in different electrolytes
[UCRL-19618] 10 p1546 N71-21146
- Design and characteristics of heat activated anode cell with anode made from one or more alloy metals and cathode made from oxidizing material
[NASA-CASE-LEW-11358] 14 p2280 N71-30809
- Crystal lattice changes and polarization current effects on nickel sulfide dissolution in sulfide solution
[NLL-TRANS-746-699-19022.401] 23 p3722 N71-36989
- Design, development, and characterization of hot and electrolytic cell with carbon anode
[NLL-M-20409-5828.4F] 23 p3773 N71-30808
- ANODE COATINGS**
- Sorption equilibrium and kinetics of water vapor to anodized aluminum
[AD-715914] 08 p1158 N71-20807
- Studying anodic oxidation of austenite on platinum gold alloys at 80 C in solutions of constant pH and salt normality
13 p3423 N71-37077
- Anodizing method for providing metal surfaces with temperature reducing coatings against flames
[NASA-CASE-XLE-00035] 16 p2093 N71-20523
- Electrochemistry of nickel-, copper-, cobalt-, and iron-sulfide anodes
18 p2885 N71-30802
- Instructions for use of anodic oxidation apparatus in conjunction with computer program to obtain electrochemically active concentration profiles of doped films
[NASA-CR-119799] 21 p3432 N71-30804
- Profiling procedure including computer program [OLS] for measuring junction depth in anodic oxidation - semiconductor fabrication reliability studies
[NASA-CR-119800] 21 p3496 N71-30806
- ANODIZING**
- Ionic currents in anodic oxidation of Ti, Zr, and Hf. Zr alloys below oxygen evolution potential and the film growth theory
[AEC-TR-7201] 09 p1402 N71-20808
- Anodization of tantalum, niobium, and silicon in hydrogen plasmas generated by both hot and cold cathode discharges
[AD-72490] 17 p3703 N71-30811
- Equipment and procedures for determining rate mechanisms in oxide film formation of plasma anodized aluminum
20 p3286 N71-30805
- ANOMALIES**
- U ABNORMALITIES**
- ANTARCTIC REGIONS**
- Salinity, temperature, and depth measurement of Weddell Sea during austral summer, 1969
[CG-73-31] 01 p0049 N71-19605
- Quantitative and qualitative characteristics of horizontal transport of snow in Antarctica
[AD-711914] 02 p0219 N71-12082
- Bibliography of geological research in Antarctic regions
[REPT-146] 03 p0369 N71-12089
- Investigation of PKP seismic waves at Byrd Station, Antarctica
[AD-712731] 03 p0371 N71-12090
- Climatology of Antarctic - Jan. 1967 - Dec. 1968
[AD-713187] 05 p0716 N71-16909
- Catalog of gravimetric measurements obtained during Antarctic expeditions
[JPRS-52123] 05 p0676 N71-15457
- Antarctic atlas and termination of drifting ice
SP-19 05 p0681 N71-15458
- Geology of Antarctica
[PB-195633] 06 p1186 N71-10977
- Temperature, salinity, oxygen, and chemical nutrient measurements in Weddell Sea
[PB-195893] 09 p1378 N71-16909
- Numerical modeling of Antarctic circumpolar current
09 p1380 N71-16909
- Survival of Antarctic desert soil bacteria exposed to various temperatures and to three years of continuous medium-high vacuum
[NASA-CR-117131] 09 p1333 N71-16909
- Growth of bacteria in soils from Antarctic dry valleys providing soil microbial ecology as Mars model
[NASA-TM-X-66963] 09 p1333 N71-16910
- High frequency absorption measurement of Antarctic region using radiometers
[GRI-NTT-75] 10 p1547 N71-30808
- Bygiene and clinical physiology of man living in Antarctica
[JPRS-52579] 11 p1678 N71-16909

SUBJECT INDEX

ANTENNA DESIGN

Arctic and Antarctic regions, ice formation, sea ice, weather forecasting, glaciology, hydrology, hydrometeorology, RV, RSTV, solar activity, and meteorological stations
[AD-70-50617] 11 p1752 N71-22901

Comparison of long period microseisms and flexural gravity waves measured at Mirny in Antarctica
11 p1753 N71-22910

Hydrological measurements of horizontal circulation of water in Pacific sector of Southern Ocean
11 p1754 N71-22922

Round-the-world echo and very far propagation of short radio waves from stations in Arctic and Antarctic
11 p1704 N71-22948

Hydrological investigation of variability of temperature and chemical properties of Lake Vanda in Antarctica
11 p1759 N71-22963

Geographic theories, morphometric parameters, and potential features of Antarctica
[N71-30015] 12 p1907 N71-23524

Cyclonic and anticyclonic ocean currents in Antarctic region of Pacific
[AD-71-0009] 12 p1907 N71-23540

Formation, melting, drift, thickness, and concentration of sea ice in Antarctic regions during different seasons
[AD-71-0907] 13 p2076 N71-23243

Soviet news releases on atmospheric processes of eastern Antarctica and hail suppression service for Central Asia
15 p2436 N71-24673

Atmospheric investigation in Arctic and Antarctic regions
16 p2629 N71-25772

Computer programs to determine quantitative morphological fit of Australia and Antarctica
18 p2915 N71-31013

Thermal satellite observations of large ice free areas in Antarctic coastal waters
18 p2916 N71-31060

Wind and turbulence structure in boundary layer over Antarctica
18 p2953 N71-31122

Quasiperiodic observations of tidal variation in Syowa station, Antarctica
20 p3261 N71-33335

Statistical analysis of effects of acclimatization on hematological of Antarctic expeditionary personnel
[RIS-52004] 21 p3302 N71-34063

Isentropic moisture transport into Antarctic interior based on Byrd station data analysis with mass transport model
21 p3303 N71-34067

Baric tide measurements by gravimeters and pendulums at ground station in Antarctic interior during winter
24 p3910 N71-37867

Relative water transparency of Indian Ocean and Antarctic waters, affected by plankton concentration and surface currents
[AD-72-057] 24 p3916 N71-37926

Observations of atmospheric turbulence in Antarctica by radioisotopes
[AD-72-070] 24 p3953 N71-38201

ANTARCTICA
U ANTARCTIC REGIONS
ANTENNA ARRAYS

HF DISTORTIBLE STEERABLE ANTENNAS
HF LINEAR ARRAYS
HF STEERABLE ANTENNAS
HF TURNSTILE ANTENNAS
HF YAGI ANTENNAS

Statistical analysis of linearly polarized arrays with short isotropic radiation patterns
[AD-71-073] 01 p0024 N71-10701

Radio receiver with array of independently steered antennas for deep space communication
[NASA-CASE-XLA-00901] 01 p0025 N71-10775

System engineering and economic analysis of testing and data relay satellite system with 16 HF antennas
[NASA-TM-X-45370] 01 p0025 N71-10800

Performance of single and multibeam antennas in ionospheric recovery plasma environment
[AD-71-047] 02 p0199 N71-11353

Wave-like structures in E-region derived from drift measurements
[AD-72-040] 02 p0220 N71-12093

Coupled dipoles as antenna elements in array
[NASA-TR-134] 03 p0334 N71-12383

Feeding network for antenna array using strip conductor
[NASA-TR-123] 03 p0334 N71-12383

Measuring time response of adaptive array antennas for communication satellites for case of strong interference in earth receiving antennas
[NASA-CR-111617] 03 p0334 N71-12387

Design of HEP antenna containing two, three, or four dipoles
[AD-72-070] 03 p0334 N71-12388

Beam procedures for compensating phased array antenna elements for impedance changes with scan angle
[NASA-CR-102955] 03 p0335 N71-12394

Characteristics of antenna horn feeds consisting of central horn with overlying peripheral horns
[NASA-CASE-GSC-10452] 03 p0335 N71-12396

Broadband constant beamwidth conical arrays
[AD-71-2676] 03 p0338 N71-12415

Mixed path propagation of very low frequency waves from antenna array in polar zone
04 p0492 N71-13710

Coupling effects on linear array for beam steering
04 p0495 N71-13917

Equipment specifications for Lunar Sounding Antenna Assembly
[NASA-CR-114797] 03 p0642 N71-14726

Performance analysis of storage array antenna system for track while scan radar equipment
[JAS-TR-70136] 03 p0644 N71-14776

Supporting research and technology for structural members used in Deep Space Network communication equipment
03 p0647 N71-14958

Constructing 210 ft diam antenna stations for Deep Space Network
03 p0647 N71-14965

Thinning algorithms on rectangular, hexagonal, and triangular arrays
[NASA-CR-110131] 06 p0803 N71-15952

Effect of interelement mutual coupling on radiation pattern of linear antenna in electric scanning
[AD-71-0881] 06 p0823 N71-16342

Microwave transmission propagation and detection
[AD-71-0995] 07 p1096 N71-18067

Radiation theory and effects of insertions in infinite planar arrays - MART program
[AD-71-0997] 08 p1161 N71-18294

Radiation theory and effects of straight insertions in infinite planar arrays - MART program
[AD-71-0998] 08 p1161 N71-18295

Numerical analysis on mutual couplings in arrays of long periodic dipole antennas
08 p1163 N71-18946

Tracking antenna system with array for synchronous satellite or ground based radar
[NASA-CASE-GSC-10553-1] 09 p1350 N71-19854

Element pattern design of large array of circular apertures on triangular grid, using rotationally symmetric and periodic antennas
[AD-71-1159] 10 p1534 N71-21212

Impedance and radiation properties of ground wave antenna analyzed using transmission line theory
[AD-71-1692] 11 p1724 N71-22657

Sharing common aperture of two plane microwave arrays for enhancing utilization of available aperture space
11 p1725 N71-22745

Optical path length stability of light beam system for local oscillator signal distribution over antenna array
11 p1714 N71-22958

Statistical model for tropospheric radio propagation loss in rough surface path between transportable and mobile antennas
12 p1878 N71-23473

Optimum number, spacing, and configuration of point sources in arrays simulating circular and square continuous-plane radiators
[AD-71-0312] 12 p1946 N71-23900

Electrical delays to define ends in directional response to conical superdirective arrays
[AD-71-0322] 12 p1967 N71-23902

Interferometric timing acquisition and tracking radar antenna systems
[NASA-CASE-XMS-09610] 13 p2044 N71-24625

Adaptive antenna array processing techniques allowing spatial signal field characterization of multiple wavefronts in background of uncorrelated noise
[AD-71-0956] 14 p2227 N71-25686

Numerical evaluation of low frequency loop antenna array resistance to ground reaction as compared to radiation resistance for electric and magnetic dipole antennas
[AD-72-0599] 14 p2331 N71-26769

Development of electronic circuit for combining input signals on two separate antennas to form two processed signals
[NASA-CASE-MSC-12265-1] 15 p2379 N71-27056

Antenna array at focal point of reflector with coupling network for beam steering
[NASA-CASE-GSC-10220-1] 15 p2381 N71-27233

Array of eight sine dipoles for studying radio signals reflected and scattered from ionospheric irregularities and meteor trails to determine wind gradients and changes at high altitudes
[AD-71-2223] 15 p2399 N71-27471

Algorithmic procedure for optimization of antenna arrays
[RE-409] 16 p2559 N71-28055

K-beta diagrams for two uniformly periodic loop antenna arrays determined from measured near field amplitudes and phase distributions of traveling waves
[AD-71-2592] 16 p2568 N71-28355

Pattern and impedance matching improvements in transversely polarized planar antennas
[NASA-CASE-XOS-02250] 16 p2563 N71-28069

Antennated bibliography on radar antennas including antenna arrays, antenna radiation patterns, types of radar antennas, and testing and evaluation
[AD-72-2200] 17 p2718 N71-29220

Possibility of obtaining arbitrary polarization in both one and two dimensional slot antennas
17 p2724 N71-29273

Problems in evaluating electromagnetic fields of linear antennas or dipole arrays in dissipative half space
[AD-72-1704] 17 p2725 N71-29480

Electronic and solid state physics, control theory, electromagnetic radiation, and antenna array research
[AD-72-2415] 17 p2853 N71-30528

Analysis of wave interaction describing antenna system
[FB-197627] 18 p2891 N71-31291

Simultaneous amplitude and phase sampling of CW signals by antenna array in over-the-horizon propagation measurements
[AD-72-2897] 18 p2892 N71-31364

Unified network analysis of antenna arrays
[AD-72-2908] 19 p3064 N71-31907

Optimization by combining antenna array coefficient for interference noise reduction
[AD-72-3428] 19 p3065 N71-31908

Analysis of multiple interelement arrays of waveguide radiators at low and high frequencies
[AD-72-3520] 19 p3084 N71-31811

Development of 16-element crossed dipole array for observations of Jupiter
[REPT-50] 19 p3088 N71-32645

Calculation of radiation patterns of antenna arrays by use of reciprocity theorem
[REPT-1971/17] 20 p3231 N71-32808

Field patterns and directivity measurements for short baseline antennas
[AD-72-4607] 20 p3241 N71-33191

Construction of antenna array and automatic recording system to measure amplitude and phase of diffraction patterns formed by ionospheric reflection of 300 kHz radio radar signals
[FNU-ILL-6C3-571] 20 p3259 N71-33207

Receiving dipole antenna array signal to noise ratio optimization based on steepest descent method
[NASA-CR-1770] 20 p3263 N71-33214

Experimental analysis of system requirements for arrays of large aperture antennas
[NASA-TM-X-45669] 20 p3264 N71-33372

Analysis of optimum parameters for radio frequency power-splitting network matched over band of frequencies
[DSC-1971/20] 20 p3266 N71-33809

Analytical determination of optimum spatial distribution of apertures for enhancing array reception
23 p3726 N71-34560

ANTENNA COMPONENTS
NT ANTENNA COUPLERS
NT ANTENNA FEEDS
ANTENNA COUPLERS
NT COUPLING CIRCUITS
NT DEPLEXERS

Coupling effects on linear array for beam steering
04 p0495 N71-13917

Numerical analysis on mutual couplings in arrays of long periodic dipole antennas
08 p1163 N71-18946

Analysis of coupling between two loaded rectangular waveguide opening in infinite conducting ground plane
11 p1728 N71-22141

Boundary value problem for impedance evaluation between coupled electrically thick folded dipoles
12 p1894 N71-24032

Low elevation recording of Early Bird satellite transmission with polarimeter, noting induction antenna coupling
24 p3914 N71-37903

ANTENNA DESIGN
Aperture antenna synthesis for HF radio signals propagated via F layer of ionosphere
[AD-71-0425] 06 p1167 N71-18252

Effect of spatiotemporal random errors on antenna performance
08 p1163 N71-18977

Radio frequency antenna theory and characteristics of antennas for space communication applications
09 p1350 N71-19847

Loss in antenna gain caused by aluminum or glass fiber support structure
11 p1701 N71-22563

Development and characteristics of low-noise multielement monopulse antenna feed system for use with microwave communication equipment
[NASA-CASE-XNP-01735] 11 p1702 N71-22570

Non-conformal heat resistant antenna comprising plurality of adjacent layers of silica net introducing paths of high thermal conductivity through oblique shims
[NASA-CASE-XMS-04312] 11 p1714 N71-22904

Applying method of moments to solution of integral equations for current induced on conducting cylinders in two-dimensional field
[NASA-CR-115222] 14 p2218 N71-26272

Development of electronic circuit for combining input signals on two separate antennas to form two processed signals
[NASA-CASE-MSC-12265-1] 15 p2379 N71-27056

- Development and characteristics of extensible dipole antenna using deformable tubular metallic strip element
[NASA-CASE-HQN-00937] 16 p2563 N71-28979
- Development of method for suppressing excitation of electromagnetic surface waves on dielectric converter antenna
[NASA-CASE-XLA-10772] 16 p2563 N71-28980
- Effects of variations of antenna parameters on radiation properties of short-backfire antenna
[AD-722048] 16 p2573 N71-29017
- Compact, self contained, symmetrical antenna for airborne use at high frequencies with capability to function in two independent modes for both transmission and reception
[AD-722736] 17 p2726 N71-29095
- Aerodynamic characteristics, rocket nozzles, spacecraft propulsion, antenna design, and internal combustion engines
[NASA-CR-119315] 18 p3014 N71-31106
- Phase velocity measurements of cigar antenna design for Mariner Venus-Mercury 1973
18 p2890 N71-31117
- Broadband active and passive radio antenna designs for use in signal transmission and reception
19 p3052 N71-31638
- Cavity-backed crossed slot antenna design for use in phased arrays with hemispherical scanning
19 p0000 N71-32341
- Development and characteristics of mechanically despun spacecraft antenna for deep space probes, tactical communications, and community broadcast applications
[NASA-TN-D-4683] 20 p3334 N71-33250
- Analysis of optimum parameters for radio frequency power-splitting network matched over band of frequencies
[BBC-1971/20] 20 p2326 N71-33809
- Proceedings of space shuttle integrated electronics conference with emphasis on power distribution, instrumentation, and communication - Vol. 2
[NASA-TM-X-59063-VOL-2] 21 p3513 N71-33034
- Design of high temperature antennas for space shuttles
21 p3514 N71-33043
- Prototype antenna design and methods of measuring and predicting antenna characteristics when mounted on space shuttle scale models
21 p3515 N71-33045
- Determination of first-order diffraction coefficients for slot-excited conical antenna
[AD-726539] 22 p3560 N71-33539
- Satellite antenna design for HF direction finder applications
[AD-726400] 22 p3561 N71-33563
- ANTENNA FEEDS**
- Feed properties and radiation patterns of conical horn antennas with small flare angles
01 p0022 N71-10474
- Development of broadband horn antennas with double ridged waveguide techniques
[AD-712299] 02 p0178 N71-11252
- Parametric tradeoff study for design of orbital low frequency radio telescope
[NASA-CR-111396] 02 p0181 N71-11271
- Design and operation of multi-feed cone Cassegrain antenna
[NASA-CASE-NPO-10539] 02 p0183 N71-11285
- Feeding network for antenna array using strip conductors
[ELAB-IR-123] 03 p0334 N71-12385
- Characteristics of antenna horn feeds consisting of central horn with overlapping peripheral horns
[NASA-CASE-GSC-10452] 03 p0335 N71-12396
- Numerical computation of linear antenna feed
[R-74] 10 p5118 N71-21053
- ANTENNA FIELDS**
- U ANTENNA RADIATION PATTERNS**
- ANTENNA RADIATION PATTERNS**
- Radiation and circuit properties of open-cavity radiator
[AD-711071] 01 p0033 N71-10457
- Feed properties and radiation patterns of conical horn antennas with small flare angles
01 p0022 N71-10474
- Numerical analysis of linearly polarized arrays with almost isotropic radiation patterns
[AD-711075] 01 p0024 N71-10701
- Integral equations for aperture fields, leading terms in near and far zone fields, admittance, and effective height of smaller slot antennas
[SC-R-70-4281] 01 p0035 N71-10794
- Feeds for reflector antenna, frequency independent conical horn antenna, and conical horn antennas with symmetrical radiation patterns
02 p0179 N71-11258
- Test facilities for satellite antennas
[ESRO-TN-97-ESTEC] 02 p0190 N71-11472
- Radiation from slot antennas on conical bodies covered by inhomogeneous plasma sheath
[AD-712049] 03 p0336 N71-12399
- Reflection coefficient, radiation pattern, gain, and efficiency of X band cavity resonators
03 p0336 N71-12401
- Theoretical investigation of ionized capsule wake interactions with circularly polarized antenna radiation while entering Martian atmosphere
03 p0353 N71-12551
- Excitation gap thickness effect on spherical antenna performance
04 p0491 N71-13708
- Electromagnetic detection of absorbing field reflected from metallic surface
04 p0492 N71-13709
- Admittance, isolation, and radiation patterns of rectangular slot antenna in simulated plasma reentry sheath
[AD-713702] 05 p0653 N71-14870
- Multiple mode horn antenna with radiation pattern of equal beamwidths and suppressed sidelobe
[NASA-CASE-XNP-01057] 06 p0813 N71-15907
- Effect of interelement mutual coupling on radiation pattern of linear antenna in electric scanning
[AD-714081] 06 p0823 N71-16342
- Electromagnetic radiation from infinite cylinder immersed in inhomogeneous medium
[AD-714575] 06 p0825 N71-16629
- Physical realizability of planar antennas
[AD-715267] 07 p0999 N71-17773
- Computerized simulation of antenna radiation patterns from current loops above conducting cone
[AD-714950] 07 p1000 N71-17936
- Radiation from infinite phased planar array of rectangular pistons with sourdled interstices
[AD-714809] 08 p1167 N71-18243
- Effect of spatiotemporal random errors on antenna performance
08 p1162 N71-18877
- High gain antenna acquisition problem during Apollo 13 flight
[NASA-TM-X-46903] 09 p1346 N71-19407
- Analysis of wave interaction during antenna system for ionospheric electron density measurements
[SR-367] 09 p1379 N71-19447
- Electromagnetic theory, antennas, microwave equipment, and radio anechoic chamber
[D-112] 10 p1517 N71-20602
- Reentry plasma effects on RAM C-1 VHF telemetry antenna radiation patterns
10 p1519 N71-21111
- Antenna radiation patterns and electron density profiles in turbulent plasma flow
10 p1519 N71-21120
- Slot antenna radiation pattern distortion produced by boundary layer plasma sheath around conical reentry vehicles
10 p1520 N71-21121
- Electromagnetic radiation detection of microwave field patterns using liquid crystals
[AD-717583] 11 p1699 N71-21923
- Shaping antenna far-field radiation patterns for uniform and nonuniform arrays, using iterative sampling and current distribution approximation
11 p1727 N71-21946
- Impedance and radiation properties of ground wire antenna analyzed using transmission line theory
[AD-717692] 11 p1724 N71-22657
- Antenna response patterns, Doppler spectra, and amplitude distributions of transhorizonal microwave scatter propagation
12 p1875 N71-23453
- Formulas for calculating depolarization effects on dipole radiation in statistically homogeneous and isotropic dielectric constant medium
12 p1876 N71-23460
- Ultrahigh frequency antenna scatter propagation disturbance by vegetation
12 p1876 N71-23461
- Point to point microwave transmission with receiving antenna wave front sampling, meteorological parameter measurements, and refractive index profiles
[AD-718272] 12 p1879 N71-23608
- Impedance and radiation properties of mesh antennas immersed in warm isotropic plasma
12 p1890 N71-23664
- Automatic antenna position control device for evaluating dome effects on radiation patterns
[AD-718288] 12 p1890 N71-23887
- Optimum number, spacing, and configuration of point sources in arrays simulating circular and square continuous-phase radiators
[AD-718312] 12 p1966 N71-23900
- Electron and solid state physics, control theory and applications, ferromagnetic and ferroelectric materials, electromagnetic phenomena, and plasma medium scattering
[AD-718117] 12 p1966 N71-23911
- Time domain solutions for transient radiation response of thin conducting wires and antennas
12 p1891 N71-24027
- Point matching and step approximation method for impedance and current distribution calculations of cylindrical antenna submerged in warm isotropic plasma
12 p1894 N71-24030
- Monopulse scanning network for scanning volumetric antenna pattern
[NASA-CASE-GSC-10299-1] 13 p2036 N71-24804
- Radiation pattern distortion for symmetrically and asymmetrically excited circumferential slot antennas on models of conical reentry vehicles
[AD-719739] 13 p2038 N71-24809
- Dynamic structural analysis on low frequency finite telescope scale model with paraboloidal antenna
13 p2170 N71-24890
- Computer program for calculating radiation pattern of ATS 6 flexible rib-reinforced retractor
13 p2088 N71-25071
- Backfire antenna research restricted to conical wave structure consisting of dipole elements
[AD-719879] 14 p2227 N71-25080
- Transmitting and receiving antennas for low frequency and very low frequency regions
[AD-719873] 14 p2227 N71-25080
- Intersection of arbitrarily oriented cone and sphere for application of finding earth coverage footprints of narrow beam satellite borne antennas
[AD-719763] 14 p2216 N71-25088
- Numerical results for Yagi backfire antennas
[AD-719809] 14 p2228 N71-25089
- High impact antennas with high radiating efficiency
[NASA-CASE-NPO-10231] 14 p2217 N71-25094
- Radiation pattern of thin, linear antenna of arbitrary length and driving point location
14 p2229 N71-25095
- Algorithmic procedure for optimization of antenna arrays
[RE-409] 16 p2359 N71-28883
- Pattern and impedance matching improvements in transverse electric triangular antennas
[NASA-CASE-XGS-02290] 16 p2363 N71-28889
- Application of Lorentz reciprocity theorem to an infield detection of buried dielectric spheres in antenna lossy half spaces
16 p2363 N71-28892
- Effects of variations of antenna parameters on radiation properties of short-backfire antenna
[AD-722048] 16 p2573 N71-29017
- Annotated bibliography on radar antennas including antenna arrays, antenna radiation patterns, types of radar antennas, and testing and evaluation
[AD-722200] 17 p2718 N71-30284
- Harmful biological effects caused by exposure to microwave radiation including radio frequency power density in vicinity of space station antennas
17 p2787 N71-30323
- Telemetry antenna radiation pattern test facility equipment for superhigh and ultrahigh frequencies
[AD-723053] 17 p2720 N71-30384
- Antenna phase and amplitude distributions shaping techniques to produce low sidelobe
[AD-722718] 17 p2721 N71-30404
- Phase shift errors in phased arrays influencing antenna radiation patterns and sidelobe reduction
[REPT-4-70] 18 p2888 N71-30888
- ESRO facility at Noordwijk, Netherlands, for testing antennas and antenna radiation patterns
[ESRO-TN-97F-ESTEC] 18 p2903 N71-31070
- Integral representations for radiation field line slots on surface of semi-infinite conducting cones
[AD-723289] 19 p3065 N71-33323
- Radiation from dielectrically coated spherical antennas determined by solving related boundary value problem
19 p3067 N71-33408
- Analysis of radiation of spherical and cylindrical antennas in incompressible and compressible plasma to detect existence of electroacoustic or longitudinal plasma wave excited by antenna
19 p3058 N71-33415
- Farfield patterns and directivity measurements for short backfire antennas
[AD-724607] 20 p3241 N71-33419
- Radiation patterns, efficiency, and bandwidth of short backfire antennas
[TP-550] 20 p3234 N71-33479
- Radiation patterns of dipole antennas in stratified medium representing lunar surface
[NASA-CR-121413] 20 p3234 N71-33488
- Mechanical and electrical characteristics of thin antennas used to measure quasi-omnidirectional radiation pattern from vehicle in 2300 MHz range
[TP-549] 20 p3235 N71-33474
- Evaluation of large reflector antennas including effects of primary reflector astigmatism and its associated through diffraction
[NASA-CR-121732] 21 p3394 N71-34157
- Input impedance and radiation patterns for equilateral, rectangular, cavity-backed aperture antenna for reentry communication
22 p3355 N71-35020
- Feasibility study of radiator and power divider for 50 to 60 GHz phased array - graphs
[NASA-CR-111949] 22 p3359 N71-35046
- NASTRAN-GAP programs for analyzing antenna radiation patterns of reflectors distorted by gravity and thermal loads
22 p3403 N71-35060
- Calculation of near fields of reflector antennas by geometrical theory of diffraction
[NASA-CR-111950] 23 p3722 N71-35062

SUBJECT INDEX

Propagation measurements on long high clearance path revealing difference between direct and ground reflected rays of about 30 wavelengths at 4 GHz (REF-4124) 23 p3722 N71-36333

Electric and magnetic field line distributions for calculating short range field around receiving antenna 23 p3723 N71-36536

Experimental and theoretical analysis of resonance properties and radiation patterns of dipole antennas symmetrically mounted on conducting spheres or cylinders 23 p3727 N71-36566

Infinite length, gap excited, thick, cylindrical dipole antenna radiation field formulations as boundary value problems based on Maxwell equations for electric and magnetic fields 23 p3734 N71-36619

Inductive gratings for compensating dielectric cylinder effects on mounted aerial (RA-67) 24 p3891 N71-37732

ANTENNAS

NT AIRCRAFT ANTENNAS

NT CASSEGRAIN ANTENNAS

NT CYLINDRICAL ANTENNAS

NT DIPOLE ANTENNAS

NT DIRECTIONAL ANTENNAS

NT FURLEABLE ANTENNAS

NT HELICAL ANTENNAS

NT HORN ANTENNAS

NT INERTIALLESS STEERABLE ANTENNAS

NT LENS ANTENNAS

NT LOG PERIODIC ANTENNAS

NT LOOP ANTENNAS

NT MICROWAVE ANTENNAS

NT MONOPOLE ANTENNAS

NT MONOPULSE ANTENNAS

NT MULTIPLE BEAM INTERVAL SCANNERS

NT OMNIDIRECTIONAL ANTENNAS

NT PARABOLIC ANTENNAS

NT RADAR ANTENNAS

NT RADIO ANTENNAS

NT RHOMBIC ANTENNAS

NT SATELLITE ANTENNAS

NT SLOT ANTENNAS

NT SPACECRAFT ANTENNAS

NT SPHERICAL ANTENNAS

NT SPIRAL ANTENNAS

NT STEERABLE ANTENNAS

NT TURNSTILE ANTENNAS

NT TWO REFLECTOR ANTENNAS

NT WAVEGUIDE ANTENNAS

NT WHIP ANTENNAS

NT YAGI ANTENNAS

Linear antenna pedestal for mobile weather radar (AW-175-41) 01 p0130 N71-10829

Radio relay communication using dual reflector antenna with offset focal axis (JRS-31721) 02 p0182 N71-11280

Electromagnetic fields produced by long, horizontal electric line source above reactive surface (AD-71857) 02 p0269 N71-12160

Reflective coefficient, radiation pattern, gain, and efficiency of X band cavity resonator 03 p0336 N71-12401

Program of measurements related to two phenomena of plasma/antenna interaction (NASA-CR-1727) 03 p0642 N71-14735

Analysis of sandwich wire antennas (AD-108) 03 p0643 N71-14736

Antenna design with self erecting mesh reflector (NASA-CASE-XGS-09190) 06 p0959 N71-16102

Electromagnetic theory, antennas, microwave components, and radio anechoic chamber (B-12) 10 p1517 N71-20602

Coupled linear antennas in inhomogeneous dispersive medium (AD-71899) 11 p1724 N71-22656

Polarization diverse S band feed cone for DSIF reflector antennas 11 p1703 N71-22778

Reflector surface distortions of 210 ft antenna and their effects on radio frequency performance 11 p1703 N71-22780

Antenna ranging angle optimization within structural member design for improved antenna performance 11 p1703 N71-22781

Analysis of integrated high frequency antenna system for F-3C aircraft radio communications (AD-71847) 12 p1887 N71-23306

High frequency antennas with high radiating efficiency (NASA-CASE-MPO-10231) 14 p2117 N71-26101

Antenna impedance measurement in compressible plasma simulating atmospheric entry (AD-72003) 14 p2322 N71-26146

Colloidal antenna beam and coaxial transmission line having inflatable inner tube (NASA-CASE-MPS-20068) 15 p2380 N71-27191

Weight error of three dimensional antenna system analyzed by plane wave spectrum representation techniques 18 p2890 N71-31098

Input impedance of aperture radiating into warm medium plasma (AD-72299) 19 p3163 N71-31678

Analysis of dynamic deflections of long flexible antenna booms on gravity gradient stabilized earth satellite by normal mode 20 p3355 N71-33892

Two antenna radiometer for localizing and tracking small radiating objects as function of temperature differences (NLL-FOBS-TRANS-2767-19022.81) 22 p3586 N71-35540

Techniques for minimizing snow and ice effects on TACAN antenna signals (FAA-RD-71-54) 22 p3617 N71-35773

NASTRAN program used to calculate gravity load distortions in 64-m antenna reflectors 22 p3683 N71-36262

ANTHERACENE

Radiation damage in single crystals of anthracene, naphthalene, and phenanthrene 08 p1283 N71-19329

ANTHROPOMETRY

Pervasive Quacina population growth physics, and pulmonary function at high altitude 02 p0155 N71-11096

Cockpit geometry evaluation program results and techniques with computer input and output samples of flight crew anthropometry (AD-716935) 09 p1321 N71-19817

Anthropometric data update for man-model used in cockpit geometry evaluation program for evaluation of flight crew interaction and compatibility with crew stations (AD-716396) 09 p1340 N71-19818

Cockpit geometry evaluation program for computer simulation of flight crew physical compatibility with crew stations based on anthropometric and environmental data for man-model movements (AD-716937) 09 p1340 N71-19819

Human factors engineering data for equipment design including anthropometry, environmental conditions, and physiological and behavioral factors (NASA-CR-114271) 14 p2269 N71-25944

Anthropometric size determination techniques and adult male and female data correlations from US, Australia, Europe, and Asia 18 p2878 N71-31481

Anthropometric survey of aviation personnel with bivariate tables noting relationships between selected variables (AD-723796) 19 p3048 N71-31942

Collection of adult anthropometry with source both domestic and foreign, male and female, military and civilian - Vol. 2 (AD-723638) 19 p3046 N71-32715

ANTIAIRCRAFT MISSILES

Computer program for analyzing and simulating attack of low flying aircraft by antiaircraft missiles and probability of aircraft survival (RAE-LIB-TRANS-1578) 24 p3896 N71-37774

ANTIBODIES

Feasibility of antigen/antibody system utilizing passive immune agglutination technique to determine microbial ecology of crew during extended space flight (NASA-CR-108587) 02 p0154 N71-11091

In vitro studies using boron-labeled antibodies and elemental boron as neutron target in therapy for tumors and cancer (NASA-CR-122925) 23 p3712 N71-36465

Electron transport, antibodies, photosynthetic membranes, and energy conservation in photosynthetic bacteria and virus infection of bacteria (NYO-3759-18) 23 p3714 N71-36474

ANTICYCLONES

Various states and development stages of northeastern extension of Siberian anticyclones during winter period 11 p1791 N71-22858

Surface effects on cumulus cloud formations in anticyclones over Russian plateau (NLL-M-20005-15828.4P) 12 p1959 N71-24272

Frequency of centers of gravity of cyclones and anticyclones for long range weather forecasting (NLL-M-20633-15828.4P) 21 p3453 N71-34574

Effect of subtropical anticyclones on development and position of intertropical convergence zone (NLL-M-20650-15828.4P) 21 p3454 N71-34583

ANTIDURETICS

Development of radioimmunoassay system for measurement of urinary antidiuretic hormone excretion 23 p3712 N71-36459

ANTIFERROMAGNETISM

Molecular field model for amorphous antiferromagnets with susceptibility variations (CALT-822-16) 07 p1069 N71-18068

Phase transitions and magnetostriiction in CaMnCl₃·2H₂O (NASA-TM-X-53997) 10 p1634 N71-21075

Ultrastrong interactions with nuclear and electron spins in antiferromagnetic insulators (AD-717190) 10 p1635 N71-21702

Magnetostatic and antiferromagnetic properties and structure of CrB compounds, emphasizing collinearity and wave vectors (ICBA-CONF-1701) 13 p2139 N71-25483

ANTIMATTER

Superficial effects on Fermi surfaces of antiferromagnetic Cr alloys with V and Mn traces, determined from de Haas-van Alphen effect (IS-T-430) 15 p2503 N71-27032

Hyperfine structure of antiferromagnetic FeC₂ using 14.4 keV Mössbauer transition in Fe-57 15 p2586 N71-27432

Theoretical and experimental investigation of electromagnetic wave propagation in antiferromagnetic MnF₂ 18 p2863 N71-31068

Thermal and magnetic behavior of electronic optical transitions in antiferromagnetic crystals at 35 K 19 p2954 N71-31137

Calculation of thermodynamic properties of two substituted anisotropic Heisenberg antiferromagnet using Green method (NASA-TN-D-6499) 21 p3487 N71-34914

Low temperature measurements of specific heat of nickel ultrate lithiuhydride and antiferromagnetic exchange interactions (AD-726425) 22 p3352 N71-32529

ANTIROLL BEARINGS

NT BALL BEARINGS

NT ROLLER BEARINGS

Grease lubricated spiral groove bearings suitable for spin axis of gyro in automatic pilots (NASA-CR-102926) 03 p0384 N71-12819

Investigating stability of steady movement of right shaft with disc on elastic rotor bearings using modified Routh procedure 06 p0893 N71-19552

Antifriction characteristics of dry bearings fabricated from various materials (AD-716512) 09 p1393 N71-19619

Rotor-bearing system analysis to determine cause of breifing failure of bearings from vibration tested PLV fans (NASA-CR-117835) 11 p1769 N71-22527

Development of hybrid bearing lubrication system with combination of standard type lubrication and magnetic thin film for earth atmosphere and space environment operation (NASA-CASE-XRP-91641) 11 p1772 N71-22997

Calculation of rotor critical speeds for two bearing rotor system from rigid body theory using film stiffness as determined from zero speed, load eccentricity data (NASA-TN-D-6350) 13 p2088 N71-25530

Designing antifriction materials for friction and wear points at elevated temperatures (AD-720367) 14 p2278 N71-25994

Development of rolling element bearing for operation in ultrahigh vacuum environment (NASA-CASE-XLE-09327-2) 14 p2262 N71-26189

Friction and wear behavior of antifriction bearings operating in ultrahigh vacuum conditions (NLL-RISLEY-TRANS-2140-0901.50P) 23 p3764 N71-36837

Effect of antiseizing and antistick additives on wear of highly loaded, small module metric gears (AD-727414) 24 p3925 N71-38031

ANTIGENS

Feasibility of antigen/antibody system utilizing passive immune agglutination technique to determine microbial ecology of crew during extended space flight (NASA-CR-108587) 02 p0154 N71-11091

Detection of antigens and genetic analysis with monoclonal hybrids (SU-326-P-36-X-2) 03 p0322 N71-12360

ANTICING ADDITIVES

Gasoline icing inhibitors for aircraft carburetors and fuel systems (LR-536) 04 p0473 N71-15414

Calculating and testing anticling systems of aircraft and helicopters (AD-719522) 14 p2197 N71-25632

Effects of corrosion inhibitors and anticling inhibitor combinations on coating properties of filter coalescer elements used to decontaminate jet engine fuels (AD-722331) 16 p3670 N71-38577

ANTIMATTER

NT ANTINEUTRINOS

NT ANTINEUTRONS

NT ANTIPARTICLES

NT ANTIPROTONS

NT POSITRONS

Hydrodynamics of matter and antimatter in contact (REF-70/38) 09 p1437 N71-20874

Cross sections and coherent final states for antineutrino deuteron interactions and related dissociation reactions at 7.0 GeV/c (TID-25610) 10 p1617 N71-21285

Cosmic antimatter annihilation and gamma ray background spectrum (NASA-TM-X-63517) 13 p2160 N71-24962

Cosmic matter-antimatter annihilation and gamma ray background spectrum (NASA-TM-X-63598) 17 p2861 N71-29926

Hydrodynamical motion of system consisting of matter-antimatter embedded in thermal radiation (REF-71/25) 20 p3328 N71-33064

Cosmological gamma ray spectrum calculations from matter-antimatter annihilations in universe [NASA-TM-X-65789] 23 p3842 N71-37395
Charge symmetry of universe and distribution of matter and antimatter 23 p3830 N71-37440
Gamma ray and neutron radiation of meteor streams in relation to antimatter comet hypothesis 23 p3830 N71-37441

ANTIMISSILE DEFENSE

Anti-intercontinental ballistic missile defense and high altitude nuclear explosions [BMVG-FW-71-1] 18 p2977 N71-36644
Phase cancellation effects on cross sections of limited irregularities related to clutter, radar target identification, jamming, and antimissile defense systems [AD-723587] 19 p3033 N71-31991
Users manual for DEANE computer program for use in ballistic missile defense analysis [AD-727645] 23 p3557 N71-33339

ANTIMONIDES

NT ALUMINUM ANTIMONIDES
NT GALLIUM ANTIMONIDES
NT INDIUM ANTIMONIDES
Hypertens fields at magnetic and nonmagnetic lattice sites measured in solid solutions of magnesium antimonide and chromium antimonide [COO-1198-800] 18 p2962 N71-30737

ANTIMONY

Consumption statistics for antimony in industry [DMAB-274] 07 p1043 N71-17519
Effect of antimony and beryllium impurities on diffusion rate of zinc in polycrystalline brass [TT-70-57086] 08 p2118 N71-19098
Production of ultrapure antimony by continuous zone recrystallization in single column vacuum apparatus 10 p1575 N71-30883
Volume and grain boundary diffusion of tin and antimony into copper 14 p2272 N71-23820
Electron irradiation induced separation of Sb from SnO₂ solutions in anhydrous alcohols, ethers, ketones, acids, esters, and aromatic hydrocarbons [NASA-TN-D-6358] 14 p2214 N71-26930
Production, consumption, and uses of antimony 17 p2762 N71-29284
Analysis and electrochemical behavior of semiconducting thin films of antimony doped tin oxide 17 p2714 N71-29695
Low temperature thermal conductivity of Sb and Ga after Te and Zn doping and electron irradiation [NRP-18836] 22 p3458 N71-36083

ANTIMONY COMPOUNDS

NT ALUMINUM ANTIMONIDES
NT ANTIMONIDES
NT GALLIUM ANTIMONIDES
NT INDIUM ANTIMONIDES
Electrical resistivity of rectifying semiconductor antimony-antimony sesquioxide diffusion junctions [AD-712941] 07 p4444 N71-13177
X ray phase analyses on vacuum sublimations of bismuth sulfide, antimony sulfide, and antimony selenide [NASA-TT-F-13461] 08 p1217 N71-19013
Dark and thermally stimulated conductivity, spectral distribution of normal and induced photoconductivity, and optical extinction of photoconductivity in Sb₂S₃ single crystals 12 p1964 N71-23266
Molecular crystals structure analyses on quinolinium antimony tetrachloride and beta picoline-N-oxide bismuth acid adduct 15 p2509 N71-27908

ANTIMONY ISOTOPIES

Directional correlation of beta-gamma decay data in Tl-208, Sb-126, Bi-214, and Nb-94 and steric effects for nuclear structure 13 p2142 N71-25558
Sorption of antimony-125 by silica gel from nitric and hydrochloric acid 23 p3794 N71-37045
Beta and electron-capture decay schemes for Sb isotopes and proton reactions of C-12, F-19, Au-197, Hg-3, Ta-181, Pb-208, and Ni-58 including angular distributions and scattering cross sections [UCLA-10-P-18-23] 23 p3816 N71-37215

ANTINEUTRINOS

Energy spectra calculations of fission fragments and antineutrino values for targets of different thickness [JINR-P3-9081] 02 p2777 N71-12134
Technique of antineutrino measurement of neutron time of flight spectrometer [JINR-P3-5119] 03 p4826 N71-12850
Ratio of neutrino to antineutrino nucleus total and differential cross sections 04 p5772 N71-13648
Mass spectra of prompt antineutrinos for neutrino induced fission of Pu-239 between 40 keV and 1.2 MeV [AWE-O-4270] 06 p9910 N71-15785

Relative measurement of antineutrino in U-235 and Pu-239 fission induced by resonance neutrons in fast neutron pulsed reactor [BNL-TR-401] 15 p2493 N71-27958
Angular correlation of neutron spin and antineutrino momentum in beta decay of polarized neutrons [IAR-1947] 23 p3807 N71-37139

ANTINEUTRONS

Calculation of nucleon-antineutrino bound states in quark models from OBE model [DESY-70-49] 15 p2488 N71-27873

ANTIOXIDANTS

Antioxidant additive for hydrocarbon oils [AD-713046] 03 p4398 N71-13400
Investigating effects of vapor space inhibitors on corrosion resistance of steam turbine oils [NRC-11644] 04 p6534 N71-14261
Determining effects of α -D-glucose acid on oxidation inhibition of steam turbine oils 04 p6534 N71-14262
Differential thermal analysis and antioxidant activity of nickel, zinc, lead, copper, and cadmium diethyldithiocarbamates [PTD-MT-23-363-70] 10 p1513 N71-31230
Chemical synthesis and lubricant tests of DNEK-P-21 (calcium) antioxidant additive [AD-727415] 24 p3944 N71-38157
Antioxidant additives for increasing thermo-oxidative stability of synthetic lubricants [AD-727691] 24 p3943 N71-38142
Extractive phenols from coal as antioxidant additive for motor fuels [AD-727438] 24 p3999 N71-38328

ANTIPARTICLES

NT ANTINEUTRINOS
NT ANTINEUTRONS
NT ANTIPROTONS
NT POSITRONS
Hyperon states in partial wave analyses of antikaon nucleus system [UCRL-19843] 06 p4934 N71-16774
Four pion and five pion final states in antiproton proton annihilations in hydrogen at 940 MeV/c [CONF-70066-49] 06 p4927 N71-16892
Heavy baryons in proton-antiproton interactions [UCI-34-P-149-1] 07 p1073 N71-17359
Isospin conservation test from antiproton interactions at 400 MeV/c from absolute and differential cross sections and differential polarizations of hydrogen bubble chamber photos 09 p1427 N71-19693

Chiral Lagrangian model of meson-baryon scattering for theory of antikaon interactions [TID-25639] 12 p1971 N71-23846

Antikaon 3 nuclei in negative baryons [EPVB-SRP-70-16] 13 p2132 N71-25109

Interaction cross sections of antikaon deuterons yields kaon Y1 Y2 [JINR-P2-5231] 14 p2314 N71-26728

Lambda and Sigma hyperon resonances, branching ratios, and lifetimes from bubble chamber analysis of antikaon nucleus reactions [CEA-2-4068] 15 p2492 N71-27951

Direct measurements of anti kaon for neutron induced fission of Pu 239 [AWE-O-8670] 16 p2655 N71-29074

Negative pion, kaon, antiproton, and antineutron production in 70 GeV proton irradiation of aluminum and beryllium nuclei [EPVB-SRP-70-38] 17 p2810 N71-30387

Antihyperon hyperon production in antiproton proton scattering, studied with absorbed Regge pole model with exchange degeneracy [N-TB-71/2] 20 p3324 N71-33877

Local models from D/D' formalism for antikaon-nucleon collisions [PAM-70-1] 22 p3636 N71-35919

ANTIPROTONS

Heavy meson resonances in antiproton proton annihilation reaction at 3.6 GeV/c [NRP-18466] 08 p1251 N71-18262
Antiproton-deuteron and proton-proton collisions with resonance decay and double pion production 10 p1625 N71-21826
Gamma ray production from cosmic proton antiproton annihilations, selection rules, and Matsuda statistical model 13 p2158 N71-24767
Relativistic magnetohydrodynamic equations of proton antiproton annihilation reactions and Klein-Alires cosmology 13 p2131 N71-25029
Antiproton annihilations at rest with bound neutrons in deuterium 13 p2141 N71-25543
Upper limit on omega meson yields 2 pion decay rate from antiproton-neutron annihilations at rest 15 p2460 N71-27873
Meson and hyperon production in antiproton proton, antiproton neutron, and antiproton deuteron annihilations at high energies 15 p2481 N71-27701
Antiproton annihilations with neutrons into final pion states 15 p2487 N71-27858

Annihilation antiproton neutron yields pions/kaons/ pions/kaons/ between 0.5 and 1.5 GeV/c and its comparison with Vassilikis model results [INPN-PD-70/2] 15 p3494 N71-37397
Final states of four-pronged antiproton deuteron interactions at 7.8 GeV/c, and cross sections for white spectator events 15 p3496 N71-37399

Large angle antiproton-proton elastic scattering - evidence for existence of local structure in functions of both beam momentum and four-momentum transfer 16 p3522 N71-38077

Properties of meson resonances in antiproton proton annihilations [SUC-P-70-1] 18 p3974 N71-38022

Mass spectra of antiproton proton annihilations into 4 or 5 pions at 3 GeV/c [NRP-18730] 18 p3974 N71-38022

Low momentum antiproton-proton interactions between 100 MeV/c and 750 MeV/c 22 p3650 N71-40022

Symmetry and possible antiprotons in primary cosmic rays 23 p3830 N71-37440

ANTIRADIATION DRUGS

Chemical and biological antiradiation drugs for space flight 08 p1153 N71-40024
Space flight radiation protection using antiradiation drugs 08 p1158 N71-40025

ANTIRADIATION WARFARE AIRCRAFT

NT P-3 AIRCRAFT
Sonic detection of submarines by helicopter and protection of flight crew hearing [AD-711910] 03 p5534 N71-12809
Sonicboom location [AD-713077] 03 p5545 N71-14013
Development and characterization of aircraft, helicopters, and airships for detecting and detecting submarines [AD-723558] 19 p3056 N71-31770

ANTISYMMETRY

Seasonal variations in antisymmetric diurnal and semidiurnal variations of cosmic rays [NASA-TT-F-135113] 09 p1462 N71-20081

ANTIKANE MINIBELS

Designing long-range antiskid/bombardment weapon system [TT-7005] 09 p1488 N71-20123

ANXIETY

Relationship of interaction of impulsiveness and anxiety to perceptual-motor performance in human beings 09 p1334 N71-20081

AO-1 AIRCRAFT

U OV-1 AIRCRAFT

APATITES

U MINERALS

APERTURES

NT IRIS (MECHANICAL APERTURES)

Gross function and expansion coefficients for entry excitation through small apertures [SC-CB-70-6099] 01 p0090 N71-14025

Apertured electrode focusing system for ion beams with nonuniform plasma density [NASA-CASE-XNP-03332] 01 p0894 N71-14026

Near electric field of rectangular aperture in infinite ground plane [AD-714574] 06 p0834 N71-14024

Physical realizability of planar antennas [AD-715267] 07 p0999 N71-17773

Element pattern design of large array of circular apertures on triangular grid, using rotationally symmetric and periodic antennas [AD-717199] 10 p1534 N71-31103

Sharing common aperture of two planar microwave arrays for enhancing utilization of available aperture space 11 p1725 N71-22940

Threshold factor aperture coupling coupling apertures for planarity of radiation, self-induced gain, and, capable of using nonconformal materials in both ends [NASA-CASE-XPR-03302] 12 p1925 N71-22944

Electromagnetic shielding effectiveness degradation from void defects in metal conducting sheets and comparison of propagation through rectangular and circular apertures [AD-721907] 16 p2569 N71-29088

Analytical determination of optimum spatial distribution of aperture for enhancing array reception 23 p3726 N71-38088

Wide and small aperture magnetic apertures using high particle energies and emphasizing precession angles and moments [SLAC-PUB-798] 23 p3759 N71-38089

Radiation impedance functions of rectangular pions and their application to sound transmission through finite depth apertures 23 p3805 N71-37710

Phase acceptance of alternating gradient double mode of quadrupoles of different apertures [CERN-71-11] 23 p3820 N71-37710

SUBJECT INDEX

APOLLO
Gas-liquid chromatography peak-shape dependence on retention time, sample volume, and column type and overpressure; peak area determination
[JPL-CE-TRANS-5578-1962.09] 23 p3721 N71-34536

APOLLO 7
RESPIRATION
Photography of Apollo 7 retrofire and service propulsion module reentry and apogee burn of Intelsat T-3 satellite 05 p0767 N71-14664

APOLLO APPLICATIONS PROGRAM
Research progress on radiation effects of nuclear power sources on spacecraft, holography application to stress analysis, composite antenna structure, and Apollo applications 01 p0128 N71-10362

Best sources for manufacturing experiments in Apollo Applications Program 02 p0305 N71-11723

Lunar fabrication for radioluminescence: best source of ATM ultraviolet micro-radiation in AAP [JPL-CE-TRANS-5578-1962.09] 10 p1561 N71-21757

Threat orbital space stations, shuttle, boost, and tugs in Apollo applications program [NASA-TM-X-67653] 11 p1830 N71-22042

APOLLO FLIGHTS
NT APOLLO 6 FLIGHT
NT APOLLO 7 FLIGHT
NT APOLLO 8 FLIGHT
NT APOLLO 9 FLIGHT
NT APOLLO 10 FLIGHT
NT APOLLO 11 FLIGHT
NT APOLLO 12 FLIGHT
NT APOLLO 13 FLIGHT
NT APOLLO 14 FLIGHT
NT APOLLO 15 FLIGHT
NT APOLLO 16 FLIGHT

Heliographic coordinates of lunar topography from Apollo 8, 10, 11, and 12 missions [NASA-TM-D-6062] 02 p0296 N71-12042

Studying simulated lunar soil for determining feasibility of proposed geotechnical tests for Apollo missions [NASA-CR-102963] 05 p0767 N71-15204

Radioisotope content in feces and urine of Apollo 7 through 13 astronauts [NASA-CR-116223] 06 p0801 N71-16358

Deep Space Network support activities for Apollo 9 through 13 flights and associated equipment [NASA-CR-118325] 13 p2168 N71-25153

Apollo range rate residuals during lunar orbits for determining lunar mass concentrations 13 p2168 N71-25153

Drilling tests for evaluating coring potential of Apollo lunar surface drill [NASA-TM-X-58057] 17 p2734 N71-29214

Activation analysis of focal samples from Apollo 7, 8, 9, and 10 astronauts to determine effects of space flight on mass balance of various elements by human body [NASA-CR-121861] 21 p3381 N71-34058

Measurement of radiation exposure of Apollo 7, 8, 9, and 10 astronauts by determination of radioisotope content of feces and urine [NASA-CR-121861] 21 p3381 N71-34059

Nutritional evaluation of Apollo diets and pathological study of mice having diets with limited substrates [NASA-CR-115124] 21 p3384 N71-34075

Red cell mass and plasma volume changes observed in astronauts on Gemini and Apollo missions 23 p3711 N71-34654

Neurological program and biochemical data from Gemini and Apollo missions 23 p3711 N71-34655

APOLLO LUNAR SURFACE EXPERIMENTS
ALSEP
Lunar ALSEP mass spectrometer for measuring composition of lunar atmosphere [NASA-CR-114774] 04 p0613 N71-14230

Design, development, fabrication, and test of lunar surface rover/rover experiment equipment for Apollo 16 [NASA-CR-114981] 10 p1645 N71-21407

Penetration manual for Apollo Lunar Surface Experiments Package describing mission, equipment, subsystems, maintenance, and operations [NASA-CR-99604] 12 p2002 N71-24292

Field maintenance manual for Apollo Lunar Surface Experiments Package [NASA-CR-114981] 13 p2004 N71-24396

Best criteria of heat flow experiment designated ALSEP Array A2 [NASA-CR-115169] 19 p3178 N71-31407

Reference of Apollo Lunar Surface Instrument Package (ALSEP) 3 band downlink telemetry signal [NASA-TM-X-65631] 19 p3857 N71-33482

APOLLO PROJECT
Material management control performance of Apollo program prime contractor 01 p0136 N71-10292

Microscopic aspects of Apollo biomedical operations 02 p0164 N71-11821

Investigating origins, structure, and composition of moon 02 p0296 N71-11951

Seak utility (Automated Seak Program) [NASA-CR-106725] 05 p0546 N71-12462

Evaluating tracking and orbit determination functions and supporting equipment for Apollo instrumentation ships [NASA-CR-111576] 05 p0455 N71-12630

Geological maps of potential Apollo landing sites on lunar surface [NASA-CR-116408] 07 p1109 N71-17497

Deep Space Network support of Manned Space Flight Network for Apollo project [NASA-CR-116891] 08 p1287 N71-18476

Apollo project technology application to orbital space station and space shuttle projects 10 p1665 N71-30830

Digital data processing and error correcting code techniques applied to Apollo unified 3 band communication system [NASA-CR-114921] 10 p1525 N71-21465

Research and development of Apollo lunar ranging retroreflectors [NASA-CR-114951] 10 p1645 N71-21466

Comparison of management techniques applied to life sustaining resources in Apollo command modules and in earth ecology 11 p1846 N71-22052

Planning for spacecraft missions and space exploration 11 p1676 N71-22392

Remote viewing of coastal areas by aerial and spaceborne photography [JAD-717936] 12 p1906 N71-23326

Penetration manual for Apollo Lunar Surface Experiments Package describing mission, equipment, subsystems, maintenance, and operations [NASA-CR-99604] 12 p2002 N71-24292

Comparison of analytical results of lunar surface materials from Surveyor, Apollo, and Luna missions 13 p2165 N71-24539

Qualification tests of lower section motors for Apollo spacecraft program launch escape system [NASA-TM-D-62955] 13 p2156 N71-25033

Computer program for simulation of nominal and anomalous operation of Apollo cryogenics storage system [NASA-CR-115022] 15 p2174 N71-25183

Statistical mechanics for wall shear turbulence in Couette flow based on Brownian motion and comparison with stochastic theory based on Navier-Stokes equation [NASA-SP-4914] 19 p3834 N71-32246

Results of world wide surface refractivity test conducted in support of Apollo program [NASA-TM-X-65647] 19 p3896 N71-32611

Determination of black and white lunar television camera performance after long storage for Apollo program [NASA-CR-115105] 19 p3858 N71-32697

Mass spectroscopy investigations of Apollo 11 and 12 soil samples [UCB-34-P-32-PB-5] 20 p3323 N71-33815

Apollo service propulsion system rocket engine biopropellant valve improvement program - valve design guide and oxygen-hydrogen technology [NASA-CR-108378] 21 p3502 N71-34946

Analysis of Apollo launch operations and applicability to space shuttle program 22 p3674 N71-36194

Evaluating Apollo oxygen tank structural performance in low g environment and capability of tank to satisfy mission requirements [NASA-CR-115143] 22 p3681 N71-36248

Results of symposium conducted to assess endocrinological changes observed in Apollo astronauts [NASA-TM-X-65647] 23 p3710 N71-34653

Review of endocrine control of fluid and electrolyte balance during Mercury, Gemini, and Apollo missions 23 p3711 N71-34656

Microbiological contamination of Apollo spacecraft components [NASA-CR-122844] 24 p3876 N71-37642

Analysis of propellant sloshing in lunar module during Apollo 14 flight and resultant erroneous indication of low level of propellant [NASA-TM-X-2562] 34 p3906 N71-37841

APOLLO SPACECRAFT
Weightlessness effects on spacecraft flammability 02 p0305 N71-11719

In-line disconnect/Automated Seak Program [NASA-CR-108735] 05 p0539 N71-12453

Computer program for processing BTD data for use by other program in Automated Seak Program System [NASA-CR-108729] 05 p0539 N71-12456

Computer program for reporting faults by operating on branch and node table data sets using indexed sequential access method [NASA-CR-108738] 05 p0539 N71-12457

Computer update program for compiling master file list from box external data [NASA-CR-108734] 05 p0542 N71-12478

Computer program for processing data on ground support equipment wiring in Apollo spacecraft [NASA-CR-106731] 05 p0542 N71-12479

Computer program for analyzing all power/power, power/ground, ground/ground, and incomplete paths in Automated Seak Program [NASA-CR-108740] 05 p0542 N71-12481

Digital computer program requirements to process Apollo spacecraft electrical data for seak circuit analysis [NASA-CR-108727] 05 p0542 N71-12482

Automated Seak Program (ASP) to generate diode, load, and special node reports which aid in drawing of circuitry paths for seak circuit analysis of Apollo spacecraft [NASA-CR-108726] 05 p0543 N71-12490

Results of simulated runs to evaluate lunar module descent performance of P46 automatic control and guidance system [NASA-CR-114787] 04 p0613 N71-14233

Hydrogen oxygen fuel cells for electric power plants and Apollo spacecraft [DLR-MIT-70-09] 06 p0796 N71-15723

Vibration tests of Apollo spacecraft positive expulsion propellant tank assemblies [NASA-CR-114811] 06 p0801 N71-16430

Characteristics of low frequency pressure oscillations in Apollo spacecraft engines [NASA-CR-114806] 06 p0801 N71-16439

Solution of command module and service module expulsion bladder repositioning problems [NASA-CR-114813] 06 p0801 N71-16481

Elimination of permeation and bubble formation in Apollo RCS positive expulsion tanks [NASA-CR-114812] 06 p0809 N71-16486

Environmental tests of design modifications for Apollo RCS positive expulsion tanks [NASA-CR-114814] 06 p0809 N71-16487

Communication system analysis techniques for Apollo unified 3 band communications [NASA-CR-116351] 07 p1081 N71-17472

Phase locked-loop tracking with sine wave modulation in Apollo communication systems [NASA-CR-116306] 07 p1081 N71-17473

Analysis of command and service module configurations and recommendations to prevent failures which occurred on Apollo 13 flight [NASA-TM-X-68932] 09 p1471 N71-19045

Physical, metallurgical, chemical, and thermodynamic surveys of high pressure tanks and plumbing systems of Apollo spacecraft [NASA-TM-X-68919] 09 p1471 N71-19046

Description of computer program for detailed stratification model of Apollo supercritical oxygen storage tank [NASA-CR-114963] 10 p1688 N71-31574

Line-of-sight deviations and ray trace analyses of Apollo side window for optical experiments [NASA-CR-114775] 13 p2175 N71-25156

Onboard optical and electronic data acquisition instrumentation for monitoring Apollo Saturn 5 launch performance [NASA-TM-X-67183] 16 p2682 N71-30172

Dynamic structural analysis, statistical analysis, and Rayleigh-Ritz methods applied to Skylab and Apollo/Saturn problems including page effects, vibration damping, and noise reduction [NASA-TM-X-64538] 16 p2688 N71-30905

Dynamic structural analysis and flow induced stress analysis of metal bellows in Apollo Saturn launch vehicle systems 16 p2688 N71-30906

Mathematical model and algorithms for Skylab docking dynamic response analysis with statistical analysis of Apollo probe/drugs docking system [NASA-CR-115143] 16 p2688 N71-30906

Acoustic vibration tests for noise reduction by helium and polyurethane foam in stainless steel cylinders for application to Skylab and Apollo vibration tests 16 p2683 N71-30161

Rocket engine biopropellant valve improvement for Apollo service propulsion system [NASA-CR-108377] 17 p3750 N71-30597

Electron microscope, electron diffraction, and electron microscope analysis of defective solid state weldment on liquid hydrogen tank from Apollo 12 fuel cell system [NASA-TM-D-6337] 18 p2857 N71-31354

Data compression and error correcting code applied to digital transmission of real time, standard format TV, along with video and other data from Apollo spacecraft 21 p3513 N71-33040

Service and shift life tests of radiation survey meter and personal radiation detector battery packs used on Apollo spacecraft [NASA-CR-115108] 23 p3717 N71-34689

APOLLO TELESCOPE MOUNT
Error study for SS-1000 ATM sensor system, effects of atmospheric refraction, atmospheric attenuation, and earth albedo [NASA-CR-108957] 04 p0611 N71-14088

APOLLO 6 FLIGHT

Linear fabrication for radiotelescope heat source of ATM ultraviolet mirror/grating in AAP (MLM-1779) 10 p1561 N71-21737

Characteristics, performance tests, and evaluation of electronic modules for fine scan sensor assembly for Apollo telescope mount used in Skylab project (NASA-TM-X-64599) 14 p2254 N71-26025

Apollo Telescope Mount experiment designed to study energy of sun from wavelength of 200 to 2000 ph /2 to 20 A/ using X ray source 17 p2730 N71-29320

Design, development, and characteristics of phototelescope for use with Apollo telescope mount mission (NASA-CR-119781) 21 p3425 N71-34374

Effect of rotation on structural and dynamic behavior of spinning body with flexible appendages, and application to Skylab Apollo telescope mount and orbital workshop 22 p3485 N71-34278

APOLLO 6 FLIGHT

Plant and soil signatures extracted by spectrophotometric analysis of Apollo 6 and earth resource survey aircraft color photography 06 p0845 N71-16149

Comparison of concurrent cloud data obtained via ATS 3 and ESSA 3 and from Apollo 6 high resolution photography (NASA-TM-D-6470) 21 p3452 N71-34366

APOLLO 7 FLIGHT

Photography of Apollo 7 retrofire and service propulsion module reentry and apogee burn of Intelsat 2 F-2 satellite (NASA-CR-115869) 05 p0767 N71-14664

Correlating color photography of Apollo 7 with natural color of surface deposits and rocks of Salar de Atacama, Chile 14 p2251 N71-26645

APOLLO 8 FLIGHT

Evaluation of flight performance of service propulsion system during Apollo 8 Mission (NASA-TM-X-66476) 02 p0290 N71-11887

Apollo 8 tracking radius data for determining lunar gravity fields 13 p2170 N71-25304

Lunar photographs from Apollo 8, 10, and 11, flights (NASA-SP-246) 17 p2842 N71-29260

APOLLO 9 FLIGHT

Multispectral terrain photography obtained from SO65 experiment aboard Apollo 9 (NASA-CR-108562) 02 p0218 N71-12060

Operational schedule for Apollo 9 command module/lunar module 3 flight plan and crew activities (NASA-TM-X-66904) 09 p1469 N71-26513

Development of meteorological information and parameters based on cloud photographs taken during Apollo 9 flight (NASA-CR-114954) 10 p1597 N71-21468

Camera and filter postflight spectrum analysis for Apollo 9 multispectral photography experiment (NASA-CR-117501) 10 p1561 N71-21469

Earth resources analyses by multispectral terrain photography with Apollo 9 cameras 13 p2082 N71-25257

System of regional agricultural land use mapping tested against Apollo 9 color infrared photography of Imperial Valley, Calif. (NASA-CR-121875) 21 p3426 N71-34375

Image enhancement techniques for detecting minute changes in Apollo 9 photographs (WDL-TR-4279) 22 p3585 N71-35532

APOLLO 10 FLIGHT

Failure analysis of recovery flaring xenon lamp on Apollo 10 flight (NASA-TM-X-66445) 02 p0298 N71-11899

Analytical aerostabilization of Apollo 10 Hasselblad photographs of moon far side (NASA-CR-115901) 13 p2081 N71-24577

Lunar geology, crater, and volcanic feature analysis from Apollo 10 visual observations and photomicrographs (NASA-SP-232) 15 p2517 N71-27871

Lunar photographs from Apollo 8, 10, and 11, flights (NASA-SP-246) 17 p2842 N71-29260

APOLLO 11 FLIGHT

Low temperature thermoluminescence of Apollo 11 material 01 p0120 N71-10079

Determining presence of porphyries in Apollo 11 and 12 soil samples by fluorescence spectrometry and analytical dematuration (NASA-CR-108671) 02 p0150 N71-11067

Evidence from comparisons with stony meteorites of solar flare proton induced radioactivity in Apollo 11 lunar rocks (NASA-CR-111348) 02 p0293 N71-11958

Luminescence of lunar rocks from Apollo 11 02 p0296 N71-11961

Nuclear emission recordings of radiation exposure of Apollo 11 astronauts on moon (NASA-CR-115804) 04 p0475 N71-13428

Developments in space science that led to Apollo 11 flight

05 p0766 N71-14613

Determination of carbon content of lunar samples from Apollo 11 flight 07 p1115 N71-17964

Investigating mineral composition of Apollo 11 and 12 lunar rock samples 08 p1289 N71-19144

Electron microprobe analysis of fine-grained igneous rocks from lunar sample 10022 from Sea of Tranquility 08 p1289 N71-19145

Electron probe microanalysis of minerals of lunar igneous rocks from Apollo 11 flight 08 p1289 N71-19146

Optical and radio frequency electrical properties and grain size analyses of Apollo 11 and 12 lunar soil samples 09 p1465 N71-19784

Activities and accomplishments of NASA from July to December, 1969 09 p1466 N71-20020

Neutron activation analysis determination of uranium and Pb-204 in Apollo 11 fines 13 p2166 N71-24560

Apollo 11 postflight analysis and mission report (NASA-SP-238) 13 p2167 N71-25042

Apollo 11 mission planning for lunar surface exploration including equipment requirements, crew/equipment interfaces, and timelines for extravehicular activities (NASA-TM-X-67180) 14 p2337 N71-26144

Analysis of anomalous jettisoning of service module during reentry of Apollo 11 14 p2345 N71-26585

Lunar photographs from Apollo 8, 10, and 11, flights (NASA-SP-246) 17 p2842 N71-29260

Chemical composition of lunar samples from Apollo 11 and 12 flights 19 p3181 N71-32388

Lunar cratering, and geologic interpretation of Apollo 11 soil samples 23 p3846 N71-37416

APOLLO 12 FLIGHT

Determining presence of porphyries in Apollo 11 and 12 soil samples by fluorescence spectrometry and analytical dematuration (NASA-CR-108671) 02 p0150 N71-11067

Cosmic radiation dosage measurement of astronauts by radiochemical techniques (BNWL-1183-4) 02 p0151 N71-11075

Chemical and isotopic analyses of Apollo 12 lunar samples (NASA-TR-R-353) 04 p0610 N71-13742

Luminescence petrography of Apollo 12 rocks and comparative features in Apollo 11 rocks, terrestrial rocks, and meteorites 07 p1110 N71-17563

Apollo 12 lunar samples studied with neutron diffraction at room and cryogenic temperatures (NASA-CR-114833) 07 p1111 N71-17565

Engineering analysis of Surveyor 3 parts returned by Apollo 12 astronauts to determine lunar environment effects 07 p1111 N71-17567

Absence of uranium, thorium, and plutonium isotopes in Apollo 12 soil and breccia samples (NASA-CR-114870) 07 p1114 N71-17868

Electron and ion microprobe analyses of Apollo 12 fines and breccias (NASA-CR-114871) 08 p1289 N71-18878

Apollo 12 flight color and black and white lunar photography indices on MERCATOR projections (NASA-TM-X-66803) 08 p1203 N71-18975

Investigating mineral composition of Apollo 11 and 12 lunar rock samples (NASA-CR-114878) 08 p1289 N71-19144

Using photomicroscope and electron microprobe for mineralogical and petrological analysis of Apollo 12 lunar sample 12013 08 p1289 N71-19147

Optical measurements on Apollo 12 soil samples from lunar mare surfaces (NASA-CR-114894) 09 p1465 N71-19780

Preliminary results from Mossbauer instrumental analysis of Apollo 12 lunar rock and soil samples (NASA-CR-114887) 09 p1465 N71-19781

Optical and radio frequency electrical properties and grain size analyses of Apollo 11 and 12 lunar soil samples 09 p1465 N71-19784

Magnetization versus field and temperature analyses of ferromagnetic material in Apollo 12 lunar samples 09 p1465 N71-19787

Determination of petrology and deformational state of pyroxene and olivines in lunar rocks returned by Apollo 12 flight 15 p2516 N71-26809

Compressibility and porosity of basalt from Apollo 12 lunar samples (UCRL-72851) 15 p2518 N71-27990

SUBJECT INDEX

Chemical composition of lunar samples from Apollo 11 and 12 flights 19 p3181 N71-32388

(NASA-TT-F-13707) 19 p3181 N71-32388

Data processing and reduction techniques for photointerpretation of Baker-Nunn photographs of venting clouds during Apollo 12 flight 20 p3257 N71-32388

(NASA-CR-121902) 20 p3257 N71-32388

Engineering tests of Surveyor 3 television camera returned to earth by Apollo 12 astronauts after 3 1/2 years on lunar surface - Vol. 1 20 p3257 N71-32388

(NASA-CR-121796) 20 p3257 N71-32388

Appendix to engineering evaluation tests of the Surveyor 3 television camera returned from moon by Apollo 12 astronauts - Vol. 2 20 p3257 N71-32388

(NASA-CR-121481) 20 p3257 N71-32388

Mineralogy and petrology of Apollo 12 lunar samples 21 p3508 N71-34369

(NASA-CR-121062) 21 p3508 N71-34369

APOLLO 13 FLIGHT

Investigation of cryogenic oxygen tank assembly in Apollo 13 flight 01 p0126 N71-10041

(NASA-TM-X-66462) 01 p0126 N71-10041

Simulation and analysis of panel separation from Apollo 13 service module 03 p0456 N71-19808

(NASA-TM-D-6087) 03 p0456 N71-19808

Abstract mission of Apollo 13 due to loss of cryogenic oxygen in service module 03 p0456 N71-19808

(NASA-TM-X-66460) 03 p0456 N71-19808

High gain antenna acquisition problem during Apollo 13 flight 09 p1346 N71-19808

(NASA-TM-X-66903) 09 p1346 N71-19808

Evaluation of effect of Apollo 13 malfunction on related subsystems 09 p1470 N71-19808

(NASA-TM-X-66928) 09 p1470 N71-19808

Analysis of anomalies, cause, and results of command service module oxygen tank failure on Apollo 13 flight 09 p1470 N71-19808

(NASA-TM-X-66922) 09 p1470 N71-19808

Thermodynamic analysis of Apollo 13 oxygen tank to describe stratification phenomenon preceding tank failure 09 p1470 N71-19808

(NASA-TM-X-66934) 09 p1470 N71-19808

Handling, processing, and cataloging of films resulting from Apollo 13 flight 09 p1389 N71-19807

(NASA-TM-X-66931) 09 p1389 N71-19807

Evaluation of corrective actions and hardware implementation for lunar module based on Apollo 13 flight incident 09 p1470 N71-19808

(NASA-TM-X-66929) 09 p1470 N71-19808

Investigation of government furnished equipment used on Apollo 13 flight and evaluation of established criticality ratings 09 p1470 N71-19808

(NASA-TM-X-66930) 09 p1470 N71-19808

Chronology of actions taken by ground control facilities following Apollo 13 flight emergency 09 p1466 N71-19808

(NASA-TM-X-66933) 09 p1466 N71-19808

Organization, activities, and recommendations of study, recovery, and quality control panel during Apollo 13 flight investigation 09 p1471 N71-19808

(NASA-TM-X-66924) 09 p1471 N71-19808

Analysis of Apollo 13 lunar module systems during emergency operation following command service module oxygen tank explosion 09 p1466 N71-19808

(NASA-TM-X-66935) 09 p1466 N71-19808

Analysis of spacecraft components and systems with potential for failures similar to Apollo 13 flight emergency 09 p1471 N71-19808

(NASA-TM-X-66918) 09 p1471 N71-19808

Survey of breathing systems design and reliability conducted by accident investigation panel following Apollo 13 flight emergency 09 p1471 N71-19808

(NASA-TM-X-66925) 09 p1471 N71-19808

Analysis of government furnished equipment and ground support equipment used on Apollo 13 flight 09 p1365 N71-19807

(NASA-TM-X-66926) 09 p1365 N71-19807

Analysis of lunar module related system descent and ascent engine used on Apollo 13 flight 09 p1471 N71-19808

(NASA-TM-X-66927) 09 p1471 N71-19808

Analysis of fabrication records of oxygen tank used on Apollo 13 flight 09 p1471 N71-19808

(NASA-TM-X-66921) 09 p1471 N71-19808

Summary of actions taken by Apollo 13 spacecraft following explosion in oxygen tank 09 p1466 N71-19808

(NASA-TM-X-66923) 09 p1466 N71-19808

APOLLO 14 FLIGHT

Apollo/Saturn 5 consolidated instrumentation plan for AS-201 (Apollo 14) 04 p0444 N71-14440

(NASA-TM-X-66907) 04 p0444 N71-14440

Predicted lunar vehicle operational trajectory and related data for Apollo 14 launch window 05 p0771 N71-12817

(NASA-TM-X-66345) 05 p0771 N71-12817

Systems design and performance tests of Apollo 14 lunar ranging retroreflecting equipment 09 p1396 N71-19799

(NASA-CR-114908) 09 p1396 N71-19799

Design, development, fabrication, and test of lunar ranging retroreflector experiment equipment for Apollo 14 flight 10 p1645 N71-31949

(NASA-TM-X-66901) 10 p1645 N71-31949

Narrative and pictures of Apollo 14 flight 10 p1646 N71-31970

(NASA-EP-91) 10 p1646 N71-31970

Deep Space Network support for Pioneer P and G missions, Helios Project, Viking Mars 1973 orbiter and lander, and Apollo 14 flight 12 p1993 N71-32388

SUBJECT INDEX

APPLICATIONS TECHNOLOGY SATELLITES

Lunar topographic, geologic, magnetic field, geophysical, and atmospheric data from Apollo 14 experiments and photography
[NASA-SP-272] 18 p3010 N71-30953

Apollo 14 lunar seismographic, geologic, magnetic field, and atmospheric data summary 18 p3010 N71-30954

Photographic equipment and film used during Apollo 14 flight in command and lunar modules and during extravehicular activity 18 p3010 N71-30955

Apollo 14 crew visual observations of earth, moon, lunar topology and geology, and astronaut maneuverability during extravehicular activity 18 p3010 N71-30956

Lunar geology based on Apollo 14 photographs and soil and rock samples 18 p3010 N71-30957

Lunar soil mechanics and properties based on Apollo 14 observations and data 18 p3011 N71-30958

Mineralogy and petrology of lunar rock and soil samples returned from Apollo 14 landing site 18 p3011 N71-30959

Isotopic signal analysis from Apollo 14 positive stasis experiment 18 p3011 N71-30960

Active seismic signal analysis from Apollo 14 seismograph and mortar detonations on lunar surface 18 p3011 N71-30961

Clumped particle lunar environment experiment of Apollo 14 detecting particle fluxes at lunar surface resulting from wide range of lunar surface, magnetospheric, and interplanetary data 18 p3011 N71-30964

Lunar ranging retroreflector deployed on lunar surface to study lunar librations for defining precisely lunar orbit and studying earth planetary structure - Apollo 14 flight 18 p3012 N71-30965

Lunar portable magnetometer experiment to measure steady magnetic field at different sites in Fra Mauro region - Apollo 14 flight 18 p3012 N71-30967

Group photographs of soil and rock on lunar surface obtained with Apollo 14 stereoscopic camera 18 p3012 N71-30968

Evolution of Apollo 14 geoscientific photography from lunar orbit including phenomenon mechanics 18 p3012 N71-30969

Apollo 14 command service and lunar module orbital velocity data from radio navigation 3-band transponder experiment for lunar gravitation effects 18 p3012 N71-30970

Geologic sketch map of candidate Apollo 14 landing site in Descartes region prepared from Apollo 14 photographs 18 p3013 N71-30975

In-flight calibration of 500-mm Hasselblad camera flown on Apollo 14 [NASA-CR-115176] 22 p3583 N71-35518

Field electrophoresis separation based on motion of particles in electric field for demonstrating near-zero viscosity condition in space - Apollo 14 [NASA-TM-X-64611] 22 p3718 N71-36506

Scientific report of Apollo 14 mission covering flight experiments, launch, lunar EVA, and recovery [NRC-00986] 23 p3845 N71-37405

APOLLO 15 FLIGHT

Predicting flight performance of cryogenic storage system for Apollo 15 [NASA-CR-115116] 19 p3183 N71-31603

Radio certification of Apollo 15 lunar ranging instrument experiment [NASA-CR-115108] 19 p3187 N71-31609

Apollo 15 radio and manual geologic exploration of lunar landing site - maps [NASA-CR-119725] 20 p3347 N71-33233

Infant names and descriptions of lunar topographic features in Apollo 15 landing region [NASA-CR-121625] 21 p3506 N71-34079

Location and distribution of nonconformities for lunar topographic features in Apollo 15 landing region [NASA-CR-121624] 21 p3506 N71-34080

Location of documented samples returned by Apollo 15 including photographs of sample sites, core locations, general rock types, and monitoring system [NASA-CR-121881] 22 p3667 N71-36148

Catalog of all pictures taken from lunar module or lunar surface during Apollo 15 mission [NASA-CR-121982] 22 p3668 N71-36149

Apollo 15 mission report to committee on science and astronautics 22 p3708 N71-36394

Primary data evaluation from Apollo 15 light and lunar surface experiments with analysis of extraterrestrial, medium, support, and communication system performance [NASA-TM-X-67381] 23 p3848 N71-37427

Photographs and descriptions of Apollo 15 at lunar base and lunar rover traverses [NASA-EP-54] 24 p4088 N71-38579

APOLLO 16 FLIGHT

Sketch map of proposed Descartes Apollo 16 lunar landing site 18 p3013 N71-30976

Determining thickness of regolith in Apollo 16 landing site by Monte Carlo method [NASA-TM-X-63099] 23 p3848 N71-37424

APPARATUS

U EQUIPMENT

APPARATUS

NT FORBARM

NT HAND (ANATOMY)

NT LBG (ANATOMY)

APPLICATION

U UTILIZATION

APPLICATIONS OF MATHEMATICS

Programming language for solving symbolic mathematical problems [AD-710746] 02 p0189 N71-11330

Limitations of formal mathematical systems 02 p0252 N71-12077

Techniques for manipulation of long Polaris series also used for SPASM 04 p0538 N71-14839

Space science training materials and motivation of high school algebra students 07 p1133 N71-17778

Apparatus for computing square roots [NASA-CASE-XOS-04748] 09 p1352 N71-19457

Index of documents on numerical calculations for algebraic and transcendental equations [ORNL-4395] 09 p1411 N71-20382

Intuitive, graphical, and simplified mathematical treatment of rotational dynamics as applied to human centrifuges 12 p1945 N71-23340

Mathematical study of unfolding problems arising in experimental nuclear physics 12 p1972 N71-23895

Concentration of negative ions in flame for checking of static configuration of flame 14 p2353 N71-26021

Approximate confidence interval and tests for products and ratios of binomial probabilities with application in investigating and comparing system reliability [NASA-CR-118511] 14 p2282 N71-26096

Mathematical formulation of biometric equations to describe motion of six degrees of freedom vibration table for use in research on human subjects [AD-726269] 14 p2210 N71-26158

Mathematical treatment of stationary thermal conductivity in piecewise homogeneous media arising in design of pebble bed reactor 15 p3467 N71-27225

Mathematical aspects of neutron physics for ITR project [NASA-TT-T-13645] 17 p2781 N71-29238

Formulas for with order derivatives of hyperbolic and trigonometric functions used in evaluating Fourier sine and cosine integrals [NASA-TN-D-6405] 17 p2773 N71-29772

Multiscale sequential hypothesis with applications in pattern recognition [NASA-CR-118959] 17 p2725 N71-29894

Analysis of summation for modal formulas of first degree and application to classical computation formalisms [NLL-RYS-3840] 17 p2774 N71-30035

Integral representation for functions holomorphic in tube domains over arbitrary proper cones 18 p2976 N71-30623

Algorithmic pattern generation with applications to isomorphic and biological structures, and other branches of mathematics and computer science [FS-197604] 18 p2947 N71-31314

Development and application of mathematical models in science 19 p3122 N71-32017

Organization of theoretical knowledge into mathematical models 19 p3122 N71-32018

Boolean algebra for application to digital electronics and relay networks [ISF-70-33] 20 p3299 N71-32970

Compilation of papers on applications of mathematics and computer programs for industry related problems [NASA-SP-399901] 21 p3447 N71-34532

Numerical treatment of some integro-differential equations, Fourier integrals, and integral equations 22 p3606 N71-35682

Correlations between observables pertaining to two different systems with applications in theoretical physics [LPTF-71/42] 22 p3645 N71-35992

Adaptive nonparametric approach to estimation and signal processing combining learning, decision, and optimization mathematical techniques 23 p3726 N71-36361

Numerical analysis of existence and impossibility of existence of various types of nonlinear differential equations 23 p3781 N71-36950

Generalization of three elementary formulas from the calculus to include fractional derivatives 23 p3783 N71-36962

Mathematical analysis of plane sound waves of finite amplitude in nondispersive medium [NRC-12146] 23 p3803 N71-37112

Mathematical foundations and identification of systems easily solved by synchro computer [AD-727657] 24 p3882 N71-37672

APPLICATIONS PROGRAMS (COMPUTERS)

Applying basic tools and techniques of industrial engineers to systems engineering [WAFD-T-2311] 04 p0202 N71-12511

Graphics applications program for computer design of printed circuit cards [UCRL-72637] 24 p3884 N71-37751

APPLICATIONS TECHNOLOGY SATELLITES

NT ATS 1

NT ATS 2

NT ATS 3

NT ATS 5

NT ATS 6

NT ATS 7

Phase recovery and calibration techniques for position location interferometer in synchronous orbit [NASA-CR-111137] 01 p0053 N71-10652

Optimization of electrical power system for ATS [NASA-CR-111140] 01 p0087 N71-10653

ATS-3 multicolor spin scan cloud camera and image detector camera systems with meteorological data catalogs from ATS-3 and ATS-1 - Vol. 2 [NASA-TM-X-64467] 02 p0254 N71-11602

Meteorological data submitted from Applications Technology Satellite observations including photographs of clouds - Vol. 3 [NASA-TM-X-64468] 02 p0254 N71-11603

Ranging tests with transponders in North Atlantic with VHF SATCOM equipment by two satellites [NASA-CR-115782] 04 p0544 N71-14492

Millimeter wave propagation utilizing ATS 3 satellite [NASA-TM-X-65004] 05 p0643 N71-14738

Design, development, and characteristics of several communications satellites [NASA-TM-X-66711] 07 p1121 N71-17771

Activities and accomplishments of NASA from July to December, 1969 [NASA-TM-X-66954] 09 p1466 N71-20020

Aircraft communication using ATS links [PFA-A-57] 10 p1646 N71-21727

Miniaturizing balloon borne radio altimeter and meteorological applications of ATS data [NASA-CR-118357] 13 p2108 N71-25424

Early bird and ATS C simultaneous recordings of F region ionospheric electron density for calibration analysis of ionospheric disturbances [AD-719872] 14 p2245 N71-25827

Reflective surface degradation data from samples flown on Applications Technology Satellites [NASA-CR-118632] 14 p2337 N71-25965

Satellite activities of organizational elements of NOAA including weather, fisheries services, and environmental research 14 p2337 N71-26107

ATS ranging and position fixing experiments with 4-day synoptic ionospheric propagation and 24-hour synoptic measurements [NASA-CR-118648] 14 p2291 N71-26713

Tropical wind flow patterns from automated analysis of streamlines, streamfunctions, divergence, and vorticity in tropics with feasibility of wind analysis using ATS data [AD-721345] 16 p3636 N71-28597

Investigation of cost effective utilization of space maintenance and repair techniques to develop Applications Technology Satellite number 5 - Vol. 1 [NASA-CR-119001] 16 p3684 N71-29161

Requirements of docking simulation necessary to establish conditions involved in depth control of Applications Technology Satellite number 5 - Vol. 2 [NASA-CR-119002] 16 p3684 N71-29162

Evaluation of capabilities of electronic display system used in analysis of ATS cloud photographs [NASA-CR-119317] 18 p0285 N71-31421

NASA balloon-circuit ranging, data and voice experiment for determining best approach for using ATS in air traffic control [NASA-TM-X-65649] 19 p3857 N71-32527

Design for Future X4 British Applications Technology Satellite 20 p3551 N71-33012

Known total electron content of ionosphere and scintillation boundary from ATS 20 p3608 N71-33830

Meteorological research in time domain data extraction, radio altimetry, and application of ATS data as hydrological tool in remote tropical regions [NASA-CR-121438] 20 p3771 N71-33670

Comparison of concurrent cloud data obtained via ATS 3 and ESSA 3 and from Apollo 6 high resolution photography [NASA-TN-D-6470] 21 p3452 N71-34546

Small Applications Technology Satellite program for developing sensors, experiments, and spacecraft technology and systems through orbital flight testing (NASA-TM-X-67239) 21 p3513 N71-35033

APPROACH

NT INSTRUMENT APPROACH

Application of approach and landing data to design of space shuttle 01 p0125 N71-10109

In-flight determination of lateral-directional dynamics for landing approach (AD-715317) 07 p0973 N71-17792

Computer graphics display program for use in terminal operations and V/STOL approach and departure path synthesis (NASA-CR-117887) 12 p1896 N71-23186

Inflight simulation with high wing landing fighter aircraft approach using FFB-520 and Pegasus aircraft (DLR-FB-71-46) 19 p3072 N71-31789

Systems and equipment for civil aircraft approach and landing (REPT-52) 20 p3299 N71-32850

Mathematical modeling of F-4 aircraft wake flow trajectories for aircraft carrier approaches (AD-727121) 23 p3708 N71-36439

Effectiveness of control towers in reducing aircraft accidents and approach time 24 p3953 N71-38213

APPROACH CONTROL

Using automatic control theory with simple pilot model for synthesizing helicopter landing approach flight director control laws (NASA-TM-X-64492) 03 p0312 N71-12224

Psychological and procedural aspects to ILS approaches and landings in visibility less than 1200 feet 03 p0405 N71-12429

Direct lift control system for producing lift without pitching moments during aircraft approach and landing 03 p0406 N71-12443

Aircraft handling characteristics during aircraft carrier approach (AD-715125) 05 p0627 N71-14558

Minimizing performance criteria to analyze ability of automatically controlled aircraft to maintain accurate flight path control during landing approach (NASA-TM-D-5236) 03 p1233 N71-18761

Environmental tests of VORLOC 2 simplified directional approach system to determine compliance with FAR-Part 171 (FAA-RD-71-12) 10 p1599 N71-20666

Speed and field length safety factors for approach and landing mechanics of Breguet aircraft 12 p1855 N71-23420

Airborne equipment for approach path control on reduced noise trajectories in Boeing transport aircraft traffic 12 p1855 N71-23425

Design and characteristics of continuous wave, microwave scanning-beam aircraft landing system operating at C band and superhigh frequencies (AD-718972) 13 p2109 N71-24555

Flight tests for controlling slope approach of short takeoff aircraft 13 p2027 N71-23850

Microwave scanning guidance system for aircraft approach and landing (DO-148-VOL-1) 15 p2365 N71-26804

Approach guidance system for side-firing tactical aircraft (AD-722412) 17 p2704 N71-29708

Vertical situation display concept for alleviating problems of inadequate guidance and display information for making steep approaches 18 p2869 N71-30770

Terminal area studies with XC-142, XV-5, Do-31, and P 1127 aircraft to develop powered lift control techniques for instrument approach 18 p2870 N71-30774

Flight simulator for studying problems of aircraft during approaches and landings at night under category 2 visual conditions (RAE-TM-AVIONICS-59[BLUE]) 24 p3873 N71-37606

Visual aids for secondary airports (FAA-NA-70-51) 02 p0198 N71-11474

Visual approach slope indicator system for long-landed aircraft (FAA-RD-70-76) 02 p0199 N71-11905

Post-1970 scanning beam guidance for approach and landing 03 p0406 N71-12435

Index of standard instrument approach procedures for domestic and foreign airports 12 p1959 N71-23233

Automatic approach and landing system with flash warning signal for Convair aircraft control 12 p1856 N71-23429

Terminal air traffic control facility for approach systems tests (AD-719104) 13 p2109 N71-24451

Design and characteristics of continuous wave, microwave scanning-beam aircraft landing system operating at C band and superhigh frequencies (AD-718972) 13 p2109 N71-24555

Approach indicator oscillation and illuminating effects on human performance of compensatory tracking tasks (NASA-CR-119640) 19 p3047 N71-31618

APPROPRIATIONS

Subsidies for American certificated air carriers 02 p0308 N71-12190

Federal support to universities and nonprofit research institutions (NSF-70-27) 04 p0433 N71-14358

Investigating impact of changes in Federal science funding patterns on academic research (NSF-70-39) 03 p0789 N71-15648

Appropriations recommended by Congress for NASA programs including project management, research and development, and construction of facilities (REPT-92-143) 12 p3019 N71-34307

Authorization hearings on NASA space flight program - Part 2, 1972 13 p2191 N71-25194

Authorization hearings on NASA space flight program - Part 3, 1972, Office of Space Science and Applications 13 p2191 N71-25195

Authorization hearings on NASA space flight program - Part 4, 1972 13 p2192 N71-25196

Testimony concerning aeronautical research and development, and DOD space-related program 14 p2361 N71-26799

Congressional hearings concerning NASA appropriations for fiscal year 1972 14 p2361 N71-26800

Senate committee recommendations concerning NASA appropriations for FY 1972 (REPT-92-146) 16 p2695 N71-29062

Recommendations by House Committee on appropriations for fiscal year 1972 (REPT-92-305) 17 p2860 N71-29385

Recommendations of Senate Committee on Appropriations for housing and urban development, NASA, Veterans administration, and other independent agencies for 1972 (REPT-92-264) 18 p3031 N71-31564

Federal budget amendment agreement recommendations for HUD appropriations (REPT-92-377) 19 p3199 N71-32657

Senate hearings on 1972 appropriations for HUD, NASA, NSF, VA, and other independent agencies 20 p3371 N71-33872

Hearings for HUD and space appropriations 20 p3371 N71-33909

NASA fiscal year 1971 appropriations for research and development, construction of facilities, and research and program management (REPT-91-83) 21 p3535 N71-35192

APPROXIMATION

NT BORN APPROXIMATION

NT CHEBYSHEV APPROXIMATION

NT FINITE DIFFERENCE THEORY

NT FINITE ELEMENT METHOD

NT HARTREE APPROXIMATION

NT LEAST SQUARES METHOD

NT MILNE METHOD

NT NEWTON-RAPHSON METHOD

NT PADE APPROXIMATION

NT RAYLEIGH-RITZ METHOD

NT RELAXATION METHOD [MATHEMATICS]

NT RITZ AVERAGING METHOD

NT SOMMERFELD APPROXIMATION

Series truncation in parametric estimation and error transformation (NASA-CR-108705) 01 p0877 N71-10979

Linear system impulse response identification from truncated input using fast Fourier transformation (AD-710630) 02 p0191 N71-11341

Successive approximations method for equation integration of laminar multicomponent boundary layer with chemical reactions including ionization (NASA-TT-F-13379) 02 p0202 N71-11532

Method for approximating certain functions with application to critical phenomena (AD-712972) 03 p0400 N71-13240

Uniqueness theorems for nonlinear approximations in strictly convex Banach spaces 03 p0401 N71-13269

Molone approximation for wave propagation in turbulent media (AD-712456) 04 p0490 N71-13485

Approximate solution for large asteroid distribution with nearest near-Earth largest class of population (NASA-CR-111738) 04 p0611 N71-15762

Two-overlapping group transport approximation for thermal neutron problems (WAPD-T-2341) 04 p0533 N71-14131

Accurate approximative solution to differential equations of oscillatory problem with perturbing damping (NASA-CR-115774) 04 p0530 N71-14147

Many body problem of elastic scattering of electrons from atoms and molecules using Green function techniques 04 p0533 N71-14150

Approximation of physical constraints (AD-712077) 04 p0539 N71-14288

Asymptotically efficient estimation of local function-parameter approximations (AD-713407) 04 p0540 N71-14309

Birkhoff-Turriton truncation problem for systems of ordinary linear differential equations (AD-715701) 05 p0714 N71-15071

Approximation model used with self-shielding data for U-238 (AARCTM-539) 06 p0911 N71-15102

Difference equations for approximating ordinary differential equations (NASA-CR-180015) 06 p0985 N71-18013

Attenuation coefficient of 0.6 to 14 micron wavebands and fog, determined with approximate equations (AD-714786) 07 p1069 N71-15710

Approximation of pressure distribution on wing body configurations at subcritical speeds 07 p1312 N71-15911

Averaging Lagrangian averaged conservation equations to hyperbolic or elliptic dispersion equations for nonlinear waveform distortion (AD-716530) 09 p1409 N71-15912

Error bounds for approximate solutions to systems of differential equations, and applications to Magnus and second order differential equations (TID-25627) 10 p1593 N71-16017

Conservation program and approximate inverse solution for nonequilibrium flow in inviscid shock layer about vehicle in hypersonic flight in arbitrary atmosphere 12 p1975 N71-20009

Shaping antenna far-field radiation pattern by uniform and nonuniform arrays, using iterative sampling and current distribution approximation 11 p1734 N71-20009

Nonlinear approximation of uniform elliptic transonic inviscid gas flow around symmetric profile 11 p1738 N71-20009

Asymptotic solution of low frequency wave equations in transonic shockless adiabatic inviscid gas flow based on complete approximation 12 p1890 N71-20009

Performance prediction of high energy rocket propellants using approximation functions (DLR-FB-70-77) 12 p1909 N71-20009

Order by order procedure for generating perturbation theory for sigma model propagators and Green function method applied to two loop approximation (NYO-2362-TA-219) 12 p1975 N71-20009

Point matching and step approximation method in impedance and current distribution calculation of cylindrical antenna submerged in warm isotropic plasma 12 p1894 N71-20009

Mean velocity profile approximation of two-dimensional incompressible turbulent boundary layer (NAL-TM-219) 13 p2067 N71-20009

Uniform type approximation of separable expansion of two T-matrix and three body problem 13 p2144 N71-20009

Approximations for off energy shell T-matrix perturbation theory 14 p2299 N71-20009

Approximations for simplified nonlinear microwave breakdown model (AD-719764) 14 p2320 N71-20009

Approximate confidence interval and tests in products and ratios of binomial probabilities with application in investigating and comparing system reliabilities (NASA-CR-118511) 14 p2282 N71-20009

Nonparametric estimation of mean and variance in random sampling with observations of varying values (NASA-CR-118512) 14 p2282 N71-20009

Approximation solution for acoustic energy transmission from vibrating rod to surrounding water (AD-720870) 14 p2286 N71-20009

Comparison of three approximation methods with Monte Carlo method for expressing resonance in terms of parameters in resonance absorption of neutrons (CNEA-246) 14 p2305 N71-20009

Approximate solution for free vibration characteristics of nonlinear systems (AARC-RM-2631) 15 p2434 N71-20009

Approximation of redundant component reliability and digital computer logic design (AD-720323) 15 p2389 N71-20009

Approximation method for turbulence effects in aircraft aerodynamic stability with B-52 example 15 p2367 N71-20009

Approximate calculations for effective freedom of delayed neutrons and instantaneous neutron lifetime for fast critical assemblies (SRARI-F-53) 15 p2473 N71-20009

Approximations for energy levels and corresponding wave functions in one dimension deduced from Milne and Schroedinger equations (CRA-R-4007) 15 p2480 N71-20009

Wardleburn equation for relating reactivity to cycle and transient reactor periods according to P1 approximation (CNAEM-73) 15 p2484 N71-20009

ARC LAMPS

Starting circuit design for initiating and maintaining arcs in vapor lamps
[NASA-CASE-XNP-01058] 03 p0331 N71-12540

Tungsten lamps, graphite arcs, and copper-point blackbodies as radiometric standards of spectral radiance 09 p1439 N71-20212

Volatiles products from photodecomposition of organic coatings exposed to sunlight and arc lamps 09 p1406 N71-20220

Design, fabrication, and evaluation of one to two kilowatt arc metal vapor arc lamp
[AD-718877] 12 p1925 N71-23299

Magnetic arc stabilization in xenon compact arc lamps by means of longitudinal magnetic fields
[NASA-CASE-NPO-10807] 21 p3402 N71-34209

ARC MELTING

Arc fusion growth and characterization of high purity MgO crystals 03 p0441 N71-12840

Russian contributions to Russo-Swedish conference on glass steels
[JVA-MEDD-169-VOL-2] 18 p2933 N71-30680

Comparison of electrode, plasma-arc, vacuum, and electron beam methods of melting nickel steels 18 p2927 N71-30682

Plasma-arc melting in refining of steels and alloys 18 p2927 N71-30684

Plasma-arc melting in water cooled molds solving gas sorption by liquid metal 18 p2927 N71-30685

Electric arc furnaces in Sweden noting design and operation and cost reduction 19 p3104 N71-31903

ARC WELDING

NT GAS TUNGSTEN ARC WELDING
NT PLASMA ARC WELDING

Weldability of tungsten base alloys and elevated temperature stability 01 p0067 N71-10353

Arc and electron beam welding techniques
[AD-711747] 01 p0061 N71-10968

Closed circuit television arc guidance adapter kit for computerized welding skate 01 p0061 N71-10974

Pulse-current arc welding processes - reviews
[AD-712364] 02 p0238 N71-12112

Post-weld autogenous treatment of deposits on standard and Hi-proof austenitic stainless steels
[PB-193290] 03 p0386 N71-13286

Activation energy for apparent gaseous diffusion of hydrogen in multi-run metal arc welding deposits 03 p0387 N71-13315

Emission spectroscopy method for contamination monitoring of inert gas metal arc welding
[NASA-CASE-XMF-02059] 06 p0062 N71-15871

Effect of argon gas on welds produced during pressurized inert gas metal-arc welding 07 p1033 N71-17184

Multiple regression analysis techniques for parameters in pressurized inert gas metal arc
[RFP-1550] 07 p1035 N71-17634

Automatic closed circuit television arc guidance control for welding joints 09 p1346 N71-19433

Development of device to prevent high voltage arcing in electron beam welding
[NASA-CASE-XMF-06322] 09 p1392 N71-19486

Effects of welding and post-weld heat treatment on microstructure and mechanical properties of QT steel
[RFP-2] 11 p1769 N71-22541

Fabrication and acceptance data for heavy section ASTM A-533 and A-543 grade B steel plates and electrodes, submerged-arc, and shielded metal-arc weldments for nuclear pressure vessel 12 p1936 N71-23165

Development of apparatus for automatically changing carriage speed of welding machine to obtain constant speed of torch along work surface
[NASA-CASE-XMF-07069] 12 p1928 N71-23815

Pulse arc welding for joining electrical connections to glass reinforced epoxy or Mylar substrates
[BDX-613-204] 13 p2829 N71-25407

Electric arc on industrial arc welding of metals 18 p2927 N71-30731

Methods for fillet welding in vertical position with manual electrodes 18 p2928 N71-30858

Utilization of penetration obtained with automatic submerged arc welding for fillet welds
[PB-197945] 18 p2928 N71-30859

Development of pulse-arc welding process for preventing cracking when joining austenitic stainless steels 23 p3762 N71-36823

Interaction of welding arc with magnetic field under various conditions
[AD-727848] 24 p3929 N71-38038

ARCHES

Numerical analysis of buckling and postbuckling of arch structures
[AD-712042] 03 p0465 N71-13162

Numerical analysis of plastic buckling of bladed arches
[TAR-119] 09 p1480 N71-20444

Numerical analysis of plastic buckling of three bladed arches in idealized geometrically perfect structure and realistic imperfect structure 13 p2184 N71-25536

Relationship between dynamic buckling and static buckling investigated with clamped shallow circular arches using high speed cameras 14 p2330 N71-26467

ARCHITECTURE

Architectural design of spaceborne computer system operating in multi-element configuration
[NASA-CR-121016] 24 p3892 N71-37737

ARCTIC OCEAN

Arctic marine geophysics and oceanography, and underwater acoustics 02 p0209 N71-11417

Mathematical models for Arctic ice dynamics
[AD-713986] 06 p0853 N71-16583

Arctic Ocean geographical studies of Alpha Cordillera and Mendeleev Ridge 08 p1193 N71-18977

Sea ice, ocean currents, climatology, and geology of Arctic Ocean and coastal areas
[AD-716416] 09 p1384 N71-19771

Mineral content of Barents Sea sediments
[NLL-WTS-564] 10 p1553 N71-21360

Water exchange variations between Arctic and Atlantic Oceans and effects on ice cover forecasts in Arctic seas 11 p1752 N71-22803

Diurnal variations of large scale current turbulence in Arctic Basin and seas 11 p1752 N71-22805

Quantitative analysis of hummocking effects on mean thickness of fast ice in Arctic seas 11 p1758 N71-22853

Total heat budget between ocean-ice-atmosphere in Arctic Basin for military utilization 12 p1906 N71-23351

Application of cartographic grid network of coordinates for solution of meteorological and hydrological plotting of fields in polar areas
[AD-720149] 16 p2588 N71-28452

Crystallization heat given off by ice to atmosphere and effect on meteorological conditions in Arctic analyzed on basis of observational data and theoretical computations 16 p2508 N71-28499

News briefs and abstracts of scientific articles concerning magnetic anomalies in Atlantic Ocean, and currents in Arctic Basin 17 p2739 N71-29402

Atmospheric models and thermodynamic effects of glaciers and Arctic Ocean in relation to causes of ice age climatology 20 p3368 N71-33884

Two-year periodic variations in Arctic sea ice formation
[NLL-M-20593-5828.4F] 21 p3422 N71-34354

ARCTIC REGIONS

Precipitation from cooling towers in cold climates 01 p0082 N71-10998

Telluric, geomagnetic, and auroral activity on Arctic drifting stations and at Pt. Barrow
[AD-711679] 02 p0291 N71-11143

Methods of designing foundations and bases on permafrost frozen soil
[AD-711909] 02 p0301 N71-12021

Long term solar radiation effects on Arctic region temperatures during winter months 03 p0402 N71-12625

Hiss, auroral electrojets, and Arctic region magnetic variations 04 p0521 N71-15780

Geodetic survey of Spitzbergen by ground station measurements and satellite triangulation 05 p0674 N71-14935

Thermal heat exchange processes between atmosphere and hydrosphere in Arctic Region
[TT-70-50091] 05 p0400 N71-15668

Climatology in extreme decades and displacement of Arctic intrusion axes 06 p0887 N71-15764

Automatic processing of Arctic pack ice data obtained by microwave sensor and remote sensors
[AD-713911] 06 p0854 N71-16620

Experimental and theoretical review of Arctic ice dynamics
[PB-195364] 08 p1186 N71-18335

Arctic ionospheric model 08 p1190 N71-18664

Research on Arctic sea ice heat and mass budget, sea ice drift, micrometeorology, radiation, atmospheric chemistry, and Arctic oceanography
[AD-715436] 08 p1190 N71-18731

Arctic marine geophysics and oceanography
[AD-715005] 08 p1190 N71-18737

Observations of carbon dioxide and plant growth in Arctic ecosystem 08 p1194 N71-18768

Arctic manpower, industrial, mineral, petroleum, and transportation resources
[AD-716413] 09 p1383 N71-19770

Effects of Arctic Basin on air temperature and precipitation over USSR
[JPRS-22736] 11 p1744 N71-21809

Arctic and Antarctic regions, ice formation, sea ice, weather forecasting, glaciology, hydrology, hydrometeorology, KGY, KGYV, solar activity, meteorological stations
[TT-70-50617] 11 p1752 N71-22804

Radiation measurements of Central Arctic Basin from US and USSR drifting stations 11 p1752 N71-22805

Long term variations of air and water temperatures in Churchill Sea 11 p1752 N71-22806

Diurnal variations of large scale current turbulence in Arctic Basin and seas 11 p1752 N71-22807

Long range forecasting of annual variations of ice cover in Arctic 11 p1752 N71-22808

Short range forecasting of navigability of close pack ice by icebreakers in Arctic 11 p1753 N71-22809

Electromagnetic measurement of water column velocities in Arctic regions 11 p1753 N71-22810

Analysis of synoptic charts of magnetic activity measured in Arctic for KGY 11 p1753 N71-22811

Analysis of radio communication conditions during Levanevskii flight in Arctic on 12-13 August 1957 11 p1704 N71-20804

Organization, functions, and research capabilities Arctic Institute of North America 11 p1733 N71-22812

Formation of thermal radiation regime of Arctic based on atmospheric circulation in Northern Hemisphere 11 p1754 N71-22813

A.A. Girs rebuttal to review of his research on role of atmospheric circulation in formation of thermal regime in Arctic 11 p1754 N71-22814

Historical review of Soviet exploration in Arctic regions 11 p1848 N71-22815

Mobilist approach to role of Arctic Basin in structural development of supercontinent Laurasia during Paleozoic era 11 p1754 N71-22816

Combined characteristics of air temperature and humidity for Arctic summer period 11 p1754 N71-22817

Predicting location of baric formation centers and evolution in Arctic and Subarctic on third day based on variations of thermal field of troposphere and surface pressure variations 11 p1755 N71-22818

Vertical temperature profile in Arctic atmosphere determined by absorption of microwave radiation by molecular oxygen 11 p1755 N71-22819

Design, operation, and accuracy of automatic radiometeorological drifting stations in Arctic 11 p1733 N71-22820

New geographical names for locations on Ross Josef Land maps 11 p1755 N71-22821

Distribution of magnetic activity in Arctic daily solar activity cycles 11 p1756 N71-22822

Economic efficiency calculations for long range forecasts for ship navigation of Northern Sea Route 11 p1757 N71-22823

Development of heavy cumulus clouds formed by forced convection in vicinity of warm fronts in Arctic regions 11 p1791 N71-22824

Round-the-world echo and very far propagation of short radio waves from stations in Arctic and Antarctic 11 p1704 N71-22825

Short range forecasting of ice formation in Arctic waters to thickness of 20-25 cm with forecasting period up to 20 days 11 p1758 N71-22826

Objective classification of synoptic processes in northern region of Yakutia during winter by expansion of pressure fields in natural orthogonal functions 11 p1758 N71-22827

Wind velocity tables for selected Soviet winter stations in Arctic 11 p1758 N71-22828

Propagation of very low frequency radio waves in Arctic region during polar cap absorption 11 p1759 N71-22829

Space-time distribution of magnetic disturbances in Arctic during KGY and KGYV 11 p1759 N71-22830

Hydrological observations of temperature, salinity, and currents of water in Dianshi Fjord 11 p1759 N71-22831

Continental drift theory applied to role of Arctic Basin in development of Laurasia structure
[AD-718068] 12 p1987 N71-22832

Seven-year cycle of Arctic ice formation due to rotation of earth axis
[NLL-M-20594-5828.4F] 12 p1994 N71-22833

Identification of Arctic ice types by measurements of solar backscatter 13 p2078 N71-25496
[NASA-CR-118340]
Solar radiation regime characteristics measured in Arctic regions 15 p2081 N71-27515
Solar radiation in heat balance of ice-covered surfaces on Franz Joseph Land and Spitzbergen 15 p2039 N71-27519
Solar radiation regime of ice-covered surfaces on Novaya Zemlya 15 p2039 N71-27530
Osteological research in Arctic Regions including solar measurement of glacier thickness 16 p2584 N71-28151
Antarctic research in Arctic and Antarctic regions 16 p2629 N71-28772
Relationship between variations of radiation fluxes and albedo on subpolar ice caps in summer (AD-721409) 16 p2628 N71-29080
Results of field work in Arctic regions using pulsed light range finder (AD-725427) 19 p3084 N71-31681
Hydrography of Arctic regions water resources (R-106464) 19 p3085 N71-31818
Geographic and paleogeographic data of terrestrial life studied by Arctic station 20 p3261 N71-33324
Investigation of tundra biogeocoenoses noting species saturation of surface layer and soil and eleven phases of turnover 20 p3223 N71-33304
Arctic field tests of prototype life rafts capable of protecting astronauts from cold water exposure for 72 hours (NASA-CR-121449) 20 p3227 N71-33718
Isotopic interactions between Arctic ice and climate (JPRS-53967) 21 p3432 N71-34343
Possibility of regulating incident and reflected solar radiation on buildings in arctic regions (JLL-M-20601-5828.4P) 21 p3505 N71-34968
Isolation of storms in southwestern Kara Sea and aluminum solar activity (JLL-M-20643-5928.4P) 22 p3616 N71-35764
One-light chromatography peak-shape dependence on retention time, sample volume, and column type and overlapping-peak area determination (JLL-CR-TRANS-5576-9022.6P) 23 p3721 N71-36326
ASTRONOMY
Meteorological and geoscientific abstracts for Argentina, Chile, and Uruguay (AD-717196) 10 p1997 N71-21243
AR-ARGON ISOTOPES
Scattering of monoenergetic argon molecular beam from solid argon surface 02 p0274 N71-11795
Sweepback-bladed centrifugal compressor overall performance in air flow (NASA-TN-D-2125) 03 p0310 N71-12209
Dissolved argon gas effects on cavitation in liquid sodium (AD-713831) 06 p0836 N71-16453
Apparatus for extracting radioactive argon from sodium containing substance 06 p0934 N71-16770
Shock tube study of cyanogen dissociation in argon (AD-70033) 06 p0927 N71-16868
Microvane and pulsed electrostatic probe measurements of argon gas ionization behind shock waves (JPRS-778-70-43) 07 p1088 N71-17111
Effect of argon gas on welds produced during preheated laser gas metal-arc welding (JPRS-1530) 07 p1083 N71-17184
Performance of axial flow compressor for Brayton gas electrical power generating system with argon (NASA-TN-D-2194) 07 p0908 N71-17082
Initiation cross section measurements of argon collisions, photon emission during argon decay, and Penning ionization discharge 09 p1420 N71-19718
Scattering distributions for argon incident on fresh silicon oil film (NASA-CR-171806) 09 p1438 N71-20194
Thermal density study in argon plasma jet, using Thomson and Rayleigh scattering (JPRS-3798) 09 p1430 N71-20376
Scattering of argon beams with incident energies up to 14 MeV from silver (111)-surfaces (JLLA-ENH-7061) 10 p1614 N71-20930
Acoustical performance of sweepback-bladed centrifugal compressor in argon as function of Mach number and inlet flow (NASA-TN-D-2509) 12 p1831 N71-23659
Some argon gas atomic dynamics using slow motion scattering 12 p1970 N71-23709
Argon plasma transport properties, including electrical and thermal conductivity, radiation source strength, and viscosity (AD-710162) 12 p1982 N71-24014

Phase-parallel experimental ionization chamber containing liquid and solid argon 13 p2130 N71-24852
[JPRS-723-5064]
Influence of aluminum on friction and wear of iron-aluminum alloys dry lubricated in argon atmosphere (NASA-TN-D-4339) 14 p2261 N71-26043
Shock tube investigation of chemical kinetics of NO-CO-Ar mixtures at temperatures from 3000 to 4300 K 14 p2214 N71-26311
Multicharged ion emission from nitrogen, argon, and neon in reflex ion source with axial extraction (LVCEM-7065) 14 p2312 N71-26703
Energy dependence of charge exchange reactions in iodine and argon ionization by exchange collisions (KFK-1265) 14 p2315 N71-26733
Ionization cross sections for neon and argon single electron loss in nitrogen, oxygen, and air between 25 and 90 keV (SC-RR-70-735) 15 p2472 N71-27436
X-ray excitation and gamma ray branching of argon at incident proton energy 15 p2475 N71-27460
Reaction kinetics and charge transfer in ionic collisions of argon ions with molecular hydrogen, deuterium, and carbon dioxide 15 p2477 N71-27578
Absorption region of SO₂ in neon and argon at 5.6 K 15 p2436 N71-27779
Density distribution measurements in rarefied argon contained between two concentric cylinders undergoing relative rotation, and heat transfer and drag measurements 16 p2583 N71-28876
Primary and secondary ionization coefficients of argon-hydrocarbon Penning mixtures (AD-722313) 17 p2714 N71-29684
Measurement of differential scattering of argon by neon and nitrogen 18 p2808 N71-31375
[JPRS-197408]
Energy spectra of ions and electrons produced in collision of argon neutral beams (AD-723685) 19 p3049 N71-32034
Experimental measurements of spread pattern of large amounts of airborne radioactivity suddenly released in DREX-reactor shall using Ar-41 (RISO-265) 19 p3153 N71-32252
Argon ion-atom collision hypothesis investigated using coincidence methods to obtain fast electron energy spectrum with known scattering angle, ion energy, and charge state 19 p3160 N71-32667
Performance test of piston shock tube with helium driven gas and argon test gas 20 p3244 N71-32957
[VKI-TN-69]
Measurement of total cross section for low energy electrons on metastable argon by atom beam recoil method 20 p3318 N71-33579
Evaluation of single collisions between nitrogen ions scattering from argon atoms at keV energies 20 p3321 N71-33744
One-electron and two-electron cavities in metal-anion solutions, electron-molecule and intermolecular reactions, and corrections for effective intermolecular pair argon potentials 21 p3389 N71-34111
Comparison of generalized phase shift treatment with classical trajectory calculations of rotational inelasticity cross sections of Ar-N₂ scattering (NASA-CR-121712) 21 p3466 N71-34671
Neon, argon, and helium density and flux distributions in laser atmosphere 21 p3506 N71-34981
Lifetimes of 2 100 state of helium-like argon using beam foil method (UCRL-30458) 22 p3641 N71-35959
Comparison of experimental data and theoretical predictions for doubly differential ionization cross sections for neon and argon collisions 22 p3650 N71-36020
Experimental investigation of nonequilibrium corner-expansion flow of ionized argon (AD-726532) 22 p3654 N71-36062
Cathode surface temperature effects in argon and neon discharges (JEDC-Q459) 24 p3924 N71-38000
Thermophysical properties of air and air components: tables and diagrams (TTT-3062) 24 p4030 N71-38755
AR-ARGON ISOTOPES
Magnetic moments and lifetimes of 7/2 minus mirror states of Ar-37 and K-37 measured from Cs-37(p,n)Ar-37 and Ca-40(p,α)Ar-37 reactions [CONF-700933-2] 11 p1803 N71-22432
Contamination measurement of radiogenic argon with atmospheric argon by neutron activation analysis using radiochemical spectroscopy (JFA-MR-33) 17 p2732 N71-29545
Concentrations and isotopic compositions of He, Ne, and Ar measured by mass spectroscopy in separated metal phase and bulk samples of 15 chondrites for cosmic ray record studies 20 p3350 N71-33973

Scattering cross sections for nuclear reactions of C-12, Ne-20, and Ar-40 induced by 14 MeV neutrons in gilded ionization chamber 21 p3480 N71-34838
He-3, p reactions with Ne-20, Ne-24, and Ne-21, and gamma-ray description of Ne-21 and Ar-41 (JPR-18042) 24 p3978 N71-32990
ARGON LASERS
Using quartz discharge tube for generating high power single-frequency argon laser 03 p0308 N71-13343
Spatial coherence measurement on argon laser beam after passage through water 04 p0534 N71-13725
Long term frequency stability of three-mirror cavity argon laser using standard frequency light source (BESRD-IN-117) 06 p1580 N71-16643
Investigating hollow cathode discharge as energy source for argon laser beams 06 p2120 N71-19163
Iodine molecular beam absorption resonance as long-term frequency reference for argon laser stabilization (NASA-CR-117528) 10 p1570 N71-21443
Multistep, modulated-wave mode argon ion laser (AD-717206) 11 p1774 N71-31896
Effect of scattering on pulse length of argon laser beam in foggy and turbulent atmosphere, and feasibility of Monte Carlo calculation of laser beam energy density distribution (AD-724280) 20 p3281 N71-33126
ARGON PLASMA
Diagnostic studies in induction-heated low density supersonic plasma jet (AD-711127) 01 p0185 N71-10555
Inverse population of argon levels in supersonic plasma jet (AD-711141) 01 p0186 N71-10593
Electron temperature and density measurements in nonequilibrium boundary layer of seeded argon plasma (AD-711669) 01 p0186 N71-10739
Electronic structure of cluster ion with 33 argon atoms in icosahedral symmetry (JFA-FT-42) 03 p0438 N71-12269
Radiation and nonequilibrium effects on heat transfer from plasma in tube flow (SU-247-15) 04 p0596 N71-13809
Spectroscopic measurements of radial temperature distribution in powder seeded argon plasma (JNR-1173) 04 p0601 N71-14640
Optical laser generation by electron beam impact in high temperature argon plasma (UCRL-TRANS-10478) 05 p0733 N71-13830
Ion current responses of Langmuir probe in presence of ion-atom collisions in weakly ionized argon plasma (NASA-TN-X-65443) 07 p1077 N71-17394
Radial distribution of RF magnetic field measured with water cooled search coil in argon induction plasma (JFA-712563) 07 p1083 N71-17817
Transverse magnetic field effects on wall heat transfer from ionized argon channel flow (NASA-CR-116800) 08 p1363 N71-16800
Shock structure in partially ionized argon plasma jet 10 p1542 N71-21281
Arc plasma thulium temperature measurement between metal electrodes in argon atmosphere (NLL-RTS-6099) 10 p1683 N71-21632
Measurements of electronic free path in argon discharge using interaction between plasma electrons and slow wave on helix (NASA-CR-117043) 11 p1812 N71-22516
Equilibrium compositions, thermodynamic properties, and partition functions for Ar-O₂ plasma between 0.01 and 10 atm, and between 2000 and 35,000 K 11 p1814 N71-23083
Electron density and temperature measurements for argon plasma arcs (AD-726554) 15 p2380 N71-27792
Simple argon model atoms used for calculating electron number densities for argon plasma discharges (NASA-TN-D-4383) 16 p2643 N71-30083
Cryopump used in magnetoplasmadynamic converters with liquid helium cooled argon plasma (DLR-MITT-71-43) 17 p2730 N71-29579
Arc ignition and plasma production in magnetoplasmadynamic driven engine 18 p2990 N71-31136
Multi-species ion acoustic dispersion relation for argon-helium plasma (NASA-CR-121721) 21 p3489 N71-34881
Ion and electron energy spectra from neutral Ar and He beam collisions with Ar and He gas respectively below 228 eV (NVO-3161-37) 24 p3978 N71-30566
Argon plasma acceleration by travelling wave magnetic field 24 p3986 N71-30583
AR-ARGON ISOTOPES
U ARGON ISOTOPES
AR-ARGON ISOTOPES
U ARGON ISOTOPES

ARGUMENTS [MATHEMATICS]

U INDEPENDENT VARIABLES

ARIEL SATELLITES

NT ARIEL 3 SATELLITE

ARIEL 3 SATELLITE

Definitive orbit for Ariel 3 computed from minitrac observations for 27.5 months
[RAE-TR-69275] 16 p2677 N71-28059

ARIP [IMPACT PREDICTION]

U COMPUTERIZED SIMULATION

U IMPACT PREDICTION

ARITHMETIC

NT FLOATING POINT ARITHMETIC

Significant digit arithmetic techniques on CDC 6600 computer
[LA-4470] 04 p2508 N71-13857

Cyclic arithmetic codes and their distance properties with demonstration of modular arithmetic weight invariance to code word cyclic shifts
[NASA-CR-117084] 12 p1947 N71-23218

ARITHMETIC AND LOGIC UNITS

Simulation and design of arithmetic and logic unit for ILLIAC-3

[COO-2118-2] 12 p1882 N71-23614

Cooperative sequential queuing for buffer pool operator in multiprogramming computer operation
[SU-STAN-CS-71-202] 12 p1885 N71-24024

ARIZONA

Studying air pollution as regional problem in Arizona

02 p0155 N71-11100

Meteorological data for Mt. Hopkins Observatory for 1968 and 1969

[NASA-CR-111740] 04 p0541 N71-14169

Application of Apollo space photography and sequential high altitude NASA aircraft photography for evaluating natural and cultural resources in southeastern Arizona - map

[NASA-CR-115096] 17 p2750 N71-29233

Meteorological data recorded at Fort Huachuca, Arizona during Oct. 1970

[AD-726345] 22 p3614 N71-35745

Atmospheric temperature and pressure, precipitation, humidity, solar radiation, and wind velocity and direction data for Yuma test range, Arizona - Oct. 1970

[AD-726358] 22 p3614 N71-35748

Budgeting, optical and mirror system, and instrumentation of 150-inch reflecting telescopes in Arizona and Chile

24 p3921 N71-37962

ARM [ANATOMY]

NT FOREARM

ARMATURES

Characteristics of superconducting alternators with iron core and iron-free armatures

[AD-713523] 05 p0631 N71-14646

Design and development of electric motor with stationary field and armature windings which operates on direct current

[NASA-CASE-XGS-65290] 14 p2228 N71-25999

ARMED FORCES

NT ARMED FORCES [FOREIGN]

NT ARMED FORCES [UNITED STATES]

NT NAVY

Stress and adaptation problems associated with large scale, long range, rapid reaction time, aerial troop deployments

09 p1336 N71-20360

Statistical analysis of Navy and Marine aircraft activity and airspace usage in Feb. and Mar. 1970 as part of National Airspace Utilization System

[AD-722698] 17 p2705 N71-30174

Paste electrolyte cell development and multikilowatt lithium/sulfur secondary batteries for electrically-driven army vehicles

[JML-7745] 21 p3380 N71-34647

ARMED FORCES [FOREIGN]

Oxygen consumption and work capacity in fitness evaluations on Canadian Armed Forces personnel

11 p1609 N71-22311

ARMED FORCES [UNITED STATES]

Alternatives to decision making goal of obtaining utility functions

[AD-712763] 03 p0400 N71-13252

Education and training of US Air Force flight surgeons

04 p0477 N71-13878

Aviation medicine training in US army

04 p0477 N71-13879

Conference on military research and sciences

[AD-713598] 05 p0787 N71-15364

Conference on military research and sciences

[AD-713593] 05 p0787 N71-15365

Conference on military research and sciences

[AD-713561] 05 p0787 N71-15366

Pure tone audiometry for monitoring hearing and determining physical profiles of persons routinely exposed to potentially hazardous noise

[AD-717446] 11 p1680 N71-22151

General aviation traffic implied densities and interaction frequencies computed with model using southern California to judge difficulty for naval air traffic

[AD-719906] 14 p2197 N71-25621

Evaluating developed structural materials of potential Air Force weapons system interest and engineering data on these heat resistant alloys
[AD-728273] 16 p3614 N71-28099

ARMOR

Design of optimum thin bumper on armor plates

[AD-712074] 02 p0248 N71-11970

Determination of Hugoniot elastic limits for light armor materials

[UCL-50901] 06 p0932 N71-15878

Ballistic properties of solidified armor plate steel

[AD-714254] 06 p0874 N71-16579

Microstructural characterization of proprietary ceramic armor

[AD-715352] 08 p1221 N71-18541

Growth of sapphire single crystals for transparent armor applications based on modified Verneuil process

[AD-715941] 09 p1452 N71-19557

Cochran method for growing aluminum oxide single crystals in plate form for transparent armor applications

[AD-716222] 09 p1405 N71-19824

Surface and structural defects in alumina ceramic armor caused by ballistic impact

[AD-717325] 11 p1781 N71-21866

Testing armored T-28B for exploring severe ball storms

[NRI-69-FR-641] 16 p2626 N71-28646

Ballistic fabrics woven of nylon and polypropylene fibers for personal body armor

[AD-726918] 23 p3779 N71-34933

AROMATIC COMPOUNDS

Electron impact behavior and mass spectra of molecular ion aromatic imide refractory materials

[RAE-TR-70047] 06 p0808 N71-15829

Using heat resistant aromatic cyanate esters as reinforced plastics

[NASA-TT-F-13454] 06 p0811 N71-16476

Differential thermal analysis and X ray data for transitions and relaxations in aromatic polymers

[AD-718343] 12 p1942 N71-23395

AROUSEAL

Neural mechanisms underlying visual perception, arousal, and attention processes in man, cat, and monkey

[NASA-CR-122941] 23 p3712 N71-36464

ARRAYS

NT ANTENNA ARRAYS

NT DIRECTIONAL STEERABLE ANTENNAS

NT LARGE APERTURE SEISMIC ARRAY

NT LINEAR ARRAYS

NT PHASED ARRAYS

NT STEERABLE ANTENNAS

NT TURNSTILE ANTENNAS

NT YAGI ANTENNAS

Rigid and space erectable solar cell array structures for spacecraft power supplies

[ESKO-TN-40] 03 p0318 N71-12270

Characteristics of convex slotted-guide array of radiators with frequency scanning

[AD-713471] 05 p0642 N71-14510

Processes for sensor arrays

[AD-713456] 05 p0645 N71-14915

Quality control of welded joints on flexible solar cell array

[ESKO-CR-17] 11 p1677 N71-21991

Self erecting solar cell array with folding tubes

[DLR-FB-71-11] 17 p2705 N71-29364

Effects of warp tension on stored blanket dynamics and in-plane structural characteristics of rollup solar arrays

[NASA-CR-121454] 20 p3213 N71-33245

NASTRAN program differential stiffness method applied to structural analysis of Apollo Telescope Mount solar array wing and results compared with static load tests

22 p3683 N71-36261

Shadow and earth albedo effect on ESRO 1 solar cell array performance in orbit

[ESRO-TN-103-ESTEC] 23 p3839 N71-37305

ARRESTING GEAR

Performance tests and evaluation of wire cable materials for use with aircraft arresting gear

[AD-724284] 22 p3359 N71-35211

ARRESTYTHMIA

Development of system for identifying dynamic heart rate response to respiration

[AD-719860] 13 p0304 N71-24953

Analog computer program and display device for detecting arrhythmia signals during electrocardiography

[AD-711899] 19 p3046 N71-31612

Electrocardiographic monitoring device with arrhythmia signal detector and step-like output of R-wave amplitude

[AD-712668] 19 p3047 N71-31622

Spontaneous cardiac arrhythmias induced by bromofluoromethane in monkeys

[AD-723645] 19 p3042 N71-31733

ARROW WINGS

Wind tunnel studies of external store induced flow field instability effects on longitudinal stability of arrow wing aircraft

09 p1319 N71-19582

Predicting aerodynamic characteristics of nose, delta, and diamond wing platforms using Prandtl-Glauert singularity

[NASA-TN-D-6343] 11 p1609 N71-20370

Experimental and analytical study of subsonic longitudinal and lateral aerodynamic characteristics of slender sharp edge 74 deg swept wings

[NASA-TN-D-6344] 18 p3885 N71-28099

ARSENIC

NT ARSENIC ISOTOPES

ARSENIC COMPOUNDS

NT ARSENIDES

NT GALLIUM ARSENIDES

NT INDIUM ARSENIDES

NT FROUSTITE

Atomic structure of amorphous arsenic selenide and germanium telluride semiconductor switches

[AD-716810] 10 p1636 N71-33085

Determination of optical constants of amorphous thin films of selenium and arsenic telluride from infrared reflectivity spectra

[AD-723633] 19 p3169 N71-33315

ARSENIC ISOTOPES

Gamma ray spectra analysis to determine assay levels in Ge-72 from radioactive decay of Ge-72 and As-72

10 p1622 N71-21778

Beta-gamma circular polarization correlation and nuclear matrix element analysis on arsenic isotopes

[COO-1746-54] 19 p3169 N71-33315

ARSENIDES

NT GALLIUM ARSENIDES

NT INDIUM ARSENIDES

NT FROUSTITE

Methods for chemical analysis of cadmium-arsenides

[AD-713662] 03 p0332 N71-13109

Thermoelectric transport phenomena measurements in semiconducting cadmium arsenide

05 p0757 N71-14080

ARTERIES

Arterial pressure characteristics of athletes

09 p1329 N71-19109

ARTERIOCLEROSIS

Arterioclerotic and electrocardiographic abnormalities in aging pilots of French Air Force

11 p1690 N71-21019

Medical examination of civil aviation flight personnel to determine predisposing factors for arteriosclerosis

16 p2547 N71-30001

Differential scanning calorimetry for determining physiological chemistry of cholesteryl ester in phospholipid-water systems and arteriosclerosis

20 p3362 N71-33811

ARTHOPODS

NT BEES

NT INSECTS

ARTICULATION

Estimating human emotional states by changes in frequency characteristics of articulation

[NASA-TT-F-137772] 18 p2875 N71-30885

ARTIFICIAL SATELLITE

NT VENERA 4 SATELLITE

ARTIFICIAL CLOUDS

Concentration and radioactive particle size distribution in effluent cloud from nuclear explosion

[PNE-330] 02 p0270 N71-11390

Procedure for identifying silver iodide particles in ice crystals as snow crystal nuclei

[PB-192754] 02 p0260 N71-11314

Investigating production and detection of artificial ice nuclei and growth of formed ice crystals

[PB-19429] 04 p0542 N71-04161

Rocket-borne, dual channel photometer for artificial cloud brightness measurements at 200 km

[BMW-FB-W-70-44] 07 p1017 N71-17119

Spectroscopic measurements of bottom clouds and spectrum of luminous cloud produced by release of diborne in rocket sounding of upper atmosphere for use in growing satellite orbit

[AD-717696] 11 p1751 N71-33810

Stereo techniques for studying spatial structure and dynamics of human releases

[AD-717722] 11 p1751 N71-33810

Optical observations following release of bubble vapor at high altitudes described in three phases

[AD-717695] 11 p1751 N71-33810

Thermoelectric densities determined from diffusion coefficient measured on aluminum oxide artificial clouds released from ESRO rockets

13 p2089 N71-30885

Thermoelectric density determined from ESRO rocket release of aluminum oxide artificial clouds

13 p2070 N71-30885

Physics of dynamic growth of maximum clouds in isolated with nuclear explosions, laboratory

[AEC/LIB-255] 13 p2159 N71-20180

Stratiform vapor cloud expansion in high atmosphere and mathematical model of transport motion in cloud diffusion phase

[BMW-FB-W-71-10] 13 p2398 N71-20180

Measurements of ionospheric electric field in equatorial and medium magnetic latitudes using balloon clouds

[MFI-PAR/EXTRATER-40/70]

SUBJECT INDEX

15 p2398 N71-2763
Detection of silver in seeded clouds by atomic spectroscopy to high sensitivity and related aircraft problems
(AD-721664) 16 p2325 N71-26456
Solutions of diffusion equation for expanding gas cloud in constant shear flow
(AD-722457) 17 p2379 N71-29649
Scoring releases from Javelin and Nike-Tomahawk surface rockets for ion cloud study of earth electric and magnetic fields
(NASA-SP-364) 17 p2740 N71-29671
Using isolated barium vapor clouds for direct measurement of electric fields in magnetosphere
(AD-727408) 17 p2748 N71-29672
Position of neutral barium clouds, position and motion of Javelin isolated cloud, and radial growth of clouds by triangulation
(AD-727408) 17 p2741 N71-29680
Electric field distribution, cloud elongation, and shift along magnetic field line of barium release from Javelin
(AD-727408) 17 p2741 N71-29681
Analysis and interpretation of photochemically induced photographic and vidicon images of chemical releases in upper atmosphere
(AD-722454) 17 p2743 N71-29629
Vertical temperature thermospheric distribution determined by analysis of aluminum oxide artificial cloud spectra during ESR0 rocket sounding in Italy
(AD-722454) 20 p3254 N71-32873

ARTIFICIAL GRAVITY

Artificial gravity system for simulating self-locomotion capability of astronauts in rotating environments
(NASA-CASE-XLA-03127) 01 p0899 N71-10776
Artistic control of dynamically balanced artificial gravity space stations
(NASA-CR-116227) 06 p0952 N71-10806
Impact of artificial gravity simulations on spacecraft design configurations and crew operational procedures
(NASA-CR-111866) 10 p1501 N71-21558
Development of method for producing artificial gravity in manned spacecraft
(NASA-CASE-XNP-02995) 11 p1830 N71-21881
Physiological effects and design criteria for artificial gravity space stations
(NASA-CR-114902) 13 p2032 N71-24454
Mechanical behavior of lunar fine soils in engineering gravity flow bins
(NASA-CR-121670) 21 p3308 N71-34993

ARTIFICIAL HEART VALVES

Design and characteristics of artificial heart control system
(NASA-TN-D-6171) 07 p0986 N71-17593
Long term percutaneous leads in artificial hearts
(P-19095) 10 p1511 N71-21641

ARTIFICIAL INTELLIGENCE

Heuristic program for solving scientific inference problems - motivation and implementation
(NASA-CR-111092) 01 p0819 N71-10741
Automata theory and iterative array computers
(AD-710402) 01 p0829 N71-10785
Maximal semantic resolution proofs based upon binary semantic trees
(AD-710402) 01 p0829 N71-10786
Parallel data processing
(AD-710402) 01 p0829 N71-10787
Deterministic realization and simulation of non-deterministic automata
(AD-710402) 01 p0829 N71-10788
Simulation of elementary ALGOL like automata
(AD-710402) 01 p0829 N71-13490
Structural properties of generalized automata and theorems
(AD-712377) 05 p0639 N71-14737
Computer synthesis for classifying natural shapes and patterns including leaves
(AD-715163) 05 p0637 N71-14833
Machine learning of structural descriptions from examples
(AD-715905) 06 p0606 N71-16285
Research activities in recognition, computational models, and artificial intelligence
(AD-714005) 06 p0607 N71-16477
Information systems and processing, linguistic, artificial intelligence, and human information processing
(P-194790) 06 p0603 N71-16897
Generalized inverse matrices for representation of trees and morphisms with probabilistic meaning
(AD-716491) 01 p3352 N71-19535
Models of living and life-like systems with applications to man-machine technology
(NASA-CR-70-34) 11 p1692 N71-23033
Basic models for pattern recognition in human and artificial brains
(AD-716491) 11 p1685 N71-23037
Pattern recognition and heuristic functions of natural and artificial intelligence
(AD-716491) 11 p1721 N71-23075
Signal and coding computer processes of artificial intelligence
(AD-716491) 11 p1721 N71-23077

Development, characteristics, and performance of learning machines, artificial intelligence, and pattern recognition techniques
(AD-718981) 12 p1045 N71-25247
Feasibility and limitations of speaker adaptation in improving performance of fixed speaker independent automatic speech recognition systems
(AD-718235) 12 p1067 N71-25416
Algorithms of self organization, artificial intelligence, and tree search applied to various practical problems
(AD-719938) 14 p2387 N71-25452
Electronic circuitry for trainable systems with application to control and recognition functions
(AD-721737) 16 p2559 N71-28358
Cybernetics including models for statistical decision making, biomechanical systems, and complex stochastic systems
(JPRS-53531) 19 p3044 N71-32888
Increased automation and development of robots capable of anthropomorphic movements and fitted with sense organs and artificial instincts
(AD-726441) 20 p3277 N71-32911
Design of learning machine and analysis of convergence characteristics during operation
(AD-726441) 21 p3400 N71-34302
Development and characteristics of prototype computer system capable of mixed-initiative man-computer dialogue
(AD-726441) 22 p3537 N71-35338
True statements theory and artificial intelligence
(AD-726393) 22 p3608 N71-35698

ARTIFICIAL RADIATION BELTS

General formula for artificial electron decay life times
(NASA-TM-X-63374) 01 p0118 N71-10768
Artificial electron cloud formation using cesium and potassium isotopes for simulation of ionospheric propagation in E region with coherent radar
(AD-728254) 15 p0406 N71-27809
Calculation of decay lifetimes of artificial electrons produced by Stanford nuclear explosion
(NASA-TN-D-6284) 17 p2841 N71-29780
Transient behavior of electrons in artificial radiation belts from satellite observations
(AD-728254) 18 p3004 N71-30922

ARTIFICIAL SATELLITES

NT ALOUETTE SATELLITES
NT ALOUETTE 1 SATELLITE
NT ALOUETTE 2 SATELLITE
NT APPLICATIONS TECHNOLOGY SATELLITES
NT ARIEL 3 SATELLITE
NT ATS 1
NT ATS 2
NT ATS 3
NT ATS 4
NT ATS 5
NT ATS 6
NT ATS 7
NT BIRACON EXPLORER A
NT BIOSATELLITE 1
NT BIOSATELLITE 2
NT BIOSATELLITE 3
NT COMMUNICATION SATELLITES
NT COSMOS SATELLITES
NT COSMOS 34 SATELLITE
NT COSMOS 140 SATELLITE
NT COSMOS 266 SATELLITE
NT COSMOS 224 SATELLITE
NT COSMOS 225 SATELLITE
NT DIADEME SATELLITE
NT DODGE SATELLITE
NT EARLY BIRD SATELLITES
NT EARTH RESOURCES TECHNOLOGY SATELLITES
NT ECHO 2 SATELLITE
NT EOS
NT ESSO SATELLITES
NT ESSO 1 SATELLITE
NT ESSO 2 SATELLITE
NT ESSA SATELLITES
NT ESSA 3 SATELLITE
NT ESSA 4 SATELLITE
NT ESSA 6 SATELLITE
NT ESSA 8 SATELLITE
NT ESSA 9 SATELLITE
NT EUROPEAN SPACE RESEARCH ORGANIZATION SAT
NT EXPLORER SATELLITES
NT EXPLORER 15 SATELLITE
NT EXPLORER 18 SATELLITE
NT EXPLORER 22 SATELLITE
NT EXPLORER 26 SATELLITE
NT EXPLORER 28 SATELLITE
NT EXPLORER 31 SATELLITE
NT EXPLORER 33 SATELLITE
NT EXPLORER 35 SATELLITE
NT EXPLORER 36 SATELLITE
NT EXPLORER 37 SATELLITE
NT EXPLORER 38 SATELLITE
NT EXPLORER 40 SATELLITE
NT GODETIC SATELLITES
NT GEOFYSICAL SATELLITES

ARTIFICIAL SATELLITES

NT GROS 1 SATELLITE
NT GROS 2 SATELLITE
NT GROS-C SATELLITE
NT GRAVITY GRADIENT SATELLITES
NT HROS A SATELLITE
NT HROS SATELLITES
NT IMP
NT IDUN SATELLITES
NT INTERSAT SATELLITES
NT IBS SATELLITES
NT IBS-B
NT LUNAR ORBITER
NT LUNAR SATELLITES
NT METEOROLOGICAL SATELLITES
NT NAVIGATION SATELLITES
NT NIMBUS SATELLITES
NT NIMBUS 2 SATELLITE
NT NIMBUS 3 SATELLITE
NT NIMBUS 4 SATELLITE
NT NIMBUS 5 SATELLITE
NT OAO
NT OGO
NT OGO-A
NT OGO-B
NT OGO-C
NT OGO-E
NT ORBITAL SPACE STATIONS
NT ORBITAL WORKSHOPS
NT OSO-F
NT OSO-H
NT OSO-I
NT OUTER PLANETS EXPLORERS
NT PAGOS SATELLITE
NT PASSIVE SATELLITES
NT POGO
NT POLYOT SATELLITES
NT PROTON 4 SATELLITE
NT RADIO ASTRONOMY EXPLORER SATELLITE
NT RELAY SATELLITES
NT SAN MARCO 3 SATELLITE
NT SAS-A
NT SAS-B
NT SAS-D
NT SYNCHRONOUS METEOROLOGICAL SATELLITE
NT SYNCHRONOUS SATELLITES
NT TELSTAR 1 SATELLITE
NT TIROS M
NT TIROS SATELLITES
NT TIBOS SATELLITES
NT TRANSIT 1B SATELLITE
NT VELA SATELLITES
NT VENERA SATELLITES
NT VENERA 5 SATELLITE
Computer programs for processing astronomical data from satellite data transmissions
(NASA-TT-F-13367) 02 p0167 N71-11317
Problems encountered when electronic orbit prediction is used with optical observations
(AD-71214) 02 p0190 N71-11886
Analysis of tracking data for recent geopotential effects obtained from 24 hour satellites
(NASA-TM-X-63382) 03 p0214 N71-11930
Artificial satellite optical tracking data, July 1970
(BOE-FTS-104) 03 p0209 N71-12801
Calculations of instants of artificial satellites crossing certain orbital circles
(NASA-TT-F-13347) 03 p0432 N71-12423
Determinations of short term atmospheric density variations from quasi-continuous visual observations of artificial satellites
(NASA-TT-F-13386) 03 p0667 N71-12748
Second order artificial satellite theory based on intermediate orbit
(NASA-CR-111537) 03 p0454 N71-13028
Orbit calculations using gravitational parameter sets
(AD-714142) 06 p0497 N71-16738
Central zone cosmographic requirements for earth observational satellites - Part 1
(NASA-CR-111816) 07 p0108 N71-17282
Central zone cosmographic requirements for earth observational satellites - Part 2
(NASA-CR-111817) 07 p0108 N71-17283
Central zone cosmographic requirements for earth observational satellites - Summary
(NASA-CR-111818) 07 p0109 N71-17284
Computation of first optical contacts for large angle attitude motions of satellite system
(AD-714142) 07 p1119 N71-16768
Satellite stationkeeping in vicinity of unstable collinear libration points
(AD-714142) 07 p1120 N71-16769
Discussion of European space projects and aspects of European and US cooperation
(NASA-TT-F-13347) 09 p0467 N71-30521
Employment of microwave beams for transferring power between satellites
(NASA-CR-105090) 11 p1723 N71-23188
Computer program for calculating velocity requirements of intercept of earth orbiting satellite by rocket fired from earth surface or from earth orbit
(AD-710421) 12 p3001 N71-30840
Formulas derived for averaged potential in artificial satellite theory
(NASA-CR-110407) 13 p2100 N71-34632

- Investigation of techniques for determining flight paths, descent trajectories, and landing sites of satellites
[AD-719849] 13 p2166 N71-34950
- Tables of artificial earth satellite launching from 1 Sep. to 31 Dec. 1970
[RAE-TR-70163-SUPPL.] 14 p2341 N71-35806
- Gravity gradient attitude control system with gravity gradiometer and reaction wheels for artificial satellite attitude control
[NASA-CASE-QSC-10555-1] 15 p2441 N71-27324
- Advances in atmospheric physics technology from sounding rocket and artificial satellite data
[JPRS-53314] 16 p2677 N71-38091
- Russian survey of satellite applications including communication, navigation, scientific, and military satellites, space stations and tracking systems
[AD-722817] 17 p2851 N71-30111
- Tables of artificial satellites for investigating magnetosphere, solar wind, electric field, and magnetic fields from 1971 to 1975
[ORI/NTP/85] 18 p3018 N71-30879
- Sounding rocket and artificial satellite launching data for 1 Jan. to 31 Dec. 1971 from World Data Center A
[NASA-TM-X-67241] 18 p3029 N71-31276
- Analysis of orbital parameters and localization of French earth satellite METEOSAT
[NASA-TT-F-13832] 18 p3016 N71-31315
- Second order solution for motion of artificial earth satellite based on intermediate orbit
18 p3016 N71-31316
- Gravity field measurement by satellite to satellite Doppler tracking, critical configurations for fundamental range networks, and improvement of triangulation systems
[NASA-CR-119356] 18 p3017 N71-31358
- Advantages of mounting manometers and mass spectrometers in artificial satellite nose cones and calculation of particle flux density passing through instrumentation orifice
19 p3103 N71-32605
- Optical satellite tracking of Cosmos and other artificial satellites, Edinburgh, Jan. 1971
[ROE-ST5-110] 20 p3350 N71-32867
- Tables of Cosmos and other artificial satellites optically tracked from Great Britain observatories, Feb. 1971
[ROE-ST5-111] 20 p3353 N71-33112
- Tables of Cosmos and other artificial satellites optically tracked from Great Britain observatories in Dec. 1970
[ROE-ST5-109] 20 p3354 N71-33159
- Small Applications Technology Satellite program for developing sensors, experiments, and spacecraft technology and systems through orbital flight testing
[NASA-TM-X-67259] 21 p3513 N71-35033
- Lifetimes, weights, dimensions, and orbital details of instrumented satellites launched before January 1969
[RAE-TR-70020-VOL-1] 21 p3525 N71-35118
- Satellite detection of energetic particles in outer space and interpretive analysis of relationships to ionospheric fields and interplanetary conditions
[NASA-CR-121908] 22 p3667 N71-36145
- Trigonometrical expansion for calculation of tidal effects on motion of artificial satellites
[NASA-TM-X-65665] 22 p3668 N71-36152
- Artificial earth satellites used in upper atmosphere and geodetic studies, and satellite orbit mechanics
22 p3676 N71-36206
- Relation of orbit stability of remote artificial planetary satellites to radius of Hill gravitational sphere
22 p3676 N71-36207
- Artificial earth satellite motion theory using zonal harmonics of terrestrial attraction
22 p3676 N71-36208
- Solar perturbations in artificial earth satellites due to atmospheric attraction
22 p3676 N71-36209
- Accuracy of synchronous plane determined by positions of artificial satellite and two observation points, used in space triangulation
22 p3677 N71-36214
- Establishment of world-wide earth satellite and ground base observation network
22 p3678 N71-36223
- Calculation of azimuth between two distant ground points from synchronous photographs taken by artificial earth satellites
22 p3678 N71-36224
- Space positional vector calculation using Baker-Nunn and Laser observations of artificial earth satellites
22 p3678 N71-36225
- Artificial satellite geodesy using least squares method
22 p3678 N71-36227
- ALGOL program for determining satellite period variations and celestial equator transit time
22 p3679 N71-36233
- Two cameras for photographing artificial earth satellites
22 p3680 N71-36238
- Parameter calculation for determining Zeiss camera axes for satellite observation
22 p3680 N71-36239
- International conference on artificial earth satellite use for upper atmosphere and geodetic studies
22 p3680 N71-36245
- Feasibility of obtaining gravity anomalies directly from analyzing artificial earth satellite orbits
23 p3733 N71-36763
- Low outgassing polymeric materials for general service and communication satellite structures
[NASA-TM-X-65705] 23 p3776 N71-36913
- Gamma and X radiation measurements by artificial earth satellites
23 p3851 N71-37447
- Algorithms for determining artificial satellite position from magnetometric measurements
23 p3839 N71-37512
- ARTILLERY**
- Internal ballistics of tube artillery and powder rockets
[AD-711270] 01 p0114 N71-10972
- Low level turbulence measurement for artillery missile trajectories mounted on towers
19 p3127 N71-31804
- Development of plating technique for electroforming gliding metal rotating bands used on 155 millimeter artillery shells
[BDX-613-236] 23 p3762 N71-36822
- ARTYL COMPOUNDS**
- U AROMATIC COMPOUNDS**
- ASBESTOS**
- Asbestos and glass reinforcing fibers and reinforced thermoplastic resins
[ERDE-TR-2] 03 p0396 N71-13254
- X ray and infrared spectroscopic analysis of zinc, zinc oxide, and asbestos weathered exterior paints on potassium bromide disks
[AD-721696] 16 p2617 N71-28506
- Using infrared spectroscopy in analysis of amphibole-asbestos
[NLL-LTI-746-658-7022.401] 16 p2598 N71-28912
- ASCENT**
- NT CLIMBING FLIGHT**
- Aerodynamic spacecraft design to minimize buffeting during atmospheric ascent
[NASA-SP-8001] 09 p1472 N71-20473
- Aerothermodynamic shock heating of space shuttle booster surface during atmospheric ascent
14 p2354 N71-26059
- ASCENT TRAJECTORIES**
- Initial data for space shuttle orbiter guidance, navigation, and control equations for preflight, boost, separation, orbit insertion, and ascent abort phases
[NASA-TM-X-67217] 19 p3133 N71-32678
- Effect of aerodynamic characteristics of combined booster/orbiter ascent configuration of space shuttle on ascent guidance and control
20 p3352 N71-33056
- Trajectory design for space shuttle noting effect of ascent fuel, structural weight requirements, booster flyback propellant requirements, and on-orbit propellant needed for orbiter abort
20 p3353 N71-33057
- Station longitude error effects on Doppler plus range and Doppler only orbit determination solutions, emphasizing Viking mission trajectory
21 p3391 N71-34129
- ASHES**
- Erosion rate of turbine blades produced by ash from caliche coal
[ARL/ME-315] 09 p1459 N71-20019
- Melting temperature measuring instrument for lubricating oil additive ashes
13 p2101 N71-25104
- ASIA**
- Comparison of aerial and spaceborne photographic methods and photointerpretation techniques using northwest Saudi Arabia geomorphology
[NASA-TM-X-65594] 17 p2749 N71-30177
- Bibliographies on nuclear mathematics and technology of eastern countries
[AED-C-12-34] 18 p2908 N71-31477
- Flux of atmospheric water, frequencies and paths of storms, and local water budget related to hydroclimate in Middle East
[RM-6267-FF] 21 p3454 N71-34584
- Technological development program for Korea
[NASA-CR-123183] 24 p4033 N71-38778
- ASPARTIC ACID**
- Stereospecific sorption technique for separating optical isomers of aspartic acid using glutamic acid
[UCRL-20471] 21 p3308 N71-34101
- ASPECT RATIO**
- NT HIGH ASPECT RATIO**
- NT LOW ASPECT RATIO**
- Low speed boundary layer separation on compressor blades of varying aspect ratios
[ARC-CF-1103] 07 p0966 N71-17108
- Determine aerodynamic characteristics of elastically deformed load bearing wing using large aspect ratio
[AD-716509] 09 p01315 N71-19559
- Initial plasma chamber noise measurement comparison of 20 inch diameter fan rotors with aspect ratios of 3.6 and 6.5
[NASA-TM-X-2191] 09 p1316 N71-30929
- Critical aspect ratios of copper matrix and tungsten fibers in reinforced composites from stress-strain and tensile tests
[NASA-TM-X-52993] 10 p1509 N71-31228
- Aspect ratio effect on oscillatory pitching motion derivatives of slender sharp-edged delta wing in incompressible flow
13 p3022 N71-30899
- Buckling of boron/aluminum and graphite/aluminum fiber composite anisotropic panels - load tests
[NASA-TM-X-67080] 18 p3022 N71-31028
- ASPHALT**
- Concrete and asphaltic materials evaluation for use on ground under loading tests
[AD-710962] 01 p0036 N71-10028
- Weighted defect densities of asphaltic and cement concrete pavement in airfield pavement condition survey, USNARS Cocl Field, Florida
[AD-721325] 16 p2577 N71-31008
- Weighted defect densities of asphaltic and cement concrete pavement in airfield pavement condition survey, USNARS Willow Grove, Pennsylvania
[AD-721324] 16 p2577 N71-31009
- Weighted defect densities of asphaltic and cement concrete pavement in airfield pavement condition survey, USNARS Charleston, Rhode Island
[AD-721323] 16 p2577 N71-31010
- Primary and secondary air pollution from asphalt plants
[PB-199355] 23 p3749 N71-30829
- ASPHENICITY**
- Spherometer measuring mirror surface sphericity of large astronomical telescopes
24 p3922 N71-37993
- ASPHYXIA**
- Proximal effects on asphyxial rigidity of cat gastrocnemius-soleus muscles and neuromuscular responses to shock
[AD-712121] 02 p0150 N71-31111
- ASPIRATION**
- U VACUUM**
- ASHAVING**
- Conversion of data from three stream chalcocite assay methods
[AM-70-13] 01 p0011 N71-10009
- Method for preparation and assay of T9 isotopes
[NASA-CR-117172] 09 p1334 N71-30828
- Automated procedure for direct count assay of bacteria in urine by bioluminescence reaction of b-cliferase when mixed with ATP
[NASA-TM-X-65521] 13 p3054 N71-32009
- High sensitivity beryllium ore assaying instrument based on neutron photoproduction method
[RT/EL-7014] 21 p3428 N71-30829
- Neutron sources and instrumentation for destructive assays for nuclear reactor safety
[LA-4605] 21 p3427 N71-30829
- Human vaccination by resin, angiotensin, and d-tetose and human physiological studies using radioimmunoassay
23 p3712 N71-30828
- Assays of hormonal control of calcium and bone metabolism
23 p3712 N71-30829
- Radioimmunochemical assay for ACTH levels in human plasma hormones
23 p3712 N71-30829
- ASSEMBLIES**
- NT SUBASSEMBLIES**
- Turbulent velocity distribution and wall shear stress in turbulent flow parallel to triangular or rectangular rod assemblies
[NLL-W-441-79091.5W] 17 p2735 N71-30828
- Compilation of information on assembly technology for efficiency and cost reduction
[NASA-SP-593401] 18 p2930 N71-31028
- ASSEMBLING**
- NT ORBITAL ASSEMBLY**
- Assembly methods for three types of aircraft gas turbine engines
[AD-719223] 13 p2154 N71-30829
- Computer programming system based on assembling techniques for geophysical data processing
[MITT-12] 19 p3080 N71-31029
- ASSEMBLY LANGUAGE**
- Extended SPL assembly language for SCC 400 computer
[NASA-CR-102590] 05 p0449 N71-14709
- PL-516 assembly language for Honeywell DDP-10 computer
[NPL-COM-SC1-44] 11 p1715 N71-30829
- ASSESSMENTS**
- NT TECHNOLOGY ASSESSMENT**
- ASSIGNMENT**
- U ALLOCATIONS**
- ASSOCIATIONS**
- U ORGANIZATIONS**

SUBJECT INDEX

ARTIFICIAL ISOTOPES
Long lived states in Fe-204 and Fe-206 based on decay of Al-204 and Al-206
[AD-71-5197] 06 p1256 N71-18383
Alpha particles and gamma rays in isotopic decay of actinides, polonium, and bismuth
[JCL-20412] 17 p2780 N71-25288
Mass transfer mechanisms reactions of Be-200 bombarded with C and N lines yielding recoil radioisotopes Al-211, Al-210, and Po-210
[AD-71-5197] 17 p2801 N71-20187
Artificial isotopes yield as function of proton energy, using alpha spectra measurements
[AD-71-5556] 24 p2972 N71-26334
Thermal conductive excitations in Al-205
[AD-71-5562] 24 p2976 N71-26345

ASTEROIDS
NE CERES ASTEROID
Space missions to asteroids, comets, and meteoroids for study of solar system evolution
[AD-71-5197] 02 p2596 N71-11953
Approximate solution for large asteroid distribution with masses near limiting largest mass of population
[NASA-CR-111738] 04 p6611 N71-17562
Soviet Project asteroids formed by asteroid collision
[JCL-20-30363/30284P] 12 p1914 N71-24834
Physical, natural evolution, comets, and asteroids related to future space missions
[AD-71-5197] 13 p2166 N71-24991
Angular velocity evolution of solar system isolated planets, asteroids, and comets
13 p2167 N71-24994
Methods for observing individual or family asteroids of solar system minor planets
13 p2167 N71-24995
Geometry of asteroid streams
[NASA-CR-121451] 20 p3348 N71-33430
Asteroid surface properties determined by photometric measurements of phase curve between 10 and 20 deg
[NASA-CR-122920] 23 p3845 N71-37404

ASTROPHYSICS
Refractive error effects on pilot performance during entry wing and fixed wing training
02 p6171 N71-11814
Orbital syntheses during slow bend rotation
[JML-2-66-4] 18 p2880 N71-31538
Evaluation of large reflector antennas including effects of primary reflector astigmatism and its measurement through diffraction
[NASA-CR-121752] 21 p3394 N71-34157

ASTROPHYSICS
ASTROPHYSICS
Astrodynamics characteristics of lunar trajectories for manned and unmanned spacecraft
[AD-71-5197] 06 p9946 N71-16744
Orbital astrodynamics and geodynamic parameters including fundamental astronomical constants, gravitational harmonic coefficients, station locations, and other geometric quantities
[NASA-TM-X-65607] 18 p3000 N71-30513

ASTROPHYSICS
Survey of southern Milky Way for stars earlier than spectral type G0 and at least as intrinsically luminous as B2 dwarf
[AD-72041] 16 p2661 N71-28836
Some comet and minor planet positions from photos taken with photographic telescopes
23 p3836 N71-37487

ASTROPHYSICS
Astrodynamics evaluation of satellite photographs
01 p6820 N71-10808

ATOMIC THERMONUCLEAR REACTOR
Injection of relativistic electrons into Astron type magnetic field configurations
[AD-711822] 04 p6598 N71-14162
Computer simulation and research development in plasma confinement, magnetic mirrors, Astron thermonuclear reactor program, and related research
[JCL-20402-70] 13 p2143 N71-25579
Two computer programs for calculating plasma stability and equilibria in Astron and minimum-B magnetic mirror systems
23 p3627 N71-37298
Injection, equilibrium, and stability of E layer and confined plasmas in Astron
[COMP-710607-11] 24 p3993 N71-38485

ASTRONAUT LOCOMOTION
Artificial gravity system for simulating self-inertion capability of astronauts in rotating environments
[NASA-CASE-XLA-63127] 01 p6039 N71-10776
Space suit with pressure-volume compensator system
[NASA-CASE-XLA-65332] 02 p8168 N71-11194
Potential space suits utilizing mechanical aids to minimize astronaut energy at bending joints
[NASA-CASE-LAR-10807-1] 02 p8168 N71-11195
Mathematical cost evaluation of self-locomotion in simulated lunar gravity using space suits and carts in reduced weight load and surface effects
[NASA-CR-1697] 10 p1364 N71-26698

Space suit using inflatable material with low leakage and providing protection against thermal extremes, physical punctures, and radiation with high mobility characteristics
[NASA-CASE-XAC-67043] 12 p1863 N71-23161
Design and performance of extravehicular astronaut thermal protection gloves
12 p1868 N71-24138
Gravity environment simulation by locomotion and restraint aid for studying manual operation performance of astronauts at zero gravity
[NASA-CASE-ARC-10153] 16 p2554 N71-26619
ASTRONAUT MANEUVERING EQUIPMENT
Space environment work simulator with portions of space suit mounted to vacuum chamber wall
[NASA-CASE-XMF-07480] 06 p1176 N71-16773
Lightweight propulsion unit for movement of personnel and equipment across lunar surface
[NASA-CASE-MFS-20130] 15 p2513 N71-27583

ASTRONAUT PERFORMANCE
Coordination of human voluntary movements during space flight
[JFBS-3102] 05 p6433 N71-14623
Man-machine systems and astronaut and onboard computer communications
[NASA-CR-102903] 05 p6651 N71-14999
Planar motion of human being subjected to action of body-fixed force
[NASA-CR-116799] 06 p1157 N71-16599
Investigating erect posture regulation of Soyuz 9 crew members before and after flight
06 p1151 N71-18006
Statistical analysis of simulated pilot ability to control lunar module approach and descent to lunar surface
[NASA-TN-D-6113] 09 p1416 N71-20144
Crew activity analysis for long duration space flight simulation test
10 p1508 N71-20981
Details of astronaut zero gravity performance evaluation program including publication of handbook, fabrication of prototype hardware, and workable performance data
[NASA-CR-1725] 11 p1692 N71-22679
Graphical predictions of human strengths for two handed IVA/EVA tasks including effects of differing gravities, populations, and space suit conditions
[NASA-CR-15014] 14 p2211 N71-26410
Biomedical test data for predicting weightlessness effects on man during long term space flight
16 p2533 N71-28542
Environmental adaptation and operational performances of humans in space missions
16 p2554 N71-28547
Gravity environment simulation by locomotion and restraint aid for studying manual operation performance of astronauts at zero gravity
[NASA-CASE-ARC-10153] 16 p2554 N71-26619
Mathematical models for control activity of human spaceflight operator
20 p3227 N71-33461
Physical and physiological aspects of visual optics in space flight
[NASA-CR-115120] 21 p3382 N71-34060
Method for evaluating work capacity of astronaut in spacecraft control, based on probability iterative techniques and linear differential transforms
24 p6815 N71-30647

ASTRONAUT TRAINING
Attitude control training device for astronauts permitting friction-free movement with five degrees of freedom
[NASA-CASE-XMS-62977] 01 p6039 N71-10746
Discussing basic principles and methods for evaluating health, functional capacity, and psychological peculiarities in cosmonaut selection
08 p1150 N71-18095
Low and zero gravity simulator for astronaut training
[NASA-CASE-MFS-10535] 09 p1364 N71-19494
Apparatus for training astronaut crews to perform on simulated lunar surface under conditions of lunar gravity
[NASA-CASE-XMS-64790] 10 p1530 N71-21474
Design and tests of astronaut tool kit and tools for in-flight space maintenance
[NASA-CR-103135] 13 p3039 N71-25533

ASTRONAUTICS
History of development of aviation and astronautics in USSR
[NASA-TT-F-15142] 13 p2191 N71-25034

ASTRONAUTS
ORBITAL WORKERS
Cosmic radiation dose measurement of astronauts by microfilm techniques
[BNWL-1103-4] 02 p6151 N71-11073
Nuclear emission recordings of radiation exposure of Apollo 11 astronauts on moon
[NASA-CR-115985] 04 p6473 N71-13438
Astronauts and manned space flight
04 p6415 N71-14297
Nerve releases on cosmonauts from Soyuz 7 and 8 and flight training
[AD-714771] 06 p6006 N71-16097

ASTRONOMICAL MAPS

Radiocesium content in feces and urine of Apollo 7 through 13 astronauts
[NASA-CR-116223] 06 p6001 N71-16036
Therapeutic motion effects on impedance measuring photostereographic signal from cosmonaut flight
[AD-715311] 07 p6083 N71-17680
Gamma ray spectrometer for measuring radiation exposure of astronauts
[NASA-CR-110807] 12 p1864 N71-24237
In-orbit assembly of space ships and stations by automation and astronaut participation
[JFBS-53381] 16 p2682 N71-26882
Human visual perception in space flight
16 p2553 N71-28545
Marsella balance studies of two astronauts during 10 day preflight phase, Gemini 7 flight of 14 days, and 4 day postflight recovery phase
20 p3216 N71-33255
Personal hygiene protocol for man in spacecraft environment
[NASA-CR-115181] 22 p3543 N71-35238
Space shuttle external crew/computer communication utilizing remote graphic displays and technology oriented vocabulary
22 p3673 N71-36282
Results of symposium conducted to assess oculo-oculomotor changes observed in Apollo astronauts
[NASA-TM-X-50848] 23 p3710 N71-34453

ASTRONOMY
Spacecraft designed with three axis orientation for historical radio communications
[NASA-TT-F-13378] 01 p6083 N71-10942
Guidance analyzer having modified spacecraft simulation system for astronaut navigation
[NASA-CASE-XNF-69572] 05 p6089 N71-15631
Astronaut navigation in Arctic and Antarctic regions
16 p2629 N71-28772

ASTRONOMICAL CATALOGS
Empirical probability distributions for astronomical water height on California coast
[AD-711564] 02 p6219 N71-13074
Cataloging data from solar X ray monitors on Vela 5 satellite
[LA-4454] 03 p6450 N71-12641
Representative list of globular and dark nebulae for use in optical and radio astronomy
03 p6453 N71-12952
Photographic data of proper motion survey of suspected white dwarf stars in Northern Hemisphere
04 p6080 N71-13554
Photographic data of proper motion survey of stars in regions G256 through G265 in Northern Hemisphere
04 p6080 N71-13555
Compiling catalog of visual binary stars with astrometric and hyperbolic orbits
05 p6767 N71-15137
Tabular data of photographic observations of minor planets, double and binary stars, and orbits of psi 312 optical CVI
05 p6767 N71-15191
Star position and motion catalog for Taurus and Orion regions
06 p6940 N71-14828
Calculations of service star declinations and motions
01 p667 N71-20312
Star catalog data for determining selective absorption in region of Milky Way galaxy
[NLL-R75-6451] 10 p1646 N71-21773
Astronomical catalog containing spectra, colors, and magnitudes of O-A stars in Milky Way galaxy
[NLL-R75-6450] 10 p1646 N71-21773
Survey of radio sources between 0 and 20 deg north declination using Ohio State University radio telescope at 615, 1415, and 2650 MHz
16 p2800 N71-28033
Astronomical catalog of cosmic X ray sources
[UCID-15632] 17 p2840 N71-29211
Position declination and motion data for international reference stars
20 p3348 N71-33292

ASTRONOMICAL COORDINATES
Meridian astronomy
05 p6769 N71-15496
Polynomial expressions for planetary ephemerides and orbit elements in relationship to earth coordinate system
[NASA-CR-116307] 06 p6948 N71-16785
Astronomical observations of fundamental star coordinates and reference faint and bright stars, and photography of minor planets and galaxies to compile catalog of faint stars
[JFBS-53156] 14 p2333 N71-25708
Drive controls for ultraviolet monitoring during stellar motion observations
24 p3924 N71-37993

ASTRONOMICAL MAPS
Photometric map of Milky Way
[BNWL-1419] 03 p6452 N71-22282
Constructing maps of planet Mars from infrared photographs of planetary surface
04 p6410 N71-13396
Radio map of the Crab nebula at 3.5 mm
[VR-47] 17 p2843 N71-29552

ASTRONOMICAL MODELS

- Physical aspects of radiation spectrum produced by stellar atmosphere 04 p0612 N71-14149
[JILA-106]
Astronomical meteoroid environment model for space missions 07 p1110 N71-17525
[NASA-SP-8038]
Light scattering in reflection nebulae models 07 p1117 N71-18077
Lunar seismic velocity models and lunar reverberation calculations 07 p1117 N71-18119
[NASA-CR-116418]
Relativistic electron diffusion from point source in Sagittarius A astronomical model 10 p1642 N71-20661
Model for ionization and heating of Gum Nebula by energetic particles from Vela X supernova 10 p1642 N71-21653
[NASA-TM-X-65486]
Structure and stability of long period variable star model envelopes 11 p1824 N71-21935
Model for self excited vibrations in pulsating stars 11 p1825 N71-22109
Cosmological models, and galactic and stellar evolution 11 p1826 N71-22412
Theoretical inhomogeneity emission models of planetary nebulae 12 p1999 N71-24317
Stellar laser model for pulsar surface emission 13 p2169 N71-25299
Model of eclipsing binary star system based on digital computers 14 p2336 N71-25962
[NASA-CR-118643]
Development and characteristics of laboratory models to explain structure and composition of comet cores 15 p2517 N71-26960
[LA-TR-70-27]
Cosmic matter-antimatter annihilation and gamma ray background spectrum 17 p2841 N71-29924
[NASA-TM-X-65598]
Astronomical model and theoretical physics of expanding universe with evolving sources effects on low energy cosmic rays 18 p3003 N71-30612
[NASA-TM-X-65623]
Survey of optical properties of Saturn ring system and establishment of physically reasonable ring models 19 p3181 N71-32424
Models for studying origin and composition of ultrahigh energy cosmic rays 23 p3841 N71-37391
[NASA-TM-X-65713]
Nonhomogeneous isotropism of centrally symmetric models of origin of universe 23 p3848 N71-37430
Derivation of cosmologic model for verification of gravitation theory 23 p3849 N71-37434
Photon propagation in perturbed Einstein-de Sitter universe model containing ionized gas 23 p3857 N71-37493

ASTRONOMICAL OBSERVATORIES

- NT HEAD
NT OAO
Observing compact radio sources with radio interferometers in US and USSR 02 p0297 N71-12153
Designing onboard digital computer for attitude control and data reduction for Astronomical Netherlands Satellite 05 p0347 N71-12624
Point star and galaxy research and instrumentation improvement [AD-712826] 05 p0455 N71-13275
History of radio telescope and interferometer design modifications at Owens Valley Radio Observatory [AD-712825] 05 p0382 N71-13296
Summary of prominence and calcium floodcan observations at Kodaikanal Observatory Jan. through June 1964 - tables and graphs 05 p0451 N71-13297
[BULL-174]
Astronomical observatory and laboratory research reports 05 p0689 N71-15581
Observations of stellar parallax from photographs taken at Royal Observatory, Greenwich during 1924 to 1939 - Vol. 3 05 p0769 N71-15603
Development and characteristics of USSR automatic solar observatory 07 p1185 N71-16068
Research projects at astronomical observatory in South Africa 09 p1368 N71-20549
Astrometric observations of fundamental star coordinates and reference faint and bright stars, and photography of minor planets and galaxies to compile catalog of faint stars 14 p2335 N71-25788
[JPRS-55154]
Design and operation of astronomical observatory telescope with 6 meter mirror [AD-72264] 18 p2923 N71-30724

Research projects and activities of Vatican Observatory during 1970 noting an atomic spectra excited by glow discharge 20 p3347 N71-33216

Model turbulence profile for predicting optical effects of turbulence on stellar observations [NASA-TR-8-369] 20 p3312 N71-33499

Stratospheric observatory using Cassegrainian telescope to obtain solar photographs as well as spectrograms 21 p3430 N71-34409

Radio and radar astronomy investigations at Haystack Observatory [NASA-CR-121846] 21 p3509 N71-34996

Eight variable stars in cygnus cloud studied at different observatories - tables and graphs 21 p3510 N71-35013

Harmonic analysis of earth inclinations by Flagstaff Astronomical Observatory 23 p3749 N71-36726

Telescope and site of astronomical observatory at Cerro Las Campanas, Chile 24 p3921 N71-37963

Canadian 157-inch Ritchey-Chretien telescope 24 p3921 N71-37964

German astronomical project with observatories in Spain and Germany 24 p3921 N71-37967

Soviet 6-m astronomical telescope with alt-azimuth mounting 24 p3921 N71-37968

Using balloons for lifting astronomical observatories to high altitudes [NASA-TT-F-12339] 24 p4008 N71-38580

ASTRONOMICAL PHOTOGRAPHY
Investigating suitability and requirements of mountain sites for high altitude IR astronomical observations 04 p0609 N71-13590

Relative measures of satellites of Uranus and Mars from astronomical photographs 04 p0610 N71-13593

Calculating orbital elements of comet Burnham-Slaughter 1934-1959 04 p0610 N71-13594

Calculating orbital elements of comet Humason 1960-1959X 04 p0610 N71-13595

Observations of stellar parallax from photographs taken at Royal Observatory, Greenwich during 1924 to 1939 - Vol. 3 05 p0769 N71-15603

Stellar spectrophotometry, meteor photography, installation of solar telescope and Schmidt camera, and lunar dust analysis 12 p1995 N71-23177

Star position and proper motions in south celestial pole region and source dependent systematic deviations in Smithsonian Astrophysical Observatory data [NASA-CR-118033] 12 p1997 N71-24225

Coefficient of electron attachment to oxygen molecules method from simultaneous photographic and radar observations applied to meteor radar echo data for 1957 to 1959 12 p1998 N71-24288

Sensors for ground based infrared sky survey [AD-720845] 14 p2336 N71-25806

Photographic measurements of Saturn and its rings [NASA-CR-118864] 15 p2518 N71-27984

Image restoration techniques applied to astronomical photography with degradation caused by atmospheric turbulence 16 p2594 N71-28522

Image restoration for processing photographs by Stratoscope 2, and orbital telescopes 16 p0000 N71-28524

Astronomical photography of zodiacal light and lunar libration clouds 18 p3014 N71-30979

Investigating photogrammetric and astronomical methods for plate reduction 19 p3098 N71-31838

Comparison of Injun 3 satellite measurements of low energy electron precipitation and ground based observations of visible auroral arcs [NASA-CR-121675] 21 p3415 N71-34300

Stratospheric observatory using Cassegrainian telescope to obtain solar photographs as well as spectrograms [NRL-M-20418-5828.4P] 21 p3430 N71-34409

Astronomical observation and photography of five old and seven new variable stars by various observatories 21 p3510 N71-35012

Computerized searches for meteor streams in photographic meteor orbits [NASA-CR-121922] 22 p3666 N71-36141

Computerized search for meteor streams in 865 precise photographic meteor orbits 22 p3667 N71-36142

Computerized search for meteor streams in 2401 photographic meteor orbits, and association with other streams or comets 22 p3667 N71-36143

Astronomical observations of free diurnal satellite amplitudes of earth 23 p3748 N71-36726

Some comet and minor planet positions from plates taken with astrigraphic telescope 23 p3856 N71-37493

ASTRONOMICAL PHOTOMETRY
NT STELLAR SPECTROPHOTOMETRY
Spectral power flux magnitude system for astronomical scaling 01 p0121 N71-10019

Supernovae remnant Vela-X 02 p0293 N71-13588

Photometric map of Milky Way [BNWL-1419] 03 p0432 N71-13589

Photometry of elliptical galaxies in Virgo Cluster [AD-712907] 03 p0434 N71-13589

Infrared photography, mapping, and orbit calculation of natural satellites, comets, and planets in solar system [NASA-CR-115785] 04 p0609 N71-13589

Selected data on physical characteristics of planet Mercury 04 p0609 N71-13589

Developing sky brightness photometer for continuous measurements of atmospherically scattered light near edge of solar disk [NCAR-TN-53] 06 p1203 N71-18169

Selenologic catalogs, lunar photometry, and Cephæus spectra [AD-719057] 13 p2164 N71-30303

OGO-D photometric airglow measurements 13 p2076 N71-32548

Conference on using TV type image sensors in astronomical photometry [NASA-SP-256] 16 p2679 N71-30309

Diode matrix silicon vidicon for astronomical photometry 16 p2679 N71-30316

Processing electronic camera images for use in astronomical photometry 16 p2570 N71-30323

Photometric studies of interstellar light obscuring media and stellar distribution in constellations Aquila and Scutum [NRL-RTS-6052] 17 p2844 N71-30978

Calcite filter for astronomical photometry, sun, and near infrared applications 22 p3584 N71-35323

Aberration and reflectance in calcite filter for photographic photometry using Schmidt telescope 22 p3584 N71-35323

Near infrared astronomical photometry using calcite-Poloid filter method 22 p3584 N71-35327

Asteroid surface properties determined by photometric measurements of phase curve between 10 and 30 deg 23 p3845 N71-37984

Instrument constants of astronomical cameras compared with object positions obtained by other methods [AD-727902] 24 p3926 N71-38912

ASTRONOMICAL SATELLITES

NT OSO-3
ASTRONOMICAL SPECTROSCOPY
Spectroscopic analyses of interstellar matter [NASA-CR-1667] 02 p0174 N71-11126

Research in upper air physics, radio astronomy, and rocket spectroscopy [NASA-CR-111376] 02 p0297 N71-12048

Narrow band photometry of dwarf Cepheid like Puppi variable star 03 p0451 N71-13079

Spectroscopic study of visual binary stars with B-type primaries 06 p0948 N71-18120

Project planning of Jansu camera for astronomical ultraviolet spectroscopy 14 p2334 N71-25808

Sensor for space astronomy applications especially diffraction limited imagery and high resolution spectroscopy 16 p2593 N71-28512

Electrical readout image tube for use on LARC Cooke spectrograph 16 p2570 N71-30310

Research projects and activities of Vatican Observatory during 1970 noting an atomic spectra excited by glow discharge 20 p3347 N71-33216

Performance and response characteristics of smoothing, image intensifier detector for low light level astronomy and optical detection [NASA-CR-121913] 22 p3558 N71-30340

ASTRONOMICAL TELESCOPES
NT APOLLO TELESCOPE MOUNT
NT SPECTROSCOPIC TELESCOPES
NT STRATOSCOPE TELESCOPES
NT X RAY TELESCOPES

Peristaltic action microfilm actuator for primary mirror active-optics system of orbiting astronomical telescope [NASA-CR-1658] 01 p0852 N71-10011

CASSIOPE system for rocket-borne astronomical telescope attitude control

02 p0363 N71-11763
Describing conceptual design for High Energy Astronomy Observatory spacecraft and major systems
[NASA-CR-109062] 05 p0771 N71-15318
Design and construction of six-meter telescope
[JPRS-52015] 05 p0686 N71-15412

Selected articles on Soviet research in space, geophysics, and astronomy
[JPRS-52183] 07 p1107 N71-16917

Reporting development of astronomical telescopes, radioastronomical observations of solar eclipses and observation of faint meteor orbits
07 p1107 N71-16918

X ray telescope of Lunokhod 1 for observations of gamma and galactic from lunar surface
07 p1027 N71-16982

Laser interferometer for monitoring and control of large telescopes
[NASA-CR-111811] 08 p1263 N71-19019

Light sensitive control system for automatically opening and closing dome of solar optical telescope
[NASA-CASR-109061] 09 p1388 N71-19568

Development of cosmic physics, and importance of Luna Chacabaya Laboratory, Bolivia
09 p1461 N71-20026

Requirement and design criteria for high resolution ultraviolet spectroscopy on SAS-D mission
[NASA-TM-X-67165] 12 p2081 N71-24070

Feasibility and scientific benefits of ultraviolet telescopes for SAS-D mission
[NASA-TM-X-67166] 12 p2081 N71-24071

Gamma ray scintillation, Compton, and pictorial detector telescopes
13 p2081 N71-24779

Abstracts of published Soviet articles concerning research in geophysics, astronomy, and space
[JPRS-52989] 15 p2396 N71-26859

Laser beam projector for continuous, precise alignment between target, laser generator, and astronomical telescope during tracking
[NASA-CASR-NPO-11067] 16 p2640 N71-29125

Deep sky survey at 2700 MHz using 210-foot telescope - measurements of positions and flux densities of sources
[JPRS-10622] 17 p2846 N71-30211

Design and operation of astronomical observatory telescope with 6 meter mirror
[AD-72624] 18 p2923 N71-30724

Aluminum infrared telescope for flux measurements of astronomical objects with spectral energy peaks occurring at wavelengths of more than 25 microns
[NASA-CR-121414] 20 p3272 N71-33285

Research projects and activities of Vedic Observatory during 1970 noting an atomic spectrum excited by glow discharge
20 p3347 N71-33216

Application of cosmographic perspectives in interpreting photographs taken in space
[NASA-TT-F-139228] 20 p3275 N71-33590

Astronomical television telescope and solar temperatures for disturbed and undisturbed regions
21 p3509 N71-34998

Effects of space shuttle on cosmic mission objectives, and operational modes of OAO/LST program
[NASA-CR-121703] 21 p3513 N71-35031

Proposal for economic study of space shuttle effect on OAO/LST program
[NASA-CR-121702] 21 p3513 N71-35032

Engineering experience and performance evaluation of telescope experiment during its operational life on OAO 2
[NASA-CR-121932] 22 p3583 N71-35520

Problems in development of mirror transit astronomical telescopes
22 p3786 N71-35542

Meteorological parameter observation, early star system analysis, and astronomical telescope mirror
22 p3670 N71-36170

Elastic deformation of telescope mirror, noting load distribution on static support system
22 p3670 N71-36172

Description of Isaac Newton Telescope Cassegrain synchrograph and results of radial velocity observations of stars near Lyra constellation
23 p3758 N71-36794

Conference papers on world astronomical telescopes noting structural design and optics
24 p3921 N71-37960

Anglo-Australian 150-inch reflecting telescope for Southern Hemisphere
24 p3921 N71-37961

Budgeting, optical and mirror system, and instrumentation of 150-inch reflecting telescopes in Arizona and Chile
24 p3921 N71-37962

French astronomical telescope project planning
24 p3921 N71-37963

Built 3.5-m telescope project and optical parameters
24 p3921 N71-37964

ESO 3.6-m telescope at La Silla, Chile
24 p3921 N71-37969

Coude optical design in astronomical telescopes

24 p3922 N71-37971
Alignment of optical system in astronomical telescopes

24 p3922 N71-37972
Spherometer measuring mirror surface sphericity of large astronomical telescopes

24 p3922 N71-37973
Light noise due to light scattering in astronomical telescope Lickman camera image corrector-receiver system

24 p3922 N71-37977
Limit magnitude of optically weak radio stars measured by large telescope electronic camera

24 p3922 N71-37978
Structural aspects of large astronomical telescope mounts

24 p3922 N71-37980
Deformation in Serrurier truss tubes in large astronomical telescopes

24 p3923 N71-37981
Removal of astronomical telescope mirrors for re-aluminizing

24 p3923 N71-37982
Structural design of astronomical telescopes using digital computers with emphasis on tubes

24 p3923 N71-37983
Telescope building and dome design

24 p3923 N71-37984
Structural design of Cassegrain cages in large astronomical telescopes

24 p3923 N71-37985
Computer control of large telescopes

24 p3923 N71-37986
Telescope control by on-line computers, including ESO 3.6-m telescope

24 p3923 N71-37987
Telescope tracking drives and controls at McDonald Observatory using 107 and 82 inch telescope

24 p3923 N71-37988
Mechanical drives of French 2 and 3.6-meter telescopes from horseshoe, noting gears

24 p3923 N71-37989
Digital computer used to control drive of 2.2-meter astronomical telescope

24 p3923 N71-37991
Image intensifiers used with television tubes for enhanced visual observations

24 p3924 N71-37992
Computer subsystem of Anglo-Australian 150-inch telescope

24 p3924 N71-37993
Anglo-Australian telescope proposed drive and control system using printed circuits

24 p3924 N71-37994
Daytime operations of large telescopes for infrared astronomy

24 p3924 N71-37996
Daytime use of telescopes, emphasizing infrared astronomy, remote control, and astronomical spectroscopy

24 p3924 N71-37997
Light beams fed into telescope laboratory

24 p3924 N71-37998
Light beams fed into telescope laboratory

24 p3924 N71-37998
Light beams fed into telescope laboratory

24 p3924 N71-37998
Light beams fed into telescope laboratory

24 p3924 N71-37998
Light beams fed into telescope laboratory

24 p3924 N71-37998
Light beams fed into telescope laboratory

24 p3924 N71-37998
Light beams fed into telescope laboratory

24 p3924 N71-37998
Light beams fed into telescope laboratory

24 p3924 N71-37998
Light beams fed into telescope laboratory

24 p3924 N71-37998
Light beams fed into telescope laboratory

24 p3924 N71-37998
Light beams fed into telescope laboratory

24 p3924 N71-37998
Light beams fed into telescope laboratory

Observation and analysis of light variations of binary stars UU Pictoris, RLM Cephei and 44 Bootis

16 p1643 N71-21233
Theory of stellar evolution applied to dying stars, neutron stars, dwarf stars, and black holes
[NASA-TM-X-65478] 16 p1644 N71-21238

Abstracts of news releases and scientific articles on geophysics, meteorology, astronomy and space
[JPRS-52385] 11 p1824 N71-21931

Soviet news releases on meteorology, oceanography, geophysics, upper atmosphere, and astronomy for 1 Mar. 1971
11 p1825 N71-22049

Soviet research in astronomy, meteorology, oceanography, geophysics, upper atmosphere, space, and Lunokhod 1 activities - No. 248
[JPRS-52634] 11 p1828 N71-22682

Lunokhod 1 design, control, and lunar geology and astronomy experiments
11 p1832 N71-22688

Soviet research on astronomy, meteorology, oceanography, geophysics, astronomy, upper atmosphere, and space program - No. 249
[JPRS-52746] 11 p1995 N71-23176

Development of method for studying transfer of resonance line radiation in media of extremely large optical thicknesses
13 p2170 N71-25436

Research projects in astronomy involving parallax measurements, proper motion and membership studies of open clusters, and development of instrumentation
[AD-719932] 14 p2334 N71-25617

Soviet research in glaciology, meteorology, astronomy, and space sciences
[JPRS-53253] 16 p2678 N71-28145

Soviet astronomical developments including structure of radio emission sources, and new improvements in constellation Virgo
16 p2678 N71-28146

Relationship of Cepheids to surrounding stars and interstellar material and interstellar observations to determine Cepheid evolution
18 p3017 N71-31339

Soviet research in astronomy, meteorology, oceanography, terrestrial geophysics, and space sciences
[JPRS-53726] 21 p3509 N71-34997

Soviet news releases on astronomy, oceanography, meteorology, geophysics, upper atmosphere, and aerospace activities
[JPRS-53818] 21 p3509 N71-35004

Astronomical observation and photography of five old and seven new variable stars by various observations
21 p3510 N71-35012

Development of techniques for obtaining metal abundance of late type stars and application to field dwarfs in solar vicinity and Hyades
22 p3672 N71-36182

Cosmic ray research and instruments used for interplanetary and astronomical studies, Vol. 2 - conference
24 p4009 N71-38382

Bibliography of abstracts concerning pulsars, neutron stars, black holes, and cosmic ray sources
[TTD-3320-SUPPL-1] 24 p4013 N71-38631

Soviet line research in astronomy, meteorology, oceanography, geology, and space sciences - 13 Sept. 1971
[JPRS-54039] 24 p4016 N71-38649

Soviet Mac research in astronomy, meteorology, oceanography, geology, and space sciences - 14 Oct. 1971
[JPRS-54246] 24 p4016 N71-38650

ASTROPHYSICS
Atmospheric models and standard orbit calculations from satellite observations
[NASA-CR-111128] 01 p0122 N71-10576

Astrophysical investigations at Malindi Space Science Laboratory
02 p0296 N71-11930

Observational evidence for galactic spiral structure
03 p0453 N71-12264

Astrophysical aspects of cosmic radiation, and radiation environment of earth
[NASA-CR-115550] 05 p0963 N71-13322

Determination of stellar magnitudes from objective prism spectra
06 p0943 N71-16732

Calibration of high energy cosmic ray experiment
[NASA-TM-X-65040] 06 p0944 N71-16739

Recent astrophysical laboratory observations of solar activity and solar structure
07 p1104 N71-16954

Determination of lunar orbital elements and other astronomical constants
07 p1111 N71-17672

Finite difference methods of numerical integration in celestial mechanics
07 p1111 N71-17673

Characteristics of synchrotron and Compton radiation below plasma frequency from particle upblowing in magnetospheres
[AD-719925] 07 p1107 N71-18076

Development of cosmic physics, and importance of Monte Chacaltaya Laboratory, Bolivia

Research in environmental sciences including seismology, oceanography and earth resources, planetary atmospheres and ionospheric physics, space physics, astrophysics, and relativity

Special problems in physics and astrophysics including thermonuclear reactions and high temperature conductivity

Geophysical and astrophysical fluid dynamics

Geophysical and astrophysical fluid dynamics, emphasizing rotating fluids

Astrophysics, extraterrestrial radiation, and magnetosphere - conference

Magnetospheric, solar, interplanetary space, and plasma physics

Development of computer program for study of short time scale phenomena in stellar evolution - eclipse

Relation of gravitation with astrophysics, and geophysics

Jupiter atmospheric entry mission rationale with environmental models, science criteria, mission and system evolution, baseline data, mission design, and illustrative sample missions

Cosmic gamma ray production processes, galactic and extragalactic gamma rays, and cosmology

Aerospace scientific and technological studies in 1969 for satellite systems and spacecraft missions

Absence anomalies in A-poc sites caused by diffusion processes, and anisotropy of elements between Si-28 and Co-59

Earth orbital research programs in atmospheric physics and space astronomy

Interpretation of data on muons in cosmic rays for relevance to high energy interactions and astrophysics

Soviet astronomical developments including structure of radio emission sources, and new supernova in constellation Virgo

Research in plasma physics including gravitational plasmas of globular star clusters

Astrophysical investigation of four classical Cepheid variable stars

Cosmic gamma radiation from pion decay in interstellar gas

Heavy leptons in neutrino astrophysics

Comparison of Smithsonian Astrophysical Observatory 1969 gravity field representations with surface gravity

Astrophysics, radio astronomy, radio sources, galaxies, cosmology, pulsars, black body radiation, universe, and electromagnetic wave propagation

Relativistic and Newtonian cosmology in understanding setting in which astrophysical phenomena occur and are observed

Photoabsorption cross sections for molecules of astrophysical interest at wavelengths less than 3000 Å

Structure, composition, evolution, and physics of stars, galaxies, and universe

Spectroscopic detection of water on celestial bodies and in interplanetary space

Astrophysics, solar physics, and dynamic processes in interplanetary space and magnetosphere

History of School for Space Physics and discussion of papers given at Sixth Meeting, Aposity, 1969

Interaction of optical and particle radiation into matter in astrophysics

Nuclear astrophysics, heavy ion induced reactions, nuclear spectroscopy, and radiative proton capture reactions

Satellite observations, radio-astronomical and optical techniques, and problems in plasma physics associated with effects of energetic particles in outer space

Gamma ray detector for astrophysical research

Investigating reaction eta-meson yields 3 pion for charge asymmetry

Asymmetry in single pion/0 photoproduction by polarized gamma rays on protons

Neutrino, electron, and proton up-down asymmetry measurements from beta decay of polarized Lambda hyperons

Trajectory computer program /SIXD/ to determine motions of asymmetric missiles emphasizing various nonlinear-induced effects associated with flamed bodies

Symmetry in physics including principles of nonobservables, transformation and conservation laws, asymmetry and observables, time reversal, and complementarity of symmetry violations

Cross sections and asymmetries measured in p, d reactions in Si-118 and Si-119 induced by polarized proton beams

Buckling and column failure interaction of thin walled compression members due to flange asymmetry

Monte Carlo procedure for detecting CP nonconserving asymmetry in $K(0)$ sub L into $\pi^0\pi^0$ decay

Pion asymmetry in earth formations and on other planets

Asymmetric confining toroidal field effect on ion velocity distribution energy in plasma generator

Asymptotic behavior and error analysis for linear integral differential difference equations

Asymptotic behavior of electron-proton scattering amplitude, spectral function of commutator of currents, and sum rules for Schwinger term

Asymptotic behavior of covariance matrix solution for discrete matrix Riccati equation

Uniform asymptotic stability of functional differential equations of neutral type

Loss due to missing data in efficiency of locally optimal test for homogeneity with respect to very rare events in supernova observations

Structure of control laws insuring asymptotic stability of control systems with unstable targets

Asymptotic results for goodness-of-fit statistics with estimated parameters

Digital computer program for asymptotic solution for short ring-reinforced oval cylinders

Applying asymptotic SU(3)/ and SU(2) symmetries to hadron systems

Asymptotically efficient estimation of local location-parameter approximations

Modified Rago representation for scattering amplitude

Using finite energy sum rules as consistency test of models for asymptotic behavior of kaon proton scattering amplitudes

Presenting proposals for implementation of subprogram for computing and manipulating asymptotic expansions

Asymptotic solution of differential equations for red oscillations at high temperatures

Asymptotic single particle distributions with pionization in multiphase model based on Feynman conjecture

Asymptotic wave functions near thresholds in presence of long range potentials

Consistency and asymptotic normality of two phase regression maximum likelihood estimates

Frequency response and design of distributed parameter networks using asymptotic approximation

Aerodynamic sound production and method of matched asymptotic expansions

Asymptotic solutions of stress and strain as functions of radial and longitudinal distance, and time for axisymmetric waves in step-function pressure-loaded hollow elastic circular cylinder

Asymptotic solution of low frequency wing oscillations in transonic oscillation elastic inviscid gas flow based on complete approximation

Existence, uniqueness, stability, and asymptotic stability conditions for solution of elliptic partial differential equations with general boundary conditions

Asymptotic convergence theorems for sequential nonlinear filters

Condition for Rago asymptotic behavior

Mathematical model and computer program for solution of asymptotic neutron transport equations in slab geometry

Analysis of effect of shear deformation on solution of this, nonhomogeneous elliptic shells using method of matched asymptotic expansions

Asymptotic expansion techniques to define pressure loading effects on wings with unbalanced control surfaces

Asymptotic relations for averaged amplitudes and generalizations of some asymptotic equalities via violating microcausality

Axiomatic proof of asymptotic relations for averaged amplitudes

Test of models for asymptotic behavior of pion-pion or pion-proton scattering amplitudes

Asymptotic method for statistical failure rate function estimators

Global and local structure of relativistic quantum systems with superselection rules

Unit disk for boundary functions and sets of asymptotic values

Large angle hadron and proton scattering and duty calculations based on mesomorphic and scattering functions, momentum transfer, and asymptotic methods

Correction for straight trailing edges for slender slender wing theory using asymptotic expansion

Asymptotic expansion procedure for effects of dissipative and dispersive mechanisms and nonlinearity on homogeneous, isotropic, wave propagation problems

Asymptotic expansion for 2-boson scattering amplitude with Pomeron singularities

Erosion of discontinuities and formation of solutions in numerical computations of discontinuous solutions of differential equations

Asymptotic expansion and Schrodinger equation for perturbed harmonic oscillator

Moldensky series and analytical continuation applied to gravimetric geodesy

Essays on cardiology in sports

Cardiac activity of athletes in quiet state

Blood circulation and state of physical training in athletes

Electrocardiography and vector cardiography of athletes

X ray methods for quantitative analysis of cardiac activity in athletes

Functional tests of cardiovascular system in athletes

Transmission and analysis of cardiological data in athletes

Clinical problems of cardiology of athletes

Arterial pressure characteristics of athletes

Cardiac rhythm disruptions in athletes

Physical overtraining effect on cardiac muscle in athletes

SUBJECT INDEX

Phonocardiographic analysis of systolic noises in athletes 09 p1329 N71-19394

Catheterization medical services for Soviet athletes 09 p1330 N71-19395

Heat tolerance of athletes during muscular exercise in various thermal environments 09 p1337 N71-20346

ATMOSPHERIC

ATMOSPHERIC ENGINEERING

Temperature microstructure of Atlantic Ocean and its effect on sound propagation (AD-710714) 01 p0048 N71-10529

Time spectra of atmospheric temperature, pressure, and wind velocity variations above Atlantic Ocean (NARS-LIB-TRANS-1472) 02 p0233 N71-11448

North Atlantic physiographic patterns of relief, slope, and topographic texture of ocean bottom (N71-11359) 02 p0231 N71-11560

Microscopic winds over Ascension Island in January (AD-711851) 02 p0237 N71-11466

Project management and experimental designs for tropical meteorological experiments in Atlantic Ocean 02 p0238 N71-11679

Feasibility of satellite navigation system for subsonic and supersonic air traffic control over North Atlantic Ocean 03 p0407 N71-12594

Abstracts of articles on oceanography including concentration of suspended matter in sea water 03 p0408 N71-13041

System of predicting waves and swells on US Continental Shelf of east coast (PB-192081) 03 p0372 N71-13324

Oceanographic observations of North Atlantic standard monitoring sections for 1964 to 1966 (PB-192296) 03 p0372 N71-13327

Range tests with transponders in North Atlantic with VHF SATCOM equipment by two satellites (NARS-CR-115782) 04 p0544 N71-14492

Off Stream flow with transient current fluctuations and detached eddy formations (ESSA-TR-REL-164-AOML-1) 05 p0679 N71-15524

News release on Soviet research in Atlantic Ocean 05 p0681 N71-15680

Atlantic Ocean gravity anomaly map 07 p1017 N71-17138

Environmental and oceanographic data for sections of Atlantic coastline (AD-714833) 07 p1022 N71-17801

Ice thickness observations along coasts of eastern Canada and southern Greenland (AD-715434) 08 p1188 N71-18503

1960 average monthly North Atlantic surface temperature gradients between 50 to 80 deg N and 0 to 60 deg W 11 p1790 N71-22403

Water exchange variations between Arctic and Atlantic Oceans and effects on ice cover forecasts in Arctic seas 11 p1752 N71-22803

Sea surface and water circulation in Drake Passage between Atlantic and Pacific Oceans during summer months 11 p1758 N71-22852

Water interchange between North Atlantic Ocean and Norwegian Sea between Scotland and Iceland (CO-375-28) 12 p1913 N71-23752

Virginia Beach environmental data and time series analysis of water table interactions with processes in fresh-ocean-atmosphere system for environmental control (AD-719923) 14 p2245 N71-25629

Project planning for observation of atmospheric circulation and heat budget over the Atlantic Ocean using international collaboration and satellite observations 15 p2437 N71-26972

News briefs and abstracts of scientific articles concerning magnetic anomalies in Atlantic Ocean, and currents in Arctic Basin 17 p2739 N71-29402

Physical properties of cloud clusters over tropical Atlantic - tropical meteorology 17 p2777 N71-29483

Long range tropical weather forecasting of cloud clusters over Atlantic using ground weather stations international cooperation and training 17 p2777 N71-29485

Analysis of deposition and erosion of ocean bottom along Middle Atlantic Continental Slope 18 p2915 N71-31011

Geophysical data and regional geology indications of existence of salt domes in Atlantic Ocean off coast of southwest Africa 18 p2915 N71-31012

Characteristics of tropical storms and path of storm across Atlantic Ocean as observed by meteorological satellites 18 p2951 N71-31016

Tropical cyclone data for North Atlantic, Caribbean, and Gulf of Mexico - charts (AD-723035) 19 p3128 N71-32058

Numerical analysis showing Atlantic Ocean influence on tidal gravity variations observed at Moulou climatic station, France 20 p3263 N71-33351

Relation between temperature anomalies in lower air level and upper water level for North Atlantic Ocean (NLL-M-20724-5828.4F) 21 p3423 N71-34353

News briefs and abstracts of scientific articles concerning oceanography 21 p3509 N71-35006

Oceanic conditions in upper 1800 meters of water column off northeastern Brazil (CO-375-34) 22 p3575 N71-35459

Free-air and vertical wind structure analysis for equatorial maritime friction layer based on surface temperature and wind profiles for Arabian Sea and Atlantic Ocean 23 p3785 N71-36978

Tidal modulation of Florida current surface flow 23 p3789 N71-37005

Fluctuations of Florida current inferred from sea level records and linear weather effects 23 p3789 N71-37006

Meteorological charts of Northern Atlantic surface temperatures (ISBN-87-7478-036-0) 23 p3792 N71-37033

Global atmospheric research program on numerical weather forecasting, Atlantic tropical experiment, and future activities 23 p3793 N71-37034

Eigenvector analysis of air temperature distributions over Atlantic Ocean (NLL-M-20364-5828.4F) 24 p3918 N71-37958

ATLAS LAUNCH VEHICLES

Spacecraft maneuvers of Atlas-Centaur 19 and 20 in 1969 Mariner Mars missions (NARS-TM-X-2378) 19 p3185 N71-32496

ATMOSPHERIC EXPLORER B

U. EXPLORER 32 SATELLITE

ATMOSPHERES

Basic methods of measuring atmospheric electric fields (TT-70-50125) 03 p0367 N71-12357

Analysis of submarine atmosphere and instrumentation for deep submergence ocean array applications 17 p2944 N71-29426

Analysis of trace contaminant composition in submarine atmospheres 17 p2713 N71-29427

ATMOSPHERIC ABSORPTION

U. ATMOSPHERIC ATTENUATION

ATMOSPHERIC ATTENUATION

NT. AURORAL ABSORPTION

Atmospheric attenuation and sky emission measurements using microwave radiometers (ESSA-TR-REL-156-WPL-11) 01 p0023 N71-10596

Data evaluation for ATS 5 millimeter wave measurements of meteorological parameters (NARS-TM-X-65371) 01 p0023 N71-10654

Infrared radiation atmospheric attenuation controlled by heat balance tests in presence or absence of carbon dioxide and water vapor in solar simulation (ESRO-TN-94-BSTEC) 03 p0371 N71-13288

Mesosphere atmospheric attenuation of solar radiation by oxygen and ozone 04 p0522 N71-13825

Error study for SS-1080 ATM sensor system, effects of atmospheric refraction, atmospheric attenuation, and earth albedo (NARS-CR-102957) 04 p0611 N71-14098

Atmospheric optical properties - tables and charts (AD-715270) 07 p1022 N71-17814

Stationary phase for beam of radio waves propagating in absorptive ionosphere as function of some directions of real and imaginary parts of wave vector (GRI-TP-95) 08 p1187 N71-18470

Atmospheric absorption effects on spectroscopic analyses and electromagnetic radiation transmission (AD-715482) 08 p1191 N71-18835

Atmospheric heat budget calculator from solar radiation characteristics in clear and cloudy conditions (TT-70-50035) 11 p1822 N71-22043

Radar doppler frequency system for estimating microwave attenuation by hydrometeors 12 p1880 N71-23930

Influence of temperature, ozone, and water vapor on atmospheric absorption by 15 micron bands of carbon dioxide 15 p2401 N71-27503

Transmission functions in 15 micron carbon dioxide band 15 p2401 N71-27503

Laser radiation absorption in lower atmosphere 15 p2419 N71-27506

Degradation effects of atmospheric absorption of 10.6 micron laser beam with kinetic model for vibrational relaxation process and numerical analysis of vibrational ray displacement (RB-350) 17 p2759 N71-30153

Derivation of equations for Rylov and Born approximations in turbulent atmospheric attenuation and scattering of coherent light (AD-723473) 17 p2789 N71-30229

Effect of microwave absorption and dielectric radio noise in Jovian atmosphere on radio communication in 1 to 10 GHz frequency band 18 p2963 N71-30739

Ionospheric rates due to atmospheric absorption of solar protons and alpha particles in upper atmosphere (AD-723627) 19 p3175 N71-31824

D region electron density profiles at geomagnetic equator based on radar and absorption experiments (ESD-57) 20 p3267 N71-33538

Influence of atmosphere on performance of thermal imaging systems 20 p3299 N71-33985

Temporal and spatial distribution of atmospheric transmissivity coefficients based on long-term monthly mean flux densities of direct solar radiation for 1954 to 1963 in USSR (NLL-M-20697-5828.4F) 21 p3422 N71-34352

Spatial distribution of absorbed atmospheric radiation over whole earth (NLL-M-20721-5828.4F) 23 p3842 N71-37397

Remote radar sensing of ocean surface, atmospheric laser transmission near 5 microns, and various elements in electronics, mathematics, meteorology, nuclear and atomic physics, ocean technology, optics, solid state physics, and space antenna system 23 p3855 N71-37476

Atmospheric transmission of infrared radiation near 5 microns 23 p3855 N71-37478

Development of four dimensional atmospheric models from global data for predicting atmospheric attenuation encountered by earth resources observation sensors (NARS-CR-61362) 24 p3951 N71-38189

Radiation attenuation due to aerosols (NLL-M-20965-5828.4F) 24 p4004 N71-38537

ATMOSPHERIC BOUNDARY LAYER

Measurement of maximum nocturnal winds at White Sands Missile Range, New Mexico (AD-712325) 03 p0269 N71-12187

Vertical momentum and heat transfer determinations in atmospheric boundary layers at sea (AD-711376) 03 p0361 N71-12173

Limited area seven layer physical and numerical model for lower troposphere 05 p0403 N71-12050

Similarity model for atmospheric turbulence structure in planetary boundary layer (AD-713569) 05 p0667 N71-14695

Meteorological data for developing engineering boundary layer wind model of gust loads on structures (NARS-TM-X-66547) 05 p0777 N71-15305

Technique for determining wind and temperature vertical gradients in surface boundary layer (AD-714366) 06 p0891 N71-16319

Hydrodynamic theory applied to climatology and general atmospheric circulation and numerical analysis of micro-atmospheric processes (AD-716023) 12 p1955 N71-23838

Numerical variational analysis of wind, pressure, temperature, and moisture values for atmospheric boundary layer forecast model and prediction of equal line formation 12 p1955 N71-23841

Autocorrelation and cross correlation of high frequency atmospheric boundary layer temperature and velocity fluctuation measurements (AD-721540) 16 p2587 N71-20408

Radiosonde and radar echo measurements on area of air/sea interactions over tropical ocean surface with numerical weather forecasting (NARS-CR-119764) 19 p3199 N71-32731

Oceanographic and meteorological research on sea/air interactions over tropical ocean surface 19 p3200 N71-32732

Oceanographic and meteorological measurements on air/sea energy flux in atmospheric boundary layer over tropical ocean region 19 p3200 N71-32733

Mass and energy budget calculations for atmospheric boundary layer over tropical ocean surface 19 p3131 N71-32734

ATMOSPHERIC CHEMISTRY

Simultaneous measurement of atmospheric dust by laser and balloon sounding (NARS-CR-111790) 01 p0045 N71-10042

Research on Arctic sea ice heat and mass budget, sea ice drift, micrometeorology, radiation, atmospheric chemistry, and Arctic oceanography (AD-715450) 08 p1190 N71-18731

Characterization of chemically generated waves in dilute, isothermal atmosphere and numerical analysis of chemical reactions involved (NARS-TM-X-65478) 10 p3142 N71-21285

Atmospheric radiochemistry and radioactive fallout and deposition from nuclear explosions (ORO-2529-28) 11 p1822 N71-22430

Development of theoretical mechanism for producing reactions and conditions involved in air pollution 11 p1897 N71-22649

Fluorine absorption processes of gases important in upper atmospheric chemistry and physics, mainly in the stratospheric region (AD-723507) 18 p2921 N71-31590

Bibliographies of air pollution emission sources created by municipal incineration
[AD-92] 20 p3268 N71-33787

ATMOSPHERIC CIRCULATION

Tidal motions in E region as source of daily variation of geomagnetic field
[AD-71782] 01 p0051 N71-10849

Long term variability of tropical heat budget of Pacific Ocean and effects on atmospheric circulation
[AD-71308] 05 p0252 N71-11140

Atmospheric radiation investigations using atmospheric circulation model
02 p0257 N71-11673

Wave-like structures in E-region derived from drift experiments
[AD-712346] 02 p0230 N71-12093

Numerical simulation of atmospheric flow over idealized mountains
[AD-712785] 05 p0403 N71-13049

Satellite observation of atmospheric energetics
[PB-192447] 05 p0403 N71-13174

Fluorescent particle diffusion test for determining atmospheric model of chemical warfare agents in forest area
[AD-713609] 05 p0404 N71-13376

Grey gas approximation of thermal radiation effect on Venus atmospheric model circulation
[NASA-CR-111736] 04 p0612 N71-14179

Meteorological parameters in lower atmosphere
[AD-713783] 05 p0715 N71-14520

Meridional flow, relative angular momentum, and energy flux calculations for International Geophysical Year
[MFT-O-808C] 05 p0673 N71-14878

Atmospheric circulation and hydrodynamic weather forecasting
[AD-713775] 05 p0718 N71-15397

Climatological and circulation epochs in Northern Hemisphere in first half of 20th century
[TT-70-50556] 06 p0886 N71-15760

Atmospheric circulation variations and mean monthly air temperature anomalies in Northern Hemisphere
06 p0886 N71-15761

Statistical analysis of elementary circulation mechanisms during Northern Hemisphere winter
06 p0886 N71-15762

Atmospheric energy processes in winter over Northern Hemisphere
06 p0887 N71-15763

Climatology in extreme decades and displacement of Arctic intrusion axes
06 p0887 N71-15764

Winter circulation and temperature conditions in Far East sector of Northern Hemisphere during two epochs
06 p0887 N71-15765

Atmospheric circulation and temperature fluctuation in eastern Siberia
06 p0887 N71-15766

Precipitation amounts in East Siberia during two circulation epochs
06 p0887 N71-15767

Comparison of extremal periods of circulation epochs over European USSR and West Siberia
06 p0888 N71-15768

Circulation conditions and monthly average temperature and precipitation anomalies over European USSR
06 p0888 N71-15769

Atmospheric circulation relationships and Moscow weather during January
06 p0888 N71-15770

Numerical methods for dynamic meteorology and weather forecasting problems, and atmospheric circulation dynamics
[AD-714749] 06 p0890 N71-15982

Stationary nonlinear model of atmospheric circulation
[AD-714763] 06 p0890 N71-16045

Potential energy model for computing diabatic processes in multilayer atmospheric circulation
06 p0896 N71-16796

Energy of auroral charged particles drawn from solar wind, earth rotation, and atmospheric circulation, and infrared generation from electric current interactions
07 p1014 N71-16930

Model of global circulation induced by solar radiation and auroral heating, for determining semiannual effect in atomic oxygen concentration
[NASA-TM-X-65443] 07 p1018 N71-17261

Numerical analysis of frontal motion in atmosphere
[AD-715068] 07 p1054 N71-17734

Mean monthly tropospheric circulation and cloudiness over Southeast Asia
[AD-715912] 08 p1230 N71-18671

Development and characteristics of global atmospheric circulation model
08 p1231 N71-18996

Lecture papers from symposium on general ocean circulation theory
[NCAR-TN-51] 09 p1379 N71-19501

Numerical modeling of Antarctic circumpolar current
09 p1380 N71-19505

Solutions to theoretical problems in oceanography
09 p1380 N71-19506

Transient ocean circulation models for Gulf of Mexico
09 p1380 N71-19507

Numerical models of ocean circulation
09 p1381 N71-19509

Meander circulation patterns of Gulf Stream
09 p1381 N71-19513

Ocean circulation modeling technology
09 p1381 N71-19514

Trajectory model data for numerical weather forecasting
[AD-716811] 10 p1593 N71-20645

Harmonic analysis of seasonal variations of atmospheric circulation in Northern Hemisphere
11 p1552 N71-22006

Formation of thermal radiation regime of Arctic based on atmospheric circulation in Northern Hemisphere
11 p1754 N71-22817

A.A. Girs rebuttal to review of his research on role of atmospheric circulation in formation of thermal regime in Arctic
11 p1754 N71-22818

Improved accuracy of long range forecasting through prediction of sign of frequency anomaly of atmospheric circulation
11 p1754 N71-22823

Influence of solar corpuscular radiation emissions on changes of meridional forms of atmospheric circulation
11 p1756 N71-22838

Tropospheric model for air mass circulation effect on ultrahigh frequency transmission
11 p1820 N71-22951

Synoptic weather maps of Northern Hemisphere for August, 1970
12 p1932 N71-23249

Synoptic weather maps of Northern Hemisphere for January through March, 1969
[QR-1-PT-1] 12 p1933 N71-23290

Total heat budget between ocean-atmosphere in Arctic Basin for military utilization
[AD-717967] 12 p1906 N71-23351

Thermospheric wind circulation excited during magnetic storm shown as effective mechanism for removing atomic oxygen at high latitudes
[NASA-TM-X-65508] 12 p1906 N71-23366

Synoptic weather maps of Northern Hemisphere for September, 1970
12 p1933 N71-23680

Seasonal variations of geophysical process interaction in Northern and Southern Hemispheres in total atmospheric circulation
[AD-718477] 12 p1911 N71-23686

Salt particle origins, jetstream into air, inland transport, impingement, incrustment, dry or precipitative fallout, and return to sea in sea-salt atmospheric cycle - bibliography
[AD-718613] 12 p1913 N71-23732

Hydrodynamic theory applied to climatology and general atmospheric circulation and numerical analysis of macro-atmospheric processes
[AD-718623] 12 p1955 N71-23838

Solar corpuscular streams and atmospheric circulation influenced by seasonal variations
[NASA-TT-F-13625] 12 p1993 N71-23894

Nonexpanding reflecting balloon for radar measurement of stratospheric circulation
[NLL-M-20296-5828.4F] 12 p1857 N71-23934

Atmospheric model of circulation epochs and long range predictions for Northern Hemisphere
[NLL-M-20296-5828.4F] 12 p1957 N71-24018

Stratospheric meteorological charts of daily constant pressure level heights and temperatures from rawinsonde-rocketsonde data and polar, middle, and tropical circulation for 1970
[QR-3-PT-3] 12 p1958 N71-24104

Long term variations of atmospheric circulation over Northern Hemisphere and its sectors
[NLL-M-20676-5828.4F] 12 p1959 N71-24334

Planning of GARP tropical experiments noting tropospheric motions and cloud clusters
13 p2105 N71-24469

Spectral model of winter stratospheric circulation, radiative effects including solar absorption by ozone and Newtonian approximation to infrared cooling
13 p2106 N71-25827

Numerical atmospheric modeling of planetary circulation over limited region
[AD-719867] 13 p2106 N71-25861

Measurement of upper atmospheric wind circulation
13 p2074 N71-25864

Nimbus 2 high resolution infrared radiometer data on cloud motion for determining wind velocities
13 p2108 N71-25261

Ionic hydrogen to oxygen transition level variations caused by atmospheric winds
13 p2108 N71-25266

Polar front jet stream maintenance, and numerical simulation of stratospheric trace substance transfer and ozone transport
[AD-719893] 14 p2286 N71-25682

Horizontal neutral air winds arising from diurnal variation of atmospheric pressure during seasonal and solar cycle changes
[AD-720347] 14 p2349 N71-30008

News releases concerning assimilation of Arctic ice, and solar activity effect in atmosphere
15 p3436 N71-30009

Project planning for observation of atmospheric circulation and heat budget over the Atlantic Ocean using international collaboration and satellite observation
15 p3437 N71-30071

Atmospheric energy transport over North America calculated from radiosonde data
15 p3399 N71-32707

Radiation influence on atmospheric circulation
15 p3438 N71-32708

Radiation processes for atmospheric dynamic models
15 p3440 N71-32717

Circulation patterns at 850, 700, 500, and 200 mb over Eastern Hemisphere from 40 day epoch to 40 day epoch during May and June, 1956 to 1960
[MET-O-806D] 15 p3440 N71-32811

Data processing methods for improving F70-16 radar/lidar system measurements of atmospheric motion
[NASA-CR-118997] 16 p3624 N71-30002

Autocorrelation and cross correlation of high frequency atmospheric boundary layer temperature and velocity fluctuation measurements
[AD-721548] 16 p3587 N71-30006

Statistical data plan for reduction of raw data from Barbados Oceanographic and Meteorological Experiment, BOMEX
[COM-71-01018] 16 p3626 N71-30007

Relationship between atmospheric cause content and stratospheric warming
[NLL-M-9270-5828.4F] 16 p3589 N71-30006

Review of numerical experimentation related to global atmospheric research program
17 p3777 N71-30008

Atmospheric and meteorological aspects of air pollution - survey of USSR air pollution literature
[PB-190661] 17 p3742 N71-30011

Vertical air mass exchange in troposphere studied by isotopic labeling
[NLL-M-9265-5828.4F] 17 p3744 N71-30007

Radiation measurements from polar and synchronous satellites applied to problems of atmospheric circulation and energetics
[NASA-CR-119240] 18 p2910 N71-30002

Numerical analysis of ring convection parameters and effect of variable resolution on cellular convection
18 p2915 N71-30004

Graphic analysis to determine probability of tropical storm location at specific times
18 p2952 N71-30010

Multilevel primitive equation model for simulating development of tropical cyclones
[ESSA-TM-5811-TM-NIELL-82] 18 p2952 N71-30015

Analysis of hemispheric circulation and monthly patterns when tropical storms reach hurricane intensity
[ESSA-TM-WB-TM-SR-46] 18 p2953 N71-30010

Frequency density spectra of atmospheric motion
18 p2916 N71-30009

Variations of atmospheric circulation in Northern Hemisphere
[AD-722840] 18 p2954 N71-30016

Traveling ionospheric disturbance studies by CW Doppler phase-path sounding array
[AD-723518] 19 p3083 N71-30079

Upper and lower level wind data tables from rawinsonde soundings over Palmyra, Fanning, and Christmas Islands
[NCAR-TN/STR-35-VOL-2] 19 p3129 N71-30070

Air pollution in relation to certain atmospheric and meteorological conditions and methods employed in survey and analysis of air pollutants
[PB-198327] 19 p3086 N71-30080

Atmospheric circulation and aerosol pollution transport noting role of temperature inversions
[IPA-RDP-56] 20 p3215 N71-30080

Atmospheric circulation in Northern Hemisphere and possible effects of polar ice destruction on climate and climatology
[NLL-M-20595-5828.4F] 21 p3422 N71-30040

Surface layer stability parameter distribution over USSR and over time
[NLL-M-20714-5828.4F] 21 p3423 N71-30039

Effect of subtropical anticyclones on development and position of intertropical convergence zone
[NLL-M-20650-5828.4F] 21 p3454 N71-30039

Effect of solar activity on distribution curves for natural relaxation oscillations
[NLL-M-20596-5828.4F] 21 p3393 N71-30070

Chemical composition, meteorological parameters, cloud layer, atmospheric circulation, upper atmosphere, and origin and evolution of Venusian atmosphere
[NASA-TT-F-137722] 21 p3397 N71-30080

SUBJECT INDEX

Mathematical model of atmospheric circulation around Venus based on hydrodynamic equations of spheres and Greenhouse effect
[NASA-750983] 21 p3510 N71-35015

Computer program for predicting atmospheric shear-layer instability and clear air turbulence induced by mountain waves
[NASA-CR-122841] 22 p3489 N71-35701

Cloud seeding technological development and effects on cloud growth with applications
23 p3786 N71-36981

Analysis of synoptic scales of atmospheric motion by means of synoptic network supplemented by satellite cloud observations
[AD-726525] 23 p3791 N71-37020

Global atmospheric research program on numerical weather forecasting, Atlantic tropical experiment, and storm activities
23 p3793 N71-37034

Tables of synoptic meteorological observations - Hawaiian and selected North Pacific coastal marine area
[AD-727909] 24 p3953 N71-38203

Two-dimensional numerical model of large scale mountain-plate circulation including sloping plain effects for analysis of convective patterns in the Colorado Rockies
24 p3954 N71-38208

Differential heating effects on steady-state tropical cyclone dynamics and energetics based on diagnostic quasigeostrophic model in isentropic coordinates
24 p3954 N71-38209

Analysis of influence exerted by solar activity on changes in circulation in earth atmosphere
[NL-4-20041-5828.47] 24 p4004 N71-38555

ATMOSPHERIC COMPOSITION
BY ATMOSPHERIC COMPOSITION
BY ATMOSPHERIC COMPOSITION

Simultaneous measurement of atmospheric dust by laser and balloon sounding
[NASA-CR-111798] 01 p0045 N71-10042

Review of knowledge on upper atmosphere
[AD-716953] 01 p0048 N71-10460

Steady-state nondivergent Ginzburg computer model for simulating air quality in region of New York City
[NS-3932] 01 p0013 N71-10712

Radio acoustic sounding system for remote measurement of atmospheric parameters
[AD-712352] 02 p0179 N71-11261

Selected articles on space exploration, lunar landing vehicles, and atmospheric parameters
03 p0297 N71-12157

Atmospheric fine structure effect on aerosol vertical distribution in mountainous regions
[AD-713824] 03 p0402 N71-12259

Measurement of atmospheric ozone using satellite infrared observations in 9.6 micron band
[NASA-CR-111566] 03 p0509 N71-13089

Chemical and environmental factors affecting ozone concentrations in lower troposphere
[NS-PUBL-234] 03 p0570 N71-13125

Resonance fluorescence techniques for determining upper atmosphere hydrogen radical
[NASA-CR-115883] 05 p0639 N71-14744

Seasonal intensity of F-region explained in terms of ionization changes in lower atmosphere
[NASA-TM-X-65410] 05 p0669 N71-14804

Development of meridional model of oxygen-hydrogen atmosphere
[AD-713821] 05 p0672 N71-14866

Optical radar observations of stratosphere and mesosphere
05 p0672 N71-14869

Lidar observations of lower troposphere over BOMBAY area
[IND-35532] 05 p0673 N71-14900

Measurement of molecular and aerosol backscatter from stratosphere by ground-based ruby laser
05 p0677 N71-15488

Program design and methodology data summary for atmospheric reaction studies in Los Angeles, California-Bad. V-61
[NS-409651] 05 p0678 N71-15506

Radio measurements in atmosphere or in sea
[NS-40404] 05 p0678 N71-15520

Atmospheric contamination by Kr-85
[NSA-COMP-1350] 06 p0911 N71-15799

Mass concentration and particle size distribution within nuclear condensing cloud during first four hours after formation
[NSCL-59044] 06 p0949 N71-15846

Abstracts and book outlines on Soviet meteorology
06 p0972 N71-16512

Statistical analysis of simultaneous two-station meteorological readings
[AD-714192] 06 p0983 N71-16571

Air pollution and soiling index for Saint Louis, Missouri, 1968
[NS-154703] 06 p0984 N71-16655

Air pollution and soiling index for District of Columbia, 1968
[NS-154703] 06 p0985 N71-16656

Air pollution and soiling index for Denver, 1968
[NS-154703] 06 p0985 N71-16657

Air pollution and soiling index for Philadelphia, Pennsylvania, 1968
[NS-154701] 06 p0985 N71-16658

Air pollution and soiling index for Cincinnati, 1968
[NS-154708] 06 p0985 N71-16726

Air pollution and soiling index for Chicago, 1968
[NS-154767] 06 p0985 N71-16745

Abstracts on Soviet meteorological research
07 p1652 N71-16957

Air pollution in southern Alaska
[NS-154074] 07 p1016 N71-16999

Air pollution control in Kanawha Valley, West Virginia
[NS-154881] 07 p1016 N71-17000

Development and characteristics of detectors for analysis of planetary atmospheres
[NASA-CR-116406] 07 p1116 N71-18020

Characteristics of low energy gamma rays in atmosphere
[AD-713271] 07 p1106 N71-18035

Survey on mechanisms of atmospheric precipitation scattering
[BNWL-SA-3450] 08 p1185 N71-18263

Biosphere sinks for carbon monoxide emissions to atmosphere
[NS-155433] 08 p1186 N71-18307

Diurnal variations of atomic and molecular oxygen concentration in 65 to 200 km altitude range
08 p1195 N71-19129

Rocket measurements of nitric oxide density profile in upper atmosphere with scanning ultraviolet spectrometers aboard Nike-Apache rocket vehicle
[NASA-CR-16808] 08 p1195 N71-19135

Atmospheric propagation studies with phase-path Doppler sounder array
[AD-716541] 09 p1379 N71-19444

Atmospheric pollution by platinum in comparison with aerosol composition
[NSA-CR-1701] 09 p1385 N71-20185

Concentrations of principal ions in ionosphere at 100 to 200 kilometer altitude and factors which affect ion formation
10 p1553 N71-21482

Procedure for processing atmospheric composition data obtained through use of sweeping quadrupole mass spectrometer on OGO-4 satellite
[NASA-CR-117325] 10 p1529 N71-21544

Atmospheric factors in ice fog formation
[NS-156977] 10 p1598 N71-21617

Techniques and equipment for industrial air pollution monitoring and sampling
[IPRS-52566] 11 p1747 N71-22055

Kinetic methods for analyzing organic compounds using catalytic reactions
11 p1695 N71-22062

Freibach, launch, and inflight earth orbital environment data for HRAO spacecraft
[NASA-TM-X-64576] 11 p1831 N71-22178

Transformation in air components due to marked increase in temperature during reentry shock wave
11 p1813 N71-22640

Development of theoretical mechanism for producing reactions and conditions involved in air pollution
11 p1697 N71-22669

Atmospheric models of tropospheric refractive index structure for predicting phase deviations at very high frequencies
11 p1712 N71-22945

Atmospheric composition effects on electromagnetic wave propagation and precision of radio and optical locating systems
11 p1712 N71-22948

Tropospheric composition induced errors in ESSA microwave distance and angular position tracking measurements over water surface
11 p1712 N71-22949

Radio-optical path length measurements for determining atmospheric water vapor density and temperature
11 p1714 N71-22959

Atmospheric distribution of CO₂, O₂, O₃, water vapor, and other chemical tracers and global transport processes
[TID-25314] 12 p1911 N71-23656

Neutral helium, atomic oxygen, and molecular nitrogen densities measured by Explorer 32 mass spectrometers
[NASA-TD-D-7043] 12 p1997 N71-24084

Description of projects for determining effect of atmospheric pollutants on weather and climate
[NSA-TR-ERL-185-APCL-15] 12 p1998 N71-24115

Thermosphere composition and density variations
13 p2070 N71-24564

Atmospheric cycles analyzed to determine sources, abundance, and fate of gaseous atmospheric pollutants
13 p2075 N71-25147

Design and fabrication of measuring system to determine concentration and mobility of atmospheric ions
[NAS-LIB-TRANS-1435] 13 p2075 N71-25148

Aluminum 3 infrared detectors for remote sensing of global ozone
13 p2162 N71-25258

ATMOSPHERIC COMPOSITION

Atmospheric corrosion and air pollution effects
[FOA-1-C-1333-92] 14 p2279 N71-36239

Effects of atmospheric gas and moisture concentration, temperature, pressure, and wind velocity on human performance and skin water loss rate
[NASA-CR-115824] 14 p2286 N71-36385

Performance data of undersea atmospheric sensor system to monitor and display atmospheric conditions
[NASA-CR-111800] 14 p2258 N71-36607

Electron and rotational transitions in ozone molecules and Zeeman and Stark effects on microwave spectra in atmospheric molecular composition
[AD-721187] 15 p2376 N71-36841

Investigation of optical properties of earth's atmosphere noting excitation of stellar objects, transparency of atmosphere, and twilight observation techniques
15 p2516 N71-36882

Atmospheric oxygen, water vapor, and carbon dioxide concentration effects on drop size and sodium compound structures in sodium laser networks
[AERB-B-6-6468] 15 p2377 N71-27448

Relationship between atmospheric ozone content and stratospheric warming
[NLL-4-5270-5828.47] 16 p2589 N71-38866

Remote air sampling and monitoring system for gas analysis of radioactive isotopes in containment atmosphere after loss of coolant tanks
17 p2744 N71-29045

Application of remote air sampling and monitoring system to nuclear power industrial safety and analysis of radioactive isotopes in containment atmosphere
17 p2744 N71-29046

Atmospheric sampling and analysis of ozone, water vapor, krypton, carbon dioxide, and radon radioactivity by thermal absorption and gas chromatography
17 p2746 N71-29067

Functionality measurements of atmospheric particle diffusion through high efficiency dust filters and relationships with dielectric polarization
17 p2744 N71-29071

Meteorological charts for air space over Toulouse-Mignac
18 p3951 N71-30952

Spectrophotometric ozone measurements for July through September 1968 in Belgium
18 p2916 N71-31041

Model studies on formation of organic compounds in simple atmospheric gases by electric discharges
[NASA-TT-F-13757] 18 p2887 N71-31312

Correlation between solar radiation and hourly and seasonal variations for calculating atmospheric turbidity
18 p3007 N71-31517

Tables of aerological ozone soundings over Germany
[AD-72406] 19 p3126 N71-31716

Correlation between ozone in earth atmosphere and cosmic ray cosmic intensity measurements
[AD-723330] 19 p3175 N71-31941

Data tables from aerological ozone soundings by German meteorological observatory for 1970
[AD-723487] 19 p3130 N71-32580

Data tables from aerological ozone soundings by German meteorological observatory for 1969
[AD-723437] 19 p3130 N71-32631

Simulation of radon removal from atmosphere by means of artificial fog
20 p3237 N71-33038

Scintillation counter for radon ion density measurements in atmosphere
[JFA-RDP-32] 20 p3271 N71-33040

Spectrophotometric ozone measurements for second quarter of 1968 from Belgian weather station
20 p3260 N71-33287

Meteorological and atmospheric electric data from Bombay observatory for 1967
20 p3269 N71-33969

Investigation of ultraviolet glow of atmosphere at wavelength of 1304 angstrom from Comet 315 satellite
21 p3428 N71-34332

Inventory of automatic sampler-analyzer, mechanical samplers, and static samplers used for air pollution monitoring in US and Puerto Rico
[NS-156329] 21 p3428 N71-34334

Composition of upper ionosphere as shown by magnetic mass spectrometer flown on Explorer 31
[NASA-CR-121663] 21 p3426 N71-34379

Estimation of governmental and private expenditures for prevention and control of air pollution
[S-DOC-92-4] 21 p3532 N71-35175

Application of aerospace and defense industry resources and technology to solution of environmental problems
21 p3533 N71-35180

Composition of planetary boundary layer and representation by boundary layer along gas phase
[TID-25465] 22 p3469 N71-34143

Forecasting of atmospheric processes by assessment of rhythmic recurrence frequencies
[NLL-4-20441-5828.47] 23 p3792 N71-37020

Development of mathematical meteorological diffusion models for analysis and solution of urban air pollution problems
[NLL-M-20342-5828.4F] 23 p5792 N71-37031

Composition of planetary atmospheres and comets
23 p5846 N71-37413

Pressure and temperature determination in Venus atmosphere from decimeter and millimeter wave radio transmission from Venus probes
[PB-16] 23 p5835 N71-37479

Flight sampling of flora using atmospheric probes
[NASA-CR-114378] 24 p3920 N71-37938

ATMOSPHERIC CONDITIONS

U METEOROLOGY

ATMOSPHERIC CONDUCTIVITY

NT IONOSPHERIC CONDUCTIVITY

ATMOSPHERIC DENSITY

Developing models of atmospheric density to formulate algorithms for control of spacecraft motion in atmosphere
[NASA-TT-F-13359] 01 p0045 N71-10046

Observation and measurement of ground visibility for meteorological purposes
01 p0078 N71-10119

Review of knowledge on upper atmosphere
[AD-710693] 01 p0048 N71-10460

Measuring variations in density of upper atmosphere and effects on satellite orbits near earth
[RAE-TR-69102] 02 p0208 N71-11392

Measuring atmospheric density above 180 km by variations in satellite orbits
[RAE-TR-69054] 02 p0208 N71-11394

Seasonal model for density in altitude range 45 to 90 km at Woomera [31 deg S]
[WRE-TN-E8A-174] 02 p0213 N71-11700

Determination of short term atmospheric density variations from quasi-simultaneous visual observations of artificial satellites
[NASA-TT-F-13288] 1 p0367 N71-12748

Atmospheric density and rotation below 195 km from high resolution drag analysis of OV-1 satellite
[AD-72688] 03 p0374 N71-13382

Atmospheric densities from satellite drag data
[NASA-CR-115998] 05 p0671 N71-14845

Deriving criteria for optimum detector by analyzing threshold conditions of vision from standpoint of information theory
[TT-70-50053] 05 p0719 N71-15513

Multivariate regression analysis of atmospheric density in region 30 to 100 km
[NASA-CR-115895] 05 p0679 N71-15533

Air density distribution in stratosphere
[NASA-TT-F-13456] 06 p0851 N71-16502

Mass spectroscopy rocket sounding data on neutral particle densities in Canadian lower thermosphere
[BBMW-FB-W-70-55] 07 p1018 N71-17151

Wavelet variations in ionosphere
[AD-714993] 07 p1023 N71-17874

Representation of heterospheric semiannual variation as density variation with amplitudes as functions of altitude
[NASA-CR-117137] 09 p1413 N71-19765

Atmospheric density changes observed from nine soundings over three and one half hour period, and determination of sensor random error
[AD-716995] 10 p1551 N71-21204

Frequencies of cyclonic vortices, mean air density, and horizontal air temperature gradients over Northern Hemisphere
11 p1755 N71-22826

Atmospheric density annual variations obtained from North Africa upper atmosphere radio probing
[GEOPHYSRDBW-FP/165-P7-10] 12 p1912 N71-23692

Thermospheric densities deduced from diffusion coefficient measured on aluminum oxide artificial clouds released from ESSO rockets
13 p2069 N71-24406

Thermosphere composition and density variations
13 p2070 N71-24564

Thermospheric density determined from ESSO rocket releases of aluminum oxide artificial clouds
13 p2070 N71-24568

Coordinated auroral electron observations from synchronous and polar satellites
[NASA-CR-118319] 13 p2074 N71-25082

Atmospheric density models for 30 N latitude for January and July for use in entry studies of Skylab command module
[NASA-TM-X-50600] 15 p2520 N71-27950

Phase and amplitude scintillations of microwave signals over elevated atmospheric path for obtaining atmospheric density profiles
[NASA-CR-111926] 16 p2561 N71-28431

Number density profiles for oxygen and nitrogen profiles in lower thermosphere compatible with US standard atmosphere for winter, summer, and equinox at 15, 30, 45, and 60 degrees N
[CON-71-50601] 16 p2580 N71-28498

Effects of atmospheric particles on fireball observations calculated for thermodynamic model showing mass of meteoritic material vaporized in fireball less than one pound per megaton bomb
[AD-722051] 16 p2588 N71-28608

Construction of N₂, O₂, and O densities in US standard atmosphere in 80 to 120 km range
[BSSA-TR-E8L-184-SDL-17] 17 p2738 N71-29304

Determination of heavy nuclear charge in atmosphere from formation density of delta electrons
[NASA-TT-F-13743] 17 p3005 N71-30395

Three-axis accelerometer for determination of atmospheric density with low altitude research satellites
[AD-722064] 18 p2926 N71-31470

Upper atmosphere density deduced from Cosmos satellite deceleration and applied to atmospheric models
19 p3097 N71-32784

Mesospheric ozone density measured by spectrophotometry of near ultraviolet radiation absorption during rocket sounding
[ADP-160] 20 p3256 N71-32938

Computation of atmospheric density variations at high altitude from Doppler observations made on polar satellites
[AD-724638] 20 p3256 N71-32986

Atmospheric density variations at 140 km deduced from precise satellite radar tracking data
[NASA-TM-X-64616] 21 p3416 N71-34304

Analysis of air density relationships to solar activity and geomagnetic disturbances based on ATS 2 orbital data
[RAE-TR-70084] 21 p3420 N71-34336

Analysis of orbits of five satellites to determine semiannual variation in air density in upper atmosphere
[RAE-TR-69254] 21 p3421 N71-34341

Method for estimating gravity wave density variation from wind speed profiles between 60 km and 100 km
[NASA-CR-61359] 22 p3572 N71-35436

Interpolation of synoptic and climatological atmospheric density profiles from constant pressure surfaces for use in ballistic trajectory calculations
[AD-726994] 22 p3580 N71-35498

Design, development, and characteristics of gamma backscatter atmosphere density sensor
[NASA-CR-111933] 22 p3583 N71-35519

Atmospheric density variations from satellite observations correlated to solar activity
22 p3678 N71-36228

Upper atmospheric density variations and solar activity analysis and correlation
22 p3679 N71-36230

Atmospheric density measurements by artificial satellites and comparison with atmospheric models
22 p3679 N71-36232

Two-dimensional time dependent diffusion model for phase delay between thermospheric density and temperature
[NASA-TM-X-65694] 23 p3747 N71-36719

Diurnal and semiannual variations of upper atmosphere density determined from Cosmos satellite drag data
[D-18] 23 p3751 N71-36744

Upper atmosphere atomic hydrogen density evaluation by comparison of high and low altitude electron content
24 p3915 N71-37912

ATMOSPHERIC DIFFUSION

Atmospheric diffusion of Ra-220 from point source of Th-228
[NP-18349] 04 p0575 N71-13680

Diffusion of aerosols in atmosphere near earth surface
07 p1052 N71-16923

Characteristics of chemically generated waves in dilute, isothermal atmosphere and numerical analysis of chemical reactions involved
[NASA-TM-X-65478] 10 p1542 N71-21303

Hyperbolic diffusion equation derived from classical parabolic equation
[AD-718616] 12 p1949 N71-23578

Atmospheric diffusion effects on ground surface pollution in northwestern Bohemia
[NLL-M-20310-5828.4F] 12 p1959 N71-24223

Atmospheric diffusion of tritium and other radioactive materials, fast neutron spectra of Cf-252, radiation rate of Cf-252 in D₂O spheres, and Co-60 gamma dose distribution
[UCRL-50067-70-2] 13 p2144 N71-25583

Atmospheric models for determining radioactive and marine aerosol particle diffusion into troposphere
[NP-18609] 15 p2405 N71-27700

Solutions of diffusion equation for expanding gas cloud in constant shear flow
[AD-72437] 17 p2739 N71-29649

Atmospheric and meteorological aspects of air pollution - survey of USSR air pollution literature
[PB-190061] 17 p2742 N71-29831

Numerical analysis of ring convection parameters and effect of variable reaction on cellular convection
18 p2915 N71-31014

Statistical analysis of long term atmospheric turbulence data for predicting atmospheric diffusion
[BC-DC-713920] 18 p2955 N71-31557

Theory of atmospheric diffusion in fog conditions and relation to air pollution
[AD-724104] 20 p3295 N71-32976

Mathematical and diffusion models for atmosphere and control of air pollution over urban areas
[PB-190400] 20 p3260 N71-32980

Comparison of turbulence intensity and stability ratio measurements and diffusive properties of a mesosphere
[BC-DC-70-5443] 23 p3575 N71-35498

Two-dimensional time dependent diffusion model for phase delay between thermospheric density and temperature
[NASA-TM-X-65694] 23 p3747 N71-36719

Atmospheric diffusion of beryllium exhaust gas from solid propellant rocket engines correlated to meteorological parameters
[AD-726999] 23 p3840 N71-36980

Derivation of diffusion equations under condition of no wind
[NLL-M-20351-5828.4F] 24 p3954 N71-37912

ATMOSPHERIC ELECTRICITY

NT AURORAL ELECTROJETS

NT ELECTROJETS

NT EQUATORIAL ELECTROJET

NT IONOSPHERIC CURRENTS

Atmospheric electricity criteria guidelines for spacecraft design
[NASA-TM-X-64549] 02 p0259 N71-11700

Atmospheric electricity measurement near the detector and correlation with VHF atmospheric [PB-4] 03 p0372 N71-13382

Geomagnetism, radioactivity, ionospheric parameters, cosmology, cosmic rays, and atmospheric electricity - Mar. 1970
06 p0840 N71-15513

Dourbes geophysical observatory, Belgium, data on geomagnetism, ionospheric propagation, cosmology, cosmic rays, and atmospheric electricity, April 1970
06 p0840 N71-15513

Atmospheric electricity, ionospheric conditions, cosmology, and geomagnetism, and cosmic ray data, Belgium, June 1970
07 p1018 N71-17150

Atmospheric electricity, ionospheric sounding, cosmology, and geomagnetism, and cosmic ray data, Belgium, June 1970
07 p1018 N71-17150

Analysis of reported incidences of ball lightning
[NASA-TT-F-13228] 07 p1036 N71-17150

Injun 5 double probe measurements of dc field in magnetosphere
[NASA-CR-116791] 08 p1187 N71-18880

Atmospheric potential gradient and cloud to ground lightning monitoring system design
[AD-716534] 09 p1412 N71-18880

Collection, reduction, and evaluation of electric field phenomena and geomagnetic field data at low and high altitudes
11 p1748 N71-35498

Hourly values of atmospheric and earth-surface potential gradients at Kakioka, Japan, for 1965
[REPT-71] 11 p1749 N71-35498

Effect of low frequency periodic perturbations of height of conducting surface on earth local electric field normal component
[AD-719428] 13 p2124 N71-30887

Tubulated upper air data obtained over Japan by radioondes for dew point, atmospheric electricity, and long wave radiation for 1966 and 1967
13 p2169 N71-30887

Simulation and measurement of electrical properties of lightning discharge by use of long sparks produced under laboratory conditions
[FAA-D8-69-16] 14 p2287 N71-25583

Validity of using laboratory produced sparks in evaluating properties of atmospheric lightning of description of parameters of primary importance
14 p2287 N71-25583

Qualitative analysis, quantitative analysis, and the dependent model of high speed time-resolved spectroscopic study of lightning return strokes
14 p2287 N71-25583

Determination of lightning temperature by spectroscopic channel capacity, temperature profile, and energy state distribution
14 p2287 N71-25583

Theoretical determination of temperature decay of lightning channel during interstroke period and the interval between lightning strokes and inhibition of jet leaders
14 p2287 N71-25583

Relationships between atmospheric electricity and meteorological parameters, noting vertical air motion and ionization
17 p2776 N71-29831

Dourbes Geophysical Observatory, Belgium, data on geomagnetism, ionospheric propagation, cosmology, cosmic rays, and atmospheric electricity, Feb. 1970
19 p3091 N71-31014

Upper atmospheric geophysical data for March 1970
20 p3256 N71-32976

Meteorological and atmospheric electric data from Bombay Observatory for 1967
20 p3269 N71-32980

SUBJECT INDEX

Evaluation of ball lightning observations and hypotheses concerning its theoretical interpretation and experimental reproduction
[NASA-TT-1-19932] 23 p3573 N71-35443

Development and characteristics of device for deployment of long wires as method of reducing loads due to lightning during spacecraft launches
[NASA-TM-X-63683] 23 p3756 N71-36772

Lightning and ball lightning phenomena in weapons systems; aerohydrodynamics and meteorology
[AS-DC-713590] 23 p3791 N71-37034

ATMOSPHERIC REENTRY
U AIRGLOW
ATMOSPHERIC ENTRY
NT HYPERBONIC REENTRY
NT REENTRY
NT SPACECRAFT REENTRY
Had shield technology for extraterrestrial atmosphere
[NASA-CR-111377] 02 p3045 N71-12057

Photography of Apollo 7 retrofire and service propulsion module reentry and apogee burn of Intelsat [S2] satellite
[NASA-CR-113089] 05 p0767 N71-14664

Attenuation, isolation, and radiation patterns of rectangular slot antenna in simulated plasma reentry flow
[AD-715702] 05 p0653 N71-14676

Reentry spacecraft for flight into space, atmospheric entry, and landing at selected sites
[NASA-CASE-XAC-62058] 05 p0794 N71-16087

Variable lift control of space vehicle during reentry in Martian atmosphere
06 p0952 N71-16085

Examining three-dimensional motion of flying vehicle entering atmosphere at low angles of attack
07 p0945 N71-16091

Shock wave formation and propagation during large spacecraft entry into atmosphere
[AD-715337] 08 p1191 N71-18008

Attitude technology for planetary entry heat shield
[NASA-TM-X-62946] 09 p1484 N71-20563

Development of method for measuring electron density gradients of plasma sheath around space vehicle during atmospheric entry
[NASA-CASE-XLA-62323] 09 p1451 N71-20563

Atmospheric model and on-line Mars atmospheric parameter measurement updating ahead of entry vehicle
[AD-717168] 10 p1643 N71-21065

Causes, effects, and diagnostic techniques of early plasma sheath
[AD-716423] 12 p1980 N71-23919

Science, navigation and trajectory, mechanical systems, and telecommunications design trade studies for Jupiter atmospheric entry mission planning
[NASA-CR-110821] 12 p1995 N71-24337

Higher atmospheric entry mission rationale with computational models, science criteria, mission and avionics evolution, baseline data, mission design, and alternative sample missions
[NASA-CR-110822] 12 p1999 N71-24338

Unmanned planetary and technical reentry vehicles for Jupiter atmospheric entry mission in 1978 using WEP or Pioneer F/G spacecraft
[NASA-CR-110823] 12 p2080 N71-24339

Analysis of surface mounted aperture antenna for measurement of microwave reentry plasma diagnostics
[AD-716961] 13 p2146 N71-24593

Aerodynamic and heating problems of spacecraft entry into Mars and Venus atmospheres
[AD-717285] 13 p2172 N71-24705

Streamline ovalization by laminar boundary layers
[AD-717940] 13 p2065 N71-24743

Penetration of electrons from high temperature shock layer of blunt reentry vehicle at high altitude
[AD-717938] 13 p2067 N71-25171

Effect of reentry plasma sheath on very high frequency and superhigh frequency telemetry signal propagation
[AD-717940] 13 p2067 N71-25185

Analysis of radioactively structured shock wave flow around reentry vehicle
[AD-720021] 14 p2239 N71-25927

Ring control method for space shuttle orbital entry recovery guidance
14 p2344 N71-26071

Orbital entry trajectory analysis for rigid glide descent of space shuttle to landing site
14 p2344 N71-26072

Science impedance measurements in compressible plasma during atmospheric entry
[AD-720263] 14 p2322 N71-26146

Reentry device for observing entry direction
[NASA-CR-36] 15 p2513 N71-27102

Study on impact dispersion of winds and density changes from standard atmosphere derived by solution of approximate equations
[AD-721351] 16 p2678 N71-28317

Development of motion control algorithm for spacecraft under atmospheric entry conditions at hypersonic speed
[AD-722385] 17 p2849 N71-29531

Determining heat transfer to space vehicles entering planetary atmospheres for proper design and thermal protection
[NASA-SP-09642] 18 p3025 N71-31179

Numerical method of intensity adjustment for calculating inviscid flow fields about convex and concave shapes on atmospheric entry with obstacles
[NASA-CR-121371] 20 p3363 N71-32801

Navigational requirements for space shuttle reentry noting effects of plasma sheath and restrictions on distance from selected landing area
20 p3300 N71-33058

Development of perturbation method to calculate optimal three dimensional reentry trajectories for Apollo vehicles
21 p3511 N71-33022

Analysis of reentry protection performance of silver impregnated zirconium oxide from material with lithium hydride backup
[TID-254565] 22 p3594 N71-35593

Approximate optimal atmospheric entry trajectories maximizing terminal function of velocity, heading angle, flight path angle, and altitude
[NASA-CR-113145] 22 p3669 N71-36158

Preliminary feasibility of depositing atmospheric entry probe from flyby mission to Jupiter
[NASA-TM-X-23358] 22 p3670 N71-36166

Analytic functions solving equations of motion in Newton theory for ballistic trajectory in atmospheric reentry
[DLR-FB-71-16] 22 p3670 N71-36168

Control of angular motion of space vehicle during atmospheric reentry
23 p3839 N71-37311

Science and engineering tradeoffs for Jupiter atmospheric entry probe mission
[NASA-CR-123120] 24 p4006 N71-38363

ATMOSPHERIC ENTRY SIMULATION
Wind tunnel method for simulating flow fields around blunt vehicles entering planetary atmospheres without involving high temperatures
[NASA-CASE-LAR-11158] 09 p1578 N71-20436

Facility for simulating reentry flow fields over blunt-nosed bodies
11 p1740 N71-22634

Dynamic flight control simulation for straight wing space shuttle booster entry
14 p2343 N71-26069

Laboratory means to measure diffusion coefficient for characterization of turbulent plasma in reentry simulation
[AD-726731] 23 p3829 N71-37312

ATMOSPHERIC HEAT BUDGET
International studies on air pollution, atmospheric heat budget, and real time data processing operations
06 p086 N71-15755

Atmospheric heat budget calculator from solar radiation characteristics in clear and cloudy conditions
[TT-70-50055] 11 p1822 N71-22043

Project planning for observation at atmospheric circulation and heat budget over the Atlantic Ocean noting international collaboration and satellite observation
15 p2437 N71-26972

Radiation measurements from polar and synchronous satellites applied to problems of atmospheric circulation and energetics
[NASA-CR-119240] 18 p2910 N71-30742

ATMOSPHERIC HEATING
Joule heating of upper atmosphere caused by geomagnetic perturbations
[NASA-TM-X-64508] 08 p1189 N71-18631

Influence of gravity waves on transient heating rates of upper atmosphere
[AD-716961] 13 p2069 N71-24425

Mathematical model for impulsive heat release by chemically generated waves in atmosphere
[NASA-TM-X-65500] 15 p3441 N71-27044

Electric power plant cooling tower effluent effect on urban atmospheric composition
[WB-197542] 18 p2920 N71-31487

One dimensional model for analytical solution to problem of impulsive heat release by chemically generated waves in dense, isothermal atmosphere
[NASA-TM-X-65641] 19 p3128 N71-32347

Radiative flux densities and heating rates in atmosphere calculated using pressure and temperature dependent cross-sections
21 p3423 N71-34359

Thermospheric heating by solar radiation in Schumann-Runge band as function of altitude and particle density
[D-14] 23 p3751 N71-36743

Genesis of sudden stratospheric warmings and related climatic cycles
[NASA-TD-D-6322] 24 p3953 N71-38282

ATMOSPHERIC IMPURITIES
U AIR POLLUTION
ATMOSPHERIC IONIZATION
NT AURORAL IONIZATION

ATMOSPHERIC MODELS

Abstracts of research on upper atmosphere and space
03 p0454 N71-13043

Investigating positive ions created in atmospheric air at pressures from 10 to 200 torr by glow discharge or by alpha irradiation from Po-210
[NP-10409] 06 p1252 N71-18505

Pulse radar for measuring wind speed in upper atmosphere by observing drift of ionized smoke trails
[AD-715922] 08 p1462 N71-18555

Concentrations of principal ions in ionosphere at 100 to 200 kilometer altitude and factors which affect ion formation
10 p1353 N71-21482

Production of electrons from high temperature shock layer of blunt reentry vehicle at high altitude
[AD-719730] 13 p2067 N71-25171

Failure of rocket flow electron accelerator to create artificial aurora
13 p0876 N71-25269

Aurora formation by electron injection and drift in upper atmosphere
13 p0876 N71-25272

Physiological effects of ionized air on mice acetylcholine/cholinesterase system
16 p2343 N71-28252

Radiation absorption in shock front of hypersonic air flow around blunt reentry body
[NASA-TT-F-13572] 16 p2382 N71-28837

Relationship between atmospheric electricity and meteorological parameters, noting vertical air currents and ionization
17 p2776 N71-29304

Transonic deceleration of solar wind via planetary, cometary, and interstellar gas, noting ionization processes
[TRITA-EFT-71-01] 22 p3454 N71-30800

Comparison of atmospheric lightning measurements under various meteorological and environmental conditions
[JPLA-CP-224] 23 p3790 N71-37016

ATMOSPHERIC MODELS
NT BREADBOARD MODELS
NT DYNAMIC MODELS
NT REFERENCE ATMOSPHERES
Constructing atmospheric models of Jupiter and Saturn for space vehicle design criteria
01 p0121 N71-10233

Theoretical van der Waals growth curves for pure absorption in Schuster-Schwarzschild atmospheric model
01 p0075 N71-10396

Calculating profiles of Stokes parameters and degrees of linear and circular polarization using narrow band blurring filter
[NASA-TM-X-64541] 01 p0075 N71-10439

Solar models for baroclinic and Rossby waves in magnetic fields, Rossby wave dynamics, thermal convection and rotation and shear flow, and magnetic reconnection instabilities
[AD-716629] 01 p0122 N71-10494

Atmospheric models and standard earth calculations from satellite observations
[NASA-CR-111128] 01 p0122 N71-10576

Model of global climate and ecology
[AD-711498] 01 p0079 N71-10732

Atmospheric radiation investigations using atmospheric circulation model
02 p0257 N71-11673

Seasonal model for density in altitude range 45 to 90 km at Woomera [31 deg S]
[WRE-TN-253A-174] 02 p0213 N71-11700

Numerical simulation of atmospheric flow over idealized mountains
[AD-712785] 03 p0403 N71-13049

Limited area seven layer physical and numerical model for lower troposphere
[AD-713808] 05 p0485 N71-17030

Grey gas approximation of thermal radiation effect on Venus atmospheric model circulation
[NASA-CR-111794] 06 p0812 N71-14179

Seasonal model for wind field in altitude range 35 to 75 km at Woomera, Australia
[WRE-TN-253A-172] 06 p0717 N71-15153

Transactions on numerical weather forecasting
[AD-713777] 06 p0718 N71-15220

Climate modification problems including ocean models, atmospheric radiation, convective and cumulus cloud models, and numerical weather prediction
[AD-713428] 06 p0718 N71-15252

Steady-state nonlinear model of atmospheric circulation
[AD-714763] 06 p0809 N71-16045

Electrical structure model of D and E regions, based on dynamic current theory
[AD-714365] 06 p0849 N71-16333

Analogs for refining numerical weather forecasts, and semiempirical model for forecasting hemispheric geopotential parameters
[AD-714425] 06 p0852 N71-16443

Stability of finite-difference methods to forecasting equations for barotropic motion in incompressible hydrostatic field
[NOAA-TM-JW8-NMC-49] 06 p0853 N71-16777

ATMOSPHERIC MODELS

Potential energy model for computing diabatic processes in multilayer atmospheric circulation

06 p0856 N71-16799
Turbulence effects and stochastic processes in three dimensional scatter simulation of tropospheric propagation

06 p0856 N71-16799
Lower atmosphere gravity wave propagation in stratified atmospheric models for pressure and wind variations

07 p1053 N71-17165
Reflection of transient VLF signals from stratified magnetospheric model of ionosphere

07 p0993 N71-17706
Atmospheric optical properties - tables and charts

[AD-715270] 07 p1022 N71-17814
Full wave solutions for ULF and ELF transmission through ionosphere

[AD-715301] 07 p1022 N71-17835
Computerized simulation of dispersion models for airport air pollution

[RE-3983] 07 p1055 N71-17923
Multiple source urban atmospheric dispersion model for Chicago air pollution

[ANL-RC-CC-7] 08 p1185 N71-18296
Exponential power law method for wind profile prediction in surface boundary layer

[AD-715349] 08 p1186 N71-18349
Arctic ionospheric model

[AD-715893] 08 p1190 N71-18664
Three dimensional primitive equation model from Boussinesq equations for application to mesoscale atmospheric phenomena

[AD-715547] 08 p1231 N71-18730
Development and characteristics of global atmospheric circulation model

08 p1231 N71-18998
Vertical eddy thermal transport and global energy budgets of mesosphere and lower thermosphere

[NASA-CR-117047] 09 p1379 N71-19465
Lecture papers from symposium on general ocean circulation theory

[NCAR-TN-51] 09 p1379 N71-19501
Linear theory for response of two-layer ocean model to moving hurricane

09 p1380 N71-19502
Numerical modeling of Antarctic circumpolar current

09 p1380 N71-19503
Free oscillations of fluid on hemisphere bounded by meridians of longitude

09 p1380 N71-19504
Modeling longshore currents from obliquely incident sea waves

09 p1380 N71-19505
Solutions to theoretical problems in oceanography

09 p1380 N71-19506
Transient ocean circulation models for Gulf of Mexico

09 p1380 N71-19507
Calculations on aggressive turbulence interactions

09 p1380 N71-19508
Numerical models of ocean circulation

09 p1381 N71-19509
Climate calculation with combined ocean and atmosphere model

09 p1381 N71-19510
Numerical oceanographic models of baroclinic flow

09 p1381 N71-19511
Ocean circulation modeling technology

09 p1381 N71-19514
Physicochemical properties and condensation growth rate equation for hygroscopic materials

[AD-716384] 09 p1413 N71-19659
Ionospheric irregularity characteristics from Explorer 22 Faraday readings of 40 MHz transmissions

[RSD-553] 09 p1384 N71-20047
Thermospheric density response to auroral heating during geomagnetic disturbance

[NASA-TM-X-65463] 09 p1385 N71-20284
Atmospheric models and synchronization time signal propagation delay

[NASA-TM-X-65460] 09 p1385 N71-20285
Hydrogen line blanketed stellar model atmospheres

[NASA-SP-3065] 09 p1462 N71-20410
Atmospheric model for investigating fronts and predicting frontal rainfall

[MET-O-836] 09 p1414 N71-20553
OGO-D atmospheric composition data for polar thermospheric storm model

[NASA-CR-183080] 10 p1546 N71-20638
Concentric sphere model of ionosphere for takeoff angle and length determinations in complex ray configurations

[AD-716963] 10 p1517 N71-20631
Atmospheric photochemical model for polar regions summer mesosphere and lower thermosphere

10 p1546 N71-20712
Atmospheric models for magnetospheric instabilities and magnetopause fine structure

[NASA-CR-117471] 10 p1547 N71-20853
Sound-gravity wave natural modes in solar atmosphere models

10 p1643 N71-20911
Atmospheric model and on-line Mars atmospheric parameter measurement updating each of entry vehicle

[AD-717108] 10 p1643 N71-21065
Ammonia and water properties in modelling Jupiter and Saturn atmospheres

10 p1644 N71-21340
Three fluids circulation model for analysis on tropospheric structure and dynamics

10 p1553 N71-21411
Atmospheric transport of X ray determination using liquid nitrogen to simulate air

[AD-716801] 10 p1555 N71-21736
Examination of deep space Doppler data for terrestrial media contamination

11 p1703 N71-22773
Propagation model for diurnal amplitude and phase variations of very low frequency transmission path

11 p1705 N71-22907
Thermospheric wind circulation excited during magnetic storm shown as effective mechanism for removing atomic oxygen at high latitudes

[NASA-TM-X-65500] 12 p1906 N71-23366
Atmospheric circulation model for analyzing tropospheric ultrahigh frequency signal fading

12 p1875 N71-23456
Auroral electrojet current model for polar magnetic substorms

12 p1908 N71-23554
Kelvin-Helmholtz wave model for predicting maximum amplitude, breaking mode, and turbulent kinetic energy

[AD-718841] 12 p1911 N71-23687
Transmission model effects on water vapor mixing ratios and radiance calculations for infrared horizon scanners

[NASA-TN-D-6112] 12 p1912 N71-23694
Numerical variational analysis of wind, pressure, temperature, and moisture values for atmospheric boundary layer forecast model and prediction of equal line formation

12 p1955 N71-23841
Numerical techniques for solving meteorological equations

[NOAA-TM-NWS-NMC-50] 12 p1957 N71-24004
Atmospheric model of circulation epochs and long range predictions for Northern Hemisphere

[NLL-M-30298/5828-AP] 12 p1957 N71-24018
Laboratory model of radio star signal diffraction by ionosphere or solar wind using 40 kHz airborne ultrasonic radiation and warm turbulent air diffracting screen

12 p1999 N71-24313
Jupiter atmospheric entry mission rationale with environmental models, science criteria, mission and system evolution, baseline data, mission design, and illustrative sample missions

[NASA-CR-118022] 12 p1999 N71-24338
Calcium K line formation in nonhomogeneous solar chromosphere

13 p2166 N71-24941
Numerical atmospheric modeling of planetary circulation over limited region

[AD-719867] 13 p2106 N71-25061
Flux-corrected radiative atmospheric models and metal abundances for R Cygnus

13 p2167 N71-25066
Atmospheric model for effects of water vapor, liquid water, and ice upon radiative transfer processes at microwave frequencies and in far infrared

[NASA-CR-61348] 13 p2106 N71-25079
Atmospheric model with damped gravity waves from vertical atmospheric sounding analyses

13 p2076 N71-25264
Atmospheric model for thermal plasma near equatorial plasmapause

13 p2076 N71-25270
Upper ionospheric electron density profiles calculated from lower ionosphere data

14 p2247 N71-25890
Reference atmosphere for Vandenberg AFB, California based on current annual tabulation of thermodynamic quantities

[NASA-TM-X-64590] 15 p2437 N71-26074
Radiation processes for atmospheric dynamic models

15 p3440 N71-27557
Simplified dynamic atmospheric model for radiative heat transfer eliminating use of absorption functions

15 p2440 N71-27559
Vertical spectral distribution of radiative flux divergence in infrared range computed for five atmospheric models

15 p2440 N71-27559
Atmospheric models for tenuous cloud effects on atmospheric heat infrared radiation flux

15 p2403 N71-27561
Atmospheric models for determining radiocative and marine aerosol particle diffusion into troposphere

[NP-18609] 15 p2403 N71-27760
Three dimensional thermospheric model developed from solar XUV radiation and corpuscular heating during geomagnetic storms of atmospheric system

[NASA-TM-X-65579] 15 p2406 N71-27774
Atmospheric density models for 30 N latitude for January and July for use in entry studies of Earth command module

[NASA-TM-X-58060] 15 p2520 N71-27800
Global cloud model for computerized simulation of earth-viewing space missions

[NASA-CR-61345] 15 p2518 N71-27800
Atmospheric model of Venus based on results of temperature, pressure, and gas composition measurements made by Venus satellites in troposphere of planet

[NASA-TT-P-13697] 16 p2677 N71-28000
Number density profiles for oxygen and nitrogen profiles in lower thermosphere compatible with standard atmosphere for winter, summer, and spring/fall at 15, 30, 45, and 60 degrees N

[COSM-71-50004] 16 p2588 N71-28000
Digital computerized simulation of transmission size wave transmission with tropospheric scattering including atmospheric model using meteorological parameters

16 p2562 N71-28000
Models of thermospheric neutral composition using molecular and turbulent diffusion

[D-4] 17 p2739 N71-28000
Solutions of diffusion equation for expanding gas cloud at constant shear flow

17 p2739 N71-28000
Research results on high latitude sporadic E layer plotted and displayed in corrected geomagnetic latitude and corrected geomagnetic time

[AD-722435] 17 p2740 N71-28000
Model of interaction of tropospheric fronts with tropopause based on analysis of 56 vertical sections of high fronts

[WLL-RTS-6362] 17 p2778 N71-28000
Critical survey of six thermodynamic and transport properties of air for range of pressures and temperatures corresponding to conditions experienced by aircraft

[AD-722402] 17 p2741 N71-28000
Interpretation of vertical wave patterns in winter atmosphere at high latitudes in terms of gravity wave theory

[NASA-TM-X-65605] 17 p2745 N71-28000
Atmospheric models for relating precipitation rate to monthly climatology

[AD-722684] 17 p2778 N71-28001
Studying diurnal oscillations of wind in planetary boundary layer using theoretical model

18 p2953 N71-31087
Standard, wet summer and winter, and dry summer and winter model atmospheric radiative heat flux spectral distributions

[NASA-TT-P-13824] 18 p2917 N71-31087
Model studies on formation of organic compounds in simple atmospheric gases by electric discharge

[NASA-TT-P-13757] 18 p2887 N71-31087
Interpolated meteorological charts used for atmospheric models in numerical weather forecasting

19 p3125 N71-31087
Conference papers on low level turbulence models to determine influence on aircraft stability and flight trajectories

[DLR-MITT-70-12] 19 p3036 N71-31087
Low level turbulence models for determining standard deviation of ballistic missile trajectories

19 p3127 N71-31087
Atmospheric turbulence models showing gust load influence on aircraft yaw motion

19 p3037 N71-31087
Electromagnetic field disturbance models for clear air turbulence detection in atmosphere

[AD-723312] 19 p3091 N71-31087
Correlation between muons in earth atmosphere and cosmic ray muon intensity measurements

19 p3175 N71-31087
Generation and propagation of tidal waves in three dimensional spherical model of thermospheric dynamics

[NASA-TM-X-65632] 19 p3179 N71-31087
One dimensional model for analytical solution of problem of impulsive heat release by chemically generated waves in dilute, isothermal atmosphere

[NASA-TM-X-65641] 19 p3128 N71-31087
Collisionless Boltzmann equation for model of rotating and nonuniform planetary exosphere

[NASA-TM-X-65662] 19 p3094 N71-31087
Magnetospheric model for dynamic plasma flows in polar magnetosphere

[NASA-R-119780] 19 p3095 N71-31087
Atmospheric effects on infrared multiplexed sensing of sea-surface temperature from space

[NASA-CR-18358] 19 p3130 N71-31087
Atmospheric models and strong-line profiles in pure absorption for late-type dwarf stars in 3200 to 3200 Å effective temperature range

19 p3182 N71-31087
Atmospheric models for observing air-sea, air-land interactions of Lesser Antilles

19 p3201 N71-31087
Upper atmosphere density deduced from COSMOS satellite deceleration and applied to atmospheric models

[D-80] 19 p3097 N71-31087

SUBJECT INDEX

SUBJECT INDEX

Thermospheric models accounting for diurnal variation of temperature and density during eclipses [P4] 20 p3254 N71-32821

Mathematical and diffusion models for abatement and control of air pollution over urban areas [P2-10409] 20 p3250 N71-32330

Two dimensional thermospheric model for ionospheric data, planetary waves, and magnetic disturbance 20 p3266 N71-33443

TR code dependence of 10 MeV proton cutoff latitude in image dipole model magnetosphere [WASA-TM-X-45676] 20 p3316 N71-33444

Model turbulence profiles for predicting optical effects of turbulence on stellar observations [NASA-TN-B-369] 20 p3312 N71-33499

Local thermospheric model for simulating earth's climate and testing ion age theories [NCAR-72085] 20 p3267 N71-33521

Atmospheric models of radiative processes, energy, and effects in mesosphere and thermosphere [NASA-CR-121468] 20 p3342 N71-33732

Atmospheric models and thermodynamic effects of global and Arctic Ocean in relation to causes of ice age climatology 20 p3368 N71-33804

Revised static models of thermosphere and ionosphere with empirical temperature profiles [NASA-CR-3352] 21 p3414 N71-34296

Analysis of N2A 3 Sigma positive molecular decays in aurora using atmospheric model based on ionospheric measurements [NASA-CR-121671] 21 p3415 N71-34301

Three-dimensional computer model of Venus-like atmosphere for calculating thermodynamic profiles [NASA-CR-121745] 21 p3415 N71-34302

Spectrum analysis of four O-type stars towards tails for thermospheric models of stars RZ 44, plus 25 qd 495, and HD 127495 21 p3311 N71-33019

Thermal stability of stellar chromosphere model 21 p3311 N71-33021

Evolution of ball lightning observations and hypotheses concerning its theoretical interpretation and experimental reproduction 21 p3373 N71-35445

Monte Carlo calculations of photoelectron motion in ionosphere 21 p3373 N71-35465

Convective instability in fluid layer with electromagnetic effects applied to earth and stellar atmospheres 22 p3672 N71-36183

Atmospheric density measurements by artificial satellites and comparison with atmospheric models 22 p3679 N71-36232

Lower atmosphere of Mars, Venus, and Jupiter 23 p3846 N71-37412

Development of four dimensional atmospheric model from global data for predicting atmospheric situation encountered by earth resources observation means [NASA-CR-61362] 24 p3951 N71-38189

ATMOSPHERIC MOISTURE

Measurement of atmospheric water vapor content over ocean surface 02 p0220 N71-12121

Design modifications to Mars atmospheric water detection spectrophotometer [NASA-CR-115091] 05 p0689 N71-15561

Effect of atmospheric humidity on characteristics of radio signals 07 p1103 N71-17728

Infrared detectors for balloon sounding of aerosols and atmospheric moisture [NASA-CR-61339] 08 p1302 N71-18930

Remotely sensed weather forecasting based on hydrodynamic and thermodynamic equations and accounting for atmospheric moisture transfer and radiative effects [AD-71607] 09 p1412 N71-19482

Lump, dust, and sulfate containing atmospheric sulfur number concentrations for aerosol air pollution New Mexico 10 p1551 N71-31165

Ice particle origins, injection into air, island transport, impingement, increment, dry or precipitative loss, and return to sea in sea-salt atmospheric cycle [AD-71607] 12 p1913 N71-23732

Radiation absorption by volcanic dust and its influence on atmospheric temperature and moisture [NASA-CR-30099-1828-4P] 12 p1914 N71-24175

Remote meteorological measurements of water vapor in atmosphere over selected mountain sites in southeast 14 p2338 N71-26216

High speed, and high resolution sensors for meteorological measurements of atmospheric temperature and moisture [AD-72056] 16 p2626 N71-28645

Atmospheric estimates in Germany from visibility measurements, noting influence of wind and atmospheric moisture 17 p2776 N71-29577

Pulsed ruby laser radar for studying water vapor distribution by atmospheric transmissivity [PB-197917] 17 p2778 N71-29747

Statistical correlation between atmospheric moisture content, aerosol particle size, and visual range [NLL-M-9267-1928-4P] 17 p2744 N71-29809

Comparison of radiances and laser backscatter data of atmospheric humidity [AD-723501] 19 p3125 N71-31677

Atmospheric temperature and moisture radiances tables and data reduction techniques used in analysis of atmospheric thermodynamics over Palmyra, Fanning, and Christmas Islands [NCAR-TN/STR-35-VOL-1] 19 p3129 N71-32506

Cosmos 243 thermal radio emission measurements of atmospheric moisture over ocean 19 p3130 N71-32575

Correction curves for humidity effects and flashover voltages in spark gaps [NLL-CE-TRANS-5347-1942.00] 19 p3088 N71-33705

Analysis of fluctuations in moisture content of troposphere based on division into large scale and small scale variations [POA-3-A-5729-68] 22 p3578 N71-35487

Improved pulsed laser radar system for spectroscopic measurement of spatial water vapor distribution in atmosphere 22 p3611 N71-35718

Atmospheric moisture transport into Antarctic interior based on Byrd station data analysis with mass transport model 23 p3785 N71-36977

ATMOSPHERIC NEUTRON FLUX DENSITY

U. ATMOSPHERIC RADIATION

U. NEUTRON FLUX DENSITY

ATMOSPHERIC NOISE

U. ATMOSPHERICS

ATMOSPHERIC OPTICS

Statistical characteristics of transverse beam displacements in turbulent atmosphere [AET-70-208-BULL.] 07 p1052 N71-16924

Activities related to atmospheric physics at IFA, Italy, during 1969 including surveying, atmospheric radiation, and atmospheric optics [IFA-TR-29] 15 p2396 N71-27062

Transmission functions in 15 micron carbon dioxide band 15 p2401 N71-27365

Monte Carlo method applied to some problems of atmospheric optics by narrow light scattered beams 15 p2403 N71-27359

Computer programming for atmospheric optics using Monte Carlo method 15 p2403 N71-27342

Atmospheric optics problem solving using Fredholm equations of first kind 15 p2403 N71-27343

Complex instrumentation for investigation of atmospheric optics 15 p2410 N71-27350

Soviet news releases on atmospheric optics, astrometry conference, and expanded high speed service 18 p2940 N71-30790

ATMOSPHERIC PHYSICS

NT CLOUD PHYSICS

Low-altitude satellite interaction study of neutral gases and Monte Carlo computer techniques for describing flow field and spacecraft interactions [NASA-CR-111194] 01 p0049 N71-10611

Distribution of temperatures, pressures, and densities in upper atmosphere 02 p0215 N71-11947

Satellite observation of atmospheric optics [PB-192447] 03 p0403 N71-13174

Detection of atmospheric regions of disturbed index refraction [PB-192345] 05 p0672 N71-14865

Abstracts on Soviet space program and atmospheric, ionospheric, and interplanetary research 07 p1020 N71-17491

Solar atmospheric physics and radiation effects on earth [AD-715456] 08 p1286 N71-18919

Project planning for quasi stationary meteorological satellite and orbital research laboratory experiments on atmospheric physics, temperature profiles, and horizon sensing [BMRW-FB-W-70-70] 11 p1831 N71-22181

Planning of first GARP experiment to study atmospheric circulation and physics and meteorological parameters in tropo- and stratosphere 13 p2105 N71-24467

Clear air turbulence in stratosphere and effects on weather formation, atmospheric physics, and supersonic flights [JPBS-53133] 14 p2346 N71-25746

Satellite data on upper atmospheric physics, and solar and stellar spectra 14 p2247 N71-23087

Earth orbital research program in atmospheric physics and space astronomy [NASA-EP-83] 15 p2517 N71-26991

ATMOSPHERIC PRESSURE

Activities related to atmospheric physics at IFA, Italy, during 1969 including surveying, atmospheric radiation, and atmospheric optics [IFA-TR-29] 15 p2396 N71-27062

Advances in atmospheric physics technology from sounding rocket and artificial satellite data [JPBS-53514] 16 p0677 N71-30891

Atmospheric budget equations for mass, momentum, and energy derived for Baruch Oceanographic and Meteorological Analysis Program (BOMAP) [COM-71-00195] 16 p2625 N71-28313

Aerospace problems for atmospheric dynamics study with three dimensional convection models, Ekman layer convergence, inertial stability, influence of horizontal wind shear, and boundary dynamics [COM-71-00216] 16 p2656 N71-28390

Determination of heavy metal changes in atmosphere from formation density of delta electrons [NASA-TT-F-15743] 17 p2805 N71-30395

Infrared spectrometry for meteorological and atmospheric physics studies [IFA-EP-81] 19 p3951 N71-36875

Fluxion absorption processes of great importance in upper atmospheric chemistry and physics, mainly in the ultraviolet region 19 p3127 N71-32802

Solar and atmospheric phenomena and global wind and fog investigations 19 p3127 N71-32802

Research projects, facility development, and organizational mechanism of National Center for Atmospheric Research 19 p3075 N71-32461

Subsolar red arc producing mechanism based on ionospheric and atmospheric equations [NASA-TM-X-45600] 21 p3416 N71-34303

Optical propagation measurements in inhomogeneous atmosphere at Escondido Lake, California for optical propagation theory validity testing [NASA-CR-11735] 23 p3732 N71-36733

Error analysis of Monte Carlo calculation for three structure of short duration light pulses reflected by atmosphere surface [NLL-M-20553-1980-4P] 24 p3932 N71-38358

ATMOSPHERIC PRESSURE

Peculiarities of human heat exchange under reduced atmosphere pressure and sufficient oxygen supply [NASA-TT-F-15374] 01 p0010 N71-10607

Time spectra of atmospheric temperature, pressure, and wind velocity variations above Atlantic Ocean [RAE-LIB-TRANS-1472] 02 p0253 N71-11448

Applying Kalman filtering to problems of barometric pressure and inertial height in navigation [RAE-TR-49131] 03 p0262 N71-11763

Atmospheric pressure and oxygen tensions effects on mice infections 02 p0163 N71-11813

Strain gauges on superpressure balloons flights from Christchurch, New Zealand - Jul 1968 to Dec. 1969 [NASA-CR-111410] 02 p0214 N71-11906

Global ground and 630 mb maps for Northern Hemisphere for period 1 Jan. to 31 Mar. 1970 04 p0542 N71-14275

Temperature, pressure, and related climatological data for Australia - tables for July 1970 05 p0672 N71-14061

Temperature, pressure, and related climatological data for Australia - tables for June 1970 05 p0716 N71-15088

Daily height and temperature analyses of constant pressure levels for Northern Hemisphere for second quarter 1970 06 p0809 N71-15933

Daily height and temperature analyses of constant pressure levels for Northern Hemisphere for second quarter 1970 06 p0809 N71-15936

Daily height and temperature analyses of constant pressure levels for Northern Hemisphere for first quarter 1970 06 p0809 N71-15937

Daily height and temperature analyses of constant pressure levels for Northern Hemisphere [OR-1-TT-1] 06 p0809 N71-15938

Current breakdown on stations in standard planetary atmosphere and atmospheric pressure 06 p0817 N71-16433

Lower atmosphere gravity wave propagation in stratified atmospheric models for pressure and wind variations 07 p1053 N71-17145

Effects of barometric pressure fluctuations on data recorded by inertial seismic equipment [AD-715896] 08 p1190 N71-18736

Infrared microbarometric phenomena correlation with long period seismograph signals [AD-716333] 09 p1302 N71-19638

Predicting location of baric formation centers and evolution in Arctic and Subarctic on third day based on variations of thermal field of troposphere and surface pressure variations 11 p1755 N71-23825

Possible effect of deformation forces on diurnal state of baric field and subsequently for short range weather forecasting 11 p1756 N71-23836

Atmospheric pressure annual variations obtained from North Africa upper atmosphere radio probing [GEOPHYSBDBW-FM/163-PT-8]

Monthly and annual tables of mean atmospheric pressure with monthly mean maps for Finland in 1931 - 1960 [REPT-21]

Solar corpuscular streams and atmospheric circulation influenced by seasonal variations [NASA-TT-F-13425]

Changes in surface pressure during polar cap and auroral absorption [NLL-M-20599-5828-4P/]

Upper atmosphere and rain data for Oahu and 500 mb trough effects on tradewind rainfall including seasonal variations [MIG-70-28]

Mariner 6 and 7 occultation data for determining temperature and pressure of Martian atmosphere [13 p168 N71-25277]

Results of radiosonde ascents from aerological station in Berlin, Germany including extreme and mean values of temperature, pressure, wind data, geopotential and other meteorological data [14 p228 N71-25884]

Meteorological charts and data tables for July through September, 1970 from Berlin [QR-3-PT-3]

Martian atmospheric temperature and pressure and temperature gradient determination by least squares differential correction of satellite photometric solar eclipses data [NASA-TN-D-6258]

Spatial coherence of 1 to 5 min acoustic waves from two nuclear explosions along with atmospheric pressure background noise for same period measured at low altitude [AD-720853]

Earth atmosphere pressure measurement using satellite network and radio microwave occultation technique [15 p2400 N71-27488]

Diurnal mean tropospheric heights data for North America [NOAA-TM-NWS-TDL-41]

Vertical accelerometers for observing ground motion caused by ocean tides, low frequency ocean waves, and atmospheric pressure [AD-723869]

Isentropic atmospheric pressure minimum seasonal migration due to oscillation of earth axis [AD-724501]

Drift of horizontal pendulums at Kanne, Belgium, in east-west direction noting atmospheric pressure effect [20 p3263 N71-33354]

Meteorological charts for Northern Hemisphere containing ground level and 850-mb height and temperature data for third quarter of 1970 [QR-3]

Meteorological charts for Northern Hemisphere containing ground level and 850-mb height and temperature data for fourth quarter of 1970 [QR-4]

Atmospheric-lithostatic pressure ratio effects on extensive crater dimensions in dry soil [NASA-TN-R-346]

Deformation anomalies of ocean surface related to atmospheric pressure distribution for potential long range weather forecasting technique [NLL-M-20599-5828-4P/]

Stratospheric weather maps of Northern Hemisphere containing daily height and temperature analysis of constant pressure levels [AD-721909]

Phase distribution, amplitude, and amplitude distribution in relation to latitude for 11 year fluctuations of atmospheric pressure caused by sun [NLL-M-20631-5828-4P/]

Pulse amplitude determination in air pulsed columns as function of air pressure reservoir and pulse frequency [BNWL-B-51]

Statistical analysis of tropical cloudiness and rainfall in relation to semidiurnal atmospheric tide and pressure variations [23 p3784 N71-36974]

Fluctuations of Florida current inferred from sea level records and linear weather effects [23 p3789 N71-37006]

Temperature, pressure, and related climatological data for Australia - tables for March 1971 [23 p3792 N71-37025]

Neutron component measurement and multi-channel recording of atmospheric pressure [24 p4012 N71-38614]

ATMOSPHERIC RADIATION

NT AIRGLOW
NT AURORAL ARCS
NT AURORAS
NT DAWN CHORUS
NT DAYGLOW
NT IONOSPHERIC NOISE
NT NIGHTGLOW
NT RED ARCS
NT SKY RADIATION

NT STRATOSPHERIC RADIATION

NT TROPOSPHERIC RADIATION

NT TWILIGHT GLOW

NT WHISTLERS

Atmospheric radiation investigations using atmospheric circulation model [02 p0257 N71-11673]

Millimeter wave radiometer for remote sensing of atmospheric stability in first mile of atmosphere [AD-723333]

Flow of radiation in earth atmosphere [AD-712699]

Radiative transfer in planetary atmospheres [AD-712590]

Abstracts and bibliographies of meteorological articles [11 p1788 N71-21953]

Theory and design of aspiration counters and atmospheric-ion current measurement [TT-68-50499]

Activities related to atmospheric physics at IFA, Italy, during 1969 including aeronomy, atmospheric radiation, and atmospheric optics [IFA-TR-29]

Radiation influence on atmospheric circulation [15 p2438 N71-27485]

Measurement of free atmosphere water vapor radiation angular distribution at 60 to 120 km altitude [15 p2400 N71-27498]

Radiation processes for atmospheric dynamic models [15 p2440 N71-27557]

Upper atmosphere helium fluorescence due to cycles of electron flux, solar ultraviolet radiation, and geomagnetic activity [NRC-TT-1458]

ATMOSPHERIC REFRACTION

NT RADIO WAVE REFRACTION

Radio sources and atmospheric effects on interferometer operating at 2695 MHz [01 p0120 N71-10151]

Observations of visible shock waves in atmosphere [AD-711123]

Remote probing of earth atmosphere by refraction measurements of microwaves propagated between occultation satellites [02 p0256 N71-11623]

Atmospheric refraction and reflection in sonic booms [NASA-TT-F-13409]

Atmospheric refraction and temperature profiles in lower atmosphere over Bay of Helligoland [REPT-12]

Error study for SS-1090 ATM sensor system, effects of atmospheric refraction, atmospheric attenuation, and earth albedo [NASA-CR-102957]

Detection of atmospheric regions of disturbed index refraction [PB-192345]

Atmospheric optical properties - tables and charts [AD-715270]

Influence of atmospheric refraction on minitrac interferometer system and correction procedures for computation accuracy [NASA-TN-D-5966]

Climatology and atmospheric refraction models for worldwide radio wave propagation [05 p0672 N71-14865]

Ray tracing techniques for examination of refractivity profile sensitivity in tropospheric range and Doppler effects on profile shape [11 p1751 N71-22772]

Atmospheric turbulence effects on propagation of high frequency electromagnetic tracking wave [NASA-CR-117804]

Radio-optical paths lengths measurements for determining atmospheric water vapor density and temperature [11 p1712 N71-22946]

Variability of atmospheric refraction coefficient for ultrashort radio waves in lower 1.5-km layer of troposphere over Gazi station, USSR in Sept. 1964 [AD-719830]

Sonic boom pressure signature variations as function of distance to ground due to atmospheric refraction [16 p2535 N71-28389]

Degradation effects of atmospheric absorption of 10.6 micron laser beam with kinetic model for vibrational relaxation process and numerical analysis of vibrational lag ray displacement [RR-350]

Charts giving mean atmospheric refractivity in Mediterranean Europe [IEA-STR-13]

Relationship between disturbed gradients of index of refraction, layer echoes by vertically pointing radar, clear air turbulence and synoptic meteorological conditions [PB-197765]

[18 p2955 N71-31411]

Radiative transfer in turbid atmosphere and atmospheric refractivity determinations [AD-722338]

Errors in Doppler geodetical measurements from coherent frequencies for correcting ionospheric refraction [22 p3680 N71-3680]

ATMOSPHERIC SCATTERING

NT TROPOSPHERIC SCATTERING

Calculating high energy anisotropic transport in the response functions in atmosphere [NASA-TN-D-6010]

Tabulated computations of scattering of visible and infrared waves by water droplets [AZT-70-238-RULL]

Balloons borne polar nephelometer measurements of atmospheric scattering angle, polarization, and wavelength [AD-712691]

Measurement of molecular and aerosol backscatter from stratosphere by ground-based ruby laser [05 p0677 N71-21980]

Developing sky brightness photometer for continuous measurements of atmospherically scattered light near edge of solar disk [08 p1203 N71-14880]

Atmospheric propagation studies with phase-patch Doppler scatter array [AD-716341]

Atmospheric stratifications causing anomalous signal propagation at 170 and 5000 MHz over sea surface beyond horizon [10 p1524 N71-21409]

Perturbation method for calculating surface roughness effects on electromagnetic wave propagation in inhomogeneous atmosphere [10 p1525 N71-21412]

Development of computable electromagnetic theory model for lunar reflectivity problem - Vol. 3 [NASA-CR-115084]

Computer programs for calculating visible and infrared atmospheric transmission, absorption, and scattering, and reflection [AD-727131]

Optical heterodyning with reference beam for diminishing atmospheric turbulence effects on signal to noise ratio [19 p3143 N71-32206]

Effect of scattering on pulse length of argon laser beam in foggy and turbulent atmosphere, and feasibility of Monte Carlo calculation of laser beam energy density distribution [AD-724200]

Effect of coherence and multiple scattering on laser radar air pollution measurements [NASA-CR-121673]

Light impulse backscattering for determining wind range in atmosphere [23 p3750 N71-36778]

ATMOSPHERIC SHELLS

U ATMOSPHERIC STRATIFICATION

Measuring stratospheric temperature inversions in air pollution and weather forecasting [NLL-M-9143-5828-4P/]

Investigating structure of upper atmosphere layers to solve problems of rocket and satellite motion at high altitudes [JPRS-51990]

Climatological values of lower atmosphere temperature and wind stratification [08 p1230 N71-14839]

Tropospheric stratification effects on radio propagation and signal distortion [10 p1523 N71-21405]

Radio reflectivity calculations for tropospheric elevated layers during transhorizon propagation [10 p1524 N71-21404]

Electromagnetic pulse propagation in duct between ground and atmospheric layer [10 p1524 N71-21405]

Ducting in microwave propagation on transmission path over sea [10 p1524 N71-21407]

Ray tracing analysis on duct effect in line of sight wave propagation above sea surface [10 p1524 N71-21408]

Atmospheric stratifications causing anomalous signal propagation at 170 and 5000 MHz over sea surface beyond horizon [10 p1524 N71-21409]

Tropospheric scatter propagation and prediction of radio transmission characteristics [AGARD-CP-70-71]

Scanning forward scatter mapping and analysis layer model for tropospheric scatter propagation analysis [12 p1873 N71-21404]

Mathematical model for partial reflection from tropospheric layers in radio transmission propagation [12 p1875 N71-21407]

Radio attenuation prediction method using stratified atmospheric level indices [12 p1877 N71-21408]

SUBJECT INDEX

Ultraviolet absorption by atomic oxygen layer in earth atmosphere 13 p2108 N71-25263

Atmospheric oxygen absorption spectra and construction of growth curves for stratified atmosphere 13 p2401 N71-27507

Aerosol concentration within different layers of atmosphere derived from pyroellometric and optical measurements 13 p2402 N71-27530

Transmission and extinction of solar radiation in atmospheric stratification 18 p3006 N71-31042

Radiation pattern of dipole antenna in stratified medium representing lunar surface (NASA-CR-121413) 20 p3234 N71-33538

ATMOSPHERIC TEMPERATURE

NT KINOSPHERIC TEMPERATURE

Molecular beam sampling technique for temperature measurement of earth thermosphere 01 p0093 N71-10301

Time spectra of atmospheric temperature, pressure, and wind velocity variations above Atlantic Ocean (NAS-LIB-TRANS-1472) 02 p2533 N71-11448

Time dependence calculation of exospheric temperature of Venus (NAS-455-VOL-35-NO-15) 02 p0295 N71-11917

Investigating mesometeorological processes, climate modification, hail suppression, thermal emission, and humidity variations 02 p0260 N71-12154

Heat emission reduction into atmosphere (NWFL-SA-3552) 03 p0321 N71-12291

Long term solar radiation effects on Arctic region temperatures during winter months 03 p0402 N71-12625

Measurement of air temperature and wind velocity from one to eighty centimeters above sea surface (AD-760856) 03 p0404 N71-13336

Five scale temperature structure of upper atmosphere measured by continuous recording sonde (AD-712211) 04 p0541 N71-13942

Temperature, pressure, and related climatological data for Australia - tables for July 1970 05 p0672 N71-14861

Temperature, pressure, and related climatological data for Australia - tables for June 1970 05 p0716 N71-15088

Thermal heat exchange processes between atmosphere and hydrosphere in Arctic Region (IT-76-50091) 05 p0680 N71-15668

Atmospheric circulation variations and mean monthly air temperature anomalies in Northern Hemisphere 06 p0886 N71-15761

Atmospheric circulation and temperature fluctuation in eastern Siberia 06 p0887 N71-15766

Circulation conditions and monthly average temperature and precipitation anomalies over European USSR 06 p0888 N71-15769

Variations in phenological events and climatic spectra in European USSR 06 p0889 N71-15771

Solar cycle variation of planetary exospheric temperature (NASA-TM-X-65419) 06 p0942 N71-15886

Statistical long range forecasting of mean monthly air temperature (AD-714623) 06 p0891 N71-16320

Wind velocity, air temperature, and wave height measurements from floating laboratory instrument platform in West Indies (AD-713608) 06 p0892 N71-16425

Climatological values of lower atmosphere temperature and wind stratification 08 p1230 N71-18339

Upper atmospheric temperature profiles obtained from ground glow cloud spectra recorded by Echelle spectrometer with image intensifier (NASA-TN-161) 06 p1195 N71-19127

Atmospheric temperature distribution in turbulent flow (AD-716507) 09 p1413 N71-19660

French/English/NASA rocket sounding using Nike-Centaur rocket vehicle for high altitude wind and upper atmospheric temperature investigations over polar region (NAS-44-X-6911-24) 10 p1597 N71-21271

Geostrophic turbulence and horizontal temperature measured at supersonic transport altitudes by B-77 aircraft (AD-716421) 10 p1552 N71-21284

Effects of Arctic Bush on air temperature and humidity over USSR (NAS-455-VOL-35-NO-15) 11 p1744 N71-21889

Planetary ozone and temperature decrements for upper atmosphere (NASA-TN-188A-179) 11 p1832 N71-22507

Long term variations of air and water temperatures in Chukchi Sea 11 p1732 N71-22804

Predicting location of basic formation centers and evolution in Arctic and Subarctic on third day based on variations of thermal field of troposphere and surface pressure variations 11 p1733 N71-22825

Frequencies of cyclonic vortices, mean air density, and horizontal air temperature gradients over Northern Hemisphere 11 p1733 N71-22826

Atmospheric temperature annual variations obtained from North Africa upper atmosphere radio probing (GROPHYSDDBW-FM/164-PT-9) 12 p1912 N71-23691

Atmospheric temperature charts for Jan. and Apr. in Malaysia, Thailand, Vietnam, Cambodia, Laos, and Burma with analogies to Cristobal and Howard AFB, Panama (AD-718611) 12 p1954 N71-23830

Solar radiation absorption by volcanic dust and influence on atmospheric temperature and moisture (NLL-M-20999-5828-4F1) 12 p1914 N71-24175

Thermosphere and lower exosphere gas density and temperature from satellite drag measurements 13 p2070 N71-24567

Computerized simulation of wind velocity using Nimbus 3 infrared sounding data 13 p2108 N71-25262

Mariner 6 and 7 occultation data for determining temperature and pressure of Martian atmosphere 13 p2168 N71-25277

Results of radiosonde ascents from aerological station in Berlin, Germany including extreme and mean values of temperature, pressure, wind data, geopotential and other meteorological data 14 p2208 N71-25804

Measurement of nocturnal temperature distribution in Austin, Texas from August through December, 1970 (REPT-28) 14 p2248 N71-26024

Synoptic meteorological charts for Berlin in Nov. 1970 including temperature-precipitation relationships and radioactivity 14 p2288 N71-26027

Meteorological charts and data tables for July through September, 1970 from Berlin (OR-3-PT-3) 14 p2288 N71-26077

Martian atmospheric temperature and pressure and temperature gradient determination by least squares differential correction of satellite photometric solar eclipse data (NASA-TN-D-6258) 14 p2337 N71-26089

Selective chopper radiometer based on multilayer interference filter for atmospheric temperature sounding from Nimbus D satellite 15 p2410 N71-27486

Statistical estimation of atmosphere temperature and pressure height distribution from Nimbus 3 radiation measurements 15 p2400 N71-27495

Maximum likelihood estimates of atmospheric temperature profile deduced from satellite radiation measurements in cloud presence 15 p2400 N71-27496

Influence of temperature, ozone, and water vapor on atmospheric absorption by 15 micron bands of carbon dioxide 15 p2401 N71-27503

Solar radiation effects on atmospheric temperature using simplified heat flux equation 15 p2403 N71-27560

Radiative-convective equilibrium temperature calculations of Venus atmosphere 15 p2404 N71-27563

Rocket-borne temperature ozone sensor measurements in mesosphere and stratosphere with analysis of diurnal variations (AD-71309) 16 p2586 N71-28346

Computer programming manual for calculating molecular excitation due to air temperature effects including particle size distribution, wind, and thermal radiation effects (AD-722252) 16 p2586 N71-28351

Autocorrelation and cross correlation of high frequency atmospheric boundary layer temperature and velocity fluctuation measurements (AD-721540) 16 p2587 N71-28408

High speed, and high resolution sensors for micrometeorological measurements of atmospheric temperature and moisture 16 p2626 N71-28645

Relationship between atmospheric ozone constant and stratospheric warming (NLL-M-9270-5828-4F1) 16 p2589 N71-28664

Finnish atmospheric temperature and precipitation predictions from Jan. 1968 through Oct. 1970 (RR-32) 16 p2627 N71-28895

Atmospheric temperature distribution data over Finland from 1931 through 1960 (RR-31) 16 p2627 N71-28896

Model of interaction of tropospheric fronts with tropopause based on analysis of 36 vertical sections of high level clouds 17 p2778 N71-29699

ATMOSPHERIC TURBULENCE

Atmospheric and meteorological aspects of air pollution - survey of USSR air pollution literature (PB-190861) 17 p2743 N71-29831

Measurement, autocorrelation, and variance evaluation of near ground atmospheric temperature and wind velocity (MFT-20) 18 p2948 N71-30585

Atmospheric temperature and moisture rawinsonde tables and data reduction techniques used in analysis of atmospheric thermodynamics over Palmyra, Fanning, and Christmas Islands (NCAR-TN/STR-55-VOL-1) 19 p3129 N71-32506

Computer program to simplify reduction of temperature data from meteorological sounding rockets (AD-724599) 20 p3294 N71-32972

Meteorological charts for Northern Hemisphere containing ground level and 850-mb height and temperature data for third quarter of 1970 20 p3296 N71-33916

Meteorological charts for Northern Hemisphere containing ground level and 850-mb height and temperature data for fourth quarter of 1970 20 p3296 N71-33917

Relation between temperature anomalies in lower air level and upper water level for North Atlantic Ocean (NLL-M-20724-5828-4F1) 21 p3423 N71-34335

Stratospheric weather maps of Northern Hemisphere containing daily height and temperature analysis of constant pressure levels (AD-721909) 21 p3451 N71-34563

Comparison of temperature and humidity differences between mountain stations and free atmosphere over Poprad, Czechoslovakia (NLL-M-20354-5828-4F1) 21 p3453 N71-34578

Inversion frequency of atmospheric temperature over 2m region in USSR (NLL-M-20390-5828-4F1) 21 p3454 N71-34580

Effects of swell and air-sea temperature differences on momentum transfer and wave properties (SU-TI-133) 22 p3374 N71-35453

Spring breakup of snow and ice on Delta River, Alaska, and air temperature measurements (AD-724683) 22 p3374 N71-35457

Comparison of turbulence intensity and stability ratio measurements and diffusive properties of atmosphere (SC-DC-70-5443) 22 p3575 N71-35468

Daily meteorological charts showing world-wide temperature distribution and variations at 30 millibar level for last quarter of 1970 (OR-4-PT-4) 22 p3616 N71-35767

Correlation between soft solar X-rays and fortnightly thermal fluctuations in upper atmosphere 22 p3679 N71-36229

Modified expression for exospheric temperature in Jacchia static diffusion models of upper atmosphere in polar regions (NASA-TM-X-65697) 23 p3747 N71-36718

Two-dimensional time dependent diffusion model for phase delay between thermospheric density and temperature (NASA-TM-X-65694) 23 p3747 N71-36719

Computing dispersal of atmospheric pollutants near airports by use of mean wind and temperature profiles (NASA-CR-111962) 23 p3748 N71-36720

Micrometeorological field data including energy balance components, temperature profiles, and wind profiles from California (AD-726390) 23 p3790 N71-37014

Temperature, pressure, and related climatological data for Australia - tables for March 1971 23 p3792 N71-37025

Parametric method for estimating solar radiation effects on atmospheric temperature (NLL-M-20358-5828-4F1) 23 p3842 N71-37396

ATMOSPHERIC TIDES

Diurnal variation and tidal dependence of field strength on radio links in German Bight (REPT-13) 04 p0490 N71-13488

Variations of atmospheric parameters in lower thermosphere and development of upper atmosphere density models (AD-714583) 06 p0851 N71-16493

Rotation of horizontal velocity vector in atmospheric tides (NASA-TT-F-13818) 18 p2917 N71-31227

Implication of Rough function thermospheric degradation on ionospheric tidal mode structure and vertical wave propagation (NASA-TM-X-65675) 20 p3296 N71-33442

Three dimensional thermospheric model for interpreting tides, planetary waves, and magnetic disturbances (NASA-TM-X-65676) 20 p3296 N71-33443

Statistical analysis of tropical cloudiness and rainfall in relation to semidiurnal atmospheric tide and pressure variations 23 p3784 N71-36974

ATMOSPHERIC TURBULENCE

NT CLEAR AIR TURBULENCE

NT GUSTS

NT LOW LEVEL TURBULENCE

- Remote measurement of wind speed and air turbulence by laser scattering 01 p0082 N71-10208
- Multiwavelength laser scintillations due to atmospheric turbulence 02 p0238 N71-11395
- Calculating kinetic energy of atmospheric turbulence from balloon sounding data 02 p0254 N71-11568
- Turbulence data from measurements on 32 meter tower facility at White Sands Missile Range 02 p0259 N71-11769
- Incorrectness of mutual coherence function for optical wave propagation in turbulent atmosphere 02 p0369 N71-12172
- Soviet research in geophysics, astronomy and space 03 p0470 N71-13038
- News briefs and abstracts of articles on meteorology 03 p0483 N71-13040
- Turbulence and gravitational waves in upper atmosphere 03 p0374 N71-13378
- Mollere approximation for wave propagation in turbulent media 04 p0490 N71-13485
- Similarity model for atmospheric turbulence structure in planetary boundary layer 05 p0667 N71-14693
- Energy equations describing physical processes in ground atmosphere 05 p0717 N71-15144
- Turbulence measurements in and near thunderstorms correlated with aircraft stability measurements from ground based radar 05 p0717 N71-15152
- Passive optical wind and turbulence remote detection system 06 p0891 N71-16340
- Wind velocity, air temperature, and wave height measurements from floating laboratory instrument platform in West Indies 06 p0892 N71-16425
- Variations of atmospheric parameters in lower thermosphere and development of upper atmosphere density models 06 p0851 N71-16493
- Responses of balloon and falling sphere wind sensors in atmospheric turbulence, analyzed with Fourier transformation 07 p1053 N71-17479
- Calculations on aggressive turbulence interactions 07 p1380 N71-19508
- Turbulence characteristics affecting aerodynamic stability over heterogeneous terrain 09 p1382 N71-19603
- Time and space history analysis of buoyant cloud tops and heat release, cloud behavior and meteorological factor interrelationships in cloud rise 09 p1413 N71-20024
- Stratospheric turbulence and horizontal temperature measured at supersonic transport altitudes by B-57 aircraft 10 p1532 N71-21284
- Beam scintillations and atmospheric turbulence characteristics of multiwavelength laser transmission 10 p1570 N71-21718
- Atmospheric optical line of sight communication system and application of multichannel optical diversity to improve communication effectiveness 11 p1699 N71-21999
- High frequency Doppler sounding at vertical incidence of atmospheric disturbances 11 p1709 N71-22930
- Atmospheric turbulence effects on propagation of high frequency electromagnetic tracking wave 11 p1712 N71-22946
- Atmospheric turbulence effects on laser beam phase correlation during tropospheric propagation 11 p1713 N71-22953
- Atmospheric turbulence effects on phase coherence of propagating optical wave 11 p1713 N71-22954
- Refractivity measurements and effects of atmospheric turbulence on optical heterodyne reception 11 p1713 N71-22955
- Optical image distortions for measuring atmospheric turbulence fluctuations 11 p1714 N71-22956
- Holographic phase contrast measurements on optical wave propagating through turbulent atmosphere 11 p1776 N71-22957
- Fallout from nuclear explosions, atmospheric turbulence, aerosol propagation, and aerological and hydrometeorological measurements 12 p1952 N71-23178
- Computation and measurements of dynamic aircraft transfer functions to atmospheric turbulence 12 p1852 N71-23213
- Meteorological radar for detection of thunderstorms, hail, and turbulence hazardous to aviation notice aco interpretation and radar transmission 13 p2104 N71-24394
- Random process theory method for estimating response of flexible airplanes to atmospheric turbulence 13 p2026 N71-24708
- Alleviation of lateral and longitudinal gust effects on aircraft 13 p2024 N71-24709
- Analysis of empennage loads and aerodynamic response of T-tail transport aircraft in continuous atmospheric turbulence 13 p2034 N71-24996
- Atmospheric model with damped gravity waves from vertical atmospheric sounding analysis 13 p2076 N71-25264
- Atmospheric turbulence effects on gas laser communication system 13 p2090 N71-25318
- Actinometers for measuring atmospheric turbidity characteristics, resulting from general statistical analysis 14 p2247 N71-25959
- Flight evaluations using variable stability aircraft to determine effects of turbulence induced aerodynamic disturbances and lateral directional dynamics on pilot performance 14 p2196 N71-26170
- Scintillation and signal to noise ratio of heterodyne detection for carbon dioxide laser beam propagated over path 3.2 km to determine effects of atmospheric turbulence 14 p2266 N71-26419
- Temporal frequency spectra of multifrequency waves in turbulent atmosphere and correlation with wind velocity 15 p2382 N71-27357
- Effects of spanwise variation of gust velocity on alleviation system designed for uniform gust velocity across span 16 p2529 N71-28009
- Atmospheric turbulence effects on sonic boom shock wave thickness 16 p2532 N71-28367
- Atmospheric turbulence effects on sonic boom shock wave scattering 16 p2532 N71-28369
- Anomalous rise times of acoustic sonic boom waveforms caused by atmospheric turbulence 16 p2533 N71-28374
- Image restoration techniques applied to astronomical photography with degradation caused by atmospheric turbulence 16 p2594 N71-28522
- Synoptic atmospheric conditions indicative of severe storms and dynamic and thermodynamic properties of air in proximity to tornado from June 1967 Oklahoma storm system 16 p2626 N71-28599
- Observing atmospheric structure of mountain lee waves by laser radar 17 p2778 N71-30071
- Systems analysis of aircraft, aircraft guidance and control systems, and atmospheric turbulence for low visibility instrument landing system requirements 17 p2789 N71-30225
- Derivation of equations for Rytov and Born approximations in turbulent atmospheric attenuation and scattering of coherent light 17 p2789 N71-30225
- Evaluating effects of high altitude turbulence encounters on XB-70 airplane 18 p2868 N71-30718
- Flight tests to determine handling qualities of general aviation aircraft during ILS approaches in turbulent air 18 p2869 N71-30771
- Evaluating analytical models of turbulence having non-Gaussian gust distributions and effects of wind shear on aircraft operations 18 p2902 N71-30778
- Preliminary study of airplane-autopilot response to atmospheric turbulence while operating in altitude-hold and attitude-hold modes 18 p2870 N71-30780
- Aircraft design, flight characteristics, and atmospheric effects on sonic boom during supersonic and hypersonic flight 18 p2871 N71-30787
- Approximate solution of nonlinear potential equation for small disturbance in transonic range and pressure distribution on aircraft 18 p2872 N71-31061
- Wind and turbulence structure in boundary layer over Antarctica 18 p2953 N71-31122
- Estimation of lateral and longitudinal rigid body responses of aircraft structures continuous and random atmospheric turbulence 18 p2872 N71-31242
- Prediction method for performance of total pilot-vehicle system in turbulence with application to tracking tasks 18 p2873 N71-31288
- Statistical analysis of long term atmospheric turbulence data for predicting atmospheric diffusion 18 p2955 N71-31557
- Atmospheric turbulence models showing gust influence on aircraft yaw motion 19 p3037 N71-31601
- Statistical analysis of atmospheric turbulence in Cape Kennedy Launch Complex for spacecraft design 19 p3132 N71-32001
- Theoretical error analysis of radar measurements of turbulence structure function 20 p3257 N71-32001
- Analysis of helium-neon and carbon dioxide laser beam propagation in atmospheric turbulence 20 p3310 N71-32001
- Measurement and analysis of atmospheric turbulence along Pacific Coast air route in Japan 20 p3397 N71-32001
- Comparison of turbulence intensity and stability ratio measurements and diffusive properties of atmosphere 22 p3375 N71-32001
- Relation between turbulence in atmospheric boundary layer aircraft buffeting, and vertical distribution of meteorological parameters calculated from radiosonde data 23 p3703 N71-32001
- Optical propagation measurements in inhomogeneous atmosphere at Emerson Lake, California for optical propagation theory validity tests 23 p3752 N71-32001
- Photography of smoke plumes from industrial sources as means of determining characteristics of atmospheric turbulence 23 p3760 N71-32001
- Limitations imposed on resolution of coherent radar systems by atmospheric turbulence for sensing wave front or angle-of-arrival of return signal from target 23 p3760 N71-32001
- Techniques for relating transient tolerances in inlet throat Mach number and shock position to upstream unsteady frequency due to atmospheric turbulence in supersonic inlet design 24 p3965 N71-32001
- Observations of atmospheric turbulence in Antarctica by radioondes 24 p3965 N71-32001
- Optical wave phase structure and mutual coherence function for propagation in turbulent atmosphere and heterodyne detection effects 24 p3967 N71-32001
- ATMOSPHERICS
- NT DAWN CHORUS
- NT HISS
- NT IONOSPHERICS
- NT WHISTLERS
- Amplitude and time statistics of atmospheric noise made radio noise 01 p0023 N71-10208
- Atmospheric electricity measurement near the storm and correlation with VHF atmospheric (FR-4) 03 p0372 N71-13012
- Construction of coil antenna and ball antenna for extremely low frequency signal reception 04 p0492 N71-13012
- Atmospheric radio noise recordings during Atlantic Ocean crossing 04 p0492 N71-13012
- Extremely low frequency atmospheric noise measurements underwater and on ocean surface 04 p0520 N71-13014
- Measurements and characteristics of atmospheric electrical potential near earth surface 05 p0669 N71-14693
- Simultaneous magnetic and electric field measurements for extremely low frequency ionospheric disturbances and atmospheric 06 p0850 N71-16493
- Development and characteristics of global atmospheric circulation model 08 p1251 N71-21284
- Characteristics of high frequency channels used to obtain parameters for choosing appropriate statistical codes 11 p1699 N71-21999
- Statistical spectral amplitude distribution measurements on atmospheric at very low frequencies during thunderstorms 11 p1703 N71-22946
- Compilation of meteorological data for Alaska and Aleutian Islands Vol. 13 12 p1956 N71-23178
- Observation of ionospheric winds in aerosol time following release of rocket borne chemicals 14 p2246 N71-26419
- Meteorological parameters for Hunter-Liggett military reservation, California for December, 1970 23 p3770 N71-32001
- Development of weather forecasting procedure using cubic spline technique applied to two dimensional data fields and mechanics of frontal inversions under idealized conditions 23 p3771 N71-32001
- Daily and monthly synoptic weather maps of Northern Hemisphere at 5 millibar level for period October - December 1967 24 p3953 N71-32001

SUBJECT INDEX

Development of fallout interpretative code and transport model for Defense Land Pollutants Interpretative Code [AD-727613] 24 p3981 N71-38414

ATOMIC BATTERIES
U RADIOTOPES BATTERIES
ATOMIC BEAMS
 Polarization of lithium nuclei from atomic beam furnaces using high frequency transitions and polarization measurement using nuclear reaction 03 p0406 N71-13279
 Performance of mass spectrometer oxygen beam for upper atmospheric measurements 06 p0856 N71-16796
 Fast neutral injector facility for obtaining intense neutral excited hydrogen atom beam [CEA-CONF-1662] 09 p1366 N71-20192
 Determination of physical characteristics of crystal surfaces by observation of elastic and one-phonon inelastic scattering of atomic beams from surfaces [JAMP-3824-101-70U] 10 p1636 N71-21752
 Van de Graaff accelerator operation in atomic beam field spectroscopy 11 p1803 N71-22119
 Energy separation measurements in a square 2 state of atomic hydrogen by radio frequency produced field transitions between hyperfine components [IND-25596] 14 p2315 N71-26734
 Method for atomic beam ionization with storage of polarized ions in electron beam and their pulsed excitation during accelerator capture time [JAMP-29-5446] 15 p2473 N71-27443
 Dissociation rate and plasma generation in hydrogen beam electron interaction [CEA-CONF-1616] 15 p2474 N71-27457
 High energy cosmic ray interactions in emission detectors 16 p2675 N71-28042
 Atomic beam radio frequency measurement of 2H1/2 to 2P3/2 energy separation in N equals 2 state of atomic hydrogen 17 p2889 N71-30579
 Design and transmission characteristics of high pass, mechanical wave filter for fast neutral atomic or ionic beams [NASA-TN-X-3332] 18 p3980 N71-30745
 Atomic absorption spectrophotometry for rapid analysis of impurities in uranium 22 p3635 N71-33913
 Neutral beam injection in mirror systems for fast fusion plasma production [CONF-710607-98] 24 p3989 N71-38461

ATOMIC CLOCKS
 Synchronization of distant atomic clocks by microwave - Operation Systat [NBSA-TN-1657] 02 p0226 N71-11681
 Performance characteristics of portable atomic reference clock and frequency standard 06 p0460 N71-16479
 Prototype atomic hydrogen mass standard for field operation 13 p2090 N71-23338
 Atomic clock time measurements and standardization [AD-721351] 15 p2409 N71-27393
 Comparison of pulsed clock with atomic earth-based clock, noting frequency variations 18 p2924 N71-31116
 Physical basis of atomic frequency standards, and characteristics of hydrogen maser, cesium beam, and silicon gas cell [NBS-TN-369] 18 p2989 N71-31509

ATOMIC COLLISIONS
 Collisions of atoms with exponential repulsive potential of atom and harmonic oscillator [AD-711197] 01 p0101 N71-10897
 Displacement of atoms from normal lattice positions by positrons and alpha particles [NBSA-TN-3013] 02 p0273 N71-11791
 Generalized integral equation for two body scattering potential in core interactions using tensor and Coulomb forces [NBSA-TN-3746-37] 04 p0284 N71-14204
 Annotated bibliography of atomic and molecular collision research for 1969 [NBSA-AMPC-13] 07 p1074 N71-17417
 Resonance effects on high temperature vibrational absorption coefficients for atomic hydrogen collisions in hydrogen gas [NBSA-TN-4155] 07 p1076 N71-17514
 Resonance collision processes in interphases [AD-715715] 08 p1260 N71-18763
 Theoretical and experimental findings on atomic and molecular collisions [NBSA-CN-117178] 09 p1444 N71-20408
 System mechanical study of H,2 reactive scattering treated by distorted-wave Born and simplified Born approximations [NBSA-TN-360-36] 09 p1445 N71-20572
 Free structure transitions theory and low energy collisional atomic systems 10 p1618 N71-21460
 Analysis of atomic hydrogen in metastable 23S1/2 state by electron impact - polarization of Lyman alpha radiation produced by collision transfer between inert gas atoms and protons 12 p1978 N71-24234
 Threshold law for electron atom impact ionization 13 p2182 N71-25283
 Collisional effects on electron waves in non-Maxwellian Lorentz magnetoplasmas [AD-719790] 14 p2320 N71-25708
 Statistical model for electron scattering in ion atom interactions [AD-720822] 15 p2474 N71-27456
 Method for describing elastic atomic collisions based on concepts of chemical physics [NBSA-TN-1225] 15 p2484 N71-27799
 Spin-lattice relaxation and atomic motions in lithium fluoride 16 p2668 N71-28088
 Proton and alpha particle reflections from atomic and ionic chains 17 p2795 N71-29738
 Probability distribution functions for nonreactive collisions of tritium with H2, D2, HD, or Ar and of deuterium with H2 or D2, calculated with Monte Carlo method 18 p2906 N71-31258
 Quantum mechanical calculations of approximate scattering cross sections for elastic, isotropic, and rearrangement collisions of electrons, atoms, and molecules 18 p2987 N71-31349
 Limitations of merging beam method in studying ion atom collisions [IAE-2001] 19 p3146 N71-31962
 Evaluation of single collision between nitrogen ions scattering from argon atoms at keV energies 20 p3321 N71-33744
 Monte Carlo method for determining reactive collisions of fluorine atoms with hydrogen molecules [LA-4603] 21 p3388 N71-34103
 Resonance and nonresonance charge exchange probabilities of atomic collisions in molecular orbitals [JAREP-MEMO-4299] 22 p3635 N71-33967
 Elastic scattering and multiple scattering in atomic collisions based on classical mechanics [INDR-1-1217] 22 p3635 N71-33969
 Ion deuterium studies of vibrational and rotational excitation levels of molecular nitrogen target in low energy atomic collisions [NBSA-TN-1853] 23 p3811 N71-37173

ATOMIC ENERGY
U NUCLEAR ENERGY
ATOMIC ENERGY LEVELS
 Resonance light scattering for measuring spectral line transitions in cobalt isotopes spectrum 01 p0089 N71-10522
 Mechanism of nuclear reactions Be-9(p,n)Be-9 and Be-9(p,alpha)Li-6 at low energies [CEA-CONF-1499] 02 p0270 N71-11411
 Research in basic atomic properties extending useful range of electromagnetic spectrum [AD-711546] 02 p0275 N71-11914
 Low lying states of light atomic nuclei in framework of cluster model 02 p0278 N71-12178
 Static quadrupole moments measurement of first excited 2D5/2 states of Po-106 and 110 nuclei by heavy ion Coulomb excitation 03 p0429 N71-12898
 Calculating level structure of neutron-deficient lead and bismuth isotopes [INDR-11691/PL] 03 p0432 N71-12957
 Calculating binding energy of Lambda hyperon particle in nuclear matter using self-consistent Brueckner K matrix theory [INDR-11537/PL] 03 p0433 N71-12958
 Classification of calcium-49 nuclei based on reactions K-39(E,He-3,d) gamma/calcium-40 and calcium-40(p,p' gamma)/calcium-40 - conference [CEA-CONF-1335] 04 p0571 N71-13614
 Gamma ray energy measurements of transitions from first and second excited levels of Fe-58 [CONF-690818-7] 04 p0577 N71-13799
 Deriving analytic expressions for calculating phase space contour and area of quadrupole triplets from nuclear moments [CEA-TN-70-22] 04 p0588 N71-14279
 Quantum mechanical excitation measurements on ytterbium states 04 p0588 N71-14309
 Constructing model for proton elastic and inelastic scattering at isobaric analogues resonances in one-level approximation [NBSA-TN-378] 05 p0744 N71-15168
 GRAPEP program for random generation of Batch and Monte Carlo parameters for simulated unexcited resonances of fission isotopes [WAFD-TN-935] 05 p0740 N71-15281
 Excited states of Co-138 and Pr-138 determined from beta decay of Pr-138, Pr-138m, and Nd-138 [NASA-TN-D-7040] 06 p0912 N71-15837
 Excited levels of boron 10 in 7.5 MeV region [NBSA-TN-18403] 06 p0913 N71-15867
 First excited state lifetimes in thulium 169, thulium 171, and cerium 134 [IS-T-350] 06 p0917 N71-16196

ATOMIC ENERGY LEVELS

Wavelengths and energy levels of Ca/II for far ultraviolet wavelength standards 01 p0085 N71-14349 [LA-4498]
 Measuring low-lying electronic levels of impurity ions in Al2O3 and electromagnetic absorptivity of Fe using far infrared spectroscopic techniques [UCRL-15666] 06 p0852 N71-16607
 Measuring conversion electron and gamma ray spectra by decay of Th-163 to Fr-163 [JNRS-P-5132] 07 p1072 N71-17340
 Atomic energy level and multiple tables for carbon-12 through carbon-13 [NBSA-TN-363-3] 07 p1076 N71-17330
 Measuring optical spectra of highly ionized orbit in calcium tungstate using absorption and fluorescence spectroscopy [AD-715908] 07 p1079 N71-18043
 Tables of half lives for excited nuclear levels [AD-400] 08 p1269 N71-18286
 Measuring differential cross sections for inelastic electron scattering from calcium, titanium, and iron isotopes [AD-713647] 08 p1253 N71-18331
 Investigating properties of lowest even-even nuclear states of actinide region with respect to superfluid model of multipole interaction in single phonon approximation [INDR-P4-5126] 08 p1256 N71-18371
 Two particle fractional parentage coefficients for atomic spectral calculations - tables [AD-715924] 08 p1262 N71-18066
 Atomic energy levels, and atomic and molecular structure of systems in microscopic environments [AD-715798] 08 p1262 N71-18067
 Bound electron problems, involving Schrodinger theory, transition probability, and Compton scattering [IC70/34-CN-1-3] 09 p1441 N71-20337
 Measurement and analysis of differential cross sections for reaction negative pion proton yields sigma minus proton at six energies between 2.9 and 18.2 GeV/c [CEA-B-4057] 09 p1444 N71-20528
 Energy level analysis of dysprosium first and second spectra from wavelength and wave number measurements and Zeeman effect observations [UCRL-19944] 09 p1488 N71-20536
 Low lying atomic energy levels for odd-A nuclei Yb 177, Re 183, Ir 167, and Pt 239 09 p1446 N71-20578
 Neutron elastic and inelastic scattering cross sections for yttrium in 4.19 to 8.56 MeV energy range [ORNL-4552] 10 p1615 N71-21057
 Optical model of nucleus and atomic energy levels studied with tandem Van de Graaff machine, proton linear accelerator, and magnetic spectrometer [COO-1265-94] 10 p1616 N71-21170
 Experimental nuclear structure data compilation for level energies, spins, and parities of nuclei in mass region A equals 91 to 117 [ORNL-4627] 10 p1616 N71-21172
 Giant monopole state and isospin mixing in nuclear ground states [NYO-2171-350] 10 p1617 N71-21306
 Resonant structure of lithium between 2 triplet S and 2 singlet P thresholds [AD-716032] 10 p1617 N71-21374
 Nuclear energy levels of Co-133 and Pr-141 from gamma ray measurements after neutron inelastic scattering 10 p1620 N71-21738
 Levels in medium weight even-even nuclei populated by Co-66, Ga-68, Ce-132, and I-132 studied with Ge/Li detectors in singles and coincidence mode 10 p1622 N71-21760
 Measurement of low energy and high energy portions of pion/plus in kaon/plus yields pion/plus/pion/zero/pion/zero decay 10 p1623 N71-21768
 Data on Os-184,187 levels from Re-184,187 decays, Hg-200 and Au-200 levels from Au-200m decay, and Re/ptot, neutron, photon/nuclear reactions [COO-1672-21] 11 p1606 N71-22436
 Equipment and methods for neutron investigation and destructive analysis of fissionable materials [LA-4525] 13 p2119 N71-25311
 J mixing determination in Ba 139 and 112 p,d reactions by asymmetry measurements at 25.5 MeV [CEA-CONF-1635] 13 p2136 N71-25382
 Deuteron accelerated to 28 MeV for investigating iron-54(d,alpha)nickel reactions [LYCIN-7074] 14 p2308 N71-26423
 Triple differential cross sections measured in reaction proton proton yields pion/plus/nucleon proton at 630 MeV [JNRS-P-5570] 14 p2308 N71-26530
 Obtaining accurate determination of real parts of hadron-proton forward scattering amplitudes at intermediate energies [JNRS-E2-5216] 14 p2309 N71-26629
 Geometrical aberrations and transfer matrix of quadrupole lenses in guiding devices or finite extension beam matching systems and application to matching triplet study [CEA-M-1266] 14 p2311 N71-26669

Neutron cross sections and angular distributions for Li-7/a, b reactions including neutron spectra indications of atomic energy levels
[JINR-P15-3143] 14 p2313 N71-36710

Capture cross sections in keV region versus energy curves to determine gamma ray strength, S wave neutron strength, and P wave neutron strength in silver, iodine, and indium isotopes
15 p2479 N71-37634

Level structure of Sn-120 determined by Ge/Li detector and Ge/Li-NaI/TV coincidence measurements of decay of Sn-120 and Sn-120 isomers
[HP-18394] 15 p2485 N71-37815

Oscillatory strengths, lines, and lifetimes of energy levels in atomic and ionic spectra with beam-foil measurements
[AD-721604] 16 p2656 N71-39189

Low and high field level crossing experiments in 2P state of atomic hydrogen and measurement of Sommerfeld fine structure constant
16 p2657 N71-39124

Measuring average number of prompt neutrons and of relative cross sections for fission of U-235 and Pu-239 induced by neutrons within 0.3 and 1.4 MeV energy ranges
[LEB-TRANS-308] 16 p2660 N71-39196

Proton and neutron scattering cross sections for carbon, deuterium, helium, and hydrogen, and atomic energy level schemes from krypton and lead isotope alpha reactions
[UCD-CNL-125] 17 p2790 N71-39230

Matrix element tables for computing L shell fluorescence yields and electron transition rates in spin-spin coupling including Auger, Coster-Kronig, and radiative transitions
[SC-RR-710073] 17 p2791 N71-39288

Instrumentation for investigating nature of energy levels of impurity ions in crystalline solids
[AD-722411] 17 p2814 N71-39692

Level crossing and resonance spectra of excited states in lutetium 175 hyperfine structure
17 p2796 N71-39791

Hydrogen bubble chamber experiments on 10 and 19 GeV/c proton-proton interactions
[AD-7270-8] 17 p2798 N71-39005

Energy levels of Yb-176 from decay of Tm-176 and Yb-176m studied by Ge/Li detectors and gamma-gamma as well as gamma-beta coincidences
[NP-18599] 17 p2807 N71-39336

Radiative lifetime of 2 150 metastable state of helium
[UCRL-20412] 17 p2808 N71-39342

Calculation of binding energy and wave function of helium isotope by harmonic polynomial method
[ITP-70-1-E] 17 p2810 N71-39388

Photon effects in γ -gamma, α - γ , and γ -gamma, β - γ reactions in light nuclei
[JLUNP-7089] 18 p2967 N71-39404

Mechanism of He-^3 alpha particles at low energy and applications to Si-27 and S-31 levels
[NP-18464] 18 p2969 N71-39438

High resolution radiation counter design and use in study of S-32 T-2 state
[NP-18623] 18 p2972 N71-39534

Half lives and spin levels in promethium isotope determined by coincidence and gamma-gamma correlation methods
[JINR-P6-5317] 18 p2979 N71-39695

Hyperfine structures and positions of $5d_{5/2}$ $\pm 2F$ states in lanthanum I spectrum by laser-cooling method and Doppler resonance spectroscopy
18 p2983 N71-39951

Limitations of merging beam method in studying ion atom collisions
[IAE-2001] 19 p3146 N71-31962

Superficial nuclear model for calculating ground- and excited-state of odd-N nuclei
[JINR-E4-5567] 19 p3150 N71-32121

Line absorption analysis and reaction kinetics of two metastable nitrogen atomic energy levels
[NASA-CR-111963] 19 p3154 N71-32295

Data analysis methods for correcting cascade transition effects in atomic transition probability measurements
19 p3155 N71-32358

Spectroscopic analysis of nuclear reactions, atomic energy levels, and fluorescence including nuclear magnetic resonance and particle polarization
19 p3157 N71-32594

Redetermination of hyperfine structure constant by microwave transitions in H, a equals 2
19 p3158 N71-32560

Nuclear interactions and atomic energy levels for Pb-210, Bi-210, Po-210, Po-206, Tl-206, and Hg-206
[AD-724640] 20 p3314 N71-33033

Glauber and Born approximations of electron impact excitations of hydrogen atomic energy levels
[NASA-CR-121444] 20 p3319 N71-33686

Elastic proton scattering from osmium and platinum isotopes and identification of atomic energy levels
20 p3319 N71-33694

Microwave-optical measurements of atomic energy levels in ionized helium
20 p3327 N71-33950

Nuclear models of radioactive decay and shell theory for atomic energy levels of nuclei
[ORNL-2434-7] 20 p3329 N71-35989

Orientation dependence in triplet-triplet energy transfer determined by magnetophotoselection techniques
[AD-726543] 22 p3552 N71-35298

Single particle spectrum of O-17, O-16 and Ca-40 binding energies, and O and Ca isotope shifts for nucleon-nucleon interactions
[JINR-P4-5614] 22 p3631 N71-35873

Lifetime measurements of eight Ca-41 levels excited from K-41 and Ca-40 reactions using Doppler effect attenuation technique and comparison with nuclear model results
[NP-18812] 22 p3637 N71-35923

Radioactive decay and energy level study of Ta-174 using semiconductor devices
[LYCEN-7084] 22 p3641 N71-35955

Tables on atomic energy levels and multiplets of four nitrogen spectra
[NBSRS-NBS-3-SECT-4] 22 p3651 N71-36059

Scaled Thomas-Fermi method for calculating photoionization cross sections of atoms from ground level data
24 p3817 N71-37228

Glauber approximation of differential and integrated atomic hydrogen excitation cross sections at electron impact
[NASA-CR-123926] 24 p3971 N71-38527

Equipment and capabilities developed in investigation of K and L shell ionization cross sections, X ray intensity ratios, bremsstrahlung spectrum, coincidences, and isotopic electron scattering
[NASA-CR-119957] 24 p3976 N71-38368

ATOMIC EXCITATIONS
Observing Moenchauer effect after Coulomb excitation by alpha particles in Dy-161 and Eu-151
[AD-710293] 01 p0093 N71-10039

Low energy interactions of alkali metal atoms and molecules
[AD-711110] 01 p0097 N71-10571

X ray excited LMM Auger spectra of copper, iron, and nickel
[NASA-TM-X-65381] 01 p0097 N71-10584

Interaction processes between helium ions and atoms
[NASA-CR-111353] 01 p0103 N71-11000

Lifetime measurements of 2 positive rotational states in Oe-182 and 184 and of 1020 keV excited state in Bi-204
[JINR-B6-5070] 02 p0270 N71-11397

Excitation of Si-28 particle-hole states by isotopic electron scattering at high momentum transfer
[AD-712083] 02 p0276 N71-12061

Lower excited levels of Ra-225, gamma and alpha emission accompanying Th-229 decay
[ITP-748] 03 p0431 N71-12923

Absolute experimental emission cross sections for excitation of electric dipole transitions in Be ions by electron impact
[ORNL-3827-17] 04 p0570 N71-12600

Gamma ray energy measurements of transitions from first and second excited levels of Fe-58
[CONF-690818-7] 04 p0577 N71-13799

Quantum mechanical excitation measurements on ytterbium states
04 p0588 N71-14309

Measuring inelastic electron scattering form factors for proton excited states in vanadium 51
05 p0736 N71-14533

Investigating ionization processes in thermal bimolecular collisions of particles in electronically excited state
05 p0743 N71-15135

Excited levels of boron 10 in 7.5 MeV region
[NP-18458] 06 p0913 N71-15847

Applying generalized phase shift approach to rotational excitation problem to atom-right rotor case in first order approximation
[NASA-CR-116136] 06 p0916 N71-16093

Measuring ground and excited states of pyrazine for ground state equilibrium geometry of molecule
07 p0980 N71-17079

Measuring level schemes of Nb-92 and Nb-94 by p, n reaction on separated titanium targets
[NASA-CR-116429] 07 p0979 N71-18010

Tables of half lives for excited nuclear levels
[AE-400] 08 p1249 N71-18206

Thyrion trigger exciting in coils of magnetic extension of synchrocyclotron
[JINR-P9-5260] 08 p1174 N71-18218

Calculating energy loss of fast electrons passing through thin films using classical electrodynamics techniques
[IS-T-368] 08 p1255 N71-18348

Even-even isotopes of tellurium of masses between 122 and 130 studied by Coulomb excitation
[NP-18467] 08 p1257 N71-18516

Magnetic spectroscopic study of O-15 bound states and T3/2 states in C-13, O-17, and Ne-21
09 p1430 N71-19767

Conservation laws and vibrational band structure of nitrogen subjected to excitation collisions with helium and argon metastable atoms
09 p1431 N71-19989

Fast neutral injector facility for obtaining intense neutral and hydrogen atom beams
[CRA-CONF-1602] 09 p1464 N71-20079

Average energies of ground and singly ionized excited configurations in highly ionized atoms for electron numbers N equals 3 to N equals 20
[NASA-SP-3856] 09 p1444 N71-20089

Accelerator studies on proton scattering, excited atomic energy levels, and resonance charge exchange reactions
[CRA-N-1232] 09 p1446 N71-20089

Mass spectrometric investigation of collisional ionization by electronically excited helium atoms
11 p1009 N71-35889

Non-equilibrium excitation origin in sodium stars, hydroxyl radicals, or water molecules according to hydrogen-oxygen or acetylene-oxygen excitation fluid waves
[NASA-TF-15-1632] 12 p1009 N71-35889

Proceedings from conference on isotopic atom scattering with emphasis on collective excitations in disordered and magnetic systems, and lattice dynamics of high polymer substances
[JAERI-1197] 13 p2130 N71-34009

Simultaneous computer analysis of first positive band system of N2 in near infrared excited by hollow cathode discharges also analysis of existing energy level data
13 p2135 N71-34009

Quant-free electron scattering from proton with scattering calculation from harmonic oscillation and Wood-Saxon potentials for bound state proton and wave functions for final states
13 p2138 N71-34007

Further angular correlation measurements of O-192 and Pu-192 excited state magnetic moments and NMR internal field measurements of Oe-187 in Fe and Ni alloys
[COCO-1746-53] 14 p2293 N71-32374

Calculation of box diagram effects with scalar and vector resonances in intermediate state with degradation
[IPV-STR-70-34] 15 p2483 N71-37719

Hyperfine interactions of first excited 2p/2s states of Sm-154 and U-238 studied using Moenchauer effect following Coulomb excitation
15 p2485 N71-37817

Oxygen, fluorine, and sodium isotopes atomic excitation energies, spins, parities, and angular distributions using time of flight spectrometers and Born approximations
15 p2494 N71-37804

Radiative decay of naphthalene crystal phosphorescence and Chlorophyll pyrenoid-like fluorescence including atomic excitation kinetics
15 p2497 N71-37804

Monopole/Upon/ equals positive of excitation is even-even deformed nuclei
[JINR-P4-5422] 16 p2652 N71-39005

Measurement of 472 state lifetimes in ruby with fluorescent and nonfluorescent transitions and dynamic model including activation energies, Franck-Condon principle, and frequency factors
16 p2658 N71-39005

Computer program for activity calculations from high energy neutron irradiation of thin targets using atomic excitation function and neutron cross section values
[NP-18649] 17 p2791 N71-39005

Level crossing and resonance spectra of excited states in lutetium 175 hyperfine structure
17 p2796 N71-39791

Population levels of O-17 and O-19 studied experimentally by proton double-striping reactions of 8 MeV He-3, proton with N-15 and Al-27
[NP-18628] 17 p2807 N71-39336

Excitation energies, transition probabilities, and Ramanujan parameter for neutron pair vibration in ytterbium isotopes
[JINR-P4-5576] 18 p2980 N71-39695

Correlation between quasi-particle and collective excitations in nuclei, based on variational principle
[JINR-E4-5578] 18 p2983 N71-39951

Highly excited states of C-12 and O-16 from He bombardment of Be-9 and C-13
18 p2983 N71-39951

Continuous operation laser based on chemical reaction of vibrational rotational levels of hydrogen chloride produced in detonation waves stabilized by supersonic flow
18 p2983 N71-39951

Atomic excitations, ultraviolet photolysis, and microwave vapor phase atom, radical, and molecule reactions including spectroscopic analysis techniques
[AD-722641] 18 p2986 N71-39951

Kinetic excitation mechanisms of alcohols like positive and first negative radiation at high temperature
[AD-723530] 19 p3049 N71-36095

Many body theory electron correlation effects in excited and ground states
20 p3317 N71-33950

SUBJECT INDEX

Calculation of ionization-excitation cross rates in gases probed by electron fragments and alpha particles

20 p3307 N71-33667

Atomic excitation of palladium, lithium, and thallium ground states and lifetime measurement based on laser effect

20 p3320 N71-33685

Time dependent correlations in linear Heisenberg chain

20 p3325 N71-33914

Computer programs for PM cyclotron analysis comparing excitation energy of residual nuclei

21 p3470 N71-34708

Time of flight techniques in neutron spectroscopy for studying structure of highly excited states

21 p3471 N71-34717

Intermediate phenomena in nuclear reactions proceeding through intermediate isolated excited states

21 p3472 N71-34718

Measurement of excitation probability of bound atomic states by photon emission

21 p3474 N71-34736

Experimental and theoretical research in isotopic scaling, nuclear reactions, radioactive isotopes, and atomic excitation states

21 p3484 N71-34820

Comparison of angular momentum quantum number and electromagnetic de-excitation properties of ^{20}Ne , ^{21}Ne , ^{22}Ne , and ^{23}Ne nuclei for rotor, disk, and cascade model predictions

21 p3490 N71-34904

Analysis of pulsed x-discharges characterized by atomic photoconductivity in thin-layer region

21 p3492 N71-34905

Bound states of lithium investigated through final state interactions and qualitative scattering reactions on Li

22 p3543 N71-35974

Quenching excited lithium atoms and photochemical production of excited singlet oxygen species and their reactivity

22 p3644 N71-35982

Heavy body perturbation procedure for studying wave properties of interacting atoms applied to H-H and H-He systems

22 p3650 N71-36027

Inelastic scattering of vibrational and rotational excitations levels of molecular nitrogen target in low energy atomic collisions

23 p3811 N71-37173

Tables of generalized oscillator strengths for excitation and ionization of atoms He through Na

23 p3814 N71-37196

Isotopic scaling studies between 4 MeV and 6 MeV ionization Cn-40p/Cn-48

23 p3815 N71-37204

Ion decay properties of Gamow-Teller (spin) excitations in odd-odd nuclei

23 p3817 N71-37223

Pauli Thomas-Fermi method for calculating photoionization cross sections of atoms from ground states

23 p3817 N71-37228

Theory of electron bremsstrahlung in nuclear and Compton fields using distorted wave Born approximation

23 p3821 N71-37260

Further approximation of differential and integrated atomic hydrogen excitation cross sections at electron impact

24 p3971 N71-38337

Atomic excitation and photon emission by sudden change of nuclear charge during beta-minus decay

24 p3971 N71-38361

Thomson scattering excitations in Al-285

24 p3976 N71-38365

NUCLEAR EXPLOSIONS

NUCLEAR EXPLOSIONS

NUCLEAR EXPLOSIONS

NUCLEAR EXPLOSIONS

NUCLEAR EXPLOSIONS

NUCLEAR EXPLOSIONS

NUCLEAR EXPLOSIONS

Studying properties of atoms, molecules, and plasmas by radio frequency, microwave and optical spectroscopy

23 p3818 N71-37232

Existence bound calculations for atomic model by variational calculus

24 p3979 N71-38397

ATOMIC RECOMBINATION

Electronic dipole interactions among substitutional pair molecules and atoms in alkali halides

07 p1093 N71-17450

Recombination of nitrogen atoms, visible emission from oxygen atoms, and photolysis of sulfur dioxide for atmospheric studies

08 p1194 N71-19024

Recombination of iodine atoms in dilute argon solutions studied by flash photolysis

09 p1439 N71-19747

Atom recombination and molecule production from atomic hydrogen reactions on clean metal surfaces

21 p3442 N71-34494

ATOMIC SPECTRA

Absorption spectrum of boron vapor in region of autoionization from 2362 to 1700

02 p0069 N71-11144

Mathematical proof of spherical symmetry of exchange potential produced by closed shell

06 p0914 N71-15958

Rapid atomic absorption spectrophotometric analysis of group 4B, 5B, and 6B metals in uranium alloys

07 p1042 N71-17349

Boron 11 NMR spectra of B9H11 ligand derivatives

06 p1260 N71-18687

Two particle fractional partition coefficients for atomic spectral calculations - tables

06 p1262 N71-18886

Applications of plasma kinetic theory to atomic spectroscopy

09 p1449 N71-30813

Van de Graaff accelerator operation in atomic beam foil spectroscopy

11 p1803 N71-22119

Fluorescence cross section data as function of wavelength for 24 atoms

14 p2305 N71-26087

Residual interactions in quadrupole pair production and influence on atomic excitation spectra in transuranic even-even nuclei

14 p2314 N71-26718

Odd-even staggering of nuclear radii in isotope shifts of atomic and molecular spectra, calculated using pairing plus quadrupole model

15 p2408 N71-27343

Atomic absorption spectra of clouds formed by laser-induced vaporization of chromium steel

17 p2730 N71-29225

Development of atomic absorption spectrophotometric techniques for analysis of alloying elements in stainless steels

17 p2763 N71-29348

Spectral line drift measurements on alkaline earth metals in hollow cathode discharge by interferometer

19 p3166 N71-32783

ATOMIC STRUCTURE

Research in relevance and electronic structure of heterocyclic radicals

02 p0175 N71-11230

Electronic structure of cluster ion with 33 argon atoms in icosahedral symmetry

03 p0438 N71-12949

Model for carbon fiber structure

03 p0596 N71-13013

Electron scattering and atomic structure

03 p0436 N71-13574

Heat of formation of metal oxides and thermal stability related to their atomic structure

05 p0638 N71-14590

Computer program for tabulating mass differences of various molecules and for deriving empirical formulae for molecular fragment

05 p0737 N71-14620

Method for determining parameters of atomic structure in plasma radiation

05 p0743 N71-15152

Investigating short-range behavior of wave function by comparing projected Hartree-Fock spectra using basis functions having harmonic oscillator and Wood-Burns radial dependence

05 p0748 N71-15283

Description of crystal defects by point force arrays

05 p0759 N71-15376

Program for solving mixed relativistic and non-relativistic form of Hartree-Fock equations

06 p0919 N71-16247

Electronic properties of solids including atomic and band structure calculations

06 p0934 N71-16304

Structures and electromagnetic properties of magnetic polymers

06 p0982 N71-16780

Atomic structure of Cr-51 via prompt gamma ray emission and intensity measurements

07 p1077 N71-17550

Mass transport and atomic structure near metal surfaces

06 p1277 N71-18411

Atomic energy levels, and atomic and molecular structure of systems in microscopic environments

06 p1283 N71-18807

Configuration interaction wave functions and properties of atoms and diatomic molecules

06 p1284 N71-18893

Local atomic arrangements in some silver-palladium and gold-palladium alloys

06 p1289 N71-19321

Negative mass absorption by atomic structures and theoretical model of atomic molecules

06 p1443 N71-30405

Relativistic, radial expectation values, and potentials for free atoms from 2 equals 2 to 126 as calculated from relativistic Hartree-Fock-Slater atomic wave functions

10 p1614 N71-30848

Project review for experimental and theoretical investigations of light nuclei

10 p1643 N71-31066

Recent structure of lithium between 2 triplet S and 2 singlet P thresholds

10 p1617 N71-31374

Atomic structure of amorphous arsenic colloids and germanium telluride semiconductor colloids

10 p1636 N71-31806

Determination of isotopic composition and quantity of radioactive metal by gamma spectroscopy

11 p1782 N71-32264

Small cluster theory of electronic structure of disordered systems

12 p1979 N71-34330

Development of statistical model for electrons in atoms based on expansion of one-electron Orstein function in spherical harmonics

13 p2146 N71-34938

Unrestricted Hartree-Fock atomic wave functions for neutral, divalent, and trivalent transition metal atoms

13 p2131 N71-34949

Nuclear quadrupole resonance spectroscopy of nitrogen bonds in nitrate with boron, carbon, and chlorine substitution including atomic structure and lattice effects in ionic crystals

14 p2396 N71-26308

Solid state physics for calculating material parameters and characteristics

14 p2329 N71-26543

Hartree approximations of configurational energies of light nuclei with 1p and 2s-1d shells

15 p0461 N71-27808

Calculation method of identifying elements 162 and 164 and measurement of integrated angular distribution of nuclear reaction products for identifying atomic number of elements

15 p3473 N71-37441

Applying Hylleraas correlation function to Gluck-Gordon combination of Hartree-Fock orbitals for two electrons

15 p3484 N71-37790

Structural, magnetic, and spectroscopic examination of dical cuprate dihydrides

15 p3510 N71-27978

Investigating pair correlations of superconducting type in metal with A greater than 100 using Bardeen-Wood potential

16 p3661 N71-29198

Atomic structure, radiation effects on atoms, radiation detection using nonlinear of gases and solids, p-n junction detector, and practical p-n junction devices

17 p3627 N71-30103

Shell structure of light nuclei during inelastic scattering of high energy electrons accompanied by knockout of nucleons from nuclei

18 p3974 N71-38251

Time dependent perturbation theory for evaluating angular distribution of electrons emitted from inner atomic shells by proton impact

18 p3983 N71-38133

Electronic structure and optical properties of semiconductor materials used in solid state devices for aerospace environments

18 p3997 N71-31215

Conference on atomic, molecular, solid-state theory and quantum biology

19 p3197 N71-32525

Mechanism of diffusion of some elements in brass and steel - atomic transference and movement of electrons in metal lattices

20 p3284 N71-33327

Structure of hydrogen covering hydrocarbon and semiconducting processes

22 p3446 N71-30880

Hyperspherical harmonics for Hartree-Fock atoms

24 p3983 N71-38427

Atomic structure, bonding, and transport properties of various amorphous semiconductors

24 p3988 N71-38517

ATOMIC THEORY

MT. HEISENBERG THEORY

ATOMIZATION

- Exact screened calculations of atomic field bremsstrahlung
[NYO-3629-51] 02 p0272 N71-11772
- Borevsky elementary particle model of nuclei vibrations
[RLO-1925-46] 10 p1618 N71-21388
- Fine structure transition theory and low energy collisions between atomic systems
[AD-716831] 10 p1618 N71-21400
- Experimental and theoretical high energy studies also atomic, statistical, plasma, and health physics - connecting and data handling
[UCRL-28138] 14 p2301 N71-25741
- Quantum electrodynamics of atom interaction with radiation field
15 p2494 N71-27957
- Photon theory of light and matter
[NASA-TT-F-13495] 16 p2640 N71-29002
- Phenomenological approximations in atomic theory
[PAM-70-9] 18 p2943 N71-30578
- Long-range electrostatic and electromagnetic interactions between two neutral hydrogenic atoms in ground state
[NASA-TB-8-367] 18 p2982 N71-30917
- Numerical solution of Thomas-Fermi atomic model with quantum corrections
[P-4546] 20 p3291 N71-33133
- Quantum sciences and atomic, molecular, and solid state theory
[REPT-224] 22 p3699 N71-36379
- Scaled Thomas-Fermi method for calculating photoionization cross sections of atoms from ground level data
23 p3817 N71-37228

ATOMIZATION

U ATOMIZING

ATOMIZERS

- Portable cryogenic cooling system design including turbine pump, cooling chamber, and atomizer
[NASA-CASE-NPO-10467] 14 p2398 N71-26654

ATOMIZING

- Formation and movement of droplets in atomization in gas-liquid phase
[PB-1921797] 01 p0362 N71-12692
- Drop radius calculations for estimating dust sedimentation on drops formed in high-velocity gas atomization and comparison with laser diameter calculations
[ANL-TRANS-871] 12 p1901 N71-23676

ATOMS

NT METASTABLE ATOMS

NT OXYGEN ATOMS

NT RECOIL ATOMS

- Atom diffusion and diffusion-controlled processes in solids including metals, semiconductors, oxides, and piezoelectric crystals
[AD-711417] 02 p0286 N71-11926
- Thermotransport of oxygen and nitrogen in silicon beta-titanium, beta-zirconium, and tantalum
[NP-10486] 08 p1211 N71-18155
- Meteor atom and molecule effective diffusion cross sections and application to meteor theoretical physics problems
[NASA-TT-F-13493] 12 p1998 N71-24289
- Substrate mediated interaction between adsorbed atoms caused by exchange of phonons
[RLO-1308-085] 18 p2985 N71-31219
- Hot atom beam in halogens and hydrogen sources, cathode sputtering of non-metals, and hot atom reactions of alkali metals
[AD-722450] 19 p3030 N71-32107
- Isotope effect for diffusion of interstitial atoms
[ANL-TRANS-882] 22 p3643 N71-35977

ATP

U ADENOSINE TRIPHOSPHATE [ATP]

ATR REACTOR

U ADVANCED TEST REACTORS

ATROPHY

- Atrophy in monkeys due to immobilization and implications for extended manned space flight
20 p3217 N71-33260

ATS [SATELLITES]

- U APPLICATIONS TECHNOLOGY SATELLITES

ATS 1

- Meteorological data catalog for Applications Technology Satellites - Vol. 4
[NASA-TM-X-64469] 02 p0254 N71-11694
- Cloud photography from ATS 1 and ATS 3
02 p0255 N71-11614
- Quantitative radiance measurements in visible region from ATS 1 spin-scan camera
02 p0256 N71-11619
- Performance of ATS 1 spin-scan cloud cover camera equipment at Mojave ground station
[NASA-TM-X-65401] 05 p0482 N71-14801
- Data analysis on ATS-1 Suprathermal Ion Detector (SID) measurements of low energy plasma flow in magnetopause boundary
[NASA-CR-121452] 20 p3267 N71-33563
- Total electron density plots obtained at Hawaii from ATS 1 VHF telemetry - 1 Jan. to 31 Dec. 1970
22 p3575 N71-35458

- Navigation accuracy resulting from sidetone signals relayed by two synchronous ATS-1 and ATS-3 satellites and application to aircraft navigation
[NASA-CR-121577] 22 p3617 N71-35770
- ATS 1 Faraday effect data applied to Pioneer 6 space probe solar corona data
24 p3914 N71-37911

ATS 2

- Analysis of air density relationships to solar activity and geomagnetic disturbances based on ATS 2 orbital data
[RAE-TR-70084] 21 p3430 N71-34336
- Isochoric electron constant from Faraday rotation measurements of ATS 1 and Pioneer 7 space probe
24 p3914 N71-37910

ATS 3

- Applications Technology Satellite reflectometer experimental data
[NASA-CR-107063] 01 p0854 N71-10364
- ATS 3 mapping and position fixing experiments
[NASA-CR-111592] 02 p0179 N71-11255
- Meteorological data catalog for Applications Technology Satellites - Vol. 4
[NASA-TM-X-64469] 02 p0254 N71-11604
- Cloud photography from ATS 1 and ATS 3
02 p0255 N71-11614
- Cloud distributions determined using reflected radiance measurements from multicolor spin-scan cloud camera on ATS 3
02 p0256 N71-11620

- Very Long Baseline Interferometer experiments using ATS 3 and ATS 5 satellites
[NASA-TM-X-65428] 06 p0860 N71-16447

- Meteorological benefits from satellite-borne photography, ATS 3 photographic equipment, and photointerpretation of cloud photography
[NASA-BF-79] 14 p2286 N71-25782

- Meteorological data catalog for ATS 3 1 Aug. 1969 - 23 May 1970 and summary of ATS 1 operations
[NASA-CR-118653] 14 p2289 N71-26621

- Test plans for conducting very long baseline interferometer experiments using Applications Technology Satellites 3 and 5
[NASA-TM-X-65608] 18 p2921 N71-30440

- Navigation accuracy resulting from sidetone signals relayed by two synchronous ATS-1 and ATS-3 satellites and application to aircraft navigation
[NASA-CR-121577] 22 p3617 N71-35770

- Isochoric electron constant up to plasmasphere determined from Faraday results of ATS 3 data
24 p3912 N71-37888

- Total ionospheric electron content measurements with ATS 3 signal Faraday effect, noting gravity wave effects
24 p3915 N71-37915

ATS 5

- Data evaluation for ATS 5 millimeter wave measurements of meteorological parameters
[NASA-TM-X-65771] 01 p0823 N71-10654

- Analysis of coordinated observations from ATS 5 and low altitude polar satellite OVI-1
[NASA-CR-115779] 04 p0608 N71-14419

- Very Long Baseline Interferometer experiments using ATS 3 and ATS 5 satellites
[NASA-TM-X-65428] 06 p0860 N71-16447

- ATS 5 ground station magnetometer data processing program
[NASA-TM-X-65457] 08 p1166 N71-19082

- ATS 5 down link 15 GHz signal propagation compared to ground based radio and meteorological data
10 p1523 N71-21418

- Measurements on microwave attenuation by precipitation by ATS 5 satellite beacon
10 p1523 N71-21419

- Test plans for conducting very long baseline interferometer experiments using Applications Technology Satellites 3 and 5
[NASA-TM-X-65608] 18 p2921 N71-30440

- Development and characteristics of apparatus to magnetically couple artificial satellites with specific application to ATS 5 satellite
[NASA-TM-X-65615] 18 p3017 N71-30493

- ATS 5 observational data on isolated magnetospheric substorms
[NASA-CR-119773] 19 p3094 N71-32367

- Tom code range and position system adapted to L band frequency of ATS 5
[NASA-CR-121622] 21 p3455 N71-34586

ATS 6

- ATS-F Nimbus E tracking and data relay experiment
[NASA-TM-X-65400] 05 p0770 N71-14597

- Computer program for calculating radiation pattern of ATS 6 flexible rib-reinforced reflector
13 p3648 N71-23317

- Utilization prospects of ATS 6 beacon radiated frequencies
24 p3913 N71-37898

- ATS 6 radio signal receiver for measuring total electron content of ionosphere and magnetosphere
24 p3915 N71-37914

ATS 7

- System analysis and tradeoffs, spacecraft subsystems, and development of ATS 7 satellite
[NASA-CR-111199] 01 p0126 N71-10639

SUBJECT INDEX

- Design parameters and program objectives of Applications Technology Satellites 7 and 8
[NASA-CR-111149] 01 p0126 N71-10639
- Functional and performance requirements of a time control subsystem for Applications Technology Satellites 7 and 8
[NASA-CR-111150] 01 p0126 N71-10639

ATTACK AIRCRAFT

- NT A-4 AIRCRAFT
NT A-6 AIRCRAFT
NT B-52 AIRCRAFT
NT B-57 AIRCRAFT
NT B-70 AIRCRAFT
NT BUCCANER AIRCRAFT
NT F-104 AIRCRAFT
NT F-106 AIRCRAFT
NT F-111 AIRCRAFT
NT FIGHTER AIRCRAFT
NT JAGUAR AIRCRAFT
NT OV-10 AIRCRAFT
NT VJ-101 AIRCRAFT

- Inspection and structure of aerial laser camera for photographic scanning from aircraft
[AD-723620] 19 p3008 N71-31710

- Maintenance, management planning, and requirements for single seat attack/lighter aircraft
[AD-723227] 19 p3006 N71-31688

ATTENTION

- Psychophysics of human attention, and sensory and time discrimination
[NASA-CR-119023] 16 p2545 N71-30888

- Analysis of cerebral slow potentials underlying human attentive processes in central nervous system
[NASA-CR-121409] 20 p3220 N71-31688

- Neural mechanisms underlying visual perception, arousal, and attention processes in man, cat, and monkey
[NASA-CR-122941] 23 p3712 N71-36688

ATTENUATION

- NT ACOUSTIC ATTENUATION
NT ATMOSPHERIC ATTENUATION
NT AUROREAL ABSORPTION
NT MANDELSTAM REPRESENTATION
NT RADAR ATTENUATION
NT RADIO ATTENUATION
NT SHOCK WAVE ATTENUATION
NT SIDELOBE REDUCTION
NT WAVE ATTENUATION

- Characteristics of overline circular waveguide at transitions at 3-millimeter wavelengths
[AD-712378] 05 p0338 N71-12888

- Computer program for calculating fast antenna attenuation in dense material separated by water
[ORNL-TR-2357] 06 p0917 N71-16010

- Transmission, attenuation, and signal to noise calculations for RF optical communication
[PUBL-157] 09 p1350 N71-30888

- Attenuation of photonic sunlight and moonlight for TD-1 satellite baffle system
11 p1822 N71-20314

- Attenuation of photonic sunlight and moonlight at photometer channel in TD-1 satellite baffle system
11 p1822 N71-20314

- Mechanisms of underwater sound attenuation at various frequencies and environmental parameters of temperature and pressure
[AD-718350] 12 p1965 N71-20314

- Ultrasonic attenuation in liquid sodium cooled between 94 to 146 K with pressure to 5700 psi
12 p1971 N71-20314

- Effect of turbulent shear on decay of trailing vortex system behind aircraft
[AD-720852] 15 p2394 N71-37898

- Experimental techniques for determining electron attenuation lengths in metals in energy range to 50 keV
[AD-720849] 15 p2397 N71-37898

- Flow shape, steam volume fraction and pressure drop in two phase flow of water-steam determined by attenuation of gamma ray beam
[NLL-RISLEY-TRANS-1950-70091.59] 19 p3082 N71-30888

ATTENUATION COEFFICIENTS

- Attenuation coefficient of 0.6 to 14 micron wave in water and fog, determined with appropriate optics
[AD-714786] 07 p1069 N71-17875

- Method for solving transfer functions, phase and reflection factors, and attenuation coefficients in linear passive networks for component tolerances
[SC-T-70-4048] 10 p1535 N71-20314

- Temporal and spatial distribution of atmospheric transmissivity coefficients based on long-term monthly mean flux densities of direct solar radiation for 1954 to 1963 in USSR
[NLL-M-26097-19628.4P] 21 p3422 N71-30888

- Volume photometric model and photometric determination of electron attenuation lengths in copper, sodium and aluminum
[ORNL-TM-2617] 24 p3980 N71-36688

ATTENUATORS

- NT PRINTED RESISTORS
NT RESISTORS
NT THERMISTORS

SUBJECT INDEX

Investigating construction of Unibonds diodes for microwave switching and attenuation circuits
[N7-70-1] 06 p0023 N71-10891

Design and development of positive air shock wave
[AD-710013] 09 p1475 N71-19061

ATTITUDE (INCLINATION)
NT PITCH (INCLINATION)
NT ROLL
NT SATELLITE ORIENTATION
NT YAW

Investigating operation of ion orientation sensors based on perception of charged particles stream in upper atmosphere and deviation of vehicle axis from stream direction
03 p0416 N71-13179

Ballistic range test equipment for measuring model position, attitude, and velocity
[NASA-TM-X-65535] 04 p0522 N71-13582

Operation and training uses of vestibular analyzer
[N7-52173] 07 p0985 N71-16978

Rate of vestibular compensatory process in naturally labyrinthectomized rabbit
07 p0979 N71-16980

Dynamic of orientation system for space vehicles using angular position transducers as sensors
11 p1787 N71-22268

Spatial orientation of crystals in ice formed in water under with different temperature regimes
11 p1753 N71-22868

Postflight analysis of Aerobion rocket vehicle attitude determination with solar aspect sensors and magnetometers
[NASA-TM-X-65570] 15 p2442 N71-27738

Effect of mission attitude timelines on consumable requirements for proposed shuttle orbiters least rejection systems
[NASA-CR-115117] 19 p3183 N71-31602

Reaction and maneuverability for systems of axes, attitude angles, direction angles, and flight control systems for aircraft dynamics
[ARC-RM-5563-PT-3] 20 p3283 N71-32862

Total gravity variations of earth crust observed in USSR
20 p3263 N71-33348

Laboratory and on tests of gyrotheoretical marine gyroscope for measuring disturbing accelerations and its in submarine
21 p3417 N71-34316

Instrument for synchronous photographic recording of perturbing acceleration and residual axis of gyrotheoretical platform
21 p3418 N71-34320

Resonance relation for general normalized inclination functions with three parameters and axisymmetric spin for earth satellite orbits
[NASA-TM-70074] 21 p3449 N71-34548

Research attitude sensing system design with narrow-field of view sensor rotating about spacecraft x-y axis
[NASA-CASE-GSC-10890-1] 21 p3455 N71-34589

Earth tilt observations at two stations south of Hawaii
24 p3918 N71-37872

Earth tilt measurements by parallel clinometers
24 p3911 N71-37877

Gravitational influence on earth tides and clinometer observations
24 p3911 N71-37878

ATTITUDE CONTROL
NT DIRECTIONAL CONTROL
NT LATERAL CONTROL
NT LONGITUDINAL CONTROL
NT SATELLITE ATTITUDE CONTROL
NT THERUST VECTOR CONTROL

Attitude control training device for astronauts performing closed-loop movement with five degrees of freedom
[NASA-CASE-XMS-62577] 01 p0839 N71-10746

Long angle, three dimensional reconstruction of maneuvering spacecraft in real optimal manner
[AD-710706] 01 p0126 N71-10750

Photostabilizer detector of Canopus for spacecraft attitude control
[NASA-CASE-XNP-60914] 01 p0883 N71-10771

Attitude control system for Skylark rocket payloads using solar sensors
02 p0262 N71-11761

CAROUSEL system for rocket-borne astronomical telescopes attitude control
02 p0262 N71-11762

Investigating various sources of attitude errors in bank Arrow third stage and effects on accuracy of velocity increment error
[N7-70-2377] 02 p0299 N71-11969

Linear interaction problem between spacecraft attitude control and flexible appendages solved in frequency domain using Fourier transform
[NASA-CR-111530] 03 p0499 N71-13063

Control moment gyro fine attitude control system for spacecraft
[NASA-CR-106763] 03 p0410 N71-13280

Automatic balancing device for use on frictionless attitude-controlled test platforms
[NASA-CASE-LAB-10774] 04 p0513 N71-13545

Development of spacecraft experiment pointing and attitude control system
[NASA-CASE-XLA-65464] 04 p0543 N71-14132

Stability and performance characteristics of earth-orbiting, attitude-control, shock-sensor spacecraft
[NASA-TM-X-65464] 04 p0543 N71-14132

Development of attitude control system for spacecraft orientation
[NASA-CASE-XOS-64393] 04 p0543 N71-14139

System for aerodynamic control of rocket vehicles by secondary injection of fluid into nozzle exhaust stream
[NASA-CASE-XLA-61163] 05 p0721 N71-15582

Drive mechanism for operating resistance attitude control system for aerospace bodies
[NASA-CASE-XMP-61396] 05 p0721 N71-15583

Attitude detection system using stellar references for three-axis control and spin stabilized spacecraft
[NASA-CASE-XOS-63431] 05 p0721 N71-15642

Remote control device operated by movement of fluid-type for manual control of spacecraft attitude
[NASA-CASE-XAC-62460] 06 p0523 N71-16089

Developing attitude control single-axis detector for Thermoelectric Outer Planet Spacecraft
06 p0893 N71-16480

Spin axis scanning of celestial sphere for attitude control of spin stabilized spacecraft
[NASA-TM-D-5611] 06 p0940 N71-16840

Development of attitude control system for orbiting space vehicles
[NASA-CR-140206] 07 p1057 N71-17445

Development of magnetic attitude control system for High Energy Astronomy Observatory satellite
[NASA-CR-140205] 07 p1057 N71-17446

Design development, and characteristics of attitude control propulsion systems
[NASA-CR-114651] 07 p1185 N71-17566

Target and attitude control apparatus using jet nozzle in movable control surface or fin configurations
[NASA-CASE-XLE-65383] 07 p1119 N71-17629

Computation of fuel optimal controls for large angle attitude motions of satellite system
07 p1119 N71-17678

Design criteria and performance specifications for spacecraft sun sensors
[NASA-SP-6047] 07 p1032 N71-17756

Dynamic, control requirements, and optimal performance of lumped, two-body satellite attitude control system
07 p1121 N71-17784

Equilibrium states and attitude stability of dual spin spacecraft
[NASA-TM-X-342] 09 p1415 N71-20143

Principles of operation and characteristics of attitude control systems for surface-to-surface missiles
[AD-717096] 10 p1599 N71-20922

Electric propulsion engine, digital gyro system, and step motor solar electric thrust vector system for interplanetary spacecraft control
10 p1600 N71-21348

Results and description of qualification tests of attitude control system and pyro-duplex system in flight configuration as installed on DMF-1 spacecraft
[NASA-TM-X-65473] 10 p1600 N71-21349

Attitude sensor with scanning mirrors for detecting orientation of space vehicle with respect to planet
[NASA-CASE-XLA-60793] 11 p1793 N71-22880

Attitude sensors to determine motion of rocket free body precession including magnetometers and star trackers
[AD-716314] 12 p1960 N71-23043

Optimal methods for orbital recovery, maintenance, and repair of hybrid propellant rocket engine subsystem for orbiting space station attitude control
[NASA-CR-103111] 12 p1991 N71-23953

Operational description and performance data of ITOR 1 attitude control system
[NASA-TM-X-65490] 12 p2002 N71-24178

Radiation torque sources and effects on spacecraft and spacecraft attitude control system design
[NASA-SP-60577] 12 p2002 N71-24312

Development of attitude control system for aerodynamic stabilization during ballistic phase of flight
[NASA-CASE-XOS-61654] 13 p2172 N71-24750

Structural modes required to determine interaction between attitude control system and flexible deployed solar electric spacecraft
[NASA-CR-113327] 13 p2175 N71-25155

Optimal quadratic Lagrange function generating algorithm for estimating domain of equilibrium attraction of nonlinear star tracker attitude control systems for GAO stability
[NASA-CR-11729] 15 p2433 N71-26916

Absolute stability analysis of attitude control systems for large launch vehicles
[NASA-TM-X-64522] 15 p2519 N71-26951

Adaptive differential learning control system for launch vehicles
[NASA-TM-X-64518] 15 p2442 N71-27046

Design of solar powered spacecraft with three axis attitude control
[NASA-TT-P-15060] 16 p0883 N71-28949

Preliminary study of airplane-aircraft response to atmospheric turbulence while operating in altitude-hold and attitude-hold modes
18 p2870 N71-30780

AUDIO FREQUENCIES

Engineering description of TACS-3M RCS consumables program - Skylab Program
[NASA-CR-115114] 19 p3183 N71-31804

Flight simulation of hovering vertical takeoff aircraft with various attitude and speed controls
19 p3074 N71-31955

Design, development, fabrication, and acceptance test results for two flexible proportional thrusters for use in SPARC3-4
[NASA-CR-114333] 19 p3186 N71-32794

Development of voice operated controller for controlling reaction jets of spacecraft
[NASA-CASE-XLA-64463] 20 p3354 N71-33160

Computer program documentation and user manual for transient attitude attitude control propulsion systems
[NASA-CR-115162] 23 p3728 N71-34572

Computer program documentation and user manual for steady state attitude control propulsion system - vol. 1
[NASA-CR-115104] 23 p3728 N71-34573

Development of general computer simulation model for attitude control propulsion systems and computer program documentation - Vol. 2
[NASA-CR-115183] 23 p3728 N71-34574

Development of generalized, transient and steady-state simulation models for space shuttle attitude control propulsion system
[NASA-CR-115103] 23 p3839 N71-37375

Deflectable dual beam, linear video camera contact, ion thruster system design and performance testing
[NASA-CR-72989] 23 p3839 N71-37376

Development of design and programmatic data for space shuttle reaction control systems and integrated reaction control system/orbit measuring systems
[NASA-CR-123146] 24 p0016 N71-36856

ATTITUDE GYRO
NT GYRO HORIZONS

Behavior of attitude gyro and gyro busines during looping flight
03 p0413 N71-13381

Performance and nonlinear control of twin gyro attitude control system with positive compensation
07 p1058 N71-17821

ATTITUDE INDICATORS
NT GYRO HORIZONS

DMF-1 optical aspect system based on spacecraft angular relationship between sun and earth using digital solar sensor and visible-light detector
[NASA-TM-D-7000] 10 p1539 N71-21220

Hand controller operable about three respectively perpendicular axes and capable of actuating signal generators for attitude control devices
[NASA-CASE-XMS-67487] 12 p1925 N71-23255

Combined optical attitude and attitude indicating instrument for use in aircraft or spacecraft
[NASA-CASE-XLA-61907] 13 p1917 N71-23268

Postflight analysis of Aerobion rocket vehicle attitude determination with solar aspect sensors and magnetometers
[NASA-TM-X-65570] 15 p2442 N71-27738

Earth tilt measurements by parallel clinometers
24 p3911 N71-37877

ATTITUDE STABILITY
NT DIRECTIONAL STABILITY
NT GYROSCOPIC STABILITY
NT LATERAL STABILITY
NT LONGITUDINAL STABILITY

Investigating nonlinear digital control methods for attitude stabilization of VTOL aircraft
03 p0347 N71-12615

Effects of energy dissipation on systems stability of SAS-A spacecraft
[NASA-TM-X-65537] 15 p2442 N71-27706

Spin-axis attitude stability of dissipative dual spin spacecraft in force-free environment
[NASA-TM-X-65581] 21 p3483 N71-34587

AUDIO EQUIPMENT
NT MICROPHONES

Determination of real ear attenuation for Con-Fit earplugs using human subjects
[JEP-1971-6] 18 p0883 N71-30873

Distribution and other amplifiers for human voice communication
[AD-72810] 19 p0664 N71-31710

Airborne multi-video recording system design and results
[AD-727625] 22 p3549 N71-35280

AUDIO FREQUENCIES

Evaluation of frequency spectrum of human speech as method for determining degree and nature of emotional stress
[JPRS-52806] 10 p1385 N71-31725

Effect of low frequency periodic perturbations of height of conducting surface on earth local electric field normal component
[AD-719426] 13 p2124 N71-24637

High efficiency transformation amplitude modulator coupled to RF power amplifier
[NASA-CASE-GSC-10660-1] 16 p0261 N71-30430

Integrated circuits designed for audio frequency output amplifier and the output stage of television receiver
23 p3726 N71-34644

AUDIO VISUAL EQUIPMENT

Radiation impedance functions of rectangular pistons and their application to sound transmission through finite depth apertures 23 p3805 N71-37130

Construction and tests at audio frequencies of half-wave microwave rectifying circuit with theoretical efficiency of 100 percent 24 p4014 N71-38634

AUDIO VISUAL EQUIPMENT U TRAINING DEVICES U VISUAL AIDS AUDIOMETRY

Determining feasibility of using transformer and common base preamplifier impedance matching to detect very low level electrical signals from radiometers [AD-711639] 01 p0013 N71-10690

Characteristics of acoustic damage found in technical military personnel 02 p0171 N71-11808

Pure tone audiometry for monitoring hearing and determining physical profiles of persons routinely exposed to potentially hazardous noise 11 p1680 N71-22151

Feasibility of on-site audiometer calibration check [AD-718417] 12 p1866 N71-23355

Procedure for measuring auditory threshold displacements and prediction of auditory masking patterns [FAA-AM-71-1] 13 p2124 N71-24746

AUDITORY DEFECTS

Characteristics of acoustic damage found in technical military personnel 02 p0171 N71-11808

Acoustic pattern recognition neurophysiological transformation into synthetic signals by deaf persons 11 p1685 N71-23064

AUDITORY FATIGUE

Improving signal to noise ratios for speech signal processing by aircraft pilots [FAA-AM-70-6] 05 p0635 N71-14991

AUDITORY PERCEPTION

Physiological aspects of auditory perception of complex sound, combination tones, and sinusoidal tones [TDCK-56077-16] 05 p0632 N71-14571

Measurements and comparison of human visual and auditory acoustics [EZF-1976-12] 05 p0633 N71-14651

Improving signal to noise ratios for speech signal processing by aircraft pilots [FAA-AM-70-6] 05 p0635 N71-14991

Auditory perception thresholds and long term effects [NPL-AERO-AC-44] 07 p0980 N71-17098

Subjective evaluation tests of ground observers on relative noise from acoustically treated engine nacelles of Boeing 707 aircraft [NASA-CR-1717] 08 p1143 N71-18499

Real ear evaluation of earplugs using comparison of noise bands to pure tones 08 p1148 N71-18536

Visual and acoustic discrimination of dolphin under conditions of good and poor visibility [JPRS-52444] 08 p1153 N71-19023

Mass growth and recovery function for temporary threshold shifts produced by extended exposure to simulated armored vehicle 10 p1499 N71-21041

Speech discrimination test for pilot pure-tone hearing standards [AD-717232] 10 p1499 N71-21061

Pure tone audiometry for monitoring hearing and determining physical profiles of persons routinely exposed to potentially hazardous noise 11 p1680 N71-22151

Audiometric evaluation of aging pilots hearing acuity in relation to flying time 11 p1690 N71-22320

Acoustic pattern recognition neurophysiological transformation into synthetic signals by deaf persons 11 p1685 N71-23064

Auditory and tactile information transfer of biological systems 11 p1693 N71-23066

Weighting method for aircraft auditory risk limits when wearing ear protectors [AD-719061] 13 p2038 N71-25086

Analog simulation of peripheral, ascending, and central auditory perception mechanisms and band-width compression relationships to speech recognition [AD-720246] 14 p2206 N71-26261

Judgment of effects of Doppler shifts on perceived loudness of aircraft made by subjects in anechoic chamber [NASA-CR-1779] 17 p2709 N71-29980

Determination of real ear attenuation for Com-Fit earplugs using human subjects [EZF-1971-4] 18 p2883 N71-30873

Analog to digital converters for voice signal analysis [JPRS-53666] 19 p3042 N71-32009

Problems of automatic auditory patterns recognition and solutions 19 p3042 N71-32010

Psychophysical evidence of lateral inhibition in hearing [EZF-1971-4] 20 p3225 N71-33859

AUDITORY REHABILITATION

Mechanical response of frog membrane to stimulating frequencies and electrophysiological determined hearing areas [NASA-CR-123162] 24 p3877 N71-37634

AUDITORY SIGNALS

Physiological aspects of auditory perception of complex sound, combination tones, and sinusoidal tones [TDCK-56077-16] 05 p0632 N71-14571

Audio signal processing system for noise surge elimination at low amplitude audio input [NASA-CASB-MSC-12233-1] 14 p2218 N71-36181

Using statistical decision theory analysis to obtain predicted performance in discrimination of brief empty time intervals between auditory signals [NASA-CR-118996] 16 p3621 N71-28135

AUDITORY STIMULI

Comparative effects of auditory and extra auditory acoustic stimulation on human equilibrium and motor performance [AD-711046] 01 p0008 N71-10177

Long term adaptation of pursuit rotor performance to impulsive acoustic stimulation [AD-715289] 08 p1140 N71-18363

Physiological and psychological limits and ranges of human response to acoustic stimuli 09 p1335 N71-20352

Effects of long term exposure on auditory thresholds for discrete tonal signals and recovery from temporary threshold shift 09 p1335 N71-20353

Auditory stimuli effects of pistol shots during learning process noting human reactions and performance [ISVR-TR-26] 10 p1504 N71-20799

Sound and visual sensory interactions of pleasant, unpleasant, and no sound with red, green, and blue lights against white standards [AD-717715] 11 p1690 N71-22341

Effects of auditory stimuli (sonic booms) on sleep and other effects of sleep deprivation [JSAV-TR-40] 17 p2710 N71-29437

Auditory stimuli effects on human color-word distraction susceptibility test performance [FAA-AM-71-7] 17 p2708 N71-29637

Neural responses of bat cochlear nuclei to ultrasonic stimuli [JPRS-54133] 23 p3716 N71-36487

Mechanical response of frog membrane to stimulating frequencies and electrophysiological determined hearing areas [NASA-CR-123162] 24 p3877 N71-37634

AUDITORY TASKS

Measuring human performance of auditory vigilance task time shared with memory task [AD-711563] 02 p0138 N71-11119

AUGER EFFECT

X ray excited LMM Auger spectra of copper, iron, and nickel [NASA-TM-X-63381] 01 p0097 N71-10584

Auger electron spectroscopy study of surface segregation in copper-aluminum alloys [NASA-TN-D-6995] 02 p0241 N71-11430

Deriving expressions for Auger transition rates for f electrons [SC-RR-70-429] 04 p0575 N71-13686

Applying Auger emission spectroscopy to analysis of silicon surfaces 07 p0989 N71-17317

Measuring Auger spectra of simple gaseous molecules [NASA-CR-116411] 07 p1072 N71-17342

Pre-accelerating spectrograph with cylindrical symmetry for studying low energy electron spectra and Auger spectra of U-235, Te-125, Ag-109, and Fe-155 10 p1622 N71-21759

Auger spectroscopy of low alloy steel, copper bismuth alloy, and refractory metal annealing and sintering embrittlement due to grain boundary fracture, corrosion, and mobility [COO-1778-6] 07 p1087 N71-23954

Electron interactions with solid surfaces, plasmon excitations and Auger emission, and sensitivity of Auger spectroscopic data [OEO-2735-25] 13 p2127 N71-25600

Lead and Auger electron spectroscopy study of oxygen adsorption on tungsten (110) [NASA-TN-D-6399] 18 p2998 N71-31454

Auger electron velocity analyzer for use with scanning electron microscope to identify low concentrations of elements on surfaces of semiconductor devices [NASA-CR-111968] 21 p3425 N71-34371

Friction and wear apparatus incorporating Auger cylindrical mirror spectrometer [NASA-TN-D-6497] 21 p3434 N71-34433

LMM peaks in Auger spectra identified for transition metals of Fe, Co, and Ni [AERE-E-6719] 21 p3438 N71-34461

AUGMENTATION

NT THRUST AUGMENTATION

SUBJECT INDEX

Rough inside diameter tubing and internal fit testing for augmented heat transfer 05 p0782 N71-14889

Augmented ram wing vehicle performance and flow field for high speed ground transportation 18 p2867 N71-36181

Kron-proton interactions and low mass enhancement due to diffraction phenomena 23 p3651 N71-37634

Augmenting combustion flames with electric discharges to produce high temperature chemical and physical reactions in 2500 to 3000 K range [BCCR/N327] 23 p3664 N71-37634

AURORAL ABSORPTION

Latitudinal distribution of auroral absorption rate in Northern Hemisphere during solar activity cycle 11 p1623 N71-22320

Auroral magnetic substorm and high energy electron absorptions 12 p1980 N71-23066

Auroral absorption measurement during auroral substorm development at geophysical observatories separated in longitude 12 p1989 N71-23066

Auroral ionization longitudinal drift rate recorded along auroral zone 12 p1989 N71-23066

Changes in surface pressure during polar cap auroral absorption [NLL-M-2000-5828-4P] 12 p1993 N71-36181

Risometer polar cap absorption, auroral absorption, and solar flare observations and ionospheric absorption forecasting [AD-721182] 15 p2395 N71-36181

Effect of quasi-rhythmicity in geomagnetic and aeromagnetic phenomena 17 p2747 N71-36181

Auroral absorption types and thermal patterns as determined by risometer measurements 17 p2748 N71-36181

AURORAL ACTIVITY

AURORAS

AURORAL ARCS

NT RED ARCS

Stable auroral red arcs [BNWL-1484] 07 p1183 N71-14889

NO measurement in auroral arc by mass spectrometer aboard Aerobee rocket [NASA-CR-116877] 08 p1194 N71-18499

Circumauroral auroral arcs and magnetic disturbances observed from polar geophysical observatory [GRI-TR-80] 10 p1547 N71-20352

ELF noise band associated with low-energy electron precipitation events and auroral arcs based on Explorer 40 observations [NASA-CR-121676] 21 p3415 N71-34309

AURORAL ELECTROJETS

Hiss, auroral electrojets, and Arctic region magnetic variations 04 p0321 N71-11119

Sounding rocket investigating auroral phenomena's charged particle precipitation, magnetic disturbances, and electric fields 05 p0668 N71-14991

Polar cap electric field measurements, and model for Hall current auroral electrojet continuity and pole cap magnetic disturbances [NASA-TM-X-65447] 07 p1019 N71-23066

Polar upper atmospheric disturbances, auroral electron and proton precipitation, and magnetospheric substorm origin 12 p1980 N71-23066

Auroral electrojet current model for polar magnetic substorms 12 p1980 N71-23066

Auroral zone X ray events detected by means of electron precipitation balloon sounding 12 p1989 N71-23066

Electric field measuring techniques used in ionospheric and magnetospheric electrojet current studies [NASA-TM-X-65596] 17 p2748 N71-36181

AURORAL IONIZATION

AURORAS

U LIGHT EMISSION

AURORAL IONIZATION

European space research organization program for auroral magnetic storms investigation - satellite observation 12 p1980 N71-23066

Auroral ionization longitudinal drift rate recorded along auroral zone 12 p1989 N71-23066

Auroral electron and proton mass determined by auroral ionization spectroscopy aboard ESO 1 satellite 12 p1989 N71-23066

Auroral photometry used on ESO 1 (Aurora) satellite for ionospheric sounding 15 p2407 N71-32009

Auroral Lyman alpha emission cross section from hydrogen-proton collisions in upper atmosphere [AD-721462] 16 p2664 N71-36181

SUBJECT INDEX

AURORAL IRRADIATION

Electromagnetic noise and altitude variation of auroral proton microbursts and proton flux density estimates 18 p2516 N71-31082

AURORAL SPECTROSCOPY

Ball-balloon ultraviolet and visual spectroscopy with no view effects for auroral spectroscopy using the photometer tubes 03 p0372 N71-13311

Optical properties and ion composition of aurora bands determined by Aerobee rocket vehicle 04 p0608 N71-14422

Aerobee multi-filter scanning photometer data on aurora 10 p1543 N71-20618

Ball-balloon and computer programming for ESO 1 auroral spectroscopy experiment 10 p1545 N71-20621

Calibration of ESO 1 spectrometer channels for auroral spectroscopy 10 p1557 N71-20752

ESO 1 spectrometer for measuring auroral electron and proton 10 p1557 N71-21005

Auroral optical emission spectroscopy by ionospheric rocket sounding 12 p1909 N71-23565

ESO 1 satellite Arctic auroral localization spectroscopy experiments 12 p2080 N71-23569

Auroral electron and proton zones determined by ionospheric localization spectroscopy onboard ESO 1 satellite 12 p1909 N71-23570

Flux, energy spectra, and phase angle distribution of precipitated low energy hydrogen and electron from Waco-Tomahawk auroral hydrogen experiment 22 p3468 N71-36155

AURORAL ZONES

High frequency auroral noise caused by proton ionization of ionosphere 02 p0180 N71-11268

ESO 1 Geiger counter and ground geophysical observations of radiation belt electron precipitation, fine structure, and angular distribution over other stars, 03 p0172 N71-11541

High altitude balloon measurements of X ray and gamma radiation in auroral zone 03 p0372 N71-13293

Magnetic variations and auroral zones over Greenland in night and daytime 04 p0321 N71-13779

Atmospheric analysis of bromostrahlung effects in low ionosphere due to electrons penetrating into ionosphere 04 p0322 N71-13824

Auroral ionospheric electric field rocket sounding by means of Geiger counters, electrostatic probe, and balloon artificial clouds 10 p1543 N71-20634

Plasma and electric field distribution over auroral zone and polar cap 10 p1546 N71-20708

Star and lunar ionospheric currents and magnetic field variations 10 p1547 N71-20809

Individual distribution of auroral absorption zone in Northern Hemisphere during solar activity cycle 11 p1823 N71-22815

Ground-based measurements of polar magnetic storms by means of magnetometers 12 p1909 N71-23558

Geomagnetic pulsation measurement for auroral magnetospheric substorm study 12 p1909 N71-23559

VLF emission measurement in auroral zone during magnetic substorm phase 12 p1909 N71-23560

Auroral localization longitudinal drift rate recorded during auroral zone 12 p1909 N71-23562

Magnetic substorm effects on auroral electron and proton precipitation 12 p1909 N71-23566

Auroral ionospheric electric field measurements by means of gas release or electrostatic probe 12 p1909 N71-23567

Auroral ionospheric plasma diagnostics by means of electrostatic probe 12 p1909 N71-23568

Confined auroral electron observations from satellite and polar satellites 13 p2074 N71-23082

Nonstationary recordings of magnetospheric plasma in auroral zone 15 p2399 N71-27187

Auroral formation and development of polar storm in polar oval 18 p2554 N71-31162

Auroral zone VLF hiss and low energy particle observations with Injun 5 satellite 20 p3266 N71-33592

Auroral proton spectra and angular distribution from Cosmos 261 satellite observations, and polar substorm concept 23 p3750 N71-36740

Flux distribution of protons precipitating in auroral zone in range of hundreds keV, as observed from Cosmos 261 satellite 23 p3750 N71-36741

Hard and soft electron emission and periodic variations in auroral zones 23 p3853 N71-37463

Beacon Explorer A signal scintillation in auroral zone, measured with Faraday and Doppler effect 24 p3915 N71-37916

AURORAS

NT AURORAL ARCS

NT RED ARCS

Turbid, geomagnetic, and auroral activity in Arctic drifting stations and at Pt. Barrow 02 p0291 N71-11143

Geomagnetic/electric current alignment, space charge and electric field effects on particle acceleration, and auroral emissions 03 p0451 N71-13332

Alouette 1 satellite electron density data and diurnal variation of Greenland auroras 04 p0615 N71-14298

Optical properties and ion composition of aurora bands determined by Aerobee rocket vehicle 04 p0608 N71-14422

Sounding rocket investigating auroral phenomena in charged particle precipitation, magnetic disturbances, and electric fields 05 p0668 N71-14747

Ionization and excitation cross sections in proton auroras 05 p0764 N71-14908

Literature survey on auroras at composite points 05 p0765 N71-15490

Measurement of relative emission rates of auroral systems 06 p0853 N71-16389

Energy of auroral charged particles drawn from solar wind, earth rotation, and atmospheric circulation, and infrared generation from electric current interactions 07 p1014 N71-16930

Cosmos 261 observations of electron and ion interactions with solar cosmic rays in aurora and photoelectron production 07 p1014 N71-16931

Dawn chorus and auroral hiss emission in upper ionosphere and magnetosphere 07 p1017 N71-17143

Model of global circulation induced by solar radiation and auroral heating, for determining ionospheric effect in atomic oxygen concentration 07 p1018 N71-17261

Secondary electron emission measurement in aurora using Aerobee rocket vehicle 08 p1193 N71-18995

Photometer observations of auroras from CV-990 aircraft 08 p1193 N71-18996

Altitude profiles of nitrogen Vegard-Kaplan band emission in aurora, from rocket-borne UV spectroscopy 08 p1194 N71-19084

Photometric observations of pulsating aurora 08 p1195 N71-19115

Spectrophotometric results from NASA 1968 Aerobee Auroral Expedition and tentative identification of several molecular nitrogen emission bands 08 p1196 N71-19148

Thermospheric density response to auroral heating during geomagnetic disturbances 09 p1385 N71-20284

ESO 1/Aurora satellite photometric data on auroral ionospheric electron and proton precipitation and population for Oct. - Nov. 1968 - conference 10 p1549 N71-21151

ESO 1 satellite photometric data on relationship between electron and proton aurora and precipitation 10 p1549 N71-21152

Correlation between ESO 1 satellite auroral photometric data and ground based observations 10 p1549 N71-21153

Swedish/NASA rocket sounding in several D and E regions for ionospheric ion and electron density investigation using Arca and Petrel rocket vehicles 10 p1552 N71-21270

Photometric observations of auroral scattering by CV 990 aircraft 11 p1702 N71-23135

Morphology of auroral geomagnetic pulsations for low and high magnetic activity observed from Tromsø, Norway 12 p1908 N71-23557

Balloon study on auroral nitrogen emission and bromostrahlung x rays produced by electron precipitation 12 p1994 N71-24274

Aerobee rocket-borne instruments for auroral measurements, including electron and proton counters, electron density and temperature probes, X ray counter, and light photometers 13 p2161 N71-25198

Extraterrestrial ring current intensity changes and aurora dynamo model 13 p2161 N71-25380

Failure of rocket flows electron accelerator to create artificial aurora 13 p2076 N71-23280

Aurora formation by electron injection and drift in upper atmosphere 13 p2076 N71-23272

Ionospheric auroral morphology, height variations, and relationships to planetary magnetic disturbances in periods of minimum and maximum solar activity at varying latitudes 17 p2745 N71-30076

Vertical sounding and ionometer investigations of ionospheric magnetic field variations and spatial position and spectra of auroras 17 p2746 N71-30077

Aerobee photography of polar auroral band during magnetic disturbances 17 p2746 N71-30078

AR sky photography of U-shaped polar aurora in ionosphere 17 p2746 N71-30079

Effect of magnetic activity on auroral height 17 p2746 N71-30080

Photometric observation of auroral pulsation characteristics 17 p2746 N71-30081

Auroral variations during maximum and minimum cycles of solar activity 17 p2747 N71-30082

Ratio of 1 NOO2/plus and 1 POH2 emissions as function of auroral height 17 p2747 N71-30083

Ionospheric processes associated with auroral height variations as determined by scanning photometer 17 p2747 N71-30084

Spectral variability analysis on auroral aurora and aurora emission data 17 p2748 N71-30139

Comparison of VLF auroral hiss with precipitating low energy electrons studied with simultaneous OGO-4 data to determine line origin 19 p3894 N71-33413

Payload preparation and launching of Black Brant rocket to investigate aurora 20 p3351 N71-33876

Comparison of Injun 5 satellite measurements of low energy electron precipitation and ground based observations of visible auroral arc 21 p3415 N71-34300

Analysis of N2A 3 Sigma positive molecule destruction in aurora using atmospheric model based on mass spectrometer measurements 21 p3415 N71-34301

AUSTENITIC STAINLESS STEELS

Electron density and temperature probes, X ray counter, and light photometers 13 p2161 N71-25198

Extraterrestrial ring current intensity changes and aurora dynamo model 13 p2161 N71-25380

Failure of rocket flows electron accelerator to create artificial aurora 13 p2076 N71-23280

Aurora formation by electron injection and drift in upper atmosphere 13 p2076 N71-23272

Ionospheric auroral morphology, height variations, and relationships to planetary magnetic disturbances in periods of minimum and maximum solar activity at varying latitudes 17 p2745 N71-30076

Vertical sounding and ionometer investigations of ionospheric magnetic field variations and spatial position and spectra of auroras 17 p2746 N71-30077

Aerobee photography of polar auroral band during magnetic disturbances 17 p2746 N71-30078

AR sky photography of U-shaped polar aurora in ionosphere 17 p2746 N71-30079

Effect of magnetic activity on auroral height 17 p2746 N71-30080

Photometric observation of auroral pulsation characteristics 17 p2746 N71-30081

Auroral variations during maximum and minimum cycles of solar activity 17 p2747 N71-30082

Ratio of 1 NOO2/plus and 1 POH2 emissions as function of auroral height 17 p2747 N71-30083

Ionospheric processes associated with auroral height variations as determined by scanning photometer 17 p2747 N71-30084

Spectral variability analysis on auroral aurora and aurora emission data 17 p2748 N71-30139

Comparison of VLF auroral hiss with precipitating low energy electrons studied with simultaneous OGO-4 data to determine line origin 19 p3894 N71-33413

Payload preparation and launching of Black Brant rocket to investigate aurora 20 p3351 N71-33876

Comparison of Injun 5 satellite measurements of low energy electron precipitation and ground based observations of visible auroral arc 21 p3415 N71-34300

Analysis of N2A 3 Sigma positive molecule destruction in aurora using atmospheric model based on mass spectrometer measurements 21 p3415 N71-34301

Preliminary thermochemical treatment of D6AC steel during annealing and martensite transformations 04 p0528 N71-13947

Mechanical properties of some metastable austenitic alloys 04 p0529 N71-14029

Microstructure and mechanical properties of martensite transformed from precipitation hardened austenite 04 p0530 N71-14091

Stress-strain properties of metastable austenites 06 p0869 N71-15087

Anelastic behavior of austenites, martensites, and bcc refractory alloys, and dislocation-solute atom interactions and interstitial hardening in bcc alloys 06 p1211 N71-16239

Production of standard reference material containing ferrite austenite for calibrating X ray diffraction equipment by powder metallographic techniques 10 p1576 N71-21608

Steel microstructure, surface martensite and carbide formation, and diffusion coefficient measurement during chemical and thermal treatment 14 p2280 N71-25640

Austenite intergranular structure effect on self diffusion of iron 14 p2371 N71-25816

Effects of prior plastic deformation of austenite on nucleation of martensite in Fe-Ni-C alloys 15 p2423 N71-27380

Electron microscope characteristics of precipitated needles in austenite-transformed austenitic steels 22 p3642 N71-33966

AUSTENITIC STAINLESS STEELS

Fast neutron radiation effects in Type 304 stainless steel 03 p0398 N71-12604

Post-weld nitrogen content of deposits on standard and HX-proof austenitic stainless steels 03 p0396 N71-13286

Manufacturing and welding austenitic steels for reactor structures 03 p0727 N71-15160

In-pile creep behavior of austenitic steels and nickel alloys under multiaxial loads
[KFK-1152] 05 p0731 N71-15587

Stress-rupture behavior of types 304 and 316 stainless steel cladding in high temperature static sodium
[AL-ABC-12976] 06 p0970 N71-19390

Behavior of metastable austenitic steels under cyclic loading
[UCRL-19620] 06 p0872 N71-16352

Strengthening of austenitic stainless steels by internal nitridation
06 p1219 N71-19111

Stress corrosion cracking of metastable austenitic TRIP steel
[UCRL-20380] 09 p1400 N71-20083

Statistical analysis to determine unalloyed steel initial state influence on tempering ability
10 p1577 N71-21144

Carbide precipitation and equilibrium in austenitic 18% steels
[NLL-CE-TRANS-5391-19022.09] 10 p1577 N71-21216

Corrosion tests on titanium, austenitic stainless steels, chromium ferrites, and light alloys in sea water up to 150°C
[ORNL-TR-2412] 10 p1580 N71-21405

Structural stability of austenitic Cr-Ni steels under plastic deformation and extremely low temperature
[ORNL-TR-2314] 10 p1580 N71-21406

Cold working effects on creep properties of elongated cylindrical austenitic steel specimens at room temperature
[NLL-CE-TRANS-5413-19022.09] 10 p1581 N71-21478

Structural transformations and properties of high strength Cr-Mn-Ni austenitic steels
[JPRS-52877] 12 p1936 N71-23148

Irradiation induced creep in austenitic stainless steels at 45 and 370°C
[WHAN-FR-39] 14 p2267 N71-25641

Gross-section monitoring to determine stability of austenitic formed in surface layers during friction of high strength cast irons
[AD-720762] 14 p2276 N71-26661

Irradiation produced defects in microstructure of annealed austenitic stainless steels
[WHAN-FR-16] 15 p2420 N71-26921

Effect of cold working on creep properties of AISI 316 type stainless steel
[JAERI-MEMO-4123] 15 p2422 N71-27218

Design methods for light gas coil formed structural elements and members made of cold rolled austenitic stainless steel
15 p2423 N71-27327

Microstructure precipitates in austenitic steel exposed to neutron irradiation
[CEA-CONF-1638] 15 p2424 N71-27406

Grain boundary diffusion coefficients and reaction kinetics for austenitic stainless steel carburizing by carbide nuclear fuels
[JAERI-4132] 16 p2608 N71-28072

Uranium nitride and uranium-plutonium nitride fuel compatibility with austenitic stainless steel claddings of liquid metal cooled reactor
[BMJ-1095] 16 p2634 N71-28743

Carbon transport in austenitic stainless steel at temperature gradient after sodium flux exposure
[ORNL-15569] 17 p2713 N71-29204

Fabrication and testing of double vacuum melted, type 316 thin walled austenitic stainless steel tubing, for use as cladding in LMFBR fuel pins
[WARD-4135-14] 17 p2786 N71-30313

Effects of loading rate on creep properties of austenitic stainless steel type 316
[FB-197120] 18 p2934 N71-30806

Nitrogen effect on creep properties of ferritic steels and intermetallic influence on austenitic steel creep properties
19 p3111 N71-31905

Boron influence on austenitic stainless steel precipitation during creep
19 p3111 N71-31906

Kinetics of steel vacuum degassing in highly basic refractory material crucibles
19 p3111 N71-31910

Nitrogen content effect on low ductility of molybdenum alloyed austenitic stainless steel
19 p3112 N71-31921

Influence of nitrogen and sulfur content on hot ductility, flow stress, and recrystallization in austenitic stainless steel
19 p3112 N71-31922

High temperature brazing of austenitic thermocouples and pipe ducts on reactor plugs of three construction materials
[JUL-681-8X] 19 p3104 N71-32055

Titanium alloying effects on mechanical properties and microstructures of low-carbon chromium nickel iron alloys
[NLL-L71-746-668-19022.401] 19 p3115 N71-32300

Metallurgical characteristics and interactions of boron and carbon with austenitic chrome-nickel steel in sea water
[ABC-TR-7183] 19 p3118 N71-32597

Irregularities in diffusion front of nickel in polycrystalline Fe-Cr-Ni alloys
[TI-70-59111] 20 p3285 N71-33576

Effect of stress relaxation on microstructure of austenitic steels
[NLL-TRANS-746-678-19022.401] 23 p3775 N71-36902

Corrosion tests of austenitic Cr-Ni steel and nickel alloys in steam loop at 620°C and 1 atm pressure for 5000 hours, and behavior of cold-formed material surfaces
[KFK-1301] 24 p3935 N71-38077

AUSTRALIA

Seasonal model for density in altitude range 45 to 90 km at Woomers 731 deg S/
[WRE-TN-HSA-174] 02 p0213 N71-11700

Temperature, pressure, and related climatological data for Australia - tables for July 1970
05 p0672 N71-14861

Temperature, pressure, and related climatological data for Australia - tables for June 1970
05 p0671 N71-15088

Seasonal model for zonal wind in altitude range 35 to 75 km at Woomers, Australia
[WRE-TN-HSA-172] 05 p0717 N71-15153

Ionospheric data obtained over Salisbury, Australia during October, 1969
[SAD-1969/10/5] 05 p0681 N71-15484

Ionospheric daily data obtained over Salisbury, Australia during September, 1969
[SAD-1969/9/5] 05 p0681 N71-15485

Ionospheric daily data obtained over Salisbury, Australia during December, 1969
05 p0681 N71-15600

Ionospheric daily data obtained over Salisbury, Australia during November, 1969
[SAD-1969/11/5] 05 p0681 N71-15691

Hourly values of ionospheric parameters in Salisbury, Australia
[WRE-SAD-1970/11/5] 11 p1749 N71-22445

Velocity and frequency of winds of arid zone of Australia related to seasonal shift of pressure systems
[PB-196022] 18 p2951 N71-30804

Computer programs to determine quantitative morphological fit of Australia and Antarctica
18 p2915 N71-31013

Tropical cyclones in Australian Region for 1967-1968 season
20 p3296 N71-33419

Meteorological flight search for clear air turbulence in stratosphere above Australia, 1966
20 p3297 N71-33671

Ionospheric data for June 1970 from Salisbury, South Australia
[WRE-SAD-1970/6/5] 20 p3268 N71-33789

Earthquake seismographic data records from Port Moresby - June-July 1971
20 p3269 N71-33947

Propagation measurements on long high clearance path revealing difference between direct and ground reflected rays of about 50 wavelengths at 4 GHz
[REFT-4124] 23 p3722 N71-36533

Monthly cyclone parameters in Australian region, Nov. 1969 to June 1969
23 p3791 N71-37023

Temperature, pressure, and related climatological data for Australia - tables for March 1971
23 p3792 N71-37025

Anglo-Australian 150-inch reflecting telescope for Southern Hemisphere
24 p3921 N71-37961

AUSTRIA

Synoptic meteorology for airports in Spain, Austria, France, Switzerland, and Alps
[AD-720700] 15 p2440 N71-27807

AUTOCOLLIMATORS

U COLLIMATORS

AUTOCORRELATION

Investigating autocorrelation of mutual amplitude and phase fluctuation in diffracted waves on rough screen
[AD-712335] 03 p0337 N71-12405

Linear three-tap feedback shift register
[NASA-CASE-NPO-10351] 03 p0345 N71-12503

Investigating techniques for measuring random patterns in photomicrographs by studying nature of coherent light diffracted by spatial patterns
[NASA-CR-115886] 04 p0499 N71-13494

Time dependence autocorrelation of chemical liquid
[NYO-3326-29] 07 p1074 N71-17435

Mathematical models for simulation of combined stochastic processes with stationary Gaussian processes
[NASA-CR-110990] 16 p3630 N71-36902

Autocorrelation and cross correlation of low frequency atmospheric boundary layer temperature and velocity fluctuation measurements
[AD-721546] 16 p3587 N71-36902

Velocity autocorrelation functions of small velocity vectors in turbulent flow and estimation of Lagrangian field properties
15 p3580 N71-36902

Mathematical model for 1/f noise propagation along Fourier transformations, time series analysis, and autocorrelation of random noise processes
[AD-721450] 16 p3562 N71-36902

Computer programming formulas for frequency and statistical analysis of random waveform signals using Fourier analysis, probability density function, and autocorrelation
[NASA-CR-115073] 17 p3775 N71-36902

Measurement, autocorrelation, and variance estimation of near ground atmospheric temperature and wind velocity
[MITT-20] 18 p3048 N71-36902

Autocorrelation functions for diffuse cosmic X-rays
[NASA-TM-X-65668] 19 p3177 N71-36902

Transformation of input autocorrelation function for optimum filtering of noisy phase shift keyed signal
19 p3030 N71-36902

Autocorrelation and power spectrum analysis computer programs for signal analysis of X-ray and gamma ray emission spectra
[NASA-CR-121899] 22 p3582 N71-36902

Upper atmospheric density variations and solar activity analysis and correlation
22 p3670 N71-36902

AUTOKINEZATION

Absorption spectrum of barium vapor in region of autokinization from 2382 to 1700
[AD-711785] 02 p0269 N71-11144

Autokinization of H₂ near threshold
[NASA-TM-X-65434] 06 p0915 N71-15991

Existence of dielectric recombination in solar corona
[AD-715257] 07 p1115 N71-17900

Autokinization and electron transitions in chloride photoabsorption of atomic calcium
[AD-719737] 13 p2139 N71-25048

Projection operator technique for calculating autokinization states of negative helium
[NASA-TM-X-65399] 17 p2790 N71-28800

AUTOKINESIS

Measurements and comparison of human visual and auditory autokinesis
[JZP-1970-12] 05 p0633 N71-14811

AUTOMATA THEORY

Switching and automata theory using computer graphics
[AD-711080] 01 p0030 N71-10999

Automata theory and iterative array computation
[AD-711048] 01 p0029 N71-10999

Deterministic realization and simulation of nondeterministic automata
[AD-711050] 01 p0029 N71-10999

Development and applications of cybernetics theory in transportation, industry, and commerce in USSR
[JPRS-51457] 01 p0027 N71-10999

Automation and mechanization of cartography, and coordination of research and cartographic activities
[AD-711978] 02 p0212 N71-13171

Automatic computation theory and problems of program complexity, complexity measures for finite automata, algorithms for inner products, and complexity of inversion
[AD-712843] 03 p0341 N71-13479

Adaptive and goal-seeking system formulation and systems theory
[AD-712446] 03 p0341 N71-13479

Type and time bounded Turing acceptors and APL
[AD-712704] 03 p0344 N71-13496

Cybernetics, computer programming, and automata theory
[AD-709873] 03 p0352 N71-13544

Developing self-organizing control systems for application in aerodynamics
03 p0347 N71-13543

Automatic pattern recognition
[JPRS-51963] 04 p0391 N71-13580

Investigating nonstationary automatic control systems and construction of asymmetrical control systems connected with solution of combinatorial Dixon problem
[JPRS-51830] 04 p0313 N71-13580

Automatic system for radial and phase beam positioning device for 70 GeV synchrotron
[CERN-TRANS-69-34] 04 p0315 N71-13580

Analysis of large systems and theory of estimation
[JPRS-51802] 04 p0312 N71-13580

Structural properties of generalized automata and algebras
[AD-712377] 05 p0659 N71-14971

Generalized inverse matrices for representation of maps and morphisms with probabilistic meaning
[AD-716491] 09 p3152 N71-15951

Character recognition device design and applications in weather forecasting, medical diagnostics, and mail sorting
[JP83-52554] 10 p1536 N71-30681

Theorem for automatic recognition of word by Turing machine 11 p1786 N71-31904

Computer developments in USSR and industrial applications in automation and information processing [JP83-52595] 12 p1881 N71-35444

Algorithmic inaccessibility of finding asymptotic behavior of Shannon function with bounded deterministic operators based on finite system of finite automatic devices [JP83-52973] 13 p2185 N71-35281

Optimal schemes for varying structure stochastic systems 14 p2281 N71-35997

Linear, nonlinear, and hybrid updating schemes for controlling optimal 3 model 14 p2281 N71-35997

Baseometer for photographic film frequency content characteristics measurement based on semi-automatic conversion of transmission factors into effective exposure [AD-72304] 17 p2751 N71-32494

Procedure for finding suboptimality property partitions, suboptimality property covers, and cover pairs for finite state sequential machines [JP-179643] 18 p2947 N71-31378

Two dimensional periodogram for estimating spectral density of real, homogeneous, random field over rectangular area on plane 18 p2948 N71-31381

Electronic simulation of financial transactions and security for anti-fraud controls 19 p3193 N71-31645

Model for quantitatively examining performance of automatic machines with normal and disturbed functions in statistical decision making 19 p3044 N71-32009

Automation and technological change and future studies: bibliographies 19 p3198 N71-32573

Robot engineering concepts, instrumented striding information device, and planetary striding vehicle [JP83-53742] 20 p3277 N71-32910

Increased automation and development of robots capable of anthropomorphic movements and fitted with sense organs and artificial intellect 20 p3277 N71-32911

Theory of X ray diffraction for understanding atomic diffraction 20 p3277 N71-32917

Automated analysis, local forecasting, tailored meteorological support, and automated processing and evaluation of satellite data [AD-72495] 20 p3295 N71-32977

The automatic theory and artificial intelligence [AD-72695] 22 p3608 N71-35696

AUTOMATIC CONTROL

ADAPTIVE CONTROL

AUTOMATIC FLIGHT CONTROL

AUTOMATIC FREQUENCY CONTROL

AUTOMATIC GAIN CONTROL

AUTOMATIC LANDING CONTROL

CASCADE CONTROL

DYNAMIC CONTROL

FEEDBACK CONTROL

FEEDFORWARD CONTROL

LEARNING MACHINES

NUMERICAL CONTROL

OFF-ON CONTROL

OPTIMAL CONTROL

PROPORTIONAL CONTROL

SELF ADAPTIVE CONTROL SYSTEMS

SEQUENTIAL CONTROL

TIME OPTIMAL CONTROL

Pulsed energy power system for application of combustible gases to turbine controlling air voltage generation [NASA-CASE-MSC-13112] 02 p6149 N71-11057

Stochastic cybernetics, mathematical economics, industrial process control, and automatic computer design in USSR [AD-711361] 03 p6188 N71-11320

Operating characteristics of ripple correcting system for converted alternating gradient accelerators [JP83-54039] 03 p6358 N71-13156

Automatic compensation of integrated average radius fluctuation during heliostat scan [AD-72726] 03 p6381 N71-13215

Investigating nonstationary automatic control systems and construction of asymmetrical coding systems connected with solution of combinatorial flows problem 04 p6513 N71-13542

Constructing solutions of given system in form of automatic series and formulating criteria of local stability of unperturbed motion 04 p6513 N71-13543

Automatic balancing device for use on frictionless supported attitude-controlled test platforms [NASA-CASE-LAR-10774] 04 p6513 N71-13545

Operational control and performance of computer stored radar systems 04 p6498 N71-13932

Computerized radar plot extractor models for automatic air traffic control 04 p6498 N71-13936

Controlling acceleration of particles in proton accelerators by digital computers [CERN-TRANS-76-5] 04 p6586 N71-14244

Deriving equations for automatic correction of betatron oscillations in cyclic accelerators [CERN-TRANS-68-52] 04 p6587 N71-14276

Proceedings from symposium on control theory applications [NASA-TM-X-66516] 04 p6623 N71-14626

Control theory applications in nerve magnetics publishing 04 p6699 N71-14627

Technology trends in nerve magnetics publishing 04 p6699 N71-14628

Control problems in airline operations particularly air cargo handling 04 p6744 N71-14630

Computer process control applications with emphasis on oil and chemical industries 04 p6834 N71-14634

Panel discussion on control theory problems 04 p6834 N71-14638

Investigating computer program functions and test procedures for failure analysis of NAS In Route Stage A Model 1 System [RAA-NA-76-31] 05 p6786 N71-14567

Interface of PDP 8 computer control for neutron spectrometer [RT/BL/70/1] 05 p6884 N71-14830

Performance of computer controlled analytical mass spectrometer [ABCL-3470] 05 p6884 N71-14888

Automatic system for analog to digital conversion and digital recording of seismic signals [RGA-4-C-4397-28] 05 p6851 N71-14969

Control system of A-1 nuclear reactor with moving chambers [ZIE-79] 05 p6727 N71-15090

Circuitry for automatic control of alternating current motors [AD-713386] 05 p6654 N71-15482

System for regulating direct current of triphase alternator [PUBL-114] 05 p6656 N71-15514

Synchronous smooth rotor in system for automatic reduction of field current [PUBL-115] 05 p6656 N71-15516

Automated, high sensitivity, three column gas chromatograph [UCRL-30849] 05 p6688 N71-15519

Computer controlled apparatus for maintaining within tenth angle and velocity during beam tracking [NASA-CASE-XMP-63287] 05 p6683 N71-15687

Soviet cybernetics and computerized production control [AD-714048] 06 p6819 N71-16334

Describing subsystems of batch silicon epitaxy reactor and effect of chamber geometry on reactor performance 07 p1088 N71-17282

Fluid leakage detection system with automatic monitoring capability [NASA-CASE-LAR-10523-1] 07 p1089 N71-17573

System description of field test model of ARTS 2 modular alphanumeric nontracking ATC system 08 p1166 N71-18815

Interviews and conversations with officials and engineers of model scientific production association for manufacturing of electronic equipment 08 p1309 N71-19321

Light sensitive control system for automatically opening and closing doors of solar optical telescope [NASA-CASE-MSC-10866] 09 p1388 N71-19568

Automatic performance monitoring system for improved shipboard system operation 09 p1367 N71-20233

Directional antenna control system conversion from manual to dual-automatic control [AD-716961] 10 p1531 N71-20795

Perturbation expansion of Coulomb potential for determining pair distribution function in plasma [AD-717038] 10 p1527 N71-20817

Automatic control and crucible shape effects on zone recrystallization of germanium 10 p1633 N71-20886

Automatic control of two-gas atmospheric supply system for long term test on space station simulator 10 p1587 N71-20966

Automated management systems for decision making and systems control [JP83-52623] 10 p1665 N71-21086

Systems analysis and cybernetics simulation of automatic air sampling systems 11 p1728 N71-22064

Development of machine oriented languages for control of automatic machine tools [AD-717778] 11 p1768 N71-22293

Automation of control systems for processing scientific measurement data [JP83-52745] 11 p1717 N71-22726

Software problems in automation system for scientific experiments 11 p1718 N71-22728

Systems engineering planning methodology of automation systems for complex experiments 11 p1718 N71-22729

Automation system planning for experimental data processing 11 p1718 N71-22734

Technology review on temperature regulators for automatic control systems 11 p1719 N71-22742

Design, operation, and accuracy of automatic radioastronomical drifting stations in Arctic 11 p1733 N71-23831

Welding torch with automatic speed controller using speed sensing wheel and closed servo system [NASA-CASE-XMP-61730] 11 p1773 N71-23638

Automatic underwater camera system design and performance characteristics for time lapse photography of algae growth and sedimentation [NASA-TM-X-67807] 12 p1918 N71-23380

Microprocessor versatile switch with rotor position control [NASA-CASE-XMP-64507] 12 p1889 N71-23548

Automatic antenna position control device for evaluating dome effects on radiation pattern [AD-713386] 12 p1889 N71-23687

Automatically recirculating, high pressure pump for use in spacecraft cryogenic propellants [NASA-CASE-XMP-64731] 12 p1929 N71-24043

Electronic digital computer for automating 2-OeV electron lens [SLAC-TRANS-126] 12 p1976 N71-24139

Cybernetic and spontaneous movement of matter in world systems 12 p1895 N71-24216

Dynamic synthesis of computerized automatic control systems 12 p1893 N71-24217

Industry automatic control system design 12 p1893 N71-24218

Methodological and algorithmic considerations in synthesis of linear multidimensional automatic control systems 12 p1886 N71-24221

Automatic controlled thermal fatigue testing apparatus [NASA-CASE-XLA-02839] 12 p2013 N71-24276

Automatically charging battery of electric storage cells [NASA-CASE-XMP-64758] 13 p2029 N71-24685

Radar amplifiers with instantaneous automatic gain control [JP83-52891] 13 p2045 N71-24720

Use of instantaneous automatic gain control in tracking radar 13 p2045 N71-24721

High gain and low time constant requirements of LAOC amplifiers 13 p2045 N71-24722

Electric motor control system with pulse width modulation for providing automatic self cooling curve [NASA-CASE-XMP-63195] 13 p2099 N71-24661

Computer controlled automatic tracking data analysis with graphic display 13 p2052 N71-25336

Design and construction of programmer for control and automation of electric beam welding machine [BUW-4537-9] 13 p2088 N71-25528

Feasibility analysis of automatic systems as practical means of urban transportation [RAE-TB-66087-PT-1] 13 p2193 N71-25395

Inducing mechanism for cathode array substitution in electron beam tube [NASA-CASE-MPO-10625] 14 p2229 N71-26182

Voltage range selection apparatus for testing and applying voltage to electronic instruments without loading signal source [NASA-CASE-XMS-66497] 14 p2255 N71-26244

Automated fluid chemical analysis for microchemical analysis of small quantities of liquids by use of reduced pressure and vacuum methods [NASA-CASE-XMP-69451] 14 p2216 N71-26754

Spectrometer for microanalysis of condensed matter emphasizing automation and remote control of spectrometer electronics and delay systems [IMP-727] 15 p670 N71-27488

Computer programming for nuclear physics experiments [IMP-8-96] 15 p674 N71-27483

Boron trifluoride proportional neutron spectrometer control unit for automatic or manual control [IMP-707] 15 p2412 N71-27799

Approach power computer system for manual and automatic Navy carrier landing system [AD-723025] 16 p2528 N71-28541

Step input linear system modeling from nonlinear system sampled input data based on method of perturbation or quantization of automatic control systems [NASA-CR-115074] 17 p2729 N71-30036

Algorithm for automatic failure analysis of gates in logic circuitry [LAAS-G-3-E-1] 18 p2882 N71-30820

- Design and operation of complex man machine systems and heuristic solution to automatic control problems in production engineering and biomedical situations
[JPRS-53414] 18 p2882 N71-30867
- Design and evaluation of information display systems and development of operator work station stages
18 p2882 N71-30868
- Automatic monitoring of human operator state in closed, man machine systems with biomedical application
18 p2883 N71-30869
- Development and construction of automatic photometer scan and data system
[NASA-CR-115988] 18 p2925 N71-31399
- Automatic speaker identification and verification
19 p3059 N71-31635
- Program device for automatic control of weather radar systems
19 p3128 N71-32039
- Algorithm for automatic control of gauge and shape in roll forming
[PB-198368] 19 p3106 N71-32419
- Theory of logic-dynamic control systems and multi-layer theory of statistical decisions
[JPRS-53766] 20 p3288 N71-32822
- Mathematical modeling of logic-dynamic control systems
20 p3288 N71-32823
- In-flight P-111 data on total and static pressure from left inlet during automatically scheduled and manually controlled off-schedule positioning of spike at Mach 0.68 to 2.18
[NASA-TN-D-6490] 20 p3210 N71-33211
- Accuracy of earth tidal observations using tiltmeters and automatic calibration
20 p3264 N71-33364
- Belgian computerized information system applied to automatic control
[CRIF-EL-2] 20 p3370 N71-33436
- Mathematical models for control activity of human spaceship operator
20 p3227 N71-33461
- Performance tests on Brayton cycle direct current power supply circuit for automatic control
[NASA-TM-X-2349] 20 p3342 N71-33691
- Automatic tracking of Q switched laser range finders
[TP-964] 20 p3283 N71-33820
- Evaluation of automatic guidance modes and software for V/STOL aircraft flight control
[NASA-CR-121768] 21 p3375 N71-34016
- Automatic temperature control for liquid cooling garments used during astronaut extravehicular activity with external auditory means, and skin temperature as input signals
[NASA-CR-115122] 21 p3384 N71-34077
- Highway vehicle speed and cruise control system based on conversion of speeds into frequencies and resulting in greater reliability and less maintenance
[NASA-CASE-WUC-11165] 21 p3427 N71-34384
- Optimal selection of automation systems under multivariate normal model in terms of reliability, feasibility, and economy
[NASA-CR-121656] 21 p3446 N71-34524
- Computer controlled electric power distribution system for aerospace systems
21 p3514 N71-35040
- Problems of digital computer program control of milling machines
[NLI-RTS-4307] 22 p3557 N71-35340
- Developed Martin roving vehicle simulator for test platform of obstacle sensor for autonomous roving vehicle
[NASA-CR-122944] 23 p3739 N71-36665
- Design and construction of automatic timing system for neutron generator counting station
[NIM-967] 23 p3755 N71-36768
- Breadboard testing of automated anesthesia machine
[NASA-CR-122646] 23 p3761 N71-36813
- Automatic start-up system for UA-RB-1 reactor for reaching criticality from deep subcriticality in pressurized pool
[UAAE-188] 23 p3795 N71-37052
- Schematic diagram and preliminary block diagrams for start-up system in WWR-5
[UAAE-94] 23 p3800 N71-37094
- Lunar roving vehicle control system emphasizing stereoscopic sensor data processing
[D-48] 23 p3839 N71-37507
- Algorithmic simulation of ergonomic systems for designing operator-control systems
24 p3881 N71-37666
- Procedure for analysis of data representation systems for man-operator controlling complex automated object
24 p3881 N71-37667
- EE-44 computer-controlled test system for measuring electrical properties of test equipment
[SC-D8-70-862] 24 p3892 N71-37740
- Computerized real time data processing and display system for air traffic control in airspace over Belgium, Luxembourg, the Netherlands, and Germany
24 p3893 N71-37744
- Computer technology for medical information systems, in patient care, and for diagnostic purpose
24 p3893 N71-37745
- Basic requirements for computers designed for operations with control automation systems
[AD-727265] 24 p3895 N71-37739
- Selected articles on application of mathematical methods to automation of rail transportation
[AD-727267] 24 p3895 N71-37760
- Increased operating reliability of digital computers used in automatic control systems
[AD-727163] 24 p3895 N71-37762
- Computer controlled electrical measuring devices for thermoelectric generator of power plant
[AD-727461] 24 p3925 N71-38010
- AUTOMATIC CONTROL VALVES**
NT PRESSURE REGULATORS
NT RELIEF VALVES
- Design and operation of freeze, melt valve used in vacuum encapsulating column for thermionic diodes
[NASA-TM-X-2126] 01 p0086 N71-10435
- Predicting bearing fatigue failure and life in primary control check valves of advanced test reactor
[DN-1338] 04 p0557 N71-14153
- Describing metal valve plastic with encapsulated elastomeric body
[NASA-CASE-MSC-12116-1] 07 p1035 N71-17648
- Semicrobital diaphragm cavitation flow control valve
[NASA-CASE-XNP-09704] 08 p1179 N71-18615
- Relief, safety, and cryogenic check valve systems engineering with industrial applications
[NASA-SF-592701] 16 p2600 N71-28282
- AUTOMATIC DATA PROCESSING**
U DATA PROCESSING
AUTOMATIC FLIGHT CONTROL
NT AUTOMATIC LANDING CONTROL
- Considering design of digital computers for guidance and control of aerospace vehicles
[AGARD-CP-68-70] 03 p0407 N71-12601
- Investigating tasks of data processing equipment in advanced navigation systems for aircraft
03 p0408 N71-12604
- Investigating problems encountered in developing and maintaining airborne computer programs for guidance and control
03 p0346 N71-12606
- Evaluating use of airborne digital computers for guidance and control of X-15 and F-104 aircraft
[NASA-TM-X-66491] 03 p0408 N71-12610
- Developing high integrity digital flight control of variations in performance of complex systems
03 p0409 N71-12614
- Digital data processing for designing automatic flight control systems
03 p0409 N71-12616
- Investigating conversion of signals into common digital form and transmission by time division multiplexing along wire or fiber optic cable
03 p0347 N71-12621
- Optimization and estimation models for automatic navigation
[AD-714699] 06 p0894 N71-16284
- Accuracy and range of guided missile telocontrol system
[AD-714437] 06 p0894 N71-16286
- Dynamic response of vehicle and its automatic flight control system
09 p1324 N71-20334
- Operational performance of Hawker Siddeley aircraft automatic flight approach and landing control system
12 p1854 N71-23414
- Operational performance of automatic V/STOL flight control systems using jet thrust or air bleed
12 p1854 N71-23415
- Human factors and control system failures in jet upsets during turbulence encounters
12 p1853 N71-23424
- Component connection schemes of brain for trainable feedback flight control system
13 p2035 N71-25326
- Helicopter gyro displacement measurements at differing flying conditions
[FOA-2-C-2356-49-721] 14 p2199 N71-26567
- Preliminary study of airplane-autopilot response to atmospheric turbulence while operating in altitude-hold and attitude-hold modes
18 p2670 N71-30780
- Modification of bang-bang attitude control system hysteretic and threshold values to provide improved missile guidance
[FOA-2-C-2371-54] 22 p3607 N71-35800
- AUTOMATIC FREQUENCY CONTROL**
Audio signal processing system for noise surge elimination at low amplitude audio input
[NASA-CASE-MSC-12223-1] 14 p2218 N71-26181
- AUTOMATIC GAIN CONTROL**
Automatic feedback control system for controlling volume of power amplifier and measuring frequency range of background noise
[AD-721598] 16 p2548 N71-28185
- AUTOMATIC LANDING CONTROL**
Using automatic control theory with simple pilot model for synthesizing helicopter landing approach flight director control laws
[NASA-TM-X-66492] 03 p0312 N71-12609
- Developing mathematical model for tandem rotor helicopter for analysis of automatic approach and landing system
[NASA-TM-X-66493] 03 p0312 N71-12610
- Advanced ILS and automatic landing systems for conventional and V/STOL aircraft: conference
[AGARD-CP-59-70] 03 p0404 N71-12605
- All-weather automatic landing systems and previous areas
03 p0404 N71-12607
- International aviation and all-weather automatic landing systems
03 p0405 N71-12608
- Importance of aircraft speed control relative to longitudinal touchdowns dispersion
03 p0405 N71-12609
- All-weather automatic landing systems for use in aircraft carriers and training ashore
03 p0406 N71-12610
- Automatic pilot system for landing commercial aircraft
03 p0406 N71-12611
- Autopilot landing system for VC-10 aircraft
03 p0406 N71-12612
- Direct lift control system for producing lift without pitching moments during aircraft approach and landing
03 p0406 N71-12613
- Flight control systems for VTOL automatic landing
03 p0407 N71-12614
- Automatic landing system of Concorde**
03 p0407 N71-12615
- Maintaining performance criteria to analyze ability of automatically controlled aircraft to maintain cruise flight path control during landing approach
[NASA-TM-X-62396] 08 p2523 N71-15780
- Piloted beam simulation evaluation of one fully automatic and six manual low visibility landing systems for helicopters
[NASA-TM-X-5913] 09 p1324 N71-20335
- Radio frequency interference monitoring for instrument landing system in automatic landing
[RAE-TR-70776] 12 p1560 N71-23318
- Operational performance of Hawker Siddeley aircraft automatic flight approach and landing control system
12 p1854 N71-23414
- Automatic approach and landing system with lift warning signal for Caravelle aircraft control
12 p1856 N71-23419
- AUTOMATIC PATTERN RECOGNITION**
U PATTERN RECOGNITION
AUTOMATIC PICTURE TRANSMISSION
- Weather profile data and APT pictures for European area during last quarter of 1968
[QR-4] 04 p0241 N71-14117
- Infrared scanner onboard meteorological satellite for automatic picture transmission of earth and cloud surfaces
16 p1518 N71-21800
- Simple method for receiving picture signals from satellites, using ESSA 4
[AD-722045] 18 p2562 N71-28185
- ESSA 6/APT meteorological photographs of Europe for April through June 1968, and weather satellite developments
21 p3454 N71-34015
- AUTOMATIC PILOTS**
Automatic pilot and associated airborne equipment developments for automatic landing systems
03 p0405 N71-12608
- Automatic pilot system for landing commercial aircraft
03 p0406 N71-12610
- Autopilot landing system for VC-10 aircraft
03 p0406 N71-12611
- Autopilot for C-141 all-weather landing system
03 p0406 N71-12612
- Automatic pilot TAPIR
03 p0407 N71-12613
- Onion lubricated spiral groove bearings suitable for spin axis of gyro in inertial guidance platform
[NASA-CR-102265] 03 p0804 N71-12610
- Techniques for applying frequency domain optical control in practical closed loop controller synthesis
[AD-722046] 16 p2025 N71-20308
- Preliminary study of airplane-autopilot response to atmospheric turbulence while operating in altitude-hold and attitude-hold modes
18 p2670 N71-30780
- Design and characteristics of digital autopilot for man with space shuttle
20 p3353 N71-33805
- Automatic pilots for control of rotary and fixed wing aircraft
[AD-727789] 24 p3874 N71-37601

SUBJECT INDEX

AUTOMATIC ROCKET IMPACT PREDICTORS

U IMPACT PREDICTION

AUTOMATIC TEST EQUIPMENT

Automatic ultrasonic testing methods for welds

[KSA-CONF-1540] 01 p3387 N71-13314

Automatic test equipment for hydrovalves and eddy current energy dissipation in steel metal sheets

[NPL-MEMO-5] 01 p3383 N71-13343

Developing techniques for verifying operational integrity of redundant equipment without disrupting systems

[NASA-CR-111765] 04 p3131 N71-13980

Automatic test equipment for electronic components

[NASA-CR-1734] 01 p1171 N71-19223

Automatic test equipment for electronic components

[NASA-CR-1735] 01 p1300 N71-20551

Computer-controlled system for testing time domain instruments to speed up calibration process

12 p1919 N71-25630

Computer-automated calibrating system with accuracy and precision for use in Standards Laboratories

12 p1683 N71-25631

Biostatistical device for analyzing nuclear emission around low and medium energy accelerators

[KSA-8-4053] 13 p2466 N71-37283

Automatic bioassay instrument for analysis based on adenine triphosphate bioluminescent property to urine sample bacterial content

[NASA-CASE-GSC-11169-1] 15 p2373 N71-27992

Automatic apparatus for analyzing bacterial ATP in urine samples

[NASA-CASE-GSC-11169-2] 21 p3385 N71-34079

AUTOMATIC TYPEWRITERS

High speed data printer using mechanical type bars

04 p3085 N71-13835

AUTOMATION

Automation of technological processes in aircraft system production

[AD-714835] 07 p1018 N71-17532

Automated gas chromatography with improved sensitivity

11 p1763 N71-22635

Automatic, remotely controlled noise-level recorder for telecommunication equipment production, calibration, and maintenance

12 p1879 N71-25649

Description of equipment used for automatic control of road and rail transport and application to improved urban transportation system

14 p2359 N71-26128

Development and characteristics of digital recording system for automatic digitizing of map contour line data

[AD-726306] 22 p3579 N71-35493

Computer programmer manual for use with automated general purpose system for structural analysis - Vol. 3

[AD-726566] 22 p3609 N71-36316

Development of technique for finding functional degree of combination automation with complex of [AD-727974] 24 p3806 N71-37768

AUTOMOBILE ACCIDENTS

Digital computer simulation of automobile impact by flexible safety barrier, and multiple source defense system for NAE triangle wind tunnel

[NAB-197073] 01 p1363 N71-19481

Digital computer simulation of automobile impact by flexible safety barrier

01 p1473 N71-19482

Energy absorbing restraint system for automobile crash protection

17 p2754 N71-29806

Human performance in escape from vehicle accidents and escape workloads of vehicles

[PB-199772] 19 p3196 N71-33247

AUTOMOBILE ENGINES

Air pollution reduction by carbon-to-air air transportation system around New York City

[NAA-NO-70-14] 01 p3086 N71-18124

Automobile exhaust manifold thermal reactor system comparison in control of hydrocarbon and carbon monoxide emissions

[NASA-TN-X-2239] 01 p1408 N71-19946

Technology review on electric automobiles, and modified T-33 aircraft system for pyrotechnic tail ejection seats

[NAB-197044] 11 p1700 N71-22130

Technology review on electric automobiles

11 p1700 N71-22130

Public controls for automotive engine examined by turbine cycle performance with water, CO-34, and heat TP and investigation for boiler and feed pump control criteria

[NASA-CR-115065] 16 p2578 N71-28104

Air pollution sources and control procedures and US Clean Air Act summary

[PB-199479] 22 p3089 N71-34378

AUTOMOBILES

Air and land transportation noise sources and measurement, noise level scales, and individual and community responses - conference

[PB-191117] 01 p3003 N71-18049

Carbon monoxide oxidation rates for automobile exhaust manifold reactor conditions

[NASA-TN-D-7034] 02 p3066 N71-12866

Performance of hydroperoxide shock absorbers with servomechanism in automobiles

03 p3065 N71-13148

Developing molten alkali carbonate catalytic in removing lead compounds from spark ignition engine exhaust gases

[PB-194132] 04 p3084 N71-13444

Safety standards development analysis for passenger vehicles and aircraft

[AD-710997] 12 p2016 N71-23333

Acceptance tests of various upper torso restraints by automobile users with application to general aviation aircraft

[FAA-AA-71-12] 16 p2549 N71-28806

Highway vehicle speed and cruise control system based on conversion of speeds into frequencies and running in greater reliability and less maintenance

[NASA-CASE-NUC-11165] 21 p3427 N71-34384

Influence of fuel additives on automobile exhaust emissions and composition of exhaust hydrocarbons

[TPR-40] 22 p3461 N71-36109

Model of human operator reflecting known perceptual and response characteristics for automobile driving task

23 p3718 N71-36504

Low cost electronic control systems for automobiles utilizing integrated circuits

23 p3737 N71-36646

Mathematical models for analyzing automotive gas turbine and nitric oxide emissions

[PML-PUBL-71-11] 24 p3032 N71-36769

Motor vehicle noise generation, traffic noise prediction, and highway noise propagation - Vol. 4

[OST-ONA-71-1-VOL-4] 24 p3035 N71-36787

AUTONOMIC NERVOUS SYSTEM

NT SYMPATHETIC NERVOUS SYSTEM

Physical controls of autonomic nervous system by gaggle impulses

09 p1331 N71-19835

AUTOPILOTS

U AUTOMATIC PILOTS

AUTORADIOGRAPHY

Iron self diffusion parameters in Fe delta-region and in Fe alloys with small Al additions

[TT-70-57043] 02 p3040 N71-11309

Grain boundary diffusion in iron using autoradiography

[TT-70-57048] 08 p1218 N71-19006

Feasibility study of autoradiographic techniques for determining relative power densities in reactor fuel plates

[Y-OR-29] 09 p1418 N71-19009

Quantitative autoradiography of aluminum-tritium particles for danger of incorporation of tritium gas during neutron production

[KFKI-70-26-RP] 14 p2314 N71-26723

Collinear alpha for alpha autoradiograph of irradiated nuclear fuels

[LBNL-2914] 21 p3462 N71-34643

Microautoradiogram of thermal distribution in aluminum foil irradiated by thermal neutrons

[NLL-WINDSCALE-448-1991.9P] 32 p3774 N71-36898

AUTOROTATION

Experimental aerodynamic performance characteristics of rotor entry vehicle configuration - transonic

[NASA-TN-D-7047] 06 p3792 N71-16534

Airspeed, rate-of-turn, engine cycling, and gross weight effects on OH-1 C helicopter during autorotation

[AD-717047] 10 p1493 N71-21363

AUTOTOPHIES

NT HYDROGONOMONAS

Grain cereals as polyfunctional autotrophic components of closed ecological life support systems

16 p2530 N71-38253

AUXILIARY ELECTRIC POWER UNITS

U AUXILIARY POWER SOURCES

AUXILIARY EQUIPMENT (COMPUTERS)

NT PLOTTERS

NT PRINTERS (DATA PROCESSING)

Use of discrete ordinate and auxiliary program of ANEM in one dimensional neutron and gamma ray transport

[CRA-N-1338] 13 p2129 N71-24872

Pinhole computer-processed telemetry using sequence control, auxiliary memory, and system reset registers for sensors and digital data source sampling

[NASA-CASE-INFO-11358] 21 p3395 N71-34140

AUXILIARY POWER SOURCES

NT CHEMICAL AUXILIARY POWER UNITS

NT NUCLEAR AUXILIARY POWER UNITS

NT SNAP

NT SNAP 6

NT SNAP 19

AUXILIARY PROPULSION

NT SNAP 21

NT SNAP 23

NT SPACE POWER UNIT REACTORS

Analyzing computer simulation of potentially heated reacting electrical power generating system

[NASA-TN-D-6076] 01 p3086 N71-18083

Satellite auxiliary propulsion selection techniques

[NASA-CR-111408] 02 p3289 N71-11877

Evaluation of spacecraft power supply systems and auxiliary circuits including preflight analysis

05 p3290 N71-12579

Technology and configurations of hydrogen oxygen auxiliary propulsion system for space shuttle orbiter and booster

[NASA-TM-X-60894] 08 p1284 N71-10433

Three-stage potassium vapor turbine test to determine effects of vapor volume on impingement damage of different rotor blade materials

[NASA-CR-1815] 15 p3369 N71-27645

Design and development of auxiliary power unit and air breathing propulsion system for space shuttle vehicle

17 p3354 N71-35683

Program for developing hydrogen-oxygen fueled auxiliary power unit for space shuttle vehicle

17 p3358 N71-35684

Space shuttle auxiliary power unit design selection and performance evaluation

17 p3358 N71-35685

Synthesis, selection, and design of optimal auxiliary power unit for space shuttle vehicle

[SC-71-25] 17 p3358 N71-35686

Acceptance tests of nickel cadmium spacecraft cells with auxiliary electrodes for charge control

[NASA-CR-115942] 18 p2673 N71-26936

Predicting isotopic power source microstructure of Po-238O2 in thermocouple using phase diagram

[ORNL-4545] 21 p3474 N71-34742

AUXILIARY PROPULSION

Space shuttle low pressure, hydrogen oxygen auxiliary propulsion subsystem requirements, tradeoffs, and concept selection

[NASA-CR-114999] 13 p3171 N71-24676

Space shuttle high pressure, hydrogen oxygen auxiliary propulsion subsystem requirements, tradeoffs, and concept selection

[NASA-CR-103109] 13 p3172 N71-24677

Space shuttle high pressure, hydrogen oxygen auxiliary propulsion subsystem design, weight conditions, and operating performance

[NASA-CR-103110] 13 p3172 N71-24678

Prototype auxiliary propulsion subsystem with isolated single tank prepropellant feed system and 5-cm diameter ion thruster

[NASA-TN-X-67638] 13 p3155 N71-24735

Space shuttle high pressure hydrogen oxygen auxiliary propulsion subsystem conceptual and design study summary

[NASA-CR-103115] 13 p3174 N71-25868

Space shuttle low pressure, hydrogen oxygen auxiliary propulsion subsystem preliminary design

[NASA-CR-115900] 13 p3176 N71-25470

Space shuttle high pressure, hydrogen oxygen auxiliary propulsion subsystem preliminary design

[NASA-CR-103108] 13 p3176 N71-25471

Conference on auxiliary propulsion system performance and configurations for space shuttle applications - Vol. 2

17 p3036 N71-29588

Space shuttle hydrogen/oxygen auxiliary propulsion system high and low pressure thrusters

17 p3036 N71-29589

High and low chamber pressure injectors for space shuttle hydrogen oxygen APS nozzles

[AGC-4100-71] 17 p3036 N71-29590

High pressure reverse flow engine for space shuttle APS application

17 p3036 N71-29591

Design criteria for flight type gaseous hydrogen gaseous oxygen propellant shutoff valves for space shuttle APS

17 p3036 N71-29592

Design and fabrication of hydrogen oxygen propellant shutoff valves for space shuttle APS thrusters

17 p3031 N71-29593

Analytical and experimental program of design, fabrication, testing of gaseous hydrogen/oxygen spark and plasma torch ignition system for space shuttle APS

[AGC-4100-71] 17 p3036 N71-29594

Spark and auto-igniter systems for hydrogen and oxygen propellants in space shuttle APS

[SC-71-34] 17 p3037 N71-29595

Experimental and analytical evaluation of catalytic ignition system and performance of hydrogen oxygen thruster for space shuttle APS

17 p3037 N71-29596

Broad based model of space shuttle auxiliary propulsion system design and configuration

17 p3037 N71-29597

Space shuttle high and low pressure auxiliary propulsion subsystem definition

17 p3037 N71-29599

Preliminary design of high and low pressure APS for space shuttle

17 p3037 N71-29600

AVALANCHE DIODES

- Reliability and cost of electrostatic and electromagnetic character systems for satellite auxiliary propulsion [NASA-CR-115919] 18 p3501 N71-31145
- Evaluation of oxygen-hydrogen auxiliary propulsion subsystems for space shuttle booster and orbiter baseline vehicles [NASA-CR-115162] 23 p3836 N71-37370
- Pumped liquid, dual gas generation cycle for space shuttle booster and orbiter auxiliary propulsion systems [NASA-CR-115161] 23 p3838 N71-37371
- Development of requirements for auxiliary propulsion system used with baseline orbiter and booster of space shuttle system [NASA-CR-123186] 24 p4016 N71-38653
- Development of design and programmatic data for space shuttle reaction control systems and integrated reaction control system/orbit maneuvering systems [NASA-CR-123184] 24 p4016 N71-38656
- Development and characteristics of space shuttle auxiliary propulsion system based on vehicle configuration and vehicle/misison requirements [NASA-CR-123181] 24 p4017 N71-38657

AVALANCHE DIODES

- Analysis of avalanche diode microwave oscillator modes 01 p0032 N71-10215
 - InAsP α -type negative resistance microwave semiconductor development for avalanche diodes 01 p0032 N71-10216
 - Theory of multiple modes in avalanche diodes [AD-711923] 02 p192 N71-11348
 - Gallium arsenide avalanche transit time devices [AD-713599] 05 p0653 N71-14841
 - Temperature effects, polarization characteristics and failure of p-n junction transistors and avalanche diodes 06 p0826 N71-15790
 - Avalanche diodes and tunnel diode amplifier system used as radiation counters [NYO-4028-TA-1] 08 p1199 N71-18360
 - Noise characteristics of gallium arsenide p-n junction avalanche transit time oscillators [AD-716998] 10 p1332 N71-20002
 - Analysis of finite rise and fall time current excitation of TRAPATT diodes using physical approximations for plasma formation and recovery as used in previous square wave analyses [AD-717720] 11 p1724 N71-22574
 - Surface barrier and avalanche diode detectors for spaceborne particle detection 13 p2152 N71-25330
 - Radiation damage to miniature silicon avalanche diodes by high energy neutrons and electrons 14 p2326 N71-26287
 - Intermodulation distortion and gain compression in solid state microwave amplifier diodes [NASA-CR-118096] 15 p2310 N71-27969
 - Solid state pulse modulator design for use with two terminal semiconductor microwave sources using avalanche diodes [SC-CR-70-6157] 17 p2724 N71-29229
 - High efficiency mode diodes, waveform, and circuit studies for improving avalanche oscillators [SC-CR-70-6171] 17 p2725 N71-29423
 - Application of Boltzmann transport equation to statistical theory of avalanche breakdown in silicon [AD-722369] 17 p2814 N71-29542
 - Research on avalanche type semiconductor radiation detectors using video amplifiers [NYO-3246-TA-8] 20 p2328 N71-33775
 - Operating characteristics of avalanche diodes in microelectronic circuits [AD-726558] 22 p3561 N71-35362
- AVANCEMENTS**
- NT ELECTRON AVALANCHE**
 - Development of avalanche and streamer in gases in homogeneous electric field with application of Debye screening radius [JDR-P13-5504] 14 p2322 N71-26074
 - Weather and snow composition effects on avalanche formation [PB-197487] 18 p2919 N71-31490
- AVERAGE**
- NT MEAN**
 - AVIATION**
 - U AERONAUTICS**
 - AVIATORS**
 - U AIRCRAFT PILOTS**
- AVONICS**
- Lightning induced voltage in aircraft electrical circuits [NASA-TM-X-52906] 01 p0004 N71-10391
 - Considering design of digital computers for guidance and control of aerospace vehicles [AGARD-CP-65-78] 03 p0407 N71-12601
 - Investigating system requirements of airborne data processors 03 p0408 N71-12608
 - Investigating small digital processors as interface between computer and sensor in airborne systems 03 p0407 N71-12609
 - Developing self-organizing control systems for application in aerodynamics 03 p0407 N71-12613

- Data handling equipment for aerospace and ground support applications - conference [AGARD-CP-67-70] 04 p0504 N71-13826
 - Simulation model for advanced avionics digital computer [AD-714140] 06 p0004 N71-16295
 - Advanced aircraft for flight testing of integrated electronics systems for reusable space shuttle [NASA-CR-114832] 06 p0796 N71-16713
 - Space shuttle avionics technology [NASA-TM-X-66893] 08 p1292 N71-18436
 - Development and characteristics of frequency separated display devices for aircraft control [AD-715458] 08 p1144 N71-16739
 - Interference prediction model for evaluating expected interactions between avionics equipment on aircraft [AD-718997] 13 p2042 N71-34357
 - Human factor considerations applicable to aviation armament and avionics [AD-719108] 13 p2036 N71-34453
 - Development and characteristics of electronic equipment for digital processing of stochastic signals for military aircraft avionics systems [AD-719622] 13 p2046 N71-34954
 - Test methods and testing techniques for determining tactical performance and safety characteristics of ground support service avionics equipment [AD-723636] 17 p2732 N71-30258
 - Magnitudes of induced voltages and their relation to characteristics of lightning discharge and electrical properties of aircraft electrical systems 18 p2049 N71-30761
 - Simulation and modeling of advanced avionics digital computer system operation for optimum hardware configurations [AD-723521] 19 p3062 N71-32330
 - Development program planning for space shuttle avionics systems noting test beds and facilities required 20 p3352 N71-33053
 - Data bus for avionics systems of space shuttle, noting functions of interface unit, error detection and recovery, redundancy, and bus control philosophy [NASA-CR-115187] 23 p3756 N71-36771
 - Cost effectiveness, failure analysis, and design techniques for measuring reliability of avionics systems [AGARD-LS-47-71] 23 p3756 N71-36776
 - Reliability estimation, including failure effect analysis of avionics systems 23 p3757 N71-36777
 - Effectiveness of reliability programs for avionics equipment 23 p3757 N71-36779
 - Cost ownership analysis of avionics equipment 23 p3758 N71-36784
 - Analysis of functional requirements for data management systems used with space shuttle - Vol. 1 [NASA-CR-119953] 24 p4020 N71-38406
 - Space shuttle subsystem interface description, subsystems conceptual requirements, and analysis program - Vol. 2 [NASA-CR-120093] 24 p4020 N71-38687
- AVOIDANCE**
- NT COLLISION AVOIDANCE**
 - Self stimulation and avoidance reactions in rabbits when breathing virtually pure oxygen 08 p1155 N71-19872
 - Single and multiple irradiation effects on avoidance behavior in monkeys 16 p2543 N71-28187
- AVRO WHITWORTH HS-748 AIRCRAFT**
- U HS-748 AIRCRAFT**
 - AVRO 707 AIRCRAFT**
 - Boundary layer separation and longitudinal and lateral stability of Avro 707 aircraft during flight tests [ARC-CP-1107-PT-4] 07 p0909 N71-17082
 - Low speed lateral stability and control flight tests on Avro 707 aircraft [ARC-CP-1106-PT-3] 07 p0909 N71-17083
- AXIS (COORDINATES)**
- COORDINATES**
 - AXIS (REFERENCE LINES)**
 - NT AXES OF ROTATION**
 - NT EARTH AXIS**
 - Test fixture for measuring moment of inertia of irregularly shaped body with multiple axes [NASA-CASE-XOS-01023] 11 p1765 N71-22592
 - Mechanism for restraining universal joints to prevent separation while allowing bending, angulation, and lateral offset in any position about axis [NASA-CASE-XNP-02278] 16 p2604 N71-28951
- AXIS OF ROTATION**
- NT EARTH AXIS**
 - Galactic rotation model for axial alignment of interstellar disturbances 06 p0947 N71-16783
 - Spin axis scanning of celestial sphere for attitude control of spin stabilized spacecraft [NASA-TN-D-3611] 06 p0948 N71-16840
 - Electrical and electromechanical trigonometric computation assembly and space vehicle guidance system for aligning perpendicular axes of two sets of three-axis coordinate references [NASA-CASE-XMF-00684] 10 p1000 N71-31000
 - Hand controller operable about three respectively perpendicular axes and capable of actuating signal generators for attitude control devices [NASA-CASE-XMB-07487] 12 p1925 N71-23229
 - Determination of mass, variance, covariance, and correlation estimates for axes rotation of bivariate normal elliptical distributions [NASA-TM-X-44595] 15 p3434 N71-30799
 - Thermal bowing of single rods at several axial positions [TBO-3089] 21 p3458 N71-34008
 - Matrix algebra used to describe rotation about non-orthogonal axes [NASA-TM-X-40681] 22 p3485 N71-33077
 - Parameter calculation for determining Zeiss camera axes for satellite observation 22 p3486 N71-33079

SUBJECT INDEX

- AXIAL COMPRESSION LOADS**
 - Buckling of integrally stiffened cylindrical shells under axial compression [AD-712098] 03 p0460 N71-12800
 - Effect of variations in creep exponent N on buckling of circular cylindrical shells in axial compression [AD-711949] 03 p0461 N71-12800
 - Measuring abnormal mechanical properties in U-Nb-Zr nuclear fuels in uniaxial tension and compression with respect to stress, strain, and aging [Y-1752] 05 p0783 N71-15719
 - Strain energy theory of failure of oriented fiber glass reinforced plastic laminates under biaxial compression [NASA-TT-F-13444] 06 p0800 N71-16609
 - Euler buckling of clamped oval cylindrical shells under axial compression [AD-714578] 06 p0936 N71-16376
 - Plastic buckling of axially compressed thin shells of revolution with arbitrary meridional shape 06 p0936 N71-16376
 - Multiaxial stress studies on this wall tubes of rigid polyurethane foam [UCRL-50809] 07 p1048 N71-17882
 - Determining feasibility of increasing static shell loading of single stage compressor rig by bleeding or blowing station surface boundary layer [NASA-CR-54575] 08 p1142 N71-19740
 - Creep rupture strength of reinforced plastics under uniaxial compression [NASA-TT-F-13441] 08 p1300 N71-19374
 - Minimum weight design of axially compressed ring and stringer stiffened cylindrical shells [NASA-CR-1766] 17 p2853 N71-30110
 - BUSHEL - computer program used to determine buckling load of revolution shells under hydrostatic pressure, axial compression or both [WAFB-TM-809] 21 p3461 N71-34835
- AXIAL COMPRESSIONS**
- U TURBOCOMPRESSORS**
- AXIAL FLOW**
- Eliminating downstream flow blockage down to bypass air duct of turbofan engine with axial flow fan rotor [NASA-TN-D-6071] 01 p0115 N71-10537
 - Development of axial plasma flows in oscillating gas discharge 04 p0576 N71-13000
 - Design of axial flux heaters and gold spacer films on reactor cooling flow [ORAP-10186] 05 p0726 N71-15047
 - Nozzle flow theory for determining distribution function on centerline of free jet expansion [AD-714153] 06 p0636 N71-14618
 - Axial and radial aerosol diffusion in circular pipes [HSL-238] 06 p1177 N71-14581
 - Entropy and wall heat flux calculations for supersonic region aft of blunt axisymmetric bodies in hypersonic axial flow [AD-71416] 11 p1733 N71-22007
 - Effects of wave inlet distortion at high and low flow rate on performance of axial flow compressor [CUEDA-TURBO-TR-30] 11 p1738 N71-22408
 - Axial conducting gas controlled heat pipe leading to predictive capability for heat and mass transfer along heat pipe [NASA-CR-114300] 13 p2185 N71-30005
 - Axial mixing in gas and liquid phases and mass transfer coefficients for gas absorption in mechanically agitated columns 16 p2580 N71-30000
 - Shock wave boundary layer interactions in two dimensional and axially symmetric flows including surface influence 16 p2583 N71-30007
 - Analysis of flows past rectangular recesses in plate and axially symmetric bodies immersed in supersonic air stream [NASA-TT-F-13577] 16 p2594 N71-30739
 - Design of axial compressor rotor - specification of meridional velocity profile [AD-722834] 18 p3001 N71-31234

- Similar solutions for axial hypersonic flow past slender bodies with nearly elliptic cross section and slender nonsymmetric bodies
(JAL-PB-71-13) 22 p3368 N71-35412
- AXIAL FLOW COMPRESSORS**
U TURBOCOMPRESSORS
AXIAL FLOW PUMPS
NT TURBINE PUMPS
FORTRAN program for computational design of axial flow pump by blade element analysis
(NASA-CR-115174) 63 p0305 N71-13239
Design and performance of 0.5-hub-tip-ratio axial flow pump rotor with blade-tip diffusion factor of 0.63
(NASA-TN-X-2235) 69 p1377 N71-20288
- AXIAL FLOW TURBOFANS**
Water analysis on axial turbofan blade loading
(AD-710794) 61 p0081 N71-10562
Cold air tests on axial flow turbine with transpiration cooled discrete hole static blades to determine coolant flow ejection effect on turbine aerodynamic performance
(NASA-TN-X-2133) 62 p0142 N71-11010
Developing computer program for predicting performance of single-stage axial flow turbines
(AD-713116) 63 p0763 N71-15361
Design and performance of transpiration cooled axial high entry temperature axial flow turbine
(AD-711229) 67 p1129 N71-17399
Polym tests and structural analysis of axial flow compressor blade root
(JAL-TR-214) 69 p1476 N71-19873
Computer program to generate turbine aerodynamic parameters, approximate external blade geometries, and coolant flow requirements for two stage axial flow turbine
(NASA-TN-X-2225) 11 p1607 N71-22548
Cold-air tests to determine performance characteristics of single-stage turbine with static blades employing transpiration coolant ejection through wire mesh wall
(NASA-TN-X-2176) 12 p1991 N71-23980
Vibration damping capacity of blade mounting in axial flow turbomachines
(JAL-TR-218) 14 p2348 N71-26006
Unsteady flow characteristics of turbocompressors and axial flow turbines including blade vibration and damping
(TR-71) 20 p3340 N71-33760
Rotor-stator axial clearance effects on cold air performance of turbine with swept cooled stator blades
(NASA-TN-X-27914) 20 p3340 N71-33779
- AXIAL LOADS**
NT AXIAL COMPRESSION LOADS
Axial load fatigue tests on chromium-nickel-titanium test tubing with welded fish mouth type welds
(JAL/RM-323) 61 p0127 N71-10117
Finite element analysis of alternating axial loading of elastic plate pressed between two rectangular blocks with finite friction
(JEPF-110770) 62 p0360 N71-11945
In-plane creep behavior of austenitic steels and nickel alloys under multiaxial loads
(JEP-1152) 63 p0731 N71-15587
Linear elastic-plastic, and stability analysis of biaxially loaded columns
(AD-714176) 66 p0955 N71-16436
Elastic buckling of clamped oval cylindrical shells under axial loads
(AD-714579) 66 p0955 N71-16526
Coupling characteristic effects on dynamic response of axially coupled turbofan with digital computer program based on transfer matrix techniques
(AD-71770) 67 p1770 N71-22712
High temperature uniaxial tensile tests performed on diamond-graphite composites
(AD-711513) 12 p1942 N71-23402
Analysis of friction bonding process with metal coupon under high axial pressure
(AD-712528) 16 p2528 N71-31038
NASTRAN program used to calculate stress concentration caused by surface cavities in plates under tensile loading
(AD-713623) 22 p3062 N71-36235
Stability of thin cylindrical shells subject to periodic loads in three-dependent temperature field
(AD-713623) 22 p3092 N71-36238
- AXIAL STRAIN**
Cooking stress criteria for estimating strength and stability of rock formations
(JEP-75-740) 63 p0211 N71-11513
Finite element analysis for axial deformation of materials and measurement of strains produced at constant pressure up to 5 kbar
(JEP-75-740) 64 p0333 N71-13953
Axial deformation analysis of thin shell elastic cylindrical shells of uniform thickness with surface constraints
(AD-713623) 22 p3062 N71-36235
Uniaxial bond strengths of brittle matrix composites prepared from soda borosilicate glass reported as function of reactor concentration
(JEP-75-740) 64 p0333 N71-13953
Reluctivity spectrum of uniaxial stress of single crystal GaAs
(AD-713623) 22 p3062 N71-36235

- Effects of uniaxial and shear stress on conduction and valence bands of bismuth samples
(AD-713623) 22 p3062 N71-36235
Numerical analysis of properties of anisotropic waves in transversely isotropic rods
(AD-713623) 22 p3062 N71-36235
Uniaxial strain rate, creep, isotropy, and relaxation tests for characterization of polycrystalline
(AD-713623) 22 p3062 N71-36235
- AXIAL STRESS**
Axisymmetric stresses and displacements in two finite circular cylinders in contact
(NASA-TN-X-20853) 61 p0129 N71-10448
Multiaxial analytic creep theory for describing primary, secondary, and creep recovery
(JEP-75-740) 64 p0333 N71-13953
Development of numerical equations for internal shear forces, axial forces, and bending moments based on kinematics of curved beams
(AD-713623) 22 p3062 N71-36235
Effect of internal stresses on strength of chemically bonded composites with varying coefficients of thermal expansion
(JEP-75-740) 64 p0333 N71-13953
Creep of polycrystalline under varying temperature for nonlinear uniaxial stress described by multiple integral representation and modified superposition principle
(AD-713623) 22 p3062 N71-36235
Technique for testing high strength sheet steel to determine sensitivity to cold crack formation during welding under biaxial stress conditions
(AD-713623) 22 p3062 N71-36235
- AXISYMMETRIC**
Asymptotic proof of asymptotic relations for averaged amplitudes
(JEP-75-740) 64 p0333 N71-13953
AXISYMMETRIC BODIES
Prediction of flow properties in shock wave interactions on axisymmetric bodies at zero incidence and spin
(JEP-75-740) 64 p0333 N71-13953
Laminar flow past axisymmetric blunt bodies moving at hypersonic speed
(NASA-CR-115171) 63 p0361 N71-12391
Incremental variational method for determining isochoric load deformation and buckling load for shells of revolution
(AD-712522) 64 p0617 N71-13946
Turbulent boundary layer and skin friction on axisymmetric bodies in subsonic and supersonic flow
(JEP-75-740) 64 p0333 N71-13953
Perturbation theory and asymptotic expansion analysis on supersonic inviscid gas flow past axisymmetric body
(AD-713623) 22 p3062 N71-36235
Base flow analysis of axisymmetric body with conical jet
(AD-712522) 64 p0617 N71-13946
Development of aerodynamic coefficients on maximum thickness and length of axisymmetric bodies in supersonic flow
(JEP-75-740) 64 p0333 N71-13953
Singularity method for calculation of potential flow around axisymmetric rings
(AD-713623) 22 p3062 N71-36235
Structural elastic shell theory for axisymmetric half-circular cylinders
(NASA-CR-115171) 63 p0361 N71-12391
Continuum theory of slender electrostatic probes
(JEP-75-740) 64 p0333 N71-13953
Differential equations governing transient response of vibrating axisymmetric orthotropic bodies and effect of shape change
(NASA-TN-D-6220) 14 p2353 N71-26006
Instability and turbulence for various external compression axisymmetric supersonic intakes of 25 degree cone semi-angle at various turbulence, Reynolds number, and surface conditions
(JEP-75-740) 64 p0333 N71-13953
Subsonic flow wake of blunt-based axisymmetric body in uniform steady flow wind tunnel
(AD-713623) 22 p3062 N71-36235
Finite element method used for stiffness analysis of axisymmetric shells of composite materials
(AD-713623) 22 p3062 N71-36235
Computer program for analyzing transient response of vibrating axisymmetric bodies including effects of shape change
(NASA-TN-X-20853) 61 p0129 N71-10448
Kinetic equation solution in drift approximation for electric field effect on transfer processes in axially symmetric magnetic traps
(CONF-710607-50) 24 p3994 N71-30493
- AXISYMMETRIC DEFORMATION**
U AXIAL STRAIN
AXISYMMETRIC FLOW
NT ANNULAR FLOW
Measuring distortion characteristics at engine face section of axisymmetric inlet
(NASA-CR-1644) 63 p0610 N71-12211
Non-continuous axisymmetric hypersonic flow past very slender bodies
(AD-713623) 22 p3062 N71-36235

- Wave theory and axially-symmetric super-sound waves
(AD-713623) 22 p3062 N71-36235
Description of computer program for solving two dimensional and axisymmetric forms of compressible boundary layer equations for continuity, momentum, and mean total enthalpy
(NASA-TN-X-2140) 11 p1739 N71-23588
Applications of finite difference methods to subsonic, supersonic, and plane flows
(JEP-75-740) 64 p0333 N71-13953
Electrostatic coefficients of axisymmetric centered nozzle under steady, critical flow over Reynolds number range from 100 to 34,000
(AD-713623) 22 p3062 N71-36235
Harmonic functions applied to two dimensional axisymmetric flow and thermodynamics
(AD-713623) 22 p3062 N71-36235
Numerical solution of flow equations for laminar, transitional, and turbulent compressible boundary layers for plane or axisymmetric flows
(NASA-TR-R-348) 19 p0970 N71-32164
Axisymmetric flow of rotating vortex analyzed to determine conditions allowing isolated vortex breakdown to develop
(NASA-CR-1045) 19 p0970 N71-32192
Axisymmetric flows with regions of closed streamlines confined by rotational limits or electromagnetic fields, for containment for gas core reactors
(AD-713623) 22 p3062 N71-36235
Statistical minimum model of axisymmetric charged particle beams with nonzero angular velocities
(JEP-75-740) 64 p0333 N71-13953
General properties of self-similar solutions of plane and axisymmetric transonic nozzle flows
(AD-713623) 22 p3062 N71-36235
Axisymmetric, transonic plasma equilibria in Tokamak and hybrid systems examined according to MHD theory
(CONF-710607-50) 24 p3994 N71-30493
- AXISYMMETRY**
U SYMMETRY
AXIS
U SHAFTS [MACHINE ELEMENTS]
AXIS [INORGANIC]
Crystal structure and molecular dynamics of inorganic metal azides
(AD-713623) 22 p3062 N71-36235
Technique for differential thermal analysis of primary explosives
(AD-713623) 22 p3062 N71-36235
- AXISYMMETRY**
Systems design and flight tests of axisymmetric guidance orientation system
(NYO-5747-13) 63 p0346 N71-13073
Semiempirical radar look-direction analysis of faults, joint systems, and dip slopes and radar detectability of geologic features
(AD-713623) 22 p3062 N71-36235
Digital controlled radar interferometer for measuring extension of radar echoes from target trails
(AD-713623) 22 p3062 N71-36235
Tracking system for laser telescope employed in tracking large rockets and space vehicles to give information regarding azimuth and elevation
(NASA-CASE-MF-14017) 14 p2259 N71-36237
Development and testing of VHF bearings transmitter for aircraft azimuth guidance
(FAA-RD-71-65) 22 p3618 N71-33779
Synchrotron radiation observations and normalization for determining Rg-ortho azides
(AD-713623) 22 p3062 N71-36235
Calculation of azimuth between two distant ground points from synchrotron photographs taken by artificial earth satellites
(AD-713623) 22 p3062 N71-36235
Range and azimuth resolution characteristics and aircraft operation measurement capability of radar beacon-digital altimeter
(FAA-NA-71-16) 23 p3793 N71-37038
- AXISYMMETRY**
Synthesis of azide polymers for heat shields by azide-azide azide reactions
(NASA-CASE-MF-14017) 14 p2259 N71-36237
Polyphenyl-oxazones used for high temperature adhesive, laminating resin, protecting coatings, and films
(AD-713623) 22 p3062 N71-36235
Molecular structure and thermal stability of fluorinated polyimides and poly(ether-imide)s
(AD-713623) 22 p3062 N71-36235
Nuclear quadrupole resonance spectroscopy of nitrogen nuclei in azides with linear, cyclic, and chiral substitution including steric structure and kinetic effects in linear azides
(AD-713623) 22 p3062 N71-36235
- AXISYMMETRY**
Chemical synthesis and thermogravimetry of thermal resistant polyimides and poly(ether-imide)s
(AD-713623) 22 p3062 N71-36235
- AXISYMMETRY**
NT CARBATOLES
NT DIOLES

EPR and ENDOR study of free radicals produced by gamma irradiation of imidazole single crystals
[CEA-R-3758] 14 p2397 N71-26395
Corrosion inhibition in metal compounds of azole type
[AD-727853] 34 p3940 N71-38104

AZUR SATELLITE

Satellite motion simulators for space environment test budget tests, particularly for Azur satellite
03 p0356 N71-12712
Thermal space environment simulation tests of scientific satellite Azur
03 p0358 N71-12722

Systems integration of scientific satellite Azur and space environment tests
03 p0358 N71-12723

Planning and coordination of space environment simulation test programs for Azur and Dial satellites
03 p0358 N71-12724

Cost analysis and costs of satellite test programs with reference to Azur satellite
03 p0460 N71-12727

PCM telemetry system and instrument packages for sounding rockets to assist German Azur satellite observations
[BMW-FB-W-70-49] 10 p1647 N71-20788

Ray-traced distribution between supplementary sounding rockets for German Azur satellite, noting radiation counters, magnetometers, and aerol spectroscopy
[BMW-FB-W-70-40] 10 p1648 N71-20789

Conference on Europa 1 launch vehicle, Azur research satellite, Symphonie communication satellite, and German ground station-satellite communication system technology
10 p1649 N71-21520

Azur satellite experiments for measuring radiation both electron and proton energies using radiation counters
[BMW-FB-W-70-47] 11 p1825 N71-22099

Radiation counter package payload for sounding rockets supplementary to German Azur satellite
[BMW-FB-W-70-59] 11 p1831 N71-22222

Azur satellite observation of proton and electron energy in auroral zones and magnetosphere
[BMW-FB-W-70-56] 12 p1994 N71-24262

Acoustic data obtained during launch of ESRO 1-B satellite and GRS-A satellite by Scout launch vehicles
[NASA-TN-D-6369] 20 p3354 N71-33543

Azur satellite, Dial satellite, ground support systems, ELDO launch vehicle, and space environment simulation
[QB-1-71] 22 p3681 N71-36249

AZUR AIRCRAFT

U A-4 AIRCRAFT

A40 AIRCRAFT

U A-4 AIRCRAFT

B

B STARS

Atmospheric parameters, effective temperature, and surface gravity for extreme population II stars
[NP-18375] 04 p0610 N71-13744

Photoelectric and Balmer emission for B stars
03 p2166 N71-24928

Spectroscopic observation of seven neutral helium line profiles for five main sequence B stars with estimated helium abundance for upturn Orionis, HR 2154, and pi Ceti
16 p2680 N71-28786

Survey of southern Milky Way for stars earlier than spectral type GO and at least as intrinsically luminous as B2 dwarf
[AD-722041] 16 p2681 N71-28836

B-52 AIRCRAFT

Optimal bomb release intervals from B-52 aircraft bombing system
09 p1319 N71-19383

Approximation method for turbulence effects on aircraft aerodynamic stability with B-52 examples
15 p2367 N71-27320

B-57 AIRCRAFT

Stratospheric turbulence and horizontal temperature measured at supersonic transport altitudes by B-57 aircraft
[JLE-542] 10 p1532 N71-21284

Spectra of reflected solar energy from clouds, snow, and fields at 0.4 to 2.4 microns using C-47 and B-57 aircraft - graphs
[NASA-TM-X-63574] 15 p2405 N71-27649

B-70 AIRCRAFT

Measurement of engine exhaust noise during ground operation of XB-70 aircraft
[NASA-TN-D-7043] 06 p0794 N71-15830

Base pressure measurements on XB-70 aircraft at Mach numbers from 0.4 to 3.0
[NASA-TM-X-1612] 07 p0970 N71-17132

Evaluating effects of high altitude turbulence on XB-70 airplane
[NASA-TN-D-6457] 18 p2848 N71-30718

XB-70 aircraft for investigating and predicting clear air turbulence in stratosphere caused by mountain waves
[NASA-CR-1078] 18 p2954 N71-31351

B-103 AIRCRAFT

U BUCKANEER AIRCRAFT

BARBIT METAL

U BEARING ALLOYS

BAC AIRCRAFT

NT H-126 AIRCRAFT

NT VC-10 AIRCRAFT

Aerodynamic interference caused by rear fuselage mounted power plants on BAC aircraft
09 p1314 N71-19575

Low speed wind tunnel and flight stability tests of BAC 721 aircraft longitudinal balance, noting airfoil characteristics
[ARC-CP-1134] 10 p1493 N71-21205

BACILLUS

Thermal inactivation curves of *Bacillus subtilis* spores for decontamination of interplanetary space vehicle components
[NASA-CR-111367] 02 p0151 N71-11073

Survey and criteria of bacterial growth quantitative determination methods including *Bacillus coli* direct microscopic morphology and growth measurement
[NASA-TT-F-13632] 13 p2032 N71-24584

Polymerization and energy conversion efficiency of yeast and *Bacillus lactis* fermentation for biochemical fuel cells
14 p2205 N71-26245

BACKFIRE

Backfire antenna research restricted to surface wave structures consisting of dipole elements
[AD-719679] 14 p2227 N71-25653

BACKGROUND NOISE

Low frequency background noise in planar silicon transistors
[PUBL-586] 02 p0195 N71-11364

Tunnel diode amplifier circuit stability and background noise effects in terms of bias, temperature, and bandwidth variations
09 p1360 N71-20084

Transonic wind tunnel background noise measurement for analysis of Saturn 5 model protrusion test data
[NASA-CR-103064] 09 p1473 N71-20510

Space station simulator background noise effects on crew behavior during long term confinement
10 p1509 N71-20988

Adaptive antenna array processing techniques allowing spatial signal field characterization of multiple wavefronts in background of uncorrelated noise
[AD-719096] 14 p2227 N71-25686

Spatial coherence of 1 to 5 min acoustic waves from two nuclear explosions along with atmospheric pressure background noise for same period measured at low altitudes
[AD-728853] 15 p2599 N71-27216

Automatic feedback control system for controlling volume of power amplifier and measuring frequency range of background noise
[AD-712956] 16 p2568 N71-28356

Receiving dipole antenna array signal to noise ratio optimization based on steepest descent method
[NASA-CR-1778] 20 p3243 N71-33214

Techniques for extracting objects from gray value real and computer-generated pictures including noise-free extraction from noisy backgrounds
[TR-145] 21 p3400 N71-34195

BACKGROUND RADIATION

Validity of bremsstrahlung model for background radiation in galaxy and earth atmosphere
[NASA-TT-F-13615] 16 p2675 N71-28943

Cosmic electron sources of galactic background radiation
[NASA-TT-F-13611] 16 p2676 N71-29027

Energy spectra of background radiation in universe for X ray and radio regions
[NASA-TT-F-13732] 18 p3003 N71-30046

Background radiation measurements on proton synchrotron intersecting storage rings
[CERN-71-1] 18 p2903 N71-31550

Thin NaI(Tl) crystals for estimating natural terrestrial background in 17 and 60 keV energy regions from Compton continuum peak
[UCRL-72927] 22 p3644 N71-35983

Electromagnetic background radiation of universe
23 p3830 N71-37438

BACKSCATTERING

Polarization rotation effects on inhomogeneously propagated sea backscatter amplitudes
[AD-711341] 01 p0824 N71-10733

Calculating secondary backscattering for water clouds for collimated pulsed laser system
[PB-193435] 01 p0800 N71-10086

Radar studies for lunar landing sites using backscatter measurements
[NASA-CR-108666] 02 p0294 N71-11402

Classification of radar targets from polarized radar backscatter formulated as scattering matrix
[AD-712067] 02 p0105 N71-12010

Simultaneous measurements of radar backscatter and bistatic cross sections of rain and this turbulent layers
[NASA-CR-111418] 03 p0335 N71-12700

Fitted cuts and planar nucleus backscatter coefficients
[COO-364-596] 03 p0433 N71-12680

Electromagnetic wave transmission along air-sea interface and in underwater communication and optical systems
[AGARD-CP-77-70] 04 p0363 N71-12700

Spectral characteristics of resonant high frequency radio signals backscattered from sea surface
04 p0492 N71-12700

Synchronous scanning for backscatter reduction in underwater optical systems
04 p0366 N71-12700

Effect of decreasing altitude on statistics of radar backscatter from random rough surface
[NASA-CR-114083] 03 p0443 N71-12700

Scattering by imperfectly conducting spheres
[BC-3-70-4277] 03 p0746 N71-12700

Investigating polarization diversity as technique to reduce effects of target glint or angle fluctuation
[AD-713535] 03 p0704 N71-12700

Backscattering cross sections for spheres for calibrating radar receivers
[R-79] 06 p0812 N71-12700

Investigating backscattering factor as function of surface roughness of radioisotope carrier materials for remote detection of different oceanic features
[BMW-FBK-70-B-A] 06 p0914 N71-12700

Cloud structure determined from laser backscatter
07 p1033 N71-12700

Atlas of oblique incidence high frequency backscatter inhomogeneities of midlatitude ionosphere
[ESSA-TR-EEL-162-JTS-104] 07 p1026 N71-12700

Spectral response measurements of man-made targets and surfaces for frequency variation analysis of electromagnetic backscatter
[NASA-CR-117035] 09 p1346 N71-19025

Heavy particle transfer model of backward double alpha particle scattering and cluster structure of O-6 and C-12
[NYO-2171-327] 09 p1426 N71-12700

Measuring backward elastic scattering of positrons from proton and negative kaon proton events
[CEA-R-3685] 09 p1438 N71-12700

Background pressure effects on reduction of molecular beam intensity
[AD-717158] 10 p1539 N71-12700

Reliability and experimental design of optical radar system for tropospheric and ionospheric backscatter
[DLR-MITT-70-18] 10 p1518 N71-12700

Measurement of negative pion proton deep exchange at backward angles
[COO-1764-113] 10 p1613 N71-12700

Backscattered signal amplitudes of radar measurements applied to target recognition
[AD-717198] 10 p1521 N71-12700

Remote sensing of midlatitude ionosphere with narrow beam high frequency backscatter coastal scanning in azimuth and elevation
11 p1744 N71-12700

Energy spectra of backscattered electrons and positrons by Monte Carlo calculations
[UCRL-197191] 12 p1968 N71-12700

Radiometric and radar observations of dynamic ocean features including determination of sea state, spray, whitecaps, and radar backscatter cross section as function of wind speed
[AD-718773] 12 p1910 N71-12700

Backscattering in fog using pulsed laser
[DLR-FB-70-31] 13 p0808 N71-12700

Angular reflection and dissociation of molecular nitrous oxide beam incident on tungsten surface
15 p2471 N71-12700

Quantum statistics and elastic backscattering cross sections of potassium ion proton interactions between 1.0 and 2.5 MeV/c
15 p2477 N71-12700

Estimation of total ozone from Nimbus 4 satellite measurements of backscattered ultraviolet earth radiance
[NASA-TM-X-63576] 15 p2405 N71-12700

Multiple scattering model for isotropic protons and nonrelativistic high energy forward and backward scattering
[TRB-TP-2-70] 15 p2405 N71-12700

Electron temperatures measured by electron probe and radar backscatter in ionospheric nonuniform plasma for studying planetary ionospheres
[NASA-TM-X-63586] 16 p2661 N71-12700

Exchange mechanisms and polarization in backward scattering of protons on light nuclei and d plus He-4 yields He-3 plus H-3 reaction
[JHEP-P2-5496] 17 p2792 N71-12700

Dispersion model for pion-nucleon backward scattering peak amplitudes
[TTP-76-65] 17 p2811 N71-12700

SUBJECT INDEX

Mean quadratic angles of inclination of surfaces on Venus with diagrams of backscatter measured by radio waves
[NASA-TT-F-13741] 18 p3291 N71-13131

Methods for measuring backscattering, light scattering, and internal wave parameters of ocean water
19 p3292 N71-13203

Root mean square slope angles of Venus surface from radar backscattering and Venusian satellite altimetric data
19 p3183 N71-13287

Temperature and radiation dosage effects in electron induced defect backscatter of proteins and helium ions
21 p3488 N71-13493

Radar backscatter measurement to determine electron temperature dependence of F region absorption
[JRD-65] 22 p3575 N71-13544

Estimates of atomic concentration hemisphere from laser backscatter and rocket probe measurements of electron and ion temperatures and electron concentration
[NASA-CR-112648] 23 p3578 N71-13548

Light impulse backscattering for determining visual range in atmosphere
23 p3750 N71-13678

Negative pion proton yields neutral pion neutrons differential cross section measurements and baryon exchange model with absorption in pion nucleus backward scattering
[PD-1040] 23 p3886 N71-13712

Coefficient of backscatter for monochromatic electron striking target at oblique angle
[JLL-CR-TRANS-5553-1922.09] 23 p3821 N71-13723

BACKWASH
Calculation of crew radiation dosage from uranium gas nuclear rocket engine exhaust backflow of fission products
20 p3305 N71-13655

BACTERIA
NT BACILLUS
NT BACILLUS
NT HYDROGEMONOMAS
NT STREPTOCOCCUS
Bacterial mat formation and Chromatium vulnificum bacteria of hot mineral springs in Yumoto, Japan
[NASA-TT-F-12738] 02 p0156 N71-11107

Microbiological fuel corrosion by bacteria and fungi in fuel tanks
02 p0287 N71-11848

Ultraviolet radiation and high vacuum space environment disinfection for biocompatible bacteria
[NASA-PB-W-70-46] 06 p0799 N71-15724

Survival of soil bacteria during prolonged desiccation
[NASA-CR-116807] 06 p1148 N71-18562

Methods for studying biochemical properties of bacteria
[AD-71506] 06 p1149 N71-18792

Feasibility of computerized bacterial identification
[NASA-CR-116815] 06 p1156 N71-19817

Survival of Antarctic desert soil bacteria exposed to various temperatures and to three years of continuous vacuum-high vacuum
09 p1333 N71-20169

Investigation of movement of ciliary infusoria in isotonic medium
[JPRS-52581] 10 p1503 N71-21713

Structural origin of transoidal pyrites in coals
[JLL-RTS-5946] 11 p1744 N71-21891

Recombination of petroleum products with heavy water
[NASA-CASE-JNP-65835] 12 p1870 N71-23499

Temperature requirements for thermophilic bacteria growth in soil and by culture techniques
[NASA-TT-F-13458] 12 p1864 N71-23976

Artificial changes in leukocyte count of rabbits
[NASA-TT-F-13458] 13 p2053 N71-24737

Automated procedure for direct cell count of bacteria in urine by bioluminescence reaction of luciferase when mixed with ATP
[NASA-TM-X-65531] 13 p2054 N71-25053

Automatic bioassay instrument for arboviruses based on electrode triphosphate bioluminescent property to urine sample bacterial content
[NASA-CASE-GSC-11169-1] 13 p2373 N71-27992

Procedures and immunofluorescent techniques for staining *Agrobacterium tumefaciens* for bacterial infection after laser sample exposure
[NASA-CR-113664] 17 p2707 N71-29328

Characteristics of thermophilic bacteria
[NASA-TT-F-13705] 18 p2975 N71-30671

Automated apparatus for analyzing bacterial ATP in soil samples
[NASA-CASE-GSC-11169-2] 21 p3385 N71-34079

Effects of thermotolerance inactivation on *Bacillus subtilis* var. *alger* at various temperatures, and natural range in soil
[NASA-CR-121921] 22 p3469 N71-36161

Thermal transport, antibiotics, photodynamic action and energy conversion in photosynthetic bacteria and virus infection of bacteria
[NPO-3779-18] 23 p3714 N71-36474

BACTERICIDES
Germicidal activity of ethylene oxide evaluated through experiments in planetary quarantine program
[NASA-CR-122889] 23 p3715 N71-36488

BACTERIOLOGY
Investigating effects of thermal environments and acidity on growth of bacteria and blue green algae
07 p0983 N71-17988

Application of environmental microbiology to spacecraft quarantine procedures
[NASA-CR-119638] 19 p3841 N71-31001

Biogeography of scientific publications and presentation relating to planetary quarantine for year 1970 - Vol. 5
[NASA-CR-121325] 19 p3844 N71-32231

Effect of hard impact and median erosion on release of microorganisms from geological formations
[NASA-CR-121707] 21 p3381 N71-34056

BACTERIOPHAGES
Characteristics of X irradiated lambda phages
[NYO-3779-16] 03 p0652 N71-14373

Method for preparation and assay of T4 bacteriophage
[NASA-CR-117172] 09 p1334 N71-20236

Neopharyngeal bacterin cultures of spacecrew during long duration space station simulation
10 p1498 N71-20992

BAFFLES
Studies of propellant sloshing under low gravity conditions
[NASA-CR-102891] 01 p0041 N71-10320

Comparison of flexible and rigid ring baffles for slosh suppression
01 p0041 N71-10322

Analytical and experimental investigations of oscillations in rocket baffle cavities
[AD-71428] 02 p0289 N71-11878

Light baffles with oblate hemispherical surface and sloshing fluids
[NASA-CASE-NPO-10357] 03 p0669 N71-15604

Flexible ring slosh damping baffle for spacecraft fuel tank
[NASA-CASE-LAR-10317-1] 06 p0954 N71-16103

Submerged fuel tank baffles to prevent sloshing in liquid propellant rocket flight
[NASA-CASE-XLA-04665] 06 p0954 N71-16106

Vertical motion of static loads over baffles during landing operations using ground effect machines
[NPL-ROVERCRAFT-TM-31] 07 p0970 N71-17160

Baffle geometry, subsonic estimation, and connector failure analysis for ion thruster of solar electric propulsion system
10 p1639 N71-21557

Attenuation of photophosphoric sunlight and moonlight for TD-1 satellite baffle system
11 p1822 N71-22114

Attenuation of photophosphoric sunlight and moonlight at photometer channel in TD-1 satellite baffle system
11 p1822 N71-22122

Tables on natural and self acoustic radiation impedance for pistons in plane baffles and baffle
[AD-718313] 12 p1987 N71-23940

Analysis of aluminum and nonmetallic baffles for use with liquid oxygen containers to prevent sloshing
[NASA-CR-11800] 21 p3413 N71-34204

BAGS
NT GAS BAGS
BALANCE
Structural parameters effect on tapered cantilever and lower beam yield strength
[AD-710709] 01 p0067 N71-10561

BALANCE
U DEGRASSING
BALANCE EQUATIONS
U EQUATIONS
BALANCING
Flexible rotor balancing by exact point-speed influence coefficient method
[NASA-CR-72774] 01 p0857 N71-10021

Automatic balancing device for use on frictionless supported attitude-controlled test platforms
[NASA-CASE-LAR-10774] 04 p0513 N71-11545

General method for dynamic stiffness and force balancing of spatial mechanisms
12 p1950 N71-24132

Force balanced throttle valve for fuel control in rocket engines
[NASA-CASE-NPO-10886] 15 p3416 N71-27432

Direct comparison methods for calibrating piston gas weights for use with equal arm balances and single pan balances
[NBS-TN-577] 16 p2594 N71-28652

Automatically balanced air bearing standards for testing satellite attitude control system
[ESRO-CR-18] 17 p2779 N71-29971

Subsonic static characteristics of slender wing configurations using magnetic suspension and balance system
[NASA-CR-1796] 17 p2701 N71-29775

Capacitor system for load balancing in SNAP-8
[NASA-CR-72508] 24 p3661 N71-36253

BALL BEARINGS
Evaluation of ceramic-hybrid rolling element bearing
[NASA-TN-D-7011] 03 p0449 N71-13471

Determination of bearing torques for ballasted methylalumoxane disulfide ball bearings
[NASA-TN-D-7023] 03 p0653 N71-15149

Ball bearing economy on design and performance of roller, ball, and needle bearings
[NASA-TM-X-66477] 05 p0693 N71-15626

Testing materials for use in cages, balls, and races in cryogenic hydrogen-cooled 110-mm ball bearing
[NASA-CR-72279] 06 p0666 N71-16487

High temperature ball bearing design for turbopump casings
[NASA-TM-X-53938] 06 p0666 N71-16554

Rolling element fatigue lives of AISI T-1, AISI M-42, AISI 52100, and Inconel at 150 F
[NASA-TN-D-6179] 07 p1084 N71-17529

Performance of high speed bearings with cylindrical ball bearings
[NASA-TN-D-7007] 08 p1207 N71-18630

Durability and service life of ball bearings
[NASA-TT-F-13460] 08 p1208 N71-19880

High temperature fatigue tests of steel ball bearings with synthetic paraffinic oil lubricant in low oxygen environment
10 p1567 N71-21666

Stearic acid additives in lubricants for improved contact fatigue life of ball bearing steel
[AD-717628] 11 p1703 N71-22079

Use of scanning electron microscopy for following localized surface alterations in ball bearings during running
[AD-717959] 12 p1936 N71-23771

Surface evaluation of stainless steel grove bearings manufactured by various hardening techniques
[NASA-CR-114980] 12 p1939 N71-23949

Development and characterization of test equipment for measuring friction moment and friction losses in ball bearings under various radial load conditions
[AD-719110] 13 p2084 N71-24433

Design and application of tool-steel ball bearings to turbocharger and mercury pump of SNAP-8 electrical generator
[NASA-CR-72825] 15 p2414 N71-28910

Wide angle rotating mirror scan system design for laser display system and synchronous motor gas and ball bearing performance tests
[AD-721484] 16 p0886 N71-30071

Combination guide and rotary bearing for freely moving shaft
[NASA-CASE-XLA-08013] 16 p0885 N71-30136

Elastohydrodynamic film thickness between rolling disks with synthetic paraffinic oil at temperatures from 339 to 509 K
[NASA-TN-D-6411] 18 p2930 N71-31228

Effect of surface inclusions on ball bearing steel durability involving surface contact
19 p1817 N71-31819

Shear strength of solidified oil lubricant in ball bearing
[JPRS-198321] 19 p1816 N71-31706

Vaporized oil ball bearings for satellite antennas
[BMSW-PB-W-71-11] 20 p3278 N71-33061

Space environment vacuum simulation of ball bearing with Monte Carlo analysis of friction zone
[D-61] 20 p2272 N71-33115

Design and basic characteristics of bearings for gyroscopic devices for aerodynamic and aerostatic bearings
[JPRS-53083] 21 p3428 N71-34597

Tests of ball bearings of various material combinations in liquid hydrogen
[NASA-CR-72280] 23 p3762 N71-34818

BALLISTIC MISSILES
NT INTERCONTINENTAL BALLISTIC MISSILES
Design of guided ballistic missiles with liquid or solid propellant rocket engines
[AD-711138] 01 p0629 N71-10592

Design and test procedures for ballistic missiles and missile complexes
[JPRS-51016] 03 p0453 N71-13004

Ballistic missile design methods
06 p0456 N71-13002

Design and optimization of ballistic missile complexes
03 p0456 N71-13003

Experimental development and testing of ballistic missiles during design stages
03 p0456 N71-13004

Low level turbulence models for determining standard deviation of ballistic missile trajectories
19 p3127 N71-31887

BALLISTIC RANGES
Conference on ballistic range techniques and equipment
[AGARDGRAPH-138] 04 p0514 N71-12576

Modern ballistic range facilities and research applications
[NASA-TM-X-66530] 04 p0514 N71-12577

Light gas gun model launcher for ballistic range research
[NASA-TM-X-66531] 04 p0515 N71-12578

Hypervelocity impact research in ballistic ranges
[NASA-TM-X-66533] 04 p0515 N71-12580

BALLISTIC TRAJECTORIES

Ballistic range test equipment for measuring model position, attitude, and velocity
[NASA-TM-X-46535] 04 p0522 N71-13582

Aerodynamic characteristics of free flight bodies in ballistic ranges
[NASA-TM-X-46536] 04 p0472 N71-13583

Shadow, schlieren, and interferometer photographs and uses in ballistic ranges
[NASA-TM-X-46537] 04 p0523 N71-13584

Techniques and instrumentation for optical radiation measurements in ballistic ranges
[NASA-TM-X-46538] 04 p0524 N71-13585

Microwave techniques and equipment used in ballistic ranges
[NASA-TM-X-46539] 04 p0525 N71-13586

Convective heat transfer measurements in ballistic ranges and free flight apparatus
[NASA-TM-X-46540] 04 p0526 N71-13587

Ballistic ranges for free flight measurements of speed drag at subsonic, transonic, supersonic and hypersonic speeds in upper atmosphere
[AD-721200] 15 p2395 N71-37675

BALLISTIC TRAJECTORIES

Mean orbital element determination using Vinti spheroidal theory of drag-free satellite motion applied to ballistic trajectories
[NASA-TN-D-6069] 02 p0295 N71-11918

Wind effect on unguided rockets fired near maximum range
[AD-711834] 02 p0296 N71-11949

Diagrams for projectile trajectory calculations
[ISL-T-2749] 03 p0312 N71-12222

Accuracy in range, azimuth and elevation angle measurements to determine impact area of ballistic trajectories
[REPT-1-1969] 03 p0334 N71-12384

Bezel function solutions for low angle of attack approach of flying vehicle to atmospheric boundary and transition into vibrational motion
[AD-70949] 07 p0949 N71-16083

Measurements of yawing and rolling behavior of projectiles over long flight paths using solar aspect sensors
[AD-717002] 13 p0278 N71-24374

Air breathing engine principles for improved guided missiles and artillery projectiles
[FOA-2-C-262-1246] 14 p2332 N71-26257

Vertical flight free fall ballistic charts and theoretical analysis of translational motion
[SC-RR-70-001] 17 p2850 N71-29629

Interpolation of synoptic and climatological atmospheric density profiles from constant pressure surfaces for use in ballistic trajectory calculations
[AD-726994] 22 p3580 N71-35498

Trajectory and propulsion characteristics of spacecraft rendezvous mission opportunities to comets during 1975 to 1995
[NASA-CR-121762] 22 p3466 N71-36140

Analytic functions solving equations of motion in Newtonian theory for ballistic trajectory in atmospheric reentry
[DLR-FB-71-16] 22 p3670 N71-36168

BALLISTIC VEHICLES

Calculating carrying capacity and rigidity of design for flight vehicles
[AD-712822] 03 p0456 N71-13065

BALLISTICS

NT HYDROBALLISTICS
NT INTERIOR BALLISTICS
NT THERMAL BALLISTICS

Fractographic analysis of desulfurized ceramics and glass-ceramics ballistically impacted by caliber .30 M2 projectiles
[AD-712306] 02 p0247 N71-11656

Flight prototype electrostatic ballistic pendulum momentum transducer
[NASA-CR-114785] 05 p0686 N71-15411

Flash radiography in ballistic testing
[AD-715800] 13 p2188 N71-24444

BALLOON FLIGHT

Steady state on supersonic balloon flights from Christchurch, New Zealand - Jul. 1968 to Dec. 1969
[NASA-CR-111410] 02 p0214 N71-11906

Systems design and flight tests of astronomical gondola orientation system
[NYO-3747-13] 03 p0348 N71-13075

Upper air sampling for radioactive contaminants using balloon flights
[COO-001-162] 05 p0669 N71-14784

Response of balloons and falling sphere wind sensors in atmospheric turbulence, analyzed with Fourier transformation
[NASA-TN-D-7049] 07 p1023 N71-17479

Design modifications and flight results of balloon-borne telescopes
[AD-715299] 07 p1032 N71-17741

Balloon borne X ray survey of Cygnus region
[AD-715299] 07 p1106 N71-18054

Computerized real time simulation of atmospheric balloon environment in altitude chamber
[AD-715299] 09 p1385 N71-20217

Aerodynamic characteristics of captive balloons and other lighter than air devices
[AD-717002] 10 p1492 N71-21146

Skyhook balloon flights in 1970 at Fort Churchill, Canada
[AD-718371] 12 p1914 N71-24196

High altitude balloon flights for solar cell calibration
[NASA-CR-118372] 13 p2030 N71-24919

Balloon flight measurements of gamma ray spectra of cosmic large energy sources
[AD-719064] 13 p2161 N71-25199

Observations of galactic center radiation and possible point sources obtained by gamma ray telescope flown on three balloon flights
[NASA-TM-X-45564] 15 p2516 N71-27826

High altitude solar cell and radiometer calibrations using balloon techniques
[NASA-CR-119170] 17 p2841 N71-30845

Shutter triangulation using balloon-borne light signal equipment and Schmidt telescopes
[AD-719064] 22 p3677 N71-36215

BALLOON SOUNDING

Daily summaries of vertical echo sounding of upper atmosphere over Freiburg, Germany during July 1970
[REPT-293-F] 01 p0045 N71-10018

Simultaneous measurement of atmospheric dust by laser and balloon sounding
[NASA-CR-111790] 01 p0045 N71-10042

Determining accuracy of measuring wind aloft by tracking free rising balloons with Loren C
[ESSA-TM-WFTM-EDL-11] 01 p0078 N71-10497

Calculating kinetic energy of atmospheric turbulence from balloon sounding data
[AD-71947] 02 p0254 N71-11568

Pulse radar altimeter for atmospheric sounding balloons
[AD-71947] 02 p0226 N71-11624

Balloon measurements of cosmic ray ionization in atmosphere, 1968-70
[HASL-234] 04 p0608 N71-14236

Daily summaries for vertical echo sounding of upper atmosphere over Freiburg, Germany during Oct. 1970
[REPT-292-F] 05 p0670 N71-14814

Daily summaries for vertical echo sounding of upper atmosphere over Freiburg, Germany, for September 1970
[REPT-291-F] 05 p0672 N71-14862

Measurement of gamma ray energy spectrum at balloon altitudes
[AD-71947] 06 p0943 N71-16731

Balloon measurements of ionospheric electric fields
[NASA-CR-114818] 06 p0856 N71-16820

Infrared detectors for balloon sounding of aerosols and atmospheric moisture
[NASA-CR-61339] 08 p2702 N71-18950

Balloon sounding of radioactive air masses from nuclear test
[CEA-T-4093] 09 p1461 N71-20160

Ionospheric data from vertical echo soundings over Freiburg, Germany during November, 1970
[REPT-293-F] 10 p1555 N71-21670

Balloon sounding and mud flow warning system
[AD-71947] 11 p1780 N71-22851

Auroral zone X ray events detected by means of electron precipitation balloon sounding
[AD-71947] 12 p1909 N71-23564

Nonexpanding reflecting balloon for radar measurement of atmospheric circulation
[NLL-M-20326-5828-4P] 13 p1857 N71-23934

Soviet research and developments in meteorology including balloon soundings, radar measurement of precipitation, and numerical weather forecasting
[AD-71947] 16 p2624 N71-28147

Balloon-borne optical spark chamber for pulsed gamma ray source measurements
[CEA-CONF-1433] 16 p2675 N71-28843

Daily summaries for vertical echo sounding of upper atmosphere over Freiburg, Germany during January, 1971
[REPT-295-F] 18 p2920 N71-31495

Daily summaries for vertical echo sounding of upper atmosphere over Freiburg, Germany during March, 1971
[REPT-297-F] 18 p2920 N71-31496

Daily summaries for vertical echo sounding of upper atmosphere over Freiburg, Germany during February, 1971
[REPT-296-F] 18 p2920 N71-31497

Mobile and fixed data collection platforms for constant level balloons and remote ground locations, for platform-outside-ground station system
[NASA-CR-123174] 20 p3570 N71-32895

Gamma ray balloon-borne experiments and comparison with satellite experiments
[AD-71947] 20 p3546 N71-33071

Daily summaries for vertical echo sounding of upper atmosphere over Freiburg, Germany during April, 1971
[REPT-298-F] 20 p3566 N71-33434

Comparison of wet chemical ozone sondes for balloon sounding in free atmosphere
[REPT-120] 21 p3419 N71-34327

Equivalent specifications for balloon carried open-circuiting magnetic spectrometer to measure spectra of cosmic ray nuclei with charges ranging from protons to iron
[NASA-CR-121709] 21 p3425 N71-34370

Use of constant-level meteorological balloons for seasonal weather forecasting in Southern Hemisphere
[WMO-295] 23 p3793 N71-37908

BALLOONS

NT HIGH ALTITUDE BALLOONS
NT METEOROLOGICAL BALLOONS
NT ROBIN BALLOONS
NT SKYHOOK BALLOONS

Development and characteristics of hot air balloon deceleration and recovery system
[NASA-CR-XLA-0824-2] 02 p0146 N71-41809

Design and testing of stabilized balloon gondola in astronomical gamma ray spectrometer
[ORNL-TM-2802] 03 p0314 N71-12300

Design of electronic linear circuit using electrolytic cells
[CR-154] 06 p0797 N71-14598

Inflation system for balloon type manometer
[NASA-CR-XGB-03351] 06 p0550 N71-16008

Aerodynamic characteristics of captive balloons and other lighter than air devices
[AD-717015] 10 p1492 N71-21146

Aerobee 350 recovery system comprising parachute and extended skirt parachute deceleration device and incorporating electrical control, pyrotechnic, and pneumatic mechanisms - tests
[NASA-CR-118605] 14 p2342 N71-23800

Polyethylene balloon fabrication and flight time/time/altitude data
[NASA-CR-115030] 14 p2199 N71-20770

Design considerations for development of operational super-pressure balloon system to carry 10 pounds to 10 millibar atmospheric pressure
[NASA-CR-115027] 14 p2199 N71-20770

Thermal vacuum tests of three balloon-type sensors for thermal control of satellites
[NASA-TN-D-6234] 16 p0489 N71-26204

Discussion of cosmological horizons using the dimensional balloon model and metric models
[AD-717015] 20 p3344 N71-33044

BALLS

Initial velocity and penetration depth of explosively accelerated metal balls
[REPT-9609] 08 p1307 N71-16075

Gravimeter calibration for earth tide observations by using steel balls
[AD-717015] 20 p3344 N71-33044

BALLISTICS

Effect of strain rate and load cycling on tensile behavior and air permeability of coated fabric for inflatable decelerator system
[NASA-CR-111083] 12 p3004 N71-23319

Wind tunnel tests to determine flow patterns and pressure distributions around half airbrake in case of 120 deg cone for various separation distances at Mach 3.0
[NASA-TN-D-6281] 16 p2320 N71-28800

Mach 3 variable-density tunnel used for determination of aerodynamic heating of attached inflatable decelerator configurations
[NASA-TM-X-2355] 24 p0030 N71-30728

BALMER SERIES

Stark profile calculations for first four hydrogen Balmer lines for electron densities and temperatures
[SC-M-70-504] 05 p0745 N71-15580

Photoelectric and Balmer emission for H-beta stars
[AD-717015] 13 p2166 N71-23008

BALTIMORE

Vehicle momentum and heat transfer determinations in atmospheric boundary layers at sea
[AD-717015] 03 p0261 N71-12170

Sea roughness and wind velocity relationships in Baltic and North Seas
[AD-717015] 07 p1017 N71-17710

BANACH SPACE

Obtaining generators from conjugate of nonlinear transformations on Banach space
[AD-712066] 03 p0400 N71-12328

Uniqueness theorems for nonlinear approximations in strictly convex Banach spaces
[AD-712066] 03 p0401 N71-12329

Differentiation from simple algorithms with mapping of Banach space subset
[AD-712066] 03 p0401 N71-12329

Completeness conditions of theorems on conjugate of operators on Banach space, with bounded solutions of abstract differential equations
[AD-712066] 03 p0411 N71-12330

Lagrange multiplier in Banach space for solving optimal control in time lag system
[NASA-CR-118099] 16 p0300 N71-25000

Solution to equations in function space relating linear operator defined in subspace of Banach space and linear or nonlinear operator
[NASA-CR-118097] 16 p0321 N71-25001

Survey of recent developments in theory of nonlinear conjugate mappings including conjugate of nonlinear transformations in Banach spaces and partial differential equation applications
[AD-722700] 17 p2774 N71-30000

Fixed point method and Lagrange function for investigating problems concerning periodic and almost periodic differential systems
[NASA-TT-F-13003] 18 p2845 N71-31110

SUBJECT INDEX

Monotonic operators and iteration method for Banach spaces 23 p3782 N71-30953

Ring of holomorphic function germs in Banach space 24 p3948 N71-38148

Null hypothesis for Banach case 24 p3949 N71-38149

BAND STRUCTURE OF SOLIDS

Formal calculation of band structure of GaAs, InAs, and GaInAs alloys 01 p0108 N71-10134

Reflectivity and band structure calculations of semiconducting samples using optical reflectometer 01 p0553 N71-10286

Nonequilibrium plasma production, energy mode stability, and oscillation feedback control in electron tube plasmas [AD-716478] 01 p0771 N71-10241

Correlation effects on structure of layered bands [NASA-TN-D-6074] 01 p0110 N71-10410

X ray diffraction and scattering studies of crystal imperfections in solids [P-192604] 02 p0285 N71-11844

Existence of ground-state rotational band in ^{51}V nuclei [NUC-1925-33] 03 p0428 N71-12870

Rotational bands constructed on octapole vibrations for even-even nuclei [ITP-70-13] 03 p0433 N71-12947

Investigating band structures of crystals by studying two-photon absorption process [AD-712395] 03 p0444 N71-13234

Electrical properties of semiconducting materials [AD-713944] 05 p0594 N71-16302

Electronic properties of solids including atomic and band structure calculations 06 p0934 N71-14034

Investigating materials and microelectronics for solid state devices [AD-714079] 06 p0935 N71-16324

Spectroscopy on solid state physics including condensed matter and theoretical biology 06 p0935 N71-16363

Electronic measurements and band structures of doped aluminum silver alloys and aluminum gold alloys [UCRL-30004] 07 p1094 N71-17859

Reaction effects research program including radiation damage on semiconductor devices and materials [AD-715140] 07 p1095 N71-18045

Nuclear magnetic resonance in lead telluride [AD-715492] 07 p1096 N71-18048

Influence of hot carrier mobilities on magnetoresistance effects in forward biased Schottky junctions [AD-717062] 08 p1278 N71-18676

Electronic structure conduction mechanism in random lattices [AD-715393] 09 p1278 N71-18678

Atomic energy levels, and atomic and molecular structure of systems in microscopic environments [AD-715796] 09 p1282 N71-18697

Plasma effects in solids and low frequency effects in semiconductors 09 p1451 N71-19353

Structural and electrical properties of alkali glasses and calculations of potassium graphite band structure, Fermi surface, work functions, and electronic specific heat coefficient 09 p1483 N71-19571

Electronic structure of dilute metallic alloys and theoretical conductivity of liquid metals [AD-716389] 09 p1452 N71-19708

Monotonic and pleiotropic ultrasonic attenuation in metals [AD-716474] 09 p1453 N71-19998

Magnetoresistivity, cooperative fluorescence of rare earth ions in crystals, narrow-band and narrow-gap compounds, and related studies of rare earth compounds [AD-716478] 09 p1453 N71-20007

Spin relaxation methods for studying pseudospin semiconductor alloys [AD-716216] 09 p1453 N71-20018

Resonance method for determining magnetic tunneling in crystals in one and two band models 09 p1454 N71-20423

Influence of valence-conduction band inversion on electrical properties of lead-telluride semiconductor alloys [AD-716005] 10 p1632 N71-20772

Comments on solid state physics delivered at Banquet in 1969 including order-disorder transformation and magnetic properties of semiconducting ions [AD-716005] 10 p1632 N71-20772

Characteristics of solid state lasers and amplifiers and methods of excitation of optical generators and laser systems [AD-716005] 10 p1632 N71-20772

Magnetic properties, hyperfine field, and band structure of ferromagnetic iron 10 p1640 N71-21762

Schrodinger equation for examining energy levels in three dimensional metal crystals [AD-717002] 11 p0104 N71-22162

Band structure of n-type tellurium-doped gallium arsenide single crystals studied using Shubnikov-de Haas effect 11 p0104 N71-22162

Band structure and electrical properties of amorphous semiconductors [AD-717793] 13 p2150 N71-24382

Investigation of structure, bonding, electronic composition, and transport properties of amorphous semiconductors [AD-719419] 13 p2150 N71-24648

Electromagnetic probe measurements of optical quantum waves, optical properties, and critical points in metals [AD-719836] 13 p2151 N71-24852

Development and characteristics of semiconductor materials based on polarizability of large organic molecules, extension of band theory of solids, and transition temperatures [AD-720776] 14 p2324 N71-25764

Magnetic properties of solids including electron paramagnetic resonance in dilute magnetic alloy, hyperfine splitting of localized moment in metal, and band theory of solids [AD-720777] 14 p2325 N71-26020

Electron-photon enhancement effects on low temperature specific heat measurements of solids and transition metals 15 p2622 N71-27212

Theory of cohesion and elastic properties of solids [AD-720891] 15 p2626 N71-27393

Impurity problem in semiconductor and dynamics of Bloch electron in constant electric field [AD-721311] 16 p2664 N71-28287

Band structure of germanium analyzed by single crystal photoemission 16 p2665 N71-28332

Integrated circuit development, photolithographic interconnection of plastic integrated semiconductor chips, semiconductor testing, magnetic film engineering and computer applications [AD-722075] 16 p2665 N71-28357

Experimental investigation of electronic properties of solids [AD-722672] 16 p2665 N71-28726

Analysis of electron energy states and optical excitation processes with ultraviolet photoemission spectroscopy and optical spectra [AD-722825] 17 p2814 N71-29643

Electronic states at dislocations in semiconductor and diamond structures 17 p2825 N71-29997

Quantum mechanical model for electronic energy bands of dislocations in cadmium sulfide crystal 17 p2825 N71-30001

Ho-166 rotational bands, M1 radiative strength resonance in Cr-53 , dynamical theory, photoelectron spectroscopy of high temperature vapors [ANL-7739] 17 p2846 N71-30343

Electron-electron exchange calculations for band transfers in semiconductors 18 p2998 N71-31448

Ion mobility effects in Jost mechanism for solid state reactions [KFK-1512] 19 p3168 N71-32072

Power spectrum of V33 based on physically motivated model of conduction electron bands 20 p3316 N71-33408

Electronic band structure and physical properties of nitride metals and their compounds [COO-2185-3] 21 p3439 N71-34469

Band structure of aluminum oxide determined using basis set having 50 ion functions and 15 plane waves 21 p3445 N71-34514

Research in solid state physics including band theory, optical properties and magnetic resonance [ORNL-4608] 21 p3448 N71-34919

Applying rigid band model to metal and alloy band structure determinations [DREC-TT-1475] 22 p3393 N71-33584

Quantum mechanical calculations of shifts in optical constants for deformed single silicon crystals at different polarization directions 23 p3834 N71-37341

Use of augmented plane wave method to calculate band structure of hypothetical simple cubic tellurium [CALT-422-29] 24 p3935 N71-38073

Band structure of metals, metal compounds, and ionic crystals determined by ultrasonic and photoacoustic measurements [AD-727069] 34 p3997 N71-38312

Analysis of electrical and optical properties of vanadium oxide crystals at semiconductor-quality transition temperatures [AD-727242] 34 p3997 N71-38313

BANDPASS FILTERS

Insertion loss and pulse response of power line filters [AD-713171] 01 p0835 N71-10828

Trifield filter for detecting sound transmission under water [AD-705246] 01 p0891 N71-10878

Tripler for third harmonic voltage multiplier [NASA-CN-111784] 01 p0835 N71-10893

Using postband interference filters in multispectral photography for earth resources applications 03 p0327 N71-11987

Pulse code modulation processing of bandpass signal and error analysis of input signals [AD-718932] 13 p2043 N71-24450

Polarization of channel wavelength division multiplexing optical communication link [AD-719405] 15 p2379 N71-26080

Selective chopper reflectometer based on multiplex interference filter for atmospheric temperature sounding from Nimbus D satellite 15 p3410 N71-27486

Conversion factor for converting Colson tube count rates or ion chamber currents into units of incident X ray energy flux in specified postband in normalizing solar X ray data [NASA-TM-X-43353] 15 p3514 N71-27444

High Q bandpass resonators suitable for operation in microwave frequency range [NASA-CASE-0899-1] 16 p2570 N71-28470

Phase locked demodulator with bandwidth varying linearly with frequency [NASA-CASE-XNP-61107] 16 p2576 N71-28839

Resonance functions of sampled bandpass filter input signals for calculating constant efficiency 17 p2728 N71-29149

Methods of designing straight dielectric-forming bandpass filter [NLL-FOES-TRANS-362-7902.81/1] 17 p2721 N71-30101

Analysis of receiver performance composed of bandpass or IF filter followed by detector optimum in presence of additive white noise noise process 19 p2686 N71-33330

Design and performance characteristics of bandpass systems 19 p2688 N71-33608

Video signal processing in low signal to noise environments - bandpass filter in multi-filter phase lock loop [NASA-CN-121433] 20 p3234 N71-33413

BANDWIDTH

NT BROADBAND

NT SPECTRAL LINE WIDTH

Total radiance width analysis of nuclear neutron resonances [IDR-P-4929] 03 p0436 N71-12851

Dynamic reconstruction errors in digital to analog systems with biomedical applications [NASA-TN-D-6296] 12 p1065 N71-33140

Bandwidth compression by signal distortion using nonlinear device [SERD-70051] 12 p1074 N71-33340

Improvements in receiver of narrow bandwidth television system [NASA-CASE-3063-65740-1] 14 p2220 N71-26579

Low frequency background noise spectrum in field of effect metal oxide semiconductor transistors using adjustable bandwidth method 16 p2664 N71-38243

VEITA system for compressing television bandwidth video signals 16 p2668 N71-38084

Electronic radar data reduction and Explorer 35 reflectivity and bandwidth tables with production system [NASA-CN-119522] 16 p2664 N71-38243

Techniques and circuits used in designing AID highly flexible telemetry system comprising single channel/double channel/constant bandwidth compatible system - space application 17 p2718 N71-30923

Nuclear magnetic resonance bandwidths in metals as function of temperature - density matrix equation [AD-723914] 19 p3113 N71-32123

Real time television bandwidth compression system design for photographic data transmission [COO-1486-178] 19 p3256 N71-32226

Bandwidth control and removal of radar clutter 19 p3259 N71-32717

PCM television transmission bandwidth reduction by reduction of sampling redundancy [NLL-FOES-TRANS-362-7902.81/1] 19 p3259 N71-32779

Radiation pattern, efficiency, and bandwidth of short helical antennas [ITP-700] 20 p3234 N71-33379

RANGE-RANGE CONTROL

U OFF-ON CONTROL

BANKING FLIGHT

U TURNING FLIGHT

BARRIER APPROXIMATION

U BARRIER LAYERS

U ELECTRICAL PROPERTIES

U SURFACE PROPERTIES

BARRIER

NT BARRIER MOTORS

Absorption spectrum of barium vapor in region of autoionization from 2303 to 1700 [AD-711705] 01 p0380 N71-11144

Deposition of carbon and boron in carbon stainless steel system to predict distribution of fusion products in LMFBR system [AI-ABC-12652] 02 p0663 N71-11702

- Absolute experimental emission cross sections for excitation of electric dipole transitions in Ba ions by electron impact
[ORO-3027-17] 04 p0570 N71-13600
- Computerized analysis of data on high altitude barium release
[EOG-1183-3007] 07 p1015 N71-16997
- Electrooptic effects in ferroelectric ceramics with emphasis on electrical and optical properties of Ba, Sr, and La modified lead zirconate titanate
[EO-3-70-4353] 10 p1590 N71-21532
- Spectroscopic measurements of barium clouds and spectrum of ionospheric cloud produced by release of diborane in rocket sounding of upper atmosphere for use in predicting satellite orbit
[AD-717096] 11 p1751 N71-22689
- Stereo techniques for studying spatial structure and dynamics of barium releases
[AD-717722] 11 p1751 N71-22692
- Optical observations following release of barium vapor at high altitudes described in three phases
[AD-717093] 11 p1751 N71-22698
- Behavior of barium ion cloud at high altitudes
[NASA-NEWS-RELEASE-71-61] 12 p1953 N71-23517
- Continuous beam techniques for measuring absolute experimental cross sections for ionization of singly charged barium ions by electron impact
[ORO-3027-18] 14 p2300 N71-25725
- Hydrostatic pressure measurements on solid and liquid phase transition points for bismuth I-II and barium I-II
14 p2243 N71-26479
- Barium releases from Javelin and Nike-Tomahawk sounding rockets for ion cloud study of earth electric and magnetic fields
[NASA-SP-264] 17 p2740 N71-29671
- Using ionized barium vapor clouds for direct measurement of electric fields in magnetosphere
17 p2740 N71-29672
- Description of Javelin and Nike-Tomahawk sounding rocket used for barium release experiments
17 p2740 N71-29673
- Optical equipment operated by Max Planck Institute for barium cloud experiments
17 p2730 N71-29675
- Emission spectra of ionized barium recorded by spectrophotometer for September 24
17 p2741 N71-29677
- Photometry of barium ion emission for Javelin second release
17 p2741 N71-29678
- Position of neutral barium clouds, position and motion of Javelin ionized cloud, and radial growth of clouds by triangulation
17 p2741 N71-29680
- Electric field distribution, cloud elongation, and drift along magnetic field line of barium release from Javelin
17 p2741 N71-29681
- Barium-copper oxide/canister barium vapor release system for geomagnetospheric measurements
[NASA-CR-1739] 18 p2888 N71-31424
- Excitation and ionization cross sections for Ba(I) by electron impact, plasma diagnostics, Li energy loss in C films, and multiple charge ion sources for collision experiments
[ORO-3027-19] 23 p3827 N71-37297
- BARIUM COMPOUNDS**
- NT BARIUM FLUORIDES**
- NT BARIUM OXIDES**
- NT BARIUM TITANATES**
- Parametric tuning characteristics of barium sodium alubate
[AD-710220] 01 p0062 N71-10005
- Optical quality barium sodium alubate as harmonic generator
01 p0109 N71-10202
- Optimal conditions for obtaining solid solutions of Ba, Sr, and TiO₃
[AD-711176] 01 p0069 N71-10869
- Investigating retention of polonium 210 by refractory oxide barium cerate
[DP-1240] 08 p1268 N71-19338
- Development of single crystal barium sodium alubate as nonlinear optical material
[AD-719807] 09 p1453 N71-19996
- Diffusion coefficients and other physico-chemical properties of calcium, strontium, and barium chlorides and nitrates
[NRC-TT-1443] 10 p1513 N71-21257
- Production engineering for temperature stable dielectric constant ferroelectric composite materials in strontium tin oxide/barium titanium oxide system
12 p1547 N71-24185
- Composition and spectral reflectance data of barium sulfate polyvinyl alcohol coating
[NASA-TM-X-64653] 19 p3120 N71-32530
- Stoichiometric and compositional effects on sintering and magnetic characteristics of high purity, freeze dried, barium ferrite ceramics
23 p3780 N71-36943
- BARIUM FLUORIDES**
- Production of barium fluoride-calcium fluoride composite lubricant for bearings or seals
[NASA-CASE-XLR-08511-2] 06 p0877 N71-16105
- Low-frequency dielectric constants of alkaline earth fluorides determined by substitution method
[COO-623-154] 08 p1282 N71-19085
- BARIUM ISOTOPES**
- Quadrupole interaction of Ba-137 and Ba-135 near positive fluorine ion centers and electron paramagnetic resonance spectrum of positive trivalent Gd ions in single BaO crystals
11 p1805 N71-22402
- Oxygen and alpha beam excitation of Ba-134, 136, and 138 and Nd-150
15 p3406 N71-27970
- Nuclear structure of Co-140, La-139, and Ba-138 obtained from proton transfer reactions of (He-3, α)
17 p2794 N71-29656
- Isomeric β -transitions to α -pin/ transition in Ba-130 nucleus, and model of transition model
[JNDR-84-5407] 18 p2862 N71-30900
- Electron capture decay of Ba-131 and Li-193 nuclear energy and relative intensity measurements using coaxial Ge(Li) detector
21 p3490 N71-34063
- BARIUM OXIDES**
- Quadrupole interaction of Ba-137 and Ba-135 near positive fluorine ion centers and electron paramagnetic resonance spectrum of positive trivalent Gd ions in single BaO crystals
11 p1805 N71-22402
- Auxiliary discharge thermionic converter performance using barium oxide electrodes
16 p2633 N71-28700
- X ray diffraction, thermal, and thermogravimetric analyses of La2O3-BaO-B2O3 glass structures and properties
18 p2940 N71-31250
- BARIUM TITANATES**
- Shock wave structure in barium titanate ceramics
[AD-714673] 06 p0876 N71-16020
- Surface and grain boundary layer of barium titanate
[AD-715097] 07 p1048 N71-17848
- Ceramic BaTiO₃ disk subjected to pulsed electric field monitor
[AD-714988] 07 p1002 N71-17939
- Aging characteristics of barium titanate and lead zirconate-titanate ferroelectric ceramics
[AD-715624] 08 p1279 N71-18809
- Shock induced ferroelectric/paraelectric phase transition in barium titanate
[AD-717551] 11 p1815 N71-21960
- Heat flux sensors based on thermistors in doped polycrystalline ceramics such as barium strontium titanate showing ferroelectric resistance anomaly
11 p1764 N71-22746
- Production engineering and testing of low-power, solid state, lanthanum doped barium strontium titanate-thermistor for use in automatic electronic tuning with nonlinear dielectrics
[AD-718614] 12 p1890 N71-23611
- Effects of sintering and grain growth reactions on distribution of niobium additives in barium titanate ceramics
16 p3619 N71-20998
- Oxygen partial pressure and temperature effects on stoichiometric BaTiO₃ crystal electrical resistivity with heat of formation, electron mobility, and oxygen vacancy values
17 p2769 N71-29706
- Optical phonons for studying Raman scattering spectra in BaTiO₃ and in LaSb single crystals
20 p3335 N71-33767
- BARKHAUSEN EFFECT**
- Barkhausen nondestructive test methods for detecting stress in brittle materials
[AD-716006] 01 p0065 N71-10063
- Nondestructive inductor techniques for Barkhausen effect study
[AD-716025] 12 p1927 N71-23799
- BAROCLINITY**
- Numerical oceanographic models of baroclinic flow
09 p1381 N71-19511
- BAROMETERS**
- Uncorrected and barometer corrected data in tabular form
[ABCL-3836] 21 p3504 N71-34967
- BAROMETRIC PRESSURE**
- U ATMOSPHERIC PRESSURE**
- BAROTRAUMA**
- Pulmonary findings in sheep X rays and nasal examinations on humans after low pressure chamber exposures
02 p0163 N71-11812
- BAROTROPIC FLOW**
- Accuracy of fine mesh 500 mb barotropic predictions
[NOAA-TM-NWS-TDL-42] 21 p3451 N71-34562
- BARRELS**
- Calculation of critical diameter ratios for reverse yielding of thick-walled cylinders
[AD-717448] 10 p1452 N71-30812
- BARRIER LAYERS**
- Cross modulation in barrier layer field effect transistors
03 p0352 N71-13106
- Surface barrier and avalanche diode detectors for spaceborne particle detection
13 p2152 N71-20200
- Capacitance of surface barrier detectors made from p-type silicon
[RASC-527] 18 p2822 N71-30900
- Inversion barrier energies in NiE3 and PbE3 and calculations of electronic properties in TiO₂/silicon clusters
21 p3491 N71-34063
- BARS**
- NT ELASTIC BARS**
- NT PRISMATIC BARS**
- Radial variation of longitudinal modes in vibratory bar
[UCRL-50847] 09 p1477 N71-21939
- Analysis of axisymmetric boundary value problems for thick solid circular bar with lateral surface tractions free and end sections having prescribed transverse displacements
12 p2806 N71-30900
- Variational derivation of partial differential equations for Saint Venant torsion problem of homogeneous anisotropic bars
[R-657] 23 p3862 N71-37298
- BARYCENTER**
- U CENTER OF GRAVITY**
- BARYON RESONANCES**
- Positive kaon proton elastic scattering, Regge pole analysis, and K resonance production in scattering for Z resonances
[UCRL-19832] 03 p0420 N71-13106
- N¹⁷²⁰ production and subsequent decay to Delta hyperon/1234 pion in pion/ proton interactions at 13.1 GeV
[COO-1428-175] 03 p0431 N71-13106
- Studying various kaon/ proton interactions at 2.2 to 2.70 GeV/c for existence of two Sigma hyperon/1600 resonances
[UCRL-19834] 03 p0431 N71-13106
- Sigma⁻1 baryon states observed in production in p-p collisions
[COO-1428-208] 03 p0434 N71-13106
- Analysis of Y(1385)/ pion production near Y(1385) resonance
[NYO-3451-13] 04 p0382 N71-16020
- Constructing double Regge exchange model for kaon production in K/p reactions at 9.0 GeV/c
[COO-1428-229] 04 p0383 N71-16020
- Phenomenological model of T-violation for baryon decays of baryons as function of electron energy
[SDNP-TT-67-2] 03 p0739 N71-13106
- Resonance productions in K/pion/ proton interactions at 4.6 GeV/c and 9 GeV/c
[UCRL-19809] 07 p1074 N71-13106
- Neutral pion-electron production at Delta/1234 and π^0 and four momentum transfer of 150 eV
[DESY-70/56] 08 p1248 N71-18809
- Angular distributions of resonance decay products in reactions positive pion proton yields nucleon resonance neutral rho-meson, and nucleon resonance cascade-meson at 2.34 GeV/c
[JNDR-71-5236] 08 p1252 N71-18809
- Bubble chamber experiment for resonance states in positive pion proton interactions between 3 and 4 GeV/c
10 p1425 N71-21939
- Studying reaction negative pion proton yields nucleon/1234 negative pion negative pion at incident momentum of 4.47 GeV/c
[ITEP-767] 14 p2317 N71-30770
- Polarization of Lambda and Sigma hyperons in in-body Y-resonance production processes and the quark model with experimental methods for determining polarization moments of hyperons
[TPU-270] 14 p2320 N71-30770
- Baryon-baryon resonances in pp inelastic mechanism of 200 to 640 MeV
[JNDR-72-5055] 15 p3467 N71-31939
- Quark-nucleon model of many baryon resonances
[ITEP-799] 15 p3484 N71-31939
- Asymmetry parameters of isospin Sigma hyperon decays in negative kaon beam interactions
15 p3467 N71-31939
- Lambda and Sigma hyperon resonances, branching ratios, and lifetimes from bubble chamber analysis of antineutron nucleus reactions
[CEA-E-4060] 15 p3492 N71-31939
- Statistical evidence against isospin, 2 negative pion enhancement at 1.627 GeV/c as mass in antineutron nucleus reactions at 4.46 GeV/c
[COO-1428-235] 16 p2647 N71-30911
- Events obtained in counter and spark chamber experiment for production of baryon resonances in positive pion and proton collisions
16 p2636 N71-30911
- Electroproduction of Delta hyperon/1234 in neutral pion channel at four momentum transfer, studied from angular distribution measurements of outgoing protons
[DESY-70/45] 17 p2806 N71-30900

SUBJECT INDEX

BEAM CURRENTS

Balance on nonrelativistic bound states in nuclear-nuclear systems, and possible quasibound states of heavy mesonic resonances
[JF-1874] 19 p3139 N71-32364

Experimental estimate of total cross section for deuteron breakup by heavy mesons on nucleons from neutron or electroproduction experiments in heavy liquid bubble chamber
[JF-7178] 20 p3315 N71-33342

Quasi-atomic model of many-baryon resonances from Delta hyperon nucleus potential interaction
[JF-16779] 21 p3472 N71-34722

Nuclear spectrometer measurements of neutron resonances and gamma rays from neutron capture by Sn-147 and Sm-149
[JF-73-5635] 22 p3639 N71-33942

Resonance in trans(nucleon) proton reactions, Yrast-like states in antikaon nucleus reactions, and (n,n') resonances in 31 in deuterium chamber, and theoretical and theoretical developments
[JF-3178-4] 23 p3812 N71-37186

MEASUREMENTS
NT X-51 HELICOPTER
P wave and I wave solutions of relativistic quantum mechanics for baryon exchange with cutoff
[JF-70721] 03 p3394 N71-12987

Chiral Lagrangian model of meson-baryon scattering for theory of antikaon interactions
[JF-3178-4] 23 p3812 N71-37186

Two states, polarized targets and baryon spin determination
[JF-7171] 14 p2384 N71-36203

Spin resonance scattering amplitude calculation for antikaon-baryon-meson interactions and quark model applications
[JF-1705] 14 p2388 N71-26446

Additive quark model for decay distribution of mesons produced in meson baryon high energy interactions
[JF-1570] 14 p2316 N71-36749

Current commutators in quantum electrodynamics and mass differences of pseudoscalar mesons and baryon octets
15 p2470 N71-27380

Exchange degeneracy with SU(6) symmetry and charge conjugation in hyperon and charge exchange reactions for meson baryon scattering
[JF-36] 15 p2480 N71-27869

MEASUREMENTS
Basalt melts in simulated lunar environment
04 p6613 N71-14442

Analyzing subsurface flows of lava in eastern Iceland and recent and Pleistocene flows in neotectonic zone of central Iceland for basalt composition
07 p1625 N71-17979

Apollo 11 basalt petrographic and theoretical of lunar evolution comparing lunar and earth environments
[NASA-CR-110834] 12 p1990 N71-24389

Volcanic gas collections used to calculate chemical composition of volatile fraction of basaltic magma gas phase
[NASA-TR-8-348] 13 p3871 N71-24610

Basaltic eruptions of basaltic from craters produced by nuclear explosions and of rocks from lunar craters
13 p1618 N71-25274

Compressibility and porosity of basalts from Apollo 11 lunar samples
[JF-72851] 15 p2518 N71-27990

Mathematical models for measuring frictional behavior of basalt and diatomaceous surface in ultrahigh vacuum
16 p3682 N71-28678

Geomorphology of basaltic lava tubes from Mount St. Helens, Washington
[NASA-TR-X-62823] 20 p3257 N71-33020

Quartz, basalt, gabbro, and diatomaceous surface volume compressibilities and densities under 32,000 kg pressure
[JF-71361] 23 p3682 N71-37108

Heat transfer in base type supercritical laminar and turbulent separated flows
[JF-71057] 01 p3840 N71-16249

Heat flow analysis of axisymmetric body with conical jet
[JF-71258] 07 p1012 N71-17787

HEATING
Measurement of base heating characteristics of high speed, blunt cones at hypersonic speeds
[NASA-CR-19280] 24 p4031 N71-38746

MEASUREMENTS
Base pressure measurements on XB-70 aircraft at Mach numbers from 0.4 to 3.0
[NASA-TN-X-1612] 07 p3970 N71-17132

Flight-measured base pressures from sharp leading edge over vertical fin of X-15 aircraft compared with base data for turbulent flow at Mach numbers from 1.5 to 5.0
12 p1981 N71-33922

MEASUREMENTS
Low concentration alkaline solution treatment of aluminum with metal phosphate surface coatings to improve chemical bonding and reduce coating weight
[NASA-CASE-XLA-91955] 11 p1786 N71-23047

MEASUREMENTS
U FOUNDATIONS

BATCH PROCESSING
Investigating symbolic mathematical computation using PL/I FORMAC batch system and Scope FORMAC interactive system
[JF-684812] 00 p1227 N71-19185

Design problems in design and implementation of practical batch processing systems for performing symbolic mathematical computation
00 p1229 N71-19196

Modification to initiator which allows memory location assignment to particular initiator for batch processing
[JF-4935] 21 p3480 N71-34198

Kinetics of crystal nucleation and growth in batch copolymer crystallization
21 p3501 N71-34999

BATHS
NT SALT BATHS
BATHMETERS
Bathymetry and magnetics of region (POL-421-3) 29 day to 35 day N, 153 deg to 145 deg W - map
[JF-TR-REL-146-POL-4] 07 p1624 N71-17957

Geophysical, bathymetric, and bathymetric of Central American-Latin ridge
[JF-716271] 09 p1384 N71-19809

Operational and environmental performance tests and specifications for precision bathymetric recorder
[JF-71010] 12 p1916 N71-25217

Bathymetry measurements in deep ocean using narrow beam stabilized echo sounders and digital computer
[JF-TR-CGS-37] 18 p2911 N71-30882

Bathymetric surveys of north leader shelf of Molokai Island, Hawaii
[JF-49-21] 18 p2914 N71-31005

Geophysical and bathymetric measurements of ocean bottom and lower continental rise hills off Cape Hatteras
18 p2915 N71-31009

Magnetic and bathymetric survey profile in Pacific Ocean from Costa Rica to central California
[JF-TR-REL-179-AOML-3] 18 p2917 N71-31248

Geomagnetic, bathymetric, and gravitational field data from Indian Ocean 1964 survey
18 p2919 N71-31432

BATHMETRY
U BATHMETERS
BATHYMETROGRAPHY
Temperature microstructure of Atlantic Ocean and its effect on sound propagation
[JF-10714] 01 p0948 N71-10529

Two-part glossary of bathymetric terms in 27 languages and English equivalents
[JF-10992] 01 p0949 N71-10687

Temperature profile plotting from magnetic tape recorded aircraft expendable bathythermograph data and underwater acoustic velocity calculated from Pacific Ocean salinity data
[JF-718393] 12 p1906 N71-23385

Bathymetric data of subsurface temperature anomalies and relationship to Pacific Ocean surface temperatures
[JF-722587] 18 p2920 N71-31504

BATS
Echolocation on biologic communication systems for bats and dolphins
11 p1493 N71-23065

Neuronal responses of bat cochlear nuclei to ultrasonic stimuli
[JF-8-54133] 23 p3716 N71-36487

BATTERIES
U ELECTRIC BATTERIES
BATTERY CHARGERS
Battery charging system with coil to cell voltage boost
[NASA-CASE-XGS-65433] 09 p1325 N71-19438

Alkaline-type coulometer cell for primary charge control in secondary battery recharge circuits
[NASA-CASE-XGS-65434] 09 p1327 N71-19491

Development and characteristics of battery charging circuits with coulometer for control of available current
[NASA-CASE-XGS-10487-1] 13 p2830 N71-24719

BATTERY SEPARATORS
U SEPARATORS
BAUSCHINGER EFFECT
Bauschinger effect examined for unidirectional fiber glass reinforced plastics
[JF-717019] 10 p1587 N71-20887

Bauschinger effect in series of nickel-cobalt alloys overstrained in various amounts up to 5 percent in tension and reverse strained in compression
[JF-722333] 16 p3612 N71-26616

Uniaxial tension behavior of materials with various heat treatments and its relation to Bauschinger effect
18 p2936 N71-31139

BAUSCHINGER
Basalt production and consumption during 1968
17 p2708 N71-29278

BEARD-ALPERT SENSATION
Describing thin filament type Beard-Alpert ionization gauge with low collector buried or removed from grid structure
[NASA-CASE-XLA-67434] 00 p1380 N71-18462

BAYES THEOREM
Development and evaluation of adaptive pattern recognition schemes based on Bayesian decision theory
[JF-716673] 01 p0800 N71-10946

Bayes type sequential method for minimum random sampling problems
06 p0804 N71-15947

Bayes system for optimal signal detection in non-Gaussian noise
06 p0804 N71-15976

Bayesian filter for use in trajectory estimation and comparison of performance with Kalman filter
[NASA-CR-114897] 09 p1480 N71-15915

Bayesian decision making and learning in geometric pattern recognition problem for continuous-time Markov process
[JF-72810] 14 p2388 N71-23847

Bayesian algorithms for Markov chain pattern recognition problems
[JF-728357] 14 p2388 N71-23850

Bayesian model for group effects on individual decision making
14 p2388 N71-23871

Single chart joint detection and estimation for discrete and continuous data, and joint Bayesian detection, estimation, and system identification
[JF-722468] 18 p2396 N71-31346

BAYESIAN STATISTICS
U BAYES THEOREM
BAYS (TOPOGRAPHIC FEATURES)
Research progress in coastal engineering
[JF-11940] 02 p0319 N71-12873

Analysis of Biscayne Bay, Florida as coastal reservoir, using effects of pollution and need for environmental control
18 p2991 N71-30884

BECK HIERARCHY
Quantum mechanics of two particle interactions in homogeneous systems including kinetic and equilibrium correlation equations using BECK hierarchy
15 p2487 N71-27829

BCC LATTICES
U BODY CENTERED CUBIC LATTICES
BCH CODES
Search for best cyclic (26, 4) block codes and comparison of performance with (15, 5) BCH codes
[JF-TR-REL-174-JTS-111] 07 p0994 N71-17946

BEA
U BEACON EXPLORER A
BEA
U EXPLORER 22 SATELLITE
BEACHES
Virginia Beach environmental data and time series analysis of water table interactions with processes in beach-coast-atmosphere system for environmental control
[JF-719923] 14 p2345 N71-25620

Design of computer related information system to provide accurate data for military purposes
[JF-722427] 17 p2361 N71-25640

Analysis of effects of storm winds on southeastern shores of Lake Michigan
[JF-723932] 20 p3284 N71-32940

BEACON EXPLORER A
Geomagnetic electron content from Beacon Explorer A Faraday effect during half orbit cycles
24 p3914 N71-37986

Beacon Explorer A digital estimation in several tones, measured with Faraday and Doppler effect
24 p3915 N71-37916

BEACON EXPLORER B
U EXPLORER 22 SATELLITE
BEACON SATELLITES
NT BEACON EXPLORER A
NT EXPLORER 22 SATELLITE
BEACONS
NT RADAR BEACONS
NT RADIO BEACONS
NT RADIO DETECTION FINDERS
Performance of mean flash beacon for buoy
[JF-715872] 00 p1232 N71-18355

BEADS
Rotary bead dropper and collector for testing microelectronic transducers
[NASA-CASE-XGS-61304] 11 p1776 N71-22880

BEAGLE AIRCRAFT
Beagle 1125 training aircraft handling time
[JF-7163-PT-1] 12 p1856 N71-23496

BEAM COLUMNS
U BEAMS (SUPPORTS)
U COLUMNS (SUPPORTS)
BEAM CURRENTS
Particle accelerator beam current and position monitor which prevents beam disturbance from plasma resonance modes
[JF-728166] 19 p3167 N71-31996

Current-carrying twisted plasma column high-frequency stabilization in longitudinal magnetic fields using Tolubashvili device
[JF-728166] 19 p3167 N71-31996

BEAM PLASMA AMPLIFIERS

Reducing ion beam scattering in collector tanks of isotope separators by using stabilizing devices [CEA-R-3999] 04 p0776 N71-13709

Investigating effect of beam of electrons on Maxwellian plasma by numerical integration of Vlasov equation in one dimension [COO-2059-2] 05 p0748 N71-15274

Coupling coefficient derived for three-wave interaction in beam plasma system [NASA-CR-116783] 06 p1273 N71-18696

BEAM SPLITTERS

X-ray diffraction analysis with mechanical attenuation of primary beam and pulse counting for determining polymer molecular weight [PS-19483T] 01 p0893 N71-18089

Observing resolved linear Stark splitting for R⁺ spectroscopy line in LJP [NYO-3464-25] 05 p0739 N71-15084

Describing injector and beam optics of 6 MeV tandem Van de Graaff accelerator [CISE-N-139] 06 p1174 N71-18168

Stochastic correlation method for beam chopper optimization in neutron time of flight spectrometers [P-12596] 16 p2596 N71-28709

Far infrared Michelson gas laser with variable out-pur coupling [NBS-TN-395] 17 p2739 N71-30199

Magnet beam splitting system for external proton beam of beryllon [UCRL-20194] 19 p3150 N71-32128

Angular dependence of this film profiles for use as beam splitters for ruby laser radiation [AD-724625] 20 p3281 N71-33139

Image clearing eyepiece for calibrating acceleration transducer [AOJN/772] 23 p3759 N71-36799

BEAM SWITCHING

Using electron beam switching for brushless motor commutation [NASA-CASE-XGS-01451] 01 p0034 N71-10677

Antenna array at focal plane of reflector with coupling network for beam switching [NASA-CASE-GSC-10220-1] 15 p2381 N71-27253

BEAM WAVEGUIDES

Geometrical aberrations and transfer matrix of quadrupole lenses in guiding devices or finite emittance beam matching systems and application to matching triplet study [CEA-N-1286] 14 p2311 N71-26669

Laser machining device with dielectric functioning as beam waveguide for mechanical and medical applications [NASA-CASE-HQN-10541-2] 15 p2415 N71-27125

Optical communication system with gas filled waveguide for laser beam transmission [NASA-CASE-HQN-01054-1] 15 p2418 N71-27183

Laser beam projector for continuous, precise alignment between target, laser generator, and astronomical telescope during tracking [NASA-CASE-NP-11067] 16 p2640 N71-29125

BEAMS (RADIATION)

NT ATOMIC BEAMS

NT ELECTRON BEAMS

NT GAMMA RAY BEAMS

NT ION BEAMS

NT LIGHT BEAMS

NT MICROBEAMS

NT MOLECULAR BEAMS

NT NEUTRAL BEAMS

NT NEUTRON BEAMS

NT PARTICLE BEAMS

NT PHOTON BEAMS

NT PHOTON BEAMS

NT PHOTON BEAMS

NT PHOTON BEAMS

NT PHOTON BEAMS

NT PHOTON BEAMS

NT PHOTON BEAMS

NT PHOTON BEAMS

NT PHOTON BEAMS

NT PHOTON BEAMS

NT PHOTON BEAMS

NT PHOTON BEAMS

NT PHOTON BEAMS

NT PHOTON BEAMS

NT PHOTON BEAMS

NT PHOTON BEAMS

NT PHOTON BEAMS

NT PHOTON BEAMS

NT PHOTON BEAMS

NT PHOTON BEAMS

NT PHOTON BEAMS

NT PHOTON BEAMS

NT PHOTON BEAMS

NT PHOTON BEAMS

NT PHOTON BEAMS

NT PHOTON BEAMS

NT PHOTON BEAMS

NT PHOTON BEAMS

NT PHOTON BEAMS

NT PHOTON BEAMS

NT PHOTON BEAMS

Alternating gradient synchrotron, beam research reactor, and medical reactor development and operation and research summaries [BNL-50230] 12 p1976 N71-34210

Proton total cross sections for light nuclei between 24 and 46 MeV using beam attenuation technique [AD-714177] 12 p1979 N71-34341

Influence of high frequency fields on properties of accelerating channel and beam emittance in linear accelerator [SLAC-TRANS-128] 14 p2300 N71-25703

Continuous beam techniques for measuring absolute experimental cross sections for ionization of singly charged boron ions by electron impact [ORO-3027-10] 14 p2300 N71-25725

Method and means for recording and reconstructing holograms without use of reference beam [NASA-CASE-ERC-10020] 14 p2266 N71-26154

Beam transport program BOPIC in FORTRAN 4 for analyzing monoenergetic charged particle beams in post acceleration system [AASCTM-544] 15 p3459 N71-26981

Oxygen and alpha beam excitation of Ba-134, 136, and 138 and Nd-150 15 p3496 N71-27970

Characterization of spatial profile of laser beam before and after amplification [AD-722074] 16 p2606 N71-28400

Accelerator beam experiments, including short-lived radioactive isotopes and heavy ion on-line isotope separator [NP-18671] 16 p2660 N71-29193

Space charge influence on beamlet motion in strong focusing proton synchrotron [IPV-SKU-76-15] 18 p2901 N71-30604

Rotating radiation-resistant film target for nuclear particle beams [JINR-B13-5621] 18 p2979 N71-30700

Frequency distributions of event size in deposition of energy over small pathlengths measured after penetration of 64.3 MeV protons through thicknesses of tissue-like material [NASA-CR-111943] 18 p2984 N71-31093

Apochromatic method for measuring mean proton energy in 657 MeV beam using Vavilov-Cherenkov radiation [JINR-P3-5637] 19 p3150 N71-32131

Alternating gradient synchrotron study, including beams, high resolution spectrometers, and instrumentation [BNL-16000] 19 p3157 N71-32490

Effects of flowing water on neutron transport in beam [BNWL-TR-46] 19 p3161 N71-32673

Effect of scattering on pulse length of argon laser beam in foggy and turbulent atmosphere, and feasibility of Monte Carlo calculation of laser beam energy density distribution [AD-744000] 20 p3281 N71-33126

High energy physics, experiments, accelerator operation and colliding beam facility [CEAL-1053] 20 p3321 N71-33757

Lifetime of 2.140 state of helium-like argon using beam foil method [UCRL-20458] 22 p3641 N71-39559

Multifunctional chamber using tungsten wires for high resolution beam microscope [LAL-1246] 22 p3643 N71-39573

Beam focusing characteristics of variously shaped grid holes with application to electron bombardment ion thrusters [NASA-TM-X-67922] 22 p3662 N71-36115

Ray theory analysis of magnetostatic wave propagation in ferrimagnetic media with application to delay lines 23 p3738 N71-36653

Effect of synchrotron capture during bunching of beam outside separatrix calculated by using computer [IPV-SKU-70-20] 23 p3807 N71-37141

Phase acceptance of alternating gradient doublet mode of quadrupoles of different aperture [CERN-71-11] 23 p3820 N71-37245

Bi-gaussian charge distribution in transverse beam plane [LAL-RT-S-70] 24 p3971 N71-38330

Vacuum calculations and fast neutral beam production system for multi-injection experiments in quadrupole cells [EUR-CHA-PC-587] 24 p3994 N71-38490

BEAMS (SUPPORTS)
NT BOX BEAMS
NT CANTILEVER BEAMS
NT CURVED BEAMS
NT I BEAMS
NT RECTANGULAR BEAMS

Experimental techniques for determining support reactions in models of beams and slabs [PS-19783] 03 p0460 N71-12590

Structural analysis of composite beams and circular plates undergoing flexural vibration [AD-712765] 03 p0467 N71-13386

Computer calculation of natural frequencies and transverse vibration modes in continuous beam [RT/DNG/79/5] 04 p0570 N71-13873

Creep analysis of statically indeterminate beams [BNWL-1362] 04 p0579 N71-13870

Nonlinear vibration of buckled beams and reentrant bar plates [PS-193853] 04 p0618 N71-14086

Stress waves in beam to column connections [AD-714177] 06 p0653 N71-30600

Optimum design techniques for linear elastic beams and rods under free and forced vibration [AD-713946] 06 p0654 N71-30600

Dynamic response of supported beams to excitations by statistical pressure distributions [ISVR-TR-36] 07 p1123 N71-47122

Lumped mass finite difference analysis for loaded structural beam dynamics [AD-715112] 07 p1126 N71-47122

Plastic deformations of clamped beams by impulsive loading [AD-714083] 07 p1126 N71-47122

Shear deformation effect on optimal design of linear elastic beam with fundamental frequency of torsional vibration [AD-715021] 07 p1126 N71-47122

Beam for terminal rigidity of beam under axial thermal stress [AD-715076] 07 p1127 N71-47122

Approximate analyses of thermally induced beam and plate vibrations [AD-715077] 07 p1127 N71-47122

Elevated guideway structures using support beams and spread footing of various construction methods [TRW-00816-7005-20-00] 07 p1136 N71-47122

Minimum weight and strain optimization for optimal beam and frame structures under random loads [NASA-TT-F-13451] 08 p1206 N71-16800

Dynamic structural analysis on minimum weight beams and frames by one degree of freedom system [NASA-TT-F-13450] 08 p1206 N71-16800

Variational calculus for minimum weight loaded beam structures [NASA-TT-F-13452] 08 p1207 N71-16806

Approximation method for structural beam and plate resonances at elastic edge excitations [NASA-CR-17394] 08 p1207 N71-16807

Solving plane elastic-plastic boundary value problems for application to bending of simply supported single crystal beam [AD-715776] 08 p1208 N71-16800

Development of exact stiffness matrix for tapered beam element and assessment of errors produced by considering tapered beam as series of straight uniform beams [TT-7007] 09 p1401 N71-30022

Development of numerical expressions for internal shear forces, axial forces, and bending moments based on kinematics of curved beams 10 p1656 N71-31310

Iterative solution to large deflection problem of flexible beam springs for design of compressors and torsion springs 10 p1658 N71-31407

Numerical analysis of buckling of continuously elastic beams using Winkler model, Pasternak model, and elastic continuum [NASA-CR-118131] 13 p2183 N71-29113

Numerical solution of problems of optimal structural design for minimum static deflection, minimum dynamic deflection, maximum fundamental frequency, and maximum stability 14 p2346 N71-25919

Comparison of finite element and analytic solutions of normal uniform beam modes under various end conditions [NASA-TN-D-6326] 14 p2346 N71-25919

Dynamic problem of infinite, elastically supported beam under influence of uniformly moving single point load solved by complex variable theory [NASA-TT-F-13369] 14 p2347 N71-25919

Determination of upper and lower bounds to frequencies of uniform beams with elastically attached masses [AD-721334] 16 p0086 N71-30071

Derivation of asymptotic stability and instability conditions for elastic systems with dissipation [AD-721384] 16 p0087 N71-30071

Stochastic calculation method for design of solid beams of glass reinforced plastics on independent elastic supports [AD-722389] 17 p0053 N71-30019

Numerical analysis of torsion forces in uniform circular beam having crack along circular arc or along radius [RAE-LIB-TRANS-1559] 18 p0020 N71-30003

Expressions and graphs for estimating average modal densities for various structural elements of engineering importance including beams, rods, elastic plates, and control shells [NASA-CR-1773] 18 p0022 N71-30003

Finite element model of Timoshenko beam segment [AD-724352] 20 p3357 N71-33886

Elementary calculations for axial thermal stresses in beams constrained with those of exact theory [AD-724464] 20 p3358 N71-33886

Magnet pole stability and beam orbit operations of beryllon [UCRL-20240] 21 p3400 N71-30400

SUBJECT INDEX

Structural analysis of uniform beam under various conditions using finite element and analytic methods 22 p3403 N71-36345

Variational methods used for approximate analytic solution to problem of bending and torsion in elastic thin beams 22 p3409 N71-36311

Nonself-adjoint boundary value problem solution with dependent variable time derivatives for forced vibration of elastic beams based on Winkler method (AD-725767) 22 p3409 N71-36312

Solution obtained for problem of normal impact of elastic elastic-plastic beam by semi-analytic elastic rod (AD-725748) 22 p3409 N71-36313

General order solutions to shear stress, normal stress, horizontal displacement, and transverse deflection in multilayer Timoshenko beams (AD-727495) 24 p3406 N71-36726

COLLECTIONS

MECHANICAL ENGINEERING

Research conducted with three axis orientation for mechanical stress communication (AD-727495) 24 p3406 N71-36726

Information capacity of discrete motor responses measured for different directions and amplitudes of motion (AD-727151) 01 p0012 N71-10536

Investigating operation of ion circulation sensors based on perception of charged particle stream in upper atmosphere and deviation of vehicle axis from course direction 03 p0410 N71-13179

Microbeam interferometer with photodetector for radial direction sensing (AD-727151) 03 p0410 N71-13179

Transmitted device for observing entry direction of air shovers (AD-727151) 03 p0410 N71-13179

Unidirectional liquid filled accelerometer design with field and housing temperature compensation (AD-727151) 03 p0410 N71-13179

Flow 9 computer program for detection of incident laser radiation with PM cyclohexane analyzer (AD-727151) 03 p0410 N71-13179

MATERIALS

Effect of reactor irradiation on properties of nonferrous alloys (AD-727151) 03 p0410 N71-13179

Rolling element fatigue lives of AISI T-1, AISI M-2, AISI 52100, and M-50 (AD-727151) 03 p0410 N71-13179

Run-in sprayed, chromium carbide 'wearing' steam turbine protection using noncorrosive, nonexpensive steam seals (AD-727151) 03 p0410 N71-13179

Residuals and fatigue tests of steel bearing alloys (AD-727151) 03 p0410 N71-13179

MECHANICAL ENGINEERING

ANTIFRICTION BEARINGS

BALL BEARINGS

FLUID BEARINGS

GAS BEARINGS

JOURNAL BEARINGS

LIQUID BEARINGS

NEEDLE BEARINGS

ROLLER BEARINGS

THRUST BEARINGS

Predicting bearing fatigue failure and life in primary contact elastic valves of advanced test reactors (AD-727151) 03 p0410 N71-13179

Analysis and extreme pressure additive effects due to bearing spinning with synthesized hydrocarbon oil (AD-727151) 03 p0410 N71-13179

Extended duration testing of vapor lubricated roller bearings system and design of externally pressurized roller bearings (AD-727151) 03 p0410 N71-13179

Design and testing of prototype hydrostatic liquid lubricated roller bearings (AD-727151) 03 p0410 N71-13179

Power input, variation of operating properties, and lubricant consumption of oil lubricated roller bearings system for communication satellites with force and mass calibration (AD-727151) 03 p0410 N71-13179

Acoustic emission analysis for bearing and gear failure mode identification (AD-727151) 03 p0410 N71-13179

Multidimensional model of all wave phenomena in rotating shaft systems with incompressible fluid lubrication and analysis of apparent film bearings (AD-727151) 03 p0410 N71-13179

Experimental tests of bearing system components for dynamic response of elastic stabilized communication (AD-727151) 03 p0410 N71-13179

Heat after bearing materials for space applications (AD-727151) 03 p0410 N71-13179

Actuator and bearings for satellite lever thermal control array (AD-727151) 03 p0410 N71-13179

Low friction bearing and lock mechanism for two-axis global carrying satellite payload (AD-727151) 03 p0410 N71-13179

Pressure distribution of roller bearings with bearings of materials with low modulus of elasticity (AD-727151) 03 p0410 N71-13179

Lubricant rheology and chemistry effects on contact material fatigue (AD-727151) 03 p0410 N71-13179

Bearing requirements for liquid rocket engine turbochargers (AD-727151) 03 p0410 N71-13179

Equations for flow rate, head capacity, and friction torque for control hydrostatic bearings under laminar and turbulent flow conditions (AD-727151) 03 p0410 N71-13179

Magnetic bearing with diverse magnetic sources coupled to common air gap via different low magnetic reluctance paths for use with permanent magnets (AD-727151) 03 p0410 N71-13179

Control hydrostatic bearing optimal dimensions for friction reduction based on laminar and turbulent flow velocity, head capacity, and friction torque calculations (AD-727151) 03 p0410 N71-13179

Bearings, lubricants, and seals for lubricated and hydraulic components for space shuttle with high temperature and vacuum operating capabilities (AD-727151) 03 p0410 N71-13179

Use of infrared radiation to reveal lubrication behavior between bearing surfaces (AD-727151) 03 p0410 N71-13179

Performance of unlubricated pivot bearings made from epoxy resins and polyimide materials (AD-727151) 03 p0410 N71-13179

Flight tests of elastomeric bearings in main rotor of AH-1G helicopter (AD-727151) 03 p0410 N71-13179

Direct current motor design with magnetic bearing for use in low friction disturbance control systems (AD-727151) 03 p0410 N71-13179

Design, optimization, and test instrumentation for solid-lubricated bearings in sodium pumps and circulating auxiliaries in breeder reactors (AD-727151) 03 p0410 N71-13179

BEAT

U SYNCHRONISM

BEAT FREQUENCIES

Beat signal frequency of rotating ring gas laser (AD-727151) 03 p0410 N71-13179

BEET

Beet density studies of bed rest subjects by radiographic method (AD-727151) 03 p0410 N71-13179

Performance decrement as function of seven days complete bed rest (AD-727151) 03 p0410 N71-13179

Extravascular dehydration effects in production of cardiovascular deconditioning by bed rest simulating weightlessness - data tables (AD-727151) 03 p0410 N71-13179

Extravascular dehydration produced by bed rest simulating weightlessness - data tables (AD-727151) 03 p0410 N71-13179

Hypothalamic effects during 120-day bed confinement with drug therapy (AD-727151) 03 p0410 N71-13179

Physiological effects and acceleration tolerances after weightlessness based on space environment simulation with human centrifuge and bed rest (AD-727151) 03 p0410 N71-13179

Red cell mass and plasma volume changes noted in hypodynamic states of bed rest and water immersion compared to changes observed during earth orbital missions (AD-727151) 03 p0410 N71-13179

Bed rest and immobilization effects on oxygen transport system of human body (AD-727151) 03 p0410 N71-13179

Hemodynamic and body fluid alterations induced by varying periods of bed rest (AD-727151) 03 p0410 N71-13179

Forearm vascular responses to brachial artery infusions of tyramine and norepinephrine after two weeks bed rest (AD-727151) 03 p0410 N71-13179

Total body exercise effect on metabolic, hematologic, and cardiovascular consequences of prolonged bed rest (AD-727151) 03 p0410 N71-13179

Long term bed rest effects on mineral balance and bone density in normal individuals (AD-727151) 03 p0410 N71-13179

Effects of prolonged bed rest on bone and calcium metabolism and mineral content loss of osseous (AD-727151) 03 p0410 N71-13179

Relationship between diurnal and nocturnal urinary patterns in human kidney during bed rest (AD-727151) 03 p0410 N71-13179

Carbohydrate tolerance in human body during five weeks of bed rest (AD-727151) 03 p0410 N71-13179

Bed rest effects on glucose regulation in human beings (AD-727151) 03 p0410 N71-13179

Bed cell mass loss in human beings as result of bed rest (AD-727151) 03 p0410 N71-13179

Diurnal variation in endocrine and cardiovascular systems during prolonged bed rest (AD-727151) 03 p0410 N71-13179

BIOS (PHYSIOLOGICAL ENGINEERING)

Hydrodynamic characteristics of opening processes in fluidized beds (AD-727151) 03 p0410 N71-13179

Computer analysis of axial mass dispersion data for packed catalytic glass particle beds (AD-727151) 03 p0410 N71-13179

Iodine adsorption properties of metal-loaded ion-exchange resins for gas filtration beds in nuclear fuel processing plants (AD-727151) 03 p0410 N71-13179

Partial bed temperatures precisely calculated from flowing vertical bed-through distribution moments (AD-727151) 03 p0410 N71-13179

Carbon bed filtration system for removing particulate matter and gaseous radioactive contaminants from radioactive wastes (AD-727151) 03 p0410 N71-13179

Glass and steel microsphere opening bed properties and model for thermodynamic deposition of pyrolytic carbon from methane on nuclear fuel microspheres in spent beds (AD-727151) 03 p0410 N71-13179

Design and tests of monolithic catalyst beds for heterogeneous hydrocarbon reactions (AD-727151) 03 p0410 N71-13179

Cyclic heat transfer and static pressure drop measurements of gas flow through packed beds (AD-727151) 03 p0410 N71-13179

BIOS LAW

Multichannel photoluminescence chamber for measuring absorption, photoluminescence yield, and coefficients of gases (AD-727151) 03 p0410 N71-13179

BIOS

Documentation of petroleum products with heavy (AD-727151) 03 p0410 N71-13179

BEHAVIOR

NT HUMAN BEHAVIOR

Low-level, low-frequency electric field effects on monkey behavior and brain activity based on electroencephalography (AD-727151) 03 p0410 N71-13179

BIOS

Climatological data for Belgian weather stations for Aug. 1970 (AD-727151) 03 p0410 N71-13179

Climatological tables for Belgian weather stations - May 1970 (AD-727151) 03 p0410 N71-13179

Synoptic meteorological data tables from Belgian weather stations - July 1969 (AD-727151) 03 p0410 N71-13179

Synoptic meteorological data tables from Belgian weather stations - Aug. 1969 (AD-727151) 03 p0410 N71-13179

Sulfur oxides, smoke, and air pollution tables from Belgian weather stations, Mar. 1970 (AD-727151) 03 p0410 N71-13179

Sulfur oxides, smoke, and air pollution tables from Belgian weather stations, Feb. 1970 (AD-727151) 03 p0410 N71-13179

Meteorological parameter tables for Belgian weather stations, Sep. 1970 (AD-727151) 03 p0410 N71-13179

Douglas psychophysical observatory, Belgium, data on geomagnetism, ionospheric propagation, cosmology, cosmic rays, and atmospheric electricity, April 1970 (AD-727151) 03 p0410 N71-13179

Ionospheric sounding and cosmic ray neutron flux density tables at Dourbes, Belgium, Jan. 1970 (AD-727151) 03 p0410 N71-13179

Ionospheric sounding and cosmic ray neutron flux density tables at Dourbes, Belgium, Oct. 1970 (AD-727151) 03 p0410 N71-13179

Atmospheric electricity, ionospheric sounding, meteorology, and geomagnetism, and cosmic ray data - Belgium, May 1970 (AD-727151) 03 p0410 N71-13179

Atmospheric electricity, ionospheric sounding, meteorology, and geomagnetism, and cosmic ray data - Belgium, June 1970 (AD-727151) 03 p0410 N71-13179

Climatological data - Belgium, Oct. 1970 (AD-727151) 03 p0410 N71-13179

Climatological data - Belgium, Nov. 1970 (AD-727151) 03 p0410 N71-13179

Ionospheric sounding and cosmic ray neutron flux density tables, Dourbes, Belgium, Nov. 1970 (AD-727151) 03 p0410 N71-13179

Ionospheric sounding and cosmic ray neutron flux density tables, Dourbes, Belgium, Oct. 1970 (AD-727151) 03 p0410 N71-13179

Ionospheric sounding and cosmic ray neutron flux density tables, Dourbes, Belgium, Aug. 1970 (AD-727151) 03 p0410 N71-13179

- Ionospheric sounding and cosmic ray neutron flux density tables, Dourbes, Belgium, Sep. 1970
11 p1746 N71-21994
- Meteorological parameter tables for Belgian weather stations, Jan. 1971
11 p1788 N71-22014
- Sulfur oxides, smoke, and air pollution tables from Belgian weather stations, May 1970
11 p1788 N71-22015
- Sulfur oxides, smoke, and air pollution tables from Belgian weather stations, Sep. 1970
11 p1789 N71-22016
- Sulfur oxides, smoke, and air pollution tables from Belgian weather stations, Jul. 1970
11 p1789 N71-22017
- Sulfur oxides, smoke, and air pollution tables from Belgian weather stations, Jun. 1970
11 p1789 N71-22083
- Meteorological parameter tables for Belgian weather stations, Dec. 1970
11 p1789 N71-22084
- Sulfur oxides, smoke, and air pollution tables from Belgian weather stations, Aug. 1970
11 p1789 N71-22085
- Data tables of air pollution by smoke and sulfur dioxide at Belgian weather stations for Oct. 1970
13 p2105 N71-24442
- Data tables of air pollution by smoke and sulfur dioxide at Belgian weather stations for Nov. 1970
13 p2105 N71-24443
- Meteorological parameter tables for Belgian weather stations, Feb. 1971
15 p2437 N71-26971
- Tabulated data on atmospheric ozone density at Uccle, Belgium for 4th quarter of 1968
15 p2398 N71-27031
- Statistical analysis of turbidity from 15 years radiometric observations in Belgium
15 p2439 N71-27512
- Spectrophotometric ozone measurements for July through September 1968 in Belgium
18 p2916 N71-31041
- Meteorological parameter tables for Belgian weather stations, May 1971
19 p3125 N71-31657
- Synoptic meteorology data for weather stations, Belgium, Oct. 1969
19 p3126 N71-31686
- Synoptic meteorology data for weather stations, Belgium, Sept. 1969
19 p3126 N71-31687
- Dourbes Geophysical Observatory, Belgium, data on geomagnetism, ionospheric propagation, seismology, cosmic rays, and atmospheric electricity, Jul. 1970
19 p3091 N71-31928
- Belgian computerized information system applied to automatic control
[CRIF-EL-2] 20 p3370 N71-33436
- Meteorological parameter tables for Belgian weather stations, Apr. 1971
22 p3613 N71-35741
- Sulfur oxides, smoke, and air pollution tables from Belgian weather stations, Dec. 1970
23 p3790 N71-37012
- ### BELL AIRCRAFT
- #### NT UR-1 HELICOPTER
- Correlation studies based on wind tunnel test data and flight tests to determine performance, stability and control of XB-70-1 aircraft
[NASA-CR-114035] 21 p3373 N71-34001
- ### BELL MILITARY AIRCRAFT
- #### U MILITARY AIRCRAFT
- ### BELLMAN THEORY
- Using FORMAC system to solve optimal control problem of behavior of higher pressure derivatives of optimal value function along optimal trajectory
08 p1228 N71-19193
- ### BELLOWS
- Flexible bellows joint shielding sleeve for propellant transfer pipelines
[NASA-CASE-XMP-01855] 16 p2604 N71-28937
- Dynamic structural analysis and flow induced stress analysis of metal bellows in Apollo Saturn launch vehicle systems
16 p2608 N71-29098
- Investigation of bellows and flex hose induced vibrations in spacecraft ducting components
17 p2830 N71-29582
- Development of bellows-type tanks for long term storage of potable water for space shuttle
22 p3548 N71-35273
- Fabrication and fatigue tests of improved welded tilt-edge bellows for positive expulsion applications
[AD-726523] 23 p3762 N71-36824
- Environmental tests of cryogenic propellant effects on metallic positive expulsion bellows operating parameters
[NASA-CR-72797] 24 p3999 N71-38526
- ### BENCIES
- #### U SEATS
- ### BENDING
- #### NT ELASTIC BENDING
- Bending solution of full circular plates supported on two rings of equally spaced columns
[REPT-291] 02 p0301 N71-12013
- Bending solutions of uniformly loaded annular plates supported by columns on one boundary with other boundary simply supported
[REPT-387] 02 p0301 N71-12014
- Bending of circular plates supported on equally spaced columns under eccentric concentrated load
[REPT-286] 02 p0302 N71-12029
- Stress concentration around hole in bent plates
[AD-712109] 02 p0303 N71-12099
- Numerical solutions for bending, vibration, and buckling of laminated anisotropic rectangular plates
[AD-715200] 07 p1126 N71-17926
- Method and apparatus for boring of instrument panels to improve radio frequency shielded enclosure
[NASA-CASE-XMP-09422] 09 p1346 N71-19436
- Elastic bending stresses in out-of-round pipe due to internal pressure
[ORNL-TM-3244] 09 p1479 N71-30175
- Development of systems for automatically and continuously suppressing or attenuating bending motion in elastic bodies
[NASA-CASE-XAC-05432] 12 p2006 N71-33971
- Elbow forming in jacketed pipes while maintaining separation between core shape and jacket pipe
[NASA-CASE-XMP-10475] 13 p2003 N71-34679
- Improved multiload finite difference variant with combined ordinary modified and conventional multiload schemes for bending analysis of arbitrary cylindrical shells
[UNICIV-R-43] 17 p2835 N71-30316
- Problem of bending cylindrical shells solved using cylindrical strip elements, and rectangular circular cylindrical elements used in finite element analysis of cylindrical shells
[PB-195967] 18 p3021 N71-30906
- Fourier analysis of clamped anisotropic plates during bending under transverse load, shear and biaxial compression buckling, and natural frequencies of flexural vibrations
[AD-723287] 19 p3187 N71-31800
- Thermal bowing of single rods at several axial positions
[TRG-3089] 21 p3458 N71-34608
- Bending modes of single rods in boiling water reactor fuel assembly
[RT/ING-70124] 21 p3458 N71-34614
- Effects of combined loading on buckling of simply supported skew plates based on Rayleigh-Ritz method
[AE-299-2-PT-2] 22 p3689 N71-36308
- Bending, tensile strength, and plasticity of zirconium carbide samples
[AD-727942] 24 p3945 N71-38144
- ### BENDING DIAGRAMS
- Charged particle analyzer with periodically varying voltage applied across electrostatic deflection members
[NASA-CASE-XAC-05506-1] 06 p0917 N71-16095
- Bending force-time and bending force-deflection diagrams obtained with oscillograph during notched bar impact tests
[NLL-M-20165-5828.4P] 12 p2007 N71-24214
- ### BENDING FATIGUE
- Solution for bending of overhanging circular plate supported on columns
[REPT-280] 02 p0301 N71-12020
- Cryostat for flexure fatigue testing of composite materials
[NASA-CASE-XMP-02964] 07 p1032 N71-17659
- Effect of aging and finishing sequence on fatigue performance of maraging steel
[TN-2/70] 08 p1220 N71-19271
- Design and performance tests for reversed bending with steady torque fatigue test machine using notched steel specimens
[NASA-TM-X-67949] 23 p3761 N71-36815
- Tension and slow bend tests to determine effect of temperature and shear orientation on Al-AD3961 anodic alloy deformation
24 p3942 N71-38120
- ### BENDING MOMENTS
- Bond formability of titanium-aluminum-vanadium alloy over temperature range
[AD-710885] 01 p0059 N71-10557
- Calculation of bending moments of transverse continuous rectangular plates with matrix algorithms
03 p0400 N71-12751
- Buckling tests of two integrally stiffened circular cylinders subjected to bending loads
[NASA-TN-D-62711] 16 p2684 N71-28116
- Adaptive sampled data control of time varying bending modes of flexible airframe
[AD-723846] 18 p3020 N71-31582
- Variational methods used for approximate analytic solutions to problem of bending and torsion in anisotropic elastic beams
[NPL-MA-96] 22 p3689 N71-36311
- Analysis of stresses in torispherical shells subject to bending moments
[ORNL-TM-3201] 23 p3861 N71-37322
- Variational derivation of partial differential equations for Saint Venant torsion problem of non-homogeneous anisotropic bars
[R-45] 23 p3862 N71-37331
- ### BENDING THEORY
- Measuring simultaneous effects of pressure and temperature on modulus of elasticity of rods in slab bending tests
[NASA-TT-F-153111] 02 p0309 N71-14101
- Continuum plasticity and microstructure dissipation in elastic-plastic plane bending of crystal beam
17 p3823 N71-38100
- ### BENDING VIBRATION
- Computer program for predicting structural bending vibration data
[NASA-CR-105974] 05 p0776 N71-14508
- Memory (flex) pendulum damper for controlling bending vibration induced by wind effects
[NASA-CASE-LAR-10374-1] 07 p1001 N71-17102
- Development of method for predicting fatigue life of panels under flutter conditions with application to Saturn S launch vehicle structures
[NASA-CR-110896] 21 p3796 N71-34608
- ### BENZENE
- #### U DECOMPRESSION SICKNESS
- ### BENZOCATION
- Very high vacuum infrared mineral bandshift methods transferred to vacuum subunit of laser surface
[NASA-CR-111399] 02 p0230 N71-13100
- ### BENZENE
- Relations between crystal lattice structure and molecular and lattice structure as exemplified by benzene
03 p0440 N71-12720
- Radiation effects on sulfur compound impurities in crude oil
04 p0487 N71-13100
- Ground and excited states of benzynes by SCF and CI methods
07 p0867 N71-13100
- Using single photon counting technique to study fluorescence response and time dependence of benzene in cyclohexane excited by protons and ultraviolet radiation
[BNWL-SA-5526] 08 p3368 N71-32828
- Steady isentropic propagation data - Poling, Dec. 1970
[REPT-294-P] 10 p3536 N71-34608
- Kinetic principles of photochemical, mercury vapor mediated oxidation of benzene in gas phase
[NLL-RTS-5963] 10 p3516 N71-34608
- Benzene evaporation rate determined from film plate boiling under high temperature air flow with application to gas turbine air pollution reduction
[DLR-FB-70-38] 11 p1040 N71-30901
- Raman spectra perturbation in benzene solution of sulfur monosulfide and sulfur monochloride
12 p1672 N71-34608
- Sound ranging distance for detecting benzene-dioxane emulsions
[TZF-1971-4] 10 p3563 N71-34608
- Radiography of shock waves emanating from fast compressed frozen dielectric layer of liquid bromobenzene
[UCRL-TRANS-10507] 18 p2908 N71-31112
- Pure-benzene-quinone dioxane and concentrated mineral acid processed to yield intermediate or final product, heat transfer materials
[NASA-CASE-ARC-10304-1] 21 p3443 N71-34608
- Elastic activity of Rb-PyS2O2 and Rb-PyS2O2 catalysts in benzene hydrogenation reactions
[NLL-RTS-6448] 23 p3722 N71-34608
- Interactions between intense coherent light from Q switched ruby laser and iodine vapor, neodymium-doped glass, and benzene
23 p3885 N71-37128
- ### BENZONIC ACID
- Potentiometric titration of benzonitrilic acid derivatives in non-aqueous medium
[RAB-LIB-TRANS-1507] 19 p3630 N71-32827
- ### BERING SEA
- Geomorphology of ocean bottom structure and topography of Bering Sea and Gulf of Alaska
11 p1737 N71-28941
- Analysis of processes maintaining oceanic heat storage in 0 to 250 meter surface layer of North Pacific Ocean
[PB-197661] 18 p2948 N71-34719
- ### BERNOLLI EQUATION
- High efficiency counting of Rb-84 by liquid scintillation technique
[KR-139] 05 p0402 N71-12801
- ### BERNOULLI EQUATION
- #### U BERNOULLI THEOREM
- ### BERNOULLI THEOREM
- Number theoretical class of weak Bernoulli transformations
[BB-20/BBR/2/KM4W/1] 23 p3762 N71-34608
- ### BERYL
- Beryllium production and consumption for 1969
17 p2761 N71-38120
- ### BERYLLIUM
- #### NT BERYLLIUM ISOTOPES
- #### NT BERYLLIUM 7
- #### NT BERYLLIUM 9
- #### NT BERYLLIUM 10

SUBJECT INDEX

BETA PARTICLES

Conference on applications of beryllium in structural materials

10-710764 01 p0857 N71-10483

Measuring preferred orientation of beryllium foils by X-ray diffractionometry and sodium iodide counters

10-710765 03 p020 N71-12639

Beryllium determination in gamma activated samples

10-710766 04 p0573 N71-13650

Redeposition of magnesium and beryllium from molten salts

10-710767 08 p0216 N71-10836

Effects of selected minor alloying additions on structure and deformation of beryllium

10-710768 08 p1219 N71-19216

Integral test of inelastic scattering cross sections for measured neutron spectra from thick shells of Li, W, Mo, and Be

10-710769 09 p1444 N71-20457

Factorial design, fabrication and test of beryllium-ceramic panel of built-up beryllium structure

10-710770 10 p1495 N71-20727

Beam and pressure tests for determining thermal stability of beryllium, uranium, and tungsten

10-710771 10 p1503 N71-21700

Neutron cross sections and angular distributions for Li-7, Be-9 reactions including neutron spectra indicators of atomic energy levels

10-710772 14 p2313 N71-26710

Lithium, beryllium, and boron particle production by spallation and isotopic spin classification of scattering cross sections

10-710773 15 p2456 N71-26846

Angular neutron distribution from beryllium neutron sources

10-710774 15 p2470 N71-27383

Method for producing neutrons in Be-9 energy region utilizing gamma rays from radioactive decay to reduce photo-neutron reaction in beryllium

10-710775 16 p2630 N71-28119

Pulse count initiation and propagation in aluminum alloy boron and beryllium matrix composites

10-710776 16 p2680 N71-28181

Collisional ionization rates for lithium and beryllium ions deduced from time history of spectral lines emitted by these ions in hot plasmas

10-710777 16 p2648 N71-28637

Beryllium production and consumption for 1969

10-710778 17 p2761 N71-29279

Reduction of overall program costs for reusable space shuttle by use of beryllium as primary structural material

10-710779 17 p2848 N71-29465

Quality measurements of neutron spectra produced in bombardment of beryllium target below 8.3 MeV

10-710780 17 p2896 N71-29270

Negative pion, kaon, antiproton, and antineutrino production in 70 GeV proton irradiation of aluminum and beryllium metal

10-710781 17 p2810 N71-30387

Synchrotron radiation of carbon, boron, and beryllium and observations of K lines in ultrafast X-ray emission spectra

10-710782 19 p3151 N71-32142

Reactive arrangement of beryllium monolith with ion counter having individual discriminator and amplifier

10-710783 21 p3405 N71-34306

High sensitivity beryllium ore assaying instrument based on neutron photoproduction method

10-710784 21 p3432 N71-34392

Crystal structure and characteristics of beryllium film after coating with aluminum by electrolysis

10-710785 21 p3439 N71-34468

Evolution of mineral and chemical trends properties of beryllium foil in rolling and transverse directions to maintain yield and fracture ductility

10-710786 22 p3599 N71-35589

Ball bonding beryllium wire-metal matrix composites

10-710787 22 p3602 N71-35655

Low energy electron diffraction from zinc and boron cleavage surfaces as function of direction and energy of incident beam

10-710788 22 p3652 N71-36844

Atmospheric diffusion of beryllium exhaust gases from solid propellant rocket engines correlated with meteorological parameters

10-710789 23 p3840 N71-37383

Development of methods for improving ductility of beryllium and techniques for deforming high beryllium sheet metal

10-710790 24 p3938 N71-38094

Determining Knight shift in beryllium from hyperfine contact and dipolar interaction calculations combined with zero polarization effect

10-710791 24 p3942 N71-38119

Positivity effects on elastic and strength properties of beryllium crystals, emphasizing beryllium

10-710792 24 p4023 N71-38703

BERYLLIUM ALLOY

Dependency of age-hardening of binary beryllium alloys on beryllium content

10-710793 11 p1778 N71-22399

Analysis of cause for concentration perturbation in off-cooled aluminum-beryllium alloy caused by change in freezing rate during progressive freezing and zone melting

10-710794 13 p3092 N71-24534

Development of fluoride coating to prevent oxidation of beryllium surfaces at elevated temperatures

10-710795 20 p3285 N71-33408

BERYLLIUM COMPOUNDS

NT BERYLLIUM FLUORIDES

NT BERYLLIUM HYDRIDES

NT BERYLLIUM OXIDES

Nuclear quadrupole coupling constants and Knight shift of NMR in crystalline compounds

10-710796 07 p1075 N71-17438

Electrophysical properties and structure of chemical bond in boron, carbon, and beryllium compounds

10-710797 21 p3386 N71-34091

BERYLLIUM FLUORIDES

Preparation and handling of molten salt mixtures for molten salt reactor experiment, using LiF, BeF₂, ZrF₄, and UF₄ mixture

10-710798 10 p1603 N71-21199

BERYLLIUM HYDRIDES

Configuration interaction on ground state of beryllium hydride molecule

10-710799 21 p3492 N71-34879

BERYLLIUM ISOTOPES

NT BERYLLIUM 7

NT BERYLLIUM 9

NT BERYLLIUM 10

Alpha, 2 alpha reaction on Li-6, Li-7, Be-9, C-12, and O-16 at 35 MeV

10-710800 02 p0277 N71-12132

Excitation functions and differential cross sections for Be-9 particle interactions from 8 to 50 MeV neutrons

10-710801 14 p2311 N71-26886

Time of flight method for studying fast neutron elastic and inelastic scattering on B-10 and B-11 in 2 to 5 MeV energy region

10-710802 15 p3489 N71-27885

Energy effects in three particle proximity scattering in beryllium isotope decay

10-710803 20 p3323 N71-33044

Angular and energy distributions of neutrons produced by bombarding thick beryllium targets with 53.8-MeV deuterons

10-710804 22 p3432 N71-35877

BERYLLIUM OXIDES

Thermal neutron wave propagation in beryllium oxide

10-710805 02 p0276 N71-11559

Measurement of Li-6 diffusion from irradiated beryllium oxide

10-710806 13 p2128 N71-24474

Reactor irradiation of thermionic sheath insulators: two beryllium and two aluminum bonded trilayers

10-710807 13 p2116 N71-24635

Dynamic characteristics of commercial beryllium oxide as thermoluminescent material

10-710808 13 p2099 N71-24670

Electron spin resonance for detecting defects in beryllium oxide single crystals created by gamma or neutron irradiation

10-710809 15 p2496 N71-27972

Program package COLLI for calculating thermal neutron scattering for moderators of random structure and composition using beryllium oxide as typical example

10-710810 16 p2641 N71-28026

Thermally stimulated electron emission of ceramic beryllium oxide and calcium sulfate pure and doped with cerium, manganese, and lead: studied for dosimetric material

10-710811 16 p2642 N71-28020

Design and performance of thermal beryllium oxide and graphite neutron sources and high flux beam reactors in neutron spectrometry

10-710812 16 p2649 N71-28716

Immersion calorimeter for measuring Wigner energy in irradiated BeO, MgO, Al₂O₃, and SiO₂ at high temperatures

10-710813 19 p3156 N71-32428

Phonon optical effects on scattering properties of beryllium oxide based on crystal models, quantum mechanics, and computer program for scattering matrix calculations

10-710814 23 p3836 N71-37360

BERYLLIUM 7

Dispersed atmospheric fallout data of Be-7 and P-32 derived at Zugspitze, Germany from 1 Apr. to 15 Nov. 1970

10-710815 15 p2515 N71-27703

Air mass exchange study using atmospheric Be-7 and P-32 as tracers

10-710816 22 p3575 N71-35466

BERYLLIUM 9

Alpha alpha interaction in Be-9 yields alpha alpha pairs and gamma decay

10-710817 04 p0280 N71-14293

Quasi-free electron scattering on C-12 and Be-9 using external electron beam

10-710818 08 p1247 N71-18190

Angular distributions and total cross sections of Be-9 deuterium alpha-alpha Li-7 and Be-9 deuterium alpha-alpha Li-7/470 Be-9 reactions in 0.9 to 1.2 MeV energy range

10-710819 14 p2316 N71-26744

Rhectic scattering of proteins on Be-9 nuclei

10-710820 14 p2318 N71-26744

Asymmetrical asymmetry of reaction products produced by polarized protons and deuterons incident on beryllium 9 target measured by polarized beam from tandem Van de Graaff accelerator

10-710821 15 p2678 N71-26815

Detection, and energy and angular distributions of Li-6 recoil nuclei from Be-9 irradiated with 100 and 600 MeV protons

10-710822 15 p3480 N71-27457

Angular distributions and absolute cross sections measured for Be-9 plus 1 reaction below Coulomb barrier

10-710823 17 p2795 N71-26777

Coincidence spectra of alpha particles from reaction Be-9/alpha alpha Be-4 measured for several angular configurations at 1.55 MeV bombarding energy

10-710824 20 p3326 N71-33644

BERYLLIUM 10

Be-10, p/Be-10 reaction used for study of doublet at 3.96 MeV in Be 10

10-710825 10 p1623 N71-21764

BERYLLIUM FUNCTIONS

Recursion formula for logarithmic derivatives of spherical Bessel functions in complex plane

10-710826 08 p0252 N71-11938

Classical theory of conductive heat transfer

10-710827 05 p0469 N71-13326

Bound function solutions for low angle of attack approach of flying vehicle to atmospheric boundary and transition into vibrational motion

10-710828 07 p0609 N71-16883

Bound functions for deep inelastic e-p structure in ladder model with spin 1/2 nucleons

10-710829 07 p1073 N71-17439

BETA PARTICLES

Precision measurement of He-203 beta-gamma directional correlation

10-710830 01 p0905 N71-10416

Energy dependent beta-gamma circular polarization and nuclear matrix elements of Be-9

10-710831 01 p0909 N71-10716

Deriving equations for automatic correction of beta-ray oscillations in cyclic accelerators

10-710832 04 p0587 N71-14576

Deriving formulae for spin and angular correlations in hyperon beta decay

10-710833 05 p0747 N71-13240

Method for extraction of first-forbidden beta matrix elements from angular correlation data

10-710834 05 p0749 N71-13294

Measuring fractions of aerosol beta activity in precipitation and settled dust

10-710835 05 p0720 N71-13585

Charge distribution effects on beta decay on diffuse surface

10-710836 06 p0913 N71-15873

Isotopic in bound nuclear states, spin assignments, and electromagnetic multiple mixing deduced from beta-gamma (CP) correlation measurements in allowed transitions

10-710837 08 p2533 N71-18522

Facility and procedures for processing alpha, beta, gamma, and neutron counters

10-710838 08 p1176 N71-19542

Beta and gamma irradiation of bitumen and bitumen coated materials with dose rate and degradation analysis

10-710839 09 p1431 N71-26887

Finite nuclear size and radiative effects for Kurie plot analysis of beta spectrum decay

10-710840 10 p1417 N71-21263

Polarized hyperon beta decay in cosmic mass frames of outgoing leptons

10-710841 11 p1802 N71-22089

Q squared spectrum and asymmetry functions of hyperon beta decay

10-710842 11 p1805 N71-22092

Foot-value ratio expressions for second class currents from mirror beta decays in Be-12-N-13 system

10-710843 12 p1866 N71-23291

Angular correlations of polarized conversion electrons, vanadium isotope beta particles, and bremsstrahlung

10-710844 12 p1978 N71-33085

Measurement of 4 plan beta minus gamma coincidences in radioactivity measuring laboratory case of complex decay scheme, and accuracy obtainable in particular cases

10-710845 14 p2389 N71-26571

Delayed neutron emission probabilities and spectra using beta particle decay and gamma ray or neutron energy loss

10-710846 14 p2389 N71-26613

Beta spectrum measurement of C-14 using an effective proportional counter and gaseous C-14 sources

10-710847 15 p2462 N71-27122

Radioactive characteristics for studying these products - beta radiation and conversion electrons

10-710848 15 p2471 N71-27409

Si/Li detector in homogeneous magnetic field for beta spectrometer with electromagnetic shielding for selected electron energy level studies
[DPR-P-1227] 15 p2485 N71-27814

Time dependent analysis of thermal radiation from fission product beta and gamma radioactive decay
[IAER-MEMO-4265] 15 p2495 N71-27965

Angular distributions and correlations of alpha and beta particles, electrons, and electromagnetic radiations from oriented nuclei
[LA-4565] 16 p2455 N71-28157

Beta-gamma CPV-asymmetry coefficients in isomeric forbidden mixed beta transitions
[KFE-1249] 16 p2451 N71-28938

Alpha and beta particle range determination, using cadmium telluride detectors for gamma ray spectrometry
[CEA-R-4852] 16 p2455 N71-29072

Measurement of Co-137 radioactivity and total beta activity from nuclear explosion fallout and aerosols in air suspended over continents, mountains, and oceans
[CEA-R-3977] 17 p2738 N71-29236

Energy levels of Yb-176 from decay of Tm-176 and Yb-176m studied by Ge/Li detectors and gamma-gamma as well as gamma-beta coincidences
[NP-18599] 17 p2807 N71-30336

Beta detection efficiency curve for some radioisotopes in different thickness sources obtained by specific radiochemical separations
[CISE-N-119] 18 p2976 N71-30624

Beta particle observations between inner edge of plasma sheet to plasmasphere in midnight earth magnetosphere
[NASA-TM-X-45640] 19 p3094 N71-32436

Standardization of beta-gamma emitters by 4pi beta-gamma coincidence method for corrections and counting errors
[BAR-1240] 21 p3467 N71-34680

Beta activity in samples of atmosphere, surface waters, and drinking water supplies and content of Co-137 and Sr-90 in food samples - Italy
[PROT-SAN-13169] 21 p3473 N71-34729

Second order form factors for spin correlation analysis in beta decay of Lambda hyperon
[COO-264-568] 21 p3476 N71-34750

Weak interaction in beta decay of polarized Lambda hyperons
[COO-1701-14] 21 p3480 N71-34794

Alpha and beta radiation measurements from air, soil, vegetation, and water samples in Ames reactor environment
[IS-2541] 22 p3644 N71-35985

Beta and electron-capture decay schemes for Sb isotopes and proton reactions of C-12, F-19, Au-197, Hg-3, Te-181, Pb-208, and Ni-58 including angular distributions and scattering cross sections
[UCLA-10-P-18-23] 23 p3816 N71-37215

Feasibility of crystal growth techniques for beta alumina membranes from molybdenum, tungsten, and trifluoride
[NASA-CR-72982] 23 p3833 N71-37336

Generation of osmium stability pole nucleides in processes of stellar evolution
23 p3850 N71-37444

Air and precipitation beta radioactivity at Los Alamos, New Mexico, for 1970
[LA-4461] 24 p3951 N71-38190

Atomic excitations and photon emission by sudden change of nuclear charge during beta(minus) decay
[NRC-TT-1455] 24 p3975 N71-38361

Beta and electron capture decay in iodine and tellurium
[ANL-TRANS-883] 24 p3980 N71-38401

Search for double beta decay of Nd-150 using large aperture, low resolution magnetic spectrometer-detector in salt mine
[COO-1749-23] 24 p3981 N71-38411

Toroidal high beta experiments in compact axisymmetric configurations
[CN-28/1-2] 24 p3987 N71-38449

BETATRONS

Coherent betatron beam oscillation measurements during high energy acceleration
[CERN-TRANS-70-10] 14 p2315 N71-26732

Betatron oscillation coupling and decoupling by longitudinal magnetic compensating fields and application to storage ring longitudinal detector fields
[SLAC-TRANS-131] 21 p3483 N71-34824

BEYER-SHULTZ FORMULA

Combinatorial corrections to Bethe-Heitler cross sections for electron-nucleus bremsstrahlung
[NASA-TM-D-4836] 01 p0103 N71-10999

BEYER-SALPETER EQUATION

Lorentz symmetry of Bethe-Salpeter equation for two scalar mesons
[NP-18418] 06 p0914 N71-17091

Numerical determinations of Regge poles from Bethe-Salpeter equation with scalar couplings
[ILL-TM/17-1] 06 p0937 N71-18832

Lorentz transformation properties of Bethe-Salpeter Green function
[TR-71-101] 13 p2103 N71-34963

Two particle S wave scattering and Bethe-Salpeter equation
13 p2141 N71-25344

Approximate solutions to Bethe-Salpeter and integral equations, and applications to high energy interactions
[AD-709697] 15 p2466 N71-27265

Analysis of scalar particle scattering amplitude based on Bethe-Salpeter equation for two particle Green function
[DNR-R2-5640] 18 p2981 N71-30824

BETATRON

Betatron operation and resonant extraction studies
[UCRL-19726] 13 p2861 N71-25124

Magnet beam splitting system for external proton beam of betatron
[UCRL-30194] 19 p3150 N71-32128

Ultra-narrow, high quality, high field quadrupole magnet for use in betatron experimental area
[UCRL-30164] 20 p3246 N71-33589

Nitrogen cryogenic pumping system design for betatron refrigeration
[UCRL-30197] 20 p3247 N71-33708

Betatron pole-face windings power system with high voltage transformer actuator
[UCRL-26191] 20 p3247 N71-33889

Digital system with real time closed loop control of betatron guide field
[UCRL-26189] 20 p3247 N71-33899

Digital control of betatron acceleration cycle requiring reduction of beam and noise
[UCRL-30185] 20 p3248 N71-33980

Magnet pulse stability and beam split operations of betatron
[UCRL-28249] 21 p3408 N71-34349

BEVERAGES

Advantages of various types of liquids taken by workers under high temperature working conditions (miners, fire fighters, steelworkers)
[NASA-TT-F-14002] 23 p3713 N71-36460

BIAS

NT RESPONSE BIAS

Investigation of statistical concepts of unbiasedness and invariance as keys to deriving signal detectors
16 p2561 N71-28581

BIBLIOGRAPHIES

Meteorological bibliography for Switzerland
01 p0077 N71-10066

Nondestructive tests developed for bonded material evaluation
[AD-709962] 01 p0070 N71-10072

Stress concentration around holes and fissures including stress-strain diagrams - bibliography
[NASA-TT-F-467] 01 p0128 N71-10121

Annotated bibliography and indexes on Aerospace Medicine and Biology - Sept. 1970
[NASA-SR-7011/80] 01 p0008 N71-10125

Techniques in plating including types of plating, and materials used for plating - bibliography
[AD-709950] 01 p0038 N71-10188

Bibliography on diffusion bonding
[AD-710500] 01 p0058 N71-10197

Annotated bibliography on nonequilibrium flow
[AD-710400] 01 p0040 N71-10199

Isot gas welding - bibliographies
[AD-709900] 01 p0059 N71-10290

Aviation medicine studies - bibliography
[AM-70-1] 01 p0009 N71-10298

Bibliography of documents containing numerical data on planar lifting surfaces
[AGARD-R-574-70] 01 p0001 N71-10339

Bibliography with abstracts on materials dynamic properties
[AD-710823] 01 p0129 N71-10484

Applications of Mossbauer effect in chemical research - bibliographies
[AD-710818] 01 p0110 N71-10533

Annotated bibliography of reports related to aerospace medicine including radiobiology and stress physiology
[AD-710764] 01 p0012 N71-10594

Bibliography of compilation of articles on heat and mass transfer
[AD-711147] 01 p0134 N71-10892

Annotated bibliography of FY 1970 scientific and technical reports, articles, papers, and presentations sponsored by NASA
[NASA-TM-X-46474] 01 p0138 N71-10900

Annotated bibliography of regulations, standards, and guides for microwaves, and ultraviolet, laser, and television receiver radiation
[PB-189360] 02 p0151 N71-11074

Bibliography of research projects in air pollution for year 1969
[PB-192220] 02 p0152 N71-11077

Selective bibliography of water and air pollution for business and industry
[PB-192318] 02 p0152 N71-11078

Review and annotated bibliography of selected research on human performance
[NBS-SPEC-PUBL-319] 02 p0166 N71-11181

Bibliography on physical, life, and social sciences and engineering
02 p0307 N71-11382

Annotated bibliography on infrared photography and films - Vol. I
[AD-712100] 02 p0226 N71-11833

DDC bibliography on zone refining for May 1969 - Apr. 1969
[AD-712000] 02 p0285 N71-11833

Bibliography and index of hurricane and storm storm along coastal plains of US
[PUBL-70-3] 02 p0259 N71-11833

Annotated bibliography and indexes on Aerospace Medicine and Biology - Sept. 1970
[NASA-SR-7011/81] 03 p0322 N71-11833

Soviet cybernetics - bibliographies
[AD-709972] 03 p0332 N71-11833

Alphabetic bibliography of magnetic materials and transition temperatures
[ORNL-RR-7-REV-2] 03 p0417 N71-11833

Annotated bibliography of capital budgeting selection by mathematical programming
[TM-173] 03 p0599 N71-11833

Bibliography on existence of high temperature materials including refractory materials, ceramics, carbon, graphite, chert, and ablative materials in use in aerospace engineering
[NASA-CR-102934] 03 p0468 N71-11833

Bibliography of geological research in Antarctic regions
[REF-146] 03 p0349 N71-11833

Correlation between magnetic variation and old world and interplanetary magnetic fields
[GRI-NT-79] 03 p0451 N71-11833

Bibliography of mass spectroscopy literature for first half of 1968 - compiled by computer method
[IS-2039] 04 p0485 N71-11833

Selected bibliography of abstracts on present water power reactors
[NEEC-RR-39] 04 p0545 N71-11833

Synthesis and variational methods in nuclear reaction theory, physics, and computational methods - bibliography
[LA-4461] 04 p0549 N71-11833

Bibliography on lunar surface
[PB-194206] 04 p0613 N71-11833

Annotated bibliography and indexes on Aerospace Medicine and Biology - Nov. 1970
[NASA-SR-7011/82] 04 p0480 N71-11833

Annotated bibliography of technical literature related to nitrogen oxides and air pollution control
[PB-194429] 04 p0480 N71-11833

Annotated bibliography of information facilities and data resources available to Environmental Health Service on environmental pollution
[PB-194414] 04 p0481 N71-11833

Annotated bibliography on application of results observations to hydrology problems
[PB-194072] 05 p0467 N71-11833

Bibliography on chemical effects of nuclear transformations for year 1969
[NP-18402] 05 p0739 N71-11833

Annotated bibliography on neutral particle transport theory
[LA-4387-M3] 05 p0740 N71-11833

Annotated bibliography on plasma physics and controlled thermonuclear fusion
[TID-3557-SUPPL-C] 05 p0754 N71-11833

Bibliography of management sciences literature
[NASA-TM-X-46546] 05 p0787 N71-11833

Xeromography and related topics - bibliography
[AERE-BIB-173] 05 p0749 N71-11833

Annotated bibliography of coastal resources and seacoast development in Texas
[PB-189700] 05 p0876 N71-11833

Abstracted bibliography on meteorology, climatology, and oceanography of Caribbean region
[AD-713492] 05 p0877 N71-11833

Indexes for bibliography on meteorology, climatology, and oceanography of Caribbean Sea region
[AD-713493] 05 p0878 N71-11833

Bibliography on geophysical publications
05 p0881 N71-11833

Annotated bibliography of reports on parameters of human pattern perception for Sept. 1967 through Aug. 1969
[AD-714672] 05 p0886 N71-11833

Bibliography of computer programs on nuclear physics, reactor design, reactor operation, and reactor engineering
[ANL-7084] 06 p0819 N71-11833

Bibliography on solid state physics including condensed matter and theoretical physics
[AD-714265] 06 p0805 N71-11833

Hydrodynamic theory of lubrication applied to nuclear reactors - bibliographies
[AD-714346] 06 p0806 N71-11833

Bibliography of mass spectroscopy literature for last half of 1968 compiled by computer method
[IS-2327] 06 p0812 N71-11833

Bibliography synopsis of external ionization apparatus and techniques for cryogenic storage systems
[NASA-CR-114026] 06 p0808 N71-11833

Bibliography on urban economics and planning
[AD-714500] 06 p0803 N71-11833

Bibliography of technical literature of match and ceramics division for 1969 at Oak Ridge National Laboratory
[ORNL-4276-VOL-3] 07 p0800 N71-11833

SUBJECT INDEX

High temperature liquid metal technology - associated bibliography 07 p1043 N71-17245
[N71-17245]

Bibliography of laser publications of interest to civilian spectroscopists 07 p1039 N71-17266
[N71-17266]

Associated bibliography of atomic and molecular collision research for 1969 07 p1074 N71-17417
[N71-17417]

Associated bibliography and indexes on Aerospace Medicine and Biology - Nov. 1970 07 p0983 N71-17449
[N71-17449]

Associated bibliography and indexes on Aerospace Medicine and Biology - Dec. 1970 07 p0983 N71-17450
[N71-17450]

Associated bibliography of scientific and engineering work performed at JPL up to Aug. 1970 07 p1068 N71-17758
[N71-17758]

Selected bibliography of published papers on Surface 07 p1026 N71-18000
[N71-18000]

Bibliography on tritium hazards: emphasizing nuclear characteristics 08 p1246 N71-18134
[N71-18134]

Bibliography of technical reports on scientific and engineering studies, November 1970 08 p1286 N71-18705
[N71-18705]

Bibliography of technical reports on scientific and engineering studies, December 1970 08 p1286 N71-18706
[N71-18706]

Research effort - bibliographies 08 p1261 N71-18798
[N71-18798]

Bibliography on cold regions science and technology, November between July 1969 and June 1970 - Part 1 08 p1191 N71-18851
[N71-18851]

Bibliography on cold regions science and technology, November between July 1969 and June 1970 - Part 2 08 p1191 N71-18852
[N71-18852]

Hard Scientific and Technical Information Centre bulletin for 1970 - bibliography of accessioned books and selected abstracts of journal articles 08 p1289 N71-19325
[N71-19325]

Information - annotated bibliography for 1967 and 1968 08 p1196 N71-19340
[N71-19340]

Bibliography on chemical, physical, and nuclear properties of transplutonium elements 08 p1342 N71-19434
[N71-19434]

Remote sensing for earth resources and urban development - bibliographies 08 p1382 N71-19602
[N71-19602]

Bibliography with abstracts on carbon-carbon, metal-metal, and metal-metal composites 08 p1403 N71-19665
[N71-19665]

Telecommunications and communication equipment research - bibliography 08 p1349 N71-19739
[N71-19739]

Associated bibliography of plasma physics research papers including plasma propulsion, plasma radiation, and plasma resonance - conference 08 p1447 N71-19806
[N71-19806]

Associated bibliography of plasma physics research papers including plasma spectroscopy, crossed field plasma accelerators and electric forces on solid, and collisionless plasma - conference 08 p1448 N71-19811
[N71-19811]

Bibliography on quenching alloys from liquid state - CALT-22-17 08 p1399 N71-19907
[N71-19907]

Control theory and applications to inertial guidance and navigation, vehicle stabilization, and related - bibliography 08 p1389 N71-20002
[N71-20002]

Mathematical programming techniques applied to computer directed design - algorithmic tools, applications, and literature review 08 p1476 N71-20128
[N71-20128]

Mathematical programming applications to structural design optimization - literature review 08 p1479 N71-20132
[N71-20132]

Technology of human and animal waste products and by-products in controlled atmospheres of closed ambient systems - literature review 08 p1338 N71-20493
[N71-20493]

Selected annotated bibliography on interpretation of quantum mechanics 08 p1425 N71-20554
[N71-20554]

Associated bibliography on engineering aspects of design, construction, evaluation, testing, and performance of aircraft and associated components, materials, and systems 10 p1491 N71-20749
[N71-20749]

Telecommunication science research 10 p1516 N71-20781
[N71-20781]

Technology review on integrated linear, digital, and microwave circuits 10 p1537 N71-20893
[N71-20893]

School bibliography on technology transfer 10 p1665 N71-20921
[N71-20921]

Interdisciplinary and geosociophysical abstracts for Argentina, Chile, and Uruguay 10 p1597 N71-21243
[N71-21243]

Introduction to design and use of AM subcarrier telemetry systems, with bibliography 10 p1534 N71-21247
[N71-21247]

Associated bibliography on hydromechanics and air pollution 10 p1466 N71-21697
[N71-21697]

Thermal effluent effects and reactor safety measures - bibliography 10 p1685 N71-21748
[N71-21748]

Bibliography of electrostatic precipitators for particulate emission control 10 p1548 N71-21813
[N71-21813]

Bibliographies on natural resources including atmosphere, earth, water, climate, plants, and animal subject matter 11 p1744 N71-21894
[N71-21894]

Bibliography on remote sensing of earth resources applications with emphasis on water resources 11 p1748 N71-22243
[N71-22243]

Vapor-laser methods of film deposition - associated bibliography 11 p1749 N71-22331
[N71-22331]

Biodynamics, aerospace medicine, acoustics, stresses, human tolerance, centrifuges, test facilities, and associated bibliography 12 p1865 N71-23337
[N71-23337]

Associated bibliography of worldwide biodynamics research findings 12 p1866 N71-23344
[N71-23344]

Bibliographies of fatigue measurements 12 p1918 N71-23409
[N71-23409]

Woods Hole oceanographic research - 1970 bibliography 12 p1914 N71-23835
[N71-23835]

Graph theory and its applications - bibliography, September 1971 12 p1930 N71-23964
[N71-23964]

Bibliography of reports on variable stars for 1969 and 1970 12 p1996 N71-23991
[N71-23991]

Planetary and space research, plasma physics, wave propagation, and applicable mathematics - bibliography 12 p1996 N71-23992
[N71-23992]

Satellite observations, earth atmosphere, and solar radiation - reports received at World Data Center C1, 1 July - 31 Dec. 1970 12 p1996 N71-23993
[N71-23993]

Associated reference bibliography on aeronautical engineering documents 12 p1852 N71-24172
[N71-24172]

Associated bibliography indexes on Aerospace Medicine and Biology - Feb. 1971 12 p1864 N71-24174
[N71-24174]

JPL bibliography of technical reports released from July 1969 through June 1970 12 p2019 N71-24327
[N71-24327]

Bibliography on structural stability and buckling of conical and spherical thin walled shells 12 p2176 N71-24371
[N71-24371]

Aerodynamicity and unsteady flow problems of aircraft 13 p2023 N71-24706
[N71-24706]

Deterministic optimal control theory 13 p2026 N71-24712
[N71-24712]

Associated bibliography of translations of foreign language articles on aviation medicine, vestibular function, body temperature, and physiological effects (FAA-AM-71-5) 13 p2033 N71-24745
[N71-24745]

Bibliography on fast breeder reactors with subject index, reactor index, report index, and patent index 13 p2118 N71-24926
[N71-24926]

Bibliography on astronomical satellite system air traffic control and propagation factors 13 p2173 N71-24942
[N71-24942]

Bibliography of publications by Social Science Department of Rural Corporation - 1963 to 1970 (R-705) 13 p2191 N71-25190
[N71-25190]

Bibliography of technical literature resulting from aerospace research and development at Jet Propulsion Laboratories 13 p2192 N71-25249
[N71-25249]

Associated bibliography on human acclimation and acclimatization to heat 13 p2035 N71-25393
[N71-25393]

Environmental engineering abstracts and bibliographical data 13 p2078 N71-25480
[N71-25480]

Physics of dynamic growth of mushroom clouds, associated with nuclear explosions, bibliography 13 p2139 N71-25484
[N71-25484]

Associated bibliography and indexes on Aerospace Medicine and Biology - March 1971 14 p2283 N71-25743
[N71-25743]

Method of storing inverted film with minimum storage space and low access time for quick retrieval of nonnumerical data by computer 14 p2221 N71-25988
[N71-25988]

Computer patent searching system with automatic indexing using word truncation and similar query in on-line mode 14 p2221 N71-25981
[N71-25981]

Bibliography of phosphate coatings used in industrial processes 14 p2279 N71-26223
[N71-26223]

BIBLIOGRAPHIES

Composite materials, ceramics, textiles, and plastics for radars in radar and radar detection systems - bibliography 14 p2219 N71-26389
[N71-26389]

Bibliography of refractory coatings used in industrial processing 14 p2280 N71-26388
[N71-26388]

Remote sensing of earth resources - bibliography 14 p2230 N71-26398
[N71-26398]

Corrosion prevention by fungus-proofing - bibliography 14 p2287 N71-26638
[N71-26638]

Associated bibliography and indexes on aeronautical engineering and aerodynamics - Jan. 1971 14 p2194 N71-26709
[N71-26709]

Bibliography on radar and radio navigation 14 p2441 N71-26879
[N71-26879]

Associated bibliography on silicon recovery from silicon wafer effluents 15 p2422 N71-27132
[N71-27132]

Selected and annotated bibliography of human resources graduation in man-machine systems - Vol. 3 15 p2574 N71-27321
[N71-27321]

Environmental policy and law - bibliography 15 p2524 N71-27367
[N71-27367]

Thermophysical properties of alkali metals in liquid and vapor phases based on analysis of experimental and theoretical data from literature 16 p2536 N71-28314
[N71-28314]

Equilibria, reactions, and clustering in ternary system containing iron oxide 16 p2689 N71-28523
[N71-28523]

Literature survey on plasma instability 16 p2682 N71-28841
[N71-28841]

Tabulation of bibliographic cross section data for neutron induced reactions 17 p2780 N71-29216
[N71-29216]

Associated bibliography on radar antennas including antenna arrays, antenna radiation patterns, types of radar antennas, and testing and evaluation 17 p2718 N71-29220
[N71-29220]

Bibliographies on optical modulators 17 p2738 N71-29515
[N71-29515]

Satellite observation of earth resources 17 p2738 N71-29597
[N71-29597]

Cost/benefit model for decision making in planning German space program - bibliography 17 p2861 N71-29422
[N71-29422]

Remote sensing relating to military geography of arid lands including terrain, ground water, surface materials, cultural features, and related subjects - associated bibliography 17 p2742 N71-29838
[N71-29838]

Associated bibliography on neutron scattering cross sections for radioactive isotopes 17 p2801 N71-30122
[N71-30122]

Associated bibliography on bird aircraft hazards and accidents from Oct. 1967 to Jan. 1971 17 p2785 N71-30128
[N71-30128]

Bibliography of activation analysis publications up to 31 Jan. 1971 17 p2717 N71-30265
[N71-30265]

Activation analysis bibliography up to 31 Jan. 1971 including chemical element, methodology, matrix analysis, and author indexes 17 p2717 N71-30267
[N71-30267]

Bibliography of Soviet literature on high altitude and aerospace medicine and biology - 1965 to 1967 17 p2844 N71-30367
[N71-30367]

Bibliography on proton recoil counters for measurement of fast neutrons 18 p2871 N71-30463
[N71-30463]

Bibliography on isotope separation by ion exchange from 1938 to 1970 18 p2874 N71-30550
[N71-30550]

Associated bibliography on gas detectors compiled from DDC data bank 18 p2932 N71-30708
[N71-30708]

Bibliography on three dimensional flow dynamics 18 p2934 N71-30713
[N71-30713]

Bibliography on one dimensional flow dynamics 18 p2934 N71-30716
[N71-30716]

Space rendezvous trajectories and guidance techniques - bibliographies 18 p2989 N71-30728
[N71-30728]

Associated bibliography and indexes on Aerospace Medicine and Biology - Apr. 1971 18 p2876 N71-30836
[N71-30836]

Bibliography for uranium isotopes, cesium, strontium, plutonium, and cerium, deuterium, tritium, and helium 18 p2841 N71-30880
[N71-30880]

Bibliography of aeronautical engineering with abstracts 18 p2886 N71-30861
[N71-30861]

Plastics in composite materials - annotated bibliography 18 p2886 N71-30865
[N71-30865]

Comprehensive index for abstracts of NASA documents on aerospace medicine and biology 18 p2876 N71-31077
[N71-31077]

Associated bibliography and indexes on aerospace medicine and biology - May 1971 18 p2876 N71-31281
[N71-31281]

- Annotated bibliography and indexes on Aerospace Medicine and Biology - May 1971 19 p3276 N71-31230
- Annotated bibliography and indexes on Aerospace Medicine and Biology - June 1971 19 p3277 N71-31231
- Bibliographies of aeronautical engineering, design, production, evaluation, operation, and performance of aircraft and associated components equipment, and systems [NASA-SF-7037/04] 19 p3272 N71-31263
- Bibliographies on nuclear mathematics and technology of eastern countries [AED-C-12-34] 19 p3298 N71-31477
- Annotated bibliographies of reports relating to design and improvement of National Airspace System 19 p3193 N71-31615
- Cross-referenced directory of reports of Human Engineering Laboratories 1953 to 1970 19 p3047 N71-31617
- Goodway and cartography - bibliography [AD-723428] 19 p3065 N71-31810
- Bibliography of Arctic regions water resources [PB-190648] 19 p3085 N71-31818
- Chemical information systems including information input techniques, retrieval, dissemination, and publication bibliographies [JPRS-53523] 19 p3194 N71-31976
- Literature analysis including information aging and bibliography of books and periodical publications pertinent to chemistry 19 p3194 N71-31979
- Basic secondary publications on chemistry and chemical engineering promoting international cooperation in information dissemination 19 p3194 N71-31981
- Advantages and disadvantages of information retrieval techniques on organic chemical reactions 19 p3195 N71-31983
- Analog to digital converters for voice signal analysis [JPRS-53606] 19 p3042 N71-32009
- Problems of automatic auditory pattern recognition and solutions 19 p3042 N71-32010
- Analog to digital converters for description and recognition of voice signals 19 p3042 N71-32011
- Bibliography of structural mechanics computer programs [AD-723178] 19 p3188 N71-32026
- Annotated bibliography of aerosols and particle characteristics of air pollutants [AD-723980] 19 p3092 N71-32030
- Internal aerodynamics design manual considering internal air flow system effect on aircraft performance including bibliography 19 p3173 N71-32059
- Bibliography on fuel- and propellant-tanks [AD-723928] 19 p3172 N71-32074
- Annotated bibliography of selected wideband laser communications literature [AD-723834] 19 p3095 N71-32130
- Bibliography of oceanographic research in Pacific Ocean [AD-723848] 19 p3093 N71-32152
- Bibliography on industrial weatherproofing processes [AD-723861] 19 p3105 N71-32176
- Annotated bibliography on recent developments in radioisotopic decontamination of buildings, equipment, and personnel 19 p3152 N71-32202
- Bibliography of scientific publications and presentations relating to planetary quarantines for year 1970 - Vol. 5 [NASA-CR-121325] 19 p3044 N71-32231
- Injuries and sickness caused by radiation and radioactive decay - bibliographies [AD-722976] 19 p3044 N71-32239
- Desert climatology and geomorphology - bibliographies [AD-722962] 19 p3093 N71-32240
- Mercury lamps - bibliography [AD-722860] 19 p3105 N71-32241
- Models for using vortices for fluid dynamic containment of gaseous core nuclear reactor, bibliography [NASA-CR-1772] 19 p3079 N71-32276
- Associative or content addressable memory systems - overview, bibliography, and KWIC index [NASA-CR-119779] 19 p3062 N71-32459
- Annotated bibliography and indexes on aeronautical engineering and aerodynamics - May 1971 [NASA-SF-7037/05] 19 p3053 N71-32511
- Automation and technological change and future studies - bibliographies [P-3365-4] 19 p3198 N71-32573
- Annotated bibliographies on protective coatings and treatments for industrial processes [AD-722988] 19 p3121 N71-32671
- Tubes and bibliographic survey for BOMEX project [NASA-CR-119763] 19 p3201 N71-32765
- Bibliography of BOMEX papers and publications 19 p3201 N71-32767

- Annotated bibliography on emission sources in electric power plants and air pollution effects 20 p3255 N71-32891
- Bibliography of Canadian geomagnetism and aeronomy studies 20 p3255 N71-32914
- Annotated bibliography on photography [AD-724510] 20 p3256 N71-32950
- High lift aerodynamic and propulsion system configurations for short takeoff aircraft design - bibliographies [AD-724186] 20 p3209 N71-33015
- Test data reduction and prediction techniques for high lift aerodynamic and propulsion system configurations for short takeoff aircraft design - bibliographies [AD-724183] 20 p3209 N71-33016
- Bibliographies and abstracts on air pollution emission sources - sulfuric acid manufacturing [AP-93] 20 p3237 N71-33026
- Annotated bibliography and indexes on aeronautical engineering and aerodynamics - May 1971 [NASA-SF-7037/06] 20 p3204 N71-33036
- Bibliography of literature on environmental pollution, noise pollution, and ear protection devices [AD-724650] 20 p3236 N71-33088
- Bibliographies on Japanese, German, and Italian military aircraft during Second World War [RAE-LIB-BIB-312] 20 p3210 N71-33162
- Annotated bibliography and indexes on aeronautical engineering and aerodynamics - July 1971 [NASA-SF-7037/07] 20 p3205 N71-33174
- Bibliography on effects of gamma rays, fission fragments, and neutrons on organisms, food, tissues, and nervous system [AD-724688] 20 p3219 N71-33276
- Annotated bibliography on chemistry of radiation effects on organic, inorganic, and polymeric compounds [AD-723940] 20 p3229 N71-33277
- Literature survey and bibliography on noise pollution including sources, effects, and control [AD-724344] 20 p3311 N71-33315
- Bibliography of technologies, social systems and environment [P-4541] 20 p3370 N71-33417
- Bibliographies of air pollution emission sources created by municipal incineration [AP-92] 20 p3268 N71-33787
- International bibliography on terrestrial life research 20 p3268 N71-33839
- Annotated bibliography of aeronautical and mechanical engineering and test reports - Jan. 1971 20 p3371 N71-33948
- Annotated bibliography on use of optical radar techniques and devices in radar detection systems [AD-723930] 20 p3237 N71-33998
- Annotated bibliography on noise pollution-sonic booms [AD-722910] 21 p3376 N71-34023
- Annotated bibliography of data compression and data compaction from information theory literature [AD-723525] 21 p3395 N71-34165
- Key word in context index and bibliography on computer systems evaluation techniques [NASA-CR-121757] 21 p3398 N71-34183
- Bibliography on irradiation behavior of plastics [JUL-BIBL-15] 21 p3443 N71-34499
- Bibliography and KWIC index on mechanical theories proving and its applications [NASA-CR-121648] 21 p3446 N71-34525
- Annotated bibliography on radiation effects on semiconductor and non-semiconductor materials and devices, reliability and radiation hardening, and radiation model studies [TDCE-56709] 21 p3477 N71-34762
- Bibliographies of Atomic Energy Literature [TD-3762] 21 p3534 N71-35191
- Bibliography of remote sensor applications and study of earth resources using airborne and earth satellite techniques 22 p3577 N71-35479
- Bibliography of reports on aspects of physical quality of hot rolled steel strip 22 p3593 N71-35587
- Safety aspects of nuclear reactor design, materials, engineered safeguards, and operating procedures - bibliography [TID-3525-REV-5-SUPPL-4] 22 p3426 N71-35834
- Bibliography on ion implantation technology [JC-B-7161-6] 22 p3646 N71-35998
- Bibliography of publications and compilation of abstracts on Explorer 33 and 35 satellites 22 p3643 N71-36130
- Bibliography of nuclear reactor applications for heat pipes [AAEC/LIB/BIB-264] 22 p3695 N71-36349
- Electronic educational information dissemination and broadcast services in US including historical development and infrastructure - bibliography [NASA-CR-121910] 22 p3698 N71-36374
- Annotated bibliography and indexes on aeronautical engineering and aerodynamics - August 1971 [NASA-SF-7037/08] 23 p3706 N71-36420

- Annotated bibliography and indexes on Aerospace Medicine and Biology - Aug. 1971 23 p3716 N71-36428
- Annotated bibliography and indexes on Aerospace Medicine and Biology - Sept. 1971 [NASA-SF-7011/09] 23 p3716 N71-36429
- Annotated bibliography of theoretical papers relating to steady inviscid external transonic flows [NASA-TM-X-2363] 23 p3744 N71-36428
- Bibliography of vacuum in forced convection heat transfer in uniform and nonuniform flow systems [AAEC/LIB/BIB-286] 23 p3794 N71-36429
- Research summaries and publications for 1970 from University of New South Wales 23 p3869 N71-36429
- Annotated bibliography and indexes on aeronautical engineering and aerodynamics - September, 1971 [NASA-SF-7037/09] 24 p3872 N71-36429
- Digital computer bibliography, processing techniques and applications, and software manual, standardization and reliability [AD-727645] 24 p3896 N71-3776
- Bibliography of fusion products in fast reactors and their methods of measurement [CEA-BIB-195] 24 p3963 N71-3808
- Bibliography of abstracts concerning plasma, neutron stars, black holes, and cosmic ray secondary [TID-3520-SUPPL-1] 24 p4013 N71-3808
- Soviet technical literature relevant to explosion, soil mechanics, laser and particle beams, and treaty problems - bibliography [AD-727584] 24 p4035 N71-38078
- ### BICARBONATES
- ### U CARBONATES
- ### BILLETTS
- Jet impingement technique for rapidly heating and billeting [DIS/1/69] 02 p3043 N71-31536
- Radiographic nondestructive testing method in titanium billets for engine disk forging 02 p3032 N71-31609
- ### BIMETALS
- Application of spiral, bimetallic strip to create similar motion on mechanical shaft by change of temperature in the strip [NASA-CASE-NPO-11263] 21 p3403 N71-3801
- Thermal compensating structural member, coupling of bimetallic housing, compensator stem, and compensating drive linkage [NASA-CASE-MPS-20433] 21 p3432 N71-3803
- Influence of diffusion during heating on bond strength between bimetal layers [NLL-M-21017-3582AF] 24 p3941 N71-38115
- ### BINARY ALLOYS
- Investigating interdiffusion of W-Ta, W-Mo, and W-Nb systems in refractory temperature range [NASA-CR-111593] 04 p3030 N71-3468
- Marine transformation in Ti-Ni alloys has stabilizes caused by temperatures above 1800 K [COO-588-19] 03 p3031 N71-3484
- Mechanism superconductivity and superconductivity above and below Kondo temperature for LaCo system [IS-T-405] 05 p0733 N71-1383
- Superconductivity of intermetallic vanadium alloys and nickel-aluminum alloys [CAL-T-622-13] 07 p085 N71-1382
- Epitaxial sublimation methods for producing binary semiconductor alloys such as lead selenide in ultrahigh vacuum [AD-716211] 09 p1453 N71-3089
- Epitaxial sublimation methods for studying pseudo-binary semiconductor alloys [AD-716210] 09 p1453 N71-3089
- Sodium solubility of silver, cadmium, indium, tin, and antimony individually and in combination for silver binary sodium alloy studies [BNL-36271] 10 p1511 N71-3003
- Mathematical models for solid molecular diffusion in binary alloys and Kirkendall effect 10 p1635 N71-3110
- Electrolytic deposition of binary and ternary alloys on copper and chromium-nickel surfaces [NLL-TRANS-746-501-79822.401] 10 p1386 N71-3088
- Dependency of air-hardening of binary boron steels on boron content [NLL-TRANS-544-5286.6] 11 p1770 N71-3209
- Noble-metal binary alloy friction experiments in sliding contact with iron and alloy free energy of formation effects on friction and wear [NASA-TN-D-6311] 12 p1906 N71-3310
- Digital computer programming for phase diagrams in binary, ternary, and quaternary alloys [NPL-DCS-9] 13 p0892 N71-3089
- Gilbre free energy, enthalpy, and entropy of binary metal alloys [NPL-DCS-16] 15 p2534 N71-3089
- Statistical thermodynamics of vacancies in binary alloys using Ising model 16 p2609 N71-3089
- Mechanical properties of pure binary Ni-Cr alloys at high and low temperatures [NLL-TRANS-746-499-79822.401] 17 p3784 N71-3809

SUBJECT INDEX

Soviet research on binary alloy phase diagrams 18 p2354 N71-30688

Magnetic coupling and phase boundaries determined for series of pseudo binary alloys of C15 and 22 elements containing lanthanides 19 p3171 N71-32642

BINARY CODES

Time division relay synchronizer with master sync pulse for activating binary counter to produce signal identifying time slot for station 09 p1349 N71-19773

Optimum, simple binary nonredundant code for self information transmission in asynchronous channel consisting from linear error 10 p1329 N71-21332

Surveillance system MERMES and MAOIC for binary code system library tapes used by MC sup 2 multi-track tape section code 11 p1804 N71-22332

Binary code symbol transformations testing code 12 p1948 N71-23447

Logic circuit for generating multiple binary code used in parallel 14 p2323 N71-36183

Differential calculus applied to discrete Walsh-Hadamard functions, making techniques for binary codes 15 p3434 N71-37033

Design and development of encoder/decoder system to generate binary code which is function of outputs of binary logic elements 20 p3243 N71-33407

BINARY DATA

High accuracy time function generator using digital timing converter and field effect transistors 02 p1883 N71-11362

Optimum binary signals for frequency response tests 07 p1060 N71-17189

Logic circuit to ripple add and subtract binary numbers for synchronous counter 08 p1164 N71-18682

Sampling circuit for obtaining sum of squares of numbers 09 p1165 N71-18695

Digital synchronizer for extracting binary data in master of PSE/PCM communication system 13 p3643 N71-34613

Binary classification reaction time and human performance in data processing using decision making elements 15 p2374 N71-36885

Algorithms for solving set of linear inequalities expressed in binary variables 18 p2462 N71-30534

BINARY DIGITS

Minimal semantic resolution proofs based upon binary semantic trees 01 p0829 N71-10796

Binary number series for arranging numbers in order of magnitude 03 p0344 N71-12592

Binary sequence detector with low memory elements and minimum logic circuit complexity 09 p1357 N71-38571

Characteristics of computer circuits for comparison of binary numbers in information processing systems 12 p1881 N71-23295

Algorithms for labeling, counting, and comparing sorted objects in binary three dimensional array 17 p2774 N71-36217

Binary sequences with specified correlation properties 22 p3585 N71-35674

BINARY FLUIDS

Concentration effects on Gibbs free energy and activity of mixing of binary fluids 07 p1128 N71-17210

Thermodynamic channel flow stability of oil and water in porous media: flow profiles, disturbance amplitudes, distribution, amplification rate, and wave speed and direction 10 p1184 N71-19590

Mass transfer during binary liquid drop growth at constant capillary tubes 16 p2579 N71-28235

BINARY INTEGRATION

Binary decision graph for analyzing validation of complex information processing models 04 p0499 N71-13493

BINARY MIXTURES

NT BINARY FLUIDS

NT EUTECTIC ALLOYS

NT EUTECTICS

Relation of viscous shock layer equations for binary mixtures of oxygen atoms and molecules 05 p0548 N71-12586

Thermodynamic of colloidal azeotropic binary systems with magnesium, boron or calcium 07 p1129 N71-17332

Molar enthalpy and entropy calculations for elements of liquid phase binary systems 13 p2187 N71-25355

Thermal conductivity and viscosity measurements in binary liquid mixtures and vapor phases near critical points 15 p2395 N71-27780

Derivation of 1/omega can rules from two component uniform many body systems and large range correlations in binary solutions 18 p2996 N71-31566

Measurements of complete pool boiling heat transfer characteristics for binary mixtures and comparison with predicted results to determine parametric effects of mixture composition 20 p3367 N71-33782

Determination of pressure-temperature-composition relations of chromium-aluminum binary system by thermogravimetric technique 20 p3369 N71-33999

Stimulated Rayleigh-type light scattering in binary gas mixtures from local fluctuations and concentration 23 p3804 N71-37121

Heat exchange, theoretical considerations on cooling, and dependence of heat exchange on state of two-phase mixture in post-burnout reaction 24 p4028 N71-38748

BINARY STARS

NT ECLIPSING BINARY STARS

Astrometric tables of double stars 02 p0295 N71-11929

Computing catalog of visual binary stars with astrometric and hyperbolic orbits 05 p0767 N71-15137

Spectroscopic study of visual binary stars with B-type primaries 06 p0948 N71-16830

Data correlation for theoretical and empirical observations on compact binary systems spectral reflexions 10 p1645 N71-21515

Visual binary stars used to compare external errors and systematic differences in K line, line ratio, and H sub gamma luminosity systems 16 p3680 N71-28789

Frequency of double stars in extended solar system 20 p3330 N71-33643

BINARY SUBMATORS

U ADDING CIRCUITS

BINARY SYSTEMS (DIGITAL)

U DIGITAL SYSTEMS

BINARY SYSTEMS (MATERIALS)

NT BINARY ALLOYS

NT BINARY FLUIDS

NT BINARY MIXTURES

NT EUTECTIC ALLOYS

NT EUTECTICS

Thermodynamic properties of phase equilibria in binary and ternary systems 05 p0638 N71-14644

Investigating phase equilibria, electrical conductance, and density in system ZnCl₂ at low temperature using of SnO₂ and Bi₂O₃ system 05 p0711 N71-15584

Applying fundamental concepts of thermodynamics of irreversible processes to acoustic wave propagation in two-phase steam media 07 p1067 N71-17011

State diagram of system Dy₂O₃-Cr₂O₃ 07 p1041 N71-17134

Method for determining dispersion relations in fiber reinforced binary composite materials based on Fourier series and equations of motion 10 p1389 N71-21319

Melting point-composition and phase diagrams of thallium-iodine systems and X ray powder patterns of TlI and Tl₂I₂ 11 p1784 N71-22498

Interfacial tension in binary liquid system as function of temperature 11 p1739 N71-22584

Diffusion in two phase alloys 14 p2271 N71-25693

Metallurgical and elastic model measurements on two phase isotropic microstructures 17 p2765 N71-29885

Equations deduced relating interdiffusion coefficients of binary liquid systems with composition of system, component diffusivity coefficients, and various system parameters 18 p2806 N71-31836

Effect of particle spatial distribution on thermal conductivity of two-phase systems 18 p2948 N71-31252

Laves phases in iron binary systems with transition elements and dispersed precipitates 18 p2957 N71-31396

Construction of metallurgical phase diagrams to show eutectic equilibrium of chromium, niobium, ruthenium, and molybdenum alloys 21 p3442 N71-34492

Thermodynamic and solid state properties of manganese selenide-selenic selenide system determined from high purity single crystals 21 p3390 N71-34957

Computer program for solving two-phase equilibrium data for binary mixtures and thermodynamic functions including critical points based on Van der Waal equations of state 22 p3886 N71-38157

BINARY TO DECIMAL CONVERTERS

Design and operation of high speed binary to decimal conversion system 09 p1332 N71-19564

Binary to decimal decoder logic circuit design with feedback control and display device 13 p3852 N71-34988

BINDERS (ADHESIVES)

BINDERS (MATERIALS)

NT SOLID ROCKET BINDERS

Protein imbedded effects on color transmission of silicone rubber thermal conductive material 05 p1286 N71-18823

Polymer adhesives, optical color cell filter, and fusible antenna construction for interplanetary spacecraft 18 p1389 N71-31349

BINDING

Relativistic scalar quark model of mesons as bound states 19 p3145 N71-31930

K-harmonic method for calculating binding energy and wave functions of H-3 and He-3 neutral 19 p3149 N71-32185

BINOCLULARS

Search effectiveness with straight scope and binoculars 03 p0336 N71-11595

BIOLOGICAL COMPOUNDS

Factorization of dual amplitude and loops in coherent state model with finite set of five dimensional oscillators 14 p2393 N71-30899

BIOLOGICAL THEOREMS

Finding single defective in binomial group testing 04 p0548 N71-14570

BIOLOGICALS

Approximate confidence interval and tests for products and ratios of binomial probabilities with application in investigating and comparing system reliability 14 p2777 N71-30889

BIOACOUSTICS

Ultrasonic bioacoustic research and its results and insects 06 p0880 N71-16049

UE-IP helicopter acoustic measurements during gunfire and rocket firing including bioacoustic factors 19 p3642 N71-31613

BROADBAND

Electron microscope analysis of biological materials 01 p0184 N71-10750

Establishing detection limits for emission spectrometric approach in determination of trace metals in biological materials 03 p0331 N71-12339

Construction of unique underground whole body counter - counter 07 p1061 N71-17213

Bacterial thermodynamic equilibrium models and computerized binary system for Apollo biological data 07 p0985 N71-18026

Possibility of computerized bacterial identification 08 p1152 N71-19817

Possibility of binary spacecraft models for space station 15 p2319 N71-27188

Automatic binary instrument for analysis based on ultrasonic triphosphate bioacoustic proportionality to water content bacterial content 15 p2373 N71-27992

Procedures and interrelationships techniques for screening Apollo aquatic test animals for bacterial poisons after lunar sample exposure 17 p2797 N71-30528

BROADBAND

Nerve mechanisms of vestibular reactions - Soviet aerospace biology research 01 p0811 N71-10390

Lectures in aerospace medicine 02 p0133 N71-11085

Aerospace medicine and bioacoustic countermeasures 02 p0136 N71-11188

Bioacoustic aspects of Apollo biological operations 03 p0164 N71-11821

Physiological effects of 10 day space flight on crew of Soyuz-9 03 p0123 N71-12588

Biomedical effects of weightlessness and confinement on man and other organisms 06 p0881 N71-16288

- Transactions on space biology and medicine
[JPRS-52121] 06 p1153 N71-19051
Proceedings summary for meeting on aviation and space medicine research 06 p1156 N71-19076
Summary data on aviation and space medicine research 06 p1156 N71-19077
Consideration of bioastronautics and biological exploration of space for determination of extraterrestrial life and origin of life on earth 09 p1334 N71-20187
[NASA-TT-F-13467]
Spacecraft water reclamation and closed self contained biological cycle-closed ecological system techniques in USSR and US 12 p1866 N71-23376
[NASA-TT-F-13634]
Bioastronautical problems of orbital stations 20 p3370 N71-35474
Activation analysis of fecal samples from Apollo 7, 8, 9, and 10 astronauts to determine effects of space flight on mass balance of various elements by human body 21 p3381 N71-34058
Measurement of radiation exposure of Apollo 7, 8, 9, and 10 astronauts by determination of radioisotopic content of feces and urine 21 p3381 N71-34059
[NASA-TT-F-13666]
BIOCHEMICAL FUEL CELLS
Polarization and energy conversion efficiency of yeast and *Bacillus lactis* fermentation for biochemical fuel cells 14 p2205 N71-26245
Design and fabrication of flight-concept prototype electrochemical water recovery subsystem 23 p3718 N71-36507
[NASA-CR-111961]
BIOCHEMISTRY
NT BACTERIOLOGY
NT BIOGEOCHEMISTRY
NT ENZYMOLOGY
NT PHYSIOCHEMISTRY
Proceedings summary for symposium on bio-organic chemistry 02 p0173 N71-11217
[JPRS-51782]
Biochemical regulation of sleep-wake and temperature cycles in monkeys 02 p0165 N71-11828
Nutritional quality of *Hydrogonomonas entomophila* protein 03 p0326 N71-12326
[NASA-CR-111599]
Biochemistry of growth, gametogenesis, and fertilization in algae 05 p0635 N71-14722
[NYO-3473-24]
Methods for studying biochemical properties of bacteria 08 p1149 N71-18792
Biochemistry model for endocrine system effects on mammalian neurophysiology and human behavior 09 p1332 N71-19887
Purification and characterization of enzymes from *H. salinarum*, *H. stearothermophilus*, and *V. marisii* (RLO-2227-T-5-1) 10 p501 N71-21527
Escherichia coli cell phospholipid composition changes during sporulation formation in presence of penicillin and sucrose 11 p1683 N71-22506
[NASA-TT-F-13488]
Cytoskeletal detection of lactic dehydrogenase isoenzymes in free-living *Protona* 12 p1862 N71-23382
[NASA-TT-F-13624]
Development of separators using centrifugal force and used in agriculture and biochemistry 13 p2189 N71-24464
Separation methods such as centrifuging, ion exchange, electrophoresis, and chromatography applied to biochemical materials (gels, proteins, amino acids) 13 p2032 N71-24466
Biochemistry, molecular biology, radiochemistry, meteorology, soil science, and water pollution research and development and environmental engineering 13 p2033 N71-24489
[ARCL-3728]
Chemical and biochemical space manufacturing using scaling laws and Gibbs functions 14 p2261 N71-26013
Trends and possibilities in biochemistry, biotechnology, geology of minerals, earth resources, and man machine systems 18 p3028 N71-30839
Trends and possibilities in biochemical and biotechnical in medical science 18 p2875 N71-30840
Differential thermal analysis methods in high temperature research on biochemical, polymeric and explosive materials 20 p3361 N71-32826
[NBS-39-334]
Preparation of biochemical materials for electron microscopy 20 p3215 N71-32948
[ISS-7614]
Physics, chemistry, biochemistry, mathematics, reactors, and radiation safety research and development 21 p3532 N71-35170
[US-253]
Gas chromatograph, mass spectrometer system for chemical and biochemical determinations on Mars, and data reduction program 22 p3583 N71-35514
[NASA-CR-12036]

Hematological program and biochemical data from Gemini and Apollo missions

- 25 p3711 N71-36455
Reproducibility of gas chromatographic biochemical data and values in toxicology 24 p3079 N71-37653
[AD-727523]
Mechanism of water decomposition during process of photosynthesis related to biological oxidation and chlorophyll 24 p3085 N71-37680
[NASA-TT-F-14018]
Human acclimatization to high altitudes, monsoons, and hot, dry weather 11 p1679 N71-22001
[JPRS-52594]
Seasonal variations in physiology of old-timers and newcomers in monsoon climate 11 p1679 N71-22002
Seasonal variations in thermoregulation of residents in hot, dry climates with respect to age and sex 11 p1679 N71-22003
Phenological survey in *Grewia* to determine the correlation between life cycles of plants and prevailing meteorological and climatic factors 13 p2105 N71-24439
[AD-719728]

BIOCONTROL SYSTEMS

- Development of theory for formal nervous as mathematical basis for creation of highly reliable cybernetic systems and computers 19 p3061 N71-32015

BIODYNAMICS

- Use of computers for man machine modeling status and plans 01 p0015 N71-10080
[AD-711638]
Flight simulator tests of human behavior in roll tracking tasks in fighter and large aircraft with descriptive functional analysis 09 p1339 N71-19751
[NAL-TR-266]
Dynamic models of human body response to acceleration environments and determination of tolerance limits 10 p501 N71-21598
[NASA-TM-X-67038]
Biodynamics, aerospace medicine, acceleration stresses, human tolerances, centrifuges, test facilities, and associated bibliography 12 p1865 N71-23337
[AGARDGRAPH-150]
Equipment and facilities for biodynamic research in US and Canada 12 p1896 N71-23342
Equipment and facilities for biodynamic research in NATO European countries 12 p1896 N71-23343
Annotated bibliography of worldwide biodynamics research findings 12 p1866 N71-23344
[NASA-TM-X-67138]
Four degree-of-freedom lumped parameter model for vertical accelerations of seated human body as might be imposed by aircraft ejection systems 15 p2370 N71-26944
[AD-721225]
Biodynamic evaluation of air traffic control students from 1960 to 1963 16 p2549 N71-28005
[FAA-AM-71-8]
Biomechanics protocol for evaluating effects of environment on biological systems, including metabolic effects of different gases and oxygen toxicity 16 p2542 N71-28183
[NASA-CR-118955]

BIOELECTRIC POTENTIAL

- Changes in bioelectric potentials in brains of rabbits subjected to X ray irradiation and acceleration on centrifuge 08 p1156 N71-19094
[JPRS-52488]
Telemetric equipment for pulse code modulation and processing of biomedical data 10 p1504 N71-20683
[SI-PUBL-419]
Radial acceleration effects on spinal cord induced potentials of intact and labyrinthectomized rats 20 p3220 N71-33456
BIOELECTRICITY
Existence of electric and magnetic field component associated with transmission of neuronal impulse studied in isolated sciatic nerves of frogs 13 p2034 N71-25240
[NASA-CR-118334]
Development and characteristics of electrodes in which poisoning by organic molecules is prevented by ion selective electrolytic deposition of hydrophilic protein colloid 14 p2228 N71-26002
[NASA-CASE-XMS-04213-1]
Analysis of the effects of regional blood circulation on intensity of muscular response to stimulus 16 p2547 N71-28496
Theoretical model for neuroelectric oscillation modes in arbitrary number of nerve cells arranged in single closed loop 20 p3343 N71-33217
[R-642-BC]

BIOENGINEERING

- NT ANTHROPOMETRY
NT BIODESIGN
NT BIOMECHANICS
NT BIOTELEMETRY
NT CARDIOGRAPHY
NT ELECTROCARDIOGRAPHY
NT ELECTROENCEPHALOGRAPHY
NT ELECTRORETINOGRAPHY
NT PLETHYSMOGRAPHY
Types of biological indicators used in monitoring sterilization processes 02 p0168 N71-11192
[TR-34]

Biological control systems analysis

- 04 p0483 N71-14020
Realizable gain matrices for N-legged machines 06 p0807 N71-14001
[AD-714592]
Mechanical theory for legged locomotion systems 06 p0807 N71-14002
[AD-714591]
Dynamic stability of legged locomotion systems 06 p0807 N71-14003
[AD-714589]
Design and characteristics of artificial heart control system 07 p0906 N71-17009
[NASA-TN-D-6171]
Technology assessment of research in biological medical engineering including problem areas 10 p1499 N71-20008
[NASA-CR-117407]
Review on biometric and interdisciplinary engineering areas in aerospace research 11 p1092 N71-20009
Investigation of application of NASA developed technology to cardiovascular and pulmonary patient monitoring to improve availability of data for medical diagnosis 12 p1868 N71-23398
[NASA-CR-118030]
Program plans and cost estimates of project for application of bioelectronic technology to patient monitoring system 12 p1868 N71-23399
[NASA-CR-118033]
Semiconductor devices, quantum electrodynamics, lasers, defects in crystals, communication and other systems, bioengineering, plasmas, and other related subjects - continuing report 13 p2108 N71-24440
[AD-718927]
Standard transducers applied to bioengineering research problems 14 p2211 N71-26006
Biotechnological problems of man machine systems required for long duration space flights 16 p2551 N71-28018
[NASA-RP-205]
Development of theory for formal nervous as mathematical basis for creation of highly reliable cybernetic systems and computers 19 p3061 N71-32016

Technology utilization in biomedical areas, particularly for infants and handicapped persons

- 21 p3383 N71-34060
[NASA-CR-121627]
Development and characteristics of bioelectric system for obtaining electroencephalogram and neurophysiologic data during space missions 22 p3547 N71-35188
[NASA-CR-115132]
Enzyme reaction model of flow diffusion effect in blood coagulation in vivo 23 p3713 N71-36408
[NASA-CR-122529]
Determination of electrical charge and field strength at cell membrane of human erythrocytes 24 p3877 N71-39326
[NASA-TT-F-14007]
BIOGENESIS
U BIOLOGICAL EVOLUTION
BIOGENY

Microscopic analyses of Apollo 11 lunar rock and dust samples for biological activities

- 07 p1113 N71-17778
BIOGEOCHEMISTRY
Biogeochemical and microstructural analysis on lunar rock and dust samples for biological compounds 07 p1113 N71-17779
[NASA-CR-114839]
Microscopic analyses of Apollo 12 lunar samples for biogenic structures 07 p1113 N71-17780

Microscopic analyses of Apollo 11 lunar samples for biogenic structures

- 07 p1113 N71-17779
Biogeochemical analysis on lunar dust sample for organic compounds 07 p1113 N71-17780

Biogeochemical detection of organic matter in Precambrian charts

- 07 p1030 N71-17771
[PUBL-693]
Radiation shielding and biogeochemical process and their relevance for earth preservation 23 p3730 N71-36735
[JPRS-54091]

BIOINSTRUMENTATION

- NT BIOTELEMETRY
Electrode attached to helminths for detecting low level signals from skin of living creatures 02 p0168 N71-11195
[NASA-CASE-ARC-10043-1]
Characteristics of pressed disc electrodes for biological measurements 03 p0329 N71-12546
[NASA-CASE-XMS-04212-1]
Monitoring cardiovascular function in patients using prolonged vital electrodes 05 p0633 N71-14033
[NASA-CR-75400]
Sensing arrays using concept of involuntary human eye motion with application to photogrammetry and metrology 05 p0804 N71-14008
[AD-713568]
Development of avalanche type semiconductor radiation detector 06 p0801 N71-14007
[NYO-3366-TA-7]
Application of image intensifiers developed in high energy physics to space problems in biology 06 p0799 N71-13904
[FURC-6159-1]
Biomedical technology applications and operational descriptions of Application Team Program 06 p0803 N71-14009
[NASA-CR-116136]
Psychological stress and bioinstrumentation 07 p0901 N71-17008

SUBJECT INDEX

Operational description of Summer Institute for Biomedical Research in Technology Utilization
[NASA-CR-116416] 07 p0096 N71-17344

Describing biotechnology for monitoring in-flight physiological functions of Soyuz 9 crew members
08 p1150 N71-18001

Brain gaps testing element for measuring skeletal muscle contraction
08 p1156 N71-18074

Biomedical respiratory flowmeters and electronic instrumentation technology for measurement and analysis of metabolic quantities
[NASA-CR-114905] 09 p1540 N71-17776

Analysis of water flow around living sharks based on flow visualization and body attached flow sensor velocity profiles
12 p1808 N71-23192

Development of apparatus and method for quantitatively measuring brain activity as automatic indication of sleep state and level of consciousness
[NASA-CASR-MSC-13282-1] 13 p0307 N71-24729

Development and characteristics of electrodes in which poisoning by organic molecules is prevented by an selective electrolytic deposition of hydrophilic amino collod
[NASA-CASR-XMS-04213-1] 14 p2228 N71-26092

Radioactive equipment used in Interception Landing System, and results in remote ground, aircraft, and satellite tracking of alt and black box
[NASA-CR-121895] 22 p3546 N71-35260

Development and characteristics of biomedical system for obtaining electroencephalogram and neurophysiologic data during space missions
[NASA-CR-115152] 22 p3547 N71-35263

BIOLOGICAL ACTIVITY
U ACTIVITY (BIOLOGY)
BIOLOGICAL ANALYSIS
U BIOASSAY
BIOLOGICAL CELLS
U CELLS (BIOLOGY)
BIOLOGICAL EFFECTS
U RELATIVE BIOLOGICAL EFFECTIVENESS (RBE)
Annotated bibliography and indexes on Aerospace Medicine and Biology - Sept. 1970
[NASA-SP-7011/09] 01 p0008 N71-10125

Biological effects of radiation and mechanism of genetic and metabolic acid synthesis
[BUX-3645-49] 01 p0012 N71-10613

Increasing decrease in concentration of adenosine triphosphate in brain of rats before onset of convulsions induced by hypoxia
[AD-772432] 02 p0158 N71-11122

Neurologic flight data of weightlessness effects on biological systems
02 p0161 N71-11711

Investigating experimental and theoretical approaches to microelectroscopy, radiobiology, and single-unit stimulation systems
[NASA-CR-111626] 03 p0321 N71-12295

Model case studies of effects of DDT on human cells
[PB-194413] 04 p0481 N71-14479

Biological effects of microwaves in occupational hazards
[NASA-TT-F-633] 05 p0633 N71-14632

Toxicity and safety hazards research
[AD-774046] 06 p0799 N71-15942

Influence of electromagnetic force fields on biological systems studied on drosophila and ciliates
[AD-774071] 06 p0801 N71-16350

Weightlessness effects on man during space flight
06 p0805 N71-16321

Experimental evaluation of radiation hazard to man during prolonged space flight
06 p0842 N71-16322

Annotated bibliography and indexes on Aerospace Medicine and Biology - Nov. 1970
[NASA-SP-7011/03] 07 p0082 N71-12449

Annotated bibliography and indexes on Aerospace Medicine and Biology - Dec. 1970
[NASA-SP-7011/04] 07 p0082 N71-17450

Investigating effects of thermal environments and safety on growth of bacteria and blue green algae
07 p0905 N71-17900

Biological effects of thermal environments on growth of blue green algae and microorganisms in Iceland and Surtsey
07 p0903 N71-17909

Investigating biological effects of cold thermal stress on growth of organisms in Iceland
07 p0903 N71-17900

Investigating proliferation of insect life in harsh environments of Iceland and Surtsey
07 p0904 N71-17901

Investigating inhibitory activity of lichens on growth of root plants and ferns
07 p0904 N71-17906

Literature review on biological effects of microwaves
[UR-48-1256] 08 p1148 N71-18495

Investigating physiological and biological effects of prolonged space flight on Soyuz 9 crew members
[JPRS-52402] 08 p1149 N71-18004

Determining hemopoietic, cytological, and immunological parameters of simulated long term exposures to space radiation
08 p1150 N71-18006

Investigating long term effects of proton irradiation on ventral posterior anatomy of dogs
08 p1150 N71-18007

Determining functional changes in physiological responses of Soyuz 9 crew members after prolonged flight
08 p1151 N71-18003

Ionizing radiation effect on biological properties of food products
08 p1154 N71-19083

Effect of low power density modulated radio frequency energy on biological functions
[AD-71-0644] 09 p1330 N71-19671

Biological system analysis and biodynamic modeling of physiological and biological interrelationships in human body and mammals
[NASA-CR-1720] 09 p1330 N71-19076

Hierarchical regulation model for human biological systems
09 p1331 N71-19079

Biological and optical contamination effects in space simulating vacuum chamber
09 p1334 N71-36094

Annotated bibliography and indexes on Aerospace Medicine and Biology - Feb. 1971
[NASA-SP-7011/06] 12 p1064 N71-24174

Annotated bibliography and indexes on Aerospace Medicine and Biology - March 1971
[NASA-SP-7011/07] 14 p2203 N71-25745

Biological and therapeutic effects of magnetic fields on human organisms
[JPRS-53091] 14 p2597 N71-26327

Biomechanical protocol for evaluating effects of environment on biological systems, including metabolic effects of different gases and oxygen toxicity
[NASA-CR-110955] 16 p2542 N71-28183

Annotated bibliography and indexes on Aerospace Medicine and Biology - Apr. 1971
[NASA-SP-7011/08] 18 p2876 N71-30856

Frequency distributions of event size in deposition of energy over small pathlengths measured after penetration of 44.3 MeV protons through thicknesses of tissue-like material
[NASA-CR-111943] 18 p2904 N71-31093

Annotated bibliography and indexes on aerospace medicine and biology - May 1971
[NASA-SP-7011/09] 18 p2876 N71-31201

Annotated bibliography and indexes on Aerospace Medicine and Biology - May 1971
[NASA-SP-7011/10] 18 p2876 N71-31230

Annotated bibliography and indexes on Aerospace Medicine and Biology - June 1971
[NASA-SP-7011/11] 18 p2877 N71-31251

Technique for estimating maximum internal dose rate to man from continuous release of radionuclides to biosphere
[UCRL-50163-PT-7] 18 p2878 N71-31499

Air pollution sources, distribution, biological effects, and mathematical models
[AD-7571] 20 p3261 N71-33299

Biological effects of magnetic fields on development of pupae of fruit flies and embryos of marine algae
23 p3715 N71-36484

Annotated bibliography and indexes on Aerospace Medicine and Biology - Aug. 1971
[NASA-SP-7011/12] 23 p3716 N71-36480

Annotated bibliography and indexes on Aerospace Medicine and Biology - Sept. 1971
[NASA-SP-7011/13] 23 p3716 N71-36491

Radiation hazards of space flights and biological effects on components
24 p3679 N71-37649

BIOLOGICAL EVOLUTION
Investigating mechanism by which inorganic and mineral phosphate groups become part of cellular structure
01 p0014 N71-10810

Studying geology, geochemistry, and biology of Iceland and Surtsey as examples of new and extreme environments
07 p1024 N71-17966

Determining transport and climatological factors affecting colonization of life on remote islands
07 p1024 N71-17969

Investigating Surtsey and Iceland as natural laboratories for testing planetary life detection techniques
07 p1024 N71-17973

Investigating effects of lava outpouring on primary colonization by organisms
07 p0904 N71-17993

Investigating algal plain of Icelandic glacier for terrestrial and aquatic plant succession
07 p0904 N71-17994

Considering lack of development of endemic species in Iceland
07 p0904 N71-17995

BIOMEDICAL DATA

Searching for *Proteobacteria* reflect photoregulation in Iceland
07 p0004 N71-17990

Mathematical models of survival of flint during biological evolution
[LA-4573] 12 p1083 N71-30490

Amino acid synthesis by heating formaldehyde and ammonia mixtures in molecular evolution research
[NASA-CR-110011] 12 p1072 N71-30422

Amino acids produced by long UV irradiation of gas mixtures using hydrogen sulfide as initial photosynthetic starting protobacterial earth conditions
[NASA-CR-110309] 13 p0940 N71-30861

Formulation for measuring low field permeability of rocks used to study origin of life
[NASA-CR-110921] 16 p2585 N71-30330

Mathematical models of microbiological production processes
[JPRS-53634] 16 p2577 N71-31271

Development of scientific principles of protecting and transforming nature for improving environment and control use of natural resources
[JPRS-53743] 20 p3223 N71-33561

Analysis and definition of tasks in field of biogeography
20 p3223 N71-33562

Multiple coding mechanism for evolution of genetic code
[NASA-CR-131896] 23 p3543 N71-33537

Biological effects of magnetic fields on development of pupae of fruit flies and embryos of marine algae
23 p3715 N71-36484

Effects of UV selection pressure on evolutionary development patterns of early eukaryotes
[NASA-CR-123193] 24 p3076 N71-37632

Perturbation of UV light in evolution of contemporary ribosomes
[NASA-CR-123164] 24 p3077 N71-37633

BIOLOGICAL MODELS
U BIONICS
BIOLOGY
Nuclear physics, nuclear chemistry, nuclear biology, and applied nuclear technology in Poland
[ABC-TR-76572] 03 p0429 N71-12809

Analysis of conduct and effectiveness of biological research projects of military research facility
[ORNL-TM-3218] 13 p0305 N71-25351

Monitoring techniques for biological and chemical atmospheric contaminants in closed environment
[NASA-CR-1206] 17 p2711 N71-29763

Lectures presented at seminar in various scientific fields
[ISS-70/20] 20 p3310 N71-33161

Role of individual components of biogeosystems in organization of structure and functions
20 p3324 N71-33309

Discussion of photosynthesis process and production of biomass
20 p3324 N71-33310

Articles concerning undergraduate education in biological sciences
[NASA-CR-121726] 21 p3381 N71-34053

Biochemical research and applications to biological and medical problems
[BM-6847-BC] 21 p3385 N71-34082

Hazards associated with laser radiation and radiation used as tool in biology and medicine
24 p3600 N71-37082

BIOLOGICAL SCIENCE
Ultraviolet radiation and high vacuum space environment simulation for biobioscience bacteria
[BMFW-FB-W-70-46] 06 p0799 N71-15724

Detection instrument for light emitted from ATP biochemical reaction
[NASA-CASR-XGS-05334] 06 p0903 N71-16335

Describing method for biophysics of biochemistry containing minimum for use in life detection reactions
[NASA-CASR-XGS-05332] 07 p0900 N71-17705

Radiative decay of supramolecular crystal phosphorescence and chlorophyll fluorescence (bioluminescence including atomic emission biology)
15 p3405 N71-27044

Bioluminescent reaction of adenosine triphosphate with enzyme luciferase for quantitative analysis of bacteria in urine samples
[NASA-CASR-GBC-11092-1] 15 p3573 N71-37991

Automatic laboratory instrument for analysis based on adenosine triphosphate bioluminescent property to make accurate bacterial count
[NASA-CASR-GBC-11149-1] 15 p3573 N71-37992

BIOCHEMISTRY
U BIODYNAMICS
BIOCHEMICAL DATA
Research progress in technology transfer by NASA Biomedical Applications Team
[NASA-CR-111131] 01 p0012 N71-10541

Biomechanical aspects of Apollo biomedical operations
02 p0044 N71-11821

Silicon radiation detecting probe design for in vivo biomedical use
[NASA-CASR-XMS-01177] 09 p1339 N71-19440

- Telemetric equipment for pulse code modulation and processing of biomedical data
[SI-PUBL-619] 10 p1504 N71-20683
- Advanced application of computers for biomedical research in manned space flight
[NASA-SP-5078] 15 p2375 N71-27719
- Biomedical telemetric systems for monitoring physiological parameters of animals
[NASA-SP-5064] 15 p2376 N71-27983
- Compact analytic solution to distribution theory of nonsteady state model illustrated with biological data dependency in compartmental analysis
[NASA-CR-115061] 16 p2620 N71-28002
- Manned 90-day performance test of regenerative life support systems in space station simulator including crew biomedical tests
[NASA-CR-111881] 16 p2554 N71-28877
- Biomedical electronics, information sciences, plasma and quantum electronics, solid state electronics, acoustics, and radio sciences
[AD-722073] 17 p2727 N71-29499
- Automatic monitoring of human operator state in closed, man machine systems with biomedical application
18 p2883 N71-30669
- Biomedical evaluations of cardiovascular and overall physical fitness of air traffic control personnel
[FAA-AM-71-19] 22 p3544 N71-35243
- Use of general purpose digital computers for analysis of biological structures and chromosomes
[JPRS-54035] 23 p3715 N71-36479
- BIOMETEOROLOGY**
U BIOCLIMATOLOGY
- BIOMETRICS**
NT ANTHROPOMETRY
NT CARDIOGRAPHY
NT ELECTROCARDIOGRAPHY
NT ELECTROENCEPHALOGRAPHY
NT ELECTRORETINOGRAPHY
NT PHONOCARDIOGRAPHY
NT PLETHYSMOGRAPHY
- Characteristics of pressed disc electrode for biological measurement
[NASA-CASE-XMS-04212-1] 03 p0329 N71-12346
- Mathematical simulation of biological subjects and construction of systems to control certain functions of biological nature
[JPRS-52300] 06 p0802 N71-16463
- Conference on biometrics noting human psychic and physical stress
[DLR-MITT-70-11] 07 p0980 N71-17237
- Human reactions to mechanical vibrations
07 p0981 N71-17238
- Application of parallel tasks for measuring psychological stress noting pilot performance
07 p0981 N71-17239
- Psychological stress and pilot performance
07 p0981 N71-17240
- Psychological stress and bioinstrumentation
07 p0981 N71-17241
- Utilizing atomic resolution capability of field ion microscope for viewing biomolecules
[NVO-3851-10] 23 p3714 N71-36475
- BIONICS**
Biological control systems analysis
04 p0483 N71-14429
- Induced fields and heating in cranial model irradiated by electromagnetic plane wave
[AD-712845] 04 p0479 N71-14469
- Statistical characteristics of spontaneous electrical activity of nerve units that exhibit stochastic dead time following impulses
[NASA-TM-X-62007] 05 p0635 N71-14917
- Radio signal generation, solid state receivers, information theory, and biological principles in radioelectronics
[AD-714411] 06 p0613 N71-16084
- Two hybrid computer identification techniques for use in manual control research
[NASA-CR-116514] 07 p0986 N71-17442
- Biological systems analysis and biodynamic modeling of physiological and biological interrelationships in human body and mammals
[NASA-CR-1720] 09 p1330 N71-19676
- Biological systems analysis for developing dynamic physiological models
09 p1331 N71-19677
- Physiological and behavioral parameters in design of dynamic human biological system
09 p1331 N71-19678
- Hierarchical regulation model for human biological systems
09 p1331 N71-19679
- Summary of design parameters for models of dynamic biological systems
09 p1331 N71-19680
- Physical controls of autonomic nervous system by ganglia impulses
09 p1331 N71-19683
- Biological models for mammalian cardiovascular systems
09 p1331 N71-19684
- Neurophysiological model for interactions between nervous system, cellular mechanisms, and human behavior synthesis
09 p1332 N71-19686
- Biochemistry model for endocrine system effects on mammalian neurophysiology and human behavior
09 p1332 N71-19687
- Processing of visual imagery by model derived for recognition of visual patterns
[AD-717157] 10 p1503 N71-20603
- Synapsis circuit design and applications in bionics, cybernetics, and electronic robots
[AD-716821] 10 p1504 N71-20735
- Bionics modeling of enzyme analysis of toxic compounds and olfactory system simulation
11 p1686 N71-22065
- Distributed parameter mathematical model of human body in dynamic mechanical environments
[AD-717764] 11 p1696 N71-22130
- Hydrodynamics, marine biology, bionics, dolphins, sharks, porpoises, traveling waves, fluid flow, viscous fluids, nervous system, skin structure, swimming
[JPRS-52605] 11 p1687 N71-22201
- Bionics of living and life-like systems with application to man machine technology
[AGARD-CP-44] 11 p1692 N71-23053
- Review on bionics and interdisciplinary bioengineering areas in aerospace research
11 p1692 N71-23054
- Structures of biological information processing and pattern recognition in living systems
11 p1685 N71-23056
- Pattern recognition and classification in biological systems
11 p1721 N71-23058
- Bionic model for adaptive flight control system
[NASA-CR-117807] 11 p1693 N71-23060
- Social and industrial applications of learning response patterns
11 p1721 N71-23061
- Neural mechanism of human cerebral cortex for speech functions
11 p1685 N71-23063
- Echolocation as bionic communication systems for bats and dolphins
11 p1693 N71-23065
- Auditory and tactile information transfer of biological systems
11 p1693 N71-23066
- Bionic oscillating propulsion system of fishes
11 p1694 N71-23071
- Neurophysiological mechanisms of learning and memory as biological adaptation to environment
11 p1694 N71-23074
- Critical analysis and predicted developments in bionics science
11 p1694 N71-23078
- Application of dynamic programming and theory of control processes to biological phenomena including evolution of consciousness
[TR-71-17] 14 p2204 N71-25937
- Algorithmic pattern generation with application to inorganic and biological structures, and other branches of mathematics and computer science
[PB-197604] 18 p2847 N71-31314
- Development of theory for formal neurons as mathematical basis for creation of highly reliable cybernetic systems and computers
19 p3061 N71-32015
- Cybernetics including models for statistical decision making, biomechanical systems, and complex stochastic system
[JPRS-53531] 19 p3044 N71-32088
- Model for quantitatively examining performance of automatic machines with normal and disturbed functions in statistical decision making
19 p3044 N71-32089
- Dynamic reactions of operators with random vibrational stimuli and biomechanical systems
19 p3044 N71-32090
- Reviewing continuous system simulation techniques with emphasis on interactive, graphic-oriented systems
[P-4503] 19 p3061 N71-32281
- Encoding function of neurophysiological synapses
[AD-724072] 20 p1327 N71-33329
- BIOPHYSICS**
NT HEALTH PHYSICS
- Biophysical research at Laboratory for Agricultural Remote Sensing, Purdue University
06 p0066 N71-16153
- Bibliography on solid state physics including condensed matter and theoretical biology
[AD-714265] 06 p0935 N71-16363
- Neutron dosimetry, biophysics and biological effectiveness, genetic effects, repair and recovery, and modifying factors of neutrons in radiobiology
[CONF-691106] 09 p1332 N71-30010
- Radiology, radiobiology, radiophysics, and biophysics research
[NYO-2740-7] 10 p1499 N71-21167
- Neuron modeling, electrophysiology, and biophysics involved in information processing along nervous system
[AD-727770] 24 p3082 N71-37673
- Particle accelerator, nuclear physics, and biophysics research
[NF-18683] 24 p3970 N71-39977
- BIOREGENERATIVE LIFE SUPPORT SYSTEMS**
U CLOSED ECOLOGICAL SYSTEMS
- BIOATELLITE 1**
Bioattellite flight data of weightlessness effects on biological systems
02 p0161 N71-11711
- BIOATELLITE 2**
Bioattellite flight data of weightlessness effects on biological systems
02 p0161 N71-11711
- BIOATELLITE 3**
Testing for trace contaminants in Bioattellite 3 spacecraft atmosphere and their effects on occupants
[NASA-TM-X-62004] 10 p1510 N71-21110
- BIOATELLITES**
NT BIOATELLITE 1
NT BIOATELLITE 2
NT BIOATELLITE 3
- BIOENRONS**
U BIOINSTRUMENTATION
BIOSIMULATION
U BIONICS
BIOSPHERE
U EARTH HYDROSPHERE
U LOWER ATMOSPHERE
BIOINTERFACES
Biological effects of radiation and mechanism of protein and nucleic acid synthesis
[HUX-2643-40] 01 p0012 N71-11640
- Investigating methods of synthesizing alpha glycerols from waste gases in spacecraft
[NASA-CR-114276] 07 p0990 N71-17005
- Investigating theory of chemical evolution on Sary Island and relationship to life detection techniques for other planets
07 p1024 N71-17001
- Problems of mathematical modeling in microbiological processes
[JPRS-53452] 17 p2707 N71-30025
- BLOT METHOD**
Curves for determining elastic modulus of mineral and dry sandstones
[NASA-TT-F-13749] 17 p2749 N71-30047
- BIO TECHNOLOGY**
Survival training in Royal Netherlands Air Force
04 p0483 N71-14429
- Applications of aerospace technology in biology and medicine
[NASA-CR-115888] 05 p0636 N71-16460
- Investigation of application of NASA developed technology to cardiovascular and pulmonary patient monitoring to improve availability of data for medical diagnosis
[NASA-CR-118030] 12 p1868 N71-23060
- Program plans and cost estimates of project for application of biotechnology to patient monitoring systems
[NASA-CR-118035] 12 p1868 N71-23060
- Biotechnological aspects of Gemini flight for future manned space flight technology
16 p2551 N71-28227
- Technology transfer and applications in medicine and biology
[NASA-CR-119161] 17 p2709 N71-30029
- Trends and possibilities in biotechnology, biotechnology, geology of minerals, earth resources, and man machine systems
18 p2828 N71-31329
- Trends and possibilities in biochemical and biotechnical in medical science - heart transplantation
18 p2875 N71-30040
- BIO TELEMETRY**
Biotelemetry apparatus with dual voltage generation for implants in animals
[NASA-CASE-XAC-65706] 03 p0328 N71-12346
- Telemetric equipment for pulse code modulation and processing of biomedical data
[SI-PUBL-619] 10 p1504 N71-20683
- Radiation hardened transmitter optical implantation in animals for electrocardiogram biotelemetry in radiation environments
[AD-718151] 12 p1866 N71-23078
- Biomedical telemetric systems for monitoring physiological parameters of animals
[NASA-SP-5064] 15 p2376 N71-27983
- Prototype device for monitoring sleep during manned space flight including performance tests
[NASA-CR-115071] 17 p2711 N71-30030
- Radiotelemetry equipment used in Interrogative Recording Location System, and results in remote ground, aircraft, and satellite tracking of oil and blood bases
[NASA-CR-121831] 22 p3546 N71-33080
- Development of MMFEL telemetry system to inventory cycle time burst system
[AD-724406] 22 p3549 N71-33077
- BIOPROPELLANTS**
U LIQUID ROCKET PROPELLANTS
- BIRDS**
NT CHECKERBERRIES
NT PIGEONS

BLACKOUT (PROPAGATION)

- NT ATMOSPHERICS
NT COSMIC NOISE
NT DAWN CHORUS
NT ELECTROMAGNETIC NOISE
NT HISS
NT IONOSPHERIC NOISE
NT IONOSPHERICS
NT THERMAL NOISE
NT WHISTLERS
- Circuits, equipment, and experimental approach used for analysis of blackout from X band microwave pulse incident on shock-produced plasma
(AD-715974) 05 p4439 N71-13190
- Electron removal from ionospheric fields by dissociative attachment for blackout alleviation
10 p1520 N71-21129
- Spatial nonuniformity effects on high temperature plasma breakdown over X band waveguide aperture including continuous wave and pulsed breakdown in air and nitrogen
(AD-716412) 12 p1961 N71-23965
- Wind tunnel tests of plasma covered antenna to determine transmission and radiation characteristics and effects of injecting chemicals into boundary layer
(AD-718976) 13 p2643 N71-24357
- Analysis of surface mounted aperture antenna for measurement of microwave reentry plasma diagnostics
(AD-718981) 13 p2146 N71-24393
- Analysis of self and mutual admittances for axial rectangular slot antennas in echelon configuration for cylindrical body clad with radially inhomogeneous plasma
(AD-719734) 13 p3038 N71-25202
- Microwave breakdown predictions for rectangular aperture antenna including lateral diffusion
(AD-721203) 15 p2386 N71-27205
- Effect of near field on breakdown of antenna radiation capability in reentry vehicles
(AD-724655) 19 p3858 N71-32664
- Spectral degree of blackness for certain reentry vehicles at high temperatures, dependent on composition, structure, and surface cleaning or radiating materials
(AD-727473) 24 p3943 N71-38126
- BLADDERS
NT EXPULSION BLADDERS
BLADDERS (MECHANICS)
U DIAPHRAGMS (MECHANICS)
- BLADE TIPS
- Numerical solution of Fredholm equation for air duct vortices of shrouded propeller with tip clearance
(DLR-FB-71-15) 19 p3033 N71-31788
- BLADES (CYLINDERS)
Machine tool wear caused by cutting of porous ceramic materials
(AD-718488) 12 p1944 N71-23766
- BLASTOFF
U ROCKET LAUNCHING
- BLASTS
Numerical analysis of curved characteristics behind strong blast waves
(NASA-CR-111908) 13 p2066 N71-24929
- BLEED-OFF
U PRESSURE REDUCTION
- BLENDING
U MIXTURES
- BLINDNESS
NT FLASH BLINDNESS
- BLOCK BAND
Computer program for evaluating Bloch-Grüneisen parameters of metals and evaluating transition electrical resistivity as function of temperature
(NASA-TM-X-2320) 17 p2816 N71-29922
- BLOCKING
Simulating downstream flow blockage doors in bypass air duct of turbofan engine with axial flow fan rotor
(NASA-TN-D-6971) 01 p1015 N71-10537
- Flow blockage effects on heat transfer in bottom cooling system of fuel assembly
(WCAP-5353) 13 p2187 N71-25357
- BLOCKS
Foldable blocks for construction of structures in remote areas lacking building materials
(NASA-CASE-MSC-12233-2) 18 p3022 N71-31415
- BLOOD
NT ERYTHROCYTES
NT LEUKOCYTES
NT LYMPHOCYTES
Storage stability of human blood cholesteroles
(AM-70-4) 01 p1009 N71-10274
- Influence of pericapillary plasma on chemical exchange from blood to tissue
(NASA-TN-D-6227) 08 p1148 N71-18421
- Effects of positive G_y acceleration on blood oxygen saturation and plasma pressure relations in dogs breathing air and liquid fluorocarbons in whole body water immersion respirator
(NASA-CR-117199) 09 p1336 N71-30058
- Human physiology, thermoregulation, and harmonic oscillation of blood glucose levels
(NASA-CR-1806) 16 p2542 N71-28206

- Prolonged bed rest effects on human chromosomes during space flight simulation and actual space flight
20 p3221 N71-33462
- Hemoglobin compound identification, oxygen involvement, and major breakdown products of monomethylhydrazine effect on blood, in vitro
(AD-727528) 24 p3879 N71-37651
- BLOOD CIRCULATION
NT CARBOXYHEMOGLOBIN
NT ISCHEMIA
NT PULMONARY CIRCULATION
- Circulatory impairment during exposure to ambient pressures of 4 mm Hg and 55 mm Hg
(AD-712160) 02 p0156 N71-11103
- Viscous flow of deformable liquid drops in suspension in circular cylindrical tubes
(AD-711633) 02 p0203 N71-11563
- Fluid dynamics of blood circulation and respiratory flow
(AGARD-AR-36-70) 03 p0521 N71-12290
- Clinical evaluation of rheographic measurements on subjects during underwater activity
(NASA-TT-3-13423) 04 p0481 N71-14483
- Investigating blood flow of living tissue for application to thermal control of protective clothing
(NASA-CR-116873) 08 p1152 N71-18926
- Correlations between diurnal indices of cerebral and systemic circulation
08 p1155 N71-19049
- Blood circulation and state of physical training in athletes
09 p1328 N71-19583
- Applying flow characteristics in constricted tube to arterial stenoses
(PB-193172) 09 p1371 N71-19618
- Application of cinechiroangiography to study of microcirculation hemodynamics and related physiological studies of man and animal
(AD-719401) 13 p2036 N71-24684
- Clinical and experimental investigations of effect of motor activity restriction on cardiac function in human and animal subjects
16 p2547 N71-28493
- Analysis of the effects of regional blood circulation on intensity of muscular response to stimulus
16 p2547 N71-28496
- Effects of posture on body fluid circulation and long term immersion effects on physiological mechanisms
20 p3219 N71-33273
- Hypokinesia effects on nasal blood circulation of man
20 p3221 N71-33464
- Hypoxia affecting circulatory responses in dogs, such as cardiac output, left ventricular d₀/dt, and stroke volume
(NASA-CR-121665) 21 p3580 N71-34051
- Water-salt metabolism during space flight and microanalysis of actively circulating blood volume
(NASA-TT-F-14028) 24 p3877 N71-37638
- BLOOD COAGULATION
Analysis of problems associated with effects of surfaces on blood clotting and on theory of blood clot regulation
(AD-721207) 15 p2372 N71-27475
- Thrombi growth in stagnation point flow of fresh blood
(NASA-CR-121668) 21 p3580 N71-34053
- Enzyme reaction model of flow diffusion effect on blood coagulation in vivo
(NASA-CR-122929) 23 p3713 N71-36470
- BLOOD FLOW
Flow of neutrally buoyant suspensions of rigid spheres and disks through narrow tubes, simulating non-Newtonian blood flow
14 p2341 N71-26299
- Pressure sensors, blood flow transducers, pH electrodes, and photographic recording of biological data for use in aerospace medicine
(NASA-CR-119024) 16 p2550 N71-28284
- Transverse acceleration effects on blood flow in human veins
20 p3221 N71-33463
- Enzyme reaction model of flow diffusion effect on blood coagulation in vivo
(NASA-CR-122929) 23 p3713 N71-36470
- BLOOD PLASMA
Influence of pericapillary plasma on chemical exchange from blood to tissue
(NASA-TN-D-6227) 08 p1148 N71-18421
- Radiobiological plasma and blood volume measurements on humans and rats
(CEA-R-4831) 13 p2053 N71-24627
- Red cell mass and plasma volume changes noted in hypodynamic states of bed rest and water immersion compared to changes observed during ortho orbital missions
20 p3216 N71-33253
- Development and characteristics of automated fluorometric procedures for analyzing monophosphates and adenosine content of blood plasma and urine
(FAA-AM-71-15) 22 p3543 N71-35241
- Red cell mass and plasma volume changes observed in astronauts on Gemini and Apollo missions
23 p3711 N71-36454

BLOOD PRESSURE

- Blood pressure changes in heart cavities and large vessels in dogs during acceleration in water deceleration
02 p0159 N71-11103
- Alveolar gas exchange and cardiovascular function during respiratory inhibition
(PB-194025) 07 p0990 N71-13309
- Arterial pressure characteristics of athletes
09 p1329 N71-19583
- Development of indirect blood pressure measuring device and method for rapid determination of blood pressure
(FAA-AM-70-21) 11 p4678 N71-28206
- Mathematical functional model for cerebral blood pressure control system
(AD-717047) 11 p1080 N71-25000
- Electrocardiographic and blood pressure changes of physical fitness for aging pilots
11 p1089 N71-25000
- Blood pressure measuring system for rapidly recording dc and ac pressure signals of Korotkoff sounds
(NASA-CASE-XMS-60661) 12 p1045 N71-28206
- Human pressure distribution measurements in healthy subjects engaged in manual work
20 p3222 N71-33464
- BLOOD VESSELS
NT ARTERIES
NT CAPILLARIES (ANATOMY)
- Investigating high frequency wave propagation in blood vessels as function of dynamic instability of brachial artery during systolic phase of unsteady measurement
07 p0983 N71-13309
- BLOWDOWN WIND TUNNELS
Test facilities, wind tunnels and tests at Malvern Aircraft Center
(ONERA-TN-146) 02 p0196 N71-13309
- Calebrimetric and thermocouple pyrometer heat measurements in blowdown wind tunnels
(ONERA-TN-159) 02 p0385 N71-23965
- Error analysis for pressure measurements in blowdown supersonic wind tunnel models
(NPL-AERO-1506) 07 p1003 N71-19583
- Somehow blowdown and emergency case study project test report
(DN-1993) 07 p1009 N71-19583
- Investigating effects of leading-edge blurring on aerodynamic characteristics of jet impinged diffuser
07 p0960 N71-19583
- Results of two-phase blowdown experiments with straight tube test section and steam-water mixture
(ARL-3644) 08 p1176 N71-28206
- Nozzle flow calibration in blowdown wind tunnel
(WEB-TN-85A-171) 08 p1176 N71-28206
- Flow control system design for blowdown wind tunnels and disturbance effects on reentry vehicle
(NAL-TN-22) 11 p1552 N71-28206
- Hypervelocity blowdown nitrogen wind tunnel air gas turbine resistance heater nozzle, nozzle, diffuser, and calibration
(IC-AERO-71-01) 13 p3061 N71-30058
- Support systems and operational design of nitrogen hypervelocity blowdown wind tunnel
(AD-722345) 17 p2731 N71-28206
- BLOWERS
Flow-induced vibration of bellows with heated cryogenic fluid flows
(NASA-CR-102955) 09 p0644 N71-13309
- Radial blowers, shut-down, valves, and seal performance in helium atmosphere of AVR experimental gas cooled reactor
(NLL-EE-TRANS-1953-3774.5) 21 p3462 N71-34051
- BLOWING
Wind tunnel study of augmented ram-wing vehicle with various blowing arrangements
(PB-18435) 12 p1830 N71-28206
- Laminar boundary layer on wing and body of revolution in presence of blowing
(NASA-TT-F-13637) 12 p1903 N71-28206
- Low-speed wind tunnel longitudinal stability test on sweptback wing model with blowing at leading edge slots and trailing edge flaps for Deacon aircraft performance
(ARC-R/4-3655) 13 p0822 N71-28206
- Blowing effect on static efficiency of two dimensional air foils with momentum injection in boundary layer control form
(ARC-R/4-3656) 15 p2564 N71-28206
- Blowing effects on flow around models analyzed by flow visualizations produced in water tunnel
(NASA-TT-F-13743) 21 p3089 N71-28206
- Theoretical analysis of trailing edge blowing effect on circulation around airfoils based on iterative solutions with lift coefficients
(AD-726454) 23 p3336 N71-28206
- BLADE GREEN ALGAE
Biochemical effects of thermal treatments on disposal of blue green algae and microorganisms in Iceland and Turkey
07 p0983 N71-19583

SUBJECT INDEX

BLUNT BODIES

- Drug in turbulent wake behind blunt bodies measured directly and compared with measurements obtained from von Karman equation
[NACA-TR-1140] 10 p1491 N71-20483
- Unsymmetrical nose bluntness effect on stability derivatives of slender cone at Mach 14
[AD-71921] 10 p1412 N71-11008
- Time-dependent method for calculating supersonic blunt body flow field with sharp corners and conical shock waves
[NACA-TR-D-4031] 10 p1412 N71-11533
- Characteristics of magnetoacoustic flow around blunt bodies
[AD-71921] 10 p1412 N71-11533
- Measuring low-density flow over two-dimensional blunt bodies in hypersonic arc tunnel
[NACA-TR-D-4017] 10 p1411 N71-12215
- Isolation of viscous shock layer at stagnation point of blunt body
[AD-71921] 10 p1411 N71-12287
- Isolation of chemical nonequilibrium boundary layer flow of hypervelocity in earth atmosphere
[AD-71921] 10 p1411 N71-12588
- Laminar flow past axisymmetric blunt bodies moving at hypersonic speed
[NACA-CN-11571] 10 p1411 N71-12591
- Effects of reattachment located at apex of 140 deg blunt cone at Mach numbers of 3.00, 4.50, and 6.00
[NACA-TR-D-4002] 10 p1411 N71-14614
- Coupled flow effects on pressure contour of blunt body in hypersonic flow
[NACA-TR-D-4002] 10 p1411 N71-14614
- Numerical analysis of blunt body electrostatic probe plasma flow
[NACA-TR-D-4002] 10 p1411 N71-14614
- Investigating supersonic viscous gas flow around blunt bodies
[AD-71921] 10 p1411 N71-14692
- Hypersonic flow fields around cylindrical body with blunt nose
[NACA-TR-199] 10 p1372 N71-19761
- Navier-Stokes equations for calculating viscous radiative cooling gas flow around blunt bodies
[NACA-TR-T-15531] 10 p1378 N71-20343
- Wind tunnel method for simulating flow fields around blunt vehicles entering planetary atmospheres without involving high temperatures
[NACA-CASE-LAR-11158] 10 p1578 N71-20436
- Numerical analysis of supersonic blunt body viscous flow - constant viscosity results
[AD-71921] 10 p1540 N71-21014
- Finite difference method for unified solutions to inviscid supersonic flow distribution about blunt bodies
[AD-71921] 10 p1540 N71-21114
- Low Reynolds number viscous flow at stagnation angles of blunt bodies during hypersonic reentry
[AD-71921] 10 p1541 N71-21127
- Isobathy and wall heat flux calculations for stagnation region of blunt axisymmetric bodies in hypersonic flow
[AD-71921] 10 p1733 N71-22867
- Heat bluntness effect on aerodynamic characteristics of blunt body in supersonic wind tunnel
[NACA-TR-221] 10 p1679 N71-22160
- Separated flow over flat plate with blunt fin at small angle of attack
[AD-71921] 10 p1679 N71-22590
- Pushy for simulating reentry flow fields over blunt-nosed bodies
[AD-71921] 10 p1740 N71-22634
- Aerodynamic characteristics of large angle blunt nose with and without fence-type afterbodies
[NACA-TR-D-4209] 12 p2001 N71-34083
- Hypersonic heat transfer to flat plates and conical and blunt bodies in boundary layer flow
[NACA-TR-D-4209] 12 p2001 N71-34083
- Reentry flowfield by laminar boundary layers
[NACA-TR-D-4209] 12 p2001 N71-34083
- Time dependent numerical techniques for solving equations governing two dimensional viscous flow about blunt bodies with discontinuous curvatures
[AD-71921] 10 p2241 N71-36371
- Aerodynamic heat determination on blunt bodies in hypersonic flow with force and pressure measurements
[NACA-TR-D-4209] 12 p2001 N71-34083
- Simple integral method for calculating real gas turbulent boundary layers with variable edge velocity and edge temperature showing effect of nose bluntness at low Mach
[NACA-TR-D-4209] 12 p2001 N71-34083
- Isolation of viscous shock layer at stagnation point of blunt body
[AD-71921] 10 p1411 N71-12287
- Isolation of chemical nonequilibrium boundary layer flow of hypervelocity in earth atmosphere
[AD-71921] 10 p1411 N71-12588
- Laminar flow past axisymmetric blunt bodies moving at hypersonic speed
[NACA-CN-11571] 10 p1411 N71-12591
- Effects of reattachment located at apex of 140 deg blunt cone at Mach numbers of 3.00, 4.50, and 6.00
[NACA-TR-D-4002] 10 p1411 N71-14614
- Coupled flow effects on pressure contour of blunt body in hypersonic flow
[NACA-TR-D-4002] 10 p1411 N71-14614
- Numerical analysis of blunt body electrostatic probe plasma flow
[NACA-TR-D-4002] 10 p1411 N71-14614
- Investigating supersonic viscous gas flow around blunt bodies
[AD-71921] 10 p1411 N71-14692
- Hypersonic flow fields around cylindrical body with blunt nose
[NACA-TR-199] 10 p1372 N71-19761
- Navier-Stokes equations for calculating viscous radiative cooling gas flow around blunt bodies
[NACA-TR-T-15531] 10 p1378 N71-20343
- Wind tunnel method for simulating flow fields around blunt vehicles entering planetary atmospheres without involving high temperatures
[NACA-CASE-LAR-11158] 10 p1578 N71-20436
- Numerical analysis of supersonic blunt body viscous flow - constant viscosity results
[AD-71921] 10 p1540 N71-21014
- Finite difference method for unified solutions to inviscid supersonic flow distribution about blunt bodies
[AD-71921] 10 p1540 N71-21114
- Low Reynolds number viscous flow at stagnation angles of blunt bodies during hypersonic reentry
[AD-71921] 10 p1541 N71-21127
- Isobathy and wall heat flux calculations for stagnation region of blunt axisymmetric bodies in hypersonic flow
[AD-71921] 10 p1733 N71-22867
- Heat bluntness effect on aerodynamic characteristics of blunt body in supersonic wind tunnel
[NACA-TR-221] 10 p1679 N71-22160
- Separated flow over flat plate with blunt fin at small angle of attack
[AD-71921] 10 p1679 N71-22590
- Pushy for simulating reentry flow fields over blunt-nosed bodies
[AD-71921] 10 p1740 N71-22634
- Aerodynamic characteristics of large angle blunt nose with and without fence-type afterbodies
[NACA-TR-D-4209] 12 p2001 N71-34083
- Hypersonic heat transfer to flat plates and conical and blunt bodies in boundary layer flow
[NACA-TR-D-4209] 12 p2001 N71-34083
- Reentry flowfield by laminar boundary layers
[NACA-TR-D-4209] 12 p2001 N71-34083
- Time dependent numerical techniques for solving equations governing two dimensional viscous flow about blunt bodies with discontinuous curvatures
[AD-71921] 10 p2241 N71-36371
- Aerodynamic heat determination on blunt bodies in hypersonic flow with force and pressure measurements
[NACA-TR-D-4209] 12 p2001 N71-34083
- Simple integral method for calculating real gas turbulent boundary layers with variable edge velocity and edge temperature showing effect of nose bluntness at low Mach
[NACA-TR-D-4209] 12 p2001 N71-34083
- Isolation of viscous shock layer at stagnation point of blunt body
[AD-71921] 10 p1411 N71-12287
- Isolation of chemical nonequilibrium boundary layer flow of hypervelocity in earth atmosphere
[AD-71921] 10 p1411 N71-12588
- Laminar flow past axisymmetric blunt bodies moving at hypersonic speed
[NACA-CN-11571] 10 p1411 N71-12591
- Effects of reattachment located at apex of 140 deg blunt cone at Mach numbers of 3.00, 4.50, and 6.00
[NACA-TR-D-4002] 10 p1411 N71-14614
- Coupled flow effects on pressure contour of blunt body in hypersonic flow
[NACA-TR-D-4002] 10 p1411 N71-14614
- Numerical analysis of blunt body electrostatic probe plasma flow
[NACA-TR-D-4002] 10 p1411 N71-14614
- Investigating supersonic viscous gas flow around blunt bodies
[AD-71921] 10 p1411 N71-14692
- Hypersonic flow fields around cylindrical body with blunt nose
[NACA-TR-199] 10 p1372 N71-19761
- Navier-Stokes equations for calculating viscous radiative cooling gas flow around blunt bodies
[NACA-TR-T-15531] 10 p1378 N71-20343
- Wind tunnel method for simulating flow fields around blunt vehicles entering planetary atmospheres without involving high temperatures
[NACA-CASE-LAR-11158] 10 p1578 N71-20436
- Numerical analysis of supersonic blunt body viscous flow - constant viscosity results
[AD-71921] 10 p1540 N71-21014
- Finite difference method for unified solutions to inviscid supersonic flow distribution about blunt bodies
[AD-71921] 10 p1540 N71-21114
- Low Reynolds number viscous flow at stagnation angles of blunt bodies during hypersonic reentry
[AD-71921] 10 p1541 N71-21127
- Isobathy and wall heat flux calculations for stagnation region of blunt axisymmetric bodies in hypersonic flow
[AD-71921] 10 p1733 N71-22867
- Heat bluntness effect on aerodynamic characteristics of blunt body in supersonic wind tunnel
[NACA-TR-221] 10 p1679 N71-22160
- Separated flow over flat plate with blunt fin at small angle of attack
[AD-71921] 10 p1679 N71-22590
- Pushy for simulating reentry flow fields over blunt-nosed bodies
[AD-71921] 10 p1740 N71-22634
- Aerodynamic characteristics of large angle blunt nose with and without fence-type afterbodies
[NACA-TR-D-4209] 12 p2001 N71-34083
- Hypersonic heat transfer to flat plates and conical and blunt bodies in boundary layer flow
[NACA-TR-D-4209] 12 p2001 N71-34083
- Reentry flowfield by laminar boundary layers
[NACA-TR-D-4209] 12 p2001 N71-34083
- Time dependent numerical techniques for solving equations governing two dimensional viscous flow about blunt bodies with discontinuous curvatures
[AD-71921] 10 p2241 N71-36371
- Aerodynamic heat determination on blunt bodies in hypersonic flow with force and pressure measurements
[NACA-TR-D-4209] 12 p2001 N71-34083
- Simple integral method for calculating real gas turbulent boundary layers with variable edge velocity and edge temperature showing effect of nose bluntness at low Mach
[NACA-TR-D-4209] 12 p2001 N71-34083

- based on time dependent finite difference theory and method of characteristics
[NACA-TR-D-4209] 12 p2001 N71-34083
- Mathematical model of supersonic flow around blunt-nosed body with sharp leading edge including comparison with schlieren photographs and cooling Mach number dependence
[REPT-1771] 19 p3033 N71-31658
- Aerodynamic characteristics at Mach numbers 1.0 to 2.16 of blunt-nose missile model having triangular cross section and fixed trim fin
[NACA-TR-X-2348] 19 p3033 N71-32211
- Pressure distributions and shock wave shapes during hypersonic flow over 18 deg semi-angle cone with rounded leading edge
[AFL-AN-530] 20 p3240 N71-32902
- Reduction of radiative and convective heat transfer at stagnation points due to blowing expressed in terms of shock standoff-distance ratio for blunt-nosed bodies
[NAL-TR-224] 20 p3364 N71-33240
- Determination of transonic aerodynamic characteristics of spherically blunted 35 and 60 degree half-cones in ballistic range tests
[NACA-TR-D-4405] 20 p3286 N71-33344
- Computer program for determining inviscid flow around blunt bodies at supersonic and hypersonic speeds - users manual
[NACA-TR-X-2348] 20 p3252 N71-33670
- Subsonic near wake of blunt-based axisymmetric body in uniform steady flow wind tunnel
[NACA-TR-X-2348] 20 p3252 N71-33811
- Influence of parameter variability in shock layer on heat flux in nonequilibrium viscous flow of multicomponent gas near stagnation point of blunt body
[AD-71921] 21 p3412 N71-34277
- Pressure distribution over 10 deg cone in hypersonic wind tunnel at Mach-14 for various angles of attack
[AD-72633] 22 p3337 N71-35280
- Hypersonic flow around blunt object by nonviscous gas current accounting for radiation transfer in shock layer
[NACA-TR-X-2348] 22 p3566 N71-35400
- Computer program for determining radiating nonequilibrium inviscid flow over blunt body by integral equations
[NACA-TR-X-2348] 22 p3786 N71-36417
- Numerical analysis of relaxation and nonequilibrium radiation properties behind shock waves in air
[SC-T-13506] 23 p3743 N71-36496
- Correlation of local nonequilibrium heat transfer rate and pressure ratio for blunt cones at angle of attack
[AD-72787] 24 p4022 N71-38490
- Measurement of base heating characteristics of high angle, blunt cones at hypersonic speed
[NACA-TR-1920] 24 p4031 N71-38766
- BLUNTNESS
UO-166 HELICOPTER
Use of UO-166 helicopter for in-flight simulation of VISTOL aircraft
[AD-71921] 19 p3037 N71-31960
- BOARDS (PAPER)
Variations in crushing strength of paper honeycomb
[AD-71557] 10 p1679 N71-22160
- Developing digital magnetic compass based on Hall effect for small boats
[AD-71547] 10 p1679 N71-22590
- BOSSIES OF REVOLUTION
NT CELESTIAL SPHERE
NT CONICAL BODIES
NT CYLINDRICAL BODIES
NT PARABOLIC BODIES
NT POINCARÉ SPHERES
NT ROTATING CYLINDERS
NT ROTATING SPHERES
NT SPHERICAL CONES
NT SPHERES
NT TORUSES
- Evaluating methods of numerically integrating equations of motion for nonlinear dynamic analyses of shock of revolution by matrix displacement method
[NACA-TR-10639] 10 p1679 N71-10166
- Computation of Green function for bodies of revolution
[AD-71099] 10 p1691 N71-10861
- Boundary layer transition studies of several pointed bodies of revolution at supersonic speeds
[NACA-TR-D-4663] 10 p1692 N71-11530
- Laminar boundary layer calculations on bodies of revolution in hypersonic flow
[AD-71099] 10 p1691 N71-10861
- Digital computer program for computing vibration characteristics of ring-stiffened orthotropic shells of revolution - users manual
[NACA-TR-X-2130] 10 p2462 N71-13093
- Investigating spectrum of set of axisymmetric vibration equations for shells of revolution
[AD-71099] 10 p2466 N71-13228
- Computer program for finite difference solutions of shells of revolution under asymmetric dynamic loading
[NACA-TR-D-4659] 10 p1700 N71-13540

BODY CENTERED CUBIC LATTICES

- Finite element program for determining stiffness and mass matrices of shells of revolution - users manual
[NACA-TR-11400] 10 p1692 N71-10861
- DYNASOR-2 finite element program for dynamic nonlinear analysis of shells of revolution
[NACA-TR-11400] 10 p1692 N71-10861
- Measuring values of entropy on surface of body of revolution at various angles of attack
[AD-71921] 10 p1411 N71-12287
- Turbulent values of flat and rounded cylindrical bodies acting with development
[AD-71921] 10 p1411 N71-12287
- Computer program using finite element method for computing temperature distributions in thin shells of revolution
[NACA-TR-D-4100] 10 p1503 N71-10746
- Wind tunnel vortex flow study on body of revolution with or without wings
[AD-71921] 10 p1511 N71-15933
- Integration of Karman equations to determine stressed state of slightly shaping shells of revolution under high degree of displacement
[AD-71921] 10 p1652 N71-20023
- Measurements of scale beam pressure distribution of bodies of revolution at Mach 2.50, 3.00, and 4.00 in U-tube flow wind tunnel
[NACA-TR-D-4100] 11 p1669 N71-12161
- Supersonic combustion, fuel injection, and recuperation in hydrogen hypersonic external combustion at flat plates and bodies of revolution
[AD-71921] 11 p1680 N71-22129
- Schlieren method for three dimensional axially symmetric problems on sound diffraction and reflection from general class of bodies of revolution
[AD-71921] 11 p1797 N71-22143
- Comparing profiles for supersonic surfaces of revolution with inflatable tubes
[NACA-CASE-XGS-01023] 11 p1770 N71-22705
- Test fixture for measuring moment of inertia of irregularly shaped body with multiple axes
[NACA-CASE-XGS-01023] 11 p1763 N71-22992
- Laminar boundary layer on wing and body of revolution in presence of blowing
[NACA-TR-T-15407] 12 p1902 N71-23796
- Application of continuum, second order differential equations to solution of calorimetric data of revolution
[AD-71921] 12 p2008 N71-34083
- Matched asymptotic investigation of steady, axisymmetric, supersonic flow past cone of revolution
[AD-71921] 12 p1903 N71-24125
- Computer programs to calculate characteristic currents and gas patterns of conducting bodies of revolution
[AD-71921] 13 p3043 N71-34416
- Fluid element effect on vibration frequencies of elastically shells of revolution
[AD-71921] 13 p1213 N71-23363
- Application of special isoperimetric finite elements for elastic-plastic analysis of shells of revolution
[AD-71921] 14 p2008 N71-20086
- Aerodynamic drag of many bodies of revolution in supersonic flow
[AD-71921] 14 p2008 N71-20086
- Slurry solutions using free parameter technique for laminar flow of viscous, incompressible fluid between rotating coaxial surfaces of revolution
[AD-71921] 20 p3253 N71-33783
- Development of near-field method for determining supersonic flow properties about bodies of revolution
[NACA-TR-D-4500] 23 p3785 N71-36413
- Pressure distributions and drag coefficients of 18 constant length and volume slender bodies of revolution at zero incidence for Mach numbers 2.0 to 12.0 - graphs
[NACA-TR-D-4500] 23 p3785 N71-36416
- Numerical analysis and design of thin walled shells of revolution
[AD-72769] 24 p4027 N71-38731
- BOY CENTERED CUBIC LATTICES
Neutron irradiation effect on dislocation of two metals and cold solutions at low temperatures
[CONF-70019-3] 10 p1692 N71-10861
- Scavenging and weakening in two cold solutions
[CONF-70019-4] 10 p1692 N71-10861
- Irradiation strengthening of two metals and cold solutions - annealing mechanism in two metals
[ORO-3612-7] 10 p1692 N71-10861
- Analytic behavior of amorphous, crystalline, and two refractory alloys, and dislocation-solute atom interaction and interstitial hardening in two alloys
[COO-1676-13] 10 p1692 N71-10861
- Lattice theory of face-center and diamond-like crystals in body centered cubic crystal phases
[AD-71566] 10 p1692 N71-10861
- Microscopic determination in body centered cubic metals and cold solutions and analysis of lattice defects in real metals and interstitial impurities on dislocation motion controls
[CONF-70045-1] 10 p1692 N71-10861
- Characterization of self diffusion of body centered phosphorus under hydrostatic pressure of zero to twenty kilobars
[CRA-CONF-1435] 10 p1514 N71-21408

- Mathematical procedure for Born stability determination of body centered cubic crystal lattice tunnel properties
[AD-717696] 11 p1817 N71-23423
- Electron energy bands for body centered cubic vanadium for several different electron exchange approximations using augmented-plane-wave method
12 p1970 N71-24351
- Activation volume for self diffusion, under hydrostatic pressure, of body centered cubic Fe
[CRA-CONF-1698] 15 p2477 N71-27384
- Zero point motion effect on Peierls stress in body centered cubic crystals
17 p2818 N71-29943
- Interaction between screw dislocation and carbon in body centered cubic iron using model with pairwise interatomic potential matching
17 p2818 N71-29947
- Iron screw dislocation for slip behavior in body centered cubic materials
17 p2819 N71-29948
- Role of ductility brittleness transition in body centered cubic lattice of iron polycrystals
19 p3112 N71-31913
- Computer program [KRISTALL] for studying dynamics of radiation damage in face centered cubic lattices, body centered cubic lattices, and diamonds
[IAB-2002] 21 p3496 N71-34998
- Nuclear magnetic susceptibility in bcc solid He-3 with Neel temperature and negative exchange interaction energy calculations and impurity effects
22 p3652 N71-36041
- BODY COMPOSITION [BIOLOGY]**
- Diet and altitude effects on body composition of growing rats
[AD-712239] 02 p0155 N71-11098
- Body structure effects on fish hydrodynamic characteristics
[JPRS-52299] 08 p1148 N71-18492
- Gas bubble growth and compression in body physical systems and tissues
08 p1155 N71-19070
- Biomedical body fluid and composition data from spacecover during long term space station simulation
18 p1498 N71-20995
- Measuring instruments for in vivo bone mineral content and body composition measurement
[NASA-CR-121415] 20 p3215 N71-33223
- BODY FLUIDS**
- NT BLOOD
- NT ERYTHROCYTES
- NT LEUKOCYTES
- NT LYMPHOCYTES
- NT SALIVA
- NT SWEAT
- NT URINE
- Determination of surface tension in biologic fluids for susceptibility to desiccation sickness
[NASA-CR-111382] 02 p0154 N71-11092
- Influence of electromagnetic force fields on biological systems studied on dunaliella and ciliates
[AD-714071] 06 p0081 N71-16350
- Biomedical body fluid and composition data from spacecover during long term space station simulation
18 p1498 N71-20995
- Performance of impedance cardiograph for measuring heart rate and body fluids
[NASA-CR-114985] 12 p1864 N71-24173
- Hemodynamic and body fluid alterations induced by varying periods of bed rest
20 p3217 N71-33263
- Effects of posture on body fluid circulation and long term immersion effects on physiological mechanisms
20 p3219 N71-33273
- Review of endocrine control of fluid and electrolyte balance during Mercury, Gemini, and Apollo missions
23 p3711 N71-36456
- BODY KINEMATICS**
- Kinematic analysis of inaccessible three-dimensional mechanism for application to human skeletal kinematics
02 p0153 N71-11083
- Dynamic model for microvascular system control of mammal body kinematics
09 p1331 N71-19082
- BODY MEASUREMENT [BIOLOGY]**
- NT ANTEROPOSMITY
- BODY TEMPERATURE**
- Human heat stress tolerance indications
02 p0160 N71-11406
- Wind tunnel tests with human subjects to determine effects of whole body and bare hand cooling at high wind speeds as might be encountered in air-to-air rescue operations
[AD-719766] 09 p1330 N71-19013
- Celestial temperature response of rats to oxygen at high pressure
[AD-716965] 10 p1497 N71-20776
- Microthermistor measurements of temperature distribution on body surface of dolphins
11 p1682 N71-22216
- Daily oral temperature measurements for circadian rhythm analysis on human body
[NASA-TT-P-13636] 12 p1864 N71-34019

- Thermoregulating with cooling flow pipe network for humans
[NASA-CASE-XMS-10369] 12 p1868 N71-24147
- Steady state and dynamic experiments to determine thermoregulatory heat production in human subjects
[AD-720831] 14 p2204 N71-25766
- Metabolic work loads of long duration exercise at moderate work loads including tables of heart rate, rectal temperature, minute volume, water balance, and respiratory quotient
15 p2372 N71-27784
- Dynamic mathematical model of physiological regulation of body temperature in human beings
[NASA-CR-1855] 20 p3220 N71-33401
- Effects of exercise on elevation of body temperature in human subjects and response of subject to temperature variations
[NASA-TT-P-13972] 23 p3716 N71-36486
- BODY TEMPERATURE [NON-BIOLOGICAL]**
- U TEMPERATURE
- BODY TEMPERATURE REGULATION**
- U THERMOREGULATION
- BODY WEIGHT**
- Relationships between cardiac volume, body weight, physical work capacity, and blood volume in healthy men and women with varying range of performance
[NASA-TT-P-13439] 08 p1148 N71-18573
- Intraspecific relationships between lean weight and wing length for migratory birds
[NLL-RTS-6197] 16 p2545 N71-28352
- BODY-WING AND TAIL CONFIGURATIONS**
- Aerodynamic interference characteristics of airframe-propulsion systems of transport and military aircraft
[AGARD-CP-71-71] 09 p1311 N71-19353
- Computerized prediction of aerodynamic lifting characteristics for wing-horizontal tail and canard wing configurations
[NASA-TM-X-66886] 09 p1312 N71-19361
- Calculation methods for wing-body interference drag on supersonic aircraft in stationary or nonstationary flow
09 p1312 N71-19362
- Approximation of pressure distribution on wing-body configurations at subcritical speeds
09 p1312 N71-19364
- Numerical calculation of steady three dimensional potential flow around lifting nonplanar aerodynamic configurations based on surface distribution of quadrilateral vortex rings
[TT-7009] 09 p1317 N71-20115
- Wind tunnel investigation of hypersonic transport model aerodynamic characteristics at Mach numbers to 6-graphs
[NASA-TN-D-6191] 12 p1852 N71-23127
- Wind tunnel study of augmented ram-wing vehicle with various blowing arrangements
[PB-109425] 12 p1850 N71-23283
- Calculation of shock inclination angle and surface pressure coefficient in vertical plane of symmetry of bodies at angle of attack related to delta wing-body space shuttle orbiter
[NASA-TM-X-62031] 15 p2394 N71-27662
- Procedures for calculating normal wash in non-planar configurations and interference between wings and bodies
17 p2698 N71-29340
- Subsonic static characteristics of slender wing configurations using magnetic suspension and balance system
[NASA-CR-1796] 17 p2701 N71-29775
- Subsonic stability, control, and performance of shuttle concept with blended wing-body
[NASA-TM-X-2341] 18 p3018 N71-31254
- Pressure distributions on planar delta wings attached to cylindrical bodies in supersonic flow - theoretical results for sonic leading edge, angle of attack case
[WRE-TN-HSA-186] 20 p3207 N71-33699
- Comparisons of theoretical and experimental pressure distribution over wing-body model at high supersonic speeds
[NASA-TN-D-6480] 22 p3537 N71-35197
- Low speed wind tunnel tests of 1/25 scale models of reusable orbital spacecraft for subsonic aerodynamic data at Mach 0.17
[NASA-CR-119982] 24 p4019 N71-38674
- BOEING AIRCRAFT**
- NT B-52 AIRCRAFT
- NT BOEING 707 AIRCRAFT
- NT BOEING 727 AIRCRAFT
- NT BOEING 747 AIRCRAFT
- NT CH-46 HELICOPTER
- Airframe equipment for approach path control on reduced noise trajectories in Boeing transport aircraft traffic
12 p1855 N71-23425
- Low wing load logSTOL transport ride smoothing using Boeing aircraft
[NASA-CR-111819] 13 p3026 N71-24586
- Aircraft accident investigation of Alaska Airlines Flight 186 on Sept. 4, 1971
[BB-71-87] 23 p3708 N71-36434

- BOEING MILITARY AIRCRAFT**
- U MILITARY AIRCRAFT
- BOEING 707 AIRCRAFT**
- Turbofan nacelle modifications to minimize the compressor noise radiation of Boeing 707 aircraft - Vol. 1
[NASA-CR-1711] 05 p0639 N71-24489
- Cockpit and center of gravity accumulation data tabular of Boeing 707 aircraft
[ABC-CR-11290] 06 p0793 N71-25773
- Static tests to determine effects of thrust line concepts on forward-radiated fan noise of 707-320B aircraft
[NASA-CR-1715] 07 p0971 N71-27488
- BOEING 727 AIRCRAFT**
- Aircraft accident investigation of United Air Lines Boeing 727-22C near Los Angeles, 18 Jan. 1969
[PB-196812] 01 p0606 N71-06061
- Congressional hearings on Boeing 727 use of Washington National Airport
07 p1084 N71-27488
- Analysis of Boeing 727 aircraft impact on environment, passenger processing, passenger loading trends, and scheduled and total operation trends
11 p1672 N71-22998
- BOEING 747 AIRCRAFT**
- Boeing 747 aircraft crash landing in Washington caused by pilot error
[NTSS-AAR-70-19] 01 p0605 N71-06051
- Planning for expected civil aviation developments caused by change-over to Boeing 747 aircraft and supersonic transport
11 p1674 N71-22998
- Planning for civil aviation operations including Boeing 747 aircraft and supersonic aircraft
11 p1675 N71-22998
- Market forecasts and traffic control technologies of Boeing 747 aircraft and supersonic aircraft operations
11 p1675 N71-22998
- Civilian airline operations with Boeing 747 aircraft and supersonic aircraft
11 p1675 N71-22998
- Flight tests of Boeing 747 aircraft and operational analysis for supersonic transport
11 p1675 N71-22998
- Planning for Boeing 747 aircraft integration to Israel airline operations
11 p1675 N71-22998
- BOGOLUBOV THEORY**
- Finite quantum mechanics for four fermion spin field interactions based on Bogolubov theory and spin-tensor functions with Federbusch model example
14 p2304 N71-30239
- Investigating charged Bose gas interactions function using Bohm-Pines and Bogolubov formalisms
15 p2690 N71-29340
- Hartree-Bogolubov theory and application to neutron proton pairing problem
[NP-18338] 17 p2800 N71-30144
- BOILERS**
- Acoustic leak detection in water cooled liquid sodium steam generators
[AFDA-256] 01 p0084 N71-10084
- Leak detection systems development for sodium heated LMFBR steam generators
[AFDA-255] 03 p0414 N71-11820
- SNAP-8 boiler performance degradation and two phase flow heat and momentum transfer models
[NASA-CR-72739] 04 p0619 N71-12980
- Mathematical model of sodium-water reactions related to steam generators
[AFDA-257] 04 p0559 N71-14978
- Vapor generating boiler system for turbine motor
[NASA-CASE-XLE-00785] 06 p0558 N71-14978
- Leak detection method for water and sodium systems applied to boilers of liquid sodium-cooled fast reactors
[ANL-TRANS-837] 06 p0901 N71-10775
- Dynamic analysis of nonequilibrium, forced convective, boiling liquid metal flows
[NASA-CR-117034] 09 p1372 N71-19964
- Experimental evaluation of four transfer functions for single tube boiler and demonstration of function being independent of exit restrictions
[NASA-TM-X-2247] 09 p1376 N71-19964
- Performance and transient testing of single tube potassium boiler for Rankine nuclear power plant system
[NASA-TM-X-52996] 10 p1661 N71-21119
- Shell side hydraulic characteristics of full-scale SNAP 8 multiple-tube model boiler over turbulent Reynolds number from 18,000 to 38,000
[NASA-CR-72830] 11 p1795 N71-20023
- On-line monitoring of impurities in sodium and leak detection in boilers
[ANL-ST-4] 12 p1915 N71-23628
- Heat transfer coefficients and transition point in functions of steam in high pressure boiling flow steam generator
[EUR-4561-E] 13 p1817 N71-24586
- Thermal design analysis on tubular/annular shell forced convection mercury boiler for SNAP 8 system
[NASA-CR-72760] 15 p2453 N71-28585

SUBJECT INDEX

Experimental data on subcooled and not-quality boiling heat transfer to low pressure water in electrically heated tubes
[NASA-TN-D-4402] 17 p3857 N71-29711

SNAP 8 refractory boiler development - corrosion of oxygen contaminated tungsten in NaK
[NASA-CR-1520] 17 p5764 N71-29773

Thermal and hydraulic performance of prototype SNAP-8 mercury boiler - design, fabrication, and preliminary evaluation
[NASA-TN-D-4451] 19 p3041 N71-32280

Destructive tests of Inconel 600 tubes from H reactor steam generator 6A
[NBS-BA-149] 20 p3360 N71-35933

Heat transfer and fluid flow during forced convection boiling of wetted mercury with application to design and optimization of once-through boilers for Space Power Reacting Cycle Systems - SNAP-8
[NASA-CR-72807] 22 p3621 N71-35796

Digital simulation with lumped parameter system of once-through supercritical steam generator
[NASA-CR-72901] 23 p3689 N71-35759

SNAP 8 double containment boiler evaluation for accident conditions
[NASA-CR-72923] 24 p3959 N71-36243

Performance testing of SNAP 8 boiler
[NASA-CR-72940] 24 p3959 N71-36244

Low refractory double containment boiler for SNAP 8 power conversion system utilizing mercury, sodium, zirconium, and type 304 stainless steel materials
[NASA-CR-72918] 24 p3960 N71-36247

Heat and momentum transfer analysis for SNAP 8 condenser NaK to Hg boiler using IBM 360 computer code
[NASA-CR-72977] 24 p4018 N71-36647

Development, characteristics, and performance test of turbine alternator assembly system and component parts
[NASA-CR-72917] 24 p4028 N71-36743

HT FILM BOILING
HT LIQUID-PROST PHENOMENON
HT NUCLEATE BOILING
Self control model through boiling in power excursion of water cooled reactor
[NBS-BA-151] 05 p0416 N71-12890

Boiling and heat transfer characteristics of aqueous hydrogen flows in straight and annular tubes
[NASA-TN-D-6159] 07 p1152 N71-17955

Boiling of liquid alkali metals in tubes
[NBS-BA-155] 09 p1303 N71-18314

Heat transfer phenomena associated with pool boiling from flat horizontal surface
[NBS-BA-156] 08 p1306 N71-19298

Information on parameters associated with generation of acoustic energy by boiling bubbles
[NBS-BA-157] 10 p1089 N71-21778

Heat transfer and hydrodynamic behavior for subcooled flow boiling of Freon 113 for use in cooling electronic components
[NBS-BA-158] 14 p2352 N71-27805

Interacting effect of gravity and size on peak and minimum pool boiling heat fluxes
[NASA-CR-118638] 14 p2353 N71-27843

Reactor local boiling characteristics analysis using digital detection
[NASA-CR-118638] 16 p2633 N71-28699

Low gravity incident boiling heat transfer in closed cylindrical container
[NBS-BA-159] 17 p2631 N71-29612

Analysis of mechanism of boiling, evaporation, and heat transfer in fluids
[NASA-CR-118638] 17 p2859 N71-30187

Mechanism of boiling and characteristics of heat transfer in boiling of metals
[NASA-TT-F-620] 17 p2859 N71-30188

Thermal characterization data used to determine sodium phase boiling point
[NBS-BA-160] 20 p3285 N71-33645

Hydrodynamics of boiling heat flux and dynamics and stability of small gravity and capillary waves
[NASA-CR-121467] 20 p3346 N71-33746

Use of thermocouples for temperature measurement during boiling metal heat transfer experiments
[NBS-BA-161] 23 p3369 N71-33753

Measuring surface material, surface condition and geometry, contact duration, and contact geometry and surface contact effects on heat transfer in boiling of metal
[NBS-BA-162] 23 p3369 N71-33753

MEASURING WATER REACTORS
HT BALDWIN BOILING WATER REACTOR
HT BERTH REACTOR
Cooling temperature and material effects on emergency core cooling system in boiling water reactor
[NBS-BA-163] 01 p0066 N71-10645

Effects of gadolinium added to fuel in boiling water reactor
[NBS-BA-164] 03 p0416 N71-12921

Activity, power distribution, temperature effects, and fuel quality in BWR core
[NBS-BA-165] 05 p0416 N71-12976

Heat transfer in simulated BWR fuel bundle cooled by spray under loss-of-coolant conditions
[ORNL-1908] 04 p0545 N71-13566

Hydrodynamic and heat transfer measurements on full-scale simulated 36-rod Marviken fuel element with nonuniform radial heat flux distribution
[PROG-3] 04 p0547 N71-13634

Aerodynamic system compared with other types of neutron flux detectors in boiling water reactor
[EPRI-120] 04 p0507 N71-13635

Response of simulated BWR fuel bundle cooled by flooding under loss of coolant conditions
[ORNL-1917] 04 p0548 N71-13677

Molybdenum filament performance in BWR emergency cooling heat transfer tests
[ORNL-19092] 04 p0548 N71-13676

Accident evaluation studies for water cooled reactors postulating loss of coolant
[NBS-1083] 04 p0551 N71-13656

Safety studies of blowdowns from bottom outlet of pressure vessels, simulating loss of coolant accidents in pressurized water and boiling water reactors
[BNWL-1411] 04 p0552 N71-13663

Performance data for uranium oxide and plutonium oxide/uranium oxide fuel cores of boiling water reactors
[BNWL-1379] 05 p0726 N71-15045

Investigation of pitting corrosion on molybdenum stainless steel control rod push rods in La Crosse boiling water reactor
[ACNP-70502] 05 p0729 N71-15211

Literature survey on scaling laws for heat transfer and burnout in two phase flow with application to boiling water reactors
[RISO-207] 05 p0784 N71-15555

Simultaneous multiple functional failures in critical safety and protection equipment in boiling water reactors
[NBS-10189] 06 p0899 N71-16681

Probability analysis of pipe failure and low-cycle fatigue in reactor cooling systems
[ORNL-19097] 06 p0900 N71-16738

Using computer code to study behavior of vapor transport fuel pin in boiling water reactor
[NASA-TN-D-6162] 07 p1064 N71-17463

Boiling water reactor accident radiolysis and containment spray system design
[ORNL-TM-2412-PT-8] 08 p1239 N71-18711

Water cooled reactor power gain by intensified heat transfer using artificial roughness
[AD-715461] 08 p1241 N71-18833

Two phase steam-water critical flow data obtained at moderate pressures
[ANL-7240] 09 p1419 N71-19974

Critical heat flux and pressure drop tests of electrically heated nuclear fuel rod bundles with ferrous hydrazine slurry crud deposits
[WAFD-TM-918] 09 p1421 N71-20288

Accident analysis for pressurized and boiling water nuclear steam supply systems loss of coolant situations
[NBS-10897] 13 p2122 N71-25441

Development of differential, regional boiling water reactor model for prediction of volumetric properties of fluid state of gaseous effluents and liquid methanes
[NBS-10897] 14 p2355 N71-26264

Plutonium fuels use and recycling in boiling water reactors
[NBS-10897] 16 p2632 N71-28642

Boiling water reactor fuel test assembly irradiation
[EPRI-132] 16 p2633 N71-28697

Diameter profiles of Zircaloy-clad UO₂ fuel rods from boiling water reactor for defect evaluation
[ORNL-19287] 17 p2782 N71-29368

Pressurized water and boiling water reactor coolant blowdown simulation for reactor safety including temperature and pressure measurements
[BNWL-1463] 18 p2960 N71-30647

FORTRAN computer code for transient flow data analysis and critical cooling deficiency prediction in boiling system of reactor core
[ORNL-19221] 19 p3192 N71-32117

Performance testing and design parameters evaluated for UO₂-Zr fuel assemblies in boiling water reactor
[RISO-6-1350] 21 p3457 N71-34604

Computer program (COGTA-X-BOL) for analysis of intermediate accidents or severe operational transients for BWR and PWR nuclear reactors
[NBS-4497-3] 21 p3458 N71-34612

Bonding modes of single rods in boiling water reactor fuel assembly
[RYTENG-7020] 21 p3458 N71-34614

Three types of uranium oxide-fuel clad charring investigation investigated by X ray fluorescence analysis of two fuel elements after high burnup in VAK reactor
[NBS-4497-3] 21 p3458 N71-34612

Cooling of simulated reactor fuel element by heat transfer from element to boiling water
[UARS-110] 23 p3796 N71-37064

Mathematical evaluation of simulated BWR emergency core cooling tests
[IN-1433] 23 p3796 N71-37076

BOLTZMANN TRANSPORT EQUATION

Use of existing data to analytically describe boiling water and pressurized water reactor coolant
[NBS-1904] 23 p3790 N71-37077

Experimental loop for two phase heat transfer in simulated BWR fuel element
[UARS-81] 24 p4088 N71-38739

BOLIVIA
Astronomical observations and experiments conducted during total solar eclipse of November 12, 1968 in Bolivia
[NBS-1904] 09 p1468 N71-38849

BOLKOW AIRCRAFT
NT BO-105 HELICOPTER
BOLKOW BO-105 HELICOPTER
U BO-105 HELICOPTER
BOLSHAKOV
U BOLOMETERS
BOLSHAKOV
Low temperature silicon thermometer and bolometer
[AD-715908] 02 p0224 N71-11598

High impedance shunting current sensing transformer device between two bolometers for measuring insertion loss of test component
[NASA-CR-100193] 06 p0827 N71-10857

Bolometric measurement of copper, aluminum, and stainless steel emissivities at cryogenic temperatures
[NBS-1904] 11 p1783 N71-23045

Automated system for cost reduction in calibrating bolometer mounts by cutting power measurement time
[NBS-1904] 12 p1919 N71-23632

This film capacitive bolometer and capacitance temperature interchange sensor
[NASA-CR-100193] 15 p2306 N71-37232

Operational superconducting bolometer for use in vacuum characterized and for infrared regions
[NASA-CR-121672] 21 p3426 N71-34377

Platinum-film four glass bolometer development, radiation centers in boron glasses, local order in liquid chalcogenides, and chalcogenide glass bolometers for infrared and microwave detection
[AD-726416] 22 p3483 N71-35657

BOLIVIA
Analysis of bolt loads by ultrasonic techniques
[NASA-CR-100193] 03 p0461 N71-12945

Prestrained bolt joining and prestrain effect under static and dynamic loads
[CRIP-MT-63] 10 p1453 N71-21031

Split nut and bolt separation device
[NASA-CR-100193] 10 p1567 N71-31489

Analysis of physical properties and yield strength of bolts used as shear connectors in concrete on steel composite beams
[NBS-1904] 10 p1459 N71-31807

Investigation of variables affecting joint prestrain proportion of installed structural bolts and nuts used in fabrication and construction of spacecraft components
[NASA-CR-100193] 14 p2364 N71-36548

Ultrasonic, pulse echo interferometric method for measuring bolt prestrain
[NBS-1904] 16 p2590 N71-28818

Device for measuring together structural members with axially stretched bolt and nut
[NASA-CR-100193] 21 p3432 N71-34422

Materials, manufacture, quality control, and mechanical properties of bolted joints under static and dynamic stresses
[NBS-1904] 22 p3590 N71-35563

Prediction of bolted joint heat transfer in spacecraft applications
[NASA-CR-119533] 22 p3604 N71-34346

BOLTZMANN DISTRIBUTION
Considering quantum-mechanical status as Boltzmann ensemble
[AD-715125] 08 p1246 N71-19289

BOLTZMANN TRANSPORT EQUATION
User manual for DOT-TW discrete ordinate transport computer code
[WAFD-TM-1982] 01 p0101 N71-10833

Optimization to non-Hilbert space of interior boundary value problem for Boltzmann equation
[ONERA-TP-903] 02 p0251 N71-11639

Two-overlapping group transport approximation for thermal neutron problems
[WAFD-T-5341] 04 p0283 N71-14831

One dimensional, discrete ordinate neutron transport technique for use with neutron reactor shielding methods, modification, updating, and data input preparation - Vol. 4
[NASA-CR-100193] 05 p0729 N71-15165

Two dimensional, discrete ordinate transport technique for use with neutron reactor shielding methods, modification, updating, and data input preparation - Vol. 5
[NASA-CR-100193] 05 p0729 N71-15166

Neutron transport equation solutions
[NBS-1904] 05 p0806 N71-15715

Quantum theory of density corrections to gaseous transport coefficients
[NASA-CR-116137] 06 p0808 N71-15934

Flux synthesis methods to obtain detailed neutron flux from lower-order calculations
[LA-4472] 06 p0808 N71-16289

Derivation of hydrodynamic equations for gas mixtures using Boltzmann transport equations and Onsager symmetry relations

07 p1006 N71-16049

Using Monte Carlo method for calculating constant variance of neutron for every point in phase space [CEA-CONF-1567]

06 p1252 N71-16297

Transport analysis of thermionic diode plasma [AD-719228]

09 p1373 N71-18371

Boltzmann transport equations for flow of heat between parallel plates in rarefied gas

06 p1183 N71-18986

Local potential of Boltzmann-type equations used in kinetic theory of gas shock waves [IPI-101]

09 p1369 N71-19423

Determination of local thermodynamic equilibrium by zero-order Boltzmann collision equation [CEA-CONF-1629]

09 p1450 N71-20283

Solutions to integral transport equations for particle density using spherical geometry

11 p1810 N71-23038

Turbulent transport equations to determine turbulent flow and increase predictive capability in mean velocity field closure

12 p1902 N71-23757

Linear Boltzmann operator for multiple scattering processes in electron and neutron transport theory [AD-718665]

12 p1973 N71-23936

Finite difference techniques peculiar to solution of Boltzmann transport equation in two dimensional spherical geometry - FORTRAN program [LA-4567]

12 p1980 N71-24347

Review of Monte Carlo method applications for calculation of radiation transport

14 p2301 N71-25730

Three dimensional photon transport calculations based on Boltzmann transport equation and Neumann series for photon scattering densities

14 p2307 N71-26392

Boltzmann transport equation for calculating triple collision effects on thermal conductivity and viscosity of moderately dense gases

14 p2215 N71-26639

Mathematical model and computer program for solution of asymptotic neutron transport equations in slab geometry

14 p2312 N71-26707

Neutron behavior in multiplying medium, Boltzmann equation application, and derivation of related kinetic equations

15 p2486 N71-27819

Integral Boltzmann transport equation for nonequilibrium neutrons solved by direct kernel decomposition [JEP-70/27]

16 p2643 N71-28083

Derivation of kinetic equations for slightly dense and dilute short range gases, Boltzmann equation related to short range gas equations, and role of collision events in system evolution

17 p2733 N71-29623

Boltzmann transport equation for elastic scattering of electrons in solids

19 p3167 N71-31708

Three dimensional integrals for stationary neutron transport equation with spherical symmetry

19 p3149 N71-32103

Collisionless Boltzmann equation for model of rotating and nonspherical planetary exospheres [NASA-TM-X-45662]

19 p3094 N71-32391

Numerical solution of linear integral Boltzmann equation as applied to reactor core and shield neutron and photon transport problems

20 p2392 N71-33677

Variational synthesis method applied to steady state Boltzmann neutron transport equation [ORNL-TM-3200]

21 p3477 N71-34766

Transport equation including nonlinear induced scattering effects for photon flux (speed of light time density)

21 p3484 N71-34817

Boltzmann models for hydrodynamic equations, transport coefficients, and light scattering by simple fluids

22 p3570 N71-35429

Stationary one-group neutron transport equation with application to transport calculations for multidimensional, heterogeneous reactor configurations [ANL-7779]

22 p3646 N71-35997

Fluctuation enhanced conductivity of superconductors, and evaluation of Maki graph based on Boltzmann equation

22 p3657 N71-36080

Transport equations for determining cosmic ray phenomena of galaxy

22 p3665 N71-36129

SNAP radiation shielding design using computer programs with numerical solutions to transport equation [ORNL-TM-3364]

23 p3797 N71-37871

Monte Carlo method for studying deep penetration of neutrons by means of biasing system

[CEA-R-4145]

23 p3807 N71-37140

Numerical solution of Boltzmann equation applied to problems of shock structure in gas of elastic spheres [NYO-1488-173]

23 p3814 N71-37195

BOMBARDMENT

Quality measurements of neutron spectra produced by bombardment of beryllium target below 0.5 Mev

17 p2804 N71-30270

BOMBER AIRCRAFT

NT A-4 AIRCRAFT

NT A-4 AIRCRAFT

NT B-52 AIRCRAFT

NT B-57 AIRCRAFT

NT B-70 AIRCRAFT

BOMBS [ORDNANCE]

Optimal bomb release intervals from B-52 aircraft bombing system

09 p3139 N71-19383

BOMBS [PRESSURE GAGES]

U PRESSURE GAGES

BOMBS [SAMPLERS]

U SAMPLERS

BONDING

NT ADHESIVE BONDING

NT CERAMIC BONDING

NT EXPLOSIVE WELDING

NT METAL BONDING

NT METAL-METAL BONDING

NT RESIN BONDING

Nondestructive tests developed for bonded material evaluation

[AD-709962]

01 p0070 N71-10072

Nondestructive tests for evaluating bonded materials

[AD-709963]

01 p0071 N71-10174

Nondestructive test development for bonded materials evaluation

[AD-709964]

01 p0071 N71-10302

Activated gas plasma spraying of polymers for adhesive bonding

[AD-711011]

01 p0039 N71-10363

Effect of oil films on adhesion of polymers to metal surfaces

[AD-713450]

05 p0710 N71-15370

Evaluation of characteristics and integrity of casting

05 p0711 N71-15662

Intermetallic diffusion and bonding characteristics of Zircaloy with niobium and tungsten

[AD-714499]

05 p0706 N71-15699

Beam lead technology for microcircuit interconnections with applications to metallization, passivation, and bonding

[NASA-CR-111838]

09 p1362 N71-19422

Compilation of technical information including technology, electrical repair, fabrication techniques for coating, bonding and brazing, and electron beam welding

[NASA-SP-5925/01]

13 p2087 N71-25026

Influence of core to sleeve bonding on fracture of hydrostatic extrusion of hard core clad rod

[NYO-4078-3]

18 p2938 N71-31559

Roll Bonding beryllium wire-metal matrix composites

[AD-726423]

22 p3602 N71-35655

Properties of composite structures bonded by epoxy resins with various hardening agents

[AD-727600]

24 p3944 N71-38134

BONE MARROW

Effects of gamma radiation on cell division processes and chromosomes in bone marrow of dogs

[AD-726423]

02 p0161 N71-11497

Evaluating bone tissue optical density and calcium content in blood serum and urine of Soyuz 9 crew members

06 p1151 N71-18904

Survey of radiological science research and development in Japan in 1969, with program emphasis on internal plutonium exposure and clinical aspects of bone marrow transplantation

[NIHS-9]

18 p2876 N71-31853

Neutron dose distributions at bone tissue interfaces in human body

[ORNL-TM-5329]

21 p3382 N71-34066

BONES

NT CRANIUM

NT SCIATIC REGION

NT SKULL

NT VERTEBRAE

Age and exercise factors influencing osteoporosis, bone strength, and acceleration tolerance investigated using rhino monkeys

[AMRL-TR-70-74]

09 p1336 N71-20359

Measuring instruments for in vivo bone mineral content and body composition measurement

[NASA-CR-121415]

20 p3215 N71-33223

Conference on aerospace environments, manned space flight, weightlessness simulation, musculoskeletal and cardiovascular systems, bone loss, mineral metabolism, and hematology

[NASA-SP-269]

23 p3216 N71-33251

Measurement of bone density loss during manned space flight

20 p3216 N71-33254

Measurement of bone mass loss as result of immobilization

20 p3216 N71-33256

Effects of inactivity or immobilization on bone loss

20 p3216 N71-33258

Nondestructive measurement of density, tensile strength, and modulus of elasticity of bones

20 p3217 N71-33259

Long term bed rest effects on mineral balance and bone density in normal individuals

20 p3218 N71-33260

Effects of prolonged bed rest on bone and calcium metabolism and mineral content loss of os calcis

20 p3218 N71-33261

Research and development, weightlessness simulation, calcium metabolism, manned space flight, pressure suits, immobilization, and aerospace medicine

20 p3219 N71-33262

Assays of hormonal control of calcium and bone metabolism

23 p3712 N71-36080

Effects of space flight on bone metabolism as visualized by analyzing peptides hormones in urine

23 p3712 N71-36081

Structural development of bone in rats under earth gravity, simulated weightlessness, hypergravity, and mechanical vibration

[NASA-CR-18523]

24 p3879 N71-38080

BOOLEAN ALGEBRA

NT BOOLEAN FUNCTIONS

Boolean algebra and vector spaces for pattern recognition, pulse communication, switching, and information theory

[NPL-DES-4]

03 p0342 N71-12569

Boolean matrices for optimization of functional covering problems

04 p0536 N71-11800

Boolean algebra applied to logic counting circuits

18 p1528 N71-25140

Finite approximability of superintendible classes of propositions

11 p1786 N71-20800

Geometric properties of nonbinary switching functions which are direct generalizations of Boolean functions of binary logic

11 p1729 N71-20801

Algebraic formulation of single layer printed circuit wiring problem with triple connectivity based on simultaneous Boolean equations

[AD-718804]

12 p1887 N71-20802

Boolean algebra for application to digital electronics and relay networks

[ISS-70/18]

20 p3290 N71-33099

BOOLEAN FUNCTIONS

Fast algorithm for minimization of Boolean functions to two level and-or form

[NASA-CR-102918]

02 p0187 N71-11314

Models for solving pseudo-Boolean linear equations and inequalities

10 p1592 N71-30800

Boolean function derivatives and series

[LAAS-NI-700-PT-1]

18 p2945 N71-31111

Synthesizing logic circuits and Boolean function cubes with not more than three variables

[AD-727972]

24 p3896 N71-37780

BOOMS [EQUIPMENT]

Elastic stability and equilibrium configuration of earth pointing gravity gradient satellites with long appendages

[CRC-1204]

01 p0127 N71-10865

Orbital expansion thrust effect on shape of INS satellite boom

[NASA-CR-652]

05 p0771 N71-11801

Thermodynamic boom actuator and fuelable antenna for Thermoelectric Outer Planet Spacecraft

10 p1566 N71-33035

Performance test on rolling solar array system and thermal bending tests on deployable boom

[NASA-CR-118006]

12 p1860 N71-25114

Collapsible antenna boom and conical trusslike line having inflatable laser tube

[NASA-CASP-MPS-30008]

15 p2280 N71-27099

Torsional rigidity measurements on different satellite boom configurations

[NASA-TN-D-6175]

19 p3180 N71-32848

Influence of ship on boom and rawinsonde temperature measurements during BOMEX

[NOAA-TM-ERL-BOMEX-6]

22 p3574 N71-35800

NASTRAN computer program used to calculate internal deflections of weak spacecraft antenna booms to determine stiffness at small angles

22 p3482 N71-34825

BOOST

U ACCELERATION [PHYSICS]

BOOSTER ROCKETS ENGINES

Aerodynamic drag effects on ramjet missile booster rocket engine

[DLR-FB-70-45]

07 p1117 N71-11800

Low altitude longitudinal aerodynamic characteristics of twin body space shuttle booster configuration using low turbulence pressure tunnel - graphs

[NASA-TM-X-21462]

12 p1890 N71-25114

Technology development for low cost rocket boosters and estimates of total cost reduction obtainable by implementation

[NASA-TM-X-67912]

20 p3340 N71-33070

Low speed wind tunnel tests of subsonic, laminar and cruise aerodynamic characteristics of space shuttle booster with exhaust effect simulation

[NASA-CR-119773]

24 p4019 N71-38080

SUBJECT INDEX

BOOSTER ROCKETS

- Asymmetrical shock loading of space shuttle booster surfaces during atmospheric ascent 14 p2354 N71-38059
- Separation systems for reusable space shuttle booster configurations 14 p2343 N71-38068
- Dynamic flight control simulation for straight wing space shuttle booster entry 14 p2343 N71-38069
- Booster wing geometry effects on space shuttle design requirements 14 p2344 N71-38070

BOOSTERS

- Life-off procedures for space booster 07 p1118 N71-17994

BORANES

- NT CARBORANES
- NT PENTABORANES
- Reactions and low temperature mass spectrometry of carboranes 02 p0173 N71-11222

BORATES

- Procedures for determining boron in borates, boron hydrides, organo-boron compounds, elemental boron, and refractory borides and thrust standardization 12 p1870 N71-33520
- Effects of nuclear dipole-dipole interaction on nuclear magnetic resonance powder pattern studied by computer techniques using thin-film borate glasses and polycrystalline monocrystals 15 p2483 N71-27768

- Biological properties of alkali borate glass melts and influence of water on rheological properties of borate oxide glass and two sodium borate glasses 21 p3443 N71-34594
- Thermodynamic properties of four crystalline sodium borates 22 p3530 N71-35290

- Potential-free laser glass development, radiation source in borate glasses, local order in liquid chalcogenides, and chalcogenide glass biomaterials for infrared and microwave detection 22 p3482 N71-35657

BORON FLAKES

- Thermal dilatation dynamics and plastic flow in crystal lattices 17 p2834 N71-35990

BORON

- Analysis of space group symmetry, polytypism, layer twisting, and stacking for application to aluminum borate structures 14 p2336 N71-36348

- Tables on fracture mechanics of notched bars of boron composites and carbon bonded boron carbide 15 p2435 N71-27783

- Heat treatment of carbide and boride strengthened aluminum alloys to improve tensile and creep rupture strength 18 p2933 N71-36676
- Development of techniques for borizing machine oil and parts in powdered mixtures 24 p3929 N71-38036

BORON MACHINES

- Automatic controlled drive mechanism for portable turbo 20 p3279 N71-35518

BORON APPROXIMATION

- Ultimate parameters in Born model of rubidium lattice 03 p0435 N71-12999
- Investigating structure factors, Born approximation, nuclear and magnetic cross-sections, and polarization analysis in neutron physics 04 p0573 N71-13687

- Proving uniqueness of Chan-Pao SU(5) factor for hadron terms involving nonexotic mesons 04 p0508 N71-14310

- Born approximation for inelastic electron scattering in alkali gas atoms 05 p0747 N71-15230

- Computer coupled channel and distorted wave Born approximation optical model parameters in 2e-14 scattering from inelastic nuclear scattering 05 p0746 N71-15282
- Quantum mechanical study of H₂ reactive scattering, treated by distorted-wave Born and simplified wave Born approximations 09 p1445 N71-30572

- Differential ionization cross section in Born approximation 10 p1613 N71-30827

- Mathematical models for solving scattering by weak volume inhomogeneities 10 p1609 N71-31753

- Determining high energy peripheral collisions by measuring Born approximation by phase shift factors of nuclei scattering 11 p1806 N71-32523
- Optical potential spin-orbit effects on the inelastic proton detector asymmetry with polarized protons from deuterated wave Born approximation 14 p2317 N71-36756

- Polarization of protons from C-12 α pC-13 reaction at 12.4 MeV and distorted wave Born approximation comparisons 15 p2481 N71-27891

- Orbital, fluorine, and sodium isotope atomic excitation energies, spins, parities, and angular distributions using time of flight spectrometers and Born approximations 15 p2484 N71-27954

- Neutron scattering cross sections for T₂, H₂O-4 reactions and spin-orbit interactions including polarization effects and distorted wave Born approximations 17 p2792 N71-39443

- Derivation of equations for Klystron and Born approximations in turbulent atmospheric attenuation and scattering of coherent light 17 p2789 N71-36229

- Low energy theorems for Compton scattering off arbitrary spin targets with scattering amplitudes dominated by Born approximation 17 p2809 N71-36564

- Using Born-Green-Yvon 2 theory for describing low and moderately dense fluids 18 p2903 N71-31889

- Glimmer and Born approximations of electron impact excitations of hydrogen atomic energy levels 20 p3515 N71-35806
- Numerical analysis of inelastic scattering of neutrons from Li-7 using distorted wave Born approximation 21 p3492 N71-34876

- Distorted wave Born approximation code adaptation for IBM 360/30 computer 22 p3634 N71-35994
- Theory of deuteron breakup in nuclear and Coulomb fields using distorted wave Born approximation 23 p3621 N71-37260

- ANU-SP-307

- 23 p3621 N71-37260

- 23 p3621 N71-37260

- 23 p3621 N71-37260

- 23 p3621 N71-37260

- 23 p3621 N71-37260

- 23 p3621 N71-37260

- 23 p3621 N71-37260

- 23 p3621 N71-37260

- 23 p3621 N71-37260

- 23 p3621 N71-37260

- 23 p3621 N71-37260

- 23 p3621 N71-37260

- 23 p3621 N71-37260

- 23 p3621 N71-37260

- 23 p3621 N71-37260

- 23 p3621 N71-37260

- 23 p3621 N71-37260

- 23 p3621 N71-37260

- 23 p3621 N71-37260

- 23 p3621 N71-37260

- 23 p3621 N71-37260

- 23 p3621 N71-37260

- 23 p3621 N71-37260

- 23 p3621 N71-37260

- 23 p3621 N71-37260

- 23 p3621 N71-37260

- 23 p3621 N71-37260

- 23 p3621 N71-37260

- 23 p3621 N71-37260

- 23 p3621 N71-37260

- 23 p3621 N71-37260

- 23 p3621 N71-37260

BORON COMPOUNDS

- Interface effects on off-axis and transverse tensile properties of boron-reinforced aluminum alloys 18 p2885 N71-38104
- Developing thermally stable adhesives for bonding titanium alloy and boron composite substrates 17 p2770 N71-38771

- Effects of boron concentration in water on environment pollution 18 p2882 N71-38998
- Boron influence on amorphous titanium steel precipitation during creep 19 p3111 N71-31896

- Synchronous radiation of carbon, boron, and beryllium and observations of K lines in ultraviolet X-ray emission spectra 19 p3151 N71-32142
- Crack propagation in aluminum alloys reinforced with boron and stainless steel fibers 20 p3285 N71-33590

- Effects of boron on plasticity and structure of carbon composite, strength and density - properties of synthetic graphite 20 p3285 N71-33590
- Design, fabrication and tests of boron-graphite reinforced structures for CR-548 rail cars 21 p3574 N71-34813

- Structural analysis of tail cone of CR-548 helicopter reinforced with boron-graphite composites 21 p3575 N71-34814
- Steam pyrolysis treatment for purifying boron and potassium fluoride powders 21 p3444 N71-34511

- Monte Carlo codes for evaluating efficiency of boron-cadmium in the neutron center 21 p3471 N71-34715
- Electron affinity calculations for Li, B, O, F, C, N and self consistent field equations for multiple open shells 21 p3482 N71-34876

- Boron effects on ductility and strength of Inconel 600 and Tycron 304 and 316 stainless steel at hot metal working temperatures 22 p3594 N71-35591
- Boron proportional counter with low gamma ray sensitivity for measuring thermal neutron flux in fast neutron reactors 22 p3635 N71-35910

- Nuclear structure of boron 11 studied by high energy electron scattering 22 p3636 N71-35921
- Crytalllographic positions and boron shifts of boron in boron determined by Mossbauer spectroscopy 22 p3640 N71-35946

- Electronic potential and spectroscopic determination of boron fluoride, chlorine, and boron in phosphorus oxide fuels after pyrolysis of boron 23 p3681 N71-37899
- Fabrication and testing of one-third scale boron-graphite tubular reactor thrust structure 24 p3687 N71-38818

- Filament tensile strength and pressure-strain characteristics of high modulus, high-strength, boron-fiber-reinforced-carbon composites pressure vessel at ambient and cryogenic temperatures 24 p3688 N71-38823
- Mechanical properties of continuous composition of boron fibers magnesium metal matrix 24 p3696 N71-38152

- Supersonic combustion chemistry and mixing of high energy density fuels related to advanced aircraft engine design, using boron particles 24 p3690 N71-38530

- AD-72762

- 24 p3690 N71-38530

- 24 p3690 N71-38530

- 24 p3690 N71-38530

- 24 p3690 N71-38530

- 24 p3690 N71-38530

- 24 p3690 N71-38530

- 24 p3690 N71-38530

- 24 p3690 N71-38530

- 24 p3690 N71-38530

- 24 p3690 N71-38530

- 24 p3690 N71-38530

- 24 p3690 N71-38530

- 24 p3690 N71-38530

- 24 p3690 N71-38530

- 24 p3690 N71-38530

- 24 p3690 N71-38530

- 24 p3690 N71-38530

- 24 p3690 N71-38530

- 24 p3690 N71-38530

- 24 p3690 N71-38530

- 24 p3690 N71-38530

- 24 p3690 N71-38530

- 24 p3690 N71-38530

- 24 p3690 N71-38530

- 24 p3690 N71-38530

- 24 p3690 N71-38530

BORON FLUORIDES

NT BORON CARBIDES
NT BORON FLUORIDES
NT BORON HYDRIDES
NT BORON NITRIDES
NT CARBORANE
NT DIBORANE
NT ORGANIC BORON COMPOUNDS
NT PENTABORANES

Highly reactive boron compound cryosynthesis and theoretical reaction kinetics at cryogenic temperatures using molecular orbital methods

Development of boron diffusion process to diffuse large quantities of stress-free, high efficiency, radiation resistant solar cells

Metamagnetic and antiferromagnetic properties and structures of CrB compounds, emphasizing collinearity and wave vectors

Electrophysical properties and structure of chemical bond in boron, carbon, and beryllium compounds

Electrical conductivity of boron and silicon compounds produced by hot pressing and sintering of cold-pressed pellets

In vitro studies using boron-labeled antibodies and elemental boron as neutron target in therapy for tumors and cancer

Boron trifluoride proportional neutron spectrometer control unit for automatic or manual control

BORON NITRIDES
NT BORANES
NT CARBORANE
NT PENTABORANES

Procedures for determining boron in borates, boron hydrides, organo-boron compounds, elemental boron, and refractory borides and titan standardization

Space vehicle oxygen fluoride/boron hydride tank nuclear thermal control design for Javelin mission

BORON ISOTOPES
NT BORON 10

Decay mode and He-4 coherent interference data for B-11 (p, γ) He-4 reaction at proton beam energies of 0.675, 1.00, and 1.388 MeV

Foot-value ratio expressions for second class currents from mirror beta decays in B-12-N-12 systems

Excited states in boron 10 decay between 18 and 22 MeV

In vitro studies using boron-labeled antibodies and elemental boron as neutron target in therapy for tumors and cancer

Advantages and use of ion exchange resins for separating boron, nitrogen, and uranium isotopes

He-3, p reactions with Ne-20, N-14, and B-11, and gamma de-excitation of Ne-21 and Ar-41

BORON NITRIDES
Boron nitride effect on tungsten friction and wear

High temperature stability and electrical properties of pyrolytic boron nitride capacitors

Determination of boron and nitrogen in pure boron nitride by controlled fusion of boron nitride with sodium carbonate followed by potentiometric titration of resulting boric acid

BORON TRIFLUORIDE
U BORON FLUORIDES
BORON 10

Mechanism of nuclear reactions Be-9/p/Be-9 and Be/p/alpha/Li-6 at low energies

Excited levels of boron 10 in 7.5 MeV region

Energy spectra of neutron pairs from pion capture in carbon 12 boron 10 reaction

Cyclotron for measuring angular distributions from 15 deg to 165 deg for transitions in B-10 states - reaction mechanism and capture structure

BORONICACATE GLASS
Determination of viscosity of standard borosilicate glass

Lead oxide immiscibility in lead borosilicate glass for opaque glazes

Light scattering effect for determining phase separation in sodium borosilicate glasses

Fracture energy and strength behavior of sodium borosilicate glass A202 composite materials system

BORONICACATE GLASS FATIGUE AND SOLUBILITY IN SILICATES

BOSE GEOMETRY
Inhomogeneous Bose gas interactions with ion impurities, walls, and vortices

BOSE-CHANDRASEKHAR-BOCQUENHIEUX CODES
U BCH CODES
BOSE-EINSTEIN STATISTICS
U QUANTUM STATISTICS
BORON FIELDS

Group theory and Lagrange multipliers generated by boson fields and vector current algebra

BOSONS
NT ALPHA PARTICLES
NT ETA-MESONS
NT KAONS
NT LIGHT BEAMS
NT MESON RESONANCES
NT MESONS
NT PHOTONS
NT PIONS

Heavy bosons in proton-antiproton interactions

Hadronic decay modes of weak intermediate bosons produced by high energy neutrinos

Call model of boson quantum system in three phases

Heisenberg ferromagnetism at low temperatures with boson theory of angular momentum including spin operators

Current algebraic model for asymptotic weak spectral functions and hadronic decays of intermediate vector bosons

Second quantized nonrelativistic time-dependent scattering theory describing identical bosons interacting via two body forces and generalizing in-out formalism

Spinor field theory of Dirac fermions interacting with bosons at infinite momentum based on perturbation theory and tree-graph approximation

Pion shielding and muon background minimization from pions and gamma quanta in IHEP accelerator and W boson experiments in nucleon-nucleon interactions

Estimation of muon scattering cross sections in nucleon-nucleon interactions and W-bosons

Lambda phi cubed interaction with boson fields using nuclear models

Investigating charged Bose gas intermediate densities using Bohm-Pines and Bogoliubov formalisms

Construction of axial vector current in boson sigma model using perturbation theory

Quadratically divergent terms in amplitudes of weak nonleptonic processes with photon emission studied in theory with intermediate boson

Asymptotic expansion for 2-boson scattering amplitude with Pomeron singularities

Asymptotic SU(3) symmetry, nonet boson coupling sum rules, and ninth pseudoscalar mesons

Unitarity used to calculate imaginary part of elastic scattering amplitude for identical bosons

Hypersonic-nucleon interaction using crossed channel boson exchange model

BOTTLES
Materials tests on bottles for oxygen, air, and other gases to be used as airborne equipment, noting filament viscosities

BOUQUET LAW
Bouquet anomalies in ocean

BOUNDARIES
NT FLUID BOUNDARIES
NT FREE BOUNDARIES
NT GAS-SOLID INTERFACES
NT GRAIN BOUNDARIES
NT JET BOUNDARIES
NT LIQUID-LIQUID INTERFACES
NT LIQUID-SOLID INTERFACES
NT LIQUID-VAPOR INTERFACES

Wall porosity effect on stability of quasi-periodic laminar flow over plane compliant boundaries

Monte Carlo techniques using regressive analog computer for estimating lowest eigenvalues for certain partial differential equations with Dirichlet boundary conditions

Analytic model of boundary conditions for heat transfer coefficients through porous walls

Formalism describing space dependence of acoustic resonance self shielding at boundaries of homogeneous zones in nuclear reactors

Integral equation formulations of scattering from two dimensional inhomogeneities in conductive media

Existence bound calculations for atomic model by variational calculus

BOUNDARY LAYER COMBUSTION
Velocity profiles for subsonic turbulent boundary layer with mass addition, combustion, and pressure gradients

Shock-induced combustion in explosive mixtures of hydrogen and air or oxygen by high speed shots at low pressures

BOUNDARY LAYER CONTROL
NT POROUS BOUNDARY LAYER CONTROL
Feasibility study of counter incompressible aircraft with suction boundary layer control

Lift and pressure distribution on leading edge and trailing-edge flaps of wing profile with boundary layer control

High lift wing characteristics - wing with plain hinged flaps and boundary layer control, and wing with drag and high lift devices extended

Low speed wind tunnel tests of ground proximity effects on static longitudinal characteristics and boundary layer control of short takeoff aircraft

Operational performance and handling safety requirements for single engine boundary layer controlled aircraft in STOL mode

Blowing effect on static efficiency of two dimensional air intakes with momentum injection in boundary layer control form

Unsteady airfoil stall characteristics using state data input for predicting stall flutter boundaries of space shuttle wing

Velocity profile control tests of diffuser wall bend to control combustor inlet airflow distribution

Determination of aircraft longitudinal motion during takeoff and landing after loss of lift from boundary layer control system

Feasibility study of combined laminar and turbulent boundary layer control system using distributed suction with application to low-speed research aircraft of glass reinforced plastic

BOUNDARY LAYER FLOW
NT BOUNDARY LAYER SEPARATION
NT REATTACHED FLOW
NT SECONDARY FLOW
NT SEPARATED FLOW

Successive approximations method for equation integration of laminar multicomponent boundary layer with chemical reactions including ionization

Effects of rotation on boundary layers in turbomachine rotors

AGARD conference on connecting and chemistry reacting viscous flows over hypersonic at hypersonic conditions

Solution of chemical nonequilibrium boundary layer flow of hypersonic in earth atmosphere

High order boundary layer effects on rare lift drag of spherical bodies

Numerical results for ideal gas boundary layer flow for asymptotic half-angle hypersonic

Determination of boundary layer diffusion in forced convection flow

Investigating gas dynamical aspects of combustion in hybrid rocket motors

Boundary layer measurements in accelerated flow with and without heat transfer

SUBJECT INDEX

Air flow over roughness discontinuity
 [AD-712113] 05 p0465 N71-15465
 Boundary layer flow over rough surface, and
 surface transport
 [AD-714021] 06 p0836 N71-16132
 Flowed boundary layer flow in converging channel
 06 p0839 N71-16852
 Numerical analysis of boundary layer equations in
 two-dimensional section for laminar flow
 [NASA-TN-D-6152] 07 p1089 N71-17416
 Investigating transonic rotational flow around con-
 ventional airfoils
 [AD-717797] 08 p1178 N71-18455
 Boundary layer characteristics of particulate flow in
 ducts
 [AD-717721] 08 p1179 N71-18454
 Velocity distributions in turbulent channel flow with
 glass wall layers
 08 p1179 N71-18594
 Limits of hypersonic boundary layer theory, and
 laminar and turbulent flow phenomena in laminar hyper-
 sonic boundary layer
 09 p1373 N71-19833
 Hypersonic laminar boundary layer growth over
 concave and convex surfaces
 09 p1374 N71-19834
 Finite difference method for solving equations for
 compressible turbulent boundary layers on swept in-
 clined cylinders
 [NASA-TN-D-6303] 10 p1339 N71-20709
 Surface density and temperature in laminar flow
 and nozzle-wall boundary layer, measured with con-
 tact film-voltage and swept-voltage RAM probes
 10 p1620 N71-21115
 Visualized flow patterns of polystyrene films to mea-
 sure vortex formation and air and water boundary
 layer effects
 [AD-725791] 10 p1544 N71-21646
 Analytical techniques for determining flow
 conditions in boundary layer of aerodynamic self-
 propelled models and individual aquatic animals
 11 p1699 N71-22211
 Determination of flow properties of turbulent bound-
 ary layers with negligible wall stress
 11 p1739 N71-22587
 Techniques for generating artificially thickened
 laminar flow on flat plates
 [NASA-TN-D-6238] 11 p1742 N71-22681
 Solution of general self-similar boundary layer
 equations and parametric investigation of several
 cases of boundary layer flow
 11 p1743 N71-22759
 Correlation between characteristic viscous length
 and shear stress gradient in retransitional flow
 [N7186] 12 p1902 N71-23826
 Development and tests of slots and ejectors for in-
 vestigating additive solutions in aqueous boundary
 layer to reduce turbulent frictional resistance
 [AD-719573] 13 p2065 N71-24636
 Hypersonic heat transfer to flat plates and conical
 and blunt bodies in boundary layer flow
 [ARC-RM-3637] 13 p2065 N71-24714
 Hydrodynamics and gas dynamics of boundary
 layer flow including mass transfer and convective and
 radiative heat transfer of bodies in fluids
 [AD-720728] 14 p2244 N71-26539
 Relation to boundary layer problems in laminar
 subsonic flow with aerodynamic chemical reactions
 16 p2582 N71-28868
 In-flight use of traversing boundary layer probe
 tubes with mechanical and electrical features and
 simple boundary layer profiles
 [NASA-TN-D-6428] 16 p2530 N71-28872
 Shock wave boundary layer interactions in two
 dimensional and axially symmetric flows including
 viscous influences
 16 p2583 N71-28897
 Second order effects on wave structures associated
 with planar and conical bodies in supersonic flow
 17 p2734 N71-29486
 Boundary effects on heat transfer in non-Newtonian
 fluid flow through plane cracks
 18 p3087 N71-31450
 Numerical solution of flow equations for laminar,
 transitional, and turbulent compressible boundary
 layer for slender or axisymmetric flows
 [NASA-TN-D-5-568] 19 p3078 N71-32164
 FORTRAN 4 computer program for design of
 deep-angled throat supersonic nozzles with boundary
 layer correction
 [NASA-TN-D-2543] 19 p3083 N71-32793
 Statistical analysis of atmospheric turbulence at
 Cape Kennedy Launch Complex for spacecraft design
 [NASA-CR-1089] 19 p3132 N71-32796
 Numerical analysis of structure of nonequilibrium
 laminar flow along flat plate in partially ionized gas
 at heating conditions
 [AD-720254] 20 p3329 N71-33851
 Stability of three dimensional waves moving in
 boundary layer flow on flat plate rotating about lead-
 ing edge
 20 p3253 N71-33861
 Numerical analysis of shock induced boundary
 layer flow on semi-infinite flat plate - Part 2
 [NASA-CR-131743] 21 p3410 N71-34280

Measurements in boundary layer of flat plate using
 helium or argon injection and supersonic flow mea-
 surement with hot-wire anemometer
 [NASA-TT-8-12929] 21 p3410 N71-34283
 Measurement of flow characteristics behind
 backward facing step to demonstrate flow in reat-
 tachment region
 [IC71/105] 21 p3411 N71-34272
 Hexagonal convection flow in internally heated
 fluid layers and bifurcation phenomena
 [AD-728016] 21 p3531 N71-35159
 Integral equations for solution of three dimensional
 laminar boundary layer problems
 [NASA-TT-F-13567] 22 p3567 N71-35403
 Wind tunnel investigation of laminar, transitional,
 and turbulent boundary layer profiles on wedge at
 hypersonic speed to confirm theoretical analysis
 [NASA-TN-D-6463] 22 p3569 N71-35417
 Composition of planetary boundary layer and
 representation by boundary layer along flat plate
 [TD-25465] 22 p3669 N71-36163
 Design, construction, and performance of water
 tunnel for two dimensional testing of pitching airfoils
 [D180-14130-1] 24 p3904 N71-37827
 Performance tests and efficiency measurement of
 hub-shaft-coupled stage in single stage compressor
 [NASA-CR-120023] 24 p3945 N71-37834
 Theoretical and experimental analysis of laminar
 shock-boundary layer interactions
 [IC71/116] 24 p3908 N71-37832
BOUNDARY LAYER NOISE
U AERODYNAMIC NOISE
U BOUNDARY LAYERS
BOUNDARY LAYER SEPARATION
 Heat transfer in base type supersonic laminar and
 turbulent separated flows
 [AD-710347] 01 p0049 N71-10249
 Three dimensional flow patterns obtained during
 boundary layer separation on airfoils
 [NPL-AERO-1305] 02 p0143 N71-11014
 Separation point study of incompressible laminar
 boundary layers around parabolic bodies at angle of
 attack
 [AD-712084] 02 p0201 N71-11519
 Investigating flow field in rear wake behind rear-
 ward facing step in supersonic flow and heat transfer
 distribution along reattachment surface downstream
 of step
 03 p0311 N71-12216
 Correlation of criterion for air flow separation from
 wind waves and relationship between surface
 roughness and wind stress
 [AD-712706] 03 p0370 N71-13175
 Techniques for analyzing three dimensional bounde-
 ry layer separation
 07 p1006 N71-16938
 Laminar and turbulent boundary layer separation in
 three dimensional flow
 07 p1007 N71-16967
 Boundary layer separation and longitudinal and
 lateral stability of Avro 707 aircraft during flight tests
 [ARC-CP-1107-PT-4] 07 p0969 N71-17082
 Low speed boundary layer separation on compres-
 sor blades of varying aspect ratios
 [ARC-CP-1103] 07 p0966 N71-17108
 Turbulent supersonic boundary layer separation
 [DLR-FB-70-33] 07 p1008 N71-17141
 Breakup of laminar capillary jet of nonnewtonian
 fluid
 [NASA-CR-116408] 07 p1008 N71-17326
 Horizontal boundary layer calculations for density
 stratified fluid flow
 08 p1182 N71-18932
 Method of integral relations application to bounde-
 ry layer problems including separation
 [NASA-CR-117051] 09 p1373 N71-19832
 Supersonic, turbulent boundary layer interaction
 with compression corner at very high Reynolds
 number
 [NASA-CR-117052] 09 p1374 N71-19834
 Turbulent separated and reattaching flow on flat
 plate-compression corner at supersonic and hyper-
 sonic speeds
 09 p1374 N71-19835
 Attached and separated laminar boundary layer
 characteristics over high cooled, curved compression
 surfaces in hypersonic airflow
 09 p1374 N71-19837
 Laminar two dimensional boundary layer separation
 measurements at moderately hypersonic speeds
 09 p1376 N71-19845
 Interaction of nozzle-mounted supersonic propul-
 sion system with circulated wing boundary layer
 [NASA-TN-D-2184] 09 p1316 N71-19853
 Flow separation concepts under high Mach conditions
 09 p1316 N71-20035
 Representations of flow separation bubbles near air-
 foil leading edges
 09 p1323 N71-20064
 Supersonic laminar boundary layer separation mea-
 surements near compression corner at Mach numbers
 near 2.5
 10 p1541 N71-21255

BOUNDARY LAYER TRANSITION

Boundary layer separation in viscous flow around
 rigid bodies
 [AD-717772] 11 p1736 N71-32241
 Magnetic field suppression of magnetohydrodyna-
 mic boundary layer separation and inviscid flow equa-
 tions
 12 p1983 N71-34088
 High lift and boundary layer separation behavior of
 sweptback wing airfoil profile using trailing and lead-
 ing edge stall patterns
 [ARC-RM-3648] 13 p3021 N71-34408
 Flat plate aspect ratio effects on ramp-induced,
 adiabatic, boundary layer separation at supersonic
 and hypersonic speeds
 [AD-719747] 13 p3065 N71-34744
 Separation and flow phenomena in three dimen-
 sional boundary layer
 [SC-T-71-3697] 13 p3088 N71-35462
 Tertiary flow injection system for thrust vectoring
 of propulsive nozzle flow
 [NASA-CASE-MPB-28831] 16 p2673 N71-39153
 Integral method for estimating influence of initial
 boundary layer on development of two dimensional,
 isobaric, turbulent, free shear layer
 [D72-42242] 18 p2985 N71-30892
 High speed photographic techniques to study
 impinging streams of propellants in experimental in-
 vestigation of reactive stream separation
 [NASA-CR-119343] 18 p2923 N71-30844
 Computer program used for design criteria of stall
 characteristics of straight wing aircraft
 [NASA-CR-16446] 18 p2867 N71-31154
 Mathematical models for incompressible laminar
 boundary layer flow inside and outside of liquid spher-
 ical moving through liquid
 19 p3088 N71-32376
 Transonic buffeting flow on cone-cylindrical missile
 body
 [TP-942] 20 p3387 N71-33040
 Laminar and turbulent boundary layer separation in
 three dimensional flow
 [SC-T-71-3610] 21 p3411 N71-34247
 Supersonic turbulent boundary layer step induced
 separation, and incompressible flow model for pre-
 dicting upstream flow field in channels
 21 p3414 N71-34292
 Determining limiting conditions of flow in separation
 zones with large Reynolds number
 [NASA-TT-F-13992] 23 p3742 N71-36681
BOUNDARY LAYER STABILITY
 Deriving boundary layer structure from addition of
 axial magnetic field to rotating viscous fluid and
 resulting modification in the caused by distortion of
 field lines
 07 p1010 N71-17640
 Generalizing continuous surface boundary layer
 problem using similarity theory
 [AD-715822] 08 p1178 N71-18454
BOUNDARY LAYER TRANSITION
 Boundary layer transition studies of several pointed
 bodies of revolution at supersonic speeds
 [NASA-TN-D-6053] 01 p0302 N71-11520
 Hypersonic boundary layer transition and hyper-
 sonic heat transfer on cylindrical shells, cones and flat
 plates
 [KRPET-1104/70] 04 p0472 N71-13408
 Effects of unit Reynolds number and incidence on
 boundary layer transition in supersonic wind tunnels
 [NPL-AERO-1381] 04 p0472 N71-13409
 Comparison of spherical and triangular boundary
 layer trips on flat plates at supersonic speed
 [NASA-TN-X-2146] 04 p0518 N71-13763
 Fourier transformation for precursor wave study
 from continuous transition layer in sound speed
 profile
 [AD-713601] 05 p0731 N71-14553
 Boundary layer optimization for small turbine blade
 design with curved trailing edge
 07 p1100 N71-17380
 Boundary layer interactions with turbulent heated
 compressed flows from hypersonic inlets
 09 p1376 N71-19932
 Spherically symmetric phase change problem solved
 by least balance integral method using appropriate
 conservation profiles
 [AD-718151] 12 p1899 N71-23321
 Laminar boundary layer transition, separation and
 streamlines direction on rotating helicopter blades
 [NASA-TN-D-6321] 12 p1851 N71-23770
 Boundary layer transition thermodynamic test data
 for space shuttle configuration and trajectory analysis
 14 p2340 N71-28855
 Effect of spark discharges into laminar boundary
 layer at supersonic free stream Mach numbers
 [NASA-TN-D-6370] 15 p2363 N71-26930
 Transition in oscillating boundary layers including
 role of stability theory and transient vorticity distri-
 bution
 [AD-720293] 16 p2382 N71-28875
 Solving equations of motion to produce equilibrium
 flow consisting of modified Ekman spiral flow and
 helical secondary flow
 17 p3735 N71-39827

- Influence of artificially induced turbulence upon boundary layer transition in supersonic flows
[AD-723322] 18 p2908 N71-31586
- BOUNDARY LAYERS**
- NT **ATMOSPHERIC BOUNDARY LAYER**
- NT **COMPRESSIBLE BOUNDARY LAYER**
- NT **HYPERSONIC BOUNDARY LAYER**
- NT **LAMINAR BOUNDARY LAYER**
- NT **SUPERSONIC BOUNDARY LAYERS**
- NT **THERMAL BOUNDARY LAYER**
- NT **THREE DIMENSIONAL BOUNDARY LAYER**
- NT **TURBULENT BOUNDARY LAYER**
- Numerical interpretation of wind, temperature, and specific humidity profiles for surface boundary layer of atmosphere
[AD-711599] 02 p0258 N71-11741
- Chemical nonequilibrium effects in boundary layer and transport properties in rocket engine nozzles
[RFB-TR-7073] 02 p0885 N71-12058
- Influence of solid surface on relaxation and cross-linking processes in polymer boundary layers
[JPRS-51683] 02 p0248 N71-12086
- Nonequilibrium plasma boundary layer over cathode in presence of magnetic field
[NASA-CN-11611] 03 p0437 N71-12679
- Survey of heat transfer to near-critical fluids
[NASA-TN-D-5886] 03 p0468 N71-13035
- Boundary layer development and swirling flow in conical diffusers
05 p0660 N71-14767
- Mach 2 slender wing boundary layer effects on Concorde aircraft engine inlets
[ARCC-1122] 06 p0792 N71-15708
- Isentropic and thermal nonequilibrium in MHD boundary layer in potassium seeded, nitrogen plasma accelerator
[AD-715272] 07 p1084 N71-17961
- Determining feasibility of increasing rotor blade loading of single stage compressor rig by bleeding or blowing suction surface boundary layer
[NASA-CR-54573] 08 p1142 N71-15749
- Mathematical connection between solutions of Navier-Stokes system and Prandtl boundary layer system
08 p1184 N71-19020
- Eddy transfer of active and passive contaminants in atmospheric boundary layer
[AD-716359] 09 p1413 N71-19825
- Analysis of effect of terrain irregularity on turbulence and diffusion in surface boundary layer
[NYO-4140-1] 09 p1367 N71-20591
- Boundary layer velocity and temperature profiles measured in near critical nitrogen
[NASA-TM-X-52988] 10 p1540 N71-21080
- Eddy diffusivity ratios in boundary layer parameters
[AD-716982] 10 p1598 N71-21593
- Longitudinal curvature and displacement speed of effects on incompressible boundary layer flow past circular cylinder
[AD-717071] 10 p1544 N71-21613
- Stereophotogrammetric current meter prototype for observing turbulence in and above ocean bottom boundary layer
[AD-717638] 11 p1762 N71-22165
- Turbulence diffusion above flow during boundary layer and hypersonic flow interaction
[NASA-TT-F-13522] 12 p1899 N71-23312
- Boundary layer techniques applied to two-dimensional couple-stress theory of linear elasticity
[AD-717864] 12 p3004 N71-23494
- Application of research in panel flutter and boundary layer thickness to space shuttle
13 p2179 N71-24660
- Flow meter for measuring stagnation pressure in boundary layer around high speed flight vehicle
[NASA-CASE-XPR-03007] 13 p2065 N71-24692
- Structure of electric double layer at solid metal solution interfaces
[AD-721718] 16 p2557 N71-28353
- Lower atmosphere vertical distribution of boundary layer wind shear annual variations as observed in Canada
18 p2949 N71-30829
- Studying diurnal oscillations of wind in planetary boundary layer using theoretical model
18 p2953 N71-31067
- Wind and turbulence structure in boundary layer over Antarctica
18 p2953 N71-31122
- Soviet news releases on boundary layer physics, reflectivity profile effects, and climate of polaronic age
21 p3510 N71-33006
- Numerical solution of elliptic equations over irregular regions
[USC-113P19-10] 23 p3407 N71-35094
- Calculation of simultaneous transient developing mass and momentum boundary layers in moving-wall problem from fluid flow through channels with dissolving walls
[ANL-7797] 29 p3743 N71-36687
- Model for calculating condensation effects in boundary layer on mass transfer from rotating disks
23 p3746 N71-36714
- Particle motion at neutral layer boundary in magnetoplasma tail
23 p3854 N71-37473
- Technique for improving calibration accuracy standards from boundary layer calculations
[JC71/23] 24 p3908 N71-37851
- Least square method for determining Love wave scattering upon boundary irregularity in elastic layer over rigid half space
24 p3918 N71-37944
- BOUNDARY LUBRICATION**
- Qualitative model and calculations of interaction energy in thin film rheology study of boundary lubricating surface films
[AD-721176] 15 p0452 N71-27755
- Additive effects on boundary lubricant-metal surface interactions during friction process
[AD-727863] 24 p3929 N71-38037
- BOUNDARY VALUE PROBLEMS**
- NT **NEUMANN PROBLEM**
- Axiymmetric stresses and displacements in two fluids circular cylinders in contact
[NASA-TM-X-3052] 01 p0129 N71-10448
- Mathematical model for acoustic radiation from free-floating ring transducers
[AD-710745] 01 p0900 N71-10551
- Series-perturbation technique for stress solutions of two-point boundary value problems
01 p0976 N71-10620
- Radios and Fourier integral transformations applied to boundary value problem solution of neutron transport theory
[SRAIR-P-57] 02 p0269 N71-11148
- Nonlinear pulse system dynamics, control laws insuring control system asymptotic stability, and continuous variable ordered sampling functions
[JPRS-51622] 02 p0196 N71-11370
- Point transformation analysis of nonlinear pulse system dynamics with linear distributed link
02 p0196 N71-11371
- Generalization to non-Hilbert space of interior boundary value problem for Boltzmann equation
[ONERA-TP-665] 02 p0251 N71-11659
- Application of Ritz method to this elastic shell analysis
[AD-711962] 02 p0301 N71-12023
- Boundary value problems of forced diffusion in semi-infinite region with mobile boundary
[TT-76-57857] 03 p0442 N71-12914
- Four theorems characterizing optimal filtered and smoothed estimates for linear parabolic systems
[AD-712404] 03 p0399 N71-12995
- Finite element method for solving differential equations in boundary value problems of plastic flow in rod metal drawing
[REPT-12] 03 p0466 N71-13346
- Frequency domain criteria for system stability modeled by certain partial differential equations
[NASA-TM-X-66514] 04 p0338 N71-14165
- Examining characteristics of systems of stationary macroscopic equations for plasma resistivity and viscosity
[JPR-6784] 05 p0754 N71-15184
- Solutions of Krook equation of kinetic theory
[AD-712684] 05 p0665 N71-15466
- Boundary value problems and resonant vibrations of liquid surfaces in tanks with pressure chambers
[NPL-MA-89] 06 p0833 N71-15787
- Free boundary value problems of heat flow around aerodynamic bodies
[AD-714621] 06 p0938 N71-15963
- Convergence and mean square error estimation in solution of boundary value problems for elliptic equations by finite line method
[NASA-TT-F-11452] 06 p0884 N71-16496
- Finite difference solution to mixed boundary value problem for Laplace equation
[NASA-CR-116225] 06 p0885 N71-16497
- Numerical solution of boundary value problem for linearized Navier-Stokes equations
07 p1006 N71-16957
- Orbital boundary value problems using oscillatory solutions
[BMW-FB-W-70-52] 07 p1108 N71-17219
- Electric field produced by long horizontal electric line across bare homogeneous surface
[AD-714791] 07 p0994 N71-17764
- Regular perturbation approach to nonlinear periodic waves in bounded medium
[AD-714997] 07 p1012 N71-17786
- Modified quasilinearization method for solving nonlinear, two point boundary value problems
[NASA-CR-116198] 07 p1051 N71-17790
- Difference scheme for solving initial value problem for one dimensional Vlasov equation
[COO-3879-3] 06 p1272 N71-18395
- Solving plane elastic-plastic boundary value problems for application to bending of simply supported single crystal beam
[AD-715778] 08 p1298 N71-18810
- Describing analytical technique for solving electromagnetic boundary value problems of suboptical resonators with grating mirrors
08 p1203 N71-19078
- Boundary value problems for temperature and the fluid inside and around paraboloidal needle and paraboloidal crystal during growth
08 p1282 N71-19088
- Characteristics of three dimensional nonlinear wave motion of incompressible viscous fluid
[AD-715958] 09 p1369 N71-19704
- Solution of mixed boundary value problems involving three dimensional equations for thermodynamic shells
[AD-716015] 09 p1478 N71-20008
- Numerical solution of initial value problems for boundary and partial differential equations using differential quadrature and long-term integrations
[TID-25616] 10 p1594 N71-20704
- Invariant imbedding method for reducing two point boundary value problems for vector-matrix systems of linear difference equations to initial value problems
[TID-25609] 10 p1594 N71-20708
- Solution method for three dimensional axially symmetric problems on sound diffraction and reflection from general class of bodies of revolution
[AD-717394] 11 p1777 N71-23640
- Imbedding nonlinear differential equations in minimizing boundary value problems to initial value problems for computerized computation
11 p1788 N71-23689
- Analysis function theory, superposition, and gain matching used to determine non-Hermitian contact stresses between cylinders of dissimilar cross sections
11 p1838 N71-23838
- Asymptotic solution of low frequency wave conditions in transonic shockless subsonic inviscid gas flow based on complete approximation
12 p1898 N71-23818
- Boundary value problem in electromagnetic wave radiation from flanged waveguide
[AD-718497] 12 p1892 N71-23848
- Analysis of axisymmetric boundary value problems for finite solid circular bar with lateral surface traction free and end sections having prescribed traction and displacements
12 p2006 N71-23884
- Boundary value problem for Laplace equation between coupled electrically thin folded dipole
12 p1894 N71-23882
- Existence, uniqueness, stability, and asymptotic stability conditions for solution of elliptic partial differential equations with general boundary conditions
[NASA-CR-118036] 12 p1950 N71-24089
- Second order differential equations for free boundary condition of heat equation
12 p1951 N71-24087
- Boundary value problem application to determining capillary surface of volume of liquid partially filling right circular cylinder
[NPL-MA-95] 13 p2182 N71-24079
- Numerical analysis of axially symmetric boundary value problems in elastic dissimilar layered media
13 p2181 N71-24078
- Stability of solitary waves in nonlinear Schrödinger equation and solitary wave formation from initial disturbances
[RIFP-117] 13 p2048 N71-23946
- Boundary problems at phase interface between vacuum and plasma, anisotropic plasma described by linearized Vlasov equation
[AD-719926] 14 p2321 N71-25711
- Ritz-Galerkin residual convergence in boundary value problems including trigonometric, polynomial, and spline coordinate functions
14 p2304 N71-25705
- Thermomechanical dissipation analysis of the servocyclic solid by finite element method
[AD-720887] 15 p2521 N71-25706
- Approximate solution for time dependent boundary value problems including Couette flow, Rayleigh problems, oscillating wall flow, and sound propagation using Chapman-Enskog theory
15 p2393 N71-27202
- Numerical integration method for solving two point boundary value equations
[AD-721210] 15 p2434 N71-27786
- Finite elements theory applied to elastic wave propagation equations
[AD-722887] 16 p2585 N71-28888
- Algorithm proposed for approximate integration of specific boundary value problem of nonlinear system of differential equations with delayed argument and satisfying Lipschitz conditions
[NASA-TT-F-13694] 16 p3822 N71-38828
- Numerical analysis of aerodynamic loads on wing and tail surfaces with oscillations in steady supersonic and subsonic flow including transonic flow
[AGARD-CP-60-71-PT-1] 17 p2697 N71-38828
- Aerodynamic load predicting for control surfaces in unsteady supersonic and subsonic flow
17 p2697 N71-38834
- Numerical analysis of aerodynamic loads and coefficients for tandem and T tail surfaces harmonically oscillating in subsonic flow
17 p2698 N71-38835
- Wing interference lift line lattice simulation and application to aerodynamic loads on tandem wings in steady flow
17 p2698 N71-38836

SUBJECT INDEX

BRANCHING [PHYSICS]

Approximation and error estimation method for solving second order boundary value problem
17 p2773 N71-27720

Variational and boundary value problems and differential properties of corresponding generalized solutions of integro-differential equations
[NASA-TT-F-13745] 17 p2773 N71-29014

Asymptotic computer solution of elliptic boundary value problems
17 p2773 N71-29048

Differential correction processes for solution of multiple point boundary value problems in powered spacecraft trajectory determinations
17 p2845 N71-30664

Solution of initial value problem in linear transport theory obtained by monotonicity methods minimizing in this case with infinite reflector and isotropic scattering
[NASA-TR-8-357] 17 p2805 N71-36298

Hydrodynamics and boundary value problems in all phase field theory based on classical and quantum methods
17 p2808 N71-30354

Formulation of Volterra equations describing fatigue problem, and algorithm based on Kruok equation
[TR-36] 17 p2773 N71-30372

Formulation of Volterra equations describing nonlinear plate problem, and algorithm based on Kruok equation
[TR-37] 17 p2773 N71-30373

Iteration phenomena for nonlinear perturbations in singular self-adjoint boundary value problems
[AD-722622] 18 p2946 N71-31235

Boundary value problems associated with small circles or injection through discrete point on viscous flow in field, circular tube
18 p2907 N71-31382

Value propagation in nonlinear viscoelastic rods of finite length and subject to homogeneous boundary conditions
[AD-722770] 18 p2907 N71-31393

Fourier analysis of boundary value problems for bounded equation of ocean waves
[AD-722698] 18 p2919 N71-31440

Isolating algorithm for solution of two-point boundary value optimization problems
[AD-723441] 19 p3122 N71-31823

Two boundary value problems on semi-infinite strips solved with eigenvector expansions
19 p3123 N71-32257

Radiation from dielectrically coated spherical antenna determined by solving related boundary value problem
19 p3067 N71-32483

Construction of approximates for solution of elliptic boundary problems and analysis of resulting errors
19 p3123 N71-32449

Unit disk for boundary functions and sets of asymptotic values
19 p3124 N71-32497

Nonlinear boundary value problem of Strum-Liouville type for two dimensional system of ordinary differential equations
[AD-724173] 20 p3280 N71-32983

Indirect effects in boundary value problem for connecting star like observations
20 p3263 N71-33355

Constructing normal modes for bounded systems from infinite dispersion relation roots for interpretation of plasma wave and instability studies on finite observations
20 p3292 N71-33529

Design of computational algorithms for optical control by Hilbert space methods, and involving cost function
[NASA-TN-D-6266] 21 p3449 N71-34531

Boundary value conditions and solutions for stability and vibration problems of shells of revolution
21 p3528 N71-35140

Laminar gas flow at transonic speeds with subsonic and supersonic regions
[AD-725092] 22 p3540 N71-35422

Functional equations for solving boundary value problems including Dirichlet problem, Green function, harmonic function, and nonorthogonal functions
[NASA-TT-F-639] 22 p3487 N71-35487

Integral equation methods for calculating sound radiation and scatter from arbitrary closed surfaces
[AD-725464] 22 p3430 N71-35963

Ray-trace method in solving two-dimensional steady state theory of elasticity for cases of specified stress on boundary
[NASA-TT-F-13564] 22 p3481 N71-36252

Nonself-adjoint boundary value problem solution with dependent variable time derivatives for forced vibration of elastic beams based on Williams method
[AD-724376] 22 p3489 N71-36312

Finite element method applied to heat transfer problem, and transient two dimensional heat transfer with convection and radiation boundary conditions
[AD-726371] 22 p3497 N71-36343

Finite element method applied to solid heat conduction with radiation-convection, nonlinear heat-flux boundary conditions
[AD-726376] 22 p3497 N71-36346

Infinite length, gap etched, thick, cylindrical dipole antenna radiation field formulations as boundary value problems based on Maxwell equations for electric and magnetic fields
23 p3734 N71-36619

Finite cylindrical dipole antenna of arbitrary orientation in gyrotropic media solved as boundary value problem
23 p3734 N71-36622

Polynomial roots, boundary value problems of nonlinear equations, and eigenvalue problems of linear ordinary differential operators treated with continuation method using fast computers
[TAB-123] 23 p3782 N71-36938

Boundary conditions for adjacent stresses of cold plasma in magnetic field
[UARS-76] 23 p3823 N71-37282

Dynamic response of slender circular cylinders in axial flowing fluid with base excited motion
23 p3863 N71-37541

BOUSSON TUBES
Numerical analysis of effect of cross section shape on behavior of Bourdon tubes
07 p1028 N71-17273

BOUSSON APPROXIMATION
Three dimensional primitive equation model from Boussinesq equations for application to mesoscale atmospheric phenomena
[AD-715347] 08 p1231 N71-18730

BOW SHOCK WAVES
U BOW WAVES
V BOW WAVES
W BOW WAVES
Interplanetary magnetic field role in counterstreaming ion-ion instability in ion thermalization process for earth bow shock
[NASA-CR-111420] 02 p0282 N71-12032

Average and unusual locations of magnetopause and bow shock positions observed by IMF spacecraft
[NASA-TM-X-65429] 06 p0351 N71-16509

External source radiation effects on bow shock structure of stagnation point detaching with convection
07 p1011 N71-17008

Analysis of multiple earth bow shock crossings at large geocentric distances from Pioneer 6 magnetic field data
[NASA-TM-X-65474] 10 p1554 N71-21541

Magnetopause, magnetosheath, and bow shock studied using Explorer 33 and 35 MIT plasma experiment data
[NASA-CR-123195] 24 p4007 N71-38371

BOX BEAMS
Determining optimal shape and optimum distribution of cross sections along statically determinate and statically indeterminate beams using calculus of variations
[NASA-TT-F-13449] 06 p1224 N71-18419

BOXES [CONTAINERS]
Glove box vacuum system for radiologic targets
[ORNL-TM-5209] 10 p1616 N71-21132

Sealed storage container for chemical carriers with mounted miniature electronic components
[NASA-CASE-MPB-20073] 14 p2229 N71-26133

BRAGG ANGLE
Research in Bragg diffraction from magnetoelectric waves using acoustic surface waves
[AD-711101] 01 p0091 N71-10837

Dual crystal X ray telescope using single crystals in Bragg reflection
[NFF-PAR/EXTRATER-30] 07 p1105 N71-17217

Double diffraction between Bragg reflections and double intensity planes observed with high energy electron diffraction
[AD-715373] 08 p1213 N71-18521

Imaging techniques for ultrasonic radiation using Bragg diffraction principle
16 p3638 N71-28417

Acoustic-optical imaging techniques using Bragg diffraction by sound lenses to produce optical image for detection studies
[AD-723595] 18 p2967 N71-31594

Sit resonantly using high purity aluminum single crystals for high precision measurements of X ray Bragg reflections
[COO-1041-18] 21 p3497 N71-34912

Diffraction of light with ultrasonic waves for oblique incidence of light on sound wave front - Bragg reflection
[NASA-TT-F-13994] 23 p3801 N71-37182

BRAIN
NT BRAIN STEM
NT CEREBRAL CORTEX
NT HIPPOCAMPUS
Describing and comparing resolution characteristics of rectilinear brain scanner
[ACR-1006-190] 02 p0169 N71-11197

Changes in bioelectric potentials in brains of rabbits subjected to X-ray irradiation and acceleration on centrifuge
[JPRS-52088] 08 p1156 N71-19094

Low-level, low-frequency electric field effects on monkey behavior and brain activity based on electroencephalography
[AD-717100] 10 p1500 N71-21222

Biologic models for pattern recognition in human and artificial brains
11 p1083 N71-23037

Biologic neural model integration into functional learning networks of brain
11 p1093 N71-23048

Quantitative analysis of gamma aminobutyric acid in brain after locomotion and pure oxygen breathing
[DLR-FR-71-03] 13 p2852 N71-24534

Component connection schemes of brain for trainable feedback flight control system
13 p2853 N71-25326

Monamine oxidase inhibitors and neuropharmacology decrease by receptors affecting brain action in aldehyde exposed rats
[AD-720469] 14 p2284 N71-23837

Induced fields and static heating patterns within multilayer spherical model of primate cranial structure
[AD-720280] 14 p2285 N71-26140

Model describing symmetrical information processing along visual pathways of brain
[NASA-CR-118317] 14 p2285 N71-26284

Measurement of brain and heart accumulation of bromotrifluoromethane for evaluation as potential fire extinguisher chemical
[AD-721211] 15 p2371 N71-27299

Synaptic junction model for memory in brain
[NASA-TN-D-6436] 19 p3043 N71-33474

Single cell responses within cat models during constant angular accelerations
[AD-724628] 21 p3383 N71-34089

BRAIN DAMAGE
Toxic effects of cyanide on brain functions of aerial applicator personnel
[FAA-AM-70-11] 03 p0321 N71-12299

Effects of carbon monoxide on brain cellular metabolism in monkeys
[AD-715609] 05 p0632 N71-14375

Tolerances of human brain to impact shock and concussion
[FAA-AM-71-13] 17 p2708 N71-29636

BRAIN STEM
Possibility of focused ultrasound to act locally on brain structures of animals and man without opening skull
15 p2370 N71-26894

BRAKES [FOR ARRESTING MOTION]
NT AERODYNAMIC BRAKES
NT AIRCRAFT BRAKES
NT BALLUTES
NT LEADING EDGE SLATS
NT TRAILING-EDGE FLAPS
NT WING FLAPS
Design, fabrication and static testing of attached inflatable decelerator models for supersonic wind tunnel evaluation
[NASA-CR-111831] 11 p1676 N71-22534

Sensor, decelerator, telemetry and rocket vehicle technological developments for 30 km to 200 km meteorological rocket sounding systems
[NASA-CR-1790] 14 p2289 N71-26692

Automatic braking device for rapidly decelerating humans or materials from elevated locations
[NASA-CASE-XKS-07814] 15 p3414 N71-27067

Trajectory, thermodynamic, and stress analysis of spacecraft inflatable decelerators in Mars and Earth atmospheres
[NASA-CR-111950] 19 p3191 N71-32083

Adhesive and coating material formulations and manufacturing processes for lightweight low-permeability brines for use in high altitude decelerators
[NASA-CR-111964] 22 p3350 N71-33208

BREAKING
Direct current electromagnetic system for regenerative braking of electric motor
[NASA-CASE-XMP-00866] 06 p0826 N71-16030

Linear magnetic braking system with nonuniformly wrapped primary coil producing constant braking force on secondary coil
[NASA-CASE-XLB-03679] 07 p1036 N71-17652

Anemometer with braking mechanism to prevent rotation of wind driven elements
[NASA-CASE-XMP-05224] 12 p1921 N71-25726

Elastic response and characteristics of thin ply aircraft tires subjected to braking forces and simple static flexure
[NASA-TN-D-6406] 21 p3375 N71-24827

Evaluation of braking performance of light, twin engine airplane on grooved and ungrooved runway surfaces
[NASA-TN-D-6444] 23 p3787 N71-36431

BRANCHING [MATHEMATICS]
Existence and extendability of continuous eigenvalue branches and application of nonlinear programming algorithms to nonlinear heat generation and rotating disk problems
[NASA-CR-119020] 16 p2633 N71-28430

BRANCHING [PHYSICS]
Lifetime and branching ratio studies of B-28 in search of excited proton resonant bands
[KLO-1925-34] 03 p0420 N71-12643

Production, decay, and branching ratio for Lambda hyperon (1528) - cascade
[UCRL-19743] 03 p0427 N71-12633

- Neutral branching ratios of eta meson using energy spectrum of gamma rays
[PUBC-459-3] 04 p0580 N71-14021
- Elastic KN scattering and charge exchange taking branching into account
[ITEP-754] 04 p0585 N71-14231
- Alpha particle energies, half lives, and alpha branching of short-lived rare earth isotopes
[BNL-TL-356] 05 p0758 N71-14721
- Experimental limit on branching ratio for neutral kaon to L yields lepton antilepton
[UCRL-20078] 06 p0924 N71-16759
- Kaon/ π yields positron neutrino to kaon/ π yields muon/neutrino
[UCRL-20079] 06 p0925 N71-16837
- Reconstruction of Ti-45 decay to Sc -45 resolve branching ratio discrepancies
[ANU-P-309] 13 p2143 N71-23554
- Neutral eta meson decay modes evaluation, including branching ratios
[JINR-EI-5256] 14 p2318 N71-26742
- Lambda and Sigma hyperon resonances, branching ratios, and lifetimes from bubble chamber analysis of antineutron nucleus reactions
[CEA-R-4068] 15 p2492 N71-27931
- Branch curvature in dislocations at free surfaces from image force and concept of line tension
17 p2816 N71-29928
- Kaon pion pion/kaon pion decay branching ratio of kaon resonance
[UR-475-332] 17 p2798 N71-30008
- Branching of proton-proton reactions at 19 GeV/c with production of two and three pions
[USIP-70-4] 17 p2805 N71-30299
- Branching ratio and relative rates of positive kaon decays, and upper limit for structure dependent radiation in kaon decay into electron neutrino photon
19 p3162 N71-32778
- Spark chamber and spectrometric analysis of kaon decay branching ratios for electron neutrino events and vector-axial theory test for weak interactions
[UCRL-20031] 21 p3485 N71-34826
- BRASSES**
- Mechanism of stress corrosion cracking in brass
[AD-712327] 02 p0245 N71-12195
- Crystal orientation and material processing effects on fatigue crack propagation in brass and stainless steel
08 p1282 N71-19306
- Physical properties and ordering process in beta brass alloys based on quasi-chemical approximation
[TT-70-59079] 14 p2269 N71-25667
- Determination of diffusion coefficient of zinc in brass by evaporation
[DMDC-5757] 14 p2271 N71-25700
- Plastic deformation and mechanical properties of gamma brass phase Ag₂Zn and CuAl single and polycrystals and temperature effects on crystal lattices
14 p2276 N71-26615
- Plastic deformation in tool engagement and cutting of 70/30 brass
18 p2929 N71-31222
- Improved corrosion resistance of aluminum brass for use in sea water conversion plants
[PB-190643] 19 p3110 N71-31730
- Effects of quenching, plastic deformation, and neutron and electron irradiation defects on order-disorder transformations in beta-brass
19 p3117 N71-32539
- Effects of elevated temperature on deformation resistance of steel and brass
[AD-727841] 24 p3939 N71-38102
- BRAYTON CYCLE**
- Experimental performance of 2-15 kilowatt Brayton cycle power system using mixture of helium and xenon
[NASA-TM-X-52936] 03 p0316 N71-12252
- Performance evaluation of Brayton cycle power system 400-hertz inverters
[NASA-TM-X-2141] 03 p0317 N71-12266
- Parametric data of heat exchanger size and weight for nuclear reactor Brayton cycle space power systems
[NASA-CR-77783] 04 p0555 N71-14037
- Thermal analysis for predicting internal temperatures in isotropic Brayton power system operation
[NASA-TM-X-52948] 05 p0783 N71-15324
- Nuclear Brayton cycle heat exchanger and duct assembly
[NASA-CR-72816] 05 p0785 N71-15638
- Plate-fin heat exchangers for nuclear reactor Brayton cycle
[NASA-CR-72815] 06 p0899 N71-16560
- Motoring tests of single shaft turbine compressor altimeter
[NASA-TM-X-2154] 07 p0975 N71-17570
- Evaluation of vapor chamber/heat pipe/radiator for Brayton cycle space power system
[NASA-CR-1677] 07 p0976 N71-17581
- Motor-starting characteristics of modified Lundell alternator for single shaft, Brayton cycle, space power system
[NASA-TM-X-2200] 07 p0976 N71-17664
- Performance of axial flow compressor for Brayton cycle electrical power generating system with argon
[NASA-TM-X-2194] 07 p0988 N71-17882
- Transfer functions for primary loop of conceptual nuclear Brayton cycle space power plant
[NASA-TM-X-2193] 07 p1066 N71-17993
- Steady state and transient operating characteristics of lithium cooled primary flow loop of nuclear Brayton cycle space power plant
[NASA-TM-X-2161] 08 p1241 N71-18066
- Dynamic electrical characteristics of 400 Hz Brayton cycle turboalternator and controls for space applications
[NASA-TN-D-6185] 11 p1677 N71-22364
- Motor start of 2 to 10 kilowatt Brayton rotating unit operating on gas bearings in closed loop test facility
[NASA-TM-X-2266] 11 p1678 N71-22570
- System integration computer study to determine compatibility and interactions of Brayton power system and integrated life support system operating in integrated mode
[NASA-TM-X-2207] 12 p1801 N71-23859
- Environmental tests of electrical subsystem of 2-40-15 kW Brayton power conversion system
[NASA-TM-X-67814] 12 p1963 N71-23928
- Comparison of turbo-MHD cycle with Brayton-MHD and turboelectric cycles
[NASA-TM-X-67829] 13 p2116 N71-24578
- Design point characteristics of 15-80 kW nuclear reactor Brayton cycle power system
[NASA-TM-X-67811] 13 p2116 N71-24609
- Predicted performance of 15-80 kW reactor Brayton power system over range of operating conditions
[NASA-TM-X-67833] 13 p2116 N71-24609
- Motor starting techniques for 2-15 kW Brayton cycle power system
[NASA-TM-X-67819] 13 p2117 N71-24691
- Low temperature radiator for rejecting thermal power from isotope Brayton power system
[NASA-TM-X-67822] 13 p2186 N71-25090
- Component and system performance tests of Brayton cycle power conversion system in 2 to 15 kW sub-a range
[NASA-TM-X-67835] 13 p2157 N71-23550
- Post test analysis of closed Brayton cycle space electric power conversion system for space
[NASA-TM-X-67841] 13 p2157 N71-23567
- Computer controlled durability test of 50,000 hour life Brayton power conversion system for space applications
[NASA-TM-X-67830] 13 p2157 N71-23568
- Voltage transients due to phase angle switching of speed control power for Brayton cycle alternator examined by computerized simulation
[NASA-TM-X-2291] 13 p2031 N71-25420
- Brayton cycle turbogenerator performance tests using helium xenon gas mixture including gas turbine engine, turbocompressor, coolant pump, and heat exchanger power efficiencies
[NASA-TM-X-67846] 15 p2570 N71-27713
- Foil journal bearings for Brayton cycle turboalternator
[NASA-CR-72864] 15 p2617 N71-27772
- Thermal steady state analyses for predicting isotopic heat source performance in Brayton thermodynamic cycle
[NASA-TM-X-67853] 15 p2525 N71-27864
- Half-size shock and sinusoidal vibration tests of gas bearing supported rotor assembly and effects on mechanical performance of Brayton cycle space power turbomachinery
[NASA-CR-71762] 20 p3278 N71-33215
- Performance tests on Brayton cycle direct current power supply circuit for automatic control
[NASA-TM-X-2349] 20 p3242 N71-33491
- Preliminary test results of heat transfer/thermal storage tube design for solar Brayton cycle power system under simulated orbital conditions
[NASA-TM-X-67904] 20 p3367 N71-33785
- Nondestructive tests of aluminum isotopic heat source for use in Brayton power system
[NASA-TM-X-2374] 21 p3439 N71-34621
- Gas management subsystem using xenon-helium venting fluid designed for Brayton cycle power system
[NASA-CR-72631] 21 p3502 N71-34948
- Design, development, and performance of 35 to 150 kilowatt Brayton power conversion module and application to nuclear reactor powered systems
[NASA-TN-D-6525] 22 p3542 N71-35223
- Development of combined turbine-magnetohydrodynamic generator operating in Brayton cycle with NERVA nuclear reactor for space and ground applications
[NASA-TN-D-6513] 23 p3710 N71-36450
- Power and load priority control concept for Brayton cycle power system providing speed control and field current control for alternator and load simulation which includes energy storage
[NASA-TN-D-6478] 23 p3710 N71-36452
- BRAZING**
- Brasileira agriculture remote sensing research projects
[LAF-132] 05 p0690 N71-15653
- Oceanic conditions in upper 1800 meters of water column off northeastern Brazil
[CO-373-34] 22 p3575 N71-33409
- BRAZING**
- Brazing processes and equipment for producing metal and alloy joints
02 p2333 N71-14140
- Development of optimum fabrication techniques for brazed stainless steel transition joints
[NASA-CR-72746] 05 p0804 N71-13200
- Radiography on brazing techniques in industrial processing
[AD-714080] 06 p0865 N71-14057
- Fabrication and structural evaluation for representative coated panels - tensile tests, creep rupture, and fracture tests of brazed plate-fin specimens
[NASA-CR-1651] 06 p1305 N71-14904
- Joining titanium to stainless steel by bonding titanium coatings onto titanium coated stainless steel and brazing titanium to titanium/titanium coated steel
[NASA-CASE-MFS-07360] 09 p1395 N71-30405
- Heat transfer and flow friction characteristics of compact heat exchanger surfaces with and without brazing processes
[AD-717661] 11 p1768 N71-32706
- Brazing alloy adapted for brazing corrosion resistant steel to refractory metals, also for brazing refractory metals to other refractory metals
[NASA-CASE-XNP-03063] 12 p1997 N71-32508
- Cooling rate and yield strength effects on tensile properties of brazed joints
13 p2094 N71-34022
- Compilation of technical information including metallurgy, electrical repair, fabrication techniques for coating, bonding and brazing, and electron beam welding
[NASA-SF-5923/01] 13 p2087 N71-32508
- Isostatic brass units for repair and assembly of stainless steel materials on space missions
[NASA-CR-163169] 14 p2261 N71-26004
- Strength evaluation of brass alloys used for linear accelerator components
[LA-4584] 16 p3085 N71-30701
- Vacuum brazing, vacuum heat treatment, gas quenching process for fabricating hardware items with helium leak-tight joints
[AD-727398] 17 p2756 N71-30013
- High temperature brazing of austenitic thermocouples and pipe ducts on reactor plugs of these construction materials
[JUL-481-RX] 19 p3104 N71-32805
- Welding of various metals by different brazing alloys
[EUK-4637-R] 24 p3933 N71-36844
- BREATHBOARD MODELS**
- Design, manufacture, and tests of high reliability radar set AN/TPS-17 XN-1
[AD-712530] 05 p0338 N71-12414
- Breathboard miniature carbon dioxide sensor units model and function manual
[NASA-CR-114799] 05 p0082 N71-14759
- Phonocardiographic preprocessor using breathboard circuit consisting of full wave rectifier with sample-and-hold capacity filtering
[NASA-TM-X-65420] 06 p0085 N71-13040
- Design and development of breathboard model of airborne radar
[AD-713004] 06 p0859 N71-16214
- Analysis and breathboarded performance of parallel energy storage units for power systems
[NASA-CR-116510] 07 p0975 N71-13971
- Linear modulator, demodulator, and phase locked loops breathboard test procedures and results
[NASA-CR-103002] 10 p1537 N71-31540
- Design, operation, and alignment of single channel breathboard modulator, demodulator, and phase locked loops for double sideband signals
[NASA-CR-103116] 13 p2057 N71-34000
- Expiry system used to determine degree of sole consistent curve in printed circuit board fabrication
[BDC-613-233] 15 p2082 N71-30468
- Breathboard model of high power UHF oscillator for space communication satellite
[NASA-CR-115005] 17 p2717 N71-30233
- Bread board model of space shuttle auxiliary propulsion system design and components
17 p2807 N71-30097
- Breadboard model of digitally controlled very high frequency synthesizer for use in aviation navigation receiver
[NASA-TN-D-6309] 21 p3595 N71-34444
- BREAKAWAY**
- BOUNDARY LAYER SEPARATION**
- BREAKDOWN**
- Space charge electron avalanches in nitrogen and hydrogen breakdowns
17 p2785 N71-30710
- Multi-pulse breakdown by secondary electron current on cavity walls
[DSS-4449] 20 p3243 N71-33580
- Toroidal discharge breakdown in argon and oxygen/nitrogen mixtures caused by current amplification
20 p3311 N71-33291
- BREAKERS (ELECTRIC)**
- U CIRCUIT BREAKERS**

SUBJECT INDEX

BREAKING

- Five models for three dimensional chip curl, chip breaking, and chip control in metal cutting process
17 p2734 N71-29345
- Nondestructive measurement of density, breaking strength, and modulus of elasticity of bones
26 p3217 N71-33361
- Relationship of breaking load, elongation, and tear strength of fabrics to properties of component yarns
33 p5604 N71-35646

BREATHING APPARATUS

- NT OXYGEN MASKS
NT UNDERWATER BREATHING APPARATUS
Physiological consideration in preventing instability in oxygen breathing systems
03 p0171 N71-11822

- Survey of breathing systems design and reliability conducted by accident investigation panel following Apollo 13 flight emergency
09 p1471 N71-19644

- Three-port transfer valve with one port open continuously suitable for manned space flight
11 p1773 N71-23051

- Extrapolation of animal tolerance of air contaminants to human tolerance for driver breathing under hazardous conditions
17 p2470 N71-29359

BRUCCA

- Abundance of uranium, thorium, and plutonium isotopes in Apollo 12 soil and breccia samples
07 p1114 N71-17668
- Electron and ion microprobe analyses of Apollo 12 soil and breccia
08 p1289 N71-18678

U CLOSURES

BREEDER REACTORS

- NT EXPERIMENTAL BREEDER REACTOR 1
NT EXPERIMENTAL BREEDER REACTOR 2
Theoretical treatment of conceivable various accidents at fast breeder reactors in context of Buta-Tu method
04 p0546 N71-13568

- Positron product removal from cover gas of vented fuel tubes
04 p0577 N71-13774

- FFTP closed loop test characteristics
04 p0551 N71-13955

- Operational design analysis for breeder reactor core
04 p0552 N71-13970

- Design limit and transient survival criteria for typical fuel elements of large liquid metal fast breeder reactor
04 p0553 N71-14002

- Reactor core technology for LMFBR
04 p0557 N71-14122

- Development of shielding for liquid metal fast breeder reactor
05 p0722 N71-14650

- Neutron cross sections for materials for breeder reactor physics
05 p0740 N71-15095

- Preliminary study of chopper for complete fuel element bundles of ENR-Na2 in WAX
05 p0731 N71-15574

- In-pile creep behavior of austenitic steels and nickel alloys under mechanical loads
05 p0731 N71-15587

- Research on nuclear reactors and fuels
05 p0807 N71-15876

- Isolator lubricated bearing technology for high torque pumps used in fast breeder reactors
05 p1285 N71-18328

- High temperature gas cooled reactor, gas cooled breeder reactor, and pressurized concrete pressure vessel developments
06 p1238 N71-18548

- Research on behavior of fast neutrons in breeder reactors
06 p1242 N71-19210

- U-Pu-Zr alloys prepared by conventional melting and casting techniques for fast breeder reactor applications
06 p1416 N71-19392

- Isolation and thermal hydraulics of sodium boiling and reflux and transport of neutrals and energy in sodium combustion accidents in liquid metal fast breeder reactors
06 p1419 N71-20009

- Research and development in LMFBR physics program
06 p1421 N71-20309

- One dimensional static physics design and analysis code (FARAD) for fast breeder reactor project development
11 p1795 N71-22425

- Shield test models related to LMFBR piping systems including X ray diffraction, strain gages, leak testing, and isotopic interdiffusion
12 p1963 N71-23636

- Survival and testing of liquid sodium piping in LMFBR
12 p1963 N71-23947

- Research and development recommendations for the design of LMFBR piping
12 p1963 N71-23987

- LMFBR environmental effects on type 304 and 316 stainless steels and Co-Mo alloy piping materials
12 p1963 N71-24055

- Scalability of inert gases in liquid sodium and related safety problems for primary circuits of fast sodium cooled breeder reactor
13 p2117 N71-30009

- Bibliography on fast breeder reactors with subject index, reactor index, report index, and patent index
13 p2110 N71-30095

- Research in reactor technology for gas cooled fast breeder reactors
13 p2122 N71-35516

- Nondestructive nuclear assay, calorimetric, gamma, and neutron instrumentation techniques for nuclear fuel element fabrication in breeder reactors
14 p2253 N71-25631

- Accident prevention and safety devices for water cooled reactors compared with liquid metal cooled, fast breeder reactor safety
14 p2291 N71-25684

- Mechanical properties of stainless steel type 304 for LMFBR cladding
14 p2291 N71-25691

- Apparatus for in-pile compressive creep studies of LMFBR ceramic fuels during irradiation
14 p2292 N71-25713

- Core experiments for optimizing sodium-cooled fast breeder reactors by nonlinear programming methods
14 p2293 N71-25720

- Results of irradiation test of Zircaloy clad wiretied UO₂-Fe₂O₃ fuel in BR-2 reactor
14 p2295 N71-26738

- Design guide for LMFBR sodium piping system
15 p3444 N71-36975

- Influence of calculational methods on void effect and multiplication factor for large fast sodium cooled breeder reactors
15 p3445 N71-37012

- Control and order dimensions of storage and mixing containers for plutonium-containing fuels used in breeder reactors
15 p3446 N71-37168

- Temperature and neutron and nitrogen alloying effects on creep and creep rupture tests of AISI type 316 stainless steel and welds in high temperature environments for breeder reactor use
15 p3425 N71-37252

- Creep and fatigue tests of type 316 stainless steel and Inconel 800 for use in breeder reactors
16 p0612 N71-20610

- Discrete element analysis of creep and stress properties of stainless steel tubing for LMFBR
16 p0613 N71-20801

- Technological development work for fast sodium breeder reactors
17 p2784 N71-30059

- Broader reactor research and development including nuclear fuel elements, reactor safety, monitors, and radiation effects on environment
18 p2960 N71-30995

- Effects of irradiation induced metal growth on core components for LMFBR design
19 p3135 N71-31620

- Flow characteristics in primary and secondary loops of LMFBR and failure probabilities
19 p3138 N71-32248

- Optimization of sodium cooled fast breeder reactors by nonlinear programming methods
19 p3139 N71-32599

- Evaluation of sodium cooled breeder reactor technology and instrumentation in German, French, and British facilities
19 p3140 N71-32565

- Methods and models for LMFBR accident analysis and safety system design
19 p3140 N71-32569

- Progress in development of fuel elements, fuel, cooling systems, core monitoring systems, and core design for fast breeder reactors
19 p3141 N71-32772

- Analysis of existing instrumentation systems to protect LMFBR core integrity and recommendations for improvement
20 p3383 N71-33544

- Higher fuel performance in breeder reactors after irradiation
20 p3387 N71-33782

- Welding, radiation effect, and refractory metal alloy research and development for nuclear fuel element and reactor materials for fast breeder reactors including nondestructive testing
20 p3388 N71-33729

- Static load tests on self-welding structural materials for gas-cooled fast breeder reactors
21 p3456 N71-34595

- Uranium and plutonium oxide properties and fabrication methods for ceramic oxide fuels applied to fast breeder reactors
21 p3460 N71-34624

- Design, optimization, and test instrumentation for sodium-lubricated bearings in sodium pumps and circulating auxiliaries in breeder reactors
21 p3461 N71-34626

- Program for accurate determination of nuclear fuel burnup in fast breeder
21 p3462 N71-34640

- Noncritical publication on breeder reactor developments in US
22 p3622 N71-35080

- Development and technology of fast breeder reactors
23 p3622 N71-35080

- Processing method for removing fission and corrosion products and fission materials from molten salt breeder reactor fuel
23 p3634 N71-35018

- Fast breeder fuel element spacer assemblies based on spacer geometry and operating conditions
23 p3636 N71-35036

- Thermal expansion for fuel element chidding in fast breeder reactors
23 p3796 N71-37057

- Quantitative analysis of spatial effects in transfer function measurements of LMFBR based on open-loop reactor model and Galerkin method
23 p3799 N71-37064

- Neutron energy dependent cross sections of LMFBR determined by foil activation methods
23 p3816 N71-37216

- Natural frequencies, vibration modes, and damping of nuclear fuel pins in model of sodium cooled fast breeder reactor
24 p3956 N71-38218

- Pyrochemical bond and conception for fast breeder fuel processing
24 p3956 N71-38224

BREGUET AIRCRAFT

- NT BREGUET 941 AIRCRAFT
Speed and fuel length safety factors for approach and landing mechanics of Breguet 941 aircraft
12 p1855 N71-23420

BREGUET 941 AIRCRAFT

- Establishment of take-off and landing safety margins for Breguet 941
07 p0971 N71-17441

- Possibility of inter-metropolitan transport system using Breguet 941 STOL aircraft
07 p0974 N71-18184

BRUCCA-2000

- Computer corrections to Buta-Tu cross sections for electron-cyclotron bremsstrahlung
01 p0103 N71-10999

- Exact screened calculations of atomic field bremsstrahlung
02 p0272 N71-11772

- Characteristics and operation of electron linear accelerator
03 p0273 N71-11790

- Bremsstrahlung contribution in shielding of gamma rays having energies less than 10 MeV
03 p0489 N71-12884

- Laboratory survey to determine bremsstrahlung production from X irradiation in electronic products
03 p0435 N71-13189

- Automatic analysis of bremsstrahlung effects in lower ionosphere due to electron penetrating into auroral zone
04 p0522 N71-13824

- Energy losses, range, and bremsstrahlung yield for 10 keV to 100 MeV electrons in some simple elements and some chemical compounds
04 p0589 N71-13969

- Isotaxial in satellite linear by bremsstrahlung produced by Van Allen electron clouds
04 p0585 N71-14223

- Electron interaction with matter and differential cross section measurements for bremsstrahlung produced in coincidence with isotactically captured electrons
05 p0923 N71-14699

- Fast variation of hydrocarbon amplitudes and gamma quanta bremsstrahlung
07 p1061 N71-18136

- Vacuum-SI/gamma, electron-atom-71 reaction initiated with second electron after electron irradiation with bremsstrahlung energy between 40 and 65 MeV
08 p1265 N71-19206

- Kinematical gamma ray spectra from Compton interactions and bremsstrahlung production
13 p2159 N71-34776

- Experimental techniques and comparison of theory and experiment for nuclear-neutron bremsstrahlung
13 p2162 N71-35046

- Electronic detection measurements in hot electron matter confined plasma by bremsstrahlung spectra
13 p2167 N71-35076

- Regenerational gamma bremsstrahlung cross sections calculated by Wolkenstein-Williams method
14 p2203 N71-23994

- Bremsstrahlung diagnosis of electron ion beams produced by accelerating heavy atoms to high energies
15 p3460 N71-34670

- Motographic gamma ray spectra calculated for relativistic electron beam bremsstrahlung interactions
15 p3515 N71-37466

- Measuring wide angle bremsstrahlung by electron-photon coincidences using electron synchrotron
15 p2483 N71-37780
- Calculation of electron and bremsstrahlung dose deposition with energy deposition, transmission, and reflection coefficients for electron
[NASA-TN-D-6385] 16 p2674 N71-28127
- General theory of bremsstrahlung of relativistic plasma particles
[NP-16758] 19 p3163 N71-31924
- Bremsstrahlung effect from relativistic particles in turbulent plasma
[NP-18759] 19 p3164 N71-31963
- High energy bremsstrahlung-induced γ - μ reactions in Au-197
[LUNP-7108] 19 p3159 N71-32628
- Magnetic fields, bremsstrahlung, and synchrotron emission in solar flares of October 24, 1969
[NASA-CR-121620] 21 p3583 N71-34954
- Iterative method for interpreting bremsstrahlung spectra
[RT/71-7014] 22 p3631 N71-35869
- Electron-ion bunch diagnostics by bremsstrahlung, using heavy atom acceleration to high energies
[UCRL-TRANS-1440] 23 p3808 N71-37155
- Calculation of radiation cross section for relativistic suprathermal proton bremsstrahlung to determine contribution to cosmic gamma rays
[NASA-TM-X-65469] 23 p3811 N71-37171
- X ray spectral measurements of bremsstrahlung emissions from thick tungsten targets in 12 to 300 kV range
[LA-4624] 23 p3813 N71-37192
- Cross section measurements of proton-proton bremsstrahlung at 20 MeV
23 p3821 N71-37257
- Equipment and capabilities developed in investigation of K and L shell ionization cross sections, X ray intensity ratios, bremsstrahlung spectrum, coincidence, and inelastic electron scattering
[NASA-CR-119957] 24 p3976 N71-38368
- BREWSTER ANGLE**
Angles significant for radio propagation - wave tilt of total field electrical vector, wave tilt of surface waves, Brewster angle, and Norton limiting angle
[AD-711946] 02 p0179 N71-11259
- BRIDGES (STRUCTURES)**
Prototype integrated bridge design subsystem for solving computational problems and generating plotting parameters
14 p2226 N71-36557
- BRIDGMAN METHOD**
Neutral defects in mercury telluride single crystals grown by Bridgman method in mercury vapors
07 p1047 N71-17125
- Numerical analysis of plastic deformation and dislocation density in crystals grown by Bridgman method
[AD-719575] 13 p2151 N71-25180
- BRIGHTNESS**
Magnitude estimates of brightest stars in Large Magellanic Cloud
[SAO-SPEC/L-REPT-320] 01 p0122 N71-10365
- Airborne filter colorimeter measurements of atmospheric thermal glow brightness
01 p0049 N71-10587
- Microvane radiometer and polarimeter measurements of sun surface
02 p2027 N71-11164
- Modulating and controlling intensity of light beam from high temperature source by servocontrolled rotating cylinders
[NASA-CASE-XMS-04300] 09 p1357 N71-19479
- Light scattering calculations for brightness effect in Mars atmosphere caused by aerosols
13 p2148 N71-25278
- Earth brightness deduced from Cosmos 149 measurement of solar radiation reflected by earth
15 p2514 N71-27501
- Visual flash duration discrimination and decision theory analysis of effects of temporal and brightness differences
[NASA-CR-118998] 16 p2541 N71-28068
- Reconstruction of ultraviolet brightness of stars by SAO from video data obtained in Celestec experiment
16 p2679 N71-28520
- Correlation of zero phase brightness surge - heliograph with lunar surface roughness
18 p3013 N71-30977
- Solar radial brightness distribution as determined from 3 mm observations of March 1970 total eclipse
[ER-622] 19 p3182 N71-32651
- Brightness and life of pointed cold cathodes for electron microscope applications
[NRC-TT-1473] 22 p3539 N71-35351
- BRIGHTNESS DISCRIMINATION**
Video signal processing system for sampling video brightness levels
[NASA-CASE-NPO-10140] 13 p2045 N71-24742
- Signal and stimulus ratio effects on long term human responses to light signal intensity differences
[RSC-503] 13 p2038 N71-24953
- Luminance density distribution effects on television picture perception
23 p3723 N71-36534
- BRIGHTNESS TEMPERATURE**
Infrared radiometer for measuring lunar brightness temperature
[NASA-TM-X-64539] 01 p0053 N71-10275
- Measured quiet sun/new moon brightness temperature ratios at 6 mm
[AD-713114] 05 p0769 N71-15359
- Measuring brightness temperature of simulated ocean surface using microwave radiometer
06 p0848 N71-16179
- Correlation of sea surface roughness with vertically polarized microwave radiometric brightness temperature
[AD-719447] 13 p2069 N71-24393
- Radio spectrum analysis of two active regions based on Laplace transform and brightness temperatures from Nov. 12, 1966 solar eclipse data
[NASA-TM-X-64543] 22 p3664 N71-36127
- BRILLOUIN EFFECT**
Investigating quantum statistical properties of electromagnetic radiation
[AD-714683] 06 p0917 N71-16188
- Elastic, photoelastic, and photoacoustic constants for light scattering with hypersonic waves and Brillouin effects in ferroelectric lithium niobate crystals using helium-neon lasers
13 p2125 N71-24906
- High resolution spectroscopy, resonant reflectors, and Brillouin and other light scattering phenomena
[AD-720571] 20 p2574 N71-33476
- Measurement of hypersonic sound speeds in methanes at moderate pressure and comparison with ultrasonic speed data
[NASA-CR-121577] 20 p3274 N71-33477
- Analysis of vibrational relaxation in carbon tetrachloride
20 p3275 N71-33482
- BRILLOUIN ZONES**
Acoustic phonon lifetime of fused silica and Brillouin scattering - time and temperature dependence
17 p2082 N71-30130
- Numerical analysis of transport parameters for point defect scattering in nearly free electron model metals
22 p3640 N71-36098
- Brillouin scattering and infrared spectroscopy of C2H2 and HF dimer
[AD-721122] 24 p3967 N71-38297
- BRIS**
Devices to regulate flashing brine flow through flash evaporators
[ORNL-TM-2746] 07 p1008 N71-17269
- Hydrographic and meteorological survey of Red Sea revealing brine holes and related hot lakes - Oceanographic expedition
23 p3788 N71-37000
- BRISTOL-SIDDELEY OLYMPUS 593 ENGINE**
Efficiency of air cooling blade design for Olympus 593 gas turbine engine
07 p1099 N71-17376
- BRITISH AIRCRAFT CORP AIRCRAFT**
U BAC AIRCRAFT
BRITTLE MATERIALS
Structural data on brittle nonmetallic materials for use in designing reentry vehicles
[AGARD-AO-152-71] 09 p1406 N71-30027
- Measurement of stress pulses resulting from fracture of brittle circular rods under uniaxial tension and mechanical properties of materials at high rates of shearing strain
14 p2349 N71-26253
- Micromechanism of crack propagation in brittle materials and description of motion of crack zone during crack propagation
14 p2349 N71-26258
- Stress-strain diagrams for crack loading of brittle bodies weakened by pointed concentrators
[AD-720959] 15 p2523 N71-27865
- Fracture mechanics and statistical failure analysis of brittle materials and erosion and abrasion machining processes
18 p2929 N71-31209
- Development of method for testing resistance of brittle material to fracture when subjected to shock wave loading
[RFP-1554] 21 p3529 N71-35146
- Discrete element model for predicting deformation and failure mode of stressed brittle materials
23 p3065 N71-37554
- BRITTLENESS**
Bartholomew nondestructive test methods for detecting stress in brittle materials
[AD-710808] 01 p0045 N71-10063
- Describing machine for testing strength and safety of large structures
[ZJR-62] 05 p0776 N71-15193
- Brittle fracture of alloyed, high density, fine grained, and pure aluminum
[AD-715988] 09 p1405 N71-19803
- Brittleness and surface crack initiation in steel castings
10 p1562 N71-30703
- Brittleness and microcrack initiation in chromium steel piston heads
10 p1572 N71-30819

- Effect of internal stresses on strength of elastically bonded composites with varying coefficients of thermal expansion
[UCRL-26995] 15 p2428 N71-30900
- Static and cyclic fatigue characteristics of brittle polymers using machines to provide zero mean stress with alternating tension and compression stresses
[COO-1794-7] 15 p2522 N71-32968
- Analysis of fracture mechanism that occurs during penetration of rigid wedge into elastic, brittle, anisotropic material
16 p3086 N71-30886
- Systems analysis to simplify brittle fracture tests of metals
[AD-72876] 18 p2958 N71-31022
- Role of ductility brittleness transition in body centered cubic lattice of iron polycrystals
19 p3112 N71-32903
- Steel brittleness related to low cycle fatigue, brittle failure prediction calculations
[AD-727422] 24 p3957 N71-36869
- Poreosity effects on elastic and strength properties of brittle materials, emphasizing beryllium
[AWR-O-2571] 24 p0023 N71-30270
- BROADBAND**
Predicting wideband frequency modulated signal by waveform generator
[AD-710832] 01 p0033 N71-10018
- Development of broadband horn antennas with double ridged waveguide techniques
[AD-712299] 02 p0178 N71-11258
- Broadband constant beamwidth conical arrays
[AD-712676] 03 p0338 N71-12045
- Broadband radiometers for quantitative analysis of electromagnetic radiation
[T-3849] 03 p0300 N71-12144
- Short axial length broadband horn design for S band
[AD-714954] 07 p1080 N71-17801
- Anerodynamic broadband noise mechanism applicable to axial compressors
[NASA-CR-1743] 07 p1013 N71-17818
- Flexible monopole antenna with broad bandwidth and low voltage standing wave ratio
[NASA-CASE-MSC-12101] 08 p1169 N71-18220
- Broadband frequency discriminator with variable capacitive inductive networks
[NASA-CASE-NPO-10096] 13 p2043 N71-24883
- Broadband microwave waveguide window to compensate dielectric material filling
[NASA-CASE-XNP-40880] 13 p2056 N71-24888
- Comb type traveling wave mass amplifier for improved high gain broadband output
[NASA-CASE-NPO-10548] 13 p3089 N71-34821
- Broadband hot carrier diode mixers - analysis of intermodulation and cross modulation distortions
[AD-721244] 15 p2585 N71-26889
- Wideband voltage controlled oscillator with high phase stability
[NASA-CASE-XLA-43895] 15 p2588 N71-27271
- Broadband signal encoding device with circular scanning cathode ray tube
[JPRS-53353] 16 p2562 N71-28706
- Broadband current preamplification for obtaining simultaneous high resolution energy and time information from nuclear radiation detectors
[ORNL-TM-3252] 17 p2799 N71-30022
- Broadband active and passive radio systems design for use in signal transmission and reception
19 p3052 N71-31610
- Modified broadband nonconcentric sliding short circuit for moderating microwave measurements
[NBS-TN-602] 19 p3065 N71-32263
- Organic dye laser as high power optical carrier for broadband data transmission and diagnostic applications during nuclear research test events
[EGG-1183-2262] 21 p3455 N71-36445
- Broadband quartz resonator with thin film piezoelectric transducer
23 p3731 N71-36570
- Broadband sound wave delay line with low insertion losses
23 p3731 N71-36580
- BROADBAND AMPLIFIERS**
Broadband model of broadband pulse width modulated amplifier
[NASA-CR-102997] 06 p0824 N71-16199
- Iron doped resistive wideband mass amplifier with low signal-to-noise ratio
13 p2080 N71-25337
- Solid state broadband stable power amplifier
[NASA-CASE-XNP-10854] 14 p2233 N71-26311
- Broadband distribution amplifier with complementary pair transmitter output stages
[NASA-CASE-NPO-10003] 14 p2234 N71-26415
- Broadband parametric amplifier for space communication
17 p2725 N71-26891
- Procedural description for computerized design of broadband amplifier
[NLL-TRANS-2734-19022.81] 22 p3563 N71-35371
- Experimental quadrature two-channel modulation system for video signals operating at VHF
[RSC-197170] 23 p5776 N71-36538

SUBJECT INDEX

broadband differential amplifier having gain of 16
 from dc to 150 MHz 24 p0897 N71-37779
BROADCASTING
 Communication theory and research applied to
 processing emergency Civil Defense broadcasting
 system messages 02 p0162 N71-11277
 Construction of satellite broadcasting network
 systems 07 p0992 N71-17466
 Effects of nuclear electromagnetic pulses on AM
 radio broadcast stations in emergencies 11 p1096 N71-31854
 Radio construction, broadcasting, and training in
 USSR 12 p1073 N71-32374
 Data handling method for satellite TV broadcast
 system design, and data analysis and plotting by com-
 puter techniques 16 p2561 N71-28427
 Digital and analog UHF antennas for home TV
 reception via satellite broadcast relay system 16 p2561 N71-28428
 Digital coding techniques used for satellite televi-
 sion broadcasts 21 p3396 N71-34169
 Multichannel signaling in digital color circuits for
 automatic control of broadcasting network 23 p3725 N71-36555
NUCLEAR BROMIDES
 Raman, infrared, and far infrared spectra of laser
 excited sulfur monochloride and sulfur monobromide 12 p1872 N71-34062
 Raman and far infrared spectra of laser excited sul-
 fur monobromide 12 p1872 N71-34064
 Vibrational spectra of sulfur monochloride and sul-
 fur monobromide excited by laser 12 p1873 N71-34066
 Computer calculations of Raman line intensities,
 angles of polarization, and scattering cross sections
 for sulfur monochloride and sulfur monobromide 12 p1873 N71-34069
 Electro deposition of palladium from amino-palladi-
 um hydroxide, bromide, and sulfamate electrolytes
 and electrolyte properties 22 p3599 N71-35562
 Computer assisted assignment and analysis method
 for vibration-rotation spectra of methyl bromide 24 p3983 N71-38424
NUCLEAR BROMINE ISOTOPES
 Chemical reduction of Br₂ molecules in argon heat
 bath 07 p1073 N71-17413
 Resonance potential analyzer used with vacuum
 monochromator for recording photoelectron spectra
 of iodine and bromine 13 p2041 N71-25345
NUCLEAR COMPOUNDS
NUCLEAR BROMIDES
NUCLEAR POTASSIUM BROMIDES
NUCLEAR ISOTOPES
 Reaction cross section measurement of Ge-71, Br-
 79 and Br-79 isomeric states using 14.8 MeV neutrons
 15 p2483 N71-27083
 Nuclear processes activated by isomeric transition
 of Br-82m and I-130m 15 p2488 N71-27076
NUCLEAR U BROMINE ISOTOPES
NUCLEAR U BROMINE ISOTOPES
NUCLEAR TUNGSTEN
NUCLEAR TRACERS
 Low temperature mechanical properties of various
 alloys of high strength and corrosion resistant 12 p1930 N71-33793
 Electrical and magnetic properties of potassium
 methylsulfate bromide 17 p2765 N71-29650
NUCLEAR MOVEMENTS
 Reversible motion of interstitial grains and mass
 quantum displacement calculations 11 p1824 N71-32300
NUCLEAR METROLOGY
 Comparison of aluminum 26 radioactivity of Bro-
 chidion chondrites, lunar rocks, and schists 15 p2517 N71-27670
NUCLEAR PHENOMENA
 Production of saturated impurity semiconductor
 layers for electrical energy transfer 07 p1094 N71-17018
NUCLEAR REACTIONS
 Exposure of 15 foot detector filled bubble
 chamber to positive pion meson beam at 40 GeV/c
 04 p0681 N71-14060
 Daily film measuring system for bubble and spark
 chambers 05 p0883 N71-14036

Bubble chamber on-line film plane digitizing system
 using CDC 3100 computer 05 p0683 N71-14082
 Scanning measuring equipment for processing bul-
 ble chamber and oscillogram films 05 p0683 N71-14083
 Investigating development and components of bul-
 ble chambers for elementary particle research 05 p0741 N71-15120
 Development of on-line video scanning system for
 rapid cycle bubble chambers 05 p0680 N71-15510
 Lecture series on elementary particle interactions
 and bubble chamber technology 06 p0832 N71-16256
 Neutral kaon resonance production in positive pion
 deuterium interactions within bubble chamber 06 p0823 N71-16812
 Mass, photon, and neutron detectors to study in-
 elastic interactions of neutrinos in hydrogen bubble
 chamber 06 p0826 N71-16853
 Mass identification in neutrino interactions in bul-
 ble chamber 06 p0827 N71-16891
 High energy interactions in spark and bubble cham-
 bers 07 p1071 N71-17035
 Heat exchange and thermoisolation for 2-meter
 liquid hydrogen bubble chamber of ITEP 06 p1174 N71-16230
 Bubble chamber study of two body channels of
 positive and negative Sigma hyperons and pions from
 scattering negative kaon beam 09 p1425 N71-19475
 Hydrodynamical processes and parameters of glass
 motion in large bubble chamber 09 p1365 N71-19916
 Precision scintillator and positron recognition device,
 bubble chamber, photon problems, and cathode ray
 tube devices—conference 09 p1445 N71-20555
 Digital automatic pattern recognition system to find
 and measure events in bubble chambers 10 p1612 N71-20723
 NAL 15 ft hydrogen bubble chamber, stress analy-
 sis of 22 ft vacuum tank, and failure mode analysis of
 hydrogen bubble chamber 12 p1895 N71-32129
 Radiation induced ionization of bubbles caused by
 alpha particles in superheated water 12 p1908 N71-23136
 Data acquisition from bubble chamber photographs
 of nuclear reactions 13 p2129 N71-24671
 Propose bubble chamber photographic analysis of
 kaon tau decays and calculation of final state pion
 energy distributions with comparison to nuclear
 resonance models 13 p2142 N71-25556
 Reaction pion/minor proton yields rho-meson /
 pion/minor proton with momentum studied in liquid
 hydrogen bubble chamber at 4.45 GeV/c 14 p2316 N71-26745
 Testing fast valve operating at pressure of 100 atm
 for use in bubble chamber 15 p2413 N71-27118
 Electronic circuit for detecting gas bubble
 discharge in liquids 15 p2479 N71-27635
 Positive kaon negative pion elastic scattering from
 positive kaon proton interaction at 5.43 GeV/c in 80-
 inch bubble chamber 15 p2482 N71-27745
 Lambda and Sigma hyperon resonances, branching
 ratios, and lifetimes from bubble chamber analysis of
 antiproton nucleus reactions 15 p2492 N71-27951
 Gamma ray probability in Monte Carlo generation
 of neutral negative pion proton interactions at 5 GeV/c
 in propane bubble chamber 16 p2649 N71-28316
 Searching method for kink and track parameter
 determination of particles scattered in bubble chamber
 for reconstruction 16 p2650 N71-28379
 Hydrogen bubble chamber experiments on 10 and 19
 GeV/c proton-proton interactions 17 p2790 N71-30005
 Hardware system for measurements of bubble
 chamber films on-line 17 p2723 N71-30013
 Distortion effects in geometrical reconstruction of
 events in CERN 2m hydrogen bubble chamber 17 p2809 N71-30008
 Photo-reproduction of four proton reactions in
 hydrogen bubble chambers including particle trajec-
 tory reconstruction and analysis of particle production
 mechanisms 17 p2801 N71-30115
 Hydrogen bubble chamber study of polarized
 gamma proton yields pion/kaon/pion/minor proton at
 2.8 and 4.7 GeV produced by Compton backscattering
 17 p2804 N71-30266

Analog models to measure two-dimensional and
 three-dimensional distribution of magnetic flux den-
 sity of magnet for bubble chamber 18 p3060 N71-30414
 Precise determination of particle coordinates in
 proportional multiwire chambers with potentiometric
 readout 18 p3070 N71-30461
 Computer program for photo-interpreting and anal-
 ysis of multi-particle production in bubble chambers 18 p3072 N71-30469
 Design of ITEP 2-meter liquid hydrogen bubble
 chamber and calculation for chamber body expansion
 system, vacuum tank, and nitrogen shielding 19 p3073 N71-32238
 Superconducting magnet for giant bubble chamber
 at CERN 21 p3464 N71-34654
 Hyperon hyperon decay measurements and two
 decay mode search in bubble chamber 21 p3476 N71-34751
 Scattering cross section for pionic/plasma/plasma
 yields pionic/plasma/plasma/plasma/plasma
 proton determined from 2454 hydrogen bubble
 chamber events 21 p3480 N71-34845
 Operating properties of liquid hydrogen bubble
 chamber and cooling system 22 p3635 N71-35908
 Methods for approximating particle tracks and mag-
 netic field strength in bubble chambers 22 p3638 N71-35935
 Computer techniques for photo-interpretation of
 neutral pion and gamma quanta events in bubble
 chamber filled with heavy liquids 22 p3641 N71-35958
 Charged pion production in 40,000 isotopic proton-
 neutron interactions in hydrogen bubble chamber
 between 13 and 28.5 GeV/c 22 p3645 N71-35954
 Correlation of eta and omega meson production
 from pion neutron reactions in bubble chamber with
 exchange models 22 p3649 N71-36025
 Neutrino physics and bubble chamber properties—
 Vol. 1 23 p3815 N71-37211
 Bubble chamber research and progress—Vol. 3 23 p3816 N71-37212
 Heavy gas-liquid mixture bubble chamber with 70
 liter volume and hydrogen internal target for use with
 electron-activated gamma beams 24 p3920 N71-37951
 Applications of bubble chamber to study of ionized
 particles 24 p4012 N71-38618
BUBBLES
 Mass transfer in gas flow through fluidized bed 01 p0843 N71-10491
 Delayed bubble movement on airfoil during
 helicopter stall 02 p0441 N71-11005
 Radial bubble distribution in heated turbulent flow
 in sodium cooled reactors 03 p0416 N71-12922
 Calculation of bubble rise velocities in multibubble
 systems under reduced gravity conditions 03 p0446 N71-13103
 Spray, mist, bubbles, and foam in sodium heat
 transfer experiments 04 p0538 N71-14161
 Far field holography for determining bubble spec-
 trum in cavity tunnel 04 p0525 N71-14271
 Elimination of permeation and bubble formation in
 Apollo RCS positive expulsion testings 04 p0609 N71-14866
 Bubble effects in candle fuel and cooling and gas
 releases 07 p1029 N71-17027
 Asymmetric convection bubble collapse near solids
 (PB-195-027) 08 p1177 N71-18318
 Measuring bubble size distribution by light scatter-
 ing 08 p1177 N71-18366
 Gas bubble growth and compression in body phys-
 ical systems and tissues 08 p1155 N71-18970
 Mass transfer and drag coefficients of bubbles rising
 in dilute aqueous solutions 08 p1245 N71-19030
 Representations of flow separation bubbles near air-
 foil leading edge 09 p1323 N71-20064
 Dynamics and stability of obtaining and interpreting
 bubble contour images and detachment diameter 10 p1512 N71-20779
 Time-dependent motion of small gas bubbles in
 smoothly deforming liquid including bubble slip
 functions 10 p1543 N71-21447
 Information on parameters associated with genera-
 tion of acoustic energy by boiling bubbles 10 p1609 N71-21778

BUCCANEER AIRCRAFT

SUBJECT INDEX

Spherically symmetric phase change problem solved by least balance integral method using appropriate temperature profile
[AD-718151] 12 p189 N71-23321

Numerical estimates of intensity, scale, duration, and repetition rates of surface attack from individual bubble collapse and cavitation damage relationships to corrosion-fatigue
[UMICR-083371-7-7] 12 p1900 N71-23339

Stability of bubble growth in nucleate boiling and electrolysis
[NASA-CR-118641] 14 p2332 N71-23902

Gas dynamics and thermodynamics of single vapor bubbles in liquid hydrogen and ultrasonic radiation effects
[JNRP-113-5327] 15 p2392 N71-27085

Flowing solution of air bubbles and droplets of equal radius to mineral particle surface
[NLL-RTS-6134] 17 p2786 N71-29269

Asymmetric and thermodynamic effects on cavitation bubble collapse, modes of collapse, and causes of cavitation damage
[PB-198046] 17 p2734 N71-29733

Isenthalpic bubble motion under influence of varying high-g body forces, low gas flow rate isenthalpic bubble formation, and coefficients of drag for planar elliptical bubbles
18 p2887 N71-31368

Krypton and helium bubble migration on dislocations in copper foil, and measurement of root mean square random migration distances during isothermal annealing
[RD/RN-1858] 19 p3146 N71-31964

Reaction kinetics for fission gas bubble growth, nucleation, and resolution
[GEAP-12148] 20 p3322 N71-33762

Microscopic foundation of bubble model for excess electron in liquid lithium
20 p3325 N71-33905

High-voltage isolator design for injecting hydrogen bubbles into liquid metal feed lines to interrupt electrical continuity
[NASA-CASE-NPO-11075] 21 p3402 N71-34208

High speed photography of bubble collapse close to rigid boundary, flexible boundary, and second bubble
[PB-199464] 21 p3413 N71-34286

Formation of fission gas bubbles in solids during reactor irradiation
[AERE-R-6595] 21 p3467 N71-34679

Size of fission product gas bubbles released from simulated break in fuel-element cladding
[ANL-7789] 21 p3479 N71-34778

Numerical analysis of asymmetric collapse of vapor bubble in viscous incompressible liquid using modified Marker and Cell technique
[PB-199568] 22 p3567 N71-35406

Newtonian viscous flow in infinitely long wavy wall tube with gas bubbles along centerline
22 p3571 N71-35431

Electron microscope scanning of re-solution of gas from bubbles and sintering pores during UO₂ irradiation at high temperature
[RD/RN-1716] 22 p3621 N71-35797

Analysis of Preact-113 bubble growth and collapse in constant-diameter, vertical channels with oscillatory initial temperature profiles
[ANL-7746] 22 p3623 N71-35813

Effect of gas bubbles entrained in sodium coolant examined on LMFBR fuel rods
[CONF-700608-36] 22 p3625 N71-35827

Effects of gas bubbles in ocean bottom sediments on behavior of sound waves
[AD-726712] 23 p3752 N71-36751

Comparison of bubble method and cmf measurements of Al and Cu activities in molten Al-Cu alloy reactions with AlCl₃
[NLL-RTS-6273] 23 p3774 N71-36899

Analysis of pressure disturbances associated with growth of isolated bubble in pool of boiling liquid
23 p3802 N71-37107

Mathematical model for motion of small drops and bubbles considering absorption, diffusion, and convection in interfacial region
[NVO-2007-91] 24 p3996 N71-38306

BUCCANEER AIRCRAFT

Low-speed wind tunnel longitudinal stability tests on sweptback wing model with blowing at leading edge slots and trailing edge flaps for Buccaneer aircraft performance
[ARC-RM-3635] 13 p2022 N71-24563

BUCKLING

NT CREEP BUCKLING

NT ELASTIC BUCKLING

NT BULGE BUCKLING

NT THERMAL BUCKLING

Using Rayleigh-Ritz method to calculate buckling of orthotropic skew plates under direct and shear loading
[AE-264-5] 02 p3032 N71-12081

Buckling of integrally stringer-stiffened cylindrical shells under axial compression
[AD-712090] 03 p0460 N71-12869

Investigating plastic behavior and design methods of welded structures
[AD-712121] 03 p0460 N71-12951

Effect of variations in creep exponent N on buckling of circular cylindrical shells in axial compression
[AD-711949] 03 p0461 N71-12966

Numerical analysis of buckling and postbuckling of arch structures
[AD-712042] 03 p0465 N71-13162

Numerical method for obtaining minimum weight design of structures with requirements imposed on stresses and natural frequencies
[EAS-432-VOL-35-NO-10] 03 p0466 N71-13227

Experimental and theoretical studies of thin-walled circular cylindrical buckling
[DLR-MITT-70-10] 03 p0466 N71-13345

Incremental variational method for determining inelastic load deformation and buckling load for shells of revolution
[AD-712322] 04 p0617 N71-13946

Theoretical and experimental vibration and buckling results for blunt truncated conical shells with ring supported edges
[NASA-TN-D-7003] 04 p0617 N71-14056

Nonlinear vibration of buckled beams and rectangular plates
[PB-193885] 04 p0618 N71-14300

Critical buckling data for design of skew plates subjected to loads
[AE-248-5] 05 p0775 N71-15151

Exact buckling criterion for eccentrically stiffened multilayered circular cylindrical shells of materials having different orthotropic moduli in tension and compression
[AD-713113] 05 p0779 N71-15319

Plastic buckling of axially compressed thin shells of revolution with arbitrary meridional shape
06 p0936 N71-16842

Numerical solutions for bending, vibration, and buckling of laminated anisotropic rectangular plates
[AD-713280] 07 p1126 N71-17926

Equilibrium equations for plastic buckling and deformation behavior of steel plates
08 p1296 N71-18612

Buckling of eccentrically stiffened thin-walled circular cylinders under axial loads
[DLR-FB-70-48] 08 p1297 N71-18643

Buckling strength of fiber glass reinforced plastic bars
08 p1300 N71-19174

Wall motions in circular thin-walled cylindrical shells under combined loading
08 p1301 N71-19282

Numerical analysis of vibration and buckling in web stiffened sandwich structures
[AD-716394] 09 p1475 N71-19860

Numerical analysis of plastic buckling of hinged arches
[TAE-119] 09 p1480 N71-20464

Buckling and post-buckling behavior of thin elastic plate subjected to compressive forces along the edge
10 p1657 N71-21396

Perturbation method extension for nonlinear panel flutter to include fifth-order nonlinear terms effect, flutter-buckling interaction, and small damping terms
[NASA-CR-117504] 10 p1658 N71-21672

Application of curved triangular finite elements in buckling analysis of arbitrary shell
[AD-717766] 11 p1836 N71-22337

Buckling of simply supported skew plates under combined loading with in-plane stresses expressed in terms of orthogonal components
[AE-290-5] 11 p1836 N71-22366

Finite element analysis of response of structures exhibiting bifurcation change of state from pre-buckling to post-buckling equilibrium configuration
12 p2080 N71-24275

Optimum design for buckling prevention in cylindrical shells under lateral pressure
13 p2178 N71-24648

Structural analysis and design data for buckling of simply supported skew plates with stresses expressed in terms of oblique components
[AE-294-S-PT-1] 13 p2183 N71-25414

Numerical analysis of influence of fiber orientation on mechanical properties of cylindrical shells in initial postbuckling region
[AD-720231] 14 p2349 N71-26252

Relationship between dynamic buckling and static buckling investigated with clamped shallow circular arches using high speed camera
14 p2350 N71-26467

SNAP - computer program for solving finite difference form of group diffusion equations in two dimensions
[TRG-1990] 15 p3493 N71-27944

Analytical evaluation of buckling modes of shell configurations to determine imperfection sensitivity of optimum structural designs for Mars entry capsule
[NASA-CR-1800] 16 p2684 N71-28031

Influence of in-plane boundary conditions on buckling of clamped conical shells under external pressure
[AD-721475] 16 p2684 N71-28056

Buckling tests of two integrally stiffened circular cylinders subjected to bending loads
[NASA-TN-D-6271] 16 p2684 N71-28116

Effect of in-plane boundary conditions on buckling loads of simply supported ring stiffened cylindrical shells
[AD-721473] 16 p2685 N71-28119

Buckling and column failure interaction of thin-walled compression members due to flange asymmetry
[VTN-160] 17 p2851 N71-30006

Flat rectangular plate buckling analysis using finite element method
[VTN-161] 17 p2853 N71-30006

Buckling coefficients of clamped skew plates under individual loading with in-plane stresses expressed in orthogonal components
18 p3021 N71-31004

Buckling of boron/aluminum and graphite/aluminum fiber composite anisotropic panels - load tests
[NASA-TM-X-67890] 18 p3022 N71-31201

Fourier analysis of clamped anisotropic plates under bending under transverse load, shear and lateral compression buckling, and natural frequencies of lateral vibrations
[AD-723287] 19 p3187 N71-31800

Buckling of trusses with arbitrary supports or all beams with bracing against lateral deviation
19 p3187 N71-31804

Design for determining buckling strength of structural plates for spacecraft
[NASA-SP-9068] 20 p3358 N71-33318

Dynamic structural analysis of clamped skew plate buckling under various loads
[AE-296-5] 20 p3360 N71-33821

BUSHEL - computer program used to determine buckling load of revolution shells under hydrostatic pressure, axial compression or both
[WAFB-TM-500] 21 p3461 N71-34635

Stress analysis and deformation of perforated thin elements subjected to compressive buckling
[NASA-CR-121669] 21 p3526 N71-35127

Local and overall buckling interactions in relation to structural failure in built-up columns
[WTHD-23] 21 p3528 N71-35139

NASTRAN computer program applied to buckling problem of reinforced cylindrical shells with opening
22 p3682 N71-36319

Effects of combined loading on buckling of stiffened supported skew plates based on Rayleigh-Ritz method
[AE-299-S-PT-2] 22 p3689 N71-36908

Statistical model for buckling of isotropic structures by considering material properties as random parameters with known joint probability density functions
22 p3693 N71-36936

Lateral buckling coefficient curves for rectangular beams bent in plastic range
[AEL/SM-NOTB-354] 23 p3660 N71-37318

Design curves and computer program for investigating post buckling behavior of stiffened plates with small initial curvature under combined loads
[AD-726455] 23 p3661 N71-37325

Dynamic buckling of thin elastic shells of cylindrical, spherical, and conical shape
[AD-726597] 24 p4024 N71-36709

BUDGETING

NT FEDERAL BUDGETS

Research and development in State government agencies
[NSF-70-22] 01 p0138 N71-10977

Program budgeting role in US government guiding and managing social, economic, and environmental systems
[AD-711903] 02 p0187 N71-11883

Annotated bibliography of capital budgeting/project selection by mathematical programming
[TM-173] 03 p0399 N71-12817

Federal fund allocations for research and development and other scientific activities for FY 1960, 1961, and 1971
[NSF-70-38] 05 p0788 N71-15081

Contents and scope of AGARD technical program and budget for 1972
[AGARD-BUL-71/2] 14 p2361 N71-26570

Congressional hearing on budgeting authorization for continuation of Fire Research and Safety and Standard Reference Data Act
22 p3689 N71-36883

Budgeting, optical and mirror system, and instrumentation of 150-inch reflecting telescopes in Adams and Chile
24 p3821 N71-37980

BUDGETS

Science policy for United States of America
01 p0000 N71-10817

BUFFER STORAGE

Feasibility design of billion-gate computer
[AD-714089] 06 p0619 N71-14966

Cooperative sequential queuing for buffer pool operator in multiprogramming computer operation
[SU-STAN-CS-71-262] 12 p1885 N71-36606

Data acquisition and processing system with buffer storage and timing device for magnetic tape recording of PCM data and timing information
[NASA-CASE-NPO-12107] 15 p2083 N71-27253

Adaptive approach to dynamic allocation and release of buffer storage within computer systems
[NASA-CR-119765] 21 p3397 N71-34871

SUBJECT INDEX

ABSTRACTING

Determination of steady forces during wind tunnel test of elastic model by placing wind tunnel model in feedback circuit of servosystem
[NASA-CR-114287] 00 p1316 N71-19796

Aeroblastic spacecraft design to minimize buffeting and atmospheric ascent
[NASA-SP-2061] 00 p1472 N71-30473

Transonic flutter and buffeting for elastic wind tunnel models of straight wing proposed for space station
13 p2179 N71-34659

Buffet response of straight wing and delta wing model of space shuttle launch configuration
13 p2179 N71-34642

Transonic buffeting flow on cone-cylindrical models
13 p2179 N71-34642

Relation between turbulence in stratosphere coming through buffeting, and vertical distribution of meteorological parameters calculated from radioonde data
[NASA-TT-F-15961] 23 p3783 N71-36396

Horizontal temperature and wind distribution effects on aircraft buffeting in stratosphere
[NASA-TT-F-15978] 24 p3872 N71-37600

BUILDING MATERIALS

U CONSTRUCTION MATERIALS

STEEL STRUCTURES

U BUILDINGS

Standards and measurement methods for building and electronic technology, systems analysis, motor vehicle safety, and engineering materials
01 p0137 N71-10511

Basic beam and explosive shock wave effects on buildings and structural members
02 p0146 N71-11035

Shadowgraph photography and differential laser interferometry for studying aircraft boom effect on buildings
[NRL-T-7376] 03 p0315 N71-12347

Wind effect criteria for structural design and engineering of buildings
05 p0776 N71-15301

Structural building design criteria for dynamic wind loads
05 p0777 N71-15302

Wind load consideration in building wall design
05 p0777 N71-15303

Meteorological data for developing engineering boundary layer wind model of gust loads on structures
[NASA-TM-X-64547] 05 p0777 N71-15305

Wind loading moments produced on scale models of tall buildings in wind tunnel tests
05 p0777 N71-15306

Wind pressure measurements on high building for wind tunnel modeling of structural aerodynamics
05 p0778 N71-15307

Gust factor for determining dynamic wind effects on buildings
05 p0778 N71-15310

Aerostatic wind effects for dynamic design of tall buildings
05 p0778 N71-15311

Aerostatic response of tall buildings to vortex shedding and gust loading
05 p0778 N71-15312

Differentiation in dynamic structural analysis for buildings subjected to wind loads
05 p0778 N71-15313

Aerostatic wind tunnel modeling and three dimensional structural analysis for dynamic building response prediction to wind loads
05 p0778 N71-15314

Meteorological wind data for determining gust loads on engineering structures
05 p0779 N71-15315

Economic equipment and layout planning of windmills using computerized simulation methods
10 p1665 N71-20770

Ground and aerial surveys of building damages caused by tornadoes
[NBS-TN-338] 10 p1652 N71-20661

Probabilistic theory for analyzing response and safety of buildings subjected to seismic loading
10 p1656 N71-21268

Transfer functions for calculating coupled aeroelastic response of structures in seismic motion
15 p2354 N71-28380

Yield of US facilities capable of sustaining nuclear chain reactions
[TID-4280-REV-23] 16 p2578 N71-28782

Expandable space frames for three dimensional or shear building structures
[NASA-CASE-XRC-10945] 16 p3083 N71-30948

Structural damage in response to underground nuclear explosion
[AD-75-76] 19 p3092 N71-33115

Probability of regulating incident and reflected solar radiation on buildings in arctic regions
[NRL-82-26001-328.47] 21 p3925 N71-34068

BULGARIA

P wave velocity and compressive strength of Bulgarian rock specimens at hydrostatic pressure up to 5000 kg/cm²
[NASA-TT-F-15309] 01 p2289 N71-11423

Synchronous satellite observations and normalization for determining RSO-topo altitudes
23 p3577 N71-36216

BULK MODULES

Calculation of bulk modulus, shear modulus, and thermal expansion of composite materials using Van der Waals theory
[CL-71/53] 11 p1836 N71-23400

Flux cylinder assembly for diamagnetic and ultrasonic high pressure measurements on solids and liquids
14 p2327 N71-26478

Thermal and vibrational approximations of high pressure/volume relations in sodium chloride bulk modules
14 p2327 N71-26478

Theory of cohesion and elastic properties of solids
[AD-720991] 15 p2588 N71-27593

Simple empirical relation based on adiabatic compressibility, adiabatic bulk modulus, and reduced temperature for liquid argon, krypton, and xenon, and application to mercury
[NVO-4176-4] 15 p2378 N71-27982

BULKHEADS

Stress analysis and design of cylindrical shell bulkhead for spacecraft
[NASA-CR-114047] 07 p1134 N71-15338

Mixing fluids in confined cylindrical geometry similar to rocket configuration with simulated bulkhead failure mode
14 p2240 N71-26219

BUNCHING

NT ELECTRON BUNCHING

Design and development of package for transporting Cesium tube unrelaxed fuel bundles
[ABCL-2083] 19 p3139 N71-32286

Chopper for complete fuel elements bundles of SNR-Na2 in WAK
[ORNL-TN-2414] 21 p3468 N71-34629

COBRA heat transfer code extensions for large liquid Na cooled pin bundles and coolant mixing effects due to fuel pin spacer wires
[WPAFB-44-76] 23 p3798 N71-37880

BUOYANCY

Diving techniques and equipment for eliminating neutral buoyancy in space environment testing
09 p1367 N71-28248

Removal of instability in free convection problem
[BPTN/A/35] 12 p1902 N71-23827

Booyancy effect on cryogenic hydrogen film boiling during upward and downward flows
15 p2325 N71-27664

Effect of buoyancy on fuel containment in open-cycle gas-core nuclear rocket engine
[NASA-TM-X-67924] 22 p3628 N71-35794

BUOYS

Directional wave buoy for obtaining sea surface statistics up to 15 Hz
[AD-712554] 03 p0355 N71-12665

Engineering and design criteria for Totem buoy, including two-point mooring system
[AD-712772] 03 p0359 N71-13250

U.S. Coast Guard buoy development conference
[AD-712833] 03 p0359 N71-13316

Characteristics and performance of interception, recording, and location subsystem free-floating buoy
[AD-712948] 06 p0853 N71-16567

Performance of xenon flash beacon for buoys
[AD-715872] 06 p1232 N71-18355

Low power data processing approach for reduction in sonobuoy complex problems
[AD-717046] 11 p1792 N71-21967

Diurnal variations of large scale current turbulence in Arctic Basin and seas
11 p1752 N71-22085

Wave reflection and electromagnetic absorption influence on radio transmission from salvage buoys, noting waves propagation for target acquisition
15 p2306 N71-27157

Spar buoy as instrument platform for measuring ocean temperatures
[AD-722418] 17 p2777 N71-28475

Reflected waves method for seismic investigations of sedimentary strata in oceans and development of hydrophones, radiobuoys, and related instruments
[JPLR-53-422] 18 p2910 N71-30702

Seismic investigations studied in open oceans on large oceanographic ships and seismic instrument development of hydrophones, radiobuoys, and related instruments
18 p2910 N71-30703

Cost effectiveness model applicable to national data buoy systems and other national marine environmental data collection systems
[AD-722594] 19 p3091 N71-31945

BUREAU OF ORGANIZATIONS
Goals, organization, and programs of National Bureau of Standards
[NBS-SP-348] 08 p1291 N71-19269

BURNOUT

Testimony in support of creation of National Oceanic and Atmospheric Administration
11 p1848 N71-23899

Survey of air pollution by Federal facilities in Milwaukee air control region
22 p3577 N71-35482

Headings on National Bureau of Standards organizational structure
23 p3708 N71-34291

BURNING EQUATION

Determination of Burger vectors, glide planes, and densities of crystal dislocations by various Burgers angle sequence micrograph and dynamic electron diffraction analysis
[NYO-5087-19] 12 p1907 N71-23957

Validity ranges of simple wave approximations for nonlinear, diffusive, and dispersive wave equations using Burger and Korteweg-de Vries equations
21 p3448 N71-34544

BURNERS

Calculating penetration depth of one-row round jet system developed in limited cross wind under conditions most typical for gas burners
[NASA-TT-F-15756] 17 p2355 N71-29815

BURNING

U COMBUSTION

BURNING PROCESS

U COMBUSTION

BURNING RATE

Utilization of Doppler microwave interferometer for measuring solid propellant burning rates
[NASA-CR-111797] 01 p0852 N71-10043

Tests of polyethylene plastic propellant giving reduced burning rates
[OSR/CSR/55] 02 p0286 N71-11880

Determining burning characteristics of fuel elements for Halden Boiling Heavy Water Reactor
[EPRI-116] 04 p0539 N71-14217

Measurements of cathode heating in Penning discharge in strongly inhomogeneous magnetic mirror field
[NPL-10416] 04 p0291 N71-14386

Acoustic instability of burning in solid fuel rocket engines associated with reflections from burning surface
[AD-713753] 03 p0761 N71-13323

Measuring microwave burning rate of solid propellants under conditions of rapidly changing pressure
06 p0254 N71-16687

Mathematical models for unsteady periodic combustion and composite propellant burning rate mechanism
07 p1096 N71-18066

Monodimensional burning code for reactor core also radial distribution of short-lived activations
[FN-B-109] 06 p2408 N71-18196

Experimental and theoretical results of critical pressure number of fuel droplets
[NASA-CR-72834] 09 p1483 N71-28532

Tests for analysis of acceleration-induced transient burning rate augmentation of ablated solid rocket propellant
10 p1497 N71-21522

Pressurized gas injection for burning rate control of solid propellants
[NASA-CASE-XLR-43494] 10 p1036 N71-21819

Low pressure burning rates of solidified solid propellant during spacecraft orbit insertion
11 p1519 N71-22355

Gas composition, electrical ignition hazards, and combustion products from fire resistant material in diving atmosphere
[AD-720552] 14 p2289 N71-23925

Computerized simulation and analysis of combustion chamber length instability for solid rocket propellant and effects of burning rate
[AD-723606] 19 p3171 N71-31881

Numerical analysis of energy release rates during combustion caused by periodic flow field disturbances
[NASA-TM-X-67892] 20 p3365 N71-33617

BURNING TIME

Model for predicting thrust-time curve during entire ignition transient of solid propellant rocket engine with head-and-igniter layout
17 p2840 N71-30376

Procedure for computing gravity losses over a burn underestimates escape trajectories of specified final energy and prediction of optimal burn schedules for nuclear rocket escape maneuvers
[NASA-CR-115144] 23 p3471 N71-34478

BURNOUT

Change in thermal conductivity of oxide fuel element during burn and estimation of porosity and change in stoichiometry as well as heat transfer coefficient
[KFK-1245] 15 p2446 N71-27138

Determining effects of variations in core coolant flow, system pressure, core lifetime, and coolant temperature on burnout of FM-3A Type 4 plutonium core
[NIT-465] 16 p2636 N71-28864

Bibliography on burnout in forced convection heat transfer in uniform and nonuniform heat systems
[AARCLIN/818-204] 23 p3776 N71-37859

BURNS [INJURIES]

- Evaluation of eye hazards from nuclear detonations
[AD-713152] 05 p0635 N71-14834
- Combined effects of optical absorption and thermal conduction in retinal tissue calculated for establishing thresholds for eyeburns in imaging intense light sources in lasers and nuclear explosions
[LA-4651] 24 p3878 N71-37643

BURSTS

- NT RADIO BURSTS
NT SOLAR RADIO BURSTS
NT TYPE 3 BURSTS
NT TYPE 4 BURSTS
- Effect of quasi-rhythmicity in geomagnetic and aeromagnetic phenomena
17 p2747 N71-30083

- Electromagnetic noise and altitude variation of natural protein microbursts and proton flux density distributions
18 p2916 N71-31062

BUS CONDUCTORS

- Electronic control for spacecraft power supplies based on maximum power point tracking
[ESEO-CR-15] 02 p0147 N71-11044
- Preboost main bus regulator for IMP satellite power system
[NASA-TM-X-65463] 10 p1536 N71-21612
- Data bus for avionics system of space shuttle, including functions of interface unit, error detection and recovery, redundancy, and bus control philosophy
[NASA-CR-115187] 23 p3756 N71-36771

BUTADIENE

- Preparation and characteristics of free radical and ionic solution of one-ferrocenyl-one, three-butadiene
[AD-729933] 20 p3228 N71-33996

BUTENES

- Cobalt and copper ferrite spinels as catalysts in oxidative dehydrogenation of butenes
[NASA-CR-116082] 08 p1161 N71-19238
- Characterization, optimization, production, and performance of cellulose acetate butyrate membranes
[PB-198956] 22 p3401 N71-35649

BUTT JOINTS

- Fatigue tests on transverse butt welded joints containing porosity
[CRP-MT-53] 10 p1652 N71-21015

BUTTERFLY VALVES

- NT DAMPERS [VALVES]

BUTYLENE

- U BUTENES

BUTYRIC ACID

- Quantitative analysis of gamma aminobutyric acid in brain after locomotion and pure oxygen breathing
[DLR-FB-71-03] 13 p2852 N71-24456

BY-PRODUCTS

- Effect of organic iron chelate, ligand structure on oxidation product formation and autooxidation rate of cumene
[FOA-I-B-1155-92] 24 p3886 N71-37698

BYPASSES

- Servomechanism design of high-response multilooped bypass valving system for supersonic inlets
[NASA-TN-D-60811] 02 p0150 N71-11061
- Numerical study on controlling dynamic properties of supersonic inlet using bypass bleed
[NASA-TN-D-6144] 05 p0626 N71-14669

- Two-line transmission line terminated at both ends by resistors investigated for signal dependence on line load conductance and termination
[UCRL-50991] 17 p2724 N71-29298

- Two dimensional radiative-convective analysis of bypass flow in uranium plasma rocket
20 p3304 N71-33632

- Switching circuit, bypass, and power conditioning circuit tests for TOPS electrical system
[NASA-CR-121478] 20 p3355 N71-33721

- Current regulating voltage divider design with load current sharing
[NASA-CASE-MPS-30935] 21 p3403 N71-34212

C

C BAND

- C and X band dual function microwave oscillators
[AD-711560] 02 p0193 N71-11330
- Atmospheric density and rotation below 195 km from high resolution drag analysis of OV-1 satellite
[AD-712688] 03 p0374 N71-13382
- Airborne measurements on radio attenuation and radar reflectivity by precipitation by microwave frequencies
10 p1523 N71-21417

- Fabrication and integration of C band modules mechanically and electrically interchangeable with X band modules in magnetron radio to provide operation in 4.4 to 5.0 GHz band
[AD-727377] 17 p2720 N71-29047

- Estimation of C band radar station positions and is-range distances
19 p3854 N71-31842

- Data processing for calibration of C band radar global tracking network using GEOS 2 satellite data
19 p3809 N71-31853

- C band tracking radar used to obtain more accurate geodetic data for downrange MISTRAM/MBR sites
19 p3854 N71-31863

- GEOS 2 C band radar technique for determining geometry and orientation of underwater acoustic transponders
19 p3854 N71-31864

- Shipborne C band radar tracking of GEOS 2 for precise ship positioning
19 p3854 N71-31866

- Integrated solid state C band parametric amplifier for use in space shuttle communication receiver
21 p3515 N71-33047

- Doppler signal processing and instrumentation for modified Perceples C band weather radar
[AD-727776] 23 p3725 N71-36551

- C band radar transmitter for airborne radar system
[AD-727808] 24 p3887 N71-37707

- Focusing and tuning considerations for high CW power C band klystron amplifier for tropospheric scattering applications
[AD-727901] 24 p3889 N71-37717

C-5 AIRCRAFT

- Interior sound pressure measurements in C-5A aircraft
[AD-719746] 13 p2627 N71-23040

- Ditching behavior of dynamic C-5A model
18 p2868 N71-30757

- Tests on scale model configurations of C-5 aircraft to obtain data correlation on three transonic wind tunnels
[AD-727006] 23 p3704 N71-36408

C-47 AIRCRAFT

- Spectra of reflected solar energy from clouds, snow, and fields at 0.4 to 2.4 microns using C-47 and B-37B aircraft graphs
[NASA-TM-X-65474] 15 p2405 N71-27649

C-54 AIRCRAFT

- Aircraft accident at Miami, Florida involving Republic of Ecuador C-54D during climb following instrument takeoff
[NTSB-AAR-71-2] 14 p2197 N71-26032

- Aircraft accident report for Republic C-54 at Miami International Airport 14 April 1970
[PB-199330] 21 p3377 N71-34031

C-120 AIRCRAFT

- Flight service effects on residual tensile properties of C-130 aircraft center wing plate sections
[NASA-CR-111828] 12 p1857 N71-24021

C-141 AIRCRAFT

- Autopilot for C-141 all-weather landing system
03 p0406 N71-12442

- Identification and control of aeromedical factors associated with aircraft noise and acoustic measurements during C-141 operational missions
[AD-718977] 12 p1837 N71-23748

CABIN ATMOSPHERES

- NT SPACECRAFT CABIN ATMOSPHERES
- Cabin air conditioning for passenger aircraft seating air purification and recirculation, odor control, and pressurization requirements
[ARC-CP-1136] 10 p1692 N71-20049

- Using miniature pigs for analysis of altitude decompression sickness and relative decompression hazards of various cabin atmospheres of least gases
[NASA-CR-114353] 18 p2875 N71-30847

CABLE FORCE RECORDERS

- Design and characteristics of device for showing amount of cable payed out from winch and load imposed
[NASA-CASE-MSC-12052-1] 13 p2084 N71-34599

CABLES

- Swaged mineral-insulated cable for high temperature sensor detector
[AERW-R-498] 09 p1389 N71-20258

- Review on synthetic fiber ropes for deep water mooring lines
17 p2771 N71-30178

CABLES [ROPES]

- Publications survey on mechanical wire rope and wire rope systems to review literature on mechanical responses of stranded cables
[AD-718004] 01 p0129 N71-10492

- Development program for methods of terminating flat conductor cable to small electrical components used on electrical displays and control panels
[NASA-CR-108703] 04 p0510 N71-13525

- Crack formation in aluminum speaker cables of F84 F aircraft
[TDCE-53807] 05 p0704 N71-15267

- Force separation rigid tethering device using cables
[NASA-CASE-XLA-82332] 07 p1125 N71-17669

- Derivation of stability boundaries in wind tunnels for bodies towed by cables
[ARC-RM-3644] 08 p1140 N71-18461

- Support for flexible conductor cable between drawers or racks holding electronic equipment and cabinet assembly housing drawers or racks
[NASA-CASE-XMP-07367] 08 p1207 N71-16701

- Cabling and connectors for use on nuclear stage, environmental and related tests
[NASA-CR-103656] 09 p1360 N71-19873

- Design and construction of satellite appendage tie-down cord
[NASA-CASE-XOS-82534] 10 p1648 N71-21064

- Quick attach mechanism for moving or stationary wires, ropes, or cables
[NASA-CASE-XPF-85421] 11 p1772 N71-22049

- First order motion of cable towed and tethered bodies for predicting aircraft dynamic stability performance
[VLI-TN-68] 20 p3285 N71-30814

- Performance tests and evaluation of wire cable materials for use with aircraft arresting gear
[AD-724804] 22 p3539 N71-30811

- Fixed wing aircraft employing free fall and climbing line techniques in rescue of personnel and retrieval of equipment
[AD-727087] 22 p3541 N71-30328

- Axial fatigue tests in air conducted on wire rope, strand, and single wires
[AD-726457] 23 p3763 N71-36023

- Rotating cable pulser for pulsed-propulsion space vehicles
[LA-4666] 23 p3840 N71-37719

- Commercial and governmental flat conductor cable for connecting and terminating hardware
[NASA-TM-X-64613] 24 p3896 N71-37970

CADMIUM

NT CADMIUM ISOTOPES

- Electrodeposited cadmium interaction with cadmium substrate
[TT-70-57036] 03 p0332 N71-12008

- Bonding parameters and quality control for cadmium-stainless steel clad fuel post containment vessel production
[NASA-CR-111573] 03 p0367 N71-13020

- Thin cadmium layer for holography and optical communication
[ON-3] 04 p0327 N71-14040

- Reflectivity and absorptivity of cadmium crystal
[IS-T-395] 07 p1067 N71-47082

- Statistical analysis of standard deviations in interlaboratory measurements on vapor pressure of cadmium and silver
[NBS-SP-260-21] 06 p1214 N71-10597

- Ordering effect on Cd diffusion in MgCd alloy
[TT-70-57051] 06 p1218 N71-19489

- Neutron scattering measured in tungsten, rhodium, and platinum 239 in resonance region below 1400 eV
06 p1438 N71-19489

- Morphology and capacity of cadmium electrodes on repeated charge and discharge
[NASA-CR-72777] 10 p1535 N71-21320

- Fermi surface model compared to size-dependent oscillatory magnetoresistance in cadmium
10 p1608 N71-21397

- Duration of cadmium molecules on surface during condensation at varied temperatures measured on mica, copper, glass, and plexiglas before being reflected
[NASA-TT-F-34609] 16 p0446 N71-28223

- Electrochemical impregnation of cadmium electrodes for storage batteries
16 p2330 N71-28040

- Addition of precharge to negative cadmium electrode during cell assembly to account for capacity loss due to fading
16 p2339 N71-28043

- Production, consumption, and uses of cadmium
17 p2762 N71-29097

- Critical magnetic field curves of superconducting molybdenum and cadmium above 0.93 K using Shubnikov field curve as thermometer
16 p2594 N71-31118

- Trace determination of cadmium by neutron activation applied to air-borne particulates, hair, and food stuffs
[RCN-136] 21 p3483 N71-34800

- Thermal resistance of cadmium and magnesium at temperatures from 3 to 100 K
22 p3660 N71-30899

- Cyclic leaching process for cadmium and silver recovery from nickel cadmium scrap battery waste
[RM-RE-7366] 23 p3772 N71-30803

CADMIUM ALLOYS

- Density of electron states, electron phonon coupling constants, and Debye characteristic temperatures of alpha-phase In alloys containing Cd and Sn
[UCRL-15681] 07 p1078 N71-47294

- Liquid quenching effects on martensitic transformation of metastable Au-Cd alloy
[AD-716045] 08 p0408 N71-30806

- Electrodeposited zinc and cadmium alloy coatings for corrosion protection of steel to marine and industrial conditions
[NLL-TRANS-746-890-19222-401/1] 10 p1582 N71-31408

- Isotropic and anisotropic Knight shift, line width, and quadrupole coupling frequency measurements of In-113 NMR in dilute In-Cd, In-Sn, and In-Tl alloys
10 p1583 N71-31394

- Plastic deformation in single crystals of zinc cadmium and copper aluminum alloy systems
15 p2508 N71-23882

CADMIUM COMPOUNDS

NT CADMIUM Selenides

NT CADMIUM SULFIDES

NT CADMIUM TELLURIDES

SUBJECT INDEX

Methods for chemical analysis of cadmium-zinc arsenides
[AD-713842] 03 p0332 N71-12369

Thermomagnetic transport phenomenon measurement in semiconducting cadmium arsenides
05 p0757 N71-14583

Exciton interaction in cadmium sulfide and cadmium selenide
[AD-713811] 05 p0757 N71-13800

Development of non-magnetic, stable, cadmium electrodes for silver cadmium cells
[NASA-CR-720053] 07 p0975 N71-17259

Oxide and red shaped crystals of semiconducting ferromagnetic chalcogenide optical copper cadmium chromates - energy converting materials
[AD-722765] 18 p2599 N71-31458

Analysis of carrier density fluctuations in mercury cadmium telluride and causes of electromagnetic noise in photoconductors
19 p3171 N71-32617

Cadmium compound photoconductors for laser lighting
[AD-727079] 24 p3967 N71-38301

CADMIUM ISOTOPES

Electric and isotopic proton scattering functions from Cd-110, Cd-112, and Cd-114 based on shell theory and elastic scattering in cadmium isotopes for isotopic mixing resonances
13 p2141 N71-25473

Determination effect of gamma ray angular distribution in Cd isotopes caused by Compton excitation
13 p2141 N71-25540

Nuclear resonance fluorescence and neutron capture gamma rays for studying excited levels in nickel and cadmium isotopes
15 p3478 N71-37627

CADMIUM NICKEL BATTERIES

CADMIUM NICKEL BATTERIES

CADMIUM NICKEL BATTERIES

Recombined anodes in II-VI semiconducting compounds and gain curves for CdSe
[AD-710906] 01 p0111 N71-10684

Electrical properties and photoconductivity of semiconducting ferromagnetic cadmium chromates
[AD-726767] 15 p2510 N71-37936

Determination of low temperature antiferromagnetic thermal conductivity of cadmium sulfide crystals using doubly powered multidirectional steady state thermal conductivity equipment
20 p3336 N71-38098

Thermodynamic and solid state properties of manganese selenide-cadmium selenide system determined from high purity single crystals
21 p3590 N71-38937

Vapor phase growth of CdTe, CdSe, ZnTe, and CdS single-crystal boules by seed-growth method with analysis of multiple twinning
22 p3659 N71-36089

Radiation effects in semiconducting laser materials including cadmium selenide, cadmium sulfide, and cadmium chloride
23 p3766 N71-36844

NMR study of cadmium selenide and cadmium telluride with Knight shift and spin-lattice relaxation times measured for Cd-113 in indium doped cadmium telluride
[AD-726099] 23 p3835 N71-37346

CADMIUM SILVER BATTERIES

CADMIUM SILVER BATTERIES

CADMIUM SULFIDES

This film cadmium sulfide solar cell fabrication parameter study
[AD-710634] 01 p0606 N71-10436

Thermally annealed interferometric modulation of light in cadmium sulfide crystals illuminated by gas laser radiation
01 p0691 N71-10749

X ray and electron damage of cadmium sulfide
[NASA-CR-71708] 01 p0112 N71-10926

Surface areas of thermally treated cadmium sulfide films
[MRS-71-7008] 02 p0209 N71-12114

Optical transmission characteristics of copper sulfide layers formed on cadmium sulfide films
[NASA-TM-X-2143] 05 p0459 N71-12572

Development of cadmium sulfide films for fabrication of solar cells
[NASA-CR-720083] 05 p0590 N71-12599

Properties of p-n junctions in cadmium sulfide and measurement of photoelectric transmission
[AD-712595] 05 p0444 N71-13221

Vaporization kinetics of zinc oxide and cadmium sulfide single crystals
[JCL-19167] 04 p0602 N71-14008

Presenting results of research effort to improve quality of cadmium sulfide photoelectric cells
[NASA-CR-710542] 07 p0108 N71-17759

Degradation of CdS thin film solar cells in different environments
[AD-715931] 07 p0795 N71-17785

Thermal cycling test of cadmium sulfide, thin film, solar cells in various stages
[NASA-TM-X-2231] 06 p1147 N71-19109

Photoelectric properties of CdS-CdSe heterojunctions
09 p1361 N71-19405

Electron mobility in cadmium sulfide crystals and thin films
[ELAB-78-120] 10 p1533 N71-31055

Nonlinearity of current versus voltage due to resistance heating in CdS thin films
11 p1799 N71-22761

Diffusion of Yb into CdS as function of temperature and sulfur pressure
[AD-718797] 12 p1906 N71-23757

Open circuit and bias degradation tests in copper and cadmium sulfide thin film solar cells
[NASA-TN-D-6362] 13 p0031 N71-35994

Effect of cell voltage and certain testing procedures on degradation of cadmium sulfide thin film solar cells
[NASA-TM-X-2292] 13 p0031 N71-35334

This film cadmium sulfide-cadmium telluride polycrystal solar cells
[BMSW-FB-W-71-07] 15 p2340 N71-27162

This film CdS-CdSe solar cells thermally cycled for 10,000 cycles under simulated orbital conditions
[NASA-TM-X-47047] 15 p2340 N71-27496

Operating and failure mechanisms in CdS thin film solar cells
[AD-722112] 16 p2530 N71-28436

Crystal lattice effects on thermal conductivity and specific heat of zinc sulfide and cadmium sulfide single crystals
17 p2837 N71-29717

Quantum mechanical model for electronic energy bands of dislocations in cadmium sulfide crystal
17 p2825 N71-30001

Vibrational and electronic resonance Raman effect in cadmium sulfide and garnet crystals
[AD-722701] 17 p2827 N71-30148

Effect of isotope-electric domains on transmission of monochromatic light through cadmium sulfide for various crystallographic orientations
18 p2996 N71-31160

Electron paramagnetic resonance spectra of Cd / Si / Ga / In in single crystals of cadmium sulfide observed at liquid nitrogen temperature
18 p2996 N71-31342

Stationary and moving electric fields in silver- and gold-doped cadmium sulfides
18 p2941 N71-31468

Flight testing of cadmium sulfide thin film solar cells for stability and efficiency
[AD-723315] 19 p3041 N71-31939

Excess Cd induced CdS crystal defects determined by Hall effect and electrical resistivity measurements in high temperature environments
19 p3169 N71-32270

Performance tests on cadmium sulfide and cadmium telluride thin film solar cells to be used in aerospace environments
[ONERA-N702/1970] 20 p3213 N71-33189

Effects of manufacturing process variations on CdS solar cell performance and effect of temperature and time exposure during evaporation
[NASA-CR-720069] 21 p3378 N71-34037

Vapor phase growth of CdTe, CdSe, ZnTe, and CdS single-crystal boules by seed-growth method with analysis of multiple twinning
[AD-727048] 22 p3659 N71-36089

Radiation effects in semiconducting laser materials including cadmium selenide, cadmium sulfide, and cadmium chloride
[AD-727061] 23 p3766 N71-36844

Field electron emission from CdS as function of temperature and exposure with current voltage characteristics and excimer laser observations
[NLL-TRANS-2751-19022.81] 23 p3836 N71-37358

Effects of photooxidation and traps on thermally stimulated conductivity in cadmium sulfide
24 p3999 N71-38322

CADMIUM TELLURIDES

Investigating light modulation by strong electrical field in thin CdTe layers
01 p0111 N71-10644

Design and fabrication of 15.5 micron mercury cadmium telluride photodetectors for operation at 105 K
[NASA-CR-715959] 05 p0690 N71-15790

Single crystal high resistivity cadmium telluride for use as gamma-ray spectrometer
[BANS-349-0] 06 p0933 N71-16016

Prediction of cadmium telluride single crystals for use in infrared modulators
[AD-714284] 06 p0935 N71-16449

This film cadmium sulfide-cadmium telluride polycrystal solar cells
[BMSW-FB-W-71-07] 15 p2340 N71-27162

Alpha and beta particle range determination, using cadmium telluride detectors for gamma ray spectrometry
[CRA-E-4832] 16 p2655 N71-28072

Growth of single crystals of cadmium telluride by modified Bridgman technique to improve infrared modulator devices
[AD-723599] 19 p3167 N71-31736

CALCIUM FLUORIDES

Electron tunneling characteristics of metal contacts on n-type CaF₂ and p-type LaF₃
19 p3871 N71-32666

Performance tests on cadmium sulfide and cadmium telluride thin film solar cells to be used in aerospace environments
[ONERA-N702/1970] 20 p3213 N71-33189

High speed (100 ns) photodiode detectors sensitive to 16.6 microns radiation with operating temperature range of 77 to 90 K
[NASA-CR-121764] 21 p3482 N71-32085

Vapor phase growth of CaF₂, CdSe, ZnTe, and CdS single-crystal boules by seed-growth method with analysis of multiple twinning
[AD-727048] 22 p3659 N71-36089

NMR study of cadmium selenide and cadmium telluride with Knight shift and spin-lattice relaxation times measured for Cd-113 in indium doped cadmium telluride
[AD-726099] 23 p3835 N71-37346

CADMIUM 114

CADMIUM ISOTOPES

CALCIATION

ROASTING

CALCITE

X ray diffraction analyses on quartz, calcite, and dolomite
[JCL-19021] 07 p1004 N71-17838

Calcite filter for astronomical photography, errors, and near infrared applications
22 p3584 N71-35525

Near infrared astronomical photometry using calcite-Poloid filter method
22 p3584 N71-35527

CALCIUM

NT CALCIUM ISOTOPES

Time-of-flight facility for submillimeter resonance analysis of total neutron cross sections of Na 23 and Ca
[EURPFR-776] 01 p0055 N71-10409

Spectrophotometric determination of calcium in zirconium and titanium powders using ureazide
[AD-711883] 02 p0172 N71-11214

Thermal neutron capture in natural calcium using Ge/Li spectrometers
[NP-12506] 03 p0425 N71-13842

Molecular calcium atom orientation by optically pumped sodium atom clouds
06 p0914 N71-13948

Calcium K line formation in neodymium-sodium chromophore
13 p2166 N71-34041

Autoionization and electron transitions in ultraviolet photoabsorption of atomic calcium
[AD-719757] 13 p2139 N71-35486

Effects of prolonged heat treatment on bone and calcium metabolism and mineral content loss of rat
20 p3210 N71-33267

Magnetohydrodynamic wave propagation and dissipation in relation to calcium ionization in chromosphere
21 p3586 N71-34976

CALCIUM CARBONATES

NT CALCITE

Monomeric diatomic vs. calcium carbonate processes for decomposition of radioactive wastes
[CRA-8-3821] 09 p1420 N71-30145

CALCIUM CHLORIDES

Metal and oxide solubilities in calcium chloride melts
04 p0535 N71-14324

Effect of lithium and calcium ions on acetylcholinesterase activity of erythrocytes
[NASA-TT-P-13476] 09 p1333 N71-30179

CALCIUM COMPOUNDS

NT CALCITE

NT CALCIUM CARBONATES

NT CALCIUM CHLORIDES

NT CALCIUM FLUORIDES

NT CALCIUM OXIDES

NT CALCIUM SULFIDES

NT CALCIUM TUNGSTATES

NT PEROVSKITES

NT SCHERLITE

Diffusion coefficients and other physico-chemical properties of calcium, strontium, and barium chlorides and sulfates
[NRC-TT-1443] 10 p1513 N71-21257

Thermally stimulated electron emission of cerium boron oxides and calcium telluride films and doped with cerium, manganese, and lead studied for detector material
[RTI/70157] 16 p2643 N71-30830

Adiabatic elastic model of viscous calcium silicates to 3.5 kilobars
23 p3780 N71-37804

Comparative tests on kinetics of formic acid decomposition in presence of calcium hydroxide
[NASA-TT-P-14001] 24 p3085 N71-37809

Chemical synthesis and lubricant tests of INEL-P-21 (calcium) sulfonate additive
[AD-727413] 24 p3944 N71-38137

CALCIUM FLUORIDES

Production of barium fluoride-calcium fluoride composite lubricant for bearings or seals
[NASA-CR-XLR-08311-2] 06 p0877 N71-14105

CALCIUM ISOTOPES

Low-frequency dielectric constants of alkaline earth fluorides determined by substitution method
[COO-623-154] 06 p1282 N71-19305
Carbon dioxide lasers, CaF₂H experiment, light scattering from semiconductors associated with impurities, and far infrared radiation
[AD-721654] 16 p2607 N71-38508
Preparation, spectrum analysis, and crystal structure determination of CaF₂-Nd doped complex
[NYO-6075-10] 18 p2999 N71-31525
Nuclear spin in CaF₂ and lattice relaxation via paramagnetic centers in rotating reference frame
22 p3652 N71-36042

CALCIUM ISOTOPES

Chemical scandium isotope separation from calcium compounds containing radioactive calcium 48
01 p6894 N71-10311
Asymmetries produced by 28 MeV vector polarized deuterons in elastic scattering on C-12, Ss-28 and Ca-40
[LYCHEN-7021] 03 p0277 N71-12131
Purity violation search in polarized Ca-41 after polarized thermal neutron capture
[KFE-1160] 02 p0277 N71-12133
Classification of calcium-40 nuclei based on reactions K-39/He-3, γ -Ca-40 and calcium-40/ γ -p/gamma-calcium-40 conference
[CEA-CONF-1335] 04 p0571 N71-13614
Quasi-elastic scattering from calcium 40 and calcium 48 excitation spectra
09 p1442 N71-20414
Asymmetric measurement of isotopic scattering of polarized protons by Ca 40 at 24.5 MeV
[CEA-CONF-1456] 13 p2134 N71-25177
Cross section and asymmetry measurements of Ca-48 and Ti-49 in p,d reactions with polarized proton beams
[CEA-CONF-1455] 13 p2135 N71-25206
Reaction mechanism and distortion of γ -p in reactions C-12/p, γ -p/11 in ^{17}O state and Ca-40/ γ -p/K-39 in ^{28}Si state at 156 MeV
[INP-18476] 16 p2598 N71-30426
Single particle spectrum of O-17, O-16 and Ca-40 binding energies, and O and Ca isotope shifts for nucleus-nucleon interactions
[IDNB-F4-5614] 22 p3631 N71-33873
Lifetime measurements of eight Ca-40 levels excited from K-41 and Ca-40 reactions using Doppler effect attenuation technique and comparison with nuclear model results
[INP-18812] 22 p3637 N71-33923
Isobaric analog states between 4 MeV and 8 MeV for reaction Ca-40(p,p')Ca-48
[NP-18824] 23 p3815 N71-37204

CALCIUM METABOLISM

Bone density studies of bed rest subjects by radiographic method
[NASA-CR-114784] 04 p0481 N71-13434
Evaluating bone tissue optical density and calcium content in blood serum and urine of Soyuz 9 crew members
08 p1151 N71-18904
Conference on aerospace environments, manned space flight, weightlessness simulation, musculoskeletal and cardiovascular systems, bone loss, mineral metabolism, and homeostasis
[NASA-SP-269] 20 p3216 N71-33251
Research and development, weightlessness simulation, calcium metabolism, manned space flight, pressure suits, immobilization, and aerospace medicine
20 p3219 N71-33275
Assays of hormonal control of calcium and bone metabolism
23 p3712 N71-36461

CALCIUM OXIDES

Analyzing spectroscopic constants of low-lying electronic states of CaO
[UCRL-19649] 06 p0922 N71-16408
Vibronic absorption and emission spectra of F centers in calcium oxide
11 p1818 N71-22898

Color center and substitutional impurity point defects in magnesium, calcium, and strontium oxide insulators
[AD-726647] 23 p3835 N71-37351

CALCIUM SULFIDES

Copper sulfate-calcium sulfide thin film solar cell for space applications
[NASA-TN-X-67846] 15 p2369 N71-27678

CALCIUM TUNGSTATES

Measuring optical spectra of triply ionized erbium in calcium tungstate using absorption and fluorescence spectroscopy
[AD-715808] 07 p1079 N71-18043

CALCIUM 48

U CALCIUM ISOTOPES

U COMPUTATION

Input/output devices and MOS-LSI circuits for desk calculator systems
23 p3735 N71-36629

CALCULUS

NT ASYMPTOTIC SERIES
NT COLLINEARITY
NT CONTINUITY (MATHEMATICS)

NT DIFFERENTIAL CALCULUS

NT FOURIER SERIES
NT FOURIER-BESSEL TRANSFORMATIONS
NT INTEGRAL CALCULUS
NT LIMITS (MATHEMATICS)
NT PADE APPROXIMATION
NT POWER SERIES
NT SERIES (MATHEMATICS)
NT VECTOR ANALYSIS
NT VORTICITY

Finite approximability of superstationary calculus of propositions

Strategies and theorem proofs for predicate calculus using resolution principle
[NLL-RTS-5857] 17 p2774 N71-30818
Specializations for deducing classical calculus of predicate formula with functional edges
[NLL-RTS-5858] 19 p3124 N71-32582
Theory and computer applications of subre replacement systems
[NASA-CR-121635] 21 p3446 N71-34523
Generalization of three elementary formulas from the calculus to include fractional derivatives
23 p3783 N71-36962

CALCULUS OF VARIATIONS

Correction to variational calculation of tritium nucleus binding energy
[ITP-70-35] 02 p0270 N71-11179
Numerical solutions in simplest problem of calculus of variations
[AD-712543] 03 p0399 N71-12800
Circular plates in sandwich structures with edge loading analyzed by calculus of variations
[REPT-112078] 03 p0466 N71-13351
Application of multivariable search techniques to design of low sonic boom overpressure
[NASA-CR-73496] 05 p0625 N71-14613
Variational flux synthesis in space-time neutron diffusion theory
[ANL-7096] 07 p1076 N71-17534
Determining optimal shape and optimum distribution of cross sections along statically determinate and statically indeterminate beams using calculus of variations
[NASA-TT-F-13440] 08 p1234 N71-18419
Variational calculus for minimum weight loaded beam structures
[NASA-TT-F-13452] 08 p1297 N71-18646
Solution of trajectory optimization problems by calculus of variations, dynamic programming, and Pontryagin's Principle
[NASA-CR-114964] 10 p1594 N71-21573
Monosymmetric neutron transport in homogeneous slabs based on calculus of variations and Chandrasekhar equation
[AABCTM-534] 15 p2459 N71-26992
Comparison of integration techniques applicable to determination of orbits of Jovian sixth and twelfth satellites with variation of parameters integration experimentation
16 p2680 N71-28787

Minimum variance estimates of signal derivatives with application to case of aircraft descent rate in instrument landing systems
[NASA-CR-111928] 17 p2705 N71-30241
Variants of calculus of variations with equality and functional symbols
[NLL-RTS-5964] 17 p2775 N71-30362
Multiple value differential equations for optimal solutions
21 p3449 N71-34550
Processes and applications of calculus of variations in optimal control theory
[NASA-CR-121907] 22 p3405 N71-35671
Dimension and shape calculations of light nuclei with neutron surpluses based on variational method for one-particle wave functions of three dimensional anisotropic harmonic oscillators
[ITP-70-83-E] 22 p3436 N71-35918

CALCULATING

NT WIND TUNNEL CALIBRATION

Calibration of laboratory standard microphones in diffuse sound fields to establish primary specifications
01 p0088 N71-10801
Phase recovery and calibration techniques for position location interferometer in synchrotron orbit
[NASA-CR-111137] 01 p0855 N71-10852
Stellar standards at 10 microns
[AD-711364] 01 p0123 N71-10731
Computer optimization of thermocouple calibration
[AD-710761] 01 p0129 N71-10870
Photographic calibrations for emission spectroscopy using small computer
[BM-R1-7447] 01 p0857 N71-10876
High altitude solar cell and radiometer calibrations using balloon techniques
[NASA-CR-111421] 02 p0227 N71-11935
Tilt method for calibrating shipborne horizontalized gravimeters
02 p0221 N71-12156

Activation technique for absolute calibration of standard long counter in neutron energy range from 50 to 1200 keV
[AERE-R-4429] 05 p0432 N71-12935

SUBJECT INDEX

Panoramic exposure assembly for accurate time-comparisons and routine calibration of dosimeters
[BARC-400] 04 p0386 N71-10801
Calibration of impedance meters and bridges to 500 kHz
[UCRL-72485] 05 p0452 N71-14704
Calibration of high intensity flash X-ray machine by Compton effect measurements
[BGO-1183-2230] 05 p0742 N71-18123
Measuring dynamic response of thermistors at liquid hydrogen temperatures
[RSP-70-65400] 05 p0887 N71-32977
Techniques for calibrating infrared pyrometer
[UCRL-19645] 07 p1091 N71-17966
Calibration techniques and neutron exposure characteristics of JFDR in-core monitor system
[JAERI-4114] 08 p1257 N71-18270
Evaluation of gyroscopes on precision counting using counter rotating platform
[AD-715906] 08 p1232 N71-18055
Reference transfer for vacuum gauge calibration
09 p1389 N71-30880
Calibration of HERO 1 spectrometer channels for x-ray spectroscopy
[KOO-PREPRINT-70-312] 10 p1357 N71-30912
Solid rocket multicomponent test stand design, calibration, and error analysis for secondary injection thrust vector control mechanism studies
[NAL-TR-255] 11 p1730 N71-23237
Procedures for calibration of test section of single jet, flexible nozzle supersonic wind tunnel at supersonic speeds
[TAB-110] 11 p1731 N71-23200
Development and characteristics of self-calibrating displacement transducer for measuring magnitude and frequency of displacement of bodies
[NASA-CASE-XLA-00701] 11 p1726 N71-23209
Combination pressure transducer-calibrator assembly for measuring fluid
[NASA-CASE-XNP-01660] 11 p1746 N71-23206
Calibration and test service documentation for National Bureau of Standards
[NBS-SP-250] 12 p1895 N71-33123
Feasibility of units radiometer calibration check
[AD-718417] 12 p1866 N71-33325
Advance in precision metrology, calibration, optimization, and standards laboratory techniques
[NBS-SP-335] 13 p1918 N71-33266
Responsibilities of standards laboratories, tradeoff decisions, and advanced calibration
12 p1919 N71-33328
Computer-controlled system for testing time domain instruments to speed up calibration process
12 p1919 N71-33330
Computer-automated calibration system with accuracy and precision for use in Standards Laboratories
13 p1902 N71-33331
Calibration system specification requirements and approval
12 p1917 N71-33333
Cost data contributions for calibration and maintenance cost reduction
12 p1917 N71-33336
Optimization of calibration intervals and cost reduction
13 p1919 N71-33337
Intervals by exception for calibration interval control
12 p1919 N71-33338
Two-method system of optimizing calibration intervals for instrument reliability
12 p1919 N71-33339
Calibration history of instrument family used to calculate optimum calibration interval for desired level of confidence
12 p1920 N71-33340
Breakthrough techniques for cost reduction, and measurement and calibration services
12 p1917 N71-33340
Computerized test equipment control system for inventory, costs, and calibration management
12 p1917 N71-33340
Computer techniques for improved accuracy and precision in standard calibration procedures
12 p1920 N71-33347
Adjusting and calibrating mass standards, and designing and manufacturing precision balances in India
12 p1920 N71-33348
Control system for pressure balance device used in calibrating pressure gauges
[NASA-CASE-XNP-04134] 12 p1921 N71-33375
Alignment and calibration of windtunnel load measuring unit using accelerometer, gyroscope, and optical filtering techniques
[RE-47] 12 p1940 N71-33387
Calibration of commercial physical sciences thermometer using Z function interpolation
[NASA-TM-X-67815] 12 p1922 N71-33389
Calibration of cryogenic densimeter for mass density measurements of upper atmosphere
[NASA-CR-1019] 12 p1922 N71-33389
Fluorescence simulator predicting electrical voltage waves to control amplitude and duration between simulated trends
[NASA-CASE-XKS-10004] 13 p3004 N71-36886

SUBJECT INDEX

High altitude balloon flights for solar cell calibration
[NASA-CR-113272] 13 p2030 N71-34919

Calibrator for measuring and modulating or
demonstrating laser outputs 14 p2363 N71-32914

[NASA-CASR-XLA-03410] 14 p2363 N71-32914

Phase transformation transition points on high pressure
scale for precise pressure measurement standards
[NBS-SP-526] 14 p2342 N71-36476

Research equilibrium boundaries and upper pressure
limitation point 14 p2336 N71-36480

Thermal noise and thermocouple temperature measurements
in high pressure cell 14 p2356 N71-36488

Paramagnetic Curie temperature shifts for calibrating
high pressure gauges up to 90 kbar 14 p2397 N71-36504

Insoluble phase transformations versus pressure of
various materials for high pressure sensor calibration
14 p2338 N71-36506

High pressure covalent-ionic transition in pressure
calibrating point at high temperatures 14 p2338 N71-36507

Isotopic transition parameters of biomass and
salinity of high temperatures for high pressure
calibration points 14 p2338 N71-36508

Mercury melting curve equation of state for high pressure
measurements 14 p2257 N71-36511

Post test reactor simulation oven development and
fusion and rhodium/uranium ceramic thermocouple
calibration [NVO-3995-12] 13 p2406 N71-36584

Equivalent measurements, observability, and
sensitivity accuracy limits in linear estimation and
adaptation to orbital position estimation
[NASA-TN-D-4358] 15 p3433 N71-36970

Empirical formula for calibrating radiometric
poles presented as function of soil bulk density, soil
chemical composition, source detector spacing, and
vegetation parameters 15 p2405 N71-37467

Direct comparison methods for calibrating piston
gauge weights for use with equal arm balances and
slip-gate balances [NBS-TN-577] 16 p2394 N71-36652

Methods for calibration of proton recoil
proportional counter 17 p2798 N71-36699

High altitude solar cell and radiometer calibrations
using balloon techniques [NASA-CR-119170] 17 p2841 N71-36845

Distortion effects in geometrical reconstruction of
events in CERN 2m hydrogen bubble chamber
[NBS-70-6] 17 p2880 N71-36996

Calibration procedure for Coulter counter allowing
for effects of particle shape for particle size
determination [NBS-TRANS-3196-1/556] 17 p2880 N71-36996

PORTRAM 4 program for correction and calibration
of neutron isotopic scattering data including
background, air attenuation, detection efficiency, and
sample thickness [NBS-559-8] 18 p2972 N71-36514

GEOS-3 altimeter bias recovery simulation using
range and angle tracking data [NASA-TN-X-65619] 18 p2922 N71-36592

Design and operation of seismic type linear
acceleration strain gage 18 p2924 N71-31074

Miniaturized system self calibration scheme feasibility
based on GEOS 2 satellite tracking data 19 p3089 N71-31851

Data processing for calibration of C band radar
global tracking network using GEOS 2 satellite data
19 p3089 N71-31853

Angle calibration from GFTF computer program
and in near real time sensor to obtain improved radar
calibration test data 19 p3054 N71-31865

Design, fabrication, and testing of dissolved oxygen
cell [NBS-556-6] 19 p3100 N71-32132

Partial pressure analyzer calibration and techniques for
measuring gas mixtures and leakage [NBS-DR-70-275] 19 p3078 N71-32227

Fluxmeter transfer used as absolute standard for
calibrating and intercomparing vacuum gauges in 10 to
20 micron range [NASA-TM-X-67889] 19 p3101 N71-32274

Photographic film sensitivity calibration for use in
lensless aerial color and infrared photography
[NASA-CR-121572] 20 p2778 N71-32815

Performance characteristics of static and dynamic
load sensors [NASA-TN-82-117] 20 p2772 N71-33117

Field control, vibration, and calibrating equipment,
recorder programs, and data reduction techniques -
calibration [NASA-SP-5936/81/7] 20 p2778 N71-33142

Optical measurement of size distribution of spray
[NBS-DR-70-275] 20 p3111 N71-33290

Development of low range moisture generator for
use in laboratory and field calibration operations
[Y-1791] 20 p3246 N71-33236

Calibration constants of quartzometer and thick
walled ion chamber [NBS-TR-66] 21 p3470 N71-34706

Pointing calibration of high resolution, millimeter
wave, parabolic antenna by star observation
[AD-726077] 22 p3500 N71-35340

Calibrated infrared emission spectra of earth and
atmosphere using high resolution interferometer spectro-
radiometer on Nimbus 4 satellite [NASA-TM-X-65087] 22 p3583 N71-35517

In-flight calibration of 300-mm Hasselblad camera
flown on Apollo 14 [NASA-CR-115176] 22 p3583 N71-35518

Calibration method for hot-wire probes [AD-727049] 22 p3586 N71-35538

Flight calibration device for absolute measurements
of photometer at Lyman alpha wavelength on OGO-6
and other satellites [AD-726507] 22 p3645 N71-36136

Silicon photovoltaic cells for calibrating photoelectric
accelerometers [AQD/77] 23 p3759 N71-36796

Image clearing eyepiece for calibrating acceleration
transducers [AQD/77] 23 p3759 N71-36799

Calibration of diaphragm condenser microphones for
micrometeorological impact gauge [UTIAS-TR-157] 23 p3759 N71-36800

Universal machine for testing full scale structural
components and applying force necessary for calibrating
large force measuring devices 23 p3764 N71-36821

STADAM reducing antenna calibration at 137, 402,
and 1702 MHz using absolute flux density from Cygnus
A [NASA-TM-X-67579] 23 p3844 N71-37402

Technique for improving calibration accuracy
standards from boundary layer calculations [IC/71/23] 24 p3908 N71-37851

Application of ground-truth data to monitor ocean
calibrations for Earth Resources Technology Satellite
[NBS-SP-355] 24 p3919 N71-37945

Methods for determining mass flow rates of gases
for use in calibrating gas flowmeters [NASA-CR-72896] 24 p3920 N71-37954

Star selection and bias error eliminating calibration
for five onboard optical measurements used to determine
spacecraft trajectories [NASA-TN-D-65311] 24 p3954 N71-38212

Focal image method for calibration in calculating
characteristic curve for comets 24 p4009 N71-38385

CALIFORNIA

Summary of synoptic meteorological observations
for North American coastal marine areas of San Francisco
and Point Mugu, California - Vol. 8 [AD-710771] 01 p0880 N71-10905

Aircraft accident investigation of United Air Lines,
Boeing 727-22C near Los Angeles, 16 Jan. 1969
[PB-194812] 01 p0886 N71-10914

Empirical probability distributions for astronomical
water levels on California coast [AD-711946] 02 p0219 N71-12074

Air pollution problems in California and methods for
air quality forecasting [PB-194128] 04 p0475 N71-13429

Data analysis and methods improvement for Los
Angeles Basin [PB-194060] 04 p0542 N71-14274

Engineering aspects of Santa Rosa, California
earthquake, 1 Oct. 1969 05 p0674 N71-14968

Atmospheric reaction studies in Los Angeles Basin
El Monte area - Vol. 3 [PB-194863] 05 p0678 N71-15390

Airborne data from atmospheric studies in Los Angeles
Basin, California Basin - Vol. 4 [PB-194864] 05 p0678 N71-15399

Light scattering measurements off San Diego Coast,
California [AD-714481] 06 p0985 N71-16337

Geologic value of small scale aerial photographs and
correlation of high altitude oblique and vertical
photographs of California 06 p1197 N71-19239

Aerial and satellite-borne photography of Imperial
Valley agricultural land use characteristics 06 p1198 N71-19265

Factors affecting weather conditions at Midway Air
Force Base, California 09 p1412 N71-19442

Air pollution monitoring and pollutant source
surveillance system, and effective regulations and
enforcement means for San Francisco Bay area
[NASA-CR-114292] 10 p1552 N71-21298

Large scale effects of cloud cooling in Santa Barbara,
California 12 p1953 N71-23991

General aviation traffic implied densities and
interaction frequencies computed with model using

CALIFORNIA ISOTOPES

Southern California to judge difficulty for naval air
traffic [AD-719966] 14 p2197 N71-25821

Synoptic meteorological charts and ocean current
data for southern California from 1949 to 1970
[AD-721117] 15 p0437 N71-30912

Tables and graphs of wind data for Lawrence Livermore
Laboratory - Berkeley 17 p3796 N71-37266

Analysis of magnetic anomalies in ocean bottom off
central California coast 18 p2912 N71-30906

Magnetic and bathymetric survey profile in Pacific
Ocean from Costa Rica to central California
[SSA-TR-BRL-179-AGRL-3] 18 p2917 N71-31268

Magnetic survey of Baja and southern California
coast and continental shelf including magnetic
anomaly map of Pacific Ocean [NOAA-MOS-DE-12] 18 p2919 N71-31438

Pacific Ocean influence upon seasonal precipitation
patterns of western US and Baja, Calif. [PB-198126] 19 p1316 N71-31713

Impact of jet aircraft emissions on air quality in
vicinity of Los Angeles International Airport
[PB-198099] 19 p3056 N71-31779

Aircraft measurements in Los Angeles (California)
area 19 p3057 N71-32528

Remote sensing inventories and socio-economic studies
of water resources and management in California
[NASA-CR-121370] 20 p3255 N71-32896

System of regional agricultural land use mapping
tested against Apollo 9 color infrared photography of
Imperial Valley, Calif. [NASA-CR-121873] 21 p3406 N71-34375

Economic aspects and regional planning for international
airport facility at Ontario, California [PB-199052] 23 p3565 N71-35391

Precipitation, atmospheric pressure and temperature,
humidity, and wind velocity data for meteorological
stations in California - Nov. 1970 [AD-726099] 22 p3615 N71-35730

Precipitation, atmospheric pressure and temperature,
humidity, and wind velocity data for meteorological
stations in California - Dec. 1970 [AD-726098] 22 p3615 N71-35734

Meteorological parameters and wind profile
measurements for Hunter-Liggett Military Reservation,
California during October 1970 [AD-726354] 22 p3615 N71-35735

Precipitation, atmospheric pressure and temperature,
humidity, and wind data for meteorological
stations in California - Oct. 1970 [AD-726346] 22 p3615 N71-35738

Airborne remote sensing of Mojave Desert playas
for use as natural landing areas [AD-727031] 23 p3751 N71-36748

Meteorological parameters for Hunter-Liggett
military reservation, California for December, 1970
[AD-726356] 23 p3750 N71-37013

Meteorological field data including energy
balance observations, temperature profiles, and wind
profiles from California [AD-726390] 23 p3770 N71-37014

Damage resulting from San Fernando, California
earthquake of 9 Feb. 1971 [PB-735] 24 p3917 N71-37933

CALIFORNIA ISOTOPES

Using CI-252 as neutron source for neutron
activation analysis of terrestrial, ocean floor, and planetary
surfaces [BNWL-SA-3003] 19 p3093 N71-32230

Solubility and leach rates of isotopic californium
ceramic nuclear fuel element [ORNL-6439] 19 p1401 N71-28644

Determining coefficients of CI 252 as source for
particle thermal neutron radiography [BNWL-SA-3169] 21 p1968 N71-33154

Delayed neutron fission yields and half life curves
from time of flight spectroscopy of He-3 and He-4
induced fission of U-238, Th-232, and Pu-239 and CI-252
spontaneous fission 12 p1977 N71-24228

Guide for fabricating and handling CI-252 sources
including health physics procedures, shielding requirements,
containment and ventilation requirements, and
purification techniques [ORNL-153] 13 p2143 N71-25545

Atmospheric diffusion of tritium and other radioactive
materials, flux neutron spectra of CI-252, radiation
rate of CI-252 in D2O spheres, and Co-60 gamma
dose distribution 13 p2144 N71-25585

Calculation of neutron and gamma ray dose rates for
CI-252 shielding materials [DP-1246] 18 p3084 N71-31373

Standardized measurements of X-ray and neutron
emission and elastic angles of CI-252 fission fragments
[CEA-R-4131] 19 p3149 N71-32101

Kinetic energy distributions of CI-252 fission
products as function of fission product mass ratios
[ORNL-TR-3453] 21 p3075 N71-34746

- Design and fabrication of Cf-252 portable device for neutron radiography 21 p3475 N71-34747
[BNWL-1329]
- Cross correlation measurements of unmoderated and polyethylene moderated uranium assemblies with prompt neutron decay constants, using Cf-252 as neutron source 21 p3482 N71-34802
- Measuring spatial distribution of sodium activation in water using Cf-252 source with results compared with computer program calculations 23 p3413 N71-37187
- Thermal fission cross sections and fission resonance integral measurements for Cf-249 and Cm-244 to Cm-248 made in core and thermal column of research reactor 23 p3816 N71-37218
- Effects of delayed gamma rays, systematic and random coincidences, and scattered neutrons on Maxwellian temperature value from time of flight measurements of Cf-252 fission neutron spectrum 24 p3971 N71-38332
- Specific energy loss and effective charge of fission products in metal absorbers using Cf-252 fission source and semiconductor detector 24 p3975 N71-38344
- Computerized enhancement calculations for thermal neutron flux from californium isotope source 24 p3977 N71-38381
- CALIFORNIUM 252**
U CALIFORNIUM ISOTOPES
CALORIC REQUIREMENTS
Human caloric requirements when working in extreme climatic environments 09 p1337 N71-30367
- CALORIC STIMULI**
High fat diet effects on caloric intake, body weight, and heat escape responses in normal and hypothyroid rats 11 p1684 N71-22979
- CALORIMETERS**
Calorimetric and thermocouple pyrometer heat flux measurements in blowdown wind tunnels 02 p3043 N71-32639
- Calorimetric determination of absorbed dose rate of epoxy resin irradiated in JER-4 04 p5083 N71-4232
- Developing calorimeters for measurement of gamma radiation intensity in reactor structural materials 05 p7277 N71-15099
- Test equipment design for measuring heat generated in U fuel element in nuclear fuel plant 06 p1234 N71-18177
- Development of high temperature calorimetry techniques for solid ionic systems 06 p1221 N71-18530
- Heat of formation for CuCa and HCa and adiabatic calorimetric measurements from 10 to 400 K 10 p1572 N71-20725
- Thin film thermometer and thin film calorimeter techniques for surface heat flux rates of microsecond duration 11 p1843 N71-22005
- Heat of reaction for flameless combustion of M-2 double-base propellant / 20 percent nitroperoxy 77 percent nitrocellulose, 3 percent other ingredients/ at varying pressures 11 p1844 N71-22697
- Adiabatic calorimetric enthalpy measurements for alpha, beta, and gamma phases of U-238 and heats of alpha yields beta and beta yields gamma transformations 12 p2009 N71-23173
- Development of calorimeter for spacecraft batteries comprising pressurized vessel, heat sink, and copper conductor 12 p1923 N71-24129
- Calorimeter for measuring heat generation rates in nonfissionable materials by gamma and thermal neutron interactions in nuclear reactor test facility environment 13 p2113 N71-24524
- Nondestructive nuclear assay, calorimetric, gamma, and neutron instrumentation techniques for nuclear fuel element fabrication in breeder reactors 14 p2253 N71-25631
- Air flow thermal balance calorimeter for measuring heat evolved by spaceborne nickel cadmium cells 14 p2253 N71-25748
- Construction and characteristics of adiabatic, microthermal differential calorimeter for investigation of properties of temperature deformed copper specimens 14 p2275 N71-26523
- Development and characteristics of calorimeter with integral heat sink for maintenance of constant temperature 16 p3693 N71-29051
- Isothermal calorimetric determination of plutonium 239 half life based on alpha zero energy and recoil energy 17 p3799 N71-30820
- Direct measurement of thermal power input to servo-controlled calorimeter 18 p3963 N71-31229

- Immersion calorimeter for measuring Wigner energy in irradiated BeO, MgO, Al₂O₃, and SiO₂ at high temperatures 19 p3156 N71-32428
- Calorimetric determinations of thermodynamic properties of Na₂O/4-PeO₃ up to 1200 K 19 p3051 N71-32643
- Differential thermal analysis methods in high temperature research on biochemical, polymeric and explosive materials 20 p3361 N71-32826
- Thermodynamics and operation of differential calorimeters using intermittent heating 20 p3362 N71-32828
- Differential thermal analysis and high temperature calorimetry dynamics 20 p3362 N71-32830
- Differential scanning calorimetry for determining physiological chemistry of cholesterol esters in phospholipid-water systems and arteriosclerosis 20 p3362 N71-32831
- Instrumental and thermal time constants of differential scanning calorimeter 20 p3362 N71-32832
- Thermogravimetry and calorimetric experiments to study phenomenology of synsperic system for catalysis of ammonium nitrate decomposition in solid rocket propellants 20 p3337 N71-33084
- Design and development of adiabatic calorimeter for measuring specific heat of aqueous solutions of electrolytes up to 150 C 20 p3362 N71-32831
- [JLL-CE-TRANS-5634-1982.09]
- Calorimeter and recording system for measuring heat generation in reactor holes 24 p3926 N71-38015
- [LEB-3017]
- CALORIMETRY**
U HEAT MEASUREMENT
CALUTONS
U CYCLOTRONS
Performance and acoustic near field measurements on variable chamber propeller having STOL applications 24 p3958 N71-38233
- CAMBERED WINGS**
Aerodynamic coefficients, pressure, load and force distributions on cambered delta wings 07 p6966 N71-17112
- Aerodynamic characteristics of thin, highly cambered airfoils in incompressible flow 17 p2701 N71-25893
- CAMERA SHUTTERS**
Magnetically opened diaphragm design with camera shutter and expansion tube applications 10 p1564 N71-21060
- CAMERA TUBES**
NT IMAGE DISSECTOR TUBES
NT IMAGE ORTHICON
NT VIDICONS
Development of pattern threshold recognition device 02 p0191 N71-11543
- CAMERAS**
NT FRAMING CAMERAS
NT HIGH SPEED CAMERAS
NT LALLEMAND CAMERAS
NT SCHMIDT CAMERAS
NT TELEVISION CAMERAS
ATS-3 multicolor spin scan cloud camera and image detector camera systems with meteorological data output from ATS-3 and ATS-1, Vol. 2 02 p6254 N71-11602
- Satellite tracking camera performance 03 p0376 N71-12675
- Satellite tracking by use of K-24 aerial camera and Polaroid film 03 p0376 N71-12695
- Performance of ATS 1 spin-scan cloud cover camera system at Mojave ground station 05 p0682 N71-14081
- Camera and filter photoflight spectrum analysis for Apollo 9 multiband photoflight experiment 10 p1561 N71-21609
- Mechanism for measuring nanosecond time differences between luminous events using streak camera 12 p1967 N71-23976
- Project planning of Jans camera for astronomical ultraviolet spectroscopy 14 p2334 N71-25638
- Camera adapter design for image magnification including lens and filterometer 14 p2256 N71-26474
- Application of Guinier-Hagg focusing camera for X ray analysis of powder diffraction 16 p2594 N71-28603
- Longitudinal film gate and lock mechanism for securing film in motion picture cameras under vibration and high acceleration loads 16 p2596 N71-28935
- [NASA-CASE-LAR-10066]
- Evaluation of high altitude balloon aerial photography for earth resources and oceanography including

- photographic formats and camera systems and techniques 17 p3753 N71-34006
- [NASA-TM-X-2208]
- Study of the side upland volcanism of lunar surface using Hasselblad camera 18 p0013 N71-30912
- Image intensifier camera, infrared imagery, and high sensitivity vidicon for use in police night surveillance 19 p0070 N71-31040
- Long distance infrared surveillance camera with searchlight and flash lamp for obtaining photographic documentation in total darkness 19 p0090 N71-31040
- Installation and structure of aerial laser camera for photographic scanning from aircraft 19 p0090 N71-31070
- [AD-72426]
- Performance comparisons of cameras used in photographic tracking of GEOS 1 satellite 19 p0089 N71-30912
- Present status and future requirements of geostationary satellite geodesy using simultaneous optical distance observations with lasers and cameras 19 p0090 N71-31040
- Converting powder diffraction camera into back reflection camera for X ray diffraction studies 20 p3270 N71-32886
- [AD-724147]
- Design and characterization of laser camera system with diffraction filter of small particles with average diameter larger than wavelength of laser light 20 p3281 N71-33010
- [NASA-CASE-NPO-10417]
- Design requirements for streak camera with narrow angle optics for use in underwater photography 22 p3383 N71-33004
- [FOA-2-C-2384-51]
- Two cameras for photographing artificial earth satellites 22 p3680 N71-36800
- Parameter calculation for determining Zeiss camera sizes for satellite observation 22 p3680 N71-36800
- Limit magnitudes of optically weak radio stars measured by large telescope electronic cameras 24 p3922 N71-37970
- Instrument constants of astronomical cameras compared with object positions obtained by other methods 24 p3926 N71-38015
- CAMOUFLAGE**
Visual detection and identification tests of geometric shapes with olive green and mottling camouflage adhesive camouflage paint 10 p1510 N71-21020
- CAMS**
Apollo service propulsion system bipropellant test with can flow seals 05 p0092 N71-14006
- CANADA**
Aeromedical training in Canadian facilities 04 p0777 N71-13977
- Canadian aircraft operational aeromedical testing 04 p0882 N71-13980
- Assessment of STOL technology for establishment of Canadian transport system 05 p0639 N71-14706
- Mass spectroscopy rocket sounding data on neutral particle densities in Canadian lower thermosphere 07 p01018 N71-17151
- Ice thickness observations along coasts of eastern Canada and southern Greenland 08 p1188 N71-16709
- [AD-715424]
- Equipment and facilities for biodynamic research in US and Canada 12 p1896 N71-23342
- Tables on magnetic activity observed in Canada Agincourt Observatory for 1968 and Jan. to Mar. 1969 12 p1906 N71-23406
- Tables on magnetic field observations made at Alert Observatory of Canada 12 p1907 N71-23406
- North, east, and vertical magnetic flux data and synoptic tables from Baker Lake, Canada for 1968 12 p1911 N71-23877
- Tables of magnetic elements observed at Alert Observatory of Canada 12 p1912 N71-23877
- Skyhook balloon flights in 1970 at Fort Churchill, Canada 12 p1914 N71-24016
- [AD-718371]
- Canadian west coast strong motion seismograph network for determining basic ground motion data earthquakes 13 p0377 N71-23889
- Lower atmosphere vertical distribution of boundary layer wind shear annual variation as observed in Canada 18 p2949 N71-28889
- Wind shear vertical distribution periodic variation at three Canadian airport towers 18 p2949 N71-28889
- Horizontal intensity, declination, and vertical intensity by hour, day, month, and year at Victoria Magnetic Observatory - 1969 20 p3257 N71-33047
- [M70-4166]
- Mapping Canadian gravitational fields 22 p3380 N71-33800

SUBJECT INDEX

Chemistry, geography, geology, and history of Texas Territory, Canada and Chihuahua, New Mexico (AD-74645) 23 p3613 N71-37962

Canadian power reactor operation economics and safety test transport system, valve development (ARC-3838) 23 p3796 N71-37961

Canadian 157-inch Ritchey-Chretien telescope 24 p3921 N71-37964

Canadian National Science Council research in low speed aerodynamics, machine learning, and turbulent air flow 24 p4013 N71-38635

Canadian National Science Council goals in low speed aerodynamics - Canada 24 p4013 N71-38637

CANADIAN CR-104 AIRCRAFT
U F-104 AIRCRAFT
CANALS

Canine fauna and benthic shell-slope communities of Lake Erie 06 p0841 N71-15967

Application of structural control models extended to rail sections of canals, airports and airports, network of street crossings, and other large systems 21 p3448 N71-34338

CANAL CONFIGURATIONS

Flow and attitude control apparatus using jet nozzles in variable mass surface or film configurations (NASA-CASE-X-42085) 07 p1119 N71-17629

Wind tunnel static longitudinal stability and control characteristics of cruciform delta winged models with various horizontal canards and trailing-edge flap control (NASA-TN-X-2367) 23 p3705 N71-36415

Pulse longitudinal, directional, and lateral characteristics and control surface effectiveness of scale model of open static canard booster at Mach 0.25 (NASA-CR-115970) 24 p4008 N71-38608

CANINEA BOMBER
U B-57 AIRCRAFT
CANCELLATION

Effects of reductions in NASA contracts on management of aerospace employees (NASA-CR-118374) 13 p2191 N71-34001

CANCER
NT LEUKEMIAS

In vivo corneal radiation therapy and application of laser accelerators in cancer therapy (JCL-TRANS-1422) 17 p2787 N71-29249

In vivo studies using boron-labeled antibodies and chemical boron as neutron target in therapy for tumor and cancer (NASA-CR-122925) 23 p3712 N71-36465

CANINE
U CANES
CANIONS
U GUINIS (ORDNANCE)
CANINEAL FORMS

Refraction of square matrices to Jost's canonical form (JMA-P-C-6238-11) 05 p0712 N71-14344

Analysis of conical correlation to forecasting statistics of meteorological fields (AD-73774) 05 p0718 N71-15263

Modification of canonical form of general relativity theory for advancement of quantum theory of gravitational fields 22 p3406 N71-35086

Quantum and semiclassical equilibrium of infinite chains of coupled harmonic oscillators 23 p3823 N71-37270

CANINE

Aerodynamic and deployment characteristics of high lift air-lifted paratrooper rig with several variations of parachute canopy and suspension line loading system (NASA-TN-D-6306) 18 p2865 N71-30748

MASTRAM computer program differential stiffness and static load analysis methods compared for aircraft tail air opening complex 22 p3482 N71-35269

CANINE

Design and characteristics of device for cooling engines under high vacuum conditions (NASA-CASE-XLA-01446) 10 p1567 N71-21520

On kinetic and vacuum physics to analyze for system operating rates minimum pressure ranges attainable by spacecraft canister - tables (NASA-TN-X-6406) 18 p3819 N71-31255

Back-surface condensation heat transfer vapor release from gas-permeable membranes 23 p3880 N71-31434

CANINE

SLOPED
CANTILEVER BEAMS

Further toughness of graphite double cantilevered beam specimens (NWL-CC-74) 04 p0533 N71-13012

Characteristics of crack stability in cantilevered double cantilever beam specimens (AD-713512) 05 p0779 N71-15340

Parametric cantilever beams and platforms for space vehicle structures (NASA-CASE-XLA-01731) 10 p1653 N71-21045

Numerical analysis of small amplitude transverse oscillations of three-variable length cantilever beam 11 p1839 N71-23019

Development of approximate theory for rectangular plates clamped on one edge and free on the opposite and subjected to chordwise bending vibrations (AD-722720) 17 p2852 N71-20781

Effects of variations in location of concentrated masses on transverse flutter characteristics of swept-back thin cantilever wings (NAL-TN-226) 20 p3305 N71-33173

CANTILEVER MEMBERS
NT CANTILEVER BEAMS

Optimization of pie-joint frames, cantilever members, and machine tool structures (ARC-RM-3432) 06 p0933 N71-15797

Dynamic stability of cantilever model subjected to following pulsating loading 06 p1301 N71-19119

CANTILEVER WINGS
U WINGS
CAPACITANCE

Capacitive and inductive couplings for surge voltage distribution optimization in layered windings 01 p0836 N71-10515

Parametric using varactors as nonlinear circuit elements 05 p0453 N71-14006

Moment of dielectric constant of nonlinear dielectrics as function of electric field strength (AD-713971) 06 p0903 N71-15961

Investigating techniques for measuring doping profiles using capacitance-voltage measurements based on C square root V law for step junction 07 p1089 N71-17295

Capacitance calculation for diffused p-n junction with exponential doping gradient (NASA-TN-X-2179) 07 p1094 N71-17806

Capacitance study of solar cells and panels using swept loading techniques (NASA-CR-116622) 08 p1147 N71-18063

Static dielectric constant of solids determined by substitution method with techniques for refining capacitance measurements (COO-623-150) 08 p1282 N71-19304

Capacitive gap accuracy and stability for high pressure measurement 08 p1282 N71-19307

Acceptance tests including capacity, cell short, high vacuum leak, overcharge, and internal resistance of nickel-cadmium secondary cells with nickel brass ceramic seals for spacecraft (NASA-CR-117318) 09 p1327 N71-20325

Doping impurity distribution in p-n junctions determined from capacitance measurement 10 p1632 N71-20794

Device for measuring two orthogonal components of force with gallium flotation of measuring target for use in vacuum environments (NASA-CASE-XAC-04085) 12 p1922 N71-23790

Nuclear radiation effects on junction capacitance of silicon p-n diode (NASA-TN-D-6330) 13 p3059 N71-25389

Hall, capacitance, and time-dependent measurements of radiation hardened LJ-AlGaAs solar cells 14 p2201 N71-26229

Thin film capacitive bolometer and capacitance temperature interchange sensor (NASA-CASE-NFO-10607) 15 p2386 N71-27332

Nondestructive measurement of OAO battery plate weights and capacities 16 p2539 N71-28664

Addition of precharge to negative cathode electrode during cell assembly to account for capacity loss due to fading 16 p2539 N71-28665

Capacitance of surface barrier detectors made from p-type silicon (BARC-527) 18 p2922 N71-30470

Electromagnetic radiation measuring instrument utilizing a p-n junction diode capacitance (NASA-CASE-LW-11159-1) 18 p2934 N71-31137

Capacitance distance gap for differential measurement with digital readout or direct computer processing (V-1783) 19 p3101 N71-32343

Absolute capacitance microcopy and dimensional stability measuring system (NASA-TN-X-2046) 22 p3585 N71-35330

Formulas, tables, and graphs for calculation of electrical capacitance (AD-721101) 24 p3968 N71-38304

CAPACITANCE SWITCHES

Feedback integrating circuit with grounded capacitor for signal processing (NASA-CASE-XAC-10607) 12 p1809 N71-23669

CAPACITIVE FUEL GAGES

Ullage volume and capacitive fuel gages for satellite attitude control propellant tanks (BSRO-CR-19) 03 p0459 N71-13331

CAPACITORS

Capacitor sandwich structure containing metal sheets of heavy thickness for counting penetration rates of neutrons (NASA-CASE-XLE-01246) 01 p0856 N71-10797

CAPE KENNEDY LAUNCH COMPLEX

Capacitor requirements for static power conversion systems (BSRO-0007) 03 p0333 N71-12353

Capacitor fabrication by solidifying mixture of ferromagnetic metal particles, nonmagnetic particles, and dielectric material (NASA-CASE-LW-10064-1) 04 p0310 N71-13522

Prototype capacitive electrode for electroforming mask (PS-10404) 06 p0470 N71-13999

Measuring coil for determining permeability of solids, liquids, and gases between 100 kHz and 100 MHz (FRL-1976-10) 04 p0208 N71-14296

Terminated capacitor discharge firing of electrovacuum devices (NASA-CR-116792) 06 p1160 N71-18702

Planar linear circuit construction from capacitors and differential voltage controlled current sources (AD-716531) 06 p1357 N71-19429

Technology review on capacitors 06 p1358 N71-19377

High temperature stability and electrical properties of pyrolytic boron nitride capacitors (NASA-CR-11799) 09 p1236 N71-30186

Periodically reverse-switched capacitors or inductors in feedback networks, resulting in linear subharmonic filter 11 p1725 N71-22004

Metal thin film sandwich structures used as microindustrial capacitors, noting tunneling current theory, electron work function, vacuum deposition, and volt-ampere characteristics 12 p1908 N71-23513

Mechanism for measuring nanosecond time differences between luminous events using streak camera (NASA-CASE-XLA-01907) 12 p1967 N71-23976

Feasibility of producing thin metal and oxide-film capacitors with stable electrical properties in high temperature environments (NASA-CR-72779) 12 p1891 N71-23983

Spraying process for producing thin dielectric ceramic film capacitors 12 p1891 N71-24026

Electrochromic electrodes with silicon-silicon oxide half-cells (AD-719538) 13 p2064 N71-24413

Possible electron irradiated failure modes of MOS microelectronic capacitor detectors (NASA-CR-111892) 16 p2391 N71-30025

Steady state radiation effects on electrical insulating materials and capacitors - handbook (NASA-CR-11977) 17 p2736 N71-29776

Formulas for calculating conductivity and dielectric constants of capacitors made up of composite bodies extended to more than two components (NASA-TT-F-13725) 17 p2727 N71-30044

Quality control of polystyrene capacitor (BCR-10) 18 p2097 N71-30643

Screenable dielectric constant ceramic glass paste for thick film capacitors in microcircuits (AD-725404) 19 p2064 N71-31714

Silicon control rectifier three phase bridge for regulation of high voltage capacitor bank (ITEX-761) 19 p2065 N71-32040

Capacitor field calculations for capacitive displacement measurement of open mesh structures such as radio telescopes and radar receivers (NASA-TN-D-6341) 20 p2275 N71-33397

Design and testing of ac polycarbonate capacitors for aerospace power systems (NASA-CR-10697) 21 p3579 N71-34046

Microcomputer analyzer using arrays of interconnected capacitors and ion detectors (NASA-CASE-ARC-10443-1) 21 p3437 N71-34082

Computer-aided data reduction techniques for extracting time dependent conductivity of dielectric material from test circuit recorded responses (AD-726359) 22 p3560 N71-35357

Firing unit with 12.5KJ capacitor bank (BSRO-71-33) 23 p2728 N71-36791

Capacitor system for load balancing in SNAP 8 (NASA-CR-72936) 24 p3963 N71-38253

CAPACITY

Methodology for evaluating capacity of air traffic control systems (FAA-RD-70-69) 03 p0708 N71-13358

CAPE KENNEDY LAUNCH COMPLEX

Statistical analysis of wind distribution probabilities at Cape Kennedy (NASA-CR-105972) 03 p0717 N71-15130

Improved accounting control over equipment at Kennedy Space Center (B-10636) 03 p0609 N71-13379

Characterization of bacterial spore population from Cape Kennedy soil (NASA-CR-116462) 06 p0799 N71-13940

AZURA GDS computer program (AZORD) for Kennedy Space Center electrical trajectory computation (NASA-TN-X-6005) 09 p1332 N71-19333

NASA launching operations summary for Cape Kennedy complex (NASA-TN-X-6038) 09 p1473 N71-30089

- High altitude mesospheric wind data taken by meteorological sounding rockets at Cape Kennedy, Florida
[NASA-TM-X-64578] 12 p1958 N71-34039
- Analysis of bonding and grounding measures for minimizing hazards from electrical fault, lightning, explosion, and electromagnetic radiation MRC - Vol. 1
[NASA-CR-118494] 14 p2238 N71-26598
- On-site evaluation of bonding and grounding of electrical equipment at KSC to minimize hazards from electrical fault, lightning, explosion, and radiation - Vol. 2
[NASA-CR-118492] 14 p2238 N71-26599
- Preventive maintenance instructions for bonding and electrical grounding systems to prevent equipment damage by electrical faults, lightning, and radiation - Vol. 3
[NASA-CR-118491] 14 p2238 N71-26600
- Territorial environment/climate criteria guidelines for use in NASA space vehicles and associated equipment development with major emphasis on Kennedy Space Center launch area
[NASA-TM-X-64580] 17 p2737 N71-29235
- Statistical analysis of atmospheric turbulence at Cape Kennedy Launch Complex for spacecraft design
[NASA-CR-1899] 19 p3132 N71-32796
- History of Cape Kennedy launch complex noting origin, initial construction, organization, launching sites, ground support equipment, and significant accomplishments
[NASA-TM-X-67274] 20 p3247 N71-33771
- Fire prevention, protection, and fighting systems at KSC for space shuttle operations 22 p3676 N71-36205
- Statistical summary of ground wind data recorded at 150-m tower on Merritt Island, Kennedy Space Center
[NASA-TM-X-64612] 24 p3951 N71-38187
- CAPILLARIES**
- Capillary containment system designs for low gravity propellant control in cryogenic vehicles
[NASA-CR-102900] 01 p0116 N71-10653
- Influence of hypoxia on pulmonary microcirculation
[AD-714671] 06 p0801 N71-16200
- CAPILLARIES (ANATOMY)**
- Influence of pericapsular plasma on chemical exchange from blood to tissue
[NASA-TN-D-6227] 08 p1148 N71-18421
- CAPILLARY CIRCULATION**
- U CAPILLARY FLOW**
- Capillary radiator for carrying heat transfer liquid in planetary spacecraft structures
[NASA-CASE-XLE-03307] 04 p0620 N71-14035
- Breakup of laminar capillary jet of nonwetting fluid
[NASA-CR-116480] 07 p1006 N71-17326
- Streaming potentials of fine-pore capillary systems and Donnan hindrance of electrolyte transfer through ion-selective permeable membranes
[NRC-TT-1442] 10 p1513 N71-21259
- Lubrication for bearings by capillary action from oil reservoir of porous material
[NASA-CASE-XNP-02972] 11 p1773 N71-23048
- Soldering device particularly suited to making high quality wiring joints for aerospace engineering utilizing capillary attraction to regulate flow of solder
[NASA-CASE-XLA-00911] 15 p2416 N71-27214
- Experimental model of heat transfer to two phase, fluid particle flow in tubes for use in analysis of capillary blood flow 19 p3193 N71-32401
- Qualitative hydrodynamic model of dynamic angle hysteresis for fluid-field interface being driven through capillary tube by applied pressure gradient
[AD-726635] 22 p3570 N71-35424
- CAPILLARY TUBES**
- Low gravity propellant control by capillary devices in cryogenic vehicles - screen flow tests, bubble dynamics, residual analysis, settling, and surface tension properties
[NASA-CR-102902] 01 p0043 N71-10764
- Steady gas flow in capillary tubes using Knudsen law
[PB-1905687] 02 p0301 N71-11504
- Capillary matrix and fuel cell development study
[NASA-CR-106757] 03 p0318 N71-12272
- Low gravity propellant control using capillary devices in large scale cryogenic vehicles
[NASA-CR-102879] 04 p0604 N71-14227
- Tubular flow restrictor for gas flow control in reaction
[NASA-CASE-NPO-10117] 05 p0695 N71-15608
- Development of liquid separating systems using capillary device connected to flexible bladder storage chamber
[NASA-CASE-XMS-13052] 09 p1390 N71-20427
- Interrupter switching device utilizing electrodes and mercury filled capillary tubes in which current flow vaporizes mercury as circuit breaker
[NASA-CASE-XNP-02231] 10 p1540 N71-20896
- Pressure difference induced across stainless steel capillary tube by temperature gradient used to predict thermal transpiration effect 11 p1844 N71-22709

- Boundary value problem application to determining capillary surface of volume of liquid partially filling right circular cylinder
[NPL-MA-95] 13 p2102 N71-34370
- Turbulent flow drag reduction by dilute polyethylene oxide solutions in capillary tubes
[AD-726688] 14 p2241 N71-26347
- Mass transfer during binary liquid drop growth at nonwetting capillary tubes 16 p2579 N71-28235
- Capillary condensation and evaporation in porous adsorbents 16 p2648 N71-28438
- Low gravity propellant control, using capillary devices in large scale cryogenic vehicles 17 p2831 N71-30611
- Anomalous water from cleaned and annealed capillary tubes, from weak H₂O₂ solutions, and from water extractions of crushed glass
[AD-726761] 23 p3720 N71-36517
- Effects of capillary grooves on surface wetting and evaporation characteristics related to cross section shape of grooves
[AD-727200] 24 p4031 N71-38762
- CAPILLARY WAVES**
- NT GRAVITY WAVES**
- Meteorological capillary wave instrument recording and analysis of power spectra from wind velocity and direction and air/water temperature data
[AD-726617] 16 p2911 N71-30798
- Hydrodynamics of boiling heat flux and dynamics and stability of small gravity and capillary waves
[NASA-CR-121467] 20 p3566 N71-33746
- CAPSULES**
- Oxidation of refractory metals considered for isotope capsule structural members
[SC-DR-70-164] 08 p1220 N71-19331
- Capsule rig for temperature control and irradiation of structural material in SM-2 reactor 24 p3957 N71-38226
- CAPSULES (SPACECRAFT)**
- U SPACE CAPSULES**
- CAPTIVE TESTS**
- NT STATIC FIRING**
- NT STATIC TESTS**
- Possibility of burning fuel-rich combustible exhaust gas mixtures by injection of either gaseous oxygen or gaseous carbon dioxide into exhaust stream
[AD-721209] 15 p2512 N71-27261
- Captive-fired testing of solid rocket motors for design criteria
[NASA-SP-6041] 18 p3000 N71-30866
- CAPTURE CROSS SECTIONS**
- U ABSORPTION CROSS SECTIONS**
- CAPTURE EFFECT**
- Thermal neutron capture in natural calcium using Ge(Li) spectrometers
[NPL-10290] 03 p0425 N71-12842
- Nuclear model for pion absorption by light nuclei
[NPL-10446] 06 p1235 N71-18362
- Evaluating changes in 26th group fission cross sections of U-235 and capture cross sections of U-238 from critical mass of ZPR-3 reactor 06 p1261 N71-18790
- Study of high isospin states in several light self-conjugate nuclei by isospin forbidden radiative capture reactions 13 p2131 N71-25041
- Westcott formalism and neutron capture by reactor materials
[LFEN-NI-45-A] 13 p2134 N71-25173
- Muon capture neutron yield in oxygen, sulfur, calcium, and lead
[JINR-P15-5324] 18 p2979 N71-30701
- Neutron capture and total cross section measurements of V, Ni, and Cr isotopes
[RPI-328-380] 20 p3322 N71-33806
- Two particle-on-hold shell model calculation for five neutron system applied to deuterium-tritium photocapture 20 p3327 N71-33953
- Methods for calculating reference cross sections for radiative neutron capture by U-238
[INDC(CCP)-11/U] 21 p3496 N71-34909
- Production of spontaneously fissionable isomer U-236 by radiative thermal neutron capture
[JINR-P7-5497] 22 p3639 N71-35943
- Elastic scattering, radiative capture, gamma ray production, and related information from nuclear data file for hydrogen in .00001 eV to 20 MeV range
[LA-4574] 23 p3813 N71-37193
- High energy proton capture effect and geomagnetism 23 p3852 N71-37458
- Semi-empirical evaluation of fast neutron radiative capture cross sections
[CCDN-NW-10] 24 p3976 N71-38269
- CARAVELLE AIRCRAFT**
- U SE-10 AIRCRAFT**
- CARBAMATES (TRADENAME)**
- NT URETHANES**
- Differential thermal analysis and antioxidant activity of nickel, zinc, lead, copper, and cadmium dialkyl-dithiocarbamates
[FTD-HT-23-363-70] 10 p1513 N71-21230

- Mass spectra of alkyl carbamates derived from primary, secondary, and tertiary alcohols by use of isotopic labeling and high resolution mass spectrometry
[NASA-CR-125196] 24 p3484 N71-34909
- CARBAZOLES**
- Method of producing output voltage from photoconductive cell using poly-N-vinyl carbazole compound with iodine
[NASA-CASE-NPO-10373] 06 p1146 N71-14018
- Analysis of decaying photoconductor in polyvinylcarbazole to determine charge transport and trapping states 23 p3837 N71-37920
- CARBIDES**
- NT BORON CARBIDES**
- NT CHROMIUM CARBIDES**
- NT HAFNIUM CARBIDES**
- NT MOLYBDENUM CARBIDES**
- NT NIOBIUM CARBIDES**
- NT SILICON CARBIDES**
- NT TANTALUM CARBIDES**
- NT TITANIUM CARBIDES**
- NT TUNGSTEN CARBIDES**
- NT URANIUM CARBIDES**
- NT VANADIUM CARBIDES**
- NT ZIRCONIUM CARBIDES**
- Thermodynamic properties of ternary refractory carbides
[NASA-CR-111123] 01 p0072 N71-10000
- Fast reactor mixed-carbide fuel element development program in EBR-2 02 p2264 N71-13287
- Revealing tests on friction and wear of materials in sodium
[LMRC-70-10] 03 p0390 N71-13800
- Preparation, properties, and phase diagram for plutonium carbides
[LA-4415] 04 p0539 N71-14005
- Self-diffusion of metallic atoms in monocarbides of transition metals 05 p0701 N71-13807
- Mass spectroscopy of vaporization of boronides and scandium carbides
[NASA-TN-D-7039] 06 p0809 N71-13800
- Mechanical properties of carbides and nitrides in fast reactor fuels
[LA-4452] 07 p1061 N71-17700
- Additional improving properties and facilitating manufacture of U-Pu-C-M fuel-conformers
[CEA-COINP-1632] 08 p1233 N71-18800
- Working points of metallic elements and selected compounds including nitrides, borides, carbides, borides, and sulfides
[AD-715908] 08 p1159 N71-18800
- Bibliography with abstracts on carbon-carbon, metallic-carbide, and metal-matrix composites
[ORNL-4596] 09 p1403 N71-19044
- Reactor technology and fuel element development for nuclear research and test reactors including mechanical and thermal analysis of oxide, carbide, and nitride fuels
[BML-1086] 09 p1418 N71-19000
- Carbide electrolysis extraction from high temperature resistant stainless steels with 20 percent Ni and 5 percent Cr 10 p1577 N71-21116
- Carbide precipitation and equilibrium in stainless steel
[NLL-CR-TRANS-5391-1902.09] 10 p1577 N71-31216
- Phase diagrams, thermal conductivity, and Young modulus of carbide compounds
[CEA-COINP-1589] 10 p1515 N71-31108
- Experimental methods for determining heat of formation energies of plutonium carbides
[CEA-COINP-1508] 10 p1516 N71-30808
- Technique for carbiding optical pyrometers of aluminum, molybdenum, and tungsten in large batch
[AD-719783] 13 p3089 N71-34077
- Steel microstructure, surface oxidation and carbide formation, and diffusion coefficient measurement during chemical and thermal treatment
[TT-70-59089] 14 p2269 N71-32868
- Magnetic permeability, electrical resistivity, and specific heat measurements on oxides carbides and nitrides carbides
[CEA-B-4113] 15 p0471 N71-27813
- Grain boundary diffusion coefficients and reaction kinetics for austenitic stainless steel carburizing by carbide nuclear fuels
[JAERI-4132] 16 p3008 N71-30071
- Superconducting properties of transition metal carbides and nitrides 16 p3663 N71-30803
- Oxide and carbide metal matrix composites with thermal shock resistance for use in aerospace environments
[AD-721667] 16 p3618 N71-30803
- Activation enthalpy of carbon self diffusion in metal carbides
[LA-TB-71-13] 16 p2667 N71-30807
- Heat treatment of carbide and boron strengthened aluminum alloys to improve tensile and creep rupture strength
[NASA-CR-72883] 18 p2333 N71-30808

SUBJECT INDEX

Preoxidation with refractory metal carbides for
resistant chromium-base alloys
[NASA-CR-72874] 18 p2934 N71-30809

Heat of formation and entropy of formation of
phenyl carbides
[KFK-71-71-21] 20 p3368 N71-33951

Oxygen contamination, chemical roles, non-
contamination of solid solution, second phase, and
carbon and nitrogen distribution in UC-UN solid solution
[ILL-WINDSCALE-443-1091.591] 21 p3801 N71-37100

CARBOHYDRATE METABOLISM
Aldehyde effects on drug action in glucose metabolism
and ACTH release in dogs
07 p2962 N71-17660

Monoethylhydrazine effects on glucose carbon
metabolism and effects of pure oxygen inhalation in
rat
[AD-727068] 22 p3346 N71-35239

CARBOHYDRATES
ADENOSINE TRIPHOSPHATE [ATP]
CELLULOSE
FATS
GLUCOSE
LACTOSE
MONOSACCHARIDES
SUGARS
Effects of 4-amphetamine on carbohydrate
metabolism at ground level and elevated high altitudes
[AD-715726] 05 p0633 N71-14641

Decomposition of petroleum products with honey
[NASA-CASE-XNP-03835] 12 p1670 N71-23459

Carbohydrate interference in human body during two
weeks of bed rest
20 p3218 N71-33269

Chromatographic and spectrographic extractions
for determining concentrations of anabolic reductants
in animal plasma electrolytes
[NLL-T-71-746-725-19022.401] 22 p3389 N71-35560

Determination of physical and chemical properties
of fuels gelled with carbohydrate resins to evaluate of
effectiveness in reducing aircraft fire hazards
[FAA-WA-71-18] 23 p3336 N71-37369

CARBON
CARBON ISOTOPES
CARBON 12
CARBON 13
CARBON 14
CHARCOAL
Optical method for estimation of amorphous content
in pyrolytic carbon
[SC-T-70-4023] 01 p0699 N71-10710

Carbon tracing of mineral forming processes
[NASA-TT-F-13184] 02 p0214 N71-11967

Monitoring techniques for carbon contaminants in
air
[MSAR-70-34] 02 p0267 N71-12189

Properties of carbon fibers
[NAS-LIB-TRANS-1417] 02 p0249 N71-12191

Field ion microscopy of tantalum-carbon alloys to
give measure of interstitial order
[UCRL-19639] 03 p0389 N71-12660

Electrical conductivity measurements through
carbon on wood/carbon/metal thin films of sandwich
structure
[AD-712073] 03 p0441 N71-12835

Model for carbon fiber structure
[SC-T-70-4030] 03 p0396 N71-13013

Aluminum performance of graphite carbons,
pyrolytic graphite, and artificial graphite in stagnation
pressure range 0.835 to 15 atm
[NASA-TN-D-7005] 04 p0534 N71-14138

Procedure for extinguishing fires in activated
carbon adsorbents used in air cleaning systems
[UCRL-72494] 04 p0517 N71-14499

Experimental determination of absolute cross
sections for elastic scattering from carbon
05 p0735 N71-14530

Phase diagram for W-C ternary alloy system
[AD-711514] 05 p0700 N71-14857

Phase diagram for Ti-V-C system
[AD-713198] 05 p0700 N71-14858

Red ring carbon-graphite materials for aircraft
gas
[NASA-CR-72799] 05 p0692 N71-14890

Thermal imager transducer, infrared scanning, and
high power broadband ultrasonic methods for non-
destructive tests of carbon-carbon composites
[BMVL-SA-3654] 05 p0707 N71-15053

Optimization of thin carbon films for electron
microscopy
[NTO-4142-1] 05 p0708 N71-15062

Effect of counterforce on friction and wear of carbon
fiber reinforced thermosetting resins
[BAE-71-7015] 05 p0693 N71-15433

Compressive and fracture strengths of carbon fiber
reinforced plastics
[NASA-CR-1131] 06 p0876 N71-15742

Carbon chemical activity in sodium measured by
electrochemical carbon meter
[NLL-14508] 06 p0837 N71-15900

Manufacturing process for large diameter carbon
base monofilaments by chemical vapor deposition
[NASA-CR-72770] 07 p1834 N71-17328

Atomic energy level and multiplet tables for carbon
I through carbon/VII
[NSRDS-NBS-3] 07 p1076 N71-17330

Determination of carbon content of lunar samples
from Apollo 11 flight
[NASA-SF-237] 07 p1115 N71-17964

Additional improving properties and facilitating
manufacture of U-Pu-C-M fuel-coniference
[CRA-COMP-1332] 08 p1235 N71-18210

Uranium distribution and uranium diffusion through
pyrocarbon coating in UO₂ coated particles
[EUR-4530-K] 08 p1235 N71-18214

Absorption of halogen 4 on activated carbon
[CRA-COMP-1505] 08 p1221 N71-18389

Properties of cast columbian carbide-carbon alloys
stapling in carbon content from 12 to 17 weight percent
compared with hot pressed composites of similar composition
[BM-81-7479] 08 p1213 N71-18479

Large diameter graphite/carbon composite
monofilaments produced by pyrolysis
[NASA-CR-72709] 08 p1222 N71-18748

Relationship with abstracts on carbon-carbon,
metallic-carbide, and metal-metal composites
[ORNL-4598] 09 p1485 N71-19645

Properties, microstructure, and irradiation behavior
of carbonaceous and graphitic reactor materials
[GA-9975] 09 p1476 N71-19918

Uranium-base niobium alloy and silicic acid reactions
and alloy explosive behavior due to two-phase
microstructure and high carbon content
[RFP-1575] 10 p1511 N71-20700

Synthesis and structure of MnPC alloy and inter-
ference, atomic distribution, and radial distribution
functions for structural model
[CALT-422-31] 10 p1580 N71-21394

Actinide concentration effect on uranium and thorium
diffusion in columnar pyrocarbons
[ORNL-TM-2899] 10 p1591 N71-21637

Microstructural research on carbon and graphite for
use as engineering materials
[NASA-CR-117494] 10 p1591 N71-21841

Shock tube decomposition of iron pentacarbonyl to
yield hydrogenated relaxed carbon
[AD-717742] 11 p1695 N71-22171

Total cross section of carbon for standard measurement
of neutron cross sections
[KAPL-P-3901] 11 p1803 N71-22274

Optical analysis of crushing mode of pyrocarbon
coated fuel particles
[EUR-4501] 13 p2117 N71-24851

Core support graphite and carbon composites for
reactor core and reflector of Fort St. Vrain reactor
plant
[GA-9641] 13 p2121 N71-25245

Synthesis and thermal properties of fluorocarbon
silicon and carbon polymers for space use
[NASA-CR-111884] 13 p2041 N71-25364

Research on carbonization, radiation effects,
chemical properties, and mechanical properties of
graphite and carbon compounds
[NRL-1716-100] 14 p2276 N71-25679

Carbon effect on iron self diffusion in iron nickel
system
[TT-70-57655] 14 p2272 N71-25821

Comparison of charged particle activation analysis
and infrared spectroscopy for carbon and oxygen
trace contaminant determination in silicon and aluminum
14 p2214 N71-26362

Gas chromatographic method for determining
carbonate carbon in rocks and minerals
14 p2251 N71-26646

Carbon content effects on aluminum alloy deformation
[AD-720932] 15 p3419 N71-26812

Mechanical properties of polycrystalline nickel-
copper and nickel-copper-carbon alloys at tempera-
tures from 78 to 523 K
15 p3422 N71-27222

Nondestructive tests of carbon-carbon test cases
using thermal detectors
[SC-DK-70-864] 15 p3409 N71-27480

Interfacial reactions of boron fibers and carbon
fibers in chromium matrices at elevated temperatures
[ARL/MET-83] 15 p3432 N71-27620

Solubility of carbon in sodium with indicators of
carbon dissolving in single steps
[TRG-REPORT-1506] 15 p3278 N71-27663

Differential cross sections for elastic scattering of
neutrons from carbon measured at primary energies
between 0.30 and 2.00 MeV in steps of 30 keV
[EUR-4538-B] 15 p3491 N71-27899

Analysis of high temperature oxidation rate of carbon
for use as reentry material
[NASA-TN-D-6310] 16 p3616 N71-28012

Carbon equilibrium loop work including data on
electrochemical meters, cover gas analysis, and oxygen
determination and mass transfer models in sodium
[WARD-4210-T-1-1] 16 p3634 N71-28724

CARBON MONOXIDE
CARBON
Activation cathode of carbon and diffusion in cubic
carbides
[LA-TR-71-13] 16 p3667 N71-28847

Carbon transport in austenitic stainless steel at temperature
gradient after sodium flow exposure
[ORAR-15469] 17 p2713 N71-29304

Development and testing of carbon/carbon composites
fabricated by chemical vapor infiltration of fibrous
wound substrates
[SC-DC-70-5369] 17 p2768 N71-29385

Development of reusable oxidation resistant carbon-carbon
laminates and surface oxidation materials for thermal
protection systems
17 p2856 N71-29452

Cosmic ray data from cloud and ionization chambers,
and carbon and free plates
[AD-721714] 17 p2840 N71-29472

Flight test of chemical vapor deposited felt and filament
wound carbon composite heat shields
[SC-DC-71-3833] 17 p2769 N71-29516

Effect of gamma radiation on adsorption of iodine
and methyl iodide on activated carbon exposed to
flowing mixtures of steam and air
17 p2715 N71-29836

Activated carbon in reactor containment systems to
remove radionuclides from effluent gases in event of
nuclear accident
17 p2713 N71-29837

Carbon bed filtration system for removing particulate
matter and gaseous radioactive contaminants from radioactive
wastes
17 p2770 N71-29870

Testing of fire extinguisher for activated carbon
adsorbers in air cleaning systems
17 p2721 N71-29875

Interaction between curve dislocation and carbon in
body centered cubic iron using model with pairwise
interatomic potential matching
17 p2818 N71-29947

Feasibility of fabricating carbon/carbon honeycomb
using woven carbon cloth
[BDC-613-535] 18 p2399 N71-30562

Oxygen 18 labeling used for detection of desorption
of iron-carbon melts in vacuum systems
18 p2394 N71-30486

Three 27 kg solid propellant engines, using static
firing and all-carbon radiating nozzle
18 p3001 N71-31111

Effect of acidic surface oxides on carbon sorption of
pollutant type molecules from aqueous solutions
[PUB-194519] 19 p3030 N71-32133

Synchrotron radiation of carbon, boron, and beryllium
and observations of k lines in ultraviolet X ray emission
spectra
[DESY-70/39] 19 p3151 N71-32142

Nickel, carbon, and aluminum oxide particle
velocity measurement after injection into air plasma
jets
[LA-TR-71-27] 19 p3165 N71-32239

Thermodynamic, precipitation, swelling, creep
resistance, strength, and reliability effects of carbon on
Types 304 and 316 stainless steels
[NLL-RESELY-TRANS-2055-7091.591] 19 p3117 N71-32586

Thermogravimetric analysis of carbon black oxidation
characteristics in elastomer compounds and vulcanizates
20 p3363 N71-32835

Electrochemical properties and structure of chemical
bond in boron, carbon, and beryllium compounds
[LA-TR-71-30] 21 p3386 N71-34091

Microstructural study of physical and mechanical
properties of carbon and graphite
[LA-4714-M23] 21 p3442 N71-34496

Teflon-carbon mixture identified as air equivalent
material and suitable for cavity ionization chambers
[CRA-B-4173] 21 p3443 N71-34498

Irradiation of nuclear graphite and model carbons
[GA-10533] 21 p3444 N71-34606

Glass and steel microsphere sputtering bed properties
and model for thermomechanical deposition of pyrolytic
carbon from methane on nuclear fuel microsphere in
sputtered beds
21 p3463 N71-34646

On phase electron diffraction projection and carbon
scattering determination using molecular dynamics
21 p3491 N71-34845

Theoretical model for electronic stopping power of
heavy ions compared with experimental results for
carbon and nitrogen targets
21 p3493 N71-34880

Process for reduction of aluminum pentoxide with
limpstone in vacuum at high temperatures
22 p3601 N71-35642

Design, development, and characteristics of fuel
and electrolysis cell with carbon anode
[NLL-M-26489-1928.491] 23 p3773 N71-36091

Thermal, chemical, and wear properties of carbon-
graphite and ring materials at air temperature to 1300
F
[NASA-CR-72906] 23 p3776 N71-36010

Development, test, and evaluation of carbon and
carbon composite heat shields
[CONP-718152-1] 23 p3778 N71-36822

- Reentry simulation test data with performance analysis of pyrolytic carbon and hafnia coatings [GA-8994-SUPPL-B] 23 p3775 N71-36936
- Shaping carbon section dependence on carbon foil thickness and scattering angle [GPR-41] 23 p3815 N71-37285
- Excitation and ionization cross sections for [Bulgas] by electron impact, plasma diagnostic, Li energy loss in thin C films, and multiple charge ion sources for collision experiments 23 p3827 N71-37297
- Mechanical properties of this liquid films analyzed by study of anomalies observed in flow of fluids through porous ceramic and carbon filters [NASA-TT-F-19999] 24 p3905 N71-37831
- Carbon resistors as cryogenic thermometers [AD-727187] 24 p3925 N71-38005
- Research and development on carbon and graphite to determine properties and behavior as engineering materials [NASA-CR-123171] 24 p3942 N71-38123
- CARBON ARCS**
- For ultraviolet spectral intensities of energetic vacuum carbon arc [NASA-TM-X-52566] 08 p1243 N71-18747
- CARBON COMPOUNDS**
- NT BORON CARBIDES
- NT CALCITE
- NT CALCIUM CARBONATES
- NT CARBIDES
- NT CARBONATES
- NT CHROMIUM CARBIDES
- NT DOLOMITE (MINERAL)
- NT HAFNIUM CARBIDES
- NT LEXAN (TRADEMARK)
- NT MOLYBDENUM CARBIDES
- NT NIOBIUM CARBIDES
- NT POLYCARBONATES
- NT SILICON CARBIDES
- NT SODIUM CARBONATES
- NT TANTALUM CARBIDES
- NT TITANIUM CARBIDES
- NT TUNGSTEN CARBIDES
- NT URANIUM CARBIDES
- NT VANADIUM CARBIDES
- NT ZIRCONIUM CARBIDES
- CFA carbonaceous molding material development for ablative nozzles on solid rocket engines [NASA-CR-72766] 01 p0071 N71-10427
- Comparing effects of irradiation on dimensional stability of high and low temperature isotropic carbons used in reactor materials [FB-191701] 05 p0708 N71-15059
- Vapor deposited laminated nitride-silicon coating for corrosion protection of carbonaceous surfaces [NASA-CASE-XLA-00284] 06 p0664 N71-16075
- Manufacturing of improved carbon and graphite materials [NASA-CR-117315] 09 p1407 N71-20373
- Solid state structure of carbon metal-carbides determined by analysis of X ray diffraction patterns 11 p1695 N71-22103
- Microinjections of carbide in anterior preoptic hypothalamic area of rats inducing hyperthermia 11 p1684 N71-22977
- Thermal stability of eta carbides of alloys containing iron, nickel, cobalt, molybdenum, and tungsten [ORNL-TR-2425] 13 p2101 N71-25437
- Nuclear magnetic relaxation times of deuterium and fluorine nuclei in liquid CDF₃ 15 p2496 N71-27969
- Structural, magnetic, and spectroscopic examination of nickel selenate dihydrate [IS-T-432] 15 p2510 N71-27978
- Uranium carbonyls as high efficiency fuel - preparation and irradiation properties [JUL-703-RU] 18 p2939 N71-30528
- Mechanical properties of advanced filament wound carbon composites 19 p3120 N71-32216
- CARBON DIOXIDE**
- Conversion tables for Beckman CO₂ analyzers [models IR-215 and IR-315A] [AD-711330] 01 p0035 N71-10714
- Carbon dioxide content changes in atmosphere [NLL-M-9147-5828.4P] 03 p0367 N71-12864
- Equilibrium normal shock properties for vibrationally excited CO₂-N₂-He gas mixtures [AD-712518] 03 p0364 N71-13155
- Infrared radiation atmospheric attenuation controlled by least balance tests in presence or absence of carbon dioxide and water vapor in solar simulators [ESRO-TN-24-ESTBC] 03 p0371 N71-13288
- Ion and electron production in proton and hydrogen atom collisions with carbon monoxide, carbon dioxide, methane, and ammonia 03 p0436 N71-13377
- DF-CO₂ and C₂H₂-O₂ CO₂ laser research, electrode configuration efficiency, and CO₂/N₂/H₂ rate of deactivation by DF and HF [AD-712564] 03 p0438 N71-13396
- Electron scattering spectrum of carbon dioxide including scattering processes through formation of short lived negative molecule-ion compound states 04 p0592 N71-14393
- Dissipated power in graphite and CO₂ of graphite reactor cell of NAIADE 2 subcritical assembly [CEA-R-3985] 04 p0583 N71-14414
- Broadband miniature carbon dioxide sensor scale model and instruction manual [NASA-CR-114799] 05 p0602 N71-14799
- Diffraction of strong shock waves by sharp compressive corner [AD-714584] 06 p0637 N71-16491
- Measuring average absorption coefficients of carbon dioxide gas as function of temperature and pressure 07 p1128 N71-17041
- Nonequilibrium solubility of carbon dioxide near 4.3 microns and shock wave molecular relaxation [ARC-CP-11116] 07 p1007 N71-17000
- Laser fluorescence method for rate constant determination of vibrationally excited carbon dioxide dissociation [AD-715376] 07 p1009 N71-17767
- Lamb dip spectroscopy and carbon dioxide frequency stabilization on sulfur hexafluoride [AD-715314] 07 p1040 N71-17772
- Experimental method for determining parameters for rate of reaction of CO₂ with solid carbon [BM-81-7476] 08 p1159 N71-18589
- Observations of carbon dioxide and plant growth in Arctic ecosystem 08 p1149 N71-18768
- Kinetic studies of electrolytic reduction of carbon dioxide on various metals 08 p1216 N71-19001
- Carbon dioxide concentration control in pressure chamber during atmospheric regeneration by Chlorine 08 p1153 N71-19052
- Work intensities with greatest endurance reduction due to inspiratory resistance and carbon dioxide inhalation [AD-716380] 09 p1330 N71-19720
- Spectral reflectance measurements on carbon dioxide cryodroplets at infrared wavelengths 09 p1434 N71-20211
- Physiological responses to interacting stresses of exercise and hypercapnia under acute and chronic exposure to ambient P sub CO₂ of 21 mm Hg 09 p1336 N71-20370
- Stability of molecular sieve as regenerative carbon dioxide and water absorber in closed controlled atmosphere [AD-716748] 10 p1503 N71-20629
- Carbon dioxide distribution in mixture with argon in graphite channel at high temperatures [NLL-RTS-5839] 10 p1514 N71-21318
- Kinetics of reaction between graphite and carbon dioxide in flow tubes at atmospheric pressure and high temperatures [NLL-RTS-5838] 10 p1514 N71-21331
- Chemisorption of O₂, CO, and CO₂ on solid fuel under static and dynamic conditions [NLL-RTS-5837] 10 p1638 N71-21746
- Decay in fluorescence from asymmetric stretching vibrational level of CO₂ after excitation by Q switched CO₂ laser 11 p1803 N71-22111
- Ionization cross sections for helium and neon positive ion collisions with nitrogen, oxygen, and carbon dioxide molecules at 3 to 200 eV [AD-717690] 11 p1808 N71-22711
- Atmospheric distribution of CO₂, O₂, O₃, water vapor, and other chemical tracers and global transport processes [TD-25314] 12 p1911 N71-23656
- Dissociation and output of platinum catalyzed CO₂ laser [AD-718424] 12 p1933 N71-23705
- Thermodynamics of reaction of incandescent tungsten filaments with oxygen and carbon dioxide at 1500 to 3500 K [NASA-TT-F-13546] 12 p2012 N71-24198
- Closed Sabatier system for oxygen recovery from carbon dioxide [NASA-CR-118025] 12 p1868 N71-24256
- High temperature reaction of MoS₂ with CO₂ [RAE-LIB-TRANS-1494-PT-3] 12 p2040 N71-25125
- Mariner 6 and 7 occultation data for determining temperature and pressure of Martian atmosphere 13 p2168 N71-25277
- Determination of vibrational relaxation time in CO₂ and CO using relatively driven acoustic waves [AD-720406] 14 p2239 N71-25938
- Mathematical model for computerized evaluation of Sabatier reaction kinetics in oxygen recovery from carbon dioxide [NASA-CR-115826] 14 p2211 N71-26295
- News briefs, and abstracts of scientific articles concerning oceanography 15 p2396 N71-26862
- Calculating vibrational excitation of CO₂ for anharmonic coupling and normal mode at high temperature [NASA-CR-16411] 15 p2450 N71-26940
- Atmospheric oxygen, water vapor, and carbon dioxide concentration effects on drop size and sodium compound structures in sodium fire aerosol [AERE-R-4460] 15 p2377 N71-27468
- Influence of temperature, ozone, and water vapor on atmospheric absorption by 15 micron bands of carbon dioxide 15 p2481 N71-27609
- Reaction kinetics and charge transfer in tests of oxides of argon loss with molecular hydrogen, deuterium, and carbon dioxide 15 p2477 N71-27670
- Mass spectroscopic analysis of positive ionization diffusion in carbon dioxide [AD-720997] 15 p2378 N71-27688
- Zirconium oxidation in carbon dioxide atmosphere above 500 C and corrosion protection by copper cladding to prevent oxygen dissolving into metal [CEA-CONF-1726] 16 p2011 N71-28004
- High power uniform electric discharge to produce laser action in mixture of nitrogen, carbon dioxide, and helium [AD-721590] 16 p2086 N71-28004
- Carbon dioxide lasers, CaF₂ experiment, light scattering from semiconductors associated with impurities, and for infrared radiation [AD-721654] 16 p2087 N71-28004
- Sound velocity in low temperature carbon dioxide (TRG-2070) 16 p2562 N71-28004
- Design, temperature, carbon dioxide, and current density effects on alkaline hydrogen oxygen fuel cell performance [NASA-CR-72906] 16 p2573 N71-31110
- Hydrodynamic model for slug flow mass transfer in carbon dioxide/water two phase flow 16 p2586 N71-31110
- Characteristics of high speed flowing N₂-CO₂ gas lasers - effects of viscosity and diffusion 16 p2592 N71-31110
- Stress effects of intermittent exposure to 3 per cent CO₂ on acid-base balance and electrolyte excretion in rhesus monkey [AD-722663] 16 p2577 N71-31228
- Characteristics of chemical reactions between mercury alloy and gases of carbon dioxide, water vapor, nitrogen, and oxygen [ISC-DB-710124] 16 p2593 N71-31408
- Enhancement output power of CO₂ laser controlled by electric discharge and irradiated by neutron obtained from nuclear reactor 20 p3382 N71-35088
- Proportional feedback control to replace signal servocontrol unit for controlling carbon dioxide concentration and relative humidity in Null point compensating system for plant measurements [UCLA-L-82-813] 21 p3433 N71-35088
- Low temperature photodetachment of carbon dioxide, ammonia, and nitrous oxide condensed gas molecules utilizing ultraviolet light [NASA-CR-121958] 22 p3428 N71-35088
- Measurements of angular dependence of scattered X ray intensity from carbon dioxide near critical point 22 p3467 N71-35088
- Breathing metabolic simulator design for test and evaluation of breathing and life support equipment [NASA-CR-122948] 23 p3717 N71-36008
- Viscosity of carbon dioxide between 293 and 190 K [NLL-RISLEY-TRANS-2129-19091.9P] 23 p3721 N71-36002
- Delayed oxidation of molybdenum dichloride during reaction with carbon dioxide [RAE-LIB-TRANS-1494] 23 p3775 N71-36008
- Development of light scattering apparatus for determining power law dependencies and application to measuring critical opalescence phenomenon in carbon dioxide 23 p3777 N71-36008
- CARBON DIOXIDE CONCENTRATION**
- Performance of carbon dioxide concentrator in long duration spacecraft cabin atmosphere simulation 10 p1583 N71-20739
- Accurate and precise titrimetric analysis of oxides in nuclear fuels by dissolving material in orthophosphoric and nitric acids for analysis in carbon dioxide atmosphere [RCN-126] 15 p2378 N71-27700
- Physiological effects of high carbon dioxide concentrations in helium/oxygen and argon/oxygen atmospheres on rats at ambient temperatures 16 p2543 N71-28008
- CARBON DIOXIDE LASERS**
- Thermal defocusing of CO₂ laser beam in air duct with SP6 [AD-710743] 01 p0063 N71-10407
- Gas discharge analysis of CO₂ and B₂H₆ lasers [AD-711523] 01 p0063 N71-10408
- Gaseous reactions in passive CO₂ laser cells as indicated by emission in visible region [AD-711522] 01 p0063 N71-10408
- Pulsing techniques for CO₂ lasers [AD-712117] 02 p0238 N71-11158
- Production of plasmas by long wavelength carbon dioxide lasers [MATT-786] 03 p0436 N71-13283
- Using double expansion nozzle in shock tube facility to study population inversions in carbon dioxide gas [AD-713497] 03 p0607 N71-15340

SUBJECT INDEX

Production of carbon dioxide laser pulsing by cavity length modulation 05 p0897 N71-15368
[AD-715770]
Self-mode-locking of cross-excited electrically pumped CO₂ laser 06 p0888 N71-14213
[AD-714023]
Velocity dependence of gain of carbon dioxide laser [AD-715136] 07 p1859 N71-17642
Focusing experiments with high power modulated carbon dioxide lasers 07 p1859 N71-17643
[AD-715139]
Flow and stationary systems of glow discharge in carbon dioxide laser 08 p1209 N71-14533
[AD-715353]
Small signal series multistage protection quantum amplifier [AD-716091] 10 p1569 N71-20912
Infrared inspection of free surface wear on lathes using carbon dioxide lasers 10 p1563 N71-20945
[AD-TL-132]
Single-mode continuous-wave carbon dioxide laser intensity fluctuation variance and power spectrum measured by photomultiplier detector 10 p1570 N71-21674
[AD-716047]
Chase air turbulence pulse Doppler laser radar design including analysis of mechanical vibration effects on laser transmitter and receiver [NASA-CR-183091] 11 p1774 N71-22131
Carbon dioxide lasers, optical frequency tuning by geometric operation, tunable Raman effect in crystals, and impedance analysis of interactions in semiconductor 12 p1993 N71-23404
Infrared nondestructive testing techniques employed for laser heating for thermal images to detect voids and defects 13 p2088 N71-24440
[AD-715941]
Rapidly pulsed wavelength selective carbon dioxide laser [NASA-CASE-ERC-10178] 13 p2089 N71-24832
Radio frequency stabilization of carbon dioxide laser beam 13 p2090 N71-25319
Performance of mercury photoelectric infrared mixer for ATR 6 carbon dioxide laser communication system 13 p2048 N71-25320
Development of simultaneous mode locking and gain coupling of carbon dioxide laser using single gallium arsenide element 14 p2265 N71-25618
[AD-719917]
Gallium arsenide infrared window materials for high power carbon dioxide lasers 14 p2265 N71-25874
[AD-720050]
Development of radiative ignition apparatus based on carbon dioxide laser to examine effects of radiant flux, pressure, oxygen concentration, and absorptivity on ignition delay of polymers 14 p2355 N71-26332
Vibrational kinetics of high pressure CO₂ laser mixtures 16 p2686 N71-28322
[AD-721735]
Nonlinear propagation and chirping of carbon dioxide laser pulses 17 p2759 N71-30200
[AD-722652]
Detecting clear air turbulence using CO₂ laser Doppler system 18 p2991 N71-30763
Carbon dioxide laser with vacuum pump and oven for use in molecular laser physics without chemical reaction or charged particle effects 18 p2991 N71-31129
Numerical analysis of coherent dynamic effects and absorption coefficient measurements for carbon dioxide subjected to low intensity source of radiation 19 p3189 N71-32684
Analysis of helium-neon and carbon dioxide laser laser propagation in atmospheric turbulence [NASA-TR-8-370] 20 p3310 N71-33222
Characterization of carbon dioxide laser radiation emitting in atmosphere and application as remote sensing probe [NASA-CR-121663] 21 p3435 N71-34439
Influence of collisions on radiative excitation and Lamb dip formation in CO₂ molecular lasers 21 p3436 N71-34449
Application of holographic techniques for measurement of chemiluminescence effects using gas and infrared laser 22 p3591 N71-35372
Ionization rate measured in glow discharge in gas mixture commonly used in carbon dioxide lasers [NIST-443] 23 p3766 N71-36848
Feasibility analysis for use of long-wavelength high-powered lasers for controlled thermonuclear fusion [CONF-710077-40] 23 p3767 N71-36849
Optical properties of gallium arsenide infrared window material and evaluation of CO₂ laser [AD-726743] 24 p3951 N71-38091
CARBON DIOXIDE REMOVAL
Carbon dioxide concentrator subsystem for closed loop space oxygen system [NASA-CR-73397] 02 p0170 N71-11204

Catalytic carbon dioxide reduction cartridge for oxygen recovery to life support systems of long term manned space flights [NASA-CR-1682] 03 p0327 N71-12333
Reaction deconvolution technology for carbon dioxide control in manned spacecraft 07 p0887 N71-17945
Membrane of aqueous carbonate solution with catalyst for hydrolysis of CO₂ for removal of CO₂ in life support systems [AD-715978] 08 p1340 N71-17772
Oxygen recovery from exhaled carbon dioxide in spacecraft cabin atmosphere by chemical reactor with toxin burner unit 10 p1596 N71-20960
Amino absorbent for carbon dioxide concentrator in long term life support system 10 p1596 N71-20961
CARBON DIOXIDE TENSION
NT HYPERCAPNIA
CARBON INSULIN
DF-CO₂ and CS₂-O₂ CO laser research, electrode configuration efficiency, and CO₂/O₂ ratio of dissociation by DF and HF [AD-712564] 03 p0368 N71-13396
CARBON FIBERS
Third derivative reinforcement of carbonized composites [BDD-413-144] 06 p0879 N71-16370
Electron microscopy, radiography, electrical resistivity, thermal expansivity, and X ray diffraction of fibrous carbon-carbon composite dynamic characteristics [Y-1752] 11 p1783 N71-22475
Mechanical properties and physical, chemical, and thermal tests of polybenzimidazole and carbon fabric laminates for spacecraft thermal insulation [NASA-CR-1723] 15 p2427 N71-26915
Thermal degradation of polyacrylonitrile polymers for conversion to high modulus carbon and graphite reinforcement fibers 17 p2769 N71-29546
Strength of adhesive of carbon fiber composite bonded to metal [DLR-FB-71-31] 20 p3287 N71-33100
Interface structure and effects of carbon fiber microstructure on shear strength of carbon-epoxy composites 21 p3445 N71-34516
Tensile tests on lap-joints carbon fiber reinforced plastics [AB-727034] 23 p3779 N71-36934
Proceedings of International conference on carbon fibers [AD-726673] 23 p3779 N71-36935
Effect of voids on mechanical properties of two graphite fiber composites [AD-727256] 24 p3943 N71-38127
Yield and stability of pyrolytic carbon fiber products improved by chemical modification of cellulose fibers and metal additives [AD-727141] 24 p3943 N71-38128
CARBON ISOTOPES
NT CARBON 12
NT CARBON 13
NT CARBON 14
Asymmetry produced by 28 MeV vector polarized deuterons in elastic scattering on C-12, Si-28 and Ca-40 [LYCEN-7021] 02 p0277 N71-12131
Alpha, 2 alpha reaction on Li-6, Li-7, Be-9, C-12, and O-16 at 35 MeV [LYCEN-7089] 02 p0277 N71-12132
Chemical fate of nascent C-11 atoms induced by proton irradiated water and aqueous solutions in terms of hot and thermal reactions 04 p0484 N71-13441
[INF-18376]
Carbon isotope separation and thermal diffusion [MLM-1768] 10 p1612 N71-20722
Using Fokker-Planck equation for studying model of three rigid alpha particles for nucleus of C-12 13 p2144 N71-23588
Alpha, deuteron, and helium 3 activation determination of carbon isotopes [ORO-3922-2] 16 p2660 N71-29191
Apparatus for studying radiolytic carbon deposition of C-labeled gas mixtures at high temperature and pressure [RD/RN-1748] 17 p2804 N71-30209
Scattering cross sections for nuclear reactions of C-12, Ne-20, and Ar-40 induced by 14 MeV neutrons in grafted insulation chamber 21 p3490 N71-34858
Irradiation yield curves and angular distributions for Li-4-C-12 reaction 21 p3491 N71-34869
CARBON MONOXIDE
Transfer reactions in carbon monoxide oxidation 01 p0018 N71-10514
Infrared measurement on vibrational relaxation rate of carbon monoxide in argon shock tube wave [NASA-CR-111570] 02 p0201 N71-11453

CARBON MONOXIDE POISONING

Laser power at 5 microns from carbon monoxide pyrolytic expansion 02 p0239 N71-11468
[NASA-TM-X-63066]
Effects of carbon monoxide containing cable atmospheres on performance of human and primate [AMRL-TR-69-19] 02 p0162 N71-11804
Carbon monoxide oxidation rates for automobile exhaust manifold reactor conditions [NASA-TN-D-7024] 02 p0206 N71-12066
Stratospheric photochemical and hydrophobic CO oxidation and tropospheric CO reaction with ozone as atmospheric CO sinks 03 p0366 N71-12093
[PB-195188]
Ion and electron production in proton and hydrogen atom collisions with carbon monoxide, carbon dioxide, methane, and ammonia [AD-712689] 03 p0436 N71-13377
Sampling by frontal analysis for determination of carbon monoxide in air [NASA-TT-F-13434] 04 p0485 N71-13434
Oxidation of carbon monoxide/methane mixtures in shock waves [AD-712531] 04 p0485 N71-13435
Effects of chemisorption of CO on catalytic reaction [AD-715283] 07 p0990 N71-17754
Spectral coincidences between oxidation lines of CO laser and absorption lines of nitrogen oxides [AD-715293] 07 p1041 N71-18033
Biophore shims for carbon monoxide oxidations to atmosphere [PB-195433] 08 p1186 N71-18307
Removing sulfur dioxide by carbon monoxide reduction [BM-82-7403] 08 p1160 N71-18979
Chemisorption of O₂, CO, and CO₂ on solid fuel under static and dynamic conditions [DILL-878-3837] 10 p1630 N71-31746
Studying static and time dependent catalytic functions for liquids of carbon monoxide and nitrogen using computer simulated molecular dynamics 11 p1883 N71-22112
Effect of carbon monoxide on human performance including heart rate and galvanic skin response [AD-717716] 11 p1883 N71-22399
Carbon monoxide accumulator cell for spacecraft mass spectrometer atmospheric sensor system [NASA-CR-111815] 11 p1764 N71-22669
High temperature kinetics of photochemical mercury decomposition of nitrous oxide in carbon monoxide methane mixtures 12 p1871 N71-23783
Signal gain coefficient and spectral characteristics of electrically excited carbon monoxide laser [AD-718463] 12 p1924 N71-23801
Vibration energy transfer in N₂-CO and N₂-NO mixtures [AD-718093] 12 p1976 N71-34160
Determination of vibrational relaxation time in CO₂ and CO using radiatively driven acoustic waves [AD-726486] 14 p2322 N71-23938
Infrared reflectance spectra of CO and O₂ absorbed on oxidized nickel films 14 p2274 N71-36325
Shock tube investigation of chemical kinetics of NO-CO-Ar mixtures at temperatures from 3000 to 4500 K 14 p2214 N71-36311
Carbon monoxide purity standards for gas breathing apparatus of divers and toxic hazards under controlled hyperbaric atmospheres [AD-721666] 17 p2787 N71-29358
Carbon monoxide chemisorption on alpha and beta activated iron precipitation catalysts 17 p2714 N71-29687
Iron film adsorption of carbon monoxide, hydrogen and their mixtures 17 p2714 N71-29688
Reduction in smoke level and carbon monoxide emissions resulting from air-cooled fuel nozzles in jet aircraft exhaust pollutant tests 18 p2871 N71-30784
Dissociative excitation of CO₂ 3 pi and other metastable fragments such as O(3P) produced by electron impact on CO₂ 21 p3466 N71-34670
[NASA-CR-121714]
Energy distribution of electron-impact dissociated carbon monoxide ions from plasmas 21 p3488 N71-34831
Toxicological evaluation of carbon monoxide, atmospheric contaminants, and pollutants in environmental pollution [AD-727022] 22 p3506 N71-35258
Mercury photochemical oxidation of CO at 273 C [PBU-BRL-SCI-570] 23 p3719 N71-36869
CARBON MONOXIDE POISONING
Effects of carbon monoxide on brain cellular metabolism in monkeys 05 p0632 N71-14575
Circulating blood volume changes after lower body negative pressure exposure 06 p1154 N71-19309

CARBON STEELS

- Composition and heat treatment effects on wear resistance and fatigue strength of carbon steels [AD-71157] 01 p0868 N71-10630
- Weld heat affected zone notch impact properties of normalized C-Mn steel and fully killed A1 grain refined C-Mn steel [MAT-1] 02 p0240 N71-11429
- Static and cyclic strain aging effects on Charpy impact properties of carbon steel plates [GEAP-10140] 03 p0391 N71-12918
- Decomposition of reactors containing carbon steel piping [BNWL-CC-2639] 04 p0530 N71-13757
- Carbon steel corrosion and mechanical wear of equipment [AD-712951] 04 p0527 N71-13785
- Austenitic formation and dendritic liquification of silicon, nickel, copper, and molybdenum in low carbon iron alloys [NLL-TRANS-746-510-79022.401/] 10 p1582 N71-21497
- X ray diffraction analysis of crystal defects caused by martensitic transformations in iron nickel and iron carbon steels 10 p1583 N71-21571
- Microstructure and mechanical properties of boronized medium carbon steels [NLL-TRANS-746-527-79022.401/] 10 p1584 N71-21604
- Industrial process for producing steel sheets of low carbon steel with high degree of strength and stiffness [NLL-M-20179/5828.4P/] 12 p1940 N71-24191
- Effect of temper rolling on elimination of yield point in vacuum-treated low-carbon steels 18 p2927 N71-30687
- Technique of surface carburization prior to extrusion reported for two C-Mn-Si steels 18 p2927 N71-30744
- Effects of machining parameters on carbon steel wear inhibiting layer of tools [PB-198063] 18 p2927 N71-30797
- Factors affecting scatter of elongation values obtained from rupture tests on silicon killed, aluminum treated carbon steel [PB-197140] 18 p2935 N71-30881
- Fatigue testing of carbon and stainless steel boiling water reactor cooling system pipes including failure probability and fracture mechanics analyses [GEAP-10207-23] 19 p3134 N71-31711
- Influence of carbon and stainless steel refining processes on inclusions 19 p3104 N71-31909
- Corrosion of polished carbon steels at inclusions noting effect of manganese sulfide 19 p3122 N71-31917
- X ray analysis of residual stresses in electron beam welded carbon steel structures [RAE-LIB-TRANS-1556] 20 p3361 N71-33986
- Analysis of true stress variation as function of degree of deformation based on tensile tests of aluminum, copper, and unalloyed steels with varying carbon contents [RAE-LIB-TRANS-1587] 22 p3608 N71-36306
- CARBON TETRACHLORIDE**
- Effects of carbon tetrachloride on microstructure of metal alloys 02 p0159 N71-11480
- Reaction kinetics of carbon tetrachloride with complex transition metal fluorides 04 p0488 N71-13469
- Arithmetic all shift correction for laser excited Raman spectra of carbon tetrachloride and methanol 12 p1934 N71-24068
- Analysis of vibrational relaxation in carbon tetrachloride 20 p3275 N71-33482
- CARBON 12**
- Multipole formation for calculating angular distribution of proton scattering on carbon 12 nuclei [ITF-76-18] 02 p0271 N71-11501
- Decay of C-12 into 3 alpha [CEA-CONF-1498] 03 p0432 N71-12930
- Polarization measurements of doubly charged scattered deuterons on C-12 for energies between 41 and 51 MeV [INF-18301] 04 p0574 N71-13669
- Quasi-free electron scattering on C-12 and Be-9 using external electron beam 06 p1347 N71-18190
- Center of mass energies for C 12 plus C 12 and C 12 plus O 16 reaction cross sections [ANU-P7515] 12 p1979 N71-24302
- Reaction of pions with C-12 at 73 MeV pion energy and zero degree proton angle 13 p2144 N71-23584
- Elastic scattering of high energy hadrons from deformed carbon 12 nuclei calculated using multiple collision theory and deformation oscillator wave functions [BIP-721] 14 p2308 N71-26422
- Report of experiments including neutron polarization, elastic and inelastic scattering of neutrons on C-

- 12, and angular distribution of fission fragments in U-238 neutron reaction 15 p2459 N71-27047
- Energy spectra of neutrons from pion capture in carbon 12 boron 10 reaction 15 p2472 N71-27418
- Polarization of protons from C-12/d,p-C-13 reaction at 12.4 MeV and distorted wave Born approximation comparisons [INF-711] 15 p2481 N71-27691
- Differential cross sections of elastic and inelastic angular distributions of neutrons scattered from C-12 and excited states of C-13 at angles from 15 deg to 135 deg 15 p2489 N71-27884
- Proton polarization in reaction C-12/He-3, proton sub 0/0-14 [JINR-P15-5156] 15 p2497 N71-27995
- Oxygen and carbon elastic form factor calculations based on liquid drop nuclear model with quadrupole surface oscillations [RLO-1388-397] 17 p2790 N71-29270
- Reaction mechanism and distortion of p,p in reactions C-12/ p,p -B-11 in $1P_{3/2}$ state and C-40/ p,p -K-39 in $2S_{1/2}$ state at 156 MeV [INF-18476] 18 p2968 N71-30426
- Computation of elastic and inelastic pion C-13 scattering using distorted wave impulse approximation [COO-1051-45] 18 p2971 N71-30487
- Coincidence methods for measuring decay of C-12 into 3 alpha particles 18 p2975 N71-30574
- Angular distributions and absolute cross sections for C-12 triton reactions at triton energies between 0.5 and 1.9 MeV, and excitation curves [CEA-R-4153] 18 p2981 N71-30897
- Highly excited states of C-12 and O-16 from He-3 bombardment of Be-9 and C-13 18 p2983 N71-31039
- Multipole analysis of polarization and asymmetry from elastic and inelastic neutron scattering by C-12 [ITF-70-87-P] 19 p3146 N71-31972
- Emissions of He-4 during fission of U-235 and Au-197 by C-12 and O-16 at 82 and 137 MeV [KFK-TR-352] 19 p3157 N71-32535
- Differential cross section and vector polarization for elastic scattering of 41 to 51 MeV deuterons on carbon-12 21 p3469 N71-34701
- Extrapolation of C-12 plus C-12 and C-12 plus O-16 reaction cross sections below 4 MeV [ANU-P-515] 22 p3642 N71-33967
- Beta and electron-capture decay schemes for Sb isotopes and proton reactions of C-12, F-19, Au-197, He-3, Ta-181, Pb-208, and Ni-58 including angular distributions and scattering cross sections [UCLA-10-P-18-23] 23 p3816 N71-37215
- CARBON 13**
- Production of algae containing 93 percent C-13 [LA-4496] 05 p0779 N71-15913
- Magnetic spectroscopic study of O-15 bound states and T3/2 states in C-13, O-17, and Ne-21 09 p1430 N71-19767
- Polarization of protons from C-12/d,p-C-13 reaction at 12.4 MeV and distorted wave Born approximation comparisons [INF-711] 15 p2481 N71-27691
- Differential cross sections of elastic and inelastic angular distributions of neutrons scattered from C-12 and excited states of C-13 at angles from 15 deg to 135 deg 15 p2489 N71-27884
- Reduction of C-13,H Overhauser polarization with added paramagnetic species - theoretical and experimental confirmation [AD-721732] 16 p2636 N71-29105
- Directly bonded nuclear spin-spin coupling constant between Ge-73 and C-13 measured in tetramethylgermane [AD-721717] 17 p2793 N71-29514
- Nuclear magnetic resonance analysis on C-13 mono- and di-substituted molecules 18 p2867 N71-31318
- CARBON 14**
- Measuring energy spectrum of electrons from C-12 up to 16 MeV for three different excitation combinations at each of three values of momentum transfer 03 p0735 N71-14332
- Studies in nuclear physics research, radiation research, isotope geochemistry, carbon 14 variations, and isotope applications 06 p1349 N71-18207
- Radioactive age determination by carbon 14, errors including isotopic effects and geochemistry [CEA-CONF-1618] 06 p1185 N71-18219
- C 14 diffusion coefficients during annealing of titanium wire between 1223 to 1923 K [IT-70-57649] 14 p2270 N71-25681
- Diffusion coefficients of C-14 in W and W-Re alloys over 1500 to 1800 C temperature range 14 p2272 N71-25801
- Both spectrum measurement of C-14 using multichannel proportional counter and gaseous C-14 sources [KFK-1222] 15 p2462 N71-27122

- Water sampler for measuring radiocarbon in sea [RLO-2223-T-20-3] 22 p3375 N71-34000
- Geiger counter detection of carbon 14 for upper limit determination 24 p4013 N71-38000
- CARBONACEOUS ROCKS**
- NT COAL**
- Ultrasonic wave propagation in carbonaceous and siliceous rocks 09 p1386 N71-30800
- [NASA-TF-F-13477] 09 p1386 N71-30800
- Thermodynamic data for carbonaceous materials used in high temperature reactor technology [GAAD-9355] 12 p1961 N71-23044
- CARBONATES**
- NT CALCITE**
- NT CALCIUM CARBONATES**
- NT DOLOMITE (MINERAL)**
- NT LEXAN (TRADEMARK)**
- NT POLYCARBONATES**
- NT SODIUM CARBONATES**
- Membrane of aqueous carbonate solution with catalyst for hydrolysis of CO2 for removal of CO2 in life support systems 09 p1340 N71-30770
- Cathodoluminescence and X ray induced fluorescence of manganese activated carbonates 17 p2770 N71-30800
- Refinement of X ray data on arsite using La Alamos Crystal Structure Least Squares program GENLES [PRNC-145] 21 p3499 N71-34000
- CARBONYL COMPOUNDS**
- Investigation of structure of manganese(I) and rhodium(I) carbonyl halides by infrared and mass spectroscopy, photolysis reactions, and conductivity measurements 01 p0019 N71-10000
- Chemical characteristics and synthesis of polyoxalanes with carbonyl groups in polymers [AD-716742] 16 p1388 N71-30800
- Competitive reaction of O/SP atoms with oxen and carbonyl sulfide in temperature range 197 K - 299 K [NASA-CR-114046] 16 p1551 N71-32218
- Tables on vapor pressure of iron pentacarbonyl, nickel carbonyl, and nickel carbonyl system [NLL-TRANS-746-515-79022.401/] 10 p1386 N71-31821
- Shock tube decomposition of iron pentacarbonyl to yield vibrational relaxed carbon [AD-717742] 11 p1095 N71-32071
- CARBORANS**
- Synthesis of carborene-transition metal phenoxides of side C2B4H6-2/ and cyclic C2B2H2-2 ligands from iron pentacarbonyl and 2,3-dichloro-4,5-difluorobenzene 03 p0333 N71-10278
- Gamma ray induced polymer formation of carborenes [ORO-3781-7] 06 p0882 N71-10278
- Diisopropyl alkylcarborane adhesives with high temperature stability for steel-on-steel bonding [NASA-CR-114837] 06 p0882 N71-10278
- Thermal behavior of polycarborene siloxane 10-11 dimethoxy from C2B2H2 10 p1587 N71-30800
- Solid state structure of carbon metalloboranes determined by analysis of X ray diffraction patterns 11 p1095 N71-32071
- Synthesis of carborene siloxane polymers by a cobalt catalyst of bis-chlorodimethylsilyl carborenes [AD-724350] 20 p3286 N71-33970
- CARBOXYHEMOGLOBIN**
- Circulating blood volume changes after lower body negative pressure exposure 06 p1154 N71-10278
- CARBOXYHEMOGLOBIN TEST**
- Spacecrew blood carboxyhemoglobin estimation in long duration space station simulation 10 p1409 N71-30800
- CARBOXYL GROUP**
- Carboxyl terminated polyester propylene and foams produced from propylene and materials [NASA-CASE-NPO-10596] 14 p2213 N71-25680
- CARBONYLATION**
- Thermodynamic carbon/oxygen equilibria in liquid nickel and liquid nickel copper alloys 13 p2957 N71-31318
- CARBONYLIC ACIDS**
- NT ACETIC ACID**
- NT ASPARTIC ACID**
- NT BENZOIC ACID**
- NT ETHYLENEDIAMINETETRAACETIC ACID**
- NT LACTIC ACID**
- NT OLEIC ACID**
- NT OXALIC ACID**
- Pressure effects on ferric hydroxamate and ferrioxamine A based on electromagnetic absorption and Mossbauer resonance [COO-1196-777] 11 p1704 N71-23000
- CARBOSTEONS**
- Gasoline icing inhibitors for aircraft carburetors and fuel systems [LR-536] 04 p0573 N71-13404

SUBJECT INDEX

CARBONIZING

- Quin boundary diffusion coefficients and reaction kinetics for austenitic stainless steel carburizing by carbonaceous fuels
[NASA-4132] 16 p3008 N71-20972
- Technique of surface carburization prior to extrusion needed for two C-Mn-Si steels
[PB-17125] 18 p2927 N71-30744
- Analysis (modeling) of chromium carburizing steel using production tests and tool wear
19 p3104 N71-31915

CARCINOMA

U CANCER

- Procedure for determining functional state of human heart right side
02 p0100 N71-11409

CARDIOGRAMS

- Electrocardiography and vector cardiography of athletes
09 p1329 N71-19585

CARDIOGRAPHY

- NT ELECTROCARDIOGRAPHY
NT PHONOCARDIOGRAPHY
Cardio-respiratory functional tests reliability in military pilot selection
02 p0164 N71-11018

- Methods for measuring mechanical aspects of cardiac activity and vessel functional state
09 p1329 N71-19586

- Signal cardiostimulator incorporating circuit for measuring heart rate of subject over prolonged periods of one minute also converting rate to beats per minute
[NASA-CASR-XM5-62399] 11 p1092 N71-22896

CARDIOLOGY

- Essays on cardiology in sports
[NASA-TT-F-462] 09 p1328 N71-19580

- Cardiac activity of athletes in quiet state
09 p1328 N71-19581

- Cardiac activity under stress of physical work
09 p1328 N71-19582

- Technology review on cardio and hemodynamics
09 p1328 N71-19584

- X ray methods for quantitative analysis of cardiac activity in athletes
09 p1329 N71-19587

- Functional tests of cardiovascular system in athletes
09 p1329 N71-19588

- Transmission and analysis of cardiographic data on athletes
09 p1329 N71-19589

- Clinical problems of cardiology of athletes
09 p1329 N71-19590

- Cardiac rhythm disruptions in athletes
09 p1329 N71-19592

- Physical overexertion effect on cardiac muscle in athletes
09 p1329 N71-19593

- Cardiological medical services for Soviet athletes
09 p1330 N71-19595

- Development of system for identifying dynamic heart rate responses to respiration
[AD-719008] 13 p2034 N71-24953

- Hardware and techniques for studying human circulatory performance in space environment
[NASA-CR-121665] 21 p3380 N71-34032

CARDIOLOGISTS

- Development of cooled Pb-210 sources for implanted cardiac pacemakers
[PB-10503] 15 p3375 N71-27732

CARDIOVASCULAR SYSTEM

- NT ARTERIES
NT BLOOD VESSELS
NT CAPILLARIES (ANATOMY)
NT CARDIAC VENTRICLES
NT ERYTHROCYTES
NT HEART
NT HEMATOPOIESIS
NT LYMPHOCYTES
NT MYOCARDIUM
NT SYSTOLE

- Investigating effects of gravitational and inertial forces on cardiovascular and respiratory dynamics
[NASA-CR-111695] 09 p0321 N71-12294

- Cardiovascular reactions of flying personnel to flight
[PB-1238] 04 p0476 N71-13433

- Measuring cardiovascular function in primates under prolonged weightlessness
[NASA-CR-71498] 05 p0633 N71-14633

- Intervascular dehydration effects in production of microvascular deconditioning by bed rest simulating microgravity
[NASA-CR-114668] 06 p0804 N71-16702

- Relationships between cardiac volume, body weight, physical work capacity, and blood volume in healthy men and women with varying range of performance
[NASA-TT-F-13439] 06 p1148 N71-18373

- Studying cardiovascular effects of prolonged confinement in Soyuz 9 simulator during normal and modified work and rest cycles
08 p1152 N71-18912

Essays on cardiology in sports

- [NASA-TT-F-462] 09 p1328 N71-19580
- Functional tests of cardiovascular system in athletes
09 p1329 N71-19588

Biological models for mammalian cardiovascular systems

- 09 p1331 N71-19594
- Conditioning unit for normal function of increased cardiovascular system in gravity environment
[NASA-CASR-XLA-62896] 09 p1341 N71-20268

- Cardiac and neural effects of UHF radio energy on frogs
09 p1335 N71-20354

- Physiological effects of gravitational overloads of immersion of sorts, struts, and vessel curves
[PB-179916T] 10 p1562 N71-21640

- Comparison of ground level rats to rats exposed to altitude of 18,000 feet to determine cardiovascular responses
[AD-717851] 11 p1082 N71-22240

- Exercise effects on physical fitness and cardiovascular system of aging pilot
11 p1609 N71-22313

- Rat estimator for monitoring blood oxygenation and pressure, pulse rate, and pressure pulse curve, using dog and rat
[NASA-CASR-XAC-65422] 12 p1961 N71-23183

- Effect of weightlessness on cardiovascular and urtic functions in human subjects
[AD-717970] 13 p2034 N71-20997

- Physiological effects of positive acceleration on cardiovascular system based on requirements for cardiovascular stimulation
[AD-715902] 14 p2203 N71-23674

- Species comparison of cardiac hypertrophy in animals chronically exposed at sea level, 5,380, 11,140, and 14,110 feet
[AD-720594] 14 p2203 N71-26167

- Clinical and experimental investigations of effect of motor activity restriction on cardiac function in human and animal subjects
16 p2547 N71-28493

- Spontaneous cardiac arrhythmias induced by bromocriptine in monkeys
[AD-723445] 19 p3042 N71-31733

- Conference on aerospace cardiovascular, manned space flight, weightlessness simulation, micro-isolated and cardiovascular systems, bone loss, mineral metabolism, and hematology
[NASA-SP-249] 20 p3216 N71-33231

- Physiological changes in cardiovascular and musculoskeletal systems during manned space flight
20 p3216 N71-33232

- Bed rest and immobilization effects on oxygen transport system of human body
20 p3217 N71-33262

- Total body exercise effect on metabolic, hematologic, and cardiovascular consequences of prolonged bed rest
20 p3218 N71-33265

- Deconditioning and its prevention by simulating hydrostatic gradient by use of cardiovascular conditioning suit
20 p3219 N71-33274

- Biomedical evaluations of cardiovascular and overall physical fitness of air traffic control personnel
[FAA-AM-71-19] 22 p3544 N71-33293

CARBS

NT PUNCHED CARDS

CARBET WINGS

- Receptor and control wing units in supersonic and hypersonic turbulent flow for hypersonic vehicles
[ABC-874-3624] 07 p0965 N71-17183

CARGO

NT AIR CARGO

NT AIR MAIL

- Technical and engineering investigation of transportation of hazardous materials
[AD-69182] 01 p0015 N71-10386

- Legal aspects of air and surface carrier interactions in freight transportation
02 p0308 N71-12119

- Freight transportation in Great Lakes Area for year 2000
06 p1308 N71-19520

- Human factors study of IVA cargo transfer from shuttle to space station
[NASA-CR-160118] 14 p2543 N71-25936

- Cargo handling, transfer, and storage under weightlessness conditions of space shuttle
22 p3548 N71-33270

- Solutions to legal constraints to international cargo transportation
[AD-726777] 22 p3781 N71-34097

- Economic, administrative, and legal factors affecting freight lines and damage
24 p4035 N71-37708

CARGO AIRCRAFT

NT BERGUEY 941 AIRCRAFT

NT C-3 AIRCRAFT

NT C-47 AIRCRAFT

NT C-54 AIRCRAFT

NT C-119 AIRCRAFT

NT C-141 AIRCRAFT

CARRIER FREQUENCIES

- Report of aircraft accident due to forward shift of improperly secured cargo
[NTSS-AAR-71-4] 05 p1143 N71-19941

CARGO SHIPS

- Graphical solution to stay time of commercial fleet vessels in region of icing
11 p1739 N71-22601

- Contributions of oceanography toward solving problems affecting the United States Merchant Marine
18 p3911 N71-38083

CARIBBEAN SEA

- Meteorological, climatological, and physical/chemical oceanography for Caribbean Sea - annotated bibliography
03 p0323 N71-12197

- Meteorology, climatology, and physical/chemical oceanography for Caribbean Sea - indices
02 p0323 N71-12198

- Marine biology and geology of Caribbean Sea
[PB-180697T] 03 p0373 N71-13343

- Lidar observations of lower troposphere over BOMEX area
[TD-25323] 05 p0673 N71-14900

- Abstracted bibliography on meteorology, climatology, and oceanography of Caribbean region
[AD-719422] 05 p0677 N71-15904

- Indices for bibliography on meteorology, climatology, and oceanography of Caribbean Sea region
[AD-715493] 05 p0678 N71-15505

- Meteorological radar study of Caribbean Sea from May through July 1969
[AD-714191] 06 p0892 N71-16597

- High precision, high resolution sound speed and temperature profile measurements in and near deep regions of eastern Caribbean
[AD-716945] 09 p1434 N71-30146

- Tabulation of B-57 aerial cloud photography of tropical convection systems for 11 to 28 July 1969 with flight path over Barbados Islands
[NASA-TM-BRL-TM-BOMAP-1] 12 p1921 N71-23746

- Geomorphology, biological activity, and hydrology of Gulf of Mexico and Caribbean Sea as determined from Soviet-Cuban oceanographic expeditions
[JPBS-53412] 18 p2509 N71-30604

- Geomorphology and bottom sediment characteristics in Gulf of Mexico and Caribbean Sea as determined by Soviet-Cuban oceanographic expeditions
18 p2509 N71-30605

- Geomorphology of southern Gulf of Mexico and Cuban shore areas as determined from Soviet-Cuban oceanographic expedition
18 p2509 N71-30606

- Soviet-Cuban oceanographic expeditions in Gulf of Mexico and Cuban shore area to determine geologic characteristics and biological productivity
18 p2509 N71-30607

- Hydrological characteristics of upper layers of Caribbean Sea and Gulf of Mexico as determined by Soviet-Cuban oceanographic expeditions
18 p2509 N71-30608

- Isostatic gravity map of Antilles Islands and Venezuela Basin
18 p2912 N71-30908

- Velocity divergence computation for Barbados Oceanographic and Meteorological Experiment from flights at different heights
[NOAA-TM-BRL-BOMAP-5] 18 p2904 N71-31225

- Inventory of high level cloud photography collected results during oceanographic and meteorological experiment in Barbados area
[NOAA-TM-BRL-BOMAP-4] 18 p2905 N71-31283

- Climatology of tropical storms in North Atlantic Caribbean and Gulf of Mexico
[NASA-CR-61335] 18 p2955 N71-31437

- Tropical cyclone data for North Atlantic, Caribbean, and Gulf of Mexico - charts
[AD-722655] 19 p0128 N71-32838

- Oceanographic and meteorological measurements on aircraft energy flux in atmospheric boundary layer over tropical ocean region
19 p3280 N71-32733

- BMAP plans for BOMEX area experiment
[NASA-CR-115760] 19 p3280 N71-32731

- Current status of BOMEX experiments
19 p3097 N71-32733

- Establishment of BOMAP advisory panel, and planned BOMEX activities
19 p3280 N71-32734

- Acquisition of data in Caribbean related to energy exchange between ocean surface and atmosphere - Project BOMEX
20 p3309 N71-32806

- Transition of BOMEX to BOMAP with objectives and structure
[NASA-CR-121431] 20 p3309 N71-33304

CAROTID BLOOD FLOW

- Mathematical functional model for carotid blood pressure control system
[AD-717647] 11 p1600 N71-22104

CARRIER FREQUENCIES

NT BARBADOSE GENERATIONS

- Demonstrator for characteristics dissemination of two modulating on signal carrier class in frequency
[NASA-CASR-XM5-61106] 03 p0184 N71-11930

Experimental quadrature two-channel modulation system for video signals operating at VHF
[BBC-1971/30] 23 p3726 N71-36558
Theory and analysis of demodulating suppressed carrier AM based in noise and recorder filter
24 p3890 N71-37729

CARRIER INJECTION

Iron doping effects on growth kinetics and electron spin resonance of aluminum oxide single crystals
23 p3834 N71-37342

CARRIER MOBILITY

NT ELECTRON MOBILITY

NT HOLE MOBILITY

Investigating backscattering factor as function of surface roughness of radiolotope carrier material for metals of different atomic numbers
[BMBW-FBE-70-4-A] 06 p0914 N71-15972

Measuring incremental sheet resistivity for determining impurity distribution in silicon after diffusion
07 p1088 N71-17289

Interaction between slow electromagnetic waves and drifting carriers in semiconductors
08 p1163 N71-19118

Broadband hot carrier diode mixers - analysis of intermodulation and cross modulation distortions
[AD-721244] 15 p2385 N71-26898

Production of carrier-free radioisotopes 5r-45 by irradiation in U-120 cyclotrons
[JUY-2431-CB] 18 p2970 N71-30462

Plasma waves and superconductivity in quantizing semiconductor /semimetal/ films and layered structures with high mobility of free carriers
[NASA-TT-F-13747] 18 p2995 N71-30850

Model description of polycrystalline semiconductor film assuming different conductivities and Hall mobilities for grains and boundaries
[NASA-TT-F-13680] 18 p2995 N71-31094

Quantum mobility and nuclear spin echo damping in impure crystals
[NUP-2069] 18 p2999 N71-31486

Neutron damage effects in Step Recovery Diode frequency multipliers
[SC-RR-710188] 20 p3329 N71-33991

Diffusion mechanisms responsible for charge carrier mobility in doped silicon, studied to determine impurity band effects on electrical conductivity
[N-816] 21 p3497 N71-34916

Precipitates and flux line pinning in superconducting Pb-Na alloy investigated by electron microscopy
[NLL-CE-TRANS-5559-19022.091] 24 p3968 N71-38365

CARRIER MODULATION

U MODULATION

CARRIER ROCKETS

U LAUNCH VEHICLES

CARRIER WAVES

Modulated sub-carrier system for precise measurement of attenuation at X band
01 p0021 N71-10231

Investigating propagation of helicon and carrier waves through medium of free carriers in semiconductor
08 p1170 N71-18938

Analysis of errors in independent subcarrier and harmonic subcarrier methods of radio telemetry on FM radio carrier
[SC-RR-70-6092] 10 p1526 N71-21756

Variable frequency subcarrier oscillator with temperature compensation
[NASA-CASE-XNP-03919] 16 p2571 N71-28810

Acoustoelectric surface wave amplifier with net terminal gain, low power dissipation, and stable continuous drift field operation
23 p3837 N71-37365

CARRIERS

Selecting and processing solid carriers for organophosphorus compounds using gas chromatography
[JPRS-53065] 13 p2040 N71-25137

Sealed storage container for channel carriers with mounted miniature electronic components
[NASA-CASE-MFS-38075] 14 p2229 N71-36133

Fluid motion in two dimensional Cartesian or cylindrical coordinates by following Lagrangian energy cells
[LA-4464] 04 p0585 N71-14243

Versatile FORTRAN 4 computer program for producing Cartesian plots suitable for publication using CalComp plotter
[AD-715279] 07 p0997 N71-18012

Design and development of random function tracer for obtaining coordinates of points on contour maps
[NASA-CASE-XLA-01401] 10 p1565 N71-21179

Cartesian coordinate system for direction finding of satellite sea bottom instruments
[AD-717966] 12 p1911 N71-23688

Modified computer program HEATING 3 for solving heat conduction problems in one, two, or three dimensional Cartesian or cylindrical coordinates
[JORN-TM-3208] 13 p2188 N71-25492

Displacement equations in Cartesian coordinates for solving deflection response of flat membranes
14 p2347 N71-25807

Accuracy of Cartesian and spherical coordinates of GROS 2 determined by synchronous observation from Riga and Vitorod
22 p3677 N71-36221

Method of characteristics for analysis of elastic wave equations in Cartesian coordinates
[NASA-CR-123178] 24 p4023 N71-38703

CATOGRAPHY

U MAPPING

CARTRIDGE ACTUATED DEVICES

U ACTUATORS

U EXPLOSIVE DEVICES

CARTRIDGES

Endless loop tape transport mechanism for driving and tensioning recording medium in magnetic tape recorder
[NASA-CASE-XGS-01223] 01 p0023 N71-10609

Catalytic carbon dioxide reduction cartridges for oxygen recovery in life support systems of long term manned space flights
[NASA-CR-1682] 03 p0327 N71-12333

CARTS

Metabolic cost evaluation of self-locomotion in simulated lunar gravity using space suits and carts including weight load and surface effects
[NASA-CR-1697] 10 p1504 N71-20898

CASCADE CONTROL

Reversible ring oscillator using cascaded single silicon controlled oscillator stages
[NASA-CASE-XGS-01473] 01 p0034 N71-10673

Cascade synthesis of logic functions
[AD-711154] 02 p0186 N71-11310

Constant key weight cascades for multicomponent isotope separation
[ABCOF-330] 03 p0419 N71-12561

Cation cascade controlling electron multiplication within straight channel photomultiplier tubes
10 p1557 N71-20856

Low energy component of secondary particles based on cascade- evaporative model
[JINR-P2-5549] 14 p2305 N71-26324

Synchronous dc direct-drive system comprising multiple-loop hybrid control system controlling load directly connected to actuator
[NASA-CASE-GSC-10065-1] 15 p2388 N71-27136

FORTRAN 4 computer program for design application of stagger angle replacing inlet flow angle for given blade cascade
[NASA-CR-121679] 21 p3410 N71-34262

CASCADE FLOW

Trajectories and velocities of solid particles entrained by fluid flows in cascade nozzles
[AD-711121] 01 p0043 N71-10546

Testing low reaction jet turbine stator blades in cascade annular cascade
[NASA-CR-1675] 03 p0312 N71-12227

Boundary layer characteristics of particulate flow in cascade nozzles
[AD-715721] 08 p1179 N71-18542

Gas particle flow properties in blade to blade stream surface of cascade nozzle calculated theoretically
[AD-715711] 09 p1372 N71-19762

Integral equations of kinematics of cascade decay and energy distribution
[JINR-P1-4926] 09 p1443 N71-20450

Acoustic resonant frequency computation of two and three dimensional cascade flow
[REPT-1007/71] 11 p1734 N71-21988

Directional correlations of gamma ray cascades in Hg-200 using TI-200 source and coincidence spectrometer arrangement
[NP-18613] 14 p2369 N71-26587

Structure of three dimensional transonic shear flow in turbomachine cascade examined in context of time dependent computer experiment
[NASA-CR-1816] 15 p2363 N71-27004

Cascade model of space distribution of alpha clusters in light nuclei
[JINR-P4-5479] 16 p2649 N71-28812

Unsteady flow in aerodynamic cascades of turbomachines
[AD-721959] 16 p2583 N71-29927

Singularity method for calculating incompressible potential flow in plane profile cascade stage
[NASA-TT-F-13922] 23 p3742 N71-36688

Noise reduction studies involving variable geometry inlet guide vanes for choking using two-sector cascade apparatus with three inlet configurations
[NASA-TM-X-2392] 24 p3872 N71-37601

CASCADES

Two dimensional cascade test of jet flap turbine rotor blade
[NASA-TM-X-2183] 07 p0967 N71-17589

Aerodynamic forces produced in turbine stage by vane cascade of cascade series
[NASA-TT-F-13631] 14 p2330 N71-25998

Cascade model for resonance effects produced in intranuclear particle collisions
[JINR-P2-5546] 18 p2957 N71-30474

Estimate of knock-out coefficient from uranium fission product collision cascade calculations and electron microscopic study of dependence of uranium oxide layer thickness
[NEMI-B-165] 24 p3979 N71-38395

CASCADES (FLUID DYNAMICS)

U FLUID DYNAMICS

CASCODE MORFET

U FIELD EFFECT TRANSISTORS

CASE BONDED PROPELLANTS

Quasi-static stress and strain analysis of viscoelastic hollow cylinder encased in elastic cylindrical shell with sliding pressurized cavity
[DLR-FB-70-61] 11 p1835 N71-28979

Analysis of bond stress in viscoelastic case bonded solid propellant rocket assembly during thermal shock
[NASA-CR-117891] 12 p1988 N71-29871

CASE HISTORIES

Model case studies of effects of DDT on human environment
[PB-194413] 04 p0481 N71-14429

Development, use, and application of information retrieval systems in geology and controlled medical records
[AD-716231] 09 p1383 N71-19882

Case history of Chodak-Higuchi disease with characteristic Friedreich hereditary spinal ataxia and histologic, neurologic, and genetic characteristics
[NASA-TT-F-13537] 12 p1863 N71-23209

Cost benefit analysis and technology assessment in civil aviation research and development with case histories
[NASA-CR-1808] 15 p2366 N71-27006

Geological uses of earth-orbital photography with case histories
[NASA-TM-X-45682] 22 p3583 N71-33034

Computer technology for medical information systems, in patient care, and for diagnostic purposes
24 p3893 N71-37700

CASES (CONTAINERS)

NT ROCKET ENGINE CASES

Nonmagnetic hermetically sealed battery case made of epoxy resin and woven glass tape for use with diaphragmed cells in spacecraft
[NASA-CASE-XGS-50890] 02 p0148 N71-11088

Radioactive isotope capsule container design for atmospheric reentry protection and heat transmission in spacecraft
[NASA-CASE-LEW-11227-1] 21 p3530 N71-35113

CASPIAN SEA

Yearly, monthly and ten-day changes in position of ice edge in North Caspian Sea
[AD-724672] 20 p3259 N71-33197

CASSEGRAIN ANTENNAS

Design and operation of multi-feed cone Cassegrain antennas
[NASA-CASE-NFO-10539] 02 p0183 N71-11328

Beam optimization in large Cassegrain antennas with parabolic horn reflector feeds
[NASA-CR-113369] 06 p0812 N71-15776

Modified Cassegrain feed paraboloidal and conical antenna designs for spacecraft
11 p1701 N71-22562

Synchronous detection system for detecting weak radio astronomical signals
[NASA-CASE-NXP-09832] 12 p1996 N71-27373

CASSEGRAIN OPTICS

Rocket-borne Cassegrain telescope for measuring stellar microwave radiation
[ARU-BIS-1] 02 p0224 N71-11323

Laser interferometer for monitoring and control of large telescopes
[NASA-CR-11811] 08 p1203 N71-19810

Thermal active optics technique for correcting optical distortions in space telescope mirror via analytical demonstration on beryllium paraboloid
[NASA-TM-X-67620] 10 p1600 N71-31514

Stereoscopic observatory using Cassegrain telescope to obtain color photographs as well as spectrograms
[NLL-M-20418-15828-4F] 21 p3430 N71-34409

Description of Isaac Newton Telescope Cassegrain spectrograph and results of radial velocity observations of stars near Lyrae constellation
23 p3758 N71-30709

Structural design of Cassegrain cages in large astronomical telescopes
24 p3923 N71-37805

CASULLANO VARIATIONAL THEOREM

Casullano theorem validity in variable medium elasticity theory of anisotropic body subjected to plane stressed state
[AD-726606] 22 p3680 N71-38009

CASTING

NT INVESTMENT CASTING

NT SLP CASTING

Nozzle plugging mechanisms occurring in casting aluminum containing steel
[BAR-7] 03 p0993 N71-11328

Ceramic coatings for casting plutonium and plutonium alloys
[LA-4495] 06 p0882 N71-14087

Hydraulic apparatus for casting and molding of liquid polymers
[NASA-CASE-XNP-07639] 11 p1690 N71-23975

Radiochemical measurement techniques for minimum wall thickness of small castings, using 5r-90 beta radioactive measurements
12 p1919 N71-23207

SUBJECT INDEX

Development of furnace design, operating, coating, and annealing procedures to improve structural properties of fused-cast aluminum oxide articles 12 p1946 N71-34895

Poling and coating of titanium alloys (AD-719416) 13 p3895 N71-32863

Composition, properties, and applications of superalloys and techniques for vacuum melting and vacuum casting procedures (NASA-SP-3695) 14 p2273 N71-32891

Use of photographic film coating techniques using gel flow viscosity for maintaining interlayer suspension in solution (NASA-TT-F-136711) 16 p2392 N71-38869

Decoding and vacuum casting effect on plastic properties of nickel-chromium steels noting corrosion resistance 18 p2927 N71-36881

Identification of ingots noting crystal structure 19 p3112 N71-31914

Extensible metal and grafted pattern coating of metal to metal (JPL-53572) 19 p3105 N71-34332

Low-alloy 12 percent chromium steel replacing nickel for nitrogen to improve casting and mechanical properties (JPL-5746-748-0022-404) 21 p3443 N71-34483

Effects of combined changes on dimensions of welded parts occurring during transfer molding processes (AD-613-283) 23 p3762 N71-36821

Effect of electromagnetic mixing on ingot grain size during continuous casting of magnesium alloys (AD-721777) 24 p3937 N71-38866

CATHODES

NET INGOITS

Alternative wear resistance of manganese cast iron in welded with carbon and studied with K2S4-B method (AD-711156) 01 p0868 N71-10633

Feasibility of preheated fluidity models for cobalt in alloy castings (AD-711936) 03 p0243 N71-11871

Weighted composite casting of structural materials in space manufacturing 02 p0235 N71-11722

Properties of cast columbium carbide-carbon alloys using in carbon content from 12 to 17 weight percent measured with hot pressed compounds of similar composition (JPL-53-7479) 06 p1213 N71-18479

Intermetallic and surface crack inhibition in steel castings 10 p1562 N71-30703

Neodymium formation and feeding for sand cast aluminum alloy sheets 10 p1576 N71-21012

Investment casting titanium alloy development (AD-721366) 16 p2568 N71-28191

Variability of mechanical properties of construction metals, casting alloys, aluminum alloys, and castings (ARC-BM-3654) 17 p2833 N71-30044

Development of structural models made by scanning strain gage networks in epoxy (JPL-52-742) 18 p2926 N71-31441

Weldability and formation of alloyed coatings on iron castings (JPL-52-31816-3828-4P) 21 p3441 N71-34485

Optimal points, crack formation, and shrinkage characteristics for castings of Co-Ni, Co-Mn, and Mn steel (JPL-TRANS-746-399-0022-401) 22 p3597 N71-35611

CATALYSTS

Monomethylhydrazine effects on glucose carbon monoxide and effects of pure oxygen inhibition in air (AD-727008) 22 p3546 N71-35259

CATALOGS

Catalog of electronic devices of USSR (NASA-TN-52-BEV) 02 p0194 N71-11358

CATALOGS (PUBLICATIONS)

ASTRONOMICAL CATALOGS

Meteorological data tabulated from Applications Technology Satellite observations including photographs of clouds - Vol. 3 (NASA-TM-X-66468) 02 p0254 N71-11603

Atlas of total electron content plots for 1959 - Vol. 5 (AD-727008) 02 p0254 N71-11603

Catalog of geophysical measurements obtained during the Antarctic expeditions (JPL-53-7123) 05 p0676 N71-15437

Catalog of red-draw and transfer functions from RED-3 runs 25 through 30A (JPL-7542) 10 p1403 N71-31183

Level proper motion survey in Northern Hemisphere of G magnitude stars, including 8991 stars brighter than magnitude 8 with motions greater than 0.5 seconds per year 12 p1930 N71-34338

Catalog of NASA special publications issued before 1971 (NASA-TM-X-67163) 12 p2030 N71-34332

Supplement to Data Catalog of Satellite Experiments (NASA-TM-X-67163) 14 p2338 N71-36321

Catalog of rocket and satellite reports and reports at World Data Center C 20 p3571 N71-33957

Catalog of reprints of scientific papers in Pauli collection with author index and cross references (CERN-5128-8) 21 p3473 N71-34731

World Data Center catalog of rocket and satellite launchings, and satellite sightings 22 p3676 N71-36165

Computer based cataloging and subject indexing system (NIST-32) 22 p5089 N71-36381

European sounding rocket catalog (ESRO-SP-39-ESTEC-VOL-1) 23 p3839 N71-37589

CATALYSTS

Waste of catalytic flat plate in low density dissociation gas flow (AD-711291) 01 p0844 N71-10975

Hydrogen tritium and hydrogen deuterium exchange reaction in alkyl aromatics during catalytic hydrogenation (SC-T-70-4031) 03 p0270 N71-11599

Catalytic surface effects on thermocouple combustion gas temperature measurements in jet engines 07 p1025 N71-17379

Effects of organic compounds on catalytic nickel plating of steel plates (NLL-TRANS-746-513-0022-401) 10 p1586 N71-21846

Dissociation and output of platinum catalyzed CO2 laser (AD-710424) 12 p1933 N71-32785

Physicochemical synthesis of sugar by formaldehyde condensation with lacticamide hydronide catalysts for space flight feeding 16 p2555 N71-36256

Catalytic deoxygenation process for irradiated organic reactor coolants (JPL-4631) 18 p2957 N71-30459

Thermogravimetric and calorimetric experiments to study phenomenology of synergistic system for catalysis of ammonium nitrate decomposition in solid rocket propellants (AD-724317) 20 p3337 N71-33884

CATALYSTS

Electronic effects of chemisorption on powdered zinc oxide catalyst (AD-712856) 03 p0330 N71-12356

Effect of oxidation-reduction potential on metal salt-catalyzed autooxidation of styric polypropylene (AD-711629) 05 p0333 N71-12375

Propellant decomposition catalysts for hydrazine engines and gas generators - conference papers (DLR-MIT-49-59) 07 p1097 N71-17192

Propellant decomposition in hydrazine engines and gas generators using noble metal catalysts 07 p1097 N71-17193

Scanning electron microscope study of hydrazine liquid rocket propellant catalysts 07 p1097 N71-17194

Nickel catalysts for hydrazine fuel cells 07 p1097 N71-17195

Hydrazine propellant decomposition with noble metal catalysts for quick ignition 07 p1097 N71-17196

Catalysts for hydrazine and hydrogen peroxide in hydrazine engines and gas generators 07 p1097 N71-17197

Amide catalyst effects on compressive strength of rigid urethane foams (BDX-613-170) 07 p1047 N71-17360

Delayed action accelerator for curing chloroprene resins (SD-153) 07 p0869 N71-17664

Metal oxide catalysts for air-oxygen electrode in electrochemical fuel cells and zinc oxygen batteries (AD-715707) 08 p1146 N71-18463

Effects of chemical catalysts, heat curing, chemical manufacturing techniques, operating conditions, and chemical handling procedures on hydrazine peroxide (NASA-CR-114094) 09 p1345 N71-19914

Effect of catalysts on decomposition, pressure loss, start transient, and lifetime of hydrogen peroxide monopropellant in reactor 09 p1456 N71-20116

Development of device for detecting hydrogen in solid environments (NASA-CASE-MPS-11577) 09 p1391 N71-20442

Effects of high temperature and composition gradients along external surface of catalyst particle behavior 10 p1513 N71-21275

Process industrial catalyst studies comprising structure and composition of platinum surface by low electron diffraction and molecular beam scattering under high vacuum conditions 15 p3493 N71-37946

Molecular spectroscopic studies of low Y zeolite and effects of oxidation catalysts (AD-721528) 16 p2555 N71-38177

CATHODE RAY TUBES

Carbon monoxide chemisorption on silver and beta activated iron propylene catalysts 17 p2714 N71-32867

Protein synthesis by catalytic polymerization of aminoacetonitrile and effects of ammonia and various catalysts (NASA-TT-F-15713) 18 p3884 N71-38510

Effects of oxygen on polymerization of ethylene in presence of supported chromium oxide catalysts (AD-723582) 19 p3540 N71-31773

Measurement of surface diffusion in porous hydrocarbon catalyst for three binary gas systems 19 p3851 N71-32518

Chemical analysis of organic trace contaminants in simulated space station atmospheres described from molecular sieve, silicon gel, and catalyst beds (NASA-CR-111956) 20 p5220 N71-33143

Quantitative measurements of liquid hydrogen resistance to mass fraction of absorbed gas residues of catalyst and liquid hydrogen control catalysts (NASA-CR-121964) 22 p3540 N71-33281

Design and tests of monolithic catalyst beds for monoperfluorinated hydrazine reactors (NASA-CR-122644) 23 p5719 N71-36988

Catalytic activity of osmium electrode catalyst and effects of weight and thickness of osmium during reaction of hydrazine (NLL-CTS-746-719) 23 p3721 N71-36524

Electrochromic factor calculation technique for monomolecular catalysts taking into account mass and heat transfer effects at boundary film and in particle interiors (NLL-RTS-6472) 23 p3722 N71-36527

CATALYTIC ACTIVITY

Carbon chemical activity in sodium measured by electrochemical carbon motor (NLL-14508) 06 p0857 N71-15960

Macromolecular chemistry research including polymers, photochemistry, and catalytic activity (AD-714831) 06 p0859 N71-16071

Kinetics of catalytic hydrogenation of methylcyclohexane at 600, 650, and 700 deg F and 3 atm pressure (AD-715936) 08 p1383 N71-18729

Effect of lithium and calcium ions on acetylcholinesterase activity of acrylamide (NASA-TT-F-13476) 09 p1333 N71-20179

Catalytic decomposition of five extinguishants, bromochlorodifluoromethane, in confined area (AD-716757) 10 p1513 N71-21291

Kinetic methods for analyzing organic compounds using catalytic reactions 11 p1495 N71-22862

Mass spectrometry, free radicals, and transient intermediates originating from heated catalytic surfaces (AD-716757) 11 p1497 N71-22864

Prediction of aminoacetonitrile model chain of copper, zinc, nickel, and cobalt and catalytic action of metal chains in hydrazine and glyoxime oxidation (NASA-TT-F-15711) 17 p2716 N71-36212

Kinetic activity of Rh-Pt/SiO2 and Rh-Pt/SiO2 catalysts in benzene hydrogenation reactions (NLL-RTS-6448) 23 p3722 N71-36528

CATHODES

Activation analysis to identify materials for use as cathodes for microelectronics (NASA-CR-108777) 03 p0434 N71-13199

Evaluation tests to demonstrate feasibility of increasing efficiency of linear beam microwave tubes using novel depressed collector (NASA-TM-X-2322) 19 p3867 N71-33465

CATHODEIZATION

Transducer circuit design with single channel coils for input and output connections including hyperbolic beam microchannel cathode transducer (NASA-CASE-ARC-10132-1) 19 p3853 N71-34597

CATHODE RAY TUBES

Computer graphics terminal using storage CRT (NCR-TN-623) 01 p0008 N71-10835

Cathode ray oscilloscopes for analyzing chemical waveforms representing amplitude distribution of time function (NASA-CASE-ONP-01363) 01 p0094 N71-10839

Developing 32 by 30 resolution digital address this display tube for man pack reader (AD-713025) 03 p0337 N71-13486

Information display from access storage of digital computer on cathode ray tube screen (AD-713025) 03 p0340 N71-13486

Development of cathodoluminescent phosphor for cathode ray tubes with fiber optic fiberoptic (AD-713031) 06 p0800 N71-16481

Cathode ray tube display unit connected to on-line computer used in acquiring and analyzing nuclear physics data (LYCEN-7053) 07 p1080 N71-18121

Protonic conductor and pattern recognition devices, bubble chamber physics problems, and cathode ray tube display - conference (NIST-500-400) 09 p1443 N71-20335

Cathode ray tube system for displaying scan and trace in binary wave form (NASA-CASE-XGS-04067) 09 p1337 N71-20571

- Feasibility of utilizing color cathode ray tubes for aircraft crew station displays
[AD-717635] 11 p1673 N71-32174
- Fiber optics in electron optical devices such as cathode ray tubes, image intensifiers, and image converters
[AD-717638] 11 p1798 N71-22470
- Beam penetration cathode ray tube for high performance color display systems
[AD-718423] 12 p1889 N71-23549
- Cathode ray tube display and recorder interface to provide graphical output for small digital computers
[NASA-CR-118011] 12 p1883 N71-23967
- Digital address thin display tube for man-pack radar
[AD-719282] 13 p2042 N71-24401
- Development and characteristics of cathode ray tubes, image iconoscope, image orthicon, and color kineoscopes for television equipment
[AD-720386] 14 p2228 N71-26601
- Indexing mechanism for cathode array substitution in electron beam tube
[NASA-CASE-NPO-10623] 14 p2229 N71-26182
- Pattern threshold recognition device comprising cathode ray tube with image converter input, flood-gun for suppressing background information, and read-gun output of information
[AD-721021] 15 p2367 N71-27747
- Display effectiveness factors for solid state flat panel displays
[AD-721307] 16 p2567 N71-28219
- Development of rectangular display cathode ray tube with low power drain suitable for battery operation
[AD-722287] 16 p2568 N71-28348
- Broadband signal encoding device with circular scanning cathode ray tube
[JPRS-53333] 16 p2562 N71-28595
- Color television system utilizing single gun current sensitive color cathode ray tube
[NASA-CASE-ERC-10090] 16 p2570 N71-28618
- Digital address thin cathode display tube for portable radar
[AD-723413] 19 p3053 N71-31676
- Aircraft indicating instruments with digital cathode ray tube display
[DLR-FB-71-27] 19 p3064 N71-31695
- Digital video display system for display of image, alpha numeric, and other data on cathode ray tubes with economical raster scan and 2, 4, or 8 gray shades
[NASA-CASE-NPO-11342] 20 p3540 N71-33103
- Analysis of feasibility of using shadow-mask tubes with increased luminance for display in color film telecording
[BBC-1971/23] 20 p3276 N71-33748
- Visual performance compared using highly illuminated CRT similar to those encountered in high altitude flight in direct sunlight
[NASA-CR-114361] 21 p3364 N71-34073
- Development and characteristics of display system for space shuttle and cost effectiveness analysis of cathode ray tube system
21 p3317 N71-33662
- CATHODES**
- NT CELL CATHODES
- NT COLD CATHODE TUBES
- NT COLD CATHODES
- NT FREQUENCY MODULATION PHOTOMULTIPLIERS
- NT HOLLOW CATHODES
- NT HOT CATHODES
- NT PHOTOCATHODES
- NT PHOTOMULTIPLIER TUBES
- NT PHOTOTUBES
- NT THERMIONIC CATHODES
- NT TUBE CATHODES
- Operating temperature of ion thruster hollow cathodes and performance tests of convergent supersonic nozzle
01 p0115 N71-10266
- Nonequilibrium plasma boundary layer over cathode in presence of magnetic field
[NASA-CR-111611] 03 p0437 N71-12679
- Investigating cathodoluminescent phosphors for light output response under high electron beam voltage and extreme power input
[AD-712978] 04 p0532 N71-13808
- Measurements of cathode heating in Penning discharge in strongly inhomogeneous magnetic mirror field
[NP-18416] 04 p0591 N71-14386
- Fabrication and properties of press sintered lanthanum, yttrium, and gadolinium hexaboride cathodes
[AD-718423] 04 p0591 N71-14391
- Electric and magnetic field measurements in cathode region of quasi-steady magnetoplasma dynamic arcjet
[NASA-CR-117040] 09 p1448 N71-19984
- Electronic cathodes for use in electron bombardment ion thrusters
[NASA-CASE-XLE-04501] 12 p1886 N71-23190
- Corrosion characteristics and response to cathodic protection of copper alloys in quiescent sea water
[AD-718310] 12 p1938 N71-23793

- Hollow cathode for ion propulsion
[DLR-FB-70-72] 13 p2155 N71-24674
- Design and characteristics of heat activated electric cell with anode made from one or more alkali metals and cathode made from oxidizing material
[NASA-CASE-LEW-11358] 14 p2200 N71-26084
- Cathode environment characteristics in glow discharge
[SC-RE-710122] 19 p3070 N71-32219
- Survey of various cathodes used in Kaufman ion thruster
[NASA-TM-X-67918] 20 p3339 N71-33300
- Mercury vapor fed hollow cathodes for electron bombardment ion thrusters
[NASA-CR-121631] 21 p3502 N71-34943
- Numerical analysis of double cathode electronic tube operation at high frequencies
22 p3539 N71-35350
- Determination of quantitative laws of joint discharge of ions under conditions of electrowinning of pure metals
[NLL-LTI-746-663-19022.401] 22 p3590 N71-35565
- Cathode surface temperature effects in argon and ammonia discharges
[MDC-Q0450] 24 p3924 N71-38000
- CATIONS**
- NT FERRIC ION
- NT METAL IONS
- Relative cation mobilities in silver bromide-potassium bromide melts
[NYO-3608-11] 05 p0631 N71-14691
- Current-voltage characteristics of continuum flash-mounted electrostatic probes in presence of negative ions
[SC-RR-70-413A] 06 p0857 N71-15852
- Rare earth cation excitation at electrodes
[AD-714235] 06 p0810 N71-16422
- Cation cascade controlling electron multiplication within straight channel photomultiplier tubes
10 p1557 N71-20856
- Cation energy distribution within straight channel photomultiplier tubes
10 p1558 N71-21039
- Cation distribution in cinnoylpropane, olivine, and feldspar separated from Apollo 11 and 12 rocks determined with Mossbauer spectroscopy of Fe-57
[NASA-CR-114941] 10 p1635 N71-21451
- Oxidation of refractory metals in presence of alkali cations studied by differential thermal and thermogravimetric analyses
[RE-405] 10 p1584 N71-21605
- Oxidation and reduction half wave potentials, and electron spin resonance of positive and negative ion radicals
18 p2987 N71-31340
- Structural factors in formation of polymer properties and cationic polymerization
[AD-723595] 19 p3119 N71-31747
- Equatorial D region positive ion composition studies by rocket payloads
[NASA-TM-X-65451] 19 p3095 N71-32501
- CATS**
- Otolithic reactions in rabbits and cats after intravenous injection of sodium bicarbonate
08 p1155 N71-19071
- Compensatory capabilities of vestibules, hypothalamus, and central nervous system toward gravitational effects on cats during orthostatic
20 p3321 N71-33458
- CAUSES**
- Electromagnetic corrections to pion(minus) proton reaction to determine causality in rho meson system
[TR-72-003] 23 p3819 N71-37239
- Possible causes of Tunguska explosion and its effects on surrounding region
24 p4009 N71-38390
- CAUSTICS**
- U ALKALIES
- CAVITATION**
- U CAVITATION FLOW
- CAVITATION CORROSION
- Pressure, temperature and gas content effect in vibratory cavitation test
[NEL-438] 01 p0039 N71-10096
- Destructive effects on metal surfaces in diesel engines due to liquid cavitation corrosion caused by opposite oscillating plates
02 p0231 N71-11583
- Destruction effects on metal surfaces in diesel engines due to liquid cavitation corrosion caused by opposite oscillating plates
02 p0231 N71-11584
- Electrochemical method of protecting hydrocarbons against cavitation corrosion
[PB-194587] 02 p0231 N71-11597
- Vibratory cavitation for metal and supralloy etching in distilled water
[NASA-TM-X-52929] 03 p0392 N71-12961
- Hydroabrasive wear of metals under cavitation
[PB-192268] 03 p0393 N71-13051
- Asymmetric cavitation bubble collapse near obstacles
[PB-195427] 08 p1177 N71-18318

- Cavitation damage resistance of iron alloys, steel alloys, and cobalt alloys in liquid sodium and mercury
- review of NASA program
[NASA-TN-X-52956] 08 p1215 N71-18400
- CAVITATION FLOW**
- Radiation induced acoustic cavitation in scintillation liquid
[AD-711286] 01 p0092 N71-10000
- Calculating cavitation characteristics in converging channels of different shape using Borda-Carnot theorem
[NASA-TT-F-13346] 02 p0300 N71-14000
- Cavitation and noncavitation performance of 70 deg helical inducer in liquid hydrogen
[NASA-TN-X-2131] 02 p0203 N71-11800
- Cavitation performance of 84 deg helical inducer in water and hydrogen
[NASA-TN-D-7016] 03 p0339 N71-12300
- Decreased density of small pits after applied stress on early stages of cavitation damage
[KAPL-P-3045] 04 p0334 N71-14002
- Far field holography for determining bubble spectrum in cavity tunnel
[TDCC-53967] 04 p0323 N71-14000
- Observations and analyses of cavitation flow in Venturi systems using water and mercury as working fluids for plastic and stainless steel Venturis
05 p0662 N71-14000
- Cavitation data analysis for liquefied cryogenic hydrogen and nitrogen
[NASA-CR-116804] 06 p0833 N71-18000
- Dissolved argon gas effects on cavitation in liquid sodium
[AD-718351] 06 p0836 N71-18000
- Suction and pressure head and temperature effects on cavitation flow in aircraft fuel pumps
[AR-CR-1128] 07 p1007 N71-17000
- Hydraulic performance and cavitation characteristics of electromagnetic helical induction pump operating with potassium at 1500 F and with lithium at 2200 F
[ORNL-TN-2995] 08 p1205 N71-18000
- Semitoroidal diaphragm cavitating flow control valve
[NASA-CASE-XNP-09704] 08 p1179 N71-18000
- Tabulated values of cavitation b-factor for helium, H2, N2, F2, O2, refrigerant 114, and H2O
[NASA-CR-116821] 08 p1160 N71-18000
- Describing formation and growth of gas bubbles in crosslinked elastomers as function of superatmospheric pressure
08 p1160 N71-18000
- Hydrodynamic parameters effect on hydraulic cavitation erosion intensity
[AD-716053] 09 p1372 N71-19711
- Validation of mathematical model for wall effect correction in cavitation flow
[AD-717393] 11 p1736 N71-32010
- Substantially asymmetric phase change problem solved by least squares integral method using appropriate temperature profile
[AD-718151] 12 p1899 N71-23321
- Linear theory for two dimensional supercavitating flow past flat hydrofoil
[AD-718816] 12 p1899 N71-23308
- Numerical estimates of intensity, scale, duration, and repetition rates of surface attack from individual bubble collapse and cavitation damage relationships to corrosion rate
[UMICR-003371-7-T] 12 p1900 N71-23309
- Porco coefficients and cavity detachment points under various cavitating conditions on two similar convex hydrofoils
[AD-718564] 12 p1900 N71-23308
- Pressure and thermodynamic effects on cavitation performance for helical inducers operated in liquid hydrogen
[NASA-TN-D-6361] 14 p2239 N71-25000
- Effects of waves on ventilation of surface piercing strut models of one-foot chord length with leading edge radius 1.82 percent of chord length
[AD-712173] 16 p2579 N71-28004
- Development and verification of analytical model to predict cavitation compliance in turbopump design
17 p2630 N71-28000
- Asymmetric and thermodynamic effects on cavitation bubble collapse, modes of collapse, and causes of cavitation damage
17 p2734 N71-28000
- One dimensional equations describing noncavitating and cavitating flow in liquid-to-liquid jet pumps programmed for computer use
[NASA-TN-D-6453] 18 p2931 N71-31800
- Effect of wire screen roughness on wall shear stress and cavitation characteristics during fluid flow in hydraulic test tunnel
19 p3077 N71-31800
- Simulation and testing techniques for high speed underwater projectile cavitation and trajectory calculations
[SC-DC-71-713982] 21 p3411 N71-34000
- Numerical analysis of asymmetric collapse of vapor bubble in viscous incompressible liquid using modified Marker and Cell technique
[PB-199560] 22 p3567 N71-35000

Balloon flight measurements of gamma ray spectra of celestial large energy sources
[AD-719864] 13 p2161 N71-25199

Upper atmospheric investigations and motion picture images of celestial bodies
19 p3179 N71-32001

Simple formulae for calculating time variations of instantaneous osculating orbital parameters and celestial body range rate
[NASA-CR-119691] 19 p3181 N71-32405

Mathematical model for thermal behavior and surface temperatures of celestial bodies in solar system
[NASA-CR-121471] 20 p3342 N71-33567

Spectroscopic detection of water on celestial bodies and in interplanetary space
[NASA-TT-F-13935] 23 p3848 N71-37425

CELESTIAL GEODESY
Applications of solid trigonometry of tetrahedrons to celestial geodesy
22 p3677 N71-36219

CELESTIAL MECHANICS
Stellar perturbation problems in earth-moon space
[AD-710729] 01 p1122 N71-10544

Adiabatic perturbation theory in celestial mechanics
[NASA-TM-X-63379] 01 p0976 N71-10589

Hydrodynamic analysis in celestial mechanics
[NASA-CR-111364] 02 p0294 N71-11414

Astrometrical tables of double stars
02 p0295 N71-11929

Nikolajev-Helvan space direction between tracking stations studied at long distances by photographic observations of Echo 2 satellite
[NASA-TT-F-13340] 03 p0452 N71-12284

Calculations of instants of artificial satellites crossing certain celestial circles
[NASA-TT-F-13347] 03 p0452 N71-12423

Stability of periodic orbits in restricted three body problem
[AD-717225] 03 p0454 N71-13180

Tracking and data system support for Pioneer project, Pioneer 9 periscope through June 1969
[NASA-CR-111561] 03 p0459 N71-13296

Analytical solutions to swigby trajectory
[NASA-CR-116197] 06 p0947 N71-16765

History, present state, and future possibilities of extra-atmospheric submillimeter astronomy
[AZT-76-195-BULL.] 07 p1108 N71-17016

Finite difference methods of numerical integration in celestial mechanics
07 p1111 N71-17673

Astrometrical phenomena for year 1973
[AD-715224] 07 p1115 N71-17922

Modified quadratization used with method of particular solutions for determining several periodic orbits of the earth-moon system
[AD-717192] 10 p1647 N71-21801

Mean motions of node and perigee evaluated using improved lunar ephemeris numerical values
[AD-717282] 11 p1624 N71-21905

Almanac of astronomical ephemerides for 1970
12 p1996 N71-23850

Developmental history of adiabatic invariance including contributors to radiation energy transfer and celestial mechanics concepts
[NASA-TM-X-65498] 12 p1968 N71-24056

Modern techniques in celestial mechanics and astrophysics
[AD-718963] 13 p2164 N71-24354

Formulas derived for averaged potential in artificial satellite theory
[NASA-CR-118367] 13 p2102 N71-24632

Research projects in astronomy involving parallel measurements, proper motion and membership studies of open clusters, and development of instrumentation
[AD-719932] 14 p2334 N71-25617

Data collection by Pioneer 7 of interplanetary phenomena
[NASA-CR-118339] 14 p2336 N71-25814

Tables of interplanetary high energy particles, solar phenomena, and plasma taken by Pioneer 7 space probe
[NASA-CR-117961] 14 p2336 N71-25815

Algebraic solutions of linear equations for secular perturbations of planetary ephemerides and longitudes
[NASA-TT-F-13466] 16 p2621 N71-28134

Model for growth of planets in solar nebula and postformation dynamic evolution of planets
16 p2680 N71-28788

Development of approximations for motion of one massive body in trajectory which passes close to one member of double mass system
17 p2845 N71-29824

Development of procedures for midcourse and approach guidance of moon to earth trajectories based on optical angular measurements and onboard calculations
[NASA-TN-D-6343] 18 p2955 N71-30523

Comparison of analytical relative motion theory with numerical solutions for equations of planet motion for two satellites of oblate planet
[NASA-TM-X-65633] 19 p3180 N71-32173

Virtual mass techniques for numerically integrating a-body solution like spacecraft trajectories
[NASA-CR-121749] 21 p3447 N71-34528

Numerical analysis of three body problem and application to stability of captured comets with respect to various planets
22 p3672 N71-36184

Stellar triangulation using balloon-borne light signal equipment and Schmidt telescopes
22 p3677 N71-36215

Algorithm and subroutine for solving Kepler equation for elliptical orbits
[NASA-CR-122933] 23 p3848 N71-37426

CELESTIAL NAVIGATION
ASTRONAVIGATION
Development of star intensity measuring system which minimizes effects of outside interference
[NASA-CASE-XNF-06510] 12 p1922 N71-23797

Automatic pattern recognition system to locate Mars pole star for unmanned surface vehicle navigation
[NASA-CR-119635] 14 p2339 N71-26442

Pressure deformations of spacecraft windows and angular line-of-sight deviations of light rays from three windows causing errors in celestial navigation sightings - graphs
[NASA-CR-114310] 14 p2345 N71-26445

Position declination and motion data for international reference stars
20 p3348 N71-33292

CELESTIAL OBSERVATION
U ASTRONOMY
CELESTIAL REFERENCE SYSTEMS
Spin axis scanning of celestial sphere for attitude control of spin stabilized spacecraft
[NASA-TN-D-5611] 06 p0948 N71-16860

Astrometric observations of fundamental star coordinates and reference faint and bright stars, and photography of minor planets and galaxies to compile catalog of faint stars
[JPRS-53136] 14 p2335 N71-25788

CELESTIAL SPHERE
ALGOL program for determining satellite period variations and celestial equator transit time
22 p3679 N71-36233

CELL ANODES
Heat activated emf cells with aluminum anode
[NASA-CASE-LEW-11359] 16 p2536 N71-28579

CELL CATHODES
Electrodeposited cadmium interaction with cathode substrate
[TT-76-57026] 03 p0332 N71-12368

CELLS
Separation cell with permeable membranes for fluid mixture component separation
[NASA-CASE-XMS-02952] 10 p1587 N71-20742

CELLS (BIOLOGY)
NT CARBOXYHEMOGLOBIN
NT CHROMOSOMES
NT ERYTHROCYTES
NT HEMATOPOIESIS
NT HEMOGLOBIN
NT LEUKOCYTES
NT LYMPHOCYTES
NT MITOCHONDRIA
NT NEURONS

Investigating mechanism by which inorganic and mineral phosphate groups become part of cellular structure
01 p0014 N71-10810

Design and operation of cell-volume analyzer, glass, glass, and etched die effects on bioassays
[NASA-CR-111384] 02 p0225 N71-11537

Functional synchronization of neurosecretory cells of supra-optical nucleus of dehydrated and rehydrated rat
[NASA-TT-F-13419] 03 p0332 N71-12301

Effects of ultraviolet radiation and X rays on mammalian cells
[UCSF-10-F-2-114] 05 p0634 N71-14668

Electron microscopic studies of nerve membrane ultrastructure
08 p1156 N71-19313

High resolution electron microscopes for cell membrane and multi-enzyme complex studies
08 p1157 N71-19314

Dynamic models for cell membrane functions in molecular biology
09 p1331 N71-19881

Electron microscopic analysis of outer sensing cell microstructure
15 p2371 N71-27159

Theoretical model for neuroelectric oscillation modes in arbitrary number of nerve cells arranged in single closed loop
[R-642-BC] 20 p3243 N71-33217

Low temperature cytophysiological adaptations of human and mammalian cells
20 p3220 N71-33455

Radiation effects on cytoplasmic structure and differential activity of genes
[NYO-2356-43] 20 p3225 N71-33934

Control of mitosis in biological cells through isopropyl ion hierarchy of cells involved
[NASA-CASE-LAR-10773-1] 21 p3382 N71-34061

Single cell responses within cat medulla during constant angular accelerations
[AD-724628] 21 p3383 N71-34069

Proceedings of conference on interaction between atmospheric environment and human system at all levels
[AD-720601] 22 p3545 N71-36088

Microspectrophotometer for study of living cell chemistry and organic compound identification
[NASA-CR-122066] 22 p3583 N71-36089

Control of aging processes in human body cells
[NASA-TT-F-13964] 23 p3713 N71-36955

CELLULOSE
Measuring effects of flame retardants on thermal degradation of alpha-cellulose in nitrogen using prediction of Parker-Lipka model
[AD-715411] 06 p1222 N71-28889

Chemical properties of cellulose acetate gels in both dry and gel states
[NRC-TT-14099] 10 p1512 N71-28889

Utilization of xerographic nonfluorescent cellulose acetate, fibrous, and composite materials in structural aircraft refurbishment
18 p3886 N71-36955

Factors affecting combustion of small vertically oriented catalytic cylinders of circular cross section
18 p3896 N71-36955

Beach scale models of improved cellulose acetate membranes for reversed osmosis
[FB-190932] 21 p3444 N71-34089

Characterization, optimization, production, and performance of cellulose acetate bipolymer membranes
[FB-190936] 22 p3681 N71-36955

Yield and stability of pyrolytic carbon fiber products improved by chemical modification of carbon fibers and metal additives
[AD-727141] 24 p3943 N71-36955

CELLULOSE NITRATE
Spectrophotometric sulfate determination in cell reagent propellants and nitrocellulose
[AD-711084] 02 p0287 N71-11889

Thermochemistry of cellulose nitrate binary explosive mixtures with magnesium, boron or aluminum
[JPRS-7770] 07 p1120 N71-27189

Investigating insulating particle deposition in cellulose nitrate and mechanisms explaining alpha particle track formation in plastic detectors
[WP-10411] 08 p1239 N71-18889

Cellulose nitrate for alpha autoradiography of β -radiated nuclear fuels
[LBG-2916] 21 p3462 N71-36955

Etching in cellulose nitrate used as radiation counters for particle trajectories in particle accelerators vacuum chambers, noting temperature effects
23 p3738 N71-36955

CELSIUS TEMPERATURE SCALE
U TEMPERATURE SCALE
CEMENTS
Concrete and asphaltic materials evaluation for use in great under landing mats
[AD-710932] 01 p0810 N71-10889

Slotted diamond compacts using cobalt as binder
[NASA-CR-116419] 07 p1049 N71-17889

Weighted defect densification of asphaltic and cement concrete pavement in airfield pavement condition survey, USAF Willow Grove, Pennsylvania
[AD-713324] 16 p2577 N71-26089

Laboratory tests of polymeric latex modified bitum C-1 cement for repair of damaged runway pavements
[AD-727278] 24 p3943 N71-36955

CESAR SYSTEM
U CENTRAL ELECTRONIC MANAGEMENT SYSTEM
CENTAUR LAUNCH VEHICLE
Centaur launch vehicle for Jupiter and Saturn orbiters missions using solar electric propelled spacecraft
[NASA-CR-111422] 02 p0309 N71-12389

Spacecraft maneuvers of Atlas-Centaur 19 and 20 1969 Mariner Mars missions
[NASA-TM-X-2278] 19 p3185 N71-32089

Numerical analysis of acceleration flight data of Mariner Mars 69, OAO 2, and A7B to determine disturbing forcing function of Centaur engine at main engine cutoff
[NASA-CR-119689] 19 p3185 N71-32089

Control of acceleration flight data of Mariner Mars 69, OAO 2, and A7B showing selected global axis forcing functions and dynamic response of Centaur main engine cutoffs
[NASA-CR-119693] 19 p3185 N71-32089

Mathematical models for prediction of acceleration responses and reaction forces and moments at base of Mariner Mars 71 and Viking spacecraft from Centaur main engine cutoff
[NASA-CR-121673] 20 p3355 N71-30789

CENTAUR VEHICLE
U CENTAUR LAUNCH VEHICLE
CENTER OF GRAVITY
Cockpit and center of gravity acceleration (delta) takeoff of Boeing 707 aircraft
[ARC-CP-1120] 06 p0793 N71-11539

Center of gravity vertical acceleration and wing stream of Boeing 720-B aircraft
[TB-67-1970] 07 p0870 N71-17189

SUBJECT INDEX

Frequency of centers of gravity of cyclones and an-
ticyclones for long range weather forecasting
[JLL-M-20653-1928-AP] 21 p3453 N71-34574

CENTER OF PRESSURE
Control flow effects on pressure center of blunted
nozzle bodies in hypersonic flow
[NPL-ASRO-NOTE-1065] 66 p0033 N71-15708

CENTRIFUGAL TEMPERATURE SCALE
U TEMPERATURE SCALES
CENTRAL ELECTRONIC MANAGEMENT SYSTEM
Data processing facilities for Black Knight rocket
measurements in Great Britain
[NSA-3-C-3616-68] 14 p2237 N71-26258

CENTRAL NERVOUS SYSTEM
NT BRAIN
NT BRAIN STEM
NT CEREBRAL CORTEX
NT HYPOTHALAMUS
NT SPINAL CORD
NT SPINE
Functional state of central nervous system during
development of epilepsy and sarcosis in man and
which subjected to increased pressures of oxygen
and inert gases 02 p0158 N71-11116

Low intensity microwave effects on central nervous
system [AD-72694] 04 p0481 N71-14482

Mechanical molecular model for metabolic energy
transfer from mammalian organs to central nervous
system 09 p1331 N71-19085

Adaptive patterns in central nervous system learning
process [NSA-CR-117006] 11 p1692 N71-23639

Signal transformation by central nervous system for
anatomical pattern construction in postural adjust-
ment 11 p1694 N71-23672

Neurophysiological mechanisms of learning and
memory as biological adaptation to environment 11 p1694 N71-23674

Analysis of cerebral slow potentials underlying
transient electroencephalographic changes in central nervous system
[NASA-CR-121409] 20 p3320 N71-33437

CENTRIFUGAL COMPRESSORS
Cooling water system for compressor of supersonic
wind tunnel [AD-710711] 01 p0038 N71-10679

Overall performance of 6-inch radial-bladed cen-
trifugal compressor with various diffuser vane setting
angles [NASA-TM-X-2107] 03 p0310 N71-12208

Swoptch-bladed centrifugal compressor overall
performance in argon 03 p0310 N71-12209

Flow distribution and performance of supersonic
wind diffusers for centrifugal compressors
[NASA-TT-P-13428] 03 p0384 N71-12541

Technical feasibility and aerodynamic effective-
ness of rotating vaned diffuser [AD-716370] 09 p1315 N71-19558

Theory, calculation, and design of centrifugal
compressor machines [AD-717767] 12 p1925 N71-23297

Aerodynamic performance of swoptch-bladed
centrifugal compressor in argon as function of
applied weight flow [NASA-TM-X-2209] 12 p1851 N71-23639

Visualized flow patterns of airflow in centrifugal
rotor with thin plate blading and with thick airfoil
blades [AD-7234] 23 p3705 N71-36410

Single-back vane impeller tested on low speed cen-
trifugal compressor rig [AD-72620] 24 p3871 N71-37596

CENTRIFUGAL FORCE
Centrifugal barrier penetration factors used in
mass defect kinematics [NSC-19056] 03 p0421 N71-12653

Development of separators using centrifugal force
and used in agriculture and biochemistry 13 p2189 N71-34464

Development of separators using centrifugal force
for agricultural and other uses 13 p2189 N71-34465

Separation and containment of liquid-gas mixtures in
dual cyclone separator [AD-718992] 13 p3063 N71-34476

Theoretical analysis of centrifugally driven,
radially inward, rotating flows and gravitational insta-
bility in bounded rotating fluids 16 p2581 N71-28720

CENTRIFUGAL PUMPS
Performance of coolant-salt centrifugal pumps for
nuclear salt reactor experiment [ORNL-TM-2767] 05 p0723 N71-41717

Calculation of pressure head loss in centrifugal
pumps [NASA-TT-P-13465] 07 p1034 N71-17481

Block and vibration tests of SNAP 8 centrifugal
pump assembly [NASA-TM-X-25990] 10 p1002 N71-21049

Design, fabrication, and testing of improved thian-
ium impeller for high pressure liquid hydrogen pump-
ing [BC-71-26] 17 p2836 N71-26583

Laboratory and in-plant tests for increasing wear re-
sistance of slurry pump parts [AD-72695] 22 p3580 N71-35555

Development of facility for experimental evaluation
of centrifugal pump operating under periodic fluctua-
tions of inlet pressure and flow [NASA-TN-D-6543] 24 p3908 N71-37857

CENTRIFUGES
NT HUMAN CENTRIFUGES
Linear motion of accelerometers on centrifuge
03 p0412 N71-13213

Liquid-gaseous centrifugal separator for weightless-
ness environment [NASA-CASE-XLA-00415] 06 p0865 N71-16079

Evaluation of gyroscopes on precision centrifuge
using counter rotating platforms [AD-715906] 09 p1232 N71-18525

Conference on design and development of gas cen-
trifuges, and Navier Stokes equations in calculating in-
compressible flow in centrifuges 13 p2866 N71-24870

Development of techniques for analyzing size of
fine particles using Coulter counter and Joyce cen-
trifuge [REF-433] 20 p3288 N71-33897

Development of methods for calculating the flow
processes in gas centrifuges [NLL-CA-TRANS-251-19091.9P] 23 p3745 N71-36703

Equations of motion for determining slip flow in one
dimensional gas centrifuges [NLL-CA-TRANS-250-19091.9P] 23 p3745 N71-36705

Calculation of flow processes in gas centrifuges
based on continuum concept and non-steady Navier-
Stokes equations [CONF-700557-4] 24 p3905 N71-37833

CENTRIFUGING
High speed centrifugal determination of mechanical
properties of small iron and other ferromagnetic
crystals and whiskers [AD-711582] 02 p0244 N71-11698

Summary of AFDA sodium technology program in-
cluding impurity monitoring devices and removal
processes such as cold-trapping, hot-trapping, and
centrifuging [AFDA-259] 02 p0265 N71-11783

Computer program for determining solvent solubility
in cesium chloride isopycnic density gradient cen-
trifuging [LA-4416] 06 p0822 N71-16851

Separation methods such as centrifuging, ion
exchanging, electrophoresis, and chromatography ap-
plied to biochemical materials (gels, proteins, amino
acids) 13 p2032 N71-24466

CEPHIED VARIABLES
Shallow envelopes, hydrodynamic calculations for
Cepheid variable star model 12 p1998 N71-24257

Color indices for stellar spectrophotometry of
Cepheid variables and supergiant stars [NASA-TM-X-65543] 14 p2336 N71-25948

Astrophysical investigation of four classical
Cepheid variable stars [INP-18720] 17 p2845 N71-30014

Relationship of Cepheids to surrounding stars and
interstellar material and interpretation of observations
to determine Cepheid evolution 18 p3017 N71-31559

CERAMAL PROTECTIVE COATINGS
U CERMISTS
U PROTECTIVE COATINGS
CERAMALS
U CERMISTS
CERAMIC BONDING
Plasma spraying gas for forming diffusion bonded
metal or ceramic coatings on substrates [NASA-CASE-XLE-61064-2] 05 p0895 N71-15610

Method of forming ceramic to metal seals imper-
vious to gaseous and liquid mercury at high temperature
[NASA-CASE-XNP-61263-2] 14 p2263 N71-26312

Fabrication and burst testing of reaction-bonded sil-
icon carbide tubes [ABCL-3462] 23 p3781 N71-36812

CERAMIC COATINGS
Water tests of ceramic coatings for aluminum alloys
exposed by flame and plasma spraying and etching
[AD-712365] 02 p0247 N71-11663

Ceramic coatings for casting photoconductor and photo-
conductor alloys [LA-4495] 06 p0882 N71-16807

Spraying process for producing thin titanium diox-
ide ceramic film capacitors 12 p1091 N71-24026

Unfired ceramic insulation for protection from radi-
ation heating environments 13 p2185 N71-24858

Ceramic structural burn and performance test of
abraded, diffusion welded thianium pump impellers
for liquid hydrogen pump applications [NASA-CR-100124] 14 p2352 N71-26428

CERAMIC NUCLEAR FUELS

Cermet for nuclear fuel constructed by pressing
metal coated ceramic particles in die at temperature to
cause bonding of metal coatings, and tested for ther-
mal stability [NASA-CASE-XLE-10219-1] 16 p3418 N71-28729

CERAMIC NUCLEAR FUELS
Electron microscope analysis of irradiated ceramic
nuclear fuel and cladding materials [EUR-4504-D] 04 p0548 N71-13645

Heterogeneous coated fuel element, vitreous ceramic
nuclear fuels, and radiation effects on electrical resis-
tivity, dimensional changes, and thermal diffusivity
[IPA-MN-11] 04 p0550 N71-13795

Synthesis and cladding of nuclear ceramic fuels,
UO₂ and UC [IPA-MN-10] 04 p0550 N71-13796

Ceramic fuel fabrication and irradiation behavior
for heavy water reactors 04 p0552 N71-13986

Fuel, core, and cladding developments and safety
experiments for fast ceramic reactors [ORAF-10028-33] 04 p0552 N71-13988

Investigating performance of stainless steel clad and
plutonium-uranium oxide fuel elements in fast
breeder reactors [ORAF-10028-34] 04 p0557 N71-14154

Research and development on fuel cycle technology
for Arg. through Jan. 1970 [ANL-7735] 07 p1063 N71-17339

Mechanical properties of uranium and plutonium
based ceramic fuels [ORNL-TN-2380] 07 p1066 N71-17081

Addition improving properties and facilitating
manufacture of U-Pu-C-M fuel - composites [CRA-CONF-1632] 08 p1255 N71-18210

Uranium oxides and ceramic nuclear fuels
[AD-715459] 08 p1259 N71-18770

Quantitative analysis of uranium-based ceramic
materials by X ray diffraction [EUR-4516] 09 p1406 N71-30170

Solubility and leach rates of isotopic californium
ceramic nuclear fuel element [ORNL-4639] 10 p1601 N71-20644

Fabrication and assembling of laminated and ceram-
ic fuel elements [NLL-WINDSCALE-453-70091.9P] 12 p1964 N71-24102

Apparatus for obtaining data on compressive creep
of ceramic nuclear fuels during irradiation 13 p2112 N71-24513

Technology of production and testing ceramic
nuclear fuels [WHAN-SA-70] 13 p2130 N71-25320

Sodium cooled reactors fast ceramic reactor
development program review [ORAF-10028-35] 13 p2132 N71-25478

Apparatus for in-situ compressive creep studies of
LMFBR ceramic fuels during irradiation [BME-1804] 14 p2292 N71-25713

Test mechanism for gas release from ceramic
nuclear fuels based on literature review [SRAEP-P-73] 15 p2443 N71-26854

Cyclotron injection of helium into ceramic nuclear
fuels for studying fission gas evolution [AI-ABC-12304] 15 p2446 N71-27165

Creep rate of plutonium-based fuel ceramics at high
temperature, and effects of composition, porosity,
and neutron irradiations [CRA-CONF-1670] 15 p2446 N71-27167

Cermet for nuclear fuel constructed by pressing
metal coated ceramic particles in die at temperature to
cause bonding of metal coatings, and tested for ther-
mal stability [NASA-CASE-XLE-10219-1] 16 p3418 N71-28729

Uranium nitride and uranium-plutonium nitride fuel
compatibility with austenitic stainless steel cladings
of liquid metal cooled reactor [BML-1805] 16 p3634 N71-29743

Space power unit fuel reactor design with ceramic
UH fuel elements, lithium coolant, and thianium alloy
[NASA-TM-X-67839] 16 p3636 N71-29805

Thermal conductivity of ceramic nuclear fuels as
function of porosity [NLL-WINDSCALE-TRANS-449-7001.1] 16 p3692 N71-29807

Induction plasma torch reactor for converting uran-
ium dioxide/graphite powder to uranium carbide
spheres [ANL-7671] 17 p2811 N71-29301

Theoretical properties of ceramic fuel rods of
uranium and plutonium oxide in pellet and vitreous-
bonded form for CVRANUM reactors [RT/BNQ-70/15] 17 p2808 N71-29323

Solid processes for preparation of ceramic fuels in
PNC, Japan [NP-14630] 18 p2854 N71-30423

Development of fast reactors using ceramic fuels
particularly mixed plutonium-uranium oxides [ORAF-10028-37] 19 p3155 N71-31800

Parameters influencing solid state densification for
obtaining ceramic nuclear fuels from ceramic grade
powders [RT/BNQ/70/11] 19 p3130 N71-32380

- Venting device for sodium cooled fast reactor with ceramic fuel elements [KT/ING-70]29 21 p3457 N71-34605
- Uranium and plutonium oxide properties and fabrication methods for ceramic oxide fuels applied to fast breeder reactors [GEAF-13583] 21 p3469 N71-34634
- Thorium ceramics data manual including information on thorium carbides, uranium carbides, and plutonium carbides with application to nuclear fuels [ORNL-4308(VOL-3)] 22 p3634 N71-35823
- Replica preparation for electron microscopy of irradiated uranium-plutonium dioxide nuclear fuel [ANL-7790] 24 p3962 N71-38261
- ### CERAMICS
- #### NT CERAMIC NUCLEAR FUELS
- Fractographic analyses of densified ceramics and glass-ceramics ballistically impacted by caliber .30 M2 projectiles [AD-712004] 02 p0247 N71-11656
- Microstructural and fractographic studies of boron carbide ceramics subjected to ballistic impact and static flexural loading [AD-712907] 02 p0247 N71-11664
- Low gravity manufacturing of metals and ceramics in space laboratories 02 p0234 N71-11706
- Nucleation phenomena in glass-ceramic materials [AD-712094] 03 p0441 N71-12804
- High voltage electron microscopy for ceramic substructure and biological radiation damage studies [UCRL-19628] 03 p0381 N71-13216
- Comparator for measuring micro-step motion using piezoelectric ceramics [RRE-TN-751] 03 p0382 N71-13295
- Balanced oscillator method for measuring thermal conductivity of ceramic fuels and gas conductors [KFK-1125] 04 p0459 N71-13752
- Thermal diffusivities of dense polycrystalline ceramic materials [PB-192253] 04 p0536 N71-14372
- Roll forming ceramic strip from oxide powders [BM-R1-7463] 05 p0092 N71-14930
- Improved efficiency of drilling ceramics and glass using liquid environments [AD-713593] 05 p0710 N71-15361
- Shock wave structures in barium titanate ceramics [AD-714673] 06 p0876 N71-16020
- Assessment of surface and subsurface damage in ceramics caused by semi-finish grinding machines [AD-714491] 06 p0879 N71-16395
- Bibliography for technical literature of metals and ceramics division for 1969 at Oak Ridge National Laboratory [ORNL-4270-VOL-2] 07 p1060 N71-17191
- Chemical, ceramic, and metallurgical aspects of nuclear fuels - conference [INR-1194] 08 p1236 N71-18216
- Microstructural characterization of proprietary ceramic armor [AD-715352] 08 p1221 N71-18541
- Research in ceramic materials including mechanical properties, crystallography, and deformation [NASA-CR-116809] 08 p1222 N71-18654
- Open-circuit sensitivities of axially polarized ferroelectric ceramic cylinders 08 p1222 N71-18780
- Aging characteristics of barium titanate and lead zirconate-titanate ferroelectric ceramics [AD-715624] 08 p1297 N71-18809
- Measurement of strains induced at ceramic bicrystal grain boundaries [AD-715447] 08 p1280 N71-18862
- Deformation processes in forging polycrystalline oxide ceramics 08 p1224 N71-19225
- Density control in mixed U-Pu oxide fuel pellets by ceramic processing techniques [WHAN-FR-7] 09 p1417 N71-19478
- Surface finishing effects on ceramic mechanical, electrical, optical, and magnetic properties [AD-716806] 10 p1565 N71-21221
- Mechanical property determination of ceramic covered uranium and plutonium, using modules of elasticity [CSA-COMP-1620] 10 p1590 N71-21501
- Electrooptic effects in ferroelectric ceramics with emphasis on electrical and optical properties of Ba, Sr, and La modified lead zirconate titanate [SC-R-70-4353] 10 p1590 N71-21532
- Mixing, firing, and aging methods for titanate and oxide ceramic materials with high dielectric constants, low loss, and thermal stability [AD-717086] 11 p1783 N71-22353
- Characteristics of foamed-in-place ceramic refractory insulating material and method of fabrication [NASA-CASE-XGS-02435] 11 p1785 N71-22998
- Process for fiberizing ceramic materials with high fusion temperatures and tensile strength [NASA-CASE-XNP-00397] 11 p1786 N71-23008
- Effects of glazing and quenching on physical and mechanical properties of ceramic materials [AD-717983] 12 p1941 N71-23282
- High drive properties of disk specimens of whisker reinforced, composite ceramic, piezoelectric transducer material [AD-718387] 12 p1946 N71-24013
- Determination of mechanical properties of ceramic materials used in piezoelectric transducers [AD-717964] 12 p1946 N71-24094
- Improvement in heat exchanger efficiency through use of pyroceramic inserts, or other dielectric materials in place of metallic surfaces [AD-718287] 12 p2015 N71-24349
- Nondestructive testing of composites and ceramics to determine surface defects by infrared and induction heating methods [WHAN-SA-42] 13 p2101 N71-25215
- Compressive surface glazing for improved strengths of ceramic materials 13 p2101 N71-25315
- Dynamic piezoelectric shell theory for polarized ferroelectric ceramic orthotropic material 13 p2155 N71-25364
- Research and development in ceramic engineering, chemical engineering, chemistry, mathematics and computer science, metallurgy, physics, and reactor materials and technology [IS-2300] 13 p2193 N71-25396
- Sintering of reactive MgAl₂O₄ spinel ceramic, devitrification, and improved cordierite compositions [AD-720383] 14 p2278 N71-26015
- Development of model for initiation of branching fractures in stressed glass and glass ceramics [SC-RR-70-766] 15 p2428 N71-26949
- Properties and selective applications of ceramic materials 15 p2429 N71-27041
- Ceramic optical voltage sensors operating from remote location by transmitting light through flexible light guides [SC-RR-70-593] 15 p2408 N71-27111
- Production, annealing, detection of crystal lattice point defects caused by neutron irradiation of ceramic materials [KFK-1215] 15 p2469 N71-27370
- Properties of molten ceramics at 3000 C [BNWL-SA-3579] 15 p2431 N71-27426
- Factors influencing stress-strain behavior of single crystals in ceramic systems [UCRL-20383] 15 p2433 N71-27977
- Effects of sintering and grain growth reactions on distribution of niobium additives in barium titanate ceramics 16 p2619 N71-28998
- Method for coating through-holes in ceramic substrates used in fabricating miniaturized electronic circuits [NASA-CASE-XMF-03999] 16 p2604 N71-29032
- Open circuit sensitivity of radially polarized ferroelectric ceramic hollow spheres treating ceramic as anisotropic material [AD-723401] 17 p2726 N71-29732
- Test of this wall channel with ceramic lining in liquid aluminum induction pump [AD-72310] 17 p2737 N71-30246
- Eutectic microstructures of high temperature ceramic oxides [AD-723818] 18 p2942 N71-31592
- Screenable dielectric constant ceramic glass paste for thin film capacitors in microcircuits [AD-723404] 19 p3064 N71-31714
- Application of dielectric and anelastic loss techniques for determining defects in ceramic materials [AD-723834] 19 p3120 N71-32007
- Design, fabrication and tests of alumina ceramic envelope for cryogenic electrically-suspended cryocooler [NASA-CR-119885] 19 p3102 N71-32356
- Flexural strength of alumina ceramics increased by reduction of crystal anisotropy [AD-724315] 20 p3287 N71-33085
- Design and operation of extrusion can for use in extruding ceramics under heat and pressure [NASA-CASE-NPO-10812] 21 p3433 N71-34428
- Occurrence of explosion-like processes during high powered pulsed electron bombardment of diamonds, glass, and ceramics [SC-T-71-3017] 21 p3434 N71-34435
- Interdisciplinary research on properties of ceramic materials with emphasis on refractory surface insulation [NASA-CR-121090] 22 p3596 N71-35618
- Chemical, X ray diffraction, electron microscopic, and structural analysis of silicon carbide ceramics for open cycle magnetohydrodynamic generators 22 p3596 N71-35623
- Analysis of rate of evaporation and erosion of silicon carbide ceramics in air at high temperatures 22 p3598 N71-35634
- Effects of temperature on electrical resistivity of silicon, carbon, and metal compounds 22 p3598 N71-35625
- Structure-property relationships in liquid ceramics heated to temperatures as high as 3000 C [AD-726401] 22 p3603 N71-35658
- Application of unidirectional solidification technique for reinforcement of metallic or ceramic materials [NLL-LT-746-703] 23 p3774 N71-36909
- Development of techniques for measuring electrical resistivity of ceramic materials at high temperatures from 1,000 to 1,700 degrees centigrade [NASA-TT-F-13944] 23 p3776 N71-36914
- Stoichiometric and compositional effects on sintering and magnetic characteristics of high purity, fused, dried, barium ferrite ceramics 23 p3780 N71-36917
- Mechanical properties of this liquid films analyzed by study of anomalies observed in flow of films through porous ceramic and carbon filters [NASA-TT-F-139991] 24 p3983 N71-37888
- Application of ground ruby holographic techniques to tests of ceramic materials [AD-727160] 24 p3931 N71-38009
- Determining threshold damage in slip cast fused silica by discrete impact in ballistics range [AD-728050] 24 p3945 N71-38010
- Reinforcement of ceramic materials with refractory metal fibers [NLL-LB/G-3074-0901-9F1] 24 p3946 N71-38018
- ### CEREBRAL CORTEX
- Investigating state of brain and muscles during high altitude acclimation and effects of physical training on heat tolerance of man 07 p0980 N71-17086
- Investigating changes in brain cortex and gastrocnemius muscle functions during adaptation to high mountainous altitudes 07 p0980 N71-17089
- Correlations between diurnal indices of cerebral and systemic circulation 08 p1155 N71-18009
- Neural mechanism of human cerebral cortex for speech functions 11 p1685 N71-28803
- Computerized simulation of cerebral neuron pattern recognition model [AD-722651] 18 p2875 N71-30811
- Analysis of cerebral slow potentials modeling human attentive processes in central nervous system [NASA-CR-121409] 20 p3220 N71-33007
- ### CERENKOV COUNTERS
- Energy spectra of multi-charged nuclei measured by Cerenkov counters onboard Cosmos 225 satellite [NASA-TT-F-135111] 09 p1462 N71-30812
- Gamma ray scintillation, Cerenkov, and photodiode detector telescopes 13 p2081 N71-30779
- Narrowband pulses of photomultiplier in differential-threshold Cerenkov counter [NAL-TR-1] 13 p2082 N71-31019
- High resolution, differential, Cerenkov gas counter using helium [NAL-TR-3] 13 p2083 N71-31018
- Electron and positron scattering from negative pion-nucleon interactions at 275 MeV using scintillation and Cerenkov counters, absorption spectrometers, and spark chambers [JINR-P1-5598] 14 p2317 N71-30728
- Positive to negative pion ratios as functions of incident photon energy using Cerenkov counter, spark chamber, and magnetic spectrometry of the photoproduction 15 p2476 N71-31020
- High resolution gas Cerenkov counter operational characteristics [NAL-TR-2] 15 p2492 N71-31019
- Diode switching circuit for pulse amplitude gain compensation in Cerenkov and scintillation counters at fast shaper triggering moments [IPVE-SRP-69-44] 16 p2571 N71-30777
- Measurement of charged particle spectra in interplanetary space by Cerenkov counter on Pioneer 8 spacecraft 20 p3341 N71-31018
- Heavy and ultrahigh nuclei observations of cosmic rays using ionization chamber-Cerenkov counter system [NASA-CR-123197] 24 p4002 N71-38014
- Optical and spectral characteristics of Cerenkov and scintillation counters 24 p4012 N71-38019
- ### CERENKOV EFFECT
- #### U CERENKOV RADIATION
- #### CERENKOV RADIATION
- Cerenkov light detection system at Monte Chacabuco, Bolivia, and chemical composition of primary cosmic rays 10 p1641 N71-31511
- Focused Cerenkov radiation detection system for measuring beam energy and energy spread of cosmic 600-MeV proton beam [NASA-TN-D-6194] 11 p1886 N71-32006
- Design and construction of electron-pumped Cerenkov laser [AD-718409] 12 p1933 N71-32008
- Two day laser action and tunable Cerenkov laser for wavelengths shorter than 3000 A [AD-718408] 12 p1934 N71-32009

- Low-frequency charge waves to explain Compton and Smith-Purcell radiation 24 p3902 N71-37811
- CEMENT ASTEROID**
Solar electric propulsion performance and trajectory data for indirect solar probes, extra-solar missions, and rendezvous with Ceres, D-Arrest, and others [NASA-CR-118312] 13 p2167 N71-25043
- CERAM**
NT CESIUM ISOTOPES
Low temperature specific heat of cesium and cesium-uranium alloys 05 p0701 N71-15065
Curium/III-coated cerium/III luminescence in cerium-orthophosphate 07 p1082 N71-18144
Annealing preparation and superconducting behavior of CeRu₂ and its Gd, Mn, Co, and Ni containing mixed phases (LA-TN-71-26) 20 p3334 N71-33621
- CERAM COMPOUNDS**
Electrical conductivity of single crystal cerium dioxide as a function of temperature and oxygen pressure (COO-1441-11) 06 p0932 N71-15893
Positron of ammonium nitrate with cerium compounds for solid propellants 07 p1096 N71-17230
Molten 4 impurities and magnetic field effect on surface boundary resistance between powdered cerium magnesium nitrate and liquid helium 3 at very low temperatures (UCSD-34-P-143-35) 13 p2127 N71-23463
- CERAM ISOTOPES**
Excited states of Ce-138 and Pr-138 determined from beta decay of Pr-138, Pr-138m, and Nd-138 [NASA-TN-D-7040] 06 p0912 N71-15837
Gamma-gamma coincidences in Ce-140 [JNEA-275] 13 p2133 N71-25223
Gamma ray spectrometric comparisons of cerium isotopes to neutron activation cross section values and S values of Be-74, 78, 80, Br-81, I-127, Te-130, Ce-140, 142, and Ba-138 [JNEA-274] 13 p2140 N71-25505
Nuclear structure of Ce-140, La-139, and Ba-138 obtained from proton transfer reactions of He-3/d 17 p2784 N71-29636
Nuclear structure of isotones Ce-140, Pr-141, and Nd-142 determined by α , He-3/d and He-3/d reactions 18 p2983 N71-31126
- CERMET**
Plutonium 238 space electric power fuel development program emphasizing solid solution cermets (LA-4776) 03 p0414 N71-12690
Interaction of cerium sesquioxide with refractory metal matrices in pressed and sintered cermet compositions (AF-M3-70-10) 05 p0710 N71-15271
Freeze coating of metal ceramic and refractory composites into plastic slips [NASA-CASE-XLE-00106] 06 p0864 N71-16076
Machine tool wear caused by cutting of porous cermet materials (AD-718408) 12 p1944 N71-23766
Mathematical models for determining electrical conductance in cermet films 14 p2234 N71-26435
Balors evaporation unit for thermal treatment of C80 cermet thin films (US-587) 14 p2281 N71-26590
Empirical relationship for high density, distended fluoropolymer cermet (SC-DE-70-908) 16 p2632 N71-28641
Cermet for nuclear fuel constructed by pressing metal coated ceramic particles in die at temperature to cause bonding of metal coatings, and tested for thermal stability [NASA-CASE-LEW-10219-1] 16 p2618 N71-28729
High temperature compatibility tests on platinum and cerium combinations with refractory metals, and aluminum/molybdenum cermets (MDC-G-2033) 17 p2760 N71-29202
Materials tests of cermet materials based on refractory carbides to determine melting point, oxidation resistance, emissivity, and weldability 22 p3600 N71-35641
- CERTIFICATION**
Personnel of conference to train personnel in conducting aircraft noise certification tests (NRC-TR-300-SUPPL-1) 14 p2198 N71-26303
Guide to private and commercial multigrade aircraft pilot certification (FAA-AC-61-4C) 23 p3708 N71-36438
- CERUM**
NT CESIUM VAPOR
NT CESIUM 133
NT CESIUM 134
NT CESIUM 137
NT CESIUM 144
Development of cesium seeding techniques, large MED magnets, plasma diagnostic techniques, and thermionic electrodes compatible with shock tube MED generators (AD-711511) 01 p0107 N71-10992

- Deposition of cesium and barium in sodium stainless steel system to predict distribution of fission products in LMFBR system [AI-ABC-12952] 02 p0265 N71-11782
Determining high temperature saturated liquid and vapor phase densities and critical density and temperature of cesium (CU-2660-56) 03 p0389 N71-12562
Absolute total cross sections for low energy electron scattering by rubidium, cesium, and potassium 04 p0594 N71-14452
Vacuum encapsulation of cesium for out-of-core thermionic diodes [NASA-TM-X-2152] 06 p0896 N71-15815
Direct electromagnetic generation and detection of acoustic waves reported for cesium and mercury near room temperature (NYO-2150-45) 11 p1799 N71-22536
Cesium adsorption measurements in thermionic energy conversion (AD-724007) 14 p2280 N71-25956
Heated tungsten filter for removing oxygen impurities from cesium [NASA-CASE-XNP-04263-2] 14 p2276 N71-26773
Cesium ionization by simultaneous absorption of three ruby laser quanta 15 p2418 N71-27189
Sorption of cesium by graphite and charcoal reducing volatility of cesium and rendering it fully stable in sodium at 500 C and in air at same temperature [AERE-B-6481] 15 p2492 N71-27932
Forbidden transition absorption spectra in cesium and rubidium atoms due to rare gas presence 16 p2648 N71-28439
Photoionization cross sections for excited cesium states in triple crossed beam experiment, temperature tuning of pulsed GaAs laser, and optical pumping of Cs by pulsed GaAs laser (AD-721370) 16 p2606 N71-28459
Sorption properties of cesium by tungsten and graphite between 600 and 800 C and vapor pressure from .01 to 30 mm Hg for use in thermionic converter reservoirs (EUR-4549) 19 p3121 N71-32584
Nuclear magnetic resonance in cesium-graphite inclusion compounds with optically relaxation times and line shapes for C-13 and Cs-133 species 21 p3445 N71-34515
Collisional ionization between cesium atoms and NO₂, N₂O, and O₂ molecules (ORNL-TM-2620) 21 p3475 N71-34743
- CERUM COMPOUNDS**
NT CESIUM FLUORIDES
NT CESIUM HALIDES
NT CESIUM IODIDES
NT CESIUM OXIDES
Production of cesium telluride for measurement of ultraviolet radiation intensity (AD-711614) 03 p0375 N71-12658
- CERUM DIODES**
Research and development in thermionic conversion [AD-714253] 06 p0798 N71-16710
Ionization of cesium diode discharge by laser heating [AD-715883] 08 p1274 N71-18817
Energy transfer involving thallium phenomena in thallium electrode, cesium gas filled diode 06 p1266 N71-19203
Thermionic cesium diode converter with cavity emitters [NASA-CASE-MPO-10412] 16 p2570 N71-28421
Numerical analysis of relationship between current, voltage, emitter temperature, and collector temperature of cesiated thermionic converter [NASA-TM-X-2398] 21 p3380 N71-34048
Computer analysis of performance of chemically vapor-deposited tungsten, niobium thermionic converter based on temperatures of emitter, collector and cesium reservoir [NASA-TM-X-2373] 21 p3380 N71-34049
- CERUM ENGINES**
Cesium bombardment ion engine system design, modification, and testing [NASA-CR-111381] 02 p0288 N71-11464
Cesium ion microthrusters with beam deflection and optimal control for synchronous satellite attitude control 03 p0438 N71-13251
Fabrication and testing of bonded metal-ceramic, glass-coated metal, and glass-coated ceramic bonded to metal composite electrodes for cesium bombardment ion thrusters [NASA-CR-119695] 19 p3175 N71-32516
Microporous extended range thrust test stand design and cesium engine calibrating standards [NASA-TN-D-7029] 20 p3339 N71-33396
- CERUM FLUORIDES**
Electron emission from fluoride ion in shock heated mixtures of cesium fluoride and argon (AD-715994) 09 p1442 N71-28306
- CERUM HALIDES**
NT CESIUM FLUORIDES
NT CESIUM IODIDES

- Computer program for determining solvent solubility in cesium chloride isopycnic density gradient centrifugation (LA-4416) 06 p0822 N71-16831
Equation of state based on ultrasonic bulk modulus measurements for cesium halides 14 p2327 N71-26497
- CERUM IODIDES**
HRAO CsI crystal activation for measurement of gaseous gamma and cosmic particle energy spectra (RM-507) 16 p2674 N71-28167
Light yield measurements of CsI(Tl) crystal bombarded with protons, deuterons, and tritons, dependent linearly on energy (JINR-P1-3482) 21 p3468 N71-34609
- CERUM ION**
Research and developments on cesium ion thrusters including measuring, testing, and calculation techniques [ONERA-TP-974] 20 p3340 N71-33800
Electric field shift parameters of prosoodymium and cesium ions directly substituted for barium magnesium double nitrate 20 p3327 N71-33948
Deflectable dual beam, linear strip cesium contact, ion thruster system design and performance testing [NASA-CR-72509] 23 p3839 N71-37376
- CERUM ISOTOPES**
NT CESIUM 133
NT CESIUM 134
NT CESIUM 137
NT CESIUM 144
CERUM OXIDES
Optical and photoelectric properties of thin cesium oxide films on glass, silver, and palladium 03 p0396 N71-13391
Defect structure of stoichiometric cesium oxide (COO-1441-12) 06 p0932 N71-16004
Thermochemistry of cesium-oxygen solutions and their gaseous atmospheres estimated from phase diagram [NASA-TM-X-2157] 06 p0811 N71-16546
- CERUM PLASMA**
Design and operation of freeze, melt valve used in vacuum crucible for melting cesium for thermionic diodes [NASA-TM-X-2126] 01 p0086 N71-10455
Heat conduction and ionization properties of thermionic reactors for spacecraft and reaction potential of plutonium fuel (K-12) 04 p0539 N71-14209
Helicon resonances in low pressure cesium plasma discharge in external cross-magnetic field (REPT-4458) 05 p0752 N71-14509
Multiple-grid probe separating currents flowing from plasma to collector into their electron and ion components (IPP-2/83) 08 p1271 N71-18266
Transport analysis of thermionic diode plasmas (AD-715928) 06 p1273 N71-18571
Ion sampling measurements in high pressure cesium discharges (AD-720713) 15 p2504 N71-27927
- CERUM VAPOR**
Thermochemistry of cesium-oxygen solutions and their gaseous atmospheres estimated from phase diagram [NASA-TM-X-2157] 06 p0811 N71-16546
Design technology for ion cesium microthrusters [ONERA-TP-947] 08 p1284 N71-18732
Thermodynamic diffusion of cesium vapors in helium (TT-70-57072) 08 p1160 N71-19097
- CERUM 133**
Nuclear energy levels of Cs-133 and Pr-141 from gamma ray measurements after neutron isotopic scattering 10 p1620 N71-21738
- CERUM 134**
First excited state lifetimes in thallium 169, thallium 171, and cesium 134 (IS-T-330) 06 p0917 N71-16196
- CERUM 137**
Relationship of cesium-137 and iron-59 elimination rates to metabolic rates of small rodents (ORNL-4568) 03 p0523 N71-12311
Deformation in rectangular Cs-137 sources (ORNL-TM-3069) 03 p0414 N71-12746
Gamma radiation attenuation gaps for measuring alkali metal vapor or liquid density (ORO-3604-6) 09 p1397 N71-19446
Measurements of Cs-137 radioactivity and total beta activity from nuclear explosion fallout and aerosols in air suspension over continents, mountains, and oceans (CEA-R-3977) 17 p2738 N71-29236
Error analysis of thickness measuring devices with Am-241 and Cs-137 sources including errors due to chemical composition of steel, temperature distribution, and statistical variation (PB-193469) 19 p3102 N71-32420
Does uniformity ratios and minimum dose data in cobalt 60 and cesium 137 rectangular source irradiators (BNL-50145-REV) 20 p3328 N71-33983

- Beta activity in samples of atmosphere, surface waters, and drinking water supplies and content of Cs-137 and Sr-90 in food samples - Italy
[PROT-SAN-13169] 21 p3473 N71-34729
- CESTUM 144**
Statistical analysis of cesium 144 half life determinations
[AERB-R-6529] 15 p2471 N71-27411
- CESSNA MILITARY AIRCRAFT**
U MILITARY AIRCRAFT
CEYLON
Physical properties and absolute age determination for some rocks of India and Ceylon
[NASA-TT-F-13416] 05 p0670 N71-14839
Analysis of bathymetric and geophysical survey of ocean bottom off Ceylon
18 p2912 N71-30989
- CF-104 AIRCRAFT**
U F-104 AIRCRAFT
CH-46 HELICOPTER
Flight control software package for digital flight control and landing system of CH-46C helicopter
[NASA-CR-110903] 01 p0027 N71-10283
Guidance software package for digital flight control and landing system of CH-46C helicopter
[NASA-CR-111025] 01 p0028 N71-10284
Systems performance/design requirements specifications for CH-46C helicopter digital flight control and landing system
[NASA-CR-110889] 01 p0003 N71-10294
Systems analysis of flight control and guidance of CH-46C helicopter
[NASA-CR-111024] 01 p0003 N71-10297
Using automatic control theory with simple pilot model for synthesizing helicopter landing approach flight director control laws
[NASA-TM-X-66492] 03 p0312 N71-12224
- CH-54 HELICOPTER**
Flight simulation for evaluating proposed stabilization system to ensure helicopter hovering precision during cargo loading
[AD-710948] 01 p0003 N71-10564
Design, fabrication and tests of boron/epoxy reinforced stringers for CH-54B tail cone
[NASA-CR-111929] 21 p3374 N71-34013
Structural analysis of tail cone of CH-54B helicopter reinforced with boron/epoxy stringers
[NASA-CR-111930] 21 p3375 N71-34014
- CH-113 HELICOPTER**
U CH-46 HELICOPTER
CHAFF
Doppler radar measurements of flow generated by wing tip vortices using reflective chaff dispensed into vortices
[NASA-CR-111877] 10 p1491 N71-20630
- CHAIR**
U SEATS
CHALCOGENIDES
NT ALUMINUM OXIDES
NT BARIUM OXIDES
NT BERYLLIUM OXIDES
NT BISMUTH SULFIDES
NT CADMIUM SELENIDES
NT CADMIUM SULFIDES
NT CADMIUM TELLURIDES
NT CALCIUM OXIDES
NT CALCIUM SULFIDES
NT CARBON DIOXIDE
NT CARBON DISULFIDE
NT CARBON MONOXIDE
NT CESIUM OXIDES
NT CHROMITES
NT CHROMIUM OXIDES
NT COBALT OXIDES
NT COPPER OXIDES
NT COPPER SULFIDES
NT DIOXIDES
NT DISULFIDES
NT GALLIUM SELENIDES
NT GERMANIUM OXIDES
NT HAFNIUM OXIDES
NT HEAVY WATER
NT HEMATITE
NT HYDROGEN PEROXIDE
NT HYDROGEN SULFIDE
NT INORGANIC PEROXIDES
NT IRON OXIDES
NT LANTHANUM OXIDES
NT LEAD OXIDES
NT LEAD SELENIDES
NT LEAD SULFIDES
NT LEAD TELLURIDES
NT LITHIUM OXIDES
NT MAGNESIUM OXIDES
NT MAGNETITE
NT MANGANESE OXIDES
NT MERCURY OXIDES
NT MERCURY TELLURIDES
NT METAL OXIDES
NT MOLYBDENUM DISULFIDES
NT MOLYBDENUM OXIDES
NT NICKEL OXIDES
NT NIOBIUM OXIDES
NT NITRIC OXIDE
NT NITROGEN DIOXIDE
- NT NITROGEN OXIDES
NT NITROGEN TETROXIDE
NT NITROUS OXIDES
NT OXIDES
NT PEROXIDES
NT PHOSPHORUS OXIDES
NT PLUTONIUM OXIDES
NT POLYSULFIDES
NT POTASSIUM OXIDES
NT POTASSIUM PEROXIDES
NT PYRITES
NT PYROXENES
NT QUARTZ
NT RUTILE
NT SAPPHIRE
NT SCHEELITE
NT SELENIDES
NT SILICON DIOXIDE
NT SILICON OXIDES
NT SILVER OXIDES
NT SULFIDES
NT SULFUR OXIDES
NT TANTALUM OXIDES
NT TELLURIDES
NT THORIUM OXIDES
NT TIN OXIDES
NT TIN TELLURIDES
NT TITANIUM OXIDES
NT TUNGSTEN OXIDES
NT URANIUM OXIDES
NT VANADIUM OXIDES
NT YTTRIUM OXIDES
NT ZINC OXIDES
NT ZINC SELENIDES
NT ZINC SULFIDES
NT ZINC TELLURIDES
NT ZINCBLENDE
NT ZIRCONIUM OXIDES
- Temperature and pressure dependence of optical and electrical gap in chalcogenide glasses
[AD-713288] 05 p0757 N71-14639
Phase diagrams of germanium-sulfur, germanium-selenium, and germanium-tellurium systems
07 p1046 N71-16945
Chemical synthesis and crystal growth of pure and doped europium chalcogenides, including magnetic moment, transport properties, and photoconductivity data
[AD-713669] 11 p1816 N71-22120
Semiconducting and transmission properties of chalcogenide glass
[NLL-M-20394-5828.4F] 12 p1966 N71-23836
Lithium/chalcogen cells applied to secondary batteries for vehicular propulsion
[ANL-7756] 14 p2199 N71-25651
Platinum-free laser glass development, radiation centers in borate glasses, local order in liquid chalcogenides, and chalcogenide glass bolometers for infrared and microwave detection
[AD-726416] 22 p3602 N71-35657
- CHAMBERS**
Hermetically sealed chambers for accurate earth tide registrations by pendulums and gravimeters
24 p3910 N71-37869
- CHANCE-VOUGHT MILITARY AIRCRAFT**
U MILITARY AIRCRAFT
CHANDRASEKHAR EQUATION
Characteristics of collisional kinetic equations and solutions using constants of motion method including Chandrasekhar, Hamiltonian, Vlasov, and Langevin formulations
[NASA-TM-X-65493] 12 p1970 N71-23302
Monoenergetic neutron transport in homogeneous slabs based on calculus of variations and Chandrasekhar equation
[AAEC/TM-554] 15 p2459 N71-26992
- CHANNEL CAPACITY**
Systematics of elastic scattering
01 p0100 N71-10754
Patterns in direct channel helicity amplitudes caused by crossed channel exchanges
01 p0100 N71-10755
Theory of channelling effect
[IAE-1878] 02 p0276 N71-11997
Frequency correlation measurements on multipath tropospheric scatter propagation
12 p1876 N71-23465
Impulse response measurements and radio test link for evaluating tropospheric scatter propagation channel capacity
12 p1877 N71-23466
Design of 6-channel stereomicrophone amplifier prototype
[ILEA-292] 18 p2897 N71-30587
- CHANNEL FLOW**
NT OPEN CHANNEL FLOW
Effect of random fluctuations in pressure gradient on channel flow
[NASA-TM-X-52960] 06 p0837 N71-16528
Skewed boundary layer flow in converging channel
06 p0839 N71-16852
Heated element sensor for fluid flow detection in thermal conductive conduit with adaptive means to determine flow rate and direction
[NASA-CASE-MSC-12084-1] 07 p1009 N71-17569

- Velocity distributions in turbulent channel flow with viscous wall layers
08 p1179 N71-18095
Superimposition of fluctuating velocity on steady incompressible channel flow by randomly fluctuating pressure gradients
[NASA-TN-D-6213] 08 p1225 N71-18092
Transverse magnetic field effects on wall heat transfer from ionized argon channel flow
[NASA-CR-116800] 08 p1303 N71-18088
Rectangular channel flow stability of oil and water including mean flow profiles, disturbance amplitude distributions, amplification rate, and wave speed and numbers
[REPT-70-006] 06 p1184 N71-19009
Finite difference scheme of unsteady flow in open channels
[PB-196159] 09 p1369 N71-19408
Determining characteristics of jet elements whose operation is based on jet interaction with turbulent or laminar flow in control channels
[AD-716519] 09 p1371 N71-19409
Numerical analysis of turbulent characteristics of velocity field associated with mean velocity profile in turbulent channel flow
11 p1742 N71-22606
Velocity fields and hydraulic resistance of turbulent fluid flow in channels formed by clusters of annular fuel rods
[AEC-TX-7189] 15 p2444 N71-26880
Liquid film disruption in air-water adiabatic channel flow with and without obstacles with wall shear stress and film thickness measurement for reactor core designs
[GEAP-10248] 15 p2394 N71-27401
Computer program for thermodynamic and hydraulic analysis of water cooled reactor channel flow operating under static conditions
[BUR-4533] 19 p3140 N71-32578
Velocity and temperature distribution of laminar free convection flow in vertical heated channel
20 p3368 N71-33972
Randomly fluctuating, non-Gaussian pressure gradient effect on steady, incompressible channel flow
[NASA-TX-F-67881] 21 p3409 N71-34255
Hydrodynamics of two-phase parallel boiling water channel flow after heat flux increase
21 p3410 N71-34261
Calculation of hydrodynamic entrance length and flow characteristics in channels of varying cross sections
[NLL-M-20388-5828.4F] 21 p3413 N71-34260
Calculation of simultaneous transient developing mass and momentum boundary layers in moving-wall problem from fluid flow through channels with dissolving walls
[ANL-7797] 23 p3743 N71-36857
- CHANNELS**
Critical channel length of Hall-type MHD generator
[INR-1159] 03 p0317 N71-12844
Design of optimal detectors for detection of propagating signal in time variable channels
14 p2234 N71-26416
Principle channels for information transfer and assessment of their effectiveness
[NLL-RISLEY-TRANS-2116-9501.9F] 16 p0000 N71-29118
Test of thin wall channel with ceramic lining in liquid aluminum induction pump
[AD-722310] 17 p2757 N71-30246
Double channel pulse shaper
[JENR-P13-5669] 21 p3467 N71-34677
General mathematical laws for electromagnetic field-conductive fluid interactions in rectangular channels
24 p3968 N71-38308
- CHANNELS (DATA TRANSMISSION)**
Equipment for multiplexing telegraph channels of various speeds and formats using time division techniques
04 p0507 N71-13839
Multimegabit transmission system for troposcatter channel
04 p0507 N71-13839
Characterization and modeling of real communication channels
[AD-715288] 07 p0995 N71-18013
Error correction circuitry for binary signal channels
[NASA-CASE-XNP-63263] 08 p1170 N71-18010
Channel punch code-converter for telegraph systems to transmit information manually and automatically
[AD-717035] 10 p1517 N71-30979
Calibration of ESRO 1 spectrometer channels in several spectroscopy
[KGO-PREPRINT-70-312] 10 p1557 N71-30754
Error analysis for mean linear error of nonrandom code in asymmetrical channel without memory
[NLL-RTS-6038] 10 p1530 N71-26460
Information preserving data compression systems with coding algorithm developed for noiseless channel conditions
[NASA-CR-117846] 11 p1716 N71-32549

SUBJECT INDEX

- Ultra-high frequency communication system with automatic channel selection and selective calling
[NASA-3-A-5731-63] 14 p2219 N71-36334
- Reliability of channel selection devices and automatic channel communication link
[AD-721053] 15 p2379 N71-36890
- Description criteria for pulse transmission channels with memory for tropospheric scatter communications
[AD-720664] 15 p2381 N71-37310
- Reduction ratio for deep space onboard equipment in telemetry frame, taking into account active channel probability distributions
[D-54] 17 p2718 N71-27930
- Method to quantify effect of speech transmission channel on speech intelligibility on basis of simple speech measurements
[AD-1978-23] 18 p2889 N71-31876
- Apparatus for measuring speech transmission index of communication channels by means of artificial speech with measuring time below 3 sec
[N71-1971-2] 18 p2890 N71-31879
- Phase locked loop data carrier with quadrature channel
[NASA-CASE-NPO-11282] 20 p3342 N71-33165
- Master data model for characterizing error sources in digital channels with memory
[NASA-CR-121429] 20 p3357 N71-33551
- Multichannel telemetry system for high-rate and low-rate data communications
[NASA-CASE-NPO-11572] 21 p3394 N71-34159
- Studying information channels and their use by mathematical models and data simulation
[NASA-C-3616-63] 22 p3557 N71-35335
- Channel and nonchannel estimation theory for non-linear random vector channels, for radar tracking and diversity communications
23 p3726 N71-36559
- Median speed multiplexer system for interfacing radio channels to bit series computer
[N71-1460-171] 23 p3729 N71-36580
- Modification of coupled-channel code [JUPITOR I] including expansion of deformed optical potential in terms of Legendre polynomials and Coulomb excitation
[N71-3433] 23 p3811 N71-37170
- CHAPMAN-SHERR LAYER
U SHERR LAYERS
CHAPMAN-SHERR THEORY
Quantum theory of density corrections to gaseous transport coefficients
[NASA-CR-116157] 06 p6008 N71-15934
- Chapman-Enskog theory used to determine macroscopic contribution to reaction rate of internal multicomponent system
[N71-3700-31] 09 p1345 N71-20580
- Approximate solution for time dependent boundary value problems including Couette flow, Rayleigh problem, oscillating wall flow, and sound propagation using Chapman-Enskog theory
15 p2395 N71-27322
- CHAPMAN-JOUBERT FLAMES
U CHEMICAL EQUILIBRIUM
U DETONATION
U FLAME PROPAGATION
CHARACTER RECOGNITION
Computerized simulation of character recognition for rates using PDP 11 computer
[N71-32151] 03 p0329 N71-12349
- Self-organizing networks including threshold and logic networks, photonic perception, dialog systems, character recognition, and programming by simulated selection
[AD-716796] 10 p1536 N71-20680
- Character recognition device designs and applications in weather forecasting, medical diagnostics, and mail sorting
[N71-32151] 10 p1536 N71-20681
- Optimization and data input format of geomagnetic field data
[N71-32151] 17 p2739 N71-28434
- Computerized simulation of character recognition including use of reading machines and implementation of decision trees in pattern processing
[N71-32151] 20 p3328 N71-33121
- Automatic reading of handwritten Hebrew using binocular marking grids
24 p3894 N71-37750
- CHARACTERISTIC EQUATIONS
U EIGENVALUES
U EIGENVECTORS
CHARACTERISTIC FUNCTIONS
U EIGENVALUES
U EIGENVECTORS
CHARACTERISTIC METHOD
U METHOD OF CHARACTERISTICS
CHARACTERS
U SYMBOLS
CIRCULAR
Analysis of motion by graphic and chemical reduction of velocity of motion and rendering of fully visible in air at 500 C and in air at same temperature
[N71-32151] 15 p3492 N71-37952

- In-place testing of charcoal adsorbent bed filters with methyl iodide as test pollutant using pyrolytic-microcoulomb detector
17 p2743 N71-29834
- In-place test results of M reactor charcoal confinement filters using iodine tagged with iodine 131 tracer
17 p2743 N71-29835
- Computer code for estimating maximum temperatures in charcoal bed by fusion product decay heat
17 p2859 N71-29873
- Physics of carbon adsorbents
17 p2770 N71-30135
- Numerical analysis of radioactive decay heat generation and effects on charcoal adsorbents for reactor accident simulation
[ORNL-4402] 20 p3309 N71-33908
- Physicochemical factors affecting activated charcoal adsorption of contaminants using mathematical models - tables
[NASA-CR-115302] 24 p3688 N71-37457
- CHARGE CARRIERS
NT HOLES (ELECTRON DEFICIENCIES)
NT MINORITY CARRIERS
Electron mobility of indium arsenide phosphide for charge carriers
01 p0100 N71-10212
- Radio frequency impedance resonances for determining charge carrier properties in gallium arsenide band
01 p0089 N71-10512
- Two carrier model for electronic properties of single crystal band
[ORNL-3651-5] 03 p0390 N71-12963
- Impact ionization, bulk negative differential conductivity and other nonequilibrium carrier phenomena in GaAs
[AD-721404] 03 p0443 N71-13370
- Electromagnetic wave and charge carrier interaction in crossed fields
[AD-713399] 05 p0635 N71-14883
- Carrier recombination and laser processes in semiconductors, mainly gallium arsenide
[AD-714333] 06 p0667 N71-16180
- Investigating effects of high energy proton irradiation on carrier lifetimes of junction diodes and solar cells
[N71-18472] 06 p1239 N71-18669
- Spatial distribution of slow electrons and negative ions in irradiated organic liquids
[N71-133-70-02] 06 p1263 N71-18915
- Interaction between slow electromagnetic waves and drifting carriers in semiconductors
06 p1163 N71-19118
- Positive and negative charge carrier mobilities in organic liquid - 2 under pressure
[N71-25587] 06 p1267 N71-19234
- Electron beam recombination time and diffusion length of metals, and carrier density role at ohmic metal-semiconductor boundaries
[ORNL-3651-7] 09 p1455 N71-20580
- Hydrostatic pressure effects on excess carrier lifetimes of n and p type germanium
12 p1967 N71-24303
- Ultrasonic resonator responses used to measure phonon charge carrier interactions in metals and semiconductors
13 p2141 N71-25552
- Ambipolar diffusion coefficient in elemental semiconductors determined by measurement of ambipolar diffusion length and excess carrier lifetime
[ORNL-3651-8] 19 p3170 N71-32317
- CHARGE DISTRIBUTION
Nuclear charge distribution determinations of even neodymium isotopes by electron scattering
[AD-712062] 02 p0277 N71-12062
- Investigating reaction cross-section yields 3 plan for charge distribution method
[N71-177] 04 p0591 N71-14589
- Isotope shift of nuclear charge distribution, statistical theory of deformed nuclei, and validity of Strutt's shell correction theory
[UCRL-10-P-11-105] 05 p0730 N71-15334
- Charge distribution effects on beta decay on diffuse surface
[N71-32151] 06 p0913 N71-15473
- Charge distribution of heavy nuclei of cosmic rays in region 2 greater than or equal to 36 determined by photoemission method
[NASA-TT-P-13510] 09 p1463 N71-20409
- Operation of vidicon tube for scanning optical charge density pattern
[NASA-CASE-NXP-04628] 12 p1886 N71-23109
- Low energy fluxes of thorium-232 studied with 11.3 MeV protons and 17.5 MeV deuterons
12 p1976 N71-34897
- Determination of dipole antenna electric impedance in isotropic media using charge distribution on radio frequency impedance probe surface
15 p3453 N71-27650
- Target nuclei charge distribution effects on high energy electron small angle multiple scattering distributions based on Mott's formula and elastic form factors
15 p3478 N71-27687

CHARGE EXCHANGE

- Determination of heavy metal charges in atmosphere from formation density of delta electrons
[NASA-TT-P-13743] 17 p3685 N71-30393
- Scattering of electromagnetic waves by systems of unknown charge distribution
[N71-3700-27] 19 p3154 N71-32326
- Mass yields and charge distributions of 26 Ag, Cd, In, Sn, and Sb isotopes from U-238 fission with protons
[COO-1167-10] 20 p3328 N71-33967
- Ground state charge distribution and physical properties of some low-lying states in Nd-142, Nd-144, and Nd-150 produced by electron scattering
21 p3488 N71-34834
- Dependence of intensity of characteristic X-radiation on charge of electron
[AD-726754] 23 p3816 N71-37231
- At-gas-phase charge distribution in transverse beam photo
[LAL-ET-8-70] 24 p3971 N71-38330
- CHARGE EXCHANGE
NT RESONANCE CHARGE EXCHANGE
Nuclear models used for studying nuclear reactions, nuclear fusion, isotopic scattering, and charge exchange - contents
[ANS-1970-2] 01 p0106 N71-12832
- Investigating ion collision using isotopes separated with two magnetic stages and an electrostatic stage
[N71-3433] 04 p0576 N71-15989
- Constructing double Ranges charge exchange model for heavy production in K/A reactions at 9.0 GeV/c
[COO-1436-229] 04 p0583 N71-14177
- Elastic K/N scattering and charge exchange taking bremsstrahlung into account
[N71-3433] 04 p0585 N71-14231
- Mathematical proof of optical symmetry of exchange potential produced by closed shells
[NASA-CR-116125] 06 p0814 N71-15938
- Measurement of negative pion proton charge exchange at backward angles
[COO-1764-113] 10 p1613 N71-20836
- Preliminary investigation to eliminate or reduce concentrated charge exchange ion erosion of accelerator grid supports for electron bombardment ion thrusters
[NASA-TM-X-676-02] 14 p2331 N71-25694
- Obtaining dense beam of hydrogen atoms with particle energies above 1 keV by means of charge exchange in magnetron vapor target from plasma clusters generated by coaxial plasma gun
[UCRL-TRANS-10497] 14 p2321 N71-25768
- Pion proton and pion proton reactions analyzed by charge exchange model with four Regge poles
[N71-3433] 14 p2320 N71-25768
- Kinematics of neutral kaon 3 electron decay with analysis of charge exchange and strangeness
15 p3084 N71-27781
- Charge exchange degeneracy with SU(3) symmetry and absorptive corrections in hypercharge and charge exchange reactions for meson baryon scattering
[N71-3433] 15 p3085 N71-27781
- This falls as charge exchange model for neutral injection into controlled thermonuclear fusion devices
[UCRL-28253] 17 p2800 N71-30400
- Pion neutron charge exchange polarization and violation of Pomeranchuk theorem
[N71-3433] 17 p2806 N71-30400
- Consecutive ion-molecule reactions in acetylene ion-activated by charge exchange mass spectroscopy as function of energy transfer during ionization
[AD-722470] 18 p2804 N71-30719
- Spectroscopic factors and charge exchange effects of single neutron transfer reactions on silicon and methylsilicon isotopes
19 p3004 N71-31052
- Constant behavior of total cross section above 30 GeV, pion-nucleon charge exchange scattering, and pion regeneration amplitude on hydrogen
[N71-3433] 19 p3005 N71-31180
- Substrate mediated interaction between aliphatic radicals caused by exchange of plasmons
[RLO-1380-005] 19 p3085 N71-31219
- Electron-positive ion pair production in copper foil by electron energy exchange effects
19 p3086 N71-31219
- Small angle differential charge exchange measurements for He/He⁺ on He, Ne, and Kr at 1 keV to 3 keV range
[N71-3433] 20 p3318 N71-33574
- Asymptotic generalized optical electron model and Regge theory combined in model for high energy pion nucleon charge exchange scattering
20 p3323 N71-33816
- Using particle conservation equations for fast hydrogen atoms, slow hydrogen molecules, and charged particles for calculating fast atomic hydrogen flux produced by charge exchange in high temperature plasmas
[N71-3433] 21 p3494 N71-34887
- Resonance and nonresonance charge exchange probabilities of atomic collisions in molecular orbitals
[N71-3433] 22 p3635 N71-35987
- Single and double pion production and charge exchange reaction from positive heavy proton and positron

CHARGE SEPARATION

Use known deuteron interactions at 1585 MeV/c in 25-
inch bubble
[UCRL-20628] 22 p3639 N71-35937
Proper time dependence of charge and neutral decay
modes for K and L decays into 2 neutral pions and K
and 3 decays into 2 neutral pions
22 p3649 N71-36020

CHARGE SEPARATION
U POLARIZATION [CHARGE SEPARATION]
CHARGE TRANSFER

Electronic counter circuit utilizing magnetic core
and low power consumption
[NASA-CASE-XRP-69836] 03 p0348 N71-12515
Charge collection in silicon detectors for strongly
ionizing particles
[UUIP-711] 04 p0595 N71-13611
Development of room temperature polymeric super-
conductors
[AD-714139] 06 p0811 N71-16626
Orbital initiation pressures of explosives by shock
waves
[UCRL-TRANS-10490] 06 p0960 N71-16882
Charged particle energy transfer for assessing stimu-
lation of accelerated radiation tests
09 p1439 N71-20233

Total cross sections for formation of excited
hydrogen atoms by charge exchange in proton colli-
sions with Ar, He, H₂, N₂
[ORO-2591-51] 10 p1612 N71-20756

Switch-on times and charge transfer mechanism ef-
fects on concentrated MOS transistors
[NLL-TRANS-2657-1922-81/1] 10 p1534 N71-21236

Reaction kinetics and charge transfer in ionic colli-
sions of argon ions with molecular hydrogen, deuteri-
um, and carbon dioxide
15 p2477 N71-27578

Model Hamiltonian for charge parity violation in
positronium decay
[AD-720834] 15 p2480 N71-27660

Total cross section measurements for formation of
metastable hydrogen atoms by charge transfer of
proton traversed targets of helium, argon, nitrogen,
and oxygen
[NASA-CR-118863] 15 p2492 N71-27925

Charge transfer characteristics of ion recombination
in phase boundary of germanium surface with electro-
lyte
18 p2998 N71-31326

Distorted even-even nuclei formation by ground
band rotational transitions in rare earth nuclei
18 p2989 N71-31521

Analysis of decaying photocurrents in polyvinylcar-
bazole to determine charge transport and trapping
states
23 p3837 N71-37364

X ray diffraction and charge transfer in reduced
stoichiometric titanium oxide at various tempera-
tures for defect ordering effects
[AD-727600] 24 p3998 N71-38515

CHARGED PARTICLES

NT ALPHA PARTICLES
NT ANIONS
NT ANTIPROTONS
NT ARGON PLASMA
NT ARTIFICIAL RADIATION BELTS
NT BETA PARTICLES
NT CATIONS
NT CESIUM PLASMA
NT COLD FUSIONS
NT COLLISIONLESS PLASMAS
NT CONDUCTION ELECTRONS
NT COSMIC PLASMA
NT DEUTERIUM PLASMA
NT DEUTERONS
NT ELECTRON PLASMA
NT ELECTRONS
NT FERRIC ION
NT FREE ELECTRONS
NT HELIUM PLASMA
NT HIGH ENERGY ELECTRONS
NT HIGH TEMPERATURE PLASMAS
NT HOT ELECTRONS
NT HYDROGEN PLASMA
NT INNER RADIATION BELT
NT MAGNETICALLY TRAPPED PARTICLES
NT METAL IONS
NT METALLIC PLASMAS
NT NONEQUILIBRIUM PLASMAS
NT NONUNIFORM PLASMAS
NT OUTER RADIATION BELT
NT PHOTOELECTRONS
NT PI-ELECTRONS
NT PLASMA CLOUDS
NT PLASMA LAYERS
NT PLASMA SHEATHS
NT PLASMA SLABS
NT PLASMAS (PHYSICS)
NT POLARONS
NT POSITRONS
NT PROTON BELTS
NT PROTONS
NT RADIATION BELTS
NT RAREFIED PLASMAS
NT RECOIL PROTONS

NT RELATIVISTIC PLASMAS

NT ROTATING PLASMAS
NT SOLAR PROTONS
NT SOLAR WIND
NT THERMAL PLASMAS
NT TOROIDAL PLASMAS
NT TRITONS
Method of forming thin window drifted silicon
charged particle detector
[NASA-CASE-XLB-00808] 01 p0097 N71-10560
Approximate density-effect correction for ioniza-
tion loss of charged particles
[NASA-CR-111652] 01 p0103 N71-10981
Magnetic and drift surfaces of charged particle of
stellarator field
[EPJ-95] 02 p0279 N71-11458
Motion characteristics of charged particles in mag-
netosphere
[REPT-70-23] 02 p0292 N71-11921
Research in nuclear chemistry including isomer
ratios in charged particle induced fission
[RLO-2050-8] 03 p0427 N71-12058
Neutron and charged particle cross section data
relevant to nuclear energy program
[WASH-1136] 03 p0434 N71-12971
Eta meson minus neutral pion mixing in positive
kaon yields positive pion neutral pion decay
[NYO-2171-316] 03 p0434 N71-12974
Direct conversion of fusion-reactor charged particle
energy to electrical form
[UCRL-72487] 04 p0569 N71-13547
Coordinate lattice method used to calculate two
dimensional magnetic fields for charged particle trans-
port in accelerators
[JINR-P5-5013] 04 p0573 N71-13667
Computer program TRANSPORT/360 for designing
charged particle beam transport systems
[SLAC-91] 04 p0580 N71-13990
Nonlinear interactions of intensive beam of charged
particles with accelerating field
[KFK-TR-318] 04 p0587 N71-14278
Motion and radiation of charged particles in strong
electromagnetic waves in plane and spherical waves
[NASA-CR-111535] 05 p0744 N71-15178
Use of conformal mapping to improve uniformity of
electric fields
[IPJ-T-4] 05 p0657 N71-15375
Charged particle analyzer with periodically varying
voltage applied across electrostatic deflection mem-
bers
[NASA-CASE-XAC-05506-1] 06 p0917 N71-16095
Generating first and second order matrix elements
by tracking charged particles in magnetic fields
[UCRL-19823] 06 p0923 N71-16725
Characteristics of energetic interplanetary particles
and X rays produced by solar activity
[NASA-TM-X-65439] 06 p0944 N71-16749
Neutron physics, nuclear reactions with charged
particles, beta and gamma spectroscopy, and kinetics
of neutron and photon gases
[NYO-73-293] 06 p0927 N71-16856
Dipole expansion technique for particle simulation
of plasmas
[AD-715075] 07 p1084 N71-18090
Fast charged particle scattering on Coulomb and
short range potentials and amplitude expressions
[IPVE-STP-49-106] 07 p1080 N71-18122
Photoemissions of 60 GeV negative pion-meson in-
teraction with nucleons and nuclei
[JINR-P1-5336] 08 p1246 N71-18182
Charged particle motion in stellarator magnetic field
[NR-18475] 08 p1255 N71-18361
Absorbed dose microdistribution in heavy charged
particle track
08 p1263 N71-19061
Evidence for angular momentum fractionation in
decay of compound nuclei
08 p1264 N71-19092
Partial cross sections and angular distributions for
negative kaon P interactions
09 p1426 N71-19522
Controlled charged particle emission from
synchrotron satellites for plasma diagnostics and in-
teractions in magnetosphere
[JONLAB-P-26] 10 p1626 N71-20610
Mathematical models for onboard electrostatic
analyzer measuring low energy charged particles
[KGO-PREPRINT-70-311] 10 p1536 N71-20635
Distribution and charge composition of ionized heli-
um and other heavy ions in auroral zone
[AD-717154] 10 p1640 N71-20773
Equilibrium equations for small ions in region of
synchronous and nonresonant clouds, and reducing at-
mospheric concentration of charged particles by
aerosols
[IPRS-52562] 10 p1535 N71-21066
Empirical and phenomenological aspects of weak
interactions of pure leptonic, semi-leptonic, and non-
leptonic types
10 p1635 N71-21701
Negative pion deuteron interactions at 2.5 GeV/c
10 p1625 N71-21844
Relativistic quantum mechanics for hyper-
critical particles endowed with electric and magnetic charges
[NYO-3629-45] 11 p1802 N71-23008

SUBJECT INDEX

Electron concentration and charged particle con-
centrations in ionosphere
11 p1746 N71-2380
Probe measurements of charged particle concentra-
tions and ionization relaxation phenomena in low den-
sity supersonic gas flows
11 p1808 N71-2380
High rate charged particle detector for use on Sand
Scientific Satellite for measuring directional intensity
of electrons and protons
11 p1764 N71-2370
Ionization of multi-electron atoms by fast charged
particles and electron and proton impact
[NASA-TM-X-655502] 12 p1970 N71-2350
Design and fabrication of charged-particle detectors
with high counting efficiency for neutron, recoil ion
laboratory study of magnetospheric boundary regions
[AD-718110] 12 p1922 N71-2370
Impact acceleration study of charged beam colli-
sions by coherent method
[UCRL-TRANS-1421] 12 p1974 N71-2370
Motion of medium composed of neutral and positive
particles at high electric Reynolds numbers
[RAB-LB-TRANS-1515] 13 p0466 N71-2380
Low energy, heavy cosmic ray ionosphere study
with high resolution, Loran charged particle detector
13 p1243 N71-2380
Development of crystal structure for charged par-
ticle acceleration
[ANL-TRANS-825] 13 p1514 N71-2380
Radiation emitted when charged particles cross
boundary between vacuum and metal
13 p1444 N71-2380
Turbulence effects on charged particle mobility
[AD-720834] 14 p2322 N71-2380
High velocity apparatus for investigating energy
distribution of charge particles of 10 to 15th and 16th
power eV
[KFKI-70-21-HEP] 14 p2314 N71-2370
Penetration and cascade phenomena at low and very
high energies
[ANL-7727] 15 p2463 N71-2370
Numerical calculations for strong particle inter-
action dynamics
15 p2480 N71-2370
Determining solar absorption stability of un-
tilized Teflon second surface mirror thermal control
coatings as function of electron, proton, and UV
radiation dosage
[NASA-TM-X-65559] 15 p2482 N71-2370
Investigating charged Bose gas intermediate densi-
ties using Bohm-Pines and Bogoliubov formalisms
15 p2490 N71-2370
Generally covariant, nondivergent equations of mo-
tion including self field effects of charged particles
15 p2493 N71-2370
Fractional percentage coefficients occurring in
matrix elements for various particle interactions and a
p shell model for deuterons and other particles colli-
cated by ELLIOTT SU-3
[LYCEN-7078] 16 p2642 N71-2007
Heavy charged particle energy loss rate into
nuclear elastic scattering
[LA-4543] 16 p2645 N71-2011
Photon theory of light and matter
[NASA-TT-F-13495] 16 p2640 N71-2008
Temporal variations in charged particle population
of inner radiation zone as measured by satellite
16 p2676 N71-2008
Mathematical model for composite magnetic of
electrostatic charged particle beam analyzer trans-
mission
[NASA-TT-F-13617] 16 p2659 N71-2007
Alpha, deuteron, and helium 3 activation determina-
tion of carbon isotopes
[ORO-2922-2] 16 p2660 N71-2008
Approximate calculation of ionization energy loss
and range of fast charged particles
[JINR-P1-5676] 18 p2968 N71-3003
Proton determination of particle coordinates in pro-
portional multiwire chambers with potentiometer
readout
[JINR-P1-5628] 18 p2970 N71-3004
Heavy leptons in neutrino astrophysics
[JINR-E2-5387] 18 p3007 N71-3007
Fast charged particle beam scattering by dipole
crystals
[RISO-239] 18 p2995 N71-3008
Charged particle motion in plasma during propaga-
tion of magnetohydrodynamic shock wave
[NASA-TT-F-13815] 18 p2992 N71-3008
Charged particle lunar environment experiment of
Apollo 14 detecting particle fluxes at lunar orbit
resulting from wide range of lunar surface, magne-
tospheric, and interplanetary data
18 p3011 N71-3004
Adiabatic equations for charged particle trajectories
in geomagnetic tail null zone
20 p3314 N71-3008
Effect of charge transport on disintegration of light
jets studied by comparison of calculated and experi-
mental values of size of drops formed from elevated
jets
[AD-724334] 20 p3363 N71-3008

SUBJECT INDEX

CHEMICAL ANALYSIS

Auroral zone VLF hiss and low energy particle observations with Injun 5 satellite
 (NASA-CR-121418) 20 p3246 N71-33392

Measurement of charged particle spectra in interplanetary space by Cerenkov counter on Pioneer 8 spacecraft
 20 p3541 N71-33485

Study of events with two or four charged prongs from 2.5 GeV/c pion pion interactions
 20 p3526 N71-33943

Photoproduction of charged and neutral pions using photon beams produced by diamond monocrystal
 NYO-4115-1 21 p3480 N71-34785

Using particle conservation equations for fast hydrogen atoms, slow hydrogen molecules, and charged particles for calculating fast atomic hydrogen gas produced by charge exchange in high temperature plasmas
 (AERE-MEMO-0403) 21 p3494 N71-34887

Measurement and analysis of heavy cosmic rays with high altitude balloons
 21 p3506 N71-34977

Search for particles with fractional charge (quarks) produced by protons in 70 GeV accelerator
 CERN-TRANS-71-4 22 p3535 N71-35912

Coherent interactions of negative pions with photoemission nuclei at 17 GeV
 (N71-35555) 22 p3641 N71-35954

Application of Riemann method to inverse problem of charged particle scattering
 (IIT-70-96-2) 22 p3643 N71-35975

Charged pion production in 40,000 isotopic proton-proton interactions in hydrogen bubble chamber between 13 and 28.5 GeV/c
 (UCRL-20632) 22 p3645 N71-35994

Isolation effects in cyclotron resonance oscillators with emphasis on generation and amplification of millimeter waves
 (NASA-CR-121294) 23 p3731 N71-36394

Scattering chamber, detection telescopes, electronics, and computer characteristics of multidetector system for charged particle coincidence measurements
 (K-3) 23 p3756 N71-36775

Pulse energy sum rules on hyperbolae and backward pion nucleus scattering
 (T-72-01) 23 p3783 N71-36963

Pulse energy sum rules on hyperbolae and nucleon-nucleon pion-pion reactions
 (T-72-012) 23 p3783 N71-36964

Effect of optical parameters of refractive index on field and angular distribution of transition radiation of relativistic charged particles
 (IOP-74-574) 23 p3807 N71-37138

Fermion models for describing interactions of high velocity photons with hadronic matter
 (JHEP-71-5) 23 p3808 N71-37148

Statistical nonlinear model of axisymmetric charged particle beams with nonzero angular velocity
 (NP-18866) 23 p3815 N71-37206

Charge symmetry of universe and distribution of matter and antimatter
 23 p3830 N71-37440

Beam design studies based on use of mirror-concentrated zones fed by neutral beam injectors and shifting driver converters for charged particle energy recovery
 (EDM-710607-127) 24 p3961 N71-38256

Satellite observations, radio-astronomical and optical techniques, and problems in plasma physics associated with effects of energetic particles in outer space
 (NASA-CR-123150) 24 p4007 N71-38572

Charged particle showers and electromagnetic radiation from stationary and nonstationary sources
 24 p4010 N71-38595

Fluctuations due to particle scattering in interplanetary magnetic field
 24 p4011 N71-38601

CHARPY IMPACT TEST
 Comparison of Charpy impact test with drop-weight test for structural steels
 02 p3043 N71-11585

Static and cyclic strain aging effects on Charpy impact properties of carbon steel plates
 (NIAAP-10140) 03 p3091 N71-12918

Fracture toughness prediction and method for relating transition temperature and Charpy transition temperature changes
 (AD-716599) 09 p3199 N71-19987

Results and impact properties of thick-section plates and welds used for pressure vessels
 (KORNL-TM-3211) 12 p3603 N71-33138

Charpy impact test and irradiation tests of domestic Steady 2 charring materials in JFDR
 (AERE-MEMO-4192) 13 p2119 N71-25205

CHARMING
 Analysis of charging inhibition with description of associated computing program
 (NASA-TN-D-6083) 02 p3504 N71-11127

Determination of energy transfer in char zone of charging shifter
 02 p0175 N71-11232

Mathematical model for predicting erosion of charging shifter in aerodynamic environment
 09 p1484 N71-26248

Ablation sensor for measuring char layer recession rate using electric wires
 (NASA-CASE-XLA-01794) 10 p1663 N71-21586

Thermochemical and thermophysical properties and ablation test data for three charring shiflers
 (NASA-CR-111834) 16 p3691 N71-30795

CHARTS
 NT FLOW CHARTS
 NT GRAPHS (CHARTS)
 NT METEOROLOGICAL CHARTS
 NT MOLLIER DIAGRAM
 Two-part glossary of bathymetric terms in 27 languages and English equivalents
 (AD-710952) 01 p0049 N71-10887

Development of generalized digital contouring program
 (NASA-TN-D-6022) 03 p0649 N71-14654

Summary descriptions of NASA graphic arts techniques and equipment
 (NASA-SP-5919/1) 12 p0819 N71-34285

Revised periodic table for incorporating actinides and lanthanides
 (UCRL-TRANS-10510) 15 p2376 N71-26886

In-control probability properties of variables control charts for mean population surveillance
 (NASA-CR-110868) 15 p3435 N71-37727

CHEBYSHEV APPROXIMATION
 Deriving incommensurate gamma functions for various applications and using Chebyshev polynomial approximations for solution of Lane-Emden equation
 01 p0774 N71-10254

Deriving algorithms for computations involving sparse matrices
 (NASA-CR-115777) 04 p0536 N71-15758

Computer program for electric propelled spacecraft trajectory, flyby, and rendezvous trajectory optimization based on Chebyshev approximation and polynomial representations
 (NASA-CR-114354) 18 p3008 N71-30678

CHECKOUT
 Compact computer control system for shipborne missile checkout and launch
 04 p0506 N71-13843

Digital computer system for automatic prelaunch checkout of spacecraft
 (NASA-CASE-XKS-08012-2) 03 p0772 N71-15566

Checkout and data reduction procedures for acceptance test of sealed, absolute, gaseous, and differential strain gage pressure transducers
 (NASA-TM-X-46003) 06 p0662 N71-16746

Development of onboard checkout equipment for space shuttle propulsion systems
 (NASA-CR-116427) 07 p1122 N71-18060

Computer methods for fault isolation in systems checkout
 (NASA-CR-1758) 08 p1167 N71-19117

Results and description of qualification tests of altitude control system and yo-yo despin system in flight configuration as installed on TMP-1 spacecraft
 (NASA-TM-X-45473) 10 p1600 N71-21859

Development of onboard checkout equipment and performance monitoring capability for space shuttles - Vol. 1
 (NASA-CR-119037) 17 p2834 N71-29521

Description of design reference model for space shuttle propulsion system onboard checkout and monitoring equipment to establish design criteria - Vol. 2
 (NASA-CR-119840) 17 p2834 N71-29522

Criteria and concepts for onboard checkout and monitoring system for space shuttle propulsion system - Vol. 3
 (NASA-CR-119038) 17 p2834 N71-29523

Space shuttle propulsion systems onboard checkout and monitoring systems development study - appendices
 (NASA-CR-119039) 21 p3518 N71-35071

Concepts and requirements analysis for automated onboard checkout of manned space station
 (NASA-CR-115128) 21 p3519 N71-35076

Language and executive software requirements for automated onboard checkout of manned space station
 (NASA-CR-115129) 21 p3519 N71-35077

Logic device for readiness assessment and checkout of airborne and ground equipment mechanical components
 22 p3674 N71-36197

Checkout and verification of space shuttle system redundant components without disrupting systems
 22 p3675 N71-36198

NASTRAN program for input data checkout and undeformed structure plotting
 22 p3686 N71-36287

Technical aviation handbook covering aircraft maintenance, navigation aids, altimetry, lubricants, piston and gas turbine engines, and checkout procedures
 (AD-727195) 24 p0774 N71-37643

Design, development, fabrication, test, checkout, and support activities for delivery of integrated X ray and alpha particle spectrometer systems for lunar orbiter
 (NASA-CR-115216) 24 p3921 N71-37959

CHECKOUT EQUIPMENT
 U TEST EQUIPMENT
 CHELATE COMPOUNDS
 CHELATES
 CHELATES
 Investigating kinetics of crystal growth of copper compounds in magnetic and electric fields
 (AD-704356) 03 p0440 N71-12755

Ammonium perchlorate composite propellant with organic Cu/II chelate catalyst additive
 (NASA-CASE-LAR-10173-1) 04 p0604 N71-14880

Using photochemical titration and color exchange methods to study formation of postvalent platinum and selenium chelates with alpha-keto acids
 (LIBTRANS-261) 05 p0736 N71-14580

Solid state spectrum analysis of cerium chelates
 (UCRL-77707) 05 p0641 N71-15595

Vapor pressure and heat of vaporization of metal bismuth chelates measured by gas-liquid chromatography
 (AD-710628) 12 p1870 N71-23479

Differential scanning calorimetry and analysis by thermogravimetry of some metal chelates and some subjects of these metal chelates
 (ORO-2124-34) 13 p0890 N71-25320

Synthesis and properties of metal chelates for polymerization studies
 21 p3388 N71-34105

CHEMICAL ANALYSIS
 NT GAS ANALYSIS
 NT GAS SPECTROSCOPY
 NT MICROANALYSIS
 NT NEUTRON ACTIVATION ANALYSIS
 NT OZONOMETRY
 NT POTENTIOMETRIC ANALYSIS
 NT QUALITATIVE ANALYSIS
 NT QUANTITATIVE ANALYSIS
 NT SPECTROSCOPIC ANALYSIS
 NT URINALYSIS
 NT VOLUMETRIC ANALYSIS
 Ni-Ti-C system analysis by X ray and chemical methods
 (AD-709460) 01 p0566 N71-10228

Isotopic lead and thallium analysis of rocks, meteorites, and lunar samples
 01 p0617 N71-10209

Summary of lunar sample chemical analysis scheme
 01 p0617 N71-10313

Mass spectrometric analyses of meteoritic and lunar samples containing lead and thallium
 01 p0633 N71-10314

Irradiation, microanalysis of lithium, rhodium, ruthenium and platinum
 (NASA-TT-F-13357) 01 p0647 N71-10351

Research and development of standard reference materials in chemical analysis
 (NBS-TN-546) 01 p0619 N71-10675

Effects of inhomogeneities in explosives on critical diameter of detonation
 (LA-TN-70-7) 01 p0114 N71-10756

Flexibility and capability of electron microprobe analysis for measuring pollutant aerosol particles in atmosphere
 (PB-189282) 02 p0130 N71-11668

Electron microprobe X ray analysis of atmospheric aerosol particles
 (PB-189283) 02 p0132 N71-11679

Food and drug chemical analysis
 (PB-189284) 02 p0152 N71-11680

Chemical analysis of thiamine metabolism in man
 (AD-712238) 02 p0155 N71-11699

Chemical analysis of gold and tantalum thin films
 (RAE-TB-69036) 02 p0771 N71-17208

Chemistry program review including work in kinetics, electrochemistry, chemical lasers, trace element analysis, photoinitiation, and photochemical spectroscopy
 (AD-705364) 02 p0172 N71-11213

Chromatographic separation and spectrophotometric determination of uranium
 (IS-T-382) 03 p0330 N71-12358

Methods for chemical analysis of carbon-taric compounds
 (AD-713062) 03 p0332 N71-12349

Mass spectra of phenolic polymethine compounds of p-cresol and formaldehyde
 (RAE-LIB-TRANS-1406) 03 p0333 N71-12381

Harvesting of algae through chemical flocculation and flotation
 (REPT-321) 04 p0647 N71-13482

Chemical and isotopic analyses of Apollo 12 lunar samples
 (NASA-TB-3-353) 04 p0610 N71-13742

Design and performance of high resolution nuclear magnetic resonance spectrometer
 (DIS-4233) 05 p0732 N71-14509

Chemical analysis of neodymium-cadmium hydride phase system
 (IS-T-616) 05 p0838 N71-14621

Determination of rare earth impurities in purified barium oxide using infrared spectroscopy
 (BARC-472) 05 p0839 N71-14697

Spectrographic determination of rare earth impurities in erbium oxide and ytterbium oxide
 (BARC-471) 05 p0839 N71-14708

- Spectrographic method for determining cerium and yttrium in rare earth mixtures [BARC-476] 05 p0639 N71-14769
- Automatic colorimetric determination of nitrogen in low weight steel samples [BNW/C7/3] 05 p0639 N71-14710
- Selected reports on standards for food and drug purity [PB-190941] 05 p0639 N71-14728
- Spectrographic analysis of pure bismuth [BARC-486] 05 p0700 N71-15023
- Estimation of plutonium by chemical analysis [BARC-464] 05 p0725 N71-15040
- Using gas sheathed tubular electrode arc for alloy analysis [AD-713696] 05 p0705 N71-15214
- Continual monitoring of sister mixtures [MG/D/389/68] 05 p0640 N71-15447
- Automated, high sensitivity, three column gas chromatograph [UCRL-30849] 05 p0668 N71-15519
- Chemical analysis techniques for metals, alloys, and other materials [AD-715977] 06 p0610 N71-16275
- Pacific Northwest Laboratory manual of procedures for analysis of metallic sodium [BNWL-MA-76-BEV-3] 06 p0811 N71-16625
- Determination of trace impurities in high purity materials by anodic stripping voltammetry 07 p0908 N71-17069
- Chemical analyses of boron in elemental boron, boron carbides, and boron mixtures, and of impurities in boron [TID-25190] 08 p1253 N71-18323
- Electrochemistry, organic and inorganic chemistry, and chemical analysis [TT-69-5106/2-4] 06 p1161 N71-19334
- Low temperature chemical thermodynamics and solid state behavior [COO-1149-180] 10 p1631 N71-20626
- Oxidation of refractory metals in presence of alkali cations studied by differential thermal and thermogravimetric analyses [RE-465] 10 p1584 N71-21665
- Development and operation of mass spectrometer for analysis of highly reactive fluorine compounds at subambient temperatures 11 p1697 N71-22670
- Chemical analysis of polyimides using pyrolysis-gas chromatograph-mass spectrometer system [RAE-TR-70177] 12 p1870 N71-23432
- Procedures for determining boron in borates, boron hydrides, organo-boron compounds, elemental boron, and refractory borides and titan standardization [UCRL-56948] 12 p1870 N71-23520
- Analytical test apparatus and method for determining oxygen content in alkali liquid metal [NASA-CASE-XLB-01997] 12 p1871 N71-23527
- Purification and chemical analysis of organometallic solvents [AD-718189] 12 p1871 N71-23588
- Microradiation, dimensional, and chemical analysis of neutron irradiated UN fuel specimens 13 p2114 N71-24541
- Spectrochemical techniques for determination of impurities and of tantalum in zirconium alloy and Zircaloy 2 [EUB-4541-F] 13 p2093 N71-24819
- Physical properties and ordering process in beta brass alloys based on quasi-chemical approximation [TT-76-59079] 14 p2269 N71-25667
- Quantitative analysis of motor oil additives based on dependence of surface tension on temperature and additive content [AD-720377] 14 p2277 N71-25886
- Comparison of atomic fluorescence flame spectrometry with atomic absorption flame spectrometry 14 p2214 N71-26218
- Automated fluid chemical analyzer for microchemical analysis of small quantities of liquids by use of selected reagents and analyzer units [NASA-CASE-XNP-49451] 14 p2216 N71-26734
- Chemical recovery and analysis of trace elements from irradiated silicon carbide coated plutonium dioxide fuel [KR-140] 15 p2452 N71-27849
- Photoelectron spectroscopy for chemical analyses on doped metals and alloys [CEA-COMF-1725] 15 p2495 N71-27959
- Broad spectrum of materials chemistry under extreme conditions, including ionizing radiation, high vacuum, high pressure, and high temperature [AD-726095] 16 p2557 N71-28437
- Detection of silver in sealed clouds by atomic evaporation to high sensitivity and related aircraft sampling problems [AD-721740] 16 p2625 N71-28456
- NASA/GSFC workshop on materials processing, chemical analysis, cell processing, and testing of biomaterials for aerospace applications [NASA-TM-X-67260] 16 p2538 N71-28459
- Chemical analysis of active materials of nickel cadmium battery plates 16 p2538 N71-28461
- Chemical analysis and electrical performance tests of nickel cadmium batteries for Intelat 4 program 16 p2539 N71-28462
- Chemical analysis of Intelat 4 nickel cadmium battery electrolyte 16 p2539 N71-28463
- Development and application of techniques and equipment for conductive measurement of nuclear materials in fuel cycles [GULF-RT-10511] 17 p2794 N71-29635
- Chemical analysis of polymerization products in alpha-aminopropionitrile equilibrium reaction and chemical properties [NASA-TT-F-13712] 18 p2804 N71-30509
- Chemical and X ray analysis of phase diagrams of Th-U-O ternary systems for ThO₂-UO₂-U₃O₈ [KPK-1297] 18 p2933 N71-30646
- Facility and equipment manual for chemical and failure analysis [NASA-TM-X-67342] 18 p2886 N71-31181
- Detection and determination of chemical characteristics of trace constituents in sea water and air [MIT-905-162] 18 p2888 N71-31567
- Analysis of dried polyethylene terephthalate and its degradation products [NLL-M-9262/5828-AP/1] 19 p3050 N71-32090
- Computer plotted soft X ray spectra to facilitate chemical combination studies with electron microbeam probe [AD-723635] 19 p3050 N71-32249
- Chemical analysis of organic trace contaminants in simulated space station atmospheres desorbed from molecular sieve, silicon gel, and catalyst beds [NASA-CR-111936] 20 p3528 N71-33143
- Apparent ages of Rb-87 and Sr-87, and contents of K, Rb, Sr, Y, and rare earths in lunar soil from Mare Fecunditatis [NASA-TT-F-13945] 20 p3349 N71-33608
- Noninvasive infrared gas analyzer [NASA-CASE-ARC-10308-1] 21 p3386 N71-34050
- Comparison of wet chemical ozone sensors for balloon sounding in free atmosphere [REPT-120] 21 p3419 N71-34327
- Test methods and procedures for determining effect of chemical and physical forces at magnetic head/tape interface of magnetic tape recorders [NASA-CR-121649] 21 p3424 N71-34364
- Chemical and physical forces at magnetic head/tape interface of satellite tape recorders [NASA-CR-121700] 21 p3424 N71-34365
- Micrometeoroid analyzer using arrays of interconnected capacitors and ion detector [NASA-CASE-ARC-10443-1] 21 p3427 N71-34382
- Osmium dioxide single crystal growth and electrical transport measurements, and analysis of osmium tetroxide and phosphoric acid reaction products 21 p3490 N71-34930
- Electrochemical dissolution of zinc oxide single crystals and measurement of dissolution rates as function of potential 21 p3500 N71-34938
- Development and characteristics of automated fluorometric procedure for analyzing noradrenaline and epinephrine content of blood plasma and urine [FAA-AM-71-15] 22 p3543 N71-35241
- Gas chromatograph, mass spectrometer system for chemical and biochemical determinations on Mars, and data reduction program [NASA-CR-122038] 22 p3583 N71-35514
- Atomic absorption spectrophotometry for determining constituents in minerals, slags, and matters from smelting, evaporative furnaces, and other sources [NLL-CR-TRANS-5496/5922-09] 22 p3597 N71-35612
- Chemical, X ray diffraction, electron microscopic, and structural analysis of silicon carbide ceramics for open cycle magnetohydrodynamic generators 22 p3600 N71-35623
- Chemical and structural analysis techniques for materials suitable for aircraft structures [AD-727017] 22 p3691 N71-36323
- Modification of theory of diffusion-controlled particle coarsening to account for volume fraction of precipitate [UCLA-34-P-172-2] 23 p3719 N71-36512
- Determination of energy and size conformal parameters and application to excess properties of simple liquids 23 p3746 N71-36713
- Chemical and X ray analysis of ferroplutonium from Norilsk deposits [NASA-TT-F-19966] 23 p3768 N71-36857
- Chemical analysis of amine curing agent used in adhesives manufacturing to determine compliance with specifications [BDX-613-085] 23 p3777 N71-36918
- Characteristics of oxazepam and occurrence as metabolite in metabolism of diazepam in human organisms [RAD-LIB-TRANS-1583] 24 p3886 N71-37697
- Emission spectral methods for determining content of mineral admixtures in fuels, oils, and lubricants [AD-727197] 24 p3886 N71-37699
- Corrosion tests of austenitic Cr-Ni steel and nickel alloys in steam loop at 630 C and 1 atm pressure for 5000 hours, and behavior of cold-formed material surfaces [KFE-1301] 24 p3885 N71-38077
- Phase analysis of nickel alloys, selection of electrolyte, and electrochemical behavior [AD-727861] 24 p3909 N71-38106
- Problems of chemical analysis in connection with lunar surface and landforms 24 p3889 N71-38209
- Chemical analysis of meteorites [ORO-3585-22] 24 p3813 N71-38263
- CHEMICAL ATTACK
- NT INTERGRANULAR CORROSION
- Corrosion of nickel heat pipes containing liquid potassium [ORNL-TM-3077] 10 p1572 N71-28809
- Corrosive mass transfer of structural materials and radioactive isotopes in sodium cooled reactor [GEAP-13539-15] 17 p2780 N71-29206
- Mass transfer and stainless steel corrosion in sodium cooled reactors [GEAP-13539-16] 17 p2780 N71-29207
- Chemical attack of laboratory equipment, and preparation of corrosion resistant materials for construction of chemical apparatus 22 p3596 N71-35508
- Effects of dry heat and chemicals on long term survival rates of bacteria spores under varying temperatures and humidity conditions [NASA-CR-122068] 23 p3713 N71-36407
- CHEMICAL AUXILIARY POWER UNITS
- Development of antimicrobial porous media model for analyzing effects of fluid motion in fuel cell cavities [AD-727861] 24 p3813 N71-38263
- Development and characteristics of ion-exchange membranes and electrode assembly for fuel cells in electrolysis cells [NASA-CASE-XMS-03063] 16 p2541 N71-28044
- CHEMICAL BONDS
- NT HYDROGEN BONDS
- Investigating Sillard-Chalmers processes in organic compounds with direct multiple bonds between heavy activated atom and carbon atoms of organic radical [PRIC-139] 04 p0906 N71-14235
- Electron microbeam probe identification of bonding and chemical combinations [AD-713711] 05 p0640 N71-14094
- Investigating existence of chemically bound neutrons in lithium fluoride crystals [ANL-7729] 08 p1283 N71-19540
- Effects of chemical bonding between phases of glass-metal composite on strength and fracture behavior 11 p1783 N71-23810
- Theoretical aspects of semiconductivity in amorphous semiconductors from viewpoint of chemical bonding [RM-505] 13 p2153 N71-25401
- Nuclear quadrupole resonance spectroscopy of nitrogen bonds in amines with boron, amine, and chlorine substitution including atomic structure and lattice effects in ionic crystals 14 p2306 N71-35338
- Variable-reduced-mass model for describing long amplitude bending and K-type rotation of triatomic molecules 14 p2307 N71-35405
- Prediction of unimolecular rate constants of copper, zinc, nickel, and cobalt and catalytic action of metal chains in Sorbital and glyoxime oxidation [NASA-TT-F-137111] 17 p2716 N71-30113
- Electrophysical properties and structure of chemical bond in boron, carbon, and beryllium compounds [LA-TR-71-30] 21 p3586 N71-34609
- Variation method, and binding energy and structure of atoms and molecules 23 p3720 N71-36518
- Heat resistance of titanium examined by formation of solid solutions and compounds with varying degree of disorder and chemical bond strength [AD-727424] 24 p3937 N71-38000
- High temperature electron swarm apparatus for investigating electron attachment to polyatomic molecules 24 p3903 N71-38420
- CHEMICAL CLEANING
- Nitric acid-hydrofluoric acid pickling effects on stress corrosion cracking of mild-tempered Ni-Cr-Pb alloy in pure water at 660 F [WAPD-TM-944] 07 p1045 N71-10839
- Electrochemical procedure for removal of surface oxidation products on uranium alloys [RFP-1596] 17 p2763 N71-28517
- Specifications for cleaning, fusion welding, and postwelding treatment and aluminum alloys [NASA-TM-X-67679] 18 p2956 N71-31115
- Surface preparation, materials, solution, and operating conditions for electro-brightening and chemical brightening 20 p3312 N71-33640
- CHEMICAL COMPOSITION
- NT CARBON DIOXIDE CONCENTRATION

SUBJECT INDEX

Viscosity and chemical composition of dispersion medium affecting aromatic hydrocarbons in lithium process
[AD-711177] 01 p0072 N71-10683

Luna-16 soil samples
[NASA-TT-F-13432] 03 p0452 N71-12556

Post-weld nitrogen content of deposits on standard and H₂-proof austenitic stainless steels
[PB-195290] 03 p0386 N71-13286

Chemical composition changes of mitochondria during cardiac hypertrophy and hypoxia
[ACR-1000-199] 06 p0002 N71-16367

Chemical composition of copper-silver binary alloys using X ray fluorescent analysis
[AD-713936] 06 p0873 N71-16437

Composition and properties of high energy hyper-elastic rocket propellants
[AGARD-AD-141-70] 07 p1098 N71-17841

Investigating composition and ages of Icelandic lavas to determine validity of sea floor spreading
07 p1025 N71-17975

Mass and infrared spectroscopic and gas chromatographic analysis of air samples from space station simulator during 90 day manned test
[NASA-CR-111851] 09 p1413 N71-19636

Chemical composition of copper clad laminates and resin used for printed circuit insulation, impregnation, and protection
10 p1511 N71-20684

Composition of trace contaminants in space station simulator atmosphere during long term operation
10 p1506 N71-20962

Chemical composition and structure of low silica sodium hydraluminoalicates determined by IR spectroscopy
[NLL-RRE-TRANS-288/8036.47] 10 p1513 N71-21239

Chemical composition of nuclear particles in extensive isomeric storms
10 p1641 N71-21550

Cernikov light detection system at Monte Chacaltay, Bolivia, and chemical composition of primary cosmic rays
10 p1641 N71-21551

X ray diffraction measurement of crystal composition profiles, structure, and misorientations in nickel and gold electrodeposited diffusion zones of copper(111) single crystals
10 p1583 N71-21588

Evolution and structure of metal rich stars
11 p1826 N71-22110

Chemical synthesis and crystal growth of pure and doped europium chalcogenides, including magnetic moment, transport properties, and photoconductivity data
[AD-717369] 11 p1816 N71-22120

Escherichia coli cell phospholipid composition changes during spheroplast formation in presence of antibiotics and sucrose
[NASA-TT-F-13480] 11 p1683 N71-22506

Composition and atomic ordering effects in Fe-Co alloy systems using Mossbauer spectroscopy and measurement of effective magnetic field at Fe nuclei, inner shift, and quadrupole splitting
11 p1780 N71-22794

Interstitial concentration, solvent composition, stress, and temperature gradient effects on interstitial diffusion in metals based on hydrogen diffusion in titanium
11 p1780 N71-22795

Chemical composition and bending strengths of lithium-potassium and lithium-sodium silicate glass systems under melting conditions
11 p1783 N71-22893

Chemical composition, electromagnetic properties, raw materials, and production techniques for various types of ferrites
[PB-325922] 12 p1965 N71-23285

Chemical composition of gaseous nebulae, and atmospheres of normal stars and objects with unusual metal to hydrogen ratios
[AD-716411] 12 p1997 N71-24287

Chemical composition and radioactivity analyses of lunar surface materials
[NASA-CR-114976] 13 p2165 N71-24558

Comparison of analytical results of lunar surface materials from Surveyor, Apollo, and Luna missions
13 p2165 N71-24559

Chemical composition and energy spectra of primary cosmic radiation
[AD-728410] 14 p2334 N71-25911

Oil viscosity and chemical composition effects on oil bearing lubricant efficiency
15 p2415 N71-26836

Medium density and chemical composition and measurement geometry effects on accuracy of neutron neutron measurement method
[BQ-709] 16 p2659 N71-29172

Chemical composition of odorants in diesel engine exhaust
[PB-198072] 17 p2839 N71-29786

Rubber composition for expulsion bladders and diaphragms for use with hydrazine
[NASA-CASE-NPO-11433] 18 p2940 N71-31140

Chemical composition of lunar samples from Apollo 11 and 12 flights
[NASA-TT-F-13787] 19 p3181 N71-32388

Composition, and chemical, physical, and concentration properties of human urine
[NASA-CR-1802] 19 p3045 N71-32520

Air pollution sources, distribution, biological effects, and mathematical models
[P-4571] 20 p3261 N71-33299

Argon, krypton, and xenon heating analysis, electron microprobe analysis for chemical composition, and depth studies of cosmogenic gases of lunar rocks
[NASA-CR-121722] 21 p3587 N71-34983

Chemical composition, meteorological parameters, cloud layer, atmospheric circulation, upper atmosphere, and origin and evolution of Venusian atmosphere
[NASA-TT-F-13722] 21 p3587 N71-34988

Lusckhod-1 RIFMA instrument for analyzing chemical composition of lunar soil
[NLL-M-20428-(5828.4F)] 21 p3526 N71-35122

Crystal composition, melt composition, growth temperature, and phase diagram of Ge-Al-As ternary grown by liquid epitaxy
23 p3837 N71-37362

Atmospheric precipitation composition in various Soviet regions
[AD-727957] 24 p3953 N71-38200

Gamma logging data interpretation techniques for radioactive elements in individual borehole layers
[CSIRO-TRANS-10088] 24 p3974 N71-38350

Control and chemical composition of aircraft fuels, lubricants, and special liquids
[AD-727199] 24 p4000 N71-38531

CHEMICAL COMPOUNDS
Low gravity manufacturing of vaccines and chemicals in space laboratory by unit separation
02 p0235 N71-11712

Industrial chemical manufacture in spacecrafts
02 p0177 N71-11731

Directed crystallization of compounds during impurity exchange of liquid phase with crucible and atmosphere
10 p1634 N71-20890

Chemical reaction kinetics in qualitative changes of substances
14 p2215 N71-26454

Characteristics of superpure compounds and establishment of classification based on behavior of impurities not described by laws of chemical thermodynamics
16 p2555 N71-28291

Effects of foreign contaminants on superpurification processes and limitations imposed on production of semiconductor devices
16 p2555 N71-28292

Manual and mechanized methods of retrieving information on chemical compounds from data retrieval systems
19 p3195 N71-31984

Problems of retrieving data on chemical compounds and materials using manual data retrieval system
19 p3195 N71-31985

Equations and computer program for calculating chemical equilibria in thermodynamic states of complex systems
[NASA-SP-273] 24 p3897 N71-37775

CHEMICAL EFFECTS
Bibliography on chemical effects of nuclear transformations for year 1969
[NP-18402] 05 p0739 N71-15852

Preparation and characteristics of indium arsenide films grown by coplanar chemical transport used for commercial production of thin film Hall generators
11 p1814 N71-21939

CHEMICAL ELEMENTS
NT ACTINIDE SERIES
NT ALKALINE METALS
NT ALKALINE EARTH METALS
NT ALUMINUM
NT ALUMINUM ISOTOPES
NT ALUMINUM 26
NT ALUMINUM 27
NT AMERICIUM
NT AMERICIUM ISOTOPES
NT AMERICIUM 241
NT ANTIMONY
NT ARGON
NT ARGON ISOTOPES
NT ARSENIC ISOTOPES
NT ASTATINE ISOTOPES
NT BARIUM
NT BARIUM ISOTOPES
NT BERYLLIUM
NT BERYLLIUM ISOTOPES
NT BERYLLIUM 7
NT BERYLLIUM 9
NT BERYLLIUM 10
NT BISMUTH
NT BISMUTH ISOTOPES
NT BORON
NT BORON ISOTOPES
NT BORON 10
NT BROMINE

CHEMICAL ELEMENTS

NT BROMINE ISOTOPES
NT CADMIUM
NT CADMIUM ISOTOPES
NT CALCIUM
NT CALCIUM ISOTOPES
NT CALIFORNIUM
NT CALIFORNIUM ISOTOPES
NT CARBON
NT CARBON ISOTOPES
NT CARBON 12
NT CARBON 13
NT CARBON 14
NT CERIUM
NT CERIUM ISOTOPES
NT CESIUM
NT CESIUM VAPOR
NT CESIUM 133
NT CESIUM 134
NT CESIUM 137
NT CESIUM 144
NT CHARCOAL
NT CHLORINE
NT CHROMIUM
NT CHROMIUM ISOTOPES
NT COBALT
NT COBALT ISOTOPES
NT COBALT 58
NT COBALT 60
NT COPPER
NT COPPER ISOTOPES
NT CURIUM
NT CURIUM ISOTOPES
NT CURIUM 244
NT DEUTERIUM
NT DEUTERIUM PLASMA
NT DYSPROSIUM
NT DYSPROSIUM ISOTOPES
NT ELEMENT 104
NT ELEMENT 105
NT ERBIUM
NT ERBIUM ISOTOPES
NT EUROPIUM
NT FLUORINE
NT GADOLINIUM
NT GALLIUM
NT GALLIUM ISOTOPES
NT GERMANIUM
NT GERMANIUM ISOTOPES
NT GOLD
NT GOLD ISOTOPES
NT HAFNIUM
NT HAFNIUM ISOTOPES
NT HALOGENS
NT HELIUM
NT HELIUM ATOMS
NT HELIUM FILM
NT HELIUM ISOTOPES
NT HOLMIUM
NT HOLMIUM ISOTOPES
NT HYDROGEN
NT HYDROGEN ATOMS
NT HYDROGEN IONS
NT HYDROGEN ISOTOPES
NT HYDROGEN PLASMA
NT INDIUM
NT INDIUM ISOTOPES
NT IODINE
NT IODINE 125
NT ITRIDIUM
NT ITRIDIUM ISOTOPES
NT IRON
NT IRON ISOTOPES
NT IRON 57
NT IRON 59
NT ISOTOPES
NT KRYPTON
NT KRYPTON 65
NT LANTHANUM
NT LANTHANUM ISOTOPES
NT LAWRENTIUM
NT LEAD (METAL)
NT LEAD ISOTOPES
NT LIGHT ELEMENTS
NT LIQUID HELIUM
NT LIQUID HYDROGEN
NT LIQUID NITROGEN
NT LIQUID POTASSIUM
NT LIQUID SODIUM
NT LITHIUM
NT LITHIUM ISOTOPES
NT LUTETIUM
NT LUTETIUM ISOTOPES
NT MAGNESIUM
NT MAGNESIUM ISOTOPES
NT MANGANESE
NT MANGANESE ISOTOPES
NT MERCURY (METAL)
NT MERCURY ISOTOPES
NT MERCURY VAPOR
NT METALLOIDS
NT MOLYBDENUM
NT NEODYMIUM
NT NEODYMIUM ISOTOPES
NT NEON
NT NEON ISOTOPES

CHEMICAL ENERGY

NT NEPTUNIUM
NT NEPTUNIUM ISOTOPES
NT NICKEL
NT NICKEL ISOTOPES
NT NIOBIUM
NT NIOBIUM ISOTOPES
NT NITROGEN
NT NITROGEN ATOMS
NT NITROGEN IONS
NT NITROGEN ISOTOPES
NT NITROGEN 15
NT NITROGEN 16
NT NOBELIUM
NT NUCLIDES
NT ORTHO HYDROGEN
NT OSMIUM
NT OSMIUM ISOTOPES
NT OXYGEN ISOTOPES
NT OXYGEN 18
NT PALLADIUM
NT PHOSPHORUS 32
NT PLATINUM
NT PLATINUM ISOTOPES
NT PLUTONIUM
NT PLUTONIUM ISOTOPES
NT PLUTONIUM 238
NT PLUTONIUM 239
NT PLUTONIUM 240
NT PLUTONIUM 241
NT POLONIUM ISOTOPES
NT POLONIUM 210
NT POTASSIUM
NT POTASSIUM ISOTOPES
NT POWDERED ALUMINUM
NT PRASEODYMIUM
NT PRASEODYMIUM ISOTOPES
NT PROMETHIUM ISOTOPES
NT PROTACTINIUM ISOTOPES
NT RADIOACTIVE ISOTOPES
NT RADIUM
NT RADIUM ISOTOPES
NT RADIUM 226
NT RADON
NT RADON ISOTOPES
NT RARE EARTH ELEMENTS
NT RARE GASES
NT REFRACTORY METALS
NT RHODIUM
NT RHODIUM ISOTOPES
NT RUBIDIUM
NT RUBIDIUM ISOTOPES
NT RUBIDIUM 86
NT RUTHENIUM
NT RUTHENIUM ISOTOPES
NT SAMARIUM
NT SAMARIUM ISOTOPES
NT SCANDIUM
NT SCANDIUM ISOTOPES
NT SELENIUM
NT SILICON
NT SILICON ISOTOPES
NT SILVER
NT SILVER ISOTOPES
NT SODIUM
NT SODIUM ISOTOPES
NT SODIUM VAPOR
NT SOLID NITROGEN
NT STRONTIUM
NT STRONTIUM ISOTOPES
NT STRONTIUM 88
NT STRONTIUM 89
NT STRONTIUM 90
NT SULFUR
NT SULFUR ISOTOPES
NT TANTALUM
NT TECHNETIUM
NT TECHNETIUM ISOTOPES
NT TELLURIUM
NT TELLURIUM ISOTOPES
NT TERBIUM
NT TERBIUM ISOTOPES
NT THALLIUM
NT THALLIUM ISOTOPES
NT THORIUM
NT THORIUM ISOTOPES
NT THULIUM
NT THULIUM ISOTOPES
NT TIN
NT TIN ISOTOPES
NT TITANIUM
NT TITANIUM ISOTOPES
NT TRACE ELEMENTS
NT TRANSURANIUM ELEMENTS
NT TRITIUM
NT TUNGSTEN
NT TUNGSTEN ISOTOPES
NT URANIUM
NT URANIUM ISOTOPES
NT URANIUM 232
NT URANIUM 233
NT URANIUM 235
NT URANIUM 238
NT VANADIUM
NT XENON
NT XENON ISOTOPES
NT XENON 133

NT XENON 135
NT YTTERBIUM
NT YTTERBIUM ISOTOPES
NT YTTRIUM
NT YTTRIUM ISOTOPES
NT ZINC
NT ZINC ISOTOPES
NT ZIRCONIUM
NT ZIRCONIUM ISOTOPES
Inert - sulfuric acid of iridium, rhodium, ruthenium and platinum
[NASA-TT-F-13357] 01 p0047 N71-10351
Creation of chemical elements by nuclear reactions in exploding stars 01 p0124 N71-10957
Analysis of proposition that chemical elements were created by nuclear reactions in stars
[AD-716097] 06 p0946 N71-16240
X ray analysis, metallographic, and electron microprobe analyses of reaction-diffusion in metal-metal binary and multicomponent systems of Ti/SiC and Ti-6Al-4V/SiC 10 p1586 N71-21820
Bibliography of activation analysis publications up to 31 Jan. 1971
[NBS-TN-467-PT-1] 17 p2717 N71-30266
Activation analysis bibliography up to 31 Jan. 1971 including chemical element, methodology, matrix analysis, and author indexes
[NBS-TN-467-PT-2] 17 p2717 N71-30267
Express extraction and universal precipitation methods for radiochemical determination of Pu, Am, Cm, Cf, Bk, and fission products in irradiated materials
[SRARI-P-81] 18 p2976 N71-30575
Values of solar abundances of 65 elements, and isotope ratios for 8 elements
[AD-723633] 19 p3178 N71-31795
Activation analysis of fecal samples from Apollo 7, 8, 9, and 10 astronauts to determine effects of space flight on mass balance of various elements by human body
[NASA-CR-121861] 21 p3381 N71-34058
Determining micro amounts of elements contained in natural water by means of neutron-activation analysis
[RT/CHI-70/33] 23 p3812 N71-37179
Spectrum analysis of chemical elements existing in solar atmosphere 24 p4014 N71-38632
Thermochemical properties of chemical elements and compounds - tables 24 p4033 N71-38775
CHEMICAL ENERGY
NT ENERGY OF FORMATION
Hazardous conditions associated with electrical, chemical, and radiated energies
[AD-718783] 12 p2019 N71-24107
CHEMICAL ENGINEERING
Chemical research relating to nuclear fuel elements and reactor materials
[CEA-N-1241] 01 p0102 N71-10924
Chemical engineering and research for nuclear fuel technology
[ANL-7630] 04 p0553 N71-13975
Chemical recovery and refinement procedures in electromagnetic separation of isotopes
[ORNL-4583] 04 p0584 N71-14186
Research and development in chemical engineering
[TT-68-50056/5-7] 05 p0639 N71-14777
Research progress in various aspects of applied mathematics, metallurgy, engineering, nuclear physics, and optical measurement 05 p0679 N71-15544
Chemical technology applications to nuclear reactor fuels
[ORNL-4572] 07 p1065 N71-17665
Research and development in ceramic engineering, chemical engineering, chemistry, mathematics and computer science, metallurgy, physics, and reactor materials and technology
[IS-2300] 13 p2193 N71-25596
Chemical analysis techniques and equipment for nuclear chemistry
[CEA-N-1341] 15 p2377 N71-27202
Basic secondary publications on chemistry and chemical engineering promoting international cooperation in information dissemination 19 p3194 N71-31981
Major Soviet information institutes on chemistry and chemical technology providing single classification system for information service system 19 p3195 N71-31982
Production operation planning and control theory for complex chemical engineering system 21 p3406 N71-34231
CHEMICAL EQUILIBRIUM
NT ACID BASE EQUILIBRIUM
Solution of chemical nonequilibrium boundary layer flow of hypoboloid in earth atmosphere 03 p0361 N71-12588
Equilibrium normal shock properties for vibrationally excited Co₂-N₂-He gas mixtures
[AD-712510] 03 p0364 N71-13155

SUBJECT INDEX

Investigating phase equilibria, electrical conductance, and density in system ZnCl₂ as low temperature analog of SiO₂ and BeF₂ system
[COO-2008-2] 05 p0711 N71-15304
Sorption equilibrium and kinetics of water vapor on anodized aluminum 08 p1158 N71-18497
[AD-715914]
Acid-base equilibrium in aluminum chloride melts and electrochemical measurements 09 p1343 N71-19546
Volcanic gas collections used to calculate chemical composition of volatile fraction of basaltic magma gas phase
[NASA-TR-X-348] 13 p2071 N71-24610
Derivation of equations for coupled gas species concentrations equations in chemical equilibrium using free energy and equilibrium methods for specific heat and acoustic velocity calculations
[AD-720004] 14 p2213 N71-25941
Equilibrium, reactions, and sintering in ternary system containing iron oxide 16 p6009 N71-28123
Chemical analysis of polymerization products in alpha-aminopropionitrile equilibrium reaction and chemical properties
[NASA-TT-F-13712] 18 p2884 N71-30260
Numerical analysis of chemical thermodynamic reactions to find equilibrium composition of chemical systems
[P-4638] 19 p3193 N71-32335
Numerical scheme for solution of general turbulent tube flow problem with surface mass transfer and nonequilibrium chemical reactions 23 p3746 N71-36711
Equations and computer program for calculating chemical equilibria in thermodynamic states of complex systems
[NASA-SP-273] 24 p3897 N71-37775
CHEMICAL EXPLOSIONS
NT GAS EXPLOSIONS
Behavioral aspects of hexanitrostilbene in small charges
[SC-CR-70-6076] 01 p0100 N71-10795
Analysis of procedures for determining fire or explosion hazards of materials exposed to liquid or gaseous oxygen
[NASA-TM-X-66926] 09 p1470 N71-19956
Analysis of thermal radiation frost propagation from point explosion using radiation diffusion approximation techniques
[FOA-4-C-4402-23/25/1] 13 p2187 N71-25407
Development of technique for charging and exploding large amounts of trinitro explosive to simulate mechanical and thermal effects of nuclear explosions
[FOA-4-C-4408-26] 22 p3696 N71-30362
CHEMICAL EXTINGUISHERS
U FIRE EXTINGUISHERS
CHEMICAL FUELS
NT AEROSOL
NT AIRCRAFT FUELS
NT GASOLINE
NT HYDROCARBON FUELS
NT HYDROGEN FUELS
NT JET ENGINE FUELS
NT JP-5 JET FUEL
NT METAL FUELS
NT SLURRY PROPELLANTS
Chemical and physical properties of aircraft fuels gelled with hydrocarbon resins
[FAA-HA-71-17] 19 p3172 N71-32878
Comparison of nuclear space power unit reactor principles with chemical fuels, solar cells, and radioisotope systems 22 p3621 N71-33882
CHEMICAL KINETICS
U REACTION KINETICS
CHEMICAL LASERS
Chemistry program review including work in kinetics, electrochemistry, chemical lasers, trace element analysis, photoionization, and photoelectron spectroscopy
[AD-705264] 02 p0172 N71-11213
Hydrocarbon-air laser, and thermodynamics of flame structure
[AD-711581] 02 p0239 N71-11598
CW chemical laser development, N₂-C₂ electrically excited fluid mixing laser techniques, and gas dynamic mixing behind shock waves
[NASA-CR-117503] 10 p1571 N71-31840
Theoretical analysis of continuous chemical laser emphasizing constant gain method of solution and strong coupling in cavity between radiation and chemistry
[AD-720794] 14 p2265 N71-25944
Atomic iodine photodissociation and UP₂-H₂ hydrogen fluoride chemical lasers for studying vibrational energy distribution in reaction products and chemical reactivity 14 p2266 N71-26313
CHEMICAL MACHINING
NT ELECTROCHEMICAL MACHINING
Manufacturing process and construction methods for fluidator laminates using chemical milling
[FK-49111] 05 p0664 N71-14090

SUBJECT INDEX

Cosmic thunderstorm data analyzed for universal time variations and comparison of chemical polishing and etch pitting on sapphire 16 p2694 N71-28201

Analysis of three dislocation etchants and two chemical polishes for effective temperature and orientation ranges on sapphire and comparison of etchants effectiveness on dislocation pitting 16 p2664 N71-28203

CHEMICAL MILLING
U CHEMICAL MACHINING
CHEMICAL PROPERTIES
 NT ACIDITY
 NT HEAT OF COMBUSTION
 NT HEAT OF FORMATION
 NT HEAT OF VAPORIZATION
 NT SALINITY
 NT THERMOCHEMICAL PROPERTIES
 Synthesis and properties of cobalt complexes containing bidentate binding ligand [AD-716758] 02 p0175 N71-11234
 Effects of unusual environmental conditions on characteristics and stability of drugs 02 p0161 N71-11495
 Structure and properties of unidirectionally solidified superalloys 02 p0242 N71-11632
 Properties, preparation, structure, and uses of solids [AD-712413] 03 p0333 N71-12371
 Alpha decay, and chemical properties of isotopes of element 104 [UCRL-18633] 03 p0421 N71-12647
 Development of meridional model of oxygen-hydrogen atmospheres [AD-719421] 05 p0672 N71-14066
 Physical, chemical, and mechanical property data of silicon carbide [ORNL-4583-VOL-1] 05 p0708 N71-15063
 Preparation and properties of polycrylonitrile fibers with difluoro as comonomer [RAE-LIB-TRANS-1464] 05 p0709 N71-15175
 Solid state chemistry of rare earth oxides [COO-1109-32] 06 p0931 N71-15877
 Materials science research on lasers, high pressure effects, superconductors, crystal structure, and chemical and physical properties [AD-713909] 06 p0961 N71-16331
 Physical and chemical properties of metallic elements and inorganic compounds at high temperatures [NYO-4176-3] 07 p1130 N71-17636
 Chemical properties of polyquinoxalines containing nitroaryl groups [AD-716025] 09 p1403 N71-19667
 Chemical treatment of glass surfaces to improve wetting strength, resistance to abrasion and chemical action, and hydrophobic reaction [NASA-TT-F-13477] 09 p1406 N71-20089
 Chemical and mechanical properties and synthesis of 4-vinylphenyl-isoprene ABA block copolymers for permeation and propellant binder studies [NASA-CR-117305] 09 p1344 N71-20152
 Chemical, mechanical, and physical property data for thorium ceramics [ORNL-4503-VOL-2] 09 p1408 N71-20594
 Method for producing alternating ether-alkene copolymers with stable properties when exposed to elevated temperatures and UV radiation [NASA-CASE-XMP-42584] 10 p1512 N71-20905
 Chemical characteristics and synthesis of polyquinoxalines with carbonyl groups in polymers [AD-716742] 10 p1580 N71-21029
 Chemical properties of cellulose acetate gels in both dry and gel states [BRC-T-1439] 10 p1512 N71-21208
 Effects of high temperature and composition gradients along external surface of catalyst particle behavior 10 p1513 N71-21275
 Synthesis and chemical properties of elastomeric polymers resistant to effects of fluorine, oxygen, alcohols, nitrogen tetroxide, and similar agents [NASA-CR-117498] 10 p1511 N71-21499
 Physical and chemical effects on reactivity of artificial graphite used for electrode technology [BRL-TR-5841] 10 p1580 N71-21583
 Design and fabrication of shield block for series of organic fluid capsule tests to evaluate combined effects of temperature and radiation [ORNL-TM-3214] 10 p1496 N71-21608
 Chemical and magnetic properties of single alpha manganese crystal structure 11 p1814 N71-21862
 Double-point method and gas content method for determining helium saturation level of AeroZINE-50 as stress indicator [NASA-TN-D-4249] 11 p1832 N71-22612
 Hydrological investigation of variability of temperature and chemical properties of Lago Vanda in Antarctica 11 p1759 N71-22863
 Oxygen difluoride hazards, chemical and physical properties, decontamination methods, and transfer to other toxic substances manual [NASA-CR-72401] 12 p1925 N71-23149

Hydride physico-chemical and chemical properties, reactions, purification, isolation, and analysis techniques [AD-718179] 12 p1870 N71-23519
 Investigation of structure, bonding, electronic composition, and transport properties of amorphous semiconductors [AD-719419] 13 p2150 N71-24640
 Analysis of cathodoluminescent properties of polycrystalline powdered phosphors of yttrium and europium 13 p2039 N71-24726
 Research on carbonization, radiation effects, chemical properties, and mechanical properties of graphite and carbon compounds [NYO-1710-108] 14 p2276 N71-25679
 Preparation and properties of polyfunctional polymeric lubricant additives [AD-720369] 14 p2278 N71-25895
 Periodicity of lanthanide and actinide properties [DNR-1212] 14 p2303 N71-26201
 Production engineering and chemical, mechanical, and thermodynamic properties of thorium dispersed nickel chrome alloys for space shuttle thermal protection applications [NASA-TM-X-64602] 15 p2428 N71-27008
 Properties and selective applications of thermosetting and thermoplastic polymers 15 p2429 N71-27042
 Chemical properties and half life of selenium [ORNL-TR-2428] 15 p2460 N71-27071
 Characteristics of superpure compounds and establishment of classification based on behavior of impurities not described by laws of chemical thermodynamics 16 p2555 N71-28291
 Chemical analysis of polymerization products in alpha-aminopropionitrile equilibrium reaction and chemical properties [NASA-TT-F-13712] 18 p2884 N71-30509
 Composition, and chemical, physical, and constructive properties of human urine [NASA-CR-1802] 19 p3045 N71-32520
 Lectures presented at seminar in various scientific fields [ISS-70/20] 20 p3310 N71-33161
 Synthesis and properties of metal chelates for polymerization studies 21 p3388 N71-34105
 Computational approach for measuring and evaluating heat effects in liquid chemical samples with elevated temperature differential scanning calorimetry 21 p3389 N71-34110
 Chemical and physical properties and mass response to nitrogen oxides in atmosphere [AF-84] 22 p3612 N71-35730
 Mechanical, physical, and chemical properties of Indite SA synthetic foam systems [BDD-613-177] 23 p3777 N71-36921
 Effect of temperature of infrared overtones spectra of D2O and HOD in liquid state under saturation conditions into supercritical region [NLL-CE-TRANS-5458-0022-09] 24 p3968 N71-38306

CHEMICAL PROPULSION
 Comparative performance of solid core nuclear and cryogenic chemical space propulsion systems [NASA-TM-X-2532] 18 p3082 N71-31246

CHEMICAL REACTION CONTROL
 Control of hydrogen absorption in electroplating 02 p0231 N71-11634
 Analysis of high temperature oxidation rate of carbon for use as reentry material [NASA-TN-D-4310] 16 p2616 N71-28012
 Numerical analysis of chemical thermodynamic reactions to find equilibrium composition of chemical system [P-4538] 19 p3193 N71-32555
 Oxygen reactivity effects on cosmic NaK alloy and SNAP 8 system including oxygen contamination sources, oxide solubility, and oxide control methods [NASA-CR-72653] 24 p3959 N71-38342

CHEMICAL REACTIONS
 NT ATOMIC RECOMBINATION
 NT CARBOXYLATION
 NT CHLORINATION
 NT COPOLYMERIZATION
 NT DEHYDROGENATION
 NT DENITROGENATION
 NT DEOXYDIZING
 NT DESULFURIZING
 NT ELECTROCHEMICAL OXIDATION
 NT EXOTHERMIC REACTIONS
 NT FERMENTATION
 NT FLUORINATION
 NT HALOGENATION
 NT HYDROGENATION
 NT HYDROGENOLYSIS
 NT HYDROLYSIS
 NT ION RECOMBINATION
 NT NITRATION
 NT NITRIDING
 NT OXIDATION
 NT OXYGENATION
 NT PHOSPHORYLATION

CHEMICAL REACTIONS

NT PHOTOCHEMICAL REACTIONS
 NT PHOTOCHEMISM
 NT PHOTOCOMPOSITION
 NT PHOTOLYSIS
 NT PHOTOSYNTHESIS
 NT PYROHYDROLYSIS
 NT PYROLYSIS
 NT RADIOLYSIS
 NT REDUCTION (CHEMISTRY)
 NT SABATER REACTION
 NT THERMAL DISSOCIATION
 NT TITRATION
 Optimal conditions for obtaining solid solutions of Ba, Sr, and TiO₂ [AD-711176] 01 p0889 N71-10889
 Effect of structure on rate and mechanism of addition of dihalomethide ions to methyl acrylate [AD-710991] 02 p0172 N71-11210
 Development of molecular orbital methods for applications to organic systems [AD-711100] 02 p0172 N71-11211
 Preparation and characterization of heteropoly tungstates [AD-711290] 02 p0172 N71-11215
 Effect of water vapor on ozone synthesis in photo-oxidation of alpha-phenols [REPT-70-122] 02 p0172 N71-11216
 Synthesis and polymerization of beta-alkylstyrenes [AD-711097] 02 p0173 N71-11218
 Chemical properties of optically active compounds containing germanium or silicon bonded to platinum [AD-712371] 02 p0173 N71-11220
 Determination of heat of formation of gibbsite from alpha-alumina and water 02 p0173 N71-11221
 Explicit time dependence of perturbed distribution functions for chemically reacting diffusing particles [AD-710748] 02 p0175 N71-11231
 Synthesis and properties of cobalt complexes containing bidentate binding ligand [AD-710758] 02 p0175 N71-11234
 Process for interfacial polymerization of pyromellitic dianhydride and tetraamino benzene [NASA-CASE-XLA-63104] 02 p0175 N71-11235
 Synthesis of polymeric Schiff bases by Schiff-base exchange reactions [NASA-CASE-XMP-06651] 02 p0175 N71-11236
 Preparation of ordered poly(arylimidazole)s/polymers [NASA-CASE-XMP-10733] 02 p0176 N71-11237
 Synthesis and chemical properties of imidazopyrrolone/imide copolymers [NASA-CASE-XLA-08802] 02 p0176 N71-11238
 Integral equations of inviscid hydrodynamics applied to viscous, heat conducting, chemically reacting, radiating shocked flows [AD-711954] 02 p0201 N71-11583
 Chemical nonequilibrium effects in boundary layer and transport properties in rocket engine nozzles [RFE-TR-705] 02 p0305 N71-12058
 Temperature and pressure distributions of sodium reactions [RFE-1034] 02 p0266 N71-12128
 Gel-solubility process chemical studies in EBR-2 [BAW-3714-17] 02 p0266 N71-12186
 Effects of fluorine substitution on properties and reaction rates of monocyclidyl ethers [AD-712507] 03 p0331 N71-12362
 Properties, preparation, structure, and uses of solids [AD-712413] 03 p0332 N71-12371
 Synthesis of carbazone-transition metal complexes of tetrakis(2,4,6-trimethylphenyl)-2,3,5-triazine-4,6-dione from iron pentacarbonyl and 2,3-dichloro-4,6-dibenzotriazine 8 [AD-712540] 03 p0333 N71-12378
 Derivation of chemical reaction rate constants from complex concentration-time data [RFE-TR-493] 03 p0333 N71-12380
 AGARD conference on measuring and chemically reacting viscous flows over hypersonic at hypersonic conditions [AGARDGRAPH-147] 03 p0340 N71-12582
 Physical and chemical reactions of impure and flared elastomers between -150 C and 150 C [NASA-TN-D-6116] 03 p0396 N71-12745
 Synthesis of oil additives, action mechanisms, and production techniques for motor and lubricating oils [AD-712630] 03 p0397 N71-13181
 Research on turbulent flows with chemical reactions [AD-712727] 03 p0365 N71-13313
 Manufacturing flame resistant polyurethane foams by foaming organic diisocyanates in organic compounds with interchangeable hydrogen [NASA-TT-F-12735] 04 p0534 N71-14049
 Structural effect on radiation chemical reactivity of water [AD-713551] 05 p0736 N71-14334
 Kinetics of bimolecular reactions in frozen solutions [AD-713623] 05 p0638 N71-14643
 Radiochemical separation of lanthanum, cerium, and gadolinium from tungsten and selenium irradiated by 14-MeV neutrons [ORNL-TM-32598] 05 p0738 N71-14725
 Mechanism of addition of singlet oxygen to olefins 05 p0640 N71-15409

- Thermal stresses in chemically hardened elastic media and applications to molding processes [NASA-CR-115878] 05 p0781 N71-15627
- Pulse radiolysis studies of fast reactions in molecular systems [COD-1763-16] 06 p0908 N71-15744
- Chemical reactions in molecular flow reactors at high temperatures [AD-714103] 06 p0809 N71-16018
- Project SQUID research in fluid mechanics, chemical reactions, and combustion physics [AD-714236] 06 p0836 N71-16398
- Literature survey and experimental evaluation of graphite properties in high vacuum environment [NASA-CR-111829] 06 p0881 N71-16396
- Technology and procedures for chemical vapor deposition [AD-714517] 06 p0867 N71-16622
- Reactions of selected halogens and interhalogens activated by radiative neutron capture and isomeric transition [COD-1617-26] 07 p0989 N71-17162
- Composition and process for improving definition of resin masks used in chemical etching [NASA-CASE-XGS-04993] 07 p1029 N71-17574
- Comparison of 3D classical trajectory and transition state theory reaction cross sections [JHUX-3780-29] 07 p0990 N71-17890
- Kinetic studies of hydrogen and bromine interactions and surface generation for alkali halide dimers [JHUX-3780-33] 07 p0990 N71-17891
- Investigating theory of chemical evolution on Surtsey Island and relationship to life detection techniques for other planets 07 p1024 N71-17972
- Reactions between liquid dinitrogen tetroxide and titanium alloy that result in stress corrosion cracking [NASA-CR-116796] 08 p1158 N71-18490
- Experimental method for determining parameters for rate of reaction of CO₂ with solid carbon [BM-R1-7476] 08 p1159 N71-18589
- Reaction kinetics of formation of zinc dithionite [NRC-TT-1435] 08 p1159 N71-18842
- Discussing chemistry of dihalides of Group 4B elements as intermediates in liquid and gas phase reactions [NASA-CR-116844] 08 p1161 N71-19168
- Mechanical properties, thermal stability, and synthesis of aromatic polyimides, amide-imides, ester-imides, and pyrrones [RAE-LIB-TRANS-1499] 09 p1343 N71-19631
- Use of solid state reactions and phase transformations to alter structure of solids 09 p1452 N71-19728
- Nickel plaque impregnation to form nickel-cadmium battery plates by nitrate conversion to hydroxides and Fleischer methods [NASA-CR-117306] 09 p1327 N71-20270
- Procedures for submitting and requesting programs to Quantum Chemistry Program Exchange and available literature descriptions [AD-717162] 10 p1511 N71-20694
- Uranium-base niobium alloy and nitric acid reactions and alloy explosive behavior due to two-phase microstructure and high carbon content [RFP-1575] 10 p1511 N71-20700
- Chemical characteristics and synthesis of polyquinolines with carbonyl groups in polymers [AD-716742] 10 p1588 N71-21029
- Characteristics of chemically generated waves in dilute, isothermal atmosphere and numerical analysis of chemical reactions involved [NASA-TM-X-65478] 10 p1542 N71-21303
- Synthesis and structure of MnPC alloy and interferences, atomic distribution, and radial distribution functions for structural model [CALT-822-21] 10 p1580 N71-21394
- Kinetic model of enzyme monomolecular enzyme reactions with substrate and product inhibition and possibility of self oscillation [NLL-RTS-5991] 10 p1500 N71-21401
- Preparation of inorganic solid film lubricants with long wear life and stability in aerospace environments [NASA-CASE-XMF-07988] 10 p1566 N71-21403
- Studying reaction N₂/plus/ plus O₂ yields NO₂/plus/ plus O as function of collision energy using crossed beams [NASA-CR-117527] 10 p1619 N71-21714
- Potential energy surfaces for singlet states of H₂/plus/ [NASA-CR-117500] 10 p1516 N71-21715
- Kinetics mechanisms of step-growth polymerization of polyimides, polybenzimidazoles, and polyquinolines [AD-717641] 11 p1781 N71-21937
- Synthesis and thermochemical properties of organometallic complexes of titanium, zirconium, hafnium, and nickel 11 p1695 N71-21945
- Experimental design and operational problems of ozone difluoride manufacturing in chemical reactions [DLR-FB-70-55] 11 p1696 N71-22292
- Warm fog seeding to determine potential of various sized and unsized hygroscopic chemicals for fog dissipation [NASA-CR-17311] 11 p1790 N71-22619
- Transformation in air components due to marked increase in temperature during reentry shock wave 11 p1813 N71-22640
- Quadrupole mass spectrometer for study of photolytic and heterogeneous reactions 11 p1697 N71-22643
- Synthesis of high purity diaminosilanes [NASA-CASE-XMF-06409] 12 p1869 N71-23230
- Report of research activities including chemistry, reaction kinetics, and crystal structure [AD-714864] 12 p1941 N71-23261
- Hydride physico-chemical and chemical properties, reactions, purification, isolation, and analysis techniques [AD-718179] 12 p1870 N71-23519
- Synthesis and chemical properties of imide-quinoline copolymers 13 p2099 N71-24602
- Synthesis of aromatic diamines and dialdehyde polymers using Schiff base [NASA-CASE-XMF-03074] 13 p2039 N71-24740
- Crystal structure of aluminum alloys, neutron capture cross sections for deuterium, reactor fuels, electron microscopy, and radiation effects on semiconductors [AECL-3776] 13 p2040 N71-24998
- High temperature reaction of MoS₂ with CO₂ [RAE-LIB-TRANS-1494-PT-2] 13 p2040 N71-25125
- Selecting and processing solid carriers for organophosphorus compounds using gas chromatography [JPRS-53065] 13 p2040 N71-25137
- Chemical reactions for producing histidine esters by means of acyl migration from one amino acid to another [NASA-TT-F-13645] 14 p2212 N71-25727
- Conversion of histidine with carboxyl group to peptide bond by synthesizing peptide from acetylated amino acids to histidine [NASA-TT-F-13672] 14 p2212 N71-25728
- Influence of radiation on thermal explosion limit in exothermal chemical reactions 14 p2352 N71-25760
- Atomic iodine photodissociation and UFG-H2 hydrogen fluoride chemical lasers for studying vibrational energy distribution in reaction products and chemical reactivity 14 p2266 N71-26313
- Chemical reaction kinetics in qualitative changes of substances 14 p2215 N71-26454
- Reaction kinetics of elementary, gaseous phase, and condensed phase chemical processes 14 p2215 N71-26463
- Numerical analysis of chemically reacting and diffusing fluid mixtures including longitudinal and transverse wave dispersion and thermodynamics 14 p2242 N71-26472
- Developments in radiation chemistry to include electron in condensed phases, application of cyclotron resonance to chemical reactions, and effects of low temperature 15 p2459 N71-26959
- Pyrochemical processing techniques for recovery and purification of Pu-238 from various fuel materials [ANL-7709] 15 p2447 N71-27180
- Chemical synthesis of hydroxy terminated perfluoroethers as intermediates for highly fluorinated polyurethane resins [NASA-CASE-NPO-10768] 15 p2377 N71-27254
- Particle accelerator design with sputtering radiation source for neutral particle monoenergetic beam study of elementary chemical reactions and kinetics [JUL-674-RC] 15 p2467 N71-27289
- Chemical interferences and ionization in high temperature flame spectroscopy [IS-T-417] 15 p2409 N71-27352
- Chemical synthesis of thermally stable organometallic polymers with divalent metal ion and tetraphenylphosphonium units [NASA-CASE-HQN-10364] 15 p2377 N71-27363
- Apparatus and process for volumetrically dispensing reagent quantities of volatile chemicals for small batch reactions [NASA-CASE-NPO-10070] 15 p2416 N71-27372
- Synthesis of bis-(gamma-aryloxy-beta-chloropropyl) sulfides and disulfides by reacting sulfur chlorides with allyl esters, and their use as additives [AD-720943] 15 p2431 N71-27400
- Pumping effect in oxygen reaction with hot tungsten cathode, and spectrometric measurements of formation energies for volatile species in gas-solid chemical reactions [NASA-CR-118897] 15 p2389 N71-27988
- Quantitative comparison of reactive and nonreactive Mach stems for understanding detonation structure [AD-721465] 16 p2578 N71-28015
- Description of methods for chemical production of superpure inorganic substances [JPRS-53256] 16 p2555 N71-28290
- Characteristics of superpure compounds and establishment of classification based on behavior of impurities not described by laws of chemical thermodynamics 16 p2555 N71-28291
- Description of processes of crystallization and precipitation from chemical solutions and use in production of superpure inorganic materials 16 p2555 N71-28292
- Characteristics and application of adsorption purification methods for production of superpure inorganic materials 16 p2555 N71-28293
- Characteristics and application of rectification methods for production of superpure inorganic materials 16 p2555 N71-28294
- Development of theoretical aspects and practical application of extraction method for purification of inorganic materials 16 p2555 N71-28297
- Chemical transport reactions applied to production of superpure inorganic materials 16 p2555 N71-28340
- Description and numerical analysis of thermal diffusion process of purification 16 p2555 N71-28391
- Removal of microimpurities from substances by chemico-physical methods 16 p2555 N71-28392
- Synthesis of 12 hydroxystearic acid esters of tri 1,1,2-methyl aziridinyl phosphine oxide at 100 C or less [AD-721655] 16 p2557 N71-28354
- Infusible polymer production from reaction of polyfunctional epoxy resins with polyfunctional aziridine compounds [NASA-CASE-NPO-10701] 16 p2557 N71-28620
- Thermal behavior of amorphous poly (4,4'-oxydiphenylene/ pyromellitimide [AD-721934] 16 p2558 N71-28742
- Process for preparing high molecular weight polyoxyalanes from lower molecular weight forms [NASA-CASE-XMF-08674] 16 p2558 N71-28807
- Organometallic compounds of niobium and tantalum useful for film deposition [NASA-CASE-NXP-04023] 16 p2558 N71-28808
- Solutions to boundary layer problems in laminar surface flow with exothermic chemical reactions 16 p2582 N71-28808
- Spectrophotometry of trivalent Fe, divalent CrO₄, and hydroxyl ion complexing in aqueous solution at various oxalic acid concentrations and pH values [NLL-CE-TRANS-5509/9022.091] 17 p2714 N71-29649
- Survey of errors in sampling shock tube gas with mass spectrometer for study of chemical reaction rates at high temperatures 17 p2735 N71-29782
- Analysis of concurrent adsorption and chemical reaction 17 p2715 N71-29941
- Chemical reactions between alkali-lead oxide silica glasses and acid solution at low temperature 18 p2940 N71-31264
- Characteristics of chemical reactions between Methyl alcohol and gases of carbon dioxide, water vapor, nitrogen, and oxygen [SC-DR-710124] 18 p2938 N71-31402
- Developments in production of nylon fabric to improve garment comfort and thermal resistance through diffusion and copolymerization of polyacrylic acid [AD-722913] 19 p3119 N71-31731
- Advantages and disadvantages of information retrieval techniques on organic chemical reactions 19 p3195 N71-31983
- Chemical reaction between polytetrafluoroethylene chips, liquid sodium, potassium, and sodium potassium alloy [TRG-2104] 19 p3120 N71-32045
- Symmetry in chemical reactions with single transition matrix [AD-723997] 19 p3147 N71-32052
- Hot atom beam in halogen and hydrogen sources, cathode sputtering of non-metals, and hot atom reactions of alkali metals 19 p3050 N71-32187
- Numerical analysis of chemical thermodynamic reactions to find equilibrium composition of chemical system [P-4628] 19 p3193 N71-32355
- Synthesis of carbosiloxane polymers by alcoholysis of bis-chlorodimethylsilyl carbosiloxane [AD-724350] 20 p3286 N71-32979
- Preparation and characteristics of free radical and ionic solution of one-ferrocenyl-one, three-butadiene [AD-723963] 20 p3228 N71-33090
- Polyurethane resins derived from hydroxy terminated perfluoroethers or diols [NASA-CASE-NPO-10768-2] 20 p3230 N71-33516
- Spectrophotometric determination of platinum plus 4 and iridium using bromine as reagent 20 p3230 N71-33622
- Q switched laser induced gas breakdown used in hydrogen atom detection, spectral analysis, and chemical reactions [NASA-CR-121646] 21 p3385 N71-34084

SUBJECT INDEX

Synthesis and properties of metal chalcides for polymerization studies 21 p3388 N71-34105

Reaction between chlorosilyl material and aluminum yielding silicon-chalcogen compound 21 p3389 N71-34109

Starch fulgins in glass from thermally activated chemical reaction (SCL-RR-710010) 21 p3444 N71-34310

Developmental history of chemical synthesis of diamonds and hydrogen diamond synthesis in USSR (NLL-M-20593-5028.4P) 21 p3444 N71-34512

Chemical processes for producing oxygen and water from lunar rocks and soils (NASA-TM-X-30061) 21 p3306 N71-34978

Technical criteria for prevention of criticality in chemical processing facilities (AER-405-REV) 22 p3364 N71-35387

Analysis of chemical and electrolytic processes for deposition of copper layers on stainless steel surfaces (NLL-L-71-746-751-5022.401) 22 p3589 N71-35561

Effects of organic substances and determination of products of conversion in electrolytes during electrocatalysis of metals with examples of controlling technique (NLL-L-71-746-727-5022.401) 22 p3397 N71-35617

Process for reduction of silicon peroxide with hydrogen in vacuum at high temperatures 22 p3601 N71-35642

Development of technique for preparing foam materials to be used as thermal structural components in aerospace applications (NASA-CR-1791) 22 p3402 N71-35652

Preparation of benzobistriazole isophenanthroline polymer by polycondensation (AD-726545) 22 p3603 N71-35662

Synthesis of ladder and spine polymers resistant to decomposition (AD-726596) 22 p3603 N71-35663

Chemical analysis of crack propagation in glass (AD-726710) 22 p3603 N71-35664

Differential approximation extension for process gain in pharmacokinetics and fitting by means of experimental data for compartmental models (TR-71-32) 22 p3607 N71-35692

Catalytic activity of common electrolyte catalyst and effects of weight and thickness of medium during reaction of hydrogenation (NLL-L-71-746-719) 23 p3721 N71-36324

Numerical scheme for solution of general turbulent flow problem with surface mass transfer and nonequilibrium chemical reactions 23 p3746 N71-36711

Fabrication and burst testing of reaction-bonded silicon carbide tubes (ABCL-3462) 23 p3761 N71-36812

Delayed oxidation of methylbenzene hydrocarbons during reaction with carbon dioxide (RAE-LIB-TRANS-1494) 23 p3773 N71-36888

Effects of rate of inclusion of sulfur in silicon deposits and consumption of α -chloromethylbenzene (NLL-TRANS-746-730-5022.401) 23 p3780 N71-36939

Analysis of rate of oxidation of petroleum products in water under conditions where nitrogen, phosphorus, and potassium are present (NLL-NSTC-TRANS-3474-6180.591) 24 p3806 N71-37701

Chemical synthesis and inherent tests of ENKs-P-21 (nitro) nitrobenzene additive (AD-727413) 24 p3844 N71-38137

CHEMICAL REACTORS

Nitric oxide-chloride chlorination kinetics in flow reactors utilizing sequential statistical design (IS-7-576) 01 p0068 N71-10700

Weightlessness manufacturing of vaccines and fermenter design for orbital workshop 02 p0161 N71-11713

Describing subsystems of batch silicon epitaxy reactor and effect of chamber geometry on reactor performance 07 p1008 N71-17282

Describing reactor for growing optical silicon films in resistance heated system 07 p1010 N71-17283

Orthogonal collocation method applied to plug flow model of packed bed reactor to predict heat transfer coefficient 12 p1963 N71-33890

Determination of pH CSTR dynamic equations based on acetic acid-cacodylate hydrolysis neutralization and equilibrium equations for chemical reactors 13 p2040 N71-33046

Computerized simulation and time optimal control of pH in acetic acid-cacodylate hydrolysis CSTRs and comparison with Ziegler-Nichols controller for chemical reactors 13 p2046 N71-33047

Developmental history of chemical synthesis of diamonds and hydrogen diamond synthesis in USSR (NLL-M-20593-5028.4P) 21 p3444 N71-34512

Design and tests of monolithic catalyst beds for nonequilibrium hydrogen reactors (NASA-CR-126644) 23 p3719 N71-36598

CHEMICAL REACTION

U MOLECULAR RELAXATION

CHEMICAL REACTION

U CHEMICAL EQUILIBRIUM

CHEMICAL TESTS

NT CHEMICAL ANALYSIS

NT GAS ANALYSIS

NT GAS SPECTROSCOPY

NT MICROANALYSIS

NT NEUTRON ACTIVATION ANALYSIS

NT OZONOMETRY

NT POTENTIOMETRIC ANALYSIS

NT QUALITATIVE ANALYSIS

NT QUANTITATIVE ANALYSIS

NT SALT SPRAY TESTS

NT SPECTROSCOPIC ANALYSIS

NT URINALYSIS

NT VOLUMETRIC ANALYSIS

Mechanical properties and physical, chemical, and thermal tests of polybenzoxazines and carbon fabric laminates for spacecraft thermal insulation (NASA-CR-1793) 15 p3427 N71-26915

Test results of using synthesized dialkylbenzyl sulfides as oil additives (AD-720942) 15 p3431 N71-27401

Chemical spot test for identification of titanium and titanium alloys for aerospace use (NASA-CASE-LAR-10359) 21 p3437 N71-34457

Chemical spot tests for identifying alloying elements in aluminum alloys (BM-RI-7544) 23 p3769 N71-36863

CHEMICAL WARFARE

Fluorescent particle diffusion test for determining atmospheric motion of chemical warfare agents in forest area (AD-713089) 03 p0044 N71-13376

Summary reports and abstracts including nuclear reactions, chemical and biological warfare, applied physics, telecommunication, and systems analysis (RAE-LIB-TRANS-1454) 21 p3532 N71-35173

Flight tests of airborne dissemination devices for chemical warfare (AD-726358) 22 p3540 N71-35218

Title and abstract translations of papers on nuclear reactions, chemical and biological warfare, applied physics, electronics, biotechnology, military psychology, and psychological defense (RAE-LIB-TRANS-1570) 22 p3700 N71-36390

CHEMICALS

Poor land use and hydrologic practices and physical and chemical pollution of Anacostia river valley (NASA-TM-X-65549) 15 p3405 N71-27630

Monitoring techniques for biological and chemical atmospheric contaminants in closed environment (NASA-CR-1026) 17 p2711 N71-29743

CHEMILUMINESCENCE

Photomultiplier tubes for ozone chemiluminescent study (PB-194116) 04 p0533 N71-14210

Monitoring water sterility in spacecraft water storage and supply systems using porphyrin initiated chemiluminescence technique (NASA-CR-114779) 04 p0615 N71-14270

Engineering drawings for chemiluminescent ozone meter (PB-194118) 05 p0683 N71-14813

Analysis of cathodoluminescent properties of polycrystalline powdered phosphors of yttrium and europium 13 p2039 N71-26726

Luminescent processes in solids during interaction with gas 14 p2326 N71-29455

Characteristics of chemiluminescence in flames and combustion in solid rocket propellants (NASA-CR-10263) 16 p2609 N71-28560

Instruction manual for chemiluminescent ozone meter for continuous air monitoring (PB-190863) 17 p2752 N71-29744

Metal oxide infrared emission, and detection of vibrationally excited metal oxide molecules by laser induced fluorescence (AD-725819) 18 p2808 N71-31597

CHEMISORPTION

Electronic effects of chemisorption on powdered zinc oxide catalyst (AD-712834) 03 p0330 N71-12356

Mechanism of adsorption of amino-type corrosion inhibitors (AD-710293) 04 p0408 N71-13472

Effects of chemisorption of CO on methylalumoxane surfaces (AD-715283) 07 p0990 N71-17754

Chemisorption of O₂, CO, and CO₂ on solid fuel under static and dynamic conditions (NLL-RTR-5037) 10 p1630 N71-21746

Carbon monoxide chemisorption on alpha and beta activated iron precipitation catalysts 17 p2714 N71-30487

Iron film adsorption of carbon monoxide, hydrogen and their mixtures 17 p2714 N71-30488

Physics of carbon adsorption 17 p2770 N71-30435

Infrared study of chemisorbed sulfur compounds on platinum and germanium films 18 p2807 N71-31257

Josephson junction formation, and chemisorption of carbon on Pb surface (NASA-CR-123733) 21 p3402 N71-36394

CHEMISTRY

Solid state physics, metallurgy, solid mechanics, geology, and chemistry (AD-712433) 03 p0445 N71-13381

Progress committee on research in chemistry, geology, geology, and physics (AD-715150) 08 p0307 N71-16761

Abstracts on chemical research reports (AD-710661) 07 p0307 N71-17040

Nuclear energy, molecular biology, microbiology, chemistry, and metallurgy research (NIP-10700) 10 p2000 N71-31565

Computer-based chemical information system (PB-191795) 19 p3194 N71-31777

Chemical information systems including information input techniques, retrieval, dissemination, and bibliography (JPRS-53523) 19 p3194 N71-31976

Computer applications in chemical information systems and journal publications 19 p3194 N71-31978

Literature analysis including information aging and bibliography of books and periodical publications pertinent to chemistry 19 p3194 N71-31979

Information system as useful tool for furthering chemical research and selective dissemination of results to various branches of chemistry 19 p3194 N71-31980

Basic secondary publications on chemistry and chemical engineering promoting international cooperation in information dissemination 19 p3194 N71-31981

Major Soviet information institutes on chemistry and chemical technology providing single classification system for information service system 19 p3194 N71-31982

Formulation for particle density distribution in quantum chemistry 20 p3229 N71-33386

Chemistry, physics, metallurgy, and engineering related problems in provision and use of defense material 23 p3836 N71-37488

Curriculum supplement to assist general chemistry teachers in updating instruction materials with aerospace developments (NASA-EP-67) 24 p3885 N71-37691

CHEMOCATALYTIC PROPULSION

U CHEMICAL PROPULSION

U NUCLEAR PROPULSION

CHEMOCATALYTIC PROPULSION

Chemical signal interpretation by olfactory information systems of living organisms 11 p1093 N71-23070

CHEMOTHERAPY

Physiological effects of phenanthrene hydrocarbons on animals at simulated high altitude (AD-711554) 03 p0433 N71-11082

Aeromedical aspects of manned space flight (JPRS-52309) 06 p0803 N71-14530

Onboard medication for space flight crew 06 p0809 N71-14533

Effect of binocular therapy on pilot performance (AD-721634) 16 p2545 N71-30280

CHECKERS

Low locomotor process effects on human and chicken erythrocyte active sodium efflux 02 p0155 N71-11897

CHEILIDEN

Directional cognition in two-dimensional space of children from 3 to 8 years old (NLL-RTR-6334) 12 p1063 N71-23774

CHILE

Meteorological and geostrophical abstracts for Argentina, Chile, and Uruguay (AD-717104) 16 p1597 N71-31243

Night cloud cover and meteorological parameters determined at La Silla, Chile, during 1969 25 p3670 N71-36171

Redesigning, optical and mirror systems, and instrumentation of 150-inch reflecting telescopes in Argentina and Chile 24 p3821 N71-37942

Telescope and site of astronomical observatory at Cerro Las Campanas, Chile 24 p3821 N71-37943

ESO 3.6-m telescope at La Silla, Chile 24 p3821 N71-37944

Surface finishing of ESO (Chile) telescope mirror defects using grinding machine 24 p3822 N71-37976

CHILLING

U COOLING

CHEERS

U AUDITORY SIGNALS

CHIMNEYS

Wind tunnel aerodynamic stability tests on chimneys with plan and helical winding stabilizers
[NPL-AERO-1310] 07 p1233 N71-17334

Measurement of wind induced oscillations of tall cylindrical bodies with emphasis on vortex excited motion
[TT-7008] 09 p1482 N71-20543

Amplitude of vibration and aerodynamic drag of chimneys fitted with vertical fins for vibration damping
[CAIP-MT-69] 15 p2364 N71-27150

CHIMPANZEES

NT HUMAN BEINGS

NT MONKEYS

CHINA

History of rocketry in China including structure of rockets, advantages and disadvantages of various rockets, and capabilities of intercontinental missiles
[AD-730382] 14 p3343 N71-26022

CHIPS

Five models for three dimensional chip curl, chip breaking, and chip control in metal cutting processes
17 p2754 N71-29345

Evaluation of nondestructive tensile testing of chip and wire bonds in semiconductor devices
[NASA-CR-122643] 23 p3860 N71-37516

CHIRAL DYNAMICS

Algebraic theory for elementary particle dynamics
[AD-711441] 01 p0100 N71-10736

Investigating chiral symmetry of multiple charged pion amplitudes
[COO-264-552] 01 p0420 N71-12637

Research in elementary particle theory
[NYO-3399-226] 03 p0423 N71-12740

Models of chiral symmetry in meson states
03 p0424 N71-12773

Theoretical investigation of problems in soft pion and Regge theory
[AD-712746] 03 p0435 N71-13244

Chiral SU(2) x SU(2) hard pion current algebra models
[NUB-2029] 04 p0339 N71-14242

Broken chiral and conformal symmetry and Kuo transformation
[IC7-0911] 04 p0587 N71-14266

Proving uniqueness of Chan-Paton SU(3) factor for dual Born terms involving nonexotic mesons
04 p0588 N71-14310

Developing non-Lagrangian field theory for equal time commutators from broken conformal invariance and chiral U(1) symmetry
[UPT-71-770] 06 p0912 N71-15818

Veneziano model compatibility with current algebra and chiral symmetry
[UHS-511-79-70] 06 p0924 N71-16773

Mass spectrum in chiral model of pseudoscalar and scalar mesons
[SU-1206-230] 07 p1071 N71-17265

Symmetry breaking in chiral model using mass spectra of spin-zero mesons
[SU-1206-228] 07 p1073 N71-17358

Defining super propagator for any mass in field theory with exponential interaction Lagrangian
[DESY-70/50] 08 p1249 N71-18223

Extending model of partially conserved axial current breakdown to higher order on basis of hard meson current algebra
[NUB-2823] 08 p1258 N71-18623

Chiral symmetry coupling of soft pions
[RLO-1388-589] 09 p1431 N71-19892

Chiral dynamics calculations of single pion production in pion-nucleon inelastic scattering
12 p1975 N71-24049

Eta prime meson decay rate calculated from chiral symmetry breaking
[TR-71-189] 13 p2141 N71-25552

Chiral SU(2) times SU(2) dynamics for A1 mesons, rho mesons, and pions
[JINR-E2-5249] 14 p2318 N71-26768

Chiral dynamics of vector meson field coupling and true approximations of scattering amplitudes in Veneziano models
[DEMO-71/1] 15 p3489 N71-27882

Spontaneous breakdowns theory of conformal and chiral symmetry
[CALT-68-295] 16 p3630 N71-28878

Algebra of nonlinear chiral SU(3) x SU(3) symmetry
[JINR-P2-5692] 18 p2977 N71-30637

Broken SU(3) sum rules derived from chiral algebra
18 p2945 N71-31141

Application of algebraic realizations to pion-meson couplings in chiral dynamics and Yang-Mills field theory
[JINR-P2-5759] 22 p3640 N71-35950

Scalar and pseudoscalar fields interaction studied by means of the [SU(3)] sigma model with nonderivative chiral SU(3) x SU(3) invariant and any symmetry breaking
[SU-1206-241] 23 p3814 N71-37199

Current algebra sum rules in neutrino scattering and scale dimension of chiral symmetry breaking Hamiltonian
[TR-72-054] 23 p3819 N71-37244

Chiral symmetry breaking of vacuum

[NYO-2262-TA-243] 24 p3977 N71-38378

CHIRP

NT CHIRP SIGNALS

CHIRP SIGNALS

Nonlinear propagation and chirping of carbon dioxide laser pulses
[AD-722812] 17 p2759 N71-30200

CHLORELLA

Production of algae containing 93 percent C-13
[LA-4496] 06 p0799 N71-15913

Carbon dioxide concentration control in pressure chamber during atmospheric regeneration by Chlorella
08 p1153 N71-19652

Chlorella cultivation for purifying isolated environments of toxic gaseous contaminants
08 p1153 N71-19653

Relative biological effectiveness of multicharged ions during single irradiation of Chlorella
08 p1154 N71-19662

Radioactive decay of naphthalene crystal phosphorescence and Chlorella pyrenoidosa bioluminescence including atomic excitation kinetics
15 p2493 N71-27964

Quantitative analysis of lipid, protein, and carbohydrate content in Chlorella cultivation by pyrolysis and gas chromatography
16 p2543 N71-28255

Combined vibration and gamma irradiation effects on Chlorella culture yield
20 p3223 N71-33472

CHLORIDES

NT ALUMINUM CHLORIDES

NT AMMONIUM CHLORIDES

NT CALCIUM CHLORIDES

NT CARBON TETRACHLORIDE

NT COPPER CHLORIDES

NT HYDROCHLORIC ACID

NT HYDROCHLORIDES

NT LEAD CHLORIDES

NT LITHIUM CHLORIDES

NT MAGNESIUM CHLORIDES

NT PHOSGENE

NT POTASSIUM CHLORIDES

NT SILVER CHLORIDES

NT SODIUM CHLORIDES

NT SULFUR CHLORIDES

NT TETRACHLORIDES

NT TITANIUM CHLORIDES

Nickel oxychloride chlorination kinetics in flow reactors utilizing sequential statistical design
[IS-T-376] 01 p0668 N71-10760

Complexing ability of trivalent lanthanides and actinides in chloride solution
[ORNL-TR-2342] 04 p0484 N71-13442

Physicochemical study of ZnCl₂ based on binary molten salt systems
[COO-2006-3] 05 p0730 N71-15227

Specific heat measurements on trichloride borohydrides of gadolinium, terbium, holmium and isotopes
[IS-T-378] 06 p0883 N71-16786

Presenting results of experiments on methods for preparation of uranyl chlorides
[NP-18248] 07 p0987 N71-16961

Gold transport by complex metal chloride vapors
[BM-R1-7489] 08 p1219 N71-19138

Stress corrosion cracking in iron nickel chromium alloy system in chlorides
[COO-2069-3] 09 p1399 N71-19799

Analysis of crystal-field splittings, Zeeman effect, and line strengths for GdCl₃·6H₂O magnetic dipole transition
[AD-716040] 09 p1454 N71-20094

Impurity behavior during zone melting of lower indium chlorides
10 p1574 N71-20877

Precipitation of nickel and cobalt sulfides from chloride solutions at atmospheric pressure by hydrogen sulfide
[NLL-TRANS-746-542-7022.401] 10 p1513 N71-21257

Diffusion coefficients and other physico-chemical properties of calcium, strontium, and barium chlorides and nitrides
[NRC-TT-1443] 10 p1513 N71-21257

Protonic spin-lattice relaxation time measurements in antiferromagnetic nickel chloride and cobalt chloride crystals
11 p1808 N71-22971

Raman scattering of phosphorus oxychloride and phosphorus oxychloride/zirconium tetrachloride/trivalent neodymium
[SC-RE-78-762] 12 p1978 N71-24301

Oxidation reaction of iron in solutions containing chloride and/or iron(III) at 300 C, studied by hydrogen effusion method
[AD-719887] 14 p2267 N71-25626

Electron irradiation induced separation of Sb from SbCl₃ solutions in anhydrous alcohols, ethers, ketones, acids, esters, and aromatic hydrocarbons
[NASA-TN-D-6358] 14 p2214 N71-26030

Effect of chloride ions on stress corrosion cracking behavior of U-7 1/2 weight percent Nb-2 1/2 weight percent Zr and U-4 1/2 weight percent Nb alloys
[SC-RE-70-660] 17 p2761 N71-20221

Angular distribution and velocity analysis of alkali chloride reactions
21 p3490 N71-34061

CHLORINATION

Nickel oxychloride chlorination kinetics in flow reactors utilizing sequential statistical design
[IS-T-376] 01 p0668 N71-10760

Metallurgy and preparation of titanium materials for chlorination
[AD-717831] 11 p1777 N71-22328

Application of chlorination process to water sanitation for advanced life support systems
[NASA-CR-111854] 15 p2374 N71-30800

Chlorine generator for purifying water in life support systems of manned spacecraft
[NASA-CASE-14-0815] 16 p2596 N71-28093

CHLORINE

Apparatus for extracting radioactive argon from chlorides containing substance
[BNL-TX-364] 06 p0924 N71-16770

Studies of f electron systems in single crystals, including electron nuclear double resonance lines for La and Ce
[COO-294-10] 10 p1624 N71-37770

Measurement of reaction Cl-35(n,gamma)Cl-36 using three-crystal pair and anti-Compton spectrometer
[PH-2] 14 p2317 N71-30773

Chlorine ion implantation of ZnTe crystals to create n-type layers
[CEA-CONF-1719] 14 p2330 N71-30770

Electrode potential and spectrophotometric determination of trace fluorine, chlorine, and boron in plutonium oxide fuels after pyrohydrolytic separation
[KFK-1360] 23 p3801 N71-37000

CHLORINE COMPOUNDS

NT ALUMINUM CHLORIDES

NT AMMONIUM CHLORIDES

NT AMMONIUM PERCHLORATES

NT CALCIUM CHLORIDES

NT CARBON TETRACHLORIDE

NT CHLORIDES

NT CHLORINE FLUORIDES

NT COPPER CHLORIDES

NT DICHLORODIPHENYL-

TRICHLOROETHANE

NT HYDROCHLORIC ACID

NT HYDROCHLORIDES

NT LEAD CHLORIDES

NT LITHIUM CHLORIDES

NT MAGNESIUM CHLORIDES

NT PERCHLORATES

NT PHOSGENE

NT POTASSIUM CHLORIDES

NT POTASSIUM PERCHLORATES

NT SILVER CHLORIDES

NT SODIUM CHLORIDES

NT SULFUR CHLORIDES

NT TETRACHLORIDES

NT TITANIUM CHLORIDES

Potential surface estimates for E-Cl-Cl
[AD-719123] 05 p0736 N71-14153

Preparation of additives containing phosphorus, sulfur, and chlorine from the ethers of glycerol alpha-monochlorohydrate
[AD-718693] 12 p1943 N71-23671

Stoichiometric dichloro-difluoromethane-fluorine combustion reaction
[AD-718375] 12 p2011 N71-24110

Analysis of subvalent Hg ion discovered in molten chloroalkanes
[CONF-701-204-1] 14 p2212 N71-25087

Nuclear magnetic resonance of chlorinated hydrocarbon molecules in excited triplet states using Hammett-type for electron spin-spin, nuclear quadrupole, and hyperfine interaction
[UCRL-20590] 17 p2791 N71-28071

Preparation of new covalent inorganic phosphates from chlorine perchlorate, iodine fluorosulfate preparation, chlorine fluoride reactions, and other inorganic halogen oxidizer investigations
[AD-724331] 20 p3229 N71-33112

CHLORINE FLUORIDES

Agrotoxic materials toxicity screening tests and effects of ethylene glycol, monomethylhydrazine, NF₃, OF₂, and ClF₃
[NASA-CR-111394] 02 p0153 N71-11807

Low temperature fluorine chemistry of chlorine, nitrogen, and oxygen
[AD-727659] 23 p3720 N71-36314

CHLOROTETRAHYDRENE

Radiochemistry for uranium isotopes, uranyl nitrate, uranyl acetate/UFA mixtures, and uranium dioxide/tetrachloroethane
[LAECIL-BIS-245] 18 p2981 N71-30800

CHLOROPHYLLS

High frequency modulated flash scanner for photometric measurements of photochemical reactions
17 p3752 N71-29795

SUBJECT INDEX

CHLOROPRENE RESINS

Delayed action accelerating agent for curing Neoprene compounds 07 p0909 N71-17638

Delayed action accelerator for curing chloroprene resins (RD-153) 07 p0909 N71-17664

(Use of Akroflex AZ as an antioxidant for Neoprenes) 12 p1869 N71-23318

CHLOROPROMAZINE

Chloropromazine and althide effects on conditioned responses of rate to visual and auditory stimuli (AD-71264) 03 p0332 N71-12305

CHOICE

U SELECTION

CHOICES

Program for calculating parameters of optical choice by digital computer (NLL-RT-4155) 17 p2726 N71-29422

CHOICES (RESTRICTIONS)

Shadowgraph photography of shock waves, wave fronts, wave reflection, and Mach cones in one dimensional channel flow passing through chokes (REPT-970) 13 p2021 N71-34481

CHOLESTEROL

Third-harmonic generation in cholesterol, for infrared generation by ultrashort pulses, and self focusing of light as examples of nonlinear optical effects (JCL-36558) 10 p1009 N71-21800

Differential scanning calorimetry for determining physiological chemistry of cholesterol esters in phospholipid-water systems and arteriole disease 20 p3362 N71-32831

CHOLESTEROL

Storage stability of human blood cholesterol esters (AM-70-4) 01 p0009 N71-16374

Conversion of data from three serum cholesterol assay methods (AM-70-13) 01 p0011 N71-10449

Effect of lithium and calcium ions on anticholinesterase activity of erythrocytes (NABA-TT-F-13474) 09 p1333 N71-20179

Physiological effects of ionized air on mice anticholinesterase system 16 p2543 N71-28252

CHOLESTEROL

Storage stability of human blood cholesterol esters (AM-70-4) 01 p0009 N71-16374

Conversion of data from three serum cholesterol assay methods (AM-70-13) 01 p0011 N71-10449

Effect of lithium and calcium ions on anticholinesterase activity of erythrocytes (NABA-TT-F-13474) 09 p1333 N71-20179

Physiological effects of ionized air on mice anticholinesterase system 16 p2543 N71-28252

CHOLESTEROL

Storage stability of human blood cholesterol esters (AM-70-4) 01 p0009 N71-16374

Conversion of data from three serum cholesterol assay methods (AM-70-13) 01 p0011 N71-10449

Effect of lithium and calcium ions on anticholinesterase activity of erythrocytes (NABA-TT-F-13474) 09 p1333 N71-20179

Physiological effects of ionized air on mice anticholinesterase system 16 p2543 N71-28252

CHOLESTEROL

Storage stability of human blood cholesterol esters (AM-70-4) 01 p0009 N71-16374

Conversion of data from three serum cholesterol assay methods (AM-70-13) 01 p0011 N71-10449

Effect of lithium and calcium ions on anticholinesterase activity of erythrocytes (NABA-TT-F-13474) 09 p1333 N71-20179

Physiological effects of ionized air on mice anticholinesterase system 16 p2543 N71-28252

CHOLESTEROL

Storage stability of human blood cholesterol esters (AM-70-4) 01 p0009 N71-16374

Conversion of data from three serum cholesterol assay methods (AM-70-13) 01 p0011 N71-10449

Effect of lithium and calcium ions on anticholinesterase activity of erythrocytes (NABA-TT-F-13474) 09 p1333 N71-20179

Physiological effects of ionized air on mice anticholinesterase system 16 p2543 N71-28252

CHOLESTEROL

Storage stability of human blood cholesterol esters (AM-70-4) 01 p0009 N71-16374

Conversion of data from three serum cholesterol assay methods (AM-70-13) 01 p0011 N71-10449

Effect of lithium and calcium ions on anticholinesterase activity of erythrocytes (NABA-TT-F-13474) 09 p1333 N71-20179

Physiological effects of ionized air on mice anticholinesterase system 16 p2543 N71-28252

CHOLESTEROL

Storage stability of human blood cholesterol esters (AM-70-4) 01 p0009 N71-16374

Conversion of data from three serum cholesterol assay methods (AM-70-13) 01 p0011 N71-10449

Effect of lithium and calcium ions on anticholinesterase activity of erythrocytes (NABA-TT-F-13474) 09 p1333 N71-20179

Physiological effects of ionized air on mice anticholinesterase system 16 p2543 N71-28252

CHOLESTEROL

Storage stability of human blood cholesterol esters (AM-70-4) 01 p0009 N71-16374

Conversion of data from three serum cholesterol assay methods (AM-70-13) 01 p0011 N71-10449

Effect of lithium and calcium ions on anticholinesterase activity of erythrocytes (NABA-TT-F-13474) 09 p1333 N71-20179

Physiological effects of ionized air on mice anticholinesterase system 16 p2543 N71-28252

CHOLESTEROL

Storage stability of human blood cholesterol esters (AM-70-4) 01 p0009 N71-16374

Conversion of data from three serum cholesterol assay methods (AM-70-13) 01 p0011 N71-10449

Effect of lithium and calcium ions on anticholinesterase activity of erythrocytes (NABA-TT-F-13474) 09 p1333 N71-20179

CHOLESTEROL

Storage stability of human blood cholesterol esters (AM-70-4) 01 p0009 N71-16374

Rare earth chelates and organic solvents as paramagnetic shift reagent for nuclear magnetic resonance spectral chromatography (AD-72344) 10 p2085 N71-30012

Analysis of phenol formaldehyde condensates by chromatography on polyethylene glycol (ONERA-TT-171) 19 p3049 N71-31701

Development and characteristics of automated fluorometric procedure for analyzing tetrahydrocannabinol and epinephrine content of blood plasma and urine (PAA-AM-71-15) 22 p3543 N71-35241

Chromatographic and spectroscopic extractions for determining concentrations of acetic acid reduction products in nickel plating electrolytes (NLL-LTT-746-725-1922.401) 22 p3589 N71-35360

Electrophoretic and chromatographic analysis of lactate dehydrogenase isoenzyme activity in fetal, neonatal, and adult human thymus and spleen lymphocytes (NABA-TT-F-13991) 23 p5715 N71-36482

Chromatographic isolation of pure phenanthrene 238 from radiolytic reaction products 23 p3818 N71-37229

CHROMIUM

U CHROMIUM

CHROMIUM

State diagram of system Dy2O3-Cr2O3 07 p1041 N71-17124

CHROMIUM

NT CHROMIUM ISOTOPES

Increase of chromium-1 concentration in X ray irradiated ruby during isothermal annealing measured by EPR technique (NABA-TN-D-6079) 02 p0285 N71-11888

Temperature effects on magnetic permeabilities of chromium-chromium alloys with rhodium, osmium, ruthenium, molybdenum, and tungsten (DSS-4179) 05 p0732 N71-14020

Low temperature heat capacities of dilute solutions of Fe and Cr in Cu (JCL-15605) 07 p1132 N71-17924

Single particle mode peak of inelastic neutron scattering cross section for antiferromagnetic chromium at low temperatures 08 p1279 N71-18089

Liquid hyperfine spin-orbit interactions in chromium, molybdenum, and tungsten oxyhydrides 12 p1970 N71-23685

Fine structure of ground state levels of first four neighbor exchange coupled Cr3+ spin pairs in ruby 13 p2135 N71-25178

Temperature dependence of self diffusion coefficient of iron, chromium, and cobalt in steel with 8 percent carbon (DMEC-5795) 14 p2271 N71-25093

Interfacial reactions of boron fibers and carbon fibers in chromium matrices at elevated temperatures (ARL/MT-83) 15 p2432 N71-27620

Polarization of protons inelastically scattered on Mg-24, Cr-52, and Ni-58 (NIP-18532) 15 p2490 N71-27894

Neutron capture and transmission measurements in Fe-V region on chromium, nickel, and vanadium (RFS-528-223) 17 p2005 N71-30300

Diffusion coefficient of chromium in Fe-Cr alloys annealed at 1200 C determined by evaporation in vacuum (TT-70-59105) 20 p3284 N71-33177

Rare earth and thorium alloying of chromium and mechanism for controlling nitrogen embrittlement (NABA-CR-72892) 20 p3285 N71-33399

Determination of pressure-temperature-composition relations of chromium-nickel binary system by thermogravimetric technique 20 p3369 N71-33999

Trivalent chromium ion X-ray fluorescence electron spin resonance spectra in single MgO crystals 21 p3499 N71-34931

Low temperature density and high temperature strength of pure chromium and chromium-thorium alloy prepared from vapor deposited powders (NABA-CR-72901) 22 p3592 N71-35380

CHROMIUM ALLOYS

NT CHROMIUM STEELS

Microprobe analysis of diffusion layers with application to chromium-nickel bonded 713 (ONERA-TT-636) 02 p0341 N71-11564

Measuring oxidation resistance of thin dispersion strengthened nickel-chromium alloys for aircraft applications (NABA-CR-11087) 02 p0341 N71-11573

Stress corrosion cracking of Fe-Cr-Ni alloys in chloride environments 04 p0528 N71-13940

Temperature effects on magnetic permeabilities of chromium and chromium alloys with rhodium, osmium, ruthenium, molybdenum, and tungsten (DSS-4179) 05 p0732 N71-14020

Chromium palladium silicon foil thermometer for low temperature measurements (CAL-T-822-14) 06 p0802 N71-16788

Neutron diffraction analysis on magnetic structures of chromium alloys 07 p1069 N71-18037

CHROMIUM

NT CHROMIUM ISOTOPES

Increase of chromium-1 concentration in X ray irradiated ruby during isothermal annealing measured by EPR technique (NABA-TN-D-6079) 02 p0285 N71-11888

Temperature effects on magnetic permeabilities of chromium-chromium alloys with rhodium, osmium, ruthenium, molybdenum, and tungsten (DSS-4179) 05 p0732 N71-14020

Low temperature heat capacities of dilute solutions of Fe and Cr in Cu (JCL-15605) 07 p1132 N71-17924

Single particle mode peak of inelastic neutron scattering cross section for antiferromagnetic chromium at low temperatures 08 p1279 N71-18089

Liquid hyperfine spin-orbit interactions in chromium, molybdenum, and tungsten oxyhydrides 12 p1970 N71-23685

Fine structure of ground state levels of first four neighbor exchange coupled Cr3+ spin pairs in ruby 13 p2135 N71-25178

Temperature dependence of self diffusion coefficient of iron, chromium, and cobalt in steel with 8 percent carbon (DMEC-5795) 14 p2271 N71-25093

Interfacial reactions of boron fibers and carbon fibers in chromium matrices at elevated temperatures (ARL/MT-83) 15 p2432 N71-27620

Polarization of protons inelastically scattered on Mg-24, Cr-52, and Ni-58 (NIP-18532) 15 p2490 N71-27894

Neutron capture and transmission measurements in Fe-V region on chromium, nickel, and vanadium (RFS-528-223) 17 p2005 N71-30300

Diffusion coefficient of chromium in Fe-Cr alloys annealed at 1200 C determined by evaporation in vacuum (TT-70-59105) 20 p3284 N71-33177

Rare earth and thorium alloying of chromium and mechanism for controlling nitrogen embrittlement (NABA-CR-72892) 20 p3285 N71-33399

Determination of pressure-temperature-composition relations of chromium-nickel binary system by thermogravimetric technique 20 p3369 N71-33999

Trivalent chromium ion X-ray fluorescence electron spin resonance spectra in single MgO crystals 21 p3499 N71-34931

Low temperature density and high temperature strength of pure chromium and chromium-thorium alloy prepared from vapor deposited powders (NABA-CR-72901) 22 p3592 N71-35380

CHROMIUM ALLOYS

NT CHROMIUM STEELS

Microprobe analysis of diffusion layers with application to chromium-nickel bonded 713 (ONERA-TT-636) 02 p0341 N71-11564

Measuring oxidation resistance of thin dispersion strengthened nickel-chromium alloys for aircraft applications (NABA-CR-11087) 02 p0341 N71-11573

Stress corrosion cracking of Fe-Cr-Ni alloys in chloride environments 04 p0528 N71-13940

CHROMIUM COMPOUNDS

Plasma sprayed chromium nitride coatings for improved oxidation resistance of chromium alloys (NABA-CR-72763) 08 p1223 N71-18927

Stress corrosion cracking in low nickel chromium alloy system in magnesium chloride, for water cooled reactors (COO-2689-6) 10 p1571 N71-26069

Viscosity measurement of molten metal and some chromium chromium alloys 10 p1580 N71-31304

Corrosion tests on titanium, ceramic titanium steels, chromium ferrites, and light alloys in sea water up to 150 C (ONRL-TR-3412) 10 p1580 N71-31403

Thermomechanical processing effects on crystal microstructure, texture, and high temperature strength of dispersion strengthened and fine nickel-based Cr, Ti-6Al-4V, and W alloys 10 p1583 N71-31509

Electrochemical and vacuum evaporation of yttrium oxide-chromium oxides coating of chromium alloys for aircraft embrittlement protection (NABA-CR-72847) 12 p1956 N71-23136

LMFBR environmental effects on type 304 and 316 stainless steels and Cr-Mo alloy piping materials (SAN-701-228-REV-1) 12 p1963 N71-30833

High temperature characterization of ferrocenyl alloys (TT-70-58193) 14 p2270 N71-25677

Oxidation resistance of aluminum-chromium alloys on nickel-chromium alloy 14 p2278 N71-25943

Mechanical properties of dispersion strengthened chromium-base alloy with magnesium oxide additive (AD-728505) 14 p2274 N71-26159

Production engineering and chemical, mechanical, and thermodynamic properties of thin dispersed nickel-chromium alloys for space shuttle thermal protection coatings (NABA-TM-X-44682) 15 p2628 N71-27008

Spectroscopic effects on Fermi surfaces of antiferromagnetic Cr alloys with V and Mn ions, determined from de Haas-van Alphen measurements (IS-7-428) 15 p2953 N71-27852

Kanadan gaps and mass spectrometer measurements of vanadium, titanium, and chromium binary alloys in bcc phase (AD-728267) 16 p2611 N71-28202

Oxidation kinetics of stainless chromium alloys and oxidation resistance due to chromium oxide transformation (AD-723521) 16 p2614 N71-28921

Mechanical properties of Ni-Cr alloys in light of stoichiometric composition NiCr (NLL-LTT-746-639-1922.401) 16 p2614 N71-28931

Development and fabrication of precipitation hardened Ti-NiCr structures for use in high temperature environments 17 p2648 N71-29446

Oxidation mechanism and morphology of scale formation on Ni-Cr-Al alloys at 1000 to 1200 C 17 p2764 N71-29683

Mechanical properties of pure binary Ni-Cr alloys at high and low temperatures (NLL-TRANS-746-639-1922.401) 17 p2764 N71-29684

Heat treatment of carbide and boride strengthened chromium alloys to improve tensile and creep rupture strength (NABA-CR-72803) 18 p2823 N71-30576

Precipitation with refractory metal carbides for creep resistant chromium-base alloys (NABA-CR-72874) 18 p2894 N71-30809

Diffusion coefficient of chromium in Fe-Cr alloys annealed at 1200 C determined by evaporation in vacuum (TT-70-59105) 20 p3284 N71-33177

NMR for determining distribution of hyperfine fields at cobalt nuclei in dilute alloys of Co-V, Co-Cr, and Co-Mn (COO-1350-71) 20 p3319 N71-33649

Creep behavior of 1Cr-Mn-V steels under cyclic loads (RD/RH-1089) 21 p3441 N71-34482

Compatibility of UIC compounds and iron nickel chromium alloys, and nuclear fuel clad failure (SURF/RH-424) 22 p3523 N71-35807

Electrochromic of yttrium, barium, and lanthanum coatings for preventing oxidation embrittlement of chromium alloys at high temperatures (NABA-TM-D-4528) 23 p3772 N71-38086

CHROMIUM COMPOUNDS

Techniques for preparation of single phase chromium oxides for determination of electrochemical and corrosion characteristics (AD-715879) 08 p0877 N71-16121

Plasma sprayed, chromium carbide bearing steam corrosion protection using amorphous, uncoated polymer coats (AD-728866) 10 p2617 N71-28474

CHROMIUM COMPOUNDS

NT CHROMIUM

CHROMIUM

CHROMIUM

CHROMIUM

CHROMIUM

CHROMIUM

CHROMIUM

CHROMIUM

CHROMIUM

CHROMIUM

CHROMIUM

CHROMIUM

CHROMIUM

CHROMIUM

CHROMIUM

CHROMIUM

CHROMIUM

CHROMIUM

CHROMIUM

CHROMIUM

CHROMIUM

CHROMIUM

CHROMIUM

CHROMIUM

CHROMIUM

CHROMIUM

CHROMIUM

CHROMIUM

CHROMIUM

CHROMIUM

CHROMIUM

CHROMIUM

CHROMIUM

CHROMIUM

CHROMIUM

CHROMIUM

CHROMIUM

- Alloy softening in chromium, molybdenum, and tungsten metals alloyed with chromium
[NASA-TN-D-7600] 02 p0403 N71-11662
- Photochemical aqueous reactions of chromium(III) complexes
[USC-113-P-10-X-1] 04 p0487 N71-13463
- Structure and environment effects on transition probabilities of luminescent chromium complexes
[COO-773-21] 06 p0673 N71-16795
- Magnetomagnetic and antiferromagnetic properties and structures of CrII compounds, emphasizing collinearity and wave vectors
[CEA-COMP-1701] 13 p2139 N71-25483
- Lattice parameters and compressibilities of high pressure phases of lead chalcogenides, manganese antimony, manganese tellurium, chromium antimony, and chromium tellurium compounds
14 p2327 N71-26495
- Magnetic properties of chromium and vanadium nitride binary mixtures, noting concentration and temperature effect
[ONERA-TP-719] 15 p2420 N71-26996
- Electrical properties and photoconductivity of semiconducting ferroelectric cadmium chromium selenides
[AD-72070] 15 p2510 N71-27936
- Hyperfine fields at magnetic and nonmagnetic lattice sites measured in solid solutions of manganese antimonide and chromium antimonide
[COO-1196-800] 18 p2962 N71-30737
- Scanning electron microscope used to determine surface morphology of TD-NiCr oxidized at 800 to 1200 deg for up to 64 hours
[NASA-TM-X-67807] 18 p2936 N71-31153
- Oxide films and red shaped crystals of semiconducting ferroelectric chalcogenide spiral copper cadmium chromium selenides - energy converting materials
[AD-722785] 18 p2999 N71-31458
- Thermodynamics of oxide reduction on heat exchanger, chromium as alloying component, sulphate and hydrogen chloride corrosion, and silicon sulphide phenomena
[NLL-CE-TRANS-5605-1902.09] 22 p3697 N71-36370

CHROMIUM ISOTOPES

- Threshold photoelectron cross sections for nuclei of Mg, Cr, Fe, and Pb isotopes
[UCRL-30902] 06 p0921 N71-16397
- Total positron cross sections of Ti-49 and Cr-53
[EURPNE-741] 07 p1070 N71-16928
- Atomic structure of Cr-51 via prompt gamma ray energy and intensity measurements
[COO-1530-21] 07 p1077 N71-17550
- Ho-166 rotational bands, M1 radiative strength resonance in Cr-53, Dyamitron research, photoelectron spectroscopy of high temperature vapors
[ANL-7739] 17 p2808 N71-30343
- Neutron capture and total cross section measurements of V, Ni, and Cr isotopes
[RPI-528-340] 20 p3322 N71-33806

CHROMIUM OXIDES

- NT CHROMITES
Techniques for preparation of single phase chromium carbides for determination of electrochemical and corrosion characteristics
[AD-713879] 06 p0677 N71-16121
- Electrochroming and vacuum evaporation of yttrium oxide-chromium oxide coating of chromium alloys for nitrogen embrittlement protection
[NASA-CR-72047] 12 p1936 N71-23136
- Effects of oxygen on polymerization of ethylene in presence of supported chromium oxide catalyst
[AD-723853] 19 p3049 N71-31773

CHROMIUM STEELS

- Brittleness and microcrack initiation in chromium steel piston heads
10 p1572 N71-30819
- Structural transformations and properties of high strength Cr-Mn-Ni austenitic steels
[JPRS-52877] 12 p1936 N71-23148
- Martensitic transformations in low carbon austenitic chromium-nickel steels examined by X ray, metallographic, magnetic, and dilatometric techniques
[ORNL-TR-3623] 15 p2426 N71-27002
- Atomic absorption spectra of clouds formed by laser-induced vaporization of chromium steel
[NASA-TT-F-13605] 17 p2758 N71-29225
- Reaction contributions to Ramo-Swedish conference on clean steel
[JVA-MEDD-169-VOL-2] 18 p2933 N71-30480
- Deoxidizing and vacuum casting effect on plastic properties of nickel-chromium steels noting corrosion resistance
18 p2937 N71-30681
- Flame-out testing in refining of steels and alloys
18 p2937 N71-30684
- Interfacial tensions and density measurement of chromium steel and vanadium slag noting effect of flux on phase transformations
18 p2934 N71-30689
- Milling (machining) of chromium carburizing steel noting production tests and tool wear
19 p3104 N71-31915

- Low-alloy 12 percent chromium steel replacing nickel for nitrogen to improve casting and mechanical properties
[NLL-LT-746-748-1902.401] 21 p3442 N71-34493

- Changes in mechanical properties and internal friction during aging of stainless, dispersion hardened chromium steels
[NLL-LT-746-680-1902.401] 22 p3596 N71-35608

- Suitability of Nb stabilized Cr-Mo steel as structural material in sodium cooled reactor plants after neutron irradiation
[NLL-RISLEY-TRANS-2118-1901.97] 22 p3596 N71-35609

- Critical points, crack formation, and shrinkage characteristics for castings of Cr-Ni, Cr-Mn, and Mn steels
[NLL-TRANS-746-293-1902.401] 22 p3597 N71-35611

- Intergranular fractures along grain boundaries of quenched low tempered manganese silicon-chromium steel
[NLL-CE-TRANS-5362-1902.09] 22 p3597 N71-35616

- Microstructural changes as criterion for assessing operational reliability and high temperature resistance of chromium steels
[NLL-CE-TRANS-5369-1902.09] 23 p3774 N71-36896

- Corrosion tests of chromium and chromium-nickel steels in molten lead at 575, 650, and 750 C for 3250 hr
[JUL-604-RW] 24 p3935 N71-38078

CHROMOBOMES

- Effects of ionizing radiation on chromosomes
[AI-AEC-12974] 02 p0152 N71-11081
- Effects of gamma radiation on cell division processes and chromosomes in bone marrow of dogs
02 p0161 N71-11497
- Chromosomal aberrations in persons exposed to repeated occupational irradiation
[ORNL-TR-2332] 03 p0634 N71-14696
- Prolonged bed rest effects on human chromosomes during space flight simulation and actual space flight
20 p3221 N71-33462
- Use of general purpose digital computers for analysis of biological structures and chromosomes
[JPRS-54053] 23 p3715 N71-36479

CHROMOSPHERE

- Measuring transition of photoelectric spectrum into chromospheric and vice versa during total solar eclipse of 15 Feb. 1961
03 p0370 N71-13158
- Structure and energy distribution of chromospheric-corona transition region
[NASA-CR-116872] 08 p1286 N71-19294
- Solar corona physics including spiral topology of chromospheric fibrils and filaments near sunspots
[AD-717636] 11 p1824 N71-21928
- Calcium K line formation in nonhomogeneous solar chromosphere
13 p2166 N71-24941
- Collisional processes for determining kinetic temperature distribution and heating of chromosphere
13 p2077 N71-25282
- Correlation of calcium H and K line profiles with sunspot numbers and Mg 5172 A line position shifts in relation to chromospheric activity
19 p3176 N71-32254
- Existence of 5 minute oscillations in solar photospheric and low chromospheric magnetic fields
[NASA-CR-115606] 19 p3177 N71-32512
- Velocity fields in magnetically disturbed regions of H alpha chromosphere measured by Doppler and Zeeman maser pairs
20 p3342 N71-33867

- High resolution H-alpha photographs for studying chromospheric fine structure at active region polarity boundaries
[NASA-CR-121619] 21 p3580 N71-34955

- Magnetohydrodynamic wave propagation and dissipation in relation to calcium emission in chromosphere
21 p3586 N71-34976

- Thermal stability of stellar chromosphere model
21 p3511 N71-35021

- Ground and Coosmo 361 satellite observation of isospheric disturbances due to chromospheric flare of 27 Dec. 1968
[D-23] 23 p3750 N71-36742

- Physical properties and processes of solar interior, photosphere, chromosphere, and corona
23 p3845 N71-37407

- CHROMOTOGRAPHY
NT THIN LAYER CHROMATOGRAPHY
CHROMOLOGY
Physical properties and absolute age determination for some rocks of India and Ceylon
[NASA-TT-F-13416] 05 p0870 N71-14839

- Structural analysis and chronology of micrometeorite crystals on lunar rocks
[NASA-TM-X-66707] 07 p1109 N71-17498

- Pu/Xe and I/Xe decay intervals for three chondrites from xenon content and isotopic composition determinations
18 p2089 N71-31410

- Apparent ages of Rb-87 and Sr-87, and contents of K, Rb, Sr, Ba, and rare earths in lunar soil from Moon Percutite
[NASA-TT-F-13945] 20 p3349 N71-33100

- Concentrations and isotopic compositions of Rb, Ne, and Ar measured by mass spectroscopy in separated metal phase and bulk samples of 15 chondrites for cosmic ray record studies
20 p3350 N71-33173

- Galaxy cluster detection of carbon 14 for upper age limit determination
24 p4013 N71-39015

- Chronology of Ranger project events - 1957 through 1965
[NASA-CR-123168] 24 p4021 N71-39000

- CHRONOPHOTOGRAHY
Time and space history analysis of basaltic dikes tops and heat release, closed behavior, and conductivity factor interrelationships in closed rim
[BNL-56244] 09 p1413 N71-26016

- Automatic underwater camera system design and performance characteristics for time lapse photography of algae growth and sedimentation
[NASA-TM-X-67007] 12 p1918 N71-23009

- Photodiode recorder with electric-optical converter for recording ultraviolet light pulses
[AD-719451] 15 p3779 N71-36100

- Techniques for serial time-lapse closed photographic analysis, Doppler navigation data analysis, and photogrammetric data acquisition
23 p3787 N71-36100

CHRONOTRONS

- U PULSE RATE
U TIME LAG
CRUCKISH SEA
Long term variations of air and water temperatures in Chukchi Sea
11 p1752 N71-22800

- Annual variations of winter hydrological characteristics in surface waters of East Siberia and Chukchi sea due to salinity and temperature anomalies
11 p1756 N71-22810

- Graphic method of forecasting nonperiodic oscillations of sea level in East Siberia and Chukchi sea
23 p3758 N71-22814

CRUDDING

- U COMBUSTION STABILITY
CRUTES
Formation of fusion gas bubbles in solids during reactor irradiation
[AERE-R-4395] 21 p3467 N71-34079

- CINEFLUOROGRAPHY
U MOTION PICTURES
U RADIOGRAPHY
CINEMATOGRAPHY
Drug of fine falling spheres in water for Reynolds numbers in critical regime using orthocornal cinematography
[AD-717492] 11 p1753 N71-22816

- Photometric and cinematographic studies of aquatic domain processes in ferromagnetic materials
[AD-717669] 11 p1783 N71-22818

- Application of cinematography to study of microcirculation hemodynamics and related physiological studies of man and animal
[AD-719401] 13 p3806 N71-36104

- Large synchronous impairment in 16 mm film presentation by television
[BBC-1971/25-PT-2] 23 p3725 N71-36107

- CINERADIOGRAPHY
U MOTION PICTURES
U RADIOGRAPHY
CINTEBOLITES
Performance specification and test procedure for cinebolites capable of 2-arc-second dynamic range accuracy
[AD-728379] 22 p3883 N71-35104

- CIRCADIAN RHYTHMS
Circadian determination of rectal and cutaneous temperature in man while resting in controlled environment
[NASA-TT-F-13400] 01 p0011 N71-10460

- Characterization of voluntary cardiac eye movements and importance for pilot performance
02 p0164 N71-11825

- Circadian rhythms of pilot performance in flight simulator and effects on time sleep
02 p0165 N71-11827

- Neurochemical regulation of sleep-wake and temperature cycles in monkeys
02 p0165 N71-11829

- Biological investigations in space environments including circadian rhythms
[NASA-CR-115083] 04 p0470 N71-15809

- Circadian rhythm of light sensitivity in visual perception threshold of man
[AD-714044] 06 p0001 N71-10013

- Circadian rhythms of psychological functions under different conditions
07 p0107 N71-10016

NT SWITCHING CIRCUITS
NT THRESHOLD GATES
NT TRANSISTOR CIRCUITS
NT TRANSMISSION CIRCUITS
NT TRIGGER CIRCUITS
NT VARACTOR DIODE CIRCUITS
NT WHEATSTONE BRIDGES
NT WIRE BRIDGE CIRCUITS

Production engineering and materials evaluation for thick film circuit manufacture
[BCR-12] 02 p0194 N71-11362

Algorithm for synthesis of distributed systems to solve circuit design problems
[NASA-CR-111009] 02 p0197 N71-11379

Rapid computer aided analysis of nonlinear electronic circuits
02 p0197 N71-11381

Path redundancy/Automated Sneak Program
[NASA-CR-108723] 03 p0343 N71-12486

Sneak circuit analysis handbook
[NASA-CR-108721] 03 p0343 N71-12487

Compact transistorized pulse unit
[NASA-TT-F-13351] 03 p0351 N71-12537

Starting circuit design for initiating and maintaining arcs in vapor lamps
[NASA-CASE-XNP-01058] 03 p0351 N71-12540

Utilization of ternary logic in calculating no failure probability of reserved systems with two forms of failure process
[AD-712804] 03 p0401 N71-13354

Analysis of negative impedance converter circuit
[AD-713161] 05 p0644 N71-14853

Circuitry for automatic control of alternating current motors
[AD-71386] 05 p0654 N71-15482

Circuit and electrode tests of low voltage breakdowns in nitrogen, water vapor, and mixtures of nitrogen and water vapor
06 p0825 N71-16637

Measurements and analysis of lightning-induced voltages in aircraft electrical circuits
[NASA-CR-1744] 08 p1170 N71-19122

Voltage drift compensation circuit for analog-to-digital converter
[NASA-CASE-XNP-04780] 09 p1353 N71-19687

High voltage driver system for attenuating high voltages to convenient levels suitable for introduction to measuring circuits
[NASA-CASE-XLE-02008] 19 p1535 N71-21583

Rejection of magnetic fields produced by this water-like circuit elements in space vehicles
[NASA-CASE-XGS-03590] 12 p1858 N71-23187

Alternating current gated flip-flop implementation in sequential circuit design
12 p1880 N71-23787

Split Path Nonlinear (SPAN) filter compared with lead-lag network and optimal linear controller
12 p1893 N71-23873

Stability of inert gases in liquid sodium and related safety problems for primary circuit of fast sodium cooled breeder reactor
[EURFNR-785] 13 p2117 N71-24909

Internal circuit excitation by electromagnetic field transmission through shielded missile skin
[SC-R-70-4339] 13 p2048 N71-25346

Circuits for controlling reversible dc motor
[NASA-CASE-XNP-7477] 14 p2229 N71-26092

Evaluation of conductor material compatibilities and production finishing processes for thick film circuits
[BCR-20] 14 p2250 N71-26548

Control arm and safety circuits for high flux research reactor
[AAEC/M-10] 15 p2451 N71-27683

Device for rapid adjustment and maintenance of temperature in electronic components
[NASA-CASE-XNP-02792] 16 p2596 N71-28958

Pulse generating circuit for operation at very high duty cycles and repetition rates
[NASA-CASE-XNP-00745] 16 p2576 N71-28960

Development of electric circuit for production of different pulse width signals
[NASA-CASE-XLA-07788] 16 p2573 N71-29139

Digital registered data array module and performance characteristics of its electronic circuits
[NASA-TM-X-3314] 17 p2250 N71-29904

Performance of gallium lubricated slipring assembly in ultrahigh vacuum for 500 hours
[NASA-TN-D-6436] 19 p3105 N71-32137

Design and circuitry of torquemeter for measuring magnetic torques on spacecraft
[NASA-TN-D-6387] 19 p3102 N71-32476

Ozone formation by electric discharges discussing photochemical process, circuits, results
[TI-71-E-19] 20 p2577 N71-32819

Sensing circuit for instantaneous reaction to power overloads
[NASA-CASE-GSC-10467-1] 20 p3242 N71-33129

Capacitance and 4000-tps data circuits of GCP SPOF communications terminal subsystem high-speed data assembly
21 p3393 N71-34143

Development of computer memory system for automated attendance accounting system
[NASA-CASE-NPO-11456] 21 p3399 N71-34189

Electronic control circuitry of servomotor curve tracer
[ARL/SYS-25] 21 p3405 N71-34229

Operating characteristics of avalanche diodes in microelectronic circuits
[AD-726550] 22 p3561 N71-35362

Steady state analysis of lightly damped nonlinear circuits, such as harmonic multipliers and oscillators
[AD-726912] 22 p3561 N71-35367

Performance data and specifications for amplifiers and signal analyzers for nuclear instruments
[JAERI-MEMO-4303] 22 p3584 N71-35524

Simultaneous signalling in digital sound circuits for operational control of broadcasting network
[BBC-1971/26] 23 p3725 N71-36555

Design structure of various primary circuits in sodium cooled reactors
[KFE-1379] 23 p3796 N71-37058

Electrical fluctuations of thermal origin in quasi-stationary circuits
23 p3804 N71-37122

Development and characteristics of energy injection circuit for ac power continuity device
[AD-727581] 24 p3899 N71-37795

CIRCULAR CONES
Inviscid hypersonic flow of chemically relaxing air about pointed circular cones
05 p0659 N71-14748

Investigating formation of circular structures of volcanic, meteoritic, and nuclear origin on earth for correlation with cratering on moon and inner planets
[NASA-TT-F-13457] 07 p0109 N71-17412

General kinetic problem for collisionless flow of neutral, monatomic, unexcited gas past circular cone
07 p0101 N71-17674

Interferometric holographic analysis of density flow fields around half-angle conical bodies in supersonic wind tunnels with 10 deg angle of attack
[AD-721543] 16 p2529 N71-28411

Effect of viscosity on supersonic flow around circular semicones placed on plane plate
[NASA-TT-F-13578] 18 p2904 N71-30801

CIRCULAR CYLINDERS
Axisymmetric stresses and displacements in two finite circular cylinders in contact
[NASA-TM-X-38052] 01 p0129 N71-10448

Circulation control by slot suction on circular cylinder
[LR-530] 02 p0141 N71-11002

Laminar near wake characteristics behind circular cylinder in Mach 6 rarefied air stream
[REPT-1108/70] 02 p0142 N71-11012

Viscous flow of deformable liquid drops in suspension in circular cylindrical tubes
[AD-711633] 02 p0203 N71-11563

Liquid oscillation frequency measurement in inclined right circular cylinder
[NASA-TM-X-44540] 03 p0362 N71-13006

Thermostructural materials data for optimal design of thin circular cylinders
03 p0464 N71-13138

Experimental and theoretical studies of thin walled circular cylinder buckling
[DLR-MITT-70-10] 03 p0466 N71-13345

Crosspower spectral density of unsteady surface pressure around circular cylinder in two dimensional flow
[NASA-CR-114132] 05 p0664 N71-15309

Analytical and numerical calculations for cylinder-vortex combination in incompressible flow noting pressure distribution and downwash
[NLR-TR-69057-U] 05 p0666 N71-15548

Analysis for creep buckling of tubes under external pressure
[WAFD-TM-956] 06 p0956 N71-16836

Numerical analysis of flow field around right circular cylinder in Mach 2 airstream
07 p1012 N71-17761

Buckling of eccentrically stiffened thin walled circular cylinders under axial loads
[DLR-FB-70-48] 08 p1297 N71-18643

Structural elastic shell theory for axisymmetric hollow circular cylinders
[NASA-CR-116457] 08 p1299 N71-19160

Modulating and controlling intensity of light beam from high temperature source by servcontrolled rotating cylinders
[NASA-CASE-XMS-04300] 09 p1357 N71-19479

Separated flow numerical method applied to problem of two dimensional plane flow around right circular cylinder at supersonic speeds
09 p1375 N71-19840

Smooth double-slotted circular cylinder aerodynamic force characteristics measured for circulation control by slot suction
[NRC-11714] 09 p1377 N71-20196

Characteristics of viscoelastic plastic hollow circular cylinder in state of plane strain for compressible and incompressible conditions
10 p1657 N71-21399

Energy conversion and thermomechanical coupling in nonisothermal viscoelastic circular cylinder solids
11 p1839 N71-22885

Numerical analysis of wave propagation in cylindrical shells based on application of general dynamic equation
12 p2006 N71-23975

Boundary value problem application to determining capillary surface of volume of liquid partially filling right circular cylinder
[NPL-MA-95] 13 p2102 N71-34178

Acoustically excited, incompressible, turbulent, subsonic Couette air flow around circular cylinder
13 p2866 N71-25809

Determination of upper and lower bounds to limit pressure for circular cylinders containing axial slots and relation to brittle fracture problem
14 p2349 N71-26318

Buckling tests of two integrally stiffened circular cylinders subjected to bending loads
[NASA-TN-D-63711] 16 p2684 N71-28116

Drag force, pressure distribution, and separation angle measured on circular cylinders in flow of aqueous solutions of dilute polymers
[AD-722807] 16 p2578 N71-28178

Development of linear theory for dynamic interaction of solid elastic circular cylinder bonded to thin shell of different material
17 p2852 N71-29888

Pair interaction energies for screw and edge dislocations in circular cylinder
17 p2824 N71-29910

Theoretical analysis of viscous, incompressible fluid flow oscillations around circular cylinder between closely spaced parallel plates based on successive approximations and inner-outer expansion
22 p3571 N71-35401

Tabular data for electrostatic structure of distorted region behind moving bodies in collisionless plasma for sphere and long circular cylinder
[NASA-CR-121963] 22 p3673 N71-36187

Current load calculations for transmission lines terminating parallel to and near infinite length circular conducting cylinders in incident fields
[SC-B-713230] 23 p3757 N71-36440

Series truncation method with novel coordinate system used for calculation of flow about circular cylinder at low Reynolds numbers
[AD-726447] 23 p3743 N71-36808

Momentum and heat transfer measurements for low Reynolds number shear flow past rotating circular cylinders
23 p3746 N71-36780

Dynamic response of slender circular cylinders in axial flowing fluid with base excited motion
23 p3863 N71-37340

Multiple scattering and signification solutions for electromagnetic scattering from cylinders over and embedded in dielectric half spaces
24 p3890 N71-37770

High structural strength in welded joints of cylinders made of high strength thin sheet steels
[AD-727897] 24 p3930 N71-38080

Experimental determination of oscillatory forces generated by gravity waves interacting with rigid horizontal circular cylinder near simulated ocean bottom
[AD-727691] 24 p4025 N71-38721

CIRCULAR ORBITS
NT STATIONARY ORBITS
Terrestrial and orbital launched spacecraft maneuvers for orbital rendezvous with space stations in circular orbit
14 p2336 N71-23924

Communication satellite circular orbit network providing earth surface coverage
[RAE-TR-70211] 17 p2719 N71-29409

Altitude estimation and control of earth pointing satellites in circular orbit
[DLR-FB-70-75] 17 p2849 N71-29408

Calculation of topocentric trajectory of circular satellite orbits, and correlation between topocentric coordinates and time
22 p3676 N71-34010

CIRCULAR PLATES
Bending solution of full circular plates supported on two rings of equally spaced columns
[REPT-291] 02 p0301 N71-12813

Solution for bending of overhanging circular plate supported on columns
[REPT-288] 02 p0301 N71-12810

Bending of circular plates supported on equally spaced columns under eccentric concentrated load
[REPT-286] 02 p0302 N71-12809

Circular plates in sandwich structures with edge loading analyzed by calculus of variations
[REPT-1126/70] 03 p0466 N71-13151

Structural analysis of composite beams and circular plates undergoing flexural vibration
[AD-712765] 03 p0467 N71-13160

Oscillation of disk fixed to flat plate with isotropic fluid
[PUBL-3] 03 p0775 N71-16726

Mathematical models for modulus and elasticity of circular plates and rectangular or square beams
[CRIF-MC-37] 06 p1297 N71-18644

SUBJECT INDEX

- Experimental investigation to determine stability, surface deformation characteristics, and extent of plastic yielding associated with surface cracks in plates subjected to tensile loading
[NASA-CR-114934] 13 p2181 N71-34820
- Expressions and graphs for estimating average modal densities for various structural elements of importance including beams, rods, circular plates, and conical shells
[NASA-CR-11773] 18 p3022 N71-31483
- Stability of circular cylindrical sandwich shell reinforced by internal ring-type diaphragms
[AD-723548] 19 p3189 N71-32336
- Nonlinear oscillation in edge loaded circular plates and large strain plate theory
19 p3191 N71-32704
- Acoustic pressure distribution from forced harmonic vibrations of clamped circular plate in acoustic field
23 p3865 N71-37555
- Thermoelastic solutions for determining thermal stress distributions in circular plates with circular holes
24 p4027 N71-38737
- CIRCULAR POLARIZATION**
Polarization rotation effects on ionospheric propagation and backscatter amplitude
[AD-711341] 01 p0024 N71-10733
- Measuring dependence of emission power and polarization of helium-neon laser on transverse magnetic field
[AD-712104] 02 p0238 N71-11567
- Left and right hand circular electromagnetic polarization excitation by phase shifter and hybrid network
[NASA-CASE-GSC-10021-1] 13 p2054 N71-34595
- Gamma quantum detection of electromagnetic interaction which yield neutrino, antineutrino, and photon particles emphasizing photon circular polarization and shower observation
[NP-18558] 14 p2317 N71-26759
- Non-gamma circular polarization measurements on odd metal transitions in mercury 203 cascade
[NP-18644] 19 p3348 N71-32069
- Non-gamma circular polarization correlation and nuclear matrix element analysis on arsenic isotope
[COO-1746-34] 19 p3149 N71-32113
- CIRCULAR SHELLS**
Buckling analysis of elastic ring confined to uniformly contracting circular boundary
[AD-71682] 10 p1639 N71-21804
- Development and characteristics of test equipment for measuring creep buckling of moderately thin-walled circular cylindrical shells under axial compression loads
[AD-709767] 14 p2348 N71-26097
- CIRCULAR TUBES**
Laminar heat transfer and wall temperature distribution for high temperature gases and nitrogen plasma in circular tubes and over flat plates
[NRP-70-3] 04 p0519 N71-13791
- Analyzing structural response of casing and pipe at different levels in emplacement hole of underground nuclear tests
[UCRL-50657] 06 p1302 N71-19337
- Structural design of astronomical telescopes using digital computers with emphasis on tubes
24 p3923 N71-37963
- CIRCULATION**
NT **ATMOSPHERIC CIRCULATION**
NT **BLOOD CIRCULATION**
NT **CARBOXYHEMOGLOBIN**
NT **ISCHEMIA**
NT **PULMONARY CIRCULATION**
Two dimensional recirculation flow of viscous fluid
[AD-71826] 01 p0400 N71-10173
- Hydrological measurements of horizontal circulation of water in Pacific sector of Southern Ocean
11 p1734 N71-22822
- Tidal, rotational, solar activity, and circulation effects on global state of oceans
11 p1758 N71-22851
- Zero surface and water circulation in Drake Passage between Atlantic and Pacific Oceans during summer months
11 p1758 N71-22852
- Technical and economic aspects of recycling plutonium in thermal light water reactors
[BUREAU-2145] 13 p2118 N71-24961
- Internal recirculating air cleaning loop tests in containment systems
[WRAN-SA-59] 13 p2121 N71-25309
- Plutonium fuels use and recycling in boiling water reactors
[NEDC-12152] 16 p3632 N71-28642
- Computer programs for solving two dimensional multi-group neutron diffusion equations and for solving or recycle of isotopic compositions and related problems
[NAP-13672] 22 p3647 N71-34007
- CIRCULATORS (PHASE SHIFT CIRCUITS)**
Development of electromagnetic wave transmission line circulator and application to parametric amplifier
[NASA-CASE-XNP-02140] 11 p1727 N71-23097

- Development of microwave frequency yttrium-iron garnet filter and circulator
19 p3064 N71-31696
- CIRCULATORY SYSTEM**
NT **ARTERIES**
NT **BLOOD VESSELS**
NT **CAPILLARIES (ANATOMY)**
NT **VASCULAR SYSTEM**
Circulating blood volume changes after lower body negative pressure exposure
08 p1154 N71-19029
- Medical examination of civil aviation flight personnel to determine predisposing factors for atherosclerosis
16 p2547 N71-28491
- CIRCUMLUNAR TRAJECTORIES**
Aborted mission of Apollo 13 due to loss of cryogenic oxygen in service module
[NASA-TM-X-66449] 03 p0456 N71-13073
- CIRCUMPOLAR WETTERLINES**
Numerical modeling of Antarctic circumpolar current
09 p1380 N71-19503
- CIRRUS CLOUDS**
Relationship of cirrus cloud formation/marine tails and jet streams in troposphere examined for aerial navigation application
[NASA-TT-F-13606] 12 p1933 N71-23350
- Calculation of infrared radiation emerging from earth atmosphere in presence of cirrus clouds using remote sensing
15 p2402 N71-27531
- CIRCULAR SPACE**
OGO 3 experiment to measure physical parameters of program size dust particles in circular and near earth space
[NASA-CR-121477] 20 p3276 N71-33768
- CITIES**
NT **MOSCOW**
Microclimatological measurements in new building development in northern Leningrad
[NLL-M-9144-(5828.AB)] 02 p0259 N71-11798
- Technology Applications Program for transferring aerospace technology to cities
[NASA-CR-122035] 22 p3696 N71-36375
- CIVIL AVIATION**
Systems approach to accident investigation in civil aviation and homes
01 p0002 N71-10115
- Demonstration plan for Western Region Short Haul Air Transportation Program
[ATR-71-7198-1-VOL-1] 01 p0003 N71-10279
- Technical studies for Western Region Short Haul Air Transportation Program
[ATR-71-7198-1-VOL-2] 01 p0003 N71-10280
- Air carrier demand for slots particularly in area of Washington-Baltimore
[PB-193350] 01 p0038 N71-10347
- National Aviation Facilities Experimental Center history and programs
01 p0038 N71-10356
- Statistical analysis of direct rail rapid transit system impact on transportation to Cleveland airport
01 p0137 N71-10570
- File formats and code descriptions for analysis of direct rail rapid transit system impact on transportation to Cleveland airport
01 p0028 N71-10571
- FAA statistical handbook of aviation 1958-1968
01 p0003 N71-10572
- Statistical tabulation of United States civil aircraft accident histories for 1969
[PB-196792] 01 p0006 N71-10932
- Statistical tabulation of United States civil aircraft accident histories in 1968
[PB-196811] 01 p0006 N71-10933
- Evaluating current and future requirements and resources for pilots and mechanics in US civil aviation
02 p0167 N71-11187
- Legal aspects of air and surface carrier interactions in freight transportation
02 p0308 N71-12119
- Possible benefits of local and trunk air carrier mergers
02 p0308 N71-12120
- Subsidies for American certificated air carriers
02 p0308 N71-12190
- Analysis of New York air transportation system and recommended improvements
[PB-3] 04 p0515 N71-13777
- Analysis of air transportation facilities in Gulf Coast region of US - Vol. 1
[PB-194359] 04 p0516 N71-13805
- Analysis of civil aviation facilities in Gulf Coast region of US - Vol. 2
[PB-194340] 04 p0516 N71-13804
- Organizational structure and operational procedures of USSR civil aviation
[AD-713415] 05 p0627 N71-14553
- Airline meteorological radar operational policies and procedures
[AD-715636] 05 p0714 N71-14623
- Problems of local airlines in providing service to rural communities
05 p0787 N71-15390

CIVIL AVIATION

- Survey of Hanterville pattern of commercial air traffic
[NASA-CR-115800] 05 p0788 N71-15533
- Problem areas for jet fan propulsion for civil VTOL transports
[NASA-TM-X-52907] 04 p0795 N71-16558
- Cost reduction procedures for aircraft turbine engines used in civil aviation
[NASA-TM-X-52951] 06 p0841 N71-16592
- US general aviation and supplemental air carrier accident statistical tables for 1969
[NTSB-BA-70-4] 07 p0971 N71-17475
- Congressional hearings on Boeing 727 use of Washington National Airport
07 p1004 N71-17697
- Civil aeronautics operations review
07 p1133 N71-17779
- Employment opportunities for economists and air transportation analysts with Civil Aeronautics Board
07 p1134 N71-17798
- Problems in civil air transportation and law
07 p1134 N71-17799
- Reporting career opportunities as economist or auditor with Civil Aeronautics Board
07 p1134 N71-18004
- Problems facing local air transport industry, communities, and government agencies
07 p1135 N71-18078
- Market research and management planning for optimization of civilian airline operations in France
[RREP-19707-II] 07 p1136 N71-18093
- Cybernetic and economic international study group for civil aviation in France
07 p1136 N71-18094
- Economics and cybernetics in civil aviation market research for air traffic prediction
07 p1136 N71-18097
- Air transport supply on scheduled services in Europe-Mediterranean and Southeast Asia regions
[RREP-19707-III] 07 p1138 N71-18112
- Benefits and problems of using hand-up displays in commercial and general aviation aircraft
[NASA-CR-117135] 09 p1308 N71-19732
- Transportation management, regional planning, and commercial aviation development for state of Texas
[PB-196952] 10 p1404 N71-21627
- Characteristics of VISTOL aircraft for commercial transportation system and applications to Texas
[PB-196954] 10 p1404 N71-21632
- Evaluation of short takeoff aircraft for commercial shuttle flight applications to reduce traffic congestion in San Francisco, California area
11 p1671 N71-21874
- Analysis and statistics of airports, air carrier fleet operation, aircraft production, and status of civilian pilot personnel for September, 1970
11 p1672 N71-21977
- Analysis of Boeing 727 aircraft impact on environment, passenger processing, passenger boarding trends, and scheduled and total capacity trends
11 p1672 N71-21978
- Planning for expected civil aviation developments caused by change-over to Boeing 747 aircraft and supersonic transport
11 p1674 N71-22381
- Economics and operational planning for future civil air transportation
11 p1675 N71-22384
- Civilian airline operations with Boeing 747 aircraft and supersonic aircraft
11 p1675 N71-22385
- Planning parameters for high capacity international airport system
11 p1676 N71-22389
- Integrated systems approach for developing requirements of increased civil aviation in Israel
11 p1676 N71-22391
- Weather factors in fatal civil transport aircraft accidents
12 p1856 N71-25431
- Air transportation system and Civil Aeronautics Board decisions
12 p1857 N71-25728
- General aviation traffic implied decisions and limitations from economic comparison with model using southern California to judge difficulty for naval air traffic
[AD-719904] 14 p2197 N71-25621
- Aircraft maintenance for civil aviation
[AD-720346] 14 p2197 N71-25953
- Analysis of magnitude, growth, and carrier participation of passenger traffic in major short-haul markets
14 p2199 N71-26528
- Controlling institutional factors and options for civil aviation research and development
[NASA-CR-18077] 15 p2366 N71-27809
- Cost benefit analysis and technology assessment in civil aviation research and development with case histories
[NASA-CR-18080] 15 p2366 N71-27810

Comparison of fatal aircraft accidents with medical personnel as pilots against aircraft accident fatalities among general aviation pilots
[FAA-AM-71-9] 15 p2367 N71-27428

Investigation and conclusions concerning metal fatigue in aircraft components as cause of civil aircraft accidents
15 p2368 N71-27429

Selected aircraft accident reports in brief form occurring in US civil aviation operations during 1970
[NTSB-BA-71-1] 16 p2531 N71-28189

Analysis of current status and future outlook of US consumer airline industry
[AD-718871] 16 p2531 N71-28216

Airline operations, costs, effects on aircraft industry, and cooperation with CAB
17 p2860 N71-29256

Review of policies affecting civil aviation, problems confronting it, and potential for future contributions to national benefits
[NASA-SP-265] 18 p2867 N71-30506

Civil aviation research and development projects noting characteristics and growth to date, current problems, future requirements, potential solutions, and recommendations
[NASA-SP-266] 18 p2868 N71-30507

Analysis of 79,000 hours data obtained from NASA V-G/VGH flight recorders installed on 734 general aviation aircraft engaged in eight types of operations
18 p2871 N71-30782

Performance tests on liquid explosive emergency exit for civil aircraft
[FAA-RD-71-33] 18 p2872 N71-31064

Annotated bibliography of reports relating to design and improvement of National Aerospace System
19 p3193 N71-31615

Investigation of air charter operations utilizing large airplanes to fulfill demands of aircraft capacity and speed, cargo type and size, as well as frequency of operation
[PB-197636] 19 p3193 N71-31624

Mathematical simulation and queuing models for air traffic control systems
[AD-721726] 19 p3132 N71-32065

Systems and equipment for civil aircraft approach and landing
[JREPT-52] 20 p3299 N71-32850

Pros and cons of SST aircraft for civil airline operations
[BL-147] 20 p3211 N71-33438

Development of data for commercially viable hypersonic transport aircraft
[NASA-TM-F-13793] 20 p3212 N71-33625

Centralized flow control concepts and applications in air traffic control
21 p3456 N71-34594

Civil Aeronautics Board regulatory actions taken fiscal year 1970
21 p3534 N71-35186

Aircraft accident briefs for 1969 including date, location, aircraft data, injuries, flight purpose, and pilot data
[NTSB-BA-71-2] 23 p3708 N71-36433

Statistical, cause/factor and injury tables, accident rates, and briefs of accidents involving US carriers in 1969
[NTSB-ARC-71-1] 23 p3708 N71-36437

Planning short-haul intercity commercial air transportation with STOL aircraft
[WRCN-2] 24 p3873 N71-37605

Senior aviation medical examiners conducting FAA first-class medical examinations
[FAA-AM-71-38] 24 p3884 N71-37683

Survey of domestic air passenger trip length including number of passengers and aircraft types
24 p3896 N71-38795

CIVIL DEFENSE

Communication theory and research applied to prewarning emergency Civil Defense broadcasting system messages
[AD-712332] 02 p0182 N71-11277

Effects of nuclear electromagnetic pulses on AM radio broadcast stations in emergencies
[AD-717319] 11 p1698 N71-21854

Acquisition of data on federal R and D efforts related to command and control center design and law enforcement communications for civil disturbances
[NASA-CR-121639] 21 p3389 N71-34112

CL-595 HELICOPTER

U XH-51 HELICOPTER

CLADDING

Preliminary results of BWR-FLECHT internally pressurized, Zircaloy-clad bundle, spray cooling test
[NEDO-13064] 01 p0086 N71-10599

Cladding temperature and material effects on emergency core cooling system in boiling water reactor
[NEDO-10179] 01 p0086 N71-10645

Research and development of nuclear fuels, cladding, and other structural materials for fast reactors, space power reactors, and general reactors
[ORNL-4520] 01 p0087 N71-10920

Performance tests of stainless steel, and Zircaloy cladding for nuclear fuel assemblies
[IN-1378] 02 p0264 N71-11733

Implementation manual of computer program for calculating fission product corrosion in liquid metal clad breeder reactor cladding
[AI-ABC-12957] 03 p0415 N71-12841

Micromachining methods for studying samples of fission products and cladding in irradiated fuel elements
[CBA-CONF-1564] 04 p0546 N71-13612

Electron microscope analysis of irradiated ceramic nuclear fuel and cladding materials
[EUR-4504-D] 04 p0548 N71-13645

Chemical decladding of nonirradiated, stainless steel canned uranium dioxide fuel elements
[BLG-435] 04 p0551 N71-13817

Fuel, core, and cladding developments and safety experiments for fast ceramic reactors
[OEAP-10928-33] 04 p0552 N71-13968

Performance and isotopic composition of Zircaloy clad uranium oxide fuel elements
[OEAP-10160] 04 p0553 N71-13973

Fast breeder reactor advanced fuel element cladding fabrication
[OEAP-745] 04 p0553 N71-13994

Cladding effects on heat transfer to liquid metals, forced circulation stainless steel loops, and neutron cross section studies
[BNWL-50205] 04 p0589 N71-14314

Zirconium alloys for fuel cladding or structural materials of water cooled reactors
[BARC-463] 05 p0702 N71-15097

Metallographic analysis of heater rods, cladding, and metal-water reactions
[WCAP-7444] 06 p0897 N71-15874

Stress-rupture behavior of types 304 and 316 stainless steel cladding in high temperature static sodium
[AI-ABC-12976] 06 p0870 N71-15930

Embrittlement of Zircaloy under high temperature conditions simulating loss of coolant accident in reactors
[IN-1389] 06 p0898 N71-16192

Advanced reactor stainless steel materials cladding development
[OEAP-4135-12] 06 p0874 N71-16698

Radiation effects on mechanical properties of cladding materials
[BM1-1899] 07 p1065 N71-17552

Two step process for cladding nuclear fuels with tungsten
[NASA-CASE-XNP-03704] 07 p1037 N71-17695

Chemical aspects of reactor safety including release and transport of fission products, aerosol behavior, and chemical reactions of metal cladding
[HMI-B-99] 08 p1235 N71-18213

Zircaloy clad uranium dioxide fuel rod evaluation
[OEAP-10204] 08 p1238 N71-18345

Zircaloy-clad uranium dioxide fuel rod burnup, crud thickness, surface roughness, and cracks
[OEAP-10217] 10 p1601 N71-20607

Materials for reactor cores, control rods, fuel, cladding, and moderators
[BNWL-SA-3426] 10 p1601 N71-20608

Mechanical properties data for LMFB reactor materials, and irradiation effects on cladding and structural alloys
[BM1-1891] 10 p1602 N71-21084

Optimum grid spacing in fuel rod support systems
[WAPD-TM-714] 10 p1603 N71-21184

Tensile and fatigue properties and liquid oxygen compatibility of bilaminar stainless steel-clad titanium prepared by vacuum deposition and explosive welding
[NASA-CR-72841] 10 p1581 N71-21437

Stress strain limits in evaluating built-up rod-type fuel elements to sustain up-power transients inducing high strain rates in cladding
[WAPD-TM-979] 11 p1794 N71-22351

Progress report including removal of stainless steel cladding, development of fluid bed process for reduction of nuclear fuel oxide to metal
[ANL-7755] 12 p1961 N71-23194

Simulation of thermal effects of fuel elements with resistance heater, thermocouples, and cladding
[NLL-RISLEY-TRANS-1805-9091.9F] 12 p1964 N71-24103

Combined ultrasonic/induction testing for Zircaloy cladding tubes
[NLL-WINDSCALE-446-9091.9F] 12 p1940 N71-24122

Comparison of neutronic and thermal environments for stainless steel-clad uranium- or plutonium oxide fuel rod in proposed reactor with test conditions currently available
13 p2111 N71-24510

Lithium filled heat pipe for obtaining near isothermal conditions axially along cladding of in-pile fast-neutron reactors
13 p2185 N71-24512

First generation uranium dioxide fuel, tungsten clad, test capsule data
13 p2114 N71-24542

Charpy impact test and irradiation tests of domestic Zircaloy 2 cladding materials in JPDR
[JAERI-MEMO-4192] 13 p2119 N71-25205

Electrochemical properties of aluminum, nickel-based, and stainless steel cladding alloys for nuclear fuels examined by galvanostats
[IN-1295] 13 p2120 N71-25204

Postirradiation examination of tantalum cladding from EBIR-2 photoneutron startup sources for oxidation and changes in microstructure and chemical content
[ANL/EBIR-31] 14 p2291 N71-25800

Mechanical properties of stainless steel type 304 for LMFB cladding
[WHAN-SA-8] 14 p2291 N71-25800

Development of oxidation resistant hafnium alloys as cladding for niobium and tantalum base alloys
[AD-720724] 14 p2274 N71-26131

Results of irradiation test of Zircaloy clad uranium dioxide fuel rods in BR-2 reactor
[EUR/ABC-2146] 14 p2295 N71-26170

Compatibility tests at 900 C on Fe-Ni-Cr alloys and UC with varying carbon content and with Cr, V, and VC stabilizers for fuel cladding reactions
[KFK-1213] 15 p2446 N71-27166

High quality weld of cladding during hot rolling of VAD-23 alloy sheets
[AD-721034] 15 p2416 N71-27228

Application of flame metal spraying to bonding gas-tight alloy cladding to uranium nuclear fuel elements
[CEA-CONF-1625] 15 p2448 N71-27228

Thermal cycling tests of Cr, Al, Si, Fe, and Y alloy clad nichel alloy at 1040 and 1090 C and time, cycle frequency, and film thickness effects on oxidation resistance
[NASA-TN-D-6276] 16 p2688 N71-28010

Fuel rod failure experiment in TREAT facility using Zircaloy clad UO₂ fuel rods in flowing steam atmosphere
[ORNL-4635] 16 p2631 N71-28010

Processes designed for decladding and dissolution of UO₂ and PuO₂ fuels clad with stainless steel or Zircaloy
[CEA-BIB-191] 16 p2637 N71-28009

Reactor safety experiments including fuel pin performance tests, cladding failure, and fuel pin loss of coolant
[EUR/FNR-884] 17 p2782 N71-28008

Research in fuel cycle technology including rearing stainless steel cladding, and fluid bed process for converting uranyl and plutonium nitrate to oxide forms
[ANL-7767] 17 p2786 N71-28026

Fabrication and testing of double vacuum melted, type 316 thin walled austenitic stainless steel tubing for use as cladding in LMFB fuel pins
[WAPD-4135-14] 17 p2786 N71-28011

Fuel pin failure detection in sodium cooled reactors by delayed neutron transit time measurements as claddings
[INF-18778] 19 p3137 N71-32071

Code for calculating mechanical and thermal stresses in cladding of fuel elements
[EUR-4562-F] 19 p3137 N71-32080

Sodium carbonate inhibitor for preventing coolant corrosion and pitting in magnesium cladding of water cooled fuel rods
[NLL-CE-TRANS-5440-9002.09] 19 p3138 N71-32074

Corrosion of steel claddings of nuclear fuel elements in sodium cooled fast breeder reactor
[NLL-RISLEY-TRANS-2015-9091.9F] 19 p3115 N71-32200

Comparison of high-resolution gamma ray scanning and mass spectrometry for use in failure analysis of encapsulated fast reactor fuel element cladding
[LA-4675-365] 21 p3463 N71-34619

Reactor safety including failure modes of Zircaloy clad fuel rods
[ORNL-4647] 21 p3479 N71-34777

Size of fission product gas bubbles released from simulated break in fuel-element cladding
[ANL-7789] 21 p3479 N71-34778

Oxidation protection of superalloys by the claddings of Ni-Cr-Al-Si and Fe-Cr-Al-Y alloys examined and compared with commercial stainless coatings
[NASA-TM-X-67925] 22 p3592 N71-35979

Effects of fast breeder reactor core conditions in type 316 stainless steel fuel cans
[CONF-700211-7] 22 p3626 N71-35985

Reactor and electron microscope analysis of fast neutron flux effects on metal cladding material microstructure
[RD/BN-1812] 22 p3635 N71-35911

Titanium-vanadium for fuel element cladding in fast breeder reactors
[CONF-700211-9] 23 p3796 N71-37807

Fuel rod, cladding, and canning materials for superheated water reactors
[BMFW-FBK-70-22] 24 p3955 N71-39016

Storage and handling of highly irradiated fast breeder reactor fuel in hybrid sodium organic coolant storage pool, and Bz-Ca liquid metal dissolution for decladding
[EUR-4613-B] 24 p3956 N71-39023

SUBJECT INDEX

CLAMPING CIRCUITS

Clamped amplifier circuit for barium counter
modeling amplifiers and accurate measurement of
qualified parameters
[NASA-CASE-308-01794] 10 p1536 N71-30782

CLAMPS

Hydraulic clamping of sheet stock apparatus
[NASA-CASE-354-00100] 67 p1687 N71-37496

Thermal concept clamping assembly design for
support structure and control system mounting
[NASA-CASE-XMS-02184] 10 p1563 N71-30813

Design and development of module joint clamping
device for application to solar array construction
[NASA-CASE-TNF-02341] 10 p1567 N71-31531

Quick attach mechanism for moving or stationary
video camera or camera
[NASA-CASE-CFR-05421] 11 p1772 N71-32994

Influence of in-plane boundary conditions on buckling
of clamped circular shells under external pressure
[AD-721075] 16 p2684 N71-30836

Theoretical study of nonlinear flutter behavior of
clamped plate subjected to various loads
21 p3374 N71-34810

CLARK V AIRFOIL

U AIRFOIL PROFILES
[NASA-CASE-354-00100] 67 p1687 N71-37496

CLASICAL MECHANICS
[NASA-CASE-354-00100] 67 p1687 N71-37496

ASTRODYNAMICS
[NASA-CASE-354-00100] 67 p1687 N71-37496

CELESTIAL MECHANICS
[NASA-CASE-354-00100] 67 p1687 N71-37496

KEPLER LAWS
[NASA-CASE-354-00100] 67 p1687 N71-37496

ORBITAL MECHANICS
[NASA-CASE-354-00100] 67 p1687 N71-37496

Limiting transition from nonrelativistic quantum
mechanics to classical mechanics
[JPL-TR-354] 67 p1678 N71-17777

Electrodynamics and boundary value problems in
all plane field theory based on classical and quantum
mechanics
17 p2888 N71-30354

Pair distribution function in classical statistical
mechanics
18 p2986 N71-31239

Comparison of quantum electrodynamics and classical
mechanics for gravitational effects on Mercury or
[JPL-TR-354] 20 p2340 N71-33882

Classical trajectory study of rotationally inelastic
scattering of hydrogen molecules by collisions with
helium ions
[NASA-CR-121729] 21 p3306 N71-34087

Generation of particles in classical relativistic
mechanics
[NASA-TT-F-13734] 22 p3634 N71-35901

Electric scattering and multiple moments in atomic
collisions based on classical mechanics
[JPL-TR-354] 22 p3635 N71-35909

CLASSIFICATIONS

NT HIERARCHIES
[NASA-CASE-354-00100] 67 p1687 N71-37496

NT INDEXES (DOCUMENTATION)
[NASA-CASE-354-00100] 67 p1687 N71-37496

Computerized classification of meteorological
charts and development of forecast aids
[AD-712676] 65 p6073 N71-12758

Classification and signal analysis of pulse width
modulated signals
[NASA-CR-100009] 94 p2609 N71-13517

Classification of calcium-40 model based on reaction
K-39/Fe-54, gamma/calcium-40 and calcium-
40, gamma/calcium-40 - conference
[CAL-CONF-1333] 64 p5771 N71-13614

Systematic classification of meteorite impact
sites for lunar and planetary craters
[NASA-CR-116898] 65 p1194 N71-19083

Automatic identification and classification of wheat
from airborne multispectral data in agricultural remote
sensing
[JPL-TR-354] 12 p1913 N71-23731

Heavy classification reaction time and human
performance in data processing using decision making
experiments
[AD-721198] 15 p2374 N71-34885

Major Soviet information institutions on chemistry
and chemical technology providing single classification
system for information service system
[JPL-TR-354] 15 p2375 N71-34886

Classification of coordinate transformations and
the vector-tensor calculus
[JPL-TR-354] 15 p2376 N71-34887

Methods for classifying atmospheric ice crystals
according to geometric form
21 p3452 N71-34545

Development of techniques for homogeneity studies
of gold-silver and gold-copper alloys for standard
calibration potential classification
[JPL-TR-354] 22 p3594 N71-35594

Handbook presenting classification of electronic
and nuclear computers and sensing devices
[AD-722822] 24 p3885 N71-37758

Structure and classification scheme of hydrogen
methyl chloride
[JPL-TR-354] 24 p3890 N71-38321

CLASSIFICATION
[NASA-CASE-354-00100] 67 p1687 N71-37496

CLASIFICACION
[NASA-CASE-354-00100] 67 p1687 N71-37496

CLASIFICACION
[NASA-CASE-354-00100] 67 p1687 N71-37496

CLASIFICACION
[NASA-CASE-354-00100] 67 p1687 N71-37496

CLASIFICACION
[NASA-CASE-354-00100] 67 p1687 N71-37496

CLASIFICACION
[NASA-CASE-354-00100] 67 p1687 N71-37496

CLASIFICACION
[NASA-CASE-354-00100] 67 p1687 N71-37496

CLASIFICACION
[NASA-CASE-354-00100] 67 p1687 N71-37496

CLASIFICACION
[NASA-CASE-354-00100] 67 p1687 N71-37496

CLASIFICACION
[NASA-CASE-354-00100] 67 p1687 N71-37496

Examination by nuclear resonance in saturated clay
shale - Project Pro-Quartz 2
[AD-720083] 14 p2340 N71-30106

CLEAN ROOMS

Horizontal laminar flow clean room complex for
microphotography
[AD-711936] 62 p0199 N71-11535

Laminar airflow and airborne contamination control
concepts with clean room specifications and laminar
flow facility design
[NASA-CR-116185] 69 p1548 N71-30423

Standards for clean rooms in vacuum electronics
manufacturing for precision instruments
[JPL-TR-354] 69 p1549 N71-30530

Clean room fire caused by gas heating element thermal
failure in liquid nitrogen system
[NASA-TM-X-67293] 17 p3731 N71-35880

CLEANING
[NASA-CASE-354-00100] 67 p1687 N71-37496

NT AIR FILTERS
[NASA-CASE-354-00100] 67 p1687 N71-37496

Device for back purging thrust engines
[NASA-CASE-XMS-04036] 16 p3672 N71-38849

CLEANING
[NASA-CASE-354-00100] 67 p1687 N71-37496

Internal recirculating air cleaning loop tests in
contaminated systems
[NASA-CR-116185] 13 p2121 N71-35300

Planar cleaning techniques for removing contaminants
from optical surfaces in spacecraft
[NASA-CR-121733] 21 p3519 N71-35074

Development of gas plasma cleaning techniques for
removing contaminants from optical surfaces in space
environments
[NASA-CR-116185] 21 p3519 N71-35075

CLEANING
[NASA-CASE-354-00100] 67 p1687 N71-37496

Classification control effects on aircraft components
and instrument vacuum production in Sweden
[FOA-C-1325-76] 14 p2312 N71-36566

Ultraviolet radiation and quartz crystal
microbalance analysis of vacuum chamber cleanliness
and effects of chamber use history and pumping
mechanism on contamination
[NASA-TM-X-63571] 15 p2392 N71-27708

CLEAR AIR TURBULENCE
[NASA-CASE-354-00100] 67 p1687 N71-37496

High resolution forward scatter system to detect
refractive index fluctuations caused by clear air
turbulence
[AD-712688] 62 p0285 N71-11130

Description of clear air turbulence by radar
[JPL-TR-354] 62 p0286 N71-11131

Synoptic meteorological conditions for clear air
turbulence and turbulence effects on aircraft flight
characteristics
[JPL-TR-354] 67 p0290 N71-17145

Airborne photostatic particle counter for mapping
clear air turbulence
[NASA-CR-116185] 69 p1414 N71-30390

Clear air turbulence pulse Doppler radar
design including analysis of mechanical vibration effects
on laser transmitter and receiver
[NASA-CR-105991] 11 p1774 N71-22131

Airborne laser-radar measurements of atmospheric
clear air turbulence by optical diffraction patterns
11 p1776 N71-22960

Clear air turbulence in stratosphere and effects on
weather formation, atmospheric physics, and
supersonic flight
[JPL-TR-354] 14 p2346 N71-25746

Detecting clear air turbulence using CO2 laser Doppler
system
16 p2951 N71-30763

XE-70 aircraft for investigating and predicting clear
air turbulence in stratosphere caused by mountain
waves
[NASA-CR-10789] 18 p2954 N71-31251

Relationship between disturbed gradients of index
of refraction, layer echoes by vertically pointing
radar, clear air turbulence and synoptic meteorological
conditions
[JPL-TR-354] 18 p2955 N71-31411

Synoptic meteorological conditions for clear air
turbulence and turbulence effects on aircraft flight
characteristics
[JPL-TR-354] 19 p3127 N71-31781

Synoptic meteorological conditions for clear air
turbulence and turbulence effects on aircraft flight
characteristics
[JPL-TR-354] 19 p3127 N71-31782

Electromagnetic field disturbance models for clear
air turbulence detection in atmosphere
[AD-723121] 19 p3091 N71-31996

Meteorological flight search for clear air turbulence
in stratosphere above Australia, 1966
20 p3399 N71-33671

Computer program for predicting atmospheric
clear-air layer instability and clear air turbulence induced
by mountain waves
[NASA-CR-122041] 22 p3680 N71-37961

Clear-air layer and clear-air effects on cold air
performance of turbine with vent cooled starter blades
[NASA-TM-X-67914] 20 p3340 N71-33779

CLASIFICACION
[NASA-CASE-354-00100] 67 p1687 N71-37496

CLASIFICACION
[NASA-CASE-354-00100] 67 p1687 N71-37496

CLASIFICACION
[NASA-CASE-354-00100] 67 p1687 N71-37496

CLASIFICACION
[NASA-CASE-354-00100] 67 p1687 N71-37496

CLASIFICACION
[NASA-CASE-354-00100] 67 p1687 N71-37496

CLASIFICACION
[NASA-CASE-354-00100] 67 p1687 N71-37496

CLASIFICACION
[NASA-CASE-354-00100] 67 p1687 N71-37496

CLASIFICACION
[NASA-CASE-354-00100] 67 p1687 N71-37496

CLASIFICACION
[NASA-CASE-354-00100] 67 p1687 N71-37496

CLASIFICACION
[NASA-CASE-354-00100] 67 p1687 N71-37496

CLASIFICACION
[NASA-CASE-354-00100] 67 p1687 N71-37496

CLASIFICACION
[NASA-CASE-354-00100] 67 p1687 N71-37496

CLASIFICACION
[NASA-CASE-354-00100] 67 p1687 N71-37496

CLASIFICACION
[NASA-CASE-354-00100] 67 p1687 N71-37496

CLASIFICACION
[NASA-CASE-354-00100] 67 p1687 N71-37496

CLERSC-GORDAN COEFFICIENTS

Clerse-Gordan coefficients for crystallographic
space groups
69 p1472 N71-19847

CLIMATE

Description of projects for determining effect of
atmospheric pollutants on weather and climate
[ESSA-TR-SRL-185-APCL-15] 12 p1998 N71-34115

Research in basic physical processes which control
weather and climate
13 p2188 N71-25412

Zonal atmospheric model for simulating earth
climate and testing ice age theories
[UCRL-72885] 20 p3267 N71-33521

CLIMATOLOGY
[NASA-CASE-354-00100] 67 p1687 N71-37496

NT MICROCLIMATOLOGY
[NASA-CASE-354-00100] 67 p1687 N71-37496

Model of global climate and ecology
[AD-711408] 61 p0679 N71-16732

Climatology analysis of Southeast Asia for month of
August
[AD-711386] 62 p2577 N71-11677

Climatological data for Belgian weather stations for
Aug. 1970
62 p2528 N71-11607

Climatological tables for Belgian weather stations -
May 1970
62 p2529 N71-11601

Investigating mesometeorological processes, climate
modification, hail suppression, thermal inversions,
and humidity variations
62 p2530 N71-12154

Archiving and climatological applications of
meteorological satellite data
[ESSA-TR-NESC-33] 61 p0361 N71-12181

History of meteorological satellites launched to
date, and type of data acquired from TIROS, ESSA,
and Nimbus for climatological applications
61 p0362 N71-12182

Archival procedures, and available meteorological
satellite data for climatology
61 p0363 N71-12183

Meteorological, climatology, and physical/chemical
oceanography for Caribbean Sea - annotated bibliography
61 p0364 N71-12184

Meteorology, climatology, and physical/chemical
oceanography for Caribbean Sea - indexes
61 p0365 N71-12185

News briefs and abstracts of articles on meteorology
61 p0366 N71-12186

Meteorological data for Mt. Hopkin Observatory
for 1968 and 1969
[NASA-CR-111748] 64 p541 N71-14149

Long term climatological and atmospheric effects of
air pollution
[JPL-TR-354] 64 p5222 N71-14493

October climate of Southeast Asia
[AD-713128] 65 p0714 N71-14519

Climatology of Antarctic - Jan. 1967 - Dec. 1968
[AD-713187] 65 p0716 N71-14729

Temperature, pressure, and related climatological
data for Australia - tables for July 1970
65 p0722 N71-14861

Temperature, pressure, and related climatological
data for Australia - tables for June 1970
65 p0716 N71-15088

Climate modification problems including ocean
models, atmospheric radiation, convective and cumulus
cloud models, and numerical weather prediction
[AD-713428] 65 p0718 N71-15252

Climatological and circulation aspects in Northern
Hemisphere in first half of 20th century
[TT-76-5820] 65 p0805 N71-15708

Atmospheric circulation variations and mean
monthly air temperature anomalies in Northern Hemisphere
65 p0806 N71-15761

Climatology in extreme deserts and displacement
of Arctic intrusion runs
65 p0807 N71-15764

Water circulation and temperature conditions in
Far East sector of Northern Hemisphere during two
epochs
65 p0808 N71-15765

Atmospheric circulation and temperature fluctuations
in eastern Siberia
65 p0809 N71-15766

Precipitation amounts in East Siberia during two
circulation epochs
65 p0810 N71-15767

Comparison of estimated periods of circulation
epochs over European USSR and West Siberia
65 p0811 N71-15768

Circulation conditions and monthly average temperature
and precipitation anomalies over European USSR
65 p0812 N71-15769

Atmospheric circulation relationships and Moscow
weather during January
65 p0813 N71-15770

Variations in phenological events and climatic epochs in European USSR

Snow cover climatology and physical properties at Lebeson, New Hampshire

December climate of Southeast Asia

November climate of Southeast Asia

Climatological data - Belgium, Oct. 1970

Climatological data - Belgium, Nov. 1970

Wind observations and derived wind stresses for North Pacific

Sea level meteorological properties and heat exchange processes for North Pacific

Discussing geological, topographical, and climatological features of Iceland and effects on human habitation

Determining transport and climatological factors affecting colonization of life on remote islands

Climatological values of lower atmosphere temperature and wind stratification

Mean monthly tropospheric circulation and cloudiness over Southeast Asia

Charts of digitized global monthly means of ocean surface temperature

Remote sensing of land uses, urban growth and environmental quality, climatology, census data, and thematic maps

Climate calculation with combined ocean and atmosphere model

Sea ice, ocean currents, climatology, and geology of Arctic Ocean and coastal areas

Aeronautical climatological conditions at Kajani Airport, Finland

Aeronautical climatological conditions at Kruunukylä Airport, Finland

Climatology for North American coastal areas from Vancouver to Alaska

Climatology and atmospheric refraction models for worldwide radio wave propagation

Surface climatological data for twenty selected launch, landing, and alternate landing sites for space shuttle system

Climatology at Rovaniemi Airport, Finland

Climatology at Maarianhamina Airport, Finland

Climatology at Vaasa Airport, Finland

Climatology at Turku Airport, Finland

Climatology at Oulu Airport, Finland

Glacio-climatological observations on Lomonosov glacier plateau

Climatological ground effects on subsurface radio wave propagation

Meteorological radioonde data from aerological station in Berlin, Germany, for December 1969

Meteorological radioonde data from aerological station in Berlin, Germany, for February 1970

Meteorological radioonde data from aerological station in Berlin, Germany, for March 1970

Meteorological radioonde data from aerological station in Berlin, Germany, for April 1970

Hydrodynamic theory applied to climatological and general atmospheric circulation and numerical analysis of macro-atmospheric processes

Computerized simulation of meteorological parameters and transmissibility in Sigeau area

Climatological data summary for Greenland during 1958

Urban development effects on climatology of Paris

Solar activity cycles and heliostatimetry in long range forecasting

Methods for long range weather forecasting of monthly and seasonal mean values of climatological elements analyzed in terms of synoptic climatology

Interaction between atmosphere and terrain in producing climate for US

Airfield climatology for European Low Countries and British Isles

Airfield climatology for Scandinavia and northern Europe

Meteorological charts and data tables for July through September, 1970 from Berlin

Daytime measurements of precipitable water vapor in atmosphere over selected mountain sites in southwest

Climatic cooling effects on earth surface

Tropical weathering effects on soil formation and erosion

Tables on climatology of ionosphere measured by ionosondes

Meteorological parameter tables for Belgian weather stations, Feb. 1971

Climatology at Post Flux Test Facility, Washington

Conferences on solar radiation, instrumentation, spectroscopy, and radiation climatology

Survey of 1962-1965 satellite observation of earth atmosphere radiation climatology

Radiation climatology applied to numerical models

Tables on climatological conditions for airfields and climatic areas of Mediterranean region

Finnish meteorological parameters for Jan. 1971

Utilization of climatological data for tropical weather forecasting

Atmospheric models for relating precipitation rate to monthly climatology

Occurrence frequency of poor ceiling and visibility conditions in Southeast Asia and Korea

Climatology of tropical storms in North Atlantic Caribbean and Gulf of Mexico

Acquisition and storage of militarily significant data on climatology, hydrology, soils, and ecology of humid tropical regions

Desert climatology and geomorphology - bibliography

Climatological experiments concerning interaction with sea surface

Topography, weather conditions, climatic side, and local forecast studies at Chamite AFB, Illinois

Results of systematic measurements of geomagnetism and meteorological summaries

Meteorological data from Berlin weather station for fourth quarter of 1970

Daily meteorological charts from Swiss weather stations for 1969

Atmospheric models and thermodynamic effects of glaciers and Arctic Ocean in relation to causes of ice age climatology

Mutual interactions between Arctic ice and climate

Atmospheric circulation in Northern Hemisphere and possible effects of polar ice destruction on circulation and climatology

Occurrence of frost conditions in North Germany with emphasis on meteorological parameters and seasonal variations

Analysis of rhythmic activity of atmosphere for forecasting extreme temperature ranges over USSR

Soviet news releases on boundary layer physics, reflectivity profile effects, and climate of paleozoic age

Observations of yearly wind conditions and climatology of Denmark

Precipitation, atmospheric pressure and temperature, solar radiation, and wind velocity data for Fort Greely, Alaska - Oct. 1970

Atmospheric temperature and pressure, precipitation, humidity, solar radiation, and wind velocity and direction data for Yuma test range, Arizona - Oct. 1969

Climatology, precipitation, atmospheric temperature, and wind direction and velocity data for Fort Wainwright, Alaska - Nov. 1970

Climatology, geography, geology, and history of Yukon Territory, Canada and Chukotka Pen., Alaska

Temperature, pressure, and related climatological data for Australia - tables for March 1971

International cooperation in global atmospheric research program on weather forecasting

Meteorological data for Wanger expedition with daily surface synoptic charts

Atmospheric phenomena for 1968 at Canadian Center for Nuclear Studies, Italy

Basic physical processes controlling weather and climate

Location of Aleutian low center, and pressure at center

Climatology and landing approach noise measurements for three engine turbofan transport aircraft

Aircraft accident at Miami, Florida involving Republic of Ecuador C-340 during climb following instrument takeoff

Flight simulator evaluation of aircraft instrument approach procedures

To-134 aerodynamic characteristics during climb, climb, horizontal flight, landing stability and maneuverability, and strength under various loads

Investigating wear processes in hip prostheses after brief use

Clinical problems of cardiology of athletes

Cardio-vascular medical services for Soviet athletes

Technology assessment of research in biological and medical engineering including problem areas

Systems management with computers and television aids in medicine including physical examination, patient isolation, data processing, and electrocardiographic diagnosis

Artificial changes in leukocyte count of rabbits

Biological and therapeutic effects of magnetic field on human organisms

Applications of X ray photography to diagnosis of cardiovascular and respiratory system diseases

Technology transfer and applications in medicine and biology

Clinical neurology and neurophysiology of vestibulo-ocular reflexes

Opto theory, information system for direct data needs, and model of workspace systems

Computerized method for input of disease history information and retrieval for diagnosis

Bioelectronic research and applications to biological and medical problems

Computer technology for medical information systems, in patient care, and for diagnostic research

Chopper distortion of two narrow band pass signals

Chopper distortion of two narrow band pass signals

Chopper distortion of two narrow band pass signals

Chopper distortion of two narrow band pass signals

Chopper distortion of two narrow band pass signals

Chopper distortion of two narrow band pass signals

Chopper distortion of two narrow band pass signals

Chopper distortion of two narrow band pass signals

Chopper distortion of two narrow band pass signals

Chopper distortion of two narrow band pass signals

Chopper distortion of two narrow band pass signals

Chopper distortion of two narrow band pass signals

Chopper distortion of two narrow band pass signals

Chopper distortion of two narrow band pass signals

Chopper distortion of two narrow band pass signals

Chopper distortion of two narrow band pass signals

Chopper distortion of two narrow band pass signals

Chopper distortion of two narrow band pass signals

Chopper distortion of two narrow band pass signals

Chopper distortion of two narrow band pass signals

Chopper distortion of two narrow band pass signals

Chopper distortion of two narrow band pass signals

Chopper distortion of two narrow band pass signals

Chopper distortion of two narrow band pass signals

Chopper distortion of two narrow band pass signals

Chopper distortion of two narrow band pass signals

Chopper distortion of two narrow band pass signals

Chopper distortion of two narrow band pass signals

Chopper distortion of two narrow band pass signals

Chopper distortion of two narrow band pass signals

Chopper distortion of two narrow band pass signals

Chopper distortion of two narrow band pass signals

Chopper distortion of two narrow band pass signals

Chopper distortion of two narrow band pass signals

Chopper distortion of two narrow band pass signals

Chopper distortion of two narrow band pass signals

SUBJECT INDEX

Low frequency time signals for clock synchronization 11 p1707 N71-22915

Geophysical effects on superposed clock synchronization using low frequency ground waves 11 p1708 N71-22922

Time synchronization system for spacecraft using clocks at remote locations with master clock using space reflected optical signals 14 p2235 N71-26326

Check for measuring wide range of pulse rates by utilizing high capacity counter 15 p2388 N71-27137

Aircraft mechanical and battery operated clocks resistant to high intensity magnetic fields 23 p3707 N71-34436

GLIDING

U FLUODING

CLOUDED CIRCUIT TELEVISION

Cloud circuit television and guidance adapter kit for suspended landing state 01 p0964 N71-10974

Computer-aided operations measuring machine with closed circuit TV viewing system for inspecting closed circuit monitors 03 p0376 N71-12770

CLOUD CYCLES

Cloud-cycle regulator development program 03 p0329 N71-12352

Cloud cycle magnetohydrodynamic power generation with two channels 12 p1981 N71-23932

CLOUDS ECOLOGICAL SYSTEMS

Feasibility of satellite/satellite system utilizing passive infrared radiance techniques to determine abundance ecology of crew during extended space flight 02 p0154 N71-11091

Possible water reclamation from human waste in zero-G environment 02 p0170 N71-11207

Thermoplastic films of human oral cavity during prolonged confinement 08 p1154 N71-19065

Inhabitable vehicle for testing simulation of closed ecological space station system 09 p1367 N71-20328

Toxicology of human and animal waste products and by-products in controlled atmosphere of closed ecological systems - literature review 09 p1338 N71-20493

Oxygen recovery from animal carbon dioxide in spacecraft cabin atmosphere by chemical reactor with waste burner tank 10 p1506 N71-20960

Ambient absorbent for carbon dioxide concentration in long term life support system 10 p1506 N71-20961

Oxygen production efficiency of water electrolysis systems in long term regenerative life support system 10 p1506 N71-20965

Water regeneration by extraction of organic and inorganic impurities in closed ecological systems 10 p1548 N71-21009

Aerofact water reclamation and closed self contained biological oxygenated closed ecological system techniques in USSR and US 12 p1866 N71-23376

Ominicure as polyfunctional autotrophic components of closed ecological life support systems 16 p2550 N71-28253

Evaporation and filtration systems for water management in manned space vehicles 16 p2552 N71-28336

Monitoring techniques for biological and chemical atmospheric contaminants in closed environment 17 p2711 N71-29763

Statistical analysis model for ocean ecological system and measurement methods for phytoplankton production 22 p3577 N71-35477

Cloud ecological systems, water reclamation, astronaut work capacity, and psychological stress experiments - conference 24 p3015 N71-30642

Water reclamation from human and other wastes for prolonged space flights 24 p3015 N71-30645

CLOUD LOOP SYSTEMS

U FEEDBACK CONTROL

Design and characteristics of device for closing nozzles under high vacuum conditions 16 p1567 N71-21528

Close technique for retention of grease in large bearing on F-40 aircraft wheels 19 p3104 N71-31744

Design and characteristics of 28-inch diameter seals for bearing propulsion system - Part I 23 p3659 N71-37374

CLOTHES

U FABRICS

NT COTTON FIBERS

NT FLIGHT CLOTHING

NT GARMENTS

NT GLOVES

NT GOGGLES

NT HELMETS

NT PRESSURE SUITS

NT PROTECTIVE CLOTHING

NT SMOGERS

NT SPACE SUITS

NT SUITS

Zen gravity clothes washer utilizing principles of fluidics to provide washing action and reduction in number of components and model 13 p2096 N71-24455

Flammable Polymer program reporting standards for carpets and rugs, blankets, mattresses, and apparel for children 23 p3776 N71-30914

CLOUD CHAMBERS

Cosmic ray data from cloud and ionization chambers, and carbon and iron plates 17 p2340 N71-29472

CLOUD COVER

Comma 12 cloud photograph of cloud cover and photostereopairs for weather forecasting 01 p0061 N71-10991

Cloud distributions determined using reflected radiance measurements from multicolor spin-scan cloud camera on ATS 3 02 p0156 N71-11620

Performance of ATS 1 spin-scan cloud cover camera mounted at Mojave ground station 03 p0082 N71-14001

Cloud cover distribution on days with and without precipitation 06 p0080 N71-16109

Mean monthly tropospheric circulation and cloudiness over Southeast Asia 06 p1230 N71-18671

Temperature and spatial correlation functions for cloud cover over European Russia, calculated from satellite data observations 09 p1414 N71-20342

Satellite cloud cover observations for determining radio and radar propagation characteristics 10 p1522 N71-21414

Calculations of clear channel radiances using infrared temperature profile radiometer measurements taken by Convair-590 over partly cloudy areas 10 p1542 N71-21842

Abstracts and bibliographies of meteorological articles 11 p1708 N71-21953

Behavior of barium ion cloud at high altitudes 12 p1953 N71-23517

Planning of GARP tropical experiments testing tropospheric motions and cloud clusters 13 p1405 N71-24469

Radar weather index used for forecasts of cloud cover and precipitation in Southeast Asia 15 p2436 N71-26822

Simulation of sensor spatial resolution effects on estimates of cloud cover from satellites 15 p2496 N71-26925

Location, optical instrumentation at observational sites, and weather conditions for testing flights 17 p2552 N71-29679

Numerical analysis of 500 surface geopotential heights from satellite-observed cloud patterns in Northern Hemisphere 20 p2597 N71-33618

Effect of clouds on laser communication between space and earth determined by simulated operation 21 p3435 N71-34443

Effects of ionosphere in observations toward horizon on direct solar radiation and radiation direction calculations 21 p3465 N71-34969

Chemical composition, meteorological parameters, cloud layer, atmospheric circulation, upper atmosphere, and origin and evolution of Venusian atmosphere 21 p3507 N71-34988

Analysis of cloud clusters and probability of seeing them for application to ERTS 21 p3508 N71-34990

News briefs and abstracts of scientific articles concerning meteorology including statistical forecasting and climatic characteristics of cloud cover 21 p3509 N71-34999

Night cloud cover and meteorological parameters determined at La Silla, Chile during 1968 22 p3670 N71-36171

CLOUD GLACIATION

Venus halo and photometric evidence for ice in Venus clouds 06 p0843 N71-10834

Electrical force potential for deep supercooling and development and dissipation of clouds and fog 09 p1413 N71-19661

Weather modification for increasing high elevation snowfall in northern Rocky Mountains 22 p3611 N71-35725

Cloud seeding technological development and effects on cloud growth with applications 23 p3706 N71-36961

CLOUD PHOTOGRAPHY

CLOUD HEIGHT INDICATORS

Computer program for determining tall convective cloud occurrence and altitude and comparison with radar precipitation echoes in stratosphere 06 p1413 N71-19622

Spectrometer measurement of cumulus cloud reflection in 0.70 micron band of oxygen for cloud height determination 13 p2096 N71-24455

Using Rayleigh scattering to measure height of cloud tops from geostationary satellite 19 p3181 N71-32384

CLOUD PHOTOGRAPHY

Time-lapse ESSA satellite photographs of tropical cloud formations 03 p0777 N71-15134

Cloud growth and rainfall analysis after precipitation silver iodide cloud seeding in Florida based on meteorological radar data and cloud photographs 14 p2250 N71-25779

Meteorological interpretation of infrared cloud photographs from satellite observations 15 p2440 N71-27400

Evaluation of capabilities of electronic display system used in analysis of ATS cloud photographs 16 p2523 N71-28141

ESSA 9 television cloud photographs of North and Southern Hemisphere - Apr. 1-June 30, 1969 20 p2597 N71-33618

Vertical momentum transport over mountainous terrain based on Apollo 9 cloud photographs, gravity waves, and wind data for southwestern US 20 p2597 N71-33618

Satellite in meteorological research and weather forecasting with typical cloud photographs 24 p3016 N71-30651

CLOUD PHOTOGRAPHY

Cloud analysis from meteorological satellite television and infrared pictures 01 p0070 N71-10993

Machine analysis of infrared cloud images obtained by Comma-122 satellite 01 p0070 N71-10993

Meteorological data of cloud measurements, sea surface temperatures, and BOMEX flight data 01 p0070 N71-10993

Photostereopairs of Comma 122 satellite television photographs of wave clouds and statistical analysis of rainbands wind and temperature data for simulation 02 p0154 N71-11091

Convective cloud cells as observed from artificial earth satellites 02 p0154 N71-11091

Satellite cloud photography and terrestrial radiation measurements 02 p0154 N71-11091

Cloud photography from ATS 1 and ATS 3 02 p0154 N71-11091

Convective heat and mass transport over tropical mid-Pacific outlined from satellite cloud photographs 02 p0154 N71-11091

Causes of cloud systems over tropical Pacific Ocean from satellite photographs 02 p0154 N71-11091

Cloud cover taking over control and western Pacific Ocean from satellite photographs 02 p0154 N71-11091

Computer processing of satellite cloud pictures 02 p0154 N71-11091

Current operational products from National Environmental Satellite Center 02 p0154 N71-11091

Performance of ATS 1 spin-scan cloud cover camera mounted at Mojave ground station 03 p0082 N71-14001

Very short range binocular forecasting using satellite observations 06 p1230 N71-18671

Tabulation of 3-57 aerial cloud photography of tropical convection systems for 11 to 20 July 1969 with flight path over Barbados Islands 12 p1981 N71-23932

Meteorological benefits from satellite cloud photography, ATS 3 photographs, computer, and photostereopairs of cloud photography 14 p2250 N71-25779

Satellite activities of operational elements of NOAA including weather, marine service, and environmental research 16 p2550 N71-28253

Meteorological data obtained for ATS 3 1 Aug. 1969 - 15 May 1970 and summary of ATS 1 operations 14 p2250 N71-25779

Tables of meteorological satellite data - ESSA 9 television cloud photography - 1 Jan. 1969 to 31 Mar. 1969 20 p2597 N71-33618

Abstracts of BOMEX related conference papers, sample products from BOMEX cloud photography and radar surveillance, and description of BOMEX data processing and results 19 p3284 N71-32735

Description and statistics of high level cloud photography during BOMEX 19 p3463 N71-35737

- Data processing and reduction techniques for photointerpretation of Baker-Nunn photographs of seeding clouds during Apollo 12 flight [NASA-CR-121952] 23 p3237 N71-33018
- Comparison of convective cloud data obtained via ATS 3 and ESSA 3 and from Apollo 6 high resolution photography [NASA-TN-D-6470] 21 p3452 N71-34566
- Cloud photography and meteorological description of cloud holes observed over Miami, Florida on 1 Dec. 1967 23 p3785 N71-36976
- Temperature, water content, and photographic analysis of seeded clouds over Florida with mathematical model of cloud physics [ESSA-TM-ERLTM-APCL-8] 23 p3786 N71-36984
- Aerial and satellite photography and radar echo analysis of convective cloud dynamics and effects of cloud seeding over Florida on 16 May 1968 [ESSA-TM-ERLTM-APCL-7] 23 p3787 N71-36989
- Techniques for aerial time-lapse cloud photographic analysis, Doppler navigation data analysis, and photogrammetric data acquisition 23 p3787 N71-36990
- Analysis of subsynoptic scales of atmospheric motion by means of synoptic network supplemented by satellite cloud observations [AD-726624] 23 p3791 N71-37020
- CLOUD PHYSICS**
- Calculating secondary backscattering for water clouds for simulated paired lidar system [PB-193435] 01 p0890 N71-10836
- Convective cloud cells as observed from artificial earth satellites [NASA-TT-F-13363] 02 p0254 N71-11465
- Feasibility of convective cloud management for precipitation [PB-192259] 05 p0716 N71-13073
- Climate modification problems including ocean models, atmospheric radiation, convective and cumulus cloud models, and numerical weather prediction [AD-713428] 05 p0718 N71-12522
- Using radar to distinguish hail-producing clouds for determining probability of modifications in convective clouds [AD-713468] 05 p0718 N71-12562
- Calculating probability of appearance of thunderstorms from data on vertical distribution of radar echo intensity [D-70-70-82] 07 p1052 N71-10962
- Cloud structure determined from laser backscatter 07 p1053 N71-17171
- Measuring effects of evaporative cooling at base of dense clouds and obscuring clouds using Doppler and conventional radars 07 p1053 N71-17421
- Abstracts on Soviet meteorological research 07 p1054 N71-17488
- Survey on mechanisms of atmospheric precipitation scattering [BNWL-SA-3456] 08 p1185 N71-18263
- Time and space history analysis of low-level cloud type and limit relations, cloud behavior, and meteorological factor interrelationships in cloud rise [BNWL-50244] 09 p1413 N71-20024
- Cloud droplet growth theory and diffusional interaction between growing droplets 11 p1790 N71-22360
- Freezing rate and solute specie and concentration effects on charge separation at advancing surfaces of growing ice related to cloud physics [AD-718359] 12 p1910 N71-23655
- Statistical distribution of radar parameter in different cloud systems with liquid precipitation [NLL-M-20891-(5828.4F)] 12 p1957 N71-24037
- Optical properties of clouds with emphasis on radiation transfer, reflection, and transmission [AD-719089] 13 p2106 N71-23855
- Aerospace scientific and technological studies in 1969 for satellite systems and operational missions [NASA-SP-251] 13 p2192 N71-25256
- Summary of research in cloud physics and weather modification in Soviet Union [TT-70-50141] 20 p3296 N71-33236
- Collisionless cloud waves and factors influencing linear stability of baroclinic clouds [NASA-CR-121437] 20 p3330 N71-33445
- Numerical simulation of airflow over ERM models for determining cloud physics parameters related to any cloud 22 p3612 N71-37277
- Cloud seeding effects on cloud physics and precipitation and ocean current analyses with tidal predictions 23 p3784 N71-36975
- Mathematical model of cumulus cloud growth and effects of silver iodide seeding 23 p3786 N71-36983
- Temperature, water content, and photographic analysis of seeded clouds over Florida with mathematical model of cloud physics [ESSA-TM-ERLTM-APCL-8] 23 p3786 N71-36984
- Precipitation and cloud dynamics analyses of silver iodide pyrotechnic cloud seeding in Florida during May 1968 [ESSA-TM-ERLTM-AOML-2] 23 p3786 N71-36986

- Aerial and satellite photography and radar echo analysis of convective cloud dynamics and effects of cloud seeding over Florida on 16 May 1968 [ESSA-TM-ERLTM-APCL-7] 23 p3787 N71-36989
- Clouds of lower Venezuelan atmosphere [NASA-CR-125303] 24 p0006 N71-38362
- CLOUD SEEDING**
- Measurements of artificially seeded and unseeded winter storms over Cascade Mountains [PB-195443] 01 p0890 N71-10894
- Mechanism by which precipitation develops in winter storms over Washington 02 p0257 N71-11665
- Mathematical model for calculating precipitation over orographic barrier [PB-192757] 02 p0360 N71-12108
- Procedure for identifying silver iodide particles in ice crystals as snow crystal nuclei 02 p0360 N71-12124
- Statistical results of winter orographic cloud seeding experiment over Park Range barrier in Colorado [PB-192768] 02 p0360 N71-12125
- News briefs and abstracts of articles on meteorology 03 p0400 N71-13040
- Dynamic seeding experiments on supercooled cumulus clouds 03 p0404 N71-13222
- Investigating production and detection of artificial ice nuclei and growth of formed ice crystals [PB-194129] 04 p0542 N71-14216
- Mathematical model for droplet growth rate in cloud seeding [AD-713559] 05 p0719 N71-15399
- Dry ice effects on dispersal of supercooled stratus and stratocumulus clouds 05 p0890 N71-16199
- Investigating cloud characteristics, atmospheric thermal energy, rain formation in clouds, and uses of radar in meteorology 07 p1052 N71-16919
- Computerized analysis of data on high altitude barium release [BGG-1183-3807] 07 p1015 N71-16997
- Cumulus cloud modification by injecting powdered surface active substances [PB-195264] 10 p1546 N71-20679
- Technology review on electric automobiles, and modified T-33 aircraft system for pyrotechnic hail suppression seeding [DME/NAE-1979/4] 11 p1768 N71-22198
- Modified T-33 aircraft system for pyrotechnic hail suppression seeding 11 p1840 N71-22200
- Tropical storm and hurricane modification - Project Secondary [AD-717498] 11 p1790 N71-22362
- Worm fog seeding to determine potential of various sized and modified hygroscopic chemicals for fog dissipation [NASA-CR-1731] 11 p1790 N71-22619
- Large scale effects of cloud seeding in Santa Barbara, California [AD-718814] 12 p1933 N71-23391
- Cloud seeding for forest fire fighting and heavy rainfall prevention [NLL-M-30360-(5828.4F)] 12 p1956 N71-23969
- Cloud growth and rainfall analysis after pyrotechnic silver iodide cloud seeding in Florida based on meteorological radar data and cloud photographs [COM-71-00184] 14 p2286 N71-25779
- Detection of silver in seeded clouds by atomic evaporation to high sensitivity and related aircraft sampling problems 16 p3625 N71-28456
- Tables of condensation nuclei growth rates under various super saturations for worm fog or cloud modification [AD-721591] 17 p3776 N71-29443
- Process for encapsulating hygroscopic cloud seeding agents [AD-722448] 18 p3939 N71-30805
- Silver iodide cloud seeding for rainfall augmentation over Philippine Islands [AD-723815] 18 p3935 N71-31591
- Weather/Weather modification experiments - Secondary project 19 p3127 N71-31822
- Computerized effectiveness model for predicting artificial precipitation through pyrotechnical cloud seeding [AD-723842] 19 p3128 N71-32056
- Developing and managing water resources of Western US 23 p3609 N71-35705
- Detecting changes in large scale precipitation patterns of randomized seeding 23 p3609 N71-35704
- Using seeded topographic models and laboratory techniques to study transport and dispersion of cloud seeding material over mountainous terrain 23 p3609 N71-35705
- Ecological consequences of winter cloud seeding in San Juan area of Colorado River Basin 23 p3609 N71-35706

- Steady state ice nuclei generator for field application 22 p3608 N71-35699
- Techniques for determining hydrologic stability of regions considered for precipitation management 23 p3609 N71-35700
- Statistical analysis and numerical results of 1968 South Florida cumulus seeding project 23 p3610 N71-35701
- Precipitation augmentation during winter season for Sierra Nevada 23 p3610 N71-35702
- Quantitative estimates of the potential effects of cloud seeding on crop production 23 p3610 N71-35703
- Seeding isolated cumuli to increase precipitation in Arizona 23 p3610 N71-35704
- Randomized seeding in Sierra Nevada and Santa Mountains, New Mexico during winter 23 p3610 N71-35705
- Methods for beneficially modifying precipitation from convective clouds over Great Plains Region 23 p3611 N71-35706
- Feasibility of increasing and redistributing rainfall by cloud seeding in Cascade Mountains 23 p3611 N71-35707
- Studying characteristics of warm cumulus clouds below freezing levels in Texas to assess feasibility of warm cloud management as water resource 23 p3611 N71-35708
- Ice nuclei generators suitable for cloud seeding 23 p3611 N71-35709
- Research in atmospheric water resources for developing management techniques for application to Nevada water system 23 p3612 N71-35710
- Processing and analyzing data from airborne and ground-based cloud seeding 23 p3612 N71-35711
- Cloud seeding effects on cloud physics and precipitation and ocean current analyses with tidal predictions 23 p3784 N71-36975
- Analysis of cloud liquid-water content, drop size, and temperature effects of tropical cumulus clouds for artificial glaciation with silver iodide 23 p3785 N71-36980
- Cloud seeding technological development and effects on cloud growth with applications 23 p3786 N71-36986
- Mathematical model of cumulus cloud growth and effects of silver iodide seeding 23 p3786 N71-36983
- Temperature, water content, and photographic analysis of seeded clouds over Florida with mathematical model of cloud physics [ESSA-TM-ERLTM-APCL-8] 23 p3786 N71-36984
- Development, testing, and utilization of silver iodide pyrotechnic cloud seeding system [ESSA-TM-ERLTM-APCL-5] 23 p3786 N71-36985
- Precipitation and cloud dynamics analyses of silver iodide pyrotechnic cloud seeding in Florida during May 1968 [ESSA-TM-ERLTM-AOML-2] 23 p3786 N71-36986
- Large scale precipitation effects of silver iodide pyrotechnic seeding of single clouds over southern Florida during May 1968 [ESSA-TM-ERLTM-AOML-3] 23 p3787 N71-36988
- Aerial and satellite photography and radar echo analysis of convective cloud dynamics and effects of cloud seeding over Florida on 16 May 1968 [ESSA-TM-ERLTM-APCL-7] 23 p3787 N71-36989
- Radar data on cumulus cloud seeding experiments [ML-71-608] 23 p3792 N71-37027
- Effect of liquid water content on nucleation efficiency of cloud seeding generators from sizes 5 to sizes 12 C [AD-727183] 34 p3932 N71-30809
- CLOUDS**
- ARTIFICIAL CLOUDS
- NT CIRRUS CLOUDS
- NT CLOUDS (METEOROLOGY)
- NT CUMULONIMBUS CLOUDS
- NT CUMULUS CLOUDS
- NT ELECTION CLOUDS
- NT NOCTUCLUCENT CLOUDS
- NT PLASMA CLOUDS
- NT STRATOCUMULUS CLOUDS
- NT STRATUS CLOUDS
- Aircraft mounted infrared detectors for remote measurements of optical cloud properties 13 p2107 N71-23856
- Nimbus 2 high resolution infrared radiometer (in cloud modes) for determining wind velocity 13 p2108 N71-23858
- Origin and evolution of radiative clouds from nuclear explosions [CLOS-81/2] 19 p3155 N71-32040
- CLOUDS (METEOROLOGY)**
- NT ARTIFICIAL CLOUDS
- NT CIRRUS CLOUDS
- NT CUMULONIMBUS CLOUDS
- NT CUMULUS CLOUDS
- NT NOCTUCLUCENT CLOUDS

SUBJECT INDEX

NT STRATOCUMULUS CLOUDS

NT STRATUS CLOUDS

Structural features of clouds and wind fields in cyclones by pictures from Cosmos-122
[NASA-TT-F-13361] 01 p0882 N71-10993

Abstracts on Soviet meteorological research
07 p1052 N71-14957

Underwater acoustic prospecting, microwave probing of soils, and laser backscatter study of cloud composition
[NBS-52148] 07 p1067 N71-17168

Meteorological radar equipment and data analysis of clouds and precipitation
07 p1053 N71-17187

Computer program for determining total convective cloud occurrence and altitude and comparison with precipitation echoes in stratosphere
[AD-716394] 09 p1412 N71-19622

Time and space history analysis of buoyant cloud tops and heat release, cloud behavior, and meteorological factor interrelationships in cloud rise
[NRL-50244] 09 p1413 N71-20024

Infrared scanner onboard meteorological satellite for automatic picture transmission of earth and cloud surfaces
10 p1518 N71-21054

Optical polarization techniques for use with laser detection and ranging system to differentiate between dust returns and target returns
[AD-717077] 11 p1775 N71-22278

Cloud three-dimensional anemology program
[AD-71653] 11 p1790 N71-22363

Performance tests and characteristics of four fog detecting instrument systems operating under natural atmospheric conditions
[NBS-10186] 11 p1762 N71-22454

Spectral albedo of snow and ice cover under differing cloud conditions and solar elevations
11 p1757 N71-22446

Determining microstructure of clouds and fogs by light scattering
[NBS-LIB-TRANS-1529] 12 p1952 N71-23237

Convective cloud prognosis technique for computer forecasting of shower and thunderstorm activity including meteorological parameters and tests of instability indices over Germany
12 p1958 N71-24103

Digital optical detectors for cloud data processing aboard satellite using Fourier analysis
13 p2126 N71-25321

Measurement of sparking potential of gaps in low pressure air between two electrodes, with plane water surface as cathode, to simulate lightning strokes and safe sites
[AD-720771] 14 p2247 N71-23856

Maximum likelihood estimates of atmospheric temperature profile deduced from satellite radiation measurements in cloud presence
15 p2400 N71-27496

Cloud distribution over Indian Ocean at beginning of monsoon deduced from Nimbus 2 satellite radiation measurement
15 p2438 N71-27497

Barth surface and cloud temperature determination by measurement of terrestrial infrared radiation
15 p2401 N71-27500

Light scattering and absorption parameters of clouds and aerosols
15 p2402 N71-27523

Light scattering in water clouds, fog, and haze
15 p2439 N71-27524

Visible and infrared radiation transfer in clouds
15 p2402 N71-27533

Multiple anisotropic polarized and unpolarized light scattering in plane parallel homogeneous cloud layers
15 p2402 N71-27535

Spectrometer-radiometer for infrared cloud transmission measurements
15 p2410 N71-27547

Atmospheric models for tenuous cloud effects on atmospheric heat infrared radiation flux
15 p2403 N71-27561

Global cloud model for computerized simulation of each-cloud-type mass mixtures
[NASA-CR-41545] 15 p2518 N71-27975

Optical and impedance coupling methods for sizing and counting water droplets in clouds for use in sampling from aircraft
[AD-721677] 16 p2635 N71-28457

Behavior of night fog characteristics and development of mathematical model for design of night fog detection device
[AA-ED-45-VOL-2] 17 p2729 N71-29310

Physical properties of cloud clusters over tropical Atlantic - tropical meteorology
17 p2777 N71-29483

Long range tropical weather forecasting of cloud clusters over Atlantic using ground weather stations international cooperation and training
17 p2777 N71-29485

Astronomical photography of zodiacal light and lunar breville clouds
18 p3014 N71-30979

Me infrared radiation scattering function data for dusts, micrometeorites, and stratocumulus clouds
01 p0846 N71-16308

including extinction, scattering, and absorption cross sections
[NOAA-TR-NBSS-57] 18 p3007 N71-31466

Formula for calculating rate of condensation growth of drops in clouds considering latent heat of condensation
[AD-724105] 20 p3294 N71-32803

Sulfate ion as dominant constituent in cloud and fog condensation nuclei for aerosol areas
[AD-724610] 20 p3294 N71-32809

Numerical analysis of 500 millibar geopotential heights from satellite-observed cloud patterns in Northern Hemisphere
[NOAA-TR-NBSS-55] 20 p3297 N71-33618

Static electrification of aircraft when flying through clouds and precipitation
[AD-726581] 22 p3541 N71-35225

Statistical analysis of tropical cloudiness and rainfall in relation to semidiurnal atmospheric tide and pressure variations
23 p3784 N71-36974

Cloud condensation nuclei effects on rainfall during spring droughts in Florida from pest, algae, seaweeds, and leaf fire smoke
[BSSA-TM-BRL-TM-AOML-4] 23 p3784 N71-36975

Cloud photography and meteorological description of cloud holes observed over Miami, Florida on 1 Dec. 1967
23 p3785 N71-36976

Analysis of cloud liquid-water content, drop size, and temperature profiles of tropical maritime clouds for artificial glaciation with silver iodide
23 p3785 N71-36980

Cloud seeding technological development and effects on cloud growth with applications
23 p3786 N71-36981

Determination of aspects of convective thunderstorm behavior by radar observations at Brisbane, Australia
24 p3952 N71-38193

Relationships among cloudiness, precipitable water vapor, water vapor flux, stability, and precipitation for Texas high plains
24 p3954 N71-38207

CLUMPS
Cluster expansion applications for alpha particle-matter mixture, He-3/He-4 mixture and impurity problem
13 p2137 N71-25402

Cluster decomposition techniques for analyzing hydrodynamic perturbation theory amplitudes at high energy
[ILL-(TH)-71-10] 23 p3830 N71-37251

CLUSTERS
U CLUMPS
CLUTCHES

Testing capacity of clutch with rubber elastic toroidal element for longevity under shaft displacements and loads
14 p2260 N71-23854

CLUTTER
Computerized radar signal processing for stationary ground target detection in clutter environment
02 p0180 N71-11269

Detection and estimation of complex radar missile system targets in noise and clutter environment
03 p0538 N71-12412

Radar clutter generation by ocean surface wave reflection
04 p0493 N71-13717

Digital techniques and components for signal detection in clutter by advanced radar systems
[AGARD-CP-46-70] 04 p0493 N71-13901

Coherent and noncoherent signal bandwidth methods for radar target detection in clutter
04 p0495 N71-13911

Switched capacitor storage arrays for radar signal processing and moving target indication in presence of clutter
04 p0496 N71-13923

Digital techniques for monopulse radar signal determination in clutter environment
04 p0497 N71-13927

Sea state effects on radar echo clutter
[AD-713595] 05 p0644 N71-14085

Computerized simulation of performance and probability of MTI in aircraft detection in clutter
[NRL-TN-739] 12 p1878 N71-23508

Reduction of radar clutter and improved target acquisition by cross-polarized Ku band radar during rain conditions
[AD-721627] 16 p2360 N71-28335

Phase cancellation effects on cross sections of limited irregularities related to clutter, radar target identification, jamming, and antisatellite defense systems
[AD-723597] 19 p3055 N71-31991

Bandwidth control and removal of radar clutter
19 p3059 N71-32717

COAGULATION

NT BLOOD COAGULATION

Comparison of iron 57 Mossbauer spectra of iron containing compounds and coal
01 p0846 N71-16308

Bacterial origin of framboidal pyrites in coals
[NRL-RTS-5946] 11 p1744 N71-31891

COALESCENCE

U COALESCING

COALESCING

Corrosion inhibitor effects on water condensing characteristics of DOD type filter/condenser elements
[AD-712999] 03 p0445 N71-13670

Effects of corrosion inhibitors and anti-foul inhibitor combinations on condensing properties of filter condenser elements used to deaerate jet engine fuels
[AD-722231] 16 p3670 N71-38577

COANDA EFFECT

Acoustically excited, incompressible, turbulent, subsonic Coanda air flow around circular cylinder
13 p2066 N71-23809

Switching dynamics of bistable fluid amplifiers
[AD-723632] 19 p3079 N71-32328

COARSENING

Effect of dislocations on coarsening of particles by pressure waves, coarsening in nickel aluminum alloys, and in situ recrystallization
[NRL-CE-TRANS-5081-7022.00] 17 p2815 N71-29737

Mathematical model for estimating particle size distribution and volume fraction effects on coarsening rates during precipitation hardening with Ni-Cr-Al and Ni-Al alloys
[UCLA-54-P-173-1] 19 p3115 N71-33332

COASTAL ECOLOGY

Aerial photography for studying coastal ecology
02 p0208 N71-11170

Annotated bibliography of coastal resources and seacoast development in Texas
[PB-189708] 05 p0676 N71-15459

Aerial infrared imagery and radiometric survey of coastal areas
06 p0844 N71-16142

Aerial photography as technique for remote sensing of hydrobiological features in swamp and coastal regions
06 p0846 N71-16171

Environmental and oceanographic data for sections of Atlantic coastline
[AD-714833] 07 p1022 N71-17001

Aerial photography of coastal waters of New York and Long Island
[AD-715804] 08 p1186 N71-18334

Evaluating scientific and engineering requirements for research related to coastal wastes management
[PB-195861] 09 p1330 N71-19653

Coastal ecology and effects of industrial pollution on coastal zones
18 p2911 N71-30983

COASTING FLIGHT

Exponential downweighting of past data in single stage, weighted least squares trajectory processor for coasting spacecraft
[NASA-CR-114979] 13 p2165 N71-34359

COASTS

Summary of synoptic meteorological observations for North American coastal marine areas of San Francisco and Point Mugu, California - Vol. 8
[AD-710771] 01 p0800 N71-10906

Summary of synoptic meteorological observations for North American coastal marine areas of Galveston and Corpus Christi, Texas and New Orleans, Louisiana - Vol. 6
[AD-710770] 01 p0801 N71-10907

Summary of synoptic meteorological observations for North American coastal marine areas of Astoria, Oregon and Seattle, Washington - Vol. 10
[AD-710825] 01 p0801 N71-10908

Thermal erosion of permafrost on Beaufort Sea coast in Alaska
[AD-711344] 02 p0213 N71-11562

Bibliography and index of hurricanes and severe storms along coastal plains of US
[PUBL-78-2] 02 p0239 N71-11847

Nimbus 2 and 3 HIRER measurements of upwelling along Somali coast
[NASA-TM-X-45387] 03 p0369 N71-13008

Two dimensional model for radio wave propagation across land/sea boundaries
04 p0491 N71-13703

Aerial radar and infrared imagery of coastal geology in Oregon and Washington
05 p0844 N71-16141

Light scattering measurements off San Diego Coast, California
[AD-714481] 06 p0803 N71-16337

Synoptic meteorological data for Mediterranean coast
06 p0803 N71-16370

Photomagnetic study of coastal geology on Hawaii
[PB-195634] 08 p1187 N71-18335

Aerial multispectral and infrared scanning of Massachusetts coastline
[NASA-CR-116782] 08 p1187 N71-18402

Remote sensing techniques as applied to coastal sedimentation in south Texas
08 p1197 N71-19257

Sea ice, ocean currents, climatology, and geology of Arctic Ocean and coastal areas
[AD-716416] 09 p1304 N71-19771

Microwave radiometry, spaceborne and aerial photography, and oceanographic data from ships evaluated for remote sensing of coastal oceans
[NASA-CR-117316] 09 p1387 N71-20422

Mean sea level and periodic variation at Danish coast
10 p1546 N71-20639

Systems management and control of demographic and technological change within coastal regions of US and resource management
11 p1847 N71-22035

Aerial reconnaissance of Northern California and Oregon coastlines to determine extent of erosion
[AD-717359] 11 p1747 N71-22152

Data tables of synoptic marine surface meteorology for Bristol Bay and St. Paul Island, Alaska
[AD-718345] 12 p1954 N71-23832

Data tables of synoptic marine surface meteorology for Nainivak, St. Matthew, and St. Lawrence Islands, Cape Lisianski, and Barrow, Alaska
[AD-718346] 12 p1954 N71-23833

Earth Resources Technology Satellites E and F orbits and remote sensor instruments for coastal oceanographic data collection
[NASA-CR-111623] 16 p2586 N71-23828

Design of computer assisted information system to provide uncoastal data for military purposes
[AD-722427] 17 p2861 N71-25660

Computer graphic mapping of Maryland coasts from aerial color and infrared photographic remote sensors including microdensitometer analysis
[RM-5085] 17 p2749 N71-30176

Generalized characteristics of coastal currents based on statistical analysis of aerial photographs of areas of Black Sea and Baltic Sea
[NOD-TRANS-486] 18 p2918 N71-31374

Synoptic meteorological tables for marine coastal areas including Hawaii and Pacific Islands
[AD-725798] 19 p3130 N71-32682

Computer applications to tide and current analysis in coast and geodetic surveys
23 p3789 N71-37008

Sensible heat flux and momentum flux in turbulent boundary layer of coastal winds
[REFT-29] 23 p3791 N71-37018

Synoptic meteorological data for Ponce, Truk, and Pohna North Pacific Island coastal marine areas
[AD-726740] 23 p3791 N71-37019

Interpretation of color infrared photography of Florida tidewater coastline
[AD-726300] 24 p3916 N71-37924

Tables of synoptic meteorological observations - Hawaiian and selected North Pacific coastal marine areas
[AD-727900] 24 p3953 N71-38203

COATING

NT ANODIZING
NT ELECTROPLATING
NT ENCAPSULATING
NT METALLIZING

Solder coating process for printed copper circuit protection
[NASA-CASE-XMF-01599] 10 p1531 N71-20705

High thermal emittance black surface coatings and process for applying to metal and metal alloy surfaces used in radiative cooling of spacecraft
[NASA-CASE-XLA-04199] 13 p2086 N71-24875

Sol-gel processes and remote handling equipment for coating particles, preparation of thorium, uranium, and plutonium fuels, and accelerated life testing of nuclear fuel elements
[ORNL-4629] 15 p2447 N71-27201

COATINGS

NT ALUMINUM COATINGS
NT ANODIC COATINGS
NT CERAMIC COATINGS
NT ELECTROPLATING
NT ENAMELS
NT ENCAPSULATING
NT GLASS COATINGS
NT GLAZES
NT GOLD COATINGS
NT INORGANIC COATINGS
NT LACQUERS
NT MAGNETIC FILMS
NT METAL COATINGS
NT METALLIZING
NT NICKEL COATINGS
NT PAINTS
NT PLASTIC COATINGS
NT PRIMERS [COATINGS]
NT PROTECTIVE COATINGS
NT RUBBER COATINGS
NT SPRAYED COATINGS
NT THERMAL CONTROL COATINGS
NT ZINC COATINGS

Thermal coatings of granola payloads
[NHO-5747-12] 01 p0071 N71-10496

Calculation of radiative heat transfer and optimization of spacecraft fin-tube radiator with and without coatings
03 p0458 N71-13260

Reduced burnup characteristics and long life performance of regenerative coating material /90 percent

U-234 and 10 percent U-235/ in developing thermal neutron detectors for reactor
[WHAM-FR-37] 15 p2458 N71-26937

Microwave system evaluated as nondestructive means of measuring thickness of conformal coatings
[BDC-413-245] 15 p2428 N71-27013

Microwave system evaluated as nondestructive means of measuring thickness of conformal coatings
[BDC-413-257] 15 p2428 N71-27014

Coating of fuel particles and model investigations of conical fluidized beds noting effect of gas current and gas distribution particle load, and nozzle geometry
[JUL-669-RW] 15 p2448 N71-27339

Film thickness of dip-coated layers
16 p2617 N71-28361

Masked eddy current probe for crack detection in Rover fuel element coating
[LA-4590] 16 p2635 N71-28758

Silicon carbide and pyrocarbon coating of nuclear fuel particles including preparation techniques and neutron irradiation effects
[JUL-667-RW] 18 p2938 N71-30496

Wettability and formation of alloyed coatings on iron coatings
[NLL-M-21010-5328.4F] 21 p3441 N71-34485

Determining distribution of fission products in fuel particle coatings by sputtering technique using ion beams
[SGAB-PH-96/1970] 21 p3458 N71-34615

Sodium silicate disk for transmission measurements in magnesium oxide coated integrating sphere
[NASA-TM-X-2393] 22 p3629 N71-35856

Relationship between microhardness of materials and thickness of wear resistant coatings
[AD-727416] 24 p3944 N71-38136

COAXIAL CABLES

Time and frequency measurements of miniature superconducting coaxial transmission lines
[UCRL-72574] 04 p0512 N71-13536

Radio frequency breakdown in 50-ohm coaxial transmission lines
06 p0628 N71-16652

Design and development of device for cooling linear conductor of coaxial cable
[NASA-CASE-XNP-09775] 09 p1360 N71-20445

Design and development of electric connectors for rigid and semirigid coaxial cables
[NASA-CASE-XNP-04732] 10 p1532 N71-20851

Transducer circuit design with single coaxial cable for input and output connections including incorporation into miniaturized catheter transducer
[NASA-CASE-ARC-10132-1] 13 p3055 N71-24597

Design of multichannel communication system using digital cable transmission
[AD-719688] 13 p2047 N71-25101

Signals or noise in in-vessel detector cables within reactor core environment
[WHAM-SA-18] 13 p2122 N71-25406

Outgassing of sample material, e.g. aluminum foil, coaxial cables
[REFT-710-229/70] 14 p2267 N71-25616

Collapsible antenna boom and coaxial transmission line having inflatable inner tube
[NASA-CASE-MFS-20064] 15 p2380 N71-27191

Flashovers across dielectric spacers in compressed gases of coaxial cylinder system with insulation recommendations
[NLL-CE-TRANS-5434-7022.09] 17 p2787 N71-29634

Onset of microwave breakdown in air-filled coaxial transmission lines and rectangular waveguides predicted by mathematical models
[AD-727719] 18 p2896 N71-31369

Early current measurements using coil encircling coaxial two-conductor rod and solution of electromagnetic induction problem
[Y-1787] 19 p3071 N71-32327

Special diagnostic devices designed to solve particular positioning and measurement problems in fusion research engineering
[MATT-838] 23 p3828 N71-37905

COAXIAL FLOW

Transverse mode stability characteristics of coaxial and hyperthin injectors in transverse excitation chamber
[NASA-CR-117033] 09 p1460 N71-20500

Fluid mechanics experiments to investigate methods for reducing mixing between confined coaxial flows in cylindrical chambers for application to open-cycle gaseous-core nuclear reactors
[NASA-CR-1851] 16 p2579 N71-28403

Vortex and coaxial flow of argon and helium plasmas heated inductively, and strong magnetic field effects on turbulent plasma mixing, for gas core reactors
20 p3330 N71-33635

Effect of inlet conditions on flow and containment characteristics of coaxial flows for gas core nuclear reactors
20 p3363 N71-33636

Interfacial stability at thin flexible partition between fuel and propellant flows for gas core nuclear reactors
20 p3304 N71-33639

COAXIAL TRANSMISSION

U COAXIAL CABLES

U TRANSMISSION

COBALT

NT COBALT ISOTOPES
NT COBALT 58
NT COBALT 60

Dilatometer in cobalt ferrite spinels
[UCRL-19198] 04 p0300 N71-1400

Martensitic conversion in Fe-Ni-Co alloys
[SC-T-70-4036] 03 p0786 N71-1352

Acceptance test for nickel-cadmium cells with cobalt additive
[NASA-CR-115708] 06 p0796 N71-1370

Internal magnetic fields of Co impurity in Au, Cu, and Au-Cu alloys determined by neutron orientation of Co-60
[COO-1569-47] 07 p1079 N71-1790

Sintered diamond compacts using cobalt as binder
[NASA-CR-116419] 07 p1049 N71-1791

Numerical values for neutron elastic and inelastic scattering cross sections for natural Co, Co-59 in range 4.19 to 8.36 MeV
[ORNL-4549] 13 p2131 N71-3449

Temperature dependence of self diffusion coefficient of iron, chromium, and cobalt in steel with 8 percent carbon
[DMDC-3795] 14 p2271 N71-3280

Extended ellipsometry method used for electrochemical and optical measurements on electrochemically induced passivity of cobalt
[AD-721719] 16 p2537 N71-3004

Radioactive tracers used in determination of diffusion coefficients of cobalt in polycrystalline austenite Fe-Cr-Ni alloys
[TT-70-59110] 20 p3284 N71-3218

Irradiated cobalt and tantalum tracers measured by activation analysis in river and sea sediment transport studies
[RI-133-70-06] 20 p3316 N71-3340

LMD peaks in Auger spectra identified for transition metals of Fe, Co, and Ni
[AERE-R-6719] 21 p3438 N71-3448

Nuclear spin-lattice relaxation and nuclear magnetic resonance in Fe, Co, and Ni
22 p3652 N71-3810

Analysis of isochronal annealing behavior of radiation defects in germanium crystals after irradiation with cobalt-60
[AD-726993] 23 p3835 N71-3746

Microwave study of magnetocrystalline anisotropy of Ni-Co for application to manufacture of permanent magnets
[AD-726991] 23 p3835 N71-3747

COBALT ALLOYS

Thermal fatigue data on 15 nickel and cobalt base alloys
[NASA-CR-72738] 01 p0065 N71-1007

Evaluation of cobalt base alloy made by extrusion of gasified powders
[NASA-TN-D-6072] 01 p0066 N71-1008

Temperature dependence of initial permeability of ferromagnetic amorphous Co-P alloy
[AD-711087] 01 p0092 N71-1009

Crimp rupture tests on cobalt alloy weldments
[ORNL-3028] 04 p0531 N71-1410

High strength, corrosion resistant cobalt-base alloys for aerospace structures
[NASA-CASE-XLE-00726] 05 p0706 N71-1544

High temperature cobalt-base alloy resistant to corrosion by liquid metals and to oxidation in vacuum environment
[NASA-CASE-XLE-02991] 06 p0670 N71-1800

Investigating effect of surface preparation on oxidation of W-52 by high temperature X ray diffraction
[NASA-TN-D-6148] 06 p0670 N71-1800

Cobalt and nickel based alloy metallurgy for high temperature gas turbine materials
07 p1101 N71-1780

Using thin-film electron microscopy to study effects of cold working and aging on substructure and precipitation in cobalt-base alloy L-605
[NASA-TN-D-7051] 07 p1043 N71-1744

Friction and wear determination of cobalt-chromium solid solution alloy in air and in vacuum
[NASA-TN-D-6145] 07 p1036 N71-1780

Modification of high temperature cobalt-chromium alloys for improved stability
[NASA-TN-D-6147] 08 p1213 N71-1800

Corrosion damage resistance of iron alloys, nickel alloys, and cobalt alloys in liquid sodium and mercury - review of NASA program
[NASA-TM-X-52936] 08 p1213 N71-1800

Discontinuous precipitation of gamma phase in nickel-cobalt-chromium alloys by transmission electron microscopy
08 p1220 N71-1800

Oxidation resistance determined for cobalt and nickel based alloys by isothermal and cyclic tests in static furnace air
[NASA-TM-X-3195] 09 p1399 N71-1903

Oxidation of cobalt-nickel-chromium alloys at 1200 K to 1429 K
[BM-BL-7496] 09 p1401 N71-3004

Decomposition of internal stresses of electroplated deposited polycrystalline-cobalt alloy
[NLL-TRANS-744-512-7022.001] 10 p1578 N71-3323

SUBJECT INDEX

CODES

Composition and atomic ordering effects in Fe-Co alloy systems using Mössbauer spectroscopy and measurement of effective magnetic field at Fe nuclei, inner shift, and quadrupole splitting

11 p1780 N71-22794

High temperature ferromagnetic cobalt-base alloy for electrical power generating equipment

12 p1937 N71-33248

Matrix and face lattice precipitation phase conditions and quantity determinations of Co-Al alloy coercive force

[NLL-CR-TRANS-5523-19022.00/]

Dynamic deformation and fracture strength of tungsten carbide-cobalt alloys at elevated temperatures

13 p2096 N71-25114

Precipitate hardening of CuCo and CuCoZn alloys and particle size and temperature effects on creep properties and edge dislocations

15 p2425 N71-27652

Response of cast Co-Cr-Mo alloy to impulsive thermochemical fatigue conditions present during flight of automatic weapons

16 p3610 N71-28453

Reinforcing effect in series of nickel-cobalt alloys overstrained in various amounts up to 5 percent in tension and reverse strained in compression

16 p2612 N71-28616

Cleaved Fermi surfaces in NiB₁₂ order-disorder transformations when alloyed with Ni₃Fe and Ni₃Co

[NLL-LT-746-638-19022.00/]

Electrodeposition of nonporous Co-Ni coating on magnetic recording drums

[NLL-LT-746-641-19022.00/]

Distribution of particles of gamma phase with homogeneous precipitation in supersaturated solid solutions of titanium in cobalt

[NLL-CR-TRANS-5524-19022.00/]

Hydrogen solubility in liquid iron-cobalt-nickel alloys including free energy and enthalpy increments

18 p2936 N71-31131

Use of samarium cobalt as permanent magnet material for field excitation in 100 kW generator

18 p274 N71-31289

Processing rare earth-cobalt intermetallic compounds for use in permanent magnets

19 p3141 N71-31720

Room analysis of cobalt heat treatment alloy tubes internally pressurized with helium after creep testing to failure

19 p3113 N71-32143

Steel and cobalt-nickel alloy compression and corrosion tests after precipitation hardening at cryogenic temperatures for increased yield strength and corrosion resistance

19 p3115 N71-32321

MRSA for determining distribution of hyperfine fields at cobalt nuclei in dilute alloys of Co-V, Co-Cr, and Co-Mn

20 p3319 N71-33669

Thermodynamic study of cobalt-platinum solid solutions with alloys exhibiting negative excess free energy of mixing

20 p3368 N71-33918

Are join tests of thin dispersed nickel base alloys and nickel base alloys for space shuttle metallic thermal protection systems

24 p3934 N71-38068

COBALT COMPOUNDS

WT COBALT OXIDES

Synthesis and properties of cobalt complexes containing ketone bonding ligand

02 p0175 N71-11234

Kinetics of autooxidation of steric polypropylene in presence of cobalt salts by infrared spectroscopy

03 p0331 N71-12363

Thermal expansion of nickel and cobalt systems and their solid solutions

07 p1042 N71-17330

Precipitation of nickel and cobalt sulfides from dilute solutions at atmospheric pressure by hydrogen sulfide

07 p1042 N71-17330

Formation of spin-lattice relaxation time measurements in antiferromagnetic nickel chloride and cobalt chloride crystals

10 p1513 N71-21230

Optical and characterization of iron radiation damage in ferromagnetic cobalt ferrite determined by electron microscopy

11 p1808 N71-22971

Production of antineutrino-like metal chains of copper, silver, nickel, and cobalt and catalytic action of metal chains in ferrihydrite and glycerol oxidation

17 p2716 N71-30212

Effects of temperature and magnetic fields on thermal conductivity of cobalt chloride single crystals

20 p3336 N71-33891

COBALT ISOTOPES

WT COBALT 58

WT COBALT 60

Resonance light scattering for measuring spectral line transitions in cobalt isotope spectrum

01 p0609 N71-10522

Structure and photoelectron cross section of Co-59

04 p0572 N71-13632

Excitation function measurement of α, γ reaction on Co-59 using single foils and stacked foil arrangement

05 p0751 N71-15419

Aircraft altimeter containing X ray source

07 p1027 N71-16995

Use of thallium and cobalt isotopic indicators to study electrodeposition conditions of ternary alloy systems

19 p3114 N71-32183

COBALT OXIDES

Temperature and doping effects on cobaltous oxide and nickelous oxide structures

07 p1006 N71-17024

Oxidation constant drop of mixed oxides (Co, MgO and Co, NiO)

10 p1578 N71-21217

Thermodynamic properties of FeO, CoO and NiO in sodium disulfate over temperature range from 700 to 1100 C

23 p3781 N71-36945

COBALT 58

Computer program for calculating neutron spectra from activated cobalt isotopes

15 p2470 N71-27382

COBALT 60

Cobalt 60 radiation field calculation of directionally radiation point source of gamma quanta with method of moments

04 p0580 N71-14022

Electrical and photoluminescence measurements on liquid spinel nickel arsenide irradiated at room temperature by 1.25 MeV Co-60 gamma rays

06 p0924 N71-16189

Co-60 contamination effect on structural steel with background counting rate of proposed shadow shield, whole body monitor

08 p1262 N71-18829

Long term radiation induced conductivity in polystyrene terephthalate

08 p1161 N71-19112

Atmospheric diffusion of tritium and other radioactive materials, fast neutron spectra of Cf-252, radiation rate of Cf-252 in D₂O spheres, and Co-60 gamma dose distribution

13 p2144 N71-25583

Computer program for calculating neutron spectra from activated cobalt isotopes

15 p2470 N71-27382

Test data for designing, fabricating, and operating Co-60 heat sources

15 p2449 N71-27567

Effects of gamma radiation on lifetime of red blood cells and bone marrow production in dogs exposed to cobalt 60 irradiation for two and one half years

16 p2545 N71-28480

Dose uniformity ratios and minimum dose data in cobalt 60 and cesium 137 rectangular source irradiators

20 p3328 N71-33983

COBOL

Development of machine translation system

01 p0026 N71-18816

Users manual for COBOL compiler validation system

01 p0029 N71-18941

Requirements for Automated Spoken Program written in COBOL for IBM 360 computer

03 p0339 N71-12454

Automated Spoken Program written in COBOL for circuit analysis on IBM 360 computer

03 p0340 N71-12459

COBOL program for providing reports on circuit analysis

03 p0340 N71-12460

Path redundancy/Automated Spoken Program written in COBOL for IBM 360 computer

03 p0342 N71-12463

North American processors/Automated Spoken Program written in COBOL for IBM 360 digital computer

03 p0342 N71-12464

COCELEA

Neurophysiological model for cochlear function in auditory nervous system information processing

11 p1721 N71-23062

Neuronal responses of bat cochlear nuclei to ultrasonic stimuli

23 p3716 N71-36487

COCKPIT REGULATORS

Pilot evaluation of movable and rigid cockpit control sticks

01 p0083 N71-10184

Controlled visibility device for simulating poor visibility conditions in training pilots in instrument landing and flight procedures

01 p0083 N71-10184

Evaluation of transfer of training effectiveness for two cockpit simulators differing greatly in physical fidelity and cost

05 p0636 N71-14683

Human factors in aircraft simulation

06 p0830 N71-16888

Human factors in Concordia cockpit simulation

06 p0831 N71-16885

Human factors in developing a piloted simulation program for evaluating aircraft handling aspects

06 p0832 N71-16889

Television-type, cut-window visual simulation image generator design and specifications for aircraft or spacecraft manual flight simulation

12 p1897 N71-34126

Major and critical component specifications for construction of simulator cruise scene visual attachment for manned spacecraft or aircraft flight simulation

12 p1898 N71-34127

Cruise scene visual attachment system assembly and detail design drawings for manned spacecraft or aircraft flight simulators

12 p1898 N71-34128

Jet vertical takeoff aircraft piloted cockpit simulator for controlling aircraft flight performance

13 p2027 N71-25063

Definition of night fog characteristics and development of mathematical model for design of night fog simulator device

17 p2729 N71-29910

Cockpit simulators without visual or motion cues in pilot training

19 p3074 N71-31952

Flight simulation of short takeoff aircraft and Dornier-31 aircraft, and results using cockpit simulator with 6 degrees of freedom for DO-31

19 p3074 N71-31956

COCKPITS

Cockpit and center of gravity acceleration during takeoff of Boeing 707 aircraft

06 p0793 N71-15721

Aircraft pilot thermal environment, thermal comfort and cockpit air conditioning

07 p0965 N71-17096

Cockpit geometry evaluation program results and techniques with computer input and output samples of flight crew anthropometry

09 p1321 N71-19817

Anthropomorphic data update for man-model used in cockpit geometry evaluation program for evaluation of flight crew interaction and compatibility with crew stations

09 p1340 N71-19818

Cockpit geometry evaluation program for computer simulation of flight crew physical compatibility with crew stations based on anthropometric and environmental data for man-model movements

09 p1340 N71-19819

Cockpit display of automatic radar control system data

09 p1415 N71-19848

Model design for vertical takeoff aircraft cockpit seating navigation aids, visual displays, and console configurations

11 p1674 N71-22196

Routine unprojected exposure to acoustic noise within cockpits of trainer aircraft presenting potential hazardous stress

11 p1796 N71-22426

Methods for predicting speech interference within cockpits of fixed wing and rotary wing aircraft

12 p1870 N71-23528

Vibrational responses of VC-10 aircraft during takeoff taxi, noting cockpit accelerations

20 p3288 N71-32811

Pilot performance in recognizing electronic display systems under varying display and color conditions in cockpits

24 p3873 N71-37621

Environmental and performance tests of voice-activated cockpit control and interrogation system

24 p3889 N71-37723

COCKPIT

Speech recognition tests of continuous variable shape delta code-decoder using continuous recognition for radio communication

16 p2581 N71-26818

Counting circuit studies for timing code generator

20 p3270 N71-33932

Design and development of encoder/decoder system to generate binary code which is function of outputs of plurality of binary elements

20 p3343 N71-33487

Optical-mechanical marine gravimeter with manual pulse coding device

31 p3418 N71-34317

N-F junction diode detector used in design of radiofrequency source non-coherent oscillator

34 p3830 N71-37936

COCKS

Virtual algorithm for decoding convolutional codes for space channel application

11 p1720 N71-22773

- RSYN and 3DB codes for flux and bulk parameter computation of fast reactors
[WHAAN-IR-48] 12 p1964 N71-24152
- CODING**
- NT DECODING
- NT REDUNDANCY ENCODING
- NT SIGNAL ENCODING
- Algorithms for tree threading for encoder traversal
[AD-70231] 01 p0026 N71-10014
- Pseudo-noise addressing system analysis for multiple access communication with applications of error correcting codes
[AD-711001] 01 p0022 N71-10535
- Digital waveform encoding methods for speech
[AD-712304] 02 p0178 N71-11253
- Cascaded tree codes for sequential decoding in presence of noise
[NASA-CR-111349] 02 p0181 N71-11270
- Use of circuit codes in analog to digital conversion
[AD-711944] 02 p0189 N71-11327
- Majority logic decoding for duals of primitive polynomial codes, and maximality of Euclidean geometry codes
[AD-711791] 02 p0190 N71-11337
- Conventional coding techniques including constructing inverses, algorithms, and code comparing for sequential decoding
[NASA-CR-111601] 03 p0343 N71-12488
- Computer codes for solving kinetic neutron diffusion equations in reactor safety program
[BMM-1888] 04 p0532 N71-13972
- CALIB, three dimensional flux synthesis code, for fast management studies in SGHWR
[AEWE-R-620] 04 p0563 N71-14486
- Coding related to speed and accuracy of recall
[AD-714639] 06 p0759 N71-15929
- Application of address coding guide ACC/DIME to transportation planning problems
[PB-191488] 07 p1135 N71-18041
- Univac 1108 and IBM 360 codes for calculating energy emission of unstable negative beta nuclides
[CEA-N-1285] 08 p1251 N71-18249
- Development of digital encoding methods for improved military communication systems
[AD-715998] 09 p1349 N71-19673
- High temperature gas cooled reactor design and development including cesium and strontium diffusion in graphite, reprocessing cycles, and fission product transport coding
[GA-10288] 09 p1419 N71-19937
- Lattice cell code, WIMS, for predicting neutron physics of heavy water moderated rod clusters
[AEWE-R-549] 09 p1420 N71-20154
- FREADM-1 code, fast multichannel accident analysis program, restricted to accidents within annular or cylindrical coaxial core regions
[GEAP-13608] 10 p1604 N71-21251
- Error analysis for mean linear error of nonredundant code in asymmetrical channel without memory
[NLL-RTS-6058] 10 p1530 N71-21669
- RABID, integral transport theory code, for thermal neutron slowing down in slab cells with repeating boundary conditions
[ANL-7645] 11 p1802 N71-22091
- Characteristics of high frequency channels used to obtain parameters for choosing appropriate convolutional codes
[AD-717599] 11 p1699 N71-22132
- Description of error correcting methods for use with digital data computers and apparatus for encoding and decoding digital data
[NASA-CASE-XNP-02748] 11 p1719 N71-22749
- Cyclic arithmetic codes and their distance properties with demonstration of modular arithmetic weight invariance to code word cyclic shifts
[NASA-CR-117884] 12 p1947 N71-23218
- Mean global distributions of Secchi disc water transparency measurements and Forel-Ule water color codes including seasonal variations for Sea of Japan and Indian Ocean
[AD-718333] 12 p1910 N71-23592
- Parameterization of human speech for encoding into information units
[AD-717599] 12 p1880 N71-23929
- Description and utilization of Monte Carlo code Puker
[CEA-N-1308] 13 p2128 N71-24473
- Nuclear data processing from TIMOC Monte Carlo library ENDF/B file using CODAC FORTRAN 4 program
[EUR-4521-E] 13 p2134 N71-25163
- Conventional encoding and decoding developments, and applications in deep space communication
[NASA-TM-X-65536] 14 p2220 N71-25719
- Near-orthogonal codes for multiple-short keying communication systems
[AD-720822] 14 p2216 N71-25848
- Problem of deterministic source encoding with fidelity criterion using computational work
[NASA-CR-118656] 14 p2224 N71-26343
- Analog coding in nonlinear data transmission systems
[AD-721228] 15 p2380 N71-27177

- Computer program modifications and lattice coding for hydrogous systems including transport corrections for self-scatter cross sections and collision probability
[AEWE-M-952-REV] 15 p3467 N71-37287
- Treating coding problem as critical problem in combinatorial geometry
[AD-722080] 16 p2622 N71-28199
- DULCINEE code for water cooled reactor at low pressure
[CEA-N-1378] 17 p2781 N71-29295
- Applications and methods for improving data coding device
[NLL-FORS-TRANS-2687-9022.81] 17 p2720 N71-29844
- Optimal prefix codes for ensembles of N equiprobable messages using binary alphabet
[PB-197642] 18 p2895 N71-31292
- M-ary block code with bit-by-bit decisions for probability of error signal analysis
[AD-723519] 19 p3053 N71-31682
- Comparison of concatenated and sequential decoding systems and convolutional code structural properties
[NASA-CR-114358] 19 p3063 N71-32505
- Bit-plane encoding and other aperture methods for data redundancy removal for onboard spacecraft data management
[AD-723519] 19 p3063 N71-32543
- Development of hydrodynamic code for representing shocks by discontinuities whose jump conditions and propagation velocities satisfy Hugoniot relations
[P-4556] 19 p3081 N71-32606
- Combinatorial coding for discrete stationary sources
[AD-724072] 20 p3299 N71-32946
- Encoding function of neurophysiological synapses
[AD-724072] 20 p3277 N71-33329
- Radiation distribution image analysis and multiplex coding techniques including Fourier, Fresnel, and Walsh-Hadamard transformations
[TP-972] 20 p3293 N71-33759
- Weights in third-order Reed-Muller codes applied to space communication
[AD-726685] 21 p3391 N71-34132
- Development of arithmetic unit for decoding data encoded by convolutional encoding with fewer channels than prior units
[NASA-CASE-NPO-11371] 21 p3399 N71-34187
- TIMOC, general purpose Monte Carlo code written in FORTRAN 2, for stationary and time dependent neutron transport
[EUR-4519-E] 21 p3473 N71-34727
- DBLSCAT, FORTRAN 4 computer code, for double scattering corrections of slow neutrons
[ANL-7780] 21 p3482 N71-34801
- All digital communications signal design using convolutional coding and PSK modulation for two-way transmission of voice and data between space shuttle and ground
[AD-726685] 21 p3515 N71-35048
- Convolutional coding, sequential coding, subband coding, and inverse systems for data protection
[NASA-CR-121917] 22 p3555 N71-35322
- Information theory and coding with communications applications
[POA-3-A-3733-63] 22 p3556 N71-35334
- Neutron spectra determination from activation data using RP01 only for threshold detectors and RP07 codes
[KFKI-70-30-RPT] 22 p3631 N71-35875
- FLANGE-AI code for Oier computer for calculating scattering kernels and cross sections of polycrystalline moderators
[DNR-1260] 22 p3633 N71-35896
- RAFFLE Monte Carlo code for obtaining correlated estimates of collapsed cross sections using uniform interval number tables
[CONF-710302-11] 22 p3646 N71-35996
- Coding considerations for implementation of general isoparametric solid elements into NASTRAN displacement method program for stress analysis
[AD-726685] 22 p3688 N71-36304
- TENSOR code for two-dimensional stress-induced adiabatic flow
[UCRL-50987] 22 p3689 N71-36310
- CORBA heat transfer code extensions for large liquid Na cooled pin bundles and coolant mixing effects due to fuel pin spacer wires
[WHAAN-5-76] 23 p3798 N71-37080
- Coded mask for improved signal to noise ratio in scanning optical systems
[NASA-CR-123155] 24 p3887 N71-37705
- One-dimensional code adaptation for electron transport
[NASA-CR-123118] 24 p3976 N71-38370
- Problems in nuclear data processing by computer code
[CONF-710302-3] 24 p3977 N71-38382
- PEARLS, FORTRAN code, for solution of neutron slowing down equations in multiplication lattices of resonance absorbers using IBM 360/5081 computer
[AEC/R-213] 24 p3981 N71-38407

COEFFICIENT OF FRICTION

- Concentration dependence of translational friction coefficient of macromolecules solution
[AD-710294] 01 p0016 N71-10000
- Tables of coefficient of friction versus Reynolds number for ship hull scale models
[NPL-SHIP-142] 03 p0362 N71-12700
- Prediction of friction and heat transfer coefficients with large variations in fluid properties
[NASA-TM-X-2145] 04 p0620 N71-10001
- Effect of rate macromolecular movement on coefficient of progressive friction
[AD-714745] 06 p0809 N71-19099
- Models for coefficient of friction on plastic contact
[AD-716970] 10 p1631 N71-20797
- Coefficient of friction for materials used in cinema equipment
[AD-720376] 14 p2254 N71-23900
- Horizontal static forces exerted by men standing in common working positions on various surfaces including coefficients of friction between different floor and shoe materials
[AD-720252] 14 p2210 N71-23816
- Measurement of local skin friction coefficient and combined effect of favorable pressure gradient and free stream turbulence on local skin friction coefficient
[AD-720376] 14 p2254 N71-23900
- Velocity fields and hydraulic resistance of turbulent fluid flow in channels formed by clusters of smaller fuel rods
[AEC-TR-7189] 15 p2444 N71-26000
- Mathematical models for measuring frictional behavior of basalt and aluminum surfaces in ultrahigh vacuum
[AD-720376] 16 p2602 N71-28073
- Parametric effects on static and dynamic coefficients of friction of thermoplastics
[NLL-RISLEY-TRANS-1928-9091-59] 19 p3105 N71-32100
- Coefficient of friction of high polymers as function of pressure determined by shear strength measurements
[AD-726685] 23 p3778 N71-38007
- Estimating coefficient of friction during initial stage of upsetting of cylindrical specimen through oil packing
[AD-727884] 24 p4026 N71-38778
- COEFFICIENTS**
- NT ACCOMMODATION COEFFICIENT
- NT AERODYNAMIC COEFFICIENTS
- NT ATTENUATION COEFFICIENTS
- NT BINOMIAL COEFFICIENTS
- NT CLEBSCH-GORDAN COEFFICIENTS
- NT COEFFICIENT OF FRICTION
- NT COHERENCE COEFFICIENT
- NT CORRELATION COEFFICIENTS
- NT COUPLING COEFFICIENTS
- NT DIFFUSION COEFFICIENT
- NT DISCHARGE COEFFICIENT
- NT FLOW COEFFICIENTS
- NT HEAT TRANSFER COEFFICIENTS
- NT IONIZATION COEFFICIENTS
- NT NOZZLE THRUST COEFFICIENTS
- NT RECOMBINATION COEFFICIENT
- NT REGRESSION COEFFICIENTS
- NT SCATTERING COEFFICIENTS
- NT STRUCTURAL INFLUENCE COEFFICIENTS
- NT WIGNER COEFFICIENT
- Generation and application of sensitivity coefficients
[NASA-CR-102912] 02 p0197 N71-11190
- K-conversion coefficient of 897-keV transition in Pb-207
[INP-15288] 03 p0425 N71-10000
- Extrapolation based on coefficients for data reduction and data transmission
[DRL-FB-70-49] 08 p1162 N71-10077
- Path integral formulation and derivation of space-time correlation functions for calculating transport coefficients
[NYO-1480-160] 08 p1264 N71-19194
- Complex optimization techniques applied to value sensitivity coefficient determination for distributed lumped-active networks
[NASA-CR-117757] 11 p1787 N71-22017
- Derivation and charts of spherical harmonics coefficients and isopropic charts for International Geomagnetic Reference Field for 1965
[NASA-TM-X-65664] 17 p2745 N71-20000
- Effects of surface roughness on conduction heat at millimeter wavelengths determined by optical techniques and resonator quality factors
[NASA-CR-121859] 21 p3390 N71-34816
- Weights in third-order Reed-Muller codes applied to space communication
[AD-726685] 21 p3391 N71-34132
- Determination of first-order diffraction coefficients for slot-excited conical antennas
[AD-726539] 22 p3560 N71-35100
- Boltzmann models for hydrodynamic equation, transport coefficients, and light scattering by simple fluids
[AD-726539] 22 p3570 N71-35100

SUBJECT INDEX

Electrical and thermal transport coefficients of thin single crystals 22 p3660 N71-3686

Prediction models for turbulent dispersion of rigid spherical particles of differing sizes and densities 23 p3746 N71-36712

Estimate of incoherent coefficient from transient fluxes of electron cascade calculations and electron microscopic study of dependence of electron cascade layer thickness 24 p3979 N71-36295

Transmission coefficient calculation for double-lens potential 24 p3979 N71-36296

Upper limits for transport coefficients due to plasma fluctuations and convective cells based on quasi-linear approximations of diffusion across magnetic fields in toroidal devices 24 p3980 N71-36439

Thermodynamic coefficient equation and coefficient derivation for neutron component of cosmic rays 24 p4011 N71-36882

Determination of partial coefficient equation and coefficient calculation for cosmic radiation 24 p4011 N71-36883

Coincidence effect and thermodynamic coefficient for various neutron reactions 24 p4012 N71-36811

COUPLED

IN THERMAL

COUPLED

Characteristics of convective force of this magnetic field consisting of two neomagnetic inductive layers (AD-714433) 06 p0933 N71-16072

Matrix and free lattice precipitation phase conditions and quality determinations of Cu-Al alloy convective flow 12 p1999 N71-34090

COUPLED

Human cognition, involving man-machine interaction directions 09 p1339 N71-19063

Neurological cognition in two-dimensional space of children from 3 to 8 years old 12 p1863 N71-33774

Cosmological explanation of quantum mechanics and its application to microcosm 19 p3136 N71-33426

Conceptual functions and information properties of devices used to understand cognitive mechanisms of man 21 p3399 N71-34192

COUPLED

Coherent effects in slow neutrons scattering on liquid vibrations 06 p0989 N71-15778

Coherent production of kaon states and study of their decay into neutral pions 23 p3889 N71-37136

COUPLED COEFFICIENT

Incorrectness of mutual coherence function for optical wave propagation in turbulent atmosphere (AD-711307) 02 p0269 N71-12172

Optimization by combining antenna array coefficient for interference noise reduction (AD-723281) 19 p3065 N71-31888

COUPLED ACOUSTIC RADIATION

Attenuation and spatial coherence of underwater acoustic signals generated by explosion in rough sea (BMVQ-PW71-71-4) 18 p3289 N71-31134

COUPLED ELECTROMAGNETIC RADIATION

NT COHERENT LIGHT

Design of folded traveling wave maser structure (NARA-CASE-XNP-65219) 05 p0098 N71-13350

Development of focused image holography with external sources 05 p0098 N71-13350

NARA-CASE-HRC-10019 05 p0098 N71-13351

Interaction between focused, pulsed laser radiation and copper or gold targets 10 p1569 N71-31278

Hypothesis to level crosshairs and coherence scattering in microwave resonance radiation 20 p3318 N71-33396

Effect of laser beam impingement on metal surface and determination of ratio of liquid and gaseous phases (NARA-TT-P-139649) 23 p3768 N71-36858

COUPLED LIGHT

Simulation of second harmonic light in transparent media by pulsed ruby laser 01 p0064 N71-10047

Investigating techniques for measuring random pattern in photomicrographs by studying nature of coherent light diffracted by spatial pattern (NARA-CR-115085) 06 p0489 N71-13494

Investigating various methods for modulation of the second harmonic coherent light waves (PDA-3-C-3345-52) 05 p0732 N71-14682

Liquid biological system using reference, transmitted, and reflected beams simultaneously (NARA-CASE-MFP-38074) 06 p0489 N71-13545

Interaction between focused, pulsed laser radiation and copper or gold targets 10 p1569 N71-31278

Development of apparatus for amplitude modulation of diode laser by periodic discharge of direct current power supply (NARA-CASE-XM3-04368) 11 p1776 N71-32885

Computer generation and plotting of synthetic holograms, binary holograms, and spatial filters 16 p3007 N71-30815

Coherent light beam device and method for measuring gas density in vacuum chambers (NARA-CASE-XER-11283) 16 p3299 N71-30894

Derivation of equations for Rylov and Born approximations in turbulent atmospheric attenuation and scattering of coherent light 17 p3789 N71-36229

Developing visible CW optical parametric oscillators 23 p3767 N71-30833

Interactions between intense coherent light from Q-switched ruby laser and iodine vapor, neodymium-doped glass, and benzene 23 p3805 N71-37128

Transmission of coherent light in nonlinear systems (AD-723739) 24 p3932 N71-30856

COHERENT RADAR

Laboratory coherent radar system design for evaluating digital MTI subsystems (JCR-T-426) 01 p0020 N71-10020

Coherent and noncoherent signal bandwidth methods for radar target detection in clutter 04 p0495 N71-15911

Atmospheric instability effects on wideband coherent tracking radar accuracy 11 p1712 N71-23847

Upwind-downwind dependence of Doppler spectra of radar sea echo using coherent radar data (AD-719333) 13 p2043 N71-24713

Artificial electron cloud formation using cesium and potassium isotopes for simulation of ionospheric propagation in E region with coherent radar (AD-720934) 15 p2406 N71-27809

Coherent radar system for determining radar altimeter bias from GLOB-C tracking 19 p3655 N71-31869

Effect of coherence and multiple scattering on laser radar air pollution measurements (NARA-CR-121873) 21 p3435 N71-34441

Incoherent and coherent pulse radar operation and characteristics 24 p3888 N71-37711

Portable, frequency-coherent spectrum analyzer for spectral analysis of radar echoes (NOAA-TT-BRL-384-AL-3) 24 p3889 N71-37726

COHERENT RADIATION

NT COHERENT ACOUSTIC RADIATION

COHERENT ELECTROMAGNETIC RADIATION

NT COHERENT LIGHT

Thermally scanned interferometric modulation effect in cadmium sulfide crystals illuminated by gas laser radiation (AD-710954) 01 p0081 N71-10749

Measuring correlation characteristics of signals at photomultiplier output in presence of monochromatic background (AD-712231) 02 p0269 N71-11778

Radiative emission from N-S point contacts (AD-712662) 03 p0367 N71-12418

Nonlinear interactions of intensive beams of charged particles with accelerating field (KFK-T-318) 04 p0367 N71-14378

Physiological effects produced by laser radiation (JPRS-32274) 07 p1039 N71-17484

Variation of refractive index during optical pumping in ruby laser 08 p1210 N71-18653

Coherent optical processing of motion-degraded images (AD-716779) 10 p1557 N71-30852

Modern optics for problem solving in generation, propagation, properties, and uses of coherent electromagnetic radiation (AD-717775) 11 p1774 N71-22329

Applications of coherent state representations of minimizing particles to magnetization theory using Heisenberg model with 1/2 spin case 15 p3401 N71-27822

Characteristics of photon echo resonances determined by application of two brief laser pulses to transient absorbing system 16 p3665 N71-30539

Propagation of coherent radiation in cylindrical plasma channels considering laser beam refraction (NARA-CR-1899) 17 p3736 N71-30812

Characteristics of far field power distribution for circular apertures with Gaussian illumination (AD-720431) 19 p3108 N71-32889

Characterization of carbon dioxide laser radiation scattering in atmosphere and application as remote sensing probe (NARA-CR-121663) 21 p3435 N71-34439

Coherent frequencies of transverse oscillations in electron model of ring cyclotron for magnetic field variants (JPRS-P-5677) 21 p3473 N71-34728

Effect of ruby laser beam impact on mirror coating of sighting prism 22 p3391 N71-35569

Measurements of off-axis intensities produced by laser beam in water 23 p3391 N71-35573

Data analysis for incoherent laser radiometry (AD-726514) 23 p3766 N71-30843

Electroretroactive self-triggering of piezoelectric laser pulse trains (AD-726521) 23 p3766 N71-30843

Development of methods for obtaining high power coherent emission at various wavelengths using conventional lasers as primary sources 23 p3766 N71-30847

Limitations imposed on resolution of coherent radar systems by atmospheric turbulence for scanning wave front tilt or angle-of-arrival of return signal from target (RMA-526) 24 p3880 N71-37727

Phase formation upon laser irradiation of transparent dielectric materials below damage threshold (AD-727145) 24 p3882 N71-30852

Efficient laser-pumped 10-micron infrared quantum counter conversion in rare earth doped crystals (AD-727152) 24 p3882 N71-30853

Extending tuning range of parametric oscillators into infrared, visible, and ultraviolet regions (AD-727127) 24 p3887 N71-30836

Optical wave phase structure and mutual coherence function for propagation in turbulent atmosphere and heterodyne detection effects 24 p3867 N71-30842

COHERENT SCATTERING

Phase-coherent laser interactions including multiplicity of charged particles, distribution over multiplicity, and angular distribution (JINR-P1-5072) 03 p0427 N71-12860

Spatial coherence measurement on argon laser beams after passage through water 04 p0524 N71-13723

Investigating coherent transverse stability of short beam interacting with low-quality resonator (KFK-T-319) 04 p0506 N71-14045

Small angle scatter filter for measuring coherent neutron inelastic scattering amplitude (JINR-E3-5371) 15 p2468 N71-27874

Molecular dynamics of coherent function of Lennard-Jones fluids in liquid and gas phases 16 p3641 N71-30823

Coherent production of positive ions, positive plasmas, negative plasmas by negative ions of neon, neon, 5.5, 16.6, and 12.7 GeV on Ne, C, F, and Br nuclei (LAL-1242) 18 p3975 N71-30509

Coherent state method for high energy hadron scattering related to quark models 18 p3981 N71-30823

Use of semiconductor telescopes for detecting recoil nuclei in proton-light nuclei scattering at high energy (LYCEN-7065) 21 p3472 N71-34724

Coherent (n,2n) scattering amplitude on heavy nuclei at low energies based on infinite mass nuclei approximation (JPR-70-55-5) 21 p3487 N71-34839

Determination of structural amplitude phases for polarized neutron diffraction and limiting neutron flux density (JINR-P3-5334) 22 p3468 N71-33949

Coherent interaction of negative plasmas with photoemission model at 17 GeV (JINR-P1-5365) 22 p3641 N71-33954

Hartree-Fock theory for calculating coherent X-ray scattering factors (JRG-1165-1468) 22 p3645 N71-33990

Neutron electron coherent scattering amplitude of W-186 studied by neutron diffraction (JINR-E3-5713) 23 p3886 N71-37135

COHERENT SOUND

U COHERENT ACOUSTIC RADIATION

U SOUND WAVES

COHERENT SOURCES

U COHERENT RADIATION

U RADIATION SOURCES

COHERENT TRANSMISSION

U COHERENT RADIATION

COHERENT

Studying Laser Coherent photomicrographs of bubble tracks left on laser surface to determine cell cohesion and angle of internal friction (NARA-CR-102508) 05 p0768 N71-15085

Summary data on thin film physics, collective properties of crystals, and solid state theory (COO-625-156) 08 p1278 N71-14637

Theory of electron and chain processes of cells (AD-728941) 15 p3288 N71-37370

Form of ion coherence with atoms related to type of materials, surface roughness, structure and rate of natural heat, and surface temperature (AD-722106) 16 p3612 N71-30730

One electron theories of coherence on ion pair potentials in metals, using Fourier transformation and integral equations (MFC-1147) 17 p3810 N71-35948

COBOMOLOGY

- Cohesion effects in superfluids, such as liquid helium and superconductors 20 p3333 N71-33045
- COBOMOLOGY**
U ROMOLOGY 01 p3333 N71-33045
- COILS**
Superconducting coil for storing energy and restoring it in about one millisecond [LA-TR-70-11] 02 p0286 N71-11924
High voltage test of large cryogenic coil for magnetic energy storage system [LA-4469] 06 p0903 N71-10821
Particle accelerator beam steering coils using printed circuit boards [UCRL-20165] 19 p3142 N71-31995
Measured coil impedance in eddy current testing [ARL/MET-NOTE-79] 23 p3731 N71-36398
- COIN AIRCRAFT**
NT OV-10 AIRCRAFT
COINCIDENCE CIRCUITS
Two coincidence units with three independent twofold channels gated by one common signal [CERN-70-25] 08 p1168 N71-18042
Solid state X ray/alpha coincidence counter for measuring radioactive decay on transuranic elements [BNWL-SA-1514] 10 p1536 N71-20738
Quantized random signal correlator output signal to noise ratio expression and comparison with output ratios of analog and polarity coincidence correlators [AD-718053] 12 p1892 N71-23378
Gamma/gamma angular coincidence measurements on thallium lead crystal electric fields 15 p2472 N71-27417
Two dimensional analyzer for half life measurements of nucleus of excited states by gamma-gamma delayed coincidence method on basis of computer Mink 2 [JINR-P13-5485] 16 p2655 N71-29073
Coincidence Mossbauer studies of solid state phenomena 18 p2999 N71-31510
Standardization of beta-gamma emitters by dual beta-gamma coincidence method for corrections and counting errors [DTR-1240] 21 p3467 N71-34600
- COKE**
Experimental method for determining parameters for rate of reaction of CO₂ with solid carbon [BM-R1-7474] 08 p1159 N71-18589
Heat sink capabilities of Jet-A fuel - heat transfer and cooling studies [NASA-CR-72951] 18 p3027 N71-31482
- COLD ACCLIMATION**
Hypoxia and clinical physiology of men living in Antarctica [JPRS-52579] 11 p1678 N71-21888
Physical training, cold adaptation, and adaptation pharmacokinetics for increased physiological stress resistance in rats 20 p3220 N71-33454
- COLD CATHODE TUBES**
NT FREQUENCY MODULATION PHOTOMULTIPLIERS
NT PHOTOTUBES
Long-term performance tests of neon gas filled, high-temperature ceramic voltage-regulator tubes [NASA-CR-1813] 12 p1858 N71-23120
Low frequency oscillation measurements on spherical magnetized cold cathode direct current discharge by plasma probes [NASA-CR-118028] 12 p1966 N71-23877
Cold cathode gaps for measuring amount of gas present in lunar atmosphere 18 p3011 N71-30963
Cold cathode glow discharge tube for detecting meteoroid puncture of pressurized cells [NASA-TN-D-6447] 21 p3429 N71-34405
Cold cathodes, Penning discharge, heavy ion source, power supply in lanthanous cyclotron [ORNL-TN-3591] 21 p3481 N71-34800
- COLD CATHODES**
Production and performance of silicon cold cathodes [AD-719718] 13 p2999 N71-25408
Brightness and life of pointed cold cathodes for electron microscope applications [NRC-TT-1473] 22 p3559 N71-35551
Cold cathode emission obtained from bleated silicon p-n junctions activated to negative electron affinity [AD-726644] 23 p3733 N71-36612
- COLD FLOW TESTS**
Cold air tests on axial flow turbine with transpiration cooled discrete hole stator blades to determine coolant flow ejection effect on turbine aerodynamic performance [NASA-TN-X-3133] 02 p0142 N71-10101
- COLD FORMING**
U COLD WORKING
Cold gas and high temperature gas rocket engines and ion engines for satellite attitude control [DLR-MIT-70-14] 07 p1118 N71-47158
- COLD HOLDING**
U COLD PRESSING

- COLD NEUTRONS**
Cold neutron beam intensity for differently shaped moderator chambers in tangential beam tube of reactor Triga Mark-3 [US-571] 14 p2303 N71-26049
Extraction of ultracold neutrons from stationary reactor [JINR-P3-5392] 17 p2792 N71-29473
- COLD PLASMAS**
Alfvén theory of critical velocity in neutral gas and magnetized plasma interactions [REPT-70-30] 02 p0280 N71-11837
Laboratory analysis of space charge potentials formed by cold plasmas in magnetic field [REPT-70-14] 02 p0281 N71-11869
Characteristics of collisionless damping of electromagnetic waves in region of intense inhomogeneity of cold plasma [KHPT-69-53] 03 p0437 N71-12891
Computerized simulation of high temperature plasmas [UCB-34-F-128-18] 07 p1083 N71-17056
Numerical solutions of full wave equations in inhomogeneous cold plasma slab near lower hybrid resonance [CEA-CONF-1613] 06 p1272 N71-18505
Cold plasma density and collisional frequency measurements in presence of magnetic fields for cyclotron radiation plasma diagnostics [COO-1789-1] 10 p1627 N71-20803
Radio wave scattering from random electron density fluctuations in cold anisotropic magnetoplasma [NASA-CR-118332] 13 p2407 N71-25085
Radio spectra, synchrotron self-absorption, free-free absorption, cold plasma effect, stimulated emission, and quasi-stellar sources 20 p3344 N71-32841
Ion-ion hybrid resonance in cold collisionless plasma 22 p3656 N71-36074
Boundary conditions for adjacent streams of cold plasma in magnetic field [UAAEE-78] 23 p3825 N71-37282
- COLD PLATES**
U COLD SURFACES
COLD PRESSING
Preparation of uranium mononitride pellets of different densities by cold pressing and sintering using fine power particles [ORNL-TR-2365] 10 p1603 N71-21197
- COLD ROLLING**
Measuring stress distribution across width of steel strip in cold mill to predict shape of finished product [PB-194445] 04 p0531 N71-14215
Performance tests on laboratory cold rolling mill [ORNL-TN-3085] 05 p0693 N71-14997
Description of techniques used in design of cold rolling mills for optimum operation [AD-717401] 11 p1767 N71-22137
Design methods for light gauge cold formed structural elements and members made of cold rolled austenitic stainless steel 15 p2423 N71-27327
Effect of temper rolling on elimination of yield plateau in vacuum-treated low-carbon steels 18 p2927 N71-30687
Electron microscopic analysis of cold rolled zirconium microstructure [INIS-MF-15] 19 p3113 N71-32112
Stress deformation due to cold rolling of splines on shafts [AD-727926] 24 p3929 N71-38035
- COLD SURFACES**
Environmental simulation of low space temperatures using cold walls 03 p0356 N71-12706
- COLD TOLERANCE**
Wind tunnel tests with human subjects to determine effects of whole body and head lined cooling at high wind speeds as might be encountered in air-to-air rescue operations [AD-719716] 09 p1330 N71-19813
Establishment of relationship between skin temperature and ability to tolerate cold and hot environments for human subjects [FAA-AM-71-4] 13 p2037 N71-24748
- COLD TREATS**
Summary of AFDA sodium technology program including impurity monitoring devices and removal processes such as cold-trapping, hot-trapping, and centrifuging [AFDA-529] 02 p0265 N71-11783
Design and performance testing of dual patch multi-element radiant cooler with cold trap [NASA-CR-121476] 20 p3346 N71-33715
- COLD WALLS**
U COLD SURFACES
U COLD SURFACES
U COLD SURFACES
Origin and history of permafrost and effect on recharge, discharge, movement, and storage of ground water in geologic environments 03 p0367 N71-12775

SUBJECT INDEX

- Arctic field tests of prototype life rafts capable of protecting occupants from cold water exposure for 24 hours [NASA-CR-121449] 20 p3327 N71-33710
- COLD WEATHER**
Occurrence of frost conditions in North Germany with emphasis on meteorological parameters and seasonal variations 21 p3451 N71-34600
- COLD WEATHER TESTS**
Cold weather testing of equipment durability [AD-710611] 01 p0015 N71-10000
Bibliography on cold regions science and technology, accession between July 1969 and June 1970 - Part 1 [AD-715769] 06 p1191 N71-14900
Bibliography on cold regions science and technology, accession between July 1969 and June 1970 - Part 2 [AD-715717] 06 p1191 N71-14900
Cold weather tests to determine effectiveness of resonant combustor as power source for starting aircraft engines [AD-724123] 20 p3338 N71-33388
- COLD WORKING**
NT COLD ROLLING
NT EXPLOSIVE FORMING
Elastic anisotropy effects on cold drawing of metals [ONERA-TN-158] 02 p0230 N71-11100
Using thin-film electron microscopy to study effects of cold working and aging on substructure and precipitation in cobalt-base alloy L-605 [NASA-TN-D-7051] 07 p1043 N71-17000
Effects of cold working by hydrostatic extrusion on mechanical properties of high strength steels [NASA-TN-D-6186] 07 p1034 N71-11888
Influence of cold shearing of steel plates on welded joint mechanical properties [CRIP-MT-46] 06 p1206 N71-18002
Cold working effects on creep properties of elongated cylindrical austenitic steel specimens at room temperature [NLL-CR-TRANS-5413-9002.09] 10 p1581 N71-31470
Effects of cold work on irradiation induced density changes in types 316 and 304 stainless steel and mild steel [WHAAS-A-9] 14 p2267 N71-25009
Cold metal hydroforming techniques using epoxy molds for constructing crop or stretch [NASA-CASE-XLE-02641-1] 14 p2363 N71-30346
Effect of cold working on creep properties of AISI 316 type stainless steel [NASA-MEMO-4125] 15 p3422 N71-27210
Comparison of cold working and roll forming of machine shafts and effects on wear resistance [AD-722095] 17 p2755 N71-29408
Deformation criteria in cold extrusion of metals with equation for calculating extrusion pressure from material parameters 17 p2854 N71-30110
Relative stress relaxation behavior at 300 C of cold worked Zircaloy-2, cold worked Zr-2.5 wt percent Nb, and heat treated Zr-2.5 wt percent pressure tube materials [ABCL-3782] 18 p3021 N71-30904
Influence of cold work and heat treatment on tensile and fatigue strengths - fatigue properties of stainless and titanium alloys - Part 3 [RAE-LIB-TRANS-1319-PT-3] 18 p2935 N71-30804
Thermomechanical processing of nickel alloy is relation to yield and creep rupture strength [NASA-TN-D-6418] 21 p3454 N71-34402
Heat treatment and cold work effects on oxidation of Zr-1 percent Nb alloy in air and pressurized steam at 450-650 C [UAAEE-72] 24 p3933 N71-38041
- COLLAPSES**
Program for computing collapse loads of basins, irregularly loaded spherical shells in closed form [SC-DG-70-218] 07 p1124 N71-17071
Asymmetric and thermodynamic effects on cavitation bubble collapse, modes of collapse, and causes of cavitation damage [PB-198040] 17 p2754 N71-29715
High speed photography of bubble collapse close to rigid boundary, flexible boundary, and second bubble [PB-199464] 21 p3413 N71-34006
Analysis of Freese-113 bubble growth and collapse in constant-diameter, vertical channels with nonuniform initial temperature profiles [ANL-7746] 22 p3633 N71-33113
- COLLECTORS**
U ACCUMULATORS
COLLECTORS
U UNIVERSITIES
COLLECTION
Collimation method of identifying elements 103 and 104 and measurement of integral angular distribution of nuclear reaction products for identifying small number of elements [KFK-TR-529] 15 p3473 N71-33446

COLLOCATION

- Aircraft accident report on midair collision involving DC-9 commercial aircraft and Marine Corps F-4B aircraft near Durie, California on June 8, 1971 [E8-71-42] 19 p3839 N71-32491
- Analysis of 34 Army midair collisions which occurred during period Jan. 1963 to Nov. 1969 with conclusions and recommendations [AD-724882] 20 p3210 N71-33278
- Computer simulation of aircraft collision-hazard warning radar techniques in terminal area 21 p3394 N71-34170
- Effects of plasma compressibility, collision frequency, and sheath on antenna current, input impedance, and maximum driving voltage 23 p3832 N71-37331

COLLOCATION

- Mathematical model for acoustic radiation from free-flooding ring transducers [AD-710745] 01 p0090 N71-10551
- Box collocation method for calculating aerodynamic loads on tandem delta wings with oscillation in supersonic flow 17 p2686 N71-29537
- Boundary collocation for two dimensional stress analysis of cracks emanating from or from near holes with various shapes [NASA-TN-D-5376] 19 p3189 N71-32306
- COLLOIDAL GENERATORS
- Analysis of insulating properties of alkali metallic colloids and problem of charge generation by contact ionization [AD-721197] 13 p2368 N71-26896
- Steady state ice nuclei generator for field application 22 p3609 N71-35707
- Ice nuclei generators suitable for cloud seeding 22 p3611 N71-35723

COLLOIDAL PROPELLANTS

- Problems encountered when electrostatic colloid propulsion integrated with operational spacecraft [AD-721114] 02 p0296 N71-11896
- Development of colloid thruster system with array of emitters [NASA-CR-111417] 02 p0291 N71-12076
- Liquid hydrogen propellant containing hydrocarbon colloids for nuclear propulsion systems [NASA-CR-115918] 04 p0562 N71-14417
- Vacuum chamber tests on silt and liquid propellant of colloid rocket engine for propulsion system performance [E8RO-CR-23] 12 p1989 N71-23707
- Research in optimization of performance, and performance characteristics of annular silt colloid thruster [NASA-TN-D-7001] 12 p1990 N71-23925
- Electrostatic microthruster propulsion system with annular silt colloid thruster [NASA-CASE-GSC-10709-1] 13 p2156 N71-25213

COLLOIDING

- Collection efficiency of water droplets freely falling through oiler chloride aerosol determined by light scattering [NYO-3847-2] 17 p2798 N71-30015

COLLOIDS

- NT AEROSOLS
- NT COLLOIDAL PROPELLANTS
- NT FOG
- Synergistic effect of detergent and antioxidant additives during colloidal dissolution [AD-711152] 01 p0072 N71-10597
- Ester emulsion analysis and colloidal molecular weight determination by gel chromatography 03 p0330 N71-12353
- Equation of state and static correlations for ferro-magnetic colloid [AD-722713] 17 p2789 N71-30210
- Colloid core nuclear rocket engine concept [AD-724139] 20 p3301 N71-32919

COLOR

- Electrical properties of quartz as related to impurities and electrolytic coloring 02 p0287 N71-12008
- Visual effects from moving achromatizing lens in front of eye while viewing achromatic pattern [AD-710877] 12 p1865 N71-23394
- Beam penetration cathode ray tube for high performance color display systems 12 p1089 N71-23549
- Mean global distributions of Soviet sea water transparency measurements and Ford-Uls water color codes including seasonal variations for Sea of Japan and Indian Ocean 12 p1910 N71-23592
- Design, fabrication, and evaluation of three-color plasma-panel display device and multiple intensity operating techniques [AD-713668] 12 p1890 N71-23612
- Effects of acid end groups and structural anomalies on thermal coloration of polyacrylonitrile [RAE-LIB-TRANS-1095] 13 p3041 N71-25138
- Psychophysiological stimulation of humans, monkeys and rats by color schemes for spacecraft cabin interiors 16 p2550 N71-28239

- Relationship between albedo of water surface of small lakes and chrominance and transparency of water mass [NLL-M-9264-3828-4F/1] 16 p2591 N71-29173
- Twilight glow and twilight sky color determinations from Soyuz 5 spectrophotometry and photography [NASA-TT-F-13082] 18 p2916 N71-31084
- Effect of sequentially changing background color during target detection 19 p3054 N71-32325
- Color and luminance effects on visual space perception [AD-72572] 20 p3236 N71-33158
- Development of plasma panel display device having three color capability and three levels of intensity [AD-725983] 21 p3403 N71-34217
- Computerized pseudocolor transformations from black and white to chromatic images with density separations [R-767-NIR] 23 p3730 N71-36588

COLOR MATERIALS

U COLOR VISION

COLOR CENTERS

- Vibronic absorption and emission spectra of F centers in calcium oxide 11 p1818 N71-22598
- F to M center conversion and equilibrium in X ray irradiated KCl crystals 11 p1810 N71-23002
- Color centers and magnesium oxide crystal defects from proton irradiation and impurities [NASA-CR-118965] 16 p2642 N71-29044
- Individual dynamic properties of off-center ions in crystal lattices and electron phonon interaction effects [AD-728399] 17 p2828 N71-36075
- Effect of electric field and temperature on relative lifetimes of excited F center in KCl, KF, and NaF [NYO-3463-23] 18 p2996 N71-31568
- Heat treatment and irradiation effects on rare earth ions in crystal color centers 19 p3168 N71-31988
- Spectral sensitivity and dominance of color center cones in macaque monkeys based on flicker electroretinography [IEF-1971-10] 20 p3225 N71-33823
- F2 color center formation in potassium chloride crystals irradiated with near ultraviolet radiation [TT-70-57054] 20 p3355 N71-33845
- Use of F centers in potassium iodide as crystal for selective absorption optically pumped maser [AD-726760] 23 p3591 N71-35574
- Platinum-free laser glass development, radiation centers in borate glasses, local order in liquid chalcogenides, and chalcogenide glass bolometers for infrared and microwave detection [AD-726416] 22 p3602 N71-35657
- Color center and substitutional impurity point defects in magnesium, calcium, and strontium oxide insulators [AD-726647] 23 p3835 N71-37351

COLOR PERCEPTION

U COLOR VISION

COLOR PHOTOGRAPHY

- Reflectometers for color aerial photography [AD-710978] 01 p0256 N71-10745
- Infrared and color photography for water inlet survey in Alaska 02 p0205 N71-11153
- Aerial synoptic sensing by infrared imagery and color photography of lake areas in Florida 02 p0206 N71-11155
- Remote airborne measurements of ocean color 02 p0208 N71-11167
- Aerial multispectral sensing test on submerged body in ocean 02 p0208 N71-11168
- Multispectral additive color viewing devices for earth resources applications 02 p0227 N71-11988
- Color aerial photography of Douglas fir forest with color density 02 p0221 N71-12164
- Pseudocolor image enhancement by two-separation photographic process [AD-712658] 03 p0381 N71-13163
- Creating color preservation in photographic emulsion by alternating dark and light layers within and parallel to emulsion 05 p0684 N71-14871
- Aerial color photography for detecting stressed forest vegetation 05 p0677 N71-15882
- Plant and soil signatures extracted by spectrophotometric analysis of Apollo 6 and earth resource survey aircraft color photography 06 p0845 N71-16149
- Computer produced microfilm in pseudocolor transformations [AD-713901] 06 p0859 N71-16291
- Color photointerpretation of interference colors reflected from thin film oil-coated components in service maps for gas flow visualization [NASA-CASE-XMP-91779] 10 p1539 N71-20015

SUBJECT INDEX

- Correlating color photography of Apollo 7 was natural color of surface deposits and roots of Lake Titicaca, Chile 14 p2351 N71-30409
- Quantitative evaluation of multiband photographic techniques using combination of black and white and color photos [NASA-CR-115955] 17 p2751 N71-30017
- Oceanographic pictures from Gemini and Apollo 9 sun color photography enhanced by photographic means producing false color outlines of small changes in density [AD-723682] 17 p2743 N71-30009
- Computer graphic mapping of Maryland coast from aerial color and infrared photographic remote sensing including microdensitometer analysis [RLM-388] 17 p2549 N71-30016
- Color photogrammetry for Nimbus infrared satellite data analysis [NASA-TM-X-65614] 18 p3049 N71-30016
- High speed photographic techniques to study impinging streams of propellants in experimental visualization of reactive stream separation [NASA-CR-119346] 18 p2923 N71-30044
- Rotational and vibration effects in ion dipole cells demonstrated in color motion picture [NASA-TM-X-67678] 16 p2983 N71-31196
- Time lapse photographic techniques for recording seasonal contrasts in eastern Mojave Desert [AD-722738] 19 p3127 N71-30016
- Evaluation of enhancement of light intensity (fluorescence) on color aerial photographs and thermal infrared imagery [NASA-CR-121408] 20 p3260 N71-31089
- Photoreproduction of aerial color infrared photography for analysis of urban land use [NASA-CR-121652] 21 p3424 N71-34009
- Graphical method for deriving day-layer densities of color infrared image elements from known reflectance curves, and analysis of CIR photography film spectral windows [NASA-CR-121650] 21 p3424 N71-34009
- Range measurement in color infrared aerial photography and phenology of vegetation [PB-197226] 21 p3429 N71-34009
- Geological uses of earth-orbital photography with case histories [NASA-TM-X-65682] 22 p3583 N71-35596
- Multicolor photography for investigating infrared and ultraviolet radiation excesses of young jet clusters containing T Tauri stars 22 p3669 N71-36148
- COLOR TELEVISION
- Color design for SECAM color television system and stereotelevision system using time parallel [JPRS-51782] 02 p0183 N71-11097
- Selecting color design for SECAM color television system 02 p0183 N71-11097
- Optimum phosphor phosphor filter pair for FM transmission of Laser Communications Relay Unit color television [NASA-CR-108676] 02 p0183 N71-11097
- Magnitude of frequency division in SECAM system on parameter determining quality of reproduced color image [JPRS-51918] 04 p0268 N71-14008
- Possibility of utilizing color cathode ray tubes for aircraft ground vision displays [AD-716555] 11 p1673 N71-32318
- Color television graph plotter for use with PDP-9 digital computers [NASA-CR-118015] 12 p1883 N71-23008
- Color television system utilizing single gun camera sensitive color cathode ray tube [NASA-CASE-ERC-10090] 16 p2570 N71-29880
- Methods of estimating tolerance errors in color television transmission systems [BBC-1971/21] 20 p3257 N71-30009
- Mathematical model of color television display for assessment of random noise [BBC-1971/22] 23 p3725 N71-30018
- COLOR VISION
- Color vision of dichromatic in humans [PB-196467] 02 p0466 N71-11110
- Color and subjective distance [AD-712804] 03 p0321 N71-12008
- Statistical analysis of structure of color vision test for standardization of test methods and procedures [IEF-1970-17] 05 p0733 N71-15889
- Sound and visual sensory interrelations of pitch, loudness, and hue sound with red, green, and blue light against white standards 11 p1089 N71-23549
- Achromatic pattern recognition model for processing chromatic objects [AD-722853] 17 p2712 N71-30009
- Correlation of color blindness tests with ability to recognize variation color signal light flashes [FAA-AIR-71-27] 22 p3543 N71-30009
- Development of computer program for calculation color coordination and color differences for color matching [FOA-3-C-2386-51] 22 p3439 N71-30009

SUBJECT INDEX

- Tests of color defective vision in predicting performance under day and night conditions
[FAA-AM-71-32] 23 p3716 N71-36489
- COLORADO**
Comparison of ozone observations at Switzerland and Colorado
[LAPATH-1] 02 p2315 N71-11956
Statistical results of winter orographic cloud seeding experiment over Park Range barrier in Colorado
[R-192768] 02 p2060 N71-12125
Air pollution and soiling index for Denver, 1968
[W-197460] 06 p0835 N71-16657
Studying crop-hall insurance records for northeastern Colorado for designing hail experiment
[W-197644] 18 p2955 N71-31444
Transmission loss data tabulations based on propagation experiments in 230 to 9200 MHz frequency range over irregular terrain in Colorado
[NSA-TR-BRL-45-ITS-58-3 FT-3] 19 p3057 N71-32480
Snow cover and moisture content data from survey of mountains in Colorado and New Mexico, Jan. - Jun. 1971
24 p3911 N71-37881
Hydrologic forecasting of snow melt runoff from mountain cover in central Colorado
[NSA-FSRP-RM-66] 24 p3953 N71-38304
- COLORADO**
U COLOR
COLORIMETRY
Automatic colorimetric determination of nitrogen in low weight solid samples
[BWIC/73] 05 p0639 N71-14710
Chemical analysis techniques for metals, alloys, and other materials
[AD-713977] 06 p0810 N71-16275
Fluorimetric gas analysis methods and equipment
11 p1761 N71-22057
Reduction oxidation reactions for colorimetric analysis of atmospheric toxicity
11 p1695 N71-22061
Color indices for stellar spectrophotometry of Coudé variable and supergiant stars
[NASA-TM-X-65343] 14 p2336 N71-25948
Performance and colorimetry standards for glass optical filters used in air, railroad, and highway traffic signal control systems
[NBS-TN-564] 17 p2770 N71-30095
Determination of alpha-tocopherol in freeze dried feeds by modified colorimetric procedure
[AD-713829] 19 p3041 N71-31610
Effect of interfering substances on performance of Satchi iodine colorimeter
[NASA-CR-115155] 22 p3550 N71-35284
Development of computer program for calculating color coordinates and color differences from colorimeter values
[FOA-2-C-286-51] 22 p3629 N71-35838
- COLUMBIUM**
U NIOBIUM
COLUMBIUM (PROCESS ENGINEERING)
Design and performance of automatic sequential chromatographic apparatus for purification of lipid extracts
[UCRL-30861] 01 p0011 N71-10480
Feasibility of extractive fractional distillation as separation method for volatile rare earth complexes
[AD-712876] 03 p0331 N71-12364
Column method of counterflow crystallization of alky in molten state
10 p1573 N71-20868
- COLUMNS (SUPPORTS)**
NT TAPERED COLUMNS
Parametric study of uniformly loaded annular slabs supported between edges with equally spaced columns
[NIST-292] 02 p0301 N71-12012
Bending solution of full circular plates supported on two steps of equally spaced columns
[NIST-291] 02 p0301 N71-12013
Bending solutions of uniformly loaded annular plates supported by columns on one boundary with other boundary simply supported
[NIST-297] 02 p0301 N71-12014
Analysis of static behavior in long rectangular plates supported by three parallel rows of equidistant columns
[NIST-285] 02 p0301 N71-12019
Relation for bending of overhanging circular plates supported on columns
[NIST-288] 02 p0301 N71-12020
Bending of circular plates supported on equally spaced columns under eccentric concentrated load
[NIST-286] 02 p0302 N71-12029
Annular slab supported on columns along inner boundary and fixed at outer boundary
[NIST-293] 02 p0303 N71-12094
Effect of eccentric load forces and different stress-strain relationships on stiffness of columns
03 p0466 N71-13350
Stress strains in beam to column connections
[AD-714777] 06 p0955 N71-16455
Link, elastic-plastic, and stability analysis of biaxially loaded columns
06 p0955 N71-16456

- Nonlinear Euler buckling model for slender columns
[AD-713997] 06 p0955 N71-16458
Behavior of structural subassemblies with laterally unsupported columns
[AD-714516] 06 p0957 N71-16849
Systems analysis of nonlinear rigid columns with 6 degrees of freedom for electronic equipment protection from underground nuclear explosion ground shocks
[UCRL-50973] 16 p2682 N71-28648
Buckling and column failure interaction of thin walled compression members due to flange asymmetry
[VTH-160] 17 p2851 N71-29486
Local and overall buckling interactions in relation to structural failure in built-up columns
[WTHD-23] 21 p3528 N71-35139
- COMBAT**
Simulation of aerial combat
[RAE-LIB-TRANS-1367] 03 p0787 N71-15372
- COMBINATORIAL ANALYSIS**
NT BINOMIAL COEFFICIENTS
NT FACTORIALS
NT PARTITIONS (MATHEMATICS)
NT PERMUTATIONS
Investigating nonstationary automatic control systems and construction of asymmetrical coding systems connected with solution of combinatorial Dixon problem
[JPRS-51830] 04 p0513 N71-13542
Proving Haswood conjecture for nonorientable surfaces
[AD-712714] 04 p0537 N71-13807
Aliasing schemes and construction of fractional replicates
[AD-715696] 05 p0714 N71-15279
Results on redundancy and testability of combinatorial logic networks
[AD-714157] 06 p0827 N71-16457
Apparatus for computing square roots
[NASA-CASE-XGS-84768] 09 p1352 N71-19437
Large scale integration microelectronic wafer and package testing including parametric and functional tests of combinatorial and sequential logic circuits
[NASA-CR-103166] 14 p2336 N71-26704
Treating coding problem as critical problem in combinatorial geometry
[AD-722080] 16 p2622 N71-28199
Combinatorial coding for discrete stationary sources
20 p3290 N71-32946
- COMBINED STRESS**
Wall motions in circular thin-walled cylindrical shells under combined loading
08 p1301 N71-19282
Reliability factors in rotary machine steel shaft design including materials fatigue, combined stress, and strain rates
[AD-716071] 09 p1477 N71-20029
- COMBUSTIBILITY**
U FLAMMABILITY
COMBUSTIBLE FLOW
Photographic recording and analysis of detonation waves produced by nitromethane-acetone mixes
[UCRL-72160] 09 p1485 N71-20525
Examination of two dimensional combustion flow field upstream of inert and chemically reactive transverse jets
[DI-82-1066] 19 p3079 N71-32264
- COMBUSTION**
NT AFTERBURNING
NT BOUNDARY LAYER COMBUSTION
NT DEFLAGRATION
NT FUEL COMBUSTION
NT HYPERSONIC COMBUSTION
NT METAL COMBUSTION
NT PROPELLANT COMBUSTION
NT SOLID PROPELLANT IGNITION
NT SPONTANEOUS COMBUSTION
NT SUPERSONIC COMBUSTION
Turbulence and stirred reactor concepts of combustion
[AD-710231] 01 p0132 N71-10187
Combustion of boron particles at elevated pressures
[AD-710747] 01 p0133 N71-10548
Composition distribution and equivalent body shape for reacting, coaxial, supersonic hydrogen air flow
[NASA-TN-D-6123] 05 p0783 N71-15639
Nonequilibrium excitation origin in sodium atoms, hydroxyl radicals, or water molecules occurring behind hydrogen-oxygen or acetylene-oxygen combustion shock waves
[NASA-TT-F-15622] 12 p1949 N71-23264
Interdependence of combustion processes and physical-mechanical behavior of solid fuel materials for rocket engines
[AD-720834] 14 p2353 N71-25952
Tritium determination in metals derived by burning trinitrated water sample in sealed quartz tube filled with oxygen and heated to high temperature
06 p0955 N71-16455
Factors affecting combustion of small vertically oriented cellular cylinders of circular cross section
18 p3026 N71-31346

COMBUSTION CHAMBERS

- Deficiencies in combustion technology, and 5 year research and development plan for air pollution control by combustion process modification
[PB-190666] 19 p3192 N71-31908
Augmenting combustion flames with electric discharges to produce high temperature chemical and physical reactions in 2500 to 3000 K range
[BCRC/N327] 23 p3866 N71-37562
Supersonic combustion chemistry and mixing of high energy density fuels related to advanced air-breathing engine design, using boron particles
[AD-727022] 24 p4000 N71-38330
- COMBUSTION CHAMBERS**
Turbulence and stirred reactor concepts of combustion
[AD-710521] 01 p0132 N71-10187
Film vaporizing combustor for gas turbines
[NASA-TT-F-15272] 01 p0115 N71-10382
Comprehensive analysis of liquid rocket combustion
[AD-710634] 01 p0133 N71-10437
Sweep frequency nozzle pressure oscillation effects on turbulent combustion dynamics
[NASA-TN-D-6064] 01 p0117 N71-10982
Swirl-can modular turbojet combustor burning natural gas fuel
[NASA-TN-D-7020] 03 p0448 N71-12421
Shortening transition liner to decrease overall length of ram induction combustor
[NASA-TN-D-7021] 03 p0448 N71-12422
Feasibility of measuring chamber temperature of solid propellant rocket motors using microwave attenuation measurements
[AD-715703] 03 p0447 N71-13375
Upgrading computer program for determining nozzle admittance to eliminate double-root solution and to fit resultant admittance data curves by statistical means
[NASA-CR-102830] 04 p0567 N71-14213
Convective heat transfer in steady uniform air flow between parallel plates, and organ pipe combustion oscillations of premixed gases in variable length combustor
05 p0661 N71-14769
Performance of short modular turbojet combustor segment with ASTM-A1 fuel
[NASA-TN-D-6167] 07 p1022 N71-17414
Jet engine combustion chamber burn-through fire and methods for controlling damage
[FAA-RD-70-68] 07 p1022 N71-17483
Effect of fuel distribution and flame stabilization techniques on combustion stability limits for swirl-can combustor modules
[NASA-TM-X-2185] 07 p1103 N71-17724
Effect of multiple length on combustor stability in ramjet combustors
07 p1103 N71-17725
Combustion stability limits for swirl-jet combustor modules combining air swirl and impinging jet atomization of ASTM A-1 fuel
[NASA-TM-X-2218] 08 p1284 N71-18580
Effect of various diffuser designs on performance of experimental turbojet combustor insensitive to radial distortion of inlet airflow
[NASA-TM-X-2216] 08 p1303 N71-18561
Annular diffuser and combustor assembly in full scale direct burner for supersonic turbine engine
[NASA-TN-D-6163] 08 p1304 N71-18882
Performance tests and characteristics of short length, double annular ram induction turbojet combustion chambers for supersonic flight
[NASA-TN-D-6254] 09 p1439 N71-20291
Combustion characteristics of turbojet combustion chambers with variations of inlet air pressure, temperature, and velocity
[NAL-TR-204] 09 p1439 N71-20247
Conversion of experimental turbojet combustor from ASTM A-1 fuel to natural gas fuel
[NASA-TM-X-2241] 09 p1466 N71-20333
Rocket combustion chamber stability by controlling transverse instability during prestart combustion
[NASA-CASE-XLB-04683] 10 p1663 N71-21507
Simulation of supersonic ramjet combustion chamber in shock tunnel
11 p1740 N71-22630
Differential equations and numerical analysis of combustion chambers similar to cylindrical shells using special boundary conditions
[JCT-1408] 12 p2084 N71-23495
Determination of combustion stability limits with hydrogen-oxygen combustor of variable length
[NASA-TN-D-6328] 12 p2081 N71-23713
Regenerative cooling system for rocket combustion chamber using coolant tubes in convergent-divergent nozzle
[NASA-CASE-XLB-04857] 12 p1991 N71-23048
Rocket engine injector orifice to accommodate changes in density, velocity, and pressure, thereby maintaining constant mass flow rate of propellant into rocket combustion chamber
[NASA-CASE-XLB-03157] 13 p2156 N71-24736
Calculation of wall temperature in presence of chemical reactions by considering heat transfer

- between thermally dissociated gaseous oxidant and cooling fluid
[AD-719785] 13 p2186 N71-24971
- Sampling point decrease effects on computed annular combustor parameters and exhaust nozzle temperature profile analysis of thermocouple location
[NASA-TN-D-6352] 14 p2351 N71-25683
- Aircraft gas turbine combustion chamber design
[NAL-TR-208] 14 p2352 N71-26298
- High frequency pressure variations in internal rocket engine probes for combustion instability environment
14 p2256 N71-26365
- Gas turbine combustor liner film cooling for slot geometries in presence of high free stream turbulence
[NASA-TN-D-6360] 17 p2353 N71-26941
- Velocity profile control tests of diffuser wall bleed to control combustor inlet airflow distribution
[NASA-TN-D-6435] 18 p3000 N71-30817
- Use of air-assist fuel nozzle to reduce exhaust emissions from a gas turbine combustor at simulated life conditions - J-57 engine
[NASA-TN-D-6404] 18 p3002 N71-31456
- Computerized simulation and analysis of combustion chamber length instability for solid rocket propellant and effects of burning rate
[AD-725488] 19 p3171 N71-31801
- Operational methods for control of air pollution emissions from aircraft turbine engine combustor
[NASA-TN-X-67887] 19 p3174 N71-32484
- Cold weather tests to determine effectiveness of resonant combustor as power source for starting aircraft engines
[AD-724125] 20 p3338 N71-32804
- Stabilizing influence of acoustic cavities on acoustic modes of combustion instability in rocket engines
[NASA-TN-D-15087] 20 p3363 N71-32897
- Modified wind tunnel tests of supersonic combustion chamber for hydrogen burning ramjet
[TP-924] 20 p3340 N71-33841
- Low cost, lightweight ignition system for hydrogen oxygen engine system incorporating multicomponent thrust chambers
[NASA-CR-119928] 21 p3530 N71-35152
- Primary and secondary mixing performance of combustors under high inlet air pressures
[NASA-TN-D-6491] 22 p3463 N71-36119
- Design, characteristics, and test firing of radiation and film cooled 25 pound thrust graphic thrust chamber with liquid cryogenic propellant
[NASA-CR-72855] 24 p4000 N71-38534
- Textbook on combustion chambers of gas turbine engines
[AD-727960] 24 p4002 N71-38542
- Mathematical solution of nonlinear transverse combustion instability problems in thin annular liquid propellant rocket chambers
[NASA-CR-120781] 24 p4025 N71-38746
- Ablation cooling in rocket engine with combustion chamber liner and nozzle constructed of silica phenolic ablative material
[NASA-CR-120798] 24 p4029 N71-38749
- Variational-iterational technique for predicting wave motion and instability frequencies in baffled combustion chambers
[NASA-CR-72879] 24 p4029 N71-38750
- Combustion efficiency and performance of swirl can modules under conditions simulating operation of 10,000 pound thrust lift engine for vertical takeoff
[NASA-TN-D-6542] 24 p4032 N71-38767
- COMBUSTION CONTROL**
- Developing experimental information and analytical methods for design and safety analysis of sodium cooled fast reactors
[AI-ABC-12970] 04 p0554 N71-14017
- Pressurized gas injection for burning rate control of solid propellants
[NASA-CASE-XLE-03494] 10 p1638 N71-21819
- Controlled-flow igniter for low thrust burning rate of solid propellant rocket engine
11 p1819 N71-22556
- Solid propellant rocket motor with igniter operating in vacuum and maintaining burning of propellant below normal combustion limit
[NASA-CASE-NPO-11559] 21 p3502 N71-34049
- COMBUSTION EFFICIENCY**
- Combustion kinetics of particulate boron
[AD-713121] 05 p0781 N71-14506
- Combustion efficiency of hydrocarbon fuels with ammonium nitrate propellant additive and solidified oxygen and fluorine gas oxidizers
[BMW-FB-W-70-47] 07 p1098 N71-17227
- Effects of engine design and propulsion system configurations on combustion efficiency
09 p1457 N71-19455
- Throttling and heat sterilization effects on hydrazine reactor efficiency and bottle geometry for combustion chamber stability
10 p1639 N71-21858
- Qualitative selection of combustion additives for fuel oil efficiency
[NLL-CR-TRANS-5408-9802.09] 10 p1638 N71-21856
- Gas-air mixture requirements for turbine and injection burner combustion efficiencies
[AD-719354] 13 p2187 N71-25399
- Development and testing of ablative rocket engine with selected 7.62 cm (3.0 in.) diameter throat inserts, and testing of titanium-reinforced with tungsten-rhenium wire for throat insert material
[NASA-TM-X-2315] 17 p2839 N71-29921
- Preliminary sector tests at 920 K of three afterburner concepts proposed for inlet temperatures of 1260 F and comparison of results with conventional V-gutter flame holder
[NASA-TN-D-6457] 19 p3192 N71-32191
- Hybrid and decomposition combustion of hydrazine fuels using flat flame burner to provide high temperature gaseous environment for burning drops of liquid fuel
[NASA-CR-72977] 22 p3695 N71-36352
- Thermal decomposition and combustion of explosive substances - handbook
[AD-726573] 23 p3867 N71-37565
- Projects and techniques including mass spectrometry, gas chromatography, combustion carbon analysis, atomic absorption spectrophotometry, and related analytical chemistry methods
[UCRL-50086-71] 24 p3885 N71-37693
- Combustion efficiency and performance of swirl can modules under conditions simulating operation of 10,000 pound thrust lift engine for vertical takeoff
[NASA-TN-D-6542] 24 p4032 N71-38767
- COMBUSTION HEAT**
- U HEAT OF COMBUSTION**
- COMBUSTION INSTABILITY**
- U COMBUSTION STABILITY**
- COMBUSTION PHYSICS**
- Velocity profiles for subsonic turbulent boundary layer with mass addition, combustion, and pressure gradients
[AD-710308] 01 p0132 N71-10169
- Combustion characteristics and safety factors for hydrogen-diffusion flames in flare stack operations
[NASA-CR-114141] 02 p0506 N71-12103
- User manual for computer programs to determine high frequency instability in baffled annular liquid propellant rocket engines - Vol. 2
[NASA-CR-115871] 05 p0760 N71-14630
- High frequency nonlinear combustion instability in baffled annular liquid propellant rocket engines - Vol. 1
[NASA-CR-115872] 05 p0760 N71-14631
- Combustion kinetics of tetrafluoroethylene
[AD-713144] 05 p0784 N71-15396
- Combustion and physical properties of hydrocarbons
[AD-714674] 06 p0958 N71-16043
- Project SQUID research in fluid mechanics, chemical reactions, and combustion physics
[AD-714236] 06 p0836 N71-16398
- Characteristics of unsteady liquid rocket propellant combustion processes
[NASA-CR-116245] 06 p0941 N71-16716
- Combustion chemistry and mixing in supersonic flow
[AD-714109] 06 p0961 N71-16886
- Performance of short modular turbojet combustor segment with ASTM-A1 fuel
[NASA-TN-D-6167] 07 p1102 N71-17414
- Effect of fuel distribution and flame stabilization techniques on combustion stability limits for swirl-can combustor modules
[NASA-TM-X-2185] 07 p1103 N71-17724
- Mathematical models for ammonium perchlorate combustion and composite propellant burning rate mechanism
07 p1098 N71-18066
- Combustion stability limits for swirl-jet combustor modules combining air swirl and impinging jet atomization of ASTM-A1 fuel
[NASA-TM-X-2218] 08 p1284 N71-18560
- Combustion characteristics of turbojet combustion chambers with variations of inlet air pressure, temperature, and velocity
[NAL-TR-204] 09 p1459 N71-20347
- Combustion of large magnesium particles during pressure change in ambient medium within range from 100 to 760 mm Hg
[NASA-TT-F-13503] 09 p1485 N71-20531
- Experimental and theoretical results of critical pressure burning of fuel droplets
[NASA-CR-72834] 09 p1485 N71-20532
- Nondestructive testing of solid, low pressure combustion of metal propellants, and laser beam detection
10 p1637 N71-21355
- Interaction between shockwaves and burning or nonburning fuel droplets in pure oxygen
11 p1740 N71-22631
- Computer program for equilibrium equations, combustion temperature, and combustion efficiency of explosive and propellant combustions
[ICT-370] 12 p3010 N71-23357
- Theoretical and experimental analysis of flame spreading across pools of liquid fuels and ignitability under quiescent and flowing environments
[AD-718864] 12 p3010 N71-23492
- Determination of combustion stability limits with hydrogen-oxygen combustor of variable length
[NASA-TN-D-6328] 12 p2011 N71-23711
- Combustion physics and ignition of hydrogen in a person stream of vitiated air or inert gases with stopped swirl injection procedure
[NASA-TM-X-67840] 13 p2188 N71-25399
- Combustion physics of gas jet in turbulent water to bind stabilizer
[AD-721026] 13 p2525 N71-27070
- Characteristics of detonation phenomenon in heterogeneous system of decane droplets in oxygen-methane
16 p2690 N71-28071
- Prediction of combustion temperature, product species, and air specific impulse values as function of total equivalence ratio for slurry fueled propulsion systems
[AD-721665] 16 p2671 N71-28072
- Combustion mechanism of composite propellant during desiccation
[AD-722084] 16 p2670 N71-28073
- Characteristics of combustion of premixed gases in stagnation flow condition
16 p2692 N71-28074
- Determination of ignition temperature, ignition delay times of various combustible mixtures, and the effect of gas flow on ignition process
16 p2692 N71-28075
- Numerical analysis and development of model for effect of ignition energy and coupling of reaction kinetics with shock front
16 p2692 N71-28076
- Analysis of mechanisms of energy addition from propellant spray combustion to steady flow fields and pressure disturbance
[AD-722473] 17 p2838 N71-32897
- Mathematical models of nonlinear combustion instabilities in liquid propellant rocket engine
[NASA-CR-119182] 17 p2860 N71-34048
- Pyrometric temperature measurements on silica decomposition products during combustion of silica reinforced plastics
[TP-962] 20 p3365 N71-35146
- Combustion dynamics of air/methane supersonic diffusion flame in duct
[TP-961] 20 p3365 N71-35149
- Momentum loss and heat transfer in deflagrant propane jet flow during combustion
20 p3251 N71-33578
- Mathematical models for computer calculations of two dimensional hydrodynamic nonlinear combustion instability flow
[NASA-CR-121472] 20 p3365 N71-35177
- Numerical analysis of energy release rates during combustion caused by periodic flow field disturbances
[NASA-TM-X-67892] 20 p3365 N71-35177
- Analysis of metal combustion using isolated aluminum particles ignited by laser and burning in controlled mixture of oxygen and argon
20 p3366 N71-35178
- Injection, mixing, and chemical reactions of modified slurry fuels in high speed air stream to determine ignition and combustion properties
[AD-726639] 22 p3662 N71-36110
- Numerical analysis of effects of transient response in catalytic ignition system to promote hydrogen-oxygen combustion
[NASA-CR-120799] 23 p3865 N71-37575
- Selected articles on kinetics and aerodynamics of diffusive combustion
[AD-726575] 23 p3866 N71-37574
- Analysis of burning stability conditions in free jet flames and influence of turbulence and intermittency
[NLL-M-20389-5828.4F] 23 p3868 N71-37576
- Analysis of fundamental combustion characteristics of polymers contained in solid rocket propellants using diffusion flame technique
[AD-727990] 24 p4000 N71-38023
- Operation of liquid propellant rocket engines with nonstationary conditions and derivation of formula for determination of combustion delay
[AD-727969] 24 p4001 N71-38024
- COMBUSTION PRODUCTS**
- Air pollution, and condensation nuclei measurement in Rome
[IPA-TR-28] 03 p0404 N71-13170
- Air pollution problems in California and methods for air quality forecasting
[PB-194128] 04 p0475 N71-14023
- Development of methods for analyzing rates of sulfur dioxide and sulfur trioxide in jet exhaust streams
[AD-713222] 05 p0638 N71-14088
- Contamination free separation and eliminating combustion products from ambient surroundings generated by solid firing
[NASA-CASE-XGS-01971] 06 p0863 N71-19102
- Spectroscopic measurements of properties of combustion products in ramjet burner employing benzene loaded catalyst in primary rocket
[AD-716331] 09 p1483 N71-20531
- Radioactive-convective heat transfer of high temperature flow of gas in channel
10 p1660 N71-28077

SUBJECT INDEX

Normal or oblique plane detonation waves producing combustion products in supersonic flow [ABC-RM-3636] 10 p1661 N71-29398
 Carburization effects of simulated jet turbine exhaust products on nickel and chromium turbine stator blades [ARL/ME-319] 12 p1948 N71-34999
 Diffusion in combustion technology, and 5 year research and development plan for air pollution control by combustion process modification [PB-19896] 19 p1512 N71-31900
 Survey of air pollution by Federal facilities in Milwaukee air control region 22 p3577 N71-35482
 Thermal and dynamic properties of combustion products from various gases and heat transfer to flat plates from high-temperature combustion product jets [NLL-RTS-6531] 22 p3697 N71-36368
 Temperature and oxygen percentage effects on liquid sodium combustion and X ray analysis of combustion products [NLL-RTS-TRANS-2115-19691.9F1] 23 p3588 N71-37374
COMBUSTION STABILITY
W FLAME STABILITY
 Parametric study of rocket motor combustion instability [AD-710312] 01 p0115 N71-10123
 Gas dynamic stability and damping of detonation waves in aerosols [AD-711753] 01 p0044 N71-10943
 Guidelines for designing combustion stability control devices [NASA-CR-111405] 02 p0290 N71-11884
 Computer program for determining combustion stability limits of bipropellant rocket engine [NASA-TN-D-7026] 04 p0605 N71-14038
 User manual for computer programs to determine high frequency instability in buffed annular liquid propellant rocket engine - Vol. 2 [NASA-CR-115871] 05 p0760 N71-14630
 High frequency nonlinear combustion instability in buffed annular liquid propellant rocket engine - Vol. 1 [NASA-CR-115872] 05 p0760 N71-14631
 Convective heat transfer in steady uniform air flow between parallel plates, and organ pipe combustion oscillations of premixed gases in variable length combustor 05 p0661 N71-14769
 Acoustic instability of burning in solid fuel rocket engines associated with reflections from burning surface [AD-719753] 05 p0761 N71-15321
 Field mechanics approach to acoustic liner design [NASA-CR-728077] 06 p0940 N71-16948
 Characteristics of unsteady liquid rocket propellant combustion processes 06 p0941 N71-16716
 Effect of fuel distribution and flame stabilization techniques on combustion stability limits for swirl-can combustor modules [NASA-TM-X-2185] 07 p1103 N71-17724
 Cause and effect of pressure oscillations at acoustic frequencies in solid propellant rocket engine and methods for inhibiting unstable combustion [NRC-100] 09 p1460 N71-20348
 Computerized stability design of time lag combustion system for liquid propellant rocket engine [NASA-CR-120096] 09 p1460 N71-20415
 Computer programs for determining combustion stability of liquid propellant rocket engines 09 p1460 N71-20416
 Computerized analysis of gas-tapeoff cycle stability with gaseous hydrogen and gaseous oxygen 09 p1578 N71-20417
 Time lag theory for longitudinal high frequency stability analysis on staged combustion cycles of liquid propellant rocket engines 09 p1460 N71-20418
 Transverse mode stability characteristics of coaxial and hyperbolic injectors in transverse excitation chamber [NASA-CR-117033] 09 p1460 N71-20500
 Combustion instability in liquid rocket engines [NASA-CR-728048] 10 p1662 N71-21316
 Rocket combustion chamber stability by controlling transverse instability during propellant combustion [NASA-CR-728049] 10 p1663 N71-21307
 Mathematical models for chemical thermodynamics of oscillatory combustion 11 p1844 N71-22708
 Project summary of research on combustion stability of solid rocket propellants [AD-710857] 12 p1908 N71-33617
 Determination of combustion stability limits with hydrogen-oxygen combustor of variable length [NASA-TN-D-4538] 12 p2011 N71-33713
 Approximate models for amplification by wave detection of dynamic response of vaporization limited combustion 12 p2013 N71-34243
 Damping devices for controlling combustion oscillations in rocket thrust chambers 17 p2835 N71-29581

Low frequency analysis of rocket engines using compressible propellants 17 p2835 N71-29584
 Suppression of acoustic modes of combustion instability in space shuttle engines by use of cavity resonators [BC-71-28] 17 p2837 N71-29601
 Computerized simulation and analysis of combustion chamber length instability for solid rocket propellant and effects of burning rate [AD-725690] 19 p3171 N71-31801
 Substituting influences of acoustic cavities on acoustic modes of combustion instability in rocket engines [NASA-CR-115067] 20 p3363 N71-32897
 Numerical analysis of energy release rates during combustion caused by periodic flow field disturbances [NASA-TM-X-67092] 20 p3365 N71-33617
 Analytical techniques for solving nonlinear combustion problems associated with liquid propellant rocket engines 21 p3501 N71-34941
 Mathematical solution of nonlinear transverse combustion instability problems in thin annular liquid propellant rocket chambers [NASA-CR-120781] 24 p4029 N71-38746
 Variational-functional techniques for predicting wave motion and instability frequencies in buffed combustion chambers [NASA-CR-72879] 24 p4029 N71-38750
COMBUSTION TEMPERATURE
 Catalytic surface effects on thermocouple combustion gas temperature measurements in jet engines 07 p1029 N71-17579
 Combustion chamber temperature measurement using sodium 4-line reversal [DLR-FB-70-70] 12 p2010 N71-23362
COMBUSTION WAVES
U FLAME PROPAGATION
COMBUSTION WIND TUNNELS
 Advanced jet engine combustor test facility [NASA-TN-D-6009] 01 p0057 N71-10069
 Test section of combustion wind tunnel for jet propulsion [DLR-MITT-71-48] 19 p3073 N71-31812
COMBUSTORS
U COMBUSTION CHAMBERS
COMETS
 Observations of formation of scattering agencies by solar wind in Comet Ikeya-Seki 03 p0451 N71-13096
 Infrared photography, mapping, and orbit calculation of natural satellites, comets, and planets in solar system [NASA-CR-115785] 04 p0609 N71-13589
 Photographing and measuring orbit of comet Beaster 1946k-1947 04 p0609 N71-13592
 Calculating orbital elements of comet Burnham-Slaughter 1958e-1959 04 p0610 N71-13594
 Calculating orbital elements of comet Hannuana 1960e-1959X 04 p0610 N71-13595
 Random distribution of radial moments in central gravitational field, Newtonian mechanics, and comet orbits about sun [NASA-TM-X-65414] 06 p0902 N71-15864
 Light distribution dependence along single EL line of comet as function of frequency and amplitude of applied voltage [AD-714631] 06 p0907 N71-16769
 Radio detection of mother molecules in comets using microwave lines [LA-4542] 06 p1287 N71-18338
 Comets, meteorites, lunar geology, cosmic rays, radiation measuring instruments, and data processing - conference [NASA-TT-F-630] 11 p1826 N71-22415
 Properties, photometry, and dynamic processes of comets, lunar morphology, and Tunguska meteorite blast 11 p1827 N71-22416
 Intensity of gas production in comets based on photometric parameters [NASA-TT-F-13492] 12 p1998 N71-24344
 Angular velocity evolution of solar system isolated planets, asteroids, and comets 13 p2167 N71-34994
 Solar electric propulsion performance and trajectory data for indirect solar probes, extra-solar missions, and rendezvous with Ceres, D-Arrest, and Echo [NASA-CR-118312] 13 p2167 N71-23043
 Calculating definitive orbit for Comet 1940A-1940V 14 p2338 N71-36310
 Calculating definitive orbit of Comet Neowin with consideration of planetary perturbations 14 p2338 N71-36311
 Development and characteristics of laboratory models to explain structure and composition of comet cores [LA-TN-70-27] 15 p2517 N71-36960
 Using 85-foot telescope to detect 22,235 MHz transition of H2O during appearance of Comet Bennett [NASA-TM-X-65536] 15 p2518 N71-37949

COMMAND MODULES

Range-Kutta analysis of hypothetical comet motion from Jovian surface, and possible origin of short-lived comets in Jovian surface eruptions [NASA-TT-F-13708] 20 p3348 N71-33406
 Characteristics and capabilities of solar electric propulsion for missions to Halley's comet due to return 1983-1986 21 p3386 N71-34992
 [NASA-CR-123099] 21 p3386 N71-34992
 Trajectory and propulsion characteristics of spacecraft rendezvous mission opportunities to comets during 1975 to 1995 [NASA-CR-121762] 22 p3666 N71-36148
 Computerized search for meteor streams in 3000 photographic meteor orbits, and association with other streams or comets 22 p3667 N71-36143
 Numerical analysis of three body problem and application to stability of captured comets with respect to various planets 22 p3672 N71-36184
 Electrically propelled spacecraft designs using thermionic reactors to electrical power sources investigated for Halley Comet rendezvous mission [NASA-CR-123028] 23 p3699 N71-37377
 Composition of planetary atmospheres and comets 23 p3696 N71-37413
 Gamma ray and neutron radiation of meteor streams in relation to antimeteor comet hypothesis 23 p3830 N71-37441
 Some comet and minor planet positions from plates taken with astrophysical telescope 23 p3836 N71-37487
 Comet characteristics and composition in relation to kinetics 24 p0089 N71-38583
 Sublimation of ice in connection with comet phenomena 24 p0089 N71-38584
 Focal image method for calibration in calculating characteristic curve for comets 24 p0089 N71-38585
 Comets as indicators of conditions in interplanetary space 24 p0089 N71-38586
 Comet luminosity variations and spectral properties in relation to interplanetary medium 24 p0089 N71-38587
 Comet and magnetosphere streamlining by solar wind 24 p0089 N71-38588
COMFORT
 Environmental tests of V/STOL vibration effects on human comfort [NASA-TM-X-68956] 09 p1333 N71-38036
COMMAND AND CONTROL
 Description of Air Force tactical air control and communications system 06 p0895 N71-16492
 Describing operations of Deep Space Network command system 07 p0893 N71-17623
 Prototype management decision system for planning and control [AD-715633] 08 p1306 N71-12664
 Fundamental processes, problems, and operations in control of space vehicle flight 08 p1290 N71-19320
 Automated command and control dispatch system for deployment of police units 19 p3052 N71-31630
 Formulation and development of analytical model based on queuing theory to improve concepts of military communication systems [AD-724340] 20 p3231 N71-32954
 Acquisition of data on federal R and D efforts related to command and control center design and low enforcement communications for civil disturbances [NASA-CR-121639] 21 p3389 N71-34112
 Multiple-mission command system for installation in DSH for command and control of spacecraft 21 p3395 N71-34147
 DSH command system operation from Space Flight Operations Facility supporting Mariner Mars 1971 mission 21 p3393 N71-34130
 Design, development, and operation of communications system for command and control of unmanned spacecraft during exploration of deep space [NASA-CR-121684] 22 p3533 N71-35004
COMMAND GUIDANCE
 Design criteria for guidance and control computer computer selection including physical and functional characteristics and reliability [NASA-SF-8070] 20 p3229 N71-33679
COMMAND MODULES
 Command module configuration and operation for Soviet spacecraft 05 p0770 N71-14062
 Analysis of command and service module configurations and recommendations to prevent failures which occurred on Apollo 13 flight 09 p1471 N71-19043
 Summary of actions taken by Apollo 13 spacecraft following explosion in oxygen tank [NASA-TM-X-68923] 09 p1466 N71-19970

COMMAND SERVICE MODULES

Atmospheric density models for 30 N latitude for January and July for use in entry studies of Skylab command module
[NASA-TM-X-59060] 15 p2520 N71-37950

PORTMAN 5 digital computer program for predicting dynamic response of Apollo command module to earth impact
[NASA-TN-D-65359] 23 p3730 N71-36389

COMMAND SERVICE MODULES

Analysis of anomalies, cause, and results of command service module oxygen tank failure on Apollo 13 flight
[NASA-TM-X-66922] 09 p1470 N71-19954

Analysis of command and service module configurations and recommendations to prevent failures which occurred on Apollo 13 flight
[NASA-TM-X-66932] 09 p1471 N71-19965

COMMAND SYSTEMS

U COMMAND GUIDANCE

COMMAND-CONTROL

U COMMAND AND CONTROL

COMMERCIAL

Characteristics and cost analysis of nuclear powered air cushion vehicles for oceanic commercial operations
[NASA-TM-X-2293] 14 p2293 N71-25783

Contributions and effects of commercial airline service on growth of manufacturing facilities in urban areas below 40,000 population
14 p2199 N71-26529

Contributions of oceanography toward alleviating problems affecting the United States Merchant Marine
18 p2911 N71-30985

Congressional testimony of nationally representative groups regarding U.S. conversion to metric system
[NBS-SP-345-12] 19 p1396 N71-32352

Growth rate of US air cargo markets - tables
24 p4036 N71-38794

COMMERCIAL AIRCRAFT

NT BOEING 707 AIRCRAFT

NT BOEING 727 AIRCRAFT

NT BOEING 747 AIRCRAFT

NT CV-440 AIRCRAFT

NT CV-990 AIRCRAFT

NT DC 3 AIRCRAFT

NT DC 8 AIRCRAFT

NT DC 9 AIRCRAFT

NT EUROPEAN AIRBUS

NT F-28 TRANSPORT AIRCRAFT

NT SE-210 AIRCRAFT

NT SUPERSONIC COMMERCIAL AIR TRANSPORT

NT TU-134 AIRCRAFT

NT VC-10 AIRCRAFT

FAA statistical handbook of aviation 1958-1968
01 p0003 N71-10372

Aircraft incident report and investigation of Air France Boeing 747, St. Jean, Canada, August 17, 1970
[NTSB-AAR-70-26] 01 p0004 N71-10531

Influence of gravel depth and tire inflation pressure on soft-ground arresting of civil aircraft
[RAE-TR-69001] 02 p0147 N71-11040

Legal aspects of air and surface carrier interactions in freight transportation
02 p0308 N71-12119

Possible benefits of local and trunk air carrier mergers
02 p0308 N71-12120

Automatic pilot system for landing commercial aircraft
03 p0406 N71-12440

Aeronautical climatological tables of international commercial airports
05 p0717 N71-15143

Survey of Huntsville pattern of commercial air traffic
[NASA-CR-115880] 05 p0788 N71-15553

Problems facing local air transport industry, communities, and government agencies
07 p1135 N71-18078

US commercial aircraft export strategy and recommendations for financing and expansion
07 p1136 N71-18087

Midair collision hazards, incidents, and recommendations for safe aircraft operations
07 p0974 N71-18103

Computerized simulation of alternate logistics for overhaul and expensive parts inventory procedures of commercial airlines
07 p1818 N71-18118

Parametric engine study for Mach 0.98 commercial air transport with supercritical wing
[NASA-TM-X-52961] 06 p1284 N71-18733

Propulsion technology for STOL and V/STOL commercial aircraft
09 p1457 N71-19456

Benefits and problems of using head-up displays in commercial and general aviation aircraft
[NASA-CR-117135] 09 p1388 N71-19752

Ditching of DHC-6 turboprop aircraft in Long Island Sound near Waterford, Connecticut on February 16, 1970
[NTSB-AAR-71-1] 10 p1493 N71-21607

Tabulation data on United States commercial aircraft accidents during 1958 to 1952
[PB-196672] 10 p1493 N71-21624

Transportation management, regional planning, and commercial aviation development for state of Texas
[PB-196933] 10 p1494 N71-21627

Characteristics of V/STOL aircraft for commercial transportation system and applications to Texas requirements
[PB-196934] 10 p1494 N71-21632

Tabulation data on United States commercial aircraft accidents during 1953 to 1957
[PB-196673] 10 p1494 N71-21663

Tabulation data on United States commercial aircraft accidents during 1958 to 1963
[PB-196674] 10 p1494 N71-21665

B-evaluation of short takeoff aircraft for commercial shuttle flight applications to reduce traffic congestion in San Francisco, California area
11 p1671 N71-21874

Analysis and statistics of airports, air carrier fleet operation, aircraft production, and status of civilian pilot personnel for September, 1970
11 p1672 N71-21977

Material specifications, flammability, safety considerations, and design criteria for materials used in construction of commercial aircraft interiors
12 p1941 N71-23232

Safety standards development analysis for passenger vehicles and aircraft
[AD-718397] 12 p2016 N71-23333

Air transportation system and Civil Aeronautics Board decisions
12 p1857 N71-23720

Analysis of magnitude, growth, and carrier participation of passenger traffic in major short-haul markets
14 p2199 N71-26528

Utilization of aerospace nonflammable cellular elastic, fibrous, and composite materials in commercial aircraft refurbishment
18 p2866 N71-30759

Senate hearings on Federal anti-air-kicking program
18 p3031 N71-31511

Trends in air transportation and airline industry operations from 1970 to 1980
18 p3031 N71-31512

Commercial aircraft performance and cost analysis data for 1968 and 1969 in US
19 p3035 N71-31611

Civil Aeronautics Board regulatory actions taken fiscal year 1970
21 p3534 N71-35186

Survey of domestic air passenger trip length including number of passengers and aircraft types
24 p4036 N71-38795

COMMERCIAL AVIATION

U CIVIL AVIATION

U COMMERCIAL AIRCRAFT

COMMUNITION

NT CRUSHING

NT GRINDING (COMMUNITION)

COMMUNITIES

Characteristics and information requirements of staple, fashion, and big ticket merchandise inventory management and management information systems for retail stores
11 p1847 N71-22038

Weight and Measures Labeling Handbook for use in packaging and labeling commodities and enforcing state laws and regulations
[NBS-HB-108] 16 p2601 N71-28568

COMMUNICATING

NT AIRCRAFT COMMUNICATION

NT CONVERSATION

NT GROUND-AIR-GROUND COMMUNICATIONS

NT INFORMATION DISSEMINATION

NT INTERSTELLAR COMMUNICATION

NT POINT TO POINT COMMUNICATIONS

NT UNDERGROUND COMMUNICATION

NT VERBAL COMMUNICATION

Spacecraft crew function classification and methods for communicating with onboard computers
[NASA-CR-102903] 01 p0028 N71-10526

Vocabulary for spacecrew communication with spaceborne computers with graphic display devices
[NASA-CR-103171] 14 p2221 N71-23922

Man machine system using computer for decision making in information retrieval
14 p2222 N71-23983

Principle channels for information transfer and assessment of their effectiveness
[NLL-RISLEY-TRANS-2116-9091.9F] 16 p0000 N71-29116

Space shuttle onboard crew/computer communication utilizing remote graphic displays and technology oriented vocabulary
22 p3675 N71-36202

COMMUNICATION

NT INFORMATION DISSEMINATION

NT UNDERWATER COMMUNICATION

NT VERBAL COMMUNICATION

Continuous-access VHF waveguide for coordinating communications with high speed truck vehicles
[PB-191028] 07 p0995 N71-18111

Circularity for developing autocorrelation function continuously with signal receiving period
[NASA-CASE-XNP-69746] 10 p1526 N71-21476

Estimation of error density function for optimum pulse modulation communication systems using Monte Carlo simulations
16 p2563 N71-28790

Project organization and communications for training Korean personnel in technology transfer methods and resources
[NASA-CR-121785] 21 p3532 N71-35167

Information theory and coding with communications applications
[FOA-3-A-3733-63] 22 p3556 N71-35334

COMMUNICATION CABLES

NT BEAM WAVEGUIDES

NT COAXIAL CABLES

NT WAVEGUIDES

Research progress in developing shielded flat-cable and termination method
[AD-724636] 05 p0691 N71-14819

Underwater electrical connector and cable system designed for delivering large amounts of electric power for use underwater - photographs
05 p0690 N71-15012

Method of making molded electric connector for use with flat conductor cables
[NASA-CASE-XMF-03498] 06 p0864 N71-15986

Frost heave effects on communication cables in cold regions
[AD-724636] 20 p3340 N71-33089

Thermal insulation of communications cables for frost heave protection
[AD-724636] 20 p3323 N71-33125

COMMUNICATION EQUIPMENT

NT CLOSED CIRCUIT TELEVISION

NT DIGITAL SPACECRAFT TELEVISION

NT DIPLEXERS

NT RADIO RECEIVERS

NT SATELLITE TELEVISION

NT SPACECRAFT TELEVISION

NT STEREO TELEVISION

NT TRANSMITTER RECEIVERS

NT WHISTLER RECORDERS

Design and fabrication of personal communication system for spacecrews
[NASA-CR-111572] 02 p0180 N71-11263

Astronaut-LM and moon-earth communication systems and equipment
[NASA-CR-106667] 02 p0185 N71-11596

Open cycle hydrocarbon-air fuel cell power plant
[AD-713328] 05 p0631 N71-14689

Equipment specifications for Lunar Sounder Antenna Assembly
[NASA-CR-114797] 05 p0642 N71-14776

Design and fabrication of underwater communication set
[JPRS-52138] 05 p0648 N71-15564

Modifications and evaluation of narrow band, broad bandwidth optical communication system
[NASA-CR-103013] 07 p1059 N71-17547

Selection of circuit parameters for connecting photo receiver and electronic loop in optical communication systems
06 p1173 N71-19131

System selection criteria of microwave and laser systems for communication and tracking - Vol. 2
[NASA-CR-16677] 09 p1347 N71-19638

Design of space communication systems based on space mission, data requirements, and time duration
09 p1470 N71-19639

General optimization procedures and design methodology for optical and radio communication systems
09 p1348 N71-19640

Computer programs for determining interrelation of communication system parameters of range, transmitter power, antenna gain, and electromagnetic noise
09 p1348 N71-19640

Development of digital encoding methods for improved military communication system
[AD-715998] 09 p1349 N71-19673

Telecommunications and communication equipment research - bibliography
[DSIS-B14] 09 p1349 N71-19739

Multiplexed communication system design including automatic correction of transmission errors introduced by frequency spectrum shifts
[NASA-CASE-XNP-01306] 10 p1518 N71-30814

Error effects on antenna gain and pattern degradation tolerances of parabolic reflectors and lenses
10 p1521 N71-21540

Oceanographic electronic equipment including solar systems, sensors, shipboard computers, and communication and navigation systems
[AD-716499] 10 p1534 N71-31542

Serial synchronous communication method for short distances without using modems
11 p1721 N71-23707

Communications control group teletype line switching equipment for space stations
11 p1703 N71-22790

SUBJECT INDEX

COMMUNICATION THEORY

- Procedures for qualitative evaluation of frequency accuracy and stability of communication-electronics equipment [AD-718794] 13 p1678 N71-23529
- Altitude and temperature-altitude effects on performance of electronic and communication equipment under environment simulation tests [AD-718653] 13 p1688 N71-23535
- Equipment and software for common channel international telephone and telemetry system field trial [BEP-4567] 12 p1800 N71-23979
- Determination of communication-electronics equipment power requirement and its compatibility with power sources [AD-719099] 13 p2053 N71-24396
- Voice communication, direction finding, and radio locating equipment development for search and rescue by air [AD-715318] 13 p2054 N71-24414
- Procedures for testing communication security equipment under simulated tactical conditions [AD-718903] 13 p2043 N71-24438
- Tests to determine presence of electromagnetic interference and qualitative effect on communication-electronic equipment [AD-718949] 13 p2054 N71-24496
- Binary data decoding device for use at receiving end of communication channel [NASA-CASE-NPO-10118] 13 p2045 N71-24741
- Design and characteristics of photo receiver and electronic lamp installed in optical communication systems [AD-719836] 13 p2046 N71-24956
- Computer design technique of electron gun for use in spacecraft transmitter [NASA-CR-118415] 14 p2227 N71-25931
- Communication, surveillance, and airborne electronic equipment performance testing in tropical environments [AD-720577] 14 p2218 N71-26176
- Data processing system for meteor trail radio communication equipment [FOA-3-C-3597-63] 14 p2219 N71-26333
- Communication equipment for tropospheric propagation link [FOA-3-C-3684-63] 14 p2219 N71-26342
- Long distance high capacity communication using simulated circular waveguide [BEP-4494] 13 p2363 N71-27463
- Application of game theory for determining optimum allocation of radio communication resources [AD-721540] 16 p2540 N71-28336
- Procedures for service test of communication and electronic equipment under adverse weather conditions [AD-720629] 17 p2721 N71-28335
- General procedure for analysis of communication system applied to performance of optical receiver [AD-720629] 17 p2721 N71-28335
- Formulation and development of analytical model based on queuing theory to improve concepts of military communication systems [AD-720540] 20 p2521 N71-28354
- Three algorithms for Ford sequence generation of length 2 to the nth power, a large for digital communication equipment [AD-720540] 20 p2521 N71-28354
- GCP DSS communications equipment subsystem high-speed data assembly for data conversion to satellite form for transmission [AD-720540] 21 p3391 N71-34131
- Capabilities and 4090-kHz data circuits of GCP DSS communications terminal subsystem high-speed data assembly [AD-720540] 21 p3393 N71-34143
- GCP one communications terminal subsystem high-speed data regeneration assembly for routing and controlling all communications entering and leaving [AD-720540] 21 p3393 N71-34144
- Performance tests and evaluation of military communication equipment during transmission [AD-720540] 22 p3562 N71-35370
- Development of analysis techniques for determining cause for airport congestion and interaction of various modes [FAA-RD-71-55] 22 p3565 N71-35393
- Space communication, waveguide transmission, and development of associated electronic equipment research projects conducted by Australian research facilities [BEP-4541] 23 p3460 N71-37582
- COMMUNICATION SATELLITES
- NT EARLY BIRD SATELLITES [NASA-CR-118415] 14 p2227 N71-25931
- NT INTELSAT SATELLITES [NASA-CR-118415] 14 p2227 N71-25931
- NT RELAY SATELLITES [NASA-CR-118415] 14 p2227 N71-25931
- USF switch developed for LRS-4 satellite [AD-718653] 01 p0831 N71-10071
- Station hopping of high power communication satellite [NASA-TM-X-4136] 02 p0177 N71-11245
- Developments in worldwide communication satellite network [NASA-CASE-XNP-021809] 16 p2543 N71-28080

- Measuring time response of adaptive array antennas for communication satellites for case of strong interference in earth receiving antennas [NASA-CR-111617] 03 p0334 N71-12587
- Cost analysis of joint NASA-European space program involving navigation and communication satellites for civil air traffic control [BEP-4567] 03 p0489 N71-12734
- Solar radiation measurements from Intersat-1 satellite [AD-718653] 03 p0438 N71-13276
- Multipath operation of low altitude satellite using data relay satellite system [NASA-CR-115813] 04 p0489 N71-13478
- Analysis of low altitude satellite operating in conjunction with data relay satellite system - Phase 2 [NASA-CR-115814] 04 p0489 N71-13479
- Second order coherent multiple access technique for communication satellite users [AD-713674] 05 p0443 N71-14745
- Overview on satellite VHF navigation and communication systems [NASA-CR-115813] 06 p0814 N71-16227
- Ionospheric propagation aspects of VHF navigation and communication satellite systems [NASA-CR-115813] 06 p0814 N71-16228
- German/French Symposium communication satellite systems [BEP-4567] 07 p0991 N71-17070
- Technical and cost analysis for communication systems using satellites in geostationary orbits [FB-154782] 07 p0991 N71-17120
- European aerospace and electronic equipment industrial cooperation for air traffic control and communication satellites [NASA-CR-115813] 07 p1132 N71-17181
- Construction of satellite broadcasting network system [NASA-TT-F-428] 07 p0992 N71-17466
- Design of low-cost microwave adapter suitable for television reception from high-power communications satellites [NASA-CR-115813] 07 p0994 N71-17607
- Design, development, and characteristics of several communication satellites [NASA-TM-X-46711] 07 p1121 N71-17771
- Two-signal primer for Fourier analysis of random access communication system [BEP-4567] 07 p0993 N71-17947
- Satellite relationship to satellite communications in F region [AD-715991] 08 p1162 N71-18534
- European Space Research Organization meteorological, communication and air traffic satellite program [AD-715991] 08 p1293 N71-18640
- Doppler shift considerations in naval satellite communication systems employing synchronous satellites [AD-716745] 10 p1517 N71-20693
- Program review on Symposium French-German communication synchronous satellites [AD-716745] 10 p1447 N71-20783
- Conference on Europa 1 launch vehicle, Amer research satellite, Symposium communication satellite, and German ground station-satellite communication system technology [AD-716745] 10 p1447 N71-20783
- Analysis of requirements for longrange repeaters in synchronous equatorial orbit [NASA-TM-X-2238] 11 p1708 N71-22624
- Problems of communication and navigation systems in VLF and UHF produced by small irregularities in electron density in F region [AD-717094] 11 p1731 N71-22693
- Development of antenna system for spin stabilized communication satellites for electronic reception and transmission of data [NASA-CASE-XGS-02407] 11 p1833 N71-23089
- Environmental tests of bearing system components for spin-stabilized antennas of spin stabilized communication satellites [BEP-4567] 12 p1924 N71-23147
- Preliminary report on European space program in communication satellites, noting satellite television, telegraph systems, telephony, and data transmission [CSB-CR-71(1)] 13 p2042 N71-24082
- Discussion of tracking occultation problems occurring during continuous monitoring of interplanetary satellites by using Earth orbiting communication satellites [NASA-CASE-XAC-40225-1] 13 p2173 N71-24813
- Survey of very high and ultrahigh frequency utilization in US atmosphere for communication satellite frequency assignment [NASA-TM-X-45527] 14 p2217 N71-25920
- Communication satellite directional antenna spin reduction mechanism [NASA-TM-X-45527] 15 p2280 N71-27138
- Satellite radio communication system with remote accessible antennas [NASA-CASE-XNP-021809] 16 p2543 N71-28080

- Broadband model of high power UHF transmitter for space communication satellites [NASA-CR-115813] 17 p2717 N71-28213
- Communication satellite circular orbit network providing earth surface coverage [NASA-TM-X-45527] 17 p2719 N71-28439
- Technical and cost factors for implementation of Alaskan communication satellite system [NASA-TM-X-45527] 18 p2880 N71-30093
- Analysis of technological and cost factors affecting feasibility of television broadcast satellites during 1970 to 1975 period - Vol. 1 [NASA-CR-115813] 18 p2889 N71-31406
- Specifications and guidelines for launch vehicle, spacecraft, orbit and coverage, transmission, and receiving systems for television broadcast satellites - Vol. 2 [NASA-CR-115813] 18 p2889 N71-31407
- Communications system design, service description, and coverage requirements for television broadcast satellite system - Vol. 3 [NASA-CR-115813] 18 p3019 N71-31408
- Power conditioning, telemetry and command, cost of up-link ground terminal, and up-link receiver for television broadcast satellite system - Vol. 4 [NASA-CR-115813] 18 p3019 N71-31409
- Synthesis and optimization computer program for design of television broadcast satellite system Vol. 5 [NASA-CR-115813] 18 p3019 N71-31410
- Communications satellite applications in education in US [NASA-CR-115813] 19 p3197 N71-32375
- Design and development of control system for spin axis alignment of communication satellite along orbital axis [AD-724609] 20 p3351 N71-32871
- Evolution of signal processing and communication techniques for transmission and reception of image type data via millimeter wave relay satellites [NASA-CR-121753] 21 p3394 N71-34156
- Technology assessment of communication mode and educational technology including future trends utilizing communication satellites, television, and computer-aided instruction [NASA-CR-121753] 22 p3553 N71-35306
- Status of high power technology for educational satellites and recommendations for expansion to rural and remote areas [NASA-TM-X-47953] 22 p3673 N71-36190
- Orbits 2 satellite distribution system for television, data, newspaper and facsimile, multichannel telephony, and radio broadcasting transmission [AD-727448] 23 p2725 N71-36540
- Compatibility of European communication satellites with United States [AD-727448] 23 p2725 N71-36540
- Status, cost-effectiveness, and telecommunications requirements of computer-based instruction [NASA-CR-122943] 23 p3069 N71-37583
- Audio-Visual Satellite Instruction System (AVSIS) for USA - preliminary considerations [NASA-CR-122943] 23 p3069 N71-37584
- Satellite navigation and communication applied to maritime and commercial services [AD-727448] 24 p3915 N71-37918
- COMMUNICATION SYSTEMS
- U. TELCOMMUNICATION
- COMMUNICATION THEORY
- NT SYLLABLES
- NT WORDS (LANGUAGE)
- Feasibility of continuous communication system [AD-710949] 01 p0825 N71-10889
- Communication theory and research applied to prewarning emergency civil defense broadcasting system [AD-712332] 02 p0182 N71-11277
- Mathematical difficulties in communication theory [NASA-TM-X-46495] 03 p0338 N71-12413
- Functional operations in dynamic programming associated with communication theory [NASA-TM-X-46495] 06 p2225 N71-18095
- Application of system theory to provide conditions to describe communications modulation and demodulation implementation [AD-710949] 09 p1340 N71-15640
- Handbook containing radar theory, engineering, control systems, communications, and instruments [AD-716408] 09 p1340 N71-15774
- Digital filter realizations of arbitrary loss and delay functions applicable for any type of frequency in space communication channels [AD-717101] 10 p1534 N71-21246
- Estimating parameters of chi square and related distributions using quantiles, for data compression of space telemetry [NASA-CR-119318] 18 p2945 N71-31161
- Causes and successful estimation theory for nonlinear random vector channels, for radar tracking and diversity communication [AD-717101] 23 p3726 N71-36559
- Determining signal set with minimum probability of error, and dependence of optimal signal set on signal to noise ratio [AD-717101] 23 p3727 N71-36564

COMMUNITIES

Community physical, psychological, and social reactions to aircraft noise around 7 US international airports
[NASA-CR-111316] 02 p0146 N71-11032

Problems of local airlines in providing service to rural communities 05 p0787 N71-15390

Cost, time, and social burdens created by need for commuting to work and suggestions for eliminating problems
[NASA-TM-X-67243] 14 p2357 N71-25761

Community values and social problems associated with construction of air and surface transportation facilities 15 p2525 N71-26802

Relations between aircraft and road traffic noise and noise tolerance in communities 21 p3375 N71-34019

Compressed bearings on airline service to small communities and towns 22 p3700 N71-36395

COMMUTATION

Commutative operators of singular integral equations 17 p2772 N71-29691

COMPUTATORS

Plan low-energy photo and electroproduction with equal-time commutators 02 p0273 N71-11787

Current commutator derivation of mass difference relations
[NYO-2171-315] 03 p0424 N71-12807

Operational expansion of product of two currents determining derivatives of current equal-time commutators 06 p0902 N71-15822

Constraints on equal time commutators from Lorentz covariance
[IPFT-5/70] 06 p0883 N71-15831

Comparison of magnetic moment and electric dipole sum rules for testing validity of current and field algebra commutators 10 p1592 N71-21002

Dispersion theory and current algebra commutator studies proving single pole dominance for spin one parts of vector or axial vector currents inconsistent with current algebra 14 p2302 N71-25743

Variable speed commutatorless electric machine drive system with speed-torque characteristics suitable for application to industrial drive and vehicle propulsion systems 14 p2230 N71-26413

Approximation method for dynamic properties of commutative control element in converter servomechanisms 17 p2728 N71-30125

Fourier transformation calculation and validation of sum rules and Ward identities using equal-time commutator in axiomatic quantum field theory 18 p2967 N71-30412

Nucleon sigma commutator and nucleon-nucleon cross sections
[NYO-2262-7A-243] 24 p3977 N71-38377

COMPACTING

Compaction study during packing of titanium powder
[AD-711145] 01 p0067 N71-10509

Reproducibility of soil classification and compaction test data
[PB-194134] 05 p0667 N71-14694

Powder metallurgy compaction 05 p0702 N71-15101

Evaluating slurry compaction process for fabrication of metal matrix composites
[NASA-TN-D-6107] 06 p0874 N71-16504

Direct and liquid absorption methods of testing ceramic insulator compaction in sheathed thermocouples
[ORNL-4439] 06 p1242 N71-19346

Traction, compaction, and friction loss predictions of vehicle wheel performance in soft soil 10 p1565 N71-21312

Effectiveness of superimposed vibrating forces in reducing die wall friction during powdered metal compaction
[SRO-475-10] 16 p2614 N71-28898

Hot isostatic compaction at 3000 F and 30,000 psi used for successfully preparing single phase bulk graphite for electron testing 17 p2768 N71-29219

Finite difference techniques for compactness of function sequences in L sub p spaces
[SAC-RE-70-452] 19 p3124 N71-32467

Metal powder compaction calculations using kinetic constants for entire sintering period including initial heating and isothermal soaking
[NLL-LT-746-743-1902.401] 22 p3397 N71-35614

Utilization of vibrational compaction for nuclear fuels
[KJ/TMO-70/22] 23 p3794 N71-37043

Deformation mechanisms in compacting metal powders
[AD-727851] 24 p3940 N71-38105

COMPACTNESS

U VOID RATIO

COMPARATORS

Describing frequency discriminator using digital logic circuits and supplying single binary output signal
[NASA-CASE-MF8-14322] 08 p1165 N71-13692

Development of pulsed differential comparator circuit
[NASA-CASE-XLE-03804] 09 p1363 N71-19471

Optical image comparator for examination of field ion micrographs 02 p0224 N71-11506

Comparator for measuring micro-step motion using piezoelectric ceramics
[RRE-TN-731] 03 p0582 N71-13295

Photometric flow meter with comparator reference means
[NASA-CASE-XGS-01331] 11 p1766 N71-22996

Characteristics of comparator circuits for comparison of binary numbers in information processing system
[NASA-CASE-XNF-04019] 12 p1881 N71-23295

Optical comparator and hydraulic gaging methods for obtaining underwired dimensional measurements of irradiated fuel elements 13 p2113 N71-24527

Computer calculations of pressure distributions on swept wings
[NLR-TN-T-109] 02 p0143 N71-11015

Comparison of flight simulation techniques and costs 19 p3074 N71-31954

Comparing and integrating NASTRAN with other finite element computer programs 22 p3686 N71-36284

COMPARTMENTATION

U COMPARTMENTS

COMPARISONS

NT AIR LOCKS

NT ANECHOIC CHAMBERS

NT COMMAND MODULES

NT PRESSURE CHAMBERS

NT SPACECRAFT CABINS

NT TEST CHAMBERS

NT VACUUM CHAMBERS

In-flight vesting of space shuttle vehicles investigated using delta wing booster and high cross-range orbiter vehicles as configurations 15 p2520 N71-27804

Models for permitting continuous purging of impurities from gas compartments of fuel cell 17 p2706 N71-29694

COMPASSES

NT GYROCOMPASSES

NT MAGNETIC COMPASSES

Low power data processing approach for reduction in sonobuoy compass problems
[AD-717406] 11 p1792 N71-21967

Mechanical and radiological tests of levitic compasses modified with sealed tritium gas luminous sources 22 p3618 N71-35781

COMPATIBILITY

Plutonium and curia compatibility tests 04 p0559 N71-14192

Compatibility of structural materials with sodium
[WARD-4173-2] 05 p0701 N71-15024

Plutonium/curia compatibility testing 05 p0725 N71-15038

Compatibility of Pu-238 dioxide with plutonium and plutonium-rhodium alloys 07 p1061 N71-17221

Agreements between US and USSR on spacecraft design and systems compatibility
[NASA-NEWS-RELEASE-70-210] 07 p1116 N71-18021

Tensile and fatigue properties and liquid oxygen compatibility of bismuthine stainless steel-clad titanium prepared by vacuum deposition and explosive welding
[NASA-CR-72841] 10 p1581 N71-21437

Ammonia decontaminant control of oxygen difluoride and static and dynamic compatibility tests with plastic and elastomer materials
[NASA-CR-72380] 12 p1869 N71-23167

Liquid and gaseous oxygen difluoride compatibility tests with plastic and metal orifices and metal ignition temperature data 12 p1869 N71-23168

Procedures for evaluating compatibility of aviation material with related equipment
[AD-719107] 13 p2025 N71-24457

Compatibility tests at 900 C on Fe-Ni-Cr alloys and UC with varying carbon content and with Cr, V, and V-C stabilizers for fuel cladding reactions
[KFK-1213] 15 p2446 N71-27166

Uranium nitride and uranium-plutonium nitride fuel compatibilities with austenitic stainless steel claddings of liquid metal cooled reactor
[BM1-1895] 16 p2634 N71-28743

High temperature compatibility tests on plutonia and curia combinations with refractory metals, and plutonia/molybdenum cermet
[MDC-G-2053] 17 p2760 N71-29302

High temperature refractory alloy compatibility with plutonia 17 p2760 N71-29302

Crack propagation and compatibility of toughness, low strength steels with N2O4 and UDMH propellants
[AD-726540] 22 p3595 N71-33209

Compatibility of UC compounds and iron based chromium alloys, and nuclear fuel stabilizer effect
[EURFR-426] 22 p3595 N71-33209

Compatibility of European community metals with isotopic oxidizers 23 p3859 N71-37205

Uranium and plutonium monocarbide products and compatibility with steel canning materials for utilization as fuels for fast nuclear reactors
[NLL-RISLEY-TRANS-2184-1901.9F1] 24 p3963 N71-38208

COMPENSATION

Compensation of resonance perturbations in nuclear magnetic field
[INR-18477] 08 p1246 N71-12810

Proportional chamber for compensation of counter geometry in time of flight measurements
[JINR-P3-5472] 13 p2081 N71-24049

Particle beam energy distribution compensation techniques for particle accelerator sections under current test including phase velocity changes
[SLAC-TRANS-129] 17 p2792 N71-29018

COMPENSATORS

Digital fluidic compensator for analog field systems
[AD-713026] 03 p0963 N71-13108

Generalized digital compensators for sampled-data systems 06 p1166 N71-11800

Computer-aided compensator design program for increasing relative stability of control systems
[NASA-CR-103862] 09 p1563 N71-19712

Compensator for automatically maintaining power radiated from reentry vehicles 12 p1880 N71-23940

Time coordinate compensator design for time of flight spectrometers with long plastic scintillation counters 15 p3408 N71-37005

Feedback compensator for time-time levelation system insensitive to parameter variations
[NASA-CR-117998] 16 p2565 N71-30110

Approach power compensator system for manual and automatic Navy carrier landing system
[AD-722023] 16 p2828 N71-30204

User guide for use of compensator design program /COMPDES/- Vol. 4
[NASA-CR-1119912] 20 p3294 N71-33905

Compensator improvement program with application to large space vehicles and tactics noting relative stability versus frequency response
[NASA-CR-1119959] 24 p3901 N71-37810

COMPENSATORY TRACKING

Effects of motion cues and motion scaling on one and two axis compensatory control tasks with application to flight simulators
[NASA-TN-D-6110] 05 p0637 N71-14889

Optimal control theory and systems analysis of man-machine systems and operator performance prediction model for compensatory tracking tasks
[NASA-CR-1753] 18 p2800 N71-31107

Approach indicator oscillation and eliminating effects on human performance of compensatory tracking tasks
[NASA-CR-119640] 19 p3047 N71-31610

COMPILE (COMPUTERS)

U COMPILERS

COMPILE PROGRAMS

U COMPILERS

U COMPILERS

Users manual for COBOL compiler validation system
[AD-711369] 01 p0029 N71-10941

JOVIAL Compiler Validation System - instruction manual
[AD-711370] 02 p0180 N71-11154

Space programming language for translating source statements into machine or assembly language code
[AD-711787] 02 p0189 N71-11153

Algorithms for accessing symbol tables in compiler
[NASA-CR-711723] 09 p1352 N71-19019

Intermediate code and table driven processor for translating retrieval question to users original language
[AD-712769] 14 p2221 N71-28017

Feasibility of unified compilers for outboard code
[NASA-CR-119863] 18 p2896 N71-30770

Higher order programming language and compiler for advanced computer software systems to be used with manned space flights between 1972 and 1980
[NASA-CR-115126] 21 p3398 N71-34104

COMPLEX NUMBERS

Linear commutativity problem in complex space
[AD-712769] 03 p0599 N71-13104

COMPLEX SYSTEMS

Developing high integrity digital flight control of variations in performance of complex systems 05 p0600 N71-12804

Binary decision graph for analyzing validity of complex information processing models 04 p0499 N71-13105

A-190

SUBJECT INDEX

- Presenting techniques for assessing utility of complex alternatives in transportation problems
[EN-508-DOT/BC] 07 p1134 N71-18017
- Examining principles of structural systems analysis and identification of complex systems in cybernetics
[WRS-52496] 08 p1173 N71-18076
- Two dimensional peridogram for estimating spectral density of real, homogeneous, random field over spatial lattice on plane
[WRS-53548] 18 p2948 N71-18181
- Cybernetics including models for statistical decision making, biomechanical systems, and complex stochastic system
[WRS-53531] 19 p3044 N71-18208
- Methods for determining characteristic of any combination of stochastic systems
19 p3123 N71-18201
- Principles of stochastic control and practical aspects of stochastic control models for complex systems
[WRS-53913] 21 p3448 N71-18256
- Formal generative and transformational grammars for constructing model for complex systems
21 p3448 N71-18257
- COMPLEX VARIABLES**
- NT ANALYTIC FUNCTIONS
- NT BESSEL FUNCTIONS
- NT CONFORMAL MAPPING
- NT ELLIPTIC FUNCTIONS
- NT ENTIRE FUNCTIONS
- NT EXPONENTIAL FUNCTIONS
- NT GAMMA FUNCTION
- NT HARMONIC FUNCTIONS
- NT HYPERBOLIC FUNCTIONS
- NT LAURENT FUNCTIONS
- NT LOGARITHMS
- NT MATHEU FUNCTION
- NT MEROMORPHIC FUNCTIONS
- NT ORTHOGONAL FUNCTIONS
- NT RATIONAL FUNCTIONS
- NT SINGULARITY [MATHEMATICS]
- NT SPHERICAL HARMONICS
- Functional iteration of functions of several variables
02 p0252 N71-11937
- Dynamic problem of infinite, elastically supported beam under influence of uniformly moving single point load solved by complex variable theory
[NASA-TT-F-13549] 14 p2347 N71-13802
- Algorithm for simultaneous minimization of multiple Boolean functions with application in telemetry systems
[NASA-CR-119630] 17 p2723 N71-30096
- Even-type p -harmonic functions on Riemann surface
[AD-72281Q] 17 p2775 N71-30053
- Dynamic model for optimization of wide utility in engineering sciences
22 p3408 N71-15609
- Complex analytical structures of Hilbert space relations
24 p3949 N71-38170
- COMPLEXITY**
- NT TASK COMPLEXITY
- Automatic computation theory and problems of program complexity, complexity measures for finite automata, algorithms for linear products, and complexity of iteration
[AD-712843] 03 p0341 N71-12649
- COMPLIANCE (ELASTICITY)**
- U MODULUS OF ELASTICITY
- COMPLICATION**
- U COMPLEXITY
- COMPONENT RELIABILITY**
- Expendable erosion of thermoelectric elements in type thermoelectric generators
[NCR-70-554] 02 p0147 N71-11045
- Concrete program for production of high reliability electronic components
02 p0194 N71-11560
- Nondestructive magnetic field testing methods for reliability engineering of aerospace components
02 p0232 N71-11643
- Quality and reliability assurance methods for LSI circuits
03 p0384 N71-12633
- Testing methods for components of inertial guidance systems
[AARDGRAPH-128] 03 p0410 N71-13201
- Testing methods for sensors of inertial reference systems
03 p0411 N71-13202
- Acceptance testing of inertial equipment in platform assembly system
03 p0412 N71-13206
- Expendable and Phenix components of sodium circuits for sodium cooled fast reactors
[KORC-19007-S] 04 p0546 N71-13643
- Isolated nickel-cadmium battery assembly BB-455
[AD-714563] 06 p0797 N71-16349
- Large scale integrated circuit testing using test probe and additional logic
[AD-714511] 06 p0824 N71-16342

- Fabrication voids in aluminum base fuel dispensers applicable to high flux isotope reactor and advanced test reactor
[ORNL-4611] 07 p1063 N71-17361
- Probability concepts applied to sequential equipment operation
[NASA-TN-D-6306] 09 p1326 N71-19652
- Automatic test equipment for electronic components
[NASA-CR-17355] 09 p1360 N71-20331
- Experimental and prototype SHAP 23 development and testing
[DDMM-4187-1] 12 p1838 N71-23118
- Prompt effects of weapon effects display system, including flight components
[UCRL-50892-VOL-4-PT-2] 12 p1916 N71-23152
- Conference on fatigue life in helicopter components
[DLR-MITT-70-61] 13 p2024 N71-24385
- Dynamic tests of helicopter components
13 p2025 N71-24388
- Structural stability tests of helicopter components
13 p2025 N71-24390
- Self-organization methods for complex linear dynamic systems to compensate for component failures
[NASA-CR-118314] 13 p2103 N71-24874
- Component and system performance tests of Brayton cycle power conversion system in 2 to 15 kW scale range
[NASA-TN-D-67835] 13 p2157 N71-25330
- Aluminide coatings for nickel-base superalloy developed for high temperature jet engine components
[NASA-CR-72843] 13 p2897 N71-25454
- Classless control effects on aircraft components and immobilization vaccine production in Sweden
[FOA-A-C-1325-70] 14 p2312 N71-26566
- Approximation of redundant component reliability and digital computer logic design
[AD-720332] 15 p2389 N71-27287
- Derivation of minimum test sets for waste function logic circuit failure analysis and component reliability
[AD-720330] 15 p2389 N71-27288
- Reliability evaluation of plastic-encapsulated integrated circuits including long-term tests and short-term highly accelerated tests
[AD-722493] 16 p2569 N71-29405
- Reliability improvement using redundant components suitable for binary logic circuits
[RAE-TR-69045] 17 p2722 N71-29442
- Microleakage and reliability of plugging and target mechanisms and magnets in Hasedro thin section extraction systems
[RIHEL/R-209] 18 p2959 N71-30409
- Reliability, cumulative damage, and redundancy in multicomponent systems
[AD-724499] 18 p2944 N71-30894
- Lubrication by boundary, elastohydrodynamic, and fluid films, wear due to fretting, erosion, scuffing, and pitting, and friction in aircraft
[NASA-TM-X-67672] 18 p2929 N71-31134
- Compilation of information on assembly technology for efficiency and cost reduction
[NASA-SP-593401] 18 p2930 N71-31394
- Evaluation of three component electronic wind tunnel balance installed in 3.5 by 5.0 ft subsonic tunnel
[AD-722571] 18 p2925 N71-31400
- Parallel standbys redundancy subject to both open and short circuit failures - extension of branch and bound algorithms
[AD-723095] 19 p3067 N71-32471
- Statistical mechanics and computer programs for estimating component reliability
[NLL-CE-TRANS-5427-1982.09] 19 p3186 N71-32658
- Component characteristic and failure mode recording and data acquisition system design for determining component reliability
[NLL-BISLEY-TRANS-1928-1981.50] 19 p3106 N71-32718
- Design criteria for guidance and control spacecraft computer selection including physical and functional characteristics and reliability
[NASA-SP-8070] 20 p3259 N71-33679
- Profiling procedures including computer program [OLS] for measuring junction depth in anodic oxidation - semiconductor fabrication reliability studies
[NASA-CR-119000] 21 p3496 N71-34906
- Handbook on use of radio-measurement instruments
[AD-726385] 22 p3361 N71-33584
- Safety aspects of nuclear reactor design, materials, engineered safeguards, and operating procedures - bibliography
[TID-523-REV-5-SUPPL-4] 22 p3436 N71-35834
- Checkout and verification of space shuttle system redundant components without disrupting systems
22 p3575 N71-36198
- Calculating current voltage and capacitance voltage characteristics in production of Schottky diodes for integrated circuits
[NLL-FORS-TRANS-2768-1982.81] 23 p3733 N71-36617

COMPOSITE MATERIALS

COMPOSITE FUNCTIONS

Formulas and algorithms for computing partitions of numbers and derivatives of composite functions
[UCRL-20215] 16 p2635 N71-28740

COMPOSITE MATERIALS

NT CERAMICS

NT COMPOSITE PROPELLANTS

NT LAMINATES

NT METAL MATRIX COMPOSITES

NT PLASTICS

NT REINFORCED PLASTICS

NT THREE DIMENSIONAL COMPOSITES

NT WHISKER COMPOSITES

Static and dynamic elastic moduli and real moduli of glass fiber-epoxy and boron fiber-aluminum composites
[AD-710590] 01 p0070 N71-10022

Characteristics and applications of polyphenylene composites
[AD-710504] 01 p0070 N71-10033

Optical properties of silicon solar cell component material
[NASA-CR-111004] 01 p0107 N71-10048

Stress concentrations in filament-reinforced sheets of finite length
[NASA-TN-D-5947] 01 p0128 N71-10438

Standard reference materials prices and availability listing
[NBS-260-SUPPL.] 01 p0072 N71-10722

Computer program for analysis of folding strains on composite bladder structures
[NASA-CR-111133] 01 p0130 N71-10837

Fatigue life prediction of composite bladder structures
[NASA-CR-111306] 01 p0131 N71-10838

Omniview method of composite fabrication of graphite filaments and mechanical properties of fabrics
[NASA-CR-102916] 02 p0246 N71-11441

Metal and alloy reinforcing fibers grown in-situ, including tensile strength and creep analysis
[ONERA-TP-625] 02 p0246 N71-11576

Solid state diffusion growth of composite materials containing continuous Kevlar fibers in aluminum matrices from hot-pressed aluminum embedded nickel wires
[AD-711346] 02 p0246 N71-11591

Fiber reinforced plastic structures
02 p0247 N71-11633

Ultrasonic velocity and gamma radiometric measurements for testing mechanical properties and chemical composition of composites
[AVSD-4823-70-FR] 02 p0232 N71-11642

Polyimide resin and steel reinforced composites
[NASA-CR-72633] 02 p0247 N71-11657

Developing large-diameter carbon base monofilaments for reinforcing metal matrix composites
[NASA-TM-X-52922] 02 p0247 N71-11686

Weightless solidification of multicomponent superconducting systems in space laboratory
02 p0283 N71-11707

Response of mixed materials to one dimensional shock waves
[AD-712062] 02 p0248 N71-11972

Spin and isospin effects on pion scattering by composite materials using Glauber formalism
[BLO-1384-570] 03 p0424 N71-12005

Theoretical maximum compression strength determination for reinforced materials
[AD-712937] 03 p0497 N71-13182

Statistical isotropic deformation of elastic solid of composite materials
[AD-712814] 03 p0467 N71-13383

Magnetic properties of magnetic composite materials
[AD-712523] 04 p0266 N71-13843

Design and materials engineering for aircraft turbine engines
[NASA-TT-F-13398] 04 p0306 N71-14188

Mechanical properties of mixed boron/graphite composites
[NASA-CR-102944] 04 p0355 N71-14267

Analytical procedures for predicting mechanical properties of fiber reinforced composites
[AD-713675] 05 p0787 N71-14540

Method for arranging filamentary, load bearing material to approximate stress condition in an envelope of free floating balloons for maximizing structural efficiency
[AD-713181] 05 p0530 N71-14811

Thermal image transducer, infrared scanning, and high power broadband ultrasonic methods for non-destructive tests of carbon-carbon composites
[BNWL-SA-3534] 05 p0787 N71-15023

Stiffness and expansion of oriented random fiber reinforced composite materials
[AD-713099] 05 p0711 N71-15085

Process coating of metal ceramic and refractory composite powders into plastic alloys
[NASA-CASE-XLE-08106] 06 p0804 N71-16076

Preparation and characteristics of lightweight reinforced composites
[NASA-CASE-XMP-63279] 06 p0777 N71-16134

Flexible composite membrane structure impervious to extremely reactive chemicals in rocket propellant
[NASA-CASE-XNP-00837] 06 p0878 N71-16218

- Third direction reinforcement of carbonized composites
[BDX-413-144] 06 p0879 N71-16370
- Fatigue damage indicator for composite material with particle filled matrix
[AD-714258] 06 p0860 N71-16433
- Finite element analysis of interlaminar shear in fibrous composites
[RM-492] 06 p0880 N71-16466
- Theoretical limits of compression strength of reinforced materials
[NASA-TT-F-13443] 06 p0881 N71-16503
- Development and fabrication of filament composite nondestructive test standards
[NASA-CR-103011] 06 p0881 N71-16593
- Performance of low density silicone-phenolic and commercial ablative composites
[NASA-TN-D-4130] 06 p0960 N71-16872
- Stress concentration in composite materials with damaged reinforcing fiber
[NPL-MA-68] 07 p1046 N71-17122
- Flow characteristics of wire-form and laminate-form porous materials
[NASA-TM-X-3111] 07 p0966 N71-17130
- Material characteristics and methods for predicting mechanical properties of graphite
[ORNL-3191] 07 p1047 N71-17203
- Crystal for flexure fatigue testing of composite materials
[NASA-CASE-XMF-02964] 07 p1032 N71-17659
- Evaluation of protective coatings for heat resistant alloys
[NASA-CR-72813] 07 p1043 N71-17669
- Determining feasibility of using laser beam holography for detection and characterization of bond defects in composite material structures
[NASA-CR-111836] 07 p1039 N71-17757
- Strength and elastic behavior of composite nuclear fuel bodies
[RD/N-1622] 06 p1236 N71-18228
- Thermally induced stress waves in laminated composites
[AD-715896] 08 p1221 N71-18485
- Oblique propagation of time-harmonic waves in periodically laminated composite materials
[AD-715895] 08 p1222 N71-18461
- Large diameter graphite/carbon composite monofilaments produced by pyrolysis
[NASA-CR-72769] 08 p1222 N71-18748
- Plastic deformation effect on tensile strength, and deformability of fiber reinforced material
08 p1298 N71-19140
- Measurements of shock Hugoniot in unidirectional fiber reinforced composites
[AD-716560] 09 p1403 N71-19491
- Artificial characteristics of dry bearings fabricated from various materials
[AD-716512] 09 p1393 N71-19619
- Bibliography with abstracts on carbon-carbon, metallic-carbide, and metal-matrix composites
[ORNL-4598] 09 p1403 N71-19665
- Behavior of various alloys, polymers and composites
09 p1474 N71-19729
- Longitudinal strength of unidirectional fibrous composites
[AD-716629] 09 p1405 N71-19804
- Numerical analysis of thermo mechanical constraints of materials reinforced with cords
[AD-716037] 09 p1474 N71-19828
- Collocated interfacial elastic stress intensity for finite, bi-material plates
[AD-716334] 09 p1476 N71-19919
- Crank-Nicolson finite difference method for TEPLD, heat conduction code, for thermal explosion studies in laminar composites
[LA-4511] 10 p1639 N71-20606
- Continuum theory for determination of macroscopic equations for reinforcing fiber composites
[NPL-MA-92] 10 p1630 N71-20665
- Large deflection of a-layered rectangular plates with clamped edges and uniformly distributed load
[AD-717245] 10 p1632 N71-21010
- Quantitative analysis of aliasing in systems which produce single pictures by superposition of several periodic samplings using single detector array
[AD-717619] 11 p1797 N71-21974
- Calculation of bulk modulus, shear modulus, and thermal expansion of composite materials using Van der Pauw theory
[CL-71/53] 11 p1836 N71-22400
- Electron microscopy, radiography, electrical resistivity, thermal expansivity, and X ray diffractometry of fibrous carbon-carbon composite dynamic characteristics
[Y-1752] 11 p1783 N71-22475
- Development of method for producing metallic composites reinforced with ceramic and refractory hard metals that are filled in place
[NASA-CASE-XLE-03925] 11 p1783 N71-22894
- Effects of chemical bonding between phases of glass-metal composites on strength and fracture behavior
11 p1783 N71-23010
- Magnetic coupling in composite ferromagnetic structures consisting of two permalloy films /81.7 percent Ni and 18.3 percent Fe/ with thin separation layer of chromium and/or gold
11 p0000 N71-23014
- Material specifications, flammability, safety considerations, and design criteria for materials used in construction of commercial aircraft interiors
12 p1941 N71-23332
- Development and characteristics of diffusion bonded boron coated titanium foil sheets
[AD-717968] 12 p1941 N71-23279
- Preparation of thermally stable polyimides from solutions of monomeric reactions
[NASA-TM-X-67803] 12 p1069 N71-23367
- Double torsion technique to determine fracture energy of epoxy resin
[AD-718864] 12 p1942 N71-23379
- High temperature uniaxial tensile tests performed on aluminum-graphite composites
[AD-718153] 12 p1942 N71-23402
- Development of aluminum-graphite composite
[AD-718409] 12 p1943 N71-23619
- Abstracts of papers presented at US Air Force materials symposium held at Miami Beach, Florida in May, 1978
[AD-718432] 12 p1943 N71-23625
- Stress-strain behavior of aluminum alloys under ambient temperature conditions and fracture mechanics of copper-aluminum eutectic alloys
[AD-718360] 12 p1944 N71-23765
- Materials science research including trace element studies, composite catalysts and polymers, crystal growth, radiation damage, and related subjects
[AD-718821] 12 p1945 N71-23794
- Dynamic model for stress wave propagation in composite material containing dispersed rigid spherical inclusions
[AD-718087] 12 p1945 N71-23806
- Investigation of impact resistance of unidirectional fiber composites using Izod impact tests
[NASA-TM-X-67802] 12 p1946 N71-24010
- Production engineering for temperature stable dielectric constant ferroelectric composite materials in strontium tin oxide/barium titanium oxide system
[AD-718944] 12 p1947 N71-24185
- Stress analysis of central transverse crack in stiffened fiber reinforced composite panel under tension
[AD-719696] 13 p2099 N71-24429
- Analysis of cause for concentration perturbation in off-eutectic aluminum-beryllium alloy caused by changes in freezing rate during progressive freezing and zone melting
[AD-718964] 13 p2092 N71-24554
- Stress analysis of elastic plate, composite plates with holes, fiber reinforced plates, and thin walled shells
[NASA-CR-111891] 13 p2177 N71-24642
- Stress concentration on five ply, fiber reinforced plates with circular holes
13 p2177 N71-24644
- Stress-strain diagram for nonhomogeneous composites with circular inclusion using Hooke's law
13 p2177 N71-24645
- Stress analysis of unidirectionally reinforced, composite plates with holes
13 p2178 N71-24646
- Hot firing tests with FLOX/methane propellants for evaluating pyrolytic refractory composite materials for thrust chambers
[NASA-CR-118321] 13 p2101 N71-24974
- Theoretical elasticity solutions for determining bond stresses in multifiber composite materials due to uniform tension
13 p2181 N71-25121
- Numerical analysis of axially symmetric boundary value problems in elastic dissimilar layered media
13 p2181 N71-25126
- Nondestructive testing of composites and ceramics to determine surface defects by infrared and induction heating methods
[WHAM-SA-42] 13 p2101 N71-25215
- Determination of static and fatigue characteristics of graphite epoxy composite materials with variations in temperature, stress mode, and stress ratio
[AD-728396] 14 p2277 N71-25885
- Numerical analysis of influence of fiber orientation on mechanical properties of cylindrical shells in initial postbuckling region
[AD-728231] 14 p2349 N71-26252
- Computer program for design and analysis of composite filament wound, axisymmetric pressure vessels considering orthotropic construction of vessel
[NASA-CR-118669] 14 p2358 N71-26366
- Effects of composition, particle size, and component thermal properties on effective thermal conductivity of composite solids
14 p2356 N71-26469
- Irradiation effects on mechanical properties of epoxy resin/glass composites
[BREL/R-200] 15 p2427 N71-26815
- Mechanical properties of fiber reinforced materials
15 p2429 N71-27043
- Relationship between morphological factors and elevated temperature stability of eutectically made fiber composites
[ORSO-3947-5] 15 p2429 N71-27015
- Feasibility of boron-epoxy reinforced aluminum alloy for horizontal stabilizer structure of DC-6 aircraft and recommendations for demonstration program
[NASA-CR-111913] 15 p2360 N71-23640
- Electronic methods to control placement and orientation of short graphite fibers in fiber composite and fiber structures
[SC-CR-69-3277] 15 p2432 N71-23809
- Thermal treatment for nondestructive testing of carbon-carbon composites and metal-nonmetal bonds
[BNWL-SA-3289] 15 p2367 N71-23779
- Profilometer equations for load absorption by discontinuous filament in fiber reinforced composite
[AD-721999] 16 p2417 N71-20110
- Decomposition sintering of titanium hydride powder yielding matrix composites of titanium and titanium and wire reinforcement
[AD-722258] 16 p2411 N71-20120
- Development and testing of carbon/carbon composites fabricated by chemical vapor infiltration of filament-wound substrate
[SC-DC-70-5369] 17 p2768 N71-20100
- Acoustic emission analysis of material properties and defect structure
[UCRL-72657] 17 p2786 N71-20108
- Flight test of chemical vapor deposited felt and filament wound carbon composite heat shields
[SC-DC-71-3853] 17 p2769 N71-20170
- Developing thermally stable adhesives for bonding titanium alloy and boron composite substrates
[NASA-CR-1824] 17 p2770 N71-20171
- Fracture energy and strength behavior of sodium borosilicate glass A12O3 composite materials system
[AD-723349] 17 p2771 N71-20180
- Calculations of flow induced in adjoining slabs of PMMA and aluminum as shock wave propagates through composite slabs
[AD-723344] 17 p2771 N71-20182
- Utilization of aerospace nonflammable cellular elastomer, fibrous, and composite materials in commercial aircraft refurbishment
18 p2868 N71-20179
- Plastics in composite materials - associated bibliography
[AD-722404] 18 p2940 N71-20085
- Composite organic semiconductors from pyrolytic ion exchange resins
18 p2940 N71-20120
- Preparing composite materials based on silver and synthetic mica - physicochemical and synthetic characteristics
[AD-722819] 18 p2941 N71-20108
- Mathematical models for dynamic elastic properties of fiber reinforced viscoelastic materials
[AD-723389] 19 p3118 N71-31718
- Theoretical prediction of phase reduction of plane stress waves in fiber reinforced elastic solid
[AD-723390] 19 p3119 N71-31719
- Mathematical models for quasi-static behavior of fiber glass reinforced viscoelastic plastics
[AD-723388] 19 p3119 N71-31718
- Mechanical properties of advanced filament wound carbon composites
[SC-DR-710192] 19 p3120 N71-31716
- Impact resistant unidirectional fiber composite design based on micro and macro-mechanics, load impact tests, and residual stress and structural analysis
[NASA-TN-D-4463] 19 p3108 N71-32203
- Torsional shear strength and stiffness of filament wound, glass epoxy tubes, with helical or alternating helical and circumferential windings
[NASA-TN-D-6140] 19 p3189 N71-32204
- Nondestructive testing and failure analysis of composite construction materials in load bearing structural modifications
[AD-72854] 19 p3190 N71-32010
- Fabrication and testing of bonded metal-ceramic, glass-coated metal, and glass-coated ceramic bonded to metal composite electrodes for sodium bombardment ion thrusters
[NASA-CR-119695] 19 p3175 N71-32316
- Propagation of plane harmonic waves in a anisotropic elastic media in two dimensions only
[AD-723417] 19 p3172 N71-32315
- Fourier series solution to free edge effects in measurement of composite in plane shear properties
[AD-724140] 20 p2527 N71-32979
- Strength of adhesive of carbon fiber composite material bonds
[DLR-FB-71-31] 20 p2527 N71-32978
- Effect of process conditions on tensile properties of LOBEA and phenol novolac resin resins with addition of methylene dianiline and phthalic anhydride
[NRC-M3-132] 20 p2527 N71-32978
- Crack propagation in aluminum alloys reinforced with boron and stainless steel fibers
[UCRL-28524] 20 p2528 N71-32978
- Stress waves induced in anisotropic fiber composite plates by transverse, short-duration impact forces
[NASA-TN-D-8357] 20 p3359 N71-32972

SUBJECT INDEX

Proportion and phase transformations of fibrous composite materials with metal matrix [ONERA-NT-170] 20 p3288 N71-37273
Design, fabrication and tests of boron/epoxy reinforced stringers for CR-548 tail cone [NASA-CR-111929] 21 p3374 N71-34013
Electrically coupled individually encapsulated coil matrix [NASA-CASE-NPO-11190] 21 p3379 N71-34044
Application of spiral, bimetallic strip to create circular motion on mechanical shaft by change of temperature in the strip [NASA-CASE-NPO-11283] 21 p3403 N71-34213
Analysis of aluminum and nonmetallic buffers for use with liquid oxygen containers to prevent clacking [NASA-CR-1890] 21 p3413 N71-34284
Diffusion bonded graphite reinforced aluminum composites [NASA-CASE-MPS-21077] 21 p3443 N71-34502
Transient and harmonic wave effects on composite materials [JCR-R2-710034] 21 p3444 N71-34509
Interface structure and effects of carbon fiber microstructure on shear strengths of carbon-epoxy composites 21 p3445 N71-34516
Analysis of failure mechanisms of carbon-epoxy composite materials and methods of predicting performance under load conditions [NASA-CR-121621] 21 p3526 N71-35123
Critical equilibrium of two-component composite with crack originating along diameter of round inclusion and entering with one tip into binder [NASA-TT-F-13934] 21 p3527 N71-35131
Three dimensional analysis of statics and dynamics of orthotropic laminates and application to rectangular plates and laminates [AR-272-5] 21 p3528 N71-35136
Development and evaluation of refractory water-proof, external insulation materials for use on earth orbiting shuttle 22 p3537 N71-35547
Analysis of structural phase state in composite metal-ceramic of nickel and sulfur with application to thermal-vacuum deposition of metallic and nonmetallic materials [NLL-LT-746-742-19022.401] 22 p3596 N71-35610
Development and evaluation of high temperature materials for use in magnetohydrodynamic generators [WFS-53599] 22 p3598 N71-35621
Analysis of resistivity of refractory concretes and reinforcing materials based aluminum and boron-aluminum cements and bonding agents 22 p3599 N71-35633
Development of analytical model to calculate axial and transverse stress distribution in axially aligned tapered wire-reinforced lead composite system [T-788] 22 p3602 N71-35630
Determination and stress field determination within piezoelectric elastic bodies with prescribed internal loads and boundary conditions [AD-726425] 22 p3602 N71-35634
Roll Bonding beryllium wire-metal matrix composites [AD-726423] 22 p3602 N71-35635
Elastic behavior of composite materials influenced by shape of dispersed particles [AD-726561] 22 p3602 N71-35636
Formulation of mathematical stress wave model for predicting effects of sandwich plates subjected to high velocity impact [NASA-CR-121892] 22 p3603 N71-36251
Finite element method used for stiffness analysis of axisymmetrical shells of composite materials 22 p3603 N71-36338
Manufacturing process for production of high temperature, low density, thermal insulation equipment [MDX-615-313] 23 p3709 N71-36446
Application of unidirectional solidification technique for reinforcement of metallic or ceramic materials [NLL-LT-746-740] 23 p3774 N71-36900
Flexural, shear, bending, tensile, and impact strengths of high modulus, high strength, glass fiber-reinforced resin composites [NASA-CR-122775] 23 p3775 N71-36907
Determination of thermodynamic properties of volume foam by thermogravimetric analysis, differential thermal analysis, and thermomechanical analysis [MDX-615-406] 23 p3777 N71-36917
Development, test, and evaluation of carbon and carbon composite heat shields [CONF-71012-1] 23 p3778 N71-36922
Proceedings of international conference on carbon fibers [AD-726673] 23 p3779 N71-36935
Development of technique for measuring forces involved in powder pressing operation to account for internal pressure, binding, and plastic deformation [NLL-TRANS-746-695-19022.401] 23 p3780 N71-36938
Predicting time-temperature behavior of epoxy resin and epoxy composites in any loading mode 23 p3780 N71-36942

Effect of voids on mechanical properties of two graphite fiber composites 24 p3943 N71-38127
Stability of oxides in metal or metal alloy matrices determined by interaction between sapphire filaments and nickel alloys [AD-727781] 24 p3944 N71-38138
Empirical methods for determining longitudinal residual stresses in reinforced composite materials [AD-727208] 24 p3945 N71-38143
Reinforcement of ceramic materials with refractory metal fibers [NLL-LB/O-3074-19091.5P] 24 p3946 N71-38151
COMPOSITE PROPELLANTS
Homogeneous constitutive equations for describing failing microstructure of polymeric materials with plastic memory 01 p0114 N71-10689
Ammonium perchlorate composite propellant with organic Cu/II chelate catalytic additive [NASA-CASE-LAR-10173-1] 04 p0604 N71-14090
Stress analysis and fracture mechanics of dovetail, isotropic, composite propellants [AD-720596] 14 p2331 N71-26079
Development of theoretical model for calculation of shear modulus, bulk modulus, and thermal expansion behavior of two phase composite materials by Van der Poel theory [AD-721576] 16 p2618 N71-28734
Combustion mechanism of composite propellants during depressurization 16 p2670 N71-28784
Composite and double base rocket propellant extinguishing by rapid pressure reduction and propellant property and additive effects on combustion extinction 17 p2832 N71-29809
Surface flame spreading characteristics of ICRBP reference composite propellant composed of ammonium perchlorate with polyurethane binder 18 p3026 N71-31427
Statistical evaluation of brittle point embrittlement temperature tests of composite propellants [AD-727038] 23 p3838 N71-37368
COMPOSITE STRUCTURES
NT LAMINATES
NT FLYWOOD
Shrouded composite propulsion system configuration [NASA-CASE-XLA-01043] 01 p0116 N71-10780
Matrix method for computerized design optimization of framed structures subjected to loads [AD-711279] 01 p0131 N71-10931
High velocity impact tests conducted with polyethylene tetraphthalate projectiles and flexible composite wall panels [NASA-TN-D-6135] 09 p1481 N71-20515
Determination of efficiency of joint absorption of honeycomb structure attached to collecting base surface on which incoming solar energy impinges directly on base surface [NASA-TN-D-6337] 13 p2187 N71-25466
Electrostatic methods to control placement and orientation of short graphite fibers in fiber composites and fiber structures [SC-CR-49-3277] 15 p2432 N71-27699
Development of linear theory for dynamic interaction of solid elastic circular cylinder bonded to thin shell of different material 17 p2852 N71-29803
Formulas for calculating conductivity and dielectric constants of capacitors made up of composite bodies extended to more than two components [NASA-TT-F-13725] 17 p2727 N71-30244
Operational functions and electrical properties of metal oxide semiconductor structures [REF-1-628] 20 p3335 N71-33848
Mechanical analysis of composites structural members subjected to pure torsion 23 p3864 N71-37350
Properties of composite structures bonded by epoxy resin with various hardening agents [AD-727600] 24 p3944 N71-38134
COMPOSITES
U COMPOSITE MATERIALS
COMPOSITION (PROPERTY)
NT ATMOSPHERIC COMPOSITION
NT ATMOSPHERIC MOISTURE
NT BODY COMPOSITION (BIOLOGY)
NT CARBON DIOXIDE CONCENTRATION
NT CHEMICAL COMPOSITION
NT CONCENTRATION (COMPOSITION)
NT GAS COMPOSITION
NT IONOSPHERIC COMPOSITION
NT LUNAR COMPOSITION
NT METEORIC COMPOSITION
NT METEOROID CONCENTRATION
NT MOISTURE CONTENT
NT PLANETARY COMPOSITION
NT PLASMA COMPOSITION
Measurement of effective stabilizer content in propellants [TL-1970-17] 05 p0761 N71-15139

COMPRESSIBLE BOUNDARY LAYER

Composition distribution and equivalent body shape for reacting, coaxial, supersonic hydrogen air flow [NASA-TN-D-4123] 05 p0785 N71-15630
Ultrasonic spectroscopy used to determine composition fluctuations on structural relaxation in glass 13 p2180 N71-24947
Analysis of trace contaminant composition in sub-marine atmospheres 17 p2713 N71-29427
Aluminum foils for measuring solid wire loss composition 18 p3012 N71-30946
Handbook of standard samples issued in USSR for determining properties and composition of substances and materials [NBS-SP-260-30] 18 p3029 N71-31338
Utilization of gamma rays as nondestructive method of determining elemental composition of rocks and minerals 20 p3342 N71-33902
Mixed oxide nuclear fuel element porosity, grain structure, and composition distribution measurements for EBR-2 subassemblies [HEDL-TME-71-45] 22 p3624 N71-35334
Influence of fuel additives on automobile exhaust emissions and composition of exhaust hydrocarbons (TPR-40) 22 p3661 N71-36109
COMPOUND HELICOPTERS
Normal and compound helicopters to be used as short haul aircraft in view of burden on today's air traffic control 11 p1673 N71-32189
COMPRESSED AIR
Stabilized air pumping with diode type gas-iron pumps 03 p0351 N71-12338
Gas gun utilizing compressed air and helium for investigating office flow velocity [REF-1-469] 05 p0365 N71-13289
COMPRESSED GAS
NT HIGH PRESSURE OXYGEN
Statistical analysis on thermodynamic properties of dense gas normal paraffins 12 p2013 N71-24278
Flashovers across dielectric spacers in compressed gases of coaxial cylinder system with insulation recommendations [NLL-CE-TRANS-5434-19022.09] 17 p2787 N71-29634
Development history and application of free piston engine 19 p3175 N71-32621
Some aspects of propulsion for supersonic wind concept [NASA-TT-F-14005] 24 p4001 N71-38535
COMPRESSIBILITY
Static compressibility measurements of Cedar City tonalite using equations of state [AD-713175] 05 p0676 N71-15440
Young modulus, shear modulus, and compressibility of Fe-Ni (fcc) alloys [NASA-TT-F-13479] 08 p1299 N71-19151
X ray diffraction measurements on lithium fluoride compressibility and thermal expansion at high pressures and high temperatures 14 p2327 N71-26496
Simple empirical relation based on adiabatic compressibility, adiabatic bulk modulus, and reduced temperatures for liquid argon, krypton, and xenon, and application to mercury [NYO-4176-6] 15 p2378 N71-27982
Computer program for reduction of isothermal Burnett compressibility data [BM-IC-4491] 17 p2722 N71-29524
Compression corrections for Acme thread gages using graphs and formulas 21 p3428 N71-34393
Creep, break, gabbro, and diatom isochoric volume compressibilities and densities under 32,000 kg pressure [SC-T-713031] 23 p3082 N71-37168
COMPRESSIBILITY EFFECTS
Supersonic laminar boundary layer response to moving pressure field and solution of partial differential systems 10 p1543 N71-21342
This critical shell stability subjected to dynamical longitudinal compression [AD-719651] 13 p2182 N71-25352
Isothermal and adiabatic compressibility of liquid metals, particularly lead, from melting point to critical region [NYO-4176-4] 15 p2425 N71-27482
Compressibility and porosity of basalt from Apollo 12 lunar samples 15 p2518 N71-27990
Compressible heat transfer in low speed flow with small temperature differences [NPL-ABRO-1325] 21 p3390 N71-33135
COMPRESSIBLE BOUNDARY LAYER
Velocity distributions in compressible turbulent boundary layers with air injection in supersonic flow [ARC-RM-3627] 06 p0833 N71-15709

Model equations for studying compressible turbulent boundary layers

[NASA-CR-116781] 00 p1177 N71-18426

Finite difference method for solving equations for compressible turbulent boundary layers on swept infinite cylinders

[NASA-TN-D-6203] 10 p1539 N71-26709

Evaluation of turbulent shear models and prediction of compressible turbulent boundary layers by method of extended models

[NASA-CR-118079] 12 p1903 N71-24140

Compressible turbulent boundary layer flow past wind tunnel walls noting conductive heat transfer and ablation

[VKI-TN-67] 13 p2022 N71-24499

Compressible turbulent boundary layer predictions with heat transfer from flat plates in gas tunnel at Mach 9

[IC-AERO-70-05] 17 p2697 N71-29318

Numerical solution of flow equations for laminar, transitional, and turbulent compressible boundary layers for planar or axisymmetric flows

[NASA-TN-D-368] 19 p3078 N71-32164

Mechanics of free piston engine, aspects of human factors engineering, and compressible boundary layer studies at high Reynolds numbers

[DME/NAS-1971/11] 19 p3198 N71-32620

Streamwise pressure gradient effects upon two dimensional compressible boundary layers at high Reynolds numbers

19 p3082 N71-32623

Three methods for calculation of compressible turbulent boundary layer with pressure gradient and internal flow heat transfer with reference to supersonic nozzles

[TT-7104] 20 p3253 N71-33818

COMPRESSIBLE FLOW

NT TRANSONIC FLOW

Turbulent mixing between two compressible streams in constant area duct

[AD-71064] 01 p0839 N71-10010

Numerical simulation of instability growth rates in compressible inviscid fluid

[UCRL-30845] 01 p0043 N71-10476

Theoretical solution for pressure distribution over arbitrarily shaped periodic waves using Fourier series

[NASA-TN-D-3964] 02 p2082 N71-11548

Turbulent mixing between two compressible streams in constant area duct and with eccentric primary flow jet

03 p0362 N71-12762

Numerical study of shock formation of compressible fluid flow in cylindrical and two dimensional shock tubes

[ISAS-451-VOL-35-NO-9] 03 p0364 N71-13004

Diffraction of strong shock waves by sharp compressive corner

[AD-714584] 06 p0837 N71-16491

Analysis of compressible flow across shaft face seals

[NASA-TM-X-52599] 06 p0837 N71-16527

Subsonic compressible gas flow around semi-infinite plate in channel

07 p1006 N71-16946

The continuity equation of compressible flow with flow velocity distortions and gas density variations

[DLR-MITT-70-13] 07 p1008 N71-17167

Energy estimates for equations of compressible flow initial value problems

[LA-4525] 08 p1182 N71-18943

Supersonic laminar boundary layer separation measurements near compression corner at Mach numbers near 2.5

10 p1541 N71-21235

Computer program for analysis of compressible fluid flow across sealing dam consisting of two closely spaced parallel rings

[NASA-TN-D-5345] 10 p1566 N71-21434

Physical properties and rotational effects on isothermal compressible flow across shaft seals

[NASA-TM-X-52991] 12 p1898 N71-23102

Analytical model for run-out of flow instability and start of compressible transition

[AD-719759] 14 p2238 N71-25655

Antenna impedance measurements in compressible subsonic flow over atmospheric entry

[AD-720623] 14 p2322 N71-26146

Numerical analysis of compressible turbulent boundary layer skin friction with arbitrary pressure gradient and criteria for boundary layer flow separation

[AD-720627] 14 p2342 N71-26307

Flow generator design for compressible flow visualization and high pressure Mollier diagram

[AD-721193] 15 p2592 N71-26881

Finite difference theory using time and space step calculations for transient two-phase compressible flow in pressurized water reactors

[AABC/TM-558] 15 p2592 N71-26882

Turbulent boundary layers in compressible flow and their interactions with normal shock waves in zero and adverse pressure gradients

[ARL/ME-321] 15 p2594 N71-27602

Energy-integral prediction of hypersonic and laminar heat transfer in thermal boundary layer around blunt-nosed cones and of compressible flow with heat transfer

17 p2838 N71-29807

Computerized pressure transducer and thermocouple system for compressible flow measurements

[GAT-T-1649] 18 p2598 N71-31549

Holographs applied to calculation of compressible flow on turbomachine blades and use of visualization terminal display

[ONERA-TN-179] 19 p3076 N71-31706

Operational Mach number increase by vortex flow compression

[AD-723279] 19 p3077 N71-31935

Method for predicting compressible turbulent boundary layers in adverse pressure gradients applied to hypersonic air breathing propulsion

[NASA-TM-X-2302] 19 p3078 N71-32210

Three dimensional axisymmetric ducts with axial velocity distributions in compressible flow

[TAB-123] 21 p3410 N71-34264

Analysis of compressible turbulent mixing of parallel coaxial hydrogen-air jets at supersonic speed for outer jet and subsonic speed for inner jet

[NASA-TN-D-6467] 21 p3413 N71-34283

Numerical solution of Navier-Stokes equations for compressible viscous gas in near-wake behind trailing face of flat plate in supersonic flow

[NASA-TT-F-13993] 23 p3742 N71-36678

Numerical solution of partial differential equations governing initial development of general nonisothermal compressible free shear layer

[NASA-CR-1828] 24 p3906 N71-37842

COMPRESSIBLE FLUIDS

Apparatus for tensile strength testing of specimens by pressurized fluid

[NASA-CASE-XKS-06250] 05 p0689 N71-15600

Compressible circular jet instabilities with respect to spatially growing disturbances

[DLR-FB-70-51] 08 p1178 N71-18471

Computer program for analysis of compressible fluid flow across sealing dam consisting of two closely spaced parallel rings

[NASA-TN-D-5345] 10 p1566 N71-21434

Wave propagation through compressible fluid from transient pulsations of spherical elastic shell

[ARL/SM-352] 12 p1968 N71-24155

System of nonlinear equations of motion for isotropic, compressible fluid solved by cyclic relaxation method for subsonic and transonic regimes

16 p2580 N71-26888

Calculation of dynamic and thermal characteristics of gas circuit in variable flow conditions with application to studying reactor under natural convection flow conditions

[NLL-CB-TRANS-3375-19022.09] 17 p2733 N71-29574

Low frequency analysis of rocket engines using compressible propellants

17 p2835 N71-29584

Properties of three dimensional compressible fluid flows obtained by application of invariant transformation to equations of motion

[AD-719333] 24 p3907 N71-37849

Coupling of monochromatic elastohydrodynamic waves propagating in compressible fluids

[AD-719352] 24 p3995 N71-38500

COMPRESSION

Adiabatic compressional cooling of He 3 to millikelvin temperatures

[UCSD-34-F-143-27] 08 p1305 N71-19050

Method and apparatus for producing very low temperature refrigeration based on gas pressure balance

[NASA-CASE-XNP-18877] 11 p1773 N71-23025

Bandwidth compression by signal distortion using nonlinear device

[SRDE-70051] 12 p1674 N71-23360

Recompressing underwater long wave acoustic signals distorted by surface waves

[BMVG-FBWT-71-3] 18 p2889 N71-30641

Electron rings and compression cycles at high and low intensities

[UCRL-20183] 21 p3481 N71-34799

Ultrahigh frequency heating and adiabatic compression of plasma in Tuman-2 facility

[CONF-710697-141] 23 p3826 N71-37287

COMPRESSION BECKLING

U BECKLING

COMPRESSION LOADS

NT AXIAL COMPRESSION LOADS

NT IMPACT LOADS

Measuring electrical resistance and pressure behavior of actinide elements

[FOA-4-C-4434-23] 05 p0701 N71-15060

Lower critical load of conical shell under longitudinal compression

[AD-714768] 06 p0954 N71-16040

Creep buckling of plates under compressive loads

07 p1127 N71-17954

Stress analysis of spherical shell compressed between rigid plates with axisymmetric postbuckling and nonsymmetric buckling

[AD-716791] 10 p1655 N71-21190

Development of model for behavior of foams under uniaxial and multiaxial loads and extension to post-yield behavior of foams under compression

10 p1807 N71-31399

Dislocation density dependence on compressive shear stress measured by etch-pit techniques in high purity and Mg doped, strain hardened LIP single crystals

[NRC-TN-1447] 12 p1987 N71-32020

Dielectric constant of polyethylene under shock compression in pressure range 16 to 246 kb

[AD-718033] 12 p1947 N71-34229

Buckling coefficients of clamped shear plates under individual loading with in-plane stresses expressed in orthogonal components

18 p3021 N71-31850

Stress analysis and deformation of perforated plate elements subjected to compressive buckling

[NASA-CR-121669] 21 p3526 N71-35137

Effects of combined loading on buckling of clay supported shear plates based on Rayleigh-Ritz method

[AE-299-S-PT-2] 22 p3489 N71-36308

COMPRESSION TESTERS

U COMPRESSION TESTS

COMPRESSION TESTS

Deformation of crystals of alpha plutonium in compression - conference

[UCRL-72597] 03 p0499 N71-13609

Compression tests on FFTF fuel subelements

[WEAN-FR-16] 07 p1044 N71-17580

Averaging for in-pile compressive creep studies of LMPFR ceramic fuels during irradiation

[BML-1894] 14 p2292 N71-25711

Compression tests on SD 505 polystyrene head foam

[UCRL-50952] 15 p0428 N71-20023

Compression tests for establishing possible thermal effect of tectonic deformation of rocks

[NASA-TT-F-13707] 16 p2585 N71-28220

Transient pressure, temperature, and density measurement of high temperature dense gas during compression tests

[VKI-TN-23] 20 p3349 N71-32355

Recording of flow curves in tensile tests and compression tests with and without preloading

[RAE-LB-TRANS-1549] 20 p3204 N71-33228

Mylar, Teflon, and Kapton film effects at elevated temperatures on compression sets of cellular silicon rubbers used to cushion dissimilar weapons-related components

[BDX-613-410] 23 p3778 N71-36925

COMPRESSION WAVES

Measuring acoustic parameters of volcanic rocks from compressional and shear wave velocities

[USGS-474-49] 06 p0831 N71-16080

Using two-fluid collisionless plasma model to describe behavior of fully ionized gas under axially symmetric radial compression

08 p1275 N71-19048

Theoretical analysis of seismic compression waves and comparison with experimental results from underground nuclear explosions in Sahara

[CEA-R-4105] 15 p3399 N71-2474

Temperature effects on microwave frequency compression wave attenuation in aluminum oxide and ruby crystals

17 p2721 N71-29912

Calculation of ground motions generated by air waves from surface explosions

[UCRL-TRANS-10529] 21 p3421 N71-34340

COMPRESSION STRENGTH

Mechanical twinning of titanium single crystals

[AD-710699] 01 p0110 N71-10085

P wave velocity and compressive strength of Italian rock specimens at hydrostatic pressures up to 5000 kg/cm²

[NASA-TT-F-13209] 02 p0289 N71-11423

Coulomb strength criteria for estimating strength and stability of rock formations

[BM-R-7449] 02 p0211 N71-11513

Variations in crushing strength of paper honeycombs

[AD-711557] 02 p0248 N71-12981

Theoretical maximum compression strength determinations for reinforced materials

[AD-712937] 03 p0197 N71-13181

Compressive and fracture strengths of carbon fiber reinforced plastics

[ARC-CP-1132] 06 p0876 N71-19702

Theoretical limits of compression strength of reinforced materials

[NASA-TT-F-13443] 06 p0881 N71-16093

Amine catalyst effects on compressive strength of rigid urethane foams

[BDX-613-170] 07 p1947 N71-17280

Conical shell stability under dynamical longitudinal compression

08 p1309 N71-19162

Effects of selected minor alloying additions on structure and deformation of beryllium

08 p1219 N71-15016

Creep rupture strength of reinforced plastics under uniaxial compression

[NASA-TT-F-13441] 08 p1309 N71-19274

Longitudinal strength of unidirectional fibrous composites
[AD-716629] 09 p1402 N71-19004

Numerical analysis of compression of elastic cylinder between two smooth, flat, and parallel rigid plates
[AD-719376] 13 p2177 N71-34616

Compressive surface glazing for improved strength of ceramic materials
13 p2181 N71-35315

Stress range components and creep fatigue behavior of steel related independently to cyclic life by equations in both tension and compression
[NASA-TM-X-67838] 13 p2523 N71-37945

Mechanism impregnation and polymerization effects on sandstone and volcanic tuff compressive strength and elastic properties
[BM-81-7343] 19 p3097 N71-32729

Production of refractory concretes and determination of compressive and tensile strength at various temperatures
22 p3408 N71-35636

COMPRESSOR BLADES

Heat flux measurements on fixed turbine and compressor blades in supersonic flow
[ONERA-TP-871] 02 p0505 N71-11135

Manufactured elastot pressure sensor for this purpose
[ONERA-TP-800] 02 p0226 N71-11682

Swirlback-bladed centrifugal compressor overall performance in argon
[NASA-TM-X-2129] 03 p0310 N71-12209

Supplementary data tables for single stage experimental evaluation of compressor blade with slots and vortex generators
[NASA-CR-72778] 05 p0426 N71-14672

Data and performance of stage four of compressor blades with slots and vortex generators
[NASA-CR-72741] 05 p0626 N71-14740

Evaluation of range and distortion tolerance for high Mach number transonic flow stages - Vol. 1
[NASA-CR-72767-VOL-1] 05 p0462 N71-14851

Evaluation of range and distortion tolerance for high Mach number transonic flow stages - Vol. 2
[NASA-CR-72767-VOL-2] 05 p0462 N71-14852

Aerodynamic design of symmetrical blading for stage three axial flow compressor test rig
[AD-714385] 06 p0793 N71-16565

Low speed boundary layer separation on compressor blades of varying aspect ratios
[AEC-CR-1185] 07 p0966 N71-17108

Interference effect between oscillating and distorted inlet flow on compressor stall
09 p1313 N71-19370

Additional plot and flow fence effects on aerodynamic characteristics of single stage compressor blading
[NASA-CR-72635] 11 p1734 N71-21995

Rotated blades and vane and rotor tip design for highly loaded, low speed fan stage applicable to low noise aircraft engines
[NASA-CR-72895] 16 p2671 N71-28315

PORTMAN 4 computer program for design application of stagger angle replacing inlet flow angle for given blade cascade
[NASA-CR-121679] 21 p3410 N71-34262

Resistance welding to join compressor and turbine parts reducing weight and cost of jet engines
[NASA-CASE-LAW-10533-1] 21 p3433 N71-34424

Vibration strength of compressor blade steels, titanium alloys, and aluminum alloys at high temperatures
[AD-727951] 24 p3936 N71-38096

COMPRESSOR EFFICIENCY

Additional slot and flow fence effects on aerodynamic characteristics of single stage compressor blading
[NASA-CR-72635] 11 p1734 N71-21995

COMPRESSOR ROTORS

Simulating downstream flow blockage down in bypass air duct of turbine engine with axial flow fan rotor
[NASA-TN-D-6071] 01 p0115 N71-10671

Effects of rotation on boundary layers in turbomachinery rotors
[PB-192316] 03 p0309 N71-12202

Data and performance of stage four of compressor blades with slots and vortex generators
[NASA-CR-72741] 05 p0626 N71-14740

Experimental data and performance of honeycomb rotor shroud configuration to improve stall margin of 0.5 inch tip radius stage compressor
[NASA-CR-72880] 05 p0762 N71-15328

Flow distribution data for solid and honeycomb rotor shrouds to improve stall margin of 0.5 inch tip radius stage compressor
[NASA-CR-72889] 05 p0762 N71-15329

Design and tests of WTP-46 single rotor compressor rotor
[AD-715626] 08 p1204 N71-18001

Thin plasma chamber noise measurement comparison of 26 inch diameter fan rotors with aspect ratio of 3.6 and 6.6
[NASA-TM-X-2191] 09 p1316 N71-19707

Slotted blades and vane and rotor tip design for highly loaded, low speed fan stage applicable to low noise aircraft engines
[NASA-CR-72895] 16 p2671 N71-28315

Design of axial compressor rotor - specification of meridional velocity profile
[AD-72824] 18 p3001 N71-31214

Resistance welding to join compressor and turbine parts reducing weight and cost of jet engines
[NASA-CASE-LAW-10533-1] 21 p3433 N71-34424

Visualized flow patterns of airflow in centrifugal rotors with thin plate blading and with thick airfoil blades
[BM-82-238] 23 p3785 N71-36410

Performance tests and efficiency measurement of hub-diffusion stage in single stage compressor
[NASA-CR-128003] 24 p3905 N71-37836

COMPRESSOR ROTORS

NT CENTRIFUGAL COMPRESSORS

NT SUPERCHARGERS

NT SUPERSONIC COMPRESSORS

NT TRANSONIC COMPRESSORS

NT TURBOCOMPRESSORS

Nuclear Brayton turboalternator compressor with turbine inlet temperature consistent with SNAP 8 capabilities
[NASA-CR-111565] 03 p0417 N71-13064

Thermal pump-compressor for converting solar energy
[NASA-CASE-XLA-00377] 07 p1130 N71-17410

Isentropic-compression tube techniques producing hypersonic flow in wind tunnels including isentropic flow and free-piston shock tube modes
[AD-717727] 11 p1731 N71-22158

Influence of disc valve springs on action of valves and functioning of compressor
[NLR-RTS-958] 17 p2756 N71-29825

Compressor vacuum chambers for electron ring accelerator research
[UCRL-20177] 19 p3153 N71-32206

Dynamic models of negative mass instabilities in particle accelerator electron ring compressor
[UCRL-20208] 20 p3323 N71-33833

Effects of synchrotron radiation from electrons in compressors for electron ring accelerators
[UCRL-TRANS-1435] 21 p3464 N71-34823

Efficiency estimates of turbine and compressor components of Brayton rotating unit during hot closed loop operation
[NASA-TM-X-2350] 22 p3542 N71-35252

COMPTON EFFECT

Photon monochromator with Compton-scattered gamma rays as energy source
[IS-2335] 03 p0423 N71-12741

Photofluorescence of U-235 and U-238 using Compton scattering monochromator
[IS-T-375] 03 p0425 N71-12831

Resonance product estimated from superconvergent sum rule obtained from helicity flip amplitude of pion-Compton scattering
[BLL-2041-42] 05 p0742 N71-15122

Calculating resonance contributions to deep inelastic electron scattering using semiempirical model of electron spectrum
[NYO-4075-2] 05 p0742 N71-15123

Calibration of high intensity flux X ray machine by Compton effect measurements
[BGG-1183-2230] 05 p0742 N71-15127

Electric field due to polarization of air during progress of Compton currents excited by photons
07 p1014 N71-16932

Gamma ray spectrometer design for intense gamma fields incorporating Compton spectral detector
[NASA-CR-103046] 08 p1204 N71-19136

Extrinsic gamma ray spectra from Compton interactions and bremsstrahlung production
13 p2159 N71-24776

Charged pion lifetimes, photoabsorption cross sections for complex nuclei, and Compton scattering
[UCSB-34-P-135-12] 13 p2132 N71-25110

Continuous moment sum rule for calculating Compton scattering at high energies
[TUBP-71-2] 13 p2140 N71-25500

Off-axis hyperbolic etching method for Ge/Li detectors and anti-Compton spectrometers
[NP-18653] 14 p2528 N71-26592

Measurement of Compton scattering on protons at 6 GeV and small momentum transfer
[DESY-70/46] 15 p3463 N71-27173

Isotactic diffractive neutral pion photoproduction via diffractive rho-isobar production and Compton scattering
[DESY-70/45] 15 p3467 N71-27363

Differential cross sections for proton Compton effect at 66, 75, and 90 deg for incident photon energies from 600 to 850 MeV
16 p3653 N71-29010

Computer programs for reduction of Compton recoil electron energy distribution measurements to continuous gamma spectra
[ANL-7611] 17 p2793 N71-29446

Hydrogen bubble chamber study of polarized gamma production yields pion/pion⁰/pion⁺/pion⁻ proton at 2.8 and 4.7 GeV produced by Compton backscattering
[UCRL-19890] 17 p2804 N71-30226

Kinetic theory of Compton scattering by relativistic electrons with induced scattering
[NASA-TT-F-15738] 17 p3229 N71-30281

Validity of Cottingham formula relating electromagnetic self mass of hadrons to integrals over forward virtual spin averaged Compton scattering
[TR-71-125] 17 p775 N71-30541

Low energy theorems for Compton scattering off arbitrary spin targets with scattering amplitude dominated by Born approximation
17 p3889 N71-30664

Cyclotron radiation, relativistic velocities, angular distribution, total power, electron distribution, and inverse Compton scattering
20 p3444 N71-32840

Nuclear Compton effect sum rule calculation from dispersion relation and low energy theorems
[JHEP-P2-5679] 22 p3633 N71-35089

Integrated Compton cross section and its effect in Monte Carlo schemes
[LA-4952] 22 p3638 N71-35934

Thin Ba(Ti) crystals for estimating natural terrestrial background in 17 and 40 keV energy regions from Compton continuum peak
[UCRL-72927] 22 p3644 N71-35963

Destruction of low energy theorems for Compton-type scattering of strong magnetic vector and axial vector currents and neutron-nucleon sum rules
[BIRP-127] 22 p3647 N71-36011

COMPUTATION

NT ORBIT CALCULATION

PORTMAN program for computing coordinates of circular arc single and tandem turbomachinery blade sections on plane
[NASA-TM-D-6050] 01 p0001 N71-10411

Automatic computation theory and problems of program complexity, complexity measures for finite automata, algorithms for linear products, and complexity of iterations
[AD-712843] 03 p0341 N71-13409

Computational work and efficient computation on general purpose machines
[NASA-CR-115828] 04 p0208 N71-13499

Calculation of digital current distribution systems on micron type cores
[AD-714748] 06 p0822 N71-15936

PORTMAN program for computation of group tables, alphanumeric display
[NASA-TM-X-2172] 07 p1051 N71-17338

Apparatus for computing square roots
[NASA-CASE-XGS-04765] 09 p3332 N71-19437

RSYN and SDB codes for flux and bulk parameter computation of fast reactors
[WHAIR-TR-40] 12 p1964 N71-24152

Nuclear, theoretical, and neutron physics research and computation
[ARCL-3467] 16 p0657 N71-29121

Design of computational algorithms for optical control by Hilbert space methods, and involving cost function
[NASA-TN-D-6269] 21 p3449 N71-34551

COMPUTER COMPONENTS

NT COMPUTER GRAPHICS

Reviewing development of digital computer systems and components for aerospace vehicles
03 p0346 N71-12682

Inspection device with warning system for RW 330 computer near CARI reactor
[CBA-N-1274] 04 p0547 N71-13638

Recovery algorithms and avoidance of deadlocks in application of cellular array logic to LSI
04 p0502 N71-13657

Classification and survey of computer system performance evaluation techniques
04 p0503 N71-13661

Computerized control system with linear calculator for control computer experiments
[RT/EL/60/12] 04 p0506 N71-14237

Multiaccess computer memory with cyclic service allocation
[UCRL-72640] 10 p1530 N71-21657

Computer circuit performing both counting and shifting logic operations also capable of miniaturization and integration in basic circuits
[NASA-CASE-XOP-04753] 11 p1721 N71-22897

Development in integrated circuit production and utilization as computer components
[JPRS-53659] 12 p2901 N71-31555

Analog signal processing using analog computer components
[DRL-MITT-71-46] 19 p3660 N71-31697

Reliability optimization for series-parallel systems and specially connected 1-out-of-n type systems, with cost constraints and reliability considerations
[NASA-TM-X-67910] 20 p3291 N71-33429

Projected developments for computer systems technology
24 p3893 N71-37743

Equipment specifications for interactive program system for image processing with IBM 360 and PDP 8 computer components
[JCOO-2115-3] 24 p3894 N71-37753

COMPUTER DESIGN

Advances in electronic and timing computers
[JPRS-51323] 01 p0020 N71-10504

- Development and characteristics of electronic keyboard calculator [AD-711753] 02 p0186 N71-11308
- Design of analog computer with constant diagnostic monitoring [AD-711144] 02 p0186 N71-11309
- Cascade synthesis of logic functions [AD-711154] 02 p0186 N71-11310
- Design and characteristics of matrix oriented cellular computer [AD-711305] 02 p0187 N71-11311
- Mutual exclusion or interlock problem applied to computer operations [NASA-CR-111401] 02 p0188 N71-11319
- Computer designing and programming [NASA-CR-115819] 04 p0382 N71-13654
- Unified hardware/software design for computer systems optimization 04 p0503 N71-13662
- Design of special purpose computer using FFT to perform speech analysis in real time 04 p0503 N71-13663
- Application of domain logic in designing associative processors for spaceborne use [NASA-CR-113865] 05 p0652 N71-15535
- Photocardiographic preprocessor using breadboard circuit consisting of full wave rectifier with simple resistance capacity filtering [NASA-TM-X-65420] 06 p0805 N71-15848
- Simulation model for advanced avionics digital computers [AD-714140] 06 p0894 N71-16295
- Functional analysis of graphic computer [D-1-70-01] 07 p0996 N71-17090
- Technical summary of reconfigurable guidance and control computer for space station application - Vol. 1 [NASA-CR-114679] 09 p1354 N71-19788
- Design and development of reconfigurable guidance and control computer for space station applications - Vol. 2 [NASA-CR-114880] 09 p1354 N71-19789
- Requirements for performance of reconfigurable guidance and control computer for space station applications - Vol. 3 [NASA-CR-114881] 09 p1354 N71-19790
- Design and development of input/output processor and voter-comparator switch concept of guidance and control computer for space stations - Vol. 4 [NASA-CR-114882] 09 p1354 N71-19791
- System analysis and computer requirements derivation of guidance and control computer for space station applications - Vol. 5 [NASA-CR-114883] 09 p1354 N71-19792
- D-200 computer family, system error analysis, reliability derivation, and power converter design for reconfigurable guidance and control computer - Vol. 7 [NASA-CR-114885] 09 p1354 N71-19794
- Development of eclectic information processing system for computer design [NASA-CR-117304] 09 p1355 N71-19923
- Design, development, and test of ferrite memory system for application as computer storage device [AD-714140] 09 p1358 N71-11233
- Characteristics of self-powered, multichannel digital data buffer designed to expand input capability of electronic scope generator [NASA-CR-114925] 10 p1529 N71-21463
- Development of programming languages, syntax, algorithms, and subroutines for digital computers [AD-714686] 10 p1529 N71-21561
- Deep 1 general purpose computer system 11 p1718 N71-22733
- General purpose digital computer system using Deep 1 control components and Minsk 2 magnetic tape units 11 p1719 N71-22739
- Computer designing and programming, and man machine systems - conferences 14 p2223 N71-26186
- Experience with Extendable Computer System Simulator as special-purpose language for computer systems modeling [NASA-CR-118688] 15 p2384 N71-27722
- Airborne/spaceborne computer design and techniques for space shuttle data management systems [NASA-CR-118832] 15 p2384 N71-27782
- Computer and data processing developments [CERN-71-6] 18 p2892 N71-30484
- Feasibility of unified compilers for network analysis [NASA-CR-119663] 18 p2896 N71-31370
- Development of theory for formal neurons as mathematical basis for creation of highly reliable cybernetic systems and computers 19 p3061 N71-32015
- Design criteria for guidance and control spaceborne computer selection including physical and functional characteristics and reliability [NASA-SP-0070] 20 p3329 N71-33679
- Development of arithmetic unit for decoding data encoded by convolutional encoding with fewer channels than prior units [NASA-CASE-NPO-11371] 21 p3399 N71-34187
- Development of computer memory system for automated attendance accounting system [NASA-CASE-NPO-11456] 21 p3399 N71-34189
- Advantages and disadvantages of some radical computer designs 21 p3399 N71-34191
- Design, development, and characteristics of modular spaceborne data processors for space shuttle applications 21 p3516 N71-35053
- Application of redundancy techniques for improved computer system reliability 21 p3516 N71-35054
- Design and development of subsystem interface unit, bus control unit, and supporting equipment for space shuttle data processing equipment 21 p3516 N71-35055
- Characteristics and advantages of data bus to facilitate data handling process on space shuttle 21 p3517 N71-35056
- Procedures for development and verification of complex software used in space shuttle data management system 21 p3517 N71-35059
- Development and characteristics of executive software for application to space shuttle data management system 21 p3517 N71-35060
- Development and characteristics of prototype computer system capable of mixed-initiative man-computer dialogue [AD-726441] 22 p3557 N71-35338
- Architectural design of spaceborne computer system operating in multi-element configuration [NASA-CR-121016] 24 p3892 N71-37377
- Projected developments for computer systems technology 24 p3893 N71-37743
- Basic requirements for computers designed for operations with control automation systems [AD-727265] 24 p3895 N71-37759
- Executive routine primitives and process control for spaceborne computer functional design specification - Vol. 3 [NASA-CR-1869] 24 p3897 N71-37777
- COMPUTER GRAPHICS
- NT DATA PROCESSING TERMINALS
- NT PLOTTERS
- Algorithms for tree threading for scanner traversal [AD-709231] 01 p0026 N71-10014
- Computer graphics terminal using storage CRT [CRC-TN-625] 01 p0026 N71-10035
- Combining conversational programming system and programmer oriented graphics operations with PL-1 computer language [AD-709905] 01 p0027 N71-10061
- Design of interactive graph reduction and analysis system [AD-709927] 01 p0028 N71-10621
- Switching and automata theory using computer graphics [AD-711080] 01 p0028 N71-10700
- PDP-1 computer graphics, man machine interfaces, and complex organic molecule synthesis [AD-711392] 01 p0028 N71-10752
- Use of computers for man machine modeling studies [AD-711638] 01 p0015 N71-10880
- Computer-aided coordinate measuring machine with closed circuit TV viewing system for inspecting printed circuit masters [SC-M-70-46] 03 p0376 N71-12770
- Computer graphic system for three dimensional structural design analysis 03 p0348 N71-13139
- Man machine system for finite element structural analysis with computer graphics 03 p0465 N71-13140
- Computer graphics terminal for disc profile design of gas turbine engine 03 p0348 N71-13141
- RAND video graphic system - approach to general user/computer graphic communication system 04 p0506 N71-13844
- Sophisticated graphic display system - GRACE 04 p0506 N71-13845
- Computer synthesis for classifying natural shapes and patterns including leaves 05 p0637 N71-14833
- Application of computer graphics to multiharmonic analysis of structural shells [AD-713101] 05 p0679 N71-15350
- Graphical method of removing outlier values from analytical data [BM-83-7472] 05 p0651 N71-15427
- Photocardiographic preprocessor using breadboard circuit consisting of full wave rectifier with simple resistance capacity filtering [NASA-TM-X-65420] 06 p0805 N71-15848
- Comparison of moving map display and two graphics with hand-held maps [AD-714061] 06 p0894 N71-16294
- Digital data processing techniques and supporting facsimile plotter hardware [AD-714378] 06 p0849 N71-16321
- AUPLLOT 2, set of callable subroutines for computer graphics [NASA-CR-116218] 06 p0820 N71-16508
- Topological manipulation of line drawings using pattern description language 06 p0821 N71-16460
- Functional analysis of graphic computer [D-1-70-01] 07 p0996 N71-17090
- Computer technology applied to optical systems analysis [AD-715263] 07 p1069 N71-17200
- Versatile FORTRAN 4 computer program for producing Cartesian plots suitable for publication using CalComp plotter [AD-715279] 07 p0997 N71-17082
- Literature survey on contour map and terrain invisibility processing [AD-715311] 08 p1185 N71-20202
- Characteristics of computer-aided mathematical analysis operating system 08 p1185 N71-20202
- Dual graph for maximal flow capacity of network [AD-715546] 08 p1172 N71-18808
- Computer graphics for satellite antenna geographic mappings [NASA-CR-116814] 08 p1146 N71-17022
- Parallel processing and graph program simulation [TID-25393] 09 p1335 N71-19705
- Discriminator algorithm for computer pattern generation and texture recognition [NASA-TN-D-5933] 09 p1390 N71-20244
- Computer controlled interactive graphic display system for hydrologic analysis [BNWL-1525] 11 p1716 N71-22208
- Oncological data processing system using general purpose computer and graphic input device 11 p1719 N71-22277
- Computer graphics display program for use in terminal operations and VSTOL approach and departure path synthesis [NASA-CR-117887] 12 p1896 N71-23106
- Testing of conic and hyperbolic multiquadrant topography consisting of geomorphologically derived areas for computer graphics [AD-718038] 12 p1905 N71-23380
- Digital simulation, digital filters, PDP 9 computers, on-line programming, hybrid computers, computer graphics, plotters, analog computers, optimization, and integrated circuits [RIEFT-29-7-70-400] 12 p1882 N71-23062
- Cathode ray tube display and recorder interface to provide graphical output for small digital computers [NASA-CR-118011] 12 p1883 N71-23067
- Color television graph plotter for use with PDP 9 digital computers [NASA-CR-118015] 12 p1883 N71-23068
- Computer controlled automatic tracking data analysis with graphic display 13 p2052 N71-25316
- Graphic computer program for plotting engineering drawings [RIEFT-70-8] 13 p2053 N71-23142
- FORTRAN for animated reconstruction of telemetry [AD-719741] 13 p2053 N71-23171
- Vocabulary for spacecrew communication with spaceborne computers with graphic display device [NASA-CR-103171] 14 p2221 N71-23922
- Computer graphics patching of failed flying spot digitizer events for a spark chamber EP experiment [RIEFT-205] 14 p2308 N71-24488
- AGNOS language to allow IBM 360/44 FORTRAN programmer access to Adage graphics facilities without recourse to computational facilities [TR-71-19] 14 p2224 N71-24611
- Computer programming for time sharing systems and graphic displays 14 p2225 N71-24640
- Designing visibility quality in highways by computer graphics 14 p2226 N71-24650
- Perspective highway viewing program for designing safe roads 14 p2226 N71-24651
- Using computer graphics for producing computer program forms, and for highway perspective 14 p2226 N71-24652
- CMPLLOT FORTRAN subroutine for graph and diagram plotting using CalComp 835 CRT plotter [TRITA-EPP-71-03] 15 p2383 N71-27134
- Oscilloscope, analog and logic units, generation of visual function, and method of associated dialing for nuclear physics visualization unit adapted to C3-90-10 computer [CRA-N-1363] 15 p2467 N71-27379
- CONPLOT 2 contour generating program with output of large cartographic quality contour map designed to form larger maps by combining other maps [AD-721018] 15 p2384 N71-27773
- Prompt effects computer program for weapons effect display system (WEIDS MOD 2) [UCRL-50892-VOL-6] 15 p2384 N71-27774
- Integrated circuit development, photolithographic interconnection of plastic imbedded semiconductor chips, semiconductor testing, magnetic film engineering and computer applications [AD-722075] 16 p2465 N71-28517

- Mathematical representation of kinematic structure of mechanisms and kinematic chains as abstract, linear graph
[AD-751357] 16 p3284 N71-20085
- Computer generation and plotting of synthetic holograms, binary holograms, and spatial filters
16 p3287 N71-20085
- Computer graphics of vibrational effects in ion particles collisions including electron ionizing excitation, nuclear capture, and molecular excitation and relaxation
[NASA-TN-D-6487] 17 p2795 N71-29749
- Computer graphic mapping of Maryland costs from solid color and infrared photographic remote sensing including microcomputer analysis
[AD-750501] 17 p3749 N71-30176
- Real machine hardware problems in graphic display including applications in various fields
[NASA-TT-2-1301Q] 18 p3284 N71-31081
- Software for computer aided design of logical circuits for study of interactive computer graphics
[AD-722895] 18 p3284 N71-31412
- Reviewing continuous systems simulation techniques with emphasis on interactive, graphic-based systems
[P-6953] 19 p3681 N71-33281
- Computer plots of accelerating flight data of Nuclear Navy O, OAO 2, and ATB showing selected initial axis forcing functions and dynamic response of Center main engine cutoffs
[NASA-CR-119593] 19 p3381 N71-33271
- Computer graphics on-line programming for synthesis of natural shapes and patterns with nose and tail sections
[AD-724134] 20 p3237 N71-33813
- On-line computer graphics program for on-line data of aircraft drive variables
[AD-724622] 20 p3238 N71-32985
- Pattern recognition, speech recognition, man-machine systems for computer graphics, information systems, and data communications
[NPL-COM-SCI-48] 20 p3238 N71-33213
- Graphic flow simulation and motion picture flow visualization of reactor blowdown calculations
[DOE-TF-10502-4] 20 p3251 N71-33556
- Techniques for extracting objects from gray value and color computer-generated pictures including selection criterion from noisy backgrounds
[P-145] 21 p3409 N71-34195
- Methodology of computer graphics to include graphics applications, animation, graphics languages and interactive packages, and graphic text manipulation
[P-4028] 21 p3400 N71-34197
- Modified computer graphics program for rapid data input and display
[AD-722877] 22 p3556 N71-33527
- On-line computer graphics program applied to NASA-TM for checking finite element models prior to detailed analysis
22 p3587 N71-36295
- Interactive graphic instructional program illustrating basic concepts of systems analysis - INSGRINT
[N7-71-21] 22 p3498 N71-36371
- Factor routines for IBM 1800 computers performing graphic presentation of data with minimum programming effort
[NASA-TM-X-57708] 23 p3728 N71-36576
- Computer graphic techniques, computer systems and management, and digital waveform processing for medical man/machine communications
[AD-726623] 23 p3738 N71-36587
- Interactive graphics for computerized design of integrated circuit layouts
23 p3736 N71-36637
- Graphical display computer program for OAO2 nonlinear scheduling system
[NASA-TM-X-57723] 24 p3882 N71-37736
- Subroutines for PDP-10/0010 4000 graphic line plotter for hybrid and digital simulation
[N7L-5-55] 24 p3882 N71-37741
- Graphics applications program for computer design of integrated circuit cards
[N7L-7257] 24 p3884 N71-37751
- COMPUTER METHODS**
- COMPUTER PROGRAMS**
- COMPUTER PROGRAMMING**
- LANGUAGE PROGRAMMING**
- MICROPROGRAMMING**
- MULTIPROGRAMMING**
- ON-LINE PROGRAMMING**
- SYMBOLIC PROGRAMMING**
- Real time with list processing capability
[P-6953] 21 p3681 N71-33281
- Subroutine of program for certain AFL
[NASA-CR-111118] 21 p3681 N71-33281
- Low-altitude satellite interaction study of second and third order Cule computer techniques for simulating flow field and spacecraft interaction
[NASA-CR-111136] 21 p3681 N71-33281
- Research achievements in simulation mathematics, and languages - review
[NASA-TM-X-57708] 21 p3681 N71-33281

- Analysis of charting abilities with description of associated computing program
[NASA-TM-D-5883] 22 p3894 N71-11137
- Description and flow chart of PDP 7/9 communication package
[AD-711377] 22 p3878 N71-11349
- Manual for implementing general purpose computer
[NASA-TM-D-530] 22 p3878 N71-11354
- Minimal evaluation or internal problem applied to computer operations
[NASA-CR-111491] 22 p3878 N71-11359
- Concepts of Space Programming Language
[AD-711706] 22 p3878 N71-11358
- Programming language for solving symbolic mathematical problems
[AD-716446] 22 p3878 N71-11358
- Design of parallel processor for Data Classification Recognition (DCR) decoding
[AD-711366] 22 p3878 N71-11352
- Recognizable and representation of parallel processes in stream in computer program
[NASA-CR-109354] 22 p3878 N71-11353
- Computer programming requirements in support of solar astronomy experiment on manned space station
[NASA-CR-102917] 22 p3878 N71-12638
- Automatic computation theory and problems of program complexity, complexity measures for finite automata, algorithms for linear problems, and complexity of iterations
[AD-712843] 23 p3431 N71-12469
- Design and construction of flexible and efficient interactive programming systems
[AD-717211] 23 p3431 N71-12473
- Computer program for selection, editing, and dissemination of engineering and scientific educational literature from NASA technical reports
[NASA-CR-111613] 23 p3432 N71-12477
- Digital computer program requirements to process Apollo spacecraft electrical data for small circuit analysis
[NASA-CR-108727] 23 p3432 N71-12482
- Conventional coding techniques including constructing inverse, algorithms, and code comparing for nonparallel decoding
[NASA-CR-111601] 23 p3432 N71-12486
- Cybernetics, computer programming, and automatic theory
[AD-708673] 23 p3532 N71-12544
- Investigating problems encountered in developing and maintaining airborne computer programs for guidance and control
23 p3546 N71-12686
- Investigating data word and instruction format factors for selecting common word length in aerospace computers
23 p3547 N71-12687
- Computerized classification of meteorological charts and development of forecast aids
[AD-712678] 23 p3548 N71-12738
- Outlining theorem-proving approach to automatic programming synthesis using recursive and heuristic methods
[NASA-CR-115811] 24 p3691 N71-13508
- Applying basic tools and techniques of industrial engineering to computer engineering
[WAFD-2-2511] 24 p3692 N71-13511
- Describing design and implementation of NPS LISP 1.5 VERB 1 programming system
[AD-712779] 24 p3692 N71-13512
- Computer designing and programming
[NASA-CR-115819] 24 p3692 N71-13654
- Significant digit arithmetic techniques on CDC 6800 computer
[LA-4476] 24 p3698 N71-13657
- Computerized control system with linear calculator for neutron spectrometer experiments
[ETRL-10/12] 24 p3698 N71-13657
- Computer process control applications with emphasis on oil and chemical industries
24 p3694 N71-14434
- Hardware development and standardized software for process control systems
24 p3694 N71-14435
- Programming documentation for extended capability of FORTRAN-PORTAN matrix abstraction
[AD-712640] 25 p3774 N71-14537
- Storing user data for extended capability of FORTRAN-PORTAN matrix abstraction techniques of structural analysis
[AD-713727] 25 p3774 N71-14538
- Computerized optimization of self acting harpoon-jaw bearing for maximum radial load capacity
[NASA-TM-X-52945] 25 p3691 N71-14608
- Deriving algorithm for floating point arithmetic using single length arithmetic register for most accurate approximation
[AD-713697] 25 p3713 N71-15249
- Empirical and analytical techniques for determining thermal radiation interchange factors
[NASA-CR-115862] 25 p3783 N71-15432

- Machine learning of structural descriptions from cases
[AD-713642] 25 p3691 N71-14608
- Computer produced algorithms in postorder transformation
[AD-713641] 25 p3692 N71-14601
- Mathematical of mass spectrometry literature for last half of 1968 compiled by computer method
[IS-3327] 25 p3692 N71-16713
- Verification of data structure - CAME
[AD-710553] 25 p3692 N71-16833
- Applying growing theory, network synthesis, and signal modeling to information systems
[JPRS-51962] 27 p1081 N71-16873
- Proving theorem of coding statements in arbitrary languages
27 p3696 N71-16976
- Design networks having prescribed driving-point impedance in Brown ladder
[AD-713534] 27 p3699 N71-17774
- Determining optimal dynamic output feedback controller for linear discrete systems
[NASA-CR-109382] 27 p3699 N71-16862
- Characteristics of computer-aided mathematical analysis operating system
[AD-713535] 28 p3165 N71-18742
- Computer program using finite element method for computing temperature distributions in thin shells of revolution
[NASA-TM-D-6108] 28 p3283 N71-18746
- Feasibility of computerized lateral life-cycle estimation
[NASA-CR-116815] 28 p3152 N71-19017
- Computer methods for fault isolation in systems checkout
[NASA-CR-1738] 28 p3167 N71-19117
- Presenting proposals for implementation of subprogram for computing and manipulating asymptotic expansion
28 p3228 N71-19199
- Experimental and computerized observation of measurements in fused sodium chloride channels
[NASA-CR-117854] 28 p3162 N71-19542
- Pulse polygraphy and chemometrics measurements for electrochemical measurements in fused salts
28 p3163 N71-19543
- Parallel processing and graph program simulation
[TSD-25295] 28 p3153 N71-19585
- Data reduction of chemically reacting gases
[NASA-TT-2-15486] 28 p3164 N71-20089
- Unconstrained minimization formulation of constrained problem, and penalty functions
28 p3140 N71-20134
- Computerized position scanning of short-lined radioluxes for studies of pulmonary physiology and blood flow in other organs
[N7O-3007-2] 28 p3146 N71-20615
- Data reduction and computer programming for ESR0 several production experiments
[EEO-FR-10017-70-315] 28 p3145 N71-20601
- Computer programming for manually controlled machine tools
[CRIF-MC-53] 28 p3152 N71-20644
- Self-organizing networks including threshold and logic networks, photoacoustic perception, dining systems, character recognition, and programming by essential selection
[AD-716796] 28 p3156 N71-20649
- Computerized solution of nonlinear differential equations for lateral navigation systems
[AD-717028] 28 p3159 N71-20763
- Perturbation expansion of Coulomb potential for determining pair distribution function in plasma
[AD-717835] 28 p3157 N71-20817
- User machine-oriented languages for simple data processing
28 p3157 N71-20822
- Supersubstituted high, strong polymer, and automatic word recognition
[JPRS-52589] 28 p3178 N71-21081
- Formulation of problem of dining production units in terms of regular scheduling
28 p3178 N71-21085
- Computer programming techniques for determining displacements and stresses of large complex structural systems
28 p3184 N71-21084
- Cloud three dimensional optical data processing
[AD-716533] 28 p3178 N71-21083
- Basic parameters for application of laser Doppler velocimeter, cross beam techniques in three modes of operation obtained by computer programming
[NASA-TM-D-6125] 28 p3177 N71-21085
- Software programs in automatic system for vehicle experiments
28 p3178 N71-21085
- Energy deposition in beam, computer revised code including multiplicity calculation, bodies of revolution, and geometry data facility
[AD-716002] 28 p3182 N71-23219
- Analysis of computer requirements for linear filtering algorithms
[AD-716416] 28 p3189 N71-23577
- Computerized image evaluation program, POLYTAGOS, using Fourier techniques
[AD-716865] 28 p3189 N71-23974

- Cooperative sequential queuing for buffer pool operator in multi-programming computer operation [SU-STAN-CR-71-222] 12 p1085 N71-34034
- Digital computer programming for phase diagrams in binary, ternary, and quaternary alloys [NPL-DCS-9] 13 p2092 N71-34497
- Aerospace engineering and computer programming manual for space shuttle synthesis program to simulate spacecraft trajectories and weight analysis for performance prediction [NASA-CR-114966] 13 p1173 N71-34823
- Space shuttle synthesis program manual including deck setup, input parameters, and symbolic operations for trajectory and performance predictions [NASA-CR-114964] 13 p1173 N71-34824
- Space shuttle synthesis program manual including weight, geometry, and trajectory simulation output data and error detecting codes for spacecraft performance prediction [NASA-CR-114965] 13 p1173 N71-34825
- Aerospace engineering weight-volume manual for space shuttle synthesis program trajectory and performance predictions [NASA-CR-114967] 13 p1173 N71-34826
- Computer codes for reactor shielding calculations [DBP/SEFP-894/70] 13 p1117 N71-34854
- Computing power of finite machines [NASA-CR-118636] 14 p2220 N71-35869
- Encoders designed to generate comma free international Reed-Muller type code comprising conversion of 64 6-bit words into 64 32-bit data for communication purposes [NASA-CASE-N70-10595] 14 p2232 N71-35917
- Conference on information retrieval and management information systems including construction of dictionaries, analysis of query formulations, and computer programming 14 p2221 N71-35976
- Syntax oriented data formatting to facilitate information input and retrieval 14 p2221 N71-35979
- Pattern recognition applied to extraction of documentation indexes from text - KWIC indexes 14 p2222 N71-35988
- Information system as subject of information science and informatics - terminological aspects 14 p2223 N71-35992
- EURATOM automatic documentation system, noting structure of index, information retrieval strategies, and performance evaluation 14 p2223 N71-35995
- Computer designing and programming, and man machine systems - conferences 14 p2223 N71-36166
- Research studies in chemical reaction kinetics, laser generation of plasmas, soil science, magnetohydrodynamics, tropical meteorology, computer programming, and imaging techniques [JPRS-51284] 14 p2339 N71-36452
- Computer programming for time sharing systems and graphic displays 14 p2323 N71-36460
- Adressable interface unit for computerized visual information processing system of earth resources information data [NASA-CR-114997] 14 p2226 N71-36463
- Iterative method for solving Marcian function by computer programming 15 p2379 N71-37029
- Computer programming for nuclear physics experiment control [IMI-B-96] 15 p2474 N71-37455
- Computer programming for atmospheric optics using Monte Carlo method 15 p2403 N71-37542
- CONFLOT 2 contour generating program with output of large curvilinear quality contour map designed to form larger maps by combining other maps [AD-721018] 15 p2384 N71-37733
- Computer programming manual for calculating nuclear explosion dust and air temperature effects including particle size distribution, wind, and thermal radiation effects [AD-72252] 16 p2586 N71-38351
- Real time capability, satellite monitoring, and system reliability of satellite recording and data base system - Tables of costs and studies [COM-71-06220] 16 p2590 N71-38874
- PROD computer programming for predicting satellite orbit decay under long term effects [RAE-TB-71097-PT-1] 17 p2844 N71-39418
- Computer programming for earth satellite orbit determination [RAE-TB-SPACE-156] 17 p2844 N71-39487
- Solving multicriteria problems of industrial plant controls with convex programming 17 p2713 N71-39538
- Updating of Mk 3 Mod 0 diagnostic program for Polaris submarine AN/EX-1 satellite navigation system [AD-72405] 17 p2779 N71-39670
- Algorithm for simultaneous minimization of multiple Beale's functions with application to telemetry system [NASA-CR-119830] 17 p2723 N71-39896
- Computer programming formulas for frequency and statistical analysis of random waveform signals including Fourier analysis, probability density functions, and autocorrelation [NASA-CR-115975] 17 p2775 N71-39857
- Programming computers to make decisions in management information systems [NASA-CR-119100] 17 p2863 N71-39268
- User's manual giving information on writing data for electric channel using computer program LHS 2 [RLAB-TT-135] 18 p2893 N71-39630
- Users manual for computer programming of distribution networks of water supply systems 18 p2893 N71-39642
- Photographic processing and pattern recognition using computer programming and photographic processing equipment [BMVG-FWVT-70-3] 18 p2894 N71-39673
- Algorithmic pattern generation with applications to isomeric and biological structures, and other branches of mathematics and computer science [PB-197604] 18 p2847 N71-31314
- Computer solution of allocation problem having 5600 variables, and Dantzig algorithm for solving convex function minimized over closed convex set [AD-722584] 18 p2895 N71-31344
- Feasibility of unified compilers for network analysis [NASA-CR-119863] 18 p2896 N71-31370
- Computer programming manual for calculating stress distributions in structural members and frames using iterative solution and matrix methods 19 p3186 N71-31655
- Computer programming system based on assembling techniques for geographical data processing [MITT-12] 19 p3060 N71-31780
- Angle calibrations from GPT computer program used in near real time sense to obtain improved radar calibration test data 19 p3054 N71-31865
- Capacitance distance gauge for dimensional measurement with digital readout or direct computer processing [Y-1783] 19 p3101 N71-32343
- Numerical method for restoration of planar image algorithm for use on digital computers [UCRL-73080] 19 p3062 N71-32469
- Introductory information for equations to perform guidance, navigation, and control onboard computation functions for space shuttle orbiter [NASA-TM-X-67218] 19 p3133 N71-32677
- Algorithm for local minimum of indefinite quadratic convex programming [NPL-DNAC-1] 20 p3238 N71-32869
- Game theory, information system for disease diagnosis, and model of warehouse system [JPRS-53701] 20 p3389 N71-32877
- Automatic testing of logic integrated circuits including computer program [LAAS-PUBL-747-748] 20 p3240 N71-32939
- Computer language for implementation of graphic tessellation algorithms [NASA-CR-119723] 20 p3239 N71-33564
- Monitor in telemetry playback system for automatic pulse code modulation processing [BC-DB-710211] 21 p3395 N71-34163
- Adaptive approach to dynamic allocation and release of buffer storage within computer systems [NASA-CR-119765] 21 p3397 N71-34171
- Listing for and tabulation of LIFTING ROBOT program results [NASA-CR-119923] 21 p3398 N71-34178
- Description of NONAME program and system for determining and analyzing satellite orbits and estimating geodetic parameters [NASA-CR-121662] 21 p3397 N71-34985
- Development of test and flight engineer language for space shuttle system [NASA-CR-121616] 21 p3312 N71-35027
- Briefing aids used for oral presentation describing development of test and flight engineer oriented computer language for space shuttle system [NASA-CR-121657] 21 p3312 N71-35029
- LIFTING ROBOT minimum Hamiltonian-stopover ascent multistage lifting booster optimization program input and example problem for mission planning [NASA-CR-119922] 21 p3318 N71-35069
- Computer programming of chess games 22 p3545 N71-35249
- Radiation chemistry of high polymers and computer techniques for data reduction [ORD-4659-1] 22 p3550 N71-35286
- Flow diagrams and comparison capabilities for software interfacing of flight data [NASA-CR-61360] 22 p3555 N71-35321
- Instructional strategies for optimizing learning processes and application of such principles to practical course of instruction in computer science [NASA-CR-121956] 22 p3556 N71-35326
- Distorted wave Born approximation code adaptation for IBM 360/50 computer use [ANU-P-367] 22 p3634 N71-35904
- New element preprocessor for NASTRAN programming to generate tables and routines for new elements 22 p3687 N71-36292
- Automatic generation of finite element input, load transparency, and symbolic parameters for NASTRAN simplification and error reduction 22 p3687 N71-36294
- Automated general purpose system for structural analysis using finite element method - Vol. 1 [AD-726564] 22 p3689 N71-36484
- Computer programmer manual for use with automated general purpose system for structural analysis - Vol. 3 [AD-726566] 22 p3689 N71-36486
- Computer program documentation and user manual for transient analysis attitude control propulsion systems [NASA-CR-115182] 23 p3728 N71-36777
- Computer program documentation and user manual for steady state attitude control propulsion system - Vol. 1 [NASA-CR-115184] 23 p3728 N71-36779
- Development of general computer simulation programs for attitude control propulsion systems and computer program documentation - Vol. 2 [NASA-CR-115185] 23 p3728 N71-36780
- Algorithms for operator identification in ALGOL 68 23 p3728 N71-36781
- Computer graphic techniques, computer system and management, and digital waveform processing for graphical man-machine communication [AD-726623] 23 p3730 N71-36789
- FORTRAN 4 program for generating fast neutron spectra and average multigroup constants utilizing cross section data from library - FERG [IN-1435] 23 p3715 N71-37110
- Computer program development for potential lift calculation about lifting bodies [AD-726628] 24 p3671 N71-37599
- Methods for improving and extending WIDOCMB MB computer code [AD-727627] 24 p3689 N71-37716
- Modified thermal analyzer digital computer program for heat transfer problems [NASA-CR-72944] 24 p3691 N71-37710
- Computer programming manual for calculating temperatures and reactant concentrations as functions of time and axial position in catalyzed continuous flow hydrogen-oxygen reactors [NASA-CR-120008] 24 p3692 N71-37719
- Automatic data processing systems for air traffic control, health services, operations research, management planning, information systems, and mobile machines 24 p3692 N71-37720
- Projected developments for computer system technology 24 p3693 N71-37720
- Characteristics and application of problem oriented language to mathematical programming and data processing 24 p3693 N71-37720
- Computer system language for job construction and control 24 p3693 N71-37720
- Advanced avionic digital computer development program [AD-727607] 24 p3695 N71-37720
- Digital computer bibliography, programming techniques and applications, and software standardization and reliability 24 p3696 N71-37720
- Conversion of computational algorithms for decreasing length of word format of code of computer for aircraft [AD-727917] 24 p3696 N71-37720
- Computer program for analyzing and simulating attack of low flying aircraft by anti-aircraft missiles and probability of aircraft survival [RAE-LIB-TRANS-1976] 24 p3696 N71-37724
- Executive routine primitives and process control for spacecraft computer functional design specifications - Vol. 3 [NASA-CR-18009] 24 p3697 N71-37777
- Computer programming for figuring large telescope mirrors 24 p3698 N71-37779
- Utilization of data processing equipment in business and application to decision making process [RAE-LIB-TRANS-1501] 24 p3698 N71-37780
- COMPUTER PROGRAMS
- NT COMPILERS
- NT COMPUTER SYSTEMS PROGRAMS
- NT EDITING ROUTINES (COMPUTERS)
- NT INPUT/OUTPUT ROUTINES
- NT MULTIPLE OUTPUT PROGRAMS
- NT OPERATING SYSTEMS (COMPUTERS)
- NT SUBROUTINE LIBRARIES (COMPUTERS)
- NT SUBROUTINES
- Liquid propellant rocket engine performance computer program with distributed energy scheme [NASA-CR-111006] 01 p0114 N71-40017
- Development and characteristics of automatic language processing system 01 p0126 N71-40015
- Development of machine translation system 01 p0126 N71-40016

SUBJECT INDEX

System analysis in computer programs responding to input data structures 01 p0027 N71-10145

Isolation and retrieval of facts through on-line computer terminal 01 p0027 N71-10147

Tracking error propagation and orbit prediction program for space surveillance system (AD-711077) 01 p0120 N71-10194

Flight control software package for digital flight control and landing system of CR-46C helicopter (NASA-CR-110995) 01 p0027 N71-10283

Guidance software package for digital flight control and landing system of CR-46C helicopter (NASA-CR-111023) 01 p0028 N71-10304

Computer parameter study of viscoelastic stress analysis and extension of cumulative damage relation in creep-fatigue 01 p0113 N71-10399

FORTRAN program for computing coefficients of aerodynamic drag and random turbulent boundary layer on airfoil 01 p0091 N71-10411

Computer-aided design of linear networks in memory domain (NASA-CR-111103) 01 p0036 N71-10426

Calculation method for large numbers of digital and analog function probabilities (NASA-TN-D-5967) 01 p0095 N71-10428

FORTRAN program for calculating aerodynamic forces from pressure or velocity distributions on blade (NASA-TM-X-3123) 01 p0001 N71-10467

Computer program for stability analysis on system of interconnected compartments (JNHL-TM-2413) 01 p0096 N71-10475

Computer program arrangements in library using the ratio analysis (TS-4) 01 p0075 N71-10506

Time share FORTRAN 4 program for calculating reaction pattern interplanar spacing (Y-729) 01 p0096 N71-10521

Program for calculating neutron ages using ENDF/B library (WAPD-TM-422-ADD-1) 01 p0008 N71-10635

User manual for DOT-3W discrete ordinates transport computer code (WNL-TM-1902) 01 p0101 N71-10833

Computer program for mixed analysis of variance and based on maximum likelihood (NASA-CR-109704) 01 p0076 N71-10834

Computer program for analysis of folding strains on composite bladder structure (NASA-CR-111133) 01 p0130 N71-10837

Computer optimization of thermocouple calibration (AD-710761) 01 p0029 N71-10870

Photographic calibration for emission spectroscopy using small computer (NBS-21-7447) 01 p0057 N71-10876

Computer program for harmonic analysis of curved folded plate structures using finite element method (TS-19535) 01 p0131 N71-10883

Equations controlling wave transmission in lower ionosphere and computer program for integrating numerical solution (NASA-CR-111125) 01 p0052 N71-10971

Applied and research activities at Center for Computer Sciences and Technology 01 p0030 N71-10978

Computerized calculations of adiabatic nuclear boundary layer and shock wave interactions using Shallow method (NBS-TM-70) 02 p0143 N71-11017

Computer program for pattern recognition of acoustic signals (AD-712009) 02 p0145 N71-11175

Computerized radar signal processing for stationary ground target detection in clutter environment 02 p0100 N71-11240

Analysis of pattern description language for describing line drawings 02 p0106 N71-11305

Library of models for parallel computer (NASA-CR-111412) 02 p0107 N71-11312

Analysis of parallel systems (NASA-CR-111415) 02 p0107 N71-11313

Analytical procedures for system modeling and control of real time computer networks 02 p0107 N71-11316

Computer programs for processing telemetric data from satellite data transmission (NASA-TT-F-13367) 02 p0107 N71-11317

Overview of evolution of space programming language (TS-711709) 02 p0100 N71-11321

Building language subject, form, and highlights of new programming language 02 p0100 N71-11322

FORTRAN computer program for IBM 2250 display job (AD-711008) 02 p0109 N71-11329

Registration and representation of parallel processing in computer programs (NASA-CR-109534) 02 p0100 N71-11333

Computer analysis of logic circuits (LAAS-9143-514) 02 p0196 N71-11374

Developing digital computer program for converting soft parameters of thermal network by Kalman filtering method (NASA-CR-108081) 02 p0300 N71-11403

Computer programs and predictor displays for solving air traffic control problems (NASA-CR-111573) 02 p0302 N71-11466

Move code for use in multiple-point and point ray Monte Carlo transport code (AD-711941) 02 p0374 N71-11853

Computer programs for solid propellant orthogonality by rapid desuperization (AD-712116) 02 p0388 N71-11881

Computer programs for dynamic structural analysis (AD-711519) 02 p0380 N71-11944

Manual of computer programs for generating characteristics of earth satellites (JAE-TM-59164) 02 p0396 N71-11960

Digital simulation of seismic rays (AD-712092) 02 p0315 N71-11963

Finite element method for obtaining approximate three-dimensional stress solutions for laminated plates (AD-711399) 02 p0340 N71-12176

Intersect node/Automated Snark Program (NASA-CR-108724) 02 p0339 N71-12450

Local path report/Automated Snark Program (NASA-CR-108741) 02 p0339 N71-12451

Description of Node Report Data Generation Program (NASA-CR-108743) 02 p0339 N71-12452

Initial disconnect/Automated Snark Program (NASA-CR-108735) 02 p0339 N71-12453

Regeneration-1/Automated Snark Program written in COBOL for IBM 360 computer (NASA-CR-108739) 02 p0339 N71-12454

Computer program for processing BED data for use by other programs in Automated Snark Program System (NASA-CR-108729) 02 p0339 N71-12456

Computer program for reporting paths by operating on branch and node table data sets using indexed sequential access method (NASA-CR-108738) 02 p0339 N71-12457

Automated Snark Program written in COBOL for check analysis on IBM 360 computer (NASA-CR-108723) 02 p0340 N71-12459

Branch/Cross Reference Table program written in COBOL for IBM-360 computer (NASA-CR-108737) 02 p0340 N71-12461

Snark utility/Automated Snark Program (NASA-CR-108725) 02 p0340 N71-12462

Gradient version of Schubert-Schupf N-Body program for computation of solar system orbits (NASA-TM-X-43598) 02 p0348 N71-12464

ISAM table generated/Automated Snark Program (ASPI) (NASA-CR-108744) 02 p0341 N71-12471

Computer program to satisfy data requirements of Path Derivation Program (NASA-CR-108736) 02 p0341 N71-12473

TAP and SCRAP - programs for processing data from automatic gas analysis equipment using PDPA/1 computer (JNHL-TM-1301) 02 p0342 N71-12476

Computer update program for compiling minor wins list from test aircraft data (NASA-CR-108734) 02 p0342 N71-12478

Computer program for processing data on ground support equipment wiring in Apollo spacecraft (NASA-CR-108731) 02 p0342 N71-12479

Path redundancy/Automated Snark Program written in COBOL for IBM 360 computer (NASA-CR-108722) 02 p0342 N71-12483

North American preprocessor/Automated Snark Program written in COBOL for IBM 360 digital computer (NASA-CR-108730) 02 p0342 N71-12484

Groundwork pre-processor program to create LM wire list (NASA-CR-108733) 02 p0342 N71-12485

Path redundancy/Automated Snark Program (NASA-CR-108720) 02 p0343 N71-12486

Computer code for prediction of hydrometeor impact on high speed sphere-cone vehicles (SC-DB-79-373) 02 p0343 N71-12489

Automated Snark Program (ASPI) to generate diode, band, and special mode reports which aid in drawing of circuit paths for analog circuit analysis of Apollo spacecraft (NASA-CR-108736) 02 p0343 N71-12490

Time series analysis in economics using computer programs (SAJAOH/1976) 02 p0343 N71-12493

Computer program for on-line pattern recognition (AD-712677) 02 p0343 N71-12495

Software used with signature data processing system for automatic extraction of spectral information from multipoint laser tomograms - Vol. 2 (NASA-CR-108741) 02 p0343 N71-12509

Implementation manual of computer program for calculating fluidic product conversion in liquid metal cooled breeder reactor cladding (AI-ABC-13597) 02 p0415 N71-12641

COMPUTER PROGRAMS

Two-body relativistic kinematics code written in FORTRAN (LA-640) 02 p0407 N71-12829

Principles of nuclear, thermal, and hydraulic performance calculations for water cooled reactors (AEEW-3-491) 02 p0416 N71-12880

PROF GROUND-C - processing code for group constants for fast reactor (JAERI-1192) 02 p0416 N71-12894

Method of calculating sampling errors (JAE-TM-49170) 02 p0409 N71-12904

Digital computer program for computing vibration characteristics of ring-stiffened cylindrical shells of revolution - theory manual (NASA-TM-X-2136) 02 p0412 N71-12909

Parallel tangent and steepest descent algorithm with computer implementation for application to partially linear models (AD-712481) 02 p0400 N71-13167

FORTRAN program for computerized design of axial flow pump by blade element method (NASA-CR-111574) 02 p0385 N71-13230

Computer program for deriving total stress concentration factor caused by branch pipe connection to main pipe under internal pressure (AD-712449) 02 p0446 N71-13248

Computer program predictions of stacking fault images at high voltages (JPS-592166) 02 p0445 N71-13274

Computer program for reconstruction of Shylark rocket vehicle thrust curve (JRSO-TM-17-330C) 02 p0439 N71-13317

Computer program for calculation of variables of state of fuel gas mixtures with logarithmic linearization of nonlinear equations (DLR-MITT-69-27) 02 p0409 N71-13372

Reliability of mass spectroscopy literature for first half of 1960 - compiled by computer (JIS-2609) 02 p0403 N71-13432

Computer program for calculating convective heat transfer coefficients from laminar incompressible oscillation (NASA-TM-X-2147) 02 p0390 N71-13496

Modification of NUALGAM and BEREAD codes (NASA-CR-115089) 02 p0390 N71-13497

Computer programs for this calculation in toluene reactor (JNHL-TM-2354) 02 p0404 N71-13539

FORTRAN 4 calculator program for production of data of creep collapse of thin walled tubes (JNP-10354) 02 p0405 N71-13543

Inspection device with warning system for RW 330 computer near CABRI reactor (CRA-N-1274) 02 p0407 N71-13638

Design of FORTRAN parallel task recognizer program 02 p0388 N71-13635

Survey of techniques for recognizing parallel processable streams in computer (JAE-10323) 02 p0383 N71-13656

Heat exchanger program MICRED (JERM-725) 02 p0383 N71-13664

Computer calculation of natural frequencies and transverse vibration modes in continuous beams (JNHL-TM-7025) 02 p0378 N71-13675

Computer program for smoothing and differentiation of data from multichannel spectrum (UCRL-15963) 02 p0337 N71-13644

Digital computer program for stress distribution in ring of semi-circular cross section under uniform radial load (AD-712516) 02 p0416 N71-13644

RELAP3 computer program for reactor blowdown analysis including pump failure, power transients, or loss of coolant (IN-1331) 02 p0331 N71-13694

Computer program TRANSPORT for designing chemical particle beam transport systems (SLAC-91) 02 p0390 N71-13699

Digital computer program for symmetric solution for short ring-reinforced oval cylinders (AD-712519) 02 p0317 N71-14009

Computer program for Monte Carlo simulation of fast cross in analysis of large complex systems (NASA-CR-111566) 02 p0337 N71-14006

Computer program for determining confidence interval limits of the theoretical distribution (NASA-TM-D-704) 02 p0405 N71-14028

Computer subroutines for Romberg-Kutta integration of differential equations (BSCR/N261) 02 p0338 N71-14076

ALGOL program for calculating scattered gamma ray energy spectra in shielding slab (JNHL-TS-2533) 02 p0396 N71-14078

Application of ray tracing method to computer program for collection of sound intensity from vibrating space vehicle (NASA-CR-102948) 02 p0416 N71-14081

FORTRAN 5 for TIME computer program for finance determination with time varying rates (BNWL-1408) 02 p0388 N71-14112

Developing computer program for optimum economic parameters of conceptual 1000 MWt nuclear reactor (WARD-388-94) 02 p0378 N71-14113

- Updating computer program for determining nozzle similarities to eliminate double-root solution and to fit resultant abundance data curves by statistical means
[NASA-CR-102338] 05 p0367 N71-14213
- Digital analysis of liquid sloshing in rotational symmetric tanks under weak gravitational fields - Vol. 2
[NASA-CR-111739] 04 p0604 N71-14236
- Computer program for partial wave expansion for scattering amplitude and density matrix element
[CEA-N-1391] 04 p0392 N71-14392
- Three dimensional multi-group diffusion-burnup program BDDT
[LA-4396] 04 p0561 N71-14408
- Investigating computer program functions and test procedures for failure analysis of NAS IIa Route Stage A Model 1 System
[PAA-NA-76-31] 05 p0706 N71-14567
- Mathematical method and FORTRAN program for routine interpretation of gamma-logarithm in stratiform deposits
[CEA-N-1279] 05 p0736 N71-14577
- Computer program for tabulating mass differences of various molecules and for deriving empirical formula for molecule fragment
[POA-C-1319-34] 05 p0737 N71-14620
- Development of generalized digital contouring program
[NASA-TN-D-6022] 05 p0649 N71-14654
- COBRA, few group, one dimensional neutron diffusion program in FORTRAN 4 language
[IN-1416] 05 p0737 N71-14720
- Computer program for calculation of electron scattering and photoionization cross sections of atomic systems with configuration $h\nu/q$
[REPT-70-858] 05 p0649 N71-14781
- Computerized analytic triangulation for compiling topographic maps from aerial photographs
05 p0683 N71-14842
- Computer programs for solving electromagnetic radiation and scattering from thin wires
[AD-713154] 05 p0654 N71-14856
- Computer program for finite group presentations
[AD-713697] 05 p0659 N71-14873
- Computer program for solving finite difference analogs to differential equations of motion in wave propagation
[SC-DR-70-315] 05 p0659 N71-14875
- Performance of computer controlled analytical mass spectrometer
[NASA-CR-1470] 05 p0684 N71-14888
- Measurement of amount of nonlinearity introduced by amplitude dependent time delay computer model
[BGG-1183-533] 05 p0645 N71-14918
- Updated FORTRAN program for waveguide propagation allowing for vertical and horizontal dipole excitation
[AD-713168] 05 p0655 N71-14925
- Computer program for heat transfer and temperature distribution analysis on multidimensional systems
[WANL-TME-1872] 05 p0702 N71-15027
- Extending COBRA 2 computer program for thermal and hydraulic analysis in large bundles of fuel pins
[BNWL-1422] 05 p0726 N71-15072
- Computer program for calculating concentrations of chemical species in set of radiation-induced chemical reactions with homogeneous kinetics
[ANL-7693] 05 p0741 N71-15105
- Computer program for normalization of scattering differential cross sections
[COO-335-413] 05 p0742 N71-15128
- Computer manual for implementing digital program in space station dynamics simulation
[NASA-CR-102971] 05 p0771 N71-15139
- Analysis of data systems and computer programs for nuclear rocket shielding methods, modification, updating, and data input preparation - Vol. 1
[NASA-CR-102964] 05 p0728 N71-15162
- Computation of neutron and photon cross section data using computer programs developed for nuclear rocket shielding methods, modification, updating, and input data preparation - Vol. 2
[NASA-CR-102963] 05 p0728 N71-15163
- Cross section generation and data processing techniques for nuclear rocket shielding methods, modification, updating, and input data preparation - Vol. 3
[NASA-CR-102966] 05 p0728 N71-15164
- One dimensional, discrete ordinate transport techniques for use with nuclear rocket shielding methods, modification, updating, and data input preparation - Vol. 4
[NASA-CR-102967] 05 p0729 N71-15165
- Two dimensional, discrete ordinate transport techniques for use with nuclear rocket shielding methods, modification, updating, and data input preparation - Vol. 5
[NASA-CR-102968] 05 p0729 N71-15166
- Point kernel techniques for use with nuclear rocket shielding methods, modification, updating, and data input preparation - Vol. 6
[NASA-CR-102969] 05 p0729 N71-15167
- Improved reconstruction of high momentum tracks using double precision version TVGP
[UR-875-315] 05 p0744 N71-15185
- Computer program for predicting structural bending theoretical data
[NASA-CR-102974] 05 p0776 N71-15193
- ENDRUN-1 program for calculating multi-group constants from ENDF/B data
[OEAP-13392] 05 p0746 N71-15217
- Finite difference scheme for calculating problems in three space dimensions and time
[UCRL-72634] 05 p0733 N71-15233
- GRAMP program for random generation of Reich and Moore parameters for multilevel unresolved resonances of fission isotopes
[WAFD-TM-935] 05 p0740 N71-15281
- TIBRO-GENERAL computer program for calculating precise trajectories of charged particles in de magnetic fields
[UCRL-50916] 05 p0749 N71-15295
- Exact buckling criterion for essentially stiffened uniaxially curved cylindrical shells of materials having different orthotropic moduli in tension and compression
[AD-713113] 05 p0779 N71-15319
- Monte Carlo calculation, computer programs, and flow charts for neutron scattering
[ORNL-TR-2360] 05 p0730 N71-15335
- Developing computer program for predicting performance of single-stage axial flow turbines
[AD-713116] 05 p0763 N71-15381
- Software for on-line controlled triple-axis spectrometer
[RT/BL/70/2] 05 p0687 N71-15450
- Computer programs for oceanographic data processing
[AD-713491] 05 p0679 N71-15522
- Computer program for finite difference solutions of shells of revolution under asymmetric dynamic loading
[NASA-TN-D-6059] 05 p0780 N71-15569
- Computer programs for analysis of optimal selection of mass centers from billets
[SC-RR-70-306] 05 p0772 N71-15624
- Use of UK nuclear data library in Monte Carlo program MONK
[AHSB/SR-184] 06 p0997 N71-15727
- Subroutine ALLMAT for eigenvalues and eigenvectors of general complex matrix
[NASA-TN-D-7032] 06 p0818 N71-15833
- Rapid, flexible computer program for Earth-Mars trajectory and mission analysis
[NASA-TN-D-5957] 06 p0945 N71-15903
- TRESTRAN subroutine package in FORTRAN 4 for manipulation of tree structured data
[NASA-CR-116145] 06 p0818 N71-15911
- Computer program for predicting motion and appendage stresses of spacecraft during deployment maneuvers
[NASA-CR-116148] 06 p0818 N71-15965
- Investigating computer programs for deriving molecular rotational constants and energy levels from observed rotational spectra of asymmetric rotor molecules
[AD-714566] 06 p0816 N71-16094
- Computer program for calculating fast neutron attenuation in dense material separated by water
[ORNL-TR-2357] 06 p0917 N71-16191
- Program for solving mixed relativistic and non-relativistic form of Hartree-Fock equations
[AD-714873] 06 p0919 N71-16247
- Bibliography of computer programs on nuclear physics, reactor design, reactor operation, and reactor engineering
[ANL-7604] 06 p0819 N71-16271
- Computer program for calculating slowing down spectrum of neutron group
[BNWL-1432] 06 p0819 N71-16272
- Revised THERMOS program for computing thermal neutron density, flux, and spectra over 0 to 0.683 eV in slab or cylindrical geometry
[NASA-1434] 06 p0896 N71-16282
- Discrete angle scattering, angular importance sampling incorporated into Monte Carlo neutron transport code
[ORNL-TM-2031] 06 p0921 N71-16301
- FORTRAN 4 for ANDYIG3 and ANDYIG2 Monte Carlo programs for time dependent mesoscopic particle transport in general geometries and separating arrays
[LA-4416] 06 p0921 N71-16308
- Computer program for resolution band model prediction of heat transfer from rocket exhaust plumes
[NASA-CR-102998] 06 p0909 N71-16420
- Combination test generation program for any non-redundant fault in combinational logic test
[NASA-CR-116199] 06 p0820 N71-16432
- Modal analysis computer program package for finding frequencies and mode shapes of any linear discrete system governed by generalized eigenvalue equation
[NASA-CR-116178] 06 p0820 N71-16439
- Procedures for using FORTRAN 4 computer program to simulate GERT networks
[NASA-CR-116177] 06 p0820 N71-16439
- Computer programs for fitting experimental solid state physics data to parametrized theory
[AD-714199] 06 p0836 N71-16470
- Computerized landmark navigation position updating techniques for lunar roving vehicles
06 p0895 N71-16482
- Computer programs for calculating trajectories to Mars and Jupiter
06 p0921 N71-16494
- Finite element program for determining stresses and mass matrices of shells of revolution - user manual
[NASA-CR-116024] 06 p0936 N71-16496
- Digital computer program for solving isotropic two dimensional plane and axially symmetric problems in CDC 6600 computer
[WAFD-TM-956] 06 p0904 N71-16504
- Hartree-Fock computer program to calculate molecular wave functions of light metal diatomic hydrides, oxides, and halides
[AD-713977] 06 p0923 N71-16504
- Computerized design and operation of laser position screen video with alternate line resolution
[COO-1018-1214] 06 p0921 N71-16505
- Computer program for determining static and dynamic response of symmetrically loaded shell orthotropic shells of revolution
[NASA-TN-D-6150] 06 p0937 N71-16506
- DYNASOR-2 finite element program for dynamic nonlinear analysis of shells of revolution
[NASA-CR-116023] 06 p0930 N71-16508
- User manual for NOISYI program to calculate space dependent spectral density functions of noise in nuclear reactors
[BNWL-1260] 07 p0928 N71-16504
- Computer calculations of water wave refraction and diffraction effects
[PS-194468] 07 p0915 N71-16505
- Digital computer program for calculation of heat temperature and mass flux in cooling channels of jet elements
[ANL-TRANS-638] 07 p0839 N71-17000
- Calculating collision matrix in nuclear symmetric clusters by numerical integration
[RISO-M-1209] 07 p0850 N71-17000
- ALGOL computer programs for linear system data dependence
[ABC-CR-1124] 07 p0906 N71-17113
- Characteristics and operation of automatic file scanning device used with digital computer
[UCRL-18042] 07 p0906 N71-17116
- Computer program IRESINT to calculate response integrals
[NP-18281] 07 p0971 N71-17125
- Monte Carlo superposition code for calculation of resonance integrals in reactor cell
[RISO-M-1257] 07 p0862 N71-17123
- Computer programs for processing two-dimensional analyzer pulse height data for automatic separation of gamma and neutron counts
[NASA-TM-X-2181] 07 p0862 N71-17130
- GBOSTAR-2 multiple area geopotential coefficient and station position recovery system
[NASA-TM-X-65441] 07 p0907 N71-17150
- User guide for Langley time series analysis computer program used in analyzing random, stationary time series
[NASA-TM-X-2160] 07 p0907 N71-17151
- Vortex-lattice FORTRAN program for aerodynamic subsonic aerodynamic characteristics of complex planforms
[NASA-TN-D-6142] 07 p0907 N71-17150
- Using computer code to study behavior of vapor transport fuel pin in boiling water reactor
[NASA-TN-D-6162] 07 p0864 N71-17160
- Manual for Mark 4 Error Propagation Program operation in CDC 6600 computer search of isentropic trajectories
[NASA-CR-111892] 07 p0907 N71-17160
- User manual for 1DX, 2DX, 3DX, PERT-3 web package for reactor data processing
[BNWL-1412] 07 p0864 N71-17150
- Digital computer programs for evaluating low temperature vibrational characteristics of chemical systems
[NASA-CR-103941] 07 p1127 N71-16988
- Computerized simulation for engineering analysis of high speed ground transportation system
[PRA-RT-76-35] 07 p0907 N71-16991
- Venture FORTRAN 4 computer program for predicting Cartesian plots suitable for publication using CalComp plotter
[AD-715279] 07 p0907 N71-16992
- Computer program for estimating cost for gas road profile
[TRW-6018-W004-B0-60] 07 p1136 N71-16998
- Approximate modeling of large-amplitude plasma oscillations - computer experiments
[AD-715074] 07 p1084 N71-16999
- Computer program for estimating costs of constructing complicated tunnel-shaft systems
[PS-193373] 07 p0908 N71-16999

SUBJECT INDEX

Computer program (PROPIA) to evaluate fusion product concentrations in fuel irradiated under various conditions
[CEA-R-3967] 07 p1066 N71-18143

Investigating fast group constants and processing program using UNDF/A format
[NARS-1195-PT-1] 08 p1233 N71-18169

Monodimensional burnup code for reactor core also radial distribution of short-lived activations
[JN-3-109] 08 p1248 N71-18196

Computer program for calculating magnitudes in single production of pions from nucleons
[LNF-49/39] 08 p1249 N71-18222

Computer code SESYPHUS for solving low-group neutron diffusion equations in two dimensions using finite difference method - users manual
[AFKJ-70-13-BPT] 08 p1236 N71-18237

Computer program for calculating fusion product activity according to experimental conditions
[CEA-N-1308] 08 p1254 N71-18347

Computer code for subcooled pressure predictions in subcooled pressure vessel simulations
[DN-1431] 08 p1238 N71-18358

Comprehensive computer program for predicting star coil performance
[NASA-TM-X-2220] 08 p1164 N71-18474

Analytic computer program for turbomachinery-driven cryogenic systems in helium, including porous heat exchanger
[AD-715724] 08 p1206 N71-18537

FORTRAN computer program for generating geometrical data of heat transfer code
[NASA-TM-X-2254] 08 p1303 N71-18621

MCFLARE code to calculate probable flow losses concentrated on intersectorial mixing
[NASA-TM-X-2271] 08 p1283 N71-18754

SAMBO, computer routine package for Monte Carlo codes
[ORNL-TM-3203] 08 p1261 N71-18776

Describing operating characteristics and costs of de-aerated heat exchangers and condensers for industry
08 p1304 N71-18812

System description of field test model of ARTS 2 modular alphanumeric tracking ATC system
08 p1166 N71-18815

VISCCEL computer program user manual for analysis of linear viscoelastic structures
[NASA-CR-116823] 08 p1166 N71-18931

Computer program for indexing X ray metal powder patterns
[NLCO-1066] 08 p1263 N71-18941

Computer program for processing respiratory dust sampling data
[BM-3C-3504] 08 p1166 N71-19029

ATS 5 ground station magnetometer data processing program
[NASA-TM-X-25457] 08 p1166 N71-19082

Computer program for design of low pass filters with uniform or nonuniform dissipation
[WRB-TD-193] 08 p1170 N71-19172

Investigating interaction between FORMAC data organization and algorithm design
08 p1227 N71-19187

Describing experimental on-line interactive symbol in prototype Scope FORMAC language implemented on IBM 2250 graphic display unit
08 p1228 N71-19189

Discussing problem of symbolic numeric conversion in solving quantum mechanical eigenvalue problems with FORMAC
08 p1228 N71-19192

Computer subroutines to determine photometric magnitudes of planets and their satellites
[NASA-CR-114826] 08 p1290 N71-19233

Fast Fourier transform programs for EAI-640 digital computer
[RBC-11477] 08 p1167 N71-19332

Computer program for determining low speed interference effects of flow fields about arbitrary bodies by superposition
08 p1314 N71-19377

Computerized prediction of flow field interference forces and moments on aircraft stores at subsonic speeds
08 p1319 N71-19385

AZUSA ODPS computer program (AZGDZ) for Kennedy Space Center theoretical trajectory computation
[NASA-TM-X-24095] 08 p1332 N71-19333

Computer program description for applying pulses to electrochemical system and yielding current time plots as output
08 p1332 N71-19566

Computer program access protection by self-aware computing systems
[NASA-CR-117126] 08 p1333 N71-19599

Computer program for determining tail convective flow occurrence and altitude and comparison with radar precipitation echoes in stratiform clouds
[AD-716368] 08 p1412 N71-19622

Pin-film combination model for flow visualization studies of pin combustors partially immersed in turbulent boundary layer at Mach 5
[AD-710819] 08 p1423 N71-19657

Reliability prediction computer program and applications to organic Rankine-cycle engine generator systems
[AD-715945] 08 p1326 N71-19719

Mathematical models and computer programs for equalizing West German part in European triangulation net
08 p1353 N71-19724

Computer program for assessing ambient and disturbed day and night ionospheric effects on radio wave reflection and transmission
[AD-716679] 08 p1349 N71-19748

Computer programs for simulation of reconfigurable engine and control system operation - Vol. 6
[NASA-CR-114884] 08 p1354 N71-19793

Cockpit geometry evaluation program results and techniques with computer input and output samples of flight crew anthropometry
[AD-716393] 08 p1321 N71-19817

Library routines and macros for FDP hybrid software system
[BNWL-8-36] 08 p1355 N71-20110

Digital computer program for studying transient performance of pressure fed rocket engine
[NASA-CR-114915] 08 p1459 N71-20173

Digital computer program description with updating case data mode and extended force method matrix generation capability
[AD-715923] 08 p1356 N71-20180

SYSTID computer program for system time-domain simulation program in FORTRAN 5 for Univac 1108 computer
[NASA-CR-114914] 08 p1356 N71-20280

Computer program for numerical analysis of flow and pressure distribution in idealized spiral grooved pumping seal
[NASA-TD-D-6183] 08 p1394 N71-20399

Computer programs for predicting inducer blade pressure loading, stress distribution, and vibration characteristics of turbine pumps
[NASA-CR-22712-VOL-2] 08 p1460 N71-20404

Computer manual for calculating dynamic vector control of dual spin space station
[NASA-CR-117310] 08 p1473 N71-20483

Computer program for cellular structures of arbitrary plan geometry designed to capture behavior of deck and web components
[PB-196143] 08 p1481 N71-20517

Users manual for FORTRAN 4 computer program for analysis of multilayered fiber composites
[NASA-TM-D-7013] 08 p1481 N71-20530

Computer program for calculating structure invariants from crystal lattice parameters
[AD-717466] 08 p1435 N71-20600

Computer programs for static and dynamic deformation of structures with straight axis
[CRIP-MC-32] 10 p1451 N71-20687

Procedures for submitting and reviewing programs to Quantum Chemistry Program Exchange and available literature descriptions
[AD-717162] 08 p1511 N71-20694

Assessment of computer programs for structural response of shallow spherical shell
[AD-716813] 10 p1451 N71-20726

Computer program for least squares determination of crystal structure factor phases
[AD-716747] 10 p1431 N71-20733

Computer programs for analyzing crack propagation in cyclic loaded structures
[AD-717150] 10 p1451 N71-20776

Test problems and results for OMNITAB 2 computer program
[NBS-TN-551] 10 p1527 N71-20843

Computer program enabling nonprogrammer to perform data, statistical, and numerical analysis
[NBS-SPEC-PUBL-339] 10 p1527 N71-20844

Analytical triangulation program in FORTRAN 5 for frame photography including free formatting input/output routines, and least squares adjustment
[AD-717105] 10 p1548 N71-20906

Photogrammetric data preparation manual for analytical triangulation program, MUSAT 4
[AD-717106] 10 p1548 N71-20907

Program structure, external data sets, and subroutines of analytical triangulation program, MUSAT 4
[AD-717107] 10 p1548 N71-20908

Examining fuel cycle codes using different techniques for fuel cost calculations
[BNWL-SA-3605] 10 p1602 N71-21050

Numerical computation of linear antenna feed
[R-74] 10 p1518 N71-21053

Finite difference model and computer program for predicting large deflection elastoplastic response of shell structures
[AD-717085] 10 p1635 N71-21192

Real time digital simulation program preprocessor
[NASA-TM-X-7018] 10 p1528 N71-21305

Description of general purpose digital computer program (NASTRAN) for analysis of elastic structures under various loading conditions using finite element method approach
[NASA-SP-260] 10 p1658 N71-21559

Nucleon-neutron transport code NHTC to compute transport of muons below 3.5 GeV and muons and charged pions below 2.5 GeV
[NASA-CR-117496] 10 p1618 N71-21562

COMPUTER PROGRAMS

Description of algorithm for performing automated closed form integration of formulas in elliptic motion
[NASA-CR-114963] 10 p1594 N71-21572

Computer program for analysis of magnetic field problems involving ferromagnetic materials
[AD-716992] 10 p1608 N71-21631

Computer program for converting IBM FORTRAN to CDC 6600 computer use
[LA-4553] 10 p1530 N71-21638

Coordinate displacement computer program for adjusting triangulation networks
[REPT-120] 10 p1530 N71-21673

Computer program for predicting fuel element performance and models for fuel pin design
[TID-25599] 10 p1603 N71-21712

Recursive calculation of linearly rising stage trajectory in single channel, single trajectory model when dispersion relations are separately written
10 p1623 N71-21770

Microcomputer designed to emulate variety of parallel and sequential computers
[TID-25623-APP-4] 10 p1530 N71-21809

Computer program and approximate inverse solution for non-equilibrium flow in inviscid model layer about vehicle in hypersonic flight in arbitrary atmosphere
11 p1734 N71-21919

Computer programs for dynamic design and analysis of mechanisms composed of beams and/or springs with up to 48 degrees of freedom
[AD-717650] 11 p1834 N71-21933

Orbit prediction models and computer program for satellite tracking using bores
[BMW-FB-W-76-64] 11 p1825 N71-22040

Development of computer system capable of numerical and algebraic manipulations to eliminate changes necessary in translating formal mathematical expressions
11 p1715 N71-22101

Models and computer program for vibration of oil-shafted uniform filament with changed ends as related to piping systems
11 p1835 N71-22236

Mathematical background and application of two computer programs obtaining smooth group delay characteristics from moderate number of specific points
[REPT-4146-ADD-1] 11 p1716 N71-22283

Example solutions obtained from circulation curves method of calculating flow through turbomachinery for several operating points of Rolls-Royce compressor
[CUEDA-TURBO/TR-19] 11 p1737 N71-22294

FORTRAN 4 code for predicting in-pile behavior of cylindrical fuel reactor fuel elements
[ANL-7736] 11 p1793 N71-22323

Three programs for two dimensional hydrodynamics in spherical, pure Eulerian coordinate system
[AD-717708] 11 p1737 N71-22326

Computer program for steady hydrodynamics and hydrofoil servocontrol near free surface
[AD-717681] 11 p1737 N71-22328

Evaluation of computer program for prediction of laminar flow by solution of elliptic partial differential equation
[BITN/B/31] 11 p1737 N71-22330

Computer program and mathematical model for temperature variance measurements on satellite
11 p1840 N71-22335

IBM computer program for temperature distribution computation by method of zones
11 p1841 N71-22336

Service routines MERMC2 and MAGIC for binary cross section library tapes used by MC up 2 multi-group cross section code
[ANL-7654] 11 p1894 N71-22332

Monte Carlo general purpose shielding computer program in FORTRAN 4 for IBM 7094 computer
[NASA-TN-D-6170] 11 p1794 N71-22378

One dimensional static physics design and analysis code (FARED) for fast breeder reactor project development
[BAW-3867-A-VOL-1-REV-1] 11 p1795 N71-22425

Computer oriented information management system for earth physics program
[NASA-CR-117842] 11 p1730 N71-22478

Component specifications and computer program for intermediate water recovery system on manned spacecraft
[NASA-CR-114961] 11 p1691 N71-22514

Computer program for symbolic analytical expressions in relativistic mathematics
11 p1788 N71-22535

Computer program to generate turbine aerodynamic requirements, approximate external blade geometries, and coolant flow requirements for two stage axial flow turbine
[NASA-TM-X-2229] 11 p1670 N71-22548

Coupling characteristic effects on dynamic response of axially coupled turbomachinery with digital computer program based on transfer matrix method
11 p1770 N71-22712

Computer program giving transient characterization of four different types of dispersion also transient response waveform
11 p1729 N71-22747

COMPUTER PROGRAMS

SUBJECT INDEX

Mark 3A simulation center EMR 6050-Univac 1108 computer interface 11 p1720 N71-22782

Real time on-line diagnostics routines developed for IBM 360/75 computers 11 p1720 N71-22785

Analytic procedures and computer codes for prediction of weight optimized radioisotope thermoelectric generator shields for unmanned spacecraft [NASA-CR-117698] 12 p1961 N71-23258

Mathematical model for computer program to determine vibratory response of finite plates and associated acoustic radiation to fully developed turbulence excitation [AD-718815] 12 p2004 N71-23309

Computer program for equilibrium equations, combustion temperature, and combustion efficiency of explosive and propellant combustion [JCT-370] 12 p2010 N71-23357

Document update, editing, search, authority file creation program. Setup instructions manual for Radiation Shielding Information Center [CTC-INF-1017] 12 p1881 N71-23445

Computerized simulation of performance and probability of MTI in aircraft detection in clutter [RRE-TN-759] 12 p1878 N71-23508

Simulation and design of arithmetic and logic unit for ILLIAC 3 [COO-2118-2] 12 p1882 N71-23614

Computer program for solving equations of motion governing pipe oscillations [NASA-CR-103101] 12 p1882 N71-23666

ALGOL program for detection and correction of data errors using TR4 computer [RAE-LIB-TRANS-1544] 12 p1882 N71-23667

FORTAN program for calculating probability of locating elliptical targets with square, hexagonal, or rectangular grid of any size [GJO-918-4] 12 p1882 N71-23804

On-line FORTAN 4 digital computer program for solving ordinary differential equations 12 p1883 N71-23866

Computer program for numerical solution of unsteady Navier-Stokes equations and application to flow in rectangular cavity with moving wall [NASA-TN-D-6312] 12 p1883 N71-23915

Mathematical techniques and computer programs for inversion of de Haas-van Alphen data on closed Fermi surfaces [ANL-7659] 12 p1972 N71-23921

FORTAN program for computing two dimensional magnetic field components for conduction geometries [ORNL-TM-2444] 12 p1968 N71-24006

Altitude and elevation angle determination from UNH/APCRL meteor trails interferometric radar, using computer processing [AD-718165] 12 p1997 N71-24111

Model and computer program to predict film usage time of Skylab missions 12 p1924 N71-24197

Computer programs for studying infrared band contours of perpendicular symmetric top molecules 12 p1977 N71-24251

Manual of computer program for probabilistic optimal launch vehicle assignment and budget smoothing model [NASA-CR-114285] 12 p2003 N71-24320

Computer program using numerical integration techniques for computation of meteoroid impact and angular distributions over complex geometric spacecraft configurations [NASA-CR-105162] 12 p2003 N71-24335

Computer programs to calculate characteristic currents and gain patterns of conducting bodies of revolution [AD-718969] 13 p2042 N71-24416

Description and utilization of Monte Carlo code Puker [CEA-N-1388] 13 p2128 N71-24473

Low aerodynamic drag airfoil designed by Lightbulb method [ARC-R/M-3618] 13 p2021 N71-24498

Computer performance test program for assessing computer indexing operations [NBS-TN-572] 13 p2049 N71-24580

Space-held thermal analysis of oblate spheroid tank mounted multilayer insulation configurations by computer including programs [NASA-TN-D-4228] 13 p2049 N71-24594

Self testing and repairing computer comparing control and diagnostic unit and rollback points for error correction [NASA-CASE-MPO-10567] 13 p2049 N71-24633

FORTAN program for stresses in anisotropic elastic plate with circular hole 13 p2178 N71-24647

Characteristics of computerized management analysis and planning system for planning and scheduling engineering project work [NASA-TN-D-4189] 13 p2049 N71-24716

Computer programs to calculate and analyze plasma and neutron interaction within prescribed medium and OPER 3C Transport Code [NASA-TM-X-2158] 13 p2157 N71-24723

Two-dimensional reactor lifetime program with local and spectrum dependent depletion for IBM 360 computer based on spatial modal expansion and finite difference theory [EUR-4539] 13 p2118 N71-24924

Computerized design procedures for development of rocket propelled sled [AD-719731] 13 p2061 N71-24957

Control of spacecraft descent for accurate impact following atmospheric entry by computer control of spacecraft trajectory [AD-719795] 13 p2109 N71-24973

Computer program for simulation of nominal and anomalous operation of Apollo cryogenics storage system [NASA-CR-115022] 13 p2174 N71-25103

Computer program for calculating concentration of fission products - HERETRA [DEMO-70/10] 13 p2135 N71-25182

NASA computer program for dynamic structural analysis in stress and thermal deformation problems 13 p2182 N71-25387

Computer program for calculating radiation pattern of ATS 6 flexible rib-reinforced reflector 13 p2048 N71-25317

Test facility and computer programs for control of digital tape drive functions 13 p2062 N71-25341

Graphic computer program for plotting engineering drawings [RREP-70-8] 13 p2053 N71-25342

Computer program for predicting frequency interference between transmitters and receivers [RGO-1183-1509] 13 p2048 N71-25344

Description of facilities and sensors used in high altitude nuclear detection studies [AD-719619] 13 p2077 N71-25383

Finite element computer program for three dimensional analysis on radial flow impeller [IC/71/09] 13 p2053 N71-25410

Symmetry optimization program for toroidal magnet currents [UCRL-50944] 13 p2127 N71-25453

Finite difference equations for TRANZIT program for multigroup time dependent transport in $r/\theta, z$ cylindrical geometry [LA-4575] 13 p2138 N71-25481

Modified computer program HEATING 3 for solving heat conduction problems in one, two, or three dimensional Cartesian or cylindrical coordinates [ORNL-TM-3208] 13 p2188 N71-25492

GROG12 spin dependent nuclear evaporation code for following deexcitation of compound nuclei [BNL-58246] 13 p2141 N71-25541

Computer program for determination of optimal herringbone journal bearings for maximum radial load capacity [NASA-TN-D-6351] 14 p2260 N71-25665

Computer programs for electron and proton radiation dose spatial distribution during satellite orbits [ONERA-NT-02/20/70] 14 p2341 N71-25669

Development of computer program to increase on-site analysis capabilities of experimental optical and meteorological parameters 14 p2286 N71-25791

Mathematical analysis of Vuilleumier refrigerator and use of computer program for solution of resulting equations [NASA-TM-X-65534] 14 p2352 N71-25812

Statistical algorithms and computer programs for remote sensor multispectral data analysis [NASA-CR-103182] 14 p2220 N71-25921

Airborne computer architecture and organization for executing computer programs written in space programming language [AD-720796] 14 p2221 N71-25930

Computer program for processing automatically collected navigational and sounding data on Minak-22 computer 14 p2248 N71-25972

Computer program for linked file information retrieval including semantics, syntax, and outline of search program 14 p2221 N71-25978

Computer program simulating generation of flected forms of irregular verbs in German for use in dictionaries and grammars 14 p2222 N71-25982

Computer program for linguistic data processing including translating text from Russian into English 14 p2222 N71-25984

Automatic dictionary for creating indexes for information retrieval through computer programs 14 p2222 N71-25985

Integration of text processing and written communication into management information system 14 p2223 N71-25991

Computer program for measurements of electron drift velocity in silicon at high fields [AD-720543] 14 p2325 N71-26147

Problem of deterministic source encoding with fidelity criterion using computational work [NASA-CR-118656] 14 p2224 N71-26343

Nonlinear Volterra equations for describing temperature and power output of nuclear reactor 14 p2284 N71-26009

GBRT nomenclature for describing project plan in system operating policy [NASA-CR-110490] 14 p2224 N71-26011

Computer program user manual for thermal design analysis in temperature control systems [NASA-CR-110649] 14 p2356 N71-26040

Pilot system of integrated design programs for TMS software compatibility 14 p2266 N71-26050

Mathematical formulation of Double Precision Orbit Determination Program (DFODP) for linear and planetary mission spacecraft trajectories [NASA-CR-110673] 14 p2340 N71-26060

COMRA, computer program for coolant boiling in rod arrays in Scl-1905 computer [KFKI-70-30-BPT] 14 p2294 N71-26088

Computer programs for Hartree-Fock wave function calculations and for rotational band spectrum calculations [LYCEN-7050] 14 p2312 N71-26071

Computer program for calculation of neutron propagation according to straight line anisotropic model by determining displacement cross section values in spherical geometry [CEA-N-1312] 14 p2310 N71-26077

Mathematical model and computer program for solution of asymptotic neutron transport equations in slab geometry [KFKI-70-14-BPT] 14 p2312 N71-26079

Computer program for storage and processing of available data on spacecraft waste control and description of search and retrieval capabilities - Vol. 3 [NASA-CR-115038] 15 p2373 N71-26086

Instruction manual for BOOST on-line computer program for estimating powered rocket performance [AD-721189] 15 p2159 N71-26101

QHAZ - computer program for statistical calculation of environmental hazards from nuclear reactors [LA-1266] 15 p2443 N71-26109

Monte Carlo calculations of neutron transport in cylindrical and spherical geometry by ELP program [ORNL-TR-2409] 15 p2458 N71-26179

Modifications of CYGRO-2 computer program for mechanical analysis of irradiated nuclear fuel pin subjected to swelling due to fission products [NASA-TM-X-2150] 15 p2444 N71-26199

Computer program for correlation and spectral analysis of reactor flow data statistics [DP-1244] 15 p2444 N71-26200

Beam transport program BOPTIC in FORTRAN 4 for analyzing monoenergetic charged particles beam in post acceleration system [AAEC/TM-544] 15 p2459 N71-26204

Computer program for optimum flight path and by flight test investigation of performance characteristics (excess thrust, fuel flow, and climb potential of F-104D aircraft [NASA-TN-D-6398] 15 p2366 N71-27068

Structure of three dimensional transient shear flow in turbulent cascade examined in context of time dependent computer experiment [NASA-CR-1816] 15 p2363 N71-27084

Computer codes for calculating lattices and lattice evolution in natural uranium graphite moderated gas cooled reactors [CEA-N-1344-1] 15 p2446 N71-27164

Monte Carlo computer code, equivalent to two dimensional solution of transport equation, for analyzing double-differential neutron scattering cross section data [RPI-328-211] 15 p2466 N71-27206

Computer program modifications and lattice coding for hydrodynamic systems including transport corrections for self-scatter cross sections and collision probability [AEEW-M-952-REV] 15 p2467 N71-27207

Program connecting measuring microscopes PUCB with computer Minak-2 [IPE-SFK-68-53] 15 p2384 N71-27208

W-MESSEUR - Computer program for analysis of portion of two dimensional figure into mesh cell network [WANL-TM-2721] 15 p2454 N71-27278

Computer program for calculating neutron spectra from activated cobalt isotopes [IN-1446] 15 p2470 N71-27382

Computer program and techniques for solving on dimensional multigroup reactor equations based on diffusion coefficients and transport theory [AE-1598] 15 p2469 N71-27391

Computer-aided, ultrasonic test system for graphite billets to select optimum location of reentry vehicle nose tip [SC-D8-70-693] 15 p2431 N71-27421

Computer program for calculating resonant integrals and nuclear cross sections [KFKI-70-12-RPT] 15 p2474 N71-27426

Trajectory computer program (SDXO) to determine motions of asymmetric missiles explaining vector nonlinear-induced effects associated with fluid bodies [SCL-RR-70-121] 15 p2364 N71-27613

SUBJECT INDEX

Drakulski method for determining eigenvalues of matrices with real elements programmed in FORTRAN (AERL-3M-349) 15 p2434 N71-27619

Prompt effects computer program for weapons effect display system (WEDS MOD 2) (JCRIL-50892-VOL-6) 15 p2384 N71-27734

Computer program for analysis and design of critical experiments with fast nuclear reactor (JAERI-MEMO-4215) 15 p2451 N71-27740

Computer program for discovery of excited states according to Ritz combination principle (JNFK-1247) 15 p2483 N71-27765

Effects of nuclear dipole-dipole interaction on nuclear magnetic resonance powder patterns studied by computer techniques using thallium borate glasses and polycrystalline metamaterials 15 p2483 N71-27766

Comparative performance of Monte Carlo and discrete one dimensional transport codes in iron built shield calculation (KCA-CONF-1669) 15 p2484 N71-27789

Accident analysis of light water reactor by digital computer program NURLOC-1.0 (JAERI-4194) 15 p2451 N71-27831

Computer program for control rod calculations in two flux reflected reactor (JRR-164) 15 p2452 N71-27851

SNAP - computer program for solving finite difference form of group diffusion equations in two dimensions (TRG-1990) 15 p2493 N71-27944

Program package COLLI for calculating thermal neutron scattering for moderators of random structure and composition using beryllium oxide as typical example (JUL-648-B0) 16 p2641 N71-28026

Fractional parenting coefficients occurring in matrix elements for various n-particle operators and in a shell model for deuterium and other particles calculated by RELIOTT-SU-3 (JVCEN-7078) 16 p2642 N71-28027

Computer program for transfer orbit trajectory optimization based on Lagrange multipliers, Newton-Raphson method, and power series (NASA-TN-D-6120) 16 p2677 N71-28089

PUMBLE - computer code for fast power reactor fuel management and burnup calculations (ORAP-15599) 16 p2630 N71-28106

CONTRAN program and users manual update for space communication system performance testing (NASA-CR-119003) 16 p2560 N71-28162

Computer code MINIGASKET for thermal neutron scattering law in polycrystals based on free translation and isotropic harmonic vibration with continuous frequency spectrum (JRR-1186) 16 p2646 N71-28212

NEB - computer program for analysis and interpretation of experimental fusion data (AD-721-011) 16 p2647 N71-28238

Computer programs for optimization of nonlinear booster inductor alternators (AD-721515) 16 p2537 N71-28278

Manipulation errors in computer solution of critical dimension structural equations using finite element method (NASA-CR-1784) 16 p2655 N71-28279

Analysis of stratospheric balloon programs using geophysical and flight data for transcription, graphing, and mathematical computations with computer program and hand and machine plotting (AD-722876) 16 p2625 N71-28473

Reactor shielding calculations by Monte Carlo and discrete ordinates methods with example calculations of neutron flux in thermal and fast columns and neutron current near heat exchangers (KCA-CONF-1730) 16 p2631 N71-28589

TOMOF - code for describing thermohydrodynamics of two-fluid mixtures in studies of boiling and ejection of coolant from reactor channel due to direct contact with hot molten fuel (JRR-4592-E) 16 p2632 N71-28590

BODOL - code for processing isotopic diffusion measurements from spent uranium or plutonium fuel samples into information descriptive of nuclear transformation within sample (JRWL-1553) 16 p2632 N71-28591

LMPFR physics programs including VIM code development, Doppler coefficients for BCRL, ZPR-3, ZPR-4, and ZPR-9, BCRL core 20 fuel element assembly, and related topics 16 p2632 N71-28621

Computer program for tracing cosmic rays and their interaction and absorption through complex two-dimensional geological models (JRR-197303) 16 p2589 N71-28622

Computer programs for characteristic modes of vibration of arbitrary shape (AD-722862) 16 p2566 N71-28632

Development of information system for data reduction of wide range image spectrometer program raw field data on water pollution including of optical (AD-721205) 16 p2597 N71-28731

Comparison of coefficient modification, chain rule, and function methods for computing gravitational

potential derivatives with chain rule subroutines for CDC 6600 computer (COM-71-0013) 16 p2589 N71-28764

Algorithms and FORTRAN coding program permitting efficient convergence and high degree of non-machine interactions in steady state process systems analysis 16 p2566 N71-28791

Objective assessment of fusion product yields by compilation of library of all published neutron induced fusion product yields maintained and interrogated by computer methods (JAERI-E-6642-PT-1) 16 p2630 N71-28918

Two dimensional analyzer for half life measurements of nucleus of excited states by gamma-gamma delayed coincidence method on basis of computer Mimic 2 (JINR-P13-5483) 16 p2635 N71-29073

Dynamic and static structural analysis computer program for one and two dimensional elastic bodies 16 p2607 N71-29099

LFEN-FR6 program for calculating spatial neutron flux distribution variation following reactivity perturbations (JFEN-NI-48-A) 16 p2657 N71-29120

Computer program for reduction of isothermal Burnett computerability data 17 p2722 N71-29254

Computer program for activity calculations from high energy neutron irradiation of thin targets including atomic excitation functions and neutron spectra values (JN-18649) 17 p2791 N71-29281

Computer programs for evaluating subsonic flow over wing-tail, wings with folded tips, T tails, and cruciform tail surfaces 17 p2699 N71-29341

Computer programs for calculating airframe coefficients of wing horizontal tail and fin horizontal tail oscillating in subsonic flow 17 p2699 N71-29342

MSBR heat exchanger computer programs - PRIDEX for primary heat exchangers, RETEX for re-heaters, and SUFEK for steam generator superheaters (ORNL-TM-2815) 17 p2782 N71-29367

Computer program using parts of ALGOL to be used with Univac operating system 17 p2732 N71-29440

Computer programs for reduction of Compton recoil electron energy distribution measurements to continuous gamma spectra 17 p2792 N71-29446

ALGOL computer program for estimation of maximum of analytical functions with arbitrarily small error bound 17 p2772 N71-29482

CLUP 77 - FORTRAN program for numerical integration of collision probabilities for square cluster assembly (JAERI-1196) 17 p2793 N71-29530

Stability of synchronized induction motors with feedback control system using digital computer (NLL-RTS-6232) 17 p2725 N71-29662

Neutron activation analysis of silicate rocks with chemical separation techniques and computer code for elimination of interference by low abundance elements 17 p2741 N71-29727

Program for calculating parameters of optimal choices by digital computer (NLL-RTS-6155) 17 p2726 N71-29822

Computer code for estimating maximum temperatures in charcoal bed by fusion product decay heat 17 p2859 N71-29873

Digital computer program manual for design, analysis, and performance prediction of heat pipes with wickless tubes including input/output routines and Runge-Kutta methods (NASA-CR-114306) 17 p2735 N71-29908

Computer program for evaluating Bloch-Grüneisen parameters of metals and evaluating transition electrical resistivity as function of temperature (NASA-TM-X-2320) 17 p2816 N71-29922

Simulation of single-server model for paging drum channel system (NASA-CR-123375) 17 p2774 N71-30023

Computer program for performing corrections on X ray diffraction profile before Fourier analysis (NBS-TN-696) 17 p2723 N71-30030

Computer codes for determining neutron flux spectrum in SIFER target region (ORNL-TM-3322) 17 p2800 N71-30046

Distortion effects in geometrical reconstruction of events in CERN 2m hydrogen bubble chamber (USIP-70-6) 17 p2800 N71-30096

HYLAS codes for predicting heavy element composition of irradiated reactor fuels 17 p2785 N71-30142

IBM S/360 FORTRAN 4 G program to compute homogeneous resonance integrals for fission and non-fission reactions 17 p2724 N71-30147

COMPUTER PROGRAMS

Computer program for reducing radar tracking data magnetic tape numbers for data storage by editing and low pass filtering (NASA-CR-119176) 17 p2748 N71-30149

Machine algorithm for establishing detectability in classical calculus using inverse methods (NLL-RTS-9856) 17 p2724 N71-30163

Nondestructive test methods and techniques including computer programs and data reduction (NASA-SP-5931/61) 17 p2802 N71-30183

Hydraulic pump jet propulsion unit for destroyer, and incorporated computer program 17 p2840 N71-30339

Fast reactor nuclear fast burnup computer code using M4, U, and Pu mass spectrometric data (ORAP-5335-A-REV) 18 p2535 N71-30442

Computer program for evaluation of pollution experiments and reactivity calculations (JUV-2381-EP) 18 p2892 N71-30453

Burnup of nuclear fuel determined by measuring abundance of neodymium-148 - computer program (JINR-1195) 18 p2722 N71-30464

Computer program for photomicroscopy and analysis of multi-particle production in bubble chamber (JSC-T-70-3) 18 p2972 N71-30489

Two-body orbit analysis computer program to evaluate resulting state vector and covariance matrix for orbit after one coast and one burn maneuver (NASA-TM-X-45620) 18 p2807 N71-30511

FORTRAN 4 program for correction and calibration of neutron isotopic scattering data including background, air attenuation, detection efficiency, and sample thickness (JRR-4593-E) 18 p2972 N71-30514

Computer program for automatic analysis of gamma ray spectra (ICBA-N-1381/1-PT-1) 18 p3002 N71-30516

SYNTHRON - computer code for reactor problems involving three dimensional neutron flux calculations (JRR-M-1346) 18 p2974 N71-30548

Computer program for hydrodynamic analysis of this vessel structure (NASA-TM-X-45617) 18 p2893 N71-30609

FORTRAN computer program for determination of rocket and gas propellant performance (JCT-970) 18 p3000 N71-30615

Computer program for calculation of solid angles and angular acceptances with particular application to camera telescopes 18 p2894 N71-30657

Computer program for electric powered spacecraft interplanetary, flyby, and rendezvous trajectory optimization based on Chebyshev approximation and polynomial representations (NASA-CR-114354) 18 p3008 N71-30678

FORTRAN computer program for calculating prolate spheroidal radial functions of first and second kind and their first derivatives (AD-722649) 18 p2844 N71-30713

FORTRAN computer program for calculating oblate spheroidal radial functions of first and second kind and their first derivatives (AD-722649) 18 p2844 N71-30714

Computer program for calculating thermal neutron scattering kernels by phonon expansion of coherent and incoherent scattering approximations (JAERI-MEMO-4211) 18 p2800 N71-30732

Computer code for calculating radiation environments in predicting neutron activation (NASA-CR-61356) 18 p2804 N71-30755

Computer programs of LFEN-FR6 for numerical calculation of experimental results of rod drop in nuclear reactors (JFEN-NI-49/ALPHA) 18 p2840 N71-30821

Heuristic decision making programs for man machine systems 18 p2803 N71-30872

Computer program and finite element method for recognizing structural stiffness matrix to improve computational efficiency 18 p2895 N71-31114

Computer program used for design criteria of stall characteristics of straight wing aircraft (NASA-CR-16446) 18 p2807 N71-31154

Optimal control system design for multivariable processes using computer programs and digital simulation 18 p2895 N71-31168

CAFO code for studying equations of state/opacity of isolated gases 18 p2893 N71-31343

Computer program for open-loop error analysis of low thrust interplanetary trajectories (NASA-CR-119375) 18 p3016 N71-31296

Segmented two-body low thrust interplanetary trajectory and performance optimization program (NASA-CR-119362) 18 p3016 N71-31297

Modification to interplanetary trajectory program for providing capability of generating optimum low-thrust trajectory in N-body field (NASA-CR-119377) 18 p3016 N71-31298

Computer editing routine for data abnormalities in meteorological statistical analysis (NASA-TN-D-6472) 18 p2896 N71-31371

COMPUTER PROGRAMS

One dimensional equations describing noncavitating and cavitating flow in liquid-to-liquid jet pumps programmed for computer use
[NASA-TN-D-6453] 18 2931 N71-31395

Computer program system for failure analysis data acquisition systems with on-line programming capabilities
[NASA-TM-X-2331] 18 2896 N71-31398

Software for computer aided design of logical circuits for study of interactive computer graphics
[AD-722895] 18 2896 N71-31412

Computer program for analyzing energy effects in hypervelocity impact on rocks
[SC-8-70-4622] 18 2920 N71-31553

TOPLER - two dimensional thermal energy transport code for computation of temperature distribution in large water bodies resulting from power plant condenser coolant water discharges
[HRL-7ME-71-39] 18 2928 N71-31570

Engineering description of TACS-3M RCS computer program - Skylab Program
[NASA-CR-113114] 19 3183 N71-31604

Analog computer program and display device for detecting arrhythmia signals during electrocardiography
[AD-711039] 19 3046 N71-31612

Hybrid computer program for determination of Euler angle sequence transient response
[DLR-FB-71-19] 19 3060 N71-31662

Geometric survey program package for digital frequency analysis of time series
[KGO-705] 19 3084 N71-31692

Computational model for fast reactor disassembly analyses - VENUS computer code
[ANL-7701] 19 3134 N71-31735

Computer programs for broadening X ray diffraction peaks of hexagonal close-packed metals
[AD-721911] 19 3167 N71-31737

SASIA - computer code for analyzing power and flow transients for large LMPBR cores
[ANL-7607] 19 3134 N71-31776

Formulation of general equations of motion of thrust alleviated gyroscopes given missile motion, and computer code for integrating resulting differential equations
[AD-723426] 19 3132 N71-31799

Computer program for predicting curved beam sensor transducer shell dynamic responses to shock waves
[AD-723826] 19 3187 N71-31806

Bibliography of structural mechanics computer programs
[AD-723178] 19 3188 N71-32026

Program device for automatic control of weather radar antenna
[AD-723298] 19 3128 N71-32039

STOWA - code for calculation of flux distribution in reactor sub-regions with generalized multiple collision probabilities
[EURPFR-898] 19 3148 N71-32096

Code for calculating mechanical and thermal stresses in cladding of fuel elements
[EUR-4562-F] 19 3137 N71-32109

FORTRAN computer code for forming nuclear cross section data tapes
[ORNL-TM-3266] 19 3061 N71-32118

Computer program and thermalization models for temperature distribution calculation in water cooled reactor cores
[EUR-4554] 19 3138 N71-32141

Computer experiments for proving theory of non-linear evolution of beam cyclotron instability
[AD-723572] 19 3164 N71-32145

Computer program with predictor-corrector numerical integration subroutine for fast trajectory analysis
[NASA-TM-X-45435] 19 3180 N71-32172

FORTRAN 4 program /FITLOS/ for fitting low-order polynomial splines of two and three degrees by least squares method
[NASA-TN-D-6401] 19 3061 N71-32188

Two dimensional axisymmetric transient heat conduction material ablation computer program
[SC-DB-70-510] 19 3192 N71-32342

Third-order interpolation technique for continuous path, numerically controlled machines and data reduction
[Y-1782] 19 3123 N71-32344

FORTRAN 4 code to perform extended variational approximation for light and intermediate nuclei
[AEC-3881] 19 3155 N71-32400

SCEPTRE program for analyzing multibeam loop control system
[AD-723437] 19 3067 N71-32411

Computer programs for calculating electron bombardment energy and gamma yields based on Vavilov theory of proton loss distributions
[AD-723188] 19 3156 N71-32417

Computer oriented approach to statistical analysis and general factorial design programs
[TR-71-18] 19 3062 N71-32493

FORTRAN-based version, FORAAL, of graph algorithmic language GRAAL
[NASA-CR-119778] 19 3062 N71-32494

Errors in PERT analysis and critical path method, and computer program for error elimination
[NASA-CR-119777] 19 3197 N71-32495

COREGRAF code for calculation of graphite moderated lattices compared to experiment with adjustments to U-238 resonance integral and U-235 fission cross section resulting
[CEA-N-1344-2] 19 3158 N71-32536

ETOX - code for calculating group constants for fast nuclear reactor calculations
[HRL-TME-71-36] 19 3159 N71-32568

Computer program for thermodynamic and hydraulic analysis of water cooled reactor channel flow operating under static conditions
[EUR-4553] 19 3140 N71-32576

Computer program for calculating steel package temperature after thermal tests for radioactive material transport
[AEC-3882] 19 3140 N71-32581

Procedures for estimating control costs and emissions reductions for specified air pollution sources - users manual
[PB-196779] 19 3198 N71-32589

On-line and off-line computer analysis of complex particle and gamma ray spectra with programs for performing all basic reduction functions
[ANU-P-467/2] 19 3063 N71-32600

Statistical mechanics and computer programs for estimating component reliability
[NLL-CE-TRANS-5437-9022.09] 19 3106 N71-32658

Nuclear planning of reactor core using Wigener program with average thermal and epithermal cross sections
[EUR-4555-I] 19 3161 N71-32675

Misalignment estimation software system for calibrating in-flight slew angle scale factors and drift rates of OAO gyros
[NASA-TM-X-45667] 19 3133 N71-32680

Two computer programs for investigation of wide variety of lagged planetary landing gear configurations
[NASA-CR-111919] 19 3185 N71-32690

Computer program utilizing IBM 360-40 computer for transforming correlation functions of three particle decay
[TR-1] 19 3162 N71-32726

FORTRAN 4 program for solving neutron transport problems with isotropic scattering in bare spheres and homogeneous slabs by j sub N method
[EUR-4601] 19 3162 N71-32727

FORTRAN 4 computer program for design of sharp-edged-throat supersonic nozzles with boundary layer correction
[NASA-TM-X-2343] 19 3083 N71-32793

Computer program for calculating effects of washplate stiffness on helicopter rotor system dynamics and stability
[NASA-CR-1818] 19 3039 N71-32797

Program for computing free vibration modes and natural frequencies of thin plates with clamped and rotational supports and cylindrical curvature
[AD-724642] 19 3136 N71-32937

Computer program to simplify reduction of temperature data from meteorological sounding rockets
[AD-724599] 19 3294 N71-32972

FORTRAN computer program for selective information retrieval from articles and reports
[AD-724611] 19 3299 N71-32987

Users manual for 3 computer programs for predicting aerodynamic interference between lifting surfaces and lift and cruise fans in transport-type aircraft
[NASA-CR-114332] 19 3204 N71-33002

Computer program for aerodynamic characteristics evaluation of multiple-component airfoils in subsonic, viscous flow
[NASA-CR-1843] 19 3205 N71-33140

Fluid control, filtration, and calibrating equipment, computer programs, and data reduction techniques - technology utilization
[NASA-SP-5938/01] 19 3278 N71-33142

Computerized analysis of single peaked hydrographs using transformation of incomplete gamma function and weighted least squares method
[PB-196899] 19 3258 N71-33153

Comparison of differenced Doppler and range tracking data-types for process noise problem solutions and computer programs for orbit and failure rate calculations
19 3347 N71-33166

Digital television system, computer programs, high-speed data subassemblies and performance, multiple-mission telemetry and command systems, and phase shifter and data decoders for DSN
19 3333 N71-33167

Computer program for calculating lifting force distributions on symmetrical and cambered wings in subsonic flow based on numerical integration and lifting surface theory
19 3306 N71-33220

Computer program for calculating propellant dynamics in two dimensional and axisymmetric tanks during spacecraft docking
[NASA-CR-119904] 19 3337 N71-33243

FORTRAN computer programs to evaluate semiconductor materials in conjunction with Schottky barriers
[AD-724106] 19 3333 N71-33314

SUBJECT INDEX

Computer programs for calculation of thermodynamic and transport properties of cryogenic fluids
[NASA-TM-X-67895] 20 3338 N71-33339

POPOF library and codes for preparing secondary gamma ray production cross sections
[ORNL-TM-3367] 20 3317 N71-33373

Mathematical models for computer calculations of two dimensional hydrodynamic nonlinear convection instability flow
[NASA-CR-121472] 20 3345 N71-33375

Derivation of difference equations for MATH hydrodynamic computer program, and computation of flows containing plastic and elastic effects
[LA-4601] 20 3339 N71-33375

Computer program for determining inviscid flow around blunt bodies at supersonic and hypersonic speeds - users manual
[NASA-TM-X-2334] 20 3252 N71-33378

Digital computer program for calculation of one heat transfer in power reactors during loss of coolant accidents
[CONF-710302-2] 20 3307 N71-33379

Computer program for calculating nuclear fuel element transient responses to transient loads
[ORNL-TM-3293] 20 3309 N71-33384

User guide for use of computerized design programs /COMPDES/ - Vol. 4
[NASA-CR-119912] 20 3294 N71-33388

Computer program /MCNA/ to solve elastic neutron transport equation by coupled sampling with Monte Carlo method
[LA-4488] 20 3337 N71-33390

Evaluation of automatic guidance modes and software for BTOL aircraft flight control
[NASA-CR-121768] 21 3375 N71-33404

Mark 3A simulation center diagnostic software for EMR 6058-Univac 1108 interface
21 3392 N71-33410

DSIF telemetry and command processing operational program for providing software to Mariner Mars 1971 mission
21 3394 N71-33411

Computer program for transmission electron diffraction pattern analysis
[AEC-5729] 21 3394 N71-33418

Simulation of piping drum channel system by ALGO and SIMULA programs on Univac 1108
[NASA-CR-121633] 21 3397 N71-33412

Description and operation of outer planet data presentation computer program
[NASA-CR-121748] 21 3398 N71-33411

Sample data cases for outer planet data presentation computer program
[NASA-CR-121747] 21 3398 N71-33412

Bibliography of computer graphics to include graphics applications, animation, graphics language and subroutine packages, and graphic text manipulation
[P-4629] 21 3400 N71-33419

FORTRAN 4 computer program for design application of stagger angle replacing inlet flow angle in given blade cascade
[NASA-CR-121679] 21 3410 N71-33418

Development of computer program for calculation of minimum path lengths from many sources
[NLL-M-20634-5828.4F1] 21 3423 N71-33418

Instructions for use of acoustic oxidation apparatus in conjunction with computer program to obtain directly active concentration profiles of droplet sized aerosols
[NASA-CR-119799] 21 3432 N71-33411

Compilation of papers on applications of mathematics and computer programs for industry related problems
[NASA-SP-5938/01] 21 3447 N71-33412

Computer program for function optimization on the segments by golden section
[UCID-30002] 21 3447 N71-33413

Computer program for calculating concentration and burnoff profiles in section of graphite being irradiated by water
[AERE-M-2403] 21 3457 N71-33418

XBWR - computer program for analysis of mass transfer in boiling nuclear reactors
[EUR-4603-B] 21 3457 N71-33418

Slab reactor program, SHOVAV, for solving for group, space-time dependent diffusion equation with temperature feedback
[LA-1217] 21 3458 N71-33411

Computer program [COSTAX-BOL] for analysis of intermediate accidents or severe operating transients for BWR and PWR nuclear reactors
[EUR-4607-B] 21 3458 N71-33412

RELAP/ASME code for analyzing reactor core and loop thermal hydraulics during blowdown
[CONF-710302-6] 21 3459 N71-33417

ANCON code for solving point reactor kinetic equations including thermal feedback
[LA-4616] 21 3460 N71-33418

BUSSEL - computer program used to determine buckling load of revolution shells under hydrostatic pressure, axial compression or both
[WAFD-TM-690] 21 3461 N71-33418

SUBJECT INDEX

Program for accurate determination of nuclear fuel burnup in fast breeder 21 p3482 N71-34840

FRANK, computer program, for analysis of time-of-flight spectra using least squares method 21 p3487 N71-34884

FRP-9 program for IBM FM cyclotron beam control and program loading profile used 21 p3479 N71-34787

Computer program for FM cyclotron analyzer comparing electron energy of residual nuclei 21 p3479 N71-34786

Optical-matrix search code including spin with time in estimating and absorption potentials for spin-1 and spin-1 particles 21 p3473 N71-34732

Computer code incorporating level density and correction factor to estimate compound nucleus cross sections with Hauser-Feshbach theory 21 p3473 N71-34733

Computer program and thermal correction formulae for Fe , NiO , CSE , COH , and ZrSi obtained from lattice dynamics models 21 p3478 N71-34778

FOR-9 computer program for detection of incident ion direction with FM cyclotron analyzer 21 p3483 N71-34887

Program for resolving Moseley's spectra by Gauss surface regression procedure 21 p3485 N71-34827

Computer program for solving MIXED equations for free fluids in one dimension and application to particularized hydrograph or ballistics problems 21 p3485 N71-34885

Building procedures including computer program (BAP) for measuring junction depth in amorphous silicon-semiconductor fabrication reliability studies 21 p3486 N71-34886

Computer program (KRISTALL) for studying kinetics of radiation damage in face centered cubic lattice, body centered cubic lattice, and diamond 21 p3486 N71-34886

Basic, implementation, and type of digital computer program for determining dynamic behavior of dual spin space vehicles - Vol. 1 21 p3512 N71-35080

Hardware for development and verification of complex software used in space shuttle data management system 21 p3517 N71-35089

Development and characteristics of executive software for application in space shuttle data management system 21 p3517 N71-35089

Development of computer programming language for use on space shuttle 21 p3517 N71-35081

Characteristics of Space shuttle data management system for data transmission and service for avionics equipment and other subsystems 21 p3518 N71-35045

Development of structural analysis for fast and small operations involving space shuttle ground support equipment 21 p3518 N71-35045

LEPTON ROBOT minimum Manhattan-transport unit controlling flying boomer optimization program based on dynamic programming for mission planning 21 p3518 N71-35046

Large and sensitive software requirements for structural analysis of space shuttle 21 p3519 N71-35077

Methods of structural dynamic systems using IBM computer and FORMAPORTMAN Matrix 21 p3527 N71-35128

Computer program for evaluating vibrational distortion of concentrated structural systems subjected to random excitation of arbitrary structure 21 p3527 N71-35129

Removal of photomicrographic mission identification with emphasis on global block adjustment matrix - Vol. 2 21 p3533 N71-35334

Flow and temperature manual for NASA-70 digital computer program 21 p3534 N71-35325

Structural analysis graphics program for rapid solution and display 21 p3534 N71-35327

Computer program for system history of geostationary orbit in orbit diagrams 21 p3534 N71-35329

Development and application of computer program for design of microwave cavity in electro-optical system 21 p3534 N71-35331

Development of digital systems for picture processing 21 p3534 N71-35333

Computer program RETRAN to solve five dimensional steady state heat conduction on shielded tube containing fluid 21 p3537 N71-35336

FORTRAN computer program to implement fast Fourier transform algorithm for multi-2 transform (AD-726339) 21 p3537 N71-35337

Users manual for DRANE computer program for use in ballistic missile defense analysis (AD-727045) 21 p3537 N71-35339

Computer-aided data reduction techniques for extracting time dependent conductivity of dielectric materials from fast shock recorded responses (AD-726339) 21 p3537 N71-35337

Computer program for predicting abundances of slowly converging particles and acoustic lines in three dimensional acoustic field (NASA-CR-115941) 21 p3547 N71-35483

Computer program for calculating flow through conical turbine cascades with variations of existing blade design to reduce shock strengths and performance loss (IVK1-TM-37) 21 p3548 N71-35410

Computer analysis and forecasts of tides (IPA-CF-208) 21 p3574 N71-35431

Autocorrelation and power spectrum analysis computer programs for digital analysis of X ray and gamma ray emitting patterns 21 p3582 N71-35398

Computerized work and compensation delay required by machines to compute functions (NASA-CR-121593) 21 p3587 N71-35486

Geometrical interpretation of Sandwich theorem related to geometry and algorithm and program for achieving solutions (AD-726403) 21 p3588 N71-35484

Computer program for predicting atmospheric short-layer instabilities and clear air turbulence induced by aircraft wakes (NASA-CR-122041) 21 p3589 N71-35701

Developing computer programs for use in real time decision making tool by precipitation measurement 21 p3611 N71-35724

Manned shuttle comprehensive optimization and targeting program (MASCOT) 21 p3616 N71-35768

ZODIAC-C code for multigroup, multigroup neutron flux burnup analysis (BRLW-1529) 21 p3621 N71-35801

Computer code for predicting and analyzing irradiation performance of stainless steel clad (U-Pu)O₂ fuel pins (ORNL-TM-3586) 21 p3623 N71-35828

Computer program for calculating transient heat transfer performance of reactor coolant channel during accidental power excursions 21 p3627 N71-35843

Development of computer program for calculating color coordinates and color differences from colorimeter values (FOA-2-C-2386-51) 21 p3629 N71-35828

FLAMOR-AL code for Gler computer for calculating scattering kernels and cross sections of polycrystalline moderators (INR-1260) 21 p3633 N71-35886

Computer programs for calculating penetration and diffusion of neutrons and associated bremsstrahlung through extended media 21 p3634 N71-35889

Preparation of particle identification system using ORTEC 423 with block diagrams of circuits and graphs (ANU-P-514) 21 p3634 N71-35903

FORTRAN computer program for automatic analysis of gamma ray spectra from Ge(Li)-detectors (LJNR-7101) 21 p3634 N71-35905

FORTRAN program for gamma radiation dosimetry in arbitrary shapes and target geometry (ORNL-TM-3596) 21 p3638 N71-35953

Description and use of ARES4 discrete ordinates program and subroutines for reactor physics applications (ORNL-TM-3619) 21 p3642 N71-35965

RAD surveying system for nuclear data acquisition utilizing a digital program (IFUC-47-504) 21 p3644 N71-35978

Computer program for solving five dimensional multigroup neutron diffusion equations and for solving or recycle of isotopic compositions and related problems (ORNL-13672) 21 p3647 N71-36087

User manual for Monte Carlo direct simulation (NASA-CR-115131) 21 p3649 N71-36157

Computer program for calculating infrared surface transmittance and heat transfer on space shuttle configurations (NASA-CR-111981) 21 p3673 N71-36186

Survey of NASTRAN applications in static and dynamic structural analysis problems (NASA-TM-X-5787) 21 p3682 N71-36253

Development, maintenance, and future capabilities of NASTRAN - NASA Structural Analysis computer program 21 p3682 N71-36254

NASTRAN program used to calculate stress concentration caused by surface cavities in plates under biaxial loading 21 p3682 N71-36255

COMPUTER PROGRAMS

NASTRAN computer program used to calculate lateral deflections of vent spawners systems beam to determine stiffness of small vessels 21 p3682 N71-36256

NASTRAN computer program application in stress analysis performed on Skyline hardware 21 p3682 N71-36257

Accuracy, adequacy, and limitations of NASTRAN computer program static load structural analysis solution 21 p3682 N71-36258

NASTRAN computer program applied to localized problem of reinforced cylindrical shells with openings 21 p3682 N71-36259

NASTRAN computer program differential stiffness and static load analysis methods compared for stress-tension side opening examples 21 p3682 N71-36260

NASTRAN program differential stiffness method applied to structural analysis of Apollo Telescope Mount solar array wing and results compared with static load tests 21 p3683 N71-36261

NASTRAN program used to calculate gravity load distortions in 64-m antenna reflectors 21 p3683 N71-36262

NASTRAN-GAP program for analyzing antenna radiation patterns of reflectors distorted by gravity and thermal loads 21 p3683 N71-36263

Comparison of ASKA and NASTRAN program analyses of space shuttle hot stress test article deformed under thermal and mechanical loads 21 p3683 N71-36264

NASTRAN application to static stress and dynamic modal problems of horizontal stabilizer of F-14A aircraft 21 p3684 N71-36269

NASTRAN program for calculating structural vibration characteristics of plate configurations 21 p3684 N71-36272

Application of NASTRAN to structural analysis of space shuttle orbital flight element model with over 3000 joint degrees of freedom 21 p3685 N71-36279

Use of NASTRAN as analysis tool in structural design optimization process applied to aircraft fuselage type structure 21 p3685 N71-36280

Structural analysis and design optimization of spacecraft using NASTRAN 21 p3686 N71-36281

Evaluation of NASTRAN system based on large complex aerospace analysis 21 p3686 N71-36282

Management, standards, and maintenance of NASTRAN documentation reviewed with emphasis on specifications in style and format 21 p3686 N71-36283

Comparing and integrating NASTRAN with other finite element computer programs 21 p3686 N71-36284

Computer program technology transfer and COSMIC evaluation and dissemination functions 21 p3686 N71-36285

Accuracy, usability, and economics of using NASTRAN program 21 p3686 N71-36286

NASTRAN program for input data check and undeformed structure plotting 21 p3686 N71-36287

Training and installation procedures for NASTRAN program 21 p3686 N71-36288

NASTRAN installation and implementation on CDC 6600, IBM 360, and UNIVAC 1108 21 p3686 N71-36289

Evaluating current NASTRAN discrete element models for monocoque and semi-monocoque structures 21 p3687 N71-36290

Comparison of worksheet computing and hand-work computing using NASTRAN program for relative comparison of structural models 21 p3687 N71-36291

New element preprocessing for NASTRAN programming to generate tables and routines for new elements 21 p3687 N71-36292

Comparison of finite element computer programs for analysis of clamped flat plate and built-up wing vibration frequencies 21 p3687 N71-36293

NASTRAN generation of motion pictures for analysis of elastic structure transient response under continuous deformation conditions 21 p3687 N71-36294

On-line computer graphics program applied to NASTRAN for checking finite element models prior to structural analysis 21 p3687 N71-36295

Automatic generation of finite element input, mesh transparency, and symbolic parameters for NASTRAN simplification and error reduction 21 p3687 N71-36296

COMPUTER SIMULATION

Auxiliary computer routines for generating, checking, and displaying NASTRAN input and output data for analysis of aerospace vehicle structures
22 p3687 N71-36297

Pre-processor, post-processor, and multiple level substructuring routines for data management in support of NASTRAN finite element structural analysis of spacecraft
22 p3688 N71-36298

NASTRAN static, modal, and transient analyses plotting techniques with delta wing examples
22 p3688 N71-36299

NASTRAN post-processor routines for space-truss structural frameworks
22 p3688 N71-36300

NASTRAN flat plate finite element convergence properties for stress analysis of cylindrical and conical shells
22 p3688 N71-36301

NASTRAN and substructuring techniques for structural analysis of complex space shuttle structures
22 p3688 N71-36302

Module design modification requirements for incorporating aerodynamic capabilities into NASTRAN structural analysis program
22 p3688 N71-36303

Coding considerations for implementation of general isoparametric solid elements into NASTRAN displacement method program for stress analysis
22 p3688 N71-36304

Reduction of proliferation and maintainability of finite element method computer programs
22 p3688 N71-36305

Computer program for analyzing stresses, strains, and displacements in layered elastic structure under action of vertical loads on top surface
22 p3689 N71-36309

Computer user manual for use with automated general purpose system for structural analysis - Vol. 2
22 p3689 N71-36315

Computer program for solving two-phase equilibrium data for binary mixtures and thermodynamic functions including critical points based on Van der Waal equations of state
22 p3689 N71-36357

Interactive graphic structural program illustrating basic concepts of systems analysis - INSHOIT
22 p3689 N71-36371

Computer based cataloging and subject indexing system
22 p3689 N71-36381

Computer program for numerical integration of downwash aerodynamic flow about rectangular planforms, for different aspect ratios
22 p3704 N71-36485

Computer program for determining radiating nonequilibrium inviscid flow over blunt body by integral equations
22 p3706 N71-36417

Development of computer program to predict performance from specified cell characteristics in lithium-diffused silicon solar cells
22 p3709 N71-36444

Program for calculating saturation curves and condensation characteristics of gaseous mixtures of binary organic vapor and air
22 p3720 N71-36519

IBM 360 TELOR3 program for testing, editing, and listing information on ORBSA tape
22 p3728 N71-36571

Computer program [DIODE] for comprehensive evaluation of gamma spectra with options ranging from simple printout of spectrum to complete analysis
22 p3728 N71-36575

User manual for computer system to analyze high resolution spectrum - Vol. 1
22 p3728 N71-36577

PAGE computer program for space framework analysis using piping systems of refinement and power plants
22 p3729 N71-36579

FORTRAN computer program for simulation of movement using set of time dependent differential equations and plotting curve
22 p3729 N71-36585

Computerized pseudocolor transformation from black and white to chromatic images with density operations
22 p3730 N71-36588

FORTRAN 5 digital computer program for predicting dynamic response of Apollo command module to earth impact
22 p3730 N71-36589

Computer program for solving eddy-current problems encountered in nondestructive testing including operating instructions and examples
22 p3737 N71-36648

Computer program for calculating corona thresholds in nonuniform electrical fields
22 p3738 N71-36654

Machine parameters and computer programs for superconducting synchrotron cool analysis
22 p3740 N71-36669

Multi-material Eulerian program [HELP] for flow in two space dimensions and time
22 p3743 N71-36692

FORTRAN listing of multi-material Eulerian program [HELP] for compressible fluid and elastic-plastic flow in two space dimensions and time
22 p3744 N71-36693

Program for tidal measurements in a plastic area
22 p3767 N71-36992

Computer applications to tide and current analysis in coast and geodetic surveys
22 p3769 N71-37008

Two group code [SAVE] for reflector savings of completely reflected cylindrical reactor utilizing iterative techniques
22 p3795 N71-37068

Multigroup multiregion one dimensional criticality calculation diffusion code for IBM 1130 computer - UARAE-90
22 p3795 N71-37069

Four groups, four regions, one dimensional criticality calculation diffusion code for IBM 1620 computer - UARAE-85
22 p3795 N71-37050

Two group, two region, one dimensional neutron diffusion code for nuclear reactor criticality calculations
22 p3795 N71-37051

Physical-mathematical model [NEMI] for sodium boiling in core channel during loss of flow or power excursion accident
22 p3795 N71-37053

One dimensional, multigroup diffusion code for use in fast reactor criticality and kinetics parameter analyses
22 p3796 N71-37063

SNAP radiation shielding design using computer programs with numerical solutions to transport equation
22 p3797 N71-37071

Computer program for nuclear fuel burnup calculations and preliminary fuel cycle cost analysis
22 p3799 N71-37083

Manual for ORSAC computer program for calculating power plant combinations to provide given electrical capacities in US with minimum cost
22 p3799 N71-37083

IBM 1620 code for calculating multigroup, constant and neutron fluxes in 2 and 3 group diffusion approximations for homogeneous multigroup reactor
22 p3799 N71-37088

Programs for management and processing of neutron diffraction data
22 p3806 N71-37133

Multigroup time independent neutron diffusion code for IBM-1130 - RAM-1
22 p3808 N71-37150

Modification of coupled-channel code [JUPITER 1] including expansion of deformed optical potential in terms of Legendre polynomials and Coulomb excitation
22 p3811 N71-37170

Measuring spatial distribution of neutron activation in water using Cf-252 source with results compared with computer program calculations
22 p3813 N71-37187

MECC-3 code instructions for calculating nuclear reactions involving incident particles of high energy on complex nuclei
22 p3816 N71-37213

Monte Carlo code written in FORTRAN for estimating high energy neutron spectra
22 p3820 N71-37246

Monte Carlo program for thermal neutron thermalization spectrum estimates and errors associated with beams within and leaving source blocks
22 p3820 N71-37247

Computer programs for qualitative and quantitative neutron activation analysis using monoenergetic gamma ray spectra
22 p3822 N71-37261

Two computer programs for calculating plasma stability and equilibria in Astron and minimum-B magnetic mirror systems
22 p3827 N71-37298

Computer code for calculating radial transport profiles in toroidal discharge plasmas
22 p3830 N71-37318

Development of computer program for analyzing flow conditions and performance of turbomachinery at design and off-design conditions
22 p3840 N71-37385

Design curves and computer programs for investigating post buckling behavior of stiffened plates with small initial curvatures under combined loads
22 p3881 N71-37526

FORTRAN program for calculating free vibrational frequencies and mode shapes for smooth arc of arbitrary shape and varying cross sections
22 p3882 N71-37529

Development of polyhedral subdivision concepts and application to structural analysis of spheres, hemispheres, and domes - Part I
22 p3882 N71-37535

Computer program for analyzing transient response of oblique axisymmetric bodies including effects of shear flow
22 p3887 N71-37569

SUBJECT INDEX

Computerized KWIC system for retrieval of microfilm research files
22 p3879 N71-37578

Modified thermal analyzer digital computer program for heat transfer problems
22 p3881 N71-37578

Computer program for solving a one-dimensional transient or steady state heat flow problem by using electrical analogy of problem and solving by finite difference method
22 p3882 N71-37578

MUFAN program for determining processes, rates, and pressure drops in systems involving one dimensional incompressible steady state fluid flow
22 p3882 N71-37578

Graphical display computer program for GDS operations scheduling system
22 p3882 N71-37578

Computerized management information systems for accounting and control activities
22 p3884 N71-37578

Digital computer bibliography, programming techniques and applications, and software standardization and reliability
22 p3886 N71-37578

Equations and computer program for calculating chemical equilibria in thermodynamic states of complex systems
22 p3887 N71-37578

Computer program for inductive inference problems in organic chemistry
22 p3887 N71-37578

Computer program for JMT fuel atomization
22 p3887 N71-37578

Numerical method and computer program for determining stresses and strains in complex structures
22 p3887 N71-37578

UNAMIT - computer code for calculating temperature water unit shield weights for 250 megawatt reactors
22 p3887 N71-37578

Problems in nuclear data processing by computer
22 p3887 N71-37578

Computer code in FORTRAN 4 for thermal neutron absorption calculations in spherical and cylindrical neutron sources
22 p3887 N71-37578

TRACE 66 program for analysis of satellite orbit trajectories and tracking systems
22 p3887 N71-37578

ERLESC finite element program for electrolysis, photo stress, and photo stress, orthotropic elastic tensor dependent material properties
22 p3887 N71-37578

COMPUTER SIMULATION
U. COMPUTERIZED SIMULATION
COMPUTER STORAGE DEVICES
NT BUT-ER STORAGE
NT CORE STORAGE
NT DELAY LINES [COMPUTER STORAGE]
NT FLIP-FLOPS
NT MAGNETIC CORES
NT MAGNETIC DRUMS
NT MAGNETIC TAPES
NT RANDOM ACCESS MEMORY
NT REGISTERS [COMPUTERS]
NT SHIFT REGISTERS
Computer graphics terminal using storage CRT [CSC-TN-625]
01 p3887 N71-37578
Feasibility of 50 nanosecond cycle time bit-to-bit magnetic film storage
01 p3887 N71-37578
Data storage with fast processing capability
01 p3887 N71-37578
Information display from access storage of light computer on cathode ray tube screen
01 p3887 N71-37578
Magnetic matrix memory system for nondestructive reading of information contained in matrix
01 p3887 N71-37578
Binary sequence detector with few memory elements and minimum delay
01 p3887 N71-37578
Feasibility study for using holographic techniques for read/write optical memory
01 p3887 N71-37578
Computational work and efficient computers in general purpose machines
01 p3887 N71-37578
Core, magnetic, transistor, and BORAN chips and memory devices
01 p3887 N71-37578
Core, magnetic film, and semiconductor memory techniques
01 p3887 N71-37578
High speed core, magnetic, semiconductor, or laser storage systems
01 p3887 N71-37578
Permanent read only memory
01 p3887 N71-37578
Mass memory system for advanced computers
01 p3887 N71-37578
Application of digital associative machines in pattern processing methods
01 p3887 N71-37578

SUBJECT INDEX

- Investigating holographic techniques for high capacity read/write optical memory having no moving parts
[NASA-CR-102973] 05 p0096 N71-15136
- Application of domain tip logic in designing associative processors for spaceborne use
[NASA-CR-115966] 05 p0522 N71-15533
- Feasibility design of billion-gate computer
[AD-714099] 06 p0019 N71-16316
- Development and characteristics of most memory subsystems for spacecraft applications
[NASA-CR-116242] 06 p0021 N71-16572
- Applying waveguide transverse filters to playback of digital tape recorder signals and complementary-symmetry MOSFET memory for outer planet spacecraft
06 p0021 N71-16604
- Pulsed magnetic core memory element with feedback for regeneration without loss of digital information
[NASA-CR-RG-89393] 06 p1164 N71-18395
- Investigating nonlinear radiation effects on domain tip film elements used as data storage devices
[AD-715913] 06 p1222 N71-18636
- Reliable techniques for page storage
[NASA-CR-117122] 06 p1353 N71-19598
- Capacity of holographic memory systems with laser system, coherent-optic beam deflector, block data computer and synthesizer
[NASA-CR-103026] 06 p1354 N71-19773
- Requirements for memory units in digital computers for long reliability
06 p1355 N71-19801
- Associative memory system for mass storage using integrated elements and array organization
[NRL-34519] 06 p1355 N71-20124
- High level computer programming language (BAM-III) and parallel processing system to implement it
[NASA-CR-117134] 06 p1358 N71-20332
- Metal oxide semiconductor and magnetic memory as computer data storage devices for European research organization meteorological satellites
10 p1528 N71-21693
- Design, development, and test of ferrite memory system for application as computer storage device
10 p1528 N71-21693
- Multiaccessing computer memory with cyclic address
[NRL-72644] 10 p1530 N71-21657
- Reliable magnetic core circuit operates with application in selection matrices for digital memories
[NASA-CR-RX-01316] 11 p1739 N71-23033
- Photoreactive memory for computer applications giving improved signal to noise ratio and reading and retention of stored information during slight light loss
[AD-718391] 12 p1881 N71-23222
- Feasibility, design, and algorithms of integrated circuit content addressable memories
12 p1891 N71-24025
- Time division multiplexed telemetry transmitting circuit for use with programmed memory
[NASA-CR-RG-10131-1] 12 p2044 N71-24624
- Serial digital decoder design using square wave clock and serial memory storage units
[NASA-CR-RX-01050] 12 p2049 N71-24630
- Visual memory management system with working as model suitable for microprogramming
[NASA-CR-118316] 13 p2620 N71-24915
- Computer program for linked list information retrieval including semantics, syntax, and outline of search program
14 p2221 N71-23978
- Method of storing inverted file with minimum storage space and low access time for quick retrieval of astronomical data by computers
14 p2221 N71-23980
- Description and characteristics of automatic information storage and retrieval system using batch processing mode on IBM 360 computer
[NRL-70927] 14 p2224 N71-26306
- Visual memory system with multiple switch circuit for batch processing location
[NASA-CR-RX-01446] 14 p2234 N71-26434
- Computer compilation of high energy physics data generated by graphs or tables
[NRL-80000-N71] 15 p2467 N71-27286
- Signal to noise ratio effects on digital computer data transmission and storage operations including test, cross coupling, and switching circuits
16 p2575 N71-28767
- Robust memory for enhanced reliability of digital data processing system
[NASA-CR-RG-10264] 16 p2576 N71-29135
- Magnetic power for making computer storage devices
17 p2723 N71-30023
- Vulnerability of remote accessible computerized information systems to electronic crime
19 p3059 N71-31634
- Associative or content addressable memory systems using holography, and KWC index
[NASA-CR-117772] 19 p3062 N71-32459
- Memory chain model for determining error sources in digital channels with memory
[NASA-CR-121439] 20 p3259 N71-33551

- Adaptive approach to dynamic allocation and release of buffer storage within computer systems
[NASA-CR-117905] 21 p3397 N71-34171
- Development of computer memory system for automated attendance accounting system
[NASA-CR-RX-011456] 21 p3399 N71-34189
- Modification to inhibitor which allows memory location assignment to particular inhibitor for batch processing
[P-4585] 21 p3400 N71-34198
- Flow diagram and compression capabilities for software interfacing of flight data
[NASA-CR-61346] 22 p3535 N71-35321
- Computational work and computational delay required by machines to compute functions
[NASA-CR-121908] 22 p3607 N71-35688
- High concentration integrated computer storage devices
[REPT-1413] 23 p3729 N71-36582
- Ferrite wireform computer storage devices with increased size and storage capacity
23 p3729 N71-36583
- Design, operation, and calibration of signal amplitude measuring system for computer secondary standard magnetic tapes by reference tapes
[NBS-SP-268-29] 23 p3730 N71-36590
- Reference matrix effects associated with high speed magnetic tapes and computer flying head
[AD-726444] 23 p3744 N71-36694
- Using control computer to analyze beam quality of MeV proton linear accelerator
[UAAAB-76] 23 p3823 N71-37283
- Dynamic memories constructed as circulating shift registers with enhanced data access
[AD-727116] 24 p3895 N71-37763
- COMPUTER SYSTEMS PROGRAMS
NT INPUT/OUTPUT ROUTINES
NT OPERATING SYSTEMS (COMPUTERS)
NT SUBROUTINE LIBRARIES (COMPUTERS)
Advances in electronic and analog computers
[JPLR-51522] 01 p0026 N71-10594
- Analysis and simulation of computer center performance
[AD-711293] 02 p0190 N71-11338
- On-line, real time, whole body counter computer system
[BIRW-FBS-70-6] 03 p0339 N71-12449
- Computer program ADMAQ for analog to digital conversion of data on XDS 930 computer
[AD-72674] 03 p0344 N71-12498
- Computer designing and programming
[NASA-CR-115019] 04 p0382 N71-13654
- Classification and survey of computer system performance evaluation techniques
04 p0383 N71-13661
- Unified hardware/software design for computer systems optimization
04 p0585 N71-15662
- FORMAL programming system with language capability for performing symbolic algebraic manipulations
[NASA-CR-116149] 06 p0818 N71-16086
- Computer program SUPPER for console execution of utility programs on IBM S/360 computer
[NASA-TM-X-45501] 12 p1081 N71-23331
- Computer systems hardware and software operations review
[CDD-1014-1287] 13 p0052 N71-25192
- Computerized inventory control system for highway department of Pennsylvania
14 p2225 N71-26553
- Highway integrated computer system with subsystems for decision making, management, and technical services
14 p2225 N71-26554
- Experiments with Extendable Computer System Simulator as special-purpose language for computer systems modeling
[NASA-CR-118048] 15 p2384 N71-27722
- Transmission system for data generated by flying spot device into Radian-3 computer
[ITR-779] 18 p0893 N71-30589
- Computer program for generating cross reference index in operating system of IBM 360 computer
[NASA-TM-X-45611] 18 p0895 N71-30610
- Modification to inhibitor which allows memory location assignment to particular inhibitor for batch processing
[P-4585] 21 p3400 N71-34198
- Computer system language for job construction and control
24 p3893 N71-37748
- COMPUTER TECHNIQUES
Computerized cartography
[FB-194570] 07 p1013 N71-16994
- Computerized analysis of data on high altitude burst release
[BOO-1183-3007] 07 p1015 N71-16997
- Characteristics of computer-aided mathematical analysis operating system
[AD-715382] 08 p1143 N71-18742
- Computerized techniques incorporating adaptive pilot training concepts and means of predicting student performance
[AD-716473] 09 p1340 N71-19796

COMPUTER TECHNIQUES

- Computerized ruler equipment for automatic meter scale readings
[REPT-70-14] 09 p1390 N71-20563
- Perturbation theory of single liquids and its comparison to computer results
[LPTER-71/5] 16 p1543 N71-31315
- Technology revolution and educational system management planning
11 p1847 N71-22803
- Systems management with computers and television aids in routine including physical examination, patient histories, data processing, and electrocardiographic diagnosis
11 p1847 N71-22807
- Algorithm using ALOOL 68 type language for automated determination of three dimensional path for automated control of machine tools
[AD-717777] 11 p1760 N71-22238
- Computer research techniques including information systems, language programming, and statistical analysis
[COD-2004-3] 11 p1716 N71-22422
- Automation of control systems for processing satellite measurement data
[JPLR-50743] 11 p1717 N71-22726
- Automation system planning for experimental data processing
11 p1718 N71-22734
- Data processing system parameters for complex experiments
11 p1718 N71-22735
- Two way information exchange in experimental data processing system
11 p1719 N71-22736
- Data reduction techniques for automated scientific experiments
11 p1719 N71-22738
- Optimal experimental data input to local storage units
11 p1719 N71-22740
- State of the art review on computerized processing of scientific data
11 p1719 N71-22744
- Digital computer enhancement by use of techniques of interpretation rather than compilation of higher order languages
[NASA-CR-117901] 12 p1881 N71-23435
- Computer-controlled system for testing time domain instruments to speed up calibration process
12 p1881 N71-23436
- Computer-estimated calibration system with accuracy and precision for use in Standards Laboratories
12 p1882 N71-23631
- Computerized test equipment control system for inventory, control, and calibration management
12 p1887 N71-23643
- Computer techniques for improved accuracy and precision in standard calibration procedures
12 p1888 N71-23647
- Dynamic synthesis of computerized automatic control systems
12 p1885 N71-24217
- Methodological and algorithmic considerations in synthesis of linear multidimensional automatic control systems
12 p1886 N71-24221
- Literature survey on programmed instruction technology and cybernetics
12 p1882 N71-24222
- Recent revised system usage, software and hardware development, and cost analysis, and model theory educational program
[DITRIN-PR-11] 12 p1896 N71-24323
- Computer systems hardware and software operations review
[CDD-1014-1287] 13 p0052 N71-25192
- Research and development in ceramic engineering, chemical engineering, chemistry, mathematics and computer science, metallurgy, physics, and reactor materials and technology
[IS-2208] 13 p2193 N71-25296
- Quantitative surface finish characterization by computer evaluation of scanning electron microscope images
[AD-719925] 14 p2289 N71-23624
- Applications of computer technology in state highway systems - conference
14 p2328 N71-26651
- Advanced applications of computers for biomedical research in manned space flight
[NASA-SP-5070] 15 p2375 N71-27719
- PDP 8 computer techniques in nuclear physics including data acquisition and reduction of absorption cross sections, radiation, pulse-time, and neutron lifetime and reactivity measurements
[RT/77-70/16] 15 p2451 N71-27799
- Airborne/spaceborne computer design and techniques for space shuttle data management systems
[NASA-CR-115023] 15 p2504 N71-27762
- Computer oriented electronics instruction effectiveness in comparison with classroom training
[AD-720509] 16 p2550 N71-28194

COMPUTERIZED DESIGN

- Computer facilities capable of providing substantive aid in human decision maker concerned with complex unstructured problems
[AD-721618] 16 p2583 N71-38277
- Data handling method for satellite TV broadcast system design, and data analysis and plotting by computer techniques
[NASA-CR-119631] 16 p2561 N71-38427
- Dynamic and static structural analysis computer program for one and two dimensional elastic bodies
16 p2689 N71-39099
- Computer techniques used in information theory, industrial controls, solutions to Fredholm equations, and simulating spreading of epidemic
[JFR-53401] 17 p3727 N71-39036
- Self-classifiers and algorithms for use with digital computers
17 p3723 N71-39070
- Computer techniques for trafficability and visibility analysis of linear surface in mission planning for saving vehicles
[NASA-CR-1081] 16 p3008 N71-30661
- Structure of neutron deficient boron and dysprosium nuclei investigated using Ge/Li detectors and computer methods
[BMBW-FBK-70-30] 18 p3979 N71-30729
- Man machine interface problems in graphic display including specifications in various fields
[NASA-TT-F-13816] 18 p3894 N71-31081
- Equivalence of perturbation theories of Hori and Dupin, based on Poisson brackets, and computer calculations through sixth order
[NASA-CR-119564] 18 p2945 N71-31205
- Engineering, finance, and personnel management methods and computer techniques for cost reduction and reliability in project planning
[NASA-SP-595301] 18 p3031 N71-31516
- Proceedings of conference on electronic crime countermeasures
[PB-190309] 19 p3069 N71-31628
- Computer-aided system for automated, high speed identification of human fingerprints
19 p3060 N71-31647
- Computer system for high speed processing of non-numerical information in criminal investigations
19 p3060 N71-31648
- Computer applications in chemical information systems and journal publications
19 p3194 N71-31978
- Computerized method for input of disease history information and retrieval for diagnosis
20 p3389 N71-32882
- Computerized system for processing hydrogeological data
[WMO-275] 20 p3294 N71-32958
- Utilization of electronic and computerized techniques for undergraduate medical education
[RM-6180-NLM] 21 p3385 N71-34061
- Computer system and processing of chemical data for subject indexes and index files
21 p3387 N71-34093
- Computer system for recording and organizing information in subject indexes of chemical documents
21 p3387 N71-34094
- Organization of subject index for chemistry and conversion from manual to computer system
21 p3387 N71-34095
- Computerized processing of chemical data for indexes and index files
21 p3387 N71-34096
- Configuration control for SUDC microcomputers allowing for periodic changes in operational modes
[NASA-CR-119926] 21 p3397 N71-34174
- Key word in context index and bibliography on computer systems evaluation techniques
[NASA-CR-121757] 21 p3398 N71-34183
- Theory and computer applications of submicron implantation systems
[NASA-CR-121655] 21 p3446 N71-34523
- Computer-controlled instrumentation for Danish DR-2 reactor
[RISO-M-1206] 21 p3430 N71-34613
- On-line computer techniques for reactor physics applications
[EURPHE-883] 22 p3432 N71-35065
- Computer calculation of vacancy and interstitial migration using post-interactive procedure in small computer techniques
[CRA-2-5049] 22 p3434 N71-35962
- Computer techniques for photoacoustic detection of neutral plasma and gamma quanta events in bubble chamber filled with heavy liquids
[ITEP-753] 23 p3441 N71-35958
- Computer-aided interface using interactive man/computer tasks and techniques for qualitative planning
23 p3770 N71-36391
- Magnetic mass spectrometer with programmable magnetic field analyzer for measuring isotopic isotopes
23 p3857 N71-37492
- Static, cost-effectiveness, and telecommunication facilities requirements of computer-based instruction
[NASA-CR-122945] 23 p3869 N71-37583

- Automatic data processing systems for air traffic control, health services, operations research, management planning, information systems, and reading machines
24 p3892 N71-37742
- Computerized real time data processing and display system for air traffic control in airspace over Belgium, Luxembourg, the Netherlands, and Germany
24 p3893 N71-37744
- Computer technology for medical information systems, in patient care, and for diagnostic purposes
24 p3893 N71-37745
- Neuritic resource allocation for network scheduling operational analysis
24 p3893 N71-37746
- Computer search techniques used to determine microwave frequencies used in indirect sensing by laser
[NOAA-TR-EEL-302-WPL-14] 24 p3917 N71-37904
- Introduction to numerical computer techniques for scientists
[ORNL-TR-71-1] 24 p3949 N71-38175
- Computer techniques for solving nonlinear partial differential equations for one-dimensional solid state device analysis
24 p3999 N71-38523
- COMPUTERIZED DESIGN
- Optimization of distributed-lumped-active networks
[AD-711059] 01 p0056 N71-10097
- Computer aided integrated circuit mask production
01 p0054 N71-10223
- Computer-aided design of linear networks in frequency domain
[NASA-CR-111103] 01 p0036 N71-10436
- Computer aided analysis and synthesis of fourth-order high pass filter
[AD-710733] 01 p0033 N71-10530
- Matrix method for computerized design optimization of framed structures subjected to loads
[AD-711279] 01 p0131 N71-10931
- Optimization techniques in aircraft configuration design
[AD-711410] 02 p0144 N71-11023
- Computer aided manufacturing and numerical control impact on management disciplines
02 p0233 N71-11652
- Computerized scaling data design analysis for gas film seal of turbohaft
02 p0237 N71-12009
- Computerized design of LSI systems particularly MOS arrays
03 p0354 N71-12629
- Computer based methods in man machine interaction for dynamic structural design optimization of stressed-skin structures and structural members
[AGARD-CP-34-70] 03 p0462 N71-13125
- Computerized optimization of structural design and engineering problems
03 p0463 N71-13127
- Feasibility direction methods for nonlinear programming in structural optimization
03 p0468 N71-13128
- Computer system for optimal design of aircraft structures
03 p0464 N71-13132
- Sequential convergence for full stress design synthesis of optimal truss structures
03 p0464 N71-13133
- Matrix methods in computer-aided design optimization of aircraft structures
03 p0464 N71-13135
- Linear programming for computerized minimum mass layout design of trusses
03 p0464 N71-13136
- Computer program for structural design optimization of horizontal stabilizer of supersonic aircraft
03 p0464 N71-13137
- Computer graphic system for three dimensional structural design analysis
03 p0440 N71-13139
- Computer graphics terminal for disc profile design of gas turbine engine
03 p0448 N71-13141
- FORTRAN program for computerized design of axial flow pump by blade element analysis
[NASA-CR-111574] 03 p0485 N71-13239
- Improving feedback control design by using digital computer techniques
[NASA-CR-116771] 04 p0508 N71-13301
- Techniques for optimizing structural design by using computer
[NASA-CR-115880] 04 p0500 N71-13302
- Computer aided design of microwave triode cavity oscillators
[SC-70-497] 04 p0511 N71-13333
- Microelectronics, large scale integrated arrays, electronic packaging, thin film optics, computerized design, radar equipment
[NASA-CR-107754] 04 p0512 N71-13339
- Computerized optimization of airport runway design
04 p0495 N71-13913
- Operational feasibility of computerizing reactor design data
[ORNL-TM-2928] 04 p0552 N71-13971

SUBJECT INDEX

- Computer method for evaluating optical properties of selection detector assemblies
[JUIP-679] 04 p0592 N71-14000
- Electrical, structural, and technological requirements for producing printed circuits
[AD-713615] 05 p0656 N71-14071
- Matrix method and stiffness matrix algorithms in numerical integration for computer aided network design programming
[NASA-CR-111857] 05 p0651 N71-14080
- Feasibility design of billion-gate computer
[AD-714060] 05 p0615 N71-14084
- Design and performance of logic circuit chips in computerized design of MOS integrated circuit arrays
[NASA-CR-116440] 07 p0104 N71-15100
- Computerized optimization of thermal resistant turbine blades
07 p1129 N71-15100
- Design networks having prescribed driving-point impedance in three fashion
[AD-715334] 07 p0699 N71-15771
- Computer program for design of low pass filter with minimum nonuniform distribution
[WRE-TD-159] 08 p1170 N71-16171
- Computerized prediction of aerodynamic lift characteristics for wing-horizontal tail and control wing configurations
[NASA-TM-X-64086] 09 p1312 N71-16184
- Methods for finding numerical models suitable for use in algorithms for computer-aided analysis and design of bipolar junction devices
[AD-716539] 09 p1358 N71-16188
- Computer-aided control system design program for increasing relative stability of control system
[NASA-CR-103064] 09 p1363 N71-16192
- Mathematical programming techniques applied to aerospace structural design - algorithmic tools, applications, and literature review
[AGARD-AG-140-71] 09 p1478 N71-16203
- Basic concepts of mathematical programming applied to structural design of aerospace vehicles
09 p1478 N71-16203
- Assessment of structural design philosophy in combining conceptual structural analysis with mathematical programming
09 p1479 N71-16203
- Mathematical programming applications to structural design optimization - literature review
09 p1479 N71-16203
- Computer programs for optimum, least weight design of complex elastic aerospace structures
09 p1526 N71-16213
- Computerized design of off-axis cylindrical shells and solving composite heat shells
09 p1410 N71-16217
- Computer and optimization techniques in design design
09 p1479 N71-16218
- Computerized stability design of time lag combustion system for liquid propellant rocket engine
[NASA-CR-120896] 09 p1460 N71-16219
- Dependence of computer aided circuit analysis methods and circuit design dependence on design of transistor models
[NLL-TRANS-3646-1982.81] 10 p1520 N71-16219
- Internal logic manual for programmed control systems controller for connecting teletypewriter terminals to multiple spectrometer control system
[BNL-15437] 10 p1526 N71-16219
- Computer aided design and analysis of dome fire
[AD-717307] 11 p1722 N71-16219
- Geometric programming for engineering design problems of constrained maximization of polynomial and determination of efficient points for constrained minimization
11 p1707 N71-16219
- Computer simulation for design of integrated microwave linear amplifiers
11 p1723 N71-16219
- One dimensional static physics design and analysis code (FARAD) for fast breeder reactor power development
[BAW-3067-A-VOL-1-REV-1] 11 p1795 N71-16219
- Computer program for calculating space data fields in design optimization of traveling wave tube
11 p1724 N71-16219
- Computer program to generate turbine aerodynamic requirements, approximate external blade geometry, and coolant flow requirements for two stage axial flow turbine
[NASA-TM-X-2239] 11 p1670 N71-16219
- Numerical processes in computer-aided design of switching circuits and semiconductor devices
[AD-718152] 12 p1807 N71-16219
- Simulation and design of arithmetic and logic unit for ILLIAC-2
[CDO-2118-2] 12 p1802 N71-16219
- Computerized design procedures for development of rocket propelled sled
[AD-719751] 13 p2061 N71-16219
- CIRCL-2, second generation on-line circuit design program
[NASA-CR-118643] 14 p2232 N71-16219

SUBJECT INDEX

Computer design technique of electron gun for use in nuclear light bulb engines
[NASA-CR-110415] 14 p2227 N71-25931

Hypersonic theoretical/experimental correlations of aerodynamic characteristics for space shuttle design
14 p2195 N71-26066

Computerized design of delta body space shuttle
14 p2343 N71-26067

Integrated system of computer procedures for aiding engineers in designing highways
14 p2223 N71-26356

Prototype integrated bridge design subsystem for solving computational problems and generating plotting parameters
14 p2226 N71-26357

Computerized multivariate design analysis for low sonic boom overpressure supersonic transport configuration
16 p2535 N71-26386

Structural analysis and computerized design of space shuttle structures
17 p2848 N71-29463

Computerized propeller design considered flow field distortion by hub
17 p2704 N71-29690

Telecommunications at Hirst Research Center including filter design, computer aided circuit design, and systems theory
17 p2726 N71-29731

Software for computer aided design of logical circuit for study of interactive computer graphics
[AD-72205] 18 p2896 N71-31412

Computerized design of integrated circuit boards using Lee algorithm
19 p3063 N71-31656

Digital computer graphics program for on-line design of electric drive vehicles
[AD-72462] 20 p3238 N71-32905

Computerized design of high frequency amplifiers
[AD-72496] 20 p3241 N71-33136

Computer surface algorithm for optimum search procedure in automated design
20 p3361 N71-33971

QCF high-speed data system design and implementation for 1971-1972, including doubled data transmission, block demultiplexing, and positive labeling of error-free blocks
21 p3392 N71-34141

Applications of electronic computers for computation involved in ship design and construction
[PB-55966] 21 p3480 N71-34199

Design, implementation, and use of digital computer program for determining dynamic behavior of dead ship space vehicles - Vol. I
[NASA-CR-121723] 21 p3512 N71-35030

Development and application of computer program for design of microwave cavities in electro-optical equipment
[DA-3-C-2376-51] 22 p3556 N71-35331

Procedural description for computerized design of broadband amplifier
[RL-TRANS-2734-19022.81] 22 p3562 N71-35372

Inter chip design curves for collection efficiency
[NASA-CR-122921] 23 p3709 N71-36440

Computerized design of MOS circuits
23 p3736 N71-36634

Computerized design of Micromosaic integrated circuit arrays
23 p3736 N71-36636

Interactive graphics for computerized design of integrated circuit layouts
23 p3736 N71-36637

Computerized design of integrated selective amplifiers to feedback structure or as net-work topology
23 p3739 N71-36660

BNAP radiation shielding design using computer programs with numerical solutions to transport equations
23 p3797 N71-37071

Graphics applications program for computer design of printed circuit cards
[JCL-72637] 24 p3804 N71-37751

Reliable synthesis in automatically designing digital systems
[AD-72724] 24 p3895 N71-37761

Use of miniature general-purpose digital computers for design of digital control systems
[AD-72719] 24 p3895 N71-37764

Computer for designing machines
[AD-72780] 24 p3896 N71-37771

COMPUTERIZED SIMULATION
NT ANALOG SIMULATION
NT DIGITAL SIMULATION

Computerized aerodynamic optimization of aircraft
[AD-710036] 01 p0002 N71-10122

Construction and simulation of gas dynamic laser
[AD-70996] 01 p0052 N71-10196

Computerized simulation of control systems for nuclear light bulb engine during start-up and at sustained full power operation
[NASA-CR-111097] 01 p0085 N71-10404

Simulating radiant heating of propellant stream of nuclear light bulb engines
[NASA-CR-111099] 01 p0085 N71-10405

Pseudo-noise addressing system analysis for multiple access communication with applications of error correcting codes
[AD-711001] 01 p0022 N71-10535

Mass data storage requirements for radar image simulation of urban area from aerial photographs
[AD-711365] 01 p0024 N71-10665

Steady-state nondrifting Gaussian computer model for simulating air quality in region of New York City
[RE-3923] 01 p0013 N71-10712

Analog computer simulation of perennally loaded rotating electrical power generating system
[NASA-TN-D-6070] 01 p0080 N71-10963

Computer calculations of pressure distributions on swept wings
[NLK-TN-T-189] 02 p0143 N71-11015

Computerized modeling of ultraviolet and thermal radiation distribution of spores
[NASA-CR-111386] 02 p0130 N71-11066

Analysis and simulation of computer center performance
[AD-711293] 02 p0190 N71-11338

Computer analysis of logic circuits
[LAAS-613-614] 02 p0196 N71-11374

Continuous random pressure field simulation using signals generated at several point sources
[BSV-TR-32] 02 p0267 N71-11773

Using automatic control theory with simple pilot model for precision helicopter landing approach flight director control laws
[NASA-TM-X-66492] 03 p0312 N71-12224

Computerized simulation of character recognition layer sets using PDF 8 computer
[PB-192138] 03 p0329 N71-12349

Integrated time shared instrumentation display for aerospace vehicle simulators
[NASA-CASE-XLA-01952] 03 p0345 N71-12507

Computer program for numerical simulation of plasma
[AD-712562] 03 p0437 N71-12752

Computer calculations of 184-inch synchrotron magnetic field and field changes produced by change in coil excitation
[UCRL-10082] 03 p0417 N71-12875

Computer systems analysis and simulation studies on design, development, and management of complex computer systems
[NASA-CR-115807] 04 p0501 N71-13504

Supervisory controlled manipulation system for complex manipulation tasks on unmanned space vehicles using AND TREE computer data structure
[NASA-CR-115812] 04 p0501 N71-13507

Computer aided analysis of receiving and transmitting properties of thin wire circular loop antenna
[SC-RL-70-433] 04 p0511 N71-13534

Computerized simulation of radiation damage processes in metals
[JUL-653-MA] 04 p0527 N71-13641

Computerized simulation of quasi-electrostatic plasma in cylindrical geometry with azimuthal symmetry
[SU-IFR-373] 04 p0596 N71-13960

Computer program for Monte Carlo simulation of fault trees in analysis of large complex systems
[NASA-CR-111364] 04 p0537 N71-14036

Orbital position estimation error analysis and earth orbital mission simulation
[NASA-CR-108708] 04 p0543 N71-14050

Computerized simulation of human visual perception based on spatial filtering and allowing for scale changes in input stimuli
[AD-712065] 04 p0480 N71-14475

Analog simulation in nuclear power engineering
[AD-713273] 05 p0222 N71-14543

Computerized analysis of consolidation cell test data
[PB-194036] 05 p0667 N71-14608

Investigating various materials and components for liquid metal applications
[LMBC-70-13] 05 p0702 N71-15103

Computer manual for implementing digital program in space station dynamics simulation
[NASA-CR-102971] 05 p0771 N71-15159

Computer simulation of fracture
[UCRL-72640] 05 p0779 N71-15359

Computer simulation of random response induced by complex, organic, Gaussian excitation as function of response spectral densities
[AD-713141] 05 p0779 N71-15393

Computerized simulation of LP and VLP radio wave propagation with spherical wave functions of integer order
[ESSA-TR-ERL-165-ITS-104] 05 p0640 N71-15451

Technical and human engineering requirements for simulating pilot flight
06 p0631 N71-16066

Computerized simulation of finnae swelling and gas release model for solids
[WAFD-TM-942] 06 p0917 N71-16195

COMPUTERIZED SIMULATION

Procedures for using FORTRAN 4 computer program to simulate GERT networks
[NASA-CR-116177] 06 p0630 N71-16459

Computerized simulation analysis of temperature transients in reactor rod-drop experiments
[ANL-7664] 06 p0901 N71-16834

Computerized simulation of high temperature plasmas
[UCB-34-P-128-16] 07 p1083 N71-17050

Analysis of ALQOL computerized simulation statistics at NPL, Great Britain
[NPL-CCU-11] 07 p0994 N71-17071

Computerized simulation of neutron attenuation in shielding geometries
[CEA-COMP-1566] 07 p1068 N71-17095

Computerized precipitation probability prediction for United States of America
[NOAA-TM-NWS-TDL-39] 07 p1054 N71-17517

Hybrid simulation of N-reactor
[BNWL-B-4] 07 p1065 N71-17533

Theoretical analyses and computer calculations of microwave breakdown in nonuniform plasmas
[AD-715259] 07 p1083 N71-17807

Simulating seismic rays, computer travel times, and approximating amplitudes in earth models
[AD-715316] 07 p1022 N71-17815

Computerized simulation of dispersion models for airport air pollution
[RE-3583] 07 p1053 N71-17923

Computerized simulation of antenna radiation patterns from current loops above conducting cone
[AD-714990] 07 p1080 N71-17936

Computer program for satellite rendezvous and docking maneuver simulations
[NASA-CR-103037] 07 p1059 N71-18006

Computerized simulation for engineering analysis of high speed ground transportation system
[FRA-RT-70-34] 07 p0997 N71-18011

Application of address coding guide ACG/DIME to transportation planning problems
[PB-191408] 07 p1135 N71-18041

Dipole expansion technique for particle simulation of plasmas
[AD-715075] 07 p1084 N71-18090

Computer program for modeling response of elevated roadway to passing of heavy and two-axle trucks
[PB-190635] 07 p1138 N71-18102

Computerized simulation of alternate logistics for overhaul and expensive parts inventory procedures of commercial airlines
07 p1138 N71-18118

Investigating direct electrical heating of UO₂ fuel rod for fast reactor
[BURNER-773] 08 p1234 N71-18170

Radiation energy releases in experimental channels of RB-2 reactor
[SABRI-P-69] 08 p1224 N71-18174

Spontaneous study of graphite gas power reactor on hybrid computer - conference
[CEA-COMP-1580] 08 p1235 N71-18208

Computerized simulation of RF heating and confinement of plasmas
[CEA-COMP-1617] 08 p1271 N71-18387

Coefficient determination of flight dynamics multivariable systems by means of computer simulated aircraft dynamic models
[DRL-78-30] 08 p1144 N71-18586

Computerized prediction of suspected store trajectories dropped from bomber aircraft at high speed
09 p1310 N71-19579

Computerized prediction of interference flow field for wing-fuselage store location on bomber aircraft
09 p1319 N71-19581

Digital computer simulation of automobile impacting flexible safety barrier, and multiple source criterion system for NAE vehicle wind tunnel
[DMB/NAS-1979/31] 09 p1363 N71-19401

Digital computer simulation of automobile impacting flexible safety barrier
09 p1473 N71-19402

Anthropomorphic data update for man-model used in cockpit geometry evaluation program for evaluation of flight crew interaction and compatibility with crew stations
[AD-714396] 09 p1340 N71-19818

Cockpit geometry evaluation program for computer simulation of flight crew physical compatibility with crew stations based on anthropometric and environmental data for man-model movements
[AD-714397] 09 p1340 N71-19819

Mathematical link-system model for computerized simulation of human movement in cockpit geometry evaluation program for flight crew physical compatibility with crew stations
[AD-716398] 09 p1341 N71-19820

Validation criteria and performance evaluation of human movement computerized simulations used in cockpit geometry evaluation program for flight crew physical compatibility with crew stations
[AD-716399] 09 p1341 N71-19821

Developing basic methodology for predicting aircraft stopping distance on wet runway using computerized simulation
[FAA-NA-70-51] 09 p1323 N71-20048

COMPUTERIZED SIMULATION

SUBJECT INDEX

Noise reduction in closed loop servo systems in computerized simulations 09 p1363 N71-20178 [AE-404]

Transient surface heating of large solids subject to surface heat loss 09 p1483 N71-20184 [AD-715924]

Space simulation technology for determining space environment effects on materials, spacecraft, and man 09 p1366 N71-20201 [NBS-SP-336]

Computerized simulation and analysis of residual gas composition spectra of space simulator 09 p1344 N71-20210 [AD-715924]

Computerized real time simulation of atmospheric balloon environment in altitude chamber 09 p1385 N71-20217

Computerized simulation of aerospace systems for advanced spacecraft design 09 p1367 N71-20224

Computer controlled micrometeoroid impact simulation system 09 p1368 N71-20253 [NASA-TM-X-66947]

Dynamic formation and computer program for multiple space vehicle attitude and control simulations 09 p1480 N71-20482 [NASA-CR-117358]

Simulation software for space station X r:y polarimeter experiment PFB 5.1 10 p1526 N71-20622 [NASA-CR-103076]

Computerized analysis of image data processing techniques supporting space station X ray imaging solar telescope PFE 3.3A 10 p1526 N71-20623 [NASA-CR-103077]

Modifications to computerized simulation system for space shuttle and space station applications 10 p1527 N71-20624 [NASA-CR-103078]

Computer simulation of galium arsenide limited space charge accumulation relaxation oscillations in microwave iris circuit 10 p1631 N71-20744

Experimental and computerized simulation of e-type gallium arsenide operating in limited space charge accumulation mode 10 p1631 N71-20745

Economic equipment and layout planning of warehouses using computerized simulation methods 10 p1665 N71-20770

Computerized models for nuclear reactor accident analysis 10 p1602 N71-21035 [BML-1090]

Computer code for numerical solution of laminar boundary layer and thin shock layer equations predicting electron density around reentry vehicle 10 p1628 N71-21113

Dynamic simulation digital code for EBR-2 plant protective system response to hypothetical malfunctions in reactor system 10 p1605 N71-21371 [ANL-7665]

Edge structure and representation of pictures in digital form using human visual system 11 p1699 N71-21398

Studying static and time dependent correlation functions for liquids of carbon monoxide and nitrogen using computer simulated molecular dynamics 11 p1803 N71-22112

Graphical computer simulation of incompressible flow about airfoil 11 p1715 N71-22149 [TN-71-2]

Mark 3A simulation center EMR 6050-Univac 1108 computer interface 11 p1720 N71-22782

Performance evaluation of two real time operating systems using simulation models 11 p1720 N71-22784

Computerized simulation of lateral inhibitory networks of visual afferences 11 p1693 N71-23067

Chemical signal interpretation by olfactory information systems of living organisms 11 p1693 N71-23070

Computerized simulation of electrical generator system in human heart 11 p1686 N71-23079

Materials research programs including computer simulation of creep, and nuclear magnetic resonance 11 p1683 N71-23371 [AD-714793]

Computerized simulation of sinusoidal reflecting surface effects on radio wave transmission in ionosphere 12 p1874 N71-23446 [AD-718166]

Computerized simulation of tropospheric scatter channel distortion using Monte Carlo method 12 p1877 N71-23467

Computerized simulation of performance and probability of MTI in aircraft detection in clutter 12 p1878 N71-23508 [RRE-TN-759]

Simulation and design of arithmetic and logic unit for ILLIAC 3 12 p1882 N71-23614 [COO-2116-2]

Computer animated display device for diagnosis of heart disease 12 p1867 N71-23751 [NASA-NEWS-RELEASE-71-58]

Computerized simulation of meteorological parameters and trafficability in Salinas area 12 p1955 N71-23853 [AD-718115]

Hybrid computer simulation of detection of phase coherent RF pulse train of unknown phase in additive random noise 12 p1884 N71-23869 [NASA-CR-118012]

Computerized space mission simulation for measuring spacecraft cabin thermal control system performance 12 p1885 N71-23883 [AD-718992]

Computerized simulation of tether docking by orbiting spacecraft 12 p2002 N71-24271 [NASA-CR-103163]

Computerized probabilistic model for optimal cost assignment of launch vehicle programs to advanced space missions 12 p2003 N71-24319 [NASA-CR-114284]

Solar electric propulsion performance and trajectory data for indirect solar probes, extra-orbital missions, and rendezvous with Ceres, D'Arrest, and Eureka 13 p2073 N71-25013

Computerized simulation and time optimal control of pH in acetic acid-sodium hydroxide CSTRS and comparison with Ziegler-Nichols controller for chemical reactors 13 p2040 N71-25047

Computerized life cycle cost model of cost predictions for electronic equipment 13 p2058 N71-25227 [AD-719709]

Computerized simulation of wind velocity using Nimbus 3 infrared sounding data 13 p2108 N71-25262

Computer assisted management simulation exercise for training of personnel as project managers 13 p2192 N71-25472 [NASA-TN-D-6347]

Computer simulation and research development in plasma confinement, magnetic mirrors, Astron thermonuclear reactor program, and related research [UCRL-50002-70] 13 p2143 N71-25579

Computer modeling of hippocampus and studies involving pattern recognition and information compression 14 p2289 N71-25864 [AD-720816]

High energy shock tube production of very strong, ionizing shock waves in high temperature plasmas 14 p2321 N71-25906 [AD-720838]

Digital computer simulation of steady-state and transient engine performance of gas turbine propulsion system 14 p2331 N71-25910 [AD-720803]

Computer program simulating generation of flexed forms of irregular verbs in German for use in dictionaries and grammars 14 p2222 N71-25982

Stochastic model for computerized simulation of closed man machine system operated by crew 14 p2210 N71-26076 [AD-720354]

Computerized simulation of plasma heating from electron cyclotron resonance including ion trapping and magnetohydrodynamic instability 14 p2322 N71-26078 [AD-720675]

Engine-airframe contribution to combat aircraft maneuverability 14 p2211 N71-26371 [AD-720238]

Digital computer program for simulating vehicle flow on freeways 14 p2225 N71-26352

Computerized simulation model for communication network jamming 14 p2235 N71-26612 [FOA-3-A-5727-43]

Computerized simulation of meteor orbit and atmospheric trajectory from parameters of impacted fragments 14 p2341 N71-26755 [CRA-8-4045]

Computer simulation and laboratory studies made of quantitative analysis obtained by overlapping two or more chromatograms 15 p3377 N71-27125 [COO-1222-43]

Computerized simulation of subharmonic resonance in limit cycling voltage regulator 15 p3380 N71-27127 [AD-720701]

Computerized simulation of experimental breeder reactor 2 dynamic response to sodium-fluxion and PuO₂-UO₂ fuel including specific heat and thermal conductivity effects 15 p2449 N71-27368 [AD-720742]

Computer simulation results of satellite antenna bore-sight parameter estimation 15 p2387 N71-27425 [AD-720742]

Computer code (VORTEX) simulating behavior of incompressible, inviscid, homogeneous fluid in two dimensions by following motion of point vortices 15 p2394 N71-27470 [CLM-8-106]

Experiments with Extendable Computer System Simulator as special-purpose languages for computer systems modeling 15 p2384 N71-27722 [NASA-CR-118048]

Computerized simulation of autonomous satellite landmark tracking navigation system 15 p2442 N71-27845 [AD-720841]

Global cloud model for computerized simulation of earth-viewing space missions 15 p2518 N71-27975 [NASA-CR-41451]

Approximate method for predicting motion of symmetric rigid body subjected to body-fixed force 16 p2485 N71-28171 [NASA-CR-118995]

Airborne PDP 15 computerized simulation for aircraft gunnery and navigation training including head-up display and real time computer program 16 p2585 N71-28200 [AD-721673]

Electric motor off-on speed control limiter circuit for thyristor and computerized simulation 16 p2574 N71-28200 [AD-721561]

Computerized simulation of helicopter tactical maneuvers in three body, three dimensional environment including fixed wing and rotary wing aerodynamic forces 16 p2563 N71-28200 [AD-721527]

Microeconomic analysis of in-process manufacturing quality control 16 p2601 N71-28200 [AD-720998]

Mathematical model and computerized simulation of crew related factors in space station 16 p2553 N71-28200

Digital computerized simulation of transverse noise wave transmission with tropospheric scattering including atmospheric model using meteorological parameters 16 p2563 N71-28200

Computerization of magnetic spectroscopy in cryogenic probe, oxidation states of Mo compounds, ESCA spectra of metal chalcides, and related research 16 p2551 N71-28200 [RSC-445-11]

Computerized simulation of temperature distribution and heat flux in incense thermionic reactors 17 p2781 N71-28200 [NASA-TT-F-15086]

Analysis of particle distribution using bit pushing and distribution pushing techniques for solving Vlasov equation 17 p2811 N71-28200 [COO-1726-68]

Computerized simulation of influence options from one city over vast territory 17 p2786 N71-28200

One-fluid model of low pressure MDM plasmas in toroidal geometry 17 p2811 N71-28200 [MATT-81-4]

Computer simulated electron diffraction analysis of electrons passing through absorbing crystal foil 17 p2814 N71-28200 [AD-722244]

Computerized simulation of long term physiological effects of radiation, oxide inhibition on dog respiratory systems including tissues, blood, and related research 17 p2789 N71-28200

Computerized simulation of point defects and dislocations in copper 17 p2818 N71-28200

Simulation of single-server model for paging data channel system 17 p2774 N71-28200 [NASA-CR-123375]

Monte Carlo creating simulation model to determine conditions of formation of lunar magnetospheric crusts 17 p2845 N71-28200 [NASA-TM-X-62027]

Achromatic pattern recognition model to processing chromatic objects 17 p2712 N71-28200 [AD-722853]

Computerized and manned spacecraft and cloud simulator impact testing of air cushion elastic restraint system 18 p2882 N71-28200 [NASA-CR-40169]

Computer assisted teleoperator control system in making comparative performance evaluations of tactile perception 18 p2889 N71-28200 [NASA-CR-114346]

Computer simulation of adaptive classifying structures and self-correcting devices for photographic processing 18 p2893 N71-28200 [BMVG-PBWT-70-4]

Computerized simulation of cerebral cortex pattern recognition model 18 p2875 N71-28200 [AD-722651]

Computerized simulation of convection currents in atmosphere 18 p2954 N71-28200 [AD-722836]

Computer simulation analysis of suggested optimal state confidence interval for system maintainability parameters 18 p2893 N71-28200 [AD-722651]

Computerized simulation of frequency division duplex telephony radio transmission through ionosphere using Monte Carlo method 19 p3083 N71-28200 [REPT-10-70]

Computer simulation to verify energy contents in nonlinear theory of transverse electromagnetic instabilities in collisionless plasmas 19 p3163 N71-28200 [AD-723814]

Computerized simulation and analysis of combustion chamber length instability for solid state propellant and effects of burning rate 19 p3171 N71-28200 [AD-723680]

Computerized simulation of aerodynamic loads and dynamic responses for aircraft control system data based on optimal and feedback control theories 19 p3087 N71-28200 [AD-722652]

Sodium-2 neutron control studies with digital data in computer on IBM 360/45 computer 19 p3157 N71-28200 [EURPFR-535]

Computerized simulation of electromagnetic fields both sub effects on countermeasures for low ability 19 p3164 N71-28200 [AD-723525]

SUBJECT INDEX

Reviewing continuous systems simulation techniques with emphasis on interactive, graphics-oriented systems 19 p3061 N71-32281

Computerized simulation of statistical onboard data analysis for long range spacecraft 19 p3062 N71-32346

Optical heterodyne receiver design and analysis by computerized simulation with nonlinear recursive estimates 19 p3065 N71-32377

Analysis of two plans for assigning identity codes to aircraft by digital computer simulation of peak IPR traffic conditions 19 p3069 N71-32456

Effects of aircraft system noise and signal fading on pilot performance during IPR approach based on computerized simulation of XV-3 aircraft and UB-1 aircraft 20 p3209 N71-33076

Computerized simulation of character recognition including use of reading machines and implementation of decision trees in pattern processing 20 p3238 N71-33121

Simulation of wind-induced magnetic vector in ship to sea applied to ambient acoustic pressure and shallow field noise parameters 20 p3258 N71-33157

Block computer and plotter for simulating flow about fuselages 20 p3260 N71-33463

Vehicle mode model and computerized simulation of dynamic system model response 20 p3359 N71-33714

Hybrid computer simulation of hydraulic pumping system 20 p3280 N71-33629

Mark 34 simulation center diagnostic software for Bell 605-Union 1106 interface 21 p3392 N71-34140

Computer simulation of aircraft collision-based tracking radar techniques in terminal area 21 p3396 N71-34170

Simulation of pulsed drum chemical system by ALGOL and SIMULA programs on Univac 1106 21 p3397 N71-34172

Two-dimensional computer model of Venus-like atmosphere for calculating thermodynamic profile 21 p3415 N71-34302

Block-coded search code including spin orbit time in scattering and absorption potentials for optical spin-1 particles 21 p3473 N71-34732

Inter 1106 virtual mass trajectory simulation program of FORTRAN subroutines for analysis of spacecraft trajectories 21 p3508 N71-34991

Modeling information channels and their use by statistical models and data elements 22 p3557 N71-35335

Simulation of electron avalanche in life using Monte Carlo method for study of electron population growth accompanying transient phase of avalanche and related topics 22 p3558 N71-35341

Stochastic mission simulator program, using FORTRAN 22 p3564 N71-35383

Analysis of ship propulsion reactor 22 p3621 N71-35800

Hydro, theta pinch, z-pinch, plasma gun, plasma probe, computerized simulation of plasmas, and related topics in controlled thermonuclear research program 22 p3654 N71-36056

Computerized simulation of plasma injection and coupling to laser outputs 22 p3656 N71-36072

User manual for Monte Carlo direct simulation technique 22 p3668 N71-36157

Optimization of space shuttle launch operations, fuel use, facilities, and support equipment through computerized simulations 22 p3675 N71-36199

Use of computer simulation to aid in mission and component planning and decision making 22 p3675 N71-36206

Visual mode determination of RAE antenna and research for in-flight configuration using computer simulation 22 p3684 N71-36208

Stress mechanics of plastic stress and strain fields on crack tip and computer simulation of fracture growth in viscoelastic solids 22 p3691 N71-36321

Computer program for calculating IIR interference from wind tunnel test sections by vortex lattice method 22 p3704 N71-36407

Self adaptive differential pulse code modulation system with delay adaptive predictor and quantizer and system analysis using stationary Gaussian Markov process 23 p3724 N71-36346

Computerized simulation of burst A ground wave propagation pulse subjected to atmospheric perturbation 23 p3793 N71-37040

Computerized simulation of ion-sound instability as effect of electron distribution in plasma 23 p3826 N71-37289

Simulation of aircraft ground operations for Dallas-Fort Worth Regional Airport 24 p3873 N71-37087

Computerized simulation of man machine systems 24 p3881 N71-37664

Algorithmic simulation of organic systems for designing operator-control systems 24 p3881 N71-37666

Standardized methods for compact and systematized representation of sets of functionally related parameters by matrices 24 p3881 N71-37668

Subroutines for PDP-9/GOULD 4800 graphic line printer for hybrid and digital simulation 24 p3892 N71-37741

Computer program for simulating logic circuit by describing circuit topology 24 p3894 N71-37752

Computerized business games and mathematical models of optimal scientific research development 24 p3894 N71-37755

Computerized business game for training students in industrial decision making and cooperation 24 p3894 N71-37756

Computer improvement program with application to large space vehicles and failure noting relative stability versus frequency response 24 p3901 N71-37803

Digital computer simulation of SNAP 8 power conversion system G startup and shutdowns for systems analysis 24 p3960 N71-38246

Computer aided analysis of theoretical and experimental operating characteristics of insulated gate field effect transistors 24 p3999 N71-38524

NT AIRBORNE/SPACEBORNE COMPUTERS

NT ALBORG/COMPUTERS

NT CDC COMPUTERS

NT CDC 3180 COMPUTER

NT CDC 3280 COMPUTER

NT CDC 6680 COMPUTER

NT DIGITAL COMPUTERS

NT HONEYWELL ADAPT COMPUTER

NT HYBRID COMPUTERS

NT IBM COMPUTERS

NT IBM 360 COMPUTER

NT IBM 1130 COMPUTER

NT IBM 7030 COMPUTER

NT IBM 7094 COMPUTER

NT ILLIAC COMPUTERS

NT PDP COMPUTERS

NT PDP 8 COMPUTER

NT PDP 9 COMPUTER

NT SEQUENTIAL COMPUTERS

NT UNIVAC COMPUTERS

NT UNIVAC 1106 COMPUTER

Scientific research in physics, electronics, and computer technology 01 p0138 N71-10930

Applied and research activities at Center for Computer Sciences and Technology 01 p0330 N71-10978

Grumman preprocessor - Automated Sneak Program 03 p0463 N71-13469

Compact computer control system for shipboard missile checkout and launch 04 p0506 N71-13043

Soviet cybernetics and computerized production control 06 p0819 N71-16334

Specifications of CAMAC 25-MHz counter module type LEM-52/1-1 08 p1199 N71-18160

Data compression processor for monitoring analog signals by sampling procedure 08 p1167 N71-19208

Economical, technological, and time saving effects of computer revolution on man 01 p1528 N71-21257

Oceanographic electronic equipment including sensor systems, sensors, shipboard computers, and communication and navigation systems 01 p1554 N71-31542

Analysis of test equipment used for computer assemblies 12 p1881 N71-33332

Computer developments in USSR and industrial applications in automation and information processing 12 p1881 N71-33404

Cybernetics and production control systems using Soviet computers 12 p1883 N71-33916

Objectives and measurements in computer performance analysis 12 p1885 N71-34023

CONCENTRATION [COMPOSITION]

Computer system for development and application of high resolution mass spectrometry 12 p1902 N71-34052

Corrective cloud prognostic techniques for computer forecasting of shower and thunderstorm activity including meteorological parameters and tests of instability indices over Germany 12 p1908 N71-34105

Two proportional wire chambers on-line with computer 12 p2129 N71-34576

DR2 computer system, software for hybrid computer system, X ray opportunity for determining earth elements in rock surfaces, fission track autoradiography, and related nuclear research 12 p2136 N71-33253

Probability models for solution of elliptic and parabolic equations by computers 12 p2348 N71-33970

Man machine system using computer for decision making in information retrieval 12 p2322 N71-33983

Strategies for searching in data bank files adapted to query and file structure and use of theorems with small and medium computers 12 p2323 N71-33993

Synchrocyclotron particle identification and data acquisition system based on computers and multiplexed input converter 12 p2384 N71-37290

Man-computer interaction information system to simulate various problem solving environments and provide users on-line feedback of their relative effectiveness 17 p2712 N71-30218

Computer acquired performance data from physically vapor deposited tungsten-silicon thermal conductors 18 p2804 N71-36796

Estimates of lightning caused computer component damage and malfunctions 18 p2877 N71-34143

Time sharing computer system at Lawrence Radiation Laboratory 19 p3061 N71-32215

Correction of inspection data for part misalignment utilizing small computer 19 p3123 N71-32217

Human reactions to using a university computer center 20 p3369 N71-33620

Use of computer system accounting data to measure effects of system modification 20 p3338 N71-33132

Computer system performance analysis using accounting data, with availability of data and methods of conditioning and reducing data 20 p3339 N71-33427

Belgian computerized information system applied to automatic control 20 p3370 N71-33436

Computer controlled monitoring of safety system of nuclear power reactors 22 p3622 N71-35804

Advances and limitations of computers and mathematics on social sciences 22 p3704 N71-36086

Design principles of high precision measuring instrumentation system for information transmission into computer 23 p3725 N71-36330

ES-44 computer-controlled test system for measuring electrical properties of test equipment 24 p3892 N71-37748

COMBAT PROGRAM

Development and characteristics of solar cells for COMBAT program 05 p0631 N71-14711

Design, development, and characteristics of several communication satellites 07 p1121 N71-17771

CONCAVITY

Hyperbolic laminar boundary layer growth over concave and convex surfaces 09 p1374 N71-19206

Heat transfer in jet impingement cooling of convective surface in semi-enclosed environments 24 p4000 N71-36759

CONCENTRATION [COMPOSITION]

NT ATMOSPHERIC MOISTURE

NT CARBON DIOXIDE CONCENTRATION

NT MASCONS

NT METHANOL CONCENTRATION

NT MOISTURE CONTENT

Concentration dependence of translational friction coefficient of macromolecular solutions 01 p0616 N71-10908

Determining electron concentration in flowing plasma in process of accelerating and evaporating water droplets 01 p0183 N71-10436

Simultaneous donor and acceptor concentration determination in p-type semiconductors using Hall effect measurements 02 p0283 N71-11836

CONCENTRIC CYLINDERS

- Carbon dioxide content changes in atmosphere
[NLL-M-9147-5828AF] 03 p0367 N71-12864
- Recording dust concentrations in atmosphere
[NLL-M-9139-5828AF] 03 p0368 N71-12866
- Oceanographic instrumentation system for in situ carbonate autometer measurements
[TID-25476] 03 p0374 N71-13387
- Investigating existence of long-lived super-heavy elements in nature and synthesis in stars
[JINR-P-4902] 04 p0586 N71-14247
- Computer program for calculating concentrations of chemical species in set of radiation-induced chemical reactions with homogeneous kinetics
[ANL-7693] 05 p0741 N71-15105
- Determining quantity of oxygen and carbon retained by adsorption or chemical reaction on surface of high purity metals
[LIB/TRANS-299] 07 p1070 N71-17030
- Concentration effects on Gibbs free energy and entropy of mixing of binary fluids
[NPL-DCS-6] 07 p1128 N71-17210
- Investigating theory for concentration dependent diffusion phenomena based on simple assumption for impurity atom interaction in diffusion systems exhibiting solid solubility saturation
07 p1089 N71-17296
- Measuring U-235 depletion as function of Pa content in spent fuels of power reactors
[BNWL-SA-3304] 08 p1237 N71-18258
- Freezing rate and solute species and concentration effects on charge separation at advancing surfaces of growing ice related to cloud physics
[AD-718359] 12 p1910 N71-23655
- Derivation of equations for coupled gas species concentrations equations in chemical equilibrium using free energy and equilibrium methods for specific heat and acoustic velocity calculations
[AD-720004] 14 p2213 N71-25941
- Time resolved measurements of exhaust gas temperature, mass flow rate, and hydrocarbon concentration of spark ignition engine
14 p2353 N71-26004
- Tables on critical micelle concentrations of aqueous surfactant systems
[NSRDS-NBS-36] 14 p2215 N71-26740
- Cyclotron simulation of uniform concentrations of helium produced during neutron irradiation
[ORNL-TM-3299] 20 p3308 N71-33705
- Limiting current and concentration profile in stagnant diffusion cell for copper sulfate solution
[UCRL-18397-REV] 21 p3387 N71-34099
- Auger electron velocity analyzer for use with scanning electron microscope to identify low concentrations of elements on surfaces of semiconductor devices
[NASA-CR-111968] 21 p3425 N71-34371
- Chromatographic and spectrographic extractions for determining concentrations of saccharin reduction products in nickel plating electrolytes
[NLL-LT-746-725-19022.401] 22 p3589 N71-35560
- Spectrophotometric and polarographic determinations of butadiol, saccharin, and phthalimide concentrations in brackish nickel plating electrolyte
[NLL-LT-746-726-19022.401] 22 p3590 N71-35564
- Fundamentals of calculating concentration and diffusion of air pollutants
[AD-726984] 22 p3615 N71-35760
- Isobaric-isothermal potentials for lithium oxide reduction by metals and metallic impurity oxide, nitride, carbide, and hydride concentrations in liquid lithium
[NLL-RISLEY-TRANS-2169-19091.9F1] 23 p3773 N71-36892
- Computer programming manual for calculating temperature and reactant concentrations as functions of time and axial position in catalyzed continuous flow hydrogen-oxygen reactors
[NASA-CR-120800] 24 p3892 N71-37738
- CONCENTRIC CYLINDERS**
- Guns effect in devices with concentric electrodes
01 p0603 N71-10137
- Magnetic induction concentric cylinder magnetohydrodynamic generator with cryogenic cooling
[DLR-FB-70-25] 07 p1083 N71-17640
- CONCENTRICITY**
- Natural convective heat transfer between concentric spheres, construction of experimental apparatus for heat transfer and flow visualization
[RLO-2214-1] 12 p2015 N71-24340
- CONCORDE AIRCRAFT**
- Influence of Concorde powerplant operating conditions on design of Olympus 593 fuel and oil system
02 p0289 N71-11653
- Automatic landing system of Concorde
03 p0407 N71-12448
- Mach 2 slender wing boundary layer effects on Concorde aircraft engine inlets
[ARC-CP-1122] 06 p0792 N71-15708
- Human factors in Concorde cockpit simulation
06 p0831 N71-16065
- Concorde 002 aircraft equipment for flight data recording and processing
[ESS/ES-13] 10 p1492 N71-20857

- Monte Carlo general purpose shielding computer program in FORTRAN 4 for IBM 7094 computer
[PNSI-TR-70-0301-1-VOL-1] 11 p1792 N71-22379
- Simulation, analysis, and recommendations for flight profile of Concorde aircraft to predict and achieve improvements in aircraft operation - Vol. 2
[PNSI-TR-70-0301-2-VOL-2] 11 p1792 N71-22380
- Flight tests of Concorde prototypes, design modifications, and operational costs of supersonic aircraft
11 p1675 N71-22387
- Summary of flight test methods used for performance measurement of Concorde aircraft
[NASA-TT-F-13728] 19 p3039 N71-32455
- Federal funding for SST and Concorde aircraft development in 1971
20 p3370 N71-33758
- CONCRETES**
- Fast reactor fuel interaction with concrete floor after hypothetical core meltdown
[BNWL-CC-2369] 04 p0582 N71-14104
- High temperature gas cooled reactor, gas cooled breeder reactor, and prestressed concrete pressure vessel developments
[ORNL-4589] 08 p1238 N71-18348
- Distribution moments and Monte Carlo calculation of high energy gamma ray absorption in concrete, iron, and lead slabs
14 p2384 N71-26277
- Weighted defect densities of asphaltic and cement concrete pavement in airfield pavement condition survey, USNAS Cecil Field, Florida
[AD-713235] 16 p2577 N71-28422
- Weighted defect densities of asphaltic and cement concrete pavement in airfield pavement condition survey, USNAS Willow Grove, Pennsylvania
[AD-721324] 16 p2577 N71-28423
- Weighted defect densities of asphaltic and cement concrete pavement in airfield pavement condition survey, USNALT Charleston, Rhode Island
[AD-721323] 16 p2577 N71-28424
- Multiple tests with eddy current proximity gage for determining thickness of concrete pavements
[NASA-CR-119857] 18 p2923 N71-30820
- Production of refractory concretes and determination of compressive and tensile strength at various temperatures
22 p3600 N71-35636
- Thermodynamic and electrical properties of refractory materials used in magnetohydrodynamic generator channels
22 p3600 N71-35639
- Nonlinear analysis technique for planar steel and reinforced concrete frames under static and short-time loading
23 p3864 N71-37545
- CONDENSATES**
- High energy neutron-liquid helium-4 scattering and helium-4 condensate density
[RLO-1388-566] 01 p0099 N71-10697
- Superconducting transition temperatures of electron beam evaporated metals condensed on liquid helium cooled substrates
[UCRL-19624] 02 p0284 N71-11838
- Air pollution, and condensation nuclei measurement in Rome
[IFA-TR-28] 03 p0404 N71-13270
- Refrigerant forced convection condensation inside horizontal tubes
06 p0960 N71-16875
- Apparatus for determining volatile condensable material present in polymeric products
[NASA-CASE-XNP-09699] 13 p2839 N71-24607
- Hydrodynamics of superfluid condensates including equations of motion and density matrix
14 p2304 N71-26286
- Theoretical calculations of heat transfer during vapor condensation in tube based on analogy between hydraulic friction resistance and heat exchange according to Reynolds
14 p2356 N71-26333
- Spectrometer for microdynamics of condensed matter emphasizing automation and remote control of spectrometer kinematics and delay systems
[BNP-727] 15 p2470 N71-27408
- Tables of condensation nuclei growth rates under various super saturations for warm fog or cloud modification
[AD-721591] 17 p2776 N71-29443
- Analysis of phenol formaldehyde condensates by chromatography on polystyrene gels
[ONERA-NT-171] 19 p3049 N71-31701
- Elimination of condensation on observation window of test chambers
[NASA-CASE-NFO-10890] 20 p3247 N71-33868
- Acceleration of condensate drops in axial gap of turbine stage
[RAE-LIB-TRANS-1602] 24 p3906 N71-37837
- CONDENSATION**
- Kinetics and mechanisms of step-growth polymerization of polyimides, polybenzimidazoles, and polyoxazolones
[AD-717641] 11 p1781 N71-21957

SUBJECT INDEX

- Spurter condensation of alkalites and other minerals in argon glow discharge
14 p2280 N71-26815
- Reaction kinetics of elementary, gaseous phase, and condensed phase chemical processes
14 p2215 N71-26400
- Prevention of steam hammer instability and film collapse caused by condensation in steam turbine bearings
[AD-72005] 16 p2600 N71-26200
- Production of sugar by formaldehyde condensation in presence of calcium hydrosulfide
[NASA-TT-F-13709] 16 p2538 N71-26802
- Heat transfer coefficients for dropwise condensation of organic liquids on Teflon
[NASA-TN-D-4502] 17 p2859 N71-29998
- Infrared spectra of UO and UO₂ vapor condensed in rare gas mixtures at high temperatures
[COO-1182-34] 19 p3150 N71-32324
- Formula for calculating rate of condensation growth of drops in clouds considering latent heat of condensation
[AD-724105] 20 p3294 N71-32880
- Preparation of benzobistriazole polyimides from polymer by polycondensation
[AD-726551] 22 p3403 N71-33640
- Analysis of high vapor velocity condensation in tubes based on universal velocity distribution, pressure drops, and heat transfer coefficients
[DSR-72391-74] 22 p3486 N71-34043
- Model for calculating condensation effects in boundary layer on mass transfer from rotating disks
23 p3746 N71-36714
- CONDENSATION PUMPS**
- Developing thermomechanical pump for thermoelectric outer planet spacecraft
01 p0258 N71-10200
- Temperature relaxation of highly rarefied gas applied to adsorption and condensation vacuum pumps
[NASA-TT-F-13784] 19 p3192 N71-32213
- CONDENSATION TRAILS**
- U CONTRAILS**
- CONDENSER RADIATORS**
- U CONDENSERS [LIQUIFIERS]**
- U HEAT RADIATORS**
- CONDENSERS [LIQUIFIERS]**
- NET JET CONDENSERS**
- Deadhead condenser inlet pressure control method for SNAP 8 startup
[NASA-TM-X-2115] 06 p0796 N71-13840
- Heat transfer and pressure variation during flowing steam condensation in tubes
[K-TRANS-60] 06 p0959 N71-16414
- Schematized condenser cooling systems for electronic devices and components by means of boiling and condensation in liquid-filled enclosures
[TR-29077-73] 08 p1306 N71-19333
- Mercury and NaK inlet and outlet port, condenser, and attachment design modifications of power conversion system for SNAP 8
[NASA-CR-72946] 24 p3959 N71-38341
- CONDENSING**
- NT FILM CONDENSATION**
- Inventory control of mercury condensing pressure during SNAP 8 startup
[NASA-TM-X-2114] 02 p0263 N71-11770
- Heat and mass transfer during vapor condensation in presence of noncondensing gases
[AD-712446] 02 p0306 N71-12880
- Heat transfer and pressure drop during condensation of refrigerant vapors in air-cooled condensers
[K-TRANS-57] 06 p0961 N71-16880
- Physicochemical properties and condensation growth rate equation for hygroscopic materials
[AD-716384] 09 p1413 N71-19239
- Content and distribution of atmospheric aerosols over the USSR
[TT-68-50637] 14 p2252 N71-26891
- Duration of cadmium molecules on surface during condensation at varied temperatures measured in mica, copper, glass, and pectine before being collected
[NASA-TT-F-13649] 16 p3646 N71-26223
- Prevention of condensing steam in designing novel scrubbers for polluted air streams
[ORNL-4654] 20 p3345 N71-33533
- Program for calculating saturation curves and condensation characteristics of gaseous mixtures of binary organic vapor and air
[BM-EL-7563] 23 p3720 N71-36510
- Iodine/air and zinc/argon condensation tests of flowing metal-vapor-cooled gas mixtures in ducts for cavity exhaust port design of nuclear light bulb engines
[NASA-CR-123200] 24 p3984 N71-37829
- CONDITIONED RESPONSES**
- U CONDITIONING [LEARNING]**
- CONDITIONING [LEARNING]**
- Long term adaptation of pursuit rotor performance to insensitive acoustic stimulation
[AD-715282] 08 p1148 N71-18100
- CONDITIONING [TREATING]**
- U TREATMENT**
- CONDITIONS**
- NT ADIABATIC CONDITIONS**
- NT FLIGHT CONDITIONS**

SUBJECT INDEX

NT KUTTA-JOUKOWSKI CONDITION
NT LIPSCHITZ CONDITION
NT NONEQUILIBRIUM CONDITIONS
NT RUNWAY CONDITIONS
CONDUCTANCE
U RESISTANCE
CONDUCTING FLUIDS
 Substituted electromagnetic pump for conductive fluids
NASA-CASE-NPO-107353 13 p2415 N71-37084
 Techniques for collecting various pressure drops in conducting fluid flows in magnetic fields applied to liquid flow in hypothetical fusion reactor tanks
(JNCL-51049) 23 p3742 N71-36884
CONDUCTING MEDIA
U CONDUCTORS
CONDUCTION BANDS
 Calculation of conduction electronic energy bands and Γ bands in alkali halide crystals
 05 p1283 N71-19549
 Wavelength modulation spectra of semiconductor materials
(JNCL-28361) 15 p2508 N71-37041
CONDUCTION ELECTRONS
 Investigating interaction of solid-state plasmas with infrared laser radiation in large magnetic fields
 06 p2925 N71-19641
 Positive ionization and conduction electrons in diamond, aluminum, and ytterbium
(JNCL-19477) 05 p0870 N71-15902
CONDUCTION HEAT TRANSFER
 Chemical theory of conductive heat transfer
(P-1922637) 05 p0870 N71-15902
 Heat conduction in solids having temperature dependent properties
(JNCL-70-334) 04 p0820 N71-14061
 IBM 509 heat conduction program
(JNCL-70-334) 05 p0783 N71-15302
 Combined conduction, convection, and radiation effects on heat transfer of participating gases in lateral flow
(NASA-TN-616127) 06 p0834 N71-15909
 Measuring heat flow to obtain surface using infrared two-wavelength radiometer
 06 p0848 N71-16183
 Space suit body heat exchanger design composed of thermal conduction yarn and liquid coolant loops
(NASA-CASE-XMS-99371) 09 p1339 N71-19439
 Transient surface heating of large solids subject to uniform heat loss
 09 p1483 N71-30184
 Oak-Ridgely finite difference method for turbulent, heat conduction code, for thermal explosion tests in laminar combustors
(LA-511) 10 p1839 N71-20066
 Effect of heat conduction of material on temperature distribution in vicinity of wing leading edge in hypersonic flight
(JNCL-6941) 11 p1841 N71-22494
 Thermal gas conduction and radiation heat transfer assessment near liquid helium temperatures
 11 p1844 N71-22791
 Conductive heat transfer effect on temperature distribution in vicinity of wing leading edge in hypersonic flow
(JNCL-CP-1125) 13 p2184 N71-24446
 Compressible turbulent boundary layer flow past flat plate walls using conductive heat transfer and velocity
(JNCL-71-47) 13 p2622 N71-24499
 Chemical model contains for measuring heat conductivity of aqueous solutions of electrolytes, with experimental data for potassium bromide
(NASA-TT-F-15666) 13 p2185 N71-24815
 Ability conducting gas controlled heat pipe leading to predictive capability for heat and mass transfer data heat pipe
(NASA-CR-11-008) 13 p2185 N71-24866
 Numerical integration of steady state heat conduction equations representing thermal variations in upper atmosphere
(NASA-TN-X-63532) 13 p2186 N71-25089
 Modified computer program HEATING-3 for solving heat conduction problems in one, two, or three dimensional Cartesian or cylindrical geometries
(JNCL-TM-3288) 13 p2186 N71-25492
 Heat temperature distribution and solution of nonlinear heat conduction problem with boundary condition of fourth kind
(NASA-TT-F-13463) 14 p2352 N71-25756
 Conductive and/or convective radiative energy transfer in absorbing-emitting medium
 15 p3025 N71-30848
 Ocean surface roughness effects on surface temperature based on conductive heat transfer and thermal radiation model
(AD-72674) 16 p2918 N71-31270
 Two dimensional axisymmetric transient heat conduction material ablation computer program
(JNCL-70-516) 19 p3192 N71-32342
 Analytical solution of nonlinear heat conduction problem including influence of internal heat generation
 20 p3365 N71-33682

Computer program HETRAM to solve two dimensional steady state heat conduction on clad tubes with convecting fluid
(NASA-TN-X-2551) 23 p3537 N71-35336
 Differential equations and boundary conditions for finitely deformable, polarizable and magnetizable, heat conducting materials interacting with electromagnetic fields
(AD-72645) 22 p3630 N71-35864
 Finite element method applied to heat transfer problems, and transient two dimensional heat transfer with convection and radiation boundary conditions
(AD-726371) 22 p3697 N71-36343
 Finite element method applied to solid heat conduction with radiation-convection, nonlinear heat flux boundary conditions
(AD-726576) 22 p3697 N71-36346
 Solution to eigenvalue problems of thermal instability of viscous fluid heated from below in completely enclosed cylinder with arbitrarily conducting side walls
 23 p3688 N71-37378
CONDUCTIVITY
FORTRAN program for computing two dimensional magnetic field components for conduction geometries
(JNCL-TM-2484) 12 p1968 N71-24006
 Underwater sensor unit for measuring conductivity, temperature, and pressure of ocean
(JNCL-71012) 17 p2753 N71-25917
 Pressure dependence of electrolytic conductance at 30 C in presence of 3000 hpa/cm for solutions of potassium iodide and series of tetraalkyl ammonium salts
 19 p3851 N71-32308
 Fluorine enhanced conductivity of superconductors, and evaluation of Maki graph based on Boltzmann equation
 22 p3657 N71-36080
 Numerical analysis of potential in semiconductor produced by point current source and measurement of conductivity with four point probe
(NASA-TN-D-6584) 22 p3650 N71-36084
CONDUCTIVITY METERS
NT ELECTRICAL CONDUCTIVITY METERS
 Basic methods of measuring atmospheric electric fields
(TT-70-58125) 05 p0347 N71-12577
CONDUCTORS
NT AIRCRAFT ANTENNAS
NT ANTENNAS
NT BUS CONDUCTORS
NT CASSGRAIN ANTENNAS
NT DIPOLE ANTENNAS
NT DIRECTIONAL ANTENNAS
NT ELECTRIC CONDUCTORS
NT ELECTRIC WIRE
NT ELECTROLYTES
NT EXPLODING WIRES
NT FLAT CONDUCTORS
NT HELICAL ANTENNAS
NT HORN ANTENNAS
NT INERTIALLESS STEERABLE ANTENNAS
NT ION EXCHANGE MEMBRANE ELECTROLYTES
NT LENS ANTENNAS
NT LOOP PERIODIC ANTENNAS
NT LOOP ANTENNAS
NT MICROWAVE ANTENNAS
NT MOLYBDEUM SALT ELECTROLYTES
NT MONOPOLE ANTENNAS
NT MONOPULSE ANTENNAS
NT MULTIPLE BEAM INTERVAL SCANNERS
NT PARABOLIC ANTENNAS
NT PHOTOCONDUCTORS
NT RADAR ANTENNAS
NT RADIO ANTENNAS
NT RHOMBIC ANTENNAS
NT SLOT ANTENNAS
NT SPIRAL ANTENNAS
NT STEERABLE ANTENNAS
NT SUPERCONDUCTORS
NT TURNSTILE ANTENNAS
NT TWO REFLECTOR ANTENNAS
NT WAVEGUIDE ANTENNAS
NT YAGI ANTENNAS
 Integral equation formulations for electromagnetic scattering from two-dimensional inhomogeneities in conductive earth
(NASA-CR-110910) 01 p0809 N71-10783
 Integral equation formulations for electromagnetic scattering from two-dimensional inhomogeneities in conductive earth - appendices, figures, bibliography, and computer programs
(NASA-CR-110911) 01 p0809 N71-10784
 Heat aging evaluation of common coated copper conductors
(JNCL-4087) 06 p0340 N71-11390
 Scattering by imperfectly conducting spheres
(JNCL-70-477) 05 p0746 N71-13229
 Handbook of electromagnetic propagation in conducting media
(AD-714006) 06 p0817 N71-14630

Support for flexible conductive cable between drivers or units having different configurations and cabinet assembly housing drivers or units
(NASA-CASE-XMF-6757) 06 p1207 N71-16781
CONES
NT ABLATIVE NOSE CONES
NT CIRCULAR CONES
NT CONICAL BODIES
NT NOSE CONES
NT ROCKET NOSE CONES
NT SLINDER CONES
 Hypersonic boundary layer transition and hypersonic heat transfer on cylindrical shells, cones and flat plates
(JNCL-110470) 04 p0472 N71-13488
 Effects of reentry on heat transfer at apex of 140 deg blunt cone at Mach numbers of 5.0, 4.5, and 4.0
(NASA-TN-D-6952) 05 p0825 N71-14414
 Steady, three-dimensional, hypersonic aligned stagnation-point flow over cones
 07 p1813 N71-17760
 Shock body radiometer design with temperature sensing and array heat source cone winding
(NASA-CASE-XNP-69781) 14 p2257 N71-36475
 Pressure distributions and shock wave shapes during hypersonic flow over 18 deg semi-angle cone with spherical blunting
(JNCL-71012) 20 p3549 N71-33982
 Vibration tests on dual path of radiant cooling apparatus, and conductivity and reflectance analysis of cones in radiative heat transfer determination
(NASA-CR-121443) 20 p3311 N71-33284
CONFERENCE
 Air and land transportation noise control and measurement, noise level scales, and individual and community response - conference
(P-19117) 01 p0883 N71-10548
 Conference on applications of boron in structural engineering
(AD-710704) 01 p0877 N71-10483
 Symposium on spectrum formation in stars with steady state atmospheric atmospheres
(JNCL-71-312) 01 p0123 N71-10579
 Abstracts of presentations at conference on information theory
(AD-711434) 01 p0826 N71-10898
 Maintenance programs, evaluation, acceptance, and monitoring procedures for transport aircraft
 02 p0144 N71-11039
 Aerospace medicine and bioastronautics conference reports
(JNCL-51468) 02 p0156 N71-11185
 Aerial and spaceborne photography and infrared imagery in earth hydrogeology and geomorphology
(NASA-TM-X-64061) 02 p0285 N71-11131
 Describing and computing resolution characteristics of rectilinear brain scanner
(JNCL-1050-198) 02 p0160 N71-11197
 Proceedings summary for symposium on bio-organic chemistry
(JNCL-51762) 02 p0173 N71-11217
 Advanced technology for production of aerospace engines - conference
(JNCL-CP-64-70) 01 p0389 N71-11426
 Radiographic nondestructive testing method on titanium sheets for engine disk forging
 02 p0322 N71-11439
 Development of space manufacturing techniques for orbital workshops
(NASA-TM-X-64061) 02 p0324 N71-11781
 Legal, preventive, and clinical aspects of spacecraft
(JNCL-CP-61-70) 02 p0161 N71-11191
 Conference on static transport in solids and liquids
(AD-711418) 02 p0384 N71-11040
 Developing advanced multipoint heat sensors for application in remote sensing of forestry and agricultural resources
(NASA-TM-X-64061) 02 p0316 N71-11976
 Conference on information in space and oceans
(JNCL-MET-LCRD-2-50070) 02 p0376 N71-12184
 Conference on new problems in aerospace sciences
 02 p0388 N71-12104
 Reports from conference on ultraviolet temperatures
(AD-712861) 02 p0388 N71-12129
 Conference on condensed phase dynamics
(AD-712881) 02 p0388 N71-12148
 Conference on application of science and technology to problems of pollution, transportation, and environment
(P-192329) 02 p0333 N71-12306
 Advanced ILS and automatic landing systems for conventional and V/STOL aircraft - conference
(JNCL-CP-59-70) 02 p0344 N71-12304
 Conference on large storage and transmission systems for libraries
(P-192402) 02 p0344 N71-12399
 Proceedings from conference on spacecraft power conditioning and control
(JNCL-51-30) 02 p0319 N71-12378
 AGARD conference on aerodynamics and chemically reacting viscous flows over hypersonic and transonic conditions
(JNCL-DOGRAPH-147) 02 p0348 N71-12382

CONFERENCES

SUBJECT INDEX

Considering design of digital computers for guidance and control of aerospace vehicles [AGARD-CP-48-70] 03 p0407 N71-12601

Proceedings from lecture series on large scale integration in microelectronics [AGARD-LS-40-70] 03 p0354 N71-12636

Lectures on space environment simulation for improving spacecraft reliability - Vol. 1 03 p0355 N71-12701

Lectures on space environment simulation for improving spacecraft reliability - Vol. 3 03 p0357 N71-12719

Investigating possibilities and limitations of applying holographic techniques to aerospace technology [NASA-SP-248] 03 p0377 N71-12776

Nuclear models used for studying nuclear reactions, nuclear fission, isotopic scattering, and charge exchange - conference [ANS-EPD-2] 03 p0426 N71-12852

On-line calculation of beam transport systems to first and second order - conference [UCRL-9414] 03 p0427 N71-12854

Selected articles on thermal stresses in power machinery structural elements 03 p0461 N71-12996

Proceedings of conference on low gravity fluid dynamics and propellant control [DACC-63140] 03 p0457 N71-13101

Computer based methods in mass machine interaction for dynamic structural design optimization of stressed-skin structures and structural members [AGARD-CP-36-70] 03 p0462 N71-13126

Describing physical characteristics of storage ring and detection apparatus for electron synchrotron [DESY-70/24] 03 p0358 N71-13157

Testing methods for components of inertial guidance systems [AGARDGAPR-128] 03 p0410 N71-13201

Evaluation of refractory tantalum-, niobium-, and molybdenum based alloys for space power systems applications [NASA-SP-245] 03 p0393 N71-13301

Ion temperature and rotation in Penning discharge in inhomogeneous magnetic mirror [REFT-70-27] 03 p0439 N71-13341

Proceedings from symposium on redundancy in information transmission systems - Part 1 04 p0499 N71-13491

Proceedings from symposium on redundancy in information transmission systems - Part 2 04 p0499 N71-13492

Conference on ballistic range techniques and equipment [AGARDGAPR-136] 04 p0514 N71-13576

Classification of calcium-40 nuclei based on reactions $K-39/H\alpha-3,4$ gamma/calcium-40 and calcium-40/p gamma/calcium-40 - conference [CEA-CONF-1375] 04 p0571 N71-13614

Electromagnetic wave transmission along air-sea interface and in underwater communication and optical systems [AGARD-CP-77-70] 04 p0563 N71-13701

Data handling equipment for aerospace and ground support applications - conference [AGARD-CP-47-70] 04 p0504 N71-13826

High speed core, magnetic, semiconductor, and laser storage systems 04 p0504 N71-13829

Proceedings from conference on role of national laboratories and universities in solving environmental problems [CONF-690703] 04 p0476 N71-13855

Military aeronautical education, physiological training, civil aeronautical education, and survival training in various countries [AGARD-CP-75-70] 04 p0477 N71-13876

Digital techniques and components for signal detection in clutter by advanced radar systems [AGARD-CP-46-70] 04 p0493 N71-13901

Proceedings from conference on accelerator technology and operation [CONF-691101] 04 p0580 N71-14004

Proceedings of 9th annual US Army operations research symposium [AD-711942] 04 p0622 N71-14196

Production of laser glass and optical damage mechanisms in laser materials [NBS-SP-341] 04 p0525 N71-14326

Proceedings from symposium on engineering using nuclear explosives - Vol. 1 [CONF-700101-VOL-1] 04 p0562 N71-14423

Proceedings from symposium on engineering using nuclear explosives - Vol. 2 [CONF-700101-VOL-2] 04 p0562 N71-14424

Proceedings from symposium on control theory applications [NASA-TM-X-66516] 04 p0423 N71-14426

Investigating electron scattering and nuclear structure in linear accelerators [INTERIKO-70/7] 05 p0735 N71-14528

Discussing development of engineering psychology as independent science [UPRS-37004] 05 p0636 N71-14992

Wind effect criteria for structural design and engineering of buildings 05 p0776 N71-15301

Proceedings of annual land surveyors conference [PB-191326] 05 p0675 N71-15418

Human factors in aircraft simulation [AGARD-CP-79-70] 05 p0830 N71-16060

Conference on agriculture, forestry, and sensor studies related to NASA Earth Resources Program - Vol. 2 [NASA-TM-X-62563] 05 p0844 N71-16147

Investigating application of airborne remote sensors to hydrology and oceanography [NASA-TM-X-62566] 05 p0846 N71-16166

Proceedings from meeting on gas tube erosion [AD-714668] 05 p0879 N71-16435

Proceedings of conference on controlled fusion and plasma physics [AD-714617] 05 p0930 N71-16623

Corona and multipactor discharges, packaging techniques and materials, and voltage breakdown in satellite instruments - conference [NASA-CR-116173] 05 p0825 N71-16631

High voltage packaging techniques and materials 05 p0828 N71-16642

Proceedings from conference on Range poles [CONF-691203] 05 p0923 N71-16707

Proceedings of Sixth Agard Annual Meeting 05 p0962 N71-16893

Radiation counters and spectrometers for charged and neutral particle measurements - conference [TID-25473-VOL-3] 07 p1027 N71-17048

Proposed decomposition catalyst for hydrazine engines and gas generators - conference papers [DLR-MITT-69-29] 07 p1097 N71-17192

Conference on biometrics noting human psychic and physical stress [DLR-MITT-70-11] 07 p0980 N71-17237

Discussing method of quality control and materials characterization in silicon device processing [NBS-SP-337] 07 p1087 N71-17276

Advanced cooling systems and heat exchanger materials for turbine blades of high temperature aeronautical gas turbine engines [AGARD-CP-73-71] 07 p1099 N71-17372

Research projects discussed during conference on semiconductor physics [CONF-700801] 07 p1093 N71-17459

Proceedings from symposium on thermoelectric fusion reactor design [ORO-1171-1] 07 p1065 N71-17637

Conference summary on solid state devices, including LSI electronics, crystal growth, computer-aided design, microwave amplifiers, lasers, and semiconductor memories [AD-715101] 07 p0999 N71-17748

International conference on rain erosion and associated phenomena [AD-715100] 07 p0973 N71-17906

Particle accelerator research on two body interactions, and electromagnetic, electron moon, and neutrino experiments - conference [TID-25473-VOL-4] 07 p1078 N71-17927

Studying geology, geochemistry, and biology of Iceland and Surtsey as examples of new and extreme environments [NASA-TM-X-62009] 07 p1024 N71-17966

Small particle accelerator uses in education and research - conference [DWR-1556] 07 p1080 N71-18044

Market research and management planning for optimization of civilian airline operations in France [REFT-1970/7-8] 07 p1136 N71-18093

Chemical, ceramic, and metallurgical aspects of nuclear fuels - conference [ENR-1194] 08 p1236 N71-18216

Proceedings of symposium on control of hazardous water polluting substances 08 p1185 N71-18253

Conference on diagnosis of high temperature plasma including interferometry and spectroscopic methods [LA-4520-TR] 08 p1272 N71-18527

Papers presented at International Symposium on Behavioral Thermoregulation [AD-715783] 08 p1149 N71-18794

Proceedings and recommendations of conference on prevention of midair collisions [NTSB-AAS-70-2] 08 p1145 N71-19043

Schedule of AGARD conferences for 1971, and summaries of 1970 AGARD publications [AGARD-BUL-71-1] 08 p1142 N71-19114

Investigating mineral composition of Apollo 11 and 12 lunar rock samples [NASA-CR-114678] 08 p1289 N71-19144

Critical review and round table discussion data for collection on reactions between gases and solids [AGARD-AR-32-71] 08 p1285 N71-19177

Investigating symbolic mathematical computation using FLI FORMAC batch system and Scope FORMAC interactive system [PSC-69-8012] 08 p1227 N71-19185

Proceedings of conference on electrochemistry and electrodeposition of metals [TT-70-5637] 08 p1209 N71-19200

Conference on Earth Resources Program including geology and geography [NASA-TM-X-66913] 08 p1196 N71-19188

Application of computer processed multispectral data in discrimination of land collapse prone areas in Florida 08 p1196 N71-19189

Digital computer processing of visible and near-infrared scanner data for automatic computer mapping of Yellowstone National Park 08 p1197 N71-19190

Remote sensing analysis of grassland phenomena in Florida 08 p1198 N71-19191

Aerodynamic interference characteristics of airframe-propulsion systems of transport and military aircraft [AGARD-CP-71-71] 09 p1311 N71-19203

Electronic product radiation and health physics including ionizing radiation - conference [PB-195772] 09 p1328 N71-19208

Proceedings of conference on aircraft propulsion [NASA-SP-259] 09 p1456 N71-19281

Lecture papers from symposium on general ocean circulation theory [NCAR-TN-511] 09 p1370 N71-19291

Electron ring accelerator program at Lawrence Radiation Laboratory - conference [UCRL-20004] 09 p1364 N71-19316

Program and introduction for Fifth NASA Intercenter and Contractors Conference on Plasma Physics [NASA-TM-X-66953] 09 p1447 N71-19389

Annotated bibliography of plasma physics research papers including plasma propulsion, plasma radiation, and plasma resources - conference [NASA-TM-X-66952] 09 p1447 N71-19390

Program of proceedings and abstracts presented at Sixth NASA Intercenter and Contractors Conference on Plasma Physics [NASA-TM-X-66950] 09 p1448 N71-19390

Research at NASA Lewis Research Center reported at Fifth NASA Intercenter and Contractors Conference on Plasma Physics [NASA-TM-X-66949] 09 p1448 N71-19391

Annotated bibliography of plasma physics research papers including plasma spectroscopy, crossed field plasma accelerators and electric forces on satellites, and collisionless plasmas - conference [NASA-TM-X-66948] 09 p1448 N71-19391

Proceedings for symposium on viscous turbulent phenomena in supersonic and hypersonic flow [AD-714323] 09 p1373 N71-19398

Neutron dosimetry, biophysics and biological effectiveness, genetic effects, repair and recovery, and modifying factors of neutrons in radiobiology [CONF-691106] 09 p1332 N71-20010

Aerodynamics and applications of lift augmentation devices - AGARD lecture series [AGARD-LS-43-71] 09 p1321 N71-20011

Similarity between two phase liquid-vapor flows with heat exchange - conference [CEA-CONF-1648] 09 p1376 N71-20011

Space simulation technology for determining space environment effects on materials, spacecrafts, and man [NBS-SP-336] 09 p1346 N71-20011

Discussion of European space projects and impact of European and US cooperation [NASA-TT-F-13547] 09 p1467 N71-20031

North Atlantic Treaty Organization conference on adaptation and acclimatization in aerospace medicine [AGARD-CP-62-71] 09 p1334 N71-20031

Precision encoder and pattern recognition devices, bubble chamber physics problems, and cathode ray tube devices - conference [MIT-2098-660] 09 p1445 N71-20031

Data from 90-day manned test of representative life support system in space station simulator [NASA-SP-261] 10 p1304 N71-20071

Conference review on critical phenomena in alloys, magnets, and superconductors [AD-716947] 10 p1634 N71-21001

Plasma shock diagnostics and reduction for improved rocket communication - conference [NASA-SP-252] 10 p1627 N71-21016

ESRO-1/Aurora satellite photometric data on internal ionospheric electron and proton precipitation and population for Oct. - Nov. 1968 - conference [ESRO-SP-62] 10 p1549 N71-21231

Tropospheric characteristics and their effects on electromagnetic wave propagation and radio signal transmission [AGARD-CP-70-71-PT-1] 10 p1522 N71-21240

Conference on Europe 1 launch vehicle, Aurore research satellite, Symphonie communication satellite, and Gorman ground station-satellite communication system technology 10 p1649 N71-21231

Proceedings from conference on water resources utilization [PB-196731] 10 p1554 N71-21240

Proceedings of conference on radiation control, radiation hazards, and environmental effects [PB-196444] 10 p1582 N71-21240

CONFIDENCE LIMITS

Introductory remarks delivered at space shuttle integrated electronics conference conducted at NASA MSC on May 11-13, 1971

European space program on gamma ray astronomy - conference

OSO-3 observations of origin of galactic gamma rays and correlation with X ray sources

Lectures presented at seminar in various scientific fields

Conference on aerospace environments, manned space flight, weightlessness simulation, musculoskeletal and cardiovascular systems, bone loss, mineral metabolism, and hematology

Earth gravity tides - conference

Magma reservoir evidenced from tidal gravity variations observed at Hekima lava lake, Kilauea, Hawaii

Proceedings of conference on Fourier spectroscopy including topics on signal to noise ratios, interferometers, refractometers, double-beam techniques, and data handling and processing

Uranium plasmas applied to nuclear rocket engines, MHD generators, nuclear lasers, and plasma stability and flow - conference

Conference on heavy ion sources

Actions and recommendations of Ninth Meeting of Airworthiness Committee

Interaction of relativistic particle beam with itself due to beam coupling with surroundings

Proceedings of space shuttle integrated electronics conference with emphasis on power distribution, instrumentation, and communication - Vol. 2

Proceedings of space shuttle integrated electronics conference with emphasis on data systems design - Vol. 3

Interdisciplinary Communications Program conferences on populations, technology utilization, and origin of life

Proceedings of conference on licensing and control of nuclear power plants

Statement by Honorable Sec. D. Brown, chairman, CAB, presented to Port of Seattle Air Cargo Conference, January 19, 1971

Proceedings of conference on interaction between atmospheric environment and human system at cell level

Conference on space shuttle environmental control and life support systems - Vol. 2

Proceedings of conference on remote sensors for scientific geological applications

Measurement of ocean solar energy and production engineering, noting photoplankton and marine ecological system - conferences

Proceedings of conference on short light pulse lasers and interaction with matter

Solar radiation as energy sources in terrestrial hydrometeorological processes - conference

Conference on ground operations, flight operations, and safety for space shuttle program - Vol. 1

Results of symposium conducted to assess technological changes observed in Apollo astronauts

Proceedings of conference to determine specifications of Walsh functions to signal filtering, computer signal processing, voice signal compression, and multiplexing

Conference on research, development, and applications of integrated microelectronic circuits

Conferences on earth tide and earth surface phenomena

Proceedings of international conference on carbon fibers

Critical evaluation of nuclear data information in connection with reactor designs - international conference

Long duration confinement effects on crew behavior during manned space flight simulation

Activities of thirteenth British theoretical mechanics colloquium

Conference on application of satellite radio beacon for isomeric electron content determination and navigation

Conference papers on world astronomical telescopes noting structural design and optics

Conference on analytical functions and topology of algebraic spaces

Cosmic ray research and instruments used for interplanetary and astronomical studies, Vol. 2 - conference

Closed ecological systems, water reclamation, astronaut work capacity, and psychological stress experiment - conference

Physics of sun, planetary atmospheres and interiors, and earth-moon system - conference

Automatic data processing systems for air traffic control, health services, operations research, management planning, information systems, and reading machines

Activities of thirteenth British theoretical mechanics colloquium

Conference on application of satellite radio beacon for isomeric electron content determination and navigation

Conference papers on world astronomical telescopes noting structural design and optics

Conference on analytical functions and topology of algebraic spaces

Cosmic ray research and instruments used for interplanetary and astronomical studies, Vol. 2 - conference

Closed ecological systems, water reclamation, astronaut work capacity, and psychological stress experiment - conference

Histogram method of density estimation

Standard deviation estimates causing operating characteristic curves to be random variables in quality control acceptance sampling plans and methods for computing confidence limits

Confidence intervals and significance tests for means of symmetrical population with outlier observation not largest or smallest

Confidence intervals and significance tests for means of symmetrical population with smallest or largest outlier observation

Statistical mechanics for constructing confidence intervals for variance ratios in balanced and unbalanced experimental designs

Optimization techniques in aircraft configuration design

Weight reduction and configuration of fuel cell

Reaction times of subjects in tests with display control configurations typical of those used in continuous tracking tasks

Space Flight Operations Facility Configuration Control System for management control purposes

Configuration control for SUMC microprocessors allowing for periodic changes in operational modes

Innovations in techniques of joining metals and means for handling difficult weld configurations

Radioactive surface research restricted to surface wave structures consisting of dipole elements

Concentration of negative ions in flame for checking of static configuration of flame

Configuration interaction approach to improving Hartree-Fock representation of pi-electron systems

Configuration interaction on ground state of beryllium hydride molecule

Stationary one-group neutron transport equation with application to transport calculations for multidimensional, heterogeneous reactor configurations

Noble gas confinement after accidents

Air revitalization unit for sealed survival shelters without external power supply

Stress-strain characteristics of human oral cavity during prolonged confinement

Hypokinetic effects during 120-day bed confinement with drug therapy

Long duration confinement effects on crew behavior during manned space flight simulation

Catalytic decomposition of five esters, isobutylacrylate, in confined space

Human reactions to psychological stresses of confined environments using Tellico project concepts

Color and music effects on humans during prolonged isolation in confined space

Electron beam probe to measure potential and bipolar shifted spectral lines to study presence of fast particles in inertial electrostatic confinement device

Plasma confinement dependent on microwave field parameters and plasma parameters J x B type ion BICRIS and ohmic heating plasma concepts

Ion and electron plasma confinement and kinetic stabilizes in adiabatic traps

Plasma confinement in dc cathode sheath in collisional and collisionless regimes

Plasma confinement in dc cathode sheath in collisional and collisionless regimes

SUBJECT INDEX

Confinement effects on human psychomotor performance during long duration space environment simulation test

Long duration confinement effects on simulated space station on human performance during working task

Long duration confinement effects in simulated space station atmosphere on human short-term memory

Catalytic decomposition of five esters, isobutylacrylate, in confined space

Human reactions to psychological stresses of confined environments using Tellico project concepts

Color and music effects on humans during prolonged isolation in confined space

Electron beam probe to measure potential and bipolar shifted spectral lines to study presence of fast particles in inertial electrostatic confinement device

Plasma confinement dependent on microwave field parameters and plasma parameters J x B type ion BICRIS and ohmic heating plasma concepts

Ion and electron plasma confinement and kinetic stabilizes in adiabatic traps

Plasma confinement in dc cathode sheath in collisional and collisionless regimes

Plasma confinement in dc cathode sheath in collisional and collisionless regimes

Plasma confinement in dc cathode sheath in collisional and collisionless regimes

Plasma confinement in dc cathode sheath in collisional and collisionless regimes

Plasma confinement in dc cathode sheath in collisional and collisionless regimes

Plasma confinement in dc cathode sheath in collisional and collisionless regimes

Plasma confinement in dc cathode sheath in collisional and collisionless regimes

Plasma confinement in dc cathode sheath in collisional and collisionless regimes

Plasma confinement in dc cathode sheath in collisional and collisionless regimes

Plasma confinement in dc cathode sheath in collisional and collisionless regimes

Plasma confinement in dc cathode sheath in collisional and collisionless regimes

Plasma confinement in dc cathode sheath in collisional and collisionless regimes

Plasma confinement in dc cathode sheath in collisional and collisionless regimes

Plasma confinement in dc cathode sheath in collisional and collisionless regimes

Plasma confinement in dc cathode sheath in collisional and collisionless regimes

Plasma confinement in dc cathode sheath in collisional and collisionless regimes

Plasma confinement in dc cathode sheath in collisional and collisionless regimes

Plasma confinement in dc cathode sheath in collisional and collisionless regimes

Plasma confinement in dc cathode sheath in collisional and collisionless regimes

Plasma confinement in dc cathode sheath in collisional and collisionless regimes

Plasma confinement in dc cathode sheath in collisional and collisionless regimes

Plasma confinement in dc cathode sheath in collisional and collisionless regimes

Plasma confinement in dc cathode sheath in collisional and collisionless regimes

Plasma confinement in dc cathode sheath in collisional and collisionless regimes

Plasma confinement in dc cathode sheath in collisional and collisionless regimes

Plasma confinement in dc cathode sheath in collisional and collisionless regimes

Plasma confinement in dc cathode sheath in collisional and collisionless regimes

Plasma confinement in dc cathode sheath in collisional and collisionless regimes

SUBJECT INDEX

Congressional hearings on feasibility of establishing NASA aerospace museum 05 p0787 N71-15407

Report to Congress on need for improvement in management of magnetic tapes at GSPC 05 p0631 N71-15452

Congressional hearings on Boeing 727 use of Washington National Airport 07 p1004 N71-17697

Environmental control methods to reduce air and water pollution in United States of America 07 p1133 N71-18071

Congressional hearing on efforts to improve knowledge of and support for environmental and ecological projects 09 p1489 N71-20566

Congressional hearings on nuclear rocket engine development program 11 p1848 N71-22489

Tutwamy in support of creation of National Outer and Atmospheric Administration 11 p1848 N71-22899

Appropriations recommended by Congress for NASA programs including project management, research and development, and construction of facilities 12 p2019 N71-24307

Authorization hearings on NASA space flight program - Part 2, 1972 13 p2191 N71-25194

Authorization hearings on NASA space flight program - Part 3, 1972, Office of Space Science and Applications 13 p2191 N71-25195

Authorization hearings on NASA space flight program - Part 4, 1972 13 p2192 N71-25196

Procedures for informing members of Congress on technical subjects prior to enacting legislation 13 p2193 N71-25572

Tutwamy concerning astronomical research and development, and DOD space-related programs 14 p2361 N71-26799

Congressional hearings concerning NASA appropriations for fiscal year 1972 14 p2361 N71-26800

House committee recommendations concerning NASA appropriations for FY 1972 16 p2695 N71-29062

House committee investigation of Department of Defense communications 16 p2696 N71-29146

Recommendations by House Committee on appropriations for fiscal year 1972 17 p2860 N71-29385

Papers relevant to development of fuels and energy policy compatible with environmental control 17 p2861 N71-29471

Congressional hearings on chartered airline travel 17 p2861 N71-29707

Control equipment and engine development for air pollution control from jet aircraft engine emissions 18 p2919 N71-31403

Senate hearings on Federal anti-tyranny program 18 p3031 N71-31511

Management policies and management planning for operation of NASA facility 18 p3031 N71-31520

Recommendations of Senate Committee on Appropriations for housing and urban development, NASA, Veterans administration, and other independent agencies for 1972 18 p3031 N71-31564

Federal budget amendment agreement recommendation for HUD appropriations 19 p3159 N71-32657

Air piracy resolutions presented to Congress and US and worldwide air piracy statistics 19 p3159 N71-32689

Panel funding for SST and Concorde aircraft development in 1971 20 p3370 N71-33758

Congressional statements relating to Goddard Space Station with tributes to Dr. Goddard and short biography 20 p3370 N71-33800

Index for hearings before Committee on Science and Astronautics, US House of Representatives, during Ninety-second Congress 20 p3371 N71-33801

Senate hearings on 1972 appropriations for HUD, NASA, NRP, VA, and other independent agencies 20 p3371 N71-33872

Hearings for HUD and space appropriations 20 p3371 N71-33909

Panel and information index for proposed 1972 hearings before Committee on Science and Astronautics of United States Congress 20 p3371 N71-33961

Effect of private litigation on national efforts to preserve and enhance the environment 21 p3533 N71-35177

Documentation of Congressional Subcommittee testimony regarding Navy oil sludge pollution off Florida coast 21 p3533 N71-35178

Analysis of Usamery resources and review of national laws and policies which influence energy situation 21 p3533 N71-35181

Manpower and training needs for air pollution control - public and private sectors 21 p3533 N71-35182

Proceedings of Panel on Science and Technology before Committee on Science and Astronautics of US House of Representatives, Ninety-second Congress 21 p3534 N71-35190

NASA fiscal year 1971 appropriations for research and development, construction of facilities, and research and program management 21 p3535 N71-35192

Congressional hearing on budgeting authorization for continuation of Fire Research and Safety and Standard Reference Data Acts 22 p3699 N71-36383

Congressional hearing to study effects of science and technology on US and world economy 22 p3700 N71-36385

Hearings on National Bureau of Standards organizational structure 22 p3700 N71-36391

Apollo 15 mission report to committee on science and astronautics 22 p3700 N71-36394

Congressional hearings on airline service to small communities and towns 22 p3700 N71-36395

Convention for suppression of unlawful aircraft seizure and article by article analysis 23 p3870 N71-37390

CONICAL BODIES

NT SLENDER CONES

Maxwell equation for conical horn antennas [TH-70-8-10] 02 p0182 N71-11279

Boundary layer transition studies of several pointed bodies of revolution at supersonic speeds [NASA-TN-D-4063] 02 p0302 N71-11520

Flexible trailing wire effect on aerodynamic characteristics and radar cross sections of hypervelocity cones [AD-712509] 03 p0309 N71-12205

Flight assessment of trailing-cone static pressure probe at subsonic speeds 03 p0311 N71-12214

Radiation from slot antennas on conical bodies covered by inhomogeneous plasma sheath [AD-712049] 03 p0336 N71-12399

Measuring radiation from slot antennas on conical bodies covered by plasma sheath 03 p0336 N71-12402

Eddy viscosity-intermittency factor approach to numerical calculation of laminar, transitional, turbulent heating of sharp cones in hypersonic flow [AD-714058] 06 p0835 N71-16217

Pumping characteristics of rotating truncated cones [NASA-TM-X-52933] 06 p0867 N71-16576

Vibration and flutter tests of pressurized thin walled truncated conical shell 07 p1123 N71-17355

Real gas effects on drag and trajectories of nonlifting conical shell during Mars atmospheric entry [NASA-TN-D-5240] 07 p1116 N71-18015

Wake flow properties of conical bodies at supersonic speeds and various angles of attack [NASA-TM-X-21139] 08 p1178 N71-18480

Wire and probe support interference on hypersonic wakes of magnetically suspended round based conical body [ARC-CP-1133] 10 p1492 N71-20848

Numerical method for calculating steady asymmetric liquid supersonic flow past pointed conical bodies at yaw 10 p1541 N71-21269

Modified Cuspidary food paraboloidal and conical antenna designs for spacecraft 11 p1701 N71-22562

Numerical analysis of inviscid flow fields about pointed circular cone and conical wing-body configuration at various angles of attack 11 p1671 N71-22667

Wingtip tests of cylindrical and Lundell-conical rears in ambient air producing Reynolds numbers up to 100,000 for high speed altimeters [NASA-TM-X-67009] 12 p1857 N71-23116

Numerical analysis of vertical water entry of cone 2, impact prediction 12 p1899 N71-23223

Hypersonic heat transfer to flat plates and conical and blunt bodies in boundary layer flow [ARC-RM-3437] 13 p2063 N71-24714

Coating of fuel particles and model investigations of conical fluidized beds noting effect of gas current and gas distribution particle load, and nozzle geometry [JUL-660-8/W] 15 p3448 N71-27359

CONICAL SHELLS

Mathematical models for shock wave profile around conical bodies using schlieren photography interpretation [ARC-CP-1143] 15 p2365 N71-27717

Equations for flow rate, load capacity, and friction torque for conical hydrostatic bearings under laminar and turbulent flow conditions 16 p2680 N71-28046

Measurement of convective heat transfer rates on conical nozzles and hemispherical afterbody configuration at hypersonic speed [NASA-TN-D-6433] 16 p2691 N71-28062

Second order effects on wave structures associated with planar and conical bodies in supersonic flow 17 p2734 N71-28686

Mathematical model of supersonic flow around blunt conical body with sharp leading edge including comparison with schlieren photographs and noting Mach number dependence 19 p3033 N71-31658

Finite difference method for solving compressible three dimensional boundary layer flow equations of elliptical cones [AD-723280] 19 p3077 N71-31896

Integral representations for radiation field from slots on surface of semi-infinite conducting cones [AD-723289] 19 p3083 N71-32223

Theory of operation and evaluation of conical-receiver radars 19 p3102 N71-32422

Pressure distribution near center line of trailing edges of delta wings and conical bodies at high supersonic speeds [ARC-CP-1153] 20 p3203 N71-32648

Determination of transonic aerodynamic characteristics of spherically blunted 35 and 60 degree half-angle cones in ballistic range tests [NASA-TN-D-4499] 20 p3266 N71-33244

Magnus force and moment data for standard 10 degree cone calibration model as determined in supersonic wind tunnel [SC-DC-71-3821] 23 p5743 N71-36408

Formula for determining axial buckling compression stress for conical and spherical sandwich shells [AD-727056] 24 p6827 N71-38732

CONICAL FLARE U CONES

CONICAL FLOW

Flat plate pressure distribution and heat transfer in conical hypersonic flow [VKI-TN-56] 03 p0363 N71-12326

Boundary layer development and swirling flow in conical diffusers 05 p0660 N71-14767

Conical flow effects on pressure center of blunted conical bodies in hypersonic flow [NPL-ARRO-NOTE-1065] 06 p0833 N71-15708

Integral transform solution for conical diffuser flow with field extrusion through multiple slots 13 p2065 N71-24796

Sonic boom in interaction of conical field and plane shock wave 16 p2532 N71-28346

Method of finite techniques for computing flow field about conical configurations at incidences in supersonic flow [NASA-TR-R-374] 23 p3744 N71-36697

CONICAL INLETS

Boundary layer interactions with turbulent heated compressed flows from hypersonic inlets 09 p1376 N71-19932

CONICAL NOZZLES

Eigenvalues, eigenfunctions, and series coefficients for calculating Nusselt numbers of turbulent liquid/metal heat transfer in conicentric annuli [BNL-50163] 05 p0782 N71-15020

Mach number reduction in low density hypersonic wind tunnel by increasing nozzle throat area [DLR-FB-70-43] 13 p2391 N71-27060

Effects of flow rate, port location, and sonic condition of inlet in secondary injection into supersonic flow field for conical rocket nozzles [AD-724127] 20 p3249 N71-32859

CONICAL SCANNING

Frequency modulation effects on tracking errors in monophase radar and conical cone system 04 p0405 N71-13010

Comparison of system noise temperatures in radar angle tracking systems for mechanical, single pre-amplifier, and three pre-amplifier conical cone systems [AD-719735] 13 p2047 N71-25160

CONICAL SHELLS

Theoretical and experimental vibration and buckling results for blunt truncated conical shells with ring supported edges [NASA-TN-D-7003] 04 p0617 N71-14026

Acoustic reflection efficiency and structural vibration characteristics of truncated conical shells [NASA-CR-111040] 06 p0853 N71-15866

Lower critical limit of conical shell under longitudinal compression [AD-714700] 06 p0954 N71-16640

Stress analysis of thin elliptic cones and sandwich structures 07 p1135 N71-17010

Conical shell stability under dynamical longitudinal compression

06 p1300 N71-19162

Shell impact response and wave propagation in cylindrical and conical shells by experimental and analytical methods

[NASA-CR-469211] 10 p1651 N71-30701

Estimation of stability of elastic noncircular conical and cylindrical orthogonal shells

[AD-717014] 10 p1651 N71-30754

Holographic interferometry analysis of axisymmetric imperfections effect on natural frequencies and mode shapes of conical shells

10 p1569 N71-31280

Algorithms for thin-walled axisymmetrically loaded bodies of revolution elastic stability problems including cylindrical, conical, spherical, and toroidal shells

11 p1837 N71-22495

Rotary spindle lathe attachments for machining geometrical cones

[NASA-CASE-XMS-04292] 11 p1770 N71-22722

Thin conical shell stability subjected to dynamical longitudinal compression

[AD-719551] 13 p2182 N71-25352

Physical properties and mechanical strength of structural fiber glass in conical shells

[JPRS-53118] 14 p2346 N71-25757

Supersonic asymmetric flutter and divergence characteristics of truncated conical shells with ring-supported edges under three types of flow-induced instabilities

[NASA-TN-D-6223] 14 p2347 N71-25790

Analytical evaluation of buckling modes of shell configurations to determine imperfection sensitivity of optimum structural designs for Mars entry capsule

[NASA-CR-1800] 16 p2684 N71-28031

Influence of in-plane boundary conditions on buckling of clamped conical shells under external pressure

[AD-721475] 16 p2684 N71-28856

Expressions and graphs for estimating average modal densities for various structural elements of engineering importance including beams, rods, circular plates, and conical shells

[NASA-CR-1773] 18 p3022 N71-31485

CONICS

NT ELLIPSOIDS

NT HYPERBOLAS

NT PARABOLAS

Testing of conic and hyperbolic multigrid topography equations of geomorphologically diversified areas for computer graphics

[AD-718038] 12 p1905 N71-23303

CONJUGATE POINTS

Literature survey on auroras at conjugate points

[JPRS-52023] 05 p0765 N71-15490

CONJUGATES

NT CONJUGATE POINTS

CONNECTIONS

U JOINTS (JUNCTIONS)

CONNECTORS

NT ELECTRIC CONNECTORS

NT UMBILICAL CONNECTORS

Design and development of quick release connector

[NASA-CASE-XLA-01141] 04 p0524 N71-13789

Dynamics of four combinations of fluid control and load actuating components in hydraulic servoactuators having long lines or flexible metal-reinforced rubber hose connections

18 p2907 N71-31304

Commercial and governmental flat conductor cable for connecting and terminating hardware

[NASA-TM-X-64613] 24 p3898 N71-37782

CONNECTORS (ELECTRIC)

U ELECTRIC CONNECTORS

CONOIDS

U CONICAL BODIES

CONSCIOUSNESS

Development of apparatus and method for quantitatively measuring brain activity as automatic indication of sleep state and level of consciousness

[NASA-CASE-MSC-13282-1] 13 p0307 N71-24729

Application of dynamic programming and theory of control processes to biological phenomena including evolution of consciousness

[TR-71-17] 14 p2304 N71-25937

CONSTRUCTIVE EVENTS

Investigating method for measuring high-order sequential dependencies in short sequences

[JZF-1970-19] 05 p0713 N71-15069

CONSERVATION

Reporting activities of Natural Environment Research Council of Great Britain

02 p0220 N71-12090

CONSERVATION EQUATIONS

Application of equations of conservation to two phase liquid gas systems

[PB-1970-97] 05 p0663 N71-14907

External source radiation effects on bow shock structure at stagnation point determined with conservation

07 p1011 N71-17698

Isotopic conservation test from antineutrino interactions at 480 MeV/c from absolute and differential cross sections and differential polarizations of hydrogen bubble chamber photos

09 p1427 N71-19693

Numerical analysis for static multiple density correlation function of many particle system

[NUB-2053] 11 p1800 N71-21678

Binet formalism in general theory of relativity and laws of conservation considering integral and differential forms of conservation laws

[NLL-873-5731] 17 p2787 N71-29701

Expression for kinetic energy transformed into work, heat, and sound during impact of spherical reactor containment vessel model and concrete block

[NASA-TM-X-67917] 20 p3358 N71-33316

Using particle conservation equations for fast hydrogen atoms, slow hydrogen molecules, and charged particles for calculating fast atomic hydrogen flux produced by charge exchange in high temperature plasma

[JAERI-MEMO-4243] 21 p3494 N71-34887

CONSERVATION LAWS

Conservation laws and vibrational band structures of nitrogen subjected to excitation collisions with helium and argon metastable atoms

09 p1431 N71-19920

Symmetry in physics including principles of nonobservable, transformation and conservation laws, asymmetry and observables, time reversal, and complementarity of symmetry violations

[BNL-50261] 16 p2639 N71-28722

CONSOLES

NT REMOTE CONSOLES

Fast, on-line, all-digital, block diagram-based simulation system which adds simulation console to PDP 9 computer

12 p1883 N71-23864

CONSTANTS

NT GRAVITATIONAL CONSTANT

NT GRUNEISEN CONSTANT

NT SOLAR CONSTANT

NT TIME CONSTANT

Derivation of chemical reaction rate constants from complex concentration-time data

[RPE-TR-693] 03 p0333 N71-12380

CONTELLATIONS

NT CYGNUS CONSTELLATION

NT LYRAE CONSTELLATION

NT ORION CONSTELLATION

NT SAGITTARIUS CONSTELLATION

NT SCORPIUS CONSTELLATION

NT SCUTUM CONSTELLATION

CONSTITUTIONAL DIAGRAMS

U PHASE DIAGRAMS

CONSTITUTIVE EQUATIONS

Homogeneous constitutive equations for describing falling microstructure of polymeric materials with plastic memory

[AD-711657] 01 p0114 N71-10689

Continuum thermodynamic theory of nonlinear thermochemical materials with memory

[AD-711401] 02 p0304 N71-12174

Calculation of elastic, viscous, and plastic effects in materials

[UCRL-72639] 05 p0703 N71-15226

Investigating electromagnetic wave propagation in uniformly accelerated medium

06 p0946 N71-16690

Modeling soil mass as continuum using constitutive equations of continuum mechanics

[NASA-CR-103022] 07 p1048 N71-17462

Studying constitutive laws at finite strain for class of isotropic solids

[AD-718400] 12 p1937 N71-23284

Polymer physics and constitutive equations for thermoviscoelastic amorphous materials

[AD-720290] 16 p2616 N71-28182

Dislocation dynamics and formulation of constitutive equations for rate dependent elastic plastic response in isotropic metals

[AD-722314] 17 p2765 N71-30110

Derivation of constitutive equations, material symmetries, dynamical restrictions, and related topics for nonlinear and linear theories of elastic shells and plates - Part 2

[AD-722351] 17 p2854 N71-30221

Analyzing structure of constitutive relations which govern flow deformation laws used in stress analysis

[AD-722831] 18 p3022 N71-31483

Constitutive equations for analysis of elasto-viscoplastic structural materials

[ONERA-PUBL-135] 19 p3186 N71-31699

Study of relativistic constitutive equations of continua

22 p3692 N71-36335

Numerical integration solution of constitutive equations for viscoplastic strain of rate sensitive materials

23 p3864 N71-37549

CONSTRAINTS

NT METEOROLOGICAL PARAMETERS

Analytical and experimental study of limitations in using small scale models for determining spacecraft thermal behavior

[NASA-CR-102566] 01 p0133 N71-10429

Constraints on equal time commutators from Lorentz covariance

[JPTF-6770] 06 p0883 N71-15831

Engineering constraints in designing optimal and suboptimal feedback systems

[NASA-CR-116895] 08 p1173 N71-19121

Unconstrained minimization formulations of constrained problem, and penalty functions

09 p1410 N71-30134

Operational limitations of arc heaters caused by enthalpic stagnation pressures

[NASA-CR-117144] 09 p1484 N71-30229

Three stage motion restraining mechanism for restraining and damping three dimensional vibrational movement of gimbaled package during launch of spacecraft

[NASA-CASE-GSC-10306-1] 13 p2085 N71-30406

Effects of constraints on kinetic reactions of copper particles during sintering

13 p2096 N71-32509

Discrete optimization and optimal control problems with equality constraints

[CT-36] 14 p2281 N71-32002

Hybrid computer nonlinear programming with dynamic constraints and application to nuclear reactors and heat exchangers

[CEA-R-3988] 15 p2449 N71-27708

Comparison of methods for resolving problems of constraint in construction of large structures

18 p3030 N71-31416

Optimal control systems performance sensitivity differential equations including hard and soft constraints

[RM-314J] 18 p2548 N71-31014

Capabilities, constraints, and costs of Delta launch vehicle, Model 2914

[NASA-TM-X-65674] 20 p3354 N71-33406

Restraint system for argonmeter used under microgravity conditions or earth atmosphere in microgravity positions

[NASA-CASE-MPS-21046] 21 p3385 N71-34808

Context-free language generation using contextual constraints on context-sensitive grammar rules

[NASA-CR-121497] 21 p3446 N71-34828

Accuracy, adequacy, and limitations of NASTRAN computer program static load structural analysis solutions

22 p3482 N71-34818

Solutions to legal constraints to international space transportation

[AD-726797] 22 p3701 N71-36308

Algorithm for solving general quadratic programming problem with linear constraints

[NASA-CR-133214] 24 p3592 N71-37779

Theoretical and computational solutions of optimal control problems with state variable inequality constraints

24 p3982 N71-37610

CONSTRICTIONS

Neon constricted positive column in gas discharge tubes with thermal model based on thermoelectric and spectroscopic measurements

22 p3653 N71-36864

CONSTRUCTION

Quality assurance practices in construction and maintenance of molten salt reactor

[ORNL-TM-2999] 04 p0561 N71-14086

Investigating economic and engineering aspects of using dirigibles in construction

05 p0629 N71-14029

Semiempirical formula for calibrating radiometric probes presented as function of soil bulk density, soil chemical composition, source detector spacing, and construction parameters

[INP-715] 15 p2405 N71-27670

Applications of electronic computers for computations involved in ship design and construction

[JPRS-53906] 21 p3400 N71-34119

CONSTRUCTION MATERIALS

Standard reference materials price and availability listing

[NBS-260-SUPPL.] 01 p0072 N71-10772

Structure and properties of unidirectionally solidified superalloys

02 p0242 N71-11052

Electromagnetic pulse forming process for aerospace assembly manufacturing

02 p0233 N71-11772

Weightless composite casting of structural materials in space manufacturing

02 p0235 N71-11772

Thermomechanical materials data for optimal design of thin circular cylinders

03 p0664 N71-11318

Techniques for optimizing structural design by using computers

[NASA-CR-115808] 04 p0208 N71-11588

Compatibility of structural materials with sodium

[WARD-1173-2] 05 p0701 N71-12081

Elevated groundwater structures using support beams and spread footing of various construction materials

[TRW-66816-W005-R0-00] 07 p1136 N71-24802

Performance of test equipment for low temperature materials

[RHEL/R-203] 06 p1205 N71-18304

Emission measurement techniques for space data materials in high temperature environmental simulation

[NASA-CR-103071] 10 p1503 N71-21083

Loss in antenna gain caused by aluminum or glass fiber support structure

11 p1701 N71-22508

SUBJECT INDEX

Dilatometric thermal expansion measurements on high temperature structural materials
[AGARD-AR-31-71] 13 p2187 N71-25358

Plasticity and low cycle fatigue life of structural alloys
[AD-720368] 14 p2373 N71-25949

Rubber bearing material technology
13 p2413 N71-26834

Properties and selective applications of high strength steels, aluminum and titanium alloys, polymeric materials, ceramic materials, and composite materials in aerospace engineering
[AGARD-LS-51-71] 15 p2429 N71-27038

Properties and selective applications of high strength steels
15 p2421 N71-27040

Properties and selective applications of thermoplastic and thermoplastic polymers
15 p2429 N71-27042

Properties and selective applications of aluminum alloys in aerospace construction
15 p2414 N71-27044

Properties and selective applications of titanium alloys in aircraft and jet engines
15 p2421 N71-27045

Evaluating developed structural materials of potential Air Force weapons system interest and engineering data sheets on these heat resistant alloys
[AD-720778] 16 p2614 N71-28099

Expandable space frames for three dimensional or three building structures
[NASA-CASE-ER-10365] 16 p2683 N71-28048

Measuring elevated-temperature time-dependent corrosion effects of liquid metal on immersed structural materials
[NASA-TM-X-67882] 18 p2936 N71-31221

Potable blocks for construction of structures in remote areas lacking building materials
[NASA-CASE-MSC-12233-2] 18 p3022 N71-31415

Constitutive equations for analysis of elasto-viscoplastic structural materials
[ONERA-PUBL-135] 19 p3186 N71-31699

Experimental device for measuring gamma absorption cross section of materials used for nuclear construction
[DEMO-70/11] 19 p3147 N71-32042

Materials tests and radiation effects on nuclear reactor construction materials
[WRAAN-FR-40-11] 19 p3140 N71-32377

Chemical attack of laboratory equipment, and properties of corrosion resistant materials for constructing chemical apparatus
[AD-726803] 22 p3396 N71-35605

Stability of Nb stabilized Cr-Mo steel as structural material in sodium cooled reactor plants after neutron irradiation
[JLL-RESEARCH-TRANS-2118-19091.9F1] 22 p3396 N71-35609

Evaluation of metallic and nonmetallic construction material performance and reliability after long storage in O₂ and B₂H₆
[NASA-CR-122067] 22 p3661 N71-36107

Low outgassing polymeric materials for general service and communication satellite structures
[NASA-TM-X-65705] 23 p3776 N71-36913

Capable rig for temperature control and irradiation of electrical material in S₂-2 reactor
[JRG-3623] 24 p3957 N71-38226

Capable rig for irradiation of structural materials in S₂-2 reactor with temperature control by variation of gas gap size
[JRG-3613] 24 p3957 N71-38229

Service performance and irradiation embrittlement of structural materials in nuclear power plant
[JLL-CE-TRANS-5598-19022.09] 24 p3964 N71-38280

CONSUMERS
Investigation of attitudes toward and impact of U.S. conversion to metric system
[NBS-SP-345-7] 19 p3197 N71-32353

CONSUMPTION
NT FUEL CONSUMPTION
NT OXYGEN CONSUMPTION
NT WATER CONSUMPTION
Impact of technological changes on refractory material demand and supply
[JRG-3645] 17 p2768 N71-29264

Bauxite production and consumption for 1969
17 p2768 N71-29278

Bauxite production and consumption for 1969
17 p2761 N71-29279

Production, consumption, and utilization of aluminum during 1969
17 p2761 N71-29280

CONTACT RESISTANCE
Residual frictional resistance between soil-wheel interfaces in linear moving vehicle design simulation
09 p1466 N71-20216

Quality control data on lubricants for electric contacts
[NCR-40] 10 p1563 N71-21003

CONTACTORS
Preliminary calculations of centrifugal extractor of type MPB extractor
[ORNL-TR-2358] 04 p0382 N71-14105

CONTACTS [ELECTRIC]
U ELECTRIC CONTACTS
CONTAINERLESS MELTS
Production of single crystals from containerless melts in weightless space environment
02 p0283 N71-11724

CONTAINERS
Engineering design and test of packaging systems for 2171 pyroscopy platform
[AD-711584] 02 p0263 N71-12175

Bonding parameters and quality control for cadmium-stainless steel clad fuel pot containment vessel production
[NASA-CR-111573] 03 p0387 N71-13323

Dynamic behavior of liquids in elastic tanks
[LMSC-60-80-70-23] 06 p0838 N71-16529

Manufacture of fluid containers from fused coated polymer sheets having resealable septum
[NASA-CASE-NPO-10123] 13 p2086 N71-34833

Method for locating leaks in hermetically sealed containers
[NASA-CASE-ERIC-10045] 13 p2087 N71-24910

Technology utilization briefs on packaging and containers
[NASA-SP-5923/01/1] 13 p2087 N71-24967

Quantitative liquid measurements in container by resonant frequencies
[NASA-CASE-XNP-02500] 15 p2431 N71-27397

Impact response modeling for design of weapon container
[SC-RR-70-8001] 15 p2523 N71-27966

Design and construction of containers for storage of superoxide materials
16 p2556 N71-28303

Analysis of impact test results of foamed plastic cushioning systems used in military container designs
[AD-723396] 19 p3120 N71-31798

Mechanical properties of cylindrical vessels under internal pressure at high temperatures
[NLL-CE-TRANS-5321-19022.09/1] 19 p3189 N71-32412

Modified remote cell for thermal differential decomposition studies on lead azide
20 p3363 N71-32834

CONTAINMENT
Pressure and activity histories in ventilated containment for nuclear reactor during long term heat addition
[AHSB/SR-187] 07 p1059 N71-17018

Design considerations of reactor containment spray systems, also protective coating for these containment structures
[ORNL-TM-3412-PT-5] 08 p1220 N71-18304

Separation and containment of liquid-gas mixture in closed cyclone separator
[AD-710992] 13 p2063 N71-24476

Sudden release of large number of cosmic rays as supernova burst considered in relation to cosmic rays containment in galactic disk
[NASA-TM-X-65906] 13 p2160 N71-24988

Fission product transport and behavior in stainless steel lined Containment Research Installation
[ORNL-4502] 13 p2140 N71-25499

Impact tests on model nuclear reactor containment system with models weighing 350 lb to 1305 lb and impact velocities varying from 241 to 580 ft/sec
[NASA-TM-X-67856] 16 p2636 N71-28621

Remote air sampling and monitoring system for gas analysis of radioactive isotopes in containment atmospheres after loss of coolant tests
17 p2744 N71-29065

Application of remote air sampling and monitoring system to nuclear power industrial safety and analysis of radioactive isotopes in containment atmospheres
17 p2744 N71-29066

Literature survey for identifying primary containment safety features in accident and safety system analysis for liquid metal fast breeder reactor
[BAW-1352] 19 p3136 N71-32064

Axially-symmetric flows with regions of closed streamlines confined by rotational inertia or electromagnetic pinch, for containment for gas core reactors
20 p3252 N71-33637

Flooded impingement plate for blowing high expansion, long-lived foam having noble gas containment
[DUN-7221-VOL-1] 20 p3309 N71-33773

Bare refractory double containment boiler for SNAP 8 power conversion system utilizing mercury, tantalum, zirconium, and type 300 stainless steel materials
[NASA-CR-72918] 24 p3960 N71-38247

CONTAMINANTS
NT RADIOACTIVE CONTAMINANTS
NT TRACE CONTAMINANTS
Fluid transferring system design for purging toxic, corrosive, or noxious fluids and fumes from materials handling equipment for cleaning and accident prevention
[NASA-CASE-XMS-01905] 10 p1540 N71-21089

Description of spacecraft microbial contamination and techniques for reducing level of contamination
[NASA-CR-118017] 12 p1063 N71-23825

CONTAMINATION

Smog forming reactivities of exhaust aldehydes measured using test mixtures similar to exhaust at atmospheric dilution
[BM-R1-7527] 14 p2212 N71-25798

Extrapolation of animal tolerances of air contaminants to human tolerances for diver breathing under hyperbaric conditions
[AD-721681] 17 p2787 N71-29359

Environmental and materials contamination including detection and control methods for production engineering
[SC-84-70-369] 17 p2739 N71-29449

Effects of runway contaminants and pavement surface properties on runway displacements
18 p2962 N71-30767

Reductions in smoke level and carbon monoxide emissions resulting from air-cooled fuel nozzles in jet aircraft exhaust pollutant tests
18 p2871 N71-30784

Application of biotransformative phase dispersion model to estimate concentrations of air pollutants - tables and graphs
[PB-191462] 19 p3123 N71-31626

Effect of acidic surface oxides on carbon sorption of pollutant type molecules from aqueous solutions
[PB-196319] 19 p3050 N71-32133

Air pollution in relation to certain atmospheric and meteorological conditions and methods employed in survey and analysis of air pollutants
[PB-196327] 19 p3096 N71-32601

Analysis of air pollution problems, including types of pollutants, monitoring systems, and development of global air quality standards
[BGG-1183-2242] 20 p3267 N71-33537

Development of gas plasma cleaning techniques for removing contaminants from optical surfaces in space environments
[NASA-CR-119802] 21 p3519 N71-35075

Computing dispersal of atmospheric pollutants near airports by use of mean wind and temperature profiles
[NASA-CR-111962] 23 p3748 N71-36720

Remote investigation using on-line mass spectrometry and emphasizing target construction, elimination of contamination, and recording of mass spectra
[NP-18829] 23 p3811 N71-37177

CONTAMINATION
NT FUEL CONTAMINATION
NT SPACECRAFT CONTAMINATION
Monitoring techniques for carbon contaminants in sodium
[MSAR-70-54] 02 p0267 N71-12189

Portable transistorized tritium contamination monitor
[CLOR-79/D] 03 p0383 N71-13347

Manual Space Center contamination control manual - Vol. 1
[NASA-TM-X-66541] 05 p0657 N71-14929

Emission spectroscopy method for contamination monitoring of inert gas metal arc welding
[NASA-CASE-XMP-02039] 06 p0662 N71-19671

Contamination free operation and eliminating combustion products from ambient surroundings generated by solid firing
[NASA-CASE-XGS-01971] 06 p0863 N71-15922

Co-60 contamination effect on structural steel with background counting rate of proposed shadow shield, whole body monitor
[SC-83/569] 08 p1262 N71-18829

Ground water contamination by high energy proton accelerator through sealant release
[UCRL-20131] 09 p1426 N71-19537

Eddy transfer of active and passive contaminants in atmospheric boundary layer
[AD-716359] 09 p1413 N71-19825

Laminar airflow and airborne contamination control concepts with clean room specifications and laminar flow facility designs
[NASA-CR-116133] 09 p1348 N71-20425

Freezing and microwave effects on contaminated precooled frozen meal components
[AD-717833] 11 p1063 N71-22253

Apparatus and process for volumetrically dispensing reagent quantities of volatile chemicals for small batch reactions
[NASA-CASE-NPO-10670] 15 p3416 N71-27372

Accidental external irradiation and accidental radioactive contamination - rules and therapeutic procedures
[CEA-N-1365] 15 p2481 N71-27992

Effects of radiation on stability and compatibility of hydrazine and hydrazine-24 percent hydrazine nitrate in stainless steel and titanium alloy containers with O ring seals
[NASA-CR-109767-PT-2] 16 p2670 N71-29888

Contamination control checklist for manufacturing or assembly plants
[NASA-CR-121740] 21 p3432 N71-34418

Surface plasma resonance effect in diffraction gratings and relation of effect to space contamination by spacecraft instruments
[NASA-CR-121754] 21 p3508 N71-34994

Analysis of probable viable terrestrial microorganisms on Mars caused by Mariner Mars 1971 Project
[NASA-CR-122845] 24 p3878 N71-37643

CONTEXT FREE LANGUAGES

Auger electron spectroscopy, surface contamination, and silicon device parameters for microcircuits [NASA-CR-121013] 24 p3901 N71-37804
Room temperature contamination of uranium dioxide powder during storage [ORNL-4704] 24 p3962 N71-38262

CONTEXT FREE LANGUAGES

Formal semantics definition based on nonterminal symbols in context free grammar and simple programming language [AD-71529] 02 p0190 N71-11336
Definition and implementation of simple LR/k context free grammars [NASA-CR-117125] 09 p1333 N71-19600
Context sensitive grammar and generation of non-context free languages [NASA-CR-121658] 21 p3397 N71-34177
Context-free language generation using nontrivial constraints on context-sensitive grammar rules [NASA-CR-121497] 21 p3446 N71-34520

CONTINENTAL DRIFT

Investigating hypothesis of sea floor spreading and continental drift with respect to location of Iceland at lithospheric plate boundaries [AD-71564] 07 p1025 N71-17978
Reporting results of disciplinary and interdisciplinary research into geology of Iceland [AD-71564] 07 p1026 N71-17983
Continental drift theory applied to role of Arctic Basin in development of Lavras structure [AD-718068] 12 p1907 N71-23521
Appraisal of earth origins and structure based on theory of continental drift and geological observations [AD-718068] 12 p1907 N71-23521
History of earth's crust based on rheology and chemistry of upper mantle, evidence from continents, and evidence concerning drift from ocean basins [AD-718068] 12 p1907 N71-23521
Comparison of continental margins of eastern North America at Cape Hatteras and Africa coast at Cap Blanc [AD-718068] 12 p1907 N71-23521
Computer programs to determine quantitative morphological fit of Australia and Antarctica [AD-718068] 12 p1907 N71-23521
Lectures presented at seminar in various scientific fields [AD-718068] 12 p1907 N71-23521

CONTINENTAL SHELVES

System of predicting waves and swells on US Continental Shelf of east coast [PB-192201] 03 p0372 N71-13324
Temperature, horizontal current, and wind velocity measurements by moored instruments over Peru continental shelf [AD-715784] 08 p1191 N71-18804
Thermographic and current measurements from Oregon continental shelf [AD-715650] 08 p1191 N71-18924
Discussing international legal aspects of regulating continental shelves and demilitarization of ocean floor [JPRS-52585] 08 p1309 N71-19322
Response of stratified ocean model to pressure disturbance moving seaward across continental shelf [AD-715650] 08 p1191 N71-18924
Underwater research in ocean floor habitat for 60 day evaluation of supporting facilities at Virgin Islands for Tekite 1 project [NASA-CR-118333] 13 p2192 N71-25529
Analysis of deposition and erosion of ocean bottom along Middle Atlantic Continental Slope [AD-715650] 08 p1191 N71-18924

CONTINENTS

NT AFRICA
NT ASIA
NT AUSTRALIA
NT EUROPE
NT NORTH AMERICA
NT SOUTH AMERICA
Mobilist approach to role of Arctic Basin in geotectural development of supercontinent Laurasia during Paleozoic era [AD-715650] 08 p1191 N71-18924
Measurements of Cs-137 radioactivity and total beta activity from nuclear explosion fallout and aerosols in air suspension over continents, mountains, and oceans [CEA-R-3977] 17 p2738 N71-29236

CONTINGENCY

FORTAN subroutine TWOBYK for testing of hypotheses in probability theory using contingency tables [AD-715650] 08 p1191 N71-18924

CONTINUITY

Post-processor producing control tape for continuous path, numerically controlled inspection machine [Y-1723] 19 p3062 N71-32345

CONTINUITY (MATHEMATICS)

Continuous representation and kernel functions [SU-1206-227] 07 p1050 N71-17205
Error bounds of spline interpolation of piecewise-continuous functions [LA-4477] 07 p1073 N71-17356
Lorentz force, Maxwell equation, and Poisson equation in continuum electromechanics [AD-716567] 09 p1423 N71-19658

Nonlinear operator for determining complete continuity when kernel is function of variables [NASA-CR-119014] 16 p2622 N71-28404
Feasibility of overcoming local convergent nature of continuation methods for nonlinear equations [NASA-CR-119016] 16 p2623 N71-28575
Moldensky series and analytical continuation applied to gravimetric geodesy [AD-724133] 20 p3239 N71-33181

CONTINUITY EQUATION

The continuity equation of compressible flow with flow velocity distortions and gas density variations [DLR-MITT-70-13] 07 p1008 N71-17167
Continuity equation solution for diurnal variations in oxygen concentration between 65 and 200 km altitudes [AD-715643] 13 p2074 N71-25078

CONTINUOUS NOISE

Mass growth and recovery function for temporary threshold shifts produced by extended exposure to simulated armored vehicle [AD-717232] 10 p1499 N71-21041

CONTINUOUS RADIATION

CW transferred electron oscillators for Q band [AD-715643] 13 p2074 N71-25078
Single-mode continuous-wave carbon dioxide laser intensity fluctuation variance and power spectrum measured by germanium detectors [AD-716847] 10 p1570 N71-21674
Multiline, multitransverse mode argon ion laser [AD-717296] 11 p1774 N71-21896
Spatial nonuniformity effects on high temperature plasma breakdown over X band waveguide aperture including continuous wave and pulsed breakdown in air and nitrogen [AD-718412] 12 p1981 N71-23965
Theoretical analysis of 24.5/73.6 MHz rocket-to-ground CW propagation experiment for in situ electron density measurements [NASA-TM-X-65552] 15 p2382 N71-27670
Analysis of concept of spin-stabilized synchronous satellite carrying interferometer transmitting CW signals in L-band [NASA-CR-121756] 21 p3455 N71-34588
Developing visible CW optical parametric oscillators [AD-715643] 13 p2074 N71-25078

CONTINUOUS WAVE RADAR

Statistical wave front data analysis on horizontal continuous microwave transmission [AD-715643] 13 p2074 N71-25078
CW and pulse radar compared, and operating principles and characteristics of various CW radars [AD-715643] 13 p2074 N71-25078

CONTINUOUS WAVES

U CONTINUOUS RADIATION
CONTINUUM FLOW
Steady state, axisymmetric flow distribution of free expansion of supersonic plasma jet issuing from sonic orifice numerically investigated using continuum flow [AD-715643] 13 p2074 N71-25078
Diffusion of ion and gas molecules to aerosol particles in noncontinuum regions [AD-715643] 13 p2074 N71-25078
Ion density probe design for continuum flows using flat-plate electrodes for measuring ion currents and production rates [AD-715643] 13 p2074 N71-25078
Path finding schemes for energy continuation determination of energy independent pion-nucleon phase shift analysis [UCRL-20250] 21 p3475 N71-34748
Calculation of flow processes in gas centrifuges based on continuum concept and non-steady Navier-Stokes equations [CONF-700557-4] 24 p3905 N71-37833

CONTINUUM MECHANICS

Continuum mechanics of grain boundary dislocations and diffusional creep [AD-711088] 01 p0111 N71-10669
Modifying Rayleigh-Ritz method for predicting values of stress concentrations in elastic continua [RAE-TX-68273] 02 p0301 N71-12022
Continuum thermodynamic theory of nonlinear thermomechanical materials with memory [AD-711401] 02 p0304 N71-12174
Steady-profile analysis of plane shock structures in solids [AD-712059] 03 p0460 N71-12949
Superposing small elastic deformations on large ones with explicit expressions for incremental stress-strain relations for isotropy and transverse isotropy [AD-712399] 03 p0461 N71-13005
Describing induced birefringence in viscoelastic materials based on constitutive assumptions for stress and dielectric properties [NASA-CR-1703] 05 p0731 N71-14547
Description of crystal defects by point force arrays [AD-713214] 05 p0739 N71-15376
Modeling soil mass as continuum using constitutive equations of continuum mechanics [NASA-CR-103022] 07 p1048 N71-17462

SUBJECT INDEX

Hill stress rate in continuum mechanics of polycrystals including application to crystal deforming via quasi-static single slip [AD-717326] 11 p1816 N71-23172
Description of basic laws of motion of micropolar continuum and application of micropolar theory to liquid crystals [AD-717396] 11 p1696 N71-23223
Homogeneous continuum for describing mechanical behavior of laminated composite elastic solids [AD-717331] 11 p1838 N71-23217
Boundary layer techniques applied to two-dimensional couple-stress theory of linear elasticity [AD-717884] 12 p2004 N71-23404
Flat plate and cylindrical ion density probes including flow molecular flow and continuum regimes [AD-717884] 12 p1923 N71-24130
Intrinsic representation of flows with Lamb surfaces [AD-719431] 13 p2063 N71-24078
Continuous moment sum rule for calculating Compton scattering at high energies [TUBEP-71-5] 13 p2140 N71-23380
Thermodynamic theory for deducing governing equations for nonequilibrium continuum processes [AD-717884] 12 p2004 N71-23404
Constitutive equations and continuum mechanics for magnetic, kinetic, thermal, and material subsystem nonlinear interactions [AD-717884] 12 p2004 N71-23404
Unified approach to interactions of defects applicable to rigid and deformable defects [AD-721469] 16 p2664 N71-28227
Dislocation configurations in stress producing and zero stress continuum [AD-722432] 17 p2815 N71-29784
Stacking fault energy determination in dislocations in continuum elasticity [AD-721469] 16 p2664 N71-28227
Invariance and continuity of Burgers vector applied to crystalline interface dislocations [AD-721469] 16 p2664 N71-28227
Nonlinear continuum theory for analyzing crystal dislocation effects [NBS-SP-317-VOL-2] 17 p2821 N71-29948
Macroscopic continuum mechanics theory for dilatational wave interactions in crystal lattice dislocations [AD-721469] 16 p2664 N71-28227
Nonlinear elastic theory for finite inhomogeneous medium derived from crystal lattice mechanics [AD-721469] 16 p2664 N71-28227
Nonlinear variational formalism of dislocation and yielding in plastic manifold for mechanical material [AD-721469] 16 p2664 N71-28227
Statistical analysis of crystal lattices for continuum mechanics of dislocations [AD-721469] 16 p2664 N71-28227
Elastic Cosserat surface continuum with deformable strains [AD-721469] 16 p2664 N71-28227
Dynamic nonlinear theory of crystal dislocations with elastic-plastic continuum mechanics [AD-721469] 16 p2664 N71-28227
Continuum mechanics for nonlinear dynamic dislocation analysis on anisotropic elastic media [AD-721469] 16 p2664 N71-28227
Thermodynamic properties of inhomogeneous elastic bodies [NASA-CR-119065] 17 p2822 N71-29978
Geometric stress mechanics for crystal lattice defects [AD-721469] 16 p2664 N71-28227
Green function and Fourier integrals in dynamic elastic field theory of crystal dislocations and disclinations [AD-721469] 16 p2664 N71-28227
Kinematic distribution of crystal lattice defects [AD-721469] 16 p2664 N71-28227
Micromorphic and micropolar continuum dislocation theories for elastic solids [AD-721469] 16 p2664 N71-28227
Kinematics of continuum dislocations in crystal lattices [AD-721469] 16 p2664 N71-28227
Thermally activated dislocation motions in crystal lattices with surmountable barriers [AD-721469] 16 p2664 N71-28227
Strain rate effects on dislocation flow dynamics in crystal lattices [AD-721469] 16 p2664 N71-28227
Kinematics and general principles in nonlinear and linear theories of elastic shells and plates by direct approach and three-dimensional equations of classical continuum mechanics - Part I [AD-722350] 17 p2854 N71-30229
Analyzing structure of constitutive relations which govern force-deformation laws used in stress analysis [AD-722831] 18 p3022 N71-31483
Three dimensional theory of thermomechanical material developed using techniques of continuum mechanics and law of thermodynamics [NASA-CR-1795] 20 p3339 N71-33777

Interdependence of continuum mechanics and physical chemistry in failure analysis of adhesives
[NASA-CR-121857] 21 p3537 N71-33130

Analysis of infinitesimal plane stress wave propagation in fluid using continuum mechanics
22 p3571 N71-35434

Optical continuum emission of Soyfert and N-type plasmas and correlation with ionization and thermal equilibrium calculations for nonthermally ionized gas
[AD-72641] 22 p3571 N71-35177

Multi-material Eulerian program [HRLP] for flow in two space dimensions and time
[AD-72609] 23 p3743 N71-36692

FORTRAN listing of multi-material Eulerian program [HRLP] for compressible fluid and elastic-plastic law in two space dimensions and time
[AD-72646] 23 p3744 N71-36693

Continuum theory of dislocations for plastic deformation of metallic crystals
23 p3837 N71-37363

CONTINUOUS
Subsequent reducible property of being plane locally simply connected, Ponce composite
06 p0853 N71-16681

Continuum theory of slender electronic probes
[NRP-2281/3] 06 p1173 N71-19165

Continuum theory for determination of macroscopic equations for reinforcing fiber composites
[NPL-MA-92] 10 p1690 N71-20665

Finite-difference time fluxes and linear operators in discrete space
21 p3448 N71-34540

Thin MoTiCr crystals for extending material background in 17 and 80 keV energy regions from Compton scattering peak
[UCRL-72927] 22 p3444 N71-35963

Study of relativistic constitutive equations of continua
22 p3692 N71-36335

CONTOURS
Development of generalized digital contouring programs
[NASA-TN-D-60223] 05 p0649 N71-14634

Calculated thickness of thermal insulation layer on metal surface
07 p1130 N71-17502

Describing device for surveying contour of surface using X-Y plotter and traveling transducer
[NASA-CASE-XLA-68646] 07 p1030 N71-17506

Contouring program application to mapping of ionospheric parameters using electron density data from ionospheric stations for extrapolating observations
[AD-17083] 11 p1730 N71-22592

Development and characteristics of digital recording system for automatic digitizing of map contour line data
[AD-726306] 22 p3579 N71-35493

Development of curved and flat finite shell elements for higher order shell theory
24 p4037 N71-38736

CONTRACT MANAGEMENT
Materials management control performance of Apollo program prime contractor
01 p0136 N71-10292

Comprehensive investigation into contract management and development costs of TFX aircraft
[NRP-21-1496] 05 p0789 N71-15649

Project and contract management in NASA orbital space station program
[NASA-TN-X-67631] 11 p1830 N71-22041

CONTRACT NEGOTIATION
Profit analysis techniques for profit and fee negotiations
[NASA-CR-119864] 16 p2694 N71-28272

Application of life cycle costing techniques to award of contracts for hardware and related support by military procurement agencies
[AD-726976] 23 p3870 N71-37389

CONTRACTING
Effects of vertical contraction on horizontal flow of incompressible density-stratified fluid
21 p3414 N71-34290

Origin of gaseous clusters due to explosion or preheated contraction
23 p3849 N71-37433

CONTRACTS
Air mail transportation by contract operations
01 p0138 N71-10816

Compendial hearing on investigation of contract for TFX aircraft
02 p0146 N71-11034

Improving effectiveness of contractor procurement team reviews
05 p0789 N71-15695

Effects of reductions in NASA contracts on unemployment of aerospace employees
[NASA-CR-118774] 13 p2191 N71-24801

CONTRACTS
New techniques for studying spatial structure and dynamics of human releases
11 p1751 N71-32692

Optical observations following release of human test at high altitudes described in three phases
[AD-717695] 11 p1751 N71-32698

CONTRAST
NT IMAGE CONTRAST
NT PHASE CONTRAST
Reconformer for photographic film frequency contrast characteristics measurement based on automatic conversion of transmission factors into effective exposures
[AD-72394] 17 p3751 N71-28494

Television display and artificial background for showing effects of contrast and motion on target detection
[AD-723407] 17 p2711 N71-29085

CONTROL
Operational modeling of dynamic systems for control purposes
[JPRS-52308] 10 p1664 N71-20647

Space Flight Operations Facility Configuration Control System for management control purposes
11 p1733 N71-22790

Valve assembly for controlling simultaneously more than one fluid flow, and having stable qualities under loads
[NASA-CASE-XMB-65890] 12 p1086 N71-23191

Control system for pressure balance device used in calibrating pressure gauges
[NASA-CASE-XMP-64134] 12 p1921 N71-23753

Sources and control of air pollution
12 p1956 N71-23854

Cybernetics and production control systems using neural computers
[AD-710404] 12 p1885 N71-23914

International scientific cooperation for control of military technologies
13 p2190 N71-24755

External via covariance and internal via Markov process descriptions of Gaussian stochastic processes
[AD-723406] 18 p2944 N71-30816

Effects of larger Scout D and B heat shields on vehicle stability and control, structure, and ground support
[NASA-CR-111947] 20 p3334 N71-35286

Civil Aeronautics Board regulatory actions taken fiscal year 1970
21 p3534 N71-35186

Simultaneous signaling in digital sound circuits for operational control of broadcasting network
[SBC-1971/28] 23 p3723 N71-36555

CONTROL BOARDS
Development program for methods of terminating flat conductor cable to small electrical components used on electrical displays and control panels
[NASA-CR-108783] 04 p6510 N71-13525

Low cost source data terminal for technical text
[UCRL-19590] 05 p0652 N71-15578

Control board instrumentation and life support system for Soyuz command module
07 p1118 N71-17086

Isolation control system design for machining separately located ion gauge pressures on vacuum chambers
[NASA-CASE-XLE-00787] 16 p1539 N71-21080

Approximate switching surfaces for optimal control of nonlinear systems
14 p2235 N71-26578

Operator performance and control panel layout for discontinuous tasks based on sequence of use, functional grouping, and location by frequency and importance
[AD-727791] 24 p3883 N71-37676

CONTROL DATA [COMPUTERS]
Computer control of large telescopes
24 p3923 N71-37986

Telescope control by on-line computers, including ESO 3.6-m telescope
24 p3923 N71-37987

Computer subsystem of Anglo-Australian 150-inch telescope
24 p3924 N71-37993

CONTROL DEVICES
U CONTROL EQUIPMENT
CONTROL EQUIPMENT
NT CRYOSTATS
NT PRESSURE REGULATORS
NT SERVOAMPLIFIERS
NT SPEED REGULATORS
NT TELEOPERATORS
NT THERMOSTATS

Optical simulation study to determine manual instrumentation for pilot control of lunar flying vehicle
[NASA-TN-D-5963] 05 p0327 N71-12334

Proceedings from symposium on control theory applications
[NASA-TN-X-46516] 04 p0623 N71-14426

Computer process control applications with emphasis on oil and chemical industries
04 p0524 N71-14434

Hardware development and standardized software for process control systems
04 p0524 N71-14435

Numerical study on controlling dynamic properties of supercavitic jet using bypass bleed
[NASA-TN-D-6144] 05 p0626 N71-14689

Design and characteristics of artificial heart control system
[NASA-TN-D-6171] 07 p0886 N71-17593

Stepping motor control apparatus enabling winding in proper time sequence to cause motor to rotate in either direction
[NASA-CASE-QSC-10366-1] 08 p1172 N71-18772

Voltage drift compensation circuit for analog-to-digital converter
[NASA-CASE-XNP-64780] 09 p1333 N71-19687

Handbook containing radar theory, engineering, control systems, communications, and instruments
[AD-716668] 09 p1349 N71-19774

Development of attitude control system for vertical takeoff aircraft using reaction nozzles displaced from various axis of aircraft
[NASA-CASE-XAC-68972] 09 p1323 N71-20570

Numerical analysis of dynamic and thermodynamic state of plasma-type air-cushion vehicle to determine wave response and control system operating characteristics
[NASA-TN-D-4357] 11 p1739 N71-32589

Device for controlling rotary potentiometer mounted on aircraft steering wheel or altimeter control
[NASA-CASE-XAC-10810] 12 p1987 N71-23009

Light Push-Buttons (SPAN) (BNC) interlocked with load-in network and optical line receiver
12 p1893 N71-23673

Controlled release device for use in launching rockets or missiles
[NASA-CASE-XES-68330] 12 p1929 N71-24043

Fabrication and test of torque control device for rocket engine models
[BC-DE-70-911] 12 p1901 N71-24346

Control analysis of regenerative spacecraft orbit altitudes system for earth orbiting manned missions of up to 1 year duration
[NASA-TN-D-6159] 14 p2209 N71-26019

Circuit for controlling reversible dc motor
[NASA-CASE-XMP-7477] 14 p2229 N71-26802

Description of equipment used for automatic control of road and rail transport and application to improved urban transportation system
14 p2309 N71-26128

Digital memory system with multiple switch cores for driving each word location
[NASA-CASE-XNP-61466] 14 p2334 N71-26434

Superconducting internal control equipment
[AD-720740] 14 p2192 N71-36538

Performance of electric stepping motor as reactor control drum drive
[NASA-TN-X-2297] 15 p2366 N71-26979

Control arm and safety circuits for high flux research reactor
[AEC/TM-16] 15 p3451 N71-27683

Field control of jet amplifiers
[NASA-CASE-XLE-69341] 16 p2381 N71-28741

Instrumentation for control of magnetic field in ion thruster for improved starting and improved scanning of external magnetic field
[NASA-CASE-LEW-10835-1] 16 p2672 N71-28873

Design of control equipment for manned Mars roving vehicle
[NASA-CR-119360] 16 p2695 N71-28941

Aircraft structure elasticity effects on control lever deflection and control forces
18 p2872 N71-31065

Two dimensional periodogram for estimating spectral density of real, homogeneous, random field over regular lattice on plane
[JPRS-53340] 18 p2948 N71-31381

Control equipment and engine development for air pollution control from jet aircraft engine emissions
18 p2919 N71-31489

Post-processor producing control tape for continuous-path, numerically controlled inspection machine
[V-1723] 19 p3082 N71-32345

Fluid control, filtration, and conditioning equipment, computer programs, and data reduction techniques - technology utilization
[NASA-SP-5938/01] 20 p3276 N71-33142

Theoretical solution to minimum-time pulse frequency modulated regulator problem
20 p3342 N71-33774

Device for controlling terminal shock waves in supersonic jets
[NASA-CASE-LEW-11108-1] 21 p3373 N71-34817

Optimization of communications network performance and control for space shuttle orbiter
21 p3515 N71-35846

Air pollution sources and control procedures and 1970 Clean Air Act summary
[SP-159479] 22 p3699 N71-36376

Power and load priority control concept for Brayton cycle power system providing speed control and field current control for generator and load demands which includes energy storage
[NASA-TN-D-6476] 23 p3710 N71-36432

Analysis of criteria for survivable flight control system using fly-by-wire and integrated structure package techniques
[AD-727722] 24 p3874 N71-37616

Use of miniature general-purpose digital computers for design of digital control systems
[AD-727190] 24 p3885 N71-37764

Computer control of large telescopes
24 p3923 N71-37986

CONTROL MOMENT GYROSCOPES

CONTROL MOMENT GYROSCOPES

Control moment gyro fine attitude control system for spacecraft
[NASA-CR-108702] 03 p0410 N71-13200

Control system designs for USSR single-rotor helicopters including controllability characteristics, rotors with control gyroscopes, and transfer functions in closed loop systems
[NASA-TT-3-656] 10 p1492 N71-20719

Space station/base blowdown reusults system for orbit-keeping and control moment gyro deactivation - summary data
[NASA-CR-111878] 10 p1650 N71-21654

Space station/base blowdown reusults system for orbit keeping and control moment gyro deactivation - systems design
[NASA-CR-111879] 10 p1650 N71-21655

Space station/base blowdown reusults system for orbit keeping and control moment gyro deactivation - systems development
[NASA-CR-111880] 10 p1650 N71-21656

Stylab control moment gyroscope inner gimbal design and thermal vacuum and environmental tests
[NASA-TM-X-64583] 18 p2956 N71-31199

CONTROL PANELS

U CONTROL BOARDS

CONTROL ROOMS

Computer calculation of wall effect on sodium coolant temperatures in subchannels of rod bundles
[KFK-1042] 01 p0887 N71-10928

Experimental pressure loss determination in 37 rod bundle of tubes with 6 integral spiral fins per rod as spacers for economic design of nuclear fuel elements
[KFK-1038] 02 p0263 N71-11410

Hydrodynamic and heat transfer measurements on full-scale simulated 36-rod Marviken fuel element with nonuniform radial heat flux distribution
[FRIG-3] 04 p0547 N71-13634

Resonance analysis of natural zirconium calculated for rods of varying diameter and TriGen fuel elements using different resonance parameters
[TKK-F-A-106] 04 p0530 N71-13814

P sub 1 blackness theory and Rossi alpha measurements of control rods
[RT/FU705] 04 p0578 N71-13865

Correlation of rod bundle critical heat flux for water in pressure range 150 to 725 psia
[IN-1412] 04 p0554 N71-14011

Investigating fuel burnup rates, safety rods, fuel elements, and critical experiments in thermal and fast reactors
[BNWL-1381-2] 04 p0554 N71-14016

Conceptual design of packaged loop for EBR-2 control rod positions
[ANL-7538] 05 p0724 N71-14731

Extending COBRA 2 computer program for thermal and hydraulic analysis in large bundles of fuel pins
[BNWL-1422] 05 p0726 N71-15072

Investigation of pitting corrosion on malcozined stainless steel control rod push rods in La Cross bubble water reactor
[ACWP-76052] 05 p0729 N71-15211

Computerized simulation analysis of temperature transients in reactor rod-drop experiments
[ANL-7664] 06 p0901 N71-16824

Rod-drop determination of reactor feedback and stability through inverse kinetics computations
[ANL-7686] 06 p0901 N71-16825

Digital computer program for calculation of local temperature and mass flux in cooling channels of fuel elements
[ANL-TRANS-858] 07 p1059 N71-17010

Investigating direct electrical heating of UO₂ fuel rod for fast nuclear reactor
[EURFNR-773] 08 p1234 N71-18170

Burnout heat flux measurements on 3 by 3 rod bundles with nonuniform heat generation and high pressure water
[EUR-4514-E] 08 p1302 N71-18220

Zircaloy clad uranium dioxide fuel rod evaluation
[GEAP-10204] 08 p1238 N71-18345

Fabrication of non-fuel core components for experimental fast oxide reactor
[GEAP-13593] 08 p1239 N71-18508

Predicted fuel and control rod behavior of SM-1 core 3
[AD-715850] 08 p1241 N71-18827

Particle size distributions from fuel rods fragmented during power burst tests in capsule driver core
[IN-1428] 09 p1417 N71-19897

EBR-2 codes for processing reactivity data at full and reduced coolant flows using thermal expansion corrections for control rods
[ANL/EBR-20] 09 p1418 N71-19904

Critical heat flux and pressure drop tests of electrically heated annular fuel rod bundles with ferrous hydrazide slurry crud deposits
[WAPD-TM-918] 09 p1421 N71-20088

Manual control mechanism for adjusting control rod to null position
[NASA-CASE-XLA-61808] 10 p1562 N71-20740

Optimum grid spacing in fuel rod support systems
[WAPD-TM-714] 10 p1603 N71-21184

Critical mass measurements, control rod calibration, neutron and gamma flux measurement, measurement of various reactivity worths, power calibration, and xenon buildup for TRR-3
[JAERI-MEMO-4141] 13 p2119 N71-25107

EL-600 space-dependent kinetic problems, including reactor safety and control rod dropping after dead time
[CEA-CONF-1726] 14 p2294 N71-26521

Transport theory for analysis of neutron flux distribution near absorber rod in reactor
[JAERI-4238] 15 p2452 N71-27830

Computer program for control rod calculations in two flux reflected reactor
[EIR-166] 15 p2452 N71-27831

High temperature, gas cooled reactor control rod, control rod guide tube, and thermally released shut-down rod after 300 full power days of operation
[GA-10196] 16 p2631 N71-28215

Turbulent velocity distribution and wall shear stress in turbulent flow parallel to triangular or rectangular rod assemblies
[NLL-W-461-9091.9F1] 17 p2735 N71-29891

Computer programs of LFEN-FR6 for numerical calculation of experimental results of rod drop in nuclear reactors
[LFEN-NL49/ALPHA] 18 p2960 N71-30821

Operational control system for part length rod drive mechanism in pressurized water reactor
[WCAP-7406] 19 p3135 N71-31938

Heat rate efficiency calculations for irradiated fuel assembly rods using instrument measurements
[JAERI-MEMO-4248] 19 p3136 N71-32067

Rod position monitoring in pressurized water reactors
[WCAP-7571] 19 p3140 N71-32580

Thermal bowing of single rods at several axial positions
[TRG-2089] 21 p3458 N71-34608

Effect of gas bubbles entrained in sodium coolant expansion on LMFBR fuel rods
[CONF-700628-36] 22 p3625 N71-33827

Fast reactor control and absorber studies including radiation damage and reliability of absorbing materials
[SRARI-P-96] 23 p3800 N71-37092

Thermal flux distribution and reflector saving measurements in UA-RR-1 reactor core using foil activation technique
[UARAEE-99] 24 p3958 N71-38236

OPTICAL SIMULATION
Optical simulation study to determine channel instrumentation for pilot control of burner flying vehicle
[NASA-TN-D-5983] 03 p0327 N71-12334

Simulating static and dynamic responses of single-module unmanned Mars roving vehicle
[NASA-CR-111560] 03 p0457 N71-13074

Specifications of CAMAC 25-MHz counter module type LEM-521.1
[KFK-1184] 08 p1199 N71-18160

Parallel microcomputer for emulating sequential and parallel computer control structure
[SLAC-127] 09 p1355 N71-20088

Mathematical functional model for carotid blood pressure control system
[AD-717847] 11 p1680 N71-22161

Analysis of glide-slope information requirements for low visibility aircraft landing approach using Kalman filter-optimal control combination to simulate DC-8 control system
[AD-722655] 18 p2956 N71-30887

Real time computer hardware simulation for investigation of space station dynamics and control problems
[NASA-TN-D-6449] 21 p3525 N71-35119

CONTROL STABILITY
Wind tunnel and flight tests for stability and control derivatives of lifting body vehicles
01 p0124 N71-10103

Structure of control laws insuring asymptotic stability of control systems with unstable linearized
02 p0196 N71-11572

Computer-aided compensator design program for increasing relative stability of control systems
[NASA-CR-103066] 09 p1363 N71-19722

Aircraft structure elasticity effects on control lever deflection and control forces
18 p2872 N71-31085

Hypervelocity wind tunnel static stability and control tests of variable geometry configuration of space shuttle
[NASA-CR-103151] 21 p3521 N71-35088

Trisomic wind tunnel tests on static stability and controllability of NAR/GD space shuttle and booster
[NASA-CR-103196] 21 p3521 N71-35090

CONTROL SURFACES
NT AILERONS
NT ELEVATORS [CONTROL SURFACES]
NT ELEVONS
NT FLAPS [CONTROL SURFACES]
NT GUIDE VANES
NT HORIZONTAL TAIL SURFACES
NT JET FLAPS
NT JET VANES
NT LEADING EDGE SLATS
NT SPOILERS

NT TRAILING-EDGE FLAPS

NT WING FLAPS

Linear theoretical method for arbitrary wing planform and trailing edge control surfaces in low frequency oscillatory motion in subsonic flow
[NPL-AERO-1363] 02 p0143 N71-11913

Designs and data for selecting aerodynamic surface control and thrust vector control servomechanisms
[NASA-CR-106696] 02 p0149 N71-11889

Investigating various classes of thermal control surfaces for satellites
[RAE-TR-68276] 02 p0305 N71-11135

Computation of pressure induced by control surface oscillation in subsonic flow
[NASA-TT-F-13385] 03 p0311 N71-12119

Feasibility study of counter insurgency aircraft with reaction boundary layer control
[AERO-41] 04 p0473 N71-13415

Pin loads and control surface hinge moments measured in full scale wind tunnel tests on X-34A flight vehicle
[NASA-TM-X-1922] 05 p0635 N71-14086

Mathematical models for control surface wings in subsonic unsteady flow
[ONERA-TP-689] 06 p1141 N71-16075

Further suppression with dissipated energy reduced to quadratic form for control surfaces
[NASA-TN-D-5199] 11 p1671 N71-23088

Calculation of pressure distributions over wing with harmonic oscillating control surfaces using panel function method
17 p2099 N71-20944

Application of lifting surface theory to wing with control surfaces in unsteady subsonic flow
17 p2099 N71-20944

Asymptotic expansion techniques to define pressure loading effects on wings with unbalanced control surfaces
17 p2700 N71-23048

Unsteady pressure measurements on harmonically oscillating swept wing with two control surfaces in incompressible flow
17 p2700 N71-23048

Wind tunnel investigation of control surface instability of lifting body reentry vehicle configurations at Mach 15
18 p3048 N71-31044

Static longitudinal, directional, and lateral characteristics and control surface effectiveness of sub model of space shuttle canard booster at Mach 0.36
[NASA-CR-119978] 24 p0030 N71-30889

CONTROL SYSTEMS

U CONTROL

CONTROL THEORY

Proceedings from symposium on control theory applications
[NASA-TM-X-66516] 04 p0623 N71-14015

Extension of frequency response and pole-zero methods for identification of nonlinear system elements described by nonlinear differential equations
[AD-714499] 06 p0827 N71-14089

Synthesizing asymptotically stable closed system and formulation of mixed problems of optimal control theory
[NASA-TT-F-13435] 06 p0885 N71-14048

Combined optimal control in gyrobalancing stabilization circuit
07 p1057 N71-17002

Continuous parameter stochastic optimization principle using abstract variational theory
[NASA-CR-116512] 07 p1051 N71-17027

Control analysis of spinning drag free satellite controller to reduce trajectory errors from mass attraction
[NASA-CR-116516] 07 p1119 N71-17098

Linear multichannel control systems for supersonic aerospace vehicles orbiting in earth atmosphere
[AD-714796] 07 p1057 N71-17002

Stable adaptive control with gain constraints
[NASA-CR-116428] 07 p1002 N71-17071

Review and critique of procedures and results in nonlinear estimation
[AD-715631] 08 p1225 N71-18921

Suboptimal feedback control law synthesis for second order nonlinear systems
08 p1173 N71-19104

Application of optimal control theory to power systems
[AD-716552] 09 p1362 N71-19027

Stability models for weakly nonlinear dynamical systems with application to gyroscopic devices
[AD-716538] 09 p1409 N71-19088

Linear control systems designed with distributed parameter elements for determining absolute and relative stability and root location of closed loop characteristic equations
11 p1728 N71-22018

Approximations, existence, uniqueness, and stability of diffusions with discontinuous drift term in stochastic differential equations in control theory
[NASA-CR-117746] 11 p1787 N71-22088

Approximations to and local properties of diffusions with discontinuous controls expressed by stochastic differential/Itô equations
11 p1787 N71-22088

SUBJECT INDEX

- Stability and existence of diffusions with discontinuous or rapidly growing drift terms in stochastic differential equations 11 p1787 N71-22410
- Observability of continuous time systems in relation to inverse function theory 12 p1940 N71-23349 [AD-716141]
- Analysis of computer requirements for linear filter-algorithms 12 p1949 N71-23577 [AD-716410]
- Equivalent mathematical control system models for maximum principle time delay systems with feedback 12 p1893 N71-23661 [AD-716437]
- Electron and solid state physics, control theory and applications, ferromagnetic and ferroelectric materials, electromagnetic phenomena, and plasma medium scattering 12 p1966 N71-23911 [AD-716171]
- Adaptive control techniques for variable mechanical systems 13 p1802 N71-24430 [AD-719743]
- Deterministic optimal control theory 13 p2026 N71-24712
- Synthesis procedure for adaptive control systems for adjusting parameter vectors 13 p2060 N71-25140 [AD-719828]
- Method of characteristics for synthesis and identification of distributed parameter systems in control theory 13 p2284 N71-26163 [AD-720341]
- Dual control algorithms for self adaptive filters and optimal control law for linear systems with unknown input gains 16 p2573 N71-28052 [AD-721461]
- Mathematical models and optimal control for uncertain systems 16 p2620 N71-28060 [AD-721470]
- Optimal structure and adaptive estimators for continuous and discrete data Gaussian process models 16 p2622 N71-28198 [AD-722083]
- Electronic circuitry for trainable systems with application to control and recognition functions 16 p2550 N71-28358 [AD-721577]
- Techniques for applying frequency domain optimal control in practical closed loop control systems 16 p2623 N71-28563 [AD-722040]
- Control theory extended to hyperbolic distributed processes with identification strategy incorporated in closed-loop adaptive controller 16 p2575 N71-28692 [AD-722415]
- Electron and solid state physics, control theory, electromagnetic radiation, and antenna array research 17 p2663 N71-30358 [AD-722415]
- Body forces of controlled movements and related problems in differential games aspect of controlled systems theory 17 p2773 N71-30378 [AD-722415]
- Computer assisted teleoperator control system for making comparative performance evaluations of tactical perception 18 p2899 N71-30531 [AD-722415]
- Pulse time stability of linear discrete time systems and corresponding results for stochastic linear discrete time systems 18 p2944 N71-30720 [AD-722634]
- Identification of model parameters from input output data of dynamic systems with time delays 18 p2946 N71-31217 [AD-722634]
- Electronic execution of financial transactions and security for anti-fraud controls 19 p3193 N71-31645 [AD-722634]
- Mathematical models for pole assignment in linear feedback control systems 20 p3293 N71-31883 [AD-722634]
- Application of cybernetics and control theory to problems of production control in complex systems and optimum stabilization of several coordinates of plant by one controlling influence 21 p3405 N71-34230 [AD-722634]
- Production operation planning and control theory for complex chemical engineering systems 21 p3406 N71-34231 [AD-722634]
- Design method including effects of parameter uncertainties in design of linear control systems 21 p3431 N71-34414 [AD-722634]
- Principles of situation control and practical application of situational control models for complex systems including airports, drydocks, and street crossings 21 p3448 N71-34536 [AD-722634]
- Formal generative and transformational grammars for constructing model for complex systems 21 p3448 N71-34537 [AD-722634]
- Application of situational control models examined for local sections of canals, seaports and airports, network of street crossings, and other large systems 21 p3448 N71-34538 [AD-722634]
- Presence and applications of calculus of variations in general control theory 22 p3465 N71-35671 [AD-722634]
- Dynamic model for optimization of wide utility in engineering sciences 22 p3468 N71-35699 [AD-722634]
- Investigative graphic instructional program illustrating basic concepts of systems analysis - INSIGHT 22 p3468 N71-35711 [AD-722634]

- Switching-time-variation computational method for optimal control problems of bilinear systems and systems linear in control 23 p3738 N71-36459 [AD-722634]
- Optimization of systems with sensitivity constraints with emphasis on launch vehicle trajectories 24 p3901 N71-37805 [AD-722634]
- Optimal strategy construction by trial and error based on Pontryagin maximum principle 24 p3947 N71-38157 [AD-722634]
- Discrete data model and regression analysis for devaluating economic control strategy 24 p4036 N71-38799 [AD-722634]
- CONTROL UNITS (COMPUTERS)**
- Self testing and repairing computer comprising control and diagnostic unit and rollback points for error correction 13 p2049 N71-24633 [AD-722634]
- On-line computer system for surface ionization mass spectrometer scan control and data recording 15 p2456 N71-26883 [AD-722634]
- Flexible computer-aided telemetry using sequence control, auxiliary memory, and system control registers for sensors and digital data source sampling 24 p3395 N71-34140 [AD-722634]
- CONTROL VALVES**
- Control valve and coaxial variable injector for controlling bipropellant mixture ratio and flow 07 p1036 N71-17654 [AD-722634]
- Control valve for switching main stream of fluid from one stable position to another by means of electrohydraulic forces 15 p2393 N71-27332 [AD-722634]
- Force balanced throttle valve for fuel control in rocket engines 15 p2416 N71-27432 [AD-722634]
- CONTROLLABILITY**
- Assessment of lifting body vehicle handling qualities 01 p0124 N71-10104 [AD-722634]
- Flight tests of lifting reentry vehicles for controllability 05 p0627 N71-14527 [AD-722634]
- Flight testing military transport aircraft for handling and performance in STOL applications 09 p1322 N71-20060 [AD-722634]
- Control system designs for USSR single-rotor helicopters including controllability characteristics, rotors with control gyroscopes, and transfer functions in closed loop systems 10 p1493 N71-20902 [AD-722634]
- Jet transport aircraft airspeed control and controllability data obtained by flight recorders 10 p1493 N71-20902 [AD-722634]
- Maneuverability and controllability of dolphins compared to performance characteristics of manned underwater vehicles 11 p1681 N71-22209 [AD-722634]
- Stability and controllability of supersonic swept wing aircraft 13 p2027 N71-25049 [AD-722634]
- Aerodynamic stability control for reentry trajectory of space shuttle orbiter at transition maneuver 14 p2543 N71-26063 [AD-722634]
- Flight tests to determine handling qualities of general aviation aircraft during ILS approaches in turbulent air 18 p2869 N71-30771 [AD-722634]
- Local controllability, equivalence, and diffeomorphic maps for nonlinear RC and RL circuits 24 p3901 N71-37808 [AD-722634]
- CONTROLLED ATMOSPHERES**
- NT CABIN ATMOSPHERES
- NT INERT ATMOSPHERES
- NT SPACECRAFT CABIN ATMOSPHERES
- Papers presented at conference on atmospheric contamination in confined spaces 01 p0045 N71-10176 [AD-709994]
- Circadian development of rectal and cutaneous temperature in man while resting in controlled environment 01 p0011 N71-10445 [AD-712940]
- Human sleep patterns during prolonged exposure to hyperbaric nitrogen saturated atmosphere 01 p0013 N71-10723 [AD-711671]
- Life support system for Sea-Bed Observation Laboratory 03 p0329 N71-12347 [AD-712940]
- Automatic fire protection system for manned hyperbaric chamber 03 p0329 N71-12348 [AD-712940]
- Regeneration of artificial respirable atmospheres using potassium peroxide 04 p0487 N71-13463 [AD-712940]
- High voltage pulse generator for testing flash and ignition limits of aerospace materials in controlled atmosphere 04 p0509 N71-13518 [AD-712940]
- Laminar airflow and airborne contamination control concepts with clean room specifications and laminar flow facility designs 09 p1366 N71-20425 [AD-712940]

CONTROLLED FUSION

- Toxicology of human and animal waste products and by-products in controlled atmospheres of closed ecological systems - literature review 06 p1338 N71-20483 [AD-716740]
- Stability of molecular sieve as regenerable carbon dioxide and water absorber in closed controlled atmosphere 10 p1593 N71-20629 [AD-716740]
- Directed crystallization of compounds during impurity exchange of liquid phase with crucible and atmosphere 10 p1634 N71-20890 [AD-716740]
- Design and performance of mass spectrometer system for atmosphere control in manned space station simulator 10 p1597 N71-20948 [AD-716740]
- Humidity generator and atmospheric control chamber for use with optical microscopes in studying specimen changes with variations in humidity 10 p1597 N71-21244 [AD-716994]
- Aerosol behavior and filtration in high pressure environments 11 p1687 N71-22255 [AD-717733]
- System for continuous monitoring of exhalation, weighing, and cage cleaning for animal exposed to controlled atmosphere for toxic study 11 p1733 N71-22875 [AD-717733]
- Equipment and procedure for crosslinking time and exothermic temperature determination of reacting plastic compositions in controlled atmosphere 12 p1671 N71-23756 [AD-717733]
- Human fluid balance in artificial environments, and influence of ambient temperature, water vapor pressure, total barometric pressure, wind velocity, and atmospheric gas composition 13 p2008 N71-25000 [AD-719877]
- Environmental effects on surface layer stress movement during cyclic hardening and softening 14 p2346 N71-25705 [AD-719877]
- Gas composition, electrical ignition hazards, and combustion products from fire resistant material in diving atmosphere 14 p2209 N71-25925 [AD-722052]
- Humidity control, carbon dioxide removal, and oxygen regeneration in cable atmosphere during prolonged manned space flight 16 p2552 N71-28332 [AD-722052]
- Identification and control of contaminants in spacecraft cabin atmosphere 16 p2552 N71-28334 [AD-722052]
- Carbon monoxide purity standards for gas breathing apparatus of divers and toxic hazards under controlled hyperbaric atmospheres 17 p2787 N71-29358 [AD-722052]
- Methods, instruments, and performance of air filters used to cleanse contained atmospheres - conference 17 p2743 N71-29851 [AD-722052]
- Long term hyperoxia exposures effects on human respiratory physiology 17 p2789 N71-30150 [AD-722052]
- CONTROLLED FUSION**
- Research and development in plasma physics and controlled nuclear fusion 02 p0280 N71-11835 [AD-702634]
- Annotated bibliography on plasma physics and controlled thermonuclear fusion 05 p0754 N71-15196 [AD-702634]
- Notations - electrostatic instabilities in magnetoplasma - conference 06 p1271 N71-18267 [AD-702634]
- Investigating vacuum techniques for generating useful plasma lifetimes in controlled fusion experiments 06 p1276 N71-19283 [AD-702634]
- Discussing deuterium and D-T fusion confinement devices for study of collisionless and collisional plasmas 06 p1276 N71-19284 [AD-702634]
- Calculation of energy transfer in slowing down reactions with controlled fusion systems 09 p1449 N71-20014 [AD-716594]
- Fused fibers for controlled thermonuclear fusion 12 p1903 N71-23719 [AD-716594]
- Deuterium helium-3 fusion power balance calculations with inclusion of variable cyclotron radiation parameter 13 p2149 N71-25926 [AD-716594]
- Determination of boron and nitrogen in pure boron nitride by controlled fusion of boron nitride with sodium carbonate followed by potentiometric titration of resulting boric acid 15 p2429 N71-27112 [AD-716594]
- Lower energy necessary for inertially confined nuclear fusion plasmas 15 p2503 N71-27008 [AD-716594]
- Thin foils as charge exchange medium for neutral injection into controlled thermonuclear fusion devices 17 p2080 N71-30100 [AD-716594]
- One dimensional laser heating of stationary plasmas for application to controlled thermonuclear fusion 19 p3169 N71-32139 [AD-716594]
- Research in plasma physics and controlled thermonuclear fusion 20 p3329 N71-33136 [AD-716594]

Analysis of processes occurring and computations involved with lasers and controlled thermonuclear fusion

[NASA-TT-F-13700] 21 p3435 N71-34442
Review on plasma physics and controlled thermonuclear research in USSR
[ARC-TR-7185] 21 p3479 N71-34774

Scylla, theta pinch, z-pinch, plasma gun, plasma physics, computerized simulation of plasmas, and related topics in controlled thermonuclear research program
[LA-4385] 22 p3654 N71-36656

Feasibility analysis for use of long-wavelength high-powered lasers for controlled thermonuclear fusion
[CONF-710607-48] 23 p3767 N71-36849

CONTROLLED STABILITY

U CONTROL

U STABILITY

CONTROLLERS

NT SERVOMECHANISMS

NT SERVOMECHANISMS

NT SERVOMOTORS

First evaluation of movable and rigid cockpit control sticks
[AD-709954] 01 p0003 N71-10184

Control analysis of spinning drag free satellite controller to reduce trajectory errors from mass attraction
[NASA-CR-116516] 07 p1119 N71-17398

Hand controller operable about three respectively perpendicular axes and capable of actuating signal generators for attitude control devices
[NASA-CASE-3065-07487] 12 p1925 N71-23255

Theory extended to hyperbolic distributed processes with identification strategy incorporated in closed-loop adaptive controller
[AD-725707] 23 p3737 N71-36652

Modular system-oriented discharge-charge controller for automated space power-source evaluation
[NASA-TM-X-65648] 19 p3068 N71-32609

Effects of display gain and signal bandwidth on visual sources of human controller response
[AD-727807] 23 p3717 N71-36500

Tuning, application, optimal switching times, and comparison of optimal and suboptimal controllers for feedback and feedforward control
[AD-727807] 23 p3737 N71-36652

CONVAIR MILITARY AIRCRAFT

U MILITARY AIRCRAFT

CONVAIR 440 AIRCRAFT

U CV-440 AIRCRAFT

CONVAIR 590 AIRCRAFT

U CV-590 AIRCRAFT

CONVECTION

NT FORCED CONVECTION

NT FREE CONVECTION

Numerical solution of partial differential equations on convection
[AGARD-OGRAPH-146] 03 p0362 N71-12673

Computer study of weakly ionized plasma convection in nonuniform magnetic field
[NASA-TM-X-65396] 04 p0597 N71-14128

Impurity distribution and convection in liquid phase during zone recrystallization of tellurium tetrachloride
[AD-727807] 10 p1574 N71-20876

Numerical analysis of temperature distribution and phase change positions when phase change is caused by constant heating or cooling or convection to constant temperature
[AD-727807] 14 p2356 N71-26357

Finite difference formulation for differential expressions involving both first and second derivatives in problems involving transport by simultaneous convection and diffusion
[JEP-TN-A-38] 20 p3292 N71-33534

Convection electric fields observed with double probe dc electric field experiment on Explorer 40 satellite
[NASA-CR-121741] 21 p3419 N71-34324

Convective instability in fluid layer with electromagnetic effects applied to earth and stellar atmospheres
[AD-727807] 22 p3672 N71-36183

Convective and hydromagnetic mechanisms of solar spin-down
[AD-727807] 23 p3846 N71-37409

Low frequency convective oscillations in neutron stars with internal magnetic field
[AD-727807] 23 p3849 N71-37436

CONVECTION CURRENTS

Convective cloud cells as observed from artificial earth satellites
[NASA-TT-F-13363] 02 p0254 N71-11465

Meocase investigation of tornadoes and thunderstorms in Oklahoma on 10 June 1967
[AD-721242] 15 p2438 N71-27211

Computerized simulation of convection currents in atmosphere
[AD-722836] 18 p2954 N71-31287

BOMEX data reduction on sea-air interaction and tropical convective systems studies
[NASA-CR-119762] 19 p3201 N71-32760

Sea-air interaction and tropical convective systems
[AD-722836] 19 p3201 N71-32764

Two-dimensional numerical model of large scale mesoscale circulation including sloping plane effects for analysis of convective patterns in lee of Colorado Rockies
[AD-722836] 24 p3934 N71-38208

CONVECTIVE FLOW

Prediction of weightlessness effects on single crystal growth by floating zone and Czochralski methods
[AD-722836] 02 p0284 N71-11728

Determination of boundary layer diffusion in forced convection flow
[NASA-TN-D-7012] 03 p0363 N71-13043

Stability of steady finite amplitude convection in rotating fluid layer
[UPT-4/86] 08 p1178 N71-18487

Numerical study of steady, laminar, natural convection of fluids in vertical rectangular enclosure
[AD-722836] 11 p1743 N71-22725

Tubular flow reactors used for chemical kinetics over extended pressure ranges
[COO-2026-4] 12 p1870 N71-23526

Removal of instability in free convection problem
[EP/TN/A/35] 12 p1902 N71-23827

Surface effects on cumulus cloud formations in microclimates over Russian plateau
[NLL-M-20005-5828-4F/1] 12 p1959 N71-24372

Mixed convection from sphere at small Reynolds and Grashof numbers and stability of vertical natural convection boundary layers
[AD-722836] 20 p3346 N71-33684

Analysis of pulsational characteristics of low mass cepheid model to include convection effects
[AD-722836] 21 p3512 N71-35025

Stellar magnetic fields and convective processes
[AD-722836] 23 p3849 N71-37437

Convective motion in Clinean toroidal quadrupole device
[CN-28/A-4] 24 p3993 N71-38485

CONVECTIVE HEAT TRANSFER

Local potential and nonlinear stability in magnetohydrodynamics
[AD-710319] 01 p0104 N71-10300

Convective heat and mass transport over tropical mid-Pacific estimated from satellite cloud photographs
[AD-722836] 02 p0255 N71-11616

Chemical nonequilibrium effects in boundary layer and transport properties in rocket engine nozzles
[RPE-TR-70/3] 02 p0305 N71-12658

Calorimetric and thermocouple pyrometer heat flux measurements in blowdown wind tunnels
[ONERA-NT-159] 02 p0305 N71-12659

Computer program for calculation convective heat transfer coefficients from harmonic temperature oscillations
[NASA-TM-X-2147] 04 p0500 N71-13496

Convective heat transfer measurements in ballistic ranges and free flight apparatus
[NASA-TM-X-65399] 04 p0523 N71-13588

Convective heat transfer in steady uniform air flow between parallel plates, and organ pipe combustion oscillations of premixed gases in variable length combustor
[AD-722836] 05 p0661 N71-14769

Convective heat transfer in rotating thermospheres
[ARC-CP-1115] 06 p0833 N71-15807

Combined conduction, convection, and radiation effects on heat transfer of participating gases in internal flow
[NASA-CR-116127] 06 p0834 N71-15989

Convective heat transfer characteristics of M2 and M2-F2 lifting entry vehicles
[NASA-TM-X-1691] 07 p0970 N71-17131

Vaporization caused by incident boiling in forced convective flow of superheated liquid
[NASA-CR-117046] 09 p1486 N71-20593

Formulation for temperature distribution in laminar flow with radiative and convective heat transfer
[AD-722836] 10 p1663 N71-21506

Non-steady state heat propagation in solid bodies with simultaneous radiant and convective heat flows
[NLL-RTS-6022] 10 p1664 N71-21687

Numerical model of thermal convection for two dimensional laminar, nonlinear fluid, heated nonuniformly
[AD-717670] 11 p1749 N71-22358

Combined free and forced laminar convective heat transfer to nonNewtonian fluids flowing in constant wall temperature vertical tubes and controlling parameter analysis
[AD-722836] 11 p1742 N71-22702

Analysis of temperature distributions in infinite slab with one surface perfectly insulated and other surface exposed to fluid with temperature varying in specified way
[AD-718332] 12 p2010 N71-23252

Investigation of natural convection heat transfer between two isothermal concentric spheres of various diameter ratios from 1.09 to 2.81
[RLO-2214-2] 12 p2011 N71-23906

Natural convective heat transfer between concentric spheres, construction of experimental apparatus for heat transfer and flow visualization
[RLO-2214-1] 12 p2015 N71-24340

Aerodynamic and heating problems of spacecraft entry into Mars and Venus atmospheres
[AD-722836] 13 p2172 N71-26719

Hydrodynamics and gas dynamics of boundary layer flow including mass transfer and convective and radiative heat transfer of bodies in fluids
[AD-720735] 14 p2344 N71-28919

Liquid sodium or sodium potassium cooling system based on convective heat transfer from nuclear fuel elements in swimming pool reactor
[CRA-N-1348] 14 p2204 N71-28448

Thermal design analysis on test/development/forced convection mercury boiler for SNAP 8 reactor
[NASA-CR-72760] 15 p4522 N71-27813

Forced flow heat transfer coefficients for laminar film boiling interface on vertical surface
[NASA-TM-X-67860] 15 p5255 N71-27867

Flight reentry heating instrumentation required for ballistic entry simulation of radiative and convective heating rates
[NASA-TN-D-6265] 16 p2391 N71-28087

Free convection heat and mass transfer along cylindrical bodies
[AD-722836] 16 p2899 N71-30880

Measurement of convective heat transfer rates in conical nozzles and hemispherical afterbody configurations at hypersonic speed
[NASA-TR-D-6433] 16 p2891 N71-30882

Nonaxisymmetric free laminar convection flow from vertical flat plate with uniform surface heat flux
[AD-722836] 16 p2904 N71-30883

Mechanism of boiling and characteristics of heat transfer in boiling of metals
[NASA-TT-F-620] 17 p3859 N71-36888

Conductive and/or convective radiative energy transfer in absorbing-emitting medium
[AD-722836] 18 p3025 N71-31904

Principles of operation, circuits, and construction of thermal flow rate meters for liquid metals
[AD-723540] 19 p3103 N71-32391

Derivation of equations describing heat transfer by radiation and convection from annular film of isopropyl alcohol on cylinder
[AD-723974] 20 p3363 N71-33932

Holographic interferograms of laminar free convection boundary produced by vertical flat plate with isothermal wall-temperature distribution
[AD-724698] 20 p3364 N71-33930

Reduction of radiative and convective heat transfer at stagnation points due to blowing expressed in terms of shock standoff-distance ratio for blunt nosed bodies
[NAL-TR-224] 20 p3364 N71-33930

Mixed convection from sphere at small Reynolds and Grashof numbers and stability of vertical natural convection boundary layers
[AD-722836] 20 p3366 N71-33931

Numerical solution for transient temperature distribution and thermocouple stresses in homogeneous spherical fuel element with variable convective heat transfer at surface
[AD-722836] 20 p3367 N71-33931

Transient heat transfer in thermal entrance region between parallel plates with fully developed laminar velocity profile determined for low Péclet number flows
[AD-722836] 20 p3367 N71-33931

Velocity and temperature distribution of laminar free convection flow in vertical heated channel
[AD-722836] 20 p3368 N71-33931

Hexagonal convection flow in internally heated fluid layers and bifurcation phenomena
[AD-728161] 21 p3331 N71-33119

Finite element method applied to heat transfer problems, and transient two dimensional heat transfer with convection and radiation boundary conditions
[AD-726371] 22 p3607 N71-34043

Natural convection heat transfer from nonisothermal vertical flat plate immersed in temperature stratified media
[AD-727204] 24 p4031 N71-39710

CONVEGENCE

Evaluation of several ENDF/B nucleide cross sections by Monte Carlo techniques
[AL-AEC-MEMO-129153] 01 p0084 N71-10889

Quantitative analysis of adaptive control systems using random search algorithms convergence in continuous time
[RE-3963] 01 p0076 N71-10881

Using Thomas-Pearl-Direct statistical model for reducing convergence of power series solutions
[AD-712287] 02 p0250 N71-11465

Geometric convergence theory for QR, Rayleigh quotient, and power iterations
[AD-712444] 04 p0337 N71-13522

Applications of partial orderings to study of positive definiteness, monotonicity, and convergence of iterative methods for linear systems
[NASA-CR-116134] 06 p0883 N71-15949

Chaos on nonlinear functions and convergence of Gauss-Seidel and Newton-Gauss-Seidel iterations
[NASA-CR-116129] 06 p0884 N71-15950

Convergence and mean square error estimation in solution of boundary value problems for elliptic equations by straight line method
[NASA-TT-F-114572] 06 p0884 N71-15950

SUBJECT INDEX

Slowed boundary layer flow in converging channel
06 p0639 N71-16652

Asymptotic convergence theorems for sequential nonlinear filters
12 p1894 N71-24148

Weak convergence theorem for virtual waiting time queue in heavy traffic
12 p1951 N71-24247

Biz-Galerkin residual convergence in boundary value problems including trigonometric, polynomial, and spline coordinate functions
14 p2284 N71-26276

Variants of secant method for solving nonlinear system of equations comprising algorithms and related convergence theorems
15 p2436 N71-27785

Feasibility of overcoming local convergent nature of continuation methods for nonlinear equations
16 p2623 N71-28575

Existence and extendability of continuous eigenvector branches and application of nonlinear programming algorithms to nonlinear heat generation and radiating problems
16 p2623 N71-28575

Algorithms and FORTRAN coding program permitting efficient convergence and high degree of mass machine interactions in steady state process systems analysis
16 p2566 N71-28791

Convergence of iterative methods applied to large overdetermined linear and nonlinear systems of equations using least squares
18 p2946 N71-31266

Weak convergence theorem for order statistics from strong mixing processes
18 p2947 N71-31313

General convergence result for unconstrained minimization methods
21 p3409 N71-34196

Convergence of Galerkin method for constructing approximate solutions of nonlinear operator equations
21 p3447 N71-34534

Effect of tropical anticyclones on development and position of intertropical convergence zone
21 p3454 N71-34583

Convergence of centers algorithm for solving nonlinear programming problems
22 p3605 N71-35672

Acceleration of convergence of iterative methods for solution of equations including Newton method
22 p3608 N71-35700

Method for calculating convergent modified Wentzel-Kramers-Brillouin expansions
22 p3636 N71-35917

Weakly convergent operators in incomplete tensor product of Hilbert spaces
24 p3949 N71-38174

CONVERGENT NOZZLES
Nozzle lateral spreading effect on drag and performance of two jet airbody configurations with convergent nozzles at Mach 0.6 to 2.2
01 p0115 N71-10276

Acoustic and flow characteristics of subsonic and supersonic jets from convergent nozzles
05 p0664 N71-14993

Mathematical model for ideal fluid jets from convergent nozzles
10 p1541 N71-21139

Computer program for predicting admittances of divergent convergent nozzles and acoustic liners in three dimensional acoustic field
22 p3567 N71-35405

CONVERGENT-DIVERGENT NOZZLES
Transonic equations of motion for convergent-divergent nozzle
01 p0042 N71-10444

Method of finite differences used for supersonic nozzle design
09 p1316 N71-19709

Numerical solution of quasi-conservative hyperbolic systems applied to case of converging-diverging cylindrical shock waves
12 p1950 N71-23740

Representative cooling system for rocket combustion chamber using coolant tubes in convergent-divergent nozzle
12 p1950 N71-23740

Two phase critical discharge of high pressure liquid through convergent-divergent nozzle exhibiting mass behavior as water
12 p1991 N71-23968

Time-dependent calculation method for transonic flow in nozzle with or without central body
16 p2639 N71-28819

CONVERGENCE
Intelligence, speed, and conversational ability of children
08 p1156 N71-19123

CONVERSION
Congressional testimony of nationally representative groups regarding U.S. conversion to metric
19 p3196 N71-32352

Investigation of attitudes toward and impact of U.S. conversion to metric system
19 p3197 N71-32353

Impact of U.S. conversion to metric system units of measurement on current engineering standards
19 p3106 N71-32396

Conversion of US scientific and technical resources from defense and aerospace to civilian objectives
20 p3371 N71-33825

CONVERSION TABLES
Conversion of data from three serum cholinesterase assay methods
01 p0011 N71-10449

Conversion tables for Beckman CO2 analyzers
01 p0055 N71-10714

Human factors engineering manual including mathematical formulae, nomographs, conversion tables, units of measurement, and nomenclatures
14 p2209 N71-25943

CONVERTAPLANES
U/VISTOL AIRCRAFT
Photoelectric recorder with electric-optical converter for recording ultrashort light pulses
13 p2079 N71-24424

CONVEXITY
Uniqueness theorems for nonlinear approximations in strictly convex Banach spaces
03 p0401 N71-13269

Perturbation analysis of diffraction by rippled convex surface
06 p0815 N71-16288

Hyperbolic laminar boundary layer growth over concave and convex surfaces
09 p1374 N71-19836

CONVEYORS
Pulsed reactor potentialities for neutron activation analysis, using high speed specimen conveyors
14 p2318 N71-26763

CONVOLUTION INTEGRALS
Convolutional coding techniques including constructing inverse, algorithms, and code comparing for sequential decoding
03 p0343 N71-12488

Applying convolutional encoding to error control and data compression in deep space communication
07 p0993 N71-17639

Minimum convolutions and Green function in dynamic programming theory
10 p1594 N71-21662

Statistical properties of solution to deconvolution problem
10 p1595 N71-21682

Performance tests of convolutional decoder systems for high data rate telemetry links
15 p2383 N71-27786

Comparison of concatenated and sequential decoding systems and convolutional code structural properties
19 p3063 N71-32505

Convolutional Reed-Wigner signals detected by measuring instruments with Gaussian resolution functions
21 p3474 N71-34740

Convolutional coding, sequential coding, subband coding, and inverse systems for data protection
22 p3555 N71-35322

CONVOLUTIONS [MATHEMATICS]
U. CONVOLUTION INTEGRALS
COOLANTS
NT ENGINE COOLANTS
NT ORGANIC COOLANTS
Experimental pressure loss determination in 37 rod bundle of tubes with 6 integral spiral ribs per rod as spacers for economic design of nuclear fuel elements
02 p0263 N71-11410

Coolant flowmeters for measuring flow distribution in test reactor core
02 p0265 N71-11770

Heat transfer in simulated BWR fuel bundle cooled by spray under loss-of-coolant conditions
04 p0545 N71-13566

Response of simulated BWR fuel bundle cooled by flooding under loss of coolant conditions
04 p0548 N71-13677

RELAP3 computer program for reactor blowdown analysis including pump failure, power transients, or loss of coolant
04 p0551 N71-13954

Accident evaluation studies for water cooled reactors postulating loss of coolant
04 p0551 N71-13956

Assessment of safety injection strategies during loss of coolant accidents - conference
04 p0551 N71-13962

Reactor primary coolant system - rupture study on water cooled reactors
04 p0555 N71-14047

Beach type, bottom flooding, coolant injection tests for heat transfer mechanism determination in reactor cores
06 p0899 N71-16692

EBR-2 codes for processing reactivity data at full and reduced coolant flows using thermal expansion corrections for control rods
09 p1418 N71-19904

COOLING

Explosive disassembly of fast spectrum nuclear reactors, following coolant loss and gravity composition of fuel
10 p1604 N71-21369

CORRA, computer program for coolant boiling in rod arrays in Sici-1985 computer
14 p2294 N71-26636

TOMOF - code for describing thermohydrodynamics of two-fluid mixture in studies of boiling and ejection of coolant from reactor channel due to direct contact with hot molten fuel
16 p2632 N71-28390

Control of radioactive waste in coolant water from nuclear facilities
17 p2785 N71-30141

Pressurized water and boiling water reactor coolant blowdown simulation for reactor safety including temperature and pressure measurements
18 p2960 N71-30647

Effects of fast neutron irradiation on Chromel/Alumel thermocouples for FFTF coolant measurement systems
22 p3623 N71-35817

Computer program for calculating transient heat transfer performance of reactor coolant channel during accidental power excursions
22 p3627 N71-35843

COOLERS
Dual patch multi-element radiant cooler for earth oriented spacecraft
01 p0133 N71-10606

Heat transfer and pressure drop data on standard oil coolers for turbine installations
16 p2690 N71-28137

COOLING
NT AIR COOLING
NT EVAPORATIVE COOLING
NT FILM COOLING
NT GAS COOLING
NT LIQUID COOLING
NT QUENCHING [COOLING]
NT RADIANT COOLING
NT REGENERATIVE COOLING
NT SODIUM COOLING
NT SUPERCOOLING
NT SURFACE COOLING
NT SWEAT COOLING
NT THERMOELECTRIC COOLING
Preliminary results of BWR-FLECHT internally pressurized, Zircaloy-clad bundle, spray cooling test
01 p0086 N71-10599

Cladding temperature and material effects on emergency core cooling system in boiling water reactor
01 p0086 N71-10645

Microwave power receiving antenna solving heat dissipation problems by construction of elements as heat pipe devices
04 p0308 N71-13406

Numerical determination of thermal conductivity from transient cooling data
06 p0958 N71-15851

Magnetic induction concentric cylinder magnetohydrodynamic generator with cryogenic cooling
07 p1083 N71-17840

Temperature anomaly of July 1968 in Rumania
12 p1956 N71-23962

Ultrasonic vibration effects on cooldown rate of bodies in liquid nitrogen and helium
12 p1968 N71-24154

Climatic cooling effects on earth surface
14 p2251 N71-26437

Dissipative voltage regulator system for minimizing heat dissipation
14 p2251 N71-26437

INHA-Case-GSC-10091-1
Inhibition of scintillations in liquid helium by temperature reduction
15 p2487 N71-27834

Design criteria for high efficiency, high gain, high power klystron final amplifier stage operating in 4.4 to 5.0 GHz range
16 p2567 N71-28176

Heat sink capabilities of Jet-A fuel - heat transfer and coking studies
18 p3027 N71-31482

Cooling intrinsically stable superconducting magnets with supercritical helium tubes adjacent to magnet coils
21 p3465 N71-34665

Cooling of simulated reactor fuel element by heat transfer from element to boiling water
23 p3796 N71-37064

Advanced cooling concepts for gas producer axial flow turbine of small gas turbine engine
24 p4001 N71-38339

Ablation cooling in rocket engine with combustion chamber liner and nozzle constructed of silica phenolic ablative material
24 p4029 N71-38749

Solutions for transient temperature distribution in one-dimensional solid with linear heat loss
24 p4029 N71-38751

COOLING FINNS

COOLING FINNS

Calculation of radiative heat transfer and optimization of spacecraft fin-tube radiator with and without coatings

03 p0458 N71-13260

Heat transfer coefficient determination in helical-fin fins for thermal design of nuclear fuel elements [NLL-WINDSCALE-TRANS-397-1989.97]

22 p3426 N71-35836

COOLING SYSTEMS

Thermodynamic tests of helium cooled reactor fuel element loop with natural circulation under high pressures

[NASA-TT-F-13397] 01 p0087 N71-10875

Liquid metal cooling of turbine blades with thermopneumatic circulation or phase transformation

[ONERA-TT-672] 02 p0229 N71-11557

Optimization of plane fin-tube radiators for spacecraft nuclear power supplies discussing cooling circuits

03 p0458 N71-13259

Organic cooled, heavy-water moderated WR-1 research reactor capable of low pressure with high temperature in primary system and very low radiation fields near primary piping [AECL-3523]

04 p0547 N71-13640

Effects of random pressure and temperature pulsations in nuclear reactor coolant systems

[EURFNR-784] 04 p0561 N71-14082

Automatic thermal switch for improving efficiency of cooling gases below 40 K

[NASA-CASE-XNP-03796] 05 p0735 N71-15467

Differential thermopile for measuring cooling water temperature rise

[NASA-CASE-XAC-00812] 05 p0689 N71-15598

Semicalc blowdowns and emergency core cooling project test report

07 p1060 N71-17190

Experimental analysis of emergency core cooling reactor systems

[IN-1348] 07 p1060 N71-17207

Prestartup thawing of lithium coolant in nuclear reactor for space powerplant

[NASA-TM-X-2177] 07 p1064 N71-17369

Advanced cooling systems and heat resistant materials for turbine blades of high temperature aeronautical gas turbine engines

[AGARD-CP-73-71] 07 p1099 N71-17372

Effectiveness of turbine cooling systems for high temperature turbines

[NASA-TM-X-46702] 07 p1100 N71-17385

Impact cooling method for turbine rotor blades

07 p1129 N71-17397

Heat transfer in liquid metal cooled gas turbine blades

07 p1129 N71-17398

Design considerations of reactor containment spray systems, also protective coating for these containment structures

[ORNL-TM-2412-PT-5] 08 p1220 N71-18304

Boiling water reactor accident radioactivity and containment spray systems design

[ORNL-TM-2412-PT-6] 08 p1239 N71-18711

Superconductivity cool cooling of cryogenic system in full scale thermoelectric power plants

[ORNL-TM-3097] 08 p1242 N71-19236

Submerged condenser cooling systems for electronic devices and components by process of boiling and condensation in liquid-filled enclosures

[TR-29077-73] 08 p1306 N71-19333

Development of improved turbine cooling processes and facilities for conducting turbine cooling research

09 p1457 N71-19454

Semicalc blowdowns and emergency core cooling project tests for reactor safety

[IN-1404] 09 p1419 N71-20033

Single stage turbine operation with various stator cooling techniques and effects on stator, stage, and rotor efficiencies

[NASA-TM-X-52964] 09 p1460 N71-20420

Zircaloy charring failure modes in reactor coolant channels

[ORNL-TM-3108] 10 p1601 N71-20643

Evaluation of idealized paramagnetic system for magnetic cooling

[NASA-TM-X-52963] 10 p1664 N71-20943

Cooling system and thermal balance data for long duration operation of space station simulator

10 p1568 N71-20974

Pressure loss effect on cold production in two stage gas refrigerating machinery

10 p1663 N71-21505

Research to improve reliability of reactor piping

[GEAP-16207-22] 11 p1793 N71-22273

Electric power system with circulatory liquid coolant cooling system

[NASA-CASE-MPS-14114-2] 13 p2056 N71-24087

Feasibility of cryogenic heat pipe for cooling isotopic spacecraft power supply cycle

13 p2186 N71-25113

Flow blockage effects on heat transfer in bottom cooling system of fuel assembly

[WCAP-5533] 13 p2187 N71-25357

Accident analysis for pressurized and boiling water nuclear steam supply systems loss of coolant situations

[BML-1897] 13 p2122 N71-25441

Analysis of heat exchange processes of built-in heat exchangers by replacing actual values of gas discharge and temperature with average value of flow in one direction

14 p2352 N71-25739

Analysis of first stage turbine stator vane and rotor blade cooling designs for application in highspeed aircraft

[NASA-TM-X-1782] 14 p2196 N71-26355

Feasibility of superfluid helium use in tubular cooling systems with particular application to superconducting helix waveguides

[NP-18631] 14 p2264 N71-26439

Liquid sodium or sodium potassium cooling system based on convective heat transfer from nuclear fuel elements in swimming pool reactors

[CEA-N-1348] 14 p2294 N71-26618

Portable cryogenic cooling system design including turbine pump, cooling chamber, and stonizer

[NASA-CASE-NPO-10467] 14 p2298 N71-26654

Information concerning static seals commonly used in primary cooling systems of water cooled reactors

[ORNL-TM-3306] 15 p2448 N71-27340

Cooling, cooling, construction, and structural characteristics of jet fuel-cooled plug nozzle for afterburning turbojet

[NASA-TM-X-2304] 16 p2671 N71-28128

Development and characteristics of natural circulation radiator for use with nuclear power plants installed in lunar space stations

[NASA-CASE-XHQ-03637] 16 p2693 N71-29046

Development and characteristics of cooling system to maintain temperature of rack mounted electronic modules

[NASA-CASE-MSC-12389] 16 p2693 N71-29052

Development of method for cooling high temperature wall members with cooling medium having high heat absorption capability

[NASA-CASE-HQN-00938] 16 p2693 N71-29053

Apparatus for liquid spray cooling of turbine blades

[NASA-CASE-XLE-00027] 16 p2694 N71-29152

Comparison of water, convective air, and reversed air flow cooled suits for body temperature thermoregulation in high temperature environments

[FFRC-1307] 17 p2712 N71-30127

Development and characteristics of instruments for inductive measurement of liquid metal levels in cooling systems

[RD/N/N-1726] 18 p2921 N71-30427

Electric power plant cooling tower effluent effect on urban atmospheric composition

[FB-197562] 18 p2920 N71-31487

Fatigue testing of carbon and stainless steel boiling water reactor cooling system pipes including failure probability and fracture mechanics analyses

[GEAP-10207-23] 19 p3134 N71-31711

Candidate systems for emergency heat removal in LMFBR

[BAW-1351] 19 p3135 N71-31993

FORTRAN computer code for transient flow data analysis and critical cooling deficiency prediction in boiling system of reactor core

[GEAP-10221-5] 19 p3192 N71-32117

Computer code for calculating thermal response of nuclear reactor core in coolant loss accident

[IN-1445] 19 p3137 N71-32120

Design and specifications of gas refrigerator system based on thermal driver principle

19 p3193 N71-32552

Progress in development of fuel elements, fuels, cooling systems, core monitoring systems, and core design for fast breeder reactors

[EURFNR-824] 19 p3141 N71-32772

Analysis of phenomena occurring in exhaust gas spray cooler utilizing liquid injection, and mathematical model of optimum cooler

[AD-724687] 20 p3338 N71-32991

Graphic flow simulation and motion picture flow representation of reactor blowdown calculations

[CONF-710302-4] 20 p3251 N71-33556

Analysis of transpiration cooling system parameters for nose tip under supersonic conditions

[NC-DC-713922] 21 p3411 N71-34269

Site selection and cooling system requirements for FWR power plants in arid regions

[EES-35] 21 p3530 N71-35158

Analysis of wall temperatures in rocket engine cooling system using D-shaped copper and stainless steel tubes for reduction of tube-wall crest temperatures

[NASA-TN-D-6422] 21 p3531 N71-35162

Operating properties of liquid hydrogen bubble chamber and cooling system

[BSC-T-71-1] 22 p3635 N71-35908

Flow and heat transfer technology resulting from NASA turbine cooling program

[NASA-TM-X-2384] 22 p3663 N71-36120

Metallographic evaluation of simulated BWR emergency core cooling tests

[IN-1453] 23 p3798 N71-37076

Evaluation of cryogenic refrigeration systems for space applications

[NASA-CR-115192] 23 p3802 N71-37061

Performance tests and specifications for space storable regenerative cooling system with liquid oxygen and methane propellants

[NASA-CR-72704] 23 p3866 N71-37508

Effect of nuclear radiation on aluminum alloys used in water and steam-water cooling systems of MR reactor loops

[LB/G-3006] 24 p3934 N71-39067

Emergency cooling and radioactive waste disposal requirements for fusion reactors

[CONF-710607-134] 24 p3961 N71-39237

Heat exchange, theoretical considerations on cooling, and dependence of heat exchange on state of two-phase mixtures in post-burnout regime

[RT/ENG-75027] 24 p4023 N71-39700

Regenerative cooling system design for rocket engines

[NASA-CR-123117] 24 p4023 N71-39701

COORDINATE SYSTEMS

U COORDINATES

COORDINATE TRANSFORMATIONS

Examination of simple coordinate transformations in Z-plane and W-plane for root locus analysis of sampled data systems

[NASA-TM-X-65131] 04 p0339 N71-41044

Transformation of differential equations in linear theory

[NASA-TN-D-7036] 06 p0949 N71-44803

Ritz-Galerkin residual convergence in boundary value problems including trigonometric, polynomial, and spline coordinate functions

14 p2284 N71-26276

Classifications as coordinate transformations and class vector-system selection

[NLL-TRANS-2670-79022.81] 19 p3123 N71-32271

Transformation formulas in solid spherical harmonics for calculating forces between two homogeneous hemispheres with examples involving coordinate translation and rotation

[NASA-CR-115141] 22 p3606 N71-33828

Transformation properties of coordinates in isoviscous power spherical harmonic expansions

[NASA-CR-122286] 23 p3781 N71-39800

COORDINATES

NT ASTRONOMICAL COORDINATES

NT CARTESIAN COORDINATES

NT GEOCENTRIC COORDINATES

NT GEODETIC COORDINATES

NT HYPERBOLIC COORDINATES

NT LAGRANGE COORDINATES

NT POLAR COORDINATES

FORTRAN program for computing coordinates of circular arc angle and tandem turbomachinery blade sections on plane

[NASA-TN-D-6020] 01 p0001 N71-10401

Auroral oval plotter and nomogram for determining corrected geomagnetic local time, latitude, and longitude for high latitudes in Northern Hemisphere

[AD-713170] 05 p0764 N71-44857

Riemann manifold tensor analysis in general coordinates using FL1

[ESRO-TM-151-ESTEC] 07 p0997 N71-47105

Space coordinate system and clock rates specified operationally to separate coordinate and physical effects in arbitrary gravitational field

07 p1021 N71-17782

Calculation of streamline coordinates for three dimensional turbulent boundary layer in vanishing diffusor

[ARC/RM-3646] 08 p1141 N71-18408

Application of cartographic grid network of meridians for solution of meteorological and hydrological plotting of fields in polar areas

[AD-720149] 16 p2508 N71-30422

Grid choice in low beta fluid computations for high magnetic stress compared to plasma pressure

[MATT-522] 17 p2812 N71-29748

Precise determination of particle coordinates in proportional multiwire chambers with potentiometric readout

[RSDR-P13-5628] 18 p2970 N71-30401

Mathematical structure of vertical and oblique cosmographic perspectives for spaceborne global graph intersection

[NASA-TT-F-13761] 19 p3103 N71-32519

Automatic compilation of navigation coordinate using analog and digital computers

[AD-724603] 22 p3618 N71-35702

Field displacement graphical processing problems and techniques for calculating partial derivatives of displacements using moire and coordinate grid method

[NLL-M-21006-1828.4P] 24 p3950 N71-39800

COORDINATION

Coordination compounds of transition metals

[AD-712795] 03 p0333 N71-13377

Planning and coordination of space environment simulation test programs for Azar and Dial satellites

03 p0338 N71-12770

SUBJECT INDEX

- Coordination of human voluntary movements during space flights
[JPS-31499] 05 p0633 N71-14623
- COPYLOTS**
U AIRCRAFT PILOTS
COPYLIMERIZATION
Copolymerization of esters of bis allyloxymethyl phosphonic acid with methylmethacrylates
[AD-713459] 05 p0709 N71-13270
Kinetics of copolymerization reactions of ethylene and vinyl acetate at low pressure determined by sequential sampling
05 p0641 N71-15697
Radiation stability of MRC copolymer 250 and forming dielectric quality films
[AD-713417] 08 p1221 N71-18551
Kinetics of free radical initiated copolymerization of 1-vinyl-3,5-dimethyl adamantane and vinyl acetate as function of glass transition temperature
21 p3388 N71-34106
- COPYLYMERS**
NT VITON
Method for producing alternating ether-alkene copolymers with stable properties when exposed to elevated temperatures and UV radiation
[NASA-CASE-XMF-02584] 10 p1512 N71-20905
Effects of quantity and placement of copolymer units within polymeric chain on crystallization phenomena in polymers
[AD-716824] 10 p1590 N71-21524
Preparation of diacyonocetylene and vinylidene monomers using organic compounds
[NASA-CASE-XMF-03250] 12 p1870 N71-23500
Thermal and solubility properties of four ordered aliphatic imide-oxazoline copolymers to obtain strong films and fibers
[AD-720657] 14 p2279 N71-26220
Mathematical models for studying kinetics of aqueous emulsion copolymer system
14 p2215 N71-26580
Infrared spectra analysis of latex copolymers cross-linking reactions in relation to molecular weight and number of methacrylate groups
[DILL-RTS-6218] 16 p2559 N71-29055
- COPPER**
NT COPPER ISOTOPES
X ray excited LMM Auger spectra of copper, iron, and nickel
[NASA-TM-X-45381] 01 p0097 N71-10584
Fatigue crack propagation in copper and copper-aluminum single crystals
[AD-711678] 01 p0113 N71-10954
Heat aging evaluation of common coated copper conductors
[RM-6882] 02 p0340 N71-11390
Rate of hydrogen absorption by copper
[PB-190937] 02 p0243 N71-11697
Effect of trace elements on precipitation in Al-Cu alloys
[UCRL-19137] 04 p0529 N71-14007
Critical experiments of copper-reflected fast assembly with time dependent code
[AE-399] 04 p0589 N71-14316
Grain structure of high purity copper melts undisturbed before nucleation
[RIFT-374] 03 p0702 N71-15068
K sub L and K sub S resonance amplitude in copper at 2.5 GeV/c CP non-invariance
[HEVTS-184] 03 p0746 N71-15236
High temperature soft soldering system using microfil nickel coating for zinc solder spreading on copper, copper alloy, and steel substrates
[TPB-29] 06 p0862 N71-15805
Development of method for etching copper
[NASA-CASE-XGB-06306] 06 p0871 N71-16044
Wavelengths and energy levels of Cu/II for far ultraviolet wavelength standards
[LA-4080] 06 p0985 N71-16369
Correlation of dislocation structure with microstrain density in copper single crystals
[NYO-4073-2] 07 p1093 N71-17456
Piezoelectric dislocation motion in copper crystals
[UCRL-19625] 07 p1093 N71-17460
High voltage electron microscopy study of slip band growth in radiation hardened copper crystals
[UCRL-19601] 07 p1095 N71-17962
Velocity measurements of ultrasonic surface waves on single crystal copper using light-sound interaction techniques
[AD-715633] 08 p1279 N71-18683
Pulsed gas welding Kovar ribbons to copper conductors printed wiring boards
[NASA-TN-D-62362] 08 p1207 N71-18737
Effects of surfaces and environment on nucleation and growth of fatigue cracks in copper
[NASA-CR-114838] 08 p1280 N71-19031
Three-crystal spectrometer X ray line width measurements of copper, silver, and molybdenum
09 p1287 N71-19483
Chemical composition of copper clad laminates and need for printed circuit lamination, impregnation, and protection
10 p1511 N71-20684

- Critical aspect ratios of copper matrix and tungsten fibers in reinforced composites from stress-rupture and tension tests
[NASA-TM-X-52993] 10 p1589 N71-21228
Anodic potential fluctuations observed in copper dissolution in different electrolytes
[UCRL-19618] 10 p1566 N71-21365
Rheometric measurement of copper, aluminum, and stainless steel composites at cryogenic temperatures
11 p1783 N71-23045
Tritium solubility and diffusivity in cold-worked and annealed copper at 300 C
[MLM-1734] 12 p1936 N71-23137
Impact properties determined for pure copper, copper-aluminum alloy, and superalloy metal matrix composites reinforced with tungsten fibers
[NASA-TM-X-67810] 12 p1945 N71-23950
Designing and rates of evolution for copper wires in ultrahigh vacuum
13 p2094 N71-24921
Use of copper and silver as interconnecting materials in superconducting magnets
[MIT-7500-13] 13 p2127 N71-25518
Kinetic process of mutual diffusion between titanium with copper and other metals serving as galvanic coatings
[TT-75-30804] 14 p2269 N71-25646
Interdiffusion of titanium with elements forming continuous series of solid solutions and elements with limited solubility in titanium/nickel, copper, rhodium, and tungsten
[DMDC-5064] 14 p2270 N71-25687
Volume and grain boundary diffusion of tin and antimony into copper
[TT-75-57065] 14 p2272 N71-25820
Method of plating copper on aluminum to permit conventional soldering of structural aluminum bodies
[NASA-CASE-XLA-00946-1] 14 p2273 N71-25903
Effect of oxidation degree on copper emittance for application to radiation shields or multifoil insulation systems at 700 to 1400 F
14 p2274 N71-26314
Influence of this epitaxial surface film on plastic deformation of copper single crystals
14 p2326 N71-26349
High pressure formation of solid-liquid phase line in copper
14 p2328 N71-26391
Construction and characteristics of adiabatic, autothermal differential calorimeter for investigation of properties of temperature deformed copper specimens
14 p2275 N71-26523
Mobility of edge dislocations in pure copper single crystals measured as function of stress at temperatures from 66 to 373 K
14 p2330 N71-26619
Neutron cross section calculations for Cu-63, Au-197, Th-232, Th-232, and U-238 using Hauser-Feshbach statistical mechanics
[AABCTM-342] 15 p2459 N71-26948
Microdynamic slip initiation and stress-strain flow in tungsten and copper
15 p2424 N71-27403
De polycrystalline determination of Cu and Mo in Zr alloys without preliminary separation
[RT/CHI-70/14] 15 p2491 N71-27913
Optimum thickness of copper single crystal neutron monochromators determined by crystal mosaic spread
[PFE-4] 16 p3642 N71-28028
Homo-epitaxial crystallization in copper electrodeposition
16 p3609 N71-28285
Fretting corrosion of stainless steel-copper and Zn-copper in 2% NaCl at ambient temperature
[RT/DNG/70/14] 16 p3610 N71-28450
Radiation damage by electron irradiation in copper
[COO-1800-13] 16 p3612 N71-28624
Spectral reflectance of neutrons by distorted copper crystal in monochromator
16 p2596 N71-28768
Plastic deformation in microtomed thin films of copper and aluminum single crystals
16 p3646 N71-28776
Electron irradiation effects on thermal conversion of intermetallics in copper
[COO-1800-15] 17 p2760 N71-29383
Determining fast and thermal neutron fluxes by copper and indium foil activation analysis
[RFP-1464] 17 p2754 N71-29331
Slip band growth in prestrained copper crystals studied by transmission electron microscopy
[UCRL-28072] 17 p2815 N71-29738
Microstrain analysis of edge dislocation effects of strain hardening on copper single crystal initiation
17 p2815 N71-29808
Computerized simulation of point defects and dislocations in copper
17 p2818 N71-29944
Fracture characteristics of polycrystalline copper explosively loaded by two different methods
[AD-723395] 17 p2767 N71-30251
Inequity strain effects on copper diffusion in single crystal copper
18 p2997 N71-31323

COPPER ALLOYS

- Krypton and helium bubble migration on dislocations in copper foil, and measurement of root mean square random migration distances during isothermal annealing
[RD/B/N-1838] 19 p3146 N71-31964
Gaseous hydrogen embrittlement in Inconel 718, Inconel 625, AISI 321 stainless steel, Ti-5Al-25Sn ELI, and OFHC copper
[NASA-CR-119917] 19 p3116 N71-32489
Reversed creep tests on chemical lead, aluminum, and copper and creep deformation behavior under repeated stress reversals
[NASA-CR-72540] 20 p3357 N71-33204
Differential technique used to determine third and fourth order elastic constants of copper and nickel
20 p3286 N71-33932
Electrical resistivity of Al and Cu during rapid heating to melting point and fracture in investigation of metallic melting mechanisms
[NLL-M-21008-5820.4F] 21 p3441 N71-34489
Analysis of chemical and electrolytic processes for deposition of copper layers on stainless steel surfaces
[NLL-LT-746-751-19022.401] 22 p3589 N71-35561
Interpretation of Hall coefficient of pure copper, silver, and some other alloys based on microscopical Fermi surface model
[NRC-TT-1476] 22 p3592 N71-35581
Technical-economic data for copper and aluminum conductors and superconductors for high field magnets
[LNF-70/19] 22 p3657 N71-36802
Nickel and copper substructural dislocation angle dependencies on deformation, loading, and temperature
[NLL-LT-746-751-19022.401] 22 p3659 N71-36891
Analysis of true stress variation as function of degree of deformation based on tensile tests of aluminum, copper, and unalloyed steels with varying carbon contents
[RAE-LIB-TRANS-1587] 22 p3688 N71-36306
Comparison of bubble method and cast measurements of Al and Cu activities in molten Al-Cu alloys relative to Al₂O₃
[NLL-RTS-6273] 23 p3774 N71-36899
Stable surface treatments for 304 stainless steel, copper, and aluminum alloy contact with liquids
[NASA-CR-72875] 23 p3775 N71-36908
Electrochemical copper deposition at high current densities
[NLL-RTS-5647] 24 p3961 N71-38117
Neutron activation technique for determining solubility of copper in sodium
[RD/B/N-1981] 24 p3973 N71-38347
- COPPER ALLOYS**
NT BRASSES
NT BRONZES
NT MANGANIN [TRADEMARK]
Heat treatment effects on discontinuous yielding of aluminum-copper alloys
[AD-710317] 01 p0066 N71-10230
Fatigue crack propagation in copper and copper-aluminum single crystals
[AD-711678] 01 p0113 N71-10954
Auger electron spectroscopy study of surface segregation in copper-aluminum alloys
[NASA-TN-D-6095] 02 p0241 N71-11438
Thermal emittance effect on diffusion process in copper-nickel alloys
[TT-75-57061] 03 p0746 N71-15236
Steady state diffusion in copper rich Cu-Zn-Mn system
[COO-1434-36] 03 p0785 N71-15444
Copper alloy forced with tungsten filaments
[AD-714753] 06 p0879 N71-16889
Annealing behavior of Cu-based solid solutions and CuAl₃
[COO-1431-9] 06 p0873 N71-16390
Chemical composition of copper-aluminum binary alloys using X ray fluorescence analysis
[AD-713936] 06 p0873 N71-16437
Cluster and moment effects on paramagnetic to ferromagnetic transition in Cu-Ni alloys
[UCRL-72587-REV-1] 07 p1078 N71-17776
Internal magnetic fields of Cu in relation to Au, Cu, and Ag-Cu alloys determined by nuclear orientation of Cu-60
[COO-1580-47] 07 p1079 N71-17943
Low temperature magnetization of dilute copper magnetic alloys
[UCSD-34-P-143-33] 08 p1216 N71-18942
Phase diagram-based eutectic degradation of copper-aluminum system
10 p1570 N71-21218
Copper-bearing alloy replacement with aluminum alloys in diffusion dislocation photo for sea water corrosion resistance
[ORNL-TR-3413] 10 p1581 N71-31434
Potassium perchlorate electrolyte for electrodeposition of copper nickel coatings
[NLL-TRANS-746-800-76022.404] 10 p1582 N71-31485
X ray diffraction measurement of crystal composition profile, structure, and substitution in Al₂O₃

- and gold electroplated diffusion zones of copper/111/
single crystal 10 p1583 N71-21588
- Diffusion-viscous flow contribution to high tem-
perature creep of copper aluminum alloys
[NLL-CE-TRANS-5438-9022.69/1] 10 p1584 N71-21603
- Trace element influence on aluminum-copper alloy
quenching microstructure and precipitation hardening
12 p1938 N71-23718
- Corrosion characteristics and response to cathodic
protection of copper alloys in quiescent sea water
[AD-718310] 12 p1938 N71-23793
- Steady state diffusion in copper-manganese-cin-
alloys and feasibility of calculating atomic mobilities
13 p2094 N71-24917
- Kondo state as function of magnetic field and tem-
peratures in Cu-Fe alloys
[AD-719862] 13 p2126 N71-25151
- Structure and mechanical properties of ordered al-
loys (NiAlMo) and CuPt systems/
[ORO-3908-2] 13 p2153 N71-25504
- Phase diagrams and mutual thermal diffusion in
copper-gold system 13 p2094 N71-24917
- Investigation of interdiffusion in ordered alloys with
crystal lattices of Cu₃Al and CuAu type
[TT-70-59113] 14 p2269 N71-25659
- Pore development, plastic deformation, and diffu-
sion coefficients in nickel titanium and copper tita-
nium alloys 14 p2270 N71-25672
- Ionic diffusion and spectroscopic analysis of copper
alloy dendrite etching by electric discharge
[TT-70-57063] 14 p2324 N71-25706
- Characteristics of aluminum-copper alloys deter-
mined by electron microbeam probe X ray analysis of
emission spectra 14 p2275 N71-26450
- Quenching transformations in binary zirconium
copper alloys and ternary zirconium copper molyb-
denum alloys 15 p2422 N71-27130
- Precipitate hardening of CuCo and CuCo₂ alloys
and particle size and temperature effects on creep
properties and edge dislocations 15 p2425 N71-27652
- Plastic deformation in single crystals of zinc cad-
mium and copper aluminum alloy systems 15 p2508 N71-27682
- Zirconium oxidation in carbon dioxide atmospheres
above 500 C and corrosion prevention by copper alloying
to prevent oxygen dissolving into metal
[CEA-CONF-1728] 16 p2611 N71-28504
- Effects of rolling temperature and titanium content
on creep, hardness, and microstructure of zinc-titan-
ium and zinc-copper-titanium alloys 17 p2761 N71-29275
- Presence of magnetic moments in nickel copper al-
loys containing up to 70 per cent copper 18 p2965 N71-31306
- Low temperature effects on electrical resistivity of
copper aluminum alloys with trace amounts of iron
19 p3115 N71-32376
- Measurement of physical properties in phase trans-
formation of Cu-Ni-Zn alloys 19 p3116 N71-32431
- Development and characteristics of high temper-
ature soldering system for use with copper, copper al-
loys, and low carbon steel 20 p3277 N71-32849
- Auger emission spectroscopy, low energy electron
diffraction, sputtering studies, and adhesion and fric-
tion experiments on single crystals of Cu-Sn, Cu-Al,
and Cu-P alloys 20 p3284 N71-33248
- Martensitic transformation occurring in copper-iron
alloy during tensile testing with magnetic susceptibility
measurement 21 p3430 N71-34407
- Saturation and forced volume magnetostriiction of
single crystal nickel and copper-nickel alloys 21 p3441 N71-34400
- Influence of group B metals on electrical resistivity,
Hall effect, and thermophysical properties of
polycrystalline copper and silver alloys 22 p3592 N71-35582
- Development of techniques for homogeneity studies
of gold-silver and gold-copper alloys for standard
reference material classification 22 p3594 N71-35594
- COPPER CHLORIDES**
- Curie-point anomaly in linear thermal expansion
coefficient of copper potassium chloride single crystal
20 p3367 N71-35791
- COPPER COMPOUNDS**
- NT COPPER CHLORIDES
- NT COPPER OXIDES
- NT COPPER SULFIDES
- Investigating kinetics of crystal growth of copper
compounds in magnetic and electric fields
[AD-704354] 03 p0448 N71-12755
- Thermal, structural, and magnetic studies of nickel,
copper, and rare earth compounds
[NYO-3454-33] 04 p0528 N71-19992
- Spin interactions in copper compounds
[AD-713133] 05 p0756 N71-14517
- Gallium arsenide solar cell preparation by surface
deposition of cuprous iodide on thin a-type
polycrystalline layers and heating in iodine vapor
[NASA-CASE-XNP-01960] 11 p1727 N71-23027
- Copper sulfide-cadmium sulfide thin film solar cell
for space application 15 p2369 N71-27678
- This film Cu₂S-CdS solar cells thermally cycled for
10,050 cycles under simulated orbital conditions
[NASA-TM-X-67847] 15 p2369 N71-27696
- Production of aminoacetone nitrile metal chains of
copper, zinc, nickel, and cobalt and catalytic action of
metal chains in Sorbitol and glycerine oxidation
[TT-70-57111] 17 p2716 N71-30212
- Octahedral and rod shaped crystals of semiconduc-
tor ferromagnetic chalcogenide spinel copper cadmi-
um chromoselenides - energy converting materials
[AD-722785] 18 p2999 N71-31458
- Refinement of X ray data on azurite using Los
Alamos Crystal Structure Least Square program
GENLES [PKNC-145] 21 p3499 N71-34927
- COPPER ISOTOPES**
- Nuclei Cu-61, Cu-64, Ga-67, and Ga-68 studies with
 β reaction 07 p1077 N71-17595
- Perturbed angular correlations of 596-42 keV
cascade in Cu-62 measured in external and internal
magnetic fields for liquid and metallic sources of Zn-
62 [INF-734] 16 p2643 N71-28084
- COPPER OXIDES**
- Barium-copper oxide/canister barium vapor release
system for geomagnetospheric measurements
[NASA-CR-1739] 18 p2888 N71-31424
- COPPER SULFIDES**
- Coulometer titration and thermodynamic properties
of copper sulfides for solar cells [BSRO-CR-14] 03 p0318 N71-12269
- Optical transmission characteristics of copper sul-
fide barriers formed on cadmium sulfide films
[NASA-TM-X-2143] 03 p0439 N71-12572
- Photovoltaic properties of Cu₂S-CdS heterojunc-
tions 09 p1361 N71-19405
- Open circuit and bias degradation tests in copper
and cadmium sulfide thin film solar cells
[NASA-TN-D-6362] 13 p2031 N71-25394
- Limiting current and concentration profile in stag-
nant diffusion cell for copper sulfate solution
[UCRL-18597-REBVI] 21 p3387 N71-34099
- CORDERITE**
- Sintering of reactive MgAl₂O₄ spinel ceramic,
devitrification, and improved corderite compositions
[AD-720383] 14 p2278 N71-26015
- CORDEX**
- COLLOIDAL PROPELLANTS
- U DOUBLE BASE PROPELLANTS
- CORE SAMPLING**
- Soviet research in geophysics, astronomy and space
[JPRS-51657] 03 p0470 N71-13038
- Description of Luna-16 flight including automatic
station, soil drilling device, return to earth, and lunar
soil 03 p0456 N71-13044
- Radioactive dating of ocean core samples and
geochemical studies of limiting boundary conditions
[ORO-3622-9] 05 p0676 N71-15460
- Annular magnet for manual drilling of ice holes for
core sampling 11 p1771 N71-22866
- Drilling tests for evaluating coring potential of Apo-
lo lunar surface drill titanium core stems
[NASA-TM-X-58057] 17 p2754 N71-29214
- Evaluation of core scintillation counter for bulk
density measurement in marine sediment cores
18 p2912 N71-30987
- Determination of organic components in sediment
from deep ocean cores [NASA-CR-121734] 21 p3415 N71-34297
- CORE STORAGE**
- Core, magnetic, transistor, and BORAM storage
and memory devices 04 p0504 N71-13827
- Core, magnetic film, and semiconductor memory
techniques 04 p0504 N71-13828
- High speed core, magnetic, semiconductor, and
laser storage systems 04 p0504 N71-13829
- Shock data storage for Helios solar probe using ran-
dom access ferrite core storage [BMBW-FR-W-71-14] 19 p3060 N71-31667
- Branch-and-bound algorithms for core data storage
and iteration reduction [P-4459-1] 21 p3399 N71-34193
- CORES**
- NT EARTH CORE
- NT HONEYCOMB CORES
- NT MAGNETIC CORES
- NT REACTOR CORES
- Contraction stability for two body exchange central
potentials with hard cores, in light doubly magic nuclei
He-4, O-16, and Cd-40 [ITF-70-67-E] 18 p2970 N71-30434
- COROLIS EFFECT**
- Effects of rotation on boundary layers in tur-
bomachine rotors 03 p0309 N71-12262
- Numerical analysis of frontal motion in stagnation
[AD-713068] 07 p0154 N71-17774
- Examining dynamics of changes in suprapre-
nucleus of hypothalamus in rats exposed to transverse
accelerations 08 p1150 N71-18009
- Evaluation of human vestibular tolerance for
Coriolis acceleration test 16 p2544 N71-26262
- Vector analysis for estimating acceleration forces
affecting human receptors in semicircular canal dis-
turbance 16 p2544 N71-26263
- Studying oculogravic illusion and Coriolis effect in
causes of disorientation in aerospace flight
[JZF-1970-25] 18 p2883 N71-30937
- CORRE [MATERIALS]**
- Thermal conductivity, thermal expansion, and heat
capacity of high purity silicone elastomer and filled
cork from 150 K to 500 K [NASA-CR-111912] 15 p3432 N71-27746
- CORNERS**
- Non-equilibrium corner expansion flow of moist air
[AD-714210] 06 p0837 N71-16480
- Thermal stress analysis of wind tunnel corners
[ARC-CP-1117] 07 p1003 N71-17408
- Three dimensional diffraction of sonic booms by
corners of structures [NASA-CR-1728] 07 p1013 N71-18829
- Directional control capability of 18 x 5.5, type 7 air-
craft tires on wet surfaces 09 p1524 N71-28138
- Pressure pulse diffraction by three dimensional
structural corner subjected to sonic boom 16 p2533 N71-28375
- CORONA DISCHARGES**
- U ELECTRIC CORONA
- CORONAGRAPH**
- Digitized SEC vidicon for mapping outer solar
corona from OSO spacecraft, and digitized SEC
vidicon for measuring adsorption lines and mapping
solar magnetic field 16 p2593 N71-28513
- CORONAS**
- NT ELECTRIC CORONA
- NT SOLAR CORONA
- Structure and energy distribution of chromophore-
corona transition region [NASA-CR-116672] 08 p1286 N71-19294
- Flare, coronal enhancements, faculae, and
geomagnetic response of quiet and active regions of
solar magnetic sector structure [NASA-CR-121420] 20 p3341 N71-33206
- CORPUSCULAR RADIATION**
- NT BETA PARTICLES
- NT CYCLOTRON RADIATION
- NT ELECTRON BEAMS
- NT ELECTRON PRECIPITATION
- NT ELECTRON RADIATION
- NT ION CYCLOTRON RADIATION
- NT PRIMARY COSMIC RAYS
- NT RADIATION BELTS
- NT SOLAR CORPUSCULAR RADIATION
- NT SOLAR COSMIC RAYS
- NT SOLAR PROTONS
- Feasibility of using radiation resistant solar cell
cover glass to replace fused quartz [NASA-TN-D-6024] 03 p0519 N71-12278
- Weightlessness, corpuscular radiation, and mag-
netic field environmental laboratory simulation 03 p0535 N71-12794
- Simulation of space corpuscular radiation using
radiation tolerance of spacecraft electronic devices
03 p0536 N71-12790
- Energy spectra of multi-charged nuclei measured by
Cerenkov counters onboard Cosmos 225 satellite
[NASA-TT-P-13311] 09 p1462 N71-28412
- Influence of solar corpuscular radiation emission on
changes of meridional forms of atmospheric circula-
tion 11 p1756 N71-22838
- Corpuscular radiation effects on radiation belts of
earth [NASA-TT-P-4335] 17 p2842 N71-30340
- Tunnel penetration and impact multiplication
procedures for quick recording of particle tracks in
condensed media [JINR-P13-5623] 21 p3467 N71-34676
- Interaction of optical and particle radiation with
matter in astrophysics 23 p3852 N71-37468
- CORRECTION**
- NT OPTICAL CORRECTION PROCEDURE
- Validation of mathematical model for wall effect
correction in cavitation flow [AD-717393] 11 p1736 N71-22170

SUBJECT INDEX

Corrections for dead time in detection experiments on nuclear statistics using probability analysis

[CNRA-262] 13 p2134 N71-23164

Correction of propagation anomalies in Omega navigation system

[AD-721108] 15 p2441 N71-36888

Correction method for static pressure distribution measurement on spherically-bellied cones using cavity size on model with streamwise pressure gradients

[AARC-CR-1139] 15 p2363 N71-37714

Magnetic lens aberration correction in electron microscopy

16 p2592 N71-38245

Theoretical physics and mathematical model for QEOS 2 isomeric corrections using VHF range and range rate tracking data

19 p3088 N71-31849

Computer code incorporating level density and corrections with Hauser-Feshbach theory

[ANU-P-518] 21 p3473 N71-34733

Relativistic correction to Fermi-contact hyperfine Hamiltonian derived for arbitrary principle quantum number n

[NP-18818] 23 p3815 N71-37287

Derivation of corrections to K infinity in two group approximation using high temperature lattice test results

[BNWL-1568] 23 p3817 N71-37224

Correction of range errors due to isomeric electron content

24 p3914 N71-37904

CORRELATION

NT ANGULAR CORRELATION

NT AUTOCORRELATION

NT CORRELATION COEFFICIENTS

NT CORRELATION DETECTION

NT CROSS CORRELATION

NT DATA CORRELATION

NT SIGNAL ANALYSIS

NT STATISTICAL CORRELATION

Infrared vibrational spectral correlation derived from terrestrial and synthetic minerals for characterizing Apollo 11 and 12 lunar samples

[NASA-CR-114898] 09 p1466 N71-19913

Temporal and spatial correlation functions for cloud cover over European Russia, calculated from satellite and ground observations

[SC-7-70-4048] 09 p1414 N71-30342

Correlation between NRL electron storage ring fluxes and behavior of nonlinear dispersive partial differential equations

[AD-716736] 10 p1611 N71-28676

Conformal solution correlation representing excess volume, excess enthalpy, and excess Gibbs free energy for mixtures of simple liquids from simple to infinite

12 p1875 N71-24368

Simulation of radar echoes by means of electromagnetic wave filters generating clutter signals with known auto- and cross correlations

[BMVG-FWWT-70-7] 13 p2042 N71-24361

Correlation of sea surface roughness with vertically polarized microwave radiometric brightness temperature

[AD-719447] 15 p2089 N71-34393

Correlation techniques in plasma diagnostics including turbulent diffusion measurement of particle losses and diffusion coefficients and investigation of fluctuations and instabilities

[BGR-CRA-FC-578] 15 p2148 N71-25234

Energy transfer spectra in locally isotropic grid turbulence determined from third-order correlation functions

14 p2341 N71-26296

Numerical values of physical bonds for components of single and double statistical tensors for spin less fermions equal to 2

[TPU-1278] 14 p2387 N71-26394

Quantum mechanics of two particle interactions in inhomogeneous systems including kinetic and equilibrium correlation equations using BGKY hierarchies

15 p2487 N71-27829

Nonlinear equation for correlation function between lambda₁ hyperon and lambda₂ nucleon in nuclear matter

[BREM-7019] 15 p2488 N71-27878

Determination of correlation functions between events given by neutron detectors for fast thermal neutron source

16 p2645 N71-38113

Correlation method for beam pulsing in neutron line of sight spectroscopy

16 p2597 N71-38710

Phase space reformulation for quantum corrections to classical time correlation functions

16 p2659 N71-39176

Utilization of climatological data for tropical weather forecasting

[AD-721087] 17 p2776 N71-29434

Limiting relations for correlation averages in quantum statistics of four fermion interactions

[BTP-70-59] 17 p2811 N71-30399

Correlation of zero phase brightness surge - bipolarity with lunar surface roughness

18 p3013 N71-38077

Derivation of 1/omega sum rules from two component uniform many body systems and large range correlations in binary solutions

[RLO-1588-599] 18 p2998 N71-31566

Field theory approach to phase transformations, using renormalization groups, correlation functions, and scaling laws

20 p3310 N71-33108

Many body theory electron correlation effects for excited and ground states

20 p3317 N71-33523

Correlation between deformation substructure, precipitates, recrystallization state, and stress corrosion of aluminum zinc magnesium alloy

[NLL-46-28573-15828-4P] 21 p3441 N71-34488

Correlations between observations pertaining to two different systems with applications in theoretical physics

[LPTP-71143] 22 p3645 N71-35992

Necessary and sufficient conditions for rapid decay of correlations for many body systems having probability distributions obeying master equation

[AD-726763] 22 p3648 N71-36813

Tests on scale model configurations of C-5 aircraft to obtain data correlation on three transonic wind tunnels

[AD-727065] 23 p3784 N71-36408

Space-time dependent spin correlation functions for isotropic Heisenberg paramagnet with cylindrical symmetry at elevated temperature based on Ginzburg representation of diffusivity

24 p3908 N71-38307

Photomicro cross section and structure correlation

[IS-T-418] 24 p3980 N71-38402

Atomic structure, bonding, and transport properties of various amorphous semiconductors

[AD-727179] 24 p3998 N71-38517

Equipment and correlation data for cosmic ray studies

24 p4012 N71-38615

Correlation of signal processing techniques for signal to noise ratio improvement during ultrasonic inspection of dissimilar weld seams

[AD-727156] 24 p4024 N71-38713

CORRELATION COEFFICIENTS

Statistical characteristics of transverse beam displacements in turbulent atmosphere

[AZT-70-288-BULL.] 07 p1052 N71-14934

Evaluating multiple density correlation function of many particle system

[NUB-2851] 08 p1257 N71-18416

Hypersonic theoretical/experimental correlations of aerodynamic characteristics for space shuttle design

14 p2195 N71-24046

Determination of mean, variance, covariance, and correlation estimates for axes rotation of bivariate normal elliptical distribution

[NASA-TM-X-64595] 13 p3434 N71-36978

Pseudorandom and Markov sequences optimizing correlation time of light spectroscopy

[JUL-64-FF] 15 p3489 N71-27561

Theoretical correlation coefficients as functions of mixing ratio data for triple gamma ray cascades with intermediate transitions unobserved

[NP-18644] 15 p2989 N71-31514

Computer program utilizing IBM 360-48 computer for transforming correlation functions of three particle data

[TR-1] 19 p3162 N71-32726

Measurement of correlation coefficient of frequency components in tropospheric propagation

[FOA-3-C-3406-43] 22 p3554 N71-35314

Upper atmospheric density variations and solar activity analysis and correlation

22 p3679 N71-36230

CORRELATION DETECTION

Optical correlation methods for remote sensing of trace gases at high altitudes

02 p2236 N71-11093

Digital techniques and components for signal detection in clutter by advanced radar systems

[AGARD-CP-66-78] 04 p4083 N71-19881

Pulse compression and correlation for high range resolution of tracking radar

04 p4086 N71-19929

Digital correlation for signal detection in presence of interference noise

04 p5514 N71-19922

Digital techniques for monopulse radar signal detection in clutter environment

04 p4097 N71-19927

Adaptive clutter suppression filter for Doppler shifted radar signal detection

04 p4097 N71-19929

Digital filters and Fourier transformation for pulsed Doppler radar processor

04 p4097 N71-19930

Position sensitive semiconductor detectors used in measuring angular correlations for helium induced fission of uranium 238

[MTRC-5783-7] 11 p1084 N71-22275

X2/M1 multiplets mixing ratios in spherical nuclei to 124 and 126, and X₂ 126 using gamma-gamma correlation techniques

[COD-1746-51] 11 p1885 N71-22368

Landing systems signal reflection interference on correlation protected instrument landing system beams

[RAE-TR-70141] 12 p1968 N71-23341

CORRELATION FUNCTIONS

U CORRELATION

CORRELATORS

NT IMAGE CORRELATORS

UEF digital correlator and analyzer

[CRA-FC-547] 04 p2593 N71-13578

Quantized random signal correlator output signal to noise ratio expression and comparison with output ratios of analog and partially coincident correlators

[AD-710885] 12 p1892 N71-23578

Synchronous detection system for detecting weak radio astronomical signals

[NASA-CASE-XRP-6852] 12 p1994 N71-23723

Radio astronomy studies including passive linear correlators, digital correlators, and related measuring instruments also radar techniques for lunar topography

[NASA-CR-114898] 12 p2882 N71-29883

Receivers with sample correlators for signal processing when noise dominates

23 p3727 N71-36549

CORROSION

NT CAVITATION CORROSION

NT ELECTROCHEMICAL CORROSION

NT FRETTING CORROSION

NT FUEL CORROSION

NT INTERGRANULAR CORROSION

NT SCALE CORROSION

NT STRESS CORROSION

Downturn effect in liquid sodium corrosion of stainless steel

[ANL-TRANS-639] 01 p8868 N71-18824

Hydrogen embrittlement corrosion studies using electrochemical permeation method

[AD-715807] 06 p1215 N71-18789

General regulations in corrosion of metals under action of radioactive radiation

[AD-717865] 10 p1572 N71-38889

Techniques involving metal corrosion in fluorinated gases in inverse correlation plots

[NLL-CA-232-1981-SV] 11 p1780 N71-22285

Numerical estimates of intensity, amplitude, duration, and repetition rate of surface attack from individual bubble collapse and cavitation damage relationships to corrosion failure

[UMICH-683571-7-T] 12 p1980 N71-23539

Analysis of corrosion in high temperature lithium heat pipes with sodium-circumferential and stainless steel wall material

[HUR-6395-3] 13 p2882 N71-24734

Effects of superheated steam and long periods of exposure on aluminum alloys

[JER-184] 13 p2882 N71-24818

Design, fabrication, and evaluation of T-111 fuel-line system refractory alloy corrosion test loop

[NASA-CR-72853] 13 p2887 N71-25381

Atmospheric corrosion and air pollution effects

[FOA-1-C-1533-92] 14 p2279 N71-36239

Microbial corrosion emphasizing mechanisms of anaerobic corrosion produced by sulfate-reducing bacteria primarily those in gas collection devices

[AD-726683] 14 p2275 N71-36293

Corrosion of aluminum alloys at different sodium oxide levels

[PRL-201] 15 p3436 N71-37730

Determination of steady-state mass-transfer conditions in silicon alloys and prediction of nickel transport in flowing sodium at high temperatures

[ORNL-6575-VOL-1] 16 p2615 N71-29816

Pitting corrosion of stainless steels in water containing chlorine ions, sodium ions, or both, for use in processing weak chlorinated acids

[NLL-WINDSCALE-TRAPS-65-1981-1] 16 p2615 N71-29816

Electrochemical and corrosion behavior of high purity aluminum exposed to oxygen-free and oxygen-saturated sodium solutions of varying pH content

[AD-722165] 17 p2703 N71-28847

Sub-boundary corrosion in polypropylene polycarbonate aluminum containing iron and copper impurities and exposed to HF and HCl solutions

17 p2704 N71-29736

SNAP 8 electrolytic boiler development - corrosion of current constrained titanium in NaCl

[NASA-CR-1536] 17 p2704 N71-29773

Corrosion of light metals at elevated temperatures and methods to prevent corrosion

[CRA-CORP-1729] 18 p2882 N71-38438

Characterization of Shallow 2 corrosion in steam water mixture under molten reactor radiators

[CSB-8-390] 18 p2882 N71-38441

Thermodynamic heat operational performance for use in corrosion measurement in high temperature electrolysis

[NUL-6538-5] 18 p2880 N71-38253

- Measuring elevated-temperature time-dependent corrosion effects of liquid metal on immersed structural materials [NASA-TM-X-67882] 18 p2936 N71-31221
- Corrosion of polished carbon steels at incisions noting effect of manganese sulfide 19 p3112 N71-31917
- Conditions of accelerated oxidation of nickel base alloys from effects of vanadium and sodium compounds [AD-723207] 19 p3113 N71-32023
- Corrosion of steel claddings of nuclear fuel elements in sodium cooled fast breeder reactor [NLL-RISLEY-TRANS-2015-79091.9F] 19 p3115 N71-32301
- Behavior of Duganess A fine due to coolant gas induced corrosion and thermal cycling [TRG-2121] 19 p3141 N71-32592
- Assessment of cost of air pollution corrosion damage to metal systems and structures in US, both presently and by 1990 [PB-198453] 20 p3283 N71-33122
- Analysis of corrosion rates and products of depleted uranium in ocean water and hydrochloric acid [RFP-1586] 21 p3440 N71-34477
- Pitting rate of pure nickel in potassium chloride solutions containing sodium sulfate or potassium hydroxide inhibitors [NLL-TRANS-746-714-9022.401] 22 p3596 N71-35607
- Processing method for removing finion and corrosion products and fissile materials from molten salt breeder reactor fuel [ORNL-TM-3138] 22 p3624 N71-35818
- Thermodynamics of oxide reduction on heat exchanger, chromium as alloying component, sulphate and hydrogen chloride corrosion, and silicon sulphide phenomena [NLL-CE-TRANS-5605-9022.09] 22 p3697 N71-36370
- Research organizations, investigators, and programs in high temperature research from eleven NATO countries and Spain [AGARD-R-585-71] 22 p3699 N71-36382
- Characterization and prevention of filiform corrosion on aluminum [AD-726739] 23 p3771 N71-36877
- Characteristics of aluminum compression joints and methods for analyzing contact corrosion [NLL-OA-TRANS-637-6036.3] 23 p3775 N71-36906
- Advanced high-temperature pebble-bed reactor design with temperature distributions and corrosion damage in reactor core and primary circuit [JUL-725-RO] 23 p3796 N71-37062
- Electrochemical technique for remote measurement of instantaneous rate of uniform corrosion of aluminum alloys in nuclear reactor heavy water circuits [ZJB-96] 23 p3798 N71-37074
- Analytical superposition model for environmentally-assisted corrosion fatigue crack propagation in aluminum and steel alloys [UCRL-28533] 23 p3860 N71-37520
- Structural analysis of corrugated aircraft wing skin panels to determine effects of corrosion damage [AD-728099] 24 p3875 N71-37619
- Mechanical properties and metallurgical effects of circulating sodium potassium alloy on stainless steel loop [CONF-710310-1] 24 p3933 N71-38059
- Plastic deformation of fine-grained, high purity, hot pressed aluminum oxide and stress corrosion of polycrystalline magnesium oxide [AD-727618] 24 p3945 N71-38140
- ### CORROSION PREVENTION
- Ellipsometric and potentiostatic measurements of oxidation of mild steel in aqueous solutions [AD-711006] 01 p0067 N71-10628
- Corrosion inhibitor effects on water condensing characteristics of DOD type filter/condenser elements [AD-712999] 03 p0445 N71-13070
- Mechanism of adsorption of amine-type corrosion inhibitors [AD-712953] 04 p0488 N71-13472
- Rest prevention in stainless steel fluid transmission lines of nuclear engines for rocket vehicles [NASA-CR-111730] 04 p0536 N71-14077
- Investigating effects of vapor space inhibitors on corrosion resistance of steam turbine oils [NRC-11644] 04 p0534 N71-14261
- Developing laboratory glassware corrosion test method for measuring presence and effectiveness of vapor space corrosion inhibitors in oils 04 p0535 N71-14263
- Thermodynamics of corrosion inhibition of iron in Fe/H₂O, H₂O₂, O₂ system [AD-713451] 05 p0699 N71-14536
- Corrosion prevention behavior of wrapping paper for steel containers 05 p0704 N71-15330
- Vapor deposited laminated nitride-silicon coating for corrosion prevention of carbonaceous surfaces [NASA-CASE-XLA-00284] 06 p0064 N71-16075
- Corrosion inhibitors in aqueous solutions of liquid hydrocarbons [AD-714419] 06 p0071 N71-16328
- Method to prevent stress corrosion cracking in titanium alloys [NASA-CASE-NPO-10271] 06 p0073 N71-16393
- Adsorption microcell method for determining electrochemical properties of certain volatile corrosion inhibitors using mild steel samples [AD-714003] 06 p1212 N71-18312
- Method and apparatus for inducing compressive stresses in pressure vessel to prevent stress corrosion [NASA-CASE-XLA-07390] 06 p1207 N71-18616
- Protective efficiency, synergism, and polarity of ferrous and nonferrous metal, oil-soluble corrosion inhibitors including sulfonates, stibates, amines, and amides [AD-717011] 10 p1578 N71-21232
- Interfacial behavior of corrosion inhibitors on iron surfaces [AD-717030] 10 p1579 N71-21289
- Action of mixtures of inhibitors on steel corrosion [AD-717830] 11 p1778 N71-22256
- Electrochemical analysis of metal corrosion in aqueous environments to determine whether process is anodic, cathodic, or both [AD-718063] 12 p1938 N71-23674
- Development and characteristics of high strength, stress corrosion resistant aluminum alloys for aircraft structures [AD-720398] 14 p2273 N71-25876
- Development and properties of organic compounds for primers on aluminum and titanium alloys to prevent corrosion in marine environments [AD-720384] 14 p2277 N71-25877
- Preparation and properties of polyfunctional polymeric lubricant additives [AD-720369] 14 p2278 N71-25895
- Testing methods for corrosion inhibitors in tanks [FOA-1-C-1332-92] 14 p2279 N71-26149
- Atmospheric corrosion and air pollution effects [FOA-1-C-1333-92] 14 p2279 N71-26259
- Corrosion prevention by fungus-proofing - bibliography [AD-720202] 14 p2207 N71-26638
- Salt spray tests and tropical exposure studies of improved final rinse for zinc phosphate pretreatment coatings [AD-721283] 15 p2427 N71-26922
- Plasma sprayed, chromium carbide bearing steam corrosion prevention using noncorrosive, nonporous primer coats [AD-722006] 16 p2617 N71-28474
- Zincous oxidation in carbon dioxide atmospheres above 500 C and corrosion prevention by copper alloying to prevent oxygen dissolving into metal [CRA-CONF-1728] 16 p2611 N71-28504
- Effects of corrosion inhibitors and anti-leak inhibitor combinations on coalescing properties of filter condenser elements used to decontaminate jet engine fuel [AD-722311] 16 p2670 N71-28577
- Spot welding of aluminum alloy joints using primers for corrosion prevention [ID-MAT-170] 17 p2755 N71-29388
- Galvanically induced hydriding of titanium in saline solutions [PB-190639] 19 p3110 N71-31769
- Sodium carbonate inhibitor for preventing contact corrosion and pitting in magnesium cladding of water cooled fuel rods [NLL-CE-TRANS-5440-9022.09] 19 p3138 N71-32174
- Development of fluoride coating to prevent oxidation of beryllium surfaces at elevated temperatures [NASA-CASE-LEW-10327] 20 p3285 N71-33408
- Bleeter formation in corrosion protective coatings of thermosetting resins including film thickness, pigment, aging, and adhesion effects [NLL-M-36609-1828.4F] 21 p3445 N71-34513
- Corrosion inhibition in metal compounds of azole type [AD-727853] 24 p3940 N71-38104
- ### CORROSION RESISTANCE
- #### NT OXIDATION RESISTANCE
- Techniques in plating including types of plating, and materials used for plating - bibliography [AD-709530] 01 p0058 N71-10188
- Heat resistant coatings to protect against high temperature oxidation [AD-711173] 01 p0072 N71-10632
- Relation between structural constitution of Zircaloy 2 and corrosion behavior in water vapor under pressure at 400 C [WAFD-TRANS-130] 01 p0069 N71-10896
- Mechanism of iron dissolution and corrosion inhibition by galvanostatic polarization and electrical double layer capacitance measurement 02 p0174 N71-11227
- Measuring effects of prestressing on stress corrosion resistance of high strength steels [AD-711606] 02 p0242 N71-11574
- Electrochemical method of protecting hydrocarbons against cavitation corrosion [PB-1936587] 02 p0231 N71-11597
- Application of welding methods and treatment of metal surfaces to improve corrosion resistance and dimensional build up in engine production 02 p0233 N71-11611
- Mechanical, physical, technological, and corrosive properties of welded aluminum 03 p0309 N71-12529
- Carbon steel corrosion and mechanical wear of equipment [AD-712931] 04 p0527 N71-13705
- High strength, corrosion resistant cobalt-based alloys for aerospace structures [NASA-CASE-XLE-00726] 05 p0706 N71-15644
- Hydrazine monoperfluoro siloxane solder thus having corrosion resistant coating, for metals such as copper [NASA-CASE-XNP-03459-2] 05 p0711 N71-15808
- High temperature cobalt-base alloy resistant to corrosion by liquid metals and to sublimation in vacuum environment [NASA-CASE-XLE-02991] 06 p0870 N71-16053
- Corrosion resistance of polymeric petroleum lubricants against microbiological attack [AD-714133] 06 p0878 N71-16200
- Investigating component storage stability and material compatibility with liquid propellants 06 p0936 N71-16400
- Corrosion resistant, titanium alloys for shipbuilding [AD-715254] 07 p1044 N71-17025
- Corrosion resistance of aluminum-silicon alloy in relation to hydrogen content introduced by vacuum refining processes [NASA-TT-F-13506] 09 p1400 N71-20002
- Metal soldering with hydrazine monoperfluoro siloxane for corrosion resistant coatings [NASA-CASE-XNP-03459] 10 p1564 N71-21070
- Heat treatment effect on microhardness, wear, and corrosion resistance of chemically deposited nickel coatings [NLL-TRANS-746-599-9022.401] 10 p1578 N71-21210
- Copper-bearing alloy replacement with aluminum alloys in diffusion desalination plants for sea water corrosion resistance 10 p1581 N71-21438
- Electrochemical and corrosion behavior of corrosion resistant titanium base under platinum coating depending on pH [NLL-TRANS-746-561-9022.401] 10 p1583 N71-21700
- Iron nickel steels containing chromium and molybdenum as corrosion resistant materials for production of phosphoric acid [NLL-TRANS-746-514-9022.401] 10 p1587 N71-21807
- Electroplating and vacuum evaporation of yttrium oxide-chromium oxide coating of chromium alloys for nitrogen embrittlement protection [NASA-CR-72847] 12 p1936 N71-23116
- Corrosion characteristics and response to cathodic protection of copper alloys in quiescent sea water [AD-718310] 12 p1938 N71-23790
- Low temperature mechanical properties of various alloys of high strength and corrosion resistant [NASA-SR-5921/01] 12 p1939 N71-23795
- Corrosion of water reactor core materials, liquid metals, hydrogen diffusion in corrosion process, and plasma anodization [AECL-3778] 13 p2118 N71-28006
- High temperature mercury corrosion resistance of titanium, tantalum alloy, and aluminum alloy sheets after bending stress [NASA-CR-1811] 15 p2420 N71-28047
- Extended ellipsometry method used for electrochemical and optical measurements on electrochemically induced passivity of cobalt [AD-721719] 16 p2537 N71-28341
- Corrosion behavior of stainless steel, nickel alloy, and zirconium alloy fuels in nuclear reactors [NLL-RISLEY-TRANS-2014-79091.9F] 16 p2537 N71-28341
- High temperature refractory alloy compatibility with plutonium 238 [MDC-G-2034] 17 p2700 N71-29080
- Deoxidizing and vacuum casting effect on plastic properties of nickel-chromium steels noting corrosion resistance 18 p2927 N71-30088
- Development of low cost iron base alloy with corrosion resistance to hot sea water [PB-190642] 19 p3109 N71-31673
- Improved corrosion resistance of aluminum alloys for use in sea water conversion plants [PB-190643] 19 p3110 N71-31720
- Effects of silver addition on stress corrosion resistance of Al-Zn-Mg-Cu alloys [AD-723563] 19 p3110 N71-31745
- Development of iron-aluminum alloy with minimum sea water corrosion resistance and minimum dimensional constant 19 p3110 N71-31770
- Isothermal corrosion tests on Inconel 600 and nickel alloy sheets by superheated steam [NLL-RISLEY-TRANS-2093-79091.9F] 19 p3118 N71-32616

SUBJECT INDEX

Blister formation in corrosion protective coatings of thermosetting resins including film thickness, pigment, aging, and adhesion effects
[NLL-M-30438-5828.4F] 21 p3445 N71-34513

Chemical effect of laboratory equipment, and prediction of corrosion resistant materials for constructing chemical apparatus
[AD-726803] 22 p3596 N71-35405

Analysis of effect of lithium and chromium on stress corrosion resistance of aluminum-zinc-magnesium alloys
[NLL-M-30438-5828.4F] 23 p3774 N71-36895

Corrosion tests of austenitic Cr-Ni steel and nickel alloys in steam loop at 620 C and 1 atm pressure for 500 hours, and behavior of cold-formed material surfaces
[EPK-1301] 24 p3935 N71-38077

Destructive examination of Hallam Nuclear Power Facility intermediate heat exchanger emphasizing service corrosion problems
[IN-1477] 24 p3978 N71-38357

CORROSION TESTS
NT SALT SPRAY TESTS
Fabrication of Rankine system corrosion test loop components with niobium zirconium alloy
03 p5886 N71-13508

Investigation of pitting corrosion on unaluminized stainless steel control rod push rods in La Crosse boiling water reactor
[ACNP-70303] 05 p0729 N71-15211

Fabrication, operation, and posttest evaluation of T-11 Rankine System Test Loop
[NASA-CR-72782] 06 p0849 N71-15890

Evaluation of T-11 refractory alloy Rankine system corrosion test loop
[NASA-CR-72818] 07 p1043 N71-17483

Hot corrosion of TD nickel and TD nickel chromium in jet engine exhaust
[NASA-TM-X-52976] 09 p1396 N71-17900

Stress corrosion cracking in iron nickel chromium alloy system in chlorides
[COO-2869-5] 09 p1399 N71-17979

Corrosion tests on titanium, austenitic stainless steel, chromium ferrites, and light alloys in sea water up to 150 C
[NML-TR-2412] 10 p1580 N71-21405

Electrochemical analysis of metal corrosion in aqueous environments to determine whether process is anodic, cathodic, or both
[AD-710063] 12 p1938 N71-23674

Corrosion effects of simulated gas turbine exhaust products on nickel and chromium turbine stator blades
[ARL/MC-319] 12 p1940 N71-24099

Solubility and corrosion behavior of iron, steel, molybdenum, niobium, tantalum, vanadium, tungsten, and chromium in molten lead at high temperatures
[JUL-661-RW] 15 p2434 N71-27560

Measurement of elevated temperatures, their dependence on corrosion effects of liquid metals on immersed structural materials by blocked two-level factorial experiment
[NASA-TN-D-6452] 18 p2936 N71-31244

Hot sea water corrosion test performance of mild steel, low alloy steels, stainless steel wrought and cast alloys, and Alclad
[PB-19658] 19 p3109 N71-31671

Computer program for calculating concentration and burnoff profiles in section of graphite being corroded by water
[AERE-M-2403] 21 p3437 N71-34602

Corrosion tests of austenitic Cr-Ni steel and nickel alloys in steam loop at 620 C and 1 atm pressure for 500 hours, and behavior of cold-formed material surfaces
[EPK-1301] 24 p3935 N71-38077

Corrosion tests of chromium and chromium-nickel steels in molten lead at 575, 650, and 750 C for 3250 hr
[JUL-694-RW] 24 p3935 N71-38078

CORROGATED PLATES
Application of corrugated core sandwich structures to preplanned components
02 p0380 N71-11636

Mathematical model for elastic shear bonding of superadhesively corrugated plate with through hole held tightly including stiffness and stress analysis
[NASA-CR-1749] 20 p3357 N71-33141

CORROSION
Techniques for solving problem of sound transmission from harmonic monopole source through finite corrugated boundary between fluid media
[AD-722829] 16 p5638 N71-28240

CRYSTALLINE
U ALUMINUM OXIDES
CRYSTAL
U THERMOMETRIC FUNCTIONS
COSMIC DUST
NT INTERPLANETARY DUST
Origin of cosmic material fallout on earth surface and structure of cosmic dust and meteoritic material
[REPT-69/18] 15 p2396 N71-27930

System for detecting impact position of cosmic dust and similar outer space particles on detector surface
[NASA-CASB-GSC-11291-1] 16 p2663 N71-29183

Compilation of cosmic dust spatial distribution measurements from satellite and space probes
[D-72] 19 p3183 N71-32785

OGO 3 experiment to measure physical parameters of elongation size dust particles in cleaner and near earth space
[NASA-CR-121477] 20 p3276 N71-33768

COSMIC GASES
NT INTERPLANETARY GAS
NT INTERSTELLAR GAS
Intensity of gas production in comets based on photochemical parameters
[NASA-TT-F-13492] 12 p1990 N71-24244

Synthetic sensitivity of cosmic electrons in ionized interstellar space
[NASA-TM-X-65729] 24 p4000 N71-38578

COSMIC NOISE
Solar X ray and cosmic noise absorption measurements for solar flare predictions
[AD-717792] 11 p1820 N71-22376

Day-to-night ratio of cosmic noise absorption from high latitude sites in Northern and Southern Hemispheres
11 p1757 N71-22847

Calculation of radio noise absorption expected for any riometer system
19 p3178 N71-32665

Effects of solar X ray spectral distribution changes below 10 A on nature and magnitude of sudden cosmic noise absorptions
[RSD-61] 22 p3665 N71-36133

COSMIC PLASMA
Minimum temperature and power effects of cosmic plasmas interacting with neutral interstellar gas applied to solar prominences and rotating plasmas
[REPT-70-11] 02 p0279 N71-11834

Neutral gas effects on cosmic plasmas in presence of magnetic field
[NP-10421] 04 p0600 N71-14320

Cosmic plasma physics and polar system evolution
[REPT-70-39] 15 p2517 N71-27668

Simulation of ultrarelativistic cosmic plasmas in terms of photon-electron interactions in strong magnetic fields
[PR-51] 19 p3178 N71-32709

Numerical analysis of solar wind interactions with magnetospheric plasmas based on equations of magnetohydrodynamics for perfect gas
[NASA-CR-121871] 21 p3503 N71-34957

Cosmological gamma ray spectrum calculations from matter-antimatter annihilation in universe
[NASA-TM-X-65709] 23 p3842 N71-37395

COSMIC RADIATION
U COSMIC RAYS
COSMIC RADIO WAVES
U EXTRATERRESTRIAL RADIO WAVES
COSMIC RAY ALBEDO
Cosmic ray albedo neutron decay - source for equatorial neutron proton radiation belt
[MPI-PAR/EXTRATER-46] 10 p1548 N71-21057

COSMIC RAY SHOWERS
Properties of electron and muon components of extensive air showers for different models of high energy interactions
[DNR-1162] 04 p0587 N71-14258

Monte Carlo calculation of horizontal air shower size spectrum in mean nucleus interaction
[DNR-121] 05 p0742 N71-15124

Quarks and pulsars at cosmic ray shower energies
[MPI-PAR/EXTRATER-47] 06 p1204 N71-18723

High energy muons in cosmic radiation showers
10 p1554 N71-21552

Determining extent of cosmic ray shower by pointing radio antennas
10 p1554 N71-21553

Calculation of effective area times solid angle in horizontal cosmic ray showers
[DNR-123] 15 p2513 N71-26801

Quarks, large transverse momenta, and energy spectra of air showers
[MPI-PAR/EXTRATER-47] 15 p2513 N71-27049

Transistorized device for observing entry direction of air showers
[DNR-124] 15 p2513 N71-27102

Penetration and cascade phenomena at low and very high energies
15 p2463 N71-27181

HERAO CATT crystal activation for measurement of galactic gamma and cosmic particle energy spectra
[RM-307] 16 p3074 N71-28167

Space and time simulation of nuclear active and muon components in extensive air showers for primary energies from 100,000 to 10 million GeV
[INST-125] 18 p3002 N71-30406

Studying radio pulses received at large zenith angles from extensive air showers by two-fold coincident radio receiving system
[AD-727429] 24 p4003 N71-38534

Extended cosmic ray showers from high energy protons and nuclei
[NLL-M-20419-5828.4F] 24 p4004 N71-38536

COSMIC RAYS
NT COSMIC RAY SHOWERS
NT PRIMARY COSMIC RAYS
NT SECONDARY COSMIC RAYS

COSMIC RAYS

NT SOLAR COSMIC RAYS
Design of proportional counter to record location and magnitude of cosmic X ray event
01 p0853 N71-16018

Cosmic radiation at extremely high energies
[AD-710653] 01 p1177 N71-16432

Spark chamber response to incident neutral particles
[AD-711267] 01 p1519 N71-16879

Cosmic radiation dose measurement of astronauts by radiochemical techniques
[BNWL-1183-4] 02 p0151 N71-11075

Measurements of cosmic rays and high energy extraterrestrial particles
[NASA-SP-343] 02 p0294 N71-11415

Formulation and effective rigidity changes of geomagnetic cosmic ray cutoff with primary spectrum changes in equivalent geomagnetic field
[AD-712344] 02 p0293 N71-12086

X ray detector development and investigation of celestial X ray sources
[AD-712893] 02 p0293 N71-12033

Tables for cosmic ray neutron and muon monitor diurnal vectors
[ABCL-3651] 03 p0430 N71-12045

Tables for cosmic ray neutron and muon monitor diurnal vectors
[ABCL-3668] 03 p0450 N71-12046

Source abundances of cosmic ray nuclei from silicon burning process in supernovae
[NASA-TM-X-65589] 03 p0450 N71-13033

Propagation and storage of cosmic rays in interstellar magnetic fields with additional turbulent field
03 p0454 N71-13257

Two stream instability in Colgate supernovae model of cosmic ray acceleration
[UCRL-50808] 04 p0395 N71-13574

Principal investigator requirements for lunar module-borne cosmic ray detector experiment
[NASA-CR-108715] 04 p0607 N71-14041

Support requirements for lunar module-borne cosmic ray detector experiment
[NASA-CR-108712] 04 p0607 N71-14053

Reliability requirements for lunar module-borne cosmic ray detector experiment
[NASA-CR-108714] 04 p0607 N71-14053

Balloon measurements of cosmic ray ionization in atmosphere, 1968-70
[JASL-254] 04 p0608 N71-14236

Cosmic ray modulation during Perseus decreases in 1968-1969
[AD-713226] 05 p0764 N71-14563

Procedure for measuring heavy cosmic ray particles directly incident on spacecraft
[NASA-CR-114804] 05 p0836 N71-14682

Astrophysical aspects of cosmic radiation, and radiation environment of earth
[NASA-CR-115805] 05 p0765 N71-15332

Geomagnetism, radioactivity, ionospheric parameters, meteorology, cosmic rays, and atmospheric electricity - Mar. 1970
06 p0840 N71-15725

Durbach geophysical observatory, Belgium, data on geomagnetism, ionospheric propagation, cosmology, cosmic rays, and atmospheric electricity, April 1970
06 p0840 N71-15886

Upper atmosphere cosmic data observations - July 1969
06 p0842 N71-15843

Upper atmosphere cosmic data observations - August 1969
06 p0842 N71-15844

Design of experiments and systems for HEO to determine composition and spectra of high energy cosmic rays
[NASA-TM-X-65431] 06 p0842 N71-16082

Compound diffusion of cosmic rays along interstellar magnetic field lines
[NASA-TM-X-65437] 06 p0843 N71-16785

Calibration of high energy cosmic ray experiment
[NASA-TM-X-65440] 06 p0844 N71-16730

Interactions due to high Z particles in primary cosmic rays
06 p0844 N71-16731

Geophysics and space data bulletin - Vol. 7, no. 2
[AD-714412] 06 p0856 N71-16761

Analysis of data obtained from USSR lunar roving vehicle
07 p1105 N71-17085

Ionospheric sounding and cosmic ray neutron flux density tables at Durbach, Belgium, Jan. 1970
07 p1016 N71-17047

Ionospheric sounding and cosmic ray neutron flux density tables at Durbach, Belgium, Jul. 1970
07 p1046 N71-17051

Cosmic ray investigations conducted by lunar based observatories
07 p1106 N71-17074

Ionospheric sounding and cosmic ray neutron flux density data - May 1970
07 p1017 N71-17076

Atmospheric electricity, ionospheric sounding, cosmology, and geomagnetism, and cosmic ray data, Belgium, May 1970
07 p1018 N71-17149

- Atmospheric electricity, ionospheric sounding, seismology, and geomagnetism, and cosmic ray data - Belgium, June 1970 07 p1018 N71-17150
- Characteristics of low energy gamma rays in atmosphere [AD-715271] 07 p1106 N71-18035
- Charge ratio of 1-10 TeV cosmic ray muons 07 p1106 N71-18035
- Cosmic ray muon investigations [LN-70/32] 08 p1285 N71-18227
- Neutrino interactions, cosmic ray muons, and search for quarks in cosmic radiation [UCI-10-P-19-40] 08 p1285 N71-18392
- Calculating production of deuterium, He-3, boron, lithium, and beryllium by galactic cosmic rays in interstellar medium [SAO-SPECIAL-REPT-330] 08 p1285 N71-18794
- Parallel plate ionization chamber for identifying relativistic cosmic ray nuclei [NASA-CR-116874] 08 p1176 N71-18914
- Detection of cosmic gamma radiation with gamma ray telescope [AD-716492] 09 p1461 N71-19334
- Scaling and angular distribution of cosmic ray events for proton plus proton yields pion plus anything reaction [RLO-1388-587] 09 p1426 N71-19539
- Observed data by neutron monitor at Monte Chacaltaya, Bolivia from July 1968 to March 1969 [REPT-34] 09 p1461 N71-20025
- Development of cosmic physics, and importance of Monte Chacaltaya Laboratory, Bolivia 09 p1461 N71-20026
- Underground detection of cosmic ray neutrons [UCI-10-P-19-38] 09 p1461 N71-20159
- Cosmic ray distribution for analysis of nonuniform interplanetary magnetic fields during solar activities [NASA-TT-F-13514] 09 p1462 N71-20409
- Seasonal variations in anti-symmetric diurnal and semi-diurnal variations of cosmic rays [NASA-TT-F-13513] 09 p1462 N71-20411
- Charge distribution of heavy nuclei of cosmic rays in region Z greater than or equal to 26 determined by photoemulsion method [NASA-TT-F-13510] 09 p1463 N71-20490
- Solar proton observation over southern polar cap during cosmic ray event, 18 Nov. 1968 10 p1550 N71-21156
- Exposure of human subjects to fast neutron beam to determine cause of light flashes observed by astronauts on lunar missions [NASA-CR-117495] 10 p1500 N71-21509
- Summary of published data on cosmic hadron flux for various altitudes 10 p1554 N71-21554
- Tabulated hourly neutron count, and graphs of hourly variations at Chacaltaya, Bolivia 11 p1745 N71-21936
- Summaries of news releases and scientific articles on upper atmosphere and space research 11 p1745 N71-21936
- Ionospheric sounding and cosmic ray neutron flux density tables, Dourbes, Belgium, Nov. 1970 11 p1746 N71-21985
- Ionospheric sounding and cosmic ray neutron flux density tables, Dourbes, Oct. 1970 11 p1746 N71-21986
- Ionospheric sounding and cosmic ray neutron flux density tables, Dourbes, Belgium, Aug. 1970 11 p1746 N71-21993
- Ionospheric sounding and cosmic ray neutron flux density tables, Dourbes, Belgium, Sep. 1970 11 p1746 N71-21994
- Abstracts of scientific and technical papers of OGO program [NASA-CR-117758] 11 p1825 N71-22046
- Comets, meteorites, lunar geology, cosmic rays, radiation measuring instruments, and data processing - conference [NASA-TT-F-630] 11 p1826 N71-22415
- Diffuse ultraviolet X ray detection and polarization of Crab Nebula emissions [AD-717671] 11 p1822 N71-22450
- Objectives of ISIS-B including measurement of fluctuations in upper atmosphere electron density, radio and cosmic emission studies, and measurements of ionospheric magnetic particles [NASA-NEWS-RELEASE-71-41] 11 p1827 N71-22537
- Origin and propagation of galactic cosmic ray electrons in interstellar space 11 p1823 N71-22578
- Reproduction of high energy heavy ions in cosmic rays using heavy ion accelerator [PPAD-676-E] 12 p1896 N71-23183
- List of articles on cosmic and solar radiation research and their relationship to astrophysics [AD-717891] 12 p1992 N71-23263
- Design and construction of cosmic ray telescope to measure zenith angle distribution of muons and to determine zenith angle dependence 12 p1992 N71-23323
- Cosmic ray anisotropy in interplanetary space reflected in solar diurnal variation 12 p1993 N71-23893
- Homogeneity and anisotropy measurements of thermal radiation field surrounding planet Earth 12 p1993 N71-24323
- Description of photoionization cross section for helium and molecular hydrogen and effect on absorption of interstellar X rays 12 p1995 N71-24324
- Magnetometer, cosmic ray, RLP noise,rometer, solar optical and radio emission, and ionosonde data - July - Sept. 1970 13 p2049 N71-24415
- Gamma ray producing decay modes of secondary particles produced in high energy cosmic ray interactions with interstellar and intergalactic gas 13 p2159 N71-24765
- Gamma ray spectra from neutral pion decay and model for numerical calculation of spectrum below 1 GeV, for gamma rays produced by galactic cosmic ray interactions 13 p2159 N71-24769
- Cosmic gamma ray spectra from secondary particles produced by cosmic ray collisions in extragalactic space 13 p2159 N71-24774
- Sudden release of large number of cosmic rays as supernova burst considered in relation to cosmic rays contained in galactic disk [NASA-TM-X-65506] 13 p2160 N71-24988
- Monthly graphs of cosmic ray NM-64 neutron monitor data for May to Aug. 1970 13 p2161 N71-25158
- Thermal electron density and cosmic ray flux in galactic radio emissions 13 p2163 N71-25289
- Low energy cosmic radiation spectrum analysis for IMP 4 data on solar system 13 p2163 N71-25290
- Galactic origin of pulsars and cosmic radiation sources 13 p2163 N71-25291
- Extragalactic origin of ultrahigh energy cosmic rays 13 p2163 N71-25292
- Solar activity and upper atmosphere geomagnetic variations, cosmic ray, and earth current data - Feb. 1970 13 p2170 N71-25465
- Solar activity, and upper atmosphere geomagnetic variations, cosmic ray, and earth current data - Jan. 1970 13 p2170 N71-25476
- Identification of relativistic secondary particles emitted by 60 GeV pions from Serpukhov accelerator and in cosmic ray jets in nuclear emulsions [BNP-718] 14 p2311 N71-26697
- Galactic and extragalactic origin of cosmic gamma ray flux between 1 and 6 MeV [NASA-TM-X-65562] 15 p2514 N71-27639
- Effects of propagation and source distribution on cosmic ray composition and anisotropy [NASA-TM-X-65575] 15 p2515 N71-27702
- High energy interactions produced by surviving primary protons of cosmic radiation at altitude of Chacaltaya, Bolivia from 1968 to 1970 15 p2515 N71-27823
- Interpretation of data on muons in cosmic rays for relevance to high energy interactions and astrophysics [ENR-1231] 15 p2516 N71-27825
- Hadron interaction at ultrahigh energies in cosmic rays [BNP-722] 15 p2489 N71-27879
- Telescope description and results obtained on production of low energy muons by neutral components of cosmic radiation at sea level [NYO-2419-18] 16 p2674 N71-28188
- Ionization of Gum nebula by energetic charged particles from supernova Vela X with estimate of gamma ray line emission from ambient gas, energetic nuclei interaction [NASA-TM-X-65590] 16 p2674 N71-28367
- High energy cosmic ray interactions in emulsion chambers 16 p2675 N71-28942
- Astronomical catalog of cosmic X ray sources [UCID-15622] 17 p2840 N71-29211
- Cosmic ray data from cloud and ionization chambers, and cosmic and iron plates [AD-71714] 17 p2840 N71-29472
- Sea level cosmic-ray neutron spectrometer measurements for New York City [NASL-241] 17 p2841 N71-29529
- Three discrete cosmic X ray sources in Scorpius-Ara region observed with detector system sensitive to low energy X rays 17 p2841 N71-29724
- Cosmic gamma radiation from pion decay in interstellar gas [NASA-TM-X-65602] 17 p2842 N71-30069
- Xenon scintillation counter design and performance tests using alpha particles and cosmic ray muons [USIP-70-1] 17 p2753 N71-30120
- Collective interaction in collision of high energy particles referring to cosmic rays 17 p2806 N71-30523
- Astrophysical model and theoretical physics of expanding universe with evolving sources effects on low energy cosmic rays [NASA-TM-X-65623] 18 p3083 N71-30612
- Experimental and theoretical study of biologically important radiation components and dose equivalence due to galactic and solar rays at SST in high atmosphere - summary 18 p2870 N71-30779
- Production of iodine isotopes in meteorites by cosmic rays, gas proportional counting of transmuted metal X ray emitters, and radiochemical analysis of lunar samples 18 p3017 N71-31348
- Measurement and effects of radiation doses from cosmic radiation at altitudes of supersonic transport flights [ORNL-PR-2455] 18 p2878 N71-31350
- Geophysical Observations, Belgium, data on geomagnetic, ionospheric propagation, ionosonde, cosmic rays, and atmospheric electricity, Jul. 1970 19 p3091 N71-31938
- Correlation between muons in earth atmosphere and cosmic ray muon intensity measurements [AD-723330] 19 p3175 N71-31941
- Auto-correlation functions for diffuse cosmic X rays [NASA-TM-X-65668] 19 p3177 N71-32409
- Telescope for measuring nuclear component of primary cosmic radiation on Cosmos 163 19 p3178 N71-32740
- Convection-diffusion equation for closed formation of cosmic ray transport theory in solar environment [NASA-CR-121440] 20 p3341 N71-33550
- Magnetohydrodynamics of discontinuities in interplanetary medium and their relation to propagation and acceleration of cosmic rays [NASA-TM-X-65673] 20 p3342 N71-33711
- Concentrations and isotopic compositions of Fe, Ni, and Ar measured by mass spectroscopy in a separated metal phase and bulk samples of 13 chondrites for cosmic ray record studies 20 p3350 N71-33977
- Ionospheric propagation, geomagnetic, and cosmic ray data - tables for Dec. 1969 21 p3419 N71-34336
- Equipment specifications for balloon carried superconducting magnetic spectrometer to measure spectra of cosmic ray nuclei with charges ranging from protons to iron [NASA-CR-121709] 21 p3425 N71-34378
- Cosmic ray charge and energy spectra from ORO-3 experiments with details of detector design and operation [NASA-CR-121626] 21 p3503 N71-34955
- Calibration and efficiency of scintillation counter for measuring cosmic radiation during balloon flights 21 p3504 N71-34966
- Uncorrected and barometer corrected data in tabular form [AECL-3854] 21 p3504 N71-34967
- Transport equations for high energy heavy nuclei cosmic rays in interstellar medium 21 p3506 N71-34975
- Measurement and analysis of heavy cosmic rays with high altitude balloons 21 p3506 N71-34977
- Handbook of correlative data on galactic cosmic rays, solar electromagnetic radiation, solar proton, geomagnetism, ionosphere, and neutral atmosphere [NASA-TM-X-67294] 21 p3532 N71-35188
- Observations of geophysical phenomena concerning electric and magnetic states of upper atmosphere, ionosphere, cosmic rays and earth currents 22 p3574 N71-35401
- Origin of cosmic electrons with high energies from supernovas [NASA-TM-X-65689] 22 p3644 N71-36128
- Transport equations for determining cosmic ray phenomena of galaxy [NASA-CR-115178] 22 p3665 N71-36129
- Calculation of radiation cross section for relativistic suprathermal proton bremsstrahlung to determine contribution to cosmic gamma rays [NASA-TM-X-65699] 23 p3811 N71-37171
- Models for studying origin and composition of ultrahigh energy cosmic rays [NASA-TM-X-65713] 23 p3841 N71-37578
- One-dimensional diffusion model for calculating effect of interstellar magnetic field line wandering on cosmic ray parameters [NASA-TM-X-65698] 23 p3847 N71-37529
- Radioactive isotope studies in connection with cosmic rays, solar wind, and geophysical processes 23 p3855 N71-37588
- Energy and charge spectra of cosmic rays [NASA-TT-F-13731] 24 p3928 N71-37915
- Heavy and ultrahigh energy nuclei observations of cosmic rays using ionization chamber-Cosmos counter system [NASA-CR-123197] 24 p4082 N71-38044

SUBJECT INDEX

- Millisecond-time-scale atmospheric light pulses induced by solar activity
[NASA-TM-X-65716] 24 p4002 N71-38345
- Cosmic ray research and instruments used for ionospheric and astronomical studies, Vol. 2 - Conference 24 p4009 N71-38582
- Solar and galactic cosmic ray diffusion coefficients and dependencies 24 p4010 N71-38593
- Cosmic ray origin and electron density spectra 24 p4010 N71-38594
- Intensity variations of cosmic rays due to solar activity 24 p4010 N71-38599
- Barometric coefficient equation and coefficient distortion for neutron component of cosmic rays 24 p4011 N71-38602
- Cosmic ray intensity variation and Forbush decrease during solar activity maximum 24 p4011 N71-38605
- Automatic processing of cosmic ray data 24 p4012 N71-38612
- Equipment and correlation data for cosmic ray studies 24 p4012 N71-38615
- COSMOGONY**
U COSMOLOGY
COSMOLOGY
- Gravitational waves in galaxies from cosmological point of view 02 p0296 N71-11952
- Gravitational interactions, general relativity, pulsars, and cosmology [AD-714662] 07 p1115 N71-17920
- Cosmology application of mathematical modeling by symbolic computation [NASA-TT-F-13360] 08 p1287 N71-18477
- Cosmological models, and galactic and stellar evolution 11 p1826 N71-22412
- Origin of meteorites and relation to early solar system [NASA-CR-117755] 11 p1827 N71-22529
- Homogeneity and anisotropy measurements of thermal radiation field surrounding planet Earth 12 p1995 N71-24323
- Cosmic gamma ray production processes, galactic and extragalactic gamma rays, and cosmology [NASA-SP-249] 13 p2158 N71-24764
- General theory of relativity, Robertson-Walker metric, and cosmological effects in photon flux calculations 13 p2159 N71-24773
- Cosmic, isotropic gamma ray spectra, primordial gamma ray sources, and intergalactic gas density 13 p2160 N71-24778
- Cosmic antimatter annihilation and gamma ray background spectrum [NASA-TM-X-65517] 13 p2160 N71-24962
- Relativistic magnetohydrodynamic equations of proton antiproton annihilation reactions and Klein-Allyn cosmology 13 p2131 N71-25029
- Cosmic matter-antimatter annihilation and gamma ray background spectrum [NASA-TM-X-65598] 17 p2841 N71-29924
- Effect of cosmological expansion on self gravitating ensembles of particles [NASA-TM-X-67240] 18 p3015 N71-31253
- Astrophysics, radio astronomy, radio sources, galaxies, cosmology, pulsars, black body radiation, universe, and electromagnetic wave propagation [P-4294] 20 p3343 N71-32836
- Relativistic and Newtonian cosmology in understanding setting in which astrophysical phenomena occur and are observed 20 p3344 N71-32842
- Magnitude-red shift, magnitude-galaxy count, and angular diameter-red shift relations included in tests of cosmological models 20 p3344 N71-32843
- Discussion of cosmological horizons using two dimensional balloon model and metric models 20 p3344 N71-32844
- Application of cosmographic perspectives in interpreting photographs taken in space [NASA-TT-F-133928] 20 p3325 N71-33590
- Metric composition including distribution of and origin of elements and their isotopes [UCSD-34-P-43-X-9] 20 p3350 N71-33875
- Electromotive forces, magnetohydrodynamic turbulence, and stellar and planetary magnetic fields based on turbulent dynamo theory in cosmological electrodynamics [NCAR-TN/FA-60] 21 p3511 N71-35016
- Behavior of strongly interacting particles at ultrahigh temperatures related to origin of galaxies and matter [LPTHE-71/15] 21 p3530 N71-35156
- Theoretical analysis of distribution of orientation angles of apparent major axes of spiral galaxies in different zones of sky and galactic orbits [REPT-80] 22 p3671 N71-36176

COSMOS SATELLITES

- Origin of solar system and characteristics of primitive nebula 23 p3847 N71-37417
- Derivation of cosmologic model for verification of gravitation theory 23 p3849 N71-37434
- Photon propagation in perturbed Einstein-de Sitter universe model containing ionized gas 23 p3857 N71-37493
- Space environmental conditions, solar radio emission, solar spectrum, cosmic rays and terrestrial radiation [AD-727778] 24 p4014 N71-38636
- COSMONAUTS**
- Neuroendocrine heart rate analysis techniques for cosmonauts during space flight [AD-714405] 06 p0802 N71-16409
- Physiological responses of cosmonauts during training for prolonged space flights [AD-714406] 06 p0802 N71-16410
- Foodlight metabolic and renal functional shifts in Soyuz spacecraft cosmonauts 16 p2543 N71-28257
- Radiation hazards of space flights and biological effects on cosmonauts [AD-727245] 24 p3879 N71-37649
- COSMOS SATELLITES**
- NT COSMOS 54 SATELLITE 01 p0046 N71-10246
- NT COSMOS 149 SATELLITE 01 p0078 N71-10350
- NT COSMOS 206 SATELLITE 01 p0081 N71-10991
- NT COSMOS 224 SATELLITE 01 p0082 N71-10995
- NT COSMOS 225 SATELLITE 01 p0082 N71-10995
- Velocity of ordered motion of ionospheric ions at 600 km [NASA-TT-F-13358] 01 p0046 N71-10246
- Statistical structure of outgoing radiation fields measured by Cosmos 122 satellite [NASA-TT-F-13368] 01 p0078 N71-10350
- Machine analysis of infrared cloud images obtained by Cosmos-122 satellite [NASA-TT-F-13369] 01 p0081 N71-10996
- Cosmos-122 infrared photography of cloud cover and photointerpretations for weather forecasting [NASA-TT-F-13362] 01 p0081 N71-10991
- Structural features of clouds and wind fields in cyclones by pictures from Cosmos-122 [NASA-TT-F-13361] 01 p0082 N71-10995
- Filter measurements of zenith intensities for individual components of airglow [NASA-TT-F-13396] 02 p0208 N71-11393
- Convective cloud cells as observed from artificial earth satellites [NASA-TT-F-13363] 02 p0254 N71-11465
- Weather satellite data on European climate for first quarter in 1968 [QR-1-PT-1] 02 p0254 N71-11469
- Comparison of radiation measurements from Cosmos 122 satellite instruments with photointerpretation data and ground station observations [NASA-TT-F-13366] 02 p0257 N71-11676
- Performance of helium cooled superconducting device at reduced gravity onboard Cosmos 213 satellite [NASA-TT-F-13402] 02 p0292 N71-11903
- Optical satellite tracking of Samos, Nimbus, Cosmos, and Explorer 39 satellites, Edinburgh, May 1970 [ROE-STS-102] 02 p0299 N71-12001
- Passage of superlong radio waves through ionosphere to Cosmos 142 satellite [NASA-TT-F-13413] 03 p0336 N71-12398
- Tabulated tracking data for Cosmos 71 satellite - Jan. through Dec. 1967 03 p0453 N71-13010
- Tabulated data on equatorial coordinates for Cosmos 55 satellite carrier rocket 03 p0453 N71-13012
- Tabulated tracking data for Cosmos 71 satellite - Jan. through Dec. 1967 03 p0453 N71-13016
- Abstracts of research on upper atmosphere and space 03 p0454 N71-13043
- Soviet news releases on Cosmos satellites, geophysics, oceanography, meteorology, and astronomy [JPRS-51856] 05 p0769 N71-15677
- News releases of Cosmos satellites launching and lunar soil analysis 05 p0681 N71-15682
- Cosmos 142 observation of VLF wave propagation through ionosphere 06 p0857 N71-16498
- Cosmos 261 observations of electron and ion interactions with solar cosmic rays in aurora and photoelectron production 07 p1014 N71-16931
- Cosmos 184 ion sensor for measuring ion velocity at 600 km 07 p1014 N71-16948
- Cosmos 381 ionospheric sounding experiments 07 p1017 N71-17105
- Optical tracking of Cosmos and Explorer satellites, Edinburgh, Sep. 1970 07 p1118 N71-17156
- Optical tracking of Cosmos and Explorer satellites, Edinburgh, Aug. 1970 07 p1118 N71-17157
- Technology review on Soviet Cosmos satellite program 07 p1119 N71-17597
- Energy spectra of multi-charged nuclei measured by Cerenkov counters onboard Cosmos 225 satellite [NASA-TT-F-13311] 09 p1462 N71-20412
- Analysis of geophysical investigations by USSR and other East European Bloc Nations using Cosmos 348 and Cosmos 261 satellites 10 p1463 N71-20775
- Upper atmospheric physics and radio transmissions, Cosmos launches, and Lunokhod I activities 11 p1791 N71-22687
- Ionospheric soundings, Cosmos launches, and lunar exploration 12 p1993 N71-23181
- Gamma radiation spectral composition and intensity space and time distributions from Cosmos 135 including measurement of photon effects due to satellite and detector secondary emissions 12 p1992 N71-23262
- Global distribution of upper atmospheric infrared emission layers from Cosmos 65 data analysis [NASA-TT-F-13400] 12 p1905 N71-23304
- Analysis and interpretation of rocket sounding investigations of infrared radiation layers in upper atmosphere 12 p1994 N71-24264
- Intensity variations and spectral composition of gamma radiation in near earth space measured by Cosmos 135 14 p2334 N71-25799
- Abstracts of scientific articles concerning upper atmosphere and space research, and announcement of Cosmos satellite launches 15 p2396 N71-26864
- Soviet news releases on radio astronomy, synoptic meteorology, oceanography, and Cosmos satellites [JPRS-52898] 15 p2396 N71-26871
- Soviet news releases on launching of Cosmos 400 and 401 and Lunokhod-I activities 15 p2396 N71-26876
- Flights to other planets, Cosmos satellites, international space law, and USSR space achievements 15 p2397 N71-26906
- Satellite optical tracking of Cosmos and other artificial satellites, Edinburgh, Nov. 1970 15 p2519 N71-27032
- Launching of Cosmos, Soyuz, and Mars spacecraft and ionization in E layer 17 p2739 N71-29404
- Cosmos 261 satellite program for observation of low energy electrons and ions [FR-4-PT-1] 17 p2749 N71-30201
- Cosmos 261 satellite observation of upper atmosphere low energy electrons, including scintillation spectrometer description [FR-7-PT-2] 17 p2749 N71-30202
- Cosmos 261 observation of upper atmosphere low energy ions, including ion trap spectrometer description [FR-9-PT-3] 17 p2749 N71-30203
- Cosmos 261 observation of upper atmosphere middle- and high-energy electrons and protons, and instrumentation description [FR-9-PT-4] 17 p2749 N71-30204
- Soviet news releases on Lunokhod lunar roving vehicle and launching of Cosmos 419, 420, and 421 18 p2910 N71-30793
- Cosmos 381 scientific satellite for ionospheric sounding 19 p3185 N71-32661
- Telescope for measuring nuclear component of primary cosmic radiation on Cosmos 163 19 p3178 N71-32741
- Upper atmosphere density deduced from Cosmos satellite deceleration and applied to atmospheric models [D-80] 19 p3097 N71-32784
- Tables of Cosmos and other artificial satellites optically tracked from Great Britain observatories, Mar. 1971 [ROE-STS-112] 20 p3350 N71-32833
- Tables of Cosmos and other artificial satellites optically tracked from Great Britain observatories, Feb. 1971 [ROE-STS-111] 20 p3353 N71-33112
- Tables of Cosmos and other artificial satellites optically tracked from Great Britain observatories in Dec. 1970 [ROE-STS-109] 20 p3354 N71-33159
- Investigation of ultraviolet glow of atmosphere at wavelength of 1304 angstrom line by Cosmos 215 satellite 21 p3420 N71-34332
- Comparison of Cosmos-215 and OGO-8 observations of airglow in 1225 to 1350 Å range at low geomagnetic latitudes 21 p3420 N71-34333

COSMOS 54 SATELLITE

Soviet news releases on Lunokhod 1, Soyuz 11 flight crew, and launching of Cosmos 425 21 p3510 N71-35009

Auroral proton spectra and angular distribution from Cosmos 261 satellite observations, and polar sub-atom concept 23 p3750 N71-36740

Pitch distribution of protons precipitating in auroral zone in range of hundreds keV, as observed from Cosmos 261 satellite 23 p3750 N71-36741

Ground and Cosmos 261 satellite observation of ionospheric disturbances due to chromospheric flare of 27 Dec. 1968 23 p3750 N71-36742

COSMOS 54 SATELLITE

Tabulated tracking data for Cosmos 54 satellite - Jan. through Dec. 1967 03 p0453 N71-13009

Tabulated tracking data for Cosmos 54 satellite - Jan. through Dec. 1967 03 p0453 N71-13011

COSMOS 149 SATELLITE

Characteristics of Cosmos 149 instruments for measurement of solar and infrared radiation emerging from earth 15 p2410 N71-27490

Earth brightness deduced from Cosmos 149 measurement of solar radiation reflected by earth 15 p2514 N71-27501

COSMOS 206 SATELLITE

Weather satellite data on European climate for first quarter in 1968 02 p0254 N71-11469

COSMOS 234 SATELLITE

Cosmos 234 measurements of nitric oxide vertical profile in E and F regions at low sun zenith angles 07 p1014 N71-16934

COSMOS 225 SATELLITE

Electron flux with energy higher than 300 MeV at 250 to 500 km altitudes, observed by Cosmos 225 [NLL-RTS-6033] 16 p2674 N71-28286

Hypothesis on movement of magnetically trapped particles based on Cosmos 225 electron data at 200 to 300 km 24 p4003 N71-38553

COSSERAT SURFACES

Elastic Cosserat surface continuum with deformable strains 17 p2822 N71-29975

Structural analysis of gridwork models for cases of edge loads and distributed moment loads based on Cosserat continuum 23 p3863 N71-37542

COST ANALYSES

Statistical data on delays and cost of delays at airline terminals 01 p0003 N71-10366

Incidence and costs of pilot disorientation Army aircraft accidents during fiscal year 1967 [AD-710987] 01 p0013 N71-10695

Cost analysis of air pollution effects on electric contacts [PB-192478] 03 p6350 N71-12525

Cost analysis and costs of satellite test programs with reference to Azur satellite 03 p0460 N71-12727

Cost analysis of joint NASA-European space program involving navigation and communication satellites for civil air traffic control [ESRO-SP-41] 03 p0409 N71-12756

Cost analysis of accelerator magnet system [NP-18357] 04 p0547 N71-13628

Developing computer programs for optimum economic parameters of conceptual 1000 MW/n LMFBR [WARD-2000-96] 04 p0558 N71-14183

Cost experience of weapon system procurement [AD-712457] 04 p0623 N71-14361

High cost haffium for interaction with transition metals [AD-713778] 05 p0704 N71-15332

Cost analysis of increased ESSA services for estuarine dynamic study in Gulf Coast [PB-194077] 05 p0676 N71-15455

Congressional investigation into contract management and development costs of TFX aircraft [REPT-91-1496] 05 p0789 N71-15649

Critical evaluation and cost analysis of reactivity methods of nuclear materials assay [BNL-30251] 06 p0897 N71-15826

Results of 1968 survey of industrial research and development [NSF-78-29] 06 p0962 N71-16896

Weight, cost and spacecraft reliability analyses of hydrazine and aerosol spin stabilized communication satellite orientation devices 07 p1118 N71-17057

Technical and cost analyses for communications systems using satellites in geostationary orbits [PB-194782] 07 p0991 N71-17120

Reporting financing, accounts, and progress in research and development for atomic energy program in Great Britain [RP-18112] 07 p1063 N71-17365

Refurbishment cost study to identify costs associated with inspection, repair, and replacement of components for space shuttle thermal protection systems [NASA-CR-111830] 07 p1122 N71-18088

Cost analysis of future European space programs with or without NASA cooperation 08 p1307 N71-18708

Low cost launch vehicle system for economical space exploration [NASA-CR-116902] 08 p1294 N71-18726

Analysis of research and development costs by federal and nonfederal agencies [NSF-70-46] 09 p1489 N71-20565

Thermal vacuum and ultraviolet vacuum tests on adhesives, thermoplastic resins, and polymeric films with cost analysis 10 p1664 N71-20673

Examining fuel cycle codes using different techniques for fuel cost calculations 10 p1602 N71-21050

Cost analysis in vertical takeoff aircraft operation for short haul traffic noting influence of airport operation 11 p1674 N71-22193

Flight tests of Concorde prototypes, design modifications, and operational costs of supersonic aircraft 11 p1675 N71-22387

Cost effectiveness in recording experimental data 11 p1718 N71-22732

Cost analysis of data reduction and retrieval methods 11 p1719 N71-22741

Aerospace price indexes for component and material cost changes 12 p2019 N71-24108

Cost distributions and facility and tooling cost impact on unit production costs for 2 and 20 per year production rates in state of art, improved, and advanced manufacturing technologies [NASA-CR-114281] 12 p1931 N71-24180

Computerized life cycle cost model of cost predictions for electronic equipment [AD-717099] 13 p2058 N71-25227

Cost benefit analysis and technology assessment in civil aviation research and development with case histories [NASA-CR-18086] 15 p2366 N71-27010

Nuclear and economic performance calculations for nichium and molybdenum in LMFBR cores [ORNL-TM-3271] 16 p2633 N71-28643

Cost and weight data for space shuttle booster heat sink structural concept 17 p2847 N71-29459

Cost and failure analyses and acceptability data from electronic equipment testing of various electronic components [NASA-CR-119001] 18 p2897 N71-30630

Research and development program evaluation techniques including cost analysis, technology forecasting, market research, and decision making for project management planning 18 p3030 N71-31389

Commercial aircraft performance and cost analysis data for 1968 and 1969 in US 19 p3035 N71-31611

Cost comparison of ground effect machines using box, inverted-tee, and channel cross section tracks [PB-197501] 19 p3036 N71-31782

Comparison of flight simulation techniques and costs 19 p3074 N71-31954

Cost benefit analysis of metrication on commercial weight and measure units activities [NBS-SP-345-3] 19 p3199 N71-32720

Cost analysis and effects of metrication within DOD [NBS-SP-345-9] 19 p3199 N71-32721

Redundancy optimization for series-parallel systems and serially connected k-out-of-n type subsystems, with cost constraints and reliability considerations [NASA-TM-X-67910] 20 p3291 N71-33429

Capabilities, constraints, and costs of Delta launch vehicle, Model 2914 [NASA-TM-X-65674] 20 p3354 N71-33446

Algorithm for cost and potential benefit assessment of TV networking as mode of disseminating information to biomedical communities [BM-6204-NLM] 21 p3395 N71-34166

Cost sensitivity analysis technique applied to developing annual operating costs for ground sensor system [P-4361] 21 p3408 N71-34248

Design of computational algorithms for optical control by Hilbert space methods, and involving cost function [NASA-TN-D-6260] 21 p3449 N71-34551

Effects of space shuttle on costs, mission objectives, and operational modes of OAO/LST program [NASA-CR-121703] 21 p3513 N71-35031

Proposed for economic study of space shuttle effect on OAO/LST program [NASA-CR-121702] 21 p3513 N71-35032

SUBJECT INDEX

Summary of experiment performance options and cost for orbital research centrifuge compatible with Skylab, Space Station, and space shuttles [NASA-CR-111937] 22 p3563 N71-33379

Experiment performance options and cost comparisons of orbital research centrifuge for Skylab and Space Station [NASA-CR-111938] 22 p3563 N71-33380

Cost comparisons and experiment performance options for space shuttle orbital research centrifuge [NASA-CR-111939] 22 p3564 N71-33381

Machine parameters and computer programs for superconducting synchrotron cost analysis [UCRL-20299] 23 p3740 N71-36640

Cost ownership analysis of avionic equipment 23 p3758 N71-36704

Computer program for nuclear fuel burnup calculations and preliminary fuel cycle cost analysis [BNWL-462] 23 p3799 N71-37803

Payload analysis and impact of space transportation system on unmanned satellite costs in 1978 to 1990 23 p3857 N71-37846

Application of life cycle costing techniques to award of contracts for hardware and related support by military procurement agencies [AD-726978] 23 p3870 N71-37850

Performance and costs of nuclear aircraft used in transoceanic commerce [NASA-TM-X-2386] 24 p3964 N71-38277

COST EFFECTIVENESS

System engineering and economic analysis of tracking and data relay satellite system with 16 GHz ground antennas [NASA-TM-X-65370] 01 p0025 N71-10800

Cost effectiveness of LSI circuits 03 p0354 N71-12604

Cost effectiveness of pulse Doppler radar in airborne aircraft of early warning system 04 p0621 N71-13919

Analysis of planning, programming, and budgeting systems [AD-712455] 04 p0623 N71-14333

Equivalent algorithms for optimal planning and scheduling of project networks [DISS-4355] 05 p0713 N71-14670

Investigating repair and maintenance with respect to cost effectiveness and quality [FTL-A-A08-5] 05 p0713 N71-14677

Investigating distribution criteria, effectiveness and cost models in management of resources [FTL-A-A08-7] 05 p0713 N71-14679

Investigating technology and analytic techniques for solving inter-airport transportation problems [AD-707738] 05 p0657 N71-14811

Report to Congress on need for improvement in management of magnetic tapes at GSPC [PB-164392] 05 p0651 N71-15453

Low cost source data terminal for technical test [UCRL-193900] 05 p0652 N71-15578

Cost effectiveness determination for design and maintenance of ultra reliable pulsed Doppler surveillance radar [AD-715064] 07 p0994 N71-17033

Optimizing propulsive/lift system for turboprop STOL aircraft considering cost effectiveness 09 p1459 N71-28662

Cost effectiveness of closer tolerances in manufacturing [UCRL-72380] 09 p1393 N71-28180

Fabrication of low cost ablative heat shield push for space shuttles [NASA-CR-111835] 09 p1473 N71-28012

Economic equipment and layout planning of warehouses using computerized simulation methods 10 p1665 N71-20770

Cost effectiveness in recording experimental data 11 p1718 N71-22731

Cost distributions and facility and tooling cost impact on unit production costs for 2 and 20 per year production rates in state of art, improved, and advanced manufacturing technologies [NASA-CR-114281] 12 p1931 N71-24180

Computerized probabilistic model for optimal assignment of launch vehicle programs to advanced space missions [NASA-CR-114284] 12 p2063 N71-24019

Manual of computer program for probabilistic optimal launch vehicle assignment and budget smoothing model [NASA-CR-114285] 12 p2063 N71-24020

Cost benefit models for German space program, noting technology transfer from space programs to physical sciences and industries - Part 1 [BMBW-FB-W-71-01-PT-1] 14 p2357 N71-25079

Cost benefit models for German space program, noting technology transfer from space programs to physical sciences and industries - Part 2 [BMBW-FB-W-71-02-PT-2] 14 p2357 N71-25079

Cost effectiveness as critical selection requirement for small gas turbines in military and commercial operations 15 p2511 N71-28053

SUBJECT INDEX

- Cost effectiveness and quality control in German scientific satellite space programs 15 p2526 N71-27104
- Investigation of adverse effects of producing QH-50 helicopters prior to completion of development and flight tests 17 p2862 N71-30301
- Technical and cost factors for implementation of Alaskan communication satellite system (NASA-TM-X-45609) 18 p2889 N71-30393
- Review and assessment of documents concerning cost and benefits of ERS satellites, and value of these studies in directing R and D activities (NASA-CR-119363) 18 p3015 N71-31279
- Mathematical methods in production planning with cost effectiveness optimization 18 p3031 N71-31578
- Cost effectiveness model applicable to national data buoy systems and other national marine environmental data collection systems 19 p3091 N71-31965
- Cost effectiveness study of VSTOL versus CTOL aircraft systems (P-4587) 19 p3099 N71-32574
- Economic desirability of space shuttles and cost reducing concepts for payloads (NASA-CR-121499) 21 p3512 N71-35028
- Cost effectiveness, failure analysis, and design techniques for measuring reliability of avionics systems (AGARD-LS-47-71) 23 p3756 N71-36776
- Cost effectiveness of built in test provisions in aircraft operations 23 p3757 N71-36780
- Application of life cycle costing techniques to award of contracts for hardware and related support by military procurement agencies (AD-722996) 23 p3870 N71-37589
- COST ESTIMATES**
- Annual report on marine sources and engineering development from President of US to Congress 01 p0407 N71-10400
- High speed access system evaluation for transportation from jetport to Miami with cost estimates and network descriptions (P-192842) 01 p0038 N71-10417
- Air mail transportation by contract operations 01 p0138 N71-10816
- Subsidies for American certificated air carriers 02 p0308 N71-12190
- Harvesting of algae through chemical flocculation and flotation (REF-321) 04 p0487 N71-13462
- Storage tubes 04 p0505 N71-13838
- Investigating relationship of conversion efficiency to fixed and variable costs in fusion reactors (UCRL-72349) 05 p0730 N71-15242
- Contemporary instrument technology (JPRS-51883) 05 p0687 N71-15470
- Computer program for estimating cost for given road profile (TRW-06818-WD04-R0-00) 07 p1136 N71-18081
- Investigating alternative high speed ground transportation systems for late 1970s or early 1980s (TRW-06818-6041-R0-00) 07 p1138 N71-18106
- Computer program for estimating costs of constructing complicated tunnel-shaft systems (PB-193272) 07 p0998 N71-18110
- Cost estimates and means of funding information analysis centers 09 p1347 N71-19528
- Economic analysis of intercity short-haul business passenger travel (NASA-TM-X-2228) 09 p1488 N71-20114
- Evaluating cost of four processes for production of oxygen difluoride - fluorine-caustic least expensive (NASA-CR-117317) 09 p1345 N71-20266
- Program plans and cost estimates of project for application of bioelectronic technology to patient monitoring systems (NASA-CR-118035) 07 p1868 N71-23849
- Fabrication of prototype low density ablative heat shield panels for space shuttles with production cost estimates (NASA-CR-111874) 12 p2015 N71-24333
- Lunar base synthesis, mission analysis, shelter design, and cost and resource estimates - summary (NASA-CR-103127) 14 p2236 N71-25857
- Cost and resource estimates for lunar shelters and scientific, mobility, and power supply equipment for lunar base (NASA-CR-103132) 14 p2237 N71-25862
- Satellite directional antenna array reduction mechanism design (JED-TP-7213) 15 p2380 N71-27156
- Systems analysis and cost estimates of satellite borne remote sensing for wheat crop and fungus disease control and water management (NASA-CR-1119011) 16 p2387 N71-28445
- Mathematical models for application of satellite borne multispectral remote sensors to water and wheat production management and wheat fungi control in-shedding cost estimates (NASA-CR-1119012) 16 p2588 N71-28446

- Reliability and cost of electrostatic and electromagnetic thruster systems for satellite auxiliary propulsion (NASA-CR-119319) 18 p3091 N71-31146
- Procedures for estimating control costs and emission reductions for specified air pollution sources - summary (PB-198779) 19 p3196 N71-32589
- Costs of target cost underarm for stage one of Saturn 5 launch vehicle 19 p3200 N71-32740
- Assessment of cost of air pollution corrosion damage to metal systems and structures in US, both presently and by 1980 (PB-198453) 20 p3283 N71-33122
- Cost estimates, noise constraints, and supercritical wing compatibility in optimization of turbofan engines for Mach 0.90 to Mach 0.98 commercial air transports (NASA-TM-X-47906) 20 p3338 N71-33246
- Cost estimates and feasibility of compression molded plastic motor cases and nozzles for solid rocket motors (NASA-CR-111951) 20 p3369 N71-33328
- Conceptual design for high energy electron ring accelerator allowing mass production techniques and ensuring low cost (UCRL-20169) 20 p3248 N71-33965
- Cost estimates of national projects for international cooperation in meteorological World Data Center (WMO-289) 20 p3299 N71-33997
- Preliminary research requirements analysis and design and cost synthesis of ground research facilities for hypersonic aircraft (NASA-CR-114323) 21 p3406 N71-34236
- Comparison of logistics problems and cost aspects in selection of aircraft for earth resources surveys (NASA-TM-X-3418) 24 p3917 N71-37928
- Weight and cost estimation for pressurization systems for hydrogen, oxygen, and nitrogen storage (NASA-CR-115284) 24 p3927 N71-38621
- Integrated air-path program analysis and cost techniques to assess multiple program decision impacts on program cost (NASA-TM-X-44620) 24 p4033 N71-38777
- Determining faculty necessary for accredited engineering curriculum as function of faculty workload, number of students, and curriculum characteristics with cost estimates (NASA-CR-123114) 24 p4034 N71-38780
- COST REDUCTION**
- Thermal reactor cost reduction by uniform stress arrangement of fuel elements (EIR-182) 02 p0265 N71-11739
- Space shuttle for space transportation and cost reduction of space missions - international cooperation (NASA-TM-X-46388) 02 p0298 N71-11932
- Cost reduction by reliable performance life testing of gyroscopes 03 p0411 N71-13204
- Low cost design study for turbopump concepts (NASA-CR-102923) 04 p0406 N71-14064
- Flight simulations for accelerated development of aircraft at reduced cost 06 p0831 N71-16062
- Cost reduction procedures for aircraft turbine engines used in civil aviation (NASA-TM-X-52951) 06 p0941 N71-16592
- Discussing techniques for improving quality and reducing cost of silicon chips used in integrated circuits 07 p1087 N71-17277
- Development and characteristics of low cost engines for general aviation aircraft 09 p1457 N71-19458
- Mariner Mars 1971 mission support plan modifications and cost reductions by DSN 11 p1829 N71-22768
- Automated system for cost reduction in calibrating bolometer mounts by cutting power measurement time 12 p1919 N71-23632
- Cost data contributions for calibration and maintenance cost reduction 12 p2017 N71-23636
- Optimization of calibration intervals and cost reduction 12 p1919 N71-23637
- Breakthrough techniques for cost reduction, and measurement and calibration services 12 p2017 N71-23641
- Data system for improving instrument reliability and reducing costs 12 p1920 N71-23644
- Computer system for development and application of high resolution mass spectrometer 12 p1922 N71-24052
- Performance of nickel and iron heat block-shields for Isotope Kilowatt Program evaluated for both organic and steam Rankine cycle systems and for thermoelectric systems (ORNL-TM-3213) 13 p2087 N71-25455
- Potential feasibility of safe, practical, and economical air breathing nuclear propulsion system for aircraft and air cushion vehicles (NASA-TM-X-67837) 13 p2123 N71-25524

COUETTE FLOW

- Reduction of overall program costs for reusable space shuttle by use of beryllium as primary structural material 17 p2848 N71-29465
- Congressional hearings on charged airline travel 17 p2861 N71-29707
- Compilation of information on assembly technology for efficiency and cost reduction (NASA-SP-5934/01) 18 p2930 N71-31394
- Technology development for low cost rocket boosters and estimates of total cost reduction obtainable by implementation (NASA-TM-X-67912) 20 p3340 N71-33578
- Resistance welding to join compressor and turbine parts reducing weight and cost of jet engines (NASA-CASE-LEW-10533-1) 21 p3433 N71-34424
- Economic desirability of space shuttles and cost reducing concepts for payloads (NASA-CR-121499) 21 p3512 N71-35028
- Minimization of space shuttle maintenance costs through application of commercial airline maintenance concepts 22 p3674 N71-36195
- COSTA RICA**
- Magnetic and bathymetric survey profile in Pacific Ocean from Costa Rica to central California (ESSA-TR-ERL-179-AOML-3) 18 p2917 N71-31268
- COSTS**
- NT LOW COST**
- Differences in policies and practices of DOD, AEC, and NASA in paying corporate expenses at government-owned contractor-operated plants 01 p0135 N71-10013
- Low cost turbopump design and development (NASA-CR-102923) 02 p0299 N71-11911
- Low cost, ablative heat shield for space shuttles (NASA-CR-111795) 02 p0306 N71-12067
- Cost analysis and costs of satellite test programs with reference to Azar satellite 03 p0469 N71-12727
- Profile construction, cost benefits, economics, and user surveys in transfer of technology and selective dissemination of information 12 p1867 N71-23596
- Technology and data used to generate thermionic reactor experiment cost estimate (GSRB-2123) 13 p2123 N71-25537
- Airline operations, costs, effects on aircraft industry, and cooperation with CAB 17 p2860 N71-29256
- Minimal 2-arc connected graph on a nodes for synthesizing minimum communication networks (P-2371-1) 19 p3123 N71-33212
- Costs and benefits of nuclear hardness criteria and system design specifications (AD-727010) 23 p3818 N71-37235
- Status, cost-effectiveness, and telecommunication/satellite requirements of computer-based instruction (NASA-CR-122945) 23 p3869 N71-37583
- Models for single-server queueing systems with intermittent service and economic measure of system performance (AD-728006) 24 p3950 N71-38179
- COTTON FIBERS**
- Elastic bonding, tearing, and breaking of cotton fiber and nylon fabrics with rubber and plastic coatings (RAB-TR-70112) 06 p0876 N71-15741
- Equivalent rigidity of cotton, wool, and nylon fibers increased in parallel electric field (NLL-RTS-5749) 16 p2616 N71-28285
- COUCHES**
- Shock absorbing articulated multiple couch assembly (NASA-CASE-MSC-11253) 03 p0328 N71-12343
- COUETTE FLOW**
- Thermal conductivity of humid-vacuum insulation and heat transfer during sublimation in rarefied gas medium for Couette flow (AD-715233) 07 p1130 N71-17727
- Variational formulation of turbulent Couette flow 08 p1181 N71-18159
- Characteristics of Couette flow of radiating ionized gas and development of absorption coefficient model 14 p2346 N71-26602
- Approximate solution for time dependent boundary value problems including Couette flow, Rayleigh problems, oscillating wall flow, and second propagation using Chapman-Enskog theory 15 p2393 N71-27322
- Density distribution measurements in rarefied gases contained between two concentric cylinders undergoing relative rotation, and heat transfer and drag measurements 16 p2583 N71-28076
- Statistical mechanics for wall shear turbulence in Couette flow based on Brownian motion and comparison with stochastic theory based on Navier-Stokes equation (NASA-CR-119607) 19 p3079 N71-32245
- Physical and numerical experiments on viscous, time dependent rotational Couette flow (PB-196599) 19 p3080 N71-32332

Finite integral method of solving elliptic differential equations for steady Couette flows in two dimensional domains [EFT/NA-33] 20 p3250 N71-33332

COULOMB COLLISIONS

Static quadrupole moments measurement of first excited $2p$ states of Fe-106 and 110 nuclei by heavy ion Coulomb excitation [COO-1746-32] 03 p0429 N71-12898

Deriving Fokker-Planck equation for Coulomb scattering into loss cone in presence of ambipolar potential [CRA-CONF-1609] 07 p1085 N71-18148

Accurate treatment of Coulomb interaction associated with localized center [AD-716730] 10 p1606 N71-20825

Strength distribution for coulomb mixing of isospin state 12 p1977 N71-24250

Reorientation effect of gamma ray angular distribution in Cd isotopes caused by Coulomb excitation 13 p2141 N71-25540

Coulomb three body interaction for calculating muon meson transitions in collisions with hydrogen isotopes [JINR-P4-5039] 15 p2464 N71-27199

Nonrelativistic mechanics for time dependent scattering of two spinless particles with application to Coulomb potentials 15 p2476 N71-27574

Hyperfine interactions of first excited $2p$ states of Sm-154 and U-238 studied using Mossbauer effect following Coulomb excitation 15 p2485 N71-27817

Hydrodynamic equations for arbitrary anisotropic plasma allowing for Coulomb collisions among plasma particles [DP-17112] 15 p2503 N71-27891

Angular distributions and absolute cross sections measured for Be-9 plus t reaction below Coulomb barrier [CRA-R-4117] 17 p2793 N71-29477

Negative pion-nucleon Coulomb scattering cross sections including angular distributions, transverse momentum distributions, and comparisons with nuclear models 17 p2797 N71-29802

Perturbation method for solving collision problem in three body interactions according to Coulomb law [JINR-P4-5068] 17 p2810 N71-30384

Modification of coupled-channel code [JUPITOR 1] including expansion of deformed optical potential in terms of Legendre polynomials and Coulomb excitation [KFK-1333] 23 p3811 N71-37170

COULOMB POTENTIAL

He-3/H-3 charge form factor and He-3 Coulomb energy [RLO-1388-575] 01 p0099 N71-10711

Coulomb corrections to Bethe-Heitler cross sections for electron-surface bremsstrahlung [NASA-TD-D-6038] 01 p0103 N71-10999

Energy level calculations for spherical and deformed Woods-Saxon potentials with Thomas type spin-orbit coupling [LA-4329] 03 p0424 N71-12806

Generalized integral equation for two body scattering potential in core interactions using tensor and Coulomb forces [COO-1746-37] 04 p0384 N71-14204

Statistical models of electrons in atoms using Coulomb approximation [AD-712719] 04 p0594 N71-14450

Fast charged particle scattering on Coulomb and short range potentials and amplitude expressions [IPVE-STF-69-106] 07 p1080 N71-18122

Even-even isotopes of tellurium of masses between 122 and 130 studied by Coulomb excitation [INP-18447] 08 p1257 N71-18516

Applying Green function theory to calculation of longitudinal and transverse dielectric functions in neutral, isotropic, equilibrium plasma 08 p1275 N71-19249

Permeability of one dimensional potential barriers in chemical reactions 09 p1429 N71-19745

Perturbation expansion of Coulomb potential for determining pair distribution function in plasmas 10 p1631 N71-21817

De-excitation of gamma rays following Coulomb excitation of Bi-211 and 153 using Ge/Li spectrometer 11 p1810 N71-23835

Application of Faddeev and Coulomb T-matrix to electron capture in hydrogen 12 p1975 N71-24050

Nonrelativistic mechanics for time dependent scattering of two spinless particles with application to Coulomb potentials 15 p2476 N71-27574

Expansion of scattering amplitude and solutions to multi-Coulomb type equations using generators and Casimir operators of invariance groups 17 p2772 N71-29697

Hyperfine interactions in research fields including perturbed angular correlation, NMR, Coulomb recoil

implantation, rotational states, and electric monopoles - lectures 19 p3157 N71-32478

[NP-18702]

Elastic scattering processes using nonlocal separable interactions with general expression for transition amplitude [LYCN-7069] 22 p3639 N71-35938

Three-dimensional Green function solution for field emission from spherical tip with arbitrary perturbative potentials 22 p3651 N71-36033

Theory of deuteron breakup in nuclear and Coulomb fields using distorted wave Born approximation 23 p3821 N71-37260

COULOMETERS

Coulometer titration and thermodynamic properties of copper sulfides for solar cells [ESRO-CR-14] 03 p0318 N71-12269

Alkaline-type coulometer cell for primary charge control in secondary battery recharge circuits [NASA-CASE-XGS-05434] 09 p1327 N71-20491

Polarographic, coulometric, and photographic gas analyzers for air pollution measurements 11 p1761 N71-22058

Development and characteristics of battery charging circuits with coulometer for control of available current [NASA-CASE-GSC-10487-1] 13 p2030 N71-24719

COULOMETRY

Research progress on acidity measurements, pH measurements, calibration of ion selective electrodes, and high precision coulometry [NBS-TN-543] 04 p0486 N71-13456

Controlled potential coulometric and potentiometric titrations of uranium and plutonium in mixed oxide, carbide, and nitride ceramic-type materials [LA-4537] 10 p1511 N71-20654

COUNTERFLOW

Counterflow test facilities for high velocity research [NASA-TM-X-66534] 04 p0515 N71-13581

Flooding phenomena in cryogenic heat pipe with vertical two phase counterflow [CEA-CONF-1496] 05 p0724 N71-14973

Computerized design and operation of sodium-water counterflow heat exchanger [CEA-CONF-1592] 09 p1486 N71-20564

Column method of counterflow crystallization of alloys in molten state 10 p1573 N71-20668

Counterstream continuous gas chromatography distillation of nitrogen/liquid system [NLL-RTS-6323] 17 p2716 N71-30213

COUNTERMEASURES

NT CRAFT

NT ELECTRONIC COUNTERMEASURES

NT JAMMING

Industrial noise and countermeasures - research methods and measuring devices [AD-720414] 14 p2296 N71-25878

COUNTERS

NT CERENKOV COUNTERS

NT ELECTRON COUNTERS

NT GEIGER COUNTERS

NT NEUTRON COUNTERS

NT NEUTRON SPECTROMETERS

NT PARTICLE TELESCOPES

NT PROPORTIONAL COUNTERS

NT QUANTUM COUNTERS

NT RADIATION COUNTERS

NT SCINTILLATION COUNTERS

NT SPARK CHAMBERS

Reducing noise in multiplier of quadrupole mass spectrometer when operating in ion counting mode [NASA-CR-1747] 07 p1033 N71-18032

Use of Pioneer 7 and 8 cosmic dust detectors in Apollo 17 lunar ejecta and micrometeorite experiment to measure meteoroid fluxes on moon [NASA-CR-118663] 14 p2339 N71-26441

Circuit for measuring wide range of pulse rates by utilizing high capacity counter [NASA-CASE-XNP-06234] 15 p2338 N71-27137

Calibration procedure for Coulter counter allowing for effects of particle shape for particle size determination [NLL-TRANS-5196-11556/1] 17 p2808 N71-30353

Gas phase diffraction unit employing particle counting techniques for molecular structure investigations requiring small sample quantities [COO-2058-2] 18 p2980 N71-30740

Reliability of Coulter counter particle sizing techniques - sampling reproducibility and statistical analysis of pellet differences [MLM-1810] 19 p3101 N71-32314

Development of techniques for analyzing size of fine particles using Coulter counter and Joyce centrifuge [REF-833] 20 p3288 N71-33897

COUNTING

Mainframe data counting and time tagging [NASA-TM-X-65391] 04 p0612 N71-14124

Counting interval for pulsed beams [RLO-1925-42] 05 p0745 N71-15709

Counting probability methods for estimating whether particles with given initial wave functions will

be in given volumes at least once between two distinct fixed times 19 p3142 N71-32379

COUNTING CIRCUITS

NT SCALERS

Reversible ring counter using cascaded single electron controlled rectifier stages [NASA-CASE-XGS-01473] 01 p0034 N71-10607

Capacitor sandwich structure containing metal sheets of known thickness for counting penetration rates of meteoroids [NASA-CASE-XLE-01246] 01 p0056 N71-10709

Electronic counter circuit utilizing magnetic core and low power consumption [NASA-CASE-XNP-06636] 03 p0348 N71-12513

Synchronous counter design incorporating cascaded binary stress drivers by previous stages and inputs through NAND gates [NASA-CASE-XGS-02440] 09 p1331 N71-20492

Boolean algebra applied to logic counting circuits 10 p1528 N71-21140

Digital cardiometer incorporating circuit for measuring heartbeat rate of subject over predetermined portion of one minute also converting rate to beats per minute [NASA-CASE-XMS-02399] 11 p1692 N71-22806

Reversible logic performing both counting and shifting logic operations also capable of minifunction and integration in basic circuits [NASA-CASE-XNP-01753] 11 p1721 N71-22807

Noninterruptible digital counter circuit design with display device for pulse frequency modulation [NASA-CASE-XNP-09739] 13 p2052 N71-24801

Counter-timer system using dead time and pulse repetition rate [NP-18655] 14 p2258 N71-26511

Scalar readout and control for radiation counter measurements [DMS-TN-67] 15 p2461 N71-27808

Counting circuit satellite for timing code generator [RAE-TN-70242] 20 p3270 N71-33932

Fabrication of high speed logic counting circuits using bipolar processes 23 p3737 N71-36844

Bi-directional counter for operation with model OM Gold hot-wire anemometer systems [AD-727602] 24 p3925 N71-38888

COUPLED MODES

Mode coupling and energy cascades in turbulent spectrum of thermal ionized plasma [NASA-TM-X-52919] 02 p0279 N71-11460

Analysis of mode coupling conditions in ionosphere for solar radio waves [NASA-CR-118640] 14 p2216 N71-23913

Calculating vibrational excitation of CO₂ for microwave coupling and normal mode at high temperature [NASA-CR-1841] 15 p2458 N71-28040

Far infrared Michelson gas laser with variable output coupling [NBS-TN-395] 17 p2759 N71-30199

COUPLED

NT ANTENNA COUPLERS

NT COUPLING CIRCUITS

NT DIPLEXERS

COUPLING

NT CROSS COUPLING

NT GYROSCOPIC COUPLING

NT MICROWAVE COUPLING

NT OPTICAL COUPLING

NT SPIN-SPIN COUPLING

NT THERMODYNAMIC COUPLING

Energy level calculations for spherical and deformed Woods-Saxon potentials with Thomas type spin-orbit coupling [LA-4329] 03 p0424 N71-12806

Superpropagator of fields with exponential coupling [DESY-7026] 04 p0294 N71-14435

Air-coupling acoustic energy into and through oil with emphasis on shear wave propagation [AD-716342] 07 p1434 N71-19351

This perfectly conducting fences used to reduce mutual coupling of two parallel plane waveguides [NASA-TN-D-5914] 09 p1350 N71-20610

Spin-orbit coupling and energy shifts in single crystal anisotropic graphite 10 p1634 N71-21894

Perturbation expansion of Coulomb potential for determining pair distribution function in plasmas 10 p1631 N71-21817

Magnetic coupling in composite ferromagnetic structures consisting of two permalloy films 70.7 percent Ni and 18.3 percent Fe with thin separation layer of chromium and/or gold 11 p0000 N71-32014

Isosensor couplings in electromagnetic interactions including energy distributions 12 p1978 N71-26235

Coupling resonance effects on vertical emission in electron beam distributions 14 p2312 N71-30706

Chiral dynamics of vector meson field coupling and true approximations of scattering amplitudes in Veneziano models [DEMO-71/1] 15 p3489 N71-37803

SUBJECT INDEX

- Equilibrium and saddle point gauge vibration of deformed nuclei and effects on quadrupole coupling constant
[JNR-P-1201] 16 p2359 N71-29173
- Application of algebraic realizations to pion-nucleon couplings in chiral dynamics and Yang-Mills field theory
[JNR-P-5759] 22 p3840 N71-35950
- Resolutive effects of alpha-particle hypersonic coupling laser in NIBSCONHO radical formed from gamma-irradiated hydroxyacrylate crystals
[JNR-18449] 24 p3971 N71-38329
- Coupling Circuits**
Coupling network for high power pulse NMR
05 p3551 N71-12536
- Effect of interelement mutual coupling on radiation pattern of linear antennas in electric coupling
[AD-74081] 06 p0822 N71-16342
- Interconnector and current driver circuit for combination of transistor flip-flop circuit
[NASA-CASE-X08-69054] 09 p1363 N71-19547
- Antenna complex prototype for improving communication under severe radio interference
[AD-716475] 09 p1559 N71-19946
- Design and characteristics of photo receiver and electronic loop installed in optical communication system
[AD-719509] 13 p2046 N71-24956
- Antenna array at focal plane of reflector with coupling network for beam switching
[NASA-CASE-GSC-10220-1] 15 p2381 N71-27233
- Planar modulator with tunable variable length electrical lines including coupling and vectorial delay elements
[NASA-CASE-MSC-13201-1] 16 p2561 N71-28429
- High efficiency transformerless amplifier modulator coupled to RF power amplifier
[NASA-CASE-GSC-10668-1] 16 p2561 N71-28430
- Coupling Coefficients**
Capacitive and inductive couplings for surge voltage distribution optimization in layered windings
01 p0854 N71-18515
- Deriving dual theory of processes involving external and internal acoustic hydrogens in form of quantal balance principle
[KOO-254-556] 04 p0579 N71-13980
- Resonance product estimated from superconvergent sum rules obtained from helicity flip amplitudes of pion-nucleon scattering
[RLQ-2041-42] 05 p0742 N71-15122
- Using wave functions of strong coupling constant as test functions for calculating three nucleon ground state energy
[JTF-70-31] 06 p0910 N71-15782
- PORTMAN 4 subroutines for coupling coefficients and matrix elements in quantum mechanical theory of nuclear moment
[NASA-TN-D-6173] 07 p0150 N71-17337
- Coupling coefficient derived for three-wave interaction in beam plasma system
[NASA-CR-116783] 08 p1273 N71-18696
- Recursive functions and coupling coefficients of fractional percentages for a yields a minus 2 for like nucleus-nucleon interactions based on shell theory
[UCRL-10061] 15 p2138 N71-25474
- Three components of D spin for rule selection in beta coupling
[KOO-364-570] 14 p2388 N71-23723
- Rho-proton coupling constant and rho-nucleon scattering amplitudes determined by Glauber model of multiple scattering
[JNR-P-1166] 16 p2654 N71-29837
- Calculation of quadrupole interaction constant ratio in solid hydrogen based on isotropic neutron scattering distributions
[JPR-1527] 21 p3470 N71-34794
- Scalar and pseudoscalar meson mass formulas, coupling constants, and pion pion scattering lengths from delta meson formation of direct products of SU(2) and SU(2) and SU(3) and SU(3)
[JL-72-023] 23 p3819 N71-37240
- Couplings**
Quick-release coupling for fueling rocket vehicles and cryogenic propellants
[NASA-CASE-X08-61903] 01 p0880 N71-10782
- Load distribution on gear tooth couplings
06 p0862 N71-15736
- Impact mechanism for high speed operation at impact loading
[NASA-CASE-MPB-12805] 07 p1837 N71-17805
- Ball nut and ball separation device
[NASA-CASE-X08-6014] 10 p1347 N71-21480
- Coupling characteristic effects on dynamic response of stability coupled turbomachinery with digital computer program based on transfer matrix techniques
11 p1770 N71-22712
- Quick disconnect duct coupling device for straight-hand operation
[NASA-CASE-MPB-20395] 13 p2086 N71-24903
- Couplings**
U. PATER
COVARIANCE
Covariant quantum geometrodynamics
02 p0274 N71-18557

- Covariance matrix for deflections of vertical and meridians based on arcual gravity data
[AD-713351] 02 p0222 N71-12168
- CPT and inelastic-component fields and covariance analysis of quantized fields
[JNR-32-5140] 04 p0588 N71-14283
- Constraints on equal time commutators from Lorentz covariance
[JPR-74-470] 06 p0853 N71-19831
- Random errors in a twenty-four hour orbit analysis navigation system, air navigation and covariance matrices
[DLR-FB-76-36] 07 p1856 N71-17121
- Recursive computation of uncoupled and filtered least squares estimates for lumped signal processing in additive white noise given covariance functions
[AD-716477] 09 p1363 N71-20336
- Mean estimation of multivariate normal distribution with covariance matrix on identity and sum of squared error loss
[AD-710536] 10 p1394 N71-21675
- Statistical equation relating mean values of pressure, temperature, and density with correction term proportional to covariance between density and temperature
[NASA-TR-R-365] 11 p1747 N71-22066
- Development of Machine theory of inertia and gravitation
12 p1912 N71-23696
- Quantum Bianchi Monotonic and field equations derived from Lagrangian for general relativity
[AD-718977] 13 p2128 N71-24365
- Covariant density matrix for arbitrary spin particles
[JNR-P-4951] 15 p2464 N71-27197
- Quantization of interacting covariant massless fields using Lagrangian formalism with prescribed asymptotic field data
15 p2476 N71-27472
- Two-body error analysis computer program to evaluate residual state vector and covariance matrix for orbit after one coast and one burn maneuver
[NASA-TM-X-45620] 18 p0807 N71-30511
- Subroutine WSHRT for generating matrix of variances and covariances of Wishart distribution
[NASA-CR-121888] 22 p3684 N71-35670
- Connection between conformal covariance and gauge invariance of interactions
[JNR-72-5716] 23 p3087 N71-37143
- Analyticity, covariance, and unitarity in quantum field theories regularized by finite mass, indefinite norm states
[JNR-3992-26] 23 p3814 N71-37282
- Covariance analysis of relative velocity response spectra derived from horizontal ground motion
[INVO-1163-TM-34] 24 p3912 N71-37882
- COVERINGS**
High vacuum ion beam sputtering of integral coverings for solar cell utilization
[NASA-CR-121468] 20 p3214 N71-33685
- Interferometric test method for lunarlander chamber cover glass conformity to planarity specifications
[NBS-TN-579] 23 p3739 N71-36802
- COVERS**
U. RAYS (TOPOGRAPHIC FEATURES)
COWELL METHOD
U. NUMERICAL INTEGRATION
CRAB NEBULA
Mechanism of relativistic electron injection in Crab Nebula
[CSTRO-TRANS-10122] 04 p0687 N71-13625
- Small angular size point-like source in Crab Nebula
[CSTRO-TRANS-10211] 04 p0688 N71-14444
- Diffuse ultraviolet X ray detection and polarization of Crab Nebula emissions
[AD-717671] 11 p1822 N71-23450
- Radio map of the Crab nebula at 3.5 mm
[JPR-47] 17 p2043 N71-29352
- CRACK FORMATION**
U. CRACK INITIATION
CRACK INITIATION
Analysis of crack initiation in solder joints on printed circuit boards
[NASA-TM-X-53963] 01 p0834 N71-10409
- Investigating effects of surface and through cracks on failure of pressurized thin-walled aluminum cylinders
[NASA-TN-D-6899] 02 p0302 N71-12050
- Stress hour framing camera for photographs of growth and effects of crack formation of materials stressed by explosives
[UCRL-72543] 03 p0347 N71-13628
- Crack initiation and arrest beneath restraints of A533 grade B class 1 pressure vessel steel
[JESTP-74-4] 04 p0331 N71-14288
- Plastic deformation, notch tests, crack initiation, and strain concentration in flat steel plates
[TU-84-1970] 07 p1124 N71-17523
- Thermal elastic stresses and crack initiation and propagation in flat glass plates
[JESTP-74-70] 07 p1124 N71-17535
- Crack initiation in stress corrosion cracking of aluminum base alloys
[SC-ER-76-718] 08 p1212 N71-18277

CRACK PROPAGATION

- Deformation mechanisms of crack initiation in structurally loaded joints under loads
[AD-715712] 09 p1286 N71-18322
- Crack initiation in heat affected zone of low alloyed high strength steels during weld and tensile tests
[CRIP-MT-63] 06 p1214 N71-18385
- Hydrogen embrittlement of titanium as related to stress-corrosion cracking
[NASA-CR-117177] 09 p1465 N71-20462
- Brittleness and surface crack initiation in steel castings
10 p1562 N71-20703
- Brittleness and microcrack initiation in chromium steel piston heads
10 p1572 N71-20819
- High temperature crack initiation and propagation in aluminum and aluminum alloys with emphasis on grain size effects
10 p1576 N71-21013
- Determining cyclic deformation and strain concentration factor at notch root of flat specimens by extensometer
[TUE-94/1970] 11 p1836 N71-23477
- Fracture mechanics evaluation of stress intensity factors for various crack geometries and loading conditions
[WAFD-TM-976] 12 p3884 N71-33163
- Crack initiation and propagation modes of roller contact bearing heads
15 p2413 N71-28833
- Fracture toughness data utilizing small notched round tensile steel specimens with hydrogen embrittlement as crack starter
15 p2425 N71-27618
- Stress-strain diagrams for crack loading of brittle bodies weakened by pointed concentration
[AD-720979] 15 p2523 N71-27865
- Fatigue crack initiation and propagation in aluminum alloy bones and beryllium matrix composites
[AD-722005] 16 p2688 N71-30181
- Masked eddy current probe for crack detection in Rover fuel element casing
16 p2685 N71-28738
- Thermodynamics of crack initiation in dry operating graphite ring seals
17 p2756 N71-30824
- Stress intensity factor and shape of edge crack in plate under tension
[NASA-TM-X-47091] 19 p3188 N71-32229
- Stress concentration and fracture mechanics for isotropically pressurized thick-walled cylinders with cracks and effects of cyclic loads
[AD-726641] 20 p3357 N71-33034
- Critical points, crack formation, and shrinkage characteristics for castings of Cu-Ni, Cu-Mn, and Mn steels
[NLL-TRANS-746-295-[5082.001]] 23 p3597 N71-35611
- Aluminum concentration effects on stress corrosion cracking of titanium alloys at ambient temperatures in aqueous solutions of salt
[NASA-CR-122935] 23 p3749 N71-36862
- Hydrogen embrittlement of titanium alloy surface in hot salt corrosion cracking
[NASA-CR-1239] 23 p3772 N71-36882
- Crack formation and yield phenomena during plastic deformation of steels
[AD-727233] 24 p3956 N71-38083
- Techniques for testing high strength steel used to determine resistivity to cold crack formation during welding under biaxial stress conditions
[AD-727609] 24 p3940 N71-38110
- CRACK PROPAGATION**
Mathematical crack problems concerning square and hexagonal holes with small symmetrical corner cracks
[AD-709048] 01 p0129 N71-10442
- Fatigue crack propagation in copper and copper-aluminum single crystals
[AD-711676] 01 p0113 N71-10954
- Investigating low-cycle fatigue crack propagation in titanium alloys exposed to air and hot water environments
[AD-712056] 02 p0240 N71-11332
- Ductile fracture in anisotropic solids studied by Dugdale model
[AD-712122] 02 p0280 N71-12100
- Heat treatment studies of aluminum alloy type 7079 forgings including tensile strength, fatigue and crack resistance and stress corrosion resistance
[NLR-TR-69058-L3] 02 p0345 N71-12126
- Photograph and yielding in low stress steels
[JPR-192306] 03 p0362 N71-12981
- Stress corrosion cracking of Inconel 600 titanium base alloy
[SC-ER-76-371] 04 p0329 N71-14068
- Inhibition and extent of ductile pipe rupture
[BMJ-1087] 04 p0610 N71-14145
- Plane element stress analysis of crack in bi-material plate
[AD-713593] 05 p0775 N71-14598
- Metallographic studies including electropolishing, anodic etching, and crack propagation
[CONF-69054] 05 p0699 N71-14688

Considering methods for evaluating fracture toughness of structural materials
[MGA/5368] 05 p0776 N71-15194

Crack growth rate dependence on stress intensity factor in hot rolled banded steel plate
[AD-713536] 05 p0704 N71-15331

Characteristics of crack stability in contoured double cantilever beam specimens
[AD-713512] 05 p0779 N71-15340

Computer simulation of fracture
[UCRL-72640] 05 p0779 N71-15359

Investigating alloy effects on stress corrosion cracking of Fe-Cr-Ni base alloys in boiling MgCl₂ solutions
[COO-1319-81] 05 p0785 N71-15367

Crack growth rates under reversed tension-compression, strain controlled load in nuclear piping steels
[GEAP-10181] 06 p0670 N71-15901

Fracture, fatigue, and crack propagation of aluminum alloy sheet and flat plates
[AD-714019] 06 p0872 N71-16330

Investigating mesh materials for deployable antennas, radiation tolerance of solar array components, and crack propagation threshold for isopropyl alcohol and titanium alloy
06 p0826 N71-16681

Densification of plutonium and uranium dioxides, radiation effects on fission gas release, and crack formation during reactor power rise
[ORNL-TR-2387] 06 p0901 N71-16810

Thermal elastic stresses and crack initiation and propagation in flat glass plates
[REPT-570] 07 p1124 N71-17535

Measurement of fatigue crack propagation in aluminum alloys at high stress
[NASA-CR-1732] 07 p1127 N71-18002

Crack propagation in aluminum alloy sheet materials under flight simulation loading
[AD-715331] 08 p1211 N71-18245

Fatigue mechanics of aluminum alloy and steel crack tip regions
[AD-715421] 08 p1297 N71-18645

Effects of surfaces and environment on nucleation and growth of fatigue cracks in copper
[NASA-CR-116859] 08 p1280 N71-19031

Fatigue mechanisms in fracture of glasslike polymers
08 p1300 N71-19173

Dynamic crack propagation according to nonlinear atomic separation laws
08 p1266 N71-19211

Crystal orientation and material processing effects on fatigue crack propagation in brass and stainless steel
08 p1282 N71-19306

Crack arrest in transversely loaded elastic plates
[UCRL-72335] 09 p1477 N71-20000

Steady pH region at tips of stress corrosion cracks in aluminum alloys associated with onset of precipitation
[AD-716480] 09 p1400 N71-20091

Structural analysis of circular crack partially embedded in solid of finite thickness
[NASA-CR-114240] 09 p1482 N71-20544

Computer programs for analyzing crack propagation in cyclic loaded structures
[AD-717150] 10 p1651 N71-20776

Development of fracture model to predict rate of crack propagation under high temperature low cycle fatigue conditions based on creep rupture principle
12 p2008 N71-24283

Fracture and crack growth for welded joints of SAl-2.5Sn titanium in environment of low pressure, high purity hydrogen
[NASA-CR-114859] 13 p2091 N71-24378

Stress analysis of central transverse crack in stiffened fiber reinforced composite panel under tension
[AD-719694] 13 p2099 N71-24429

Prediction of critical length of fatigue cracks based on concepts of linear elastic fracture mechanics
[AD-719757] 13 p2182 N71-25141

Determination of conditions leading to fracture arrest by circular hole ahead of propagating crack by dynamic photoelasticity technique
[AD-719934] 13 p2183 N71-25398

Fracture mechanics and anisotropy of fatigue crack propagation in hot rolled banded steel plate
13 p2183 N71-25444

Stress intensity factor calculated for cracked sheet with riveted and uniformly spaced stringers
[NASA-TR-358] 14 p2273 N71-25934

Micromechanism of crack propagation in brittle materials and description of motion of crack zone during crack propagation
14 p2349 N71-26358

Crack initiation and propagation modes of roller contact bearing fatigue
15 p2413 N71-26833

Crack propagation and tensile and yield strengths of stainless steels
[TD-25664] 15 p2421 N71-27059

Stress corrosion crack arrest and crack propagation in titanium alloys proving crack arrest stress intensities higher than those for crack initiation when testing thin materials
[AD-728235] 15 p2426 N71-27748

Stress wave emission as measure of crack growth in materials failure
[ARL/NET-72] 15 p2522 N71-27857

Effects of surface layer on plastic deformation and rate of crack propagation of metals used in pressure vessels
[AD-721292] 16 p2608 N71-28131

Fatigue crack initiation and propagation in aluminum alloy boron and beryllium matrix composites
[AD-722099] 16 p2608 N71-28181

Effect of orientation and specimen thickness on fatigue crack growth rate of 4340 steel
[AD-722728] 17 p2763 N71-29812

Fatigue crack length relationship with aircraft inspection intervals and structural reinforcement, high strength materials, and aircraft usage effects
18 p3021 N71-30783

Measurement of crack propagation velocities in silicon and germanium using ultrasonic fractography
[REPT-770] 19 p3109 N71-31704

Fracture mechanics for predicting fatigue crack propagation and velocity in aluminum alloy
[AD-723285] 19 p3187 N71-31778

Structural response and acoustic transmission characteristics of glass pane and standard wood frame construction wall panels subjected to static loads
[NASA-CR-111925] 19 p3190 N71-32488

Stress conditions and behavior of materials with sharp cracks subjected to thermal and mechanical loads
[NASA-TT-F-13699] 19 p3190 N71-32554

Crack propagation in aluminum alloys reinforced with boron and stainless steel fibers
[UCRL-20524] 20 p3288 N71-33598

Strain hardening and stress relaxation effects on crack propagation with problem notes on plasma physics, communication sciences, electronics, metallurgy, and ocean and space technology
20 p3360 N71-33871

Critical equilibrium of two-component composite with crack originating along dislocation of round inclusion and entering with one tip into binder
[NASA-TT-F-13934] 21 p3527 N71-35131

Studying fracture surface striations and crack propagation in aluminum alloy by electron microscope
[NLR-MP-69014-U] 21 p3529 N71-35149

Effects of hydrogen and hydrogen-oxygen mixtures on fracture of high strength steel in precracked configuration
[NYO-3975-3] 22 p3594 N71-35590

Crack propagation and compatibility of high toughness, low strength steels with N2O4 and UDMH propellants
[AD-726540] 22 p3595 N71-35598

Clinical analysis of crack propagation in glass
[AD-726710] 22 p3603 N71-35664

Fracture mechanics of plastic stress and strain fields near crack tip and computer simulation of fracture spreading in viscoelastic solid
[AD-726745] 22 p3691 N71-36321

Analytical superposition model for environmentally-assisted corrosion fatigue crack propagation in aluminum and steel alloys
[UCRL-20538] 23 p3840 N71-37520

Plastic deformation at tip of fatigue crack in high strength steels
24 p4024 N71-38715

X-ray microbeam studies of plastic zone at tip of fatigue crack
24 p4025 N71-38716

Kinetic theory of fatigue propagation based on vacancy condensation mechanism
24 p4025 N71-38718

CRACKING (FRACTURING)
Abstract journal on stress corrosion cracking
[AD-709903] 01 p0065 N71-10168

Stress corrosion cracking technology review
[AD-711599] 02 p0243 N71-11696

Stress corrosion cracking of stainless steels
[EUR-4080-F] 03 p0391 N71-12822

Nickel zirconium alloy cracking during fabrication of Rankine cycle system components
03 p0395 N71-13309

Stress corrosion cracking of Fe-Cr-Ni alloys in chloride environments
[COO-1319-82] 04 p0528 N71-13940

Standardization of test methods for stress corrosion cracking
[AGARD-AR-25-70] 05 p0899 N71-14611

Method to prevent stress corrosion cracking in titanium alloys
[NASA-CASE-NPO-10271] 06 p0873 N71-16393

Nitric acid-hydrofluoric acid pickling effects on stress corrosion cracking of uniaxially rolled Ni-Cr-Fe alloy in pure water at 660 F
[WAFD-TM-644] 07 p1045 N71-18028

Reactions between liquid dinitrogen tetroxide and titanium alloy that result in stress corrosion cracking
[NASA-CR-116796] 08 p1158 N71-18490

Low frequency excitation for inducing stress and cracking in metal samples applied to ultrasonic pulse-echo crack detection
[AD-716642] 09 p1396 N71-19614

Stress corrosion cracking in iron nickel chromium alloy systems in chlorides
[COO-2089-5] 09 p1399 N71-19770

Stress corrosion cracking of metastable austenitic TRIP steel
[UCRL-203008] 09 p1400 N71-20000

Stress corrosion cracking in iron nickel chromium alloy system in magnesium chloride, for water cooled reactors
[COO-2089-6] 10 p1571 N71-30000

Fractographic analysis on fatigue crack mechanisms and fracture tolerance of pressurized vessels
[AD-717301] 11 p1833 N71-31300

Analysis of fracture mechanism that occurs during penetration of rigid wedge into elastic, brittle, anisotropic material
16 p2686 N71-28833

Corrosion behavior of stainless steel, nickel alloy, and aluminum alloy fuels in sodium reactors
[NRL-RISLEY-TRANS-2014-0601-97] 16 p2637 N71-28813

Heat treatment and stress corrosion analyses on aluminum alloy single- and bicontinuous microstructures
[NASA-CR-115849] 17 p2766 N71-30131

Analysis of effects of environment on strength of glass materials
[AD-722692] 17 p2771 N71-30226

Fatigue crack repair in notched steel sheets by vacuum methods
[NLR-TR-70029-U] 17 p2766 N71-30131

Transgranular cracking of Zircaloy 2 and Zircaloy 4 in hot and forced salts
[AECL-3799] 18 p2933 N71-30600

Electric eddy current probe for nondestructive crack detection in tubes
[AD-728938] 18 p2923 N71-30720

EPR and fracture mechanics applied to stress cracking in rubber
18 p2940 N71-31224

Analysis of gross strain crack tolerance in A53-B steel with plots of displacement measurements versus temperature
[HSST-TR-14] 22 p3393 N71-33300

Susceptibility of aluminum alloys to stress corrosion cracking during precipitation hardening
[AD-726713] 22 p3393 N71-33300

Electrochemistry of freshly generated titanium surfaces and stress corrosion cracking in aqueous solutions and in molten salts
[NASA-CR-122399] 23 p3768 N71-30010

Effects of dimethyl-dichloroethyl phosphate and sodium chloride solution on stress corrosion cracking of aluminum and steel
[NASA-TM-X-64617] 24 p3933 N71-30800

Stress corrosion cracking of titanium alloys, velocity of cracking in aqueous and methanol solutions and halogenated organic solvents, concentration of TiCl₃ in cracks
[NASA-CR-123165] 24 p3934 N71-30800

Metal corrosion effects on stress corrosion cracking of titanium alloys in nitrogen tetroxide, water, and salt
[NASA-CR-11846] 24 p3934 N71-30800

CRACKS
NT MICROCRACKS
Mechanism of stress corrosion cracking in brass
[AD-712327] 02 p0245 N71-12195

Boundary effects on heat transfer in non-Newtonian fluid flow through plane crack
18 p3827 N71-31400

Boundary collocation for two dimensional stress analysis of cracks emanating from or from near hole with various shapes
[NASA-TN-D-6376] 19 p3189 N71-33000

Damage control systems for detecting and locating overboard and onboard leak and damage modes in space stations
[NASA-CR-111963] 23 p3857 N71-30800

Photoelastic determination of dynamic stress intensity factor for five crack length to pulse length ratios
[NASA-CR-123179] 24 p3823 N71-30800

CRAFT
U VEHICLES
CRANUM
Induced fields and hunting in cranial model irradiated by electromagnetic plane wave
[AD-712645] 04 p0479 N71-14400

CRASH PHENOMENA
Analysis of aircraft structures which cause majority of injuries in aircraft accidents and recommendations for structural improvement to reduce accident severity
[FAA-AW-71-3] 19 p0838 N71-25010

CRASH LANDING
NT DITCHING (LANDING)
Jet aircraft crash during instrument approach due to electrical systems failure
[NTSB-AW-70-52] 01 p0805 N71-20010

Boeing 747 aircraft crash landing in Washington caused by pilot error
[NTSB-AAR-70-19] 01 p0805 N71-20010

SUBJECT INDEX

- Crash fire hazard evaluation of jet fuel
[AA-NA-70-44] 06 p0938 N71-16864
- Investigation of aircraft crash landing caused by engine failure and aircrew error
[NTSB-ACC-70-17] 07 p0969 N71-17063
- Evacuation tests from 280-passenger SST mock-up through different type exits
[FAA-AM-70-19] 09 p1321 N71-19812
- Landing accidents investigations for Hawker Siddeley 748 aircraft with performance measurements on rough surfaces
12 p1854 N71-23417
- Accident investigation of Alitalia Airlines Douglas DC-8-42 at J.F.K. International Airport 15 Sept. 1970
[NTSB-ACC-71-9] 21 p3377 N71-34029
- Aircraft accident investigation of fatal DC-8 crash at Kennedy Airport, New York during ferry flight on September 8, 1970
[NTSB-ACC-71-12] 21 p3377 N71-34030
- CRASH LANDING**
NT DITCHING [LANDING]
Cause and result of transport aircraft accident
[NTSB-ACC-70-27] 07 p0972 N71-17512
- Statistical compilation of annual aircraft accident data of US general aviation for 1969
[NTSB-ARG-71-1] 19 p3038 N71-32454
- Aircraft accident report on Convair 440 aircraft crash at New Haven, Connecticut on June 7, 1971
[NTSB-71-55] 19 p3039 N71-32500
- Design criteria for crashworthy aircraft fuel systems for military aircraft
[AD-723008] 20 p3209 N71-32992
- CRATERING**
NT PROJECTILE CRATERING
Radioactive fallout data from nuclear cratering experiment, Short Denny Bay
[OR-1818] 04 p0392 N71-14399
- Formation of crater due to expansion of gaseous explosive products following rock crushing by direct and reflected waves
[UCRL-TRANS-10476] 05 p0743 N71-15131
- Mass concentration and particle size distribution within nuclear cratering cloud during first four hours after formation
[UCRL-50844] 06 p0840 N71-15846
- Structural analyses and chronology of microcrater craters on lunar rocks
[NASA-TM-X-64707] 07 p1109 N71-17498
- Air erosion after nuclear cratering detonation in Project Schooner
[UCRL-72534] 10 p1624 N71-21792
- Recovery by nuclear explosives in saturated clay shale - Project Pro-Gondola 2
[AD-726003] 14 p2248 N71-26106
- Wave propagation and crater growth characteristics in hypervelocity impact on hard and soft aluminum alloys analyzed using two dimensional Eulerian numerical models
[AD-71468] 16 p2612 N71-28748
- CRATERS**
NT LUNAR CRATERS
NT METEORITE CRATERS
NT TYCHO CRATER
Laboratory simulation of impact cratering with high explosives
[NASA-TM-X-62016] 05 p0675 N71-14995
- Atmospheric-lithostatic pressure ratio effects on explosive crater dimensions in dry soil
[NASA-TR-8-366] 21 p3419 N71-34330
- CRACKS**
U SURFACE CRACKS
CRACKING
U CREATIVITY
Psychotechnical analysis of creativeness in research personnel based on personal interviews for personnel management applications
[NLL-TRANS-746-301-19022.401] 24 p3880 N71-37656
- CRACK ANALYSIS**
Metal and alloy reinforcing fibers grown in-situ, including tensile strength and creep analysis
[ONR-TR-433] 02 p0246 N71-11576
- Random material parameters effect on nonlinear steady creep solutions for 3-bar stress
[AD-712857] 03 p0463 N71-13161
- Creep analysis of statically indeterminate beams
[BNWL-1562] 04 p0579 N71-13985
- Mathematical models for complex loaded cylinder creep analysis taking into account viscoelasticity
[ONR-TR-7-546] 08 p1297 N71-18642
- Physical model for neutron flux enhanced creep rate
[AD-719905] 14 p2324 N71-25707
- Strain rate components and creep fatigue behavior of metals related independently to cyclic life by equation in both tension and compression
[NASA-TM-X-67838] 15 p2523 N71-27945
- Effects of rolling temperature and titanium content in creep, hardness, and microstructure of zinc-titanium and zinc-copper-titanium alloys
[BM-85-7322] 17 p2761 N71-29275
- Creep analysis of metallic thermal protection system under simulated mission environments
17 p2847 N71-29435

X ray diffraction method for determining high temperature creep in Ni-base structure
[NLL-TRANS-746-339-19022.401] 17 p2765 N71-29688

Numerical integration of integrodifferential equations for creep analysis of thick-walled shells
[REPT-NA-70-19] 20 p3291 N71-33144

In-pile and out-of-pile creep rates of enriched uranium dioxide at various temperatures, stress ranges, and fluence rates
20 p3307 N71-33673

Dislocation glide, deformation twinning and grain boundary sliding in compressive creep of single and bicrystalline aluminum oxide
21 p3300 N71-34932

Approximation equations for calculating loss and storage components of viscoelastic data from experimental stress relaxation and creep data without differentiation
[NASA-TT-F-14032] 24 p3947 N71-38158

Determining effective stresses under conditions of cyclic loading
[AD-727263] 24 p4024 N71-38711

CREEP BUCKLING
FORTRAN 4 calculator program for predetermination of creep buckling of thin walled tubes
[NP-18354] 04 p0545 N71-13565

Analysis for creep buckling of tubes under external pressure
[WP-DM-956] 06 p0956 N71-16836

Creep buckling of plates under compressive loads
07 p1127 N71-17954

Instantaneous and time dependent collapse of externally pressurized circular tubes with initial out-of-roundness due to creep deformation
[GAMD-8219-REV] 12 p2004 N71-23162

Numerical analysis of critical times for creep buckling in series of circular cylindrical shells under pure bending stress
[AD-720764] 14 p2348 N71-26094

Strain rate equations for secondary creep deformation of thick-walled tubes operated at high temperatures
[NASA-TM-X-2339] 19 p3191 N71-32799

CREEP DIAGRAMS
Steady-state creep rates in refractory metals and alloys - tungsten, titanium, and niobium
[AD-726848] 22 p3596 N71-35604

CREEP PROPERTIES
NT SHEAR CREEP
NT STEADY STATE CREEP
NT TENSILE CREEP

Analytical model for creep of T-111 fuel capsule
[AI-AEC-12943] 03 p0413 N71-12559

Self consistent polycrystalline model for creep under combined stress states
[AD-712046] 03 p0461 N71-12967

Creep properties of niobium, tantalum, molybdenum, and tungsten refractory alloys in ultrahigh vacuum
03 p0394 N71-13305

Heat treatment effects on creep properties and microstructure of tantalum base alloy
03 p0394 N71-13306

In-pile creep behavior of austenitic steels and nickel alloys under multiaxial loads
[KFK-1152] 05 p0731 N71-15587

Thermal, swelling, and irradiation creep effects on fast reactor core components
[BNWL-1430] 06 p0899 N71-16283

Materials considered critical to reactor design and performance - effects of radiation on creep, hardening, fracture, and swelling - conference
[BNWL-SA-3495] 08 p1238 N71-18343

Irradiation induced swelling and creep in fast reactor materials - conference
[BNWL-SA-3283] 08 p1238 N71-18344

Creep-rupture properties of tungsten thermionic capsule materials
[ONR-TR-3202] 09 p1325 N71-19389

Calculations on plasticity and creep properties of elementary structures
[SC-T-70-4047] 09 p1453 N71-19921

Cold working effects on creep properties of elongated cylindrical austenitic steel specimens at room temperature
[NLL-CE-TRANS-5413-19022.09] 10 p1581 N71-21478

Diffusion-viscous flow contribution to high temperature creep of copper aluminum alloy
[NLL-CE-TRANS-5438-19022.09] 10 p1584 N71-21403

Creep mechanisms and structure dependence of high temperature deformation of metals and alloys
[SU-326-P-17-X-1] 10 p1584 N71-21616

Friction and creep effects in rail transportation
[PB-196707] 10 p1568 N71-21786

Uranium-plutonium nitride fuels for LMFBFR, fast reactor fuels, and reactor fuel material creep properties
[BM-1893] 11 p1794 N71-22419

Stress for one percent creep strain at temperature range 1800 to 4000 F for powder metallurgy tungsten-rhenium-molybdenum alloys
[NASA-TN-D-6285] 12 p1936 N71-23110

CREEP PROPERTIES

Materials research programs including computer simulation of creep, and nuclear magnetic resonance
[AD-714793] 12 p1983 N71-23571

Creep properties of iron doped polycrystalline tungsten oxide and iron and chromium doped polycrystalline aluminum oxide between 1500 and 1800 C
[JCOO-1591-3] 12 p1943 N71-23951

Apparatus for obtaining data on compressive creep of ceramic nuclear fuels during irradiation
13 p2112 N71-24513

Dislocation mechanisms involved in low stress-high temperature creep of metals
13 p2094 N71-23058

Irradiation induced creep in austenitic stainless steels at 43 and 370 C
[WHAN-FB-30] 14 p2267 N71-23641

Numerical analysis of critical times for creep buckling in series of circular cylindrical shells under pure bending stress
[AD-720768] 14 p2348 N71-26094

Microvoid and creep in stationary and rotating contact surfaces of cylindrical bodies
15 p2453 N71-30829

Silicon and germanium alloying effects on creep properties and strength of vanadium-titanium and vanadium-titanium-niobium alloys in high temperature environments
[KFK-1193] 15 p2420 N71-37007

Creep rates of plutonium-based fuel ceramics at high temperatures, and effects of composition, porosity, and sintering irradiation
15 p2446 N71-27167

Effect of cold working on creep properties of AISI 316 type stainless steel
[JAERI-MEMO-4125] 15 p2422 N71-27218

Fission product swelling, gas evolution, and creep properties of uranium dioxide nuclear fuels
[TRG-1957/52] 15 p2449 N71-27388

Precipitate hardening of Cu-Cu and Cu-CuZn alloys and particle size and temperature effects on creep properties and edge dislocations
[IS-T-422] 15 p2425 N71-27652

Discrete element analysis of creep and stress properties of stainless steel tubing for LMFBFR
[ONR-TR-3254] 16 p2613 N71-28001

Short-term creep properties of OT-4 alloy in high speed air flows under aerodynamic vibrations
[NASA-TT-F-13658] 16 p2614 N71-28032

Weathering effects on creep properties of glass fiber reinforced polyester resin laminates under bending stress
[NLL-LBB-COMM-5196-11553] 17 p2768 N71-29503

Creep deformation of lithium fluoride single crystals at 650 to 730 C
[UCRL-20350] 17 p2815 N71-29757

Numerical analysis of plane stress problem with creep including creep strain predictions, load and temperature effects, multiaxial stress flow criterion, and numerical approximations
17 p2853 N71-30667

Effects of loading rate on creep properties of austenitic stainless steel type 316
[PB-197128] 18 p2934 N71-30006

Notch sensitivity of creep-rupture properties of Waspalloy between 1000 to 1400 F
[NASA-CR-1849] 18 p2936 N71-31180

Thermal treatment, thermal equilibrium, and microstructural effects on intergranular creep in sintered and fused cast aluminas
18 p3022 N71-31367

Nitrogen effect on creep properties of ferritic steels and interstitial influence on austenitic steel creep properties
19 p3111 N71-31985

Boron influence on austenitic stainless steel precipitation during creep
19 p3111 N71-31986

Short term creep of nickel in vacuum and high speed air flow at high temperatures
[NASA-TT-F-13661] 19 p3114 N71-32234

Creep and other mechanical properties of extruded zinc-30 percent aluminum alloys containing magnesium
[BM-81-7530] 19 p3116 N71-32395

Development of computer program for predicting creep and stress rupture strength of steel
[PB-196562] 19 p3118 N71-32662

Development of uranium-plutonium nitride fuels for LMFBFR applications, studies of high temperature fuels for advanced fast reactors, and studies of creep of reactor fuel materials
[BM-1890] 20 p3309 N71-33946

Creep behavior of 1Cr-Mo-V steels under cyclic loads
[RD/B/N-1089] 21 p3441 N71-34483

Viscoelastic analysis of irradiated graphite with variable creep coefficient for molten salt breeder reactor core
[ONR-TR-3242] 21 p3459 N71-34618

Effect of grain size on creep of plutonium-rhenium alloys at high temperature
[NLL-LT-746-744-19022.401] 22 p3597 N71-35615

CREEP RESISTANCE

- Electron microscopy creep properties study of beta NIAI thin film specimens from deformed single crystals [COO-1489-10] 23 p3770 N71-38669
- Plastic deformation on creep characteristics of aluminum-type alloy [AD-72785] 24 p3938 N71-38695
- Viscoelastic creep and relaxation in filamentary single-ply laminates with numerical results for boron-epoxy and graphite epoxy plastics [AD-727126] 24 p3943 N71-38129
- Mx-4, -4, and -10 uniaxial creep machines in NRX and NRU reactors [ABCL-3738] 24 p3956 N71-38220
- ### CREEP RESISTANCE
- #### U CREEP STRENGTH
- ##### CREEP RUPTURE STRENGTH
- Creep rupture properties and tensile strength of stainless steels exposed to high temperature sodium and solubility for reactor materials [MSAR-76-76] 02 p0242 N71-11575
- Short-time stress rupture of prestressed titanium alloys under rapid heating conditions [NASA-TN-D-6053] 02 p0243 N71-11669
- Precipitation strengthening of lead-cadmium-antimony alloys [BM-RI-7453] 02 p0244 N71-12003
- Physicochemical theory of heat resistance and new heat resistant titanium alloys [AD-712810] 03 p0295 N71-13334
- Creep rupture tests on cobalt alloy weldments [ORNL-3028] 04 p0331 N71-14191
- Stress-rupture behavior of types 304 and 316 stainless steel cladding in high temperature static sodium [AI-ABC-12976] 06 p0670 N71-15930
- Nickel base alloy with resistance to oxidation at high temperatures and superior stress-rupture properties [NASA-CASE-XLE-02082] 06 p0670 N71-16026
- Facility and procedure for studying short term tensile impact and compression strength, creep, and ductility of graphite at 300 to 3500 K [LA-4462-72] 07 p1047 N71-17127
- Uniaxial and biaxial creep rupture of type 316 stainless steel after fast reactor irradiation [BNWL-SA-3295] 08 p1212 N71-18311
- Modification of high temperature cobalt-tungsten alloys for improved stability [NASA-TN-D-6147] 08 p1213 N71-18515
- Creep rupture strength of reinforced plastics under uniaxial compression [NASA-TT-F-13441] 08 p1300 N71-19274
- Past neutron irradiation effects on stainless steel creep rupture properties [ORNL-TM-3169] 10 p1576 N71-21016
- Specialized model for analysis of creep-rupture data by minimum commitment, station function approach with general time-temperature-stress relation to include all commonly used parameters [NASA-TM-X-52999] 10 p1655 N71-21215
- Critical aspect ratios of copper matrix and tungsten fibers in reinforced composites from stress-rupture and tension tests [NASA-TM-X-52993] 10 p1589 N71-21228
- Tensile, fatigue, and creep rupture properties of extruded nickel-based aluminum, titanium carbide, and boron nitride alloys and aluminum-based silicon, copper, and iron alloys [NASA-CR-117582] 10 p1583 N71-21587
- Comparison of creep-rupture properties of electron beam-melted polycrystalline and powder-metallurgy rhodium sheets at 2200 to 4200°F and 4 to 40 ksi [NASA-TN-D-6291] 12 p1936 N71-23114
- Development of fracture model to predict rate of crack propagation under high temperature low cycle fatigue conditions based on creep rupture principle [AD-727898] 12 p2008 N71-24283
- Tensile stress and tensile time-to-rupture relation determined from cyclic creep rupture tests on high temperature titanium alloy, cobalt alloy, and stainless steel [NASA-TN-D-6309] 14 p2268 N71-25645
- Temperature and aluminum and aluminum alloying effects on creep and creep rupture tests of AISI type 316 stainless steel and welds in high temperature environments for breeder reactor use [JAERI-MEMO-0097] 15 p2423 N71-27252
- Analysis of creep rupture properties of metals and application to predicting useful life and occurrence of damage [UCRL-11489] 17 p2851 N71-29541
- Thermodynamic, precipitation hardening, creep rupture strength, and solubility effects of carbon on Types 304 and 316 stainless steels [NLL-RESELY-TRANS-2039-70091.99] 19 p3117 N71-32586
- Thermomechanical processing of nickel alloy in relation to yield and creep rupture strength [NASA-TN-D-6418] 21 p3434 N71-34432
- Platinum-thorium oxide alloy for resistor-thrustor showing increase in stress rupture life [NASA-CR-111959] 22 p3598 N71-35619

CREEP STRENGTH

- Multiaxial analytic creep theory for describing primary, secondary, and creep recovery [WTHD-32] 02 p0244 N71-12025
- Effect of variations in creep exponent N on buckling of circular cylindrical shells in axial compression [AD-711949] 03 p0461 N71-22966
- Evaluation of refractory tantalum-, tungsten-, niobium-, and molybdenum based alloys for space power systems applications [NASA-SP-243] 03 p0593 N71-13301
- Ultra-high vacuum chamber for determining deformation strength of simulated lunar rocks [NASA-CR-117139] 09 p1366 N71-20215
- Thermocyclic creep, rupture strength, and elastic properties of aluminum, tantalum, and molybdenum based refractory materials [AD-719833] 13 p0593 N71-24936
- Development and conduct of national and international programs to determine variations in creep test techniques and establishment of standard creep test procedures [AGARD-R-581-71] 13 p2184 N71-25449
- Numerical analysis of critical times for creep buckling in series of circular cylindrical shells under pure bending stress [AD-720768] 14 p2348 N71-26094
- Estimating characteristics of stress rupture strength of heat resistant alloys [AD-720947] 15 p2424 N71-27398
- Precipitation with refractory metal carbides for creep resistant chromium-base alloys [NASA-CR-72674] 18 p2934 N71-30809
- Forming and bonding metallic lining onto inside surface of metal tube [AD-720947] 19 p3114 N71-32161
- Biaxial creep strength of T-111 (tantalum alloy) tubing in high temperature, high vacuum environment [NASA-CR-72846] 19 p3114 N71-32162
- Development of computer program for predicting creep and stress rupture strength of steel [PB-198362] 19 p3118 N71-32662
- Correlation equation relating creep deformation of tubes to stress and temperature functions, and application to design of heat exchanger tubes [NASA-TM-X-2372] 21 p3529 N71-35147
- Absolute capacitance microcreep and dimensional stability measuring system [NASA-TM-X-2046] 22 p3585 N71-35530
- Creep strength and solidification rate of Al-Al₃Si eutectic whisker composites [AD-727615] 24 p3937 N71-38091
- High temperature tests of creep in structural graphite [AD-727898] 24 p3946 N71-38147
- ### CREEP TESTS
- Development of creep tester for metals and alloys with electromechanical and servomechanical instrumentation [BM-RI-7456] 02 p0244 N71-12004
- Large radioisotope heat source capsule design, fabrication, and materials compatibility and creep tests [AI-AEC-12948] 03 p0415 N71-12873
- Electrical resistance, magnetic coercivity, and mechanical property measurement for investigation of structural changes in steels under creep test [AD-720947] 03 p0467 N71-13353
- Strength and creep of laminated plastics [NASA-TT-F-461] 05 p0709 N71-15176
- Experimental biaxial steady-state creep data for tantalum and molybdenum alloys [NASA-TN-D-6149] 06 p0874 N71-16498
- Creep rate correlation in solution-treated type 304 and 316 stainless steels [WHAN-FR-25] 07 p1044 N71-17894
- Steady state creep test on model pressure vessel containing four nozzles in spherical cap [RD/RN-1668] 08 p1295 N71-18315
- Refractory alloy creep test data for molybdenum base alloy TZM, pure tantalum, and tantalum base alloys T-111 and ASTAR-811C at elevated temperatures in ultrahigh vacuum [NASA-CR-72619] 09 p1482 N71-20458
- Creep tests on CrNiNb and CrNi at 600°C and at different stresses [NLL-CE-TRANS-5414-9022.09] 10 p1586 N71-21833
- Creep tests used to determine viscoelastic behavior of nonlinear fiber reinforced plastic [AD-718978] 13 p2099 N71-24410
- Steady state creep tests to measure deformation enhanced diffusion in iron and iron alloys at elevated temperatures [NLL-CE-TRANS-5414-9022.09] 13 p2099 N71-24410
- Apparatus for in-pile compressive creep studies of LMFBR ceramic fuels during irradiation [BM-RI-1804] 14 p2292 N71-25713
- Tests to determine short-term creep of metals and alloys under conditions of aerodynamic heating with high velocity air flow [NASA-TT-F-13633] 14 p2272 N71-25822
- Development and characteristics of test equipment for measuring creep buckling of moderately thin-

SUBJECT INDEX

- walled circular cylindrical shells under axial compression loads [AD-720767] 14 p2348 N71-26094
- Failure creep tests on glass fiber reinforced epoxy resins for four polymerization reaction conditions [CRIF-PL-1] 15 p2423 N71-3092
- Temperature and aluminum and aluminum alloying effects on creep and creep rupture tests of AISI type 316 stainless steel and welds in high temperature environments for breeder reactor use [JAERI-MEMO-0097] 15 p2423 N71-27252
- Creep and fatigue tests of type 316 stainless steel and Inconel 800 for use in breeder reactors [BM-1894] 16 p2612 N71-30810
- Stress analysis of cobalt heat resistant alloy tube internally pressurized with helium after creep testing to failure [NASA-TM-X-2346] 19 p3113 N71-32161
- Reversed creep tests on chemical lead, aluminum, and copper and creep deformation behavior under repeated stress reversals [NASA-CR-72674] 20 p3357 N71-3204
- Creep and creep rupture deformation and tensile tests of nickel alloys [AD-720768] 22 p3937 N71-38091
- Uniaxial strain rate, creep, isotropy, and relaxation tests for characterization of polycarbonates [AD-720768] 22 p3937 N71-38091
- ### CREOSOLS
- Mass spectra of phenolic polynuclear compounds of p-cresol and formaldehyde [RAE-LIB-TRANS-1486] 03 p0333 N71-1200
- Confirmation of chain structure of polynuclear compounds formed from p-ion-cresol and formaldehyde [RAE-LIB-TRANS-1486] 05 p0641 N71-1301
- ### CRESTATIONS
- #### U TRAVELING WAVE TUBES
- ### CRESTS
- #### U WAVES
- ### CREVATES
- #### NT GLACIERS
- ### CREVICES
- #### U CRACKS
- ### CREWS
- #### NT FLIGHT CREWS
- #### NT SPACECREWS
- Stochastic model for computerized simulation of closed man machine system operated by crew [AD-720334] 14 p2210 N71-3084
- Crew performance measurement relationship for automated air to air intercept weapon system testing simulator [AD-727739] 24 p3882 N71-3785
- ### CRITERIA
- Solving multicriteria problems of industrial plant controls with convex programming [AD-720334] 17 p2713 N71-2958
- Simulation studies for development of certification criteria applicable to SST taken off and on-line failure [AD-720334] 18 p2870 N71-3077
- Criteria and recommended practices for design, selection, analysis, and testing of duplicate aerodynamic deceleration systems [NASA-SP-8066] 18 p2873 N71-3138
- Techniques for selecting performance criteria for voice, video, and digital data systems [NASA-CR-115079] 21 p3390 N71-34115
- Accelerated life test models, criteria for model selection, and extrapolation in creep tests [NASA-CR-121645] 21 p3526 N71-35114
- Microstructural changes as criterion for assessing operational reliability and high temperature resistance of chromium steels [NLL-CE-TRANS-5569-9022.09] 23 p3774 N71-3086
- ### CRITICAL EXPERIMENTS
- Survey of heat transfer to near-critical fluids [NASA-TN-D-5886] 03 p0468 N71-13301
- Uncontrollable prompt critical excursions in fast reactor cooled by sodium [RT/INO/70/2] 04 p0548 N71-1307
- Relativistic electron beam and plasma instabilities and critical current problem [UCRL-TRANS-10470] 04 p0596 N71-1308
- Uranium metal criticality, Monte Carlo calculations, and nuclear criticality safety [IV-CDC-7] 04 p0528 N71-1309
- Investigating fuel burnup rates, safety rods, fuel elements, and critical experiments in thermal and fast reactors [BNWL-1301-2] 04 p0534 N71-1406
- Critical experiments of copper-reflected fast assembly with time dependent rods [AE-359] 04 p0599 N71-1406
- Subcritical experiments for Japanese power reactor [DP-1219] 05 p0724 N71-1406
- Critical evaluation and cost analysis of recently methods of nuclear materials testing [BNL-50251] 06 p0697 N71-1406
- Critical initiation pressures of explosives by shock waves [UCRL-TRANS-10490] 06 p0666 N71-1406
- Results of two-phase blowdown experiments with straight tube test section and steam-water mixtures [ABCL-3664] 08 p1177 N71-3086

SUBJECT INDEX

Apparatus for use in liquid helium cryostat for measurement of small magnetic field changes occurring within detection chamber 08 p1244 N71-19010

Neutron sensitive criticality alarm system for detection and warning - conference 08 p1176 N71-19328

Particle size distributions from fuel rods fragmented during power burst tests in capsule driver core (JNL-1428) 09 p1417 N71-19897

Similarity between two phase liquid-vapor flows with heat exchange - conference 09 p1376 N71-20118

Critical experiments in integral neutron thermalization (JNL-10223) 10 p1615 N71-21021

Fe-240 as convertible poison in critical experiments of Phoenix fuel in MTR mockup (JNL-1481) 13 p2120 N71-25208

Criticality for energy dependent transport in slab geometry 13 p2143 N71-25580

Apparatus and process for volumetrically dispensing reagent quantities of volatile chemicals for small batch reactions (NASA-CASE-MPO-10070) 15 p2416 N71-27372

Computer program for analysis and design of critical experiments with fast neutron reactors (JAERI-MEMO-4215) 15 p2451 N71-27740

Design and experiments with compact fast spectrum reactor for generating electric power in space (NASA-TM-X-67857) 16 p2655 N71-28820

State-of-the-art review on nuclear parameters of fast critical experiments (JURNPR-838) 16 p2654 N71-28957

Critical experiments, uranium production, and radioactive isotope research (JNL-16726) 17 p2780 N71-29224

Penetration of induction electrical fields and losses in superconducting type 2 superconductors having surface currents (JNL-TR-3475) 20 p3337 N71-33979

Mockup of coaxial flowing gas cavity reactor for space nuclear propulsion, performed with critical experiment (NASA-CR-72577) 21 p3456 N71-34597

Criticality experiments using spherical gas core to provide benchmark results for cold conditions of typical nuclear rocket concept (NASA-CR-72781) 21 p3456 N71-34598

Critical tests to determine physics parameters of UO₂-2 wt percent PuO₂ fuel elements in batch core experiment (JNL-1553) 21 p3462 N71-34641

Technical criteria for prevention of criticality in chemical processing facilities (JNL-468-REV) 22 p3564 N71-35387

Critical experiment for cylindrical core with central air gap in FRO fast reactor (JNL-4-4412-22) 22 p3624 N71-35825

Vibrometric description of supercritical magnetoacoustic compression pulse (JNL-1113) 22 p3653 N71-36048

Criticality evaluation of hydrogenous enriched lattices using three group model for reactor design (UAREB-84) 23 p3794 N71-37047

Neutronic multigroup one dimensional criticality calculation diffusion code for IBM 1130 computer - UAREB-90 23 p3795 N71-37049

Four groups, four regions, one dimensional criticality calculation diffusion code for IBM 1620 computer - UAREB-85 23 p3795 N71-37050

Automatic start-up system for UA-RR-1 reactor for reaching criticality from deep subcriticality in prescribed period (UAREB-108) 23 p3795 N71-37052

Pile oscillator technique for measuring Doppler effect with heated small samples in critical zero energy lattices for fast thermal reactors (JNL-1350) 23 p3800 N71-37093

CRITICAL FLOW

Two phase steam-water critical flow data obtained at moderate pressures (JNL-7740) 09 p1419 N71-19974

Experiments for mass flow of methane and natural gas mixtures through critical flow nozzles, including real gas effects (NASA-TM-X-52994) 10 p1543 N71-21330

FORTRAN computer code for transient flow data analysis and critical cooling deficiency prediction in boiling system of reactor core (JNL-10221-5) 19 p3192 N71-32117

CRITICAL FREQUENCIES

Neutronic propagation charts of predicted median critical and maximum stable frequencies in F2 region, Feb. - Jan. 1971 (JNL-8172) 11 p1747 N71-22067

Neutron values of ionospheric propagation data for July - June 1969 (JNL-1169) 21 p3416 N71-34308

Neutron values of ionospheric propagation data for July 1969 (JNL-1170) 21 p3416 N71-34309

Ionospheric propagation data for E and F regions, July - October 1969 (JNL-1171) 22 p3575 N71-35460

Ionospheric propagation data for E and F regions, India - September 1969 (JNL-1172) 22 p3575 N71-35461

Ionospheric propagation data for E and F regions, India - Aug. 1969 (JNL-1173) 22 p3575 N71-35462

Ionospheric propagation data for E and F regions, India - Dec. 1969 (JNL-1174) 23 p3575 N71-36752

Ionospheric propagation data for E and F regions, India - Nov. 1969 (JNL-1175) 23 p3575 N71-36753

CRITICAL LOADING

Torsion-resistant prestressed perforated plate stress analysis for supercritical loading 02 p0300 N71-11946

Critical buckling data for design of skew plates subjected to loads (JNL-248-5) 05 p0775 N71-15151

Lower critical load of conical shell under longitudinal compression (JNL-47600) 06 p0954 N71-16040

Stress-strain diagrams for crack loading of brittle bodies weakened by pointed concentrators (JNL-720939) 15 p2523 N71-27865

Critical equilibrium of two-component composite with crack originating along diameter of round inclusion and entering with one tip into binder (NASA-TT-P-13934) 21 p3527 N71-35131

Critical tensile strength curve determination for orthotropic two-layer fiber glass shells in plane stress corresponding to therapeutic pressure chambers 24 p3902 N71-37816

CRITICAL MACH NUMBER

U CRITICAL VELOCITY

U MACH NUMBER

CRITICAL MASS

Deriving empirical model for calculating safe nuclear criticality parameters for complex arrays of intersecting pipes containing enriched uranyl nitrate solution (JNL-1553) 05 p0638 N71-14699

Development of wall-less proton recoil proportional detector for neutron spectroscopy in critical assemblies (JNL-578-P-33-18) 05 p0730 N71-15244

Critical assemblies, radiation detectors, and reactor control elements (JNL-3647-18-RT-3) 09 p1421 N71-20551

Fast reactor systems characterized by high specific impulse and relatively low specific mass (NASA-TM-X-67826) 13 p2116 N71-24688

Critical mass measurements, control rod calibration, neutron and gamma flux measurement, measurement of various reactivity worths, power calibration, and xenon buildup for TRR-2 (JAERI-MEMO-4141) 13 p2119 N71-25107

Critical and safe dimensions of storage and mixing containers for plutonium-containing fuels used in breeder reactors (JNL-1192) 15 p2446 N71-27168

Adiabatic approximation of gas reactor critical mass during nuclear fuel density oscillations (JNL-1964) 17 p2783 N71-29528

Critical mass experiments to establish design calculation standards for modular cavity reactors of gas core nuclear rocket engines 21 p3456 N71-34599

Critical assembly models for fast reactor research and determination of critical mass, reactivity coefficients, and fission distribution (JNL-201) 22 p3619 N71-35786

Criticality study of ZPR-1 and ZPR-2 with 25.4-cm diameter cylindrical stainless steel cores (NASA-TM-X-2381) 22 p3624 N71-35822

Two group, two region, one dimensional neutron diffusion code for nuclear reactor criticality calculations (UAREB-79) 23 p3795 N71-37051

One dimensional, multigroup diffusion code for use in fast reactor criticality and kinetics parameter analyses (JAERI-MEMO-4331) 23 p3796 N71-37063

CRITICAL PATH METHOD

Computer program for analyzing all power/power, power/ground, ground/ground, and incomplete paths in Automated Search Program (NASA-CR-108740) 03 p0342 N71-12481

Errors in PERT analysis and critical path method, and computer program for error elimination (NASA-CR-119777) 19 p3197 N71-32495

Calculation of b-k shortest paths and k greater than 2 modification for improved algorithm efficiency (JNL-4638) 21 p3449 N71-34545

CRITICAL POINT

Conference review on critical phenomena in alloys, magnets, and superconductors (JNL-710497) 10 p1634 N71-21067

Boundary layer velocity and temperature profiles measured in near critical nitrogen (NASA-TM-X-52963) 10 p1540 N71-21080

CROSS CORRELATION

Anomalous behavior model for prediction of thermal conductivity of fluids in critical region (NASA-TM-X-52953) 12 p0809 N71-23196

Droplet evaporation in liquid-vapor critical region (AD-719946) 13 p2184 N71-24363

Thermal conductivity and viscosity measurements in binary liquid mixtures and vapor phases near critical points (AD-720718) 15 p2595 N71-27709

Critical heat flux in liquid helium 2 close to lambda transition 19 p3193 N71-32542

Phase transformation thermodynamics and equations of state near critical points 20 p3346 N71-33754

Critical points, crack formation, and shrinkage characteristics for castings of Cr-Ni, Cr-Mn, and Mn steels (NLL-TRANS-746-293-19022.401) 22 p3597 N71-35611

Measurements of angular dependence of scattered X ray intensity from carbon dioxide near critical point 22 p3647 N71-36606

Fermi system phase transition model analysis near critical point for two, three, and many body interactions with comparison to classical theory 23 p3823 N71-37271

CRITICAL PRESSURE

Experimental and theoretical results of critical pressure burning of fuel droplets (NASA-CR-72834) 09 p1485 N71-20532

CRITICAL REYNOLDS NUMBER

U CRITICAL VELOCITY

U REYNOLDS NUMBER

CRITICAL SPEED

U CRITICAL VELOCITY

CRITICAL STRESS

U CRITICAL LOADING

CRITICAL TEMPERATURE

Critical temperatures of superconducting transition metal films on helium cooled substrates (JNL-192667) 02 p0287 N71-12122

Superconductivity, solid state physics, and low temperature physics (COP-1569-59) 06 p0930 N71-15740

Transitions in high critical temperature superconductors, tunneling in Ga and Al single crystals, and critical temperature enhancement (ORO-3665-23) 06 p0868 N71-15751

Sum rules in hydrodynamic scaling approach for near critical temperature liquid helium 10 p1571 N71-20482

Critical velocity and attenuation changes for longitudinal and shear ultrasound in rare earth metals, insulators, and Cr at magnetic transition temperature 20 p3313 N71-33751

CRITICAL VELOCITY

Determining critical speeds of hydraulic unit shafts (JNL-193634T) 02 p0236 N71-11755

Aliven theory of critical velocity in neutral gas and magnetized plasma interactions (JNL-70-36) 02 p0280 N71-11837

Viscous damping and harmonic disturbing forces in rotors with critical speed, support deflection, and support phase angle determinations (NASA-TM-X-67896) 20 p3358 N71-33247

CROCCO METHOD

Mathematical connection between solutions of Navier-Stokes system and Prandtl boundary layer system 08 p1184 N71-19020

CROW GROWTH

Studying interaction of electromagnetic radiation with plants, soils, and water, and wavelengths and procedures for discriminating agricultural crops 02 p0217 N71-11981

Applying advanced remote sensing and processing techniques to agricultural resources 02 p0217 N71-11982

CROSS CORRELATION

Kalman extension of filtering and optimization of linear stochastic systems with cross correlated noise (JNL-717869) 01 p0137 N71-10819

Optical cross correlation technique for nondestructive testing and lifetime prediction of printed circuit boards 03 p0379 N71-12791

Dynamic response of F-2 aircraft using cross correlation and power spectra (ARC-CR-1121) 06 p0793 N71-15720

Cross correlation of speech signals and signal transmission time (AD-717869) 12 p1878 N71-23536

Comparison of pseudorandom and time of flight analysis in cross correlation for quantum statistics applications in nuclear physics (LYCEN-7032) 14 p2310 N71-24655

Autocorrelation and cross correlation of high frequency atmospheric boundary layer temperature and velocity fluctuation measurements (AD-721540) 16 p2587 N71-28408

Nonlinearity and signal transduction delay effects on feedback control systems based on random input signal analysis and cross correlation 16 p2576 N71-28226

CROSS COUPLING

- Cross correlation function for estimating structural frequency response
[ISVR-TR-33] 17 p2771 N71-29312
- Cross correlation measurements of unmoderated and polyethylene moderated uranium assemblies with prompt neutron decay constants, using Cf-252 as neutron source
[Y-DR-41] 21 p3482 N71-34802

CROSS COUPLING

- Calculating level structure of neutron-deficient lead and bismuth isotopes
[INR-1169/PL] 03 p0432 N71-12937
- Hyperpolarizabilities for Hartree-Fock atoms
24 p3983 N71-38427

CROSS FLOW

- Transportation cooling near stagnation line of cylindrical body in cross flow
[AD-710739] 01 p0133 N71-10568
- Turbulent air and water polluting plumes in laminar cross flow
[FML-PUBL-70-8] 04 p0520 N71-14312
- Interference phenomenon of subsonic turbulent jet exhausts from flat plate in low speed cross flow
[AD-710798] 12 p1899 N71-23314
- Wind tunnel investigation of jet exhausting into cross flow - data for three jet configurations
[AD-718123] 13 p2064 N71-24491
- Wind tunnel investigation of jets exhausting into cross flow - description and data analysis
[AD-718122] 13 p2064 N71-24492
- Analytical investigation of three dimensional turbulent boundary layers on helicopter rotors including cross flow derivatives and effects of centrifugal and Coriolis forces
[NASA-CR-1845] 15 p2363 N71-27003
- Free stream turbulence effects on local heat and mass transfer rate across laminar, forward stagnation boundary layer on circular cylinders in cross flow
1. p2393 N71-27321

- Calculating penetration depth of one-row round jet system developing in limited cross wind under conditions most typical for gas burners
[NASA-TT-F-13726] 17 p2735 N71-29815
- Experiments on turbulent circular jets issuing into cross flow from both heated and unheated jets
[NASA-CR-72893] 17 p2735 N71-29806
- Wind pressure and cross flow velocity profiles for short takeoff aircraft building roof airports
18 p2902 N71-30776
- Mean temperature difference for cross flow in tube bundle heat exchangers
18 p3025 N71-31132

- Steady turbulent flow and heat transfer downstream of sudden enlargement in pipe of circular cross section
[EF-TN-A-39] 20 p3251 N71-33495
- Hypervelocity wind tunnel investigation of turbulent boundary layer undergoing adverse pressure gradient and cross flow along plane of symmetry
[NASA-CR-121635] 21 p3409 N71-34257

CROSS RELAXATION

- Cross relaxation dynamics for Li-F/Li-7 system in LiF based on rotating frame nuclear double magnetic resonance
18 p2983 N71-31047

CROSS SECTIONS

- Excitation of carbon monoxide fourth positive band system by electron impact on carbon monoxide and carbon dioxide
[NASA-CR-116141] 06 p0809 N71-15980
- Numerical analysis of effect of cross section shape on behavior of boundon tubes
07 p1028 N71-17273
- Compilation of fission product cross sections for reactor burnup calculations
[AARC/TM-549] 15 p2460 N71-27079
- Tubulation of bibliographic cross section data for neutron induced reactions
[UCRL-50400-VOL-2] 17 p2790 N71-29210
- Partial cross section and resonance production of strange particles measured in deuteron filled bubble chamber exposed to negative kaon beam
19 p3159 N71-32599
- Cross sections in double resonance reaction positive pion proton yields neutral rho-meson positive positive Delta hyperon at 11.7 GeV/c
[DESY-71/8] 19 p3161 N71-32787
- Production cross sections for He I, He II, H-alpha, and H-beta emissions
20 p3318 N71-33573
- Analysis of extinction cross-sections for grains composed of water ice, quartz, and silica surrounded by ice mantle with application to stellar composition
21 p3512 N71-35026
- Graphs and tables of negative pion induced reaction cross sections
[CERN/HERA-70-7] 22 p3632 N71-35883
- Computer program for calculating lift interference factors of wind tunnel test sections by vortex lattice method
[TAE-124] 23 p3704 N71-36407
- CROSSED FIELD AMPLIFIERS
- Design and performance of injected beam crossed field amplifier
[NASA-CR-72810] 06 p0823 N71-16578

CROSSED FIELD TRAVELING WAVE AMPLIFIERS IN SEMICONDUCTORS

- [ELAB-AE-117] 10 p1533 N71-21032
- Design of S band axial injection cross field amplifier for satellite borne transmitter
[NASA-CR-72876] 23 p3731 N71-36593
- CROSSED FIELD
- Ion motion in crossed fields with resonance charge exchange ionic collisions
[REPT-70-15] 04 p0600 N71-14301
- Electromagnetic wave and charge carrier interaction in crossed fields
[AD-713399] 05 p0655 N71-14883
- Mathematical model for cross mode excitation structures in synchrocyclotron acceleration
[CERN-70-13] 05 p0742 N71-15129
- Crossed field MHD plasma generator-accelerator
[NASA-CASE-XLA-03374] 05 p0755 N71-15562
- Acoustic amplification in high mobility extrinsic semiconductors in presence of crossed dc electric and magnetic fields
11 p1798 N71-22468

- Low frequency 1 to 100 KHz oscillations in hot cathode Penning discharge plasmas caused by density waves moving in plasma drift direction in crossed electric and magnetic fields
[NASA-TT-F-13641] 12 p1981 N71-23966
- Broadband, high gain photomultiplier - dynamic crossed field electron multiplier for sampling photocurrent once each cycle of RF electric field
17 p2728 N71-29663
- Crossed field investigation of plasma formation processes and resulting guide field spatial and energy distributions
17 p2813 N71-30195

- Crossed field instabilities and turbulent ion heating calculated in mirror machine
[CONF-710607-67] 24 p3988 N71-38458

CROSSLINKING

- NT VULCANIZING
- Influence of solid surface on relaxation and cross-linking processes in polymer boundary layers
[JPRS-51683] 02 p0248 N71-12086
- Equipment and procedure for crosslinking time and exothermic temperature determination of reacting plastic compositions in controlled atmosphere
[NRC-11845] 12 p1871 N71-23756
- Infrared spectra analysis of latex copolymers cross-linking reactions in relation to molecular weight and number of methylolamide groups
[NLL-RTS-6218] 16 p2559 N71-29055
- Resin crosslinking effects on anion exchange separation of rare earth-EDTA complexes at tracer loadings
[INR-P-1209] 16 p2659 N71-29189
- Crosslinking effects on thermal conductivity of polystyrene
18 p2996 N71-31157

CRUCIBLES

- Automatic control and crucible shape effects on zone recrystallization of germanium
10 p1633 N71-20886
- Impurity distribution in tellurium as function of direction of travel of zone in vertical crucible zone recrystallization
10 p1633 N71-20888
- Directed crystallization of compounds during impurity exchange of liquid phase with crucible and atmosphere
10 p1634 N71-20890

CRUCIFORM WINGS

- Effects of nose bluntness on static aerodynamic characteristics of cruciform wing missile at Mach 1.50 to 2.86
[NASA-TM-X-2289] 18 p2866 N71-30813

CRUDE OIL

- Radiation effects on sulfur compound impurities in crude oil
04 p0487 N71-13468
- Decontamination of petroleum products with honey
[NASA-CASE-XNP-03835] 12 p1870 N71-23499
- Measures for providing financial responsibility liability limitations for vessels and offshore and offshore facilities in oil pollution cases
19 p3198 N71-32624
- Legal, economic, and technical aspects of liability and financial responsibility of oil pollution
[PB-198776] 19 p3198 N71-32625
- Statistical analysis of world reserves of solid fuel, crude oil, uranium, and natural gas in year 2000
[NLL-TRANS-1166-19022.9] 22 p3580 N71-35501
- Analysis of rate of oxidation of petroleum products in water under conditions where nitrogen, phosphorus, and potassium are present
[NLL-NSTC-TRANS-2474-6180.59] 24 p3886 N71-37701

CRUISING FLIGHT

- Subsonic wind tunnel investigation of rotary wing configurations for VTOL aircraft in cruise mode
[NASA-TN-D-5945] 02 p0145 N71-11025
- Configuration optimization and performance of air breathing hypersonic cruise vehicles
[AD-721471] 16 p2529 N71-28580

SUBJECT INDEX

- Low speed wind tunnel test to define space shuttle model cruise and landing aerodynamic characteristics
[NASA-CR-119835] 21 p3322 N71-33090
- Aerodynamic characteristics of scale model of space shuttle booster at cruise and landing speed of Mach 0.2
[NASA-CR-119974] 24 p4019 N71-36379
- CRUSADER AIRCRAFT
U F-8 AIRCRAFT
- CRUSHING
- Optical analysis of crushing mode of pyrocarbon coated fuel particles
[EUR-4501] 13 p2117 N71-34851
- CRUSTS
- NT EARTH CRUST
NT LUNAR CRUST
- CRYOCYCLE PRINCIPLE
- Possibility of cryogenic heat pipe for cooling interspacecraft power supply cycle
13 p2186 N71-25911
- CRYODEPOSITS
- Sorption for cryodeposited frosts of hydrogen
[AD-712373] 02 p0687 N71-11775
- Using interference techniques to measure density and refractive index of water and carbon dioxide deposits as function of wavelength
06 p1244 N71-19129
- Spectral reflectance measurements on carbon dioxide cryodeposits at infrared wavelengths
09 p1424 N71-38211
- CRYOGENIC EQUIPMENT
- Cryochemical pump study and behavior of sublimation gases at low temperatures
[NASA-CR-111799] 01 p0559 N71-14008
- High voltage test of large cryogenic coil for magnetic energy storage system
[LA-4469] 06 p0903 N71-14023
- Mathematical modeling of cryogenic heat pipes
[NASA-CR-116175] 06 p0961 N71-14007
- Thermodynamic properties of insulated liquid methane fuelage tanks for supercruise cruise aircraft
[NASA-TM-D-61577] 07 p1102 N71-17056
- Method and apparatus for removing plastic contamination from wire using cryogenic equipment
[NASA-CASE-MF3-10340] 07 p1035 N71-17028
- Cryogenic heat pipe measurements of film condensation heat transfer coefficients
[CEA-CONF-1634] 08 p1302 N71-18137
- Cryogenic device for leakage detection using helium
[CEA-CONF-1506] 08 p1285 N71-16996
- High voltage, high resolution electron microscope with superconducting lenses operating with superfluid helium refrigerator
06 p1245 N71-19513
- Liquid nitrogen circulating pump problems and solutions including pump performance curves
[NBS-9777] 10 p1567 N71-21444
- Temperature scales, and cryogenic resistance and magnetic thermometers
11 p1842 N71-23081
- Calibration of cryogenic densimeter for mass density measurements of upper atmosphere
[NASA-CR-1819] 12 p1922 N71-30808
- Variable temperature Dewar for operation in temperature range from 77 to 400 K
[SRDE-70048] 13 p2079 N71-3400
- Dual solid cryogenics for spacecraft refrigeration insuring low temperature cooling for extended periods
[NASA-CASE-GSC-10168-1] 13 p1214 N71-34725
- Mathematical analysis of Vaisala refrigeration and use of computer program for solution of cooling equations
[NASA-TM-X-65334] 14 p2352 N71-23011
- Bellevue, metallic diaphragm, and pulsed valve subcritical transfer systems designs and high pressure systems analyses for orbital space station cryogenics
[NASA-CR-119831] 16 p2669 N71-30841
- Development of analytic model for determining relative heat transfer characteristics of conings in cryogenic surfaces
[AD-722720] 17 p2820 N71-30823
- Performance tests of low temperature desiccant refrigeration systems with bellows 4 and modifs
[NASA-CR-119184] 17 p2709 N71-30809
- Cryogenic flow measurement facility performance evaluation and accuracy statements for mass and volumetric flow
[NBS-TN-686] 19 p3075 N71-32720
- Nitrogen cryogenic pumping system design for bevatron refrigeration
[UCRL-201977] 20 p3247 N71-33708
- Thermal analysis of electrical cylindrical conductor used for multilayer insulation thermal conductivity tests - Vol. 1
[NASA-CR-119843] 21 p3463 N71-34848
- Empirical analysis of thermophysical properties of multilayer insulation composite materials in cryogenic storage equipment - Vol. 2
[NASA-CR-119844] 21 p3463 N71-34849
- Analysis of heat transfer characteristics of vacuum cryogen tank - Vol. 3
[NASA-CR-119845] 21 p3463 N71-34850
- Development of toroidal Dewar having lead shielding on glass epoxy and fibreglass substructure
[MATT-946] 23 p3828 N71-37708

SUBJECT INDEX

Cryotransformer design for use in laboratory
(AD-727901) 24 p3876 N71-37629

CRYOGENIC FLUID STORAGE
Investigation of cryogenic oxygen tank anomaly on
Apollo 13 flight 01 p0126 N71-10614
(NASA-TM-X-64462)
Pressurization collapse in cryogenic propellant
tanks due to subcooled vapor bubbles 03 p0446 N71-13107

Mathematical models for external insulation
systems of cryogenic fuel storage tanks
(NASA-CR-114627) 06 p0881 N71-16600
Bibliography synopsis of external insulation mate-
rials and techniques for cryogenic storage systems
(NASA-CR-114626) 06 p0938 N71-16645
Fabrication of filament wound propellant tank for
cryogenic storage
(NASA-CASE-XLE-03803-2) 07 p1035 N71-17651
Design of thermal control system for cryogenic fluid
storage tanks 07 p1121 N71-17918
(NASA-CR-114626)
Data on external refrigeration systems for space
storage of cryogenics for long periods
(NASA-CR-114920) 09 p1424 N71-20279
Description of computer program for detailed
multidimensional model of Apollo supercritical oxygen
storage tank 10 p1608 N71-21574
(NASA-CR-114963)
Prefabricated multilayered self-evacuating insula-
tion panels using gas with low vapor pressure at
cryogenic temperatures for application to storage of
cryogenics
(NASA-CASE-XLE-04222) 11 p1799 N71-22881
Tests of cryo-formed spheres to determine suitability
as replacements for titanium helium storage bottles
in liquid hydrogen tanks of eastern S-40 stage
(NASA-CR-61343) 12 p2002 N71-24179
Thermal cycling tests of ground and space liquid
hydrogen storage tank heat shielding with multilayer,
rigid substrate, thermal insulation blankets
(NASA-TN-D-6331) 13 p2173 N71-24822
Multilayer insulation panels for cryogenic liquid
containers
(NASA-CASE-MPS-14023) 13 p2186 N71-25351
Bellevue, metallic discharges, and paddle vortex
electrical transfer systems design and high pressure
systems analysis for orbital space station cryogenics
(NASA-CR-119831) 16 p2669 N71-28342
Development of thermal insulation material for insu-
lating liquid hydrogen tanks in spacecraft
(NASA-CASE-XMF-45046) 16 p2691 N71-28892
Development of cryogenic storage systems for
 manned space flight 18 p2963 N71-30910
(NASA-SP-247)
Predicting flight performance of cryogenic storage
system for Apollo 15 19 p3183 N71-31603
(NASA-CR-13116)
Analysis of aluminum and nonmetallic baffles for
use with liquid oxygen containers to prevent sloshing
(NASA-CR-1880) 21 p3463 N71-34284
Evaluation of liquid methane storage and transfer
problems for future supersonic aircraft cryogenic fuel
systems
(NASA-CR-72952) 21 p3463 N71-34648
Thermal analysis of electrical cylindrical calorime-
ter used for multilayer insulation thermal conductivity
test, Vol. 1 21 p3463 N71-34649
(NASA-CR-119043)
Empirical analysis of thermophysical properties of
multilayer insulation composite materials for
cryogenic storage equipment - Vol. 2 21 p3463 N71-34650
(NASA-SP-119044)
Analysis of heat transfer characteristics of venting
oxygen tank - Vol. 3 21 p3463 N71-34651
(NASA-CR-119045)
Insulation for light-weight, cryogenic gas storage
systems 21 p3464 N71-34653
(NASA-CR-115123)
Design and parametric analysis of passive rota-
tion/translation system for subcritically stored
cryogen during low-g 22 p3461 N71-36105
(NASA-CR-115140)
Development of passive rotation/expulsion system for
subcritical storage of cryogenic material during
low gravity situations 22 p3461 N71-36106
(NASA-CR-115149)
Developing apollo oxygen tank stratified per-
formance in low g environment and capability of tank
liquid motion requirements 22 p3461 N71-36248
(NASA-CR-115143)
Design and storage tests of 200 lb aluminum shipping
container including storage time, volumetric loading,
and pressure-temperature limitations 23 p3761 N71-36810
(NASA-CR-122952)
Evaluation of cryogenic refrigeration systems for
space applications 23 p3802 N71-37104
(NASA-CR-115192)
Insulation and optimization of space cryogenic
storage tank 23 p3802 N71-37105
(NASA-CR-115191)
Handbook of external refrigeration systems for long
term cryogenic storage 23 p3866 N71-37561
(NASA-CR-115190)

Analysis of recirculating type external pressuriza-
tion systems for use in pressure control of cryogenic
hydrogen, oxygen, and nitrogen storage systems
(NASA-CR-115205) 24 p3999 N71-38527

CRYOGENIC FLUIDS
NT FERMIL LIQUIDS
NT FLOX
NT LIQUID HELIUM
NT LIQUID HYDROGEN
NT LIQUID NITROGEN
NT LIQUID OXYGEN
NT SOLIDIFIED GASES
Film boiling on vertical surfaces in turbulent regime
using cryogenic fluids 01 p0132 N71-10064
(NASA-CR-110977)
Feasibility of rotational destratification of cryogenic
fluids 03 p0446 N71-13110
Flooding phenomena in cryogenic heat pipe with
vertical two phase counterflow
(CEA-CONF-1496) 05 p0734 N71-14973
Automatic thermal switch for improving efficiency
of cooling gases below 40 K
(NASA-CASE-XNF-03796) 05 p0735 N71-15467
Mathematical models for two phase cryogenic chok-
ing flow of hydrogen and nitrogen
(NASA-CR-116003) 06 p0833 N71-15808
Cavitation data analysis for liquefied cryogenic
hydrogen and nitrogen 06 p0833 N71-15809
(NASA-CR-116004)
Descriptive synopses for separating gas from
cryogenic liquid under zero gravity and for venting gas
from fuel tank
(NASA-CASE-XLE-00586) 06 p0864 N71-15968
Development of apparatus for measuring thermal
conductivity
(NASA-CASE-XGS-01052) 06 p0858 N71-15992
Method and apparatus for producing fine particles
in cryogenic liquid bath for gelled rocket propellants
(NASA-CASE-NFO-10250) 06 p0904 N71-16312
Application and characteristics of cryogenic fluids
for air breathing gas turbine engines 09 p1415 N71-19463
Summary data on thermodynamic and transport
properties of fluids and solids for cryogenic applica-
tions
(NASA-CR-117407) 10 p1606 N71-20734
Microscopic theory of quasi-particle spin fluctua-
tions in low temperature, dense Fermi liquids
10 p1618 N71-21440
Superconducting alternator design with cryogenic
fluid for cooling windings below critical temperature
(NASA-CASE-XLE-02823) 12 p1887 N71-23443
Flow angle sensor and remote readout system for
use with cryogenic fluids 13 p2081 N71-24864
(NASA-CR-116050)
Computer programs for calculation of ther-
modynamic and transport properties of eight
cryogenic fluids
(NASA-TM-X-67895) 20 p3238 N71-33318
Operation and accuracy of research facility for
measuring flow of cryogenic fluids using positive displace-
ment volumetric flowmeters
(NBS-TN-605) 22 p3585 N71-35531
Critical points of magnetic substances and
cryogenic fluids derived from equations of state, not-
ing deviations in thermodynamic properties 22 p3629 N71-35857
Design, characteristics, and test firing of radiation
and film cooled 25 pound thrust graphic thrust
chamber with liquid cryogenic propellants
(NASA-CR-72845) 24 p4080 N71-38534

CRYOGENIC GYROSCOPES
Survey of unconventional gyroscopes including
cryogenic gyroscopes, electrostatic gyroscopes, fluid
rotor gyroscopes, and optical gyroscopes
(DLR-MITT-71-42) 17 p2779 N71-29370
Design, fabrication and tests of alumina ceramic
envelopes for cryogenic electrically-suspended gyroscopes
(NASA-CR-119085) 19 p3102 N71-32386

CRYOGENIC MAGNETS
Performance of helium cooled superconducting
device at reduced gravity onboard Cosmos 213 satel-
lite
(NASA-TT-F-13402) 02 p0292 N71-11903
Design of cryogenic high frequency acceleration
system in ringotron 14 p2314 N71-26730
(JDR-PP-5408)
Wide-range nuclear magnetic resonance probe
design including integrated circuit, RF coil, and coaxial
cable for use with high field cryogenic magnets
(NASA-TN-D-6338) 15 p2585 N71-26908
Design of proton synchrotron using superconduct-
ing or cryogenically cooled aluminum magnets
(BNL-15438) 15 p2391 N71-27133
Tests of the quadrupole magnets, superconducting
as dipole magnet designs with ferromagnetic return
yokes, and analysis of Kohler's rule in pure aluminum
tapes
(RFE-1316) 21 p3464 N71-34657
Pulse dipole cryogenic magnets for superconducting
proton synchrotron
(UCRL-30403) 21 p3481 N71-34798

CRYOGENICS

CRYOGENIC ROCKET PROPELLANTS
Low gravity propellant control using capillary
devices in large scale cryogenic vehicles
(NASA-CR-102901) 01 p0116 N71-10602
Capillary containment system designs for low gravi-
ty propellant control in cryogenic vehicles
(NASA-CR-102900) 01 p0116 N71-10653
Low gravity propellant control by capillary devices
in cryogenic vehicles - seven flow tests, bubble
dynamics, residual analysis, settling, and surface ten-
sion properties 01 p0843 N71-10764
(NASA-CR-102902)
Quick-release coupling for fueling rocket vehicles
with cryogenic propellants 01 p0868 N71-10782
(NASA-CASE-XLS-01963)
Ignition characteristics and delivered performance
of gaseous hydrogen-oxygen reaction control thrusters
at cryogenic temperatures 02 p0291 N71-12097
(NASA-CR-72765)
Vehicle-scale analysis of fluorine-hydrogen main
tank injection pressurization system 03 p0437 N71-13100
(NASA-CR-72756)
Pressurization collapse in cryogenic propellant
tanks due to subcooled vapor bubbles 03 p0446 N71-13107
Techniques for determining cryogenic propellant
destratification 03 p0446 N71-13108
Effects of low Bond number sloshing on thermal
stratification of cryogenic fluids 03 p0446 N71-13109
Feasibility of rotational destratification of cryogenic
fluids 03 p0446 N71-13110
Development and characteristics of thermodynamic
vapor-liquid separator for cryogenic rocket propel-
lants 03 p0447 N71-13113
Hot-wire liquid level detector for cryogenic propel-
lants
(NASA-CASE-XLE-00454) 07 p1068 N71-17002
Glass fiber tubing for cryogenic rocket propellant
system
(NASA-CR-72797) 11 p1781 N71-21984
Molecular transfer of cryogenic propellants for orbit-
ing space stations using shuttle system
(NASA-CR-103083) 11 p1819 N71-22398
Automatically reciprocating, high pressure pump
for use in spacecraft cryogenic propellants
(NASA-CASE-XNF-04731) 12 p1929 N71-24042
Evaluation of throttling injector concepts applicable
to advanced cryogenic engines
(NASA-CR-103183) 14 p2332 N71-26411
Measurement of cryogenic propellant quantity
under conditions of weightlessness 21 p3514 N71-35036
Design, characteristics, and test firing of radiation
and film cooled 25 pound thrust graphic thrust
chamber with liquid cryogenic propellants
(NASA-CR-72845) 24 p4080 N71-38534

CRYOGENIC STORAGE
Vapor volume entrained in liquid due to boundary
layer boiling under reduced gravity conditions 03 p0446 N71-13104
Light weight plastic foam thermal insulation for
cryogenic storage 12 p1943 N71-23458
(NASA-CASE-XLE-02647)
Development of foam insulation for filament wound
cryogenic storage tank
(NASA-CASE-XLE-03803) 12 p1928 N71-23816
Weight and cost estimation for pressurization
systems for hydrogen, oxygen, and nitrogen storage
(NASA-CR-115204) 24 p3927 N71-38021

CRYOGENICS
Mechanical properties of cryogenically stratched
type 301 stainless steel and aluminum alloys 2021-T81
and X7007-T6
(NASA-CR-72733) 01 p0067 N71-10447
Characteristics of superconducting flux pump
(AD-711569) 02 p0195 N71-11352
Low temperature silicon thermometer and bolome-
ter
(AD-711940) 02 p0224 N71-11588
Thermal insulation for cryogenic applications in
aerospace technology 02 p0249 N71-12091
Reports from conference on ultralow temperatures
(AD-712061) 02 p0268 N71-12129
Friction and wear tests of steels, hard alloys, and
polymer materials at low temperatures
(AD-712947) 03 p0390 N71-12697
Fusion trends in cryoelectrical technology
(LA-TB-70-10) 03 p0418 N71-12867
Fluid-induced vibration of bellows with internal
cryogenic fluid flows 03 p0464 N71-13001
(NASA-CR-102953)
Phase behavior in fluid mixtures at high pressures
(AD-713540) 05 p0438 N71-14645
Cryogenic mechanical properties of aluminum al-
loys, titanium alloys, and stainless steels - Vol. 1
(AD-713419) 05 p0752 N71-14685

Cryogenic mechanical properties of superalloys, fiber reinforced plastics, seals, and gaskets - Vol 2 [AD-713620] 05 p0732 N71-14686

Free precession nuclear gyroscopes in zero magnetic fields at cryogenic temperature [AD-713633] 05 p0732 N71-14657

Testing materials for use in cages, balls, and races in cryogenic hydrogen-cooled 110-mm ball bearing [NASA-CR-72279] 06 p0866 N71-14647

Cryogenic gravity meter [AD-714569] 06 p0860 N71-14632

Magnetic induction concentric cylinder magnetohydrodynamic generator with cryogenic cooling [DLR-FB-70-25] 07 p1083 N71-17840

Feasibility of superconducting and cryogenic electrotransmission lines [AD-714797] 07 p1000 N71-18051

Magneto-optical technique to measure spin-lattice relaxation time of paramagnetic ions in crystal lattice as function of static magnetic field strength [AD-71448] 08 p1278 N71-18679

Tabulated values of cavitation b-factor for helium, H₂, N₂, F₂, O₂, refrigerant 114, and R23 [NASA-CR-115621] 08 p1160 N71-18930

Summary data on thermodynamic and transport properties of fluids and solids for cryogenic applications [NASA-CR-117407] 10 p1606 N71-20734

High strength aluminum casting alloy for cryogenic applications in aerospace engineering [NASA-CASE-XMF-02786] 10 p1572 N71-20743

Mass and volumetric flow accuracy of cryogenic flow research facility [NBS-9778] 10 p1538 N71-21480

Bolometric measurement of copper, aluminum, and stainless steel emittances at cryogenic temperatures 11 p1785 N71-23045

Low temperature mechanical properties of various alloys of high strength and corrosion resistance [NASA-SP-5921/01] 12 p1939 N71-23795

Computer program for simulation of nominal and anomalous operation of Apollo cryogenics storage system [NASA-CR-115022] 13 p2174 N71-25103

Turbulent diffusion, acceleration, confinement, and heating of plasma, properties of plasmas, cryogenic pumping, high power oscillators, drift instabilities, and related studies [EUR-CEA-FC-542-PT-2] 13 p2148 N71-25183

Noise level of Josephson junction amplifier at cryogenic temperatures [AD-720385] 14 p2228 N71-25947

Portable cryogenic cooling system design including turbine pump, cooling chamber, and atomizer [NASA-CASE-NPO-10467] 14 p2298 N71-26654

Test of rolling element fatigue life with fluorinated ether lubricant at cryogenic temperature using five ball fatigue tester [NASA-TN-D-6367] 16 p2600 N71-28038

Relief, safety, and cryogenic check valve systems engineering with industrial applications [NASA-SP-5921/01] 16 p2600 N71-28282

High density nickel-zinc ferrite with high Q factor and high permeability for RF application developed by utilizing cryogenic crush procedure [AD-721387] 16 p2569 N71-28407

Characteristics of electromagnetic superconductor devices, and magnetic alloys under low temperature conditions [AD-720683] 16 p2665 N71-28558

Use of semiconductors for storage and discharge of electrical energy [NASA-TF-P-13559] 16 p2639 N71-28888

Qualitative analysis of shuttle cryogen technology 17 p2831 N71-29610

Low gravity propellant control, using capillary devices in large scale cryogenic vehicles 17 p2831 N71-29611

Cryogenic components and insulation for shuttle cryogen technology program 17 p2831 N71-29618

Service life, instrumentation, and cryogenic technology applications [NASA-SP-5921/01] 18 p2962 N71-30707

Thermal insulation materials and techniques for high temperature and cryogenic environments - technology utilization [NASA-SP-5930/01] 18 p3024 N71-30851

Cryogenic deformation of single zirconium crystal structures 18 p2996 N71-31158

Steel and cobalt-nickel alloy compression and corrosion tests after precipitation hardening at cryogenic temperatures for increased yield strength and corrosion resistance [NASA-CR-72798] 19 p3115 N71-32321

Development and characteristics of dilution refrigerator capable of producing and holding temperatures near absolute zero 19 p3197 N71-32458

Low temperature and ultralow temperature research on superfluid helium and superconductivity [AD-724633] 20 p3333 N71-33154

Cryogenic porous media bed for trapping rare gases in airstreams [DUN-7221-VOL-2] 20 p3308 N71-33763

Determination of length and volume changes in solid nitrogen at zero pressure and 4.2 to 40 degrees K 20 p3335 N71-33804

Determination of thermal conductivity and electrical resistivity of solids at cryogenic temperatures [NASA-CR-121706] 21 p3463 N71-34652

Development of equation of state for solid hydrogen for pressures up to 112 K-bars [NYO-3699-52] 21 p3465 N71-34663

Cryogenic shock tube used for study of low temperature shock waves in molecular and para hydrogen [AD-726652] 22 p3570 N71-35423

High response, drag-body flowmeters for cryogenic gas application [NASA-CR-115144] 22 p3584 N71-35521

Derivation and analysis of Josephson effect in superconducting weak links [AD-726537] 22 p3658 N71-36085

Design and development of prototype static cryogenic heat transfer system utilizing heat pipe with wetting arterial wick and nitrogen as working fluid [NASA-CR-121939] 22 p3693 N71-36355

Carbon resistors as cryogenic thermometers [AD-727187] 24 p3925 N71-38005

Multilayer dielectric film reflector applied to cryogenic insulation materials [NASA-CR-115203] 24 p3966 N71-38289

CRYOPUMPING

Vacuum system model study for 500 MeV H⁻/cyclotron [TR-69-7] 03 p0359 N71-13344

Space simulator with cryosorption vacuum pump 09 p1367 N71-20243

Hydrogen vapor pressure observed at 2.8 K during cryopumping [LA-TR-71-15] 15 p2392 N71-27775

Cryopump used in magnetoplasma dynamic converters with liquid helium cooled argon plasma [DLR-MITT-71-03] 17 p2730 N71-29379

Vacuum cryopumping of heavy ion source in high voltage terminal of accelerator injector [UCL-20620] 19 p3150 N71-32119

CRYOSORPTION

U SORPTION

CRYOSTATS

Optimization of high current leads suitable for cryostats 01 p0068 N71-10144

Characteristics of right angle helium crystal incorporating high field superconducting solenoid [NBS-TN-562] 05 p0734 N71-15284

Cryostat for flexure fatigue testing of composite materials [NASA-CASE-XMF-02964] 07 p1032 N71-17659

Investigating design parameters and costs of simplified helium cryostat superconducting dipole and quadrupole magnets [UCL-19764] 08 p1242 N71-18272

Apparatus for use in liquid helium cryostat for measurement of small magnetic field changes occurring within detection chamber 08 p1244 N71-19010

Specific heats of H₂ and D₂ solid mixtures down to 0.5 K, adsorption isotherms of He-3 and He-4 at low temperatures, and development of He-3 dilution refrigerator and liquefier [AD-717623] 11 p1815 N71-21941

Cryostat for use with horizontal fatigue testing machines at low temperatures [NASA-CASE-XMF-10968] 12 p1924 N71-24234

Design and performance of cryostat for single crystal and X ray diffraction analyses [AERE-R-6532] 15 p2509 N71-27910

Helium-3 cryostat for specific heat measurements at 0.5 to 4.2 K [UUIP-677] 18 p2921 N71-30449

Cryostat for keV heavy ion irradiation and isochronal annealing at 77 to 300 deg K to study lattice defects in metals by Mossbauer spectroscopy and other experiments [RD/B/M-1753] 18 p2973 N71-30544

X ray spectrometer with cooled Si(Li) detector and field transistor in chamber cryostat [JENR-P13-5707] 22 p3633 N71-35887

CRYSTAL DEFECTS

NT CRYSTAL DISLOCATIONS

NT EDGE DISLOCATIONS

NT FRENKEL DEFECTS

NT POINT DEFECTS

NT SCREW DISLOCATIONS

NT VACANCIES (CRYSTAL DEFECTS)

X ray diffraction and scattering studies of crystal imperfections in solids [PB-192684] 02 p0283 N71-11844

Computer program predictions of stacking fault images at high voltages [PB-192186] 03 p0445 N71-13274

Method for nondestructive determination of nature of flaws by ultrasonic examination [ORNL-TM-3056] 04 p0616 N71-13945

Dosimeter techniques for neutron produced defects in ammonium salts, hydrocarbons, and organic materials [COO-1105-153] 04 p0579 N71-13976

Electron radiation effects in ruby laser crystals [NASA-TN-D-7025] 04 p0602 N71-13982

Production of laser glass and optical damage mechanisms in laser materials [NBS-SP-341] 04 p0525 N71-14526

Crystal defects caused by photoelectron excitation 04 p0568 N71-14535

Surface damage to optically nonlinear crystals by Q switched lasers [NASA-CR-111767] 04 p0526 N71-14537

Raman spectroscopy of laser produced damage in crystalline quartz 04 p0535 N71-14538

Defects and their role in determining luminescence and electrical properties of crystals [AD-714620] 06 p0933 N71-14007

Investigating mechanical properties of solids, relaxation processes in polymers, and properties of crystals [AD-713923] 06 p0933 N71-14012

Investigating spin-lattice relaxation of paramagnetic defects in crystals of II-VI compounds [AD-713964] 06 p0934 N71-14019

Temperature and doping effects on cobaltous oxide and nickelous oxide structures [NASA-CR-116435] 07 p1006 N71-17034

Neutral defects in mercury telluride single crystals grown by Bridgman method in mercury vapors 07 p1047 N71-17125

Growing silicon crystals with minimum defects using Czochralski method 07 p1067 N71-17278

Examining aspects of epitaxial growth of silicon films and relationship to process technology 07 p1087 N71-17279

Investigating structural defects in silicon material after epitaxial layer formation and diffusion 07 p1091 N71-17304

Measuring defects in silicon wafers induced by residual strain during processing 07 p1091 N71-17308

Methods for determining characteristics of bulk silicon used in production of semiconductor devices 07 p1091 N71-17311

Measuring surface damage on silicon caused by shaping operations 07 p1092 N71-17313

Investigating methods for chemical treatment of silicon surfaces to reduce oxide impurities 07 p1092 N71-17314

Crystal defect chemistry of sintering and ferroelectric properties of lead zirconate titanate ceramics [UCL-206309] 07 p1048 N71-17085

Transport and defect properties of thin tungsten, platinum, and nickel wires [COO-1247-21] 07 p1044 N71-17094

Mass transport and atomic structure near metal surfaces [AD-715291] 08 p1277 N71-18411

Describing instrumentation and methods used in study of radiation damage in lithium-diffused silicon [NASA-CR-116790] 08 p1257 N71-18417

Influence of defects created by neutron irradiation at 80 K on elastic moduli and internal friction of germanium [CEA-CONF-1621] 08 p1213 N71-18445

Investigations on magnetic flux and interaction and crystal defects in type 2 superconductors [NYO-4060-5] 08 p1278 N71-18636

Quantum mobility, configurational entropy, and Mossbauer spectroscopy of impurity atoms in crystals [NUB-2049] 08 p1279 N71-18690

Thermoluminescence of single thorium oxide crystals having lattice defects [AD-715885] 08 p1280 N71-18823

Radiation damage in single crystals of anthracene, naphthalene, and phenanthrene 08 p1283 N71-18939

Infrared spectra with frequency shifts in crystal defect resonance modes [NYO-2391-119] 09 p1436 N71-20045

Gaseous exposure experiments of lunar soil with microchemical, microphysical, and adhesion analysis [NASA-CR-114916] 09 p1467 N71-20277

X ray diffraction analysis of crystal defects caused by martensitic transformations in iron nickel and iron carbon steels 10 p1583 N71-21571

X ray diffraction measurement of crystal composition profiles, structure, and misorientations in nickel and gold electroplated diffusion zones of copper/nickel single crystals 10 p1583 N71-21598

Photoconductivity energy spectra of defects in lithium-doped gallium arsenide monocrystals [NLL-TR-5904] 10 p1637 N71-21610

Crystal defects in diamonds and semiconductor fabrication [IPR-5-5245] 11 p1816 N71-22102

Crystalline structure defects of diamonds caused by lithium ion injection 11 p1816 N71-22103

Defect properties of semiconductor materials as function of impurity concentration and ionizing radiation [AD-717773] 11 p1817 N71-22247

SUBJECT INDEX

Radioactive trace diffusion of AuZn and FeCo species isotopes with measurement of correlation and aging effects in crystal lattice defects
(AD-71737) 11 p1778 N71-22353

Ultrasonic measurements on paramagnetic impurities in small hollows compared with predictions of tunneling model
(NYO-2471-47) 11 p1784 N71-22591
Low temperature volume expansion of LBR/LIT by self damage due to beta decay of negative tritium ion
11 p1889 N71-23031

Determining nature of defects responsible for degradation in solar cells by studying radiation effects in silicon-diffused bulk silicon after neutron and electron irradiation
(NASA-CR-118009) 12 p1860 N71-23404

Defect motion in crystals and numerical solution of the time-dependent Schrödinger equation
(AD-71953) 13 p2130 N71-24348

Semiconductor devices, quantum electrodynamics, laser, defects in crystals, communication and radar systems, laser-scattering, plasmas, and other related subjects - continuous report
(AD-71952) 13 p2180 N71-24445

Phonon and electron induced transition effects on superconductor of transition metals, and impurity effects on crystal lattice dynamics
13 p2154 N71-23549

Characteristics of some of displacements of defects in graphite from neutron irradiation
(CNA-1574) 14 p2281 N71-24522

Microscopic and X ray crystallographic analysis of corrosion in body centered cubic aluminum phosphorus alloys during aqueous hardening
(CNA-CONF-1408) 15 p2422 N71-27129

Microstructure precipitates in austenitic steel exposed to neutron irradiation
(CNA-CONF-1438) 15 p2424 N71-27406

Ion pair absorption phenomena observed between heavily doped ions in ionic crystals
(AD-71971) 15 p2506 N71-27428

Neutron, magnesium, and aluminum annealing effects on neutron irradiated iron crystal defects in low temperature environments
(CNA-CONF-1481) 15 p2472 N71-27437

Neutron spin resonance for detecting defects in hydrogen oxide single crystals created by gamma or neutron irradiation
(CNA-CONF-1486) 15 p2496 N71-27972

Color centers and magnesium oxide crystal defects from neutron irradiation and impurities
(NASA-CR-118045) 16 p2642 N71-28044

Spectral reflectance of neutrons by distorted copper crystal in monochromator
16 p2596 N71-28708

Defects introduced into Ge and Si by electron irradiation at low temperature
(COO-125-56) 16 p2666 N71-28735

Metal content, plastic deformation, and stacking fault effects on martensitic formation in iron chromium alloys at cryogenic temperatures
(NRL-RTS-6180) 16 p2613 N71-28806

Isolation absorption and crystal defects in alkali and alkaline earth halides
(NRL-RTS-62-23) 17 p2792 N71-29349

Thermal elimination of discontinuities in thin films of gold formed by evaporation in vacuum
(NRL-PORT-TRANS-2674-7022.81) 17 p2764 N71-29608

Crystal lattice effects on thermal conductivity and specific heat of zinc sulfide and cadmium sulfide single crystals
17 p2857 N71-29717

Nonlinear elasticity theory for dragging forces on moving defects by strain-field phonon scattering
17 p2819 N71-29932

Point on intrinsic and physical properties of dislocation theory
17 p2821 N71-29968

Quasistatic stress mechanics for crystal lattice defects
17 p2823 N71-29980

Dislocation flow through point and line obstacles during alloy precipitation hardening
17 p2823 N71-29987

Mathematical model for dislocation stacking fault energy and partial dissociation in crystal defect dislocations
17 p2824 N71-29991

X ray analysis of transformation-induced defects in cubic nickel single crystals
17 p2828 N71-30172

Individual dynamic properties of off-center ions in crystal lattices and electron phonon interaction effects
(AD-72287) 17 p2828 N71-30273

Step gradient analysis for measuring optical transfer functions
(NARA-TN-D-6434) 18 p2893 N71-30358

Luminescent intensity formulae and polarized neutron diffraction patterns including effects of crystal defects
(NRL-1228) 18 p2979 N71-30786

Cryogenic deformation of single zirconium crystal samples
18 p2996 N71-31158

Quantum mobility and nuclear spin echo damping in impure crystals
(NUS-2089) 18 p2999 N71-31486

Heat treatment and irradiation effects on rare earth ions in crystal color centers
(AD-72353) 19 p3168 N71-31988

Application of dielectric and acoustic loss techniques for determining defects in ceramic materials
(AD-723838) 19 p3120 N71-32007

Resonance Cd induced CdS crystal defects determined by Hall effect and electrical resistivity measurements in high temperature environments
19 p3169 N71-32270

Nature, size, and distribution of lattice defects in type 3 superconductor NbZr2S and their influence on critical current density
(NRL-CE-TRANS-5350-7022.09) 19 p3168 N71-32282

Slip, twinning, and deformation bands in indium single crystals under tensile strain at varying temperatures
19 p3170 N71-32482

Interaction between acoustic phonons and tunneling defect states in KCl-Li using resonant pumping of tunneling states with microwaves and scattering of heat phonons
(NYO-2391-111) 19 p3162 N71-32743

Defect structure of Al-Zn alloy induced by quenching and low temperature aging
(AD-72632) 22 p3595 N71-33599

Intercrystalline fracture along grain boundaries of quenched low temperature manganese silicon-chromium steel
(NRL-CE-TRANS-5342-7022.09) 22 p3597 N71-33616

Electron microscopy creep properties study of beta NiAl thin film specimens from deformed single crystals
(COO-1409-10) 23 p3770 N71-34840

Iron doping effects on growth kinetics and electron spin resonance of aluminum oxide single crystals
23 p3834 N71-37342

Analysis of isochronal annealing behavior of radiation defects in germanium crystals after radiation with cobalt-60
(AD-726993) 23 p3835 N71-37345

X ray diffraction and charge transfer in reduced monochalcogenite uranium oxide at various temperatures for defect ordering effects
(AD-727100) 24 p3998 N71-38515

CRYSTAL DISLOCATIONS

NT EDGE DISLOCATIONS

NT SCREW DISLOCATIONS

Continuum mechanics of grain boundary dislocations and diffusional creep
(AD-71088) 01 p0111 N71-10669

Dislocation mobility and density in metallic crystals
(CALT-767-P-3-14) 03 p0760 N71-15096

Neutron irradiation effect on dislocation of bcc metals and solid solutions at low temperatures
(CONF-700819-3) 06 p0609 N71-15868

Mobility of basal dislocations interacting with non-basal dislocations in zinc
(CALT-767-P-3-11) 06 p0872 N71-16353

Investigating misfit dislocations in silicon induced by diffusion of phosphorus and boron
07 p1090 N71-17298

Correlation of dislocation structure with microstrain damping in copper single crystals
(NYO-4073-2) 07 p1093 N71-17454

Anisotropic behavior of austenite, martensite, and bcc refractory alloys, and dislocation-oxide stress interaction and intermetallic hardening in bcc alloys
(COO-1676-13) 08 p1211 N71-18239

Dislocation glide at high temperatures and glide recovery model for steady state creep
08 p1299 N71-19161

Dislocations and radiation damage in alpha-uranium using electropolished thin foils
(CEA-R-3407) 09 p1437 N71-20105

Dislocation structure of refractory metals of Group 6A produced by electron beam and zone melting methods
10 p1633 N71-20683

Electron diffraction contrast effects from dislocations and dislocations in ordered superlattice alloy interfaces
(ORO-355-4) 11 p1779 N71-22481

Observation of void formation induced by electron irradiation in single crystal and bicrystal Au films and polycrystalline Al films
(NYO-4185-1) 11 p1708 N71-22583

Dislocation density dependence on compression shear stress measured by etch-pit technique in high purity and Mg doped, strain hardened LIP single crystals
(NRC-TT-1447) 12 p1967 N71-23958

Matrix and fcc lattice precipitation phase condition and quantity determinations of Co-Al alloy coercive force
(NRL-CE-TRANS-5352-7022.09) 12 p1939 N71-24096

CRYSTAL DISLOCATIONS

Impurity caused grain boundary sliding in aluminum ceramics during compression
(ORO-3328-17) 15 p2308 N71-27905

Edge, screw, and crystal dislocations
(NBS-SP-317-VOL-1) 17 p2816 N71-29936

Stacking fault energy determination in discrete dislocations in continuous dislocations
17 p2816 N71-29937

Computerized simulation of point defects and dislocations in copper
17 p2818 N71-29944

Dynamic theories of signification in dislocated crystal using Lagrangian formalism
17 p2819 N71-29949

Invariance and continuity of Burgers vector applied to crystalline interface dislocations
17 p2820 N71-29958

Structural and elastic properties of screw twin dislocations in anisotropic crystals
17 p2820 N71-29959

Nonplanar dislocations and Burgers vector of twinning dislocations
17 p2820 N71-29960

Crystal glide dislocation through internal grain boundaries with symmetrical fit
17 p2820 N71-29961

Basis vector pair and triplet of dislocations in surface and conventional crystals
17 p2820 N71-29963

Dislocation theory applied to liquid crystals in mesomorphic media
17 p2821 N71-29965

Nonmetric connections, quasidifferential and quasidifferential applied to noncommutative stress theory in crystals
17 p2821 N71-29966

Nonlinear continuum theory for analyzing crystal dislocation effects
(NBS-SP-317-VOL-2) 17 p2821 N71-29968

Macroscopic continuum mechanics theory for dislocation wave interactions in crystal lattice dislocations
17 p2821 N71-29970

Nonlinear variational formulation of dislocation and yielding in plastic manifold for mechanical material
17 p2822 N71-29975

Statistical analysis of crystal lattices for continuum mechanics of dislocations
17 p2822 N71-29974

Elastic Cosserat surface continuum with deformable strains
17 p2822 N71-29975

Dynamic nonlinear theory of crystal dislocations with elastic-plastic continuum mechanics
17 p2822 N71-29976

Continuum plasticity and microstructure dislocation in elastic-plastic phase modeling of crystal lattices
17 p2822 N71-29979

Green function and Fourier integrals in dynamic elastic field theory of crystal dislocations and disclinations
17 p2823 N71-29981

Kinematics of continuous dislocations in crystal lattices
17 p2823 N71-29984

Thermally activated dislocation motion in crystal lattices with nonreversible barriers
17 p2823 N71-29985

Dislocation flow through point and line obstacles during alloy precipitation hardening
17 p2823 N71-29987

Strain rate effects on dislocation flow dynamics in crystal lattices
17 p2824 N71-29988

Strain effects on plastic cross slip of hardening dislocations in two phase alloys
17 p2824 N71-29989

Thermal dislocation dynamics and plastic flow in crystal lattices
17 p2824 N71-29990

Mathematical model for dislocation stacking fault energy and partial dissociation in crystal defect dislocations
17 p2824 N71-29992

Resonance line broadening by crystal dislocations
17 p2824 N71-29993

Fourier transform of X ray diffraction line profiles from crystals with dislocations
17 p2825 N71-29995

Dislocation formation energy effects on thermodynamic properties of solids
17 p2825 N71-29996

Electronic states at dislocations in semiconductor and diamond structures
17 p2825 N71-29997

Electron scattering by stacking faults in metal crystals
17 p2825 N71-29998

Mathematical model for surface states on crystal stacking faults
17 p2825 N71-29999

Dynamic model for vibrating dislocation interaction with conduction electrons in metals
17 p2825 N71-30000

- Quantum mechanical model for electronic energy bands of dislocations in cadmium sulfide crystal 17 p2825 N71-30001
- Energy dissipation in electron interaction with moving crystal dislocations 17 p2826 N71-30002
- Formulation and applications of dislocation theory in crystal physics 17 p2826 N71-30003
- Model for migration of dislocation arrays in ionic crystals based on dislocation climb in vacancy concentration gradients by action of external electric field at array sites 17 p2826 N71-30004
- Dislocation mobility in doped silicon single crystals, analyzed by amplitude dependent internal friction 17 p2827 N71-30171
- Electron microscopic analysis of cold rolled zirconium microstructure [JNHS-MF-15] 19 p3113 N71-32112
- Magnetic field neutron scattering analysis of tension induced nickel single crystal dislocation [JUL-675-PF] 19 p3161 N71-32709
- Crystal defect effects on ultrasonic attenuation and phonon scattering in germanium [AD-74328] 20 p3332 N71-33017
- Dislocation glide, deformation twinning and grain boundary sliding in compressive creep of single and bicrystalline aluminum oxide 21 p3500 N71-34932
- Nickel and copper substructural disorientation angle dependencies on deformation, loading, and temperature [NLL-LT-746-728-[9022.40]] 22 p3659 N71-36091
- Analysis of extraneous grain boundary dislocations in high angle [110] twist boundaries in thin film gold bicrystals [NYO-3504-58] 23 p3834 N71-37340
- Quantum mechanical calculations of shifts in optical constants for deformed single silicon crystals at differing polarization directions 23 p3834 N71-37341
- Analysis of structure and behavior of dislocations in grain boundaries and Burgers vectors of lattice dislocations in Fe-Mn alloys [NLL-M-20645-[5828.4F]] 23 p3836 N71-37357
- Continuum theory of dislocations for plastic deformation of metallic crystals 23 p3837 N71-37363
- ### CRYSTAL FILTERS
- Techniques for fabrication of quartz filter crystals with mode control and frequencies up to 280 MHz [AD-719175] 13 p2054 N71-24418
- ### CRYSTAL GROWTH
- NT CZOCHRALSKI METHOD
- NT EPITAXY
- NT HYDROTHERMAL CRYSTAL GROWTH
- NT TRAVELING SOLVENT METHOD
- NT VERNEUIL PROCESS
- Differential equations describing nucleation in crystal growth 01 p0100 N71-10132
- Electrical properties of single crystals of Prosulite 01 p0109 N71-10143
- Gallium arsenide bulk crystal growth from solution [AD-710812] 01 p0110 N71-10493
- Solid state diffusion growth of composite materials containing continuous NIAI fibers in aluminum matrices from hot-pressed aluminum embedded nickel wires [AD-711346] 02 p0346 N71-11591
- Development of space manufacturing techniques for orbital workshops [NASA-TM-X-66486] 02 p0234 N71-11701
- Low gravity manufacturing of potassium sodium nitrate crystals in earth orbiting laboratory 02 p0283 N71-11704
- Planned experiment on weightless crystal growth from solutions in orbital workshop 02 p0283 N71-11717
- Nondestructive tests to evaluate and characterize weightless grown gallium arsenide crystals 02 p0283 N71-11718
- Production of single crystals from containerless melts in weightless space environment 02 p0283 N71-11724
- Weightlessness effects on solidification processes in space manufacturing 02 p0284 N71-11725
- Low gravity manufacturing of single crystals from melts 02 p0284 N71-11726
- Low gravity effects on crystal whisker growth in orbital workshop 02 p0284 N71-11727
- Prediction of weightlessness effects on single crystal growth by floating zone and Czochralski methods 02 p0284 N71-11728
- Mathematical theory for geometrical selection of crystals [AD-711886] 02 p0284 N71-11842
- Production of filamentary diamond monocrystals from carbon containing media 02 p0287 N71-12009
- Electric field effect on crystal growth rate of molecular solids [A69-10140] 03 p0324 N71-12314
- Investigating kinetics of crystal growth of copper compounds in magnetic and electric fields [AD-704356] 03 p0440 N71-12755
- Arc fusion growth and characterization of high purity MgO crystals [ORNL-4547] 03 p0441 N71-12840
- Characteristics of crystals grown from molten silicon [AD-712022] 03 p0442 N71-12909
- Reaction kinetics of crystal growth in mixed solid solutions [PB-189374] 03 p0442 N71-12989
- Absorption spectra of gadolinium /32- in crystals of alkaline earth fluorides at laser D energy levels [AD-712687] 04 p0380 N71-14010
- Thermodynamic significance of interface potential increase during crystal growth from solution [REPT-4164] 05 p0756 N71-14582
- Growth of selenium and selenium-tellurium alloy crystals with determination of optical absorption and photoconductivity [NASA-CR-111825] 05 p0757 N71-14640
- Interparticle interference effects in diffusion controlled growth [NYO-3678-3] 05 p0758 N71-15297
- Statistical theory of interfacial thermal conductivity and crystal growth under weightlessness [NASA-CR-102989] 05 p0784 N71-15601
- Solid state chemistry of rare earth oxides [COO-1109-52] 06 p0931 N71-15877
- Investigating crystal growth and dendritic character of chalcogenides of transition metals in aluminum alloys [AD-714420] 06 p0935 N71-16323
- Investigating magnetic susceptibility of small crystallites of nickel and nickel-iron ferrite as function of hydrothermal growth and frequency [AD-714485] 06 p0906 N71-16405
- Production of cadmium telluride single crystals for use in infrared modulators [AD-714284] 06 p0935 N71-16449
- Investigating morphology of extended chain crystals of polyethylene, polytetrafluoroethylene, and polyoxymethylene under elevated pressure 07 p1047 N71-17136
- Mechanism of growth of whiskers from gas phase of silicon, germanium, and other semiconductors [AD-714799] 07 p1096 N71-18047
- Growth and evaluation of bismuth titanate single crystal also growth of thick single crystals of related compounds [AD-715312] 08 p1277 N71-18420
- Boundary value problems for temperature and flux fields inside and around parabolic needle and parabolic platelet crystals during growth 08 p1282 N71-19295
- Development of single crystal barium sodium nitrate as nonlinear optical material [AD-715987] 09 p1453 N71-19996
- Hamiltonian method for determining magnetic tunneling in crystals in one and two band models 09 p1454 N71-20423
- Crystal growth and galvanomagnetic properties of Mg2Pb 09 p1454 N71-20438
- Production of crystals with lattice spacing gradients for neutron monochromators [ORNL-TR-2401] 09 p1455 N71-20547
- Zone melting, recrystallization, single crystals, impurities, crystal growth, fluxes, magnetic fields, X ray analysis, and mixing [JPRS-52552] 10 p1573 N71-20866
- Distribution of lead, copper, and zinc impurities in KCl single crystals grown from melt 10 p1632 N71-20878
- Growth of chemically homogeneous single crystals of alloys 10 p1633 N71-20829
- Phase transitions and magnetostriiction in CaMnCl₂ 2H₂O [NASA-TM-X-52997] 10 p1634 N71-21075
- Chemical synthesis and crystal growth of pure and doped europium chalcogenides, including magnetic moment, transport properties, and photoconductivity data [AD-717369] 11 p1816 N71-22120
- Design and construction of steady state crystal growth system suitable for growth of rare earth compounds with magnetic properties [AD-717311] 11 p1816 N71-22163
- Growth and properties of single crystal materials for optoelectronics including lasers [AD-717684] 11 p1817 N71-22395
- Diamond crystals of high chemical and mechanical perfection for research in electronic devices [AD-717691] 11 p1819 N71-23093
- Mass transport properties, crystal growth, and self-diffusion rates for magnesium oxides 12 p1942 N71-23227
- Growth form for polyelectrolyte macromolecules resulting in large unit spherulites [AD-718420] 12 p1943 N71-23408
- Characterization of mechanisms involved in growth processes of inorganic whiskers [AD-718248] 12 p1986 N71-23774
- Improved encapsulating glass drying and polishing techniques for growing bulk gallium arsenide crystals [AD-718138] 12 p1987 N71-24013
- Mechanism of crystal nucleation in gels, and heterogeneous nuclei and gel structure [AD-718964] 13 p2130 N71-24094
- Numerical analysis of plastic deformation and dislocation density in crystals grown by Bridgman method [AD-719575] 13 p2151 N71-25108
- Growth of p-type semiconducting diamond by vapor phase deposition using methane-diborane doping gas mixture in presence of diamond seed crystals [NASA-TM-X-67866] 14 p2324 N71-27702
- Production of pure silicon single crystals and effects of gamma radiation on crystal structure [AD-720753] 14 p2329 N71-26609
- Growth parameters for zinc single crystals grown at controlled rate from melt [IS-T-441] 15 p2505 N71-27228
- Optimization for zero gravity experiment on solution growth of gallium arsenide and design of equipment package for melt growth of indium antimonide crystals [NASA-CR-119792] 15 p2510 N71-27916
- Nucleation of damage centers in single crystal silicon held at room temperature and bombarded in random direction with light ions [RISO-236] 16 p2642 N71-28014
- Homo-epitaxial crystallization in copper electrodeposition 16 p2669 N71-28085
- Evaluation of optical density measurements in method for monitoring and controlling vapor concentrations used for crystal growth [AD-721590] 16 p2665 N71-28732
- Chalcocite single crystal growth [AD-722097] 16 p2667 N71-28844
- Optical measurements and crystal growth for development of chalcocite crystals [AD-722058] 16 p2667 N71-28844
- Temperature effects on growth and nucleation rates in mixed suspension crystallization 16 p2668 N71-28849
- Numerical analysis of solvent reorganization energy and method for prevention of dendritic crystal growth and zinc electrode surface area decrease in silver batteries [NASA-CR-119247] 18 p2873 N71-30827
- X ray and thermal conductivity measurements of unidirectional growth and recrystallized hexagonally close packed bismuth 18 p2883 N71-31020
- Growth of single crystals of cadmium telluride by modified Bridgman technique to improve infrared modulator devices [AD-723859] 19 p3167 N71-31776
- Crystal growth of cinnabar, prosselite, and lead selenide, experimental work in HgS-Hg₂ phase diagram, and electro-optic coefficients of zincblende structure compounds [AD-721201] 19 p3168 N71-32007
- Optical, dielectric properties, and growth of alpha-monoclinic selenium 19 p3170 N71-32007
- Kinetics of crystal nucleation and growth in bulk evaporation crystallization 21 p3501 N71-34999
- Preparation of compound semiconductors by controlled diffusion mechanism with gel growth optimization of single crystals of lead sulfide and other group 2-6 compounds [AD-727035] 22 p3638 N71-36089
- Vapor phase growth of CdTe, CdSe, ZnTe, and CdS single-crystal boules by seed-growth method with analysis of multiple twinning [AD-727048] 22 p3659 N71-36089
- Feasibility of crystal growth techniques for beta alumina membrane from molybdenum, tungsten, and iridium [NASA-CR-72962] 23 p3833 N71-37376
- Iron doping effects on growth kinetics and domain spin resonance of aluminum oxide single crystals 23 p3834 N71-37376
- Properties determination of rutile in areas of crystal growth, sample preparation, semiconductor devices, and Hall effect [AD-726752] 23 p3835 N71-37376
- Development of theory for replacement partition function for crystals based on nucleation theory [AD-726758] 23 p3835 N71-37376
- Analysis of crystals to be grown in space with emphasis on dislocations and stacking faults [NASA-TN-D-4505] 24 p3990 N71-38512
- ### CRYSTAL LATTICES
- NT BODY CENTERED CUBIC LATTICES
- NT CUBIC LATTICES
- NT FACE CENTERED CUBIC LATTICES

SUBJECT INDEX

Applications of Moseley effect in chemical research - bibliographies 01 p0110 N71-10553

Displacement of atoms from normal lattice positions by neutrons and alpha particles 02 p0273 N71-11791

Monte Carlo computation of volume effects in macromolecules for chains in cubic lattice 02 p0274 N71-11854

Measuring preferred orientation of beryllium foil by X ray diffractometry and sodium iodide counters 03 p0420 N71-12639

Relationship between crystal index surfaces and surface and lattice structure as exemplified by tungsten 03 p0440 N71-12754

Effect of lattice parameter and melting point of metal on solid state diffusion 03 p0442 N71-12908

Energy transferred to zirconium lattice by neutron radiation 04 p0575 N71-13584

Electronic and vibrational spectra of ionic solids, lattice dynamics of solids, high pressure research, fluorescence of hydrocarbons and optical spectra 04 p0577 N71-13749

Effects of low temperature on lattice structure, X ray scattering, mobility of electrons and quantum hydrodynamics 04 p0569 N71-14418

Inscription of crystal defects by point force arrays 05 p0739 N71-15376

Using isomorphous and phase rule concepts to obtain accurate thermodynamic and solubility in mixed crystals for propellants 05 p0761 N71-15378

Forward angular correlation techniques for studying effect of cubic lattice on electronic levels of erbium in HoAl₂ 06 p0909 N71-15780

Quantitative phase analysis and precise lattice parameter measurements by X ray diffraction in thin films 06 p0934 N71-16383

Influence of lattice vacancies and impurities on electrical resistivity of noble metals 06 p0937 N71-16700

Parasitic and paramagnetic behavior of dipole centers in crystals 06 p0937 N71-16720

Variations in length and crystal parameters of alpha, beta, and delta phases of plutonium at low temperatures due to self-irradiation 08 p1256 N71-18386

Using X ray powder diffraction line profiles to study stacking fault probability in hexagonal close-packed titanium aluminum alloys 08 p1214 N71-18601

Atomic mobility in crystal lattices in liquid metals 08 p1282 N71-19292

Crystal orientation and material processing effects on fatigue crack propagation in brass and stainless steel 08 p1282 N71-19306

Electromagnetic interaction energy expansion using tensor spherical harmonics and matrix element densities on crystal dynamical matrix eigenvalues and acoustic wave functions 09 p1427 N71-19694

Magneto-optical study of magnetic field dependence of spin-lattice relaxation time of paramagnetic ions in crystal lattice 09 p1432 N71-19929

Mossbauer studies of recoilless fractions, isomer shifts, and magnetic properties of gold and gold alloys at high pressure effects on Kondo copper-iron alloys 09 p1400 N71-20012

Piled carbon source for graphite lattice analysis 09 p1442 N71-20383

Characteristics of alkali hydride lattice energies for ions Born-Mayer potential 09 p1454 N71-20394

Reduction of crystals with lattice spacing gradients forming monocrystalline 09 p1455 N71-20547

Annual report of materials research activities at Northwestern University, from October 1969 to September 1970 09 p1588 N71-20916

Structure and structure of Mn-PC alloy and intermetallic, atomic distribution, and radial distribution functions for structural model 10 p1580 N71-21394

Schrodinger equation for examining energy levels between dimensional metal crystals 11 p1816 N71-22162

Neutron diffraction contrast effects from antiphase boundaries and dislocations in ordered superlattice structures 11 p1779 N71-22481

Determination of Burgers vectors, glide planes, and density of crystal dislocations by various Bragg angle

sequence micrograph and dynamic electron diffraction equation analysis 12 p1967 N71-23957

Thermodynamically consistent equations of state for alpha and omega phases of iron 13 p2092 N71-24563

Elastic, piezoelectric, and photoelastic constants for light scattering with hypersonic waves and Brillouin effects in ferroelectric lithium niobate crystals using helium-neon lasers 13 p2125 N71-24906

Debye-Waller factor of Herring structure theory for model of solid with vacant lattices 13 p2152 N71-25451

Calculation of lattice-constant change for helium induced strain in ErT₂ and BeT₂ 13 p2154 N71-25531

Face centered to body centered cubic lattice transformations in vacuum deposited thin iron films 13 p2154 N71-25548

Lattice dynamics calculations for high pressure shock compression analysis on solid crystal 14 p2327 N71-26490

Computer program modifications and lattice coding for hydrogenous systems including transport corrections for self-scatter cross sections and collision probability 15 p2467 N71-27297

Production, annealing, detection of crystal lattice point defects caused by neutron irradiation of ceramic materials 15 p2469 N71-27370

Atomic location, bond state, and magnetic properties of compounds and minerals by neutron diffraction 15 p2477 N71-27583

Molecular crystals structure analysis on quinolinol monohydrate/monohydrate and beta picoline-N-oxide fumaric acid adduct 15 p2509 N71-27908

Structural, magnetic, and spectroscopic examination of nickel square dihydrate 15 p2510 N71-27978

Spin-lattice relaxation and atomic motions in lithium fluoride 16 p2668 N71-28988

Microstress analysis of edge dislocation effects of strain hardening on copper single crystal lattices 17 p2815 N71-29808

Fourier transformation for lattice statics method for distortion 17 p2818 N71-29942

Lattice theory model for screw dislocation and Peierls energy calculations 17 p2818 N71-29946

Dynamic theories of eigenfrequencies in dislocated crystal using Lagrangian formalism 17 p2819 N71-29949

Macroscopic continuum mechanics theory for dilatational wave interactions in crystal lattice dislocations 17 p2821 N71-29970

Nonlinear elastic theory for finite inhomogeneous medium derived from crystal lattice mechanics 17 p2821 N71-29971

Dilation theory of elasticity for crystal lattice interaction mechanics 17 p2821 N71-29972

Statistical analysis of crystal lattices for continuum mechanics of dislocations 17 p2822 N71-29974

Formulation and solution of sixteen vertex general lattice statistical model 17 p2826 N71-30031

Solution of Ising model with two and four spin interactions and critical properties of model in various regions of parameter space 17 p2826 N71-30032

Individual dynamic properties of off-center ions in crystal lattices and electron phonon interaction effects 17 p2828 N71-30275

Hyperfine fields at magnetic and nonmagnetic lattice sites measured in solid solutions of magnesium nitride and chromium antimonide 18 p2962 N71-30737

Lattice mechanics in electron-phonon scattering in solids 18 p2962 N71-30913

Determination of stress induced crystal lattice imperfections in polycrystalline materials by density measurement, precision lattice parameter measurements and X ray diffraction analysis 18 p2996 N71-31188

Application of dielectric and acoustical loss techniques for determining defects in ceramic materials 19 p3120 N71-32007

Mossbauer study of BiP₃ type ordering in monobasic iron alloys containing up to 25 percent gallium 19 p3171 N71-32776

Crystallographic positions and isomer shifts of iron in boron determined by Mossbauer spectroscopy 22 p3640 N71-35946

Crystal lattice changes and polarization current effects on electrical resistance in sulfide anodes 22 p3640 N71-35946

Sequence micrograph and dynamic electron diffraction equation analysis 22 p3640 N71-35946

Thermodynamically consistent equations of state for alpha and omega phases of iron 22 p3640 N71-35946

Elastic, piezoelectric, and photoelastic constants for light scattering with hypersonic waves and Brillouin effects in ferroelectric lithium niobate crystals using helium-neon lasers 22 p3640 N71-35946

Debye-Waller factor of Herring structure theory for model of solid with vacant lattices 22 p3640 N71-35946

Calculation of lattice-constant change for helium induced strain in ErT₂ and BeT₂ 22 p3640 N71-35946

Face centered to body centered cubic lattice transformations in vacuum deposited thin iron films 22 p3640 N71-35946

Lattice dynamics calculations for high pressure shock compression analysis on solid crystal 22 p3640 N71-35946

Computer program modifications and lattice coding for hydrogenous systems including transport corrections for self-scatter cross sections and collision probability 22 p3640 N71-35946

Production, annealing, detection of crystal lattice point defects caused by neutron irradiation of ceramic materials 22 p3640 N71-35946

Atomic location, bond state, and magnetic properties of compounds and minerals by neutron diffraction 22 p3640 N71-35946

Molecular crystals structure analysis on quinolinol monohydrate/monohydrate and beta picoline-N-oxide fumaric acid adduct 22 p3640 N71-35946

Structural, magnetic, and spectroscopic examination of nickel square dihydrate 22 p3640 N71-35946

Spin-lattice relaxation and atomic motions in lithium fluoride 22 p3640 N71-35946

CRYSTAL STRUCTURE

Oxygen contamination, chemical rates, non-stoichiometry of solid solution, second phases, and carbon and nitrogen distribution in UC-UN solid solution lattices 23 p3722 N71-36529

Analysis of structure and behavior of dislocations in grain boundaries and Burgers vectors of lattice dislocations in Fe-Mn alloys 23 p3801 N71-37180

Heat resistance of titanium examined by formation of solid solutions and compounds with varying degrees of disorder and chemical bond strength 23 p3836 N71-37357

Theoretical models and phonon dispersion measurements for analysis of rutile lattice dynamics 24 p3937 N71-38090

Analysis of crystals to be grown in space with emphasis on dislocations and stacking faults 24 p3996 N71-38508

Effects of photoexcitation and traps on thermally stimulated conductivity in cadmium sulfide 24 p3999 N71-38532

Dual crystal X ray telescope using single crystals in Bragg reflection 07 p1105 N71-17217

Prescan integrals for wave diffraction in crystals 11 p1799 N71-22704

Heat capacity data for calculating Debye-Waller factor of tungsten 15 p2460 N71-27609

Edge gradient analysis for measuring optical transfer functions 18 p2893 N71-30558

Optics of linear media formulated in terms of integrodifferential equations and extended to spatially dispersive media 19 p3143 N71-32607

Quantum mechanical calculations of shifts in optical constants for deformed single silicon crystals at differing polarization directions 23 p3834 N71-37341

Manual for analyzing diffraction patterns of face centered cubic crystals for unit members of surface structures in hexagonal, square, and rectangular shapes 23 p3836 N71-37356

Valence forces potential for calculating crystal vibrations in silicon 05 p0760 N71-15446

Prismatic edge dislocation motion in copper crystals 07 p1093 N71-17460

Describing crystal oscillator instrument for detecting condensable gas contaminants in vacuum apparatus 07 p1093 N71-17460

High stability temperature compensated crystal oscillators 09 p1358 N71-19567

Developing viable CW optical parametric oscillators 23 p3767 N71-36853

Justification for use of series transistor banks for improvement of silicon controlled rectifier power supply current regulation in beam transport magnets 14 p2235 N71-26531

Optical activity as weak perturbation of ordinary dispersive properties of continuous medium 01 p0109 N71-10141

Quantum mechanics and electron exchange effects on excitation spectrum 01 p0096 N71-10524

Standard X ray diffraction patterns from high purity powders 01 p0111 N71-10539

Molecular interactions and crystal structures at low temperature emphasizing Proton 22 01 p0111 N71-10539

Preparation and characterization of heteropoly tungstates 02 p0172 N71-11215

Electronic charge density in diamond structure crystals from X ray diffraction form factors 02 p0285 N71-11839

Localized one-electron states in perfect crystals of hydrogen atoms 02 p0285 N71-11891

Characteristics of phonons in amorphous solids and collective motion in simple liquids 02 p0286 N71-11975

Production of filamentary diamond monocrystals from carbon containing media 02 p0287 N71-12009

Electric and magnetic fields effect on liquid crystal structure 03 p0324 N71-12313

Standard X ray diffraction patterns from high purity powders 03 p0324 N71-12313

Molecular interactions and crystal structures at low temperature emphasizing Proton 22 03 p0324 N71-12313

Preparation and characterization of heteropoly tungstates 03 p0324 N71-12313

Electronic charge density in diamond structure crystals from X ray diffraction form factors 03 p0324 N71-12313

Localized one-electron states in perfect crystals of hydrogen atoms 03 p0324 N71-12313

Characteristics of phonons in amorphous solids and collective motion in simple liquids 03 p0324 N71-12313

Production of filamentary diamond monocrystals from carbon containing media 03 p0324 N71-12313

Electric and magnetic fields effect on liquid crystal structure 03 p0324 N71-12313

Standard X ray diffraction patterns from high purity powders 03 p0324 N71-12313

Molecular interactions and crystal structures at low temperature emphasizing Proton 22 03 p0324 N71-12313

Preparation and characterization of heteropoly tungstates 03 p0324 N71-12313

Electronic charge density in diamond structure crystals from X ray diffraction form factors 03 p0324 N71-12313

Localized one-electron states in perfect crystals of hydrogen atoms 03 p0324 N71-12313

Characteristics of phonons in amorphous solids and collective motion in simple liquids 03 p0324 N71-12313

Production of filamentary diamond monocrystals from carbon containing media 03 p0324 N71-12313

- Absence of helical inversion in single component cholesteric liquid crystals 03 p0325 N71-12322
- Inorganic structure and spectra and paramagnetic anisotropy in complexes 03 p0332 N71-12373
- Deformation of crystals of alpha plutonium in compression - conference 03 p0439 N71-12669
- Structure and properties of solid solutions [COO-916-17] 03 p0390 N71-12686
- Conditional probability distribution of crystal structure invariants [AD-712767] 03 p0443 N71-13067
- Investigating band structures of crystals by studying two-photon absorption process [AD-712395] 03 p0444 N71-13234
- Crystal structure and molecular dynamics of inorganic metal azides 05 p0756 N71-14562
- Chemical analysis of neodymium-neodymium hydride phase system [IS-T-416] 05 p0638 N71-14621
- Investigating orientation relationships between major grains radiating from single nucleation event into highly undercooled copper [REPT-343] 05 p0708 N71-15056
- Studying motions of atoms in crystalline solids with models of interpolation schemes 05 p0758 N71-15299
- Direct solution of complex crystal structures by electron microscopy [AD-713554] 05 p0759 N71-15309
- Recording of X ray profiles with 3-crystal diffractometer [SC-T-70-4037] 05 p0653 N71-15413
- Experimental re-evaluation of two-crystal scanning geometry for whole body counting with log-shape placement of crystals [BARC-498] 06 p0931 N71-15756
- Cyclotron resonance techniques for determining electronic structure of metals [AD-714104] 06 p0933 N71-16038
- Polymorphism of oxides of rare earth elements 06 p0878 N71-16125
- Materials science research on lasers, high pressure effects, superconductors, crystal structure, and chemical and physical properties [AD-713990] 06 p0961 N71-16331
- Characteristics of niobium crystals determined by nuclear magnetic resonance 06 p0937 N71-16719
- Computing characteristics of carbon-vacancy and carbon-interstitial complexes in nickel from radiation effects [ORO-3912-3] 06 p0900 N71-16739
- Deriving relationship between macroscopic second order elastic constants and microscopic interatomic potential in crystals [KAPL-M-7131] 06 p0923 N71-16740
- Structural changes in briefly treated uranium dioxide with and without neutron irradiation as aid in determining temperature distribution in fuel elements for nuclear reactors [BNWL-TR-55] 06 p0900 N71-16762
- Breakdown of crystal lattice structure due to shock effects [NASA-TM-X-66703] 07 p1086 N71-17178
- Analyzing dopant semiconductor surface layers using elastic ion-backscattering data 07 p1089 N71-17291
- Cryogenic cooling of single crystals and X ray structures of water containing tantalum chloride and photodimer crystals [IS-T-423] 07 p1094 N71-17837
- Decomposition of stabilized polyoxymethylene under elevated pressure 07 p1049 N71-17956
- Radiation effects research program including radiation damage on semiconductor devices and materials [AD-715140] 07 p1095 N71-18045
- Determining crystal and molecular structure of selected organometallic compounds [IS-T-390] 07 p1096 N71-18063
- Summary data on thin film physics, cohesive properties of crystals, and solid state theory [COO-423-156] 08 p1278 N71-18637
- Affect of systematic errors on measurement of crystal lattice constants 08 p1278 N71-18677
- Structure and intrinsic stress of platinum thin films [COO-423-151] 08 p1281 N71-19033
- Elastic displacements produced by point defect in cubic medium by Fourier transform method 08 p1281 N71-19279
- Research in structural characterization, solid state reactions, phase transformations, and mechanical properties of materials [NASA-CR-117134] 09 p1474 N71-19726
- Research in structural characterization of materials with emphasis on polymers 09 p1404 N71-19727
- Use of solid state reactions and phase transformations to alter structure of solids 09 p1452 N71-19728
- Crystal structure and phase transitions of KIRCl6 09 p1452 N71-19800
- Clebsch-Gordan coefficients for crystallographic space groups 09 p1452 N71-19847
- Analysis of texture and crystalline orientation of lunar rock samples [NASA-TT-F-13561] 09 p1468 N71-20327
- Analysis and determination of strain-rate effects in crystalline materials [UCRL-30320] 09 p1453 N71-20582
- Computer program for calculating structure invariants from crystal lattice parameters [AD-716746] 09 p1453 N71-20600
- Computer program for least squares determination of crystal structure factor phases [AD-716747] 10 p1631 N71-20733
- Chemical composition and structure of low silica sodium hydroaluminosilicates determined by IR spectroscopy [NLL-RRE-TRANS-288-7036-477] 10 p1513 N71-21239
- Kinetics of melting metals and mechanism of long to short range atomic ordering in liquid metals [NLL-TRANS-746-560-7022-401] 10 p1579 N71-21307
- Correlation between structural modifications and superconducting properties of thin silicon films 10 p1636 N71-21751
- Comparison of electron diffraction and X ray diffraction analyses on crystalline structure of glycine [UCRL-20139] 10 p1636 N71-21805
- Angular dependence of cyclotron resonance in single thallium crystals 11 p1800 N71-21673
- Anisotropy and crystal structure of Ni-Fe alloy thin films, and Lorentz microscopic study of magnetic microstructure 11 p1815 N71-21948
- Quantitative analysis of alasing in systems which produce single pictures by superposition of several periodic samplings using single detector array [AD-717619] 11 p1797 N71-21974
- Solid state structure of carbon metalloboranes determined by analysis of X ray diffraction patterns 11 p1695 N71-22103
- Mathematical procedure for Born stability determination of body centered cubic crystal lattice tensile properties [AD-717698] 11 p1817 N71-22423
- Composition and atomic ordering effects in Fe-Co alloy systems using Mossbauer spectroscopy and measurement of effective magnetic field at Fe nuclei, isomer shift, and quadrupole splitting 11 p1780 N71-22794
- Spatial orientation of crystals in ice formed in water bodies with different temperature regimes 11 p1753 N71-22808
- Particle size effects and intensity calculations from Debye scattering equation for face centered cubic crystal 11 p1817 N71-22887
- F to M center conversion and equilibrium in X ray irradiated KCl crystals 11 p1818 N71-23062
- Thermodynamic stability, crystal structure, and properties of ternary lead-oxygen systems 11 p1783 N71-23011
- Report of research activities including chemistry, reaction kinetics, and crystal structure [AD-714864] 12 p1941 N71-23261
- Birefringence, optical polarization, and crystal structure of tellurium and selenium compounds 12 p1965 N71-23346
- Mineral composition, textural and structural characteristics, metamorphism type, and secondary changes effects on elastic properties of Krivoy Rog Basin metamorphic rocks [NASA-TT-F-13548] 12 p1907 N71-23442
- Influence of crystal chemistry factor in separation of rare earth elements in silicate crystallization differentiation [NASA-TT-F-13647] 13 p2151 N71-24821
- Numerical analysis of plastic deformation and dislocation density in crystals grown by Bridgman method [AD-719575] 13 p2151 N71-25180
- Empirical pseudopotential method for exploring electronic structure and dielectric properties of face-centered cubic semiconductors [UCRL-20377] 13 p2153 N71-25488
- Numerical analysis of constitutive relations describing response of single crystals of triclinic, monoclinic, rhombic, tetragonal, and hexagonal crystal systems 13 p2153 N71-25489
- Preparation and characteristics of metallic solid solutions in which small metal atoms (Al) interstitial sites in host metal composed of larger atoms [AD-719940] 13 p2154 N71-25539
- Development of crystal structure for charged particle acceleration 13 p2154 N71-25547
- Phonon and electron induced transition effects on thermopower of transition metals, and impurity effects on crystal lattice dynamics 13 p2154 N71-25549
- Development and characteristics of semiconductor materials based on polarizability of large organic molecules, extension of band theory of solids, and transition temperatures 14 p2324 N71-23794
- Polyethylene terephthalate film diffraction patterns from low angle X ray irradiation and analysis of crystal and molecular structure 14 p2213 N71-24009
- Characteristics of zones of displacements of defects in graphite from neutron irradiation [CEA-R-1374] 14 p2381 N71-24262
- Production of pure silicon single crystals and effects of gamma radiation on crystal structure [AD-720753] 14 p2329 N71-24600
- Distribution and density of dislocation loops in crystal boundaries produced by fast neutrons in silicon and copper 14 p2330 N71-24608
- Crystalline structures of rare earth elements and nickel compounds [CEA-CONF-1704] 15 p2503 N71-27200
- Kinetics of NH3 reduction of alpha and beta phases in UO2, and reactivity of UO2 with oxygen and hydrofluoric acid [CEA-R-4074] 15 p2468 N71-27320
- Antiferromagnetic resonance measurements on neopropyl telluride crystals as function of direction 15 p2508 N71-27928
- Structural compositions and fast neutron damage thresholds of germanium selenide and germanium telluride amorphous semiconductors [AD-720754] 15 p2509 N71-27968
- Electrophysics and chemical reactions of metal surfaces including mechanical properties and crystal structures [AD-722613] 16 p2611 N71-28006
- Crystal structure and morphology of hydrous oxides and hydroxides in lanthanide and actinide series [ORO-3955-2] 16 p2667 N71-28079
- Significance of stereoisomerism in organic molecules and relationship to determination of origin of earth life [NASA-TT-F-13677] 16 p2548 N71-28090
- Determination of chemical properties of zirconium and zirconium dioxide system at high temperatures and controlled oxygen partial pressures 16 p2615 N71-28091
- Structural properties of sodium silicate glass 16 p2619 N71-28099
- Phase transformations involving interstitial ordering in vanadium-nickel systems containing less than 15 atomic percent nitrogen [COO-1196-796] 17 p2763 N71-29520
- Spectral properties of natural silicate garnets with structural and chemical interpretations of spectra in optical range of 0.3 to 5.0 microns and to 300 microns in infrared 17 p2814 N71-29713
- Heat treatment and stress corrosion analyses on aluminum alloy single- and bi-crystal microstructures [NASA-CR-119609] 17 p2766 N71-29911
- Development of spin Hamiltonian theory for very low symmetry systems with matrix-diagonalization programs and tensorial notation for analysis of ESR spectra 17 p2828 N71-29925
- Effects of atomic repulsive potential in ferroelectric crystals in terms of temperature, pressure, and crystal structure [AD-722449] 18 p2993 N71-30728
- Determination of stress induced crystal lattice imperfections in polycrystalline materials by density measurement, precision lattice parameter measurements and X ray diffraction analysis 18 p2996 N71-31100
- Effect of polymer crystallinity and density on permeability to carbon dioxide and water vapor of polyethylene, polypropylene, and cellulose acetate 18 p2997 N71-31109
- Stationary and moving electric fields in silver and gold-doped cadmium sulfides 18 p2941 N71-31408
- Preparation, spectrum analysis, and crystal structure determination of CaF2-Np doped complex [NYO-4075-10] 18 p2999 N71-31310
- Structural semiconductor analysis by ion implantation and Hall and channeling effect measurements [AD-723308] 19 p3168 N71-31881
- Magnetic coupling and phase boundaries determined for series of pseudo binary alloys of C15 and R structure containing lanthanides 19 p3171 N71-32040
- Analysis of wurtzite-type SiC whiskers obtained by sublimation and thermal stability of basic SiC polytypes [AD-724103] 20 p3332 N71-32090
- Effect of aluminum doping on thermal stability of silicon carbide polytypes in 2000 to 3000 C range [AD-724102] 20 p3333 N71-32090
- Initial structure and texture effects and influences of cooling rate from beta region on preferred orientation of uranium after heat treatment [UWV-2523-M] 21 p3438 N71-34400

SUBJECT INDEX

- Correlation between deformation substructure, precipitates, recrystallization state, and stress corrosion of aluminum zinc magnesium alloy (NLL-M-20372-5828.4F) 21 p3441 N71-34488
- Nuclear magnetic resonance spectra of platinum 195 in tetragonal complexes 21 p3499 N71-34935
- Correlation of supramolecular solid and liquid crystal phase structure of poly- γ -benzyl-L-glutamate and its properties 21 p3500 N71-34935
- Crystal structure of four complexes of sulfur containing ligands with metallic ions using three dimensional single crystal X ray diffraction techniques 21 p3500 N71-34935
- X ray analysis and representation of preferred orientations of grains in monomineralic aggregates 22 p3581 N71-35505
- Structural and mechanical properties of AlZnMg, AlMgSi, and AlCuMg alloys as function of natural aging prior to artificial aging (NLL-M-20408-5828.4F) 22 p3596 N71-35606
- Electro-optical effect in LiNbO₃ crystal at 6328 angstroms (FOA-I-C-2377-51) 22 p3629 N71-35860
- Isotope effect for diffusion of interstitial atoms (AHL-TRANS-882) 22 p3643 N71-35977
- X-ray technique for determining structural changes in relation to metal substructures and their mechanical properties (AD-727420) 23 p3773 N71-36889
- Analysis of extraneous grain boundary dislocations in high angle (110) twist boundaries in this film gold bicrystals (NYO-3504-58) 23 p3834 N71-37340
- Mechanism study of magnetocrystalline anisotropy of Nd-Co₅ for application to manufacture of permanent magnets (AD-726991) 23 p3835 N71-37347
- Manual for analyzing diffraction patterns of face centered cubic crystals for unit meshes of surface structures in hexagonal, square, and rectangular shapes (HEPT-10-156) 23 p3836 N71-37356
- Determination of low energy electron diffusion resulting from absorption on single crystal planes (NLL-FOBS-TRANS-2706-19022.81) 23 p3837 N71-37361
- Analysis of chemically pure zirconium dioxide by electron microscope and roentgenographic techniques (AD-727973) 24 p3945 N71-38139
- Tables of magnetic structures determined by neutron diffraction with emphasis on rhombohedral and hexagonal systems (DP-1845) 24 p3970 N71-38319
- Differential conductance curves based on electron tunneling measurements of single and polycrystalline pure bulk thorium and analysis of crystal structure in tunnel junction regions (AD-72404) 24 p3996 N71-38507
- CRYSTAL SURFACES
- Mathematical model for chemical activity increase in crystal surface caused by mechanical impact 01 p0018 N71-10513
- Examination of molybdenum disulfide with L²ED and Auger emission spectroscopy (NASA-TN-D-7010) 03 p0332 N71-12366
- Relations between crystal index surfaces and molecular and lattice structure as exemplified by benzene 03 p0440 N71-12754
- Single crystal surface work function and desorption studies (NASA-CR-111564) 03 p0443 N71-13069
- Scattering of argon beams with incident energies up to 20 eV from silver (111)-surfaces (UCLA-ENG-7061) 10 p1614 N71-20930
- Determination of physical characteristics of crystal surfaces by observation of elastic and one-phonon-inelastic scattering of atomic beams from surfaces (AEP-3824-101-70U) 10 p1636 N71-21752
- Mathematical models for surface modes of vibration and optical properties of ionic crystal slab (US-T-407) 15 p2505 N71-27237
- Mathematical model for surface states on crystal melting faults 17 p2825 N71-29999
- Diffraction of helium atoms from tungsten (112) crystal surface and measurement of time of flight distribution of deuterium molecules desorbed from nickel surface (NASA-CR-121985) 22 p3634 N71-35900
- CRYSTALLINITY
- Select states in glassy and crystalline silicates studied by optical spectroscopy and electron paramagnetic resonance (AD-719303) 01 p0111 N71-10661
- Optical method for estimation of amorphous content in pyrolytic carbon (UC-T-70-4023) 01 p0099 N71-10710
- Effects of composition on glass forming tendency of amorphous metal systems (AD-72942) 15 p2426 N71-27753

Structure of graphite materials subjected to intensive wear at various pressures (NLL-RISLEY-TRANS-1990-9091.9F) 16 p2619 N71-29160

Instrumentation for investigating nature of energy levels of impurity ions in crystalline solids (AD-722411) 17 p2814 N71-29492

Thermodynamic properties of four crystalline sodium borates (BM-R-7351) 22 p3530 N71-35250

Electrical and magnetic properties of palladium base amorphous alloys containing small concentrations of transition metals 24 p3901 N71-37807

CRYSTALLITES

NT SPHERULITES

Effects of natural chemical impurities and crystallite orientation on erosion behavior of artificial graphite (NASA-TN-D-6023) 01 p0070 N71-10070

Orientations and distribution of crystallites in molded artificial graphite 12 p1941 N71-23108

Effect of crystallite size, crystallite orientation, and density on dimensional and property changes in irradiated graphite and isotropic materials (GA-10433) 14 p2277 N71-25480

CRYSTALLIZATION

NT RECRYSTALLIZATION

Vapor deposited titanium dioxide thin films - some properties as function of crystalline phase (NASA-CR-111559) 03 p0443 N71-13068

Physical chemistry and crystallization of linear high polymers under high pressure 07 p1049 N71-17858

Aging time and temperature effects on silicon precipitation from aluminum silicon alloy (NYO-2394-40) 08 p1216 N71-18922

Clebsch-Gordan coefficients for crystallographic space groups 09 p1452 N71-19647

Mathematical model of crystallizer based on physicochemical velocity rates for subprocesses involved 10 p1592 N71-20820

Column method of counterflow crystallization of alloys in melted state 10 p1573 N71-20868

Intensification of crystallization processes in liquid phase using mobile magnetic field 10 p1574 N71-20880

Influence of heating methods on efficiency of directed crystallization of germanium in vacuum apparatus 10 p1633 N71-20887

Directed crystallization of compounds during impurity exchange of liquid phase with crucible and atmosphere 10 p1634 N71-20890

Effects of quantity and placement of copolymer under within polymeric chain on crystallization phenomena in polymers 10 p1590 N71-21524

Crystallization of BSX solvents from nitromethane, acetonitrile and acetone by evaporation of saturated solutions studied by X ray diffraction (ERDE-TN-18) 12 p1871 N71-23574

Influence of crystal chemistry factor in separation of rare earth elements in silicate crystallization differentiation (NASA-TT-F-13647) 13 p2151 N71-24821

Sintering of reactive MgAl₂O₄ spinel ceramic, devitrification, and improved cordierite compositions (AD-720383) 14 p2278 N71-24015

Homo-epitaxial crystallization in copper electrodeposition 16 p2609 N71-28205

Description of processes of crystallization and precipitation from chemical solutions and use in production of superpure inorganic materials 16 p2555 N71-28293

Production of superpure inorganic substances by zone melting or zone recrystallization 16 p2556 N71-28290

High temperature microscopy of crystallization processes in molten iron, steel, and eutectic containing iron carbon alloy steels 18 p2997 N71-31321

Kinetics of crystal nucleation and growth in batch evaporation crystallization 21 p3501 N71-34939

Markov model for application of uniform withdrawal assumption in continuous crystallizer design equations to continuous mixing vessel equations 21 p3501 N71-34940

Devitrification kinetics of glass containing calcium, aluminum, magnesium oxide, and silicon oxide under influence of iron and chromium (PB-199222) 22 p3601 N71-35648

Dilatometric and vacuum drying techniques for selective crystallization studies and solvent concentration, viscosity, and dielectric constant effects on nucleation (UTCHE-7111) 23 p3721 N71-36521

Theoretical mechanisms for crystallization, super-saturation, and nucleation (NLL-RISLEY-TRANS-2168-5091.9F) 24 p4032 N71-38772

CRYSTALLOGRAPHY

Theoretical model of thermionic converter surface crystallographic and atomic parameters (AD-711352) 02 p0150 N71-11064

Radio frequency size effect for determination of molybdenum Fermi surfaces (IS-T-356) 02 p0206 N71-11934

Experimental re-evaluation of two-crystal scanning geometry for whole-body counting with log-phase placement of crystals (BARC-498) 06 p0931 N71-15756

Resistive transition and current-voltage characteristics of single crystal tin whiskers (NYO-3029-44) 06 p0931 N71-15757

Low-energy electron diffraction for surface crystallography (AD-714691) 06 p0934 N71-16216

Grain boundary faceting of 10-10 tilt boundaries in zinc crystals grown from melt (AD-714227) 06 p0935 N71-16361

Breakdowns of crystal lattice structure due to shock effects (NASA-TM-X-66703) 07 p1086 N71-17178

Research in ceramic materials including mechanical properties, crystallography, and deformation (NASA-CR-116009) 08 p1222 N71-18654

Research by Nuclear Chemistry Division, University of California for 1969 (UCRL-19530) 09 p1436 N71-20048

Analysis and determination of strain-rate effects in crystalline materials 09 p1435 N71-20582

Effect of surface potential with periodic variations on anisotropic tunneling probabilities on crystallographic plane 11 p1808 N71-22882

Plastic yielded iron-nickel single crystal martensite crystallography 12 p1939 N71-24077

Numerical analysis of constitutive relations describing response of single crystals of triclinic, monoclinic, rhombic, tetragonal, and hexagonal crystal systems 13 p2533 N71-25480

Growth of p-type semiconducting diamond by vapor phase deposition using methane-diborane doping gas mixture in presence of diamond seed crystals (NASA-TM-X-67066) 14 p2324 N71-25762

Crystallographic techniques and data transmission electron microscopy of zirconium (AABC/B-204) 15 p2505 N71-26996

Design and performance of crystal for single crystal and X ray diffraction analysis (AERIE-B-4532) 15 p2509 N71-27910

Monochromatic X rays for crystallographic and radiographic studies (CEA-BIB-194) 16 p2654 N71-29036

Electron paramagnetic resonance of Co₂/ph₂/Ni₂/ph₂ and Cu₂/ph₂/ph₂ in hydrated single crystals at temperatures from 300 to 1.2 K (UCRL-20386) 17 p2814 N71-29725

Magnetic crystallographic orientation produced in ferrites by hot working (AD-723558) 18 p2931 N71-31580

Calculated intensities in indexing of X ray powder patterns. Reissinger effect during X ray analysis of solid solution crystals, and computer plotting in stereophotography (AD-718094) 19 p3169 N71-32205

Nuclear reactor applications to crystallography, phase transitions in organometallic compounds, proton dynamics, and neutron activation analysis (NBS-TN-567) 20 p3382 N71-33390

Properties and phase transformations of fibrous composite materials with metal matrix (ONERA-MT-170) 20 p3288 N71-33725

Nuclear magnetic resonance of deuterons in hydrazinium sulfate noting electric quadrupole coupling constants and electrical conductivity 20 p3335 N71-33864

Analysis of impurity, strain, temperature, and size dependence of transverse magnetoresistance of polycrystalline potassium (NYO-2150-48) 20 p3336 N71-33890

Determination of low temperature anisotropic thermal conductivity of cadmium selenide crystals using doubly guarded unidirectional steady state thermal conductivity equipment 20 p3336 N71-33890

Crystal structure of four complexes of sulfur containing ligands with metallic ions using three dimensional single crystal X ray diffraction techniques 21 p3500 N71-34935

Crystallographic data, cation distributions, magnetic transition temperatures, and magnetic structure of tetragonal systems determined by neutron diffraction (NF-18783) 22 p3631 N71-35874

Programs for management and processing of neutron diffraction data (AABC/TM-578) 23 p3804 N71-37133

CRYSTALS

Analysis of crystals to be grown in space with emphasis on dislocations and stacking faults
[NASA-TN-D-6505] 24 p3998 N71-38521

CRYSTALS

NT CRYSTAL OSCILLATORS
NT CRYSTALLITES
NT DENDRITIC CRYSTALS
NT IONIC CRYSTALS
NT LIQUID CRYSTALS
NT METAL CRYSTALS
NT MICROCRYSTALS
NT MIXED CRYSTALS
NT PIEZOELECTRIC CRYSTALS
NT POLYCRYSTALS
NT QUARTZ CRYSTALS
NT SINGLE CRYSTALS
NT SPHERULITES
NT WHISKERS (SINGLE CRYSTALS)

Phosphorescence and delayed fluorescence of naphthalene in mixed crystals 08 p1280 N71-18848

Transformation of form and displacement of air inclusions in ice due to molecular rearrangement of ice crystals and temperature gradients 11 p1759 N71-22862

Brushless dc tachometer design with Hall effect crystals and output voltage magnitude proportional to rotor speed
[NASA-CASE-MFS-20385] 13 p2057 N71-24994

Calculation of crystal field splittings of trivalent neodymium ion in yttrium aluminum garnet
[BARC-505] 15 p2469 N71-27349

Semipermanent method for positioning crystals in multidetector-stretcher geometry for whole-body counters using Lagrange multipliers including computer program
[BARC-505] 15 p2469 N71-27349

Equations for describing noncollinear phase matching in uniaxial crystals 15 p2454 N71-27376

Methods and standards for measuring quartz crystals
[AD-721584] 16 p2574 N71-28416

Computer simulated electron diffraction analysis of electrons passing through absorbing crystal foil
[AD-722244] 17 p2814 N71-29693

Theoretical phonon research in crystals and liquids
[NYO-3699-53] 21 p3474 N71-34739

Disappearance of inelastic channel of nuclear reaction in resonant nuclear scattering of gamma rays in perfect crystal
[IAE-1966] 22 p3640 N71-35948

Thin NaI(Tl) crystals for estimating natural terrestrial background in 17 and 60 keV energy regions from Compton continuum peak
[UCRL-72927] 22 p3644 N71-35983

Tunable stimulated far infrared and visible emission from polariton modes in crystals 23 p3823 N71-37269

Effect of electromagnetic mixing on ingot grain size during continuous casting of magnesium alloys
[AD-727177] 24 p3937 N71-38086

Dynamic characteristics of optical and surface crystal properties
[AD-727327] 24 p3997 N71-38509

CUBIC EQUATIONS

Scattering of slow neutrons by ortho hydrogen in cubic phase
[JUL-724-FF] 22 p3641 N71-35957

CUBIC LATTICES

NT BODY CENTERED CUBIC LATTICES
NT FACE CENTERED CUBIC LATTICES

Theoretical and experimental determinations of elastic constants for magnesium
[COO-1198-756] 06 p0875 N71-16781

Elastic displacements produced by point defect in cubic medium by Fourier transform method
[COO-1198-756] 06 p0875 N71-16781

Superconducting metastable simple cubic alloys and rapid quenching from liquid state
[CALT-822-22] 11 p1817 N71-22375

Metals and compounds crystallizing in cubic system determined by neutron diffraction tables
[NP-18718-PT-1] 16 p2655 N71-29071

Series representations of elastic Greens tensor for cubic media with point defects 17 p2817 N71-29935

Quantum mechanics of vibrational transitions in nonreactive collinear collisions and dynamics of cubic anharmonic oscillator 21 p3491 N71-34868

CUES

Visual flash duration discrimination and analysis of temporal and energy cue models, and memory effects
[NASA-CR-119009] 16 p2541 N71-28136

Cockpit simulators without visual or motion cues in pilot training 19 p3074 N71-31952

Motion cues and pilot error in simulated instrument landing system approach 19 p3074 N71-31953

CULTIVATION

Chlorella cultivation for purifying isolated environments of toxic gaseous contaminants 08 p1153 N71-19053

CULTURE [SOCIAL SCIENCES]

Discussion of effects of increased population on environment, resources, and standard of living with recommendations for specific study areas to develop understanding of situation 19 p3198 N71-32531

CULTURE TECHNIQUES

Selecting algae, seeds, and seedlings of higher plants and establishing tissue cultures for Lunar Receiving Laboratory
[NASA-CR-108764] 03 p0321 N71-12296

Chromosomal aberrations in persons exposed to repeated occupational irradiation
[ORNL-TR-2332] 05 p0634 N71-14696

Production of algae containing 93 percent C-13
[LA-4495] 06 p0799 N71-15913

Modification of Berman-Slavsky method for neutrophil digestive capability determination
[NASA-TT-F-13553] 09 p1333 N71-20150

Temperature requirements for thermophilic bacteria growths in soil and by culture techniques
[NASA-TT-F-13650] 12 p1864 N71-23978

Survey and critique of bacterial growth quantitative determination methods including Bacillus coli direct microscopic morphology and growth measurement
[NASA-TT-F-13652] 13 p2032 N71-24584

Microbial corrosion emphasizing mechanisms of anaerobic corrosion produced by sulfate-reducing bacteria primarily those in genus desulfovibrio
[AD-720693] 14 p2275 N71-26393

Optimal mineral composition in nutrient for autotrophic Hydrogenomonas cultivation 20 p3222 N71-33471

CUMULONIMBUS CLOUDS

Evolution of cumulonimbus clouds and wind, temperature, and vertical current perturbations near and in clouds
[TT-70-50020] 01 p0080 N71-10795

Development and meteorological aspects of thunderstorms
[ESSA-PI-670004] 01 p0080 N71-10811

Structure of air currents including jet streams, turbulence in cumulonimbus, and variability of wind velocity
[AD-717052] 10 p1597 N71-21242

CUMULUS CLOUDS

Dynamic seeding experiments on supercooled cumulus clouds 03 p0404 N71-13222

Feasibility of convective cloud management for precipitation
[PB-192259] 05 p0716 N71-15073

Cumulus cloud modification by injecting powdered surface active substances 10 p1546 N71-20679

Development of heavy cumulus clouds formed by forced convection in vicinity of warm fronts in Arctic regions 11 p1791 N71-22845

Surface effects on cumulus cloud formations in anticyclone over Russian plateau
[NLL-M-20005/5828.4F1] 12 p1959 N71-24272

Spectrometer measurement of cumulus cloud reflectance in 0.76 micron band of oxygen for cloud top altitude determination 15 p2400 N71-27491

Numerical model of isolated cumulus clouds formed by surface heating
[AD-722216] 17 p2777 N71-29506

Seeding isolated cumuli to increase precipitation in Arizona 22 p3610 N71-35716

Methods for beneficially modifying precipitation from convective clouds over Great Plains Region 22 p3611 N71-35719

Studying characteristics of warm cumulus clouds below freezing levels in Texas to assess feasibility of warm cloud management as water resource 22 p3611 N71-35722

Mathematical model of cumulus cloud growth and effects of silver iodide seeding 23 p3786 N71-36983

Radar data on cumulus cloud seeding experiments
[ML-71089] 23 p3792 N71-37027

CURIE TEMPERATURE

Alphabetic bibliography of magnetic materials and transition temperatures
[ORNL-RMTC-7-REV-2] 03 p0417 N71-12597

Perturbed angular correlation measurements on Rh-100 in nickel host near Curie temperature
[TID-25597] 09 p1402 N71-20449

Hyperfine field of Sc-44 in Ni host from 80 K to Curie point, obtained from perturbed angular correlations
[CONF-700933-4] 09 p1446 N71-20584

Hyperfine field of Rh-100 in Ni host near Curie point, obtained from perturbed angular correlations
[CONF-700933-3] 09 p1446 N71-20585

Ferromagnetic Curie temperature shifts for calibrating high pressure gauges up to 90 kbar 14 p2297 N71-26504

Curie-point anomaly in linear thermal expansion coefficient of copper potassium chloride single crystal 20 p3367 N71-33799

CURIE-WEISS LAW

Susceptibility of liquid He-3 with comparison to Curie susceptibility 11 p1809 N71-23828

CURING

Irradiation curing process for producing pyrotechnic materials - flares
[AD-724652] 20 p3287 N71-33194

CURIUM

NT CURIUM ISOTOPES
NT CURIUM 244

Plutonia/curia compatibility testing for nuclear fuels
[MDC-G1665] 04 p0556 N71-14995

Plutonia and curia compatibility tests
[MDC-G1675] 04 p0559 N71-14992

CURIUM ISOTOPES
NT CURIUM 244

Interaction of curium sesquioxide with refractory metal matrices in pressed and sintered cermet compacts
[DP-MS-70-10] 05 p0710 N71-15271

Thermal fission cross sections and fission resonance integral measurements for Cf-249 and Cm-244 to Cm-248 made in core and thermal column of research reactor
[DP-MS-70-95] 23 p3816 N71-37218

Fission and radiative capture cross sections of curium isotopes using Physics 8 nuclear explosion in neutron source 24 p3980 N71-38400

CURIUM 244

Investigating temperature and pressure characteristics of curium fuel capsules
[ORNL-45977] 05 p0724 N71-15916

Plutonia/curia compatibility testing
[MDG-G-1700] 05 p0725 N71-15918

Self-radiation damage in Cm-244 oxide and aluminate including lattice swelling, metamict state formation, and phase transformation
[DP-MS-70-44] 12 p1969 N71-21301

Plutonium 238 and curium 244 oxide compatibility tests with refractory metal alloys for use in Plow heat source
[MDC-G2026] 16 p2612 N71-28749

High temperature compatibility tests on plutonia and curia combinations with refractory metals, and plutonia/molybdenum cermets
[MDC-G-2033] 17 p2760 N71-29202

Metallographic examination of container material for Cm-244/203
[ORNL-4663] 17 p2785 N71-30206

CURL [MATERIALS]
Five models for three dimensional chip curl, chip breaking, and chip control in metal cutting processes 17 p2754 N71-29505

CURL [VECTORS]
NT VORTICITY

CURRENT ALGEBRA
Current commutator derivation of mass difference relations
[NYO-2171-315] 03 p0424 N71-12007

Using current algebra and vector meson dominance methods for S-wave kaon-nucleon scattering
[SINP-TH-67-17] 03 p0739 N71-15021

Developing non-Lagrangian field theory for equal time commutators from broken conformal invariance and chiral U(3) symmetry
[IFPHT-7/70] 06 p0912 N71-15818

Operational expansion of product of two currents determining derivatives of current equal-time commutators
[IFPHT-5/70] 06 p0902 N71-15822

Considering relationship between nonleptonic hadron decay and current x current theory
[UH-511-73-70] 06 p0923 N71-16740

Veneziano model compatibility with current algebra and chiral symmetry
[UH-511-79-70] 06 p0924 N71-16771

Extending model of partially conserved axial current breakdown to higher order on basis of hard mass current algebra
[NUB-2023] 08 p1258 N71-18023

Necessity of Schwinger terms in ground state Fock brackets for classical boson currents containing terms linear in canonized variable
[RLO-1388-584] 10 p1610 N71-20640

Comparison of magnetic moment and electric dipole sum rules for testing validity of current and field algebra commutators 10 p1592 N71-21002

Contribution of rho meson in calculation of low energy pion-nucleon partial wave scattering parameters 10 p1621 N71-21753

Current algebra for determining form factors and divergences of mass in electromagnetic interactions 10 p1624 N71-21814

Current algebraic model for asymptotic weak spectral functions and hadronic decays of intermediate vector boson 12 p1972 N71-22007

Isotopic spin analysis and current algebra kinematics of positive kaon decay modes from propane bubble chamber photographs of pion emission

13 p1311 N71-25930

Dispersion theory and current algebra commutator studies proving single pole dominance for spin one parts of vector or axial vector currents inconsistent with current algebra

14 p2302 N71-25743

Group theory and Lagrange multipliers generated by boson fields and vector current algebra

15 p2434 N71-27433

Current algebra for weak interactions in elementary particle physics

15 p2475 N71-27465

Current algebra for nonleptonic kaon decay modes

15 p2479 N71-27637

Current algebra and sum rules for pion nucleon elastic scattering amplitude low energy theorems and nuclear structure interpretations

15 p2491 N71-27898

Mathematical models for investigating vertex functions in current algebra

15 p2491 N71-27912

Particle physics research including theoretical studies, kinematical investigations, Regge poles, and current algebra

16 p2648 N71-28638

Solving functional differential equations for local current algebras

17 p2772 N71-29330

Meson current algebra for calculating form factor and coupling constant in gamma - 3 pion amplitude in pion-pion interaction

17 p2774 N71-30061

Integral representation for functions holomorphic in tube domains over arbitrary prisms

18 p2976 N71-30623

Broken scale invariance, current algebra, and massive gravitons in formalism describing meson interactions at intermediate energies and below

22 p3481 N71-36018

Representations of local currents and related algebras, emphasizing infinite parameter Lie algebras

22 p3481 N71-36018

Improved solution for S wave pion pion scattering amplitudes to satisfy crossing relations - current algebra beyond tree approximation

23 p3813 N71-37190

Current algebra sum rules in neutron scattering and scale dimension of chiral symmetry breaking Hamiltonian

23 p3819 N71-37244

Vector currents and current algebra in zero width model of hadron bootstrap

23 p3822 N71-37262

CURRENT AMPLIFIERS

NT FREQUENCY MODULATION PHOTOMULTIPLIERS

XT PHOTOMULTIPLIER TUBES

External operating characteristics, current and voltage amplification ratios, and electric power efficiency of electrodynamic energy converter

14 p2244 N71-26605

Phase sensitive detector and commercial Hall probe combined with control current amplifier to provide sensitive, low field magnetometer for use from room to liquid helium temperatures

16 p2593 N71-26497

Broadband current preamplification for obtaining simultaneous high resolution energy and time information from nuclear radiation detectors

17 p2799 N71-30022

CURRENT DENSITY

Critical current enhancement in superconducting lead samples of varying cross section

01 p0090 N71-10691

Correlations of fluctuation in electric field intensity and current density for nonequilibrium isotropic plasma

06 p0928 N71-15738

Microscopic expansion of electromagnetic current density in classical electrodynamics

09 p1425 N71-20316

Mathematical representation of ion beam current density profiles

10 p1638 N71-20940

Transfer processes in ECM at high current densities

10 p1565 N71-21290

Current diffusion in cylindrical wires and fuses during microsecond electrical pulses

10 p1607 N71-21233

Potential polarization, potentiostatic current-voltage behavior, and electron microscopy of nickel dissolution surface topology in dilute acid solutions from 25 to 300 C

10 p1581 N71-21438

Current density and electrolyte agitation rate effects in nickel phosphorus electrodeposition

11 p1585 N71-21816

Fugacity sum rules in nuclear physics, using double commutators of various current density operators

11 p1802 N71-22090

Current density induced in pinched plasma discharge by penetration of plasma by pulsed intense relativistic electron beam

12 p1981 N71-23920

Flow equation for representing ion beam current density profile from bombardment ion thrusters

12 p1990 N71-23924

Operational characteristics and entrance conditions of high current relativistic electron beam accelerator

12 p1897 N71-23946

Repeated current discharge role in Z pinch dynamics

13 p2145 N71-24366

Extraterrestrial ring current intensity changes and aurora dynamics model

13 p2161 N71-25200

Superconducting injection laser and temperature dependent threshold current density of tantalum

13 p2090 N71-25231

Current density and electrode drop distributions in cross sectional plane of electrode in conducting wall generators

16 p2540 N71-28803

Design, temperature, carbon dioxide, and current density effects on alkaline hydrogen oxygen fuel cell performance

18 p2873 N71-31150

Nature, size, and distribution of lattice defects in type 3 superconductor Nb₃Zr₂S and their influence on critical current density

19 p3071 N71-32468

Current collection characteristics of moving cylindrical and spherical electrostatic probes applied to velocities in earth satellites and planetary probes

20 p3337 N71-33979

Electrochemical copper deposition at high current densities

24 p3941 N71-38117

Field-current identity formalism for stress tensor with scale invariance and scale breaking condition of meson couplings to stress tensor

24 p3982 N71-38417

CURRENT DISTRIBUTION

Current distribution for continuous source antenna with specified side lobe levels on both sides of main beam

03 p0337 N71-12407

Integral vectorial equation for calculating current distribution on antenna

04 p0491 N71-13707

Electron bombardment ion rocket engine with improved propellant introduction system

05 p0763 N71-15661

Calculation of digital current distribution systems on micron tape cores

06 p0822 N71-13936

Reversible current directing circuitry for reversible motor control

08 p1172 N71-18724

Electrical power distribution systems for space vehicle with isotropic/Brayton source

09 p1472 N71-20474

Shaping antenna far-field radiation patterns for uniform and nonuniform arrays, using iterative sampling and current distribution approximation

11 p1727 N71-21946

Tokamak plasma current distribution measurement using magnetic field angles

11 p1810 N71-22117

Coupled linear antennas in inhomogeneous dispersive medium

11 p1724 N71-22636

Electric circuit for reversing direction of current flow

12 p1891 N71-23271

Functional analysis on stability of distributed reverse current electrical networks having nonlinear elements

12 p1893 N71-24029

Repeated current discharge role in Z pinch dynamics

13 p2145 N71-24366

Theory of second class currents in weak interactions

14 p2300 N71-25720

Theoretical models of high current relativistic electron beam propagation studies

15 p2306 N71-27306

Potential and current distributions throughout MPD are indicated that anode fall voltage varies inversely with local anode current density

17 p2813 N71-30326

Analogue models to measure two-dimensional and three-dimensional distribution of magnetic flux density of magnet for bubble chamber

18 p2960 N71-30414

Analytic model of crossed field MHD accelerators based on turbulent boundary layers, current density distributions, and fluid properties

18 p2994 N71-31519

Phenomenology of weak interactions, including CP violation, second class currents, and inelastic neutrino reactions

19 p3151 N71-32166

Laplace equation for controlling parameters of current distributions in cylindrical geometries

19 p3142 N71-32236

Mathematical models for inelastic electron proton scattering indicating current amplitudes with nonlinearity characteristics

20 p3324 N71-33881

Current load calculations for transmission lines terminating parallel to and near infinite length circular conducting cylinders in incident fields

23 p3737 N71-36649

Plasma confinement and cross section shapes in Tokamak plasma columns with beta sub 1 much greater than 1 and arbitrary current distribution

23 p3832 N71-37328

CURRENT REGULATORS

Power supplies for very high current control and stabilization in high magnetic field laboratories

01 p0033 N71-10222

Electronic control of spacecraft power supplies

03 p0319 N71-12577

System for regulating direct current of triphase alternator

05 p0656 N71-15514

Synchronous smooth rotor in system for automatic regulation of field current

05 p0656 N71-15516

Bridge circuit for digital resistance measuring circuits with electronic self adaptive controls at direct current

06 p0826 N71-15950

Describing magnetic core current switching device for steering tipical current pulses to memory units

08 p1163 N71-18694

Circuit design for determining amount of photomultiplier tube light detection utilizing variable current sources and dark current signals of opposite polarity

10 p1558 N71-21008

Switching series regulator with gating control network

12 p1887 N71-23316

Justification for use of series transformer banks for improvement of silicon controlled rectifier power supply current regulation in beam transport magnets

12 p1900 N71-23610

Magnetic current regulator for saturable core transformer

13 p2055 N71-24800

Automatic power supply circuit design for driving inductive loads and minimizing power consumption including solenoid example

13 p2057 N71-24892

Linear regulator problem solution using Euler equations of motion, Laplace transformations, and Hamilton-Jacobi equation for stochastic control

14 p2235 N71-26644

Turn on current transient limiter for controlling peak current flow in high capacity load

14 p2235 N71-26531

Solid state power supply with stabilized output and overload protection

18 p2898 N71-31066

Current regulating voltage divider design with load current sharing

21 p3403 N71-34212

CURRENT SHEETS

Transient magnetospheric current sheet generation of magnetohydrodynamic waves and geomagnetic micropulsations

05 p0675 N71-15420

Slow third-order, resonant beam, extraction failure, using current sheets

09 p1445 N71-20560

Current sheet magnetic model to calculate quiet large-scale magnetic field in solar corona compared with accuracy of other models

12 p1992 N71-23433

Magnetosphere electric current sheet model

14 p2245 N71-25637

Mathematical models for electromagnetic noise in neutral current sheet of geomagnetic tail

19 p3175 N71-31802

CURRENT STABILIZERS

U CURRENT REGULATORS

CURRENTS

Seasonal variations of current and salinity of Dnestrovskiy liman induced by changes in wind and rain

11 p1744 N71-21858

Hydrological observations of temperature, salinity, and currents of water in Dniestrskiy Fjord

11 p1759 N71-22867

Mechanical energy balance equations for describing secondary currents in turbulent flow through straight conduit

23 p3742 N71-36483

CURTIS-WRIGHT MILITARY AIRCRAFT

U MILITARY AIRCRAFT

CURVATURE

Glass neutron guide with 300 m curvature

02 p0209 N71-11149

- Wake curvature and correction to Kutta-Joukowski condition
[AD-713436] 05 p0662 N71-14855
- Apparatus and method for spin forming tubular elbows with high strength, uniform thickness, and close tolerances
[NASA-CASE-XMF-01083] 11 p1770 N71-22723
- Mathematical model for two-dimensional, long-wave propagation in curved acoustic ducts determining vibrational velocity distribution and variation and phase of motion at any point in system
[NASA-TM-X-67184] 14 p2219 N71-26338
- Branch curvature in dislocations at free surfaces from image force and concept of line tension
17 p2816 N71-29928
- Long acoustic wave propagation in curved ducts and junctions between straight and curved ducts utilizing Bessel functions for steady and decaying fields of motion
[NASA-TM-X-67944] 23 p3801 N71-37103
- Design curves and computer program for investigating post buckling behavior of stiffened plates with small initial curvature under combined loads
[AD-726455] 23 p3861 N71-37526
- Incompressible skewed turbulent boundary layer on end wall of curved two dimensional diffuser with aspect ratio of 1.5 and area ratio of 1.56
24 p3909 N71-37859

CURVE FITTING

- Simulating voltage-current characteristic curves of solar cell panel with different operational parameters
[NASA-CASE-XMS-01554] 01 p0037 N71-10578
- Curve fitting of sigmoid- or bell-shaped curves by least squares method
[PB-192315] 04 p0540 N71-14355
- Computer programs for fitting experimental solid state physics data to parametrized theory
[AD-714199] 06 p0936 N71-16475
- Examining solutions obtained from streamline curvature method of calculating flow through turbomachines for several operating points of Rolls-Royce compressor
[CUEDEA-TURBO/TR-19] 11 p1737 N71-22294
- Low velocity layers within earth crust of Ukrainian shield calculated by travel time curves of refracted and reflected waves at interfaces within earth crust
[NASA-TT-F-13356] 12 p1906 N71-23364
- CNPLLOT 2 contour generating program with output of large cartographic quality contour map designed to form larger maps by combining other maps
[AD-721018] 15 p2384 N71-27733
- Finite and gauge-invariant computation of electron self-charge and self-mass in quantum version of curved space and time
[IC71/3] 18 p2972 N71-30535
- Least square distance curve fitting method
[NASA-TN-D-6374] 18 p2943 N71-30579
- Adjusting satellite directions determined from BC-4 photographic plates in short orbit mode
19 p3098 N71-31839
- FORTRAN 4 program /FITLOS/ for fitting low-order polynomial splines of two and three degrees by least squares method
[NASA-TN-D-6401] 19 p3061 N71-32188
- Exact expressions for curved characteristics behind strong blast waves
[AD-722777] 19 p3080 N71-32472
- Doppler weather radar observing methods and data processing techniques
[AD-727138] 24 p3952 N71-38197

CURVED BEAMS

- Computer program for harmonic analysis of curved folded plate structures using finite element method
[PB-193535] 01 p0131 N71-10885
- Investigating buckling behavior of flanges of horizontally curved plate girders using finite element method
[PB-192901] 04 p0616 N71-13864
- Two methods for analyzing warping torsion in curved beams of H-section
11 p1837 N71-22483
- Free vibration determination of curved sandwich beams, using finite element displacement method
[ISVR-TR-45] 20 p3357 N71-33043

CURVED PANELS

- Influence of thermal and elastic variations on distribution of thermal stresses in flat plates and curved panels
02 p0304 N71-12144
- Fabrication of curved reflector segments for solar mirror
[NASA-CASE-XLE-08917] 05 p0694 N71-15597
- Method and apparatus for bowing of instrument panels to improve radio frequency shielded enclosure
[NASA-CASE-XMF-09422] 09 p1346 N71-19436
- Space erectable rollup solar array of arcuate solar panels furled on tapered drum for spacecraft storage during launch
[NASA-CASE-NPO-10188] 09 p1327 N71-20273
- Forming mold for polishing and machining curved solar magnetron reflector with reinforcing ribs
[NASA-CASE-XLE-08917-2] 13 p2086 N71-24836

- Finite element displacement method for estimating static stresses in curved sandwich plates subjected to uniformly distributed pressure
[ISVR-TR-48] 20 p3356 N71-32860

CURVED SURFACES

- U CONTOURS
U SHAPES
U SURFACES
CURVES (GEOMETRY)
NT CYCLOIDS
NT S CURVES
- Theoretical van der Held growth curves for pure absorption in Schuster-Schwarzchild atmospheric model
01 p0875 N71-10396
- Necessary conditions for optimality of junctions between singular and nonsingular subarcs for singular optimal control problems
[NASA-CR-108664] 02 p0250 N71-11406
- Möbius plane ordering functions and algebraic groups
04 p0539 N71-14284
- Edges and curve detection in textured regions related to visual scene analysis
[AD-713159] 05 p0637 N71-14832
- Measurements of electronic free paths in argon discharge using interaction between plasma electrons and slow wave on helix
[NASA-CR-117843] 11 p1812 N71-22516
- Designing visually quality in highways by computer graphics
14 p2226 N71-26560
- Acoustic wave front reflection from caustic for predicting sonic boom pressure distribution
16 p2533 N71-28371
- Sonic boom cusped shock wave near focusing ray system of supersonic wing flow field
16 p2533 N71-28373
- Finite difference method for predicting sonic boom overpressure signature near caustic
16 p2535 N71-28390
- Mathematical model for free vibration of arc with varying radius of curvature
[AD-724318] 20 p3357 N71-33134
- Arcs and closed curves in digital pictures with thinning algorithms
[NASA-CR-121715] 21 p3397 N71-34175
- Spiral structure of interplanetary magnetic fields and solar cosmic rays
23 p3852 N71-37452

CUSHIONRAFT GROUND EFFECT MACHINE

- Management planning of cushioncraft rapid transit system
[PB-196980] 10 p1494 N71-21639

CUSHIONS

- Computerized and manned spacecraft and aircraft simulator impact testing of air cushion elastic restraint systems
[NASA-CR-60169] 18 p2882 N71-30401
- Environmental, drop, and vibration tests for investigating fatigue of cushion materials for packaging
[ECR-09] 18 p2939 N71-30614
- Nonflammable polyurethane foam for ejection seat cushions and statistical analysis of its mechanical properties
[AD-723302] 19 p3119 N71-31775

CUSPS

- Thomson scattering and cusped containment geometries - Chalice project
[SET-2582-34] 04 p0593 N71-14445
- IMP 5 magnetic field measurements at high geomagnetic latitudes to observe broad depressed field region centered on polar or dayside cusp
[NASA-TM-X-65642] 19 p3093 N71-32149
- CUSPS (MATHEMATICS)
NT DOUBLE CUSPS
CUT-OUTS
U OPENINGS
CUTANEOUS PERCEPTION
U TOUCH
- Description of device for aligning stacked sheets of paper for repetitive cutting
[NASA-CASE-XMS-04178] 11 p1771 N71-22798
- Portable cutting machine for piping weld preparation
[NASA-CASE-XKS-07933] 14 p2261 N71-26134
- Remote temperature sensor for cutting tools and application to adaptive control systems
[Y-DA-4098] 17 p2751 N71-29277

CUTTING

- NT METAL CUTTING
NT MILLING (MACHINING)
NT PLANING
NT SHEARING
NT SPARK MACHINING
- Research and development of high speed liquid jets for cutting or breaking materials
[DME/NAE-19702/1] 01 p0089 N71-10424
- Ellipsograph for describing and cutting ellipses with minimal axial dimensions
[NASA-CASE-XLA-03102] 10 p1558 N71-21079

CV-440 AIRCRAFT

- Aircraft accident report on Convair 440 aircraft crash at New Haven, Connecticut on June 7, 1971
[SB-71-65] 19 p3039 N71-32800

CV-990 AIRCRAFT

- Photometer observations of auroras from CV-990 aircraft
[NASA-CR-116835] 08 p1193 N71-18996
- Calculations of clear column radiances using infrared temperature profile radiometer measurements taken by Convair-990 over partly cloudy areas
[NOAA-TM-NESS-28] 10 p1562 N71-21842
- Photometric observations of auroral scattering by CV-990 aircraft
[NASA-CR-117466] 11 p1762 N71-22139

CW RADAR

U CONTINUOUS WAVE RADAR

CYANATES

- Using heat resistant aromatic cyanate esters as reinforced plastics
[NASA-TT-F-13454] 06 p0811 N71-16475
- Physiological effects of cyanate ions in renal malfunctions
11 p1684 N71-22537
- Using Raman effect to give fast and definite indication for isomeric structures of cyanate
[NASA-TT-F-13636] 12 p1973 N71-24079

CYANIDES

- NT HYDROGEN CYANIDES
Heat of formation for CuCN and HCN and adiabatic calorimetric measurements from 10 to 400 K
[BMRI-7499] 10 p1572 N71-20725

CYANO COMPOUNDS

NT ISOCYANATES

- Viscoelastic cross linking behavior of elastomers, energy transfer in bipyridinium herbicides, and electrical properties of tetracyano quinodimethane polymeric salts
10 p1514 N71-21356

CYANOPHYTA

U BLUE GREEN ALGAE

CYBERNETICS

- Development and applications of cybernetics theory in transportation, industry, and economics in USSR
[JPRS-15457] 01 p0037 N71-10598
- Economic cybernetics, mathematical economics, industrial process control, and automatic computer design in USSR
02 p0188 N71-11339
- Soviet cybernetics - bibliographies
[AD-709872] 03 p0352 N71-12542
- Cybernetics, computer programming, and automata theory
[AD-709873] 03 p0352 N71-12544
- Analysis of disturbances in industrial operations and resulting effects on production systems determined by cybernetic methods
03 p0386 N71-13286
- Investigating nonstationary automatic control systems and construction of asymmetrical coding systems connected with solution of combinatorial Dixon problem
[JPRS-51830] 04 p0513 N71-13542
- Biological control systems analysis
04 p0483 N71-14629
- Soviet cybernetics and computerized production control
[AD-714068] 06 p0819 N71-16334
- Relationship between cybernetic and psychological approaches to human thought
[JPRS-52199] 06 p0803 N71-16541
- Investigating relationship of cybernetics and human management of large systems
[AD-715251] 07 p0987 N71-17009
- Examining principles of structural systems analysis and identification of complex systems in cybernetics
[JPRS-52496] 08 p1173 N71-19076
- Biological systems analysis and biodynamic modelling of physiological and biological interrelationships in human body and mammals
[NASA-CR-1720] 09 p1330 N71-19076
- Summary of design parameters for models of dynamic biological systems
09 p1331 N71-19080
- Syneurist circuit design and applications in bionics, cybernetics, and electronic robots
[AD-716821] 10 p1504 N71-20775
- Psychophysiological analysis of management, control type of work processes based on concepts of cybernetics
[JPRS-52752] 11 p1679 N71-21890
- Systems analysis and cybernetics simulation of automatic air sampling systems
11 p1728 N71-22004
- Bionics of living and life-like systems with application to man machine technology
[AGARD-CP-44] 11 p1692 N71-23003
- Cybernetic modelling of neuropsychological information processes in human nervous system
11 p1692 N71-23003
- Cybernetics and production control systems using Soviet computers
[AD-718404] 12 p1885 N71-23916
- Developments in engineering cybernetics and application to Latvian scientific and technical progress
[NIL-M-20340/58284P/1] 12 p1894 N71-24139

SUBJECT INDEX

- Cybernetics and spontaneous movement of matter in world system 12 p1893 N71-24216
- Literature survey on programmed instruction methodology and cybernetics 12 p1895 N71-24222
- Mathematical models for cybernetic diagnosis of dynamic systems (AD-719776) 13 p2103 N71-25118
- Double-valued threshold logic for obtaining solutions to problems in digital devices and cybernetics (JPRS-52974) 13 p2103 N71-25142
- Component connection schemes of brain for training feedback flight control system 13 p2035 N71-25326
- Algorithms of self organization, artificial intelligence, and tree search applied to various practical problems (AD-719950) 14 p2207 N71-25432
- Analysis of theory of thinking and application to cybernetics development (JPRS-53423) 17 p2728 N71-30036
- Program variable logic calculations and biological principles of data processing applied to digital cybernetics systems having many outputs (JPRS-53669) 18 p2500 N71-31417
- Cybernetics research involving neuron network simulation and synthesis of optimal scanning systems 19 p3043 N71-32033
- Cybernetics including models for statistical decision making, biomechanical systems, and complex automatic system 19 p3044 N71-32088
- Design of learning machine and analysis of convergence characteristics during operation 21 p3400 N71-34202
- Application of cybernetics and control theory to problems of production control in complex systems and optimum stabilization of several coordinates of object by one controlling influence (JPRS-53983) 21 p3405 N71-34230
- Thinking, cybernetics, and information theory 22 p3544 N71-35248
- Coordinated control mechanism in cybernetic group systems (JPRS-54046) 23 p3714 N71-36478
- Varying viewpoints on controversial and unsolved problems in cybernetics (AD-726790) 23 p3718 N71-36501
- Neuron modeling, electrophysiology, and biochemistry involved in information processing along neuron system (AD-727770) 24 p3882 N71-37673
- CYCLES**
- NT ACTIVITY CYCLES (BIOLOGY)
- NT BRAYTON CYCLE
- NT OTTO CYCLE
- NT RANKINE CYCLE
- NT SOLAR CYCLES
- NT STRESS CYCLES
- NT SUNSPOT CYCLE
- NT THERMODYNAMIC CYCLES
- NT WORK-REST CYCLE
- Long range forecasting of climatic factors determined by cyclic behavior of oscillations in mobile envelopes of earth (NLL-M-9141-(5828.4F)) 02 p0260 N71-12145
- Therion fuel cycle development including materials irradiation, uranium-233 reprocessing, and refabrication development (ORNL-TM-3088) 03 p0413 N71-12600
- Therion fuel cycle development including materials irradiation, head-end reprocessing, and refabrication development (ORNL-TM-3112) 03 p0414 N71-12609
- Multicrossing computer memory with cyclic nerve allocation (UCRL-72648) 10 p1530 N71-21657
- Cyclic arithmetic codes and their distance properties with demonstration of modular arithmetic weight relations to code word cyclic shifts (NASA-CR-117844) 12 p1947 N71-23218
- Sub particle origins, jetion into air, inland transport, impaction, sacramento, dry or precipitative fall, and return to sea in sea-salt atmospheric cycle (JPRS-51613) 12 p1913 N71-23732
- Development and application of techniques and equipment for nondestructive measurement of nuclear materials in fuel cycles 17 p2794 N71-29653
- Automatic target cycling system for p-p and n-d fuel cross sections (PDR-4197-7) 19 p3148 N71-32053
- CYCLIC ACCELERATORS**
- NT BETATONS
- NT BEVATRON
- NT SYNCHROCYCLOTRONS
- NT SYNCHROTRONS
- Deriving equations for automatic correction of between oscillations in cyclic accelerators (JPRS-TRANS-49-32) 04 p0587 N71-14276
- CYCLIC HYDROCARBONS**
- NT ANTHRACENE

- Para-benzoquinone dioxime and concentrated mineral acid processed to yield intumescent or fire resistant, heat insulating materials (NASA-CASB-ARC-10304-1) 21 p3443 N71-34501
- CYCLIC LOANS**
- Behavior of metastable autotonic steels under cyclic loading (UCRL-19630) 06 p0872 N71-14352
- Cyclic yield behavior of polycrystalline nickel (AD-714819) 08 p1211 N71-18244
- Computerized stability design of time lag combustion system for liquid propellant rocket engines (NASA-CR-120095) 09 p1460 N71-20415
- Computerized analysis of gas-turbine cycle stability with gaseous hydrogen and gaseous oxygen 09 p1578 N71-20417
- Time lag theory for longitudinal high frequency stability analysis on staged combustion cycle of liquid propellant rocket engine 09 p1484 N71-20418
- Computer programs for analyzing crack propagation in cyclic loaded structures (AD-717150) 10 p1651 N71-20776
- Fatigue life and deformation of riveted or bolted joints (JPRS-1239) 11 p1837 N71-22308
- Effect of strain rate and load cycling on tensile behavior and air permeability of coated fabric for inflatable decelerator system (NASA-CR-111083) 12 p2004 N71-23197
- Automatic controlled thermal fatigue testing apparatus (NASA-CASB-XLA-02059) 12 p2013 N71-24276
- Evaluation of helicopter flight loading and structural stability 13 p3023 N71-24389
- Static and cyclic fatigue characteristics of brittle polymers using technique to provide zero mean stress with alternating tension and compression stresses (COO-1794-7) 15 p2522 N71-27805
- Strain range components and creep fatigue behavior of metals related independently to cyclic life by equations in both tension and compression (NASA-TM-X-67838) 15 p2523 N71-27945
- Temperature and stress histories recorded for glass fiber reinforced plastic specimens subjected to torsional oscillations (AD-721522) 16 p2618 N71-28383
- Creep behavior of Cr-Mo-V steels under cyclic loads (RD/BN-1809) 21 p3441 N71-34482
- Determining effective stresses under conditions of cyclic loading (AD-727653) 24 p4024 N71-38711
- CYCLING**
- U CYCLES
- CYCLOHEXANE**
- Kinetics of catalytic dehydrogenation of methylcyclohexane at 600, 650, and 700 deg F and 5 atm pressure (AD-715926) 08 p1037 N71-18729
- Chemical analysis of aniline and cyclohexane mixtures to determine viscosity in critical region 20 p3230 N71-33753
- CYCLOID**
- Symmetry properties of cycloids and envelope curves 03 p0401 N71-13394
- CYCLONES**
- NT HURRICANES
- NT TYPHOONS
- Divergence, vertical velocity, and energy conversion in west Mediterranean during cyclone development of 24 Oct. 1964 (TT-49-51019) 01 p0879 N71-10651
- Small disturbances of vertical velocity in asymmetric atmospheric vortex (NASA-TT-P-13365) 02 p0259 N71-12005
- Frequencies of cyclonic vortices, mean air density, and horizontal air temperature gradients over Northern Hemisphere 11 p1735 N71-22826
- Relationship of cyclones in stratosphere and troposphere and ocean surface temperature during early winter with mildness or severity of Russian winters (NLL-M-9269-(5828.4F)) 17 p2739 N71-29627
- Frequencies of centers of gravity of cyclones and anticyclones for long range weather forecasting (NLL-M-20653-(5828.4F)) 21 p3453 N71-34574
- Atlantic tropical cyclone strike probabilities for selected stations during September (NASA-CR-61361) 22 p3616 N71-35765
- Energy and momentum transfer distributions in sea-air exchangers relative to model of traveling frontal cyclones in middle latitudes 23 p3786 N71-36982
- Monthly cyclone parameters in Australian region, Nov. 1967 to June 1969 23 p3791 N71-37023
- Location of Aleutian low center, and pressure at center (NLL-M-20744-(5828.4F)) 24 p3953 N71-38285

CYCLOTRON RESONANCE

- Differential heating effects on steady-state tropical cyclone dynamics and energetics based on diagnostic axisymmetric model in barotropic coordinates 24 p3954 N71-38289
- CYCLOTRON FREQUENCY**
- Electric and magnetic field ratio frequency heated hydrogen plasma diagnostics at cyclotron frequencies 18 p2993 N71-31046
- Ion cyclotron instabilities in finite plasma and finite temperature effects 23 p3833 N71-37332
- CYCLOTRON RADIATION**
- Cyclotron and synchronous wave devices (AD-712323) 02 p0193 N71-11354
- Describing precision time-of-flight spectrometer for tuning incident charged particle beam from compact cyclotron around target with path of emerging neutrons remaining fixed (FTB-270) 03 p0749 N71-15325
- Isotachronous cyclotron beam, beam handling, and monochromator systems at Juelich facility (JUL-465-KP) 09 p1366 N71-20151
- Cold plasma density and collisional frequency measurements in presence of magnetic fields for cyclotron radiation plasma diagnostics (COO-1709-1) 10 p1637 N71-20805
- Deuterium helium-3 fusion power balance calculations with inclusion of variable cyclotron radiation parameter (NASA-TM-X-2289) 13 p3149 N71-25526
- Computer experiments for proving theory of nonlinear evolution of beam cyclotron instability (AD-723527) 19 p3164 N71-32143
- Comparison of Aluminite-3 and COO-5 observation of turbulence of magnetospheric electrostatic electron cyclotron harmonic waves (NASA-TM-X-65600) 19 p3099 N71-32442
- Cyclotron radiation, relativistic velocities, angular distribution, total power, electron distribution, and inverse Compton scattering 20 p3344 N71-32840
- Radio spectra, synchrotron self-absorption, free-free absorption, cold plasma effect, stimulated emission, and quasi-stellar sources 20 p3344 N71-32841
- PDP 9 computer program for detection of ionospheric beam direction with FM cyclotron analyzer (INS-TL-109) 21 p3483 N71-34807
- Anomalous transmission and reflection of ion cyclotron waves based on linearized Vlasov-Maxwell equation expansions 23 p3833 N71-37333
- CYCLOTRON RESONANCE**
- Magnitude and wavelength dependence of resonance radiation emission caused by thermal excitation (AD-711828) 03 p0437 N71-12602
- Cyclotron resonance in indium antimonide using infrared laser (AD-713094) 03 p0729 N71-15373
- Investigating cyclotron resonance in solid-state plasma and nonlinear friction in servomechanisms 06 p0902 N71-15800
- Investigating interaction of solid-state plasma with far infrared laser radiation in large magnetic fields 06 p0929 N71-15801
- Cyclotron resonance techniques for determining electronic structure of metals (AD-714104) 06 p0933 N71-16008
- Microwave power amplification and generation utilizing linear beam devices (NASA-CR-116490) 07 p0996 N71-17346
- Relativistic motion of single particle undergoing cyclotron resonance in magnetic mirror trap (AD-714837) 07 p1083 N71-17816
- Investigating cyclotron-resonance interaction between electromagnetic waves and plasmas for velocity distribution which yield algebraic dispersion relation (DI-42-1010) 07 p1085 N71-18030
- Investigating effect of high frequency plasma spreading along magnetic field at microwave power near electron cyclotron harmonics (NPL-18303) 07 p1085 N71-18133
- Magnetic moment of proton in nuclear magnetons determined from cyclotron resonance frequency of ions 10 p1621 N71-21749
- Angular dependence of cyclotron resonance in single thallium crystal 11 p1808 N71-21873
- Electron cyclotron resonance and anisotropic energy distribution excitation of plasma instabilities and waves (COO-1695-32) 11 p1811 N71-22443
- Performance of Filadelfia-type cyclotron resonance devices in producing intense beams of energetic neutral particles (EUR-CBA-FC-567) 13 p2147 N71-24970
- Computerized simulation of plasma heating from electron cyclotron resonance including ion trapping and magnetohydrodynamic instability (AD-726675) 14 p2322 N71-36878

- Electron cyclotron resonance plasma density, energy, and lifetime measured in stellarator
[IPP-2/85] 15 p2300 N71-27317
- Doppler shifted cyclotron resonance absorption of helicon waves in indium and Gantmakher-Kaner oscillations 15 p2477 N71-27577
- Bounce frequency effects on negative mass instability in ion plasma 15 p2504 N71-27920
- High frequency oscillation research and related electronics problems including open resonator applications in electromagnetic fields and paramagnetic and cyclotron resonances 17 p2725 N71-29667
- Cyclotron and bounce resonance scattering of electrons trapped in earth magnetic field 18 p3004 N71-30924
- Enhanced transmission of strong right hand circular wave near cyclotron resonance in afterglow helium slab plasma occurring earlier than corresponding weak electromagnetic field 19 p3166 N71-32596
- Cyclotron particle extraction systems with emphasis on resonance and acceleration methods 20 p3314 N71-33048
- Electron-cyclotron wave resonance in inductively coupled HF ring discharges 20 p3235 N71-33738
- Saturation effects in cyclotron resonance oscillators with emphasis on generation and amplification of millimeter waves 23 p3731 N71-36594
- Bremsstrahlung measurements to determine plasma instabilities and excited waves from anisotropic energy distribution caused by electron cyclotron resonance [COO-1695-33] 23 p3830 N71-37315
- ### CYCLOTRONS
- #### NT MICROCOTRONS
- #### NT OAK RIDGE ISCHRONOUS CYCLOTRON
- #### NT SYNCHROCYCLOTRONS
- Nuclear research with cyclotron particles, fast electrons, beta and gamma ray spectroscopy, and radio and nuclear chemistry 01 p0095 N71-10395
- Nuclear physics research and cyclotron operation [PUC-937-378] 01 p0098 N71-10660
- Residual radiation calculations for carbon, iron, copper, aluminum, and tantalum in cyclotron structure [ORNL-TM-2834] 03 p0424 N71-12744
- Research progress on cyclotron operations, nuclear magnetism, properties of nuclei, and molecular beam research 03 p0435 N71-13235
- Vacuum system model study for 500 MeV H⁻/cyclotron [TRI-69-7] 03 p0359 N71-13344
- Monochromatization system design of external beam of 2.4 m isochronous cyclotron [IAE-1898] 04 p0572 N71-13649
- Research progress in operation of Karlsruhe isochronous cyclotron in 1969 [JNP-18358] 04 p0550 N71-13759
- Isochronous cyclotron with separated orbits and turns, and acceleration by nonsinusoidal form of radio frequency field 04 p0578 N71-13870
- Particle energy and cyclotron utilization [COO-1760-3] 04 p0589 N71-14345
- Cyclic accelerators with magnetic field harmonic analyzer using digital systems [AD-714767] 06 p0915 N71-16010
- Section-focusing cyclotron [AD-715109] 07 p1005 N71-17852
- Electron cyclotron harmonic waves in magnetically confined low pressure gas discharge [JPP-2/84] 08 p1270 N71-18251
- Axial injection of polarized protons into Grenoble cyclotron [CEA-R-3729] 09 p1437 N71-20078
- Multichannel system of two-directional communication for cyclotron facility measuring center with TeVM computer type M-220A [IAE-1953] 09 p1350 N71-20168
- Changing field gradients in isochronous ring cyclotron, using shaped magnets [KFK-1264] 09 p1445 N71-20561
- Research work with variable energy cyclotron in nuclear physics and nuclear chemistry [ORO-3396-26] 10 p1623 N71-21765
- External injection and acceleration of 600 microamp electron beam to final radius of ring cyclotron with strong focusing [JINR-P-5453] 17 p2793 N71-29518
- Performance characteristics of existing and proposed accelerators for heavy ions with description of super HILAC progress and discussion of isochronous cyclotrons 17 p2793 N71-29625
- Research in nuclear structure and nuclear reactions performed on Van de Graaff accelerator and cyclotron, and equipment modifications [RLO-1380-121] 17 p2810 N71-30395
- Production of carrier-free radioisotopes Sr-85 by irradiation in U-120 cyclotron 18 p2970 N71-30462
- Method of solution of ion motion in median plane of cyclotron and results obtained using method with U-120 cyclotron 18 p2901 N71-30658
- Conditions of formation and heating dynamics of fast particles and main electron plasma component during electron cyclotron heating [NIP-18635] 18 p2992 N71-30667
- Beam optics calculations based on beam phase space characteristics for cyclotron-tandem injection system [ANU-P-519] 19 p3146 N71-31967
- Penning ion gauge (PIG) type heavy ion source on axial injection line of 88 inch cyclotron [UCRL-20406] 19 p3153 N71-32207
- Cyclotron particle extraction systems with emphasis on resonance and acceleration methods 20 p3314 N71-33048
- Development and characteristics of cyclotron and supporting equipment [AD-724651] 20 p3314 N71-33097
- Cyclotron simulation of uniform concentrations of helium produced during neutron irradiation [ORNL-TM-3299] 20 p3308 N71-33705
- Nuclear physics and experimental research with cyclotron 20 p3327 N71-33952
- Development and characteristics of internal conversion electron spectrometer applied to gamma ray spectroscopy and nuclear structure research 21 p3430 N71-34412
- PDP-9 programs for INS FM cyclotron beam analyzer and program loading problems and usage [INS-TL-107] 21 p3470 N71-34707
- Computer programs for FM cyclotron analyzer computing excitation energy of residual nuclei [INS-TL-108] 21 p3470 N71-34708
- Coherent frequencies of transverse oscillations in electron model of ring cyclotron for magnetic field variants 21 p3473 N71-34728
- Cyclotron for measuring angular distributions from 15 deg to 165 deg for transitions in B-10 states - reaction mechanism and cluster structure 21 p3488 N71-34846
- Formation stages of magnetic field in model of accelerator sector electromagnet [JINR-P-5669] 22 p3633 N71-35895
- Cyclotron characteristics and types of ion source injectors for use in high-energy, heavy-ion cyclotrons [UR-NSRL-38] 22 p3642 N71-35962
- Empirical methods for calculating magnet pole tip shape and finding field inside magnet air gap [TRI-70-4] 22 p3642 N71-35968
- Research in experimental nuclear physics, tandem Van de Graaff accelerators and cyclotrons [ANL-7728] 24 p3990 N71-38404
- Turbulent heating and anomalous diffusion in pinch plasmas related to drift instability in electron cyclotrons [CONF-710607-66] 24 p3989 N71-38460
- ### CVGNUS CONSTELLATION
- Balloon borne X ray survey of Cygnus region 07 p1106 N71-18054
- Evidence for multiple periodicity confirmed in X ray data from rocket-borne exposure to Cyg X-1 [NASA-TM-X-65494] 12 p1992 N71-23448
- Flux-corrected radiative atmospheric models and metal abundances for R Cygnus 13 p2167 N71-25066
- X ray spectra of discrete sources in Cygnus data from rocket-borne proportional counter [NASA-TM-X-65661] 19 p3176 N71-32277
- Search for high energy gamma rays from Cygnus region with discussion of mechanisms for gamma ray production 19 p3178 N71-32668
- Eight variable stars in cygnus cloud studied at different observatories - tables and graphs 21 p3510 N71-35013
- ### CYLINDERS
- Analytic function theory, superposition, and point matching used to determine non-Hertzian contact stresses between cylinders of dissimilar cross section 11 p1838 N71-22714
- Elastic/perfectly plastic torsion analysis of doubly-connected cylinders using finite difference theory 22 p3691 N71-36325
- ### CYLINDRICAL AFTERBODIES
- ### U AFTERBODIES
- ### U CYLINDRICAL BODIES
- ### CYLINDRICAL ANTENNAS
- Electrical impedance of cylindrical and monopole antennas 06 p0812 N71-15719
- Impedance behavior of short cylindrical antenna used as diagnostic probe in isotropic and magnetized plasmas 10 p1519 N71-21105
- Applying method of moments to solution of integral equations for current induced on conducting cylinders in two-dimensional field 14 p2218 N71-26271
- Analysis of radiation of spherical and cylindrical antennas in incompressible and compressible plasmas to detect existence of electroacoustic or longitudinal plasma wave excited by antenna 19 p3058 N71-33611
- ### CYLINDRICAL BODIES
- ### NT ROTATING CYLINDERS
- Transpiration cooling near stagnation line of cylindrical body in cross flow 01 p0133 N71-10408
- Finite element analysis of K-shaped tubular joints [FB-193560] 01 p0131 N71-10446
- Elastic-plastic analysis of open-end isotropic tubes under internal pressure 02 p0299 N71-11118
- Experimentally determined aerodynamic noise environment analysis for three nose-cylinder configurations [NASA-CR-102933] 03 p0310 N71-12218
- Development and testing of cylindrical thermocouple conversion 03 p0319 N71-12277
- Characteristics of oversize circular waveguide and transitions at 3-millimeter wavelengths [AD-712378] 03 p0338 N71-12410
- Investigating electromagnetic scattering by cylinders using Rayleigh-Gans theory [NASA-TM-X-64545] 03 p0417 N71-12580
- Comparison of space and simulated environment conditions using temperature inaccuracy of hollow cylinder 03 p0357 N71-12718
- Whitman theory of shock wave diffraction tested for sphere and cylinder diffraction [REF-T-270] 03 p0365 N71-13729
- Knudsen flow and Mach number effects on hypersonic and supersonic wakes of cylindrical bodies and spheres [REF-69-7] 04 p0471 N71-13480
- Vibration properties of ring stiffened honeycomb cylinders [NASA-TN-D-6090] 05 p0780 N71-15423
- Vertical force on infinitely long circular cylinder in oblique sea [AD-713302] 07 p1006 N71-18015
- Calculation of neutron intracell transport in reactor cylindrical cells [AD-1258] 07 p1078 N71-17807
- Performance of high speed bearings with cylindrically hollow balls [NASA-TN-D-7007] 08 p1207 N71-18418
- Supersonic flow fields around cylindrical body with blunt nose [NAL-TR-199] 09 p1372 N71-19701
- Computer programs using cylindrical finite elements to solve for large nonlinear deflection [TT-7003] 09 p1401 N71-20521
- Finite difference method for solving equations for compressible turbulent boundary layers on swept finite cylinders [NASA-TN-D-6203] 10 p1539 N71-20700
- Resonant sound transmission in unstiffened cylindrical bodies noting sound waves and transmission loss [ISVR-TR-38] 10 p1606 N71-20713
- Calculation of critical diameter ratios for reverse yielding of thick-walled cylinders [AD-717248] 10 p1652 N71-20811
- Dynamic fracture in metal hollow cylinder under biaxial strain conditions 10 p1577 N71-21320
- Longitudinal propagation of axially symmetric waves in semi-infinite cylindrical body restrained in radial direction by thin elastic shell 10 p1655 N71-21320
- Longitudinal curvature and displacement speed effects on incompressible boundary layer flow past circular cylinder [AD-717071] 10 p1544 N71-21411
- Determination of pressure characteristics and flow properties of cylindrical bodies in aqueous solutions of polyethylene oxide [AD-717584] 11 p1733 N71-21589
- Fluid motion for incompressible fluid between two long eccentric cylinders [AD-717566] 11 p1734 N71-21570
- Lift coefficient for wind induced vibration of slender cylindrical body [AD-717739] 11 p1735 N71-21589
- Differential equation solution for thermal simulation of reciprocating cylindrical body temperature distribution under space environment and comparison to full rotation in actual flight [DLR-FB-70-59] 11 p1731 N71-22250
- Acoustic field of plane wave incident on elastic cylinder in contact with liquid 11 p1798 N71-22437
- Numerical analysis of small displacement, elastic independent torsionless axisymmetric behavior of cylinders 11 p1839 N71-22801

SUBJECT INDEX

CYLINDRICAL SHELLS

Wingtip tests of cylindrical and Lundell-conical rovers in ambient air producing Reynolds numbers up to 100,000 for high speed aircraft
[NASA-TM-X-67009] 12 p1857 N71-23116

Vit plate and cylindrical low density probes including flow molecular flow and continuum regimes
12 p1923 N71-24130

Effects of using resistance thermometers to measure temperatures of cylindrical walls bounding test field in thermophysical properties instrument
12 p1923 N71-24131

Amplifying interferometric and narrow multiple beam band measurement of molybdenum carbide pressure cylinder diameters
[NLL-M-20171-5828.4P] 12 p1931 N71-24226

Derivation of theory for unsymmetric deformation of nonhomogeneous, anisotropic, elastic cylindrical shells. Part I
[REPT-69-8-PT-1] 12 p2008 N71-24294

Nonexistence theorem for solution of Poisson differential equation for viscous flow around cylindrical bodies
[REPT-11/1971] 13 p2021 N71-24490

Numerical analysis of compression of elastic cylinder between two smooth, flat, and parallel rigid plates
[AD-719576] 13 p2177 N71-24616

Numerical analysis of vibrations of spheres and cylinders submerged in fluids subjected to plane acoustic waves
14 p2347 N71-25758

Statistical energy analysis to predict response of stringer stiffened cylinder to acoustical and mechanical excitation
[NASA-CR-103172] 14 p2348 N71-25964

Development and characteristics of test equipment for measuring creep buckling of moderately thin-walled circular cylindrical shells under axial compression loads
[AD-726767] 14 p2348 N71-26097

Microviscosity and creep in stationary and rolling contact surface of cylindrical bodies
15 p2453 N71-26429

Free stream turbulence effects on local heat and mass transfer rate across laminar, forward stagnation boundary layer on circular cylinders in cross flow
15 p2393 N71-27321

Vortex induced hydroelastic vibrations of spring supported cylinder in steady fluid stream
[AD-721073] 15 p2522 N71-27860

FORTRAN 4 digital codes for thermal dynamics of cylindrical nuclear fuel rod with or without distributed heat generation
[N71/NO/70/8] 16 p2630 N71-28117

Free convection heat and mass transfer along cylindrical bodies
16 p2690 N71-28200

Density distribution measurements in rarefied argon contained between two concentric cylinders undergoing relative rotation, and heat transfer and drag measurements
16 p2593 N71-28876

Mean square stresses for random distributions of debondings in cylindrical body
17 p2824 N71-29994

Dynamic plastic behavior of hollow cylinders using spinning wire technique for investigation of elastic/plastic constitutive theory
17 p2854 N71-30157

Moving long cylindrical model for aerobreaking tests at high speed in drop wire facility
18 p2867 N71-31109

Collisionless plasma flow around cylinder for application to ionospheric sounding probe
[N71/NO-PUBL-137] 19 p3072 N71-31693

Comparison of predicted and experimental wall temperatures for cylindrical ejector exhaust nozzle cooled with turbojet gas generator
[NASA-TN-D-6465] 19 p3174 N71-32156

Polynomial approximation and linear anisotropic diffusion in one-dimensional cylindrical geometry
[RE-108] 19 p3151 N71-32178

Pressure distributions on planar delta wings attached to cylindrical bodies in supersonic flow - theoretical results for sonic leading edge, angle of attack case
[NRE-TN-HSA-186] 20 p3207 N71-33699

Analysis of stationary collisionless plasma sheath around conducting cylinder
20 p3332 N71-33438

Transonic buffeting flow on cone-cylindrical missile body
[TR-92] 20 p3307 N71-33440

Phase guide for millimeter waves, measurements on matched fence guide terminations, and experimental study of one-conical cylindrical resonator
[NASA-CR-121763] 21 p3394 N71-34155

Dynamics and stability of flexible and rigid submerged towed cylinders
[N71/NO-70-4] 21 p3411 N71-34273

Production of circular cylindrical surfaces on lathe using piezoelectric torch
[N71/NO-70/134] 21 p3433 N71-34431

Wind tunnel investigation of static pressure distributions along cylindrical surface behind shallow, three-dimensional, rearward facing step of various heights
[NASA-TM-X-24042] 22 p3537 N71-35199

Criticality study of ZPR-1 and ZPR-2 with 23.4-cm diameter cylindrical stainless steel cores
[NASA-TM-X-2381] 22 p3624 N71-35822

Experimental and theoretical analysis of resonance properties and radiation patterns of dipole antennas symmetrically mounted on conducting spheres or cylinders
23 p3727 N71-36566

Drag coefficient measurements in flow around rectangular cylinders
[IC-AERO-71-15] 23 p3744 N71-36695

Two group code [SAVE] for reflector savings of completely reflected cylindrical reactor utilizing iterative techniques
[UAREE-96] 23 p3795 N71-37048

Analysis of incompressible deformations of cylindrical membranes composed of elastic, homogeneous, isotropic, and incompressible material
[AD-720022] 24 p4027 N71-38733

CYLINDRICAL CHAMBERS

Fracture toughness test method for thick-walled cylinder material
[AD-721626] 16 p2685 N71-28208

Fluid mechanics experiments to investigate methods for reducing mixing between confined coaxial flows in cylindrical chambers for application to open-cycle gas-core nuclear rockets
[NASA-CR-1851] 16 p2579 N71-28403

CYLINDRICAL SHELLS

Static and dynamic properties of thin shells, elastic and plastic theories, and study methods for stress and fracture conditions
[AD-711129] 01 p0129 N71-10591

Transient response of ring-reinforced cylindrical shell, immersed in fluid, to axisymmetric pulses
[RE-395] 01 p0150 N71-10719

Numerical determination of nonlinear displacement behavior of complete circular cylindrical thin shell subjected to uniform radial pressure
[AD-721111] 02 p0302 N71-12051

Buckling of integrally stringer-stiffened cylindrical shells under axial compression
[AD-712090] 03 p0460 N71-12849

Effect of variations in creep exponent N on buckling of circular cylindrical shells in axial compression
[AD-711949] 03 p0461 N71-12966

Investigating spectrum of set of axisymmetric vibration equations for shells of revolution
03 p0466 N71-13228

Hyperbolic boundary layer transition and hyperbolic heat transfer on cylindrical shells, cones and flat plates
[REPT-110470] 04 p0472 N71-13408

Incremental variational method for determining inelastic load deformation and buckling load for shells of revolution
[AD-712522] 04 p0617 N71-13946

Digital computer program for asymptotic solution for short ring-reinforced oval cylinders
[AD-712519] 04 p0617 N71-14009

Exact buckling criterion for eccentrically stiffened multilayered circular cylindrical shells of materials having different orthotropic moduli in tension and compression
[AD-713113] 05 p0779 N71-15319

Elastic buckling of clamped oval cylindrical shells under axial loads
[AD-714579] 06 p0955 N71-16526

Euler buckling of clamped oval cylindrical shells under axial compression
[AD-714578] 06 p0956 N71-16536

Applying nonclassical equations of cylindrical shell dynamics to study of short wave processes in shells
[AD-715971] 07 p0991 N71-16940

Stress analysis and design of cylindrical shell bulkhead for spacecraft
[NASA-CR-114847] 07 p1124 N71-17558

Vibrational response of stiffened cylindrical shell to reverberant acoustic fields
[NASA-CR-114852] 07 p1124 N71-17562

Stress distribution around openings in circular cylindrical shell
07 p1126 N71-17811

Design optimization for cylindrical shell subjected to reentry loads and heating
07 p1127 N71-18022

Singular solutions for cylindrical shell equation and relationships to mechanical or thermal loads
07 p1128 N71-18024

Wall motions in circular thin-walled cylindrical shells under combined loading
08 p1301 N71-19822

Numerical analysis of strength, rigidity, and stability of thin walled shells under various load conditions
[AD-716527] 09 p1475 N71-19858

Elastic properties of hollow spherical shells under internal pressure and torsion properties of solid circular cylinders
[AD-716550] 09 p1475 N71-19872

Computerized design of stiffened cylindrical shells and ablating composite heat shields
09 p1410 N71-20137

Analysis of free vibration characteristics of clamped/free and clamped/clamped stiffened cylindrical shells by digital computer solution
[TT-7001] 09 p1480 N71-20497

Effect of elastic end rings on eigenfrequencies of finite length thin cylindrical shells
[NASA-CR-117312] 09 p1481 N71-20516

Measurement of wind induced oscillations of tall cylindrical bodies with emphasis on vortex excited motion
[TT-7008] 09 p1482 N71-20543

Shell impact response and wave propagation in cylindrical and conical shells by experimental and analytical methods
[NASA-CR-66921] 10 p1651 N71-20701

Estimation of stability of elastic noncircular conical and cylindrical orthogonal shells
[AD-717014] 10 p1651 N71-20754

Fourier-Bessel analysis of forced torsional vibration of concentric cylindrical shells
[AD-717902] 11 p1833 N71-21809

Quasi-static stress and strain analysis of viscoelastic hollow cylinder enclosed in elastic cylindrical shell with ablating pressurized cavity
[DLR-FB-70-61] 11 p1835 N71-22179

Procedure to determine proper geometry of anisotropic and laminated cylinders with elastic stress gradients reduced to predetermined limit
[AD-717708] 11 p1836 N71-22367

Algorithms for thin-walled axisymmetrically loaded bodies of revolution elastic stability problems including cylindrical, conical, spherical, and toroidal shells
[AD-717708] 11 p1837 N71-22405

Effect of static stress and edge restraint on vibration of nearly cylindrical shells with circular cross section and slight meridional curvature
[NASA-TN-D-6133] 11 p1838 N71-22617

Differential equations and numerical analysis of combustion chambers similar to cylindrical shells noting special boundary conditions
[JCT-14609] 12 p2004 N71-23395

Determination of axial buckling load of circular cylindrical shells formed by process of plastic expansion due to internal pressure
[NASA-TN-D-6322] 12 p2085 N71-23733

Structural analysis of thermal buckling of orthotropic, multilayered, stiffened cylindrical shell using finite differences and determinant plotting or modal iteration
[NASA-TN-D-6332] 12 p2085 N71-23734

Numerical analysis of wave propagation in cylindrical shells based on application of general dynamics equation
12 p2086 N71-23975

Application of theory for unsymmetric deformation of nonhomogeneous, anisotropic, elastic shells to layered shells - Part 2
[REPT-70-3-PT-2] 12 p2088 N71-24299

Numerical analysis of behavior of finite cylindrical shell in fluid flow with linearized hydrodynamics equations
12 p2088 N71-24295

Optimum design for buckling prevention in cylindrical shells under lateral pressure
13 p2178 N71-24648

Natural vibration of closed cylindrical shell with solid elastic core
14 p2347 N71-25794

Numerical analysis of critical times for creep buckling in series of circular cylindrical shells under pure bending stress
[AD-720768] 14 p2348 N71-26094

Mixing fluids in confined cylindrical geometry similar to rocket configuration with simulated bulkhead failure mode
14 p2349 N71-26219

Numerical analysis of influence of fiber orientation on mechanical properties of cylindrical shells in initial postbuckling region
[AD-728231] 14 p2349 N71-26252

Numerical analysis of elastic general instability problem of hydrostatically loaded simply supported cylindrical shell with conical ends
14 p2349 N71-26359

Effect of in-plane boundary conditions on buckling loads of simply supported ring stiffened cylindrical shells
[AD-721473] 16 p2685 N71-28139

Effect of spatial and temporal shapes of pressure pulses on fluid deformation of circular cylindrical shells under axially varying pressure loads
[ANL-7738] 16 p2685 N71-28571

Analysis of behavior of thin elastic shells subjected to initial mechanical stresses and nonuniform heating and dynamic interaction with surrounding fluid
[AD-721400] 16 p2687 N71-28886

Analysis of dynamic snap-through stability of nonlinear, elastic, plane strain, free vibration of shallow circular cylinder
17 p2852 N71-29646

Study of cylindrical stress waves using exploding wires in long hollow thick walled shells

17 p2853 N71-29638
Minimum weight design of axially compressed ring and stringer stiffened cylindrical shells
[NASA-CR-1766] 17 p2853 N71-30118

Improved multilocal finite difference variant with combined ordinary modified and conventional multilocal schemes for bending analysis of arbitrary cylindrical shells
[UNICIV-R-43] 17 p2855 N71-30316

Analysis of natural frequencies and mode shapes for vibrations of stiffened cylindrical shells with or without end caps
[AD-722465] 18 p3021 N71-30904

Problem of bending cylindrical shells solved using cylindrical strip elements, and rectangular circular cylindrical elements used in finite element analysis of cylindrical shells
[PB-195987] 18 p3021 N71-30906

Supersonic panel flutter and aerodynamic load stress analysis of finite cylindrical shells based on Galerkin method and aerodynamic equilibrium equations
[AD-722447] 18 p2905 N71-31183

Scattering of plane waves from thin rigid porous elliptic cylindrical shells and Mathieu function
[NASA-TN-D-6340] 18 p2966 N71-31435

Dynamic plastic behavior of aluminum alloy cylindrical shells subjected to impulse loads on inner surface
[AD-723431] 19 p3188 N71-32028

Stability of circular cylindrical sandwich shell reinforced by lateral ring-type diaphragms
[AD-723548] 19 p3189 N71-32336

Dynamic and static analysis of axially nonuniform, thin cylindrical shells based on finite element type theory
[MERL-70-9-PT-1] 20 p3360 N71-33819

Derivation of governing differential equations of mixed formulation for linear, dynamic problem of thermoelectric laminated anisotropic arbitrary cylindrical shells
[UNICIV-R-59] 20 p3361 N71-33960

Application of finite difference variant method for bending analysis of various cylindrical shells
[UNICIV-R-58] 21 p3528 N71-35137

Free flexural vibration of thin cylindrical shells using hybrid finite element method
[MERL-70-10] 21 p3528 N71-35138

NASTRAN computer program applied to buckling problem of reinforced cylindrical shells with openings
[AD-726765] 22 p3662 N71-36259

Dynamic response of cylindrical shell excited by simulated turbulent boundary layer pressure field determined by NASTRAN
[AD-726765] 22 p3662 N71-36259

Stability of thin cylindrical shells subject to periodic axial loads in time-dependent temperature field
[AD-726765] 22 p3662 N71-36259

Discrepancies in minimum volume design of sand-wich axisymmetric cylindrical shells under Tresca and Mises yield criteria
[AD-726765] 22 p3662 N71-36259

Numerical analysis of displacement of mid-surface of thin cylindrical shell of finite length, simply supported at both ends, subjected to time dependent surface loads
[AD-726765] 22 p3662 N71-36259

Predictions of mode shapes and natural vibrational frequencies of circular cylindrical shell with stiffeners and end plates
[AD-726765] 22 p3662 N71-36259

Nonlinear analysis of forced vibrations of cylindrical shells in vacuum or submerged
[AD-726765] 23 p3862 N71-37533

Stiffness matrix of nonconforming triangular finite element for static and dynamic analyses of thin cylindrical shells
[AD-726765] 23 p3862 N71-37533

Laplace method for investigating dynamic stability of cylindrical shells and folded plates subjected to stochastic excitations
[AD-726765] 23 p3862 N71-37533

Sound radiation of vibrating cylindrical shell with impedance coating under hydroacoustic conditions
[AD-726765] 24 p3966 N71-38291

CYLINDRICAL TANKS

Experimental and theoretical studies of liquid sloshing at simulated low gravity
[AD-726765] 01 p0041 N71-10723

Simulated low gravity sloshing in cylindrical tanks including effects of damping and small liquid depth
[AD-726765] 01 p0041 N71-10724

Nuclear safety analysis of moderation-controlled fast, L.A. heavy wall UFG cylinders
[K-L-6255] 04 p0557 N71-14156

Plastic deformation and rupture influence on dimensions of cylindrical flat-bottomed steel pressure vessels subjected to internal pressure
[CRIF-MT-58] 08 p1295 N71-18460

Mathematical models for minimum wall thickness of cylindrical horizontal storage tank on two saddle supports
[CRIF-MT-61] 08 p1296 N71-18591

Stress analysis of cylindrical degassing tank, noting support interference effects
[CRIF-MT-57] 10 p1652 N71-21030

Liquid propellant sloshing in tilted axisymmetric cylindrical tanks for space shuttle applications
[NASA-CR-119891] 20 p3337 N71-32898

Equations derived for liquid motion in cylindrical tank with elastic bottom and subject to longitudinal excitation of sinusoidal form
[AD-726765] 22 p3693 N71-36339

CYLINDROIDS

U CYLINDRICAL BODIES

CYTOGENESIS

International control for experimentation with human eggs
[AD-726765] 13 p2033 N71-24763

CYTOLOGY

Morphological and cytological aspects of hypokinesis in rat muscles
[NASA-TT-F-13376] 01 p0009 N71-10341

Electron microscopic analysis of odor sensing cell microstructure
[AD-726765] 15 p2371 N71-27159

Low temperature cytophysiological adaptation of human and mammalian cells
[AD-726765] 20 p3220 N71-33453

CYTOPLASM

Radiation effects on cytoplasmic structure and differential activity of grass
[NYO-2356-43] 20 p3225 N71-33994

CZECHOSLOVAKIA

Design and operation of experimental gas loop for nuclear reactor
[ZB-48-48] 02 p0366 N71-12179

Analysis of centralized data processing system in Czechoslovakia
[JPRS-52674] 10 p1665 N71-21063

Atmospheric diffusion effects on ground surface pollution in northwestern Bohemia
[NLL-M-20310-5828.4F] 12 p1959 N71-24223

Integrated information system and popularization in Czechoslovakia
[JPRS-53047] 14 p2360 N71-26164

Czechoslovak information system for reducing research duplication
[AD-726765] 14 p2360 N71-26165

Popularization versus payment system for scientific and technical production in Czechoslovakia
[AD-726765] 14 p2360 N71-26166

Comparison of temperature and humidity differences between mountain stations and free atmosphere over Poprad, Czechoslovakia
[NLL-M-20356-5828.4F] 21 p3453 N71-34578

CZOSRALSKI METHOD

Large oxide single crystal growth equipment for Czochralski method
[AD-726765] 01 p0107 N71-10127

Czochralski growth of tungstate and molybdate selenides
[AD-726765] 02 p0284 N71-11841

Growing silicon crystals with minimum defects using Czochralski method
[AD-726765] 07 p1087 N71-17278

Czochralski method for growing aluminum oxide single crystals in plate form for transparent armor applications
[AD-726765] 09 p1405 N71-19824

Czochralski method for investigating yttrium orthobismuthate as optically pumped laser host material
[AD-726765] 13 p2008 N71-24426

D

D LAYER

U D REGION

D LINES

Combustion chamber temperature measurement using sodium d-line reversal
[DLR-FB-70-70] 12 p2010 N71-23362

Nonlinear least squares fitting of resonance parameters to 5 to 100 keV neutron capture cross sections including λ , ρ , and δ wave graphs of neutron strength functions
[AAEC/E-194-SUPPL-1] 13 p2130 N71-24687

D REGION

Electrical structure model of D and E region, based on dynamic current theory
[AD-714365] 06 p0849 N71-16335

Characteristics of D and E regions of ionosphere
[NASA-CR-116441] 07 p1016 N71-17052

Vertical distribution of D region electrons and energetic spectra of solar X rays during solar flares and periods of quiet sun
[AD-726765] 08 p1195 N71-19130

Coordinated rocket, satellite, aircraft, and ground measurement program studying physical chemistry of ionospheric D region - PCA 69
[AD-716385] 09 p1382 N71-19575

Daytime D region positive ion composition measurements for solar zenith angles of 53.2 and 27.8 degrees
[NASA-TM-X-65464] 09 p1385 N71-20289

Swedish/NASA rocket sounding in auroral D and E regions for ionospheric ion and electron density investigation using Arcas and Petrel rocket vehicles
[REFR-S3-X-68-44] 10 p1532 N71-31129

Ion detection and monopole mass spectrometer performance tests with transverse magnetic field and titanium getter pump pumping capacity for D region ion composition analysis
[NASA-CR-117985] 12 p1921 N71-25708

D region electron density distribution and energy spectra of solar X rays during quiet periods and solar flares of 30 Oct. 1969
[AD-719841] 13 p2161 N71-25157

Near infrared radiometer for use on small sounding rockets to observe radiation emission in D region during daytime
[NASA-TM-X-65548] 15 p2411 N71-27045

Electron and positive ion densities and their relationship to ionization sources in equatorial D region
[NASA-TM-X-65635] 19 p3095 N71-32679

Equatorial D region positive ion composition studies by rocket payloads
[NASA-TM-X-65631] 19 p3095 N71-32208

D region electron density profiles at geomagnetic equator based on riometer and absorption experiments
[RSD-57] 20 p3267 N71-33528

Low frequency vertical pulsed sounder design with digital integration and pseudo-random phase coding for ionospheric D-region sounding
[AD-727013] 22 p3580 N71-35409

Development of method for deriving electron density profiles in D region of ionosphere during solar flares
[RSD-62] 22 p3463 N71-36112

Absorption and group delay data from equatorial station used to model electron density profile in D and E regions of ionosphere
[NASA-TM-X-65730] 24 p3909 N71-37803

Paradise rotation technique for determining electron densities in D region
[NOAA-TR-ERL-203-SEL-21] 24 p3917 N71-37819

DACRON (TRADEMARK)

Mechanical properties of Dacron parachute fabric in simulated Martian atmosphere
[NASA-TN-D-6242] 16 p2616 N71-28132

DARNO (DATA ANALYSIS)

U DATA PROCESSING

U DATA REDUCTION

U DATA TRANSMISSION

DAKOTA AIRCRAFT

U C-47 AIRCRAFT

DAMAGE

NT IMPACT DAMAGE

NT METEORITIC DAMAGE

NT PROTON DAMAGE

NT RADIATION DAMAGE

NT RAIN IMPACT DAMAGE

Reliability, cumulative damage, and redundancy in multicomponent systems
[AD-722469] 18 p2944 N71-36894

Estimates of lightning caused computer component damage and malfunctions
[AD-722675] 18 p2897 N71-31413

Structural engineering and meteorological analysis of damage resulting from Lubbock, Texas storm of 11 May 1970
[PB-198377] 19 p1329 N71-31406

Statistical, cause/factor and injury tables, accident rates, and briefs of accidents involving US carriers in 1969
[NTSB-ARC-71-1] 23 p3708 N71-34407

Damage control systems for detecting and locating overboard and onboard leak and damage modes on space stations
[NASA-CR-111963] 23 p3857 N71-37495

Damage resulting from San Fernando, California earthquake of 9 Feb. 1971
[PP-733] 24 p3917 N71-37803

Economic, administrative, and legal factors affecting freight loss and damage
[AD-726765] 24 p4035 N71-36708

DAMPERS (VALVES)

Mathematical model for predicting damping time of mercury damper
[AD-722603] 17 p2851 N71-29431

DAMPING

NT ELASTIC DAMPING

NT LANDAU DAMPING

NT VIBRATION DAMPING

NT VISCOUS DAMPING

Elastic stability and equilibrium configuration of earth pointing gravity gradient satellites with long pendulums
[CRC-1206] 01 p0127 N71-10918

Techniques for determining resonant frequencies, mode shapes, and damping coefficients of modal structures
[SC-D8-70-72] 01 p0130 N71-10912

Coherent stability and damping of detonation wave in aerosols
[AD-71753] 01 p0044 N71-10940

Damping of coherent oscillations in synchronous beam excitations
[ANL-TRANS-846] 03 p0420 N71-12945

Anelastic study of dislocation damping in gold
[COO-1196-725] 03 p0440 N71-13980

Estimation of momentum transfer dependent damping of motions from factors due to pseudocubic pions [JVO-2262-TA-224] 07 p1070 N71-17034

Anomalous damping of large-amplitude electron plasma oscillations - computer experiments [AD-715074] 07 p1084 N71-18091

Model for Hamiltonization and quantization of relatively damped systems 08 p1227 N71-19156

Establishment of conditions for existence of normal modes of damped, nonlinear systems with many degrees of freedom 10 p1637 N71-21396

Perturbation method extension for nonlinear panel flutter to include fifth-order nonlinear terms effect, flutter-backing interaction, and small damping terms [NASA-CR-117504] 10 p1658 N71-21672

Utilization of momentum devices for forming attitude control and damping system for spacecraft [NASA-CASE-XLA-02551] 10 p1600 N71-21708

Effects of sound damping elements in subsonic wind tunnels [RAE-LIB-TRANS-1465] 11 p1796 N71-21885

Spacecraft attitude damping stability by means of dual spin stabilized system [ESRO-CR-24] 12 p1960 N71-23717

Support theory based on magneto-fluid-mechanics turbulent damping [J-4567] 12 p1993 N71-24192

Three stage motion restraining mechanism for restraining and damping three dimensional vibrational movement of gimbaled package during launch of spacecraft [NASA-CASE-GSC-10306-1] 13 p2085 N71-24694

Asymptotic model with damped gravity waves from vertical atmospheric sounding analyses 13 p2076 N71-25264

Iris disk slot geometry effects on waveguide dispersive properties and wave damping coefficients [KFK-TR-334] 14 p2231 N71-26775

Materials damping measurements of glass fiber-reinforced and boron fiber-aluminum composites [AD-721191] 15 p2427 N71-26821

Dual-spin spacecraft stability noting nutation damping and uniform stabilization [JES-55-52] 15 p2519 N71-27152

Derivation of asymptotic stability and instability conditions for elastic systems with dissipation [AD-721384] 16 p2687 N71-28717

Mathematical model for predicting damping time of mercury damper [AD-722093] 17 p2851 N71-29421

Structural damping in Saturn vehicles and scale models of liquid propelled rocket vehicles [NASA-TM-X-64667] 18 p3018 N71-31145

Quantum mobility and nuclear spin echo damping in impure crystals [WUB-2069] 18 p2999 N71-31486

Nonlinear angular velocity aerodynamic damping coefficient effects on statically stable missile configurations and internal mass distribution effect based on wind tunnel stability tests [AD-721131] 24 p4022 N71-38697

BALANCE FACTOR

DAMPING

DAMPING IN FITCH

U DAMPING

U FITCH [INCLINATION]

DAMPING IN ROLL

U DAMPING

U ROLL

DAMPING IN YAW

U DAMPING

U YAW

DAMPERS

U MOISTURE CONTENT

DAMP

Computerized sealing dam design analysis for gas flow seal of turbohaft 02 p0237 N71-12039

DANGER

U HAZARDS

MET TURBOFAN ENGINES

U TURBOFAN ENGINES

MAR HELICOPTER

U QR-30 HELICOPTER

DATA ACQUISITION

Digital computer system hardware for data acquisition and control of 60 ft X beam parabolic antenna [AD-705999] 01 p0027 N71-18020

Measurement of delayed neutron energy spectra [JLO-2215-1] 01 p0009 N71-18717

Permuting and transmission of data from oceanographic sensors [AD-71336] 03 p0223 N71-11386

Research progress on multispectral data collection and infrared instrumentation for specially configured aircraft 03 p0227 N71-11984

History of meteorological satellites launched to date, and type of data acquired from TIROS, ESSA, and Nimbus for climatological application 02 p0361 N71-12182

Signal data acquisition and processing of environmental test objects 03 p0357 N71-12714

Technique for improving quality and acquisition of frequency response and vibration data [NASA-TN-D-7022] 03 p0460 N71-12734

Functions of NASA Office of Tracking and Data Acquisition [NASA-TM-X-64529] 04 p0489 N71-13482

Airborne data acquisition system incorporating recycling metal tape flight data recorder 04 p0505 N71-13836

Remote data acquisition terminals for aerospace vehicles 04 p0505 N71-13837

Real time data acquisition and processing unit installed at Linell for carrying out nuclear experiments [CEA-CONF-1522] 04 p0508 N71-13856

Airborne multispectral data collection and ground based reproduction facilities [NASA-CR-108717] 04 p0516 N71-14467

Data collection of aviator knowledge, skill, and satisfaction in combat readiness training [AD-713115] 05 p0636 N71-14665

A2/NOSET - CONSISTENCY OF DATA [UCRL-19845] 05 p0741 N71-15119

Software for on-line controlled triple-axis spectrometer [RT/EL/70/2] 05 p0687 N71-15450

Meteorological data collected by buoy in Gulf of Mexico [AD-713479] 05 p0679 N71-15523

Meteorological radar data acquisition and processing equipment [AD-714764] 06 p0890 N71-16015

Development of telemetry system for position location and data acquisition [NASA-CASE-GSC-10083-1] 06 p0945 N71-16090

Hypervelocity wind tunnel data acquisition [DLR-FB-70-44] 07 p1003 N71-17046

Deep Space Network tracking and data acquisition and scientific instruments for Pioneer 6 09 p1464 N71-19413

On-line data acquisition system using LINC-8 computer for plasma physics experiment [CLM-R-104] 09 p1448 N71-19983

Data acquisition system used with electron linear accelerator for neutron capture gamma ray experiments - metallurgical and other program notes 10 p1528 N71-20901

Reference frequency generator and modulator for airborne data acquisition system [AERL/F-44] 11 p1724 N71-22441

On-line real time system for experimental data collection and processing using IBM 1800 DACS [TB-69] 11 p1716 N71-22545

Data acquisition from bubble chamber photographs of nuclear reactions [CEA-N-1397] 13 p2129 N71-24671

Data dissemination activities of Environmental Data Service and Weather Bureau 13 p2071 N71-25003

Tracking and data acquisition, scientific events and measurements, and engineering support for Pioneer 8 space probe [NASA-CR-118328] 13 p2174 N71-25128

Instrumented orbital platforms for remote data acquisition and location systems 13 p2110 N71-25331

On-line digital computer system for real time acquisition and processing of data at Materials Analysis Section of Quality and Reliability Assurance Laboratory 13 p2053 N71-25392

Tables of interplanetary high energy particles, solar phenomena, and plasmas taken by Pioneer 7 space probe [NASA-CR-117961] 14 p2336 N71-25815

Tsunami wave reporting and data acquisition manual for tide observers [COM-71-00170] 14 p2251 N71-26541

Data acquisition system for converting displayed analog signal to digital values [NASA-CASE-NFO-10344] 14 p2235 N71-26544

MIDAS double computer system for controlling acquisition, processing, and storing of measured nuclear data [JNF-18562] 14 p2227 N71-26727

Data acquisition and processing system with buffer storage and timing device for magnetic tape recording of PCM data and timing information [NASA-CASE-NFO-12107] 15 p2383 N71-27255

Synchrocyclotron particle identification and data acquisition system based on computers and multiple input converter [LYCEN-7049] 15 p2384 N71-27298

PDP 8 computer techniques in reactor physics including data acquisition and reduction of absorption cross section, radiation, noise-time, and neutron lifetime and reactivity measurements [RT/F-78/16] 15 p2451 N71-27739

Optical tracking data from geodetic satellites for deep space station coordinates [NASA-TM-X-65559] 15 p2442 N71-27847

Manual for human psychometric data acquisition and human reactions to psychological stress in Telitile project [AD-713163] 16 p2554 N71-28549

Cutoff sampling of data for repetitive surveys [BM-IC-8516] 17 p2880 N71-29259

Variety and hierarchy of data extraction methods in nuclear reactor noise analysis with systematic approach to data collecting and data handling problem [TKK-F-A-137] 17 p2706 N71-30314

Data acquisition system for US-2A aircraft training flight evaluations [AD-722983] 18 p3096 N71-31547

Computer program system for failure analysis data acquisition systems with on-line programming capabilities [NASA-TM-X-2331] 18 p2896 N71-31398

Electronically controlled camera system for optical satellite triangulation data acquisition 19 p3099 N71-31873

Acquisition and storage of militarily significant data on climatology, hydrology, soils, and ecology of humid tropical regions [AD-723066] 19 p3193 N71-32829

Computer characteristic and failure mode recording and data acquisition system design for determining component reliability [NRL-RLISLEY-TRANS-1928-7001-99] 19 p3106 N71-32718

BOMAP plans for BOMEX core data acquisition and analysis 19 p3200 N71-32752

Abstracts of conference papers on preliminary results from BOMEX and methods and techniques used to collect data 19 p3201 N71-32756

Acquisition of data in Caribbean related to energy exchange between ocean surface and atmosphere - Project BOMEX 20 p3369 N71-32886

Mobile and fixed data collection platforms for constant level balloons and remote ground locations, for platform-satellite-ground station system [NASA-CR-121374] 20 p3270 N71-32895

Nuclear reactor, nuclear structure, data acquisition, proportional and spark counters, accelerator performance, and health physics 20 p3324 N71-33878

Acquisition of data on federal R and D efforts related to command and control center design and law enforcement communications for civil disturbances [NASA-CR-121639] 21 p3389 N71-34112

Description and operation of outer planet data presentation computer program [NASA-CR-121748] 21 p3398 N71-34181

Sample data cases for outer planet data presentation computer program [NASA-CR-121747] 21 p3398 N71-34182

Air data sensors and measurement system for integration into space shuttle vehicles 21 p3513 N71-35035

Measurable qualities of basic sciences in Turkey from 1933 to 1966 [PUBL-17] 21 p3532 N71-35171

Application of optically diagnosed noise information toward development of filtering subroutines for improvement of digital sensing data type quality - Vol. 1 [NASA-CR-121978] 22 p3582 N71-35510

RAD swapping system for nuclear data acquisition utilizing set of Symbol programs [PUC-937-396] 22 p3644 N71-35978

Application of ground-truth data to monitor sensor calibrations for Earth Resources Technology Satellites - Vol. 2 [NASA-CR-121979] 24 p3919 N71-37945

Reliability data acquisition on spacecraft life support systems during ground and orbital experiments 24 p0015 N71-38646

DATA ADAPTIVE EVALUATOR/MONITOR

U DATA PROCESSING

U DATA REDUCTION

U DATA TRANSMISSION

DATA ANALYSIS

U DATA PROCESSING

U DATA REDUCTION

DATA COMPRESSORS

U DATA REDUCTION

U DATA TRANSMISSION

DATA CONTROL SYSTEMS

U DATA SYSTEMS

DATA CONVERSION ROUTINES

NT SUBROUTINES

DATA CONVERTERS

NT ANALOG TO DIGITAL CONVERTERS

NT BINARY TO DECIMAL CONVERTERS

NT DIGITAL TO ANALOG CONVERTERS

Development and testing of meter for measuring watt-hours and ampere-hours over wide range of voltages and currents [NASA-CR-115797] 04 p0510 N71-13523

Describing line to pulse height converter with timing compensation for p-i-n detectors [CEA-N-1334] 04 p0574 N71-13473

Channel punch code-converter for telegraph systems to transmit information manually and automatically [AD-717805] 10 p1317 N71-30730

Synchrocyclotron particle identification and data acquisition system based on computers and multiplexed input converter 15 p2384 N71-27298
[LYCEN-7049]

High reliability, low input voltage converter with synchronous rectifying transistors for dc to ac to dc conversion [NASA-CASE-GSC-11126-1] 16 p2569 N71-28419

DATA CORRELATION

NT SIGNAL ANALYSIS

Comparison of ionospheric sounding electron concentration and electron and ion temperature data in F region 01 p0046 N71-10228

Investigating remote sensing applications to simple geological features using microwave radiometers 02 p0227 N71-11990

Various statistical tests for trends in data based on variation in run length 04 p0501 N71-13503

Correlation of rod bundle critical heat flux for water in pressure range 150 to 725 psia [IN-1412] 04 p0554 N71-14011

Reproducibility of soil classification and compaction test data 05 p0667 N71-14694

Correlation of plutonium enriched reactor core data [BNWL-1453] 05 p0723 N71-14714

Constructing digital correlation measuring device from 1 to 15 MHz for measurement of electron-density correlations in reverse-brush cathode plasma [IPJP-DT-16] 05 p0753 N71-15182

Applying canonical correlations to forecasting characteristics of meteorological fields [AD-713774] 05 p0718 N71-15263

Gamma-gamma directional correlation and intensity studies of electromagnetic transitions of Ta-181 [COO-1746-46] 07 p0177 N71-17551

Correlations between diurnal indices of cerebral and systemic circulation 08 p1155 N71-19069

Infrasound microbarometric phenomena correlation with long period seismograph signals [AD-716533] 09 p1382 N71-19628

Comparison of solid propellant nozzle heat transfer coefficients with predicted data [NASA-TM-X-66997] 10 p1661 N71-21201

Computer program for correlation and spectral analysis of reactor flow data statistics [DP-1244] 15 p2444 N71-26980

Design of automatic data correlation system for Earth Resources Program [NASA-CR-115063] 16 p2564 N71-28003

Program summary for implementation of automatic data correlation system for Earth Resources Program [NASA-CR-115062] 16 p2564 N71-28004

Nuclear reactor transfer functions based on inter-correlation of responses from two neutron counters [LFEN-NI-58-A] 17 p2783 N71-29527

Formulation of theorems for obtaining correlation averages for wide class of model systems with four fermion interaction [ITE-70-53] 18 p2973 N71-30539

Anthropometric size determination techniques and adult male and female data correlations from U.S., Australia, Europe, and Asia 18 p2878 N71-31481

Multiple correlation of university and flight training biographical information as management tool in personnel selection for pilot training [AD-717941] 19 p3047 N71-31620

Pilot training performance data correlation in performance and probability estimation of training completion for advanced training personnel selection [AD-718448] 19 p3047 N71-31621

Neutron detector data correlations for determining kinetic parameters of nuclear reactor [CEA-N-1406] 19 p3136 N71-32068

Correlation of calcium H and K line profiles with sunspot numbers and Mg 5172 A line position shifts in relation to chromospheric activity 19 p3176 N71-32254

Calculations and data correlation procedures for Fraunhofer line discriminator operating over open water [NASA-CR-121427] 20 p3272 N71-33202

Measurement and correlation of gas-particle heat transfer coefficients in packed and fluidized bed processors by frequency response techniques [RPI-3639-16] 21 p3411 N71-34268

Handbook of correlative data on galactic cosmic rays, solar electromagnetic radiation, solar protons, geomagnetism, ionosphere, and neutral atmosphere [NASA-TM-X-67294] 21 p3532 N71-35168

Correlation of calculated and experimental product yields as functions of gas molecule residence time, power, gas pressure, and allyl alcohol in electrosynthesis of hydrazine from ammonia [ICRC/N343] 23 p3719 N71-36510

Comparison of performance data envelopes for thermionic diodes with various tungsten or rhenium emitters and sodium or molybdenum collectors [NASA-TM-X-67935] 23 p3731 N71-36595

Atmospheric diffusion of beryllium exhaust gases from solid propellant rocket engines correlated with meteorological parameters [AD-726999] 23 p3840 N71-37383

DATA HANDLING SYSTEMS

U DATA SYSTEMS

DATA LINKS

Systems engineering and economic analysis of tracking and data relay satellite system with 16 GHz ground antenna [NASA-TM-X-65370] 01 p0025 N71-10800

Performance tests of convolutional decoder systems for high data rate telemetry links [NASA-CR-114270] 15 p2383 N71-27786

PDP 9 interface for data transfers between nuclear experiments and computer [HMI-B-102] 16 p2899 N71-30481

Transmission system for data generated by flying spot device into Razdan-3 computer [ITEF-779] 18 p2893 N71-30589

Data bus for avionics system of space shuttle, noting functions of interface unit, error detection and recovery, redundancy, and bus control philosophy [NASA-CR-115187] 23 p3756 N71-36771

DATA MANAGEMENT

Discriminant analysis model for rating research and development data programs [AD-716812] 10 p1665 N71-21043

Performance evaluation of two real time operating systems using simulation models 11 p1720 N71-22784

Data processing facilities for Black Knight rocket measurements in Great Britain [FOA-3-C-3616-68] 14 p2237 N71-26258

System configuration and executive requirements specifications for reusable shuttle and space station base [NASA-CR-1820] 15 p2383 N71-27018

Airborne/spaceborne computer design and techniques for space shuttle data management systems [NASA-CR-115032] 15 p2584 N71-27782

Bin-plane encoding and other aperture methods for data redundancy removal for onboard spacecraft data management 19 p3063 N71-32543

Modification to initiator which allows memory location assignment to particular initiator for batch processing [P-4585] 21 p3400 N71-34198

Design and development of subsystem interface unit, bus control unit, and supporting equipment for space shuttle data processing equipment 21 p3516 N71-35055

Characteristics and advantages of data bus to facilitate data handling process on space shuttles 21 p3517 N71-35056

Development and application of data bus techniques for space shuttle data management systems 21 p3517 N71-35057

Application of self-sequencing data bus techniques for space shuttle data management system 21 p3517 N71-35058

Procedures for development and verification of complex software used in space shuttle data management system 21 p3517 N71-35059

Development and characteristics of executive software for application to space shuttle data management system 21 p3517 N71-35060

Development of computer programming language for use on space shuttle 21 p3517 N71-35061

Analysis of bulk storage data requirements and methods for visual display of information on space shuttle display devices 21 p3517 N71-35062

Characteristics of Space shuttle data management system for data transmission and service for avionics equipment and other subsystems 21 p3518 N71-35065

Failure effects analysis of guidance, navigation, and control, data management, and communications subsystems [NASA-CR-115131] 21 p3519 N71-35079

Pre-processor, post-processor, and multiple level substructuring routines for data management in support of NASTRAN finite element structural analysis of spacecraft 22 p3688 N71-36298

Scattering cross section preparation and testing for evaluated nuclear data file and JOSEPHUS system data management and communication [ITD-25600] 23 p3816 N71-37214

DATA PROCESSING

NT BATCH PROCESSING

NT CENTRAL ELECTRONIC MANAGEMENT SYSTEM

NT DATA CORRELATION

NT DATA REDUCTION

NT DATA RETRIEVAL

NT DATA SMOOTHING

NT DATA STORAGE

NT OPTICAL DATA PROCESSING

NT PARALLEL PROCESSING [COMPUTERS]

NT SIGNAL ANALYSIS

NT SIGNAL PROCESSING

NT VOICE DATA PROCESSING

Meteorological satellite data processing and interpretation [NASA-TT-F-511] 01 p0077 N71-10000

Computer processing of meteorological satellite data 01 p0077 N71-10001

Cloud analyses from meteorological satellite television and infrared pictures 01 p0078 N71-10099

Data evaluation for ATS 5 millimeter wave measurements of meteorological parameters [NASA-TM-X-65371] 01 p0023 N71-10604

Parallel data processing [AD-711651] 01 p0029 N71-10707

Use of computers for man machine modeling studies and plans [AD-711638] 01 p0015 N71-10808

Task analysis reduction technique for analyzing human performance and man machine interface [AD-711807] 02 p0169 N71-11110

Impact of technological trends on improving information network systems [PB-192494] 02 p0213 N71-11196

Set theory and processing of large data bases [AD-711060] 02 p0191 N71-11340

Ground data handling aspects of EROS Program from users viewpoint [PB-193666] 02 p0213 N71-11196

Reviewing research on processing data from multispectral band scanners for agricultural applications 02 p0191 N71-11190

Radar and data processing techniques for designing space radars for earth resources applications 02 p0185 N71-11199

Real time processing of acoustical and oceanographic data aboard research vessel [AD-711598] 02 p0221 N71-12140

Computer processing of satellite cloud pictures 02 p0261 N71-12181

Interact node/Automated Sneak Program [NASA-CR-108724] 03 p0339 N71-12459

Description of Node Report Data Generation Program [NASA-CR-108742] 03 p0339 N71-12452

Computer program to satisfy data requirements of Path Derivation Program [NASA-CR-108736] 03 p0341 N71-12477

TAP and SCRAP - programs for processing data from automatic gas analysis equipment using PDP/9 computer [RD/B/N-1581] 03 p0342 N71-12478

Grumman preprocessor - Automated Sneak Program [NASA-CR-108732] 03 p0343 N71-12490

Investigating system requirements of airborne data processors 03 p0408 N71-12608

Digital data processing for designing automatic flight control systems 03 p0409 N71-12614

Evaluating tracking and orbit determination functions and supporting equipment for Apollo instrumentation ships [NASA-CR-111576] 03 p0455 N71-12620

PROF GROUCH-G - processing code for group constants for fast reactor [JAERI-1192] 03 p0416 N71-12696

Radar meteorology and data processing for Doppler radar systems [PB-191960] 03 p0403 N71-13116

Automatic computation of integrated average radius deviation during latitude scan [Y-1730] 03 p0381 N71-13015

Data processing and display system for terminal guidance of X-15 aircraft [NASA-CASE-XPR-00756] 04 p0474 N71-13431

Binary decision graph for analyzing validation of complex information processing models 04 p0499 N71-13493

Centralized on-line data processing system providing concurrent service for five test facilities [NASA-TN-D-6088] 04 p0502 N71-13580

Digital computer processing of OSIRIS research reactor [CEA-CONF-1569] 04 p0548 N71-13644

Activities of Australian National University Department of Physics for 1969 [ANUP-P-484] 04 p0574 N71-13688

Real time data acquisition and processing unit installed at Limerick for carrying out nuclear experiments [CEA-CONF-1522] 04 p0508 N71-13759

Systems analysis for data processing in industry 04 p0508 N71-13759

Computer control of phased array radar system for simultaneous multiple target tracking 04 p0498 N71-13718

Statistical comparison of computer logics for controlled radar tracking of air traffic 04 p0498 N71-13715

Computerized radar plot extractor module for automatic air traffic control 04 p0498 N71-13716

- Data processing, man machine systems, and solid state physics and devices
[AD-712699] 04 p0623 N71-13964
- Midrange data counting and time tagging
[NASA-TM-X-45391] 04 p0612 N71-14124
- Airborne multispectral data collection and ground based reproduction facilities
[NASA-CR-109717] 04 p0516 N71-14467
- Computerized analysis of consolidation soil test data
[PB-194036] 05 p0667 N71-14698
- Adaptive learning computer system for raw data processing
[AD-713543] 05 p0650 N71-14874
- Application of digital associative machine in information processing methods
[AD-713769] 05 p0650 N71-14950
- Cross section generation and data processing techniques for nuclear rocket shielding methods, modification, updating, and input data preparation - Vol. 3
[NASA-CR-109966] 05 p0728 N71-15164
- Descriptions and indexes of data contained in Solar-Geophysical Data publication
05 p0765 N71-15405
- Acquisition and processing of X ray data from Southern Hemisphere sky
[NASA-CR-115596] 05 p0765 N71-15491
- Selection of techniques and equipment for analysis of random and unique data
[ARL/ME-312] 05 p0652 N71-15499
- Computer programs for oceanographic data processing
[AD-713491] 05 p0679 N71-15522
- Study visit for exchanging information on data processing applicable to rocket testing
05 p0652 N71-15529
- Meteorological data processing, laser meteorology, and distribution functions
05 p0720 N71-15679
- International system for neutron nuclear data compilation and evaluation
[BUNFNR-782] 06 p0907 N71-15729
- International studies on air pollution, atmospheric heat budget, and real time data processing operations
06 p0806 N71-15755
- Using adjustable values for processing aerial photographs in photogrammetric instruments
05 p0857 N71-15774
- TREESTAR subroutine package in FORTRAN 4 for manipulation of tree structured data
[NASA-CR-116145] 06 p0818 N71-15911
- Data processing program activities at Laboratory for Agricultural Remote Sensing, Purdue
06 p0845 N71-16154
- Data processing and interpretation of remote sensed data for agricultural purposes
06 p0846 N71-16163
- Digital data processing techniques and supporting hardware
[AD-714378] 06 p0849 N71-16321
- Information systems and processing, linguistics, artificial intelligence, and human information processing
[PB-194796] 06 p0963 N71-16897
- Data recordings and computer codes for airport field transit access system study
[PB-195048] 07 p1002 N71-16989
- Computerized analysis of data on high altitude barion release
[BROG-1183-3007] 07 p1015 N71-16997
- Hypervelocity wind tunnel data acquisition
[DLR-FB-70-44] 07 p1003 N71-17046
- Characteristics and operation of automatic film scanning device used with digital computer
[UCRL-19842] 07 p0996 N71-17163
- Characteristics of automated quantometer data handling system
[Y-1740] 07 p1027 N71-17183
- Weather outline generators for producing contours around radar weather clutter for all weather air navigation
[FAA-NA-70-42] 07 p1054 N71-17527
- FORTRAN code for verifying ENDF/B photon production data
[LA-4506] 07 p1078 N71-17608
- Sequential estimation with process noise for processing DSN tracking data during planetary orbiters and Doppler determinations of polar motion using satellites
07 p0993 N71-17615
- Simulating seismic rays, computing travel times, and approximating amplitudes in earth models
[AD-715134] 07 p1022 N71-17813
- Year real time ionospheric MOF forecasting over 60 km path
[AD-714993] 07 p1023 N71-17859
- Data processing summary for OGO radio astronomy experiments
[NASA-CR-116434] 07 p0998 N71-18058
- Controlled processing of picture data from astronomical satellites
[AD-715092] 08 p1230 N71-18459
- Timeliness ground station descriptions
[NRL-MITT-70-17] 08 p1175 N71-18466
- Effects of barometric pressure fluctuations on data recorded by inertial seismic equipment
[AD-715886] 08 p1190 N71-18756
- ATS 5 ground station magnetometer data processing program
[NASA-TM-X-45457] 08 p1166 N71-19082
- Feasibility and applications of scientific and technical information analysis centers
[AGARD-CP-78-71] 09 p1346 N71-19536
- Concept, mission, and operation of scientific and technical information analysis centers
09 p1347 N71-19527
- Transmission and analysis of cardiological data on athletes
09 p1329 N71-19589
- Peak strip and normalizes subroutines for analyzing gamma ray spectra
[MLM-1773] 10 p1611 N71-20096
- User machine-oriented languages for simple data processing
10 p1527 N71-20822
- Photogrammetric data preparation manual for analytical triangulation program, MUSAT 4
[AD-717168] 10 p1548 N71-20907
- Analysis of centralized data processing system in Czechoslovakia
[JPRS-52674] 10 p1665 N71-21063
- Multiple perception element construction method for recognition of photograph patterns
[AD-717056] 10 p1559 N71-21149
- Procedures for processing atmospheric composition data obtained through use of sweeping quadrupole mass spectrometer onOGO-4 satellite
[NASA-CR-117325] 10 p1529 N71-21544
- Mathematical filter for eliminating persistence in meteorological data
11 p1788 N71-21940
- Low power data processing approach for reduction in sonobuoy compass problems
[AD-717406] 11 p1792 N71-21967
- Atmospheric optical line of sight communication system and application of multichannel spatial diversity to improve communication effectiveness
11 p1699 N71-21999
- Cloud three dimensional nephelometry program
[AD-717653] 11 p1790 N71-22363
- Data processing procedures and instrument development for space radiation measurements
11 p1827 N71-22418
- Off-line processing of chromatographic data from fatty acid methyl ester mixtures by digital computer
[UCRL-72393] 11 p1716 N71-22548
- Automation of control systems for processing scientific measurement data
[JPRS-52745] 11 p1717 N71-22726
- Algorithm elements for closed cycle control of complex scientific experiments
11 p1718 N71-22727
- Systems engineering planning methodology of automation systems for complex experiments
11 p1718 N71-22729
- Machine algorithm statistics for processing experimental data
11 p1718 N71-22730
- Data processing algorithm for real time digital modeling of dynamic systems
11 p1718 N71-22731
- Automation system planning for experimental data processing
11 p1718 N71-22734
- Data processing system parameters for complex experiments
11 p1718 N71-22735
- Two way information exchange in experimental data processing system
11 p1719 N71-22736
- Oncological data processing system using general purpose computer and graphic input device
11 p1719 N71-22737
- State of the art review on computerized processing of scientific data
11 p1719 N71-22744
- Provisional model of visual information processing with sequential inputs
11 p1720 N71-22764
- Deep Space Network functions, facilities, operations, and research for support of space communications and flight programs
[NASA-CR-117649] 11 p1829 N71-22766
- Structures of biological information processing and pattern recognition in living systems
11 p1683 N71-23056
- Computer developments in USSR and industrial applications in automation and information processing
[JPRS-52809] 12 p1881 N71-23444
- Research projects in electronic data technology and solid state physics
[AD-718149] 12 p1892 N71-23542
- Data acquisition and reporting from remote test station interfaced with CDC-3300 computer
[Y-1748] 12 p1882 N71-23594
- Automatic identification and classification of wheat from airborne multispectral data in agricultural remote sensing
[REPT-779] 12 p1913 N71-23731
- Analysis of sampled data reconstruction errors from digital data processing
12 p1884 N71-23872
- Computer system for development and application of high resolution mass spectrometer
12 p1922 N71-24052
- Azimuth and elevation angle determination from UNH/AFRL motor trails interferometric radar, using computer processing
[AD-718165] 12 p1997 N71-24111
- Scientific and technical information processing and dissemination nationally and internationally
[NLL-M-20529-5828.4P/1] 12 p2019 N71-24270
- Design of observation and data processing systems for use in first Global Atmospheric Research Program (GARF) experiment
13 p2104 N71-24423
- Fourier transformable properties of paraboloidal mirror segments also experimental results of spatial filtering
[NASA-TM-X-45320] 13 p2125 N71-24887
- Automatic processing of hydrometeorological data for information retrieval system
[AD-719857] 13 p2107 N71-25136
- Nuclear data processing from TIMOC Monte Carlo library ENDF/B file using CODAC FORTRAN 4 program
[EUR-4521-E] 13 p2134 N71-25163
- Digitalized optical detectors for cloud data processing onboard satellite using Fourier analysis
13 p2126 N71-25321
- Stored program computer for onboard spacecraft data processing
13 p2052 N71-25325
- Computer processed performance data for thermionic converter with etched rhenium emitter and nichium collector
[NASA-TM-X-45262] 13 p2053 N71-25388
- On-line digital computer system for real time acquisition and processing of data at Materials Analysis Section of Quality and Reliability Assurance Laboratory
[NASA-TM-X-44587] 13 p2053 N71-25392
- Hybrid analog computer for magnetogram data processing
13 p2053 N71-25409
- Spatial processing characteristics in perception of brief visual arrays
[AD-719797] 14 p2207 N71-25423
- Algorithms of self organization, artificial intelligence, and tree search applied to various practical problems
[AD-719930] 14 p2207 N71-25452
- Encoders designed to generate comma free biorthogonal Reed-Muller type code comprising conversion of 64 6-bit words into 64 32-bit data for communication purposes
[NASA-CASE-NPO-10595] 14 p2332 N71-25917
- Statistical algorithms and computer programs for remote sensor multispectral data analysis
[NASA-CR-103182] 14 p2320 N71-25921
- Computer program for processing automatically collected navigational and sounding data on Minck-22 computer
14 p2348 N71-25972
- Computer program for linguistic data processing including translating text from Russian into English
14 p2222 N71-25984
- Integration of text processing and written communication into management information systems
14 p2223 N71-25991
- Information system as subject of information science and informatics - terminological aspects
14 p2223 N71-25992
- Model describing symmetrical information processing along visual pathways of brain
[NASA-CR-118517] 14 p2205 N71-26204
- Data processing system for meteor trail radio communication equipment
[FOA-3-C-3597-43] 14 p2219 N71-26533
- Evaluating requirements for data plotting equipment for Florida highway department
14 p2226 N71-26563
- Electro-optical measurement and data processing techniques
[FOA-3-C-3614-42] 14 p2290 N71-26596
- MIDAS double computer system for controlling acquisition, processing, and storing of measured nuclear data
14 p2327 N71-26737
- Production of a high altitude urban land use map and data base for Boston sector of Massachusetts
[NASA-CR-118678] 14 p2252 N71-26796
- Binary classification routine time and human performance in data processing using decision making experiments
[AD-721199] 15 p2374 N71-26883
- Data acquisition and processing system with buffer storage and timing device for magnetic tape recording of PCM data and timing information
[NASA-CASE-NPO-12107] 15 p2363 N71-27235
- Comparison of multivariate statistical analysis techniques for multibeam selection indices
[NASA-CR-115868] 16 p2630 N71-28001

- Data processing methods for improving FPS-16 radar/limb system measurements of atmospheric motion
[NASA-CR-118997] 16 p2624 N71-28062
- Display system information content characteristics and relationships with operator performance and psychophysiological factors in data processing
[JPRS-53244] 16 p2541 N71-28093
- Maintenance and improvements associated with operation of NRL Van de Graaff accelerator
[AD-721329] 16 p2577 N71-28175
- Experimental data analysis on forward elastic pion /plus or minus/ proton scattering in model-independent way
[JINR-E2-5561] 16 p2647 N71-28239
- Data handling method for satellite TV broadcast system design, and data analysis and plotting by computer techniques
[NASA-CR-119831] 16 p2561 N71-28427
- Reconstruction of ultraviolet brightness of stars by SAO from video data obtained in Telescope experiment
16 p2679 N71-28520
- Effect of spaced data interpolation upon harmonic coefficients
[AD-721593] 16 p2623 N71-28565
- Tropical wind flow patterns from automated analysis of streamlines, streamfunctions, divergence, and vorticity in tropics with feasibility of wind analysis using ATS data
[AD-721365] 16 p2626 N71-28597
- Digital data handling circuits for pulse amplifiers
[NASA-CASE-XNP-01068] 16 p2573 N71-28739
- Composition and mass data analysis of meteoroids in 1 milligram to 1 gram range using NASA LRC Paint Meteor Spectra Patrol data
[NASA-TN-D-6298] 16 p2578 N71-28802
- Real time capability, satellite monitoring, and system reliability of satellite recording and data base system - Tables of costs and schedules
[COM-71-00220] 16 p2590 N71-28874
- Data processing techniques and equipment used in analysis of Lunar Orbiter 1 and 3 and Explorer 35 bi-static-radar data
[NASA-CR-119033] 16 p2564 N71-29063
- Statistical analysis of Saturn 5 test data for determination of safety factor requirements of untested structures
16 p2688 N71-29096
- Experimental determination of data on liquid-vapor equilibrium systems
[NLL-RTS-5746] 17 p2713 N71-29218
- Sensor magnetometric data processing including magnetic field and radial velocity distributions
[NLL-RTS-6194] 17 p2840 N71-29282
- Organization and data input format of geomagnetic World Data Center
[REPT-7] 17 p2739 N71-29434
- Onboard optical data processing for earth resource spacecraft and planetary spacecraft
[NASA-TM-X-65603] 17 p2723 N71-29683
- Computer and data processing developments
[CERN-71-45] 18 p2892 N71-30484
- Color photogrammetry for Nimbus infrared radiation data analysis
[NASA-TM-X-65614] 18 p2909 N71-30590
- Composite parts of compression coefficient in data processing systems
[NASA-TT-F-13790] 18 p2894 N71-30857
- Reliability, cumulative damage, and redundancy in multicomponent systems
[AD-722469] 18 p2944 N71-30894
- Reduction and analysis of data from Explorer 15 and Explorer 26 satellites
[NASA-CR-119286] 18 p3003 N71-30919
- Particle detection equipment and particle data processing systems used with Explorer 15 and Explorer 26 satellites
18 p2923 N71-30932
- Compilation and comparative analysis of observations of lunar transient phenomena
[NASA-TM-X-65528] 18 p3014 N71-31092
- Computer calculations of time dependent light scattering in plane parallel atmospheres, using FORTRAN 4 language
[AD-722714] 18 p2918 N71-31284
- Data processing algorithms for investigating functional organization and operational principles of visual system
[JPRS-53644] 18 p2895 N71-31329
- Program variable logic calculations and biological principles of data processing applied to digital cybernetics systems having many outputs
[JPRS-53649] 18 p2900 N71-31417
- Analog to digital and digital data processing of temperature and velocity fluctuations recorded above tidal mud flat to produce power spectra
[AD-722592] 18 p2897 N71-31436
- Walsh orthogonal functions applied to image processing, and obtaining W-H transforms of two dimensional discrete pictures in real time
[AD-722663] 18 p2897 N71-31599
- Computer system for high speed processing of non-numerical information in criminal identifications
19 p3060 N71-31648
- Measuring instrument used at Fort-Archambault for ionospheric drift including geophysical data processing
[GRI/NTF/06] 19 p3084 N71-31703
- Computer programming system based on assembling techniques for geophysical data processing
[MITT-12] 19 p3060 N71-31780
- GEOS 2 satellite range and range rate tracking and minitrack optical tracking systems data proving and quality control for information dissemination
19 p3088 N71-31848
- Data processing for calibration of C band radar global tracking network using GEOS 2 satellite data
19 p3089 N71-31853
- Estimation method for real compression coefficient of spacecraft data processing system
[NASA-TT-F-13792] 19 p3061 N71-32170
- Digital photographic data processor and display system
[AD-723657] 19 p3101 N71-32335
- Data analysis methods for correcting cascade transition effects in atomic transition probability measurements
19 p3155 N71-32358
- Automatic real-time scoring of simultaneous sleep electroencephalograms
[NASA-CR-1840] 19 p3062 N71-32398
- Abstracts of BOMEX related conference papers, sample products from BOMEX cloud photography and radar surveillance, and status summaries of BOMEX data processing and reduction
[NASA-CR-119761] 19 p3201 N71-32755
- Status summaries of BOMEX data processing and data reduction as of 15 June 1970
19 p3063 N71-32759
- Computerized system for processing hydrometeorological data
[WMO-275] 20 p3294 N71-32958
- Data processing and reduction techniques for photointerpretation of Baker-Nunn photographs of evening clouds during Apollo 12 flight
[NASA-CR-121382] 20 p3257 N71-33018
- Phase locked loop data carrier with quadrature channel
[NASA-CASE-NPO-11282] 20 p3242 N71-33105
- Deep Space Network operations, monitoring system, and telemetry system
20 p3347 N71-33164
- Quantitative and comparative analysis of inorganic photochromic materials for coherent optical data processing applications
[NASA-CR-121453] 20 p3311 N71-33375
- Belgian computerized information system applied to automatic control
[CRIF-EL-2] 20 p3370 N71-33436
- Computer system and processing of chemical data for subject indexes and index files
21 p3387 N71-34093
- Computer system for recording and organizing information in subject indexes of chemical documents
21 p3387 N71-34094
- Organization of subject index for chemistry and conversion from manual to computer system
21 p3387 N71-34095
- Computerized processing of chemical data for indexes and index files
21 p3387 N71-34096
- Monitor in telemetry playback system for automatic pulse code modulation processing
[SC-DR-710211] 21 p3395 N71-34163
- Adaptive approach to dynamic allocation and release of buffer storage within computer systems
[NASA-CR-119705] 21 p3397 N71-34171
- Remote multispectral sensing and data processing techniques for agricultural applications
[NASA-CR-121769] 21 p3416 N71-34305
- Automatic processing of high frequency stellar spectrophotometric data using Gauss function model
21 p3430 N71-34408
- Point estimates of standardized variances of independent and correlated measurements using least squares method
[NLL-M-20658-[S828.4F]] 21 p3450 N71-34553
- Radiometric data analysis techniques for measuring air temperature profiles
[PB-199412] 21 p3452 N71-34567
- Program for finding synoptic telegrams in general meteorological information flow over communication channels
[NLL-M-20659-[S828.4F]] 21 p3453 N71-34577
- Flow diagrams and compression capabilities for software interfacing of flight data
[NASA-CR-61360] 22 p3555 N71-35321
- Convolutional coding, sequential coding, subband coding, and inverse systems for data protection
[AD-721917] 22 p3555 N71-35322
- Simplified computer graphics program for rapid data input and display
[AD-722827] 22 p3556 N71-35327
- Punch card modifiable logic design and intersection control for evaluating cellular logic concepts for multifunctional data processing systems
[AD-726996] 22 p3562 N71-35371
- Electronic module used to compute error statistics for simulations of photogrammetric schemes involving more than one lunar mission
[NASA-CR-115173] 22 p3565 N71-35376
- Application of optically diagnosed noise information toward development of filtering subroutines for improvement of digital sensing data tape quality - Vol. 1
[NASA-CR-121978] 22 p3562 N71-35376
- Research and development in solid state physics for data processing systems
[AD-726353] 22 p3568 N71-35386
- Evaluation of NASTRAN system based on large complex airplane analysis
22 p3686 N71-36232
- Comparing and integrating NASTRAN with other finite element computer programs
22 p3686 N71-36234
- Auxiliary computer routines for generating, checking, and displaying NASTRAN input and output data for analysis of aerospace vehicle structures
22 p3687 N71-36237
- Plotter routines for IBM 1800 computers permitting graphic presentation of data with minimum programming effort
[NASA-TM-X-65708] 23 p3728 N71-36276
- User manual for computer system to analyze high resolution spectrum - Vol. 1
[ORNL-4605] 23 p3728 N71-36277
- Optimum techniques for linear feature extraction based on pattern recognition
23 p3734 N71-36421
- Data formats and procedures for evaluated nuclear data file neutron cross section library with illustrations for elastic scattering by natural He
[BNL-50274(T-401)] 23 p3817 N71-37228
- Neuron modeling, electrophysiology, and biophysics involved in information processing along nervous system
[AD-727770] 24 p3882 N71-37670
- Main machine techniques for processing data from sonar display systems
[AD-727609] 24 p3883 N71-37677
- Characteristics and application of problem oriented language to mathematical programming and data processing
24 p3893 N71-37747
- Basic requirements for computers designed for operations with control automation systems
[AD-727265] 24 p3895 N71-37778
- Executive routine primitives and process control for spaceborne computer functional design specifications - Vol. 3
[NASA-CR-1869] 24 p3897 N71-37777
- Effect of coefficient rounding in floating point digital filters
[AD-727073] 24 p3898 N71-37794
- Doppler weather radar observing methods and data processing techniques
[AD-727158] 24 p3932 N71-38197
- Problems in nuclear data processing by computer code
[CONF-710302-3] 24 p3977 N71-38382
- Automatic processing of cosmic ray data
24 p4012 N71-38412
- Computer system for generating input data for structural analysis of three-dimensional elastostatic problems using isoparametric finite elements
[AD-727171] 24 p4024 N71-38714
- DATA PROCESSING EQUIPMENT**
- NT AIRBORNE/SPACEBORNE COMPUTERS
- NT ANALOG COMPUTERS
- NT AUXILIARY EQUIPMENT (COMPUTERS)
- NT CDC COMPUTERS
- NT CDC 3100 COMPUTER
- NT CDC 3200 COMPUTER
- NT COMPUTERS
- NT DATA PROCESSING TERMINALS
- NT DIGITAL COMPUTERS
- NT HONEYWELL ADEPT COMPUTER
- NT HYBRID COMPUTERS
- NT IBM COMPUTERS
- NT IBM 360 COMPUTER
- NT IBM 1130 COMPUTER
- NT IBM 7030 COMPUTER
- NT IBM 7094 COMPUTER
- NT ILLIAC COMPUTERS
- NT PDP 8 COMPUTER
- NT PDP 9 COMPUTER
- NT PRINTERS (DATA PROCESSING)
- NT SEQUENTIAL COMPUTERS
- NT UNIVAC COMPUTERS
- NT UNIVAC 1106 COMPUTER
- Data tables on ionospheric drift and turbulence soundings
[AD-710701] 01 p0047 N71-10882
- Methods for coordinating asynchronous events
[AD-711763] 02 p0186 N71-11307
- Automatic data processing resource estimating procedures
[AD-711117] 02 p0188 N71-11333
- Hardware design implementation for time shared computing facility
[AD-711085] 02 p0191 N71-11339

- Clock output waveform external synchronization system for satellite applications [RAE-78-09185] 02 p2225 N71-11531
- Monolithic COS/MOS large scale parallel processor array [NASA-CR-111462] 03 p3340 N71-12465
- Data processor having multiple sections activated at different times by selective power coupling to sections [NASA-CASE-X08-04767] 03 p3343 N71-12494
- Investigating tasks of data processing equipment in advanced navigation systems for aircraft 03 p3358 N71-12604
- Investigating small digital processors as interface between computer and sensor in airborne systems 03 p3347 N71-12609
- Data acquisition and reduction system for time-of-flight mass spectrometer used in routine analysis of products from gamma radiolysis of organic compounds [ORO-3106-33] 04 p4486 N71-13458
- Mass spectrometers from mass spectrometers [CEA-CONF-1542] 04 p3770 N71-13371
- Speech data interface with all digital transmission systems 04 p3507 N71-13853
- Processes for sensor arrays [AD-713456] 05 p0645 N71-14915
- System facility of elementary machine of Minsk 22 computer system [AD-713776] 05 p0450 N71-14948
- Using universal system for automatic numerical encoding of data for photogrammetric measurements 06 p0557 N71-15775
- Meteorological radar data acquisition and processing equipment [AD-714764] 06 p0890 N71-16015
- Development and characteristics of onboard processor system [NASA-CR-116239] 06 p0834 N71-16508
- Automatic processing of Arctic pack ice data obtained by submarine sonar and remote sensors [AD-715911] 06 p0854 N71-16620
- Procedure for identifying spikes in radioisotope angular data and synthesizing replacement values [AD-715351] 07 p1054 N71-17732
- Investigating fast group constants and processing program using ENDF/B format [AERE-1195-PT-1] 08 p1233 N71-18169
- On-line closed loop processor for reducing topographic data to electron density profiles [NASA-TN-D-6204] 08 p1187 N71-18406
- Computer analysis of multichannel scanning electron microscopy and X ray images from fine particles [AD-716562] 09 p1425 N71-19445
- Development of demodulation system for removing amplitude modulation from two quadrature displaced data bearing signals [NASA-CASE-XAC-04030] 09 p1363 N71-19472
- System analysis and computer requirements derivation of guidance and control computer for space station applications - Vol. 5 09 p1354 N71-19992
- Development of electronic information processing system for computer design [NASA-CR-117304] 09 p1355 N71-19923
- Concorde 002 aircraft equipment for flight data monitoring and processing [ESS/BS-13] 10 p1492 N71-20857
- Characteristics of self-powered, multichannel digital data buffer designed to expand input capability of electronic sensor generator [NASA-CR-114923] 10 p1529 N71-21463
- Characteristics of on-line IBM 360 computer processing system with telephone as complete terminal device 11 p1715 N71-22107
- On-line real time system for experimental data collection and processing using IBM 1800 DACS [TR-69] 11 p1716 N71-22545
- Mathematical models of numerical weather forecasting and analysis of meteorological parameters [AD-716262] 12 p1936 N71-23944
- Development of one dimensional magnetotelluric inversion techniques for determining frequency range of data necessary to define geological profile [AD-719392] 13 p2079 N71-24604
- Development and characteristics of electronic equipment for digital processing of stochastic signals for military aircraft avionics systems [AD-719822] 13 p2046 N71-24934
- Developments in automatic processing of data obtained from sensors of nuclear explosions and capabilities of nuclear detection systems [AD-719620] 13 p2075 N71-25170
- Computer systems hardware and software operations review [ODD-1018-1207] 13 p0452 N71-25192
- Description of facilities and sensors used in high altitude nuclear detection studies [AD-719619] 13 p2077 N71-25383
- Development of computer program to increase on-line analysis capabilities of experimental optical and meteorological parameters [AD-720625] 14 p2286 N71-25791
- Multichannel pattern recognition in unstructured situations using a set of discriminant functions which partition feature space into regions [AD-720812] 14 p2288 N71-25841
- Summary and coordination of several digital computer algorithms for information compression, structure analysis, and decision making [AD-720811] 14 p2288 N71-25842
- Development and characteristics of rate augmented digital to analog converter for computed time-dependent data [NASA-CASE-XLA-07838] 15 p2383 N71-27057
- ISIS - computer program for analysis and interpretation of experimental fusion data [AD-721481] 16 p2647 N71-28238
- Development of mass machine subsystem for military management information system and evaluation of display capability integrated into large scale computer [AD-720853] 18 p2877 N71-31335
- IFP-Ther - system for retrieving information in chemistry of fluorogenic compounds 19 p3195 N71-31906
- Ionosonde using data processing systems for continuous ionospheric soundings [AD-723290] 19 p3093 N71-32204
- Sampling functions and their effects in computing quantities used to evaluate optical system performance [AD-724265] 20 p3310 N71-32904
- Data processor with plural register stages for selectively interconnecting with each other to effect multiplicity of operations [NASA-CASE-GSC-10186] 20 p3238 N71-33110
- Analysis of three APT processors on IBM 360 computer [NASA-CR-114360] 21 p3399 N71-34186
- Design, development, and characteristics of modular spectroscopic data processors for space shuttle applications 21 p3516 N71-35053
- Application of redundancy techniques for improved computer system reliability 21 p3516 N71-35054
- Characteristics and advantages of data bus to facilitate data handling process on space shuttles 21 p3517 N71-35056
- Development and application of data bus techniques for space shuttle data management systems 21 p3517 N71-35057
- Low frequency vertical pulsed sounder design with digital integration and pseudo-random phase coding for ionospheric D-region sounding [AD-727013] 22 p3580 N71-35499
- Computer user manual for use with automated general purpose system for structural analysis - Vol. 2 [AD-726565] 22 p3699 N71-36315
- Computer programmer manual for use with automated general purpose system for structural analysis - Vol. 3 [AD-726566] 22 p3699 N71-36316
- Development and characteristics of mass machine systems for detection, recognition, transmission, and perception of information - Vol. 3 [AD-727611] 24 p3683 N71-37679
- Information processing, research projects, mathematical modeling, and analysis of computer systems [AD-727809] 24 p3896 N71-37770
- Photographic data processing, management, and dissemination system to support Earth Resources Technology Satellite program - Vol. 3 [NASA-CR-121900] 24 p3919 N71-37946
- Utilization of data processing equipment in business and application to decision making process [RAE-LIB-TRANS-1581] 24 p4035 N71-36791
- DATA PROCESSING TERMINALS
- Computer graphics terminal using storage CRT [CSC-TN-423] 01 p0026 N71-10035
- Man-machine interaction at remote console of time shared computer [AD-712693] 04 p0501 N71-13506
- User manual in form of interactive, functionally dependent time series programs accessible in any order from remote terminal [NASA-CR-116179] 06 p0620 N71-16431
- Developing digital data systems for Ground Communications Facility of DSN 07 p1004 N71-17620
- Design 1 general purpose computer system 11 p1718 N71-22753
- General purpose digital computer system using Design 1 control components and Minsk 2 magnetic tape units 11 p1719 N71-22759
- JOSHUA terminal system for mobile recording and data manipulation by remote display systems [TUD-25691] 21 p3460 N71-34626
- DATA PROCESSORS
- DATA PROCESSING EQUIPMENT
- DATA REDOUT SYSTEMS
- DATA SYSTEMS
- DISPLAY DEVICES
- DATA RECORDERS
- Airborne data acquisition system incorporating recycling metal tape flight data recorder 04 p4385 N71-15816

- Data recorder for producing digital magnetic tapes for radio transmission experiments 04 p0805 N71-15830
- Description of system for recording and reading out data related to distribution of occurrence of plurality of events [NASA-CASE-XNP-04067] 11 p1717 N71-32707
- Variable and modular acquisition system for recording similar experimental data [PFI-1] 14 p2316 N71-36748
- Equipment and correlation data for cosmic ray studies 24 p4012 N71-38615
- DATA RECORDING
- Recording dual concentration in atmosphere [NLL-M-9139-5828-471] 03 p0348 N71-12866
- Mechanical resonators for vibrating mirrors to deflect laser beams in optical data recording system 07 p1058 N71-17036
- Seismic station equipment for recording strong earthquakes [IPST-5834] 08 p1195 N71-19107
- System for recording and reproducing PCM data from data stored on magnetic tape [NASA-CASE-X08-01821] 10 p1528 N71-21042
- Description of system for recording and reading out data related to distribution of occurrence of plurality of events [NASA-CASE-XNP-04067] 11 p1717 N71-32707
- Development of data storage system for storing digital data in high density format on magnetic tape [NASA-CASE-XNP-04778] 11 p1717 N71-32710
- Cost effectiveness in recording experimental data 11 p1718 N71-32732
- Optimal experimental data input to local storage units 11 p1719 N71-32740
- Onboard data acquisition for improved aircraft design and operational flight safety 12 p1853 N71-23412
- Galvanometer for automatic recording of deformation measurement process [TT-70-59121] 14 p2253 N71-25664
- Transient video signal tape recorder with expanded playback [NASA-CASE-ARC-10083-1] 14 p2227 N71-25846
- On-line computer system for surface location mass spectrometer scan control and data recording [AAEC/TM-548] 15 p2486 N71-26883
- Meteorological radar echo amplitude modulator for continuous data recording [AD-712490] 15 p2300 N71-27178
- Real time capability, satellite monitoring, and system reliability of satellite recording and data base system - Tables of costs and checklists [COM-71-00228] 16 p2590 N71-28874
- Component characteristics and failure mode recording and data acquisition system design for determining component reliability [NLL-BIBLEY-TRANS-1926-5901-59] 19 p1466 N71-32718
- Construction of antenna array and automatic recording system to measure amplitude and phase of diffraction patterns formed by ionospheric reflection of 300 kHz pulsed radio signals [PFSU-IRL-SC-371] 20 p2529 N71-33207
- Logic problems for programming video disk recorder with single and multiple fields [LA-4582] 20 p2536 N71-33797
- Polar ionospheric geophysical data recording at Kiruna, Sweden during Jan. - Mar. 1970 20 p2530 N71-33857
- Development and characteristics of digital recording system for automatic digitizing of map contour line data [AD-726386] 22 p3579 N71-35493
- Eighty line optical camera for recording nuclear medical data with scintillation camera [UCRL-20699] 22 p3585 N71-35529
- Neutron component measurement and multichannel recording of atmospheric pressure 24 p4012 N71-38614
- DATA REDUCTION
- DATA SMOOTHING
- Interpretation of radiation data obtained by meteorological satellites for long range weather forecasting 01 p0077 N71-10091
- Data reduction techniques for digital spectrum analysis of meteorological radar echoes 01 p0821 N71-10227
- Data reduction techniques and computer programs for meteorological information obtained from Hobbs balloons [AD-711405] 04 p0879 N71-10707
- Random process model and feature reduction of spontaneous and alpha frequency electroencephalograms [NASA-CR-111385] 04 p0867 N71-11185
- Reproducible analyzing method and apparatus for determining subjects oxygen consumption in exercise carriage [NASA-CASE-XPR-04403] 02 p0400 N71-11202

- Computer program for reporting paths by operating on branch and node table data sets using indexed sequential access method
[NASA-CR-106738] 03 p0339 N71-12457
- Digital analysis of random data records by successive accumulation of time averages
[NASA-TN-D-6073] 03 p0400 N71-12466
- Computer update program for compiling master wire list from box external data
[NASA-CR-106734] 03 p0342 N71-12478
- Minimum time delay unit for conventional time-multiplexed data compression channels
[NASA-CASE-XNP-08832] 03 p0345 N71-12506
- Technique for analysis and computerized data reduction of time of flight distributions of free jet expansions
[AD-712572] 03 p0423 N71-12729
- Analysis of wind component data from rawinsonde and rocketsonde observations over Battery MacKenzie, C.Z.
[KN-70-64-FR/1] 03 p0402 N71-12818
- Research study on reduction, analysis, and interpretation of radiation balance measurements from ESSA weather satellites
[PB-192427] 03 p0404 N71-13243
- Tracking and data system support for Pioneer project, Pioneer 9 prelaunch through June 1969
[NASA-CR-111561] 03 p0459 N71-13298
- Nondestructive activation analysis of environmental samples, and computerized data reduction
[COO-1705-6] 04 p0581 N71-14074
- Data analysis and methods improvement for Los Angeles Basin
[PB-194060] 04 p0542 N71-14274
- Analyzing data from Explorer 33 and 35 on energetic solar particles in interplanetary medium and terrestrial particle fluxes in magnetopause bow shock regions
[NASA-CR-115775] 04 p0590 N71-14378
- Research on data and analytical systems for preparing national water assessments
[PB-192118] 03 p0666 N71-14692
- Data reduction processes for spinning flat-plate satellite-borne radiometers
[ESSA-TR-NESC-32] 03 p0649 N71-14779
- Reductions for correcting gravity measurements for terrain in vicinity of station
[PUBL-63] 03 p0670 N71-14822
- Selection of techniques and equipment for analysis of random and unique data
[ARL/ME-312] 03 p0652 N71-15499
- Progress report on Saxton plutonium project including data reduction on core post-irradiated data, isotopic data, and related subjects
[WCAP-3355-24] 06 p0898 N71-16279
- Checkout and data reduction procedures for acceptance test of sealed, absolute, gage, and differential strain gage pressure transducers
[NASA-TM-X-66603] 06 p0862 N71-16746
- User guide for Langley time series analysis computer program used in analyzing random, stationary time series
[NASA-TM-X-2160] 07 p0997 N71-17411
- Procedure for identifying spikes in radioisotope angular data and synthesizing replacement values
[AD-715351] 07 p0154 N71-17732
- Analysis of multi-sensor data obtained by Earth Resources Aircraft Program
[NASA-CR-116425] 07 p0132 N71-17870
- Extrapolation based on coefficients for data reduction and data transmission
[DLR-FB-70-49] 08 p1162 N71-18577
- Data compression processor for monitoring analog signals by sampling procedure
[NASA-CASE-NPO-10068] 08 p1167 N71-19288
- Wide range analog data compression system
[NASA-CASE-XGS-02612] 09 p1352 N71-19435
- Feasibility and applications of scientific and technical information analysis centers
[AGARD-CP-78-71] 09 p1346 N71-19526
- Concept, mission, and operation of scientific and technical information analysis centers
09 p1347 N71-19527
- Geometric adjustment technique for Pacific SECOR observations based on least squares method
[NASA-CR-117043] 09 p1347 N71-19546
- Data reduction and computer programming for ESRO auroral spectroscopy experiment
[KGO-PREPRINT-70-313] 10 p1545 N71-20621
- Data analysis of test to determine relationship of intergroup organizational climate with communication and joint decision making between task-interdependent R and D groups
10 p1666 N71-21100
- Studies related to Pioneer 8 and 9 data tape analysis
[NASA-CR-117526] 10 p1641 N71-21565
- Collection, reduction, and evaluation of electric field phenomena; and geomagnetic field data at both low and high altitudes
[AD-717779] 11 p1748 N71-22343
- Service routines MERMC2 and MAGIC for binary cross section library tapes used by MC 2 multi-group cross section code
[ANL-7654] 11 p1804 N71-22352
- Information preserving data compression systems with coding algorithm developed for noiseless channel conditions
[NASA-CR-117846] 11 p1716 N71-22549
- Editing system for large general time sharing computer including dynamic editing display technique and static microfilm method
[NASA-TM-X-2264] 11 p1716 N71-22575
- Description of system for recording and reading out data related to distribution of occurrence of plurality of events
[NASA-CASE-XNP-04067] 11 p1717 N71-22707
- Data reduction techniques for automated scientific experiments
11 p1719 N71-22738
- Cost analysis of data reduction and retrieval methods
11 p1719 N71-22741
- Data reduction techniques for deriving aerodynamic forces and moments in absence of support interference
[NASA-CR-111844] 12 p1895 N71-23122
- Gravimetric and satellite tracking data reduction to determine dimensionless harmonic coefficients and gravity anomalies
[AD-715152] 13 p2069 N71-24392
- Wind tunnel investigation of jets exhausting into cross flow - description and data analysis
[AD-718122] 13 p2064 N71-24492
- Shadow band phenomenon observed during solar eclipses and visible only minutes preceding and following totality
[NASA-TM-X-65545] 14 p2335 N71-25754
- PDP 8 computer techniques in reactor physics including data acquisition and reduction of absorption cross section, radiation, noise-time, and neutron lifetime and reactivity measurements
[RT/FI-70/16] 15 p2451 N71-27739
- Decoding algorithms for data reduction and transmission through noisy space channels using sequential and hybrid computers
[NASA-CR-114277] 16 p2564 N71-28088
- Analysis of coceanic thunderstorm data to determine universal time variations of ocean area effects
16 p2624 N71-28202
- Evaluation of neutron data for fissile or fertile nuclei in range of resolved or unresolved resonances with mass number above 230
[NASA-TT-F-13692] 16 p2646 N71-28210
- Self reducing optical range finder with magnetic tape recorder
16 p2592 N71-28269
- Statistical data plan for reduction of raw data from Barbados Oceanographic and Meteorological Experiment, BOMEX
[COM-71-00188] 16 p2626 N71-28601
- Bistatic-radar data reduction and Explorer 35 reflectivity and bandwidth tables with polarization spectra
[NASA-CR-119032] 16 p2564 N71-29064
- Data compression techniques for space flight data transmission systems using Telemetry Redundancy Analyzer
17 p2722 N71-29322
- Redundancy reducing signal encoding and application to pulse code modulation
[DLR-FB-70-56] 17 p2718 N71-29328
- Reduction ratio for deep space onboard equipment data in telemetry frame, taking into account active channel probability distributions
[D-54] 17 p2718 N71-29360
- Redundant data reduction in spacecraft instrument grouping
[D-63] 17 p2719 N71-29535
- Computer program for reducing radar tracking data magnetic tape numbers for data storage by editing and low pass filtering
[NASA-CR-119176] 17 p2748 N71-30149
- Nondestructive test methods and techniques including computer programs and data reduction
[NASA-SP-5931/01/1] 17 p2862 N71-30183
- Composite parts of compression coefficient in data processing system
[NASA-TT-F-13790] 18 p2894 N71-30857
- Reduction and analysis of electron content measurements permitting inference of electron density in solar wind
[NASA-CR-114356] 18 p3003 N71-30896
- Reduction and analysis of data from Explorer 15 and Explorer 26 satellites
[NASA-CR-119286] 18 p3003 N71-30919
- Compilation and comparative analysis of observations of lunar transient phenomena
[NASA-TM-X-65528] 18 p3014 N71-31092
- Development and construction of automatic photometer scan and data system
[NASA-CR-115098] 18 p2925 N71-31399
- Abstracts on electrical engineering and data compression
[TR-EE-70-45] 18 p2900 N71-31479
- Free flight stability tests on half cones in hypervelocity wind tunnels including data reduction program
[VKI-TN-66] 19 p3075 N71-31663
- Geomagnetic survey in 0.01 to 10,000 Hz including data reduction and instrumentation
[KGO-706] 19 p3084 N71-31669
- Investigating photogrammetric and astronomical methods for plate reduction
19 p3098 N71-31818
- C-band, SECOR, and TRANET radio tracking and laser tracking data analyses for 35 GEOS 2 satellite passes including preprocessing data correction effects
19 p3107 N71-31864
- Comparison of ionospheric refraction data sources and error correcting formulas using Wallops Island collocation experiment data
19 p3088 N71-31867
- GEOS 2 satellite tracking accuracy comparisons of SAO laser and NASA mobile ruby laser systems including data analysis procedures
19 p3107 N71-31869
- Geocentric coordinate determinations for station locations using optical observations of Pegasus balloon satellites
19 p3090 N71-31871
- Effect of sequentially changing background color during target detection
[AD-722572] 19 p3056 N71-32325
- Third-order interpolation technique for continuous path, numerically controlled machines and data reduction
[V-1782] 19 p3123 N71-32324
- Computerized simulation of statistical onboard data analyses for long range spacecraft
[NASA-TT-F-13791] 19 p3062 N71-32326
- Error correcting codes and data compression techniques for PCM adaptive telemetry systems - abstracts
[NASA-CR-119679] 19 p3057 N71-32388
- Atmospheric temperature and moisture rawinsonde tables and data reduction techniques used in analysis of atmospheric thermodynamics over Palmyra, Fanning, and Christmas Islands
[NCAR-TN/STR-55-VOL-1] 19 p3129 N71-32386
- Quantitative and qualitative analyses of BOMEX weather radar data collected by aircraft and land based radars
19 p3059 N71-32778
- Status summaries of BOMEX data processing and data reduction as of 15 June 1970
19 p3063 N71-32779
- BOMEX data reduction on sea-air interaction at tropical convective systems studies
[NASA-CR-119762] 19 p3201 N71-32780
- BOMEX data reduction and processing studies, including rawinsonde data and radiation analysis
19 p3063 N71-32781
- Digitization of BOMEX data reduction and processing
19 p3131 N71-32782
- Computer program to simplify reduction of temperature data from meteorological sounding rockets
[AD-724599] 20 p3258 N71-32972
- Test data reduction and prediction techniques for high lift aerodynamic and propulsion system configurations for short takeoff aircraft design - bibliographies
[AD-724185] 20 p3209 N71-33016
- Data processing and reduction techniques for photointerpretation of Baker-Nunn photographs of venting clouds during Apollo 12 flight
[NASA-CR-121382] 20 p3257 N71-33018
- Fluid control, filtration, and calibrating equipment, computer programs, and data reduction techniques - technology utilization
[NASA-SP-5938/01/1] 20 p3278 N71-33142
- POP04 library and codes for preparing secondary gamma ray production cross sections
[ORNL-TM-3367] 20 p3317 N71-33332
- Tracking and scientific measurement data analyses for Pioneer missions from July 1969 to July 1970
[NASA-CR-121383] 20 p3246 N71-33357
- Data analysis on ATS-1 Suprathermal Ion Detector (SID) measurements of low energy plasma flow in magnetosheath boundary
[NASA-CR-121452] 20 p3267 N71-33340
- Thermodynamic data program involving phosphorus and uranium at high temperatures
[GEAP-12153] 20 p3367 N71-3378
- Meteorological research in time domain data extraction, radio altimetry, and application of ATS data in hydrological tool in remote tropical regions
[NASA-CR-121438] 20 p3371 N71-3378
- Annotated bibliography of data compression and data compression from information theory literature
[AD-723525] 21 p3395 N71-34015
- Digital slope threshold data compressor
[NASA-CASE-NPO-11630] 21 p3399 N71-34018
- Composition of upper ionosphere as shown by magnetic mass spectrometer flows on Explorer 31
[NASA-CR-121865] 21 p3426 N71-34079
- Data compression and error correcting codes applied to digital transmission of real time, standard format TV, along with voice and other data from Apollo spacecraft
21 p3315 N71-34080

SUBJECT INDEX

Radiation chemistry of high polymers and computer techniques for data reduction 22 p3550 N71-35286
[OEO-4659-11]
Flow diagrams and compression capabilities for software interfacing of flight data 22 p3555 N71-35321
[NASA-CR-61360]
Data compression algorithms for processing electrocardiogram and vectorcardiogram signals 22 p3555 N71-35323
[NASA-CR-115177]
Computer-aided data reduction technique for extracting time dependent conductivity of dielectric material from test circuit recorded responses 22 p3560 N71-35357
[AD-726359]
Data acquisition and reduction methods in investigating large-amplitude, high-wave number, total magnetic field variations over exposed basic volcanic rocks 22 p3573 N71-35450
[NOAA-TR-ERL-201-ESL-15]
Reduction and analysis of selected spectral emission observations at polar cap station 22 p3580 N71-35500
[AD-726615]
Gas chromatograph, mass spectrometer system for chemical and biochemical determinations on Mars, and data reduction program 22 p3583 N71-35514
[NASA-CR-122038]
Reduction of topocentric satellite data from satellite tracking stations 22 p3678 N71-36225
Procedures for accurate condensing of eigenvalue solutions in structural analysis using Guyan reduction solutions 22 p3683 N71-36266
Application of NASTRAN to structural analysis of space shuttle orbiter finite element model with over 300 joint degrees of freedom 22 p3685 N71-36279
Computer reduction and nondestructive tests for determining material characteristics of surface fault zones 23 p3729 N71-36378
[BC-DR-710222]
Review of worldwide gravity tide data showing scatter in observations caused by ocean loading 23 p3733 N71-36764
Critical evaluation of nuclear data information in connection with reactor designs - international conference 23 p3800 N71-37091
[BDC(NDS)-29-U]
Spectroscopic observations of planets showing absorption variations in NE3 and CE4 bands 24 p4007 N71-38573
[NASA-CR-123152]
DATA RETRIEVAL
Data retrieval system using syntax techniques 01 p0027 N71-10146
Program for national information system for physics and astronomy 1971 to 1975 02 p0307 N71-11150
[PB-192717]
Magnetic matrix memory system for nondestructive reading of information contained in matrix 03 p0345 N71-12504
[NASA-CASE-XMP-03835]
Electronic microprobe and holographic methods for data condensing and retrieval, and microprobe 08 p0205 N71-19317
Cost analysis of data reduction and retrieval methods 11 p1719 N71-22741
Photocopy memory for computer applications giving improved signal to noise ratio and reading and regeneration of stored information during single light pass 12 p1881 N71-23222
Nuclear data processing from TIMOC Monte Carlo heavy ENDF/B file using CODAC FORTRAN 4 program 13 p2134 N71-25163
[BUR-4521-E]
World Data Center A upper atmosphere data retrieval information on extraterrestrial radiation and cosmogenics 18 p3007 N71-31460
[UAG-15]
Radioactive isotopes, accession number, and neutron-induced reaction indices for data retrieval 18 p3090 N71-31556
[UCL-5000-VOL-3]
Chemical information systems including information input techniques, retrieval, dissemination, and publication bibliographies 19 p3194 N71-31976
[PES-35523]
Problems of retrieving data on chemical compounds and materials using manual data retrieval system 19 p3195 N71-31985
UPR-flux system for retrieving information in chemistry of fluorocarbon compounds 19 p3195 N71-31986
Data retrieval language with ability to define data structures, describe environments, address data by content, manipulate data structures, and offer computational power comparable to FORTRAN 19 p3063 N71-32714
[NBS-TR-390]
Standard methods for storage and retrieval of meteoric data 24 p3897 N71-37776
[AD-70653]
DATA SAMPLING
Data sample consisting of mean wind speed and direction, also highest recorded gust for central Oklahoma, June 1964 - May 1967 01 p0079 N71-10615
[NSA-TR-ERL-TM-NSSL-48]

Graphical analysis of ten-year sampling of suspended particulate matter over urban and nonurban sites 02 p0151 N71-11069
[PB-192223]
Analysis of nonlinear sampled data systems with nonzero sampling duration by means of associated recursive functions 02 p0250 N71-11609
Solutions to nonlinear recursive functions and application to sampled data systems 02 p0251 N71-11610
Developing alternative test for equality of variances and comparison with F-test by data sampling 02 p0251 N71-11660
[AD-711801]
Interim results and progress on use of space and aircraft photography for range resource inventories 02 p0216 N71-11979
Method of calculating sampling errors 03 p0399 N71-12904
[RAE-TR-69178]
Examination of simple coordinate transformations in Z-plane and W-plane for root locus analysis of sampled data systems 04 p0539 N71-14184
[NASA-TM-X-66313]
Generalized digital compensators for sampled-data systems 08 p1166 N71-18869
Investigating Fourier transform estimation from unknown parameters using sequential algorithm 08 p1236 N71-19008
Computer program for processing respiratory dust sampling data 08 p1166 N71-19029
[BM-IC-8304]
Monitoring circuit design for sampling circuit control and reduction of time-bandwidth in video communication systems 11 p1714 N71-23026
[NASA-CASE-XNP-02791]
Analysis of sampled data reconstruction errors from digital data processing 12 p1884 N71-23872
Sequence reconstruction of ordered linear polymer from fragment data 12 p1951 N71-24249
[OOO-1018-1219]
Sampling circuit for signal processing in multiplex transmission by Fourier analysis 13 p2044 N71-24622
[NASA-CASE-NPO-10388]
Application of Z-transforms to sampled-data systems 13 p2102 N71-24631
[NASA-CR-61349]
Video signal processing system for sampling video brightness levels 13 p2045 N71-24742
[NASA-CASE-NPO-10140]
Algorithm for solving Popov stability criterion applied to sampled data systems 14 p2282 N71-26042
[NASA-TM-X-64606]
Cutoff sampling of data for repetitive surveys 17 p2860 N71-29259
[BM-IC-8316]
Error estimating technique for experimental data based on finite difference theory and standard deviations 17 p2772 N71-29448
[ABCL-3781]
Step input linear system modeling from nonlinear system sampled noisy data based on method of perturbation or quasilinearization of automatic control system data 17 p2729 N71-30356
[NASA-CR-115074]
Adaptive sampled data control of time varying bending modes of flexible airframe 18 p3020 N71-31582
[AD-723846]
Sampling functions and their effects in computing quantities used to evaluate optical system performance 20 p3310 N71-32904
[AD-724626]
Computer program (MCNA) to solve adjoint neutron transport equation by coupled sampling with Monte Carlo method 20 p3327 N71-33967
[LA-4468]
DATA SMOOTHING
Four theorems characterizing optimal filtered and smoothed estimates for linear parabolic systems 03 p0399 N71-12595
[AD-712404]
Computer program for smoothing and differentiation of data from multichannel analyzers 04 p0537 N71-13941
[UCL-19903]
Analyzing pulse-by-pulse return signal from on-board X-band telemetry system in RAM C-1 and C-2 payloads 07 p0992 N71-17126
[NASA-CR-111810]
Oceanographic data smoothing and hydrological station spacing 09 p1384 N71-19910
[AD-716272]
Topographic corrections for lunar gravity data 10 p1644 N71-21339
Derivation and evaluation of algorithms for error analysis, sensitivity of filtering, and smoothing solutions to nonlinear estimation problems 19 p3071 N71-32441
Optimum estimate for degree of approximating polynomial for smoothing experimental measurements 23 p3783 N71-36968
[NLL-M-20367-(SR28.4F)]
Data adjustment for neutron component analysis of primary cosmic rays 24 p0811 N71-38610
[TRF-779]
DATA STORAGE
Data storage with list processing capability 01 p0079 N71-10224
[NSA-TR-ERL-TM-NSSL-48]

DATA STORAGE

Hierarchical associative memories for parallel computation 02 p0189 N71-11331
[AD-711091]
Archival procedures, and available meteorological satellite data for climatology 02 p0361 N71-12185
Magnetic matrix memory system for nondestructive reading of information contained in matrix 03 p0345 N71-12504
[NASA-CASE-XMP-03835]
Applying method of dual-sources holographic interferometry to comparison of optical components and measurement of small phase deviations 03 p0370 N71-12706
Operation of scientific information and data analysis center with computer base and associated communications network 04 p0500 N71-13496
[ORNL-TM-3078]
Application of plasma display technique to computer memory system 04 p0602 N71-13510
[AD-712698]
Storage of high density information using holographic method 04 p0524 N71-13831
Storage tubes 04 p0505 N71-13838
Describing design, hardware, and software for large data storage and retrieval system using CDC 6600 computers 05 p0649 N71-14579
[UCL-19757-REV]
ENDRUN-I program for calculating multigroup constants from ENDF/B data 05 p0746 N71-15217
[GEAP-13992]
Development and characteristics of mass memory technologies for spacecraft applications 06 p0821 N71-16572
[NASA-CR-116342]
Applying nondestructive transversal filters to playback of digital tape recorder signals and conventional symmetry MOSFET memory for outer planet spacecraft 06 p0821 N71-16684
Variation of data structure - CAMA 06 p0822 N71-16833
[AD-714033]
Discussing REDUCE system and approach to substitution in design of symbolic mathematics systems 08 p1228 N71-19186
Properties of holograms and applications of holography 08 p1211 N71-19224
Tape guidance system for multichannel digital recording system 09 p1331 N71-19420
[NASA-CASE-XNP-09453]
System design of information storage and retrieval system 09 p1333 N71-19754
[AD-715963]
Event recorder with constant speed motor which rotates recording disk 10 p1557 N71-21006
[NASA-CASE-XLA-01832]
System for recording and reproducing PCM data from data stored on magnetic tape 10 p1528 N71-21042
[NASA-CASE-XGS-01831]
Development of data storage system for storing critical data in high density format on magnetic tape 11 p1717 N71-22710
[NASA-CASE-XNP-02778]
Optimal experimental data input to local storage units 11 p1719 N71-22740
MOSFET shift register for data storage 13 p2152 N71-25324
Stored program computer for onboard spacecraft data processing 13 p2052 N71-25325
Syntax oriented data formatting to facilitate information input and retrieval 14 p2221 N71-25979
Method of storing inverted file with minimum storage space and low access time for quick retrieval of nonnumerical data by computers 14 p2221 N71-25980
Properties of information retrieval and management information systems including data structure, hierarchy generation, and searching 14 p2222 N71-25987
Compilation of dictionaries for information retrieval systems from vocabularies from different fields of science 14 p2223 N71-25990
MIDAS double computer system for controlling acquisition, processing, and storing of measured nuclear data 14 p2227 N71-26727
[NPL-18562]
Multiple pattern holographic information storage and readout system 16 p2407 N71-29131
[NASA-CASE-ERC-10151]
Feasibility study for German materials data bank - conference 17 p2762 N71-29287
Computer program for reducing radar tracking data magnetic tape numbers for data storage by editing and low pass filtering 17 p2740 N71-30149
[NASA-CR-119176]
Transmission system for data generated by flying spot device into Radcan-3 computer 18 p3083 N71-30509
[TRF-779]
Block data storage for Helios solar probe using random access ferrite core storage 19 p3060 N71-31467
[BMW-FB-W-71-14]

- Acquisition and storage of militarily significant data on climatology, hydrology, soils, and ecology of humid tropical regions
[AD-72360] 19 p3195 N71-32029
- Branch-and-bound algorithms for core data storage and iteration reduction
[P-4459-1] 21 p3399 N71-34193
- Momentum wheel design for spacecraft attitude control and magnetic drum and head system for data storage
[NASA-CASE-NPO-11481] 21 p3435 N71-34591
- Library tape for storage of model parameters of semiconductor devices
[SC-M-716210] 21 p3498 N71-34918
- Design, development, and characteristics of modular spaceborne data processors for space shuttle applications
21 p3516 N71-35053
- Design and development of subsystem interface unit, bus control unit, and supporting equipment for space shuttle data processing equipment
21 p3516 N71-35055
- Characteristics and advantages of data bus to facilitate data handling process on space shuttles
21 p3517 N71-35056
- Analysis of bulk storage data requirements and methods for visual display of information on space shuttle display devices
21 p3517 N71-35063
- Characteristics of Space shuttle data management system for data transmission and service for avionics equipment and other subsystems
21 p3518 N71-35065
- Fabrication of memory devices using MOS transistors
23 p3736 N71-36638
- Integrated memory cell circuits for solid state storage
23 p3736 N71-36639
- System design criteria for semiconductor memories
23 p3736 N71-36640
- Dynamic memories constructed as circulating shift registers with enhanced data access
[AD-727116] 24 p3895 N71-37763
- Standard methods for storage and retrieval of aerometric data
[AFPD-6663] 24 p3897 N71-37776
- ### DATA SYSTEMS
- Display console for tactical situation radar display requirements and data management
[AD-712116] 02 p0177 N71-11247
- Formulation of design rules for PCM telemetry frame synchronization
[NASA-CR-111391] 02 p0178 N71-11248
- Program requirements for DRAFT 2 system
[NASA-CR-108662] 02 p0189 N71-11326
- TAPECLIP data system for processing isograms from sensing magnetic tape
02 p0190 N71-11334
- Set theory and processing of large data bases
[AD-711066] 02 p0191 N71-11340
- Analysis of nonlinear sampled data systems with nonzero sampling duration by means of associated recursive functions
02 p0250 N71-11609
- Telemetry system with data redundancy reduction by systemization and analysis of data sources
02 p0221 N71-12147
- Computer program ADMAG for coding to digital conversion of data on XDS 930 computer
[AD-712674] 03 p0344 N71-12498
- Signature data processing system for automatic extraction of spectral information from multispectral band scanners - Vol. 1
[NASA-CR-108760] 03 p0345 N71-12508
- Software used with signature data processing system for automatic extraction of spectral information from multispectral band scanners - Vol. 2
[NASA-CR-108761] 03 p0345 N71-12509
- Signal processing specifications of signature data processing system for automatic extraction of spectral information from multispectral band scanners - Vol. 3
[NASA-CR-108762] 03 p0346 N71-12510
- Plutonium 239 neutron cross section data in unresolved resonance region
[GEAP-13591] 03 p0424 N71-12808
- Data handling equipment for aerospace and ground support applications - conference
[ASARD-CP-67-70] 04 p0304 N71-13826
- Data handling and message switching in ATC - communication oriented computer system
04 p0306 N71-13842
- Analysis of data systems and computer programs for nuclear rocket shielding methods, modification, updating, and data input preparation - Vol. 1
[NASA-CR-102964] 05 p0728 N71-15162
- Selection of techniques and equipment for analysis of random and unique data
[ARL/MS-512] 05 p0652 N71-15499
- Analysis of centralized data processing system in Cuckoo's-nest
[UPRS-52674] 10 p1645 N71-21063
- Utility transformation of Hermitian matrix to symmetric triangular matrix
10 p1592 N71-21341
- Magnetic tape recorders, data systems, and Jupiter radiation effects on metal oxide semiconductors of Thermoelectric Outer Planet Spacecraft
10 p1560 N71-21353
- Automated meteorological data processing practiced at Air Force global weather center
[AD-717652] 11 p1790 N71-22269
- Viking mission support by tracking and data system of DSN
11 p1829 N71-22769
- Control systems and instrument development for use with liquid metal fast breeder and high flux isotope reactors, Van de Graaff and linear accelerators, and in-pile loops
[ORNL-4630] 12 p1895 N71-23166
- Data system for improving instrument reliability and reducing costs
12 p1920 N71-23644
- Description and characteristics of automatic information storage and retrieval system using batch processing mode on IBM 360 computer
[PB-188957] 14 p2224 N71-26306
- Theory and techniques applicable to design, analysis, and fault diagnosis of reliable spacecraft data systems
[NASA-CR-118664] 14 p2224 N71-26361
- Functions of environmental data collection and processing facility, project management, data base maintenance, information retrieval, and environmental simulation system
[AD-720592] 14 p2360 N71-26451
- System configuration and executive requirements specifications for reusable shuttle and space station/bases
[NASA-CR-1820] 15 p2383 N71-27018
- Development and characteristics of rate augmented digital to analog converter for computed time-dependent data
[NASA-CASE-XLA-47828] 15 p2383 N71-27057
- Design of automatic data correlation system for Earth Resources Program
[NASA-CR-115063] 16 p2564 N71-28003
- Program summary for implementation of automatic data correlation system for Earth Resources Program
[NASA-CR-115062] 16 p2564 N71-28004
- Onboard optical and electronic data acquisition instrumentation for monitoring Apollo Saturn 5 launch performance
[NASA-TM-X-67185] 16 p2682 N71-28172
- National Oceanographic Data Center activities and services
17 p2750 N71-30394
- Computer and data processing developments
[CERN-71-6] 18 p2892 N71-30484
- Composite parts of compression coefficient in data processing systems
[NASA-TT-F-13790] 18 p2894 N71-30857
- Manual and mechanized methods of retrieving information on chemical compounds from data retrieval systems
19 p3195 N71-31984
- Environmental data service facility for dissemination of Barbados oceanographic and meteorological sea/air information
19 p3200 N71-32738
- Assembly and contents of comprehensive solar physics and solar activities data base
[AD-724011] 20 p3345 N71-32964
- Consequences of introduction of spacecraft computers on data handling in conjunction with telemetry equipment and transmitter receiver operations
[D-64] 20 p3338 N71-33039
- Deep Space Network mission support activities, telemetry, and data systems for Pioneer, Helios, Viking, and Mariner 71 spacecraft telemetry data systems
[NASA-CR-121378] 20 p3346 N71-33163
- Deep Space Network support for Pioneer, Helios, Viking, and Mariner 71 spacecraft telemetry data systems
20 p3347 N71-33165
- Tracking and scientific measurement data analyses for Pioneer missions from July 1969 to July 1970
[NASA-CR-121385] 20 p3346 N71-33557
- Techniques for selecting performance criteria for voice, video, and digital data systems
[NASA-CR-115079] 21 p3390 N71-34115
- GCF high-speed data system design and implementation for 1971-1972, including doubled data transmission, block demultiplexing, and positive labeling of error-free blocks
21 p3392 N71-34141
- GCF DSS communications equipment subsystem high-speed data assembly for data conversion to suitable form for transmission
21 p3393 N71-34142
- Capabilities and 4800-bps data circuits of GCF SFOF communications terminal subsystem high-speed data assembly
21 p3393 N71-34143
- GCF area communications terminal subsystem high-speed data regeneration assembly for routing and conditioning all communications entering and leaving
21 p3393 N71-34144
- GCF high-speed data system performance and error statistics at 4800 bps
21 p3393 N71-34145
- Data decoder assembly for Pioneer F and G space probes
21 p3393 N71-34146
- Development of arithmetic unit for decoding data encoded by convolutional encoding with fewer channels than prior units
[NASA-CASE-NPO-11371] 21 p3399 N71-34100
- Development of computer memory system for automated attendance accounting system
[NASA-CASE-NPO-11456] 21 p3399 N71-34101
- Computer subroutine for processing meteorological flight data by plot on peripheral printer of up to 16 parameters with curve separation and automatic scaling
[NOAA-TR-ERL-199-APCL-17] 21 p3452 N71-34509
- Proceedings of space shuttle integrated electronics conference with emphasis on data systems design - Vol. 3
[NASA-TM-X-50863-VOL-3] 21 p3516 N71-35061
- Design and development of subsystem interface unit, bus control unit, and supporting equipment for space shuttle data processing equipment
21 p3516 N71-35063
- Development and application of data bus techniques for space shuttle data management systems
21 p3517 N71-35067
- Application of self-sequencing data bus techniques for space shuttle data management system
21 p3517 N71-35068
- Procedures for development and verification of complex software used in space shuttle data management system
21 p3517 N71-35069
- Development and characteristics of executive software for application to space shuttle data management system
21 p3517 N71-35070
- Design concept for integrated display system suitable for computer management and optimized for pilot acceptability applied to space shuttle
21 p3517 N71-35074
- Characteristics of Space shuttle data management system for data transmission and service for avionics equipment and other subsystems
21 p3518 N71-35086
- Development of time shared data bus concept for use with space shuttle guidance, navigation, and control system
[NASA-CR-1792] 21 p3525 N71-35128
- Documentation of photogrammetric mission simulator program with emphasis on global block adjustment module - Vol. 2
[NASA-CR-115172] 22 p3555 N71-35334
- Codification, management, and data systems used by NATO for control of material
[FTL-A-460-1] 22 p3700 N71-36092
- Three-dimensional reproduction of information based on photochromism
24 p3882 N71-37609
- Application of linear gas discharge displays on control panels to data representation systems
24 p3882 N71-37630
- Survey of digital baseband signaling techniques for space shuttle data bus
[NASA-TM-X-44615] 24 p3887 N71-37788
- Performance evaluation of automatic flight recorder strip cutter and loader used in air traffic control facility
[ACTEL-330] 24 p3955 N71-38215
- Analysis of functional requirements for data management systems used with space shuttle - Vol. 1
[NASA-CR-119953] 24 p4020 N71-38808
- Discrete data model and regression analysis for devaluating economic control strategy
24 p4036 N71-38799
- ### DATA TRANSMISSION
- #### NT AUTOMATIC PICTURE TRANSMISSION
- #### NT CHANNELS [DATA TRANSMISSION]
- Developing digital systems and solar electric propulsion technology for thermoelectric outer planet spacecraft
01 p0883 N71-30880
- Automatic equalization for data communications using telephone lines
[AD-710646] 01 p0882 N71-30871
- Freeze-frame addressing system analysis for multiple access communication with applications of error correcting codes
[AD-711061] 01 p0882 N71-30870
- Description and flow chart of PDF 7/P communications package
[AD-711379] 02 p0178 N71-12509
- Comparative performance of common and special grade Asovon transits
[AD-712367] 02 p0179 N71-12510
- Principles for design and selection of modems in data transmission sets
[AD-712125] 02 p0179 N71-12510
- Unified theory for design of optimum coherent digital communication systems
[NASA-CR-111388] 02 p0184 N71-12517

SUBJECT INDEX

Formatting and transmission of data from oceanographic sensors
[AD-711326] 02 p0223 N71-11386

Investigating digital bit synchronization phase locked loops employing binary phase error quantization and sequential loop filtering
[AD-711957] 03 p0336 N71-12403

Minimum time delay unit for conventional time multiplexed data compression channels
[NASA-CASE-XNP-08832] 03 p0345 N71-12506

Analysis of low altitude satellite operating in conjunction with data relay satellite system - Phase 2
[NASA-CR-115814] 04 p0489 N71-13479

Proceedings from symposium on redundancy in information transmission systems - Part 1
04 p0499 N71-13491

Proceedings from symposium on redundancy in information transmission systems - Part 2
04 p0499 N71-13492

Digital radar data transmission system for use in air traffic control
04 p0505 N71-13840

Data transmission and switching system
04 p0507 N71-13849

Error detector/corrector codes adaptable to transmission of numerical data
04 p0507 N71-13851

Speech data interface with all digital transmission systems
04 p0507 N71-13853

Advanced design for development of high reliability aerospace ultrahigh frequency command voice/data transmitter
04 p0508 N71-13854

ATS-F Nimbus E tracking and data relay experiments
[NASA-TM-X-65400] 05 p0770 N71-14597

Circuit schemes and subroutine programs for DNEPR I computer using telephone and telegraph channels
05 p0630 N71-14937

System facility of elementary machines of Minsk 222 computer system
05 p0650 N71-14948

Clustering in discrete stochastic processes with application to transmission channels having memory
[AD-714624] 06 p0813 N71-16051

Describing operations of Deep Space Network command system
07 p0993 N71-17623

Search for best cyclic 720, 80 block codes and comparison of performance with 15, 51 BCH code
[NASA-TR-ERL-174-ITS-111] 07 p0994 N71-17946

Analysis of modulation techniques for HF data transmission for JGOSS telecommunication network
[NASA-TR-ERL-174-ITS-110] 07 p0996 N71-18130

Extrapolation based on coefficients for data reduction and data transmission
[DLR-FB-70-49] 08 p1162 N71-18577

Data compression processor for monitoring analog signals by sampling procedure
[NASA-CASE-NPO-10064] 08 p1167 N71-19288

Wide range analog data compression system
[NASA-CASE-XGS-02612] 09 p1352 N71-19435

Transmission and analysis of cardiographic data on athletes
09 p1329 N71-19589

Pure channel data transmission system with quadrature modulation and complementary demodulation
[NASA-CASE-XAC-06302] 09 p1333 N71-19763

High speed data transmission system for remote data acquisition using data bus
[NASA-CR-103073] 09 p1351 N71-20281

Tropospheric turbulence effects on superhigh frequency transmissions at low elevation angles
10 p1523 N71-21422

Error analysis for mean linear error of nonuniform data in asymmetrical channel without memory
[NLL-RTS-4058] 10 p1530 N71-21649

High data transmission by PCM system
11 p1720 N71-22755

Mark 3A computer configuration of inbound high speed and wideband data synchronizers
11 p1720 N71-22783

Serial synchronous communication method for short distances without using modems
11 p1721 N71-22787

Monitoring circuit design for sampling circuit control and reduction of time-bandwidth in video communication systems
[NASA-CASE-XNP-02791] 11 p1714 N71-23026

Functions, facilities, and operations control system for Deep Space Network
12 p1896 N71-23202

Frequency shift keying apparatus for use with pulse code modulation data transmission system
[NASA-CASE-XGS-01537] 12 p1874 N71-23405

Data transmission reliability and error analysis over radio relay channels
[AD-71483] 12 p1879 N71-23537

Binary data decoding device for use at receiving end of communication channel
[NASA-CASE-NPO-10118] 13 p2045 N71-24741

Near-orthogonal codes for multiple-short keying communication systems
[AD-720822] 14 p2216 N71-25848

Coschokovsk information system for reducing research duplication
14 p2360 N71-26165

Analog coding in nonlinear data transmission systems
[AD-721228] 15 p2380 N71-27177

Long distance high capacity communication using overmoded circular waveguide
[REPT-6494] 15 p2382 N71-27603

Decoding algorithms for data reduction and transmission through noisy space channels using sequential and hybrid computers
[NASA-CR-114277] 16 p2564 N71-28088

Data transmission from Mars and Venus automatic surface vehicles
[D-6] 17 p2718 N71-29362

Data transmission system for coherent reception in channels with frequency shifts
[DISS-4349] 17 p2719 N71-29333

Redundant data reduction in spacecraft instrument grouping
[D-52] 17 p2719 N71-29335

METEOSAT - PCM transmission of satellite photographs
[NASA-TT-F-13830] 18 p2891 N71-31328

Channel capacity for nonorthogonal multiple access communications
[AD-723661] 19 p3053 N71-31725

Information flow model for visual sonal displays
[AD-723180] 19 p3053 N71-32129

Real time television bandwidth compression system design for photographic data transmission
[COO-1469-178] 19 p3056 N71-32226

Synchronous multiplexing for transmission of digital encoded television pictures
[DISS-4516] 20 p3234 N71-33289

Encoding function of neurophysiological synapses
[AD-724072] 20 p3227 N71-33329

Subcarrier frequency multiplexing to separate independent PCM data streams on common carrier by using digital circuits
[NASA-CASE-NPO-11338] 20 p3237 N71-33923

Pioneers F and G with data return capability from Jupiter vicinity
21 p3390 N71-34122

Annotated bibliography of data compression and data connection from information theory literature
[AD-723525] 21 p3393 N71-34165

Digital slope threshold data compressor
[NASA-CASE-NPO-11630] 21 p3399 N71-34188

Organic dye laser as high power optical carrier for broadband data transmission and diagnostic applications during nuclear research test events
[EEO-1183-2262] 21 p3435 N71-34445

Data compression and error correcting codes applied to digital transmission of real time, standard format TV, along with voice and other data from Apollo spacecraft
21 p3515 N71-35049

Analyzing effects of bandlimiting on performance of digital transmission corrupted by additive white Gaussian noise by averaging and series expansion
[NASA-CR-115160] 22 p3553 N71-35508

Telecommunication network exclusively for transmission of digital information
[NLL-POBS-TRANS-2712-1902.811] 22 p3555 N71-35519

Electro-optical link between electroluminescent diode and photomultiplier for temporal transmission
[CEA-N-1431] 22 p3634 N71-35807

Tracking and data system support for Mariner Mars 1969 mission from midcourse maneuver through end of nominal mission
[NASA-CR-122008] 22 p3671 N71-36174

Design principles of high precision measuring television system for information transmission into computer
[AD-72172] 23 p3725 N71-36550

Survey of digital baseband signaling techniques for space shuttle data bus
[NASA-TM-X-64615] 24 p3887 N71-37703

Linear transformation of vector of unquantized signal samples to improve accuracy of reception or measurement
[AD-727900] 24 p3889 N71-37720

Information processing, research projects, mathematical modeling, and analysis of computer systems
[AD-727909] 24 p3896 N71-37770

Image input and output unit for Minsk-2 computer
[AD-727946] 24 p3896 N71-37773

DAYTIME
U CHRONOLOGY
U TIME MEASUREMENT
DATUM (ELEVATION)
News briefs concerning terrestrial geophysics
21 p3509 N71-35081

DAWN CHORUS
Dawn chorus and auroral hiss emission in upper ionosphere and magnetosphere
07 p1017 N71-17143

DEACTIVATION

DAYGLOW
Dayglow measurements of ionized magnesium using rocket-borne ultraviolet spectrometer
[NASA-CR-116853] 08 p1192 N71-18966

DAYTIME
Magnetic variations and auroral zones over Greenland in night and daytime
04 p0521 N71-13779

Day-to-night ratio of cosmic noise absorption from high altitude sites in Northern and Southern Hemisphere
11 p1757 N71-22847

Near infrared radiometer for use on small sounding rockets to observe radiation emission in D region during daytime
[NASA-TM-X-65548] 15 p2411 N71-27685

Daytime operations of large telescopes for infrared astronomy
24 p3904 N71-37996

Daytime use of telescopes, emphasizing infrared astronomy, remote control, and astronomical spectroscopy
24 p3924 N71-37997

DC (CURRENT)
U DIRECT CURRENT
DC 3 AIRCRAFT
Aircraft accident involving Federal Aviation Administration DC-3 aircraft at La Guardia airport, New York in January, 1971
[NTSB-AAR-71-11] 18 p2873 N71-31333

DC 8 AIRCRAFT
Psychosocial evaluation of modifications to DC-8 aircraft nacelles to reduce fan-compressor noise - Part 6
[NASA-CR-1710] 05 p0628 N71-14591

Economic impact of modifications to DC-8 aircraft nacelles to reduce fan-compressor noise - Part 5
[NASA-CR-1709] 05 p0628 N71-14592

Static tests of noise suppressor configurations of DC-8 aircraft nacelle modifications to reduce fan-compressor noise levels - Part 3
[NASA-CR-1707] 05 p0628 N71-14593

Modifications to reduce fan-compressor noise level of DC-8 aircraft - Part 2
[NASA-CR-1706] 05 p0628 N71-14594

Modifications to reduce fan-compressor noise level of DC-8 aircraft - Part 1
[NASA-CR-1705] 05 p0628 N71-14595

Preliminary report of aircraft accident of DC-8 at Anchorage, Alaska
[SB-71-3] 06 p0794 N71-16059

Flight acoustical and performance evaluations of DC-8 nacelle modifications to reduce fan-compressor noise in airport communities
[NASA-CR-1708] 06 p0796 N71-16627

Feasibility of boron-epoxy reinforced aluminum alloy for horizontal stabilizer structure of DC-8 aircraft and recommendations for demonstration program
[NASA-CR-111913] 15 p2368 N71-27664

Analysis of glide-slope information requirements for low visibility aircraft landing approach using Kalman filter-optimal control combination to simulate DC-8 control system
[AD-722655] 18 p2956 N71-30887

Analysis of flight crew duties and operations during flight of DC-8 aircraft with recommended changes to improve safety
[NLL-TR-215] 20 p3212 N71-33585

Aircraft accident investigation of fatal DC-8 crash at Kennedy Airport, New York during ferry flight on September 8, 1970
[NTSB-AAR-71-12] 21 p3377 N71-34030

DC 9 AIRCRAFT
Investigation of Douglas DC-9 accident at Hartlepool, Texas, on 11 Jan. 1970
[NTSB-AAR-70-28] 07 p0971 N71-17476

Aircraft accident report involving DC-9 type aircraft damage incurred when aircraft contacted water surface during approach to Martha's Vineyard airport
[SB-71-64] 19 p3039 N71-32460

Aircraft accident report on midair collision involving DC-9 commercial aircraft and Marine Corps F-4B aircraft near Duarte, California on June 6, 1971
[SB-71-63] 19 p3039 N71-32491

DBT
U DICHLORODIPHENYL-TRICHLOROETHANE
DE HAVILLAND AIRCRAFT
Preliminary report of aircraft accident of DHC-6 at LaCrosse, Wisconsin
[SB-71-4] 06 p0794 N71-16070

Investigation of Mississippi Valley Airways De Havilland DHC-6, N954SM crash at LaCrosse, Wisconsin Nov. 9, 1970
[NTSB-AAR-71-10] 17 p2704 N71-29914

DE LAVAL NOZZLES
U CONVERGENT-DIVERGENT NOZZLES
U DECELERATION
U ACCELERATION
DEACTIVATION
Thermal inactivation curves of Bacillus subtilis spores for decontamination of interplanetary space vehicle components
[NASA-CR-111367] 02 p0151 N71-11073

DEAD RECKONING

Analysis of NZA 3 Sigma u positive molecule deactivation in aurora using atmospheric model based on mass spectrometer measurements
[NASA-CR-121671] 21 p3415 N71-34301

Effects of thermodynamic inactivation on *Bacillus subtilis* var. niger at various temperature, and natural spores in soil
[NASA-CR-121921] 22 p3669 N71-36161

DEAD RECKONING

Laboratory and field tests of dead reckoning system for lunar roving vehicles
[NASA-TM-X-64551] 04 p0544 N71-14425

Field tests of simulated remote navigation control system for lunar surface vehicle
[NASA-TM-X-64567] 06 p0895 N71-16822

DEADWEIGHT

U STATIC LOADS

DEAFNESS

U AUDITORY DEFECTS

DEATH

Comparison of risk of death by meteoroids, weather, or supernovae and electrification in industry (TP-4602) 19 p3199 N71-32708

DEBRIS

NT RADIOACTIVE DEBRIS

NT SPACE DEBRIS

Ingestion of debris into aircraft engine inlets during takeoff

[ARC-CP-1114] 07 p0969 N71-17084

DEBRUING

U CHECKOUT

DEBYE LENGTH

Procedure to replace electron correlation effects with Debye shielded interaction including classical path broadening functions for Stark effects
[NASA-TM-X-67149] 12 p1975 N71-23999

Development of avalanche and streamer in gases in homogeneous electric field with application of Debye screening radius
[JINR-P1-5504] 14 p2322 N71-26074

DEBYE TEMPERATURE

U SPECIFIC HEAT

DEBYE-SCHERRER METHOD

Particle size effects and intensity calculations from Debye scattering equation for face centered cubic crystal 11 p1817 N71-22887

DECEMETRIC WAVES

Analysis of intensity fluctuations produced by interaction of Jovian decametric radio emission with interplanetary medium 19 p3176 N71-32357

Measurement of two circular polarization components of Jovian decametric radiation, and evidence for existence of fourth LH source 19 p3182 N71-32517

DECAY

NT ALPHA DECAY

NT BIOLUMINESCENCE

NT CHEMILUMINESCENCE

NT ELECTROLUMINESCENCE

NT ELECTRON EMISSION

NT EMISSION

NT FIELD EMISSION

NT FLUORESCENCE

NT HALF LIFE

NT INCANDESCENCE

NT ION EMISSION

NT LIGHT EMISSION

NT LUMINESCENCE

NT LUNAR LUMINESCENCE

NT NEUTRON DECAY

NT NEUTRON EMISSION

NT NUCLEAR FISSION

NT OPTICAL RESONANCE

NT PARTICLE EMISSION

NT PHOSPHORESCENCE

NT PHOTOELECTRIC EFFECT

NT PHOTOELECTRIC EMISSION

NT PHOTOIONIZATION

NT PHOTOLUMINESCENCE

NT PHOTOPRODUCTION

NT PLASMA DECAY

NT RADIO EMISSION

NT RADIOACTIVE DECAY

NT SECONDARY EMISSION

NT SOLAR RADIO BURSTS

NT SOLAR RADIO EMISSION

NT SPECTRAL EMISSION

NT STIMULATED EMISSION

NT STRANGENESS

NT THERMAL EMISSION

NT THERMIONIC EMISSION

NT THERMOLUMINESCENCE

NT TYPE 3 BURSTS

NT TYPE 4 BURSTS

NT X RAY FLUORESCENCE

Regge pole approximation in pion model for kaon decay
[NYO-2262-TA-233] 12 p1971 N71-23878

Pole model for nonelectronic hyperon decays with exchanged particles of all spins
[SU-1206-258] 12 p1971 N71-23883

Current algebraic model for asymptotic weak spectral functions and hadronic decays of intermediate vector boson
[NYO-4204-7] 12 p1972 N71-23897

Gamma ray producing decay modes of secondary particles produced in high energy cosmic ray interactions with interstellar and intergalactic gas
[JINR-P1-5542] 13 p2159 N71-24765

Cosmic gamma ray energy spectra caused by hyperon and nucleon isobar decays for gamma ray energies above 1 GeV, and differential production cross section 13 p2159 N71-24770

Positron annihilation gamma ray spectra, positron and positronium production, and equilibrium spectrum of secondary galactic positrons from pion decay
[JINR-P1-5542] 13 p2159 N71-24771

Current algebra for weak interactions in elementary particle physics
[KFKI-70-24-HEP] 15 p2475 N71-27465

Search for positive muon decay yielding two positrons and one electron using cylindrical spark chamber in 4300 Oe magnetic field
[JINR-P1-5542] 16 p2658 N71-29164

Kaon⁰ sub s lifetime and CP violating parameter phase from 3725 kaon⁰ yields pion⁺/pion⁻/pion⁰/decays
[JINR-P1-5542] 19 p3158 N71-32538

Lack of CP invariance violation in kaon decay into tau mode
[PURC-4159-24] 21 p3481 N71-34795

Delta 1 equals 1 mass shift, kaon electromagnetic mass shift, and eta meson yields 3 pion decay amplitude
[SU-1206-245] 21 p3482 N71-34803

Lambda⁰ hyperon polarization along sigma⁻ hyperon decay plane by violating time reversal invariance in electromagnetic interactions of kaon⁰ (minus) or sigma⁻ (minus) with protons
[SU-1206-245] 21 p3487 N71-34842

Beta and electron capture decay in iodine and tellurium
[ANL-TRANS-883] 24 p3980 N71-38401

Neutral decay analysis of mesons
[PURC-4159-29] 24 p3980 N71-38403

Plasma confinement in dc octopole decays in collisional and collisionless regimes
[CONF-710607-3] 24 p3988 N71-38455

DECAY RATES

NT ELECTRON DECAY RATE

Test of change in S equals change in Q rule in neutral kaon sub e3 decay
[CALT-68-251] 03 p0425 N71-12827

Three body decays of neutral K mesons
[COO-1195-187] 03 p0425 N71-12828

Neutron deficient members of A equals 139 decay chain for neodymium 139
[COO-1779-15] 03 p0429 N71-12899

N⁷¹/120 production and subsequent decay to Delta hyperon/1236 pion in pion/ proton interactions at 13.1 GeV
[COO-1428-175] 03 p0431 N71-12911

Production and decay angular distributions of Delta/ hyperons from pion/ proton reactions
[COO-1428-232] 04 p0579 N71-13978

Single gamma spectrum used for investigating decay of Lu-170 to Yb-170
[UCRL-TRANS-10467] 04 p0582 N71-14108

Investigating contribution of Pb impurities to alpha spectrum in measurement of decay rates for element 104
[KFKI-TR-327] 04 p0587 N71-14277

Estimating decay rate of 8.88 MeV state of O-16 with parity-violating force involving rho exchange
[RLO-1388-569] 04 p0589 N71-14344

Investigating possibility of octet of 0/ scalar mesons and onset of 1/ axial vector mesons forming 35-plet SU(6) supermultiplet
[SINP-TH-67-1] 05 p0739 N71-15029

Phenomenological model of T-violation for leptonic decays of baryons as function of electron energy
[SINP-TH-67-2] 05 p0739 N71-15030

Investigating neutral decays of eta-meson using cubical array of lead plate spark chambers for conversion of gamma rays
[UCRL-20039] 05 p0740 N71-15104

Investigating development and components of bubble chambers for elementary particle research
[UCRL-19870] 05 p0741 N71-15120

Measuring ground state decay of Re-190 and isomer ratio in photoneuclear reactions
[IS-T-363] 05 p0746 N71-15230

Deriving formulas for spin and angular correlations in hyperon beta decay
[COO-264-548] 05 p0747 N71-15240

Measuring fractions of aerosol beta activity in precipitation and settled dust
[REPT-9] 05 p0720 N71-15585

Considering relationship between nonelectronic hadron decay and current x current theory
[UH-511-73-70] 06 p0923 N71-16743

Test of Delta S equals Delta Q selection rule in kaon sub e3 decay
[COO-1195-195] 06 p0926 N71-16839

SUBJECT INDEX

Measuring conversion electron and gamma ray spectra in decay of Tm-163 to Er-163
[JINR-P6-5132] 07 p1072 N71-17340

Measuring level schemes of Nb-92 and Nb-94 by p, n/ reaction on separated zirconium targets
[NASA-CR-116429] 07 p1079 N71-18010

Establishing nuclear level scheme of Nd-141 from decay of Pm-141 to Nd-141 using gamma ray spectroscopy
[LYCEN-7051] 07 p1082 N71-18107

Burnup analysis in thermal reactor system - decay chain of fission products
[JAERI-1194] 08 p1236 N71-18234

Measuring decay of Ru-95 to levels in Tc-103 using Ge/Li detectors singly and in coincidence
[IS-T-391] 08 p1254 N71-18340

Measuring decay of Nb-90 to levels in Zr-90 using three-crystal gamma ray spectrometer
[IS-T-395] 08 p1255 N71-18340

Examining assumption of pion, eta-meson, and sigma-meson dominance of weak and electromagnetic decays of K meson using hard meson current algebra
[NUB-2048] 08 p1257 N71-18418

Extending model of partially conserved axial current breakdown to higher order on basis of hard meson current algebra
[NUB-2023] 08 p1258 N71-18623

Decay mode and He-4 coherent interference data for B-11 p/3 He-4 reaction at proton beam energies of 0.675, 1.00, and 1.388 MeV
[JINR-P1-5542] 10 p1621 N71-21740

Solar sensor with coarse and fine sensing elements for matching preirradiated cells on degradation rates
[NASA-CASE-XLA-01584] 12 p1917 N71-23240

Strength distribution for coulomb mixing of isospin state
[JINR-P1-5542] 12 p1977 N71-24230

Eta prime meson decay rate calculated from chiral symmetry breaking
[TR-71-109] 13 p2141 N71-25332

Upper limit on omega meson yields 2 pion decay rate from antiproton-neutron annihilations at rest
[JINR-P1-5542] 15 p2460 N71-27873

Calibration factor Plopton⁺/ for measuring fast fission rate in annular fuel region of Mx 3 gas cooled reactor fuel elements
[AEW-W-975] 15 p2447 N71-27258

Duality FSR method for predicting eta meson yields pion⁰/ gamma gamma decay rate
[DEMO-71/2] 15 p2487 N71-27833

Decay rate and branching ratio R3 of hypertriton, calculated with spatial wave functions
[TID-25665] 16 p2646 N71-28176

Delta S equals 2 transition for obtaining decay rates and asymmetry parameters in nonelectronic hyperon decays
[RIFP-120] 17 p2806 N71-30305

Branching ratio and relative rates of positive kaon decays, and upper limit for structure dependent radiation in kaon decay into electron neutrino photon
[JINR-P1-5542] 19 p3162 N71-32778

Structure of nomograph and slide rule methodology useful in characterizing decay schemes
[AD-726934] 23 p3782 N71-34956

DECCA NAVIGATION

Operating instructions of Decca Mark 19 navigation system 20 p3299 N71-32861

Functions and development of Decca Navigation radio position fixing system 20 p3299 N71-32892

Operating instructions for Decca Mark 25 navigation system 20 p3299 N71-32917

Characteristics of Omega navigation system installed in Norway and installation of navigation system in Sweden
[FOA-3-C-3613-65] 22 p3618 N71-35778

DECELERATION

NT SPIN REDUCTION

Development and characteristics of hot air balloon deceleration and recovery system
[NASA-CASE-XLA-0624-2] 02 p0146 N71-11037

Histopathological and biochemical effects of decelerations on mice physiology
[JINR-P1-5542] 02 p0162 N71-11007

Zero gravity apparatus utilizing pneumatic decelerating means to create payload subjected to zero gravity conditions by dropping its height
[NASA-CASE-XMF-06515] 12 p1916 N71-23217

Development of analytical model for determining spacecraft impact velocity and orientation relative to impact surface for variable dynamic conditions
[NASA-TN-D-6325] 13 p2175 N71-25399

Aerobics 350 recovery system comprising parabolic and extended skirt parachute deceleration devices and incorporating electrical control, pyrotechnic, and pneumatic subsystems - tests
[NASA-CR-118628] 14 p2342 N71-25851

Computerized and manned spacecraft and aircraft simulator impact testing of air cushion elastic restraint systems
[NASA-CR-60169] 18 p2882 N71-30808

Performance tests of convolutional decoder systems for high data rate telemetry links
[NASA-CR-114278] 15 p2383 N71-27786
Comparison of concatenated and sequential decoding systems and convolutional code structural properties
[NASA-CR-114358] 19 p3063 N71-32505
Design and development of encoder/decoder system to generate binary code which is function of outputs of plurality of bistable elements
[NASA-CASE-NPO-10342] 20 p3243 N71-33407

DECODING

Cascaded tree codes for sequential decoding in presence of noise
[NASA-CR-111389] 02 p0181 N71-11270
Majority logic decoding for duals of primitive polynomial codes, and maximality of Euclidean geometry codes
[AD-711791] 02 p0190 N71-11337
Decoding projective geometry codes
[AD-712682] 03 p0341 N71-12474
Constructing algorithms for majority-logic decoding for linear block codes
[AD-712683] 04 p0300 N71-13495
FORTRAN subroutine to decode trace recorded digital data from Randle Cliff Radar
[AD-715336] 07 p0994 N71-17793
Viterbi algorithm for decoding convolutional codes for space channel application
11 p1720 N71-22775

Direct sequential encoding and decoding for digital data sources
11 p1721 N71-23094

Binary data decoding device for use at receiving end of communication channel
[NASA-CASE-NPO-10118] 13 p2045 N71-24741
Decodability of small topographic objects in large scale aerial photography of forests
[AD-726765] 14 p2249 N71-26267
Decoding algorithm for maximum likelihood detection of uniform convolutional codes transmitted with white random noise
15 p2381 N71-27319

Decoding algorithms for data reduction and transmission through noisy space channels using sequential and hybrid computers
[NASA-CR-114277] 16 p2564 N71-28088
Amplitude fluctuation in underwater acoustic pulses and its effect on binary decoding
[AD-722404] 17 p2788 N71-29770
Blizard decoding algorithm for binary linear error correcting codes
21 p3392 N71-34134

Data decoder assembly for Pioneer F and G space probes
21 p3393 N71-34149

DECOMPOSITION

NT HYDROGENOLYSIS
NT PHOTODECOMPOSITION
NT PHOTODISSOCIATION
NT PHOTOLYSIS
NT PROPELLANT DECOMPOSITION
NT RADIOLYSIS
Decomposition in vapor quenched aluminum-silver alloys
02 p0174 N71-11228

Unimolecular decomposition and intramolecular energy relaxation in supra-high pressure region
[AD-714020] 06 p0923 N71-16609
Decomposition of stabilized polyoxymethylene under elevated pressure
[AD-714863] 07 p1049 N71-17956

Use of N-15 as tracer to study decomposition of hydrazine on Shell 405 catalyst
[RPE-TR-69/10] 20 p3230 N71-33473
Synthesis of ladder and spiro polymers resistant to decomposition
[AD-726396] 22 p3603 N71-35663

Decomposition of supersaturated solid solution of tantalum in nickel alloy
[NLL-M-21009-5828.4F] 23 p3773 N71-36893
Mechanism of water decomposition during process of photosynthesis related to biological oxidation and chlorophyll
[NASA-TT-F-14018] 24 p3885 N71-37690

Thermal degradation of flexible polyurethane foam, polyethylene trash containers, and polystyrene packaging material
[Y-1734] 24 p3885 N71-37694

DECOMPRESSION

U PRESSURE REDUCTION

DECOMPRESSION SICKNESS

Relative decompression risk studies of spacecraft cabin atmospheres using miniature pigs
[NASA-CR-1694] 02 p0152 N71-11076
Determination of surface tension in biologic fluids for susceptibility to decompression sickness
[NASA-CR-111382] 02 p0154 N71-11092
Theoretical models related to Hills alternative to naval decompression concepts
[AD-711899] 02 p0155 N71-11095
Saturation excursion diving operations for testing extrapolated tables for repetitive no-decompression excursion from helium-oxygen atmospheres
[AD-718907] 12 p1862 N71-23352

Initial evaluation of revised helium-oxygen decompression tables
[AD-719388] 13 p3033 N71-24683

Using miniature pigs for analysis of altitude decompression sickness and relative decompression hazards of various cabin atmospheres of inert gases
[NASA-CR-114355] 18 p2875 N71-30847

Acoustic-optical imaging technique using Bragg diffraction by sound beam to produce optical image for decompression studies
[AD-723596] 18 p2967 N71-31596

HeO2 saturation dives to verify no-decompression repetitive excursion format of Deep Submergence Systems project
[AD-723721] 19 p3046 N71-32602

Repetitive excursion dives from saturated depths using helium-oxygen mixtures to eliminate decompression sickness
[AD-723733] 19 p3046 N71-32632

No-decompression repetitive excursion dive format testing at 150 and 200 ft using helium-oxygen mixtures
[AD-723711] 19 p3046 N71-32770

DECONTAMINATION

NT SPACECRAFT STERILIZATION
Computerized modeling of ultraviolet and thermal radiation inactivation of spores
[NASA-CR-111386] 02 p0150 N71-11066

Decontamination of reactors containing carbon steel piping
[BNWL-CC-2659] 04 p0550 N71-13757

Manganese dioxide vs. calcium carbonate processes for decontamination of radioactive wastes
[CEB-R-3821] 09 p1430 N71-20145

OGO-6 surface contamination by outgassing in space environment and decontamination by sputtering and desorption
[NASA-CR-117138] 09 p1400 N71-20207

Decontamination of petroleum products with honey
[NASA-CASE-XNP-03835] 12 p1870 N71-23499
Annotated bibliography on recent developments in radiocesium decontamination of buildings, equipment, and personnel
[AED-C-15-7] 19 p3152 N71-32202

Planetary quarantine, decontamination, microbial release probabilities, and contamination logs for Venus and Mars
[NASA-CR-121423] 20 p3215 N71-33221

Decontamination of spacecraft components with ethylene oxide as function of parameters of gas concentration, time, temperature, and relative humidity
[NASA-CR-121764] 21 p3381 N71-34057

Molten-salt fluoride volatility process for recovering decontaminated uranium from aluminum clad fuel elements
[ORNL-4574] 22 p3624 N71-35819

Analysis of storage stability of intermediate moisture foods for space flight feeding with tables of foods and types of manufacture
[NASA-CR-115194] 24 p3880 N71-37658

DECOUPLING

NT SPIN DECOUPLING
Feedback decoupling of time delay differential systems
[NASA-CR-111415] 02 p0196 N71-11375

Decoupling and pole assignment in linear multivariable systems by dynamic compensation
[NASA-TM-X-66510] 04 p0538 N71-14175
Flight testing devices for discharging static electricity from aircraft without production of radio interference
07 p0974 N71-18114

State variable feedback for decoupling of time delay differential equations
12 p1894 N71-24149

Decoupling and pole placement via transfer matrix synthesis
[NASA-CR-123163] 24 p3947 N71-38156

DECREMENTING

U REDUCTION

DEDUCTION

Symbolic logic - sentential and quantificational logic, and deduction
[PUBL-7-DOL-1] 21 p3449 N71-34547

DEEP SPACE

NT INTERPLANETARY SPACE
NT INTERSTELLAR SPACE
Examination of deep space Doppler data for terrestrial media contamination
11 p1703 N71-22773

Extragalactic origin of ultrahigh energy cosmic rays
13 p2163 N71-25292

Reduction ratio for deep space onboard equipment data in telemetry frame, taking into account active channel probability distributions
[D-54] 17 p2718 N71-29360

Third-order phase-locked receivers applied to deep space communication and tracking
18 p2890 N71-31118

Large aperture, phased array, and steerable antennas for high data rate deep space communication systems
[NASA-CR-111941] 18 p2890 N71-31167

Spatial and spectral energy distribution properties of low energy gamma rays in atmosphere and space
23 p3851 N71-37446

Techniques for obtaining magnetic cleanliness in deep space missions to allow interplanetary magnetic field mapping
[NASA-TR-R-373] 24 p0022 N71-3970

DEEP SPACE INSTRUMENTATION FACILITY

Development and implementation of communications equipment for Deep Space Instrumentation Facility
05 p0647 N71-1480

Describing operations in radio astronomy, signal to noise ratio predictions, and tropospheric scattering refraction models for DSIF
05 p0647 N71-1480

Operations and research development of Deep Space Network facilities
[NASA-CR-116517] 07 p0992 N71-17012

Describing operation and facilities of Deep Space Network
07 p0992 N71-17012

DSIF operations and development of wideband data systems for Deep Space Network
07 p1031 N71-17012

DSIF operations for testing theory of general relativity by very long baseline interferometers and for study of polar polarization
07 p0993 N71-17012

Deep Space Network, Ground Communications Facility, Space Flight Operations Facility, and Deep Space Instrumentation Facility research and development - Vol 2
[NASA-CR-117893] 12 p1896 N71-33208

Functions, facilities, and operations control system for Deep Space Network
12 p1896 N71-33208

Deep Space Network, Space Flight Operations Facility, Ground Communications Facility, and Deep Space Instrumentation Facility systems development
12 p1896 N71-33208

Deep Space Network, Ground Communications Facility, and Deep Space Instrumentation Facility operations and engineering
12 p1880 N71-33208

Optical tracking data from geodetic satellites for deep space station coordinates
[NASA-TM-X-65530] 15 p2442 N71-2740

Progress report, block diagrams, and processing of multiple-mission telemetry of Deep Space Instrumentation Facility
21 p3393 N71-34146

Mathematical model of DSIF Doppler tracking system phase noise
21 p3393 N71-34146

DSIF operations support of Mariner Mars 1971 mission, including launches of H and J spacecraft
21 p3394 N71-34149

DSIF telemetry and command processing question program for providing software to Mariner Mars 1971 mission
21 p3394 N71-34146

DEEP SPACE NETWORK

High performance antenna systems for deep space communication
[NASA-CR-115865] 05 p0642 N71-1480

Describing systems and facilities for Deep Space Network
[NASA-CR-115868] 05 p0646 N71-1480

Describing Deep Space Network for communication with unmanned spacecraft traveling planetary distances
05 p0646 N71-1480

Using modeling techniques in design of complex systems for Deep Space Network
05 p0646 N71-1480

Tracking support by Deep Space Network to Mariner Mars 1969 extended operations and Mariner Mars 1971 missions
05 p0647 N71-1480

Transmission media effects on DSN navigational accuracy and tropospheric effects on navigation error
05 p0720 N71-1480

Using digital techniques in communications system research for Deep Space network
05 p0647 N71-1480

Communications elements research on reception and radiometers for Deep Space Network
05 p0647 N71-1480

Supporting research and technology for structural members used in Deep Space Network communications equipment
05 p0647 N71-1480

Developing digital television and data transmission equipment for Space Flight Operations Facility
05 p0647 N71-1480

Developing wideband digital data system for Ground Communications Facility for Deep Space Network
05 p0647 N71-1480

Development and implementation of communications equipment for Deep Space Instrumentation Facility
05 p0647 N71-1480

Real-time selection and validation of telemetry in SFOF and tracking system operations in Deep Space Network
05 p0647 N71-1480

SUBJECT INDEX

DEFLATING

Investigating application of advances in man machine interaction to problems of post-1971 SPOF system 03 p0647 N71-14963

Describing operations in radio astronomy, signal to noise ratio prediction, and tropospheric scattering refraction models for DSIF 03 p0647 N71-14964

Constructing 210 ft diam antenna stations for Deep Space Network 03 p0647 N71-14965

Computer programs for calculating trajectories to Mars and Jupiter 06 p0821 N71-16674

Calibration activity of Deep Space Network in support of Mars encounter phase of Mariner Mars 1969 mission [NASA-CR-116208] 06 p0949 N71-16881

Operations and research development of Deep Space Network facilities [NASA-CR-116317] 07 p0992 N71-17612

Describing operation and facilities of Deep Space Network 07 p0992 N71-17613

Reporting DSN support of active and planned interplanetary missions by Pioneer spacecraft 07 p0993 N71-17614

Sequential estimation with process noise for processing DSN tracking data during planetary orbital missions and Doppler determinations of polar motion using satellites 07 p0993 N71-17615

Reporting advanced engineering research on communications systems for Deep Space Network 07 p0993 N71-17616

Developing communications elements for Deep Space Network 07 p0993 N71-17617

Reporting supporting research and technology for Deep Space Network 07 p0993 N71-17618

Investigating video image display assembly and durability of cathode ray tube gray shades for SPOF development 07 p1004 N71-17619

Developing digital data systems for Ground Communications Facility of DSN 07 p1004 N71-17620

DSIF operations and development of wideband data systems for Deep Space Network 07 p1031 N71-17621

Describing code for automated reporting of DSN status to management and to individual flight project 07 p0993 N71-17622

Describing operations of Deep Space Network command system 07 p0993 N71-17623

Describing modifications and facilities to convert Deep Space Station 61/63 to 85-ft-diam/210-ft-diam antenna complex 07 p1034 N71-17623

Deep Space Network support of Manned Space Flight Network for Apollo project [NASA-CR-116081] 08 p1287 N71-18476

Deep Space Network tracking and data acquisition and scientific instruments for Pioneer 6 09 p1464 N71-19413

Chronology of actions taken by ground control facilities following Apollo 13 flight emergency [NASA-TM-X-64933] 09 p1466 N71-19960

Deep Space Network functions, facilities, operations, and research for support of space communications and flight programs 11 p1829 N71-22766

Deep Space Network functions, and facility operations 11 p1829 N71-22767

Mariner Mars 1971 mission support plan modifications and cost reductions by DSN 11 p1829 N71-22768

Viking mission support by tracking and data system of DSN 11 p1829 N71-22769

Inherent accuracy of DSN as radio navigation instrument for lunar and planetary missions 11 p1733 N71-22770

Deep Space Network, Ground Communications Facility, Space Flight Operations Facility, and Deep Space Instrumentation Facility research and development - Vol. 2 [NASA-CR-117895] 12 p1896 N71-23201

Functions, facilities, and operations control system for Deep Space Network 12 p1896 N71-23202

Deep Space Network support for Pioneer F and G missions, Helios Project, Viking Mars 1975 orbiter and lander, and Apollo 14 flight 12 p1995 N71-23203

Deep Space Network, space tracking and navigation, communications elements and systems, and supporting research and development 12 p1992 N71-23204

Deep Space Network, Space Flight Operations Facility, Ground Communications Facility, and Deep Space Instrumentation Facility systems development 12 p1896 N71-23205

Deep Space Network, Ground Communications Facility, and Deep Space Instrumentation Facility operations and engineering 12 p1880 N71-23206

Deep Space Network support activities for Apollo 9 through 13 flights and associated activities [NASA-CR-118323] 13 p2168 N71-25153

Deep Space Network telecommunication and ground support equipment for planetary and interplanetary flight projects [NASA-CR-118895] 15 p2518 N71-27911

Deep Space Network mission support activities, telemetry, and data systems for Pioneer, Helios, Viking, and Mars 71 projects [NASA-CR-121378] 20 p3346 N71-33163

Deep Space Network operations, monitoring system, and telemetry system 20 p3347 N71-33164

Deep Space Network support for Pioneer, Helios, Viking, and Mariner Mars 71 spacecraft telemetry data systems 20 p3347 N71-33165

Comparison of differenced Doppler and range tracking data-types for process noise problem solutions and computer programs for orbit and failure rate calculations 20 p3347 N71-33166

Digital television system, computer programs, high-speed data subassemblies and performance, multiple-mission telemetry and command systems, and phase shifter and data decoders for DSN 20 p3333 N71-33167

Deep Space Network operations for Mars 71 project, mathematical model for Doppler tracking system, and third-order phase locked system transient response analysis 20 p3347 N71-33168

Deep Space Network progress report, including mission support, development and implementation, and operations and facilities [NASA-CR-121717] 21 p3390 N71-34118

DSN functions and facilities, including Deep Space Instrumentation Facility, Ground Communications Facility, and Space Flight Operations Facility 21 p3390 N71-34119

Real time and near real time functions of DSN telemetry system 21 p3390 N71-34120

DSN monitor system changes after using IBM 360/75 computers 21 p3390 N71-34121

DSN requirements for Mariner Mars 1971 mission support 21 p3391 N71-34124

DSN support for Viking Mars program 21 p3391 N71-34125

Twenty-six and sixty-four meter antenna station experiments in DSN 21 p3391 N71-34126

DSN research and technology support, including radiometric observations, polar observations, precision antenna gain measurement, and clock synchronization transmissions 21 p3392 N71-34136

S band planetary radar receiver for Mars Deep Space Station and Venus radar mapping experiments 21 p3392 N71-34137

Multiple-mission command system for installation in DSN for command and control of spacecraft 21 p3393 N71-34147

DSN command system operation from Space Flight Operations Facility supporting Mariner Mars 1971 mission 21 p3393 N71-34150

Design, development, and operation of communications system for command and control of unmanned spacecraft during exploration of deep space [NASA-CR-121898] 22 p3553 N71-35304

Tracking, telemetry, and command operations of Deep Space Network in support of Mariner Mars project [NASA-CR-123068] 22 p3469 N71-36159

Tracking and data system support for Mariner Mars 1969 mission from midcourse maneuver through and beyond Mars orbit [NASA-CR-123088] 23 p3671 N71-36174

Facilities, functions, and projects of Deep Space Network [NASA-CR-123843] 24 p4006 N71-38564

Summary of objectives, functions, and organization of Deep Space Network 24 p4006 N71-38565

Role of DSN in support of Pioneer, Helios Mariner Mars 1971, Viking, and Apollo missions and in support of radio science experiments 24 p4006 N71-38566

Development and implementation of Space Flight Operations Facility and Ground Communications Facility for DSN 24 p4007 N71-38568

Mission support area in DSN for Pioneer F and G probes 24 p4007 N71-38569

NT CRYSTAL DISLOCATIONS

NT EDGE DISLOCATIONS

NT FRENKEL DEFECTS

NT INCLUSIONS

NT POINT DEFECTS

NT SCREW DISLOCATIONS

NT SURFACE DEFECTS

NT VACANCIES (CRYSTAL DEFECTS)

Defect states in glassy and crystalline materials studied by optical spectroscopy and electron paramagnetic resonance 81 p0111 N71-10661

Study of defect structures with field ion microscope [NASA-CR-113771] 04 p0603 N71-14151

Visual defects related to transfer-molded parts of epoxy and diethylphthalate compounds [BDX-613-166] 10 p1366 N71-21364

Electromagnetic shielding effectiveness degradation from weld defects in metal conducting sheets and comparison of propagation through rectangular and circular apertures 16 p2549 N71-28410

Weighted defect densities of asphaltic and cement concrete pavement in airfield pavement condition survey, USNAP Cecil Field, Florida [AD-721323] 16 p2577 N71-28422

Weighted defect densities of asphaltic and cement concrete pavement in airfield pavement condition survey, USNAP Charleston, Rhode Island 16 p2577 N71-28424

Qualitative analysis of radiographs and their importance for evaluating effects of defects on fatigue properties of welds [NLL-CE-TRANS-5451-7022.09/1] 16 p2605 N71-29170

Diameter profiles of Zircaloy-clad UO₂ fuel rods from boiling water reactor for defect evaluation [GBAF-10257] 17 p2782 N71-29368

Radiographically detected weld defects in steels and effects of brittle fracture, mechanical stresses, and weld defects on weld seams during fabrication and operational conditions [NLL-CE-TRANS-5486-7022.09/1] 17 p2753 N71-29722

Ultrasonic surface waves for detecting near-surface flaws in nondestructive testing of metal plates [AD-73258] 19 p3187 N71-31944

Quantitative determination of optical imperfection by mathematical analysis of Foucault knife edge test pattern in large orbiting telescope [NASA-TN-D-6119] 19 p3142 N71-32184

Effects of quenching, plastic deformation, and neutron and electron irradiation defects on order-disorder transformations in beta-brass 19 p3117 N71-32539

Temperature and radiation dosage effects in niobium lattice defect buccinator of protons and helium ions 21 p3498 N71-34923

Damage control systems for detecting and locating overboard and onboard leak and damage modes on space stations [NASA-CR-111963] 23 p3857 N71-37495

SNAP 8 double containment boiler evaluation for metallurgical defects [NASA-CR-72962] 24 p3959 N71-38243

DEFENSE

Chemistry, physics, metallurgy, and engineering related problems in provision and use of defense material 23 p3856 N71-37488

DEFENSE COMMUNICATIONS SYSTEM (DCS)

House committee investigation of Department of Defense communications 16 p2696 N71-29146

DEFENSE INDUSTRY

Results of 1968 survey of industrial research and development [NSF-70-29] 06 p0962 N71-16896

Defense in-house laboratories, emphasizing R and D management [AD-715213] 07 p1153 N71-17726

Reporting congressional testimony on independent research and development 07 p1134 N71-18016

Military scientific research and development program review [DR-206] 13 p2193 N71-23549

Conversion of US scientific and technical resources from defense and aerospace to civilian objectives [GUPS-MON-8] 20 p3571 N71-33825

DEFENSE PROGRAM

Abstracts of research studies performed at Saadiah Research Institute for National Defense [RAB-LD-TRANS-1542] 13 p2193 N71-23550

DEFLAGRATION

Gas flow during and after deflagration of spherical cloud of fuel air mixture [AD-716339] 09 p1370 N71-19555

Theoretical and experimental determination of combustion properties and steady state deflagration of double base solid propellant 11 p1829 N71-22883

DEFLATING

U INFLATABLE STRUCTURES

U PRESSURE REDUCTION

DEFLECTION

DEFLECTION

- Calculations and measurements of strain distribution and deflection on model swept wings
[NAL-TR-195] 02 p0300 N71-11950
- Orbital expansion thrust effect on shape of ISIS satellite boom
[CRC-TR-632] 05 p0771 N71-15160
- Use of conformal mapping to improve uniformity of electric fields
[IPI-7-T-4] 05 p0657 N71-15575
- General numerical large deflection solution of coaxial ring circular glass plate flexure problem
[AD-714154] 06 p0878 N71-16344
- Helicopter application studies of variable deflection thruster jet flaps
[AD-715071] 07 p0973 N71-17907
- Iterative solution to large deflection problem of flexible beam springs for design of compression and torsion springs
10 p1658 N71-21647
- Displacement equations in Cartesian coordinates for solving deflection response of flat membranes
14 p2347 N71-25807
- Design and fabrication of electron beam X-Y deflection system for retrofit on welding guns
[NASA-CR-119841] 17 p2729 N71-29234
- Difference equations solved for determining large deflection response of circular, rectangular, and polygonal flat membranes
[AD-723538] 19 p3188 N71-32027
- Calculation of aerodynamic loads acting on flechettes and sabot projectiles resulting from shock waves
[AD-724178] 20 p3203 N71-32814
- NASTRAN computer program used to calculate lateral deflections of weak spacecraft antenna boom to determine stiffness at small strains
22 p3682 N71-36256
- Second order solutions to shear stress, normal stress, horizontal displacement, and transverse deflection in multilayer Timoshenko beams
[AD-727640] 24 p4026 N71-38726
- DEFLECTORS**
- Retrodiffractive interferometric holography in wind tunnels including displacement and deformation of deflectors
[ONERA-TP-852] 02 p0201 N71-11510
- Deflecting modes of disk-loaded waveguides for CERN RF separator
[CERN-70-26] 06 p1247 N71-16184
- Particle separation in system of conventional S-band iris-loaded deflectors interspersed with alternate gradient magnets of strong focusing channels
[BNL-15436] 11 p1804 N71-22286
- Ion beam deflector system for electronic thrust vector control for ion propulsion yaw, pitch, and roll forces
[NASA-CASE-LEW-10689-4] 14 p2332 N71-26173
- Particle separation using deflectors with crossed electric and magnetic fields
[NP-18786] 24 p3976 N71-38371
- DEFOCUSING**
- Thermal defocusing of CO₂ laser beam in air doped with SF₆
[AD-710743] 01 p0063 N71-10487
- Mathematical model for self-defocusing of light beam in fluid
[AD-710741] 01 p0090 N71-10573
- Optical retrodirective modulator with focus spearing reflector driven by modulation signal
[NASA-CASE-GSC-10062] 05 p0690 N71-15605
- Nonlinear optics of thermal laser beam defocusing in gases
[AD-720311] 15 p2418 N71-27395
- DEFORMATION**
- NT AXIAL STRAIN**
- NT ELASTIC BENDING**
- NT ELASTIC BUCKLING**
- NT ELASTIC DEFORMATION**
- NT NUCLEAR DEFORMATION**
- NT PLASTIC DEFORMATION**
- NT STATIC DEFORMATION**
- NT TENSILE DEFORMATION**
- NT WAVE FRONT DEFORMATION**
- Characteristics of materials for simulation of hot forging processes
[AD-711303] 02 p0229 N71-11528
- Viscous flow of deformable liquid drops in suspension in circular cylindrical tubes
[AD-711633] 02 p0203 N71-11563
- Large quadrupole forces of deformed nuclei with iterative calculation
02 p0275 N71-11908
- Inelastic deformation of aluminum alloys under combined stress at high temperature
[AD-712047] 02 p0244 N71-12063
- Shear deformation in heterogeneous anisotropic plates
[AD-711920] 02 p0304 N71-12105
- Deformation in rectangular C-137 sources
[ORNL-TM-3069] 03 p0414 N71-12746
- Uniqueness and convergence of discrete aggregate model in polycrystalline plasticity
[AD-712060] 03 p0441 N71-12838

- Analysis of symmetric bladder deformation due to symmetric inversion pressures
03 p0462 N71-13116
- Deformation processes in forging polycrystalline oxide ceramics
[NASA-CR-116896] 08 p1224 N71-19225
- Gas gun and piezoelectric gage for measuring high velocity deformations in shocked metal crystals
09 p1454 N71-20231
- Development and application of theory of elasticity for layer with circular cylindrical hole subjected to nonuniform radial displacement
[NASA-TM-X-58056] 09 p1480 N71-20463
- Deformation behavior of alloys and stress-strain relationships for ductile metals
[RAE-LIB-TRANS-1491] 10 p1582 N71-21519
- Crimp mechanisms and structure dependence of high temperature deformation of metals and alloys
[SU-326-P-17-X-1] 10 p1584 N71-21616
- Analysis of finite deformations of incompressible elastic solids by finite element method with formulations of higher order approximations and curvilinear elements
[AD-717768] 11 p1835 N71-22237
- Possible effect of deformation forces on diurnal state of baric field and subsequently for short range weather forecasting
11 p1756 N71-22836
- Time dependent mechanical behavior of Solihane 113 and stress and deformation analysis of thick wall cylinders of nonlinear elastic materials under internal pressure
11 p1839 N71-23020
- Investigation of characteristics of deformation and rupture of polymer materials and glass reinforced plastics
[AD-719780] 13 p2100 N71-24972
- Development of exact tensor and physical component equations for symmetrical circular plates with large deflections
13 p2181 N71-25106
- Numerical analysis of axially symmetric boundary value problems in elastic dissimilar layered media
13 p2181 N71-25126
- Effects of plastic deformation during shock loading of zinc monocrystals
[AD-719536] 13 p2096 N71-25134
- Effect of plastic deformation on distribution of microcracks and structure of mild steel
[AD-719832] 13 p2096 N71-25159
- Galvanometer for automatic recording of deformation measurement process
[TT-70-59121] 14 p2253 N71-25664
- Effect of hydrostatic pressure on deformation of NaCl single crystals
[AD-720415] 14 p2325 N71-25912
- Deformation measuring apparatus with feedback control for arbitrarily shaped structures
[NASA-CASE-LAR-10098] 14 p2351 N71-26681
- Carbon content effects on niobium alloy deformation
[AD-720932] 15 p2419 N71-26812
- Fundamental characteristics of dynamic slip-band propagation determined from high strain rate deformation of niobium single crystals
15 p2422 N71-27213
- Compression tests for establishing possible thermal effect of tectonic deformation of rocks
[NASA-TT-F-13707] 16 p2585 N71-28220
- Effect of spatial and temporal shapes of pressure pulses on final deformation of circular cylindrical shells under axially varying pressure loads
[ANL-7738] 16 p2685 N71-28571
- Analysis of effect of shear deformation on solutions of thin, nonshallow spherical shells using method of matched asymptotic expansions
16 p2687 N71-28647
- Monopole /lupion/ equals positive 0/ excitations in even-even deformed nuclei
[JINR-P4-5422] 16 p2652 N71-28985
- Acoustic emission analysis of material properties and defect structure
[UCRL-72657] 17 p2786 N71-29268
- Theoretical analysis of stiffness, stresses, and deformations of corrugated shear webs
20 p3356 N71-32884
- Plate theory structural analysis of variable thickness axisymmetric plate contact with smooth rigid surfaces including thickness and shear transverse deformation effects
20 p3361 N71-33949
- Stress analysis of aluminum and copper at high temperatures using theory of thermally activated deformation of metals
[EP-195611] 21 p3439 N71-34473
- Influence of deformation rate on yield stress of nickel-base alloys
[NLL-M-21012-5828.4F] 21 p3441 N71-34486
- Correlation between deformation substructure, precipitates, recrystallization state, and stress corrosion of aluminum zinc magnesium alloy
[NLL-M-38372-5828.4F] 21 p3441 N71-34488
- Saxon-Woods potential for describing spherical and deformed nuclei in transuranium region
[BNL-TR-416] 21 p3475 N71-34744

SUBJECT INDEX

- Formulation of large deformation elastoviscoplastic theory for thick walled spherical shells
[AD-722867] 21 p3528 N71-33141
- Application of Green function to elastic displacement caused by unit force in infinitely extended anisotropic media
[COO-2034-S] 21 p3529 N71-33141
- Correlation equation relating creep deformation of tubes to stress and temperature functions, and application to design of heat exchanger tube
[NASA-TM-X-5372] 21 p3529 N71-33141
- Photographic technique for determining region and intensity of strain zone, changes in strain rate, and deformation at any point during metal cutting
[NRC-TT-1471] 22 p3588 N71-33548
- Crimp and creep rupture deformation and tensile tests of nickel alloys
22 p3592 N71-33577
- Comparison of ASKA and NASTRAN program analyses of space shuttle hot electron test cells deformed under thermal and mechanical loads
22 p3683 N71-36256
- Stresses and deformations in multiply bent pneumatic aircraft tires subjected to inflation pressure loading
22 p3693 N71-36256
- Horizontal extensometer for measuring deformation caused by earth tides
23 p3749 N71-36707
- Gravimetric instruments for recording deformation of earth crust and earth surface caused by earth tides
24 p3969 N71-37804
- Deformation in Serrurier truss tubes in large astronomical telescopes
24 p3923 N71-37801
- Development of technique for determining toughness and inelastic resistance of tires in tangential direction
[AD-727470] 24 p3928 N71-38007
- Effect of rate of deformation on mechanical properties of metals and propagation of stress and strain waves in metal
[AD-727203] 24 p3938 N71-38007
- Analysis of deformation, stresses, and irreversible absorbing energy during thermal fatigue cyclic tests
[AD-727945] 24 p3939 N71-38007
- Deformation mechanisms in compacting metal powders
[AD-727851] 24 p3940 N71-38007
- Tension and slow bend tests to determine effect of temperature and strength orientation on Al-Al₃Si₃ intermetallic alloy deformation
24 p3942 N71-38007
- Plastic deformation of fine-grained, high purity, hot pressed aluminum oxide and stress corrosion of polycrystalline magnesium oxide
[AD-727611] 24 p3945 N71-38007
- Deformation of structural shells during welding
[AD-727943] 24 p4026 N71-38726
- Analysis of axisymmetric deformations of cylindrical membrane composed of elastic, homogeneous, isotropic, and incompressible material
[AD-728022] 24 p4027 N71-38726
- DEFORMATIONS**
- Deformations and extensometers for measuring earth crust deformations
24 p3910 N71-37801
- DEFOGGING**
- Test procedures for aircraft defogger/defewer equipment
[AD-719109] 13 p2025 N71-24482
- DEGASSING**
- NT DEOXYGENATION**
- Gas control in liquefied materials during weightless manufacturing in orbital workshop
02 p0203 N71-11771
- Partial degassing heat measurement for molten dross and slag at 2000 K
[CEA-CONF-1516] 03 p0391 N71-12880
- Stress analysis of cylindrical degassing tank, with support interference effects
[CRIF-MT-57] 10 p1453 N71-23889
- Degassing and rates of evolution for copper under a ultrahigh vacuum
13 p2094 N71-24881
- Reaction kinetics of degassing hydrogen and nitrogen from iron and steel
[TT-70-58193] 14 p2268 N71-25540
- Solar wind, meteoric volatilization, and thermal degassing contributing to lunar rarified atmosphere, and transient contributions produced by rocket gas during lunar missions
[NASA-CR-110630] 14 p2335 N71-25706
- Kinetics of steel vacuum degassing in highly heat refractory material crucibles
19 p3111 N71-33599
- DEGENERATIVE FEEDBACK**
- NT NEGATIVE FEEDBACK**
- DEGRADATION**
- NT THERMAL DEGRADATION**
- Evaporative erosion of thermoelectric aluminum some thermoelectric generators
[SC-RR-70-534] 02 p0147 N71-11908

- Susceptibility of polyurethane foam to deterioration by impurities or contaminants in ethylene glycol monomethyl ether
[AD-715313] 07 p0997 N71-17355
- Pulse superconducting magnet, niobium/titanium were selected, ac transmission loss, degradation effect, and inductance measurements for ac dipole conductors
[KFK-1217] 13 p2125 N71-34999
- Open circuit and bias degradation tests in copper and cadmium sulfide thin film solar cells
[NASA-TN-D-6362] 13 p2031 N71-25394
- Space environment radiation effects on solar cell degradation
[NASA-CR-121614] 21 p3378 N71-34036
- Degradation of Ti/Ag contacts in Si solar cells, and deposition of Ti/Ag contacts on Si wafers
[NASA-CR-121725] 21 p3378 N71-34039
- Electronic component degradation due to electromagnetic pulse transients
[AD-726923] 24 p3898 N71-37783
- MEANS OF FREEDOM**
- Astronaut control training device for astronauts performing friction-free movement with five degrees of freedom
[NASA-CASE-XMS-02977] 01 p0309 N71-10746
- Measuring effect of transmission time delay on performance of manipulation tasks with six degrees of freedom master-slave manipulator
[NASA-CR-116694] 08 p1208 N71-19134
- Mathematical formulation of kinematic equations to describe motion of six degrees of freedom vibration table for use in research on human subjects
[AD-720269] 14 p2210 N71-26158
- Tuned damped vibration absorber for mass vibrating in more than one degree of freedom for use with wind tunnel models
[NASA-CASE-LAR-10083-1] 15 p2414 N71-27006
- Dynamic aspects of fission as two-dimensional process with quadrupole and hexadecapole degrees of freedom in microscopic theory
[DNR-F-1230] 16 p2632 N71-29005
- Flight simulation of short takeoff aircraft and Dornier-31 aircraft, and results using cockpit simulator with 6 degrees of freedom for DO-31
19 p3074 N71-31956
- Single degree of freedom roll response due to vertical random two dimensional vertical gusts
[NASA-CR-111966] 23 p3706 N71-36421
- REHYDRATED FOOD**
- Feasibility of storing and dispensing rehydratable food aboard space vehicle
[AD-715096] 06 p1157 N71-18364
- Human immunology on prolonged diet of dehydrated foods
08 p1154 N71-19064
- Fabrication and evaluation of dehydrated food bars produced by compression and molding processes
[AD-717289] 11 p1686 N71-21900
- Compressed, cooked, freeze dried, nonsweet, cheese and meat flavored snack cubes for Apollo food system
[NASA-CR-114996] 13 p2038 N71-25001
- REHYDRATION**
- Functional synchronization of neurosecretory cells of supra-optical success of dehydrated and rehydrated rat
[NASA-TT-F-13419] 03 p0322 N71-12301
- Extravascular dehydration effects in production of cardiovascular deconditioning by bed rest simulating weightlessness
[NASA-CR-114808] 06 p0804 N71-16702
- Extravascular dehydration produced by bed rest simulating weightlessness - data tables
[NASA-CR-114809] 06 p0804 N71-16703
- Metabolic imbalances and body hypohydration during food deprivation for 10 days
09 p3137 N71-20368
- Chemical properties of cellulose acetate gels in both dry and gel states
[NRC-TT-1439] 10 p1512 N71-21208
- REHYDROGENATION**
- Kinetics of catalytic dehydrogenation of methylcyclohexane at 600, 650, and 700 deg F and 5 atm pressure
[AD-715936] 06 p1303 N71-18729
- Cobalt and copper ferrite spinels as catalysts in oxidative dehydrogenation of butenes
[NASA-CR-116882] 06 p1161 N71-19238
- RESEARCH**
- Environmental tests of deicing techniques for ship structures
[NRC-11872] 11 p1847 N71-22405
- Test procedures for evaluating capability of anticollision equipment aboard aircraft
[AD-724622] 20 p3209 N71-33005
- RESEARCH**
- Calculating and testing anticollision systems of aircraft and helicopters
[AD-719922] 14 p2197 N71-25622
- RESEARCH SYSTEMS**
- U DEICERS
- RELATIONS
- U COUNTERS

- DELAY**
- Statistical data on delays and cost of delays at airline terminals
01 p0083 N71-10366
- Effects of nonequilibrium free-radical content and composition variation of supersonic streams entering air breathing engines on ignition points and delays
[NASA-CR-111371] 02 p0288 N71-11467
- Nonlinearity and signal transmission delay effects on feedback control systems based on random input signal analysis and cross correlation
16 p2576 N71-28826
- Long-delayed echo observations, boxes and their recognition, and extraterrestrial origin hypothesis
[AD-726735] 23 p3724 N71-36543
- DELAY CIRCUITS**
- Development of pulsed differential compactor circuit
[NASA-CASE-XLE-03804] 09 p1362 N71-19471
- Delay circuits for pulse compression in airborne FM demodulator
[RAE-T-70110] 12 p1874 N71-23363
- Electrical delays to define nulls in directional response to acoustical superdirective arrays
[AD-718322] 12 p1967 N71-23902
- Pulse duration control device for driving slow response time loads in selected sequence including switching and delay circuits and magnetic storage
[NASA-CASE-XGS-04224] 14 p2234 N71-26418
- DELTA LINES**
- NT ACOUSTIC DELTA LINES**
- NT DELTA LINES [COMPUTER STORAGE]**
- Development and characteristics of solid state acoustic variable time delay line using direct current voltage and radio frequency pulses
[NASA-CASE-ERC-10032] 14 p2232 N71-25900
- DELTA LINES [COMPUTER STORAGE]**
- Mathematical background and application of two computer programs obtaining smooth group delay characteristics from moderate number of specific points
[REPT-6106-ADD-1] 11 p1716 N71-22283
- DELTA LINES**
- Ray tracing to delineate radio propagation to large distances by ducting under super refracting conditions in troposphere, ionosphere, or magnetosphere
[AD-726977] 23 p3723 N71-36541
- DELIVERY**
- Aerial delivery system for dropping emergency pumping equipment to distressed boats - Phase I
[AD-712288] 03 p0327 N71-12337
- Aerial delivery system for dropping emergency pumping equipment to distressed boats - Phase 2
[AD-712289] 03 p0328 N71-12338
- DELTA DART AIRCRAFT**
- U F-106 AIRCRAFT
- DELTA FUNCTION**
- Fredholm solution of delta function model for two electron helium like ions
[NASA-CR-117893] 12 p1969 N71-23286
- DELTA LAUNCH VEHICLE**
- Computerized design of delta body space shuttle orbiter
14 p2343 N71-26067
- Research, development, and design of velocity trim system for third stage of Delta launch vehicle
[NASA-CR-118488] 14 p2345 N71-26370
- Capabilities, constraints, and costs of Delta launch vehicle, Model 2014
[NASA-TM-X-65674] 20 p3354 N71-33446
- DELTA MODULATION**
- Delta modulation techniques for analog to digital conversion of speech signals
[SRDE-69822] 03 p0343 N71-12492
- Quantizing noise analysis in delta modulators applied to first order Markov sources
[AD-717221] 10 p1533 N71-21081
- Applications and methods for improving delta coding
[NLL-PORS-TRANS-2687-19022.81/1] 17 p2720 N71-29844
- Method of analogically controlling step size in band compression
[NLL-TRANS-2681-19022.81/1] 19 p3056 N71-32337
- Models for internally generated noise in delta modulators and stability criteria for nonrandom inputs
23 p3739 N71-36662
- DELTA WINGS**
- Leading edge effect on aerodynamic characteristics of 70 deg swept delta wing
[AD-712087] 02 p0142 N71-11007
- Aerodynamic characteristics of large-scale model with lift fin mounted in 5 percent thick triangular wing
[NASA-TN-D-7031] 03 p0626 N71-14638
- Aerodynamic performance of shuttle-orbiter configuration with variable delta wing geometry in low turbulence subsonic wind tunnels
[NASA-TM-X-2206] 05 p0626 N71-14943
- Low subsonic aerodynamic characteristics of space shuttle-orbiter concept with blended delta wing-body
[NASA-TM-X-2209] 05 p0772 N71-15485

- Avoidance of disrupting effects in dynamic tests on semispan delta wing models in transonic slotted and perforated wing tunnels
[ARC-R/M-3634] 06 p0791 N71-15701
- Aerodynamic coefficients, pressure, load and force distributions on cambered delta wings
[ARC-CP-1129] 07 p0966 N71-17112
- Aerodynamic heating and structural analyses for radiatively cooled delta wing of hypersonic aircraft
[NASA-TN-D-4138] 07 p1128 N71-18023
- Wall pressure and heat transfer distribution on delta wings in supersonic hypersonic flow
[REPT-70-9] 08 p1339 N71-18423
- Lift and drag interference characteristics of delta winged half cones with leading edges
09 p3132 N71-19359
- Viscous interacting flow in hypersonic streams, including flow over flaps, corners, delta wings, and wing-body combinations
[NASA-TM-X-66014] 09 p3373 N71-19831
- Aerodynamic characteristics of slender delta wing aircraft and response to vertical and lateral gusts during landing approach
[RAE-LIB-TRANS-1524] 10 p1093 N71-21223
- Predicting aerodynamic characteristics of arrow, delta, and diamond wing platforms using Prandtl-Glauert transformation
11 p1669 N71-21973
- Numerical analysis of influence coefficients, natural frequencies, and mode shapes of vibration of triangular inflatable wing
11 p1671 N71-22666
- Analysis of supersonic and hypersonic flow of inviscid ideal gas over conical wings with sharp leading edges and attached shock waves by three dimensional method of characteristics
[NASA-CR-1738] 11 p1671 N71-22672
- Angle of incidence effect on delta wing leading-edge vortices with cross flow visualization in hydraulic test tunnel
[ARC-R/M-3645] 13 p2063 N71-24482
- Flow measurement of Nonlinear delta wing in hypersonic slip flow
[DLR-FB-70-46] 13 p2022 N71-34500
- Oscillatory pitching moment derivatives measurement on delta wings in incompressible flow
[ARC-R/M-3628-PT-1-4] 13 p2022 N71-24569
- Measurements of oscillatory pitching moments on round leading edge delta wing in incompressible flow noting vortex flow development
13 p2022 N71-24570
- Measurement of oscillatory pitching moment derivatives on sharp-edged delta wing at vortex breakdown angle of attack
13 p2023 N71-24572
- Buffet response of straight wing and delta wing model of space shuttle launch configuration
13 p2179 N71-24662
- Aerodynamic characteristics of delta wing space shuttle configurations
14 p2193 N71-26062
- Box collocation method for calculating aerodynamic loads on tandem delta wings with oscillations in supersonic flow
17 p2698 N71-29337
- Active and passive thermal protection system weights for delta body space shuttle for crossrange up to 1500 n.m.
17 p2847 N71-29460
- Predicted and measured aerodynamic characteristics for blended delta-wing orbiter at hypersonic speeds
[NASA-TM-X-62046] 19 p3184 N71-32106
- Pressure distribution near center line of trailing edges of delta wings and conical bodies at high supersonic speeds
[ARC-CP-1153] 20 p2083 N71-32868
- Pressure distributions on planar delta wings attached to cylindrical bodies in supersonic flow - theoretical results for sonic leading edge, angle of attack case
[WRE-TN-HSA-106] 20 p3207 N71-33699
- Low speed wind tunnel measurement of induced drag characteristics of three 50 degree delta wings with different leading edge spanwise distributions
[KTH-AERO-TN-57] 21 p3373 N71-34083
- Wind tunnel stability tests of variable dihedral delta wing spacecraft configuration at hypersonic speed
[NASA-TM-X-2391] 21 p3374 N71-34080
- Subsonic aerodynamic stability characteristics of NAR 1348 delta wing space shuttle
[NASA-CR-103193] 21 p3522 N71-35093
- Trinomic wind tunnel static stability tests on straight wing and delta wing space shuttle models
[NASA-CR-119066] 21 p3523 N71-35100
- Low speed wind tunnel tests of directional stability characteristics for M/DAC delta wing booster
[NASA-CR-103157] 21 p3523 N71-35105
- Low speed wind tunnel tests on longitudinal and lateral stability of high cross range delta wing space shuttles
[NASA-CR-119857] 21 p3524 N71-35109
- Low speed wind tunnel tests of straight wing and delta wing configuration space shuttle booster models
[NASA-CR-103162] 21 p3524 N71-35110

Comparison of finite element computer programs for analysis of clamped flat plate and built-up wing vibration frequencies

22 p3687 N71-36293

NASTRAN static, modal, and transient analyses plotting techniques with delta wing examples

22 p3688 N71-36299

Aerodynamic heating distributions on model of space shuttle delta wing orbiter with twin wing-tip vertical tails

[NASA-TM-X-42057] 22 p3689 N71-36344

Aerodynamic heating of space shuttle delta-wing booster at free Mach stream 7.4

[NASA-TM-X-42058] 22 p3695 N71-36354

Wind tunnel static longitudinal stability and control characteristics of cruciform delta winged missile with various horizontal canards and trailing-edge flap control between Mach 1.50 and 4.65

[NASA-TM-X-2347] 22 p3705 N71-36415

Methods for prediction of centerline shock layer thickness and pressure distribution on delta wing body configurations

[NASA-TN-D-4550] 23 p3706 N71-36418

Hypersonic wind tunnel test of two delta wing orbiter models

[NASA-CR-119984] 24 p4018 N71-38663

Hypervelocity wind tunnel tests at Mach 10 of delta wing space shuttle models

[NASA-CR-119988] 24 p4018 N71-38670

DEMAND [ECONOMICS]

Consumption statistics for antimony in industry

[NMAB-274] 07 p1043 N71-17519

Production, consumption, and uses of antimony

17 p2762 N71-29284

Production, consumption, and uses of cadmium

17 p2762 N71-29297

Production, consumption, and uses of platinum group metals

17 p2762 N71-29300

Survey of yttrium and thorium properties, resources, industry, production, consumption, trade, technology, and history

[BM-IC-876] 22 p3601 N71-35647

DEMINGALIZING

Effects of prolonged bed rest on bone and calcium metabolism and mineral content loss of os calcis

20 p3218 N71-33267

DEMOLUTION

Determining power spectrum of PN codes and effect of predemodulation filtering on correlation and error signals in space communication systems

01 p0021 N71-10257

Pseud channel data transmission system with quadrature modulation and complementary demodulation

[NASA-CASE-XAC-06302] 09 p1353 N71-19763

Theory and analysis of demodulating suppressed carrier AM baseband in noise and recorder flutter

24 p3890 N71-37729

DEMOLUTORS

NT PHASE DEMOLUTORS

NT PHASE LOCK DEMOLUTORS

Principles for design and selection of modern or data transmission sets

[AD-712125] 02 p0179 N71-11262

Frequency shift keyed demodulator - circuit diagrams

[NASA-CASE-XGS-02889] 02 p0182 N71-11282

Demodulation for simultaneous demodulation of two modulating ac signal carriers close in frequency

[NASA-CASE-XMF-01160] 02 p0184 N71-11298

Development of demodulation system for removing amplitude modulation from two quadrature displaced data bearing signals

[NASA-CASE-XAC-04030] 09 p1363 N71-19472

Linear modulator, demodulator, and phase locked loops broadband test procedures and results

[NASA-CR-103082] 10 p1537 N71-21543

Analysis and measurement of characteristics of wide band frequency trackers and design and fabrication of all angle laser Doppler velocimeter

[NASA-CR-103088] 11 p1775 N71-22407

Delay circuits for pulse compression in airborne P4 demodulator

[RAE-TR-70118] 12 p1874 N71-23363

Design, operation, and alignment of single channel broadband modulator, demodulator, and phase locked loops for double sideband signals

[NASA-CR-103116] 13 p3057 N71-24883

Calculator for measuring and modeling or demodulating laser outputs

[NASA-CASE-XLA-03410] 14 p2365 N71-25914

Errors associated with demodulator technique for eddy current testing

[ARL-MR-82] 20 p3242 N71-32903

Threshold extension device for improving operating performance of frequency modulation demodulators by eliminating click-type noise impulses

[NASA-CASE-MSC-12165-1] 20 p2325 N71-33696

Development and characteristics of 1200 band frequency shift keying demodulator for use in digital integrated circuits

[PHL-1971-12] 20 p3276 N71-33749

DEMONSTRATION

U PROVING

DENDRITIC CRYSTALS

Nozzle plugging mechanisms occurring in casting aluminum containing steel

[SAR-2] 03 p0393 N71-15282

Investigating orientation relationships between major grains radiating from single nucleation event into highly undercooled copper

[REPT-365] 05 p0708 N71-15056

Investigating crystal growth and dendritic character of aluminum of transition metals in aluminum alloys

[AD-714420] 06 p0935 N71-16323

Boundary value problems for temperature and flux fields inside and around paraboloidal needle and parabolic platelet crystals during growth

08 p1282 N71-19295

Austenite formation and dendritic liquefaction of silicon, nickel, copper, and molybdenum in low carbon iron alloys

[NLL-TRANS-746-510-7002.401] 10 p1582 N71-21497

Effect of cooling rates on dendrite structure of maraging 300 alloy, size and distribution of inclusions related to tensile and fatigue properties

[AD-718902] 12 p1937 N71-23389

Ionic diffusion and spectroscopic analysis of copper alloy dendrite etching by electric discharge

[TT-70-57063] 14 p2324 N71-25706

DENDROGENATION

Particle size control by jet grinding in fluidized bed

[DN-1439] 09 p1378 N71-20597

DENMARK

Oceanographical observations from Danish light vessels and coastal stations - tables

01 p0046 N71-10192

Data tables of magnetic variations, Skov Skov, Denmark, 1967

04 p0522 N71-13787

Mean sea level and periodic variation at Danish coast

10 p1546 N71-20639

Copenhagen explication of quantum mechanics and its application to microworld

[ITF-70-62-E] 19 p1516 N71-32426

Ocean current, temperature, salinity, and surface data from Denmark for 1970

20 p3268 N71-33730

Observations of yearly wind conditions and climatology of Denmark

[ISBN-87-7478-002-6] 22 p3612 N71-35733

Atmospheric pressure and temperature, wind velocity, humidity, cloud cover, and precipitation data for Denmark and Faroe Islands in 1965

[ISBN-87-7478-025-3] 23 p3784 N71-36972

DENSIFICATION

Intermediate stage densification kinetics of alumina hot pressed in vacuum

[AD-710608] 01 p0059 N71-10650

Densification of plutonium and uranium dioxides, radiation effects on fission gas release, and crack formation during reactor power rise

[ORNL-TR-2387] 06 p0901 N71-16810

Parameters influencing solid state densification for obtaining ceramic nuclear fuels from ceramic grade powders

[RT/DNG/70/21] 19 p3139 N71-33209

DENSITOMETERS

NT MICRODENSITOMETERS

Calibration of cryogenic densitometer for mass density measurements of upper atmosphere

[NASA-CR-1819] 12 p1922 N71-24092

Densitometer for high intensity particle measurement in proton beams, using nuclear emulsions for comparison standard

[CEBN-70-27] 13 p2133 N71-25112

Soviet news releases on earth tremors and densitometers

18 p2910 N71-30792

Alpha-particle densitometer with variable response tailored to energy distribution of alpha source

[RE-4137] 18 p2924 N71-31124

DENSITY [MASS/VOLUME]

NT ATMOSPHERIC DENSITY

NT GAS DENSITY

NT SPACE DENSITY

Behavioral aspects of hexanitrotelluride in small charge

[SC-CR-70-6076] 01 p0100 N71-10793

Determining high temperature saturated liquid and vapor phase densities and critical density and temperature of cesium

[CU-2640-56] 03 p0389 N71-12562

Surface tension and density of molten alumina

[AD-711964] 03 p0396 N71-12814

Differential interferometry for determining wake density behind hypersonic spherical projectile

[ISI-T-12709] 03 p0418 N71-12982

Corrosion prevention behavior of wrapping paper for steel specimens

[M70-607] 05 p0704 N71-15330

X ray determination of density variations in polystyrene foam

[BDX-613-180] 08 p1223 N71-18945

Density control in mixed U-Pu oxide fuel pellets by ceramic processing techniques

[WHAN-FR-7] 09 p1417 N71-15428

Effect of crystallite size, crystallite orientation, and density on dimensional and property changes in L-radiated graphite and isotropic materials

[GA-10435] 14 p2277 N71-25940

Relation between moon density function, figure, external gravitational potential, and physical function constants

[NASA-CR-118892] 15 p2517 N71-37818

Low density and adequate mechanical properties of surface compression strengthened glasson permitting their use in weapons and other lightweight structures for long periods

[AD-721327] 16 p2618 N71-30815

Medium density and chemical composition and measurement geometry effects on accuracy of neutron moisture measurement method

[INP-709] 16 p2659 N71-29712

Adiabatic approximation of gas reactor critical mass during nuclear fuel density oscillations

[IAR-1964] 17 p2783 N71-29808

Interfacial tensions and density measurement of chromium steel and vanadium slag molten silicon effect on phase transformations

18 p2934 N71-34001

Measurement of bone density loss during manual space flight

20 p3216 N71-33251

Long term bed rest effects on mineral balance and bone density in normal individuals

20 p3218 N71-33267

Structure-property relationships in liquid crystals heated to temperatures as high as 3000°C

[AD-726401] 22 p3603 N71-35647

Utilization of vibrational compaction for nuclear fuels

[RT/DNG/70/22] 23 p3794 N71-37940

Granite, basalt, gabbro, and granite isotropic volume compressibilities and densities under 32,000 lb pressure

[SC-T-713031] 23 p3802 N71-37718

Galactic formation and density, velocity, and mass properties of expansion process

23 p3849 N71-37011

Lunar surface layer density determination from lunar satellite radar data on centimeter and millimeter waves

[D-17] 23 p3855 N71-37808

Viscosity and normal density measurements at lambda point intervals for pure helium-4 and helium-4 mixtures with helium-4

[NASA-TN-D-6516] 24 p3966 N71-34209

Unbounded turbulent jets for measurement of fluid velocity and density

24 p4013 N71-38263

DENSITY [NUMBER/VOLUME]

NT ELECTRON DENSITY [CONCENTRATION]

NT ELECTRON DENSITY PROFILES

NT ELECTRON DISTRIBUTION

NT ION DENSITY [CONCENTRATION]

NT IONOSPHERIC ELECTRON DENSITY

NT IONOSPHERIC ION DENSITY

NT MAGNETOSPHERIC ELECTRON DENSITY

NT MAGNETOSPHERIC ION DENSITY

NT MAGNETOSPHERIC PROTON DENSITY

NT METEOROID CONCENTRATION

NT PACKING DENSITY

NT PARTICLE DENSITY [CONCENTRATION]

NT PLASMA DENSITY

NT PROTON DENSITY [CONCENTRATION]

NT SPACE DENSITY

High energy neutron-liquid helium-4 scattering and helium-4 condensate density

[RLO-1388-566] 01 p0099 N71-10077

Velocity, temperature, density, and electron population measurements in projectile wakes

04 p0523 N71-13507

Determination of density matrix components by multiconfiguration wave functions and Hamiltonian interaction method

[NASA-CR-116885] 08 p1265 N71-31017

Large, giant, and sulfate containing atypical particle number concentrations for aerosol air pollution in New Mexico

[AD-716999] 10 p1551 N71-31161

DENSITY [RATE/AREA]

U FLUX DENSITY

DENSITY DISTRIBUTION

Evaluation of several ENDF/B nucleide cross sections by Monte Carlo technique

[AI-AEC-MEMO-12915] 01 p0094 N71-10078

Using fast Fourier transforms for analysis of structural vibration

[NASA-TM-X-53997] 02 p0251 N71-11008

Defining distribution functions for sets of a cavity in hard particle system using concept of equilibrium

02 p0268 N71-11777

Constructing digital correlation measuring device from 1 to 15 MHz for measurement of electron-density correlations in reverse-brush cathode plasma

[IPPI-DT-16] 05 p0753 N71-15310

Air density distribution in stratosphere

[NASA-TT-F-13456] 06 p0851 N71-18888

SUBJECT INDEX

Process pion nucleus yields omega-meson nucleus at high energies
(JTF-70-39) 06 p1246 N71-18151

Evaluating multiple density correlation function of many particle system
(NUB-2051) 06 p1257 N71-18416

Horizontal boundary layer calculations for density stratified flow
(JTF-70-39) 06 p1182 N71-18932

Numerical analysis for static multiple density correlation function of many particle system
(NUB-2051) 11 p1880 N71-21878

Latitudinal density distribution of gases in upper atmosphere
(JTF-70-39) 13 p2076 N71-23267

Thomas-Fermi approximation of nuclei energies with different neutrons and proton density distributions
(JTF-70-39) 14 p2305 N71-26337

Local gas density distribution in rarefied gases at rest between parallel plates at 79 K and 294 K, respectively
(JTF-70-39) 15 p2387 N71-27776

Photointerpretation of radar photography of New Bedford Sound for population density distribution
(NASA-CR-121-626) 20 p3233 N71-33212

Neon, argon, and helium density and flux distributions in lunar atmosphere
(NASA-CR-121-633) 21 p3506 N71-34981

Study of temperature and density dependence of local magnetic field in xenon gas using nuclear magnetic resonance laser precession techniques
(JTF-70-39) 22 p3630 N71-35866

Synthetic ozone density profiles for drop-out behavior prediction
(JTF-70-39) 24 p3917 N71-37931

DENSITY MEASUREMENT

NT X RAY DENSITY MEASUREMENT

Variability in depth and density of snow cover
(AD-711868) 02 p2122 N71-11516

Electron beam measurements of gas densities and rotational temperatures in viscous nozzle flow
(NASA-CR-116247) 06 p0538 N71-16586

Plasma density measurements using electrostatic probe parallel to magnetic field
(JTF-70-39) 08 p1269 N71-18180

Two phase hydrogen density measurements using open ended microwave cavity
(JTF-70-39) 08 p1166 N71-18889

Gamma radiation attenuation gaps for measuring alpha metal vapor or liquid density
(JTF-70-39) 09 p1397 N71-19446

Calibration of cryogenic densimeter for mass density measurements of upper atmosphere
(NASA-CR-16119) 12 p1922 N71-24092

Hydrodynamics of superfluid condensate including effects of motion and density matrix
(JTF-70-39) 14 p2304 N71-26286

Piston cylinder assembly for dilatometric and ultrasonic high pressure measurements on solids and liquids
(JTF-70-39) 14 p2257 N71-26478

Design and calibration of neutral gas spectrometer with impact ion source for atomic oxygen density measurement in upper atmosphere
(JTF-70-39) 15 p2391 N71-27075

Isentropic electron density measurements at magnetic equator, 1964 to 1966
(JTF-70-39) 17 p2738 N71-29311

Experiments on turbulent circular jets issuing into cross flow from both heated and unheated jets
(NASA-CR-72893) 17 p2735 N71-29896

Resonant frequency measurement systems used in conjunction with open-ended microwave cavity to continuously monitor density of liquid hydrogen in flow system
(NASA-TN-D-6415) 18 p2922 N71-30721

Nondestructive measurement of density, breaking strength, and modulus of elasticity of bones
(JTF-70-39) 20 p3217 N71-33261

Design, development, and characteristics of gamma backscatter atmospheric density sensor
(NASA-CR-111933) 22 p3583 N71-35519

Electron beam technique for rotational and vibrational temperature and density measurements in free stream hypersonic wind tunnel
(JTF-70-39) 23 p3740 N71-36671

DETERMINATION

Progress summaries on research in chemistry, astronomy, geology, and physics
(AD-711598) 05 p0707 N71-14761

DETERMINING

Reduction oxidation reactions for colorimetric analysis of atmospheric toxicity
(JTF-70-39) 11 p1695 N71-22061

Russian contributions to Russo-Swedish conference on clean steel
(JTF-70-39) 19 p3111 N71-31901

Influence of stirring on oxygen content of steels after deoxidation by aluminum, silicon and manganese
(JTF-70-39) 19 p3111 N71-31904

Deoxidizing and desulfurizing of titanium steels using electroslag refining
(JTF-70-39) 19 p3104 N71-31908

Deoxidation of liquid iron studied by electromagnetic force measurements noting removal of inclusions
(JTF-70-39) 19 p3111 N71-31911

Kinetics of removal from iron of inclusions produced by manganese silicon aluminum complex deoxidation
(JTF-70-39) 19 p3112 N71-31912

DEOXYGENATION

Catalytic deoxygenation process for irradiated organic reactor coolants
(JTF-70-39) 18 p2957 N71-30459

DEOXYRIBONUCLEIC ACID

Characteristics of X irradiated lambda phages
(JTF-70-39) 05 p0632 N71-14573

DEPENDENCY

NT SPATIAL DEPENDENCIES

NT TIME DEPENDENCIES

Solar and galactic cosmic ray diffusion coefficients and dependencies
(JTF-70-39) 24 p4010 N71-38593

DEPENDENCY

U DEPENDENCY

DEPENDENT VARIABLES

Combined transfer scattering matrix concept for calculating space-energy-angular dependent zero power reactor kinetic equations
(JTF-70-39) 10 p1602 N71-20946

Numerical study of steady, laminar, natural convection of fluids in vertical rectangular enclosure
(JTF-70-39) 11 p1743 N71-22725

Performance sensitivity minimization for optimal control problem variations by steepest descent algorithm
(JTF-70-39) 12 p1951 N71-24186

Optimum estimation model for noise using instrument-parameter variables
(JTF-70-39) 12 p1951 N71-24248

Feedback compensator for linear-time invariant system insensitive to parameter variations
(NASA-CR-119798) 16 p2565 N71-28160

Mathematical determination of number of independent data equivalent to number of dependent data and application to meteorological data in USSR
(JTF-70-39) 16 p2624 N71-29143

DEPLOYMENT

Stresses and adaptation problems associated with large scale, long range, rapid reaction time, aerial troop deployments
(JTF-70-39) 09 p1336 N71-20360

Satellite orientation during deployment established in order to achieve maximum strength of higher rotational locks for satellites in elliptic orbits
(NASA-TM-X-63555) 15 p2517 N71-27764

Flight tests of cross, modified ringtail, and disk-gapped parachute deployment performance from low altitudes with structural load data
(NASA-TM-X-2221) 16 p2530 N71-28021

Aerodynamic and deployment characteristics of twin lock all-flexible parawing rig with several variations of multistage canopy and suspension line netting system
(NASA-TN-D-63061) 18 p2865 N71-30748

Comparing automatic vehicle monitoring system dispatching police vehicles to conventional system for deployment of police units
(JTF-70-39) 19 p3069 N71-31629

Automated command and control dispatch system for deployment of police units
(JTF-70-39) 19 p3052 N71-31630

High altitude flight test of reefed 12.2-meter-diameter disk-gapped parachute with deployment at 2.5 Mach number
(NASA-TN-D-6469) 21 p3376 N71-34026

Mathematical models of planar librational stability conditions for deploying satellites
(JTF-70-39) 24 p4005 N71-38559

DEPOLARIZATION

Formulas for calculating depolarization effects on dipole radiation in statistically homogeneous and isotropic dielectric constant medium
(JTF-70-39) 12 p1876 N71-23460

Depolarization parameter measurements for elastic proton scattering in nuclear reactions
(CEA-CONF-1650) 13 p2132 N71-25093

Synchrotron electron beam resonant depolarization during particle acceleration
(JTF-70-39) 18 p2961 N71-30500

Depolarization in 612 MeV elastic p-n scattering and nucleus-nucleon scattering amplitude 600 to 650 MeV
(JTF-70-39) 23 p3086 N71-37134

DEPOLARIZERS

U DEPOLARIZATION

DEPOSITION

NT ANODIZING

NT ELECTRODEPOSITION

NT ELECTROPLATING

NT VACUUM DEPOSITION

DESCENT TRAJECTORIES

NT VAPOR DEPOSITION

Deposition of cesium and barium in sodium stainless steel system to predict distribution of fission products in LMFR system
(AI-ABC-12552) 02 p0365 N71-11782

Thermal oxidation of pyrocarbon coatings of fuel particles and associated compacting material by carbon dioxide and water vapor
(JTF-70-39) 03 p0415 N71-12879

Vapor-ion methods of film deposition - annotated bibliography
(RFP-1568) 11 p1789 N71-22331

Energy deposition in lasers, computer revised code including multifrequency calculation, bodies of revolution, and geometry debug facility
(AD-711802) 12 p1932 N71-23319

Statistical analysis of distribution pattern for major types of depositional environments in Mississippi River delta region
(AD-711946) 13 p2075 N71-25172

Metallizing parameters developed for sequential deposition of manganese, aluminum, and tantalum alloys as protective coatings for superalloys
(NASA-CR-72852) 13 p2096 N71-25580

Thermal deposition and electrical properties of silicon dioxide passivity layers on silicon wafers in oxygen and nitrogen dry atmospheres and effects of moisture and impurities
(AD-721377) 16 p2570 N71-28594

Apparatus for studying radiolytic carbon deposition of C-labeled gas mixtures at high temperature and pressure
(JTF-70-39) 17 p2804 N71-30269

Glass and steel microsphere sputtering bed properties and model for thermochemical deposition of pyrolytic carbon from methane on nuclear fuel microspheres in sputted beds
(JTF-70-39) 21 p3463 N71-34646

Optical method for measuring thin film deposition on reflecting substrates
(ECRC/N328) 21 p3834 N71-37339

DEPOSITS

NT CRYODEPOSITS

DEHYDRATION

U PRESSURE REDUCTION

DEHYDRATION

NT SENSORY DEPRIVATION

NT SLEEP DEPRIVATION

DEPTH MEASUREMENT

Salinity, temperature, and depth measurement of Weddell Sea during austral summer, 1969
(CG-373-31) 01 p0849 N71-10625

Aerial photography of water wave refraction for depth determination
(JTF-70-39) 02 p0208 N71-11169

Variability in depth and density of snow cover
(AD-711868) 02 p2122 N71-11516

Measurement of water depth by remote sensing techniques
(AD-714001) 06 p0855 N71-16463

Oceanographic pictures from Gemini and Apollo 70 mm color photography enhanced by photooptical means producing false color contours of small changes in density and color
(AD-72482) 17 p2742 N71-29810

Deep sea sounding and depth measurement using primitive equipment and repeating actions of original oceanographic expeditions
(JTF-70-39) 18 p2913 N71-30995

Development of instrument for measuring depth of liquid on plane surface and application to measuring depth of water on airport runway surfaces
(NASA-CASE-LAR-10576-1) 21 p3427 N71-34385

Shallow ocean depth measurements by aerial photographs of wave refraction and wavelength changes and by multispectral scanning of wave reflection
(NASA-CR-123194) 24 p3909 N71-37862

DEPTH PERCEPTION

U SPACE PERCEPTION

DERIVATION

Least squares method and iteration technique for obtaining aerodynamic stability derivatives
(JTF-70-39) 13 p2023 N71-24703

Derivation of partial coefficient equation and coefficient calculation for cosmic radiation
(JTF-70-39) 24 p4011 N71-38603

DERIVATION CALCULUS

U DIFFERENTIAL CALCULUS

DERMATITIS

Histopathology and clinical study of chronic X ray dermatitis and cancer of fingers
(NASA-TT-F-13664) 16 p2418 N71-29200

DESALINATION

Copper-bearing alloy replacement with aluminum alloys in distillation desalination plants for sea water corrosion resistance
(JTF-70-39) 10 p1381 N71-21436

DESCENT

NT PARACHUTE DESCENT

En route aircraft flap control during descent and holding
(ARB-TN-99) 13 p2027 N71-24920

DESCENT TRAJECTORIES

NT REENTRY TRAJECTORIES

Leak jet crash during instrument approach due to descent below path profile
[NTSB-AAR-70-21] 01 p0005 N71-10813

Computerized prediction of separated store trajectories dropped from bomber aircraft at high speed
09 p1318 N71-19379

Fuel-optimal retrothrust soft landing of airdrops through atmosphere
[AD-718405] 12 p1856 N71-23487

Effects on impact dispersion of winds and density deviations from standard atmosphere derived by solution of approximate equations
[AD-721336] 16 p2678 N71-28317

Game approach to problem of controlling descent of reentry vehicle during entry into atmosphere
[JPRS-53839] 20 p3292 N71-33580

Nonlinear control optimization for gliding descent trajectory of winged reentry vehicle coming from circular orbit onto runway
[AD-727450] 24 p4022 N71-38699

DESCRIPTORS

Arc heated plasma jet wind tunnel description
[DLR-FB-70-35] 07 p1003 N71-17140

DESCRIPTIVE GEOMETRY

Space shuttle synthesis program manual including weight, geometry, and trajectory simulation output data and error detecting codes for spacecraft performance prediction
[NASA-CR-114983] 13 p2173 N71-24825

DESERTS

Diurnal cycles of high temperature during equipment performance tests in desert
[AD-713466] 01 p0800 N71-10843

Surface and terrain features of Yuma Proving Ground desert area
[AD-715363] 08 p1190 N71-18675

Survival of Antarctic desert soil bacteria exposed to various temperatures and to three years of continuous medium-high vacuum
[NASA-CR-117313] 09 p1333 N71-20169

Remote sensing relating to military geography of arid lands including terrain, ground water, surface materials, cultural features, and related subjects - annotated bibliography
[AD-723061] 17 p2742 N71-29830

Velocity and frequency of winds of arid zone of Australia related to seasonal shift of pressure systems
[PB-196022] 18 p2951 N71-30884

Time lapse photographic techniques for recording seasonal contrasts in eastern Mojave Desert
[AD-722738] 19 p3127 N71-32037

Desert climatology and geomorphology - bibliographies
[AD-723062] 19 p3093 N71-32240

Site selection and cooling system requirements for PWR power plants in arid regions
[EES-33] 21 p3530 N71-35158

Airborne remote sensing of Mojave Desert playas for use as natural landing areas
[AD-727031] 23 p3751 N71-36748

DESICCANTS

Test on effects of curing temperature and relative humidity on dimensional stability of molded molecular sieve desiccant
[BDX-613-380] 18 p2884 N71-30581

Development of method for calculating equilibrium vapor pressure in closed desiccated systems
[SC-DK-710074] 23 p3802 N71-37109

DESICCATION

U DRYING

DESIGN

Empirical iteration model for optimal design procedures
[ECR-17] 02 p0250 N71-11468

DESIGN OF EXPERIMENTS

U EXPERIMENTAL DESIGN

DESORPTION

Single crystal surface work function and desorption studies
[NASA-CR-111564] 03 p0443 N71-13069

Heatless desorption technology for carbon dioxide control in manned spacecraft
[GR-2-CSS-70] 07 p0967 N71-17945

Gas dynamic techniques for study of desorption rates in one and two component systems
10 p1543 N71-21335

Metallic surface interaction - ion microscope adsorption and mass spectrometry desorption analyses, and field emitted electron energy distribution measurements
[COO-1383-11] 13 p2041 N71-25191

Theories of adhesion and bond failure mechanism caused by water desorption
[SC-RR-70-915] 15 p2453 N71-27119

Performance tests of low temperature desorption refrigeration systems with helium 4 and zeolite
[NASA-CR-119184] 17 p2789 N71-30291

Energy distribution of electron-impact desorbed carbon monoxide ions from tungsten
21 p3488 N71-34851

DESPINNING

U SPIN REDUCTION

DESTABILIZATION

Aerodynamic characteristics of large angle blunt cone with and without fence-type afterbodies
[NASA-TN-D-6269] 12 p2001 N71-24083

DESTRUCTION

Ground and aerial surveys of building damages caused by tornado
[NBS-TN-558] 10 p1652 N71-20861

DESTRUCTIVE TESTS

Nondestructive and destructive testing of Zircaloy tubes in K reactors
[DUN-SA-144] 07 p1065 N71-17611

Burnout heat flux measurements on 3 by 3 rod bundles with nonuniform heat generation and high pressure water
[EUR-4514-E] 08 p1302 N71-18220

Research, development, support, and test activities in aerospace nuclear safety program with stress analysis of Pioneer heat shield and Have Sinew-1 program progress
[SC-PR-70-982] 16 p2683 N71-28837

Laminated steel pressure vessel design, trial production, and destructive testing
[NLL-RTS-5936] 17 p2855 N71-30334

Destructive and nondestructive tests on nuclear fuel burnup
[INIS-MF-29] 19 p3136 N71-32041

Destructive tests of Inconel 600 tube from N reactor steam generator 6A
[DUN-SA-149] 20 p3309 N71-33933

Destructive examination of Hallam Nuclear Power Facility intermediate heat exchanger emphasizing crevice corrosion problems
[IN-1477] 24 p3978 N71-38387

DESULFURIZING

Swedish contribution to Russo-Swedish conference on clean steel
[IVA-169-1] 19 p3111 N71-31901

Desulfurizing of steels using silicon, aluminum, calcium, and cesium alloy vapor injection
19 p3111 N71-31902

Dioxidizing and desulfurizing of titanium steels using electroslag refining
19 p3104 N71-31908

DETACHMENT

Theoretical calculations on electron detachment of hydrogen ions by electron collision with Coulomb effect
[NASA-TM-X-65491] 12 p1970 N71-23396

DETECTION

NT AIRCRAFT DETECTION

NT CORRELATION DETECTION

NT FOREST FIRE DETECTION

NT MISSILE DETECTION

NT RADAR DETECTION

NT SIGNAL DETECTION

NT TARGET RECOGNITION

Analysis of US efforts for detection and prevention of air piracy with application to foreign countries
01 p0135 N71-10236

High resolution forward scatter system to detect refractive index fluctuations caused by clear air turbulence
[AD-712088] 02 p0205 N71-11130

Breadboard miniature carbon dioxide sensor scale model and instruction manual
[NASA-CR-114799] 05 p0682 N71-14799

Application of acoustic-boiling-detection techniques to liquid metal cooled reactors
[ANL-74609] 07 p1062 N71-17249

Heated element sensor for fluid flow detection in thermal conductive conduit with adaptive means to determine flow rate and direction
[NASA-CASE-MSC-12084-1] 07 p1009 N71-17569

Fluid leakage detection system with automatic monitoring capability
[NASA-CASE-LAR-10323-1] 07 p1009 N71-17573

Sound ranging distance for detecting benzene and diesel engines
[IZF-1971-6] 18 p2963 N71-30898

Single shot joint detection and estimation for discrete and continuous data, and joint Bayesian detection, estimation, and system identification
[AD-722460] 18 p2896 N71-31346

One dimensional numerical simulation of dual wavelength radar hail detector
[LAP-TR-24] 20 p3295 N71-33022

Digital computer fault detection procedures for combinational logic circuits with algorithms for efficient generation of minimum fault test schedules
[AD-726383] 22 p3563 N71-35375

Design of logic circuit to facilitate electrical fault detection in digital computers
[AD-726382] 22 p3563 N71-35376

Development of four dimensional atmospheric models from global data for predicting atmospheric attenuation encountered by earth resources observation sensors
[NASA-CR-61362] 24 p3951 N71-38189

Direct measurements of low energy solar protons and solar particle spectra
24 p4010 N71-38591

DETECTORS

Pressurized cell micrometeoroid detector
[NASA-CASE-XLA-00936] 05 p0685 N71-14996

Experimental re-evaluation of two-crystal scanning geometry for whole-body counting with top-shape placement of crystals
[BARC-498] 06 p0991 N71-15756

Development of positive ion detectors to measure ion characteristics in directed pulse plasmas
[SC-RR-70-583] 06 p0929 N71-15820

Development of large area micrometeoroid impact detector panels
[NASA-CASE-XLA-05906] 06 p0950 N71-16221

Development of pulse-activated polarographic hydrogen detector
[NASA-CASE-XMF-06531] 07 p1029 N71-17575

Electro-optical detector for determining position of light sources
[NASA-CASE-XNP-01059] 10 p1610 N71-21821

Applications for small current amplifying device including solid state sensors, Schottky junctions, and other low noise devices
[AD-719740] 13 p2054 N71-24648

Method for locating leaks in hermetically sealed containers
[NASA-CASE-ERC-10045] 13 p2087 N71-24919

Precipitation detector and mechanism for stopping and restarting machinery at initiation and cessation of rain
[NASA-CASE-XLA-2619] 14 p2233 N71-36336

Masked eddy current probe for crack detection in Rover fuel element coating
[LA-4590] 16 p2635 N71-28726

System for detecting impact position of cosmic dust and similar outer space particles on detector surface
[NASA-CASE-GSC-11291-1] 16 p2663 N71-29183

Solid state, three axis recording magnetometer with fluxgate type magnetic detectors
22 p3586 N71-35540

DETERGENTS

Reliability of testing oils with added detergents in single cylinder engines
[AD-711740] 01 p0073 N71-10978

Addition of pyrophosphates to lubricants for detergent purposes
[AD-720743] 14 p2280 N71-26108

DETERRATION

Condition survey of military airfield runways and taxiways
[AD-724069] 20 p3244 N71-33995

DETERMINANTS

Existence of generators for certain AFL
[NASA-CR-111110] 01 p0028 N71-10777

DETERMINATION

U MEASUREMENT

DETONABLE GAS MIXTURES

Effect of transverse magnetic field on propagating plane gaseous detonation wave
08 p1305 N71-18886

Shock-induced combustion in explosive mixtures of hydrogen and air or oxygen by high speed shots at low pressures
11 p1843 N71-22632

Characteristics of detonation phenomena in heterogeneous system of decane droplets in oxygen atmospheres
16 p2090 N71-28571

Machine for breaking wire carrying electric current in flammable atmosphere
23 p3764 N71-36835

DETONATION

Effects of inhomogeneities in explosives on critical diameter of detonation
[LA-TR-70-7] 01 p0114 N71-10756

Conference on condensed phase detonation
[AD-712081] 02 p0204 N71-12148

Shock initiation of LX-07-2 and LX-10-4
[UCRL-50851] 03 p0467 N71-12087

Characteristics of heterogeneous shock initiation of explosive 5404
[LA-4475] 07 p1130 N71-17955

Critical appraisal of design, development, and operation of UTIAS implosion-driven shock tubes and hypervelocity launchers
[NASA-CR-117856] 11 p1845 N71-23888

Formation mechanism of electrical pulse during detonation of ordinary explosive substances
[RAE-LB-TRANS-1528] 13 p2134 N71-23161

Quantitative comparison of reactive and nonreactive Mach stems for understanding detonation structure
[AD-721463] 16 p2578 N71-28815

Molecular structure, detonation, acoustic velocity, density, and pyrolysis of isomeric dinitro methane and propane
[AD-722463] 17 p2715 N71-28887

Analysis of acetylene oxygen detonation spectra in 3000-6000 Å
[MEJA-71-1] 20 p3364 N71-33488

DETONATION WAVES

Behavioral aspects of hexanitroethane in wall charges
[SC-RR-70-6076] 01 p0108 N71-10799

Gas dynamic stability and damping of detonation wave in nozzles
[AD-711753] 01 p0044 N71-10940

Determining impulse generation characteristics of reconstructed sheet explosives
[SC-RR-70-432] 03 p0460 N71-12951

SUBJECT INDEX

Investigating nonsteady effects in gas phase of liquid and solid explosives under different physical and chemical conditions
[AD-713541] 05 p0781 N71-14566

Formation of crater due to expansion of gaseous reaction products following rock crushing by direct and indirect waves
[UCRL-TRANS-10476] 05 p0743 N71-15131

Detonation pressure measurements in TNT and OCTOL
[AD-713547] 05 p0783 N71-15395

Effect of transverse magnetic field on propagating plane gaseous detonation wave
08 p1305 N71-18890

Photographic recording and analysis of detonation waves produced by nitromethane-acetone mixtures
[UCRL-72160] 09 p1485 N71-20525

Normal or oblique plane detonation waves producing combustion products in supersonic flow
[ARC-RM-3638] 10 p1661 N71-20938

Two phase detonation waves in liquid gas systems
[NASA-CR-722664] 11 p1841 N71-22509

Detonation reaction engine comprising outer housing enclosing pair of inner walls for continuous flow
[NASA-CASE-XMP-66926] 11 p1821 N71-22983

Explosive detonation velocity, explosive welding to hardware configurations, and flange buckling of explosively formed dome
[AD-710679] 12 p1926 N71-23758

Deformation of drops in reactive zone during homogeneous detonation of fuel mixtures consisting of liquid drops of fuel and gaseous oxidizer
[NASA-TT-F-13579] 13 p2185 N71-24933

Characteristics of detonation phenomena in heterogeneous system of decane droplets in oxygen atmospheres
16 p2690 N71-28574

Active seismic signal analysis from Apollo 14 bumper and mortar detonations on lunar surface
18 p3011 N71-30961

Continuous operation laser based on chemical excitation of vibrational rotational levels of hydrogen chloride produced in detonation waves stabilized in supersonic flow
18 p2932 N71-31420

Shock propagation model for low velocity detonation in liquid propellants, fuels, and explosives
[AD-723677] 19 p3172 N71-32073

Measurement of flow field behind plane detonation wave by observing motion of metal foils placed between explosives
[LA-4256] 21 p3413 N71-34282

Development of method for determining flow field behind detonation wave formed by acetylene-oxygen detonation based on wall heat transfer - Vol. 3
[NBSA-71-3] 23 p3867 N71-37571

Measurement of heat transfer from acetylene-oxygen detonation in shock tube - Vol. 2
[NBSA-71-2] 23 p3868 N71-37572

Propagation and characteristics of shock wave generated in air by small explosive charges
[AD-727083] 24 p3906 N71-37839

DETONATORS

Measurement of dynamic pressures produced by exploding wires
[N-1486] 04 p0513 N71-13540

Measurement of electric detonator insensitivity to electrostatic charge of human body
[AD-726903] 22 p3697 N71-36367

DEUTERIUM

Reaction kinetics of excited oxygen deuterium atoms with ozone and nitrous oxide in upper atmosphere
[NASA-CR-111378] 02 p0210 N71-11452

Total cross section for photoproduction of neutrons and deuterons on deuterium between 1.0 and 6.4 GeV
[DESY-70-177] 03 p0430 N71-12905

Energy transfer in interactions between laser beams and solid deuterium
[NBSA-1-1337] 04 p0574 N71-13670

Equation of state of hydrogen and deuterium between 3 and 10 cc/mole to 10,000 K
[UCRL-30911] 05 p0743 N71-15133

Proton-neutron scattering cross section energy in neutron trapping by proton impact
[NLSO-1388-126] 07 p1076 N71-17515

Neutron yields and energy spectra for hot deuterium-nitrogen plasmas
[NPP-1107] 08 p1271 N71-18388

Expectation values and kinetic energy for vibrational-rotational levels of ground states of H₂, HD, and D₂
09 p1429 N71-19744

Deuterium in slow neutron radiography of biological media
[BP-1209] 10 p1497 N71-20729

Pulse reactors at 200 kG and ion temperature of 10 MeV with lithium and deuterium as primordial fuel
[NBSL-TM-3207] 10 p1613 N71-20637

Alpha-deuteron isotope effects on solvolysis rate of 2,2,2-trifluoroethylsulfonate
[NLSO-1068-15] 10 p1630 N71-21732

Deuterium and tritium effects on organic reaction rates with solvolytic mechanisms
[NLSO-1088-16] 10 p1624 N71-21791

Alpha-deuteron isotope effects on solvolysis rate as function of leaving group, including interconversion of ion pairs
[COO-1008-13] 10 p1624 N71-21808

Deuterium-helium-3 fusion power balance calculations with inclusion of variable cyclotron radiation parameter
[NASA-TM-X-2280] 13 p2149 N71-25526

Antiproton annihilations at rest with bound neutrons in deuterium
13 p2141 N71-25543

Reaction kinetics and charge transfer in ionic collisions of argon ions with molecular hydrogen, deuterium, and carbon dioxide
15 p2477 N71-27578

Nuclear magnetic relaxation times of deuterium and fluorine nuclei in liquid CDF₃
15 p2496 N71-27969

Soviet stratospheric observatory for studying deuterium/hydrogen ratio in solar atmosphere
[NASA-TT-F-13675] 17 p2840 N71-29255

Research on field theory using nuclear models, and interaction of deuterium with pions
[COO-1810-7] 17 p2791 N71-29291

Neutron-proton, deuteron, and alpha scattering cross sections for H₂, D₂, He, Be, C, Al, Fe, Co, Cd, W, Pb, and U at 4.0 and 5.7 GeV/c
17 p2796 N71-29780

Probability distribution functions for nonreactive collisions of lithium with H₂, D₂, HD, or Ar and of deuterium with H₂ or D₂, calculated with Monte Carlo method
18 p2906 N71-31258

Kinetics of homogeneous, isotope exchange reactions D₂ plus CH₄, D₂ plus H₂S, and HD plus HD in single-pulse shock tubes
18 p2907 N71-31350

Partial cross section and resonance production of strange particles measured in deuterium filled bubble chamber exposed to negative kaon beam
19 p3159 N71-32599

Deuterium vertical distribution in upper atmosphere as function of thermospheric temperature
20 p3257 N71-33044

Polarization measurements of 16.5 MeV and 22.1 MeV neutrons elastically scattered from liquid tritium and liquid deuterium
20 p3326 N71-33931

Ionization study of metastable hydrogen atomic beams and polarized deuterium ions with Lamb-shift source
[KFK-1256] 21 p3468 N71-34690

Parabolic events in neutron neutron interactions based on D(n,n_p) reactions at 14.5 MeV
[CEA-R-3726] 21 p3486 N71-34835

Absolute cross section and angular distribution of deuterium photodisintegration
21 p3489 N71-34855

Magnetic spectrometer system for detecting negative pion differential cross sections in liquid deuterium
[INSJ-126] 22 p3633 N71-35893

Diffraction of helium atoms from tungsten (112) crystal surface and measurement of time of flight distribution of deuterium molecules desorbed from nickel surfaces
[NASA-CR-121985] 22 p3634 N71-35900

Equation of state calculations for solid H₂, D₂, He-3, He-4, and Ne-20 at high densities in harmonic approximations
[NYO-3699-51] 23 p3802 N71-37110

Total loss cross sections for D₂ molecules passing through H₂ gas in light ion accelerator
[UCRL-20099] 23 p3812 N71-37181

Resonance in kaon[minus] proton reactions, Veneziano model in antiproton nucleus reactions, kaon[minus] beams in π^- deuterium chamber, and related technical and theoretical developments
[NYO-3178-8] 23 p3812 N71-37186

DEUTERIUM COMPOUNDS

DEUTERIUM

DF-CO₂ and CS₂-O₂ CO laser research, electrode configuration efficiency, and CO₂/1001 ratio of deuterium by DF and HF
[AD-712544] 03 p0388 N71-13596

Experimental design using single ultrashort pulses for triggering Kerr cells and producing laser radiation to heat lithium deuteride targets for high temperature plasma generation
[NASA-TT-F-13662] 13 p2088 N71-24641

Preparation and deuterium quadrupole coupling constants of deuterio-organometallic compounds
[NYO-5965-3] 13 p2145 N71-25590

Ion-molecule reactions of CH₃-CD₃ mixtures at high pressures in ion source of quadrupole mass filter
[AD-722687] 17 p2717 N71-30210

Line spectra shifts in HF and in first overtone band of DF induced by HF pressures
[NASA-CR-121411] 20 p3233 N71-33172

Mass-spectrometric stirred-reactor technique to measure rate of reaction of hydrogen chloride and deuterium chloride with atomic oxygen
[NASA-TM-D-6495] 21 p3386 N71-34092

Effect of temperature of infrared overtone spectra of D₂O and ROD in liquid state under saturation conditions into supercritical region
[NLS-CE-TRANS-5458-19022-09] 21 p3386 N71-34092

Mass-spectrometric stirred-reactor technique to measure rate of reaction of hydrogen chloride and deuterium chloride with atomic oxygen
[NASA-TM-D-6495] 21 p3386 N71-34092

Effect of temperature of infrared overtone spectra of D₂O and ROD in liquid state under saturation conditions into supercritical region
[NLS-CE-TRANS-5458-19022-09] 21 p3386 N71-34092

Mass-spectrometric stirred-reactor technique to measure rate of reaction of hydrogen chloride and deuterium chloride with atomic oxygen
[NASA-TM-D-6495] 21 p3386 N71-34092

Effect of temperature of infrared overtone spectra of D₂O and ROD in liquid state under saturation conditions into supercritical region
[NLS-CE-TRANS-5458-19022-09] 21 p3386 N71-34092

Mass-spectrometric stirred-reactor technique to measure rate of reaction of hydrogen chloride and deuterium chloride with atomic oxygen
[NASA-TM-D-6495] 21 p3386 N71-34092

DEUTERONS

24 p3948 N71-38306

DEUTERIUM OXIDES
U HEAVY WATER
DEUTERIUM PLASMA

Time resolved neutron spectra applied to those pinch for anisotropy and relaxation analysis of deuterium velocity distributions in deuterium plasmas
[IIP-1109] 15 p2499 N71-27200

Vacuum ultraviolet spectroscopic measurement of deuterium plasma electron energy
15 p2499 N71-27204

Time resolved neutron measurement of anisotropy and relaxation of deuterium velocity distribution
[ORNL-TR-2429] 21 p3479 N71-34780

DEUTERIUM IRRADIATION

Scattering cross sections for deuterium irradiation of Tc-181 yielding Tc-182 and W-181 using stacked foil to reduce neutron energies to threshold
[CNBA-269] 15 p2462 N71-27148

Angular distribution vector analysis of polarized deuterium elastic scattering from helium 4 at energies between 3 to 11 MeV
15 p2476 N71-27575

Vector analysis of stripping reactions and elastic scattering from deuterium irradiation of O-16, Cr-52, Fe-54, and Zn-90 targets
15 p2406 N71-27827

Delayed fission of Pu-237 produced by low energy deuterium bombardment of Np-237
[ITD-25639] 18 p2906 N71-31234

Two-neutron transfer reactions Fe-54(α ,n)Mn-52 and V-51(α ,n)Cr-53 produced by 28 MeV deuterons
[LYCEN-7067] 23 p3806 N71-37137

DEUTERONS

Double scattering in quasielastic interactions of pions with deuterons
[NASA-TT-F-13384] 01 p0094 N71-10383

Microscopic analysis theoretical model for elastic scattering of deuterons and alpha particles
[CTC-32] 01 p0100 N71-10744

Schrodinger equation used to compute energy parameters of deuteron ground state
[AD-711283] 01 p0102 N71-10904

Asymmetries produced by 28 MeV polarized deuterons in elastic scattering on C-12, Si-28 and Ca-40
[LYCEN-7021] 02 p0277 N71-12131

Investigating photoproduction of rho-mesons/W in deuterium reactions between 1 and 5 GeV
[DESY-7016] 03 p0432 N71-12936

Polarization measurements of doubly elastically scattered neutrons on C-12 for energies between 41 and 51 MeV
[NPP-18301] 04 p0574 N71-13669

Coherent Q meson production in positive kaon deuterium interactions at 9 GeV/c
[COO-1428-226] 04 p0581 N71-14024

Scattering and polarization of neutrons and deuterons
[ANU-P/497] 05 p0743 N71-15141

Direct measurement of α -p and α -d total sections from 700 MeV/c to 2900
[FURC-4159-7] 05 p0746 N71-15228

Lambda hyperon-nucleon interactions in deuterium
[UCRL-30977] 06 p0927 N71-14688

Least squares method for gamma ray angular distribution of radiative capture of deuterium
[ORNL-TM-3164] 07 p1077 N71-17549

Silicon 28 deuteron/proton silicon 29 interaction at low energy
[LYCEN-7013] 06 p1251 N71-18285

Elastic scattering of fast neutrons by deuterons
[LYCEN-7026] 06 p1256 N71-18374

Neutron-deuteron scattering length calculations with realistic potentials using two-particle t-matrices and Faddeev equations
[JINR-P-5000] 09 p1440 N71-20302

Deuteron and alpha particle acceleration in synchrotron
[JINR-P-5311] 09 p1441 N71-20317

Polarization power of impacting polarized deuteron beam on emitting particles from unpolarized deuterated polyethylene target
09 p1441 N71-20374

Momentum spectra in high energy hadron deuterium interactions
[COO-1764-115] 10 p1611 N71-20686

Antiproton-deuteron and proton-neutron collisions with resonance decay and double pion production
10 p1625 N71-21826

Negative pion deuterium interactions at 2.3 GeV/c
10 p1625 N71-21844

Magnetic energy spectra of deuterons and tritons in product nuclei decay of helium irradiated lithium 7-beryllium 3 and lithium 7-beryllium 7 targets
12 p1971 N71-23882

Low energy fission of thorium-232 studied with 11.3 MeV protons and 17.5 MeV deuterons
12 p1976 N71-24097

Peak to valley ratios for proton and deuterium fission of uranium 238 measured as function of particle energy
12 p1976 N71-24098

Elastic nucleon-nucleon and nucleon-deuteron scattering [JINR-P2-5444] 13 p2130 N71-24802

Mixing determination in Sn 199 and 118 p/d reactions by asymmetry measurements at 25.5 MeV [CEA-CONF-1653] 13 p2138 N71-25382

Manufacturing tests of tritiated lithium targets to obtain optimal procedure for their use and preparation under deuteron irradiation [EUR-4286-PT-2] 13 p2138 N71-25450

Nuclear reactions of protons and deuterons on Zr-90 at 22.9 MeV and Mo-92 at 24.5 MeV [CEA-CONF-1654] 13 p2140 N71-25523

Spin tensor moments of deuterons emitted from Mg d/d elastic scattering reaction [ANU-P498] 13 p2141 N71-25545

Deuterons accelerated to 28 MeV for investigating iron-54 α reaction [LYCEN-7074] 14 p2308 N71-26423

Compilation of cross sections of reactions produced by protons on targets of protons, neutrons, deuterons, and helium [CERN/HERA-70-2] 14 p2309 N71-26586

Interaction cross sections of antikaon deuteron yields kaon Y1 Y2 [JINR-P2-5231] 14 p2314 N71-26728

Optical potential spin-orbit effects on the isotope proton deuteron asymmetry with polarized protons based on distorted wave Born approximation [CEA-CONF-1652] 14 p2317 N71-26756

Angular distribution of n final state interaction of np yields p reaction studied with 52 MeV deuterons [INP-18561] 14 p2319 N71-26794

Quasi-elastic scattering of particles on deuterons including double interaction effect of particle with deuteron nucleons [JINR-P2-5343] 15 p2461 N71-27113

Mathematical model for neutron deuteron scattering above inelastic threshold 15 p2470 N71-27386

Deuteron acceleration and extraction from proton synchrotron, and facility improvements [JINR-P9-5442] 15 p2473 N71-27444

Arithmetic asymmetry of reaction products produced by polarized protons and deuterons incident on beryllium 9 target measured by polarized beam from tandem Van de Graaff accelerator 15 p2478 N71-27615

Polarization of protons from C-12/ d , p/C -13 reaction at 12.4 MeV and distorted wave Born approximation comparisons [INP-711] 15 p2481 N71-27691

Final states of four-pronged antiproton deuteron interactions at 7.6 GeV/c, and cross sections for visible spectral events 15 p2496 N71-27979

Compilation of cross sections of reactions by negative kaons on protons, neutrons, and deuterons [CERN/HERA-70-6] 16 p2659 N71-29166

Comparison of integrated scattering cross sections of $3/2$ states in Mg-25/ d , α /Na-23 and Al-23/ d , α /Mg-25 reactions [NASA-TN-D-6412] 17 p2795 N71-29779

Neutron-proton, deuteron, and nucleus scattering cross sections for H2, D2, He, Be, C, Al, Fe, Cu, Cd, W, Pb, and U at 4.0 and 5.7 GeV/c 17 p2796 N71-29780

Production of 14 MeV neutron nanosecond pulse with Td/n He-4 reaction by accelerating deuterons with electron beams [UCRL-50935] 17 p2798 N71-30010

Differential and total scattering cross sections for neutron proton yields deuteron neutron pion for neutron energies from threshold to first resonance peak 17 p2799 N71-30019

Experimental results on kaon/ p deuteron interaction from 865 to 1365 MeV/c incident beam momentum [UCRL-20244] 17 p2803 N71-30216

Strange particle production in positive pion deuteron interactions at 5.1 GeV/c - 2-body and quasi-2-body reactions [INP-18629] 17 p2807 N71-30330

Ge/Li detectors for gamma ray spectroscopy, and spectral study of d , p , and t produced by deuteron bombardment of C-12 at high energies [INP-18570] 18 p2968 N71-30417

Investigation of $e d$ yields $e p n$ scattering reaction with scattered electrons measured with spark chamber spectrometer and recoil protons detected with counter telescope [INP-18725] 19 p3156 N71-32443

Deuteron acceleration in second drift multiplicity in proton linear accelerator with grid focusing [JINR-P9-5610] 19 p3157 N71-32463

Cross section for elastic-deuteron scattering and electron neutron form factor at four momentum transfers [DESY-71/7] 19 p3159 N71-32634

Electron capture cross sections into $3p$ and $3d$ states of hydrogen for 30-120 keV proton and deuteron impact on gas targets 20 p3325 N71-33919

Two particle-one hold shell model calculation for five nucleon system applied to deuteron-triton photocapture 20 p3327 N71-33953

Angular distributions for nuclear reaction $Sn-124$ plus deuteron yields $Sn-125$ plus proton [ANU-P5111] 20 p3328 N71-33977

Emission of deuterons in interactions of 9 GeV protons with lead nuclei [INR-P-1256] 21 p3469 N71-34693

Characteristics of fast deuterons with nuclei in photoemulsion 21 p3469 N71-34700

Differential cross section and vector polarization for elastic scattering of 41 to 51 MeV deuterons on carbon-12 [KFK-1357] 21 p3469 N71-34701

Spectroscopic analysis of deuteron angular distributions in titanium isotopes using (b,d) and (p,t) reactions 21 p3489 N71-34856

Excitation functions for Tb-159 deuteron interaction [CNEA-283] 22 p3631 N71-35870

Excitation functions for deuteron-induced reactions in gold using statistical model [LYCEN-7092] 22 p3634 N71-35898

Relativistic model for photoproduction of pions on deuterons [LPTHE-71/9] 22 p3639 N71-35940

Theory of deuteron breakup in nuclear and Coulomb fields using distorted wave Born approximation 23 p3821 N71-37260

Angular distributions for neutron polarizations in $[d,n]$ and $[He-3,n]$ stripping reactions of Li, Be, B, and C at energies from 2.1 to 3.9 MeV 23 p3822 N71-37266

Compilation of reaction cross sections produced by positive kaons on proton, neutron, and deuteron targets [CERN-HERA-70-4] 24 p3971 N71-38331

Compilation of reaction cross sections produced by positive pions on proton, neutron, and deuteron targets [CERN-HERA-70-5] 24 p3973 N71-38345

Cross sections and angular distributions in kaon(minus) deuteron yields kaon(minus) deuteron and kaon(minus) neutron yields kaon(minus) neutron interactions [INP-18891] 24 p3974 N71-38354

Reactions of Pb-204, Pb-206, Pb-208, and Bi-209 with deuterons from synchrocyclotron, and single particle states and nuclear potentials of Pb-208 [INP-18876] 24 p3974 N71-38355

DEVELOPERS [PHOTOGRAPHY]

U PHOTOGRAPHIC DEVELOPERS

DEVELOPMENT

Development, maintenance, and future capabilities of NASTRAN - NASA Structural Analysis computer program 22 p3682 N71-36254

DEVIATION

Improved accuracy of long range forecasting through prediction of sign of frequency anomaly of atmospheric circulation 11 p1754 N71-22823

DEVICES

Gnosological functions and information properties of devices used to understand cognitive mechanisms of man [JPRS-53910] 21 p3399 N71-34192

DEVITRIFICATION

U CRYSTALLIZATION

DEW

Regression analysis for predicting surface dew point temperatures from prognostic charts and upper atmospheric data [NOAA-TM-NWS-TDL-37] 07 p1054 N71-17518

DEWAR SYSTEMS

U CRYOGENIC EQUIPMENT

DEWETTING

U DRYING

DIABATIC PROCESSES

U HEAT TRANSFER

DIADROME SATELLITE

Geodetic survey by means of mobile stations of Q switched laser range finders and Diadrome satellite [ONERA-NT-156] 15 p2398 N71-27054

Laser reflectors, stabilization, and thermal control of geodetic satellites Diadrome D-1C and D-1D [RAE-LIB-TRANS-1501] 16 p2681 N71-28051

DIAGNOSIS

Electronic device for monitoring electrocardiogram and diagnosing high or low heart rate [AD-710221] 01 p0014 N71-10006

Character recognition device designs and applications in weather forecasting, medical diagnostics, and reading automata [JPRS-52554] 10 p1536 N71-20681

Diagnostic and functional measurements of human physical fitness 11 p1467 N71-22303

Diagnostic chronological and physiological criteria in geriatrics 11 p1489 N71-22312

Computer animated display device for diagnosis of heart disease [NASA-NEWS-RELEASE-71-58] 12 p1867 N71-23751

Applications of X ray photography to diagnosis of cardiovascular and respiratory system diseases [AD-706296] 17 p2708 N71-29981

Computerized method for input of disease history information and retrieval for diagnosis 20 p3289 N71-32802

Computer technology for medical information systems, in patient care, and for diagnostic purposes 24 p3993 N71-37745

DIAGRAMS

NT BENDING DIAGRAMS

NT CIRCUIT DIAGRAMS

NT CREEP DIAGRAMS

NT FEYNMAN DIAGRAMS

NT MOLLIER DIAGRAM

NT PHASE DIAGRAMS

NT S-N DIAGRAMS

NT STRESS-STRAIN DIAGRAMS

Diagram for projectile trajectory calculations [ISL-T-2769] 05 p0312 N71-12222

Graphical technique for analyzing series-parallel networks by rectangular diagrams in solving power distribution problems 06 p0883 N71-13941

Calculation rules for loop diagrams in dual resonance theories with nonlinear trajectories [RILO-1368-592] 10 p1610 N71-26819

CMPLOT FORTRAN subroutine for graph and diagram plotting using CalComp E35 CRT plotter [TRITA-EPP-71-03] 15 p2383 N71-27314

Calculation of box diagram effects with scalar and vector resonances in intermediate state with singularities [IFVE-STF-70-34] 15 p2483 N71-27700

Mean quadratic angles of inclination of surfaces on Venus with diagrams of backscatter measured by radio waves 18 p2891 N71-31111

Techniques for calculating risk of structural failure diagrams [ORNL-TR-2133] 19 p3190 N71-32800

Progress report, block diagrams, and processing of multiple-mission telemetry of Deep Space Instrumentation Facility 21 p3393 N71-34046

DIAL SATELLITE

Planning and coordination of space environment simulation test programs for Azur and Dial satellites 03 p0358 N71-12778

Azur satellite, Dial satellite, ground support systems, ELDO launch vehicle, and space environment simulation [QB-1-71] 22 p3681 N71-36309

DIALYL COMPOUNDS

Visual effects related to transfer-molded parts of epoxy and diallyl phthalate compounds [BDX-613-166] 10 p1566 N71-21344

DIALYSIS

NT ELECTRODIALYSIS

DIAMAGNETISM

Characteristics of temperature-dependent diamagnetism in superconductors [AD-713242] 05 p0756 N71-14880

Testing various organic compounds and semiconducting polymers for Meissner effect [AD-713501] 05 p0734 N71-15355

Determining Knight shift in beryllium from hyperfine contact and diamagnetism calculations combined with core polarization effect 24 p3942 N71-38119

Plasma diamagnetism, resistivity, and electron thermal conductivity anomalies in Tokamak discharges based on two-fluid MHD theory, ion and electron heat flow, and Maxwell equations [CONF-710607-26] 24 p3992 N71-38679

DIAMETERS

Amplifying interferometric and narrow multi-beam band measurement of molybdenum cathode pressure cylinder diameters [NLL-M-20171-5828.4F1] 12 p1931 N71-30328

Planetary diameter and flattening measurement 13 p2166 N71-25879

Reflected radio signals from solar corona and effective solar diameter theory 23 p3853 N71-37402

DIAMINES

Preparation of elastomeric diamine diamine polymers [NASA-CASE-XMF-04133] 10 p1512 N71-30017

Use of Abrolax AZ as antizoonant for Mosquitoes 12 p1869 N71-31888

Synthesis of aromatic diamines and dialdehydes polymers using Schiff base [NASA-CASE-XMF-03074] 13 p2039 N71-30000

DIAMOND WINGS

U LOW ASPECT RATIO WINGS

U SWEPT WINGS

DIAMONDS

Production of filamentary diamond monocrystals from carbon containing media 02 p0287 N71-12800

SUBJECT INDEX

Stirred diamond compacts using cobalt as binder
(NASA-CR-116419) 07 p1049 N71-17952

Effect of lubricants with fillers on wear of diamond
instrument during cold drawing of wire
(AD-716523) 09 p1405 N71-19623

Crystral defects in diamonds and semiconductor
fabrication
(JPRS-52545) 11 p1816 N71-22182

Crystalline structure defects of diamonds caused by
nitrogen ion injection
(AD-717681) 11 p1816 N71-22183

Diamond crystals of high chemical and mechanical
perfection for research in electronic devices
(AD-717681) 11 p1819 N71-23095

Process and apparatus for making diamond abra-
sives
(NASA-TM-X-44543) 12 p1927 N71-23775

Growth of p-type semiconducting diamond by vapor
phase deposition using methane-diborane doping gas
mixture in presence of diamond seed crystals
(NASA-TM-X-47866) 14 p2324 N71-25762

Electronic states in dislocations in semiconductor
and diamond structures
(AD-717681) 17 p2823 N71-29997

Association of olivine, garnet, and chromo-diopside
in Yakut diamond
(NASA-TT-P-138119) 18 p2995 N71-31091

Occurrence of explosion-like processes during high
powered pulsed electron bombardment of diamonds,
gases, and ceramics
(SC-71-5017) 21 p3434 N71-34435

Revelation of history of chemical synthesis of
diamonds and fluorine diamond synthesis in USSR
(NLL-M-20583-5428-4F1) 21 p3444 N71-34512

Computer program (KRISTALL) for studying
dynamics of radiation damage in face centered cubic
lattice, body centered cubic lattices, and diamonds
(JPRS-52545) 21 p3496 N71-34908

Application of diamonds for recording and retaining
information on irradiation conditions for materials in-
vestigation in nuclear reactors
(JPRS-52545) 24 p3979 N71-38399

DIAPHRAGMS (MECHANICAL)
Viscous damping techniques and high overload pro-
tection for low pressure transducers
(JPRS-52545) 02 p0224 N71-11530

Knife structure for controlling rupture of shock tube
diaphragms
(NASA-CASE-XAC-00731) 06 p0830 N71-15960

Magnetically opened diaphragm design with camera
diaphragm and expansion tube applications
(NASA-CASE-XLA-03640) 10 p1564 N71-21060

Design and development of inertia diaphragm pres-
sure transducer
(NASA-CASE-XAC-02981) 10 p1558 N71-21072

Punch and die device for forming convolution series
in thin gas metal hemispheres
(NASA-CASE-XNP-05297) 12 p1927 N71-23811

Rebar composition for explosion bladders and
diaphragms for use with hydrazine
(NASA-CASE-NP-11433) 18 p2940 N71-31140

DYNAMIC MOLECULES
Three dimensional collision-induced vibrational
transitions in homonuclear diatomic molecules
(NASA-TR-R-355) 01 p0096 N71-10453

Atomization of H₂ near threshold
(NASA-TM-X-45434) 06 p0915 N71-15991

Hartree-Fock computer programs to calculate
molecular wave functions of light metal diatomic
hydrides, oxides, and halides
(AD-713977) 06 p0925 N71-16814

Thermal dissociation affecting oscillations of
diatomic molecules
(SC-71-4045) 06 p1265 N71-19158

Isotomeric potentials and dissociation energies of
atomic hydrogen and halogen molecules studied with
spectroscopy and potential curves
(NASA-CR-116978) 09 p1428 N71-19737

Dissociation energy and long range potential of
atomic gas molecules from vibrational spacings of
higher levels
(AD-713977) 09 p1428 N71-19739

Dissociation energies and long range potentials of
atomic halogen molecules from vibrational spacings
(AD-713977) 09 p1428 N71-19740

Approximation of scattering resonance energies and
widths of ground state of molecular hydrogen from
study dependence of atomic collisional time delay
lengths
(AD-713977) 09 p1429 N71-19743

Expectation values and kinetic energy for vibra-
tional-rotational levels of ground states of H₂, HD,
and D₂
(AD-713977) 09 p1429 N71-19744

Ground state dissociation energies for diatomic
halogen from vibrational spacings near dissociation
limit
(AD-713977) 09 p1429 N71-19746

Plasma stream reaction dynamics, intermolecular
potentials from high resolution differential cross sec-
tion, and collision induced dissociations of diatomic
molecules
(SC-71-4045) 11 p1096 N71-22421

Differential scattering cross sections for He colli-
sions with rare gas and diatomic molecules
(AD-717675) 12 p1974 N71-23988

Investigation of fundamental laser processes with
computation of vibration-rotation and electric dipole-
moment matrix elements of diatomic molecules
(AD-723696) 17 p2759 N71-30161

Vibration-rotation interaction effects in calculated
band strengths studied by asymptotic expansion
method
(AD-723811) 17 p2803 N71-30215

Mathematical models for electron attachment to
molecules with negative ion formation
(AD-723642) 19 p3144 N71-31717

Quantum mechanical expression for relaxation time
of low density gas with rotating diatomic molecules
(PB-196661) 19 p3144 N71-31724

Transport properties of rotating, nonvibrating,
diatomic molecules of low density gas
(PB-196282) 19 p3156 N71-32430

Development of theory for vibrational dissociation
of diatomic molecules to neutral atoms due to direct
excitation in strong collision
(AD-723756) 24 p3982 N71-38415

DIBORANE
Spectroscopic measurements of barium clouds and
spectrum of barium cloud produced by release of
diborane in rocket sounding of upper atmosphere for
use in predicting satellite orbits
(AD-717686) 11 p1731 N71-22689

Clogging tests on liquid diborane and liquid oxygen
diffusion propellants in orifice flows
(NASA-CR-121282) 19 p3172 N71-32475

Evaluation of metallic and nonmetallic construction
material performance and reliability after long storage
in CDP and B236
(NASA-CR-122067) 22 p3661 N71-36107

Design and storage tests of 200 lb diborane shif-
ting container including storage time, volumetric loading,
and pressure-temperature limitations
(NASA-CR-122952) 23 p3761 N71-36810

DICHLORODIPHENYLTRICHLOROETHANE
Model case studies of effects of DDT on human en-
vironment
(PB-194413) 04 p0481 N71-14479

Using helicopter for spray dusting forests with DDT
for tick borne encephalitis
(AD-703998) 17 p2703 N71-29557

DICHLOROMETHANE
Color vision of dichromats in humans
(PB-190416T) 02 p0166 N71-11183

DICTIONARIES
Thesaurus for high temperature research
(AD-710092) 01 p0132 N71-10038

Two-part glossary of bathymetric terms in 27 lan-
guages and English equivalents
(NASA-710092) 01 p0049 N71-10687

Glossary of Air Force weather forecasting ter-
minology
(AD-715932) 06 p1230 N71-18544

Revised illustrated dictionary of snow and ice terms
(AD-715932) 11 p1755 N71-22834

Conference on information retrieval and manage-
ment information systems including construction of
dictionaries, analysis of query formulations, and com-
puter programming
(AD-715932) 14 p2221 N71-25976

Computer program simulating generation of finned
forms of irregular verbs in German for use in dictio-
naries and grammars
(AD-715932) 14 p2222 N71-25982

Automatic dictionary for creating indexes for infor-
mation retrieval through computer programs
(AD-715932) 14 p2222 N71-25985

Compilation of dictionaries for information retrieval
systems from vocabularies from different fields of
science
(AD-715932) 14 p2223 N71-25990

Strategies for searching in data bank files adapted to
query and file structure and use of thesaurus with
small and medium computers
(AD-715932) 14 p2223 N71-25993

Dynamic characteristics of dictionaries and docu-
mentation indexes for information retrieval
(AD-715932) 14 p2223 N71-25994

List of approximately 110 terms and definitions for
use in activities associated with fissionable materials
safeguards
(WASH-1162) 15 p2458 N71-26936

Glossary of terms used in identification and predic-
tion of mechanical failure
(AD-713534) 16 p2685 N71-28123

Hunfacts system thesaurus containing words and
phrases which reflect concepts to be indexed in human
factors engineering information retrieval system
(AD-716157) 16 p2550 N71-28119

DIELECTRIC CONSTANT
U DIELECTRIC PROPERTIES
DIELECTRIC MATERIALS
U DIELECTRICS
DIELECTRIC POLARIZATION
Dynamic piezoelectric shell theory for polarized fer-
roelectric ceramic orthotropic material
(AD-716157) 13 p2155 N71-23564

DIELECTRIC PROPERTIES
Electric field effects on dielectric properties and
molecular arrangements of cholesteric liquid crystals
(A70-11352) 03 p0324 N71-12317

DIELECTRIC PROPERTIES

Dipole relaxation and molecular arrangements in
liquid crystals
(A70-26459) 03 p0325 N71-12320

Dielectric constants measurements and magnetic
field effects on compressed cholesteric liquid
crystals
(A70-17324) 03 p0325 N71-12521

Dielectric properties of glass
(D-MAT-158) 03 p0397 N71-13054

Measuring coil for determining permittivity of
solids, liquids, and pastes between 100 kHz and 100
MHz
(PHL-1970-10) 04 p0360 N71-14296

Dielectric field computations in semiconductor
oxide integrated circuits
(AD-713476) 05 p0635 N71-14923

Particle diffusion and plasma dielectric constant in
uniform electric field transverse to spatially uniform
magnetic field
(JPP-4/5) 05 p0733 N71-15081

Studying motions of atoms in crystalline solids with
models of interpolation schemes
(TH-1409) 05 p0758 N71-15299

Measurement of dielectric constant of nonlinear
dielectrics as function of electric field strength
(AD-713871) 06 p0903 N71-15961

Investigating ferroelectric insulators, alloys, and
magnetic impurities with respect to transport theory
(AD-714096) 06 p0904 N71-16211

Processing results of experiments on methods for
preparation of vinyl chlorides
(JPRS-52545) 07 p0967 N71-16961

Measuring and controlling chemical, physical, and
electrical properties of dielectric films during fabrica-
tion of semiconductor devices
(AD-714096) 07 p1087 N71-17281

Birefringence properties of viscoelastic materials
(AD-714998) 07 p1125 N71-17783

Low frequency dielectric constants of LiF, NaF,
NaCl, NaBr, KCl, and KBr by substitution method
(COO-623-153) 08 p1280 N71-19032

Properties and interface characteristics of silicon
nitride films deposited on silicon
(AD-715932) 08 p1234 N71-19135

Static dielectric constant of solids determined by
substitution method with techniques for refining
capacitance measurements
(COO-623-150) 08 p1282 N71-19304

Low-frequency dielectric constants of alkaline earth
fluorides determined by substitution method
(COO-623-154) 08 p1282 N71-19305

Capacitive gas accuracy and stability for high pres-
sure measurement
(COO-623-155) 08 p1282 N71-19307

Development of laboratory apparatus for deter-
mination of dielectric properties of polymer films
(AD-716041) 09 p1365 N71-19715

Dielectric properties of sea ice and FM superhigh
frequency radar measurement of ice thickness in
Sweden and Greenland
(R-83) 10 p1546 N71-20637

Shock induced ferroelectric/paraelectric phase
transition in barium titanate
(AD-717551) 11 p1815 N71-21948

Influence of thermal treatments on dielectric prop-
erties of lithium-aluminum-silica glasses using electric
measurements and X ray and electron microscopy
techniques
(AD-717551) 11 p1783 N71-22344

Selection of materials for electrical connectors com-
patible with future space missions
(NASA-CR-103092) 12 p1087 N71-23383

Time-varying modulation of dielectric constant ef-
fects on semiconductor laser modes
(NASA-CR-118038) 12 p1935 N71-24185

Dielectric constant of polyethylene under shock
compression in pressure range 16 to 246 kbar
(AD-718033) 12 p1947 N71-24239

Empirical pseudopotential method for exploring
electronic structure and dielectric properties of fac-
centered cubic semiconductors
(UCRL-20377) 13 p2153 N71-25408

Abstracts of scientific articles on terrestrial
geophysics including mathematical models of earth
crust, and effect of high pressure and temperature on
dielectric constants
(AD-718033) 15 p2396 N71-26863

Approximative formula for internal friction coeffi-
cient of ice
(AD-720935) 15 p2399 N71-27804

Linear surface radar reflectance measurements and
variations of dielectric constant
(PB-4) 17 p2944 N71-29419

Formulas for calculating conductivity and dielectric
constants of capacitors made up of composite bodies
extended to more than two components
(NASA-TT-F-13725) 17 p2727 N71-30244

Physical properties, dielectric properties, and struc-
ture of several experimental types of glass
(AD-718033) 18 p2961 N71-31277

Screenable dielectric constant ceramic glass paste
for thick film capacitors in microelectronics
(AD-723404) 19 p3864 N71-31714

- Dielectric properties of selected polymers determined by skewed circular arc method of analysis
19 p3051 N71-32286
- Optical, dielectric properties, and growth of alpha-monoclinic selenium
19 p3170 N71-32387
- Dielectric properties and microwave radiometry of rocks and minerals in western US
[PB-198378] 19 p3094 N71-32418
- Spectroscopic analysis to determine effect of phase angle, compactness of material, and particle size on total reflectivity of various inorganic materials
[AD-724311] 19 p3171 N71-32702
- Calculating electrical resistance of rutile crystals from dielectric loss data
[AD-724311] 20 p3332 N71-32928
- Analysis of apparent variation of effective dielectric constant of microstrip transmission lines
22 p3559 N71-35349
- Differences, simulations, and interrelationships between insulation resistance and dielectric strength testing
[AD-726924] 22 p3561 N71-35346
- Synergistic effects of slip ring-brush design and fabrication for vacuum application determined by friction, wear, electrical noise, and dielectric strength data
[NASA-CR-122988] 23 p3740 N71-36666
- Inductive gratings for compensating dielectric cylinder effects on mounted aerial
[RA-87] 24 p3891 N71-37732
- Measuring dielectric constant of materials used in millimeter and submillimeter wave range
[AD-727941] 24 p3945 N71-38145
- Formulas, tables, and graphs for calculation of electrical capacitance
[AD-727198] 24 p3968 N71-38304
- DIELECTRICS**
- NT RADOME MATERIALS**
- Radio frequency sputtering of dielectric films
01 p0058 N71-10157
- Optical properties of vapor deposited dielectric and reflecting multiple layer systems
01 p0090 N71-10523
- Field characteristics of dielectrically loaded parallel-waveguides
02 p0184 N71-11294
- Simulation of high altitude ionized air with artificial dielectric
[AD-713531] 05 p0658 N71-15429
- Measurement of dielectric constant of nonlinear dielectrics as function of electric field strength
[AD-713871] 06 p0903 N71-15961
- Electromagnetic radiation from infinite cylinder immersed in inhomogeneous medium
[AD-714575] 06 p0825 N71-16629
- Calculations on electromagnetic radiation from infinitely long wire in dielectric material over conducting ground plane
[AD-713537] 08 p1168 N71-18446
- Radiation from open-ended parallel-plate waveguide into dielectric or plasma slab
08 p1162 N71-18876
- Charge injection mechanism from metal to dielectric liquid with applied electric field
[AD-716471] 09 p1424 N71-19930
- Shock induced electrical signals with positive and negative components examined in polyethylenes
[AD-716329] 09 p1406 N71-19950
- Energy gap for excitonic insulator in presence of persistent currents
[AD-716749] 10 p1634 N71-20919
- Nose cone mounted heat resistant antenna comprising plurality of adjacent layers of silica not introducing paths of high thermal conductivity through ablative shield
[NASA-CASE-XMS-04312] 11 p1714 N71-22984
- Polarization phenomena in dielectric structure of titanium-titanium dioxide metal
[AD-717893] 12 p1944 N71-23672
- Effect of permanent and alternating electric fields on heat transfer in fluid dielectrics
[NASA-TT-F-13560] 12 p2011 N71-24059
- Broadband microwave waveguide window to compensate dielectric material filling
[NASA-CASE-XNP-06880] 13 p2056 N71-24808
- Effects of surface roughness on reflection of radiation from vacuum deposit interface of CO₂ cryodeposits studied by angular distribution measurements of radiant flux from glass samples
[AD-728002] 14 p2296 N71-25898
- Dielectric matter and vector D analysis
[AD-721181] 15 p2452 N71-26823
- Laser machining device with dielectric functioning as beam waveguide for mechanical and medical applications
[NASA-CASE-HQN-10541-2] 15 p2415 N71-27135
- Application of Lorentz reciprocity theorem to near field detection of buried dielectric spheres in antenna lossy half spaces
16 p2563 N71-28822
- Quasi-optical microwave circuit with dielectric body for use with overlayer waveguides
[NASA-CASE-ERC-10011] 16 p2564 N71-29065

- Flashovers across dielectric spacers in compressed gases of coaxial cylinder system with insulation recommendations
[NLL-CE-TRANS-5434-9002.09/] 17 p2787 N71-29634
- Application of dielectric and anelastic loss techniques for determining defects in ceramic materials
[AD-723838] 19 p3120 N71-32007
- Radiation from dielectrically coated spherical antennas determined by solving related boundary value problem
19 p3067 N71-32403
- Electron drainage current from dilute plasma through holes in high voltage dielectric probes
[NASA-TM-X-67890] 19 p3166 N71-32483
- Selection of materials having suitable thermal and dielectric properties to cover flush mounted space shuttle antennas
21 p3515 N71-35044
- Computer-aided data reduction technique for extracting time dependent conductivity of dielectric material from test circuit recorded responses
[AD-726359] 22 p3560 N71-35357
- Differential equations and boundary conditions for finitely deformable, polarizable and magnetizable, heat conducting insulators interacting with electromagnetic fields
[AD-726450] 22 p3630 N71-35864
- Properties of ZnO powder and intergranular region between particles studied using dielectric relaxation
22 p3660 N71-36100
- Polar and ionic adsorbates, classical image force laws, electron gas dielectrics, and related surface chemistry and physics topics
[AD-726653] 23 p3720 N71-36515
- Polymer temperatures measured by thermistors, photoelectric receivers, and dielectric methods
[AD-727340] 23 p3760 N71-36803
- Multiple scattering and eigenfunction solutions for electromagnetic scattering from cylinders over and imbedded in dielectric half spaces
24 p3890 N71-37730
- Plasma formation upon laser irradiation of transparent dielectric materials below damage threshold
[AD-727143] 24 p3932 N71-38052
- Ionization in dielectric liquids produced by gamma radiation and ionization inhibition by electron scavengers
[NP-18875] 24 p3973 N71-38348
- DIENES**
- NT BUTADIENE**
- DIES**
- Punch and die device for forming convolution series in thin gate metal hemispheres
[NASA-CASE-XNP-05297] 12 p1927 N71-23811
- Development and characteristics of frusto-conical die nib for extrusion of refractory metals
[NASA-CASE-XLE-06773] 12 p1928 N71-23817
- Effectiveness of superimposed vibrating forces in reducing die wall friction during powdered metal compaction
[SRO-475-10] 16 p2614 N71-28898
- DIESEL ENGINES**
- Destructive effects on metal surfaces in diesel engines due to liquid cavitation corrosion caused by opposite oscillating plates
02 p0231 N71-11583
- Destruction effects on metal surfaces in diesel engines due to liquid cavitation corrosion caused by opposite oscillating plates
02 p0231 N71-11584
- Numerical analysis of gas turbine supercharging in multi-cylinder four cycle engines
[AD-713873] 06 p0941 N71-16225
- Photochemical reactivity of diesel exhaust hydrocarbons
[BMRI-7514] 10 p1661 N71-20931
- Comparison of small gas turbine and diesel engine power plants for aircraft and ground vehicle propulsion
15 p2512 N71-26958
- Chemical composition of odorants in diesel engine exhaust
[PB-198072] 17 p2839 N71-29786
- Sound ranging distance for detecting benzene and diesel engines
[IZF-1971-6] 18 p2963 N71-30898
- Exhaust emission characteristics of diesel engines, noting emissions of smoke, odor, hydrocarbons, nitrogen oxides, carbon monoxide, and aldehydes
[BM-R1-7530] 19 p3174 N71-32492
- Modifying air intake and fuel injection parameters to reduce diesel engine nitrogen oxide emissions
[BM-R1-7579] 23 p3841 N71-37386
- Theoretical and experimental analyses of surges in air charging systems of supercharged diesel engines
[TB-72] 23 p3841 N71-37388
- Thermodynamic analysis of cycle of pulse-charged turbo-supercharged two stroke marine diesel engine to assess performance deterioration
[ARI/ME-128] 24 p4001 N71-38536

- DIETS**
- Diet and altitude effects on body composition of growing rats
[AD-712239] 02 p0155 N71-11006
- Nutritional properties of unicellular algae compared to soya protein
02 p0161 N71-11046
- Investigating effects of liquid diets on subjects in space environment simulators
[NASA-CR-116253] 06 p0804 N71-16796
- Human immunology on prolonged diet of dehydrated foods
08 p1154 N71-19904
- Glycerol food additive for spacecrew feeding
10 p1507 N71-20971
- Hyperthermia, dietary, and desalination effects on thermoregulation in rats
[NASA-CR-117831] 11 p1684 N71-22879
- High fat diet effects on caloric intake, body weight, and heat escape responses in normal and hyperphagic rats
11 p1684 N71-22879
- Determination of growth patterns in rats fed on balanced diets differing by the presence of either oxidized or unoxidized fat
[NASA-CR-114998] 13 p2032 N71-24553
- DIFFERENCE EQUATIONS**
- Asymptotic behavior and error analysis for linear integral differential difference equations
03 p0401 N71-11352
- Difference equations for approximating ordinary differential equations
[NASA-CR-103015] 06 p0885 N71-16571
- Difference methods for hyperbolic equations using space and time split difference operators of third order accuracy
[UCRL-72806] 09 p1409 N71-19928
- Invariant imbedding method for reducing two point boundary value problems for vector-matrix systems of linear difference equations to initial value problems
[TID-25609] 10 p1594 N71-21480
- Numerical analysis of Lax-Wendroff difference method with artificial viscosity and its two variations by two-step method
[NAL-TR-217] 13 p2068 N71-23538
- Difference equations solved for determining large deflection response of circular, rectangular, and polygonal flat membranes
[AD-723338] 19 p3188 N71-32827
- Derivation of difference equations for MAGE hydrodynamic computer program, and computation of flows containing plastic and elastic effects
[LA-4601] 20 p3359 N71-33575
- Difference scheme for numerical solution of mixed boundary value problems in electrostatics
[NASA-TT-F-13565] 22 p3627 N71-35846
- Numerical methods for variable permeability magnetostatic field problems - difference equations solved iteratively
22 p3630 N71-35846
- Difference method in solving two-dimensional steady state theory of elasticity for case of specified strain on boundary
[NASA-TT-F-13566] 22 p3681 N71-36252
- Second difference of phase shift method for measuring ionospheric electron density
24 p3913 N71-37095
- Difference schemes with splittable operator for systems of first order hyperbolic equations of mixed type for which Cauchy problem periodic in space variable posed and stability proved
24 p3949 N71-38177
- DIFFERENCES**
- Difference scheme for solving initial value problem for one dimensional Vlasov equation
[COO-2059-5] 08 p1272 N71-14995
- DIFFERENTIAL ALGEBRA**
- U DIFFERENTIAL CALCULUS**
- U MATRICES [MATHEMATICS]**
- DIFFERENTIAL AMPLIFIERS**
- Stepping motor control apparatus exciting windings in proper time sequence to cause motor to rotate in either direction
[NASA-CASE-GSC-10366-1] 06 p1172 N71-16772
- Finite linear circuit construction from capacitor and differential voltage controlled current sources
[AD-716563] 09 p1357 N71-19023
- Broadband differential amplifier having gain of 16 from dc to 150 MHz
[CEA-N-1448] 24 p3897 N71-37779
- DIFFERENTIAL ANALYZERS**
- U ANALOG COMPUTERS**
- DIFFERENTIAL CALCULUS**
- Exponential bound for growth of norm for derivative of strong solution of inhomogeneous abstract wave equation
09 p1409 N71-19946
- Differential calculus applied to discrete Walsh-Paley functions, noting usefulness for binary codes
[NPL-DES-3] 15 p2434 N71-27910
- Comparison of coefficient modification, chain rule and function methods for computing gravitational potential derivatives with chain rule subroutine
[CDC 6660 computer] 16 p2589 N71-29744
- [COM-71-00185]

SUBJECT INDEX

DIFFERENTIAL EQUATIONS

- Strict estimation of derivative values
 Machine algorithm for establishing derivability in
 chemical calculus using inverse method
 [NLL-RTS-5556] 17 p3738 N71-29373
 [NLL-RTS-5556] 17 p3734 N71-30163
- DIFFERENTIAL EQUATIONS**
 NT BURGER EQUATION
 NT CHANDRASEKHAR EQUATION
 NT ELLIPTIC DIFFERENTIAL EQUATIONS
 NT FOKKER-PLANCK EQUATION
 NT GAUSS EQUATION
 NT HELMHOLTZ VORTICITY EQUATION
 NT LAME WAVE EQUATIONS
 NT LOUVILLE EQUATIONS
 NT PARABOLIC DIFFERENTIAL EQUATIONS
 NT PARTIAL DIFFERENTIAL EQUATIONS
 NT POISSON EQUATION
 NT VLASOV EQUATIONS
 Differential equations describing nucleation in
 crystal growth
 Uniform asymptotic stability of functional dif-
 ferential equations of neutral type
 [NASA-CR-111113] 01 p0074 N71-10359
 Neutral equations with fixed point property
 [NASA-CR-111114] 01 p0074 N71-10376
 Solvability of differential equations in spaces
 given to delta power/Omega
 [AD-710428] 01 p0076 N71-10765
 Feedback decoupling of time delay differential
 systems
 [NASA-CR-111415] 02 p0196 N71-11375
 Generation and application of sensitivity coeffi-
 cients
 [NASA-CR-102912] 02 p0197 N71-11380
 Applications of general method of calculating turbu-
 lent shear layers
 [ICP-7066] 02 p0201 N71-11475
 Nonlinear logarithmic amplifiers as function genera-
 tors and logarithmic multipliers for nonlinear dif-
 ferential equations
 03 p0353 N71-12590
 Finite difference solution of first order boundary
 layer equations
 03 p0360 N71-12584
 Digital computerized solution of ordinary dif-
 ferential equations
 [RAB-TM-SPACE-26] 03 p0399 N71-13053
 Set of states attainable by all solutions of control
 system or generalized differential equation
 [AD-712737] 03 p0399 N71-13185
 Mathematical logic differential equations solved by
 Web functions
 [NRL-DES-1] 03 p0400 N71-13235
 Asymptotic behavior and error analysis for linear in-
 tegral differential difference equations
 03 p0401 N71-13329
 Computer subroutines for Runge-Kutta integration
 of differential equations
 [NRL-DES-2] 04 p0538 N71-14076
 Accurate approximative solution to differential
 equations of oscillatory problem with perturbing
 forcing
 [NASA-CR-115774] 04 p0538 N71-14147
 Stability regions of discretization methods for dif-
 ferential equations
 [AD-712711] 04 p0539 N71-14289
 Computer program for solving finite difference
 analog to differential equations of motion in wave
 propagation
 [IC-DR-70-315] 05 p0650 N71-14875
 Bifurcation-truncation problem for systems of
 ordinary linear differential equations
 [AD-713701] 05 p0714 N71-15277
 Extremal problems related to eigenvalues of linear
 differential operators
 [AD-713706] 05 p0714 N71-15278
 Linear ordinary logical differential equations and
 Web functions
 [NRL-DES-2] 06 p0883 N71-15712
 Extension of frequency response and pulse test
 methods for identification of nonlinear system ele-
 ments described by nonlinear differential equations
 [AD-714489] 06 p0887 N71-16389
 Difference equations for approximating ordinary
 differential equations
 [NASA-CR-103015] 06 p0885 N71-16573
 Development of methods for treatment of basic
 nonlinear partial differential equations of theoretical
 physics
 [AD-714981] 06 p0885 N71-16617
 Transformation of differential equations in lunar
 theory
 [NASA-TN-D-7036] 06 p0949 N71-16863
 General theory of dissipative periodic processes for
 systems defined by partial, functional, or neutral dif-
 ferential equations
 [NASA-CR-110311] 07 p1051 N71-17408
 Numerical calculations of density and temperature
 profiles in cylindrical plasmas preionized by UV
 radiation
 [N7-1106] 08 p1270 N71-18250
 Investigating Lyapunov stability properties of so-
 lutions of Volterra integrodifferential equations
 [NASA-CR-116797] 08 p1225 N71-18497
- Coefficient determination of flight dynamics mul-
 tivariant systems by means of computer simulated
 aircraft dynamic models
 [DLR-FB-70-30] 08 p1144 N71-18586
 Writing programs in interactive FORMAC language
 to implement Picard iteration in solving systems of or-
 dinary differential equations
 08 p1228 N71-19190
 Asymptotic solution of differential equations for
 rod oscillations at high temperatures
 [SC-T-70-4042] 08 p1302 N71-19327
 Theorem proving for optimal control of stationary
 diffusion processes with natural boundaries and
 discounted cost
 [RR-24/RM/5] 09 p1410 N71-20011
 Optimization of aeroleastic constraints for aircraft
 design using differential equation idealization and
 finite element approximation
 [NASA-CR-117158] 09 p1479 N71-20139
 Distribution of passage times for nonsingular one
 dimensional diffusion satisfying stochastic differential
 equation
 09 p1410 N71-20200
 Relaxed solutions to stochastic differential equa-
 tions with discontinuous drift
 09 p1411 N71-20275
 Compactness condition of theorem on semigroup of
 operators on Banach space, with bounded solutions of
 abstract differential equations
 09 p1411 N71-20304
 Error bounds for approximate solutions to operator
 differential equation, and applications to Magnus and
 second order differential equations
 [TTD-25627] 10 p1593 N71-21477
 Numerical solution of initial value problems for or-
 dinary and partial differential equations using dif-
 ferential quadrature and long-term integration
 [TTD-25616] 10 p1594 N71-21578
 Approximations, existence, uniqueness, and stability
 of solutions with discontinuous drift terms in
 stochastic differential equations in control theory
 [NASA-CR-117746] 11 p1787 N71-22408
 Approximations to and local properties of diffusions
 with discontinuous controls expressed by stochastic
 differential/Itô equation
 11 p1787 N71-22409
 Stability and existence of diffusions with discon-
 tinuous or rapidly growing drift terms in stochastic dif-
 ferential equations
 11 p1787 N71-22410
 Imbedding nonlinear differential equations in re-
 formulating boundary value problems to initial value
 problems for computerized computation
 [TAE-112] 11 p1788 N71-22497
 On-line FORTRAN 4 digital computer program for
 solving ordinary differential equations
 12 p1883 N71-23866
 Scale and conformal invariance differential equa-
 tions applied to single particle matrix elements of two
 fields and false analytic assumptions when stress ten-
 sors carry momenta
 [RLO-1388-598] 12 p1975 N71-23998
 State variable feedback for decoupling of time delay
 differential equations
 12 p1894 N71-24149
 Second order differential equations for free bound-
 ary condition of heat equation
 12 p1951 N71-24187
 Formal solutions of first order functional equations
 [TR-71-110] 13 p2103 N71-24935
 Development and numerical integration of dif-
 ferential equations of spacecraft motion used in Double
 Precision Trajectory Program
 [NASA-CR-117938] 13 p2168 N71-25152
 Computer program for calculating concentration of
 fusion products - HERETRA
 [DEMO-70/10] 13 p2135 N71-25182
 Numerical solutions of differential equations for
 ecosystem models
 [ORNL-IBP-70-4] 13 p2104 N71-25428
 Differential equations for solving time dependence
 parameter in JFT-2 joule heating
 [JAERI-MEMO-4186] 13 p2149 N71-25575
 Probability models for solution of elliptic and
 parabolic equations by computers
 14 p2248 N71-25970
 Differential equations governing transient response
 of abating axisymmetric orthotropic bodies and effect
 of shape changes
 [NASA-TN-D-6220] 14 p2353 N71-26035
 Stability and control of processes described by
 stochastic functional differential equations
 14 p2284 N71-26205
 Integrator design to provide subroutines for numeri-
 cal solution of ordinary differential equations
 [NASA-CR-118521] 14 p2224 N71-26381
 Application of quasilinearization to Riccati-type
 nonlinear differential equations and stability of non-
 linear stochastic systems
 14 p2285 N71-26616
 Properties of solutions for stochastic differential
 equations
 [TR-71-12] 14 p2285 N71-26675
- Global inverse and implicit function theorems
 equivalent to existence and uniqueness of certain ordi-
 nary differential equations
 [AD-720894] 15 p2434 N71-27256
 Green function in solving linear and nonlinear
 second order ordinary differential equations including
 examples in finding rendezvous and periodic orbits of
 restricted three body system
 [NASA-CR-118993] 16 p2621 N71-28103
 Theorems on extremal strategies and aftereffects in
 differential game theory
 [JPRS-53310] 16 p2621 N71-28153
 Theorems on extremal strategies in differential
 game theory
 16 p2631 N71-28154
 Theorems on theory of differential games of
 systems with aftereffects associated with conflict
 problem
 16 p2622 N71-28155
 Algorithm proposed for approximate integration of
 specific boundary value problem of nonlinear system
 of differential equations with delayed argument and
 satisfying Lipschitz condition
 [NASA-TT-F-13694] 16 p2622 N71-28221
 Solving functional differential equations for total
 current algebra
 [NYO-2171-336] 17 p2772 N71-29330
 Survey of concepts and theorems of causality
 problems and indefinite metric in quantum field theory
 [NYO-3829-58] 17 p2787 N71-29513
 Bimetric formalism in general theory of relativity
 and laws of conservation considering integral and dif-
 ferential form of conservation laws
 [NLL-RTS-5731] 17 p2787 N71-29701
 Variational and boundary value problems and dif-
 ferential properties of corresponding generalized solu-
 tions of integrodifferential equations
 [NASA-TT-F-13745] 17 p2773 N71-29814
 Three simultaneous differential equations applica-
 ble to any strain energy function for problems of large
 elastic deformations of axisymmetric membranes
 17 p2854 N71-30156
 Solving Volterra integral equations modeled after
 finite difference methods for ordinary differential
 equations
 [TR-38] 17 p2775 N71-30374
 Rendezvous of controlled movements and related
 problems in differential games aspect of controlled
 systems theory
 [JPRS-53450] 17 p2775 N71-30378
 Logarithmic norms of matrices for error analysis in
 numerical integration of differential equations
 [NA-70-10] 18 p2943 N71-30597
 Asymptotic behavior of covariance matrix solution
 for discrete matrix Riccati equation
 [AD-722597] 18 p2944 N71-30880
 Fixed point method and Liapunov function for in-
 vestigating problems concerning periodic and almost-
 periodic differential systems
 [NASA-TT-F-13803] 18 p2945 N71-31169
 Optimization for minimum matrix norms noting solu-
 tion of differential equations
 [NA-70-26] 18 p2945 N71-31172
 Local behavior of autonomous neutral functional
 differential equations
 [NASA-CR-119360] 18 p2945 N71-31206
 Optimal control systems performance sensitivity
 differential equations including hard and soft con-
 straints
 [RM-5143] 18 p2948 N71-31434
 Mathematical model for computerized strict error
 estimation in differential equation systems
 18 p2948 N71-31461
 Formulation of general equations of motion of
 thrust alleviated gyroscope given missile motion, and
 computer code for integrating resulting differential
 equations
 [AD-723420] 19 p3132 N71-31799
 Problem solving in linear differential games
 [JPRS-53645] 19 p3122 N71-32047
 Game problem for reducing motion to given set for
 linear systems with aftereffects
 19 p3123 N71-32048
 Linear differential games of pursuit in presence of
 delays
 19 p3123 N71-32049
 Optics of linear media formulated in terms of in-
 tegrodifferential equations and extended to spatially
 dispersive media
 19 p3143 N71-32607
 Differential game theory with guaranteed estimates
 and terminal payoff
 20 p3289 N71-32878
 Generalized differential game theory of particle mo-
 tion in n-dimensional Euclidean space
 20 p3289 N71-32880
 Minimax principles in differential games without
 saddle points
 20 p3289 N71-32881
 Nonlinear boundary value problem of Strum-Liou-
 ville type for two dimensional system of ordinary dif-
 ferential equations
 [AD-724175] 20 p3290 N71-32985

- Numerical integration of integrodifferential equations for creep analysis of thick-walled shells [REPT-NA-70-19] 20 p3291 N71-33144
- Finite difference formulation for differential equations involving both first and second derivatives in problems involving transport by simultaneous convection and diffusion [EFT-TN-A-38] 20 p3292 N71-33534
- Derivation of governing differential equations of mixed formulation for linear, dynamic problem of thermoelectric laminated isotropic arbitrary cylindrical shells [UNICITV-R-59] 20 p3361 N71-33960
- Nonlinear optimization techniques in dynamic programming and solution of ordinary nonlinear differential equations by Runge-Kutta method [NASA-CR-121673] 21 p3398 N71-34179
- Jordan decompositions for n-dimensional vector space and geometric properties of solutions to a prime equals Ax differential systems [ORNL-4686] 21 p3449 N71-34549
- Multiple value differential equations for optimal solutions 21 p3449 N71-34550
- Averaging technique applied to variational equations describing rotational motions of rigid triaxial body in elliptical orbit [NASA-CR-121986] 22 p3604 N71-35668
- Numerical treatment of some integro-differential equations, Fourier integrals, and integral equations 22 p3606 N71-35682
- Differential game with vector function and prescribed duration [JPRS-53973] 22 p3606 N71-35683
- Differential approximation extension for process space in pharmacokinetics and fitting by sums of exponentials for compartmental models [TR-71-32] 22 p3607 N71-35692
- Interactive graphic instructional program illustrating basic concepts of systems analysis - INSIGHT [TR-71-21] 22 p3698 N71-36371
- FORTAN computer program for simulation of movement using set of time dependent differential equations and plotting curve [DRS/9079/TS] 23 p3729 N71-36585
- Differential equation with optimal feedback control for stochastic control system 23 p3739 N71-36663
- Numerical analysis of existence and impossibility of existence of various types of nonlinear differential equations 23 p3781 N71-36950
- Averaging technique using Jacobi elliptic functions for solving nonlinear differential equations with periodic nonhomogeneous solutions [NASA-TM-X-45710] 23 p3783 N71-36967
- Analysis of frontal model using nonlinear differential equations [AD-726617] 23 p3791 N71-37021
- Differential equations for calculating eddy current losses caused by rapidly varying magnetic fields [CTO/754/909L-9F] 23 p3805 N71-37126
- Erosion of discontinuities and formation of oscillations in numerical computations of discontinuous solutions of differential equations 24 p3949 N71-38176
- Differential equations of motion for kinematics and dynamics of proportional navigation 24 p3950 N71-38180
- DIFFERENTIAL GEOMETRY**
- NT LIE GROUPS
- NT RIEMANN MANIFOLD
- NT SPINOR GROUPS
- NT TENSOR ANALYSIS
- Geometrical interpretation of scale invariance in inelastic electron proton scattering [LNF-70/34] 04 p0578 N71-13863
- Differential forms in general relativity 04 p0539 N71-14273
- DIFFERENTIAL INTERFEROMETRY**
- Schlieren photography and differential interferometry for free flight tunnel photography [ISL-T-39/69] 05 p0312 N71-12223
- Shadowgraph photography and differential interferometry for studying aircraft boom effect on bud-bug shell [ISL-T-2/70] 05 p0315 N71-12247
- Device for determining acceleration of gravity by interferometric measurement of travel of falling body [NASA-CASE-XMF-05844] 07 p1030 N71-17587
- DSIF operations for testing theory of general relativity by very long baseline interferometers and for study of pulsar polarization 07 p0993 N71-17624
- Differential interferometric radiowave refraction measurement for monitoring columnar ionospheric electron content 24 p3914 N71-37907
- DIFFERENTIAL OPERATORS**
- U DIFFERENTIAL EQUATIONS
- U OPERATORS (MATHEMATICS)

DIFFERENTIAL PRESSURE

- Chord and rotary wing span differential pressure distribution effects on high frequency aerodynamic noise propagation from helicopters [AD-721661] 16 p2536 N71-28507

DIFFERENTIAL THERMAL ANALYSIS

- Metallurgical, X ray diffraction, and differential thermal analysis of plutonium silver system [UCRL-72225] 03 p0390 N71-12377
- Physical and chemical reactions of isoprene and fluorel elastomers between -150 C and 150 C [NASA-TN-D-6116] 03 p0396 N71-12745
- Techniques for differential thermal analysis of primary explosives 06 p0959 N71-16461
- Differential thermal analysis and antioxidant activity of nickel, zinc, lead, copper, and cadmium dialkyl-dithiocarbamates [FTD-HT-23-363-70] 10 p1513 N71-21230
- Computer programs for solution of kinetic equations and construction of thermographs during thermogravimetric analysis of ablative materials [AD-716825] 10 p1589 N71-21310
- Differential thermal analysis and X ray data for transitions and relaxations in aromatic polymers [AD-718834] 12 p1542 N71-23395
- Differential scanning calorimetry and analysis by thermogravimetry of some metal chelates and some adducts of these metal chelates [ORO-2124-24] 13 p2098 N71-23520
- Thermal analysis of lower array for satellite temperature control [TASS-70-Y-0719] 14 p2351 N71-25699
- Vacuum furnace and differential thermal analysis equipment for evaluating magnetic properties of rare earth-transition metal alloys for use as permanent magnets [AD-720660] 17 p2763 N71-29502
- Differential thermal and electrical conductivity studies of phase transitions in Li₂/V2O5, single crystals of WO₃ and WO₃ minus x, and metal-ammonia systems 18 p2887 N71-31365
- Differential thermal analysis methods in high temperature research on biochemical, polymeric and explosive materials [NBS-SP-338] 20 p3361 N71-32826
- Standardization of test methods in differential thermal analysis for materials 20 p3362 N71-32827
- Thermodynamics and operation of differential calorimeters using intermittent heating 20 p3362 N71-32828
- Evaluation of materials as temperature scale standards for differential thermal analysis 20 p3362 N71-32829
- Differential thermal analysis and high temperature calorimetry dynamics 20 p3362 N71-32830
- Differential scanning calorimetry for determining physiological chemistry of cholesterol esters in phospholipid-water systems and arteriosclerosis 20 p3362 N71-32831
- Instrumental and thermal time constants of differential scanning calorimeter 20 p3362 N71-32832
- Thermal volatility apparatus with differential condensation for evaporation rate measurements on thermally degrading materials 20 p3362 N71-32833
- Modified remote cell for thermal differential decomposition studies on lead azide 20 p3363 N71-32834
- Phase diagram for vanadium-vanadium oxide system based on melting points and thermal differential, metallographic, and X ray analyses [IS-T-448] 24 p3935 N71-38074
- Differential heating effects on steady-state tropical cyclone dynamics and energetics based on diagnostic axisymmetric model in isentropic coordinates 24 p3954 N71-38209
- DIFFERENTIATION (BIOLOGY)**
- Radiation effects on cytoplasmic structure and differential activity of genes [NYO-2356-43] 20 p3225 N71-33934
- DIFFRACTION**
- NT ELECTRON DIFFRACTION
- NT FRESNEL DIFFRACTION
- NT NEUTRON DIFFRACTION
- NT PULSE DIFFRACTION
- NT WAVE DIFFRACTION
- NT X RAY DIFFRACTION
- Perturbation analysis of diffraction by rippled convex surface [AD-714091] 06 p0815 N71-16288
- Vector analysis for exact solution to electromagnetic field diffraction by plane angular sector 11 p1797 N71-22022
- Highly stable optical mirror assembly optimizing image quality of light diffraction patterns [NASA-CASE-EBC-10001] 13 p1244 N71-24668
- Heat capacity data for calculating Debye-Waller factor of tungsten 15 p2460 N71-27069

- Estimated diffractonal peak width for scattering on Gaussian potential [IFVE-STF-69-83] 15 p2464 N71-27240
- Multiparticle production processes noting limited behavior of cross sections and diffractive dissociation [PURC-4159-19] 18 p2590 N71-31565
- Spectrum analysis of diffractively produced multimeson systems [UB-875-537] 21 p3481 N71-34797
- Determination of first-order diffraction coefficients for slot-excited conical antennas [AD-726539] 22 p3540 N71-35629
- Diffraction of helium atoms from tungsten (112) crystal surface and measurement of time of flight distribution of deuterium molecules desorbed from sputter surfaces [NASA-CR-121985] 22 p3634 N71-35980
- Kron-proton interactions and low mass enhancement due to diffraction phenomena 22 p3651 N71-36084
- Calculation of near fields of reflector antennas by geometrical theory of diffraction [NASA-CR-111950] 23 p3722 N71-34532
- Triple Raman coupling related to low mixing meson spectrum in diffraction dissociation [UCSD-10-P-10-78] 23 p3812 N71-37185
- DIFFRACTION GRATINGS**
- U GRATINGS (SPECTRA)
- DIFFRACTION PATTERNS**
- Double diffraction between Bragg reflections and diffuse intensity phases observed with high energy electron diffraction [AD-715373] 06 p1213 N71-10321
- Optimal multiple access systems and tropospheric path parameters for space communications 10 p1523 N71-21421
- Troposphere effects on microwave propagation over diffraction paths 10 p1525 N71-21430
- Very high frequency signal fading in diffraction scatter path propagation 10 p1525 N71-21431
- Diffractive Pomeron bootstrap and multiparticle fragmentation [UCSD-10-P-10-77] 21 p3481 N71-34799
- Diffraction of light with ultrasonic waves for oblique incidence of light on sound wave front - Bragg reflection [NASA-TT-F-13994] 23 p3801 N71-37182
- DIFFRACTION PATTERNS**
- Time-share FORTRAN 4 program for calculating diffraction pattern interplanar spacings [Y-1729] 01 p0096 N71-10521
- Standard X ray diffraction patterns from high purity powders [NBS-MONOGRAPH-25-SEC-8] 01 p1111 N71-10519
- Schlieren photography for optical measurements on transparent objects [ISL-T-42/69] 03 p0311 N71-12210
- Stabilizing fringe pattern in holographic system in presence of vibration and drift 03 p0379 N71-12793
- Fringe interpretation in stress-holography interferometry [AD-712669] 03 p0381 N71-31646
- Study of defect structures with field ion microscope [NASA-CR-115771] 04 p0603 N71-14151
- Investigation of deterioration in automatic power level control due to violation of assumption of time-invariance in underwater acoustic imaging [SC-CR-70-6102] 05 p0735 N71-15444
- Investigating diffraction by phase screen with random transmissivity 07 p1067 N71-17012
- Laser interferometer for monitoring and control of large telescope [NASA-CR-111811] 08 p1203 N71-19019
- Describing analytical technique for solving electromagnetic boundary value problems of suboptimal resonators with grating mirrors 08 p1203 N71-19070
- Computational method for electron diffraction intensity using s-beam theory and applied to gold microcrystal calculations 10 p1621 N71-21742
- Framing camera performance predictions from drug and diffraction image degradation source analysis [EOG-1183-530] 13 p0682 N71-25189
- Satellite orbit determination and diffraction pattern level size distribution from ionospheric irregularities [NASA-TM-X-45406] 13 p1241 N71-25210
- Polyethylene terephthalate film diffraction pattern from low angle X ray irradiation and analysis of crystal and molecular structure 14 p2213 N71-30859
- Development and evaluation of instrumented system for measuring interference fringe spacing in scattered light photoelasticity 14 p2258 N71-30824
- Digital sensor for counting fringes produced by interferometers with improved sensitivity and an photomultiplier tube to eliminate alignment problem [NASA-CASE-LAR-10204] 15 p2480 N71-27313

SUBJECT INDEX

Optical correction procedure for diffraction pattern and temperature effects on Kerr cell high voltage measurements 15 p2386 N71-27253
 Fixed pole diffraction models for Pomeranchuk 16 p2444 N71-28110
 Luminous intensity formulas and polarized neutron diffraction patterns including effects of crystal defects 18 p2579 N71-30706
 Construction of antenna array and automatic modeling system to measure amplitude and phase of diffraction patterns formed by inhomogeneous reflection of 300 kHz pulsed radio signals 20 p3259 N71-33207
 High contrast diffraction patterns by juxtaposing of half-wave plates with crossed neutral lines 20 p3313 N71-33624
 Computer program for transmission electron diffraction pattern analysis 21 p3394 N71-34158
 Manual for analyzing diffraction patterns of face centered cubic crystals for unit meshes of surface structures in hexagonal, square, and rectangular shapes 23 p3836 N71-37356
 Parabolic pulse for production of microsecond pulsed ion beams 24 p3969 N71-38313
INFRARED TELESCOPES
U SPECTROSCOPIC TELESCOPES
HYPERTELESCOPES
 Recording of X ray profiles with 3-crystal diffractometer 05 p0653 N71-15413
NUCLEAR RADIATION
 Radiation measurements of Central Arctic Basin from US and USSR drifting stations 11 p1752 N71-22802
 Theory of diffuse reflectance of particulate media including garnet, glass, corundum powders, and mixtures 17 p2816 N71-29925
 Neutral pion decay, and diffuse gamma-background relation from galactic and metagalactic sources 18 p3015 N71-31260
DIFFUSERS
 Design criterion for arbitrary diffusers (AD-70909) 01 p0040 N71-10244
 Boundary layer development and swirling flow in conical diffusers 05 p0660 N71-14767
 Integral transform solution for conical diffuser flow with fluid extraction through multiple slots 13 p2065 N71-24796
 Design, characteristics, and performance tests of short two-dimensional curved wall diffusers using suction slots 22 p3567 N71-35404
DIFFUSION
NT AMBIPOLAR DIFFUSION
NT ATMOSPHERIC DIFFUSION
NT ELECTRON DIFFUSION
NT GASEOUS DIFFUSION
NT IONIC DIFFUSION
NT MAGNETIC DIFFUSION
NT MOLECULAR DIFFUSION
NT PARTICLE DIFFUSION
NT PLASMA DIFFUSION
NT SELF PROPAGATION
NT SURFACE DIFFUSION
NT THERMAL DIFFUSION
NT TURBULENT DIFFUSION
 Diffusional flow in superplastic magnesium alloy (AD-711348) 01 p0069 N71-10997
 Iron self diffusion parameters in Fe delta-region and in Fe alloys with small Al additions 02 p0240 N71-11389
 Solid state diffusion growth of composite materials containing continuous NiAl fibers in aluminum matrices from hot-pressed aluminum embedded nickel wires (AD-711346) 02 p0246 N71-11591
 Conference on atomic transport in solids and liquids (AD-711418) 02 p0284 N71-11840
 Atom diffusion and diffusion-controlled processes in solids including metals, semiconductors, oxides, and piezoelectric crystals 02 p0286 N71-11926
 Lithium diffused radiation resistant solar cells (NASA-CR-111581) 03 p0316 N71-12257
 Effects of diffusion redistribution of phosphorus on characteristics of silicon solar cells (NASA-TN-X-2143) 03 p0318 N71-12271
 Fast neutron irradiation effects on diffusion phenomena in Al-Mg system 03 p0429 N71-12885
 Effect of lattice parameter and melting point of metals on solid state diffusion 03 p0442 N71-12908
 Three element valence effect on diffusion process in copper-zinc alloys (AD-715761) 03 p0392 N71-12978
 Determination of boundary layer diffusion in forced convection flow (NASA-TN-D-70121) 03 p0363 N71-13045

Vacuum system model study for 300 MeV H⁻ cyclotron (TRF-69-7) 03 p0359 N71-13344
 Thermotransport and self diffusion in liquid metals (COO-641-20) 04 p0483 N71-13449
 Ionization, recombination, and diffusion rates in nonequilibrium plasmas 04 p0596 N71-14248
 Anisotropic diffusion and electromigration research (RPI-1044-24) 05 p0706 N71-15538
 Flux synthesis methods to obtain detailed neutron flux from lower-order calculations 06 p0896 N71-16280
 Spin-echo technique of nuclear magnetic resonance used to determine activation energy of aluminum (IS-T-410) 07 p1079 N71-17944
 Solution of thermalization problems by quasi-diffusion method (IAE-1675) 08 p1302 N71-18156
 Uranium distribution and uranium diffusion through pyrocarbon coating in UO₂ coated particles (EYR-4530-E) 08 p1235 N71-18214
 Axial and radial aerosol diffusion in circular pipes (HASL-238) 08 p1177 N71-18261
 Mechanism and kinetics of diffusion processes in metals (TT-70-50030) 08 p1219 N71-19184
 Technology review on investigations of diffusion in solids (TT-70-57079) 08 p1281 N71-19199
 Distribution of passage times for nonsingular one dimensional diffusion satisfying stochastic differential equation 09 p1410 N71-20200
 Carbon dioxide distribution in mixture with argon in graphite channel at high temperatures (NLL-RTS-5839) 10 p1514 N71-21318
 Characteristics of self diffusion of body centered plutonium under hydrostatic pressure of zero to twenty kilobars (CEA-CONF-1635) 10 p1514 N71-21448
 Diffusion-viscous flow contribution to high temperature creep of copper aluminum alloys (NLL-CE-TRANS-5438-19022-09) 10 p1584 N71-21603
 X ray analysis, metallographic, and electron microprobe analyses of reaction-diffusion in metal-nonmetal binary and multicomponent systems of Ti/SiC and Ti-6Al-4V/SiC 10 p1586 N71-21820
 Metallic film diffusion for boundary lubrication in aerospace engineering (NASA-CASE-XLE-10337) 12 p1929 N71-24046
 Measurement of Li-6 diffusion from irradiated beryllium oxide (JUL-677-RG) 13 p2128 N71-24474
 Rate equation for thermal decomposition in diffusion kinetic region for reversible reaction of solid into solid-gas mixture (UCRL-TRANS-10506) 14 p2299 N71-25609
 Structure and phase composition of diffusion layer formed by interdiffusion of iron and aluminum (TT-70-58191) 14 p2268 N71-25647
 Kinetic process of mutual diffusion between titanium with copper and other metals serving as galvanic coatings (TT-70-59084) 14 p2269 N71-25666
 Diffusion techniques for lithium-diffused silicon solar cells and cell electrical properties 14 p2201 N71-26227
 Numerical analysis of chemically reacting and diffusing fluid mixtures including longitudinal and transverse wave dispersion and thermodynamics 14 p2242 N71-26472
 Wafer and diffusion lot dependence of surface effects resulting from ionizing radiation of transistors (AD-721096) 15 p2385 N71-26899
 Self-diffusion rates determined for oxygen in uranium dioxide using spectrum analysis of alpha particles in O-18/p, alpha-N-15 reaction (CEA-R-4095) 15 p2466 N71-27275
 Self diffusion properties in alpha phase of large grains of plutonium prepared by using high hydrostatic pressures (CEA-R-4092) 15 p2478 N71-27614
 SNAAP - computer program for solving finite difference form of group diffusion equations in two dimensions (TRG-1990) 15 p2493 N71-27944
 Effect of dislocations on coarsening of particles by pressure waves, coarsening in nickel aluminum alloys, and in situ recrystallization (NLL-CE-TRANS-5601-19022-09) 17 p2815 N71-29737
 Microstructure and frequency effects in fatigue enhanced diffusion (INVO-4097-2) 18 p3023 N71-31571
 Krypton and helium bubble migration on dislocations in copper foil, and measurement of root mean square random migration distances during isothermal annealing (RDB/N-1850) 19 p3146 N71-31964
 First-order correction of diffusion length for neutrons in medium with small absorption (RCN-134) 19 p3149 N71-32104

DIFFUSION COEFFICIENT

Progress in growth of ultra-pure Al₂O₃ crystals as laser material, measurement of oxygen diffusion in oxides, and measurement of laser beam damage threshold energy in glass 20 p3287 N71-33128
 Mechanism of diffusion of some elements in iron and steels - atomic transference and movement of electrons in metal lattices 20 p3284 N71-33327
 Diffusion of nonlinearly scattered light by etched glass in experiments using Fabry-Pérot interferometer in conjunction with laser light source 20 p3374 N71-33479
 Finite difference formulation for differential equations involving both first and second derivatives in problems involving transport by simultaneous convection and diffusion (EP-TN-A-38) 20 p3292 N71-33534
 Diffusion mechanisms responsible for charge carrier mobility in doped silicon, studied to determine impact head effects on electrical conductivity (N-816) 21 p3497 N71-34916
 Variations in electrical conductivity in sunspot structure analyzed using cylindrical models of sunspot field diffusion 21 p3505 N71-34973
 Feasibility of simultaneous solid state diffusion in manufacturing integrated circuits from doped silicon films (AD-726553) 22 p3561 N71-35361
 Fundamentals of calculating concentration and diffusion of air pollutants (AD-726964) 22 p3615 N71-35768
 Isotope effect for diffusion of interstitial atoms (ANL-TRANS-882) 22 p3643 N71-35977
 Computer programs for solving two dimensional multigroup neutron diffusion equations and for makeup or recycle of isotopic compositions and related problems (GEAP-13672) 22 p3647 N71-36007
 Multigroup multiregion one dimensional criticality calculation diffusion code for IBM 1130 computer - UARAE-90 23 p3795 N71-37049
 Four groups, four regions, one dimensional criticality calculation diffusion code for IBM 1620 computer - UARAE-45 23 p3795 N71-37050
 Multigroup time independent neutron diffusion code for IBM-1130 - RAM-1 (UARAE-107) 23 p3808 N71-37150
 Diffusion of diluted drag reducing polymers and effect of diffusing polymers on boundary layer development (AD-727632) 24 p3907 N71-37844
 Turbulent heating and anomalous diffusion in pinch plasmas related to drift instability in electron cyclotrons (CONF-710607-46) 24 p3969 N71-38460
DIFFUSION BONDING
U DIFFUSION WELDING
DIFFUSION COEFFICIENT
 Benoit cell diffusion coefficient corrections for CAOR-type lattices (RDB/N-1645) 02 p0270 N71-11412
 Iron diffusion in tungsten, tantalum, niobium, and silver 02 p0270 N71-11412
 Self diffusion coefficient measurement for gold using radioactive isotopes 03 p0391 N71-12821
 Monte Carlo calculations of thermal neutron diffusion area in fuelled cell (RDB/N-1674) 04 p0578 N71-13816
 Investigating interdiffusion of W-Ta, W-Mo, and W-Nb systems in refractory temperature range (NASA-CR-111593) 04 p0330 N71-14140
 Transferring neutron diffusion coefficient for infinite homogeneous media to general heterogeneous systems (REPT-4-49) 06 p0912 N71-15810
 Pressure effect on titanium diffusion into beta titanium (COO-1198-749) 06 p0875 N71-16778
 Investigating kinetics and technology of impurity diffusion into silicon 07 p1087 N71-17280
 Evaluating determined diffusion coefficients for Group 3A, 4A, and 5A elements in silicon 07 p1089 N71-17292
 Investigating orientation dependence of boron diffusion in silicon 07 p1090 N71-17297
 Oxygen diffusion coefficient determination in tungsten oxides (AD-715006) 07 p1045 N71-17937
 Investigating helium plasma decay in circular two-path stellarator with magnetic field variations from 6 to 12 kG (NP-18502) 07 p1085 N71-18149
 Describing techniques for measuring Th-232 diffusion in thorium and uranium oxides 08 p1234 N71-18171

Hybrid program for solving space-time dependent diffusion equation in four energy groups
[CEA-CONF-1582] 08 p1246 N71-18173
Longitudinal and transverse diffusion coefficients of gaseous ions in electric fields
[AD-715373] 08 p1274 N71-18716
Diffusion coefficient of neutral hyperfine particles in gas
[NP-18413] 08 p1260 N71-18774
Diffusion coefficients determined for hydrogen in some liquid metals
08 p1217 N71-19004

Diffusion processes in iron alloys
[TT-70-50031] 06 p1219 N71-19176
Oxidation kinetics data used for calculation of oxygen diffusion coefficient in alpha titanium at temperatures from 750 to 900 C
[NASA-TT-F-13504] 09 p1401 N71-20306
Transport equation for thermal diffusion column coefficients for separation of N_2 - $14/2$ - N_2 - $14/N$ - 15 and O - $16/2$ - O - $16/O$ - 18
[MLM-1439-REV] 10 p1660 N71-20724
Effects on high temperature microwave antenna breakdown of ionization frequency, collision frequency, diffusion coefficient, and breakdown parameters
10 p1520 N71-21126

Diffusion coefficients and other physico-chemical properties of calcium, strontium, and barium chlorides and nitrates
[NRC-TT-1443] 10 p1513 N71-21257
Actinide concentration effect on uranium and thorium diffusion in columnar pyrocarbons
[ORNL-TM-2989] 10 p1591 N71-21637
Measurements of diffusion coefficients and vapor pressure in LiOH solutions for determination of gas solubilities in fuel cell electrolytes
[NASA-CR-117906] 12 p1859 N71-23345
Impurity tracer diffusion coefficients in aluminum and dilute aluminum alloys including ion core and electrostatic effects in vacancy-impurity interactions
[ORO-2036-21] 12 p1940 N71-24209
Thermodynamic densities deduced from diffusion coefficient measured on aluminum oxide artificial clouds released from ESRO rockets
13 p2069 N71-24406

Radiation resistance and lithium concentrations of lithium doped solar cells with varying lithium diffusion times and temperatures
[NASA-CR-118317] 13 p2030 N71-24963
Temperature and manganese effects on self diffusion coefficients of iron in gamma-phase iron manganese alloys
[TT-70-57056] 14 p2268 N71-25648
Penetration depth and diffusion coefficient for gaseous diffusion in metals
[TT-70-59120] 14 p2268 N71-25658

Steel microstructure, surface austenite and carbide formation, and diffusion coefficient measurement during chemical and thermal treatment
[TT-70-59099] 14 p2269 N71-25660
Volumetric and grain boundary effects on silver isotope diffusion into aluminum single and polycrystals during annealing
[TT-70-57045] 14 p2269 N71-25661
Diffusion coefficients for molybdenum and tungsten isotopes in 35 atomic percent molybdenum tungsten alloy between 1500 and 2400 C
[TT-70-57052] 14 p2269 N71-25662
Investigation of interdiffusion in ordered alloys with crystal lattice of Cu_3Au and $CuAu$ type
[TT-70-59086] 14 p2270 N71-25675
C 14 diffusion coefficients during annealing of titanium wire between 1223 to 1923 K
[TT-70-57049] 14 p2270 N71-25681

Pore development, plastic deformation, and diffusion coefficients in nickel titanium and copper titanium alloys
[TT-70-59063] 14 p2270 N71-25682
Interdiffusion of titanium with elements forming continuous series of solid solutions and elements with limited solubility in titanium/nickel, copper, rhodium, and tungsten
[DMDC-5804] 14 p2270 N71-25687
Temperature dependence of self diffusion coefficient of iron, chromium, and cobalt in steel with 8 percent carbon
[DMDC-5795] 14 p2271 N71-25693
Diffusion in two phase alloys
[DMDC-5800] 14 p2271 N71-25695
Determination of diffusion coefficient of zinc in brass by evaporation
[DMDC-5757] 14 p2271 N71-25700
Diffusion coefficients of Cu in W and W-Re alloys over 1500 to 1800 C temperature range
14 p2272 N71-25831

Phase diagram of infinite diluted plutonium diffusion in body centered cubic beta titanium solid solutions
[CEA-CONF-1487] 15 p2421 N71-27128
Self-diffusion rates determined for oxygen in uranium dioxide using spectrum analysis of alpha particles in O-18/p/alpha-N-15 reaction
[CEA-R-4095] 15 p2466 N71-27275

Determination of limiting solubilities of uranium in nickel using heterodiffusion coefficient and vacuum apparatus
[CEA-CONF-1689] 15 p2423 N71-27350
Computer program and technique for solving one dimensional multi-group reactor equations based on diffusion coefficients and transport theory
[IAE-1938] 15 p2449 N71-27391
Activation volume for self diffusion, under hydrostatic pressure, of body centered cubic Pu
[CEA-CONF-1690] 15 p2477 N71-27584
Three dimensional analysis of ambipolar radio frequency diffusion coefficient in semiconductor
[ORO-3651-9] 15 p2509 N71-27915
Grain boundary diffusion coefficients and reaction kinetics for austenitic stainless steel carburizing by carbide nuclear fuels
[JAERI-4132] 16 p2608 N71-28072
Multigroup one dimensional approximation for physics calculation of ZRR experimental fast reactor
[UJV-2408-RF] 16 p2635 N71-28800
Nuclear magnetic resonance measurement of self diffusion coefficients and temperature effects in liquid lithium 6 and 7 and sodium 23
17 p2805 N71-30289

Volume and grain boundary diffusion coefficient measurements of Fe-Cr alloys, alpha gamma phase transformations, and effects of carbon impurities
[CEA-R-4023] 18 p2982 N71-30902
Empirical approach to three-invariant violation for radial diffusion of outer zone electrons
18 p3006 N71-30931
Equations deduced relating interdiffusion coefficients of binary liquid systems with composition of system, components self-diffusion coefficients, and various system parameters
18 p2886 N71-31036

Impurity atom effects on copper diffusion in single nickel crystals
18 p2997 N71-31323
Turbulent diffusion coefficient increase with increased pitch/diameter ratio of rod bundle in reactor core coolant water flow
[EUR-4552] 19 p3137 N71-32140
Determination of diffusion coefficient of iron in magnetite
[TT-70-59100] 20 p3283 N71-33091
Diffusion coefficient of chromium in Fe-Cr alloys annealed at 1200 C determined by evaporation in vacuum
[TT-70-59105] 20 p3284 N71-33177
Radioactive tracers used in determination of diffusion coefficient of cobalt in polycrystalline austenitic Fe-Cr-Ni alloys
[TT-70-59110] 20 p3284 N71-33178
Irregularities in diffusion front of nickel in polycrystalline Fe-Cr-Ni alloys
[TT-70-59111] 20 p3285 N71-33576
Nuclear magnetic resonance spin echo method used to determine self diffusion activation energy in aqueous solutions of electrolytes
20 p3230 N71-33623

Nonlinear effects of recombination and collective diffusion associated with nuclear seeded plasmas using helium isotopes in gas cooled reactors
20 p3306 N71-33665
Steel and its alloys used for determination of self diffusion in metals in area of phase transitions
[TT-70-59112] 20 p3285 N71-33688
Fuel cell electrolyte studies on vapor pressures of ternary systems, partial molal volumes of dissolved gases, and diffusion coefficients of gases
[NASA-CR-121628] 21 p3378 N71-34034
Analysis of diffusion behavior in ternary systems by method in which matrix of diffusion coefficients is replaced by relative penetration tendencies
[AD-726458] 23 p3770 N71-36871
Effect of nonuniform burnup on reactor lifetime
[UARAEE-83] 23 p3794 N71-37046
Laboratory means to measure diffusion coefficient for characterization of turbulent plasma in reentry simulation
[AD-726751] 23 p3829 N71-37312
Solar and galactic cosmic ray diffusion coefficients and dependencies
24 p4010 N71-38593

DIFFUSION EFFECT

U DIFFUSION

DIFFUSION FLAMES

Combustion characteristics and safety factors for hydrogen diffusion flames in flare stack operations
[NASA-CR-111419] 02 p3036 N71-12103
Combustion dynamics of air/methane supersonic diffusion flame in duct
[TP-961] 20 p3365 N71-33449
Selected articles on kinetics and aerodynamics of diffusive combustion
[AD-726575] 23 p3866 N71-37564
Activation temperature analysis with diffusion flames and supersonic combustion
[AD-726662] 23 p3867 N71-37568

DIFFUSION PUMPS

Using jet flap diffuser for recovery of ejector jet kinetic energy
[AD-726596] 22 p3664 N71-36123

DIFFUSION THEORY

Boundary value problems of forced diffusion in semi-infinite region with mobile boundary
[TT-70-57057] 03 p1442 N71-12814
Group diffusion theory, reactor kinetic equations, and space-independent kinetics
[WAFD-TM-960] 04 p2547 N71-13627
Plasma diffusion in closed systems of L-1 stellarator
[CONF-490619-15] 04 p2598 N71-14041
Three dimensional multi-group diffusion-burnup program 3DDT
[LA-4396] 04 p3561 N71-14046
Investigating high rate of plasma diffusion in closed systems in L-1 stellarator
[AEC-TR-7157] 05 p2752 N71-15814
Interparticle interference effects in diffusion controlled growth
[NVO-3678-3] 05 p2758 N71-15297
Marker motion studies in diffusion couples for determining atomic mobilities and vacancy wind terms in multicomponent alloys
[COO-1436-27] 05 p2751 N71-15816
Investigating misfit dislocations in silicon induced by diffusion of phosphorus and boron
07 p1090 N71-17298

Use and limitations of spreading resistance technique for evaluating buried collector layer structures in integrated circuits
07 p1090 N71-17298
Variational flux synthesis in space-time neutron diffusion theory
[ANL-7696] 07 p1076 N71-17354
Comparison of diffusion and transport theories for neutron transport from point sources in slabs
[AD-715563] 08 p1262 N71-18885
Investigating retention of polonium 210 by refractory oxide barium cerate
[DP-1240] 08 p1268 N71-19338
Magnetic field line structure in individual supergranules
09 p1422 N71-19498

Theorem proving for optimal control of stationary diffusion processes with natural boundaries and discounted cost
[RR-24/RM/3] 09 p1410 N71-20061
Cloud droplet growth theory and diffusional interaction between growing droplets
[AD-717788] 11 p1790 N71-22340
Diffusion kinetics of radiochemistry in aqueous solutions after passage of high energy radiation
[CALT-767-P-73] 15 p2458 N71-26878
Theories of adhesion and bond failure mechanism caused by water desorption
[SC-R-70-915] 15 p2453 N71-27119
Slow electrons and negative ions in organic liquids yielding information about spatial distribution and charged species treated with classical diffusion theory
[IRI-133-70-2] 15 p2483 N71-27762
X ray irradiation effects on diodes and transistors based on scattering parameters, diffusion theory, invariant embeddings, and quantum mechanics
[AD-720661] 17 p2725 N71-29800
Polynomial approximation and linear anisotropic diffusion in one-dimensional cylindrical geometry
[EIR-188] 19 p3151 N71-32178
Dispersion equation for studying electromagnetic surface waves in adjacent plasma flows
[UARAEE-97] 23 p3824 N71-37728

DIFFUSION WAVES

Barodiffusion processes in supersonic stream of argon-helium mixture in vacuum using beam of electrons
[NASA-TT-F-13583] 13 p2064 N71-24065

DIFFUSION WELDING

Bibliography on diffusion bonding
[AD-710500] 01 p0058 N71-10197
Structure of diffusion zone in titanium welding
[DMDC-5767] 14 p2267 N71-25631
Ceramic stresscoat burst and performance test of shrouded, diffusion welded titanium pump impeller for liquid hydrogen pump applications
[NASA-CR-103124] 14 p2332 N71-30623
Development of method of diffusion welding of butt joints in air without vacuum furnace or hot press
[NASA-TN-D-6409] 18 p2933 N71-38534
Development of technique for diffusion welding of TD-NiCr metal sheets and analysis of mechanical properties
[NASA-TN-D-64953] 21 p3439 N71-34879
Diffusion bonded graphite reinforced aluminum composites
[NASA-CASE-MFS-21077] 21 p3443 N71-34938
Diffusion bonded electroless nickel plate for wear resistance coating for titanium alloys
[AD-726954] 23 p3779 N71-36911

DIFFUSIVITY

Theoretical technique for determining gas diffusivity in plastic foam
[BDX-613-229] 06 p0879 N71-16872
Double diffraction between Bragg reflections and diffuse intensity planes observed with high energy electron diffraction
[AD-715373] 08 p1213 N71-18531

SUBJECT INDEX

DIGITAL COMPUTERS

Matrix analysis of double disc and heat shield methods for diffusivity measurement at very high temperatures
(AD-715908) 08 p1303 N71-18718
Trisublimability and diffusivity in cold-worked and annealed copper at 300 C
(NLM-1734) 12 p1936 N71-23137
Laser flash diffusivity measurement of thermal conductivity in oxide nuclear fuel materials
(WHAN-SA-40) 13 p2121 N71-25379
Equilibrium sorption isotherms and diffusivities of gases flowing through polymeric membranes
14 p2241 N71-26297
High temperature measurements of thermal diffusivity of graphite
(AD-72652) 22 p3403 N71-35640
Space-time dependent spin correlation functions for isotropic Heisenberg paramagnet with cylindrical symmetry at elevated temperature based on Gaussian representation of diffusivity
24 p3968 N71-38307

FLUORIDES
NT CALCIUM FLUORIDES
Theoretical and experimental investigation of electromagnetic wave propagation in antiferromagnetic CaF_2
18 p2963 N71-31068
Evaluation of metallic and nonmetallic construction material performance and reliability after long storage in OF2 and B2H6
(NASA-CR-122867) 22 p3461 N71-36107

FLUORO COMPOUNDS
NT PERFLUOROALKANE
NT POLYTETRAFLUOROETHYLENE
Ammonia decontaminant control of oxygen diffusive and static and dynamic compatibility tests with plastic and elastomer materials
(NASA-CR-72360) 12 p1869 N71-23167
Liquid and gaseous oxygen diffusive compatibility tests with plastic and metal orifices and metal ignition temperature data
(NASA-CR-72357) 12 p1869 N71-23168
Oxygen diffusive hazards, chemical and physical properties, decontamination methods, and transfer and storage techniques manual
(NASA-CR-72401) 12 p1925 N71-23169

HEATING
Modification of Berman-Sivazkaya method for metabolic digestive capability determination
(NASA-TT-F-13533) 09 p1333 N71-20150

INGESTIVE SYSTEM
NT GASTROINTESTINAL SYSTEM
NT INTESTINES
NT MOUTH
NT RECTUM
Investigating effects of weightlessness on enzyme secretion function of digestive system of Soyuz 9 crew members
08 p1151 N71-18909

MILITARY COMMAND SYSTEMS
Design of space base digital command system
(NASA-CR-114817) 06 p0821 N71-16575
Digitally controlled frequency synthesizer for pulse frequency modulation telemetry systems
(NASA-CASE-XGS-02317) 12 p1588 N71-23525
System for maintaining motor at predetermined speed and digital pulses
(NASA-CASE-XMP-66892) 13 p2056 N71-24805
Digital filter for reducing jitter in digital control systems
(NASA-CASE-NPO-11088) 16 p2566 N71-29034
Equations to determine tracking performance for second order, phase locked loop used for subcarrier synchronization on digital command system
(NASA-CR-122776) 23 p3722 N71-36530

MILITARY COMMUNICATION
U PULSE COMMUNICATION
DIGITAL COMPUTERS
NT CDC 1100 COMPUTER
NT CDC 3300 COMPUTER
NT CDC 6400 COMPUTER
NT IBM 360 COMPUTER
NT IBM 1130 COMPUTER
NT IBM 7030 COMPUTER
NT IBM 7094 COMPUTER
NT ILLAC COMPUTERS
NT PDP COMPUTERS
NT PDP 8 COMPUTER
NT PDP 9 COMPUTER
NT SEQUENTIAL COMPUTERS
NT UNIVAC 1106 COMPUTER
Computer processing of meteorological satellite data
01 p0077 N71-10092
Digital computer system hardware for data acquisition and control of 60 ft X band parabolic antenna
(AD-70909) 01 p0027 N71-10280
Digital computer oriented analysis method for losses from graphs
(AD-70997) 01 p0076 N71-10048
Parallel data processing
(AD-711051) 01 p0029 N71-10787
Design and characteristics of matrix oriented cellular computer
(AD-713505) 02 p0187 N71-11311

Analysis and synthesis of self repair techniques for digital computers
02 p0188 N71-11318
Program requirements for DRAFT 2 system
(NASA-CR-108662) 02 p0189 N71-11326
Computer acquired performance map of etched-rhodium, nichium planar diode
(NASA-TM-X-52926) 02 p0194 N71-11363
Rapid computer aided analysis of nonlinear electronic circuits
02 p0197 N71-11381
On-line statistical analysis of surface roughness with small digital computer
02 p0229 N71-11556
Computer processing of satellite cloud pictures
02 p0261 N71-12183
Information display from access storage of digital computer on cathode ray tube screen
(AD-712805) 03 p0340 N71-12463
Binary number sorter for arranging numbers in order of magnitude
03 p0344 N71-12502
Binary sequence detector with few memory elements and minimized logic circuit complexity
(NASA-CASE-NPO-10112) 03 p0345 N71-12505
Digital modeling method applied to circuit design
(AD-712105) 03 p0346 N71-12512
Reviewing development of digital computer systems and components for aerospace vehicles
03 p0346 N71-12602
Historical review of growth of guidance and control systems based on use of digital computers for manned aircraft
03 p0408 N71-12603
Calculating delivery errors of automatically released bombs caused by onboard computer and attitude/air data sensor errors
03 p0408 N71-12612
Designing self testing and repairing computers for long term unmanned interplanetary missions
(NASA-CR-111577) 03 p0455 N71-12618
Integrated circuits for digital applications in high dc noise systems
(NASA-CR-73487) 03 p0576 N71-12769
Digital computerized solution of ordinary differential equations
(RAE-TM-SPACE-126) 03 p0599 N71-13055
Digital computer program for computing vibration characteristics of ring-stiffened orthotropic shells of revolution - users manual
(NASA-TM-X-2138) 03 p0462 N71-13093
Digital fluidic compensator for analog fluid systems
(AD-713026) 03 p0365 N71-13383
Fast multiplication cellular arrays for LSI implementation
04 p0503 N71-13658
Heuristic optimization algorithm for arranging N page open string
04 p0503 N71-13660
Aircraft echoes and clutter signals obtained by digital surveillance radar
04 p0494 N71-13906
Digital computer processing of phased array radar data
04 p0497 N71-13931
Operational control and performance of computer steered radar systems
04 p0498 N71-13932
Digital plotting of primary radar data from aircraft echoes
04 p0498 N71-13933
Digital computer program for stresses distribution in ring of nonuniform cross section under uniform radial load
(AD-712518) 04 p0616 N71-13944
Extended SPL assembly language for SCC 4700 computer
(NASA-CR-102990) 05 p0649 N71-14778
Adaptive learning computer system for raw data processing
(AD-713543) 05 p0650 N71-14874
Circuit schemes and subroutines programs for DNEPR 1 computer using telephone and telegraph channels
(AD-713787) 05 p0650 N71-14937
System facility of elementary machine of Minsk 222 computer system
(AD-713776) 05 p0650 N71-14948
Structural methods for increasing productivity of digital computers
(AD-713773) 05 p0650 N71-14949
Application of digital associative machine in information processing methods
(AD-713769) 05 p0650 N71-14950
Selection of computers for flight control
(AD-713786) 05 p0651 N71-14977
IBM 360 fast conduction program
(CPC-INT-980-ADD-1) 05 p0783 N71-15382
Digital computer system for automatic prelaunch checkout of spacecraft
(NASA-CASE-XKS-08012-2) 05 p0772 N71-15566
Power spectral analysis of magnetic fields using Time/Data 100 system
(NASA-TM-X-65413) 06 p0818 N71-15842
Digital logic design for spectrometer
(NASA-TM-X-65417) 06 p0805 N71-15896

Simulation model for advanced avionics digital computers
(AD-714140) 06 p0894 N71-16295
Feasibility design of billion-gate computer
(AD-714005) 06 p0819 N71-16316
Development of high performance, digital microcircuits, and their application to data processor systems
(AD-714000) 06 p0823 N71-16416
Time sharing computers in ARPA network
(AD-714234) 06 p0816 N71-16418
Research activities in recognition, computational principles, and artificial intelligence
(AD-714608) 06 p0807 N71-16477
Determining optimal time-invariant output feedback controllers for linear dynamic systems
(NASA-CR-100332) 07 p1002 N71-18062
Small digital computer for calculating axially averaged neutron fluxes and channel powers
(RD/BN-1749) 08 p1251 N71-18248
Fast Fourier transform programs for EAI-640 digital computer
(NRC-11747) 08 p1167 N71-19332
Digital computer simulation of automobile impacting flexible safety barrier
09 p1473 N71-19482
Improved techniques for paging computer memory
(NASA-CR-117123) 09 p1353 N71-19598
Requirements for memory units in digital computers including reliability
(AD-716674) 09 p1355 N71-19801
On-line data acquisition system using LINC-8 computer for plasma physics experiment
(CLM-R-104) 09 p1448 N71-19983
Multichannel system of two-directional communication for cyclotron facility measuring center with TVM computer type M-228A
(IAB-1953) 09 p1350 N71-20148
Digital computer program for studying transient performance of pressure fed rocket engines
(NASA-CR-114915) 09 p1459 N71-20173
Perturbation expansion of Coulomb potential for determining pair distribution function in plasma
(AD-717038) 10 p1527 N71-20817
Development of programming languages, syntax, algorithms, and subroutines for digital computers
(AD-714406) 10 p1529 N71-21561
Off-line processing of chromatographic data from fatty acid methyl ester mixtures by digital computer
(UCRL-72393) 11 p1716 N71-22548
Computer controlled interactive graphics display system for hydraulic analysis
(BNWL-1525) 11 p1716 N71-22580
Dnepr 1 general purpose computer system
11 p1718 N71-22733
Oncological data processing system using general purpose computer and graphic input devices
11 p1719 N71-22737
General purpose digital computer system using Dnepr 1 control components and Minsk 2 magnetic tape units
11 p1719 N71-22739
Description of error correcting methods for use with digital data computers and apparatus for encoding and decoding digital data
(NASA-CASE-XMP-02748) 11 p1719 N71-22749
Mark 3A computer configuration of inbound high speed and wideband data synchronizers
11 p1720 N71-22783
Digital and analog computer processes of artificial intelligence
11 p1721 N71-23077
Digital computer enhancement by use of technique of interpretation rather than compilation of higher ordered languages
(NASA-CR-117901) 12 p1881 N71-23435
Apparatus for determining high frequency signal phase stability by autocorrelation
(NASA-CASE-XGS-01118) 12 p1893 N71-23662
Table-lookup/interpolation fast function generation with small fixed point digital computers
(NASA-CR-118010) 12 p1883 N71-23665
On-line FORTRAN 4 digital computer program for solving ordinary differential equations
12 p1883 N71-23866
Cathode ray tube display and recorder interface to provide graphical output for small digital computer
(NASA-CR-118011) 12 p1883 N71-23867
Electronic digital computer for automating 2-GeV electron line
(SLAC-TRANS-126) 12 p1976 N71-24139
Serial digital decoder design with square circuit matrix and serial memory storage units
(NASA-CASE-NPO-10150) 13 p2049 N71-24650
On-line digital computer system for real time acquisition and processing of data at Materials Analysis Section of Quality and Reliability Assurance Laboratory
(NASA-TM-X-64587) 13 p2053 N71-25392
Feasibility of computerized Doppler radar tracking system
(AD-726832) 14 p2216 N71-25870
Model of coupling binary star system based on digital computers
(NASA-CR-118643) 14 p2336 N71-25963

Digital computer algorithm for determining gain bandwidth properties of distributed parameter loads
14 p2230 N71-26547

Digital computer program for simulating vehicle flow on freeways
14 p2225 N71-26552

Approximation of redundant component reliability and digital computer logic design
[AD-720332] 15 p2389 N71-27287

Algorithmic method for optimal flight vehicle design using digital computers
[AD-720915] 15 p2519 N71-27330

FORTRAN 4 digital codes for thermal dynamics of cylindrical nuclear fuel rod with or without distributed heat generation
[RT/ING/70/8] 16 p2630 N71-28117

Movable neutron detectors for reliable control of materials testing reactor
[UJV-2375-RPA] 16 p2634 N71-28756

Signal to noise ratio effects on digital computer signal transmission and storage operations including logic, cross coupling, and switching circuits
16 p2575 N71-28767

Digital magnetic core memory with sensing amplifier circuits
[NASA-CASE-XNP-01012] 16 p2566 N71-28925

Redundant memory for enhanced reliability of digital data processing system
[NASA-CASE-GSC-10564] 16 p2576 N71-29135

Airborne nucleonics equipment design for indicating helicopter lift capability using X ray backscatter from K_α-S₂₅ temperature sensor, and digital computer
[SAN-805-1] 17 p2702 N71-29215

Heuristic system and plastic memory of digital computers
[JPRS-53399] 17 p2722 N71-29301

Digital computers as complex heuristic systems
17 p2722 N71-29302

Stability of synchronized induction motors with phase compensating system using digital computer
[NLL-RTS-6232] 17 p2725 N71-29662

Self-simulators and algorithms for use with digital computers
17 p2723 N71-29670

Program for calculating parameters of optimal chokes by digital computer
[NLL-RTS-6155] 17 p2726 N71-29822

Mathematical models for automated environmental control of acoustic test facility inside chamber
[NASA-CR-115072] 17 p2732 N71-30355

Bathymetry measurements in deep ocean using narrow beam stabilized echo sounders and digital computers
[ESSA-TR-CGS-37] 18 p2911 N71-30982

Use of block-circuit method for synthesis of microprograms
[AD-722829] 18 p2900 N71-31294

Automatic plotter for use with M-20 digital computer
[AD-722820] 18 p2896 N71-31345

Program variable logic calculations and biological principles of data processing applied to digital cybernetics systems having many outputs
[JPRS-53460] 18 p2900 N71-31417

Analogue and digital techniques for computation of shock and Fourier spectra compared on bases of speed, accuracy, and ease of use
[AD-723536] 19 p3061 N71-31990

Simulation and modeling of advanced avionics digital computer system operation for optimum hardware configurations
[AD-723521] 19 p3062 N71-32330

Numerical method for restoration of planar image algorithm for use on digital computers
[UCRL-73080] 19 p3062 N71-32469

Boolean algebra for application to digital electronics and relay networks
[ISS-70/18] 20 p3290 N71-32970

Digital signal processing computer structures for radar
[AD-724685] 20 p3232 N71-32999

Texture tone study applied to automated image interpretation technique using digital computers
[AD-724117] 20 p3271 N71-33078

High resolution, power spectral analysis using digital computer
[NASA-CASE-NPO-10748] 20 p3273 N71-33321

User guide for use of compensator design program /COMPDES/- Vol. 4
[NASA-CR-119912] 20 p3294 N71-33963

Digital computer control of meteorological observational data using Fourier series and Lagrange polynomials
[NLL-M-20718-5828-4F] 21 p3399 N71-34194

Biquadratic approximation used in drawing of isopleths for two dimensional fields by digital computers
[NLL-M-20891-5828-4F] 21 p3400 N71-34201

Iterative digital computer algorithm for solving optimization problems for linear stochastic systems
[NASA-CR-119706] 21 p3446 N71-34521

Computer controlled electric power distribution system for aerospace systems
21 p3514 N71-35040

Synthesis of structural dynamic systems using digital computer and FORM/FORTRAN Matrix Analysis
[NASA-CR-119877] 21 p3527 N71-35128

Problems of digital computer program control of milling machines
[NLL-RTS-6307] 22 p3557 N71-35340

Digital computer analysis of integrated logic circuit transient behavior
[REPT-1143] 22 p3562 N71-35374

Digital computer fault detection procedures for combinational logic circuits with algorithms for efficient generation of minimum fault test schedules
[AD-726383] 22 p3563 N71-35375

Design of logic circuit to facilitate electrical fault detection in digital computers
[AD-726382] 22 p3563 N71-35376

Automatic computation of navigation coordinates using analog and digital computers
[AD-726603] 22 p3618 N71-35782

Use of general purpose digital computers for analysis of biological structures and chromosomes
[JPRS-54035] 23 p3715 N71-36479

Computer graphic techniques, computer systems and management, and digital waveform processing for graphical man/machine communications
[AD-726623] 23 p3730 N71-36587

Polynomial roots, boundary value problems of nonlinear equations, and eigenvalue problems of linear ordinary differential operators treated with continuation method using fast computers
[TAE-123] 23 p3782 N71-36958

Distributions and mean values of inelasticity coefficient K for neutral pions in lead and graphite determined by digital computer
[ITT-5] 23 p3808 N71-37154

Modified thermal analyzer digital computer program for heat transfer problems
[NASA-CR-72944] 24 p3891 N71-37733

Handbook presenting classification of electronic and analog computers and analog devices
[AD-727282] 24 p3895 N71-37758

Basic requirements for computers designed for operations with control automation systems
[AD-727265] 24 p3895 N71-37759

Reliable synthesis in automatically designing digital machines
[AD-727234] 24 p3895 N71-37761

Increased operating reliability of digital computers used in automatic control systems
[AD-727163] 24 p3895 N71-37762

Use of miniature general-purpose digital computers for design of digital control systems
[AD-727190] 24 p3895 N71-37764

Digital computer bibliography, programming techniques and applications, and software standardization and reliability
[AD-727605] 24 p3896 N71-37766

Development of technique for finding functional diagram of combination automaton with complex of faults
[AD-727974] 24 p3896 N71-37768

Information processing, research projects, mathematical modeling, and analysis of computer systems
[AD-727989] 24 p3896 N71-37770

Compensator improvement program with application to large space vehicles and tables noting relative stability versus frequency response
[NASA-CR-119959] 24 p3901 N71-37803

Structural design of astronomical telescopes using digital computers with emphasis on tubes
24 p3923 N71-37983

Computer control of large telescopes
24 p3923 N71-37986

Telescope control by on-line computers, including ESO 3.6-m telescope
24 p3923 N71-37987

Telescope tracking drives and controls at McDonald Observatory using 107 and 82 inch telescope
24 p3923 N71-37988

Digital computer used to control drive of 2.2-meter astronomical telescope
24 p3923 N71-37991

Anglo-Australian telescope proposed drive and control system using printed circuits
24 p3924 N71-37994

Digital computation of sensitivity for optical control systems
24 p3946 N71-38150

DIGITAL DATA

Digital analysis of random data records by piecewise accumulation of time averages
[NASA-TN-D-6073] 03 p0340 N71-12466

Digital data processing for designing automatic flight control systems
03 p0409 N71-12616

Fundamental possibilities of digital phase measurement
[RAE-LIB-TRANS-1428] 04 p0513 N71-13541

Data recorder for producing digital magnetic tapes for radio transmission experiments
04 p0505 N71-13839

Digital radar data transmission system for use in air traffic control
04 p0505 N71-13840

Comparison of legibility of three types of electronic digital display
[OR/NF/1769] 05 p0649 N71-14830

Characteristics of wideband microwave digital data communication systems
[EGG-1183-4030] 05 p0645 N71-14821

Developing digital television and data transmission equipment for Space Flight Operations Facility
05 p0647 N71-14899

Developing wideband digital data system for Ground Communication Facility for Deep Space Network
05 p0647 N71-14899

FORTRAN subroutine to decode tape recorded digital data from Randle Cliff Radar
[AD-715336] 07 p0994 N71-17790

Algorithm for digital resolution of range for V/STOL aircraft
[NASA-TN-D-6232] 08 p1144 N71-18546

Tape guidance system for multichannel digital recording system
[NASA-CASE-XNP-09453] 09 p1351 N71-19420

Combined word and bit synchronization signals for PCM telemetry of experimental data
10 p1517 N71-20677

Digital telemetry system apparatus to reduce tape recorder wow and flutter noise during playback
[NASA-CASE-XGS-01812] 11 p1714 N71-23960

Direct sequential encoding and decoding for digital data sources
11 p1721 N71-23960

ALGOL program for detection and correction of data errors using TM4 computer
[RAE-LIB-TRANS-1544] 12 p1882 N71-23847

Analysis of sampled data reconstruction errors from digital data processing
12 p1884 N71-23872

Optimum receivers for continuous phase digital frequency modulated signals
[RR-71-1] 13 p2048 N71-25340

Algorithm for solving Popov stability criterion applied to sampled data systems
[NASA-TM-X-64600] 14 p2282 N71-28802

Methods for eliminating double-sided intersymbol interference in digital data systems
14 p2218 N71-28328

Digital data processor for use with large scale integrated circuit technology and spaceborne computer application
[NASA-CASE-GSC-10975-1] 16 p2565 N71-28819

Digital data handling circuits for pulse amplifiers
[NASA-CASE-XNP-01068] 16 p2575 N71-28779

Synchronous multiplexing for transmission of digital encoded television pictures
[DSS-4516] 20 p3234 N71-32329

Techniques for selecting performance criteria for voice, video, and digital data systems
[NASA-CR-115079] 21 p3390 N71-34115

Flexible computer-accessed telemetry using sequence control, auxiliary memory, and system control registers for sensors and digital data source sampling
[NASA-CASE-NPO-11358] 21 p3395 N71-34118

Analysis of effects of bandlimiting on performance of digital transmission corrupted by additive white Gaussian noise by averaging and series expansion
[NASA-CR-115160] 22 p3553 N71-35340

Telecommunication network exclusively for transmission of digital information
[NLL-PORS-TRANS-2712-19022.81] 22 p3555 N71-35319

Survey of digital baseband signaling techniques for space shuttle data bus
[NASA-TM-X-64613] 24 p3887 N71-37768

DIGITAL FILTERS

Analogue/digital method for realizing matched filter for radar signal processing
04 p0308 N71-13934

Digital filter for moving target indicator display
04 p0497 N71-13925

Design of digital moving target indicator for air traffic control radar system
04 p0497 N71-13926

Coherent Doppler radar with digital filter for range and radial speed measurements on targets
04 p0497 N71-13928

Adaptive clutter suppression filter for Doppler shifted radar signal detection
04 p0497 N71-13929

Digital filters and Fourier transformation for pulsed Doppler radar processor
04 p0497 N71-13930

Contributions to theory of digital filtering
[TN-1411] 04 p0537 N71-13957

Kolmogoroff-Smirnov test for digital filtering and spectral comparison using Fourier transform
[CTC-44] 05 p0655 N71-14905

Design and characteristics of nonrecursive digital filters
[AD-717163] 10 p1531 N71-20616

Adaptive procedure for removing multimodal power spectra using cascade transversal digital filters
[AD-716974] 10 p1532 N71-20604

Design and development of signal detection and tracking apparatus
[NASA-CASE-XGS-03502] 10 p1537 N71-20652

SUBJECT INDEX

Digital filter realizations of arbitrary loss and delay functions applicable for any type of frequency in signaling communication channels
[AD-71701] 10 p1534 N71-21246

Edge structure and representation of pictures in digital form using human visual system
11 p1699 N71-21996

Optimum design of two dimensional nonrecursive digital filters
[UCRL-72653] 12 p1549 N71-23711

Digital simulation, digital filters, PDP 9 computers, on-line programming, hybrid computers, computer graphics, plotters, analog computers, optimization, and integrated circuits
12 p1882 N71-23862

On-line interactive program to empirically determine performance of fixed point digital filters
12 p1884 N71-23873

Self-organization methods for complex linear dynamic systems to compensate for component failures
[NASA-CR-118314] 13 p3103 N71-24874

Adaptive digitalized learning control system for launch vehicles
[NASA-TM-X-64518] 15 p2442 N71-27846

Comparison of standard Z transform and algebraic substitution synthesis methods for digital filters
[AD-721571] 16 p2569 N71-28397

Digital filter for reducing jitter in digital control systems
[NASA-CASE-NPO-11068] 16 p2566 N71-29034

Analog filter noise simulation using white noise processes by mathematical models
[NBS-TN-694] 19 p3048 N71-32747

Digital integrated circuitry in 1200 baud PSK modulator using frequencies of 1300 and 2100 Hz
[NRL-1971-11] 20 p2776 N71-33860

Ordering relationship of ultrafilter topology
23 p3782 N71-36954

Effect of coefficient rounding in floating point digital filters
[AD-727073] 24 p3896 N71-37784

DIGITAL INTEGRATORS
Digital circuit switches for tactical communication system
04 p0507 N71-13848

Linear algebra for characterization and synthesis of digital circuits
[REPT-4341] 05 p0712 N71-14508

Bridge circuit for digital resistance measuring circuits with electronic self adaptive controls at direct current
06 p0826 N71-15950

Technology review on integrated linear, digital, and mechatronic circuits
10 p1537 N71-20893

Piecewise linear and step approximating converter for producing functional quanta through elementary gates
11 p1715 N71-22044

Design and performance of galvanovoltammetric detector with digital readout for electric current flow measurements
17 p2753 N71-29886

Determination of real-time mean hourly values of magnetic field using electronic integration and fluxgate magnetometer
[M76-4177] 20 p3256 N71-32988

DIGITAL NAVIGATION
Developing digital magnetic compasses based on Hall effect for small boats
[AD-712547] 04 p0544 N71-14342

Simulation and modeling of advanced avionics digital computer system operation for optimum hardware configurations
[AD-723521] 19 p3062 N71-32330

Range and azimuth resolution characteristics and aircraft separation measurement capability of radar laser-digital subsystem
[FAA-NA-71-16] 23 p3793 N71-37038

Advanced avionics digital computer development program
[AD-727607] 24 p3895 N71-37765

DIGITAL RADAR SYSTEMS
Digital techniques and components for signal detection in clutter by advanced radar systems
[AGARD-CP-66-78] 04 p0493 N71-13901

Adaptive clutter suppression filter for Doppler shifted radar signal detection
04 p0497 N71-13929

Operational control and performance of computer moved radar systems
04 p0498 N71-13932

Computerized radar plot extractor module for automatic air traffic control
04 p0498 N71-13936

Digital controlled radio interferometer for measurements of radar echoes from meteor trails
[AD-717776] 11 p1699 N71-23148

Digital address thin cathode display tube for portable radar
[AD-723413] 19 p3053 N71-31676

DIGITAL SIMULATION
Survey of models for parallel computing
[NASA-CR-111412] 02 p0187 N71-13132

Magnetic field effect on magnetic satellite attitude control and digital simulation of satellite motion
03 p0357 N71-12720

Digital simulation of ferromagnetic material hysteresis for ESSRO I satellite attitude control
[ESSRO-SR-12-ESTEC] 03 p0458 N71-13253

Digital simulation of large waves in shallow water using Navier-Stokes and Poisson equations
[AD-713444] 05 p0671 N71-14048

Digital simulation for error analysis of numerical integration schemes
[NASA-CR-102958] 05 p0713 N71-15091

Real time digital simulation program preprocessor
[NASA-TM-X-67018] 10 p1528 N71-21305

Data processing algorithm for real time digital modeling of dynamic systems
11 p1718 N71-23701

Digital simulation, digital filters, PDP 9 computers, on-line programming, hybrid computers, computer graphics, plotters, analog computers, optimization, and integrated circuits
[REPT-29-7-76-409] 12 p1882 N71-23862

Economical and convenient all-digital on-line simulation of dynamical systems using PDP 9 computers
12 p1883 N71-23863

Fast, on-line, all-digital, block diagram-based simulation system which adds simulation console to PDP 9 computer
12 p1883 N71-23864

Space shuttle trajectory performance data for east and west test range launch simulations
[NASA-TM-X-64596] 14 p2337 N71-26036

Analysis and digital simulation of nonlinear behavior of phase locked loops with input signal frequency modulated by sawtooth, normally distributed waveforms
16 p2575 N71-28805

Digital simulation of random numbers and prediction analysis techniques
19 p3061 N71-31886

Development and application of mathematical models, digital simulations of social factors and production planning methods
[FPRS-53464] 19 p3122 N71-33016

Organization of theoretical knowledge into mathematical models
19 p3122 N71-33018

Social planning by numerical forecasting methods
19 p3195 N71-33019

Digital computer simulation of two strapdown system attitude algorithms by response to angular input rates
[NASA-CR-121731] 21 p3447 N71-34527

Simulation evaluation and analysis of strapdown laser seeker guidance concept
[AD-726376] 22 p3618 N71-35780

Digital simulation and implementation techniques for Doppler radar altimeter signal processing
[NASA-CR-1776] 23 p3724 N71-36548

Digital simulation of augmented rainfall and hydrologic response of watershed
23 p3793 N71-37037

Digital simulation of energy spectra and mean inelasticity coefficients of high energy particle interactions
[ITJ-3] 23 p3808 N71-37152

Digital simulation with lumped parameter system of once-through supercritical steam generator
23 p3869 N71-37579

Subroutines for PDP-9/GOULD 4800 graphic line printer for hybrid and digital simulation
[BNWL-B-58] 24 p3892 N71-37741

DIGITAL SPACECRAFT TELEVISION
Digital coding techniques used for satellite television broadcasts
[BBC-1971/25] 21 p3396 N71-34169

DIGITAL SYSTEMS
NT DIGITAL NAVIGATION
NT DIGITAL RADAR SYSTEMS
Nichols and tentacles with large electro-optic coefficient for use in digital light deflection
01 p0109 N71-10263

Research progress on communication coding and synchronization, optimum modulation indexes, phase tracking, and speech security
01 p0021 N71-10255

Determining power spectrum of PN codes and effect of pseudomodulation filtering on correlation and error signals in space communication systems
01 p0021 N71-10257

Systems performance design requirements specifications for CH-46C helicopter digital flight control and landing system
[NASA-CR-110889] 01 p0003 N71-10294

Feedback averaging method for amplitude modulated digital laser communications system
[AD-710946] 01 p0023 N71-10567

Digital waveform encoding methods for speech
[AD-712504] 02 p0178 N71-11253

Principles for design and selection of modems or data transmission aids
[AD-712125] 03 p0179 N71-11262

Plasma physics, quantum and solid state electronics, information systems, and digital systems
[AD-711816] 03 p0307 N71-12040

DIGITAL SYSTEMS

Investigating digital bit synchronization phase locked loops employing binary phase error quantization and sequential loop filtering
[AD-711957] 03 p0336 N71-12403

Developing 32 by 30 resolution element digital address thin display tube for man pack radar
[AD-719825] 03 p0337 N71-13406

High speed PPM/digital telemetry system design for use on sounding rockets
[NASA-TM-X-65384] 03 p0341 N71-13472

Noise cleaning in binary-valued digital pictures using propagation processes
[NASA-CR-115810] 04 p0500 N71-13568

Aerobial system compared with other types of motion flux detectors in boiling water reactors
[NPR-126] 04 p0547 N71-13635

Magnetic digital recorder Remanence
04 p0504 N71-13833

Evaluation of interactive input devices associated with computer driven displays
04 p0506 N71-13846

Multimagnet transmission system for troposcatter channel
04 p0507 N71-13853

Speech data interface with all digital transmission systems
04 p0507 N71-13853

Diagnosability and recovery from massive faults in digital systems
[NASA-CR-115067] 05 p0649 N71-14732

Calculation of digital current distribution systems on micro tape cores
[AD-714768] 06 p0822 N71-15936

Digital data processing techniques and supporting facilities plotter hardware
[AD-714378] 06 p0849 N71-16321

Development of digital system for on-line control of airbreathing propulsion systems
[NASA-TM-X-2168] 07 p1102 N71-17585

Random sampling approach to digital detection using Fourier transformation
08 p1163 N71-18925

Development of digital encoding methods for improved military communication systems
[AD-715998] 09 p1349 N71-19673

Associative memory system for mass storage using integrated circuits and array organization
[BNL-14519] 09 p1355 N71-20124

Computer code for analysis of digitized seismic signals
[UCRL-50939] 10 p1446 N71-20892

Digital automatic pattern recognition system to find and measure events in bubble chambers
[UCRL-20126] 10 p1612 N71-20723

Directional antenna control system conversion from manual to digital-automatic control
[AD-716961] 10 p1531 N71-20795

Digital transponder for sequential ranging, phase shift keying/phase modulated communication system and combinatorial coding analysis
10 p1521 N71-21343

Digital data transmission by PCM systems
11 p1720 N71-22755

Digital modulator for reshaping partially degraded digital waveforms
11 p1726 N71-22777

Digital telemetry system approach to reduce tape recorder wow and flutter noise during playback
[NASA-CASE-XGS-01812] 11 p1714 N71-23001

Reliable magnetic core circuit apparatus with application in selection matrices for digital memories
[NASA-CASE-XNP-01318] 11 p1730 N71-23863

Digital system for measuring temperature-depth profile of ocean and predicting effects of this medium on underwater sound propagation
[AD-718822] 12 p1963 N71-23374

Conversion of manually operated antenna to digital autotracking antenna system using servomechanism
13 p2054 N71-24388

R and D in plasma physics, quantum electronics, radioelectronics, solid state electronics, systems theory, and digital and information systems
[AD-719408] 13 p2191 N71-24807

Noninterchangeable digital counter circuit design with display device for pulse frequency modulation
[NASA-CASE-XNP-09739] 13 p2052 N71-24091

Design of multichannel communication system using digital cable transmission
[AD-719688] 13 p2067 N71-25101

Methods for eliminating double-sided intersymbol interference in digital data systems
14 p2218 N71-26248

Digital memory system with multiple switch cores for driving each word location
[NASA-CASE-XNP-01446] 14 p2234 N71-26434

Comparison of analog and digital waveform discriminators for radiation counters
[JUL-648-2E] 15 p3468 N71-27513

Mathematical model of bipolar transistor for digital monolithic integrated circuits with low signal levels
[NILE-PORS-2709-0022.81/1] 17 p2720 N71-30485

Optical control system design for multichannel processes using computer programs and digital simulation
18 p2893 N71-31168

- Feasibility of generalized integrated circuit for digital circuit requirements
[SC-DR-710033] 19 p3070 N71-32208
- Digital photographic data processor and display system
[AD-723657] 19 p3101 N71-32335
- Digitalization of BOMEX data reduction and processing
19 p3131 N71-32763
- Digital television system, computer programs, high-speed data subassemblies and performance, multiple-mission telemetry and command systems, and phase shifter and data decoders for DSN
20 p3233 N71-33167
- Modular type MOD 2 sequential function generator for multibit binary sequence
[NASA-CASE-NPO-10636] 20 p3292 N71-33493
- Binary coded sequential acquisition ranging system for very distant objects
[NASA-CASE-NPO-11194] 20 p3239 N71-33869
- Digital system with real time closed loop control of beavron guide field
[UCRL-20189] 20 p3247 N71-33899
- Digital control of beavron acceleration cycle requiring reduction of hum and noise
[UCRL-20185] 20 p3248 N71-33900
- Subcarrier frequency multiplexing to separate independent PCM data streams on common carrier by using digital circuitry
[NASA-CASE-NPO-11338] 20 p3237 N71-33923
- Digital period detector oscilloscope trigger for multitrace display
21 p3191 N71-34130
- Three algorithms for Ford sequence generation of length 2 to the nth power, a large for digital communication equipment
21 p3391 N71-34131
- SFOF digital television display subassembly providing continuous television compatible video output
21 p3392 N71-34138
- SFOF digital television hardcopy equipment, consisting of system control unit, 12 copy request units, display image buffer, and 12 hardcopy printers
21 p3392 N71-34139
- Arcs and closed curves in digital pictures with thinning algorithms
[NASA-CR-121715] 21 p3397 N71-34175
- Proceedings of space shuttle integrated electronics conference with emphasis on power distribution, instrumentation, and communication - Vol. 2
[NASA-TM-X-58063-VOL-2] 21 p3513 N71-35034
- All digital communications signal design using convolutional coding and PSK modulation for two-way transmission of voice and data between space shuttle and ground
21 p3515 N71-35048
- Data compression and error correcting codes applied to digital transmission of real time, standard format TV, along with voice and other data from Apollo spacecraft
21 p3515 N71-35049
- User and programmer manual for NASA-70 digital circuit analysis program
[NASA-CR-121933] 22 p3556 N71-35325
- Punched card modifiable logic design and interconnection control for evaluating cellular logic concepts for multifunctional data processing systems
[AD-726996] 22 p3562 N71-35371
- Development and characteristics of digital recording system for automatic digitizing of map contour line data
[AD-726366] 22 p3579 N71-35493
- Delay adaptive differential pulse code modulation system with delay adaptive predictor and quantizer and system analysis using stationary Gaussian Markov signal
[AD-726668] 23 p3734 N71-36546
- Fabrication of high speed logic counting circuits using bipolar processes
23 p3737 N71-36644
- Digital control of processes, and dynamic programming to calculate optimal feedback control for nonlinear systems
23 p3738 N71-36658
- Digital computerized drive for reflecting telescopes
24 p3923 N71-37990
- DIGITAL TECHNIQUES**
- Developing digital systems and solar electric propulsion technology for thermoelectric outer planet spacecraft
01 p0063 N71-10260
- Digital processing for speech synthesis, and homomorphic methods for correcting helium speech
[AD-712345] 02 p0181 N71-11276
- Developing digital computer program for correcting soft parameters of thermal network by Kalman filtering method
[NASA-CR-100681] 02 p0305 N71-11405
- Considering design of digital computers for guidance and control of aerospace vehicles
[AGARD-CP-68-70] 03 p0407 N71-12601
- Investigating federated and integrated approaches to digital computer design for aerospace vehicles
03 p0346 N71-12605

- Investigating system requirements of airborne data processors
03 p0408 N71-12608
- Investigating small digital processors as interface between computer and sensor in airborne systems
03 p0347 N71-12609
- Evaluating use of airborne digital computers for guidance and control of X-15 and F-104 aircraft
[NASA-TM-X-66491] 03 p0408 N71-12610
- Describing digital computer used in navigation and attack system of Jaguar aircraft
03 p0408 N71-12611
- Developing high integrity digital flight control of variations in performance of complex systems
03 p0409 N71-12614
- Investigating nonlinear digital control methods for attitude stabilization of VTOL aircraft
03 p0347 N71-12615
- Discussing digital inertial guidance system for ELDO launch vehicle
03 p0409 N71-12617
- Investigating simplified guidance computation schemes for on-line operation
03 p0347 N71-12619
- Evaluating use of digital computers in aided navigation systems to make optimum estimates of system state or to perform coordinate transformation function in strapdown systems
03 p0409 N71-12622
- Investigating general purpose digital computers for fault isolation capabilities in guidance and control systems
03 p0409 N71-12623
- Improving feedback control design by using digital computer techniques
[NASA-CR-116771] 04 p0500 N71-13501
- Elimination of phase distortion in filters using digital techniques
[Y-DA-3314] 04 p0512 N71-13538
- Digital computer processing of OSIRIS research reactor
[CEA-COINF-1569] 04 p0548 N71-13644
- Digital registration of radar echo vector on magnetic tape
04 p0504 N71-13834
- Digital techniques for adaptive signal processing
[NASA-CR-115815] 04 p0493 N71-13860
- Digital techniques and components for signal detection in clutter by advanced radar systems
[AGARD-CP-66-70] 04 p0493 N71-13901
- Space scanning by radiation pattern of coded time modulated array antenna
04 p0495 N71-13914
- Digital correlation for signal detection in presence of interference noise
04 p0514 N71-13922
- Statistical comparison of computer logics for controlled radar tracking of air traffic
04 p0498 N71-13935
- Controlling acceleration of particles in proton synchrotron by digital computers
[CERN-TRANS-70-5] 04 p0586 N71-14244
- Programming documentation for extended capability of FORMAT-FORTRAN matrix abstraction technique of structural analysis
[AD-713840] 05 p0774 N71-14537
- Engineering users data for extended capability of FORMAT-FORTRAN matrix abstraction technique of structural analysis
[AD-713727] 05 p0774 N71-14538
- Using digital techniques in communications systems research for Deep Space network
05 p0647 N71-14956
- Automatic system for analog to digital conversion and digital recording of seismic signals
[FOA-4-C-4397-20] 05 p0651 N71-14989
- Constructing digital correlation measuring device from 1 to 15 MHz for measurement of electron-density correlations in reverse-brush cathode plasma
[FPF-DT-16] 05 p0753 N71-15182
- Combination test generation program for any non-redundant fault in combinational logic net
[NASA-CR-116199] 06 p0820 N71-16432
- Computer refreshed display for processing video information with digital computer to enhance video data
06 p0821 N71-16675
- Investigating digital techniques, telemetry systems, and genetic code inversion
06 p0817 N71-16676
- Applying nonadaptive transversal filters to playback of digital tape recorder signals and complementary-symmetry MOSFET memory for outer planet spacecraft
06 p0821 N71-16684
- Search for best cyclic /20, 8/ block codes and comparison of performance with /15, 5/ BCH code
[ESSA-TR-ERL-174-ITS-111] 07 p0994 N71-17946
- Describing frequency discriminator using digital logic circuits and supplying single binary output signal
[NASA-CASE-MFS-14322] 08 p1165 N71-18092
- Constructing Exclusive-Or digital logic circuit in single module
[NASA-CASE-XLA-07732] 08 p1165 N71-18751

- Generalized digital compensators for sampled-data systems
08 p1166 N71-18809
- Computer program enabling nonprogrammer to perform data, statistical, and numerical analyses
[NBS-SPEC-PUBL-339] 10 p1527 N71-20041
- Horizon sensor design with digital sampling of spaced radiation-compensated thermopile infrared detectors
[NASA-CASE-XNP-06937] 10 p1558 N71-21008
- Digitized, analyzed and plotted data from strong motion earthquake accelerograms
[PB-196823] 10 p1555 N71-21770
- Digital cardiotelemetry incorporating circuit for measuring heartbeat rate of subject over predetermined portion of one minute also converting rate to beats per minute
[NASA-CASE-XMS-02399] 11 p1692 N71-22006
- Digital synchronizer for extracting binary data to receiver of PSK/PCM communication systems
[NASA-CASE-NPO-10851] 13 p2003 N71-26401
- Radio astronomy studies including sensitive interferometers, digital correlators, and related measuring instruments also radar techniques for lunar topography
[NASA-CR-114669] 13 p2003 N71-25900
- Double-valued threshold logic for obtaining solutions to problems in digital devices and cybernetics
[JPRS-52974] 13 p2103 N71-25140
- Digital sensor for counting fringes produced by interferometers with improved sensitivity and on photomultiplier tube to eliminate alignment problem
[NASA-CASE-LAR-10204] 15 p2408 N71-27703
- Digital time code generator for airborne use comprising solid state visual display of time and synchronization with another time code generator
[ARL-F-45] 15 p2411 N71-27802
- Digital image processing for rectification of TV camera distortions
16 p2565 N71-28521
- Image restoration techniques applied to astronomical photography with degradation caused by atmospheric turbulence
16 p2594 N71-28522
- Applying digital techniques in real time processing of video images
16 p2565 N71-28523
- Specifications and performance tests for digital pressure transducers designed for spacecraft application
17 p2751 N71-29322
- Digital regulated solar array module and performance characteristics of its electronic circuits
[NASA-TM-X-2314] 17 p2728 N71-29904
- Digital time discrete method for running short time frequency analysis
[PRL-1970-17] 18 p2886 N71-31004
- Design criteria for real time digital videomicrograph at Aerospace San Fernando Solar Observatory
[NASA-CR-113113] 19 p3090 N71-31006
- Problems in designing speech privacy systems for law enforcement agencies
19 p3069 N71-31032
- Aircraft indicating instruments with digital cathode ray tube display
[DLR-FB-71-27] 19 p3064 N71-31085
- Third-order interpolation technique for continuous, numerically controlled machines and data motion
[Y-1782] 19 p3123 N71-31344
- Ordered search techniques for digital template matching
[TR-166] 20 p3291 N71-33413
- Digital coding techniques used for satellite television broadcasts
[BBC-1971/25] 21 p3396 N71-34109
- Digital slope threshold data compressor
[NASA-CASE-NPO-11630] 21 p3399 N71-34108
- Analysis and definition of digital techniques for signal processing
[NASA-CR-121393] 21 p3399 N71-34109
- Development of automatic contrast follower based on combination of television and digital circuit techniques
[FOA-2-C-2370-52] 22 p3554 N71-35313
- Development of digital systems for picture processing
[FOA-2-C-2369-52] 22 p3556 N71-35313
- Application of optically diagnosed noise reduction toward development of filtering subsection for improvement of digital sensing data tape quality - Vol. 1
[NASA-CR-121978] 22 p3582 N71-35310
- Photon counting digital image recorder using television camera
24 p3924 N71-37990
- DIGITAL TO ANALOG CONVERTERS**
- High accuracy sine function generator using digital to analog converters and field effect transistors
02 p0183 N71-11380
- Dynamic reconstruction errors in digital to analog systems with biomedical applications
[NASA-TN-D-6296] 12 p1865 N71-23100

SUBJECT INDEX

- Development and characteristics of rate augmented digital to analog converter for computed time-dependent data
[NASA-CASE-XLA-67028] 15 p2383 N71-27057
- U ANALOG TO DIGITAL CONVERTERS**
- UNITARY**
- NT BINARY DIGITS**
- UNITARY ANGLE**
- Wind tunnel tests to determine effects of wing dihedral angle on aerodynamic characteristics of highly swept fixed-wing configuration
[NASA-TM-X-2261] 11 p1671 N71-22622
- Wind tunnel stability tests of variable dihedral delta wing aircraft configuration at hypersonic speed
[NASA-TM-X-2391] 21 p3374 N71-34008
- UNITARY EFFECT**
- U LATERAL STABILITY**
- UNITARY**
- Experiments on dimide oxalic acid dihydrazine as hybrid rocket propellant
[JLR-70-7-52] 13 p2510 N71-27101
- UTATION**
- U STRETCHING**
- UTATION WAVES**
- Applying normal product quantization to construct energy-momentum tensor of Thirring model as local function of Thirring fields
[NYO-3629-61] 08 p1254 N71-18341
- Microscopic continuum mechanics theory for mechanical wave interactions in crystal lattice dislocations
17 p2821 N71-29970
- Elasticity theory of elasticity for crystal lattice interaction mechanics
17 p2821 N71-29972
- UTATION**
- U EXTENSIONMETERS**
- UTATION**
- Metastable transformations in low carbon austenitic stainless steels examined by X ray, metallographic, magnetic, and dilatometric techniques
[JENL-TR-2423] 15 p2426 N71-27002
- Dilatometric and vacuum drying techniques for adhesive crystallization studies and solvent concentration, viscosity, and dielectric constant effects on adhesion
[UTCH-71-11] 23 p3721 N71-36521
- UTATION**
- Neurotoxic protocol for evaluating effects of environment on biological systems, including metabolic effects of chemical agents and oxygen toxicity
[NASA-CR-118955] 16 p2542 N71-28183
- UTATION**
- Performance degradation of dilution refrigerator
[UCSD-3-P-143-32] 08 p1383 N71-18393
- Properties of liquid He-3 and dilute solutions of He-3 in superfluid He-4 for dilution refrigerators
[UCSD-3-P-143-29] 08 p1246 N71-19343
- UTATION ANALYSIS**
- Computer code (VORTEX) simulating behavior of incompressible, inviscid, homogeneous fluid in two dimensions by following motion of point vortices
[JLNL-8-186] 13 p2394 N71-27470
- Dimensional analysis and particle size distribution of lamellae from Pennsylvania including optical and mechanical properties as Mars simulation material
[RIS-5122] 17 p2846 N71-30333
- UTATION MEASUREMENT**
- Interferometric measurement of dimensional and refractive-index changes in optical materials exposed to space environment
[NASA-TM-X-66949] 09 p1424 N71-20255
- Amplifying interferometric and narrow multiple beam laser measurement of molybdenum carbide pressure cylinder diameters
[JLNL-36-26171-5828-4P] 12 p1931 N71-24226
- Optical comparator and hydraulic gaging methods for detecting underlayer dimensional measurements of laminated fuel elements
13 p2113 N71-24527
- Techniques for dimensional measurement, and chemical and metallographic microanalysis of irradiated nuclear fuel specimens
13 p2128 N71-24532
- Neutron radiography used to determine fuel specimen dimensional changes and integrity of key components in research reactors
13 p2128 N71-24537
- Microstructure, dimensional, and chemical analysis of neutron irradiated UN fuel specimens
13 p2114 N71-24541
- Planetary diameter and flattening measurement
13 p2166 N71-24993
- Regression analysis procedure for evaluating reliability of nondestructive refractory coating thickness measurements
[NASA-TM-X-64594] 14 p2271 N71-23817
- Dynamic tests on tangential pipe fittings differing in type and dimensions
[JENL-TR-1991] 19 p3105 N71-32214
- Capacitance distance gage for dimensional measurement with digital readout or direct computer processing
[J-783] 19 p3101 N71-32343

- Fluoroplastic system for rapid presentation of single plane body sections with reduced X ray exposure to patients
[NASA-CR-118944] 21 p3434 N71-34363
- UNITARY STABILITY**
- NT SHELL STABILITY**
- NT STRUCTURAL STABILITY**
- Calculating changes in shape of solid fuel charges for ramjet engines after hardening in steel and Duranex castings
[FOA-2-C-2337-46] 05 p0775 N71-14618
- Classification and physical aspects of processes in dimensional stabilization of wood
[VFA-X-63] 05 p0708 N71-15058
- Comparing effects of irradiation on dimensional stability of high and low temperature isotropic carbons used in reactor materials
[PB-191701] 05 p0708 N71-15059
- Evaluation of Zircaloy clad fuel rods to determine geometrical and environmental variable effects on post irradiation dimensional changes
[WAFD-TM-506] 12 p1964 N71-24153
- Dimensional stability and mechanical properties of solids
[AD-711198] 15 p2522 N71-27854
- Test on effects of curing temperature and relative humidity on dimensional stability of molded molecular sieve desiccant
[BDX-613-388] 18 p2894 N71-30581
- Absolute capacitance microcopy and dimensional stability measuring system
[NASA-TM-X-2046] 22 p3585 N71-35530
- UNITARY STABILITY**
- NT FROUDE NUMBER**
- NT LAVAL NUMBER**
- NT MACH NUMBER**
- NT NUSSELT NUMBER**
- NT PECLET NUMBER**
- NT PRANDTL NUMBER**
- NT REYNOLDS NUMBER**
- NT SCHMIDT NUMBER**
- UNITARY STABILITY**
- NT DIAMETERS**
- NT FILM THICKNESS**
- NT HEIGHT**
- NT LENGTH**
- NT RADIUS**
- NT TARGET THICKNESS**
- NT THICKNESS**
- NT WIDTH**
- Structural analysis of sandwich structures to determine dimensions for minimum structural weight for various load carrying capability
[AD-715909] 09 p1476 N71-19674
- Influence of icebreaker hull dimensions on ice resistance when moving at low speed in compact ice
11 p1771 N71-22864
- Dimension and shape calculations of light nuclei with neutron purposes based on variational method for one-particle wave functions of three dimensional anisotropic harmonic oscillators
[ITP-70-33-E] 22 p3636 N71-35918
- Film dimension defects in relation to image horizontal stability and geometric parameters of 35 mm motion picture film
[AD-72752] 24 p3925 N71-38004
- UNITARY STABILITY**
- Far infrared and Raman spectra of gaseous dimers calculated for many models and reported as functions of reduced temperatures
[NASA-CR-119028] 16 p2650 N71-28828
- Shock wave reaction kinetics of dimethylhydrazines with oxygen
[DLR-FE-70-34] 07 p1097 N71-17226
- UNITARY STABILITY**
- U REDUCTION**
- UNITARY STABILITY**
- Sensitivity properties of diethylalkanes
[AD-713747] 05 p0783 N71-15344
- UNITARY STABILITY**
- DIODES**
- NT AVALANCHE DIODES**
- NT CESIUM DIODES**
- NT CRYSTAL RECTIFIERS**
- NT GERMANIUM DIODES**
- NT JUNCTION DIODES**
- NT PHOTO DIODES**
- NT PLASMA DIODES**
- NT THERMIONIC DIODES**
- NT TUNNEL DIODES**
- NT VARACTOR DIODES**
- Semiconductor junction impurity measuring instrument using capacitance variation with applied voltage in sample diode junctions
01 p0031 N71-10154
- Microstrip substrates and Schottky barrier diode development for microwave integrated circuits
01 p0031 N71-10158
- Current oscillations in long Zn-doped Si p-n diodes
04 p0603 N71-14231
- Investigating construction of Unistroke diodes for microwave switching and attenuation circuits
[MW-70-1] 06 p0823 N71-16091
- Microwave mixer diode impedance calculations
[AD-714909] 07 p0999 N71-17479

- Radiation effects research program including radiation damage on semiconductor devices and materials
[AD-715140] 07 p1093 N71-18045
- Optical studies of radiation damage processes using high dose rates available from electron linear accelerators and fast optical techniques
07 p1095 N71-18046
- Current-voltage characteristics of fast electron transport in vacuum deposited thin film oxidation gold magnesium oxide diodes
09 p1361 N71-19419
- Variation with temperature of tunable, resonant resonant cavity gallium arsenide Gunn diode oscillator
[SRDE-70042] 10 p1632 N71-20763
- Dependence of computer aided circuit analysis methods and circuit design dependence on diode and transistor models
[NLL-TRANS-2644-7022.51/1] 10 p1528 N71-21240
- Temperature dependence of high frequency noise measured between 10 MHz and 22 MHz on double injection silicon diodes
10 p1537 N71-21285
- Silicon carbide semiconductor diode light source for indicator elements
10 p1535 N71-21387
- Electrical properties of biased diode bridge and application to improvement of rise time in feedback amplifier
11 p1725 N71-22640
- Single electrical circuit component combining diode, fuse, and blown indicator with elongated tube of heat resistant transparent material
[NASA-CASE-KKS-63381] 11 p1726 N71-22796
- Maintaining current flow through solar cells with open connection using shunting diodes
[NASA-CASE-XLE-44353] 12 p1859 N71-23354
- Digital substructuring system, CW TRAPATT diodes, and problems concerning hydrophobic and epoxy composites in water
13 p2054 N71-24587
- Continuous wave microwave semiconductor diode design for TRAPATT thermally limited device
13 p2054 N71-24589
- Nuclear radiation effects on junction capacitance of silicon p-n diode
13 p2059 N71-25389
- Fluctuations on one dimensional p-n junctions at high injection levels
14 p2326 N71-26350
- Semiconductor devices and performances, and ion implantation technology for semiconductors
[FOA-3-C-3608-61] 14 p2330 N71-26594
- Broadband hot carrier diode mixers - analysis of intermodulation and cross modulation distortions
[AD-721244] 15 p2385 N71-26898
- Thermal and electrical theories for analysis of second breakdown phenomena, mechanisms, and damage in semiconductor junction devices
[AD-721294] 16 p2567 N71-28218
- Diode switching circuit for pulse amplitude spread compression in Corvair and scintillation counters
[JFVSE-SEP-69-44] 16 p2571 N71-28737
- Design handbook for steady state radiation effects on semiconductor diodes
[NASA-CR-1783] 16 p2572 N71-28811
- Neutron dosimetry by semiconductor detectors and hydrogenous radiator assembly to determine energy dependence and accuracy of both methods
[KFKI-70-29-HP] 16 p2655 N71-29086
- X ray irradiation effects on diodes and transistors based on scattering parameters, diffusion theory, invariant imbeddings, and quantum mechanics
[AD-727051] 17 p2725 N71-29493
- Determination of radiation effects on gate-controlled diodes with dielectric passivation systems
[AD-72695] 17 p2828 N71-30245
- Approximate solution for propagation shifts and noise in phase diode with Maxwellian distribution
18 p2896 N71-31451
- Recombination and hysteresis losses in frequency multiplier with semiconductor diodes
18 p2900 N71-31532
- Neutron damage effects in Step Recovery Diode frequency multipliers
[SC-RR-710188] 20 p3329 N71-33991
- High-speed switching diode test system for developing diode test techniques in 400-picosecond time range
[BDX-613-315] 21 p3484 N71-34222
- Electrical properties and operation of Gunn diodes
[FOA-3-A-3754-61] 22 p3560 N71-35353
- Research and development of microwave oscillators, Gunn effect, diodes, space charge, and solid state devices
[AD-727058] 22 p3562 N71-35389
- Electro-optical link between electrochromic diodes and photomultiplier for temporal transmission
[CEA-N-1431] 22 p3634 N71-33997
- Calculating current voltage and capacitance voltage characteristics in production of Schottky diodes for integrated circuits
[NLL-TRANS-2766-7022.51/1] 23 p3733 N71-36617

Production and characteristics of Schottky barrier diode clamped TTL circuits 23 p3735 N71-36627
Fast luminescent decay of silicon light-emitting diode [NASA-TM-X-45721] 24 p3965 N71-38285

DIORITE

Aeromagnetic anomalies and granulite bodies in Pend Oreille area, Idaho for metamorphic and structural studies 21 p3419 N71-34529

DIOXIDES

NT CARBON DIOXIDE
NT HYDROGEN PEROXIDE
NT PYROXENES
NT QUARTZ
NT SILICON DIOXIDE
Sintering kinetics of uranium dioxide using three different types of powder [LIB/TRANS-267] 04 p0546 N71-13606
Chemical dechlorination of nonirradiated, stainless steel canned uranium dioxide fuel elements [BLO-435] 04 p0531 N71-13817

DIPLEXERS

Improvement in properties of lubricating greases by addition of diaryl and triaryl dithiophosphates [AD-71848] 12 p1944 N71-23706

DIPLEXERS

Performance tests and numerical analysis of differential line length diplexers and long stub waveguide filters [AD-721231] 15 p2386 N71-27229

DIPLOE ANTENNAS

Wave channel type antenna design with modulated phase velocity [JPRS-51649] 01 p0025 N71-10822
Crossed dipoles as antenna elements in arrays [ELAB-IR-154] 03 p0334 N71-12383
Multiband HF antenna containing two, three, or four dipole array [AD-712976] 03 p0334 N71-12388
Antenna radiation and wave propagation in sea water 04 p0491 N71-13706

Integral vectorial equation for calculating current distribution on antenna 04 p0491 N71-13707

Boundary value problem for impedance evaluation between coupled electrically thick folded dipoles 12 p1894 N71-24032

Backfire antenna research restricted to surface wave structures consisting of dipole elements [AD-71879] 14 p2227 N71-25653

Numerical evaluation of low frequency loop antenna array resistance to ground reaction as compared to radiation resistance for electric and magnetic dipole antennas [AD-720599] 14 p2231 N71-26769

Array of eighty nine dipoles for studying radio signals reflected and scattered from ionospheric irregularities and meteor trails to determine wind gradients and changes at high altitudes [AD-721223] 15 p2399 N71-27471

Numerical analysis of electromagnetic fields from buried magnetic dipole antennas and applications to radio direction finders and underground communication [AD-721196] 15 p2383 N71-27757

Problems in evaluating electromagnetic fields of linear antennas or dipole arrays in dissipative half space [AD-721706] 17 p2725 N71-29480

Development of 16-element crossed dipole array for observation of Jupiter [REFT-30] 19 p3058 N71-32645

Radiation patterns of dipole antenna in stratified medium representing lunar surface [NASA-CR-121413] 20 p2324 N71-33558

Electric and magnetic field line distributions for calculating short range field around receiving antenna [AD-721706] 23 p2723 N71-36536

Experimental and theoretical analysis of resonance properties and radiation patterns of dipole antennas symmetrically mounted on conducting spheres or cylinders 23 p3727 N71-36566

Infinite length, gap excited, thick, cylindrical dipole antenna radiation field formulations as boundary value problems based on Maxwell equations for electric and magnetic fields 23 p3734 N71-36619

Finite cylindrical dipole antenna of arbitrary orientation in gyrotropic media solved as boundary value problem 23 p3734 N71-36622

Effects of plasma compressibility, collision frequency, and sheath on antenna current, input impedance, and maximum driving voltage 23 p3832 N71-37331

Dipole antenna and fluctuation of far electric field intensity over stationary and time-varying irregular surfaces [AD-728033] 24 p3899 N71-37791

DIPLOE MOMENTS

NT ELECTRIC MOMENTS

NT MAGNETIC MOMENTS

Calculation method for large numbers of dipole and quadrupole transition probabilities [NASA-TM-D-59871] 01 p0095 N71-10428

Computation of Green function for bodies of revolution [AD-711099] 01 p0091 N71-10861

Updated FORTRAN program for waveguide propagation allowing for vertical and horizontal dipole excitation [AD-713166] 05 p0655 N71-14925

Parasitic and parasitic behavior of dipole centers in crystals [AD-714595] 06 p0937 N71-16720

Microwave spectra of divinyl ether and a, b, and c-type rotational transitions of one conformer 07 p0988 N71-17078

Expressing intermediate and long-range force interactions in crystals using Solbrig cell-dipole method [BN-1410] 07 p1079 N71-18009

Dipole expansion technique for particle simulation of plasmas [AD-715075] 07 p1084 N71-18090

Electron affinity and dipole moment of N132 and H2S molecules having C_{2v} symmetry 06 p1267 N71-19299

Dielectric matter and vector D analysis [AD-721181] 15 p2452 N71-26823

Rotational and vibration effects in ion dipole collisions demonstrated in color motion picture [NASA-TM-X-67878] 18 p2983 N71-31194

Intermolecular force constants of highly polar gases determined for six different models of Lennard-Jones potential 20 p3526 N71-33942

Pulsed dipole and dc dipole transport magnet designs and testing for superconducting synchrotron application [UCRL-20188] 21 p3408 N71-34252

Splitting in A2 meson fit to diplicity parameter for measuring dipole structure [UCRL-20622] 21 p3480 N71-34791

Nucleon Compton effect sum rule calculation from dispersion relation and low energy theorem [JINR-P2-5679] 22 p3633 N71-35889

DIPLOE

Factorization theorems, matrix poles, and unitarity [PAM-70-7] 15 p2474 N71-27453

DIPPING

Film thickness of dip-coated layers 16 p2617 N71-28361

DIRAC EQUATION

Dirac equation solution for spin in elastic low energy electron scattering from gaseous atoms [AD-711666] 01 p0101 N71-10842

Vector field theory of Dirac fermions interacting with bosons at infinite momentum based on perturbation theory and tree-graph approximation 14 p2304 N71-26278

Nonrelativistic transformations applied to Dirac equation [JINR-P2-5314] 14 p2298 N71-26589

Relating existence of ghost with zero mass in quantization of vector field coupled to Dirac current [PAM-70-3] 15 p2490 N71-27896

Calculating transition radiation from Dirac magnetic monopoles and experimental applications in searching for monopoles in accelerators and cosmic radiation [RE-410] 16 p2638 N71-28142

Dirac monopole - magnetic charge theory and interaction with matter [BNL-TR-410] 21 p3464 N71-34658

DIRECT CURRENT

Heating of uranium dioxide rods by direct electric current [KFK-1031] 02 p0264 N71-11413

Electrical conductivity of igneous rocks of Kola Peninsula at high temperature based on dc transmission [NASA-TT-F-13214] 02 p0210 N71-11440

Direct current conductivity in turbulent cylindrical discharge tube plasma [ORNL-TM-3038] 02 p0281 N71-11862

Thermionic diode switch for use in high temperature region to chop current from dc source [NASA-CASE-NPO-10404] 03 p0316 N71-12255

Twelve-volt dc switching device [AD-712584] 03 p0349 N71-12523

Brushless dc motor design and performance tests [NASA-CR-102942] 03 p0351 N71-12433

Direct current motor with magnetically suspended rotor [NASA-CR-115793] 04 p0509 N71-13513

Modification of dc motor with magnetically suspended rotor to increase momentum storage capacity [NASA-CR-115792] 04 p0509 N71-13514

Generating direct current with regulated constant voltage by using feeder with negative impedance output 05 p0654 N71-14760

System for regulating direct current of triphase alternator [PUBL-114] 05 p0656 N71-15514

Detection of dc voltage breakdown and breakdown processes in space flight environments 06 p0828 N71-16645

Transistorized dc-coupled multivibrator with modulated output [NASA-CASE-XNP-09450] 06 p1171 N71-1872

Stepping motor control apparatus exciting windings in proper time sequence to cause motor to rotate in either direction [NASA-CASE-GSC-10366-1] 06 p1172 N71-1872

Frequency control network for current feedback oscillators converting dc voltage to ac or higher dc voltages [NASA-CASE-GSC-10041-1] 09 p1361 N71-19118

Apparatus for dc electrical measurement of Hall and photo-Hall effects in high resistivity semiconductors 09 p1367 N71-19118

Magnetic field determination of nonlinear dc generator [AD-716437] 09 p1399 N71-19118

Direct current powered self repeating plasma accelerator with interscanned anular and linear discharge channels [NASA-CASE-XLA-03103] 10 p1630 N71-31408

Conversion of positive dc voltage to positive dc voltage of lower amplitude [NASA-CASE-XMF-14301] 12 p1806 N71-33318

Converting output of positive dc voltage source to negative dc voltage across load with common reference point [NASA-CASE-XMF-08217] 12 p1858 N71-33320

Blood pressure measuring system for separately recording dc and ac pressure signals of Korotkoff sound [NASA-CASE-XMS-00061] 12 p1863 N71-33317

Radio frequency cutoff filter to provide dc isolation and low frequency signal rejection in audio amplifier [NASA-CASE-XGS-01418] 12 p1889 N71-33317

Brushless dc tachometer design with Hall effect crystals and output voltage magnitude proportional to rotor speed [NASA-CASE-MFS-20383] 13 p2057 N71-34018

Direct current motor with magnetically suspended rotor for attitude control 13 p2058 N71-34018

Self powered fast neutron detectors for use in motor cores [WHAN-SA-23] 14 p2291 N71-2570

Inverters for changing direct current to alternating current [NASA-CASE-XGS-06226] 14 p2322 N71-2595

Circuit for controlling reversible dc motor [NASA-CASE-XNP-7477] 14 p2329 N71-26012

Maximum length of arc in altitudes up to 9500 ft is 200 volt ac and dc electric aircraft system [RAE-TR-69259] 16 p2573 N71-28010

Feedback control for direct current motor to achieve constant speed under varying loads [NASA-CASE-MFS-14610] 16 p2572 N71-28010

Load insensitive dc to dc power converter with solid state circuitry [NASA-CASE-XER-11046] 16 p2572 N71-28010

High dc switch for causing abrupt, cyclic, decrease of current to operate under zero or varying gravity conditions [NASA-CASE-LEW-10155-1] 16 p2573 N71-28010

Coordinating fuses for protection of solid state device without large safety factor and high voltage dc circuits [MATT-715] 17 p2727 N71-2931

Broadband, high gain photomultiplier - dynamic crossed field electron multiplier for sensing photocurrent once each cycle of RF electric field 17 p2728 N71-29480

Optimum parameters for 12 cm bore superconducting dc quadrupole lens [KFK-1218] 19 p3142 N71-32377

Design and emission characteristics of economical dc arc plasma jet spectroscopic excitation source for solution analysis 19 p3166 N71-32344

Adjustable output voltage dc-to-dc converter for non-type satellite attitude control and orbit transfer using electrostatic deflection of ion thruster beams [PUBL-196] 20 p3300 N71-32996

Nondestructive tests of motor drivers for delta wound dc brushless motors [NASA-CR-121498] 21 p3402 N71-34318

Time constant measurements in cascade dc on or local thermodynamic equilibrium [TR-71-E-18] 21 p3406 N71-34320

Convection electric fields observed with double probe dc electric field experiment on Explorer 33 satellite [NASA-CR-121741] 21 p3419 N71-34320

Direct current motor design with magnetic bearing for use in low friction disturbance control systems [NASA-CASE-XCS-07805] 21 p3432 N71-34320

Switching power supply for bidirectional control of dc permanent magnet motors [RM-521] 24 p3900 N71-37777

Analysis of rare earth impurities in yttrium oxide using dc arc burning in open air [BARC-521] 24 p3942 N71-38123

DIRECT LIFT CONTROLS
Aircraft pilot direct lift control for aircraft landing and reducing gust load effects [ARC-R/M-3629] 07 p0909 N71-17116

SUBJECT INDEX

Guest load reduction by feedback control using direct and tuned left controls 19 p3037 N71-31889

DIRECT POWER GENERATORS

NT ALKALINE BATTERIES
NT BIOCHEMICAL FUEL CELLS
NT ELECTROSTATIC GENERATORS
NT FUEL CELLS
NT HYDROGEN OXYGEN FUEL CELLS
NT MAGNESIUM CELLS
NT MAGNETOHYDRODYNAMIC GENERATORS
NT METAL AIR BATTERIES
NT NICKEL ZINC BATTERIES
NT PRIMARY BATTERIES
NT RADIOISOTOPE BATTERIES
NT REGENERATIVE FUEL CELLS
NT SNAP 19
NT SNAP 21
NT SNAP 23
NT SOLAR CELLS
NT THERMIONIC CONVERTERS
NT THERMOELECTRIC GENERATORS
NT ZINC-OXYGEN BATTERIES

Describing general characteristics of system for direct conversion of thermal into electrical energy by thermodynamic analysis

Regulating high voltage in direct current generators by using tripping dynamo (PUBL-23) 05 p0656 N71-15518

Thermal pump-compressor for converting solar energy (NASA-CASE-XLA-00377) 07 p1130 N71-17610

Direct power conversion by magnetohydrodynamics of thermal energy into electrical energy (CEA-R-4062) 07 p0977 N71-18125

Converting output of positive dc voltage source to negative dc voltage across load with common reference point (NASA-CASE-MP-08217) 12 p1858 N71-23239

Unstabilizing magnetic core transformer design with varying signal for electrical power processing equipment (NASA-CASE-ERC-10125) 13 p2057 N71-24893

Steady state generation of rotating multipoles for plasma experiments in MCR range with application to plasma beam acceleration and direct energy conversion for plasma turbines (JUL-667-PP) 14 p2323 N71-26426

Portable dc power generator design including power supply, limiter, and switching circuits for voltage regulation point (AD-721570) 16 p2568 N71-28342

Rectification efficiency and reliability of driven transistor synchronous rectifiers (NASA-TM-X-65395) 17 p2726 N71-30097

Development of reliable dc power supply from silicon controlled rectifier and analog signal to discrete sine wave converter (AD-727639) 24 p3876 N71-37628

Peak fitness fast breeder cavity reactor mathematical models for control and stability analysis 24 p3964 N71-38274

Experimental and computational investigations of direct conversion of plasma energy to electricity (CONF-710607-126) 24 p3989 N71-38463

Variability of direction of closure currents of western electrojet in region of geomagnetic poles 11 p1757 N71-22849

DIRECTION FINDERS (RADIO)

U RADIO DIRECTION FINDERS

NT DIPOLE ANTENNAS
NT HELICAL ANTENNAS
NT HORN ANTENNAS
NT INERTIALESS STEERABLE ANTENNAS
NT LENS ANTENNAS
NT LOG PERIODIC ANTENNAS
NT LOOP ANTENNAS
NT PARABOLIC ANTENNAS
NT RADAR ANTENNAS
NT RHOMBIC ANTENNAS
NT SLOT ANTENNAS
NT STEERABLE ANTENNAS
NT TWO REFLECTOR ANTENNAS
NT YAGI ANTENNAS

Current distribution for continuous source antenna with specified side lobe levels on both sides of main beam (AD-712768) 03 p0337 N71-12407

Constructing 210 ft diam antenna stations for Deep Space Network 05 p0647 N71-14965

Ultrahigh frequency directional spiral aircraft antenna for spacecraft communication (RAE-TR-70662) 08 p1162 N71-18519

Computer graphics for satellite antenna geographic mapping (NASA-CR-114814) 08 p1146 N71-19022

Weatherproof helix antenna (NASA-CASE-XKS-08485) 09 p1346 N71-19493

Tracking antenna system with array for synchronous satellite or ground based radar (NASA-CASE-GSC-10533-1) 09 p1350 N71-19854

Directional antenna control system conversion from manual to digital-automatic control (AD-714961) 10 p1531 N71-20795

Automatic antenna position control device for evaluating dome effects on radiation pattern (AD-718288) 12 p1896 N71-23887

Electrical delays to define nulls in directional responses to acoustical superdirective arrays (AD-718322) 12 p1967 N71-23902

Drive system for parabolic tracking antenna with reversible motion and minimal backlash (NASA-CASE-NPO-10173) 13 p2085 N71-24696

Radiation pattern of thin, linear antenna of arbitrary length and driving point location 14 p2229 N71-26352

Satellite directional antenna spin reduction mechanism design (HSD-TR-72131) 15 p2380 N71-27156

Communication satellite directional antenna spin reduction mechanism 15 p2380 N71-27158

DIRECTIONAL CONTROL

NT THRUST VECTOR CONTROL

Is-flight determination of lateral-directional dynamics for landing approach (AD-715317) 07 p0973 N71-17792

Directional control capability of 18 x 5.5, type 7 aircraft tires on wet surfaces (NASA-TN-D-6202) 09 p1324 N71-20158

Wind tunnel investigation of helicopter directional control in rearward flight in ground effect (NASA-TN-D-41181) 09 p1346 N71-20191

Computer manual for calculating dynamic vector control of dual spin space station (NASA-CR-117310) 09 p1473 N71-20483

Flight evaluations using variable stability aircraft to determine effects of turbulence induced aerodynamic disturbances and lateral directional dynamics on pilot performance (NASA-CR-1718) 14 p2196 N71-26170

System analysis of directional control, rotary wing vibratory loads, lift shoring, and fuselage vibration and damping during helicopter maneuvers 18 p2870 N71-30775

DIRECTIONAL STABILITY

NT GYROSCOPIC STABILITY

CASSIOPEE system for rocket-borne astronomical telescope attitude control 02 p0262 N71-11762

Nonsteady flight test program on Siebel 204 D-1 aircraft for determining lateral directional stability and control derivatives (NLR-TR-70038-U) 15 p2367 N71-27109

Low speed wind tunnel tests of lateral longitudinal, and directional stability of MDC STS high cross range shuttle orbiter (NASA-CR-103163) 21 p3521 N71-35091

Wind tunnel tests on longitudinal and lateral directional stability of HARQD delta wing orbiter mated to Saturn 5 S-IC booster (NASA-CR-103200) 21 p3523 N71-35101

Low speed wind tunnel tests of directional stability characteristics for M/DAC delta wing booster (NASA-CR-103157) 21 p3523 N71-35105

Subsonic longitudinal and lateral directional stability investigation of MDAC LCR orbiter, unpowered and powered - graphs 24 p4017 N71-38665

Longitudinal, lateral, and directional static stability and control characteristics of delta wing space shuttle orbiter models 134D and 134C at Mach 0.26 (NASA-CR-119979) 24 p4020 N71-38681

DIRECTIVITY

Farfield patterns and directivity measurements for short backfire antenna (AD-724607) 20 p3241 N71-33191

DIRECTORIES (DOCUMENTATION)

U INDEXES

Dirichlet solution for thin airfoil problems (NASA-TT-F-13471) 07 p0967 N71-17468

Monte Carlo technique using repetitive analog computer for estimating lowest eigenvalues for certain partial differential equations with Dirichlet boundary conditions 12 p1884 N71-23870

Applications of Dirichlet theory to superposition of infinite number of Regge poles (CNBS-CPT-70-P-330) 15 p2461 N71-27114

Methods of generating random distribution functions, and comparison of their relative merits with those of Dirichlet 16 p2623 N71-28908

DIRIGIBLES

U AIRSHIPS

DISASTERS

Solving crop-hail insurance records for northeastern Colorado for designing hail experiment (FB-197644) 18 p2955 N71-31444

Communication processes and problems during natural disasters (AD-723993) 20 p3233 N71-33114

DISCONTINUITY

DISCHARGE

Use of semiconductors for energy storage, discharge, and transfer processes (CEA-CONF-1736) 22 p3559 N71-35347

DISCHARGE COEFFICIENT

Orifice flow and discharge coefficient of liquid propellant rocket engine fuel injectors (DLR-FB-70-38) 06 p0939 N71-15824

Discharge coefficients of axisymmetric conical nozzle under steady, critical flow over Reynolds number range from 100 to 34,000 16 p2580 N71-28687

DISCHARGE TUBES

U GAS DISCHARGE TUBES

DISCHARGERS

NT STATIC DISCHARGERS

Analysis of pulsed z-discharges characterized by anomalous plasma conductivity in skin-layer regime (NF-16775) 21 p3493 N71-34886

Plasma focus experiments using neocylindrical Z pinch in Filippov discharge chamber 22 p3657 N71-36877

DISCOLORATION

Effects of radiation on stability and compatibility of hydrazine and hydrazine-24 percent hydrazine nitrate in stainless steel and titanium alloy containers with O ring seals (NASA-CR-109767-PT-2) 16 p2670 N71-29088

DISCONNECT DEVICES

Remotely actuated quick disconnect mechanism for umbilical cables (NASA-CASE-XLA-00711) 03 p0316 N71-12258

Remotely actuated quick disconnect for tubular umbilical conduits used to transfer fluids from ground to rocket vehicle (NASA-CASE-XLA-01396) 03 p0316 N71-12259

Design and development of quick release connector (NASA-CASE-XLA-01411) 04 p0524 N71-13799

Split nut and bolt separation device (NASA-CASE-XNP-06914) 10 p1567 N71-21489

Electrical circuit selection device for simulating stage separation of flight vehicle (NASA-CASE-XKS-64631) 12 p1893 N71-23663

Quick disconnect duct coupling device for single-hand operation (NASA-CASE-MFS-20395) 13 p2086 N71-24903

DISCONNECTORS

U DISCONNECT DEVICES

DISCONTINUITY

NT SHOCK DISCONTINUITY

Comments on waves and discontinuities in solar wind (NASA-TM-X-65411) 05 p0765 N71-15327

Surface roughness effects on shear strength of discontinuities or joints in rocks (AD-714244) 06 p0850 N71-16374

Characteristics of directional discontinuities in interplanetary magnetic field (NASA-TM-X-65430) 06 p0947 N71-16757

Microstructure of solar wind and interplanetary medium (NASA-TM-X-65468) 09 p1463 N71-20469

Elastic instability in pure shear effect in limiting plastic strain, particularly at discontinuities (COO-2048-1) 10 p1658 N71-21696

Stress field effect on ultrasonic energy from discontinuities in solids (AD-719434) 13 p2181 N71-24845

Servocontrol system for measuring local stresses at geometric discontinuity in stressed material (NASA-CASE-XLA-08330) 13 p2182 N71-25360

Numerical analysis of laminar boundary layer problems on porous plates with discontinuity in gas injection (REF-71-1) 17 p2732 N71-29491

Rotational discontinuities in solar wind derived from Mariner 5 plasma and magnetic field data (NASA-CR-119172) 17 p2842 N71-30261

Tangential discontinuities in solar wind derived from Mariner 5 plasma and magnetic field data (NASA-CR-119173) 17 p2842 N71-30262

Hydrodynamic equations for determining rotational discontinuities in solar wind (NASA-TT-F-13811) 18 p3006 N71-31089

Magnetization reversal discontinuities of high performance transition metal-rare earth magnets for critical applications (AD-722772) 18 p2957 N71-31353

Large velocity discontinuities in solar wind in anisotropic medium (NASA-TM-X-65464) 19 p3177 N71-32392

Magnetohydrodynamics of discontinuities in interplanetary medium and their relation to propagation and acceleration of cosmic rays (NASA-TM-X-65673) 20 p3342 N71-33717

Theoretical study of magnetopause current layer from kinetic theory of warm collisionless plasma 23 p3832 N71-37330

Erosion of discontinuities and formation of oscillations in numerical computations of discontinuous solutions of differential equations 24 p3949 N71-38176

Interpretation proposal for inclusive cross sections using discontinuity equations for scattering amplitudes (NYO-2262-TA-240) 24 p3977 N71-38376

DISCOVERING

DISCOVERING

U EXPLORATION DISCRETE FUNCTIONS

- Zoom discrete Fourier transformation of sampled signals
[CRC-TN-431] 01 p0074 N71-10037
- Stability regions of discretization methods for differential equations
[AD-712711] 04 p0539 N71-14289
- Fast Fourier transform programs for EAI-640 digital computer
[NRC-11747] 06 p1167 N71-19332
- Kalman filtering for spectral factorization and matrix solution to spacecraft tracking problem
10 p1645 N71-21359
- Linear discriminant function selection, using random variables
[AD-716956] 10 p1593 N71-21570
- Use of discrete ordinates and auxiliary programs of AMHSN in one dimensional neutron and gamma ray transport
[CEA-N-1358] 13 p2129 N71-24672
- Discrete optimization and optimal control problems with equality constraints
[CT-36] 14 p2281 N71-25852
- Method for determining outcomes and optimum strategy for all players in discrete N-person game theory with independently chosen strategies
[NASA-CR-118153] 14 p2282 N71-26111
- Error vector propagation method for solving discretized Poisson equation
[SC-RR-70-579] 15 p2433 N71-26934
- Differential calculus applied to discrete Walsh-Paley functions, nothing usefulness for binary codes
[NPL-DES-3] 15 p2434 N71-27033
- Discrete two person game theory based on median value considerations
[NASA-CR-118891] 15 p2435 N71-27730
- Discrete element analysis of creep and stress properties of stainless steel tubing for LMFBFR
[ORNL-TM-3294] 16 p2613 N71-28801
- Procedures for calculating normal wash in non-planar configurations and interference between wings and bodies
17 p2698 N71-29340
- Finite time stability of linear discrete time systems and corresponding results for stochastic linear discrete time systems
[AD-722654] 18 p2944 N71-30720
- Finite state discrete parameter Markov chain representation of ionospheric communication error sequences
19 p3057 N71-32561
- Evaluating current NASTRAN discrete element models for monocoque and semimonocoque structures
22 p3687 N71-36290
- Discrete element method for plates or slabs on non-linear foundations
23 p3864 N71-37546

DISCRIMINATION

- NT BRIGHTNESS DISCRIMINATION
- NT SENSORY DISCRIMINATION
- NT TACTILE DISCRIMINATION
- NT VISUAL DISCRIMINATION
- Temperature drift and peak current degradation in tunnel diodes used for amplitude discrimination
24 p4013 N71-38622

DISCRIMINATORS

- NT FRAUNHOFER LINE DISCRIMINATORS
- Difference indicating circuit used in conjunction with device measuring gravitational fields
[NASA-CASE-XNP-08274] 04 p0512 N71-13537
- Describing frequency discriminator using digital logic circuits and supplying single binary output signal
[NASA-CASE-MFS-14322] 08 p1165 N71-18692
- Circuit design for determining amount of photomultiplier tube light detection utilizing variable current source and dark current signals of opposite polarity
[NASA-CASE-XMS-03478] 10 p1558 N71-21040
- Characteristics of comparator circuits for comparison of binary numbers in information processing system
[NASA-CASE-XNP-04819] 12 p1881 N71-23295
- Comparison of analog and digital waveform discriminators for radiation counters
[JUL-660-2E] 15 p2468 N71-27312
- De coupled 200 MHz pulse amplitude discriminator
[CEA-N-1447] 24 p3897 N71-37780

DISEASES

- NT ARTERIO-SCLEROSIS
- NT CANCER
- NT CARBON MONOXIDE POISONING
- NT DERMATITIS
- NT ENCEPHALITIS
- NT EPILEPSY
- NT HEART DISEASES
- NT INFECTIOUS DISEASES
- NT INFLUENZA
- NT KIDNEY DISEASES
- NT LEUKEMIAS
- NT NEPHRITIS
- NT RESPIRATORY DISEASES
- NT THROMBOSIS

NT TOOTH DISEASES NT TOXIC DISEASES NT TUBERCULOSIS NT TUMORS NT ULCERS

- Laboratory-acquired infections, oncogenic viruses, allergy to animal dander and sera, and carcinogenesis
[ORNL-TM-2854] 03 p0321 N71-12298
- Developing spectral signature indicators of root disease in large forest areas
06 p0800 N71-16158
- Aerial and ground surveillance of southern corn leaf blight in Corn Belt States during 1971
[NASA-NEWS-RELEASE-71-129] 17 p2709 N71-30175
- Computerized method for input of disease history information and retrieval for diagnosis
20 p3289 N71-32882

DISHES U PARABOLIC REFLECTORS

- DISINTEGRATION
- Experimental and theoretical analysis of breakup of liquid sheets and jets in supersonic gas stream
19 p3082 N71-32618
- Calculation of Si-28 photodisintegration rate from Al-27 [γ , gamma]Si-28 and Mg-24 [α , gamma]Si-28 reactions
21 p3487 N71-34844
- Absolute cross section and angular distribution of deuterium photodisintegration
21 p3489 N71-34855

DISKS

- Influence of disc valve springs on action of valves and functioning of compressor
[NLL-RTS-5938] 17 p2756 N71-29825

DISKS (SHAPES)

- NT ROTATING DISKS
- Measurements of hypersonic, rarefied flow field of disk
[AD-710641] 01 p0042 N71-10461

- Computer graphics terminal for disc profile design of gas turbine engine
03 p0348 N71-13141

- Potential energy of electrostatic field in double disk plasma probe
[AD-715889] 08 p1275 N71-18819

- Iris disk slot geometry effects on waveguide dispersion properties and wave damping coefficients
[KFK-TR-334] 14 p2321 N71-26775

- Disk shaped discharge chamber for dense plasma focus formation
17 p2812 N71-30134

- Stress analysis in axisymmetric perforated shells and equivalent disk noting use of FORTRAN
[ONERA-NT-172] 19 p3186 N71-31700

- Antenna parameters and input admittance from numerical analysis of radiation fields of slotted circular disks
19 p3071 N71-32288

- Unit disk for boundary functions and sets of asymptotic values
19 p3124 N71-32497

- Surface pressure fluctuations on circular disk in turbulent air near stagnation point
[NBS-TN-543] 21 p3412 N71-34279

- Spherical and planar galaxy systems in relation to elastic and inelastic evolutionary processes
23 p3849 N71-37432

- Finite difference method for testing optimum design of disks and shells subjected to pressure and inertial forces
24 p4027 N71-38738

DISLOCATIONS [MATERIALS]

- NT CRYSTAL DISLOCATIONS
- NT EDGE DISLOCATIONS
- NT SCREW DISLOCATIONS

- Interaction of moving dislocations with electrons and phonons in aluminum
[AD-709940] 01 p0093 N71-10057

- Dislocations in cobalt ferrite spinels
[UCRL-19198] 04 p0580 N71-14020

- Lithium fluoride dislocation in high speed impact
[AD-713624] 05 p0707 N71-14824

- Theoretical analysis of energy storage in dislocation pile-ups and stress fields of dislocation cells
[ORO-3108-102] 05 p0706 N71-15655

- Dislocation mobility in germanium at high stresses and low temperature
[AD-714267] 06 p0872 N71-14329

- Oxygen concentration effect on internal stress and dislocation arrangements in alpha titanium
[AD-716787] 10 p1571 N71-20710

- Dislocation mechanisms involved in low stress-high temperature creep of metals
13 p2096 N71-25096

- Nonequilibrium defects in metals including point defects, line defects, surface defects, volume defects, and dislocations occurring during solidification or nucleation from impurities
[UCRL-19066] 15 p2419 N71-26919

- Irradiation produced defects in microstructure of annealed austenitic stainless steels
[WHAN-FR-16] 15 p2420 N71-26921

- Dislocation of Ni and Fe foils caused by electron irradiation
[CEA-CONF-1680] 15 p2489 N71-27880

- Unified approach to interactions of defects applicable to rigid and deformable defects
[AD-721469] 16 p2664 N71-28227

- Effect of dislocations on coarsening of particles by pressure waves, coarsening in nickel aluminum alloys, and in situ recrystallization
[NLL-CE-TRANS-5401-19022/09] 17 p2815 N71-29737

- Dislocation configurations in stress producing and zero stress continuum
[AD-722432] 17 p2815 N71-29794

- Branch curvature in dislocations at free surface from image force and concept of line tension
17 p2816 N71-29928

- Dislocation in semi-infinite isotropic media
17 p2816 N71-29910

- Subsonic, supersonic, and transonic dislocations moving on interface separating two isotropic media of differing elastic properties
17 p2817 N71-29923

- Inversion formulas for singular integral equations for linear dislocation arrays
17 p2817 N71-29936

- Dislocation pileup problem solving, using orthogonal polynomials and singular integral equations
17 p2817 N71-29937

- Phonon scattering by dislocations and its influence on lattice thermal conductivity and on dislocation mobility at low temperatures
17 p2819 N71-29939

- Phonon scattering by Cottrell atmospheres affecting dislocations
17 p2819 N71-29941

- Harmonic model of thermal energy trapping by steady moving dislocations
17 p2819 N71-29951

- Reradiation of elastic waves limiting dislocation resonance
17 p2819 N71-29954

- Thin walls of mobile dislocations emitting macroscopic sound waves
17 p2819 N71-29953

- Anharmonic properties of vibrating dislocations in terms of nonlinear stress-strain relation
17 p2820 N71-29956

- Plastic deformation of disclination and dislocation density tensors
17 p2821 N71-29967

- Panel on intrinsic and physical properties of dislocation theory
17 p2821 N71-29968

- Mean square stresses for random distributions of dislocations in cylindrical body
17 p2824 N71-29994

- Dislocation dynamics and formulation of constitutive equations for rate dependent elastic plastic response in isotropic metals
[AD-722314] 17 p2765 N71-30110

- Krypton and helium bubble migration on dislocations in copper foil, and measurement of root mean square random migration distances during isothermal annealing
[RD/N-1850] 19 p3146 N71-31944

- Measurement of stresses and displacements in this films due to presence of periodic distribution of screw dislocations and edge dislocations
[ICO-2034-6] 21 p3496 N71-34920

DISORDERS

- Aspects of mouth disorders in space flight and space flight training
[JPRS-33594] 21 p3382 N71-34862

DISORIENTATION

- NT DISORDERS
- Incidence and costs of pilot disorientation Army aircraft accidents during fiscal year 1967
[AD-710987] 01 p0013 N71-10055

- Techniques for familiarizing flying personnel with disorientation effects
[FAA-AM-70-17] 07 p0981 N71-17255

- Human performance under low frequency vibration and effects on whole body orientation
07 p0982 N71-17267

- Incidence and costs of orientation-error accidents Army UH-1 helicopter operations
[AD-715107] 07 p0973 N71-17264

- Studying oculogravic illusion and Coriolis effect as causes of disorientation in aerospace flight
[IZF-170-25] 16 p2883 N71-30087

DISPERSING

- Investigating water transport scheme for dispersal of thermophilic microorganisms to Surtsey from mainland areas
07 p0985 N71-17269

- Collisionless shocks in plasmas, dispersion and dispersion in determining shock structure
[NASA-CR-117077] 09 p1450 N71-30048

- Method for determining dispersion relations in fiber reinforced binary composite materials based on Fourier series and equations of motion
10 p1589 N71-31140

- Apparatus for mechanically dispersing ultrafine metal powders subjected to shock waves
[NASA-CASE-XLE-04946] 13 p2094 N71-34011

SUBJECT INDEX

- Metereological and chemical aspects of air pollution and propagation and dispersal of air pollutants - survey of USSR air pollution literature**
 [PB-190064] 17 p2743 N71-29434
- Global stratospheric dispersion of supersonic transport exhaust**
 [D18-12981-1] 21 p3376 N71-34021
- Elastic behavior of composite materials influenced by shape of dispersed particles**
 [AD-725611] 22 p3402 N71-35456
- Long waves along single-topography in semi-infinite uniformly rotating ocean calculated using Kelvin-type dispersions**
 23 p3788 N71-36997
- DIFFUSION**
 Dispersion theory and current algebra commutator studies proving single pole dominance for spin one parts of vector or axial vector currents inconsistent with current algebra 14 p2302 N71-27443
- DIFFUSION PRECIPITATION HARDENING**
U PRECIPITATION HARDENING
- DIFFUSIONS**
 NT AEROSOLS
 NT COLLOIDAL PROPELLANTS
 NT COLLOIDS
 NT EMULSIONS
 NT FOG
 NT LIQUID-GAS MIXTURES
 NT NUCLEAR EMULSIONS
 NT PHOTOGRAPHIC EMULSIONS
 NT SMOKE
- Film formation from polymer dispersions**
 Computerized simulation of dispersion models for airport air pollution 04 p0487 N71-13467
- Dispersion models for airport air pollution**
 [RB-3983] 07 p1055 N71-17923
- Multiple source urban atmospheric dispersion model for Chicago air pollution**
 [ANL-ES-CC-7] 08 p1185 N71-18296
- Ice nuclei dispersion systems development**
 [PB-196149] 09 p1413 N71-19714
- Correlation between NRL electron storage ring /Suzutro/ and behavior of nonlinear dispersive partial differential equations**
 [AD-716734] 10 p1611 N71-20676
- Particle size distribution in dispersions determined from scattered light intensity with aid of digital computer**
 [RAE-TN-70151] 13 p2123 N71-24408
- Atomic and molecular motions in oriented polytetrafluoroethylene studied by slow neutron inelastic scattering to obtain dispersion relations**
 15 p2742 N71-27439
- Turbulent liquid-liquid dispersions in stirred containers**
 16 p2690 N71-28213
- Polymer entropic repulsion**
 22 p3551 N71-35295
- DISPLACEMENT**
 Axisymmetric stresses and displacements in two finite circular cylinders in contact
 [NASA-TN-X-58052] 01 p0129 N71-10448
- Information capacity of discrete motor responses compared for different directions and amplitudes of displacement**
 [AD-710713] 01 p0012 N71-10536
- Wall motions in circular thin-walled cylindrical shells under combined loading**
 08 p1301 N71-19282
- Displacement measurement on numerically controlled machine tools using transducers positioning devices**
 [CRIF-MC-31] 10 p1564 N71-21004
- Brownian motion of interstellar grains and mean quadratic displacement calculations**
 11 p1824 N71-22900
- Magnetic field measuring probe displacement and positioning effect on optical system**
 [DF-18519] 14 p2298 N71-26671
- Expressions for state of stress and displacement for half space deduced from general basic formulas for three dimensional thermoelastic problem**
 [PB-197273] 18 p3024 N71-30882
- Displacement and stress field determination within axisymmetric elastic bodies with prescribed internal loads and boundary conditions**
 [AD-726425] 22 p3402 N71-35654
- Field displacement graphical processing provisions and techniques for calculating partial derivatives of displacements using matrix and coordinate grid methods**
 [NLL-M-21096-5828.4F] 24 p3950 N71-38183
- DISPLACEMENT MEASUREMENT**
 Measurement of micro-displacements by laser interferometry
 [DRIET-76-7541] 02 p0239 N71-11600
- Measuring linear and angular displacements using double exposure and real time holographic interferometry**
 03 p0379 N71-12789
- Experimental techniques for determining support reactions in models of beams and slabs**
 [PB-197703] 03 p0406 N71-12930

- Mirror movement analysis by holographic interferometry for calibration to speckle interferometry**
 [NASA-TN-X-2227] 09 p1396 N71-19633
- Development and characteristics of self-calibrating displacement transducer for measuring magnitude and frequency of displacement of bodies**
 [NASA-CASE-XLA-90781] 11 p1726 N71-22999
- Gas bearing for model support with capacity for measuring angular displacement of model in bearing**
 [NASA-CASE-XLA-90346] 16 p3602 N71-28740
- Capacitor field calculations for capacitive displacement measurement of open mesh structures such as radio telescopes and radar receivers**
 [NASA-TN-D-6341] 20 p3373 N71-33397
- Measurements and analysis of solid propellant rocket vibrations obtained during captive flight of Nike rocket**
 [NASA-TN-D-6317] 23 p3863 N71-37539
- DISPLAY DEVICES**
 NT ANEMOMETERS
 NT APPROACH INDICATORS
 NT FLOW DIRECTION INDICATORS
 NT GYRO HORIZONS
 NT HOT-FILM ANEMOMETERS
 NT HOT-WIRE ANEMOMETERS
 NT KINOFORM
 NT POSITION INDICATORS
 NT RADARSCOPES
 NT RADIO DIRECTION FINDERS
 NT SPACECRAFT POSITION INDICATORS
 NT TACHOMETERS
 NT WIND VANES
- Human factors in use of terminal radar /analog/ display systems**
 [FAA-NA-70-55] 01 p0010 N71-10381
- District of Columbia air quality display model for comparing seasonal concentration estimates**
 [PB-189194] 02 p0151 N71-11072
- Display console for tactical situation radar display requirements and data management**
 [AD-712101] 02 p0177 N71-11247
- Program requirements for DRAFT 2 system**
 [NASA-CR-108652] 02 p0189 N71-11326
- FORTRAN computer program for IBM 2250 display unit**
 [AD-711009] 02 p0189 N71-11329
- Amorphous semiconductor switches for control elements in electroluminescent display panel**
 [AD-712366] 02 p0192 N71-11349
- Developing 32 by 50 resolution element digital address thin display tube for man pack radar**
 [AD-713025] 03 p0337 N71-12406
- Information display from access storage of digital computer on cathode ray tube screen**
 [AD-712805] 03 p0340 N71-12463
- Integrated time shared instrumentation display for aerospace vehicle simulator**
 [NASA-CASE-XLA-01952] 03 p0345 N71-12507
- Investigating conversion of signals into common digital form and transmission by time division multiplexing along wire or fiber optic cables**
 03 p0347 N71-12621
- Data processing and display system for terminal guidance of X-15 aircraft**
 [NASA-CASE-XFZ-00756] 04 p0474 N71-13421
- Application of plasma display technique to computer memory system**
 [AD-712698] 04 p0502 N71-13510
- Sophisticated graphic display system - GRACE**
 04 p0506 N71-13845
- Evaluation of interactive input devices associated with computer driven displays**
 04 p0506 N71-13846
- Input communication on target simulation systems**
 [AD-713179] 04 p0506 N71-13847
- Display relationship problems applied to presentation of aircraft attitude and guidance information**
 [AD-713179] 05 p0637 N71-14743
- Comparison of legibility of three types of electronic digital display**
 [DF-NP/17169] 05 p0649 N71-14830
- Flight test of fire control system in AR-10 helicopter**
 [AD-714670] 06 p0794 N71-16019
- Data displays of Radio Astronomy Explorer I**
 [NASA-TN-X-45415] 06 p0946 N71-16239
- Comparison of moving map display and two graphics with hand-held maps**
 [AD-714061] 06 p0994 N71-16294
- Reaction times of subjects in tests with display control configurations typical of those used in continuous tracking tasks**
 [NASA-TN-D-6132] 06 p0907 N71-16506
- Computer refreshed display for processing video information with digital computer to enhance video data**
 06 p0921 N71-16675
- Functional analysis of graphic computer**
 [D-1-70-01] 07 p0996 N71-17090
- FORTRAN program for computation of group tables, alphanumeric display**
 [NASA-TN-X-21172] 07 p1051 N71-17338
- Cathode ray tube display unit connected to on-line computer used in acquiring and analyzing nuclear physics data**
 [LYCEN-7053] 07 p1080 N71-18121

- Investigation of angle of attack information display for pilots to increase efficiency of general aviation aircraft operations**
 [NASA-TN-D-6210] 08 p1143 N71-18442
- Fluidic-thermochemical display device**
 [NASA-CASE-ERC-10031] 08 p1179 N71-18603
- Development and characteristics of frequency separated display devices for aircraft control**
 [AD-715458] 08 p1144 N71-18739
- Automated visual sensitivity meter for detecting scotomas, phosphenes, and changes in retinal sensitivity**
 [NASA-TN-D-6190] 08 p1302 N71-18971
- Display systems, fluid amplification techniques, stochastic processes, and thrust vector control systems**
 [NASA-CR-103049] 08 p1233 N71-19045
- Investigating optical characteristics of plane mirror, prism, and rotating wedge scanners used in thermal viewers**
 08 p1203 N71-19131
- Selection of scanning systems for aircraft thermal viewers**
 08 p1204 N71-19220
- Effect of cockpit lighting systems on multicolored instrument displays**
 [AD-716610] 09 p1339 N71-19710
- Benefits and problems of using head-up displays in commercial and general aviation aircraft**
 [NASA-CR-117152] 09 p1388 N71-19752
- Cockpit display of automatic radar control systems data**
 [AD-716425] 09 p1415 N71-19848
- Cathode ray tube system for displaying ones and zeros in binary wave train**
 [NASA-CASE-XGS-04987] 09 p1357 N71-20571
- Universal aircraft flight simulator/trainer system definition**
 [AD-717179] 10 p1503 N71-20604
- Development of improved surveillance and communication subsystems for automated air traffic control system**
 [AD-716816] 10 p1599 N71-20774
- Optical projector system for establishing optimum arrangement of instrument displays in aircraft, spacecraft, other vehicles, and industrial instrument cockpits**
 [NASA-CASE-XNP-03853] 11 p1796 N71-21882
- Feasibility of utilizing color cathode ray tubes for aircraft crew station displays**
 [AD-717655] 11 p1673 N71-22174
- Effect of several variations of two types of TV display visual simulation systems on subjective pilot evaluations and objective measures of performance in landing approach**
 [NASA-TN-D-6274] 11 p1667 N71-22270
- Editing system for large general time sharing computer including dynamic editing display techniques and static microfilm method**
 [NASA-TM-X-2264] 11 p1716 N71-22575
- Computer controlled interactive graphics display system for hydrologic analysis**
 [BNWL-1525] 11 p1716 N71-22580
- Prompt effects of weapons effects display system, testing faulty components**
 [UCRL-50092-VOL-4-PT-2] 12 p1916 N71-23152
- Fallout display portion of weapons effects display system**
 [UCRL-50092-VOL-4-PT-1] 12 p1916 N71-23153
- Optical monitor panel consisting of translucent screen with text or meter information projected onto it from rear for application in control rooms of missile launching and tracking stations**
 [NASA-CASE-XKS-03509] 12 p1916 N71-23175
- Sweeping receiver system providing visual display of received signals in frequency range from 33 to 140 GHz and frequency markers**
 [AD-717799] 12 p1874 N71-23308
- Beam penetration cathode ray tube for high performance radar display systems**
 [AD-718423] 12 p1899 N71-23549
- Design, fabrication, and evaluation of three-color plasma-panel display device and multiple intensity coding techniques**
 [AD-718268] 12 p1890 N71-23612
- Two and three dimensional simulated target detection and recognition by pilots and TV gamma and gray scale transmission effects on target acquisition in flight simulators**
 [AD-718321] 12 p1867 N71-23750
- Computer simulated display device for diagnosis of heart disease**
 [NASA-NEWS-RELEASE-71-58] 12 p1867 N71-23751
- Cathode ray tube display and monitor interface to provide graphical output for small digital computers**
 [NASA-CR-118011] 12 p1803 N71-23867
- Binary to decimal decoder logic circuit design with feedback control and display device**
 [NASA-CASE-XKS-06167] 13 p0053 N71-34090
- Noninterruptible digital counter circuit design with display device for pulse frequency modulation**
 [NASA-CASE-XNP-00759] 13 p0652 N71-34091
- Vocabulary for spaceborne communication with spaceborne computers with graphic display devices**
 [NASA-CR-183171] 14 p1221 N71-25922

DISPLAY SYSTEMS

- Data acquisition system for converting displayed analog signal to digital values
[NASA-CASE-NPO-10344] 14 p2235 N71-26544
- Phosphor noises compensation in projection tube for television display systems
[AD-726751] 14 p2220 N71-26640
- Design and operation of linear gas discharge devices permitting continuous visual monitoring of parametric variations
[JPRS-53182] 14 p2259 N71-26666
- Development and construction of engineering model large screen multicolor projector designed to use reflective photoplastic film immediately after recording
[AD-721227] 15 p2407 N71-27037
- Digital time code generator for airborne use comprising solid state visual display of time and synchronization with another time code generator
[ARL/F-45] 15 p2411 N71-27622
- Prompt effects computer program for weapons effect display system /WEDS MOD 2/
[UCRL-50892-VOL-6] 15 p2384 N71-27734
- Display system information content characteristics and relationships with operator performance and psychophysiological factors in data processing
[JPRS-53244] 16 p2541 N71-28093
- Display effectiveness factors for solid state flat panel displays
[AD-721307] 16 p2567 N71-28219
- Development of rectangular display cathode ray tube with low power drain suitable for battery operation
[AD-722207] 16 p2568 N71-28348
- Mathematical models of nuclear effects and fallout calculations for weapons effects display system
[UCRL-50892] 16 p2566 N71-28631
- Integrated sensor array warning systems for base defense, including radar, remote sensors, and display devices
[AD-721555] 16 p2562 N71-28658
- Plastic lenses providing virtual image of flight scene for use in flight simulator with Schmidt projection system or television monitor
[NASA-TM-X-32377] 16 p2596 N71-28889
- Development and application of heads up aircraft instrument display for improvement in aircraft safety during adverse weather
[FAA-NA-71-9] 17 p2702 N71-29305
- Television display and artificial background for showing effects of contrast and motion on target detection
[AD-722407] 17 p2711 N71-29685
- Vertical situation display concept for alleviating problems of inadequate guidance and display information for making steep approaches
[AD-722609] 18 p2869 N71-30770
- Design and evaluation of information display systems and development of operator work station stages
[AD-722609] 18 p2882 N71-30668
- Man machine interface problems in graphic display including applications in various fields
[NASA-TT-F-13816] 18 p2894 N71-31081
- Evaluation of capabilities of electronic display system used in analysis of ATS cloud photographs
[NASA-CR-119317] 18 p2925 N71-31421
- Analog computer program and display device for detecting arrhythmia signals during electrocardiography
[AD-711639] 19 p3046 N71-31612
- Production engineering and electrical operation of phototransistor sensing array system and display device including large scale integration and logic circuitry
[NASA-CR-119765] 19 p3167 N71-31642
- Digital address thin cathode display tube for portable radar
[AD-723431] 19 p3053 N71-31676
- Aircraft indicating instruments with digital cathode ray tube display
[DLR-87-71-27] 19 p3064 N71-31695
- Helicopter payload capability indicator in terms of gas generator speed
[AD-723436] 19 p3098 N71-31723
- Information flow model for visual sound displays
[AD-723180] 19 p3055 N71-32129
- Computerized simulation for evaluating mosaic patterned, photoconductive near-infrared image conversion panels
[AD-723524] 19 p3066 N71-32329
- Digital photographic data processor and display system
[AD-723657] 19 p3101 N71-32335
- Capacitance distance gage for dimensional measurement with digital readout or direct computer processing
[Y-1783] 19 p3101 N71-32343
- Mathematical model and information display system for flight control and monitoring aircraft and pilot performance
[AD-724051] 19 p3045 N71-32566
- Digital video display system for display of image, alpha numeric, and other data on cathode ray tube with sequential raster scan and 2, 4, or 8 gray shades
[NASA-CASE-NPO-11342] 20 p3240 N71-33103

- Human factors engineering in optimizing visual perception of sonar and radar displays
[AD-723992] 20 p3227 N71-33187
- Discrete element magneto-optic display
[AD-724603] 20 p3241 N71-33190
- Quantitative and comparative analysis of inorganic photochromic materials for coherent optical data processing applications
[NASA-CR-121453] 20 p3311 N71-33375
- Plasma-fluidic hybrid display system combining high brightness and memory characteristics
[NASA-CASE-ERC-10100] 20 p3242 N71-33519
- Development of plasma panel display device having three color capability and three levels of intensity
[AD-723985] 21 p3403 N71-34217
- JOSHUA terminal system for module execution and data manipulation by remote display systems
[TID-25691] 21 p3460 N71-34626
- Development and characteristics of display system for space shuttle and cost effectiveness analysis of cathode ray tube system
[AD-723985] 21 p3517 N71-35062
- Analysis of bulk storage data requirements and methods for visual display of information on space shuttle display devices
[AD-723985] 21 p3517 N71-35063
- Design concept for integrated display system suitable for computer management and optimized for pilot acceptability applied to space shuttle
[AD-723985] 21 p3517 N71-35064
- Tests to determine effectiveness of two linear rare-field displays for use as flight instruments
[AD-726643] 22 p3460 N71-35229
- Human factors considerations in design, development, and tests of sonar display devices
[AD-726711] 22 p3554 N71-35317
- Mathematical model of color television display for assessment of random noise
[BBC-1971/27] 23 p3725 N71-36553
- Airborne traffic situation display system for use with radar control terminal system
[AD-727669] 23 p3794 N71-37042
- Pilot performance in recognizing electronic display systems under varying dazzle and color conditions in cockpits
[RAE-LIB-TRANS-1545] 24 p3875 N71-37621
- Application of linear gas discharge displays on control panels to data representation systems
[AD-727772] 24 p3882 N71-37670
- Television display systems for slant range target detection and recognition
[AD-727772] 24 p3882 N71-37674
- Man machine techniques for processing data from sonar display systems
[AD-727609] 24 p3883 N71-37677
- Pilot transition from conventional visual cross pointer display to aural glide slope cues
[FAA-AM-71-24] 24 p3883 N71-37682
- Equipment specifications for interactive programming system for image processing with Iliac, IBM 360, and PDP 8 computer components
[COO-2118-3] 24 p3894 N71-37753
- Use of thermoluminescent lithium fluoride dosimeters for radiation dose control purposes providing rapid readout procedure
[AEEW-M-962] 24 p3973 N71-38343
- Display requirements and concepts for space shuttle recovery and landing
[NASA-CR-123151] 24 p4020 N71-38683
- ### DISPLAY SYSTEMS
- #### U DISPLAY DEVICES
- #### DISPOSAL
- #### NT WASTE DISPOSAL
- #### DISSIPATION
- #### NT ENERGY DISSIPATION
- #### NT OHMIC DISSIPATION
- Collisionless shocks in plasmas, dissipation and dispersion in determining shock structure
[NASA-CR-117307] 09 p4150 N71-20465
- Dissipative voltage regulator system for minimizing heat dissipation
[NASA-CASE-GSC-10091-1] 14 p2235 N71-26626
- Asymptotic expansion procedure for effects of dissipative and dispersive mechanisms and nonlinearity on homogeneous, isotropic, wave propagation problems
[RE-4022] 22 p3692 N71-36331
- #### DISSIPATORS
- #### U DISSIPATION
- #### DISSOCIATION
- #### NT AUTOIONIZATION
- #### NT GAS DISSOCIATION
- #### NT PHOTODISSOCIATION
- #### NT THERMAL DISSOCIATION
- Kinetic energy of ionic products from electron impact dissociation of molecules
[AD-711690] 01 p0102 N71-10919
- Dissociative electron attachment to polyatomic molecules and negative ion lifetimes
[ORNL-TM-2614] 05 p0746 N71-15237
- Shock tube study of cyanogen dissociation in argon
[RE-4022] 06 p0927 N71-14668
- Quadrupole rotation-vibration spectrum of hydrogen and predissociation rates of B state of iodine
[NASA-CR-116176] 06 p0927 N71-14669

SUBJECT INDEX

- Effects of small amounts of impurities on process of dissociation of super saturated solid solutions
[TT-70-57078] 08 p1219 N71-19108
- Fluorine atom reaction dynamics, intermolecular potentials from high resolution differential cross sections, and collision induced dissociations of diatomic molecules
[COO-2092-1] 11 p1696 N71-23221
- Mass spectrometer for dissociation measurement of oxygen in shock heated molecular beams
[AD-723985] 11 p1807 N71-22646
- Dissociative recombination rate measurements in partially ionized gases within shock tube at elevated temperatures
[AD-718434] 12 p1933 N71-23705
- Dissociation and output of platinum catalyzed CO laser
[AD-718434] 12 p1933 N71-23705
- Calculation of dissociation stresses in lithium and potassium peroxides
[NASA-TT-F-13629] 16 p2358 N71-29961
- Nonplanar dissociations and Burgers vector of twinning dislocations
[AD-723985] 17 p2820 N71-29968
- Vacancy on nonpolar pure screw dislocation dissociating into set of kinks
[AD-723985] 17 p2820 N71-29962
- Mathematical model for dislocation stacking fault energy and partial dissociation in crystal defect dislocations
[AD-723985] 17 p2824 N71-29961
- Multiparticle production processes involving limited behavior of cross sections and diffractive dislocations
[PURC-4159-19] 18 p2990 N71-31554
- Uses of spin-unrestricted Hartree-Fock method in approximating potential energy curves for molecular dissociation in hydrogen compounds and nitridon
[AD-723985] 19 p3050 N71-32161
- Dissociative excitation of CO (3 Pi) and other metastable fragments such as O(5S) produced by electron impact on CO₂
[NASA-CR-121714] 21 p3466 N71-34678
- Angular and energy distributions during molecular dissociation due to electron bombardment
[AD-723985] 22 p3651 N71-34831
- Triple Resonance coupling related to low missing mass spectrum in diffraction dissociation
[UCSD-10-P-10-78] 23 p3812 N71-37185
- Development of theory for vibrational dissociation of diatomic molecules to neutral atoms due to direct excitation in strong collision
[AD-723985] 24 p3982 N71-38415
- ### DISSOLUTION
- #### U DISSOLUTION
- #### DISSOLVING
- Synergistic effect of detergent and antioxidant additives during colloidal dissolution
[AD-711152] 01 p0072 N71-10997
- Anode potential fluctuations observed in copper dissolution in different electrolytes
[JCL-19618] 10 p1566 N71-21343
- Zincium oxidation in carbon dioxide atmosphere above 500 C and corrosion prevention by copper alloying to prevent oxygen dissolving into metal
[CEA-CONF-1728] 16 p2611 N71-28294
- Processes designed for dechlorinating and dissolving of UO₂ and PuO₂ fuels clad with stainless steel or Zircaloy
[CEA-BIB-191] 16 p2637 N71-29819
- Model for predicting rate of dissolution of network polymers by chemical degradation
[AD-723985] 17 p2716 N71-30224
- Storage and handling of highly irradiated fast breeder reactor fuel in hybrid sodium organic coolant storage pool, and Sb-Cu liquid metal dissolution for dechlorinating
[EUR-4615-E] 24 p3956 N71-38223
- ### DISSYMMETRY
- #### U ASYMMETRY
- #### DISTANCE
- #### NT DEBYE LENGTH
- #### NT MISSILE RANGES
- #### NT RADAR RANGE
- #### NT RANGE AND RANGE RATE TRACKING
- Sonic boom pressure signature variations as function of distance to ground due to atmospheric refraction
[AD-723985] 16 p2355 N71-28380
- Noise exposure from supersonic transport operations and estimates of changes in noise levels
[AD-722346] 19 p3036 N71-31770
- Survey of domestic air passenger trip length including number of passengers and aircraft types
[AD-723985] 24 p4056 N71-38795
- ### DISTANCE MEASURING EQUIPMENT
- #### NT ALTIMETERS
- #### NT GEODIMETERS
- #### NT LASER RANGE FINDERS
- #### NT OPTICAL RANGE FINDERS
- #### NT RADIO ALTIMETERS
- #### NT RANGE FINDERS
- Capacitance distance gage for dimensional measurement with digital readout or direct computer processing
[Y-1783] 19 p3101 N71-32340

SUBJECT INDEX

Single station lightning distance measuring device based on ratio of magnetic field to electric field (NOAA-TR-ERL-195-APCL-16) 20 p3268 N71-33734

Evaluation of precision distance measuring equipment for space shuttle landing navigation (NASA-CR-115138) 22 p3617 N71-33775
Tail speed and distance measuring equipment concept of modified shield detector, electronic conversion circuitry, and cockpit readout instrumentation (FAA-NA-71-19) 23 p3779 N71-36797

SPACE PERCEPTION
U SPACE PERCEPTION

Feasibility of extractive fractional distillation as a separation method for volatile rare earth compounds (AD-712076) 03 p0331 N71-12364
Radiolabeled distillation system for reclaiming potable water from urine on prolonged space flight (AM-718945) 13 p3035 N71-24412
Distillation instrument measuring radiation balance as effective pyranometer 15 p2410 N71-27544

Countercurrent continuous gas chromatography distillation of nitrogen/liquid system (NLL-RTS-6323) 17 p2716 N71-30213
Various distillation techniques for producing ultra-pure water 20 p3285 N71-33764
Willard-Winter distillation and spectrophotometric determination of 2 to 7 micromole fluoride (FOA-C-4416-24) 22 p3351 N71-35291

DISTILLATION EQUIPMENT

Investigating feasibility of using liquid metal vacuum distillation to separate Po-210 from bismuth (DO-1222) 04 p0494 N71-13446
Design of isotopic fueled distillation and filtering system for potable water recovery from human waste during space simulation tests 10 p1505 N71-20957

Equipment for demonstrating low pressure distillation of molten fluoride mixtures from MSRE and experiment tests (ORNL-4454) 10 p1603 N71-21198

Copper-bearing alloy replacement with aluminum alloys in distillation desalination plants for sea water conversion (ORNL-TR-2413) 10 p1581 N71-21436

Utilization of solar radiation by solar still for converting salt and brackish water into potable water (NASA-CASB-XMS-04533) 11 p1773 N71-23086
Purification apparatus for vaporization and fractional distillation of liquids (NASA-CASB-XNP-08124) 15 p2416 N71-27184

DISTORTION

NT FLOW DISTORTION
NT SIGNAL DISTORTION
NT SURFACE DISTORTION

Elimination of phase distortion in filters using digital techniques (YDA-3514) 04 p0512 N71-13538

Diffractional field distortion and cross talk in simultaneous optical multibeam transmission of off-axis Gaussian beams (AD-718615) 12 p1967 N71-23904

Least squares method for describing irradiated fuel disk distortion (AEC-3688) 13 p2117 N71-24853

Diffraction efficiency and image distortion properties of volume transmission holograms 13 p2126 N71-25071

Fourier transformation for lattice statics method for distortion 17 p2818 N71-29942

Distortion effects in geometrical reconstruction of events in CERK 2m hydrogen bubble chamber (USIP-70-6) 17 p2800 N71-30098

Distorted wave Born approximation code adaptation for IBM 360/50 computer use (AMU-P-507) 22 p3634 N71-33904

MASTRAN program used to calculate gravity load distortions in 64-m antenna reflectors 22 p3683 N71-36262

MASTRAN-GAP program for analyzing antenna radiation patterns of reflectors distorted by gravity and thermal loads 22 p3683 N71-36263

Barometric coefficient equation and coefficient distortion for neutron component of cosmic rays 24 p4011 N71-38602

DISTORTED AMPLIFIERS

Leading effects due to input and output reactances of individual transistors in distributed amplifiers 08 p1170 N71-18891

Broadband distribution amplifier with complementary pair transistor output stages (NASA-CASB-NFO-10083) 14 p2234 N71-26415

DISTRIBUTION

Intensity distribution and convection in liquid phase during zone crystallization of lithium tetrachloride 10 p1574 N71-20876

Distribution of lead, copper, and zinc impurities in KCl single crystals grown from melt 10 p1632 N71-20878

Distributions and mean values of inelasticity coefficient K for neutral pions in lead and graphite determined by digital computer (ITF-5) 23 p3808 N71-37154

DISTRIBUTION (PROPERTY)

NT ANGULAR DISTRIBUTION

NT ANTENNA RADIATION PATTERNS

NT BOLTZMANN DISTRIBUTION

NT CHARGE DISTRIBUTION

NT CURRENT DISTRIBUTION

NT DIFFRACTION PATTERNS

NT ELECTRON DENSITY PROFILES

NT ELECTRON DISTRIBUTION

NT ENERGY DISTRIBUTION

NT FLOW DISTRIBUTION

NT FORCE DISTRIBUTION

NT FREQUENCY DISTRIBUTION

NT HOLE DISTRIBUTION (MECHANICS)

NT INTERFERENCE LIFT

NT ION DISTRIBUTION

NT LOAD DISTRIBUTION (FORCES)

NT MASS DISTRIBUTION

NT MOMENT DISTRIBUTION

NT NEUTRON DISTRIBUTION

NT PRESSURE DISTRIBUTION

NT RADIAL DISTRIBUTION

NT RADIATION DISTRIBUTION

NT SPATIAL DISTRIBUTION

NT SPECTRAL ENERGY DISTRIBUTION

NT STAR DISTRIBUTION

NT STRESS CONCENTRATION

NT TEMPERATURE DISTRIBUTION

NT VELOCITY DISTRIBUTION

NT VERTICAL DISTRIBUTION

Pattern of magnetic flux penetration in superconducting films (AD-703658) 03 p0444 N71-13223

Global distribution of upper atmospheric infrared emission layers from Cosmos 65 data analysis (NASA-TT-F-13600) 12 p1985 N71-23304

Orographic effects on precipitation distribution in Uppala (NLL-M-20094-5828-4F/1) 12 p1957 N71-24036

Strength distribution for coulomb mixing of isospin state 12 p1977 N71-24250

Swespot magnetometric data processing including magnetic field and radial velocity distributions (NLL-RTS-6194) 17 p2840 N71-29282

Users manual for computer programming of distribution networks of water supply systems 18 p2893 N71-30642

Air pollution sources, distribution, biological effects, and mathematical models (P-4571) 20 p3261 N71-33299

Monte Carlo and numerical integration methods of calculating distribution functions for electron transport in semiconductors 01 p0108 N71-10135

Nonlinear pulse system dynamics, control laws in saturating control system asymptotic stability, and continuous variable ordered sampling functions (JPRS-51622) 02 p0196 N71-11370

Properties of continuous logic functions which generalize out of a voting functions and threshold functions of binary variables to continuous variables 02 p0196 N71-11373

Developing alternative test for equality of variances and comparison with F-test by data sampling (AD-711801) 02 p0251 N71-11660

Technique for analysis and computerized data reduction of time of flight distributions of free jet expansions (AD-712572) 03 p0423 N71-12729

Distribution classes applied to age and block replacement with renewal theory implications (AD-712405) 03 p0383 N71-13219

Finding system of self-consistent equations for radial distribution function and excitation spectrum of many-body system using method of retarded Green function (INP-705) 04 p0576 N71-13698

Meteorological data processing, laser meteorology, and distribution functions 03 p0720 N71-15679

Electromagnetic simulation of plane and three dimensional fields by electric rotational field and variable magnetic ultrasonic frequency field (AD-714727) 06 p0903 N71-15977

Nozzle flow theory for determining distribution function on contourline of free jet expansion (AD-714155) 04 p0836 N71-16318

Evaluating multiple density correlation function of many particle system (NUS-2051) 08 p1237 N71-18416

Synthesis and identification of tapered distributed parameter systems by network approach (TR-70-38) 09 p1236 N71-18008

Synthesis and structure of MnPc alloy and interference, atomic distribution, and radial distribution functions for structural model (CALT-822-31) 10 p1580 N71-21394

DISTURBANCE THEORY

Perturbation expansion of Coulomb potential for determining pair distribution function in plasma 10 p1631 N71-21817

Periodic oscillations and momentum distribution functions for interacting fermions in magnetic field 10 p1636 N71-21849

Exact distributions of intermediate roots of class of random matrices 12 p1949 N71-23579

Effect of transverse momentum distribution in parton model for inelastic lepton-nucleon scattering (BU-1206-225) 13 p2140 N71-23501

Estimating continuous target distributions density (S-38-1971) 14 p2217 N71-26088

Solutions for multipoint distribution functions in homogeneous isotropic incompressible turbulent flow (SC-RR-70-812) 15 p2302 N71-27043

Compact analytic solution to distribution theory of nonsteady state model illustrated with biological data - age dependency in compartmental analysis (NASA-CR-115061) 16 p3620 N71-28002

Equilibrium distribution functions for electrons in ionospheric plasma calculated for energy interval of 0 to 15 eV utilizing data collected in pulse probe experiment (NASA-CR-119031) 16 p2588 N71-28508

Methods of generating random distribution functions, and comparison of their relative merits with those of Dirichlet 16 p2623 N71-28908

Pair distribution function in classical statistical mechanics 18 p2906 N71-31239

Asymptotic method for statistical failure rate function estimators (PB-197482) 18 p2946 N71-31275

Weak convergence theorem for order statistics from strong mixing processes (AD-722833) 18 p2947 N71-31313

Two dimensional periodogram for estimating spectral density of real, homogeneous, random field over regular lattice on plane 18 p2947 N71-31380

Characteristics of far field power distribution for circular aperture with Gaussian illumination (AD-722433) 19 p1108 N71-32093

Formalism for particle density distribution in quantum chemistry 20 p2229 N71-33386

Tables of distribution functions for analysis of intensity distribution patterns from Fabry-Perot interferometer (NRC-TT-1446) 20 p2373 N71-33418

Calculation of light scattering from aerosols for two assumed particle distribution functions (LA-4641) 20 p2367 N71-33540

Two particle microscopic distribution function for studying extended collision model in kinetic theory of gases 20 p2353 N71-33713

Reliability testing of aerospace problems including sampling, distribution functions, and accelerated life tests (NASA-TM-X-67877) 21 p3432 N71-34415

Effect of solar activity on distribution curves for natural relaxation oscillations (NLL-M-20596-5828-4F/1) 21 p3505 N71-34970

Two particle distributions in dual resonance model (TUEP-71-29) 22 p3642 N71-35963

Necessary and sufficient conditions for rapid decay of correlations for many body systems having probability distributions obeying master equation (AD-726762) 22 p3648 N71-36013

Nonlinear echo phenomena in plasma and distribution function oscillations (ITF-70-56) 23 p3828 N71-37306

DISTRIBUTION MOMENTS
NT MEAN
NT STANDARD DEVIATION
NT VARIANCE (STATISTICAL)

Distribution moments and Monte Carlo calculation of high energy gamma ray absorption in concrete, iron, and lead slabs 14 p2304 N71-26277

Patched bed interparticle porosity calculation from flowing aerosol breakthrough distribution moments 17 p2797 N71-29844

DISTRICT OF COLUMBIA
District of Columbia air quality display model for computing seasonal concentration estimates (PB-189144) 02 p0151 N71-11872

Air pollution and zoning index for District of Columbia, 1968 (PB-194763) 06 p0855 N71-16636

Congressional hearings on Boeing 727 use of Washington National Airport 07 p1084 N71-17097

Feasibility of rail access to Friendship International Airport from Wash., D.C. and Baltimore, Md. (PB-186033) 06 p1364 N71-18434

Four lead use and hydrologic practices and physical and chemical pollution of Anacostia river valley (NASA-TM-X-65549) 15 p2485 N71-27430

DISTURBANCE THEORY
U PERTURBATION THEORY

DISULFIDES

NT CARBON DISULFIDE

Electron interaction ferromagnetics in transition metal disulfide systems
[NUB-2039] 07 p1048 N71-17516

Lubrication properties of disulfides and diselenides of transition metals at high temperatures in air, nitrogen, and argon media
[AD-719746] 13 p2100 N71-24879

Test results of using synthesized dialkylbenzyl disulfides as oil additives
[AD-720942] 15 p2431 N71-27401

DITCHING [EXCAVATION]

U EXCAVATION

DITCHING [LANDING]

Ditching of DHC-6 turboprop aircraft in Long Island Sound near Waterford, Connecticut on February 10, 1970
[NTSB-AAR-71-1] 10 p1493 N71-21607

Aircraft accident report of DC-9 civilian aircraft ditching near St. Croix, Virgin Islands, May 1970 following fuel exhaustion
[NTSB-AAR-71-4] 17 p2705 N71-30029

DITHIOALS

U THIOLS

DIURETICS

Decreased diuresis in response to thiazide diuretic at simulated altitude
[AD-713609] 05 p0635 N71-14702

Nonlinear relationship in lactic dehydrogenase and leucine amino peptidase enzyme activities in urine related to increased and decreased diuresis
[NASA-TT-F-13557] 12 p1863 N71-23388

DIURETICS

Decreased diuresis in response to thiazide diuretic at simulated altitude
[AD-713609] 05 p0635 N71-14702

DURNAL RHYTHMS

U CIRCADIAN RHYTHMS

DURNAL VARIATIONS

Daily summaries of vertical echo sounding of upper atmosphere over Freiburg, Germany during July 1970
[REPT-289-F] 01 p0045 N71-10018

Airborne filter colorimeter measurements of atmospheric diurnal glow brightness
01 p0049 N71-10587

Diurnal cycles of high temperature during equipment performance tests in desert
[AD-71366] 01 p0080 N71-10843

Tidal motions in E region as source of daily variation of geomagnetic field
[AD-71782] 01 p0051 N71-10849

Measuring diurnal variations and probability distributions of total polarization rotation at transverse region of ionosphere using synchronous satellites
[AD-711403] 01 p0026 N71-10951

Film measurements of zenith intensities for individual components of airglow
[NASA-TT-F-13396] 02 p0208 N71-11393

Diurnal variation of Martian exospheric temperature
[ISAS-456-VOL-35-NO-12] 02 p0296 N71-11933

Diurnal variation of neutral temperature profile at Areco from incoherent scattering measurements and its relevance to 1400 hour density maximum
[NASA-CR-111416] 02 p0215 N71-11964

Tables for cosmic ray neutron and muon monitor diurnal vectors
[AEC-3651] 03 p0450 N71-12945

Tables for cosmic ray neutron and muon monitor diurnal vectors
[AEC-3608] 03 p0450 N71-12946

Diurnal variation and tidal dependence of field strength on radio links in German Night
[REPT-13] 06 p0490 N71-13488

Daily ground and 850 mb maps for Northern Hemisphere for period 1 Jan. to 31 Mar. 1970
04 p0542 N71-14275

Alouette 1 satellite electron density data and diurnal variation of Greenland aurora
04 p0615 N71-14298

Cosmic ray modulation during Forbush decreases in 1968 - 1969
[AD-713226] 05 p0764 N71-14563

Seasonal anomaly of F-region explained in terms of composition changes in lower atmosphere
[NASA-TM-X-65410] 05 p0669 N71-14804

Daily summaries for vertical echo sounding of upper atmosphere over Freiburg, Germany during Oct. 1970
[REPT-292-F] 05 p0670 N71-14814

Daily summaries for vertical echo sounding of upper atmosphere over Freiburg, Germany, for September 1970
[REPT-291-F] 05 p0672 N71-14862

Electromagnetic wave propagation characteristics for North West Cape, Australia
[AD-713596] 05 p0644 N71-14903

Aerial infrared imagery of geological region in southern California taken during pre-dawn and post-sunrise hours
06 p0643 N71-16136

Correlations between diurnal indices of cerebral and systemic circulation
08 p1153 N71-19069

Diurnal variations of atomic and molecular oxygen concentration in 65 to 200 km altitude range
08 p1155 N71-19129

Determining cycle in air pollution in urban environment by measuring solar radiation
[REPT-27] 05 p1286 N71-19297

Coordinated rocket, satellite, aircraft, and ground measurement program studying physical chemistry of ionospheric D region - FCA 69
[AD-716385] 09 p1483 N71-20892

Effects of orientation, lunation, and location on performance of lunar radiator - design studies
[NASA-TM-X-1846] 09 p1483 N71-20892

Polar and lower latitude ionospheric currents and magnetic field variations
[GRI-NT-81] 10 p1547 N71-20899

Underground observations of diurnal variations of solar cosmic rays since 1958 in Bolivia and New Mexico
10 p1640 N71-21546

Observations of diurnal sidereal variations of cosmic radiations by underground moon telescopes
10 p1641 N71-21547

Ionospheric data from vertical echo soundings over Freiburg, Germany during November, 1970
[REPT-293-F] 10 p1533 N71-21670

Hourly ionospheric propagation data - Freiburg, Dec. 1970
[REPT-294-F] 10 p1536 N71-21834

Components of terrestrial magnetic field with graphs of diurnal variations
11 p1745 N71-21932

Hourly ionospheric propagation data tables, Salisbury - Feb. 1970
[SAD-1970/2/5] 11 p1746 N71-22047

Ionospheric absorption measurement, snapshot observations, and short wave fadeout reported from optical tracking stations in Greece (Athens) - tables
11 p1823 N71-22502

Objectives of ISIS-B including measurement of fluctuations in upper atmosphere electron density, radio and cosmic emission studies, and measurements of ionospheric energetic particles
[NASA-NEWS-RELEASE-71-41] 11 p1827 N71-22537

Diurnal variations of large scale current turbulence in Arctic Basin and seas
11 p1752 N71-22805

Possible effect of deformation forces on diurnal state of baric field and subsequently for short range weather forecasting
11 p1756 N71-22836

Propagation model for diurnal amplitude and phase variations of very low frequency transmission path
11 p1705 N71-22907

Diurnal frequency variations in oblique high frequency ionospheric radio signal
11 p1711 N71-22939

Auroral ionization longitudinal drift rate recorded along auroral zone
12 p1909 N71-23562

Polar diurnal variations of proton belts and precipitation detected by ESRO 1 satellites
12 p1910 N71-23571

Cosmic ray anisotropy in interplanetary space reflected in solar diurnal variation
12 p1993 N71-23893

Statistical data of diurnal temperature variations of Kofu from 1956 to 1964
[NLL-M-20311-5828.4F] 12 p1957 N71-24002

Radar echo returns from meteors observed in USSR for IGY-IGC 1957 to 1959 including diurnal and annual variations
12 p1998 N71-24290

Continuity equation solution for diurnal variations in oxygen concentration between 65 and 200 km altitude
[AD-719843] 13 p2074 N71-25078

Numerical integration of steady state heat conduction equations representing diurnal variations in upper atmosphere
[NASA-TM-X-65522] 13 p2186 N71-25089

Dynamic diffusion concept for calculating diurnal thermospheric temperature characteristics
13 p2100 N71-25265

Diurnal variations of atomic hydrogen in thermosphere derived from Explorer 32 data and correlated with solar cycle, solar rotation, and earth rotation
[NASA-TM-X-65544] 14 p2246 N71-25747

Solar wind, meteoric volatilization, and internal degassing contributing to lunar rarified atmosphere, and transient contributions produced by rocket gases during lunar missions
14 p2335 N71-25796

Horizontal neutral air winds arising from diurnal variation of atmospheric pressure during seasonal and solar cycle changes
[AD-720247] 14 p2249 N71-26268

Diurnal, directional, and latitudinal effects of meteor influx rates determined from airborne observations of meteors at high latitudes
[NASA-TN-D-6303] 15 p2517 N71-26969

Measurement results of diurnal variation of radiation and skylight polarization
15 p2402 N71-27528

Analysis of cosmic thunderstorm data to determine universal time variations of ocean area effects
16 p3624 N71-30028

Rocket-borne temperature ozone sensor measurements in mesosphere and stratosphere with analysis of diurnal variations
16 p3504 N71-30046

Relating ionospheric electron content to electrospheric propagation effects along transionospheric paths and measurements of diurnal variations of electron content
[AD-721509] 16 p2309 N71-30050

Small rockets with proton spectrometer and Faraday rotation experiment to measure diurnal proton spectrum and electron density variations during solar proton events in polar cap studies
[COM-71-50002] 16 p2309 N71-30050

Ionospheric propagation data for E and F regions, Bangkok - Aug. 1970
[AD-720326] 16 p2589 N71-30084

Ionospheric propagation data for E and F regions, Bangkok - Sept. 1970
[AD-720327] 16 p2589 N71-30084

Relationships between atmospheric electricity and meteorological parameters, noting vertical air currents and ionization
17 p2776 N71-30085

Properties of low energy particle impacts in pole domains at dawn and daybreak hours
[NASA-TM-X-65593] 17 p2745 N71-30086

Airborne photography of polar auroral band during magnetic disturbances
17 p2746 N71-30086

Auroral variations during maximum and minimum cycles of solar activity
17 p2747 N71-30087

Auroral absorption types and seasonal patterns as determined by ionometer measurements
17 p2748 N71-30087

Active region MacMath no. 8905 producing 16 distinct electron events associated with solar flares during passage across solar disk
[NASA-TM-X-65613] 18 p3007 N71-30011

Studying diurnal oscillations of wind in planetary boundary layer using theoretical model
18 p2953 N71-31007

Northern Hemisphere map of ionospheric F-layer propagation and electron density diurnal variations with fluctuation zones for magnetically quiet and disturbed days
[NASA-TT-F-13821] 18 p2916 N71-31007

Quiet-time electron increases - measure of conditions in outer solar system
[NASA-TM-X-65623] 18 p3006 N71-31010

Daily summaries for vertical echo sounding of upper atmosphere over Freiburg, Germany during January, 1971
[REPT-293-F] 18 p2920 N71-31010

Daily summaries for vertical echo sounding of upper atmosphere over Freiburg, Germany during March, 1971
[REPT-297-F] 18 p2920 N71-31010

Daily summaries for vertical echo sounding of upper atmosphere over Freiburg, Germany during February, 1971
[REPT-296-F] 18 p2920 N71-31010

Beta particle observations between inner edge of plasma sheet to plasmapause in midnight arc magnetosphere
[NASA-TM-X-65640] 19 p3094 N71-32005

Air pollution in relation to certain atmospheric and meteorological conditions and methods employed in survey and analysis of air pollutants
[PB-198527] 19 p3096 N71-32005

Diurnal forecasting of radio transmission via troposphere using meteorological parameters
[REPT-4/70] 20 p3231 N71-32007

Thermospheric models accounting for diurnal variations of temperature and density during equinox
[D-91] 20 p3234 N71-32007

Isoline frequency charts of diurnal variation of ionospheric thunderstorm activity over US
[AD-724645] 20 p3236 N71-32010

Tests on radiosonde humidity error resulting from solar heating in low latitude regions
[NOAA-TR-ERL-194-AOML-4] 20 p3273 N71-32010

Daily summaries for vertical echo sounding of upper atmosphere over Freiburg, Germany during April, 1971
[REPT-298-F] 20 p3266 N71-32009

Seasonal dependence of solar cycle variation of EUV solar flux from calculation of electron production rates during winter for different values of solar activity
[RSD-55] 20 p3341 N71-32010

Diurnal variations in spectra of solar hydroxyl emission in relation to helium emission intensity
[NRC-TT-1457] 21 p3418 N71-34010

Surface layer stability parameter distribution over USSR and over time
[NLL-M-20714-5828.4F] 21 p3423 N71-34010

Radio wave propagation, diurnal variations, and frequency and phase modulation
[AD-726528] 22 p3354 N71-32010

SUBJECT INDEX

Durnal temperature variations in middle ionosphere and electron density in E, E-F, and F1 regions
22 p3675 N71-34331

Durnal and unimodal variations of upper atmosphere density determined from Cosmo satellite drag data
23 p3751 N71-34744

Hourly, durnal, and annual data on geomagnetic declination and intensity, Hartland, England - 1962, 1963, and 1964
23 p3753 N71-34760

Durnal and annual variations of scintillation measured during Intelsat 2 and ATS 3 transmission
24 p3912 N71-37885

Photometric measurements of diurnal variations in brightness of north sky and horizon sky and sea during daylight
24 p3916 N71-37921

DIVERGENCE
17 **MAGNETIC CHARGE DENSITY**
Divergence, vertical velocity, and energy conversion in west Mediterranean during cyclone development of 24 Oct. 1964
(TT-49-51019) 01 p0079 N71-10631

Flux and divergence of four low mass ratio hydrofoil model configurations
(AD-715891) 14 p2238 N71-25603

Quantum electrodynamics and field theories with bounded and temperate interaction examples without divergences
(TFTU-1370) 14 p2308 N71-26445

Velocity divergence computation for Barbados Oceanographic and Meteorological Experiment from flights at different heights
(NOAA-TM-ERL-BOMAP-5) 18 p2954 N71-31225

Partial elimination of infrared divergences in scalar charged field model with self-action in two-dimensional space-time and degenerated vacuum
(JNR-52-5760) 23 p3807 N71-37142

DIVERSITY
Ternative stellarator configuration with toroidal field created by helical current and application to fusion reactor diverter problems
(CRA-CONF-1664) 09 p1365 N71-30095

DIVING (MATHEMATICS)
Stochastic matrix method for linearization of analytical handles and in series convergence
24 p3948 N71-38167

DIVING (UNDERWATER)
Experimental dives for ADS-4 decompression schedules
(AD-711842) 02 p0154 N71-11093

Theoretical models related to ERL alternative to naval decompression concepts
(AD-711809) 02 p0155 N71-11095

Investigating causes of polycythemia and decrease hemoglobin in underwater workers
(NASA-TT-F-13622) 04 p477 N71-13668

Rescue ventilation rates determined for Mark 5 diving helmet as part of low pressure underwater breathing apparatus
(AD-713395) 05 p0637 N71-14705

Diving instrument development and sealab underwater research program review
07 p1020 N71-17492

Diving techniques and equipment for simulating neutral buoyancy in space environment testing
09 p1367 N71-20240

Physiological measurements on divers in underwater drilling facility to determine work-rest cycle characteristics
(JPRS-52697) 10 p1500 N71-21472

Hydrostatic factors affecting diving capabilities of dolphins
11 p1681 N71-22210

Structure and innervation of Black Sea dolphin skin and protection provided internal organs and tissues during deep dives from high hydrostatic pressure
11 p1682 N71-22213

Stationary excursion diving operations for testing extrapolated tables for repetitive no-decompression ascents from helium-oxygen atmospheres
(AD-719077) 12 p1862 N71-23352

Regulation of vocal intensity at low fundamental frequencies with voice communication of Navy divers
(AD-718057) 12 p1874 N71-23390

Effect of immersion on exchange of oxygen in lung at simulated depth of 5 feet of sea water using hyperbaric chamber
(AD-719309) 13 p2003 N71-24482

Human reactions to psychological stresses of confined environments using Teklon project aquanauts
(AD-721364) 16 p2534 N71-28550

Carbon monoxide purity standards for gas breathing apparatus of divers and toxic hazards under controlled breathing atmospheres
(AD-721686) 17 p2707 N71-29358

Retropulsion of animal tolerances of air contaminants to human tolerances for diver breathing under hyperbaric conditions
(AD-721681) 17 p2707 N71-29359

Speech intelligibility of divers as function of high ambient pressures and helium-oxygen breathing atmosphere
(AD-723771) 17 p2720 N71-29658

Improved respiratory magnetometer with high reliability and ease of operation in laboratory and diving studies
(AD-723661) 18 p2922 N71-30711

Repetitive excursion dives from saturated depths using helium-oxygen mixtures to eliminate decompression sickness
(AD-723173) 19 p3046 N71-32632

No-decompression repetitive excursion dive format testing at 150 and 200 ft using helium-oxygen mixtures
(AD-723171) 19 p3046 N71-32770

Revised tables for conversion of water depth and partial pressure combination into appropriate oxygen percentages for diver decompression
(AD-724282) 20 p3226 N71-33125

DIME-A SATELLITE
U EXPLORER 31 SATELLITE
DNA
U DBOXYRIBONUCLEIC ACID
DO-31 AIRCRAFT
Flight duration of short takeoff aircraft and Do-31 aircraft, and results using cockpit simulator with 6 degrees of freedom for DO-31
19 p3074 N71-31956

DOCKING
U SPACECRAFT DOCKING
DOCUMENT STORAGE
Describing device for flagging punched business cards
(NASA-CASE-XLA-02705) 05 p0818 N71-15908

NASA Regional Documentation Center service and file description
(NASA-CR-117175) 09 p1355 N71-30120

Operation and equipment of remote on-line documentation retrieval system
(AD-720900) 15 p2527 N71-27868

Synoptic meteorological reference file for weather forecasting at landing field
(AD-723676) 19 p3127 N71-31937

Catalog of reprints of scientific papers in Pauli collection with author index and cross references
(CERN-R12-9) 21 p3473 N71-34731

DOCUMENTATION
OENL decentralized Nuclear Science Abstracts preparation, and cost and time comparison with centralized preparation
(PB-190501) 02 p0275 N71-11910

Compilation of major recommendations from five studies relating to national scientific and technical information systems
(PB-193545) 04 p0622 N71-14197

Bibliography on geophysical publications
05 p0681 N71-15672

Organization, methods, and effectiveness of specialized documentation center
09 p1347 N71-19529

Development and operational planning documentation for reusable space tug designs and missions
(NASA-CR-114940) 10 p1649 N71-21457

Historical development of meteorology - Vol. 1
(TT-49-55186) 11 p1709 N71-22263

EURATOM automatic documentation system, noting structure of index, information retrieval strategies, and performance evaluation
14 p2223 N71-25995

Operations research for West German governmental information retrieval system, noting law application and decision making
14 p2223 N71-25997

Documentation and equipment specifications for German scientific satellite programs
15 p2526 N71-27151

Compilation of nuclear cross section measurements
(LA-4632) 21 p3478 N71-34769

Documentation of Congressional Subcommittee testimony regarding Navy oil sludge pollution off Florida coast
21 p3533 N71-35178

Management, standards, and maintenance of NAS-TRAN documentation reviewed with emphasis on specifications in style and format
22 p3686 N71-36283

DOCUMENTS
NT ABSTRACTS
NT BIBLIOGRAPHIES
NT CATALOGS (PUBLICATIONS)
NT ENGINEERING DRAWINGS
NT HANDBOOKS
NT INSTALLATION MANUALS
NT MANUALS
NT PAPERS
NT PERIODICALS
NT PROCEEDINGS
NT TEXTBOOKS
NT TEXTS
Annotated reference bibliography on aeronautical engineering documents
(NASA-SF-7037/01) 12 p1852 N71-24172

Cross-reference directory of reports of Human Engineering Laboratories 1953 to 1970
19 p3047 N71-31617

Computer applications in chemical information systems and journal publication
19 p3194 N71-31976

Basic secondary publications on chemistry and chemical engineering promoting international cooperation in information dissemination
19 p3194 N71-31981

Nuclearchemical publication on breeder reactor developments in US
22 p3422 N71-35003

DODGE SATELLITE
Gravity gradient stabilization and performance of DODGE satellite
(AD-716772) 10 p1448 N71-20928

DOGS
Respiratory heat exchange in trachea of dogs
(AD-711844) 02 p0153 N71-11006

Blood pressure changes in heart cavities and large vessels in dogs during acceleration in various directions
02 p0159 N71-11477

Prolonged gamma irradiation of dogs
(AD-714407) 06 p0800 N71-16092

Investigating long term effects of proton irradiation on renal pathologic anatomy of dogs
06 p1130 N71-16097

Proton irradiation of dogs to determine value of shielding body organs
08 p1153 N71-19556

Effects of positive O₂ accumulation on blood oxygen saturation and pleural pressure relations in dogs breathing air and liquid fluorocarbons in whole body water immersion respirator
09 p1334 N71-20358

Radiation absorption and radiobiology of dogs
(UCD-472-117) 09 p1338 N71-20546

Hypoxemia effects on erythrocyte system of splenectomized dogs
16 p2344 N71-32266

Effects of chronic and repeated gamma radiation on morphological structure of peripheral blood and bone marrow in dogs following exposure for one year
16 p2546 N71-28481

Effect of anisotropy and edema in trisphosphate toward increasing central body radioresistance and inactivation of postulated recovery in dogs
16 p2546 N71-28485

Analysis of uteroplacental excretion in dogs under influence of simulated flight stress conditions
16 p2547 N71-38495

Toxicology of dogs after inhaling plutonium-239 compounds
(BNWL-SA-3469) 17 p2707 N71-29417

Long term biological and physiological effects of plutonium compound inhalation in dogs and plutonium translocation in respiratory system
17 p2709 N71-29868

Computerized simulation of long term physiological effects of plutonium oxide inhalation on dog respiratory system including tissue, blood, and excretion data
17 p2709 N71-29869

Abdominal and head shielding effects on blood serum protein metabolism of gamma irradiated dogs
20 p2321 N71-33457

Hypoxia affecting circulatory responses in dogs, such as cardiac output, left ventricular output, and stroke volume
(NASA-CR-121665) 21 p3380 N71-34851

DOLOMITES (MINERAL)
X ray diffraction analyses on quartz, calcite, and dolomite
(UCRL-50921) 07 p1084 N71-17038

Elastic wave anisotropy in marble, dolomite, and limestone crystals based on ultrasonic tests and X ray analysis
(NASA-TT-F-13673) 14 p2585 N71-28280

DOLPHINS
Using underwater photography to demonstrate formation of mobile roughness in skin of humans and dolphins due to external hydrodynamic forces
(JPRS-51614) 01 p0014 N71-10952

Echolocation capabilities of dolphins
(JPRS-51511) 03 p0323 N71-12569

Visual and acoustic discrimination of dolphins under conditions of good and poor visibility
(JPRS-52444) 06 p1153 N71-19823

Intelligence, speed, and environmental ability of dolphins
(JPRS-52395) 08 p1156 N71-19123

Hydrodynamics, marine biology, bioacoustics, dolphins, sharks, porpoises, traveling waves, fluid flow, viscous fluids, nervous system, skin structure, swimming
(JPRS-52465) 11 p1087 N71-22281

Resonance characteristics of dolphin swimming and locomotion verified by underwater photography
11 p1087 N71-22286

Physiological investigation of Grays porpoise on locomotion of dolphins under turbulent flow conditions
11 p1087 N71-22287

Maneuverability and controllability of dolphins compared to performance characteristics of manmade underwater vehicles
11 p1087 N71-22289

Hydrostatic factors affecting diving capabilities of dolphins
11 p1087 N71-22290

- Radio telemetry technique for determining flow conditions in boundary layer of autonomous self-propelled models and individual aquatic animals 11 p1699 N71-22211
- Morphological examination of nervous system and muscular functions in dolphin tail during locomotion 11 p1682 N71-22212
- Structure and innervation of Black Sea dolphin skin and protection provided internal organs and tissues during deep dives from high hydrostatic pressure 11 p1682 N71-22213
- Morphological investigation of neural structures of frontal cushion of dolphins 11 p1682 N71-22214
- Microthermistor measurements of temperature distribution on body surface of dolphins 11 p1682 N71-22216
- Underwater acoustic measurements of dolphin and harbor porpoise activity under various situations and conditions 11 p1682 N71-22217
- Echolocation as bionic communication systems for bats and dolphins 11 p1693 N71-23065
- DOMAIN WALL**
- Determination of mechanical properties of ceramic materials used in piezoelectric transducer [AD-717964] 12 p1946 N71-24094
- DOMAINS**
- NT MAGNETIC DOMAINS**
- Development of general finite difference approximation for general domain 02 p0250 N71-11172
- Frequency domain criteria for system stability modeled by certain partial differential equations [NASA-TM-X-66514] 04 p0538 N71-14165
- Attraction domains for nonequilibrium oscillations in weakly nonlinear dynamical systems 11 p1796 N71-21884
- Constructing Lyapunov functions for nonlinear autonomous continuous time systems 11 p1788 N71-23013
- Effect of acousto-electric domains on transmission of monochromatic light through cadmium sulfide for various crystallographic orientations 18 p2996 N71-31100
- Effect of impurities on properties of slowly propagating domains in gallium arsenide 19 p3066 N71-32361
- Direct solution to finite difference approximation of Poisson equations on irregular regions [LA-4553] 23 p3782 N71-36952
- DOMES [STRUCTURAL FORMS]**
- NT RADOMES**
- Telescope building and dome design 24 p3923 N71-37984
- DONNELL EQUATIONS**
- Derivation of theory for unsymmetric deformation of nonhomogeneous, anisotropic, elastic cylindrical shells - Part I [REF-69-5-PT-1] 12 p2008 N71-24294
- DONOR MATERIALS**
- Simultaneous donor and acceptor concentration determination in n-type semiconductors using Hall effect measurements [ONERA-NT02/1670] 02 p0285 N71-11856
- Discrepancies in hyperfine constants of shallow donor materials in silicon [UR-3389-21] 03 p0435 N71-13000
- First-order radiative transition rate electron transfer from neutral donors to neutral acceptors in silicon at low temperatures 09 p1432 N71-19927
- Infrared spectra of implanted high energy nitrogen ionization energy in silicon 13 p2154 N71-25562
- Electronic transitions in infrared absorption spectrum of aluminum antimonide 13 p2155 N71-25568
- Kinetics of radiative recombination processes between donor and acceptor impurities in silicon 13 p2143 N71-25581
- Analysis of interaction between lithium and residual donor in indium antimonide 19 p3117 N71-32548
- DOORS**
- Design and specifications of emergency escape system for spacecraft structures [NASA-CASE-MSC-12086-1] 03 p0328 N71-12345
- Performance tests on liquid explosive emergency exit for civil aircraft [FAA-RD-71-33] 18 p2872 N71-31064
- DOPING [ADDITIONS]**
- U ADDITIVES**
- DOPPLER EFFECT**
- NT DOPPLER-FIZEAU EFFECT**
- Simultaneous measurement of dispersive Doppler shift, Faraday rotation, and ionospheric refraction [AD-711944] 02 p0205 N71-11147
- Physical concepts in diffraction of light by ultrasonic waves and specific form of laser acoustic delay lines [AD-712975] 03 p0418 N71-13047

- Determining local Doppler displacements of solar spectra using lines of different mean depth in Doppler comparator 03 p0451 N71-13172
- X band- and K band-Doppler spectra measurements in microwave backscattering from wind waves 04 p0493 N71-13719
- Three-dimensional laser Doppler velocimeter for measuring local mean and fluctuating gas velocities [NASA-CR-102948] 04 p0524 N71-14048
- Ionospheric electron content measurements using Explorer 22 data on Faraday and differential Doppler effects 06 p0814 N71-16231
- Uranium 238 Doppler effect in fast thermal reactor assemblies [CEA-R-4035] 07 p0662 N71-17246
- Ionospheric electron density determination over Finland using Explorer 22 signals and Faraday/Doppler method [BMW-FB-W-70-50] 08 p1189 N71-18592
- Doppler ion temperature measurements in rotating high frequency plasma pinch field [LRP-4070] 08 p1189 N71-18610
- Describing laser Doppler velocimeter for measuring mean velocity and turbulence of fluid flow [NASA-CASE-MFS-30386] 08 p1233 N71-19212
- Doppler shift considerations in naval satellite communication systems employing synchronous satellites [AD-716745] 10 p1517 N71-20693
- Determination of ion temperatures from half-width of Doppler-broadened spectral lines in plasma columns with small rotational velocity [SC-T-71-3001] 10 p1630 N71-21227
- Doppler line superradiant emission from uniform spherical gaseous medium [AD-717744] 11 p1805 N71-22368
- Analysis and measurement of characteristics of wide-band frequency trackers and design and fabrication of all angle laser Doppler velocimeter [NASA-CR-103088] 11 p1775 N71-22407
- Basic parameters for application of laser Doppler velocimeter, cross beam technique in three modes of operation obtained by computer programming [NASA-TN-D-4125] 11 p1775 N71-22615
- Ray tracing techniques for examination of refractivity profile sensitivity in tropospheric range and Doppler effects on profile shape 11 p1751 N71-22772
- Examination of deep space Doppler data for terrestrial media contamination 11 p1703 N71-22773
- Airborne Doppler shift measurements on lower ionospheric instability 11 p1707 N71-22921
- Doppler shift recordings of ionospheric disturbances 11 p1709 N71-22929
- High frequency Doppler sounding at vertical incidence of atmospheric disturbances 11 p1709 N71-22930
- Ray tracing method for correlating Doppler and Faraday differential effects in determining ionospheric disturbances by artificial satellite 11 p1712 N71-22944
- Applications of laser Doppler techniques for measurements in large flow systems [AD-718818] 12 p1932 N71-23324
- Antenna response patterns, Doppler spectra, and amplitude distributions of transhorizon microwave scatter propagation 12 p1875 N71-23453
- Upwind/downwind dependence of Doppler spectra of radar sea echo using coherent radar data [AD-719333] 13 p2045 N71-24713
- Radio direction finding technique for application to matched filter Doppler direction finding system [AD-720699] 14 p2217 N71-26104
- Measurements of thorium Doppler coefficient on lattices 1 and 2 of HTLTK [GAMM-10231] 15 p2444 N71-26994
- Neutron cross section calculation techniques including review of data and nuclear reactions, Breit-Wigner and R matrix theories, and Doppler effects and shielding of resonances 15 p2469 N71-27348
- Absorptivity and emissivity hydrodynamic equations for suprathermal electrons gyrating in magnetized plasma including Doppler effect with solar radio emission examples [AD-721337] 16 p2662 N71-28966
- Judgment of effects of Doppler shifts on perceived noisiness of aircraft made by subjects in anechoic chamber [NASA-CR-1779] 17 p2709 N71-29900
- Wing tip vortex test demonstrating use of Laser Doppler Velocimeter system for measuring gas velocities with high spatial and temporal resolution [NASA-CR-119004] 17 p2737 N71-30278
- Doppler reactivity measurement and analysis for uranium 238, tantalum, niobium, tungsten, dysprosium oxide, and samarium oxide 18 p2957 N71-30443

- Experiment for measuring periodic relativistic Doppler shift using quartz crystal oscillator [NASA-CR-119378] 18 p3015 N71-31178
- Gravity field measurement by satellite to satellite Doppler tracking, critical configurations for fundamental range networks, and improvement of triangulation system [NASA-CR-119356] 18 p3017 N71-31128
- Angle and Doppler measurements of specular and scattered components of over-the-horizon propagated microwaves [AD-722088] 18 p2891 N71-31340
- High eccentricity orbit for satellite measurements of periodic relativistic Doppler shifts [AD-716773] 19 p3176 N71-32075
- Computation of atmospheric density variations at high altitude from Doppler observations made on polar satellites [AD-724638] 20 p3256 N71-32306
- Velocity fields in magnetically disturbed regions of H alpha chromosphere measured by Doppler and Zeeman movie pairs 20 p3342 N71-33007
- Symmetrical method of optical heterodyning of Doppler shifted scattered laser radiation for velocity measurement with minimal spectral broadening and high signal to noise ratio [NASA-CR-121072] 21 p3426 N71-34376
- Errors in Doppler geodesical measurements from coherent frequencies for correcting ionospheric refraction 22 p3680 N71-36301
- Relativistic effects and optimal satellite inclination for Doppler determination of geodesic coordinates 22 p3480 N71-36302
- Robbins-Monro stochastic approximation algorithm for Doppler frequency estimation of radar echoes 23 p3727 N71-36679
- Optical response of laser-Doppler sensing instrument in measurements of high velocity particle-in-training flows 23 p3767 N71-36832
- Pile oscillator technique for measuring Doppler effect with heated small samples in critical zero energy assemblies for fast thermal reactors [KFK-1350] 23 p3800 N71-37095
- Relativistic Doppler effect and group velocity in homogeneous nonlinear and inhomogeneous plasmas [DEMO-71/65] 23 p3824 N71-37275
- Using laser Doppler anemometry for velocity measurements in two phase flow 24 p3904 N71-37828
- Ionospheric total electron content determined from satellite transmission Doppler shift and compared with Faraday effect 24 p3912 N71-37857
- Receiver for direct measurement of differential Doppler frequency in satellite transmission 24 p3913 N71-37894
- Second-order phase path difference calculations for ionospheric Faraday and Doppler effect 24 p3914 N71-37908
- Beacon Explorer A signal scintillation in auroral zone, measured with Faraday and Doppler effect 24 p3915 N71-37916
- Doppler position finding error analysis using GEOS 2 satellite data 24 p3915 N71-37917
- DOPPLER NAVIGATION**
- Chandler wobble determinations by US Navy Doppler satellite observations [AD-712658] 02 p0220 N71-12141
- Sequential estimation with process noise for processing DSN tracking data during planetary orbit missions and Doppler determinations of polar orbits using satellites 07 p0993 N71-17615
- Development and evaluation of double sided Doppler VOR system with high level reference modulation and improved receiver compatibility [FAA-NA-71-36] 14 p2290 N71-25085
- Error analysis of integrated inertial/Doppler satellite navigation system with continuous and multiple satellite coverage 14 p2290 N71-26101
- Random error reduction for Doppler observation made during satellite pass by doubling measurement interval [AD-721070] 15 p2383 N71-27771
- Accuracy of Doppler determinations of satellite observing station positions [AD-722172] 17 p2846 N71-29283
- Optimized Doppler tracking system for geodesic satellite ranging 19 p3090 N71-31074
- Techniques for aerial time-lapse cloud photographic analysis, Doppler navigation data analysis, and photogrammetric data acquisition 23 p3767 N71-36909
- DOPPLER RADAR**
- Performance characteristics of Bendix type BNA-13 airborne Doppler radar system [FAA-NA-70-50] 01 p0822 N71-10794

SUBJECT INDEX

Design, fabrication, and evaluation of high reliability radar component 02 p0180 N71-11264 [AD-711354]
 Unified theory for design of optimum coherent digital communication systems 02 p0184 N71-11297 [NASA-CR-111380]
 Cooperative Doppler radar system for avoiding midair collisions 02 p0363 N71-11766 [NASA-CASE-LAR-10403]
 Radar meteorology and data processing for Doppler radar systems 03 p0403 N71-13164 [PB-193196]
 Special radar project 3 at National Severe Storms Laboratory - R meter 04 p0489 N71-13480 [FAA-RD-70-78]
 Design, construction, and test analysis of Doppler surveillance radar 04 p0489 N71-13481 [AD-712325]
 Chatter frequency spectra determination for radar system design and control 04 p0494 N71-13904
 Adaptive clutter suppression filter for Doppler shifted radar signal detection 04 p0497 N71-13929
 Digital filters and Fourier transformation for pulsed Doppler radar processor 04 p0497 N71-13930
 Cost effectiveness of pulse Doppler radar in air-tube aircraft of early warning system 04 p0621 N71-13939
 Design, construction, tests, and inspection of pulse Doppler surveillance radar 05 p0645 N71-14912 [AD-713707]
 Doppler radar observations of drop size distribution in thunderstorms 06 p0692 N71-16519 [TR-18]
 Doppler radar measurements of flow generated by wing tip vortices using reflective chaff dispersed into vortices 10 p1491 N71-20630 [NASA-CR-111877]
 Satellite to satellite Doppler tracking with high resolution of gravity field 10 p1548 N71-21019 [NASA-CR-117404]
 Analysis of limitation on motor trail radar wind measurements imposed by uncertainty principle 10 p1643 N71-21191 [AD-716996]
 Clear air turbulence pulse Doppler laser radar system including analysis of mechanical vibration effects on laser transmitter and receiver 11 p1774 N71-22131 [NASA-CR-183091]
 Reliable miniaturized X band pulse Doppler radar development 11 p1701 N71-22325 [AD-717672]
 Feasibility and design criteria of laser Doppler system for detecting and mapping turbulence levels and wind or velocity profiles in various applications 12 p1935 N71-24081 [NASA-CR-185165]
 Feasibility of computerized Doppler radar tracking system 14 p2216 N71-25870 [AD-720832]
 Confidence testing of radar set AN/FP-17(XN-1) 15 p2379 N71-26816 [AD-719912]
 Design, test and manufacture of high reliability radar set AN/FP-17(XN-1) 15 p2380 N71-27195 [AD-719911]
 Doppler radar wind field measurements during test 15 p2440 N71-27843 [AD-720872]
 Detecting clear air turbulence using CO2 laser Doppler system 16 p2391 N71-30763
 OBOS I satellite orbit calculations from Doppler radar and optical tracking data including comparisons of rms of fits and ephemerides for both data sets 19 p3089 N71-31852
 Methods for determining characteristics of rain and snow using vertically pointing Doppler radar 20 p3295 N71-33021 [LAP-TR-32]
 Comparison of differenced Doppler and range tracking data-types for process noise problem solutions and computer programs for orbit and failure rate calculations 20 p3347 N71-33166
 Deep Space Network operations for Mars II project, mathematical model for Doppler tracking system, and third-order phase locked system transient response analysis 20 p3347 N71-33168
 Station longitude error effects on Doppler plus range and Doppler only orbit determination solutions, emphasizing Viking mission trajectory 21 p3391 N71-34129 [AD-719911]
 Mathematical model of DSIF Doppler tracking system phase noise 21 p3393 N71-34151
 Numerical evaluation of transient response for third-order phase-locked system for possible use in tracking high Doppler rates 21 p3394 N71-34152 [NASA-CR-1776]
 Digital simulation and implementation techniques for Doppler radar altimeter signal processing 23 p3724 N71-36548 [NASA-CR-1776]
 Doppler signal processing and instrumentation for modified Perseus C band weather radar 23 p3725 N71-36551 [AD-727796]

Doppler weather radar observing methods and data processing techniques 24 p3932 N71-38197 [AD-727138]
DOPPLER-FEELAU EFFECT
 Methods of measuring fluid velocity from Doppler Pizeau shift of scattered laser radiation, and optimization of optical system geometry 11 p1775 N71-22610
DORNIER AIRCRAFT
 NT DO-31 AIRCRAFT
 Rotary wing structural stability of Dornier high temperature gas jet helicopter 13 p2024 N71-24387
DORNIER DO-31 AIRCRAFT
 U DO-31 AIRCRAFT
DOSAGE
 NT RADIATION DOSAGE
 Dose measurements by ferrous-ferric, ferrous-ferric with copper added and oxalic acid dosimeters [INR-1164] 06 p0908 N71-15743
 Neutron dose distributions at bone tissue interfaces [ORNL-TM-3329] 21 p3382 N71-34066
 Human exposure to emergency exposure limit concentrations of monomethylhydrazine to determine suitability for use 24 p3879 N71-37652 [AD-727527]
DOSE
 U DOSAGE
DOSIMETERS
 NT THRESHOLD DETECTORS (DOSIMETERS)
 Intrinsic efficiency of thermoluminescent dosimetry phosphors [AD-711588] 01 p0096 N71-10637
 Investigating experimental and theoretical approaches to microdosimetry, radiobiology, and single-cell television systems 03 p0321 N71-12295 [NASA-CR-111820]
 Neutron dosimeter study based on electrical resistivity changes - tungsten dosimeter [CEA-N-1208] 04 p0573 N71-13651
 Dosimeter techniques for neutron produced defects in ammonium salts, hydrocarbons, and organic materials [COO-1105-135] 04 p0579 N71-13976
 Proceedings from conference on accelerator dosimetry and operation [CONF-691101] 04 p0580 N71-14004
 Procedure for measuring heavy cosmic ray particles directly incident on spacecrafts [NASA-CR-114804] 05 p0636 N71-14602
 Microdosage instrument for entomological investigations [AD-713473] 05 p0653 N71-14984
 Reader for radio photoluminescent-thermoluminescent dosimeters 05 p0745 N71-15188 [SPL-A13]
 Dose measurements by ferrous-ferric, ferrous-ferric with copper added and oxalic acid dosimeters [INR-1164] 06 p0908 N71-15743
 Optical absorption by excipients in alkali halides, personnel accident dosimeters, electromagnetic wave propagation in atmosphere, metallurgy, and related research 06 p0908 N71-15747
 LiF-Teflon disks laminated between plastic layers of identification pass for personnel accident dosimeters 06 p0804 N71-15749
 Dosimetry technique using thermally stimulated exoelectron emission with lithium fluoride [HASL-236] 06 p0927 N71-16857
 Performance tests on lithium fluoride thermoluminescent dosimeter [BNWL-CC-2633] 08 p1199 N71-18287
 Radiation stability of MRC copolymer 250 and forming dosimeter quality films 08 p1221 N71-18551 [AD-715417]
 Gamma ray logging of drill holes using thermoluminescence dosimeters [RISO-219] 09 p1441 N71-20310
 Development of dosimeter for measuring absorbed dose of high energy ionizing radiation [NASA-CASE-XLA-03645] 09 p1391 N71-20430
 Dosimetry of large radiation sources by optical changes in polymethyl methacrylate and evaluation as irradiation technique [JAERI-MEMO-4121] 09 p1443 N71-20454
 High power electronics including electrodynamic theory of grids, cathode losses in magnetrons, closed resonance chains, and electromagnetic vibration dosimeters [AD-717029] 10 p1537 N71-21300
 Spark chamber and discharge counter for space radiation studies, radiation shielding, and dosimetry [AD-716843] 10 p1641 N71-21620
 Measuring gamma dose rate in Plum Brook Reactor using oxalic acid 13 p2112 N71-24318
 Damage function analysis of neutron energy, effect on radiation embrittlement of steels, and need for detailed, accurate neutron dosimetry measurements of fast and thermal fluxes 13 p2128 N71-24334

DOUGLAS AIRCRAFT

Dosimetric characteristics of commercial beryllium oxide as thermoluminescent material [RT/PROT-70/23] 13 p2099 N71-24670
 Dose distribution calculations from tritium and iodine 125 sources using energy spectra 15 p2475 N71-27446 [JUL-688-ME]
 Radioactive waste disposal, radiation physics, and dosimetry related to health physics 15 p2482 N71-27744 [ORNL-4584]
 Thermally stimulated electron emission of ceramic beryllium oxide and calcium sulfate phosphor and doped with samarium, manganese, and lead studied for dosimeters material 16 p2642 N71-28030 [RT/FU/70/37]
 Moderation of fast neutrons in polyethylene and their use in neutron dosimetry 16 p2645 N71-28118 [RUB-4548-D]
 Application of nuclear emulsions in design of dosimeters used in detection of radiation exposure inside spacecraft 16 p2648 N71-28487
 Neutron dosimetry by semiconductor detectors and hydrogenous radiator assembly to determine energy dependence and accuracy of both methods [KFKI-70-29-HP] 16 p2655 N71-29086
 Sensitivity variations of TLD LiF dosimeter rods annealed at 500 C 18 p2959 N71-30504 [RD/BN-1872]
 Characteristics of radiation dosimetry conducted by polymer electret depolarization [NYO-3409-9] 18 p2996 N71-31187
 Timing properties of nuclear radiation detectors for subnanosecond spectroscopy 19 p3145 N71-31949 [INR-1213]
 Evaluation of radiation quality, mixed radiation fields, radiation direction, and absorption dose in phosphor glass dosimetry 19 p3148 N71-32095 [NP-18747]
 Dosimetric properties of silver activated phosphate glass photoluminescent dosimeter systems [NP-18746] 19 p3100 N71-32136
 X and gamma thermoluminescent dosimeter for accidental personnel dosimetry 19 p3155 N71-32339 [CLOD-52/D]
 Performance of LiF thermoluminescent dosimeters [COO-1105-120] 21 p3443 N71-34503
 FORTRAN program for gamma radiation dosimetry in arbitrary source and target geometry [ORNL-TM-3398] 22 p3638 N71-35913
 Maintenance of beta gamma ion chamber exposure dosimeters [CEA-N-1435] 22 p3811 N71-37174
 Development of method of direct correlation of radiation damage with time-integrated activation of neutron dosimeters [NASA-TN-D-6564] 24 p3964 N71-34279
 Problems of high temperature annealing of PTFE/LiF discs used for ionizing radiation dosimetry [AEEW-M-991] 24 p3973 N71-38344
DOSIMETRY
 U DOSIMETERS
DOUBLE BASE PROPELLANTS
 NT DOUBLE BASE ROCKET PROPELLANTS
 Heat of reaction for flameless combustion of M-2 double-base propellant 70 percent nitroglycerin 77 percent nitrocellulose, 3 percent other ingredients at various pressures 11 p1844 N71-22697 [NASA-TN-D-6105]
DOUBLE BASE ROCKET PROPELLANTS
 Theoretical and experimental determination of combustion properties and steady state deflagration of double base solid propellant 11 p1820 N71-22883
 Composite and double base rocket propellant extinguishing by rapid pressure reduction and propellant property and additive effects on combustion extinction 17 p2832 N71-29609
DOUBLE CUPS
 Simple formula for calculating time variations of instantaneous occulting orbital parameters and celestial body range rate [NASA-CR-115991] 19 p3181 N71-32405
DOUBLE SIDEBAND TRANSMISSION
 Design, operation, and alignment of single channel beat-note modulator, demodulator, and phase locked loops for double sideband signals [NASA-CR-103116] 13 p2857 N71-24083
 Comparison of constant bandwidth FM/FM and double sideband/FM telemetry systems [SC-DR-70-686] 15 p3379 N71-26041
 Techniques and circuits used in designing AM highly flexible telemetry system comprising single sideband/double sideband/constant bandwidth compatible system - space application 17 p2718 N71-29323
DOUGLAS AIRCRAFT
 NT A-4 AIRCRAFT
 NT C-47 AIRCRAFT
 NT C-54 AIRCRAFT
 NT DC 3 AIRCRAFT
 NT DC 8 AIRCRAFT
 NT DC 9 AIRCRAFT
 Aircraft accident report for Douglas DC-8-63P [NTSB-AAR-70-24] 04 p0475 N71-13417

DOUGLAS DC-3 AIRCRAFT

DOUGLAS DC-3 AIRCRAFT

U DC 3 AIRCRAFT

DOUGLAS DC-9 AIRCRAFT

U DC 9 AIRCRAFT

DOUGLAS MILITARY AIRCRAFT

U DOUGLAS AIRCRAFT

U MILITARY AIRCRAFT

DOVAP

U DOPPLER EFFECT

DOWNWASH

Analytical and numerical calculations for cylinder-vortex combination in incompressible flow noting pressure distribution and downwash

[NLR-TR-69057-U] 05 p0666 N71-15548

Numerical analysis of downwash interference on wings of missile tails

09 p1312 N71-19360

Aircraft wake turbulence with downwash loading of wing tips

[AD-718024] 12 p1851 N71-23660

Numerical evaluation of downwash integral for wing loading of lifting rectangular planform

[NPL-MA-90] 13 p2101 N71-24483

Numerical method for evaluating discontinuous downwash distribution for steady flow over swept and rectangular wings

17 p2700 N71-29349

Survey on different methods for lifting rotor downwash analysis

[DLR-MITT-70-23] 17 p2702 N71-29395

Mathematical model for induced velocity distribution of lifting rotor in horizontal flight

[DLR-MITT-70-22] 17 p2705 N71-30039

Rotary wing downwash influence on fixed wing flow using magnetic induction vortex model

[DLR-FB-70-42] 17 p2101 N71-30040

Wind tunnel tests of downwash aerodynamic surface incidence angles on Saturn S-1C booster coupled to Grumman C-4 orbiter shuttle

[NASA-CR-103193] 21 p3525 N71-35114

Computer program for numerical integration of downwash subsonic flow about rectangular planforms, for different aspect ratios

[NPL-MA-99] 23 p3704 N71-36405

DRAFTING [DRAWING]

Summary descriptions of NASA graphic arts techniques and equipment

[NASA-SP-591901] 12 p2019 N71-24205

DRAG

NT AERODYNAMIC DRAG

NT FRICTION DRAG

NT INTERFERENCE DRAG

NT MINIMUM DRAG

NT PRESSURE DRAG

NT SATELLITE DRAG

NT SUPERSONIC DRAG

NT VISCOUS DRAG

Flow from steady rotation of gravitating sphere in monostatic gas at rest, and drag of body moving transversely through confined stratified fluid

07 p1011 N71-17689

Mass transfer and drag coefficients of bubbles rising in dilute aqueous solutions

06 p1245 N71-19339

Drag of free falling spheres in water for Reynolds numbers in critical region using orthonormal cinematography

[AD-717492] 11 p1735 N71-22096

Framing camera performance predictions from drag and diffraction image degradation source analysis

[EGG-1183-530] 13 p2082 N71-25193

Accelerator for launching hypervelocity projectile by drag force of jet produced by gaseous explosive products

[NASA-CR-115067] 17 p2729 N71-29227

Nonlinear elasticity theory for dragging forces on moving defects by strain-field phonon scattering

17 p2819 N71-29952

Isobaric bubble motion under influence of varying high-g body forces, low gas flow rate isobaric bubble formation, and coefficients of drag for planetary ellipsoidal bubbles

18 p2887 N71-31368

Near flow field data for tube-vehicle systems and drag coefficient relationships with relative Mach numbers and relative flow velocity ratios to vehicle velocity

[GASL-TR-70-749] 24 p3908 N71-37856

DRAG BALANCE

U LIFT DRAG RATIO

DRAG COEFFICIENT

U AERODYNAMIC COEFFICIENTS

U DRAG

DRAG DEVICES

NT AERODYNAMIC BRAKES

NT BALLUTES

NT LEADING EDGE SLATS

NT SPOILERS

NT TRAILING-EDGE FLAPS

NT WING FLAPS

DRAG EFFECT

U DRAG

DRAG MEASUREMENT

Electric analog for measuring induced drag on non-planar airfoils

[NASA-CASE-XLA-00755] 04 p0472 N71-13410

Electric analog for measuring induced drag on non-planar airfoils

[NASA-CASE-XLA-05828] 04 p0472 N71-13411

Aerodynamic drag measurements on VC-10 aircraft subsonic wind tunnel models

[ARC-CP-1125] 07 p0969 N71-17118

Calculation of profile drag of airfoils at low Mach numbers by predicting instability and transition points

[NAL-TR-198] 09 p1317 N71-20101

Impact energy absorber with decreasing absorption rate

[NASA-CASE-XLA-01530] 11 p1767 N71-23092

Measurement of lift and drag forces experienced by ejector in wind tunnel and correlation with geometry and static performance of device

[AD-721192] 15 p2363 N71-26920

Ballistic range for free flight measurements of sphere drag at subsonic, transonic, supersonic and hypersonic speeds in upper atmosphere

[AD-721208] 15 p2395 N71-27675

Procedures for calculating normal wash in non-planar configurations and interference between wings and bodies

17 p2698 N71-29340

Pressure distributions and drag coefficients of 18 constant length and volume slender bodies of revolution at zero incidence for Mach numbers 2.0 to 12.0 - graphs

[NASA-TM-D-6536] 23 p3705 N71-36416

Drag coefficient measurements in flow around rectangular cylinders

[IC-AERO-71-15] 23 p3744 N71-36695

Comparison of blockage corrections in porous tunnel wall to closed wall tunnel at subsonic Mach numbers

[ARA-19] 24 p3908 N71-37853

DRAG REDUCTION

Determination of pressure characteristics and flow properties of cylindrical bodies in aqueous solutions of polyethylene oxide

[AD-717584] 11 p1733 N71-21909

Measurement of drag reduction of polymer solution at various stages of degradation in simulated long pipe

12 p1904 N71-24156

Minimizing drag and increasing performance of optimum shapes at hypersonic flight

13 p2023 N71-24704

Drag reduction and adsorption of polyethylene in aqueous solutions

[AD-719385] 13 p2067 N71-25230

Turbulent flow drag reduction by dilute polyethylene oxide solutions in capillary tubes

[AD-726688] 14 p2241 N71-26247

Drag force, pressure distribution, and separation angle measured on circular cylinders in flow of aqueous solutions of dilute polymers

[AD-722007] 16 p2578 N71-28178

Position indicators and guidance sensors for drag-free heliocentric sounding device on solar orbits

[ONERA-NT-1/1673-SY] 17 p2849 N71-29488

Effects on turbulent diffusion by distributed injection of polymer solution through porous wall adjacent to fully developed turbulent pipe flow of water

[AD-723860] 19 p3076 N71-31740

Surface roughness effects on drag reduction of flat plates moving in homogeneous polymer solutions

[AD-724288] 20 p3249 N71-32971

Theoretical analysis of polymer solution laminar flow near infinite extent flat plates for drag reduction effects

[AD-726414] 22 p3569 N71-35418

High response, drag-body flowmeters for cryogenic gas application

[NASA-CR-115144] 22 p3584 N71-35521

Diffusion of diluted drag reducing polymers and effect of diffusing polymers on boundary layer development

[AD-727632] 24 p3907 N71-37844

DRAGULATORS

U BRAKES [FOR ARRESTING MOTION]

DRAINAGE

Investigation of snow thawing and drainages using radioactive isotopes

[AD-711907] 02 p0219 N71-12071

Investigating radar imagery for application in terrain analysis of drainage basins

06 p0847 N71-16175

Mathematical model for river basin drainages systems based on hexagonal nature of geological ridges

[AD-722022] 16 p2584 N71-28207

DRAINING

U DRAINAGE

DRAWINGS

NT ENGINEERING DRAWINGS

DRIFT

Pressure gradient driven drift waves in collision-free low-pressure plasma

[CEA-CONF-1612] 15 p2498 N71-27099

DRIFT [INSTRUMENTATION]

Correction formulas for effect of ambient temperature drift on hot-wire anemometer measurements in incompressible flow

[NPL-AERO-1302] 02 p0225 N71-11544

Scale factor measurement of motors

03 p0412 N71-17311

Table 10g and requirements of gyroscopic materials under acceleration

03 p0412 N71-17311

Thermal stability and electromotive drift of noble metal and refractory metal thermocouple wires

[NASA-TN-D-7827] 05 p0483 N71-14040

Developing system for automatic compensation of signal dc level drift in laser interferometers

[Y-1737] 05 p0697 N71-15332

Large aperture Fabry-Perot spectrophotometer with helium-neon laser to reduce instrument drift

13 p0879 N71-26410

Thermal and fast neutron irradiation effects on helium-neon environment irradiated and unirradiated tungsten rhenium thermocouples at 2000 K and drift measurements

[NASA-TM-X-67818] 13 p2081 N71-26420

Long-term drift of noble and refractory metal thermocouples at 1600 K in air, argon, and vacuum

[NASA-TM-X-67813] 13 p2082 N71-25321

Metrological scatter characteristics of Manganin resistance gauges in high pressure measurements

14 p2257 N71-26403

Paired rubidium magnetometer providing reliable mapping of quasi-static total magnetic field changes to 0.1 gamma between stations to 1/2 km separation with differential drift correction

[COM-71-50005] 16 p2509 N71-28740

High sensitivity and stability characteristics of light scattering photometer for measuring aerosol concentrations

[LA-4627] 20 p3275 N71-33520

Instrument drift in earth inclination observation made by Engelhart Astronomical Observatory

23 p3749 N71-36720

Instrument constants of astronomical cameras compared with object positions obtained by other methods

[AD-727902] 24 p3926 N71-38012

Temperature drift and peak current degradation in tunnel diodes used for amplitude discrimination

24 p4013 N71-38622

DRIFT RATE

Magnetic and drift surfaces of charged particle of stellarator field

[IUPJ-95] 02 p0279 N71-11458

Investigating kinetic theory of anomalous diffusion due to drift dissipative instability

[CEA-CONF-1596] 08 p1269 N71-18152

Dispersion relation of drift instabilities in collisionless plasma

[EUR-CEA-FC-565] 09 p1448 N71-19989

Auroral ionization longitudinal drift rate recorded along auroral zone

12 p1909 N71-23562

Toroidal electric field effects on single particle radial drift in axisymmetric systems

[CLM-R-105] 14 p2313 N71-26780

Particle and field oscillations and electron heating due to drift mirror instability in magnetosphere

18 p3005 N71-36938

Drift oscillations in collisionless alkali metal Q device plasma

18 p2993 N71-31140

Misalignment estimation software system for calibrating in-flight slew angle scale factors and drift rates of OAO gyro

[NASA-TM-X-65667] 19 p3133 N71-32880

Digital computer simulation of two stepdown system attitude algorithms by responses to angular input rates

[NASA-CR-121731] 21 p3447 N71-34327

Experiments on linear and nonlinear feedback and dynamic stabilization of drift and transverse Kolmogorov instabilities

[CONF-710607-24] 24 p3991 N71-36478

Accelerated longitudinal drift regimes of oceanic 12 hour orbits due to resonant geopotential

[NASA-TM-X-65722] 24 p4021 N71-36840

DRILL BITS

Comparison of two drill bits and two lubricants for aluminum alloy drilling

10 p1564 N71-31148

Drilling tests for evaluating coring potential of Apollo lunar surface drill titanium core stems

[NASA-TM-X-58057] 17 p2754 N71-29314

DRILLING

Improved efficiency of drilling ceramics and glass using liquid environments

[AD-713595] 05 p0710 N71-15344

DRILLS

Annular auger for manual drilling of ice holes for core sampling

11 p1771 N71-22866

Field maintenance manual for Apollo Lunar Surface Drill

[NASA-CR-114969] 13 p2084 N71-26396

SUBJECT INDEX

IMPRINTING

Advantages of various types of liquids taken by workers under high temperature working conditions (miners, fire fighters, steelworkers) [NASA-TT-F-14002] 23 p3713 N71-36469

DRIVERS

Driver modifications for improved performance of electric arc shock tube 11 p1732 N71-22534

INVERTERS

Inverter drive circuit for semiconductor switch [NASA-CASE-LEW-10233] 15 p2388 N71-27126

PROPAGATION

U TOWED BODIES

WINGS HELICOPTERS

U HELICOPTERS

PROP SIZE

Moisture separator development and drop size measuring and separating techniques [NASA-49-192] 03 p0355 N71-12699

Determination of droplet size sprayed from hollow cone nozzles [PB-1921367] 03 p0365 N71-13193

Collection role in determining raindrop size distribution 04 p0542 N71-14181

Mathematical model for droplet growth rate in cloud seeding [AD-7135359] 05 p0719 N71-15399

Doppler radar observations of drop size distribution in thunderstorms [TR-18] 06 p0692 N71-16519

Wind tunnel photography for determining water droplet size in breakup of water jets [NASA-CR-1146820] 06 p1183 N71-18962

Cloud droplet growth theory and diffusional interaction between growing droplets [AD-717788] 11 p1790 N71-22360

Characteristics and operating principles of instrument for measuring size of fog droplets and aerosol particles [NLL-M-20291-5828.4F] 12 p1923 N71-24190

Deformation of drops in reactive zone during heterogeneous detonation of fuel mixtures consisting of liquid drops of fuel and gaseous oxidizer [NASA-TT-F-13579] 13 p2185 N71-24933

Radar reflectivity, rainfall rate, and drop size distribution measurements [AD-719787] 14 p2287 N71-25810

Atmospheric oxygen, water vapor, and carbon dioxide concentration effects on drop size and sodium compound structures in sodium fire aerosols [AERE-R-6466] 15 p2377 N71-27468

Optical and impact sampling methods for sizing and counting water droplets in clouds for use in sampling from aircraft [AD-721677] 16 p2625 N71-28457

Formula for calculating rate of condensation growth of drops in clouds considering latent heat of condensation [AD-724105] 20 p3294 N71-32803

Effect of charge transport on disintegration of liquid jets studied by comparison of calculated and experimental values of size of drops formed from electrified jets [AD-724334] 20 p3363 N71-32973

Analysis of cloud liquid-water content, drop size, and temperature profiles of tropical maritime clouds for artificial glaciation with silver iodide 23 p3785 N71-34900

PROP TESTS

Drop and impact tests for improving crashworthiness of integral fuel tanks [FAA-NA-70-46] 02 p0144 N71-11019

Comparison of Charpy impact test with drop-weight test for structural steels 02 p0242 N71-11385

Instrumentation and drop testing techniques for investigating flight vehicle and personnel protective systems [NASA-TM-X-2149] 05 p0682 N71-14780

Pitman RTG heat source drop tests to obtain terminal velocity and reduced trajectory data [SC-DR-70-540] 06 p0793 N71-16628

Photographic recording of aerodynamic interference in wind tunnel simulation of jetted drop loads from aircraft 09 p1314 N71-19378

Environmental, drop, and vibration tests for investigating fatigue of cushion materials for packaging [BCR-69] 18 p2399 N71-30614

PROP WEIGHT TESTS

U DROP TESTS

PROP (LIQUIDS)

NT RAINDROPS

Tabulated computations of scattering of visible and infrared waves by water droplets [AET-70-258-RULL] 01 p0092 N71-10922

Viscous flow of deformable liquid drops in suspension in circular cylindrical tubes 02 p0203 N71-11563

Formation and movement of droplets in atomization in gas-liquid phase [PB-1921707] 03 p0362 N71-12692

Determination of droplet size sprayed from hollow cone nozzles [PB-1921367] 03 p0365 N71-13193

Holography used to determine water droplet characteristics in engine test facility [AD-715916] 08 p1201 N71-18488

Fluorescence characteristics study of transuranium elements using liquid drop model 08 p1257 N71-18518

Electrical force potential for drop supercooling and development and dissipation of clouds and fog [AD-713632] 09 p1413 N71-19661

Hollow drop formation from molten UO₂ and water contact [EURFNR-811] 09 p1428 N71-20133

Evaporation from spherical liquid drop into vacuum or into pure vapor under strong nonequilibrium conditions 10 p1543 N71-21336

Interaction between shockwaves and burning or nonburning fuel droplets in pure oxygen 11 p1740 N71-23631

Drop radius calculations for estimating dust sedimentation on drops formed in high-velocity gas atomization and comparison with Sauer diameter calculations [ANL-TRANS-871] 12 p1901 N71-23676

Characteristics and operating principles of instrument for measuring size of fog droplets and aerosol particles [NLL-M-20291-5828.4F] 12 p1923 N71-24190

Sound propagation characteristics in gas media with droplets or particles based on linearized hydrodynamic equations [NASA-TT-F-13581] 13 p2064 N71-24619

Aluminum particle motion photographs for examining internal flow patterns of forming liquid drops [IS-T-440] 13 p2392 N71-27066

Mass transfer during binary liquid drop growth at nonwetted capillary tubes 16 p2579 N71-28235

Oxygen and carbon elastic form factor calculations based on liquid drop nuclear model with quadrupole surface oscillations [RLO-135-597] 17 p2790 N71-29270

Collection efficiency of water droplets freely falling through silver chloride aerosol determined by light scattering [NVO-3847-2] 17 p2798 N71-30015

Numerical models for calculating terminal velocity of water drops [F-4564] 19 p3129 N71-32407

Mathematical prediction of evaporating water droplet wetting dynamics on stainless steel, Lucite, Teflon, and copper surfaces [NASA-TM-X-67913] 20 p3312 N71-33553

Noise attenuation by injection of evaporating droplets into subsonic duct flow [NASA-CR-111905] 20 p3312 N71-33560

Application of photonic and liquid drop models to symmetric binary photofission processes 21 p3489 N71-34853

Numerical analysis of flow patterns, impact pressure, and velocities resulting from impact of spherical water drop on rigid plane surface [UMICH-633710-10-1] 23 p3744 N71-36700

Interfacial tension pressure change measurements of mass transfer effects on droplet interface motion 23 p3780 N71-36941

Acceleration of condensate drops in axial gap of turbine stage [RAE-LIB-TRANS-1602] 24 p3906 N71-37837

Mathematical model for motion of small drops and bubbles considering absorption, diffusion, and convection in interfacial region 24 p3996 N71-38386

DROPS

Vertical profiles of upper atmosphere pressure and temperature obtained by dropsondes in 1968 and 1969 [WRE-TM-HSA-170] 02 p0258 N71-11678

Photometric ozone and temperature dropsondes for upper atmosphere [WRE-TM-HSA-179] 11 p1832 N71-22587

Ultraviolet photometer for optical sensor in dropsonde system [WRE-TM-HSA-168] 24 p3917 N71-37930

Synthetic ozone density profiles for dropsonde behavior prediction [WRE-TM-HSA-153] 24 p3917 N71-37931

BROWNS

U SLEEP

DROG THERAPY

U CHEMOTHERAPY

DROG

NT ANESTHETICS

NT ANTIHYPERTENSIVES

NT ANTIARRHYTHMICS

NT ANTIADIPATIN DRUGS

NT NOREPINEPHRINE

NT RESERPINE

NT TRANQUILIZERS

Food and drug chemical analysis [PB-192020] 02 p0152 N71-11000

Effects of unusual environmental conditions on characteristics and stability of drugs 02 p0161 N71-11493

Decreased diuresis in response to thiazide diuretic at simulated altitude 03 p0635 N71-14702

Onboard medication for space flight crew 06 p0803 N71-16523

Effects of spacecraft environment on oxidative drug metabolism [NASA-CR-114821] 06 p0804 N71-16704

Effects of drop on performance of flight personnel following unusual sleep patterns 07 p0978 N71-16908

Altitude effects on drug action in glucose metabolism and ACTH release in dogs 07 p0982 N71-17660

Unilateral labyrinthectomy model for evaluating drug effects on vestibular function in guinea pigs 08 p1153 N71-19057

Hypoclozine effects during 120-day bed confinement with drug therapy 08 p1155 N71-19067

Pharmacokinetics with uncertainties in rate constants [TR-70-60] 09 p1408 N71-19519

Effects of education and pharmacodynamics on adaptability of human beings to degraded sensorial environments 09 p1337 N71-20364

Physical training, cold adaptation, and adaptive pharmacokinetics for increased physiological stress resistance in rats 20 p3220 N71-33454

DRUMS (CONTAINERS)

Simulation of piping drum channel system by ALOOL and SIMULA programs on Univac 1108 [NASA-CR-121653] 21 p3397 N71-34172

DRY CELLS

NT MAGNESIUM CELLS

NT NICKEL ZINC BATTERIES

DRY FRICTION

Changes in dislocation density in surface layers of high strength cast iron with ferritic and pearlitic structure by action of dry and lubricated friction [AD-719733] 13 p2893 N71-24878

Antifriction characteristics of graphite due to its mechanical properties and self lubricating nature [NLL-RISLEY-TRANS-1881-7091.9F] 16 p2602 N71-28727

Thermodynamics of crack initiation in dry operating graphite ring seals 17 p2756 N71-30024

DRY HEAT

Effects of dry heat and chemicals on long term survival rates of bacteria spores under varying temperatures and humidity conditions 13 p2893 N71-24878

[NASA-CR-122008] 23 p3713 N71-34467

DRYDOCKS

Application of situational control models examined for lock sections of canals, airports and airports, network of street crossroads, and other large systems 21 p3448 N71-34538

DRYERS (EQUIPMENT)

U DRYING APPARATUS

DRYING

NT DEHYDRATION

Dryout tests on internally heated annulus with variation of axial heat flux [AEEW-R-578] 04 p0561 N71-14400

Survival of soil bacteria during prolonged desiccation [NASA-CR-114687] 08 p1148 N71-18562

Tensile strength of extruded tungsten made from freeze dried and dispersion strengthened tungsten powders [BM-BI-7485] 08 p1218 N71-19016

Stress analysis and fracture mechanics of degradable, isotropic, composite propellants [AD-720666] 14 p2331 N71-26079

DRYING APPARATUS

Gas permeant dry box glove reducing permeation of air or moisture into dry box or isolator by diffusion through glove [NASA-CASE-XLE-02531] 11 p1694 N71-23080

DRIF (INSTRUMENTATION FACILITY)

U DREF SPACE INSTRUMENTATION FACILITY

DRIF

U DREF SPACE INSTRUMENTATION FACILITY

DRIF

U DREF SPACE INSTRUMENTATION FACILITY

DRIF

U DREF SPACE INSTRUMENTATION FACILITY

DRIF

U DREF SPACE INSTRUMENTATION FACILITY

DRIF

U DREF SPACE INSTRUMENTATION FACILITY

DRIF

U DREF SPACE INSTRUMENTATION FACILITY

DRIF

U DREF SPACE INSTRUMENTATION FACILITY

DRIF

U DREF SPACE INSTRUMENTATION FACILITY

DRIF

U DREF SPACE INSTRUMENTATION FACILITY

DRIF

U DREF SPACE INSTRUMENTATION FACILITY

DRIF

U DREF SPACE INSTRUMENTATION FACILITY

DRIF

U DREF SPACE INSTRUMENTATION FACILITY

DRIF

U DREF SPACE INSTRUMENTATION FACILITY

DRIF

U DREF SPACE INSTRUMENTATION FACILITY

DRIF

U DREF SPACE INSTRUMENTATION FACILITY

DRIF

U DREF SPACE INSTRUMENTATION FACILITY

DRIF

U DREF SPACE INSTRUMENTATION FACILITY

DRIF

U DREF SPACE INSTRUMENTATION FACILITY

DRIF

U DREF SPACE INSTRUMENTATION FACILITY

DRIF

U DREF SPACE INSTRUMENTATION FACILITY

DRIF

U DREF SPACE INSTRUMENTATION FACILITY

DRIF

U DREF SPACE INSTRUMENTATION FACILITY

DRIF

U DREF SPACE INSTRUMENTATION FACILITY

Annular diffuser and combustor assembly in full scale duct burner for supersonic turbofan engine [NASA-TN-D-6163] 08 p1304 N71-18882

DUCTED FLOW
NT KNUDSEN FLOW

Space-time structure of sound waves in ducted flow [ONERA-TP-844] 02 p0267 N71-11774
Measurements of neutron streaming through cylindrical bent ducts in water [EUR-4498-E] 08 p1237 N71-18286
Navier-Stokes equations and velocity distributions for two dimensional, unsteady, incompressible, laminar flow of Newtonian fluids in annular, circular, and rectangular ducts 14 p2242 N71-26473

Total pressure, static pressure, surface shear stress, and yaw angle measurements of 5 curved ducted flow [IC-71-10] 17 p2737 N71-30264

Development of method for predicting properties of confined, turbulent, axisymmetric duct flow with flame diffusion [CCK/TN/A16] 20 p3249 N71-32872

Energy transport velocity model for classification of all possible acoustic modes propagating in uniform, inviscid, homogeneous, time independent ducted air flow [ONERA-TP-965] 20 p3251 N71-33530

Two finite difference procedures for computation of steady, three dimensional boundary layers in ducts [EP/TN/A40] 20 p3251 N71-33581

Calculation of hydrodynamic entrance length and flow characteristics in channels of varying cross sections [NLL-M-20388-5828AF] 21 p3413 N71-34288

Velocity and turbulence characteristics of air flow in three ratios of concentric annuli by location of zero shear position [RD-B-N-1878] 22 p3566 N71-35401

Thermal neutron flux distributions in air-filled water-shielded ducts perpendicular to reactor beam channels [UARAE-66] 24 p3970 N71-38318

Effect of variable fluid properties on MHD flow in electrically insulated rectangular duct 24 p3995 N71-38502

DUCTED PROPELLERS
U SHROUDED PROPELLERS

DUCTILITY
Determining mechanical properties and air-oxidation behavior of chromium-base compositions at temperatures up to 2400 F [NASA-CR-72731] 01 p0065 N71-10047

Effects of helium on high temperature ductility of Sandvik 12R-72HV and Inco IN-744X [AI-AEC-12960] 02 p0244 N71-12111

High strength stainless steel of Cr, Mo, and Co with improved toughness and ductility [AD-712724] 03 p0395 N71-13367

Hot working effect on room temperature strength and ductility of gallium delta-stabilized plutonium alloy [UCRL-72547] 04 p0530 N71-14069

Facility and procedure for studying short term tensile impact and compression strength, creep, and ductility of graphite at 300 to 3500 K [LA-4462-TR] 07 p1047 N71-17127

Fracture ductility of aluminum and titanium alloys and steels as function of stress state [AD-715320] 07 p1044 N71-17844

Properties of cast columbium carbide-carbon alloys ranging in carbon content from 12 to 17 weight percent compared with hot pressed compositions of similar composition [BM-R1-7479] 08 p1213 N71-18479

Effects of selected minor alloying additions on structure and deformation of beryllium 08 p1219 N71-19216

Additions of nickel and niobium to improve ductility of APC-77 steel for rivet material [AD-716677] 09 p1393 N71-19735

Metallographic and ductility effects of lithium on tungsten-lined titanium alloy clad uranium mononitride cylinders after long term exposure [NASA-TM-X-52998] 10 p1602 N71-20948

High temperature tensile tests on uranium alloys containing carbon, iron, silicon, and aluminum [NLCO-1068] 10 p1577 N71-21051

Static ductile deformational processes in deformed quartz, olivine, pyroxene, and plagioclase [NASA-CR-119174] 17 p2828 N71-30274

Role of ductility brittleness transition in body centered cubic lattice of iron polycrystals 19 p3112 N71-31913

Nitrogen content effect on hot ductility of molybdenum alloyed austenitic stainless steel 19 p3112 N71-31921

Influence of nitrogen and sulfur content on hot ductility, flow stress, and recrystallization in austenitic stainless steel 19 p3112 N71-31922

Model for erosion of ductile materials by impaction of solid particles [AD-724116] 20 p3283 N71-33113

Analytical and experimental investigation of ductile fracture of polymers using adaptation of Dugdale model [NASA-CR-121416] 20 p3360 N71-33778

Gerard-Papirno method for measuring loss of ductility in high strength AISI 4340 steel [COO-2048-2] 21 p3438 N71-34464

Magnesium alloy plates deformed by oblique explosive loading for hardening without ductility loss [RFF-1649] 21 p3439 N71-34474

Ring tests for determining transverse ductility of fuel element canning [AE-412] 21 p3458 N71-34610

Low temperature ductility and high temperature strength of pure chromium and chromium-titanium alloy prepared from vapor deposited powders [NASA-CR-72901] 22 p3592 N71-35580

Boron effects on ductility and strength of Inconel 600 and Types 304 and 316 stainless steel at hot metal working temperatures [ORNL-TM-3316] 22 p3594 N71-35591

Multiaxial stress state effect on fracture ductility of solids [AD-726443] 22 p3690 N71-36320

Development of methods for improving ductility of beryllium and techniques for deforming ingot beryllium into sheet form [AD-727747] 24 p3938 N71-38094

DUCTS
NT ACOUSTIC DUCTS

NT AIR DUCTS
Turbulent mixing between two compressible streams in constant duct area and with eccentric primary flow jet [AD-712333] 03 p0362 N71-12762

Electromagnetic pulse propagation in duct between ground and atmospheric layer 10 p1524 N71-21423

Ray tracing analysis on duct effect in line of sight wave propagation above sea surface 10 p1524 N71-21428

Quick disconnect duct coupling device for single-handed operation [NASA-CASE-MFS-20395] 13 p2086 N71-24903

Investigation of bellows and flex hose induced vibrations in spacecraft ducting components 17 p2830 N71-29582

Monte Carlo method for neutron and photon trajectory determination through metal plate ducts [BMVG-FBWT-71-9] 19 p3144 N71-31702

Nuclear light bulb reactor propellant duct absorption of thermal radiation and simulation experiments 20 p3306 N71-33660

Three dimensional axisymmetric ducts with axial velocity distributions in compressible flow [TAB-122] 21 p3410 N71-34264

Slow neutron transmission in water shield ducts of nuclear reactor [UARAE-104] 24 p3970 N71-38320

DUMMY LOADS
U IMPEDANCE
DUNALIELLA
Influence of electromagnetic force fields on biological systems studied on dunaliella and ciliates [AD-714071] 06 p0801 N71-16350

DUNGEYS WIND SHEAR MECHANISM
U WIND SHEAR
DUNITZ
Granite, basalt, gabbro, and dunitz isothermic volume compressibilities and densities under 32,000 kg pressure [SC-T-713031] 23 p3802 N71-37108

DUOCHROMATORS
Optical properties and efficiency of duochromators in slow neutron spectrometry 16 p2596 N71-28706

DUOPLASMATRONS
Design and operation of duo-plasmatron ion source providing hydrogen ion currents [AD-717398] 11 p1801 N71-21959

Experimental design and performance of plasmatron - ionic pulverization device [ONERA-NT-02-22] 13 p2979 N71-24405

Investigation of ion beam injection system using duo-plasmatron with electron oscillation in anode plasma [JPP-2/87] 15 p2500 N71-27316

DUPLICATING
U REPRODUCTION [COPYING]

DURABILITY
In pile and out of pile durability tests and characteristics of 30 kW circulating helium fuel capsules in Plum Brook Reactor [NASA-TM-X-52676] 16 p2636 N71-28967

Effect of sulfide inclusions on ball bearing steel durability noting sulfur content 19 p3187 N71-31919

DURATION
U TIME

DUST
NT COSMIC DUST

NT INTERPLANETARY DUST
NT LUNAR DUST
NT TERRESTRIAL DUST BELT
Simultaneous measurement of atmospheric dust by laser and balloon sounding [NASA-CR-111798] 01 p0045 N71-10042

Absorption characteristics of major components of dust clouds in infrared region [AD-712909] 03 p0366 N71-12730

Recording dust concentrations in atmosphere [NLL-M-9139-5828AF] 03 p0368 N71-12844

Comparative tests of fine dust masks [LA-4459-TR] 06 p0805 N71-15985

Computer program for processing respiratory dust sampling data [BM-IC-3504] 08 p1166 N71-19029

Drop radius calculations for estimating dust sedimentation on drops formed in high-velocity atomization and comparison with Sauter diameter calculations [ANL-TRANS-871] 12 p1901 N71-23816

Effects of flow containing dust on results of hypersonic wind tunnel experiments [NASA-TT-F-13529] 12 p1901 N71-23790

Vessel size and shape effects on gas and dust explosions in closed containers [BM-R1-7307] 12 p2013 N71-24679

Analysis of Sr-90, Cs-137, and fission products in atmospheric dust and rainfall in Great Britain up to mid 1970 [AERE-R-6556] 15 p2495 N71-27966

Computer programming manual for calculating nuclear explosion dust and air temperature effects including particle size distribution, wind, and thermal radiation effects [AD-722252] 16 p2586 N71-28531

Periodic variations of air pollution dust and sulfur dioxide particle densities for urban areas of Ohio [NOAA-TM-NWS-ER-39] 16 p2627 N71-29001

Radiation attenuation of dust layer in stratosphere or upper troposphere [NLL-M-20598-5828AF] 21 p3422 N71-34039

DUST COLLECTORS
Analysis of electrostatic precipitator systems application in industrial dust control [PB-198150] 17 p2755 N71-29088

Volume, diaphragm elasticity and area, orifice area, and L/D ratio effects on pulsation dampener efficiency for smoothing personal respirable dust sampler flows [BM-R1-7545] 22 p3548 N71-35524

DWARF STARS
NT WHITE DWARF STARS

Spectral line intensity data for visual region of white dwarf star 01 p0122 N71-10077

Atmospheric models and strong-line profiles in pure absorption for late-type dwarf stars in 5200 to 3200 deg effective temperature range 19 p3182 N71-32780

Spectrum analysis of four O-type subdwarfs as basis for atmospheric models of stars HZ 44, plus 75 deg 4655, and HD 127493 21 p3511 N71-33009

Development of technique for obtaining number abundance of late type stars and application to field dwarfs in solar vicinity and Hyades [AD-726568] 22 p3672 N71-34102

DYES

Infrared difference frequency generation using tunable dye laser [AD-715700] 08 p1210 N71-18766

Nonlinear absorption properties of organic dye molecules used with ruby lasers [AD-717095] 10 p1571 N71-21707

Dye penetrant and technique for nondestructive tests of solid surfaces contacted by liquid oxygen [NASA-CASE-XMF-02221] 15 p2450 N71-27178

Laser beam filtering by saturable dyes [UCRL-51006] 20 p3282 N71-33538

Fluid electrophoresis separation based on motion of particles in electric field for demonstrating near-similarity condition in space - Apollo 14 [NASA-TM-X-64611] 23 p3718 N71-34606

Development of operational system for measuring ocean surface current from aircraft using floats and fluorescent dyes [AD-726568] 24 p3916 N71-37912

DYNAMIC CHARACTERISTICS

NT AERODYNAMIC DRAG
NT AERODYNAMIC STABILITY
NT AIRCRAFT STABILITY
NT ATTITUDE STABILITY
NT BOUNDARY LAYER STABILITY
NT COMBUSTION STABILITY
NT CONTROL STABILITY
NT DIRECTIONAL STABILITY
NT DRAG
NT DYNAMIC PRESSURE
NT DYNAMIC STABILITY
NT FLAME STABILITY
NT FLOW CHARACTERISTICS
NT FLOW DISTRIBUTION
NT FLOW STABILITY
NT FLOW VELOCITY
NT FREQUENCY STABILITY
NT FRICTION DRAG
NT GYROSCOPIC STABILITY
NT HOVERING STABILITY
NT INTERFERENCE DRAG
NT INTERFERENCE LIFT
NT JET LIFT
NT LATERAL STABILITY
NT LIFT
NT LONGITUDINAL STABILITY

SUBJECT INDEX

- NT LOW SPEED STABILITY
 NT MAGNETOHYDRODYNAMIC STABILITY
 NT MINIMUM DRAG
 NT MOTION STABILITY
 NT PRESSURE DRAG
 NT ROTARY STABILITY
 NT ROTOR LIFT
 NT SATELLITE DRAG
 NT SPACECRAFT STABILITY
 NT SUPERSONIC DRAG
 NT TRANSIENT RESPONSE
 NT VISCOUS DRAG
 NT ZERO LIFT
- Dynamics of collisions between shock interactions and wave configurations in gases and condensed explosives
 [NASA-CR-111107] 01 p0042 N71-10421
 Bibliography with abstracts on materials dynamic properties
 [AD-710623] 01 p0129 N71-10484
 Static and dynamic properties of thin shells, elastic and plastic theories, and study methods for stress and failure conditions
 [AD-711129] 01 p0129 N71-10591
 Dynamic properties of materials with emphasis on metals
 [AD-712847] 03 p0390 N71-12685
 Dynamic characteristics of pneumatic transmission lines
 03 p0384 N71-13147
 Universal dynamic flow without holdovers
 [PB-19992] 03 p0401 N71-13335
 Linear dynamic systems in Hilbert space
 05 p0712 N71-14513
 General properties of linear dynamic systems in Hilbert space
 05 p0712 N71-14515
 Numerical study on controlling dynamic properties of aerodynamic inlet using bypass bleed
 [NASA-TN-D-6144] 05 p0626 N71-14669
 Numerical methods for dynamic meteorology and weather forecasting problems, and atmospheric circulation dynamics
 [AD-714749] 06 p0890 N71-15992
 Dynamic characteristics and linear control theory for aircraft simulation
 06 p0831 N71-16061
 Effect of design factors on frequency response of short pressure probes
 [NASA-TN-D-61531] 06 p0861 N71-16390
 Basic parameter influence on dynamic coefficient of friction thermoplastics
 [AD-714878] 07 p1049 N71-17960
 Dynamic characteristics of human skeletal muscle modeled from surface stimulation
 [NASA-CR-16911] 08 p1156 N71-19125
 Field dynamic properties of turbulent swirl flows in burner ducts
 [AD-716453] 09 p1370 N71-19608
 Dynamics of orientation system for space vehicles using angular position transducers as sensors
 11 p1787 N71-22268
 Dynamic characteristics of circular fully developed laminar free jet
 [NASA-TN-D-6304] 12 p1898 N71-23103
 Dynamic synthesis of computerized automatic control systems
 12 p1885 N71-24217
 Mathematical models for cybernetic diagnosis of dynamic systems
 [AD-719776] 13 p2103 N71-25118
 Dynamical theory of Kikuchi electrons based on two beam theory
 [UCRL-19631] 13 p2139 N71-25482
 Dynamic characteristics of dictionaries and documentation indexes for information retrieval
 14 p2223 N71-25994
 Fast nuclear reactor physics technology assessment using dynamic and performance characteristics, neutron shielding, power efficiency, fuel cycles, reactivity, and numerical analysis
 [BARC-38] 17 p2783 N71-29550
 Calculation of dynamic and thermal characteristics of gas circuit in variable flow conditions with application to studying reactor under natural convection flow conditions
 [NLL-CE-TRANS-5375-PROZ.09] 17 p2733 N71-29574
 Identifying linear dynamic systems with state and observation noise with application to flight control
 [AD-721108] 17 p2773 N71-29733
 Dynamic development characteristics of geomagnetic instabilities in earth magnetosphere
 17 p2742 N71-29788
 Dynamic plastic behavior of hollow cylinders using existing flow techniques for investigation of elastoviscoplastic constitutive theory
 17 p2834 N71-30157
 Dynamic characteristics of wind and temperature profile vertical distribution over Paris-north airport site
 18 p2940 N71-30831

- Dynamic range, signal level intensity, and resolving power deterioration from photofilms in radar systems with synthesized aperture
 [JPRS-35670] 18 p2891 N71-31274
 Dynamics of various types of samplers used on ITR project
 [NASA-TT-F-137081] 18 p2988 N71-31476
 Hydrodynamic and frequency response of semicircular canals compared in yaw, pitch, and roll
 [AMRU-R-66-1] 18 p2879 N71-31527
 Notation and nomenclature for systems of area, altitude angle, direction angles, and flight control systems for aircraft dynamics
 [ARC-R/M-3562-PT-2] 20 p3203 N71-32862
 Notation and nomenclature for equation of motion of aircraft dynamics
 [ARC-R/M-3563-PT-3] 20 p3204 N71-32875
 Dynamic characteristics of Ankara gravimeters upon measurement of phase lags in tidal observations at varying times
 20 p3265 N71-33367
 Analysis of nuclear light bulb startup and engine dynamics including transient responses to perturbations at full power operating level
 20 p3305 N71-33657
 Static and dynamic experiments with repetitively pulsed booster in which rotating beryllium reflector moved past unreflected core surface
 [Y-D] 21 p3459 N71-34619
 Synthesis of structural dynamic systems using digital computer and FORM/FORTRAN Matrix Analysis
 [NASA-CR-119877] 21 p3527 N71-35128
 Dynamic characteristics of space shuttle determined by NASTRAN
 22 p3685 N71-36277
 Dynamic behavior and design procedures for spacecraft control system utilizing hybrid coordinates
 [NASA-CR-122918] 23 p3858 N71-37497
 Dynamic characteristics of optical and surface crystal properties
 [AD-727327] 24 p3997 N71-38509
 David-Greenstein effect on rigid body dynamics of interplanetary dust grains
 24 p4006 N71-38561
- DYNAMIC CONTROL
 Dynamic pressure feedback compensation of resonance in liquid rocket thrust vector control system
 [NAL-TR-213] 11 p1820 N71-22460
 Mathematical modeling of aircraft structural response modes to active control system
 12 p1852 N71-23212
 Dynamic flight control simulation for straight wing space shuttle booster entry
 14 p2343 N71-26069
 Approximation method for dynamic properties of commutative control element in converter servomechanism
 17 p2728 N71-30125
- DYNAMIC LOADS
 NT AEROYNAMIC LOADS
 NT CYCLIC LOADS
 NT GUST LOADS
 NT IMPACT LOADS
 NT LANDING LOADS
 NT ROLLING CONTACT LOADS
 NT SHOCK LOADS
 NT THRUST LOADS
 NT TRANSIENT LOADS
 NT VIBRATORY LOADS
 NT WING LOADING
- Cumulative frequency distributions of aircraft landing gear loads in determining fatigue life
 [RAE-LIB-TRANS-1462] 01 p0128 N71-10273
 Motion bounds of lumped structural parts subjected to dynamic loads and perturbations
 [AD-710787] 01 p0129 N71-10565
 Design of guided ballistic missiles with liquid or solid propellant rocket engines
 [AD-711130] 01 p0129 N71-10592
 Transient response of ring-reinforced cylindrical shell, immersed in fluid, to axisymmetric pulses
 [RE-393] 01 p0150 N71-10719
 Nonlinear stress waves in dynamic loading of solids
 [AD-712911] 03 p0467 N71-13399
 Computer program for finite difference solutions of shells of revolution under asymmetric dynamic loading
 [NASA-TN-D-4659] 05 p0700 N71-15569
 Dynamic loads on F-104 aircraft landing gear
 [PB-82-1969] 08 p1143 N71-18532
 Mathematical models for complex loaded cylinder cross analysis taking into account viscoplasticity
 [ONERA-TP-946] 08 p1297 N71-10642
 Computer programs for static and dynamic deformation of structures with straight axis
 [CRIF-MC-32] 10 p1651 N71-20687
 Multilooped support system for wind tunnel test models subjected to thermal dynamic loading
 [NASA-CASE-XLA-61326] 10 p1538 N71-21481
 Finite element analysis for response behavior of stiffened rectangular plates subjected to dynamic loads
 11 p1834 N71-21942

DYNAMIC MODELS

- Apparatus for measuring load on cable under static or dynamic conditions comprising pulleys pivoting structure against restraint of tension stress
 [NASA-CASE-XMS-04545] 11 p1772 N71-22878
 Thin conical shell stability subjected to dynamical longitudinal compression
 [AD-719851] 13 p2182 N71-23352
 Dynamic problem of infinite, elastically supported beam under influence of uniformly moving single point load solved by complex variable theory
 [NASA-TT-F-13560] 14 p2347 N71-23802
 Load-equivalence parameters for dynamic loading of structures in plastic range
 [ANL-7677] 15 p2321 N71-27238
 Fixed and variable stiffness models for simulating instantaneous dynamic loads on gear tooth
 16 p2802 N71-28611
 Analytical method for determining radial loads of effects in dynamic plastic deformation
 17 p2354 N71-30154
 Dynamic stress concentration at chamfered change of section between two plates in same phase
 [RD/B/N-1795] 17 p2855 N71-30517
 Analyzing structure of constitutive relations which govern force-deformation laws used in stress analysis
 [AD-722331] 18 p3022 N71-31483
 Dynamic surface loading of elastic half space
 [REP-470] 19 p3184 N71-31728
 Survey of NASTRAN applications in static and dynamic structural analysis problems
 [NASA-TM-X-2578] 22 p3482 N71-36253
 Equations of motion for elastic plate foundation system under dynamic load applied to aircraft landing
 23 p3864 N71-37543
- DYNAMIC MODELS
 Dynamic modeling of pressurization system and pneumatic pressure regulator in pressure fed liquid propulsion systems
 [NASA-CR-111612] 03 p0448 N71-12281
 Dynamic interaction between structure and liquid propellants in space shuttle vehicle models
 [NASA-CR-111801] 03 p0362 N71-12746
 Dynamic model of fog duration
 [AD-714625] 06 p0838 N71-16605
 Dynamic model for gas phase concentrations in porous fuel cell electrodes
 [NASA-TN-D-6166] 07 p0975 N71-17467
 Modified peaking strip method for measurements of slowly varying low field
 [SIC-A-70-5] 08 p1167 N71-18162
 Solution for ferroelectric crystal in staggered field at all temperatures
 [NUB-2045] 08 p1158 N71-18486
 Coefficient determination of flight dynamics multivariable systems by means of computer simulated aircraft dynamic models
 [DTR-FB-70-30] 08 p1144 N71-18586
 Design, fabrication, and test of research model roller-gear drive consisting of transmission driven by dc motor
 [NASA-CR-103057] 09 p1393 N71-19862
 Dynamic models for cell membrane functions in molecular biology
 09 p1331 N71-19881
 Dynamic model for microvascular system control of mammal body kinematics
 09 p1331 N71-19882
 Biodynamic modeling of biosystems by physical and biological parameters
 09 p1332 N71-19888
 Distributed parameter mathematical model of human body in dynamic mechanical environments
 [AD-717764] 11 p1686 N71-22130
 Data processing algorithm for real time digital modeling of dynamic systems
 11 p1718 N71-22731
 Dynamic model for stress wave propagation in composite material containing dispersed rigid spherical inclusions
 [AD-718087] 12 p1945 N71-23806
 Extraterrestrial ring current intensity changes and aurora dynamics model
 13 p2161 N71-25200
 Fluter and divergence of four low mass ratio hydrofoil model configurations
 [AD-719891] 14 p2238 N71-25603
 Stochastic Markov processes for modelling dynamic power systems
 [FTL-A-A08-9] 14 p2285 N71-26364
 Thermodynamic and dynamic properties for calculating liquid structures
 15 p2413 N71-26831
 Rheological models for evaluating effects of lubricant film thickness and frictional traction
 15 p2413 N71-26832
 Radiation processes for atmospheric dynamic models
 15 p2440 N71-27357
 Simplified dynamic atmospheric model for radiative heat transfer eliminating use of absorption function
 15 p2440 N71-27358
 Temperature effects on thermionic diode with space charge model including emitter and anode electron emission
 [NASA-CR-72682] 16 p2648 N71-28326

- Flow model for turbulent heat transfer in Otto cycle engine 17 p2857 N71-29718
- Dynamic model of semicircular cable affected by angular velocity 18 p2881 N71-31543
- Model of peripheral air jets in air cushion vehicles hovering over water surface 19 p3075 N71-31688
- Heavy-slow model parameter change, speed gas addition, and reflective end-wall effects on nuclear light bulb engine calculations of fuel region radiation emission spectra 20 p3305 N71-33658
- Dynamic models of negative mass instabilities in particle accelerator electron ring compressor [UCRL-20208] 20 p3323 N71-33833
- Calculation of ground motions generated by air waves from surface explosions 21 p3421 N71-34343
- Three suboptimal control policies using reduced dimensional aggregated state vectors 21 p3450 N71-34555
- Dynamic model for optimization of wide utility in engineering sciences 22 p3608 N71-35699
- Technique for conducting landing impact tests at simulated planetary gravity for Mars lander spacecraft - dynamic models [NASA-TN-D-6459] 22 p3681 N71-36247
- Computer learning algorithm to improve parameter search efficiency in system modeling with man-machine interaction 23 p3718 N71-36505
- Dynamic models for ESRO 1 attitude control system using equations of spinning motion [ESRO-TR-5-ESTEC] 23 p3859 N71-37508
- Meson-nucleon interactions and mass distribution compared with Regge pole exchange model [ITEF-790] 24 p3973 N71-38349
- Model for spark chamber breakdowns and shower efficiency determination [JINR-P13-5810] 24 p3979 N71-38393
- Plane wave approximation and shell model for particle-hole states in zirconium 24 p3983 N71-38428
- Dynamic model for ionospheric plasma with interhemispheric coupling [NASA-TM-X-65727] 24 p4008 N71-38576
- DYNAMIC PRESSURE**
- Jet to free-stream dynamic pressure ratio effects on penetration and mixing of hydrogen injected normal to supersonic airstreams [NASA-TN-D-6114] 09 p1377 N71-20195
- DYNAMIC PROGRAMMING**
- Application of multivariable search techniques to design of low sonic boom overpressure [NASA-CR-73-496] 05 p0625 N71-14613
- Functional equations in dynamic programming associated with communication theory [TR-70-48] 08 p1223 N71-18893
- Sequential search problem with dynamic programming for continuous time Markov processes 08 p1226 N71-18961
- Minimum convolutions and Green function in dynamic programming theory [TID-25612] 10 p1594 N71-21662
- Nonlinear and dynamic programming for identification problems [TID-25617] 10 p1595 N71-21794
- Application of dynamic programming and theory of control processes to biological phenomena including evolution of consciousness [TR-71-17] 14 p2204 N71-25937
- Dimensional reduction of potential equations by dynamic programming [USC-113-P-19-8] 14 p2286 N71-26676
- Solving two problems of optimal control in flight vehicles [AD-722280] 17 p2703 N71-29431
- Identification of model parameters from input output data of dynamic systems with time delays [AD-722864] 18 p2946 N71-31217
- Selection of optimal information structure in context of decision theory [AD-719605] 18 p3029 N71-31337
- Fuzzy dynamic programming for use in synthesis of flight control system, and computer algorithm for obtaining guaranteed cost function [AD-722458] 18 p2947 N71-31379
- Nonlinear filters and optimal control in dynamic programming of stochastic processes [AD-722875] 18 p2948 N71-31433
- Parallel standbys redundancy subject to both open and short circuit failures - extension of branch and bound algorithms [AD-723095] 19 p3067 N71-32471
- Pure integer programming and K-th shortest paths [P-4592] 19 p3125 N71-32583
- Theory of logic-dynamic control systems and multi-layer theory of statistical decisions [JPRS-53766] 20 p3288 N71-32822
- Mathematical modeling of logic-dynamic control systems 20 p3288 N71-32823

- Nonlinear optimization techniques in dynamic programming and solution of ordinary nonlinear differential equations by Runge-Kutta method [NASA-CR-121673] 21 p3396 N71-34179
- Calculation of k-th shortest paths and k greater than 2 modification for improved algorithm efficiency [P-4638] 21 p3449 N71-34545
- Dynamic programming procedure for recognizing continuous speech signals composed of words from known dictionary [JPRS-53975] 22 p3556 N71-35328
- Digital control of processes, and dynamic programming to calculate optimal feedback control for nonlinear systems 23 p3738 N71-36658
- DYNAMIC PROPERTIES**
- U DYNAMIC CHARACTERISTICS**
- DYNAMIC RESPONSE**
- Computerized simulation of control systems for nuclear light bulb engine during start-up and at nominal full power operation [NASA-CR-111097] 01 p0085 N71-10404
- Experimental analysis of Fitzgerald dynamic compliance machine [NASA-TM-X-52917] 02 p0283 N71-11457
- High impact dynamic response analysis of nonlinear structures [NASA-CR-111404] 02 p0301 N71-12024
- Steady-profile analysis of plane shock structures in solids [AD-712059] 03 p0460 N71-12949
- Analytical and experimental study of dynamic responses of structures with nonlinear and nonproportional damping [NASA-CR-102939] 03 p0462 N71-13098
- Dynamic aspects of concentrated magnetic systems [COO-1488-21] 04 p0566 N71-13959
- Discrete methods for linear dynamic response of elastic and viscoelastic solids [PB-194286] 04 p0618 N71-14286
- Analysis of pulsed wire anemometer to determine errors caused by finite yaw response of probe [REPT-70-07] 05 p0687 N71-15471
- Measuring dynamic response of thermistors at liquid hydrogen temperatures [REPT-69-01460] 05 p0687 N71-15477
- Dynamic response of F-2 aircraft using cross correlation and power spectra [ARC-CP-1121] 06 p0793 N71-15720
- Flat frequency response pressure transducer system [AD-714602] 06 p0861 N71-16611
- Computer program for determining static and dynamic response of symmetrically loaded elastic orthotropic shells of revolution [NASA-TM-D-6158] 06 p0957 N71-16846
- DYNASOR-2 finite element program for dynamic nonlinear analysis of shells of revolution [NASA-CR-114823] 06 p0958 N71-16883
- Static and dynamic stability and dynamic response of differential pressure sensor with electromechanical or electroacoustic feedback [RAE-TR-70120] 07 p1027 N71-17134
- Optimum binary signals for frequency response testing [ORNL-TM-3198] 07 p1060 N71-17189
- Dynamic response of supported beams to excitation by statistical pressure distributions [ISVR-TR-30] 07 p1123 N71-17212
- Responses of balloon and falling sphere wind sensors in atmospheric turbulence, analyzed with Fourier transformation [NASA-TN-D-7049] 07 p1053 N71-17479
- Dynamic response of vehicle and its automatic flight control system 09 p1324 N71-20334
- Shell impact response and wave propagation in cylindrical and conical shells by experimental and analytical methods [NASA-CR-46921] 10 p1651 N71-20701
- Finite difference model and computer program for predicting large deflection elastoplastic response of shell structures [AD-717005] 10 p1655 N71-21192
- Analytical treatment of problems of dynamic response of linearly elastic structural members with changing boundaries based on amplitude perturbation scheme 10 p1655 N71-21260
- Dynamic models of human body response to acceleration environments and determination of tolerance limits [NASA-TM-X-67038] 10 p1501 N71-21598
- Coupling characteristic effects on dynamic response of axially coupled turbomotors with digital computer program based on transfer matrix techniques 11 p1770 N71-22712
- Asymptotic solutions of stress and strain as functions of radial and longitudinal distance, and time for axisymmetric waves in step-function pressure-loaded hollow elastic circular cylinder 11 p1836 N71-22793
- Transfer functions in modelling human pilot and dynamic structural aircraft responses [AGARD-R-380-71] 12 p1830 N71-23210

- Human factors for defining transfer functions in pilot modelling 12 p1861 N71-23214
- Mathematical model for computer program to determine vibratory response of finite plates and associated acoustic radiation to fully developed turbulence excitation [AD-718815] 12 p2004 N71-23289
- Eigenvalue and deflection quantities of structural systems with material, geometric discontinuities, boundary conditions, and external loadings with probabilistic distributions 12 p2007 N71-24119
- Approximate models for amplification by wave distortion of dynamic response of vaporization limited combustion [NASA-TN-D-6287] 12 p2013 N71-24262
- Dynamic response of thermal protection system panel for space shuttle 13 p2179 N71-24844
- Alleviation of lateral and longitudinal gust effects in aircraft 13 p2024 N71-24709
- Formula for determining response of infrared scanner [AD-719647] 13 p2126 N71-23140
- Pressure sensor network for measuring fluid dynamic response in flight including fuel tank excitation, liquid slosh amplitude, and fuel depth monitoring [NASA-CASE-XLA-05541] 14 p2242 N71-26007
- On-line monitoring of characteristic structural response of space shuttle wing flutter model for failure detection and repair [NASA-TM-X-62041] 15 p2521 N71-28892
- Anticoherence function of dynamic systems including white noise and applications to oscillators [LIRBA-TN-3] 15 p2579 N71-27110
- Computerized simulation of experimental breeder reactor 2 dynamic responses to uranium-fission and PuO₂-UO₂ fuels including specific heat and thermal conductivity effects [ANL-7673] 15 p2449 N71-27708
- Mathematical model and algorithms for Stylo docking dynamic response analysis with simulated analysis of Apollo probe/drogue docking system 16 p2609 N71-29900
- Response analyzing apparatus for liquid vapor interface sensor of sloshing rocket propellant [NASA-CASE-MPS-11204] 16 p2399 N71-28814
- Application of linear control of systems with random inputs to gust response control of aircraft dynamics in atmospheric turbulence [ONERA-F-131] 17 p2701 N71-30884
- Dynamic psychological and ergonomic aspects of mental imagery [IEZF-1970-21] 18 p2676 N71-31080
- Human dynamic response to impact acceleration minus G sub x - measurements on head and neck [AD-717130] 19 p3046 N71-31616
- Statistical analysis of terrain-vehicle speed and dynamic response of wheeled vehicles [AD-723405] 19 p3072 N71-31722
- Computer program for predicting curved beam sensor transducer shell dynamic responses to shock waves [AD-723826] 19 p3183 N71-31886
- Analysis of SERT 2 spacecraft attitude response including magnetic, solar pressure, and ion thruster disturbance torques [NASA-TM-X-2324] 19 p3184 N71-32119
- Computer plots of acceleration flight data of Mariner Mars 69, OAO 2, and ATS showing selected signal axis forcing functions and dynamic response of Centaur main engine cutoffs [NASA-CR-119693] 19 p3185 N71-32070
- Computer program for calculating effects of subplate stiffness on helicopter rotor system dynamics and stability [NASA-CR-1818] 19 p3039 N71-32797
- Vibrational responses of VC-16 aircraft during takeoff runs, noising cockpit accelerations [ARC-CP-1149] 20 p3288 N71-32811
- Scheme for servomechanism with variable amplifier and dynamic response with nonlinear parameters 20 p3288 N71-32811
- Primary emission neutron activated detector for measuring system working at high temperature with fast response [AERE-R-6732] 21 p3471 N71-34076
- Evaluation of three methods for determining response analysis of plate and shell structures under random acoustic excitation [NASA-CR-119982] 21 p3526 N71-33015
- Assessment of nonlinear response of aerospace structures with nonideal characteristics under vibration conditions [ARL/SM-355] 21 p3527 N71-33814
- Development of specialized quadrupole mass spectrometer with high resolution and dynamic range increase [NASA-CR-121906] 22 p3582 N71-35500
- Nuclear reactor mathematical model matching of open loop dynamic response with experimental data [AEEW-M-1012] 22 p3620 N71-35704

SUBJECT INDEX

Dynamic response of cylindrical shell excited by distributed turbulent boundary layer pressure field determined by NASTRAN 22 p3685 N71-36375

Solutions for dynamic response of simply supported rectangular plate and shallow shell of rectangular planform 22 p3692 N71-36329

Useful frequency response variations and viscous damping in short pressure probe tubes 23 p3759 N71-36795

Dynamic response of gas lubricated thrust bearing with shrouded Raleigh-step pads 23 p3761 N71-36809

Dynamic response of hydrophobic spherical shell predicted by finite element model 23 p3861 N71-37528

Dynamic response of slender circular cylinders in axial flowing fluid with base excited motion 23 p3863 N71-37541

Equations for variation with frequency of voltage output from hydrophone exposed to constant acoustic pressure field 24 p3967 N71-38300

DYNAMIC STABILITY

NT AERODYNAMIC STABILITY 11 p1834 N71-21942

NT AIRCRAFT STABILITY 11 p1834 N71-21942

NT ATTITUDE STABILITY 11 p1834 N71-21942

NT BOUNDARY LAYER STABILITY 11 p1834 N71-21942

NT COMBUSTION STABILITY 11 p1834 N71-21942

NT CONTROL STABILITY 11 p1834 N71-21942

NT DIRECTIONAL STABILITY 11 p1834 N71-21942

NT FLAME STABILITY 11 p1834 N71-21942

NT FLOW STABILITY 11 p1834 N71-21942

NT FREQUENCY STABILITY 11 p1834 N71-21942

NT GYROSCOPIC STABILITY 11 p1834 N71-21942

NT HOVERING STABILITY 11 p1834 N71-21942

NT LATERAL STABILITY 11 p1834 N71-21942

NT LONGITUDINAL STABILITY 11 p1834 N71-21942

NT LOW SPEED STABILITY 11 p1834 N71-21942

NT MAGNETOHYDRODYNAMIC STABILITY 11 p1834 N71-21942

NT MOTION STABILITY 11 p1834 N71-21942

NT ROTARY STABILITY 11 p1834 N71-21942

NT SPACECRAFT STABILITY 11 p1834 N71-21942

Physical failure analysis of integrated circuits containing metal oxide semiconductors and its application to analog gates 02 p0194 N71-11359

Dynamic stability derivatives of twin-jet fighter model for angles of attack from -10 deg to 110 deg 06 p0954 N71-16332

Dynamic stability of fast reactor with in-core thermoelectric converters 05 p0724 N71-14732

Thermoelectric instability of frictional contacts 06 p0954 N71-16332

Dynamic stability of legged locomotion systems 06 p0907 N71-16553

Static and dynamic stability and dynamic response of differential pressure sensor with electromechanical or electroacoustic feedback 07 p1027 N71-17134

Dynamic stability of cantilever model subjected to following pulsating loading 08 p1301 N71-19319

Stability models for weakly nonlinear dynamical systems with application to gyroscopic devices 09 p1409 N71-19688

Dynamic stability criteria for continuous system states in energy, adjacent equilibrium, or Gibbs sense 10 p1662 N71-21471

Stability of decentralized linear dynamic systems with proportional feedback control 10 p1593 N71-21502

Changes in topological structure of dynamic system when system itself is changing 11 p1786 N71-21902

Stability, foam flow, and wave effects on hovercraft during power failure 11 p1690 N71-22448

Mathematical model of oil whip phenomenon in rotating shaft systems with incompressible fluid lubrication and analysis of squeeze film bearings 11 p1770 N71-22724

Relationship between dynamic buckling and static buckling investigated with clamped shallow circular arches using high speed cameras 14 p2358 N71-26467

Aerodynamic forces and dynamic stability of high-speed, magnetically suspended rocket sled moving down to stationary wall 15 p2390 N71-26943

Network of analytical methods and stability data for determining dynamic stability and control characteristics of powered single-engine compound helicopter configurations 16 p2531 N71-28338

Mathematical model of satellite with continuous elastic components comprising moment free rigid carrier attached to elastic membranes 17 p2779 N71-29700

Linear and nonlinear dynamic stability coefficient using biphenyl wind tunnel, free flight system 18 p2687 N71-31107

Configurational stability theory of fluid menisci contacting solid surfaces 19 p3083 N71-32723

Mathematical models for calculating flexible swash-plate effects on vibratory and mechanical stability characteristics of helicopter rotor systems 20 p3211 N71-33593

Hydrodynamic lubrication of journal bearing with one or two axial oil grooves, with power loss, load capacity, oil flow, and stability charts for design of minimum power loss, stable bearing 20 p3280 N71-33799

Application of cybernetics and control theory to problems of production control in complex systems and optimum stabilization of several coordinates of object by one controlling influence 21 p3405 N71-34230

Optimum stabilization of several coordinates of object in linear system by one controlling influence 21 p3406 N71-34232

Laplace method for investigating dynamic stability of cylindrical shells and folded plates subjected to stochastic excitations 23 p3865 N71-37533

Dynamic stabilization of helical in equals 1 instability characteristic for high bolt screw pinch 24 p3985 N71-38440

Experiments on linear and nonlinear feedback and dynamic stabilization of drift and transverse Kelvin-Helmholtz instabilities 24 p3991 N71-38476

Computer programs for dynamic structural analysis 02 p0300 N71-11944

Techniques for random vibration equalization using versatile laboratory apparatus 02 p0304 N71-12148

Computer based methods in man machine interaction for dynamic structural design optimization of stressed-skin structures and structural members 03 p0462 N71-13126

Finite element method for dynamic structural analysis in vertical takeoff aircraft design 03 p0464 N71-13134

Computer graphic system for three dimensional structural design analysis 03 p0348 N71-13139

Man machine system for finite element structural analysis with computer graphics 03 p0465 N71-13140

Dynamic stress analysis of axisymmetric structures under arbitrary loading 04 p0616 N71-13819

Mathematical model with error correction for calculating optimal solid bed reactor dimensions 05 p0639 N71-14821

Wind effect criteria for structural design and engineering of buildings 05 p0776 N71-15301

Structural building design criteria for dynamic wind loads 05 p0777 N71-15302

Aeroelastic wind effects for dynamic design of tall buildings 05 p0778 N71-15311

Aeroelastic responses of tall buildings to vortex shedding and gust loading 05 p0778 N71-15312

Deficiencies in dynamic structural analyses for buildings subjected to wind loads 05 p0778 N71-15313

Aeroelastic wind tunnel modeling and three dimensional structural analysis for dynamic building response prediction to wind loads 05 p0778 N71-15314

Measurement of dynamic stress and strain in rotational triaxial loading 06 p0857 N71-15853

Lumped mass finite difference analysis for loaded structural beam dynamics 07 p1126 N71-17886

Plastic deformations of clamped beams by impulsive loading 07 p1126 N71-17887

Minimum weight and strain equations for optimal beam and frame structures under random loads 08 p1296 N71-18619

Dynamic structural analyses on minimum weight beams and frames by one degree of freedom system 08 p1296 N71-18620

Variational calculus for minimum weight loaded beam structures 08 p1297 N71-18646

Sonic velocity and startup considerations in heat pipe design 08 p1303 N71-18944

Dynamic stability of cantilever model subjected to following pulsating loading 08 p1301 N71-19319

Swept wing body configurations for reduced drag at supersonic speed 09 p1312 N71-19558

Aerodynamic configuration effects of propulsion system integration into supersonic transport design 09 p1436 N71-19373

DYNAMIC STRUCTURAL ANALYSIS

Digital computer program description with updating case data mode and extended force method matrix generation capability 09 p1356 N71-20100

Analytical treatment of problems of dynamic response of linearly elastic structural members with changing boundaries based on amplitude perturbation scheme 10 p1655 N71-21260

Dynamic stability of simply-supported rectangular and circular cylinders and/or structures under uniformly distributed periodic edge loads 10 p1655 N71-21261

Probabilistic theory for analyzing response and safety of buildings subjected to seismic loading 10 p1656 N71-21268

Determination of structural stability and deformation of infinite plates and shallow shells under doubly periodic surface loads 10 p1658 N71-21262

Computer programs for dynamic design and analysis of mechanisms composed of beams and/or springs with up to 48 degrees of freedom 11 p1834 N71-21933

Finite element analysis for response behavior of stiffened rectangular plates subjected to dynamic loads 11 p1834 N71-21942

Transfer functions in modelling human pilot and dynamic structural aircraft response 12 p1850 N71-23210

Power spectrum method for determining gust frequency response functions in dynamic aircraft design 12 p1850 N71-23211

Mathematical modelling of aircraft structural response modes to active control systems 12 p1852 N71-23212

Computation and measurement of dynamic aircraft transfer functions to atmospheric turbulence 12 p1852 N71-23213

Determination of Burger vectors, glide planes, and densities of crystal dislocations by various Bragg angle sequence micrograph and dynamic electron diffraction equation analysis 12 p1967 N71-23957

Dynamic structural analysis on low frequency radio telescope scale model with parabolic antenna 13 p2170 N71-25305

Dynamic thermal oscillation analysis on satellite boom rod 13 p2175 N71-25306

NASA computer program for dynamic structural analysis in stress and thermal deformation problems 13 p2182 N71-25307

Critical pressure loads and structural bending stability of variable thickness shell 13 p2182 N71-25361

Vibrational data for analytical modal path model of structural dynamics 15 p2522 N71-27858

Structural dynamics of heliogyro solar cell device 15 p2523 N71-27999

Aluminum panel flutter tests at supersonic Mach numbers 16 p2685 N71-28161

Air flow thermodynamics for low sonic boom design of supersonic transport configuration 16 p2685 N71-28161

Dynamic structural analysis, statistical analysis, and Rayleigh-Ritz methods applied to Skylab and Apollo/Saturn problems including pogo effects, vibration damping, and noise reduction 16 p2688 N71-29095

Statistical analysis of Saturn S-2 test data for determination of safety factor requirements of untested structures 16 p2688 N71-29096

Rayleigh-Ritz iterative solution techniques for structural modal response analysis under static loads using IBM 7094 computer 16 p2688 N71-29097

Dynamic structural analysis and flow induced stress analysis of metal bellows in Apollo Saturn launch vehicle systems 16 p2688 N71-29098

Dynamic and static structural analysis computer program for one and two dimensional elastic bodies 16 p2689 N71-29099

Vibration tests and dynamic structural analysis of pogo effects in Saturn S-2 stage burn on Apollo flights 16 p2689 N71-29102

Cross correlation function for estimating structural frequency response 17 p2771 N71-29312

Dynamic structural analysis on resonant cavity for superconducting low energy proton linear accelerator 18 p2981 N71-30662

Computer program for hydroelastic analysis of thin walled structures 18 p2983 N71-30669

Evaluating effects of high altitude turbulence encounters on X-29 airplane 18 p2988 N71-30718

- Static and dynamic thread parameter effects on deformation of loaded screw connections
18 p2930 N71-31322
- Vibration mode model and computerized simulation of dynamic system modal response
[UCRL-72818-REV-1] 20 p3359 N71-33714
- Dynamic structural analysis of clamped skew plate buckling under various loads
[AE-296-5] 20 p3360 N71-33822
- Electrical analog for sonic boom indoor pressure wave effect on structural members
[UTIAS-TN-158] 20 p3312 N71-33964
- Structural dynamic analysis of electronic assemblies subjected to random vibration loads
22 p3685 N71-36274
- Effect of rotation on structural and dynamic behavior of spinning body with flexible appendages, and application to Skylab Apollo telescope mount and orbital workshop
22 p3685 N71-36278
- Application of NASTRAN to structural analysis of space shuttle orbiter finite element model with over 3000 joint degrees of freedom
22 p3685 N71-36279
- Use of NASTRAN as analysis tool in structural design optimization process applied to aircraft fuselage type structure
22 p3685 N71-36280
- Evaluation of NASTRAN system based on large complex airframe analysis
22 p3686 N71-36282
- Management, standards, and maintenance of NASTRAN documentation reviewed with emphasis on specifications in style and format
22 p3686 N71-36283
- NASTRAN installation and implementation on CDC 6600, IBM 360, and UNIVAC 1108
22 p3686 N71-36289
- Evaluating current NASTRAN discrete element models for monocoque and semimonocoque structures
22 p3687 N71-36290
- Comparison of wavefront sequencing and bandwidth sequencing using NASTRAN program for relative compactness of structural models
22 p3687 N71-36291
- NASTRAN generation of motion pictures for analysis of elastic structure transient responses under continuous deformation conditions
22 p3687 N71-36294
- Dynamics of periodically stiffened beams and plates using wave approach
[AD-726570] 22 p3690 N71-36317
- Nonlinear analysis technique for planar steel and reinforced concrete frames under static and short-time loading
23 p3864 N71-37545
- DYNAMIC TESTS**
- Hydraulic support apparatus for dynamic testing of space vehicles under near free flight conditions
[NASA-CASE-XMF-03248] 01 p0038 N71-10604
- Avoidance of disrupting effects in dynamic tests on semispan delta wing models in transonic slotted and perforated wind tunnels
[ARC-RM-3636] 06 p0791 N71-15701
- Dynamic tear tests to determine thick-section steel fracture strength
[NRL-7056] 06 p0869 N71-15850
- Generalized digital compensators for sampled-data systems
08 p1166 N71-18869
- Chemisorption of O₂, CO, and CO₂ on solid fuel under static and dynamic conditions
[NLL-RTS-5837] 10 p1638 N71-21746
- Low-inertia flow-direction vane static and dynamic wind tunnel tests at subsonic and supersonic speeds for in-flight measurement of burst velocities
[NASA-TN-D-6193] 12 p1915 N71-23115
- Conference on fatigue life in helicopter components
[DLR-MTT-79-01] 13 p2024 N71-24385
- Dynamic tests of helicopter components
13 p2025 N71-24388
- Structural stability tests of helicopter components
13 p2025 N71-24390
- Dynamic deformation and fracture strength of tungsten carbide-cobalt alloys at elevated temperatures
13 p2096 N71-25114
- Ditching behavior of dynamic C-5A model
18 p2868 N71-30757
- Dynamic tests on tangential pipe fittings differing in types and dimensions
[ORNL-TR-1991] 19 p3105 N71-32214
- DYNAMICS**
- Particle equations of motion for solving problems in electrodynamics, gas dynamics, hydrodynamics, and solid state physics
[NASA-TT-F-670] 18 p2948 N71-31492
- DYNAMO THEORY**
- Velocity and stress distributions in earth mantle due to secular variation of geomagnetic field
05 p0669 N71-14796
- Electrical structure model of D and E region, based on dynamic current theory
[AD-714365] 06 p0849 N71-16335

Electric currents and fields produced in ionosphere by highly varying horizontal winds
10 p1553 N71-21313

DYNAMOMETERS

Hydraulic grip dynamometer for study of elevated gravitational effects on flight crews
[AD-719111] 08 p1157 N71-18415

Development of thrust dynamometer for measuring performance of jet and rocket engines
[NASA-CASE-XLB-05260] 09 p1391 N71-20429

DYNAMOS**U ROTATING GENERATORS****DYNODES**

Transmission secondary emission multipliers using silicon high gain secondary emitters
[NYO-4100-3] 08 p1264 N71-19102

DYSPROSIUM**NT DYSPROSIUM ISOTOPES**

Yttria and dysprosia high temperature thermistor materials
[BM-RI-7458] 02 p0249 N71-12113

Internal fields and relaxation effects for dysprosium in ferromagnetic TbAl₂ studied by perturbed angular correlation
[UIUP-684] 06 p0909 N71-15752

State diagram of system Dy₂O₃-Cr₂O₃
07 p1041 N71-17124

Energy level analysis of dysprosium first and second spectra from wavelength and wave number measurements and Zeeman effect observations
[UCRL-19944] 09 p1408 N71-20536

Magnetic properties of gadolinium, terbium, dysprosium, and holmium hydroxides at cryogenic temperatures
20 p3313 N71-33755

X ray diffraction and metallographic phase study of UO₂-Dy₂O₃
[JAERI-1203] 22 p3620 N71-35789

DYSPROSIUM ISOTOPES

Half life of first excited levels of main and rotational band in even-even nuclei of Os, Er, and Dy
[JINR-P6-5201] 08 p1230 N71-18232

Structure of neutron deficient holmium and dysprosium nuclei investigated using Ge/Li detectors and computer methods
[BMBW-FBK-70-30] 18 p2979 N71-30729

DYSPROSIUM 161**U DYSPROSIUM ISOTOPES****E****E LAYERS****U E REGION****E REGION****NT SPORADIC E LAYER**

Gun and rocket emplaced alkali plasma cloud in E region
[AD-710742] 01 p0048 N71-10486

Tidal motions in E region as source of daily variation of geomagnetic field
[AD-711782] 01 p0051 N71-10849

Ionospheric vertical sounding data of F and E regions from Freiburg, Germany for August 1970
[REPT-290-F] 02 p0214 N71-11864

Wave-like structures in E-region derived from drift experiments
[AD-712346] 02 p0220 N71-12093

Development of model of E and F regions of ionosphere
[NASA-CR-115894] 05 p0668 N71-14759

Electrical structure model of D and E region, based on dynamo current theory
[AD-714365] 06 p0849 N71-16335

Cosmos 224 measurements of nitric oxide vertical profile in E and F regions at low sun zenith angles
07 p1014 N71-16934

Characteristics of D and E regions of ionosphere
[NASA-CR-116441] 07 p1016 N71-17052

Ion convergence production in E region by vertical neutral gas motions
[ESSA-TR-ERL-175-ITS-112] 07 p1114 N71-17914

Swedish/NASA rocket sounding in auroral D and E regions for ionospheric ion and electron density investigation using Arcas and Petrel rocket vehicles
[REPT-53-K48-44] 10 p1552 N71-21270

Artificial electron cloud formation using cesium and potassium isotopes for simulation of ionospheric propagation in E region with coherent radar
[AD-720934] 15 p2406 N71-27809

Ionospheric propagation data for E and F regions, Bangkok - Aug. 1970
[AD-720326] 16 p2589 N71-28864

Ionospheric propagation data for E and F regions, Bangkok - Sept. 1970
[AD-720327] 16 p2589 N71-28865

Launching of Cosmos, Soyuz, and Mars spacecraft and ionization in E layer
17 p2739 N71-29404

Ionospheric propagation data for E and F regions, India - October 1969
[RTRC-A173] 22 p3575 N71-35460

Ionospheric propagation data for E and F regions, India - September 1969
[RTRC-A172] 22 p3575 N71-35461

Ionospheric propagation data for E and F regions, India - Aug. 1969
[RTRC-A171] 22 p3575 N71-35462

Diurnal temperature variations in middle ionosphere and electron density in E, E-F, and F₂ regions
22 p3579 N71-36231

Annual variation of ionospheric drift in E region at Garchy, France using signal fading method
[ORI/NTF/87] 23 p3750 N71-30779

Ionospheric propagation data for E and F regions, India - [Dec. 1969]
[RTRC-A173] 23 p3752 N71-30782

Ionospheric propagation data for E and F regions, India - Nov. 1969
[RTRC-A174] 23 p3752 N71-30783

Absorption and group delay data from ground station used to model electron density profile in D and E regions of ionosphere
[NASA-TM-X-65730] 24 p3909 N71-37843

EAR**NT COCHLEA****NT LABYRINTH****NT SEMICIRCULAR CANALS****NT VESTIBULES**

Ear oximeter for monitoring blood oxygenation and pressure, pulse rate, and pressure pulse curve, using dc and ac amplifiers
[NASA-CASE-XAC-05422] 12 p1861 N71-23116

EAR PROTECTORS

Sound attenuation characteristics of military ear protective devices and helmets
02 p0171 N71-11891

Noise problems in air evacuation operations and effectiveness of ear protective devices
[AD-713882] 06 p0801 N71-14204

Real ear evaluation of earplugs using comparison of noise bands to pure tones
[AD-715748] 08 p1148 N71-18536

Good-fidelity earplug evaluation, emphasizing noise reduction and speech intelligibility
[AD-716356] 09 p1399 N71-19844

Direct person-to-person voice communication in rotary wing aircraft improved by use of earplugs
[AD-716768] 10 p1497 N71-20828

Optimal fitting of flight helmets for noise reduction
[AD-718327] 12 p1866 N71-23109

Weighting method for aircraft auditory risk limits when wearing ear protectors
[AD-719861] 13 p2038 N71-25906

Bibliography of literature on environmental pollution, noise pollution, and ear protection devices
[AD-724650] 20 p3226 N71-31868

EARLY BIRD SATELLITES

Early bird and ATS C simultaneous recordings of F region ionospheric electron density for scientific analysis of ionospheric disturbances
[AD-719872] 14 p2245 N71-25427

Low elevation recording of Early Bird satellite transmission with polarimeter, noting induction antenna coupling
24 p3914 N71-37840

EARLY STARS**NT T TAURI STARS**

Meteorological parameter observation, early star spectrum analysis, and astronomical telescopes
22 p3670 N71-36170

Spectrum analysis of early stars with extended atmosphere, noting supergiant and main sequence stars
22 p3670 N71-36171

EARLY WARNING SYSTEMS

Cost effectiveness of pulse Doppler radar in airborne aircraft of early warning system
04 p0621 N71-19199

EARTH (PLANET)

Combination of satellite and gravity data for position and gravity field determination
[AD-712348] 02 p0222 N71-12091

Earth gravity data used in determining gravitational potential vector, for satellite orbit calculation
[AD-712349] 02 p0222 N71-12090

Spaceborne photographs of earth atmosphere, lands, and waters, with photographs of sun, moon, and planets
[NASA-SP-350] 03 p0366 N71-12508

Mathematical modeling of world geodetic system
05 p0672 N71-14870

Numerical analysis of nonlinear interaction in rotating, stratified fluid with free surface
[AD-719940] 13 p3067 N71-32044

Radiation danger of Kr-83 in troposphere and lower stratosphere from worldwide nuclear power plants
[JPRS-33174] 14 p2251 N71-26013

Fine structure observation in high frequency radio signals propagated around world using obliqueograms
[AD-721703] 16 p2561 N71-30468

Apollo 14 crew visual observations of earth, moon, lunar topography and geology, and astronaut maneuverability during extravehicular activity
18 p3010 N71-30808

SUBJECT INDEX

- History of earth's crust based on rheology and chemistry of upper mantle, evidence from continents, and evidence concerning drift from ocean basins 18 p2512 N71-30993
- Investigation of solar wind interaction with earth's magnetic dipoles and shape of magnetosphere including tail and collisionless shock wave investigated by magnetic probe 18 p2564 N71-31095
- [NASA-TT-F-13734] 18 p2564 N71-31095
- Vertical accelerometers for observing ground motion caused by ocean tides, low frequency ocean waves, and atmospheric pressure 19 p3084 N71-31726
- [AD-723869] 19 p3084 N71-31726
- Approximate reduction of gravity formula describing earth shape to Taylor series 19 p3091 N71-31927
- [AD-723515] 19 p3091 N71-31927
- Gravitometric and pendulum data of terrestrial tides obtained by Arctic station 20 p3261 N71-33324
- [BULL-4/1] 20 p3261 N71-33324
- Gravitometric tides in earth gravity field 20 p3266 N71-33387
- Zonal atmospheric model for simulating earth's climate and testing ice age theories 20 p3269 N71-33851
- [UCRL-72803] 20 p3269 N71-33851
- International bibliography on terrestrial tide research 20 p3268 N71-33839
- Topographic mapping of gravitational field data [NEFT-179] 20 p3269 N71-33851
- Infrared satellite photographs for studying hydrology, glaciology, oceanography, volcanology, and radiation balance of earth 21 p3426 N71-34378
- [NASA-TT-F-13930] 21 p3426 N71-34378
- Creation of high negative potential on screened spacecraft for protection of equipment, materials and crew from electron radiation belts of earth [NASA-TT-F-13903] 21 p3504 N71-34959
- Earth tide tables 22 p3573 N71-35449
- Astronomical observations of free diurnal nutation amplitudes of earth 23 p3748 N71-36725
- Underground laboratory for studying variations in earth tides 23 p3749 N71-36727
- Elastic earth tide inclinations observed at Talgar 23 p3749 N71-36728
- Instrument drift in earth inclination observations made by Engelhart Astronomical Observatory 23 p3749 N71-36729
- Earth tide observations and measuring instruments 24 p3910 N71-37871
- Earth tilt measurements by parallel clinometers 24 p3911 N71-37877
- Estimation of interplanetary shock speed and surface normal for 8 July 1966 shock in vicinity of earth [NASA-TM-X-65720] 24 p4008 N71-38574
- EARTH ALBEDO**
- Satellite measured albedo and long wave radiation study of Indian monsoons 02 p0256 N71-11622
- Error study for SS-1090 ATM sensor system, effects of atmospheric refraction, atmospheric attenuation and earth albedo 04 p0611 N71-14008
- [NASA-CR-102957] 04 p0611 N71-14008
- Gemini 3 flight data on earth radiation at 2.2 microns 15 p2400 N71-27492
- High energy neutron detector for measuring solar neutron flux in earth radiation environment during quiet or active sun conditions 18 p3009 N71-30891
- [AD-72467] 18 p3009 N71-30891
- Global annual averages of earth albedo and radiation used to estimate long term effects on space vehicle environment and surfaces 20 p3258 N71-33104
- [NASA-SP-8067] 20 p3258 N71-33104
- Harmonic analysis of temporal and meridional variations of albedo and absorbed solar radiation zonal means derived from digitized satellite pictures taken in 1967 21 p3505 N71-34974
- Shadow and earth albedo effect on ESRO 1 solar cell array performance in orbit [ESRO-TM-103-ESTEC] 23 p3859 N71-37505
- EARTH ATMOSPHERE**
- ARTIFICIAL RADIATION BELTS**
- D REGION**
- E REGION**
- EXOSPHERE**
- F REGION**
- F 2 REGION**
- FREE ATMOSPHERE**
- HETEROSPHERE**
- INNER RADIATION BELT**
- IONOSPHERE**
- LOWER ATMOSPHERE**
- LOWER IONOSPHERE**
- MAGNETOPAUSE**
- MAGNETOSPHERE**
- MESOPAUSE**
- MESOSPHERE**
- OUTER RADIATION BELT**
- PROTON BELTS**
- RADIATION BELTS**
- SPORADIC E LAYER**
- THERMOSPHERE**

- NT TROPOPAUSE**
- NT TROPOSPHERE**
- NT UPPER IONOSPHERE**
- Numerical interpretation of wind, temperature, and specific humidity profiles for surface boundary layer of atmosphere 02 p0258 N71-11741
- [AD-71539] 02 p0258 N71-11741
- Long range forecasting of climatic factors determined by cyclic behavior of oscillations in mobile envelopes of earth 02 p0260 N71-12145
- [NLL-M-9141-5828.4F/1] 02 p0260 N71-12145
- Solution of chemical nonequilibrium boundary layer flow of hypersonic in earth atmosphere 03 p0361 N71-12588
- Carbon dioxide content changes in atmosphere [NLL-M-9147-5828.4F/1] 03 p0367 N71-12864
- Recording dust concentrations in atmosphere [NLL-M-9139-5828.4F/1] 03 p0368 N71-12866
- Theoretical analysis of geological processes affecting evolution of earth atmosphere 03 p0670 N71-14826
- Flow of radiation in earth atmosphere [AD-715269] 07 p1022 N71-17813
- Search for flux of high energy solar neutrons at earth 07 p1107 N71-18150
- Radiative transfer in planetary atmospheres [AD-715290] 08 p1287 N71-18337
- Recombination of nitrogen atoms, visible emission from oxygen atoms, and photolysis of sulfur dioxide for atmospheric studies 08 p1194 N71-19024
- Electromagnetic wave transmission in earth atmosphere from 3 kHz to 3000 THz with emphasis on earth to space paths up to Jan. 1970 [NASA-CR-117173] 09 p1350 N71-20121
- Computerized real time simulation of atmospheric balloon environment in altitude chamber 09 p1383 N71-20217
- Analysis of multiple earth bow shock crossings at large geocentric distances from Pioneer 8 magnetic field data [NASA-TM-X-65474] 10 p1554 N71-21541
- Variable spectrum of colors of earth as viewed from space [JPRS-52615] 11 p1744 N71-21887
- Bibliographies on natural resources including atmosphere, earth, water, climate, plants, and animal subject matter [AD-717253] 11 p1744 N71-21894
- Earth atmosphere and meteorological parameters, and radioisotope Meteorit 2 11 p1791 N71-22684
- Possible effect of multiannual variations in tide generating forces of moon and sun on oceans and atmosphere 11 p1754 N71-22821
- Testimony in support of creation of National Oceanic and Atmospheric Administration 11 p1848 N71-22899
- Ablation sensor for measuring surface ablation rate of material on vehicles entering earth atmosphere on entry into planetary atmospheres [NASA-CASE-XLA-01791] 11 p1765 N71-22991
- Satellite observations, earth atmosphere, and solar radiation - reports received at World Data Centre C1, 1 July - 31 Dec. 1970 12 p1996 N71-23993
- Description of method for determining visibility in earth atmosphere 13 p2104 N71-24375
- Seasonal profiles of radiative heating and thermal cooling of earth's atmosphere. 13 p2077 N71-25401
- [MIT-2241-58] 13 p2077 N71-25401
- News briefs, and abstracts of scientific articles concerning oceanography 15 p2396 N71-26662
- Investigation of optical properties of earth's atmosphere noting occultation of stellar objects, transparency of atmosphere, and twilight observation technique 15 p2516 N71-26802
- Survey of 1962-1965 satellite observation of earth atmosphere radiation climatology 15 p2514 N71-27493
- Climatology of net radiation of earth surface atmosphere system deduced from satellite actinometric measurements 15 p3400 N71-27494
- Calculation of infrared radiation emerging from earth atmosphere in presence of cirrus clouds using remote sensing 15 p2402 N71-27531
- Twilight glow brightness calculation of real terrestrial atmosphere 15 p2403 N71-27536
- Mathematical models for investigating stability of thermally stratified shear flow in atmosphere [NASA-CR-119026] 16 p2579 N71-28321
- Validity of bremsstrahlung model for background radiation in galaxy and earth atmosphere [NASA-TT-F-13615] 16 p2675 N71-28943
- Earth atmospheric thermal radiation spectra and angular distributions and satellite borne moisture and temperature measuring instruments [NASA-TT-F-636] 17 p2752 N71-29778

- EARTH CRUST**
- Atmosphere ozone measurements using filter spectrophotometer and noting Rayleigh scattering 18 p2909 N71-30628
- Computerized simulation of convection currents in atmosphere [AD-722834] 18 p3354 N71-31287
- Beta particle observations between lower edge of plasma sheet to magnetopause in midnight earth magnetosphere [NASA-TM-X-65640] 19 p3084 N71-32436
- Similarity solutions for gas expansion in rarefied atmosphere [P-4562] 19 p3081 N71-32540
- Acquisition of data in Caribbean related to energy exchange between ocean surface and atmosphere - Project BOMEX 20 p3360 N71-32886
- Depletion of atmospheric ozone by nitric oxide from SST exhausts 20 p3311 N71-33439
- Origin and structure of primitive terrestrial atmosphere and Venus and Mars atmospheres [BEP-70-444] 20 p3349 N71-33712
- Restraint system for argument used under zero gravity conditions on earth atmosphere in unconventional positions [NASA-CASE-MPS-21046] 21 p3385 N71-34080
- Radiative flux densities and heating rates in atmosphere calculated using pressure and temperature dependent emissivities 21 p3423 N71-34539
- Rocket and balloon measurements of energy spectra and fluxes of fast neutrons, gamma rays, and X rays in atmosphere [NASA-CR-121629] 21 p3503 N71-34952
- Geographical coordinates of geostrophic height, pressure, temperature, density, and potential energy levels in earth atmosphere [NASA-CR-121664] 21 p3507 N71-34966
- Design, development, and characteristics of gamma backscatter atmosphere density sensor [NASA-CR-111933] 22 p3583 N71-35519
- State-of-the-art review of earth and planetary atmospheres 22 p3670 N71-36169
- Convective instability in fluid layer with electromagnetic effects applied to earth and stellar atmospheres 22 p3672 N71-36183
- Secular perturbations in artificial earth satellites due to atmospheric attraction 22 p3676 N71-36209
- Radiation shielding and biogeological process and their maintenance for earth preservation [JPRS-54059] 23 p3750 N71-36735
- Composition and evolution of Earth, Mars, Venus, and Jupiter atmospheres 23 p3847 N71-37418
- Spatial and spectral energy distribution properties of low energy gamma rays in atmosphere and space 23 p3851 N71-37446
- Neutron intensities and amplitude variations in atmosphere and magnetic field of earth 24 p4010 N71-38597
- EARTH AXIS**
- Seven-year cycle of Arctic ice formation due to rotation of earth axis [NLL-M-20304-5828.4F/1] 12 p1914 N71-24100
- Icelandic atmospheric pressure minimum seasonal migration due to oscillation of earth axis [AD-724501] 20 p3296 N71-33675
- EARTH CORE**
- Travel times of PcP interpreted in terms of variations in radius of earth core configuration [AD-712673] 03 p0374 N71-13366
- Seismological application of shock waves to determine geophysical properties of minerals, metals, and alloys in interior of earth [UCRL-72770] 10 p1552 N71-21256
- Reflection and refraction of magnetohydrodynamic waves at liquid-solid interface, with earth core and mantle applications 15 p2406 N71-27948
- Earth rotation influence on diurnal tides in core 24 p3911 N71-37879
- EARTH CRUST**
- Summary of complex data on earth crust and upper mantle [AD-712106] 02 p0212 N71-11358
- Bouguer anomalies in ocean 02 p0218 N71-13055
- Lithology and geochemistry of weathering crust [ITT-49-55031] 03 p3367 N71-12730
- Analysis of latitude observations for detection of earth crust movements [NASA-CR-111567] 03 p3368 N71-13086
- Composition of earth upper mantle studied by petrography, analytical, and synthetic techniques [AD-713405] 05 p0675 N71-15417
- Alaskan earth tides, crustal failure, and microseisms [BLO-2095-2] 07 p1019 N71-17272
- Ground heating as functions of time, ground depth, and time from point neutron sources with fission spectrum or 12.2 to 15 Mev energy band [ORNL-4636] 09 p1426 N71-19524

- Low velocity layers within earth crust of Ukrainian shield calculated by travel time curves of refracted and reflected waves at interfaces within earth crust [NASA-TT-F-13536] 12 p1906 N71-23364
- Telemetry network and borehole installations for measurements of crustal deformation release, failure, and tilt in Alaska [AD-719846] 13 p2074 N71-25074
- Ray tracing in generally homogeneous medium based on calculus of variations and Fermat principle of stationary time and application to earth structure determination [AD-720795] 14 p2246 N71-25845
- Developments in terrestrial geophysics by Soviets including marine gyro-stabilized gravimeter and frequency of earthquakes 16 p2584 N71-28149
- Earth-crust waveguide propagation mode parameter calculations including phase velocity and excitation factors of dominant modes 16 p2560 N71-28412
- Deep seismic sounding methods for studying structure of earths crust and upper mantle 19 p3092 N71-32004
- Characteristics of earth tides and earth crust movements near North Pole - Project Spitsbergen 20 p3223 N71-32899
- Earth gravity tides - conference 20 p3261 N71-33333
- Tidal tilt study in Tien-Shan for crustal movements and earthquakes 20 p3262 N71-33345
- Tidal gravity variations of earth crust observed in USSR 20 p3263 N71-33348
- Slow and tidal gravity variations of earth crust measured by gravimeters at Sayany tilt station 20 p3263 N71-33349
- Temperature effect on tidal gravity of earth crust 26 p3263 N71-33350
- Indirect effects on earth crust tidal variations 20 p3263 N71-33352
- Laser interferometer for studying earth crust strain 20 p3264 N71-33358
- Wave attenuation calculations for two-layer earth crust waveguide model for underground electromagnetic propagation [AD-726754] 22 p3554 N71-35318
- Gravimetric instruments for recording deformation of earth crust and earth surface caused by earth tides 24 p3509 N71-37864
- Deformographs and extensometers for measuring earth crust deformations 24 p3910 N71-37866
- Earth tide measurements by gravimeters and pendulums at ground station in Antarctic interior during winter 24 p3910 N71-37867
- Geophysical classification of earth crust tides as affected by temperature and atmospheric pressure 24 p3910 N71-37868
- Hermetically sealed chambers for accurate earth tide registrations by pendulums and gravimeters 24 p3910 N71-37869
- Performance of borehole pendulums for earth tide registration 24 p3911 N71-37874
- EARTH CURRENTS**
- U TELLURIC CURRENTS**
- EARTH ENVIRONMENT**
- Earth environmental noise fields problems in inertial component testing 05 p0720 N71-14542
- Theoretical analysis of geological processes affecting evolution of earth atmosphere 05 p0670 N71-14826
- Apollo 11 basalt petrogenesis and theories of lunar evolution comparing lunar and earth environments [NASA-CR-118034] 12 p1998 N71-24309
- National and international environmental monitoring activities - directory 14 p2247 N71-25889
- Environmental policy and law - bibliography [ORNL-NSF-EP-2-VOL-1] 15 p2526 N71-27267
- Study of environment sciences and recommendations for national program, priorities, funding, and university disciplines 17 p2750 N71-36294
- High energy neutron detector for measuring solar neutron flux in earth radiation environment during quiet or active sun conditions [AD-722467] 18 p3009 N71-30891
- System of geosection indices for identification of environmental data associated with observation stations on earth surface [NASA-CR-121661] 21 p3397 N71-34176
- Definition and identification of geosections for coordinating human activities with respect to earth environment [NASA-CR-121639] 21 p3431 N71-34413
- Human and environmental natural and fallout radioactivity data [NASA-242] 21 p3484 N71-34815
- EARTH FIGURE**
- U GEODESY**

EARTH HYDROSPHERE

- Stratospheric photochemical and hydrospheric CO oxidation and tropospheric CO reaction with ozone as atmospheric CO sinks [PB-192108] 03 p0366 N71-12693
- Investigating relationship of man and biosphere with respect to food production and toxic chemical pollution [JPRS-52325] 07 p0981 N71-17429
- Discussing relationship between numerical growth and expanding industrial and technological power of man and biosphere 07 p0981 N71-17430
- Biosphere sinks for carbon monoxide emissions to atmosphere [PB-195433] 08 p1186 N71-18307
- Approaches to biogeocenotic research based on internal dynamic organization and phenomena which ultimately determine the laws of life of the biosphere 20 p3223 N71-33503
- Investigation of tundra biogeocenoses noting species saturation of surface layer and soil and eleven phases of turnover 20 p3223 N71-33504
- Analysis of natural zones and space ecosystems noting relationships of living animals and biosphere 20 p3224 N71-33505
- Radiation shielding and biogeochemical process and their maintenance for earth preservation [JPRS-54059] 23 p3750 N71-36735
- EARTH MANTLE**
- Summary of complex data on earth crust and upper mantle [AD-712106] 02 p0212 N71-11538
- Velocity and stress distributions in earth mantle due to secular variation of geomagnetic field 05 p0669 N71-14796
- Composition of earth upper mantle studied by petrography, analytical, and synthetic techniques [AD-713405] 05 p0675 N71-15417
- Low frequency discriminants for small events [AD-715328] 07 p1021 N71-17873
- Estimation of geodetic parameters describing earth gravity field and positions of satellite tracking stations in geocentric reference 19 p3086 N71-31828
- Deep seismic sounding methods for studying structure of earths crust and upper mantle 19 p3092 N71-32004
- EARTH MOTION**
- Cybernetics and spontaneous movement of matter in world system 12 p1895 N71-24216
- Canadian west coast strong motion seismograph network for determining basic ground motion during earthquakes 13 p2077 N71-25419
- Investigation of the role of water in tectonic processes and occurrence of hydrodynamic anomaly in hypocentral region of natural origin 15 p2397 N71-26905

EARTH MOVEMENTS

- NT EARTHQUAKES**
- Analysis of peak ground motions generated by underground nuclear detonations [NVO-1163-TM-20] 02 p0221 N71-12143
- Microseismic rock noise rates for determining slope stability in pit mining [BM-81-7470] 05 p0677 N71-15501
- Alaskan earth tides, crustal failure, and microseisms [RLO-2095-2] 07 p1019 N71-17272
- Simulating seismic rays, computing travel times, and approximating amplitudes in earth models [AD-715316] 07 p1022 N71-17815
- Low frequency discriminants for small events [AD-715328] 07 p1023 N71-17873
- Characteristics of earth tides and earth crust movements near North Pole - Project Spitsbergen 20 p3255 N71-32899
- Calculation of ground motions generated by air waves from surface explosions [UCRL-TRANS-10529] 21 p3421 N71-34343
- Monitoring seismicity of Aleutian/Amchitka areas after nuclear detonations [COS-746-10] 22 p3577 N71-35480
- Laser interferometer for earth strain measurements 23 p3753 N71-36761
- Covariance analysis of relative velocity response spectra derived from horizontal ground motion [NVO-1163-TM-24] 24 p3912 N71-37882
- EARTH ORBITING SPACE STATIONS**
- U BOSS**
- EARTH ORBITS**
- NT APOLLOS**
- NT PERIGEEES**
- Linear multichannel control systems for superseismic aerospace vehicles orbiting in earth atmosphere [AD-714796] 07 p1057 N71-17747
- Intensity variations and spectral composition of gamma radiation in near earth space measured by Cosmos 135 14 p2334 N71-25799
- Algorithm for rotating orbital plane of satellite in central and noncentral earth gravitational field [NASA-TT-F-13613] 16 p2681 N71-28976

- Low speed wind tunnel tests of GAC 3A earth orbiting shuttle aerodynamic characteristics [NASA-CR-103153] 21 p3523 N71-35100
- Aerodynamic characteristics of GAC 518 earth orbital shuttle at Mach .170 [NASA-CR-103158] 21 p3523 N71-35100
- Geological uses of earth-orbital photography with case histories [NASA-TM-X-65682] 22 p3583 N71-35576
- Long term equations of motion for earth-moon system including solar and lunar tidal torques 23 p3847 N71-37409

EARTH PLANETARY STRUCTURE

- Integral equation formulations for electromagnetic scattering from two-dimensional inhomogeneities in conductive earth [NASA-CR-110910] 01 p0049 N71-10701
- Integral equation formulations for electromagnetic scattering from two-dimensional inhomogeneities in conductive earth - appendices, figures, bibliography, and computer programs [NASA-CR-110911] 01 p0050 N71-10701
- Geodetic gravity approach for determining earth geopotential on grid [AD-711265] 01 p0051 N71-10806
- Using deep seismic sounding data to measure elastic wave velocities in rocks of Pechanga region of California [NASA-TT-F-13207] 02 p0209 N71-11402
- Abstracts on Soviet terrestrial geophysics research 06 p0832 N71-16014
- Investigating geomagnetism, seismic properties, and tectonic structure of earth crust 07 p1014 N71-16021
- Investigating formation of circular structures of volcanic, meteoritic, and nuclear origin on earth for correlation with cratering on moon and inner planets [NASA-TT-F-13457] 07 p1019 N71-17402
- Mobile approach to role of Arctic Basin in geotectonic development of supercontinent Laurasia during Paleozoic era 11 p1734 N71-23219
- Seismic wave propagation, geomagnetic features, and earth structure 12 p1905 N71-23110
- Continental drift theory applied to role of Arctic Basin in development of Laurasia structure [AD-710606] 12 p1907 N71-23521
- Response of elastic earth to loads located in parallel plane to bounding surface [SC-DR-70-836] 15 p2400 N71-27079
- Laser ranging retroreflector deployed on lunar surface to study lunar librations for defining precisely lunar orbits and studying earth planetary structure - Apollo 14 flight 18 p3012 N71-30805
- Appraisal of earth origins and structure based in theory of continental drift and geological observations 18 p2912 N71-30902
- Seismology and physics of earths interior in New Zealand 22 p3578 N71-35480
- Polar asymmetry in earth formations and on other planets [NASA-TT-F-139313] 22 p3668 N71-36118
- EARTH RADIATION**
- U TERRESTRIAL RADIATION**
- EARTH RESOURCES**
- NT COAL**
- NT CRUDE OIL**
- NT DESERTS**
- NT FARM CROPS**
- NT FORESTS**
- NT GLACIERS**
- NT GRAINS (FOOD)**
- NT GRANITE**
- NT ICEBERGS**
- NT LAKES**
- NT LAND ICE**
- NT LAVA**
- NT LIMESTONE**
- NT RANGE RESOURCES**
- NT RIVERS**
- NT ROCKS**
- NT SANDS**
- NT SANDSTONES**
- NT SHALES**
- NT VEGETATION**
- Instrument for studying electron stimulated luminescence of terrestrial, extraterrestrial, and synthetic materials - luminoscope 01 p0052 N71-10806
- Presentations at conference on color of ocean with application to survey of earth resources by satellite observation and aerial reconnaissance [NASA-CR-111570] 03 p0369 N71-11800
- Bibliography of geological research in Antarctic regions [REPT-146] 03 p0369 N71-11800
- Sources of rare earths, also current and anticipated usage in various applications including nuclear research and electrical engineering [NMAB-266] 04 p0553 N71-14800

SUBJECT INDEX

EARTH RESOURCES SURVEY AIRCRAFT

Biological oceanography and ocean food resource development using satellite observation 04 p0522 N71-14436

Application of remote sensors to determining, conserving earth resources 05 p0673 N71-14916

Photogrammetry techniques applicable to earth resources analyses and interpretation [NASA-TM-X-64546] 05 p0685 N71-15409

Verification of geography in Rio de Janeiro by using airborne equipment [LAFE-133-VOL-2] 05 p0680 N71-15546

Surveying natural resources of Brazil by remote sensors [LAFE-126] 05 p0688 N71-15552

Earth observations program [NASA-TM-X-64568] 05 p0682 N71-15694

Inventory of native vegetation and related resources from spaceborne photography 06 p0846 N71-16162

Orbital mechanics and observation tradeoffs for earth resources satellite [NASA-TM-X-2136] 06 p0895 N71-16733

Remote sensing for earth resources and urban development - bibliographies [PB-195748] 09 p1382 N71-19602

Arcic manpower, industrial, mineral, petroleum, and transportation resources [AD-716451] 09 p1383 N71-19770

Research in environmental sciences including climatology, oceanography and earth resources, planetary atmospheres and ionospheric physics, space physics, astrophysics, and relativity 09 p1385 N71-20149

Nimbus 3 high resolution infrared radiometer photographs of inland delta of Niger River demonstrating use in earth resources studies [PB-192863] 10 p1532 N71-21296

Proceedings from conference on water resources utilization [PB-196731] 10 p1554 N71-21625

Bibliographies on natural resources including atmosphere, earth, water, climate, plants, and animal subject matter [AD-717255] 11 p1744 N71-21894

Bibliography on remote sensing of earth resources applications with emphasis on water resources [PB-192863] 11 p1748 N71-22245

Water resources, distribution, pollution, quality control, and uses in USA 12 p1905 N71-23199

Earth resources analyses by multispectral terrain photography with Apollo 9 cameras 13 p2082 N71-25257

Microwave emission characteristics of natural materials and environment, including sea ice, soils, and oceans [AD-720388] 14 p2247 N71-25960

International data on ecological problems 14 p2249 N71-26200

Photointerpretation of remote infrared imagery of North Carolina including isopleth mapping, Pierson correlation coefficient, and multiple linear regression analysis [AD-719761] 14 p2249 N71-26263

Remote sensing of earth resources - bibliography [NASA-CR-118489] 14 p2250 N71-26398

Scientific and economic results of geologic, hydrologic, and topographic studies 14 p2251 N71-26644

Operational and technical aspects of earth resources satellite projects [RAE-TS-62119] 16 p2682 N71-28126

Space engineering, exploration, and communication, and spaceborne observations of earth resources and astronomy [PWS-53280] 16 p2696 N71-29148

Scientific observation of earth resources [RAE-LIB-BIB-314-PT-2] 17 p2738 N71-29397

Evaluation of high altitude balloon aerial photography for earth resources and oceanography including photographic formats and camera systems and scheduling [NASA-TM-X-2208] 17 p2753 N71-29910

Aerial and ground surveillance of southern corn leaf blight in Corn Belt States during 1971 [NASA-NEWS-RELEASE-71-129] 17 p2709 N71-30175

Management planning in Sweden for natural gas as industrial energy source [IVA-MEED-167] 18 p3028 N71-30522

Trends and possibilities in biochemistry, biotechnology, geology of minerals, earth resources, and man machine systems 18 p3028 N71-30839

Geology of minerals as space age earth resource possibility 18 p3011 N71-30841

Geodetic survey techniques for study of earth natural resources and use of methods for similar studies of other planets [NASA-TT-F-13810] 18 p3017 N71-31147

Accomplishments of geodetic satellite and earth survey programs during period July to December 1970 [NASA-CR-119557] 18 p3016 N71-31295

Requirements for natural resources management information system and potential application of remote sensing technology to resource programs by Bureau of Indian Affairs [SD-70-351] 18 p2919 N71-31425

Environmental engineering and management for natural environment - regional plan for water, sewage, air, and refuse comparing automatic vehicle monitoring system dispatching police vehicles to conventional system [PB-190290] 19 p3083 N71-31627

Remote sensing inventories and socio-economic studies of water resources and management in California [NASA-CR-121370] 20 p3235 N71-32896

Integrated approach to water management by remote sensing in California [NASA-CR-121460] 20 p3268 N71-33827

Remote multispectral sensing and data processing techniques for agricultural applications [NASA-CR-121749] 21 p3416 N71-34305

System of regional agricultural land use mapping tested against Apollo 9 color infrared photography of Imperial Valley, Calif. [NASA-CR-121875] 21 p3426 N71-34375

Bibliography of remote sensor applications and study of earth resources using airborne and earth satellite techniques 22 p3577 N71-35479

Developing and managing water resources of Western US 22 p3609 N71-35703

Ecological consequences of winter cloud seeding in San Juan area of Colorado River Basin 22 p3609 N71-35706

Precipitation augmentation during winter season for Sierra Nevada 22 p3610 N71-35713

Randomized seeding in Sierra Nacimiento and Jemez Mountains, New Mexico during winter 22 p3610 N71-35717

Utilization of remotely sensed data in Thesis project [AD-726946] 23 p3751 N71-36746

EARTH RESOURCES PROGRAM

Systems design of national system for management of scientific and technological information, including prototype subsystem for handling earth resources data [NASA-CR-61533] 01 p0138 N71-10086

Developing airborne multispectral band scanners for application in remote sensing of forestry and agricultural resources [NASA-TM-X-66484] 02 p0216 N71-11976

Comparing user requirements with remote sensing capabilities for inventory of vegetation resources 02 p0216 N71-11977

Multistage sampling technique for conducting timber inventories using spaceborne photography 02 p0216 N71-11978

Interim results and progress on use of space and aircraft photography for range resource inventories 02 p0216 N71-11979

Evaluating potential for making broad land use maps and earth resource surveys from spaceborne and airborne photography 02 p0217 N71-11980

Studying interaction of electromagnetic radiation with plants, soils, and water, and wavelengths and procedures for discriminating agricultural crops 02 p0217 N71-11981

Applying advanced remote sensing and processing techniques to agricultural resources 02 p0217 N71-11982

Reviewing research on processing data from multi-spectral band scanners for agricultural applications 02 p0191 N71-11983

Research progress on data processing, interpretation, and utilization of remote sensor information 02 p0217 N71-11986

Using passband interference filters in multispectral photography for earth resources applications 02 p0227 N71-11987

Multispectral additive color viewing devices for earth resources applications 02 p0227 N71-11988

Failure analysis of recovery flashing xenon lamp on Apollo 10 flight 02 p0227 N71-11989

Radar and data processing techniques for designing space radars for earth resources applications 02 p0185 N71-11991

Optical correlation methods for remote sensing of trace gases at high altitudes 02 p0228 N71-11993

Earth Resources Research Data Facility Index [NASA-TM-X-66487] 02 p0223 N71-12199

Applying photographic techniques to obtain ground truth data from earth resources and geodetic astronomy 03 p0380 N71-12798

Earth Resources Observation Satellite image utility at state and university level 03 p0671 N71-14846

Aerial multispectral sensing for determining geological and geographic aspects in Earth Resources Aircraft Program [NASA-TM-X-62564] 06 p0842 N71-16126

Conference on agriculture, forestry, and sensor studies related to NASA Earth Resources Program - Vol. 2 [NASA-TM-X-62563] 06 p0844 N71-16147

Photographic applications of NASA Earth Resources Survey Program 06 p0839 N71-16148

Wildland vegetation resource inventories under Earth Resources Survey Program 06 p0845 N71-16157

Application of remote sensing to inventory and management of ranges resources 06 p0846 N71-16161

Investigating application of airborne remote sensors to hydrology and oceanography [NASA-TM-X-62564] 06 p0846 N71-16166

Using remote sensors for detection, analysis, and mapping of snow and ice 06 p0846 N71-16167

TRIAD, preliminary design of operational earth resources survey system [NASA-CR-116208] 06 p0852 N71-16548

Coastal zone oceanographic requirements for earth observatory satellites - Part I [NASA-CR-111814] 07 p0108 N71-17262

Coastal zone oceanographic requirements for earth observatory satellites - Part 2 [NASA-CR-111817] 07 p0108 N71-17263

Coastal zone oceanographic requirements for earth observatory satellites - Summary [NASA-CR-111818] 07 p0109 N71-17264

Conference on Earth Resources Program including geology and geography [NASA-TM-X-60913] 08 p0196 N71-19251

Earth resources cartographic applications program 08 p0196 N71-19261

Evaluation of earth resources observation opportunities from orbiting satellite in Skylab program [NASA-TM-X-64598] 15 p2397 N71-27023

Design of automatic data correlation system for Earth Resources Program [NASA-CR-115063] 16 p2564 N71-28003

Program summary for implementation of automatic data correlation system for Earth Resources Program [NASA-CR-115062] 16 p2564 N71-28004

Application of Apollo space photography and sequential high altitude NASA aircraft photography for evaluating natural and cultural resources in southeastern Arizona - map [NASA-CR-115056] 17 p2750 N71-29233

Remote aerial sensing and automatic mapping for forest resources information system [NASA-CR-122922] 23 p3755 N71-36770

Development of four dimensional atmospheric models from global data for predicting atmospheric attenuation encountered by earth resources observation sensors [NASA-CR-61362] 24 p3951 N71-38189

EARTH RESOURCES SURVEY AIRCRAFT

Research progress on multispectral data collection and infrared instrumentation for specially configured aircraft 02 p0227 N71-11984

Identifying rock types by aircraft equipped with various types of infrared detectors 02 p0217 N71-11985

Investigating remote sensing applications to simple geological features using microwave radiometers 02 p0227 N71-11990

Photographic applications of NASA Earth Resources Survey Program 06 p0839 N71-16148

Plant and soil signature extracted by spectrophotometric analysis of Apollo 6 and earth resource survey aircraft color photography 06 p0845 N71-16149

Crop and soil identification from aerial photography 06 p0845 N71-16150

Identification of western forest species by means of aerial remote sensing 06 p0880 N71-16160

Radar scatterometer and imaging radar applications in Earth Resources Aircraft Program 06 p0814 N71-16164

Infrared scanner use for thermal mapping and multispectral sensing in Remote Sensing Aircraft Program 06 p0839 N71-16165

Using airborne radar scatterometry to determine high sea states 06 p0847 N71-16177

Describing development of scatterometer and imaging radar for earth resources aircraft 06 p0849 N71-16185

Investigating infrared scanners for thermal mapping and multispectral sensing 06 p0839 N71-16186

Analysis of multi-sensor data obtained by Earth Resources Aircraft Program [NASA-CR-116425] 07 p0102 N71-17870

Application of Apollo space photography and sequential high altitude NASA aircraft photography for evaluating natural and cultural resources in southeastern Arizona - map [NASA-CR-115056] 17 p2750 N71-29233

Comparison of logistics problems and cost aspects in selection of aircraft for earth resources surveys
[NASA-TM-X-3418] 24 p3917 N71-37928

EARTH RESOURCES TECHNOLOGY SATELLITES
Ground data handling aspects of EROS Program from users viewpoint
[PB-193666] 02 p0213 N71-11594

Evaluation of analog techniques for image registration of vidicon television cameras on ERTS-A
14 p2529 N71-26651

Earth Resources Technology Satellites E and F orbits and remote sensor instruments for coastal oceanographic data collection
[NASA-CR-111823] 16 p2586 N71-28328

Onboard optical data processing for earth resource spacecraft and planetary spacecraft
[NASA-TM-X-65603] 17 p2723 N71-29883

Geology of minerals as space age earth resource possibility
18 p2911 N71-30841

Review and assessment of documents concerning cost and benefits of ERS satellites, and value of these studies in directing R and D activities
[NASA-CR-119363] 18 p3015 N71-31279

Analysis of cloud statistics and probability-of-seeing values for application to ERTS
[NASA-CR-121770] 21 p3508 N71-34990

Application of optically diagnosed noise information toward development of filtering subroutines for improvement of digital sensing data tape quality - Vol. 1
[NASA-CR-121978] 22 p3582 N71-35510

Variations in image boundaries of ERTS multispectral scanner and return beam vidicon systems
[NASA-TM-X-65684] 22 p3668 N71-36153

Application of ground-truth data to monitor sensor calibrations for Earth Resources Technology Satellites - Vol. 2
[NASA-CR-121979] 24 p3919 N71-37945

Photographic data processing, management, and dissemination system to support Earth Resources Technology Satellite program - Vol. 3
[NASA-CR-121980] 24 p3919 N71-37946

EARTH ROTATION
Chandler wobble determinations by US Navy Doppler satellite observations
[AD-712058] 02 p0220 N71-12414

Velocity and stress distributions in earth mantle due to secular variation of geomagnetic field
05 p0669 N71-14796

Energy of auroral charged particles drawn from solar wind, earth rotation, and atmospheric circulation, and infrared generation from electric current interactions
07 p1014 N71-16930

Earth rotation rate values from observations on stellar occultation by moon from 1627 to 1860
07 p1117 N71-18057

Long term effect of earth tides on earth rotation
20 p3265 N71-33370

Using laser tracking systems to detect motion of pole of rotation for earth
[NASA-TM-X-65696] 23 p3765 N71-36840

Interaction of magnetosphere and electric field with respect to earth rotation
25 p3853 N71-37464

Earth rotation influence on diurnal tides in core
24 p3911 N71-37879

EARTH SATELLITES
NT ALOUETTE SATELLITES

NT ALOUETTE 1 SATELLITE

NT ALOUETTE 2 SATELLITE

NT APPLICATIONS TECHNOLOGY SATELLITES

NT ARIEL 3 SATELLITE

NT ATS 1

NT ATS 2

NT ATS 3

NT ATS 4

NT BEACON EXPLORER A

NT BIOSATELLITE 1

NT BIOSATELLITE 2

NT BIOSATELLITE 3

NT COMMUNICATION SATELLITES

NT COSMOS SATELLITES

NT COSMOS 34 SATELLITE

NT COSMOS 149 SATELLITE

NT COSMOS 206 SATELLITE

NT COSMOS 224 SATELLITE

NT COSMOS 225 SATELLITE

NT DIADEME SATELLITE

NT DODGE SATELLITE

NT EARLY BIRD SATELLITES

NT EARTH RESOURCES TECHNOLOGY SATELLITES

NT ECHO 2 SATELLITE

NT E055

NT ESSO SATELLITES

NT ESSO 1 SATELLITE

NT ESSO 2 SATELLITE

NT ESSA SATELLITES

NT ESSA 3 SATELLITE

NT ESSA 4 SATELLITE

NT ESSA 6 SATELLITE

NT ESSA 8 SATELLITE

NT ESSA 9 SATELLITE

NT EUROPEAN SPACE RESEARCH OR-

GANIZATION SAT

NT EXPLORER SATELLITES

NT EXPLORER 15 SATELLITE

NT EXPLORER 18 SATELLITE

NT EXPLORER 22 SATELLITE

NT EXPLORER 26 SATELLITE

NT EXPLORER 28 SATELLITE

NT EXPLORER 31 SATELLITE

NT EXPLORER 32 SATELLITE

NT EXPLORER 33 SATELLITE

NT EXPLORER 34 SATELLITE

NT EXPLORER 35 SATELLITE

NT EXPLORER 37 SATELLITE

NT EXPLORER 38 SATELLITE

NT EXPLORER 40 SATELLITE

NT GEODETIC SATELLITES

NT GEOGRAPHICAL SATELLITES

NT GEOS 1 SATELLITE

NT GEOS 2 SATELLITE

NT GEOS-C SATELLITE

NT HEOS A SATELLITE

NT HEOS SATELLITES

NT IMP

NT INJUN SATELLITES

NT INTELSAT SATELLITES

NT ISIS-B

NT METEOROLOGICAL SATELLITES

NT MOON

NT NAVIGATION SATELLITES

NT NIMBUS SATELLITES

NT NIMBUS 2 SATELLITE

NT NIMBUS 3 SATELLITE

NT NIMBUS 4 SATELLITE

NT NIMBUS 5 SATELLITE

NT OAO

NT OGO

NT OGO-B

NT OGO-D

NT OGO-E

NT OGO-F

NT OGO-H

NT OUTER PLANETS EXPLORERS

NT PAGEOS SATELLITE

NT POGO

NT POLYOT SATELLITES

NT PROTON 4 SATELLITE

NT RADIO ASTRONOMY EXPLORER SATELLITE

NT RELAY SATELLITES

NT SAN MARCO 2 SATELLITE

NT SYNCHRONOUS METEOROLOGICAL SATELLITE

NT TELSTAR 1 SATELLITE

NT TIROS M

NT TIROS SATELLITES

NT TRANSIT SATELLITES

NT TRANSIT 1B SATELLITE

NT VELA SATELLITES

NT VENERA SATELLITES

NT VENERA 4 SATELLITE

NT VENERA 5 SATELLITE

Analysis of radar signatures of earth satellites

01 p0021 N71-10234

Dual patch multi-element radiant cooler for earth oriented spacecraft

[NASA-CR-111134] 01 p0133 N71-10606

Visible probability of earth satellite in elliptic orbit from ground station

[ISAS-454-VOL-35-NO-12] 02 p0295 N71-11896

Manual of computer program for generating ephemerides of earth satellites

[RAE-TR-69104] 02 p0296 N71-11960

Geomagnetic field simulation and magnetic measurements of earth satellites

03 p0356 N71-12711

Simulation equipment for satellite vibration tests

03 p0357 N71-12715

Stages in environmental tests of satellites

03 p0357 N71-12716

Uranium sphere equipped with laser retroreflector array as satellite for determining accurate position of ground stations

[SAO-SPECIAL-REPT-329] 04 p0614 N71-14116

Electron density and electrostatic potential field of ionosphere satellite

06 p0927 N71-16670

Survey of USSR earth satellite, space probe, and spacecraft launches from 1957 through 1964

07 p1118 N71-17104

Temperature distribution of thin-walled, transparent, spherical earth satellite assuming negligible lateral and radial conduction and steady state fixed position for satellite

[NASA-TN-D-7035] 10 p1662 N71-21279

Lifetimes, weights, dimensions, and orbital details for artificial earth satellites

[RAE-TR-70111-VOL-2-PT-1] 11 p1831 N71-22333

Tables of artificial earth satellite launching from 1 Sep. to 31 Dec. 1970

[RAE-TR-70163-SUPPL.] 14 p2341 N71-23966

Earth orbital research programs in atmospheric physics and space astronomy

[NASA-EP-83] 15 p2517 N71-26991

Computer programming for earth satellite orbit determination

[RAE-TM-SPACE-156] 17 p2844 N71-29807

Swathing patterns of earth-sensing satellites and their control by orbit selection and modification

[NASA-TM-X-65627] 19 p3179 N71-32100

Current collection characteristics of moving cylindrical and spherical electrostatic probes applied to velocities in earth satellites and planetary probes

[NASA-TM-X-65639] 19 p3071 N71-33400

Artificial earth satellites used in upper atmosphere and geodetic studies, and satellite orbit mechanics

22 p3676 N71-36200

Artificial earth satellite motion theory using zonal harmonics of terrestrial attraction

22 p3676 N71-36200

Geocentric and osculating orbital element calculations for satellites according to visual base and asynchronous observations

22 p3676 N71-36211

Determination of difference between quasi-draconic and draconic periods of earth satellite revolutions

22 p3676 N71-36211

Accuracy of synchronous plane determined by positions of artificial satellite and two observation points, used in space triangulation

22 p3677 N71-36214

Determination of direction cosines of line connecting two observation stations from quasi-simultaneous observations of artificial earth satellites

22 p3677 N71-36220

Least squares method generalized for space triangulation compensation, for determining satellite position from ground station coordinates

22 p3678 N71-36222

Calculation of azimuth between two distant ground points from synchronous photographs taken by artificial earth satellites

22 p3678 N71-36226

Reduction of topocentric satellite data from satellite tracking stations

22 p3678 N71-36225

Space positional vector calculation using Baker-Nunn and Laser observations of artificial earth satellites

22 p3678 N71-36228

Determination of variations in quasi-draconic satellite periods from visual observations

22 p3679 N71-36234

Two cameras for photographing artificial earth satellites

22 p3680 N71-36238

International conference on artificial earth satellite use for upper atmosphere and geodetic studies

22 p3680 N71-36245

Feasibility of obtaining gravity anomalies directly from analyzing artificial earth satellite orbits

23 p3753 N71-36760

Gamma and X radiation measurements by artificial earth satellites

23 p3851 N71-37407

Tables of artificial earth satellite launching from 1 Sep. to 31 Dec. 1970

[RAE-TR-70163-SUPPL.] 14 p2341 N71-23966

Earth orbital research programs in atmospheric physics and space astronomy

[NASA-EP-83] 15 p2517 N71-26991

Computer programming for earth satellite orbit determination

[RAE-TM-SPACE-156] 17 p2844 N71-29807

Swathing patterns of earth-sensing satellites and their control by orbit selection and modification

[NASA-TM-X-65627] 19 p3179 N71-32100

Current collection characteristics of moving cylindrical and spherical electrostatic probes applied to velocities in earth satellites and planetary probes

[NASA-TM-X-65639] 19 p3071 N71-33400

Artificial earth satellites used in upper atmosphere and geodetic studies, and satellite orbit mechanics

22 p3676 N71-36200

Artificial earth satellite motion theory using zonal harmonics of terrestrial attraction

22 p3676 N71-36200

Geocentric and osculating orbital element calculations for satellites according to visual base and asynchronous observations

22 p3676 N71-36211

Determination of difference between quasi-draconic and draconic periods of earth satellite revolutions

22 p3676 N71-36211

Accuracy of synchronous plane determined by positions of artificial satellite and two observation points, used in space triangulation

22 p3677 N71-36214

Determination of direction cosines of line connecting two observation stations from quasi-simultaneous observations of artificial earth satellites

22 p3677 N71-36220

Least squares method generalized for space triangulation compensation, for determining satellite position from ground station coordinates

22 p3678 N71-36222

Calculation of azimuth between two distant ground points from synchronous photographs taken by artificial earth satellites

22 p3678 N71-36226

Reduction of topocentric satellite data from satellite tracking stations

22 p3678 N71-36225

Space positional vector calculation using Baker-Nunn and Laser observations of artificial earth satellites

22 p3678 N71-36228

Determination of variations in quasi-draconic satellite periods from visual observations

22 p3679 N71-36234

Two cameras for photographing artificial earth satellites

22 p3680 N71-36238

International conference on artificial earth satellite use for upper atmosphere and geodetic studies

22 p3680 N71-36245

Feasibility of obtaining gravity anomalies directly from analyzing artificial earth satellite orbits

23 p3753 N71-36760

Gamma and X radiation measurements by artificial earth satellites

23 p3851 N71-37407

EARTH SHAPE

U GEODESY

EARTH SURFACE

Spectrophotometry of earth by manned spacecraft with data from Soyuz 7 and Soyuz 9

02 p0222 N71-12148

Literature review on electromagnetic wave transmission in absorbing media

04 p0491 N71-13780

Photointerpretation of satellite observations of earth surface

06 p1230 N71-18451

Solar cosmic ray particle acceleration during solar flares and neutron flux and photon densities at earth surface

[MPI-PAE/EXTRATERR-48] 06 p1285 N71-18710

Electromagnetic signal propagation along the ionosphere waveguide

08

Electric ground property effects on radio navigation system operations on earth surface

11 p708 N71-22926

Surface effects on cosmic cloud formations in astrophysics

[NLL-M-20005-3828-4F] 12 p1859 N71-24272

Geomagnetic and polarization plane rotation effects on electromagnetic signal transmission along spherical waveguide formed by earth surface and ionosphere

[AD-719644] 13 p2046 N71-33058

Satellite-borne photography of earth surface

[AD-719781] 13 p2075 N71-35123

Impact tests of fuel capsule response to simulated earth impact following reentry from orbit

[SC-DR-76-127] 13 p2123 N71-35522

Biological and geological aspects of soil science

14 p2207 N71-36456

Climatic cooling effects on earth surface

14 p2251 N71-36457

Origin of cosmic material fallout on earth surface and structure of cosmic dust and meteoric materials

[REPT-69/18] 15 p2398 N71-27600

Characteristics of Cosmos 149 instruments for measurement of solar and infrared radiation emerging from earth

15 p2410 N71-27490

Earth surface and cloud temperature determination by measurement of terrestrial infrared radiation

15 p2401 N71-27500

Earth subsurface electromagnetic field disturbances due to subsurface rock electrical properties

16 p2585 N71-28248

Communication satellite circular orbit network

[BAE-TN-70211] 17 p2719 N71-29439

Geological examination and topographic analysis of Rhot and Fomelyst domes in central Mauritania

18 p2913 N71-30994

Polarization radiation measurements by aircraft of cometary waves reflected from various surfaces on ground

[NASA-TT-F-13812] 18 p2917 N71-31090

Geodetic survey techniques for study of earth natural resources and use of methods for similar studies of other planets

[NASA-TT-F-13810] 18 p2917 N71-31147

Comparison of Smithsonian Astrophysical Observatory 1969 gravity field representation with surface gravity

19 p3086 N71-31830

Results of world wide surface refractivity test conducted in support of Apollo program

[NASA-TM-X-65647] 19 p3096 N71-32611

System of geospatial indices for identification of environmental data associated with observation stations on earth surface

[NASA-CR-121661] 21 p3397 N71-34176

Results of combined fully instrumented subsatellite geophysical experiment including spectrophotometry of earth surface

[JPRS-53895] 21 p3419 N71-34328

FORTRAN 5 digital computer program for predicting dynamic response of Apollo command module to launch

[NASA-TN-D-65339] 23 p3730 N71-36389

Conferences on earth tide and earth surface phenomena

23 p3748 N71-36722

Climometer for measuring inclinations of earth surface near Moscow

23 p3748 N71-36723

Spatial distribution of absorbed atmospheric radiation over whole earth

[NLL-M-20721-3828-4F] 23 p3842 N71-37397

Comparison of Mariner 10 and topographic features with earth and moon based on Mariner 6 and 7 photographs

[NASA-TM-X-65693] 23 p3847 N71-37421

Gravitometric instruments for recording deformation of earth crust and earth surface caused by earth tides

24 p3909 N71-37864

EARTH-MOON TRAJECTORIES

Optimal strategy for orbit calculation with example for Earth-Moon trajectory

[D-5] 17 p2844 N71-29380

EARTH-MOON SYSTEM

Observing growth rhythms in shells of fossil marine invertebrates and relationship to tidal cycles in earth-moon system

[NASA-CR-111608] 03 p0323 N71-12312

Nomenclature of earth-moon orbits

[NASA-TN-D-5949] 04 p0611 N71-14057

Gravitational tide effects on rotating fluid in earth

07 p1010 N71-17630

Physics of sun, planetary atmospheres and interiors, and earth-moon system - conference

[NASA-TM-X-65702] 23 p3845 N71-37406

Long term equations of motion for earth-moon system including solar and lunar tidal torques

23 p3847 N71-37419

EARTH-MOON TRAJECTORIES

Predicted launch vehicle operational trajectory and initial data for Apollo 14 launch window

[NASA-TM-X-66365] 05 p0771 N71-15317

EARTHQUAKES

Observation of elastic shocks during transition of ammonium fluoride to substantiate phase transition hypothesis of earthquake occurrence

[NASA-TT-F-13325] 01 p0047 N71-10338

Research digest for exchanging information among investigators in earthquake engineering in North America

[PB-193507] 01 p0051 N71-10887

Measuring electrical resistance of rocks and minerals for predicting potential earthquake centers

[NASA-TT-F-13212] 02 p0209 N71-11434

Investigation of PKP seismic waves at Byrd Station, Antarctica

[AD-718731] 03 p0371 N71-15242

Earthquakes induced by hydraulic fracturing for radioactive waste disposal

[ORNL-TM-1354] 03 p0674 N71-14039

Solar and lunar effects on earthquake periodicities

03 p0674 N71-14042

Engineering aspects of Santa Rosa, California earthquakes, 1 Oct. 1969

05 p0674 N71-14068

Abstract reports for 1969 earthquakes

[NOAA-NOS-MSA-143] 05 p0682 N71-15669

Describing eruptions in region of Mt. Hecla, Iceland and toxic hazards from volcanic ash

07 p1024 N71-17968

Earthquakes in United States, Panama Canal Zone, Puerto Rico, and Virgin Islands during 1968

08 p1194 N71-19025

Optical seismograph for recording intense earthquakes

[TT-76-50123] 08 p1203 N71-19067

Seismic station equipment for recording strong earthquakes

[DPT-5854] 08 p1195 N71-19107

Simple recording installation for instrument observations in epicenter zones of intense earthquakes

[TT-76-50122] 08 p1204 N71-19219

Technical approach for study of methods to predict soil behavior at nuclear power plant sites under earthquake loading conditions

[TT-76-50120] 09 p1365 N71-20287

Digitalized, analyzed and plotted data from strong motion earthquake accelerograms

[JPRS-196223] 10 p1555 N71-21729

Earthquake and seismological studies - conference papers

[BSSA-TR-ERL-182-ESL-11] 12 p1914 N71-24167

Status of oceanographic research projects, ocean waves, stabilized platforms, seismometers, underwater earthquakes, and sedimentation

[AD-719628] 13 p0071 N71-24639

Telemetry network and borehole installations for measurements of crustal deformation, release, failure, and tilts in Alaska

[AD-719640] 13 p0074 N71-25074

Frequency dependent P wave amplitude and distance curve measurement using earthquake spectra

[AD-719674] 14 p2245 N71-25656

Soviet news releases on earthquake prediction and computer analysis of seismic waves

15 p2396 N71-26875

Investigation of the role of water in tectonic processes and occurrence of hydrodynamic anomaly in hypocentral region of natural origin

15 p2397 N71-26905

Developments in terrestrial geophysics by Soviets including marine gyro-stabilized gravimeter and frequency of earthquakes

16 p2584 N71-28149

Measurement of vertical crustal movement of sea floor following Alaska earthquakes

18 p2914 N71-31004

Atmospheric propagation studies including ionospheric motions caused by nuclear tests, spacecraft launching, and earthquakes

[AD-723519] 19 p3084 N71-31680

Tidal tilt study in Tiao-Shan for crustal movements and earthquakes

20 p3362 N71-33345

Principal New Zealand earthquakes for 1965

20 p3369 N71-33907

Seismological readings for Japanese earthquakes of 24 May 1966, and analysis of aftershocks

20 p3269 N71-33908

Earthquake seismographic data records from Port Moresby - June-July 1971

20 p3260 N71-33947

News briefs concerning terrestrial geophysics

21 p3509 N71-35001

Microseismic analysis of Denali fault in Alaska and under ground nuclear explosions and microseismic survey of Nevada, Utah, Idaho, Montana, and Wyoming

22 p3580 N71-35504

Summary of earthquakes occurring in US during 1969

23 p3749 N71-36734

Analysis of energy release problem for earthquakes and explosions

[UCL-TRANS-10434] 23 p3752 N71-36754

Possible movement variations before earthquakes

24 p3911 N71-37876

Damage resulting from San Fernando, California earthquakes of 9 Feb. 1971

[PP-733] 24 p3917 N71-37933

EATING

Relationship between diurnal and meal driven excretory patterns in human kidney during bed rest

20 p5218 N71-33268

EARTH SPECTROMETERS

Automated infrared spectrometer with Ebert monochromator

01 p0052 N71-10205

Spark chamber and Ebert spectrometer determination of ruthenium in silicious radioactive wastes coated with iron oxide

[BARC-504] 15 p4330 N71-27346

Design of satellite grid spectrometer for measurement in 15-15 micron range

15 p3411 N71-27552

EEB-1 REACTOR

U EXPERIMENTAL BREEDER REACTOR 1

EEB-2 REACTOR

U EXPERIMENTAL BREEDER REACTOR 2

EMULSION

U BOILING

ECCENTRIC ORBITS

Developing general analytical methods for predicting planar and three dimensional attitude motion of gravity gradient spacecraft in elliptical orbits

[NASA-TR-R-350] 04 p0611 N71-14005

IMP - launch window and secondary injection into eccentric orbit

[NASA-TM-X-65450] 08 p1293 N71-18649

Algebraic solutions of linear equations for secular perturbations of planetary eccentricity and longitude

[NASA-TT-F-13640] 16 p3621 N71-38134

High eccentricity orbit for satellite measurements of periodic relativistic Doppler shifts

[AD-716773] 19 p1376 N71-32075

Accelerated longitudes drift regions of eccentric 12 hour orbits due to resonant geopotential

[NASA-TM-X-65722] 24 p4021 N71-38688

ECCENTRICITY

Experimental and analytical vibration study of elliptical cylindrical shells of constant mass with varying cross-sectional eccentricity

[NASA-TN-D-6009] 06 p0597 N71-16830

Eccentricity effects in absolute determination of alpha emitter in low geometry counters

[NP-18664] 18 p2975 N71-30573

ECHO SATELLITES

NT ECHO 2 SATELLITE

ECHO 2 SATELLITE

Nikolajev-Haivan space direction between tracking stations studied at long distances by photographic observations of Echo 2 satellite

[NASA-TT-F-13348] 03 p0452 N71-12284

Synchronous satellite observations and normalization for determining Riga-sofia azimuth

22 p3677 N71-36216

Satellite period calculation on basis of photographic observations of Echo 2 and Pagosa

22 p3679 N71-36236

ECHOES

NT ANGELS

NT CLUTTER

NT LUNAR RADAR ECHOES

NT RADAR ECHOES

NT RADIO ECHOES

NT SIGNAL REFLECTION

NT SOLAR RADAR ECHOES

Ecological capabilities of dolphins

[JPRS-51511] 03 p0323 N71-12309

Echo scanning for equalizing linear signal distortion in data transmission channels

17 p2720 N71-29783

Effects of time echo in relativistic electron plasma

[NASA-TT-F-13785] 19 p3164 N71-32233

Nuclear magnetic resonance spin echo method used to determine self diffusion activation energy in aqueous solutions of electrolytes

20 p3230 N71-33623

Nonlinear echo phenomena in plasma and distribution function oscillations

[JTP-76-56] 23 p3828 N71-37306

ECLIPSES

NT LUNAR ECLIPSES

NT SOLAR ECLIPSES

ECLIPSING BINARY STARS

Observation and analysis of light variations of binary stars UU Picinus, EM Cephei and 44 Bootis

10 p1643 N71-21253

Relationship between luminosity and mass ratio in eclipsing variable star system with asymptotic

[NLL-RTS-3999] 10 p1646 N71-31774

Model of eclipsing binary star system based on digital computers

[NASA-CR-118643] 14 p2336 N71-25942

ECOLOGICAL SYSTEMS

U ECOLOGY

ECOLOGY

NT COASTAL ECOLOGY

Research planning in environmental health science

01 p0042 N71-10075

Model of global climate and ecology

[AD-711698] 01 p0079 N71-10732

Remote aerial sensing and multispectral data processing for hydrobiological survey in Florida 02 p0206 N71-11159

Multidisciplinary oceanography including physical, geological, geophysical, chemical, biological, and radioecological studies 02 p0219 N71-12083
(AD-710765)

Statistical analysis of ecological variables across grassy geological surface 03 p0322 N71-12304
(COO-1821-2)

Conference on application of science and technology to problems of pollution, transportation, and employment 03 p0323 N71-12306
(PB-192329)

Proposed environmental laboratories handling urban and rural problems and staffed by natural and social scientists, engineers, and information specialists 03 p0358 N71-13076
(PB-189691)

Phytosociological and taxonomical listings of forest and vegetation types along proposed canal through Durian, Panama 05 p0671 N71-14847
(BML-171-37)

Investigating processes of chemical and biochemical weathering of primary volcanic rock and role of phosphorus in primary productivity of natural systems on Surtsey 07 p0126 N71-17985

Observations of carbon dioxide and plant growth in Arctic ecosystem 06 p1149 N71-16768
(AD-715789)

Growth of bacteria in soils from Antarctic dry valleys providing soil microbial ecology as Mars model 09 p1333 N71-20172
(NASA-TM-X-66965)

Congressional hearing on efforts to improve knowledge of and support for environmental and ecological projects 09 p1489 N71-20566

Comparison of management techniques applied to life sustaining resources in Apollo command modules and in earth ecology 11 p1846 N71-22032

Ecological effects of electromagnetic fields and ELF global communication systems 12 p1862 N71-23381
(AD-718828)

Numerical solutions of differential equations for ecosystem models 13 p2104 N71-25428
(ORNL-IBP-70-4)

International data on ecological problems 14 p2249 N71-26200

Inhibitor effects of pilosins, MnO₂, and D2O on substances existing in nature to determine performance of terrestrial organisms in extreme and unusual gaseous and liquid environments 15 p2372 N71-27743
(NASA-CR-118883)

Susceptibility or resistance to gas and smoke of various arboreal species grown under diverse environmental conditions in industrial regions 17 p2742 N71-29832
(PB-190663)

Effects and symptoms of air pollutants on vegetation noting resistance and susceptibility of various plant species in various habitats and relation to plant utilization for shelter belts 17 p2742 N71-29833
(PB-190662)

Systemic approach to ecology, trophodynamics, biocenosis, and biogeocenosis 17 p2710 N71-30391
(JPRS-53376)

Acquisition and storage of militarily significant data on climatology, hydrology, soils, and ecology of humid tropical regions 19 p3195 N71-32029
(AD-723060)

Human reactions to air pollution and responses to ecology and environmental control 19 p3093 N71-32258
(UCRL-73063)

Bibliography of technologies, social systems and environment 20 p3370 N71-33417
(P-4541)

Analysis and definition of tasks in field of biogeocenology 20 p3223 N71-33502

Approaches to biogeocenotic research based on internal dynamic organization and phenomena which ultimately determine the laws of life of the biosphere 20 p3223 N71-33503

Applications of radiotopes in experimental biogeocenology to determine fertilizer turnover during growth of crops 20 p3224 N71-33506

Role of individual components of biogeocenosis in organization of structure and functions 20 p3224 N71-33509

Discussion of photosynthesis process and production of ctenos 20 p3224 N71-33510

Characteristics of water environment and relationship to biogeocenology 20 p3224 N71-33511

Effect of solar radiation on energy balance of biogeocenosis 20 p3224 N71-33512

Application of biogeocenology principles to land reclamation activities 20 p3224 N71-33513

Effect of private litigation on national efforts to preserve and enhance the environment 21 p3533 N71-35177

Proceedings of conference on interaction between atmospheric environment and human system at cell level 22 p3545 N71-35256
(AD-720601)

Development of system for identification of pollution reduction methods and selection of alternate methods for optimum effectiveness 22 p3548 N71-35414
(PB-199332)

Electrical analogy model for ocean ecological system and measurement methods for phytoplankton production 22 p3577 N71-35477

Ecological consequences of winter cold seeding in San Juan area of Colorado River Basin 22 p3609 N71-35706

Responsibilities of engineers in environmental and pollution control 22 p3700 N71-36386

Uranium mining, chemical reprocessing, transportation of spent fuel, and reactor systems waste products related to environmental pollution 23 p3796 N71-37065
(NP-18842)

Ecological transfer matrices for various terrestrial and aquatic systems 24 p3878 N71-37648
(ORNL-IBP-71-3)

Introduction to numerical computer techniques for ecologists 24 p3949 N71-38175
(ORNL-IBP-71-1)

TECHNICAL ANALYSES
Technical and cost analyses for communications systems using satellites in geostationary orbits 07 p0991 N71-17120
(PB-194782)

Economic analysis of airport construction in north central Texas region, emphasizing employment and dollar value of purchases 07 p1005 N71-18099

Cost effectiveness of closer tolerances in manufacturing 09 p1393 N71-20109
(UCRL-72380)

Objective and methodology of forecasting economic and scientific research and development 10 p1666 N71-21615
(NLL-KTS-4095)

Economic analysis of facilities, tooling, premanufacturing and manufacturing operations, and quality control labor in aluminum aerospace industry base on Saturn/Apollo data 12 p1931 N71-24181
(NASA-CR-114282)

Industry automatic control system design 12 p1885 N71-24218

Economic analysis of aeronautical R and D efforts in US and aeronautical contributions to noise and air pollution, including technology assessment and data analysis techniques 15 p2366 N71-27011
(NASA-CR-1809)

Microeconomic analysis of in-process manufacturing quality control 16 p2601 N71-28432
(AD-720098)

Effect of scientific and technical progress in controlling national economy and evaluation of effectiveness of science 16 p2695 N71-29066
(JPRS-53271)

Cost/benefit model for decision making in planning German space program - bibliography 17 p2861 N71-29422
(BMBW-FB-W-71-04-PT-3)

Economic analysis of rain stimulation over Israel 19 p3129 N71-32556
(P-4524)

Measures for providing financial responsibility liability limitations for vessels and offshore and offshore facilities in oil pollution cases 19 p3198 N71-32624
(PB-198775)

Legal, economic, and technical aspects of liability and financial responsibility of oil pollution 19 p3198 N71-32625
(PB-198776)

Congressional hearing to study effects of science and technology on US and world economy 22 p3700 N71-36385

ECONOMIC FACTORS
Investigating effects of Hecla volcano eruption on environment and economy of Iceland 07 p1026 N71-17982

Economic and safety factors of nuclear powered surface vehicles and aircrafts in transoceanic commerce 08 p1239 N71-18628
(NASA-TM-X-52963)

Increased satisfaction of user needs and increased economics in operation of information systems 12 p2816 N71-23504
(NASA-TM-X-67142)

Economic analysis of facilities, tooling, premanufacturing and manufacturing operations, and quality control labor in aluminum aerospace industry base on Saturn/Apollo data 12 p1931 N71-24181
(NASA-CR-114282)

Manufacturing factors and technologies in aluminum aerospace industry base on Saturn/Apollo data 12 p1931 N71-24182
(NASA-CR-114283)

Effects of reductions in NASA contracts on unemployment of aerospace employees 13 p2191 N71-24801
(NASA-CR-118374)

Effect of scientific and technical progress in controlling national economy and evaluation of effectiveness of science 16 p2695 N71-29066
(JPRS-53271)

Economic and radiation problems of upper atmosphere and space exploration - Russia 19 p3092 N71-32005

Technology and economics of isotopic electricity generators 19 p3065 N71-32122
(CEA-BIB-190)

Economic factors affecting decision to build ground station support equipment for communication with Intelsat satellite 20 p3235 N71-33807

Conversion of US scientific and technical resources from defense and aerospace to civilian objectives (GUPS-MON-8) 20 p3371 N71-33823

Economic factors of custom or customer designed integrated circuits 23 p3736 N71-36455

ECONOMICS
NT DEMAND [ECONOMICS]
Economic cybernetics, mathematical economics, industrial process control, and automatic computer design in USSR 02 p0188 N71-11529
(AD-711361)

Time series analysis in economics using computer programs 03 p0343 N71-12489
(SA/AOH/17/0)

Twisted turnpike theorem and bounded, nonconstant normalized production possibilities 04 p0510 N71-12554
(AD-713696)

World Bank operations and economic growth of less developed countries 04 p0624 N71-14032

Control theory applications in solving socio-economic problems 04 p0624 N71-14033

Economic impact of modifications to DC-8 aircraft nacelles to reduce fan-compressor noise - Part 5 [NASA-CR-1709] 05 p0628 N71-14936

Bibliography on urban economics and planning [AD-714508] 06 p0982 N71-18624

Reporting career opportunities as economist or auditor with Civil Aeronautics Board 07 p1134 N71-18086

Economic, technological, and time saving effects of computer revolution on man 10 p1528 N71-21237

Economics and operational planning for future civil air transportation 11 p1675 N71-22286

Economic efficiency calculations for long range air forecasts for ship navigation of Northern Sea Route 11 p1737 N71-22845

Profile construction, cost benefits, economics, and user surveys in transfer of technology and selective dissemination of information 12 p1867 N71-23336

Irrigation and weather modification studies of Economic Research Service 13 p2072 N71-23808

Cost, time, and social burdens created by need for commuting to work and suggestions for eliminating problems [NASA-TM-X-67243] 14 p2357 N71-25744

Marxist social and material economic bases of contemporary stage of scientific-technical revolution [AD-720916] 15 p2526 N71-28014

Profit analysis techniques for profit and fee negotiation [NASA-CR-119004] 16 p2694 N71-29272

Distribution of funds for federal academic science support and scientific activities conducted with allocated funds 17 p3262 N71-30876
(NSF-71-7)

Flying, technical, and economic characteristics of helicopters noting contribution to national economy of USSR [AD-723594] 19 p3035 N71-31770

Monte Carlo analysis of importance of collinearity as problem in applied econometrics 19 p3124 N71-32540
(P-4588)

Economic aspects and regional planning for international airport facility at Ontario, California 22 p3565 N71-33591
(PB-199695)

Accuracy, usability, and economics of using NAS-TRAN program 22 p3686 N71-34208

Economic, administrative, and legal factors affecting freight loss and damage 24 p4035 N71-38700

Discrete data model and regression analysis for devaluating economic control strategy 24 p4036 N71-38701

ECONOMY
Government planning in technological society 07 p1135 N71-18070

EDDIES
U VORTICES
EDDY CURRENTS
Large scale motion of turbulent boundary layer with zero and favorable pressure gradient [AD-712330] 02 p0205 N71-12140

Thickness measurements on plates using eddy current technique [ARL/MET-80] 03 p0353 N71-12540

Evaluation of eddy current tester for detecting seams in rolled uranium rods [MLCO-1059] 03 p0383 N71-12150

SUBJECT INDEX

Automatic test equipment for hysteretic and eddy current energy dissipation in steel metal sheets (NPL-MEMO-5) 03 p0383 N71-13363

Multiparameter eddy current nondestructive testing for tube flaws in support regions (NHWL-1468) 04 p0616 N71-13818

Oil Stream flow with transient current fluctuations and detached eddy formations (EESA-TR-ERL-164-AQML-1) 05 p0679 N71-15524

Applying vector space concept to identification of test specimen parameters in nondestructive tests (NWL-1406) 06 p0629 N71-16737

Analysis of jet stream structure and energetics using objective scheme that calculates normal and parallel wind components for determining eddy currents (AD-72121) 15 p2438 N71-27270

Eddy-current loss in closed current loops caused by mixed magnetic fields (IP-4/00) 15 p2455 N71-27778

Eddy current measurements using coil encircling coupled two-conductor rod and solution of electromagnetic induction problem (V-1/87) 19 p3071 N71-32327

Errors associated with demodulator technique for eddy current testing (ADL-MR-82) 20 p3242 N71-32903

Eddy formation in energy transport of electromagnetic wave fields in waveguide 21 p3485 N71-34825

Measured coil impedance in eddy current testing (JALLMET-NOTR-73) 23 p3731 N71-36598

Computer programs for solving eddy-current problems encountered in nondestructive testing including operating instructions and examples (JORNLT-MR-5293) 23 p3737 N71-36648

Differential equations for calculating eddy current losses caused by rapidly varying magnetic fields (Q7574-1995L-9F) 23 p3805 N71-37126

EDDY DIFFUSION

U TURBULENT DIFFUSION

EDDY VISCOUSITY

EDDY transfer of active and passive contaminants in atmospheric boundary layer (AD-716359) 09 p1413 N71-19825

EDGE DISLOCATIONS

Prismatic edge dislocation motion in copper crystals (UCRL-19625) 07 p1093 N71-17460

High voltage electron microscopy study of slip band growth in radiation hardened copper crystals (JNLT-19601) 07 p1095 N71-17962

Non-basal slip in alumina at high temperatures and pressures (AD-716788) 10 p1631 N71-20611

Determination of Burger vectors, glide planes, and densities of crystal dislocations by various Bragg angle spectroscopy micrograph and dynamic electron diffraction equation analysis (NYO-3687-19) 12 p1987 N71-23957

Mobility of edge dislocations in pure copper single crystals measured as function of stress at temperatures from 66 to 373 K 14 p2330 N71-26619

Fundamental characteristics of dynamic slip-band propagation determined from high strain rate deformation of aluminum single crystals (AD-720083) 15 p2422 N71-27215

Precipitation hardening of CuCo and CuCoZn alloys and particle size and temperature effects on creep properties and edge dislocations (IS-T-422) 15 p2425 N71-27652

Slip band growth in prestrained copper crystals studied by transmission electron microscopy (UCRL-20372) 17 p2815 N71-29738

Microstress analysis of edge dislocation effects of strain hardening on copper single crystal lattices 17 p2815 N71-29808

Edge, screw, and crystal dislocations (NBS-SP-317-VOL-1) 17 p2816 N71-29926

Theoretical calculations on extension of 1/2, 110, 111/ edge and screw dislocations in isotropic fcc metals into Shockley partials 17 p2816 N71-29931

Planar and free edge dislocations in infinite elastic solid 17 p2817 N71-29938

Atomic calculations of edge and screw dislocations in liquid krypton 17 p2818 N71-29945

Pair interaction energies for screw and edge dislocations in circular cylinder 17 p2824 N71-29993

EDGE LOADING

Structural analysis of fiber reinforced, laminated composite plates subjected to edge and thermal loads (NCL-DE-48-115) 02 p3032 N71-12065

Circular plates in sandwich structures with edge loading analyzed by calculus of variations (NBS-112070) 03 p0466 N71-13351

Stress analysis on orthotropic shell of revolution subjected to varying edge loads 07 p1126 N71-17888

Approximation method for structural beam and plate members at elastic edge excitations (NASA-CR-1736) 08 p1297 N71-18647

Large deflection of n-layered rectangular plates with clamped edges and uniformly distributed load (AD-717245) 10 p1652 N71-21810

Effect of static stress and edge restraint on vibration of nearly cylindrical shells with circular cross section and slight meridional curvature (NASA-TN-D-6133) 11 p1838 N71-22617

Stress intensity factor and shape of edge crack in plate under tension (NASA-TM-X-67891) 19 p3188 N71-32229

Nonlinear oscillation in edge loaded circular plates and large strain plate theory 19 p3191 N71-32704

EDGES

NT LEADING EDGES

NT SHARP LEADING EDGES

NT TRAILING EDGES

Edges and curve detection in textured regions related to visual scene analysis 05 p0637 N71-14832

Edge durability data for machine tools in metal cutting processes (TN-7) 10 p1563 N71-20910

Comparison of flat plate sharp and blunt edge effects on heat transfer in supersonic flow and heat transfer coefficient dependence on Reynolds number (AD-717825) 11 p1735 N71-22156

EDITING ROUTINES [COMPUTERS]

Editing system for large general time sharing computer including dynamic editing display technique and static microfilm method (NASA-TM-X-2264) 11 p1716 N71-22575

Computer editing routine for data abnormalities in multivariate statistical analysis (NASA-TM-D-6472) 18 p2896 N71-31371

EDTA

U ETHYLENEDIAMINETETRAACETIC ACIDS

EDUCATION

NT ASTRONAUT TRAINING

NT EJECTION TRAINING

NT FLIGHT TRAINING

NT GUNNERY TRAINING

NT PILOT TRAINING

NT SPACE FLIGHT TRAINING

Summary of ocean engineering programs in educational institutions (PS-193566) 02 p0211 N71-11509

National Science Foundation survey for 1969 of scientific activities of institutions of higher education (NSF-70-16) 04 p0622 N71-14066

Educational and research activities of Ford Nuclear Reactor (COO-385-3) 04 p0560 N71-14290

Small particle accelerator uses in education and research - conference (DWR-1556) 07 p1080 N71-18044

Effects of education and pharmacodynamics on adaptability of human beings to degraded sensorial environments 09 p1337 N71-20364

National Science Foundation activities in science research, education, institutes, computation, and information systems (NSF-71-1) 10 p1665 N71-21094

Systems engineering and management applied to urban development, education, water management, inventory management, Saturn-Apollo project, and ecology (NASA-TM-X-64575) 11 p1846 N71-22026

Technology revolution and educational system management planning 11 p1847 N71-22033

Implications of Saturn 5 systems approach to education and other programs (NASA-CR-61347) 12 p2018 N71-24080

Preparation of test plans used to evaluate performance of flight simulation trainers (AD-720301) 17 p2731 N71-30237

Methods and techniques for training personnel for operation and test of aviation equipment, subsystems, and related accessories 17 p2712 N71-30254

Communications satellites applications in education in US (NASA-CR-119680) 19 p3197 N71-32375

Role of education in US shift to metric system, and advantages, costs, and methods of changeover in schools (NBS-SP-345-6) 19 p3197 N71-32421

Description of facilities and resources at Smithsonian Institution for advanced study and research 19 p3199 N71-32760

Articles concerning undergraduate education in biological sciences (NASA-CR-121726) 21 p3381 N71-34055

Utilization of electronic and computerized techniques for undergraduate medical education (RM-6180-NLM) 21 p3385 N71-34081

Manpower and training needs for air pollution control - public and private sectors (S-DOC-91-98) 21 p3533 N71-35182

Technology assessment of communication media and educational technology including future trends

EFFICIENCY

utilizing communication satellites, television, and computer-assisted instruction (NASA-CR-122037) 22 p3533 N71-35306

Instructional strategies for optimizing learning processes and application of such principles to practical course of instruction in computer sciences (NASA-CR-121936) 22 p3536 N71-35326

Meteorological training in Italy and program for Mediterranean meteorology (IFRA-RDP-31) 22 p3612 N71-35731

Status of high power technology for educational satellites and recommendations for expansion to rural and remote areas (NASA-TM-X-67933) 22 p3673 N71-36190

Training and installation procedures for NASTRAN program 22 p3686 N71-36288

Interactive graphic instructional program illustrating basic concepts of systems analysis - INSIGHT (TR-71-21) 22 p3698 N71-36371

Electronic educational information dissemination and broadcast services in US including historical development and infrastructure - bibliography (NASA-CR-121910) 22 p3698 N71-36374

Status, cost/effectiveness, and telecommunication/satellite requirements of computer-based instruction (NASA-CR-122945) 23 p3689 N71-37583

Curriculum supplement to assist general chemistry teachers in updating instruction materials with aerospace developments (NASA-EP-57) 24 p3885 N71-37691

Determining faculty necessary for accredited engineering curriculum as function of faculty workload, number of students, and curriculum characteristics with cost estimates (NASA-CR-123114) 24 p4034 N71-38780

EDUCATIONAL TELEVISION

Satellite television for educational purposes in Argentina 20 p3236 N71-33836

International aspects of educational TV by satellite 20 p3236 N71-33837

Audio-Visual Satellite Instruction system (AVSIN) for USA - preliminary considerations (NASA-CR-122946) 23 p3689 N71-37584

EEG (ELECTROENCEPHALOGRAMS)

U ELECTROENCEPHALOGRAPHY

EFFECTIVENESS

NT COST EFFECTIVENESS

NT SYSTEM EFFECTIVENESS

Planning provisioning and maintenance by adjusting modifications in use against need for resources (FTL-A-A06-6) 05 p0732 N71-14678

Influence of lateral motion on effectiveness of flight simulators in training air transport pilots 18 p3002 N71-30772

Effectiveness factor calculation technique for nonisothermal catalysts taking into account mass and heat transfer effects at boundary film and in particle interiors (NLL-RTS-6472) 23 p3722 N71-36527

Effectiveness of reliability programs for avionics equipment 23 p3757 N71-36779

EFFECTORS

U CONTROL EQUIPMENT

EFFECTOR NERVOUS SYSTEMS

Measurement of ozone and some effects of ozone and nitrogen oxides on motor activity of rats 07 p0862 N71-17666

Variability in timing of simple motor responses (AD-721213) 15 p2371 N71-27198

Environmental chambers for testing human work performance under thermal stress (AD-721595) 16 p2545 N71-28447

Analogy between human motor functions and mechanical legs for planetary striding vehicle 20 p3277 N71-32913

EFFICIENCY

NT COMBUSTION EFFICIENCY

NT COMPRESSOR EFFICIENCY

NT ENERGY CONVERSION EFFICIENCY

NT NOZZLE EFFICIENCY

NT POWER EFFICIENCY

NT PROPELLER EFFICIENCY

NT PROPULSIVE EFFICIENCY

NT THERMODYNAMIC EFFICIENCY

NT TRANSMISSION EFFICIENCY

Power and efficiency of continuous hydrogen fluoride chemical laser (AD-711067) 01 p0862 N71-10433

Neutron detector with weak dependence of neutron registration efficiency for studying photoelectric reactions (AD-717402) 11 p1760 N71-21969

Computer performance test program for assessing complex indexing operations (NBS-TN-572) 13 p3049 N71-24580

Blowing effect on static efficiency of two dimensional air intakes with momentum injection in boundary layer control form (ARC-RM-3656) 15 p2364 N71-27149

- Geometric efficiency of lithium 6 suspended target type semiconductor spectrometers calculated for isotropic neutron fluxes
[IAERE-R-6318] 15 p2479 N71-27635
- Compilation of information on assembly technology for efficiency and cost reduction
[NASA-SP-593401/1] 18 p2930 N71-31394
- Efficiency and performance characteristics of low temperature two phase liquid metal MHD power systems
[AD-721087] 19 p3173 N71-31757
- Monte Carlo code for evaluating efficiency of boron-sodium iodine neutron counter
[KFK-1182] 21 p3471 N71-34715
- Model for spark chamber breakdowns and shower efficiency determination
[JINR-P13-5810] 24 p3979 N71-38393
- EFFLUENTS**
- Developing experimental information and analytical methods for design and safety analysis of sodium cooled fast reactors
[AI-AEC-12970] 04 p0554 N71-14017
- Thermal effluent effects and reactor safety measures - bibliography
[ORNL-NSIC-81] 10 p1603 N71-21748
- Activated carbon in reactor confinement systems to remove radiolodine from effluent gases in event of nuclear accident
17 p2715 N71-29857
- Aerial photography for monitoring and evaluating effluents from ocean waste disposal processes
[REPT-120408BY] 22 p3584 N71-35528
- EGCR (REACTOR)**
- U EXPERIMENTAL GAS COOLED REACTORS**
- EGYPT**
- Soviet and French programs for establishing astrometric schools and stations in Egypt for space geodesy
22 p3680 N71-36243
- EIGENFUNCTIONS**
- U EIGENVECTORS**
- EIGENSTATES**
- U EIGENVECTORS**
- EIGENVALUES**
- Fractional iteration of functions of several variables
02 p0252 N71-11937
- Bifurcation from simple eigenvalues with mapping of Banach space subset
[AD-712438] 03 p0401 N71-13389
- Digital analysis of liquid sloshing in rotational symmetric tanks under weak gravitational fields - Vol. 2
[NASA-CR-111739] 04 p0604 N71-14226
- Eigenvalues for point and space kinetics model comparison in uranium-hydride reactor
[FBI-177] 04 p0589 N71-14317
- Extremal problems related to eigenvalues of linear differential operators
[AD-717066] 05 p0714 N71-15278
- Asymptotic distribution of eigenvalues of random matrices
[ORNL-4603] 05 p0714 N71-15590
- Subroutine ALLMAT for eigenvalues and eigenvectors of general complex nature
[NASA-TN-D-7032] 06 p0818 N71-15833
- Optimum relaxation factor for SOR method with complex eigenvalues of Jacobi method
[AD-715001] 07 p1051 N71-17827
- Discussing problem of symbolic numeric conversion in solving quantum mechanical eigenvalue problems with FORMAC
08 p1228 N71-19192
- Effect of elastic end rings on eigenfrequencies of finite length thin cylindrical shells
[NASA-CR-117312] 09 p1481 N71-20516
- Eigenvalues, radial expectation values, and potentials for free atoms from Z equals 2 to 126 as calculated from relativistic Hartree-Fock-Slater atomic wave functions
[ORNL-4614] 10 p1614 N71-20840
- Monte Carlo technique using repetitive analog computer for estimating lowest eigenvalues for certain partial differential equations with Dirichlet boundary conditions
12 p1884 N71-23870
- Eigenvalue and deflection quantities of structural systems with material, geometric dimensions, boundary conditions, and external loadings with probabilistic distributions
12 p2007 N71-24119
- Nuclide transport models for clad spherical fuel particle calculation in high temperature reactors
[JUL-685-PA] 13 p2128 N71-24475
- Eigenvalues passing through hyperbolic fixed points for area-preserving mapping
[TR-1] 14 p2282 N71-26109
- Algorithms for calculation of eigenvalues and two center problem of quantum mechanics
[JINR-P4-5040] 15 p2468 N71-27544
- Daniilevsky method for determining eigenvalues of matrices with real elements programmed in FORTRAN
[ARL/SM-349] 15 p2434 N71-27619

- Stiffness, damping, and inertia change effects on eigenvalues and eigenvectors of linear vibration systems
17 p2788 N71-30057
- Eigenvalues and corresponding sets for group of permutations
[IAE-1988] 18 p2942 N71-30480
- Optimal control models for design of structures with weights minimized by constraints involving fixed eigenvalues
[NASA-CR-121458] 20 p3358 N71-33447
- Procedures for accurate condensing of eigenvalue solutions in structural analysis using Guyan reduction solutions
22 p3683 N71-36266
- Development of method for calculating resonant modes and eigenvalues of laser cavity
23 p3767 N71-36854
- Polyaomial roots, boundary value problems of non-linear equations, and eigenvalue problems of linear ordinary differential operators treated with continuation method using fast computers
23 p3782 N71-36958
- Solutions to eigenvalues problems of thermal instability of viscous fluid heated from below in completely enclosed cylinder with arbitrarily conducting side wall
23 p3868 N71-37578
- Focal image method for calibration in calculating characteristic curve for comets
24 p4009 N71-38585
- EIGENVECTORS**
- Subroutine ALLMAT for eigenvalues and eigenvectors of general complex nature
[NASA-TN-D-7032] 06 p0818 N71-15833
- Method of singular eigenfunctions developed to study transverse propagation of neutron waves in medium with isotropic scattering
14 p2310 N71-26659
- Existence and extendability of continuous eigenvector branches and application of nonlinear programming algorithms to nonlinear heat generation and rotating string problems
[NASA-CR-119020] 16 p2623 N71-28630
- Eigenfunction expansion techniques for determining resonances of ferrite-filled spherical resonator
16 p2640 N71-29126
- Stiffness, damping, and inertia change effects on eigenvalues and eigenvectors of linear vibration systems
17 p2788 N71-30057
- Two boundary value problems on semi-infinite strips solved with eigenvector expansions
19 p3123 N71-32257
- Implication of Hough function thermospheric degeneration on latitudinal tidal mode structure and vertical wave propagation
[NASA-TM-X-65675] 20 p3266 N71-33442
- Numerical analysis of displacement and stress fields caused by eigenstrains distributed uniformly inside domain
[COO-2034-4] 21 p3259 N71-35145
- Multiple scattering and eigenfunction solutions for electromagnetic scattering from cylinders over and imbedded in dielectric half spaces
24 p3890 N71-37730
- Eigenvector analysis of air temperature distributions over Atlantic Ocean
[NLL-M-20364-5828.4F] 24 p3918 N71-37938
- Focal image method for calibration in calculating characteristic curve for comets
24 p4009 N71-38585
- EIKONAL EQUATION**
- Eikonal model of elastic scattering and production processes derived from unitary correction application to Veneziano model
[UCSD-10-P-10-76] 06 p0925 N71-16811
- Deriving multiple high energy scattering amplitudes by eikonal approximation in Regge pole model
[TUEP-71-1] 10 p1622 N71-21761
- Eikonal approximation for high energy interactions
[JINR-E2-5244] 14 p2503 N71-26038
- Eikonal representation of scattering amplitudes from high energy interactions in field theory nuclear models
[JINR-P2-5577] 18 p2976 N71-30622
- Phi cube theory for studying impact picture and eikonal approximation
[DESY-71/6] 19 p3145 N71-31899
- Electron proton inelastic scattering form factors for massive quantum electrodynamics calculated from eikonal-like equations
[ILL-TH-71-9] 19 p3157 N71-32509
- Quantum electrodynamics study of high energy scattering amplitudes in phi pi 3 theory, including breakdown of eikonal approximation
[DESY-71/13-PT-1] 21 p3482 N71-34806
- Functional integration and Regge-eikonal representation of high energy particle scattering amplitudes
[JINR-P2-5768] 23 p3807 N71-37144
- EINSTEIN EQUATIONS**
- Geometrical properties of spherical space and relationships in Einstein space-time universe and planetary or test particle orbits in that universe
[NASA-TM-X-65711] 23 p3856 N71-37490

EJECTION

NT STELLAR MASS EJECTION

- Tests at Mach number 6 to investigate results of ejected liquid fuel/air and two dimensional, zero pressure gradient boundary layer for wedge model
[AD-721448] 16 p2381 N71-30922

EJECTION INJURIES

- Survey on vertebral fractures of flying personnel caused by ejection from Navy aircraft
02 p0163 N71-11911

EJECTION SEATS

- Feasibility of using flexible rotor blades for ejection systems
[AD-711642] 02 p0144 N71-11902
- Requirements for ejection seat systems
[IAE-LIB-TRANS-1471] 02 p0147 N71-11906
- Evaluating psychological and physiological factors in designing ejection seats and parachutes
[AD-711928] 02 p0158 N71-11912
- Development of pneumatic ejection seat training equipment
04 p0483 N71-12001

- Ejector for separating astronaut from ejection seat during prelaunch or initial launch phase of flight
[NASA-CASE-XMS-04625] 10 p1504 N71-20770
- Four-degree-of-freedom lumped parameter model for vertical accelerations of seated human body as might be imposed by aircraft ejection systems
[AD-721225] 15 p2370 N71-30105
- Nonflammable polyurethane foam for ejection seat cushions and statistical analysis of its mechanical properties
[AD-723302] 19 p3119 N71-31770
- Design, fabrication, and tests of energy absorbing seat integrated with extraction tractor rocket for space shuttle
22 p3547 N71-35208

EJECTION TRAINING

- Development of pneumatic ejection seat training equipment
04 p0483 N71-12001

EJECTORS

- Applied gas dynamics including data on subsonic and supersonic injectors
[AD-712821] 03 p0363 N71-12609
- Potential momentum thrust performance of three augmenting ejectors
[AD-713634] 05 p0762 N71-14022
- Performance of auxiliary inlet ejector nozzle with floating inlet doors and floating single hinge trailing edge flaps
[NASA-TM-X-2173] 07 p1102 N71-17594
- Auxiliary inlet ejector nozzle designed for supersonic cruise aircraft
[NASA-TM-X-2182] 08 p1284 N71-18863
- Ejector for separating astronaut from ejection seat during prelaunch or initial launch phase of flight
[NASA-CASE-XMS-04625] 10 p1504 N71-20770
- Latching mechanism with pivoting catch and self-contained spring ejector
[NASA-CASE-XLA-03538] 13 p2086 N71-26097

EKMAN LAYER

BOUNDARY LAYER TRANSITION

- ELASTIC ANISOTROPY**
- Elastic anisotropy effects on cold drawing of metals
[ONERA-NT-158] 02 p0230 N71-11550
- Variational methods used for approximate analysis of solutions to problem of bending and torsion in anisotropic elastic beams
[NPL-MA-96] 22 p3689 N71-36111
- ELASTIC BARS**
- Solution to axisymmetric equations of motion in elastic bars containing discontinuities
[AD-716547] 09 p1477 N71-19779
- Pressure pulse wave analysis in an elastomeric polyethylene bar using laser strobe interferometry
[REPT-2/71] 19 p3186 N71-31804
- One dimensional approximate theory for elastic circular rod with nonuniform cross section and axisymmetric transient wave propagation
[RE-415] 24 p4023 N71-38708

ELASTIC BENDING

- Elastic bending, tearing, and breaking of cotton fiber and nylon fabrics with rubber and plastic coatings
[RAE-TR-70112] 06 p0876 N71-15704
- Elastic bending and fracture mechanics of reinforced fiber epoxy resins using scanning electron microscope
[NPL-IMS-11] 07 p1047 N71-17114
- Mathematical model for elastic shear bending of trapezoidally corrugated plate with trough lines and straight including stiffness and stress analysis
[NASA-CR-1749] 20 p3357 N71-33114
- Tensile stretching and bending of elastic plate containing surface crack
[NASA-CR-121428] 20 p3359 N71-33168
- ELASTIC BODIES**
- Discrete methods for linear dynamic response of elastic and viscoelastic solids
[TPB-194286] 04 p0618 N71-14205

- Determination of unsteady forces during wind tunnel test of elastic model by placing wind tunnel model in feedback circuit of servosystem
[NASA-CR-114287] 09 p316 N71-19796
- Analysis of propagation of flexural waves in piezoelectric, elastic bars with and without prestressing
[AD-716466] 09 p474 N71-19829
- Description of general purpose digital computer program (NASTRAN) for analysis of elastic structures under various loading conditions using finite element method approach
[NASA-SP-260] 10 p1658 N71-21559
- Numerical analysis of transverse vibrations of elastic vertical rods of circular section in fluids
[NLL-RTS-5849] 10 p1658 N71-21690
- Analysis of finite deformations of incompressible elastic solids by finite element method with formulations of higher order approximations and curvilinear elements
[AD-715464] 11 p1835 N71-22327
- Development of systems for automatically and continuously suppressing or attenuating bending motion in elastic bodies
[NASA-CASE-XAC-05632] 12 p2006 N71-23971
- Dynamic problem of infinite, elastically supported beam under influence of uniformly moving single point load solved by complex variable theory
[NASA-TT-F-13569] 14 p2347 N71-25802
- Gravitational stresses in elastic half-space bodies with notches or mounds
16 p2585 N71-28209
- Dynamic and static structural analysis computer program for one and two dimensional elastic bodies
16 p2689 N71-29099
- Thermodynamic properties of inhomogeneous elastic bodies
[NASA-CR-119065] 17 p2822 N71-29978
- Dynamic surface loading of elastic half space
[REPT-479] 19 p3186 N71-31728
- Unique reflection pattern of oblique shock wave incident upon plane boundary of nonlinear simple elastic solid
[AD-724137] 20 p3357 N71-33086
- NASTRAN generation of motion pictures for analysis of elastic structure transient responses under continuous deformation conditions
22 p3687 N71-36294
- Development of theory to predict low frequency standing wave characteristics and stability parameters of elastic bodies in presence of electromagnetic fields
23 p3860 N71-37519
- ELASTIC BUCKLING**
- Investigating buckling behavior of flanges of horizontally curved plate girders using finite element method
[PB-192901] 04 p0616 N71-13864
- Elastic buckling of clamped oval cylindrical shells under axial loads
[AD-714579] 06 p0553 N71-16526
- Effective use of incremental stiffness matrices in nonlinear geometric analysis
[AD-713967] 06 p0558 N71-16877
- Stress analysis of spherical shell compressed between rigid plates with axisymmetric postbuckling and nonsymmetric buckling
[AD-716791] 10 p1635 N71-21190
- Buckling analysis of elastic ring confined to uniformly contracting circular boundary
[AD-716852] 10 p1659 N71-21804
- Application of Rayleigh-Ritz mesh method to elastic buckling of orthotropic rectangular shells
[DLR-FB-70-71] 13 p2177 N71-24493
- Numerical analysis of buckling of continuously infinite beams using Winkler model, Pasternak model, and elastic continuum
[NASA-CR-118313] 13 p2183 N71-25413
- Applying Kantorovich method to elastic and plastic buckling problems of rectangular plate
[AD-720990] 15 p2521 N71-27570
- ELASTIC COLLISIONS**
- U ELASTIC SCATTERING**
- ELASTIC CONSTANTS**
- U ELASTIC PROPERTIES**
- ELASTIC CYLINDERS**
- Investigating stability of steady movement of rigid shaft with disc on elastic rotor bearings using modified Ritz procedure
06 p0893 N71-15952
- Derivation of generalized Fourier series for calculating stresses in semi-infinite elastic strips and cylinders
[AD-716538] 09 p1477 N71-19975
- Asymptotic solutions of stress and strain as functions of radial and longitudinal distance, and time for axisymmetric waves in step-function pressure-loaded hollow elastic circular cylinder
11 p1838 N71-22793
- Natural vibration of closed cylindrical shell with rigid elastic core
14 p2347 N71-25794
- ELASTIC DAMPING**
- Numerical determination of nonlinear displacement behavior of complete circular cylindrical thin shell subjected to uniform radial pressure
[AD-712111] 02 p0302 N71-12051

- ELASTIC DEFORMATION**
- NT ELASTIC BENDING**
- NT ELASTIC BUCKLING**
- Measuring shear-creep compliance of solid and liquid materials used in spacecraft components
[NASA-CASE-XLE-01481] 01 p0056 N71-10781
- Continuous thermodynamic theory of nonlinear thermomechanical materials with memory
[AD-711401] 02 p0304 N71-12174
- Superposing small elastic deformations on large ones with explicit expressions for incremental stress-strain relations for isotropy and transverse isotropy
[AD-712399] 03 p0461 N71-13005
- Statistical isotropic deformation of elastic solid of composite materials
[AD-712814] 03 p0467 N71-13385
- Finite element analysis of interlaminar shear in fibrous composites
[RM-492] 06 p0880 N71-16466
- Elastic energy and magnitude determination for underground explosions in tuff and rhyolite
[NVO-1163-208] 06 p0854 N71-16066
- Elastic deformation of sandwich structures with load distributions on one side
07 p1122 N71-17209
- Satellite attitude control mathematical models, inertia, radiation pressure, elastic deformation, and magnetic effects
[ESRO-SP-17-VOL-2] 07 p1119 N71-17258
- Hardness and high pressure deformation mechanisms of glass
08 p1223 N71-19154
- Elastic displacements produced by point defect in cubic medium by Fourier transform method
08 p1281 N71-19279
- Axial deformation analysis of thin shallow elastic spherical shells of uniform thickness with surface constraints
10 p1659 N71-21767
- Algorithms for thin-walled axisymmetrically loaded bodies of revolution elastic stability problems including cylindrical, conical, spherical, and toroidal shells
11 p1837 N71-22495
- Homogeneous continuum for describing mechanical behavior of laminated composite elastic solids
[AD-717311] 11 p1838 N71-22517
- Development of systems for automatically and continuously suppressing or attenuating bending motion in elastic bodies
[NASA-CASE-XAC-05632] 12 p2006 N71-23971
- Derivation of theory for deformation of elastic track roadway with no side limits under loads moving with uniform horizontal velocity
[NASA-TT-F-13619] 12 p2006 N71-24116
- Derivation of theory for unsymmetric deformation of nonhomogeneous, anisotropic, elastic cylindrical shells. Part I
[REPT-69-B-PT-1] 12 p2008 N71-24294
- Lagrangian formulation for large elastic deformations of thin shells, suitable for finite element analysis
[AD-721256] 15 p2521 N71-26946
- Stress and strain equations for deflections in rotating spherical shells
[ARKL-ME-318] 15 p2522 N71-27856
- Unified approach to interactions of defects applicable to rigid and deformable defects
[AD-721469] 16 p2664 N71-28227
- Linear elasticity, elastic-plastic deformations, and deformation-fracture interactions in fracture analysis of axially symmetric solids
17 p2852 N71-29751
- Deflection analysis of heated thermorheologically simple viscoelastic disks with inclusion of temperature dependence of viscoelastic modulus and other material properties
17 p2852 N71-29752
- Nonlinear continuum theory for analyzing crystal dislocation effects
[NBS-SP-317-VOL-2] 17 p2821 N71-29969
- Nonlinear elastic theory for finite inhomogeneous medium derived from crystal lattice mechanics
17 p2821 N71-29971
- Dilation theory of elasticity for crystal lattice interaction mechanics
17 p2821 N71-29972
- Dynamic nonlinear theory of crystal dislocations with elastic-plastic continuum mechanics
17 p2822 N71-29976
- Continuum mechanics for nonlinear dynamic dislocation analysis on anisotropic elastic media
17 p2822 N71-29977
- Thermodynamic properties of inhomogeneous elastic bodies
[NASA-CR-119065] 17 p2822 N71-29978
- Micromorphic and micropolar continuum dislocation theories for elastic solids
17 p2823 N71-29983
- Kinematics of continuum dislocations in crystal lattices
17 p2823 N71-29984
- Mean square stresses for random distributions of dislocations in cylindrical body
17 p2824 N71-29994

- Three simultaneous differential equations applicable to any strain energy function for problems of large elastic deformations of axisymmetric membranes
17 p2854 N71-30156
- Analyzing structure of constitutive relations which govern force-deformation laws used in stress analysis
[AD-722831] 18 p3022 N71-31483
- Transmission electron microscopy for studying deformation substructure in polycrystalline alumina
[ORO-3328-13] 18 p2999 N71-31560
- Buckling of trusses with arbitrary supports or of beams with bracing against lateral deviation
19 p3187 N71-31816
- Stress function analysis of elastic deformation of thin membrane structures
19 p3191 N71-32710
- Ocean tide effect upon earth crust tidal variations
20 p3263 N71-33353
- Elastic stress effects on indium alloy Fermi surface topology measured on alloy whiskers
20 p3334 N71-33569
- Determination of elastodynamic response of free-free quarter-plane following single concentrated pulse load applied to one of edges at distance from corner
20 p3360 N71-33866
- Effect of yield criterion on stresses and displacements on elastic/viscoplastic flow of solids
20 p3361 N71-33904
- Deformations of paraboloidal shell subjected to axisymmetric thermal loads
[NASA-TN-D-64711] 21 p3529 N71-35148
- Elastic deformation of telescope mirror, noting load distribution on static support system
22 p3670 N71-36172
- Elastic/perfectly plastic torsion analysis of doubly-connected cylinders using finite difference theory
22 p3691 N71-36325
- Development of dynamic theory of anisotropic heterogeneous elastic plates based on large deflection assumptions
22 p3693 N71-36340
- Feasibility of using elastic deformation to predict heat transfer rates across joined smooth-metal surfaces under high vacuum conditions and light loads
[NASA-TM-X-2385] 22 p3696 N71-36361
- Incremental finite element analysis of large elastic deformation problems
[AD-726727] 23 p3861 N71-37527
- Deformographs and extensometers for measuring earth crust deformations
24 p3910 N71-37866
- Field displacement graphical processing problems and techniques for calculating partial derivatives of displacements using moiré and coordinate grid methods
[NLL-M-21006-5828.4F] 24 p3950 N71-38185
- Method for large deflection inelastic analysis of plate grillages under normal and axial loads
[AD-727601] 24 p4025 N71-38722
- ELASTIC MEDIA**
- Reflection of oblique shock waves in elastic solids
[AD-710968] 01 p0130 N71-10836
- Thermal stresses in chemically hardened elastic media and applications to molding processes
[NASA-CR-115878] 05 p0781 N71-15627
- Program for computing collapse loads of heated, arbitrarily loaded spherical shells in elastic medium
[SC-DK-70-218] 07 p1124 N71-17571
- ELASTIC MODULUS**
- U MODULUS OF ELASTICITY**
- ELASTIC PLATES**
- Finite element analysis of alternating axial loading of elastic plate pressed between two rectangular blocks with finite friction
[REPT-110770] 02 p0300 N71-11945
- Dynamic flexure theory for elastic plates including transverse shear deformation and normal stress effects
08 p3100 N71-19175
- Collocated interfacial elastic stress intensity for finite, bi-material plates
[AD-716334] 09 p1476 N71-19919
- Crack arrest in transversely loaded elastic plates
[UCRL-72335] 09 p1477 N71-20000
- Buckling and post-buckling behavior of thin elastic plate subjected to compressive forces along the edge
10 p1657 N71-21396
- Numerical analysis of behavior of waves in infinite isotropic elastic plate covered by inviscid, incompressible fluid of finite depth
13 p2180 N71-24816
- Kinematics and general principles in nonlinear and linear theories of elastic shells and plates by direct approach and three-dimensional equations of classical continuum mechanics. Part I
[AD-722350] 17 p2854 N71-30220
- Derivation of constitutive equations, material symmetries, dynamical restrictions, and related topics for nonlinear and linear theories of elastic shells and plates. Part 2
[AD-722551] 17 p2854 N71-30221
- Equations derived for liquid motion in cylindrical tank with elastic bottom and subject to longitudinal excitation of sinusoidal form
22 p3693 N71-36339

Development of dynamic theory of anisotropic heterogeneous elastic plates based on large deflection assumptions 22 p3693 N71-36340

ELASTIC PROPERTIES

- NT AEROELASTICITY
NT ANELASTICITY
NT ELASTOPLASTICITY
NT HYDROELASTICITY
NT MAGNETOELASTICITY
NT MODULUS OF ELASTICITY
NT PHOTOELASTICITY
NT PHOTOVISCOELASTICITY
NT THERMOELASTICITY
NT THERMOVISCOELASTICITY
NT VISCOELASTICITY
- Relation between elastic and optical anisotropy for silicates
[NASA-TT-F-13324] 01 p0046 N71-10337
- Static and dynamic properties of thin shells, elastic and plastic theories, and study methods for stress and fracture conditions
[AD-711129] 01 p0129 N71-10591
- Ultrasonic pulse analysis of elastic properties of plastics at high pressures
[AD-711761] 01 p0073 N71-10851
- Inelastic deformation of aluminum alloys under combined stress at high temperature
[AD-712047] 02 p0244 N71-12063
- Steady profile analysis of plane shock structures in solids
[AD-712059] 03 p0460 N71-12949
- Collocation method for solving elastic problems of loaded plates with edge columns
[PB-193855] 05 p0776 N71-15155
- Calculation of elastic, viscous, and plastic effects in materials
[UCRL-72639] 05 p0703 N71-15226
- Determination of Hugoniot elastic limits for light armor materials
[UCRL-50901] 06 p0932 N71-15878
- Deriving relationship between macroscopic second order elastic constants and microscopic interatomic potential in crystals
[KAPL-M-7131] 06 p0923 N71-16740
- Theoretical and experimental determinations of elastic constants for magnesium
[COO-1198-756] 06 p0875 N71-16781
- Pressure and temperature dependences of elastic constants in single lithium chloride and lithium bromide crystals
[NYO-2504-78] 06 p0937 N71-16823
- Determination of elastic constants for single crystal bismuth
[RD/B/N-1622] 07 p1086 N71-17177
- Effects of pressure and temperature on elastic properties of rubidium salts
[NYO-2504-69] 07 p1087 N71-17231
- Effect of minerals on elastic properties of rocks
[NASA-TT-F-13446] 07 p1019 N71-17478
- Mechanical properties of uranium and plutonium based ceramic fuels
[ORNL-TR-2388] 07 p1066 N71-17681
- Strength and elastic behavior of composite nuclear fuel bodies
[RD/B/N-1622] 08 p1236 N71-18228
- Resilient vehicle wheel for lunar surface travel
[NASA-CASE-MFS-20400] 08 p1293 N71-18611
- Influence of precrack extension on local stresses in cracked plates under bending fields
[AD-715420] 08 p1298 N71-18884
- Isotropic elastic continuum model application to calculate energy and entropy of vacancy formation in metal crystals
[NASA-CR-116881] 08 p1281 N71-19207
- Thermal and elastic properties of polymers, and electronic properties of glasses and metals
[NASA-TT-F-13549] 09 p1404 N71-19730
- Numerical analysis of thermo mechanical constraints of materials reinforced with cords
[AD-716037] 09 p1474 N71-19828
- Elastic properties of hollow spherical shells under internal pressure and torsion properties of solid circular cylinders
[AD-716050] 09 p1475 N71-19872
- Elastic properties of alkali syenites from October Masif, Azov region
[NASA-TT-F-13549] 09 p1386 N71-20300
- Sound wave mapping for determining elastic properties and water absorption of rocks
[NASA-TT-F-13532] 09 p1386 N71-20346
- Development and application of theory of elasticity for layer with circular cylindrical hole subjected to nonuniform radial displacement
[NASA-TM-X-58056] 09 p1400 N71-20463
- Effect of elastic end rings on eigenfrequencies of finite length thin cylindrical shells
[NASA-CR-117312] 09 p1481 N71-20516
- Calculation of flexure and stability of rectangular and nonrectangular anisotropic plates by differential difference method
[AD-716979] 10 p1656 N71-21367

Constructing membrane theory of anisotropic shells by reducing three dimensional problem of theory of elasticity of shells 11 p1837 N71-22499

- Threadless fastener apparatus comprising receiving apertures for plurality of articles, self-locked condition, and capable of using nonmalleable materials in both ends
[NASA-CASE-XFR-05302] 12 p1925 N71-23254
- Mineral composition, textural and structural characteristics, metamorphism type, and secondary change effects on elastic properties of Krivoy Rog Basin metamorphic rocks
[NASA-TT-F-13548] 12 p1907 N71-23442
- Boundary layer techniques applied to two dimensional couple-stress theory of linear elasticity
[AD-717884] 12 p2004 N71-23494
- Numerical analysis of wave propagation in cylindrical shells based on application of general dynamics equation
12 p2006 N71-23975
- Experimental investigation of elastic and viscous properties of several polymer systems
12 p1904 N71-24158
- Development of mathematical model for analysis of inelastic arbitrary three dimensional solid structural systems
12 p2009 N71-24296
- Theoretical elasticity solutions for determining bond stresses in multifiber composite materials due to uniform tension
13 p2181 N71-25121
- Characteristics of elastic-plastic boundaries in homogeneous, isotropic, elastic-plastic continuum
13 p2182 N71-25132
- Changes in elasticity, magnetostriction, and electric resistance of iron-aluminum alloys during ordering
[DMDC-5793] 14 p2271 N71-25692
- Analytical method for predicting elasto-plastic bending of rectangular plates with large deflection
[AD-720844] 14 p2349 N71-26251
- Numerical analysis of elastic general instability problem of hydrostatically loaded simply supported cylindrical shell with conical ends
14 p2349 N71-26359
- Response of elastic earth to loads located in parallel plane to bounding surface
[SD-DR-70-836] 15 p2400 N71-27479
- Theory of cohesion and elastic properties of solids
[AD-720991] 15 p2508 N71-27593
- Ultrasonic wave distortion measurements of strontium titanate and potassium chloride elastic constants
15 p2486 N71-27828
- Methodology for determining elastic constants of in situ rocks during engineering and geological surveys
[NASA-TT-F-13654] 16 p2590 N71-28890
- Analysis of electrical and elastic properties of sedimentary rocks to obtain velocity profiles of electrocoring samples
[NASA-TT-F-13706] 16 p2591 N71-28973
- Mathematical model of satellite with continuous elastic components comprising moment free rigid carrier attached to elastic membrane
17 p2779 N71-29700
- Subsonic, supersonic, and transonic dislocations moving on interface separating two isotropic media of differing elastic properties
17 p2817 N71-29933
- Residual stress and incompatibility problem in linear elastic distortion of infinite anisotropic body
17 p2817 N71-29934
- Fixed and free edge dislocations in infinite elastic solid
17 p2817 N71-29938
- Elastic interaction between grain boundaries and screw dislocation pileups under constant stress
17 p2817 N71-29939
- Structural and elastic properties of zonal twin dislocations in anisotropic crystals
17 p2820 N71-29959
- Dynamic plastic behavior of hollow cylinders using exploding wire technique for investigation of elastic/viscoplastic constitutive theory
17 p2854 N71-30157
- Ultrasonic propagation in steels before and after neutron irradiation at thermal reactor temperatures
[WHAN-FR-38] 18 p2939 N71-31576
- Propagation of plane harmonic waves in an anisotropic, micropolar elastic media in two dimensions only
[AD-723417] 19 p3121 N71-32585
- Nonlinear oscillation in edge loaded circular plates and large strain plate theory
19 p3191 N71-32704
- Nonisothermal theory of large elastic-plastic deformation at finite strain
[AD-724319] 20 p3356 N71-32978
- Fourier transform solutions of quarter plane problems in elasticity
[AD-724176] 20 p3358 N71-33373
- Derivation of difference equations for MAGE hydrodynamic computer program, and computation of flows containing plastic and elastic effects
[LA-4601] 20 p3359 N71-33575

Differential technique used to determine third and fourth order elastic constants of copper and nickel 20 p3286 N71-33972

- Stress analysis of aluminum and copper at high temperatures using theory of thermally activated deformation of metals
[PB-195611] 21 p3439 N71-34403
- Angular momentum restrictions of t-channel exchanges from s-channel helicity conservation in elastic reactions
[SU-1206-248] 21 p3480 N71-34938
- Formulation of large deformation elastoviscoplastic theory for thick walled spherical shells
[AD-722867] 21 p3528 N71-35844
- Application of Green function to elastic displacement caused by unit force in infinitely extended anisotropic media
[COO-2634-5] 21 p3529 N71-35844
- Displacement and stress field determination within axisymmetric elastic bodies with prescribed internal loadings and boundary conditions
[AD-726425] 22 p3602 N71-35844
- Difference method in solving two-dimensional steady state theory of elasticity for case of specified strain on boundary
[NASA-TT-F-13566] 22 p3681 N71-36222
- Computer program for analyzing stresses, strains, and displacements in layered elastic structure under action of vertical loads on top surface
[PB-199214] 22 p3689 N71-36889
- Mathematical model for elastic stress concentration problems in fiber reinforced materials
22 p3691 N71-36934
- Numerical analysis of properties of axisymmetric waves in transversely isotropic rods
22 p3692 N71-36934
- Elastic earth tide inclinations observed at Talgar
23 p3749 N71-36978
- Spherical and planar galaxy systems in relation to elastic and inelastic evolutionary processes
23 p3849 N71-37422
- Analysis of gust penetration loads and associated elastic vehicle response of Saturn 5 launch vehicle AS-505 through AS-508 penetrating sinusoidal gusts
[NASA-CR-119944] 23 p3857 N71-37944
- Analysis of axisymmetric vibration of elastic spherical shell filled with viscous incompressible fluid
[AD-726634] 23 p3864 N71-37958
- Equations of motion for elastic plate foundation system under dynamic load applied to aircraft landing
23 p3864 N71-37958
- Development of technique for determining toughness and inelastic resistance of tires in tangential direction
[AD-727470] 24 p3928 N71-38027
- Plastic deformation of fine-grained, high purity, low pressed aluminum oxide and stress corrosion of polycrystalline magnesium oxide
[AD-727618] 24 p3945 N71-38048
- Development of hybrid coordinate equations of motion for finite element model of flexible appendage attached to rigid base undergoing unrestricted motion
[JPL-TR-32-1525 NASA-CR-132313] 24 p4023 N71-38092

ELASTIC SCATTERING

- Double scattering in quasielastic interactions of pions with deuterons
[NASA-TT-F-13384] 01 p0094 N71-18880
- Elastic scattering of O-18 by O-18
[RLO-1388-123] 01 p0097 N71-18889
- Neutron elastic and inelastic scattering cross sections for silicon in energy range 4.19 to 8.56 MeV
[ORNL-4517] 01 p0099 N71-18890
- Microscopic analysis theoretical model for elastic scattering of deuterons and alpha particles
[CTC-32] 01 p0100 N71-18890
- Systematics of elastic scattering
01 p0100 N71-18890
- Dirac equation solution for spin in elastic low energy electron scattering from gaseous atoms
[AD-711664] 01 p0101 N71-18890
- Numerical values for neutron elastic and inelastic scattering cross sections from sulfur
[ORNL-4539] 01 p0103 N71-18890
- Asymmetries produced by 28 MeV vector polarized deuterons in elastic scattering on C-12, Si-28 and Co-40
[LYCEN-7021] 02 p0277 N71-19211
- Positive kaon proton elastic scattering, Regge pole analysis, and K resonance production in searching for Z resonances
[UCRL-19832] 03 p0420 N71-19447
- Neutron elastic and inelastic scattering cross sections for Fe-56 in energy range 4.19 to 8.56 MeV
[ORNL-4515] 03 p0425 N71-19447
- Angular distributions for elastic and inelastic scattering of alpha particles by Mg-26
[RLO-1388-110] 03 p0426 N71-19447
- K plus p elastic scattering at 2.53, 2.76, and 3.0 GeV/c
[COO-1195-191] 03 p0430 N71-19447
- Elastic and inelastic scattering of 26.5 MeV alpha particles on Si-28, P-31, and S-32 nuclei
[DNP-699/PL] 03 p0432 N71-19447

- Positive kaon proton partial wave analysis at 860 to 1210 MeV/c
(UCRL-19787) 03 p0433 N71-12943
- Quantum electrodynamics of high energy electron positron elastic scattering
(LNF-70/96) 04 p0569 N71-13352
- Activities of Australian National University Department of Physics for 1969
(ANU-P-444) 04 p0574 N71-13668
- Polarization measurements of doubly elastically scattered deuterons on C-12 for energies between 41 and 51 MeV
(IP-18301) 04 p0574 N71-13669
- Absorption model for direct transfer reactions
(IUV-2433-F) 04 p0577 N71-13748
- Mary body problem of elastic scattering of electrons from atoms and molecules using Green function techniques
04 p0583 N71-14150
- Eikonal model for large angle np and pp elastic scattering at medium energies
(UW-2262-TA-223) 04 p0585 N71-14224
- Investigating muon-proton elastic scattering at 6 to 10 GeV for test of muon-electron universality
(WEV-176) 04 p0593 N71-14413
- Experimental determination of absolute cross sections for elastic scattering from carbon
05 p0735 N71-14530
- Measuring elastic scattering cross sections of lead isotopes from 40 to 80 MeV
05 p0735 N71-14531
- Measuring elastic scattering cross sections for Li-7 neutrons and 11/7/20-shell nuclei of Sc, V, and Co
05 p0736 N71-14534
- Large angle proton-proton elastic scattering at intermediate momenta
(COO-2009-15) 05 p0741 N71-15117
- Olsson theory for high energy hadron-deuteron scattering
(UCRL-19831) 05 p0743 N71-15146
- Scattering probability of fast test particles in plasma
(COO-1726-32) 05 p0749 N71-15296
- Deriving general formulae of Veneziano partial waves for 2 pion elastic scattering within group 3/2
(DEMO-70/13) 06 p0912 N71-15812
- Dual resonance model with quark spin
(COO-264-357) 06 p0915 N71-16002
- Realistic interactions and exchange effects in microscopic descriptions of elastic and inelastic neutron scattering
(TID-35904) 06 p0919 N71-16245
- Impedances of partial wave helicity amplitudes for elastic scattering process
(BU-1206-231) 06 p0924 N71-16771
- Eikonal model of elastic scattering and production processes derived from unitary correction application to Veneziano model
(UCSD-10-P-10-76) 06 p0925 N71-16811
- High energy, neutrino scattering, process study using V-A theory
(COO-266-559) 06 p0926 N71-16853
- Meson and hadron production and Bhabha scattering
(LNF-70/38) 07 p1070 N71-17004
- Discussing advances in molecular beam experiments involving two-body collisions
(NASA-CR-116434) 07 p1070 N71-17031
- Analyzing dopant semiconductor surface layers using elastic ion-backscattering data
07 p1089 N71-17291
- Calculating differential cross section for α /p, 2 shell reaction using impulse approximation
(LYCEN-70331) 07 p1082 N71-18146
- Penetration time of flight method for scattering experiments with slow neutrons
(RFE-1126) 08 p1249 N71-18204
- Investigating time-reversal invariance in electromagnetic interaction of electrons and deuterons
(LNF-70/20) 08 p1249 N71-18224
- Neutron 28 deuteron/proton silicon 29 interaction at low energy
(LYCEN-7013) 08 p1251 N71-18285
- Comparing data on elastic p-p scattering at 15 to 30 GeV with discrete values of root mean square transverse momenta
(BNL-81-5219) 08 p1252 N71-18292
- Electron-proton elastic scattering cross sections at low-momentum transfers between 1.0 and 1400 MeV/c
(DESY-70/42) 08 p1252 N71-18301
- Polarization and elastic scattering in nuclear reactions
(LA-4463) 08 p1252 N71-18308
- Elastic scattering of fast neutrons by deuterons
(LYCEN-7026) 08 p1256 N71-18374
- Axially injected, polarized proton beam for measuring He-4 scattering from 20 to 40 MeV
(BNL-19943) 08 p1258 N71-18548
- Measuring asymmetry in elastic scattering of electrons from polarized proton target
(UCRL-20093) 08 p1258 N71-18574
- High energy elastic and inelastic hadron-hadron scattering in pti-cubed theory
(ILL-TH-71-4) 08 p1261 N71-18803

- Spin effects in multiple quark scattering analysis of proton proton elastic scattering
(ILL-TH-71-3) 08 p1263 N71-18879
- Heavy particle transfer model of backward elastic alpha particle scattering and cluster structure of O-16 and C-12
(NYO-2171-327) 09 p1426 N71-19538
- Electron impact elastic, differential elastic, and differential ionization cross sections for nitrogen atoms
09 p1433 N71-19973
- Construction of potential from phase shifts for elastic scattering of particles obeying Schrödinger equation
(PM-70/3) 09 p1434 N71-19991
- Measuring backward elastic scattering of positive kaon proton and negative kaon proton events
(CEA-R-3683) 09 p1438 N71-20189
- Phi-nucleon elastic scattering amplitude real and imaginary part ratio calculations using quark models
(DESY-70/53) 09 p1438 N71-20197
- Angular distribution calculations of elastic and inelastic proton scattering by C-12 with allowance for wave function distortion in multipole formalism
(ITF-70-50) 09 p1440 N71-20296
- Elastic and inelastic scattering of atoms and ions, and sources of interference patterns
(SRIA-115-P-78-6) 09 p1440 N71-20303
- Quasi-elastic scattering from calcium 40 and calcium 48 excitation spectra
09 p1442 N71-20414
- Measurement of negative pion proton charge exchange at backward angles
(COO-1764-113) 10 p1613 N71-20836
- Neutron elastic and inelastic scattering cross sections for yttrium in 4.19 to 8.56 MeV energy range
(ORNL-4532) 10 p1615 N71-21037
- Kaon and proton elastic scattering at small angles and energies of 0.40 to 0.73 GeV/c
11 p1801 N71-21879
- Nuclear Fermi momenta from quasi-elastic electron scattering
(AD-717616) 11 p1803 N71-22235
- Optical-model analysis of neutron elastic scattering by U-238
(BNL-TR-366) 11 p1806 N71-22522
- Determining high energy peripheral collisions by multiplying Born approximation by phase shift factors of elastic scattering
(BLO-1398-595) 11 p1806 N71-22523
- Method for computing elastic scattering phase shifts for intermolecular potential calculation and analysis of twinning interference and fluctuations in total cross section
11 p1809 N71-22972
- Negative pion proton elastic scattering differential cross sections from 1.71 to 5.53 GeV/c
(NASA-CR-117852) 11 p1809 N71-23032
- Elastic scattering amplitude of protons from analog and compound states
(NYO-1062-29) 12 p1977 N71-24252
- Elastic nucleon-nucleon and nucleon-deuteron scattering
(JINR-P2-5444) 13 p2130 N71-24802
- Depolarization parameter measurements for elastic proton scattering in nuclear reactions
(CEA-COMP-1650) 13 p2132 N71-25093
- Magnetic deflection analysis of reactive scattering in crossed molecular beams of neutral species
(UCRL-19654) 13 p2138 N71-25433
- Elastic and inelastic proton scattering functions from Cd-110, Cd-112, and Cd-114 based on shell theory and elastic scattering indium isotopes for isobaric analog resonances
13 p2138 N71-25473
- Quasi-free electron scattering from protons with scattering calculation from harmonic oscillators and Wood-Saxon potentials for bound state protons and wave functions for final states
13 p2138 N71-25477
- Spin tensor moments of deuterons emitted from Mg/d,d/Mg elastic scattering reaction
(ANU-P/498) 13 p2141 N71-25545
- Calculation of two body elastic scattering amplitude for Ising model of ferromagnetic phase transition slightly above critical point as Hamiltonian field theory on lattice space
13 p2145 N71-25592
- Double partial wave expansion of elastic scattering amplitude and particle interactions
(P2299 N71-25608)
- Polarization measurement of tritons elastically scattered from He-3 established as good analyzer for tritons
(LA-4538) 14 p2301 N71-25740
- Elastic scattering of high energy hadrons from deformed carbon 12 nuclei calculations using multiple collision theory and deformed oscillator wave functions
(INF-721) 14 p2308 N71-26422
- Utilization of elastically scattered recoil ions to measure solid state track detector registration characteristics and particle trajectory analysis
(NASA-CR-118637) 14 p2308 N71-26447
- Short range dynamical correlations from elastic and quasielastic high energy electron scattering on He-4
(LNF-70/47) 14 p2311 N71-26494

- Straight line particle path approximation for description of high energy elastic and inelastic hadron scattering in quantum field theory
(JINR-E2-5217) 14 p2311 N71-26696
- Differential cross sections for elastic scattering of 104 MeV alpha particles on He-3
(KFK-1204) 14 p2312 N71-26708
- Elastic scattering of protons on Be-9 nuclei
(JINR-P1-5319) 14 p2318 N71-26764
- Report of experiments including neutron polarization, elastic and inelastic scattering of neutrons on C-12, and angular distribution of fission fragments in U-235 neutron reaction
(BNL-W-PR-70-14) 15 p2459 N71-27047
- Quasi-elastic scattering of particles on deuterons including double interaction effect of particle with deuteron nucleons
(JINR-P2-5343) 15 p2461 N71-27113
- Solution of unitarity equation for elastic scattering amplitude at high energy
(IPVIE-STP-69-45) 15 p2462 N71-27141
- Nonlocal separable potential formalism for elastic alpha scattering by helium
(LYCEN-7041) 15 p2465 N71-27241
- Mathematical model for neutron deuteron scattering above inelastic threshold
15 p2470 N71-27386
- Angular distribution vector analysis of polarized deuteron elastic scattering from helium 4 at energies between 3 to 11 MeV
15 p2476 N71-27575
- Quantum statistics and elastic backscattering cross sections of potassium ion neutron interactions between 1.0 and 2.5 BeV/c
15 p2477 N71-27579
- Target nuclei charge distribution effects on high energy electron small angle multiple scattering distributions based on Moliere formula and elastic form factors
15 p2478 N71-27607
- Positive kaon negative pion elastic scattering from positive kaon proton interaction at 5.43 GeV/c in 60-inch bubble chamber
15 p2482 N71-27745
- Method for describing elastic atomic collisions based on concepts of classical physics
(JINR-P-1225) 15 p2484 N71-27799
- Vector analysis of stripping reactions and elastic scattering from deuteron irradiation of O-16, Cr-52, Fe-54, and Zr-90 targets
15 p2486 N71-27827
- Differential cross sections of elastic and inelastic angular distributions of neutrons scattered from C-12 and excited states of C-13 at angles from 15 deg to 135 deg
15 p2489 N71-27884
- Time of flight method for studying fast neutron elastic and inelastic scattering on B-10 and B-11 in 2 to 5 MeV energy region
(AWE-CO-457/0) 15 p2489 N71-27885
- Current algebra and sum rules for pion nucleon elastic scattering amplitude low energy theorems and nuclear structure interpretations
(LYCEN-7081) 15 p2491 N71-27898
- Differential cross sections for elastic scattering of neutrons from carbon measured at primary energies between 0.50 and 2.00 MeV in steps of 50 keV
(EUR-4538-E) 15 p2491 N71-27899
- Heavy charged particle energy loss rate from nuclear elastic scattering
(LA-4543) 16 p2645 N71-28112
- Experimental data analysis on forward elastic pion /plus or minus/ proton scattering in model-independent way
(JINR-E2-5561) 16 p2647 N71-28239
- Complete solution of inverse scattering problem at fixed energy of particle obeying Schrödinger equation
(PM/71/1) 16 p2624 N71-28917
- Absorption at rest and low energy elastic scattering of negative kaons by neon with various final state interaction data
(TID-25667) 16 p2653 N71-29007
- Experimental and theoretical remarks on elastic and inelastic neutron scattering cross sections
(COO-1573-71) 16 p2654 N71-29047
- Real part of alpha nucleus potential obtained by double folding procedure
(INF-720) 16 p2657 N71-29141
- Calculation of neutron elastic and inelastic scattering cross sections and spatial transverse correlation functions for Heisenberg theory of impure ferromagnets
(BNL-TR-398) 16 p2658 N71-29144
- Proton and neutron scattering cross sections for carbon, deuterium, helium, and hydrogen, and atomic energy level schemes from krypton and lead isotope alpha reactions
(UCD-CNL-125) 17 p2790 N71-29320
- Intermolecular potential energy calculations for thermal elastic scattering of gases and comparison of Lennard-Jones and Morse potential functions
17 p2795 N71-29750
- Elastic scattering angular distributions for 13 to 27 MeV helium 3 beam from light target nuclei
17 p2802 N71-30133

Differential cross section for low momentum negative kaon helium-4 elastic scattering from 115 to 160 MeV/c

17 p2806 N71-30306

Electromagnetic form factor of nucleon derived from composite model

17 p2807 N71-30329

Partial wave analysis of positive kaon proton elastic scattering to show resonance in direct channel

[ORO-2504-151] 17 p2808 N71-30337

Solution of unitary condition for elastic scattering amplitude for high resolution energies

[ITF-70-49] 18 p2970 N71-30446

Computation of elastic and inelastic pion C-12 scattering using distorted wave impulse approximation

[COO-1051-45] 18 p2971 N71-30487

Solution of unitary condition for calculation of high energy elastic scattering amplitude of scalar particle on 1/2 spin particle with spinor particle polarization formula

[IFVE-STF-70-1] 18 p2974 N71-30549

Spin structure of two-photon exchange contribution to electron-proton elastic scattering amplitude

[JINR-P2-5629] 18 p2978 N71-30679

Regge cuts and high energy pion nucleon and kaon nucleon elastic and charge exchange scattering

[LPTHE-71/14] 18 p2985 N71-31136

Boltzmann transport equation for elastic scattering of electrons in solids

[AD-723597] 19 p3167 N71-31708

Interaction of fast neutrons with 1p, 2s, and 1d nuclei

[BNL-TR-380] 19 p3151 N71-32153

Cross section for elastic-deuteron scattering and electron neutron form factor at four momentum transfers

[DESY-71/7] 19 p3159 N71-32634

Elastic scattering of Ge-70, Zn-90, Ag-107, and Ce-140 alpha particles to resolve discrete real well depth ambiguities found in optical model analysis

20 p3317 N71-33522

Elastic scattering analysis of mass flow in supersonic fragmentation model of solar system

[LA-4343-SUPPL] 20 p3348 N71-33525

Elastic proton scattering from osmium and platinum isotopes and identification of atomic energy levels

20 p3319 N71-33694

Differential cross section and vector polarization for elastic scattering of 41 to 51 MeV deuterons on carbon-12

[KFK-1357] 21 p3469 N71-34701

Generalized Wilson approximation for application to rearrangement and elastic collisions

[JAERI-MEMO-4195] 21 p3470 N71-34710

Elastic scattering in model with Regge poles and cuts generated by multiple scattering

[INR-P-1233] 21 p3472 N71-34721

Time of flight method for studying fast neutron elastic and inelastic scattering by natural molybdenum at 1.0 to 5.0 MeV

[AWRE-O-8970] 21 p3486 N71-34836

Elastic scattering and multipole moments in atomic collisions based on classical mechanics

[INR-P-1217] 22 p3635 N71-35909

Partial wave analysis of pion-nucleon elastic scattering below 1.6 GeV, including total cross sections, angular distributions, and recoil nucleon polarizations

[CEA-R-3578] 22 p3636 N71-35916

Elastic scattering processes using nonlocal separable interactions with general expression for transition amplitude

[LYCEN-7089] 22 p3639 N71-35938

Differential cross sections and slope parameters for high energy elastic scattering

[JINR-P1-5633] 22 p3642 N71-35961

Application of Riemann method to inverse problem of charged particle scattering

[ITF-70-98-P] 22 p3643 N71-35975

Expression for differential cross sections in energy range between 22.5 and 400 MeV

[UCRL-20295] 22 p3645 N71-35986

Argand diagram analysis of Pomeron coupling to kaon nucleon and antikaon nucleon system

22 p3645 N71-35988

Depolarization in 612 MeV elastic p-n scattering and nucleon-nucleon scattering amplitude 600 to 650 MeV

[JINR-P1-5743] 23 p3806 N71-37134

Spin polarization parameters in kaon[plus] proton and kaon[minus] proton elastic scattering at 6 to 18 GeV

[INP-18830] 23 p3809 N71-37158

A and R polarization and scattering amplitudes in pion[minus] proton elastic scattering at 6 and 16 GeV/c

[INP-18873] 23 p3809 N71-37159

Amplitudes and some parameters plotted and tabulated from partial-wave analyses of pion proton elastic scattering

[TID-25726] 23 p3812 N71-37182

Elastic scattering radiative capture, gamma ray production, and related information from nuclear data file for hydrogen in 00001 eV to 20 MeV range

[LA-4574] 23 p3813 N71-37193

Isobaric analog states between 4 MeV and 8 MeV for reaction Ca-48(p,p)Ca-48

[INP-18824] 23 p3815 N71-37204

Time of flight method for determining elastic and inelastic scattering of 5.0 MeV neutrons by sodium

[AWRE-O-3711] 23 p3815 N71-37209

Experimental designs for electron elastic and inelastic scattering and mathematical expressions for electron-scattering cross sections and radiative correction

[LNF-70/57] 23 p3820 N71-37249

Comparison of angular distributions based on various models for elastic scattering of 25 MeV alpha particles

[INP-735] 23 p3820 N71-37250

Cross section measurements of proton-proton bremsstrahlung at 20 MeV

23 p3821 N71-37257

Least squares method for determining Love wave scattering upon boundary irregularity in elastic layer over rigid half space

24 p3918 N71-37944

Unitarity used to calculate imaginary part of elastic scattering amplitude for identical bosons

[NP-18823] 24 p3969 N71-38316

Measurement of ratio of positron-proton and electron-proton elastic scattering cross sections at 180 deg and large q²

[LAL-1231] 24 p3974 N71-38353

Theoretical quantum electrodynamics in higher orders at low and high energies and nuclear models for lepton hadron and photon hadron scattering

[ITF-71-S-E] 24 p3976 N71-38372

ELASTIC SHEETS

Hot forming of plastic sheets

[NASA-CASE-XMS-05516] 07 p1037 N71-17803

Numerical solutions of nonlinear problems related to transverse bending of circular and rectangular plates and flat panels under different boundary conditions

[AD-722302] 17 p2851 N71-29644

Stress function analysis of elastic deformation of thin membrane structures

19 p3191 N71-32710

ELASTIC SHELLS

Application of Ritz method to thin elastic shell analysis

[AD-711962] 02 p0301 N71-12023

Investigation of sound transmission into small enclosures, and induced coupling between shell modes

[AD-712452] 03 p0419 N71-13384

Computer program for determining static and dynamic response of symmetrically loaded elastic orthotropic shells of revolution

[NASA-TN-D-6158] 06 p0957 N71-16846

Structural elastic shell theory for axisymmetric hollow circular cylinders

[NASA-CR-116857] 08 p1299 N71-19160

Solution of mixed boundary value problem based on three dimensional equations for thermoelastic shells

[AD-716015] 09 p1478 N71-20111

Harmonic analysis of nonlinear forced vibrations of infinitely long cylindrical shells

[AD-716955] 10 p1650 N71-20636

Estimation of stability of elastic noncircular conical and cylindrical orthogonal shells

[AD-717014] 10 p1651 N71-20754

Axial deformation analysis of thin shallow elastic spherical shells of uniform thickness with surface constraints

10 p1659 N71-21767

Fourier-Bessel analysis of forced torsional vibrations of encased cylindrical shells

[AD-717021] 11 p1833 N71-21869

Constructing tensor elasticity relationships in linear theory of thin elastic shells

11 p1837 N71-22484

Wave propagation through compressible fluid from transient pulsations of spherical elastic shell

[ARL/SM-352] 12 p1968 N71-24155

Free vibration analysis for nonlinear shallow elastic shells

14 p2347 N71-25787

Shell theory using linearly exact expressions for transverse variation of displacement components in thin elastic shells

14 p2350 N71-26468

Kinematics and general principles in nonlinear and linear theories of elastic shells and plates by direct approach and three-dimensional equations of classical continuum mechanics. Part I

[AD-722350] 17 p2854 N71-30220

Derivation of constitutive equations, material symmetries, dynamical restrictions, and related topics for nonlinear and linear theories of elastic shells and plates. Part 2

[AD-722351] 17 p2854 N71-30221

Free vibrations and harmonic and aperiodic forced vibrations of elastic spherical thin shells in water

22 p3693 N71-36337

Dynamic buckling of thin elastic shells of cylindrical, spherical, and conical shape

[AD-726397] 24 p4024 N71-38709

ELASTIC STABILITY

U DAMPING

ELASTIC WAVES

NT AERODYNAMIC NOISE

NT AIRCRAFT NOISE

NT CAPILLARY WAVES

NT COHERENT ACOUSTIC RADIATION

NT COMPRESSION WAVES

NT DETONATION WAVES

NT DILATATIONAL WAVES

NT ELECTROSTATIC WAVES

NT ENGINE NOISE

NT GRAVITY WAVES

NT IONIC WAVES

NT JET AIRCRAFT NOISE

NT LAMB WAVES

NT LOVE WAVES

NT MACH CONES

NT MAGNETOACOUSTIC WAVES

NT MAGNETOELASTIC WAVES

NT MAGNETOHYDRODYNAMIC STABILITY

NT MAGNETOHYDRODYNAMIC WAVES

NT MICROSEISMS

NT NOISE (SOUND)

NT NORMAL SHOCK WAVES

NT OBLIQUE SHOCK WAVES

NT P WAVES

NT PHONON BEAMS

NT PHONONS

NT PLASMA WAVES

NT POLARIZED ELASTIC WAVES

NT RAYLEIGH WAVES

NT RIEMANN WAVES

NT ROCKET ENGINE NOISE

NT S WAVES

NT SEISMIC WAVES

NT SHOCK WAVES

NT SONIC BOOMS

NT SOUND WAVES

NT STRESS WAVES

NT THERMAL NOISE

NT ULTRASONIC RADIATION

High pressure elastic wave velocities for tracing deep structural boundary in chlorite shales from USSR

[NASA-TT-F-13206] 02 p0210 N71-11499

Solutions to axisymmetric equations of motion in elastic bars containing discontinuities

05 p0681 N71-13681

Influence of high pressures and temperature on velocity of elastic waves in certain rocks of Ukrainian shield

[AD-716547] 09 p1477 N71-19979

Transverse pressure gradient on interaction of laminar hypersonic boundary layer with corner expansion wave

[NASA-TT-F-13516] 09 p1385 N71-20044

Surface motion in solids caused by reflection of intense acoustic pulse at pressure release surface determined by surface velocity reflection coefficient

[AD-717608] 11 p1835 N71-22240

Numerical analysis of wave propagation in cylindrical shells based on application of general dynamic equations

12 p2006 N71-23975

Multiconfigurational one center expansion wave functions for computing intermolecular forces of hydrogen molecule and Helium-Ne-Feynman theorem

14 p2311 N71-26607

Elastic wave anisotropy in marble, dolomite, and limestone crystals based on ultrasonic tests and X ray analysis

[NASA-TT-F-13673] 16 p2585 N71-28230

Ultrasonic investigation of elastic wave velocity in porous sedimentary rocks

[NASA-TT-F-13655] 16 p2591 N71-28974

Oxygen and carbon elastic form factor calculations based on liquid drop nuclear model with quadrupole surface oscillations

[RL-1388-977] 17 p2790 N71-35724

Radiation of elastic waves limiting disturbance resonance

17 p2819 N71-29054

Elastic wave propagation and scattering in quarter spaces with determination of transient shear stress exerted on vertical wall by line load acting tangential to horizontal surface

19 p3142 N71-32546

Temporal and spatial velocity profiles of fluid flow produced by propagation of nonlinear pressure waves

[NASA-CR-119914] 20 p2520 N71-31800

Adiabatic elastic moduli of vitreous calcium silicates to 3.5 kilobars

23 p3789 N71-37868

Method of characteristics for analysis of elastic wave equations in Cartesian coordinates

[NASA-CR-123178] 24 p4023 N71-38700

ELASTICITY

U ELASTIC PROPERTIES

ELASTODYNAMICS

NT ELASTIC DAMPING

NT ELASTOHYDRODYNAMICS

Continuum mechanics for nonlinear dynamic distribution analysis on anisotropic elastic media

17 p2822 N71-29077

SUBJECT INDEX

- Determination of elastodynamic response of free quarter-plane following single concentrated pulse load applied to one of edges at distance from corner
20 p3360 N71-3366
- Elastohydrodynamics**
Hydrodynamic stability of viscoelastic fluid films
[NASA-CN-116438] 07 p1097 N71-1097
Film thickness, friction, and pressure distribution effects in elastohydrodynamic gear lubrication
15 p2412 N71-2412
Elastohydrodynamic lubrication effects on roller bearing design and performance
15 p2414 N71-2414
Characteristics of fluid flow in vicinity of enclosed rotating disk
16 p2582 N71-2582
Film thickness profile and traction in elastohydrodynamic lubrication of point contacts in pure sliding motion
18 p2929 N71-31006
Elastohydrodynamic film thickness between rolling disks with synthetic paraffinic oil at temperatures from 330 to 589 K
[NASA-TN-D-6411] 18 p2930 N71-31228
Isothermal elastohydrodynamic theory for full range of pressure-viscosity coefficient for heavily loaded rolling contacts
22 p3588 N71-35530
Coupling of monochromatic elastohydrodynamic wave propagating in compressible fluids
[AD-727932] 24 p3995 N71-38300
- Elastomers**
NT CHLOROPRENE RESINS
NT THIOPOLASTICS
NT VITON
Physical and chemical reactions of isoprene and butadiene elastomers between -130 C and 150 C
[NASA-TN-D-6116] 03 p6396 N71-12745
Development and characteristics of elastomeric materials for positive expansion elastomers
[NASA-CN-115902] 03 p6440 N71-14064
Performance of low density silicone-phenolic and tannin-phenolic composites
[NASA-TN-D-6130] 06 p0960 N71-10872
Describing metal valve plate with encapsulated elastomeric body
[NASA-CASE-MSC-12116-1] 07 p1035 N71-17648
Effects of space environment factors on physical, mechanical, and optical properties of selected transparent elastomers
08 p1223 N71-18934
Describing formation and growth of gas bubbles in overstressed elastomers as function of superaturation pressure
08 p1160 N71-18993
Development of apparatus for measuring successive increments of strain on elastomers
[NASA-CASE-XMF-04680] 09 p1392 N71-19489
Volume change accompanying rubber extension
[AD-716563] 09 p1403 N71-19492
Preparation of elastomeric diamine siloxane polymers
[NASA-CASE-XMF-04133] 10 p1512 N71-20717
Thermal behavior of polycarbonate siloxane SBR-1 elastomers from C28587
10 p1587 N71-20808
Viscoelastic cross linking behavior of elastomers, energy transfer in bicyclic herbicides, and electrical properties of tetracyano quinodimethane polymer-15 sils
10 p1514 N71-21356
Synthesis and chemical properties of elastomeric polymers resistant to effects of fluorine, oxygen, chlorine, nitrogen tetroxide, and similar agents
[NASA-CN-117498] 10 p1515 N71-21490
Lead resistant bonded elastomeric seal for secondary electrochemical cells
[NASA-CASE-XGS-02631] 11 p1678 N71-23086
Energy balance method for predicting elastomer behavior due to thermal stress emphasizing solid propellants
11 p1785 N71-23044
Ammonia decontaminant control of oxygen diffusive and static and dynamic compatibility tests with plastic and elastomer materials
[NASA-CN-72386] 12 p1869 N71-23167
Examination of silica-filled silicone vulcanizates using combined mechanical, swelling, and optical means to determine reinforcement mechanisms of elastomers
12 p2007 N71-24118
Development of method for measuring fatigue life of elastomeric shear mounts subjected to static load duration and vibration
[AD-726575] 14 p2262 N71-26192
Synthesis of low temperature petroleum resistant elastomers
[AD-726015] 14 p2280 N71-26384
Thermal conductivity, thermal expansion, and heat capacity of low density silicone elastomer and filled with from 150 K to 500 K
[NASA-CN-111912] 15 p2432 N71-27746

- Soil surface profiles of DuPont LRU 488 molded elastomeric seal seals
[NASA-CN-118867] 15 p2417 N71-27773
Using accelerated hydrolytic reversion data to predict service life of elastomeric potting compounds
[AD-721676] 16 p2617 N71-28466
Development of theoretical model for calculation of shear modulus, bulk modulus, and thermal expansion behavior of two phase composite materials by Van der Pol theory
[AD-721576] 16 p2618 N71-28734
Synthesis of polyamide and polyester elastomers containing phenylene-perfluoro-alkylene units noting thermal stability and glass transition temperature
[RAE-TR-70160] 17 p2717 N71-30332
Measurement of dynamic shear properties of silicone based elastomers at high temperatures
[ISVR-TR-43] 18 p3020 N71-30553
Utilization of aerospace nonflammable catholonic elastomeric, fibrous, and composite materials in commercial aircraft refurbishment
18 p3048 N71-30759
Infrared spectroscopic study of amorphous elastomer reinforcement by polymeric fillers
18 p3887 N71-31233
Flight tests of elastomeric bearings in main rotor of AH-1G helicopter
[AD-724192] 20 p3278 N71-32935
Electron spin resonance of free radicals formed in elastomers by ultraviolet irradiation
[APC-CN-97] 20 p3323 N71-33828
Assessment of molded elastomeric Teflon as seal seal material for RAD engine valve
[NASA-CN-121716] 21 p3432 N71-34417
- Elastoplastics**
Elastic-plastic analysis of open-end isotropic tubes under internal pressure
[AD-712933] 02 p6299 N71-11126
Solving plane elastic-plastic boundary value problems for application to bending of simply supported single crystal beam
[AD-715761] 08 p1298 N71-18810
Design optimization of aerospace structures made of elastic/plasticity plastic materials
09 p1479 N71-20131
Finite difference model and computer program for predicting large deflection elastoplastic response of shell structures
[AD-717003] 10 p1653 N71-21192
Welding thermal and residual stress analysis and material property and weld parameter effects on thermal stresses and elastoplastic deformation of aluminum alloys, steel, niobium, and tantalum
[NASA-CN-61351] 14 p2361 N71-26143
Continuum plasticity and microstructure dislocation in elastic-plastic plane bending of crystal beam
17 p2822 N71-29979
Dislocation dynamics and formulation of constitutive equations for rate dependent elastic plastic response in isotropic metals
[AD-722514] 17 p2765 N71-30110
Constitutive equations for analysis of elasto-viscoplastic structural materials
[ONERA-PUBL-135] 19 p3186 N71-31669
Solutions obtained for problem of normal impact of infinite elastic-plastic beam by semi-infinite elastic rod
[AD-726548] 22 p3689 N71-36313
Numerical procedure for determining elasto-plastic behavior of stiffened and unstiffened three dimensional suspension structures
23 p3865 N71-37552
- Elastostatics**
Modifying Rayleigh-Ritz method for predicting values of stress concentrations in elastic continuum
[RAE-TR-68273] 02 p0301 N71-12022
Comparison of finite element and finite difference methods in plane stress and axially symmetric elastostatic problems
20 p3292 N71-33676
Computer system for generating input data for structural analysis of three-dimensional elastostatic problems using isoparametric finite elements
[AD-727177] 24 p4024 N71-38714
- ELDO LAUNCH VEHICLE**
ELDO launch vehicle inertial guidance law
[RAE-TR-70832] 02 p0262 N71-11757
Discussing digital inertial guidance system for ELDO launch vehicle
03 p0489 N71-12617
Azur satellite, Dial satellite, ground support systems, ELDO launch vehicle, and space environment simulation
[QB-1-71] 22 p3461 N71-36349
- ELECTRETS**
Electret processes for characterizing nonluminescent and near-insulating solids
01 p0107 N71-10082
Miniaturized electret pressure sensor for thin surfaces
[ONERA-TP-430] 02 p0226 N71-11682
Aerogel filtration by electret filters
[REPT-1970-17] 04 p0509 N71-13519

ELECTRIC BATTERIES

- Characteristics of radiation dosimetry conducted by polymer electret depolarization
[NYO-3409-9] 18 p2996 N71-31187
- ELECTRIC ANALOGIES**
U ANALOGIES
ELECTRIC APPLIANCES
U ELECTRIC EQUIPMENT
ELECTRIC ARCS
NT CARBON ARCS
High speed electric arc printer design
[AD-712400] 03 p0341 N71-12468
High current electric arc characteristics magnetically driven to supersonic velocities in straight and circular channels
[NASA-TN-D-6086] 03 p0438 N71-13027
Using gas sheathed tubular electrode arc for alloy analysis
05 p0703 N71-15214
Spectral, transport, and thermodynamic properties of high pressure arcs
[AD-713131] 05 p0734 N71-15362
Rotating mirror camera for rotating electric arc photography
[DLR-MITT-70-16] 08 p1201 N71-18668
Electric arc heater with supersonic nozzle and fixed arc length for use in high temperature wind tunnels
[NASA-CASE-XAC-01677] 10 p1532 N71-20816
Driver modifications for improved performance of electric arc shock tube
11 p1732 N71-23534
Arc electrode of graphite with tantalum ball tip
[NASA-CASE-XLE-04708] 11 p1726 N71-22887
Quantum mechanics of line broadening effects in solar simulator mercury resonant arc lamp spectra
13 p2882 N71-25333
Quantitative spectroscopic analysis of temperature and electron density in long arc sparks produced by laboratory equipment
14 p2287 N71-25825
Measurement of acoustic output from long sparks produced during electrical discharge from laboratory equipment
14 p2296 N71-25826
Qualitative analysis, quantitative analysis, and time dependent model of high speed time-resolved spectroscopic study of lightning return stream
14 p2287 N71-25828
Measurement of sparking potential of gaps in low pressure air between two electrodes, with plane wire surfaces as cathode, to simulate lightning stroke and radio noise
[AD-726771] 14 p2247 N71-25836
Electron density and temperature measurements for argon plasma arcs
[AD-720856] 15 p2500 N71-27392
Maximum length of arc in altitudes up to 9300 ft in 200 volt ac and dc electric aircraft systems
[RAE-TR-69259] 16 p2373 N71-28663
Development and characteristics of thermal plasma emitter in 1100 to 3100 angstrom wave length range
[MPI-PAE/EXTRATER-29] 18 p2991 N71-30407
Electric arc furnaces in Sweden noting design and operation and cost reduction
19 p3104 N71-31903
Nonconsumable metal electric arc electrodes for producing solar simulator radiation source
[NASA-CASE-LE-11162-1] 21 p3402 N71-34210
Time constant measurements in cascade dc arc in local thermodynamic equilibrium
[TR-71-E-18] 21 p3406 N71-34233
Electron beam measurement of molecular vibrational energy transfer in expanding mixtures of N2 and CO2 heated by electric arc
[NASA-TN-D-6445] 21 p3436 N71-34446
Arc velocity and electrical properties in spark channels with current shocks
21 p3465 N71-34467
- ELECTRIC BATTERIES**
NT ALKALINE BATTERIES
NT MAGNESIUM CELLS
NT METAL AIR BATTERIES
NT NICKEL CADMIUM BATTERIES
NT NICKEL ZINC BATTERIES
NT PRIMARY BATTERIES
NT SILVER CADMIUM BATTERIES
NT SILVER ZINC BATTERIES
NT STORAGE BATTERIES
NT WET CELLS
NT ZINC-OXYGEN BATTERIES
Research progress on polymers, battery separator membranes, and evaluation of spacecraft magnetic recording tapes
01 p0016 N71-10265
Fabrication and testing of organic electrolyte cells with long shelf life
[AD-711144] 01 p0007 N71-10517
Standard family of power sources providing long life
[AD-710951] 01 p0007 N71-10845
Sealed electric storage battery with gas manifold interconnecting each cell
[NASA-CASE-XNP-03378] 03 p0148 N71-11051
Twelve-volt dc switching device
[AD-712584] 03 p0349 N71-12523

- Nuclear magnetic resonance, solubility, stability, and resistance of electrolytes for lithium batteries [NASA-CR-72803] 05 p0631 N71-14608
- Battery charging system with cell to cell voltage balance [NASA-CASE-XGS-05432] 09 p1325 N71-19438
- Conference on fuel cells and batteries [AD-71833] 12 p1859 N71-23353
- Liquid ammonia primary reserve battery design [AD-718266] 12 p1860 N71-23395
- Development and characteristics of bipolar charging circuits with coulometer for control of available current [NASA-CASE-GSC-10467-1] 13 p2030 N71-24719
- Lithium/chalcogen cells applied to secondary batteries for vehicular propulsion [ANL-7756] 14 p2199 N71-25651
- Device for sensing current applied by pulse width modulated power supply to battery or other load [NASA-CASE-GSC-10656-1] 16 p2570 N71-28471
- Heat activated emf cells with aluminum anode [NASA-CASE-LEW-11359] 16 p2538 N71-28579
- Paste electrolyte cell development and multikilowatt lithium/selenium secondary batteries for electrically-driven air vehicles [ANL-7745] 21 p3380 N71-34047
- Service and shelf life tests of radiation survey meter and personal radiation dosimeter battery packs used on Apollo spacecraft [NASA-CR-115189] 23 p3717 N71-36493
- Development and characteristics of bipolar electric battery with high power density silver oxide-zinc liquid electrode [AD-727126] 24 p3875 N71-37626
- ELECTRIC BRIDGES**
- NT WHEATSTONE BRIDGES
- NT WIRE BRIDGE CIRCUITS
- Calibration of impedance meters and bridges to 50MHz [UCRL-72483] 05 p0652 N71-14794
- Bridge circuit for digital resistance measuring circuits with electronic self adaptive controls at direct current 06 p0826 N71-15950
- Low cost high performance lock-in detector for balancing bridges with reactive and resistive components nulling simultaneously [IS-2389] 07 p1000 N71-17893
- Electrical properties of biased diode bridge and application to improvement of rise time in feedback amplifier 11 p1725 N71-22660
- Design and performance of inductive voltage divider for measuring alternating current ratios [NLL-MIN-TECH-7-4763/5809.95] 12 p1891 N71-24163
- Development and characteristics of test equipment for measuring friction moment and friction losses in ball bearings under various radial load conditions [AD-719810] 13 p2084 N71-24435
- ELECTRIC CELLS**
- Design and characteristics of heat activated electric cell with anode made from one or more alkali metals and cathode made from oxidizing material [NASA-CASE-LEW-11358] 14 p2300 N71-26084
- Development and characteristics of ion-exchange membrane cell electrode assembly for fuel cells or electrolysis cells [NASA-CASE-XM2-02063] 16 p2541 N71-29044
- ELECTRIC CHARGE**
- NT ELECTRIC DIPOLES
- NT ELECTROSTATIC CHARGE
- NT ION CHARGE
- NT SPACE CHARGE
- MIS memory transistors for long term charge storage 01 p0032 N71-10221
- Experimental study of electrically thick monopole antennas - currents, charges, and conclusions [AD-710214] 01 p0022 N71-10346
- Nondestructive test methods for determining capacity remaining in zinc-mercuric oxide batteries [SC-RR-70-333] 03 p0318 N71-12275
- Tests for determining remaining charge in zinc mercuric oxide primary batteries 03 p0319 N71-12276
- Charge ratio of 1-10 TeV cosmic ray muons 07 p1106 N71-18055
- Indicator device for monitoring charge of wet cell battery, using semiconductor light emitter and photodetector [NASA-CASE-NPO-10194] 09 p1327 N71-20407
- Relativistic quantum mechanics for hypothetical particles endowed with electric and magnetic charges [NYO-5829-65] 11 p1862 N71-22608
- Automatically charging battery of electric storage cells [NASA-CASE-XNP-04758] 13 p2029 N71-24605
- Addition of precharge to negative cadmium electrode during cell assembly to account for capacity loss due to fading 16 p2539 N71-28665
- Quantitative measurement of precharge received by OAO battery cells 16 p2539 N71-28666

- Low temperature overcharge voltage characteristics of OAO batteries and cells 16 p2539 N71-28667
- Proton and electron net charge determination for two suspended niobium bodies 17 p2802 N71-30162
- Formation time, specific gravity of solution, and overcharge amount associated with electrochemical cleaning or formation operation in manufacturing nickel cadmium cells [NASA-CR-121877] 21 p3379 N71-34040
- ELECTRIC CHOPPERS**
- Chopper for complete fuel elements bundles of SNR-Na2 in WAK [ORNL-TR-2414] 21 p3460 N71-34629
- ELECTRIC CIRCUITS**
- U CIRCUITS
- ELECTRIC COILS**
- NT MAGNETIC COILS
- Rugged nonsparking RF coil conductivity probe system for reentry plasma diagnostics 10 p1559 N71-21112
- ELECTRIC CONDUCTORS**
- Development program for methods of terminating flat conductor cable to small electrical components used on electrical displays and control panels [NASA-CR-108703] 04 p0510 N71-13525
- Conductor for connecting parallel coils into sub-modules in series to form solar cell matrix [NASA-CASE-NPO-10821] 09 p1325 N71-19545
- Electrical switching device comprising conductive liquid confined within square loop of deformable non-conductive tubing also used for leveling [NASA-CASE-NPO-10037] 09 p1358 N71-19610
- Comparison between silicon-magnesium-aluminum alloy and copper aircraft electric conductors and terminals noting types of tests [TRC-BR-19785] 12 p1889 N71-23547
- Development of calorimeter for spacecraft batteries comprising pressurized vessel, heat sink, and copper conductor [NASA-CR-118029] 12 p1923 N71-24129
- Parallel circuit analysis for skin effect in conductors [AD-719344] 13 p2123 N71-24584
- Dry electrode design with wire sandwiched between two flexible conductive discs for monitoring physiological responses [NASA-CASE-FRC-10029] 13 p2055 N71-24618
- Evaluation of conductor material compatibilities and production finishing processes for thick film circuits [ECR-20] 14 p2230 N71-26548
- Negative resistance and negative conductance device technology 16 p2567 N71-28233
- Analysis of stationary collisionless plasma sheath around conducting cylinder 20 p3332 N71-33838
- Technical-economic data for copper and aluminum conductors and superconductors for high field magnets [LNF-70/19] 22 p3457 N71-36082
- Current load calculations for transmission lines terminating parallel to and near infinite length circular conducting cylinders in incident fields [SC-R-713250] 23 p3737 N71-36649
- Device for conducting electrostatic charges from man [NLL-M-20436/5828.4F] 24 p3884 N71-37684
- ELECTRIC CONNECTORS**
- Development of flexible selected interconnection technique for monolithic circuits [NASA-CR-102908] 02 p0196 N71-11376
- Nondestructive tests of welds, interconnections, and microjoints [NASA-CR-73485] 02 p0229 N71-11529
- Underwater electrical connector and cable system designed for delivering large amounts of electric power for use underwater - photographs 05 p0680 N71-15612
- Method of making sealed electric connector for use with flat conductor cables [NASA-CASE-XMF-03498] 06 p0684 N71-15986
- Corona tests on round wires, flat wires, and connectors for spacecraft components 06 p0825 N71-16643
- Retrorocket exhaust initiation of conduction in connectors during stage separation of boosters 06 p0828 N71-16647
- Feasibility of infrared reflow soldering for circuit board connections [BDX-613-169] 06 p0867 N71-16619
- Digital pulse optimization for space compatible electric connectors [NASA-CR-103021] 07 p0998 N71-17469
- Cabling and connectors for use on nuclear stage, environmental and related tests 09 p1360 N71-19875
- Design and development of electric connectors for rigid and semirigid coaxial cables [NASA-CASE-XNP-04732] 10 p1332 N71-20851
- Baffle geometry, subsystem estimation, and connector failure analysis for ion thruster of solar electric propulsion system 10 p1639 N71-21357
- Long term percutaneous leads in artificial hearts [PB-159885] 10 p1511 N71-21641

- Connector internal force gage for measuring strength of electrical connections [NASA-CASE-XNP-03918] 11 p1767 N71-23807
- Maintaining current flow through solar cells with open connection using shunting diode [NASA-CASE-XLB-04535] 12 p1859 N71-23110
- Selection of materials for electrical connectors compatible with future space missions [NASA-CR-103092] 12 p1887 N71-23180
- Pulse are welding for joining electrical connections to glass reinforced epoxy or Kevlar substrates [BDX-613-204] 13 p2059 N71-24609
- Electrical connections for thin film hybrid micro-circuits [NASA-CASE-XMS-02182] 16 p2575 N71-28700
- Electric connectors, adapters, and cable technology transfer [NASA-SP-5936/01/1] 19 p3067 N71-32371
- Separable electrical connectors for connecting flat cables with round wire cables or with other flat cables [NASA-CASE-MFS-20757] 21 p3403 N71-34011
- Proceedings of space shuttle integrated electronics conference with emphasis on power distribution, instrumentation, and communication - Vol. 2 [NASA-TM-X-50063-VOL-2] 21 p3513 N71-35016
- Research and development of improved electrical connectors for space shuttle systems 21 p3514 N71-35016
- Characteristics of aluminum compression joints use methods for analyzing contact corrosion [NLL-OA-TRANS-637/6196.3] 23 p3775 N71-38086
- ELECTRIC CONTACTS**
- Molybdenum and gold contact materials processing for metal oxide semiconductor transistor circuits 01 p0031 N71-10131
- Characteristics of hermetically sealed electric switch with flexible operating capability [NASA-CASE-XNP-09008] 03 p0349 N71-12310
- Cost analysis of air pollution effects on electric contacts [PB-192478] 03 p0350 N71-12310
- Diffusion and structural changes in microcircuit interconnections subjected to heat treatment [NASA-CR-115903] 05 p0656 N71-14076
- Tungsten hemisphere against tungsten disk slapping assembly with liquid gallium lubrication in ultrahigh vacuum [NASA-TN-D-6184] 07 p1033 N71-17374
- Electrical and mechanical characteristics of solar cell contacts after exposure to high-temperature high-humidity environments 08 p1146 N71-18033
- Electrode connection for n-on-p silicon solar cell [NASA-CASE-XLE-04767] 09 p1328 N71-26081
- Quality control data on lubricants for electric contacts [ECR-06] 10 p1563 N71-21880
- Development of slip ring assembly with inner and outer peripheral surfaces used as electrical contact for brushes [NASA-CASE-XMF-01049] 11 p1773 N71-23800
- Contact breaking speed effects on spark quenching and gas discharge of electric inductance switch [NLL-TRANS-2662/9022.81/1] 19 p3067 N71-35016
- Electron tunneling characteristics of metal contacts on a-type CdTe and p-type InAs 19 p3071 N71-35016
- Degradation of Ti/Au contacts in Si solar cells, and deposition of Ti/Au contacts on Si wafers [NASA-CR-121725] 21 p3378 N71-34009
- Synergistic effects of slip ring-brush design and fabrication for vacuum application determined by friction, wear, electrical noise, and dielectric strength data [NASA-CR-122988] 23 p3740 N71-38086
- Effect of high humidity and temperature on electrical and mechanical properties of stored silicon solar cell contacts [NASA-CR-123185] 24 p3875 N71-38082
- Dimensionless correlation for predicting thermal contact resistance between similar metal surfaces in vacuum environment 24 p4029 N71-35748
- ELECTRIC CONTROL**
- Performance characteristics of improved servomotor for electrohydraulic control systems [NASA-TM-X-2167] 07 p0998 N71-17350
- Switching series regulator with gating control network [NASA-CASE-XNP-09352] 12 p1887 N71-23110
- Switching power supply for bidirectional control of permanent magnet motors [BM-521] 24 p3900 N71-37777
- ELECTRIC CORONA**
- Corona and multipactor discharges, packaging techniques and materials, and voltage breakdown in satellite instruments - conference [NASA-CR-116173] 06 p0825 N71-16611
- Designing corona free, high voltage, toroidal transformers for spacecraft power supplies 06 p0825 N71-16611
- High voltage packaging techniques and materials 06 p0828 N71-16612

SUBJECT INDEX

Corona tests on round wires, flat wires, and connectors for spacecraft components

Low-level corona detection in insulation systems involving from step voltages across voids in insulation

Flight testing devices for discharging static electricity from aircraft without production of radio interference

Using corona discharge mechanism for electrical loads in electrofluid dynamic generator

Effect of humidity on corona discharge in air and feasibility evaluation for use of corona cell as humidity meter

Computer program for calculating corona thresholds in nonuniform electrical fields

ELECTRIC CURRENT

ALTERNATING CURRENT

ARC DISCHARGES

AURORAL ELECTROJETS

BEAM CURRENTS

CARBON ARCS

DIRECT CURRENT

EDDY CURRENTS

ELECTRIC ARCS

ELECTRIC CORONA

ELECTRIC DISCHARGES

ELECTRIC SPARKS

ELECTRODELESS DISCHARGES

ELECTROJETS

EQUATORIAL ELECTROJET

FLASHOVER

GAS DISCHARGES

GLOW DISCHARGES

HIGH CURRENT

IONOSPHERIC CURRENTS

LIGHTNING

MULTIPLIER DISCHARGES

PENNING DISCHARGE

RADIO FREQUENCY DISCHARGE

RING CURRENTS

RING DISCHARGE

TELLURIC CURRENTS

THRESHOLD CURRENTS

TOROIDAL DISCHARGE

TOWNSEND DISCHARGE

Power supplies for very high current control and stabilization in high magnetic field laboratory

Experimental study of electrically thick monopole antennas - currents, charges, and conclusions

Including didymium hydrate in nickel hydroxide of positive electrode of storage batteries to increase anion layer capacity

CRITICAL CURRENT ENHANCEMENT IN SUPERCONDUCTING JUNCTIONS OF VARYING CROSS SECTION

Development of in-line fuse device for protection of electric circuits from excessive currents and voltages

Microampere current measuring circuit, with two semiconductor thermionic diodes with filament cathode

Polar region magnetic storms and electric currents in the magnetosphere

Current oscillations in long Zn-doped Si-p-n diodes

Electrical structure model of D and E region, based on dynamic current theory

Development of theory of characteristic modes for electric bodies

Electric currents and fields produced in ionosphere by light varying horizontal winds

Solution derived numerically for electromagnetic field due to current bearing circular loop near oblate spheroid

Analysis of finite rise and fall time current excitation of TRAPATT diodes using physical approximations for plasma formation and recovery as used in previous square wave analyses

Vertical electric fields of sea currents and utilization for measurement of current velocity

Connector internal force gaps for measuring

Electrical connection

Electric circuit for producing high current pulse having fast rise and fall time

Electric circuit for reversing direction of current flow

Maintaining current flow through solar cells with open connection using shunting diode

Phenetic oscillator for measuring electrical currents in bridge wires

Computer programs to calculate characteristic currents and gain patterns of conducting bodies of revolution

Laboratory modifications of standard electric current balance

Internal circuit excitation by electromagnetic field transmission through slotted missile skin

Magnetosphere electric current sheet model

Peak current measurement in linear electron accelerators by toroidal ferrite monitoring system with associated digital equipment

Strength and direction of electric current flow in MHD generator configurations

Critical current in electron beam of 2-GeV accelerator with radial slots in iris disk

Color television system utilizing single gun current sensitive color cathode ray tube

Current density and electrode drop distributions in cross sectional plane of electrode in conducting wall generators

Design and performance of galvanovoltammetric detector with digital readout for electric current flow measurements

Analysis of magnetic storm energy balance, including total energy, rate of arrival, and energy dissipation rate at different stages of development

Mathematical model for abnormal current in MOS transistor substrates

Deterministic errors and current impulse techniques for analyzing electrochemical kinetics of hexacyanoferrate 3/2 couple on platinum

Model for structure of electric-current-carrying discontinuity moving into nonconducting gas and leaving gas behind

Electron drainage current from dilute plasma through holes in high voltage dielectric probes

Increased output signal from platinum thin film resistance thermometer heat gauges by increase of activation current

Limiting current and concentration profile in stagnant diffusion cell for copper sulfate solution

Analysis of internal inductances in current carrying circular conductors in relation to outer inductance for unit and parallel representation of inductances

Arc velocity and electrical properties in spark channels with current shocks

Effects of leakage currents to ground in mhd generator with constant gas parameters and constant channel cross section

Machine for breaking wire carrying electric current in flammable atmosphere

Field electron emission from CdS as function of temperature and exposure with current voltage characteristics and electron line observations

Analysis of decaying photocurrents in polyvinylcarbazole to determine charge transport and trapping states

Drain current-drain voltage equations for insulated-gate and junction-gate field effect transistors and drain current sensitivity to nonpiezoelectric and piezoelectric strain effects

Temperature drift and peak current degradation in tunnel diodes used for amplitude discrimination

Electrical dipole

Absolute experimental emission cross sections for excitation of electric dipole transitions in Ba ions by electron impact

Excitation of electric dipole transitions in Ba ions by electron impact

Excitation of electric dipole transitions in Ba ions by electron impact

Excitation of electric dipole transitions in Ba ions by electron impact

Excitation of electric dipole transitions in Ba ions by electron impact

Excitation of electric dipole transitions in Ba ions by electron impact

Excitation of electric dipole transitions in Ba ions by electron impact

Excitation of electric dipole transitions in Ba ions by electron impact

Excitation of electric dipole transitions in Ba ions by electron impact

Excitation of electric dipole transitions in Ba ions by electron impact

Excitation of electric dipole transitions in Ba ions by electron impact

Excitation of electric dipole transitions in Ba ions by electron impact

Excitation of electric dipole transitions in Ba ions by electron impact

Excitation of electric dipole transitions in Ba ions by electron impact

Excitation of electric dipole transitions in Ba ions by electron impact

Excitation of electric dipole transitions in Ba ions by electron impact

Excitation of electric dipole transitions in Ba ions by electron impact

Excitation of electric dipole transitions in Ba ions by electron impact

Excitation of electric dipole transitions in Ba ions by electron impact

Excitation of electric dipole transitions in Ba ions by electron impact

Excitation of electric dipole transitions in Ba ions by electron impact

Excitation of electric dipole transitions in Ba ions by electron impact

Excitation of electric dipole transitions in Ba ions by electron impact

Excitation of electric dipole transitions in Ba ions by electron impact

Excitation of electric dipole transitions in Ba ions by electron impact

Excitation of electric dipole transitions in Ba ions by electron impact

Excitation of electric dipole transitions in Ba ions by electron impact

Excitation of electric dipole transitions in Ba ions by electron impact

Excitation of electric dipole transitions in Ba ions by electron impact

Excitation of electric dipole transitions in Ba ions by electron impact

Excitation of electric dipole transitions in Ba ions by electron impact

Excitation of electric dipole transitions in Ba ions by electron impact

Excitation of electric dipole transitions in Ba ions by electron impact

Excitation of electric dipole transitions in Ba ions by electron impact

Excitation of electric dipole transitions in Ba ions by electron impact

Excitation of electric dipole transitions in Ba ions by electron impact

Excitation of electric dipole transitions in Ba ions by electron impact

Excitation of electric dipole transitions in Ba ions by electron impact

Excitation of electric dipole transitions in Ba ions by electron impact

Excitation of electric dipole transitions in Ba ions by electron impact

Excitation of electric dipole transitions in Ba ions by electron impact

Excitation of electric dipole transitions in Ba ions by electron impact

Excitation of electric dipole transitions in Ba ions by electron impact

Excitation of electric dipole transitions in Ba ions by electron impact

Excitation of electric dipole transitions in Ba ions by electron impact

Excitation of electric dipole transitions in Ba ions by electron impact

Excitation of electric dipole transitions in Ba ions by electron impact

Excitation of electric dipole transitions in Ba ions by electron impact

Excitation of electric dipole transitions in Ba ions by electron impact

Excitation of electric dipole transitions in Ba ions by electron impact

Excitation of electric dipole transitions in Ba ions by electron impact

Excitation of electric dipole transitions in Ba ions by electron impact

Excitation of electric dipole transitions in Ba ions by electron impact

Excitation of electric dipole transitions in Ba ions by electron impact

Excitation of electric dipole transitions in Ba ions by electron impact

Excitation of electric dipole transitions in Ba ions by electron impact

Excitation of electric dipole transitions in Ba ions by electron impact

Excitation of electric dipole transitions in Ba ions by electron impact

Excitation of electric dipole transitions in Ba ions by electron impact

Excitation of electric dipole transitions in Ba ions by electron impact

Excitation of electric dipole transitions in Ba ions by electron impact

Excitation of electric dipole transitions in Ba ions by electron impact

Excitation of electric dipole transitions in Ba ions by electron impact

Excitation of electric dipole transitions in Ba ions by electron impact

Excitation of electric dipole transitions in Ba ions by electron impact

Excitation of electric dipole transitions in Ba ions by electron impact

Excitation of electric dipole transitions in Ba ions by electron impact

Excitation of electric dipole transitions in Ba ions by electron impact

Excitation of electric dipole transitions in Ba ions by electron impact

Excitation of electric dipole transitions in Ba ions by electron impact

Excitation of electric dipole transitions in Ba ions by electron impact

Excitation of electric dipole transitions in Ba ions by electron impact

Excitation of electric dipole transitions in Ba ions by electron impact

Excitation of electric dipole transitions in Ba ions by electron impact

Excitation of electric dipole transitions in Ba ions by electron impact

Excitation of electric dipole transitions in Ba ions by electron impact

Excitation of electric dipole transitions in Ba ions by electron impact

Excitation of electric dipole transitions in Ba ions by electron impact

Excitation of electric dipole transitions in Ba ions by electron impact

ELECTRIC DISCHARGES

Comparison of magnetic moment and electric dipole sum rules for testing validity of current and field algebra commutators

Vibrational perturbation effects on electronic transitions in small polyatomic molecules, and electric dipole selection rules used to ascertain forbidden transitions

Quantum mechanical sum rules for electric dipole operator

S-32 electroexcitation in dipole resonance region including form factors for isotactic scattering

Electric discharges

ARC DISCHARGES

CARBON ARCS

ELECTRIC ARCS

ELECTRIC CORONA

ELECTRIC SPARKS

ELECTRODELESS DISCHARGES

FLASHOVER

GAS DISCHARGES

GLOW DISCHARGES

LIGHTNING

MULTIPLIER DISCHARGES

PENNING DISCHARGE

RADIO FREQUENCY DISCHARGE

RING DISCHARGE

TOROIDAL DISCHARGE

TOWNSEND DISCHARGE

Theoretical evaluation of electrical insulation lifetime, noting influence of voltage and frequency using Weibull theory

Experimental studies on discharge propagation of exploding wires in high vacuum and determination of developing plasma properties

High voltage pulse generator for testing flash and ignition limits of semiconducting materials in controlled atmospheres

Electrostatic hazards during launch vehicle flight operations

Measurements of cathode heating in Penning discharge in strongly inhomogeneous magnetic mirror field

Terminated capacitor discharge firing of electroexplosive devices

Partial electric discharge influence on durability of polyethylene, Mylar, and Teflon insulating materials

Techniques for kinetic studies in shock tubes including infrared emission, electron scattering and electric discharge

Atom and free radical concentration measurement and electric discharge technique applied to propulsion systems

Time dependence analysis of current flow of condenser discharge of electrodeless MHD generator

Low frequency oscillation measurements on spherical magnetized cold cathode direct current discharge by plasma probes

Repeated current discharge role in Z pinch dynamics

Measurement of acoustic output from long sparks produced during electrical discharge from laboratory equipment

High power uniform electric discharge to produce laser action in mixture of nitrogen, carbon dioxide, and helium

Auxiliary discharge thermionic converter performance using barium oxide electrodes

Use of semiconductors for storage and discharge of electrical energy

Pulse generating circuit for operation at very high duty cycles and repetition rates

Model studies on formation of organic compounds in simple atmospheric gases by electric discharges

Onset of microwave breakdown in air-filled coaxial transmission lines and rectangular waveguides predicted by mathematical models

Ozone formation by electric discharges discussing photochemical process, circuits, spark gap

Comparison of magnetic moment and electric dipole sum rules for testing validity of current and field algebra commutators

Vibrational perturbation effects on electronic transitions in small polyatomic molecules, and electric dipole selection rules used to ascertain forbidden transitions

Quantum mechanical sum rules for electric dipole operator

S-32 electroexcitation in dipole resonance region including form factors for isotactic scattering

Electric discharges

ARC DISCHARGES

CARBON ARCS

ELECTRIC ARCS

ELECTRIC CORONA

ELECTRIC SPARKS

ELECTRODELESS DISCHARGES

FLASHOVER

GAS DISCHARGES

GLOW DISCHARGES

LIGHTNING

MULTIPLIER DISCHARGES

PENNING DISCHARGE

RADIO FREQUENCY DISCHARGE

RING DISCHARGE

TOROIDAL DISCHARGE

TOWNSEND DISCHARGE

Theoretical evaluation of electrical insulation lifetime, noting influence of voltage and frequency using Weibull theory

Experimental studies on discharge propagation of exploding wires in high vacuum and determination of developing plasma properties

High voltage pulse generator for testing flash and ignition limits of semiconducting materials in controlled atmospheres

Electrostatic hazards during launch vehicle flight operations

Measurements of cathode heating in Penning discharge in strongly inhomogeneous magnetic mirror field

Terminated capacitor discharge firing of electroexplosive devices

Partial electric discharge influence on durability of polyethylene, Mylar, and Teflon insulating materials

Techniques for kinetic studies in shock tubes including infrared emission, electron scattering and electric discharge

Atom and free radical concentration measurement and electric discharge technique applied to propulsion systems

Time dependence analysis of current flow of condenser discharge of electrodeless MHD generator

Low frequency oscillation measurements on spherical magnetized cold cathode direct current discharge by plasma probes

Repeated current discharge role in Z pinch dynamics

Measurement of acoustic output from long sparks produced during electrical discharge from laboratory equipment

High power uniform electric discharge to produce laser action in mixture of nitrogen, carbon dioxide, and helium

Auxiliary discharge thermionic converter performance using barium oxide electrodes

Use of semiconductors for storage and discharge of electrical energy

Pulse generating circuit for operation at very high duty cycles and repetition rates

Model studies on formation of organic compounds in simple atmospheric gases by electric discharges

Onset of microwave breakdown in air-filled coaxial transmission lines and rectangular waveguides predicted by mathematical models

Ozone formation by electric discharges discussing photochemical process, circuits, spark gap

Enhancement output power of CO-2 laser excited by electric discharge and irradiated by neutrons obtained from nuclear reactor

20 p3382 N71-33668
Determination of quantitative laws of joint discharge of ions under conditions of electrowinning of pure metals
[NLL-L71-746-663(9022.401)]

22 p3590 N71-35565
Lightning and ball lightning phenomena in weapon strategy, magnetohydrodynamics and meteorology
[SC-DC-713998]

23 p3791 N71-37024
Augmenting combustion flames with electric discharges to produce high temperature chemical and physical reactions in 2500 to 5000 K range
[ECRC/N327]

ELECTRIC ENERGY STORAGE

Electric current measuring apparatus design including saturable core transformer and energy storage device to avoid magnetizing current errors from transformer output winding
[NASA-CASE-XGS-62439] 09 p1387 N71-19431
Use of semiconductor for storage and discharge of electrical energy
[NASA-TT-F-13559] 16 p2639 N71-28888

ELECTRIC EQUIPMENT

Failure analysis of electric equipment due to high voltage breakdown
[AD-711559] 02 p0193 N71-11354
Catalog of electronic devices of USSR
[NBS-TN-526-REV] 02 p0194 N71-11358
Performance tests and failure analysis of homopolar electric generator
[EP-RB-32] 02 p0195 N71-11368

Development program for methods of terminating flat conductor cable to small electrical components used on electrical displays and control panels
[NASA-CR-108703] 04 p0510 N71-13525
Electrical, structural, and technological requirements for producing printed circuits
[AD-713615] 05 p0656 N71-14975

Development of liquid metal slip ring to transfer power between rotating satellite parts
[NASA-CR-72790] 06 p0798 N71-16370
Voltage breakdown in spacecraft systems from test and flight experience
06 p0825 N71-16632

Motoring tests of single shaft turbine compressor alternator
[NASA-TM-X-2154] 07 p0975 N71-17370
Characteristics of electric heaters used with SNAP 8 spacecraft power supplies
[NASA-TM-X-2186] 07 p1131 N71-17898

Design and development of electric generator for space power system
[NASA-CASE-XLE-04250] 09 p1360 N71-20446
Development of electrical system for measuring high impedance
[NASA-CASE-XMS-08599-1] 09 p1361 N71-20569

Design, development, and operating principles of power supply with starting circuit which is independent of voltage regulator
[NASA-CASE-XMS-01991] 10 p1535 N71-21449
Out-of-step tripping problems of oil circuit breaker and modifications to overcome circuit breaker deficiencies
[PB-196471] 01 p1536 N71-21677

Design, development, and test of lightweight modular electrical power supplies for teleypewriter systems
[AD-718869] 12 p1858 N71-23273

Mathematical models for analog computer representation of wheeled vehicle electric systems
[AD-718075] 12 p1927 N71-23772

Mechanical and electrical tools with potential use outside aerospace industry
[NASA-SP-5908/03] 12 p1928 N71-23910

Heat transfer and hydrodynamic behavior for subcooled flow boiling of Freon 113 for use in cooling electronic components
[DSR-71903-72] 14 p2352 N71-25805

Development of method for improving signal to noise ratio and accuracy of Wheatstone bridge type radiation measuring instrument
[NASA-CASE-XLA-02810] 14 p2254 N71-25901

Design and development of buck-boost voltage regulator circuit with additive or subtractive alternating current impressed on variable direct current source voltage
[NASA-CASE-GSC-10735-1] 14 p2322 N71-26085

Development and characteristics of electronically resettable fuse with saturable core current sensing transformer having two outside legs and center leg
[NASA-CASE-XGS-11177] 15 p2385 N71-27001

Development and characteristics of voltage regulator for connection in series with alternating current source and load using three leg, two-window transformer
[NASA-CASE-ERC-10113] 15 p2386 N71-27053

Parametric, functional, and mechanical properties of bipolar LSI devices in simulated space environment
[NASA-CR-119794] 15 p2417 N71-27771

Development of electric circuit for production of different pulse width signals
[NASA-CASE-XLA-07788] 16 p2573 N71-29139

Compilation of safety items covering personnel, electrical equipment, and fire hazards
[NASA-SP-5928/01/1] 20 p3370 N71-33592

Development of analytical model for predicting performance of small electromechanical devices
20 p3280 N71-33680

Nondestructive tests of motor drivers for delta wound dc brushless motors
[NASA-CR-121498] 21 p3402 N71-34203

Effects of heat aging on properties of polyimide insulating film used in production of high temperature flat electrical cables
[BDX-613-344] 23 p3777 N71-36919

Evaluation of design fabrication, inspection and testing of integrated circuits aimed at improving quality and reliability of hardware using these devices
[AD-726560] 24 p3896 N71-37786

Development of comparison between fluid logic circuits and electric and electronic logic circuits
[NLL-PORS-TRANS-2727(9022.81)] 24 p3908 N71-37858

ELECTRIC EQUIPMENT TESTS

Electrical testing apparatus for detecting amplitude and width of transient pulse
[NASA-CASE-XMP-06319] 03 p0349 N71-12519

In-flight testing of spacecraft power system with on-board monitoring equipment
[ESRO-TM-109-ESTEC] 03 p0458 N71-13252

Electrical and environmental tests on PCM telemetry system for earth resources aircraft
[NASA-CR-108700] 04 p0488 N71-13474

Testing of electrical detection system adaptable to spark source mass spectrometer
[IS-TRANS-52] 06 p0858 N71-15981

Variable water load for dissipating large amounts of electrical power during high voltage power supply tests
[NASA-CASE-XNP-05381] 10 p1532 N71-20842

Investigation of techniques to improve performance and service life of nickel-zinc electric batteries for application to low pollutant propulsion systems
[NASA-TM-X-67812] 13 p0309 N71-24617

Electric motor environmental and electrical test procedures including electromagnetic compatibility and maintenance
[AD-721611] 16 p2568 N71-28343

Frequency response technique for locating electrical faults
[AD-721582] 16 p2568 N71-28344

Chemical analysis and electrical performance tests of nickel cadmium batteries for Intelat 4 program
16 p2539 N71-28662

Design and testing of ac polycarbonate capacitors for aerospace power systems
[NASA-CR-1897] 21 p3379 N71-34046

High-speed switching diode test system for developing diode test techniques in 400-picosecond time region
[BDX-613-315] 21 p3404 N71-34222

Electric equipment and drive adapter endurance tests for SNAP 8
[NASA-CR-72920] 24 p3960 N71-38248

ELECTRIC FIELD STRENGTH
Solar wind, plasma waves and interplanetary electric and magnetic fields from Mariner 2 and Mariner 4 space probes
[ESRO-SP-55] 03 p0454 N71-13256

Low impedance apparatus for measuring electrostatic field intensity near space vehicles
[NASA-CASE-XLE-00820] 06 p0858 N71-16014

Space environment simulation system for measuring spacecraft electric field strength in plasma sheath
[NASA-CASE-XLE-02038] 06 p0822 N71-16086

Whistler recorder using autocorrelation and analog data - frequency and field strength variation of each whistler
[BMFW-FB-W-70-58] 08 p1189 N71-18663

Device for measuring two orthogonal components of force with gallium flotation of measuring target for use in vacuum environments
[NASA-CASE-XAC-04883] 12 p1922 N71-23790

Apparatus to determine electric field strength by measuring deflection of electron beam impinging on target
[NASA-CASE-XMF-06617] 13 p2057 N71-24843

Measurements of ionospheric electric field in equatorial and medium magnetic latitudes using barium ion clouds
[MFI-PAE/EXTRATERR-49/70] 15 p2398 N71-27063

Isotropy, electric field gradient, and specific heat determinations for ferroelectric phase transitions in PbZrO₃-PbTiO₃-BiFeO₃ ternary systems
15 p2506 N71-27314

Electric field intensities for inducing gas bubble discharge in liquids
[JINR-P13-5277] 15 p2479 N71-27655

High altitude velocity distribution of ionospheric drift and electric field strength in F₂ layer
17 p2748 N71-30091

ELECTRIC FIELDS

Amplification of acoustic waves in piezoelectric semiconductors by interaction with supersonic electrons drifted in electric field
01 p0108 N71-10140

Scanning electron microscope studies of breakdown and electric field distribution in transverse Gunn effect devices
01 p0109 N71-10111

Investigating light modulation by strong electric field in this CdTe layers
01 p0111 N71-10104

Investigating interaction between light wave and microwave frequency traveling wave in anisotropic medium in parametric approximation
01 p0092 N71-10090

Orientations of electric field gradient and susceptibility tensors determined in iron salts
[AD-711621] 02 p0303 N71-11426

Longitudinal electric field effect on toroidal diffusion in tokamak plasma confinement
[IC/70/74] 02 p0200 N71-11021

RF electric field effects of ion wave dispersion with spatially modulated pressure
[IPF1-93] 02 p0281 N71-11077

Adiabatic phenomenon of particle drift and splitting by magnetospheric electric field
[AD-712044] 02 p0292 N71-11102

Electric and magnetic cross field effects on aerodynamics and thermal regime of gas flame cones
[AD-712336] 02 p0306 N71-11205

Electric and magnetic fields effect on liquid crystal structure
[NASA-CR-111582] 03 p0324 N71-12315

Electric field effect on crystal growth rate of molecular solids
[A69-10140] 03 p0324 N71-12314

Electric field strength and helix pitch relationship in induced cholesteric-nematic phase transitions
[A69-14964] 03 p0324 N71-12316

Electric field effects on dielectric properties and molecular arrangements of cholesteric liquid crystals
[A70-11352] 03 p0324 N71-12317

Electric field effects on optical rotary power of compensated cholesteric liquid crystal
[A70-14003] 03 p0324 N71-12318

Alternating current field induced cholesteric and nematic liquid crystal phase transitions
[A70-20053] 03 p0325 N71-12319

Basic methods of measuring atmospheric electric fields
[TT-70-50125] 03 p0367 N71-12777

Lower atmosphere electric field radiocone measurements at different weather conditions
[FR-2] 03 p0371 N71-12807

Geomagnetism/electric current alignment, space charge and electric field effects on particle acceleration, and auroral motions
[REPT-70-18] 03 p0451 N71-13332

Electric analog for measuring induced drag on supersonic airfoils
[NASA-CASE-XLA-00755] 04 p0472 N71-13418

Electric analog for measuring induced drag on supersonic airfoils
[NASA-CASE-XLA-05828] 04 p0472 N71-13411

Magnetohydrodynamic flow in magnetosphere, and space charges and self consistent electric fields
[REPT-70-32-PT-1] 04 p0528 N71-13808

Accelerating field effect on electron bunch containing ions
[JINR-P9-5142] 04 p0577 N71-13790

Small perturbations for peak electric field measurement in disk-loaded, traveling wave waveguides
[SLAC-TRANS-118] 04 p0566 N71-14009

Electric field effects on optical absorption by excitons in semiconductors
04 p0603 N71-14229

Electrical and magnetic field calculation for linear accelerator inductor
[JINR-P9-5129] 04 p0567 N71-14234

Particle diffusion and plasma dielectric constant in uniform electric field transverse to spatially uniform magnetic field
[IPF-4/5] 05 p0373 N71-14801

Synchronous smooth rotor in system for automatic regulation of field current
[PUBL-115] 05 p0656 N71-15316

Use of conformal mapping to improve uniformity of electric fields
[IPF1-T-4] 05 p0657 N71-15373

Correlations of fluctuation in electric field intensity and current density for nonequilibrium isotropic plasma
[SINP-TL-68-8] 06 p0628 N71-15778

Near electric field of rectangular aperture in infinite ground plane
[AD-714574] 06 p0624 N71-16044

Balloon measurements of ionospheric electric fields
[NASA-CR-114818] 06 p0856 N71-16053

Electric field due to polarization of air during progress of Compton currents excited by photons
07 p1014 N71-16050

Electrodynamic reciprocity theorem for calculating bilinear quantities of fluctuating field
07 p1001 N71-16051

Polar cap electric field measurements, and model for Hall current auroral electrojet continuity and polar cap magnetic disturbances
[NASA-TM-X-65447] 07 p1019 N71-17229

SUBJECT INDEX

Electric field produced by long horizontal electric line source above inhomogeneous surface
[AD-714791] 07 p0994 N71-17764

Ceramic BaTiO₃ disk subjected to pulsed electric field monitor
[AD-714968] 07 p1002 N71-17939

Longitudinal diffusion coefficients of gaseous ions drifting in electric field
[AD-714968] 07 p1004 N71-18083

Modified peaking strip method for measurements of slowly varying low field
[NACA-70-5] 08 p1167 N71-18162

Injection double probe measurements of dc fields in magnetosphere
[NASA-CR-116791] 08 p1187 N71-18405

Radio observation of broadband electrostatic VLF waves in polar magnetosphere
[AD-715896] 08 p1188 N71-18501

Electrotransport of impurities in rare earth metals using pulsed current
[RM-81-7480] 08 p1213 N71-18513

Ionospheric and magnetospheric electric field measuring instruments and measurement results
[NPL-PAB/EXTRATER-44/70] 08 p1189 N71-18609

Longitudinal and transverse diffusion coefficients of gaseous ions in electric fields
[AD-715375] 08 p1274 N71-18716

Potential energy of electrostatic field in double disk plasma probe
[AD-715891] 08 p1275 N71-18819

Instrument for measuring potentials on two dimensional electric field plot
[NASA-CASE-XLA-08493] 09 p1361 N71-19421

In phase oscillating magnetrons for continuous quantum power oscillators and coupled oscillations in cavity resonators
[AD-716131] 09 p1359 N71-19625

Electrical force potential for drop supercooling and development and dissipation of clouds and fog
[AD-716352] 09 p1413 N71-19661

Drift tube diameter, length, and position error perturbation of electric field distribution in Alvarez cavity
[UCRL-19932] 09 p1427 N71-19717

Auroral ionospheric electric field rocket sounding by means of Geiger counters, electrostatic probes, and laser artificial clouds
[REPT-70-25] 10 p1545 N71-20634

Plasma and electric field distribution over auroral magnet and polar caps
[NASA-CR-117403] 10 p1546 N71-20708

N-type germanium electrical resistivity in high intensity electric fields
[LAD-AB-118] 10 p1531 N71-20798

ESRO-1 satellite experiment on magnetic field aligned electric field near or in ionosphere
10 p1550 N71-21154

ESRO-1 satellite Langmuir electrostatic probe electric field detection
10 p1531 N71-21163

Low-level, low-frequency electric field effects on memory behavior and brain activity based on electroencephalography
[AD-717100] 10 p1500 N71-21222

Electric currents and fields produced in ionosphere by light varying horizontal winds
10 p1533 N71-21313

Confinement of hot, dense fusion plasma by inertia of high energy beams of particles focused at plasma from all sides
[AD-716860] 10 p1630 N71-21614

Acoustic amplification in high mobility extrinsic semiconductors in presence of crossed dc electric and magnetic fields
11 p1798 N71-22468

Electric field generated by simulated interaction of solar wind with planets
11 p1823 N71-22519

Vertical electric fields of sea currents and utilization for measurement of current velocity
11 p1756 N71-22840

Effect of applied electric field on photoconductance of n- and p-type single crystals of InSb at low temperatures
11 p1818 N71-22963

Numerical integration of spontaneous ionization of hydrogen atom in electric field using Schroedinger equation
[NASA-CR-117894] 12 p1969 N71-23287

Auroral ionospheric electric field measurements by means of gas release or electrostatic probes
12 p1909 N71-23567

Electron beam deflection devices for measuring electric fields
[NASA-CASE-XMP-10289] 12 p1920 N71-23699

Low frequency 1 to 100 KHz oscillations in hot cathode Penning discharge plasma caused by density waves moving in plasma drift direction in crossed electric and magnetic fields
[NASA-TT-135641] 12 p1981 N71-23966

Effect of permanent and alternating electric fields on heat transfer in fluid dielectrics
[NASA-TT-135601] 12 p2011 N71-24059

Numerical analysis of velocity and electrostatic potential for turning moment and capacitance of disc viscometer and condenser
12 p1923 N71-24188

Feasibility of achieving bulk laser action in polar semiconductors pumped by impact ionization in applied electric field
[AD-719403] 13 p2089 N71-24731

Calculations on electron spatial and velocity distribution from point source in neutral gas effected by homogeneous dc electric field
13 p2131 N71-24901

Selection rules and line strengths for electric field induced spectra of axially symmetric and linear molecules
13 p2145 N71-25599

Development of avalanche and streamer in gases in homogeneous electric field with application of Debye screening radius
[JINR-P3-5504] 14 p2322 N71-26074

Fluctuations of magnetospheric electric field determined by power spectra analyses
[NASA-CR-118343] 14 p2249 N71-26300

Numerical analysis of conductivity in hot plasma and relationship between current density and electric field strength
[AD-720722] 14 p2323 N71-26641

Electrodes having array of small surfaces for field ionization
[NASA-CASE-ERC-10013] 14 p2231 N71-26678

Toroidal electric field effects on single particle radial drift in axisymmetric systems
[CLM-R-105] 14 p2313 N71-26708

Approximation for electric field in toroidal metallic chamber with sections
[NP-18505] 15 p2453 N71-26867

Gamma/gamma angular coincidence measurements on thulium ion crystal electric fields
15 p2472 N71-27417

Equivalent rigidity of cotton, wool, and nylon fibers increased in parallel electric field
[NLL-TR-5769] 16 p2616 N71-28285

Purity problem in semiconductors and dynamics of Bloch electron in constant electric field
[AD-723111] 16 p2664 N71-28287

Detecting molecular constituents in radiation transparent media by measuring intensity of light transmitted through cell while applying electrostatic or electromagnetic field
[NASA-CASE-ERC-10021] 16 p2557 N71-28635

Prebreakdown processes and sparking voltage of gas moving at angle to electric field across uniformly stressed gap
[AD-723512] 17 p2811 N71-29620

Barium releases from Javelin and Nike-Tomahawk sounding rockets for ion cloud study of earth electric and magnetic fields
[NASA-SP-264] 17 p2740 N71-29671

Using ionized barium vapor clouds for direct measurement of electric fields in the magnetosphere
17 p2740 N71-29672

Determining electric and magnetic fields by visual observations of second release from Javelin vehicle
17 p2740 N71-29676

Electric field distribution, cloud elongation, and drift along magnetic field line of barium release from Javelin
17 p2741 N71-29681

Model for migration of dislocation arrays in ionic crystals based on dislocation climb in vacancy concentration gradients by action of external electric field at array sites
17 p2826 N71-30068

Electric field measuring techniques used in ionospheric and magnetospheric electrojet current studies
[NASA-TM-X-65596] 17 p2748 N71-30094

Tables of artificial satellites for investigating magnetospheric, solar wind, electric field, and magnetic fields from 1971 to 1975
[GRI/NT/785] 18 p3018 N71-30879

Effect of electric fields on flame spread rate during ignition of solid rocket propellants
18 p3080 N71-31190

Temperature effects on transport coefficients of bulk semiconductors in magnetic and electric fields
[RM-515] 18 p2999 N71-31463

Stationary and moving electric fields in silver- and gold-doped cadmium sulfides
18 p2941 N71-31468

Effect of electric field and temperature on radiative lifetime of excited F center in KCl, KF, and NaF
[NYO-3463-23] 18 p2990 N71-31568

Electric field effects in ionosphere, including ionospheric drift, conductivity, and currents
[REPT-78-11] 20 p3255 N71-32908

Geophysical phenomena observations of upper atmosphere electric and magnetic states, and solar activity data - Apr. 1970
20 p3258 N71-33101

Capacitor field calculations for capacitive displacement measurement of open mesh structures such as radio telescopes and radar receivers
[NASA-TN-D-6341] 20 p3273 N71-33397

ELECTRIC FILTERS

Close-in electric and magnetic fields produced by gamma ray induced currents from nuclear explosion
[NORE-57] 20 p3316 N71-33416

Importance of optical tolerances and electric fields in resonant reflectors used in giant pulse laser systems
20 p3275 N71-33480

Measuring gas adsorption in electric fields by method of thermal conductivity in gaseous mixtures
[NASA-TT-F-13936] 20 p3253 N71-33700

Single station lightning distance measuring device based on ratio of magnetic field to electric field
[NOAA-TR-BR-193-APCL-16] 20 p3268 N71-33734

Electric field shift parameters of proceodymium and cesium ions dilutely substituted for lanthanum magnesium double nitrate
20 p3327 N71-33968

Penetration of induction electrical fields and losses in impure type 2 superconductors having surface current
[ORNL-TR-2475] 20 p3337 N71-33979

Field line motion accompanying rapid plasma flow during geomagnetic storms
[NASA-TM-X-67295] 21 p3415 N71-34298

Convection electric fields observed with double probe dc electric field experiment on Explorer 40 satellite
[NASA-CR-121741] 21 p3419 N71-34324

Scattering of electromagnetic waves using integral equation form of Maxwell equations for electric fields
[NASA-CR-121740] 21 p3447 N71-34530

Ionization electron avalanche in high electric field in liquid argon and xenon for this particle detector development
[UCRL-20135] 21 p3484 N71-34814

Quantum theory of particles with spin up to one in magnetic or electric fields
[NYO-3829-66] 21 p3485 N71-34830

Dynamic stabilization of drift-dissipated instability in partially ionized plasma using inhomogeneous HF electric field
[EUR-CEA-FC-581] 21 p3493 N71-34883

Laser-induced plasma instability model for electric fields oscillating near plasma frequencies
[LA-4684] 21 p3493 N71-34899

Penetration of magnetic induction, electric field, and losses in impure type-2 superconductors with surface currents and interactions
[CONF-700341-8] 22 p3657 N71-36081

Electric field induced alignment and reorientation kinetics of paraelectric impurities in alkali halide crystals, using optical and calorimetric methods
22 p3659 N71-36093

Physiological effects and growth responses in plants influenced by electric fields and production of air ions and ozone by barley plants
23 p3715 N71-36485

Infinite length, gap excited, thick, cylindrical dipole antenna radiation field formulations as boundary value problems based on Maxwell equations for electric and magnetic fields
23 p3734 N71-36619

Computer program for calculating corona thresholds in nonuniform electric fields
23 p3738 N71-36654

Electric field fluctuations in turbulent plasma produced by z-discharge
[CONF-710607-56] 23 p3826 N71-37292

Experimental investigation of quasi-stationary longitudinal ion streams in L-1 stellarator
[CN-28/H-4] 23 p3831 N71-37322

Interaction of magnetospheric and electric field with respect to earth rotation
23 p3853 N71-37464

Protection from charged particles using high voltage electric fields
23 p3853 N71-37475

Particle separation using deflectors with crossed electric and magnetic fields
[NP-18786] 24 p3976 N71-38371

Crossed field instabilities and turbulent ion heating calculated in mirror machine
[CONF-710607-67] 24 p3988 N71-38458

Kinetic equation solution in drift approximation for electric field effect on transfer processes in axially symmetric magnetic traps
[CONF-710607-28] 24 p3994 N71-38496

ELECTRIC FILTERS

NT BANDPASS FILTERS

NT CRYSTAL FILTERS

NT DIGITAL FILTERS

NT ELECTROMAGNETIC WAVE FILTERS

NT INFRARED FILTERS

NT LINEAR FILTERS

NT LOW PASS FILTERS

NT MICROWAVE FILTERS

NT OPTICAL FILTERS

NT RADIO FILTERS

NT ULTRAVIOLET FILTERS

NT WAVEGUIDE FILTERS

Determining power spectrum of PN codes and effect of predemodulation filtering on correlation and error signals in space communication systems
01 p0821 N71-10237

- Optimum filters designed for analog feedback telemetry system 03 p0337 N71-12408
- Synthesis techniques for active RC filters using operational amplifiers 03 p0350 N71-12527 [AD-712466]
- Aerosol filtration by electrolyzed fibrous filter mats 04 p0509 N71-13515
- Aerosol filtration by electret filters 04 p0509 N71-13519
- Elimination of phase distortion in filters using digital techniques [Y-DA-3514] 04 p0512 N71-13538
- Network theory and insertion loss filter design [AD-713720] 05 p0654 N71-14881
- Applying nonadaptive transversal filters to playback of digital tape recorder signals and complementary symmetry MOSFET memory for outer planet spacecraft 06 p0821 N71-16684
- Describing static inverter with single or multiple phase output [NASA-CASE-XMF-00663] 08 p1165 N71-18752
- Adaptive procedure for removing multimodal power spectra using cascade transversal digital filters [AD-716974] 10 p1532 N71-20804
- Design of two dimensional electric filters and infrared windows 10 p1533 N71-21024
- Digital filter realizations of arbitrary loss and delay functions applicable for any type of frequency in equalizing communication channels [AD-717159] 10 p1534 N71-21246
- Apparatus for filtering input signal [NASA-CASE-NPO-10198] 13 p2056 N71-24806
- Comparison of standard Z transform and algebraic substitution synthesis methods for digital filters [AD-721571] 16 p2569 N71-28397
- Low voltage aluminum electrolyte capacitors with high capacitance [ECR-16] 18 p2896 N71-31170
- Development of N path filter with passive RC circuits incorporating time-variable gyrators [AD-723566] 19 p3069 N71-32771
- Effect of coefficient rounding in floating point digital filters [AD-727073] 24 p3898 N71-37784
- Theory and formalism for derivation of transfer function of N-path filters [AD-727140] 24 p3898 N71-37787
- ELECTRIC FUSES**
- Development of in-line fuse device for protection of electric circuits from excessive currents and voltages [NASA-CASE-MSC-12135-1] 03 p0350 N71-12526
- Single electrical circuit component combining diode, fuse, and blown indicator with elongated tube of heat resistant transparent material [NASA-CASE-XKS-03381] 11 p1726 N71-22796
- Coordinating fuses for protection of solid state device without large safety factor and high voltage dc circuits [MATT-715] 17 p2727 N71-29351
- Mercury filled self-healing fuses for protecting solid state circuits from faults - design and development [NASA-CR-72868] 22 p3558 N71-35343
- ELECTRIC GENERATORS**
- NT AC GENERATORS
- NT ALKALINE BATTERIES
- NT BIOCHEMICAL FUEL CELLS
- NT DIRECT POWER GENERATORS
- NT DYNAMOMETERS
- NT ELECTROSTATIC GENERATORS
- NT FUEL CELLS
- NT HYDROGEN OXYGEN FUEL CELLS
- NT MAGNESIUM CELLS
- NT MAGNETOHYDRODYNAMIC GENERATORS
- NT METAL AIR BATTERIES
- NT NICKEL ZINC BATTERIES
- NT PRIMARY BATTERIES
- NT RADIOISOTOPE BATTERIES
- NT REGENERATIVE FUEL CELLS
- NT ROTATING GENERATORS
- NT SNAP 19
- NT SNAP 21
- NT SNAP 23
- NT SOLAR CELLS
- NT SOLAR GENERATORS
- NT THERMIONIC CONVERTERS
- NT THERMOELECTRIC GENERATORS
- NT TURBOGENERATORS
- NT ZINC-OXYGEN BATTERIES
- Steady state characteristics of voltage regulator and parasitic speed controller on 14.3-kilovolt-ampere, 1200-Hz modified Lundell alternator [NASA-TN-D-5924] 01 p0006 N71-10059
- Research progress on nuclear, thin film, and electrochemical sources for spacecraft power supplies 01 p0006 N71-10258
- Viscous torque or windage losses for Lundell generator rotor in air and turbulent flow [NASA-TM-X-52905] 01 p0006 N71-10490
- Performance tests and failure analysis of homopolar electric generator [EP-RR-23] 02 p0195 N71-11368

- Capacitor requirements for static power conversion equipment [SRDE-64007] 03 p0353 N71-12553
- Formulas for determining flying weight of aircraft electric generator systems [AD-713762] 05 p0631 N71-14649
- Generating direct current with regulated constant voltage by using feeder with negative impedance output 05 p0654 N71-14760
- Numerical analysis of flow field typical of those in combustion driven supersonic MHD generator 06 p1181 N71-18871
- Magnetic field determination of nonlinear dc generator [AD-716437] 09 p1359 N71-19755
- Shutdown characteristics of SNAP-8 mercury Rankine power conversion system [NASA-TN-D-6172] 09 p1326 N71-20135
- Design and development of electric generator for space power system [NASA-CASE-XLE-04250] 09 p1360 N71-20446
- Motor start of 2 to 10 kilowatt Brayton rotating unit operating on gas bearings in closed loop test facility [NASA-TM-X-2266] 11 p1678 N71-22570
- Development and characteristics of single or double pulse generator which produces constant width pulses in nanosecond region [NASA-CASE-XGS-03427] 11 p1729 N71-23029
- Development of slip ring assembly with inner and outer peripheral surfaces used as electrical contacts for brushes [NASA-CASE-XMF-01049] 11 p1773 N71-23049
- Conversion of positive dc voltage to positive dc voltage of lower amplitude [NASA-CASE-XMF-14301] 12 p1886 N71-23188
- High temperature ferromagnetic cobalt-base alloy for electrical power generating equipment [NASA-CASE-XLE-03629] 12 p1937 N71-23248
- Solid state integrator for converting variable width pulses into analog voltage [NASA-CASE-XLA-03356] 12 p1892 N71-23315
- Environmental tests of electrical subsystem of 2-to-15 kW Brayton power conversion system [NASA-TM-X-67814] 12 p1963 N71-23928
- Closed cycle magnetohydrodynamic power generators with two channels [NASA-TM-X-2277] 12 p1981 N71-23932
- Determination of communication-electronic equipment power requirement and its compatibility with power sources [AD-719099] 13 p2053 N71-24398
- Design and development of canned-motor pump for high temperature NaK service in SNAP-8 [NASA-CR-72823] 13 p2116 N71-24634
- Electric power system with circulatory liquid coolant cooling system [NASA-CASE-MFS-14114-2] 13 p2056 N71-24807
- Device utilizing RC rate generators for continuous slow speed measurement [NASA-CASE-XMF-02966] 13 p2060 N71-24863
- Device for voltage conversion using controlled pulse widths and arrangements to generate ac output voltage [NASA-CASE-MFS-10068] 13 p2060 N71-25139
- Component and system performance tests of Brayton cycle power conversion system in 2 to 15 kW sub e range [NASA-TM-X-67835] 13 p2157 N71-25350
- Post test analysis of closed Brayton cycle space electric power conversion system for space [NASA-TM-X-67841] 13 p2157 N71-25367
- Computer controlled durability test of 50,000 hour life Brayton power conversion system for space applications [NASA-TM-X-67830] 13 p2157 N71-25368
- Multiple varactor for generating high frequencies with high power and high conversion efficiency [NASA-CASE-XMF-04958-1] 14 p2234 N71-26414
- Circuit design for failure sensing and protecting low voltage electric generator and power transmission networks [NASA-CASE-GSC-10114-1] 15 p2389 N71-27366
- Electric power system with thermionic diodes and circulatory liquid metal coolant lines [NASA-CASE-MFS-14114] 15 p2525 N71-27862
- Design and test experiments for radioisotope power conversion systems [ORNL-TM-3292] 15 p2525 N71-27933
- Design and experiments with compact fast spectrum reactor for generating electric power in space [NASA-TM-X-67857] 16 p2635 N71-28820
- Load insensitive dc to dc power converter with solid state circuitry [NASA-CASE-XER-11046] 16 p2572 N71-28902
- Approximation method for dynamic properties of commutative control element in converter servomechanism 17 p2728 N71-30125
- Use of samarium cobalt as permanent magnet material for field excitation in 100 kW generator [AD-722872] 18 p2874 N71-31289
- Main ion thrusters, microthrusters, and characteristics of electric power supplies for ion engines [LAAS-756] 19 p3173 N71-31666

- Technology and economics of isotopic electricity generators [CEA-BIB-190] 19 p3065 N71-32122
- Switching circuit, bypass, and power conditioning circuit tests for TOPS electrical system [NASA-CR-121478] 20 p3355 N71-33722
- Development and evaluation of high temperature materials for use in magnetohydrodynamic generators [JPRS-53959] 22 p3598 N71-35018
- Isotopic electricity generator studies, including radioactive isotopes, output wattage, generator lifetime, energy conversion, and generator weight [ORNL-TR-2485] 23 p3794 N71-37004
- ELECTRIC IGNITION**
- Technology review on electric automobiles 11 p1768 N71-22119
- Method of making solid propellant rocket motor having reliable high altitude capabilities, long shelf life, and capable of firing with nozzle closure with foamed plastic permanent mandrel [NASA-CASE-XLA-04126] 14 p2333 N71-26779
- Performance tests and comparison of ignition properties for normal lead styphnate under constant current and capacitor discharge ignition [AD-721695] 16 p2690 N71-28504
- ELECTRIC IMPULSES**
- U ELECTRIC PULSES
- U ELECTRIC LEADS
- U ELECTRIC WIRE
- ELECTRIC MOMENTS**
- Electric deflection molecular beam system with mass spectrometric detector [AD-710656] 01 p0018 N71-10404
- Electric and magnetic moments of F-18 and Na-2 measured using spin rotation for validity tests of shell or collective nuclear model 03 p0436 N71-17008
- Paraelectric and paraelastic behavior of dipole centers in crystals [AD-714955] 06 p0937 N71-16728
- Harmonic analysis and nuclear model of lithium core distortion and effects on energy levels, magnetic dipole and electric quadrupole moments, and Pauli exclusion principle 15 p2494 N71-27905
- Mossbauer studies of energy levels, electric and magnetic moments, hyperfine fields, and lift times of various light nuclei [NYO-2028-5] 21 p3484 N71-34823
- ELECTRIC MOTORS**
- NT SYNCHRONOUS MOTORS
- NT TORQUE MOTORS
- Microstep motor design 01 p0031 N71-10408
- Using electron beam switching for brushless motor commutation [NASA-CASE-XGS-01451] 01 p0034 N71-10407
- Brushless dc motor design and performance tests [NASA-CR-102942] 03 p0351 N71-12533
- Direct current motor with magnetically suspended rotor [NASA-CR-115793] 04 p0509 N71-13513
- Modification of dc motor with magnetically suspended rotor to increase moment of inertia capacity [NASA-CR-115792] 04 p0509 N71-13514
- Circuitry for automatic control of alternating current motors [AD-713386] 05 p0634 N71-13402
- Using polar diagrams of asynchronous triphase diagrams for developing equivalent circuits [PUBL-116] 05 p0636 N71-13515
- Characteristics of behavior of triphase induction machine with stator and rotor connected by networks [PUBL-117] 05 p0636 N71-13517
- Direct current electromotive system for regenerative braking of electric motor [NASA-CASE-XMF-01096] 06 p0826 N71-16809
- Describing angular position and velocity sensing apparatus [NASA-CASE-XGS-05600] 07 p1030 N71-17580
- Reversible current directing circuitry for reversible motor control [NASA-CASE-XLA-09371] 08 p1172 N71-18774
- Stepping motor control apparatus exciting windup in proper time sequence to cause motor to rotate in either direction [NASA-CASE-GSC-10366-1] 08 p1172 N71-18772
- Electric and electrohydraulic stepping motor for numerically controlled machine tools [CRIP-MC-33] 10 p1562 N71-20710
- Analysis of solid rotors used in high speed induction motors for aerospace applications 11 p1677 N71-18808
- Technology review on electric automobiles, and modified T-33 aircraft system for pyrotechnic ball up precision landing 11 p1768 N71-22119
- [DMR/NAE-1970/41] 11 p1768 N71-22119
- Technology review on electric automobiles 11 p1768 N71-22119
- Alternating resonant frequency oscillation characteristics of inertial asynchronous motor [NRC-TT-1448] 12 p1891 N71-30858

SUBJECT INDEX

Electromagnetic braking arrangement for controlling rotor rotation in electric motor [NASA-CASE-XNP-06956] 13 p2085 N71-24095

Electric motor control system with pulse width modulation for providing automatic null seeking servo [NASA-CASE-XMF-05195] 13 p2059 N71-24061

Velocity limiting safety system for motor driven research vehicle [NASA-CASE-XLA-07473] 13 p2086 N71-24095

Design and development of electric motor with stationary field and armature windings which operate on direct current [NASA-CASE-XGS-05296] 14 p2228 N71-23999

Circuit for controlling reversible dc motor [NASA-CASE-XNP-7477] 14 p2229 N71-26092

Pulse duration control device for driving slow response time loads in selected sequence including switching and delay circuits and magnetic storage [NASA-CASE-XGS-04224] 14 p2234 N71-26418

Electromotive force measurements on electric motor for electric hand prosthetic device [POA-2-C-2353-54] 14 p2230 N71-26532

Performance of electric stepping motor as reactor control drum drive [NASA-TM-X-2297] 15 p2368 N71-26979

Electric motor environmental and electrical test procedures including electromagnetic compatibility and maintenance [AD-721611] 16 p2368 N71-28343

Electric motor off-on speed control limiter circuit for thyristor and computerized simulation [AD-721561] 16 p2574 N71-28349

Feedback control for direct current motor to achieve constant speed under varying loads [NASA-CASE-MPS-14610] 16 p2572 N71-28896

Digital computer graphics program for on-line design of electric drive vehicles [AD-724622] 20 p2328 N71-32905

Development of analytical model for predicting performance of small electromechanical devices 20 p3280 N71-33680

Nondestructive tests of motor drivers for delta wound dc brushless motors [NASA-CR-121498] 21 p3402 N71-34203

Direct current motor design with magnetic bearing for use in low friction disturbance control systems [NASA-CASE-XGS-07805] 21 p3432 N71-34420

Air pollution sources and control procedures and 17th Clean Air Act summary [PB-199479] 22 p3499 N71-36378

Calculation and measurement of stray losses in induction motors and comparison with results obtained from standard techniques [NRL-M-20539-5828.4F] 23 p3733 N71-36615

Designing alternating current electric wheel for military construction and cargo vehicles [AD-726956] 23 p3763 N71-36827

Operating characteristics of two phase servomotors and development of servo amplifiers using switching devices for control 24 p3900 N71-37796

Switching power supply for bidirectional control of dc permanent magnet motors [RM-521] 24 p3900 N71-37797

ELECTRIC NETWORKS

Frequency domain analysis of nonlinear networks [AD-710200] 01 p0026 N71-10873

Optimization of distributed-lumped active networks [AD-711050] 01 p0036 N71-10097

Miyata synthesis of passive driving point impedance functions [AD-709928] 01 p0037 N71-10620

Design of interactive graph reduction and analysis system [AD-709927] 01 p0028 N71-10621

Optimally insensitive active circuit synthesis of second order transfer functions [AD-712443] 03 p0353 N71-12548

Electric network for monitoring temperatures, detecting critical temperatures, and indicating critical time duration [NASA-CASE-XMF-01097] 06 p0827 N71-16038

Relationship between sensitivity model and mutually reciprocal adjoint network [AD-715564] 08 p1172 N71-18755

Method for solving transfer functions, phase and reflection factors, and attenuation coefficients in linear passive networks for component tolerance effects [BC-T-70-4048] 10 p1533 N71-21302

Sensitivity theorem for linear resistive circuits showing relation between sensitivities and instantaneous power in frequency domain [AD-717491] 11 p1722 N71-22012

Complex optimization techniques applied to various sensitivity coefficient determination for distributed-lumped active networks [NASA-CR-117757] 11 p1787 N71-22177

Development and characteristics of single or double pulse generator which produces constant width pulses in nanosecond region [NASA-CASE-XGS-03427] 11 p1729 N71-23029

Predicting service regulator with gating control network [NASA-CASE-XMS-09532] 12 p1887 N71-23316

Properties and synthesis of RC network with operational amplifier [AD-718306] 12 p1890 N71-23615

Functional analysis on stability of distributed reverse current electrical networks having nonlinear elements 12 p1893 N71-24029

Broadband frequency discriminator with resistive capacitive inductive networks [NASA-CASE-NFO-10094] 13 p2043 N71-24583

Electronic circuitry for trainable systems with application to control and recognition functions [AD-721737] 16 p2550 N71-28358

Vector representation for determining fault element in passive and active networks by external measurements [AD-721581] 16 p2574 N71-28415

Synthesis of open circuit impedance matrices and topological properties of corresponding graphs 16 p2574 N71-28673

Research on fundamental properties required of networks for automatically extracting patterns from pictorial data such as aerial photos 17 p2724 N71-30146

Transformation properties between impedance and general matrix representation of two port network [NRL-PORS-TRANS-2705-19022.11] 17 p2728 N71-30205

Subharmonic response in nonlinear network analysis [AD-723216] 19 p3122 N71-31987

Parallel standbys redundancy subject to both open and short circuit failures - extension of branch and bound algorithms [AD-723055] 19 p3087 N71-32471

Analysis of stability of two-port network to determine conditions of stability and properties of transformations of impedances [NRL-PORS-TRANS-2733-19022.81] 22 p3563 N71-35378

ELECTRIC POTENTIAL

NT BIOELECTRIC POTENTIAL

NT COULOMB POTENTIAL

NT LOW VOLTAGE

Lightning induced voltages in aircraft electrical circuits [NASA-TM-X-52506] 01 p0004 N71-10391

Simulation of Laplace transform by means of dc potential in semiconductor materials [AD-713021] 03 p0352 N71-12547

Linear electric potential pulse width amplitude conversion circuit for spacecraft power supplies [ESRO-TN-101-ESTEC] 03 p0459 N71-13318

Thermodynamic significance of interface potential increase during crystal growth from solution [REPT-4164] 05 p0756 N71-14582

Characteristics of behavior of triphase induction machine with stator and rotor connected by networks [PUBL-117] 05 p0656 N71-15527

Direct conversion of fusion energy to electricity [UCRL-72411] 06 p0928 N71-15736

Graphical technique for analyzing series-parallel networks by rectangular diagrams in solving power distribution problems [NASA-CR-116118] 06 p0883 N71-15943

Gas velocity effects on breakdown potential of argon, helium, and nitrogen 06 p0839 N71-16650

Terminated capacitor discharge firing of electroexplosive devices [NASA-CR-116792] 06 p1169 N71-18702

Battery charging system with cell to cell voltage balance [NASA-CASE-XGS-05432] 09 p1325 N71-19438

Streaming potentials of fine-pore capillary systems and Donnan hindrance of electrolyte transfer through ion-selective permeable membranes [NRC-TT-1442] 10 p1513 N71-21259

Determining critical potentials by series of point-by-point potentiokinetic and potentiostatic measurements for corrosion studies [NRL-CE-TRANS-5208-19022.09] 10 p1579 N71-21286

Electrochemical potential of high purity metals in sea water for monitoring cathodic protection systems on ship hulls [AD-717348] 11 p1776 N71-21914

Conversion of positive dc voltage to positive dc voltage of lower amplitude [NASA-CASE-XMF-14301] 12 p1886 N71-23188

Solid state integrator for converting variable width pulses into analog voltage [NASA-CASE-XLA-03354] 12 p1892 N71-23315

Quantum method of maintaining volt as SI unit using a Josephson effect in superconductors 12 p1920 N71-23444

Voltage transients due to phase angle switching of speed control power for Bryton cycle alternator examined by computerized simulation [NASA-TM-X-2291] 13 p2031 N71-25420

Investigating electric potential in cesium thermionic diode for minimum plasma-loss by electrostatic probe [NASA-CR-118519] 14 p2229 N71-26273

Devices for monitoring voltage by generating signal when voltage drop below predetermined value [NASA-CASE-XSC-10050] 15 p2349 N71-27338

ELECTRIC POWER PLANTS

Electric field intensities for inducing gas bubble discharge in liquids [JNRP-F13-5277] 15 p2479 N71-27655

Low temperature overcharge voltage characteristics of OAO batteries and cells 16 p2539 N71-28667

Numerical integration of ac generator coil equations into flux linkage equations with iterative solutions for three phase machines 16 p2604 N71-28995

Low voltage test source developed for neutral beam production on ALICE baseball 1 experiments [UCRL-50961] 17 p2808 N71-30047

Potential and current distributions throughout MFD arc indicate that anode fall voltage varies inversely with local anode current density [NASA-CR-119171] 17 p2813 N71-30326

Voltage variable phase shifter having linear voltage-to-phase characteristics 21 p3393 N71-34148

High voltage large capacity varistors as power sources for pulse generator [IPFP-DT-19] 23 p3559 N71-35348

Data analysis for isoperibol laser calorimetry [AD-726514] 23 p3766 N71-36842

Manual for ORSAC computer program for calculating power plant combinations to provide given electrical capacities in US with minimum cost [ORNL-TM-5223] 23 p3799 N71-37085

Electrode potential and spectrophotometric determination of trace fluorine, chlorine, and boron in titanium oxide fuels after pyrohydrolytic separation [KPK-1340] 23 p3801 N71-37099

Field electron emission from C60 as function of temperature and exposure with current voltage characteristics and excitation line observations [NRL-TRANS-2751-19022.81] 23 p3834 N71-37358

Drain current-drain voltage equations for insulated gate and junction-gate field effect transistors and drain current sensitivity to piezoelectric and piezoelectric strain effects 23 p3837 N71-37366

Optimum excitation voltage for X ray microanalysis of pure elements, alloys, and mixtures [NPL-10887] 24 p3933 N71-38063

ELECTRIC POWER

Optimization of electrical power system for ATS [NASA-CR-111140] 01 p0087 N71-14655

Evaluation of compact, fully enclosed chamber for impedance and power testing of VHF whip antennas during production [AD-711111] 01 p0834 N71-10731

Coupling network for high power pulse NMR 03 p0351 N71-12536

Direct conversion of fusion-reactor charged particle energy to electrical form [UCRL-72487] 04 p0569 N71-13547

Thermodynamic characteristics of electrochemical energy conversion into electrical energy [AD-713875] 06 p0810 N71-16314

Development and characteristics of lithium-doped solar cells [NASA-CR-116220] 06 p0797 N71-16472

Solid state system for advanced spacecraft electric power distribution and control [NASA-CR-114813] 06 p0798 N71-16708

Generation of electric power with use of nuclear engines for rocket vehicles (NERVA) heat source [NASA-CR-103038] 07 p1104 N71-18049

Design and performance of SERT 2 spacecraft electrical power system [NASA-TM-X-2234] 09 p1472 N71-20471

Electrical power distribution systems for space vehicle with isotopic/Bryton sources [NASA-CR-103072] 09 p1472 N71-20474

Variable water load for dissipating large amounts of electrical power during high voltage power supply tests [NASA-CASE-XNP-05381] 10 p1332 N71-20842

Electrical power distribution system and energy consumption during long duration operation of space station simulator 10 p1533 N71-20875

Development and characteristics of high voltage multichannel pulse generator with six output channels [CERN-TRANS-71-6] 21 p3484 N71-34320

Effects of radiation on efficiency of lithium doped solar cells in electrical space power system [NASA-CR-122803] 23 p3769 N71-36443

Developing suitable solid state power controllers for space vehicles electrical power systems [NASA-CR-119961] 24 p3896 N71-37741

ELECTRIC POWER CONVERSION

U ELECTRIC GENERATORS

ELECTRIC POWER PLANTS

NT NUCLEAR POWER PLANTS

Future trends in cryoelectrical technology [LA-TR-70-10] 03 p0418 N71-12987

Hydrogen oxygen fuel cells for electric power plants and Apollo spacecraft [DLR-MITT-70-09] 06 p0796 N71-15723

Application of optimal control theory to power system [AD-716152] 09 p1362 N71-19437

- Feasibility of large-scale terrestrial plants for future generation of pollution free electrical power from solar energy
[NASA-TM-X-65497] 12 p1860 N71-23700
- Evaluation of factors affecting performance of series connected magnetohydrodynamic generators
[AD-72455] 16 p2540 N71-28718
- Optimization of cell dimensional parameters of in-core thermionic fuel element and power enhancement by varying converter lengths or interconnecting lead geometries in fuel elements
[NASA-TT-F-13689] 16 p2636 N71-28939
- Energy sources in US to achieve future electric energy needs and environmental compatibility requirements
17 p2743 N71-29832
- Electric power plant cooling tower effluent effect on urban atmospheric composition
[PB-197562] 18 p2920 N71-31487
- Annotated bibliography on emission sources in electric power plants and air pollution effects
20 p3255 N71-32891
- Gas core reactors and MHD generator to solve problems of growing demand for electric power without thermal pollution
20 p3306 N71-33664
- Component design data for 1.5 kW dc, turbine driven, organic Rankine cycle power plant for jungle use
[AD-726454] 22 p3542 N71-35234
- Manual for ORSAT computer program for calculating power plant combinations to provide given electrical capacities in US with minimum cost
[ORNL-TM-3223] 23 p3799 N71-37085
- ELECTRIC POWER TRANSMISSION**
- Effects of worldwide power requirements on environment
[CONF-790810-37] 04 p0480 N71-14473
- Underwater electrical connector and cable system designed for delivering large amounts of electric power for use underwater - photographs
05 p0680 N71-15612
- Development of liquid metal slip ring to transfer power between rotating satellite parts
[NASA-CR-72790] 06 p0798 N71-16570
- Feasibility of superconducting and cryogenic electrode transmission lines
[AD-714797] 07 p1000 N71-18051
- Designing rotating transformer with contactless electric power transmission
[LRBA-NT-4670/SET/EL] 08 p1169 N71-18617
- Electric power transmission by streamer discharge propagation from bundle conductors
[PB-196147] 09 p1422 N71-19474
- Model 50-600-75 Manganin pulse power supply transmitting power to piezoresistive gages and receiving signals which result from these gages
[SCL-DR-70-130] 10 p1534 N71-21224
- Power switch with transistor type magnetic core
[NASA-CASE-NPO-10242] 13 p2056 N71-24803
- Circuit design for failure sensing and protecting low voltage electric generator and power transmission network
[NASA-CASE-GSC-10114-1] 15 p2389 N71-27366
- Computer controlled electric power distribution system for aerospace systems
21 p3514 N71-35040
- Space shuttle electrical power distribution system design and development
21 p3514 N71-35042
- Design of snap-8 electrical protective system module including fabrication and assembly drawings
[NASA-CR-72938] 24 p3960 N71-38249
- ELECTRIC PROPULSION**
- NT ARC JET ENGINES
- NT ELECTROMAGNETIC PROPULSION
- NT ELECTROSTATIC PROPULSION
- NT ION PROPULSION
- NT PLASMA PROPULSION
- Payload transport into 24 hour orbit of Europa 2 rocket and solar electric propulsion module
[RAE-LIB-TRANS-1449] 01 p0125 N71-10191
- Magnetic, electrostatic, space plasma, and electromagnetic contamination levels from electric thruster and solar array
01 p0115 N71-10441
- Design criteria for integrating electric propulsion system into SERT 2 spacecraft and future spacecraft designs
[NASA-TM-X-2082] 01 p0117 N71-10905
- Centaur launch vehicle for Jupiter and Saturn orbiter missions using solar electric propelled spacecraft
[NASA-CR-111422] 02 p0299 N71-12041
- Method for determining approximate mass and dimensions of solar electric thrust subsystems
[NASA-CR-111580] 03 p0316 N71-12254
- Theoretical analysis of electron beam array propulsion from spacecraft
[NASA-CR-116808] 06 p0940 N71-15916
- Development and characteristics of electric propulsion systems for manned and unmanned spacecraft
[NASA-TM-X-66704] 07 p1102 N71-17507

- Qualification and testing of electric propulsion system for SERT 2 spacecraft
[NASA-TM-X-2199] 07 p1121 N71-17917
- Improving payload at low power by reducing total mass of electric propulsion spacecraft
[NASA-TM-X-52900] 09 p1461 N71-20501
- Research studies on development of Thermoelectric Outer Planet Spacecraft (TOPS) and lunar exploration
[NASA-CR-117440] 10 p1644 N71-21338
- Electric propulsion engines, digital gyro system, and step motor solar electric thrust vector systems for interplanetary spacecraft control
10 p1600 N71-21348
- Baffle geometry, subsystem estimation, and connector failure analysis for ion thruster of solar electric propulsion system
10 p1639 N71-21357
- Technology review and performance estimates for fixed design multipurpose solar electric propulsion stages
[NASA-TM-X-67801] 12 p1990 N71-23761
- Theoretical analysis of performance of two-grid accelerator systems for Kaufman thrusters
[NASA-TN-D-6275] 12 p1990 N71-23762
- Solar electric propulsion performance and trajectory data for indirect solar probes, extra-terrestrial missions, and rendezvous with Ceres, D-Arrest, and Encke
[NASA-CR-118312] 13 p2167 N71-25043
- Research and development of mercury electron bombardment thrusters
[NASA-TM-X-67836] 13 p2157 N71-25366
- Lithium/chalcogen cells applied to secondary batteries for vehicular propulsion
[ANL-7756] 14 p2199 N71-25651
- Performance tests of two thermionic energy converters fueled with uranium nitride
[NASA-CR-119690] 19 p3174 N71-32279
- Versatile, multimission solar electric propulsion upper stage for high energy, unmanned interplanetary flights - summary
[NASA-TM-X-114349] 19 p3184 N71-32485
- Versatile, multimission solar electric propulsion upper stage for high energy, unmanned interplanetary flights - technical details
[NASA-CR-114350] 19 p3184 N71-32486
- Versatile, multimission solar electric propulsion upper stage for high energy, unmanned interplanetary flights - appendices
[NASA-CR-114351] 19 p3184 N71-32487
- Design and characteristics of spacecraft propulsion system using charge buildup and electric propulsion techniques
[NASA-SP-276] 20 p3350 N71-32812
- Pinch and parallel-plate discharges, and analysis of anode region of quasi-steady MPD arc
[NASA-CR-121737] 21 p3405 N71-34227
- Characteristics and capabilities of solar electric propulsion for missions to Halley's comet due to return 1985-1986
[NASA-CR-122099] 21 p3508 N71-34992
- Trajectory and propulsion characteristics of spacecraft rendezvous mission opportunities to comets during 1975 to 1995
[NASA-CR-121762] 22 p3666 N71-36140
- Electrically propelled spacecraft designs using thermionic reactors as electrical power source investigated for Halley Comet rendezvous mission
[NASA-CR-122928] 23 p3839 N71-37377
- Design and development of electrically propelled spacecraft based on external-fuel reactor concepts for thermionic reactors - Vol. 2
[NASA-CR-122927] 24 p4000 N71-38533
- ELECTRIC PULSES**
- Insertion loss and pulse response of power line filters
[AD-71317] 01 p0035 N71-10828
- Statistical characteristics of spontaneous electrical activity of nerve units that exhibit stochastic dead time following impulses
[NASA-TM-X-63007] 05 p0635 N71-14917
- Analysis of pulsed wire anemometer to determine errors caused by finite yaw response of probe
[REPT-70-07] 05 p0687 N71-15471
- News release on pulsed exciter of elastic waves
05 p0681 N71-15481
- Self-mode-locking of cross-excited electrically pulsed CO-2 laser
[AD-714023] 06 p0868 N71-16215
- Design and development of variable pulse width multiplier
[NASA-CASE-XLA-02850] 09 p1361 N71-20447
- Current diffusion in cylindrical wires and fuses during microsecond electrical pulses
[AD-717003] 10 p1607 N71-21373
- Piezoelectric transducer for monitoring sound waves of physiological origin
[NASA-CASE-XMS-05365] 11 p1766 N71-22993
- Development and characteristics of single or double pulse generator which produces constant width pulses in nanosecond region
[NASA-CASE-XGS-03427] 11 p1729 N71-23029
- Computerized simulation of electrical generator system in human heart
11 p1686 N71-23079

- Solid state integrator for converting variable width pulses into analog voltage
[NASA-CASE-XLA-03356] 12 p1892 N71-23915
- Development and characteristics of electric circuitry for detecting electrical pulses rise time and amplitude
[NASA-CASE-XMF-08804] 13 p2055 N71-24717
- Formation mechanism of electrical pulse during detonation of ordinary explosive substances
[RAE-LIB-TRANS-1528] 13 p1314 N71-25148
- Behavior of living pink fish under influence of electrical and mechanical stimulation of couple of left horizontal ampulla and semicircular canal
[NASA-TT-F-13665] 14 p2203 N71-23716
- Calculating energy losses produced in pulsed superconducting magnet of any shape wound with solid core wires
[NP-18316] 14 p2298 N71-24628
- High voltage pulses for particle track storage in spark chamber
[DESY-70/60] 15 p2460 N71-27877
- Circuit for measuring wide range of pulse rates by utilizing high capacity counter
[NASA-CASE-XNP-06234] 15 p2388 N71-27137
- Trigger pulse energy, electrode dimension, gas pressure, and prepulse voltage effects on low inductance spark gaps for high voltages in air
[BBMW-FBR-70-17] 15 p2455 N71-27633
- Pulse-potential switch for computer memories
17 p2722 N71-29930
- Half-sine wave pulse firing of electroexplosive devices
[NASA-CR-119320] 18 p3025 N71-31110
- Signal proportional to power measured continuously for determining reactor reactivity
[CEA-N-1385] 19 p3136 N71-32855
- High-dynamic range rise time to amplitude converters
[CEA-N-1430] 19 p3070 N71-32880
- Precision full wave rectifier circuit for rectifying incoming electrical signals having positive or negative polarity with only positive output signals
[NASA-CASE-ARC-10101-1] 20 p3240 N71-33110
- Time determinations for electric pulse transmission through rock samples under high pressure and temperature
[NASA-TT-F-13796] 22 p3573 N71-35465
- High voltage nanosecond pulse generators with spark dischargers, techniques for shaping pulses, and analysis of gas discharge and arc formation
[AD-726793] 23 p3737 N71-34830
- Nanosecond pulse amplifier with continuously adjustable gain, working in both polarities
[CEA-N-1439] 24 p3997 N71-37778
- ELECTRIC RELAYS**
- Radio relay communication using dual reflector antenna with offset focal axis
[JPRS-51721] 02 p0182 N71-11280
- Alarm system design for monitoring one or more relay circuits
[NASA-CASE-XMS-10984-1] 09 p1361 N71-19417
- Time division relay synchronizer with master sync pulse for activating binary counter to produce signal identifying time slot for station
[NASA-CASE-GSC-10373-1] 09 p1349 N71-19770
- Spacecraft solar cell system design including electric relays, photoresistors, and switching circuits to maintain alignment during switching
[NASA-CASE-GSC-10669-1] 16 p2537 N71-28411
- Relay circuit breaker with magnetic latching to provide conductive and nonconductive paths for current devices
[NASA-CASE-MSC-11277] 16 p2572 N71-28808
- Boolean algorithms for application to digital electronics and relay networks
[ISS-70/18] 20 p3290 N71-33978
- Pulse relay control of solar orientation system for spacecraft guidance
23 p3793 N71-37839
- ELECTRIC ROCKET ENGINES**
- NT ARC JET ENGINES
- NT CESIUM ENGINES
- NT ELECTROSTATIC ENGINES
- NT ION ENGINES
- NT PLASMA ENGINES
- NT RESISTOJET ENGINES
- Development and characteristics of electric propulsion systems for manned and unmanned spacecraft
[NASA-TM-X-66704] 07 p1102 N71-17507
- Electric rocket engine with electron bombardment ionization chamber
[NASA-CASE-XNP-04124] 10 p1639 N71-21822
- Optimization of mercury electron bombardment thrusters in SERT program
[NASA-TM-X-67915] 20 p3339 N71-33017
- Design and development of electrically propelled spacecraft based on external-fuel reactor concepts for thermionic reactors - Vol. 2
[NASA-CR-122927] 24 p4000 N71-38533
- ELECTRIC SPARKS**
- Tables of iron spark lines giving comparison of calculated and measured wavelengths
[ESRD-IN-34] 02 p0281 N71-11877
- Testing of electrical detection system adaptable to spark source mass spectrometer
[IS-TRANS-82] 06 p0858 N71-15980

SUBJECT INDEX

- Dependence of spark brightness of ionization in range of 1 is less than or equal to 1/1 min is less than or equal to 15 at P equal to 1 atm, 0.3 atm, and 0.1 atm [JVE-SEP-69-75] 09 p1437 N71-20081
- Multipass process of gas ionization in laser spark production [NRC-TT-1450] 12 p2803 N71-24277
- Ionic diffusion and spectroscopic analysis of copper alloy dendrite etching by electric discharge [TT-70-57963] 14 p2534 N71-25706
- Simulation and measurement of electrical properties of lightning discharge by use of long sparks produced under laboratory conditions [JAA-DS-68-16] 14 p2587 N71-25823
- Validity of using laboratory produced sparks for evaluating properties of atmospheric lightning and description of parameters of primary importance 14 p2587 N71-25824
- Quantitative spectroscopic analysis of temperature and electron density in long arc sparks produced by laboratory equipment 14 p2587 N71-25825
- Measurement of acoustic output from long sparks produced during electrical discharge from laboratory equipment 14 p2596 N71-25826
- Effect of spark discharges into laminar boundary layer at supersonic free stream Mach numbers [NASA-TN-D-6378] 15 p2563 N71-26950
- Electron probe microanalysis and photomicrographic studies on metal surfaces eroded by spark discharges 17 p2765 N71-29884
- Radiation processes and instrument requirements for temporally and spatially resolved study of high voltage spark discharge 19 p3063 N71-32151
- Contact breaking speed effects on spark quenching and gas discharge of electric inductance switch [NLT-TRANS-2652-79022.81/1] 19 p3067 N71-32435
- Arc velocity and electrical properties in spark channels with current shocks 21 p3463 N71-34667
- High voltage nanosecond pulse generators with spark dischargers, techniques for shaping pulses, and analysis of gas discharge and arc formation [AD-726793] 23 p3737 N71-36650
- ELECTRIC STIMULI**
- Continuous perception test involving human ability to reproduce binary patterns formed by electrical stimulation of finger tips 11 p1679 N71-21099
- ELECTRIC STRAIN GAGES**
- U STRAIN GAGES**
- ELECTRIC SWITCHES**
- NT THERMOSTATS**
- UHF switch developed for LES-6 satellite [AD-710612] 01 p0031 N71-10071
- Amorphous semiconductor switches for control elements in electroluminescent display panel [AD-712366] 02 p0192 N71-11349
- Thermionic diode switch for use in high temperature region to chop current from dc source [NASA-CASE-NPO-10040] 03 p0316 N71-12255
- Characteristics of hermetically sealed electric switch with flexible operating capability [NASA-CASE-XNP-09008] 03 p0349 N71-12518
- Electrical switching device comprising conductive liquid confined within square loop of deformable non-conductive tubing also used for levitation [NASA-CASE-NPO-10037] 09 p1358 N71-19610
- Switch-on times and charge transfer mechanism effects on concentrated MOS transistors [NLT-TRANS-2652-79022.81/1] 10 p1534 N71-21236
- System for checking status of several double-throw switches by readout indications [NASA-CASE-XLA-08799] 15 p2388 N71-27272
- Pulse generating circuit for operation at very high duty cycles and repetition rates [NASA-CASE-XNP-08745] 16 p2576 N71-28960
- High dc switch for causing abrupt, cyclic, decreases of current to operate under zero or varying gravity conditions [NASA-CASE-LEW-10155-1] 16 p2573 N71-29035
- Contact breaking speed effects on spark quenching and gas discharge of electric inductance switch [NLT-TRANS-2652-79022.81/1] 19 p3067 N71-32435
- High current and multiple contact, low current switch designs and testing with respect to hermetic sealing switches with existing configuration [NASA-CR-115118] 22 p3559 N71-35345
- High voltage large capacity switches as power sources for pulse generator [PPT-DT-15] 22 p3559 N71-35348
- Oscillographic analysis of thyristor high voltage switch gear for continuous voltage adjustment [AD-72459] 23 p3733 N71-36613
- ELECTRIC TERMINALS**
- Tool attachment for opening or moving away from elements from terminal posts during winding of elementary elements [NASA-CASE-XMF-02107] 01 p0060 N71-10009

- Electrical spot terminal assembly for printed circuit boards [NASA-CASE-NPO-10034] 07 p1036 N71-17085
- Comparison between silicon-magnesium-aluminum alloy and copper aircraft electric conductors and terminals noting types of tests [TRC-BR-19783] 12 p1089 N71-23547
- Investigation of soldered component failure in plated printed circuit boards consisting of tinlead laminates copper, plated copper, and gold overplate [NASA-TM-X-2290] 13 p2055 N71-24715
- Vacuum cryopumping of heavy ion source in high voltage terminal of accelerator injector [UCRL-26620] 19 p3150 N71-32119
- Fence guide for millimeter waves, measurements on matched fence guide terminations, and experimental study of non-confocal cylindrical resonator [NASA-CR-121763] 21 p3394 N71-34155
- ELECTRIC WELDING**
- NT ARC WELDING**
- NT ELECTRON BEAM WELDING**
- NT ELECTROSLAG WELDING**
- NT GAS TUNGSTEN ARC WELDING**
- NT PLASMA ARC WELDING**
- Development of electric welding torch with casing on one end to form inert gas shield [NASA-CASE-XMF-02350] 12 p1927 N71-23798
- ELECTRIC WIRE**
- NT EXPLODING WIRES**
- Optimization of high current leads suitable for cryostats 01 p0088 N71-10144
- Computer update program for compiling master wire list from box external data [NASA-CR-108734] 03 p0342 N71-12478
- Corona tests on round wires, flat wires, and connectors for spacecraft components 06 p0825 N71-16643
- Combustion properties of Teflon insulated wires in supercritical oxygen at normal and zero gravities [NASA-TM-X-2174] 07 p1130 N71-17896
- Calculations on electromagnetic radiation from infinitely long wire in dielectric material over conducting ground plane [AD-715357] 08 p1168 N71-18446
- Control of fusion welding through use of thermocouple wire [NASA-CASE-MPS-06074] 09 p1394 N71-20393
- Wiring lists for solid state sequencer system in command module and service module junction controllers [NASA-CR-114957] 10 p1635 N71-21461
- Ablation sensor for measuring char layer recession rate using electric wires [NASA-CASE-XLA-01794] 10 p1663 N71-21586
- Nondestructive tests to determine origin of cracking problem encountered during welding of aluminum wire [BDX-613-321] 21 p3434 N71-34438
- Fabrication process and electrical properties of high temperature flat cable [BDX-613-161] 23 p3731 N71-36597
- Development and characteristics of device for deployment of long wires as method of reducing hazards due to lightning during spacecraft launches [NASA-TM-X-62085] 23 p3736 N71-36772
- Development of pulse-arc welding process for preventing cracking when joining multistrut aluminum wires [BDX-613-320] 23 p3762 N71-36823
- ELECTRIC WIRING**
- U ELECTRIC WIRE**
- U WIRING**
- ELECTRICAL BREAKDOWN**
- U ELECTRICAL FAULTS**
- ELECTRICAL CONDUCTIVITY**
- U ELECTRICAL RESISTIVITY**
- ELECTRICAL CONDUCTIVITY METERS**
- Polarographic, coulometric, and polarographic gas analyzers for air pollution measurements 11 p1761 N71-22058
- ELECTRIC ENERGY**
- U ELECTRIC POWER**
- ELECTRIC ENGINEERING**
- Intersect node/Automated Snark Program [NASA-CR-108724] 03 p0339 N71-12450
- Legal path report/Automated Snark Program [NASA-CR-108741] 03 p0339 N71-12451
- Descriptions of Node Report Data Generation Program [NASA-CR-108742] 03 p0339 N71-12452
- Initial disconnect/Automated Snark Program [NASA-CR-108735] 03 p0339 N71-12453
- Snark circuit analysis handbook [NASA-CR-108721] 03 p0343 N71-12487
- Directory of standardized symbols for electromagnetic measurements [AGARD-R-376-70] 03 p0352 N71-12545
- Superconductivity applications in electrical engineering [ENP-70-5] 04 p0604 N71-14489
- Design networks having prescribed driving-point impedance in Bruen fashion [AD-715334] 07 p0999 N71-17774

ELECTRICAL FAULTS

- Vibrating element electrometer producing high conversion gain by input current control of elements resonant frequency displacement amplitude [NASA-CASE-XAC-62087] 11 p1727 N71-23021
- Engineering aspects of magnetohydrodynamic 14 p2323 N71-26450
- Requirement specifications for environmental laboratory test chamber complex design, fabrication, and testing [NASA-CR-115007] 14 p2345 N71-26549
- Wide-range nuclear magnetic resonance probe design including integrated circuits, RF coil, and coaxial cable for use with high field cryogenic magnets [NASA-TN-D-6338] 15 p2585 N71-29908
- Absorbers on electrical engineering and data compression [TR-EE-70-45] 18 p2900 N71-31479
- Design and performance characteristics of bandpass gyrators 19 p3068 N71-32608
- ELECTRICAL FAULTS**
- NT SHORT CIRCUITS**
- Scanning electron microscope studies of breakdown and electric field distribution in transverse Gunn effect devices 01 p0109 N71-10213
- Dead space characteristics method for potentiometer evaluation [AD-710947] 01 p0033 N71-10566
- Jet aircraft crash during instrument approach due to electrical systems failure [NTSB-AAR-70-21] 01 p0005 N71-10812
- High voltage breakdown and failure analysis of electronic equipment [AD-711358] 02 p0191 N71-11364
- Failure analysis of electric equipment due to high voltage breakdown [AD-711559] 02 p0193 N71-11354
- Influence of solar illumination on X band antenna voltage breakdown [AD-712023] 02 p0194 N71-11357
- Performance tests and failure analysis of homopolar electric generator [EP-RR-23] 02 p0195 N71-11368
- Algorithm for fault isolation of multistate electronic networks 02 p0196 N71-11377
- Snark circuit analysis handbook [NASA-CR-108721] 03 p0343 N71-12487
- Overcurrent protecting circuit for push-pull transistor amplifiers [NASA-CASE-MSC-12033-1] 04 p0511 N71-13531
- Corona and multipactor discharges, packaging techniques and materials, and voltage breakdown in satellite instruments - conference [NASA-CR-116173] 06 p0825 N71-16631
- Voltage breakdown in spacecraft systems from test and flight experience 06 p0825 N71-16632
- Corona breakdown on antennas in simulated planetary atmospheres and atmospheric processes 06 p0817 N71-16633
- Laboratory testing of breakdown on Nike-Cajun VHF quadrupole antenna 06 p0817 N71-16634
- Circuit and electrode tests of low voltage breakdown in nitrogen, water vapor, and mixtures of nitrogen and water vapor 06 p0825 N71-16637
- Detection of dc voltage breakdown and breakdown processes in space flight environments 06 p0828 N71-16645
- Retrorocket exhaust initiation of conduction in connectors during space separation of boosters 06 p0828 N71-16647
- Failure analysis of breakdown in high voltage transformer of OSO-4 pointed experiment 06 p0828 N71-16648
- Description of manual on prevention of electrical breakdown in spacecraft 06 p0828 N71-16649
- Gas velocity effects on breakdown potential of argon, helium, and nitrogen 06 p0839 N71-16650
- Breakdown in mixtures of carbon dioxide, nitrogen, and argon mixtures simulating possible Mars and Venus atmospheres 06 p0839 N71-16651
- Radio frequency breakdown in 30-cm coaxial transmission lines 06 p0839 N71-16652
- Reduction of gas discharge breakdown thresholds in ionosphere due to multipactoring 06 p0839 N71-16653
- Theoretical analyses and computer calculations of microwave breakdown in resonant plasmas [AD-715259] 07 p1083 N71-17087
- Measurements and analysis of lightning-induced voltage in aircraft electrical circuits [NASA-CR-1744] 08 p1170 N71-19122
- Effects on high temperature microwave antenna breakdown of ionization frequency, collision frequency, diffusion coefficient, and breakdown parameters 10 p1520 N71-21126

- Derivation of minimum test sets for static function logic circuit failure analysis and component reliability [AD-720330] 15 p2389 N71-27288
- Circuit design for failure sensing and protecting low voltage electric generator and power transmission networks [NASA-CASE-GSC-10114-1] 15 p2389 N71-27366
- Frequency response technique for locating electrical faults [AD-721582] 16 p2568 N71-28344
- Vector representation for determining fault element in passive and active networks by external measurements [AD-721581] 16 p2574 N71-28415
- Modified detector unit for underground cable fault locator system [NBS-10354] 17 p2752 N71-29558
- Survey of vacuum insulation with discussion of factors influencing breakdown in high voltage vacuum devices [AD-723107] 17 p2727 N71-30259
- Fault testing of field effect transistor modules [AD-723442] 19 p3070 N71-31825
- Parallel standbys redundancy subject to both open and short circuit failures - extension of branch and bound algorithms [AD-723095] 19 p3067 N71-32471
- Mercury-filled self-healing fuses for protecting solid state circuits from faults - design and development [NASA-CR-72868] 22 p3558 N71-35343
- Digital computer fault detection procedures for combinational logic circuits with algorithms for efficient generation of minimum fault test schedules [AD-726583] 22 p3563 N71-35375
- Design of logic circuit to facilitate electrical fault detection in digital computers [AD-726582] 22 p3563 N71-35376
- Design of snap-3 electrical protective system module including fabrication and assembly drawings [NASA-CR-72938] 24 p3960 N71-38249
- ELECTRICAL GROUNDING**
- Analysis of bonding and grounding measures for minimizing hazards from electrical fault, lightning, explosion, and electromagnetic radiation at KSC - Vol. 1 [NASA-CR-118486] 14 p2328 N71-26598
- On-site evaluation of bonding and grounding of electrical equipment at KSC to minimize hazards from electrical fault, lightning, explosion, and radiation - Vol. 2 [NASA-CR-118482] 14 p2328 N71-26599
- Preventive maintenance instructions for bonding and electrical grounding systems to prevent equipment damage by electrical faults, lightning, and radiation - Vol. 3 [NASA-CR-118481] 14 p2328 N71-26600
- Extension grounding electrodes for grounding electrochemical assemblies under permafrost conditions [AD-722221] 16 p2569 N71-28414
- ELECTRICAL IMPEDANCE**
- NT CONTACT RESISTANCE
- NT ELECTRICAL RESISTANCE
- NT LC CIRCUITS
- NT SKIN RESISTANCE
- Establishment of microwave impedance standards [AD-710002] 01 p0035 N71-10002
- Precise measurement technique for complex voltage reflection coefficients and impedance [AD-710213] 01 p0032 N71-10161
- Experimental study of electrically thick monopole antennas - equipment, admittances, and impedances [AD-710213] 01 p0022 N71-10345
- Kalman and Howitt equivalence transformations [AD-710725] 01 p0033 N71-10533
- Time domain response to impedance for determining electrode reaction kinetics [AD-710945] 01 p0018 N71-10572
- Evaluation of compact, fully enclosed chamber for impedance and power testing of VHF whip antennas during production [AD-711111] 01 p0034 N71-10751
- Integral equations for aperture fields, leading terms in near and far zone fields, admittance, and effective height of annular slot antennas [SC-R-70-4281] 01 p0035 N71-10794
- Characteristic impedance measurement in electronic transformers [AD-711895] 02 p0191 N71-11342
- Superconducting coil for storing energy and restoring it in about one millisecond [LA-TR-70-11] 02 p0286 N71-11924
- Design procedures for compensating phased array antenna elements for impedance changes with scan angle [NASA-CR-102955] 03 p0335 N71-12394
- Polarization/charge separation in metal oxide semiconductor field effect transistor inverters [AD-711895] 03 p0336 N71-12531
- FORTAN program for computing superconductor surface impedance** [NTP-18355] 04 p0604 N71-14490
- Program of measurements related to two phenomena of plasma/antenna interaction [NASA-CR-1727] 05 p0642 N71-14735
- Analysis of negative impedance converter circuit [AD-713161] 05 p0644 N71-14833

- Electrical impedance of cylindrical and monopole antennas 06 p0812 N71-15719
- Microwave mixer diode impedance calculations [AD-714989] 07 p0999 N71-17749
- Design networks having prescribed driving-point impedance in Brune fashion [AD-715334] 07 p0999 N71-17774
- High voltage transistor circuit [NASA-CASE-XNP-00937] 09 p1358 N71-19516
- Development of electrical system for measuring high impedance [NASA-CASE-XMS-00859-1] 09 p1361 N71-20569
- Impedance behavior of short cylindrical antenna used as diagnostic probe in isotropic and magnetized plasmas 10 p1519 N71-21105
- Shock tube measurements of admittance of RAM C-2 and RAM C-3 diagnostic antenna admittance to analyze accuracy of calculated electron density 10 p1519 N71-21110
- Characteristics of mutual electromagnetic coupling of loops over homogeneous ground determined by employing image theory [AD-717351] 11 p1723 N71-22144
- Impedance and radiation properties of ground wire antennas analyzed using transmission line theory [AD-717692] 11 p1724 N71-22657
- Impedance and radiation properties of mesh antennas immersed in warm isotropic plasmas 12 p1890 N71-22664
- Boundary value problem for impedance evaluation between coupled electrically thick folded dipoles 12 p1894 N71-24032
- Performance of impedance cardiograph for measuring heart rate and body fluids [NASA-CR-114988] 12 p1864 N71-24173
- Signaling summary alarm circuit with semiconductor switch for faulty contact indications [NASA-CASE-XLE-03061-1] 13 p2039 N71-24798
- Magnetohydrodynamic generator systems analysis including electrical impedance and power conversion efficiency calculations for various designs 14 p2323 N71-26449
- Quadrupole plasma probe simulator for simulation of transfer impedance in ionospheric plasmas [GRI/NTP-78] 15 p2407 N71-26999
- Determination of dipole antenna electrical impedance in anisotropic media noting charge distribution on radio frequency impedance probe surface 15 p2453 N71-27050
- Input impedance of aperture radiating into warm overdense plasma [AD-723299] 19 p3163 N71-31678
- Mathematical analysis of apparent admittance of coaxially driven infinite monopole [AD-723650] 19 p3163 N71-31712
- Antenna parameters and input admittance from numerical analysis of radiation fields of slotted circular disks 19 p3071 N71-32288
- Computer program for predicting admittances of slowly converging nozzles and acoustic liners in three dimensional acoustic field [NASA-CR-119941] 22 p3567 N71-35405
- Effects of plasma compressibility, collision frequency, and sheath on antenna current, input impedance, and maximum driving voltage 23 p3832 N71-37331
- Inductive gratings for compensating dielectric cylinder effects on mounted aerial [RA-87] 24 p3891 N71-37752
- Synthesis procedure for developing arbitrary rational admittance matrices using operational amplifiers and RC one ports 24 p3901 N71-37809
- Formulas, tables, and graphs for calculation of electrical capacitance [AD-727198] 24 p3968 N71-38304
- ELECTRICAL INSULATION**
- Theoretical evaluation of electrical insulation lifetime, noting influence of voltage and frequency using Weibull theory 02 p0246 N71-11588
- Using coupled theory of linearized thermoelasticity and integral transform techniques to solve problem of nonconducting half-space subjected to transient radiation [SC-RR-70-428] 03 p0440 N71-12672
- Low-level corona detection in insulation systems resulting from step voltages across voids in insulation 06 p0861 N71-16644
- Method and apparatus for removing plastic insulation from wire using cryogenic equipment [NASA-CASE-MFS-10340] 07 p1035 N71-17628
- Combustion properties of Teflon insulated wires in supercritical oxygen at normal and zero gravities [NASA-TM-X-2174] 07 p1130 N71-17896
- Electrical insulation protection in printed circuits under varying temperature and humidity conditions [ECR-14] 10 p1531 N71-20691
- Partial electric discharge influence on durability of polyethylene, Mylar, and Teflon insulating materials 10 p1532 N71-20801

- Nonconductive tube as feed system for plasma thruster [NASA-CASE-XLE-02902] 10 p1630 N71-21004
- Physical property of thin films and glassy state - insulator-metal transition theory [AD-717386] 11 p1815 N71-21910
- Radiation induced noise measurements in pulsed TRIGA reactor and proportionality to induced neutron conductivity in signal cables [WRAN-IR-82] 12 p1963 N71-24061
- Internal labyrinth and shield structure to improve electrical isolation of propellant feed source from jet thruster [NASA-CASE-LEW-10210-1] 14 p2333 N71-20708
- Steady state radiation effects on electrical insulating materials and capacitors - handbook [NASA-CR-1787] 17 p2726 N71-20708
- Semiconductors and semiconductor devices, insulating and semiconducting glasses, and measurement techniques [AD-722474] 17 p2816 N71-20808
- Survey of vacuum insulation with discussion of factors influencing breakdown in high voltage vacuum devices [AD-723107] 17 p2727 N71-30259
- Thermocouple tape of two thermoelectrically different metals applied to strip of electrical insulator [NASA-CASE-LEW-11072-1] 18 p2924 N71-31125
- Utilizing vacuum insulation for devices with synaptic cores and windings [NASA-CASE-LEW-10330-1] 18 p2998 N71-31115
- Correction curves for humidity effects on flashover voltages in spark gaps [NLL-CE-TRANS-5367-9022.09] 19 p3068 N71-32708
- Effects of fast neutrons on polycrystalline alumina electrical insulators used in thermionic converter at high temperatures 21 p3444 N71-3408
- Effect of leakage currents to ground in tubular generator with constant gas parameters and constant channel cross section [INR-1242] 21 p3493 N71-34084
- Differences, simulations, and interrelationships between insulation resistance and dielectric strength testing [AD-726924] 22 p3561 N71-35346
- Resistivity measurements of refractory oxide insulators using four-probe technique [NEDL-SA-119] 22 p3602 N71-35021
- ELECTRICAL LEADS**
- U ELECTRIC CONDUCTORS**
- ELECTRICAL MEASUREMENT**
- NT COULOMETRY**
- NT POLAROGRAPHY**
- Precise measurement technique for complex voltage reflection coefficients and impedance 01 p0032 N71-10161
- Lightning induced voltages in aircraft electrical circuits [NASA-TM-X-52906] 01 p0004 N71-10161
- Dead space characteristics method for potentiometer evaluation [AD-710947] 01 p0003 N71-10164
- Bootstrap unloading circuits for sampling transducer voltage sources without drawing current [NASA-CASE-XNP-09768] 03 p0349 N71-12516
- Development and testing of meter for measuring watt-hours and ampere-hours over wide range of voltages and currents [NASA-CR-115797] 04 p0510 N71-13320
- Micromicroampere current measuring circuit, with two subminiature thermionic diodes with filament cathodes [NASA-CASE-XNP-00384] 04 p0511 N71-13319
- Investigating development of techniques for measuring electrical quantities in high frequency and microwave ranges [FOA-3-C-3599-68] 05 p0654 N71-14751
- Testing of electrical detection system adaptable to spark source mass spectrometer [IS-TRANS-82] 06 p0858 N71-15981
- Low impedance apparatus for measuring electrostatic field intensity near space vehicles [NASA-CASE-XLE-00828] 06 p0858 N71-15984
- Apparatus for dc electrical measurement of Hall and photo-Hall effects in high resistivity semiconductor 09 p1387 N71-19408
- Electric current measuring apparatus design including saturable core transformer and energy storage device to avoid magnetizing current errors from transformer output winding [NASA-CASE-XGS-02439] 09 p1387 N71-19408
- Electric and magnetic field measurements in cathode region of quasi-steady magnetoplasma dynamic arcjet 09 p1448 N71-19408
- High voltage divider system for attenuating high voltages to convenient levels suitable for introduction to measuring circuits [NASA-CASE-XLE-02008] 10 p1535 N71-21280
- Ablation sensor for measuring char layer recession rate using electric wires [NASA-CASE-XLA-01794] 10 p1663 N71-21356

SUBJECT INDEX

ELECTRICAL PROPERTIES

Influence of thermal treatments on dielectric properties of lithium-aluminum-silica glasses using electric measurements and X ray and electron microscopy techniques

11 p1783 N71-22344

Electrical resistance measurements and stability of high temperature resistance thermometers

11 p1783 N71-22399

Current measurement by use of Hall effect generator

[NASA-CASE-XAC-01662] 11 p1766 N71-23037

Connector internal force gaps for measuring strength of electrical connection

[NASA-CASE-XNP-03918] 11 p1767 N71-23087

Automated system for cost reduction in calibrating bolometer mounts by cutting power measurement time

12 p1919 N71-23632

Electrical standards of Japan, dissemination, and traceability and measuring techniques

12 p2018 N71-23630

Design and performance of inductive voltage divider for measuring alternating current ratios

[NLL-MIN-TBCH-T-6763-5809.95] 12 p1891 N71-24163

NBS activities in developing methods of measurement for semiconductor materials, process control, and devices

[NASA-CR-118271] 13 p2151 N71-24975

Electrical property measurements on bulk silicon samples and lithium-doped solar cells

14 p2201 N71-26230

Voltage range selection apparatus for sensing and applying voltages to electronic instruments without having signal source

[NASA-CASE-XMS-06497] 14 p2255 N71-26244

Dielectric property measurements for pressure induced phase transformations in solid and liquid insulators

14 p2328 N71-26593

Electrical and optical measurement of optoelectric devices before and after submission to X ray irradiation

[JNMI-B-97] 14 p2315 N71-26741

Apparatus for measurements on superconducting short samples in fields to 52 kOe and currents to 3500 A

[JPP-4/71] 15 p2498 N71-27193

Electron irradiation effects in a-type, p-type, and high-purity silicon at 5.0 and 1.6 K using a hopping conductivity

[CDO-1196-781] 16 p2667 N71-28838

Design and performance of galvanovoltammetric detector with digital readout for electric current flow measurements

17 p2753 N71-29886

Electric eddy current probe for nondestructive crack detection in tubes

[AD-720958] 18 p2923 N71-30723

Eddy current measurements using coil encircling coaxial two-conductor rod and solution of electromagnetic induction problem

[I-1787] 19 p3071 N71-32327

Computer controlled electrical measuring devices for thermoelectric generator of power plant

[AD-72461] 24 p3925 N71-38010

Tuning and photovoltaic methods and identification of test conditions for measurement of semiconductor materials, process control, and devices

[NASA-CR-123167] 24 p3996 N71-38504

ELECTRICAL PROPERTIES

NT CAPACITANCE
NT CARRIER MOBILITY
NT CHARGE DISTRIBUTION
NT CONTACT RESISTANCE
NT DIELECTRIC PROPERTIES
NT DIELECTRIC MOMENTS
NT ELECTRICAL IMPEDANCE
NT ELECTRICAL RESISTANCE
NT ELECTRICAL RESISTIVITY
NT ELECTRON MOBILITY
NT ELECTRIFICATION
NT FERROELECTRICITY
NT HOLE MOBILITY
NT INDUCTANCE
NT IONOSPHERIC CONDUCTIVITY
NT LC CIRCUITS
NT MAGNETORESISTIVITY
NT PHOTOCONDUCTIVITY
NT PHOTOVOLTAIC EFFECT
NT PYROELECTRICITY
NT PLASMA CONDUCTIVITY
NT POLARIZATION CHARACTERISTICS
NT PYROELECTRICITY
NT SKIN RESISTANCE
NT SUPERCONDUCTIVITY

Steady-state characteristics of voltage regulator and automatic speed controller on 14.3-kilovolt-ampere, 120-Hz modified Lundell alternator

[NASA-TN-D-5924] 01 p0006 N71-10059

Electrical properties of single crystals of Praseodymium

01 p0169 N71-10143

Preparation and properties of iron phosphides

[AD-716077] 01 p0018 N71-10469

Properties of thin nitride films of hard superconductors

[AD-710900] 01 p0112 N71-10917

Analysis of ranging system for lunar surface electrical properties experiment

[NASA-CR-108673] 02 p0177 N71-11244

Electrical properties of sedimentary rock under hydrostatic pressure

[NASA-TT-F-13215] 02 p0210 N71-11451

Frequency dependence of electrical properties of igneous rocks from Kola Peninsula

[NASA-TT-F-13216] 02 p0210 N71-11498

Conference on atomic transport in solids and liquids

[AD-71418] 02 p0284 N71-11840

Electrical properties of quartz as related to impurities and electrolytic coloring

02 p0287 N71-12008

Properties of carbon fibers

[RAE-LIB-TRANS-1417] 02 p0249 N71-12191

Effects of diffusion redistribution of phosphorus on characteristics of silicon solar cells

[NASA-TM-X-2142] 03 p0318 N71-12271

Reflection coefficient, radiation pattern, gain, and efficiency of X band cavity resonators

03 p0336 N71-12401

Characteristics of oversize circular waveguides and transitions at 3-millimeter wavelengths

[AD-712378] 03 p0338 N71-12410

Electrical properties of solid state materials and devices

[AD-711948] 03 p0441 N71-12834

Facilities for testing linear antenna electrical properties in infinite, homogeneous, isotropic, dissipative medium

[NASA-CR-115817] 04 p0488 N71-13476

Computer aided analysis of receiving and transmitting properties of thin wire circular loop antenna

[SC-RR-70-435] 04 p0511 N71-13534

Development and characteristics of electron beam sources

[JAERI-1190] 04 p0516 N71-13806

Electrical properties of copper fluoride/lithium hexafluoroarsenate in methyl formate/lithium high energy primary batteries

[NASA-CR-72776] 05 p0632 N71-14947

Initial research on electrical and metallurgical properties of amorphous semiconductors

[AD-713483] 05 p0738 N71-15345

Current-voltage characteristics of continuum fluorescent mounted electrostatic probes in presence of negative ions

[SC-RR-70-413A] 06 p0857 N71-15852

Defects and their role in determining luminescence and electrical properties of crystals

[AD-714620] 06 p0933 N71-16017

Electrical properties of noncrystalline materials

[AD-713940] 06 p0934 N71-16302

Useful mechanical, electrical, and acoustic properties of Soulas

[AD-714229] 06 p0878 N71-16362

Electrical and optical properties of amorphous materials

[AD-714029] 06 p0936 N71-16473

Electrical performance of three solar thermoelectric test sections

[NASA-TM-X-2175] 07 p0975 N71-17252

Mechanical and electrical design of actuator for SERT 2 spacecraft

[NASA-TM-X-2190] 07 p0976 N71-17865

Proton irradiation effects on electrical properties of a and p silicon and germanium

[NS-18474] 08 p1277 N71-18506

Electrical and mechanical characteristics of solar cell contacts after exposure to high-temperature high-humidity environments

[NASA-CR-116805] 08 p1146 N71-18563

Electrical characteristics of discharge in hollow cathode in neon

[NRC-TT-1437] 08 p1170 N71-18858

Reduced scattering in multimode scattering waveguides

08 p1172 N71-18870

Technology review on capacitors

[AD-715522] 09 p1358 N71-19577

Voltage drift compensation circuit for analog-to-digital converter

[NASA-CASE-XNP-04700] 09 p1353 N71-19487

Thermal and elastic properties of polymers, and electronic properties of glasses and metals

09 p1404 N71-19730

Optical and radio frequency electrical properties and grain size analyses of Apollo 11 and 12 lunar soil samples

[NASA-CR-114893] 09 p1463 N71-19784

High temperature stability and electrical properties of polyethylene based capacitors

[NASA-CR-1799] 09 p1326 N71-20186

Crystal growth and galvanomagnetic properties of MgZnO

09 p1454 N71-20438

Mechanical, electrical, and optical properties, crystal defects, magnetism, thermodynamics, and piezoelectricity of solids

[NASA-CR-117401] 10 p1632 N71-20828

Surface finishing effects on ceramic mechanical, electrical, optical, and magnetic properties

[AD-716066] 10 p1563 N71-21221

Morphology and capacity of cadmium electrodes on repeated charge and discharge

[NASA-CR-77777] 10 p1535 N71-21329

Characteristics of self-powered, multichannel digital data buffer designed to expand input capability of electronic scope processor

[NASA-CR-114923] 10 p1529 N71-21463

Microstructure and electrical properties of thin epitaxial films of lead telluride and effects of microstructure on electrical properties

11 p1815 N71-22182

Dynamic electrical characteristics of 400 Hz Brayton cycle turboalternator and controls for space application

[NASA-TN-D-4185] 11 p1677 N71-22364

Phase changes in signal received on earth surface and transmitted from antenna placed into deep excavation

11 p1706 N71-22925

Electric ground property effects on radio navigation system operations on earth surface

11 p1708 N71-22926

Climatological ground effects on subsurface radio wave propagation

11 p1708 N71-22927

Characteristics of particle interactions with surfaces of semiconductors and semimetals

[AD-717960] 12 p1984 N71-23272

Feasibility of producing thin metal and oxide-film capacitors with stable electrical properties in high temperature environments

[NASA-CR-72779] 12 p1891 N71-23983

Kinetic theory for analysis on electrostatic probe properties in stationary quiescent plasma

12 p1983 N71-24369

Design and electrical properties of methanol/air battery cells operating at low current density

[AD-719239] 13 p2029 N71-24377

Band structure and electrical properties of amorphous semiconductors

[AD-716795] 13 p2158 N71-24382

Investigation of techniques to improve performance and service life of nickel-silver electric batteries for application to low pollutant propulsion systems

[NASA-TM-X-67812] 13 p2025 N71-24617

Analysis of microwave reflection and cavity methods for measuring properties of semiconductor materials

[AD-719809] 13 p2151 N71-24881

NBS activities in developing methods of measurement for semiconductor materials, process control, and devices

[NASA-CR-118271] 13 p2151 N71-24975

Thermoluminescent current investigation of electrical properties of sublimated zinc sulfide electroluminescent films

[AD-719704] 13 p2153 N71-25487

Empirical pseudopotential method for exploring electronic structure and dielectric properties of face-centered cubic semiconductors

[UCRL-26577] 13 p2153 N71-25488

Simulation and measurement of electrical properties of lightning discharge by use of long sparks produced under laboratory conditions

[FAA-DS-69-16] 14 p2287 N71-25823

Measurement of peak radiant power and total radiant energy emitted within given spectral region by single stroke lightning flash and comparison with energy of long spark

[NASA-TM-X-67182] 14 p2287 N71-25827

Investigating electrical properties of bulk semiconductor materials for application as millimeter and sub-millimeter wave detectors

[NASA-CR-118507] 14 p2325 N71-26030

Diffusion techniques for lithium-diffused silicon solar cells and cell electrical properties

14 p2201 N71-26227

Lithium-doped solar cell fabrication techniques, and statistical analysis of electrical output

14 p2202 N71-26237

Subthreshold electron irradiation effects on surface and bulk electrical properties of Li-doped and Li-free silicon photovoltaic cells

14 p2202 N71-26237

Reaction kinetics model for electrical behavior of Li-doped Li-doped solar cells

14 p2203 N71-26239

Volt-ampere characteristics of deposited thin film gold-cadmium sulfide-insulator structures at power levels less than 500 microwatts and temperatures of 200 degrees Kelvin

14 p2339 N71-26633

Development and characteristics of electronically reactable fuses with selectable core current sensing transfer arm having two outside legs and center leg

[NASA-CASE-XGS-11177] 15 p2385 N71-27001

Development and characteristics of voltage regulator for connection in series with alternating current source and load using three leg, two-window transformer

[NASA-CASE-ERC-10113] 15 p2386 N71-27053

Development of system with electrical properties which vary with changes in temperature for use with feedback loop in operational amplifier circuit [NASA-CASE-MSC-13276-1] 15 p2487 N71-27058

Numerical calculations of electrical parameters in Faraday-type MHD generator with two dimensional gas flow [DNR-11199] 15 p2393 N71-27207

Synthesis and investigation of nonequilibrium compounds with semiconductor-metal transition [AD-720888] 15 p2506 N71-27277

Quantum theory of magnetic materials including magnetic, electric, and optical properties [AD-720801] 15 p2453 N71-27371

Electrical resistivity, Hall coefficient, and reflectivity measurements of single crystals of lead-telluride semiconducting alloys 15 p2507 N71-27369

Electrical properties and photoconductivity of semiconducting ferromagnetic cadmium chromium selenides [AD-720670] 15 p2510 N71-27936

Earth subsurface electromagnetic field disturbances due to subsurface rock electrical properties 16 p2535 N71-28268

Structure of electric double layer at solid metal solution interfaces [AD-721718] 16 p2557 N71-28353

Transient measurements of field effect transistors following exposure to pulse of neutrons and observations of transient annealing of drain to source resistance in n- and p-channels [AD-721743] 16 p2569 N71-28406

Thermal deposition and electrical properties of silicon dioxide passivity layers on silicon wafers in oxygen and nitrogen dry atmospheres and effects of moisture and impurities [AD-721377] 16 p2570 N71-28594

Electrical properties of silicon nitride-gallium arsenide interface 16 p2667 N71-28794

Analysis of electrical and elastic properties of sedimentary rocks to obtain velocity profiles of electroforming samples [NASA-TT-F-13706] 16 p2591 N71-28973

Characteristics of simultaneous electronics and ionic conductivity in solids at 700 to 800 C [NLL-L-T-746-617-9022.401/] 16 p2669 N71-29158

Open circuit sensitivity of radially polarized ferroelectric ceramic hollow spheres treating ceramic as anisotropic material [AD-722401] 17 p2726 N71-29732

Electrical and magnetic properties of potassium molybdenum bronzes 17 p2765 N71-29850

Magnitude of induced voltages and their relation to characteristics of lightning discharge and electrical properties of aircraft electrical systems 18 p2869 N71-30761

Hyperfine interactions in research fields including perturbed angular correlation, NMR, Coulomb recoil implantation, rotational states, and electric monopoles - lectures [NIP-18702] 19 p3157 N71-32478

Epitaxial crystal growth for manufacturing electronic equipment and components including crystal defects and electrical properties of crystallized layers [NLL-FOBS-TRANS-2690-9022.81/] 19 p3171 N71-32534

Physical and electrical characteristics for high energy density, sealed, nickel cadmium battery assembly [AD-722978] 20 p3213 N71-33192

Mechanical models for thermal and electrical properties of bipolar transistors and effects of fabrication processes 20 p3241 N71-33420

Electrical properties determined for zinc- and tellurium-doped single crystal gallium phosphide using Van der Pauw method 20 p3334 N71-33422 [AD-724600]

Mechanical and electrical characteristics of sili- amon used to measure quasi-omnidirectional radiation pattern from vehicle in 2300 MHz range [TP-549] 20 p3325 N71-33710

Determination of superconductive properties of ex- ionic insulator by simple two-band model based on Meissner effect 20 p3236 N71-33802

Operational functions and electrical properties of metal oxide semiconductor structures [EPT-1-628] 20 p3335 N71-33848

Acceptance tests of 100 ampere-hour nickel-cadmium cells for inclusion in life cycle program of secondary spacecraft cells [NASA-CR-121618] 21 p3378 N71-34035

Electrically coupled individually encapsulated solar cell matrix [NASA-CASE-MPO-11190] 21 p3379 N71-34044

Electrophysical properties and structure of chemical bonds in boron, carbon, and very thin compounds [LA-TR-71-30] 21 p3386 N71-34091

Electrical properties of metallic layers implanted in amorphous oxide glass 21 p3405 N71-34228 [NASA-CR-111953]

Analysis of internal inductances in current carrying circular conductors in relation to outer inductance for unit and parallel representation of inductances [NLL-EE-TRANS-1931-3774.51] 21 p3406 N71-34235

High-purity tungsten lattice thermal conductivity measurements at low temperatures by magnetic field suppression of electronic thermal conductivity [NYO-2150-69] 21 p3498 N71-34921

Osmium dioxide single crystal growth and electrical transport measurements, and analyses of osmium tetroxide and hypophosphorus acid reaction product 21 p3499 N71-34930

Design and development of top-wall and branch waveguide hybrids for millimeter wavelengths and measurement of electrical characteristics [AD-726538] 22 p3560 N71-35358

Internal conversion processes for electric quadrupole transitions in deformed nuclear region 22 p3649 N71-36024

Electrical transport properties and quantum size effect oscillations in thin bismuth films 22 p3659 N71-36092

Operational characteristics of low powered klystron oscillators in three-centimeter range and in pulse mode [AD-724311] 23 p3732 N71-36606

Development of theory, conversion factors, and operating procedures for determining hybrid parameters of transistors by measuring scattering parameters [BDX-613-347] 23 p3737 N71-36647

Development and characteristics of bipolar electric battery with high power density silver oxide-zinc liquid electrode [AD-727126] 24 p3875 N71-37626

EB-44 computer-controlled test system for measuring electrical properties of test equipment [SC-DR-70-862] 24 p3892 N71-37740

Electrical and magnetic properties of palladium base amorphous alloys containing small concentrations of transition metals 24 p3901 N71-37807

Analysis of electrical and optical properties of vanadium oxide crystals at semiconductor-metal transition temperature [AD-727242] 24 p3997 N71-38513

ELECTRICAL RESISTANCE

NT CONTACT RESISTANCE

NT LC CIRCUITS

NT SKIN RESISTANCE

Use of heat pipes for electrical isolation

[NASA-TM-X-52928] 01 p0134 N71-10965

Measuring electrical resistance of rocks and minerals for predicting potential earthquake centers

[NASA-TT-F-13212] 02 p0209 N71-11434

Electrical resistance, magnetic coercivity, and mechanical property measurement for investigation of structural changes in steels under creep test

03 p0467 N71-13553

Electrical resistance strain gages using Armour D alloy in LMFBR program

[LMC-70-4] 05 p0683 N71-14837

Electrode geometry effects on series resistance in ac polarography

[AD-714235] 06 p0810 N71-16423

Influence of lattice vacancies and impurities on electrical resistivity of noble metals

[AD-714678] 06 p0937 N71-16700

Calculating correction factors for spreading resistance probe measurements on n-p/positive-p structure

07 p1088 N71-17288

Loading effects due to input and output resistances of individual transistors in distributed amplifiers

08 p1170 N71-18991

Measured and calculated electrical resistance changes in shock compressed aluminum

[AD-716328] 09 p1399 N71-19871

Electronic properties of dilute alloys including magnetic permeability, electrical resistance, and ferromagnetism

[AD-716607] 09 p1453 N71-20008

Vaporization of magnesium impurities from high purity aluminum melt in vacuum apparatus reduces electrical resistance of aluminum

10 p1575 N71-20882

Techniques for establishing true scales for high pressure measurement based on changes in electrical resistance

[LA-TR-70-26] 10 p1579 N71-21253

Application of sub-order metric space to resistive network analysis

11 p1727 N71-21947

Electrical resistance measurements and stability of high temperature resistance thermometers

11 p1763 N71-22599

Heat flux sensors based on thermistors in doped polycrystalline ceramics such as boron oxoboron titanate showing ferroelectric resistance anomaly

11 p1764 N71-22746

Error analysis of in-pile thermal conductivity and gap conductance measurements with balanced oscillators in experimental breeder reactor 2

[EURFNR-755] 15 p3450 N71-27631

Type II super conductor research on conduction of Nb-Cu and NbTi-Cu junctions, and vortex flow in weak pinning Bi II [UCLA-ENG-7109] 16 p2638 N71-28144

Thermal models investigated for upper limits on lunar radioactivity consistent with temperature distribution based on electrical conductivity of lunar interior [NASA-CR-118992] 16 p2678 N71-28154

Two-line transmission line terminated at both ends by resistors investigated for signal dependence on the slant conductance and termination [UCRL-50991] 17 p2724 N71-29218

Magnetic field level effects on silicon superconductor surface resistance [NIP-18742] 18 p2961 N71-30077

Piezoresistance of ytterbium along Hugoniot calculated from Hugoniot state temperatures and geometrical effect of phase strain on resistance [UCRL-51005] 18 p2966 N71-31511

Phase decomposition in liquid-quenched aluminum-silicon alloys and determination of changes in electrical resistance 19 p3116 N71-33638

Calculating electrical resistance of rutile crystal from dielectric loss data [AD-724311] 20 p3332 N71-32928

Measurement of electrical resistance, electron microscopy, and low temperature heat capacity of liquid gases in metals [COO-1799-6] 21 p3440 N71-34676

Electrical resistance, Hall constants and absolute thermopower of disordered series of solid solutions of nickel with elements of first long period [NRC-TT-1477] 22 p3593 N71-35383

ELECTRICAL RESISTIVITY

NT IONOSPHERIC CONDUCTIVITY

NT MAGNETORESISTIVITY

NT PHOTOCONDUCTIVITY

NT PLASMA CONDUCTIVITY

NT SUPERCONDUCTIVITY

Electron processes for characterizing weakly fluorescent and near-insulating solids 01 p0107 N71-10882

Electrical resistivity and Hall coefficient measurements of semiconductor materials 01 p0109 N71-10204

Electrical conductivity of igneous rocks of Koh Peninsula at high temperature based on dc transmission

[NASA-TT-F-13214] 02 p0210 N71-11440

Electrical conductivity of Karakhan rocks at high temperatures

[NASA-TT-F-13213] 02 p0213 N71-11604

Direct current conductivity in turbulent cylindrical discharge-tube plasma

[ORNL-TM-3038] 02 p0281 N71-11882

Conduction mechanisms in high quality GaAs studied by measuring resistivity and Hall constant

[AD-712064] 02 p0287 N71-12151

Electrical conductivity measurements through carbon on metal/carbon/metal thin films of sandwich structure

[AD-712073] 03 p0441 N71-12835

Electrical and thermal properties of impure single crystals of superconductors

[AD-712411] 03 p0442 N71-12988

Electrical resistivity of rectifying semiconductor antimony-antimony selenide diffusion junction

[AD-712941] 05 p0444 N71-13177

Neutron dosimeter study based on electrical resistivity changes - tungsten dosimeter

[CEA-N-1288] 04 p0573 N71-13651

Ionic density in sea water salinity determination from electrical conductivity measurements

04 p0521 N71-13723

Electrical resistivity of platinum thin films for shock tube surface temperature data

[ONERA-NT-168] 04 p0516 N71-13881

High temperature electrical resistivity of refractory aluminum oxides

[BNWL-1458] 04 p0533 N71-13990

Temperature and pressure dependence of optical and electrical gap in chalcogenide glasses

[AD-713288] 05 p0757 N71-14639

Plastic deformation of silver iodide related to electrical conductivity

[TT-70-57019] 05 p0757 N71-14774

Investigating effects of shock waves on valium materials

[UCRL-71846] 05 p0773 N71-15812

Measuring superconductivity and magnetic order above and below Kondo temperature for La-Cu system

[IS-T-405] 05 p0733 N71-15838

Measuring electrical resistance and pressure behavior of actinide elements

[POA-4-C-4434-23] 05 p0701 N71-15880

Investigating phase equilibria, electrical conductance, and density in system ZnCl₂ at low temperature analog of BiO₂ and BiF₃ systems

[COO-2086-2] 05 p0711 N71-15904

Electrical conductivity of single crystal cerium iodide as function of temperature and oxygen pressure

[COO-1441-11] 06 p0932 N71-15989

SUBJECT INDEX

ELECTRICITY

Defect structure of nonstoichiometric cesium oxide
[COO-141-12] 06 p0932 N71-16004

Single crystal high resistivity cadmium telluride for use as gamma-ray spectrometer
[AN-349-6] 06 p0933 N71-16016

Investigating ferromagnetic insulators, alloys, and magnetic insulators with respect to transport theory
[AD-714096] 06 p0904 N71-16211

Time and temperature dependence of thermoelectric properties of Si-Ge alloys
[NASA-CR-116221] 06 p0899 N71-16665

Magnetic properties and electrical resistivity of transition metal oxide glasses
[COO-1700-17] 06 p0883 N71-16827

Lunar surface magnetometer measurements for determining electrical conductivity and temperature of lunar core
[NASA-TM-X-62012] 06 p0949 N71-16862

Low temperature electrical resistivity
[PS-195154] 07 p1132 N71-17043

Measuring incremental sheet resistivity for determining impurity distribution in silicon after diffusion
[AD-71088] 07 p1088 N71-17289

Use and limitations of spreading resistance techniques for evaluating buried collector layer structures in integrated circuits
[AD-71090] 07 p1090 N71-17301

Considering variations of C-V techniques for determining impurity profiles in p-n junctions
[AD-71090] 07 p1090 N71-17302

Methods for determining characteristics of bulk silicon used in production of semiconductor devices
[AD-71091] 07 p1091 N71-17311

Thermal conductivity and electrical resistivity of materials for NERVA engine - Vol. 3
[NASA-CR-116519] 07 p1083 N71-17352

Measuring conductivity, freezing point, and vapor pressure characteristics of halide salts for battery technology
[NASA-CR-72791] 07 p0976 N71-17703

Describing method for vapor deposition of gallium arsenide films to manganese substrates to provide semiconductor devices with low resistance substrates
[NASA-CASB-XNP-01328] 07 p1096 N71-18064

Simulating operation of thermopile vacuum gauge tube at high and low pressures
[NASA-CASB-XLA-02758] 06 p1200 N71-18481

Electrical resistivity and Hall effect in phosphorus doped and aluminum compensated n-type silicon etched by conduction bands
[JONERA-DERTS-NT-02-17] 06 p1171 N71-18582

Electronic structure conduction mechanism in random lattices
[AD-715922] 06 p1278 N71-18678

Expressions for electrical conductivity of plasmas applied to equilibrium air at 3000 to 28,000 K
[NASA-TN-D-5977] 06 p1273 N71-18715

Measuring changes in electrical resistivity and thermoelectric power of quenched high purity platinum and Pt 10 percent Rh thermocouples
[NRC-TT-1429] 06 p1304 N71-18813

Calculating effects of relaxation field and electrochromism to derive conductance of mixed strong electrolytes at finite concentrations
[AD-71600] 06 p1160 N71-18992

Electrical conductivity and elastic moduli of pressure-treated lithium substituted nickel oxide alloys
[AD-71612] 06 p1216 N71-19002

Long term radiation induced conductivity in polyethylene terephthalate
[AD-71616] 06 p1161 N71-19112

Thermal and electrical conductivities of gold ion alloys at low temperatures
[AD-71630] 09 p1398 N71-19734

Acceptance tests including capacity, cell short, high vacuum leak, overcharge, and internal resistance of silver-cadmium secondary cells with nickel bronze ceramic seals for spacecraft
[NASA-CR-117318] 09 p1327 N71-20325

N-type germanium electrical resistivity in high intensity electric fields
[JLAB-AB-118] 10 p1531 N71-20798

Electrical resistivity versus temperature measurements on magnetic amorphous alloys
[CALT-822-38] 10 p1583 N71-21382

Research in ferromagnetism, phase transitions, and electrical conductivity
[AD-71758] 11 p1748 N71-22297

Electrical conductance and physical properties of polymers
[AD-71758] 11 p1696 N71-22439

Mixed conduction in NaCl-TiCl₄/ fused salt systems and tracer techniques for determination of diffusion solubility in solid electrolytes
[COO-1400-21] 11 p1817 N71-22500

Biactive resistivity switching properties of semiconductor glass As₂-Te₂-Ge
[AD-71807] 11 p1817 N71-22884

Optical luminescence in reaction detection at rear of power electrodes and comparison of interface reaction resistance and electrolyte ohmic resistance in zinc-air oxide batteries
[NASA-CR-118007] 12 p1860 N71-23518

Feasibility of mapping variation in rock strength on basis of electrical conductivities measured by airborne equipment
[AD-718438] 12 p1907 N71-23522

Radiation induced noise measurements in pulsed TRIGA reactor and proportionality to induced insulator conductivity in signal cables
[WHAN-IR-42] 12 p1963 N71-24054

Determination of lunar electrical conductivity profile from joint power spectral density analysis of data from Apollo 12 and Explorer 35 magnetometer data
[NASA-TM-X-62019] 12 p1997 N71-24146

Low temperature measurements on electrical resistivity, magnetic susceptibility and magnetoresistivity for amorphous iron palladium silicon alloys
[CALT-822-24] 13 p2096 N71-25515

Changes in elasticity, magnetostriction, and electric resistance of iron-aluminum alloys during ordering
[DMDC-5793] 14 p2271 N71-25692

Mathematical models for determining electrical conductance in cornet films
[AD-72234] 14 p2234 N71-26435

Induced polarization and resistivity surveys on Clear Summit, Alaska
[AD-72252] 14 p2252 N71-26468

Electrical conductivity effect on low pressure plasma equilibrium in stellarator
[MPPA-762] 15 p2503 N71-27917

Phenomena occurring during magnetic flux compression by implosion of this conducting liner
[CEA-R-4824] 15 p2456 N71-27974

Neutron irradiation of samples in swimming pool reactor and measurement of their electrical resistance using sandstone oven
[IEA-212] 16 p2663 N71-28029

Sampling and linear filter theory for direct interpretation of geoelectrical resistivity measurements
[AD-72846] 16 p2585 N71-28246

Electromagnetic shielding effectiveness degradation from weld defects in metal conducting sheets and corners of propagation through rectangular and circular apertures
[AD-721907] 16 p2560 N71-28410

Effect of various impurities in ppm range on electrical conductivity of organic coolant liquids
[EUC-4597-E] 16 p2631 N71-28564

Ferroelectricity and conduction in ferroelectric crystals
[AD-721479] 16 p2666 N71-28736

Anomalous high frequency resistivity and heating of plasmas by laser irradiation
[MATT-817] 17 p2812 N71-29630

Search for active interactions and measurements of resistivity tensor in superconducting insulator
[AD-72788] 17 p2788 N71-29703

Oxygen partial pressure and temperature effects on sintered nonstoichiometric BaTiO₃ crystal electrical resistivity with heat of formation, electron mobility, and oxygen vacancy values
[AD-72769] 17 p2769 N71-29706

Difficulties in studying chromel-sheathed thermocouples as temperature sensors
[NLL-RISLEY-TRANS-1942-9091.9F] 17 p2752 N71-29800

Steady state electromagnetic interaction of solar wind with planet Mercury computed for spectrum of electrical conductivity
[NASA-TM-X-62028] 17 p2841 N71-29923

Formulas for calculating conductivity and dielectric constants of capacitors made up of composite bodies extended to more than two components
[NASA-TT-F-15725] 17 p2727 N71-30244

Magnetic modulation spectroscopy for studying microwave surface impedance of lead films
[ISS-706] 18 p2994 N71-30472

Resistivity minimum in ferromagnets with approximate calculation of electron-magnon interaction contribution to temperature dependence of electrical resistivity
[CALT-822-25] 18 p2961 N71-30537

Linear response fluctuation criteria of superconductor to static magnetic field
[ISS-701] 18 p2961 N71-30635

Differential thermal and electrical conductivity studies of phase transitions in Li₂/V₂O₅, single crystals of WO₃ and WO₃ minus x, and metal-ammonia systems
[AD-72887] 18 p3167 N71-31365

Two current conductivity in transition metal alloys
[CALT-822-26] 18 p2938 N71-31575

Measurement of resistivity changes in high purity alpha-phenylene due to self irradiation damage
[AERE-R-6506] 19 p3153 N71-32261

Excess Cd induced CdS crystal defects determined by Hall effect and electrical resistivity measurements in high temperature environments
[AD-73169] 19 p3169 N71-32270

Low temperature effects on electrical resistivity of copper aluminum alloys with trace amounts of iron
[AD-73169] 19 p3115 N71-32376

Thermophysical properties including electrical resistivity data for Ta-10W alloy to 2600 K measured by direct heating methods
[AD-734592] 20 p3363 N71-32949

Effect of film thickness and tensile stress on electrical resistance and superconducting transition temperature of vapor deposited thin lead films
[AD-73333] 20 p3333 N71-33772

NMR and electrical resistivity measurements for studying hydrogen nuclear motions in deuterated sodium trihydrogen selenide crystals
[AD-73392] 20 p3325 N71-33921

Determination of thermal conductivity, electrical resistivity, Lorentz ratio, and thermopower for annealed specimen of Inconel 718 at temperatures from 4 to 300 K
[NASA-CR-121758] 21 p3437 N71-34452

Electrical resistivity of Al and Cu during rapid heating to melting point and fracture in investigation of metallic melting mechanisms
[NLL-M-21000-5828.4F] 21 p3441 N71-34409

Determination of thermal conductivity and electrical resistivity of solids at cryogenic temperatures
[NASA-CR-121766] 21 p3463 N71-34652

Magnetic susceptibility and electrical resistivity measurements, optical microscopy, and X ray diffraction of disordered phase transformations in near-equiatomic Ni-Ru alloys
[COO-1198-807] 21 p3486 N71-34837

Diffusion mechanisms responsible for charge carrier mobility in doped silicon, studied to determine impurity band effects on electrical conductivity
[N-816] 21 p3497 N71-34916

Variations in electrical conductivity in samarium structure analyzed using cylindrical models of samarium field diffusion
[AD-73503] 21 p3503 N71-34973

Computer-aided data reduction techniques for extracting time dependent conductivity of dielectric material from test circuit recorded responses
[AD-726359] 22 p3560 N71-35357

Influence of group B metals on electrical resistivity, Hall effect, and thermoelectric properties of polycrystalline copper and silver alloys
[NRC-TT-1474] 22 p3592 N71-35382

Effects of temperature on electrical resistivity of silicon, carbon, and metal compounds
[AD-73598] 22 p3598 N71-35625

Analysis of resistivity of refractory concretes and reinforcing materials based aluminum and boron-aluminum cements and bonding agents
[AD-73599] 22 p3599 N71-35633

Electrical conductivity of boron and silicon compounds produced by hot pressing and sintering of cold-pressed pellets
[AD-73601] 22 p3601 N71-35644

Resistivity measurements of refractory oxide insulators using four-probe technique
[HEDL-SA-119] 22 p3602 N71-35651

Measurements of electrical conductivity in n-hexane, neohexane, and polystyrene films induced by X-ray irradiation
[AD-726353] 22 p3603 N71-35659

Self-modelling solutions of high-current plasma discharge and effect of thermal conductivity
[NASA-TT-F-15569] 22 p3653 N71-36851

Numerical analysis of potential in semiconductor produced by point current source and measurement of conductivity with four point probe
[NASA-TN-D-6504] 22 p3658 N71-36884

Electrical conductivity in stable phenyl free radicals
[AD-73659] 22 p3659 N71-36995

Oxygen concentrations in tantalum solid solutions measured in relation to electrical conductivity ratios at room temperature and 77 K
[ORNL-TR-3479] 23 p3769 N71-36867

Electrical resistivity of amorphous alloys P40Ni40B10 containing Cr or Fe as function of concentration and temperature
[AD-73770] 23 p3770 N71-36868

Development of techniques for measuring electrical resistivity of ceramic materials at high temperatures from 1,000 to 1,700 degrees centigrade
[NASA-TT-F-19848] 23 p3776 N71-36911

Electrical resistivity of polyvinyl chloride measured as function of temperature before and after irradiation
[AD-726972] 23 p3778 N71-36928

Development of techniques and equipment for measuring contact resistance between two single crystals and thin film microcircuits
[AD-727980] 24 p3899 N71-37789

Theoretical calculations compared with measurements of anomalous resistivity in RF confined, high-beta plasmas
[CN-26/B-8] 24 p3906 N71-38444

Differential conductance curves based on electron tunneling measurements of single and polycrystalline pure bulk thorium and analysis of crystal structure in tunnel junction region
[IS-T-436] 24 p3996 N71-38507

ELECTRICALLY SUSPENDED GYROSCOPES
ELECTROSTATIC GYROSCOPES
ELECTRICITY
NT ALTERNATING CURRENT
NT ATMOSPHERIC ELECTRICITY
NT AURORAL ELECTROJETS
NT ELECTROJETS
NT EQUATORIAL ELECTROJET
NT GEOELECTRICITY
NT IONOSPHERIC CURRENTS

ELECTRIFICATION

- NT STATIC ELECTRICITY
NT TELLURIC CURRENTS
Thermionic converter for converting heat energy directly into electrical energy [NASA-CASE-XLE-01903] 12 p1962 N71-23599
Experimental and computational investigations of direct conversion of plasma energy to electricity [CONF-710607-126] 24 p3989 N71-38463
- ELECTRIFICATION
Comparison of risk of death by meteoroids, weather, or supernovae and electrification in industry [P-4602] 19 p3199 N71-32708
Static electrification of aircraft when flying through clouds and precipitation [AD-726581] 22 p3541 N71-35225
- ELECTRO-OPTICAL EFFECT
Investigating interaction between light wave and microwave frequency traveling wave in anisotropic medium in parametric approximation 01 p0092 N71-10961
Instrumentation for determining quantitative waveforms of individual radar pulses using electro-optical effect in crystals 16 p2668 N71-28871
- ELECTRO-OPTICAL PHOTOGRAPHY
Investigating photographic sensors and electro-optical devices for optical processing of satellite data 03 p0380 N71-12797
Optical electron beam recording system for ATS television camera 13 p2083 N71-25340
- ELECTRO-OPTICS
Niobates and tantalates with large electro-optic coefficient for use in digital light deflectors 01 p0109 N71-10203
Electro-optical video laser system for information processing 01 p0056 N71-10826
Plasmas, semiconductors, lasers, electro-optics, and related research [AD-713228] 05 p0752 N71-14581
Automatic polarimeter capable of measuring transient birefringence changes in electro-optic materials [NASA-CASE-XNP-00883] 06 p0903 N71-16101
Basic studies of liquid crystals related to electro-optical and other devices - thermal stability, aging, and oxidation resistance 09 p1343 N71-19721
Technology review on integrated linear, digital, and optoelectronic circuits 10 p1537 N71-20093
Growth and properties of single crystal materials for optoelectronics including lasers [AD-717684] 11 p1817 N71-22395
Electro-optical acceleration of oscillator tubes 17 p2752 N71-29689
Eye lid movement effects on electro-oculographic recording of vertical saccadic eye movements [AMR-71-65-5] 18 p2880 N71-31533
Crystal growth of cinnabar, proustite, and lead cesium chloride, experimental work in HgS-HgI₂ phase diagram, and electro-optic coefficients of zincblende structure compounds [AD-721201] 19 p1168 N71-32057
Development and application of computer program for design of microwave cavities in electro-optical equipment [FOA-2-C-2376-51] 22 p3556 N71-35331
Electro-optical effect in LiNbO₃ crystal at 6328 angstroms [FOA-1-C-2377-51] 22 p3629 N71-35860
Electro-optical link between chemiluminescent diode and photomultiplier for temporal transmission [CEA-N-1431] 22 p3634 N71-35897
Analysis of processes of black and white film production and electro-optical transformation in telecine projection of light-shadow contrasts [AD-727244] 24 p3888 N71-37709
Frequency characteristics of electro-optical light modulators with coupled coaxial resonators [AD-727954] 24 p3932 N71-38055
Development and characteristics of birefringent device for comparison of Foucault method with Hart transform method during observation of phase defects [NASA-TT-F-14011] 24 p3965 N71-38287
- ELECTROACOUSTIC TRANSDUCERS
NT HYDROPHONES
NT MICROPHONES
Mathematical model for acoustic radiation from free-flooding ring transducers [AD-710745] 01 p0090 N71-10551
Surface wedge electroacoustic transducers [AD-711982] 02 p0192 N71-11347
Underwater electroacoustic measurements [AD-717318] 11 p1797 N71-22113
Design and fabrication of matched longitudinal acoustic wave transducers with operation over 500 MHz bandwidth centered at 1.7 GHz [AD-720823] 14 p2229 N71-26017
Analysis of temperature distribution in hollow cylindrical ceramic element used in sonar transducer under operating conditions [AD-721678] 16 p2567 N71-28306

- Electroacoustic transducer measurements of secondary sound velocity and inertial mass as function of He-3 concentration and temperature of He-3/He-4 mixture vapor pressure 17 p2789 N71-30293
- ELECTROACOUSTIC WAVES
Unknown electron density profiles determined from electroacoustic resonance frequencies by WKB approximation 10 p1628 N71-21106
Phonocardiogram simulator producing electrical voltage waves to control amplitude and duration between simulated sounds [NASA-CASE-XKS-10004] 13 p2036 N71-24606
- ELECTROCARDIOGRAMS
U ELECTROCARDIOGRAPHY
ELECTROCARDIOGRAPHY
Electronic device for monitoring electrocardiogram and disposing high or low heart rate [AD-710221] 01 p0014 N71-10006
Prototype capacitive electrode for electrocardiography [PB-194496] 04 p0478 N71-13899
Electrocardiographic electrodes for rapid application [NASA-TM-X-65438] 06 p0808 N71-16840
Electrocardiography and vector cardiography of athletes 09 p1329 N71-19585
Computerized simulation of electrical generator system in human heart 11 p1686 N71-23079
Dynamic reconstruction errors in digital to analog systems with biomedical applications [NASA-TN-D-6296] 12 p1865 N71-23160
Radiation hardened transmitter surgical implantation in animals for electrocardiogram biotelemetry in radiation environments [AD-718315] 12 p1866 N71-23478
Real time matched filter of QRS complex by replica correlation for electrocardiograms [AD-718124] 12 p1867 N71-23587
Electrocardiograph electrodes with silicon-silicon oxide half-capacitor [AD-718958] 13 p2036 N71-24413
Phonocardiogram simulator producing electrical voltage waves to control amplitude and duration between simulated sounds [NASA-CASE-XKS-10004] 13 p2036 N71-24606
Electrocardiograph electrode placements for beat R-wave amplitude correlation with respiratory volume [AD-713833] 19 p3042 N71-31614
Electrocardiographic monitoring device with arrhythmia signal detector and staple output of R-wave amplitudes [AD-712668] 19 p3047 N71-31622
Instantaneous rate reading tachometer for measuring ECG signal [NASA-CASE-MFS-20418] 21 p3427 N71-34386
Data compression algorithms for processing electrocardiogram and vectorcardiogram signals [NASA-CR-115177] 22 p3555 N71-35323
- ELECTROCHEMICAL CELLS
NT ALKALINE BATTERIES
NT BIOCHEMICAL FUEL CELLS
NT ELECTRIC BATTERIES
NT FUEL CELLS
NT HYDROGEN OXYGEN FUEL CELLS
NT MAGNESIUM CELLS
NT METAL AIR BATTERIES
NT NICKEL CADMIUM BATTERIES
NT NICKEL ZINC BATTERIES
NT PRIMARY BATTERIES
NT REGENERATIVE FUEL CELLS
NT SILVER CADMIUM BATTERIES
NT SILVER ZINC BATTERIES
NT STORAGE BATTERIES
NT WET CELLS
NT ZINC-OXYGEN BATTERIES
Nonaqueous hermetically sealed battery case made of epoxy resin and woven glass tape for use with electrochemical cells in spacecraft [NASA-CASE-XGS-00886] 02 p0148 N71-11053
Epoxy resin sealing device for electrochemical cells in high vacuum environments [NASA-CASE-XGS-02630] 11 p1678 N71-22974
Sealed electrochemical cell with flexible casing for varying electrolyte level in cell [NASA-CASE-XGS-01513] 12 p1859 N71-23336
Voltage converter/regulator for primary and secondary power sources in deep space missions 13 p2030 N71-25309
Inorganic separator materials for integrated cell stacks capable of continuous operation in contact with molten lithium metal and fused LiCl-KCl eutectic [AD-720600] 14 p2200 N71-26016
Indium amalgam, mercury, and indium-gallium electrochemistry and sodium-oxygen electrochemical cells [AI-TRANS-287] 15 p2377 N71-27387
Elimination of two step voltage discharge property of silver zinc batteries by using divalent silver oxide capacity of cell to charge nodules to monovalent silver state [NASA-CASE-XGS-01674] 16 p2541 N71-29129

SUBJECT INDEX

- Modular system-oriented discharge-charge controller for automated space power-source evaluation [NASA-TM-X-65448] 19 p3068 N71-32640
Thermodynamic investigation of effect of electron concentration in ternary alloys based upon aluminum-zinc binary system 20 p3368 N71-33994
Electrochemical cell employing twin dropping mercury electrodes used in thin layer chromatography technique 21 p3389 N71-34108
Electrochemical concentration cell ozone-soluble for measuring atmospheric ozone [NOAA-TR-ERL-200-APCL-18] 21 p3526 N71-35121
Design and fabrication of flight-concept prototype electrochemical water recovery subsystem [NASA-CR-111561] 23 p3718 N71-34507
Entropy, enthalpy, Gibbs free energy, and energy of atomization for gallium phosphide formation in electrochemical cells based on emf measurements [NLL-BRE-TRANS-315-18036.6251] 23 p3780 N71-34857
- ELECTROCHEMICAL CORROSION
Stress and electrochemical corrosion of Fe-Cr-Ni alloy exposed to aqueous solutions of NaOH [COO-2018-11] 06 p0869 N71-15808
Electrochemical degradation of platinum electrode in cadmium air battery by cadmium ion adsorption [NASA-TM-X-2198] 07 p0977 N71-17083
Adsorption microcell method for determining electrochemical properties of certain volatile corrosion inhibitors using mild steel samples [AD-714003] 08 p1212 N71-18112
Determining critical potentials by series of point-by-point potentiokinetic and potentiostatic measurements for use in corrosion studies [NLL-CE-TRANS-5208-19022.09] 10 p1579 N71-21286
Electrochemical analysis of metal corrosion in aqueous environments to determine whether process is anodic, cathodic, or both [AD-718053] 12 p1938 N71-23634
Galvanometric corrosion of uranium alloys in hydrochloric acid and ocean water [RFP-1592] 17 p2760 N71-29212
- ELECTROCHEMICAL MACHINING
Introduction of electrochemical machining in aeronautical industry 02 p0233 N71-11467
Electrochemical treatment of gas turbine blades made of heat resistant steels and alloys [AD-712938] 03 p0387 N71-13395
Electrolytic machining processes on trepanning of test specimens in BUGBY type fuel elements [CEA-N-1251] 07 p1066 N71-18127
Transfer processes in ECM at high current densities [UCRL-19615] 10 p1545 N71-21270
- ELECTROCHEMICAL OXIDATION
Ionic currents in anodic oxidation of Ti, Zr, and Ti-Zr alloys below oxygen evolution potential and this film growth theory [AEC-TR-7201] 09 p1402 N71-20450
Surface oxidation of Pt electrodes in pure solution and resolution of various stages of oxygen uptake by Pt surfaces [NASA-CR-117192] 09 p1402 N71-20450
Profiling procedures including computer program [OLS] for measuring junction depth in anodic oxidation - semiconductor fabrication reliability studies [NASA-CR-119800] 21 p3496 N71-34806
- ELECTROCHEMISTRY
NT COULOMETRY
NT ELECTROLYSIS
Ellipsometric and potentiostatic measurements of oxidation of mild steel in aqueous solutions [AD-711008] 01 p0067 N71-10828
Electrochemical reactions of organic compounds in aqueous solutions [AD-711335] 02 p0149 N71-11050
Chemistry program review including work in kinetics, electrochemistry, chemical lasers, trace element analysis, photoionization, and photoelectron spectroscopy [AD-705264] 02 p0172 N71-12151
Measuring oxidation of n-silylphenol on rotating disk electrodes and regularities in series of volatile inorganic hydrides [JPRS-51604] 02 p0174 N71-11220
Investigating regularities of reduction potentials in series of volatile inorganic hydrides of elements in main subgroups of periodic system 02 p0174 N71-11220
Weight comparison of electrochemical device and turbine-type APUs for space shuttle orbital repropulsive power [NASA-TM-X-52938] 03 p0315 N71-12040
Electrosynthesis of hydrazine from gaseous ammonia [ECRCR264] 04 p0804 N71-13440
Carbon chemical activity in sodium measured by electrochemical carbon meter [BNL-14508] 06 p0857 N71-19800

Thermodynamic characteristics of electrochemical energy conversion into electrical energy
[AD-713675] 06 p0810 N71-16314

Electrochromatographic separations of rare earths
[UCRL-19526] 06 p0812 N71-16721

Hydrogen embrittlement corrosion studies using electrochemical permeation method
[AD-713807] 06 p1215 N71-18769

Electrodeposition of magnesium and beryllium from organic baths
[NASA-CR-111850] 06 p1216 N71-18856

Proceedings of conference on electrochemistry and electrodeposition of metals
[TT-70-50037] 06 p1209 N71-19200

Electrochemistry, organic and inorganic chemistry, and chemical analyses
[TT-49-51006/2-4] 06 p1161 N71-19354

Experimental and computerized electrochemical measurements in fused sodium aluminum chlorides
[NASA-CR-117056] 09 p1342 N71-19562

Acid-base equilibrium in aluminum chloride melts and electrochemical measurements
09 p1343 N71-19564

Pulse polarography and chronopotentiometric program for electrochemical measurements in fused salts
09 p1343 N71-19565

Computer program description for applying pulses to electrochemical system and yielding current time plots as output
09 p1352 N71-19566

Applied mechanics, material testing, fluid mechanics, and electrochemical laboratories
[BAR-1] 10 p1653 N71-21133

Measuring potentials of fine-pore capillary system and Donnan hindrance of electrolyte transfer through ion-selective permeable membranes
[JIRC-TT-1442] 10 p1513 N71-21259

Electrochemical and corrosion behavior of corrosion resistant titanium base under platinum coating depending on pH
[NLL-TRANS-746-561-9022.401/] 10 p1585 N71-21709

Electrochemical reaction of nickel with solutions of sodium chloride and sodium chloride
[AD-718900] 12 p1926 N71-23300

Electrochemistry of redox couples on lithiated solid oxide electrodes
[AD-718831] 12 p1985 N71-23613

Corrosion characteristics and response to cathodic protection of copper alloys in quiescent sea water
[AD-718310] 12 p1958 N71-23795

Electrochemical properties of aluminum, nickel-based, and stainless steel cladding alloys for nuclear fuel examined by galvanostatic
[DE-1295] 13 p1210 N71-25216

Applications of transient methods to real electrode processes
[AD-728604] 14 p2214 N71-26083

Oxygen dissolution reaction in fuel cells and properties of metal electrodes
[NASA-CR-118652] 14 p2202 N71-26289

Sodium amalgam, mercury, and sodium-galium electrolytes and sodium-oxygen electrochemical cells
[AS-TRANS-287] 15 p2377 N71-27387

Superpurification of inorganic substances by electrochemical processes
16 p2536 N71-28299

Extended ellipsometry method used for electrochemical and optical measurements on electrochemically induced passivity of cobalt
[AD-721719] 16 p2557 N71-28341

Electrochemical impregnation of cadmium electrodes for storage batteries
16 p2538 N71-28660

Preparing magnetic films of nickel alloys by electrochemical method
[NLL-LT-746-445-9022.401/] 16 p2613 N71-28830

Electrochemical procedure for removal of surface oxidation products on uranium alloys
[BFF-1596] 17 p763 N71-29517

Electrochemical and corrosion behavior of high purity aluminum exposed to oxygen-free and oxygen-saturated saline solutions of varying pH content
[AD-722165] 17 p2763 N71-29647

Analysis and electrochemical behavior of semiconducting thin films of antimony doped tin oxide
17 p2714 N71-29695

Electrochemical mechanism, solution properties, and design criteria for energy conversion devices
[AD-722384] 17 p2706 N71-29795

Numerical analysis of solvent reorganization energy and method for prevention of dendritic crystal growth and disc electrode surface area decrease in silver behavior
[NASA-CR-119247] 18 p2873 N71-30827

Determinants errors and current impulse techniques for analyzing electrochemical kinetics of hexacyanoferrate 3/2 couple on platinum
18 p2886 N71-31232

Development of ion selective electrochemical sensor for detection of calcium, sodium, sulfate, and other ions in saline and brackish water
[PB-196364] 19 p3049 N71-31729

Conditions of accelerated oxidation of nickel base alloys from effects of vanadium and sodium compounds
[AD-723097] 19 p3113 N71-32023

Mathematical model of processes occurring in electrochemical reactor part of water vapor electrolysis cell
[NASA-CR-119609] 19 p3041 N71-32046

Surface preparation, materials, solutions, and operating conditions for electro-brightening and chemical brightening
20 p3312 N71-33610

Formation time, specific gravity of solution, and overcharge amount associated with electrochemical cleaning or formation operation in manufacturing nickel cadmium cells
[NASA-CR-121877] 21 p3379 N71-34040

Electrochemical dissolution of zinc oxide single crystals and measurement of dissolution rates as function of potential
21 p3500 N71-34938

Correlation of calculated and experimental product yields as functions of gas molecule residence time, power, gas pressure, and allyl alcohol in electrolysis of hydrazine from ammonia
[BCRC/N343] 23 p3719 N71-36510

Design and development of small, semiautomated electrochemical water purification system using electrochemical flocculation, settling, and electrochemical disinfection operations
23 p3719 N71-36511

Electrochemistry of freshly generated titanium surfaces and stress corrosion cracking in aqueous solutions and in molten salts
[NASA-CR-122939] 23 p3768 N71-36861

Thermodynamic properties of FeO, CuO and NiO in sodium chloride over temperature range from 700 to 1100 C
23 p3781 N71-36945

Electrochemical techniques for remote measurement of instantaneous rate of uniform corrosion of aluminum alloys in nuclear reactor heavy water circuits
[ZJE-96] 23 p3798 N71-37074

Statistical analysis of lubricating properties of electrolytes and friction measurement in system consisting of metal and lubricating electrolyte metal
[AD-727409] 24 p3944 N71-38135

ELECTROCONDUCTIVITY
Research progress on acidity measurements, pH measurements, calibration of ion selective electrodes, and high precision coulometry
[NBS-TN-543] 04 p0486 N71-13456

Plasma turbulence in circumterrestrial space due to geomagnetic field related to dynamics of magnetosphere and electroconductivity
[NASA-TT-1-13610] 16 p2843 N71-29087

ELECTRODELESS DISCHARGES
Combination scattering of microwaves by low frequency oscillations in electrodeless induction discharge plasma
[RHEFT-69-52] 03 p0432 N71-12932

Ignition behavior of electrodeless ring discharges in homogeneous periodically oscillating magnetic field
[JUL-691-PP] 18 p3023 N71-30485

ELECTRODEPOSITION
NT ELECTROPLATING
Radio frequency sputtering of dielectric films
01 p0508 N71-10157

Electrodeposited cadmium interaction with cathode substrate
[TT-70-57026] 03 p0332 N71-12368

Electrodeposition of lead from fluoroborate, fluosulfate, and sulfamate
[UCRL-50895] 05 p0701 N71-15052

Electrocrystallization of metals in ultrasonic field
[TT-70-50036] 05 p0694 N71-15357

Investigating electrodeposition of aluminum from aluminum chloride-lithium aluminum hydride-tetrahydrofuran baths
07 p1041 N71-17009

Electrodeposition and brushing methods of applying this film targets on metal substrates for nuclear reaction studies
[REPT-ID-4-70-66] 07 p1033 N71-17106

Electrodeposition of magnesium and beryllium from organic baths
[NASA-CR-111850] 08 p1216 N71-18856

Proceedings of conference on electrochemistry and electrodeposition of metals
[TT-70-50037] 08 p1209 N71-19200

Decreasing internal stresses of electrolytically deposited palladium-cobalt alloy
[NLL-TRANS-746-512-9022.401/] 10 p1578 N71-21225

Current density and electrolyte solution rate effects on nickel phosphorus electrodeposition
[NLL-TRANS-746-526-9022.401/] 10 p1583 N71-21816

Binding layer of semiconductor particles by electrodeposition
[NASA-CASE-XNP-01959] 11 p1818 N71-23043

Magnetic properties of electrodeposited films of iron-nickel-molybdenum ternary alloys with unusual magnetic permeability
[AD-719811] 13 p2091 N71-24352

Internal stresses related to deposit structure and cathodic processes in electrodeposition of metals
[TT-68-50634] 14 p2276 N71-26486

Homo-epitaxial crystallization in copper electrodeposition
16 p2609 N71-28205

Electrodeposition and codposition of metal powder particles dispersed in electrolytic solutions
[NLL-LT-746-422-9022.401/] 16 p2559 N71-29169

Electrodeposition of nonporous Co-Ni coating on magnetic recording drums
[NLL-LT-746-441-9022.401/] 17 p2761 N71-29253

Electrochemistry of nickel-, copper-, cobalt-, and iron-sulfide anodes
18 p2885 N71-30912

Electrodeposited metal coatings application in field of electrotechnology and electronics
18 p2936 N71-31212

Use of titanium and cobalt isotopic indicators to study electrodeposition conditions of ternary alloy systems
[NLL-LT-746-431-9022.401/] 19 p3114 N71-32183

Method for deposition of silicon nitride films on silicon
[NLL-FORS-TRANS-2780-9022.81/] 19 p3186 N71-32649

Glass coating of electron bombardment ion-thruster grids by electrodeposition
[NASA-CR-72992] 20 p3377 N71-32923

Descriptions and comparison of three methods for electrodeposition of metals in fused salt media
[CEA-N-1376] 21 p3437 N71-34460

Crystal structure and characteristics of beryllium wire after coating with aluminum by electrolysis
[SC-T-71-3821] 21 p3439 N71-34468

Analysis of chemical and electrochemical processes for deposition of copper layers on stainless steel surfaces
[NLL-LT-746-731-9022.401/] 22 p3589 N71-35561

Electrodeposition of palladium from amino-palladium hydroxide, bromide, and sulfamate electrolytes and electrolyte preparations
[NLL-LT-746-732-9022.401/] 22 p3589 N71-35562

Analysis of electrodeposition of palladium from alkaline ammonium chloride electrolyte using rotating disc electrode and temperature kinetic method
[NLL-LT-746-759-9022.401/] 22 p3590 N71-35566

Effects of organic substances and determination of products of conversion in electrolytes during electrodeposition of metals with examples of controlling techniques
[NLL-LT-746-727-9022.401/] 22 p3597 N71-35617

Electrochemical copper deposition at high current densities
[NLL-RTS-5647] 24 p3941 N71-38117

Dependence of hydrogenation in nickel electrodeposition on additions of metallic salts as determined by vacuum extraction
[NLL-TRANS-746-740-9022.401/] 24 p3942 N71-38118

ELECTRODERMAL RESPONSE
U GALVANIC SKIN RESPONSE
ELECTRODES
NT ANODES
NT CATHODES
NT CELL ANODES
NT CELL CATHODES
NT COLD CATHODE TUBES
NT COLD CATHODES
NT DYNODES
NT FREQUENCY MODULATION PHOTOMULTIPLIERS
NT GLASS ELECTRODES
NT HOLLOW CATHODES
NT HOT CATHODES
NT ION SELECTIVE ELECTRODES
NT PHOTOCATHODES
NT PHOTOMULTIPLIER TUBES
NT PHOTOTUBES
NT THERMIONIC CATHODES
NT TUBE ANODES
NT TUBE CATHODES
NT TUBE GRIDS

Time domain response to impedance for determining electrode reaction kinetics
[AD-710943] 01 p0018 N71-10572

Including dihydrazine hydrate in nickel hydroxide of positive electrode of storage batteries to increase ampere hour capacity
[NASA-CASE-3038-83505] 01 p0087 N71-10606

Apertured electrode focusing system for ion sources with nonuniform plasma density
[NASA-CASE-XNP-03332] 01 p0834 N71-10618

Chemical and electrochemical reactions of lithium graphite fluoride primary cell
[AD-715231] 01 p0887 N71-10936

Electromagnetic garment, applying vectorcardiographic type electrodes to human torso for data recording during physical activity
[NASA-CASE-XPR-10856] 02 p0167 N71-11189

- Electrode attached to helmets for detecting low level signals from skin of living creatures [NASA-CASE-ARC-10043-1] 02 p0168 N71-11193
- Performance of reducing electrode for neutralizing electrically charged hydrocarbon fuel flow [AD-712368] 02 p0287 N71-11876
- Characteristics of pressed disc electrode for biological measurements [NASA-CASE-XMS-04212-1] 03 p0329 N71-12346
- Kinetics of anodic oxidation of nitrous acid and nitrite ion on platinum electrode [UCRL-TRANS-10474] 03 p0333 N71-12382
- Prototype capacitive electrode for electrocardiography [PB-194496] 04 p0478 N71-13899
- X ray flash tube with exchangeable electrode system [UIUP-704] 04 p0594 N71-14451
- Floating potential profiles, electrode drops, and electrode temperature measurements in unseeded, superionic argon magnetohydrodynamic generator [NASA-TN-D-7041] 06 p0529 N71-15856
- Rare earth cation excitation at electrodes [AD-714253] 06 p0810 N71-16422
- Electrode geometry effects on series resistance in ac polarography [AD-714255] 06 p0810 N71-16423
- Circuit and electrode tests of low voltage breakdown in nitrogen, water vapor, and mixtures of nitrogen and water vapor 06 p0825 N71-16637
- Electrocardiographic electrodes for rapid application [NASA-TM-X-45438] 06 p0808 N71-16840
- Determining surface concentration of ion adsorbates with two-electrode thin layer method [MLM-1765/TR/1] 07 p0989 N71-17225
- Development of non-magnetic, stable, cadmium electrode for silver cadmium cells [NASA-CR-72805] 07 p0975 N71-17259
- Dynamic model for gas phase concentrations in porous fuel cell electrodes [NASA-TN-D-6168] 07 p0975 N71-17467
- Measuring conductivity, freezing point, and volume characteristics of halide melts for battery feasibility [NASA-CR-72791] 07 p0976 N71-17703
- Electrochemical degradation of platinum electrode in cadmium air battery by cadmium ion adsorption [NASA-TM-X-2198] 07 p0977 N71-17883
- Gamma radiation induced currents between insulated dissimilar electrodes 08 p1167 N71-18217
- Performance tests on cylindrical diodes with fluoride tungsten-niobium electrodes [TER-4125-3] 08 p1168 N71-18278
- Remote control device for positioning isotope separator collector electrodes and controlling ion beam shape and intensity 08 p1199 N71-18378
- Metal oxide catalysts for air-oxygen electrodes in electrochemical fuel cells and zinc oxygen batteries [AD-715707] 08 p1146 N71-18463
- Kinetic studies of electrolytic reduction of carbon dioxide on various metals 08 p1216 N71-19001
- Application of electroadsorption in pulse polarography to analysis of rare earth elements [CEA-R-4040] 09 p1344 N71-20098
- Electrode connection for a on-p silicon solar cell [NASA-CASE-XLE-04787] 09 p1328 N71-20492
- Surface oxidation of Pt electrodes in pure solutions and resolution of various stages of oxygen uptake by Pt surfaces [NASA-CR-117192] 09 p1402 N71-20503
- Electroforming thin nickel foil electrodes of porous honeycomb structure to increase nickel-cadmium battery service life 10 p1495 N71-20818
- Morphology and capacity of cadmium electrodes on repeated charge and discharge [NASA-CR-72777] 10 p1535 N71-21329
- Physical and chemical effects on reactivity of artificial graphite used for electrode technology [NLL-RTS-5841] 10 p1590 N71-21585
- Arc plasma titanium temperature measurement between metal electrodes in argon atmosphere [NLL-RTS-6099] 10 p1663 N71-21652
- Arc electrode of graphite with tantalum ball tip [NASA-CASE-XLE-04788] 11 p1726 N71-22987
- Electrode sealing and insulation for fuel cells containing caustic liquid electrolytes using powdered plastic and metal [NASA-CASE-XMS-01625] 11 p1772 N71-23022
- Automatic recording McLeod gage with three electrodes and solenoid valve connection [NASA-CASE-XLE-03280] 11 p1767 N71-23093
- Optical luminescence in reaction detection at rare of porous electrodes and comparison of interface reaction resistance and electrolyte ohmic resistance in zinc-silver oxide batteries [NASA-CR-118007] 12 p1860 N71-23518
- Electrochemistry of redox couples on lithiated nickel oxide electrodes [AD-718831] 12 p1985 N71-23613
- Electrocardiograph electrodes with silicon-silicon oxide half-capacitor [AD-718958] 13 p2036 N71-24413
- Dry electrode design with wire sandwiched between two flexible conductive discs for monitoring physiological responses [NASA-CASE-FRC-10029] 13 p2055 N71-24618
- Influence of small reference electrode in Langmuir probe measurement of plasma density and temperature [NASA-TM-X-65516] 13 p2146 N71-24888
- ISOLDE type isotope separator with four electrode system for ion beam formation [JINR-P13-5369] 13 p2132 N71-25108
- Third electrode and recombination electrode in nickel cadmium battery system of spacecraft 13 p2031 N71-25310
- Development and characteristics of electrodes in which poisoning by organic molecules is prevented by ion selective electrolytic deposition of hydrophilic protein colloid [NASA-CASE-XMS-04213-1] 14 p2228 N71-26002
- Applications of transient methods to real electrode processes [AD-720604] 14 p2214 N71-26083
- Oxygen dissolution reaction in fuel cells and properties of metal electrodes [NASA-CR-118632] 14 p2202 N71-26289
- Adhesive spray process for attaching biomedical skin electrodes [NASA-CASE-XFR-07658-1] 14 p2211 N71-26293
- Electrodes having array of small surfaces for field ionization [NASA-CASE-ERC-10013] 14 p2231 N71-26678
- Internal stresses related to deposit structure and cathodic processes in electrodeposition of metals [TT-48-56634] 14 p2276 N71-26688
- Trigger pulse energy, electrode dimension, gas pressure, and prepulse voltage effects on low inductance spark gaps for high voltages in air [BMWV-FBK-70-17] 15 p2455 N71-27633
- Structure of electric double layer at solid metal solution interfaces [AD-721718] 16 p2557 N71-28353
- Extension grounding electrodes for grounding electrochemical assemblies under permafrost conditions [AD-722221] 16 p2569 N71-28414
- Electrochemical impregnation of cadmium electrodes for storage batteries 16 p2538 N71-28660
- Addition of precharge to negative cadmium electrode during cell assembly to account for capacity loss due to fading 16 p2539 N71-28665
- Characterization and control of recombination electrodes in nickel cadmium cells 16 p2539 N71-28668
- Linear array, multi-electrode, ultrasonic transducer test techniques for radioisotope encapsulation inspection [BNWL-1491] 16 p2571 N71-28681
- Auxiliary discharge thermionic converter performance using barium oxide electrodes 16 p2633 N71-28700
- Current density and electrode drop distributions in cross sectional plane of electrode in conducting wall generators [AD-722086] 16 p2540 N71-28803
- Numerical analysis of solvent reorganization energy and method for prevention of dendritic crystal growth and zinc electrode surface area decrease in silver batteries [NASA-CR-119247] 18 p2873 N71-30827
- Methods for fillet welding in vertical position with manual electrodes [PB-197944] 18 p2928 N71-30858
- Electrocardiograph electrode placements for best R-wave amplitude correlation with respiratory volume [AD-713833] 19 p3042 N71-31614
- Fabrication and testing of bonded metal-ceramic, glass-coated metal, and glass-coated ceramic bonded to metal composite electrodes for cesium bombardment ion thrusters [NASA-CR-119695] 19 p3175 N71-32516
- Evaluation of sealed nickel cadmium cells, with auxiliary electrodes, operating in synchronous orbit regime [NASA-CR-121450] 20 p3213 N71-33326
- Empirical equation for thermionic converter performance as function of electrode emission properties [NASA-TM-X-2358] 20 p3308 N71-33739
- Porous and silver oxide electrodes for zinc-silver oxide battery systems [NASA-CR-121704] 21 p3386 N71-34088
- Electrochemical cell employing thin dropping mercury electrodes used in this layer chromatography technique 21 p3389 N71-34108
- Nonconsumable metal electric arc electrodes for producing solar simulator radiation source [NASA-CASE-LEW-11162-1] 21 p3400 N71-34210
- Diagrams of volt-ampere characteristics of hollow cathode discharge device with concentric spherical electrodes [RFP-TRANS-68] 21 p3404 N71-34221
- Development and evaluation of oxide electrode materials for use with open cycle magnetohydrodynamic generator 22 p3599 N71-35027
- Optimal design and working parameters for experimental installation of magnetohydrodynamic generator 22 p3600 N71-35040
- Research on inorganic compounds for use as positive electrodes in rechargeable lithium battery [AD-726607] 23 p3710 N71-36407
- Catalytic activity of osmium electrode catalyst and effects of weight and thickness of osmium during reaction of hydrogenation 23 p3721 N71-36524
- Heat treatable low hydrogen electrode welding device for welding HY-80 steels [AD-726758] 23 p3763 N71-36828
- Analytical derivation of tool electrode wear during spark machining of cavities [AD-726642] 23 p3763 N71-36829
- Development and characteristics of bipolar electrode battery with high power density silver oxide-thin liquid electrode 24 p3875 N71-37828
- Precise determination of particle trajectories using optical spark chamber with wire electrodes [LNF-70/44] 24 p3919 N71-37929
- ELECTRODIALYSIS
- Performance of multicompartiment electrochemical system with laminar flow, and fouling of membranes surfaces by iron oxide [FML-PUBL-71-13] 24 p3886 N71-37700
- ELECTROHYDRODYNAMICS
- NT ELECTROHYDRODYNAMICS
- NT ELECTROMECHANICS
- NT QUANTUM ELECTRODYNAMICS
- Scattering amplitude of quantum electrodynamics multipole model at infinite momentum 02 p0276 N71-11995
- Quantum electrodynamics for vector mesons using six component column matrix [IS-T-392] 05 p0747 N71-15229
- Multipole expansion of electromagnetic current density in classical electrodynamics [JINR-P2-5283] 09 p1425 N71-28816
- High power electronics including electrodynamic theory of grids, cathode losses in magnetrons, closed resonance chains, and electromagnetic vibration dampers [AD-717029] 10 p1537 N71-23380
- Magnetospheric plasma diagnostics and whistler electrodynamics including direction finding techniques [AD-717781] 11 p1747 N71-22125
- External operating characteristics, current and voltage amplification ratios, and electric power efficiency of electrodynamic energy converter 14 p2444 N71-26466
- Nonlinear electrodynamics equations effect on Lamb shift [IFVE-STF-69-19] 15 p3488 N71-27875
- Quantitative study of pulsed electrodynamics based on Goldreich-Julian model 20 p3345 N71-32848
- Physical meaning of Ward-like identities in dual resonance model for string modes [NUP-A-71-5] 20 p3290 N71-32940
- Difference scheme for numerical solution of mixed boundary value problems in electrodynamics [NASA-TT-P-15565] 22 p3627 N71-35846
- Differential equations and boundary conditions for finitely deformable, polarizable and magnetizable, heat conducting insulators interacting with electromagnetic fields [AD-726530] 22 p3630 N71-35864
- ELECTRODYNAMOMETERS
- U DYNAMOMETERS
- ELECTROENCEPHALOGRAPHY
- U ELECTROENCEPHALOGRAPHY
- ELECTROENCEPHALOGRAPHY
- Random process model and feature reduction of spontaneous and alpha frequency electroencephalograms [NASA-CR-111385] 02 p0167 N71-11185
- Investigating electroencephalographic and behavioral changes in rabbits and humans exposed to acute hypoxia 08 p1152 N71-18013
- Electroencephalographic sleep patterns of crew during long duration spaceflight cabin simulation 10 p3510 N71-36889
- Low-level, low-frequency electric field effects on monkey behavior and brain activity based on electroencephalography [AD-717100] 10 p3500 N71-21223
- Computer modeling of hippocampus and studies involving pattern recognition and information compression [AD-720016] 14 p2209 N71-22804
- Use of electroencephalograms in evaluation of animal state of alertness pilot during flight [JPRS-53269] 16 p3548 N71-39140
- Prototype device for monitoring sleep during manned space flight including performance tests [NASA-CR-115071] 17 p2771 N71-30138

SUBJECT INDEX

Dynamics of electroencephalogram during sleep in human under normal and altered daily regimes of sleep and wakefulness [NASA-TT-F-13679] 17 p2712 N71-30140

Automatic real-time scoring of simultaneous sleep electroencephalograms [NASA-CR-1840] 19 p3062 N71-32398

Sequential, distribution-free pattern classification procedures tested on Gaussian and EEG patterns [NASA-CR-121750] 21 p5384 N71-34074

Development and characteristics of bio-medical systems for obtaining electroencephalogram and neuropsychological data during space missions [NASA-CR-115132] 22 p3547 N71-35263

Applying principles of pattern recognition technology to analysis of EEG [AD-726473] 23 p3714 N71-36476

ELECTRODEPOSITION

U SPARK MACHINING

U ELECTRODEPOSITIVE DEVICES

U INITIATORS (EXPLOSIVES)

ELECTROFORMING

Electromagnetic pulse forming process for aerospace assembly manufacturing 02 p0233 N71-11649

Hypersonic low density wind tunnel including auxiliary equipment for electroforming and electroplating wind tunnel models [BMW-FB-W-70-51] 08 p1175 N71-18593

Techniques for fabricating electroformed injectors for high energy space storable liquid propellants [NASA-CR-121434] 20 p3359 N71-33484

Development of plating technique for electroforming of metal rotating bands used on 155 millimeter artillery shells [AD-714326] 23 p3762 N71-36822

ELECTROGENERATORS

U ELECTRIC GENERATORS

U ELECTROHYDRAULIC CONTROL

U ELECTRIC CONTROL

U HYDRAULIC CONTROL

ELECTROHYDRODYNAMICS

Feasibility of electrodynamic probe for measuring mean and turbulent velocities [AD-710719] 01 p0054 N71-10528

Charge injection mechanism from metal to dielectric fluid with applied electric field [AD-716471] 09 p1424 N71-19930

Motion of medium composed of neutral and positive particles at high electric Reynolds numbers [BAE-LIB-TRANS-1515] 13 p2666 N71-23037

Ripple magnetic field effects on electron motion in plasma rings [UNR-PP-5394] 15 p2457 N71-26849

Mathematical model of basic electrohydrodynamic process including effects of turbulence [AD-720703] 15 p2500 N71-27305

Control valve for switching main stream of fluid from one stable position to another by means of electrohydrodynamic forces [NASA-CASE-NFO-10416] 15 p2393 N71-27332

Ion beam phase characteristic measuring devices for acoustic and conductivity measurements [DP-18507] 18 p2971 N71-30468

ELECTROJETS

U AURORAL ELECTROJETS

U EQUATORIAL ELECTROJET

Variability of direction of closure currents of western electrojet in region of geomagnetic poles 11 p1757 N71-22849

Dynamic development characteristics of geomagnetic instabilities in earth magnetosphere 17 p2742 N71-29788

ELECTROKINETICS

Potentiokinetic polarization, potentiostatic current-time behavior, and electron microscopy of nickel dissolution surface topology in dilute acid solutions from 25 to 300 C 10 p1581 N71-21438

Zeta potential flowmeter for measuring very slow to very high flows [NASA-CASE-XNP-06509] 12 p1916 N71-23226

Electrokinetic potential and electrokinetic deposition of polyethylene on Pt, Ni, Cu, Fe, and Al plates at 60 V in acetonitrile, dimethyl formamide, and ethylic alcohol [NLL-LT-746-331-79022.401/1] 16 p2609 N71-28395

Imperly doping and surface treatment effects on characteristics of silicon carbide 17 p2770 N71-29849

Lectures presented at seminar in various scientific fields [BIR-70/20] 20 p3310 N71-33161

Electron kinetics in plasmas produced by neutron irradiation of anisotropic seeded noble gases 20 p3306 N71-33662

Determination of electrical charge and field strength of cell membrane of human erythrocytes [NASA-TT-F-14007] 24 p3877 N71-37636

ELECTROLUMINESCENCE

Electroluminescent semiconductor material of indium gallium phosphide 01 p0108 N71-10131

Amorphous semiconductor switches for control elements in electroluminescent display panels [AD-712346] 02 p0192 N71-11349

Light distribution dependence along single BL line of comet as function of frequency and amplitude of applied voltage [AD-714631] 06 p0907 N71-16769

Production and optical properties of zinc selenide aluminum arsenide heterojunction and platinum zinc selenide Schottky junction 07 p1095 N71-17679

Optical studies of radiation damage processes using high dose rates available from electron linear accelerator and fast optical techniques 07 p1095 N71-18046

Feasibility of electroluminescent panels and rotor lighting for military helicopters to aid in observation by other vehicles in formation [AD-715851] 08 p1144 N71-18734

Thermally stimulated current investigation of electrical properties of sublimated zinc sulfide electroluminescent films [AD-719784] 13 p2153 N71-25487

Luminescent processes in solids during interaction with gas 14 p2326 N71-26455

Electroluminescent quantum efficiency of gallium arsenide phosphide, gallium indium phosphide, and aluminum arsenide diodes [AD-720864] 15 p2508 N71-27901

Cathodoluminescence and X ray induced luminescence of manganese activated carbonate minerals 17 p2770 N71-30060

Comparison of electroluminescent and photoluminescent bands in erbium doped zinc selenide crystals and crystal defect sites [AD-724229] 18 p2884 N71-30725

Uranium glasses with high electroluminescent and photoluminescent properties 18 p2941 N71-31280

Electroluminescence of rare earth compounds in phenylacetylene chloride through cation excitations in electrodeless process [AD-723808] 19 p3052 N71-32711

Electro-optical link between electroluminescent diode and photomultiplier for temporal transmission [CEA-N-1431] 22 p3634 N71-35897

Aluminum alloy compounds as wide band gap semiconductor for electroluminescent light sources [NASA-CR-111976] 24 p3934 N71-38070

ELECTROLUMINESCENT LAMPS

U ELECTROLUMINESCENCE

U LUMINAIRIES

ELECTROLYSIS

U COULOMETRY

Electrical properties of quartz as related to impurities and electrolytic coloring 02 p0287 N71-12008

Principles of producing coatings of titanium, vanadium, and their alloys by molten salt electrolysis [AD-712940] 03 p0386 N71-13284

Water electrolysis rocket engine with self-regulating stoichiometric fuel mixing regulator [NASA-CASE-XGS-08729] 04 p0605 N71-14044

Dynamics and stability of obtaining and interpreting bubble contact angles and detachment diameters [NASA-CR-117481] 10 p1512 N71-20779

Operation method for combined electrolysis device and fuel cell using molten salt to produce power by thermoelectric regeneration mechanism [NASA-CASE-XLE-01645] 10 p1495 N71-20904

Oxygen production efficiency of water electrolysis systems in long term regenerative life support system tests 10 p1506 N71-20965

Water electrolysis system for oxygen production during long term manned test of space station simulator 10 p1507 N71-20967

Performance tests of CO₂-H₂O solid oxide electrolyte electrolysis system for generation of oxygen for life support systems [NASA-CR-114293] 12 p1869 N71-23172

Similarity of bubble growth in nucleate boiling and electrolysis [NASA-CR-118641] 14 p2352 N71-25902

Prolonged electrical test of bonded alumina trilayer at 1323 K in vacuum environment 16 p2616 N71-28035

Electrodeposition and codposition of metal powder particles dispersed in electrolytic solutions [NLL-LT-746-622-79022.401/1] 16 p2559 N71-29169

Design, fabrication, and testing of circulating electrolyte type water electrolysis system for automatic control of spacecraft total pressure and oxygen partial pressure [NASA-CR-111911] 17 p2710 N71-29383

Design and tests of water vapor electrolysis cell for generating and regulating spacecraft oxygen and for controlling humidity [NASA-CR-115070] 21 p3379 N71-34043

ELECTROLYTES

Crystal structure and characteristics of beryllium after coating with aluminum by electrolysis [SC-T-71-3021] 21 p3439 N71-34468

Establishing solar cell array criteria for use as primary power source in lunar-based water electrolysis system [NASA-CR-119943] 23 p3709 N71-34641

Design, development, and characteristics of fuel cell and electrolysis cell with carbon anode [NLL-M-20409-5828AF1] 23 p3773 N71-34891

ELECTROLYTE METABOLISM

Prolonged immersion effects on human water/mineral metabolism 16 p2543 N71-28251

Renal sodium and calcium excretion effects on human electrolytic water-mineral metabolism during space flight 20 p3222 N71-33467

ELECTROLYTES

U ION EXCHANGE MEMBRANE ELECTROLYTES

U MOLTEN SALT ELECTROLYTES

Electrolytically regenerative hydrogen-oxygen fuel cells [NASA-CASE-XLE-04526] 02 p0140 N71-11052

Applications of electrolyte rectification in aeronautics industry 02 p0231 N71-11637

Linear theory for electrolytic model of transistor [TID-25456] 03 p0390 N71-12529

Nuclear magnetic resonance, solubility, stability, and resistance of electrolytes for lithium batteries [NASA-CR-72803] 05 p0631 N71-14608

Conformation and turbulent flow characteristics of polyelectrolytes in solution [AD-713217] 05 p0664 N71-14978

Determining suitability of aluminates for use in electrochemical systems 06 p0797 N71-16115

Investigating electrodeposition of aluminum from aluminum chloride-lithium aluminum hydride-tetrahydrofuran baths 07 p1041 N71-17609

Calculating effects of relaxation field and electrophoresis to derive conductance of mixed strong electrolytes at finite concentrations 08 p1168 N71-18992

Streaming potentials of fine-pore capillary systems and Donnan hindrance of electrolyte transfer through ion-selective permeable membranes [NRC-TT-1442] 10 p1513 N71-21259

Ionic association and solvation studied in aqueous electrolytes by Raman spectroscopy 10 p1514 N71-21262

Anode potential fluctuations observed in copper dissolution in different electrolytes 10 p1566 N71-21265

Mixed conduction in NaCl-TiCl₃/fused salt systems and tracer techniques for determination of hydrogen solubility in solid electrolytes [COO-1440-21] 11 p1817 N71-22509

Sealed electrochemical cell with flexible casing for varying electrolyte level in cell [NASA-CASE-XGS-01513] 12 p1859 N71-23336

Measurements of diffusion coefficients and vapor pressure in LiOH solutions for determination of gas solubilities in fuel cell electrolytes [NASA-CR-117906] 12 p1859 N71-23345

Freezing rate and solute specie and concentration effects on charge separation at advancing surfaces of growing ice related to cloud physics [AD-718399] 12 p1910 N71-23635

Design and electrical properties of methanol/air battery cells operating at low current density [AD-719239] 13 p2029 N71-24577

Concentric metal containers for measuring heat conductivity of aqueous solutions of electrolytes, with experimental data for potassium bromide [NASA-TT-F-13660] 13 p2185 N71-24815

Chemical analysis of latent 4 nickel cadmium battery electrolyte 16 p2539 N71-28863

Electrodeposition and codposition of metal powder particles dispersed in electrolytic solutions [NLL-LT-746-622-79022.401/1] 16 p2559 N71-29169

Low voltage aluminum electrolyte capacitors with high capacitance [ECR-16] 18 p2898 N71-31170

Stress effects of intermittent exposure to 3 per cent CO₂ on acid-base balance and electrolyte excretion in submarine personnel [AD-722665] 18 p2877 N71-31238

Charge transfer characteristics of ion recombination in phase boundary of germanium surface with electrolyte 18 p2998 N71-31336

Pressure dependence of electrolytic conductance at 30 C to pressures of 3000 kg/cm for solutions of potassium iodide and series of tetraalkyl ammonium salts 19 p3051 N71-32289

Nuclear magnetic resonance spin echo method used to determine self diffusion activation energy in aqueous solutions of electrolytes

20 p3230 N71-33623

Gas solubilities and transport properties in fuel cell electrolytes

[NASA-CR-121432] 20 p3215 N71-33826

Fuel cell electrolyte studies on vapor pressures of ternary systems, partial molar volumes of dissolved gases, and diffusion coefficients of gases

[NASA-CR-121628] 21 p3378 N71-34034

Paste electrolyte cell development and multikilowatt lithium/selenium secondary batteries for electrically-driven army vehicles

[AHL-7745] 21 p3380 N71-34047

Partial differential equations for migration evolution in supported electrolyte solutions with free convection

[UCRL-20322] 21 p3387 N71-34100

Long shelf life, organic electrolyte, lithium cells with wide operating temperature range and high energy density

[AD-726383] 22 p3543 N71-35235

Chromatographic and spectrographic extractions for determining concentrations of saccharin reduction products in nickel plating electrolytes

[NLL-LTI-746-725 [9022.401]]

Spectrophotometric and polarographic determinations of butadiol, saccharin, and phthalimide concentrations in bright nickel plating electrolyte

[NLL-LTI-746-726 [9022.401]]

Effects of organic substances and determination of products of conversion in electrolytes during electrodeposition of metals with examples of controlling techniques

[NLL-LTI-746-727 [9022.401]]

Design and development of adiabatic calorimeter for measuring specific heat of aqueous solutions of electrolytes up to 150 C

[NLL-CE-TRANS-5634 [9022.09]]

Statistical analysis of lubricating properties of electrolytes and friction measurement in system consisting of metal and lubricating electrolyte metal

[AD-727449] 24 p3944 N71-38135

ELECTROLYTIC CELLS

Electrical properties of copper fluoride/lithium hexafluoroarsenate in methyl formate/lithium high energy primary batteries

[NASA-CR-72776] 03 p0632 N71-14947

Design of electronic timer circuit using electrolytic cells

[CR-154] 06 p0797 N71-15941

Prototype organic electrolyte battery performance

[AD-714675] 06 p0797 N71-16032

Performance tests of CO₂-H₂O solid oxide electrolyte electrolysis system for generation of oxygen for life support systems

[NASA-CR-114295] 12 p1869 N71-23172

Mathematical model of processes occurring in electrochemical reactor part of water vapor electrolysis cell

[NASA-CR-115669] 19 p3041 N71-32046

Radioisotopic method for determination of mercury in electrolytic cells

[ORNL-TR-2487] 21 p3484 N71-34819

ELECTROLYTIC GRINDING

U ELECTROCHEMICAL MACHINING

ELECTROLYTIC POLARIZATION

Kinetic studies of electrolytic reduction of carbon dioxide on various metals

06 p1216 N71-19001

Carbide electrolysis extraction from high temperature resistant stainless steels with 20 percent Ni and 25 percent Cr

10 p1577 N71-21145

ELECTROLYTIC POLISHING

U ELECTROPOISHING

ELECTROMAGNETIC ABSORPTION

NT AURORAL ABSORPTION

NT MOLECULAR ABSORPTION

NT PHOTODIFFRACTION

NT POLAR CAP ABSORPTION

NT ULTRAVIOLET ABSORPTION

NT X RAY ABSORPTION

Optical absorption in transparent materials during 1.5 MeV electron irradiation

[NASA-CR-110907] 01 p0888 N71-10380

Isomeric absorption measurements over Freiburg Germany for January through July, 1970

02 p0214 N71-11865

Investigating band structures of crystals by studying two-photon absorption process

[AD-712395] 03 p0444 N71-13234

Literature review on electromagnetic wave transmission in absorbing media

04 p0491 N71-13705

Antenna radiation and wave propagation in sea water

04 p0491 N71-13706

Excitation gap thickness effect on spherical antenna performance

04 p0491 N71-13708

Electromagnetic detection of absorbing field reflected from metallic surface

04 p0492 N71-13709

Light absorption and scattering effects on underwater visibility of imaging devices in sea water

04 p0565 N71-13736

Electric field effects on optical absorption by excitons in semiconductors

04 p0603 N71-14220

High frequency electromagnetic wave transformation and absorption in plasmas

[CONF-690619-16] 04 p0599 N71-14249

Transient optical absorption by self-trapped excitons in alkali halide crystals

06 p0908 N71-15748

Measuring long-lying electronic levels of impurity ions in Al₂O₃ and electromagnetic absorptivity of Pb using far infrared spectroscopic techniques

[UCRL-19666] 06 p0922 N71-16407

Investigating conditions for validity of energy absorption of electromagnetic waves by magnetic pumping with transit time derived by linear theory

[CEA-CONF-1606] 06 p1269 N71-18153

Investigating two photon absorption by single atoms in intense electromagnetic fields

[AD-715509] 06 p1251 N71-18290

Atmospheric absorption effects on spectroscopic analyses and electromagnetic radiation transmission

[AD-715482] 06 p1191 N71-18835

Calculation of conduction electronic energy bands and L bands in alkali halide crystals

06 p1283 N71-19309

High frequency absorption measurement over Antarctic region using radiometers

[GRI-NTP-75] 10 p1547 N71-20858

Photon absorption lines in electron paramagnetic resonance spectrum of second harmonic generation in ruby

11 p1800 N71-21865

Pressure effects on ferric hydroxamate and ferriochrome A based on electromagnetic absorption and Mossbauer resonance

[COO-1198-777] 11 p1784 N71-22486

Ionospheric absorption measurement, unsatop observations, and short wave fadeout reported from optical tracking stations in Greece (Athens) - tables

11 p1823 N71-22502

Metallic materials heated by laser radiation absorption

[JPRS-52916] 12 p1931 N71-23104

Heating ferrite by pulsed laser radiation absorption, preceding thermal breakdowns

12 p1932 N71-23105

Temperature distribution in metallic solids due to laser radiation absorption

12 p1932 N71-23106

Gamma ray absorption through interactions with galactic radiation, electrons, and pair producing matter

13 p2158 N71-24768

Gamma ray absorption processes at high red shifts, and energy dependences of absorption processes in interstellar and intergalactic gas

13 p2160 N71-24777

Tropospheric and ionospheric absorption at VHF for North Atlantic aeronautical satellite system

[NASA-TM-X-65507] 13 p2046 N71-24914

Laser-radiation effects on metals including damage thermodynamics, melting and cavity formation, vapor hydrodynamics, and damage product electromagnetic absorption

[JPRS-53241] 16 p2608 N71-28180

Effects of magnetic ordering on optical absorption spectrum of rubidium nickel fluoride

16 p2641 N71-29130

Relationship between ionospheric electron currents, geomagnetic storms, and absorption bursts

17 p2747 N71-30088

Interaction of Q switched ruby laser beams on metal surfaces noting electromagnetic absorption and electron emission

[REPT-1011/71] 18 p2931 N71-30602

Calculation of radio noise absorption expected for any radiometer system

19 p3178 N71-32665

Computer programs for calculating visible and infrared atmospheric transmission, absorption, Mie scattering, and reflection

[AD-722713] 19 p3097 N71-32681

Radio spectra, synchrotron self-absorption, free-free absorption, cold plasma effect, stimulated emission, and quasi-stellar sources

20 p3344 N71-32841

Nuclear radiation pumping of certain gas lasers feasible in high fluxes provided by pulsed nuclear reactor

20 p3282 N71-33666

Ionospheric, solar, and satellite optical tracking data - Apr. 1971

20 p3343 N71-33978

Use of gas lasers to measure velocity and absorption of longitudinal hyperconvergent waves

[NASA-TT-P-13902] 21 p3464 N71-34648

Elevated temperature studies of optical absorption associated with electrons trapped in fused silica

21 p3492 N71-34671

Electromagnetic wave absorption by isothermal plasma located in field of electromagnetic wave

[MATT-TRANS-105] 21 p3495 N71-34696

Optical radar photon Rayleigh and Mie scattering and absorption model and utilization of time of flight optical radar as ocean probe

[AD-726433] 22 p3579 N71-35092

Optical transmittance of fused silica at elevated temperatures during high energy electron bombardment

[NASA-TM-X-67930] 22 p3598 N71-35098

Light absorption in molecular crystal by triplet exciton pair with singlet sum spin state

22 p3643 N71-35971

Collisionless absorption of HF plasma power and plasma heating near low hybrid resonance frequency

[CONF-710607-142] 23 p3832 N71-37321

Calculation of effective electromagnetic absorption and scattering cross sections

23 p3859 N71-37408

Pressure and temperature determination in Venus atmosphere from decametric and millimeter wave radio transmission from Venus probes

[PR-16] 23 p3855 N71-37470

Comparison of 1.5 MeV electron irradiation induced optical absorption of fused commercial silicon and optical transmission of Al₂O₃, MgF₂, NaF, LiF, and BeO

[NASA-CR-123187] 24 p3958 N71-38237

ELECTROMAGNETIC COMPATIBILITY

Electromagnetic interference control in spacecraft design and interference prediction analysis applied to Nimbus satellites

03 p0354 N71-12268

Electromagnetic compatibility and interference of spacecraft electronic components and functional testing with telemetry

03 p0376 N71-12270

Experiments on circuit board mechanical and electrical properties noting brazing, soldering, and welding of laminated printed circuits

[BMW-FB-W-70-61] 11 p1723 N71-22282

Tests for determining spectral signatures of integrated high-frequency antenna systems for F-3 aircraft

[AD-718054] 12 p1809 N71-22800

Determination of communication-electronic equipment power requirement and its compatibility with power sources

[AD-719099] 13 p2053 N71-24308

Electric motor environmental and electrical test procedures including electromagnetic compatibility and maintenance

[AD-721611] 16 p2548 N71-26048

Approximate emission spectra bounds and electromagnetic pulse compression compatibility of ship radar

[AD-724184] 19 p3059 N71-32708

ELECTROMAGNETIC CONTROL

U ELECTROMAGNETS

U REMOTE CONTROL

ELECTROMAGNETIC INDUCTION

U MAGNETIC INDUCTION

ELECTROMAGNETIC FIELDS

NT FAR FIELDS

Electromagnetic induction stirring of steel ingots in mold

[AD-711754] 01 p0061 N71-10060

Radiation from aperture in conducting plane coated with moving plasma layer

[AD-712010] 02 p0279 N71-11171

Electromagnetic field measurements on rectangular waveguide for radiometer wave control in microwave [NASA-CR-111593] 02 p0183 N71-11200

Wire spacing effects on fence guide field

02 p0184 N71-11200

Effect of time-dependent gravitational fields on superconductors and metals

[ESRIN-IN-100] 03 p0285 N71-11065

Electromagnetic fields produced by long, horizontal electric line source above reactive surface

[AD-712057] 02 p0269 N71-11040

Trajectories of Compton electrons produced by gamma rays with air in electromagnetic field [LA-4348] 03 p0421 N71-11200

Nonlinearity in photon propagation and phase splitting in electromagnetic field

[NYO-3829-54] 03 p0422 N71-11065

Using RF electromagnetic fields for confining dense high-temperature plasmas

[AD-713064] 03 p0430 N71-11065

Electromagnetic simulation of plane and three dimensional fields by electric rotational field and stable magnetic ultrasonic frequency field

[AD-714727] 06 p0983 N71-19771

Influence of electromagnetic force fields on biological systems studied on drosophila and ciliates

[AD-714071] 06 p0981 N71-19789

SUBJECT INDEX

- Multiple photon ionization of atoms by electromagnetic field [ABC-TR-7167] 06 p0924 N71-16755
- Mechanical properties of stainless steel melts, and equipment development for electromagnetic control [SU-326-P-29-5] 07 p1042 N71-17243
- Electromagnetic perturbation of pseudocolor mass spectrum in SU(3) symmetry model [SU-1206-229] 07 p1074 N71-17437
- Gamma-gamma directional correlation and intensity studies of electromagnetic transitions of Ta-181 [CXX-1746-46] 07 p1077 N71-17551
- Physical realizability of planar antennas [AD-715267] 07 p0999 N71-17773
- Development of theory of characteristic modes for conducting bodies [AD-716494] 09 p1423 N71-19534
- Formulation of self consistent 2 and 2 1/2 dimensional electromagnetic and relativistic simulations [UCRL-72613] 10 p1626 N71-20671
- Equipment for testing of electromagnetic mixing of liquid phase during zone recrystallization 10 p1575 N71-20692
- Solutions derived numerically for electromagnetic field due to current bearing circular loop near oblate spheroid [AD-717306] 11 p1796 N71-21908
- Vector analysis for exact solution to electromagnetic field diffraction by plane angular sector 11 p1797 N71-22022
- Characteristics of mutual electromagnetic coupling of loops over homogeneous ground determined by employing image theory [AD-717351] 11 p1723 N71-22144
- Electromagnetic field and electron density measurements by MHD plasma accelerators 11 p1813 N71-22652
- Ecological effects of electromagnetic fields and ELF global communication systems [AD-718828] 12 p1862 N71-23381
- Electromagnetic field and wave propagation in static gravitation [AD-718143] 12 p1966 N71-23499
- Internal circuit excitation by electromagnetic field transmission through slotted metallic skin [JC-R-70-4339] 13 p2048 N71-25346
- Experimental design for diagnostic and velocity measurements of plasma acceleration in traveling electromagnetic field [JNRRA-NT-174] 14 p2320 N71-25709
- Device for high vacuum film deposition with electromagnetic ion steering [NASA-CASE-NPO-10331] 14 p2231 N71-26701
- Relevance of nonrelativistic Hamilton-Jacobi equation in electromagnetic field [JNR-P-5373] 15 p2463 N71-27174
- Determination of electromagnetic field behavior of cavity resonators using finite difference theory [JNR-70/17] 15 p2454 N71-27374
- Numerical analysis of electromagnetic fields from heated magnetic dipole antennas and applications to radio direction finders and underground communication [AD-721196] 15 p2383 N71-27757
- Quantum electrodynamics of atom interaction with radiation field 15 p2494 N71-27957
- Earth subsurface electromagnetic field disturbances due to subsurface rock electrical properties 16 p2383 N71-28268
- Detecting molecular constituents in radiation transparent media by measuring intensity of light transmitted through cell while applying electrostatic or electromagnetic field [NASA-CASE-ERC-10021] 16 p2557 N71-28635
- Electromagnetic fields of shielded microstrip transmission lines in terms of normal modes of dielectric slab waveguide 16 p2571 N71-28790
- Problems in evaluating electromagnetic fields of linear antennas or dipole arrays in dissipative half space [AD-721706] 17 p2725 N71-29480
- High frequency oscillation research and related electronics problems including open resonator applications in electromagnetic fields and paramagnetic and cyclotron resonances 17 p2725 N71-29667
- Neutrino production of lepton pair in electromagnetic field of nucleus [RPP-121] 17 p2806 N71-30307
- Computer simulation to verify energy constants for nonlinear theory of transverse electromagnetic instabilities in collisionless plasmas [AD-723814] 19 p3163 N71-31709
- Electromagnetic field disturbance models for clear air turbulence detection in atmosphere 19 p3091 N71-31936
- Isolation of charged harmonic oscillators coupled by electromagnetic field [RPP-P-1203] 19 p3148 N71-32038
- Investigation of controlled electromagnetic fields applied to Type-304 stainless steel melts during solidification including grain boundary and metallographic studies [SU-326-P-29-X-1] 19 p3114 N71-32228
- Device for measuring ionization processes and plasma acceleration in traveling electromagnetic fields [NASA-TT-F-4971] 21 p503 N71-34951
- Differential equations and boundary conditions for finitely deformable, polarizable and magnetizable, heat conducting insulators interacting with electromagnetic fields [AD-726450] 22 p3630 N71-35864
- Nonrelativistic wave equation invariance for particles with 0 and 1/2 spin in electromagnetic field [JINR-P-5322] 22 p3633 N71-35890
- OV-3 data on particles and electromagnetic fields in magnetospheres and radiation belts [AD-726542] 22 p3666 N71-36137
- Electric and magnetic field line distributions for calculating short range field around receiving antenna 23 p3723 N71-36336
- Integral equation formulations of scattering from two dimensional inhomogeneities in conductive earth 23 p3753 N71-36762
- Characteristics of modified unipolar machine with rotor consisting of two parallel magnets imbedded in superconducting lead casting 23 p3804 N71-37120
- Electromagnetic field amplification in finite three-dimensional resonator [AD-727269] 24 p3887 N71-37708
- Interaction of high frequency electromagnetic fields with magnetized plasma, high intensity electron and ion beams, pulse discharges, and related studies - bibliography [NF-18901] 24 p3993 N71-38487
- ELECTROMAGNETIC HAMMERS
- Method and apparatus for shaping and joining large diameter metal tubes using magnetomotive forces [NASA-CASE-XMF-05114] 07 p1035 N71-17650
- Portable magnetomotive hammer for metal working [NASA-CASE-XMF-05793] 13 p2085 N71-24833
- ELECTROMAGNETIC INTERACTIONS
- NT PLASMA-ELECTROMAGNETIC INTERACTION
- High frequency auroral noise caused by proton beam excitation of ionosphere 02 p0180 N71-11268
- Studying interaction of electromagnetic radiation with plants, soils, and water, and wavelengths and procedures for discriminating agricultural crops 02 p0217 N71-11981
- Time reversal invariance in electromagnetic interactions - conference [CALT-68-264] 03 p0422 N71-12656
- Electric interaction in tin isotopes at cryogenic temperatures, noting use of Mossbauer effect 03 p0444 N71-12682
- Helicon resonances in low pressure cesium plasma discharge in external cross-magnetic field [REPT-4458] 05 p0752 N71-14509
- Table of magnetic hyperfine-structure anomalies calculated from measured moment ratios [ORNL-4411] 06 p0919 N71-16248
- Relativistic quasipotential relations in case of electromagnetic interaction [JINR-B2-5225] 08 p1246 N71-18172
- Examining assumption of pion, eta-meson, and sigma-meson dominance of weak and electromagnetic decays of K meson using hard meson current algebra [NUB-2048] 08 p1257 N71-18418
- Investigating violation of CP invariance in electromagnetic interactions of hadrons [UCRL-20041] 08 p1259 N71-18459
- Electromagnetic interaction energy expansion using vectorial spherical harmonics and matrix element dependence on crystal dynamical matrix eigenvectors and electronic wave functions 09 p1427 N71-19094
- Vacuum polarization in quantum electrodynamics implying nonlinear electromagnetic interactions 10 p1612 N71-20721
- Current algebra for determining form factors and divergences of mass in electromagnetic interactions 10 p1624 N71-21814
- Interferometric measurements in optical and microwave frequencies of electromagnetically accelerated shock waves in hydrogen 11 p1741 N71-22636
- Summary of research on scattering amplitude of electromagnetic interactions [AD-717912] 12 p1970 N71-33373
- Isoscalar couplings in electromagnetic interactions 12 p1978 N71-34235
- Nonlinear interactions of electromagnetic waves in magnetostatic plasma 12 p1983 N71-24273
- Thermoelectric emission, secondary electron emission in semiconductors, development of mass spectrometers, and collisions of atomic particles [AD-719533] 13 p2148 N71-25181
- Gamma quantum detection of electromagnetic interactions which yield neutrino, antineutrino, and photon particles emphasizing photon circular polarization and shower observation [NF-18558] 14 p2317 N71-26759

ELECTROMAGNETIC INTERFERENCE

- Influence of magnetic interactions on oscillatory de Haas-van Alphen magnetization of silver samples 15 p2453 N71-27387
- Hyperfine interactions of first excited 2p/2s states of Sm-154 and U-238 studied using Mossbauer effect following Comolomb excitation 15 p2485 N71-27817
- Steady state electromagnetic interaction of solar wind with planet Mercury computed for spectrum of electrical conductivity [NASA-TM-X-43028] 17 p2841 N71-29923
- Individual dynamic properties of off-center ions in crystal lattices and electron plasma interaction effects [AD-722859] 17 p2828 N71-30275
- Numerical analysis of Feynman diagrams and application to calculation of magnetic moment of electrons and muons [CNRS-C71-70-P-336] 18 p2969 N71-30432
- Long-range electrostatic and electromagnetic interactions between two neutral hydrogen atoms in ground state [NASA-TR-X-367] 18 p2982 N71-30917
- Long range electromagnetic interactions between neutral particles 20 p3317 N71-33524
- Ultrasonic measurements on electromagnetic interaction near dielectric superconducting transition temperature 20 p3312 N71-33571
- Electromagnetic and nuclear many body forces, and effects of three body forces on various physical properties of neutron stars 20 p3326 N71-33943
- Techniques for solving Maxwell equations and applications in induction heating and electromagnetic prospecting 21 p3483 N71-34216
- Lambda[0] hyperon polarization along sigma[0] hyperon decay plane by violating time reversal invariance in electromagnetic interactions of kaon(minus) or sigma(minus) with protons 21 p3487 N71-34842
- Measuring electromagnetic form factor of neutron by comparing neutron and electron cross sections with nuclei [JINR-P-5705] 22 p3633 N71-35888
- Developments in hadron physics, dual models and dual phenomenology, weak elementary particle interactions, and electromagnetic interaction theory - topics from nuclear research conference [CERN-71-7] 22 p3640 N71-35951
- Structure of weak and electromagnetic interactions of elementary particles [AD-724661] 23 p3818 N71-37237
- Electromagnetic corrections to pi(pi minus) proton reaction to determine causality in the meson system [TR-72-003] 23 p3819 N71-37239
- General mathematical laws for electromagnetic field-conductive fluid interactions in rectangular channels 24 p3968 N71-38303
- ELECTROMAGNETIC INTERFERENCE
- NT ATMOSPHERICS
- NT BLACKOUT (PROPAGATION)
- NT COSMIC NOISE
- NT DAWN CHORUS
- NT ELECTROMAGNETIC NOISE
- NT HISS
- NT IONOSPHERIC NOISE
- NT IONOSPHERICS
- NT JAMMING
- NT RADIO FREQUENCY INTERFERENCE
- NT THERMAL NOISE
- NT WHISTLERS
- NT WHITE NOISE
- Electromagnetic interference control in spacecraft design and interference prediction analysis applied to Nimbus satellites 03 p0354 N71-12381
- Electromagnetic compatibility and interference of spacecraft electronic components and functional testing with telemetry 03 p0376 N71-12721
- Electromagnetic wave propagation in magnetoplasma and whistler interference 07 p1083 N71-17823
- Shielded housing for protecting electronic equipment against electromagnetic interference [NASA-CASE-MSC-12168-1] 08 p1169 N71-18409
- Properties of holograms and applications of holography 08 p1211 N71-19224
- Preamplifier noise effects on spectrometer energy resolution [UCRL-72481] 10 p1611 N71-20697
- Phase modulated position lines in very low frequency Omega transmissions over large distances 11 p1705 N71-22906
- Ground and sky wave reflections and interference patterns in very low frequency radio transmission 11 p1705 N71-22908
- Landing systems signal reflection interference on correlation protected instrument landing system beams [RAE-TR-70141] 12 p1940 N71-23364

ELECTROMAGNETIC MEASUREMENT

Ultrahigh frequency antenna scatter propagation disturbances by vegetation 12 p1876 N71-23461

Tests to determine presence of electromagnetic interference and qualitative effect on communication-electronic equipment 13 p2054 N71-24486

Fokker-Planck equation used to describe process of electron loss from Van Allen zones due to pitch angle scattering by electromagnetic disturbances 18 p3004 N71-30923

Analysis of carrier density fluctuations in mercury cadmium telluride and causes of electromagnetic noise in photoconductors 19 p3171 N71-32617

Mathematical modeling techniques in analysis of environmental pollution generated by mixes of transportation modes, with detailed treatment of electrical interference [R-762-DOT/RC] 21 p3420 N71-34331

Convective instability in fluid layer with electromagnetic effects applied to earth and stellar atmospheres 22 p3672 N71-36183

ELECTROMAGNETIC MEASUREMENT

Measuring electrical resistance of rocks and minerals for predicting potential earthquake centers [NASA-TT-F-13212] 02 p0209 N71-11434

Broadband radiometers for quantitative analysis of electromagnetic radiation [T-30/69] 03 p0380 N71-13144

Numerical simulation of Welbel instability in one and two dimensions [LA-4482] 04 p0601 N71-14396

Electromagnetic measurement of shock Hugoniot of Teflon [AD-716333] 09 p1406 N71-20046

Particle velocity measurement in PMMA using electromagnetic velocity probe [AD-717346] 11 p1760 N71-21895

Varying phase reference signal technique for measuring millimeter signal phases in free space [AD-717688] 11 p1700 N71-22322

Electromagnetic measurement of water current velocities in Arctic regions 11 p1753 N71-22812

ELECTROMAGNETIC NOISE

NT ATMOSPHERICS

NT COSMIC NOISE

NT DAWN CHORUS

NT HISS

NT IONOSPHERIC NOISE

NT IONOSPHERICS

NT THERMAL NOISE

NT WHISTLERS

NT WHITE NOISE

Low frequency noise properties of mercury telluride infrared detectors 01 p0033 N71-10510

Statistical analysis of FM click event for unmodulated carrier in additive normal noise 02 p0182 N71-11278

Detection and estimation of complex radar missile system targets in noise and clutter environment 03 p0338 N71-12412

Broadband radiometers for quantitative analysis of electromagnetic radiation [T-30/69] 03 p0380 N71-13144

Correction of values in measurement of impulse noise spectra [LEA-TR-266] 03 p0418 N71-13278

Measurements of urban, suburban, and rural radio frequency noise interfering with aircraft communication [NASA-CR-72802] 05 p0643 N71-14754

High frequency noise in space charge-limited, solid state devices [AD-716579] 09 p1359 N71-19756

Description and operation of experimental plasma facility (Helios) in which electrons and lithium ions are heated by electromagnetic noise [ORO-3895-15] 10 p1626 N71-20669

Noise characteristics of gallium arsenide p-n junction avalanche transit time oscillators [AD-716998] 10 p1532 N71-20802

Quantizing noise analysis in delta modulators applied to first order Markov sources [AD-717221] 10 p1533 N71-21081

Temperature dependence of high frequency noise measured between 10 kHz and 2 MHz on double injection silicon diode 10 p1537 N71-21285

Results and analysis of combined aerial and ground ultrahigh frequency noise survey in urban area [NASA-TM-X-2244] 11 p1702 N71-22623

Radiation induced noise measurements in pulsed TRIGA reactor and proportionality to induced insulator conductivity in signal cables [WHAN-IR-42] 12 p1963 N71-24054

Noise level of Josephson junction amplifier at cryogenic temperatures [AD-720385] 14 p2228 N71-25947

Electromagnetic noise and altitude variation of auroral proton microbursts and proton flux density distributions 18 p2916 N71-31082

Add-on noise blanker for use in HF communication receivers [AD-722543] 18 p2891 N71-31357

Mathematical models for electromagnetic noise in neutral current sheet of geomagnetic tail [AD-723654] 19 p3175 N71-31802

Frequency instability and spectral purity of oscillators, and computation of very short term frequency instability of oscillators perturbed by thermal noise [ONERA-P-132] 20 p3242 N71-33724

Noise control and improved system reliability for high speed logic integrated circuits [DISS-4470] 20 p3244 N71-33893

Three parameter model of differential tracking data types applied to zero declination and process noise problems for improved orbit determination 21 p3391 N71-34127

Mathematical model of DSIF Doppler tracking system phase noise 21 p3393 N71-34151

Comparison of methods for detecting nonfluctuating targets in white normal noise [PH L-1971-3] 22 p3628 N71-35852

Light noise due to light scattering in astronomical telescope Lallemand camera image correlator-receiver system 24 p3922 N71-37977

ELECTROMAGNETIC PROPAGATION
U ELECTROMAGNETIC WAVE TRANSMISSION

ELECTROMAGNETIC PROPERTIES

NT ABSORPTANCE

NT ABSORPTIVITY

NT BIREFRINGENCE

NT BRIGHTNESS

NT COLOR

NT DICHROISM

NT FARADAY EFFECT

NT LUMINOSITY

NT OPACITY

NT OPTICAL PROPERTIES

NT OPTICAL REFLECTION

NT PHOSPHORESCENCE

NT PHOTOCONDUCTIVITY

NT PHOTOELASTICITY

NT PHOTOELECTRIC EFFECT

NT PHOTOELECTRIC EMISSION

NT PHOTOIONIZATION

NT PHOTOVISCOELASTICITY

NT PHOTOVOLTAIC EFFECT

NT RADIANCE

NT REFLECTANCE

NT REFRACTIVITY

NT SKY BRIGHTNESS

NT STELLAR LUMINOSITY

NT TRANSMISSIVITY

NT TRANSMITTANCE

NT TRANSPARENCE

NT TURBIDITY

Electromagnetic properties and propagation of microwave radiation [JPRS-52129] 05 p0648 N71-14987

Structures and electromagnetic properties of magnetic glasses [COO-1700-16] 06 p0882 N71-16780

Chemical composition, electromagnetic properties, raw materials, and production techniques for various types of ferrites 12 p1965 N71-23285

Effect of velocity profile distortion in circular transverse-field electromagnetic flowmeters [NASA-TN-D-6454] 19 p3102 N71-32448

Design, development, and electromagnetic properties of shunt driven circular loop radio antennas [AD-724343] 20 p3241 N71-33119

Noise control and improved system reliability for high speed logic integrated circuits [DISS-4470] 20 p3244 N71-33893

ELECTROMAGNETIC PROPULSION
Reliability and cost of electrostatic and electromagnetic thruster systems for satellite auxiliary propulsion [NASA-CR-119319] 18 p3061 N71-31146

ELECTROMAGNETIC PULSES

Pulsing techniques for CO₂ lasers [AD-712117] 02 p0238 N71-11582

Development of wideband electromagnetic probes for detection of transient currents [AD-712948] 02 p0228 N71-12053

Simulation of high altitude ionized air with artificial dielectric [AD-713531] 05 p0658 N71-15429

Protection of pulse measuring equipment against spurious noises [CEA-N-1353] 05 p0687 N71-15454

Characteristics of wideband photorecording instrument for analyzing electromagnetic pulses [AD-713922] 06 p0813 N71-16119

Electromagnetic pulse propagation in duct between ground and atmospheric layer 10 p1524 N71-21425

Effects of nuclear electromagnetic pulses on AM radio broadcast stations in emergencies [AD-717319] 11 p1090 N71-31054

Theoretical and experimental analysis of picosecond laser pulses [AD-719415] 13 p3089 N71-34772

Nondestructive tests of electromagnetic ferromagnetic coatings for chemical and ordnance mission work [AD-723234] 16 p3617 N71-36889

High-altitude electromagnetic pulse source systems and ionization from Compton scattering of gamma rays based on forward scattering of Compton electrons [AD-726928] 23 p3818 N71-37220

Electronic component degradation due to electromagnetic pulse transients [AD-726923] 24 p3898 N71-37703

ELECTROMAGNETIC PUMPS

Hydraulic performance and cavitation characteristics of electromagnetic helical induction pump operating with potassium at 1500 F and with lithium at 2200 F [ORNL-TM-2995] 08 p1205 N71-10754

Multiducted electromagnetic pump for conducting liquids [NASA-CASE-NPO-10755] 15 p2415 N71-27004

ELECTROMAGNETIC RADIATION

NT AIRGLOW

NT BLACK BODY RADIATION

NT BREMSSTRAHLUNG

NT CERENKOV RADIATION

NT COHERENT ELECTROMAGNETIC RADIATION

NT COHERENT LIGHT

NT CYCLOTRON RADIATION

NT DAYGLOW

NT DECA-METER WAVES

NT DECIMETER WAVES

NT ELECTROMAGNETIC PULSES

NT EXTRATERRESTRIAL RADIO WAVES

NT FAR INFRARED RADIATION

NT FAR ULTRAVIOLET RADIATION

NT GAMMA RAY BEAMS

NT GAMMA RAYS

NT GERGENSHEIN

NT H WAVES

NT INFRARED RADIATION

NT LIGHT [VISIBLE RADIATION]

NT LIGHT BEAMS

NT LONG WAVE RADIATION

NT LYMAN ALPHA RADIATION

NT MICROWAVES

NT MILLIMETER WAVES

NT MONOCHROMATIC RADIATION

NT NEAR INFRARED RADIATION

NT NEAR ULTRAVIOLET RADIATION

NT NIGHTGLOW

NT NONEQUILIBRIUM RADIATION

NT PHONON BEAMS

NT PHOTON BEAMS

NT PLANETARY RADIATION

NT POLARIZED ELECTROMAGNETIC RADIATION

NT POLARIZED LIGHT

NT RADIO BURSTS

NT RADIO EMISSION

NT RADIO WAVES

NT SHORT WAVE RADIATION

NT SKY RADIATION

NT SOLAR RADIO BURSTS

NT SOLAR RADIO EMISSION

NT SOLAR X-RAYS

NT SOMMERFELD WAVES

NT SUBMILLIMETER WAVES

NT SUNLIGHT

NT SYNCHROTRON RADIATION

NT TERRESTRIAL RADIATION

NT THERMAL RADIATION

NT TROPOSPHERIC RADIATION

NT TWILIGHT GLOW

NT TYPE A BURSTS

NT ULTRAVIOLET RADIATION

NT X RAYS

NT ZODIACAL LIGHT

Electromagnetic radiation, curves, electron microscopes, solid state devices, and plasma physics [AD-709945] 01 p0035 N71-10055

Scattering from conducting cylinder clad with anisotropic plasma [AD-716692] 01 p0105 N71-10019

Research in antennas and waves in plasma [NASA-CR-111136] 01 p0106 N71-10017

Radiation from aperture in conducting plane coated with moving plasma layer [AD-712010] 02 p0279 N71-11171

Analysis of ranging system for lunar surface optical properties experiment [NASA-CR-106673] 02 p0177 N71-11264

Surface and bulk waves on axially magnetized plasma columns [AD-711649] 02 p0208 N71-11089

SUBJECT INDEX

ELECTROMAGNETIC SCATTERING

Characteristics of power flow in plasma filled waveguides
[AD-711648] 02 p0280 N71-11861

Performance report on Project Vega Studies
[AD-711961] 03 p0330 N71-12409

Effects of quantization of electromagnetic radiation on signal waveforms and communication systems
[AD-712331] 03 p0330 N71-12411

Characteristics of collisionless damping of electromagnetic waves in region of intense inhomogeneity of cold plasma
[KIPPT-69-53] 03 p0437 N71-12891

Computer programs for solving electromagnetic radiation and scattering from thin wires
[AD-713156] 05 p0654 N71-14856

Electromagnetic wave and charge carrier interaction in crossed fields
[AD-713399] 05 p0653 N71-14883

Phase correction on small reflector in double reflector antenna
[AD-713761] 05 p0646 N71-14922

Motion and radiation of charged particles in strong electromagnetic waves in plane and spherical waves
[NASA-CR-111535] 05 p0744 N71-15178

Termin analysis by remote sensors using reflection and refraction of electromagnetic waves
[AD-713539] 05 p0677 N71-15461

Electromagnetic radiation from infinite cylinder immersed in inhomogeneous medium
[AD-714575] 06 p0825 N71-16629

Electromagnetic generation of ultrasound in metal surfaces
[NYO-2150-43] 07 p1043 N71-17633

Electromagnetic wave ducting in ionosphere
[AD-715338] 07 p1023 N71-17663

Linear transformation and absorption of plasma and electromagnetic waves
[NIP-18504] 08 p1269 N71-18165

Radiation theory and effects of interfaces in infinite planar arrays - MART program
[AD-714807] 08 p1161 N71-18294

Radiation theory and effects of nonrigid interfaces in infinite planar arrays - MART program
[AD-714806] 08 p1161 N71-18295

Calculations on electromagnetic radiation from infinitely long wire in dielectric material over conducting plane
[AD-715357] 08 p1168 N71-18446

Numerical solutions of full wave equations in inhomogeneous cold plasma slab near lower hybrid resonance
[CEA-CONF-1613] 08 p1272 N71-18505

Coupled electromagnetic and electron acoustic wave propagation in inhomogeneous plasma sheath
[AD-715916] 08 p1273 N71-18660

Propagation of electromagnetic waves in ferrite filled longitudinally magnetized elliptical waveguide
[AD-716081] 08 p1163 N71-18881

Interaction between slow electromagnetic waves and drifting carriers in semiconductors
[AD-716163] 08 p1163 N71-19118

Spectral response measurements of man-made targets and surfaces for frequency variation analysis of electromagnetic backscatter
[NASA-CR-117635] 09 p1346 N71-19425

Scattering and radiation of electromagnetic waves from radially inhomogeneous cylindrical plasma structures
[AD-716709] 09 p1447 N71-19685

Determination of scalar and vector scattering from turbulent plasmas
[AD-716877] 09 p1447 N71-19705

Electromagnetic wave transmission through normal and disturbed ionospheres, emphasizing propagation from spacecraft communication
[AD-716878] 09 p1349 N71-19753

Research in environmental sciences including climatology, oceanography and earth resources, planetary atmospheres and ionospheric physics, space physics, astrophysics, and relativity
[AD-717632] 09 p1385 N71-20149

Concentric sphere model of ionosphere for takeoff angle and length determinations in complex ray configurations
[AD-716933] 10 p1517 N71-20651

Measurement of range error in vertically arriving electromagnetic signal
[AD-716774] 10 p1552 N71-21277

High power electronics including electrodynamic theory of grids, cathode losses in magnetrons, closed resonant chains, and electromagnetic vibration dampers
[AD-717629] 10 p1537 N71-21300

Electromagnetic radiation detection of microwave field patterns using liquid crystals
[AD-717533] 11 p1699 N71-21923

Development of unified mathematical theory for normal wave propagation phenomena of classical physics
[AD-717632] 11 p1796 N71-21934

Medium optics for problem solving in geodesy, navigation, properties, and uses of coherent electromagnetic radiation
[AD-717775] 11 p1774 N71-22239

Direct electromagnetic generation and detection of acoustic waves reported for cesium and mercury near room temperature
[NYO-2150-43] 11 p1799 N71-22536

Electromagnetic surface wave propagation on yttrium-iron garnet and indium antimonide rods at microwave frequencies under axial magnetization
[AD-717629] 11 p1702 N71-22719

Electromagnetic wave propagation study within inhomogeneously filled waveguides, using Maxwell equations
[AD-717833] 12 p1703 N71-22757

Development of electromagnetic wave transmission line circulator and application to parametric amplifier circuits
[NASA-CASE-XNP-02140] 11 p1727 N71-23097

High frequency and weak acceleration of electromagnetic wave propagation in uniformly accelerated simple medium
[AD-717833] 12 p1964 N71-23200

Instabilities in system of equations describing electromagnetic wave propagation and fluid dynamics
[AD-718858] 12 p1932 N71-23298

Electron and solid state physics, control theory and applications, ferromagnetic and ferroelectric materials, electromagnetic phenomena, and plasma medium scattering
[AD-718117] 12 p1986 N71-23911

Electromagnetic radiation detectors for wavelength region 0.1 micrometer to 1 micrometer
[AD-718096] 13 p2053 N71-24397

Left and right hand circular electromagnetic polarization excitation by phase shifter and hybrid networks
[NASA-CASE-GSC-10021-1] 13 p2054 N71-24595

Development of smooth perturbation method for determining propagation of radio signals in medium with large scale inhomogeneities
[AD-719533] 13 p2046 N71-24951

Development of statistical model for electrons in atoms based on expansion of one-electron Green function in spherical harmonics
[AD-719799] 13 p2146 N71-24958

Experiments demonstrating resonant nonlinear electromagnetic wave excitation of electron plasma and ion acoustic waves in plasma column
[TR-70-36] 13 p2148 N71-25184

Normalized procedures for standardizing and determining spectral sensitivities of detectors for measuring external radiation by electromagnetic radiation
[CEA-R-40091/1] 14 p2258 N71-26569

Propagation and absorption of ionic-hybrid waves in slightly inhomogeneous plasma layer
[IAE-1949] 14 p2323 N71-26736

Change in polarization of electromagnetic wave propagating across magnetically sheared plasma column
[CEA-CONF-1608] 15 p2498 N71-27143

Transport equation for Doppler frequency shift in transport of electromagnetic waves through underdense plasma
[AD-721047] 15 p2500 N71-27318

Electromagnetic wave transmission and breakdown by nuclear explosion and ionospheric disturbance discharges
[AD-720862] 15 p2480 N71-27661

Angular distributions and correlations of alpha and beta particles, electrons, and electromagnetic radiations from oriented nuclei
[LA-4565] 16 p2645 N71-28157

Model for ferromagnetic material characteristics in diffusion of transient electromagnetic fields through saturated ferromagnetic media
[AD-721906] 16 p2638 N71-28458

Numerical calculation of electromagnetic field and resonant frequencies of resonators at Swierk, Poland proton 10 MeV linear accelerator
[INR-P-1218] 16 p2577 N71-28417

Development of method for suppressing excitation of electromagnetic surface waves on dielectric conical antennas
[NASA-CASE-XLA-10772] 16 p2563 N71-28940

Electron and solid state physics, control theory, electromagnetic radiation, and antenna array research
[AD-722415] 17 p2863 N71-30358

Development of computable electromagnetic theory model for lunar reflectivity problem - Vol. 3
[NASA-CR-115084] 18 p2890 N71-31104

Calculation of power scattered by large, homogeneous body bounded by smooth, undisturbed surface when illuminated by incident field of finite extent - Vol. 2
[NASA-CR-115083] 18 p2890 N71-31105

Electromagnetic radiation measuring instrument utilizing ac p-n junction diode capacitance
[NASA-CASE-LEW-11159-1] 18 p2924 N71-31127

Neutron, electron, proton, and electromagnetic radiation effects on transistors - handbook
[NASA-CR-1834] 18 p2898 N71-31372

Antenna parameters and input admittance from numerical analysis of radiation fields of slotted circular disks
[AD-718096] 19 p3071 N71-32288

Scattering of electromagnetic waves by systems of unknown charge distribution
[THUX-3780-27] 19 p3134 N71-32326

Enhanced transmission of strong right hand circular wave near cyclotron resonance in anisotropic hollow slab plasma occurring earlier than corresponding weak electromagnetic field
[AD-723293] 19 p3166 N71-32596

Effect of new field on breakdown of antenna radiation capability in roosty vehicles
[AD-723655] 19 p3058 N71-32664

Effects of radiation from neutrons, proton, electron, and electromagnetic sources on solid state photodevices and solar cells
[NASA-CR-1872] 19 p3068 N71-32698

Astrophysics, radio astronomy, radio sources, galaxies, cosmology, pulsars, black body radiation, universe, and electromagnetic wave propagation
[P-494] 20 p3343 N71-32836

Propagation of electromagnetic waves in galaxy and effects of intervening matter on propagation
[AD-718096] 20 p3343 N71-32837

Electromagnetic wave propagation in random interstellar media and amplitude fluctuations of radio sources
[AD-718096] 20 p3321 N71-32838

Measurement of magnetic field dependence on low temperature electromagnetic generation of ultrasonic waves in potassium
[NYO-2150-72] 21 p3465 N71-34664

Analysis of radiations encountered in space environment and manner in which interactions with matter occur
[NASA-CR-1871] 21 p3504 N71-34962

Handbook of correlative data on galactic cosmic rays, solar electromagnetic radiation, solar protons, geospectrum, ionosphere, and neutral atmosphere
[NASA-TM-X-67294] 21 p3532 N71-35148

Characteristics of radio wave propagation in troposphere, ionosphere, and along earth surface
[FOA-3-A-3730-40] 22 p3554 N71-35311

Electromagnetic plasma wave propagation along external magnetic field and transverse wave echoes determined by Vlasov-Maxwell equation
[NASA-CR-121918] 22 p3653 N71-36050

Interaction of plane p-polarized electromagnetic wave obliquely incident on hot plasma half space and plasma slab
[AD-718096] 22 p3655 N71-36049

Characteristics of wideband communication systems based on wideband excitation of hypersonic waves and application of theory to continuous signals
[JPRS-54044] 23 p3723 N71-36537

Ionization spectrometer for measuring electromagnetic surface wave excitation by charged particle beams
[ITT-6] 23 p3808 N71-37153

Group velocity and refractivity behavior of strong electromagnetic surface waves propagating along vacuum-plasma plane interface
[DEMO-71/5] 23 p3824 N71-37274

Dispersion equation for studying electromagnetic surface waves in adjacent plasma flows
[UARAE-97] 23 p3824 N71-37276

Spectral degree of blackness for certain refractories at high temperatures, dependent on composition, structure, and surface cleaning or radiating materials
[AD-727473] 24 p3901 N71-38126

Charged particle showers and electromagnetic radiation from stationary and nonstationary sources
[AD-718096] 24 p4010 N71-38393

ELECTROMAGNETIC SCATTERING

NT HALOS

NT IONOSPHERIC F-SCATTER PROPAGATION

NT LIGHT SCATTERING

NT MICROWAVE SCATTERING

NT MIE SCATTERING

NT RAMAN SPECTRA

NT RAYLEIGH SCATTERING

NT THOMSON SCATTERING

NT X RAY SCATTERING

Integral equation formulations for electromagnetic scattering from two-dimensional inhomogeneities in conductive earth
[NASA-CR-110910] 01 p0049 N71-10783

Integral equation formulations for electromagnetic scattering from two-dimensional inhomogeneities in conductive earth - appendices, figures, bibliography, and computer programs
[NASA-CR-110911] 01 p0050 N71-10794

Perturbation theory for calculation of electromagnetic wave scattering from rough surfaces
[AD-711537] 02 p0213 N71-11753

Electromagnetic scattering by periodic surface
[AD-713183] 05 p0732 N71-14823

Computer programs for solving electromagnetic radiation and scattering from thin wires
[AD-713156] 05 p0654 N71-14856

Scattering by imperfectly conducting spheres
[AD-713678] 05 p0754 N71-15219

Fourier transform of scattering diagrams and selective connection techniques
[AD-713689] 06 p0815 N71-16286

Electromagnetic wave scattering by flat surface with small, shallow roughness
[AD-713678] 07 p1067 N71-17033

ELECTROMAGNETIC SHIELDING

- Scattering and radiation of electromagnetic waves from radially inhomogeneous cylindrical plasma structure
09 p1447 N71-19685
- Numerical basis transformation, least squares, and characteristic mode techniques for thin wire electromagnetic scattering
11 p1727 N71-21861
- Classical cross sections of electromagnetic and gravitational waves scattered by static gravitational field, and agreement with quantized linearized field theory
[NYO-2262-TA-222] 11 p1806 N71-22462
- Dispersion statistics of high frequency signal propagation in ionosphere
11 p1710 N71-22938
- Computer programs to calculate characteristic currents and gain patterns of conducting bodies of revolution
[AD-718969] 13 p2042 N71-24416
- Electromagnetic radiation scattering by hydrodynamically turbulent systems via operator formalism
[AD-722323] 17 p2797 N71-29842
- Development of computable electromagnetic theory model for lunar reflectivity problem - Vol. 3
[NASA-CR-115084] 18 p2890 N71-31104
- Calculation of power scattered by large, homogeneous body bounded by smooth, undulated surface when illuminated by incident field of finite extent - Vol. 2
[NASA-CR-115083] 18 p2890 N71-31105
- Application of eikonal approach to scalar and electromagnetic wave scattering from coated perfect conductors
[P-4771] 19 p3056 N71-32221
- Scattering of electromagnetic waves using integral equation form of Maxwell equations for electric fields
[NASA-CR-121760] 21 p3447 N71-34530
- Integral equation formulations of scattering from two dimensional inhomogeneities in conductive earth
23 p3753 N71-36762
- Contributions of inelastic channels to electromagnetic form factor of pions, and production of strange particles in proton-proton scattering
23 p3821 N71-37255
- Multiple scattering and eigenfunction solutions for electromagnetic scattering from cylinders over and imbedded in dielectric half spaces
24 p3890 N71-37730
- Dipole antenna and fluctuation of far electric field intensity over stationary and time-varying irregular surfaces
[AD-728033] 24 p3899 N71-37791
- ELECTROMAGNETIC SHIELDING**
NT RADIO FREQUENCY SHIELDING
S/LA detector in homogeneous magnetic field for beta spectrometer with electromagnetic shielding for selected electron energy level studies
[INR-P-1227] 15 p2485 N71-27814
- Electromagnetic shielding effectiveness degradation from weld defects in metal conducting sheets and comparison of propagation through rectangular and circular apertures
[AD-721907] 16 p2569 N71-28410
- Model for ferromagnetic material characteristics in diffusion of transient electromagnetic fields through saturated ferromagnetic media
[AD-721906] 16 p2638 N71-28458
- Shielded flat conductor cable fabricated by electrolysis and electrolytic plating
[NASA-CASE-MPS-13667] 16 p2571 N71-28691
- ELECTROMAGNETIC SHOCK TUBES**
U SHOCK TUBES
ELECTROMAGNETIC SPECTRA
NT BALMER SERIES
NT D LINES
NT ELECTRONIC SPECTRA
NT FRAUNHOFER LINES
NT H ALPHA LINE
NT H BETA LINE
NT H GAMMA LINE
NT INFRARED SPECTRA
NT K LINES
NT LINE SPECTRA
NT LYMAN SPECTRA
NT MICROWAVE SPECTRA
NT RADIO SPECTRA
NT RAMAN SPECTRA
NT SOLAR SPECTRA
NT STELLAR SPECTRA
NT ULTRAVIOLET SPECTRA
NT VIBRATIONAL SPECTRA
X ray astronomy
[NASA-TM-X-65372] 01 p0118 N71-10610
- Research in basic atomic properties extending useful range of electromagnetic spectrum
[AD-71546] 02 p0275 N71-11914
- Theoretical interpretation of optical and electron scattering spectra of H2O
04 p0568 N71-14369
- Millimeter wave propagation utilizing ATS 5 satellite
[NASA-TM-X-65404] 05 p0643 N71-14738

- Trivalent chromium ion X-ray fluorescence electron-spin resonance spectra in single MgO crystals
21 p3499 N71-34931
- Electromagnetic background radiation of universe
23 p3850 N71-37438
- ELECTROMAGNETIC WAVE FILTERS**
NT INFRARED FILTERS
NT MICROWAVE FILTERS
NT OPTICAL FILTERS
NT ULTRAVIOLET FILTERS
NT WAVEGUIDE FILTERS
Channel filters for ideal single sideband modulation
06 p1163 N71-18960
- Mathematical filter for eliminating persistence in meteorological data
11 p1788 N71-21940
- Computerized simulation of subharmonic resonance in limit cycling voltage regulator
[AD-726701] 15 p2388 N71-27127
- Development of microwave frequency yttrium-iron garnet filter and circulator
19 p3064 N71-31696
- Design and characteristics of laser camera system with diffusion filter of small particles with average diameter larger than wavelength of laser light
[NASA-CASE-NPO-10417] 20 p3281 N71-33410
- Calcite filter for astronomical photometry, errors, and near infrared applications
22 p3584 N71-35525
- Near infrared astronomical photometry using calcite-Polaroid filter method
22 p3584 N71-35527
- Optical filters for radio pulses with linear frequency modulation and interspersed phase manipulation at radar stations
24 p3888 N71-37710
- ELECTROMAGNETIC WAVE TRANSMISSION**
NT DOUBLE SIDEBAND TRANSMISSION
NT HALOS
NT IONOSPHERIC F-SCATTER PROPAGATION
NT IONOSPHERIC PROPAGATION
NT LIGHT SCATTERING
NT LIGHT TRANSMISSION
NT MANDELSTAM REPRESENTATION
NT MICROWAVE ATTENUATION
NT MICROWAVE TRANSMISSION
NT MULTIPATH TRANSMISSION
NT RADAR TRANSMISSION
NT RADIO ATTENUATION
NT RADIO TRANSMISSION
NT SCATTER PROPAGATION
NT SHORT WAVE RADIO TRANSMISSION
NT SINGLE SIDEBAND TRANSMISSION
NT TELEVISION TRANSMISSION
NT TRANSEQUATORIAL PROPAGATION
Equations controlling wave transmissions in lower ionosphere and computer program for integrating equations of motion
01 p0052 N71-10971
- Characteristics of power flow in plasma filled waveguides
[AD-711648] 02 p0280 N71-11061
- Transmission line network describing single electromagnetic waves propagating in cylindrical waveguides
[RM-4897] 03 p0336 N71-12397
- Investigating autocorrelation of mutual amplitude and phase fluctuation in diffracted waves on rough screens
[AD-712335] 03 p0337 N71-12405
- Investigating electromagnetic scattering by cylinders using Rayleigh-Gans theory
[NASA-TM-X-64545] 03 p0417 N71-12569
- Electromagnetic wave transmission along air-sea interface and in underwater communication and optical systems
[AGARD-CP-77-70] 04 p0563 N71-13701
- Sources and mechanics of extremely low frequency wave propagation in model ionosphere and sea
04 p0490 N71-13702
- Two dimensional model for radio wave propagation across land/sea boundaries
04 p0491 N71-13703
- Acoustic or electromagnetic wave propagation in stratified sea
04 p0491 N71-13704
- Literature review on electromagnetic wave transmission in absorbing media
04 p0491 N71-13705
- Antenna radiation and wave propagation in sea water
04 p0491 N71-13706
- Program of measurements related to two phenomena of plasma/antenna interaction
[NASA-CR-1727] 05 p0642 N71-14735
- Electromagnetic wave propagation characteristics for North West Cape, Australia
[AD-713596] 05 p0644 N71-14903
- Optical absorption by excitons in alkali halides, personnel accident dosimeters, electromagnetic wave propagation in atmosphere, metallurgy, and related research
06 p0908 N71-15747

SUBJECT INDEX

- Calculation of average surface impedance in periodic surface
[AD-714090] 06 p0815 N71-16822
- Handbook of electromagnetic propagation in conducting media
[AD-714096] 06 p0817 N71-16828
- Investigating electromagnetic wave propagation in uniformly accelerated medium
06 p0946 N71-16880
- Electromagnetic wave propagation in magnetoplasma and whistler interference
07 p1083 N71-17820
- Interaction of QTX wave with density fluctuations in inhomogeneous magnetized plasma
[AD-715277] 07 p1084 N71-17884
- Electromagnetic wave diffraction in Fabry-Pérot optical resonator
08 p1302 N71-18823
- Schedule of AGARD conferences for 1971, and summaries of 1970 AGARD publications
[AGARD-BUL-71-1] 08 p1442 N71-19141
- Electromagnetic signal propagation along the earth-ionosphere waveguide
08 p1464 N71-19152
- Electromagnetic wave transmission in earth ionosphere from 3 kHz to 3000 THz with emphasis on earth to space paths up to Jan. 1970
[NASA-CR-117173] 09 p1350 N71-30021
- Computer solution of plane electromagnetic wave interaction with bounded inhomogeneous plasma slab with electron density gradient transverse to wave
10 p1520 N71-31112
- Propagation of amplitude modulated, high RF plane electromagnetic wave through anisotropic plasma
10 p1520 N71-31114
- Tropospheric characteristics and their effects on electromagnetic wave propagation and radio signal transmission
[AGARD-CP-70-71-PT-1] 10 p1522 N71-31488
- Tropospheric scattering and delay effects on electromagnetic wave propagation in space communications
10 p1522 N71-31411
- Electromagnetic pulse propagation in duct between ground and atmospheric layer
10 p1524 N71-31425
- Ray tracing analysis on duct effect in line of sight wave propagation above sea surface
10 p1524 N71-31428
- Atmospheric stratifications causing anomalous signal propagation at 170 and 5000 MHz over sea surface beyond horizon
10 p1524 N71-31429
- Perturbation method for calculating surface roughness effects on electromagnetic wave propagation in inhomogeneous atmosphere
10 p1525 N71-31432
- Development of unified mathematical theory for several wave propagation phenomena of classical physics
[AD-717632] 11 p1796 N71-31994
- Galactic and solar cosmic ray propagation, variations, and energy spectra
11 p1822 N71-32017
- Tropospheric and ionospheric compositions effect on phase and frequency degradations in propagating signals
[AGARD-CP-33] 11 p1704 N71-22901
- Phase delay variations in design of very low frequency long range navigation aids
11 p1793 N71-22902
- Propagation model for diurnal amplitude and phase variations of very low frequency transmission path
11 p1705 N71-22903
- Phase changes in signal received on earth surface and transmitted from antenna placed into deep excavation
11 p1708 N71-22905
- Atmospheric composition effects on electromagnetic wave propagation and precision of radio and optical locating systems
11 p1712 N71-22906
- Propagation of electromagnetic waves along gyrotropic cylinder in longitudinal magnetic field
11 p1800 N71-22904
- Transmission loss in tropospheric transmission propagation on 12 GHz scatter link
12 p1875 N71-23408
- Boundary value problem in electromagnetic wave radiation from flanged waveguide
[AD-718407] 12 p1892 N71-23404
- Probability distributions of effective radar reflectivities derived from electromagnetic field strength measurements compared to surface rainfall rates for radio frequency interference
[AD-718270] 12 p1879 N71-23407
- Semiconducting and transmission properties of chalcogenide glasses
[NLL-M-26294-5828/AP] 12 p1966 N71-23403
- Wind tunnel tests of plasma covered antenna to determine transmission and radiation characteristics and effects of injecting chemicals into boundary layer
[AD-719976] 13 p2043 N71-31517

SUBJECT INDEX

ELECTRON ACCELERATORS

- Investigation of periodic nature of Jupiter bursts to determine correlation with position of satellite IO and central meridian of longitude of Jupiter
[NASA-CR-118335] 13 p2170 N71-25498
- Electromagnetic shielding effectiveness degradation from weld defects in metal conducting sheets and comparison of propagation through rectangular and circular apertures
[AD-721907] 16 p2569 N71-28410
- Relating ionospheric electron content to electromagnetic propagation effects along transionospheric paths and measurements of diurnal variations of electron content
[AD-722043] 16 p2587 N71-28426
- Nonlinear programming and iterative network synthesis for transverse electromagnetic wave transmission modes
16 p2575 N71-28824
- Theoretical and experimental investigation of electromagnetic wave propagation in antiferromagnetic media
18 p2963 N71-31068
- Flow of time-varying electromagnetic energy, and wide variety of energy gain mechanisms in homogeneous, solid state plasmas
18 p2994 N71-31508 [4111]
- Enhanced transmission of strong right hand circular wave near cyclotron resonance in afterglow helium slab plasma occurring earlier than corresponding weak electromagnetic field
[AD-723253] 19 p3166 N71-32596
- Complete closed forms for amplitude and phase fluctuations in forward scattering study of electromagnetic waves transmitted through turbulent media
19 p3071 N71-32712
- Edy formation in energy transport of electromagnetic wave fields in waveguide
21 p3483 N71-34825
- Wave attenuation calculations for two-layer earth crust waveguide model for underground electromagnetic propagation
[AD-726754] 22 p3554 N71-35318
- Gravitational wave effect on electromagnetic wave transmission in physical optics approximation
23 p3803 N71-37115
- Asiatic symmetric electromagnetic wave propagation in vacuum channel in magnetoactive plasma
[JAPAE-92] 23 p3824 N71-37277
- Electromagnetic wave emission of ideally conducting sphere with variable radius and constant uniform field
[AD-727434] 24 p3967 N71-38295
- ELECTROMAGNETIC WAVES**
U ELECTROMAGNETIC RADIATION
ELECTROMAGNETICS
U ELECTROMAGNETISM
ELECTROMAGNETISM
NT MAGNETOSTATICS
Directory of standardized symbols for electromagnetic measurements
[ADAR-576-70] 03 p0352 N71-12545
- Abstracts on research in fluid dynamics, plasmas, and electromagnetics
[AD-714286] 06 p0962 N71-16612
- Electromagnetic theory, microwave and radio equipment, and optical communication
[IN-3-36-1970] 10 p5156 N71-20601
- Electromagnetic theory, antennas, microwave equipment, and radio anechoic chamber
[P-112] 10 p5157 N71-20602
- Electromagnetic correction calculations for strong π - α scattering
10 p1621 N71-21741
- Electromagnetic braking arrangement for controlling rotor rotation in electric motor
[NASA-CASE-XNP-06936] 13 p2085 N71-24695
- Electric field measuring techniques used in ionospheric and magnetospheric electron current studies
[NASA-TM-X-65596] 17 p2748 N71-30094
- Computerized simulation of electromagnetic and finite hole sub effects on counterstreaming low instability
[AD-723528] 19 p3164 N71-32150
- ELECTROMAGNETS**
NT HIGH FIELD MAGNETS
NT SUPERCONDUCTING MAGNETS
Characteristics of superconducting flux pump
[AD-711569] 02 p0193 N71-11352
- Characteristics of magnetohydrodynamic flow around blunt bodies
03 p0310 N71-12212
- Magnetic element position sensing device, using miniatured electromagnets
[NASA-CASE-XGS-07514] 06 p0903 N71-16099
- Electroexplosive safe-arm initiator using electric drive electromagnetic coils and magnets to align chips
[NASA-CASE-LAR-10372] 08 p1169 N71-18599
- Justification for use of series transistor banks for improvement of silicon controlled rectifier power supply current regulation in beam transport magnets
[AD-777-02] 12 p1090 N71-23610
- Design, construction, and operation of high-field magnet for hydrogen arc experiment
[AD-473] 13 p2453 N71-27261
- Magnetic bearing with diverse magnetic sources coupled to same air gap via different low magnetic reluctance paths for use with permanent magnets
[NASA-CASE-GBC-11079-1] 16 p2629 N71-28461
- Use of samarium cobalt as permanent magnet material for field excitation in 100 kW generator
[AD-722872] 18 p2874 N71-31289
- Formation stages of magnetic field in model of accelerator sector electron magnet
[JINR-P9-5669] 22 p3433 N71-35895
- Characteristics of modified unipolar machine with rotor consisting of two parallel magnets imbedded in superconducting lead casting
23 p3804 N71-37120
- ELECTROMECHANICAL DEVICES**
High speed electro-arc printer design
[AD-712608] 03 p0341 N71-12468
- Describing device for velocity control of electromechanical drive mechanism of scanning mirror of interferometer
[NASA-CASE-XGS-03532] 07 p1031 N71-17627
- Electromechanical acoustic underwater imaging scanner assembly
[AD-717561] 11 p1722 N71-21921
- Operation of modular gear systems in vacuum environment with and without lubrication and under no load conditions
12 p1925 N71-23276
- Mechanical actuator wherein linear motion changes to rotational motion
[NASA-CASE-XGS-04548] 12 p1929 N71-24045
- Solid state force measuring electromechanical transducers made of piezoelectric materials
[NASA-CASE-ERC-10088] 13 p2153 N71-25490
- Electromechanical devices to transfer, position, and retrieve space manufacturing equipment
14 p2261 N71-26014
- Electromechanical control actuator system using double differential screws
[NASA-CASE-ERC-10022] 14 p2264 N71-26635
- Miniature electrochemical junction transducer operating on microinjection effect and utilizing epoxy for stress coupling component
[NASA-CASE-ERC-10087] 15 p2409 N71-27334
- Design and operation of electronic combination lock system with built-in alarm features suitable for multi-unit apartment and office complexes
19 p3070 N71-31646
- Effect of electromagnetic mixing on ingot grain size during continuous casting of magnesium alloys
[AD-721771] 24 p3937 N71-38086
- ELECTROMECHANICS**
Development of creep tester for metals and alloys with electromechanical and servomechanical instrumentation
[BM-R-7456] 02 p0244 N71-12004
- Lorentz force, Maxwell equation, and Poisson equation in continuum electromechanics
[AD-716567] 09 p1423 N71-19658
- Finite data analysis and electromechanical simulation of sounding rocket stability using rigid body energy techniques
[AD-719738] 13 p2175 N71-25387
- ELECTROMETERS**
Surface rate measurement of glaciers using electrometry
[AD-711911] 02 p0215 N71-11954
- Digitalizing electrometer system using integrating amplifier
[AD-714561] 06 p0822 N71-16056
- Particle velocity measurement in PEMA using electromagnetic velocity gate
[AD-717346] 11 p1760 N71-21895
- Vibrating element electrometer producing high conversion gain by input current control of elements resonant frequency displacement amplitude
[NASA-CASE-XAC-02807] 11 p1727 N71-23021
- ELECTROMIGRATION**
Transport measurements through cation-exchange membranes by concentration clamp technique
[NASA-CR-111398] 03 p0332 N71-12370
- Anisotropic diffusion and electromigration research
[RPI-1044-24] 05 p0706 N71-15538
- Electromigration and void kinetics in silver
09 p1397 N71-19352
- Observation of void formation induced by electromigration in single crystal and bicrystal Au films and polycrystalline Al films
[NYO-4185-1] 11 p1780 N71-22583
- Isotopic enrichment by electromigration in aqueous solutions of transition metal halides
[UCRL-51063] 17 p2799 N71-36016
- ELECTROMOTIVE FORCES**
Thermodynamic properties of aqueous hydrochloric acid-sodium chloride-magnesium chloride mixtures calculated by electromotive force measurements
[ORNL-TM-3017] 01 p0019 N71-10025
- High pressure effects on thermocouple electromotive forces
14 p2257 N71-26484
- High pressure and temperature effects on electromotive forces of thermocouples
14 p2257 N71-26487
- Electromotive force measurements on electric motor for electronic hand prosthetic device
[POA-2-C-2333-34] 14 p2230 N71-36532
- Heat activated end cells with aluminum anode
[NASA-CASE-LEW-11359] 16 p2338 N71-28579
- Electromotive forces, magnetohydrodynamic turbulence, and stellar and planetary magnetic fields based on turbulent dynamo theory in cosmological electrodynamics
[NCAR-TN/A-60] 21 p3311 N71-35016
- EMF measurements of indium oxide free energy of formation between 790 and 1230 K using circular electrolytic cells
[BM-R-7549] 23 p3550 N71-35289
- Comparison of bubble method and end measurements of Al and Cu activities in molten Al-Cu alloy reactions with AlCl₃
[NLL-RT-6273] 23 p3774 N71-36899
- Entropy, enthalpy, Gibbs free energy, and energy of atomization for gallium phosphide formation in electrochemical cell based on end measurements
[NLL-REE-TRANS-315-10316-6251] 23 p3700 N71-36937
- EMF method for studying ionic conductivity of molybdenum trioxide
[NLL-M-21003-15828-4F] 24 p3961 N71-38114
- Calculation of free energy of formation and thermodynamic properties of PuFe₂ over temperature range 792 to 1104 K from end measurements
[LA-4636] 24 p4030 N71-38753
- ELECTRON ACCELERATORS**
NT BETATRONS
Characteristics and operation of electron linear accelerator
[AD-711587] 02 p0273 N71-11790
- Experimental and theoretical physics research including operation and development of electron synchrotron
[RP-16316] 03 p0470 N71-13007
- Parameters of beam injector for prototype cybernetic accelerator
[CEBN-TRANS-69-35] 04 p0516 N71-13805
- Development and characteristics of electron beam generator
[JAEI-1190] 04 p0516 N71-13806
- Terminal voltage stabilization system for Van de Graaff accelerator
[CISE-N-136] 04 p0516 N71-13823
- Status of proposal for high intensity electron accelerator with high duty cycle and maximum energy of 500 MeV - Netherlands
[REPT-7046] 05 p0659 N71-15462
- Microtron electron accelerator capable of neutron and gamma interrogation for nuclear materials assay
[BNL-50230] 06 p0913 N71-15872
- Aerobee-borne electron accelerators for ejecting electron beams into upper atmosphere
[NASA-CR-116087] 06 p0999 N71-15994
- Optical studies of radiation damage processes using high dose rates available from electron linear accelerator and fast optical techniques
[AD-715303] 07 p1093 N71-18046
- Electron ring accelerator research on ion, electron, and proton acceleration
[UCRL-20125] 10 p1538 N71-20649
- Data acquisition system used with electron linear accelerator for neutron capture gamma ray experiments - mechanical and other problems
10 p1538 N71-20601
- Accelerator and research operations report for Stanford Linear Accelerator from July to September 1970
[SLAC-128] 12 p1897 N71-23580
- Operational characteristics and entrance conditions of high current relativistic electron beam accelerator
12 p1897 N71-23946
- Electron accelerator magnet ray survey using particle telescope with micrometer and hodoscope analysis for orbit distortions
[CEAL-1052] 13 p2125 N71-24085
- Failure of rocket flown electron accelerator to create artificial aurora
13 p2076 N71-25269
- Research and design of pulsed electron beam accelerator, and preliminary beam measurements
[SC-DR-78-672] 15 p2458 N71-28639
- Peak current measurement in linear electron accelerators by modulated ferrite monitoring system with associated digital equipment
[CEA-N-1389] 15 p2463 N71-27246
- Critical current in electron beam of 2-GeV accelerator with radial slots in iris disk
[KFE-TR-335] 15 p2496 N71-27980
- External injection and acceleration of 600 microamp electron beam to final radius of ring cyclotron with strong focusing
[JINR-P9-5453] 17 p2793 N71-29518
- Compressor 2 and 3 experiments, 4 MeV 300 A electron linear induction accelerator, and electron ring accelerator research and development programs
[UCRL-20130] 17 p3731 N71-30851
- Mathematical model of plasma formation of electron ring in static magnetic field and beam properties
[ALAC-5779] 18 p2662 N71-38733
- Research work with linear electron accelerators
[LAL-1241] 18 p2903 N71-38916
- Structure of electron chamber in electron ring injector with step-like varying wave-phase velocity
[KHPY-76-17] 19 p3143 N71-31926

Radiation emission effects on dynamics of relativistic electron rings
[NP-18634] 19 p3147 N71-31975

Research in neutron physics and nuclear photoreactions at Livermore 100 MeV electron accelerator and facility
[UCRL-73675] 19 p3151 N71-32158

Electron ring accelerator research and development program
[UCRL-20611] 20 p3320 N71-33707

Pulsed electron accelerator used as injector for electron ring accelerator
[UCRL-20174] 20 p3248 N71-33935

Conceptual design for high energy electron ring accelerator allowing mass production techniques and ensuring low cost
[UCRL-20169] 20 p3248 N71-33965

Relativistic electron beams for acceleration of plasma bunches and electron rings
[UCRL-TRANS-1443] 23 p3816 N71-37217

Conference on nuclear physics and research with electron linear accelerators
[JAERI-1205] 24 p3981 N71-38410

ELECTRON ATTACHMENT

Dissociative electron attachment to polyatomic molecules and negative ion lifetimes
[ORNL-TM-2614] 02 p0746 N71-15237

Electron removal from reentry flow fields by dissociative attachment for blackout alleviation
[NASA-TT-F-13494] 12 p1998 N71-24288

Coefficient of electron attachment to oxygen molecules method from simultaneous photographic and radar observations applied to meteor radar echo data for 1957 to 1959
[NASA-TT-F-13494] 12 p1998 N71-24288

High temperature electron swarm apparatus for investigating electron attachment to polyatomic molecules
[JAERI-1205] 24 p3981 N71-38410

ELECTRON AVALANCHE

Energy distribution of electrons leaving curved channel photomultiplier tube after electron avalanche
[NP-1761] 11 p1761 N71-21992

Space charge electron avalanche in nitrogen and hydrogen breakdown
[NP-1761] 11 p1761 N71-21992

Ionization electron avalanche in high electric field in liquid argon and xenon for thin particle detector development
[UCRL-20135] 21 p3484 N71-34814

Electron avalanche multiplication in bulk silicon n-type semiconductors
[NP-1761] 11 p1761 N71-21992

Simulation of electron avalanche in He using Monte Carlo method for study of electron population growth accompanying transient phase of avalanche and related topics
[NP-1761] 11 p1761 N71-21992

Electron beam welding
[NP-1761] 11 p1761 N71-21992

Weldability of tungsten base alloys and elevated temperature stability
[NASA-CR-1611] 01 p0067 N71-10353

Arc and electron beam welding techniques
[AD-71747] 01 p0061 N71-10968

Residual stress measurements and heat treatments for electron beam welding of rotating turbine engine parts
[AD-71747] 01 p0061 N71-10968

Modern welding methods in aircraft and aerospace industry
[AD-71747] 01 p0061 N71-10968

Application of welding methods and treatment of metal surfaces to improve corrosion resistance and dimensional build up in engine production
[AD-71747] 01 p0061 N71-10968

Metals melting and exothermal heating experiments for component manufacturing in orbital workshop
[AD-71747] 01 p0061 N71-10968

Portable electron beam welding chamber
[NASA-CASE-LEW-11531] 05 p0692 N71-14932

Development of device to prevent high voltage arcing in electron beam welding
[NASA-CASE-XMF-08522] 09 p1392 N71-19486

Compilation of technical information including metallurgy, electrical repair, fabrication techniques for coating, bonding and brazing, and electron beam welding
[NASA-SP-5925/01] 13 p2087 N71-25026

Maneuverable electron beam welder for welding and cutting thin metal sheets in space environment
[AD-71747] 01 p0061 N71-10968

Design and construction of programmer for control and automation of electron beam welding machine
[EUB-4537-F] 13 p2088 N71-25528

High sensitivity ultrasonic test system for inspection of electron beam welds in stainless steel parts
[GEPP-43] 15 p2390 N71-26084

Fatigue, tensile strength, and bend testing of electron beam welded joints
[RAE-LIB-TRANS-1554] 20 p3279 N71-33490

X ray analysis of residual stresses in electron beam welded carbon steel structures
[RAE-LIB-TRANS-1556] 20 p3361 N71-33986

Technique for determining longitudinal and transverse shrinkages of titanium alloy electron beam weld seams
[RAE-LIB-TRANS-1555] 22 p3588 N71-35551

Development of process for welding carbides of zirconium and niobium to stainless steel using electron beam
[AD-71747] 01 p0061 N71-10968

Electron beams
[AD-71747] 01 p0061 N71-10968

Using electron beam switching for brushless motor commutation
[NASA-CASE-XGS-01451] 01 p0034 N71-10677

Development of flexible selected interconnection technique for monolithic circuits
[NASA-CR-102988] 02 p0196 N71-11376

Superconducting transition temperatures of electron beam evaporated metals condensed on liquid helium cooled substrates
[UCRL-19624] 02 p0284 N71-11838

Electron beam scanning system for improved image definition and reduced power requirements for video signal transmission
[NASA-CASE-ERC-10552] 03 p0351 N71-12539

Preparation and characterization of electron beam, vapor deposited, germanium films using molecular beam machine
[PB-195261] 03 p0395 N71-13349

Design and development of electron linear accelerators
[NP-18317] 04 p0545 N71-13562

Electron beam stabilization in linear accelerator
[KHFTI-49-20] 04 p0573 N71-13666

Parameters of beam injector for prototype cybernetic accelerator
[CERN-TRANS-49-35] 04 p0516 N71-13805

Development and characteristics of electron beam generator
[JAERI-1190] 04 p0516 N71-13806

Relativistic electron beam and plasma interaction and critical current problem
[UCRL-TRANS-10470] 04 p0596 N71-13981

Critical plasma density corresponding to threshold of high frequency instability during electron beam interaction with plasma
[AEC-TR-7159] 04 p0597 N71-14120

Electron beam and plasma instability in low density plasma of high current gas discharge
[AEC-TR-7165] 04 p0597 N71-14121

Influence of collisional plasma background on two-stream instability
[INR-P-1188] 04 p0598 N71-14239

Investigating ion heating from modulated electron beams, plasma density and energy in magnetic mirrors, and dispersion relations for oblique wave propagation in magnetized plasma
[UCB-34-P-128-15] 05 p0752 N71-14507

Increasing maximum energy and improving beam intensity of 85 MeV linear electron accelerator at Amsterdam
[AD-71747] 01 p0061 N71-10968

Electron beam plasma heating in magnetic mirror trap
[AEC-TR-7160] 05 p0753 N71-15020

Characteristics of relativistic electron beams extracted from electrode space of flash X ray machines
[AD-713576] 05 p0755 N71-15374

Theoretical analysis of electron beam ray propagation from spacecraft
[NASA-CR-116088] 06 p0940 N71-15916

Impulse generation in aluminum using electron beam for high energy density loading
[AD-714538] 06 p0954 N71-16402

Electron beam measurements of gas densities and rotational temperatures in viscous nozzle flow
[NASA-CR-116247] 06 p0838 N71-16586

Microwave power amplification and generation utilizing linear beam devices
[NASA-CR-116490] 07 p0998 N71-17346

Electron scattering effects in beam generated plasma
[NASA-TN-D-6150] 07 p1083 N71-17824

Trajectory observations for some spiraling electron beam systems using movable probes and targets as well as photographic techniques
[NASA-TN-D-5950] 09 p1451 N71-20466

Correlation between NRL electron storage ring (Sototron) and behavior of nonlinear dispersive partial differential equations
[AD-716761] 10 p1611 N71-20676

Impurity distribution in molybdenum single crystals produced by electron beam zone melting
[AD-716761] 10 p1611 N71-20676

Dislocation structure of refractory metals of Group 6A produced by electron beam and zone melting methods
[AD-716761] 10 p1611 N71-20676

Straight beam vs. ac deflection for electron beam welding on U-Nb-Zr alloy
[MLM-1778] 10 p1585 N71-21793

Measurements on electron beams propagating in gas filled drift tube
[AD-717399] 11 p1810 N71-22164

Electron beam fluorescence in Nylon, polytetrafluoroethylene, and polyethylene
[AD-717399] 11 p1810 N71-22164

Monte Carlo method applied to angular distribution of electron beam plural scattering for gas density measurement
[REPT-1000/71] 11 p1804 N71-22280

Nonlocal reflection in warm plasmas in presence of electron beam
[AD-717659] 11 p1811 N71-22379

Comparison of creep-rupture properties of electron beam-melted polycrystalline and powder-metallurgy rhodium sheets at 2200 to 4200 F and 4 to 40 ksi
[NASA-TN-D-6291] 12 p1936 N71-23114

Electron beam deflection devices for measuring electric fields
[NASA-CASE-XMF-10289] 12 p1920 N71-23000

Microwave technology with application to electron beam devices, quantum electronics equipment, and solid state devices
[AD-717971] 12 p1934 N71-23119

Current density induced in pinched plasma discharge by penetration of plasma by pulsed relativistic electron beam
[AD-717971] 12 p1934 N71-23119

Electron beam losses in linear induction accelerators
[UCRL-TRANS-1425] 12 p1973 N71-23061

Microwave cavity systems engineering for HeV electron beam ionization measurements
[NASA-TM-X-2279] 12 p1981 N71-23059

Broadening processes in supersonic stream of argon-helium mixture in vacuum using beam of electrons
[NASA-TT-F-13583] 13 p2064 N71-24005

Apparatus to determine electric field strength measuring deflection of electron beam impinging on target
[NASA-CASE-XMF-06617] 13 p2057 N71-24040

Transfer of energy from electron beam particles to longitudinal plasma waves studied by means of plasma kinetic theory
[AD-717971] 13 p2149 N71-25236

Computerized simulation of plasma heating from electron cyclotron resonance including ion trapping and magnetohydrodynamic instability
[AD-720675] 14 p2322 N71-24079

Coherent betatron beam oscillation measurements during beginning acceleration
[CERN-TRANS-70-10] 14 p2315 N71-24072

Theoretical models of high current relativistic electron beam propagation studies
[AD-720675] 15 p2386 N71-27706

Electron and ion pulse propagation in quiescent plasma
[AD-720649] 15 p2500 N71-27406

Method for atomic beam ionization with storage of polarized ions in electron beam and their pulsed extraction during accelerator capture time
[JINR-P-5446] 15 p2473 N71-27440

Experimental techniques for determining electron attenuation lengths in metals in energy range to 10 keV
[AD-720649] 15 p2507 N71-27447

Electron beam hydrogen ionization and hot plasma generation in magnetic mirror configuration
[CEA-CONF-1611] 15 p2502 N71-27625

Measuring wide angle bremsstrahlung by electron-photon coincidences using electron synchrotron
[AD-720649] 15 p2483 N71-27700

Adone linear operation, installations, and experiments with head-on collisions and positron and electron beam energies up to 1200 MeV
[LNF-70/48] 16 p2646 N71-28180

Design and fabrication of electron beam X-Y deflection system for retrofit on welding guns
[NASA-CR-119841] 17 p2729 N71-28234

External injection and acceleration of 600 microsecond electron beam to final radius of ring cyclotron with strong focusing
[JINR-P-5453] 17 p2793 N71-28510

Production of 14 MeV neutron anomalous pulse with T/d, He-4 reaction by accelerating deuterium with electron beams
[UCRL-50955] 17 p2798 N71-28510

Electron beam parameters for 100 MeV storage ring including synchrotron radiation interferometry and plasma oscillations
[KHFTI-69-27] 18 p2967 N71-30111

Phase shift calculations of electron beam scattered by nickel atom at 2 to 100 V
[NP-18640] 18 p2968 N71-30122

Synchrotron electron beam resonant depolarization during particle acceleration
[LNF-70/52] 18 p2961 N71-30100

Comparison of electroslag, plasma-arc, vacuum, and electron beam methods of melting nickel steels
[AD-723443] 18 p2927 N71-30082

Mathematical model of planar formation of electron ring in static magnetic field and beam properties
[AECI-3779] 18 p2962 N71-30733

Incoherent scattering of microwaves from plasma waves excited in electron beam in absence of external magnetic field
[AD-723443] 19 p3163 N71-31911

Evaluation tests to demonstrate feasibility of increasing efficiency of linear beam microwave tubes using novel depressed collector
[NASA-TM-X-2322] 19 p3067 N71-32000

SUBJECT INDEX

Methods for analyzing multistage electron beam collector schemes, with and without transverse magnetic fields, for traveling wave tubes
[NASA-CR-72598] 19 p3068 N71-32612

Heating capacity for control of cathode electron beam 20 p3341 N71-33421

Electron beam probe for measuring vibrational and rotational molecular levels in rarefied gases (JP-940) 20 p3274 N71-33430

Spl analysis of direct and exchange scattering amplitudes for describing differential inelastic electron-potential collisions 20 p3323 N71-33814

Optical properties of omniconductors determined by measurement of light absorption and reflectance with electron beam modulation 20 p3336 N71-33874

Electron beam measurement of molecular vibrational energy transfer in expanding mixtures of N₂ and CO heated by electric arc [NASA-TN-D-6445] 21 p3436 N71-34446

Coherent frequencies of transverse oscillations in electron model of ring cyclotron for magnetic field solenoid [NBS-P-5677] 21 p3473 N71-34723

Negative mass effect in dense electron beams in Adjoint model [UCRL-TRANS-1426] 21 p3479 N71-34781

Electron beam probe to measure potential and Doppler shifted spectral lines to study presence of fast particles in inertial electrostatic confinement device (NYO-4169-3) 21 p3484 N71-34818

Asymmetry of electron-ion beam oscillations and laser gain in magnetic field [MATT-TRANS-83] 21 p3494 N71-34891

Electron-ion (ion sound) oscillations in electron beam passing through rarefied gas corresponding to instability of inhomogeneous plasma [MATT-TRANS-84] 21 p3494 N71-34894

Vlasov kinetic equation for studying instability of electron beam in dense plasma [JNRL-TR-2432] 21 p3499 N71-34898

Research operations and equipment development for Stanford two-mill electron accelerator [JLAC-130] 22 p3565 N71-35392

Electron beam evaporation and recrystallization of thin films yielding high Hall mobilities [NASA-CR-126797] 22 p3592 N71-35576

Vlasov equation for solving ion-electron beam system [NBS-P-5645] 22 p3637 N71-35927

Selection of focusing system for linear induction accelerator and maintenance of beam size [NBS-P-5714] 22 p3640 N71-35952

Radiation produced by high energy electrons in dielectric waveguide 22 p3648 N71-36016

Low energy electron diffraction from zinc and beryllium cleavage surface as function of direction of energy of incident beam 22 p3652 N71-36044

Control of linear instability in electron beams injected into plasma (AD-726917) 22 p3655 N71-36065

Microtron of continuous operation, excitation of electromagnetic oscillations in open resonators, electron motion in double series magnetron, beam fluxes in linear diodes, and related topics (AD-726794) 23 p3732 N71-36608

Electron beam techniques for rotational and vibrational temperature and density measurements in free stream hypersonic wind tunnel (AD-727684) 23 p3740 N71-36671

Application of plasma cutting method for flame cutting of aluminum, copper, and stainless steel [NRL-DA-TRANS-1108-6196.3] 23 p3764 N71-36639

Intrinsic electron beams for acceleration of plasma bunches and electron rings [UCRL-TRANS-1443] 23 p3816 N71-37217

Locky wave charge waves to explain Cerenkov and Smith-Purcell radiation 24 p3902 N71-37811

Effects of high energy, pulsed electron beams on dynamic fracture induced by rapid in-depth heating of aluminum and titanium alloys (AD-727983) 24 p3938 N71-38092

Intrinsic electron beam for thermonuclear plasma fusion (KFS-502-16) 24 p3967 N71-38451

Interaction of high frequency electromagnetic fields with magnetized plasma, high intensity electron and ion beams, pulse discharges, and related studies - bibliography [NBS-1064] 24 p3993 N71-38487

Radio frequency instability associated with interaction of monoenergetic electron beam with plasma in inhomogeneous magnetic field [CONF-71067-59] 24 p3994 N71-38494

ELECTRON BOMBARDMENT

Instrument for studying electron stimulated luminescence of terrestrial, extraterrestrial, and synthetic materials - luminescence 01 p0052 N71-10086

X ray and electron damage of cadmium sulfide [NASA-CR-1700] 01 p0112 N71-10926

Electron bombardment utilized for welding diverse turbomotors and turbomachinery parts 02 p0233 N71-11645

Displacement of atoms from normal lattice positions by protons and alpha particles [JNRL-TR-3013] 02 p0273 N71-11791

Space charge limitation of secondary electron emission currents produced by high energy electrons (AD-712053) 02 p0268 N71-12146

Effects of electrostatic propulsion beam divergence effects on spacecraft surfaces [NASA-CR-111518] 03 p0445 N71-12927

Effects of backscattered material on performance of glass coated accelerator grids for electron bombardment thrusters [NASA-TM-X-52927] 03 p0449 N71-12940

Characteristics of SERT thruster with argon propellant [NASA-TM-X-52940] 03 p0449 N71-12941

Formation mechanism and properties of this organic polymeric films prepared by electron beam polymerization process [NASA-CR-115848] 04 p0487 N71-13464

Investigating cathodoluminescent phosphors for light output response under high electron beam voltage and extreme power input [AD-712578] 04 p0532 N71-13608

Interactions between electrons and surface plasma states in metals 06 p0928 N71-15739

Effects of mercury electron bombardment ion thruster exhaust products on surfaces located downstream [NASA-TN-D-7038] 06 p0940 N71-15915

Effect of high power electron beam irradiation on structure and microhardness of silicon single crystal [AD-714742] 06 p0952 N71-16005

Using ion bombardment etching technique to reduce thickness of boron carbide for transmission electron microscopy (AD-715857) 06 p1221 N71-18498

Electron bombardment hollow cathode ion thruster performance [NASA-CR-116428] 08 p1285 N71-19178

Polarization power of impacting polarized deuteron beam on emitting particles from unpolarized deuterated polyethylene target 09 p1441 N71-20374

Electron paramagnetic resonance detection of electron bombarded lithium fluoride [NASA-TM-X-52989] 10 p1616 N71-21083

Baffle geometry, subsystem estimation, and connector failure analysis for ion thruster of solar electric propulsion system 10 p1639 N71-21357

Electric rocket engine with electron bombardment ionization chamber [NASA-CASE-XNP-04124] 10 p1639 N71-21822

Low frequency plasma noise from mercury electron bombardment ion thruster studied for several magnetic field configurations [NASA-TN-D-6286] 11 p1821 N71-22613

Operational performance of electron bombardment mercury ion thruster system during life testing in space simulation for SERT 2 [NASA-CR-72789] 12 p1989 N71-23113

Electronic cathodes for use in electron bombardment ion thrusters [NASA-CASE-XLE-04501] 12 p1886 N71-23190

Aurora formation by electron injection and drift in upper atmosphere 13 p2076 N71-25272

Research and development of mercury electron bombardment thrusters [NASA-TM-X-67836] 13 p2157 N71-25366

Optimization of mercury electron bombardment thrusters in SERT program [NASA-TM-X-67915] 20 p3339 N71-33317

Occurrence of explosion-like processes during high powered pulsed electron bombardment of diamonds, glass, and ceramics [SC-T-71-5017] 21 p3434 N71-34435

Low temperature, thermal conductivity measurements, phonon scattering, and induced energy levels in electron-irradiated Sb-doped Ge in n- and p-type conversion region [CEA-CONF-1745] 21 p3468 N71-34686

Mercury vapor fed hollow cathodes for electron bombardment ion thrusters 21 p3502 N71-34943

Optical transmittance of fused silica at elevated temperatures during high energy electron bombardment [NASA-TM-X-67930] 22 p3596 N71-35620

Angular and energy distributions of neutrons produced by bombarding thick beryllium targets with 53.8-MeV deuterons 22 p3632 N71-35877

Angular and energy distributions during molecular dissociation due to electron bombardment 22 p3651 N71-36853

ELECTRON DECAY RATE

Maximum propellant utilization in electron bombardment ion thrusters using mercury for propellant [NASA-TM-X-67921] 22 p3662 N71-36113

Beam focusing characteristics of various shaped grid holes with application to electron bombardment ion thrusters [NASA-TM-X-67922] 22 p3662 N71-36115

Coefficient of backscatter for monoenergetic electron striking target at oblique angle [NRL-DA-TRANS-5332-0022.09] 23 p3821 N71-37253

Surface reactions between silver nuclei and carbon and nitrogen projectiles [NP-10674] 24 p3975 N71-38368

ELECTRON BUNCHING

Accelerating field effect on electron bunch containing [JNRL-TR-3142] 04 p0377 N71-13745

Particle bunching by additional lower frequency RF system in electron storage rings [DESY-70/34] 06 p1247 N71-18194

Electron bunching structure calculations for bunching produced by injectors with wave phase velocity stopped variations [SLAC-TRANS-127] 14 p2362 N71-23749

Scattering diagnosis of electron ion bunches produced by accelerating heavy atoms to high energies [KFK-TR-357] 15 p2458 N71-26070

Structure of electron clusters in accelerator injector with step-like varying wave-phase velocity [KFIPT-70-17] 19 p3145 N71-31926

Structure of relativistic solitons and nonlinear waves as bunches for coherent acceleration [UCRL-TRANS-1443] 24 p3980 N71-38485

ELECTRON CAPTURE

Calorimetric determination of nuclear and electronic interactions in metals [AD-712095] 03 p0448 N71-12993

Electron affinity and dipole moment of NH₂ and H₂S molecules having C_{2v} symmetry 06 p1267 N71-19239

Application of Fokker-Planck and Coulomb T-matrix to electron capture in hydrogen 12 p1975 N71-24800

Electron capture and loss cross sections in heavy ion collisions with atomic oxygen and excitation of positive helium ion 15 p2478 N71-27623

Electron capture decay lifetime 168 f min yields ytterbium 168 using germanium/thin/ and silicon/thin detectors [LYCEN-7030] 15 p2489 N71-27686

Mathematical models for electron attachment to molecules with negative ion formation [AD-723642] 19 p3144 N71-31717

Internal source scintillation method for studying orbital-electron-capture and electron-capture-to-positron-emission ratios [NP-10692] 19 p3147 N71-32043

Electron capture cross sections into 3p and 3d states of hydrogen for 30-120 keV proton and deuteron impact on gas targets 20 p3325 N71-33919

Effect of synchronized capture during bunching of beam outside separatrix calculated by analog computer [IPVE-SKU-70-20] 23 p3807 N71-37141

Beta and electron capture decay in iodine and tellurium [ANL-TRANS-883] 24 p3980 N71-38481

ELECTRON CLOUDS

Forward and backscattering of spherical overvoltage clouds for ionospheric electron density distributions [AD-717085] 11 p1700 N71-22324

Artificial electron cloud formation using cesium and potassium isotopes for simulation of ionospheric propagation in E region with coherent radar [AD-72934] 15 p2406 N71-27809

ELECTRON COLLISIONS

ELECTRON SCATTERING

ELECTRON COUNTERS

Design and fabrication of resonant detector for Mossbauer spectroscopy [NBS-TN-541] 06 p0860 N71-16545

ELECTRON DECAY RATE

General formula for artificial electron decay life times [NASA-TM-X-65376] 01 p0118 N71-10768

Measurements of electronic free paths in argon discharge using interaction between plasma electrons and slow wave on helix [NASA-CR-117843] 11 p1812 N71-22516

Photoelectric effect, polarization, hysteresis, and polarization electron decay rate in organic semiconductor [AD-721188] 15 p2504 N71-26817

Decay branching ratios of eta-mesons 15 p2674 N71-27454

Current algebra for nonrelativistic decay modes 15 p2679 N71-27637

Ultrafast apparent second-order decay of hydrated electrons following nanosecond radiation pulses in air-free alkaline solutions with related solution structure data [AD-721299] 16 p2656 N71-29110

- Calculation of decay lifetimes of artificial electrons produced by Starfish nuclear explosion
[NASA-TN-D-6284] 17 p3241 N71-29709
- ELECTRON DENSITY [CONCENTRATION]**
- NT ELECTRON DENSITY PROFILES**
- NT IONOSPHERIC ELECTRON DENSITY**
- NT MAGNETOSPHERIC ELECTRON DENSITY**
- Helicon propagation in periodic structures produced by spatial modulation of magnetic field or plasma electron density 01 p0108 N71-10139
- Comparison of ionospheric sounding electron concentration and electron and ion temperature data in F region 01 p0046 N71-10228
- Ionospheric electron content during solar cycles measured by Faraday rotation of lunar radio echoes [AD-711524] 01 p0118 N71-10708
- Electron temperature and density measurements in nonequilibrium boundary layer of seeded argon plasma [AD-711669] 01 p0106 N71-10739
- Supersonic plasma stream diagnostics using immersed microwave probes [NASA-TM-X-2132] 01 p0106 N71-10964
- Electronic charge density in diamond structure crystals from X ray diffraction form factors [AD-711931] 02 p0285 N71-11859
- Microwave power transmission ratio for estimating electron density [EP-RR-21] 02 p0282 N71-11875
- Plasma probe for Pioneer spacecraft to measure ion and electron density and angular distribution in space [NASA-CR-73446] 03 p0376 N71-12768
- Alouette 1 satellite electron density data and diurnal variation of Greenland auroras 04 p0615 N71-14298
- Calculation of growth rates of electrostatic waves in infinite homogeneous plasma [EUR-CEA-FC-541] 04 p0601 N71-14416
- Stark profile calculations for first four hydrogen Balmer lines for electron densities and temperatures [SC-M-70-584] 05 p0745 N71-15203
- Electronic densities of states from X ray photoelectron spectroscopy [UCRL-18953] 05 p0747 N71-15261
- Measuring plasma density, space potential, and current density using heavy ion beam probe [AD-713857] 06 p0930 N71-16190
- Faraday rotation data of ionospheric total electron content behavior at conjugate points and during solar eclipse [AD-714571] 06 p0942 N71-16525
- Electron density and electrostatic potential field of ionosphere satellite 06 p0927 N71-16870
- Wave-like variations in ionosphere [AD-714993] 07 p1023 N71-17874
- Numerical calculations of density and temperature variations in cylindrical plasmas preionized by UV radiation [IPP-1/106] 08 p1270 N71-18250
- Interferometric and schlieren measurements of electron density in arc plasmas using IR radiation from CO₂ laser [IPP-4/4] 08 p1271 N71-18268
- Secondary electron emission measurement in aurora using Aerobee rocket vehicle [NASA-CR-116858] 08 p1193 N71-18995
- Determination of scalar and vector scattering from turbulent plasmas 09 p1447 N71-19705
- Electron density study in argon plasma jet, using Thomson and Rayleigh scattering [CEA-R-3998] 09 p1450 N71-20376
- Intensity measurements on oxygen VII solar X ray emission lines [AD-716472] 09 p1462 N71-20385
- Electron density energy spectra of galactic cosmic rays from circular and elliptic cylindrical and ellipsoidal sources [CEA-R-3674/E] 09 p1463 N71-20541
- Swedish rocket sounding using Skua rocket vehicle for investigation of electron concentration, photodetachment, and ozone distribution during twilight glow [REF-55-346-33] 10 p1546 N71-20704
- Photon density detection for determining liquid helium excess electron absorption cross sections at infrared wave lengths 10 p1612 N71-20720
- Calculated and measured nonequilibrium flow electron density and collision frequency distributions in plasma sheath around Apollo spacecraft during hypersonic reentry 10 p1627 N71-21104
- Shock tube measurements of admittance of RAM C-2 and RAM C-3 diagnostic antenna admittance to analyze accuracy of calculated electron density 10 p1519 N71-21110
- Computer code for numerical solution of laminar boundary layer and thin shock layer equations predicting electron density around reentry vehicle 10 p1628 N71-21113
- Electron density and signal attenuation data from RAM C hypersonic reentries and theoretical calculations 10 p1628 N71-21116
- ESRO 1 satellite Langmuir electrostatic probe electric field detection 10 p1551 N71-21163
- Explorer 35 observations of solar wind electron density, temperature, and anisotropy analyzed and compared with previous measurements [NASA-TM-X-65481] 10 p1640 N71-21492
- Forward and backscattering of spherical overdense clouds for ionospheric electron density distributions [AD-717685] 11 p1700 N71-22324
- Space plasma experiments involving Alouette resonances and diagnostic techniques applied to electron density and temperature and local magnetic field strength measurement [NASA-CR-117844] 11 p1812 N71-22585
- High temperature gas radiation, and direct and electron density spectroscopic methods for gas temperature measurements 11 p1842 N71-22603
- Plasma diagnostic technique for electron density profile determination 11 p1813 N71-22651
- Electromagnetic field and electron density measurements by MHD plasma accelerators 11 p1813 N71-22652
- Electron density measurement in plasma sheath [AD-717957] 12 p1982 N71-24061
- Injection laser Thomson scattered light for timed measurement of electron density and temperature of shock fronts formed by axial plasma injection into dipole magnetic fields 12 p1982 N71-24143
- Calculations on electron spatial and velocity distribution from point source in neutral gas effected by homogeneous dc electric field 13 p2131 N71-24901
- Sudden release of large number of cosmic rays as supernova burst considered in relation to cosmic rays containment in galactic disk [NASA-TM-X-65506] 13 p2160 N71-24988
- Coordinated auroral electron observations from synchronous and polar satellites [NASA-CR-118319] 13 p2074 N71-25082
- Radio wave scattering from random electron density fluctuations in cold anisotropic magnetoplasma [NASA-CR-118332] 13 p2047 N71-25085
- Thermal electron density and cosmic ray flux in galactic radio emissions 13 p2163 N71-25289
- Dynamical theory of Kikuchi electrons based on two beam theory [UCRL-19631] 13 p2139 N71-25482
- Classical path calculations of optical broadening operator phi for Stark broadening of hydrogen line H sub alpha [AD-720817] 14 p2321 N71-25916
- Electron density and temperature measurements for argon plasma arcs [AD-720856] 15 p2500 N71-27392
- Thomson scattering from pulsed ruby laser for measuring electron energy distribution and density in toroidal plasma [ICL-M-107] 15 p2502 N71-27737
- Two nucleon potentials and nuclear saturation near empirical energy and density dependent on strong tensor force 15 p2492 N71-27923
- Simple argon model atoms used for calculating electron number densities for argon plasma discharges [NASA-TN-D-6383] 16 p2643 N71-28085
- Variations in total ionospheric electron content as indication of motion of eclipse-produced internal atmospheric gravity waves [AD-721589] 16 p2675 N71-28593
- Electron density measurement of negative glow plasma with E-band Fabry-Perot interferometer using flat plate technique [NASA-TN-D-6282] 16 p2661 N71-28818
- Temperature measurement and electron density of free ionized nitrogen jet at atmospheric pressure 16 p2663 N71-29185
- Dynamic model for partial pressure variations of electrons, ions, and neutrals in active zone of hollow cathode arc discharge [NP-18708] 17 p2813 N71-30240
- Determination of heavy nuclei charges in atmosphere from formation density of delta electrons [NASA-TT-F-13743] 17 p2805 N71-30295
- Reduction and analysis of electron content measurements permitting inference of electron density in solar wind [NASA-CR-114356] 18 p3003 N71-30896
- Theoretical analysis of end effect in current response of highly negative, cylindrical Langmuir probe under ionospheric satellite conditions [AD-723531] 19 p3167 N71-32800
- Thomson scattering measured in terms of electron concentration and temperature using Q switched laser probe [AD-724180] 20 p3280 N71-32858
- Numerical analysis of axisymmetric column of gas discharge for intermediate and high plasma densities [AD-724112] 20 p3329 N71-32914
- Investigation of current collection of negatively biased flush electrostatic probes in continuous plasma [AD-724148] 20 p3329 N71-32914
- Transverse ionizing shock wave velocity measurements and analysis of velocity variation as function of shock tube bias and drive currents and initial gas density [AD-727046] 22 p3655 N71-36863
- Diurnal temperature variations in middle ionosphere and electron density in E, E-F, and F1 regions [AD-727046] 22 p3655 N71-36863
- Spectrographs for measuring hydrogen H beta line spectral shape and determining electron density of transient plasma [NASA-CR-122932] 23 p3756 N71-36770
- Faraday rotation technique for determining electron densities in D region [NOAA-TT-205-SEL-21] 24 p3917 N71-37913
- ELECTRON DENSITY PROFILES**
- Interpolated electron number density tables from Alouette 2 ionospheric sounding data 01 p0046 N71-10228
- Determining electron concentration in flowing plasma in presence of accelerating and evaporating water droplets [NASA-TN-D-6007] 01 p0105 N71-10806
- Simultaneous measurement of dispersive Doppler shift, Faraday rotation, and ionospheric refraction [AD-711394] 02 p0205 N71-11847
- Diurnal variation of neutral temperature profile at Arecibo from incoherent scattering measurements and its relevance to 1400 hour density maximum [NASA-CR-111416] 02 p2151 N71-11064
- Tabulations of electron number density profiles from Alouette 2 ionograms 03 p0366 N71-12086
- Plasma measurements in SERT 2 spacecraft lab thruster discharge chamber using Langmuir probe [NASA-TM-X-2088] 06 p0939 N71-16130
- On-line closed loop processor for reducing topology ionograms to electron density profiles [NASA-TN-D-6204] 08 p1187 N71-14860
- Morphology of traveling ionospheric disturbances based on columnar electron content data, and relation of disturbances to polar substorms [NASA-CR-116784] 08 p1188 N71-14860
- Unknown electron density profiles determined from electrostatic resonance frequencies by WKB approximation 10 p1628 N71-21116
- Electrostatic probe determinations of electron density profiles for three RAM C hypersonic reentries 10 p1628 N71-21116
- RAM C-3 S band diagnostic antenna systems and calculations of electron density profiles**
- Electron density and temperature in inviscid flow and nozzle-wall boundary layer, measured with constant bias-voltage and swept-voltage RAM probes 10 p1519 N71-21110
- Electron density profiles in plasma sheath of shock waves determined with electrostatic probes in shock tubes 10 p1629 N71-21118
- Antenna radiation patterns and electron density profiles in turbulent plasma flow 10 p1519 N71-21110
- Computer solution of plane electromagnetic wave interaction with bounded inhomogeneous plasma slab with electron density gradient transverse to wave 10 p1520 N71-21112
- Electron energy and density profiles observed on-board ESRO 1 satellite over polar caps 10 p1551 N71-21163
- Lithium donor density gradient measurements for prediction of lithium cell behavior after electron irradiation and recoverability [NASA-CR-118005] 12 p1859 N71-23441
- Spaceborne telescope measurements of heliocentric Z gradient in primary cosmic rays 12 p1994 N71-24016
- Simultaneous observations of solar flare electron spectra in interplanetary space and within earth ionosphere measured by magnetic electron spectrometers on satellitesOGO-4 and OV-19 [AD-728006] 14 p2333 N71-25795
- Faraday effect used for electron density profile determinations in ionospheric sounding by VHF Thompson scatter radar [AD-724298] 20 p3258 N71-32818
- Plasmod model for explaining electron density and temperature of hydrogen plasma with helium and argon impurities drifting into dipole magnetic field 20 p3331 N71-33074
- Jicamarca radio observations of temperature and electron density profiles, films of Spread F structure, and nightglow emission intensities [NASA-CR-121964] 22 p3572 N71-35407
- Total electron density plots obtained at Hawaii from ATS 1 VHF telemetry 1 Jan. to 31 Dec. 1970 22 p3575 N71-35408

SUBJECT INDEX

Development of method for deriving electron density profiles in D region of ionosphere during solar flares (RSD-42) 22 p3663 N71-36132

Absorption and group delay data from equatorial station used to model electron density profile in D and E regions of ionosphere (NASA-TN-X-45750) 24 p3909 N71-37863

Cosmic ray origin and electron density spectra 24 p4010 N71-38394

ELECTRON DETECTORS

U ELECTRON COUNTERS

ELECTRON DIFFRACTION

Auger electron spectroscopy study of surface segregation in copper-aluminum alloys (NASA-TN-D-6995) 02 p0241 N71-11430

Examination of molybdenum disulfide with LEED and Auger emission spectroscopy (NASA-TN-D-7010) 03 p0332 N71-12246

Examining inelastic backscattering of low-energy electrons from tungsten surfaces (AD-713056) 04 p0590 N71-14376

Low-energy electron diffraction for surface crystallography (AD-714691) 06 p0934 N71-16216

Mass transport and atomic structure near metal surfaces (AD-715291) 06 p1277 N71-18411

Bragg diffraction between Bragg reflections and diffuse intensity planes observed with high energy electron diffraction (AD-715373) 08 p1213 N71-18521

Electron microscopy and diffraction for microbiology and microanalysis of lunar rocks (NASA-CR-116916) 08 p1204 N71-19311

High voltage electron microscopic and electron diffraction studies of pyroxenes from Apollo 11 lunar rock (AD-717056) 08 p1291 N71-19312

Low energy electron diffraction and Q spoiled laser analysis of radiation, oxidation, and diffusion on solid surfaces 10 p1569 N71-20927

Computational method for electron diffraction intensity using a beam theory and applied to gold microcrystal calculations 10 p1621 N71-21742

Comparison of electron diffraction and X ray diffraction analyses on crystalline structure of glycine (UCRL-20139) 10 p1636 N71-21805

Initial stages of omega phase transformation in Ti-V alloys examined using selected area diffraction and dark field electron microscopy (AD-717353) 11 p1777 N71-21944

Surface composition, structure, and properties of alloys using electron spectrometer (AD-717260) 11 p1762 N71-22229

Electron diffraction contrast effects from antiphase boundaries and dislocations in ordered superlattice alloy interfaces (NBS-3955-4) 11 p1779 N71-22481

Porous industrial catalysts studies comprising structure and composition of platinum surface by low electron diffraction and molecular beam scattering under high vacuum conditions 15 p2493 N71-27946

Electron diffraction analysis of fracture surface changes on molybdenum disulfide/titanium interface (NBS-3955-4) 16 p2605 N71-29114

Computer simulated electron diffraction analysis of electron passing through absorbing crystal foil (AD-722244) 17 p2814 N71-29693

On phase diffraction unit employing particle counting techniques for molecular structure investigations requiring small sample quantities (NBS-3955-4) 18 p2980 N71-30740

Electron microscope, electron diffraction, and electron microprobe analysis of defective solid state weld on liquid hydrogen tank from Apollo 12 fuel cell (NASA-TN-D-6327) 18 p2937 N71-31374

Lead and Auger electron spectroscopy study of oxygen adsorption on tungsten (110) (NASA-TN-D-6399) 18 p2998 N71-31454

Computer program for transmission electron diffraction pattern analysis (ABCL-5729) 21 p3394 N71-34158

On phase electron diffraction projection and carbon scattering determination using molecular intensities 21 p3491 N71-34863

X ray and electron diffraction pattern study of structure and size of finley ground quartz particles 21 p3496 N71-34924

Low energy electron diffraction from zinc and bismuth cleavage surface as function of direction and energy of incident beam 22 p3652 N71-36044

University proposals for surface physics research program utilizing low, high, and reflected high energy electron diffraction and Auger spectroscopy 23 p3905 N71-37106

Manual for analyzing diffraction patterns of face centered cubic crystals for unit meshes of surface

structures in hexagonal, square, and rectangular shapes (REPT-10-154) 23 p3836 N71-37356

Electron diffraction and electron microscopic analysis of as-quenched and aged omega phase in TiNb alloys (AD-723594) 24 p3737 N71-38088

ELECTRON DIFFUSION

Proton irradiation effects on electron diffusion length of minority carriers in P-type silicon (AD-711750) 01 p0112 N71-10864

Solar electron injection through magnetic field lines and magnetospheric diffusion (AD-712043) 02 p0292 N71-11904

Electron hole reaction kinetics in radiation induced free radical destruction (UCRL-19649) 03 p0423 N71-12739

Electronic structure and ionic diffusion in metals (TT-70-57031) 03 p0392 N71-12979

Electron diffusion thermoelectric power in metals and dilute alloys investigated over wide range of temperatures (COO-625-152) 08 p1281 N71-19273

Relativistic electron diffusion from point source in Sagittarius A astronomical model 10 p1642 N71-20661

Satellite observation of low altitude electron flux density 11 p1823 N71-22459

Fokker-Planck equation used to describe process of electron loss from Van Allen zones due to pitch angle scattering by electromagnetic disturbances 18 p3004 N71-30923

Cyclotron and bounce resonance scattering of electrons trapped in earth magnetic field 18 p3004 N71-30924

Empirical approach to third-invariant violation for radial diffusion of outer zone electrons 18 p3006 N71-30931

Computer programs for calculating penetration and diffusion of electrons and associated bremsstrahlung during extended media 22 p3634 N71-35899

Determination of low energy electron diffusion resulting from absorption on single crystal planes (NLL-FORS-TRANS-2706-19022.81) 23 p3837 N71-37361

Plasma heating and production of relativistic electron current layers by injection of high current electron beams into magnetic fields (CONF-710607-12) 24 p3990 N71-38468

ELECTRON DISTRIBUTION

NT ELECTRON DENSITY PROFILES

Electron content measurement in polar ionosphere using signals from Explorer 22 satellite based on Faraday rotation (BMBW-FB-W-70-39) 03 p0370 N71-13229

Electron scattering effects in beam generated plasmas (NASA-TN-D-6150) 07 p1083 N71-17824

Electron current and distribution function associated with electron plasma waves (CEA-CONF-1600) 08 p1272 N71-18494

Calculations on electron spatial and velocity distribution from point source in neutral gas effected by homogeneous dc electric field 13 p2131 N71-24901

Electron distribution measurements in hot electron mirror contained plasmas by bremsstrahlung spectra (ORNL-TM-3302) 13 p2149 N71-25576

Measuring angular and energy distributions of electrons ejected from nitrogen using crossed molecular and electron beams (SC-RR-710050) 17 p2791 N71-29290

Radioisotope measurements to determine electron distribution in planetary atmospheres (D-13) 17 p2843 N71-29313

Transient behavior of electrons in artificial radiation belts from satellite observations 18 p3004 N71-30922

ELECTRON EMISSION

NT FIELD EMISSION

NT PHOTOELECTRIC EMISSION

NT SECONDARY EMISSION

Photoelectron emission in surface damage of laser materials 04 p0526 N71-14339

Dosimetry technique using thermally stimulated exoelectron emission with lithium fluoride (NBSL-236) 06 p0927 N71-16857

Electron emission from fluoride ion in shock heated mixtures of cesium fluoride and argon (AD-715904) 09 p1442 N71-20386

Preliminary results on thermally stimulated exoelectron emission from Apollo 12 lunar materials (NASA-CR-117853) 11 p1827 N71-22528

Radioactive characteristics for studying fusion products - beta radiation and conversion electrons (CEA-N-1372) 15 p2471 N71-27409

Thermally stimulated electron emission of ceramic beryllia oxide and calcium sulfide (pure and doped with cerium, manganese, and lead) studied for dosimeters material (RT/FI/70/37) 16 p2642 N71-28030

ELECTRON ENERGY

Angular distributions and correlations of alpha and beta particles, electrons, and electromagnetic radiations from oriented nuclei (LA-4565) 16 p2645 N71-38157

Time dependent perturbation theory for evaluating angular distribution of electrons emitted from inner atomic shells by proton impact 18 p2983 N71-31133

Empirical equation for thermionic converter performance as function of electron emission properties (NASA-TN-X-2358) 20 p3308 N71-37379

Numerical analysis of double cathode electronic tube operation at high frequencies 22 p3359 N71-35350

Cold cathode emission obtained from biased electron p-a junctions activated to negative electron affinity (AD-726644) 23 p5733 N71-36612

Field electron emission from C60 as function of temperature and exposure with current voltage characteristics and excitation line observations (NLL-TRANS-2731-19022.81) 23 p5836 N71-37358

Hard and soft electron emission and periodic variations in auroral zones 23 p5853 N71-37463

Electron streams and extremely low radio frequency radiation in magnetosphere 23 p5854 N71-37471

Direct and indirect methods of electron emission analysis in stratosphere 24 p4012 N71-38613

ELECTRON ENERGY

NT ELECTRON STATES

Measurement of ion and electron temperature from 180 to 850 km by ionospheric radar 01 p0045 N71-10150

Electron temperature and density measurements in nonequilibrium boundary layer of seeded argon plasmas (AD-711649) 01 p0106 N71-10779

Electronic effects of chemisorption on powdered zinc oxide catalyst (AD-712856) 03 p0330 N71-12356

Electron tunneling into superconducting rhodium single crystals for energy gap measurements (AD-711826) 03 p0441 N71-12836

Collision effect on noncoherent scattering spectrum of plasmas with unequal electron and ion temperatures (CEA-N-1295) 04 p0594 N71-13569

Energy losses, range, and bremsstrahlung yield for 10 keV to 100 MeV electrons in some simple elements and some chemical compounds (ORNL-TR-2331) 04 p0580 N71-13989

Response of trapped electrons in periodic potential trough produced in plasma to low frequency perturbation (JPP-1-99) 04 p0599 N71-14260

Langmuir probe determinations on non-Maxwellian distribution of electron energy in plasma of electron bombardment ion engines (RM-70/3) 04 p0600 N71-14300

Electron ground states in molecular and valence-bonded crystals (IN-1420) 07 p1075 N71-17493

Measurements of energetic electrons within drift loss cone, extremely low frequency emissions, and plasma wave location 07 p1066 N71-18042

Numerical calculations of density and temperature variations in cylindrical plasmas preionized by UV radiation (JPP-1/106) 08 p1270 N71-18250

Electron current and distribution functions associated with electron plasma waves (CEA-CONF-1600) 08 p1272 N71-18494

Average energies of ground and singly and doubly excited configurations in highly ionized atoms for electron numbers N equals 3 to N equals 20 (NASA-SP-3656) 09 p1444 N71-20535

Electron density and temperature in inviscid flow and nozzle-wall boundary layer, measured with constant bias-voltage and swept-voltage RAM probes 10 p1628 N71-21115

Secondary electron emission phenomenology

ESRO I satellite observation of variations and fine structure in flux density and angular distribution of electrons with energies above 40 keV 10 p1530 N71-31150

Electron energy and density profiles observed on-board ESRO I satellite over polar caps 10 p1551 N71-21162

ESRO I satellite Langmuir electrostatic probe electric field detection 10 p1551 N71-21163

Explorer 35 observations of solar wind electron density, temperature, and anisotropy analyzed and compared with previous measurements (NASA-TN-X-45681) 10 p1640 N71-21492

Space plasma experiments involving resonant and diagnostic techniques applied to electron density and temperature and local magnetic field strength measurement (NASA-CR-117044) 11 p1812 N71-22585

SUBJECT INDEX

ELECTRON IONIZATION

ELECTRON IRRADIATION

- Optical absorption in transparent materials during 1.5 MeV electron irradiation
[NASA-TN-110907] 01 p0088 N71-10380
- Recovery characteristics of electron irradiated, lithium doped, solar cells
[NASA-CR-111579] 03 p0316 N71-12256
- Low temperature annealing of electron irradiated germanium
[COO-1196-735] 03 p0389 N71-12683
- Electron radiation effects in ruby laser crystals
[NASA-TN-D-70253] 04 p0602 N71-13962
- Irradiation in satellite interior by bremsstrahlung produced by Van Allen electrons
[JNRL-TR-2202] 04 p0585 N71-14223
- Test facilities for studying electron irradiation effects on lithium-doped silicon solar cells
[NASA-CR-115809] 05 p0631 N71-14652
- Influence of proton-electron irradiation on strength of fiber glass 07 p1046 N71-16944
- Electrical impedance measurements for determining electron irradiation effects on silicon
[COO-1196-744] 07 p1085 N71-17023
- Vanadium-51/gamma, alpha/scandium-47 reaction studied with recoil method after electron irradiation with bremsstrahlung energy between 40 and 65 MeV
08 p1266 N71-19206
- Preparation of single crystalline mica specimens support films for electron microscopy, and electron irradiation effects
[AD-717037] 10 p1610 N71-20625
- Metal oxide semiconductor X ray and electron irradiation damage and annealing effect
[JUL-592] 10 p1634 N71-21011
- Electron irradiation produced length changes in pure and doped magnesium oxide samples
11 p1800 N71-21872
- Lithium donor density gradient measurements for prediction of lithium cell behavior after electron irradiation and recoverability
[NASA-CR-118005] 12 p1859 N71-23441
- Determining nature of defects responsible for degradation in solar cells by studying radiation effects in lithium-diffused bulk silicon after neutron and electron irradiation
[NASA-CR-118009] 12 p1860 N71-23404
- Lattice parameter measurements on aluminum after electron irradiation at low temperatures
[JUL-664-PN] 13 p2091 N71-24428
- Heat transfer calorimetry in annealing of electron irradiation induced Frenkel defects in platinum below 40 K
[JUL-638-PN] 13 p2132 N71-25091
- Electron irradiation induced separation of Sb from SiO₂ solutions in anhydrous alcohols, ethers, ketones, acids, esters, and aromatic hydrocarbons
[NASA-TN-D-6358] 14 p2214 N71-26030
- Dependence on lithium of introduction and annealing of neutron and electron produced damage in lithium-diffused bulk silicon
14 p2201 N71-26232
- Subthreshold electron irradiation effects on surface and bulk electrical properties of Li-doped and Li-free silicon photovoltaic cells
14 p2297 N71-26238
- Infrared spectroscopic and photoconductivity determinations of electron irradiation effects in Li-doped fused zone and crucible grown silicon
14 p2297 N71-26238
- Radiation facility and equipment for studying Se-90 electron irradiation effects in Li-doped silicon
14 p2202 N71-26240
- Environmental facility for real-time study of electron irradiation effects on Li-doped p-n silicon solar cells
14 p2202 N71-26241
- ATG-F solar cell radiation damage experiment design and ground tests including space environment simulation and low-energy proton and electron irradiation
[NASA-CR-118460] 14 p2203 N71-26389
- Effect of electron irradiation on strength of monocrystalline bcc iron - low temperature strength during in-house lattice hardening
[KRO-1367-36] 15 p2419 N71-26918
- Techniques for determining real tridents and mean free path for tridents caused by primary electron in γ production in electron irradiated nuclear emulsion
15 p2479 N71-27642
- Mitigation of Ni and Fe foils caused by electron irradiation
[KLA-COMP-1480] 15 p2489 N71-27680
- Visible electron irradiated failure modes of MOS semiconductor capacitor detectors
[NASA-CR-111892] 16 p2391 N71-28025
- Apparatus to measure excitation cross sections of molecular nitrogen bombarded by electrons in 50 to 200 eV range with reaction rate measured by counting photon emissions
16 p2648 N71-28600
- Radiation damage by electron irradiation in copper
[KRO-1809-13] 16 p2612 N71-28624

- Defects introduced into Ge and Si by electron irradiation at low temperature
[COO-125-34] 16 p2666 N71-28735
- Electron irradiation effects in n-type, p-type, and high-purity silicon at 5.0 and 1.6 K using ac hopping conductivity
[COO-1198-711] 16 p2667 N71-28838
- Electron irradiation effects on thermal conversion of interstitials in copper
[COO-1800-15] 17 p2760 N71-29203
- Electron irradiation energy thresholds for producing damage in polycrystalline tungsten wire
[NASA-TN-D-6464] 19 p3114 N71-32242
- Electron probe inelastic scattering form factors for massive quantum electrodynamics calculated from optical-like equations
[ILL-TR-71-9] 19 p3157 N71-32509
- High energy electron irradiation effects on field effect transistors in integrated circuit devices
[NASA-CR-121623] 21 p3485 N71-34225
- ELF noise band associated with low-energy electron precipitation events and auroral arcs based on Explorer 40 observations
[NASA-CR-121676] 21 p3415 N71-34299
- Low temperature thermal conductivity of Sb and Ga after Te and Zn doping and electron irradiation
[NIP-1856] 22 p3458 N71-36083
- Lithium doped solar cell hardness to 1 MeV electron irradiation
[NASA-CR-122942] 23 p3709 N71-36442
- Isothermal annealing of 0.97 eV luminescence in electron irradiated silicon semiconductors
[AD-726916] 23 p3836 N71-37352
- Comparison of 1.5 MeV electron irradiation induced optical absorption of fused commercial silicon and optical transmission of Al₂O₃, MgF₂, BaF₂, LiF, and BeO
[NASA-CR-123187] 24 p3958 N71-38237
- ### ELECTRON MICROSCOPES
- Single crystal orientation studied with scanning electron microscopes
01 p0108 N71-10129
- Scanning electron microscope studies of breakdown and electric field distribution in transverse Gunn effect devices
01 p0109 N71-10213
- Contrast mechanisms in high resolution scanning electron microscopes
[TID-25418] 01 p0254 N71-10450
- Electron microscope analysis of biological materials
[UCRL-72513] 01 p0696 N71-10520
- Crews electron-energy-analyzing scanning microscope design
[ANL-7656] 01 p0856 N71-10762
- Electron microscope X ray analysis of atmospheric aerosol particles
[PB-19283] 02 p0152 N71-11079
- Scanning electron microscope operation and micrographs of microstructure and fracture in metals
[M&A/37/69] 02 p0224 N71-11527
- Scope and applications of stereophotographic scanning electron microscope
[SRDE-70023] 02 p0225 N71-11546
- High voltage electron microscopy for ceramic substructure and biological radiation damage studies
[UCRL-19628] 03 p0381 N71-13216
- Electron microprobe analysis of metallic inclusions in irradiated plutonium oxides at high burnups
[AERE-R-6310] 04 p0527 N71-13642
- Electron microscope analysis of irradiated ceramic nuclear fuel and cladding materials
[EUR-4504-D] 04 p0548 N71-13645
- Metal fatigue studies at ultrasonic frequency using electron microscopes
[AD-712501] 04 p0528 N71-13949
- Quantitative analysis of micrometer-size uranium alloy powders using electron microprobe X ray analyzer
[Y-1745] 04 p0591 N71-14380
- Identifying strong double refracting mineral in powder mixture using phase contrast microscope
[POA-1-C-1320-40/45] 05 p0757 N71-14628
- Electron optical metallographic instruments including electron microprobe X ray analyzer, scanning electron microscope, and transmission electron microscope
[NASA-TM-X-52849] 05 p0682 N71-14790
- Graphitization of thin carbon films for electron microscopy
[NYO-4142-1] 05 p0708 N71-15062
- Direct solution of complex crystal structures by electron microscopy
[AD-713554] 05 p0739 N71-15389
- High resolution scanning microscope for molecular biology
[COO-1721-21] 06 p0804 N71-16793
- Elastic bending and fracture mechanics of reinforced fiber epoxy resins using scanning electron microscope
[NPL-IMS-11] 07 p1047 N71-17164
- Scanning electron microscope study of hydrazine liquid rocket propellant catalysts
07 p1097 N71-17194

ELECTRON MICROSCOPES

- Scanning electron microscope as semiconductor production line quality control tool to determine integrity of metallization
[NASA-TM-X-64620] 07 p1028 N71-17389
- Using thin-film electron microscopy to study effects of cold working and aging on substructure and precipitation in cobalt-base alloy 1-405
[NASA-TN-D-7051] 07 p1043 N71-17461
- High voltage electron microscopy study of slip band growth in radiation hardened copper crystals
[UCRL-19601] 07 p1085 N71-17982
- Nucleation and growth of voids in nickel
[BNWL-SA-3300] 08 p1212 N71-18310
- Using ion bombardment etching techniques to reduce thickness of boron carbides for transmission electron microscopy
[AD-715657] 08 p1221 N71-18498
- Applying photoelectron spectroscopy to species identification and qualitative analysis of characteristic shapes and shifts in spectral lines of atoms in different chemical media
[AD-715408] 08 p1258 N71-18575
- Discontinuous precipitation of gamma prime in nickel-cobalt-nickel alloys by transmission electron microscopy
08 p1220 N71-19272
- Electron microscopy and diffraction for microbiology and microanalysis of lunar rocks
[NASA-CR-116916] 08 p1204 N71-19311
- High voltage electron microscopy and electron diffraction studies of pyroxenes from Apollo 11 lunar rock
08 p1291 N71-19312
- Electron microscopic studies of nerve membrane ultrastructure
08 p1156 N71-19313
- High resolution electron microscopes for cell membrane and multi-enzyme complex studies
08 p1157 N71-19314
- High voltage, high resolution electron microscope with superconducting lenses operating with superfluid helium refrigerator
08 p1245 N71-19315
- Mossbauer effect and high voltage electron microscopy of pyroxenes in Apollo 11 lunar rocks
08 p1291 N71-19316
- Electron microscopic and holographic methods for data condensing and retrieval, and microbiology
08 p1205 N71-19317
- Computer analysis of multichannel scanning electron microscopy and X ray images from film particles
[AD-716562] 09 p1425 N71-19445
- In-situ measurement of objective lens data for alignment of high resolution electron microscope
[NASA-TM-X-63018] 09 p1388 N71-19795
- Preparation of single crystalline mica specimen support films for electron microscopy, and electron irradiation effects
[AD-717037] 10 p1610 N71-20625
- Initial stages of omega phase transformation in Ti-V alloys examined using selected area diffraction and dark field electron microscopy
11 p1777 N71-21944
- Scanning electron microscope for time resolved frequency responses analysis on Gunn effect oscillator
11 p1761 N71-22075
- Shape from shading method applied to lunar topography and scanning electron microscopes
[AD-717336] 11 p1797 N71-22227
- Electron microscopy, nuclear fuel analysis, and spectrometry
[ORNL-4634] 11 p1696 N71-22447
- Electron microscopy, radiography, electrical resistivity, thermal expansivity, and X ray diffraction of fibrous carbon-carbon composite dynamic characteristics
[Y-1752] 11 p1783 N71-22475
- Use of scanning electron microscopy for following localized surface alterations in ball bearings during running
[AD-717959] 12 p1936 N71-23771
- Microstructure of spinodal alloys determined by electron microscopes
[UCRL-19629] 13 p2093 N71-24871
- Nucleation, growth, and abnormalities of silver films on amorphous carbon studied with electron microscope, and ultrahigh vacuum chamber development
[COO-1790-3] 14 p2324 N71-25613
- Quantitative surface finish characterization by computer evaluation of scanning electron microscope images
[AD-719925] 14 p2359 N71-25634
- Application of scanning electron microscopy to study of metal fatigue mechanisms
[AD-719927] 14 p2370 N71-25678
- Electron and ion microprobes applied in characterizing aluminate coating on IN-100 nickel alloys for high temperature oxidation resistance
[NASA-TN-D-6317] 14 p2271 N71-25488
- Evaluation of PuO₂ homogeneity in PuO₂-UO₂ fast reactor fuel by scanning electron microscope
[WHAN-SA-7] 14 p2292 N71-25712

- Electron probe microanalysis of highly radioactive materials with total security for operators and easy maintenance of shielded microprobe
[CEA-N-1340] 14 p2311 N71-26670
- Crystallographic techniques and data transmission electron microscopy of zirconium
[AABC/E-204] 15 p2305 N71-26996
- This films for transmission electron microscopy from highly irradiated cracked uranium dioxide fuel elements
[AERE-R-5677] 15 p2451 N71-27685
- Magnetic lens aberration correction in electron microscopy
16 p2592 N71-28245
- Electron microprobe analysis of solute segregation near grain boundaries in Al-Zn-Mg alloy after different quenching (brine, water, oil, and air) and aging heat treatments
[AD-722034] 16 p2610 N71-28454
- Slip band growth in prestrained copper crystals studied by transmission electron microscopy
[UCRL-20372] 17 p2815 N71-29738
- Scanning electron microscope used to determine surface morphology of TD-NiCr oxidized at 800 to 1200 deg for up to 64 hours
[NASA-TN-X-67867] 18 p2936 N71-31153
- Electron microscope, electron diffraction, and electron microprobe analysis of defective solid state weldment on liquid hydrogen tank from Apollo 12 fuel cell system
[NASA-TN-D-6327] 18 p2937 N71-31354
- Transmission electron microscopy for studying deformation substructure in polycrystalline alumina
[ORO-3328-13] 18 p2999 N71-31560
- Staining techniques for electron microscopy
[ISS-70/9] 20 p3271 N71-32966
- Preparation of biochemical materials for electron microscopy
[ISS-70/8] 20 p3215 N71-32968
- Auger electron velocity analyzer for use with scanning electron microscope to identify low concentrations of elements on surfaces of semiconductor devices
[NASA-CR-111968] 21 p3425 N71-34371
- Electron metallography of ferrous martensite substructures
[UCRL-19648] 21 p3438 N71-34465
- Flux pinning mechanisms in type-2 superconductors and specific heat measurements on annealed and deformed pure niobium samples
[NASA-CR-121867] 21 p3496 N71-34907
- Studying fracture surface striations and crack propagation in aluminum alloy by electron microscopy
[NLR-MP-69014-U] 21 p3529 N71-35149
- Brightness and life of pointed cold cathodes for electron microscope applications
[NRC-TT-1473] 22 p3539 N71-35351
- Electron microscope scanning of re-solution of gas from bubbles and sintering pores during UO₂ irradiation at high temperature
[RD/B/N-1716] 22 p3621 N71-35797
- Electron microscope characteristics of precipitated needles in neutron-irradiated austenitic steels
[EURFMR-491] 22 p3642 N71-35966
- Electron microscopy creep properties study of beta NIAI thin film specimens from deformed single crystals
[COO-1489-10] 23 p3770 N71-36869
- Electron microscope for investigating heat resistance and physicochemical properties of multicomponent nickel alloys
[AD-726735] 23 p3770 N71-36873
- Discovery of native osmium by microscopic examination of platinumiferous concentrates
[NASA-TT-F-13758] 23 p3776 N71-36912
- Electron diffraction and electron microscopic analysis of as-quenched and aged omega phase in TiNb alloys
[AD-727598] 24 p3937 N71-38088
- Analysis of chemically pure zirconium dioxide by electron microscope and roentgenographic techniques
[AD-727975] 24 p3945 N71-38139
- Replica preparation for electron microscopy of irradiated uranium-plutonium dioxide nuclear fuel
[ANL-7790] 24 p3962 N71-38261
- Estimate of knock-out coefficient from uranium fission product collision cascade calculations and electron microscopic study of dependence of uranium oxide layer thickness
[HMI-B-105] 24 p3979 N71-38395
- ELECTRON MICROSCOPY**
U ELECTRON MICROSCOPES
ELECTRON MOBILITY
Electron mobility of indium arsenide phosphide for charge carriers
01 p0109 N71-10212
- Two carrier model for electronic properties of single metallic band
[ORO-3651-5] 03 p0392 N71-12963
- Atomic mobility in crystal lattices in liquid metals
[TT-70-50029] 06 p1282 N71-19292
- Electron mobility in cadmium sulfide crystals and thin films
[ELAB-TE-120] 16 p1533 N71-21055

- Electron and ion conductivity measurements on solid silver sulfide, silver selenide, and silver telluride
[ANL-TRANS-868] 10 p1516 N71-21659
- Interior potentials for alkali metals from correlations in electron liquids
[ANL-7761] 13 p2098 N71-25512
- Far infrared photoconductivity and electron transport in high purity N-type indium antimonide
15 p2506 N71-27423
- Characteristics of simultaneous electronics and ionic conductivity in solids at 700 to 800 C
[NLL-LTI-746-617-/9022.401/] 16 p2660 N71-29138
- Electron mobility mechanisms in epitaxial growth of gallium arsenide crystals and computer program for calculating Hall effect
[AD-722630] 18 p2993 N71-30734
- Electron and hole drift mobilities in photoconducting amorphous selenium
[NASA-TN-D-6500] 21 p3499 N71-34926
- Numerical analysis of transport parameters for point defect scattering in nearly free electron model metals
22 p3660 N71-36098
- ELECTRON MULTIPLIERS**
U PHOTOMULTIPLIER TUBES
ELECTRON OPTICS
Tables of focal properties of three-element electrostatic cylinder lenses
[JILA-104] 01 p0055 N71-10601
- Describing injector and beam optics of 8 MeV tandem Van de Graaff accelerator
[CISE-139] 08 p1174 N71-18168
- Fiber optics in electron optical devices such as cathode ray tubes, image intensifiers, and image converters
[AD-717838] 11 p1798 N71-22470
- Application of Q switched lasers to optical methods of plasma diagnostics using Thomson scattering
11 p1775 N71-22638
- Electro-optical measurement and data processing techniques
[POA-3-C-3614-62] 14 p2298 N71-26596
- ELECTRON ORBITALS**
Interaction of nuclear spins with orbital and spin magnetic moments of electrons leading to spin coupling observations in NMR spectra
14 p2307 N71-26397
- Applying Hylleraas correlation function to Giesbeck-Gordon combination of Hartree-Fock orbitals for two electrons
15 p2484 N71-27790
- Internal source scintillation method for studying orbital electron-capture and electron-capture-to-position-emission ratios
[NP-18692] 19 p3147 N71-32043
- ELECTRON OSCILLATIONS**
Characteristics of longitudinal plasma waves and zero sound
[NP-18364] 04 p0596 N71-13773
- Deriving equations for automatic correction of betatron oscillations in cyclic accelerators
[CERN-TRANS-49-32] 04 p0587 N71-14276
- Physics of electron storage rings including betatron oscillations, energy oscillations, radiation damping, radiation excitation, and luminosity
[SLAC-121] 12 p1980 N71-24348
- High frequency oscillation research and related electronics problems including open resonator applications in electromagnetic fields and paramagnetic and cyclotron resonances
[AD-722279] 17 p2725 N71-29667
- Theoretical model for electronic stopping power of heavy ions compared with experimental results for carbon and nitrogen targets
21 p3493 N71-34880
- Axially symmetric electron-ion beam oscillations and instability in magnetic field
[MATT-TRANS-83] 21 p3494 N71-34891
- Electron-ion (ion sound) oscillations in electron beam passing through rarefied gas corresponding to instability of inhomogeneous plasma
[MATT-TRANS-84] 21 p3494 N71-34894
- Analysis of Hall effect in plasma oscillation to include arbitrary amplitude electron oscillations, stability of low density pinch, and oscillations in electron hole pinch
[IAE-1950] 22 p3653 N71-36049
- ELECTRON PARAMAGNETIC RESONANCE**
Increase of chromium-⁵¹ concentration in X ray irradiated ruby during isothermal annealings measured by EPR technique
[NASA-TN-D-6079] 02 p0285 N71-11888
- Far-infrared resonances in ytterbium orthoferrite near spin reorientation temperature
[NYO-2391-106] 03 p0428 N71-12881
- Electron paramagnetic resonance in strontium titanate doped with chromium to determine interactions between paramagnetic ions in neighboring lattice positions
03 p0444 N71-13261
- Hyperfine ESR linewidth in linear chains using Cu/NH₃/4SO₄-H₂O/CTSA for calculations
[COO-1488-19] 04 p0483 N71-13439

- Investigating spin-lattice relaxation of paramagnetic defects in crystals of II-VI compounds
[AD-713864] 06 p0934 N71-16499
- Electron paramagnetic resonance study of oxygen adsorption on semiconductor surfaces
[AD-714986] 07 p1096 N71-18880
- Electron spin resonance studies on irradiated heterogeneous systems - structure and reactivity of paramagnetic centers in silica gel
[NP-18478] 04 p1235 N71-12320
- Second-order solutions of Hamiltonian functions for EPR study of Jahn-Teller effect in SrCl₂-La₂ plus
[NASA-CR-116883] 08 p1282 N71-15201
- Electron paramagnetic resonance of divalent manganese in zinc perchlorate and divalent nickel in nitrofluoride with parallel and perpendicular configuration
09 p1430 N71-19907
- Using electron paramagnetic resonance spectroscopy to investigate Ti-2 plus and Mn-2 plus F²⁺ super-hyperfine interaction in alkaline earth fluorides at microwave frequencies
09 p1431 N71-19908
- NMR and ESR measurements of magnetic interaction in sodium chloride-silver chloride ion and lanthanum ethyl sulfate-trivalent cerium ion
09 p1432 N71-19910
- Electron paramagnetic resonance detection of electron bombarded lithium fluoride
[NASA-TM-X-52989] 10 p1616 N71-23803
- Studies of f electron systems in single crystals, including electron nuclear double resonance lines for La and Ce
[COO-294-10] 10 p1624 N71-23779
- Photon absorption lines in electron paramagnetic resonance spectrum of second harmonic generation in ruby
11 p1800 N71-21060
- Quadrupole interaction of Ba-137 and Ba-135 with positive fluorine ion centers and electron paramagnetic resonance spectrum of positive trivalent Gd ions in single BaO crystals
11 p1805 N71-21062
- Microwave power, saturation, and modulation amplitude effects on radical concentration measurement in reacting gases using ESR
11 p1807 N71-21064
- Microwave technology with application to solid state physics, electron paramagnetic resonance, and gamma irradiation
[AD-717876] 12 p1986 N71-23823
- Single particle exchange as approximate force law and threshold zeros in resonance approximation and application to Yukawa potential scattering
12 p1974 N71-23895
- Elastic and inelastic proton scattering function from Cd-110, Cd-112, and Cd-114 based on shell theory and elastic scattering indium isotope for isobaric analog resonances
13 p2138 N71-25407
- Electron paramagnetic resonance spectrometer operating under irradiation near reactor core and with gamma ray source
[CEA-R-4022] 14 p2254 N71-26880
- Magnetic properties of solids including electron paramagnetic resonance in dilute magnetic alloys, hyperfine splitting of localized moment in metal, and band theory of solids
[AD-720777] 14 p2325 N71-26839
- EPR study of two smectic A liquid crystals with vanadyl acetyl acetonate as paramagnetic probe
[NASA-TN-D-6289] 14 p2278 N71-26407
- Resonator for X band electron spin resonance for simultaneous measurement and electron radiation of transient free radicals
[KFK-1285] 15 p2468 N71-27328
- Electron paramagnetic studies of gamma irradiated alkali-germanate glasses and crystalline compounds
15 p2507 N71-27371
- Electron paramagnetic resonance of 102Tl/indium radical in gamma irradiated single crystals of KIO₃ at room temperature
[COO-1385-34] 15 p2486 N71-27382
- Electron spin resonance for detecting defects in beryllium oxide single crystals created by gamma or neutron irradiation
[CEA-R-3937] 15 p2496 N71-27971
- Electron paramagnetic resonance of CeO₂/plus, Ni₂/plus, and Cu₂/plus in hydrated single crystals at temperatures from 300 to 1.2 K
[UCRL-20306] 17 p2814 N71-30723
- Theory of electron paramagnetic resonance in dilute magnetic alloys
[AD-722818] 17 p2815 N71-30737
- Vibronic and electronic resonance Raman effect in cadmium sulfide and garnet crystals
[AD-722701] 17 p2827 N71-30848
- Development of spin Hamiltonian theory for very low symmetry systems with matrix-diagonalization programs and tensorial notation for analysis of ESR spectra
17 p2828 N71-30858

SUBJECT INDEX

- Rare earth chelates and organic solvents as paramagnetic shift reagent for nuclear magnetic resonance spectral chromatography (AD-723440) 10 p3285 N71-30812
- RPR and fracture mechanics applied to ozone cracking in rubber 10 p3240 N71-31224
- Oxidation and reduction half wave potentials, and electron spin resonance of positive and negative ion radicals 10 p3267 N71-31340
- Electron paramagnetic resonance spectra of Cd²⁺ in single crystals of cadmium sulfide observed at liquid nitrogen temperature 10 p3298 N71-31542
- Electron and nuclear spin interactions in solids including ferromagnetism of rare earth metals, and spin-lattice relaxation of nuclei in solid ferromagnets (AD-723327) 19 p3164 N71-31721
- Fundamental aspects of electron paramagnetic resonance spectroscopy (ANL-7764) 19 p3101 N71-32313
- Paramagnetic resonance spectra of K/CuLi using positive Li-7 and Li-6 ions (NYO-2150-59) 19 p3160 N71-32638
- Electromagnetic resonance of vanadyl perchlorate in solutions of water and heavy water (UCRL-19691) 20 p3319 N71-33599
- Electron spin resonance of free radicals formed in polymers by ultraviolet radiation (APC-CR-97) 20 p3323 N71-33828
- Electron paramagnetic resonance analysis of sulfur and selenium polymerization in liquid state 21 p3387 N71-34998
- Trivalent chromium ion X-ray fluorescence electron-spin resonance spectra in single MgO crystals (AD-723663) 22 p3444 N71-35984
- Orientation dependence in triplet-triplet energy transfer determined by magnetophotoselection spectroscopy (AD-725633) 22 p3552 N71-35298
- ESR studies of radiation effects on ammonium monofluorocarbonate and ammonium difluorocarbonate at room temperature (COO-1385-37) 22 p3644 N71-35984
- Effects of anisotropy on intensity of conduction electron spin resonance in high purity sodium 22 p3652 N71-36040
- Electron paramagnetic resonance studies of spin relaxation mechanisms in stable phenyl free radicals 22 p3659 N71-36094

ELECTRON PATHS

U ELECTRON TRAJECTORIES

ELECTRON PHOTON INTERACTIONS

- Quantum theory of anisotropic effects in electron scattering and electron photon interactions (AD-721496) 03 p0443 N71-13176
- Tunneling spectroscopy in degenerate p-type silicon (NASA-CR-115709) 04 p0485 N71-13453
- Electron photon interactions for inducing superconductivity in transition metals 09 p1435 N71-20038
- Interaction effects in solids using transition metal and rare earth ions as probes (AD-719687) 13 p2152 N71-25440
- Ultrasonic tests of superconductors, electron photon interactions, nuclear spin and electronic wave interactions, and spin-spin photon interactions in new earth elements 18 p2999 N71-31464
- Calculations of phonon contribution to electron effective mass as function of position on Fermi surface, and anisotropic superconducting energy gap in white tin 21 p3492 N71-34874

ELECTRON PHOTON CASCADES

- Electron photon cascade calculations for photon beam energy absorption in beryllium and aluminum sheets (JNRL-4631) 09 p1436 N71-20042
- Calculations for structure functions of inelastic electron-photon scattering in perturbation theory for quantum electrodynamics with massive photons 14 p2304 N71-26202
- Data analysis methods for correcting cascade transition effects in atomic transition probability measurements 19 p3155 N71-32358
- Improved intracascade cascade model for estimating cross sections in spacecraft shield design (NASA-CR-123301) 24 p3971 N71-38328

ELECTRON PLASMA

- Large amplitude steady state electron plasma, harmonic ion cyclotron amplifying waves (COO-2881-2) 04 p0597 N71-14051
- Isolation of relativistic electrons into Astron type magnetic field configurations 04 p0598 N71-14162
- Theoretical analysis of quasi-steady ion cyclotron waves (JRO-791-4) 05 p0754 N71-15224
- Resonance of state for adiabatic electron plasma (COO-2880-3) 05 p0754 N71-15225

Monte Carlo analysis of photon penetration through hot electron gas (AD-713485) 05 p0754 N71-15363

Anomalous damping of large-amplitude electron plasma oscillations - computer experiments (AD-715074) 07 p1084 N71-18091

Calculation of energy transfer in slowing down reactions with controlled fusion systems (AD-716594) 09 p1449 N71-20814

Detection and operation of experimental plasma facility (Helios) in which electrons and lithium ions are heated by electromagnetic noise (COO-3092-15) 10 p1636 N71-20469

Electron cyclotron resonance and anisotropic energy distribution excitation of plasma instabilities and waves (COO-1695-32) 11 p1811 N71-22443

Procedure to replace electron correlation effects with Debye shielded interaction including classical path braiding functions for Stark effects (NASA-TM-X-47149) 12 p1975 N71-23999

Multiparticle process of gas ionization in laser spark production (NRC-T-1450) 12 p2013 N71-24277

Experiments demonstrating resonant nonlinear electromagnetic wave excitation of electron plasma and ion acoustic waves in plasma column (TR-70-34) 13 p2148 N71-25184

Collisional effects on electron waves in non-Maxwellian Lorentz magnetoplasma (AD-719798) 14 p2320 N71-25708

Effects of this echo in relativistic electron plasma (NASA-TT-F-13785) 19 p3164 N71-32233

Longitudinal nonlinear oscillations of hot electron plasma near external magnetic field investigated by perturbation method (UABAE-58) 23 p3824 N71-37278

Instability in hot electron plasma created by adiabatic compression in pulsed magnetic field 23 p3833 N71-37335

Ion and electron plasma confinement and kinetic instabilities in adiabatic traps 23 p3853 N71-37467

Magnetohydrodynamic equilibrium and stability of high-beta relativistic electron plasmas in axisymmetric and nonaxisymmetric mirror traps (CONF-710697-91) 24 p3992 N71-38478

ELECTRON PRECIPITATION

- Discontinuous precipitation of gamma prime in nickel-cobalt-aluminum alloys by transmission electron microscopy 08 p1220 N71-19272
- Auroral low energy electron precipitation and ionospheric trough (KGO-PREPRINT-70-315) 10 p1548 N71-21056
- ESRO 1 satellite photometric data on relationship between electron and proton auroras and precipitation 10 p1549 N71-21152
- Correlation between ESRO 1 satellite auroral photometric data and ground based observations 10 p1549 N71-21153
- ESRO 1 satellite experiment on low energy electron precipitation during polar cap absorption and quiet magnetospheric conditions 10 p1550 N71-21155

Auroral magnetic substorm and high energy electron absorption 12 p1908 N71-23556

Auroral zone X ray events detected by means of electron precipitation balloon sounding 12 p1909 N71-23564

Magnetic substorm effects on auroral electron and proton precipitation 12 p1909 N71-23566

Auroral electron and proton zones determined by auroral ionization spectroscopy onboard ESRO 1 satellite 12 p1909 N71-23570

Balloon study on auroral nitrogen emission and bremsstrahlung x rays produced by electron precipitation 12 p1994 N71-24274

Relationship between ionospheric electron currents, geomagnetic storms, and absorption bursts 17 p2747 N71-30088

Comparison of VLF auroral hiss with precipitating low energy electrons studied with simultaneous OGO-4 data to determine hiss origin (NASA-TM-X-45665) 19 p3094 N71-32413

Comparison of Injun 5 satellite measurements of low energy electron precipitation and ground based observations of visible auroral arc (NASA-CR-121675) 21 p3415 N71-34300

Electron pressure and energy anisotropy effects on whistlers leading collisionless plasma shock waves 07 p1083 N71-17058

Electron pressure and energy anisotropy effects on whistlers leading collisionless plasma shock waves 07 p1083 N71-17058

Electron pressure and energy anisotropy effects on whistlers leading collisionless plasma shock waves 07 p1083 N71-17058

Electron pressure and energy anisotropy effects on whistlers leading collisionless plasma shock waves 07 p1083 N71-17058

Electron pressure and energy anisotropy effects on whistlers leading collisionless plasma shock waves 07 p1083 N71-17058

Electron pressure and energy anisotropy effects on whistlers leading collisionless plasma shock waves 07 p1083 N71-17058

Electron pressure and energy anisotropy effects on whistlers leading collisionless plasma shock waves 07 p1083 N71-17058

Electron pressure and energy anisotropy effects on whistlers leading collisionless plasma shock waves 07 p1083 N71-17058

Electron pressure and energy anisotropy effects on whistlers leading collisionless plasma shock waves 07 p1083 N71-17058

Electron pressure and energy anisotropy effects on whistlers leading collisionless plasma shock waves 07 p1083 N71-17058

ELECTRON SCATTERING

Computer program for electron microprobe analysis using simple or complex standards (CRAN-1-1289) 04 p0574 N71-13672

Electron microprobe probe identification of bonding and chemical combinations 05 p0649 N71-14994

Content mapping techniques for qualitative and semiquantitative analysis with electron microprobe probe (AD-713711) 05 p0649 N71-14994

Electron microprobe analysis of fine-grained igneous rocks from lunar sample 10022 from Sea of Tranquility 06 p0875 N71-16777

Quantification of nickel alloys determined by X ray diffraction, weight and thickness change measurements, and electron microprobe analysis (NASA-TN-D-6296) 12 p1935 N71-33101

ELECTRON RADIATION NT BETA PARTICLES NT ELECTRON BEAMS

Absorbed dose microdistribution in heavy charged particle track 08 p1263 N71-19061

Reactor for X band electron spin resonance for simultaneous measurement and electron radiation of transient free radicals (KFK-1285) 15 p2468 N71-27328

Calculation of electron and bremsstrahlung dose deposition with energy deposition, transmission, and reflection coefficients for electrons (NASA-TN-D-6385) 16 p2674 N71-28127

Neutron, electron, proton, and electromagnetic radiation effects on transistors - handbook (NASA-CR-1834) 18 p2898 N71-31372

Effects of synchrotron radiation from electrons in computers for electron ring accelerators (UCRL-TRANS-1435) 21 p2404 N71-34823

Creation of high negative potential on spacecraft for protection of equipment, materials and crew from electron radiation belts of earth (NASA-TT-F-13903) 21 p3504 N71-34959

ELECTRON RECOMBINATION NT RADIATIVE RECOMBINATION

Mathematical model for minority carrier recombination in neutron irradiated silicon semiconductor (SC-8-70-431) 07 p1693 N71-17457

Determination of ionospheric electron recombination coefficient after sudden frequency deviations 11 p1710 N71-22936

Mathematical models for ionization relaxation and nitrogen ion, electron and molecular recombination behind shock waves with 17 to 25 km/sec velocities (NASA-TT-F-13992) 18 p2905 N71-31072

ELECTRON RING ACCELERATORS U STORAGE RINGS (PARTICLE ACCELERATORS)

ELECTRON SCATTERING

Correlation effects on structure of impurity bands (NASA-TN-D-6074) 01 p0110 N71-10410

Dirac equation solution for spin in elastic low energy electron scattering from gaseous atoms (AD-711644) 01 p0101 N71-10842

Inconsistent scale effects in theory of scattering among unified particles in photon-electron interactions (AD-711681) 01 p0102 N71-10939

Excitation of Si-28 particle-hole states by inelastic electron scattering at high momentum transfer (AD-712833) 02 p0276 N71-12061

Nuclear charge distribution determinations of even asymmetric isotopes by electron scattering (AD-712022) 02 p0277 N71-12062

D and s electron interactions in iron-aluminum system diffusion (TT-70-57046) 02 p0245 N71-12149

Electron scattering and atomic structure (AD-712541) 03 p0436 N71-13374

Quantum electrodynamics of high energy electron positron elastic scattering (LNF-7076) 04 p0569 N71-13552

Inelastic scattering cross sections for electron scattered from atoms 04 p0570 N71-13599

Slow electron collision processes in gases (RPI-4144-1) 04 p0572 N71-13629

Geometrical interpretation of scale invariance in inelastic electron proton scattering (LNF-7074) 04 p0578 N71-13863

Digital calculation of cross sections of inelastic electron scattering by phase shift method (CEA-N-1259) 04 p0578 N71-13871

Many body problem of elastic scattering of electrons from atoms and molecules using Green function techniques 04 p0583 N71-14150

Models for resonant electron scattering in small atoms and molecules such as hydrogen, nitrogen and carbon monoxide 04 p0588 N71-14331

Theoretical interpretation of optical and electron scattering spectra of H₂O 04 p0588 N71-14349

- Electron scattering spectrum of carbon dioxide including scattering processes through formation of short lived negative molecule-ion compound states
04 p0592 N71-14393
- Absolute total cross sections for low energy electron scattering by rubidium, cesium, and potassium
04 p0594 N71-14452
- Investigating electron scattering and nuclear structure in linear accelerators
05 p0735 N71-14528
- Measuring inelastic electron scattering form factors for proton excited states in vanadium 51
05 p0736 N71-14533
- Measuring elastic scattering cross sections for Li-7 nucleus and 16/7/2-shell nuclei of Sc, V, and Co
05 p0736 N71-14534
- Computer program for calculation of electron scattering and photoionization cross sections of atomic systems with configuration np^q
05 p0649 N71-14781
- Born approximation for inelastic electron scattering in noble gas atoms
05 p0747 N71-15238
- Electron interaction in transition metal X ray emission spectra
06 p0909 N71-15753
- High energy electron positron scattering cross section measurements as test of quantum electrodynamic theory
06 p0910 N71-15786
- Inelastic electron scattering experiments
06 p0916 N71-16055
- High energy electron scattering from Li-6
06 p0920 N71-16268
- Electron interaction with matter and differential cross section measurements for bremsstrahlung produced in coincidence with inelastically scattered electrons
06 p0922 N71-16399
- Electron scattering effects in beam generated plasma
07 p1083 N71-17824
- Quasi-free electron scattering on C-12 and Be-9 using external electron beam
08 p1247 N71-18190
- Investigating time-reversal invariance in electromagnetic interaction of electrons and deuterons
08 p1249 N71-18224
- Numerical calculations of small angle electron scattering cross section dependence on source displacements
08 p1249 N71-18225
- Electron-proton elastic scattering cross sections at low-momentum transfers between 1.0 and 3.0 GeV/c squared
08 p1252 N71-18301
- Measuring differential cross sections for inelastic electron scattering from calcium, titanium, and iron isotopes
08 p1253 N71-18331
- Investigating violation of CP invariance in electromagnetic interactions of hadrons
08 p1259 N71-18659
- Graphical investigation and vector meson dominance of inelastic electron proton scattering
09 p1446 N71-20574
- Highly inelastic electron scattering theories
10 p1615 N71-21052
- High energy electron and positron colliding beams leading to annihilation into muon pair, annihilation into hadron pair, Bhabha scattering and multibody hadron production
10 p1623 N71-21769
- Electron scattering cross section from aligned and nonaligned Ho-165
11 p1803 N71-22234
- Nuclear Fermi momenta from quasi-elastic electron scattering
11 p1803 N71-22235
- Experimental and theoretical aspects of inelastic electron-nucleon scattering
11 p1803 N71-22248
- Forward and backscattering of spherical overdense clouds for ionospheric electron density distributions
11 p1700 N71-22324
- Origin and propagation of galactic cosmic ray electrons in interstellar space
11 p1823 N71-22578
- Techniques for kinetic studies in shock tubes including infrared emission, electron scattering and electric discharge
11 p1739 N71-22627
- Procedure to replace electron correlation effects with Debye shielded interaction including classical path broadening functions for Stark effects
12 p1975 N71-23999
- Operation of 60 MeV linac including 180 degree electron scattering, slow neutron resonance data on rhenium isotopes, s-wave resonance spins, and related maintenance and improvements
14 p2305 N71-26320
- Short range dynamical correlations from elastic and quasielastic high energy electron scattering on He-4
14 p2311 N71-26694
- Electron and positron scattering from negative pion-proton interactions at 275 MeV using scintillation and Cerenkov counters, absorption spectrometers, and spark chambers
14 p2317 N71-26758
- Ionization cross sections for neon and argon single electron loss in nitrogen, oxygen, and air between 25 and 90 keV
15 p2472 N71-27436
- Statistical model for electron scattering in ion atom interactions
15 p2474 N71-27456
- Target nuclei charge distribution effects on high energy electron small angle multiple scattering distributions based on Mollere formula and elastic form factors
15 p2478 N71-27607
- Metaplastic gamma ray spectra calculated for relativistic electron bremsstrahlung interactions
15 p2515 N71-27646
- Scattering cross sections of electroproduction data in resonance region and consequences for sigma sub 1/sigma sub t
16 p2647 N71-28273
- Inelastic electron-proton scattering cross section measurements at 18, 26, and 34 deg angles
16 p2652 N71-28984
- Small signal field analysis of double-stream interactions in finite semiconductors
16 p2668 N71-29015
- High energy scattering of protons, electrons, photons, and composite particles by nuclei
16 p2658 N71-29163
- GeLi detector for measuring energy of electrons scattered forward by proton beam in thin beryllium foil
17 p2791 N71-29296
- Electron scattering by stacking faults in metal crystals
17 p2825 N71-29998
- Dynamic model for vibrating dislocation interaction with conduction electrons in metals
17 p2825 N71-30000
- Kinetic theory of Compton scattering by relativistic electrons with induced scattering
17 p2829 N71-30281
- Modification of parton model with variable intermediate state parton mass
17 p2806 N71-30310
- Inelastic high energy electron scattering by light nuclei accompanied by knockout of nucleons
18 p2970 N71-30445
- Knocking out of nucleons by inelastic electron scattering process in light nuclei
18 p2973 N71-30547
- Shell structure of light nuclei during inelastic scattering of high energy electrons accompanied by knockout of nucleons from nucleus
18 p2974 N71-30551
- Asymptotic behavior of electron-proton scattering amplitude, spectral function of commutator of currents, and sum rules for Schwinger term
18 p2974 N71-30566
- Spin structure of two-photon exchange contribution to electron proton elastic scattering amplitude
18 p2978 N71-30679
- Lattice mechanics in electron-plasmon scattering in solids
18 p2982 N71-30913
- Quantum mechanical calculations of approximate scattering cross sections for elastic, inelastic, and rearrangement collisions of electrons, atoms, and molecules
18 p2987 N71-31349
- Boltzmann transport equation for elastic scattering of electrons in solids
19 p1617 N71-31708
- Energy spectra of ions and electrons produced in collision of argon neutral beams
19 p3049 N71-32036
- Investigation of e d yields e p n scattering reaction with scattered electrons measured with spark chamber spectrometer and recoil protons detected with counter hodoscope
19 p3156 N71-32443
- Nuclear magnetic resonance study of electron-electron interactions in palladium, palladium platinum alloys, and alkali metals
19 p3160 N71-32655
- Argon ion-atom collision hypothesis investigated using coincidence methods to obtain fast electron energy spectrum with known scattering angle, ion energy, and charge state
19 p3160 N71-32667
- Operator product expansion for studying exclusive electron proton scattering in Bjorken limit
19 p3160 N71-32672
- Measurement of total cross section for low energy electrons on metastable argon by atom beam recoil method
20 p3318 N71-33579
- Two-plane-wave models for electron-electron and electron-photon unklapp scattering with determination of their effect upon transport properties of simple metals
20 p3323 N71-33622
- Mathematical models for inelastic electron proton scattering indicating current amplitudes with oscillatory characteristics
20 p3324 N71-33626
- Electron rings and compression cycles at high and low intensities
21 p3481 N71-34070
- Ground state charge distribution and physical properties of some low-lying states in Nd-142, Nd-144, and Nd-150 produced by electron scattering
21 p3489 N71-34034
- Electron wave instabilities in non-Maxwellian Lorentz magnetoplasma caused by electron-nucleon collisions
21 p3495 N71-34080
- Microwave resonance studies in alkali halides, intracavity generated by eddy currents in potassium electron-electron scattering in tungsten, and related studies
21 p3497 N71-34091
- Nuclear structure of boron 11 studied by high-energy electron scattering
22 p3636 N71-33921
- Disappearance of inelastic channel of nuclear reaction in resonant nuclear scattering of gamma rays in perfect crystal
22 p3640 N71-33940
- Phenomenological Lagrangian model calculation of scaling properties in deep inelastic electron-proton scattering
23 p3813 N71-37180
- High-altitude electromagnetic pulse source emission and ionization from Compton scattering of gamma rays based on forward scattering of Compton electrons
23 p3818 N71-37323
- Experimental designs for electron elastic and inelastic scattering and mathematical expressions for electron-scattering cross sections and radiative corrections
23 p3820 N71-37349
- Electron pitch-angle scattering in outer zone during magnetic storms
23 p3842 N71-37399
- Schrodinger equation solution for electron scattering
24 p3950 N71-38018
- Electron and muon pair production in electron-electron and electron positron collisions and hadron production via photon photon scattering
24 p3969 N71-38032
- Measurement of ratio of positron-proton and electron-proton elastic scattering cross sections at 180 deg and large q²
24 p3974 N71-38033
- Equipment and capabilities developed in investigation of K and L shell ionization cross sections, X ray intensity ratios, bremsstrahlung spectrum, coincidence, and inelastic electron scattering
24 p3976 N71-38038
- Effect of electron-magnon interaction on magnon energy in itinerant electron ferromagnets
24 p3982 N71-38039
- ELECTRON SOURCES**
Origin of cosmic electrons with high energies from supernovae
22 p3664 N71-34123
- Increasing energy of injected electrons to facilitate trapping experiments in Astron
24 p3990 N71-38040
- ELECTRON SPIN**
Spin interactions in copper compounds
05 p0756 N71-14537
- Investigations of nuclear and electron spin waves by parallel pumping
05 p0750 N71-14534
- Isotopes in bound nuclear states, spin assignments, and electromagnetic multipole mixing determined with beta-gamma γ correlation measurements in aligned transitions
08 p1253 N71-18331
- Using electron spin-echo technique to measure spin lattice relaxation of V/4 plus paramagnetic impurities in rutile at liquid-helium temperature
09 p1426 N71-20573
- Calculation of crystal field splittings of trivalent neodymium ion in yttrium aluminum garnet
14 p2330 N71-26376
- Electron paramagnetic resonance studies of spin relaxation mechanisms in stable phenyl free radicals
22 p3659 N71-38044
- ELECTRON SPIN RESONANCE**
U ELECTRON PARAMAGNETIC RESONANCE
Localized one-electron states in perfect crystals of hydrogen atoms
02 p0285 N71-11000
- Quantum mechanical excitation measurements on ytterbium states
04 p0588 N71-14008

SUBJECT INDEX

- Density of electron states, electron-phonon coupling constants, and Debye characteristic temperature of alkali-phase in alloys containing Cd and Sn [UCRL-19681] 07 p1078 N71-17596
- Magnetic properties, hyperfine field, and band structure of ferromagnetic iron 10 p1609 N71-21762
- Helium 175 excited states in tantalum 175 decay spectrum [JINR-P6-5434] 16 p2642 N71-28033
- Mathematical model for calculating equilibrium deformations in ground and excited states of rare earth nuclei [JINR-P-1216] 16 p2642 N71-28048
- Single particle energies, wave function potentials and odd parity levels of actinide nuclei [JINR-P6-5470] 16 p2644 N71-28098
- Electronic states at dislocations in semiconductor and diamond structures 17 p2825 N71-29997
- Mathematical model for surface states on crystal smectic lamella 17 p2825 N71-29999
- Atomic beam radio frequency measurement of $2S_{1/2}$ to $2P_{3/2}$ energy separation in N equals 2 state of atomic hydrogen 17 p2809 N71-30579
- Excited states in boron 10 decay between 18 and 22 MeV 18 p2894 N71-31063
- Multiphonon field state of synchrotron radiation for electron in storage ring [JLAC-TRANS-125] 18 p2903 N71-31551
- Quasiparticle model for calculating energy spectra of helium isotopes [UW-2540-F] 19 p3149 N71-32110
- Superficial nuclear model for calculating ground- and excited-states of odd-N nuclei [JINR-B4-5567] 19 p3150 N71-32121
- Relative lifetime measurements of excited states from gas-phase pulsed radiolysis of CO_2 , CH_4 , and CO [JAL-TRANS-879] 21 p3477 N71-34765
- Polarization dependence and electron state symmetries for two-photon absorption in solids 22 p3660 N71-36101
- ELECTRON SWEEPING**
- U SWEEP FREQUENCY
- ELECTRON TELESCOPES**
- U PARTICLE TELESCOPES
- ELECTRON TEMPERATURE**
- U ELECTRON ENERGY
- ELECTRON TRAJECTORIES**
- Helix-type depressed electrostatic collector for axially focused spaceborne klystron [NASA-CR-72767] 01 p8030 N71-10020
- Trajectories of Compton electrons produced by x-ray rays with air in electromagnetic field [LA-4348] 03 p0421 N71-12649
- Simultaneous detection method for Dalitz pairs and localization of neutral pion origins [JFA-CR-40] 03 p0428 N71-12877
- Bootstrap calculation of linearly rising Regge trajectory in single channel, single trajectory model when dispersion relations are separately written 10 p1623 N71-21770
- Analyzing automatic electron trajectory tracer for studying large properties of electrostatic image tubes 21 p3404 N71-34224
- ELECTRON TRANSFER**
- Monte Carlo and numerical integration methods of calculating distribution functions for electron transport in semiconductors 01 p0108 N71-10135
- Distribution function calculations applied to electron transport properties in semiconductors 01 p0108 N71-10136
- CW transferred electron oscillators for Q band 01 p0031 N71-10138
- Method for treating metal surfaces to prevent secondary electron transmission [NASA-CASE-XNP-08469] 13 p2142 N71-25555
- Energy transfer and ionization in molecular gas discharges [AD-720478] 15 p2501 N71-27419
- Evidence for particle instability of helium 10 [JINR-B7-5492] 16 p2645 N71-28143
- French-Condou and resonance charge exchange effects on charge transfer cross sections based on mass spectroscopy of molecular ion reactions with perfluorinated alkanes, and alkene targets 17 p2801 N71-30116
- Electron-electron exchange calculations for band transfer in semiconductors 18 p2998 N71-31448
- Approximate solution for propagation shifts and noise in plane diode with Maxwellian distribution 18 p2998 N71-31451
- Mechanism of diffusion of some elements in iron and steel - atomic transference and movement of elements in metal lattices [TT-70-59107] 20 p3284 N71-33327

Electron transport, antibodies, photosynthetic membranes, and energy conservation in photosynthetic bacteria and virus infection of bacteria [NYO-3759-18] 23 p3714 N71-36474

ELECTRON TRANSITIONS

- Electron conversion ratios for 1064 keV gamma ray of ^{106}Ru [NASA-TN-D-6057] 01 p0093 N71-10066
- Atomic line transitions and radiant emission from high temperature air [AD-710799] 01 p0096 N71-10503
- Resonance light scattering for measuring spectral line transitions in cobalt isotope spectrum 01 p0099 N71-10522
- Low energy interactions of alkali metal atoms and molecules [AD-711110] 01 p0097 N71-10571
- Energy transfer in solids [AD-711063] 01 p0112 N71-10730
- Effects of pressure and temperature on electromagnetic properties of materials [AD-711615] 02 p0273 N71-11788
- K-conversion coefficient of 897-keV transition in $Po-207$ [NIP-18288] 03 p0425 N71-12825
- Stark effect of R2 transition in KCl [NYO-2150-58] 03 p0429 N71-12897
- Deriving expressions for Auger transition rates for f electrons [SC-RR-70-429] 04 p0575 N71-13686
- Absorption model for direct transfer reactions [UW-2433-F] 04 p0577 N71-13748
- Four-micron molecular laser experiments using hydrogen cyanide [AD-713193] 05 p0696 N71-14670
- Obtaining dissociation constants of N-malonic ester-substituted ureas, phthalimides, pyridones, and anilines using UV spectra 06 p0913 N71-15879
- Multiple mixing ratios of gamma transitions in even-even osmium and platinum isotopes [COO-1746-47] 06 p0917 N71-16194
- Analyzing spectroscopic constants of low-lying electronic states of CaO [UCRL-156499] 06 p0922 N71-16408
- Structure and environment effects on transition probabilities of luminescent chromium complexes [COO-773-21] 06 p0875 N71-16795
- Microwave spectra of divinyl ether and a, b, and c-type rotational transitions of one conformer 07 p0988 N71-17078
- Measuring conversion electron and gamma ray spectra in decay of $Tm-163$ to $Er-163$ [JINR-P6-5132] 07 p1072 N71-17340
- Measuring Auger spectra of simple gaseous molecules [NASA-CR-116411] 07 p1072 N71-17342
- Gamma-gamma directional correlation and intensity studies of electromagnetic transitions of Ta-181 [COO-1746-46] 07 p1077 N71-17551
- Isospin in bound nuclear states, spin assignments, and electromagnetic multipole mixing determined with beta-gamma/CP correlation measurements in allowed transitions [UCRL-72624] 08 p1253 N71-18322
- Measuring decay of Nb-90 to levels in Zr-90 using three-crystal gamma ray spectrometer [US-T-389] 08 p1255 N71-18369
- Measuring variation of transition temperature of magnetite with respect to molecular field solution of Moti-Wigner transition 08 p1258 N71-18624
- Heavy ion beams for in-beam gamma ray and conversion electron spectroscopy [UCRL-19961] 08 p1261 N71-18777
- Current-voltage characteristics of hot electron transport in vacuum deposited thin film emission gold magnesium oxide diodes 09 p1361 N71-19419
- First-order radiative transition rate electron transfer from neutral donors to neutral acceptors in silicon at low temperatures 09 p1432 N71-19927
- Transitions between ground state and excited state for Schumann-Runge band system of O_2 [AD-715995] 09 p1435 N71-20017
- Analysis of crystal-field splittings, Zeeman effect, and line strengths for $GdCl_3 \cdot 8H_2O$ magnetic dipole transitions [AD-716040] 09 p1454 N71-20094
- Characteristics of molecular lasers, vibrational population distribution of binary mixture of gases, and spectroscopic observation of laser outputs [AD-717089] 10 p1569 N71-21323
- Fine structure transitions theory and low energy collisions between atomic systems 10 p1618 N71-21400
- Interrelation of electronic structure, molecular structure, and molecular motion reflected in material properties [AD-717182] 10 p1619 N71-21592
- One and two electron transfer reactions during reduction of TiO_2 [COO-1780-14] 10 p1620 N71-21721

ELECTRON TRANSITIONS

- Vibrational perturbation effects on electronic transitions in small polyatomic molecules, and electric dipole selection rules used to ascertain forbidden transitions 11 p1806 N71-22445
- Ionic hydrogen to oxygen transition level variations caused by atmospheric winds 13 p2108 N71-25266
- Autoionization and electron transitions in levelled photoabsorption of atomic calcium [AD-719737] 13 p2139 N71-25406
- Phonon and electron induced transition effects on thermopower of transition metals, and impurity effects on crystal lattice dynamics 13 p2154 N71-25549
- Electronic transitions in infrared absorption spectrum of aluminum antimonide 13 p2155 N71-25548
- Nonlinear wave interaction laser spectroscopy for atomic transition studies 14 p2306 N71-26377
- Electromagnetic transitions from high-lying states to ground, two-quasi-particle, and phonon states of even deformed nuclei [JINR-P4-5562] 14 p2312 N71-26698
- Energy separation measurements in a equals 2 state of atomic hydrogen by radio frequency produced double transitions between hyperfine components [TID-25596] 14 p2315 N71-26734
- Electron and rotational transitions in osmium molecules and Zeeman and Stark effects on microwave spectra in atmospheric molecular composition [AD-721187] 15 p2376 N71-26841
- Angular distributions of deuterons and protons in magnesium 24 to magnesium 25 transition [JINR-B4-5350] 15 p2471 N71-27413
- Ion pair absorption phenomena observed between impurity dopant ions in ionic crystals 15 p2506 N71-27420
- Incident neutron capture to fission cross section ratio for plutonium 239 [CEA-N-1368] 15 p2475 N71-27461
- Gamma transitions in lutetium and tantalum isotopes with parity nonconserving effects [INP-714] 15 p2480 N71-27658
- Mass coefficient in nucleus collective Hamiltonian and sum rules for probabilities of E2 transitions and quadrupole moments 15 p2484 N71-27795
- Wavelength modulation spectra of semiconductor materials [UCRL-20361] 15 p2508 N71-27841
- Optical determination of electron spin-lattice relaxation mechanisms between zero field levels of lowest triplet state for pyrazine-D4 in temperature range 1.5 to 7.9 K [AD-721360] 16 p2664 N71-28228
- Apparatus to measure excitation cross sections of molecular nitrogen bombarded by electrons in 50 to 2000 eV range with reaction rate measured by counting photon emissions [AD-721579] 16 p2648 N71-28600
- Spectrometric high resolution study of helium II 6560 Å and 10124 Å line transitions 16 p2653 N71-29028
- Oscillatory strengths, lines, and lifetimes of energy levels in atomic and ionic spectra with beam-foil measurements [AD-721686] 16 p2656 N71-29109
- Measurement of 4T2 state lifetimes in ruby with fluorescent and nonfluorescent transitions and dynamic model including activation energies, Franck-Condon principle, and frequency factors 16 p2658 N71-29145
- Matrix element tables for computing L shell fluorescence yields and electron transition rates in spin-spin coupling including Auger, Coster-Kronig, and radiative values [SC-RR-71-0075] 17 p2791 N71-29208
- Investigation of fundamental laser processes with computation of vibration-rotation and electric dipole-moment matrix elements of diatomic molecules [AD-722696] 17 p2759 N71-30161
- Vibrational crystal spectra caused by electronic transition of guest molecules at low temperatures 17 p2803 N71-30214
- Thermal and magnetic behavior of electronic optical transitions in antiferromagnetic crystals at 35 K 18 p2964 N71-31137
- Kinetic excitation mechanisms of nitrogen first positive and first negative radiation at high temperatures [AD-723530] 19 p3049 N71-31992
- Symmetry in chemical reactions with single transition matrix [AD-723997] 19 p3147 N71-32052
- Beta-gamma circular polarization measurements on odd nuclei transitions in mercury 203 cascade [NIP-18694] 19 p3148 N71-32089
- Electroluminescence of rare earth compounds in phosphor chloride through cation excitations in electrode processes [AD-723888] 19 p3052 N71-32711

Electron transitions and molecular relaxation mechanisms investigated using gas lasers [AD-724167] 20 p3280 N71-32857

Relative intensities and energy measurements of 2s level in muonic Pb-208 [NASA-CR-121447] 20 p3320 N71-33711
Spin analysis of direct and exchange scattering amplitudes for describing differential inelastic electron-potassium collisions 20 p3323 N71-33814

Kinetics of emissions and absorptions of molecular nitrogen and carbon dioxide ions in ground states produced by pulsed radiolysis of N₂ and CO₂ [ANL-TRANS-881] 21 p3477 N71-34760

Lifetime measurements of eight Ca-41 levels excited from K-41 and Ca-40 reactions using Doppler effect attenuation technique and comparison with nuclear model results 22 p3637 N71-35923

Internal conversion processes for electric quadrupole transitions in deformed nuclear region 22 p3649 N71-36024

Dependence of intensity of characteristic X-radiation on charge of nucleus 23 p3818 N71-37231

Photoelectron emission spectroscopic absorption band calculations for bound-unbound transitions in solution and interpretation of unbound electron random walk with kinetic energy loss [AD-727096] 24 p3981 N71-38412

ELECTRON TUBES

NT CAMERA TUBES
NT CATHODE RAY TUBES
NT CELESCOPES
NT IMAGE DISSECTOR TUBES
NT IMAGE ORTHICONS
NT KLYSTRONS
NT MAGNETRONS
NT MICROWAVE OSCILLATORS
NT MICROWAVE TUBES
NT NIGOTRONS
NT PLANOTRONS
NT THERMIONIC DIODES
NT THYRATRONS
NT TRAVELING WAVE TUBES
NT VACUUM TUBES
NT VIDICONS

Survey of vacuum insulation with discussion of factors influencing breakdown in high voltage vacuum devices [AD-723107] 17 p7277 N71-30259
Numerical analysis of double cathode electronic tube operation at high frequencies 22 p3559 N71-35350

ELECTRON TUNNELING

Low temperature tunneling and second energy gap in superconducting niobium [AD-712072] 02 p0286 N71-12007
Electron tunneling into superconducting rhenium single crystals for energy gap measurements [AD-711826] 03 p0441 N71-12836
Tunneling spectroscopy in degenerate p-type silicon [NASA-CR-115789] 04 p0485 N71-13453
Transitions in high critical temperature superconductors, tunneling in Ga and Al single crystals, and critical temperature enhancement [ORO-3665-23] 06 p0668 N71-15751
Microwave photon assisted tunneling in superconducting tin tunnel junctions [UCRL-19653] 07 p1085 N71-17020
Hamiltonian method for determining magnetic tunneling in crystals in one and two band models 09 p1454 N71-20423
Ultrasonic measurements on paramagnetic impurities in alkali halides compared with predictions of tunneling model [NYO-2471-47] 11 p1784 N71-22581
Anisotropy measurement for superconducting energy gap behavior of single crystal rhenium by tunneling [AD-718415] 12 p1986 N71-23679
Wave functions and delta function potentials for MIS structures with interface states 12 p1988 N71-24304

Experimental investigation of electronic properties of solids [AD-720272] 16 p2665 N71-28726
Superconductive tunneling in single and polycrystalline aluminum thin films 16 p2668 N71-28990
Photon modulated tunneling in thin film MOS structure of Al-Al₂O₃-Te 17 p2827 N71-30169

Electron tunneling characteristics of metal contacts on n-type CdTe and p-type InAs 19 p3071 N71-32666
Differential conductance curves based on electron tunneling measurements of single and polycrystalline pure bulk thorium and analysis of crystal structure in tunnel junction region [IS-T-436] 24 p3996 N71-38507

ELECTRON-ION RECOMBINATION

NT RADIATIVE RECOMBINATION
Investigating hollow cathode discharge as energy source for argon ion lasers 08 p1210 N71-19163

Investigating interactions of low energy electrons with polyatomic molecules of brominated aliphatic hydrocarbons and p-benzoquinone [ORNL-TM-3163] 08 p1268 N71-19350

Electron-ion recombination effects on plasma flow of partially ionized monatomic gas from sonic orifice [RE-4121] 18 p2908 N71-31502

ELECTRONIC AMPLIFIERS

U AMPLIFIERS

ELECTRONIC CONTROL
Electronic control for spacecraft power supplies based on maximum power point tracking [ESRO-CR-15] 02 p0147 N71-11044
Electronic control of spacecraft power supplies 03 p0319 N71-12577

Concepts in LSI servocontrol electronics 04 p0512 N71-13532
Design and performance of microwave frequency phased array antenna systems for airborne and ground applications 04 p0496 N71-13919

Electronically controlled hydraulic actuating systems for accelerator extractor magnets [RPP/N-21] 08 p1174 N71-18276

Hybrid electronic controller developed for pressurization and venting systems of space propulsion system [NASA-CR-72748] 11 p1762 N71-22155
Design of electronic controlled pneumatic signal converter for fluidic device testing by sine wave generation [M/P-1] 12 p1890 N71-23886

Scanning signal phase and amplitude electronic control device with hybrid T waveguide junction [NASA-CASE-NPO-10302] 14 p2333 N71-26142

Ion beam deflector system for electronic thrust vector control for ion propulsion yaw, pitch, and roll forces [NASA-CASE-LEW-10689-4] 14 p2332 N71-26173

Electronic detection system for peak acceleration limits in vibrational testing of spacecraft components [NASA-CASE-NPO-10556] 15 p2408 N71-27185

Boron trifluoride proportional neutron spectrometer control unit for automatic or manual control [INP-707] 15 p2412 N71-27791

Electronic spin-flip chopper for polarized slow neutron beam in time of flight spectrometer 16 p2597 N71-28712

Tracking algorithm for electronically controlled radar using phased arrays based on statistical methods [BMVG-FBWT-70-5] 18 p2889 N71-30616

Electronically controlled camera system for optical satellite triangulation data acquisition 19 p3099 N71-31873

Electronic arrangement of beryllium monitors with each counter having individual discriminator and amplifier [AERE-R-6308] 21 p3402 N71-34206

Electronic control circuitry of servomotor curve tracer [ARL/SYS-25] 21 p3405 N71-34229

Low cost electronic control systems for automobiles utilizing integrated circuits 23 p3737 N71-36646

ELECTRONIC COUNTERMEASURES

NT CHAFF

Development, production, and characteristics of traveling wave tubes and microwave components used for electronic countermeasures equipment [FOA-3-A-3732-66] 22 p3560 N71-35356
Fundamental principles of radar operation to include navigation, reconnaissance, identification systems, radar beacons, and electronic countermeasures [AD-727869] 24 p3889 N71-37722

ELECTRONIC EQUIPMENT

NT AVALANCHE DIODES
NT CRYSTAL RECTIFIERS
NT ELECTRONIC FILTERS
NT ELECTRONIC MODULES
NT ELECTRONIC PACKAGING
NT ELECTRONIC RECORDING SYSTEMS
NT ELECTRONIC TRANSDUCERS
NT FIELD EFFECT TRANSISTORS
NT GALLIUM ARSENIDE LASERS
NT GERMANIUM DIODES
NT JUNCTION DIODES
NT JUNCTION TRANSISTORS
NT METAL OXIDE SEMICONDUCTORS
NT MIS (SEMICONDUCTORS)
NT NEURISTORS
NT PHOTO DIODES
NT PHOTOTRANSISTORS
NT PHOTOVOLTAIC CELLS
NT RUBY LASERS
NT SEMICONDUCTOR DEVICES
NT SEMICONDUCTOR LASERS
NT SILICON TRANSISTORS
NT SOLID STATE DEVICES
NT SOLID STATE LASERS
NT THERMISTORS
NT THYRISTORS
NT TRANSISTOR AMPLIFIERS
NT TRANSISTORS
NT VARACTOR DIODES

Past and present manned spacecraft electronics and implications for space shuttle 01 p0125 N71-10445

Development and characteristics of electronic keyboard calculator 02 p0186 N71-11398

Characteristic impedance measurement in electronic transformers 02 p0191 N71-11342

High voltage breakdown and failure analysis of electronic equipment [AD-711558] 02 p0191 N71-11344

Design of diagnosable control units for switching systems using modular integrated circuits 02 p0192 N71-11346

Catalog of electronic devices of USSR [NBS-TN-526-REV] 02 p0194 N71-11330

Concerto program for production of high reliability electronic components 02 p0194 N71-11336

Analysis of applying standardization techniques to oceanographic sensors [AD-711327] 02 p0223 N71-11387

Development of wideband electromagnetic probes for detection of transient currents [AD-712048] 02 p0228 N71-12851

Compact transistorized pulse unit [NASA-TT-F-13351] 03 p0351 N71-12537

LSI devices and techniques for electronic systems design 03 p0352 N71-12832

Literature survey to determine bremsstrahlung production from X irradiation in electronic products [PB-192888] 03 p0435 N71-13149

Airborne electronic reset fuse [NASA-CR-115791] 04 p0511 N71-13527

Research and Technology Operating Plan Summary - FY 1971 [NASA-TM-X-66566] 05 p0787 N71-15251

W values in mixtures of gases containing ammonia [ORO-2001-14] 05 p0750 N71-15358

Design and construction of six-meter telescope [JPRS-52015] 05 p0866 N71-15412

Microwave device and physical electronics research [AD-713157] 05 p0788 N71-15464

Development of pulse-activated polarographic hydrogen detector [NASA-CASE-XMF-06531] 07 p1029 N71-17975

Radio electronic equipment in marine navigation [AD-714916] 07 p1058 N71-17940

Selection of circuit parameters for connecting photo receiver and electronic loop in optical communication systems 08 p1173 N71-19153

Submerged condenser cooling systems for electronic devices and components by process of boiling and condensation in liquid-filled enclosures [TR-29077-73] 08 p1306 N71-19333

Electronic product radiation and health physics including ionizing radiation - conference [PB-195772] 09 p1328 N71-19460

Development of stable electronic amplifier adaptable for microfilm and thin film construction [NASA-CASE-XGS-02812] 09 p1357 N71-19466

Development and characteristics of oscillating static inverter [NASA-CASE-XGS-05289] 09 p1357 N71-19470

Bi-directional respiratory flowmeters and electronic instrumentation technology for measurement and analysis of metabolic quantities [NASA-CR-114905] 09 p1340 N71-19776

Passive electronic component and materials research and development project summaries 09 p1360 N71-19940

Standards for clean rooms in vacuum electronics manufacturing for precision instruments [JPRS-52528] 09 p1360 N71-20530

Computation of heat transfer in electronic equipment [ECR-15] 10 p1532 N71-20880

Literature review and data analysis for radiation effects on electronic equipment of Thermoelectric Outer Planet Spacecraft 10 p1533 N71-21351

Characteristics of self-powered, multichannel digital data buffer designed to expand input capability of electronic scene generator [NASA-CR-114923] 10 p1529 N71-21440

Field and laboratory equipment and methods for airborne electroprospecting using rotating magnetic fields and anomalous effect calculations for conductive media and irregular form bodies [IT-70-58059] 10 p1555 N71-21471

Electronic signal processing for ultrasonic non-destructive tests [AD-716803] 10 p1561 N71-21470

Description of minimum performance standards for emergency locator transmitters under standard and environmental test conditions [DO-146] 11 p1698 N71-21875

Description of minimum performance standards for emergency locator transmitters of automatic, fixed, automatic portable, and automatic deployable types [DO-147] 11 p1698 N71-21877

SUBJECT INDEX

Models for performance characterization of integrated electro-thermal circuits 11 p1725 N71-22716

Development of electromagnetic wave transmission line circulator and application to parametric amplifier circuits [NASA-CASE-XNP-02140] 11 p1727 N71-23097

Development of optimum pre-detection diversity combining receiving system adapted for use with amplitude modulation, phase modulation, and frequency modulation systems [NASA-CASE-XQS-00740] 11 p1714 N71-23098

Electronic cathodes for use in electron bombardment ion thrusters [NASA-CASE-XLE-04501] 12 p1886 N71-23190

Acoustic command system for transmitting and receiving underwater signals [JPL-71099] 12 p1917 N71-23253

Procedures for qualitative evaluation of frequency accuracy and stability of communication-electronics equipment [AD-71876] 12 p1878 N71-23329

Altitude and temperature-altitude effects on performance of electronic and communication equipment during environment simulation tests [AD-71863] 12 p1888 N71-23353

Development of electronic circuits for forming sound acoustic holograms [JRL/INST-73] 12 p1935 N71-24076

Electronic digital computer for automating 2-GeV electron linac [RLAC-TRANS-126] 12 p1976 N71-24139

Interference prediction model for evaluating expected interactions between avionics equipment on aircraft [AD-71997] 13 p2042 N71-24357

Determination of communication-electronic equipment power requirement and its compatibility with power sources [AD-71999] 13 p2053 N71-24398

Development and characteristics of electronic equipment for measuring time derivative of time-dependent frequency function and application to customer operation [XRS-70-28] 13 p2054 N71-24556

Method and apparatus for adjusting thermal conductance in electronic components for space use [NASA-CASE-NPO-05324] 13 p2185 N71-24876

Computerized life cycle cost model of cost prediction for electronic equipment [AD-71979] 13 p2058 N71-25227

Development and characteristics of solid state acoustic variable time delay line using direct current voltage and radio frequency pulses [NASA-CASE-ERC-10032] 14 p2232 N71-25900

Design and development of broadband model of low band missile tracking and ranging system [AD-720351] 14 p2265 N71-26006

Design engineering of 20 kilowatt solar array electronic simulator [NASA-CR-118506] 14 p2280 N71-26018

Voltage range selection apparatus for sensing and applying voltages to electronic instruments without having signal source [NASA-CASE-XMS-06497] 14 p2253 N71-26244

Electrical and optical measurement of optoelectronic devices before and after submission to X ray irradiation [RML-8-97] 14 p2315 N71-26741

Digital sensor for counting fringes produced by interferometers with improved sensitivity and one autoamplifier tube to eliminate alignment problem [NASA-CASE-LAR-10204] 15 p2408 N71-27215

Development of rectangular display cathode ray tube with low power drain suitable for battery operation [AD-722267] 16 p2568 N71-28342

Extension grounding electrodes for grounding electrical assemblies under permafrost conditions [AD-722221] 16 p2569 N71-28414

System analysis of nonlinear rigid column with 6 degrees of freedom for electronic equipment protection from underground nuclear explosion ground shocks [JRL-50973] 16 p2602 N71-28648

Service for rapid adjustment and maintenance of impedance in electronic components [NASA-CASE-XNP-02792] 16 p2598 N71-28958

Procedures for service test of communication and electronic equipment under adverse weather conditions [AD-720259] 17 p2721 N71-30233

Electronic photointerpretation for aerial reconnaissance systems including size, color, and temperature discrimination, and spectral reflectance in visible and infrared spectra [JPL-1976-23] 18 p2894 N71-30663

Digital frequency devices with analog rebalancing, division with PFM and PDM, and rebalancing instruments with induction eddy current converters [JPL-53642] 18 p2926 N71-31573

Proceedings of conference on electronic crime measurements [JPL-19029] 19 p3069 N71-31628

Electronic signal detection devices for security against electronic eavesdropping 19 p3069 N71-31637

Electronic execution of financial transactions and necessity for anti-fraud controls 19 p3193 N71-31645

Design and operation of electronic combination lock system with built-in alarm features suitable for multi-unit apartment and office complexes 19 p3070 N71-31646

Intrusion detector for parked aircraft using sensing technique to detect human touch 19 p3070 N71-31651

Encapsulation of strain gage transducer and thermocouple in molding compound for simultaneous pressure and temperature readings during transfer molding of electronic components [BDX-613-333] 19 p3105 N71-32316

Epitaxial crystal growth for manufacturing electronic equipment and components including crystal defects and electrical properties of crystallized layers [NLL-PORS-TRANS-2690-19022.11] 19 p3171 N71-32534

Mathematical model for determining system burn-in times in complex electronic equipment for use in reliability analysis 19 p3068 N71-32616

Analog flicker noise simulation using white noise processes by mathematical models [NBS-TN-604] 19 p3068 N71-32747

Proceedings of space shuttle integrated electronics conference - Vol. 1 [NASA-TM-X-58063-VOL-1] 20 p3351 N71-33051

Operational evaluation of capability of bright radar microwave remote sensing system to provide useful radar data in satellite control tower [FAA-RD-71-48] 20 p3236 N71-33788

Utilization of electronic and computerized techniques for undergraduate medical education [BM-6180-NLM] 21 p3383 N71-34081

Development of computer memory system for automated attendance accounting system [NASA-CASE-NPO-11456] 21 p3399 N71-34189

Computer-controlled instrumentation for Danish DR-2 reactor [RISO-M-1206] 21 p3458 N71-34613

Proceedings of space shuttle integrated electronics conference with emphasis on data systems design - Vol. 3 [NASA-TM-X-58063-VOL-3] 21 p3516 N71-35052

Development and characteristics of display system for space shuttle and cost effectiveness analysis of cathode ray tube system 21 p3517 N71-35062

Technology for implementation of onboard electronics maintenance facility for manned space station [NASA-CR-115130] 21 p3519 N71-35078

Numerical analysis of double cathode electronic tube operation at high frequencies 22 p3559 N71-35350

Electrical properties and operation of Gunn diodes [FOA-3-A-3734-61] 22 p3560 N71-35353

Design and development of top-wall and branch waveguide hybrids for millimeter wavelengths and measurement of electrical characteristics [AD-726338] 22 p3560 N71-35358

Performance tests and evaluation of military communication equipment during transportation [AD-726908] 22 p3562 N71-35370

Design, fabrication, and application of integrated microsystems for electronic equipment 23 p3735 N71-36633

Asynchronous interaction of binary circuits under marginal triggering conditions through failure of flip flop circuits to stabilize after triggering 23 p3738 N71-36655

Techniques for determining reliability of electronic equipment after acceleration tests 23 p3758 N71-36786

Space communication, waveguide transmission, and development of associated electronic equipment research projects conducted by Australian research facilities [REPT-6541] 23 p3869 N71-37582

Personnel subsystem management within Electronic Systems Division [AD-726523] 23 p3870 N71-37587

Development of technique for finding functional diagram of combination automation with complex of faults [AD-727974] 24 p3896 N71-37768

Electronic component degradation due to electromagnetic pulse transients [AD-726923] 24 p3898 N71-37783

Evaluation of design fabrication, inspection and testing of integrated circuits aimed at improving quality and reliability of hardware using these devices [AD-726560] 24 p3898 N71-37786

Characteristics of photoelectronic multiplier equipment and application to obtain optimum signal to noise ratios [AD-727878] 24 p3899 N71-37794

Development of comparison between fluid logic circuits and electric and electronic logic circuits [NLL-PORS-TRANS-2727-19022.11] 24 p3908 N71-37830

ELECTRONIC FILTERS

Analysis of functional requirements for data management systems used with space shuttle - Vol. 1 [NASA-CR-119933] 24 p3920 N71-38066

ELECTRONIC EQUIPMENT TESTS

Distortion and environmental tests of travelling wave tubes [AD-71342] 02 p0192 N71-11345

Cesium bombardment ion engine system design, modification, and testing [NASA-CR-111381] 02 p0288 N71-11464

Input intercept point testing of telemetry receiver [AD-712410] 03 p0350 N71-12528

Facilities for testing linear antenna electrical properties in infinite, homogeneous, isotropic, dispersive medium [NASA-CR-115817] 04 p0488 N71-13476

Large scale integrated circuit testing using test points and additional logic [AD-714511] 06 p0824 N71-16542

Low cost high performance lock-in detector for balancing bridges with reactive and resistive components built simultaneously 07 p0100 N71-17093

Automatic test equipment for electronic components [NASA-CR-1754] 08 p1171 N71-19223

Automatic test equipment for electronic components [NASA-CR-1755] 09 p1360 N71-20331

Linear modulator, demodulator, and phase locked loop broadband test procedures and results [NASA-CR-103082] 10 p1537 N71-21543

Electronic equipment tests for satellite instruments and rocket-borne instruments, noting reliability engineering and equipment specifications [BMW-FB-W-70-63] 11 p1761 N71-21987

Fixed direction one axis inertial sensor 11 p1723 N71-22277

Analysis of test equipment used for computer assemblies [AD-718379] 12 p1081 N71-23332

Tests for determining spectral signatures of integrated high-frequency antenna systems for P-3 aircraft [AD-718054] 12 p1089 N71-23609

Encoder/decoder design and evaluation of fail-safe and error correction capability under stationary random noise conditions for pulse communication reliability improvement [AD-720250] 14 p2218 N71-26141

Communication, surveillance, and airborne electronic equipment performance testing in tropical environments [AD-720577] 14 p2218 N71-26176

Large scale integration and metal oxide semiconductor microelectronic testing techniques including combinatorial, sequential, functional, and parametric methods [NASA-CR-103165] 14 p2235 N71-26703

Large scale integration microelectronic wafer and package testing including parametric and functional tests of combinatorial and sequential logic circuits [NASA-CR-103166] 14 p2236 N71-26704

Apparatus for automatically testing analog to digital converters for open and short circuits [NASA-CASE-XLA-06713] 16 p2996 N71-28991

Performance test procedures and results for voltage and frequency transducer for use with galvanometer recorder systems [AD-718977] 17 p2725 N71-29492

Cost and failure analyses and acceptability data from electronic equipment testing of various electronic components [NASA-CR-119801] 18 p2897 N71-30650

Automatic testing of logic integrated circuits including computer program [LAAS-PUBL-747-748] 20 p3340 N71-32939

Compilation of electronic test instrumentation and techniques derived from NASA programs [NASA-SP-5907/02] 20 p3275 N71-33593

Switching circuit, bypass, and power conditioning circuit tests for TOPS electrical system [NASA-CR-121478] 20 p3355 N71-33721

High current and multiple contact, low current switch designs and testing with respect to hermetic seal switches with existing configuration [NASA-CR-115118] 23 p3559 N71-35345

Temperature stress and electrical tests of semiconductor components for failure prediction [FTL-A-A1010-38] 22 p3560 N71-35355

Handbook on use of radio-measurement instruments [AD-726585] 22 p3561 N71-35364

Development and testing of VHF omnirange transmitter for aircraft azimuth guidance [FAA-RD-71-65] 22 p3618 N71-35779

ELECTRONIC FILTERS

Active filters for time division multiplex voice communication [ELAB-TN-125] 03 p0350 N71-12530

Resolution of pulse Doppler radar using pulse compression, noting ambiguity function, and experimental design of autocorrelation [REPT-2-70] 18 p2889 N71-30627

ELECTRONIC LEVELS

Construction of thin film active circuits using hybrid techniques 23 p3737 N71-36645

ELECTRONIC LEVELS

U ELECTRON ENERGY

U ENERGY LEVELS

ELECTRONIC MODULES

Fabrication methods for matrices of solar cell sub-modules (NASA-CASE-XNP-05821) 02 p0149 N71-11056

Solid state power modules for airborne phased arrays 04 p0496 N71-13918

Development and characteristics of cooling system to maintain temperature of rack mounted electronic modules (NASA-CASE-MSC-12389) 16 p2693 N71-29052

Design and operation of self-contained, portable, hydrate-air fuel cell power unit (AD-723440) 19 p3640 N71-31767

Electronic modules used to simulate lunar gravity potential recovery based on spherical harmonics gravity model (NASA-CR-115175) 22 p3564 N71-35380

Electronic module used to compute error statistics for simulations of photogrammetric schemes involving more than one lunar mission (NASA-CR-115175) 22 p3565 N71-35390

Development of magnetic thyristor logical elements consisting of control electrodes and magnetic cores with rectangular hysteresis loops (AD-727192) 24 p3899 N71-37790

ELECTRONIC PACKAGING

Computer aided integrated circuit mask production 01 p0036 N71-10225

System packaging of LSI circuits (NASA-CR-111646) 03 p0354 N71-12630

LSI devices and techniques for electronic systems design 03 p0352 N71-12632

Cost effectiveness of LSI circuits 03 p0354 N71-12634

Capacitor fabrication by solidifying mixture of ferromagnetic metal particles, nonferromagnetic particles, and dielectric material (NASA-CASE-LEW-10364-1) 04 p0510 N71-13522

Microelectronics, large scale integrated arrays, electronic packaging, thin film epitaxy, computerized design, radar equipment (NASA-CR-109754) 04 p0512 N71-13539

Potting compounds and techniques for plantron and high voltage power supply 06 p0825 N71-16635

Testing electrical, mechanical, and handling properties and environmental characteristics of small gap electrical wire for interplanetary spacecraft 06 p0829 N71-16683

Study program to develop packaging techniques for space electrical power assemblies (NASA-CR-114854) 07 p0976 N71-17568

Method of evaluating moisture barrier properties of materials used in electronics encapsulation (NASA-CASE-NPO-10051) 13 p2100 N71-24934

Electrical connections for thin film hybrid microcircuits (NASA-CASE-XMS-02182) 16 p2575 N71-28783

Structural dynamic analysis of electronic assemblies subjected to random vibration loads 22 p3685 N71-36274

ELECTRONIC PHOTOGRAPHY

U ELECTRO-OPTICAL PHOTOGRAPHY

Electronic recording system for spatial mass distribution of liquid rocket propellant droplets or vapors ejected from high velocity nozzles (NASA-CASE-NPO-10185) 14 p2233 N71-26339

ELECTRONIC SIGNAL MEASUREMENT

U SIGNAL MEASUREMENT

ELECTRONIC SPECTRA

Electronic and vibrational spectra of ionic solids, lattice dynamics of solids, high pressure research, chemiluminescence of hydrocarbons and optical spectra (UCLA-34-P-88-30) 04 p0577 N71-13749

Pre-accelerating spectrograph with cylindrical symmetry for studying low energy electron spectra, and Auger spectra of U-233, Te-125, Ag-109, and Pt-195 10 p1622 N71-21579

ELECTRONIC STRUCTURE

U ATOMIC STRUCTURE

ELECTRONIC SWITCHES

U SWITCHING CIRCUITS

ELECTRONIC TRANSDUCERS

Fiber optic transducers for monitoring and analysis of vibration in aerospace vehicles and onboard equipment (NASA-CASE-XMF-02433) 01 p0035 N71-10616

Engineering study of electro-fluid converter concept (AD-715102) 07 p0101 N71-17737

Optoelectronic electronic equipment including solar systems, sensors, shipboard computers, and communication and navigation systems (AD-716499) 10 p1554 N71-21542

Transducer circuit design with single coaxial cable for input and output connections including incorporation into miniaturized catheter transducer (NASA-CASE-ARC-10132-1) 13 p2055 N71-24597

Circuit design for failure sensing and protecting low voltage electric generator and power transmission networks (NASA-CASE-GSC-10114-1) 15 p2389 N71-27366

Device for sensing current applied by pulse width modulated power supply to battery or other load (NASA-CASE-GSC-10656-1) 16 p2570 N71-28471

Mobile and fixed data collection platforms for constant level balloons and remote ground locations, for platform-satellite-ground station system (NASA-CR-121374) 20 p3270 N71-32893

ELECTRONICS

Standards and measurement methods for building and electronic technology, systems analysis, motor vehicle safety, and engineering materials 01 p0137 N71-10511

Scientific research in physics, electronics, and computer technology (AD-711278) 01 p0138 N71-10930

Engineering and applied physics research projects (NASA-CR-111352) 01 p0139 N71-10963

Research projects in electronic data technology and solid state physics (AD-718149) 12 p1892 N71-23542

Magnetic permeability, electrical resistivity, and specific heat measurements on actinide carbides and actinide nitrides 15 p2471 N71-27415

Strain hardening and stress relaxation effects on crack propagation with problem notes on plasma physics, communication sciences, electronics, metallurgy, and ocean and space technology 20 p3360 N71-33871

Title and abstract translations of papers on nuclear reactions, chemical and biological warfare, applied physics, electronics, biotechnology, military psychology, and psychological defense (RAS-LIB-TRANS-1570) 22 p3700 N71-36390

Micron of continuous operation, excitation of electromagnetic oscillations in open resonator, electron motion in double series magnetron, beam fluxes in triaxial ellipsoid, and related topics 23 p3732 N71-36608

Polymer temperatures measured by thermistors, photoelectric receivers, and dielectric methods (AD-727340) 23 p3760 N71-36803

High power electronics theory and descriptions of magnetrons and planotrons 24 p3901 N71-37806

ELECTROGRAPHY

Electrographic image converters for far ultraviolet spaceborne astronomy 06 p0861 N71-16636

Prototype device for monitoring sleep during manned space flight including performance tests (NASA-CR-115071) 17 p2711 N71-30126

Limit magnitudes of optically weak radio stars measured by large telescope electronic cameras 24 p3922 N71-37978

ELECTRONS

NT CONDUCTION ELECTRONS

NT FREE ELECTRONS

NT HIGH ENERGY ELECTRONS

NT HOT ELECTRONS

NT PHOTOELECTRONS

NT PI-ELECTRONS

NT POLARONS

Interaction of moving dislocations with electrons and phonons in aluminum (AD-709940) 01 p0093 N71-10057

Effects of ionizing radiation on chromosomes (AI-AEC-12974) 02 p0152 N71-11081

Kinetics of electron cooling of beams in heavy particle storage devices (CERN-TRANS-69-18) 03 p0431 N71-12924

Relation of plasmapause position to region of enhanced fluxes of trapped energetic electrons during magnetic storm on 15 June 1965 03 p0450 N71-13025

Velocity, temperature, density, and electron population measurements in projectile wakes 04 p0523 N71-13587

Properties of electron and muon components of extensive air showers for different models of high energy interactions (JINR-1162) 04 p0587 N71-14258

Computer method for evaluating optical properties of scintillation detector assemblies (UUP-679) 04 p0592 N71-14394

Statistical models of electrons in atoms using Coulomb approximation (AD-712719) 04 p0594 N71-14430

Atlas of total electron content plots for 1969 - Vol. 5 05 p0674 N71-14994

Charge-neutral self consistent plasmas and fields studied with Vlasov equations (INYO-1480-139) 05 p0753 N71-15142

Positron electron annihilation into hadrons (LNF-70/21) 06 p0911 N71-15803

Algorithm for calculating electron and positron tracks in propane bubble chamber, accounting for radiative losses (JINR-P1-5357) 07 p1080 N71-18123

Electron cyclotron harmonic waves in magnetically confined low pressure gas discharges (IPP-2/84) 08 p1270 N71-18251

Multiple-grid probe separating currents flowing from plasma to collector into their electron and ion components 08 p1271 N71-18246

Relativistic and nonrelativistic studies of many electron systems with open and closed shells 09 p1432 N71-19971

Total cross sections for positron electron yields and 5 pions (PM-70/4) 09 p1434 N71-20005

Bound electron problems, involving Schrodinger theory, transition probability, and Compton scattering (IC70/34-CH-1-3) 09 p1441 N71-20037

Neutrino, electron, and proton wave asymmetry measurements from beta decay of polarized Lambda hyperons (CDO-1545-87) 10 p1611 N71-20776

Electron velocity distribution measurement in front and behind plasma sheath (REPT-70-31) 10 p1627 N71-20809

High energy electron and positron colliding beams leading to annihilation into muon pair, annihilation into hadron pair, Bhabha scattering and muon hadron production 10 p1623 N71-21549

X rays, gamma rays, electrons, and neutrinos in outer space and upper atmosphere 11 p1822 N71-23413

Mass spectrometric investigation of collisional ionization by electronically excited helium atoms 11 p1809 N71-23818

Energy spectra of backscattered electrons and positrons by Monte Carlo calculations (UCRL-19719) 12 p1948 N71-23135

Recombination of positive ions with electrons in nitrogen (ORC-3771-3) 14 p2301 N71-25776

Radiation damage to miniature silicon avalanche diodes by high energy neutrons and electrons 14 p2326 N71-26287

Electron propagation in pure Pd and interstitial alloy PdH_{0.5} (NYO-4062-5) 15 p2421 N71-27116

Nucleon models for interpretation of deep inelastic electron-nucleon scattering 15 p2463 N71-27172

Effect of absorption nuclear lines on transition radiation of resonance gamma quanta by relativistic electrons (JINR-P2-5042) 15 p2496 N71-27073

Cosmic electron sources of galactic background radiation (NASA-TT-F-13611) 16 p2676 N71-29027

Electron and proton populations in low altitude radiation environment 16 p2676 N71-29000

Ultrafast apparent second-order decay of hydrated electrons following nanosecond radiation pulses in nitrate alkaline solutions with related solution structure data (AD-721299) 16 p2654 N71-29110

Search for positive muon decay yielding two positrons and one electron using cylindrical spark chamber in 4500 G magnetic field (JINR-P2-5542) 16 p2658 N71-29164

Scattering cross sections of hadron production from positron electron collisions based on vector dominance model (PM/71/2) 16 p2658 N71-29171

One electron theories of cohesion on ion pair potentials in metals, using Fourier transformation and integral equations (JSC-1147) 17 p2818 N71-29948

Electron and photon spectra and fluxes in liquid ionization chambers (INF-14433) 17 p2800 N71-30106

Proton and electron net charge determination for two suspended niobium bodies 17 p2802 N71-30103

Optical spark chamber experiment to test validity of Deha S equals Deha Q selection rule in neutral kaon decay into 3 electrons 17 p2802 N71-30108

Cosmic 361 observation of upper atmosphere middle and high-energy electrons and protons, and instrumentation description (PR-9-PT-4) 17 p2749 N71-30306

Sixth-order radiative corrections to anomalous magnetic moment of electron from Feynman diagrams with vacuum polarization insertions (CNRS-CPT-70-P-339) 17 p2803 N71-30322

Finite and gauge-invariant computation of electron self-charge and self-mass in quantum version of curved space and time 18 p2972 N71-30513

Resistivity minimum in ferromagnets with approximate calculation of electron-magnon interaction 18 p2972 N71-30513

SUBJECT INDEX

variation to temperature dependence of electrical resistivity
[CALT-422-25] 18 p2961 N71-30537

Comparison of electron response in magnetosphere at L equals 5 with solar wind during magnetic storm on 17-18 Apr. 1965 18 p3005 N71-30926

Correlation of increases in electron population of outer radiation belt and interplanetary magnetic fields during two geomagnetic storms 18 p3005 N71-30927

Outer radiation belt electron fluxes during solar proton event on 5 Feb. 1965 18 p3005 N71-30928

Electronic or nucleonic many body system ground state energy calculation using Mathieu functions as orthogonal single particle wave functions 18 p2583 N71-31048

Numerical analysis of instability evolution of relativistic thin electron ring 18 p3149 N71-32102

Spin interactions between slow electrons and oriented aromatic amino acid films 18 p3149 N71-32102

Cyclotron radiation, relativistic velocities, angular distribution, total power, electron distribution, and inverse Compton scattering 20 p3344 N71-32840

Microscopic foundation of bubble model for excess electron in liquid helium 20 p3325 N71-33905

Synchrotron radiation effects on slow ejection of electrons from synchrotrons 21 p3472 N71-34723

Spark chamber and spectrometric analysis of kaon decay branching ratios for electron neutrino events and vector-axial theory test for weak interactions [JCR-20031] 21 p3485 N71-34826

Elevated temperature studies of optical absorption associated with electrons trapped in fused silica 21 p3492 N71-34873

Electron affinity calculations for Li, B, O, F, C, and H and self consistent field equations for multiple open shells 21 p3492 N71-34878

Ion heating caused by ion acoustic waves from electron drift in ion streaming plasma [JPP-104] 21 p3494 N71-34889

Measuring electromagnetic form factor of neutrino by comparing neutrino and electron cross sections with nuclei [JNR-F2-5705] 22 p3633 N71-35888

Anomalous electron-phonon transport properties of layered metals 22 p3640 N71-35947

Flux, energy spectra, and pitch angle distributions of precipitated low energy hydrogen and electrons from Nike-Tomahawk auroral hydrogen experiment [NASA-CR-121934] 22 p3668 N71-36135

Saturation effects in cyclotron resonance oscillators with emphasis on generation and amplification of millimeter waves [NASA-CR-121294] 23 p3731 N71-36394

Electron-ion bunch diagnostics by bremsstrahlung, using heavy atom acceleration to high energies [JNR-TRANS-1440] 23 p3808 N71-37155

Double arm spectrometer for stringent limit determination on decay kaon(O) sub L yields muon(plus) muon(minus), positron electron, muon(plus or minus) positron or electron [JCR-20264] 23 p3812 N71-37184

Ion and electron acceleration in unperturbed plasma 23 p3854 N71-37470

Protection from charged particles using high voltage electric fields 23 p3855 N71-37475

Van Allen belt radiation on Tiro/TOS/TITOS spacecrafts - graphs [NASA-TM-X-65717] 24 p4002 N71-38546

Measurement of suprathermal electron flux caused by solar solar eclipses of 7 Mar. 1970 [NASA-CR-123121] 24 p4003 N71-38549

Surface tension and dielectrophoretic techniques in liquid rocket propellant control 03 p0447 N71-31119

Calculating effects of relaxation field and electrophoresis to derive conductance of mixed strong electrolytes at finite concentrations 08 p1160 N71-18992

Separation methods such as centrifuging, ion exchange, electrophoresis, and chromatography applied to biochemical materials (gels, proteins, amino acids) 13 p2032 N71-24466

Electrokinetic potential and electrophoretic deposition of polyethylene on Pt, Ni, Cu, Fe, and Al plates at 80 V in nitromethane, dimethyl formamide, and diethyl acetals [NLL-TI-746-331-/9022.401/ 16 p2609 N71-28395

Electrophoresis theory for aggregation phenomenon in aqueous mixture subjected to dc discharges 19 p3165 N71-32359

Electrophoretic and chromatographic analysis of lactate dehydrogenase isoenzyme activity in fetal, neonatal, and adult human thymus and spleen lymphocytes [NASA-TT-F-13991] 23 p3715 N71-36482

Fluid electrophoresis separation based on motion of particles in electric field for demonstrating near-zero gravity condition in space - Apollo 14 [NASA-TM-X-64611] 23 p3718 N71-36506

ELECTROPHOTOMETERS
Photocolorimetric gas analysis methods and equipment 11 p1761 N71-22057

Method and photodetector device for locating abnormal voids in low density materials [NASA-CASE-MFS-20044] 16 p2598 N71-28993

Photometric measurements of diurnal variations in brightness of north sky and horizon sky and sea during daylight [AD-727118] 24 p3916 N71-37921

ELECTROPHYSICS
NT ELECTRO-OPTICS
NT MOLECULAR ELECTRONICS
Closure approximation in neutral rho meson photoproduction from deuterium and light nuclei, rho-meson electroproduction from heavy nuclei, and coupling parameters to photons and nucleons 13 p2138 N71-25475

Electrophysics and chemical reactions of metal surfaces including mechanical properties and crystal structure [AD-722013] 16 p2611 N71-28505

ELECTROPHYSIOLOGY
Procaine effects on asphyxial rigidity of cat gastrocnemius-totus muscles and neuromuscular responses to shock [AD-712121] 02 p0158 N71-11117

Neuroendocrine heart rate analysis techniques for consciousness during space flight [AD-714403] 06 p0802 N71-16409

Dry electrode design with wire sandwiched between two flexible conductive discs for monitoring physiological responses [NASA-CASE-FRC-10029] 13 p2035 N71-24618

Development of theory of neuromine sets containing recurrent inhibition and analysis of hippocampus model [AD-726815] 14 p2287 N71-23840

Neuron modeling, electrophysiology, and biophysics involved in information processing along nervous system [AD-727770] 24 p3882 N71-37673

ELECTROPLATING
Control of hydrogen absorption in electroplating 02 p0231 N71-11634

Electrocrystallization of metals in ultrasonic field [TT-70-50036] 05 p0694 N71-15537

Hypersonic low density wind tunnel including auxiliary equipment for electroforming and electroplating wind tunnel models [BMW-FB-W-70-51] 08 p1175 N71-18593

Potassium pyrophosphate electrolyte for electrodeposition of copper nickel coatings [NLL-TRANS-746-499-/9022.401/ 10 p1582 N71-21496

Electrolytic deposition of binary and ternary rhodium alloys on copper and chromium-nickel surfaces [NLL-TRANS-746-501-/9022.401/ 10 p1586 N71-21498

Electroplating and vacuum evaporation of yttrium oxide-chromium oxide coating of chromium alloys for nitrogen embrittlement protection [NASA-CR-72847] 12 p1936 N71-23134

Investigation of soldered component failure in plated printed circuit boards consisting of tin lead laminate copper, plated copper, and gold overplate [NASA-TM-X-2250] 13 p2055 N71-24715

Method of plating copper on aluminum to permit conventional soldering of structural aluminum bodies [NASA-CASE-XLA-0896-1] 14 p2275 N71-25903

Development of chemical nickelizing process for applying run-in and wear resistant coatings for machine parts made of aluminum alloy [AD-726742] 14 p2263 N71-26310

Shielded flat conductor cable fabricated by electroless and electrolytic plating [NASA-CASE-MFS-13487] 16 p2571 N71-28691

Development of method for electroplating copper on linear accelerator tanks [SJC-A-70-3] 17 p2758 N71-30390

Ion plating and radio frequency sputtering method for plating adherent alloy films on objects with complex geometries [NASA-CASE-LEW-10920-1] 18 p2935 N71-31130

ELECTROPOLISHING
Metallographic studies including electropolishing, explosive bonding, and crack propagation [CONF-690954] 05 p0699 N71-14403

ELECTRORETINOGRAPHY
Spectral sensitivity and dominance of color center cones in macaque monkeys based on flicker electroretinography [JZF-1971-16] 20 p3225 N71-33823

ELECTROSTATIC EFFECT
U ELECTRIC CURRENT

ELECTROSTATIC PRECIPITATORS

U SEISMIC WAVES
ELECTROSLAG REFINING
Russian contributions to Russo-Swedish conference on clean steel 18 p2933 N71-30480

[IVA-MEED-169-VOL-3] 18 p2937 N71-30482

Comparison of electroslag, plasma-arc, vacuum, and electron beam methods of melting nickel steels 18 p2937 N71-30482

Electroslag refining of steel ingots 18 p2937 N71-30483

Removal of non-metallic inclusions from stainless steels during electroslag refining process 19 p3111 N71-31907

Decarburizing and denitrifying of titanium steels using electroslag refining 19 p3104 N71-31908

ELECTROSLAG WELDING
Fabrication and acceptance data for heavy section ASTM A-533 and A-543 grade B steel plates and electroslag, submerged-arc, and shielded metal-arc welds for nuclear pressure vessels [ORNL-4313-3] 12 p1956 N71-33145

ELECTROSTATIC CHARGE
Electrostatic hazards during launch vehicle flight operations [NASA-CR-111727] 04 p0614 N71-14114

Examining special Bernstein-Greens-Kruskal solutions of time-independent, one-dimensional, coupled Vlasov-Poisson equations 04 p0291 N71-14379

Charged particle analyzer with periodically varying voltage applied across electrostatic deflection members [NASA-CASE-XAC-03506-1] 06 p0917 N71-16095

Propagation of electrostatic waves in cylindrical charged plasma [AD-715882] 08 p1274 N71-18518

Gas exposure experiments of lunar soil with microchemical, microphysical, and electron analysis [NASA-CR-149165] 19 p1467 N71-28277

Electrostatic charge by JP-5 jet fuel at truck fill stand with 30-second relaxation chamber and bottom loading [AD-717347] 11 p1819 N71-22232

Producing gas phase, charged intact polystyrene molecules by high voltage electrospray of solutions containing monodispersed polystyrene 11 p1806 N71-22520

Measurement of electric detector insensitivity to electrostatic charge of human body [AD-726903] 22 p3697 N71-36367

Device for conducting electrostatic charges from man [NLL-M-20436-/5828.4F/ 24 p3384 N71-37684

ELECTROSTATIC ENGINES
Electron bombardment ion rocket engine with improved propellant introduction system [NASA-CASE-XLE-02066] 05 p0763 N71-15661

Dual grid electrostatic thrust vectoring system with capability of vectoring beam from 5 cm thruster to plus or minus 10 degrees off axis [NASA-CR-72877] 14 p2332 N71-26284

ELECTROSTATIC EROSION
U SPARK MACHINING
ELECTROSTATIC FIELDS
U ELECTRIC FIELDS
ELECTROSTATIC GENERATORS
Basic methods of measuring atmospheric electric fields [TT-70-50125] 03 p0367 N71-12757

Using coronen discharge mechanism for electrical loads in electrofluidynamic generator [AD-716102] 09 p1326 N71-19802

ELECTROSTATIC GYROSCOPES
Survey of unconventional gyroscopes including cryogenic gyroscopes, electrostatic gyroscopes, fluid rotor gyroscopes, and optical gyroscopes [DLR-MITT-71-02] 17 p2779 N71-29570

ELECTROSTATIC PLASMA
U PLASMAS (PHYSICS)
ELECTROSTATIC PRECIPITATORS
Investigating contaminations caused by ion scattering on residual gas and by chromatism in electrostatic isotope separators [CEA-R-4931] 04 p0574 N71-13675

Secondary flow in electrostatic precipitators 04 p0567 N71-14229

Electrostatic precipitation of lithium ions for trace contaminant removal from spacecraft cabin atmospheres hindered by oxidation caused by thermionic emission [AD-716864] 10 p1510 N71-21486

Manual of electrostatic precipitators for particulate emission control [PB-196389] 10 p1568 N71-21811

Manual of electrostatic precipitator installations in various application areas [PB-196381] 10 p1568 N71-21812

Bibliography of electrostatic precipitators for particulate emission control [PB-196379] 10 p1568 N71-21813

High temperature nuclear reactor fuel fusion product monitoring using fine precipitation systems as radiation counters [AERE-R-4475] 13 p2118 N71-24081

Analysis of electrostatic precipitator systems application in industrial dust control (PB-198158) 17 p2755 N71-29805

ELECTROSTATIC PROBES

- Time-resolved Langmuir probe measurements in striated neon discharge (AD-710597) 01 p0104 N71-10024
- Plasma diagnostic techniques and plasma arc generation (AD-709944) 01 p0104 N71-10058
- Paired comparison tests of relative signal detected by capacitive and floating Langmuir probes in turbulent plasmas from 0.2 to 10MHz (NASA-TM-X-52914) 01 p0104 N71-10237
- Cylindrical Langmuir probe response in transition regime (AD-711093) 03 p0282 N71-12027
- Current voltage characteristics of flush-mounted electrostatic probe in presence of negative ions (SC-RR-70-413) 04 p0587 N71-14264
- Langmuir probe determinations on non-Maxwellian distribution of electron energy in plasma of electron bombardment ion engines (BM-70/3) 04 p0600 N71-14300
- Flight prototype electrostatic ballistic pendulum momentum transducer (NASA-CR-114783) 05 p0686 N71-15411
- Current-voltage characteristics of continuum flush-mounted electrostatic probes in presence of negative ions (SC-RR-70-413A) 06 p0857 N71-15852
- Low impedance apparatus for measuring electrostatic field intensity near space vehicles (NASA-CASE-XLE-00620) 06 p0858 N71-16014
- Numerical analysis of blunt body electrostatic probe plasma flow (SC-RR-70-331) 06 p0929 N71-16041
- Microwave and pulsed electrostatic probe measurements of argon gas ionization behind shock waves (BMW-FB-W-70-43) 07 p1008 N71-17111
- Development and characteristics of electrostatic analyzers and solid state particle detectors (NASA-CR-114858) 07 p1110 N71-17557
- Ion current response of Langmuir probes in presence of ion-atom collisions in weakly ionized argon plasma (NASA-TM-X-54454) 07 p1077 N71-17594
- Plasma density measurements using electrostatic probe parallel to magnetic field (EUR-CEA-FC-540) 08 p1269 N71-18180
- Continuum theory of slender electrostatic probes (REF-228115) 08 p1173 N71-19165
- Vlasov equation for calculating nonlinear coupling between three electronic plasma waves (Langmuir wave) propagating in cylindrical plasma column (CEA-R-3639) 09 p1449 N71-20117
- Mathematical models for onboard electrostatic analyzer measuring low energy charged particles (KGO-PREPRINT-70-311) 10 p1556 N71-20635
- Electrostatic probe determinations of electron density profiles for three RAM C hypersonic reentries (AD-712114) 10 p1628 N71-21108
- Electron density profiles in plasma sheath of shock waves determined with electrostatic probes in shock tubes (AD-712114) 10 p1629 N71-21118
- ESRO 1 satellite Langmuir electrostatic probe electric field detection 10 p1551 N71-21163
- Dominant theories in existence for continuum electrostatic flush probes for reentry vehicles (AD-71725) 11 p1811 N71-22243
- Abnormal glow discharge from cathode configuration for use as laboratory test bed to develop and calibrate plasma diagnostic sensors (NASA-TN-D-6136) 11 p1813 N71-22676
- Auroral ionospheric electric field measurements by means of gas release or electrostatic probes 12 p1909 N71-23567
- Auroral ionospheric plasma diagnostics by means of electrostatic probes 12 p1909 N71-23568
- Kinetic theory for analysis on electrostatic probe properties in stationary quiescent plasma 12 p1983 N71-24269
- Influence of small reference electrode in Langmuir probe measurement of plasma density and temperature (NASA-TM-X-65516) 13 p2146 N71-24883
- OGO-E electrostatic spectrometer measurements on electron flux near magnetopause 13 p2077 N71-25373
- Ionized fields in electrostatic separation of granular solids (conductors and nonconductors) also applications in separations based on surface-to-mass ratio of particles (BM-RT-7509) 14 p2302 N71-25744
- Investigating electric potential in cesium thermionic diode for minimum plasma-loss by electrostatic probe (NASA-CR-118519) 14 p2229 N71-26273
- Pumping effect in oxygen reaction with hot tungsten cathode, and spectrometric measurements of formation energies for volatile species in gas-solid chemical reactions (NASA-CR-118897) 15 p2389 N71-27988

Electron temperatures measured by electrostatic probes and radar backscatter in isotropic, nonequilibrium plasma for studying planetary atmospheres (NASA-TM-X-65586) 16 p2661 N71-28639

Positive ion densities from rocket-borne hemispherical Langmuir probe at 40 to 100 km (AD-722066) 16 p2662 N71-28648

Ion temperature determination in plasmas based on electrostatic probe measurements of ion current (AD-723529) 19 p3164 N71-32135

Current collection characteristics of moving cylindrical and spherical electrostatic probes applied to velocities in earth satellites and planetary probes (NASA-TM-X-65639) 19 p3071 N71-32468

Electron drainage current from dilute plasma through holes in high voltage dielectric probes (NASA-TM-X-67890) 19 p3166 N71-32483

Theoretical analysis of end effect in current response of highly negative, cylindrical Langmuir probe under ionospheric satellite conditions (AD-723531) 19 p3167 N71-32800

Investigation of current collection of negatively biased flush electrostatic probes in continuum regime (AD-724148) 20 p3329 N71-32920

Electron beam probe to measure potential and Doppler shifted spectral lines to study presence of fast particles in inertial electrostatic confinement devices (NYO-4169-3) 21 p3484 N71-34818

Evaluation of ion density and plasma potential from Langmuir probe data - graphs (NASA-TM-X-2369) 22 p3442 N71-35964

Langmuir probe theory for collisional plasmas with collision dominated probe sheath based on hot cathode helium discharge measurements (AD-726906) 22 p3655 N71-36064

Langmuir probe diagnostics in ELMAX plasma device to determine instability thresholds (AD-726906) 23 p3829 N71-37310

ELECTROSTATIC PROPULSION

NT ION PROPULSION

High voltage insulators for direct current in acceleration system of electrostatic thruster (NASA-CASE-XLE-01902) 01 p0116 N71-10574

Problems encountered when electrostatic colloid propulsion integrated with operational spacecraft (AD-712114) 02 p0290 N71-11886

Effects of electrostatic propulsion beam divergence effects on spacecraft surfaces (NASA-CR-111518) 03 p0445 N71-12927

Electrostatic microthruster propulsion system with annular slit colloid thruster (NASA-CASE-GSC-10709-1) 13 p2156 N71-25213

Reliability and cost of electrostatic and electromagnetic thruster systems for satellite auxiliary propulsion (NASA-CR-119319) 18 p3001 N71-31146

Dual grid accelerator system with electrostatic beam deflection capability tested on 5-cm diameter Kaufman thruster for 1000 hours (NASA-TM-X-67908) 18 p3662 N71-36112

Electrostatic WAVES

Energy and phase changes of particle gyrating in homogeneous magnetic field and perpendicularly propagating electrostatic wave (PB-195690) 02 p0277 N71-12123

Heuristic method to determine electrostatic instabilities in multicomponent plasmas (AD-712690) 03 p0439 N71-13369

Calculation of growth rates of electrostatic waves in infinite homogeneous plasma (EUR-CEA-FC-541) 04 p0601 N71-14416

Low frequency axisymmetric waves in weakly ionized magnetoplasma column (SU-IPR-366) 08 p1272 N71-18526

Propagation of electrostatic waves in cylindrical charged plasma (AD-715882) 08 p1274 N71-18818

Dispersion propagation and Landau damping of electrostatic ion waves in ionospheric plasma supported by uniform magnetic field 11 p1814 N71-22886

Stability of weak electrostatic waves in collisionless magnetoplasma supporting steady large amplitude whistler wave, and influence of trapped particles (NASA-TM-X-65572) 15 p2382 N71-27095

Thermal conduction and low frequency electrostatic waves in collisional plasmas immersed in magnetic field 23 p3833 N71-37334

ELECTROSTATICS

Tables of focal properties of three-element electrostatic cylinder lenses (JILA-194) 01 p0055 N71-10601

Focusing in electrostatic spectrometers (ESRIN-IN-93) 02 p0224 N71-11522

Mechanical filtration, electrostatic collection, and total gamma ray measurements of St. Laurent 1 reactor (CEA-N-1356) 04 p0550 N71-13797

Approximation of physical constraints (AD-712077) 04 p0539 N71-14228

Electron density and electrostatic potential field of ionosphere satellite 06 p0927 N71-16870

Nonlinear electrostatic instabilities in magnetoplasma - conference (CEA-CONF-1615) 08 p1271 N71-13820

Electrostatic methods to control placement and orientation of short graphite fibers in fiber composites and fiber structures (SC-CR-49-3277) 15 p2432 N71-27900

Application of harmonic functions to electrostatic problems and magnetostatics (AD-721903) 17 p2787 N71-29825

Applications of P-harmonic principal functions to thermodynamics and electro- and magnetostatics (AD-721904) 17 p2788 N71-29796

Electric field measuring techniques used in ionospheric and magnetospheric electrojet current studies (NASA-TM-X-65596) 17 p2748 N71-28806

Long-range electrostatic and electromagnetic interactions between two neutral hydrodynamic atoms in ground state (NASA-TR-R-367) 18 p2982 N71-30017

Computational method for determining performance of ten stage electrostatic depressed collector for klystrons (NASA-CR-119683) 19 p3067 N71-32610

Steepling of large amplitude ion acoustic waves and formation of collisionless electrostatic shocks in ionospheric plasma with electron-to-ion temperature ratios in 5 to 15 range 22 p3456 N71-30075

Tabular data for electrostatic collection of dusted region behind moving bodies in collisionless plasma for sphere and long circular cylinder (NASA-CR-121963) 22 p3673 N71-38107

Electrostatic devices for ion transport (EP-18853) 23 p3817 N71-37221

ELECTROSTRICTION

Engineering study of electro-fluid converter concept (AD-715102) 07 p1011 N71-17777

Analysis of electrostriction mechanism for new beam self focusing and track formation in transparent optical glass (AD-715937) 09 p1995 N71-19522

Electrostrictive self-trapping of picosecond laser pulses (AD-726522) 23 p3766 N71-36880

ELECTROTHERMAL ENGINES

NT ARC JET ENGINES

NT PLASMA ENGINES

NT RESISTOTW ENGINES

ELECTROWINNING

Determination of quantitative laws of ion discharge of ions under conditions of electrowinning of pure metals (NLL-LTT-746-663-[9022.401]) 22 p3590 N71-35505

ELEMENT ABUNDANCE

ELEMENT 104

Collimation method of identifying elements 102 and 104 and measurement of integral angular distribution of nuclear reaction products for identifying stable nuclei (KFK-TR-329) 15 p2473 N71-27041

ELEMENT 105

Production regularities of element 105 spontaneously fissionable isotopes (JINR-PF-5108) 03 p0426 N71-12004

Alpha decay of element 105 isotopes, produced by American 243 irradiation with neutrons 22 ions (KFK-TR-343) 19 p3150 N71-32123

ELEMENTARY EXCITATIONS

NT EXCITONS

NT MAGNONS

NT PHONON BEAMS

NT PHONONS

NT POLARONS

Calculating energy spectrum and quasi-particle wave functions of spherical nuclei (IAE-1835) 04 p0570 N71-13538

Excitation function measurement of d,n reaction in C-59 using single foils and stacked foil arrangements (KFK-1171) 05 p0751 N71-15819

Vibrational states of electronically excited, free radical molecules (AD-715740) 08 p1230 N71-18547

Microscopic theory of quasi-particle spin fluctuations in low temperature, dense Fermi liquids 10 p1618 N71-21449

Quasi-stable elementary particles in aluminum and tungsten targets irradiated by 70 GeV protons (JINR-PF-5399) 13 p3132 N71-28904

Fokker-Planck solution to Liapounov-Schroedinger integral equation for three particle scattering 13 p1312 N71-28904

Elementary processes of plasmas and ion density distribution in arc discharge (LYCEN-7061) 14 p2311 N71-28085

Alpha and gamma decay structure of highly excited complex nuclei (JINR-EA-5135) 15 p2466 N71-27785

Quasi-particle state of $^{69}Zr^{2+}$ isomeric state in Fe-202 (JINR-B6-5379) 15 p3483 N71-27752

Solution of unitary condition for elastic scattering amplitudes for high reaction energies
[JTF-70-49] 18 p2970 N71-30446

Correlations between quasi-particle and collective motions in nuclei, based on variational principle
[JNTR-84-5578] 18 p2980 N71-30754

Quasi-particle model for calculating energy spectra of indium isotopes
[JUV-2540-F] 19 p3149 N71-32110

ELEMENTARY PARTICLE INTERACTIONS

NT ELECTRON CAPTURE

Algebraic theory for elementary particle dynamics
[AD-711441] 01 p0100 N71-10736

Investigating neutron and charged particle reactions and gamma and beta ray spectroscopy of radioactive sources
[ANL-7630] 03 p0420 N71-12598

Binding energy calculations for central potentials of Lambda hyperon-nucleon interactions
[TID-25407] 03 p0421 N71-12651

Sum rules for scattering amplitudes for many spinless particle systems
[NYO-3399-223] 03 p0421 N71-12652

High energy accelerator physics and low level elementary particle physics
[CDO-1749-18] 03 p0422 N71-12668

Investigating differential range of reaction mechanisms for alpha and He-3 reactions in C-6 and energy dependence of recoil properties of products from proton reactions in U-238
[CDO-1593-42] 03 p0422 N71-12700

Elementary particle physics, nuclear structure and particle interactions
[NYO-3171-310] 03 p0423 N71-12742

Non-proton-, kaon-proton-, and pion deuteron interactions
[JNTR-347-107-104] 03 p0423 N71-12743

Differential cross section and rho-meson decay matrix elements for reaction pion/ proton yields rho-meson/ Delta/ hyperon at 13.1 GeV/c
[CDO-1428-216] 03 p0430 N71-12910

Studying various kaon/ proton interactions at 2.1 to 2.70 GeV/c for existence of two Sigma hyperon/1660 resonances
[JNTR-19244] 03 p0431 N71-12912

Operation and development of Miniro reactor and particle physics experimental program
[JNTR-19-190] 03 p0431 N71-12917

S equals -1 baryon states observed in production experiments
[CDO-1428-208] 03 p0434 N71-12968

Investigating nuclear structure on basis of shell and collective models of nucleon and meson interactions
[AD-712728] 03 p0435 N71-13188

Cross sections of pion-proton interactions with two charged secondary particles at high pion energies
03 p0436 N71-13267

Proton form factors determined from electron proton scattering cross sections
[JNTR-21-5178] 04 p0573 N71-13665

Measuring 2 pion inelastic scattering cross sections at 1 GeV invariant mass
[JNTR-511-74-70] 04 p0576 N71-13689

Deriving phase-space relativistic expressions for angular correlations of particles in final state of reaction A + B yields C + D
[LA-TN-70-15] 04 p0579 N71-13977

Investigating multiparticle correlation effects of hadronic reactions at 5.9 GeV/c
[JNTR-511-45-70] 04 p0579 N71-13979

Analysis of V/1835/ pion production near V/1520/ resonance
[NYO-3651-13] 04 p0582 N71-14106

Investigating twin meson production in K/A reaction for compatibility with simple quark model
[CDO-1428-227] 04 p0583 N71-14176

Constructing double Regge exchange model for hadron production in K/A reactions at 8 GeV/c
[CDO-1428-228] 04 p0583 N71-14177

High energy nuclear scattering
[NTP-497] 04 p0587 N71-14259

Resonance interactions of intensive beams of charged particles with accelerating field
[JNTR-31-310] 04 p0587 N71-14278

Alpha alpha interaction in Be-9 yields alpha alpha
[JNTR-4-1179] 04 p0588 N71-14293

Investigating development and components of built-in elements for elementary particle research
[JNTR-1970] 05 p0741 N71-15120

Equipment development for Stanford linear accelerator research
[SLAC-126] 05 p0747 N71-15241

Investigating elementary particle interactions in linear accelerators and reactor physics
[NYO-328-187] 05 p0750 N71-15264

Relativistic and quark structure
[CDO-264-550] 05 p0750 N71-15346

High energy electron positron scattering cross section measurements as test of quantum electrodynamics theory
[LA-1235] 06 p0910 N71-15786

Calculating average range energy relations of muons in standard rock under assumptions of cross section of muon-nucleon interaction
[NBS-120] 06 p0912 N71-15811

Investigating reaction mechanisms, nuclear moments, and hyperfine interactions using various accelerators
[BNBW-FBK-70-9] 06 p0912 N71-15814

Investigating particle interactions and accelerator technology for medium energies
[LA-4514] 06 p0904 N71-16187

Letter series on elementary particle interactions and bubble chamber technology
[TID-25473-VOL-2] 06 p0932 N71-16256

Charged and neutral recoil particle reactions following nuclear transformations
[CDO-3402-11] 06 p0922 N71-16421

Numerical determinations of Regge poles from Bethe-Salpeter equation with scalar couplings
[ILL-7TH-71-2] 06 p0937 N71-16632

Test of Delta S equals Delta Q selection rule in kaon semileptonic decay
[CDO-1185-193] 06 p0926 N71-16839

Muon, photon, and hadron detectors to study inelastic interactions of neutrinos in hydrogen bubble chamber
[JNTR-511-40-70] 06 p0926 N71-16833

Rho-meson/ omega-meson interference parameter in diffractive photoproduction of vector mesons on hydrogen
[JNTR-19753] 07 p1071 N71-17233

Resonance production in K/plus/ proton interactions at 6 GeV/c and 9 GeV/c
[JNTR-19099] 07 p1074 N71-17419

Fredholm equations for three body problem in quantum mechanics
07 p1052 N71-18120

Calculating displacements of atoms and charged particles in materials subjected to neutron irradiation
[CBA-N-1294] 07 p1081 N71-18134

Connection of neutral vector mesons photoproduction on nuclei with processes of pion and K-meson interaction with nuclei
[JTF-70-40] 07 p1082 N71-18145

Inelastic interactions of particles and nuclei at high and superhigh energies
[JNTR-82-5382] 08 p1248 N71-18199

Equality of total cross sections for interaction of particles and antiparticles at high energies
[JNTR-517-69-110] 08 p1248 N71-18200

Nuclear model for pion absorption by light nuclei
[NP-18446] 08 p1255 N71-18362

Mechanism of alpha, 2alpha/ breakup reaction in three body formation
[LYCEN-7034] 08 p1256 N71-18381

SU(3) model of CP-violation with interactions of weak mesonic currents
09 p1431 N71-19848

Total cross sections for positron electron yields 4 and 5 pions
[FM-70/4] 09 p1434 N71-20005

Neutral current in semileptonic interaction up to strength of CP violation
[JNTR-113] 09 p1445 N71-20562

Graphical investigation and vector meson dominance of inelastic electron proton scattering
[LPTHE-70/49] 09 p1446 N71-20574

Characteristics of low-entropy system of superlight particles capable of producing some protological informational functions of brain and consciousness
[JNTR-52722] 10 p1502 N71-21610

Measurement of low energy and high energy portions of pion/plus/ in kaon/plus/ yields pion/plus/ pion/zero/ pion/zero/ decay
01 p1633 N71-21768

Bubble chamber experiment for resonance studies in positive pion proton interactions between 3 and 4 GeV/c
10 p1625 N71-21832

Numerical analysis for static multiple density correlation function of many particle system
[JNTR-2053] 11 p1800 N71-21878

Determination of six prong cross sections during elementary particle interactions at 7 GeV/c
11 p1801 N71-21880

Direct channel partial waves projected from Regge exchange amplitudes for pion eta-meson yields pion eta-meson and pion eta-meson yields pion rho-meson
[JNTR-2059] 12 p1979 N71-24329

Functional integral form of Green's function for dual resonance model of hadronic interactions
[TUBP-71-3] 13 p2104 N71-25429

Theoretical research in elementary particle physics
[CDO-264-508] 14 p2380 N71-25724

Applicability of one-pion exchange model to proton proton interaction in 1 equals J equals 3/2 resonances superimposed at proton energy of 660 and 970 MeV
[JNTR-25772] 14 p2315 N71-26739

Current algebra for weak interactions in elementary particle physics
[KFKI-70-24-BEP] 15 p2475 N71-27465

Numerical calculations for strong particle interaction dynamics
15 p2480 N71-27672

Asymmetry parameters of leptonic Sigma hyperon decays in negative kaon beam interactions
15 p2487 N71-27835

Statistical evidence against neutral, 2 negative pion enhancement at 1.627 GeV/c as seen in nucleon deuteron reaction at 4.48 GeV/c
[CDO-1428-253] 16 p2647 N71-28311

Validity of soft pion limit and existence of absolute value of Delta I vector equals 1/2 rule for nonleptonic weak kaon decays, and use of Lagrangian reductio
[NYO-1932-112] 17 p2759 N71-30617

Meson current algebra for calculating form factor and coupling constant in gamma -> 3 pion amplitude in gamma-pion interaction
[NUP-2074] 17 p2774 N71-30861

Formulation of theorems for obtaining correlation averages for wide class of model systems with four fermion interaction
[JTF-70-53] 18 p2973 N71-30530

Knocking out of nucleons by inelastic electron scattering reactions in light nuclei
[JTF-70-35] 18 p2973 N71-30547

Theory of weak interactions based on possible SU(4) symmetry for hadrons
[ISS-70/16] 18 p2975 N71-30548

Interaction of fast neutrons with 1p, 2s, and 1d nuclei
[BNL-TN-380] 19 p3151 N71-32153

Phenomenology of weak interactions, including CP violation, second class currents, and inelastic neutrino reactions
[FURC-4130-22] 19 p3151 N71-32166

Many body theory of helions and helion interactions analogy to polariton theory
19 p3155 N71-32355

Broken scale invariance, current algebra, and massive gravitation in formalism describing meson interactions at intermediate energies and below
[NUP-2091] 20 p3593 N71-33922

Pion(pion) proton interactions with strange particle production at p equals 4 GeV/c represented by phenomenological quasi-two-body model of multiple particle production
[JNTR-31-5706] 22 p3632 N71-35880

Developments in hadron physics, dual models and dual phenomenology, weak elementary particle interactions, and electromagnetic interaction theory - topics from nuclear research conference
[CERN-71-7] 22 p3640 N71-35951

Argued diagram analysis of Pomeron coupling to kaon nucleon and antikaon nucleon system
22 p3645 N71-35968

Phenomenology and mathematical aspects of elementary particles and elementary particle interactions, and generalization of supermultiplet theory
[AD-726657] 23 p3818 N71-37234

Structure of weak and electromagnetic interactions of elementary particles
[AD-726661] 23 p3818 N71-37237

Cross sections and angular distributions in kaon(nu) deuteron yields kaon(nu) deuteron and kaon(nu) neutron yields kaon(nu) neutron interactions
[NP-18091] 24 p3974 N71-38354

Separation of kaon(nu) proton interactions from kaon(nu) nucleon interactions in kaon(nu) pion/plus/ yields Lambda(0) hyperon pion/plus/ reaction
[LA-82-71-2] 24 p3974 N71-38357

Cluster decomposition analysis of multiple particle reactions
[ILL-7TH-71-11] 24 p3982 N71-38421

Extended cosmic ray showers from high energy protons and nuclei
[NLL-M-20419/5828-491] 24 p4004 N71-38356

ELEMENTARY PARTICLES

NT ALPHA PARTICLES

NT ANTINEUTRINOS

NT ANTINUCLEONS

NT ANTIPARTICLES

NT ANTIPROTONS

NT BARYON RESONANCES

NT BARYONS

NT BETA PARTICLES

NT BOSONS

NT COLD NEUTRONS

NT CONDUCTION ELECTRONS

NT DEUTERONS

NT ELECTRONS

NT ETA-MESONS

NT FAST NEUTRONS

NT FERMIONS

NT FREE ELECTRONS

NT GRAVITONS

NT HADRONS

NT HIGH ENERGY ELECTRONS

NT HOT ELECTRONS

NT HYPERONS

NT KAONS

NT LEPTONS

NT LIGHT BEAMS

NT MESON RESONANCES

NT MESONS

NT NEUTRINOS

NT NEUTRON BEAMS

ELEMENTS

NT NEUTRONS
 NT NUCLEONS
 NT PHOTOELECTRONS
 NT PHOTONEUTRONS
 NT PHOTONS
 NT PI-ELECTRONS
 NT PIONS
 NT POLARONS
 NT POSITRONS
 NT PROTONS
 NT QUARKS
 NT RECOIL PROTONS
 NT TACHYONS
 NT THERMAL NEUTRONS
 Response of mineral oil based liquid scintillator to heavily ionizing particles
 [PPAR-36] 02 p0227 N71-11971
 Research on elementary particle including Regge theory and Lorentz poles
 [ORO-3992-17] 03 p0419 N71-12564
 Research in elementary particle theory
 [NYO-3399-226] 03 p0423 N71-12740
 Elementary particles in room temperature, long pulse RF beam separators
 [BNL-14974] 04 p0584 N71-14189
 High energy physics and quantum theory of elementary particles
 [AD-71708] 04 p0584 N71-14203
 Theory of s-d exchange scattering in dilute magnetic alloys
 [CALT-822-12] 05 p0751 N71-15391
 Tachyon particles with greater than light velocity
 [RT/FI/70/13] 06 p0918 N71-16203
 Relativistic classical theory pertaining to elementary particles
 [AD-713996] 06 p0921 N71-16300
 Interactions due to high Z particles in primary cosmic rays
 06 p0944 N71-16751
 Dispersion potential for calculating particle transport coefficients in flow field analysis
 [SC-RR-70-664] 09 p1435 N71-20035
 Problem of elementary particle identity due to continuous transition of properties of identical and non-identical particles
 [JINR-P-5063] 09 p1438 N71-20188
 Weak nuclear interactions and history of elementary particle discoveries
 [NYO-1932/1-186] 10 p1611 N71-20707
 Bootstrap elementary particle model theory of nuclei vibrations
 [RLO-1925-46] 10 p1618 N71-21388
 Measurement of low energy and high energy portions of pion/plus/ in kaon/plus/ yields pion/plus/ pion/zero/ pion/zero/ decay
 10 p1623 N71-21768
 Reproduction of high energy heavy ions in cosmic rays using heavy ion accelerator
 [PPAD-676-E] 12 p1896 N71-23183
 Calculations on SU3 symmetrical statistical theory of elementary particle production
 [JINR-P-5480] 13 p2130 N71-24860
 Role of gravitation in elementary particle theory, microscopic parameters and macroscopic values
 [JINR-P-52589] 14 p2310 N71-26668
 Hamiltonian implying Pauli exclusion principle applied to elementary particle considerations
 [LNF-70/22] 15 p2481 N71-27690
 Determination of bound state masses in relativistic three particle system with quasi-pair interaction
 [JINR-P-5336] 15 p2496 N71-27971
 Particle physics research including theoretical studies, kinematical investigations, Regge poles, and current algebras
 [AD-721724] 16 p2648 N71-28638
 Conditions of formation and heating dynamics of fast particles and main electron plasma component during electron cyclotron heating
 [NP-18635] 18 p2992 N71-30677
 Spin and parity of resonances with sequential decay modes
 [CERN-71-8] 19 p3154 N71-32290
 On-line and off-line computer analysis of complex particle and gamma ray spectra with programs for performing all basic reduction functions
 [ANU-P-487/2] 19 p3063 N71-32600
 Nuclear models for examination of high energy scattering reactions of elementary particles
 [IS-7-426] 20 p3322 N71-33765
 Volterra equation for coupled channel amplitude densities and modified wave functions
 [NASA-CR-121759] 21 p3447 N71-34529
 Behavior of strongly interacting particles at ultrahigh temperatures related to origin of galaxies and matter
 [LPTHE-71/15] 21 p3530 N71-35156
 Two-parameter method of calculating unitary weights in SU(3) elementary particle production
 [JINR-P-5729] 22 p3632 N71-35885
 Preparation of particle identification system using ORTEC 423 with block diagrams of circuits and graphs
 [ANU-P-314] 22 p3634 N71-35903

Representations of local currents and related algebras, emphasizing infinite parameter Lie algebras
 22 p3648 N71-36018
 Proposed experiment for identification of elementary particles bearing small magnetic charges
 [CERN-TRANS-71-10] 23 p3806 N71-37136
 Phenomenology and mathematical aspects of elementary particles and elementary particle interactions, and generalization of supermultiplet theory
 [AD-726657] 23 p3818 N71-37234
 Nonrelativistic Lagrangians for elementary particle quantum mechanics
 [ITP-71-2-P] 24 p3976 N71-38373
 ELEVATIONS
 Optimum excitation voltage for X ray microanalysis of pure elements, alloys, and mixtures
 [NP-18887] 24 p3933 N71-38063
 ELEVATION
 Tracking mount for laser telescope employed in tracking large rockets and space vehicles to give information regarding azimuth and elevation
 [NASA-CASE-MPS-14017] 14 p2259 N71-26637
 Automatic tracking device for rapidly transferring humans or materials from elevated location
 [NASA-CASE-XKS-07814] 15 p2414 N71-27067
 ELEVATION ANGLE
 Lunar surface examination using low sun elevation photography
 18 p3013 N71-30978
 Low angle signal propagation of Explorer 22 satellite transmission
 24 p3913 N71-37900
 Low elevation recording of Early Bird satellite transmission with polarimeter, noting induction antenna coupling
 24 p3914 N71-37903
 ELEVATORS [CONTROL SURFACES]
 Aircraft landing lift decay and elevator oscillation analysis
 [ARC-CP-1119] 06 p0793 N71-15722
 Low speed wind tunnel tests of effects of nacelle position, refueled fuelage, and elevator effectiveness for NAR straight wing orbiter
 [NASA-CR-105160] 21 p3524 N71-35107
 ELEVATIONS
 Supersonic or hypersonic vehicle control system comprising elevons with hinge line sweep and free of adverse aerodynamic cross coupling
 [NASA-CASE-XLA-08967] 13 p2366 N71-27088
 Comparison of ASKA and NASTRAN programs analyses of space shuttle hot elevon test article deformed under thermal and mechanical loads
 22 p3683 N71-36264
 ELIMINATION
 Relationship of cesium-137 and iron-59 elimination rates to metabolic rates of small rodents
 [ORNL-4568] 03 p0323 N71-12311
 ELLIPSES
 Ellipsograph for describing and cutting ellipses with minimal axial dimensions
 [NASA-CASE-XLA-03102] 10 p1558 N71-21079
 ELLIPSOIDS
 Geoid determination by vertical deflection calculations based on Bessel's ellipsoid
 01 p0050 N71-10807
 Fluid content effect on vibration frequencies of ellipsoidal shells of revolution
 [AD-719845] 13 p2183 N71-25363
 Orbital acceleration of ellipsoidal high altitude balloon satellite by solar radiation pressure
 [X-550-70-92] 19 p3179 N71-31870
 Ellipsoidal gravity coefficients determined from expansion of geopotential in ellipsoidal harmonics series
 [AAS-71-338] 20 p3435 N71-32924
 Determination of vector equation and formulas for geodetic coordinates and ellipsoid heights, using satellite equatorial coordinates and synchronous observations
 22 p3677 N71-36218
 Testing of prime focus correctors using ellipsoid as auxiliary mirror
 24 p3922 N71-37974
 ELLIPSOIDAL
 Literature survey on application of ellipsometry to determine contamination and defects of semiconductor surfaces
 07 p1092 N71-17318
 Optical parameters of absorbing substrate with transparent surface film determined by ellipsometry, applied to silicon and germanium
 11 p1800 N71-23017
 Ellipsometric and reflectivity measurements of proton irradiation effects on refractive index of intrinsic silicon
 14 p2279 N71-26236
 Extended ellipsometry method used for electrochemical and optical measurements on electrochemically induced passivity of cobalt
 [AD-721719] 16 p2557 N71-28341
 ELLIPTIC DIFFERENTIAL EQUATIONS
 Finite element method for elliptic differential equations
 [ORO-3443-25] 03 p0399 N71-12816

SUBJECT INDEX

Averaging Lagrangian averaged conservation equations to hyperbolic or elliptic dispersion equations for nonlinear waveform distortion
 [AD-716530] 09 p1409 N71-19570
 Theorems and examples of partial elliptic differential equations
 [NASA-TT-F-13417] 09 p1411 N71-20013
 Evaluation of computer program for prediction of laminar flow by solution of elliptic partial differential equations
 [EF/TN/A/31] 11 p1737 N71-22210
 Existence, uniqueness, stability, and asymptotic stability conditions for solution of elliptic partial differential equations with general boundary conditions
 [NASA-CR-118836] 12 p1950 N71-24609
 Error vector propagation method for solving discretized Poisson equation
 [SC-RR-70-579] 15 p2433 N71-26094
 Finite integral method of solving elliptic differential equations for steady Couette flows in two dimensional domains
 [EF/TN/A/33] 20 p3250 N71-33318
 Numerical solution of elliptic equations over irregular regions
 [USC-113519-10] 22 p3607 N71-35040
 ELLIPTIC FUNCTIONS
 Moebius phase ordering functions and algebraic groups
 04 p0539 N71-14204
 Numerical methods developed in fluid mechanics and heat transfer emphasizing elliptic flows
 [EF/TN/A/34] 11 p1737 N71-22210
 Determination of mean, variance, covariance, and correlation estimates for axes rotation of bivariate normal elliptical distribution
 [NASA-TM-X-64595] 15 p2434 N71-26094
 Symbolic computer solution of elliptic boundary value problems
 17 p2773 N71-28608
 Averaging technique using Jacobi elliptic functions for solving nonlinear differential equations with periodic nonharmonic solutions
 [NASA-TM-X-65710] 23 p3783 N71-34060
 ELLIPTIC INTEGRALS
 U ELLIPTIC FUNCTIONS
 ELLIPTICAL CYLINDERS
 Digital computer program for asymptotic solution for short-pipe-reinforced oval cylinders
 [AD-721519] 04 p0617 N71-14089
 Mathematical models for acoustic scattering by porous elliptic cylinder with nonlinear resistance
 [NASA-TM-X-67019] 10 p1607 N71-21488
 ELLIPTICAL ORBITS
 NT APOGEES
 NT PERIGEEES
 NT PERIHELIONS
 NT TRANSFER ORBITS
 Visible probability of earth satellite in elliptic orbit from ground stations
 [ISAS-434-VOL-35-NO-12] 02 p0295 N71-11896
 Photogrammetry and measuring orbit of comet Bennu 1946-1947
 04 p0609 N71-13591
 Thor Agena performance in placing OOO-6 into elliptical polar orbit
 [NASA-TM-X-2148] 06 p0950 N71-19809
 Calculating definitive orbit for Comet 1940-1940V
 14 p2338 N71-26330
 Satellite orientation during deployment established in order to achieve maximum strength of higher rotational locks for satellites in elliptic orbits
 [NASA-TM-X-65555] 15 p2517 N71-27764
 PROD computer programming for predicting satellite orbit decay under long term effects
 [RAE-TR-71007-PT-1] 17 p2844 N71-28418
 Algorithm and subroutine for solving Kepler equation for elliptical orbits
 [NASA-CR-122933] 23 p3848 N71-37406
 ELLIPTICAL POLARIZATION
 Bearing errors of loop antenna direction finding caused by elliptical polarization variations
 11 p1705 N71-22210
 Atmospheric aerosol effect on elliptical polarization of scattered skylight
 15 p2402 N71-27577
 ELLIPTICITY
 Comparison of flat plate sharp and blunt end effects on heat transfer in supersonic flow and heat transfer coefficient dependence on Reynolds number
 [AD-717823] 11 p1735 N71-22216
 Theoretical physics of ellipsoidal equilibrium figures and hydrodynamics of general relativity
 [AD-719914] 14 p2295 N71-25753
 Solutions of potential flow for two dimensional compressible flow for quasi-elliptical airfoil profile noting pressure distribution
 [NLE-TR-69028-U] 19 p3077 N71-31776
 ELONGATION
 Strain gauge measurement of elongation due to thermal and mechanically induced stresses
 [NASA-CASE-XGS-04478] 12 p1924 N71-24233
 Factors affecting scaling of elongation values obtained from rupture tests on silicon killed, aluminum treated carbon steel
 [PB-197140] 18 p2935 N71-35888

SUBJECT INDEX

Concentration dependence of tensile strength, yield point, and relative elongation of Ti-Mo-Ni alloys (JNL-TRANS-746-691 (1922.401)) 23 p3775 N71-36904

ELUTION
 Clarifying elution mechanisms in gas-liquid chromatography by study of solute adsorption on liquid-solid adsorbents 11 p1695 N71-21836

ELUTRIATION
 U ELUTION
 EMANATION
 U EMISSION
 EMBODIMENT
 Hydrodynamics of viscous internal flows with embedded particulate matter 03 p3322 N71-12399
 (AD-711818)

EMBRITTEMENT
 Control of hydrogen absorption in electroplating 02 p3231 N71-11634
 Electron microscopic analysis of embrittlement in zirconium steels (SNW/CIB-721) 05 p0699 N71-14541
 Improvement of radiation embrittlement resistance of steel by control of selected residual elements (AD-714166) 06 p0870 N71-16033
 Oxidative embrittlement of polypropylene film studied by measuring stress strain behavior, molecular weight changes, and development of carbonyl concentration in infrared spectrum (AD-714359) 06 p0878 N71-16322
 Hydrogen embrittlement during hot salt, stress corrosion of titanium alloys 07 p1042 N71-17348
 Solenoid liquid metal embrittlement of aluminum and zinc-cadmium alloys to electroactivity of participating solid and liquid metal (AD-715741) 08 p1214 N71-18552
 Hydrogen embrittlement corrosion studies using electrochemical permeation method (AD-715807) 08 p1215 N71-18769
 Effect of alloying elements on tempered martensite embrittlement and fracture toughness of low alloy high strength steels (AD-718041) 12 p1938 N71-23777
 Auger spectroscopy of low alloy steel, copper, brass alloy, and refractory metal annealing and sintering embrittlement due to grain boundary fracture, corrosion, and mobility (KOD-1778-6) 12 p1987 N71-23954
 Influence of neutron spectrum on helium atom generation by neutron irradiation of stainless steels and subsequent embrittlement 13 p2111 N71-24302
 Damage function analysis of neutron energy, effect as radiation embrittlement of steels, and need for detailed, accurate neutron dosimetry measurements of fast and thermal fluxes 13 p2128 N71-24334
 Radiation embrittlement of age hardening heat resistant steels following high temperature reactor irradiation (ABC-TR-7192) 15 p2419 N71-26907
 Fracture toughness data utilizing small notched metal tensile specimens with hydrogen embrittlement as crack starter (AD-720217) 15 p2425 N71-27618
 Effect of initial heat treatment on high temperature embrittlement of nickel alloys after neutron irradiation (SRZ-1-P-30) 16 p2607 N71-28039
 Effects of initial heat treatment on high temperature embrittlement in nickel alloys after neutron irradiation (ABC-TR-7188) 16 p2613 N71-28799
 Grain boundary segregation of impurities in steels and intergranular brittle fracture (AD-72324) 19 p3113 N71-31966
 Gaseous hydrogen embrittlement in Inconel 718, Inconel 625, AISI 321 stainless steel, Ti-3Al-2.5Sn ELI, and OFHC copper (NARA-CR-119917) 19 p3116 N71-32489
 Rare earth and thorium alloying of chromium and molybdenum for controlling hydrogen embrittlement (NARA-CR-72092) 20 p3285 N71-33399
 Deformation studies on dilute hafnium base alloys to determine effects of dispersion hardening and precipitation (NPL-5719-9) 21 p3439 N71-34467
 Hydrogen embrittlement of titanium alloy surface in hot salt corrosion cracking 23 p3772 N71-36882
 Effectiveness of yttrium, lanthanum, and hafnium coatings for preventing nitridation embrittlement of titanium alloys at high temperatures (NARA-TN-D-4528) 23 p3772 N71-36886
 Metallurgical evaluation of simulated BWR emergency core cooling tests 23 p3798 N71-37076
 Service performance and irradiation embrittlement of structural materials in nuclear power plant (POLL-CE-TRANS-5598 (1922.09)) 24 p3964 N71-38280

EMULSION
 Manual control for experimentation with human eye 13 p2853 N71-24763

EMERALD
 U BERYL
 EMERGENCIES
 Experimental analysis of emergency core cooling reactor systems 07 p1040 N71-17287
 (IN-1334)
 Guidelines for design and implementation of emergency action plans for avoiding air pollution episodes (AP-76) 20 p3365 N71-33376

EMERGENCY BREATHING TECHNIQUES
 Positive pressure breathing techniques for aircraft survival in low pressure environments 04 p0483 N71-13894
 Performance of smoke hood for protection of human respiratory system in aircraft accidents and passenger evacuation (FAA-AM-70-20) 17 p2711 N71-23640

EMERGENCY LIFE SUSTAINING SYSTEMS
 Analysis of Apollo 13 lunar module systems during emergency operation following command service module oxygen tank explosion (NASA-TM-X-66935) 09 p1466 N71-19962
 Development and characteristics of inflatable structure to provide escape from orbit for spacecrafts under emergency conditions (NASA-CASE-XMS-06162) 16 p2683 N71-28851
 Evaluation of storable propellants as sources of H₂, O₂, potable H₂O, and heat for use in emergency life support system (NASA-TM-X-2521) 17 p2711 N71-29903
 Performance tests on liquid explosive emergency exit for civil aircraft (FAA-RD-71-33) 18 p2872 N71-31064
 Design, development, and evaluation of emergency life support system to protect infants and small children during water survival situation (FAA-AM-71-37) 21 p3385 N71-34083

EMISSION
 NT BIOLUMINESCENCE
 NT CHEMILUMINESCENCE
 NT ELECTROLUMINESCENCE
 NT ELECTRON EMISSION
 NT FIELD EMISSION
 NT FLUORESCENCE
 NT HYDROXYL EMISSION
 NT INCANDESCENCE
 NT ION EMISSION
 NT LIGHT EMISSION
 NT LUMINESCENCE
 NT LUNAR LUMINESCENCE
 NT NEUTRON EMISSION
 NT OPTICAL RESONANCE
 NT PARTICLE EMISSION
 NT PHOSPHORESCENCE
 NT PHOTOELECTRIC EFFECT
 NT PHOTOELECTRIC EMISSION
 NT PHOTOIONIZATION
 NT PHOTOLUMINESCENCE
 NT RADIO BURSTS
 NT RADIO EMISSION
 NT SECONDARY EMISSION
 NT SOLAR RADIO BURSTS
 NT SOLAR RADIO EMISSION
 NT SPECTRAL EMISSION
 NT SPONTANEOUS EMISSION
 NT STIMULATED EMISSION
 NT THERMAL EMISSION
 NT THERMIONIC EMISSION
 NT THERMOLUMINESCENCE
 NT TYPE 3 BURSTS
 NT TYPE 4 BURSTS
 NT X RAY FLUORESCENCE
 Doppler line superaddition emission from uniform spherical gaseous medium (AD-717724) 11 p1805 N71-22368
 Acoustic emission analysis of material properties and defect structure (UCRL-72657) 17 p2786 N71-29268
 Effective masses of different pairs of particles emitted in positive pion, xenon interactions at 2.3 GeV/c (JINR-P1-5592) 18 p2975 N71-30570
 Unload emission behavior of materials with various heat treatments and its relation to Rauscher effect 18 p2936 N71-31139
 Annotated bibliography on emission sources in electric power plants and air pollution effects 20 p3255 N71-32891
 Determination of absolute scale for neutral silicon g_f-values with pressure driven shock tube no emission source 23 p3838 N71-37367
 Stratified charge engine tests to determine exhaust emission characteristics (AD-727745) 24 p0831 N71-38760

EMISSION SPECTRA
 Intrinsic cathodoluminescence emission from willemite single crystals 01 p0107 N71-10085
 Atomic line transitions and radiant emission from high temperature air (AD-716799) 01 p0096 N71-10083
 Photographic calibration for emission spectroscopy using small computer (BM-81-7447) 01 p0857 N71-10076

Identifying rock types by aircraft equipped with various types of infrared detectors 03 p0217 N71-11985
 Establishing detection limits for emission spectroscopic approach in determination of trace metals in biological materials (NASA-TM-X-52932) 03 p0331 N71-12359
 Intensity and spectral shape of diffuse X ray emission by gaseous disk from cosmic ray heating of interstellar hydrogen (NARA-TM-X-45308) 03 p0430 N71-13834
 Using acoustic emission techniques for flow detection in structural members of reactor pressure vessels (IN-1398) 04 p0618 N71-14099
 Temperature profiles and AJO resonant spectra of thermopiles (AD-713676) 05 p0571 N71-14848
 Investigating short-range behavior of wave function by comparing projected Hartree-Pock spectra using basis functions having harmonic oscillator and Wood-Saxon radial dependence (NARA-TM-X-52944) 05 p0748 N71-15283
 Electron interaction in transition metal X ray emission spectra (UIUP-762) 06 p0909 N71-15753
 Emission spectroscopy method for contamination monitoring of inert gas metal arc welding (NARA-CASE-XMF-42039) 06 p0862 N71-15871
 Adhesion of single crystal materials to clean iron surface studied by emission spectroscopy (NARA-TN-D-7018) 06 p0863 N71-15928
 Measurement of relative emission rates of several systems (NARA-CR-116240) 06 p0853 N71-16509
 Spectral coincidences between emission lines of CO laser and absorption lines of nitrogen oxide (AD-715293) 07 p1041 N71-18833
 Fast variation of hydroxyl amplitude and gamma quanta bremsstrahlung (ITBF-764) 07 p1081 N71-18136
 Theoretical reconstruction of gamma ray spectra fission products after thermal fission of U-235 nucleus (CEA-N-1313) 07 p1081 N71-18142
 Using single photon counting techniques to study fluorescence response and line dependence of benzene in cyclohexane excited by protons and ultraviolet radiation (BNWL-SA-3526) 08 p1248 N71-19336
 Development of light source which produces molecular spectrum analogous to band spectrum of carbonaceous stars (NASA-TT-F-13520) 09 p1463 N71-20575
 Twilight aurora helium emissions in high latitudes in relation to magnetic disturbances and solar activity (NRC-TT-1441) 10 p1551 N71-21164
 Use of CO and CO₂ lasers to detect pollutants in atmosphere between laser emission lines and infrared absorption lines of NO (AD-717171) 10 p1571 N71-21788
 Vibrational absorption and emission spectra of F centers in calcium oxide 11 p1818 N71-22898
 Excitation mechanisms of rare earth element ion emission spectra in thiolate lattices (SRDE-70028) 12 p1905 N71-23359
 VLF emission measurement in several zones during magnetic reconnection phases 12 p1909 N71-23560
 Absolute and relative sensitivity of emission spectral analysis with laser excitation source (NASA-TT-F-13542) 12 p1934 N71-24038
 Limit on line emission in X ray background at high galactic latitudes - rocket observation (NASA-TM-X-65519) 13 p2160 N71-24960
 Quantitative analysis of hafnium in zirconium oxide by emission spectroscopy (IEA-200) 13 p2136 N71-25373
 Influence of high frequency fields on properties of accelerating channel and beam emittance in linear accelerator (SLAC-TRANS-128) 14 p2300 N71-25703
 Microwave absorption and emission from magnetized afterglow plasma column in S band waveguide (AD-72522) 14 p2522 N71-26345
 Emission spectroscopy for identification of high temperature reactor fuel element spheres at 40 atmospheres of helium (JUL-671-RW) 15 p2442 N71-26824
 Scintillation separation of gamma ray spectra into neutron capture, nuclear fission, and fission product sources for use in nuclear fuel element nondestructive testing (KFK-1214) 15 p3463 N71-37144
 Orthon transmission and emission spectra at 9.6 microns computed from adjusted theoretical spectral line data 15 p0476 N71-27508
 Field and laboratory investigations of microwave emission characteristics of snow, soils, and oceanographic phenomena (AD-714855) 15 p0404 N71-27021
 Computer programs for reduction of Compton recoil electron energy distribution measurements to electron prompt spectra (ANL-7411) 17 p2792 N71-29446

- Emission spectra of ionized barium recorded by spectrophotometer for September 24
17 2741 N71-29677
- Metal oxide infrared emission, and detection of vibrationally excited metal oxide molecules by laser induced fluorescence
[AD-72319] 18 2888 N71-31597
- Internal source scintillation method for studying orbital-electron-capture and electron-capture-to-positron-emission ratios
[NP-18692] 19 3147 N71-32043
- Production cross sections for He I, He II, H-alpha, and H-beta emissions
20 3318 N71-33573
- Measurements of radiation emission properties of uranium plasma
20 3331 N71-33648
- Diurnal variations in spectra of solar hydroxyl emission in relation to helium emission intensity
[NRC-TT-1437] 21 3416 N71-34310
- K line emission spectrum of lithium for energies above and below Sommerfeld threshold determined using many body diagrammatic techniques
21 3442 N71-34491
- Measurement of excitation probability of bound atomic states by photon emission
[NRC-TT-1435] 21 3474 N71-34736
- Kinetics of emissions and absorptions of molecular nitrogen and carbon dioxide ions in ground states produced by pulsed radiolysis of N₂ and CO₂
[ANL-TRANS-831] 21 3477 N71-34760
- reduction and analysis of selected spectral emission intensities at polar cap station
[AD-72615] 22 3580 N71-35500
- Calibrated infrared emission spectra of earth and atmosphere using high resolution interferometer spectrophotometer on Nimbus 4 satellite
[NASA-TM-X-45687] 22 3585 N71-35517
- Measurement of gamma ray spectra accompanying nuclear radiative capture
[DNR-1271] 22 3631 N71-35871
- Radio spectrum analysis of two active regions based on Laplace transform and brightness temperatures from Nov. 12, 1966 solar eclipse data
[NASA-TM-X-46543] 22 3664 N71-36127
- Analysis of emission spectra of metal vapors obtained by laser irradiation
[NASA-TT-F-13967] 23 3765 N71-36841
- Field electron emission from CdS as function of temperature and exposure with current voltage characteristics and excitation line observations
[NLL-TRANS-2751-9622.81] 23 3836 N71-37358
- Emission spectral methods for determining content of mineral admixtures in fuels, oils, and lubricants
[AD-727197] 24 3886 N71-37699
- EMISSIONS**
- Nonequilibrium emissivity of carbon dioxide near 4.3 microns and shock wave molecular relaxation
[ARC-CP-1116] 07 01007 N71-17080
- Ion beam phase characteristic measuring devices for volumetric and emissivity measurements
[NP-18507] 18 2971 N71-30468
- Vibrational tests on dual patch of radiant cooling apparatus, and emissivity and reflectance analysis of cones in radiative heat transfer determination
[NASA-CR-121443] 20 3311 N71-33284
- Radiative flux densities and heating rates in atmosphere calculated using pressure and temperature dependent emissivities
21 3423 N71-34359
- Techniques and apparatus design for measuring high temperature emissivity of thermal protection materials for reentry vehicles
[NASA-CR-119920] 21 3425 N71-34368
- Delayed neutron calculations of energy spectra and precursor emission probabilities following negative beta disintegration
[LB/G-2943] 21 3483 N71-34808
- Development of procedure for determining spectral emissivity of refractory oxides and concretes in visible region of spectrum
22 3600 N71-35634
- Analysis of emissivity of refractory oxides and concretes in infrared region of spectrum at high temperatures
22 3600 N71-35635
- Thermal emission of refractory materials measured in atmospheres of argon, cesium, and vacuum
22 3601 N71-35645
- Determination of monochromatic emissivity of pyrographite at various temperatures and effect on anisotropy of emission properties
22 3601 N71-35646
- Total hemispherical emissivity of thin metallic films in 200 to 300 K range, and film thickness effect
23 3885 N71-37129
- EMISOPHAGES**
- U ACTINOMETERS
- U RECORDING INSTRUMENTS
- EMITTANCE**
- Bibliography on emittance of high temperature materials including refractory materials, ceramics,

- carbon, graphite, char, and ablative materials for use in aerospace engineering
[NASA-CR-102934] 03 0468 N71-12960
- Emission measurement techniques for space shuttle materials in high temperature environmental simulation
[NASA-CR-103071] 10 3188 N71-31025
- Bolometric measurement of copper, aluminum, and stainless steel emittances at cryogenic temperatures
11 3178 N71-32045
- High thermal emittance black surface coatings and process for applying to metal and metal alloy surfaces used in radiative cooling of spacecraft
[NASA-CASE-XLA-06199] 13 2006 N71-24875
- Effect of oxidation degree on copper emittance for application to radiation shields or multifoil insulation systems at 700 to 1400 F
14 2274 N71-26314
- Infrared flux at air-sea interface calculated to solve radiative transfer equations numerically by using flux emittance and flux reflectance as functions of sea temperature and roughness
[AD-72036] 16 2588 N71-28455
- Measurement of total hemispherical emittance for chromel and alumel thermocouple wires in inert atmosphere at high temperatures
[NASA-TM-X-2339] 21 3429 N71-34404
- EMITTERS**
- NT THERMIONIC CATHODES
- NT THERMIONIC EMITTERS
- Multiple-grid probe separating currents flowing from plasma to collector into their electron and ion components
[IPP-2/83] 08 01271 N71-18266
- Dynamics of various types of emitters used on ITR project
[NASA-TT-F-13705] 18 2988 N71-31476
- Signal flow graphs for emitter follower temperature stability and linearity analysis
[INR-1256] 21 3402 N71-34207
- Inverted geometry transistor for use with monolithic integrated circuit
[NASA-CASE-ARC-10330-1] 21 3403 N71-34214
- Standardization of beta-gamma emitters by 4pi beta-gamma coincidence method for corrections and counting errors
[INR-1240] 21 3467 N71-34680
- Design and evaluation of cylindrical out-of-pile thermionic converter test vehicle to determine performance of tungsten emitters with preferred crystal orientation
[NASA-CR-1898] 23 3710 N71-36451
- EMOTIONAL FACTORS**
- Difficulties of circumscribing danger zones for other aerial radar personnel
02 0163 N71-11810
- Measurement of effects of stress on air traffic control personnel through use of mood adjective check lists
[FAA-AM-71-21] 21 3583 N71-34067
- EMOTIONS**
- Estimating human emotional states by changes in frequency characteristics of articulation
[NASA-TT-F-13772] 18 2875 N71-30803
- EMPLOYEE RELATIONS**
- Effects of reductions in NASA contracts on unemployment of aerospace employees
[NASA-CR-118374] 13 2191 N71-24801
- EMPLOYMENT**
- Conference on application of science and technology to problems of pollution, transportation, and employment
[PB-192529] 03 06323 N71-12306
- Employment opportunities for economists and air transportation analysts with Civil Aeronautics Board
07 01134 N71-17798
- Reporting career opportunities as accountant or auditor with Civil Aeronautics Board
07 01134 N71-18004
- Economic analysis of airport construction in north central Texas region, emphasizing employment and dollar value of purchases
07 01005 N71-18099
- Employment statistics on Federal scientific, technical, and health personnel for 1969
[NSF-70-44] 08 3107 N71-18447
- Survey of scientific activities and employment in independent nonprofit institutions for 1970
[NSF-71-9] 19 3199 N71-32692
- EMULSIONS**
- NT NUCLEAR EMULSIONS
- NT PHOTOGRAPHIC EMULSIONS
- Ester emulsion analysis and colloidal molecular weight determination by gel chromatography
03 06330 N71-12553
- Particle track formation in emulsion
[COO-1671-28] 12 01969 N71-23235
- Mathematical models for studying kinetics of aqueous emulsion copolymer system
14 2215 N71-26580
- Chemical structure and properties of polymer emulsifiers
[NLL-RTS-6161] 16 2559 N71-29084

- Chemical and thermomechanical properties of emulsion polymerization with initiation in boundary layer
[NLL-RTS-6162] 16 2559 N71-29084
- Variation of gamma function with wavelength and influence of emulsions on exposing light source
[RAB-LIB-TRANS-1572] 22 3628 N71-33004
- ENAMELS**
- Static, temperature-dependent magnetization of enameled motion wire
[UCSD-34-P-143-34] 13 3083 N71-23379
- ENCAPSULATING**
- Encapsulation resonance frequencies in CW Q-band diodes for J and Q bands, and limitations on oscillation characteristics
01 0032 N71-10117
- Vacuum encapsulation of cesium for out-of-circuit thermionic diodes
[NASA-TM-X-2152] 06 0696 N71-13863
- Development of bacteriostatic conformal coating and methods of application
[NASA-CASE-OSC-10007] 06 0677 N71-14066
- Application of microencapsulation techniques to photographic emulsions
[NLL-M-20169-3828.4F/1] 12 01923 N71-34110
- Equipment and procedures for remote encapsulation of pre-irradiated fuel pins in TREAT capsules
13 2115 N71-34331
- Flexible, repairable, portable composition for encapsulating electric components
[NASA-CASE-XGS-05180] 14 2277 N71-23380
- Reliability evaluation of plastic-encapsulated integrated circuits including long-term tests and short-term highly accelerated tests
[AD-722043] 16 2569 N71-26045
- Linear array, multielectrode, ultrasonic transducer test techniques for radioisotope encapsulation inspection
[BNWL-1491] 16 2571 N71-26061
- Test chambers with orifice and helium mass spectrometer for detecting leak rate of encapsulated semiconductor devices
[NASA-CASE-ERC-10150] 16 2598 N71-26092
- Process for encapsulating hygroscopic cloud seeding agents
[AD-722448] 18 2939 N71-30085
- Ecofoam encapsulation procedure for describing characteristics of potting mold - EOLE modules
[NASA-TT-F-13814] 18 2930 N71-31272
- Encapsulation of strain gage transducer and thermocouple in molding compound for simultaneous pressure and temperature readings during transfer molding of electronic components
[BDX-613-333] 19 3105 N71-32016
- Electrically coupled individually encapsulated solar cell matrix
[NASA-CASE-NPO-11190] 21 3579 N71-34804
- Prediction and inhibition of radiolysis of water in sealed aluminum capsules at reactor facility
[NASA-TM-X-67899] 22 3559 N71-33380
- ENCEPHALITIS**
- Using helicopter for spray dusting forests with DDT for tick borne encephalitis
[AD-703996] 17 2703 N71-29357
- ENCKE METHOD**
- Spacecraft trajectory analysis in many body inverse square force field based on Kepler laws and Encke method without numerical integration
[RE-407] 16 2677 N71-26068
- ENCLOSURES**
- Method and apparatus for bowing of instrument panels to improve radio frequency shielded enclosure
[NASA-CASE-XMF-09422] 09 01346 N71-19404
- Structural design of Cassegrain cages in large astronomical telescopes
24 3923 N71-37095
- ENCODERS**
- U CODERS
- ENCODING**
- U CODING
- END PLATES**
- Pressure distribution at end plate of monom shock tube
[REPT-3/70] 03 0365 N71-13291
- ENDFIRE ARRAYS**
- NT YAGI ANTENNAS
- ENDOCRINE GLANDS**
- NT ADRENAL GLAND
- NT THYROID GLAND
- NT THYROID GLAND
- ENDOCRINE SECRETIONS**
- NT HORMONES
- Biochemistry model for endocrine system effects on mammalian neurophysiology and human behavior
09 01332 N71-19887
- ENDOCRINE SYSTEMS**
- Review of endocrine control of fluid and electrolyte balance during Mercury, Gemini, and Apollo missions
23 37111 N71-36465
- Preflight and postflight analysis of effects of Gemini 7 mission on metabolic and endocrine systems
23 37111 N71-36467
- Diurnal variation in endocrine and adrenocortical systems during prolonged bed rest
23 37111 N71-36468

SUBJECT INDEX

ENDOCRINOLOGY

Results of symposium conducted to assess endocrinological changes observed in Apollo astronauts (NASA-TM-X-30648) 23 p3710 N71-36453

ENDOGENOUS CONDITIONS

U PHYSIOLOGY

Toxic effects of endrin on brain functions of aerial applicator personnel (JAA-AM-70-11) 03 p0321 N71-12293

ENERGETIC PARTICLE EXPLORER C

U EXPLORER 15 SATELLITE

ENERGETIC PARTICLE EXPLORER D

U EXPLORER 26 SATELLITE

ENERGY

Neutron interaction at ultrahigh energies in cosmic rays (JNP-722) 15 p2489 N71-27879

Senate hearings on establishment of Commission on Pesh and Energy 17 p2862 N71-30165

Approximations for total mass coefficient and mass coefficient for absorbed gamma ray energy for atomic numbers 1 to 92 (JZE-93) 17 p2808 N71-30338

Inversion barrier energies in NH₃ and PH₃ and calculations of electronic properties in TiO₂(minus x) clusters 21 p3491 N71-34866

Collision diameters and vibrational energy transfer in thermal unimolecular structures 21 p3491 N71-34867

Variational calculation of binding energies and dimensions in H₂ and O-16 (JTF-71-1-E) 23 p3811 N71-37176

MECC-3 code instructions for calculating nuclear reactions involving incident particles at high energy on complex nuclei (JORN-4564) 23 p3816 N71-37215

ENERGY ABSORPTION

NT AURORAL ABSORPTION

NT ELECTROMAGNETIC ABSORPTION

NT MOLECULAR ABSORPTION

NT NEUTRON THERMALIZATION

NT PHOTODIFFUSION

NT POLAR CAP ABSORPTION

NT SELF ABSORPTION

NT THERMAL ABSORPTION

NT THERMALIZATION (ENERGY ABSORPTION)

NT ULTRAVIOLET ABSORPTION

NT X RAY ABSORPTION

Mathematical model for chemical activity increase at crystal surface caused by mechanical impact 01 p0018 N71-10513

Commercial application of unused NASA patents involving elevator safety, highway safety, earthquake protection, and transportation (NASA-CR-111374) 02 p0307 N71-11443

Absorption and scattering of daylight during sea water propagation 04 p0564 N71-13731

Molecular absorption and light scattering in flame spectroscopy (IS-T-335) 06 p0812 N71-16791

Design and development of double acting shock absorber for spacecraft docking operations (NASA-CASE-XMS-03722) 10 p1567 N71-21530

Nonreversible energy absorbing device comprising a ring member with plurality of recesses, cutting members, and guide member mounted in each recess (NASA-CASE-XMF-10040) 11 p1772 N71-22877

Nonlinear absorption feedback for laser power stabilization 13 p2089 N71-24837

Suspended mass oscillation damper based on impact energy absorption for damping wind induced oscillations of tall stacks, antennas, and umbilical towers (NASA-CASE-LAR-10193-1) 15 p2415 N71-27146

Cosmic ionization by simultaneous absorption of deuterium and tritium 15 p2418 N71-27189

Radiation absorption in shock front of hypersonic air flow around blunt reentry body (NASA-TT-P-13572) 16 p2582 N71-28857

Energy absorption device in high precision gear train for protection against damage to components caused by stop loads (NASA-CASE-XNP-01848) 16 p2604 N71-28959

Energy absorbing restraint system for automobile crash protection (PB-197843) 17 p2756 N71-29806

Aerospace energy absorbing gearrail concept designed for redirecting errant vehicle parallel to normal traffic flow with minimum damage to vehicle and passengers 17 p2855 N71-30296

Approximations for total mass coefficient and mass coefficient for absorbed gamma ray energy for atomic numbers 1 to 92 (JZE-93) 17 p2808 N71-30338

Spectral line profiles and energy absorption in helium plasma afterglow (WV-18748) 18 p2992 N71-30640

Thermal radiative heat transfer in absorbing, emitting, and scattering media 18 p3024 N71-30941

Theory and physics of gas radiation in absorbing, emitting, and scattering media 18 p3006 N71-30942

Thermal radiation heat transfer equations for absorbing and emitting gas 18 p3024 N71-30943

Radiative properties of gas at varying wavelengths 18 p3024 N71-30945

Extended Monte Carlo method for determining radiative heat transfer in absorbing/emitting media 18 p2945 N71-30947

Conductive and/or convective radiative energy transfer in absorbing-emitting medium 18 p3025 N71-30948

Transfer coefficients for thermal radiation in scattering and absorbing media 18 p3025 N71-30949

High energy absorption docking system design for docking large spacecraft (NASA-CASE-MPS-20863) 21 p3520 N71-35082

Design, fabrication, and tests of energy absorbing seat integrated with extraction tractor rocket for space shuttle 22 p3547 N71-35266

Region of the energy absorption by plasma at upper hybrid frequencies (JNP-15807) 22 p3632 N71-36046

Probable nuclear heating values due to radiation energy absorption (LBN-G-3016) 24 p3958 N71-38232

Silicon detector for measuring gamma radiation in materials (NLL-WHT-TRANS-312-[3091.9F]) 24 p3982 N71-38422

ENERGY BANDS

NT BLOCH BAND

NT CONDUCTION BANDS

NT FORBIDDEN BANDS

Tight binding energy bands of perovskite type transition metal oxides (IS-T-371) 01 p0100 N71-10757

Electronic effects of chemisorption on powdered zinc oxide catalyst 03 p0330 N71-12356

Spin-orbit interaction and strain effects on energy bands and optical properties of diamond type semiconductors 04 p0603 N71-14219

Calculation of energy bands in ferromagnetic nickel using combined interpolation method 11 p1810 N71-23034

Use of scattered wave method to compute molecular wave functions, augmented plane wave method for energy band calculations, and Casimir invariants as invariant operators in Lie groups (NASA-CR-111635) 14 p2325 N71-25974

Vibration-rotation interaction effects in calculated band strengths studied by asymptotic expansion method (AD-722811) 17 p2803 N71-30215

Spectroscopic band models for determining gas temperature and concentrations 19 p3048 N71-31675

Pseudo-potential calculation of energy bands and optical properties of 4-layer polypyrrole ZnS 19 p3170 N71-32351

Electronic band structure and physical properties of actinide metals and their compounds (COO-2103-3) 21 p3439 N71-34469

Angular momentum decomposition of three body problem and binding energy per particle of nuclear matter 22 p3650 N71-36030

Gross theoretical analysis of nonrelativistic and relativistic trigonal selenium energy bands (PB-197640) 24 p3977 N71-38375

ENERGY BUDGETS

NT ATMOSPHERIC HEAT BUDGET

NT HEAT BUDGET

Vertical eddy thermal transport and global energy budgets of mesosphere and lower thermosphere (NASA-CR-117047) 09 p3379 N71-19465

Climatological and micrometeorological measurements for analysis of climate and energy exchange on subpolar ice cap in summer (AD-721546) 16 p2627 N71-29076

Predictive methods for solar and atmospheric thermal energy budgets in lakes and streams (PB-197657) 18 p2920 N71-31488

Mass and energy budget calculations for atmospheric boundary layer over tropical ocean surface 19 p3131 N71-32734

Thermal simulation model of radiant energy budgets for natural temperature measurement of water flow 22 p3613 N71-35740

ENERGY CONVERSION

Abstracts of conference papers on kinetics of energy conversion (AD-717338) 03 p0332 N71-12372

Spectra power supply circuits and energy conversion 03 p0319 N71-12378

ENERGY DISSIPATION

Describing general characteristics of system for direct conversion of thermal into electrical energy by thermodynamic analysis 03 p0469 N71-13249

Direct conversion of fusion energy to electricity (UCRL-72411) 06 p0928 N71-15736

Thermodynamic characteristics of electrochemical energy conversion into electrical energy (AD-713675) 06 p0810 N71-16314

Direct power conversion by magnetohydrodynamics of thermal energy into electrical energy (CEA-R-4062) 07 p0977 N71-16125

Energy transfer involving thermal phenomena in rhodium electrodes, cesium gas filled diode 06 p1266 N71-19203

Investigating vacuum techniques for generating useful plasma lifetimes in controlled fusion experiments (UCRL-72317) 06 p1276 N71-19203

Heat release explosive processes and gas dynamics for high power energy conversion systems (AD-717188) 10 p1666 N71-31783

Energy conversion and thermomechanical coupling in semithermal viscouslike circular cylinder solids 11 p1839 N71-22883

Cesium absorption measurements in thermionic energy conversion (AD-720407) 14 p2280 N71-33936

MHD energy conversion using Joule heating (AD-728257) 14 p2322 N71-26190

Design of plasma engine with magnetic field energy conversion to ion heating by ambipolar reaction (AD-721214) 15 p2582 N71-27839

Ignition of toroidal fusion reactors and plasma confinement experiments in Tokamak machines (MATT-900) 17 p2812 N71-29661

Octahedra and rod shaped crystals of semiconductor ferromagnetic chalcogenides spinel copper cadmium chromite selenide - energy converting materials (AD-722783) 18 p2999 N71-31458

Helium solar probe power supply voltage regulators and energy converters (BMBW-FB-W-71-17) 19 p3040 N71-31785

Photochemical energy conversion research including experiments on photoreduction, isomerization, and photolysis (AD-724374) 20 p3229 N71-33424

Thermoelectric, steam Rankine cycle, and organic Rankine cycle systems as sources of radioisotope energy conversion systems (JORN-TM-3394) 22 p3623 N71-35812

Experimental and computational investigations of direct conversion of plasma energy to electricity (CONF-710607-126) 24 p3989 N71-38463

Nonchemical energy sources, release mechanisms, and conversion processes in plasma dynamics (AD-727073) 24 p3993 N71-38498

ENERGY CONVERSION EFFICIENCY

Increasing power conversion efficiency of electronic amplifiers by power supply switching (NASA-CASE-XMS-09945) 01 p0035 N71-10798

Engineering aspects of Astron fusion power reactor system including structural design, neutronics, heat transfer, and costs 05 p0728 N71-15114

Investigating relationship of conversion efficiency to fixed and variable costs in fusion reactors (UCRL-72349) 05 p0730 N71-15242

Analysis and breadboarded performance of parallel energy storage units for power systems (NASA-CR-116510) 07 p0975 N71-17471

Polarization and energy conversion efficiency of yeast and *Bacillus lactis* fermentation for biochemical fuel cells 14 p2205 N71-26245

External operating characteristics, current and voltage amplification ratios, and electric power efficiency of electrodynamic energy converter 14 p2244 N71-26405

Flight testing of cadmium sulfide thin film solar cells for stability and efficiency 19 p3041 N71-31999

Research and development on silicon solar cell with improved efficiency (NASA-CR-121751) 21 p3379 N71-30482

ENERGY CONVERTERS

U DIRECT POWER GENERATORS

ENERGY DENSITY

U FLUX DENSITY

ENERGY DISSIPATION

Superconducting effects on alpha particle differential energy loss in tin, vanadium, and lead superconductors (NASA-TM-X-52096) 01 p0110 N71-10239

Viscous torque or windage losses for Landolt generator rotor in air and turbulent flow (NASA-TM-X-52903) 01 p0806 N71-10490

Energy loss of high energy electrons in the lead and gadolinium (AD-711085) 01 p0807 N71-10534

Approximate density-effect correction for ionization loss of charged particles (NASA-CR-111652) 01 p0103 N71-10881

Operation and development of Minnow reactor and particle physics experimental program (RREL-X-198) 03 p0431 N71-12917

- Automatic test equipment for hysteresis and eddy current energy dissipation in steel metal sheets [NPL-MEMO-5] 03 p0383 N71-13363
- Energy losses, range, and bremsstrahlung yield for 10 keV to 100 MeV electrons in some simple elements and some chemical compounds [JORN-TR-2331] 04 p0580 N71-13989
- Gain loss in neodymium glass laser amplifier 04 p0526 N71-14330
- Dissipated power in graphite and CO₂ of graphite reactor cell of NALADE 2 subcritical assembly [CEA-R-3985] 04 p0562 N71-14414
- Turbulent loss of ring current protons inside plasmapause 07 p1106 N71-17780
- Radiation energy releases in experimental channels of SM-2 reactor [SRARI-P-69] 08 p1234 N71-18174
- Empirical method for calculating energy straggling in slowing down ionizing particles [KFK-1173] 08 p1249 N71-18205
- Calculating energy loss of fast electrons passing through thin films using classical electrodynamics techniques [IS-T-380] 08 p1255 N71-18368
- Energy gap for excitonic insulator in presence of persistent currents 10 p1634 N71-20919
- Impedance matcher for automatically maximizing power radiated from X band antenna on reentry vehicle by eliminating power dissipated as heat 10 p1520 N71-21123
- Flutter suppression with dissipated energy reduced to quadratic form for control surfaces [NASA-TN-D-6199] 11 p1671 N71-23091
- Light scattering dissipated in optical glass fibers causing power loss [SRDE-70064] 14 p2295 N71-25635
- Calculating energy losses produced in pulsed superconducting magnet of any shape wound with solid core wires [NP-18516] 14 p2298 N71-26628
- Effects of energy dissipation on systems stability of SAS A spacecraft [NASA-TM-X-65537] 15 p2442 N71-27606
- Inelastic energy loss spectra for proton impact on helium atoms 15 p2493 N71-27942
- Heavy charged particle energy loss rate from nuclear elastic scattering [LA-4543] 16 p2645 N71-28112
- Problems in evaluating electromagnetic fields of linear antennas or dipole arrays in dissipative half space [AD-721706] 17 p2725 N71-29480
- Energy dissipation measurement in aeroidal dissipative spinning and processing system of satellites 17 p2787 N71-29653
- Internal friction production from energy dissipation during kink motion 17 p2820 N71-29957
- Nonlinear continuum theory for analyzing crystal dislocation effects [NBS-SP-317-VOL-2] 17 p2821 N71-29969
- Energy dissipation in electron interaction with moving crystal dislocations 17 p2826 N71-30002
- Analysis of magnetic storm energy balance, including total energy, rate of arrival, and energy dissipation rate at different stages of development 17 p2747 N71-30086
- Approximate calculation of ionization energy loss and range of fast charged particles [JINR-P1-5676] 18 p2968 N71-30425
- Recombination and hysteresis losses in frequency multiplier with semiconductor diode 18 p2900 N71-31522
- Computer programs for calculating electron bombardment proton and gamma yields based on Vavilov theory of energy loss distributions [AD-723188] 19 p3156 N71-32417
- Contact breaking speed effects on spark quenching and gas discharge of electric inductance switch [NLL-TRANS-2662-9022.81] 19 p3067 N71-32435
- Spin-axis attitude stability of dissipative dual spin spacecraft in force-free environment 21 p3455 N71-34587
- Effects of parametric instabilities on conversion loss of millimeter wave mixers utilizing ion bombarded silicon and gallium arsenide [NASA-CR-111990] 24 p3887 N71-37704
- Specific energy loss and effective charge of fission products in metal absorbers using Cf-252 fission source and semiconductor detector [KFK-1349] 24 p3975 N71-38364
- Resonant frequency measurements for determining energy dissipation in turbine blade materials during vibratory tests [AD-727458] 24 p4026 N71-38727
- Calculation of rates of energy loss due to sublimation for water, carbon dioxide, argon, krypton, xenon, and oxygen [NASA-TN-D-6340] 24 p4032 N71-38768

ENERGY DISTRIBUTION

- NT SPECTRAL ENERGY DISTRIBUTION
- Liquid propellant rocket engine performance computer program with distributed energy release [NASA-CR-111008] 01 p0114 N71-10012
- Investigating electrical nature of surface states caused by defects at and near oxide-silicon interface 04 p0603 N71-14322
- Meridional flow, relative angular momentum, and energy flux calculations for International Geophysical Year [MET-O-808C] 05 p0673 N71-14878
- Increased peak power of klystrons [SLAC-PUB-894] 06 p0898 N71-16264
- Measuring energy and spatial dependence of neutron importance functions in SNEAK assemblies and determining energy spectra and intensities of neutron sources [KFK-1141] 08 p1254 N71-18333
- Numerical analysis of plasma buildup, anisotropy, and energy distribution [CEA-COMP-1604] 08 p1273 N71-18665
- Plasmatron ion source with slit geometry for electromagnetic mass separator [SGAE-F93/1970] 08 p1274 N71-18719
- Energy estimates for equations of compressible flow initial value problems [LA-4525] 08 p1182 N71-18943
- Absorbed dose microdistribution in heavy charged particle track 08 p1263 N71-19061
- Structure and energy distribution of chromosphere-corona transition region 08 p1286 N71-19294
- Angular energy distribution of particles produced in inelastic pion-nucleon and nucleon-nucleon collisions at superhigh energies [JINR-P2-5331] 09 p1433 N71-19976
- Cation energy distribution within straight channel photomultiplier tubes 10 p1558 N71-21039
- Energy distribution of electrons leaving curved channel photomultiplier tube after electron avalanche 11 p1761 N71-21992
- Plasma instability characteristics, off-resonance heating phenomena, bremsstrahlung measurements, and computer simulation of plasmas [COO-1695-31] 11 p1812 N71-22461
- Negative ion vacancy formation efficiency measurements of KBr as functions of temperature and lattice energy between 6K and 300K 11 p1808 N71-22876
- Analysis of thermal radiation front propagation from point explosion using radiation diffusion approximation techniques [FOA-4-C-4402-23/25] 13 p2187 N71-25467
- Propane bubble chamber photographic analysis of kaon tau decays and calculation of final state pion energy distributions with comparison to nuclear resonance models 13 p2142 N71-25556
- Atomic iodine photodissociation and UF₆-H₂ hydrogen fluoride chemical lasers for studying vibrational energy distribution in reaction products and chemical reactivity 14 p2266 N71-26313
- Coupling resonance effects on vertical emission including beam energy distributions [NP-18517] 14 p2312 N71-26706
- SL(2,C) representations in energy dependent basis using Fourier transformation [KFK1-70-19-HEP] 14 p2313 N71-26715
- Penetration and cascade phenomena at low and very high energies [ANL-7727] 15 p2463 N71-27181
- Thomson scattering from pulsed ruby laser for measuring electron energy distribution and density in toroidal plasma [CLM-R-107] 15 p2502 N71-27737
- Calculation of ion trajectories and energy distribution in front of field emission tip [IPF-7/2] 15 p2483 N71-27766
- Equilibrium distribution functions for electrons in ionospheric plasma calculated for energy interval of 0 to 15 eV utilization data collected in pulse probe experiment [NASA-CR-119031] 16 p2588 N71-28508
- GeLi detector for measuring energy of electrons scattered forward by proton beam in thin beryllium foil [LA-4612] 17 p2791 N71-29296
- Particle beam energy distribution compensation technique for particle accelerator sections under current surges including phase velocity changes [SLAC-TRANS-129] 17 p2792 N71-29363
- Computer programs for reduction of Compton recoil electron energy distribution measurements to continuous gamma spectra 17 p2792 N71-29363
- Energy distribution of spectroscopic gradients in the ultraviolet spectra of beta Lyrae [NLL-RTS-6031] 17 p2844 N71-29764
- Energy balance equation for turbulent pulsations of free turbulent boundary layer in incompressible fluid [NASA-TT-F-13575] 17 p2737 N71-30180

Crossed field investigation of plasma formation processes and resulting guide field spatial and energy distributions 17 p2813 N71-30180

Time of flight techniques for high signal background ratio and high count rate of neutron transmission and energy 17 p2808 N71-30180

Secondary electron emission coefficients, apparent total ion scattering, and energy distributions of secondary electrons and ions produced by positive ion irradiation of metals [NPL-18490] 18 p2969 N71-30425

Frequency distributions of event size in deposition of energy over small pathlengths measured after penetration of 44.3 MeV protons through thicknesses of tissue-like material [NASA-CR-111943] 18 p2964 N71-30180

Computer program for analyzing energy effects in hypervelocity impact on rocks [SC-R-70-4402] 18 p2920 N71-31523

Use of differential energy analyzer for field electron electron energy distribution measurements in germanium 19 p3155 N71-32394

Effect of scattering on pulse length of argon laser beam in foggy and turbulent atmospheres, and feasibility of Monte Carlo calculation of laser beam energy density distribution [AD-724200] 20 p3281 N71-33126

Rocket exhaust cloud mass-energy balance measurements for Saturn S1-C static firing [NASA-CR-61357] 20 p3364 N71-33391

Models for vector-vector-tensor meson vertex including photon coupling [DESY-71/14] 21 p3470 N71-34709

Kinetic energy distributions of Cf-252 fission products as function of fission product mass ratios [ORNL-TR-2453] 21 p3478 N71-34746

Path finding schemes for energy continuous determination of energy independent pion-nucleon phase shift analysis [UCRL-20250] 21 p3475 N71-34746

Angular and energy distributions of particles produced in inelastic pion-nucleon and N-N collisions in center of mass system at superhigh frequencies [ORNL-TR-2453] 21 p3480 N71-34746

Energy distribution of electron-impact desorbed carbon monoxide ions from tungsten 21 p3480 N71-34821

Ion energy distribution and isotropy measurements and final ion temperature dependence on initial plasma conductivity in turbulent heating of plasmas [NYO-3958-4] 21 p3495 N71-34948

Angular and energy distributions of neutrons produced by bombarding thick beryllium targets with 53.8-MeV deuterons [KFK-1288] 22 p3632 N71-35877

Fast neutron spectra analysis emphasizing resonance scattering effects and influence of anisotropic scattering on energy-spatial distribution of neutrons 22 p3639 N71-35941

Angular and energy distributions during molecular dissociation due to electron bombardment 22 p3651 N71-36015

Finite energy sum rules for hyperbolas and nucleon-nucleon pion-pion reactions [TR-72-012] 23 p3783 N71-36844

Energy and momentum transfer distributions in air exchangers relative to model of traveling front cyclones in middle latitudes 23 p3786 N71-36842

Effect of probe tube on thermal neutron spectrum energy distribution using time of flight method [UARAE-75] 23 p3810 N71-37146

High resolution energy analyzer with time of flight spectrometer for studying highly ionized hydrogen and helium plasmas [IPFP-DT-22] 23 p3826 N71-37291

Analysis of swelling data for stainless steel based on Lindhard theory of energy partition with application to reactor design [HEDL-SA-159] 24 p3962 N71-38219

Volume photoemission model and photoelectric determination of electron attenuation lengths in molybdenum and aluminum [ORNL-TM-2617] 24 p3990 N71-38466

High temperature electron swarm apparatus for investigating electron attachment to polystyrene molecules 24 p3983 N71-38469

ENERGY EXCHANGE

U ENERGY TRANSFER

ENERGY LEVELS

NT ATOMIC ENERGY LEVELS

NT ELECTRON STATES

NT GROUND STATE

NT INTERMOLECULAR FORCES

NT MOLECULAR ENERGY LEVELS

Level degeneracy of generalized N-particle dual implitudes with satellites [COO-264-551] 03 p0421 N71-12819

SUBJECT INDEX

Energy level calculations for spherical and deformed Woods-Saxon potentials with Thomas type spin-orbit coupling
[LA-5359] 03 p0424 N71-12065

Gamma energy and intensity measurements in decay of Xe-142, Cs-142, Ba-142, and La-142 nuclei
[IS-T-352] 03 p0424 N71-12011

Electron tunneling into superconducting rhodium single crystals for energy gap measurements
[AD-71126] 03 p0441 N71-12836

Energy structure of zones and excitons
[AD-712812] 03 p0444 N71-13196

Asymptotic distribution of eigenvalues of random matrices
[JORN-4603] 05 p0714 N71-15390

Total cross sections of Sc, Ti, Cr, and Ni isotopes in $h\nu$ region
[EURPFR-008] 06 p0908 N71-15745

Perturbed angular correlation technique for studying effect of cubic lattice on electronic levels of erbium ions in BaAl_2
[JUB-495] 06 p0909 N71-15780

Ion energy stabilization system for Van de Graaff accelerator
[BARC-459] 06 p1252 N71-18258

Spin-orbit coupling and energy shifts in single crystal and pyrolytic graphite
[NASA-TN-D-6252] 10 p1634 N71-21074

Gamma ray spectra analysis to determine energy levels in Ge-72 from radioactive decay of Ge-73 and As-72
10 p1622 N71-21754

Absorption coefficient measurements of semiconductor compounds at room temperature in 36 to 150 eV region
12 p1984 N71-23146

Absorption spectra and excited electronic energy levels of neptunium dioxide in $\text{Ce}_2\text{UO}_{12}\text{Cl}_4$ and $\text{Ce}_2\text{UO}_{12}\text{F}_6$
12 p1969 N71-23257

Elastic scattering amplitude of protons from analog and compound states
[NYO-1682-25] 12 p1977 N71-24252

Fine structure of ground state levels of first four neighbor exchange coupled Cr^{3+} pairs in ruby
13 p2135 N71-25178

Measuring forward current and noise current of p-n junction before and after irradiation with ionizing radiation to determine effects of energy states at Si-SiO₂ interface
[RAB-LIB-TRANS-1536] 13 p2151 N71-25108

Positive pion proton interactions at 13.1 GeV/c
[JCO-1428-223] 13 p2155 N71-25246

Nuclear reactions of protons and deuterons on Zr-90 at 22.5 MeV and Mo-92 at 24.5 MeV
[CEA-CONF-1654] 13 p2140 N71-25523

Excitation functions and differential cross sections for Be-9 particle interactions from 8 to 30 MeV neutrons
[RKF-1190] 14 p2311 N71-26686

Energy separation measurements in a equals 2 state of atomic hydrogen by radio frequency produced dipole transitions between hyperfine components
[TID-25596] 14 p2315 N71-26734

Quasi-optical wave functions for relativistic corrections to energy levels of harmonic oscillator
[JNR-82-5339] 15 p2461 N71-27083

Optical model for nuclear state structure at increased excitation energy
[JNR-84-5469] 15 p2475 N71-27462

Nuclear model for calculating ground and excited states of odd nuclei
[JNR-84-5228] 15 p2475 N71-27463

Approximations for energy levels and corresponding wave functions in one dimension deduced from Miller and Schrodinger equations
[CEA-R-4007] 15 p2480 N71-27689

Computer program for discovery of excited states according to Ritz combination principle
[KFK-1247] 15 p2483 N71-27763

Calculation of nucleon-antinucleon bound states in quantum mechanics from OBE model
[DESY-7049] 15 p2488 N71-27873

K-meson nuclear existence at low energies
[NVE-STP/KFK-70-36] 15 p2488 N71-27877

Relativistic solution of many-body problem for elastic scattering of pions for high resolution energies
[ITF-70-49] 16 p2970 N71-30446

Total cross section for photoproduction of hadrons measured at 7 nuclei at 5.4 GeV photon energy
[DESY-71/5] 16 p2972 N71-30515

Nuclear density formula for interpolating level spacing and radiation width
[AABCE-311] 16 p2978 N71-30692

Energy levels of three particle system by method of nuclear interaction parameter expansion
[ITF-70-100-F] 19 p3146 N71-31970

Energy level width measurement in nuclei using resonance scattering of nickel capture gamma rays
[NRCN-234] 19 p3152 N71-32194

Electronic energy levels of Pr^{III} V and optical absorption studies of Pr^{III}/NbO₃·6H₂O on single crystals at 77 K
19 p3158 N71-32359

Relative intensities and energy measurements of 2s level in muonic Pb-208
[NASA-CR-121447] 20 p3320 N71-33711

Determining these characteristics of protons with energy 300 MeV by recombination methods
[ORNL-TR-3060] 21 p3466 N71-34674

Computer programs for FM cyclotron analyzer computing excitation energy of residual nuclei
[DMS-TL-108] 21 p3470 N71-34708

Nucleon-nucleon problem at medium energies at LAMPF
[LA-4640] 21 p3480 N71-34783

Monte Carlo studies of energy levels, electric and magnetic moments, hyperfine fields, and life times of various light nuclei
[NYO-2028-5] 21 p3484 N71-34821

Analysis of energy levels of Ne-18, Mg-22, Si-26, S-30, Ar-34, and Ca-38 using (p,t) reaction
21 p3489 N71-34857

Electron capture decay of Ba-131 and Ir-192 nuclei energy and relative intensity measurements using coaxial Ge(Li) detector
21 p3490 N71-34863

Calculations of phonon contribution to electron effective mass as function of position on Fermi surface, and anisotropic superconducting energy gap in white tin
21 p3492 N71-34874

Multipole constants for fission product nuclides covering Pa-239, U-235, and U-238
[JAERI-MEMO-4251] 22 p3632 N71-35886

Integrated Compton cross section and its effect in Monte Carlo scheme
[LA-4592] 22 p3638 N71-35934

Expression for differential cross sections in energy range between 22.5 and 400 MeV
[UCRL-20295] 22 p3645 N71-35986

Structure of hadrons covering hadronic and semihadronic processes
[NYO-4076-L4] 22 p3646 N71-36000

Gamma ray spectroscopy studies of low energy levels in odd proton nuclides in Z equals 50 to 62, N equals 64 to 82 regions
22 p3648 N71-36017

Determination of energy and size conformal parameters and application to excess properties of simple liquids
23 p3746 N71-36713

Effect of synchronized capture during bunching of beam outside separatrix calculated by analog computer
[JFVE-SKU-70-20] 23 p3807 N71-37141

Ion detector studies of vibrational and rotational excitation levels of molecular nitrogen target in low energy atomic collisions
[NIP-10853] 23 p3811 N71-37173

Development of nonequilibrium thermodynamics and application to systems having singular surfaces containing mass, internal energy balance, and entropy
23 p3807 N71-37566

Nucleon-nucleon potential for calculating binding energy of B-3 and d-d doublet scattering length
[DINP-F-1234] 24 p3949 N71-38311

Fast neutron time of flight techniques for studying proton-rich nuclei N-12, F-16, Mg-22, Si-26, and S-30 by means of (He-3, α) reactions
[AERE-R-6473] 24 p3975 N71-38359

Experimental evidence for shape transitions in nuclei demonstrated from quadrupole motion and even-even nuclei
[UR-MRL-40] 24 p3982 N71-38416

ENERGY LOSS
U ENERGY DISSIPATION
ENERGY METHODS
NT STRAIN ENERGY METHODS
Energetics analysis of correctable gyroscope stability
07 p1056 N71-17199

Measurement of low energy and high energy portion of π^0/π^+ in π^0/π^+ yields π^0/π^+ and π^0/π^+ decay
10 p1623 N71-21768

Statistical energy analysis for studying dynamic behavior of large, complex structures and acoustic spaces
[NASA-CR-110987] 17 p2789 N71-30208

ENERGY OF FORMATION
Noble-metal binary alloy friction experiments in sliding contact with iron and alloy free energy of formation effects on friction and wear
[NASA-TT-D-6311] 12 p1926 N71-23747

Dilatation formation energy effects on thermodynamic properties of solids
17 p2825 N71-29996

EMP measurements of indium oxide free energy of formation between 790 and 1230 K using zirconia electrolyte galvanic cell
[BM-R-7549] 22 p3550 N71-35289

ENERGY SPECTRA

ENERGY REQUIREMENTS
Outbound and inbound stage weight requirements for planetary sample return mission payload and energy requirements - graphs
[NASA-CR-114913] 09 p1464 N71-28276

Electrical power distribution system and energy consumption during long duration operation of space station simulator
16 p1533 N71-28975

Factors relevant to development of fuels and energy policies compatible with environmental control
17 p2861 N71-29471

Management planning in Sweden for natural gas as industrial energy source
18 p3028 N71-30522

ENERGY SOURCES
Heat release explosive processes and gas dynamics for high power energy conversion systems
[AD-717188] 10 p1664 N71-21783

Pulse generator for synchronizing or retriggering electronic signals without requiring separate external source
[NASA-CASE-XGS-03632] 12 p1887 N71-23311

Energy sources in US to achieve future electric energy needs and environmental compatibility requirements
17 p2743 N71-29852

Evaluation of laser systems for inducing nuclear fusion processes in fusion weapons and hydrogen energy sources
[ITA-4-4449] 17 p2758 N71-29911

Disk source energy and angular distribution calculations using gamma ray transport codes
20 p3327 N71-33954

High voltage large capacity switches as power sources for pulse generator
[DPF-DT-19] 22 p3559 N71-35348

Development and distribution of natural resources to satisfy energy requirements of US industry during the 1970's
[NRC-KC-8256] 22 p3700 N71-36393

ENERGY SPECTRA
NT ELECTRONIC SPECTRA
NT NEUTRON SPECTRA
Spectral power flux magnitude system for astronomical scaling
01 p0121 N71-10319

Cosmic radiations at extremely high energies
[AD-710633] 01 p0117 N71-10432

Quantum mechanics and electron exchange effects on excitation spectrum
01 p0096 N71-10524

Measurement of delayed neutron energy spectra
[RLO-2215-1] 01 p0099 N71-10717

Calculation and comparison of photon production spectrum from proton nucleus collisions in energy range 15 to 150 MeV
[NASA-CR-111121] 01 p0100 N71-10709

Energy spectra calculations of fission fragments and antineutrino values for targets of different thicknesses
[JINR-P3-5081] 02 p0277 N71-12134

Calculating energy spectrum and quasi-particle wave functions of spherical nuclei
[IAE-1855] 04 p0570 N71-13558

Energy spectra of alpha particles induced by 16 MeV neutrons in erbium isotopes
[JINR-1175] 04 p0571 N71-13647

Measuring energy spectrum of electrons from C-12 up to 16 MeV for three different excitation combinations at each of three values of momentum transfer
05 p0735 N71-14532

Standard method for protecting energy spectra
[NASA-TM-X-52943] 05 p0747 N71-15253

Astrophysical aspects of cosmic radiation, and radiation environment of earth
[NASA-CR-115850] 05 p0765 N71-15322

Design of experiments and spectra for HEAO to determine composition and spectra of high energy cosmic rays
[NASA-TM-X-65431] 06 p0942 N71-16602

Proton recoil measurements of Pulse source neutron spectra
[NASA-TM-X-52954] 06 p0922 N71-16608

Measurement of gamma ray energy spectrum of balloons altitudes
06 p0943 N71-16731

Energy spectrum in isothermal turbulent shear flow at large wave numbers
[AD-714856] 07 p1011 N71-17743

Quarks and pulsars at cosmic ray shower energies
[MPI-PAE/EXTRATER-47] 08 p1284 N71-18725

Low energy spectrum of excited states of odd nuclei with ground state spins
[ITF-70-47] 09 p1435 N71-28082

Energy spectra of multi-charged nuclei measured by Cerenkov counters onboard Cosmos 225 satellite
[NASA-TT-F-13511] 09 p1462 N71-28042

Quasi-elastic scattering from calcium 40 and calcium 48 excitation spectra
09 p1442 N71-28044

Electron density energy spectra of galactic cosmic rays from circular and elliptic cylindrical and ellipsoidal sources
[CEA-R-3674/E] 09 p1465 N71-28041

Proton precipitation above 100 keV observed by ESRO 1 satellite in noon-midnight meridian 10 p1550 N71-21157

ESRO 1 satellite observation of variations and fine structure in flux density and angular distribution of electrons with energies above 40 keV 10 p1550 N71-21158

Measurements of 1 to 30 MeV protons during solar proton events taken onboard ESRO 1 satellite 10 p1550 N71-21160

High energy muons in cosmic radiation showers 10 p1554 N71-21552

Photoconductivity energy spectra of defects in irradiated gallium arsenide monocrystals [NLL-RTS-5984] 10 p1637 N71-21830

Energy spectra of backscattered electrons and positrons by Monte Carlo calculations [UCRL-19719] 12 p1968 N71-23155

Energy deposition in lasers, computer revised code including multifrequency calculation, bodies of revolution, and geometry debug facility [AD-718302] 12 p1932 N71-23319

Polar diurnal variations of proton belts and precipitation detected by ESRO 1 satellite 12 p1910 N71-23571

Magnetic energy spectra of deuterons and tritons in product nuclei decay of helium irradiated lithium 7-beryllium 8 and lithium 7-beryllium 7 targets 12 p1971 N71-23882

Balloon study on auroral nitrogen emission and bromestrahling a rays produced by electron precipitation 12 p1994 N71-24274

Center of mass energies for C 12 plus C 12 and C 12 plus O 16 reaction cross sections [ANU-P515] 12 p1979 N71-24302

Mass and energy spectrum analyses for photon, neutral pion, and eta-meson interactions based on Monte Carlo method [JINR-EI-5349] 13 p2129 N71-24685

Gamma ray spectra from neutral pion decay and model for numerical calculation of spectrum below 1 GeV, for gamma rays produced by galactic cosmic ray interactions 13 p2159 N71-24769

Balloon flight measurements of gamma ray spectra of celestial large energy sources 13 p2161 N71-25199

Chemical composition and energy spectra of primary cosmic radiation [AD-719864] 14 p2334 N71-25911

Atlas of momentum spectra of secondary particles produced in proton proton and proton nucleus collisions [NP-18660] 14 p2311 N71-26693

Qualitative morphology of polar cap absorption events using riometers and periodic variations in energy spectra and proton flux density in ionospheric absorption forecasting [AD-721183] 15 p2395 N71-26843

Quarks, large transverse momenta, and energy spectra of air showers [MPI-PAR/EXTRATER-47] 15 p2513 N71-27049

Energy spectra of prompt and delayed fission neutrons and reactor physics [ANL-7747] 15 p2469 N71-27369

Radioactive characteristics for studying fission products - beta radiation and conversion electrons [CEA-N-1372] 15 p2471 N71-27409

Potential high energy resolution iodine negative ion source [AD-720871] 15 p2473 N71-27445

Dose distribution calculations from tritium and iodine 125 sources using energy spectra [JUL-688-ME] 15 p2475 N71-27466

Positive to negative pion ratios as functions of incident photon energy using Cerenkov counter, spark chamber, and magnetic spectrometry of pion photoproduction 15 p2476 N71-27573

Nuclear resonance fluorescence and neutron capture gamma rays for studying excited levels in nickel and cadmium isotopes 15 p2478 N71-27627

Nuclear composition for several multicharged nuclei and energy spectra for hydrogen, helium, and medium nuclei measured in solar particle event [NASA-TM-X-65573] 15 p2514 N71-27645

Photoelectron energy and angular distribution spectra from lithium 6 and lithium 7 states 15 p2479 N71-27656

Differential cross sections for elastic scattering of neutrons from carbon measured at primary energies between 0.30 and 2.00 MeV in steps of 50 keV [EUR-4358-E] 15 p2491 N71-27899

Effect of energy spectrum on nuclear matter binding energy 15 p2493 N71-27943

HEAO CalT crystal activation for measurement of galactic gamma and cosmic particle energy spectra [RM-507] 16 p2674 N71-28167

Cosmic ray proton and helium measurements over half solar cycle 1965 to 1970 with consideration of low energy portion of cosmic ray spectrum [NASA-CR-119013] 16 p2674 N71-28308

Mathematical model for composite magnetic and electrostatic charged particle beam analyzer transmission [NASA-TT-F-13617] 16 p2659 N71-29177

Measuring angular and energy distributions of electrons ejected from nitrogen using crossed molecular and electron beams 17 p2791 N71-29290

Apollo Telescope Mount experiment designed to study energy of sun from wavelength of 200 to 2000 ph /2 to 20 A/ using X ray source 17 p2730 N71-29320

Isothermal calorimetric determination of plutonium 239 half life based on alpha zero energy and recoil energy [RPF-1469] 17 p2799 N71-30020

Nuclear reactions of neutron irradiated sodium iodide 17 p2799 N71-30038

Electron and photon spectra and fluxes in liquid ionization chambers [NP-18433] 17 p2800 N71-30106

Measurement, autocorrelation, and variance evaluation of near ground atmospheric temperature and wind velocity [MITT-30] 18 p2948 N71-30385

Energy spectra of background radiation in universe for X ray and radio regions 18 p3003 N71-30846

Observations from Apollo 14 suprathermal ion detector including ionospheric ion density, mass and energy spectra during venting in LM cabin, large ion cloud, and ion resulting from impacts 18 p3011 N71-30962

Alpha-particle dosimeter with variable response tailored to energy distribution of alpha source [RE-4137] 18 p2924 N71-31124

Model of expanding universe interpreted as uniform 4-dimensional dilatation of space-time and corresponding contraction of kinetic energy parameters [ITF-70-105-E] 19 p3146 N71-31973

Quasiparticle model for calculating energy spectra of helium isotopes [UIV-2540-F] 19 p3149 N71-32110

Spectrometer for onboard measurement of ion energy spectra in plasma of solar wind and magnetosphere [NASA-TT-F-13762] 19 p3176 N71-32230

Argon ion-atom collision hypothesis investigated using coincidence methods to obtain fast electron energy spectrum with known scattering angle, ion energy, and charge state 19 p3160 N71-32667

Measurement of charged particle spectra in interplanetary space by Cerenkov counter on Pioneer 8 spacecraft 20 p3341 N71-33485

Energy spectrum of identified protons and excitation functions following decay of Al-23 [UCRL-20436] 20 p3322 N71-33793

Delayed neutron calculations of energy spectra and precursor emission probabilities following negative beta disintegration [LBGO-2943] 21 p3483 N71-34808

Buildup factors and energy spectra through lead/water slab layers for point isotropic sources utilizing radiation transport point matrix kernels [COO-2060-10] 21 p3486 N71-34838

Cosmic ray charge and energy spectra from OSO-3 experiments with details of detector design and operation [NASA-CR-121626] 21 p3503 N71-34953

Measurement of energy spectrum and solar neutrino flux [BNL-TR-418] 21 p3504 N71-34960

Factorization technique for calculating space energy synthesis in fast reactor 22 p3627 N71-35844

Single particle spectrum of O-17, O-16 and Ca-40 binding energies, and O and Ca isotope shifts for nucleon-nucleon interactions 22 p3631 N71-35873

Flux, energy spectra, and pitch angle distributions of precipitated low energy hydrogen and electrons from Nike-Tomahawk auroral hydrogen experiment [NASA-CR-121934] 22 p3648 N71-36155

Decay of high intensity isotropic turbulence investigated behind three different perforated plates [REPT-6] 23 p3749 N71-36792

Digital simulation of energy spectra and mean inelasticity coefficients of high energy particle interactions [ITT-3] 23 p3808 N71-37152

Monte Carlo method for sampling Klein-Nishina probability distribution for incident photon energies above 1 keV [LA-4663] 23 p3813 N71-37191

Energy tables of gamma rays from [n,gamma] produced nuclides for rapid identification [AASCTM-583] 23 p3817 N71-37226

Energy and charge spectra of cosmic rays [NASA-TT-F-13731] 24 p3920 N71-37935

Ion and electron energy spectra from neutral Ar and He beam collisions with Ar and He gas respectively below 220 eV [NYO-2101-37] 24 p3978 N71-38386

Experimental evidence for shape transitions in nuclei demonstrated from quadrupole motion and even-even nuclei 24 p3982 N71-38811

Particle intensities and energy spectra for galactic cosmic rays 24 p4010 N71-38911

ENERGY STORAGE

NT ELECTRIC ENERGY STORAGE

NT HEAT STORAGE

Energy storage in superconducting short solenoid of circular cross sections [LA-TR-70-9] 02 p0275 N71-11913

Superconducting coil for storing energy and returning it in about one millisecond [LA-TR-70-11] 02 p0286 N71-11994

Low temperature tunneling and second energy gap in superconducting niobium [AD-712072] 02 p0286 N71-12009

Energy accumulation in packing of regenerator [ANL-TRANS-436] 03 p0468 N71-12094

Energy storage mode interaction mechanisms of magnetohydrodynamic waves in sea water 04 p0593 N71-13724

Theoretical analysis of energy storage in dielectric pile-up and stress fields of dielectric cells [ORO-3108-102] 05 p0706 N71-13850

Describing research on dependence of plasma form parameters on energy storage increase in capacitor bank [SC-T-70-4046] 08 p1274 N71-10763

Energy storage and release capabilities of superconductors at high power [NASA-TT-F-13585] 12 p1860 N71-23913

Research and development, test techniques, and new technology for nickel cadmium batteries, silver zinc cells, and energy storage 16 p2540 N71-20574

Use of semiconductor for energy storage, discharge, and transfer processes [CEA-COMP-17346] 22 p3559 N71-35547

Superconducting inductive energy accumulator in standby electrical energy source, as energy source for load factoring in power systems, or as source for high powered electric pulses [JPRS-54051] 23 p3710 N71-34448

ENERGY STORAGE DEVICES

U ENERGY STORAGE

U ENERGY TRANSFER

NT COUPLING CIRCUITS

NT LINEAR ENERGY TRANSFER (LET)

Energy dependent beta-gamma circular polarization and nuclear matrix elements of Rb-86 [COO-1746-42] 01 p0099 N71-10716

Energy transfer in solids 01 p0112 N71-10739

Energy transfer process in molecular lasers [AD-711614] 02 p0238 N71-11146

Determination of energy transfer in char zone of charring absorber 02 p0175 N71-11232

Infrared measurement on vibrational relaxation rate of carbon monoxide in argon shock wave [NASA-CR-111370] 02 p0201 N71-11413

Development of SEPOR energy probes for power transient measurement [KFK-1033] 02 p0226 N71-11510

Manufacturing improvement program establishing applications and limitations in closed-die forging [AD-711544] 02 p0234 N71-11675

High energy forming research including explosive forming, explosive welding, and pressure welding [AD-711548] 02 p0234 N71-11699

Energy and phase changes of particle growth in homogeneous magnetic field and perpendicularly propagating electrostatic wave [PB-19590] 02 p0277 N71-12113

Energy transfer from large amplitude whistler to electrostatic wave by trapped particles [NIT-3785-11] 03 p0421 N71-12844

Energy transfer in interactions between laser beams and solid deuterium 04 p0574 N71-13670

Energy transferred to zirconium nitride by neutron irradiation [CEA-N-1332] 04 p0575 N71-13684

Level crossing analysis on hyperfine structure of europium isotopes 04 p0576 N71-13689

Energy storage mode interaction mechanisms of magnetohydrodynamic waves in sea water 04 p0593 N71-13724

Using numerical techniques to calculate inelastic response of primary containment to high energy asymmetric excursion [ANL-7499] 04 p0584 N71-14157

Mass and energy exchange between interacting water channels [WW-15-R-158] 04 p0539 N71-14237

Energy transfer between alphas and electronically excited inert gas atoms and ions [IRE-4001] 04 p0590 N71-14332

Energy equations describing physical processes in ground atmosphere 05 p0717 N71-15144

SUBJECT INDEX

Mathematical models for energy transfer mechanisms between wind and ocean waves (AD-713469) 06 p0678 N71-13521

Angular distributions of nuclear transfer reactions between heavy ions (NP-18448) 06 p0918 N71-16302

Energy transfer in hot molecules (AD-714108) 06 p0920 N71-16269

Quantitative studies by optical spectroscopy of energy exchange mechanisms in simple gases and solids (AD-714008) 06 p0922 N71-16482

Unimolecular decomposition and intramolecular energy relaxation in super-high pressure region (AD-714020) 06 p0923 N71-16609

Classical relaxation of Br₂ molecules in argon heat bath (NASA-TN-D-6180) 07 p1073 N71-17413

Thermal and electric energy transfer within life support systems (NASA-TN-D-6207) 07 p0986 N71-17592

Measuring vibration-vibration energy exchange probability in nitrogen-carbon dioxide-argon mixtures in a shock tube (NASA-CR-1116814) 06 p1244 N71-19037

Measuring near resonant vibrational energy transfer in shock heated mixtures of N₂ and N₂O (AD-714020) 06 p1244 N71-19038

Factors influencing gain in neodymium doped laser glass (AD-714020) 06 p1244 N71-19038

Flash photolysis system for studying gas laser energy transfer mechanisms (AD-716009) 09 p1396 N71-19651

Biochemical molecular model for metabolic energy transfer from mammalian organs to central nervous system (AD-716009) 09 p1396 N71-19651

Calculation of energy transfer in slowing down reactions with controlled fusion systems (AD-716594) 09 p1499 N71-20014

Scattering distributions for argon incident on fresh epitaxial silver films (NASA-CR-117180) 09 p1438 N71-20194

Plasma energy transfer dynamics (AD-716594) 09 p1499 N71-20014

Stress-strain analysis of energy transfer in plastic deformation of rod subjected to axial impact (AD-717323) 11 p1633 N71-21864

Decay in fluorescence from asymmetric stretching vibrational level of CO₂ after excitation by Q switched CO₂ laser (AD-717323) 11 p1633 N71-21864

Ionization cross sections for helium and neon positive ion collisions with nitrogen, oxygen, and carbon dioxide molecules at 1 to 200 eV (AD-717699) 11 p1808 N71-22711

Molecular relaxation of ultrasonic nitrogen oscillators in simulated expansion flow environment with vibration-vibration and vibration-translation energy exchange (AD-717699) 11 p1808 N71-22711

Vibrational energy transfer in rapid expansions of N₂, CO₂, and Ar mixtures, using arc heating (AD-718131) 12 p1954 N71-24011

Developmental history of adiabatic inviscid inviscid controllers to radiation energy transfer and convective mechanisms (NASA-TM-X-64498) 12 p1958 N71-24056

Vibration energy transfer in N₂-CO and N₂-NO mixtures (AD-718093) 12 p1976 N71-24160

Transfer of energy from electron beam particles to longitudinal plasma waves studied by means of plasma kinetic theory (AD-718093) 12 p1976 N71-24160

Criticality for energy dependent transport in slab geometry (AD-718093) 12 p1976 N71-24160

Energy transfer spectra in locally isotropic grid turbulence determined from third-order correlation functions (AD-718093) 12 p1976 N71-24160

Energy dependence of charge exchange reactions in helium and argon ionization by exchange collisions (KFK-1265) 14 p2315 N71-36733

Beam transport program BOPTIC in FORTRAN 4 for analyzing monoenergetic charged particle beams in positron acceleration system (IAAC-PT-544) 15 p3459 N71-36901

Atmospheric energy transport over North America calculated from radiocarbon data (AD-718093) 12 p1976 N71-24160

Micrometeorological investigation of momentum, energy, and mass transfers above vegetative surfaces with von Karman constant, diabatic profile functions and eddy-transfer coefficients (AD-721301) 16 p2625 N71-28225

Submicron transfer reaction mechanisms and spectra produced by C-12, Ne-22, and Ar-40 ions on Au, Pt, and Bi (JHEP-PT-5495) 16 p2647 N71-28226

Atmospheric budget equations for mass, momentum, and energy derived for Barbados Oceanographic and Meteorological Analysis Program (BOMAP) (JOM-71-00195) 16 p2625 N71-28313

Energy exchange at ice cap snow surface during summer (AD-721490) 16 p2638 N71-29081

Infrared absorption and energy transport in gases including sulfur dioxide (AD-721490) 16 p2638 N71-29081

Convective ion-molecule reactions in cyclotron investigated by charge exchange mass spectrometry as function of energy transfer during initial ionization (AD-722470) 18 p2084 N71-30719

Half-cosine wave pulse firing of electroexplosive devices (NASA-CR-119320) 18 p3025 N71-31193

Digital measurements of neutron transfer functions on thermal reactor configurations by reactivity moderator (CEA-N-1405) 19 p3137 N71-32070

Expression for kinetic energy transformed into work, heat, and sound during impact of spherical reactor containment vessel model and concrete block (NASA-TM-X-67917) 20 p3358 N71-33316

Energy transport velocity model for classification of all possible acoustic modes propagating in uniform, inviscid, homogeneous, time independent ducted air flow (ONERA-TP-945) 20 p3351 N71-33530

Analytical solution of nonlinear heat conduction equation including influence of internal heat generation (AD-722470) 18 p2084 N71-30719

Energy effects in three particle proximity scattering in beryllium isotope decay (THESES-4469) 20 p3323 N71-33844

Time dependent correlations in linear Heisenberg chains (AD-722470) 18 p2084 N71-30719

Numerical analysis of momentum or energy exchange in turbulent flow wake by multiplying velocity or enthalpy between two regions in wake (AD-722470) 18 p2084 N71-30719

Electron beam measurement of molecular vibrational energy transfer in expanding mixtures of N₂ and CO₂ heated by electric arc (NASA-TN-D-6445) 21 p3436 N71-34446

Monte Carlo program for photon and electron transport calculations (ORNL-TR-2464) 21 p3478 N71-34767

Eddy formation in energy transport of electromagnetic wave fields in waveguide (AD-722470) 18 p2084 N71-30719

Orientation dependence in triplet-triplet energy transfer determined by magnetophotoselection techniques (AD-726563) 22 p3552 N71-35296

Use of semiconductors for energy storage, discharge, and transfer processes (CEA-CONF-1736) 22 p3559 N71-35347

Nuclear magnetic susceptibility in ice solid He-3 with Neel temperature and negative exchange interaction energy calculations and impurity effects (AD-726563) 22 p3552 N71-35296

Saturation effects in cyclotron resonance oscillators with emphasis on generation and amplification of millimeter waves (NASA-CR-121294) 23 p3731 N71-36594

FORTRAN 4 program for generating fast neutron spectra and average multiplicity constants utilizing cross section data from library - FUSION (IN-1435) 23 p3815 N71-37210

Surface reactions between silver nuclei and carbon and nitrogen projectiles (NP-18874) 24 p3975 N71-38360

Energy transfer cross sections for electrons ejected from hydrogen and nitrogen molecules by fast proton impacts (BNWL-SA-3853) 24 p3978 N71-38385

ENGINE CONTROL

NT ROCKET ENGINE CONTROL

Controlled supersonic inlet-engine control using overboard bypass doors and engine speed to control normal shock position (NASA-TN-D-6019) 03 p0449 N71-13080

Direct current electromotive system for regenerative braking of electric motor (NASA-CASE-XMP-0106) 06 p0826 N71-16030

Development of digital system for on-line control of airbreathing propulsion systems (NASA-TM-X-2168) 07 p1102 N71-17505

Dynamics and control of supersonic propulsion systems (AD-726563) 22 p3552 N71-35296

Supersonic inlet engine control using engine speed as primary variable for controlling normal shock position (NASA-TN-D-6021) 10 p1438 N71-28674

ENGINE COOLANTS

Destructive effects on metal surfaces in diesel engines due to liquid cavitation corrosion caused by opposite oscillating plates (AD-726563) 22 p3552 N71-35296

Destruction effects on metal surfaces in diesel engines due to liquid cavitation corrosion caused by opposite oscillating plates (AD-726563) 22 p3552 N71-35296

Nozzle and cavity wall cooling limitations on specific impulse of gas-core nuclear rocket engines (NASA-TM-X-67923) 22 p3621 N71-35795

ENGINE DESIGN

Microstrip motor design (AD-711737) 01 p0031 N71-16160

Aircraft gas turbine engine design and construction (AD-711737) 01 p0116 N71-16853

Value engineering effects on engine design and production in aerospace industry (AD-711737) 01 p0116 N71-16853

Development of cellulosic thrust system with array of nozzles (NASA-CR-111417) 02 p0291 N71-12876

Evaluation of range and distortion tolerance for high Mach number transonic fan stages - Vol. 1 (NASA-CR-72707-VOL-1) 03 p0663 N71-14831

Evaluation of range and distortion tolerance for high Mach number transonic fan stages - Vol. 2 (NASA-CR-72707-VOL-2) 03 p0663 N71-14832

Design of gas turbine engines for high operating temperatures (AD-711737) 01 p0116 N71-16853

Operational design criteria for gas turbine engines (AD-711737) 01 p0116 N71-16853

Computer program for design and analysis of V/STOL tip turbine fans (NASA-TN-D-6161) 07 p1103 N71-17641

Characteristics of fans and compressors for aircraft turbine engines (AD-711737) 01 p0116 N71-16853

Aerodynamic characteristics of advanced turbine engines (AD-711737) 01 p0116 N71-16853

Design requirements for air breathing aircraft engines (AD-716496) 09 p1458 N71-19488

Determining amount of smoke in exhaust of gas turbine engines (NASA-CR-117081) 09 p1459 N71-20020

Performance tests and characteristics of short length, double annular ram induction turbojet combustion chambers for supersonic flight (NASA-TN-D-6254) 09 p1459 N71-20291

Design and development of gas turbine combustion unit with variable guide vanes for introducing direct air into combustion gases (NASA-CASE-XLE-1047-1) 09 p1459 N71-20030

Construction and method of arranging pinholes of ion engines to form cluster thereby increasing efficiency and control by decreasing heat radiated to space (NASA-CASE-XNP-02923) 11 p1821 N71-23881

Fundamentals of aircraft gas turbine engines (AD-719913) 14 p2331 N71-28808

Aircraft gas turbine combustion chamber design (NAL-TR-508) 14 p2332 N71-28296

Analysis of first stage turbine cluster vane and rotor blade cooling designs for application in high speed aircraft (NASA-TM-X-7182) 14 p2396 N71-28355

Design and performance of gas turbine engines for helicopters and surface transport vehicles (AD-722253) 17 p2834 N71-29500

Design operating process of turbojet, turboprop, and turboshaft aircraft engines (AD-722253) 17 p2834 N71-29500

Space vehicle auxiliary power unit design selection and performance evaluation (AD-722253) 17 p2834 N71-29500

Synthesis, selection, and design of optimal auxiliary power unit for space shuttle vehicle (BC-71-25) 17 p2838 N71-29606

Structure, operation, and economics of rocket for meteorological sounding as designed by Polish organization (AD-722253) 17 p2838 N71-29606

Design, development, and characteristics of pulsejet engines without flap valves (AD-722253) 17 p2838 N71-29606

Engine dynamics requirements implied by thrust modulation control for VTOL aircraft (NASA-TT-P-17575) 18 p3002 N71-31455

Internal aerodynamic design manual considering internal air flow system effect on aircraft performance including bibliography (AD-722823) 19 p3173 N71-32059

Aerodynamic design manual considering internal air flow system effects on aircraft performance (AD-723824) 19 p3173 N71-32060

Internal aerodynamics manual containing tabulations for calculating internal combustion engine thermodynamic properties (AD-723824) 19 p3173 N71-32060

Engine and stage design criteria on sizing requirements of complete stage for LOX/Hydrogen engine (NASA-CR-121864) 23 p3621 N71-35795

Design and characteristics of radial inflow turbine stage for use as an alternative to stage of Brayton cycle turbo-alternator compressor unit (NASA-CR-72000) 23 p3630 N71-33772

Development of computer program for analyzing flow conditions and performance of turbomachinery at design and off-design conditions (MEJA-71-5) 23 p3840 N71-37385

Supersonic combustion chemistry and mixing of high energy density fuels related to advanced air-breathing engine design, using boron particles (AD-727702) 24 p4080 N71-38530

Analysis of gas turbine design and application to aircraft operation with description of components, safety factors, and vibration problems
[AD-727183] 24 p4001 N71-38358

ENGINE FAILURE

Investigating aircraft crash landing caused by engine failure and aircrew errors
[NTSB-AAR-70-17] 07 p0969 N71-17063

System for monitoring presence of neutrals in streams of ions - ion engine control
[NASA-CASE-XNP-02592] 09 p1444 N71-20518

ENGINE INLETS

Measuring distortion characteristics at engine face station of axisymmetric inlet
[NASA-CR-1644] 03 p0310 N71-12211

Coupled supersonic inlet-engine control using overboard bypass doors and engine speed to control normal shock position
[NASA-TN-D-6019] 03 p0449 N71-13080

March 2 slender wing boundary layer effects on Concorde aircraft engine inlets
[ARC-CP-1122] 06 p0792 N71-15708

Ingestion of debris into aircraft engine inlets during takeoff
[ARC-CP-1114] 07 p0969 N71-17084

Design and characteristics of supersonic cruise inlets
09 p1458 N71-19460

Effects of engine inlet disturbances on engine stall performance
09 p1458 N71-19460

Supersonic inlet engine control using engine speed as primary variable for controlling normal shock position
[NASA-TN-D-6021] 10 p1638 N71-20674

Experimental investigation of large scale, two dimensional, mixed compression inlet system
[NASA-TN-D-6392] 15 p2363 N71-26985

Design and characteristics of supersonic inlet control for minimizing inlet unstart
[NASA-TN-D-6408] 17 p2839 N71-30072

Velocity profile control tests of diffuser wall bleed to control combustor inlet airflow distribution
[NASA-TN-D-6435] 18 p3000 N71-30817

ENGINE MONITORING INSTRUMENTS
System for monitoring presence of neutrals in streams of ions - ion engine control
[NASA-CASE-XNP-02592] 09 p1444 N71-20518

ENGINE NOISE
NT ROCKET ENGINE NOISE
Measurement of engine exhaust noise during ground operation of XB-70 aircraft
[NASA-TN-D-7043] 06 p0794 N71-15820

Noise reduction of Boeing 707 during landing approach by modifying turbofan nacelle with polyimide fiber glass acoustic sandwich materials
[NASA-CR-1713] 06 p0794 N71-15964

Development of acoustic lining for turbofan nacelle modification to minimize fan compressor noise radiation
[NASA-CR-1712] 07 p0972 N71-17591

Flightworthy nacelle development to minimize fan compressor noise radiation - Vol. 1
[NASA-CR-1714] 07 p0972 N71-17668

Jet aircraft noise reduction near airports
07 p1133 N71-18079

Sources and characteristics of aircraft noise for conventional and V/STOL aircraft
09 p1320 N71-19457

Inlet plenum chamber noise measurement comparison of 20 inch diameter fan rotors with aspect ratios of 3.6 and 6.6
[NASA-TN-D-7191] 09 p1316 N71-19707

Solution of Lighthill gas model wave equation for engine noise generation in circular jets using cylindrical coordinate system
[DLR-FB-70-57] 11 p1669 N71-22070

Theoretical analysis of jet mixing under influence of nonconstant pressure gradient
[ARL/ME-127] 11 p1821 N71-22503

Turbofan engine designs and tests for engine noise reduction
[NASA-CR-72967-VOL-1] 16 p2673 N71-29187

Low pressure turbofan rotor, stator, frame, and exhaust nozzle designs for turbofan engine noise reduction including acoustics and engine tests
[NASA-CR-72967-VOL-2] 16 p2673 N71-29188

Application of noise reduction technology to design of propulsion system for subsonic civil transport aircraft
[NASA-TN-X-67884] 18 p3001 N71-31191

Evaluating reciprocating combustion engine noises at two different places using subjective and objective measurements
[NASA-TT-F-13943] 22 p3628 N71-35849

ENGINE PARTS

Destructive effects on metal surfaces in diesel engines due to liquid cavitation corrosion caused by opposite oscillating plates
02 p0231 N71-11583

Destruction effects on metal surfaces in diesel engines due to liquid cavitation corrosion caused by opposite oscillating plates
02 p0231 N71-11584

Advanced technology for production of aerospace engines - conference
[AGARD-CP-64-70] 02 p0289 N71-11626

Application of corrugated core sandwich structures to powerplant components
02 p0300 N71-11636

X ray fluorescence analysis for quality control of gas turbine aircraft engine parts during manufacture and overhaul
02 p0232 N71-11641

Residual stress measurements and heat treatments for electron beam welding of rotating turbine engine parts
02 p0232 N71-11644

Electron bombardment utilized for welding diverse turbomachinery and turboreactor parts
02 p0233 N71-11645

Use of lathes for fabrication of turbomachinery parts
02 p0233 N71-11648

Phenomena taking place in surface layers of metal of engine components during friction
[AD-714063] 06 p0941 N71-16305

Components for low weight/small volume aircraft gas turbine engines
15 p2512 N71-26935

ENGINE STARTERS
Motor starting techniques for 2-15 kW Brayton space power system
[NASA-TM-X-67819] 13 p2117 N71-24691

ENGINE TESTING LABORATORIES
Holography used to determine water droplet characteristics in engine test facility
[AD-715916] 08 p1281 N71-18488

ENGINE TESTS
NT COLD FLOW TESTS
NT PREFIRING TESTS
NT SPACE ELECTRIC ROCKET TESTS
NT STATIC FIRING

FLOX/polyethylene hybrid propellant rocket engine tests
[BMW-FB-W-70-54] 07 p1099 N71-17331

Effects of specific speed on experimental performance of radial inflow turbine
[NASA-TN-D-6182] 07 p0967 N71-17354

Acoustic attenuation determined experimentally during engine ground tests of XB-70 airplanes and comparison with predictions
[NASA-TM-X-2223] 07 p0974 N71-17951

Effects of turbojet engine unstart on engine operation and characteristics of stall propagation through compressor and inlet system
[NASA-TM-X-2192] 07 p1104 N71-18138

Engine bombardment hollow cathode ion thruster performance
[NASA-CR-116828] 08 p1281 N71-19178

Endurance test of turbine wheel with uncooled chromium alloy blades
[ARL/ME-320] 12 p1991 N71-24322

Qualification tests of tower jetison motors for Apollo spacecraft program launch escape systems
[NASA-TN-D-6293] 13 p2156 N71-25033

Cathode insulator modifications of radiation cooled MPD arc thruster tested in power range of 9.8 to 46.4 kW using ammonium as principal propellant
[NASA-CR-72891] 14 p2331 N71-25770

Turbofan engine designs and tests for engine noise reduction
[NASA-CR-72967-VOL-1] 16 p2673 N71-29187

Low pressure turbofan rotor, stator, frame, and exhaust nozzle designs for turbofan engine noise reduction including acoustics and engine tests
[NASA-CR-72967-VOL-2] 16 p2673 N71-29188

Exhaust emission characteristics of diesel engines, noting emissions of smoke, odor, hydrocarbons, nitrogen oxides, carbon monoxide, and aldehydes
[BM-R1-7330] 19 p3174 N71-32492

Microprocessor extended range thrust test stand design and common engine calibrating standards
[NASA-TN-D-7029] 20 p3339 N71-33396

Transonic testing of double flux engine nacelles with two separate models for air intake and afterbody
[ONERA-TP-943] 20 p3207 N71-33794

ENGINEERING
Bibliography on physical, life, and social sciences and engineering
02 p0307 N71-11382

Naval Scientific and Technical Information Centre bulletin for 1970 - bibliography of accessioned books and selected abstracts of journal articles
06 p1309 N71-19325

KWIC index of VS voluntary engineering standards
[NBS-SPEC-PUBL-329] 13 p2687 N71-24977

Impact of U.S. conversion to metric system units of measurement on current engineering standards
[NBS-SP-345-11] 19 p3106 N71-32396

Dynamic model for optimization of wide utility in engineering sciences
22 p3608 N71-35699

Chemistry, physics, metallurgy, and engineering related problems in provision and use of defense material
23 p3856 N71-37488

ENGINEERING DEVELOPMENT
U PRODUCT DEVELOPMENT

ENGINEERING DRAWINGS

Design criteria for arbitrary diffusers
[AD-709909] 01 p0040 N71-10404

Graphic illustration of lifting body design
[NASA-CASE-FRC-10063] 03 p0311 N71-12217

Specifications and drawings for semipassive optical communication system
[NASA-CASE-XLA-01090] 03 p0334 N71-12209

Conceptual design of beam transport magnets for beam line 1
[TRI-70-1] 03 p0359 N71-13110

Engineering drawings for chemiluminescent camera
[PB-194118] 05 p0683 N71-14813

Method of making molded electric connector for use with flat conductor cables
[NASA-CASE-XMF-03498] 06 p0864 N71-15986

Engineering drawing lists for solid state sequencer system in command module and service module junction controller
[NASA-CR-114956] 10 p1635 N71-21428

Cruise scene visual attachment system assembly and detail design drawings for manned spacecraft or aircraft flight simulator
[NASA-CR-114303] 12 p1898 N71-34138

Graphic computer program for plotting engineering drawings
[REPT-70-8] 13 p0853 N71-25100

Requirement specifications for environmental laboratory test chamber complex design, fabrication, and testing
[NASA-CR-115007] 14 p2345 N71-26408

Engineering drawings and performance test data for transit time accelerometers
[AD-720880] 15 p2412 N71-27799

Engineering drawings for broadband radio frequency transformer using printed circuit strip transmission line techniques
[RAE-TN-70063] 17 p2724 N71-29114

Draft designing of vertical takeoff and landing aircraft
[AD-726572] 22 p3540 N71-35219

Engineering drawings of prototype restraint system for repair and maintenance by astronaut under weightless conditions - Vol. 2
[NASA-TN-119922] 23 p3762 N71-30817

Design of snap-8 electrical protective system module including fabrication and assembly drawings
[NASA-CR-72938] 24 p3960 N71-36510

Numerical analysis and design of thin walled shaft of revolution
[AD-727859] 24 p4027 N71-38731

ENGINEERING MANAGEMENT
Discussion of symbols and units of measurement in choosing metric system for international use
[AARE-TECH-425] 13 p2188 N71-24460

Engineering, finance, and personnel management methods and computer techniques for cost reduction and reliability in project planning
[NASA-SP-5933/01] 18 p3031 N71-31516

Model for technology transfer from advanced country to underdeveloped country
[P-4509] 19 p3196 N71-32294

ENGINEERING TEST REACTORS
Calculation of ETR loop irradiation test fin power of fuel elements
13 p2114 N71-24533

Fuel capsule designs for thermal and fast neutron irradiation of JUP/P in MTR/ETR and EBR 2
13 p2114 N71-24540

Procedure for calculating certain parameters of heat producing elements of VVER type
[LAE-1942] 13 p2119 N71-24007

ENGINES
NT AIR BREATHING ENGINES
NT ARC JET ENGINES
NT BOOSTER ROCKET ENGINES
NT BRISTOL-SIDDELEY OLYMPUS 593 ENGINE

NT CESIUM ENGINES
NT DIESEL ENGINES
NT DUCTED FAN ENGINES
NT ELECTRIC ROCKET ENGINES
NT ELECTROSTATIC ENGINES
NT GAS TURBINE ENGINES
NT HELICOPTER ENGINES
NT HYBRID PROPELLANT ROCKET ENGINES
NT HYDRAZINE ENGINES
NT HYDROGEN OXYGEN ENGINES
NT INTERNAL COMBUSTION ENGINES
NT ION ENGINES
NT J-2 ENGINE
NT J-57 ENGINE
NT J-85 ENGINE
NT JET ENGINES
NT LIQUID PROPELLANT ROCKET ENGINES
NT NUCLEAR ENGINE FOR ROCKET VEHICLES
NT NUCLEAR ROCKET ENGINES
NT PISTON ENGINES
NT PLASMA ENGINES
NT PULSEJET ENGINES
NT RAMJET ENGINES
NT RETROCKET ENGINES

SUBJECT INDEX

- NT ROCKET ENGINES**
NT SOLID PROPELLANT ROCKET ENGINES
NT SUPERSONIC COMBUSTION RAMJET ENGINES
 Application of wetting methods and treatment of metal surfaces to improve corrosion resistance and dimensional build up in engine production
 02 p0233 N71-11651
 Fabrication techniques of compact fluidic control equipment for aerospace engines
 02 p0203 N71-11654
 Time resolved measurements of exhaust gas temperature, mass flow rate, and hydrocarbon concentration of spark ignition engines
 14 p2353 N71-26004
- ENGRAVING**
 Wind tunnel tests to determine helical engraving effects on aerodynamic stability of standard ammunition and models
 (AD-719235) 13 p2191 N71-24846
- ENRICHMENT**
U AUGMENTATION
ENLARGING
U EXPANSION
 Development of processes considered for European uranium enrichment and discussion of technical and economic aspects of three methods
 (ILL-CA-TRANS-249[3091.9F]) 24 p3930 N71-38043
- ENSKOG-CHAPMAN THEORY**
U CHAPMAN-ENSKOG THEORY
ENTHALPY
 Magnetic anemometer used as accelerometer for high Mach number, high enthalpy flow test facility
 (AD-710316) 01 p0038 N71-10186
 Mass-flux probe as useful diagnostic tool in high Mach number and high enthalpy flows
 (NASA-TM-X-52974) 09 p1388 N71-19699
 Operational limitations of arc heaters caused by cathodic stagnation pressures
 (NASA-CR-117144) 09 p1484 N71-20250
 Heat content and specific heat of six rock types at temperatures to 1000 C
 (JBR-7503) 10 p1543 N71-20613
 Adiabatic calorimetric enthalpy measurements for alpha, beta, and gamma phases of U-238 and heats of alpha yields beta and beta yields gamma transformations
 (LA-4321) 12 p2009 N71-23173
 Statistical analyses on thermodynamic properties of deca gas normal paraffins
 12 p2013 N71-24278
 Conformal solution correlation representing excess volume, excess enthalpy, and excess Gibbs free energy for mixtures of simple liquids from argon to ethane
 12 p1873 N71-24309
 High temperature chromization of ferrochromic alloys
 (TT-70-58195) 14 p2270 N71-25677
 Activation enthalpy of carbon self diffusion in cubic carbides
 (LA-TR-71-13) 16 p2667 N71-28847
 Measuring technique for pressure, volume, enthalpy, and resistance of equilibrium thermodynamic states of liquid metals at high temperatures and pressures
 (UCRL-51035) 22 p3696 N71-36359
 Enthalpy, enthalpy, Gibbs free energy, and energy of atomization for gallium phosphide formation in electrochemical cells based on emf measurements
 (NLL-REE-TRANS-315[8036.625]) 23 p3780 N71-36937
 Radiative effects of high enthalpy gas streams over wedge simulating space vehicle reentering earth atmosphere at supersonic velocities
 24 p4033 N71-38776
- ENTHALPY-ENTROPY DIAGRAMS**
U MOLLIER DIAGRAM
ENTIRE FUNCTIONS
 Method for studying integral functionals of stochastic processes
 (AD-712408) 04 p0536 N71-13633
 Functional integrals to express dual resonance amplitudes
 (LPTHE-71/10) 12 p1950 N71-23807
 Lagrangian functional integral formulation of dual resonance amplitudes
 (LPTHE-71/25) 20 p3291 N71-33383
- ENTHOLOGY**
 Microdevice instrument for entomological investigations
 (AD-714773) 05 p0653 N71-14984
- ENTRAPMENT**
 Retention coefficient used for computation of two dimensional incompressible turbulent boundary layers
 (ARC-R/M-3643) 08 p1139 N71-18424

ENTRAPMENT

- Vapor volume entrained in liquid due to boundary layer boiling under reduced gravity conditions
 03 p0446 N71-13104
 High expansion foam for entrapping air bearing
 (DUN-SA-141) 06 p0876 N71-15869
 Laser beam interactions with thermal media in steady state and time-varying conditions including beam trapping, self-induced frequency modulation, lens effects, and beam aberration
 23 p3768 N71-36856

ENTROPY

- Heat capacity measurements of heavy rare earth trichlorohydrates during ionic entropies and crystal field splittings
 (CONF-700493-7) 03 p0467 N71-12868
 Theory and measurements of entropy
 (PB-192128) 05 p0783 N71-15170
 Measuring value of entropy on surface of body of revolution at nonzero angle of attack
 07 p0965 N71-16903
 Concentration effects on Gibbs free energy and entropy of mixing of binary fluids
 (NPL-DCS-6) 07 p1128 N71-17210
 Heat of formation, specific heat, entropy, and Gibbs free energy of some binary metal oxides
 (NPL-DCS-7) 13 p2184 N71-24372
 Quantum mechanical entropy in tensor product of Hilbert spaces
 20 p3364 N71-33381
 Heat of formation and entropy of formation of plutonium carbides
 (KFK-TR-71-22) 20 p3368 N71-33951
 Polymer entropic repulsion
 22 p3551 N71-35295
 Conditional mean information and conditional mean entropy
 22 p3606 N71-35681
 Entropy, enthalpy, Gibbs free energy, and energy of atomization for gallium phosphide formation in electrochemical cells based on emf measurements
 (NLL-REE-TRANS-315[8036.625]) 23 p3780 N71-36937
 Development of nonequilibrium thermodynamics and application to systems having singular surfaces containing mass, internal energy balance, and entropy
 23 p3867 N71-37566

ENVELOPES

- Symmetry properties of cycloids and envelope curves
 03 p0401 N71-13394

ENVIRONMENT MODELS

- Mass transfer model for external spacecraft contamination and preventive measures
 09 p1334 N71-20205
 Evapotranspiration hydrological cycle modeling in Great Plains
 13 p2072 N71-25010
 Irrigation-oriented evapotranspiration models for Great Plains to aid farmers
 13 p2072 N71-25012
 Evapotranspiration components of watershed models for Great Plains, using mathematical models
 13 p2073 N71-25014
 Remote sensing in evapotranspiration research on Great Plains and three environment models
 (NASA-CR-118184) 13 p2073 N71-25015
 Water balance data for Great Plains and evapotranspiration reduction and model
 13 p2074 N71-25023
 Numerical solutions of differential equations for ecosystem models
 (ORNL-IBP-70-4) 13 p2104 N71-25428
 Functions of environmental data collection and processing facility, project management, data base maintenance, information retrieval, and environmental simulation system
 (AD-720592) 14 p2360 N71-26451

ENVIRONMENT POLLUTION

- NT AIR POLLUTION**
NT WATER POLLUTION
 Potential applications of NASA technology to solid waste environmental problems
 (NASA-CR-111610) 03 p0469 N71-12735
 Assessment of environmental hazard from flammability product releases
 (AHSB/R-135) 03 p0415 N71-12887
 Nuclear Safety Program at ORNL with emphasis on environment pollution
 (ORNL-TM-3601) 04 p0558 N71-14164
 Effects of worldwide power requirements on environment
 (CONF-700810-37) 04 p0480 N71-14473
 Model case studies of effects of DDT on human environment
 (PB-194413) 04 p0481 N71-14479
 Annotated bibliography of information facilities and data resources available to Environmental Health Service on environment pollution
 (PB-194414) 04 p0481 N71-14480
 Investigating relationship of man and biosphere with respect to food production and toxic chemical pollution
 (JPRS-53235) 07 p0981 N71-17429

ENVIRONMENT SIMULATION

- Hygienic effects of toxic chemical pollution on biosphere
 07 p0981 N71-17431
 Congressional hearings on proposed legislation relating to water pollution control
 07 p0100 N71-17540
 Environmental impact of supersonic transport
 07 p0972 N71-17545
 Thermodynamic processes related to pollution and environmental degradation
 (NASA-TM-X-63492) 12 p2010 N71-23346
 Remote sensing methods for terrain analysis, mineral deposits, and assessment of flammability product contamination of environment using gamma ray signatures for Thomas project
 (AD-718519) 12 p1913 N71-23808
 Effects of boron concentration in water on environment pollution
 (IVA-33) 18 p2882 N71-30598
 Environment pollution research and development cooperation in Norway, Sweden, Finland, and Denmark
 18 p3038 N71-30645
 Federal programs for air, water, and solid waste pollution control
 19 p3198 N71-32653
 Bibliography of literature on environmental pollution, noise pollution, and ear protection devices
 (AD-724656) 20 p3226 N71-33008
 Development of scientific principles of protecting and transforming nature for improving environment and optimal use of natural conditions
 (JPRS-53743) 20 p3223 N71-33501
 Annotated bibliography on noise pollution-sonic booms
 (AD-722910) 21 p3376 N71-34023
 Government, industry, banking, conservation, and law in preservation of environmental quality
 (NASA-CR-121637) 21 p3414 N71-34294
 Mathematical modeling techniques in analysis of environmental pollution generated by mixes of transportation modes, with detailed treatment of electrical interference
 (R-762-DOT/RC) 21 p3420 N71-34331
 Environmental effects of jetport near Everglades Park in southern Florida
 (PB-199159) 21 p3420 N71-34338
 Pollution management in reversal of environment pollution trends
 (PB-199180) 21 p3421 N71-34339
 Measurement of radioactivities and nuclides in environment near nuclear research center of South Africa
 (PEL-205) 21 p3467 N71-34682
 Effect of increasing populations on world environment and international cooperation to reduce extent of environmental pollution
 21 p3533 N71-35183
 Toxicological evaluation of carbon monoxide, atmospheric contaminants, and propellants in environmental pollution
 (AD-727022) 22 p3546 N71-35258
 Development of system for identification of pollution reduction methods and selection of alternate methods for optimum effectiveness
 (PB-199352) 22 p3548 N71-35414
 Uranium mining, chemical reprocessing, transportation of spent fuel, and reactor systems waste products related to environmental pollution
 (NP-18042) 23 p3796 N71-37065
 Presidential proposals for controlling environment pollution
 23 p3870 N71-37591
 Environmental pollution by mercury and other toxic substances
 24 p3883 N71-37681
 Impact of air activity on environment and federal interest in environmental studies
 24 p4033 N71-38792
- ENVIRONMENT SIMULATION**
NT ACOUSTIC SIMULATION
NT ALTITUDE SIMULATION
NT SPACE ENVIRONMENT SIMULATION
NT THERMAL SIMULATION
NT WEIGHTLESSNESS SIMULATION
 Studies of propellant sloshing under low gravity conditions
 (NASA-CR-102891) 01 p0041 N71-10520
 Lateral liquid sloshing in axisymmetric tank under low gravity conditions
 01 p0041 N71-10521
 Experimental and theoretical studies of liquid sloshing at simulated low gravity
 01 p0041 N71-10523
 Simulated low gravity sloshing in cylindrical tanks including effects of damping and small liquid depth
 01 p0041 N71-10524
 High intensity RP radiant energy source to simulate thermal environment in nuclear light bulb engine
 (NASA-CR-110909) 01 p0046 N71-10581
 Model environment of high energy protons trapped in radiation belts
 (NASA-SP-3024-VOL-4) 02 p0293 N71-12117
 Investigating effects of liquid diets on subjects in space environment simulators
 (NASA-CR-116253) 06 p0804 N71-14736

- User manual for test equipment used in simulating aerodynamic heating and acoustical environments on space shuttle thermal protection specimens [NASA-CR-103017] 07 p1004 N71-17451
- Environmental test and simulation equipment at Vernou facility, France 08 p1175 N71-18467
- Effect of simulated space cabin atmosphere of 100 percent oxygen at 5 ppa on immunological response in mice 10 p1500 N71-21333
- Shock tube simulation of nuclear fireball thermal environment [AD-717090] 10 p1662 N71-21382
- Molecular relaxation of anharmonic nitrogen oscillators in simulated expansion flow environment with vibration-vibration and vibration-translation energy exchange 11 p1742 N71-22720
- Method and apparatus for applying compressional forces to skeletal structure of subject to simulate force during ambulatory condition [NASA-CASE-ARC-10100-1] 13 p2037 N71-24738
- Gravity environment simulation by locomotion and restraint aid for studying manual operation performance of astronauts at zero gravity [NASA-CASE-ARC-10153] 16 p2554 N71-28619
- Arc heated hydrogen plasma in star atmosphere simulator [MPL-PAR/EXTRATER-38] 18 p2901 N71-30483
- Simulation of radon removal from atmosphere by means of artificial fog [IFA-RDP-33] 20 p3257 N71-33038
- Techniques and apparatus design for measuring high temperature emissivity of thermal protection materials for reentry vehicles [NASA-CR-1119920] 21 p3425 N71-34368
- ENVIRONMENTAL SIMULATORS**
- NT HIGH VACUUM ORBITAL SIMULATOR
- NT LUNAR GRAVITY SIMULATOR
- NT SOLAR SIMULATORS
- NT SPACE SIMULATORS
- Human factors engineering mock-up facility value as management tool [AD-717026] 10 p1504 N71-20797
- Space environment simulator for testing spacecraft components under aerospace conditions [NASA-CASE-NPO-11041] 13 p3061 N71-24964
- Functions of environmental data collection and processing facility, project management, data base maintenance, information retrieval, and environmental simulation system [AD-720592] 14 p2360 N71-26451
- Quadrupole plasma probe simulator for simulation of transfer impedance in ionospheric plasmas [GRI/NTF-78] 15 p2407 N71-26999
- ENVIRONMENTAL CHAMBERS**
- U TEST CHAMBERS
- ENVIRONMENTAL CONTROL**
- Portable environmental control and life support system for astronaut in and out of spacecraft [NASA-CASE-XMS-09632-1] 02 p0169 N71-11203
- Control theory and environmental control 04 p0522 N71-14437
- Annotated bibliography of technical literature related to nitrogen oxides and air pollution control [PB-194429] 04 p0480 N71-14472
- Congressional hearings on proposed legislation relating to water pollution control 07 p1020 N71-17537
- Congressional hearings on proposed legislation relating to water pollution control 07 p1020 N71-17538
- Congressional hearings on proposed legislation relating to water pollution control 07 p1020 N71-17539
- Congressional hearings on proposed legislation relating to water pollution control 07 p1020 N71-17541
- Environmental control methods to reduce air and water pollution in United States of America 07 p1135 N71-18071
- Logic circuitry, and environmental and acceptance tests for solid state sequencer system in command module and service module jettison controller [NASA-CR-114955] 10 p1635 N71-21460
- Multinational air pollution control operations [PB-196841] 10 p1667 N71-21784
- Industrial pollution properties summary including data on toxicity and control, air sampling, and gas analysis 11 p1747 N71-22856
- Portable apparatus producing high velocity molecular air column surrounding low velocity, filtered, super-clean air central core for industrial clean room environmental control [NASA-CASE-XMF-03212] 11 p1770 N71-22721
- Development and characteristics of thermal sensitive panel for controlling ratio of solar absorptivity to surface emissivity for space vehicle temperature control [NASA-CASE-XLA-07728] 11 p1845 N71-22890
- Development of environmental control system for determining effects of relative humidity and dry heat on inactivation of microorganisms [NASA-CR-118024] 12 p1868 N71-23823

- Performance of aircraft environmental control systems under simulated tactical conditions [AD-719101] 13 p2025 N71-24461
- Dual solid cryogenics for spacecraft refrigeration insuring low temperature cooling for extended periods [NASA-CASE-GSC-10188-1] 13 p2124 N71-24725
- International cooperation policy for science and technology transfer 13 p2189 N71-24751
- International scientific cooperation for environmental pollution control 13 p2189 N71-24752
- International science policy for managing social effects of technology utilization 13 p2190 N71-24761
- Virginia Beach environmental data and time series analysis of water table interactions with processes in beach-ocean-atmosphere system for environmental control [AD-719923] 14 p2245 N71-25629
- Living and sleeping quarters with controlled environment for high altitude personnel 14 p2237 N71-26214
- Feasibility of spraying flash evaporator as heat rejection device for space shuttle environmental control system [NASA-CR-114913] 14 p2263 N71-26224
- Zero-gravity absorption refrigeration system design and performance testing for space station environmental control application [NASA-CR-103114] 14 p2211 N71-26390
- Materials and thermal protection, propulsion, environmental control, life support, and crew accommodation data for space shuttle design [NASA-CR-118487] 14 p2346 N71-26780
- Vibration control of flexible bodies in steady accelerating environment [NASA-CASE-LAR-10106-1] 15 p2415 N71-27169
- Bioengineering tradeoff study for cabin atmosphere selection in manned space flight 16 p2552 N71-28531
- Microbiological life support requirements in long term manned space flights 16 p2552 N71-28537
- Systems integration for optimal regenerative environmental and life support processes in manned spacecraft 16 p2552 N71-28538
- Test chamber for determining decomposition and autignition of materials used in spacecraft under controlled environmental conditions [NASA-CASE-DSC-10198] 16 p2577 N71-28629
- Determination of oxidation resistance of various alloys for possible application as thermal control and protection system components on space shuttles [NASA-TM-X-67864] 16 p2692 N71-28904
- Design, fabrication, and testing of circulating electrolyte type water electrolysis system for automatic control of spacecraft total pressure and oxygen partial pressure [NASA-CR-111911] 17 p2710 N71-29383
- Environmental and materials contamination including detection and control methods for production engineering [SC-M-70-303] 17 p2739 N71-29449
- Factors relevant to development of fuels and energy policies compatible with environmental control 17 p2861 N71-29471
- Development of minimum and optimum requirements for environmental surveillance programs around nuclear fuel reprocessing plants 17 p2784 N71-29878
- Study of environment sciences and recommendations for national program, priorities, funding, and university disciplines 17 p2750 N71-30294
- Mathematical models for automated environmental control of acoustic test facility inside chamber [NASA-CR-115072] 17 p2732 N71-30355
- Modular space station study of environmental control and life support system for long term mission [NASA-TM-X-64603] 18 p2882 N71-30751
- Human reactions to air pollution and responses to ecology and environmental control [UCRL-73063] 19 p3093 N71-32258
- Federal programs for air, water, and solid waste pollution control 19 p3198 N71-32653
- Temperature regulator for controlling temperature environment within oven [NASA-CASE-NPO-11304] 20 p3272 N71-33106
- Application of nuclear energy to meeting needs of increasing populations and reduction in environmental pollution through use of nuclear energy [INFCIRC/139/ADD-1] 20 p3324 N71-33879
- Effect of private litigation on national efforts to preserve and enhance the environment 21 p3533 N71-35177
- Conference on space shuttle environmental control and life support systems - Vol. 2 [NASA-TM-X-47265] 22 p3547 N71-35266
- Environmental control and life support system for space shuttle orbiter 22 p3547 N71-35267

- Environmental control and life support subsystem for space shuttle orbiter 22 p3548 N71-35271
- Status of LRC program on space shuttle environmental control and life support systems 22 p3548 N71-35272
- Responsibilities of engineers in environmental and pollution control 22 p3708 N71-36306
- Radiation shielding and biogeochemical process and their maintenance for earth preservation [JPRS-54039] 23 p3750 N71-36710
- Reference matrix for evaluating and preparing environmental impact reports 23 p3752 N71-36717
- Guidelines for environmental habitability planning to facilitate individual and group stability [NASA-CR-115180] 23 p3869 N71-37520
- ENVIRONMENTAL ENGINEERING**
- Research planning in environmental health sciences 01 p0012 N71-10075
- Research progress in coastal engineering [AD-711940] 02 p0219 N71-12077
- Developing molten alkali carbonate eutectic in removing lead compounds from spark ignition engine exhaust gases [PB-194132] 04 p0484 N71-13440
- Proceedings from conference on role of national laboratories and universities in solving environmental problems [CONF-690705] 04 p0476 N71-13803
- Development and implementation of R and D and program planning capability for Environmental Health Services [PB-194410] 04 p0480 N71-14476
- Investigating information resources available to Environmental Health Service for protecting man's environment [PB-194411] 04 p0480 N71-14477
- Mathematical model for environmental transport of lead from several sources and subsequent intake by man [PB-194412] 04 p0481 N71-14478
- Thermal control wall panel with application to spacecraft cabins [NASA-CASE-XLA-01243] 11 p1845 N71-22792
- Spacecraft water reclamation and closed soil contained biological cyclized-closed ecological system techniques in USSR and US [NASA-TT-F-13634] 12 p1866 N71-23378
- Biochemistry, molecular biology, radiochemistry, meteorology, soil science, and water pollution research and development and environmental engineering [AECL-3728] 13 p2033 N71-24000
- Environmental engineering abstracts and bibliographical data [SC-R-70-4211] 13 p2078 N71-25400
- Safety problems comprising fuel element failure and long term operation of containment spray systems for water cooled power reactor with emphasis on environmental effects [ORNL-TM-3263] 16 p2630 N71-28108
- Utilization of water resources within space stations, needs of men, and effects of lunar environment 16 p2681 N71-28066
- Terrestrial environment/climatic/criteria guidelines for use in NASA space vehicles and associated equipment development with major emphasis on Kennedy Space Center launch area [NASA-TM-X-64389] 17 p2737 N71-29315
- Susceptibility or resistance to gas and smoke of various arboreal species grown under diverse environmental conditions in industrial regions [PB-190605] 17 p2742 N71-29813
- Effects and symptoms of air pollution on vegetation noting resistance and susceptibility of various plant species in various habitats and relation to plant utilization for shelter belts [PB-190602] 17 p2742 N71-29816
- Meteorological and chemical aspects of air pollution and propagation and dispersal of air pollutants - survey of USSR air pollution literature [PB-190604] 17 p2745 N71-29819
- Methods, instruments, and performance of air filters used to cleanse contained atmospheres - conference [CONF-700816-VOL-2] 17 p2743 N71-29813
- Energy sources in US to achieve future electric energy needs and environmental compatibility requirements 17 p2743 N71-29813
- Procedures for estimating control costs and emission reductions for specified air pollution sources - users manual [PB-196779] 19 p3198 N71-32300
- Federal programs for air, water, and solid waste pollution control 19 p3198 N71-32301
- Development of scientific principles of predicting and transforming nature for improving environment and optimal use of natural conditions [JPRS-53743] 20 p3223 N71-33594

SUBJECT INDEX

Analysis and definition of tasks in field of biogeology 20 p3223 N71-33502

Influence of weather conditions on radioactivity in environment of atomic energy facilities [RFX-1336] 21 p3451 N71-34558

Nuclear safety research and development in support of water cooled power reactor technology emphasizing environmental effects [ORNL-TM-3342] 21 p3460 N71-34627

Effect of private litigation on national efforts to preserve and enhance the environment 21 p3533 N71-35177

Application of aerospace and defense industry resources and technology to solution of environmental problems 21 p3533 N71-35180

Separation of krypton and xenon from reactor atmospheres by selective permeation [NYO-4057-1] 22 p3644 N71-35981

Computing dispersal of atmospheric pollutants near airports by use of mean wind and temperature profiles [NASA-CR-111963] 23 p3748 N71-36720

Potential application of remote sensing to detect some circulation problems in environmental studies 23 p3788 N71-36999

Presidential proposals for controlling environment pollution 23 p3870 N71-37591

Continuous measurement of activity concentration of radionuclides in air using NaI [6] crystal detector [EKL-71-13] 24 p3919 N71-37948

Human factors engineering data for equipment design including anthropometry, environmental conditions, and physiological and behavioral factors [NASA-CR-114271] 14 p2209 N71-25944

Reference matrix for evaluating and preparing environmental impact reports 23 p3752 N71-36757

Organization of national environmental laboratory with scientific and technological input 01 p0138 N71-10818

Weightlessness, corpuscular radiation, and magnetic field environmental laboratory simulation 03 p0355 N71-12704

Proposed environmental laboratory handling urban and rural problems and staffed by natural and social scientists, engineers, and information specialists [PB-109691] 03 p0358 N71-13076

Proceedings from conference on role of national laboratories and universities in solving environmental problems [CONF-690705] 04 p0476 N71-13855

Radiation facility and equipment for studying Sr-90 electron irradiation effects in Li-doped silicon 14 p2202 N71-26240

Environmental facility for real-time study of electron irradiation effects on Li-doped p-a silicon solar cells 14 p2202 N71-26241

Requirement specifications for environmental laboratory test chamber complex design, fabrication, and testing [NASA-CR-115007] 14 p2345 N71-26549

ENVIRONMENTAL TEMPERATURE

U AMBIENT TEMPERATURE

ENVIRONMENTAL TESTS

NT COLD WEATHER TESTS

NT CORROSION TESTS

NT HIGH TEMPERATURE TESTS

NT LOW TEMPERATURE TESTS

NT SALT SPRAY TESTS

NT UNDERWATER TESTS

Applications Technology Satellite reflectometer experimental data [NASA-CR-107063] 01 p0054 N71-10364

Cold weather testing of equipment durability [AD-711611] 01 p0015 N71-10699

Low power solid-state radio beacon tests and evaluation for snow and ice outages of compass locator systems [FAA-RD-70-38] 01 p0083 N71-10990

Distortion and environmental tests of travelling wave tubes [AD-711362] 02 p0192 N71-11345

Space environmental simulation data for spacecraft reliability and test planning 03 p0355 N71-12703

Lectures on space environment simulation for improving spacecraft reliability - vol. 2 03 p0356 N71-12710

Signal data acquisition and processing of environmental test objects 03 p0357 N71-12714

Stages in environmental tests of satellites 03 p0357 N71-12716

Systems integration of scientific satellite Azar and space environment tests 03 p0358 N71-12723

Electrical and environmental tests on PCM telemetry system for earth resources aircraft [NASA-CR-100700] 04 p0488 N71-13474

Environmental testing of silicon cell spalling and experimental confirmation of mathematical model [NASA-CR-102984] 05 p0630 N71-14606

Testing electrical, mechanical, and handling properties and environmental characteristics of small gauge electrical wire for interplanetary spacecraft 06 p0629 N71-14683

Environmental tests of design modifications for Apollo RCS positive expulsion tankage [NASA-CR-11814] 06 p0939 N71-16867

Simulated space environment test of cadmium sulfide thin film solar cell module [NASA-TM-X-2125] 07 p0975 N71-17371

Environmental test and simulation equipment at Vernon facility, France [LBA-TN-157/WDAP] 08 p1175 N71-18467

Sterilization and environmental testing of solid state rate sensor with rectangular metal beam for planetary space flight [NASA-CR-111833] 08 p1202 N71-18964

Effects of surfaces and environment on nucleation and growth of fatigue cracks in copper [NASA-CR-116839] 08 p1280 N71-19031

Conceptual fusion reactor study, including fuel cycles, environmental tests, and radiation damage [ORNL-TM-3322] 08 p1265 N71-19150

Local environmental effects on magnetic moment formation in Au-V and Cu-Ni alloys [AD-710303] 09 p1424 N71-19679

Environmental tests and materials handling processes for beam lead semiconductor devices [BDX-613-194] 09 p1454 N71-20023

Space simulation technology for determining space environment effects on materials, spacecrafts, and man [NBS-SP-336] 09 p1366 N71-20201

Detection and identification of contaminating outgassing materials during spacecraft environmental tests [NASA-TM-X-66936] 09 p1406 N71-20202

Sterilization, vacuum exposure, and simulated Martian atmosphere effects on thermal conductivity of spacecraft heat exchangers [NASA-TM-X-66938] 09 p1483 N71-20214

Measurement methods during fabrication and environmental testing of microcircuits 09 p1360 N71-20228

Human centrifuge for dynamic environmental simulations 09 p1367 N71-20237

Diving techniques and equipment for simulating neutral buoyancy in space environment testing 09 p1367 N71-20240

Space environment test facility for simulating radiation effects in solar cells [NASA-TM-X-66948] 09 p1326 N71-20254

Design and testing of 30 W/lb rollup subarray [NASA-CR-117319] 09 p1327 N71-20269

Environmental tests of VISTOL vibration effects on human comfort [NASA-TM-X-66956] 09 p1335 N71-20356

Effects of education and pharmacodynamics on adaptability of human beings to degraded sensorial environments 09 p1337 N71-20364

Heat tolerance of athletes during muscular exercise in various thermal environments 09 p1337 N71-20366

Environmental tests of VORLOC 2 simplified directional approach system to determine compliance with FAR-Part 171 [FAA-RD-71-12] 10 p1599 N71-20666

Ultraviolet radiation dosage during high vacuum ultraviolet environmental tests [RV-51] 10 p1640 N71-20715

Airfield tests of specially formulated marking paints for asphalt pavements 10 p1590 N71-21523

Fabrication and evaluation of dyed/hatched food bars produced by compression and molding processes [AD-717289] 11 p1606 N71-21900

Environmental tests of deicing techniques for ship structures [NRC-11872] 11 p1847 N71-22405

Minimum performance standards for personnel type emergency locator transmitters ELT/P under environmental test conditions [DO-145] 11 p1701 N71-22440

Natural environment support for space shuttle tests and operations - advanced design and operations concepts [NASA-CR-61346] 11 p1832 N71-22492

Multisample test chamber for exposing materials to X rays, temperature change, and gaseous conditions and determination of material effects [NASA-CASE-XMS-02930] 11 p1733 N71-23042

Operational and environmental performance tests and specifications for precision bathymetry recorder [IPS-71010] 12 p1916 N71-23217

Environmental tests of radioisotope thermoelectric generators used by US Navy [AD-710697] 12 p1858 N71-23277

Model A350 magnetic tape recording current meter design and environmental performance tests [IPS-71011] 12 p1918 N71-23370

Environmental tests of electrical subsystem of 2-to-15 kW Brayton power conversion system [NASA-TM-X-67814] 12 p1963 N71-23928

LMFBR environmental effects on type 304 and 316 stainless steel and Cr-Mo alloy piping materials [SAR-781-228-REV-1] 12 p1963 N71-24055

Evaluation of Zircaloy clad fuel rods to determine geometrical and environmental variable effects on post irradiation dimensional changes [WAPD-TM-906] 12 p1964 N71-24153

Tests of cryo-formed spheres to determine suitability as replacements for lithium halide storage bottles in liquid hydrogen tanks of stern 5-4B stage [NASA-CR-61343] 12 p2002 N71-24179

Test procedures for aircraft defogger/defroster operation [AD-719109] 12 p2025 N71-24452

Tests to determine presence of electromagnetic interference and qualitative effect on communication-electronic equipment [AD-719098] 13 p2054 N71-24486

Tests for determining suitability of tape recording and reproducing equipment for tactical use by Army [AD-719097] 13 p2054 N71-24487

Flammability test chamber for testing materials in certain procedures of environmental testing [NASA-CASE-KSC-10126] 13 p2061 N71-24985

Long-term test of noble and refractory metal thermocouples at 1600 K in air, argon, and vacuum [NASA-TM-X-67813] 13 p2082 N71-25251

Design and tests of astronaut tool kit and tools for in-flight space maintenance [NASA-CR-103153] 13 p2039 N71-25533

Effect of cell viscosity and certain testing procedures on degradation of cadmium sulfide thin film solar cells [NASA-TM-X-2292] 13 p2031 N71-25534

Surface and environmental effects on plastic flow and fracture of metals and alloys [AD-720405] 14 p2272 N71-25873

Reflective surface degradation data from samples flown on Applications Technology Satellite [NASA-CR-118632] 14 p2337 N71-25965

Communication, surveillance, and airborne electronic equipment performance testing in tropical environment [AD-720577] 14 p2218 N71-26176

Environmental testing of nickel-cadmium, silver-zinc, silver-cadmium, and zinc-oxygen batteries for spacecraft power supplies [NASA-CR-118661] 14 p2203 N71-26540

Wear tests and friction measurements between nuclear fuel elements and spacer grids in air, argon, and sodium [RFX-1290] 14 p2294 N71-26653

Environmental tests of tests developed for aviation use including installation, safety, and maintainability [AD-721153] 15 p2390 N71-26880

Mechanical properties and physical, chemical, and thermal tests of polybenzimidazole and carbon fabric laminates for spacecraft thermal insulation [NASA-CR-1723] 15 p2427 N71-26915

Development of heat-stabilizable 40-Ah sealed, non-magnetic silver zinc cell for use on Viking spacecraft [NASA-CR-1812] 15 p2349 N71-27009

Copper sulfide-cadmium sulfide thin film solar cell for space application [NASA-TM-X-67848] 15 p2369 N71-27678

Electric motor environmental and electrical test procedures including electromagnetic compatibility and maintenance [AD-721611] 16 p2568 N71-28343

NASA/GSPC workshop on materials processing, chemical analysis, cell processing, and testing of batteries for aerospace applications [NASA-TM-X-67200] 16 p2538 N71-28659

Environmental testing and handling of batteries for Mariner 71 spacecraft 16 p2539 N71-28669

NASA/GSPC workshop on battery separators, seals, test techniques, and research and development of nickel cadmium and silver zinc batteries [NASA-TM-X-67106] 16 p2540 N71-28672

Research and development, test techniques, and new technology for nickel cadmium batteries, silver zinc cells, and energy storage 16 p2540 N71-28674

Environmental simulation testing and evaluation of shuttle thermal protection materials and systems 17 p2846 N71-29461

NASA specifications for high efficiency particulate aerosol filters including testing and installation [NASA-TM-X-67249] 17 p2756 N71-29679

Procedures for service test of communication and electronic equipment under adverse weather conditions [AD-723029] 17 p2721 N71-30235

- Environmental, drop, and vibration tests for investigating fatigue of cushion materials for packaging [BCR-09] 18 p2939 N71-30614
- Skyball control moment gyroscope inner gimbal design and thermal vacuum and environmental tests [NASA-TM-X-64583] 18 p2956 N71-31199
- Environmental monitoring for determining He-3 and tritium water vapor content of ground level air [ORO-3944] 19 p3095 N71-32499
- Evaluation of sealed nickel cadmium cells, with auxiliary electrodes, operating in synchronous orbit regime [NASA-CR-121450] 20 p3213 N71-33326
- Performance tests of meteorological radiosonde conducted in wind tunnel with controlled variations in humidity and temperature [AD-724488] 20 p3296 N71-33411
- Mechanical property tests of nickel, titanium, and iron alloys in 5000 psig gaseous helium and hydrogen at various temperatures [NASA-CR-119844] 20 p3230 N71-33728
- Pulsed dipole and dc dipole transport magnet designs and testing for superconducting synchrotron application [UCRL-20188] 21 p3408 N71-34252
- Ducted propeller open water systematic series tests of flow accelerating and decelerating nozzles for application to single and double screw ship 21 p3412 N71-34278
- Laboratory and sea condition tests of accuracy of double system marine gravimeter with automatic readout 21 p3418 N71-34319
- Fabrication and environmental tests of circuit boards with polyimide plastic dielectrics and pyrolyzed polycrylonitrile conductors [NASA-CR-119934] 22 p3562 N71-35373
- Environmental tests of boilers and remote handling and viewing equipment for high temperature nuclear reactors and fast neutron effects on TMC2-UC2 coated particles and graphite [GA-10560] 22 p3625 N71-35831
- Design verification test results for umbilical hose and PLSS water and oxygen hoses [NASA-CR-115158] 23 p3717 N71-36497
- Design and fabrication of flight-concept prototype electrochemical water recovery subsystem [NASA-CR-111961] 23 p3718 N71-36507
- Development, testing, and utilization of silver iodide pyrolytic cloud seeding system [ESSA-TM-ERLTM-APCL-5] 23 p3786 N71-36985
- Acceleration, structural vibration, internal temperature, heating rate, and roll rate data obtained from two Sidewinder-Arcas sounding rocket launches [NASA-TM-X-2348] 23 p3860 N71-37514
- Environmental and performance tests of voice initiated cockpit control and interrogation system [AD-727574] 24 p3889 N71-37723
- Environmental tests of solid lubricants, liquid lubricants, and lubricant additives under high pressures up to 70 kilobars [AD-727577] 24 p3946 N71-38146
- Environmental tests of cryogenic propellant effects on metallic positive expulsion bellows operating parameters [NASA-CR-72799] 24 p3999 N71-38526
- Environmental vibration testing of SNAP 9 condenser and design evaluation for space and launch conditions [NASA-CR-72925] 24 p4023 N71-38706
- Flat plate thermal conductivity tests, long term stability tests, and interface effects on thermal performance of multilayer insulation materials for use in radioactive isotope power systems [ALO-2832-43] 24 p4029 N71-38752
- ENVIRONMENTS**
- NT AEROSPACE ENVIRONMENTS
- NT CHROMOSPHERE
- NT CISELUNAR SPACE
- NT DEEP SPACE
- NT EARTH ENVIRONMENT
- NT EXTRATERRESTRIAL ENVIRONMENTS
- NT FRICTIONLESS ENVIRONMENTS
- NT HETEROSPHERE
- NT HIGH ALTITUDE ENVIRONMENTS
- NT HIGH TEMPERATURE ENVIRONMENTS
- NT INNER RADIATION BELT
- NT INTERPLANETARY SPACE
- NT INTERSTELLAR SPACE
- NT IONOSPHERE
- NT JUPITER ATMOSPHERE
- NT LOW TEMPERATURE ENVIRONMENTS
- NT LOWER IONOSPHERE
- NT LUNAR ATMOSPHERES
- NT LUNAR ENVIRONMENT
- NT MAGNETOPAUSE
- NT MAGNETOSPHERE
- NT MARS ATMOSPHERE
- NT MARS ENVIRONMENT
- NT MESOPAUSE
- NT MESOSPHERE
- NT PLANETARY ATMOSPHERES
- NT PLANETARY ENVIRONMENTS
- NT ROTATING ENVIRONMENTS
- NT SOLAR ATMOSPHERE
- NT SPACECRAFT ENVIRONMENTS

- NT STELLAR ATMOSPHERES**
- NT THERMAL ENVIRONMENTS**
- Operational, transport, and storage environments for oceanographic and meteorological sensors [AD-711325] 02 p2223 N71-11385
- Relationship of technology assessment to environmental management [PB-19254] 02 p3037 N71-11893
- Reporting activities of Natural Environment Research Council of Great Britain 02 p2220 N71-12090
- Environmental problems including air pollution, water pollution, radioactive wastes, smog, sewage, aircraft, and garbage disposal [AD-717222] 03 p3321 N71-12297
- Resume of publications and recommendations from symposium on intestinal flora ecology in changing environments [NASA-CR-114889] 09 p1330 N71-19783
- Combined environmental stress effects on human performance 09 p1336 N71-20362
- Congressional hearing on efforts to improve knowledge of and support for environmental and ecological projects 09 p1489 N71-20566
- Outdoor aging of adhesive sealants under various environments [SC-RR-70-163] 11 p1769 N71-22530
- Work environment and task factor effects on long term aircrew effectiveness [AD-723417] 17 p2711 N71-29682
- Radiological effects of underground nuclear explosions on environment of Amchitka Island, Alaska [NVO-1229-121] 22 p3576 N71-35470
- Impact of air activity on environment and federal interest in environmental studies 24 p4035 N71-38792
- ENZYME ACTIVITY**
- NT FERMENTATION**
- Histopathological and biochemical effects of decelerations on mice physiology 02 p0162 N71-11807
- Enzyme activity in terrestrial soil in relation to exploration of Martian surface [NASA-CR-116439] 07 p0106 N71-17053
- Investigating effects of weightlessness on enzyme secretion function of digestive system of Soyuz 9 crew members 08 p1151 N71-18909
- Nonlinear relationships in lactic dehydrogenase and leucine amino peptidase enzyme activities in urine related to increased and decreased diuresis [NASA-TT-F-13557] 12 p1863 N71-23388
- Peroxidase and catalase activity and hyperoxia effects on mice organs, leukocytes, and erythrocytes in pure oxygen under pressure [ANL-TRANS-877] 15 p2371 N71-27290
- Physiological effects of ionized air on mice acetylcholine/cholinesterase system 16 p2543 N71-28252
- Abundance, persistence, and localization of enzyme activity in terrestrial soil and exploration of soils suitable for planetary life [NASA-CR-121446] 20 p3215 N71-33232
- Enzyme reaction model of flow dilution effect on blood coagulation in vivo [NASA-CR-122929] 23 p3713 N71-36470
- Electrophoretic and chromatographic analysis of lactate dehydrogenase isoenzyme activity in fetal, neonatal, and adult human thymus and spleen lymphocytes [NASA-TT-F-13991] 23 p3715 N71-36482
- ENZYMES**
- NT CHOLINESTERASE**
- Considering lack of development of endemic species in Iceland 07 p0984 N71-17995
- High resolution electron microscopes for cell membrane and multi-enzyme complex studies 08 p1157 N71-19314
- Kinetic model of enzyme monomolecular enzyme reactions with substrate and product inhibition and possibility of self oscillation [NLL-RTS-3991] 10 p1500 N71-21401
- Purification and characterization of enzymes from *H. salinarum*, *B. stearothermophilus*, and *V. marisnii* [RLO-2227-T-5-1] 10 p1501 N71-21527
- Bionics modeling of enzyme analysis of toxic compounds and olfactory system stimulation 11 p1686 N71-22065
- Cytochemical detection of lactic dehydrogenase isoenzymes in free-living Protozoa [NASA-TT-F-13624] 12 p1862 N71-23382
- Nonlinear relationships in lactic dehydrogenase and leucine amino peptidase enzyme activities in urine related to increased and decreased diuresis [NASA-TT-F-13557] 12 p1863 N71-23388
- Bioluminescent reaction of adenosine triphosphate with enzyme luciferase for quantitative analysis of bacteria in urine samples [NASA-CASE-GSC-11092-1] 15 p2373 N71-27991
- Gene frequencies of red cell acid phosphatase in random samples [NASA-TT-F-13989] 24 p3877 N71-37637

- ENZYMOLGY**
- Chemistry and enzymology of photosynthesis, oxygen evolution, energy migration, and kinetics of reaction chain [RIAS-3706-15] 05 p0634 N71-14444
- EOSS**
- Materials processing and manufacturing in earth orbital payload planning 02 p0297 N71-11776
- Experiments payloads plan for extended earth orbital missions with options [NASA-TM-X-64691] 08 p1292 N71-19318
- EPF-C**
- U EXPLORER 15 SATELLITE**
- EPF-D**
- U EXPLORER 26 SATELLITE**
- EPHEMERIDES**
- NT PLANET EPHEMERIDES**
- Manual of computer program for generating ephemerides of earth satellites [RAE-TR-69104] 02 p0296 N71-11800
- Mean motions of node and perigee evaluated using improved lunar ephemeris numerical values [AD-717282] 11 p1824 N71-21980
- Almanac of astronomical ephemerides for 1970 12 p1996 N71-23830
- Almanac for 1971 including ephemerides of sun, moon, and stars 22 p3670 N71-36164
- EPIDEMIOLOGY**
- Periodicity of epidemics and snout cycle [JPRS-51788] 04 p0476 N71-13401
- Computer techniques used in information theory, industrial controls, solutions to Fredholm equations, and simulating spreading of epidemic [JPRS-53461] 17 p2727 N71-29531
- Computerized simulation of influenza epidemic from one city over vast territory 17 p2708 N71-29540
- EPILEPSY**
- Functional state of central nervous system during development of epilepsy and narcosis in man and animals subjected to increased pressure of oxygen and inert gases 02 p0158 N71-11114
- EPINEPHRINE**
- NT NOREPINEPHRINE**
- EPITAXY**
- Epitaxial growth of ferrites by vapor deposition 01 p0108 N71-14110
- Microelectronics, large scale integrated arrays, electronic packaging, thin film epitaxy, computerized design, radar equipment [NASA-CR-109754] 04 p0512 N71-13319
- Examining aspects of epitaxial growth of silicon films and relationship to process technology 07 p1087 N71-17279
- Describing subsystems of batch silicon epitaxy reactor and effect of chamber geometry on reactor performance 07 p1088 N71-17282
- Describing reactor for growing epitaxial silicon films in resistance heated system 07 p1088 N71-17280
- Investigating techniques for producing silicon epitaxial layers with uniform thickness, resistivity control, and high surface quality 07 p1088 N71-17284
- Investigating electrical properties of thin films of silicon during epitaxial growth on sapphire or silicon 07 p1088 N71-17283
- Growing submicron single and multiple epitaxial silicon layers deposited by silane pyrolysis method 07 p1088 N71-17286
- Evaluating measurement methods for epitaxially grown layers with respect to thickness and constant phase shift 07 p1090 N71-17289
- Measuring thickness of semiconductor epitaxial layer deposited on substrate of same conductivity using infrared reflectance method 07 p1090 N71-17290
- On-line impurity profile plotter for measuring doping profiles of individual slices or finished devices 07 p1090 N71-17288
- Investigating structural defects in silicon material after epitaxial layer formation and diffusion 07 p1091 N71-17294
- Infrared spectrophotometer for automatic measurement of epitaxial layer thickness in silicon wafers 07 p1091 N71-17295
- Epitaxial sublimation methods for studying possible binary semiconductor alloys [AD-716210] 09 p1433 N71-20885
- Microstructure and electrical properties of the epitaxial films of lead telluride and effects of microstructure on electrical properties 11 p1815 N71-22118
- Film growth and thickness of lead telluride epitaxial films [AD-718323] 12 p1904 N71-23387
- Growth of epitaxial germanium films from supercooled melt [AD-718695] 12 p1986 N71-23735

SUBJECT INDEX

Influence of thin epitaxial surface film on plastic deformation of copper single crystals 14 p2326 N71-26349

Forming epitaxial film of GaAs single crystals (AD-720931) 15 p2506 N71-27402
Homo-epitaxial crystallization in copper electrodeposition 16 p2609 N71-28285

Electron mobility mechanisms in epitaxial growth of gallium arsenide crystals and computer program for calculating Hall effect (AD-722650) 18 p2993 N71-30734

Growth techniques and heat treatments for producing high quality epitaxial films of lead telluride and tin selenide (AD-722766) 18 p2996 N71-31453

Diffusion of impurities from GaAs stream in epitaxial layers of GaP grown by sandwich method (AD-723599) 19 p3167 N71-31738

Epitaxial crystal growth for manufacturing electronic equipment and components including crystal devices and electrical properties of crystallized layers (NLL-POBS-TRANS-2690-1982.81) 19 p3171 N71-32534

Epitaxial deposition of silver on polybenzidine related to heteroepitaxial nucleation (AD-726749) 22 p3659 N71-36900

Crystal composition, melt composition, growth temperature, and phase diagram of Ga-Al-As ternary grown by liquid epitaxy 23 p3837 N71-37362

Epitaxial growth of garnet films for magnetic bubble devices (AD-727070) 24 p3997 N71-38511

TIME MEASUREMENT

U. EPOXY COMPOUNDS

U. EPOXY COMPOUNDS

NT ENDURE

NT ETHYLENE OXIDE

Synthesis of siloxane containing epoxy polymers with low dielectric properties (NASA-CASE-MPS-13994-1) 02 p0176 N71-11240
Viscous effects related to transfer-molded parts of epoxy and dimethyl phthalate compounds (AD-721466) 10 p1566 N71-21364

Interface structure and effects of carbon fiber microstructure on shear strengths of carbon-epoxy composites 21 p3445 N71-34516

EPOXY RESINS

Homogeneous hermetically sealed battery case made of epoxy resin and woven glass tape for use with electrochemical cells in spacecraft (NASA-CASE-XGS-00885) 02 p0148 N71-11053

Tensile properties of flexible epoxy adhesive films (PPL-126) 02 p0248 N71-11936

Calorimetric determination of absorbed dose rate of epoxy resin irradiated in ZRE-4 (SCA-70-4) 04 p0585 N71-14232

Development of marking machine for fabrication of microconductor detectors (BARC-463) 05 p0693 N71-15430

Brittleness effects on polyethylene and fiber glass reinforced epoxy capsules (NASA-TM-X-52957) 06 p0800 N71-16499

Mo/epoxy alkylcarbamate adhesives with high temperature stability for steel-on-steel bonding (AD-7214837) 06 p0882 N71-16730

Elastic bending and fracture mechanics of reinforced fiber epoxy resins using scanning electron microscope (NPL-DM-11) 07 p1047 N71-17164

Polybution of graphite reinforced epoxy tubes (AD-715319) 07 p1048 N71-17857

Measurement of pipe friction factors during flow of dilute aqueous polyethylene-oxide solutions (AD-715556) 08 p1181 N71-18743

Fractionation of epoxy resins by alternating gel permeation chromatography 11 p1717 N71-22080

Epoxy resin sealing device for electrochemical cells in high vacuum environments (NASA-CASE-XGS-02630) 11 p1678 N71-22974

Dimple torsion technique to determine fracture energy of epoxy resins (AD-718964) 12 p1942 N71-23379

Longitudinally woven quartz fiber beam with uniform thickness using epoxy resin 12 p1943 N71-23440

Surface treatment of mechanically gridded fiber reinforced plastic rods to improve tensile properties (AD-718252) 12 p1943 N71-23740

Determination of static and fatigue characteristics of graphite epoxy composite materials with variations in temperature, stress mode, and stress ratio (AD-729996) 14 p2277 N71-25885

Cold metal hydroforming techniques using epoxy resin for constructing creep or stress relaxation rigs (NASA-CASE-XLS-8464-1) 14 p2633 N71-36346

Brittleness effects on mechanical properties of epoxy resin/glass composites (NRL-78-200) 15 p2427 N71-26815

Epoxy systems used to determine degree of resin constituent cure in printed circuit board fabrication (BDX-41-233) 15 p2385 N71-26963

Fatigue creep tests on glass fiber reinforced epoxy resins for four polymerization states (CRIP-PL-1) 15 p3428 N71-26967

Miniature electromechanical junction transducer operating on piezoelectric effect and utilizing epoxy for stress coupling component (NASA-CASE-ERC-10087) 15 p2409 N71-27334

Low temperature mechanical properties of epoxy/urethane formulations (SC-DR-70-421) 15 p2377 N71-27478

Static and cyclic fatigue characteristics of brittle polymers using machines to provide zero mean stress with alternating tension and compression stresses (COO-1794-7) 15 p2522 N71-27805

Temperature and stress histories recorded for glass fiber reinforced plastic specimens subjected to torsional oscillations (AD-721322) 16 p2618 N71-28583

Inflexible polymer production from reaction of polyfunctional epoxy resins with polyfunctional aziridine compounds (NASA-CASE-NPO-10701) 16 p2557 N71-28620

Development of structural models made by cascading strain gage networks in epoxy (BM-R1-7442) 18 p2926 N71-31441

Performance of unlubricated pivot bearings made from epoxy resins and polyimide materials 18 p2931 N71-31600

Design, fabrication and tests of boron/epoxy reinforced stringers for CR-54B tail cone (NASA-CR-111929) 21 p3374 N71-34013

Structural analysis of tail cone of CR-54B helicopter reinforced with boron/epoxy stringers (NASA-CR-111930) 21 p3375 N71-34014

Tension, biaxial, and creep tests of SA1-2.5Sn titanium alloy and computerized design for fiberglass-epoxy overwrapped titanium pressure vessel (NASA-CR-72745) 23 p3761 N71-36814

Plural shear bonding, tensile, and impact strengths of high modulus, high strength, glass fiber-epoxy resin composites (NASA-CR-122775) 23 p3775 N71-36907

Evaluation of coatings and filler materials for effectiveness in reducing moisture permeability of epoxy resins (AD-726930) 23 p3779 N71-36932

Predicting time-temperature behavior of epoxy resins and epoxy composites in any loading mode 23 p3780 N71-36942

Fabrication and testing of one-third scale boron/epoxy tubular booster thrust structure (NASA-CR-119958) 24 p3927 N71-38018

Viscoelastic creep and relaxation in filamentary angle-ply laminates with numerical results for boron-epoxy and graphite epoxy plastics (AD-727136) 24 p3943 N71-38129

Properties of composite structures bonded by epoxy resins with various hardening agents (AD-727600) 24 p3944 N71-38134

EQUATIONS

Index of documentations on numerical calculations for algebraic and transcendental equations (ORNL-4595) 09 p1411 N71-20382

Mechanical energy balance equations for describing secondary currents in turbulent flow through straight conduits (WTTD-27) 23 p3742 N71-36483

EQUATIONS OF MOTION

NT EULER EQUATIONS OF MOTION

NT HELMHOLTZ VORTICITY EQUATION

NT HYDRODYNAMIC EQUATIONS

NT KINEMATIC EQUATIONS

NT KINETIC EQUATIONS

NT NAVIER-STOKES EQUATION

NT REYNOLDS EQUATION

Evaluating methods of numerically integrating equations of motion for nonlinear dynamic analyses of shells of revolution by matrix displacement method (NASA-CR-108639) 01 p0128 N71-10166

Transonic equations of motion for convergent-divergent nozzles (NASA-CR-111104) 01 p0042 N71-10444

Cavitational wave theory applied to radiation stress phenomena (AD-710715) 01 p0048 N71-10547

Motion bounds of lumped structural parts subjected to dynamic loads and perturbations (AD-710787) 01 p0129 N71-10565

Equations controlling wave transmissions in lower ionosphere and computer program for integrating equations (NASA-CR-111125) 01 p0852 N71-10971

Calculating cavitation characteristics in converging channels of different shape using Bernoulli-Carnot theorem (NASA-TT-F-13340) 02 p0200 N71-11435

Equations of motion for deep-submergence vehicle developed and transformed into state variable form (AD-712115) 02 p0199 N71-11593

Developing mathematical model for tandem rotor helicopter for analysis of automatic approach and landing system (NASA-TM-X-64493) 03 p0312 N71-12225

EQUATIONS OF MOTION

Constructing solutions of given system in form of asymptotic series and formulating criteria of local stability of unperturbed motion 04 p0513 N71-13543

Motion of liquids enclosed in aerospace vehicle tanks under weak gravitational fields. Vol. 1 (NASA-CR-113117) 04 p0604 N71-14235

Research in general relativity including equations of motion, applications of group theory, and development of trapped surfaces (AD-713140) 05 p0712 N71-14535

Computer program for solving finite difference analogs to differential equations of motion in wave propagation (SC-DR-70-315) 05 p0650 N71-14875

Mean turbulent field closure of turbulent boundary layer equations of motion - Part 2 (SC-CR-70-6125-PT-2) 05 p0643 N71-14928

Equations of viscous fluid motion with viscous accompanying self-folding processes (NASA-TT-F-12568) 05 p0663 N71-14970

Kinematics of diffusion, fluids, and plasmas by continuous movement and finite velocities (AD-713580) 05 p0665 N71-15540

Computer programs for integrating equations of motion of ion-polar molecule collisions (NASA-TM-X-2151) 06 p0906 N71-15830

Computer program for predicting motion and appendage stresses of spacecraft during deployment maneuvers (NASA-CR-116148) 06 p0818 N71-15945

Equations of motion for weakly nonuniform potential flow (AD-714113) 06 p0835 N71-16120

Orbit calculations using gravitational parameter sets (AD-714142) 06 p0847 N71-16758

Mathematical simulation of breakdown characteristics of soft landing spacecraft (NASA-TN-D-7045) 06 p0951 N71-16768

Stability of finite-difference analogues to forecasting equations for barotropic motion in incompressible hydrostatic fluid (NASA-TM-NWS-NMC-49) 06 p0985 N71-16777

Finite difference equation for calculating motion equations of three dimensional boundary layers (SC-T-70-4038) 06 p0839 N71-16789

Determining equations of motion and aerodynamic characteristics for Magnus rotors by flight tests (AD-716345) 09 p1313 N71-19560

Equations of motion for shear response of viscoelastic specimens and effects of stress relaxation (AD-716424) 09 p1476 N71-19669

Solution to axisymmetric equations of motion in elastic bars containing discontinuities (AD-716547) 09 p1477 N71-19979

Numerical analysis of dynamic characteristics of liquid propellant rocket engines (AD-716510) 09 p1472 N71-20530

Computerized solution of nonlinear differential equations for inertial navigation systems (AD-717058) 10 p1599 N71-20765

Method for determining dispersion relations in fiber reinforced binary composite materials based on Fourier series and equations of motion (AD-717192) 10 p1589 N71-21319

Calculation of Lagrange planetary equations derived in form suitable for satellites of arbitrary eccentricity (NASA-TM-X-65476) 10 p1644 N71-21327

Time-dependent motion of small gas bubbles in smoothly decelerating liquid including bubble slip functions (RM-4998) 10 p1543 N71-21447

Modified quasilinearization used with method of particular solutions for determining several periodic orbits of the earth-moon system (AD-717192) 10 p1647 N71-21801

Derivation of motion of interplanetary irregularities from observations of interplanetary scintillations (AD-716735) 10 p1647 N71-21802

Mean motions of node and perigee evaluated using improved lunar ephemeris numerical values (AD-717282) 11 p1624 N71-21985

Fluid motion for incompressible fluid between two long concentric cylinders (AD-717366) 11 p1734 N71-21970

Dynamics of three dimensional motion of guided, rotating, and roll stabilized rockets (AD-717821) 11 p1830 N71-22018

Equations of motion of satellite orbits using Kepler laws and Euler-Lagrange equation (BMW-FB-W-70-46-PT-1) 11 p1825 N71-22039

Surface motion in solids caused by reflection of intense acoustic pulse at pressure release surface determined by surface velocity reflection coefficient (AD-717608) 11 p1835 N71-22140

Equations of motion and characteristics of invariant gyrocompass with pendulum correction 11 p1762 N71-22262

Determination of kinematic and dynamic response of elastically supported mechanical systems with interfaces subjected to mechanical excitation (AD-717711) 11 p1771 N71-22880

Accelerated supersonic motion of plane at finite angle of attack (NASA-TT-F-13525) 12 p1850 N71-23278

Computer program for solving equations of motion governing pogo oscillations
[NASA-CR-103101] 12 p1882 N71-23666

Numerical solution of quasi-conservative hyperbolic systems applied to case of converging-diverging cylindrical shock waves
[AD-717956] 12 p1950 N71-23740

Hydrodynamic theory applied to climatology and general atmospheric circulation and numerical analysis of macro-atmospheric processes
[AD-718623] 12 p1955 N71-23838

Spectral model of winter stratosphere circulation, radiative effects including solar absorption by ozone and Newtonian approximation to infrared cooling
13 p2106 N71-25027

Development and numerical integration of differential equations of spacecraft motion used in Double Precision Trajectory Program
[NASA-CR-117958] 13 p2168 N71-25152

Hydrodynamics of superfluid condensate including equations of motion and density matrix
14 p2304 N71-26286

Equations of motion for time vector calculus for aircraft lateral stability
[ARC-RM-3631] 15 p2367 N71-27097

Trajectory computer program (SIXD) to determine motions of asymmetric missiles emphasizing various nonlinear-induced effects associated with finned bodies
[SCL-RR-70-121] 15 p2364 N71-27613

Stability of finite difference solution for vibratory response of thick structural plate
[AD-721001] 15 p2522 N71-27859

Generally covariant, nondivergent equations of motion (including self field effects) of charged particles
15 p2493 N71-27939

Approximative method for predicting motion of symmetric rigid body subjected to body-fixed force
[NASA-CR-118993] 16 p1685 N71-28171

Atmospheric budget equations for mass, momentum, and energy derived for Barbados Oceanographic and Meteorological Analysis Program (BOMAP)
[COM-71-00193] 16 p2625 N71-28313

Investigation of impact of blunt body against flexible plate where high tensile impact wave velocity exceeds speed of sound in material
[AD-722281] 17 p2851 N71-29532

Mathematical models of nonlinear equations of motion of steam servomotor showing transient and steady state stability
[NLL-CE-TRANS-5261-9022-09/1] 17 p2773 N71-29736

Solving equations of motion to produce equilibrium flow consisting of modified Eckman spiral flow and helical secondary flow
17 p2735 N71-29827

Integral equations of motion and momentum for hypervelocity wind tunnel nozzle design
[AD-723446] 17 p2731 N71-29906

Relativistic equations of motion invariance with respect to Poincaré group Lie algebra and application to zero mass, spinless particle free motion equation
[ITF-70-32] 18 p2967 N71-30413

Fourier analysis of boundary value problems for linearized equation of ocean waves
[AD-722680] 18 p2919 N71-31440

Particle equations of motion for solving problems in electrodynamics, gas dynamics, hydrodynamics, and solid state physics
[NASA-TT-F-670] 18 p2948 N71-31492

Formulation of general equations of motion of thrust alleviated gyroscope given missile motion, and computer code for integrating resulting differential equations
[AD-723420] 19 p3132 N71-31799

Electromagnetic field disturbance models for clear air turbulence detection in atmosphere
[AD-723312] 19 p3091 N71-31936

Equations of motion derived for two dimensional turbulent vortex pairs in homogeneous and density stratified media
[AD-723184] 19 p3077 N71-31943

Comparison of analytical relative motion theory with numerical solution for equations of planar motion for two satellites of oblate planet
[NASA-TM-X-65633] 19 p3180 N71-32173

Nonlinear theory for describing planar, free oscillatory motion of missiles
[SCL-RR-70-119] 19 p3034 N71-32237

Notation and nomenclature for equation of motion of aircraft dynamics
[ARC-RM-3562-PT-3] 20 p2504 N71-32875

First order motion of cable towed and tethered bodies for predicting aircraft dynamic stability performance
[VKI-TN-68] 20 p2305 N71-33116

Equations of motion for horizontal pendulum with Zener suspension
20 p3264 N71-33362

Equations of motion solved for one dimensional magnetic piston problem in study of shock waves propagating perpendicular to magnetic field in collisionless plasma
20 p3332 N71-33817

Gauge invariant theory of motion of singularities in linear approximation
[NASA-CR-121431] 20 p3293 N71-33896

Equations of motion for rotating gravity gradiometer, developed for forced harmonic oscillator model
[NASA-TM-X-64605] 21 p3425 N71-34372

Linearized perturbation theory for calculating relative motion of unrestrained bodies within orbiting space stations
[NASA-CR-115142] 22 p3628 N71-33851

Analytic functions solving equations of motion in Newton theory for ballistic trajectory in atmospheric reentry
[DLR-FB-71-16] 22 p3670 N71-36168

FORTRAN computer program for simulation of movement using set of time dependent differential equations and plotting curve
[DRLS/9/07/TS] 23 p3729 N71-36585

Equations of motion for determining slip flow in one dimensional gas centrifuges
[NLL-CA-TRANS-250-19091.9F] 23 p3745 N71-36705

Hybrid coordinate equations of motion for finite element model of dynamic analysis on flexible appendage attached to rigid base
[NASA-CR-122936] 23 p3781 N71-36947

Numerical analysis of constants of motion for collisional kinetics equations
[AD-726620] 23 p3830 N71-37314

Long term equations of motion for earth-moon system including solar and lunar tidal torques
23 p3847 N71-37419

Algorithm and subroutine for solving Kepler equation for elliptical orbits
[NASA-CR-122933] 23 p3848 N71-37426

Solutions to Riccati differential equations of motion of accelerated body in medium where resistance varies as square of velocity
[AD-726929] 23 p3855 N71-37482

Dynamic models for ERSO 1 attitude control system noting equations of spinning motion
[ERSO-TM-5-ESTEC] 23 p3859 N71-37508

Equations of motion for elastic plate foundation system under dynamic load applied to aircraft landing
23 p3864 N71-37543

Equations of motion for describing weightlessness phenomena during space flight
[NASA-CR-123161] 24 p3880 N71-37660

Unified heuristic model of fluid turbulence which supplements basic equations of motion and continuity
[AD-727103] 24 p3906 N71-37840

Properties of three dimensional compressible fluid flows obtained by application of invariant transformation to equations of motion
[AD-727933] 24 p3907 N71-37849

Differential equations of motion for kinematics and dynamics of proportional navigation
24 p3950 N71-38180

Finite plane wave propagation and equations of motion in nonlinear relaxing media
[AD-727316] 24 p3966 N71-38293

Two component equations of motion with zero mass and 1/2 spin particles
[ITF-70-48-E] 24 p3977 N71-38374

Development of hybrid coordinate equations of motion for finite element model of flexible appendage attached to rigid base undergoing unrestricted motions
[JPL-TR-32-1525 NASA-CR-123213] 24 p4023 N71-38702

EQUATIONS OF STATE

NT HUGONIOT EQUATION OF STATE

Defining distribution functions for sets of a cavities in hard particle system using concept of equivalence
24 p4028 N71-11777

Determination of equation of state for solid hydrogen
[NYO-3699-43] 03 p0442 N71-12915

Computer program for calculation of variables of state of real gas mixtures with logarithmic linearization of nonlinear equations
[DLR-MITT-69-27] 03 p0469 N71-13372

Investigating effects of shock waves on various materials
[UCRL-71846] 05 p0733 N71-15012

Equation of state of hydrogen and deuterium between 3 and 10 cc/mole to 10,000 K
[UCRL-50911] 05 p0743 N71-15133

Equation of state for adiabatic electron plasma
[COO-2059-3] 05 p0754 N71-15225

Static compressibility measurements of Cedar City tonalite using equations of state
[AD-713175] 05 p0676 N71-15440

Analysis of stress theory with one nonlinear and two linear parameters
[ARL/SM-351] 09 p1481 N71-20520

Thermodynamically consistent equation of state for alpha and epsilon phases of iron
[AD-719233] 13 p2092 N71-24563

Magnetohydrodynamic generator systems analysis including electrical impedance and power conversion efficiency calculations for various designs
14 p2323 N71-26449

Calculated equations of state for solid sodium and aluminum
14 p2326 N71-26489

Lattice dynamics calculations for high pressure shock compression analysis on solid crystal
14 p2327 N71-26490

Piezoresistive shock wave profile measurements for determining aluminum alloy strength
14 p2343 N71-26491

High pressure shock and acoustic velocity data for calculating equation of state of aluminum
14 p2327 N71-26492

Equation of state based on ultrasonic bulk modulus measurements for cesium halides
14 p2327 N71-26497

Thermal and vibrational approximations of high pressure/volume relations in sodium chloride bulk modulus
14 p2327 N71-26498

Consistency and adequacy of approximations in high temperature equations of state for solids
[NASA-CR-118666] 14 p2328 N71-26500

Partition functions and equations of state of He, H, N, O, Ne, Ar, and solar plasmas - tables
[NASA-SP-206] 16 p2661 N71-28171

Equation of state and static correlations for ferromagnetic colloid
[AD-727212] 17 p2789 N71-36218

Expressions for state of stress and displacement for half space deduced from general basic formulas for three dimensional thermoelastic problem
[PB-197273] 18 p3024 N71-36802

CAPO code for studying equations of state/optical properties of ionized gases
[AD-727209] 18 p2993 N71-37426

Phase transformation thermodynamics and equations of state near critical points
20 p3366 N71-37578

Complete equation of state for metals in both solid and liquid/dense vapor phases, from ambient conditions to high pressures and temperatures
20 p3334 N71-37579

Development of equation of state for solid hydrogen for pressures up to 112 K-Bars
[NYO-3699-52] 21 p3465 N71-38463

Equations of state for calculating power output of UC and Pu-C nuclear fuels under various excursions
[NLL-RISLEY-TRANS-2143-9091.9F] 22 p3626 N71-37578

Critical points of magnetic substances and cryogenic fluids derived from equations of state, using deviations in thermodynamic properties
22 p3629 N71-37587

Data analysis for isoperibol laser calorimetry
[AD-726514] 23 p3764 N71-38462

Computer program for mixed phase equation of state for aluminum alloys to determine effects of nuclear radiation
[AD-726922] 23 p3770 N71-38471

Equation of state calculations for solid H₂, D₂, He-3, He-4, and Ne-20 at high densities in harmonic approximations
23 p3802 N71-37578

Thermophysical properties of air and air components - tables and diagrams
[TT70-50095] 24 p4030 N71-38753

Thermophysical properties of heavy water including nuclear properties, parameters of equation of state, and isotopic analysis with tables on thermodynamic properties
[TT70-50094] 24 p4030 N71-38757

EQUATORIAL ELECTROJET

Nonlinear theory of plasma turbulence in the equatorial electrojet
07 p1017 N71-17675

Measurements of ionospheric electric field in equatorial and medium magnetic latitudes using barium ion clouds
[MPI-PAE/EXTRATERR-49/70] 15 p2398 N71-27460

EQUATORIAL ORBITS

NT STATIONARY ORBITS

Momentum wheel stabilized, sun-oriented, synchronous equatorial satellites for aeronomical satellite system NETCOS
[NASA-TM-X-63509] 14 p2341 N71-33611

Conceptual design analysis of geosynchronous equatorial satellites for hybrid UHF/VHF aeronomical communication to be launched by Delta vehicles
[NASA-TM-X-63529] 19 p1884 N71-33173

Determination of vector equations and formulas for geodetic coordinates and ellipsoidal heights, using geodetic equatorial coordinates and synchronous observations
22 p3677 N71-36218

EQUATORS

NT MAGNETIC EQUATOR

Hourly equatorial magnetic variations data for 1957 to 1970
[NASA-TM-X-65645] 19 p3084 N71-32818

Equatorial D region positive ion composition studies by rocket payloads
[NASA-TM-X-65651] 19 p3085 N71-32819

Transport theory and adiabatic model for particle capture along equator of outer radiation belt
23 p3854 N71-37489

SUBJECT INDEX

Absorption and group delay data from equatorial station used to model electron density profile in D and E regions of ionosphere
[NASA-TM-X-45750] 24 p3909 N71-37083

EQUILIBRIUM

Comparative effects of auditory and extra auditory acoustic stimulation on human equilibrium and motor performance
[AD-711048] 01 p6008 N71-10177
Algorithms and FORTRAN calling program performing efficient convergence and high degree of man machine interactions in steady state process systems analysis
16 p2566 N71-28791

Variational synthesis method applied to steady state Boltzmann neutron transport equation
[ORNL-TM-3200] 21 p3477 N71-34766
Canonical and noncanonical equilibrium of infinite states of coupled harmonic oscillators
23 p3823 N71-37270

Equilibrium and stability of high beta toroidal plasmas
[CONF-710607-118] 24 p3992 N71-39481
Transfer coefficients and kinetic equilibrium for plasma confined in Tokamak at high temperatures
[CONF-710607-34] 24 p3994 N71-39495

U PHASE DIAGRAMS

EQUILIBRIUM EQUATIONS

Equilibrium states and attitude stability of dual spin spacecraft
[NASA-TM-X-362] 09 p1415 N71-30143

Dynamic stability criteria for continuous system stable in energy, adjacent equilibrium, or Gibbs sense
10 p1662 N71-21471

Equilibrium equations for small ions in region of magnetic and neutralized clouds, and reducing atmospheric concentration of charged particles by means
[JPRS-52542] 10 p1555 N71-21686

Computer program for equilibrium equations, combustion temperatures, and combustion efficiency of explosive and propellant combustion
[N71-370] 12 p2010 N71-23357

Derivation of pH CSTR dynamic equations based on acetic acid-sodium hydroxide neutralization and equilibrium equations for chemical reactions
13 p2040 N71-25046

Numerical integration of steady state heat conduction equations representing diurnal variations in upper atmosphere
[NASA-TM-X-45322] 13 p2186 N71-25089

Deterioration helium-3 fusion power balance calculations with inclusion of variable cyclotron radiation parameter
[NASA-TM-X-2280] 13 p2149 N71-25526

Radiative-convective equilibrium temperature calculations of Venus atmosphere
15 p2404 N71-27563

Quantum mechanics of two particle interactions in homogeneous systems including kinetic and equilibrium correlation equations using BBGKY hierarchies
15 p2487 N71-27629

Superconductor fluid and aerodynamic load stress analysis of finite cylindrical shells based on Galerkin method and aerodynamic equilibrium equations
[AD-72447] 18 p2905 N71-31183

Theory of equilibrium figures of rotating, homogeneous, incompressible fluid mass as applied to cosmology
[NASA-SP-186] 20 p3522 N71-33591

Development of method for calculating equilibrium vapor pressure in closed degassed systems
[N71-37064] 23 p3002 N71-37109

Two computer programs for calculating plasma stability and electron and microwave-B magnetic mirror systems
[UCRL-31030] 23 p3827 N71-37296

EQUILIBRIUM FLOW

NT FROZEN EQUILIBRIUM FLOW

NT SHIFTING EQUILIBRIUM FLOW

Development of flow property charts for pure nitrogen in quasi-one-dimensional nozzle for equilibrium, nonequilibrium, and frozen flow under hypersonic conditions
[AD-71704] 11 p1737 N71-22287

Steady state inflated shape and included volume of 36 and 30 gorr flat circular, extended skirt, porous ring disk, and porous ribbon parachutes
[AD-71806] 12 p1853 N71-23387

Harmonica 2 machine observation of magnetic flux singularities and Mercier theory equilibrium predictions of magnetohydrodynamic stability
[JPRS-CEA-PC-463] 14 p2323 N71-26448

Coupled equilibrium loop work including data on electrochemical memory, cover gas analysis, and oxygen determination and mass transfer models in sodium
[WARD-4210-T-1] 16 p2634 N71-28724

Solving equations of motion to produce equilibrium flow consisting of modified Ekman spiral flow and helical secondary flow
17 p2735 N71-29827

Stability of equilibrium state of rotor in pressurized gas bearing
[AD-722828] 18 p2929 N71-31213

EQUILIBRIUM METHODS

Nonlinear panel flutter analyses by perturbation and harmonic balance methods
[NASA-CR-111907] 13 p2183 N71-25362

Derivation of equations for coupled gas species concentrations equations in chemical equilibrium using free energy and equilibrium methods for specific heat and acoustic velocity calculations
[AD-720004] 14 p2215 N71-25941

Steady state generation of rotating multipoles for plasma experiments in Mca range with application to plasma beam acceleration and direct energy conversion for plasma turbines
[JUL-667-PP] 14 p2523 N71-26426

Experimental determination of data on liquid-vapor equilibrium systems
[NLL-RTS-5768] 17 p2713 N71-29218

Variants of calculus of predicates with equality and functional symbols
[NLL-RTS-5964] 17 p2775 N71-30362

EQUINOXES

Thermospheric models accounting for diurnal variations of temperature and density during equinoxes
[D-91] 20 p3254 N71-32821

EQUIPMENT

Inventory accounting control over equipment at Kennedy Space Center
[B-160658] 05 p0659 N71-15579

Feasibility of equalization in random vibration test for acceleration response and fatigue life of equipment
09 p1480 N71-20232

EQUIPMENT SPECIFICATIONS

Design for space qualified helium-neon laser
[NASA-CR-1663] 01 p0062 N71-10065

Systems performance/design requirements specifications for CH-46C helicopter digital flight control and landing system
[NASA-CR-110809] 01 p0003 N71-10294

Waste management system functional model for aerospace vehicles
[AD-710623] 01 p0015 N71-10472

Design of diagnosable control units for switching systems using modular integrated circuits
02 p0192 N71-11346

Specifications and drawings for semipassive optical communication system
[NASA-CASE-XLA-01090] 03 p0134 N71-12389

Sealed nickel-cadmium battery assembly BB-655
[AD-714243] 06 p0797 N71-16349

Design criteria and performance specifications for spacecraft sun sensors
[NASA-SP-8047] 07 p1032 N71-17756

Specifications of CAMAC 25-MHz counter module type LEM-52/1.1
[RKF-1184] 08 p1199 N71-18160

Atmospheric sampling apparatus design to follow changes in natural radioactive decay products of radon in free and conditioned atmosphere
[CEA-B-4048] 08 p1250 N71-18233

Field standard measuring flask specifications and tolerances
[NBS-HANDBOOK-105-2] 09 p1392 N71-19484

Functions and specifications of telemetry and associated equipment, and photographs of mobile FM/PM telemetry trailer, Ground Station H
[NASA-TM-X-65459] 09 p1350 N71-20161

Design and performance requirements for rocket-borne ozone temperature sensors
[AD-716997] 10 p1551 N71-21194

Technical descriptions and specifications of modules and subunits for space base multiple signal modem
[NASA-CR-114927] 10 p1525 N71-21459

Description of minimum performance standards for emergency locator transmitters of automatic fixed, automatic portable, and automatic deployable types
[D-147] 11 p1698 N71-21877

Criteria for evaluation of spacecraft garment systems, garment support systems, and space vehicle accessory items
[NASA-CR-114953] 11 p1646 N71-21926

Equations of motion and characteristics of invariant gyrocompass with pendulum correction
11 p1762 N71-22362

Component specifications and computer program for intermediate water recovery system on manned spacecraft
[NASA-CR-114961] 11 p1691 N71-22514

Stretcher with rigid head and neck support with capability of supporting immobilized person in vertical position for removal from vehicle hatch to exterior also useful as split stretcher
[NASA-CASE-XMF-06309] 12 p1863 N71-23159

Operational and environmental performance tests and specifications for precision bathymetric recorder
[JPRS-71010] 12 p1916 N71-23217

Instrumentation and development techniques for low velocity gas flow measurement
[NASA-CR-103096] 12 p1899 N71-23313

Major and critical component specifications for construction of simulator cruise scene visual at-

EQUIPMENT SPECIFICATIONS

tachment for manned spacecraft or aircraft flight simulation
[NASA-CR-114362] 12 p1896 N71-34137

Development and characteristics of viewing systems for thermal viewers and infrared detectors for airborne operation
[AD-719854] 13 p0046 N71-23053

Patient monitoring system design and equipment specifications with physiological response display device and warning system
[NASA-CR-118643] 14 p2309 N71-25942

Effect of acceleration, gradient, wind force, and center of gravity on design of vehicles for use in improved urban transportation system
14 p2360 N71-36130

Power requirements for vehicles used in improved urban transportation system
14 p2366 N71-36131

Requirement specifications for environmental laboratory test chamber complex design, fabrication, and testing
[NASA-CR-113007] 14 p2345 N71-26549

Documentation and equipment specifications for German scientific satellite programs
15 p2526 N71-27151

Design and fabrication of electron beam X-Y deflection system for retrofit on welding guns
[NASA-CR-119041] 17 p2729 N71-29234

Specifications and performance tests for digital pressure transducers designed for spacecraft application
17 p2731 N71-29232

Techniques and circuits used in designing AM highly flexible telemetry system comprising single sideband/double sideband/constant bandwidth compatible system - space application
17 p2718 N71-29233

Program for developing hydrogen-oxygen fueled auxiliary power unit for space shuttle vehicle
17 p2738 N71-29234

NASA specifications for high efficiency particulate aerosol filters including testing and installation
[NASA-TM-X-67249] 17 p2756 N71-29879

Development and analysis of optimal parameters for magnetic field windings in stellarator installations
[IYAR-4-70] 18 p2991 N71-30409

Design of axial compressor rotor - specification of meridional velocity profile
18 p3081 N71-31214

Occurrence research and development of equipment and instrument specifications
[AD-723247] 18 p2921 N71-31584

Analysis of problems involved in production of X ray laser
19 p3108 N71-32457

Human factors engineering for man machine systems
19 p3048 N71-32622

Ultra-narrow, high quality, high field quadrupole magnet for use in bevatron experimental area
[N71-30164] 20 p3546 N71-33589

Performance data and specifications of high resolution pion beam and spectrometer for nuclear structure research
[LA-4534] 20 p3427 N71-33742

Conceptual design for high energy electron ring accelerator allowing mass production techniques and ensuring low cost
[JUL-20160] 20 p3428 N71-33965

Configuration control for SUMC multiprocessors allowing for periodic changes in operational modes
[NASA-CR-119926] 21 p3397 N71-34174

Development of computer memory system for automated attendance accounting system
[NASA-CASE-NPO-11456] 21 p3399 N71-34189

Equipment specifications for balloon carried superconducting magnetic spectrometer to measure spectra of cosmic ray nuclei with charges ranging from protons to iron
[NASA-CR-131709] 21 p3425 N71-34370

General descriptions, specifications, circuit, and performance data for nuclear instrument module system
[JAERI-MEMO-4295] 21 p3428 N71-34390

General descriptions, specifications, circuit diagrams, and performance data for nuclear instrument module system
[JAERI-MEMO-4291] 21 p3428 N71-34391

Development of unified test equipment concept for space shuttle ground support system
[NASA-CR-72974] 21 p3502 N71-34645

Fabrication and field testing of lightweight, recoverable, air-transportable hangar
[AD-727031] 22 p3565 N71-35396

Fabrication and field testing of aircraft maintenance hangars and general purpose shelters
[AD-727047] 22 p3566 N71-35397

Performance data and specifications for amplifiers and signal analyzers for nuclear instruments
[JAERI-MEMO-4303] 22 p3584 N71-35524

Heat transfer and fluid flow during forced convection boiling of wetted mercury with application to

design and optimization of once-through boilers for Space Power Rankine Cycle Systems - SNAP-8 [NASA-CR-72897] 22 p3621 N71-35796
Techniques for determining system and equipment reliability requirements 23 p3757 N71-36783

Development of technique for evaluating effectiveness and operational utility of captured air bubble chips and ground effect machines [AD-728003] 24 p3875 N71-37620

Technical specifications and performance capabilities of Soviet and Hungarian produced GTT 6000/1920 (Drazhba) microwave system [AD-727411] 24 p3889 N71-37719

Equipment specifications for interactive programming system for image processing with Iliac, IBM 360, and PDP 8 computer components [CDD-2118-3] 24 p3894 N71-37753

EQUIPOTENTIALS

Equipotential space suits utilizing mechanical aids to minimize astronaut energy at bending joints [NASA-CASE-LAR-10007-1] 02 p0168 N71-11195

Universal dynamic flow without holdovers [PB-180992] 03 p0401 N71-13335

Instrument for measuring potentials on two dimensional electric field plot [NASA-CASE-XLA-08493] 09 p1361 N71-19421

EQUIVALENCE

Equivalence theorem and quantum mechanics in field theory [JINR-P2-5266] 09 p1411 N71-20381

Local controllability, equivalence, and diffeomorphic maps for nonlinear RC and RL circuits [AD-729011] 24 p3901 N71-37808

EQUIVALENT CIRCUITS

Kalman and Howitt equivalence transformations [AD-710725] 01 p0033 N71-10533

Using polar diagrams of asynchronous triphase diagrams for developing equivalent circuits [PUBL-116] 05 p0656 N71-15515

Equivalent circuit analysis of low frequency collector self modulation in transmitter output stage and frequency-amplitude distortion measurements [AD-716529] 09 p1373 N71-19624

Phase stability of parametric amplifiers under pumping, varactor bias, and interfering conditions, noting also equivalent circuits [REPT-3-35-1970] 10 p1531 N71-20640

Parallel circuit analogy for skin effect in conductors [AD-719234] 13 p2123 N71-24384

Silicon radiation detector production engineering for biological and medical applications and explanation of continuous absorption spectra using RC delay line as equivalent circuit [BMBW-FBK-70-15] 15 p2374 N71-26914

Equivalent circuit for 1/1 noise in planar silicon transistors and mechanism of noise generation [AD-719234] 16 p2374 N71-28214

Analysis of stability of two-port network to determine conditions of stability and properties of transformations of impedances [NLL-PORS-TRANS-2733-19022.81] 22 p3563 N71-35378

Resonance method for measuring equivalent circuits in joints between straight and uniformly bent waveguides [JPRS-54096] 23 p3732 N71-36603

Amplitude and frequency modulation characteristics and applications of CW Gunn effect oscillators [AD-719234] 23 p3734 N71-36623

ERBIUM

NT ERBIUM ISOTOPIES

Vacuum distillation technique for producing ultrapure erbium [JGEP-85] 20 p3285 N71-33764

Optical emission spectroscopy and excitation spectra of glass and YAG laser materials for improvement of plasma pumps for pulsed erbium lasers [AD-726391] 22 p3591 N71-35571

ERBIUM ALLOYS

Magnetic resonance in dilute magnetic alloys - hyperfine splitting of Ag-Er-167 [AD-722711] 17 p2829 N71-30279

ERBIUM COMPOUNDS

Spectrographic determination of rare earth impurities in erbium oxide and ytterbium oxide [BARC-4711] 05 p0639 N71-14708

Perturbed angular correlation technique for studying effect of cubic lattice on electronic levels of erbium ions in HoAl₂ [JGEP-85] 06 p0909 N71-15780

X ray diffraction analysis on erbium/hafnia system phase relations [IS-T-401] 07 p1092 N71-17453

Calculation of lattice constant change for beryllium induced strain in ErT₂ and ScT₂ [SC-RR-70-753] 13 p2154 N71-25531

Comparison of electroluminescent and photoluminescent bands in erbium doped zinc selenide crystals and crystal defect sites [AD-722429] 18 p2884 N71-30725

ERBIUM ISOTOPIES

Energy spectra of alpha particles induced by 12 MeV neutrons in erbium isotopes [INR-1175] 04 p0571 N71-13617

Half life of first excited levels of main and rotational band in even-even nuclei of Os, Er, and Dy [JINR-P2-5201] 08 p1250 N71-18232

Low lying atomic energy levels for odd-A nuclei Yb 177, Re 183, Er 167, and Pu 239 09 p1446 N71-20578

Radioactive nuclide Er-173 produced by irradiations of natural Yb and enriched Yb-176 samples [AD-727411] 18 p2986 N71-31261

Tables on nuclear decay schemes of Hf-173 and Er-161 [NYO-3950-3] 21 p3484 N71-34822

ERBIUM 169

U ERBIUM ISOTOPIES

ERBIUM 171

U ERBIUM ISOTOPIES

ERBIUM 171

ERBIUM 171

ERBIUM 171

ERBIUM 171

ERBIUM 171

ERBIUM 171

ERBIUM 171

ERBIUM 171

ERBIUM 171

ERBIUM 171

ERBIUM 171

ERBIUM 171

ERBIUM 171

ERBIUM 171

ERBIUM 171

ERBIUM 171

ERBIUM 171

ERBIUM 171

ERBIUM 171

ERBIUM 171

ERBIUM 171

ERBIUM 171

ERBIUM 171

ERBIUM 171

ERBIUM 171

ERBIUM 171

ERBIUM 171

ERBIUM 171

ERBIUM 171

ERBIUM 171

ERBIUM 171

ERBIUM 171

ERBIUM 171

ERBIUM 171

ERBIUM 171

ERBIUM 171

ERBIUM 171

ERBIUM 171

ERBIUM 171

ERBIUM 171

ERBIUM 171

ERBIUM 171

ERBIUM 171

ERBIUM 171

ERBIUM 171

ERBIUM 171

ERBIUM 171

ERBIUM 171

ERBIUM 171

ERBIUM 171

ERBIUM 171

ERBIUM 171

ERBIUM 171

ERBIUM 171

ERBIUM 171

ERBIUM 171

ERBIUM 171

ERBIUM 171

ERBIUM 171

ERBIUM 171

ERBIUM 171

ERBIUM 171

ERBIUM 171

ERBIUM 171

Propulsive performance and erosion behavior of accelerator nozzle operating as short pulse discharge or quasi-steady solid Teflon propellant plasma thruster [NASA-CR-111935] 21 p3501 N71-34902

Analysis of rate of evaporation and erosion of silicon carbide ceramics in air at high temperatures 22 p3598 N71-35604

Analysis of erosion stability of titanium dioxide stabilized with yttrium oxide at high temperature and high velocity flow of ionized combustion products 22 p3599 N71-35620

Neutralizer location for minimum accelerator erosion on 30 centimeter diameter ion bombardment thruster [NASA-TM-X-67926] 22 p3662 N71-36114

Numerical analysis of collision process between rain drop and rigid surface with variations in density, velocity, and momentum [UMICH-03371-12-T] 23 p3745 N71-36708

Models for predicting erosion of ductile and brittle target materials by natural contaminants 24 p3968 N71-38300

ERROR ANALYSIS

Human factors in use of terminal radar/analog display systems [FAA-WA-70-55] 01 p0010 N71-10001

Error analysis on oscillator measurements of in-phase fuel thermal conductivity [KFK-1140] 01 p0087 N71-10019

Instrument error analysis for visual tracking of satellites using goniometers [NASA-TT-F-13355] 03 p0452 N71-12283

Asymptotic behavior and error analysis for linear integral differential difference equations 03 p0401 N71-13329

Experimental analysis in measurement of neutron flight time [IAE-1908] 04 p0569 N71-13477

Estimating location and velocity of ship using only range readings of ship-to-satellite distance at various times [AD-712756] 04 p0542 N71-13951

Orbital position estimation error analysis and earth orbital mission simulation [NASA-CR-106708] 04 p0543 N71-14010

Error study for SS-1090 ATDM sensor system, effects of atmospheric refraction, atmospheric attenuation, and earth albedo [NASA-CR-102957] 04 p0611 N71-14006

Accuracy of X ray line intensity measurements from nonmetallic materials [MG/D-587/68] 05 p0706 N71-14539

Digital simulation for error analysis of numerical integration schemes [NASA-CR-102958] 05 p0713 N71-14501

Kantorovich theorem and error estimates for Newton's method [AD-713698] 05 p0713 N71-15216

Measuring dynamic errors of infrared radiometer used to measure ocean and sea surface temperature [JPRS-52039] 05 p0676 N71-15428

Analysis of pulsed wire anemometer to determine errors caused by finite yaw response of probe [REPT-70-07] 05 p0687 N71-15471

Laboratory intercomparison of fluorescent lamps to determine available precision in photometric and spectrophotometric measurements [NBS-TN-559] 05 p0687 N71-15476

Evaluating data error analysis and equipment performance in tests of differential loan technique [ESSA-TR-ERL-166-ITS-107] 05 p0721 N71-15511

Investigating accuracy in sighting and identifying points on aerial photographs when measuring coordinates 06 p0857 N71-15777

Error analysis of satellite ionospheric electron content measurements 06 p0849 N71-16214

Developing human error rate data bank for human reliability and engineering problems [SC-R-70-4286] 06 p0807 N71-16306

Combination test generation program for any non-redundant fault in combinational logic act [NASA-CR-116199] 06 p0820 N71-16432

Effects of input power spectra on human operator compensatory tracking [AD-714130] 06 p0806 N71-16404

Calibration activity of Deep Space Network in support of Mars encounter phase of Mariner Mars 1969 mission [NASA-CR-116248] 06 p0949 N71-16881

Deriving algorithm for solving maximum stationary flow in network having exponential error 07 p1001 N71-16875

Error analysis for pressure measurements on blowdown supersonic wind tunnel models [NPL-AERO-1306] 07 p1003 N71-17001

Stochastic process error analysis of airborne gravimetry [AD-715248] 07 p1021 N71-17771

Error analysis of Cactus high sensitivity accelerometer during flight performance tests [ONERA-TP-475] 06 p1200 N71-18450

SUBJECT INDEX

Using methods of perturbation theory to produce data on sensitivity of calculated values of critical parameters and brooding factors of fast power reactors to changes in constants 06 p1240 N71-18784

Error analysis on solution of inverse heating problem for flat plates and hemispherical shells 06 p1304 N71-18828

Mariner Venus-Mercury 1973 imaging experiment for mapping Mercury and error rates for science work 06 p1289 N71-18874

Error analysis for extraterrestrial convergent photogrammetric mapping system [NASA-CR-116624] 06 p1283 N71-19021

Numerical analysis of error bounds in digital computation of four parameters for strapdown inertial systems [NASA-CR-103650] 06 p1231 N71-19044

Incremental positioning device acceptability test, including error analysis [LRAA-PV-12-310/SEI] 10 p1563 N71-20762

Error analysis of counting accelerometer data from F-4 and RF-4 aircraft and structural fatigue analysis [AD-717151] 10 p1497 N71-20796

Error effects on antenna gains and pattern degradation tolerances of parabolic reflectors and lens antennas 10 p1521 N71-21344

Error analysis for mean linear error of nonredundant code in asymmetrical channel without memory [JLL-XT-6038] 10 p1530 N71-21469

Analysis of errors in independent subcarrier and harmonic subcarrier methods of radio telemetry on FM radio carrier [SC-CR-70-6092] 10 p1526 N71-21756

Solid rocket multicomponent test stand design, calibration, and error analysis for secondary injection thrust vector control mechanism studies [MIL-TR-203] 11 p1730 N71-22157

Computational models for estimating errors in temperature measurements in fluids and solids 11 p1842 N71-22597

Dynamic reconstruction errors in digital to analog systems with biomedical applications [NASA-TN-D-6296] 12 p1865 N71-23160

Data transmission reliability and error analysis over radio relay channels 12 p1879 N71-23537

Revised robin mass measurements, systematic and random errors, and group variances 12 p2017 N71-23634

Analysis of sampled data reconstruction errors from digital data processing 12 p1884 N71-23872

Star position and proper motions in south celestial pole region and source dependent systematic deviations in Smithsonian Astrophysical Observatory data [NASA-CR-118035] 12 p1997 N71-24225

Numerical analyses of error covariance matrix in linear filtering problem: computational errors in Kalman filtering, and coasting flight equations [NASA-CR-115010] 13 p2102 N71-24470

Analysis of errors which occur during assembly of optical instruments and methods for eliminating errors [AD-719773] 13 p2125 N71-24940

Comparison of tracking rate residuals attributed to sensors with orbital calculation effects using error containing earth force fields 13 p2168 N71-25276

Error analysis of integrated inertial/Doppler satellite navigation system with continuous and multiple satellite coverage [AD-720793] 14 p2290 N71-26197

Relative compression inhomogeneities in sodium chloride/nitrobenzene mixtures as error sources in internal standards for pressure gases 14 p2243 N71-26513

Error analysis of in-pile thermal conductivity and specific heat measurements with balanced oscillation in experimental breeder reactor 2 [EUR-TR-755] 15 p2450 N71-27631

Time-base error analysis of magnetically recorded and photo-bank digital data using tape flutter spectral density and amplitude probability distribution measurements and run time plots [NASA-CR-115029] 15 p2411 N71-27711

Manipulation errors in computer solution of critical size structural equations using finite element method [NASA-CR-1784] 16 p2565 N71-28279

System inaccuracies in telescope experiment consisting of ultraviolet television photometers in OAO 2 16 p2593 N71-28511

Validity of bremsstrahlung model for background reduction in galaxy and earth atmosphere [NASA-TT-8-13615] 16 p2675 N71-28943

Error estimating technique for experimental data based on finite difference theory and standard deviations [ABCL-3781] 17 p2772 N71-29448

Survey of errors in sampling shock tube gas with mass spectrometer for study of chemical reaction rates at high temperatures 17 p2735 N71-29782

ERROR DETECTION CODES

Error analysis of Monte Carlo calculation for time structure of short duration light pulse reflected by atmosphere surface [NLL-M-20355-1528.4F] 24 p3932 N71-38058

ERROR BAND

U ACCURACY

ERROR CORRECTING DEVICES

Pseudo-noise addressing system analysis for multiple access communication with applications of error correcting codes 01 p0022 N71-10535

Developing digital computer program for correcting soft parameters of thermal network by Kalman filtering method [NASA-CR-100811] 02 p3065 N71-11605

Error detector/corrector codes adaptable to transmission of numerical data 04 p3507 N71-13831

Error correction circuitry for binary signal channels [NASA-CASE-XNP-03263] 06 p1170 N71-18843

Multiplexed communication system design including automatic correction of transmission errors introduced by frequency spectrum shifts [NASA-CASE-XNP-81508] 10 p1518 N71-20814

Topographic corrections for lunar gravity data 10 p1644 N71-21339

Description of error correcting methods for use with digital data computers and apparatus for encoding and decoding digital data [NASACASE-XNP-02748] 11 p1719 N71-22749

ALGOL program for detection and correction of data errors using TR-4 computer [RAB-LIB-TRANS-1544] 12 p1882 N71-23467

Encoder/decoder design and evaluation of fail-safe error correction capability under stationary random noise conditions for pulse communication reliability improvement [AD-720250] 14 p2218 N71-26141

Extrapolation and error estimation method for solving second order boundary value problems 17 p2773 N71-29720

PORTMAN 4 program for correction and calibration of neutron inelastic scattering data including background, air attenuation, detection efficiency, and sample thickness [EUR-4599-E] 18 p2972 N71-30514

Computer simulation of adaptive classifying structures and self-correcting devices for photographic processing [BAGWG-FBWT-70-4] 18 p2893 N71-30603

Error correction for GEOS-C altimeter system from range and angle observations 19 p3099 N71-31878

Computer program with predictor-corrector numerical integration subroutine for fast trajectory analysis [NASA-TM-X-65635] 19 p3180 N71-32172

Error correcting codes and data compression techniques for PCM adaptive telemetry systems - abstracts [NASA-CR-119679] 19 p3057 N71-32408

Long correction procedure for radiosonde humidity measurement errors 19 p3131 N71-32737

Data compression and error correcting codes applied to digital transmission of real time, standard format TV, along with voice and other data from Apollo spacecraft 21 p3515 N71-35049

Code mask for improved signal to noise ratio in scanning optical systems [NASA-CR-123155] 24 p3887 N71-37785

Correction factors for thermal diffusivity time measurements by pulsed laser [SC-RR-10220] 24 p3946 N71-38292

ERROR DETECTING CODES

NT BCH CODES

ERROR DETECTION CODES

Calculating delivery errors of automatically released bombs caused by onboard computer and attitude/air data sensor errors 03 p0408 N71-12612

Developing high integrity digital flight control of variations in performance of complex systems 03 p0409 N71-12614

Investigating general purpose digital computers for fault isolation capabilities in guidance and control systems 03 p0409 N71-12623

Constructing algorithms for majority logic decoding for linear block codes 04 p0300 N71-13495

General method for constructing efficient coding systems correcting any given number of asymmetrical errors in advance 04 p0513 N71-13544

Error detector/corrector codes adaptable to transmission of numerical data 04 p0507 N71-13831

Design of suboptimum receiver for coded, dual diversity, frequency shift keyed transmitter [AD-714599] 06 p0817 N71-16835

Manual for Mark 4 Error Propagation Program operation in CDC 6600 computer search of interplanetary trajectories [NASA-CR-111852] 07 p0997 N71-17465

Search for best cyclic /20, 4/ block codes and comparison of performance with /15, 5/ BCH code
[ESSA-TR-ERL-174-IT8-111]

- 07 p0994 N71-17946
- Digital data processing and error correcting code techniques applied to Apollo unified S band communication system
[NASA-CR-114921] 10 p1525 N71-21465
- ALGOL program for detection and correction of data errors using TR4 computer
[RAE-LIB-TRANS-1544] 12 p1882 N71-23667
- Self testing and repairing computer comprising control and diagnostic unit and rollback points for error correction
[NASA-CASE-NPO-10567] 13 p2049 N71-24633
- Space shuttle synthesis program manual including dock setup, input parameters, and synthesis operations for trajectory and performance predictions
[NASA-CR-114984] 13 p2173 N71-24824
- Problem of deterministic source encoding with fidelity criterion using computational work
[NASA-CR-118656] 14 p2224 N71-26343
- Markov chain model for characterizing error sequences in digital channels with memory
[NASA-CR-121429] 20 p2329 N71-33551
- Blizard decoding algorithm for binary linear error correcting codes 21 p3392 N71-34134

- Elastic matching, error correction coding in natural language
[NPL-COM-SCI-46] 22 p3556 N71-35330

ERROR FUNCTIONS

- Determining distribution density of unknown stochastic vector using fixed error probability matrix
[JPBS-51739] 02 p0252 N71-12170
- Affect of systematic errors on measurement of crystal lattice constants
[AD-715354] 08 p1278 N71-18677
- Estimation of error density function for optimum pulse modulation communication systems using Monte Carlo simulations 16 p2563 N71-28792

ERROR SIGNALS

- Flow induced error frequencies in tidal wave measuring hydrophones
[AD-715181] 01 p0051 N71-10937
- Transient responses of single loop systems with quantized error signals 03 p0351 N71-12534
- Error correction circuitry for binary signal channels
[NASA-CASE-XNP-03263] 08 p1170 N71-18843
- Feedback controller for sampling error signals within single control formulation time interval
[NASA-CASE-GSC-10554-1] 16 p2566 N71-29033
- Finite state discrete parameter Markov chain representation of ionospheric communication error sequences 19 p3057 N71-32561
- Determining signal set with minimum probability of error, and dependence of optimal signal set on signal to noise ratio 23 p3727 N71-36564

ERRORS

- NT INSTRUMENT ERRORS
- NT PHASE ERROR
- NT PILOT ERROR
- NT POSITION ERRORS
- NT RANDOM ERRORS
- NT RANGE ERRORS
- NT ROOT-MEAN-SQUARE ERRORS
- NT TRUNCATION ERRORS
- NT VELOCITY ERRORS
- Multichannel scattering problem solution method with two sided error estimations
[JINR-P4-5149] 03 p0426 N71-12843
- Probability of error for orthogonal signals on fading white Gaussian channel
[AD-712707] 04 p0489 N71-13483
- Systematic errors of heterotropic and PE baroclinic progs
[AD-718111] 12 p1956 N71-23858
- Design criteria establishing upper bounds for error of simple output solutions for nonlinear feedback systems 16 p2575 N71-28693
- Mathematical model for computerized strict error estimation in differential equation systems 18 p2948 N71-31461
- Integrating sphere reflectometer for measuring absorbance of cavity type receivers
[NBS-TN-575] 18 p2892 N71-31518
- Synthesis of aircraft across track errors using mathematical models with statistical parameters
[REPT-EIC-2] 20 p3299 N71-32885
- Estimate of random errors in gravity measurements made aboard submarines using grapho-mechanical analyzer 21 p3417 N71-34315
- Calcite filter for astronomical photometry, errors, and near infrared applications 22 p3584 N71-35525
- Satellite position calculation to eliminate weak star field errors 22 p3679 N71-36237

ERTS

U EARTH RESOURCES TECHNOLOGY SATELLITES

- ERYTHROCYTES
- Low barometric pressure effects on human and chicken erythrocyte active sodium efflux
02 p0155 N71-11097
- Peroxisomes and catalase activity and hyperoxia effects on mice organs, leukocytes, and erythrocytes in pure oxygen under pressure
[ANL-TRANS-677] 15 p2371 N71-27290
- Hypoxemia effects on erythrocytic systems of splenectomized dogs 16 p2544 N71-28266
- Red cell mass and plasma volume changes noted in hypodynamic states of bed rest and water immersion compared to changes observed during earth orbital missions 20 p3216 N71-32523
- Red cell mass loss in human beings as result of bed rest 20 p3219 N71-32271
- Red cell mass and plasma volume changes observed in astronauts on Gemini and Apollo missions 23 p3711 N71-36454
- Determination of electrical charge and field strength at cell membrane of human erythrocytes
[NASA-TT-F-14007] 24 p3877 N71-37636
- Gene frequencies of red cell acid phosphatase in random samples
[NASA-TT-F-13969] 24 p3877 N71-37637

ESAKI DIODES

- U TUNNEL DIODES
- ESCAPE [ABANDONMENT]
- Crash survivability and escape possibilities from motor vehicles 19 p3196 N71-32198
- Human performance in escape from crashed vehicle environments and escape worthiness of vehicles
[PB-196772] 19 p3196 N71-32247

ESCAPE CAPSULES

- Emergency escape cabin system for launch towers
[NASA-CASE-XKS-02342] 02 p0169 N71-11199
- Safe separation criteria for external stores and jet-tisonable escape capsules for pilots
[AD-726695] 23 p3707 N71-36428

ESCAPE ROCKETS

- Design, fabrication, and tests of engine absorbing seat integrated with extraction tractor rocket for space shuttle 22 p3547 N71-35268

ESCAPE SYSTEMS

- NT LAUNCH ESCAPE SYSTEMS
- Design and specifications of emergency escape system for spacecraft structures
[NASA-CASE-MSC-12086-1] 03 p0328 N71-12345
- Automatic braking device for rapidly transferring humans or materials from elevated location
[NASA-CASE-XKS-07814] 15 p2414 N71-27067
- Space shuttle hazards, safety procedures, and escape systems 22 p3675 N71-36203

ESCAPE VELOCITY

- Second order perturbation solution to modified optimal low thrust escape problem
[NASA-CR-108665] 02 p0294 N71-11403
- Amount of material evaporated, and initial escape velocity of evaporation products of various materials used as laser targets 12 p1933 N71-23384
- Procedure for computing gravity losses over n-burn multiorbit escape trajectories of specified final energy and prediction of optimal burn schedules for nuclear rocket escape maneuvers 22 p3671 N71-36178

ESCHERICHIA

- Altitude induced changes in glucose metabolism of Escherichia coli
[AD-715212] 07 p0982 N71-17830
- Effect of radiation sensitive mutations and radiation of recombination in partially diploid derivatives of Escherichia coli
[ORO-4024-1] 10 p1497 N71-20728
- Accelerated growth of Escherichia coli in high pressure helium-oxygen atmospheres
[AD-717494] 11 p1680 N71-22115
- Freezing and microwave effects on contaminated precooked frozen meal components 11 p1683 N71-22253
- Growth and fatty acid synthesis inhibition in Escherichia coli by oxygen
[AD-717673] 11 p1683 N71-22347
- Escherichia coli cell phospholipid composition changes during sporophyll formation in presence of penicillin and saccharose 11 p1683 N71-22506
- Metabolism of magnesium deficient Escherichia coli cells under aerobic and anaerobic conditions
[NRC-TT-1472] 22 p3545 N71-35255

ESG [GYROSCOPES]

- U ELECTROSTATIC GYROSCOPES
- ESRO SATELLITES
- NT AZUR SATELLITE
- NT ESRO 1 SATELLITE
- NT ESRO 2 SATELLITE

NT HEOS A SATELLITE

- NT HEOS SATELLITES
- Infrared photography for ESRO satellite surface and solar cell temperatures and vestibular eye examinations
[ESRO-TM-150-ESTEC] 03 p0382 N71-13372
- European Space Research Organization meteorological, communications and air traffic satellites program 08 p1293 N71-18840
- Scientific results from ESRO satellites and from sounding rocket campaigns including aeronomical fields, management planning, satellite development, and telecommunication - 1969 report 13 p2188 N71-24444
- Test facilities for HEOS and ESRO satellite magnetic control - Noordwijk, Netherlands
[ESRO-TM-134F-ESTEC] 17 p3730 N71-29409
- Outgassing thermal vacuum test on materials for selection as ESRO satellite materials noting weight loss analysis 17 p2756 N71-30042
- [ESRO-TM-110-ESTEC] 17 p2756 N71-30042
- ESRO program for solar orbit satellite testing gravitation theory 18 p3019 N71-31300
- [ESRO-SM-78] 18 p3019 N71-31300
- Feasibility of future ESRO polar orbiting meteorological satellites 20 p3354 N71-33848
- Acoustic data obtained during launch of ESRO 1-B satellite and GRS-A satellite by Scout launch vehicle
[NASA-TN-D-6369] 20 p3354 N71-33848
- ESRO scientific satellite spin reduction mechanism design
[ESRO-CR-30] 23 p3858 N71-37074
- ESRO 1 SATELLITE
- ESRO 1 Geiger counter and ground geophysical observations of radiation belt electron precipitation, flux structure, and angular distribution during solar flares, 25 Feb. 1969 02 p0212 N71-11550
- [R-17] 02 p0212 N71-11550
- Digital simulation of ferromagnetic material hysteresis for ESRO 1 satellite attitude control
[ESRO-SR-12-ESTEC] 03 p0458 N71-13233
- Data reduction and computer programming for ESRO auroral spectroscopy experiment
[KGO-PREPRINT-70-313] 10 p1545 N71-28621
- ESRO 1 and ESRO 2 satellite experiments investigating polar magnetosphere 10 p1647 N71-20714
- ESRO 1 satellite flight performance 10 p1647 N71-20714
- [ESRO-TN-100-ESTEC] 10 p1647 N71-20714
- ESRO 1 spectrometer for measuring auroral electrons and protons 10 p1557 N71-21085
- [KGO-PREPRINT-70-310] 10 p1557 N71-21085
- ESRO 1/Aurora satellite photometric data on auroral ionospheric electron and proton precipitation and population for Oct. - Nov. 1968 - conference
[ESRO-SR-57-621] 10 p1549 N71-21119
- ESRO 1 satellite photometric data on relationship between electron and proton auroras and precipitation 10 p1549 N71-21152
- Correlation between ESRO 1 satellite auroral photometric data and ground based observations 10 p1549 N71-21153
- ESRO 1 satellite experiment on magnetic field aligned electric field near or in ionosphere 10 p1550 N71-21114
- ESRO 1 satellite experiment on low energy electron precipitation during polar cap absorption and quiet magnetospheric conditions 10 p1550 N71-21155
- Proton precipitation above 100 keV observed by ESRO 1 satellite in noon-midnight meridian 10 p1550 N71-21157
- ESRO 1 satellite observation of variations and flux structure in flux density and angular distribution of electrons with energies above 40 keV 10 p1550 N71-21158
- Measurements of 1 to 30 MeV protons during solar proton events taken onboard ESRO 1 satellite 10 p1550 N71-21160
- Electron energy spectra 45 to 450 keV measured onboard ESRO 1 satellite during quiet and magnetically disturbed periods over polar region 10 p1550 N71-21161
- Electron energy and density profiles observed onboard ESRO 1 satellite over polar cap 10 p1551 N71-21162
- ESRO 1 satellite Langmuir electrostatic probe electric field detection 10 p1551 N71-21163
- ESRO 1 satellite guidance sensor specifications for attitude control
[ESRO-TN-99-ESTEC] 12 p1918 N71-23476
- ESRO 1 satellite control during orbital lifetimes
[ESRO-TR-9-ESTEC] 12 p2090 N71-23534
- Magnetic substorm events and magnetospheric structure in polar auroral zones determined by rocket sounding, satellite observations, and ground-based measurements - conference 12 p1908 N71-23535
- Auroral electron and proton zones determined by auroral ionization spectroscopy onboard ESRO 1 satellite 12 p1909 N71-23536

SUBJECT INDEX

- Polar diurnal variations of proton belts and precipitation detected by ESSO 1 satellite 12 p1910 N71-23571
- Measurement and calculation of ESSO 1 satellite temperature [N71D149/158] 13 p2171 N71-24380
- Auroral photometers used on ESSO 1/Aurora satellite for ionospheric sounding 15 p2407 N71-27055
- Shadow and earth albedo effect on ESSO 1 solar cell array performance in orbit [N71D149/158] 23 p3859 N71-37505
- Dynamic models for ESSO 1 attitude control system solving equations of spinning motion [N71D149/158] 23 p3859 N71-37508
- ESSO 1 SATELLITE
- ESSO 1 and ESSO 2 satellite experiments in investigating polar magnetosphere 10 p1647 N71-20716
- ESSA SATELLITES
- NT ESSA 3 SATELLITE
- NT ESSA 4 SATELLITE
- NT ESSA 6 SATELLITE
- NT ESSA 8 SATELLITE
- NT ESSA 9 SATELLITE
- Research study on reduction, analysis, and interpretation of radiation balance measurements from ESSA weather satellites [P9-19247] 03 p0404 N71-13243
- Data reduction processes for spinning flat-plate satellite-borne radiometers [ESSA-TN-1983-52] 05 p0649 N71-14779
- Time-longitude ESSA satellite photographs of tropical cloudiness [ESSA-TN-1983-56] 05 p0717 N71-15134
- Cost analysis of increased ESSA services for scientific dynamic study in Gulf Coast [P9-194077] 05 p0676 N71-15455
- Tables of meteorological satellite data - ESSA 7 television cloud photography - 1 Jan. 1969 to 31 Mar. 1969 18 p2926 N71-31442
- ESSA 3 SATELLITE
- Comparison of concurrent cloud data obtained via ATS 3 and ESSA 3 and from Apollo 6 high resolution photography [NASA-TN-D-6470] 21 p3452 N71-34566
- ESSA 4 SATELLITE
- Simple method for receiving picture signals from satellites, using ESSA 4 [AD-722045] 16 p2562 N71-28655
- ESSA 6 SATELLITE
- ESSA 6/APT meteorological photographs of Europe for April through June 1968, and weather satellite developments 21 p3454 N71-34585
- ESSA 8 SATELLITE
- Weather satellite data and APT pictures for Europe during last quarter of 1968 [P9-4] 04 p0541 N71-14117
- Satellite-borne photography of Europe and orbital data from ESSA 8 and Nimbus 3 satellites for 1 July 1969 - 30 Sept. 1969 [P9-3] 21 p3451 N71-34564
- ESSA 9 SATELLITE
- ESSA 9 television cloud photographs of Northern and Southern Hemispheres - Apr. 1-June 30, 1969 20 p3297 N71-33835
- ETHERS
- NT ACRYLATES
- NT CARBAMATES [TRADENAME]
- NT CELLULOSE NITRATE
- NT ISOCYANATES
- NT LACTATES
- NT LEXAN [TRADEMARK]
- NT NITRATE ESTERS
- NT PHTHALATES
- NT POLYCARBONATES
- NT POLYESTERS
- NT POLYETHYLENE TEREPHTHALATE
- NT SODIUM SALICYLATES
- NT STERATES
- NT URETHANES
- Investigating ester and alkyl compounds as lubricants for use with liquid oxidizers [NASA-CR-102967] 02 p0246 N71-14119
- Rate analysis and colloidal molecular weight determination by gel chromatography 03 p0350 N71-12353
- Using best resistant aromatic cyanate esters as reinforcement plastics [NASA-TT-F-13454] 06 p0811 N71-16476
- Presence of alkyl esters of long-chain fatty acids determined for Rhinopus arthrus 08 p1161 N71-19116
- Off-line processing of chromatographic data from fatty acid methyl ester mixtures by digital computer [N71D149/158] 11 p1716 N71-22548
- Synthesis of 12 hydroxystearic acid esters of tri-1,8-naphthyl aziridinyl phosphine oxide at 100°C or less [AD-721655] 16 p2557 N71-28354
- ETIMENTS
- NT COST ESTIMATES

- Statistical models for constructing minimum variance unbiased estimates [AD-714067] 06 p0884 N71-16384
- Technology and data used to generate thermionic reactor experiment cost estimates [GBSR-2123] 13 p2123 N71-25557
- Strict estimation of derivative values 17 p2738 N71-29573
- Estimation method for real compression coefficient of spacecraft data processing system [NASA-TT-F-13752] 19 p3061 N71-32170
- Estimates of laser energy required to heat inertially confined 4-1 target in pulsed fusion reactor [CLM-R-109] 21 p3436 N71-34448
- Point estimates of standardized variances of independent and correlated measurements using least squares method [NLL-14-20658-3828.4P] 21 p3450 N71-34553
- Efficiency estimates of turbine and compressor components of Brayton rotating unit during hot closed loop operation [NASA-TM-X-2350] 22 p3542 N71-35252
- Reliability estimation, including failure effect analysis of avionics systems 23 p3757 N71-36777
- Regression analysis of estimation tests and system operating data 23 p3757 N71-36778
- Mathematical models for estimating block up-and-down design of sensory thresholds [NASA-TM-X-62090] 24 p3878 N71-37644
- Manual for development of needs estimates and capital improvement programs for airports and other intercity terminals for 1970 to 1990 [OMB-04-571002] 24 p3903 N71-37824
- ESTIMATION
- NT ORBITAL POSITION ESTIMATION
- Weight estimating and forecasting during conceptual design of spacecraft [NASA-CR-108749] 04 p0614 N71-14142
- Weight estimating and forecasting of manned space systems during conceptual design - handbook [NASA-CR-108765] 04 p0615 N71-14185
- Accuracy of estimating location of landed spacecraft on Mars from range and range rate data [NASA-TN-D-6109] 05 p0766 N71-14561
- Exact solution to adaptive linear estimation problem [AD-713098] 05 p0655 N71-14926
- Scatter factor in statistical aircraft life estimation [ARL/SM-350] 05 p0775 N71-15154
- Linear estimation model for network flow [POA-P-C-8237-13] 05 p0666 N71-15611
- Review and critique of procedures and results in nonlinear estimation [AD-715631] 08 p1225 N71-18921
- Estimation of momentum, heat transfer, and mass transfer in laminar boundary layers 12 p1903 N71-23948
- Fundamental techniques of weight estimating and forecasting for advanced manned spacecraft and space stations [NASA-TN-D-6349] 13 p2062 N71-25423
- Estimating continuous target distributions density [S-38-1971] 14 p2217 N71-26088
- Kalman formulation of minimum mean square linear estimation with random variables and unknown distributions producing biased results [NASA-CR-118465] 14 p2284 N71-26429
- Computer simulation results of satellite antenna bore-sight parameter estimation [AD-720242] 15 p2387 N71-27425
- Error estimating technique for experimental data based on finite difference theory and standard deviations [ABCL-3781] 17 p2772 N71-29448
- Attitude estimation and control of earth pointing satellites in circular orbit [DRL-FB-78-75] 17 p2849 N71-29489
- Single shot joint detection and estimation for discrete and continuous data, and joint Bayesian detection, estimation, and system identification [AD-722460] 18 p2896 N71-31346
- Mathematical model for computerized strict error estimation in differential equation systems 18 p2948 N71-31461
- Kalman filtering techniques for estimating position and velocity of spacecraft [NASA-CR-116153] 22 p3417 N71-35771
- Conical and nonconical estimation theory for nonlinear random vector channels, for radar tracking and diversity communication 23 p3726 N71-36359
- Adaptive nonparametric approach to estimation and signal processing combining learning, decision, and optimization mathematical techniques 23 p3726 N71-36561
- Wind tunnel interference estimation for model design applications using chart method [NASA-TN-D-6416] 23 p3741 N71-36675
- Statistical estimation theory applied to quantum mechanics and signal detection with optical instruments [NASA-CR-121784] 23 p3801 N71-37101

- Magnitude estimation method for determining loudness of transient sounds and effect of sounds on structures [TR-42] 23 p3803 N71-37117
- ESTIMATORS
- Development of adaptive estimators for application to numerical analysis of automatic navigation and control [AD-720394] 14 p2282 N71-26087
- ESTUARIES
- Investigating feasibility of using remote sensors for studying estuaries from aircraft or spacecraft platforms 06 p0847 N71-16172
- Color infrared photography as remote sensing techniques in investigating estuaries and marshlands 06 p0847 N71-16174
- Oceanographic data on Mississippi estuary water pollution by oil [AD-714260] 06 p0820 N71-16413
- Seasonal variations of current and salinity of Dnestrovskiy liman induced by changes in wind and rain [AD-717321] 11 p1744 N71-21858
- Estuary gravitational flow mathematical model noting turbulent mixing 12 p1910 N71-23606
- Mathematical model for optimal water quality control in estuaries [REPT-08/70] 14 p2250 N71-26379
- Development, characteristics, and evaluation of model of estuary of Columbia River to determine effects of navigation channel modifications on currents and sediments [AD-724100] 21 p3421 N71-34346
- ETA-MESONS
- Investigating reaction eta-meson yields 3 pion for charge asymmetry [NEVIS-177] 04 p0591 N71-14389
- Investigating neutral decays of eta-meson using cubical array of lead plate spark chambers for conversion of gamma rays [UCRL-20039] 05 p0740 N71-15104
- Measuring reaction photon proton yields pion/eta/eta' for photon energies from 4 to 18 GeV and four-momentum transfers between -0.1 and -1.4 GeV/c² [SLAC-124] 06 p0916 N71-16024
- Radiative decay mode measurements on neutral phi-meson yielding neutral eta-meson gamma, neutral phi-meson yielding neutral pion gamma [LAL-1240] 08 p1255 N71-18360
- Mass and energy spectrum analyses for photon, neutral pion, and eta-meson interactions based on Monte Carlo method [JINR-EI-5349] 13 p2129 N71-24685
- Decay branching ratios of eta-mesons 15 p2744 N71-27454
- Duality FSR method for predicting eta meson yields pion/eta gamma gamma decay rate [DEMO-71/2] 15 p2487 N71-27833
- ETCHING
- Microetch technique for analyzing thin layers of striated single crystals 01 p0108 N71-10128
- Vibratory cavitation for metal and superalloy etching in distilled water [NASA-TM-X-52929] 03 p0392 N71-12941
- Development of method for etching copper [NASA-CASE-XGS-06306] 06 p0871 N71-16044
- Composition and process for improving definition of resin masks used in chemical etching [NASA-CASE-XGS-06993] 07 p1029 N71-17574
- Using ion bombardment etching technique to reduce thickness of boron carbides for transmission electron microscopy [AD-715057] 06 p1221 N71-18498
- Etching aluminum alloys with aqueous solution containing sulfuric acid, hydrofluoric acid, and an alkali metal dichromate for adhesive bonding [NASA-CASE-XMF-02303] 12 p1939 N71-23828
- Selective plating of etched circuits without removing previous plating [NASA-CASE-XGS-03120] 12 p1930 N71-24047
- Nickel plating onto etched aluminum castings [NASA-CASE-XNP-04140] 13 p2093 N71-24830
- Sodium hypochlorite etching method for Ge/Li detectors and anti-Compton spectrometers [NIP-18653] 14 p2258 N71-26592
- Residual stresses in rolled steel plates by etching [VTR-155] 17 p2702 N71-29433
- Diffusion of nonlinearly scattered light by etched glass in experiments using Fabry-Perot interferometer in conjunction with laser light source 20 p3744 N71-33479
- Etching in colloidal nitrate used as radiation counters for particle trajectories in particle accelerators vacuum chambers, noting temperature effects [VTR-155] 23 p3750 N71-36792

ETHANE

Development of differential, regional boiling water reactor model for prediction of volumetric properties of fluid state of gaseous ethane and liquid methane
14 p2333 N71-26264

ETHERS

NT ACETALS
Effects of fluorine substitution on properties and reaction rates of monoglycidyl ethers
[AD-71297] 03 p0331 N71-12362

Microwave spectra of divinyl ether and a, b, and c-type rotational transitions of one conformer
07 p0968 N71-17078

Method for producing alternating ether-alkane copolymers with stable properties when exposed to elevated temperatures and UV radiation
[NASA-CASE-XMP-02584] 10 p1512 N71-20905

Chemical synthesis of hydroxy terminated perfluoroethers as intermediates for highly fluorinated polyurethane resins
[NASA-CASE-NPO-10768] 15 p2377 N71-27254

Test of rolling element fatigue life with fluorinated ether lubricant at cryogenic temperature using five ball fatigue tester
[NASA-TN-D-6367] 16 p2606 N71-28038

Polyurethane resins derived from hydroxy terminated perfluoroethers or diols
[NASA-CASE-NPO-10768-2] 20 p3230 N71-33516

Quantum mechanics of internal rotation in dimethyl silane, ethyl alcohol, and CH₂DSH molecules
09 p1430 N71-19768

ETHYL ALCOHOL
Quantum mechanics of internal rotation in dimethyl silane, ethyl alcohol, and CH₂DSH molecules
09 p1430 N71-19768

ETHYL COMPOUNDS
Presence of ethyl esters of long-chain fatty acids determined for Rhizopus arrizus
[NASA-CR-116886] 08 p1161 N71-19116

NT VINYLIDENE
Low gravity effects on catalytic polymerization of ethylene with transition metal complexes
02 p0177 N71-11730

Spectra and photochemical reactions of mercury and ethylene
[COO-584-46] 04 p0592 N71-14403

Combustion kinetics of tetrafluoroethylene
[AD-713144] 05 p0784 N71-15396

Kinetics of copolymerization reactions of ethylene and vinylacetate at low pressure determined by sequential sampling
05 p0641 N71-15697

Effects of oxygen on polymerization of ethylene in presence of supported chromium oxide catalyst
[AD-723585] 19 p3049 N71-31773

ETHYLENE COMPOUNDS
NT CHLOROETHYLENE
NT ETHYLENEDIAMINETETRAACETIC ACIDS

Susceptibility of polyurethane foam to deterioration by impurities or contaminants in ethylene glycol monomethyl ether
[AD-715313] 07 p0997 N71-17755

Macromolecular structure and distribution of monomer units in ethylene-vinyl acetate copolymers by method of infrared spectroscopy
[NLL-RTS-6071] 10 p1514 N71-21334

Turbulent flow drag reduction by dilute polyethylene oxide solutions in capillary tubes
[AD-720688] 14 p2241 N71-26247

ETHYLENE OXIDE
Ethylene oxide sterilization and encapsulating process for sterile preservation of instruments and solid propellants
[NASA-CASE-XNP-09763] 09 p1391 N71-20461

Determination of pressure characteristics and flow properties of cylindrical bodies in aqueous solutions of polyethylene oxide
[AD-717584] 11 p1733 N71-21909

Decontamination of spacecraft components with ethylene oxide as function of parameters of gas concentration, time, temperature, and relative humidity
[NASA-CR-121764] 21 p3581 N71-34057

Germicidal activity of ethylene oxide evaluated through experiments in planetary quarantine program
[NASA-CR-122099] 23 p3713 N71-34468

ETHYLENEDIAMINETETRAACETIC ACIDS
Nuclear magnetic resonance, hydrolysis, molecular structure, and reaction kinetics of nickel ethylenediaminetetraacetate in aqueous solution
[RLO-2221-T-4-5] 15 p2378 N71-27712

Resin crosslinking effects on anion exchange separation of rare earth-EDTA complexes at tracer loadings
[INR-P-1209] 16 p2659 N71-29189

ETR (REACTORS)
U ENGINEERING TEST REACTORS

ETTINGHAUSEN COOLERS
U THERMOELECTRIC COOLING

EUCLEIDIAN GEOMETRY
NT ANALYTIC GEOMETRY
NT ANGLES (GEOMETRY)
NT BRAGG ANGLE
NT BREWSTER ANGLE
NT CARTESIAN COORDINATES
NT CHORDS (GEOMETRY)
NT CIRCLES (GEOMETRY)

NT CONICS

NT CYCLOIDS

NT DESCRIPTIVE GEOMETRY

NT ELLIPSES

NT HEXAGONS

NT HYPERBOLAS

NT ICOSAHEDRONS

NT LOCI

NT MERCATOR PROJECTION

NT OBLATE SPHEROIDS

NT PARABOLAS

NT POINTS (MATHEMATICS)

NT POLYHEDRONS

NT PROJECTIVE GEOMETRY

NT PROLATE SPHEROIDS

NT PYRAMIDS

NT RADII

NT RHOMBOHEDRONS

NT S CURVES

NT SPHEROIDS

NT SQUARES (MATHEMATICS)

NT TANGENTS

NT TETRAHEDRONS

NT TORUSES

NT TRIANGLES

NT TRIANGOMETRY

Majority logic decoding for duals of primitive polynomial codes, and maximality of Euclidean geometry codes
[AD-711791] 02 p0190 N71-11337

Quantum field theory with non-euclidean space of relative momenta
[JINR-P2-5691] 22 p3633 N71-35892

Coefficient function equations for scattering matrix in Euclidean region
[ITP-70-108-B] 24 p3970 N71-38324

EUCLEIDIAN SPACE
U EUCLEIDIAN GEOMETRY
EULER BUCKLING

Nonlinear Euler buckling model for slender column
[AD-713997] 06 p0955 N71-16458

Euler buckling of clamped oval cylindrical shells under axial compression
[AD-714578] 06 p0956 N71-16536

Wave propagation and crater growth characteristics in hypervelocity impact on hard and soft aluminum alloys analyzed using two dimensional Eulerian numerical code
[AD-721468] 16 p2612 N71-28748

EULER EQUATIONS OF MOTION
Using numerical techniques to calculate inelastic response of primary containment to high energy axisymmetric excursion
[AD-71499] 04 p0584 N71-14187

Three programs for two dimensional hydrodynamics in spherical, pure Eulerian coordinate system
[AD-717708] 11 p1737 N71-22526

Linear regulator problem solution using Euler equations of motion, Laplace transformations, and Hamilton-Jacobi equation for stochastic control
14 p2235 N71-26444

Hybrid computer program for determination of Euler angle sequence transient response
[DLR-FB-71-19] 19 p3060 N71-31662

Euler equations for gyroscopes on gimbal rings mounted on moving vehicle
[AD-723419] 19 p3132 N71-31794

EULER-LAGRANGE EQUATION
Investigating nonlinear and geometric behavior of shell structure using Eulerian and Lagrangian methods
[AD-717977] 05 p0780 N71-15406

Lagrangian approach to nonlinear wave interactions in warm plasma
[SU-IPR-381] 08 p1273 N71-18528

Phenomenological Lagrangian models for nonleptonic kaon decays and application of Delta I absolute value equals 1/2 rule
[BNL-50260] 10 p1614 N71-20934

Quantum Bianchi identities and field equations derived from Lagrangians for general relativity
[AD-718957] 13 p2128 N71-24365

Formulas derived for averaged potential in artificial satellite theory
[NASA-CR-118267] 15 p2102 N71-24652

Lagrangian formulation for large elastic deformations of thin shells, suitable for finite element analysis
[AD-721256] 15 p2521 N71-26946

Finite difference integration of dynamic Lagrangian equations for impact shock wave profiles in aluminum alloys
[AD-720716] 15 p2424 N71-27467

Relation of Eulerian and Lagrangian structure of pseudosound pressure and velocity fields in turbulent shear flow to aerodynamic noise generation
[NASA-CR-119359] 18 p2906 N71-31211

Mathematical model for obtaining asymptotically decreasing Efimov amplitudes for pion pion interactions using nonpolynomial interaction Lagrangian equations
[DEMO-71/7] 21 p3470 N71-34702

Lagrange function approximation for latitudinal paths
24 p4012 N71-38616

EUROPA LAUNCH VEHICLES
NT EUROPA 1 LAUNCH VEHICLE
NT EUROPA 2 LAUNCH VEHICLE

Tests of automatic topping of LOX system for Europa F3 vehicle
[TN-DWD-27] 02 p0181 N71-11222

EUROPA 1 LAUNCH VEHICLE
Conference on Europa 1 launch vehicle, Amer research satellite, Symphonie communication satellite, and German ground station-satellite communication system technology
10 p1649 N71-21528

Configuration of second stage of Europa 1 and 2 launch vehicles - Corsile
17 p2850 N71-30807

EUROPA 2 LAUNCH VEHICLE
Payload transport into 24 hour orbit of Europa 2 rocket and solar electric propulsion module
[RAE-LIB-TRANS-1449] 01 p0125 N71-10101

Configuration of second stage of Europa 1 and 2 launch vehicles - Corsile
17 p2850 N71-30807

EUROPE
Weather satellite data on European climate for first quarter in 1968
[QR-1-PT-1] 02 p0254 N71-11409

P wave velocities at high pressures in liquid containing sedimentary rocks of Carpathian Area
[NASA-TT-P-13210] 02 p0211 N71-11409

European implications of the NASA space transportation program
02 p0299 N71-11999

Analysis of synoptic meteorology in Europe with application to theory of fronts and air masses
03 p0402 N71-12375

Satellite photointerpretation for European weather forecasting
[AD-712953] 03 p0377 N71-12771

Weather satellite data and APT pictures for European area during last quarter of 1968
[QR-4] 04 p0541 N71-14117

Climatological and meteorological parameters for central Europe during July 1970
06 p0809 N71-19909

European subsonic, supersonic, transonic, hypersonic and low density wind tunnel characteristics
07 p1003 N71-17609

Air transport supply on scheduled services in Europe-Mediterranean and Southeast Asia routes
[REPT-1970/1-B] 07 p1138 N71-18112

European hypersonic wind tunnels for testing hypersonic transport aircraft, and space shuttle aerodynamic configurations
08 p1175 N71-18032

Meteorological satellite observations above Europe, Jan. - Mar. 1968
[QR-1] 06 p1230 N71-18238

Mathematical models and computer programs for equalizing West German part in European transportation net
09 p1353 N71-19774

Relief group combinations for constructing geomorphological map of western Middle Europe
09 p1383 N71-19775

Solar activity effects on European river runoff and lake level
[NLL-M-20097-5828-4F/1] 12 p1915 N71-24318

Airfield climatology for European Low Countries and British Isles
[AD-719908] 14 p2208 N71-23979

Airfield climatology for Scandinavia and northern Europe
[AD-719907] 14 p2288 N71-23980

EURATOM automatic documentation system, using structure of index, information retrieval statistics, and performance evaluation
14 p2223 N71-23990

Molecular, theoretical, and nuclear data research in EURATOM community for Jan. to 31 Dec. 1969
[EANDC/E-127/U/1] 15 p2404 N71-27328

Photographic meteorological charts for snow and ice cover reporting satellite observation over Europe
[QR-1-PT-1] 17 p2776 N71-31502

Charts giving mean atmospheric refractivity in Mediterranean Europe
[IEA-STR-13] 18 p2949 N71-30825

Environment pollution research and development cooperation in Norway, Sweden, Finland, and Denmark
18 p3028 N71-30840

Meteorological satellite observations and European weather charts for second quarter of 1969
[QR-2] 20 p3128 N71-31815

Satellite-borne photography of Europe and orbital data from ESSA 8 and Nimbus 3 satellites for July 1969 - 30 Sept. 1969
[QR-3] 21 p3451 N71-34544

ESSA 6/APT meteorological photographs of Europe for April through June 1968, and weather satellite developments
21 p3454 N71-34545

Scientific developments in Europe involving treatment of cholera, treatment of bacterial endotoxins, automated system for epidemiological information, and air traffic control
[JPRS-53877] 21 p3534 N71-35107

SUBJECT INDEX

International cooperation in atomic research, meteorology, education, and air traffic control in Europe (JPRS-53960) 21 p3335 N71-35193
European liquid propellant rocket engine technologies 23 p3840 N71-37380

EUROPEAN AIRBUS
Wind tunnel tests with jet simulation of tailplane interference on European Airbus models 09 p1314 N71-19374

EUROPEAN SPACE PROGRAMS
Characteristics of Symphonie project of Franco-German synchronous communication satellite 02 p0181 N71-11275
Launch vehicles in seventies noting French, European, and NASA space programs 02 p0299 N71-12000
Cost analysis of joint NASA-European space program involving navigation and communication satellites for civil air traffic control (ESRO-SP-61) 03 p0409 N71-12756
European aerospace industry and NASA space shuttle and space station programs 07 p1132 N71-17159
European international cooperation in space program for NASA space shuttles and space tug program 07 p1132 N71-17180
Participation of European aerospace industry in European space programs and NASA programs 07 p1133 N71-17182
European aerospace industry role in NASA space shuttle program 07 p1118 N71-17211
International European avionics cooperation for NASA space shuttle, station, and tug programs 07 p1118 N71-17257
Possible European cooperation in NASA space shuttle transportation program (NASA-TM-X-66714) 08 p1306 N71-18431
European test vehicles and small shuttle program in NASA post Apollo program 08 p1293 N71-18639
Cost analysis of future European space programs with or without NASA cooperation 08 p1307 N71-18708
Discussion of European space projects and aspects of European and US cooperation (NASA-TT-F-13547) 09 p1467 N71-20321
Program review on Symphonie French-German communication synchronous satellite 10 p1647 N71-20783
Future European Space Organization programs 10 p1665 N71-20787
NASA and European cooperation in space shuttle transportation program 10 p1648 N71-20810
Metal oxide semiconductors and magnetic memories as computer data storage devices for European research organization meteorological satellites 10 p1528 N71-21093
Magnetic substorm events and magnetosphere structure in polar auroral zones determined by rocket sounding, satellite observations, and ground-based measurements - conference 12 p1908 N71-23551
Preliminary report on European space program in communication satellites, noting satellite television, telegraph systems, telephony, and data transmission (CSRS/71/1) 13 p2042 N71-24402
Thermospheric densities deduced from diffusion coefficient measured on aluminum oxide artificial clouds released from ESRO rockets 13 p2069 N71-24406
Thermospheric density determined from ESRO rocket release of aluminum oxide artificial clouds 13 p2070 N71-24568
Cost benefit models for German space program, noting technology transfer from space programs to physical sciences and industries - Part 1 (IMSW-FB-W-71-01-PT-1) 14 p2357 N71-25670
Cost benefit models for German space program, noting technology transfer from space programs to physical sciences and industries - Part 2 (IMSW-FB-W-71-02-PT-2) 14 p2357 N71-25671
Cost/benefit model for decision making in planning German space program - bibliography 17 p2861 N71-29422
Conference on European Mercury project and German Helios solar probe (ESRO-SP-57) 17 p2849 N71-29563
Spacecraft design, configurations, and mission profile in European Mercury probe 17 p2849 N71-29565
European Mercury spacecraft experiments for interplanetary and planetary space investigation 17 p2850 N71-29566
Onboard experiments of European flyby mission to Mercury planet - European space program 17 p2850 N71-29567
Space research program in Finland during 1970 (R-76-1971) 17 p2861 N71-29633

Geological exploration, development of ultrasonic flow detector, review of scientific developments, and tactical aircraft in Eastern Europe (JPRS-53428) 17 p2845 N71-30833
European space program and Institut - international cooperation and government/industry relations 17 p2842 N71-30832
Andoya rocket test facility and range in Norway (SAD-9-7) 18 p2903 N71-31148
ESRO facility at Noordwijk, Netherlands, for testing antennas and antenna radiation patterns (ESRO-TN-97-ESTEC) 18 p2903 N71-31173
ESRO program for solar orbit satellite testing gravitation theory (ESRO-3M-78) 18 p3019 N71-31360
Vertical temperature thermospheric distribution determined by analysis of aluminum oxide artificial cloud spectra during ESRO rocket sounding in Italy 20 p3254 N71-32875
Design for future X4 British Applications Technology Satellite 20 p3351 N71-33012
European space program on gamma ray astronomy - conference (ESRO-SP-58) 20 p3346 N71-33067
ESRO COS-B space program and gamma ray detector 20 p3346 N71-33075
Feasibility of future ESRO polar orbiting meteorological satellite 20 p3354 N71-33145
Compatibility of European communication satellite with Institut satellites 23 p3859 N71-37306
European sounding rocket catalog (ESRO-SP-39-ESTEC-VOL-1) 23 p3859 N71-37509
EUROPEAN SPACE RESEARCH ORGANIZATION
SAT
NT AZUR SATELLITE
NT ESRO 1 SATELLITE
NT ESRO 2 SATELLITE
European space research organization program for auroral magnetic storms investigation - satellite observation 12 p1908 N71-23552
European Space Research Organization synchronous satellite program for magnetosphere sounding 12 p2001 N71-23572
ESRO geodetic satellite program for investigating solar gravitational fields 18 p3047 N71-30633

EUROPIUM
NT EUROPIUM ISOTOPES
Spectrographic method for determining europium and yttrium in rare earth mixtures (BARC-470) 05 p0639 N71-14709
Stability of europium, samarium, and ytterbium monoxides at low and moderate temperatures 11 p1784 N71-22892
De-excitation of gamma rays following Compton excitation of Eu-151 and 153 using Ge/Li spectrometer 11 p1810 N71-23035
Nuclear properties of low lying Gd-152 excited levels based on beta transition probabilities of Eu-152 (INS-J-123) 17 p2802 N71-30144
Spectrographic determination of rare earth elements in high purity europium oxide (BARC-532) 24 p3884 N71-37685

EUROPIUM COMPOUNDS
Solid state spectrum analysis of europium chloride (UCRL-72707) 05 p0641 N71-15593
Chemical synthesis and crystal growth of pure and doped europium chalcogenides, including magnetic moment, transport properties, and photoconductivity data (AD-71369) 11 p1816 N71-22120
Antiferromagnetic resonance measurements on europium telluride crystals as function of direction 12 p2508 N71-27626
Magnetometric permeability measurements on europium ytterbium compounds and gadolinium doped nickel aluminum alloys 17 p2746 N71-30124

EUROPIUM ISOTOPES
Electromagnetic transition probabilities in nuclei with mass numbers between 125 and 153 based on half-life measurements of T, Te, Sm, and Eu isotopic excited states 02 p0277 N71-12135
Level crossing analysis on hyperfine structure of europium isotopes 04 p0576 N71-13095
Mössbauer effect characteristics of europium isotopes in mixed oxide structures (ORO-3603-7) 07 p1072 N71-17321
Gamma ray, gamma-gamma coincidence, and internal conversion electron spectra for Sm-153 to Eu-153 decay (NP-18835) 24 p3972 N71-38339

EUTECTIC ALLOYS
Superplastic deformation of grain boundaries in eutectic alloy of cadmium and zinc (COO-1198-483) 04 p0529 N71-13097

EVALUATION

Phase diagram-based eutectic designation of copper-nickel system 10 p1578 N71-31218
Molar enthalpy and entropy calculations for elements of liquid potassium eutectic binary systems (LA-4539) 13 p3187 N71-25355
Relationship between morphological factors and elevated temperature stability of eutectic alloy matrix fiber composites 15 p3439 N71-37115
Construction of metallurgical phase diagrams to show eutectic equilibrium of chromium, hafnium, ruthenium, osmium, and molybdenum alloys (NLL-L71-746-086-19022.401) 21 p3442 N71-38492
Solidification, structure, and properties of eutectic alloys including consideration of proper control (NASA-CR-123043) 22 p3592 N71-35578
Application of unidirectional solidification technique for reinforcement of metallic or ceramic materials (NLL-L71-746-703) 23 p3774 N71-38090
Creep strength and solidification rate of Al-Al3Ni eutectic whisker composites (AD-727615) 24 p3937 N71-38091
Tension and slow bend tests to determine effect of temperature and strength orientation on Al-Al3Ni eutectic alloy deformation 24 p3942 N71-38130
Oxygen reactivity effects on eutectic NaK alloy and SNAP 8 system including oxygen contamination sources, oxide solubility, and oxide control methods (NASA-CR-72963) 24 p3939 N71-38242

EUTECTIC DIAGRAMS
NT EUTECTIC ALLOYS
Eutectic microstructures of high temperature ceramic oxides (AD-723818) 18 p2942 N71-31592
Controlled eutectic Al-Si ingots (AD-726424) 22 p3594 N71-35595

EVACUATING (TRANSPORTATION)
Noise problems in air evacuation operations and effectiveness of air protective devices (AD-715082) 06 p0801 N71-16284
Performance of smoke hood for protection of human respiratory system in aircraft accidents and passenger evacuation (FAA-AM-70-20) 17 p2711 N71-29640

EVACUATING (VACUUM)
Sealing evacuation port and evacuating vacuum container such as space jacks (NASA-CR-XMF-03290) 12 p1925 N71-23256
Gas leak detection in evacuated systems using ultraviolet radiation probe (NASA-CR-ERC-10034) 13 p2086 N71-24896

EVALUATION
Nondestructive tests for evaluating bonded materials (AD-709963) 01 p0071 N71-10174
Relationship of technology assessment to environmental management (PB-192534) 02 p0367 N71-11893
Evaluation of eddy current tester for detecting seams in rolled uranium rods (NLCO-1059) 03 p0383 N71-13352
Evaluation of weighting functions used in small angle X ray scattering by FORTRAN 4 program WEIGHT (ORNL-TM-1950-REV-1) 08 p1264 N71-19105
Performance evaluation of two real time operating systems using simulation models 11 p1720 N71-22784
Procedures for evaluating compatibility of aviation material with related equipment (AD-719107) 13 p2025 N71-24457
High specific impulse of several hydrazine thrusters ignited by electrical heaters within thrust chamber during experimental evaluation (NASA-CR-113332) 13 p2157 N71-25237
Reevaluation of neutron cross section data for U-235 at 15 to 15 MeV (IAEA-EC-MEMO-12916) 13 p2137 N71-25430
Microvare system evaluated as nondestructive means of measuring thickness of conformal coatings (BDX-613-265) 15 p2428 N71-27013
Microvare system evaluated as nondestructive means of measuring thickness of conformal coatings (BDX-613-257) 15 p2428 N71-27014
Evaluating three component electronic wind tunnel balance installed in 3.5 by 5.6 ft subsonic tunnel (AD-722731) 18 p2925 N71-31460
Systems maintenance program evaluation conducted in central region of US 19 p3072 N71-31623
Techniques for selecting performance criteria for voice, video, and digital data systems (NASA-CR-115079) 21 p3390 N71-34115
Aerial photography for monitoring and evaluating effluents from ocean waste disposal processes (NREP-120408BY) 22 p3584 N71-35528
Evaluation of NASTRAN system based on large complex airplane analysis 22 p3606 N71-36382

Evaluating current NASTRAN discrete element models for monocoque and semimonocoque structures 22 p3487 N71-36290

Critical evaluation of nuclear data information in connection with reactor designs - international conference [INDC(NDS)-29-U] 23 p3800 N71-37991

Contextual approach to technology assessment - implications for one-factor fix solutions to complex social problems [NASA-CR-123115] 24 p4034 N71-38781

EVAPORATION

NT PROPELLANT EVAPORATION

Evaporative erosion of thermoelectric elements in some thermoelectric generators [SC-RR-70-534] 02 p0147 N71-11045

High voltage electron beam gun for thin film evaporation and welding [REPT-70-19] 02 p0229 N71-11555

Neutron spectra calculations from proton-nucleus inelastic collisions for 15 to 18 MeV protons [NASA-CR-111411] 02 p0272 N71-11786

Hydrodynamic and evaporative theories of light ion flow in polar regions 06 p0441 N71-16027

Condensation and evaporation coefficients for liquid metal vapors and relation to heat and mass transfer rates [COO-2032-4] 11 p1780 N71-22661

Evaporative erosion effects on thermoelectric element and thermoelectric generator performance including mathematical models 12 p1858 N71-23119

Amount of material evaporated, and initial escape velocity of evaporation products of various materials used as laser targets 12 p1933 N71-23184

[NASA-TT-F-15339]

Evapotranspiration in Great Plains 13 p2071 N71-25002

Evapotranspiration data for design capacity of irrigation systems by Soil Conservation Service 13 p2072 N71-25005

Evapotranspiration and water resource management by Bureau of Reclamation 13 p2072 N71-25006

Evapotranspiration data for forest and grassland management by Forest Service 13 p2072 N71-25007

Irrigated and dryland crop studies by State water resource agencies, using evapotranspiration data 13 p2072 N71-25009

Evapotranspiration hydrological cycle modeling in Great Plains 13 p2072 N71-25010

Range classification and soil moisture measurements for evapotranspiration model 13 p2072 N71-25011

Irrigation-oriented evapotranspiration models for Great Plains to aid farmers 13 p2072 N71-25012

Evapotranspiration components of watershed models for Great Plains, using mathematical models 13 p2073 N71-25014

Remote sensing in evapotranspiration research on Great Plains and three environment models [NASA-CR-118184] 13 p2073 N71-25015

Subirrigation systems or microwatersheds for soil water evaporation prevention 13 p2073 N71-25017

Water use efficiency of species, soils, climate, and fertility as related to top growth and evapotranspiration 13 p2073 N71-25018

Evapotranspiration and root growth for nonirrigated crops 13 p2073 N71-25019

Manipulation methods of evapotranspiration, including plant canopy, windbreak, and reflectants 13 p2073 N71-25020

Energy and water exchange with surroundings affected by plant canopies 13 p2074 N71-25021

Plant canopy effects on air flow and evapotranspiration 13 p2074 N71-25022

Water balance data for Great Plains and evapotranspiration reduction and model 13 p2074 N71-25023

Determination of diffusion coefficient of zinc in brass by evaporation [DMDC-5757] 14 p2271 N71-25700

Angular momentum effects on probability of compound nucleus formation and alpha particle evaporation in de-excitation of Te-120 [ORO-3924-5] 16 p2646 N71-28165

Thermal elimination of discontinuities in thin films of gold formed by evaporation in vacuum [NLL-POB-5-TRANS-2674-9022.81/1] 17 p2764 N71-29698

Analysis of mechanism of boiling, evaporation, and heat transfer in fluids 17 p2859 N71-30287

Solutions of aqueous fluorocarbon surfactants placed on surfaces of liquid hydrocarbons and hydrocarbon fuels for suppression of fuel evaporation [AD-723189] 19 p3172 N71-32050

Numerical solution of two phase flow with change of phase in flash evaporation 19 p3082 N71-32626

[KFE-1300]

Kinetics of crystal nucleation and growth in batch evaporation crystallization 21 p3501 N71-34939

Electron beam evaporation and recrystallization of InSb thin films yielding high Hall mobilities [NASA-CR-120797] 22 p3592 N71-35576

Analysis of rate of evaporation and erosion of silicon carbide ceramics in air at high temperatures 22 p3596 N71-35624

Quantitative analysis of solar radiation effect on terrestrial evaporation in natural water cycle 22 p3613 N71-35737

Radiation measurements in Africa applied to evaporation-perspiration determination in tropical region climate 22 p3613 N71-35738

Evaporation-perspiration effect of terrestrial vegetation on latent heat flux density 22 p3613 N71-35739

EVAPORATION RATE

Developing empirical equation for calculating effects of container geometry on liquid lubricant evaporation in vacuum [NASA-TM-X-65455] 08 p1206 N71-18410

Evaporation from spherical liquid drop into vacuum or into pure vapor under strong nonequilibrium conditions 10 p1543 N71-21336

Benzene evaporation rate determined from flat plate film boiling under high temperature air flow with application to gas turbine air pollution reduction [DLR-FB-70-58] 11 p1840 N71-22072

Droplet evaporation in liquid-vapor critical region [AD-718968] 13 p2184 N71-24363

Thermal volatility apparatus with differential condensation for evaporation rate measurements on thermally degrading materials 20 p3362 N71-32833

Mathematical prediction of evaporating water droplet wetting dynamics on stainless steel, Lucite, Teflon, and copper surfaces [NASA-TM-X-67913] 20 p3312 N71-33553

EVAPORATIVE COOLING

NT FILM COOLING

NT SWEAT COOLING

Using simple nomograms to calculate turbulent heat exchange and heat loss in sea-air interactions [AD-71916] 02 p0252 N71-11133

Measuring effects of evaporative cooling at base of dense cirrus and altostratus clouds using Doppler and conventional radars 07 p1053 N71-17421

Continuously operating He-4 evaporation refrigerator [UCSD-34-P-143-31] 08 p1205 N71-18336

Plant growth enhancement using windbreaks to reduce evapotranspiration from summer winds [PB-195927] 09 p1412 N71-19612

Evaporative cooling mechanisms in porous material, including experimental design and temperature distribution measurement [REPT-70-6] 10 p1660 N71-20769

Liquid and vapor cooling systems for gas turbines with application of heat pipe concept to stator blade cooling [ARC-CP-1127] 10 p1638 N71-20832

Improved microwave transmission by adding rapidly evaporating liquid droplets to plasma sheath to remove free electrons 10 p1629 N71-21131

EVAPORATORS

Correlating effect of baffles on flow stability in MSF evaporator based on submerged jet model [ORNL-TM-5120] 06 p0636 N71-16385

Devices to regulate flashing brine flow through flash evaporators [ORNL-TM-2746] 07 p1008 N71-17369

Spatier proof evaporator source design for use in vacuum deposition of solid thin films on substrates [NASA-CASE-XMF-06065] 09 p1394 N71-20395

Feasibility of spraying flash evaporator as heat rejection device for space shuttle environmental control system [NASA-CR-114913] 14 p2263 N71-26224

Vertical tube evaporator smoke tests, pressure profiles, and effects of low mass velocities [ORNL-TM-3240] 15 p2395 N71-27993

Liquid spray flash evaporator for space shuttle thermal control 22 p3547 N71-35269

Sublimation, evaporation, mixed, and hypothesized cyclic sublimation modes of porous plate sublimator-evaporator [NASA-CR-115153] 22 p3695 N71-36351

EVASIVE ACTIONS

Procedures for testing communication security equipment under simulated tactical conditions [AD-719095] 13 p2043 N71-24458

Performance of aircraft environmental control systems under simulated tactical conditions [AD-719101] 13 p2023 N71-36441

Optimum random search procedures for detecting evasive targets applied to typical submarine detection problem 19 p3058 N71-32771

EVECTION

U LUNAR ORBITS

U ORBIT PERTURBATION

U SOLAR GRAVITATION

EVEN-EVEN NUCLEI

Rotational bands constructed on octupole vibrations for even-even nuclei 03 p0433 N71-12500

Gamma-gamma directional correlations following decays of even-even isotopes of Os and Pt [COO-1746-35] 05 p0740 N71-15900

Multiple mixing ratios of gamma transitions in even-even osmium and platinum isotopes [COO-1746-47] 06 p0917 N71-16474

Half life of first excited levels of main and rotational band in even-even nuclei of Os, Er, and Dy [JINR-P6-5201] 08 p1250 N71-18222

Investigating properties of lowest even-even nucleus states of actinide region with respect to superfluid model of multipole interaction in single phonon approximation [JINR-P4-5126] 08 p1256 N71-18271

Even-even isotopes of tellurium of masses between 122 and 130 studied by Coulomb excitation [IR-18447] 08 p1257 N71-18294

Ground state bands of even-even fission products [UCRL-19949] 08 p1261 N71-18278

Levels in medium weight even-even nuclei populated by Cu-66, Ga-68, Cs-132, and I-132 studied with Ge/Li detectors in singles and coincidence mode 10 p1622 N71-21760

Nuclear level structure of even-even nuclei in mass region of permanently deformed nuclei of Gd-56 and Dy-160 10 p1626 N71-21820

Ge/Li detector and channel analyzer for detecting band mixing effects in even-even deformed Gd-154, Ba-160, and Er-168 nuclei 12 p1978 N71-24208

Residual interactions in quadrupole pair production and influence on atomic excitation spectra in transuranic even-even nuclei [JINR-P-1215] 14 p2314 N71-26718

Monopole β /l β ratio equals positive Q /excitation is even-even deformed nuclei [JINR-P4-5422] 16 p2652 N71-28066

Matrix elements of nucleon-nucleon interaction for Hartree-Fock calculations in light nuclei [IFA-FI-78] 16 p2661 N71-28099

Power series analysis of ground state bands in even-even nuclei [OV-LNS-70-2] 17 p2802 N71-30416

Distorted even-even nuclei formation by ground band rotational transitions in rare earth nuclei 18 p2989 N71-31321

Experimental evidence for shape transitions in nuclei demonstrated from quadrupole motion and even-even nuclei [UR-NSRL-40] 24 p3982 N71-38016

EVENTS

NT CONSECUTIVE EVENTS

EVOLUTION (DEVELOPMENT)

NT BIOLOGICAL EVOLUTION

NT GALACTIC EVOLUTION

NT LUNAR EVOLUTION

NT PLANETARY EVOLUTION

NT STELLAR EVOLUTION

Development, research and analysis of French space program 02 p0307 N71-11131

Observing growth rhythms in shells of fossil marine invertebrates and relationship to tidal cycles in earth moon system [NASA-CR-111604] 03 p0223 N71-12312

Theoretical analysis of geological processes affecting evolution of earth atmosphere 05 p0670 N71-14325

Origin of cosmic material fallout on earth surface and structure of cosmic dust and meteoritic materials [REPT-49/18] 15 p2596 N71-27008

Model of expanding universe interpreted as uniform 4-dimensional dilatation of space-time and corresponding contraction of kinetic energy parameter [ITP-70-105-E] 19 p3146 N71-31971

Nucleosynthesis during first 1001 seconds in evolution of big bang universe 20 p3344 N71-32846

Runge-Kutta analysis of hypothetical comet model from Jovian surface, and possible origin of short-faded comets in Jovian surface eruptions [NASA-TT-F-157788] 20 p3348 N71-33048

Nonhomogeneous isotropism of centrally symmetric fields of origin of universe 23 p3840 N71-37009

Gas flow hydrodynamics in evolution of subsequence stars 23 p3849 N71-37405

SUBJECT INDEX

Energy release and neutrino streams in evolution of
23 p3851 N71-37449

Evolutionary models and fluidity functions of
spherical, cylindrical, and planar plasmas
23 p3854 N71-37449

EVOLUTION (LIBERATION)
NT GAS EVOLUTION
WV AIRCRAFT
NT V-101 AIRCRAFT
EXACTNESS
U PRECISION
EXAMINATION
NT EYE EXAMINATIONS
EXCAVATION
NT TUNNELING [EXCAVATION]
 Numerical analysis of strain distribution in soil
around underground openings during and after ex-
cavation process to predict amount of displacement
[AD-725532] 19 p3885 N71-31809

EXCHANGING
NT CHARGE EXCHANGE
NT GAS EXCHANGE
NT ION EXCHANGE
NT RESONANCE CHARGE EXCHANGE
NT SPIN EXCHANGE
 Water exchange variations between Arctic and At-
lantic Oceans and effects on ice cover forecasts in
Arctic seas 11 p1752 N71-22805

Exchange mechanisms and polarization in backward
scattering of protons on light nuclei and α plus He-4
states [IS-5496] 17 p2792 N71-29476

One plane exchange model predictions applied to
neutron-neutron interactions [USP-76-5] 17 p2804 N71-30271

Hypersonic-exclusion interaction using crossed channel
beam exchange model [NF-1836] 24 p3971 N71-38325

EXCITATION
NT ACOUSTIC EXCITATION
NT AROMATIC EXCITATIONS
NT HARMONIC EXCITATION
NT MOLECULAR EXCITATION
NT SELF EXCITATION
NT WAVE EXCITATION
 Damping of coherent oscillations in synchrotron
beam excitations [ANL-TRANS-346] 03 p0420 N71-12545

Neutron and gamma ray emission from excited
states and high-spin states 03 p0427 N71-12857

Computed X ray fluorescence and neutron excita-
tion for obtaining rapid linear and planetary surface
element analysis [NASA-TM-X-65394] 04 p0612 N71-14113

Energy transfer between nitrogen and electronically
excited inert gas atoms and ions [RE-400] 04 p0590 N71-14352

Electron impact excitation efficiency curves for
formation of neutral metastable species [LUCEN-15994] 04 p0594 N71-14453

Ionization and excitation cross sections in proton
atoms [AD-713691] 05 p0764 N71-14908

Dynamic response of supported beams to excitation
by statistical pressure distributions [USV-TR-30] 07 p1123 N71-12121

Half life of first excited levels of main and rotational
band in even-even nuclei of Os, Ir, and Dy [JNIR-96-52801] 08 p1250 N71-18232

Excitation and deexcitation of vibration in N₂ by
oxygen atoms in upper atmosphere [AD-715794] 08 p1286 N71-18802

Determination and statistical model analyses of ex-
citation functions and recoil ion ranges from reactions
induced in gold isotopes by helium ions 08 p1264 N71-19113

Excitation spectra of ferromagnetic insulators in
presence and absence of impurities 09 p1423 N71-19500

Selective excitation spectroscopy used in plasma
diagnostics for advanced aerospace vehicles [AD-716002] 09 p1449 N71-20015

Total cross sections for formation of excited
hydrogen atoms by charge exchange in proton colli-
sions with Ar, He, Ne, and N₂ [RBO-2591-51] 10 p1612 N71-20756

Decay in fluorescence from asymmetric stretching
vibrational level of CO₂ after excitation by Q switched
CO₂ laser 11 p1885 N71-22111

De-excitation of gamma rays following Compton ex-
citation of Ba-137 and 153 using Ge/Li spectrometer
11 p1810 N71-23035

Excitation mechanisms of rare earth element ion
excitation spectra in thiolate lattices [BRO-76020] 12 p1985 N71-23359

GROFIT: a spin dependent atomic excitation code for
following deexcitation of compound nuclei [NWL-50046] 13 p2141 N71-25541

Luminescent excited states of hypermetals by means of
optical potential model [JIR-F-222] 14 p2309 N71-26574

Gamma rays and gamma-ray cascades from 26.1-keV
thallium-209 decay and excited states in Hg-199
[NP-18647] 14 p2309 N71-26481

Using 52 MeV deuterons and 104 MeV alpha parti-
cles for investigating T equals 0 excited states of He-4
[KPR-1055] 14 p2312 N71-26609

Excitation functions and cross section ratios for Y-
90m/Y-90 isomeric pair produced by deuteron proton
reactions [CNEA-276] 14 p2316 N71-26742

Excitation cross section of OI(3P) and NI(4P)
resonance states by electron impact on O₂ and N₂
measured from threshold to 150 eV [NASA-CR-118672] 14 p2316 N71-26747

Measurement of half lives of excited states with
energy of 155.5 and 227 keV in Th-153 nucleus
[JNIR-P-5644] 14 p2317 N71-26751

Dependence of potential describing average nuclear
field on excitation energy 15 p2457 N71-26835

Computer program for discovery of excited states
according to Ritz combination principle [KPR-1247] 15 p2483 N71-27765

Excitation cross section measurement of Ge-71, Ir-
76 and Bi-209 isomeric states using 14.8 MeV electrons
[JNIR-P-1091] 15 p2485 N71-27803

Oxygen and alpha beam excitation of Ba-134, 136,
and 138 and Na-23 15 p2496 N71-27970

Angular distributions and excitation functions of
pick up reactions with neutrons measured by bom-
barding nuclei with N-14 and 15 ions [JNIR-P-5494] 16 p2643 N71-28079

Critical review of theories of excitation spectrum of
superfluid helium 16 p2580 N71-28677

Light scattering applications to plasma diagnostics,
including collisionless coupling and ion excitation
[ORO-3393-5] 16 p2642 N71-28040

Hamiltonian model of superconductivity in infinite
volume for excited states 19 p3146 N71-31971

Gamma ray transition probabilities in deformed
nuclei and 15 lines of excited states in heavy nuclei
[NFI-10053] 19 p3153 N71-32260

Universal excitation due to black body radiation
20 p3344 N71-32845

Enhancement output power of CO-2 laser excited
by electric discharge and irradiated by neutrons ob-
tained from nuclear reactor 20 p3282 N71-33668

Energy spectrum of identified protons and excita-
tion functions following decay of A8-23 [UCRL-30436] 20 p3322 N71-33793

Search for high spin states in Al-27 in range of ex-
citation energies from 4.8 to 8.0 MeV [ANU-P521] 20 p3324 N71-33867

Quantum mechanical molecular energy level calcu-
lations for 3 P₁ and 1 P₁ excited states of He2 21 p3487 N71-34843

Collective and particle nature of Sr-86 states deter-
mined by Sr-86(alpha, alpha-prime) and Sr-87(4,1) reactions
21 p3492 N71-34875

Photoelectron excitation of atomic oxygen
resonance radiation in terrestrial airglow [NASA-CR-121887] 22 p3572 N71-35440

Excitation functions for Tl-199 deuteron interac-
tions [CNEA-283] 22 p3631 N71-35870

Comparison of excitation functions in Rb-85 by
alpha particles to those induced in Sr-88 by protons
[LYCEN-7091] 22 p3631 N71-35872

Excitation functions for deuteron-induced reactions
in gold using statistical model [LYCEN-7092] 22 p3634 N71-35898

Elastic scattering processes using nonlocal opti-
cal interactions with general expression for transition
amplitude [LYCEN-7089] 22 p3639 N71-35938

Fission barrier excitation states and nuclear correla-
tions of fission fragments in relation to saddle point
deformation 22 p3650 N71-36026

Structure and classification scheme of hadron
excited states [ITF-70-102-E] 24 p3970 N71-38321

EXCITED STATES
EXCITATION
EXCITONS
 Quantum mechanics and electron exchange effects
on exciton spectrum 01 p0096 N71-10534

Energy structure of zones and excitons [AD-712812] 03 p0444 N71-13196

Electric field effects on optical absorption by ex-
citons in semiconductors 04 p0485 N71-14220

Exciton interaction in cadmium sulfide and selenide
and zinc oxide 05 p0757 N71-15000

Exciton oscillator strength in silver chloride
[IS-T-374] 05 p0759 N71-15442

Optical absorption by excitons in alkali halides, per-
sonnel accident dosimeters, electromagnetic wave

EXHAUST FLOW SIMULATION
 propagation in atmosphere, ionosphere, and related
research 06 p0906 N71-15747

Transient optical absorption by self-trapped ex-
citons in alkali halide crystals 06 p0908 N71-15748

Energy gap for electronic insulator in presence of
periodic currents 10 p1634 N71-20019

Exciton mobility in pure and doped alkali halides
studied by detecting diffusion of photon-created ex-
citons 15 p3481 N71-27693

Optics of linear media formulated in terms of in-
tegral-differential equations and extended to spatially
dispersive media 19 p3413 N71-32607

Determination of superconductive properties of ex-
citonic insulator by simple two-band model based on
Meissner effect 20 p3236 N71-33802

Light absorption in molecular crystal by triplet ex-
citon pair with singlet spin up state 22 p3643 N71-35971

Field electron emission from CsB as function of
temperature and exposure with current voltage
characteristics and excitation line observations
[NLL-TRANS-2751-1922.81] 23 p3836 N71-37358

EXCRETION
 Stress effects of intermittent exposure to 3 percent
CO₂ on acid-base balance and electrolyte properties in
subhuman primate [AD-724662] 18 p2877 N71-31228

Relationship between diurnal and meal driven
secretory patterns in human kidney during bed rest
20 p3218 N71-33268

EXECUTIVE AIRCRAFT
U GENERAL AVIATION AIRCRAFT
U PASSENGER AIRCRAFT
EXERCISE (PSYCHOLOGY)
 Effect of immersion at different water temperatures
on graded exercise performance in man [PB-144222] 07 p0779 N71-17042

Techniques for exercise to counteract effects of zero
gravity on skeletal muscles of rhesus monkeys during
extended orbital spaceflight [NASA-CR-117308] 09 p1333 N71-20165

Age and exercise factors influencing osteoporosis,
bone strength, and acceleration tolerance investigated
using rhesus monkeys [AMRL-TR-70-74] 09 p1336 N71-20039

Heat tolerance of athletes during muscular exercise
in various thermal environments 09 p1337 N71-20046

Physiological responses to increasing stresses of
exercise and hypoxia under acute and chronic ex-
posure to ambient P sub CO₂ of 21 mm Hg 09 p1338 N71-20070

Physical fitness of flying personnel and aging ef-
fects on flight crew performance [AGARD-CP-81-71] 11 p1667 N71-22301

Physical fitness training schedules for Canadian
Forces flying personnel 11 p1688 N71-22305

Physical exercise effects on stress tolerances of
trained and untrained subjects 11 p1688 N71-22306

Physical exercise and fitness tests for German Air
Force flying personnel 11 p1688 N71-22307

Oxygen consumption and heart rate measurements
for estimating exercise tolerance of military personnel
11 p1688 N71-22308

Physical exercise and environmental-emotional
psychotherapeutic methods in aerospace medicine
11 p1688 N71-22310

Exercise effects on physical fitness and cardio-
vascular system of aging pilot 11 p1689 N71-22313

Aging effects on military flight crew body compo-
sitions and physical exercise performance 11 p1689 N71-22316

Metabolic effects of long duration exercise at
moderate work loads including tables of heart rate,
rectal temperature, minute volume, water balance,
and respiratory quotient [NASA-CR-115633] 15 p2372 N71-27704

Total body exercise effect on metabolic, hemosta-
tic, and cardiovascular consequences of prolonged bed
rest 20 p3218 N71-33265

Continuous measurement of potassium and sodium
level in interstitial fluid of muscles during physical ex-
ercise with ion specific microelectrodes [NASA-TT-F-15996] 24 p3677 N71-37633

EXHAUST
U PHYSICAL WORK
EXHAUST DEVICES
 Radial-inflow turbine performance with exit di-
fusers designed for linear static-pressure variation
[NASA-TN-X-2357] 19 p0304 N71-32466

EXHAUST FLOW EMULATION
NT ATMOSPHERIC ENTRY SIMULATION
NT FLIGHT SIMULATION

EXOSPHERE

- Diurnal variation of Martian exospheric temperature (NASA-456-VOL-35-NO-12) 02 p0296 N71-11933
- Solar cycle variation of planetary exospheric temperatures (NASA-TM-X-45419) 06 p0942 N71-15886
- Thermosphere and lower exosphere gas density and temperature from satellite drag measurements 13 p2070 N71-24567
- Detection of hydrogen ion flux in an exosphere existing along terrestrial magnetic lines of force 18 p2918 N71-31305
- Collisionless Boltzmann equation for model of rotating and nonuniform planetary exospheres (NASA-TM-X-45662) 19 p3094 N71-32391
- Revised static models of thermosphere and exosphere with empirical temperature profiles (JGFA-88-332) 21 p3414 N71-34296
- Multiple exospheric temperatures for Venus and Mars (NASA-TM-X-45690) 22 p3468 N71-34154

EXOTHERMIC REACTIONS

- Equipment and procedure for crosslinking time and exothermic temperature determination of reacting plastic compositions in controlled atmosphere (JRC-11849) 12 p1871 N71-33756
- Isobaric brass units for repair and assembly of stainless steel materials on space structures (NASA-CR-103109) 14 p2261 N71-34044
- Modified remote cell for thermal differential decomposition studies on lead azide 20 p3363 N71-32834

EXPANDABLE STRUCTURES

- NT BALLOONS
- NT BALLUTES
- NT BEACON EXPLORER A
- NT BELLOWS
- NT EXPLORER 23 SATELLITE
- NT GAS BAGS
- NT HIGH ALTITUDE BALLOONS
- NT INFLATABLE SPACECRAFT
- NT INFLATABLE STRUCTURES
- NT METEOROLOGICAL BALLOONS
- NT ROBOT BALLOONS
- NT SKYHOOK BALLOONS
- Performance characteristics and weight variations of large area, roll-up, solar arrays (NASA-CR-115821) 04 p0475 N71-13427
- Computer program for predicting motion and appendage stresses of spacecraft during deployment maneuvers (NASA-CR-116148) 06 p0818 N71-15965
- Expandable space frames for three dimensional or planar building structures (NASA-CASE-ERC-10365) 16 p2483 N71-28048
- Development of expandable structures concepts for application to structures used in space missions - Part 2 (NASA-CR-17355) 23 p3863 N71-37537

EXPANSION

- NT GAS EXPANSION
- NT RANDT-MEYER EXPANSION
- NT THERMAL BUCKLING
- Isentropic effects in impulsive spherical and cylindrical plastic expansion with time-cavity motion relationships, final cavity size, and total expansion time determinations 17 p2853 N71-30066
- Impedances on crossing symmetry, parameterization of pion/0-pion/0 amplitude expressed expansion coefficients (ILL-THU-71-4) 19 p3161 N71-32685
- Theoretical analysis of viscous, incompressible fluid flow oscillations around circular cylinders between closely spaced parallel plates based on asymptotic approximations and inner-outer expansions 22 p3371 N71-35433
- Analysis of Freon-113 bubble growth and collapse in constant-diameter, vertical channels with nonuniform initial temperature profiles (ANL-7746) 22 p3623 N71-35813
- Galactic formation and density, velocity, and mass properties of expansion process 23 p3849 N71-37431

EXPANSION WAVES

- U ELASTIC WAVES
- EXPERIMENTAL DESIGN
- Soviet-Cuban oceanographic expeditions in Gulf of Mexico and Cuban shore area to determine geologic characteristics and biological productivity 18 p2909 N71-30607
- Hydrographic and meteorological survey of Red Sea revealing brine holes and related hot holes - Oceanographic expedition 23 p3788 N71-37000

EXPERIMENTAL BREEDER REACTOR 1

- Research and development of steam cooled fast breeder reactors with sodium and helium cooling (EPX-1370) 24 p3963 N71-38267
- Design calculations and parameters for 1000 MW(e) ship-borne molten-salt breeder reactor 24 p3963 N71-38271

EXPERIMENTAL BREEDER REACTOR 2

- Research and development programs for zero power reactors and Experimental Breeder Reactor 2 (ANL-7608) 01 p0004 N71-10331
- Materials-sodium coolant interactions in EBR-2 (ANL-7670) 01 p0084 N71-10332
- Irradiation testing of 37-pin, EBR 2 instrumented subassembly (BNWL-1624) 01 p0085 N71-10430
- Gas-adsorption process chemical studies in EBR-2 (BAW-3714-17) 02 p0266 N71-12186
- Fast reactor mixed-carbide fuel element development program in EBR-2 (UNC-5239) 02 p0366 N71-12187
- Investigating system for transferring failed fuel from primary tank to argon cell of EBR-2 facility (ANL-EBR-026) 04 p0546 N71-15605
- Irradiation of unannealed fuel pins in EBR-2 for determining constant heat flow balance (BNWL-1420) 04 p0555 N71-14028
- LMFBR, EBR 2, and ZPR 3, 4, and 9 development programs (ANL-7726) 04 p0556 N71-14096
- Input specifications for neutronics analysis of Experimental Breeder Reactor 2 (ANL-7540) 04 p0557 N71-14133
- Testing various alloys for yield strength and density changes after irradiation in EBR-2 reactor (ANL-7682) 04 p0550 N71-14139
- Preliminary system design description of EBR-2 in core instrument test facility 04 p0560 N71-14295
- Simplified EBR-2 flow monitoring system without compromising reactor safety (ANL-EBR-18) 05 p0722 N71-14637
- Criticality data for EBR 2 stainless steel radial reflector (ANL-7441) 05 p0723 N71-14680
- Investigating flux characterization and neutron cross sections in EBR-2 using foil activation techniques (ANL-7629) 05 p0738 N71-15008
- Hazards analysis of EBR-2/TREAT transient irradiation tests series (BNWL-1368) 05 p0728 N71-15110
- Suitability of some components of EBR 2 sodium systems for operation at 62.5 MW (ANL-EBR-16) 06 p0901 N71-16764
- Mixed carbide fuel element development for EBR-2 (UNC-5233) 06 p1237 N71-18326
- Neutron irradiation effects on mixed oxide fuel elements of high temperature Experimental Breeder Reactor 2 (GA-10264) 08 p1238 N71-18357
- Physical and mechanical properties of Type-304 stainless steel of EBR-2 subassembly after irradiation (GEAP-13571) 08 p1220 N71-19237
- Radiation damage of reactor structural materials including irradiation determination for high temperature alloys in EBR 2 (AD-716405) 09 p1417 N71-19814
- Symptoms and detection of fission product release from EBR-2 fuel element - defect below fuel elevation (ANL-7676) 09 p1418 N71-19898
- Zero power reactors and experimental breeder reactor 2 research and development 09 p1416 N71-19903
- EBR-2 codes for processing reactivity data at full and reduced coolant flows using thermal expansion corrections for control rods (ANL-EBR-28) 09 p1418 N71-19904
- Catalog of rod-drop and transfer functions from EBR-2 runs 25 through 30A (ANL-7542) 10 p1603 N71-21183
- Dynamic simulation digital code for EBR-2 plant protective system response to hypothetical malfunctions in reactor system 10 p1605 N71-21371
- Operating conditions and safety of series 1 ORNL oxide fuels irradiation in EBR-2, target burnup level extended from 5 percent FIMA to 10.5 percent FIMA (ORNL-TM-2635-SUPPL.) 11 p1794 N71-22424
- Irradiation of fatigue specimen capsules in EBR-2 Mark B-7 subassembly 13 p2111 N71-24503
- Using xenon for isotopic labeling of instrumented fuel capsules in EBR-2 to detect element failure 13 p2111 N71-24506
- Feasibility of instrumented subassembly system for EBR-2 for monitoring instrument readings while reactor is operating 13 p2111 N71-24507
- Irradiation subassembly permitting irradiation temperatures above normal EBR-2 temperature 13 p2111 N71-24508
- Fuel capsule designs for thermal and fast neutron irradiation of IUPu/N in MTR/ETR and EBR 2 13 p2114 N71-24543
- Unbounded input reactivity effects on flux types of EBR-2 core configurations, using MELT-2 code for meltdown analysis (ANL-7752) 13 p2119 N71-25109
- Postirradiation examination of tantalum cladding from EBR-2 photo-neutron startup sources for corrosion and changes in microstructure and chemical content (ANL/EBR-31) 14 p2291 N71-25680
- Intergranular pore density determination in PUO2-UO2 fuel pin irradiation in EBR-2 (WHAN-SA-15) 15 p3443 N71-34038
- EBR 2 irradiation effects on biaxial stress rupture of annealed Type 316 stainless steel (WHAN-SA-3) 15 p3430 N71-34090
- Computerized simulation of experimental breeder reactor 2 dynamic responses to uranium-fission and PuO2-UO2 fuels including specific heat and thermal conductivity effects (ANL-7673) 15 p3449 N71-37348
- Error analysis of in-pile thermal conductivity and gap conductance measurements with balanced oscillators in experimental breeder reactor 2 (EUBFBR-753) 15 p3450 N71-37831
- Fabrication of PuO2-UO2 fuel rods for irradiation testing in EBR-2 (NUMEC-3524-74) 16 p3833 N71-38076
- Physical model for origin of fission-product release in experimental breeder reactor 2 (ANL-7684) 16 p3852 N71-39086
- Integrated circuitry and design of sensing reactivity meter for use with Experimental Breeder Reactor 2 (ANL-7705) 18 p2958 N71-30495
- Research and development program for EBR-2, zero power reactors, fast flux test facility, and LMFBR (ANL-7790) 20 p3307 N71-33701
- Nuclear fuel element performance analysis, lifetime codes, and irradiation of oxides for Experimental Breeder Reactor 2 and fuel element design and fabrication (WARD-4135-13) 21 p3461 N71-34637
- Irradiation of sodium-bonded (U,Pu)C fueled stainless steel clad elements to burnup in EBR-2 (LA-4469) 21 p3461 N71-34638
- Mixed oxide nuclear fuel element porosity, grain structure, and composition distribution measurements for EBR-2 subassemblies (HBDL-TIME-71-45) 23 p3434 N71-35834

EXPERIMENTAL DESIGN

- NT FACTORIAL DESIGN
- Laboratory coherent radar system design for evaluating digital MTT subsystems (CERC-TV-628) 01 p0020 N71-10028
- Experimental design of three dimensional air traffic control radar tracking system 01 p0082 N71-10164
- Experimental study of electrically thick monopole antennas - equipment, admittances, and impedances (AD-710213) 01 p0022 N71-10345
- Experimental study of electrically thick monopole antennas - currents, charges, and conclusions (AD-710214) 01 p0023 N71-10346
- Neutronic analysis using IHEP accounts (CERN-TRANS-68-26) 01 p0087 N71-10634
- Experimental design and operation of rotating wickless heat pipe 01 p0134 N71-10702
- Engineering evaluation of low temperature high rate reserve magnesium perchlorate batteries (AD-710952) 01 p0007 N71-10715
- Use of heat pipes for electrical isolation (NASA-TM-X-52928) 01 p0134 N71-10985
- Sealed electric storage battery with gas manifold interconnecting each cell (NASA-CASE-XNP-03378) 02 p0149 N71-11051
- Electrode attached to helms for detecting low level signals from skin of living creatures (NASA-CASE-ARC-10043-1) 02 p0168 N71-11193
- Cyclotron and synchronous wave devices (AD-712323) 02 p0193 N71-11356
- Laser fundamentals and experiments for high school use - textbook (PB-193563) 02 p0238 N71-11420
- Project management and experimental designs for tropical meteorological experiments in Atlantic Ocean 02 p0258 N71-11679
- Open cycle hydrocarbon-air fuel cell power plant (AD-713528) 05 p0631 N71-14407
- Analysis of sandwich wire antennas (ED-188) 05 p0643 N71-14736
- Verification experiment design for satellite-borne geodetic altimeter operating over sea (NASA-CR-115897) 05 p0669 N71-14791
- Design of experimental and cable system designed for delivering large amounts of electric power to use underwater - photographs 05 p0680 N71-15612
- Design of 20-megawatt linear plasma accelerator facility (NASA-TN-D-6115) 06 p0928 N71-15819
- Very Long Baseline Interferometer experiments using ATS 3 and ATS 5 satellites (NASA-TM-X-45428) 06 p0960 N71-16447
- Design of experiments and systems for HBAO to determine composition and spectra of high energy cosmic rays (NASA-TM-X-45431) 06 p0942 N71-16602
- Multibody photoproduction experimental facility (UN-511-01-70) 07 p1076 N71-17543

Gaseous oxygen-gaseous hydrogen rocket engine injector valve technology
[NASA-CR-114857] 07 p1034 N71-17355

Design considerations of reactor containment spray systems, also protective coating for these containment structures
[ORNL-TM-2412-PT-5] 06 p1220 N71-18304

Experimental design for soil mechanics under frost conditions for road construction problems
[REPT-70-5] 06 p1187 N71-18404

Engineering constraints in designing optimal and sub-optimal feedback systems
[NASA-CR-116895] 06 p1173 N71-19121

Experiments payloads plan for extended earth orbital missions with options
[NASA-TM-X-64691] 06 p1292 N71-19318

Conditioning suit for normal function of astronaut cardiovascular system in gravity environment
[NASA-CASE-XLA-62898] 09 p1341 N71-20268

Design of shaft face seal with self-acting lift augmentation for gas turbine engines
[NASA-TN-D-6164] 09 p1394 N71-20392

Evaluation of gas discharge transducer and associated instrumentation for asteroid belt meteoroid experiment with Pioneer probes F/G
[NASA-CR-111848] 09 p1390 N71-20401

Evaporative cooling mechanisms in porous material, including experimental design and temperature distribution measurement
[REPT-70-6] 10 p1660 N71-20769

Reliability and experimental design of optical radar system lidar for tropospheric and ionospheric backscattering
[DLR-MITT-70-18] 10 p1518 N71-20780

Earth orbiting space station experiment module design concepts
[NASA-CR-117499] 10 p1650 N71-21556

Azur satellite experiments for measuring radiation belt electron and proton energies using radiation counters
[BMW-FB-W-70-67] 11 p1825 N71-23099

Kinetics experiment for development of system for remote sensing of ionospheric motions and microstructure
[NASA-CR-117837] 11 p1750 N71-22533

Design, fabrication and static testing of attached inflatable decelerator models for supersonic wind tunnel evaluation
[NASA-CR-111831] 11 p1676 N71-22538

Nozzle operation and experimental design for molecular beam production
[NASA-CR-111831] 11 p1807 N71-22645

Space suit using nonflexible material with low leakage and providing protection against thermal extremes, physical punctures, and radiation with high mobility articulation
[NASA-CASE-XAC-67043] 12 p1865 N71-23161

Experiment to measure hard solar and celestial X rays from 0.50-5 in energy range of 15 to 250 keV
[NASA-TM-X-65504] 12 p1992 N71-23434

ESRO 1 satellite Arctic auroral ionization spectroscopy experiments
[NASA-CR-111831] 12 p2000 N71-23569

Optimum design of two dimensional nonrecurrent digital filters
[UCRL-72663] 12 p1949 N71-23711

Operational characteristics and entrance conditions of high current relativistic electron beam accelerator
[REPT-70-12] 12 p1897 N71-23946

Experimental design and performance of plasmatron-ionic pulverization device
[ONERA-NT-62-22] 13 p2079 N71-24405

Design of observation and data processing systems for use in first Global Atmospheric Research Program (GARF) experiment
[NASA-CR-111831] 13 p2104 N71-24423

Fabrication and acceptance testing, fluorine compatibility testing, valve refurbishment and testing, environmental testing, and design of space storable oxidizer valve
[NASA-CR-126960] 13 p2087 N71-25456

Experimental design for diagnostic and velocity measurements of plasma acceleration in traveling electromagnetic field
[ONERA-NT-174] 14 p2320 N71-25709

Two inlet stellarator designed for containment of plasma under very clean conditions and higher stability of magnetic field configuration
[LA-TN-70-22] 14 p2321 N71-25769

Orbiting Lunar Station feasibility and definition - Operational, experiment, and science support requirements
[NASA-CR-115015] 14 p2342 N71-25832

Statistical mechanics for constructing confidence intervals for variance ratios in balanced and unbalanced experimental designs
[NASA-CR-118654] 14 p2284 N71-26386

ATS-F solar cell radiation damage experiment design and ground tests including space environment simulation and low-energy proton and electron irradiation
[NASA-CR-118660] 14 p2203 N71-26389

Evaluation of earth resources observation opportunities from orbiting satellite in Skylab program
[NASA-TM-X-64598] 15 p2397 N71-27025

Aerodynamic heat determination on blunt bodies in hypersonic flow with force and pressure measurements
[BMW-FB-W-71-08] 15 p2364 N71-27616

Theoretical analysis of 24.5/73.6 MHz rocket-to-ground CW propagation experiment for in situ electron density measurements
[NASA-TM-X-65532] 15 p2382 N71-27670

Computer program for analysis and design of critical experiments with fast nuclear reactors
[JAERI-MEMO-4215] 15 p2451 N71-27740

Pattern threshold recognition device comprising cathode ray tube with image converter input, flood-gas for suppressing background information, and read-out output of information
[AD-71021] 15 p2387 N71-27747

Optimization for zero gravity experiment on solution growth of gallium arsenide and design of experiment package for melt growth of indium antimonide crystals
[NASA-CR-119792] 15 p2510 N71-27926

Carbon dioxide lasers, CaF₂ experiment, light scattering from semiconductors associated with impurities, and far infrared radiation
[AD-71654] 16 p2607 N71-28588

Vehicle with plasma-ion electrode engine designed for orbital flights and altitudes from 50 to 200 km using ionospheric air intake for fuel/Yantar
[NASA-TT-F-13676] 17 p2832 N71-29242

Techniques and circuits used in designing AL highly flexible telemetry system comprising single sideband/double sideband/constant bandwidth compatible system - space application
[NASA-TT-F-13676] 17 p2718 N71-29323

European Mercury spacecraft experiments for interplanetary and planetary space investigation
[NASA-TT-F-13676] 17 p2850 N71-29566

Onboard experiments of European flyby mission to Mercury planet - European space programs
[NASA-TT-F-13676] 17 p2850 N71-29567

HEOS mission, experimental design, and instruments
[ESRO-TN-104-ESTEC] 18 p3017 N71-30620

Orbital fatigue tester for Skylab program - test and design of titanium alloy and aluminum alloy specimens having various sizes
[NASA-CR-111923] 18 p2925 N71-31382

Developments in program to develop extendable retractable nozzle extension for space use
[NASA-CR-115111] 19 p3183 N71-31666

Design criteria of heat flow experiment designated as ALSEP Array A2
[NASA-CR-115109] 19 p3178 N71-31607

Design certification of Apollo 15 laser ranging retroreflector experiment
[NASA-CR-115108] 19 p3107 N71-31609

Application of statistical design and data analysis to configuration and development of space station experiments and mission
[NASA-CR-118916] 19 p3185 N71-32533

Interferometric system for solar radio emission at 3 cm wavelength at Arcetri Observatory, Italy
[NASA-CR-118916] 19 p3185 N71-32533

Design optimization for fractional factorial experiments by finite decision problem based on prior information
[NASA-TM-X-67901] 20 p3292 N71-33554

Techniques and apparatus design for measuring high temperature emissivity of thermal protection materials for reentry vehicles
[NASA-CR-119920] 21 p3425 N71-34368

Techniques and characteristics of field testing including experimental design and procedures for specific problem logistics
[P-4492] 21 p3448 N71-34542

Proposed experiment for identification of elementary particles bearing small magnetic charges
[CERN-TRANS-71-10] 23 p3806 N71-37136

Experimental designs for electron elastic and inelastic scattering and mathematical expressions for electron-scattering cross sections and radiative corrections
[LNF-70/57] 23 p3820 N71-37249

Proposed Mirror Fusion Experiment (MFX) to extend mirror confinement studies
[UCRL-51042] 23 p3827 N71-37296

Program of scientific research and biomedical experiments conducted aboard Soyuz 9 spacecraft
[NASA-TT-F-13786] 23 p3847 N71-37422

Mathematical models for estimating block up-and-down design of sensory thresholds
[NASA-TM-X-62090] 24 p3878 N71-37644

Design of scanning laser radar for spaceborne applications
[NASA-CR-121014] 24 p3931 N71-38047

Development of optimal design procedures by posing experimental design problem as finite decision problem
[NASA-TM-D-6527] 24 p3950 N71-38184

EXPERIMENTAL GAS COOLED REACTORS
Radiant blowers, shutdowns, valves, and seals performance in helium atmosphere of AVR experimental gas cooled reactors
[NLL-EE-TRANS-1933-3774.5] 21 p3462 N71-34645

EXPERIMENTATION

Information distribution and optimization for similar experiments
03 p0455 N71-12894

Development and selection of experiments to be performed during space missions
[NASA-CR-116609] 07 p1114 N71-17611

Computer programming for nuclear physics experiment control
[HMI-B-96] 15 p2474 N71-27488

Design and performance of relief valve assembly for metabolic activity system of biological experiment on orbital workshop vehicle
[NASA-CR-119177] 17 p2757 N71-30830

PDP 9 interface for data transfers between nuclear experiments and computer
[HMI-B-102] 18 p2999 N71-30801

Experimental arrangements for demonstrating behavior of candle flame during free fall
[NASA-TT-F-13940] 23 p5096 N71-36136

Optimum utilization of research reactor experimental facilities
[LB/G-3011] 24 p3957 N71-38228

EXPIRED AIR

Regeneration of artificial respirable atmosphere using potassium peroxide
[NASA-TT-F-13430] 04 p0487 N71-13460

Gaseous impurities in air exhaled by humans under extremal stress factors
16 p2544 N71-26238

Gas chromatographic study of trace contaminants in man-exposed air, and effects of physiological stress of space flights
24 p4015 N71-36446

EXPLoding CONDUCTOR CIRCUITS
U CIRCUITS
U EXPLoding WIRES

EXPLoding CONDUCTORS
U EXPLoding WIRES
EXPLoding WIRES

Experimental studies on discharge propagation of exploding wires in high vacuum and determination of developing plasma properties
[NASA-TT-F-13346] 02 p0382 N71-12065

Measurement of dynamic pressures produced by exploding wires
[IN-1406] 04 p0513 N71-13540

Explosive dynamics of liquefied nitrogen jets and solidified nitrogen wires
04 p0620 N71-13633

Exploding wires as shock wave sources
[SC-RR-70-45] 04 p0620 N71-14039

Ultra-fast thin pinch, exploding wires, laser plasma heating, and plasma-solid interactions
[AD-714619] 06 p0929 N71-14074

Current diffusion in cylindrical wires and fuses during microsecond electrical pulses
[AD-717003] 10 p1607 N71-21371

Analysis of gas generated by wires exploding in air, argon, and nitrogen mixtures at low pressures
14 p2361 N71-26254

Study of cylindrical stress waves using exploding wires in long hollow thick walled shells
17 p2853 N71-28818

Dynamic plastic behavior of hollow cylinders using exploding wire technique for investigation of elastic/viscoplastic constitutive theory
17 p2854 N71-38157

EXPLORATION
NT LUNAR EXPLORATION
NT SPACE EXPLORATION

Aeromagnetic, gravity, and electrical resistivity exploration between Palala and Pambala, Hawaii
[PB-192807] 02 p0213 N71-11680

Geothermal investigations for determining subsurface structure of petroliferous and gas bearing regions
[NASA-TT-F-13392] 02 p0218 N71-13017

Underwater acoustic efficiency of explosives for marine prospecting
07 p1057 N71-17180

Field and laboratory equipment and methods for airborne electroprospecting using rotating magnetic fields and anomalous effect calculations for conductive media and irregular form bodies
[TT-70-50059] 10 p1555 N71-21671

Historical review of Soviet exploration in Arctic regions
11 p1848 N71-22019

Historical review of Soviet refusal to permit L. Bedford Pym of British Royal Navy conduct polar exploration to search for John Franklin expedition
11 p733 N71-22829

Induced polarization and resistivity surveys on Cleary Summit, Alaska
14 p2252 N71-36460

Propagation velocity of ultrasound in natural rock impregnated with mineralized water, artificial rock prepared from sand and cement of known porosity, and sand clay water suspensions
[NASA-TT-F-13696] 16 p2384 N71-38084

Earth subsurface electromagnetic field distribution due to subsurface rock electrical properties
16 p2585 N71-38208

SUBJECT INDEX

Geology of minerals as space age earth resource possibility 18 p2911 N71-30841

Techniques for solving Maxwell equations and applications in induction heating and electromagnetic prospecting 21 p3403 N71-34216

EXPLORER SATELLITES

NT EXPLORER 15 SATELLITE 07 p1118 N71-17156

NT EXPLORER 18 SATELLITE 07 p1118 N71-17156

NT EXPLORER 22 SATELLITE 07 p1118 N71-17156

NT EXPLORER 26 SATELLITE 07 p1118 N71-17156

NT EXPLORER 28 SATELLITE 07 p1118 N71-17156

NT EXPLORER 29 SATELLITE 07 p1118 N71-17156

NT EXPLORER 31 SATELLITE 07 p1118 N71-17156

NT EXPLORER 32 SATELLITE 07 p1118 N71-17156

NT EXPLORER 33 SATELLITE 07 p1118 N71-17156

NT EXPLORER 35 SATELLITE 07 p1118 N71-17156

NT EXPLORER 37 SATELLITE 07 p1118 N71-17156

NT EXPLORER 38 SATELLITE 07 p1118 N71-17156

NT EXPLORER 40 SATELLITE 07 p1118 N71-17156

IMP 07 p1118 N71-17156

OUTER PLANETS EXPLORERS

NT RADIO ASTRONOMY EXPLORER SATELLITE 07 p1118 N71-17156

Average and unusual locations of magnetopause and bow shock positions observed by IMP spacecraft (NASA-TM-X-65429) 06 p0851 N71-16509

Optical tracking of Cosmos and Explorer satellites, Edinburgh, Sep. 1970 07 p1118 N71-17156

Optical tracking of Cosmos and Explorer satellites, Edinburgh, Aug. 1970 07 p1118 N71-17156

Analysis of missions and experiments assigned to IMP satellites 09 p1469 N71-20481

Evaluation of Planetary Explorer propulsion systems of monopropellant hydrazine type for use on Venus mission satellites (NASA-CR-118648) 14 p2332 N71-26420

Particle flux densities of radiation belts for atmospheric explorer missions C, D, and E (NASA-TM-X-65412) 18 p3003 N71-30045

Venus spin vector estimation using planetary Explorer spacecraft data (NASA-TM-X-65728) 24 p4008 N71-38577

EXPLORER 15 SATELLITE

Reduction and analysis of data from Explorer 15 and Explorer 26 satellites (NASA-CR-119286) 18 p3003 N71-30919

Trapped radiation observed by Telstar I and Explorer 15 satellites 18 p3010 N71-30920

Particle detection equipment and particle data processing systems used with Explorer 15 and Explorer 26 satellites 18 p2923 N71-30932

EXPLORER 18 SATELLITE

Results and description of qualification tests of attitude control system and go-to design system in flight configuration as installed on IMP-1 spacecraft (NASA-TM-X-65473) 10 p1600 N71-21839

Application of failure flow analysis to evaluate test program of Explorer 18 satellite (NASA-TM-X-65706) 23 p3762 N71-36819

EXPLORER 22 SATELLITE

Electron content measurement in polar ionosphere using signals from Explorer 22 satellite based on Faraday rotation (JMW-FB-W-70-39) 03 p0370 N71-13229

Iospheric electron density determination over Fohned using Explorer 22 signals and Faraday/Doppler method (JMW-FB-W-70-50) 08 p1189 N71-18592

Iospheric electron density measurements from Faraday fading of Explorer 22 satellite transmissions during low and high solar activity (JMW-FB-W-70-51) 09 p1550 N71-20080

Explorer 22 satellite measurements of ionospheric electron contents during magnetic storms (JMW-FB-W-70-52) 09 p1550 N71-20080

Low angle signal propagation of Explorer 22 satellite transmissions 24 p3913 N71-37900

EXPLORER 26 SATELLITE

Reduction and analysis of data from Explorer 15 and Explorer 26 satellites (NASA-CR-119286) 18 p3003 N71-30919

Analysis of trapped particles during magnetic storms on 18 Apr. 1965 observed by Explorer 26 18 p3004 N71-30920

Particle detection equipment and particle data processing systems used with Explorer 15 and Explorer 26 satellites 18 p2923 N71-30932

EXPLORER 28 SATELLITE

Observations of interplanetary medium by Vela 3 and IMP 3 satellites (NASA-TM-X-65416) 06 p0943 N71-16604

EXPLORER 31 SATELLITE

Accomplishments of geodetic satellite and earth survey programs during period July to December 1970 (NASA-CR-119357) 18 p3016 N71-31295

EXPLORER 31 SATELLITE

Ion mass spectrometer experimental design on Explorer 31 satellite and data processing techniques for ionospheric composition (NASA-CR-121651) 21 p3434 N71-34362

Composition of upper ionosphere as shown by magnetic mass spectrometer flown on Explorer 31 (NASA-CR-121653) 21 p3435 N71-34379

EXPLORER 32 SATELLITE

Neutral helium, atomic oxygen, and molecular nitrogen densities measured by Explorer 32 mass spectrometers (NASA-TM-D-7042) 12 p1997 N71-24084

Thermal variations of atomic hydrogen in thermosphere derived from Explorer 32 data and correlated with solar cycle, solar rotation, and earth rotation (NASA-TM-X-65544) 14 p2246 N71-23747

EXPLORER 33 SATELLITE

Analyzing data from Explorer 33 and 35 on energetic solar particles in interplanetary medium and terrestrial particle fluxes in magnetopause bow shock regions (NASA-CR-115775) 04 p0590 N71-14378

Ratio of intensity of solar protons for north polar cap to that of south polar cap, as observed by Explorer 33 and 35 satellites (NASA-CR-117809) 12 p1991 N71-23112

Explorer 33 observations of sudden impulses propagating in geomagnetic tail and magnetosheath (NASA-CR-121900) 22 p3572 N71-35439

Bibliography of publications and compilation of abstracts on Explorer 33 and 35 satellites (NASA-CR-121895) 22 p3665 N71-36130

EXPLORER 35 SATELLITE

Tesseral harmonics of Explorer 34 satellite orbit perturbation in time of perigee passage due to third harmonic of earth gravitational field (NASA-TM-X-65561) 15 p2518 N71-27872

Models for internal structure of geomagnetic tail neutral sheet deduced from Explorer 34 magnetic data (NASA-TM-X-67153) 18 p3007 N71-31380

EXPLORER 35 SATELLITE

Analyzing data from Explorer 33 and 35 on energetic solar particles in interplanetary medium and terrestrial particle fluxes in magnetopause bow shock regions (NASA-CR-115775) 04 p0590 N71-14378

Application of VHF Doppler tracking data from Goddard Range and Range Rate system to determine lunar orbits for Explorer 35 satellite (NASA-TM-X-65470) 10 p1644 N71-21325

Explorer 35 observations of solar wind electron density, temperature, and anisotropy analyzed and compared with previous measurements (NASA-TM-X-65481) 10 p1640 N71-21492

Ratio of intensity of solar protons for north polar cap to that of south polar cap, as observed by Explorer 33 and 35 satellites (NASA-CR-117809) 12 p1991 N71-23112

Data processing techniques and equipment used in analysis of Lunar Orbiter 1 and 3 and Explorer 35 bistatic-radar data (NASA-CR-119033) 16 p2564 N71-29063

Bistatic-radar data reduction and Explorer 35 reflectivity and bandwidth tables with polarization spectra (NASA-CR-119032) 16 p2564 N71-29064

Bibliography of publications and compilation of abstracts on Explorer 33 and 35 satellites (NASA-CR-121895) 22 p3665 N71-36130

EXPLORER 37 SATELLITE

Tables of periodic variations of solar X-ray flux detected from Explorer 37 satellite 20 p3341 N71-33014

EXPLORER 38 SATELLITE

Data display of Radio Astronomy Explorer 1 (NASA-TM-X-65415) 06 p0946 N71-16239

U-type solar radio burst originating in outer corona observed by RAE-1 (NASA-TM-X-65484) 10 p1641 N71-21364

Analysis of launch opportunities for Radio Astronomy Explorer-B satellite during period Mar. through Dec. 1973 (NASA-TM-X-65587) 16 p2682 N71-28318

Design, calibration, and performance of low frequency RAE-1 satellite (NASA-TM-X-65616) 18 p3018 N71-30664

EXPLORER 40 SATELLITE

Explorer 40 satellite measurement of differential energy spectrum of geomagnetically trapped protons (AD-714513) 06 p0944 N71-16748

Injun 5 double probe measurements of dc fields in magnetosphere (NASA-CR-116791) 08 p1187 N71-18405

Auroral zone VLF hiss and low energy particle observations with Injun 5 satellite (NASA-CR-121418) 20 p3266 N71-33392

ELF noise band associated with low-energy electron precipitation events and auroral arcs based on Explorer 40 observations (NASA-CR-121676) 21 p3415 N71-34299

Convection electric fields observed with double probe dc electric field experiment on Explorer 40 satellite (NASA-CR-121741) 21 p3419 N71-34324

EXPLOSIONS

NT AERIAL EXPLOSIONS

EXPLOSIVE GASES

NT CHEMICAL EXPLOSIONS

NT GAS EXPLOSIONS

NT NUCLEAR EXPLOSIONS

NT UNDERGROUND EXPLOSIONS

NT UNDERWATER EXPLOSIONS

Sonic boom and explosive shock wave effects on buildings and structural members 02 p0146 N71-11803

Shock wave propagation during explosions in Freon (AD-712751) 04 p0621 N71-14580

Numerical analysis of shock wave produced by expanding sphere (AD-714197) 06 p0836 N71-16471

Heat release explosive processes and gas dynamics for high power energy conversion systems (AD-711981) 10 p1664 N71-21781

Shadowgraph photography of shock waves, wave fronts, wave reflection, and Mach cones in one dimensional channel flow passing through chokes (REPT-9770) 13 p3821 N71-24481

Influence of radiation on thermal explosion limit in exothermal chemical reactions 14 p2352 N71-25760

Rapid failure-damage assessment technique for exploding high pressure gas containment vessels (AD-720446) 14 p2350 N71-26662

Explosion processes determined by millimeter radio propagation through explosion region (JPRS-53334) 16 p2560 N71-28174

Equations of resonant interaction between three waves in plasma in fixed-phase approximation (UIUP-722) 18 p2992 N71-30583

Height of explosion sound ranging system for supersonic rockets in jungle environments using piezoelectric electroacoustic transducers (AD-724664) 20 p3351 N71-33835

Atmospheric-lithostatic pressure ratio effects on explosive crater dimensions in dry soil (NASA-TB-3-366) 21 p3419 N71-34330

Calculation of ground motions generated by air waves from surface explosions (UCRL-TRANS-10529) 21 p3421 N71-34343

Occurrence of explosion-like processes during high powered pulsed electron bombardment of diamonds, glass, and ceramics (SC-T-71-3017) 21 p3434 N71-34435

Origin of galactic clusters due to explosion or gravitational contraction 23 p3849 N71-37433

Possible causes of Tunguska explosion and its effects on surrounding region 24 p4009 N71-38590

EXPLOSIVE DEVICES

NT BOMBS [ORDNANCE]

NT DETONATORS

NT INITIATORS [EXPLOSIVES]

NT SHAPED CHARGES

Feasibility of explosive lining in launch tube for hypervelocity projectile acceleration (NASA-CR-108699) 04 p0605 N71-14033

Hermetically sealed explosive release mechanism for actuator device (NASA-CASE-XGS-00824) 06 p0864 N71-16078

Pyrrotechnic shock data associated with structure cutting charges consisting of solid detonating fuse and flexible linear shaped charge - Vol. 2 (NASA-CR-116458) 07 p1131 N71-17901

Determination of shock loads on spacecraft structures created by explosive separation of components - Vol. 3 (NASA-CR-116401) 07 p1131 N71-17902

Compilation of shock loads on spacecraft structures produced by actuation of pyrotechnics and explosive devices - Vol. 4 (NASA-CR-116402) 07 p1131 N71-17903

Performance of valve operated by cartridge discharge pressure (UCRL-50930) 07 p1038 N71-18069

Modified one-dimensional blast wave theory and experimental shock trajectories for shock tubes with high explosive drivers (SC-RR-70-182) 09 p1368 N71-20590

Development of non-magnetic indexing device for orienting magnetic flux sensing instrument in magnetic field without generation of detrimental magnetic fields (NASA-CASE-XGS-02422) 10 p1567 N71-21529

Characteristics of compressed magnetic fields produced by implosion of tubular stainless steel liners driven by high explosives 17 p2858 N71-29821

Development and characteristics of equi-actuated explosive disconnect for release of spacecraft from launch vehicle (NASA-CASE-MPO-11330) 21 p3530 N71-35154

Rocket launching of explosive grenades to measure winds and temperatures at 28 to 150 kilometers (FOA-4-C-4414-26) 22 p3614 N71-35744

EXPLOSIVE FORMING

High energy forming research including explosive forming, explosive welding, and pressure welding (AD-711568) 02 p0234 N71-14699

Research and development in high energy forming techniques (AD-722644) 17 p2757 N71-28160

EXPLOSIVE GASES

U FLAMMABLE GASES

EXPLOSIVE WELDING

- High energy forming research including explosive forming, explosive welding, and pressure welding [AD-711368] 02 p0234 N71-11699
- Dynamic parameters for obtaining wavy bonded interfaces between metals with explosive welding [AD-714221] 06 p0865 N71-16360
- Explosive welding techniques in fabricating regeneratively cooled thrust chambers for large rocket engine requirements including ultrasonic inspection, metallography, and burst testing [NASA-CR-72878] 16 p2600 N71-28045
- Explosively bonded 316SS/tantalum tubing for SNAP 8 boiler [NASA-CR-72961] 24 p3927 N71-38017

EXPLOSIVES

NT CELLULOSE NITRATE
NT TRINITROTOLUENE

- Dynamics of collisions between shock intersections and wave configurations in gases and condensed explosives [NASA-CR-111107] 01 p0402 N71-10421
- Gap test evaluation of shock sensitivity and heat resistance of explosive materials [AD-710738] 01 p0113 N71-10569
- Effects of inhomogeneities in explosives on critical diameter of detonation [LA-TR-70-7] 01 p0114 N71-10756
- Shock initiation of LX-07-2 and LX-10-4 [UCRL-30831] 03 p0467 N71-12867
- Determining impulse generation characteristics of reconstructed sheet explosives [SC-DR-70-432] 03 p0460 N71-12953
- Crystal structure and molecular dynamics of inorganic metal azides [AD-713585] 05 p0756 N71-14562
- Investigating nonsteady effects in gas phase of liquid and solid explosives under different physical and chemical conditions [AD-713541] 05 p0781 N71-14566
- Compatibility of explosives with various structural materials [SC-M-70-355] 05 p0775 N71-14793
- Laboratory simulation of impact cratering with high explosives [NASA-TM-X-62010] 05 p0675 N71-14995
- Detonation pressure measurements in TNT and OCTOL [AD-713547] 05 p0783 N71-15395
- Techniques for differential thermal analysis of primary explosives [AD-714205] 06 p0959 N71-16461
- Critical initiation pressures of explosives by shock waves [UCRL-TRANS-10490] 06 p0960 N71-16882
- Characteristics of heterogeneous shock initiation of explosive 9404 [LA-4475] 07 p1130 N71-17895
- Initial velocity and penetration depth of explosively accelerated metal balls [REPT-9469] 08 p1307 N71-18475
- Development of facilities for preparation of high explosives and booster charges [AD-716036] 09 p1365 N71-19668
- Measurement of pressures resulting from detonation of conventional explosives [SC-RR-70-541] 09 p1486 N71-20545
- Conference on safety problems in transportation and storage of explosives [AD-716790] 10 p1662 N71-21202
- Initiation and sensitivity of solid explosives to mechanical impact [NASA-TT-F-623] 11 p1841 N71-22534
- Methods and procedures used in vacuum thermal stability tests for explosives [AD-718806] 12 p1942 N71-23390
- Individual factors which produce risk in materials handling of explosives, noting safety management, accident prevention, and damping of explosions [ICT-170] 12 p1988 N71-23450
- Explosive detonation velocity, explosive welding to hardware configurations, and flange buckling of explosively formed dome [AD-718079] 12 p1926 N71-23758
- Calculation of frictional hot-spot temperatures and distributions on surfaces of explosives [AD-718806] 12 p1930 N71-24144
- Shock pulse attenuation and Hugoniot studies of three explosives and three shock explosives [UCRL-50950] 12 p2013 N71-24235
- Formation mechanism of electrical pulse during detonation of ordinary explosive substances [RAE-LIB-TRANS-1528] 13 p2134 N71-25165
- Viscosity of heterogeneous suspensions, noting solid rocket propellants and explosives [ICT-1270] 17 p2768 N71-29317
- Differential thermal analysis methods in high temperature research on biochemical, polymeric and explosive materials [NBS-SP-338] 20 p3361 N71-32826
- Modified remote cell for thermal differential decomposition studies on lead azide 20 p3363 N71-32834

Measurement of flow field behind plane detonation wave by observing motion of metal foils placed between explosives [LA-4426] 21 p3413 N71-34282

Production of intermetallic compounds by effect of shock waves resulting from explosions and resulting compaction of powders [NASA-CASE-MFS-20861] 21 p3443 N71-34500

Development of techniques for charging and exploding large amounts of trinitro explosive to simulate mechanical and thermal effects of nuclear explosions [FOA-4-C-4406-26] 22 p3696 N71-36362

Thermal decomposition and combustion of explosive substances - handbook [AD-726573] 23 p3867 N71-37565

EXPONENTIAL FUNCTIONS

NT LOGARITHMS

Imbedded Markov chain analysis of time sharing system with homogeneous Poisson arrivals, exponential service times, and ordered priority queues [AD-712319] 03 p0340 N71-12467

Superpropagator of fields with exponential coupling [DESY-70/26] 04 p0594 N71-14455

Stability and exponential penalty function techniques in nonlinear programming [AD-716564] 09 p1408 N71-19490

Exponential bound for growth of norm for derivative of strong solution of inhomogeneous abstract wave equation 09 p1409 N71-19864

Fredholm transformations and Radon-Nikodym derivatives for evaluation of Yak-Winner integrals of exponential functions [AD-718425] 12 p1948 N71-23348

Integration of exponential functions and application to long wave radiative transfer near mesopause 15 p2404 N71-27565

High energy scattering amplitude of fermion with anomalous magnetic moment and nonexpansion [DESY-71/11] 16 p2657 N71-29122

Exponential decay law of nonstable particle in framework of quantum mechanics [ITEP-773] 21 p3468 N71-34687

Structure of monograph and slide rule methodology useful in characterizing decay schemes [AD-726934] 23 p3782 N71-36956

EXPONENTS

Algorithms to find suboptimal additive chains as optimal procedure for obtaining power of associative operator [TID-25620] 10 p1594 N71-21626

EXPORTS

U INTERNATIONAL TRADE

EXPOSURE

Effects of thermal stress, exposure time, and acclimatization on human performance [AD-711012] 01 p0009 N71-10293

Circulatory impairment during exposure to ambient pressures of 4 mm Hg and 55 mm Hg [AD-712188] 02 p0156 N71-11103

Resolvent for photographic film frequency contrast characteristics measurement based on semi-automatic conversion of transmission factors into effective exposure [AD-722304] 17 p2751 N71-29494

Adhesion tests of several solar cell adhesives after thermal exposure [BMW-FB-W-71-16] 19 p3040 N71-31786

Human exposure to emergency exposure limit concentrations of monomethylhydrazine to determine suitability for use [AD-72757] 24 p3879 N71-37652

EXPRESSIONS [MATHEMATICS]

U FORMULAS [MATHEMATICS]

EXPULSION

Development and characteristics of positive expulsion systems for liquid rocket propellant tanks 03 p0447 N71-13115

Helium gas requirements for liquid hydrogen expulsion from spherical tank [NASA-TN-D-7019] 04 p0605 N71-14046

Fabrication and fatigue tests of improved welded tilt-edge bellows for positive expulsion applications [AD-726523] 23 p3762 N71-36824

EXPULSION BLADDERS

Computer program for analysis of folding strains on composite bladder structures [NASA-CR-111133] 01 p0130 N71-10837

Fatigue life prediction of composite bladder structures [NASA-CR-111306] 01 p0131 N71-10838

Analysis of symmetric bladder deformation due to asymmetric inversion pressures 03 p0462 N71-13116

Development and characteristics of elastomeric materials for positive expulsion bladders [NASA-CR-115902] 05 p0640 N71-14986

Solution of command module and service module expulsion bladder repositioning problems [NASA-CR-114813] 06 p0951 N71-16801

Elimination of permeation and bubble formation in Apollo RCS positive expulsion tankage [NASA-CR-114812] 06 p0959 N71-16866

Environmental tests of design modifications for Apollo RCS positive expulsion tankage [NASA-CR-114814] 06 p0959 N71-16867

Design fabrication and cycle tests of polymeric film expulsion bladders for liquid hydrogen [NASA-CR-72732] 10 p1607 N71-31446

Stress-strain fatigue behavior of Teflon liquid propellant expulsion bladder material 11 p1784 N71-22339

Rubber composition for expulsion bladders and diaphragms for use with hydrazine [NASA-CASE-NPO-11433] 18 p2940 N71-31116

Solvent effects on fatigue-stress-strain behavior of Teflon expulsion bladders [NASA-CR-121474] 20 p3330 N71-33620

EXTENSION

NT PROLONGATION

Support for flexible conductor cable between drawers or racks holding electronic equipment and cabinet assembly housing drawers or racks [NASA-CASE-XMF-07587] 06 p1307 N71-18700

Neat subgroup and extension problems for Abelian groups 12 p1948 N71-23392

Developments in program to develop extendable retractable nozzle extensions for open use [NASA-CR-115111] 19 p3183 N71-31606

EXTENSOMETERS

Determining cyclic deformation and strain concentration factor at notch root of flat specimens by extensometer [TUB-84/1970] 11 p1836 N71-20077

Piston cylinder assembly for diametric and ultrasonic high pressure measurements on solids and liquids 14 p2257 N71-26478

Tidal gravity variations derived from extensometer observations in Kamikake, Japan 20 p3264 N71-33037

Horizontal extensometer for measuring deformation caused by earth tides 23 p3749 N71-36776

Deformographs and extensometers for measuring earth crust deformations 24 p3910 N71-37866

EXTERNAL STORES

NT PODS [EXTERNAL STORES]

Rotary wing aircraft external stores junction systems [AD-713872] 06 p0795 N71-16082

Computerized prediction of separated store trajectories dropped from bomber aircraft at high speed 09 p1318 N71-19779

Flight test measurements on interference and aerodynamic drag effects caused by jettisoning of external stores from F-2 aircraft 09 p1319 N71-19784

Computerized prediction of flow field interference forces and moments on aircraft stores at subsonic speeds 09 p1319 N71-19785

Wind tunnel evaluation of lifting body store configurations for captive flight drag and separation characteristics 09 p1314 N71-19786

Statistical prediction of external store separation characteristics from aircraft 09 p1320 N71-19788

Guidelines for using space shuttle configuration to determine effects of carrying ascent LH2 propellant in external drop tanks 10 p1648 N71-31317

Manufacture and dynamic testing of external store models for transonic wind tunnels [REPT-23] 22 p3539 N71-35312

Safe separation criteria for external stores and jettisonable escape capsules for pilots [AD-726695] 23 p3707 N71-36428

EXTINCTION

NT INTERSTELLAR EXTINCTION

Dark and thermally stimulated conductivity, spectral distribution of normal and induced photoconductivity, and optical extinction of photoconductivity in Sb₂Se₃ single crystals 12 p1984 N71-23346

Transmission and extinction of solar radiation in atmospheric stratification 18 p3086 N71-31862

Analysis of extinction cross-sections for gain composed of water ice, quartz, and silica surrounded by ice mantle with application to stellar composition 21 p3512 N71-35826

EXTINGUISHERS

U FIRE EXTINGUISHERS

EXTINGUISHING

Ballistic model for quenching of solid propellant combustion [AD-711436] 02 p0287 N71-11809

Composite and double base rocket propellant extinguishing by rapid pressure reduction and propellant property and additive effects on combustion extinction 17 p2832 N71-29880

EXTRACTION

NT ION EXTRACTION

NT SOLVENT EXTRACTION

SUBJECT INDEX

Apparatus for extracting radioactive argon from chlorine containing substance 06 p0924 N71-16770
[NRL-TR-364]

Development of theoretical aspects and practical application of extraction method for purification of inorganic materials 16 p2356 N71-28297

Maintenance and reliability of plunging and target mechanisms and magnets in Nimrod thin section extraction system 18 p2359 N71-30499
[JHELR-309]

Aerosol water from cleaned and uncleaned capillary tubes, from weak H2O2 solutions, and from water extractions of crushed glass 23 p3720 N71-36517
[AD-726761]

EXTRAGALACTIC LIGHT
U EXTRATERRESTRIAL RADIATION
U LIGHT (VISIBLE RADIATION)
EXTRAGALACTIC MEDIA
U INTERGALACTIC MEDIA
EXTRAPOLE
Statistical extrapolation of spectral irradiance measurements of large solar simulators 02 p0224 N71-11526
[NASA-TN-D-6094]

Extrapolation based on coefficients for data reduction and data transmission 08 p1162 N71-18577
[DLR-89-70-49]

Extrapolation and interpretation of quasi-linear operators on martingales 09 p1411 N71-20341

Contouring program application to mapping of ionospheric parameters using electron density data from ionospheric stations for extrapolating observations 11 p1750 N71-22592
[AD-717683]

Theorem proving of extrapolation using Romburg quadrature 17 p2738 N71-29390

Extrapolation and error estimation method for solving second order boundary value problem 17 p2773 N71-29720

Accelerated life test models, criteria for model selection, and extrapolation in overstress models 21 p3526 N71-35124
[NASA-CR-121645]

Extrapolation of C-12 plus C-12 and C-12 plus O-16 mass cross sections below 4 MeV 22 p3642 N71-35967
[ANU-P-515]

EXTRATERRESTRIAL ENVIRONMENTS
NT CHROMOSPHERE
NT CISLUNAR SPACE
NT DEEP SPACE
NT INTERPLANETARY SPACE
NT INTERSTELLAR SPACE
NT JUPITER ATMOSPHERE
NT LUNAR ATMOSPHERES
NT LUNAR ENVIRONMENT
NT MARS ATMOSPHERE
NT MARS ENVIRONMENT
NT PLANETARY ATMOSPHERES
NT PLANETARY ENVIRONMENTS
NT SOLAR ATMOSPHERE
NT STELLAR ATMOSPHERES
Handbook on environmental and space utilization criteria for design of extraterrestrial manned spacecraft and shelters 07 p1119 N71-17560
[NASA-CR-114864]

Error analysis for extraterrestrial convergent photogrammetric mapping system 08 p1203 N71-19021
[NASA-CR-114624]

EXTRATERRESTRIAL LIFE
Search for signals of extraterrestrial life 06 p0945 N71-16201
[AD-713900]

Biogeochemical and microstructural analyses on lunar rock and dust samples for biological compounds 07 p1113 N71-17717
[NASA-CR-114639]

Consideration of biostromatolites and biological exploitation of space for determination of extraterrestrial life and origin of life on earth 09 p1334 N71-20187
[NASA-TT-F-13467]

Feasibility analysis for future use of television microscopy to detect extraterrestrial life 17 p2753 N71-29819
[NASA-TT-F-13733]

Automatic analysis system for separating and identifying amino acids to detect extraterrestrial life 19 p3044 N71-32332
[NASA-TT-F-13765]

Solvent activities and extraterrestrial life 21 p3509 N71-35002

EXTRATERRESTRIAL MATTER
NT COSMIC GASES
NT COSMIC PLASMA
NT INTERPLANETARY GAS
NT INTERSTELLAR GAS
Instrument for studying electron stimulated luminescence of terrestrial, extraterrestrial, and synthetic materials - luminescope 01 p0052 N71-10086

Origin of cosmic material fallout on earth surface and structure of cosmic dust and meteoritic materials 15 p2398 N71-27030
[REPT-49/18]

Cosmic matter-antimatter annihilation and gamma ray background spectrum 17 p2841 N71-29924
[NASA-TM-X-65598]

Abundance, persistence, and localization of enzyme activity in terrestrial soil and exploration of soils suitable for planetary life 20 p3215 N71-33232
[NASA-CR-121446]

Behavior of strongly interacting particles at ultrahigh temperatures related to origin of galaxies and matter 21 p3530 N71-35156
[LPTHE-71/15]

EXTRATERRESTRIAL RADIATION
NT EXTRATERRESTRIAL RADIO WAVES
NT GALACTIC RADIATION
NT GEGENSCHNITT
NT INTERSTELLAR RADIATION
NT LUNAR RADIATION
NT PLANETARY RADIATION
NT PRIMARY COSMIC RAYS
NT RADIO BURSTS
NT SOLAR CORPUSCULAR RADIATION
NT SOLAR COSMIC RAYS
NT SOLAR PROTONS
NT SOLAR RADIATION
NT SOLAR RADIO BURSTS
NT SOLAR RADIO EMISSION
NT SOLAR WIND
NT SOLAR X-RAYS
NT STELLAR RADIATION
NT SUNLIGHT
NT TYPE 3 BURSTS
NT TYPE 4 BURSTS
NT ZODIACAL LIGHT
Measurements of cosmic rays and high energy extraterrestrial particles 02 p0294 N71-11415
[NASA-SP-243]

Analysis of coordinated observations from ATS 5 and low altitude polar satellite OV1-18 04 p0608 N71-14419
[NASA-TM-X-65440]

Calibration of high energy cosmic ray experiment 06 p0944 N71-16750
[NASA-TM-X-65440]

Spaceborne telescopes for extraterrestrial observations 07 p1027 N71-16981

Analysis of data obtained from USSR lunar roving vehicle 07 p1105 N71-17005

Cosmic ray investigations conducted by lunar based observatories 07 p1108 N71-17074

Background radiation in space and synchrotron X radiation in galaxy and pulsars 09 p1463 N71-20472
[NASA-TM-X-64571]

Development of instruments for measuring flux of high and ultrahigh energy particles on Proton 4 satellite during space missions 09 p1464 N71-20576
[NASA-TT-F-13533]

Spark chamber and discharge counter for space radiation studies, radiation shielding, and dosimetry 10 p1641 N71-21620
[AD-716843]

Astrophysics, extraterrestrial radiation, and magnetosphere - conference 11 p1826 N71-22411
[NASA-TT-F-629]

X rays, gamma rays, electrons, and neutrinos in outer space and upper atmosphere 11 p1822 N71-22413

Data processing procedures and instrument development for space radiation measurements 11 p1827 N71-22418

Effects of nuclear and space radiation on mechanical, thermal, and optical properties of spacecraft structural materials 13 p2161 N71-25034
[NASA-SP-8053]

Criteria and procedures for determining dosage of penetrating space radiation and design of appropriate protection for space vehicles 13 p2174 N71-25075
[NASA-SP-8054]

Extraterrestrial ring current intensity changes and aurora dynamics model 13 p2161 N71-25200

Development of method for studying transfer of resonance line radiation in media of extremely large optical thickness 13 p2170 N71-25436

Application of nuclear emulsions in design of dosimeters used in detection of radiation exposure inside spacecraft 16 p2648 N71-28487

Effect of time ordering on Lyman alpha profile and comparison of time-ordered thermal average and untime-ordered thermal average 18 p2925 N71-31251
[NBS-MONOGRAPHS-131]

World Data Center A upper atmosphere data retrieval information on extraterrestrial radiation and geomagnetism 18 p3007 N71-31460
[UAG-15]

Thermal control coatings - radiation effects design handbooks 19 p3065 N71-32280
[NASA-CR-1786]

POPOP library and codes for preparing secondary gamma ray production cross sections 20 p3317 N71-33532
[ORNL-TM-3367]

Analysis of radiations encountered in space environment and manner in which interactions with matter occur 21 p3504 N71-34962
[NASA-CR-1871]

EXTRATERRESTRIAL RADIO WAVES
NT RADIO BURSTS
NT SOLAR RADIO BURSTS
NT SOLAR RADIO EMISSION
NT TYPE 3 BURSTS
NT TYPE 4 BURSTS

EXTREMELY HIGH FREQUENCIES

Measuring neutral hydrogen absorption in galaxy M82 by radio telescope 02 p0294 N71-11137
[AD-712599]

Total intensity and linear polarization properties of radio sources 3 C 10 and 3 C 58 02 p0292 N71-11145
[AD-711611]

Mechanical and optical characteristics of airborne infrared telescopes 04 p0610 N71-13620
[NASA-CR-115780]

Geophysics and space data bulletin - Vol 7, no. 2 06 p0856 N71-16761
[AD-714412]

Thermal electron density and cosmic ray flux in galactic radio emissions 13 p2163 N71-25289

Analysis of mode coupling conditions in ionosphere for solar radio waves 14 p2216 N71-25913
[NASA-CR-118640]

Geophysics and space data bulletin for Oct., Nov. and Dec. 1970 17 p2745 N71-29913
[AD-722438]

Flux density measurements on extraterrestrial waves from faint radio sources 19 p3182 N71-32781
[AD-724181]

Galactic 21 cm line absorption in 97 radio sources using two element interferometer 19 p3182 N71-32783
[AD-724182]

North-South interferometry of extragalactic radio sources 20 p3348 N71-33237
[AD-724183]

Long-delayed echo observations, echoes and their recognition, and extraterrestrial origin hypothesis 21 p3724 N71-36543
[AD-724735]

EXTRATERRESTRIAL RESOURCES
Properties of rocks, soils, and minerals in ultrahigh vacuum facility simulating lunar environment, for extraterrestrial resource utilization 22 p3666 N71-36150
[NASA-CR-121915]

EXTRAVEHICULAR ACTIVITY
Design and specifications for advanced extravehicular space suit 02 p0166 N71-11177
[NASA-CR-108666]

Portable environmental control and life support system for astronaut in and out of spacecraft 02 p0169 N71-11203
[NASA-CASE-XMS-09632-1]

Hand-held maneuvering unit for propulsion and attitude control of astronauts in zero or reduced gravity environment 03 p0327 N71-12136
[NASA-CASE-XMS-05304]

Internal and external serpentine devices for performing physical operations around orbital space stations 06 p0951 N71-16345
[NASA-CASE-XMF-05344]

Reusable, pin-type fastener, easily operated during EVA 07 p1036 N71-17653
[NASA-CASE-ARC-10140-1]

Integrated maneuvering life support system 09 p1338 N71-19399
[NASA-TM-X-66902]

Design and performance of extravehicular astronaut thermal protection gloves 12 p1868 N71-24138
[NASA-CR-114974]

Design and development of flexible tunnel for use by spacecrews in performing extravehicular activities 13 p2037 N71-24728
[NASA-CASE-MSC-12243-1]

Apollo 11 mission planning for lunar surface exploration including equipment requirements, crew/equipment interfaces, and timelines for extravehicular activities 14 p2357 N71-26144
[NASA-TM-X-67180]

Reusable portable life support systems concepts for EVA use in 1980 and technology assessment 15 p2376 N71-27788
[NASA-CR-114320]

Space tools and equipment for EVA and IVA 16 p2549 N71-28022
[NASA-CR-17000]

Extravehicular operational activities of humans during long duration space flight 16 p2553 N71-28546

Apollo 15 mission and manned geologic exploration of lunar landing site - maps 20 p3347 N71-33233
[NASA-CR-119725]

Automatic temperature control for liquid cooling garments used during astronaut extravehicular activity with external auditory muffs, and skin temperature as input signals 21 p3384 N71-34077
[NASA-TM-X-67181]

Preliminary data evaluation from Apollo 15 inflight and lunar surface experiments with analysis of extravehicular, module, support, and communication systems performance 23 p3848 N71-37427
[NASA-TM-X-67381]

EXTREMA
U RANGE (EXTREMES)
EXTREMELY HIGH FREQUENCIES
CW transferred electron oscillators for Q band 01 p0031 N71-10138

Side-looking airborne radar for K band mapping of snowfields 02 p0207 N71-11163

Performance of uncooled lens fabricated from expanded aluminum honeycomb operating at EHF 20 p3240 N71-32994
[AD-724686]

Design and development of dual frequency radiometer operating in 37 and 94 GHz 20 p3272 N71-33094
[AD-724111]

- High frequency sudden deviations caused by extreme ultraviolet flashes from solar flares in ionosphere
[NASA-CR-121461] 20 p3342 N71-33929
- EXTREMELY LOW RADIO FREQUENCIES**
- Sensory perception of ultralow frequency sinusoidal proprioceptive stimuli
[AD-711045] 01 p0009 N71-10248
- Sources and mechanics of extremely low frequency wave propagation in model ionosphere and sea
04 p0490 N71-13702
- Construction of coil antenna and ball antenna for extremely low frequency signal reception
04 p0492 N71-13712
- Extremely low frequency electromagnetic noise at deep sea levels
04 p0520 N71-13715
- Simultaneous magnetic and electric field measurements for extremely low frequency ionospheric disturbances and atmospheric
[AD-713890] 06 p0850 N71-16377
- Full wave solutions for ULF and ELF transmission through ionosphere
[AD-715301] 07 p1022 N71-17835
- Measurements of energetic electrons within drift loss cone, extremely low frequency emissions, and plasmasphere location
[AD-715266] 07 p1106 N71-18042
- Detection of atmospheric nuclear explosions by study of extremely low frequency waves and ionospheric disturbances
[AD-716601] 09 p1383 N71-19683
- Proceedings and abstracts of presentations at symposium on long wave propagation
[AD-716739] 10 p1526 N71-21796
- Fabrication and testing of flexible loop antenna as underwater, towed, ELF receiving antennas
[AD-717710] 11 p1724 N71-22573
- Ecological effects of electromagnetic fields and ELF global communication systems
[AD-718828] 12 p1862 N71-23381
- Far-field strength measurements at extremely low frequencies for determining East-West diurnal attenuation rate
[AD-718100] 13 p2042 N71-24362
- VHF/UHF parasitic probe antenna for spacecraft communication
[NASA-CASE-XKS-09340] 13 p2044 N71-24614
- Effect of quasi-rhythmicity in geomagnetic and aeronomic phenomena
17 p2747 N71-30085
- ELF noise band associated with low-energy electron precipitation events and auroral arcs based on Explorer 40 observations
[NASA-CR-121676] 21 p3415 N71-34299
- Electron streams and extremely low radio frequency radiation in magnetosphere
23 p3854 N71-37471
- Effects of ionospheric propagation on ELF communication system
[AD-727571] 24 p3890 N71-37724
- EXTREMUM VALUES**
- NT LIMITS (MATHEMATICS)**
- NT MAXIMA**
- NT MINIMA**
- Extremal problems related to eigenvalues of linear differential operators
[AD-713706] 05 p0714 N71-15278
- Graphical method of removing outlier values from analytical data
[BM-RJ-7472] 05 p0651 N71-15427
- Cumulative frequency distributions determined by extreme value analysis used for fatigue analysis and interpretation of e.g. vertical acceleration and gust velocity measured on transport aircraft
[AGARD-R-579-71] 13 p2028 N71-25080
- Extremum value statistics computer program for evaluation of radar target acquisition
[AD-722441] 18 p2089 N71-30717
- Computer program for function optimization on line segments by golden section
[UCSD-30062] 21 p3447 N71-34535
- EXTRUDING**
- Evaluation of cobalt base alloy made by extrusion of prealloyed powders
[NASA-TN-D-6072] 01 p0066 N71-10326
- Substructural hardening and gas extrusion of metals
[JPRS-51624] 02 p0241 N71-11444
- High pressure gas medium for extrusion of materials
02 p0229 N71-11446
- Coextruded titanium-316 stainless steel bimetallic joints and tubing
[NASA-CR-72761] 03 p0384 N71-12419
- Effects of cold working by hydrostatic extrusion on mechanical properties of high strength steels
[NASA-TN-D-6186] 07 p1034 N71-17485
- Deformation criteria in cold extrusion of metals with equation for calculating extrusion pressure from material parameters
17 p2854 N71-30155
- Technique of surface carburization prior to extrusion reported for two C-Mn-Si steels
[PB-197129] 18 p2927 N71-30744

- Influence of core to sleeve bonding on fracture of hydrostatic extrusion of hard core clad rod
[NYO-4078-3] 18 p2938 N71-31559
- Precision extrusion of I and E fuel element and research on U thermal expansion anisotropy, U oxidation, U forging, and extrusion processes
[RMI-16] 20 p3309 N71-33796
- Hydrostatic extrusion of refractory materials using simple press
[NASA-CASE-NPO-10811] 21 p3433 N71-34425
- Design and operation of extrusion can for use in extruding ceramics under heat and pressure
[NASA-CASE-NPO-10812] 21 p3433 N71-34428
- EYE (ANATOMY)**
- NT NYSTAGMUS**
- NT PUPILS**
- NT RETINA**
- Statistical analysis of importance of pupil in optics of visual system
[AD-713427] 05 p0633 N71-14609
- Augmentation of human eye focus control by varying index of refraction with nematic liquid crystals
[NASA-CR-115864] 05 p0634 N71-14653
- Phenomenological theory for describing intraocular pressure regulation in normal eye and consequences of deterioration of pressure regulation in abnormal eye
06 p0799 N71-15858
- Examining dynamics of changes in supranuclear nucleus of hypothalamus in rats exposed to transverse accelerations
08 p1150 N71-18898
- Matching frequency of observer eye to frequency of visual pattern for optimum recognition
[RM-498] 10 p1500 N71-21485
- Sight switch using infrared source and sensor mounted beside eye
[NASA-CASE-XMP-03934] 11 p1726 N71-22985
- Development of apparatus for studying stabilized image properties of human eye using photomultiplier tube and magnetic core array storage system
[NASA-CR-114307] 13 p2034 N71-24931
- EYE DISEASES**
- NT ASTIGMATISM**
- NT GLAUCOMA**
- Ultraviolet radiation effects on human and animal eye
[AD-711360] 01 p0013 N71-10753
- EYE EXAMINATIONS**
- Infrared photography for ESSO satellite surface and solar cell temperatures and vestibular eye examinations
[ESRO-TM-150-ESTEC] 03 p0382 N71-13272
- Intraocular pressure distribution measurements on healthy subjects engaged in mental work
20 p3222 N71-33469
- EYE MOVEMENTS**
- NT NYSTAGMUS**
- Characteristics of optokinetic eye-movement patterns and nystagmus in man and animal
[AM-70-10] 01 p0011 N71-10425
- Human torsional eye movements analysis
02 p0153 N71-11084
- Characteristics of voluntary saccadic eye movements and importance for pilot performance
02 p0164 N71-11825
- Sensing arrays using concept of involuntary human eye motion with application to photogrammetry and metrology
[AD-713568] 05 p0684 N71-14893
- Development of apparatus for studying stabilized image properties of human eye using photomultiplier tube and magnetic core array storage system
[NASA-CR-114307] 13 p2034 N71-24931
- Head and eye movements affected by angular velocity and linear acceleration in aerospace environments
[DR-208-VOL-1] 18 p2878 N71-31526
- Anticompensatory oculomotor response during rapid head rotation at high angular velocity
[AMRU-R-64-2] 18 p2879 N71-31528
- Eye lid movement effects on electro-oculographic recording of vertical saccadic eye movements
[AMRU-R-65-5] 18 p2880 N71-31533
- Clinical neurology and neurophysiology of vestibulo-ocular reflexes
[AMRU-R-66-1] 18 p2880 N71-31535
- Stochastic model for observing motion of retinal image of target during visual fixation
[NASA-CR-121640] 21 p3393 N71-34071
- Eye movement, mental performance, and problem solving
22 p3545 N71-35250
- EYE PROTECTION**
- Development and fabrication of polycarbonate eyeshield for army flyers helmet
[AD-712313] 02 p0169 N71-11200
- Design and development of protective spectacle for Apollo pressure suits
[NASA-CR-115039] 15 p2375 N71-27742
- Operational test and evaluation of photochromic goggles for eye protection during exposure to nuclear explosion flash
[AD-726544] 22 p3549 N71-35278

EYEPIECES

- Wide angle eyepiece with long eye-relief distance
[NASA-CASE-XMS-06036-1] 13 p2124 N71-24857
- EYERING THEORY**
- Dependency factor of Eyering structure theory for model of solid with vacant lattices
[AD-719307] 13 p2152 N71-25431

F

F CENTERS

U COLOR CENTERS

F DISPLAYS

U F REGION

F LAYER

U F REGION

F REGION

NT F2 REGION

- Comparison of ionospheric sounding electron concentration and electron and ion temperature data in F region
01 p0046 N71-10222

F region internal gravity waves properties

- Satellite observation of horizontal ion density gradients in F region
01 p0117 N71-10502

- Comparing vertical distribution ionospheric soundings in F region from bottom side and topside over Ouagadougou/Upper Volta/
[GRI-NT-78] 02 p0212 N71-11542

- Ionospheric vertical sounding data of F and E regions from Freiburg, Germany for August 1970
[REPT-298-F] 02 p0214 N71-11864

- Atmospheric model computation of F region ionospheric irregularities affecting radio wave propagation
[KGO-701] 03 p0575 N71-13395

- Development of model of E and F regions of ionosphere
[NASA-CR-115894] 05 p0668 N71-14759

- Seasonal anomaly of F-region explained in terms of composition changes in lower atmosphere
[NASA-TM-X-65410] 05 p0669 N71-14804

- Ionospheric irregularities affecting radio wave propagation through F region
[AD-714203] 06 p0816 N71-16419

- Cosmos 224 measurements of nitric oxide vertical profile in E and F regions at low sun zenith angles
07 p1014 N71-16934

- Aperture antenna synthesis for HF radio signal propagated via F layer of ionosphere
[AD-714825] 08 p1167 N71-18232

- Scintillation relationship to satellite communications in F region
[AD-715891] 08 p1162 N71-18534

- Problems of communication and navigation systems in VLF and UHF produced by small irregularities in electron density in F region
[AD-717694] 11 p1751 N71-22895

- Early bird and ATSC simultaneous recordings of F region ionospheric electron density for scintillation analysis of ionospheric disturbances
[AD-719672] 14 p2245 N71-25827

- Observation of ionospheric winds in auroral zone following release of rocket borne chemicals
[AD-719676] 14 p2246 N71-25827

- Ionospheric propagation data for E and F regions. Bangkok - Aug. 1970
[AD-720326] 16 p2589 N71-28864

- Ionospheric propagation data for E and F regions. Bangkok - Sept. 1970
[AD-720327] 16 p2589 N71-28864

- Ionospheric propagation data for E and F regions. India - October 1969
[RTRC-A173] 22 p3575 N71-35440

- Ionospheric propagation data for E and F regions. India - September 1969
[RTRC-A172] 22 p3575 N71-35441

- Ionospheric propagation data for E and F regions. India - Aug. 1969
[RTRC-A171] 22 p3575 N71-35442

- Radar backscatter measurements to determine electron temperature dependence of F region absorption
[RSD-65] 22 p3575 N71-35444

- Diurnal temperature variations in middle ionosphere and electron density in E, E-F, and F1 regions
22 p3679 N71-36234

- Ionospheric propagation data for E and F regions. India - (Dec. 1969)
[RTRC-A175] 23 p3732 N71-36731

- Ionospheric propagation data for E and F regions. India - Nov. 1969
[RTRC-A174] 23 p3732 N71-36732

- F2 REGION**
- Ionospheric prediction coefficients for F region and sunspot variations during April, 1970
[TB-11-499-85/TO-31-3-28-2] 05 p0681 N71-15678

- Ionospheric propagation charts of predicted median critical and maximum usable frequencies in F2 region. Delhi - Jan. 1971
[RRC-B172] 11 p1747 N71-22607

SUBJECT INDEX

- Traveling ionospheric disturbance model of F 2 region after low altitude nuclear explosion 11 p1710 N71-22933
- High altitude velocity distribution of ionospheric drift and electric field strength in F 2 layer 17 p2748 N71-30091
- F-14 AIRCRAFT**
- NASTRAN application to static tests and dynamic modal problems of horizontal stabilizer of F-14A aircraft 22 p3484 N71-36269
- F-3 AIRCRAFT**
- Dynamic response of F-2 aircraft using cross correlation and power spectra 06 p0793 N71-15720
- Flight test measurements on interference and aerodynamic drag effects caused by jettisoning of external stores from F-2 aircraft 09 p1319 N71-19384
- F-4 AIRCRAFT**
- Optimization design procedures for development of stability augmentation systems 10 p1492 N71-20617
- Error analysis of counting accelerometer data from F-4 and RF-4 aircraft and structural fatigue analysis (AD-717151) 10 p1497 N71-20796
- Measurements of aircrew total vibration exposure during low altitude, high speed flight in F-4C aircraft (AD-726271) 14 p2205 N71-26172
- F-4E aircraft in-flight television recording system in crew training 14 p2210 N71-26174
- Closure technique for retention of grease in large bearing on F-4C aircraft wheels (AD-725679) 19 p3104 N71-31744
- Aircraft accident report on midair collision involving DC-9 commercial aircraft and Marine Corps F-4B aircraft near Duarte, California on June 6, 1971 (BB-71-62) 19 p3639 N71-32491
- Practical design procedure for F-4 aircraft engine inlet systems based on quadratic optimal control technology (AD-72584) 22 p3540 N71-33221
- Hydraulic power and actuation requirements of survivable flight control system utilizing fly by wire control for F-4 aircraft (AD-727763) 24 p3873 N71-37608
- F-4 AIRCRAFT**
- Mathematical modeling of F-4 aircraft wave off trajectories for aircraft carrier approaches (AD-727121) 23 p3708 N71-36439
- F-28 TRANSPORT AIRCRAFT**
- Aerodynamic and flutter analysis for T tail of Fokker F-28 17 p2699 N71-29344
- Experimental aerodynamic analysis to determine similarities of T-tail configuration of F-28 aircraft 21 p3573 N71-34002
- F-4 AIRCRAFT**
- U-33 AIRCRAFT
- F-4 AIRCRAFT**
- Evaluating use of airborne digital computers for guidance and control of X-15 and F-104 aircraft (NASA-TM-X-44491) 03 p0408 N71-12610
- Dynamic loads on F-104 aircraft launch gear (PB-82-1569) 08 p1143 N71-18532
- Computer program for optimum flight path defined by flight test investigation of performance characteristics (alpha zero thrust, fuel flow, and climb potential) of F-104D aircraft (NASA-TN-D-6398) 15 p2366 N71-27002
- F-106 AIRCRAFT**
- Thrust measurement system and aerodynamic drag effects of underwing J-85 engine nacelles on F-106 aircraft propulsion system performance (NASA-TM-X-2356) 19 p3174 N71-32144
- F-10 AIRCRAFT**
- U-4 AIRCRAFT
- F-10 AIRCRAFT**
- Congressional hearing on investigation of contract for TPX aircraft 02 p0146 N71-11034
- Congressional investigation into contract management and development costs of TPX aircraft (HEPT-91-1496) 05 p0789 N71-15649
- Two variations of gas generator method to calculate thrust of afterburning turbofan engines installed in F-11A aircraft 11 p1821 N71-22614
- In-flight F-111 data on total and static pressure from left inlet during automatically scheduled and manually controlled off-schedule positioning of probe at Mach 0.8 to 2.18 20 p3210 N71-33211
- FORTRAN PROGRAMMING LANGUAGE**
- FABRICATION**
- Fabrication methods for matrices of solar cell substrates (NASA-CASE-XNP-63821) 02 p0149 N71-11056
- Fabrication and testing of peak wind speed recorder (NASA-CR-102909) 02 p0253 N71-11407
- Electron bombardment utilized for welding diverse tubometers and turboreactor parts 02 p0233 N71-11645

- Use of latex for fabrication of turbomachine parts 02 p0233 N71-11648
- Fabrication techniques of compact fluid control equipment for aerospace engines 02 p0203 N71-11654
- Capacitor fabrication by solidifying mixture of ferroelectric metal particles, nonferromagnetic particles, and dielectric material (NASA-CASE-LEW-10364-1) 04 p0510 N71-13322
- Isotope separation and fabrication (ORNL-TM-3089) 04 p0593 N71-14420
- Investigating nervous system regulation of intracellular pressure and fabrication of hybrid microcircuits 06 p0902 N71-15857
- Simplified method of hybrid microelectronic fabrication based on use of leadless inverted semiconductor 06 p0626 N71-15859
- Program for developing and fabricating lithium doped silicon solar cells for spacecraft (NASA-CR-116180) 06 p0797 N71-16430
- Summary report on HPOR fuel cycle development (ORNL-TM-3284) 07 p1063 N71-17362
- Fabrication of graphite reinforced epoxy tubes (AD-715319) 07 p1048 N71-17857
- Fabrication of non-fuel core components for experimental fast oxide reactor 06 p1239 N71-18508
- Crystal defects in diamonds and semiconductor fabrication (JPRS-52565) 11 p1816 N71-22182
- Fabrication techniques for split fiber glass holder (BDX-615-198) 11 p1769 N71-22532
- Fabrication and acceptance data for heavy section ASTM A-533 and A-543 grade B steel plates and electroslag, submerged-arc, and shielded metal-arc weldments for nuclear pressure vessel (ORNL-4313-3) 12 p1936 N71-23165
- Fabrication and tests of CO2 flat plate models in the hypersonic wind tunnel (SC-CR-49-3215) 12 p2010 N71-23228
- Method and apparatus for fabricating solar cell panels (NASA-CASE-XNP-63413) 14 p2203 N71-26726
- Polyethylene balloon fabrication and flight test time/altitude data (NASA-CR-115028) 14 p2199 N71-26776
- Explosive welding techniques in fabricating regeneratively cooled thrust chambers for large rocket engine requirements including ultrasonic inspection, metallography, and burst testing (NASA-CR-72878) 16 p2600 N71-28045
- Design and fabrication of separators and seals for storage batteries 16 p2540 N71-28073
- Design and fabrication of hydrogen oxygen propellant shutoff valves for space shuttle APS thrusters 17 p2831 N71-29393
- Fabrication and performance of transmission mounted silicon surface barrier detectors (BBW-FBR-78-57) 18 p2922 N71-30469
- Fabrication and evaluation of water activated zinc air electric battery 18 p2874 N71-31498
- Fabrication of reactor fuel elements for SEFOR (GEAP-10010-27) 19 p3134 N71-31734
- Fabrication of semiconductor detectors of S/L for nuclear reactions with control of depth of total compensation zone and automatic drift control (CNEA-287) 19 p3139 N71-32627
- Analysis of plutonium, uranium, and plutonium oxide materials balance during nuclear fuel fabrication (GEAP-12114-4) 21 p3461 N71-34634
- Fabrication and environmental tests of circuit boards with polyimide plastic dielectrics and pyrolyzed polycarbonate conductors (NASA-CR-119344) 22 p3562 N71-35373
- Design and fabrication of lithium hydride shields for SNAP applications (NASA-TM-129782) 23 p3761 N71-36811
- Fabrication and testing of one-third scale bone/spine tubular booster thrust structure (NASA-CR-119358) 24 p3927 N71-38018
- FABRICS**
- NT DACRON (TRADEMARK)
- NT FELTS
- NT PARACHUTE FABRICS
- NT WOOL
- Comprehensive method of composite fabrication of graphite filaments and mechanical properties of fabrics (NASA-CR-102916) 02 p0246 N71-11441
- Test chamber for fabric flammability and heat transfer measurement 06 p0882 N71-16728
- Effect of strain rate and load cycling on tensile behavior and air permeability of coated fabric for inflatable decontamination system (NASA-CR-111083) 12 p2004 N71-23197
- Development of space suits for long duration space missions to include wardrobe definition, fabric usage, laundry system concepts, wardrobe packaging, and crewman sizing (NASA-CR-115044) 15 p2374 N71-26808
- Relationship of breaking load, elongation, and tear strength of fabrics to properties of component yarns (AD-726919) 22 p3604 N71-35666

FACSIMILE TRANSMISSION

- Flammable Fabrics program reporting standards for carpets and rugs, blankets, mattresses, and apparel for children (NBS-TN-596) 23 p3776 N71-36014
- Belted fabrics woven of nylon and polypropylene fibers for personal body armor (AD-726918) 23 p3779 N71-36033
- FABRY-PEROT INTERFEROMETERS**
- Electromagnetic wave diffraction in Fabry-Perot optical resonator 06 p1202 N71-18928
- Wave diffraction in Fabry-Perot and ring type cavity resonators 12 p1809 N71-23550
- Electron density measurement of negative glow plasma with E-band Fabry-Perot interferometer using flat plate technique (NASA-TN-D-6282) 16 p2661 N71-28018
- Satellite modulator for 15 micron infrared radiation using Fabry-Perot interferometer (ESRO-CR-24) 17 p2751 N71-29389
- Tables of distribution functions for analysis of intensity distribution patterns from Fabry-Perot interferometer (NRC-TT-1466) 20 p3373 N71-35418
- Diffusion of nonlinearly scattered light by cavity glass in experiments using Fabry-Perot interferometer in conjunction with laser light source 20 p3374 N71-35479
- Hyperfine structure and isotope effect of 30 year bimetal 207 using Fabry-Perot interferometer and monochromator measurements 20 p3321 N71-35731
- FABRY-PEROT LASERS**
- U LASERS**
- FABRY-PEROT SPECTROMETERS**
- Pressure scanning Fabry-Perot magnetometer for studying solar surface features and stellar images (NASA-CR-111004) 01 p0057 N71-10062
- Zemman-modulated resonant cavity spectrometry of gas-phase free radical microwave rotational absorption spectra (UCRL-50890) 06 p1244 N71-19101
- Large aperture Fabry-Perot spectrophotometer with helium-neon laser to reduce instrument drift 13 p2079 N71-24419
- Reduced self absorption in recording Fabry-Perot spectrometer for lithium isotope analysis (BARC-598) 21 p3466 N71-34834
- FACE (ANATOMY)**
- NT NOSE (ANATOMY)**
- FACE CENTERED CUBIC LATTICES**
- Particle size effects and intensity calculations from Debye scattering equation for face centered cubic crystal 11 p1817 N71-22887
- Matrix and face lattice precipitation phase conditions and quantity determinations of Cu-Al alloy coercive force (NLL-CR-TRANS-5523-0022-00) 12 p1939 N71-34090
- Phase diagrams of metastable face centered cubic iron rhodium alloys 13 p2098 N71-25514
- Theoretical calculations on extension of 1/2/110, 1/111 edge and screw dislocations in isotropic fcc metals into Shockley partials 17 p2816 N71-29931
- The solution calorimetry for measuring heats of formation of selected face centered cubic palladium-silver-tin system (AD-722799) 18 p2937 N71-31397
- Computer program (KRISTALL) for studying dynamics of radiation damage in face centered cubic lattices, body centered cubic lattices, and diamonds (IAB-2002) 21 p3494 N71-34908
- Free energy and orientational degrees of freedom of crystalline nitrogen phase transformations 21 p3500 N71-34934
- FACETS**
- U FLAT SURFACES**
- FACILITIES**
- Measures for providing financial responsibility liability limitations for vessels and offshore and offshore facilities in oil pollution cases 19 p3196 N71-32624
- Food handling and refuse disposal procedures, air pollutant emissions, and abatement plans for Federal facilities in counties in Kansas and Missouri 22 p3577 N71-35481
- FACSIMILE COMMUNICATION**
- NT AUTOMATIC PICTURE TRANSMISSION**
- Electronic photoconductor scanner for image sensing in facsimile transmission (AD-719953) 01 p0625 N71-10830
- Integration of text processing and written communication into management information system 14 p2223 N71-25991
- Technology assessment of communication media and educational technology including future trends utilizing communication satellites, television, and computer-aided instruction (NASA-CR-123857) 22 p3553 N71-35306
- FACSIMILE TRANSMISSION**
- U FACSIMILE COMMUNICATION**

FACTOR ANALYSIS

- Nonfactorizable expression for asymptotic multiparticle amplitude signature with Toller angle variables
[RLO-1388-591] 09 p1433 N71-20037
- Kalman filtering for spectral factorization and matrix solution to spacecraft tracking problem
10 p1643 N71-21359
- Basic theory and general linear model for analysis of variance
[TR-71-14] 14 p2286 N71-26677
- Factor analysis applied to heuristic assessment matrix for numerical weather forecasting
[NLL-M-9253-15828.4F] 19 p3130 N71-32587
- Analytic method for interface relationships between different surface geometries
[AO-4193] 20 p3291 N71-33280
- Poisson density functions and factor analysis of shock wave propagation and sonic boom spectra in turbulent flow
[NASA-CR-1879] 20 p3210 N71-33283
- Factorization technique for calculating space energy synthesis in fast reactor
22 p3427 N71-33844
- Connection between conformal covariance and gauge invariance of interactions
[JINR-P2-5716] 23 p3807 N71-37143
- Development of optimal design procedures by posing experimental design problem as finite decision problem
[NASA-TN-D-6527] 24 p3950 N71-38184
- FACTORIAL DESIGN
- Space suit with pressure-volume compensator system
[NASA-CASE-XLA-05332] 02 p0168 N71-11194
- Equipotential space suits utilizing mechanical aids to minimize astronaut energy at bending joints
[NASA-CASE-LAR-10007-1] 02 p0168 N71-11195
- Miniaturized electret pressure sensor for thin surfaces
[ONERA-TP-836] 02 p0226 N71-11682
- Altering schemes and construction of fractional replicates
[AD-713696] 05 p0714 N71-15279
- Computer oriented approach to statistical analysis and general factorial design programs
[TR-71-18] 19 p3062 N71-32493
- Design optimization for fractional factorial experiments by finite decision problem based on prior information
[NASA-TM-X-67901] 20 p3292 N71-33554
- FACTORIALS
- Factorization of dual amplitudes and loops in coherent state model with finite set of five dimensional oscillators
[JINR-E2-5568] 14 p2303 N71-26039
- FACTORIES
- U INDUSTRIAL PLANTS
- FAULAE
- Magnetic fields and spectral characteristics of small H-alpha solar flares
19 p3177 N71-32439
- Flares, coronal enhancements, faculae, and geomagnetic response of quiet and active regions of solar magnetic sector structure
[NASA-CR-121420] 20 p3341 N71-33206
- Fine structure of facular fields at different levels of solar atmosphere based on escalation method
[NLL-RTS-6412] 23 p3842 N71-37398
- Fine structure and quantitative reduction of H alpha and beta lines and K lines inside facular areas
[NLL-RTS-6401] 23 p3842 N71-37399
- FADDEEV EQUATIONS
- Generalized integral equation for two body scattering potential in core interactions using tensor and Coulomb forces
[ICOO-1746-37] 04 p0584 N71-14204
- Angular distributions and polarizations of emerging particle in three body problem using Faddeev equations
[LYCEN-7046] 08 p1248 N71-18202
- Relativistic analog of Faddeev equations for scattering amplitude, using three dimensional formulation of quantum field theory
[JINR-P2-5099] 09 p1410 N71-20001
- Neutron-deuteron scattering length calculations with realistic potentials using two-particle t-matrices and Faddeev equations
[JINR-P4-3008] 09 p1440 N71-20302
- Application of Faddeev and Coulomb T-matrix to electron capture in hydrogen
12 p1975 N71-24050
- Faddeev solution to Lippman-Schwinger integral equation for three particle scattering
13 p2132 N71-25094
- Three body Faddeev equation for trinuclear binding energy and doublet scattering length for rank two separable potentials
13 p2143 N71-25582
- Using Faddeev equations for studying model of three rigid alpha particles for nucleus of C-12
13 p2144 N71-25588
- Practical potentialities of separable expansion of partial harmonics of nucleon-nucleon potential
[JINR-P4-5510] 16 p2645 N71-28120

- Binding energy, wave function, and doublet scattering length calculations for three nucleon system using Faddeev equations
[NP-18678] 18 p2972 N71-30527
- Three dimensional formulation quantum field theory based on relativistic Faddeev equations and applied to three body problems
[JINR-P2-5661] 21 p3468 N71-34688
- Solving Faddeev equations for three-nucleon systems for local potentials with soft or hard cores
[JINR-E4-5763] 21 p3482 N71-34804
- Relativistic scattering amplitude equations for transitions in three-body interactions based on Green functions, Faddeev equations, and three-particle bound state wave functions
[JINR-E2-5771] 23 p3807 N71-37145
- FADING
- NT SIGNAL FADING
- FAHRENHEIT TEMPERATURE SCALE
- U TEMPERATURE SCALES
- FAILURE
- NT ENGINE FAILURE
- NT FAILURE ANALYSIS
- NT STRUCTURAL FAILURE
- NT SYSTEM FAILURES
- Identification, characteristics, and distribution of slope failure forms as depicted by selected remote sensor returns
05 p0667 N71-14746
- Rolling shear failure of plywood in structural components
[VP-X-67] 05 p0781 N71-15614
- Fuel failure mechanics and failure propagation related to safety characteristics of fast test reactor
[BNWL-SA-3093-VOL-2] 11 p1795 N71-22458
- Fuel failure detection system of swimming pool type reactors - JRR-4
[JAERI-MEMO-4196] 13 p2117 N71-24908
- Optimal strength and failure modes of ultrasonically bonded metals in air and vacuum
[UCRL-13486] 15 p2417 N71-27801
- Bowing and eventual failure of beryllium structural plates in Plum Brook Reactor
[NASA-TM-X-67894] 19 p3139 N71-32273
- Steel brittleness related to low cycle fatigue, brittle failure prediction calculation
[AD-727422] 24 p3937 N71-38089
- FAILURE ANALYSIS
- Relativistic evaluation of propellant behavior with nonlinear viscoelasticity and cumulative damage
[AD-710776] 01 p0113 N71-10532
- Recording and frequency analysis of vibration data using coherent optical data processing techniques with emphasis of failure detection
[AD-710809] 01 p0116 N71-10554
- Design, test evaluation, and performance failure analysis of ion mass spectrometer for OGO-F
[NASA-CR-111146] 01 p0055 N71-10588
- Failure analysis of electric equipment due to high voltage breakdown
[AD-711559] 02 p0193 N71-11354
- Physical failure analysis of integrated circuits containing metal oxide semiconductors and its application to analog gates
[PUBL-369] 02 p0194 N71-11359
- Algorithm for fault isolation of multistate electronic networks
02 p0196 N71-11377
- Failure analysis of recovery flashing xenon lamp on Apollo 10 flight
[NASA-TM-X-66485] 02 p0290 N71-11899
- Potential malfunction analysis for conceptual lithium-cooled space power fast spectrum reactor
[NASA-TM-X-2057] 03 p0413 N71-12568
- Simulation and analysis of panel separation from Apollo 13 service module
[NASA-TN-D-6087] 03 p0456 N71-13026
- Mechanical failure detection for gears
[AD-712128] 03 p0385 N71-13220
- Predicting bearing fatigue failure and life in primary coolant check valves of advanced test reactors
[IN-1338] 04 p0557 N71-14153
- Investigating categorization and formation of stress and strength factors for semiconductor diodes to provide improved failure rate prediction from mathematical models
[NASA-CR-115801] 04 p0603 N71-14311
- Multiparameter differentiation in quadratic mean and asymptotically optimal tests for failure distributions
[PB-192499] 04 p0541 N71-14461
- Fatigue failure after few cycles of biaxial stresses
[PUBL-1267] 03 p0775 N71-14790
- Application of fracture mechanics to design and failure analysis
[AD-713148] 05 p0780 N71-15570
- Failure analysis of breakdown in high voltage transformer of OSO-4 pointed experiment
06 p0828 N71-16648
- Simultaneous multiple functional failures in critical safety and protection equipment in boiling water reactors
[NEDO-10189] 06 p0899 N71-16691

- Probability analysis of pipe failure and low-cycle fatigue in reactor cooling systems
[GEAP-10307] 06 p0900 N71-14778
- Failure probabilities for log normal capacity distribution with normal demand distribution
[SC-RR-70-547] 07 p1123 N71-17571
- Investigating energy concept of adhesive failure and pressurized disk test for measuring adhesive value of bonded elastomers
08 p1223 N71-19806
- Evaluation of effect of Apollo 13 malfunction on related subsystems
[NASA-TM-X-66928] 09 p1470 N71-19951
- Optimum structural design and reliability analysis
09 p1479 N71-20130
- Rotor-bearing system analysis to determine cause of bristling failure of bearings from vibration test
[NASA-CR-117855] 11 p1769 N71-23237
- Surface impurity and structural defect analysis on thermally grown silicon oxide integrated circuit
[NASA-CR-117904] 12 p1893 N71-23713
- Fuel failure behavior during in-pile meltdown tests in water cooled thermal reactors, using high speed photography and transparent autoclave
13 p2113 N71-24918
- Post-failure examination of stainless steel in-pile section of HFR pressurized water loop
[RCN-125] 13 p2122 N71-25422
- Accident analysis for pressurized and boiling water nuclear steam supply systems loss of coolant situations
[BMM-1897] 13 p2122 N71-25440
- Fracture mechanics and failure analysis of glass under biaxial loading at elevated pressures in water and inert atmospheres
[AD-717952] 14 p2277 N71-27870
- Analysis of structural failure of liquid propellant rocket engines due to gaseous hot spots within the propellant residues formed during pulse mode operation
14 p2355 N71-26739
- Ductile fracture characteristics of anisotropic elastic, orthotropic dynamic, and anisotropic viscoelastic solids
14 p2350 N71-26477
- Analysis of anomalous jettisoning of service module during reentry of Apollo 11
[NASA-TM-X-67163] 14 p2345 N71-26385
- Rapid failure-damage assessment techniques for exploding high pressure gas containment vessels
[AD-720686] 14 p2350 N71-26462
- Derivation of minimum test sets for static function logic circuit failure analysis and component reliability
[AD-720330] 15 p2389 N71-27278
- Conference on prevention of mechanical failures including bearing failures, spectrographic oil analysis, failure mechanisms of helicopter transmissions, and related problems
[AD-721359] 16 p2684 N71-28897
- Proceedings of conference dealing with advances in decision making processes for detection, diagnosis, and prognosis of mechanical failures
[AD-721355] 16 p2685 N71-28124
- Thermal and electrical theories for analysis of second breakdown phenomena, mechanisms, and damage in semiconductor junction devices
[AD-721294] 16 p2567 N71-28218
- Frequency response technique for locating electrical faults
[AD-721582] 16 p2568 N71-28344
- Technique for predicting adhesive normal bond failure times under constant stress and low humidity
[AD-722511] 16 p2617 N71-28475
- Proceedings of conference on mechanical failure prevention
[AD-721912] 16 p2686 N71-28370
- Reactor safety experiments including fuel pin performance tests, cladding failure, and fuel pin loss of coolant
[EURFNR-884] 17 p2782 N71-29590
- Nuclear fuel burnup and failure analysis of plutonium metal oxide in sodium potassium cooled fuel capsules under liquid metal cooled reactor conditions
[GEAP-134208] 17 p2783 N71-29643
- Investigation of adverse effects of producing QW-N helicopters prior to completion of development and flight tests
17 p2862 N71-30891
- Algorithm for automatic failure analysis of gates in logic circuitry
[LAAS-G-3-E-1] 18 p2892 N71-30839
- Cost and failure analyses and acceptability test from electronic equipment testing of various electronic components
[NASA-CR-119801] 18 p2897 N71-30839
- Facility and equipment manual for chemical and failure analysis
[NASA-TM-X-67242] 18 p2886 N71-31111
- Fracture mechanics and statistical failure analysis of brittle materials and erosion and abrasion machining processes
18 p2929 N71-31200

SUBJECT INDEX

- Asymptotic method for statistical failure rate function estimators (PB-17462) 18 p2946 N71-31275
- Computer program system for failure analysis data acquisition systems with on-line programming capabilities (NASA-TM-X-2331) 18 p2896 N71-31398
- Reactivity insertion effects on reactor dynamic safety during accidental malfunctions (NASA-1560-PT-2) 19 p3136 N71-32062
- Literature survey for identifying primary containment safety features in accident and safety system analysis for liquid metal fast breeder reactor (NASA-1352) 19 p3136 N71-32064
- Fast pin failure detection in sodium cooled reactors by delayed neutron transit time measurements on shutdowns (NP-16778) 19 p3137 N71-32071
- Computer code for calculating thermal response of reactor cores in coolant loss accident (BN-1445) 19 p3137 N71-32120
- Flow characteristics in primary and secondary loops of LMFR and failure probabilities (NASA-1350-PT-1) 19 p3138 N71-32248
- Nondestructive testing and failure analysis of composite construction materials in load bearing structural applications (AD-72854) 19 p3190 N71-32416
- Proceedings of conference on identification and prevention of mechanical failures in internal combustion reciprocating engine systems (AD-721913) 19 p3191 N71-32663
- Proceedings of conference on mechanical failure prevention and development of standards in surface specification (AD-724637) 20 p3356 N71-32918
- Proceedings of conference on mechanical failure prevention (AD-72475) 20 p3356 N71-32959
- Failure analysis of halogen quenched Geiger-Müller tube operation (DUN-SA-136) 20 p3308 N71-33743
- Systematic detection policies and Monte Carlo experiments on increased failure rate 21 p3392 N71-34133
- Comparison of high-resolution gamma ray scanning and mass spectrometry for use in failure analysis of contaminated fast reactor fuel element cladding (LA-4675-MB) 21 p3462 N71-34639
- Analysis of low cycle thermal fatigue in laminated glass wall turbine vanes (NASA-CR-72954) 21 p3582 N71-34944
- Failure effects analysis of guidance, navigation, and control, data management, and communications subsystems (NASA-CR-115131) 21 p3519 N71-35079
- Analysis of failure mechanisms of carbon-epoxy composite materials and methods of predicting performance under load conditions (NASA-CR-121621) 21 p3526 N71-35123
- Interdependence of continuum mechanics and physical chemistry in failure analysis of composites (NASA-CR-121877) 21 p3527 N71-35130
- Isostatic pressure versus failure and stress analysis of thread cracks (V-1758) 21 p3527 N71-35135
- Poligee behavior and failure analysis of this surface film of indium with normal loads moving at constant speeds 22 p3692 N71-36332
- Cost effectiveness, failure analysis, and design techniques for measuring reliability of avionics subsystems (MAARD-LS-47-71) 23 p3756 N71-36776
- Reliability estimation, including failure effect analysis of avionics systems 23 p3757 N71-36777
- Application of failure flow analysis to evaluate test program of Explorer 18 satellite (NASA-TM-X-65706) 23 p3782 N71-36819
- FAILURE MODES**
- Evaluation of failure modes and redesign of SERT-2 global pin buffer (NASA-TM-X-2128) 03 p0318 N71-12267
- Systematic failure study of reactor protection (SAW-10419) 04 p0556 N71-14094
- Tensile stress and breakdown of glass laser caused by inclusion particles 04 p0526 N71-14334
- Failure modes of pointing control systems for TD-1 satellite orientation (SRO-TM-66-85TBC) 06 p0949 N71-15821
- Failure characteristics of unidirectional fiber glass reinforced plastic under compression (NASA-TT-F-13442) 06 p0956 N71-16841
- Weight, cost, and spacecraft reliability analyses of turbine and suspension spin stabilized communication satellite orientation devices (NRO-CR-20) 07 p1118 N71-17557
- Random errors in aluminum alloy fatigue tests and failure modes (ABC-CF-1123) 07 p1123 N71-17330

- Acoustic signature analyses for bearing and gear failure mode identification 09 p1393 N71-20227
- Accelerated life tests for statistical failure prediction 09 p1480 N71-20229
- Failure mechanism of pipe rupture in reactor system (GEAP-10305) 09 p1422 N71-20595
- Zircaloy cladding failure modes in reactor coolant channels (JORN-L-3188) 10 p1601 N71-20643
- Lumped parameter representation for transient fault detection in power system 11 p1728 N71-22021
- Failure prediction for stressed adhesive bonds by reaction rate analysis at high humidity (AD-717534) 11 p1782 N71-22082
- Radiation thermoelectric generator uses nuclear safety tests including failure mode and safety analysis reporting (NASA-CR-118633) 14 p2292 N71-25780
- Mixing fluids in confined cylindrical geometry similar to rocket configuration with simulated bulkhead failure mode 14 p2240 N71-26219
- Stress wave emission as measure of crack growth in metallic failure (ARL-MET-72) 15 p2522 N71-27857
- Proceedings of conference on mechanical failure prevention (AD-721912) 16 p3696 N71-28592
- Mechanisms of radiation-initiated semiconductor device failures 19 p3066 N71-32356
- Component characteristic and failure mode recording and data acquisition system design for determining component reliability (NRL-RISLEY-TRANS-1920-0901.9F) 19 p3106 N71-32718
- Discrete element model for predicting deformation and failure mode of stressed brittle materials 23 p3865 N71-37554
- FAIRCHILD MILITARY AIRCRAFT U. S. MILITARY AIRCRAFT**
- FAIRINGS**
- Device and method for calculating optimal fairings for aircraft antennas (JPRS-52608) 10 p1521 N71-21258
- System for deploying and ejecting releasable clamshell fairing sections from spinning sounding balloons (NASA-CASE-GBC-10590-1) 21 p3520 N71-35081
- FALLING SPHERES**
- Responses of balloon and falling sphere wind sensors in atmospheric turbulence, analyzed with Fourier transformation (NASA-TN-D-7049) 07 p1053 N71-17479
- Device for determining acceleration of gravity by interferometric measurement of travel of falling body (NASA-CASE-XMF-05844) 07 p1030 N71-17587
- Drag of free falling spheres in water for Reynolds numbers in critical region using orthonormal cinematography (AD-717147) 11 p1735 N71-22096
- Current collection characteristics of moving cylindrical and spherical electrostatic probes applied to velocities in earth satellites and planetary probes (NASA-TM-X-65639) 19 p3071 N71-32468
- Measuring meteorological parameters of upper atmosphere using falling spheres (WRE-TM-50) 20 p3297 N71-33831
- FALLOUT**
- Studying mixed fission products from thermal fission of U-235 to create tools for analysis of fallout from nuclear explosions (POA-C-4420-28) 04 p0577 N71-13775
- Radiometric fallout data from nuclear cratering experiment, Shot Denny Boy (FOR-1818) 04 p0592 N71-14399
- Radiative fallout program review (EASL-217) 04 p0479 N71-14470
- Collection and analysis of radioactive fallout samples (AERE-R-5898) 05 p0742 N71-15126
- Analysis of scavenging by snow and ice crystals with application to radioactive fallout (IITRL-C-6105-12) 05 p0748 N71-15266
- Scavenging efficiency of naturally precipitating snow and ice with application to radioactive fallout (IITRL-C-6105-10) 05 p0749 N71-15289
- Air circulation unit for scaled survival shelters without external power supply (AD-714163) 06 p0805 N71-15994
- Atmospheric sampling apparatus design to follow changes in natural radioactive decay products of radon in free and conditioned atmospheres (CEA-R-4048) 08 p1250 N71-18233
- Artificial radioactivity of marine medium determined by gamma spectroscopy studies from 1962-1964 (CEA-R-3698) 09 p1437 N71-20079
- Health and Safety Laboratory Fallout Program data from world monitoring activities for 1 June 1970 - 1 Sept. 1970 (EASL-237-APP) 10 p1496 N71-20612

FAR INFRARED RADIATION

- Relevant deposition of radioactive iodine and lithium tracing elements from thunderstorms above (COO-1159-19) 10 p1993 N71-20646
- Analysis of radioactive fallout and accumulation in various geographical areas (HASL-237) 10 p1903 N71-21710
- Atmospheric radiochemistry and radioactive fallout and deposition from nuclear explosions (JORD-3528-38) 11 p1822 N71-23426
- Fallout display portion of weapons effects display system (UCRL-30092-VOL-4-PT-1) 12 p1916 N71-23153
- Fallout from nuclear explosions, atmospheric turbulence, aerosol propagation, and aerological and hydrometeorological measurements 12 p1952 N71-23178
- Concentration, composition of radioactive isotopes in atmosphere near ocean surface, and density of fallout after nuclear explosions 14 p2248 N71-25969
- Diurnal atmospheric fallout data of Be-7 and P-32 monitored at Zugspitze, Germany from 1 Apr. to 15 Nov. 1970 (NYO-4061-3) 15 p2515 N71-27703
- Beta activity in samples of atmosphere, surface water, and drinking water supplies and content of Cs-137 and Sr-90 in food samples - Italy (PROT-SAN-13169) 21 p3473 N71-34729
- Off-shore fallout surveillance activities of Southwestern Radiological Health Laboratory from Jan. through June 1969 (SWRHL-97-B) 21 p3478 N71-34772
- Human and environmental natural and fallout radioactivity data 21 p3484 N71-34815
- Determination of fallout distribution in oceans (NYO-2174-129) 22 p3576 N71-35471
- Fallout survey of various radioisotopes in air, drinking water, precipitation, and milk samples for extended period in North, South, and Central America (HASL-242-APP) 22 p3638 N71-35932
- Radiation monitoring data for radioactive fallout in German Democratic Republic for 1969 (SZS-1771) 23 p3713 N71-36471
- Fixation of radioactive materials in biomass, cement, glass, and ceramic decontamination media (KFK-1346) 23 p3812 N71-37178
- Radioisotope content of food, dusts, rivers and soils of Japan for 1969 and 1970, and fallout in rain and upper atmosphere after Chinese nuclear explosion of Oct. 1970 (NIRS-RSD-29) 24 p3973 N71-38346
- Development of fallout interpretative code and transport model for Defense Land Fallout Interpretative Code (AD-727613) 24 p3981 N71-38414
- FAN IN WING AIRCRAFT**
- Aerodynamic characteristics of large-scale model with lift fan mounted in 5 percent thick airfoil wing (NASA-TN-D-7031) 05 p0626 N71-14638
- Cross flow wind tunnel performance tests of 15 in. wing installed lift fan with coaxial drive turbine for VTOL transport aircraft (NASA-TM-X-67854) 15 p3365 N71-37707
- FANLIGHT DEVICES**
- U. LIFT FANS**
- FAR FIELD**
- Two dimensional models for scale invariance and distance behavior in quantum field theory (NYO-3825-56) 09 p1456 N71-20039
- Jet noise contribution to far field sound from 1.83 meter diameter fan determined for two simulated nacelle configurations (NASA-TM-X-67823) 12 p1991 N71-34009
- Dipole antenna and fluctuation of far electric field intensity over stationary and time-varying irregular surfaces (AD-728033) 24 p3899 N71-37791
- FAR INFRARED RADIATION**
- Interferometric measurements of far infrared refractive index of sodium fluoride at low temperatures (AD-711064) 01 p0809 N71-10443
- Far infrared investigations using Fourier spectrometry (AD-712742) 01 p0832 N71-13218
- Harmonic coincidences between pairs of far infrared continuous radiation gas lasers for light speed determination (NPL-QU-8) 03 p0388 N71-13266
- Design and construction of far infrared monochromator (AD-712675) 03 p0383 N71-13345
- Far infrared analysis of pair made in MnF₂-FeF₂ (NYO-2391-120) 05 p0779 N71-15445
- Measuring low-lying electronic levels of impurity ions in Al₂O₃ and electromagnetic absorptivity of Pb using far infrared spectroscopic techniques (UCRL-19666) 06 p0922 N71-16407
- Frequency mixing experiments using infrared and far infrared lasers (AD-715040) 07 p1040 N71-17768
- Third-harmonic generation in chalcogenide, for infrared generation by ultrashort pulses, and self focusing of light on examples of nonlinear optical effects (UCRL-20358) 10 p1669 N71-21809

Molecular laser studies in far infrared for optimizing power output and efficiency
[AD-718160] 12 p1932 N71-23325

Application of far infrared interferometer to transient plasma diagnostics
[UCRL-50983] 13 p2148 N71-25224

Far infrared, thermal, and sound phenomena in solids - phonon physics
[NYO-2391-126] 15 p2469 N71-27379

Far infrared photoconductivity and electron transport in high purity N-type indium antimonide
[AD-721654] 16 p2607 N71-28588

Carbon dioxide lasers, CO_2F_2 experiment, light scattering from semiconductors associated with impurities, and far infrared radiation
[NASA-CR-116928] 16 p2650 N71-28828

Measurement of far infrared absorption spectrum of water by Fourier spectrometer
[NASA-TT-F-13746] 17 p2717 N71-30320

Operational superconducting bolometer for use in vacuum ultraviolet and far infrared regions
[NASA-CR-121672] 21 p3436 N71-34377

Far infrared generation by nonlinear polarization using Q switched ruby lasers and LiNbO₃ crystal
[AD-721654] 21 p3436 N71-34451

Two color sandwiched photoconductive mercury-cadmium-telluride far infrared detectors
[NASA-CR-121852] 22 p3582 N71-35511

Solid state laser optical emission conversion to far infrared region by nonlinear polarization and small difference frequency generation
[NASA-TT-F-13979] 23 p3766 N71-36846

Tunable stimulated far infrared and visible emission from polariton modes in crystals
[AD-721654] 23 p3823 N71-37269

FAR ULTRAVIOLET RADIATION
NT LYMAN ALPHA RADIATION

Far ultraviolet radiation from xenon discharge in microwave plasma probes
[NPL-QU-10] 03 p0418 N71-13277

Extinction coefficient and reflectance of aluminum, magnesium fluoride, and magnesium fluoride coated aluminum mirrors for far ultraviolet radiation
[NPL-QU-12] 03 p0418 N71-13319

Transient heat transfer gage for measuring total radiant intensity from far ultraviolet and ionized high temperature gases
[NASA-CASE-XNP-09802] 05 p0786 N71-15641

Wavelengths and energy levels of CuII for far ultraviolet wavelength standards
[LA-4998] 06 p0905 N71-16369

Electromagnetic image converters for far ultraviolet spectroscopic astronomy
[AD-721654] 06 p0861 N71-16636

Far ultraviolet absorption spectra of sodium vapor
[ESRIN-IN-101] 07 p1080 N71-18006

Far ultraviolet spectral intensities of energetic vacuum carbon arc
[NASA-TM-X-52966] 06 p1243 N71-18747

Shock tube data on far ultraviolet photoionizing radiation flux in precursor plasma of blunt reentry vehicles
10 p1629 N71-21117

OAO 2 satellite used to obtain far ultraviolet spectrum scans of early-type supergiants
[NASA-TM-X-45523] 13 p2160 N71-24959

Microchannel intensifier vidicon for far UV imaging
16 p2593 N71-28517

Radiation absorption and crystal defects in alkali and alkaline earth halides
[ONERA-NT-02-23] 17 p2792 N71-29369

Operational superconducting bolometer for use in vacuum ultraviolet and far infrared regions
[NASA-CR-121672] 21 p3436 N71-34377

FARADAY DARK SPACE

Diffusion mechanisms and boundary problems in electropositive and electronegative gases including plasma diffusion in electropositive negative glow and Faraday dark space
[AD-718430] 12 p1980 N71-23265

FARADAY EFFECT

Polarization rotation effects on ionospherically propagated sea backscatter amplitudes
[AD-718430] 01 p0024 N71-10733

Simultaneous measurement of dispersive Doppler shift, Faraday rotation, and ionospheric refraction
[AD-71394] 02 p0205 N71-11147

Electron content measurement in polar ionosphere using signals from Explorer 22 satellite based on Faraday rotation
[BMW-FB-W-70-39] 03 p0370 N71-13229

Describing construction and alignment of laser gyro component
[FOA-2-C-2336-51] 05 p0606 N71-14480

Ionospheric electron content measurements using Explorer 22 data on Faraday and differential Doppler effects
06 p0814 N71-16231

Faraday rotation data of ionospheric total electron content behavior at conjugate points and during solar eclipses
[AD-714571] 06 p0942 N71-16525

Ionospheric electron density determination over Finland using Explorer 22 signals and Faraday/Doppler method
[BMW-FB-W-70-50] 06 p1189 N71-18592

Magnetooptical techniques to measure spin-lattice relaxation time of paramagnetic ions in crystal lattice as function of static magnetic field strength
[AD-715468] 06 p1278 N71-18679

Infrared isolator using yttrium iron garnet, Faraday rotation, and calcite dichroic polarizers
[AD-716468] 09 p1396 N71-19822

Ionospheric irregularity characteristics from Explorer 22 Faraday findings of 40 MHz transmissions
[RSD-533] 09 p1384 N71-20047

Ionospheric electron density measurements from Faraday fading of Explorer 22 satellite transmissions during low and high solar activity
[RSD-532] 09 p1350 N71-20080

Faraday effect used for electron density profile determinations in ionospheric sounding by VHF Thompson scatter radar
[AD-724290] 20 p3258 N71-33151

Ionospheric total electron content determined from satellite transmission Doppler shift and compared with Faraday effect
24 p3912 N71-37887

Ionospheric electron content up to phosphorus determined from Faraday results of ATS 3 data
24 p3912 N71-37888

Ionospheric electron content statistical analysis from Faraday effect tapes
24 p3912 N71-37890

Geophysical results of electron density measurements by Faraday rotation and riometer experiments
24 p3913 N71-37901

Ionospheric electron content from Beacon Explorer A Faraday effect during half solar cycle
24 p3914 N71-37906

Second-order phase path difference calculations for ionospheric Faraday and Doppler effect
24 p3914 N71-37908

Ionospheric electron content from Faraday rotation measurements of ATS 1 and Pioneer 7 space probe
24 p3914 N71-37910

ATS 1 Faraday effect data applied to Pioneer 6 space probe solar corona data
24 p3914 N71-37911

Total ionospheric electron content measurements with ATS 3 signal Faraday effect, noting gravity wave effects
24 p3915 N71-37915

Beacon Explorer A signal scintillation in auroral zone, measured with Faraday and Doppler effect
24 p3915 N71-37916

Faraday rotation technique for determining electron densities in D region
[NOAA-TR-ERL-205-SEL-21] 24 p3917 N71-37935

FARADAY ROTATION
U FARADAY EFFECT
WARM CROPS
NT POTATOES

Crop and soil identification from aerial photography
06 p0845 N71-16150

Cycloidal induced changes in internal structure of cotton leaves to reflectance, transmittance, and absorbance of near infrared radiation
06 p0800 N71-16151

Irrigated and dryland crop studies by State water resource agencies, using evapotranspiration data
13 p2072 N71-25009

Soil management for increased water storage for farm crops
13 p2073 N71-25016

Evapotranspiration and root growth for nonirrigated crops
13 p2073 N71-25019

Systems analysis of agricultural and water management information systems utilizing satellite borne multi-spectral band scanner, radar, and television equipment
[NASA-CR-119010] 16 p2587 N71-28444

Systems analysis and cost estimates of satellite borne remote sensing for wheat crop and fungus disease control and water management
[NASA-CR-119011] 16 p2587 N71-28445

Mathematical models for application of satellite borne multispectral remote sensors to water and wheat production management and wheat fungi control including cost estimates
[NASA-CR-119012] 16 p2588 N71-28446

Aerial and ground surveillance of southern corn leaf blight in Corn Belt States during 1971
[NASA-NEWS-RELEASE-71-129] 17 p2709 N71-30175

Studying crop-hail insurance records for northeastern Colorado for designing hail experiment
[FB-197644] 18 p2955 N71-31444

Protection of plants and crops against weather, and effects of temperature, frosts, sunlight, precipitation, and wind
[WMO-281] 20 p3296 N71-33146

Quantitative estimates of the potential effects of cloud seeding on crop production
22 p3610 N71-35715

FAST NEUTRONS

Fast neutron irradiation effects on reactor grade thermocouple performance
[BNWL-1365] 02 p0365 N71-11740

Measuring fast neutron spectra in core and thermal column of Babcock reactor by foil activation method
[IAERU-7601] 02 p0278 N71-13101

Fast neutron radiation effects in Type 304 stainless steel
[ORNL-4580] 03 p0390 N71-13201

Energy spectra of alpha particles induced by 12 MeV neutrons in erbium isotopes
[INR-1173] 04 p0571 N71-13607

SAND-2 code for absolute neutron flux spectrum in FCRA fast neutron cavity from multiple foil activation measurements
[BNWL-1467] 04 p0572 N71-13620

Fast neutron scattering cross sections
[AAB/CTM-536] 04 p0578 N71-13609

Fast neutron flux calculation in light water reactor by ORPHEE D program
[CEA-N-1311] 04 p0593 N71-14446

Investigating elementary particle interactions in linear accelerators and reactor physics
[RF-328-187] 05 p0730 N71-15264

Fast neutron activation cross sections for isotopes of ruthenium, palladium, indium, and tellurium
[AD-713404] 05 p0749 N71-15331

FORTRAN 4 code for fast neutron radiative capture calculations - FISPRO
[RT/FI/69/44] 06 p0908 N71-19774

Fast neutron total, scattering and reaction cross sections
[EURFNR-786] 06 p0909 N71-19781

Absolute measurements of neutron beam flux above 250 keV, made with proton recoil counter and solid state detector
[EURFNR-805] 06 p0913 N71-19828

Computer program for calculating fast neutron attenuation in dense material separated by water
[ORNL-TR-2357] 06 p0917 N71-14991

Neutron transport of neutrons from A/A source through many mean free paths in liquid nitrogen
[UCRL-50836] 06 p0919 N71-16239

Unified model for analysis of compound nucleus reactions in fast neutron cross sections
[IA-AEC-12931] 06 p0920 N71-16239

Radiation effects on ion and fast neutron bombarded
[COO-1053-15] 07 p1075 N71-17404

Effect of fast neutron irradiation on mechanical properties of hafnium
[IN-1440] 06 p1212 N71-16380

Collimator system for fast neutron spectral measurements
[UCRL-50837] 06 p1253 N71-18520

Tabulating observations on angular distributions of scattered neutrons and reaction products of fast neutrons and nuclei
[BNWL-400-VOL-1] 06 p1255 N71-18576

Elastic scattering of fast neutrons by deuterium
[LYCEN-7026] 06 p1256 N71-18574

Discussing monitors for determining burnup rate of enriched uranium 235 fuel in fast neutron environment
[NASA-TM-X-2153] 06 p1259 N71-18496

Research on behavior of fast neutrons in breeder reactors
06 p1242 N71-19710

Fast neutron effects on semiconductor electronic transport properties and minority carrier and hole drift mobilities in germanium
[ORO-3451-6] 09 p1426 N71-19533

Numerical code based on double spherical harmonics approximation for analysis of coupled space-time effects in fast pulsed neutron kinetics and transport theory
09 p1432 N71-19934

Fast neutron inelastic scattering measurements to determine gamma ray production cross sections
[CEA-R-4647] 09 p1433 N71-19938

Fast neutron irradiation damage and annealing effects at different temperatures in semiconductors
[JAERI-MEMO-4149] 09 p1401 N71-30240

Fast neutron irradiation effects on stainless steel creep rupture properties
[ORNL-TM-3169] 10 p1576 N71-21046

Reactor facility with variable temperature environment in fast neutron flux for use in studying radiation damage
13 p2112 N71-24411

High flux reactor thermal and fast neutron flux density values for 45 MW core configuration with 6 lower experiment positions including S-assemblies and pulse-life facility
[RCN-119] 13 p2118 N71-24053

Yields of fission product nuclides in irradiated uranium and plutonium calculated for fast and thermal fission and expressed as atoms per 100 atoms of U-235 or Pu-239
[ANL-7678] 14 p2301 N71-25542

Proposed uranium and polyethylene standard spectra for fast neutron spectrum measurements
[EACRP-L-74] 14 p2306 N71-26374

SUBJECT INDEX

FAST NUCLEAR REACTORS

Distribution and density of dislocation loops in crystal boundaries produced by fast neutrons in nickel and copper

14 p2330 N71-26631

Fast neutron irradiation of SiC coated outer layer of particles for gas cooled reactors

[JURPNR-834] 14 p2294 N71-26644

Mathematical model and computer program for solution of asymptotic neutron transport equations in this geometry

[KFKI-70-14-RPT] 14 p2312 N71-26707

U-238 capture cross section data in 2 hV to 10 MeV neutron energy region of fast nuclear reactors

[INDO/NDS-18/N] 15 p2444 N71-27235

Energy spectra of prompt and delayed fission neutrons and reactor physics

[ANL-7477] 15 p2469 N71-27349

Measuring of fast or thermal neutron produced neutrons with half lives less than 1 minute and gamma energies between 0.01 and 10 MeV

[KFKI-70-18-NAC] 15 p2485 N71-27812

Absolute measurement of fast neutron scattering cross sections from high energy neutron deuterium reactions

[NP-10488] 15 p2486 N71-27818

Relative measurement of antineutrino in U-235 and Pu-239 fission induced by resonance neutrons in fast neutron pulsed reactor

[BNL-TR-401] 15 p2493 N71-27938

U-235 fission cross sections at 440 and 530 hV neutron energies studied with gas scintillation chamber and proton recoil detector

[KFKI-1313] 16 p2641 N71-28019

Moderation of fast neutrons in polyethylene and their use in neutron dosimetry

[BUR-4546-D] 16 p2645 N71-28118

Comparison of calculated and liquid scintillation measured fast neutron spectra in layered cylindrical shield of UOP2-water solution reactor

[NASA-TM-X-67861] 16 p2637 N71-28968

Pulsed neutron technology in Japan including pulsed reactors, reactor materials, multiplying media, wave and pulse propagation, time of flight experiments, and related topics

[JAERI-A-109] 16 p2636 N71-29106

Measuring average number of prompt neutrons and of relative cross sections for fission of U-235 and Pu-239 induced by neutrons within 0.3 and 1.4 MeV energy ranges

[JLB-TRANS-300] 16 p2660 N71-29196

Integral checks of differential cross section data of fast neutron transport in iron

[JLB-528-225] 17 p2791 N71-29229

Nuclear spectroscopy research and development with radioactive materials and fast neutron reactions

[JRO-3346-45] 17 p2801 N71-30123

Bibliography on proton recoil counters for measurement of fast neutrons

[AEC/LIB/IB-270] 18 p2971 N71-30463

Simultaneous determination of fast neutron spectra by time of flight and pulse height unfolding techniques

[AD-723181] 19 p3151 N71-32134

Isotopic fission product decay series of U-235, U-238, Pu-239, and Pu-241 determined by thermal and fast neutrons

[JF-18723] 19 p3151 N71-32146

Interaction of fast neutrons with ^{12}C , ^{16}O , and ^{14}N

[BNL-TR-380] 19 p3151 N71-32153

Effects of fast neutrons on polycrystalline alumina electrical insulators used in thermionic converters at high temperatures

[JRLN-4678] 21 p3444 N71-34308

Fast neutron transmission measurements for reactor core and shielding materials including iron, water, and concrete

[CDO-2049-4] 21 p3440 N71-34625

Fast neutron reactivity effects of reactor materials measured in thermal uranyl fluoride-water-solution reactor

[JAEA-TN-D-6494] 21 p3462 N71-34642

Time of flight method for studying fast neutron elastic and inelastic scattering by natural molybdenum at 1.8 to 5.0 MeV

[JAWRE-O-9970] 21 p3486 N71-34836

Effects of fast neutron irradiation on Chromel/Alumel thermocouples for FFTF coolant measurement system

[JEDC-SA-152] 22 p3623 N71-33817

Reactor and electron microscope analysis of fast neutron flux effects on metal cladding material microstructure

[BNL-TR-1012] 22 p3635 N71-33911

Large perturbations of fast neutron spectrum in reactor of swimming pool reactor behind Pb, Al, and Fe slabs

[JAERI-MEMO-4276] 22 p3638 N71-33931

Fast neutron spectra analysis emphasizing inelastic scattering effects and influence of isotropic scattering on energy-spatial distribution of neutrons

22 p3639 N71-33941

Neutron multiplicity for Pu-239 resonance fission using fast neutron detector

[BNL-TR-3311] 22 p3647 N71-36008

Numerical analysis of fast neutron spectra in reactor core and water reflector

[UAREE-71] 23 p3810 N71-37164

Time of flight method for determining elastic and inelastic scattering of 5.0 MeV neutrons by sodium

[JAWRE-O-371] 23 p3813 N71-37209

Fast-neutron integral capture cross section measurements of Te-99, Ag-107, Ag-109, In-115, Cs-133, Fe-141, Fe-155, and Ta-169

[CONF-710301-4] 23 p3816 N71-37219

Fast neutron spectrum measurements using time-of-flight techniques and spectral measurement methods with proton recoil detectors

[JULF-RT-10523] 23 p3817 N71-37221

Effect of solar cycle modulation on production of neutrons in atmosphere and measurement of fast neutron flux

23 p3842 N71-37408

Fast neutron time of flight techniques for studying proton-rich nuclei N-12, F-16, Mg-22, Si-26, and S-30 by means of (He^3, n) reactions

[JAERI-R-6473] 24 p3973 N71-38359

Semi-empirical evaluation of fast neutron radiative capture cross sections

[CCDN-NW-10] 24 p3976 N71-38369

FAST NUCLEAR REACTORS

NT EXPERIMENTAL BREEDER REACTOR 1

NT EXPERIMENTAL BREEDER REACTOR 2

NT FAST OXIDE REACTORS

Linear accelerator research work including neutron cross section analysis, and fast reactor physics and engineering

[RPI-328-173] 01 p0087 N71-10796

Research and development of nuclear fuels, cladding, and other structural materials for fast reactors, space power reactors, and general reactors

[ORNL-4520] 01 p0087 N71-10920

Development of SEPOR energy probes for power transient measurement

[KFKI-1033] 02 p0226 N71-11561

Detection and origin of water leaks in tests for steam generator designs for fast reactors and sodium-water reaction kinetics

[JULF-RT-10599] 03 p0413 N71-12570

PROF GROUND-G - processing code for group constants for fast reactor

[JAERI-1192] 03 p0416 N71-12896

Measuring fast reactor neutron spectra from 5 hV to 8 MeV using spectrometer of single lithium 6 sandwich

[JAERI-R-6060] 04 p0570 N71-13603

Reposable and Phenix components of sodium circuits for sodium cooled fast reactors

[CONF-700007-5] 04 p0548 N71-13643

Describing aerosol model of hypothetical LMFBR accidents

[AI-AEC-12977] 04 p0530 N71-13760

Fuel, core, and cladding developments and safety experiments for fast ceramic reactors

[GEAP-10028-33] 04 p0552 N71-13968

Fast breeder reactor advanced fuel element cladding fabrication

[GEMP-745] 04 p0553 N71-13994

Investigating fuel burnup rates, safety rods, fuel elements, and critical experiments in thermal and fast reactors

[BNWL-1381-2] 04 p0554 N71-14016

LMFBR, EBR 2, and ZPR 3, 6, and 9 development programs

[ANL-7726] 04 p0556 N71-14096

Reactor core technology for LMFBR

[AEC-12969] 04 p0557 N71-14122

Investigating performance of stainless steel cladding and plutonium-uranium oxide fuel elements in fast breeder reactors

[GEAP-10028-34] 04 p0557 N71-14154

Developing computer programs for optimum economic parameters of conceptual 1000 MW_e LMFBR

[WARD-2000-96] 04 p0558 N71-14183

Core-cladding system design for fast reactors

[BNWL-SA-2691] 04 p0559 N71-14206

Conceptual system design descriptions for 1000-MW_e LMFBR central station power plant

[BAW-1328-VOL-3] 04 p0561 N71-14374

Reference design of 1000 MW_e liquid metal fast breeder reactor - Vol. I

[AI-AEC-12792-VOL-1] 04 p0561 N71-14381

Limits and requirements survey of LMFBR component materials

[BMJ-1901] 04 p0562 N71-14409

Sodium technology applied to fast nuclear reactors

[BNWL-1200-1] 04 p0562 N71-14412

Heterogeneous effects on adjoint function in cell structure of fast reactors using collision techniques

[RTI/70/19] 04 p0563 N71-14488

Dynamic stability of fast reactor with in-core thermal converters

05 p0724 N71-14732

Fast reactor spectrum measurements

[QA-10300] 05 p0724 N71-14793

Investigating fission properties and cross section data, safety, and competition methods in fast nuclear reactors

[ANL-7610] 05 p0724 N71-15085

Investigating process development program for production of high quality mixed oxide fast reactor fuel pellets

[BNWL-1445] 05 p0726 N71-15071

Sol-gel process and related processes for preparing U/PuO₂ fast reactor fuels

[BAW-3714-10] 05 p0729 N71-15210

Preliminary study of chopper for complete fuel element function of ENR-Na2 in WARE

[NP-10451] 05 p0731 N71-15374

Research on nuclear reactors and fuels

[ANL-7675] 06 p0897 N71-15876

Thermal, swelling, and irradiation creep effects on fast reactor core components

[BNWL-1430] 06 p0899 N71-16283

Leak detection method for water and sodium systems applied to boilers of liquid sodium-cooled fast reactors

[ANL-TRANS-837] 06 p0901 N71-16775

Development of fuel elements for fast ceramic reactor, and stainless steel clad plutonium oxide elements for liquid metal fast breeder reactor

[GEAP-10028-35] 06 p0901 N71-16815

Summarizing national development programs on fast reactors and fuels

[NP-10565] 07 p1059 N71-17029

Uranium 238 Doppler effect in fast thermal reactor assemblies

[CEA-R-4835] 07 p1062 N71-17206

Flowmeter using solenoid analysis techniques for large liquid metal systems at temperatures of 1200 F

[AI-AEC-12981] 07 p1028 N71-17267

Research and development on fuel cycle technology for AGR through Jan. 1970

[ANL-7755] 07 p1063 N71-17339

Neutronic design calculations for lithium 7 cooled sodium reactor for space applications

[NASA-TN-D-61069] 07 p1064 N71-17422

Fast reactor technology, space power technology, nuclear fuels, and reactor materials

[ORNL-4570] 07 p1064 N71-17526

Investigating fast group constants and processing program using ENDF/A format

[JAERI-1195-PT-1] 08 p1233 N71-18160

Fast reactor program including reactor physics, and performance, radiation damage in core materials, corrosion behavior in cooling materials, and neutron research

[BURFNR-622] 08 p1235 N71-18215

Uniaxial and biaxial core rupture of type 316 stainless steel after fast reactor irradiation

[BNWL-SA-3295] 08 p1212 N71-18311

Investigating characteristics and efficiency of fast power reactors

[JFES-52290] 08 p1240 N71-18783

Using methods of perturbation theory to produce data on sensitivity of calculated values of critical parameters and breeding factors of fast power reactors to changes in constants

08 p1240 N71-18784

Measuring increase in reactivity of fast power reactors as function of Doppler temperature

08 p1240 N71-18787

Investigating effects of resonant self-coupling of specimen and perturbation of neutron field by specimen in BPS-16 fast reactor

08 p1241 N71-18788

Calculating value of effective number of neutrons formed by fission in reactors with hard neutron spectrum

08 p1241 N71-18789

U-Pu-Zr alloys prepared by conventional melting and casting techniques for fast breeder reactor applications

[LA-4512] 09 p1416 N71-19392

Neutron radiation induced swelling in stainless steels used in fast nuclear reactors

[CEA-N-1383] 09 p1401 N71-20390

Research and development in LMFBR physics program

[AI-AEC-12978] 09 p1421 N71-20390

Plutonium segregation in uranium-plutonium solid solutions and fast reactors at high temperatures

[GEAP-12133] 09 p1487 N71-20399

Explosive disassembly of fast spectrum nuclear reactors, following coolant loss and gravity compaction of fuel

10 p1604 N71-21360

PORTMAN 4 code for predicting in-pile behavior of cylindrical fast reactor fuel elements

[ANL-7734] 11 p1793 N71-22323

Uranium-plutonium nitride fuels for LMFBR, fast reactor fuels, and reactor fuel material group properties

[BMJ-1893] 11 p1794 N71-22419

One dimensional static physics design and analysis code (FARAD) for fast breeder reactor project development

[BAW-3667-A-VOL-1-REV-1] 11 p1795 N71-22425

Fast reactor safety practices and requirements by AEC

[BNWL-SA-3093-VOL-1] 11 p1795 N71-22437

Fast reactor neutron measurements in core, at core-reflector interface, and in reflector

[JULF-RT-10421] 12 p1962 N71-23845

High speed photographic experiments within fuel capsules in irradiated fast reactor
[ANL-7578]

RSYN and 3DR codes for flux and bulk parameter simulation of fast reactors
[WHAN-IR-48]

Comparison of neutronic and thermal environments for stainless steel-clad uranium- or plutonium oxide fuel rod in proposed reactor with test conditions currently available
13 p2111 N71-24510

Design and operation of forced convection capsules for simulating erosion, chemical, and transport effects in fast reactor canopy tests
13 p2115 N71-24546

Fast reactor program - physics, fuel tests, radiation damage and corrosion in casing materials, aerosols, heat transfer, and hydraulics
[EURFNR-855]

Bibliography on fast breeder reactors with subject index, reactor index, report index, and periodical index
[NEEC-RR-41]

Comparison between calculation and experimental reactivity worths of large samples of fuel and boron carbide control material in assemblies FTR-1 and 2
[WHAN-SA-12]

Detection of nuclear fuel element failure and shutdown in fast reactors by superheated steam test loop
[KFK-1255]

Effect of fabrication variables on disassembly of unirradiated, mechanically blended PuO₂-UO₂ fast reactor fuels
[WHAN-FR-34]

Evaluation of PuO₂ homogeneity in PuO₂-UO₂ fast reactor fuel by scanning electron microprobe
[WHAN-SA-7]

Annealing and temperature gradients effect on plutonium distribution in fast reactor fuel materials
[ANL-7703]

Models of neutron slowing down calculations in thermal and fast reactors
[EURFNR-864]

Core experiments for optimizing sodium-cooled fast breeder reactors by nonlinear programming methods
[KFK-1238]

Model for analytic fast reactor mode flux and importance spectra
14 p2295 N71-26684

Safety considerations for irradiation of FTR-2 reactor fuel capsules of UC-Pu using NaK as heat transfer medium
[EURFNR-764]

Testing of resonance absorbers for suitability as sandwich detectors for determining neutron spectra in fast reactors below 10 keV
[KFK-1233]

SNEAK assembly 3B for investigating physics parameters in steam cooled fast reactor cores
[EURFNR-848]

Approximate calculations for effective fraction of delayed neutrons and instantaneous neutron lifetime for fast critical assemblies
[SRARI-P-53]

Computer program for analysis and design of critical experiments with fast nuclear reactors
[IAERI-MEMO-4215]

Scallop proton proportional counters for measuring neutron spectra in fast reactor assemblies built in ZEBRA
[AEW-M-905]

Structure and tensile properties of AISI type 316 steel irradiated by fast reactor at measured 420 to 630 C temperature ranges
[AERE-R-6435]

Relative measurement of antineutrino in U-235 and Pu-239 fission induced by resonance neutrons in fast neutron pulsed reactor
[BNL-TR-401]

Effects of neutron energy dependence of Pu-239 fission products on burnup characteristics of fast reactors
[IAERI-4165]

Determination of correlation functions between counts given by neutron detectors for fast thermal coupled reactor
[BCM-132]

LMFBR physics and technological activities with ZPR-6, ZPR-9, and ZPPR operations, EBR-2 projects, fuel fabrication, materials, shutdowns maintenance, safety and fuel cycle chemistry
[ANL-7776]

LMFBR physics programs including VIM code development, Doppler coefficients for BCEL, ZPR-3, ZPR-6, and ZPR-9, ECEL core 20 fuel element assembly, and related topics
[AI-AEC-12985]

Neutron cross section needs for fast breeder reactor design and operation
[HEDL-SA-163]

Sodium cooled fast reactor safety factors
[NP-18487]

Slowing down model for inelastic scattering and scattering and absorption-resonances in fast nuclear reactor
[RPI-528-217]

Mathematical models for predicting mechanical stress behavior of fast reactor fuel elements
[IAERI-4516]

CAGE-BIRD-SPEC, package FORTRAN 5 system, for reduction and analysis of neutron time-of-flight spectra in fast and thermal subcritical reactors
[GULF-RT-10195]

Monte Carlo program for efficiency study of Li-6 glass scintillator detector for fast reactor spectrum measurements
[AEW-M-998]

State-of-the-art review on nuclear parameters of fast critical experiments
[EURFNR-858]

Method for presentation and systematic compilation of integral tests of differential cross section data from various fast reactor analyses
[RPI-528-219]

Fission gas disengagement from flowing sodium and transport phenomena for FFTF fuel failure detection
[ANL-7744]

Neutron spectra for reactor loading in Rux 59/1 of Dounreay fast reactor
[TRG-2118]

Research and development for LMFBR, ZPR-3, ZPR-6, ZPR-9, ZPPR, and EBR-2 including reactor fuels, fuel cycle chemistry, and reactor safety
[ANL-7783]

RAFSODIE reactor technology and core production engineering for fast reactor neutron source including performance tests
[CEA-R-3501/2]

Fast nuclear reactor physics technology assessment noting dynamic and performance characteristics, radiation shielding, power efficiency, fuel cycles, reactivity, and numerical analysis
[BARC-I-58]

Mathematical model for coolant three dimensional flow during rapid reaction-gas release in fast nuclear reactor core based on plenum chamber simulation
[ANL-7651]

Measurements of particulate filtration efficiencies of buildings for application to safety and engineering safeguards design of LMFBR
17 p2744 N71-29876

Nonlinear differential equations describing stability of fast nuclear reactor with incore thermionic converter and reactivity feedback
[NASA-CR-119150]

Fabrication and testing of double vacuum melted, type 316 thin walled austenitic stainless steel tubing, for use as cladding in LMFBR fuel pins
[WARD-4135-14]

Fast reactor nuclear fuel burnup computer code using Nd, U, and Pu mass spectrometric data
[GEAP-5355-A-REV]

Survey on properties and potentials of uranium plutonium carbide fast reactor fuels and comparison with metal and oxide fuels
[BARC-I-61]

Use of stabilized steels in PFR circuits for protection from decarburization and loss of strength on exposure to sodium
[TRG-2071]

Uranium 238 neutron resonance radiation widths measurements on pulsed fast reactor
[JINR-P2-5699]

Computational model for fast reactor disassembly analyses - VENUS computer code
[ANL-7701]

SASIA - computer code for analyzing power and flow transients for large LMFBR cores
[ANL-7607]

Development of fast reactors using ceramic fuels particularly mixed plutonium-uranium oxide
[GEAP-10028-37]

Accuracy of sandwich detectors in measurement of neutron spectra in fast reactors within 1 eV to 10 keV energy range
[EURFNR-842]

Optimization of sodium cooled fast breeder reactors by nonlinear programming methods
[EURFNR-830]

ETOX - code for calculating group constants for fast nuclear reactor calculations
[HEDL-TAE-71-36]

Methods and models for LMFBR accident analysis and safety system design
[BAW-1342]

Progress in development of fuel elements, fuels, cooling systems, core monitoring systems, and core design for fast breeder reactors
[EURFNR-824]

Investigation of coolant combustion accidents, release and transport of aerosols and energy from sodium, and effects of sodium coolant boiling on fuel elements in LMFBR safety study
[AI-AEC-12946]

Analysis of existing instrumentation systems to protect LMFBR core integrity and recommendations for improvement
[ANL-7793]

Venting device for sodium cooled fast reactor with ceramic fuel elements
[RT/ING-7029]

Program for accurate determination of nuclear fuel burnup in fast breeder
[IN-1456]

Critical assembly models for fast reactor reactor and determination of critical mass, reactivity coefficients, and fission distribution
[FBI-201]

Parametric influences on stability of uncontrolled steam-cooled fast breeder reactors
[EURFNR-813]

Development and technology of fast breeder reactors
[EURFNR-823]

Critical experiment for cylindrical core with control air gap in FRO fast reactor
[POA-4-C-4412-22]

Reactor test complex for solving fluids and materials problems critical to developing liquid metal cooled fast breeder reactors - FFTF
[WHAN-SA-104-REV]

Effects of fast breeder reactor core conditions in type 316 stainless steel fuel cans
[CONF-700211-7]

Factorization technique for calculating space energy synthesis in fast reactor
12 p3627 N71-35044

One dimensional, multigroup diffusion code for use in fast reactor criticality and kinetics parameter analysis
[IAERI-MEMO-4331]

Models for analyzing burnup effects on fuel pin thermal performance applied to fast nuclear reactors
[CONF-710414-1]

Materials irradiation tests in support of fast test reactor driver fuel development program
[HEDL-SA-81]

Fast reactor control and absorber studies including reduction damage and reliability of absorbing materials
[SABRI-P-96]

Pile oscillator technique for measuring Doppler defect with heated small samples in critical zero power assemblies for fast thermal reactors
[KFK-1350]

Liquid-solid interfacial phenomena in sodium cooled fast nuclear reactors
[RD/B/N-1721]

Storage and handling of highly irradiated fast breeder reactor fuel in hyaline sodium organic coolant storage pool, and Sb-Ca liquid metal dissolution for decoupling
[EUR-4615-E]

Natural convection irradiation device, Esther, for fast reactor fuels
[EURFNR-850]

Research and development of steam cooled fast breeder reactors with sodium and helium cooling
[KFK-1370]

Bibliography of fission products in fast reactors and their methods of measurement
[CEA-BIB-195]

Pinch fission fast breeder cavity reactor mathematical models for control and stability analysis
14 p3964 N71-38274

FAST OXIDE REACTORS

Fuel assemblies and operational maintenance for experimental fast oxide reactor
[GEAP-10010-24]

Research and development program of Southwest Experimental Fast Oxide Reactor
[GEAP-10010-25]

Fabrication of non-fuel core components for experimental fast oxide reactor
[GEAP-13595]

Pneumatic device for rapid removal of poison ships from reactor cores
[IAERI-3649]

Fabrication and design parameters of PuO₂ and UO₂ fuel rods for Southwest experimental fast oxide reactor
[GEAP-10010-26]

Fabrication of reactor fuel elements for SEFOR
[GEAP-10010-27]

FAST TEST REACTORS

NT FAST NUCLEAR REACTORS

Energy-dependent neutron cross section library for calculating integral fluxes and fluences of fast and thermal test reactor environments
[BNWL-1312]

Design for material radiation damage in FFTF
[BNWL-SA-2954]

Uncontrollable prompt critical excursions in fast reactor cooled by sodium
[RT/ING/702]

Fuel pin, subassembly, and core design for Fast Test Facility
[BNWL-1064]

Fast Flux Test Facility design and development
[BNWL-1394]

Intermediate heat exchanger design for Fast Test Facility
[WARD-4112-2-VOL-1]

Thermal and hydraulic performance analysis for fast test facility intermediate heat exchanger design
[WARD-4112-2-VOL-2]

SUBJECT INDEX

FATIGUE [MATERIALS]

Design and development of liquid sodium cooling system for fast test reactor
[BNWL-1200-4] 05 p0725 N71-15041

Fast test reactor irradiation program
[BNWL-1461] 05 p0725 N71-15042

Transfer function measurements for fast test reactor by oscillator method
[BNWL-1314] 05 p0726 N71-15044

Structural design of fast test reactor primary piping system
[BNWL-1236] 06 p0897 N71-15044

Compression tests on FFTF fuel subassemblies
[WHAN-FR-18] 07 p1064 N71-17509

Two-dimensional diffusion predictions of neutron induced reaction rates in fast test reactor and zero power photon reactor cores, reflectors, and radial shields
[WAAN-FR-12] 09 p1430 N71-19852

Nuclear design model comparison for power and flux distribution near fast test reactor core and reflector interface
[WHAN-FR-35] 10 p1618 N71-21380

Atmospheric radioactivity measurement for Fast Test Facility containment system with alarm and trip levels determined
[BNWL-1479] 11 p1794 N71-22329

Fuel failure mechanics and failure propagation related to safety characteristics of fast test reactor
[BNWL-SA-3093-VOL-2] 11 p1795 N71-22458

Model test methods related to LMFBR piping systems including X ray diffraction, strain gages, brittle coatings, and holographic interferometry
[HAN-71-234] 12 p1962 N71-23856

Servicing and testing of liquid sodium piping in LMFBR
[HAN-71-343] 12 p1963 N71-23947

Comparison of two-dimensional and three-dimensional acoustics calculations for PTR
[WHAN-SA-11] 13 p2120 N71-25217

Fast neutron irradiation effects on thermocouples for measuring coolant temperature in fast test reactor
[WHAN-SA-10] 13 p2083 N71-25369

FFTF and LMFBR reactor design, fuels, and materials development
[WHAN-FR-50] 14 p2293 N71-25786

Fast test reactor simulation oven development and structure and radiation/temperature ultrasonic thermocouple calibration
[HYO-3906-12] 15 p4206 N71-26084

Multigroup one dimensional approximation for physics calculation of ZRR experimental fast reactor
[UJV-2408-RF] 16 p2633 N71-28800

Iodine behavior and control in processing plants for fast reactor fuels and removal of radioiodine from plant effluents
17 p2784 N71-29838

Development of uranium-plutonium nitride fuels for LMFBR applications, studies of high temperature fuels for advanced fast reactors, and studies of creep of reactor fuel materials
[BNI-1890] 20 p3509 N71-33946

Thorium-vanadium for fuel element cladding in fast breeder reactors
[CONP-700211-9] 23 p3796 N71-37057

Multigroup time independent neutron diffusion code for BBN-1130-RAM-1
[UABARE-107] 23 p3808 N71-37130

FASTENERS

NT ANCHORS [FASTENERS]

NT BOLTS

NT LOCKS [FASTENERS]

NT NUTS [FASTENERS]

NT PINS

NT RIVETS

NT SCREWS

Nut and bolt fastener permitting all-directional movement of skin sections with respect to supporting structure
[NASA-CASE-XLA-01807] 01 p0068 N71-10799

Aluminum, pie-type fastener, easily operated during EVA
[NASA-CASE-ARC-10140-1] 07 p1036 N71-17653

Ultrasonic wrench for applying vibratory energy to mechanical fasteners
[NASA-CASE-MFS-20586] 07 p1036 N71-17686

Design and development of electric connectors for rigid and nonrigid coaxial cables
[NASA-CASE-XNP-04732] 10 p1532 N71-20851

Design, development, and characteristics of locking mechanisms for operation in limited access areas
[NASA-CASE-XMS-03745] 10 p1564 N71-21076

Design and development of module joint clamping device for application to solar array construction
[NASA-CASE-XNP-02341] 10 p1567 N71-21531

Threadless fastener apparatus comprising receiving apertures for plurality of articles, self-locked condition, and capable of using nonmetallic materials in bulk and
[NASA-CASE-XPR-05302] 12 p1925 N71-23254

Development of resilient fastener for attaching skin of aerospace vehicles to permit movement of skin relative to framework
[NASA-CASE-XLA-01027] 12 p2001 N71-24053

Pneumatic mechanism for releasing hook and loop fasteners from large rigid structures
[NASA-CASE-XMS-10660-1] 14 p2260 N71-25975

Structural fasteners of heat resistant alloys for high temperature applications
17 p2755 N71-29468

FATIGUE [BIOLOGY]

NT AUDITORY FATIGUE

NT FLIGHT FATIGUE

NT MUSCULAR FATIGUE

Effects of repeated maximal isometric exertions with various intertrial intervals on fatigue function and determining relationship between strength and relative decrement
[AD-714190] 06 p0802 N71-16399

Rest and activity cycles for maintaining efficiency of military flight operations personnel
[AGARD-CP-74-70] 07 p0977 N71-16905

Assessment of fatigue for flight crew members during long duration flights
07 p0978 N71-16910

Work intensities with greatest endurance reduction due to respiratory resistance and carbon dioxide inhalation
[AD-716580] 09 p1330 N71-19720

FATIGUE [MATERIALS]

NT BENDING FATIGUE

NT METAL FATIGUE

NT THERMAL FATIGUE

Composition and heat treatment effects on wear resistance and fatigue strength of carbon steels
[AD-711157] 01 p0068 N71-10630

Fatigue crack propagation in copper and copper-aluminum single crystals
[AD-711678] 01 p0113 N71-10954

Total fatigue damage estimates from ground and flight loads on fixed-wing light aircraft subjected to agricultural operations
[LTR-ST-422] 03 p0313 N71-12233

Fuel flutter and divergence as structural aeroelastic problems leading to fatigue failure
[NASA-CR-111821] 04 p0471 N71-13405

Fatigue failure after few cycles of biaxial stresses
[PUBL-1267] 05 p0775 N71-14790

Effects of surface strain hardening on wear resistance and fatigue strength of steels
[AD-713454] 05 p0705 N71-15371

Fatigue damage indicator for composite material with particle filled matrix
[AD-714258] 06 p0660 N71-16433

Evaluation of materials for use in structures subjected to random low cycle vibrations
[AD-715273] 07 p1125 N71-17783

Measurement of fatigue crack propagation in aluminum alloys at high stress
[NASA-CR-11732] 07 p1127 N71-18002

Cyclic yield behavior of polycrystalline niobium
[AD-714019] 08 p1211 N71-18244

Fatigue damage determination by nondestructive tests
[AD-715630] 08 p1215 N71-18826

Durability and service life of ball bearings
[NASA-TT-F-13460] 08 p1208 N71-19009

Effects of surfaces and environment on nucleation and growth of fatigue cracks in copper
[NASA-CR-116859] 08 p1280 N71-19031

Rise and fall statistics of plastic strain of elastic-perfectly plastic material under random loading
08 p1299 N71-19142

Fatigue mechanisms in fracture of glasslike polymers
08 p1300 N71-19173

Analysis of aircraft wheel failures to determine cause of fatigue fracture and establishment of qualification tests
[NARC-11694] 09 p1475 N71-19857

Finite element and structural analysis of axial flow compressor blade root
[NAL-TR-214] 09 p1476 N71-19873

Reliability factors in rotary machine steel shaft design including materials fatigue, combined stress, and strain rates
[AD-716017] 09 p1477 N71-20029

Error analysis of counting accelerometer data from F-4 and RF-4 aircraft and structural fatigue analysis
[AD-717151] 10 p1497 N71-20796

Thermal stability, vibration strength, and fatigue life of titanium and aluminum alloys used for gas turbine blades
[AD-717012] 10 p1575 N71-20920

Analysis of physical properties and yield strength of bolts used as shear connectors in concrete on steel composite beams
[PB-196592] 10 p1659 N71-21807

Fractographic analysis on fatigue crack mechanism and fracture tolerance of pressurized vessels
[AD-717301] 11 p1833 N71-21868

Notch sensitivity factor for fatigue of elements with transverse holes
[TAIE-114] 11 p1838 N71-22533

Stress-strain fatigue behavior of Teflon liquid propellant expansion bladder material
11 p1784 N71-22559

Numerical estimates of intensity, scale, duration, and repetition rates of surface attack from individual bubble collapse and cavitation damage relationships to corrosion-fatigue
[UMICHS-003371-7-T] 12 p1906 N71-23539

Numerical analysis of stress and fracture in shallow linear-elastic shells composed of aluminum and plastic plates
12 p2087 N71-24128

Development of fracture model to predict rate of crack propagation under high temperature low cycle fatigue conditions based on creep rupture principle
12 p2088 N71-24283

Fatigue behavior of silicone glasses determined by static and dynamic tests
[AD-717546] 13 p2086 N71-24609

Cumulative frequency distributions determined by extreme value analysis used for fatigue analysis and interpretation of c.p. vertical acceleration and gust velocity measured on transport aircraft
[AGARD-R-579-71] 13 p2028 N71-23800

Fatigue and fracture mechanics of airframes and materials including structural design and stress analysis techniques
[AD-719736] 13 p2028 N71-23902

Burner rig tests on simulated turbine blades, with and without internal cooling, to predict thermal fatigue performance
[NASA-TM-X-47630] 13 p2181 N71-23120

Prediction of critical length of fatigue cracks based on concepts of linear elastic fracture mechanics
[AD-719757] 13 p2182 N71-23141

Servocontrol system for measuring local stresses at geometric discontinuity in stressed material
[NASA-CASE-XLA-08530] 13 p2182 N71-23340

Determination of static and fatigue characteristics of graphite epoxy composite materials with variations in temperature, stress mode, and stress ratio
[AD-720396] 14 p2277 N71-23885

Development of method for measuring fatigue life of elastomeric shear mounts subjected to static load deflection and vibration
[AD-720573] 14 p2282 N71-26192

Theories of adhesion and bond failure mechanism caused by water desorption
[SC-RR-70-915] 15 p2453 N71-27119

Experimental investigation on effect of spot welded or adhesively bonded thermocouples and fatigue behavior of two titanium alloys suitable for use in high speed airplanes
[NASA-TM-X-2288] 16 p2614 N71-28891

Qualitative analysis of radiographs and their importance for evaluating effects of defects on fatigue properties of welds
[NLL-CE-TRANS-5451-1982-08V] 16 p2685 N71-29170

Response of linear spring-mass-damper system of aluminum alloy subjected to wide band random force input of constant spectral density
17 p2851 N71-29445

Effect of orientation and specimen thickness on fatigue crack growth rate of 4340 steel
[AD-722728] 17 p2965 N71-29812

Development of test procedure for accurately recording dynamic signals from instrumented test bars used to measure loads during simulated fatigue tests
[NBS-TN-578] 17 p2855 N71-30082

Analysis of crack propagation in Alclad sheet specimens under two types of random loading based on gust spectrum
[NLR-TR-71014-U] 17 p2855 N71-30093

Environmental, drop, and vibration tests for investigating fatigue of cushion materials for packaging
[BCEI-49] 18 p2939 N71-30614

Fatigue strength diagrams, increasing density of clustered materials, and hardness values related to tensile strength - fatigue properties of titanium and titanium alloys - Part 5
[RAE-LIB-TRANS-1534-PT-5] 18 p2935 N71-30885

Influence of cold work and heat treatment on tensile and fatigue strength - fatigue properties of titanium and titanium alloys - Part 3
[RAE-LIB-TRANS-1534-PT-3] 18 p2935 N71-30886

Microstructure and frequency effects in fatigue stress-strain relations
[NYO-4097-3] 18 p3023 N71-31571

Metallographical study of small strain amplitudes in titanium fatigue mechanism at ultrasonic frequency
[AD-723533] 18 p2939 N71-31594

General fatigue prediction method based on Neuber notch stresses and strains for aluminum alloy airframes
[AD-723631] 19 p3188 N71-32825

Proceedings of conference on mechanical failure prevention
[AD-724475] 20 p3356 N71-32959

Solvent effects on fatigue-stress-strain behavior of Teflon expansion bladders
[NASA-CR-121474] 20 p3338 N71-33620

Static fatigue in glass from thermally activated chemical reaction
[SCL-RR-710010] 21 p3444 N71-34510

NASTRAN computer program used to calculate lateral deflections of weak spacecraft antenna boom to determine stiffness at small strains

22 p3482 N71-36236

Modal analysis of response and fatigue of aluminum aircraft panels modal response

22 p3484 N71-36237

Fatigue behavior and failure analysis of thin surface films of indium with normal loads moving at constant speeds

22 p3492 N71-36332

Analytical superposition model for environmentally-assisted corrosion fatigue crack propagation in aluminum and steel alloys

[UCRL-20538] 23 p3860 N71-37520

Steel brittleness related to low cycle fatigue, brittle failure prediction calculation

[AD-727422] 24 p3937 N71-38009

Developing metal alloys of ultrafine grain size with improved mechanical properties

[AD-727446] 24 p3938 N71-38093

Numerical analysis of effect of biaxial tension on fatigue strength of steel components based on strength relations for complex stress-strain state

[AD-727894] 24 p3940 N71-38107

Borosilicate glass fatigue and solubility in silicates

[AD-727738] 24 p3943 N71-38131

Electric equipment and drive adapter endurance tests for SNAP 8

[NASA-CR-72920] 24 p3960 N71-38248

Determining effective stresses under conditions of cyclic loading

[AD-727263] 24 p4024 N71-38711

Plastic deformation at tip of fatigue crack in high strength steels

24 p4024 N71-38715

X-ray microbeam studies of plastic zone at tip of fatigue crack

24 p4025 N71-38716

Delayed fracture of high strength steel as stochastic process in terms of nucleation theory and delayed fracture toughness

24 p4025 N71-38717

Kinetic theory of fatigue propagation based on vacancy condensation mechanism

24 p4025 N71-38718

Durability and fatigue behavior of turbine blades

[AD-727939] 24 p4026 N71-38728

FATIGUE DIAGRAMS

U S-N DIAGRAMS

FATIGUE LIFE

Cumulative frequency distributions of aircraft landing gear loads in determining fatigue life

[RAE-LIB-TRANS-1462] 01 p0128 N71-10273

TI-6Al-4V-2Sn fatigue behavior

[AD-710635] 01 p0066 N71-10330

Fatigue life prediction of composite bladder structures

[NASA-CR-111306] 01 p0131 N71-10838

Evaluation of series-hybrid rolling-element bearing

[NASA-TN-D-7811] 03 p0449 N71-13071

Frosting and geometric stress concentration effects on fatigue life of aluminum alloy clamped joints

[REPT-1112/78] 03 p0306 N71-13265

Electron fractography for high strength steel to determine fatigue life of military aircraft parts

[NLR-TR-69043-U] 03 p0395 N71-13364

Predicting bearing fatigue failure and life in primary coolant check valves of advanced test reactors

[IN-1338] 04 p0557 N71-14153

Scatter factor in statistical aircraft fatigue life estimation

[ARL/SM-350] 05 p0775 N71-15154

Vibratory load effects on glass fiber reinforced synthetic materials

06 p0876 N71-15949

Improving load capacity and fatigue life of rolling element systems in rockets and missiles

[NASA-CASE-XLE-02999] 06 p0864 N71-16052

Determining strength of hydrofoil systems by fatigue characteristics of welded joints

[AD-714436] 06 p0954 N71-16114

Dependence of fatigue life and flow stress on microstructure of precipitation hardened Al-Cu alloys

[AD-714085] 06 p0872 N71-16343

Behavior of metastable austenitic steels under cyclic loading

[UCRL-19628] 06 p0872 N71-16352

Probability analysis of pipe failures and low-cycle fatigue in reactor cooling systems

[GEAF-10207] 06 p0900 N71-16738

Rolling element fatigue lives of AISI T-1, AISI M-42, AISI 52-100, and Halmo at 150 F

[NASA-TN-D-4179] 07 p1034 N71-17329

Investigating fatigue life of rolling elements at 150 F and 800,000 psi

[NASA-TN-D-7033] 07 p1043 N71-17409

Aluminum alloy stress cycles and fatigue life of air-frame materials

[FB-78-1949] 07 p1124 N71-17524

Steel plate fatigue life tests noting plastic coating, air, sea water immersion and lubricant influence

[CRIF-MT-64] 08 p1214 N71-18584

Feasibility of equalization in random vibration test for acceleration response and fatigue life of component

09 p1480 N71-20232

Elevated temperature effects on fatigue life of tensile stressed titanium alloys, aluminum alloys, and stainless steels

[NASA-TN-D-6145] 11 p1777 N71-22076

Review of Miner-Palgrave rule for calculating fatigue

[AD-717283] 11 p1834 N71-22134

Fatigue life and deformation of riveted or bolted joints

[RIF-1239] 11 p1837 N71-22308

Conference on fatigue life in helicopter components

[DLR-MITT-70-01] 13 p2024 N71-24385

Fatigue life of helicopter rotary wings under vibrational stresses

13 p2024 N71-24386

Fracture mechanics and anisotropy of fatigue crack propagation in hot rolled banded steel plate

13 p2183 N71-25444

Plasticity and low cycle fatigue life of structural alloys

[AD-720368] 14 p2273 N71-25949

Lubrication, wear, and design aspects of rolling contact bearings

[NASA-SP-237] 15 p2412 N71-26826

Crack initiation and propagation modes of roller contact bearing fatigue

15 p2413 N71-26833

Roller bearing material technology

15 p2413 N71-26834

Lubrication chemistry of hydrocarbon liquids and effects on bearing surface wear

15 p2414 N71-26838

Method for predicting fatigue lives of 2024 T3 and 6061 T6 aluminum alloys subjected to either constant amplitude sinusoidal or wide band random fatigue loadings

[SCL-CR-710175] 15 p2420 N71-27017

Strain range components and creep fatigue behavior of metals related independently to cyclic life by equations in both tension and compression

[NASA-TM-X-67838] 15 p2523 N71-27945

Test of rolling element fatigue life with fluorinated ether lubricant at cryogenic temperature using five ball fatigue tester

[NASA-TN-D-6367] 16 p2600 N71-28038

Determination of thermal cycling capability of non-tubular regeneratively cooled thrust chambers for use in space shuttle propulsion systems

[MAT-3] 17 p2835 N71-29586

Variability of aluminum alloy aircraft structure fatigue life under symmetric and asymmetric loads

[ARL/SM-REPORT-329] 23 p3861 N71-37524

FATIGUE TESTING MACHINES

Fatigue testing apparatus for measuring strain levels on aluminum alloys with constant force or amplitude control at 20 kHz

[MAT-3] 02 p0241 N71-11565

Dynamic characteristics of fatigue testing machine

[TT-70-50833] 08 p0108 N71-19180

Cryostat for use with horizontal fatigue testing machines at low temperatures

[NASA-CASE-XMF-10904] 12 p1924 N71-24234

Fatigue testing apparatus with light shield and infrared reflector for high temperature evaluation of loaded sheet samples

[NASA-CASE-XLA-01782] 14 p2255 N71-26136

Orbital fatigue tester for Skylab program - test and design of titanium alloy and aluminum alloy specimens having various sizes

[NASA-CR-111923] 18 p2925 N71-31382

Design and performance tests for reversed bending with steady torque fatigue test machine using notched steel specimens

[NASA-TM-X-67949] 23 p3761 N71-36815

FATIGUE TESTS

Axial load fatigue tests on chromium-molybdenum steel tubing with welded fish mouth type splices

[ARL/SM-323] 01 p0127 N71-10117

Isothermal and adiabatic analyses of axial fatigue tests on metallic structures

[AD-712990] 03 p0465 N71-15198

High frequency, high temperature fatigue behavior of molybdenum base alloy and titanium base alloy

03 p0395 N71-15307

Photoelastic analysis of fatigue behavior of welded connections

[FB-194057] 04 p0615 N71-13557

Damage threshold tests on laser glass

04 p0525 N71-14328

Fatigue tests on notched samples of pure titanium

[RAE-LIB-TRANS-1493] 05 p0703 N71-15173

Random errors in aluminum alloy fatigue tests and failure modes

[ARC-CP-1123] 07 p1123 N71-17330

Steel plate fatigue life tests noting plastic coating, air, sea water immersion and lubricant influence

[CRIF-MT-64] 08 p1214 N71-18584

Fatigue tests on heated Inconel alloy having protective chromium aluminum surface layer

[NASA-TT-F-13484] 08 p1217 N71-19014

Analysis of aircraft wheel failures to determine cause of fatigue fracture and establishment of quality tests

[NRC-11694] 09 p1475 N71-20877

Fatigue tests on transverse butt welded joints containing porosity

[CRIF-MT-53] 10 p1652 N71-21813

Tensile and fatigue properties and liquid oxygen compatibility of bimetallic stainless steel-clad titanium prepared by vacuum deposition and explosive welding

[NASA-CR-72841] 10 p1581 N71-21417

Tensile, fatigue, and creep rupture properties of extruded nickel-based aluminum, titanium carbide, and beryllium oxide alloys and aluminum-based alloys, copper, and iron alloys

[NASA-CR-117502] 10 p1583 N71-21507

High temperature fatigue tests of steel ball bearings with synthetic paraffinic oil lubricant in low oxygen environment

[NASA-TN-D-6156] 10 p1567 N71-21665

Fatigue properties of titanium and nickel alloy honeycomb core sandwich structures

[AD-716731] 10 p1609 N71-21770

Fatigue test equipment for evaluating Focher aircraft wing

[NLR-TR-70088-L] 12 p2083 N71-23137

Irreversible fatigue specimen expansion in ESR-2 Mark B-7 subassembly

13 p2111 N71-24380

Plasticity and low cycle fatigue life of structural alloys

[AD-720368] 14 p2273 N71-25949

Fatigue creep tests on glass fiber reinforced epoxy resin for four polymerization states

[CRIF-PL-1] 15 p2428 N71-26807

Stress corrosion and fatigue tests and fractographic analysis of high strength aluminum alloy cylinders

[AD-728857] 15 p2425 N71-27029

Review of cumulative damage theories aimed at predicting service life of structures under fatigue loading allowing comparison of effects of various loads and cycle ratios

[ARL/SM-REPORT-326] 15 p2532 N71-27886

Response of cast Co-Cr-Mo alloy to impulsive thermal-mechanical fatigue conditions present during firing of automatic weapons

[AD-721895] 16 p2610 N71-28410

Creep and fatigue tests of type 316 stainless steel and Incoloy 800 for use in breeder reactors

[BME-1896] 16 p2612 N71-28610

Hardness and fatigue tests of steel bearing alloys

[NASA-TM-X-67874] 16 p2603 N71-28854

Fatigue properties of titanium and titanium alloys - effects of impurities, condition of surface, test cell in relation to force, and test conditions on fatigue strength

[RAE-LIB-TRANS-1399] 17 p2767 N71-30410

Chemical vapor deposition and burst testing of silicon carbide tubes

[ABCL-3674] 18 p2927 N71-30919

Fatigue testing of carbon and stainless steel balling water reactor cooling system pipes including failure probability and fracture mechanics analyses

[GEAF-10207-32] 19 p3134 N71-31711

High temperature, low cycle fatigue tests of titanium in inert argon atmosphere

[NASA-CR-1936] 22 p3594 N71-35592

Defect structure of Al-Zn alloy induced by quenching and low temperature aging

[AD-726582] 22 p3595 N71-35599

Tests of ball bearings of various material combinations in liquid hydrogen

[NASA-CR-72280] 23 p3762 N71-30410

Fabrication and fatigue tests of improved welded till-edge ballows for positive explosion applications

[AD-726523] 23 p3762 N71-30410

Axial fatigue tests in air conducted on wire rope, strand, and single wires

[AD-726457] 23 p3763 N71-30825

Effects of resination treatment and overbaking on fatigue properties of notched and unnotched D.T.D. 6873 aluminum alloy bar

[ARL/SM-MOTTE-258] 23 p3770 N71-30879

Fatigue test calculations for dynamically stressed components subjected to statistical excitation

[NASA-TT-F-19776] 23 p3840 N71-37313

Fatigue tests and life of nickel alloy during programmed loading and elevated temperature

[AD-727842] 24 p3939 N71-38418

Statistical analysis of fatigue test data on aviation turbine lubricants

[AD-727799] 24 p3946 N71-38418

Design data for regeneratively cooled panels from low cycle fatigue evaluation of Handley X and Inconel 625 sheet and sandwich panel specimens

[NASA-CR-1084] 24 p4027 N71-38734

Determination of growth patterns in rats fed on balanced diets differing by the presence of either saturated or unsaturated fat

[NASA-CR-116998] 13 p2082 N71-24333

Intraspecific relationships between lean weight and wing length for migratory birds

[NLR-TR-6197] 16 p2543 N71-20822

SUBJECT INDEX

- Determination of trace manganese and zinc in butter using neutron activation analysis
[JRI-133-70-03] 20 p3228 N71-32940
- FATTY ACIDS**
NT OLEIC ACID
Presence of estyl esters of long-chain fatty acids detected for *Rhizopus arrizus*
[NASA-CR-116886] 06 p1161 N71-19116
Growth and fatty acid synthesis inhibition in *Escherichia coli* by oxygen
[AD-717673] 11 p1683 N71-22347
Off-line processing of chromatographic data from fatty acid methyl ester mixtures by digital computer
[UCRL-72593] 11 p1716 N71-22348
Influence of dispersion medium composition on properties of lubricants thickened with lithium soaps of synthetic fatty acids [SFA]
[AD-727432] 24 p3943 N71-38130
- HAULT MECHANICS**
U FRACTURE MECHANICS
NFM (MODULATION)
U FEEDBACK FREQUENCY MODULATION
NCL LATTICES
U FACE CENTERED CUBIC LATTICES
WEARABILITY
Feasibility study of refractory-base weld-backing materials
[AD-715854] 06 p1207 N71-18700
Research in plasma physics including plasma probe, toroidal discharge, microwave diagnostics, and engineering feasibility studies
[JOD-1726-70] 10 p1627 N71-20918
Feasibility of reusable space-based tag with modular design
[NASA-CR-114938] 10 p1649 N71-21455
Feasibility, design, and algorithms of integrated circuit content addressable memories
12 p1891 N71-24025
Feasibility of cryogenic heat pipes for cooling isotopes in spacecraft power supply cycle
13 p2186 N71-23313
Feasibility of obtaining arbitrary polarization in both one and two dimensional slot arrays
[AD-722068] 17 p2724 N71-29375
Feasibility study for diamond materials data bank - conference
17 p2762 N71-29387
Feasibility of generalized integrated circuit for digital circuit requirements
[JC-CR-710033] 19 p3670 N71-32208
Simulation and modeling of advanced synaptic digital computer system operation for optimum hardware configurations
[AD-723521] 19 p3662 N71-32330
Group point kinetics for studying feasibility of high flux trap reactor system
22 p3627 N71-35842
Feasibility of fusion drives for interstellar travel with analysis of reaction equilibrium and plasma energy balance
24 p3964 N71-38275
- FECES**
Radioisotopic content in feces and urine of Apollo 7 through 13 astronauts
[NASA-CR-116223] 06 p0801 N71-16358
Design and performance of fecal waste management system for long duration manned space flight simulation
10 p1507 N71-20669
Development of prototype waste collection system modified Hydro-John/ designed for use in either zero or one gravity environment
[NASA-CR-115040] 15 p2375 N71-27770
Activation analysis of fecal samples from Apollo 7, 8, 9, and 10 astronauts to determine effects of space flight on mass balance of various elements by human body
[NASA-CR-121061] 21 p3381 N71-34058
Measurement of radiation exposure of Apollo 7, 8, 9, and 10 astronauts by determination of radioisotopic content of feces and urine
[NASA-CR-121060] 21 p3381 N71-34059
- FEDERAL BUDGETS**
Surveys on changes in federal funding effect on universities
[NSF-70-48] 09 p1487 N71-19922
Federal budget amendment agreement recommendations for HUD appropriations
[HEPT-92-377] 19 p3159 N71-32657
Federal budgeting for research and development by Agency for fiscal year 1969
[NSF-70-49] 20 p3370 N71-33716
Federal funding for SST and Concorde aircraft development in 1971
20 p3370 N71-33758
- FEDERATIONS**
NT BUREAUS (ORGANIZATIONS)
FED SYSTEMS
Process technology required for production of zone melting feed rods of pure aluminum oxides for basic studies of laser degradation
[AD-716421] 09 p1397 N71-19948
Laboratory tests on induction plasma torch with curved permeable walls and solid feed system
[NASA-CR-1764] 09 p1430 N71-26142

- Nonconductive tube as feed system for plasma thruster
[NASA-CASE-XLE-02902] 10 p1630 N71-21694
Polarization diverse S band feed cone for DSIF reflector antennas
11 p1703 N71-22778
Method and apparatus for pressurizing propellant tanks used in propulsion motor feed system
[NASA-CASE-XNP-00550] 16 p3670 N71-28929
Effects of temperature differences, acceleration fields, and geometric variations on propellant imbalance in multiple tank rocket feed systems
24 p4080 N71-38332
- FEEDBACK**
NT NEGATIVE FEEDBACK
NT NONLINEAR FEEDBACK
NT POSITIVE FEEDBACK
Information feedback approach applied to polarization modulated laser communication systems
[AD-710935] 01 p0034 N71-10894
Improving accuracy of gyro-stabilizer using floating integrating gyroscopes with feedback
10 p1562 N71-21747
Input-output properties of feedback systems based on linear time invariant systems
[NASA-CR-117467] 11 p1728 N71-22330
Volterra functional series for reactor with delayed neutrons and linear reactivity feedback
[DNR-1206] 13 p2117 N71-24856
ANCON code for solving point reactor kinetic equations including thermal feedback
[LA-4616] 21 p3460 N71-34628
Effect of retrodirective reflections on operation of ring resonator laser
[JPRS-54108] 24 p3931 N71-38048
- FEEDBACK AMPLIFIERS**
Electrical properties of biased diode bridge and application to improvement of rise time in feedback amplifier
11 p1725 N71-22660
Development of system with electrical properties which vary with changes in temperature for use with feedback loop in operational amplifier circuit
[NASA-CASE-MSC-13376-1] 15 p2487 N71-27058
Low noise preamplifier with negative feedback for spectral resolution improvement in X ray spectroscopy
[CEA-N-1401] 15 p2472 N71-27434
Phase locked demodulator with bandwidth switching amplifier circuit
[NASA-CASE-XNP-01107] 16 p2576 N71-28859
Monostable multivibrator for producing output pulse widths with positive feedback NOR gates
[NASA-CASE-MSC-13492-1] 16 p2576 N71-28860
Null balance, fixed pendulum accelerometers with analog feedback servoamplifiers
[NAL-TR-230] 20 p3373 N71-33241
Scheme for servomechanism with saturable amplifier and dynamic response with nonlinear parameters
20 p3380 N71-33603
Computerized design of integrated selective amplifier as feedback structure or as set-work topology
23 p3739 N71-36660
- FEEDBACK CIRCUITS**
Magnetic tape characteristics in spacecraft environment and design of linear m-ary feedback shift register
01 p0027 N71-10264
Feedback averaging amplitude modulated laser communication system
[AD-710956] 01 p0025 N71-10874
Optimum filters designed for analog feedback telemetry system
03 p0337 N71-12408
Linear three-tap feedback shift register
[NASA-CASE-MPC-10351] 03 p0343 N71-12503
Characteristics of generalized pulse modulated feedback systems
[NASA-TM-X-44501] 03 p0352 N71-12546
Static and dynamic stability and dynamic response of differential pressure sensor with electromechanical or electroacoustic feedback
[RAE-TR-70120] 07 p1027 N71-17134
Frequency control network for current feedback oscillators converting dc voltage to ac or higher dc voltage
[NASA-CASE-GSC-10041-1] 09 p1361 N71-19418
Determination of unsteady forces during wind tunnel test of elastic model by placing wind tunnel model in feedback circuit of servomechanism
[NASA-CR-114287] 09 p1316 N71-17996
Application of imbedding theory to problems of linear feedback control systems and trajectory optimization
10 p1643 N71-21254
Periodically reverse-switched capacitors or inductors in feedback networks, resulting in linear subharmonic filter
11 p1725 N71-22694
Feedback integrating circuit with grounded capacitor for signal processing
[NASA-CASE-XAC-10607] 12 p1893 N71-23669
Component connection schemes of brain for transable feedback flight control system
13 p2855 N71-23326

FEEDBACK CONTROL

- NT CASCADE CONTROL**
Feedback averaging method for amplitude modulated digital laser communications system
[AD-710956] 01 p0023 N71-10547
Developing thrutable nonpropellant hydrazine motor system for planetary landing vehicles
[NASA-CR-110933] 01 p0116 N71-10763
Feedback decoupling of time delay differential systems
[NASA-CR-111415] 02 p0196 N71-11375
Identifying fluctuations and feedback control of plasma confined in toroidal stellarator
[UCRL-72473] 02 p0281 N71-11866
Transient responses of single loop systems with quantized error signals
03 p0351 N71-12534
Characteristics of generalized pulse modulated feedback systems
[NASA-TM-X-44501] 03 p0352 N71-12546
Development of linear optimal control solutions using transfer matrix
[NASA-TM-X-44508] 03 p0353 N71-12555
Investigating nonlinear digital control methods for attitude stabilization of VTOL aircraft
03 p0347 N71-12615
Improving feedback control design by using digital computer techniques
[NASA-CR-116771] 04 p0390 N71-13501
FFTP closed loop test characteristics
[BNWL-1251] 04 p0351 N71-13935
Feedback controlled variable conductance heat pipe
[NASA-CR-73475] 05 p0784 N71-15402
Feedback control of PG discharge of QP machine
[IPF-T-2] 05 p0755 N71-15665
Improving precision of gyro-stabilizer having feedback with respect to reactive moment of gyroscopes
06 p0893 N71-15953
Synthesizing asymptotically stable closed systems and formulation of mixed problems of optimal control theory
[NASA-TT-F-13435] 06 p0885 N71-16501
Deriving algorithms for finding limiting characteristics and carrying capacities of dynamic systems with feedback and internal noise
07 p0996 N71-16977
Improved feedback control of distributed parameter systems for linear landing vehicle simulator
[NASA-CR-116462] 07 p1084 N71-17345
Determining optimal time-invariant output feedback controllers for linear dynamic systems
[NASA-CR-103832] 07 p1002 N71-18062
Differential trajectory sensitivity reduction for nonlinear closed loop system
[RE-4033] 07 p1051 N71-18099
Describing continuous analog to digital converter with parallel digital output and nonlinear feedback
[NASA-CASE-XAC-94031] 08 p1164 N71-18574
Reduced magnetic core memory element with blocking oscillator feedback for interrogation without loss of digital information
[NASA-CASE-XGS-03303] 08 p1164 N71-18595
Plot describing function estimates from closed loop tracking operation data
[NASA-TN-D-6335] 08 p1171 N71-18635
Minimizing performance criterion to analyze ability of automatically controlled aircraft to maintain accurate flight path control during landing approach
[NASA-TN-D-6336] 08 p1233 N71-18761
Engineering constraints in designing optimal and suboptimal feedback systems
[NASA-CR-116895] 08 p1173 N71-19121
Suboptimal feedback control law synthesis for second order nonlinear systems
08 p1173 N71-19164
Noise reduction in closed loop servo systems in computerized simulations
[AE-404] 08 p1363 N71-30178
Optimization design procedures for development of stability augmentation systems
[AD-717108] 10 p1492 N71-38617
Control system design for USSR single-rotor helicopters including controllability characteristics, rotors with control gyroscopes, and transfer functions in closed loop systems
[NASA-TT-F-636] 10 p1492 N71-38719
Stability analysis of decentralized linear dynamic systems with proportional feedback control
[AD-710822] 10 p1293 N71-21562
Realization of near time optimal feedback controllers for linear time invariant systems
[SC-ER-70-544] 10 p1430 N71-21743
Dynamic pressure feedback compensation of resonator in liquid rocket thrust vector control system
[NAL-TR-313] 11 p1820 N71-22660
Motor start of 2 to 10 kilowatt Brayton rotating unit operating on gas bearings in closed loop test facility
[NASA-TM-X-2266] 11 p1678 N71-22570
Algorithm elements for closed cycle control of complex scientific experiments
11 p1718 N71-22727
Iteration method for output feedback control of unstable linear systems
12 p1894 N71-23631

State variable feedback for decoupling of time delay differential equations 12 p1894 N71-24149

Linear time invariant optimal control feedback for closed loop stability in plant parameter variations 12 p1895 N71-24151

Analysis and synthesis of linear feedback control systems using state vector control 13 p2026 N71-24711

Nonlinear absorption feedback for laser power stabilization 13 p2089 N71-24837

Self-reorganization methods for complex linear dynamic systems to compensate for component failures [NASA-CR-118314] 13 p2103 N71-24874

Binary to decimal decoder logic circuit design with feedback control and display devices [NASA-CASE-XKS-06167] 13 p2052 N71-24890

Synthesis procedure for adaptive control systems for adjusting parameter vectors [AD-71938] 13 p2060 N71-25140

Linear regulator problem solution using Euler equations of motion, Laplace transformations, and Hamilton-Jacobi equation for stochastic control 14 p2235 N71-26444

Explicit feedback control law for singular linear quadratic-Gaussian stochastic control [AD-720341] 15 p2389 N71-27342

Feedback compensator for linear-time invariant system insensitive to parameter variations [NASA-CR-119798] 16 p2563 N71-28160

Automatic feedback control system for controlling volume of power amplifier and measuring frequency range of background noise [AD-721596] 16 p2568 N71-28356

Algorithms for suboptimal nonlinear feedback and trajectory inequality control systems including linear, nonlinear, and quadratic programming 16 p2574 N71-28612

Voltage regulator switching circuit with feedback control and hysteresis network [NASA-CASE-LEW-11005-1] 16 p2571 N71-28768

Nonlinearity and signal transmission delay effects on feedback control systems based on random input signal analysis and cross correlation 16 p2576 N71-28826

Feedback control for direct current motor to achieve constant speed under varying loads [NASA-CASE-MPS-14610] 16 p2572 N71-28886

Feedback controller for sampling error signals within single control formulation time interval [NASA-CASE-GSC-10554-1] 16 p2566 N71-29033

Normal shock inlet control systems for supersonic mixed compression inlet using feedback loops [NASA-TN-D-6332] 17 p2839 N71-29745

Computerized simulation of aerodynamic loads and dynamic responses for aircraft control system design based on optimal and feedback control theories [AD-722652] 19 p3037 N71-31933

SCEPTR program for analyzing multifeedback loop control system 19 p3067 N71-32411

Feedback control of tilt compensation horizontal pendulums for earth tide observation 20 p3265 N71-33369

Closed loop servomechanism for variable speed tape recorders onboard spacecraft [NASA-CASE-NPO-10700] 20 p3235 N71-33613

Mathematical models for pole assignment in linear feedback control systems [NRC-ME-MK-28] 20 p3295 N71-33883

Computational algorithm to mechanize theory of optimal time-invariant output-feedback controllers - Vol. 3 [NASA-CR-119913] 20 p3294 N71-33962

Proportional feedback control to replace original servomechanism unit for controlling carbon dioxide concentration and relative humidity in Null point compensating system for plant measurements [UCLA-12-813] 21 p3433 N71-34430

Pattern search algorithm for feedback control system parameter optimization [AD-726465] 22 p3563 N71-35377

Tuning, application, optimal switching times, and comparison of optimal and suboptimal controllers for feedback and feedforward control 23 p3737 N71-36652

Differential equation with optimal feedback control for stochastic control system 23 p3739 N71-36663

Optimal feedback controller design based on model for linear plant of unknown characteristics under stochastic environment 24 p3951 N71-38186

FEEDBACK FREQUENCY MODULATION

Optimum receivers for continuous phase digital frequency modulated signals [RR-71-1] 13 p2048 N71-25343

FEEDFORWARD CONTROL

Grinding machine efficiency increase due to higher forward feed speeds noting surface roughness and wear effects [CRIF-MC-34] 10 p1563 N71-20751

Tuning, application, optimal switching times, and comparison of optimal and suboptimal controllers for feedback and feedforward control 23 p3737 N71-36652

FEEDING DEVICES

U ANTENNA FEEDS

FELDSPARS

Picagoch thermometry of igneous rocks [NASA-CR-115896] 05 p0669 N71-14803

Caloric distribution in clinoquartz, olivine, and feldspars separated from Apollo 11 and 12 rocks determined with Mossbauer spectroscopy of Fe-57 [NASA-CR-114941] 10 p1635 N71-21451

FELLOWSHIP AIRCRAFT

U F-28 TRANSPORT AIRCRAFT

FELSITE

U IGNEOUS ROCKS

FELTS

Flight test of chemical vapor deposited felt and filament wound carbon composite heat shields [SC-DC-71-3853] 17 p2769 N71-29516

FERMENTATION

Polarization and energy conversion efficiency of yeast and *Bacillus lactate* fermentation for biochemical fuel cells 14 p2205 N71-26245

FERMI LIQUIDS

Microscopic theory of quasi-particle spin fluctuations in low temperature, dense Fermi liquids 10 p1618 N71-21440

Sun rules and Landau theory of Fermi liquids, and spin density fluctuation problem [NUB-2073] 17 p2804 N71-30223

Fermi system phase transition model analysis near critical point for two, three, and many body interactions with comparison to classical theory 23 p3823 N71-37271

FERMI STATISTICS

U QUANTUM STATISTICS

FERMI SURFACES

Theoretical physics study of Fermi systems using Landau, Brueckner-Bethe, and Migdal theories [NYO-4032-23] 01 p0103 N71-10945

Fermi surface investigations in Sn and Te [AD-717197] 02 p0284 N71-11839

Radio frequency size effect for determination of molybdenum Fermi surfaces [IS-T-356] 02 p0286 N71-11934

Structural and electrical properties of alkali graphite and calculations of potassium graphite band structure, Fermi surface, work functions, and electronic specific heat coefficient 09 p1403 N71-19571

Fermi surface model compared to size-dependent oscillatory magnetoresistance in cadmium 10 p1608 N71-21597

Calculation of energy bands in ferromagnetic nickel using combined interpolation method 11 p1810 N71-23034

Mathematical techniques and computer programs for inversion of de Haas-van Alphen data on closed Fermi surfaces [ANL-7659] 12 p1972 N71-23921

Threshold theorem for expanding absorptive dispersion F sub 2v nucleon radius and establishing of Fermi energy limit from light propagation and magnetic fields neutrino sea 12 p1977 N71-24253

Electromagnetic probe measurements of special quantum waves, optical properties, and critical points in metals [AD-719856] 13 p2151 N71-24952

Superlattice effects on Fermi surfaces of antiferromagnetic Cr alloys with V and Mn traces, determined from de Haas-van Alphen measurements [IS-T-420] 15 p2505 N71-27052

Fermi surface wave function tables for single particle states of transuranium region deformed nuclei in Saxon-Woods potential [JINR-P4-5457] 16 p2646 N71-28195

Closed Fermi surfaces in N318m order disorder transformations when alloyed with NiFe and NiCo [NLL-LTI-746-638/19022.4011] 16 p2614 N71-28932

Circular model for interacting Fermi gas 16 p2657 N71-29140

Elastic stress effects on indium alloy Fermi surface topology measured on alloy whiskers 20 p3334 N71-33569

Calculations of phonon contribution to electron effective mass as function of position on Fermi surface, and anisotropic superconducting energy gap in white tin 21 p3492 N71-34874

Interpretation of Hall coefficient of pure copper, silver, gold, and some silver alloys based on anisotropic Fermi surface model [NRC-TT-1476] 22 p3592 N71-35581

Numerical analysis of transport parameters for point defect scattering in nearly free electron model metals 22 p3660 N71-36098

FERMI-DIRAC STATISTICS

U QUANTUM STATISTICS

FERMIONS

NT ANTINEUTRINOS

NT BARYON RESONANCES

NT BARYONS

NT COLD NEUTRONS

NT ETA-MESONS

NT FAST NEUTRONS

NT HYPERONS

NT LEPTONS

NT MESON RESONANCES

NT MESONS

NT NEUTRONS

NT PHOTONEUTRONS

NT PROTONS

NT RECOIL PROTONS

NT SOLAR PROTONS

NT THERMAL NEUTRONS

NT KH-51 HELICOPTER

Characteristics of low-entropy system of supralight particles capable of producing some neurological functional functions of brain and consciousness [UPRS-52722] 10 p1502 N71-21610

Periodic oscillations and momentum distribution functions for interacting fermions in magnetic field 10 p1636 N71-21800

Time dependent perturbation theory of ground state many fermion system for study of self energy and ionization problems and examination of reaction matrix expansion 11 p1801 N71-21880

Spinor field theory of Dirac fermions interacting with bosons at infinite momentum based on perturbation theory and tree-graph approximation 14 p2304 N71-26270

Finite quantum mechanics for four fermion spin field interactions based on Bogolubov theory and spin-time functions with Federbush model example 14 p2304 N71-26270

Spin test for fermion $1/2$ greater than $1/2$ decaying into spin-1/2 fermion/neutral Lambda hyperon plus spin-1 photon [KFKI-70-27-HEP] 14 p2313 N71-26717

High energy scattering amplitude of fermion with anomalous magnetic moment and noncompensation [DESY-71/1] 16 p2657 N71-29122

Limiting relations for correlation averages in quantum statistics of four fermion interaction [ITF-70-59] 17 p2811 N71-30010

Quasi-averages in quantum mechanics for negative four fermion interaction models and free energy linking expressions [ITF-70-52] 18 p2967 N71-30446

Formulation of theorems for obtaining correlation averages for wide class of model systems with four fermion interaction 18 p2973 N71-30519

Employing Hamiltonian function for definition of quasi-averages for model systems with negative four fermion interaction [ITF-70-58-P] 18 p2974 N71-30519

Perturbation theory of electromagnetic interaction connected with local fermion current by nonlocal form factors [JINR-P2-5694] 21 p3472 N71-34725

Graviton fermion interaction described by Lagrangian function of tetrad field and fermion field 23 p3823 N71-37270

FERRATES

Ferroelectric properties of bismuth ferrate and related materials [PB-192509] 03 p0440 N71-12671

Deterministic errors and current impulse techniques for analyzing electrochemical kinetics of heteroconformate 3/2 couple on platinum 18 p2886 N71-31232

FERRIC ION

Acidity effects on ferrous and ferric radiolytic oxidation and reduction rates by HO2 radicals [LIB/TRANS-282] 07 p0968 N71-17908

Pressure effects on ferric hydroxamate and ferri-hemate A based on electromagnetic absorption and Mossbauer resonance [COO-1198-777] 11 p1784 N71-22405

Effect of diffusion of ferric ions on rate of oxidation of UO2 and U3O8 in sulfuric acid medium 18 p2885 N71-31004

FERRIMAGNETIC MATERIALS

Investigating ferromagnetic insulators, alloys, and magnetic impurities with respect to transport theory [AD-714096] 06 p0904 N71-14011

Magnetic moment versus temperature curves for ferromagnetic garnets [AD-715284] 07 p1095 N71-17642

Origin and characterization of ion radiation damage in ferromagnetic cobalt ferrites determined by electron microscopy [UCRL-203469] 12 p1941 N71-23107

Development of air elutriation, magnetic separation, and screening methods for recovering metals from urban refuse [IBM-TPR-34] 16 p2695 N71-29054

FERRIMAGNETISM

Propagation of electromagnetic waves in ferrite filled longitudinally magnetized elliptical waveguide 04 p1163 N71-10801

SUBJECT INDEX

Ferrimagnetic reciprocal phase for use in phased arrays (AD-717344) 11 p1723 N71-23023

FERRITES

Epitaxial growth of ferrites by vapor deposition 01 p0100 N71-10130

Far-infrared resonances in ytterbium orthoferrite near spin reorientation temperature (NYO-2391-106) 03 p0428 N71-12881

Ferrite magnetic core magnetometer 04 p0520 N71-13637

Composite ferrite substrates for microwave integrated circuits 04 p0512 N71-13912

Dislocations in cobalt ferrite spindles (UCRL-19198) 04 p0580 N71-14020

Direct solution of complex crystal structures by electron microscopy (AD-713554) 05 p0759 N71-15389

Ferrite core fluxgate magnetometer 08 p1190 N71-19688

Cobalt and copper ferrite spindles as catalysts in oxidative dehydrogenation of butenes (NASA-CR-116882) 08 p1161 N71-19238

Heating ferrite by pulsed laser radiation absorption, preventing thermal breakdown 12 p1932 N71-23105

Origin and characterization of ion radiation damage in ferrimagnetic cobalt ferrites determined by electron microscopy (UCRL-20369) 12 p1941 N71-23107

Chemical composition, electromagnetic properties, new materials, and production techniques for various types of ferrites (AFRS-52952) 12 p1965 N71-23285

Nickel-zinc ferrite cores for magnetic heads with increased wear resistance (AD-710692) 12 p1888 N71-23491

Effects of zinc substitution on switching and hysteresis loop properties of lithium ferrite cores (AD-719174) 13 p2124 N71-24839

Magnetic recording head composed of ferrite core coated with thin film of aluminum-iron-silicon alloy (NASA-CASE-GSC-10097-1) 15 p2383 N71-27210

High density nickel-zinc ferrite with high Q factor and high permeability for RF application developed by sintering cryogenic crush procedure (AD-721587) 16 p2569 N71-28407

Expansion function technique for determining resonances of ferrite-filled spherical resonator 16 p2640 N71-29126

Magnetic crystallographic orientation produced in ferrites by hot working (AD-723538) 18 p2931 N71-31580

Nitrogen effect on creep properties of ferritic steels and interstitial influence on austenitic steel creep properties 19 p3111 N71-31905

Neutron diffraction study of magnetic structure of magnetite-substituted zinc ferrites (AD-71269) 19 p3169 N71-32220

Stabilizing ferrite cavities for alternating gradient synchrotron conversion (BNL-15722) 20 p3243 N71-33813

Ferrite wafered computer storage devices with increased size and storage capacity 23 p3729 N71-36583

Stoichiometric and compositional effects on sintering and magnetic characteristics of high purity, freeze dried, barium ferrite ceramics 23 p3780 N71-36943

FERRULES

Thermal stability of polyorganosiloxanes by means of ferrocene derivatives (AD-716621) 09 p1405 N71-19949

Molecular structures and thermal stabilities of ferrocene containing polyazines and poly-Schiff bases (AD-717648) 11 p1782 N71-22078

Preparation and characteristics of free radical and ionic solution of one-ferrocenyl-one, three-butanediols (AD-722963) 20 p3228 N71-33098

FERRULES/ELECTRICITY

Open-circuit sensitivity of radially polarized ferroelectric ceramic cylinders in hydrophones (AD-712766) 03 p0350 N71-12524

Ferroelectric properties of bismuth ferrite and related materials (PB-192909) 03 p0440 N71-12671

Growth and evaluation of bismuth titanate single crystal also growth of thick single crystals of related compounds (AD-715312) 08 p1277 N71-18420

Solution for ferroelectric model in staggered field at all temperatures (BNL-2045) 08 p1158 N71-18486

Acoustic characteristics of barium titanate and lead zirconate-titanate ferroelectric ceramics (AD-715624) 08 p1279 N71-18809

Magnetoferroelectricity, cooperative fluorescence of rare earth ions in crystals, narrow-band and narrow-band compounds, and related studies of rare earth compounds (AD-716470) 09 p1453 N71-20007

Resonance polarization in KHzPO₄ within 1 K of ferroelectric transition (AD-717298) 11 p1840 N71-21964

Heat flux sensors based on thermistors in doped polycrystalline ceramics such as barium strontium titanate showing ferroelectric resistance anomaly

Electron and solid state physics, control theory and applications, ferroelectric and ferroelectric materials, electromagnetic phenomena, and plasma medium scattering

Nuclear spin-lattice relaxation by muons in order-disorder ferroelectric transformations with decahydronitrobenzene protons crystal example (US-575) 14 p3319 N71-26785

Shear acoustic velocity of ferroelectric phase transition at 122 K of KHzPO₄ single crystals

Ionicity, electric field gradient, and specific heat determinations for ferroelectric phase transitions in PbZrO₃-PbTiO₃-BiFeO₃ ternary system

Ferroelectricity and conduction in ferroelectric crystals (AD-721479) 16 p2666 N71-28736

Selected electron shell method for X ray diffraction studies of electron polarization in ferroelectrics (AD-722067) 16 p2649 N71-28744

Open circuit sensitivity of radially polarized ferroelectric ceramic hollow spheres treating ceramic as anisotropic material (AD-722401) 17 p2726 N71-29732

Effects of atomic repulsive potential in ferroelectric crystals in terms of temperature, pressure, and crystal structure (AD-722449) 18 p2993 N71-30726

Zero-shift and remanence polarization reorientations in polycrystalline ferroelectrics used in piezoelectric shear-type accelerometers (SC-RR-70-755) 21 p3429 N71-34401

FERRULES/MAGNETIC FILMS

Feasibility of 50 nanosecond cycle time thin ferroelectric film storage 01 p0109 N71-10155

Temperature dependence of resonance linewidths of standing spin wave modes in ferroelectric thin films 18 p2996 N71-31101

FERRULES/MAGNETIC MATERIALS

NT FERROELECTRIC FILMS

NT MAONETITE

NT PERMALLOYS (TRADEMARK)

Nondestructive tests for detecting stress in ferroelectric materials (AD-710012) 01 p0065 N71-10193

Mössbauer spectra of ferroelectric materials (AD-711105) 01 p0111 N71-10668

Temperature dependence of initial permeability of ferroelectric amorphous Co-P alloy (AD-711087) 01 p0092 N71-10918

High speed centrifugal determination of mechanical properties of small iron and other ferroelectric crystals and whiskers (AD-711582) 02 p0244 N71-11696

Ferroelectric return yoke effects on field enhancement and field distribution in high field magnets (SLAC-PUB-739) 03 p0417 N71-12874

Digital simulation of ferroelectric material hysteresis for ESRO 1 satellite attitude control (ESRO-SR-12-ESTEC) 03 p0438 N71-13253

Magnetostriiction of magnetic composite materials (AD-712523) 04 p0566 N71-13943

Internal fields and relaxation effects for dysprosium in ferroelectric TbAl₂ studied by perturbed angular correlation (UUP-484) 06 p0909 N71-15752

Excitation spectra of ferroelectric insulators in presence and absence of impurities 09 p1423 N71-19500

Magnetization versus field and temperature analyses of ferroelectric material in Apollo 12 lunar samples (NASA-CR-114891) 09 p1465 N71-19787

Thermodynamics of Heisenberg ferromagnet in applied magnetic field (NASA-TM-X-52969) 10 p1661 N71-21168

Microstructure and magnetic properties of internally oxidized ferromagnet alloys for application to magnetic domain theories and high temperature tests (AD-717216) 10 p1579 N71-21301

Computer program for analysis of magnetic field problems involving ferroelectric materials (AD-716992) 10 p1680 N71-21631

Magnetic properties, hyperfine field, and band structure of ferroelectric iron 10 p1669 N71-21762

Photometric and cinematographic studies of magnetic domain processes in ferroelectric materials (AD-717669) 11 p1783 N71-22348

Magnetic coupling in composite ferroelectric structures consisting of two permalloy films /81.7 percent Ni and 18.3 percent Fe/ with their separation layer of chromium and/or gold 11 p0080 N71-23014

Calculation of energy bands in ferroelectric nickel using combined interpolation method 11 p1810 N71-23034

Magnetic-optical properties of polycrystalline and single crystal ferroelectric thin films (AD-718135) 12 p1985 N71-23653

Electron and solid state physics, control theory and applications, ferroelectric and ferroelectric materials, electromagnetic phenomena, and plasma medium scattering (AD-718117) 12 p1986 N71-23911

Implantation into ferroelectric materials by Coulomb excitation, forward angular correlation method (COO-585-7) 13 p3159 N71-25495

Temperature dependence of magnetic resonance linewidths in ferroelectric crystals 15 p2454 N71-27377

Model for ferroelectric material characteristics in diffusion of transient electromagnetic fields through saturated ferroelectric media (AD-721906) 16 p2638 N71-28458

Calculation of neutron elastic and inelastic scattering cross sections and spatial transverse correlation functions for Heisenberg theory of impure ferromagnets (BNL-TR-398) 16 p2658 N71-29144

Equation of state and static correlations for ferromagnetic colloid (AD-722712) 17 p2709 N71-30210

Calculation of specific heat anomalies caused by low concentration of impurities randomly distributed in Heisenberg ferromagnets 19 p3143 N71-32649

Effect of electron-magnon interaction on magnon energy in isolated electron ferromagnets (TR-71-2) 24 p3942 N71-38430

FERRULES/MAGNETIC RESONANCE

Transmitter voltage source with low internal impedance and high current ultrasonic signal for ferromagnetic study (AD-718334) 12 p1888 N71-23489

Three reversed spin bound states in Heisenberg model of ferromagnetic spin systems with discussion of two reversed spin subspaces 17 p2810 N71-30393

FERRULES/MAGNETISM

Investigating low-temperature ferromagnetism of amorphous alloys obtained by rapid quenching from liquid state (CALT-822-11) 05 p0703 N71-15231

Electron interaction ferromagnetics in transition metal disulfide systems (NUB-2039) 07 p1068 N71-17516

Cluster and moment effects on paramagnetic to ferromagnetic transition in Co-Ni alloys (UCRL-72567-REV-1) 07 p1078 N71-17776

Electronic properties of dilute alloys including magnetic permeability, electrical resistance, and ferromagnetism (AD-716607) 09 p1453 N71-20008

Green function used for thermodynamic model of Heisenberg ferromagnet in random phase approximation (NASA-TM-X-52982) 09 p1486 N71-20534

Spin wave perturbation theoretical analysis of Heisenberg model for impure ferromagnets (BNL-TR-399-PT-1) 10 p1837 N71-21704

Research in ferromagnetism, phase transitions, and electrical conductivity (AD-717758) 11 p1748 N71-22297

Heisenberg ferromagnetism at low temperatures with boson theory of angular momentum including spin operators 11 p1809 N71-22973

High temperature ferromagnetic cobalt-base alloy for electrical power generating equipment (NASA-CASE-XLE-03629) 12 p1937 N71-23248

Mathematical models of physical properties of cooperative assemblies including ferromagnetism (AD-718077) 12 p1967 N71-23905

Calculation of two body elastic scattering amplitudes for Ising model of ferromagnetic phase transition slightly above critical point as Hamiltonian field theory on lattice space 13 p2145 N71-25592

Ferromagnetic fluid for generating pressure forces for sea vehicle propulsion (AD-722556) 17 p2756 N71-29905

Resistivity minimum in ferromagnets with approximate calculation of electron-magnon interaction contribution to temperature dependence of electrical resistivity (CALT-822-25) 18 p2561 N71-30537

Tests of de quadrupole magnets, superconducting ac dipole magnet designs with ferromagnetic return yokes, and analysis of Kohlers rule in pure aluminum tapes (KFK-1316) 21 p3464 N71-34657

Magnetization and susceptibility of Heisenberg ferromagnet in magnetic field with expressions derived for calculating thermodynamic parameters (NASA-TN-D-6420) 21 p3497 N71-34913

Analysis of magnetic properties of MnAs using neutron diffraction and effects of high compressibility on magnetic behavior 23 p3777 N71-38913

FERROMAGNETISM

FERROUS METALS

- Acidity effects on ferrous and ferric radiolytic oxidation and reduction rates by HO_2 radicals
[LIB-TRANS-282] 07 p0988 N71-17088
- Tabulated mechanical and acoustic properties for selected ferrous, nonferrous, and plastic materials
[AD-716033] 09 p1484 N71-19676
- High temperature chromization of ferrochromic alloys
[TT-70-58195] 14 p2270 N71-25677
- Development of ferrous metallurgy and advanced methods of metal production
[JPRS-54099] 23 p3772 N71-36887
- Feasibility of applying Mossbauer spectroscopy to nondestructive measurement of surface stresses in ferrous metals
[AD-726742] 24 p4025 N71-38719

FERTILITY

- Application of microbial enzymes to problems of soil fertility
20 p3324 N71-33507

FERTILIZATION

- Biochemistry of growth, gametogenesis, and fertilization in algae
[NYO-3475-24] 05 p0635 N71-14722

FET (TRANSISTORS)

U FIELD EFFECT TRANSISTORS

FEYNMAN DIAGRAMS

- Multi-loop self energy operators in dual resonance model
[TUPE-70-27] 05 p0712 N71-14521
- Asymptotic single particle distributions with pionization in multiperipheral model based on Feynman conjecture
[RLO-1388-585] 09 p1434 N71-19994
- Finite theory of quantum electrodynamics, including modified photon and fermion fields and Feynman diagrams
[NYO-1932/2-183] 13 p2139 N71-25493
- Sixth-order radiative corrections to anomalous magnetic moment of electron from Feynman diagrams with vacuum polarization insertions
[CNRS-CPT-70-P-339] 17 p2803 N71-30222
- Numerical analysis of Feynman diagrams and application to calculation of magnetic moment of electrons and muons
[CNRS-CPT-70-P-336] 18 p2969 N71-30432
- Computer programs for calculating Feynman diagrams of scalar field interactions
[CNRS-CPT-70-P-318] 18 p2962 N71-30666
- Zero slope limit of dual resonance model
[LPTHE-71/17] 18 p2944 N71-30915
- Cross sections of N particle production and inclusive production for Feynman gas model
[N-TS-71/4] 20 p3314 N71-33118
- Feynman path integral formulation of non-relativistic quantum mechanics applied to scattering theory
20 p3324 N71-33901

FIBER OPTICS

- Fiber optics with extended ultraviolet transmission
[AD-716241] 01 p0088 N71-10004
- Fiber optic transducers for monitoring and analysis of vibration in aerospace vehicles and onboard equipment
[NASA-CASE-XMF-02433] 01 p0055 N71-10616
- Fiber optics and optical coupling of sodium salicylate phosphors to photomultiplier tubes for ultraviolet radiation detection
[NPL-QU-11] 07 p1067 N71-17155
- Fiber optics in electron optical devices such as cathode ray tubes, image intensifiers, and image converters
[AD-717838] 11 p1798 N71-22470
- Light scattering dissipated in optical glass fibers causing power loss
[SRDE-78064] 14 p2295 N71-25635
- Pulse counting spectrophotometer using phosphor output image intensifiers to single photon input
16 p2594 N71-28518

FIBER STRENGTH

- Calculation of forces in infinite length fiber with transverse impact of variable velocity
[AD-711758] 01 p0131 N71-10852
- Stretching and heat treatment effects on microstructure of polyacrylonitrile fibers
[RAE-LIB-TRANS-1598] 17 p2771 N71-30392
- Analysis of failure mechanisms of carbon-epoxy composite materials and methods of predicting performance under load conditions
[NASA-CR-121621] 21 p3326 N71-35123

FIBERGLASS

U GLASS FIBERS

FIBERS

- NT CARBON FIBERS
- NT COTTON FIBERS
- NT DACRON (TRADEMARK)
- NT GLASS FIBERS
- NT NYLON (TRADEMARK)
- NT REINFORCING FIBERS
- NT SYNTHETIC FIBERS
- NT WOOL

Static and dynamic elastic moduli and real moduli of glass fiber-epoxy and boron fiber-aluminum composites
[AD-716598] 01 p0070 N71-10022

Model for carbon fiber structure
[SC-7-70-4030] 03 p0196 N71-13013

Technology review on fiber metallurgy including whisker composites
[AD-713668] 05 p0700 N71-14762

Effect of counterface on friction and wear of carbon fiber reinforced thermosetting resins
[RAE-TR-70115] 05 p0693 N71-15433

Finite element analysis of interlaminar shear in fibrous composites
[RM-492] 06 p0880 N71-16466

Hydrodynamic stability of viscoelastic fluid filaments
[NASA-CR-116438] 07 p1007 N71-17087

Production of aluminum oxide fibers by direct melt fiberization process
[NASA-CR-72812] 09 p1393 N71-20125

Models for heat transfer during spin melting within single fibers and from single fiber to surrounding fluid
10 p1660 N71-20755

Thermal stability of fibers and polymers
[RAE-LIB-TRANS-1500] 10 p1588 N71-20926

Process for fiberizing ceramic materials with high fusion temperatures and tensile strength
[NASA-CASE-XNP-00597] 11 p1786 N71-23088

Radiation damage of fiber substructure
[RAE-LIB-TRANS-1467] 12 p1941 N71-23236

Investigation of impact resistance of unidirectional fiber composites using Izod impact tests
[NASA-TM-X-67802] 12 p1946 N71-24010

Development of crystal structure for charged particle acceleration
[ANL-TRANS-825] 13 p2154 N71-25547

Interfacial reactions of boron fibers and carbon fibers in chromium matrices at elevated temperatures
[ARL/MET-43] 15 p2432 N71-27620

Electrostatic methods to control placement and orientation of short graphite fibers in fiber composites and fiber structures
[SC-CR-69-3277] 15 p2432 N71-27699

Production of zirconium containing glass with increased chemical and thermal stability for use in thread manufacturing
[NLL-LIB-COMM-1518-5196] 16 p2619 N71-28975

Utilization of aerospace nonflammable colloidal elastomeric, fibrous, and composite materials in commercial aircraft refurbishment
18 p2868 N71-30759

Impact resistant unidirectional fiber composite design based on micro and macromechanics, Izod impact tests, and residual stress and structural analyses
[NASA-TN-D-6463] 19 p3188 N71-32243

High and low speed tensile tests of fibrous textiles
[AD-726920] 22 p3604 N71-35665

FIBERS (MATHEMATICS)

Analytical morphisms of closed transcendental spaces
24 p3948 N71-38162

Holomorphic fibers in sub-spaces of Stein space
24 p3948 N71-38164

Rings of holomorphic function germs in Banach space
24 p3948 N71-38168

FIBRIN

Photometric continuous recording of fibrinolysis and fibrinolytic
[NASA-TT-F-13405] 01 p0011 N71-10423

FIBROUS MATERIALS

U FIBERS

FICKS EQUATION

Investigating theory for concentration dependent diffusion phenomena based on simple assumption for impurity atom interaction in diffusion systems exhibiting solid solubility saturation
07 p1089 N71-17296

FIDELITY

U ACCURACY

FIELD EFFECT TRANSISTORS

High accuracy sine function generator using digital to analog converters and field effect transistors
02 p0185 N71-11302

Frequency to analog converters with unipolar field effect transistor for determining potential charge by pulse duration of input signal
[NASA-CASE-XNP-07040] 03 p0344 N71-12500

Polarization /charge separation/ in metal oxide semiconductor field effect transistor inverters
03 p0350 N71-12531

Cross modulation in barrier layer field effect transistors
03 p0352 N71-12543

Computer aided analysis model for junction field effect transistor
[SC-DR-70-366] 05 p0653 N71-14884

Gallium arsenide Schottky barrier, field effect transistors
[AD-715282] 07 p0999 N71-17850

Metal oxide silicon field effect transistors for integrated circuitry in data processing
13 p2152 N71-25322

Low neutron flux irradiation effects on MOSFET

13 p2152 N71-23321

MOSFET shift register for data storage

13 p2152 N71-23304

Voltage controlled, variable frequency relaxation oscillator with MOSFET variable current feed
[NASA-CASE-GSC-10922-1] 14 p2331 N71-23002

Low frequency background noise spectra in field effect metal oxide semiconductor transistors using adjustable bandwidth method
16 p2664 N71-28340

Transient measurements of field effect transistors following exposure to pulse of neutrons and observations of transient annealing of drain to source resistance in n- and p-channels
[AD-721743] 16 p2569 N71-28085

Radiation damage to GaAs junction field effect transistor exposed to fast neutron fluence
[AD-723303] 19 p3064 N71-31740

Fault testing of field effect transistor modules
[AD-723442] 19 p3070 N71-31825

Accurate short channel insulated gate field-effect transistor which includes drain depletion effect in triode and saturation regions
[AD-723215] 19 p3066 N71-32310

High energy electron irradiation effects on field effect transistors in integrated circuit devices
[NASA-CR-121623] 21 p3485 N71-34225

X ray spectrometer with cooled Si(Li) detector and field transistor in chamber cryostat
[JINR-P13-5707] 22 p3633 N71-35087

Drain current-drain voltage equations for insulated-gate and junction-gate field effect transistors and drain current sensitivity to piezoelectric and piezoelectric strain effects
23 p3837 N71-37946

Breadboard models of silicon carbide junction field effect transistor amplifiers
[AD-727761] 24 p3899 N71-37702

Computer aided analysis of theoretical and experimental operating characteristics of insulated gate field effect transistors
24 p3999 N71-38524

Silicon junction field effect photometer with responsivities comparable to charge-storage devices
24 p3999 N71-38525

FIELD EMISSION

Measuring dependence of emission power and polarization of helium-neon laser on transverse magnetic field
[AD-712104] 02 p0238 N71-11567

Measuring intermittent enhancement of blinking effect upon addition of neon to imaging gas in helium-tungsten field-ion microscope
[NASA-TN-D-6214] 08 p1259 N71-18628

Radiation emitted when charged particles cross boundary between vacuum and metal
13 p2144 N71-25587

Calculation of ion trajectories and energy distribution in front of field emission tip
[TFP-72] 15 p2483 N71-27746

Field ion and field emission microscopic analysis of nickel tungsten alloy photoluminescent bands
[UCRL-20330] 16 p2613 N71-28752

Surface physics and work function of emission materials
[AD-723555] 18 p3000 N71-31585

Use of differential energy analyzer for field emission electron energy distribution measurements in germanium
19 p3155 N71-32324

Three-dimensional Green function solution for field emission from spherical tip with arbitrary perturbative potentials
22 p3451 N71-34003

FIELD IONIZATION SOURCES

U BRUSHES

FIELD STRENGTH

NT ELECTRIC FIELD STRENGTH

NT MAGNETIC FLUX

Field characteristics of dielectrically loaded parallel-wall waveguides
02 p0184 N71-11294

Electric field strength and helix pitch relationship in induced cholesteric-nematic phase transitions
[R69-14964] 03 p0324 N71-12316

Diurnal variation and tidal dependence of field strength on radio links in German Right
[REPT-13] 04 p0490 N71-13488

Computation of low frequency radio transmitter field strength for underwater communications
04 p0492 N71-13711

Changing field gradients in isochronous ring accelerators using shaped magnets
[EKF-1268] 09 p1445 N71-20540

Tropospheric scattering field strength analysis by synchronously offset radio beacon transmissions
12 p1875 N71-23435

Far-field strength measurements at extremely low frequencies for determining East-West diurnal attenuation rate
[AD-718108] 13 p2042 N71-30483

Predicted and measured power density distribution of large ground microwave systems
[NASA-CR-118524] 13 p2046 N71-29804

SUBJECT INDEX

FIELD THEORY [PHYSICS]

- Method for predicting time availability of VLF field strengths using ionosphere waveguide model
[AD-720318] 15 p2380 N71-27209
- Short term forecasting of signal field strength on tropospheric scattering links involving meteorological parameters
[BEP-9778] 20 p3331 N71-32808
- Automatic magnetic field measurements of bending, quadrupole, and gradient magnets with field strengths up to 50 kG
[KFK-1220] 21 p3464 N71-34656
- FIELD THEORY [ALGEBRA]**
NT CUBIC EQUATIONS
NT QUADRATIC EQUATIONS
Investigating symbolic computations by finite field theory using FORMAC system
08 p1228 N71-19191
- Ambiguities in finite computations of renormalization constants for nonpolynomial Lagrangians in field theory
[IC/70/106] 09 p1431 N71-19895
- Algebraic theory of superselection rules applied to problem of constructing field quantities from local observables
[ITF-70-66-B] 18 p2943 N71-30567
- FIELD THEORY [PHYSICS]**
Integral equations for aperture fields, leading terms in near and far zone fields, admittance, and effective height of circular slot antennas
[SC-R-70-4281] 01 p0835 N71-10794
- Theory and application of Padé technique to sequences of approximations to single variable integrals related to quantum field theory
[AD-711604] 01 p1013 N71-10939
- Perturbation measurements and field computations for nickelium acceleration structure
[AD-712085] 02 p0270 N71-11400
- Covariant quantum geometrodynamics
02 p0274 N71-11857
- Quantum electrodynamic tests in time-like lepton region
[LNF-70/23] 04 p0569 N71-13551
- Extended particle model in general theory of relativity
[JINR-E2-5271] 04 p0588 N71-14294
- Superpropagator of fields with exponential coupling
[DESY-70/26] 04 p0594 N71-14455
- Development of methods for treatment of basic nonlinear partial differential equations of theoretical physics
[AD-714581] 06 p0885 N71-16617
- Applying correlation theory of random fields to wave propagation in media with statistical inhomogeneities
07 p0990 N71-16939
- Expansion of invariant two-point function for bilocal field of Lorentz, Poincaré, and O(4,1)/R(3,2) groups
[JINR-P2-5304] 08 p1248 N71-18203
- Defining super propagator for any mass in field theory with exponential interaction Lagrangian
[DESY-70/30] 08 p1249 N71-18223
- Small-distance behavior in quantum field theory with mass vertex insertion into Lagrangian density
[DESY-70/31] 08 p1253 N71-18329
- Applying normal product quantization to construct energy-momentum tensor of Thirring model as local function of Thirring fields
[NYO-3229-61] 08 p1254 N71-18341
- Measuring variation of transition temperature of superconductor with respect to molecular field solution of Hückel-Wigner transition
[NWB-2020] 08 p1258 N71-18634
- High energy elastic and inelastic hadron-hadron scattering in p-d-coupled theory
[ILL-TR-71-4] 08 p1261 N71-18803
- Iterative expansion technique for solving Green function in model quantum field theory
08 p1265 N71-19182
- Applying Green function theory to calculation of longitudinal and transverse dielectric functions in metal, isotropic, equilibrium plasma
08 p1275 N71-19249
- Consistency and high energy theorems in stochastic field theory associated with currents and total scattering cross sections
09 p1408 N71-19517
- Configuration space in relativistic three body problem using quantum field theory
[JINR-P2-5101] 09 p1409 N71-19995
- Relativistic analog of Padé equations for scattering amplitudes, using three dimensional formulation of quantum field theory
[JINR-P2-5099] 09 p1410 N71-20001
- Dispersion potential for calculating particle transport coefficients in flow field analyses
[IC-RR-70-644] 09 p1435 N71-20035
- Nonfactorizable expression for asymptotic multiplicity amplitude signature with Toller angle variable
[LLO-1380-591] 09 p1435 N71-20037
- Two dimensional models for scale invariance and anomalous behavior in quantum field theory
[NYO-3229-56] 09 p1436 N71-20039

- Investigating tachyons within framework of quantum field theory
[TSEP-70-31] 09 p1436 N71-20072
- Equivalence theorem and quantum mechanics in field theory
[JINR-P2-5266] 09 p1411 N71-20381
- Development of one-electron pseudo-Green function and pseudopotential of d-band metals
[ML-1930] 09 p1454 N71-20499
- Necessity of Schwinger terms in ground state Poisson brackets for classical boson currents containing terms linear in canonized variable
[LLO-1380-584] 10 p1610 N71-20648
- High energy interactions, quantum mechanics, and field theory
[NYO-3229-64] 10 p1614 N71-20903
- Formulating bootstraps in terms of vanishing renormalization constants for local field theory applications
[NYO-2171-331] 10 p1614 N71-20933
- Fourth-order gravitational potential based on quantum field theory
[RIFP-114] 10 p1549 N71-21097
- Calculation of lower critical fields and comparison with measured values for some niobium-titanium alloys
[NASA-CR-117493] 10 p1583 N71-21595
- Classical cross sections of electromagnetic and gravitational waves scattered by static gravitational field, and agreement with quantized linearized field theory
[NYO-2262-TA-222] 11 p1806 N71-22462
- Development of Machian theory of inertia and gravitation
12 p1912 N71-23496
- Isoscalar couplings in electromagnetic interactions
12 p1978 N71-24255
- Quantum Bianchi identities and field equations derived from Lagrangians for general relativity
[AD-718957] 13 p2128 N71-24365
- Finite theory of quantum electrodynamics, including modified photon and fermion fields and Feynman diagrams
[NYO-1932/2-183] 13 p2139 N71-25493
- Quantum electrodynamics and field theories with bounded and temperate interaction examples without divergences
[TJPU-13/70] 14 p2308 N71-26445
- Dependence of potential describing average nuclear field on excitation energy
[JINR-P4-5084] 15 p2457 N71-26855
- Conditions for equality of local algebras of relativistic quantum field theory
[JINR-P2-5330] 15 p2460 N71-27072
- Transformation of infinite component field with mass spectrum over nonunitary symmetry group representation
[JINR-P2-5305] 15 p2461 N71-27082
- Smooth quasipotential in eldron quantum field theory models
[JINR-P2-5365] 15 p2471 N71-27416
- Quantization of interacting covariant massless fields using Lagrangian formalism with prescribed asymptotic null data
15 p2476 N71-27472
- Lambda phi cubed interaction with boson fields using nuclear models
[NP-18549] 15 p2488 N71-27874
- Relativistic formalism for quarks in field vector interactions including Padé approximation and high order perturbation
[IFPHT-10/70] 15 p2489 N71-27881
- Chiral dynamics of vector meson field coupling and tree approximations of scattering amplitudes in Veneziano models
[DEMO-71/1] 15 p2489 N71-27882
- Relating existence of ghost with zero mass in quantization of vector field coupled to Dirac current
[PAM-70-3] 15 p2490 N71-27896
- Two nucleon potentials and nuclear saturation near empirical energy and density dependent on strong tensor force
15 p2492 N71-27923
- Nonlocal quantum field research reports from international conference
[JINR-E2-5563] 16 p2643 N71-28050
- Spectroscopic trajectory analysis in many body inverse square force field based on Kepler laws and Ecker method without numerical integration
[RE-407] 16 p2677 N71-28090
- Research on field theory using nuclear models, and interaction or deuteron with pions
[COO-1810-7] 17 p2791 N71-29291
- Survey of concepts and theorems of causality processes and indefinite metric in quantum field theory
[NYO-3229-58] 17 p2787 N71-29513
- Particle superpropagator regularizing properties under various gravitational field interactions
[JINR-P2-5569] 17 p2793 N71-29712
- Nonlinear integration of Lawden intermediate thrust area and their optimality in Newtonian central force field
[NASA-TT-F-13748] 17 p2774 N71-30131
- Magnetic resonance in dilute magnetic alloys - hydrodynamic relation of Ag-Er-167
[AD-722711] 17 p2825 N71-30279

- Electrodynamics and boundary value problems in null plane field theory based on classical and quantum mechanics
17 p2888 N71-30354
- Tree graphs in Yang-Mills field theory
[JINR-P2-5616] 17 p2889 N71-30383
- Fourier transformation calculation and validation of sum rules and Ward identities using equal-time commutator in axiomatic quantum field theory
[ITF-70-57] 18 p2967 N71-30412
- Review of recent results in quantum field theory, perturbation theory, and axiomatic quantum field theory
[ITF-70-107-E] 18 p2961 N71-30415
- Infinite order differential equation for calculating supercriticality in nonlinear quantum field theories
[JINR-P2-5657] 18 p2942 N71-30471
- Edmon representation of scattering amplitudes from high energy interactions in field theory nuclear models
[JINR-P2-5577] 18 p2976 N71-30622
- Global and local structure of relativistic quantum systems with superselection rules
[JINR-E2-5575] 19 p3154 N71-32291
- Formulation of local infinite component fields as explicit realizations of wave functions with mass-spin relations
19 p3158 N71-32544
- Nonlinear semigroup theory applied to quantum field equations in two dimensional space-time
20 p2590 N71-33111
- Field theory approach to phase transformations, using renormalization groups, correlation functions, and scaling laws
20 p3310 N71-33188
- Field theory in infinite momentum frame for deriving parton model, with transverse Galilean and longitudinal Lorentz boost invariances stressed
[LPTHE-71/24] 20 p3293 N71-33958
- Newman-Penrose constants and their invariant transformations
21 p3449 N71-34552
- Three dimensional formulation of quantum field theory based on relativistic Padé equations and applied to three body problems
[JINR-P2-5661] 21 p3468 N71-34688
- Modified scalar field equation and closed world with field sources, including Penrose equation static solution
[JINR-P2-5738] 21 p3470 N71-34705
- Method for computing scattering matrix elements in class of nonrenormalizable field theories with coupling in exponential form
[NYO-1932/2-192] 21 p3476 N71-34754
- Numerical methods for variable permeability magnetostatic field problems - difference equations solved iteratively
22 p3650 N71-35865
- Quantum field theory with non-elliptic space of relative momenta
[JINR-P2-5691] 22 p3633 N71-35892
- Generation of particles in classical relativistic mechanics
[NASA-TT-F-13736] 22 p3634 N71-35901
- Application of algebraic realizations to pion-meson couplings in chiral dynamics and Yang-Mills field theory
[JINR-P2-5759] 22 p3640 N71-35950
- Indefinite metric spaces and shadow states in relativistic quantum field theory
[ORO-3992-30] 22 p3647 N71-36004
- Three-dimensional Green function solution for field omission from spherical tip with arbitrary perturbative potentials
22 p3651 N71-36033
- Functional equation for self coupled relativistic scalar field
23 p3782 N71-36955
- Exact solution for equations of relativity in the case of conformally-plate field of asymptotic axial symmetry
[ITF-69-41] 23 p3783 N71-36966
- Partial elimination of infrared divergences in scalar charged field model with self-action in two-dimensional space-time and degenerated vacuum
[JINR-P2-5768] 23 p3807 N71-37142
- Low energy limit of dual resonance models and connection between Yang-Mills field theory
[LPTHE-71/37] 23 p3812 N71-37183
- Analyticity, covariance, and unitarity in quantum field theories regularized by finite mass, indefinite norm states
[ORO-3992-36] 23 p3814 N71-37202
- Logic of relativistic quantum mechanics and non-relativistic quantum field theory
[ITF-70-41-B] 23 p3815 N71-37208
- Atomic vector current relation associated with pseudoscalar meson and sigma model formalisms
[TR-72-019] 23 p3819 N71-37241
- Cluster decomposition techniques for analyzing hadronic perturbation theory amplitudes at high energy
[ILL-(TH)-71-10] 23 p3820 N71-37251
- Graviton fusion interaction described by Lagrangian function of tetrad field and fermion field
23 p3823 N71-37268

FIGHTER AIRCRAFT

Piecewise analytic scattering amplitude in indefinite metric quantum field theory
[ORO-3992-52] 24 p3978 N71-38384

Limiting transition to zero mass and renormalizability in massive Yang-Mills field theory
[NP-18859] 24 p3979 N71-38391

Field-current identity formalism for stress tensor with scale invariance and scale breaking condition of meson couplings to stress tensor
[NUB-2097] 24 p3982 N71-38417

Crossed field instabilities and turbulent ion heating calculated in mirror machine
[CONF-716607-67] 24 p3988 N71-38458

FIGHTER AIRCRAFT
NT F-2 AIRCRAFT
NT F-4 AIRCRAFT
NT F-8 AIRCRAFT
NT F-104 AIRCRAFT
NT F-106 AIRCRAFT
NT F-111 AIRCRAFT
NT JAGUAR AIRCRAFT
NT VJ-101 AIRCRAFT

Fighter aircraft design with consideration to armament, detection capability, thrust, speed, and load factor performance tradeoffs
[AD-710497] 01 p0002 N71-10183

Dynamic stability derivatives of twin-jet fighter model for angles of attack from -10 deg to 110 deg
[NASA-TN-D-6091] 05 p0629 N71-14634

Simulation of aerial combat
[RAE-LIB-TRANS-1367] 05 p0787 N71-15372

Transonic and supersonic dynamic stability characteristics of variable sweep wing tactical fighter aircraft
[NASA-TM-X-21653] 07 p0971 N71-17425

Feasibility of using fixed simulator to determine stall and spin characteristics of fighter aircraft
[NASA-TN-D-6117] 09 p1324 N71-20292

Kalman linear least squares filtering applied to estimation of fuel quantity and rate for fighter aircraft
[AD-717468] 11 p1672 N71-21922

Static force tests of model of twin jet fighter aircraft at various angles of attack and sideslip angles to obtain data for theoretical spin studies
[NASA-TN-D-6425] 18 p2873 N71-31330

Inflight simulation with high wing loading fighter aircraft approach using FHB-320 and Faggio aircraft
[DLR-FB-71-46] 19 p3072 N71-31789

Maintenance, management planning, and requirements for single seat attack fighter aircraft
[AD-723227] 19 p3036 N71-31805

wind tunnel performance characteristics of single-engine fighter model fitted with in-flight thrust reverser
[NASA-TN-D-6460] 23 p3940 N71-37384

FILAMENT WINDING
Tool attachment for spreading or moving away loose elements from terminal posts during winding of filamentary elements
[NASA-CASE-XMF-02107] 01 p0060 N71-10809

Fracture strength of glass fiber wound plastics
[AD-713063] 03 p0397 N71-13062

Fabrication of filament wound propellant tank for cryogenic storage
[NASA-CASE-XLE-03803-2] 07 p1035 N71-17651

Computer program for design and analysis of composite filament wound, axisymmetric pressure vessels considering orthotropic construction of vessel
[NASA-CR-118469] 14 p2350 N71-26368

Development and testing of carbon/carbon composite fabricated by chemical vapor infiltration of filament-wound substrate
[SC-DC-70-5369] 17 p2768 N71-29265

Flight test of chemical vapor deposited felt and filament wound carbon composite heat shields
[SC-DC-71-3853] 17 p2769 N71-29516

Mechanical properties of advanced filament wound carbon composites
[SC-DR-710192] 19 p3120 N71-32216

Torsional shear strength and stiffness of filament wound, glass epoxy tubes, with helical or alternating helical and circumferential windings
[NASA-TN-D-6140] 19 p3189 N71-32324

Filament tensile strengths and pressure-strain characteristics of high modulus, high-strength, boron-filament-wound/resin-composite pressure vessel at ambient and cryogenic temperatures
[NASA-CR-72879] 24 p3928 N71-38023

FILAMENT WOUND CONSTRUCTION
U FILAMENT WINDING

FILAMENTS
Stress concentrations in filament-stiffened sheets of finite length
[NASA-TN-D-5947] 01 p0128 N71-10438

Literature survey on low gravity manufacturing methods for boron filaments in space laboratory
[NASA-CR-117429] 02 p0234 N71-11705

Filament effects on Q switched glass laser fatigue
[AD-70355] 04 p0355 N71-14331

Development and fabrication of filament composite nondestructive test standards
[NASA-CR-103011] 06 p0881 N71-16595

Manufacturing process for large diameter carbon base monofilaments by chemical vapor deposition
[NASA-CR-72770] 07 p1034 N71-17328

Large diameter graphite/carbon composite monofilaments produced by pyrolysis
[NASA-CR-72769] 06 p1222 N71-18748

Measurement of heat transfer properties of polymer filaments after melt spinning
10 p1564 N71-21176

Measurement of elastic modulus and tensile strength of fine filaments and whiskers using marsh machine
[AD-720571] 14 p2278 N71-26139

FILERS
Computer program for linked file information retrieval including semantics, syntax, and outline of search program
14 p2221 N71-25978

FILLERS
Effect of lubricants with fillers on wear of diamond instrument during cold drawing of wire
[AD-716523] 09 p1405 N71-19823

Infrared spectroscopic study of amorphous elastomer reinforcement by polymeric fillers
18 p2887 N71-31233

Fracture toughness of filled polymers measured using double edge notched tensile bars
23 p3780 N71-36940

FILLETS
Methods for fillet welding in vertical position with manual electrodes
[PB-197944] 18 p2928 N71-30858

Utilization of penetration obtained with automatic submerged arc welding for fillet welds
[PB-197945] 18 p2928 N71-30859

FILLING
Hardware and fluid parameter effects on filling characteristics of manifolds in vacuum, for liquid propellant rocket engines
[AD-712063] 02 p0291 N71-12159

FILM BOILING
Film boiling on vertical surfaces in turbulent regime using cryogenic fluids
[NASA-CR-110997] 01 p0132 N71-10064

Film vaporizing combustor for gas turbines
[NASA-TT-F-13272] 01 p0115 N71-16282

Stability analysis of laminar to turbulent flow transition during film boiling from vertical flat plate
10 p1542 N71-21282

Benzene evaporation rate determined from flat plate film boiling under high temperature air flow with application to gas turbine air pollution reduction
[DLR-FB-70-58] 11 p1840 N71-22072

Analysis of film boiling data for water droplets vaporizing into air, argon, nitrogen, helium, and steam
[NASA-TM-X-67808] 11 p1845 N71-23100

Heat transfer to difluoromethane and monochloromethane refrigerants at nucleate boiling, film boiling, and supercritical condition of fluid
[BMW-FBK-70-24] 15 p2524 N71-27163

Film boiling and heat transfer from platinum wire in saturated liquid nitrogen up to critical pressure
[NASA-TM-X-67849] 15 p2525 N71-27863

Buoyancy effect on cryogenic hydrogen film boiling during upward and downward flows
[NASA-TM-X-67855] 15 p2525 N71-27866

Forced flow heat transfer coefficients for laminar film boiling interface on vertical surface
[NASA-TM-X-67860] 15 p2525 N71-27867

Turbulent film boiling tests of heated flat plate model in high speed water tunnel
17 p2733 N71-29619

Transient film growth during initial 10 milliseconds of transient film boiling in horizontal annulus filled with saturated liquid
18 p3025 N71-31362

Stagnation-point free-convection film boiling approximate solutions for Freon and water on hemispherical shells at atmospheric pressure
[P-4543] 19 p3191 N71-32510

Comparison of experimental and analytic film boiling heat transfer data for spheres immersed in liquid nitrogen at standard and reduced gravity
[NASA-TM-X-2344] 20 p3364 N71-33394

Liquid or solid spheres levitated in film boiling following metastable Leidenfrost states
20 p3313 N71-33697

Inter-relationship between high frequency oscillations and nature of nucleate and film heat transfer with forced fluid flow
[NLL-CE-TRANS-5621-19022.09] 22 p3570 N71-35426

FILM CONDENSATION
Cryogenic heat pipe measurements of film condensation heat transfer coefficients
[CEA-CONF-1634] 08 p1302 N71-18157

Film condensation and heat transfer of low pressure metal vapor on flat surfaces
[NASA-CR-117429] 10 p1661 N71-20860

Condensation and evaporation coefficients for liquid metal vapors and relation to heat and mass transfer rates
[COO-2032-6] 11 p1780 N71-22661

FILM COOLING
Integral analysis of heat transfer downstream of rearward-facing step with small coolant injection
[NASA-TN-D-5970] 03 p0468 N71-13036

SUBJECT INDEX

Velocity distributions and heat transfer with film cooling near single angled sparwise continuous injection slot
05 p0785 N71-15611

Effect of gaseous film cooling on recovery temperature distribution in rocket nozzles
06 p0900 N71-16878

Performance prediction for turbine blade film cooling with injection through holes
[NASA-CR-116376] 07 p1101 N71-17388

Film cooling of gas turbine blades by air injection through holes
07 p1009 N71-17394

Effective heat transfer coefficients in film cooling systems of gas turbine surfaces
07 p1129 N71-17395

Technological aspects of film cooling for blades in high temperature gas turbines
07 p1130 N71-17406

Heat transfer characteristics of film cooled plug nozzle with transal flow
[NASA-TN-D-6160] 07 p1102 N71-17506

Multilayer film cooled pyrolytic graphite rocket nozzle
[NASA-CASE-XNP-04389] 10 p1639 N71-28942

Short duration shock tunnel and light plane tunnel for gas turbine blade film cooling and transition cooling
[REPT-112170] 11 p1730 N71-22095

Finite difference calculation based on eddy diffusivity and mixing length flow theory to characterize supersonic turbulent boundary layer with tangential slot injection
[NASA-TN-D-62211] 11 p1670 N71-22560

Conference on high temperature turbines detailing effect of film cooling on blade profile loss
[NASA-TM-X-67123] 11 p1821 N71-22669

Gas film cooling test nonadiabatic flat plate
12 p2014 N71-24366

Injector performance, heat flux, and film cooling in hydrogen oxygen engines
17 p2837 N71-28998

Gas turbine combustor liner film cooling for hot geometries in presence of high free stream turbulence
[NASA-TN-D-63460] 17 p2858 N71-28846

Thermodynamic characteristics and mutual interaction of film cooling with coolant gas injection into supersonic stream
[IC-AERO-71-47] 17 p2859 N71-36836

FILM THICKNESS
Resonance integral of natural zirconium calculated for rods of varying diameter and Trips fuel elements using different resonance parameters
[TKK-P-A-106] 04 p0550 N71-13811

Investigating techniques for producing silicon epitaxial layers with uniform thickness, resistivity control, and high surface quality
07 p1088 N71-17281

Growing submicron single and multiple epitaxial silicon layers deposited by silane pyrolysis method
07 p1088 N71-17281

Evaluating measurement methods for epitaxially grown layers with respect to thickness and constant phase shift
07 p1090 N71-17299

Measuring thickness of semiconductor epitaxial layer deposited on substrate of same conductivity using infrared reflectance method
07 p1090 N71-17299

Deriving film thickness equations for laminar and turbulent incompressible flows in recessed circular hydrostatic thrust bearings
06 p1208 N71-19081

Helium 2 film transfer rate dependent on pressure head, film height, and substrate for filling clean glass and non-coated beakers
[COO-1574-17] 12 p1869 N71-23130

Film growth and thickness of lead tin selenide epitaxial films
[AD-718323] 12 p1984 N71-23287

Thickness measurement method for water film formed on high speed and determination of conditions for expansion of film by action of time
[NASA-TT-F-13603] 12 p1984 N71-24102

Rheological models for evaluating effects of lubricant film thickness and frictional traction
15 p2413 N71-26813

Axodic oxide coating thickness effect on fracture of aluminum single crystals and polycrystals
[ORO-3401-16] 15 p2306 N71-27981

Film thickness of dip-coated layers
16 p2617 N71-28261

Film thickness profile and traction in elastohydrodynamic lubrication of point contacts in pure sliding modes
18 p2929 N71-31086

Elastohydrodynamic film thickness between rolling disks with synthetic paraffinic oil at temperatures from 339 to 589 K
[NASA-TN-D-6411] 18 p2930 N71-31228

Stopping cross section dependence on carbon foil thickness and scattering angle
[GPR-41] 23 p3815 N71-37085

SUBJECT INDEX

- FLMS**
Vapor-ion methods of film deposition - annotated bibliography (RFP-1566) 11 p1769 N71-22531
Effects of thermodynamic fluctuations in superconductive films in perpendicular magnetic field just above transition point 13 p2153 N71-25502
Influence of surface films on plastic deformation of zinc single crystals during sliding (NASA-TN-D-4366) 16 p2599 N71-28037
Effects of wind stress and wind generated wave action on set-up of various density and viscosity cells (PB-198113) 17 p3741 N71-39753
Rotating radiation-resistant film target for nuclear particle beams (JINR-E13-5621) 18 p2979 N71-30700
Mass transfer and hydrodynamic behavior of laminar liquid films flowing over solid surfaces 23 p3746 N71-36710
- FILTRATION**
U FILTRATION
U FILTERS
Procedure for extinguishing fires in activated carbon absorbers used in air cleaning (JNCR-72496) 04 p0517 N71-14499
Solutions to optimal filtering problem in nuclear spectroscopy (LYCEN-7008) 08 p1199 N71-18289
Matched filters for optimal high speed detection of binary signals 11 p1725 N71-22776
Development of filter system for control of outgas contamination in vacuum conditions using absorbent beds of molecular sieve zeolite, silica gel, and charcoal (NASA-CASE-MPS-14711) 14 p2662 N71-26183
Heated tungsten filter for removing oxygen impurities from calcium 14 p2276 N71-26773
Performance and life of used HEPA filters under various operating conditions 17 p2756 N71-29877
Single crystal bismuth and silicon filters for thermal neutrons (JUV-3468-F) 17 p2809 N71-30375
Analytic method for measuring mean proton energy using Vavilov-Cherenkov radiation and interference filters (JINR-P13-5636) 19 p3147 N71-32044
Efficiency as function of particle size and velocity for commercial filter media (LA-4638) 24 p3881 N71-37663
Nonlinear behavior of second order phase locked loop with lead lag filter 24 p3902 N71-37813
- FILTRATION**
NT SPATIAL FILTERING
Aerosol filtration by electrified fibrous filter mats (UCLRL-72496) 04 p0509 N71-13515
Aerosol filtration by electret filters (HEFT-1970-17) 04 p0509 N71-13519
Mechanical filtration, electrostatic collection, and total gamma ray measurements of St. Laurent 1 reactor (CRA-N-1356) 04 p0550 N71-13797
Aerosol behavior and filtration in high pressure environments 11 p1687 N71-22255
Packed bed interparticle porosity calculation from flowing aerosol breakthrough distribution moments 17 p2797 N71-29064
Presentation of algorithm for filtration of mixing parameters for navigation 20 p3290 N71-32948
Laser beam filtration by saturable dyes (UCLRL-51008) 20 p3282 N71-33538
Scandium, iron, and silicon filtered neutron beam source and neutron cross section measurements for use with breeder reactors (CONR-710301-8) 20 p3321 N71-33733
WATER FILTERS
U FILTS
U STABILIZERS (FLUID DYNAMICS)
- FINANCE**
Engineering, finance, and personnel management methods and computer techniques for cost reduction and reliability in project planning (NASA-SP-5933/01/1) 18 p3031 N71-31516
Electronic execution of financial transactions and security for anti-fraud controls 19 p3193 N71-31645
FINANCIAL MANAGEMENT
International financial assistance for scientific and technological transfers to developing nations 13 p2190 N71-24760
Information retrieval and selective dissemination of information in technology transfer and financial planning of research and development 14 p2222 N71-25989
Distribution of funds for federal academic science support and scientific activities conducted with alien-owned funds (NSF-71-7) 17 p3862 N71-30276

Remarks by chairman of Civil Aeronautics Board to conference of airline finance managers 18 p2868 N71-30517

Cost sensitivity analysis technique applied to developing annual operating costs for ground sensor systems (P-4361) 21 p3408 N71-34248

FINE STRUCTURE

Alpha cluster structure of lithium 6 and lithium 7 with alpha/2 alpha reaction (NIP-18232) 03 p0430 N71-12902
Deriving expressions for Auger transition rates for f electrons (SC-BK-70-429) 04 p0575 N71-13686
Deriving analytical expressions for calculating phase space contour and area of quadrupole triplets from matrix elements (CERN-70-22) 04 p0588 N71-14279
Investigating possibility of octet of 0/ scalar mesons and none of 1/ axial vector mesons forming 35-plet SU(6) supermultiplet (SINP-TN-67-1) 05 p0739 N71-15029
AZ/NOBET - CONSISTENCY OF DATA (UCLRL-19665) 05 p0741 N71-15119
Quantum electrodynamics theory and relation to precision low energy experiments (SLAC-PUB-795) 06 p0919 N71-16246
Atomic energy level and multiplet tables for carbon-II through carbon-VII (NSRDS-NBS-3) 07 p1076 N71-17530
Fine structure, hyperfine weights, and reactivity weights in fuel cluster (RD/B/N-1724) 08 p1236 N71-18221
Magnetic field fine structure in individual supergrasses 09 p1422 N71-19498
X ray diffraction analysis of structure of single crystals produced by zone recrystallization 10 p1633 N71-20084
Fine structure of superconducting Zr-Ni alloy during plastic deformation and annealing (NLL-CE-TRANS-5329-5922.09) 10 p1579 N71-21262

X ray photographic analysis of plasma focus fine structure (LA-TN-70-25) 10 p1630 N71-21377
Using general factorization and superadditive threshold properties of multiperipheral models to demonstrate existence of damped oscillatory components for total cross sections (NYO-2262-TA-228) 11 p1802 N71-22009
Fine structure of ground state levels of first four neighbor exchange coupled Cr³⁺ pairs in ruby 13 p2135 N71-25178
Algebraic realization of unitary symmetry with sum rules derived for well established supermultiplets providing predictions for none with some established members (JINR-E2-5229) 14 p2508 N71-26545
Phenomenological relationship between fine structure constant and leptonic and gravitational processes - universal scaling factor (UCLRL-72955) 16 p2646 N71-28211
Low and high field level crossing experiments in 2P state of atomic hydrogen and measurement of Sommerfeld fine structure constant 16 p2657 N71-29124
Fine structure measurement of singly ionized helium, a equals 4 20 p3328 N71-33976
High resolution H-alpha photographs for studying chromospheric fine structure at active region polarity boundaries (NASA-CR-121619) 21 p3503 N71-34955
Test of supermultiplet model for light nuclei (LYCEN-7008) 22 p3640 N71-35945
Tables on atomic energy levels and multiplets of four alkali spectra (NSRDS-NBS-3-SECT-4) 22 p3631 N71-36039
Fine structure of facular fields at different levels of solar atmosphere based on escalation method (NLL-RTS-6412) 23 p3842 N71-37398
Structure and classification scheme of hadron excited states (ITP-70-102-E) 24 p3970 N71-38321
X ray method for observing plasma fine structure during data pinch (AD-727873) 24 p3995 N71-38501

FINE
Electron and ion microprobe analyses of Apollo 12 fines and breccias (NASA-CR-114671) 08 p1289 N71-18878
Quantitative microfluorescence analysis of lunar phases and fines (NASA-CR-114966) 13 p2146 N71-24944
Development of industrial processes for separation of fine particles (NLL-CE-TRANS-5364-5922.09) 23 p3764 N71-36838

FINGERS
Histopathology and clinical study of chronic X ray dermatitis and cancer of fingers (NASA-TT-F13664) 16 p2548 N71-29200

FINITE DIFFERENCE THEORY

Computer-aided system for automated, high speed identification of human fingerprints 19 p3060 N71-31647

FINISHES

NT ENAMELS

NT GLAZES

NT LAQUERS

Quantitative surface finish characterization by computer evaluation of scanning electron microscope images (AD-719925) 14 p2359 N71-23624

FINITE DIFFERENCE THEORY

Numerical method for solving general MHD flow problems 01 p0875 N71-10464

Relativistic evaluation of propellant behavior with nonlinear viscoelasticity and cumulative damage (AD-710776) 01 p0113 N71-10552
Development of general finite difference approximation for general domains 02 p0250 N71-11172

Finite difference solution of first order boundary layer equations 03 p0360 N71-12584
Applying finite difference method to solution of numerical stability in linear algebra problems (ORO-3443-28) 04 p0539 N71-14308
Finite difference scheme for calculating problems in three space dimensions and time (UCLRL-72634) 05 p0733 N71-15233

Computer program for finite difference solutions of shells of revolution under asymmetric dynamic loading (NASA-TN-D-6059) 05 p0780 N71-15569
Finite difference solution to mixed boundary value problem for Laplace equation (NASA-CR-116225) 06 p0885 N71-16497
Finite difference equation for calculating motion equations of three dimensional boundary layers (SC-T-70-4038) 06 p0839 N71-16789
Finite difference methods of numerical integration in celestial mechanics 07 p1111 N71-17673

Lumped mass finite difference analysis for loaded structural beam dynamics (AD-715112) 07 p1126 N71-17886

Computer code SKYFUS for solving few-group neutron diffusion equations in two dimensions using finite difference method - users manual (KFKI-70-13-RPT) 08 p1236 N71-18237

Method for controlling instability in finite difference computations of liquid saturation near borehole of recovery well (BM-R1-7487) 08 p1192 N71-18970
Finite difference scheme of unsteady flow in open channels (PB-198159) 09 p1369 N71-19408
Method of finite differences used for supercavitating nozzle design (AD-716026) 09 p1316 N71-19709
Finite difference general solution to problem of one and two dimensional melting of solids (AD-716021) 09 p1482 N71-19947

Crank-Nicolson finite difference method for TEPLIO, heat conduction code, for thermal explosion studies in laminar composites (LA-4511) 10 p1659 N71-20506

Nonphysical modifications to oscillations, fluctuations, and collisions due to space-time differencing in uniform and infinite or periodic plasma (UCLRL-72635) 10 p1626 N71-20670

Finite difference method for solving equations for compressible turbulent boundary layers on swept infinite cylinders (NASA-TN-D-6203) 10 p1539 N71-20709

Finite difference method for unified solutions to inviscid supersonic flow distribution about blunt bodies 10 p1540 N71-21114

Finite difference model and computer program for predicting large deflection elastoplastic response of thin structures (AD-717005) 10 p1655 N71-21192

Comparison of computed and measured geostrophic wind data for upper troposphere and lower stratosphere in Texas-New Mexico area (AD-717268) 11 p1788 N71-21899

Finite difference calculation based on eddy diffusivity and mixing length flow theory to characterize supersonic turbulent boundary layer with tangential slot injection (NASA-TN-D-6221) 11 p1670 N71-22349

Comparison of artificial viscosity methods for blunt body flow field analysis including thermal radiation effects based on numerical integration of unsteady flow finite difference equations 11 p1742 N71-22700

Finite difference approximation of vorticity transport equations applied to laminar flow with spatially periodic disturbances (AD-718308) 12 p1901 N71-23683

Finite difference method for calculating sonic boom overpressure signatures in vicinity of canards (AD-718335) 12 p1949 N71-23738

Finite difference techniques peculiar to solution of Boltzmann transport equation in two dimensional spherical geometry - FORTRAN program [LA-4567] 12 p1980 N71-24347

Two-dimensional reactor lifetime program with local and spectrum dependent depletion for IBM 360 computer based on spatial modal expansion and finite difference theory 13 p2118 N71-24924 [EUK-4539]

Numerical solutions for two dimensional nonequidistant inviscid compressible nozzle flows using difference schemes 13 p2067 N71-25416 [NAL-TR-205]

Finite difference solution for unsteady equations of impulsively-starting incompressible jet flow [EF/TN/A/28] 13 p2068 N71-25443

Finite difference equations for TRANZIT program for multigroup time dependent transport in $r/\theta, z/\theta$ cylindrical geometry 13 p2138 N71-25481 [LA-4575]

Finite difference method for calculating inviscid flow field around supersonic/hypersonic space shuttle 14 p2240 N71-26056

Finite rate dissociation and recombinations for supersonic, two dimensional, laminar flow 14 p2241 N71-26274

Finite difference theory using time and space step calculations for transient two-phase compressible flow in pressurized water reactors 15 p2392 N71-26882 [AAEC/TM-558]

Determination of electromagnetic field behavior of cavity resonators using finite difference theory [LNF-70/17] 15 p2454 N71-27374

Finite difference integration of dynamic Lagrangian equations for impact shock wave profiles in aluminum alloys 15 p2424 N71-27467 [AD-720716]

Applications of finite difference methods to subsonic, axisymmetric, and plane flow - [ARL/A-326] 15 p2394 N71-27601

SNAP - computer program for solving finite difference form of group diffusion equations in two dimensions 15 p2493 N71-27944 [TRG-1990]

Finite difference theory applied to seismic wave propagation equations 16 p2585 N71-28208 [AD-722067]

Mass transfer from a single sphere in Stokes flow using explicit finite difference method [DLR-FB-70-73] 17 p2732 N71-29394

Error estimating technique for experimental data based on finite difference theory and standard deviations [AECL-3781] 17 p2772 N71-29448

Comparison of finite element and finite difference methods for simple sloshing problem [TR-1] 17 p2774 N71-30187

Improved multilocal finite difference variant with combined ordinary modified and conventional multilocal schemes for bending analysis of arbitrary cylindrical shells [UNICIV-R-63] 17 p2855 N71-30316

Solving Volterra integral equations modelled after finite difference methods for ordinary differential equations 17 p2775 N71-30374 [TR-38]

Finite and gauge-invariant computation of electron self-charge and self-mass in quantum version of curved space and time [IC/71/3] 18 p2972 N71-30535

Hypersonic and supersonic angle of attack flow about asymmetric and axisymmetric blunt bodies based on time dependent finite difference theory and method of characteristics [NASA-TN-D-6283] 18 p2906 N71-31207

Finite difference method for solving compressible three dimensional boundary layer flow equations of elliptical cones [AD-723280] 19 p3077 N71-31896

Systematic iterative procedure yielding finite difference solutions to steady free boundary problems in plasma physics and fluid dynamics 19 p3123 N71-32269

Finite difference techniques for compactness of function elements in L sub p spaces [SC-RR-70-52] 19 p3124 N71-32467

Finite integral method of solving elliptic differential equations for steady Couette flows in two dimensional domains [EF/TN/A/33] 20 p3250 N71-33332

Finite difference formulation for differential expressions involving both first and second derivatives in problems involving transport by simultaneous convection and diffusion [EF-TN-A-38] 20 p3292 N71-33534

Two finite difference procedures for computation of steady, three dimensional boundary layers in ducts [EF/TN/A/40] 20 p3251 N71-33581

Comparison of finite element and finite difference methods in plane stress and axially symmetric elastostatic problems 20 p3292 N71-33676

Rayleigh wave calculations using TENSOR code and finite difference theory [UCRL-50992] 20 p3328 N71-33962

Power series expansion and finite difference techniques for solving unsteady laminar boundary layer problems 21 p3412 N71-34280 [TP-941]

Application of finite difference variant method for bending analysis of various cylindrical shells [UNICIV-R-58] 21 p3528 N71-35137

Finite difference method for two dimensional and three dimensional viscous flow problems with applications to hypersonic leading edge equation 22 p3549 N71-35420 [AD-726547]

Second order accurate difference method for systems of first order hyperbolic differential equations with cumulative error and convergence shown for elastic beam flexural wave propagation [AD-726549] 22 p3608 N71-35695

Elastic/perfectly plastic torsion analysis of doubly-connected cylinders using finite difference theory 22 p3691 N71-36325

Second-order-accurate shock fitting and finite difference techniques for solution of coupled chemical and vibrational relaxation in air with radiative transfer of molecular bands [SC-RR-710203] 23 p3743 N71-36689

Numerical scheme for solution of general turbulent tube flow problem with surface mass transfer and nonequilibrium chemical reactions 23 p3746 N71-36711

Direct solution to finite difference approximation of Poisson equations on irregular regions [LA-4553] 23 p3782 N71-36952

Finite difference method for calculating spherically symmetric nonlinear acoustic flows in unbounded ideal gas [AD-727012] 23 p3803 N71-37118

Computer program for solving 2-dimensional transient or steady state heat flow problems by creating electrical analogy of problem and solving by finite difference method [NASA-CR-72916] 24 p3892 N71-37734

Finite difference method for testing optimum design of disks and shells subjected to pressure and inertial forces 24 p4027 N71-38738

FINITE ELEMENT METHOD

Computer program for harmonic analysis of curved folded plate structures using finite element method [PB-193535] 01 p0131 N71-10885

Finite element analysis of K-shaped tubular joints [PB-193560] 01 p0131 N71-10944

Finite element analysis of alternating axial loading of elastic plate pressed between two rectangular blocks with finite friction [REPT-110770] 02 p0300 N71-11945

Application of Ritz method to thin elastic shell analysis [AD-711962] 02 p0301 N71-12023

Finite element method applied to notched specimens under tension with plastic deformation [SKB-2/M-13] 02 p0302 N71-12052

Finite element method for obtaining approximate three-dimensional stress solutions for laminated plates [AD-711999] 02 p0249 N71-12176

Finite element method for elliptic differential equations [ORO-3443-25] 03 p0399 N71-12816

Finite element method for dynamic structural analysis in vertical takeoff aircraft design 03 p0464 N71-13334

Man machine system for finite element structural analysis with computer graphics 03 p0465 N71-13140

Finite element method for solving differential equations in boundary value problems of plastic flow in rod metal drawing [REPT-12] 03 p0466 N71-13346

Constructing algorithms for majority logic decoding for linear block codes [AD-712683] 04 p0500 N71-13495

Investigating buckling behavior of flanges of horizontally curved plate girders using finite element method [PB-192901] 04 p0616 N71-13864

Discrete methods for linear dynamic response of elastic and viscoelastic solids [PB-194286] 04 p0618 N71-14286

Finite element dynamic analysis of shallow shell structures [NRC-11653] 04 p0619 N71-14319

Finite element stress analysis of crack in bi-material plate [AD-713593] 05 p0775 N71-14598

Investigating nonlinear and geometric behavior of shell structure using Eulerian and Lagrangian methods [AD-713797] 05 p0780 N71-15406

Dual structure in pion N scattering including Veneziano-type amplitude [NP-18417] 06 p0910 N71-15791

Finite element analysis of interlaminar shear in fibrous composites [RM-492] 06 p0880 N71-16466

Finite element program for determining stiffness and mass matrices of shells of revolution - users manual [NASA-CR-114824] 06 p0956 N71-16752

Effective use of incremental stiffness matrices in nonlinear geometric analysis 06 p0958 N71-16877 [AD-713967]

DYNASOR-2 finite element program for dynamic nonlinear analysis of shells of revolution [NASA-CR-114823] 06 p0958 N71-16883

Finite element program for structural analysis of arbitrary three-dimensional thin shells [GA-5952] 07 p1126 N71-17925

Computer program using finite element method for computing temperature distributions in thin shells of revolution [NASA-TN-D-6100] 08 p1303 N71-18746

Investigating symbolic computations by finite difference theory using FORMAC system 08 p1228 N71-19194

Finite element analysis of structures in plastic range [NASA-CR-16449] 08 p1301 N71-19278

Finite element computer program for estimating airplane aerodynamic interference [NASA-TN-X-64884] 09 p1311 N71-19357

Analysis of elastic strength of marine propellers by finite element method [AD-716463] 09 p1474 N71-19886

Optimization of aeroelastic constraints for aircraft design using differential equation idealization and finite element approximation 09 p1479 N71-20139 [NASA-CR-117198]

Computer program for cellular structures of arbitrary plan geometry designed to capture behavior of duct and web components [PB-196143] 09 p1481 N71-20817

Computer programs using cylindrical finite elements to solve for large nonlinear deflection [TT-7003] 09 p1481 N71-20521

FORTRAN program for Kottler-type method for finite element analysis of nonlinear structural behavior of airframes [AD-717181] 10 p1527 N71-20805

Discrete element model formulation for stress and vibration analysis of thin plates [REPT-35-01-77] 10 p1653 N71-21828

Vibration mode analysis of doubly curved honeycomb sandwich plates by finite element method [ISVR-TR-37] 10 p1653 N71-21846

Computerized finite element analysis of free vibrations of paraboloidal shells of revolution 10 p1654 N71-21175

Computerized finite element analysis of lateral pressure effects on free vibration of hyperboloidal shells of revolution 10 p1654 N71-21174

Inextensional shell theory analysis of vibrations of paraboloidal shells of revolution using finite element method 10 p1654 N71-21175

Finite element analysis for response behavior of stiffened rectangular plates subjected to dynamic loads 11 p1834 N71-21962

Computer programming technique for determining displacements and stresses of large complex structural systems 11 p1834 N71-22046

Finite element technique for analyzing folded plate structures with skewed end diaphragms 11 p1834 N71-22108

Finite element analysis of transverse shear in thick shells of revolution 11 p1835 N71-22107 [AD-717767]

Finite element analysis of small amplitude acoustic wave generation and propagation in homogeneous, loss-free, compressible fluid 11 p1797 N71-22224 [AD-717585]

Analysis of finite deformations of incompressible elastic solids by finite element method with formulations of higher order approximations and curvilinear elements [AD-717768] 11 p1835 N71-22237

Linear axisymmetric analysis of internal pressure loaded conical shell using ring type finite element model [AD-717770] 11 p1836 N71-22334

Application of curved triangular finite elements to buckling analysis of arbitrary shell [AD-717766] 11 p1836 N71-22337

Kottler method for asymptotic analysis of postbuckling behavior reformulated in finite element notation [AD-717740] 11 p1837 N71-22385

Finite element potential flow modeling for predicting round lifting jet rolled up geometry and path convergent into cross-flowing mainstream as on VTOL at STOL aircraft [AD-718121] 12 p1850 N71-22453

Derivation of several variational principles for large deformation problems and application to finite element analysis [AD-717958] 12 p2005 N71-23944

Finite element analysis of response of structures exhibiting bifurcation change of state from pre-buckling to post-buckling equilibrium configuration 12 p2080 N71-24075

Finite element method for free vibrations and non-linear response of integrally stiffened panel [ILR-544] 12 p2089 N71-24078

SUBJECT INDEX

- Finite element computer program for three dimensional analysis on radial flow impeller
[IC71109] 13 p2053 N71-25410
- Comparison of finite element and analytic solutions of normal uniform beam modes under various end conditions
[NASA-TN-D-6324] 14 p2346 N71-25704
- Finite element method to model soil half-space for calculating transfer moment in form of inertial energy of projectile penetrating soil
14 p2360 N71-26470
- Lagrangian formulation for large elastic deformations of thin shells, suitable for finite element analysis
[AD-721254] 15 p2521 N71-26946
- Applications of Dirichlet theory to superposition of infinite number of Regge poles
[CNRS-CPT-70-P-338] 15 p2461 N71-27114
- Elastic-plastic finite element analysis for three dimensional specimens with cracks and for stress and strain field near cracks
[JESTP-TR-12] 15 p2521 N71-27274
- Thermochemical dissipation analysis of thermomechanical solids by finite element method
[AD-720887] 15 p2521 N71-27294
- Manipulation errors in computer solution of critical stress structural equations using finite element method
[NASA-CR-1784] 16 p2565 N71-28279
- Application of special isoparametric finite elements for elastic-plastic analysis of shells of revolution
[AD-721317] 16 p2686 N71-28606
- Finite element analysis methods for dynamic and structural problems in solid mechanics applied to pulsatile flow including Newtonian and non-Newtonian fluids
17 p2733 N71-29464
- Flat rectangular plate buckling analysis using finite element method
[VTI-161] 17 p2853 N71-30041
- Comparison of finite element and finite difference methods for simple sloshing problem
[TR-1] 17 p2774 N71-30187
- Computer program and finite element method for sequencing structural stiffness matrix to improve computational efficiency
18 p2895 N71-31114
- Finite element displacement method for estimating static stresses in curved sandwich plates subjected to uniformly distributed pressure
[BSR-TR-48] 20 p3336 N71-32860
- Finite element model of Timoshenko beam segment
[AD-724332] 20 p3357 N71-32982
- Free vibration determination of curved sandwich beams, using finite element displacement method
[BSR-TR-45] 20 p3357 N71-33043
- Mathematical techniques using finite element method for vibration analysis of nuclear reactor
[CONF-710302-7] 20 p3302 N71-33542
- Comparison of finite element and finite difference methods in plane stress and axially symmetric elastostatic problems
20 p3292 N71-33676
- Dynamic and static analysis of axially nonuniform, thin cylindrical shells based on finite element type theory
[MERL-70-9-PT-1] 20 p3360 N71-33819
- Free flexural vibration of thin cylindrical shells using hybrid finite element method
[MERL-70-10] 21 p3528 N71-35138
- Finite element analysis of nonlinear heat transfer in axisymmetric solids
[PB-199169] 21 p3531 N71-35160
- Structural analysis of uniform beam under various end conditions using finite element and analytic methods
22 p3483 N71-36265
- Adaptation of NASTRAN program to solve acoustic mode problems of solid rocket motor cavities by finite element method
22 p3484 N71-36271
- Application of NASTRAN to structural analysis of space shuttle orbiter finite element model with over 300 joint degrees of freedom
22 p3485 N71-36279
- Comparing and integrating NASTRAN with other finite element computer programs
22 p3486 N71-36284
- Comparison of finite element computer programs for analysis of clamped flat plate and built-up wing vibration frequencies
22 p3687 N71-36293
- Automatic generation of finite element input, input transparency, and symbolic parameters for NASTRAN simplification and error reduction
22 p3687 N71-36296
- NASTRAN flat plate finite element convergence properties for stress analysis of cylindrical and conical shells
22 p3688 N71-36301
- Coding considerations for implementation of general isoparametric solid elements into NASTRAN displacement method program for stress analysis
22 p3688 N71-36304
- Reduction of proliferation and misinterpretability of finite element method computer programs
22 p3688 N71-36305

- Automated general purpose system for structural analysis using finite element method - Vol. 1
[AD-726564] 22 p3689 N71-36314
- Finite element method used for stiffness analysis of axisymmetrical shells of composite materials
22 p3693 N71-36338
- Finite element method applied to heat transfer problems, and transient two dimensional heat transfer with convection and radiation boundary conditions
[AD-726371] 22 p3697 N71-36345
- Finite element method applied to solid heat conduction with radiation/convection, nonlinear heat-flux boundary conditions
[AD-726370] 22 p3697 N71-36366
- Leading edge section of thin aerofoil theory
[ARL/SM-NOTE-360] 23 p3703 N71-36399
- Hybrid coordinate equations of motion for finite element model of dynamic analysis on flexible appendage attached to rigid base
[NASA-CR-122934] 23 p3781 N71-36947
- Incremental finite element analysis of large elastic deformation problems
[AD-726727] 23 p3861 N71-37527
- Dynamic response of hydrophobic spherical shell predicted by finite element model
[AD-726726] 23 p3861 N71-37528
- Finite element method to derive stiffness and increase flexibility in honeycomb structures
23 p3864 N71-37548
- Stiffness matrix of nonconforming triangular finite element for static and dynamic analyses of thin cylindrical shells
23 p3865 N71-37551
- Computer system for generating input data for structural analysis of three-dimensional elastostatic problems using isoparametric finite element method
[AD-727177] 24 p4024 N71-38714
- BRESC finite element program for axisymmetric, plane strain, and plane stress, orthotropic solids with temperature-dependent material properties
[AD-727702] 24 p4025 N71-38720
- Optimization of finite element grids based on minimum potential energy
[AD-727953] 24 p4026 N71-38724
- Development of curved and flat finite shell elements for higher order shell theory
24 p4027 N71-38736
- FINITE-STATE MACHINES
U. TURING MACHINES
- FINLAND
- 1969 magnetic measurements of vertical and horizontal components and declination at Nurmiarvi Geophysical Observatory, Finland
[REPT-11] 05 p0676 N71-15458
- Measuring fractions of aerosol beta activity in precipitation and settled dust
[REPT-9] 05 p0720 N71-15585
- Ionospheric electron density determination over Finland using Explorer 22 signals and Faraday/Doppler method
[BMSW-FB-W-70-50] 08 p1189 N71-18592
- Climatological tables of ceiling, visibility, surface wind, and temperature for Lappeenranta Airport, Finland
[REPT-25] 09 p1414 N71-20096
- Climatological tables of ceiling, visibility, surface wind, and temperature for Kuopio Airport, Finland
[REPT-24] 09 p1414 N71-20097
- Aeronautical climatological conditions at Kajani Airport, Finland
[REPT-21] 09 p1414 N71-20057
- Aeronautical climatological conditions at Kruunuvuori Airport, Finland
[REPT-23] 09 p1414 N71-20058
- Meteorological parameters observed and recorded at Kemi Airport, Finland, 1956 - 1961
[REPT-22] 09 p1415 N71-20583
- Climatology at Rovaniemi Airport, Finland
[REPT-20] 10 p1598 N71-21521
- Climatology at Maastricht Airport, Finland
[REPT-26] 10 p1598 N71-21537
- Climatology at Vaasa Airport, Finland
[REPT-30] 10 p1598 N71-21538
- Climatology at Turku Airport, Finland
[REPT-29] 10 p1598 N71-21539
- Climatology at Oulu Airport, Finland
[REPT-27] 10 p1598 N71-21540
- Monthly and annual tables of mean atmospheric pressure with monthly mean maps for Finland in 1931 - 1960
[REPT-21] 12 p1955 N71-23840
- Tables on mean and maximum wind velocities for Helsinki, Kuopio, and Vaasa airports in Finland - 1965
12 p1955 N71-23852
- Finnish atmospheric temperature and precipitation predictions from Jan. 1968 through Oct. 1970
[RR-32] 16 p2627 N71-28895
- Atmospheric temperature distribution data over Finland from 1931 through 1960
[RR-31] 16 p2627 N71-28896
- Finnish meteorological parameters for Jan. 1971
16 p2627 N71-29000
- Spec research program in Finland during 1970
[S-39-1971] 17 p2861 N71-29633

FIRE PREVENTION

- Meteorological data from Finland for 1969
[REPT-551-506-1-4000] 20 p3295 N71-33008
- Solar radiation data from Finland for 1967 and 1968
20 p3341 N71-33049
- Finnish geophysical station for observing earth tides
20 p3343 N71-33340
- Monthly mean values of energy balance components of earth surface in Finland
20 p3287 N71-33497
- Turbulent data on lightning discharges and thunderstorm days in Finland during 1970
20 p3297 N71-33619
- Measurement of earth magnetic field by geophysical observatory 40 kilometers northwest of Helsinki, Finland
24 p3916 N71-37923
- FINNED BODIES
- Resonance instability of finned bodies with nonlinear aerodynamic characteristics
[AD-715110] 07 p0948 N71-17733
- Interference flow field of fin-flat plate configuration in supersonic turbulent boundary layer flow channel
09 p1313 N71-15945
- Trajectory computer program /EIXD/ to determine motions of asymmetric missiles emphasizing various nonlinear-induced effects associated with finned bodies
[SCL-EE-70-121] 15 p2364 N71-27613
- Derivation of equations describing heat transfer by radiation and convection from annular fins of trapezoidal profile on cylinder
[AD-723974] 20 p3363 N71-32932
- NT COOLING FINNS
- Gase flow near flat surface fitted with fins in herring bone pattern in nuclear gas-graphite power reactors
[CEA-N-1329] 04 p0562 N71-14410
- Fin loads and control surface hinge moments measured in full scale wind tunnel tests on X-24A flight vehicle
[NASA-TM-X-1922] 05 p0625 N71-14501
- Thrust and attitude control operations using jet nozzles in movable curved surface or fin configuration
[NASA-CASE-XLB-63583] 07 p1119 N71-17629
- Fin-flat plate combination model for flow visualization studies of fin protrusions partially immersed in turbulent boundary layer at Mach 5
[AD-716823] 09 p1371 N71-19636
- Computer programs for calculating airforce coefficients of wing-horizontal tail and fin-horizontal tail oscillating in subsonic flow
17 p0699 N71-29342
- Behavior of Dargone's A fins due to coolant gas induced corrosion and thermal cycling
[TRG-2121] 19 p3141 N71-32592
- Computer program HETRAN to solve two dimensional steady state heat conduction on cladded tube with connecting fin
[NASA-TM-X-2331] 22 p3557 N71-35336
- Static aerodynamic characteristics of Scout fin with enlarged tip control at Mach numbers from 0.40 to 4.40
[NASA-TN-D-4397] 22 p3481 N71-36246
- FIRE CONTROL
- Optimization analysis of compact, lightweight laser radar
[AD-713517] 05 p0897 N71-15222
- Flight test of fire control system in AH-1G helicopter
[AD-714670] 06 p0794 N71-16019
- Statistical model for calculating effect of fire power of fragmenting HE weapons on composite targets
[RAE-LIB-TRANS-1430] 21 p3532 N71-35174
- FIRE EXTINGUISHERS
- Procedure for extinguishing fires in activated carbon adsorbers used in air cleaning systems
[UCRL-74964] 06 p0517 N71-14499
- Airplane interior materials ignition and fire extinguishing foam
[FAA-RD-70-81] 06 p0796 N71-16018
- Catalytic decomposition of fire extinguishant, bromotrifluoromethane, in confined area
[AD-716737] 10 p1513 N71-21291
- Measurement of brain and heart accumulation of bromotrifluoromethane for evaluation as potential fire extinguisher chemical
[AD-712111] 15 p2374 N71-27299
- Testing of fire extinguisher for activated carbon adsorbers in air cleaning systems
17 p2731 N71-29075
- FIRE FIGHTING
- Surveying crash fire and rescue equipment at North American and Canadian airports
07 p1003 N71-18101
- Survey conducted to develop minimum requirements for airport fire fighting and rescue services
[FAA-AS-71-1] 09 p1364 N71-19426
- Cloud seeding for forest fire fighting and heavy rainfall prevention
[NLL-M-20350-3828.4F/1] 12 p1956 N71-23900
- FIRE PREVENTION
- Fire protection tests in small fuselage mounted turbojet engine and nacelle installation
[FAA-NA-70-41] 02 p0144 N71-10101

- Automatic fire protection system for manned hyperbaric chamber
[AD-712848] 03 p0329 N71-12348
- Investigating health physics, safety factors, fire prevention, and materials handling in reactor research
[CONF-690441] 05 p0729 N71-15218
- Jet engine combustion chamber burn-through fire and methods for controlling damage
[FAA-RD-70-68] 07 p1102 N71-17483
- Conference on safety problems in transportation and storage of explosives
[AD-716790] 10 p1662 N71-21202
- Hyperbaric fire safety research, including flame spread rates in helium and nitrogen diving atmospheres and minimum oxygen concentration for combustion in hyperbaric environments
[AD-720353] 14 p2209 N71-23594
- Design, development, and flight testing of fire suppressant void filler foam kits for lower hemisphere of fuel tanks in various tactical aircraft
[AD-719711] 15 p2368 N71-27679
- Studying mechanism of flame spreading over surface of igniting polystyrene and polymethyl methacrylate for minimizing fire hazard in space capsules
18 p3019 N71-31431
- Demonstration and evaluation of crash-resistant bladder fuel tank system in full-scale aircraft wing assembly
[FAA-NA-71-34] 19 p0307 N71-32077
- Incipient fire and toxic gas caution and warning system for space shuttles
22 p3675 N71-36204
- Fire prevention, protection, and fighting systems at KSC for space shuttle operations
22 p3676 N71-36205
- Flammable Fabrics program reporting standards for carpets and rugs, blankets, mattresses, and apparel for children
[NBS-TN-596] 23 p3776 N71-36914
- Simulated JP-4 jet fuel fire tests of high temperature cabin pressure sealant and insulating plastics and rubbers
[FAA-NA-71-22] 24 p3946 N71-38149
- FIREBALLS**
- Effects of atmospheric particles on fireball emissions calculated for thermodynamic model showing mass of meteoric material vaporized in fireball less than one pound per megaton bomb
[AD-722031] 16 p2588 N71-28608
- FIREPROOFING**
- Fireproof potassium silicate coating composition, insoluble in water after application
[NASA-CASE-GSC-10072] 04 p0533 N71-14014
- Measuring effects of flame retardants on thermal degradation of alpha-cellulose in nitrogen using predictions of Parker-Lipka model
[AD-715411] 08 p1222 N71-18657
- Para-benzoquinone dioxide and concentrated mineral acid processed to yield intumescent or fire resistant, heat insulating materials
[NASA-CASE-ARC-10304-1] 21 p3443 N71-34501
- FIRES**
- Aircraft accident investigation of United Air Lines, Boeing 727-22C near Los Angeles, 18 Jan. 1969
[PB-190812] 01 p0006 N71-10914
- Remote sensing analysis of grassland fire phenomena in Florida
08 p1198 N71-19263
- Portable fire weather station for measuring and recording wind speed and direction, and wet and dry bulb temperatures
[PSW-182] 09 p1388 N71-19870
- Synoptic meteorological parameters influencing forest fires in Southeast Asia including cloud cover and precipitation
[AD-721112] 15 p2437 N71-26917
- Fire test facility with filter plenums and glovebox for studying effects of fire originating within glovebox system
17 p2730 N71-29874
- Clean room fire caused by gas heating element thermostat failure in liquid nitrogen system
[NASA-TM-X-67250] 17 p2731 N71-29880
- Heat flux distributions in pools of burning aircraft fuels for design of protective clothing for firefighting personnel
[AD-722774] 18 p3030 N71-31376
- Performance of protective clothing in large J4-4 fuel fires
[AD-724648] 20 p3226 N71-32925
- Compilation of safety items covering personnel, electrical equipment, and fire hazards
[NASA-SP-5928/01] 20 p3370 N71-33592
- Congressional hearing on budgeting authorization for continuation of Fire Research and Safety and Standard Reference Data Acts
22 p3699 N71-36383
- FIREWORKS**
- U PYROTECHNICS**
- FIRING [IGNITING]**
- NT RETROFIRING
- NT ROCKET FIRING
- NT STATIC FIRING
- NT TEST FIRING

- Contamination free separation nut eliminating combustion products from ambient surroundings generated by aquib firing
[NASA-CASE-XGS-01971] 06 p0683 N71-15922
- Terminated capacitor discharge firing of electroexplosive devices
[NASA-CR-116792] 08 p1169 N71-18702
- Response of cast Co-Cr-Mo alloy to impulsive thermal-mechanical fatigue conditions present during firing of automatic weapons
[AD-721895] 16 p2610 N71-28453
- Gas spring firing and soft recovery of hard wire instrumented 155 mm projectile
[SC-RR-70-849] 17 p2729 N71-29241
- Half-size wave pulse firing of electroexplosive devices
[NASA-CR-119320] 18 p3025 N71-31193
- Firing site with 12.5KJ capacitor bank
[MHSMP-71-33] 23 p3758 N71-36791
- FIRING TIME**
- U BURNING TIME**
- FISH**
- U FISHES**
- FISHES**
- NT SHARKS**
- Marine fauna and benthic shelf-slope communities of Lithman region
[BIM-171-38] 06 p0841 N71-15987
- Investigating feasibility of locating, identifying and quantifying surface and near-surface fish stocks from aircraft and spacecraft
06 p0848 N71-16182
- Body structure effects on fish hydrodynamic characteristics
[JPRS-52299] 08 p1148 N71-18492
- Microrespirometers to measure oxygen consumption of sprouting potato plugs, and gravitational effects on hypothalamo-hypophyseal system of fish
[NASA-CR-117179] 09 p1341 N71-20006
- Visualized flow patterns of pelagic fishes to measure vortex formation and air and water boundary layer effects
[JPRS-52790] 10 p1544 N71-21646
- Plane section method used to study hydrodynamics of thin flexible bodied fish and mammals
11 p1835 N71-22202
- Swimming speed and kinematics of Black Sea fish species
11 p1681 N71-22203
- Quantitative analysis of hydrodynamic swimming characteristics of salt water fish
11 p1681 N71-22204
- Oscillatory characteristics of swimming and locomotion of aquatic animals
11 p1681 N71-22205
- Biological efficiency of swimming fish based on oxygen consumption
11 p1681 N71-22208
- Radio telemetry technique for determining flow conditions in boundary layer of autonomous self-propelled models and individual aquatic animals
11 p1699 N71-22211
- Behavior of living pike fish under influence of electrical and mechanical stimulation of cupula of left horizontal ampulla and semicircular canal
[NASA-TT-F-13665] 14 p2203 N71-25716
- Procedures and immunofluorescent techniques for screening Apollo space test animals for bacterial pathogens after lunar sample exposure
[NASA-CR-115064] 17 p2707 N71-29228
- FISHTAILING**
- U YAW**
- FISSILE MATERIALS**
- U FISSIONABLE MATERIALS**
- FISSION**
- Swelling due to fission-gas release in uranium and uranium-molybdenum alloy during irradiation
[NASA-TT-F-13339] 02 p0264 N71-11734
- Photo-fission of U-235 and U-238 using Compton scattering monochromator
[IS-T-375] 03 p0425 N71-12831
- Measurements of prompt antineutrinos for neutron induced fission of Pu-239 between 40 keV and 1.2 MeV
[AWRE-O-4270] 06 p0910 N71-15785
- International comparison of Mn-56 activity in 1968 including nuclear reactor irradiations and neutron-source calibration
[ANL-7642] 06 p0915 N71-16001
- Feasibility study of autoradiographic technique for determining relative power densities in reactor fuel plates
[Y-DR-29] 09 p1418 N71-19899
- Macroscopic characteristics of reactions in complete fusion of nuclei
[JINR-P-5019] 09 p1440 N71-20308
- Calculation of ETR loop irradiation test fission power of fuel elements
13 p2114 N71-24533
- Measure of fast fission factor in ORGEL D2O natural U lattices
[EUR-4326] 13 p2133 N71-25162
- Examination of neutron sources and fission for non-destructive assays of nuclear materials
[BNL-50267] 15 p2456 N71-26847

- Research in nuclear and reactor chemistry including identification of short-life nuclides, activation analysis, and mass distribution in fission
[BMLW-FBK-70-19] 15 p2485 N71-27800
- U-235 fission cross sections at 440 and 530 keV neutron energies studied with gas scintillation chamber and proton recoil detector
[KFK-1313] 16 p2641 N71-28019
- Measuring average number of prompt neutrons and of relative cross sections for fission of U-235 and Pu-239 induced by neutrons within 0.3 and 1.4 MeV energy ranges
[LIB-TRANS-300] 16 p2660 N71-29196
- Nuclear chemistry of fissions, alpha decay in constant isotopes, alpha radioactivity in air samples, and nuclear levels, nuclidic masses, and lifetimes of heavy elements
[MNC-3783-9] 17 p2794 N71-29631
- Cross sections for binary fission of Bi, Au, Pb, U, and some lighter elements, produced by 0.59 to 21 GeV protons
[CERN-71-2] 18 p2979 N71-30722
- Delayed fission of Pu-237 produced by low energy deuterons bombardment of Np-237
[TID-25639] 18 p2986 N71-31234
- Long range alpha particle emission in thermal neutron induced fission of U-235
18 p2986 N71-31239
- In-pile and out-of-pile creep rates of enriched uranium dioxide at various temperatures, stress ranges, and fission rates
[BIM-1899] 20 p3807 N71-33873
- U-235 and U-238 fissioning neutron fluence distributions in Phobos-2A shield systems in relation to Monte Carlo calculations
[LA-4615] 21 p3466 N71-34675
- Direct measurements of capture cross section ratio to fission cross section using ionization chamber and neutron beams
[IAE-1985] 21 p3471 N71-34791
- Nuclear research in space and lunar materials and proton fission
[COO-1167-13] 21 p3478 N71-34770
- Measurements of central fission ratios and spatial distributions of fission rates in radial direction
[JAERI-MEMO-4356] 22 p3638 N71-35990
- Epicadmium integral fission cross section measurements for twelve heavy nuclides including plutonium and uranium isotopes
22 p3650 N71-36801
- Fission investigation using on-line mass spectrometry and emphasizing target construction, elimination of contamination, and recording of mass spectra
[NP-18829] 23 p3811 N71-37177
- Thermal fission cross sections and fission resonance integral measurements for Cf-249 and Cm-244 to Cm-248 made in core and thermal column of research reactor
[DP-MS-70-95] 23 p3816 N71-37320
- Ratio of grain boundary energy to surface energy determined from observations of intergranular fission gas bubbles in neutron irradiated uranium dioxide
[RD/B/N-1851] 24 p3963 N71-38380
- Calculations of beta energy release rates from thermal neutron fission of uranium and plutonium isotopes
[SRRC-3871] 24 p3979 N71-38394
- Fission and radiative capture cross sections of common isotopes using Physics 8 nuclear explosion in neutron source
[LA-4566] 24 p3980 N71-38400
- FISSION ELECTRIC CELLS**
- NT SNAP 8**
- FISSION PRODUCTS**
- U 235 and Pu 239 capture-to-fission ratio using neutron time-of-flight methods
[UCRL-72454] 01 p0098 N71-18847
- KeV neutron energy fission cross section of U 235 measured with high resolution
[UCRL-72472] 01 p0099 N71-18970
- Deposition of cesium and barium in sodium stainless steel system to predict distribution of fission products in LMFBR system
[AI-AEC-12952] 02 p0265 N71-11702
- Effects of radiation on reactor materials, fission product contamination, sodium effects on stainless steels, and related subjects in study of fuel cladding and structural materials
[AI-AEC-12940] 02 p0266 N71-11704
- Comprehensive tables of beta and gamma activities of fission products
[CEA-N-1269] 02 p0277 N71-12130
- Energy spectra calculations of fission fragments and antineutrino values for targets of different thickness
[JINR-P-5081] 02 p0277 N71-12134
- Isotopic fuel development and fission product studies
[BNWL-1308-2] 03 p0415 N71-13871
- Assessment of environmental hazard from fission product releases
[AHSB/R-135] 03 p0415 N71-13887
- Micromachining methods for studying samples of fission products and cladding in irradiated fuel elements
[CEA-CONF-1564] 04 p0546 N71-19313

SUBJECT INDEX

Diagrams for rapid calculation of gamma protection and attenuation of gamma radiations from fission products
[CEA-N-1209] 04 p0571 N71-13613

Fission product removal from cover gas of vented fuel
[RT/ING/707] 04 p0577 N71-13774

Studying mixed fission products from thermal fission of U-235 to create tools for analysis of fallout from nuclear explosions
[POA-4-C-4428-28] 04 p0577 N71-13775

Livermore fission fragment analyzer - conference
[UCRL-72422] 04 p0582 N71-14084

Three dimensional multi-group diffusion-burnup program 3DDT
[LA-4996] 04 p0561 N71-14408

Nuclear fuel behavior during irradiation by fission gas release
[ORNL-4694] 03 p0723 N71-14674

Developing techniques for isolating and purifying Mo-99 from fission products obtained from uranium oxide irradiated with thermal neutrons
[NSRA-267] 03 p0738 N71-15007

Collection and analysis of radioactivity fallout samples
[AERE-R-5998] 03 p0742 N71-15126

On-line mass spectrometers with negative ion fission products
[COO-1600-6] 03 p0744 N71-15149

Angular distribution measurements of fragments from neutron-induced fission
[LA-4049-TB] 03 p0751 N71-15618

Synthesis of element 105 in bombardment of Am-13 with Ne-22 ions
[JINR-P7-5164] 03 p0911 N71-15790

Measuring angular distributions and fragment yields for photo-fission of even-even nuclei near threshold
[LA-4085-TB] 03 p0920 N71-16258

Densification of plutonium and uranium dioxide, neutron effects on fission gas release, and crack formation during reactor power rise
[ORNL-TM-2387] 03 p0901 N71-16810

Elastic energy distributions of single fission fragment mass lines
[FRL-196] 07 p1070 N71-17003

Critical, perturbation distributions, and central fission ratios of UO₂ in ZPR-3 Assemblies 58 and 59
[JNL-7695] 07 p1075 N71-17452

Mobile gas partitioning in dynamic air-water systems
[BNWL-SA-3346] 07 p1085 N71-17604

Tables of fission-product gamma transitions including isotopes from Sr-87 to Pb-151 with half lives greater than one minute
[CEA-N-1250] 07 p1081 N71-18137

Theoretical reconstruction of gamma ray spectra fission products after thermal fission of U-235 nucleus
[CEA-N-1313] 07 p1081 N71-18142

Computer program /PROFIS/ to evaluate fission product concentrations in fuel irradiated under various conditions
[CEA-R-3967] 07 p1066 N71-18143

Chemical aspects of reactor safety including release and transport of fission products, aerosol behavior, and chemical reactions of metal cladding
[JNL-B-99] 06 p1235 N71-18213

Burnup analysis in thermal reactor system - decay data of fission products
[JNL-1194] 06 p1236 N71-18234

Computer program for calculating fission product activity according to experimental conditions
[CEA-N-1308] 06 p1254 N71-18347

Tabulating observations on angular distributions of scattered neutrons and reaction products of fast neutrons and nuclei
[BNL-400-VOL-1] 06 p1255 N71-18370

Uranium 235 content in U-Al alloy determined by detecting fission neutrons, emitted by slow neutron irradiation
[JAERI-MEMO-4106] 06 p1256 N71-18384

Discussing monitors for determining burnup rate of enriched uranium 235 fuel in fast neutron environment
[NASA-TM-X-2153] 06 p1259 N71-18496

Fission characteristics study of transuranium elements using liquid drop model
[RP-18407] 06 p1257 N71-18518

Ground state bands of even-even fission products
[UCRL-19499] 06 p1261 N71-18778

Calculating value of effective number of neutrons lost by fission in reactors with hard neutron spectrum
[CEA-N-1378] 06 p1241 N71-18789

Evaluating changes in 26th group fission cross sections of U-235 and capture cross sections of U-238 from critical mass of ZPR-3 reactor
[CEA-N-1378] 06 p1261 N71-18790

Calculation of radiation dosage resulting from hypothetical fission product release after reactor accident
[IC-88-76-334] 06 p1267 N71-19235

Operating instructions for Chaswep sounding robot vehicle
[UCRL-50386] 06 p1295 N71-19278

Symptoms and detection of fission product release from EBR-2 fuel element - defect below fuel elevation
[ARL-7676] 09 p1418 N71-19698

Total activity/sec of products from U-235 and Pu-239 thermal fission and U-235, U-238, and Pu-239 fast fission
[CEA-N-1376] 09 p1439 N71-20199

FISP 2 program for fission product inventories with complete input data specifications
[RD/BN-1737] 09 p1440 N71-20309

Measurements and calculations on thermal Argon gas tube cores in STEK facility
[RCN-118] 09 p1446 N71-20586

Fission product removal by sprays of recirculated liquid with sodium hydroxide
[BNWL-1485] 10 p1603 N71-21108

Natural transport effects on fission product behavior in containment systems experiment, time dependence of iodine, methyl iodide, and particulate matter in vapor and steam phases
[BNWL-1457] 11 p1804 N71-22284

Measurement of re-circulation rate of fission gases in uranium oxide nuclear fuels
[GEAP-12147] 11 p1794 N71-22377

Atmospheric radiochemistry and radioactive fallout and deposition from nuclear explosions
[ORO-2529-28] 11 p1822 N71-22420

Helium sweep gas facility design and operation for analysis of reactor fission gas-isotope release rates for space power reactor fuel element design
[NASA-TM-X-2267] 12 p1897 N71-23651

Fission gas release curves at 2, 4, 12, and 24 hr intervals during Pu-239 fission
[UCRL-9656-SUPPL.] 12 p1974 N71-23989

Peak to valley ratios for proton and deuteron fission of uranium 238 measured as function of particle energy
[JNL-7676] 12 p1976 N71-24098

Fission gas pressure transducers of fluid-filled bellows, and null-balance types
[CEA-N-1376] 13 p2079 N71-24519

Pressure transducer for continuous monitoring of fission gas release by nuclear fuel specimens during irradiation
[CEA-N-1376] 13 p2112 N71-24520

Calculation techniques for estimating host power levels of radioactive decay of fission and activation products
[CEA-N-1376] 13 p2113 N71-24531

Microprobe analysis of fission gas xenon retention by UAM and U3O8 fuels dispersed in aluminum cladding
[CEA-N-1376] 13 p2114 N71-24536

High temperature nuclear reactor fuel fission product monitoring using wire precipitation systems as radiation counters
[AERE-R-6475] 13 p2118 N71-24981

Behavior of fission products Mo, Tc, Ru, Rh, and Pd in carbide fuel element and structure of system Mo-Ru-C
[KFK-1260] 13 p2133 N71-25144

Computer program for calculating concentration of fission products - HERETRA
[DEMO-70/10] 13 p2135 N71-25182

Electron microprobe analysis of metallic fission product inclusions in irradiated mixed-oxide fuels for molybdenum
[WHAN-SA-96] 13 p2120 N71-25218

Studying aircraft accidents to determine impact angle and speed criteria for designing nuclear airplane fission product containment vessel
[NASA-TM-X-2245] 13 p2122 N71-25411

Detection of nuclear fuel element failure and shut-down in fast reactors by superheated steam test loop
[KFK-1255] 13 p2122 N71-25479

Fission product transport and behavior in stainless steel lined Containment Research Installation
[ORNL-4502] 13 p2140 N71-25499

Yields of fission product nuclides in irradiated uranium and plutonium calculated for fast and thermal fission and expressed as atoms per 100 atoms of U-235 or Pu-239
[ANL-7678] 14 p2301 N71-25742

Fission product angular distributions from C-12 ion impact with Gd-158 and O-16 ion impact with Sm-154 which yield 107 MeV excited Yb-170 compound nucleus
[CU-1019-76] 14 p2302 N71-25750

Radiation effects on fission product and plutonium migration in mixed PuO₂ UO₂ reactor fuel recycling, reactor physics, and control rod deformation measurement in lattice test reactors
[BNWL-1522-1] 14 p2292 N71-25755

Concentration, composition of radioactive isotopes in atmosphere near ocean surface, and density of fallout after nuclear explosions
[CEA-N-1376] 14 p2248 N71-25969

Fission products from stoichiometric shift in oxide fuel element at high burnup
[KFK-1181] 14 p2294 N71-26663

Trap mechanism for gas release from ceramic nuclear fuels based on literature review
[SRARI-P-73] 15 p2443 N71-26854

Modifications of CYGRO-2 computer program for mechanical analysis of irradiated nuclear fuel pins subjected to swelling due to fission products
[NASA-TM-X-2150] 15 p2444 N71-26938

Report of experiments including neutron polarization, elastic and inelastic scattering of neutrons on C-

FISSION PRODUCTS

12, and angular distribution of fission fragments in U-238 neutron reaction
[BNWL-FBK-70-14] 15 p2459 N71-27047

Completion of fission product cross sections for reactor burnup calculations
[AARE-CTM-549] 15 p2460 N71-27079

Schiffman separation of gamma ray spectra into neutron capture, nuclear fission, and fission product sources for use in nuclear fuel element nondestructive testing
[KFK-1214] 15 p2462 N71-27144

Cyclotron injection of helium into ceramic nuclear fuels for studying fission gas swelling
[AI-AEC-12804] 15 p2466 N71-27165

Calculation factor $P_{fission}/A$ for measuring fast fission ratio in annular fuel region of Mh 5 gas cooled reactor fuel elements
[AERE-W-6-975] 15 p2467 N71-27258

Burnup calculations of fission products used for studying reactor poisoning applied to fast cycle studies in thermal reactors
[JUL-678-80] 15 p2469 N71-27358

Energy spectra of prompt and delayed fission neutrons and reactor physics
[ANL-7747] 15 p2469 N71-27369

Fission product swelling, gas evolution, and creep properties of uranium dioxide nuclear fuels
[TRG-1937/87] 15 p2469 N71-27388

Radioactive characteristics for studying fission products - beta radiation and conversion electrons
[CEA-N-1372] 15 p2471 N71-27409

Effects of neutron energy dependence of Pu-239 fission products on burnup characteristics of fast reactors
[JAERI-4165] 15 p2494 N71-27953

Time dependent analysis of thermal radiation from fission product beta and gamma radioactive decay
[JAERI-MEMO-4205] 15 p2495 N71-27965

Analysis of Sr-90, Co-137, and fission products in atmospheric dust and rainfall in Great Britain to mid 1969
[AERE-R-6556] 15 p2495 N71-27966

Delayed neutron emission in radioactive isotopes formed in fission
[AERE-R-6596] 16 p2644 N71-28006

Experimental and estimated values for total chain yields for neutron fission of Th-232, U-233, U-235, Pu-239, and Pu-241 at various incident neutron energies
[ANL-7749] 16 p2644 N71-28105

Multinucleon transfer reaction mechanisms and products produced by C-12, Ne-22, and Ar-40 ions on Au, Pb, and Bi
[JINR-P7-5495] 16 p2647 N71-28236

Cross sections for production spectra of protons, deuterons, tritons, He-3, and alpha particles produced by 39 and 62 MeV protons on Bi-209
[ORNL-4638] 16 p2647 N71-28230

ISIS - computer program for analysis and interpretation of experimental fission data
[AD-721481] 16 p2647 N71-28238

Objective assessment of fission product yields by compilation of library of all published neutron induced fission product yields maintained and interrupted by computer methods
[AERE-R-6642-PT-1] 16 p2650 N71-28918

Dynamic aspects of fission as two-dimensional process with quadrupole and hexadecapole degrees of freedom in microscopic theory
[JINR-P-1230] 16 p2652 N71-29005

Cross sections of production of spontaneously fissioning isotopes of uranium, plutonium, and americium in neutron reactions
[JINR-P-3528] 16 p2653 N71-29009

Fission gas management from filtering sodium and transport phenomena for FFTF fuel failure detection
[ANL-7774] 17 p2782 N71-29509

Mathematical model for coolant three dimensional flow during rapid fission-gas release in fast nuclear reactor cores based on plenum chamber simulation
[ANL-7651] 17 p2784 N71-29666

Inorganic adsorbent materials for trapping of fission product iodine in fuel reprocessing plants and gas cleaning inside reactor containment
[CEA-N-1376] 17 p2784 N71-29839

Computer code for estimating maximum temperatures in charcoal bed by fission product decay heat
[JNL-1195] 18 p2971 N71-30464

Express extraction and universal precipitation methods for radiochemical determination of Pu, Am, Cm, Cy, Bk, and fission products in irradiated materials
[SRARI-P-81] 18 p2976 N71-30673

Calculations for obtaining heavy element content and fission product inventory in CAGR fuel
[RD/BN-1887] 18 p2978 N71-30672

Fission gas and nonvolatile fission product release measuring device based on thermodynamics for high temperature nuclear reactors
[JUL-767-RW] 18 p2960 N71-30863

- Light particle emission in fission as function of characteristic time and shape of rising neutron potential
[NRCN-252] 18 p2989 N71-31515
Operation report for Oak Ridge Research Reactor
[ORNL-TM-3360] 19 p3135 N71-31819
Simultaneous measurements of X ray and neutron emission and kinetic energies of Cf-252 fission fragments
[CEA-R-4121] 19 p3149 N71-32101
Analysis of migration of fission products during reactor operation by thermogravimetric model used to describe noble gas release from fuel pins
[CONF-710302-5] 20 p3301 N71-33306
Application of fission and charged-particle emission in calculations of nuclear reactions involving computed energies, angles, and ranges of recoil nuclei
[ORNL-TM-3179] 20 p3319 N71-33616
Gaseous fission, closed loop, MHD generator in nuclear electric power plant
20 p3303 N71-33632
Nuclear laser excited by fission fragments produced in pulsed nuclear reactor
20 p3282 N71-33633
Calculation of crew radiation dosage from uranium gas nuclear rocket engine exhaust backflow of fission products
20 p3305 N71-33635
Calculations of ionization-excitation source rates in gaseous media irradiated by fission fragments and alpha particles
20 p3307 N71-33667
Reaction kinetics for fission gas bubble growth, nucleation, and resolution
[GEAP-12148] 20 p3322 N71-33762
Fission product beta and gamma decay heating for calculating reactor safety hazards
20 p3325 N71-33915
Mass yields and charge distributions of 26 Ag, Cd, In, Sn, and Sb isotopes from U-238 fission with protons
[COO-1167-10] 20 p3328 N71-33987
Determining distribution of fission products in fuel particle coatings by sputtering technique using ion beams
[SGAE-PH-96/1970] 21 p3458 N71-34615
Formation of fission gas bubbles in solids during reactor irradiation
[AERE-R-6595] 21 p3467 N71-34679
Kinetic energy distributions of Cf-252 fission products as function of fission product mass ratios
[ORNL-TR-2453] 21 p3475 N71-34746
Recall properties of high energy Ia-181 and Bi-209 fission by 450 MeV protons
[COO-1167-16] 21 p3478 N71-34771
Size of fission product gas bubbles released from simulated break in fuel-element cladding
[ANL-7789] 21 p3479 N71-34778
Ternary fission products and scattering cross sections produced in Au-197, Bi-209, and Pu-239 by intermediate energy He-4 ions
21 p3487 N71-34841
Processing method for removing fission and corrosion products and fissile materials from molten salt breeder reactor fuel
[ORNL-TM-3138] 22 p3624 N71-35818
Multigroup constants for fission product nuclides covering Pa-239, U-235, and U-238
[JAERI-MEMO-4251] 22 p3632 N71-35886
Separation of krypton and xenon from reactor atmosphere by selective permeation
[NYO-4057-2] 22 p3644 N71-35981
Fission barrier excitation states and angular correlations of fission fragments in relation to saddle point deformation
22 p3650 N71-36026
Bibliography of fission products in fast reactors and their methods of measurement
[CEA-BIB-195] 24 p3963 N71-38268
Gamma spectroscopic measurement of fission products using Ge(Li) semiconductor
[JUL-709-RG] 24 p3973 N71-38341
Specific energy loss and effective charge of fission products in metal absorbers using Cf-252 fission source and semiconductor detector
[KFK-1360] 24 p3975 N71-38364
Radiative capture and fission cross sections for plutonium 239 measured in neutron energy range 0.1 to 30 keV
[ILBG-2876] 24 p3976 N71-38367
- FISSIONABLE MATERIALS**
Design and use of storage locations for fissile materials
04 p0547 N71-13639
Separation of U-233 from U-235 during head-end reprocessing of HGR fuels of TRISO coated fissile and fertile particles
[GA-9258] 04 p0560 N71-14357
Fast response miniature neutron detector for measuring temperature-time history of fissile materials under intense neutron irradiation
13 p2080 N71-24525
Equipment and methods for neutron interrogation and nondestructive analysis of fissionable materials
[LA-4523] 13 p2119 N71-25131
- Neutron emission and fissile material production for nuclear power technology
[JINR-P9-5285] 14 p2314 N71-26731
List of approximately 110 terms and definitions for use in activities associated with fissionable materials safeguards
[WASH-1162] 15 p2458 N71-26936
Evaluation of neutron data for fissile or fertile nuclei in range of resolved or unresolved resonances with mass number above 220
[NASA-TT-F-13692] 16 p2646 N71-28210
Qualitative safety management for control of nuclear fissionable materials
[KFK-1108] 18 p2958 N71-30477
Equivalent sample method for analyzing oscillation experiments on fissionable samples in thermal neutron reactors
[CEA-R-4152] 21 p3471 N71-34711
Single crystal targets of rubidium uranyl nitrate for aligned fissile nuclei experiment
[AERE-R-6141] 21 p3497 N71-34911
Processing method for removing fission and corrosion products and fissile materials from molten salt breeder reactor fuel
[ORNL-TM-3138] 22 p3624 N71-35818
Fluctuation factors for theoretical evaluation of average neutron cross sections of fissile nuclei in unresolved resonances region
[LA-1208] 24 p3972 N71-38337
- FITNESS**
NT FLIGHT FITNESS
NT PHYSICAL FITNESS
FITTINGS
Design and development of quick release connector
[NASA-CASE-XLA-01141] 04 p0524 N71-13789
Dynamic tests on tangential pipe fittings differing in types and dimensions
19 p3105 N71-32214
FIXED POINTS [MATHEMATICS]
Least squares integral criterion for representation of gravitational potential with fixed mass points
[NASA-CR-116806] 08 p1189 N71-18650
Table-lookup/interpolation fast function generation with small fixed point digital computers
[NASA-CR-118010] 12 p1883 N71-23865
On-line interactive program to empirically determine performance of fixed point digital filters
12 p1884 N71-23875
Fixed point theorems used for solving crossing symmetric S matrix equations for one meson Low equation
17 p2773 N71-29835
Fixed point method and Liapunov function for investigating problems concerning periodic and almost-periodic differential systems
[NASA-TT-F-13803] 18 p2945 N71-31169
- FIXED WINGS**
Design of supersonic aircraft with novel fixed, swept wing planform
[NASA-CASE-XLA-04451] 03 p0314 N71-12243
Wind tunnel tests to determine effects of wing dihedral angle on aerodynamic characteristics of highly swept fixed-wing configuration
[NASA-TM-X-2261] 11 p1671 N71-23622
Computerized simulation of helicopter tactical maneuvers in three body, three dimensional environment including fixed wing and rotary wing aerodynamic forces
[AD-721527] 16 p2565 N71-28409
Rotary wing downwash influence on fixed wing flow using magnetic induction vortex model
[DLR-FB-70-62] 17 p2701 N71-30040
Fixed wing aircraft employing free fall and circling-line techniques in rescue of personnel and retrieval of equipment
[AD-727007] 22 p3541 N71-35228
- FIXED-WING AIRCRAFT**
U AIRCRAFT CONFIGURATIONS
U FIXED WINGS
FLAME FRONTS
U FLAME PROPAGATION
FLAME HOLDERS
Turbulent mass exchange processes between recirculation zones in flame holder wake and surrounding flow
[RAE-LIB-TRANS-1418] 05 p0666 N71-15669
Afterburning flame stabilization in turbofan engines
[NASA-TT-F-13657] 17 p2840 N71-30350
Preliminary sector tests at 920 K of three afterburner concepts proposed for inlet temperature of 1260 F and comparison of results with conventional V-gutter flame holder
[NASA-TN-D-6437] 19 p3192 N71-32191
- FLAME INTERACTION**
U CHEMICAL REACTIONS
U FLAME PROPAGATION
FLAME IONIZATION
Aerosol and flame ionization techniques for air pollution sampling gas analysis
11 p1747 N71-22060
Chemical interferences and ionization in high temperature flame spectroscopy
[IS-T-417] 15 p2409 N71-27352
- FLAME PROBES**
Molecular absorption and light scattering in flame spectroscopy
[IS-T-335] 06 p0812 N71-16791
- FLAME PROPAGATION**
Flame length and laminar fuel jet combustion
[NASA-TT-F-13459] 07 p1130 N71-17570
Flame spreading over surface of igniting solid propellants in different gas mixtures at various pressures
[NASA-CR-111942] 18 p3026 N71-31426
Surface flame spreading characteristics of ICRPG reference composite propellant composed of ammonium perchlorate with polyurethane binder
18 p3026 N71-31427
Flame spread over surface of solid-fuel bed in oxygen-inert environment
18 p3026 N71-31428
Mechanism by which flame spreads over surface of condensed-phase material in quiescent gaseous environment
18 p3026 N71-31429
Flame spreading over surface of igniting solid rocket propellants at different pressures, and oxygen-nitrogen mixtures
18 p3027 N71-31430
Analysis of congressional action taken to control production and use of flammable fabrics
21 p3533 N71-35179
Analysis of burning stability conditions in free jet flames and influence of turbulence and intermittency
[NLL-M-20389-5828.4F] 23 p3868 N71-37576
- FLAME QUENCHING**
U EXTINGUISHING
U QUENCHING [COOLING]
FLAME SPRAYING
Flame or plasma spraying for molybdenum coating of carbon or graphite surfaces to prevent oxidative corrosion
[NASA-CASE-XLA-00302] 06 p0864 N71-14077
Processes of depositing heat resistant coatings on various surfaces by gas flame spraying
[NASA-TT-F-13534] 12 p1928 N71-23814
Modification of polyurethanes with alkyl halide resins, inorganic salts, and encapsulated volatile and reactive halogens for fuel fire control
[NASA-CASE-ARC-10098-1] 13 p2039 N71-24739
Studying mechanism of flame spreading over surface of igniting polystyrene and polymethyl methacrylate for minimizing fire hazard in space capsules
18 p3019 N71-31431
- FLAME STABILITY**
Afterburning flame stabilization in turbofan engines
[NASA-TT-F-13657] 17 p2840 N71-30350
Analysis of burning stability conditions in free jet flames and influence of turbulence and intermittency
[NLL-M-20389-5828.4F] 23 p3868 N71-37576
- FLAME TEMPERATURE**
Temperature measuring instrument for flame temperature in rocket exhausts, noting incandescent illuminators to use Umkehr effect
[ICT-12/68] 12 p2010 N71-23511
Temperature measurement of premixed hydrogen/oxygen flames with lithium chloride traces
[DLR-FB-70-76] 13 p2082 N71-25052
- FLAMEOUT**
Investigation of helicopter jet engine flameout due to ingestion of snow and ice
[NRC-11893] 11 p1672 N71-21927
- FLAMES**
NT DIFFUSION FLAMES
NT PREMIXED FLAMES
Luminescence of oxides by OH activation in hydrogen flames
01 p0016 N71-10003
Hydrocarbon-air laser, and thermodynamics of flame structure
[AD-711581] 02 p0239 N71-11596
Physical properties of flames regarded as ionized gases
[AD-716968] 10 p1608 N71-21304
Concentration of negative ions in flame for checking of static configuration of flame
[AD-719892] 14 p2353 N71-26025
Anodizing method for providing metal surfaces with temperature reducing coatings against flames
[NASA-CASE-XLE-00035] 16 p2693 N71-29131
Experimental arrangements for determining behavior of candle flame during free fall
[NASA-TT-F-13940] 22 p3696 N71-36336
Augmenting combustion flames with electric discharges to produce high temperature chemical and physical reactions in 2500 to 5000 K range
[ECRC/N327] 23 p3866 N71-37561
- FLAMMABILITY**
Weightlessness effects on spacecraft flammability
02 p0305 N71-11719
Flash point method for flammability hazard evaluation during flammable liquid transport
[PB-193077] 01 p0468 N71-13025
Combustion and physical properties of hydrocarbons
[AD-714674] 06 p0958 N71-14000

SUBJECT INDEX

Test chamber for fabric flammability and heat transfer measurement

(PB-194614) 06 p0882 N71-16728

Crash fire hazard evaluation of jet fuels

(JAA-NA-70-64) 06 p0938 N71-16864

Analysis of procedures for determining fire or explosion hazards of materials exposed to liquid or gaseous oxygen

(NASA-TM-X-64926) 09 p1470 N71-19956

Combustion physics and flammability of aluminum magnesium alloy aerogels

(NASA-TT-F-13505) 09 p1484 N71-20511

Full tank vapor space characteristics for simulated helicopter fuel tank and evaluation of existing potential hazard from vibration environment

(AD-753901) 10 p1660 N71-20702

Theoretical and experimental analysis of flame spreading across pools of liquid fuels and ignitability under quiescent and flowing environments

(AD-718966) 12 p2010 N71-23492

Tests of jet engine fuels to determine effects of shaking and vibration in aircraft fuel tanks on flammability hazards

(AD-718991) 12 p1989 N71-23805

Flammability test chamber for testing materials in certain predetermined environments

(NASA-CASE-KSC-10126) 13 p2061 N71-24985

Synthesis of low temperature petroleum resistant elastomers

(AD-728215) 14 p2280 N71-26384

Fire hazard classification of chemical report relative to explosion-proof electrical equipment based on study on available physical and flammability properties

(AD-720294) 16 p2690 N71-28331

Flammability and heat resistance of glass fiber reinforced polyester panels

(TDC-57264) 18 p2940 N71-30899

Small scale impact tests of aircraft fuel tanks for gas leakage to determine burning, misting, and splatter characteristics

(JAA-NA-71-12) 19 p3172 N71-32067

Analysis of congressional action taken to control production and use of flammable fabrics

21 p3533 N71-35179

Flammable fabrics program reporting standards for carpets and rugs, blankets, mattresses, and apparel for children

(NBS-TN-596) 23 p3776 N71-36914

FLAMMABLE GASES

Characteristics of combustion of premixed gases in stagnation flow condition

16 p2692 N71-28910

Measurement of heat transfer from acetylene-oxygen detonation in shock tube-Vol. 2

(NBS-A-71-2) 23 p3868 N71-37572

FLANGE WRINKLING

Investigating buckling behavior of flanges of horizontally curved plate girders using finite element analysis

(PB-192901) 04 p0616 N71-13864

FLANGES

Numerical analysis for problems of nuclear reactor vessel main flanges

(JEE-61) 04 p0546 N71-13624

Light baffle with oblate hemispherical surface and shading flange

(NASA-CASE-NPO-10337) 05 p0689 N71-15604

Explosive detonation velocity, explosive welding to hardware configurations, and flange buckling of explosively formed dome

(AD-718079) 12 p1926 N71-23758

Buckling and column failure interaction of thin walled compression members due to flange asymmetry

(NTR-160) 17 p2851 N71-29486

FLAP CONTROL

AIRCRAFT CONTROL

U FLAPS (CONTROL SURFACES)

FLAPPING HINGES

Low speed wind tunnel stability tests and flutter analysis of flapped rotary wings

(DIAL-TN-18) 15 p2368 N71-27756

FLAPS (CONTROL SURFACES)

MT JET FLAPS

MT LEADING EDGE SLATS

MT TRAILING-EDGE FLAPS

MT WING FLAPS

Evaluation of geared flap control system for tilting VTOL aircraft

(AD-712645) 03 p0313 N71-12236

Viscous interacting flow in hypersonic streams, including flow over flaps, corners, delta wings, and wing-body combinations

(NASA-TM-X-64914) 09 p1373 N71-19831

Flaps and leading edge modifications for improved aerodynamic control stability of military aircraft

12 p1850 N71-23422

Direct lift control system having flaps with slots adapted to their leading edge and particularly adapted to lightweight aircraft

(NASA-CASE-LAR-10249-1) 14 p2198 N71-26110

Flowing rate and efficiency of flaps at hypersonic speeds

(NCT-71-3016) 15 p2365 N71-27674

Pressure measurements of harmonically oscillating sweptback wing with two flaps in incompressible flow

(JAL-FB-70-47) 17 p2708 N71-29433

Potential flow solution for STOL wing propeller system presenting flow fields, pressure distribution, and lift coefficient for externally blown flap, high-lift configuration

(NASA-TN-D-6394) 17 p3701 N71-29774

Aerodynamic characteristics of twin jet, swept wing fighter aircraft model with leading edge Krueger flaps at subsonic speeds

(NASA-TM-X-2325) 23 p3707 N71-36426

FLARED BODIES

None thrustless effect on aerodynamic characteristics of flared body in supersonic wind tunnel

(NAL-TR-221) 11 p1670 N71-22160

FLARES

Irradiation curing process for producing pyroscopic materials - flares

(AD-724652) 20 p3287 N71-33194

Dust thunderstorm hypothesis for short-lived red flares on parts of lunar surface

(NLL-M-20719-[5828.4F]) 21 p3511 N71-35017

FLASH

Visual flash duration discrimination and decision theory analysis of effects of temporal and brightness differences

(NASA-CR-118998) 16 p2541 N71-28068

Visual flash duration discrimination and analysis of temporal and energy cue models, and memory effects

(NASA-CR-119009) 16 p2541 N71-28136

FLASH BLINDNESS

Evaluation of eye hazards from nuclear detonations

(AD-713152) 05 p0635 N71-14834

FLASH LAMPS

Failure analysis of recovery flashing xenon lamp on Apollo 10 flight

(NASA-TN-D-66485) 02 p0298 N71-11899

X ray flash tube with exchangeable electrode system

(UUP-704) 04 p0594 N71-14451

Compilation of optical properties data of xenon flash tubes for pilot warning indicator systems

(NASA-TN-D-6272) 10 p1559 N71-21098

Flash radiography in ballistic testing

(AD-719088) 13 p2188 N71-24444

Flash lamp with ballistic piston compressor for absorption spectroscopy measurements in ultraviolet region

(NASA-CR-120784) 21 p3405 N71-34226

FLASH POINT

Flash point method for flammability hazard evaluation during flammable liquid transport

(PB-193077) 03 p0468 N71-13225

FLASH TUBES

U FLASH LAMPS

FLASHING (VAPOORIZING)

Devices to regulate flashing brine flow through flash evaporators

(JORN-TN-2746) 07 p1008 N71-17269

FLASHOVER

Flashovers across dielectric spacers in compressed gases of coaxial cylinder system with insulation recommendations

(NLL-CE-TRANS-5434-[9022.09]) 17 p2787 N71-29634

Correction curves for humidity effects and flashover voltages in spark gaps

(NLL-CE-TRANS-5367-[9022.09]) 19 p3068 N71-32705

FLASKS

Exponential dilution flask for gas chromatography, reducing wear, alignment, and maintenance

(COO-1222-34) 01 p0034 N71-10527

Field standard measuring flask specifications and tolerances

(NBS-HANDBOOK-105-2) 09 p1392 N71-19484

SKRUZ for measuring intake in flask

(IFVE-PSU-70-6) 18 p2923 N71-30730

FLAT CONDUCTORS

Research progress in developing shielded flat-cable and termination method

(NASA-CR-102525) 05 p0091 N71-14819

Method of making molded electric conductor for use with flat conductor cables

(NASA-CASE-XMF-03498) 06 p0864 N71-15986

Shielded flat conductor cable fabricated by electrolytic and electroplating

(NASA-CASE-MFS-13667) 16 p2571 N71-28691

FLAT LAYERS

Approximation of residual thermal stresses in flat sheet molded from chemical hardening materials

(NASA-CR-116504) 07 p1125 N71-17572

FLAT PLATES

Conformal mapping technique to analyze two dimensional thin foils entering water surface vertically with ventilations

(AD-709913) 01 p0040 N71-10172

Surface heat transfer rates measured on flat plates in hypervelocity shock tunnel

(NASA-CR-1692) 01 p0134 N71-10867

Wake of catalytic flat plate in low density dissociation flow

(AD-711291) 01 p0044 N71-10975

PR-1 replacement flat plate fuel elements

(PAEC/D-699) 02 p0266 N71-12127

Influence of thermal and elastic variations on distribution of thermal stresses in flat plates and curved panels

02 p0304 N71-12146

Film and glass plate holder for NASA-3x25 camera used in satellite tracking

(NASA-TT-F-13352) 03 p0375 N71-12641

Wall pressure, hypersonic forces and hypersonic heat transfer for flat plates in low density flow

(REPT-70-4) 04 p0471 N71-13401

Hypersonic boundary layer transition and hypersonic heat transfer on cylindrical shells, cones and flat plates

(REPT-1104/70) 04 p0472 N71-13408

Three dimensional unsteady compressible laminar boundary layer equations for flat plates and rotating disks

(ONERA-NT-162) 04 p0519 N71-15790

Laminar heat transfer and wall temperature distribution for high temperature gases and nitrogen plasma in circular tubes and over flat plates

(REPT-70-3) 04 p0519 N71-15791

Measuring stress distribution across width of steel strip in cold mill to predict shape of finished product

(PB-194445) 04 p0531 N71-14215

Measuring cell for determining permittivity of solids, liquids, and pastes between 100 kHz and 100 MHz

(PRL-1970-10) 04 p0548 N71-14296

Oscillation of disk fixed to flat plate with interposed fluid

(PUBL-3) 05 p0775 N71-14724

Loads due to air and helium jets impinging normal to flat plate near vacuum and sea level ambient pressures

(NASA-TN-D-7002) 05 p0640 N71-14749

Flat plate and expansion corner models in hypersonic wind tunnel

(AD-714074) 06 p0835 N71-16290

Plastic deformation, notch tests, crack initiation, and strain concentration in flat steel plates

(TU-84-1970) 07 p1124 N71-17523

Thermal elastic stresses and crack initiation and propagation in flat glass plates

(REPT-570) 07 p1124 N71-17535

Crimp buckling of plates under compressive loads

07 p1127 N71-17954

Turbulent wakes of flat and rotationally symmetrical bodies noting width development

08 p1141 N71-18472

Sound field effects on flat plate heat transfer in turbulent boundary layer

(REPT-70-8) 08 p1243 N71-18572

Influence of cold shearing of steel plates on welded joint mechanical properties

(CRIF-MT-66) 08 p1206 N71-18587

Pressure gradient effects on turbulent boundary layer porous plate

08 p1183 N71-18949

Characteristics of flow distribution in hypersonic viscous shock layer on sharp flat plate

(AD-716485) 09 p1369 N71-19487

Turbulent separated and reattaching flow on flat plate-compression corner at supersonic and hypersonic speeds

09 p1374 N71-19835

Vibration mode analysis of doubly curved honeycomb sandwich plates by finite element method

(ISVR-TR-37) 10 p1653 N71-21046

Stability analysis of laminar to turbulent flow transition during film boiling from vertical flat plate at zero angle of attack

10 p1542 N71-21282

Nonuniform flow field sonic boom reduction device using slit jet impinging on inclined flat plate

(AD-717193) 10 p1544 N71-21623

Supersonic combustion, fuel injection, and recirculation in hydrogen hypersonic external combustion at flat plates and bodies of revolution

(DLR-FB-70-64) 11 p1840 N71-22129

Comparison of flat plate sharp and blunt edge effects on heat transfer in supersonic flow and heat transfer coefficient dependence on Reynolds number

(AD-717825) 11 p1735 N71-22156

Separated flow over flat plate with blunted fin at zero angle of attack

(AD-717171) 11 p1670 N71-22300

Techniques for generating artificially thickened boundary layer on flat plates

(NASA-TN-X-2238) 11 p1742 N71-22681

Characterization of wake behind flat plate with zero thickness aligned with flow at infinity

11 p1743 N71-22751

Fabrication and tests of CO₂ flat plate models in He hypersonic wind tunnel

(SC-CR-69-3215) 12 p2010 N71-23228

Mathematical model for computer program to determine vibratory response of finite plates and associated acoustic radiation to fully developed turbulence excitation

(AD-718815) 12 p2004 N71-23309

Interference phenomenon of subsonic turbulent jet exhausts from flat plate in low speed cross flow

(AD-718794) 12 p1899 N71-23314

Flat plate and cylindrical low density probes including free molecular flow and continuum regimes

12 p1903 N71-24130

- Gas film cooling past noneadiabatic flat plate 12 p2014 N71-24306
- Hypersonic heat transfer to flat plates and conical and blunt bodies in boundary layer flow 13 p2063 N71-24714 [ARC-RM-3637]
- Flat plate aspect ratio effects on ramp-induced, adiabatic, boundary layer separation at supersonic and hypersonic speeds 13 p2065 N71-24744 [AD-179477]
- Low speed wind tunnel test of four ft diameter circular plate model to determine static pressure distributions for jet decay characteristics of cross flow [AD-720232] 14 p2244 N71-26516
- Low speed wind tunnel test of four ft diameter circular plate model with three exhausting jets [AD-720233] 14 p2244 N71-26517
- Diffuse solar irradiance of nonhorizontal plane surface as function of sun azimuth, atmospheric turbidity, and surface orientation 15 p2401 N71-27513
- Electron density measurement of negative glow plasma with E-band Fabry-Perot interferometer using flat plate technique [NASA-TN-D-6282] 16 p2661 N71-28818
- NonNewtonian free laminar convection flow from vertical flat plate with uniform surface heat flux 16 p2584 N71-29030
- Compressible turbulent boundary layer predictions with heat transfer from flat plates in gun tunnel at Mach 9 [IC-AERO-70-05] 17 p2697 N71-29318
- Flat plate in hypersonic low density flow examined in shock formation and transition regime [DLR-FB-70-79] 17 p2700 N71-29432
- Turbulent film boiling tests of heated flat plate model in high speed water tunnel [AD-722428] 17 p2733 N71-29619
- Flat rectangular plate buckling analysis using finite element method [VTH-161] 17 p2853 N71-30041
- Notch sensitivity of flat plates used as structural members in aircraft wings tested on load testing machine [TB-89] 18 p2868 N71-30675
- Turbulent boundary layer over flat plate and compression corner models studied in hypersonic gun tunnel [IC/71/11] 18 p2904 N71-30747
- Production and characteristics of hypersonic viscous shock layer at leading edge of sharp flat plates [AD-723328] 19 p3076 N71-31751
- Surface roughness effects on drag reduction of flat plates moving in homogeneous polymer solutions [AD-724288] 20 p3349 N71-32971
- Rarefied dissociated hypersonic gas flow over flat plate with sharp leading edge [DLR-FB-70-60] 20 p3349 N71-33030
- Plate theory structural analysis of variable thickness axisymmetric plate contact with smooth rigid surfaces including thickness and shear transverse deformation effects 20 p3361 N71-33949
- Numerical analysis of shock induced boundary layer flow on semi-infinite flat plate, Part 2 [NASA-CR-121743] 21 p3410 N71-34260
- Theoretical analysis of polymer solution laminar flow near infinite extent flat plates for drag reduction effects [AD-726414] 22 p3569 N71-35418
- Comparison of finite element computer programs for analysis of clamped flat plate and built-up wing vibration frequencies 22 p3687 N71-36293
- NASTRAN flat plate finite element convergence properties for stress analysis of cylindrical and conical shells 22 p3688 N71-36301
- Numerical solution of Navier-Stokes equations for compressible viscous gas in near-wake behind trailing face of flat plate in supersonic flow [NASA-TT-F-15993] 23 p3742 N71-36678
- Interferometric test method for hemacytometer chamber cover glass conformity to planarity specifications [NBS-TN-579] 23 p3759 N71-36802
- Laminar, two dimensional boundary layer generated in immediate vicinity of plane shock wave moving over flat plate into gas initially at rest [NASA-CR-123159] 24 p3905 N71-37834
- Natural convection heat transfer from nonisothermal vertical flat plate immersed in temperature stratified media [AD-727204] 24 p4031 N71-38763
- FLAT SURFACES**
- Gas flow near flat surface fitted with fins in herring bone pattern in nuclear gas-graphite power reactors [CEA-N-1329] 04 p0562 N71-14410
- Design and fabrication of plastic vacuum probe surface sampler to determine microclimate population [NASA-CR-111796] 05 p0683 N71-14831
- Film condensation and heat transfer of low pressure metal vapor on flat surfaces [NASA-CR-117429] 10 p1661 N71-20860
- Processes of depositing heat resistant coatings on various surfaces by gas flame spraying [NASA-TT-F-13534] 12 p1928 N71-23814
- Development of curved and flat finite shell elements for higher order shell theory 24 p4027 N71-38736
- FLATNESS**
- Planar and nonplanar dynamic stability coefficient using biplanar wind tunnel, free flight system 18 p2967 N71-31107
- Interferometric test method for hemacytometer chamber cover glass conformity to planarity specifications [NBS-TN-579] 23 p3759 N71-36802
- FLATTENING**
- Flattening ratios of oblate planets within 2.05 factor based on hydrostatic model for determining satellite orbits and paths of chemical releases [AD-717687] 11 p1749 N71-22357
- Planetary diameter and flattening measurement 13 p2166 N71-24993
- Statistical analysis of temperature and power flattening of hot channel factor for reactor thermal design [EURFNR-863] 14 p2293 N71-26402
- FLAW DETECTION**
- U NONDESTRUCTIVE TESTS**
- U DEFECTS**
- FLEXIBILITY**
- Weatherproof helix antenna [NASA-CASE-XKS-08455] 09 p1346 N71-19493
- Flexible bellows joint shielding sleeve for propellant transfer pipelines 16 p2604 N71-28937
- [NASA-CASE-XNP-01855] 16 p2604 N71-28937
- Analysis of dynamic deflections of long flexible antenna booms on gravity gradient stabilized earth satellite by normal mode 20 p3353 N71-33892
- Analytical investigation of effects of blade flexibility, unsteady aerodynamics, and variable inflow on helicopter rotor stall characteristics [NASA-CR-1769] 23 p3704 N71-36404
- Finite element method to derive stiffness and increase flexibility in honeycomb structures 23 p3864 N71-37548
- FLEXIBLE BODIES**
- Flexible rotor balancing by exact point-speed influence coefficient method [NASA-CR-72774] 01 p0057 N71-10021
- Stability of motion of satellites with flexible appendages [NASA-CR-111143] 01 p0123 N71-10725
- Characteristics of hermetically sealed electric switch with flexible operating capability [NASA-CASE-XNP-09008] 03 p0349 N71-12518
- Linear interaction problem between spacecraft attitude control and flexible appendages solved in frequency domain using Fourier transform [NASA-CR-111558] 03 p0409 N71-13063
- Flexible composite membrane structure impervious to extremely reactive chemicals in rocket propellants [NASA-CASE-XNP-08837] 06 p0878 N71-16210
- Development and characteristics of self supporting space vehicle [NASA-CASE-XLA-00117] 07 p1120 N71-17680
- High velocity impact tests conducted with polyethylene terephthalate projectiles and flexible composite wall panels [NASA-TN-D-6135] 09 p1481 N71-20515
- Quality control of welded joints on flexible solar cell array [ESRO-CR-17] 11 p1677 N71-21991
- Plane section method used to study hydrodynamics of thin flexible bodied fish and mammals 11 p1835 N71-22202
- Fabrication and testing of flexible loop antenna as underwater, towed, ELF receiving antennas [AD-717118] 11 p1724 N71-22573
- Random process theory method for estimating response of flexible airplanes to atmospheric turbulence 13 p2026 N71-24708
- Design and development of flexible tunnel for use by spacecrews in performing extravehicular activities [NASA-CASE-MSC-12243-1] 13 p2037 N71-24728
- Structural modes required to determine interaction between attitude control system and flexible deployed solar electric spacecraft [NASA-CR-118327] 13 p2175 N71-25155
- Vibration control of flexible bodies in steady accelerating environments 15 p2415 N71-27169
- Flexible barrier membrane comprising porous substrate and incorporating liquid gallium or indium metal used as sealant barriers for spacecraft walls and pumping liquid propellants [NASA-CASE-XNP-08881] 16 p2612 N71-28747
- Heat sealable transparent plastic film for mounting solar cell array to flexible substrate [NASA-CASE-LEW-11069-1] 16 p0000 N71-29048
- Computer program for calculating effects of wash-plate stiffness on helicopter rotor system dynamics and stability [NASA-CR-1818] 19 p3039 N71-32797
- Mathematical models for calculating flexible wash-plate effects on vibratory and mechanical stability characteristics of helicopter rotor systems [NASA-CR-1817] 20 p3211 N71-33393
- FLEXIBLE WINGS**
- NT PARAWINGS**
- Development and characteristics of control system for flexible wings [NASA-CASE-XLA-04958] 02 p0146 N71-11820
- Determining deployment characteristics of all-fabric parawings by free flight tests 20 p3210 N71-33229
- Calculations of aerodynamic properties of flexible wing grid using Reynolds number [NT-21] 21 p3373 N71-34886
- FLEXING**
- Structural analysis of composite beams and circular plates undergoing flexural vibration [AD-712765] 03 p0467 N71-12316
- Dynamic flexure theory for elastic plates including transverse shear deformation and normal stress effects 06 p1300 N71-19175
- Analysis of propagation of flexural waves in prismatic, elastic bars with and without prestressing [AD-714666] 09 p1474 N71-19293
- FLEXOWRITERS (TRADEMARK)**
- U AUTOMATIC TYPEWRITERS**
- FLEXURE**
- U FLEXING**
- FLICKER**
- Analog flicker noise simulation using white noise processes by mathematical models [NBS-TN-604] 19 p3068 N71-32707
- FLIGHT**
- Medical acoustics and aptitude of flying 02 p0162 N71-1888
- Flow meter for measuring stagnation pressure in boundary layer around high speed flight vehicle [NASA-CASE-XPR-62007] 13 p2065 N71-24001
- High altitude flight test of roofed 12.2-meter-diameter disk-guy-band parachute with deployment at 5.8 Mach number [NASA-TN-D-6469] 21 p3376 N71-34886
- FLIGHT ALTITUDE**
- Experimental and theoretical study of biologically important radiation components and dose equivalency due to galactic and solar rays at SST in high atmosphere - summary 18 p2870 N71-30779
- FLIGHT CHARACTERISTICS**
- Proposed flying qualities specifications for space shuttle 01 p0125 N71-10111
- Synoptic meteorological conditions for clear air turbulence and turbulence effects on aircraft flight characteristics [DLR-FB-70-29] 07 p0970 N71-17145
- Flight characteristics of jet-flap STOL transport aircraft during approach and landing [NASA-TN-D-6225] 07 p0971 N71-17145
- NASA space shuttle program including spacecraft configurations and construction materials, cost and systems analysis, operational problems [POSS-618-670] 08 p1293 N71-1850
- Performance and flight data for Sandhawk rocket systems [SC-DC-70-4757A] 09 p1438 N71-1998
- Characteristic flight effects on toothache developments in aircraft pilots 11 p1688 N71-22209
- Aircraft design, flight characteristics, and atmospheric effects on sonic boom during supersonic and hypersonic flight 18 p2871 N71-30779
- Predicting flight performance of cryogenic storage system for Apollo 15 [NASA-CR-115116] 19 p3183 N71-31601
- Synoptic meteorological conditions for clear air turbulence and turbulence effects on aircraft flight characteristics [BMWG-FBWT-70-9] 19 p3127 N71-31770
- Synoptic meteorological conditions for clear air turbulence and turbulence effects on aircraft flight characteristics 19 p3127 N71-31770
- Characteristics of air motion with respect to ground and analysis of dynamics of aircraft in turbulent air [NASA-TT-F-600] 19 p3053 N71-32779
- Scout first stage jet wave effectiveness, air aerodynamic pitching and yawing moment coefficients determined from flight data [NASA-CR-111945] 20 p3351 N71-3380
- Development of method for determining angle of pitch, flight path angle, and angle of attack for aircraft during steady or nonsteady flight [VTH-156] 20 p3208 N71-33929
- Aerodynamic and flight characteristics of supersonic aircraft and spacecraft motion in planetary gravitational fields 22 p3541 N71-33229
- Flight dynamics and calculation of flight trajectories of various aircraft and spacecraft [AD-727474] 24 p3872 N71-37886
- FLIGHT CLOTHING**
- Developing high altitude protection suit of push pressure type [AD-702537] 02 p0167 N71-11818

SUBJECT INDEX

- Evaluation of protective clothing for flight crew members (AD-719106) 13 p2036 N71-24460
- Development of test methods and techniques for determining technical performance and safety characteristics of aviation tools and accessories (AD-723039) 17 p2712 N71-30238
- FLIGHT CONDITIONS**
- Influence of environmental factors in aircraft carrier landings and accidents 09 p1325 N71-20349
- Prelaunch, launch, and inflight earth orbital environment data for HEAO spacecraft (NASA-TM-X-44576) 11 p1831 N71-22178
- Physiological responses of inexperienced private pilots to cross-country flying (FAA-AM-71-23) 19 p3043 N71-32082
- Determination and application of aeromedical standards to occupant selection, aircraft design features, and operational guidelines for spacecraft design (FAA-AM-71-33) 19 p3044 N71-32083
- FLIGHT CONTROL**
- NT AUTOMATIC FLIGHT CONTROL
- NT FLY BY WIRE CONTROL
- NT POINTING CONTROL SYSTEMS
- NT THRUST VECTOR CONTROL
- Flight evaluation of movable and rigid cockpit control sticks (AD-709934) 01 p0003 N71-10184
- Flight control software package for digital flight control and landing system of CH-46C helicopter (NASA-CR-110905) 01 p0027 N71-10283
- Systems performance/design requirements specifications for CH-46C helicopter digital flight control and landing system (NASA-CR-110889) 01 p0003 N71-10294
- Systems analysis of flight control and guidance of CH-46C helicopter (NASA-CR-111024) 01 p0003 N71-10297
- Flight simulation for evaluating proposed stabilization system to ensure helicopter hovering precision during cargo loading (AD-710948) 01 p0005 N71-10564
- Self organizing control system demonstrator to obtain multivariate principles pertaining to control of flight vehicles (AD-712099) 02 p0262 N71-11760
- Historical review of growth of guidance and control systems based on use of digital computers for manned aircraft 03 p0408 N71-12603
- Aerodynamic characteristics and flight dynamics of manned missiles and spacecraft (AD-713632) 03 p0458 N71-13241
- Reliability of aircraft primary control (NASA-TT-F-12709) 04 p0473 N71-13412
- Methods for determining instantaneous values of aircraft parameters with inertial navigation systems (NASA-TT-F-614) 04 p0543 N71-14055
- Results of simulated runs to evaluate lunar module descent performance of P66 automatic control and guidance system (NASA-CR-114787) 04 p0613 N71-14233
- M2-F2 lifting body flight control system (NASA-TN-X-1809) 05 p0627 N71-14526
- Selection of computers for flight control (AD-713786) 05 p0651 N71-14977
- Simulated study of lunar flying platform control by pilot body motion (NASA-TN-D-6016) 05 p0658 N71-14981
- Investigating performance of various types of pure inertial and hybrid navigation systems (NASA-CR-115905) 05 p0721 N71-15543
- Functional requirements for ground-based trainers, helicopter response characteristics (AD-714954) 07 p1084 N71-18018
- Flight tests to determine reliability of X-15 self descriptive flight control system 08 p1143 N71-18422
- Optimal control of rotational and translational motion of flight vehicles based on torsional and flexural deformations (AD-716517) 09 p1320 N71-19696
- Human factors tests to determine effects of aircraft control placement on lightly clothed or pressure suited flight crews 09 p1341 N71-19911
- Basic model for adaptive flight control system (NASA-CR-117807) 11 p1693 N71-23060
- Aerodynamic characteristics affecting stability and controllability of supersonic aircraft (AD-718474) 12 p1856 N71-23538
- Jet vertical takeoff aircraft piloted cockpit simulator for controlling aircraft flight performance (ARC-R/M-3647) 13 p2027 N71-25065
- Complexity of supersonic aircraft systems for stability and controllability 15 p2537 N71-27354
- Effectiveness of attitude feedback and translational velocity feedback flight control system assessed for ability to provide positional stability and reduce pilot error at hover (AD-72128) 16 p2531 N71-28274

- Techniques for applying frequency domain optimal control in practical closed loop controller synthesis (AD-722040) 16 p2623 N71-28363
- Development of aircraft control system with high performance electrically controlled and mechanically operated hydraulic valves for precise flight operation (NASA-CASE-XAC-00048) 16 p2537 N71-29128
- Theory of controllability for parabolic and second order hyperbolic systems and for hereditary differentiation systems applied to stabilization of high speed aircraft in gust load disturbances (AD-722073) 17 p2703 N71-29430
- Solving two problems of optimal control in flight vehicles (AD-722280) 17 p2703 N71-29431
- Identifying linear dynamic systems with state and observation noise with application to flight control problem (AD-723108) 17 p2773 N71-29735
- Approximate solution of nonlinear potential equation for small disturbance in transonic range and pressure distribution on aircraft 18 p2872 N71-31061
- Fuzzy dynamic programming for use in synthesis of flight control system, and computer algorithm for obtaining guaranteed cost function (AD-723458) 18 p2947 N71-31379
- Mathematical model and information display system for flight control and monitoring aircraft and pilot performance (AD-723051) 19 p3045 N71-32566
- Evaluation of automatic guidance modes and software for V/STOL aircraft flight control (NASA-CR-121768) 21 p3375 N71-34016
- Practical design procedure for F-4 aircraft augmentation systems based on quadratic optimal control technology (AD-726564) 22 p3540 N71-35221
- Hydraulic power and actuation requirements of survivable flight control system utilizing fly by wire control for F-4 aircraft (AD-727763) 24 p3873 N71-37608
- Analysis of criteria for survivable flight control system using fly-by-wire and integrated actuator package techniques (AD-727762) 24 p3874 N71-37616
- Development and implementation of Space Flight Operations Facility and Ground Communications Facility for DSN 24 p4007 N71-38568
- FLIGHT CREWS**
- Physiopathology and pathology of spinal affections in aerospace medicine (AGARD-AG-140-70) 01 p0008 N71-10175
- Development and fabrication of polycarbonate eyeshield for army flyers helmet (AD-712131) 02 p0169 N71-11200
- Carbon dioxide concentrator subsystem for closed loop aircrew oxygen system (NASA-CR-73397) 02 p0170 N71-11204
- Sonar detection of submarines by helicopter and protection of flight crew bearing (AD-711910) 03 p0336 N71-12400
- Effects of drugs on performance of flight personnel following unusual sleep patterns 07 p0978 N71-16908
- Effect of work-rest cycles on performance of flight crews and supervisory personnel 07 p0985 N71-16909
- Assessment of fatigue for flight crew members during long duration flights 07 p0978 N71-16910
- Influence of duty hours on sleep patterns in flight crews during long duration flights 07 p0978 N71-16912
- Differences between military and commercial flight crews work-rest cycles and physiological stresses 07 p0979 N71-16913
- Technical evaluation of circadian rhythm disturbances and flight crew performance 07 p0979 N71-16916
- Survey of helicopter flight crew morale (AD-715015) 07 p0987 N71-17750
- Hydraulic grip dynamometer for study of elevated gravitational effects on flight crews (AD-715911) 08 p1157 N71-18415
- Onboard aircrew oxygen generating system for tactical aircraft (NASA-CR-1741) 08 p1158 N71-18935
- Cockpit geometry evaluation program results and techniques with computer input and output samples of flight crew anthropometry (AD-716395) 09 p1321 N71-19817
- Anthropomorphic data update for man-model used in cockpit geometry evaluation program for evaluation of flight crew interaction and compatibility with crew stations (AD-716396) 09 p1340 N71-19818
- Cockpit geometry evaluation program for computer simulation of flight crew physical compatibility with crew stations based on anthropometric and environmental data for man-model movements (AD-716397) 09 p1340 N71-19819

FLIGHT INSTRUMENTS

- Human factors tests to determine effects of aircraft control placement on lightly clothed or pressure suited flight crews 09 p1341 N71-19911
- Vibration effects on performance of helicopter flight crews 09 p1335 N71-20353
- Posture effects on flight crew tolerance to positive acceleration 09 p1335 N71-20357
- Application of psychotherapy in aviation psychiatry for treatment of syndromes of reactive nature 09 p1337 N71-20345
- Nasopharyngeal bacterin cultures of spacecrew during long duration space station simulation 10 p1498 N71-20592
- Physical fitness of flying personnel and aging effects on flight crew performance (AGARD-CR-81-71) 11 p1687 N71-22301
- Coronary system diseases in aging flight crews and removal from flying status 11 p1689 N71-22315
- Evaluation of protective clothing for flight crew members (AD-719106) 13 p2036 N71-24460
- Mathematical formulation of kinematic equations to describe motion of six degrees of freedom vibration table for use in research on human subjects (AD-726269) 14 p2210 N71-26158
- Measurements of aircrew total vibration exposure during low altitude, high speed flight in F-4C aircraft (AD-728271) 14 p2203 N71-26172
- Engine-airframe contribution to combat aircrew rescue simulation (AD-728238) 14 p2211 N71-26371
- Work environment and task factor effects on long term aircrew effectiveness (AD-722417) 17 p2771 N71-29682
- Aerospace environments affecting flight crew fatigue (AMRU-R-67-3) 18 p2881 N71-31542
- Aircraft recognition accuracy and decision speed comparing single observers and four-man crews (AD-714213) 19 p3047 N71-31625
- Use of new philosophy of total learning process for improved crew member training (AD-723131) 19 p3048 N71-31741
- Analysis of flight crew duties and operations during flight of De-8 aircraft with recommended changes to improve safety (NAL-TR-215) 20 p3212 N71-33585
- FLIGHT FATIGUE**
- Assessment of fatigue for flight crew members during long duration flights 07 p0978 N71-16910
- Influence of duty hours on sleep patterns in flight crews during long duration flights 07 p0978 N71-16912
- FLIGHT FITNESS**
- Physical fitness of flying personnel and aging effects on flight crew performance (AGARD-CR-81-71) 11 p1687 N71-22301
- Physical fitness assessment of older pilots in relation to flight requirements and physiological responses 11 p1687 N71-22304
- FLIGHT HAZARDS**
- NT METEOROID HAZARDS
- Electrostatic hazards during launch vehicle flight operations (NASA-CR-111727) 04 p0614 N71-14114
- Report of transport aircraft accident and probable causes (NTSB-AAR-71-4) 08 p1145 N71-19040
- Human factors and control system failures in jet upsets during turbulence encounters 12 p1855 N71-23424
- Whistling swan as potential hazard to aircraft during migration periods along Eastern flyway (AD-720869) 15 p2367 N71-27220
- Evaluation of lightning hazards to jet aircraft including possibility of fuel tank explosions (AD-724092) 20 p3209 N71-33006
- FLIGHT INSTRUMENTS**
- NT APPROACH INDICATORS
- NT ATTITUDE INDICATORS
- NT AUTOMATIC PILOTS
- NT FLIGHT TEST INSTRUMENTS
- NT GYRO HORIZONS
- NT HORIZON SCANNERS
- NT RADIO ALTIMETERS
- Display relationship problems applied to presentation of aircraft altitude and guidance information (AD-713179) 05 p0637 N71-14743
- Effect of cockpit lighting systems on multicolored instrument displays (AD-716610) 09 p1339 N71-19710
- Feasibility of utilizing color cathode ray tubes for aircraft crew station displays (AD-717653) 11 p1673 N71-22174
- Holographic imagery for aviation and space flight (JPRS-55420) 17 p2706 N71-30361
- Tests to determine effectiveness of two linear rate-field displays for use as flight instruments (AD-726645) 22 p3542 N71-35229

FLIGHT MECHANICS

- Evaluating current and future requirements and resources for pilots and mechanics in US civil aviation
[AD-713035] 02 p0167 N71-11187
- Technology review on unmanned flight vehicles
[AD-713035] 03 p0456 N71-13061
- Engineering analysis on flight mechanics for simulating pilot behavior in aircraft
06 p0832 N71-16068
- Application of overall error or uncertainty in spacecraft trajectory determinations to define a time dependent error bound for coordinates of spacecraft
[NASA-TM-X-65471] 10 p1643 N71-20929
- Analysis of space flight mechanics involving interplanetary trajectories
[AD-717829] 11 p1826 N71-22127
- Bionic oscillating propulsion system of fishes
11 p1694 N71-23071
- Accident investigations, flight control systems, and operational recordings for improved aircraft flight mechanics
[AGARD-CP-76-71] 12 p1853 N71-23410
- Operational flight data analysis for improved aviation safety levels
12 p1853 N71-23411
- Onboard data acquisition for improved aircraft design and operational flight safety
12 p1853 N71-23412
- Flight simulator and airframe test stand for evaluating operational performance of aircraft flight control system
12 p1853 N71-23413
- Design modifications on short takeoff Bronco aircraft resulting from combat operations tests
12 p1854 N71-23416
- Landing accidents investigations for Hawker Siddeley 748 aircraft with performance measurements on rough surfaces
12 p1854 N71-23417
- Safety measures to eliminate aircraft trailing vortex hazards
[NASA-TM-X-67125] 12 p1854 N71-23418
- Flight mechanics problems in accident investigations for VJ-101 aircraft
12 p1855 N71-23428
- Rigid rotating body kinematic equations for use in space flight mechanics
[NASA-CR-119361] 18 p2965 N71-31176
- FLIGHT OPTIMIZATION**
- LIFTING ROBOT minimum Hamiltonian-steepest ascent multistage lifting booster optimization program input and example problem for mission planning
[NASA-CR-119922] 21 p3518 N71-35069
- FLIGHT PATHS**
- NT GLIDE PATHS**
- Behavior of attitude gyro and gyro horizon during looping flight
03 p0413 N71-13281
- Optimization techniques for aircraft multiple flight paths
[AD-713136] 05 p0721 N71-15392
- Relaxation in scaling parameters effect on free flight path of wind tunnel model with forced ejection
[ARL/A-322] 09 p1314 N71-19391
- High intensity xenon flashtube lights for increasing conspicuity of trainer helicopters during daytime and nighttime flights
[AD-718639] 13 p2026 N71-24669
- Approach guidance system for side-firing tactical aircraft
[AD-722412] 17 p2704 N71-29708
- Statistical analysis of Navy and Marine aircraft activity and airspace usage in Feb. and Mar. 1970 as part of National Airspace Utilization System
[AD-722698] 17 p2705 N71-30174
- Application of two dimensional collision geometry to collision avoidance warning techniques for military aircraft operations
[AD-723977] 20 p3208 N71-32931
- Results of combined fully instrumented satellite geophysical experiment including spectrophotometry of earth surface
[JPRS-53895] 21 p3419 N71-34328
- Plotter subroutine for two-dimensional plots of meteorological straight line flight path and four analog traces of selected meteorological parameters
[NOAA-TR-ERL-140-APCL-10] 21 p3452 N71-34570
- Meteorological flight path plotter subroutine for plots with wind vectors, time notations, and legend
[NOAA-TR-ERL-139-APCL-9] 21 p3452 N71-34571
- Summary of instrument flight rule off-airway routes for commercial and military aviation in US and overseas areas
21 p3455 N71-34592

FLIGHT PERFORMANCE

U FLIGHT CHARACTERISTICS

FLIGHT PLANS

- Northern Hemisphere temperature field atlas for SST flight planning
[AD-712017] 02 p0145 N71-11031
- Operational schedule for Apollo 9 command module/ lunar module 3 flight plan and crew activities
[NASA-TM-X-66904] 09 p1469 N71-20513

FLIGHT RECORDERS

- Jet transport aircraft airspeed control and controllability data obtained by flight recorders
[ARC-CP-1135] 10 p1493 N71-20902
- Event recorder with constant speed motor which rotates recording disk
[NASA-CASE-XLA-01832] 10 p1557 N71-21006
- Analysis of 79,000 hours data obtained from NASA V-G/UGH flight recorders installed on 734 general aircraft engaged in eight types of operations
18 p2871 N71-30782
- Performance evaluation of automatic flight progress strip cutter and loader used in air traffic control facility
[ACTEU-330] 24 p3955 N71-38215
- FLIGHT RULES**
- NT INSTRUMENT FLIGHT RULES**
- FLIGHT SAFETY**
- Discussing major and minor tasks of safety and rescue planning for lunar missions
[NASA-CR-114401] 05 p0772 N71-15349
- Preliminary report of aircraft accident of DC-8 at Anchorage, Alaska
[SB-71-5] 06 p0794 N71-16059
- Surveying air traffic controller occupation and development of performance objectives
07 p1138 N71-18105
- Investigating statistics of aircraft accidents by region and operator
[REPT-1970/10-E] 07 p0974 N71-18115
- Maintenance and flight safety problems of space shuttle
[NASA-TM-X-52964] 08 p1293 N71-18638
- Flight safety performance of V/STOL Harrier military aircraft having jet control
12 p1855 N71-23427
- Retinal image stabilization during flight
[AMRU-W-45-2] 18 p2879 N71-31530
- Application of two dimensional collision geometry to collision avoidance warning techniques for military aircraft operations
[AD-723977] 20 p3208 N71-32931
- Physiological effects of alcohol and cockpit illumination levels on pilot performance and flying safety
[FAA-AM-71-34] 22 p3548 N71-35275
- Space shuttle hazards, safety procedures, and escape systems
22 p3675 N71-36203

FLIGHT SIMULATION

- Human factors in use of terminal radar/analog display systems
[FAA-NA-70-55] 01 p0010 N71-10381
- Loading edge effect on aerodynamic characteristics of 70 deg swept delta wing
[AD-712087] 02 p0142 N71-11007
- Fire protection tests in small fuselage mounted turbojet engine and nacelle installation
[FAA-NA-70-41] 02 p0144 N71-11018
- Flight simulation of rotor forces and flow field in vicinity of step ground plane
[AD-711955] 03 p0309 N71-12203
- Simulation and analysis of panel separation from Apollo 13 service module
[NASA-TN-D-6087] 03 p0456 N71-13026
- Flow visualization of trailing vortex wakes in towing tank
[DI-82-1004] 04 p0519 N71-13800
- Human factors in aircraft simulation
[AGARD-CP-79-70] 06 p0830 N71-16060
- Dynamic characteristics and linear control theory for aircraft simulation
06 p0831 N71-16061
- Flight simulations for accelerated development of aircraft at reduced cost
06 p0831 N71-16062
- Sensory factors of motion, vision, and hearing for piloted flight simulation
06 p0831 N71-16064
- Psychological and environmental factors in selecting pilot simulator tasks
06 p0831 N71-16067
- Engineering analysis on flight mechanics for simulating pilot behavior in aircraft
06 p0832 N71-16068
- Human factors in developing a piloted simulation program for evaluating aircraft handling aspects
[NASA-TM-X-66583] 06 p0832 N71-16069
- Vestibulometric chair and stand for objective study and training uses of vestibular analyzer
07 p0985 N71-16979
- Crack propagation in aluminum alloy sheet materials under flight simulation loading
[AD-715331] 08 p1211 N71-18245
- Wind tunnel evaluation of lifting body store configurations for captive flight drag and separation characteristics
09 p1314 N71-19386
- Television simulation for aircraft and space flight
[NASA-CASE-XFR-03167] 09 p1357 N71-19449
- Statistical analysis of simulated pilot ability to control lunar module approach and descent to lunar surface
[NASA-TN-D-6113] 09 p1416 N71-20144

- Simulation of neutron effects from radioisotope thermoelectric power generator on spacecraft electronic components
[NASA-TM-X-66937] 09 p1421 N71-20308
- Student naval aviator anxiety in simulation of first aircraft carrier landing
[AD-718326] 12 p1866 N71-23370
- Electrical circuit selection device for simulating stage separation of flight vehicle
[NASA-CASE-XKS-04631] 12 p1893 N71-23403
- Television-type, cut-window visual simulation image generator design and specifications for aircraft or spacecraft manned flight simulation
[NASA-CR-114301] 12 p1897 N71-24126
- Major and critical component specifications for construction of simulator cruise scene visual attachment for manned spacecraft or aircraft flight simulation
[NASA-CR-114362] 12 p1898 N71-24127
- Cruise scene visual attachment system assembly and detail design drawings for manned spacecraft or aircraft flight simulators
[NASA-CR-114303] 12 p1898 N71-24128
- Manned simulation of crew performance for assessing space mission reliability
16 p2553 N71-28540
- Plastic lenses providing virtual image of flight scene for use in flight simulator with Schmidt projection system or television monitor
16 p2598 N71-28549
- Crew performance of metallic thermal protection system under simulated mission environments
17 p2870 N71-30771
- Simulation studies for development of certification criteria applicable to SST takeoff and engine failure
18 p2870 N71-30771
- Aircraft recognition accuracy and decision speed comparing single observers and four-man crews
[AD-714213] 19 p3047 N71-31633
- Inflight simulation with high wing loading fighter aircraft approach using HFB-320 and F-4 Phantom II
[DLR-FB-71-06] 19 p3072 N71-31709
- Conference papers on flight simulation
[DLR-MITT-70-29] 19 p3073 N71-31951
- Motion cues and pilot error in simulated instrument landing system approach
19 p3074 N71-31952
- Comparison of flight simulation techniques and costs
19 p3074 N71-31954
- Flight simulation of hovering vertical takeoff aircraft with various attitude and speed controls
19 p3074 N71-31955
- Flight simulation of short takeoff aircraft and DC-8-31 aircraft, and results using cockpit simulator with 6 degrees of freedom for DO-31
19 p3074 N71-31956
- Evaluation of in-flight simulation of flying platform using helicopter with variable stability and maneuverability
19 p3074 N71-31957
- Simulation margins and independent variable sensitivity of in-flight simulators using root locus analysis
19 p3074 N71-31959
- In-flight simulation with HFB-320 aircraft
19 p3075 N71-31959
- Use of BO-105 helicopter for in-flight simulation of V/STOL aircraft
19 p3037 N71-31960
- Performance tests of three axis motion platform simulator for Skylab program
[NASA-TM-X-66409] 19 p3181 N71-32048
- Analysis of design concepts for mechanical simulation of flight acceleration for testing of functional requirements of arm and safety devices used in nuclear warhead adaptation kits
[AD-726926] 22 p3681 N71-34230
- FLIGHT SIMULATORS**
- NT COCKPIT SIMULATORS**
- Pilot performance and acceptance of aircraft right cockpit control system during simulation
[AD-711296] 01 p0015 N71-10804
- Research and development in training personnel with low altitude, and aviation training devices
[AD-712285] 02 p1666 N71-11176
- Circadian rhythms of pilot performance in flight simulator and effects on time phase
02 p1665 N71-11187
- Effects of motion cues and motion scaling on sea and two axis compensatory control tasks with application to flight simulators
[NASA-TN-D-6110] 05 p0637 N71-18089
- Human factors in aircraft simulation
[AGARD-CP-79-70] 06 p0830 N71-16060
- Flight simulator mathematical modeling for aircraft design
06 p0831 N71-16060
- Technical and human engineering requirements for simulating pilot flight
06 p0831 N71-16060
- Behavior of fliers in emergency situations during flight
[JPRS-52233] 06 p0803 N71-16060

SUBJECT INDEX

Developing attitude control single-axis simulator for
Thermoelectric Outer Planet Spacecraft

Functional requirements for ground-based trainers,
helicopter response characteristics

Feasibility of visual tracking to determine effect of
lag in simulated aircraft dynamics

High bypass turbofan powered propulsion simulator
for aircraft engine integration analyses at subsonic
and supersonic speeds

Flight simulator tests of human behavior in roll
tracking tasks in fighter and large aircraft with descrip-
tive functional analysis

Performance of reentry nose tip facility for missile
test transfer simulations

Universal aircraft flight simulator/trainer system
definition

Physical analog model for human vestibular organ
models in guidance and control systems

Flight simulator and aircraft test stand for evaluating
operational performance of aircraft flight control
systems

Analysis of pilot training, career, education, and
motivation related to role of research and flight simu-
lation

Regenerative space station simulator and test
procedures for 4 man, 90 day testing of life support
systems

Preparation of test plans used to evaluate per-
formance of flight simulation trainers

Influence of lateral motion on effectiveness of flight
simulators in training air transport pilots

Simulation margins and independent variable sen-
sitivity of in-flight simulators using root locus analysis

In-flight simulation with HFB-320 aircraft

Use of BO-105 helicopter for in-flight simulation of
V/STOL aircraft

Development and evaluation of experimental test
plan for solutions of motion drive problem in forma-
tion flying task with flight simulators

Behavioral science programming language for use
with flight simulator facility

Motion cue and simulation fidelity aspects of valida-
tion of general purpose airborne simulator

Flight simulator for studying problems of aircraft
during approaches and landings at night under category
I visual conditions

Analysis and validation of characteristics of general
purpose airborne simulator for simulation of aerody-
namic characteristics of large transport aircraft

Low speed wind tunnel and flight stability tests of
MAC 221 aircraft longitudinal balances, noting aileron
deflections

Evolution of helicopter flight loading and structural
stability

Flight evaluations using variable stability aircraft to
simulate effects of turbulence induced aerodynamic
disturbances and lateral directional dynamics on pilot
performance

Analysis of uropneal excretion in dogs under in-
fluence of simulated flight stress conditions

Psychological test of human reaction to simulated
flight

Psychological test of human reaction to simulated
flight

Psychological test of human reaction to simulated
flight

Psychological test of human reaction to simulated
flight

Psychological test of human reaction to simulated
flight

Psychological test of human reaction to simulated
flight

Psychological test of human reaction to simulated
flight

Results of lifting body flight tests and findings from
other related studies evaluated for application to space
shuttle system

Wind tunnel and flight tests for stability and control
derivatives of lifting body vehicles

Correlation of flight test loads with wind tunnel pre-
dicted loads on three lifting body vehicles

Low power solid-state radio beacon tests and
evaluation for snow and ice outages of compass loca-
tor systems

Flight assessment of trailing-cone static pressure
probe at subsonic speeds

Flight test program to obtain data on aided inertial
system for terminal guidance and navigation of heli-
copter in designing V/STOL avionics system

Aided inertial flight test experiments for all weather
V/STOL operations

Systems design and flight tests of azimuthal guidance
orientation system

Flight tests of lifting reentry vehicles for controlla-
bility prediction

Flight evaluation of AN/APN 191 radar altimeter

Flight test methods for determining aircraft dynamic
stability

Flight acoustical and performance evaluations of
DC 8 nacelle modifications to reduce fan-compressor
noise in airport communities

Advanced aircraft for flight testing of integrated
electronics system for reusable space shuttle

Low speed lateral stability and control flight tests on
Avco 707 aircraft

Flight tests to determine reliability of X-15 self
adaptive flight control system

HL-10 and M-2F2 lifting body flight tests

Determining equations of motion and aerodynamic
characteristics for Magnus rotors by flight tests

Flight testing military transport aircraft for handling
and performance in STOL applications

H-126 jet flap research aircraft development and
testing

Possibilities for scale effect on swept wings at high
subsonic speeds on basis of pressure plotting tests

Flight tests of Boeing 747 aircraft and operational
analysis for supersonic transport

Flight tests of Concorde prototypes, design modifi-
cations, and operational costs of supersonic aircraft

Theoretical analysis of jet mixing under influence of
nonconstant pressure gradient

Accident investigations, flight control systems, and
operational recordings for improved aircraft flight
mechanics

Design modifications on short takeoff Bronto air-
craft resulting from combat operations tests

Flight test evaluation of military aircraft low altitude
high speed performance

Beagle B125 training aircraft handling tests

Flight-measured base pressures from sharp leading
edge upper vertical fin of X-15 aircraft compared with
wind tunnel data for turbulent flow at Mach numbers
from 1.5 to 5.0

Evaluation of fuel flowmeter instrumentation con-
ducted during flight tests

Flight tests for controlling slope approach of short
takeoff aircraft

Flight data analysis and electromechanical simula-
tion of sounding rocket stability using rigid body energy
techniques

Investigation of flight path and longitudinal dynamic
characteristics of free flight rocket model

FLIGHT TESTS

High altitude aircraft test for visible laser commu-
nication and analysis of errors in optical communica-
tion experiment due to flight path inaccuracies

Comparison of pilot performance using center stick,
dual side stick, and single side stick configuration

Reflective surface degradation data from samples
flown on Applications Technology Satellite

Polyethylene balloon fabrication and flight test
time/altitude data

Nonsteady flight test program on Sibel 204 D-1 air-
craft for determining lateral directional stability and
control derivatives

Design, development, and flight testing of fire sup-
pressant void filter from bins for lower hemisphere of
fuel tanks in various tactical army aircraft

Flight tests of cross, modified ring, and disk para-
chute deployment performance from low altitudes with
structural load data

Comparative analysis of data reflecting knowledge,
skill, and satisfaction of aviators in combat readiness
training flight tests

Vertical oxygen remote sensor design and flight
testing for use on OV-1 satellites

In-flight use of traversing boundary layer probe
with mechanical and electrical features and
sample boundary layer profiles

Flight tests for evaluating effect of wing-tip vortex
wake generated by large jet transports on smaller air-
craft

Vertical situation display concept for alleviating
problems of inadequate guidance and display informa-
tion for making steep approaches

Flight tests to determine handling qualities of
general aviation aircraft during ILS approaches in tur-
bulent air

Problem of wind gust absorption by aircraft struc-
tures, and flight tests of prototype II-106

Flight test of Planetary Atmosphere Experiments
Test (PAET) spacecraft to investigate means of deter-
mining structure and composition of unknown plan-
etary atmospheres

Data acquisition system for US-2A aircraft training
flight evaluations

Helicopter pilot visual acuity determined from flight
tests

Flight testing and performance evaluation of rotary
and fixed wing aircraft for military operations

Flight test data on geometric, aerodynamic, and
kinematic characteristics of two twin leaf parawings
during deployment

Summary of flight test methods used for per-
formance measurement of Concorde aircraft

Evaluation of performance, stability, and control
characteristics of XV-11 A short takeoff aircraft

Collision avoidance system for detecting probable
aircraft accidents - France

Determining deployment characteristics of all-flexi-
ble parawings by free flight tests

Application of least squares method for determining
longitudinal aerodynamic derivatives of aircraft from
flight test data

Correlation studies based on wind tunnel test data
and flight tests to determine performance, stability
and control of X-70-1 aircraft

High altitude flight test of roofed 12.2-meter-diam-
eter disk-gap-band parachute with deployment at 2.58
Mach number

Development of test and flight engineer language for
space shuttle system

Briefing aids used for oral presentation describing
development of test and flight engineer oriented com-
puter language for space shuttle system

Small Applications Technology Satellite program
for developing sensors, experiments, and spacecraft
technology and systems through orbital flight testing

Transition, approach, and vertical landing tests for VTOL transport in terminal area [NASA-TM-X-62083] 22 p3539 N71-35209
Flight tests of airborne dissemination devices for chemical warfare [AD-726359] 22 p3540 N71-35218
Fixed wing aircraft employing free fall and circling-line techniques in rescue of personnel and retrieval of equipment [AD-727007] 22 p3541 N71-35228
All weather landing system design, development, and field and flight testing 22 p3618 N71-35777
Guide to private and commercial multiengine aircraft pilot certification [FAA-AC-61-4C] 23 p3708 N71-36438
Measurements and analysis of solid propellant rocket vibrations obtained during captive flight of Nike rocket [NASA-TN-D-6517] 23 p3863 N71-37539

FLIGHT TIME

Developing realistic mission models for food system to sustain spacecraft for extended periods of time [NASA-CR-114886] 09 p1340 N71-19785

FLIGHT TRAINING

NT SPACE FLIGHT TRAINING
Astrickness during flying training 02 p0164 N71-11823
News releases on cosmonauts from Soyuz 7 and 8 and flight training [AD-714771] 06 p0806 N71-16097
Comparative analysis of data reflecting knowledge, skill, and satisfaction of aviators in combat readiness training flight status [AD-721588] 16 p2550 N71-28340
Use of new philosophy of total learning process for improved crew member training [AD-723313] 19 p3048 N71-31741
Development of multivariate system for evaluating potential effectiveness of military aviation personnel during training 20 p3226 N71-33148
Development of procedure for predicting success of personnel in military aviation training [AD-724695] 20 p3227 N71-33149

FLIGHT VEHICLES

Radio navigation aids used to navigate flight vehicles [AD-714829] 06 p1232 N71-18299
Construction of leading edges of surfaces for aerial vehicles performing from subsonic to above transonic speeds [NASA-CASE-XLA-01486] 12 p1851 N71-23497
Vehicle with plasma-ion electrodejet engine designed for orbital flights and altitudes from 50 to 200 km using ionospheric air intake for fuel [Yantar] [NASA-TT-F-13676] 17 p2832 N71-29242
FLIP-FLOPS
Bistable multivibrator circuits operating at high speed and low power dissipation [NASA-CASE-XGS-00823] 06 p0826 N71-15910
Stepping motor control apparatus exciting windings in proper time sequence to cause motor to rotate in either direction [NASA-CASE-GSC-10366-1] 06 p1172 N71-18772
Integrator and current driver circuit for combination with transistor flip-flop circuit [NASA-CASE-XGS-03058] 09 p1363 N71-19547
Alternating current gated flip-flop implementation in sequential circuit design 12 p1880 N71-23787
Asynchronous interaction of binary circuits under marginal triggering conditions through failure of flip flop circuits to stabilize after triggering 23 p3738 N71-36655

FLOATING

Swell influence on floating rectangular elastic beam vertical vibration 10 p1654 N71-21134

FLOATING POINT ARITHMETIC

Deriving algorithm for floating point arithmetic using single length arithmetic registers for most accurate approximation [AD-713699] 05 p0713 N71-15249
Effect of coefficient rounding in floating point digital filters [AD-727073] 24 p3898 N71-37784

FLOATS

Wave energy extraction by crescent shaped column for stationkeeping of floating platforms - model and feasibility study 20 p3259 N71-33176
Design, development, and evaluation of emergency life support system to protect infants and small children during water survival situation [FAA-AM-71-37] 21 p3385 N71-34083
Development of operational system for measuring ocean surface current from aircraft using floats and fluorescent dyes [AD-726568] 24 p3916 N71-37922
FLOCCULATING
Harvesting of algae through chemical flocculation and flotation [REPT-321] 04 p0487 N71-13462

FLOORS

Fast reactor fuel interaction with concrete floor after hypothetical core meltdown 04 p0582 N71-14104
[BNWL-CC-2369]
Computer program for cellular structures of arbitrary plan geometry designed to capture behavior of deck and web components 09 p1481 N71-20517
[PB-196143]
Horizontal static forces exerted by men standing in common working positions on various surfaces including coefficients of friction between different floor and shoe materials 14 p2210 N71-26196
[AD-720523]
FLOQUET THEOREM
Floquet theorem calculation of particle resonance frequencies and dispersion relations 10 p1625 N71-21828

FLORA

U PLANTS (BOTANY)

FLORIDA
Application of computer processed multispectral data in discrimination of land collapse prone areas in Florida 06 p1196 N71-19253
Weighted defect densities of asphaltic and cement concrete pavement in airfield pavement condition survey, USNAs Cecil Field, Florida 16 p2577 N71-28422
[AD-721325]
Analysis of Biscayne Bay, Florida as natural resource, noting effects of pollution and need for environmental control 18 p2911 N71-30984
Environmental effects of jetport near Everglades Park in southern Florida 21 p3420 N71-34338
[PB-199159]
Documentation of Congressional Subcommittee testimony regarding Navy oil sludge pollution off Florida coast 21 p3533 N71-35178
Cloud condensation nuclei effects on rainfall during spring droughts in Florida from pest, algae, sawgrass, and leaf fire smoke [ESSA-TM-ERL-TM-AOML-4] 23 p3784 N71-36975
Cloud photography and meteorological description of cloud holes observed over Miami, Florida on 1 Dec. 1967 23 p3785 N71-36976
Tidal modulation of Florida current surface flow 23 p3789 N71-37005
Fluctuations of Florida current inferred from sea level records and linear weather effects 23 p3789 N71-37006
Interpretation of color infrared photography of Florida tidewater coastline 24 p3916 N71-37924
[AD-727630]

FLOTATION

Harvesting of algae through chemical flocculation and flotation 04 p0487 N71-13462
Development and characteristics of rescue litter with inflatable flotation device for water rescue application [NASA-CASE-XMS-04170] 11 p1692 N71-22748
FLOTATION SYSTEMS
U FLOATS
FLOW CHARACTERISTICS
NT BOUNDARY LAYER STABILITY
NT FLAME STABILITY
NT FLOW DISTRIBUTION
NT FLOW STABILITY
NT FLOW VELOCITY
NT MAGNETOHYDRODYNAMIC STABILITY
Determining electron concentration in flowing plasma in presence of accelerating and evaporating water droplets 01 p0105 N71-10456
[NASA-TN-D-6007]
Diffusional flow in superplastic magnesium alloy [AD-711348] 01 p0069 N71-10997
Characteristics of radial wall jet bounded by circular jump [REPT-284] 02 p0204 N71-12078
Characteristics of jet issuing from two dimensional orifice past rectangular plate 02 p0204 N71-12079
[REPT-308]
Viscous interactions and flight at high Mach numbers [AD-712075] 03 p0309 N71-12204
Sinusoidal shear flow of density stratified fluid over two dimensional barrier 04 p0519 N71-13794
[D1-42-1009]
Propagation and decay of vortex rings determined by stereoscopic photography and hot-wire anemometry 05 p0660 N71-14750
[AD-713705]
Conformation and turbulent flow characteristics of polyelectrolytes in solution 05 p0664 N71-14978
[AD-713217]
Acoustic and flow characteristics of subsonic and supersonic jets from convergent nozzles [NASA-CR-1093] 05 p0664 N71-14993
Pumping characteristics of rotating truncated cone [NASA-TM-X-52953] 06 p0657 N71-16576
Measuring sonic boom pressure distribution on models in supersonic wind tunnels 06 p0839 N71-16685

Flow characteristics of wire-form and laminar-form porous materials 07 p0966 N71-17118
[NASA-TM-X-2111]
Vertical shock layer stagnation point flow characteristics [AD-715263] 07 p1012 N71-17791
Supercritical flow characteristics of overfill with nappes subjected to different constant pressures [AD-715067] 07 p1013 N71-17791
Boundary layer characteristics of particulate flow in cascade nozzles [AD-715721] 08 p1179 N71-18052
Characteristics of separated flow regions within attitude compensating nozzles [NASA-CR-116875] 08 p1184 N71-18089
Gas flow during and after deflagration of spherical cloud of fuel air mixture 09 p1370 N71-19555
[AD-716339]
Three dimensional viscous hypersonic interaction 09 p1375 N71-19555
Smooth double-slotted circular cylinder aerodynamic force characteristics measured for circulation control by slot suction [NRC-11714] 09 p1377 N71-30916
Cavity resonance effects on dynamic and thermal characteristics of resonant cavities in low speed, turbulent, shear flow 09 p1318 N71-30916
Visualized flow patterns of pelagic fishes to measure vortex formation and air and water boundary layer effects [JPRS-52790] 10 p1544 N71-31644
Separated flow theory - Thesis project [AD-717200] 10 p1544 N71-31780
Determination of pressure characteristics and flow properties of cylindrical bodies in aqueous solutions of polyethylene oxide [AD-717584] 11 p1733 N71-23100
Determination of flow conditions under which traveling wave will propagate in self oscillating regime 11 p1736 N71-23211
Heat transfer and flow friction characteristics of compact heat exchanger surfaces with and without brazing roughness [AD-717661] 11 p1768 N71-23206
Numerical analysis of turbulent characteristics of velocity field associated with mean velocity profile of turbulent channel flow 11 p1742 N71-23201
Tube length effects on transition from supersonic to subsonic flow at low Reynolds numbers and static pressure and flow characteristics upstream and downstream 11 p1742 N71-23201
Characterization of wake behind flat plate with thickness aligned with flow at infinity 11 p1743 N71-23201
Winglike tests of cylindrical and Lundell-conical rotors in ambient air producing Reynolds numbers up to 100,000 for high speed alternators [NASA-TM-X-67009] 12 p1857 N71-23116
Measurement of drag reduction of polymer solution at various stages of degradation in simulated long pipe 12 p1904 N71-34316
Development of mathematical model for predicting maximum two phase flow rates and comparison of flow rates where peak in pressure drop occurs 12 p1904 N71-34317
Transonic wind tunnel investigation of flow characteristics and pressure fluctuation of space shuttle launch and reentry configurations 13 p2180 N71-24661
Examination of sodium pipe models using example flow and temperature transients [WHAN-FR-22] 15 p2443 N71-28979
Velocity fields and hydraulic resistance of turbulent flow in channels formed by clusters of such fuel rods [AEC-TR-7189] 15 p2444 N71-30909
Permeator for measuring low fluid permeability of rocks used to study origin of life [NASA-CR-119021] 16 p2585 N71-30916
Influence of disc valve springs on action of valve and functioning of compressor [NLL-RTS-5938] 17 p2756 N71-28025
Empirical formula for expressing leakage flow from nuclear reactor containment vessel 17 p2784 N71-30909
Inlet nozzle geometry effects on subsonic flow characteristics of miniature total pressure tubes including pitot tube static and dynamic pressure and flow velocity measurements [NASA-TN-D-4406] 18 p2905 N71-31018
Measurement of polycrystalline metal flow curves at high and room temperatures and their application to plasticity mechanics [RAE-LIB-TRANS-1531] 19 p3115 N71-32046
Flow visualization and mathematical model of peristaltic pumping including pressure and velocity measurements in two dimensional flow [AD-723870] 19 p3081 N71-37029
Recording of flow curves in tensile tests and compression tests with and without prestraining [RAE-LIB-TRANS-1569] 20 p3284 N71-33225

SUBJECT INDEX

- Digital computer and plotter for simulating flow about Joukowski airfoil
[TECH-71-4] 20 p3206 N71-33403
- Experimental determination of pressure drop and flow characteristics of dilute gas-solid suspensions in turbulent pipe flow
[NASA-CR-1894] 20 p3231 N71-33514
- Unsteady flow characteristics of turbo-compressors and axial flow turbines including blade vibration and damping
[TP-971] 20 p3340 N71-33760
- Effects of vertical contraction on horizontal flow of incompressible density-stratified fluid
21 p3414 N71-34290
- Flow characteristics in exhaust of pulsed magnetron gas fed arc examined with piezoelectric pressure transducer
[NASA-TN-X-47931] 22 p3566 N71-35402
- Computer program for determining radiating aerodynamic inviscid flow over blunt body by integral equations
[NASA-TN-X-2328] 23 p3706 N71-36417
- Flow characteristics including diffuser measurements of Langley Mach 20 high Reynolds number ball tunnel
[NASA-TN-X-2353] 23 p3741 N71-36673
- Computer program development for potential flow simulation about lifting bodies
[AD-727628] 24 p3871 N71-37397
- FLOW CHARTS**
- Universal dynamic flow without holdovers
[PB-189092] 03 p0401 N71-13335
- Multilayer eruptions associated with lunar craters Tycho and Aristarchus - lava flow charts
04 p0613 N71-14441
- Dual graph for maximal flow capacity of network
[AD-715648] 08 p1172 N71-10800
- Synthetic method for solving linear equations of flow graphs by multivariate polynomial extension of two-step integer-preserving elimination algorithm
08 p1229 N71-19197
- Development of two concepts of duality for network flow theory
[AD-715622] 09 p1363 N71-19716
- Intermediate code and table drivers processor for translating retrieval question to users original language
14 p2221 N71-25977
- Simulation of single-server model for paging drum channel system
[NASA-CR-123375] 17 p2774 N71-30023
- Flow sheet for reprocessing spent fuels from power reactors
[RT/CHI-71]3] 21 p3458 N71-34609
- Flow diagrams and compression capabilities for software interfacing of flight data
[NASA-CR-61366] 22 p3555 N71-35321
- FLOW COEFFICIENTS**
- NT DISCHARGE COEFFICIENT**
- Measurement of pipe friction factors during flow of dilute aqueous polyethylene-oxide solutions
[AD-715556] 06 p1181 N71-18743
- Tensile, mechanical, and compression properties of metals, alloys, and steels derived from flow curves
[BAE-LIB-TRANS-1523] 19 p3115 N71-32265
- FLOW DEFLECTION**
- Adjustable output voltage dc-dc converter for synoptic satellite attitude control and orbit transfer using electrostatic deflection of ion thruster beams
[PUBL-198] 20 p3300 N71-32996
- FLOW DEFLECTION INDICATORS**
- NT WIND VANES**
- Flow direction generator for testing sensitivity of flowmeter to unsteady pressure
[NASA-TN-X-52962] 08 p1180 N71-18632
- Hot-wire anemometer measurements of incompressible fluid flow direction and velocity in pipes
[NASA-TN-X-52967] 08 p1180 N71-18634
- Electric circuit for reversing direction of current flow
[NASA-CASE-XNP-60953] 12 p1891 N71-23271
- Flow angle sensor and remote readout system for wind cryogenic fluids
[NASA-CASE-XLE-04503] 13 p2081 N71-24864
- FLOW DISTORTION**
- Measuring distortion characteristics at engine face station of axisymmetric inlet
[NASA-CR-1644] 03 p0310 N71-12211
- Investigating effects of strain rate on flow stress of high purity recrystallized tantalum
[RCEL-72321] 04 p0531 N71-14141
- Inlet flow distortion testing of high Mach number transonic fan stages - Vol. 1
[NASA-CR-72766-VOL-1] 05 p0662 N71-14863
- Turbulent data derived from inlet flow distortion tests of high Mach number transonic fan stages - Vol. 2
[NASA-CR-72766-VOL-2] 05 p0662 N71-14864
- Curved boundary layer flow in converging channel
06 p0839 N71-16832
- The continuity equation of compressible flow with flow velocity distortions and gas density variations
[RLA-MITT-70-13] 07 p1008 N71-17167
- Effects of wave inlet distortion at high and low flow rates on performance of axial flow compressor
[NASA-TURBO-TR-20] 11 p1738 N71-23428

- Turbulence diffusion above flow during boundary layer and hypersonic flow interaction
[NASA-TT-F-13522] 12 p1899 N71-23312
- Computerized propeller design considered flow field distortion by hub
17 p2704 N71-29690
- Distorted velocity profile and electric potential distribution of long dc electromagnetic flowmeter for liquid metals
[NASA-TN-D-2342] 19 p3100 N71-32165
- Flow abnormalities in primary and secondary loops of LMFBFR and failure probabilities
[BAW-1350-PT-1] 19 p3138 N71-32248
- Effect of velocity profile distortion in circular transverse-field electromagnetic flowmeters
[NASA-TN-D-6454] 19 p3102 N71-32448
- Performance tests of single stage, transonic compressor for advanced aircraft
[NASA-CR-72806] 20 p3250 N71-33201
- FLOW DISTRIBUTION**
- Conformal mapping techniques to analyze two dimensional thin foils entering water surface vertically with ventilations
[AD-709915] 01 p0040 N71-10172
- Flow field in pancake region of three dimensional axisymmetric vortex tube sensor
[AD-711032] 01 p0040 N71-10182
- Measurements of hypersonic, rarefied flow field of
[AD-710641] 01 p0043 N71-10461
- Low-altitude satellite interaction study of neutral gases and Monte Carlo computer techniques for describing flow field and spacecraft interactions
[NASA-CR-111136] 01 p0049 N71-10611
- Recirculation region of flow field caused by jet in ground effect with crossflow
[AD-711645] 01 p0002 N71-10832
- Three dimensional flow patterns obtained during boundary layer separation on airfoils
[NPL-AERO-1305] 02 p0143 N71-11014
- Servosystem design of high-response multilooped bypass valving system for supersonic inlets
[NASA-TN-D-6081] 02 p0150 N71-11061
- Boundary layer transition studies of several pointed bodies of revolution at supersonic speeds
[NASA-TN-D-6063] 02 p0202 N71-11520
- Time-dependent method for calculating supersonic blunt body flow field with sharp corners and embedded shock waves
[NASA-TN-D-6031] 02 p0202 N71-11533
- Coolant flowmeters for measuring flow distribution in test reactor core
[KURRI-TR-72] 02 p0265 N71-11770
- Flight simulation of rotor forces and flow field in vicinity of step ground plane
[AD-711955] 03 p0309 N71-12203
- Investigating flow field in near wake behind rearward facing step in supersonic flow and heat transfer distribution along reattachment surface downstream of step
03 p0311 N71-12216
- Flow distribution and performance of supersonic vane diffusers for centrifugal compressors
[NASA-TT-F-13428] 03 p0384 N71-12541
- Numerical study on controlling dynamic properties of supersonic inlet using bypass bleed
[NASA-TN-D-6144] 05 p0626 N71-14669
- Flow distribution data for solid and honeycomb rotor shrouds to improve stall margin of 0.5 hub tip ratio single stage compressor
[NASA-CR-72809] 05 p0762 N71-15329
- Measurement of flow distribution caused by forward facing nozzles exhibiting near large cylindrical body at hypersonic speed
[NASA-TN-D-6103] 06 p0834 N71-15828
- Strong viscous interaction between laminar boundary layer and external hypersonic flow field on curved surfaces
[AD-714075] 06 p0835 N71-16218
- Aerodynamic characteristics of flow field about axisymmetric and two dimensional bodies in supersonic flow
[AD-713917] 06 p0835 N71-16509
- Numerical analysis of flow field around right circular cylinder in Mach 2 airstream
07 p1012 N71-17761
- Wake flow properties of conical bodies at supersonic speeds and various angles of attack
[NASA-TN-X-2139] 08 p1178 N71-18480
- Numerical analysis of flow field typical of those in combustion driven supersonic MHD generator
08 p1181 N71-18871
- Aerodynamic interference characteristics of airframe-propulsion systems of transport and military aircraft
[AGARD-CP-71-71] 09 p1311 N71-19553
- Flight and wind tunnel evaluations of flow field effects on performance of supersonic underwing exhaust nozzle at transonic speeds
[NASA-TN-X-66887] 09 p1313 N71-19346
- Wind tunnel surveys of flow fields about wing fuselage core configuration inlets of transonic and supersonic aircraft
[NASA-TN-X-66885] 09 p1313 N71-19371

FLOW DISTRIBUTION

- Aerodynamic flow field interference effects on supersonic inlets
09 p1313 N71-19372
- Characteristics of flow distribution in hypersonic viscous shock layer on sharp flat plate
[AD-716485] 09 p1369 N71-19487
- Schlieren photography of flow distribution for transverse hydrogen jets from flat plate into Mach 2.72 airstream
[NASA-CR-1794] 09 p1371 N71-19637
- Supersonic flow fields around cylindrical body with blunt nose
[NAL-TR-199] 09 p1372 N71-19761
- Summary of investigation of streamwise vortex in curved flow
[AD-716478] 09 p1376 N71-19903
- Dispersion potential for calculating particle transport coefficients in flow field analysis
[SC-RR-70-664] 09 p1435 N71-20035
- Doppler radar measurements of flow generated by wing tip vortices using reflective chaff dispensed into vortices
[NASA-CR-111877] 10 p1491 N71-20630
- Color photointerpretation of interference colors reflected from thin film oil-coated components in moving gases for gas flow visualization
[NASA-CASE-XMP-01779] 10 p1539 N71-20815
- Finite difference method for unified solutions to inviscid supersonic flow distribution about blunt bodies
10 p1548 N71-21114
- Nonuniform flow field sonic boom reduction device using slit impinging on inclined flat plate
[AD-717193] 10 p1544 N71-21623
- Study of interaction of deep water gravity waves progressing into turbulent flow field produced by finite width grid towed in wide tank
[AD-717627] 11 p1733 N71-23219
- Examining solutions obtained from streamline curvature method of calculating flow through turbomachinery for several operating points of Rolls-Royce compressor
[CURVED-TURBO/TR-19] 11 p1737 N71-23294
- Steady state, axisymmetric flow distribution of space expansion of supersonic plasma jet from nozzle orifice numerically investigated using continuum flow
11 p1814 N71-22762
- Nonequilibrium radiative gas dynamics of slender pointed bodies
[AD-719744] 13 p2063 N71-24431
- Separation and flow phenomena in three dimensional boundary layer
[SC-T-71-3007] 13 p2068 N71-25462
- Wind tunnel simulations of flow fields and aerothermodynamics of space shuttle orbiter
14 p2340 N71-26053
- Finite difference method for calculating inviscid flow field around supersonic/hypersonic space shuttle
14 p2340 N71-26036
- Flow visualization, thermocouple measurements, and analyses of shock interference heating effects on straight wing space shuttle model
14 p2354 N71-26057
- Aluminum particle motion photographs for examining internal flow patterns of forming liquid drops
[IS-T-440] 13 p2392 N71-27066
- Heat transfers in two phase flows of horizontal and vertical tube heat exchangers
[CEA-CONF-1649] 15 p2393 N71-27153
- Liquid film disruption in air-water adiabatic channel flow with and without obstacles with wall shear stress and film thickness measurement for rotor core designs
[GEAF-10248] 15 p2394 N71-27651
- Circulation patterns at 850, 700, 500, and 200 millibars over Eastern Hemisphere from 40 deg north to 40 deg south during May and June, 1958 to 1960
[MET-O-0002] 15 p2440 N71-27813
- Wind tunnel tests to determine flow patterns and pressure distributions around bluff aerobody in wake of 120 deg cone for various separation distances at Mach 3.0
[NASA-TN-D-6281] 16 p2529 N71-28007
- Computerized simulation of shock waves and flow fields behind supersonic edge delta wings and wing-body combinations
16 p2532 N71-28365
- Flow field mapping for determining sonic boom intensity from wind tunnel measurements
16 p2534 N71-28384
- Interferometric holographic analysis of density flow fields around half-angle conical bodies in supersonic flow tunnels with 10 deg angle of attack
[AD-721543] 16 p2529 N71-28411
- Tropical wind flow patterns from automated analysis of streamlines, streamfunctions, divergence, and vorticity in tropics with feasibility of wind analysis using ATS data
[AD-721545] 16 p2626 N71-28597
- Transition in oscillating boundary layers including role of stability theory and transient vorticity distribution
[AD-720291] 16 p2582 N71-28875
- Flow and heat transfer characteristics of incompressible fluid in radial diffuser using air as fluid with

- inlet Reynolds numbers from 15 to 53,500 and area ratios from .245 to 2.04 16 p2583 N71-28894
- Pressure, temperature, gas sampling, and optical measurements in two dimensional jet interaction flow field [NASA-TM-X-67862] 16 p2583 N71-28953
- Rotary wing downwash influence on fixed wing flow using magnetic induction vortex model [DLR-FB-70-52] 17 p2701 N71-30040
- Augmented ram wing vehicle performance and flow field for high speed ground transportation 18 p2857 N71-31204
- Hypersonic and supersonic angle of attack flow about axisymmetric and axisymmetric blunt bodies based on time dependent finite difference theory and method of characteristics 18 p2906 N71-31207
- Production and characteristics of hypersonic viscous shock layer at leading edge of sharp flat plates [AD-723328] 19 p3076 N71-31751
- Examination of two dimensional combustion flow field upstream of inert and chemically reactive transverse jets 19 p3079 N71-31264
- Principles of operation, circuits, and construction of thermal flow rate meters for liquid metals [AD-723540] 19 p3103 N71-32591
- Numerical analysis of shock induced boundary layer flow on semi-infinite flat plate - Part 2 [NASA-CR-121743] 21 p3410 N71-34260
- Inverse solution of two dimensional gas dynamic flow fields of rotational or irrotational character [NASA-CR-121674] 21 p3410 N71-34261
- Measurement of flow characteristics behind backward facing step to demonstrate flow in reattachment region [IC71/05] 21 p3411 N71-34272
- Measurement of flow field behind plane detonation wave by observing motion of metal foils placed between explosives 21 p3413 N71-34282
- Supersonic turbulent boundary layer step induced separation, and incompressible flow model for predicting upstream flow field in channels 21 p3414 N71-34292
- Numerical analysis of pressure distribution in flow field due to diffraction of plane shock wave by thin wings 22 p3538 N71-35203
- Approximate small time solution for strong radiating reflected shock waves when radiative cooling occurs prior to chemical relaxation [TAMR-F-71-7102] 22 p3567 N71-35409
- Flow pattern of two phase flow of water/air at ambient temperature and pressure [NLL-CE-TRANS-5472-19022.091] 22 p3570 N71-35427
- Drag coefficient measurements in flow around rectangular cylinders [IC-AERO-71-15] 23 p3744 N71-36695
- Factors affecting volume from which data originate in laser Doppler velocimeter dual scatter probe [AD-727005] 23 p3766 N71-36845
- Sound and flow field of axially symmetric free jet impinging on wall at jet exit Mach numbers upwards of 0.6 [NASA-TT-F-13942] 24 p3905 N71-37832
- Near flow field data for tube-vehicle systems and drag coefficient relationships with relative Mach numbers and relative flow velocity ratios to vehicle velocity [GASL-TR-70-749] 24 p3908 N71-37856
- ### FLOW EQUATIONS
- #### NT HELMHOLTZ VORTICITY EQUATION
- #### NT VON KARMAN EQUATION
- Successive approximations method for equation integration of laminar multicomponent boundary layer with chemical reactions including ionization [NASA-TT-F-13379] 02 p2002 N71-11532
- Computer programs to determine loss and deviation correlations of flow in turbomachinery [ME/A-70-1] 03 p3312 N71-12226
- Numerical solution of partial differential equations on convection [AGARD-GRAP-146] 03 p3363 N71-12673
- Equations of viscous fluid motion with vortices accompanying self-folding processes [NASA-TT-F-12564] 05 p0663 N71-14970
- Fundamental equations of two phase flow with interfacial tension terms [PB-1939887] 05 p0664 N71-14971
- Flow models for bounded and intersecting plane, incompressible, turbulent jets 06 p0836 N71-16396
- Temperature distribution in thin fluid films heated by hot gas and hot wall [DLR-FB-69-98-PT-1] 08 p1180 N71-18618
- Energy estimates for equations of compressible flow initial value problems [LA-4525] 08 p1182 N71-18943
- Flow equations for simultaneous flow of two immiscible fluids in porous medium including infiltration problems for several boundary conditions [AEDP-71DBMC28] 08 p1184 N71-19091
- Equations for mass flow of methane and natural gas mixtures through critical flow nozzles, including real gas effects 10 p1543 N71-21330
- Formulation for temperature distribution in laminar flow with radiative and convective heat transfer 10 p1663 N71-21506
- Description of computer program for solving two dimensional and axisymmetric forms of compressible boundary layer equations for continuity, mean momentum, and mean total enthalpy [NASA-TM-X-2140] 11 p1739 N71-22588
- Numerical analysis of axisymmetric or two dimensional viscous flow at high Mach numbers in vicinity of two dimensional curved walls 11 p1741 N71-22673
- Numerical solution of mixed supersonic and subsonic steady wake flows by time-dependent method 11 p1741 N71-22674
- Comparison of artificial viscosity methods for blunt body flow field analysis including thermal radiation effects based on numerical integration of unsteady flow finite difference equations 11 p1742 N71-22700
- Characterization of wake behind flat plate with zero thickness aligned with flow at infinity 11 p1743 N71-22751
- Solution of general self-similar boundary layer equations and parametric investigation of several classes of boundary layer flow 11 p1743 N71-22759
- Theory describing hydrostatically neutral air flow adjustment in turbulent boundary layer power portion after abrupt surface roughness change perpendicular to flow direction 12 p1901 N71-23665
- Numerical solutions of compressible laminar boundary layer heat transfer and pressure drop of gas in uniformly heated tube 12 p2010 N71-23712
- Flow equation for representing ion beam current density profile from bombardment ion thrusters [NASA-TN-D-6334] 12 p1990 N71-23924
- Magnetic field suppression of magnetohydrodynamic boundary layer separation and inviscid flow equations 12 p1983 N71-24268
- Numerical analysis of behavior of finite cylindrical shell in fluid flow with linearized hydrodynamics equations 12 p2008 N71-24295
- Finite difference solution for unsteady equations of impulsively starting incompressible jet flow [EF/TN/A/28] 13 p2068 N71-25443
- Time dependent numerical technique for solving equations governing two dimensional frozen flow about blunt bodies with discontinuous curvature 14 p2241 N71-26271
- Numerical analysis of flow of viscous, compressible gas through slender axisymmetric channels using finite difference theory 14 p2242 N71-26464
- Characteristics of Couette flow of radiating ionized gas and development of absorption coefficient model 14 p2244 N71-26602
- Mathematical model for solving hydrodynamic flow equations in nonhomogeneous magnetic field for plasma flow along field line in presence of gravitational field [NASA-TM-X-65554] 15 p2503 N71-27889
- System of nonlinear equations of motion for isotropic, compressible fluid solved by cyclic relaxation method for subsonic and transonic regimes 16 p2580 N71-28688
- Characteristics of induced shock and acceleration waves determined by application of theory of singular surfaces 16 p2582 N71-28775
- Fluid dynamics and flow properties of glass, steel, and lead particle slurries in pipelines 21 p3413 N71-34285
- Calculation of hydrodynamic entrance length and flow characteristics in channels of varying cross sections [NLL-M-20388-15828.4F] 21 p3413 N71-34288
- Analysis of viscous entrance flows and development of models for pressure drop and flow instabilities 21 p3414 N71-34289
- Analysis of pulsational characteristics of low mass cepheid model to include convection effects 21 p3512 N71-35025
- Development of fluid equations based on one-dimensional, one-particle wave equation and application to wave mechanical and fluid states 22 p3571 N71-35430
- Development of methods for calculating the flow processes in gas centrifuges [NLL-CA-TRANS-251-19091.9F] 23 p3745 N71-36703
- ### FLOW FIELDS
- ### U FLOW DISTRIBUTION
- ### FLOW GEOMETRY
- Calculating cavitation characteristics in converging channels of different shape using Borda-Carnot theorem [NASA-TT-F-13340] 02 p0200 N71-11435
- Separation problems in two-dimensional incompressible laminar flow using perturbation methods [ONERA-P-128] 02 p0202 N71-11541
- Characteristics of jet issuing from two dimensional orifice past rectangular plate [REPT-308] 02 p0204 N71-12079
- Presenting empirical data on flooding in stratified gas-liquid flow in vertical tubes and horizontal rectangular ducts [REPT-327-9] 06 p1181 N71-18045
- Numerical solution of turbulent annular swirl flow [AD-716450] 09 p1370 N71-19601
- Finite element potential flow modeling for predicting round lifting jet rolled up geometry and path convergent into cross-flowing mainstream as on VTOL or STOL aircraft [AD-718121] 12 p1850 N71-23405
- Intrinsic representation of flows with Lamb surfaces [AD-719431] 13 p2063 N71-24679
- Hypersonic flows, three dimensional boundary behavior in corner, subsonic, laminar, and turbulent mixing over lifting vehicles [AD-719766] 14 p2195 N71-25628
- Experimental investigation of large scale, two dimensional, mixed compression inlet system [NASA-TN-D-6392] 15 p2363 N71-26005
- Calculation of dynamic and thermal characteristics of gas circuit in variable flow conditions with application to studying reactor under natural convection flow conditions [NLL-CE-TRANS-5373-19022.091] 17 p2733 N71-28974
- Distortion effects in geometrical reconstruction of events in CERN 2m hydrogen bubble chamber [USIP-70-6] 17 p2800 N71-30991
- Design, characteristics, and performance tests of short two dimensional curved wall diffusers using section slots [NASA-CR-120783] 22 p3567 N71-35404
- ### FLOW GRAPHS
- Digital computer oriented analysis method for Mason flow graphs [AD-709937] 01 p0076 N71-10448
- Application of flow graphs to mechanical structures and pipeline networks 19 p3105 N71-32340
- ### FLOW MEASUREMENT
- Flow induced error frequencies in tidal wave measuring hydrophones [AD-711518] 01 p0051 N71-10077
- Computer programs to determine loss and deviation correlations of flow in turbomachinery [ME/A-70-1] 03 p3312 N71-12226
- Investigating fluid heat transfer at anode of semi compact-arc lamp using flash photography 03 p3379 N71-12794
- Microwave equipment for measuring shock wave propagation velocity and steady flow in shock tube [T-23/69] 03 p3363 N71-13609
- Simplified EBR-2 flow monitoring system without compromising reactor safety [ANL/EBR-18] 05 p0722 N71-14677
- Turbulent shear flow measurements and wave induced motion above air-sea interface [PB-194016] 06 p0667 N71-14970
- Liquid film flow and critical heat flux measurement in concentric, internally heated annulus [AECL-3656] 05 p0660 N71-14777
- Boundary layer measurements in accelerated flow with and without heat transfer [NASA-TN-D-7030] 05 p0661 N71-14806
- Supersonic, turbulent boundary layer interaction with compression corner at very high Reynolds number [NASA-CR-117052] 09 p1374 N71-19601
- Mass and volumetric flow accuracy of cryogenic flow research facility [NBS-9778] 10 p1538 N71-21440
- Instrumentation and development techniques for low velocity gas flow measurement [NASA-CR-103096] 12 p1899 N71-23313
- Flow measurement of Nonweiler delta wing in hypersonic slip flow [DLR-FB-70-46] 13 p2022 N71-26005
- Pressurization for measuring intake in flask [IFVE-SKU-70-6] 18 p2523 N71-30778
- Computerized pressure transducer and thermocouple system for compressible flow measurements [GAT-T-1649] 18 p2908 N71-31510
- Measurement of flow in subchannel of water cooled plants to determine cooling deficiencies [GEAP-10221-6] 19 p3138 N71-32547
- Measurements in boundary layer of flat plate using helium or argon injection and supersonic flow measurement with hot-wire anemometer [NASA-TT-F-13929] 21 p3410 N71-34285
- Wind tunnel investigation of static pressure distributions along cylindrical surface behind shallow, two dimensional, rearward facing step of various heights [NASA-TM-X-2402] 22 p3537 N71-35119
- Operation and accuracy of research facility for measuring flow of cryogenic fluids using positive displacement volumetric flowmeters [NBS-TN-665] 22 p3583 N71-35079

SUBJECT INDEX

- Continuous and pulsed ionization measurements of gas flow with applications
(CEA-R-3699) 22 p3636 N71-35915
- RAW NETS
Linear estimation model for network flow
(FOA-F-C-4237-13) 05 p0666 N71-15611
Topologic and geometric properties of delta channel networks
(AD-719918) 15 p2395 N71-26819
- LOW PATTERNS
U FLOW DISTRIBUTION
RAW RATE
U FLOW VELOCITY
RAW REGULATORS
NT FUEL FLOW REGULATORS
Design and operation of freeze, melt valve used in vacuum encapsulating cesium for thermionic diodes
(NASA-TM-X-2126) 01 p0086 N71-10455
Antibacklash circuit for hydraulic drive system
(NASA-CASE-XNP-01020) 03 p0317 N71-22660
Tubular flow restrictor for gas flow control in gas flow
(NASA-CASE-NFO-10117) 05 p0695 N71-15608
Fluid flow control valve for regulating fluids in molecular quantities
(NASA-CASE-XLE-00703) 06 p0663 N71-15967
Devices to regulate flashing brine flow through flash evaporators
(JORN-TM-2746) 07 p1008 N71-17269
Control of gas flow from pressurized vessel by thermal expansion of metal plug
(NASA-CASE-NFO-10298) 07 p1010 N71-17661
Spheroidal diaphragm cavitation flow control valve
(NASA-CASE-XNP-09704) 08 p1179 N71-18615
Describing device for changing flow rate of fluid in duct in response to change in temperature
(NASA-CASE-MFS-14259) 08 p1209 N71-19213
Flow control system design for blowdown wind tunnels and disturbance effects on regulating accuracy
(JAL-TN-22) 11 p1732 N71-22476
Pneumatic servoamplifier for controlling flow regulation
(NASA-CASE-MSC-12121-1) 15 p2415 N71-27147
Gas management subsystem using xenon-helium working fluid designed for Brayton space power system
(NASA-CR-72631) 21 p3502 N71-34948
- LOW RESISTANCE
NT AERODYNAMIC DRAG
NT FRICTION DRAG
NT SUPERSONIC DRAG
NT VISCOUS DRAG
Small scale hydraulic characteristics of full-scale SHAP 8 multiple-tube model boiler over turbulent Reynolds number from 18,000 to 38,000
(NASA-CR-72830) 11 p1795 N71-22512
Heat transfer coefficients, heat emission, and flow resistance in intertube space of heat exchanger
(NRL-RTS-5990) 16 p2692 N71-29043
Changes in acoustic properties of perforated plates resulting from interaction of flows normal and tangential to plate surface
(NASA-TM-X-2361) 23 p3804 N71-37119
- LOW SEPARATION
U BOUNDARY LAYER SEPARATION
U SEPARATED FLOW
LOW STABILITY
NT BOUNDARY LAYER STABILITY
NT FLAME STABILITY
NT MAGNETOHYDRODYNAMIC STABILITY
Stability of smooth two dimensional transonic flows
(AD-717202) 03 p0310 N71-12207
Numerical analysis of stability of Poiseuille pipe flow
(CEA-R-3699) 05 p0661 N71-14773
Correlating effect of baffles on flow stability in MSP evaporator based on submerged jet model
(JORN-TM-3120) 06 p0636 N71-16385
Stability of steady finite amplitude convection in rotating fluid layer
(JPP-446) 08 p1178 N71-18487
Method for controlling instability in finite difference computations of liquid saturation near borehole of recovery well
(JN-81-7487) 08 p1192 N71-10970
Stability of laminar flow in circular pipes with respect to three dimensional disturbances
(NASA-CR-72635) 08 p1183 N71-10989
Rectangular channel flow stability of oil and water including mean flow profiles, disturbance amplitude distributions, amplification rate, and wave speed and number
(NPT-70-006) 08 p1184 N71-10990
Additional slot and flow fence effects on aerodynamic characteristics of single stage compressor blades
(NASA-CR-72635) 11 p1734 N71-21995
Wall porosity effect on stability of quasi-parallel laminar flows over plane compliant boundaries
(NASA-CASE-XMP-06926) 11 p1738 N71-22576
Thermionic reaction engine comprising outer housing and pair of inner walls for continuous flow
(NASA-CASE-XMP-06926) 11 p1821 N71-22983

- Removal of instability in free convection problem
(EP/TN/A/35) 12 p1902 N71-23827
Body force effects on liquid film stability interacting with external flow
(SC-RR-70-722) 13 p2068 N71-25442
Analytical model for run-out of flow instability and start of compressible transition
(AD-719759) 14 p2238 N71-25655
Mathematical models for investigating stability of thermally stratified shear flow in atmosphere
(NASA-CR-119026) 16 p2579 N71-28321
Unified approach to stability problems for systems described by operator equations of evolution, and direct method of Ljapunov
(NASA-CR-119026) 16 p2580 N71-28628
Transition in oscillating boundary layers including role of stability theory and transient vorticity distribution
(AD-720292) 16 p2582 N71-28875
Determination of minimum B and magnetic wall depth for magnetohydrodynamic flow control
(JAE-1987) 18 p2961 N71-30424
Perturbation of steady flow in viscous incompressible fluid noting nonlinear stability
(ONERA-PUBL-136) 19 p3076 N71-31689
Interfacial stability at thin flexible partition between fuel and propellant flows for gas core nuclear rockets
(NASA-CR-119026) 20 p3304 N71-33639
Dynamic models of negative mass instabilities in particle accelerator electron ring compressor
(UCRL-20268) 20 p3523 N71-33833
Wind tunnel investigation of static pressure distributions along cylindrical surface behind shallow, three dimensional, rearward facing step of various heights
(NASA-TM-X-2402) 22 p3537 N71-35199
Aerodynamic sound radiation from lifting surfaces in smooth and turbulent flow
(NASA-CR-114370) 23 p3706 N71-36422
Hydrodynamic effects on laser beam propagation through gases and laser-induced instabilities in liquids and gases
(NASA-CR-114370) 23 p3767 N71-36850
- FLOW THEORY
NT MIXING LENGTH FLOW THEORY
Numerical analysis of stability of Poiseuille pipe flow
(NASA-CR-114370) 05 p0661 N71-14773
Two dimensional thin airfoil theory with strong inlet flow on upper surface
(AD-714076) 06 p0795 N71-16261
Effect of random fluctuations in pressure gradient on channel flow
(NASA-TM-X-52960) 06 p0837 N71-16328
Developing computational procedure to predict characteristics of inertial impactor used for collection of aerosol particles
(COO-1248-21) 06 p0923 N71-16741
Deriving algorithm for solving maximum stationary flow in network having exponential error
(NRL-RTS-5990) 07 p1001 N71-16975
Applying radioactive tracer techniques to detection of metal contaminants within components of propellant feed system
(NASA-CR-116404) 07 p1072 N71-17341
Plasma flow and magnetohydrodynamic macroscopic equations
(CEA-N-1371) 08 p1269 N71-18166
Generalizing continuous surface boundary layer problem using similarity theory
(AD-715852) 08 p1178 N71-18454
Magnetic field line structure in individual supergranules
(NASA-CR-114370) 09 p1422 N71-19498
Wake throat theory and axially-symmetric super-sonic wakes
(NASA-CR-114370) 09 p1375 N71-19841
Numerical solution of laminar separated flow problem over backward facing step at high Reynolds number
(NASA-CR-114370) 09 p1375 N71-19842
Stability analysis of laminar to turbulent flow transition during film boiling from vertical flat plate
(AD-717208) 10 p1542 N71-21282
Separated flow theory - Thesis project
(AD-717208) 10 p1544 N71-21705
Determination of flow properties of turbulent boundary layers with negligible wall stress
(NASA-CR-114370) 11 p1739 N71-22587
Description of computer program for solving two dimensional and axisymmetric forms of compressible boundary layer equations for continuity, mean momentum, and mean total enthalpy
(NASA-TM-X-2140) 11 p1739 N71-22588
Numerical analysis of inviscid flow fields about pointed circular cone and conical wing-body configuration at various angles of attack
(NASA-CR-114370) 11 p1671 N71-22667
Numerical analysis of axisymmetric or two dimensional viscous flow at high Mach numbers in vicinity of two dimensional curved walls
(NASA-CR-114370) 11 p1741 N71-22673
Numerical solution of mixed supersonic and subsonic steady wake flows by time-dependent method
(NASA-CR-114370) 11 p1741 N71-22674

FLOW VELOCITY

- Numerical analysis of turbulent characteristics of velocity field associated with mean velocity profile in turbulent channel flow
(NASA-CR-114370) 11 p1742 N71-22691
Numerical analysis of velocity profiles and pressure losses during pulsating Newtonian flow in rigid tube
(NASA-CR-114370) 11 p1743 N71-22753
Solution of general self-similar boundary layer equations and parametric investigation of several classes of boundary layer flow
(NASA-CR-114370) 11 p1743 N71-22759
Theory describing hydrostatically neutral air flow adjustment in turbulent boundary layer power partition after abrupt surface roughness change perpendicular to flow direction
(NASA-CR-114370) 12 p1901 N71-23665
Experimental and theoretical investigation of flow of density-stratified fluid about symmetric towed bodies and stability of flow induced by rotating cylinder
(NASA-CR-114370) 12 p1903 N71-24134
Numerical analysis of behavior of fluid in cylindrical shell in fluid flow with linearized hydrodynamics equations
(NASA-CR-114370) 12 p2008 N71-24295
Numerical analysis of flow of viscous, compressible gas through slender axisymmetric channels using finite difference theory
(NASA-CR-114370) 14 p2342 N71-26644
Characteristics of Couette flow of radiating nongray gas and development of absorption coefficient method
(NASA-CR-114370) 14 p2344 N71-26642
Characteristics of induced shock and acceleration waves determined by application of theory of singular surfaces
(NASA-CR-114370) 16 p2582 N71-28775
Formulation and applications of dislocation theory in crystal physics
(NASA-CR-114370) 17 p2826 N71-30003
Theory for three dimensional, incompressible, zero-mean turbulence decay based on relationship between double and triple velocity moments
(NASA-CR-114370) 19 p3079 N71-32256
Fluid dynamics and flow properties of glass, steel, and lead particle slurries in pipelines
(PB-199708) 21 p3413 N71-34285
Calculation of hydrodynamic entrance length and flow characteristics in channels of varying cross sections
(NLL-M-20388-5828-4F) 21 p3413 N71-34288
Analysis of viscoelastic entrance flows and development of models for pressure drop and flow instabilities
(NASA-CR-114370) 21 p3414 N71-34289
Development of method for solving time dependent, viscous, incompressible fluid flow from observer to center of circle
(NASA-CR-114370) 21 p3414 N71-34291
Analysis of pulsational characteristics of low mass cepheid model to include convection effects
(NASA-CR-114370) 21 p3512 N71-35925
Analysis of gas phase control of critical and near-critical two phase flow where gas and liquid flow in separate streams
(NBS-TN-608) 22 p3568 N71-35413
Development of fluid equations based on one-dimensional, one-particle wave equation and application to wave mechanical and fluid states
(NASA-CR-114370) 22 p3571 N71-35430
Determining limiting conditions of flow in separation zones with large Reynolds number
(NASA-TT-F-13992) 23 p3742 N71-36681
- FLOW VELOCITY
Velocity distributions ahead of semi-infinite Rankine body in magnetohydrodynamic flow
(NASA-CR-114370) 05 p0661 N71-14768
Air flow over roughness discontinuity
(AD-712113) 05 p0665 N71-15065
The continuity equation of compressible flow with flow velocity distributions and gas density variations
(DLR-MITT-70-13) 07 p1008 N71-17167
Hot-wire anemometer measurements of incompressible fluid flow direction and velocity in pipes
(NASA-TM-X-52967) 08 p1180 N71-18634
Effect of transverse temperature gradients on velocity and temperature profiles for laminar flow of air
(NASA-CR-114370) 08 p1182 N71-18933
Vacuum chamber study on water and water gas jets
(NASA-CR-114370) 09 p1377 N71-20232
Particle size, particle and air flow rate, and jet molecular weight effects on diffusion of particulate matter in subsonic turbulent jets when coaxially mixed with another subsonic jet
(AD-717171) 10 p1539 N71-20831
Methods of measuring fluid velocity from Doppler Fizeau shift of scattered laser radiation, and optimization of optical system geometry
(NASA-CR-114370) 11 p1775 N71-22610
Electromagnetic measurement of water current velocities in Arctic regions
(NASA-CR-114370) 11 p1753 N71-22812
Quasi-three dimensional surface velocities and choking flow for turbomachine blade rows calculated by FORTRAN program
(NASA-TN-D-6171) 12 p1849 N71-23126

Zeta potential flowmeter for measuring very slow to very high flows

[NASA-TT-F-13133] 12 p1916 N71-23226

Air flow velocity, altitude, fuel-air ratio, fuel flow velocity, and pressure effects on fuel temperature before and after preevaporation in ramjet engines

[NASA-TT-F-13133] 12 p1909 N71-24033

Device for simultaneously determining density, velocity, and temperature of streaming gas

[NASA-CASE-XLA-03375] 12 p1934 N71-24074

Doppler shifted laser beam as fluid velocity sensor

[NASA-CASE-XAC-10770-1] 13 p2089 N71-24828

Pressurized water reactor flooding rate effects on cooling heat transfer time-temperature response based on plenum chamber simulation tests

[WCAP-5352] 13 p2117 N71-24907

Flowmeters for sensing low fluid flow rate and pressure for application to respiration rate studies

[NASA-CASE-FRC-10023] 14 p2244 N71-26546

Force balanced throttle valve for fuel control in rocket engines

[NASA-CASE-NPO-10008] 15 p2416 N71-27432

Determining effects of variations in core coolant flow, system pressure, core lifetimes, and coolant temperature on burnout of PM-3A Type 4 replacement core

[RIT-463] 16 p2630 N71-28064

Autocorrelation and cross correlation of high frequency atmospheric boundary layer temperature and velocity fluctuation measurements

[AD-721540] 16 p2587 N71-28408

Characteristics of turbulent structure of mixing region near outlet of circular subsonic jet and production of jet noise

[NASA-CR-1836] 16 p2583 N71-28882

Conical hydrostatic bearing optimal dimensions for friction reduction based on laminar and turbulent flow velocity, load capacity, and friction torque calculations

[NASA-TM-X-52946] 16 p2605 N71-28887

Experiments on turbulent circular jets issuing into cross flow from both heated and unheated jets

[NASA-CR-72893] 17 p2735 N71-29896

Dimensional analysis of fluidized bed reactors on gas mixing at various velocities

[MBW-FBK-70-26] 17 p2716 N71-29915

Wing tip vortex test demonstrating use of Laser Doppler Velocimeter system for measuring gas velocities with high spatial and temporal resolution

[NASA-CR-115604] 17 p2737 N71-30278

Relaxation time and flow velocity effects on aerosol vapor deposition in pipes with turbulent air flow

18 p2905 N71-31184

Theory for three dimensional, incompressible, zero-mean turbulence decay based on relationship between double and triple velocity moments

19 p3079 N71-32256

Experimental model of heat transfer to two phase, fluid particle flow in tubes for use in analysis of capillary blood flow

19 p3193 N71-33401

Principles of operation, circuits, and construction of thermal flow rate meters for liquid metals

[AD-723540] 19 p3103 N71-32591

Interface stability during liquid inflow to partially full, hemispherical ended cylinders during weightlessness

[NASA-TM-X-2348] 19 p3083 N71-32786

Randomly fluctuating, non-Gaussian pressure gradient effect on steady, incompressible channel flow

[NASA-TM-X-67881] 21 p3409 N71-34255

Compressible heat transfer in low speed flow with small temperature differences

[NPL-AERO-1325] 21 p3530 N71-35155

Using laser Doppler anemometry for velocity measurements in two phase flow

[RISO-M-1368] 24 p3904 N71-37828

Near flow field data for tube-vehicle systems and drag coefficient relationships with relative Mach numbers and relative flow velocity ratios to vehicle velocity

[GASL-TR-70-749] 24 p3908 N71-37856

Methods for determining mass flow rates of gases for use in calibrating gas flowmeters

[NASA-CR-72896] 24 p3920 N71-37954

FLOW VISUALIZATION

NT NUMERICAL FLOW VISUALIZATION

Flow visualization study of flyable fluidic low speed wind tunnel

[NASA-CR-111808] 03 p0376 N71-12728

Investigating possibilities and limitations of applying holographic techniques to aerospace technology

[NASA-SP-248] 03 p0377 N71-12776

Investigating applications of holography to low density flow visualization, vibration mapping, particle sizing, and panel flutter

03 p0377 N71-12777

Investigating air flow in noisy wind tunnels using holographic flow visualization system

03 p0379 N71-12795

Differential interferometry and schlieren photography for hypersonic aerodynamic hologram analysis

[JSL-T-49/66] 03 p0388 N71-12985

Schlieren photography for wake visualization behind hypervelocity projectiles

[T-38/69] 03 p0380 N71-13145

Determining kinematic characteristics of turbulent flows by flow visualization and photography

[NASA-TT-F-13133] 04 p0518 N71-13768

Flow visualization of trailing vortex wakes in towing tank

[DI-42-1004] 04 p0519 N71-13800

Propagation and decay of vortex rings determined by stereoscopic photography and hot-wire anemometry

[AD-713705] 05 p0660 N71-14750

Determination of asymmetric three dimensional density fields in free jet flow by holographic interferometry

[AD-714610] 06 p0838 N71-16566

Visualization of supersonic rarefied free jet flow using electron beam scanning

[REPT-76-10] 06 p1177 N71-18400

Holography used to determine water droplet characteristics in engine test facility

[AD-715916] 08 p1201 N71-18488

Digital computer simulation of automobile inspecting flexible safety barrier, and multiple source schlieren system for NAE trisonic wind tunnel

[DME/NAE-1970/3] 09 p1363 N71-19401

Multiple-source schlieren system for NAE trisonic wind tunnel

09 p1364 N71-19403

Fin-flat plate combination model for flow visualization studies of fin protrusions partially immersed in turbulent boundary layer at Mach 5

[AD-716023] 09 p1371 N71-19456

Color photointerpretation of interference colors reflected from this film oil-coated components in moving gases for gas flow visualization

[NASA-CASE-XMF-01779] 10 p1539 N71-20815

Visualized flow patterns of pelagic fishes to measure vortex formation and air and water boundary layer effects

[JPRS-52790] 10 p1544 N71-21646

Schlieren and phase contrast methods of hypersonic flow visualization

11 p1761 N71-22637

Analysis of water flow around living sharks based on flow visualization and body attached flow sensor velocity profiles

[JPRS-52593] 12 p1898 N71-23192

Laminar boundary layer transition, separation and streamline direction on rotating helicopter blades

[NASA-TN-D-6321] 12 p1851 N71-23779

Natural convective heat transfer between concentric spheres, construction of experimental apparatus for heat transfer and flow visualization

[RLO-2214-1] 12 p2015 N71-24340

Angle of incidence effect on delta wing leading-edge vortices with cross flow visualization in hydraulic test tunnel

[ARC-R/M-3645] 13 p2063 N71-24482

Flow visualization of vortex breakdowns of rectangular planforms in towing tank

[IC-AERO-70-08] 13 p2064 N71-24590

Fog generator design for compressible flow visualization and high pressure Mollier diagram

[AD-721193] 15 p2392 N71-26881

Two dimensional visual model for simulating turbulent flow in porous material

17 p2735 N71-28992

Experimental capabilities and operating conditions of hydrodynamic wind-water tunnel including flow visualization

[NASA-TT-F-13727] 17 p2732 N71-30263

Hodographs applied to calculation of compressible flow on turbomachine blades and use of visualization terminal display

[ONERA-NT-179] 19 p3076 N71-31706

Flow visualization and mathematical model of peristaltic pumping including pressure and velocity measurements in two dimensional flow

[AD-723870] 19 p3081 N71-32529

Influence of vortex rocket engine injector design on water flow distribution for future hypergolic propellant injection performance

[RPE-TR-70/6] 20 p3338 N71-33147

Simulation of ground effect in hydrodynamic tunnel analyzed by visualizations

[NASA-TT-F-13799] 20 p3251 N71-34944

Blowing effects on flow around models analyzed by flow visualizations produced in water tunnel

[NASA-TT-F-13742] 21 p3409 N71-34254

Low-beta axisymmetric fluid model showing material flux and shock structure for stellarator or low temperature Tokamak parameters

[CONF-710607-75] 24 p3991 N71-38475

FLOWMETERS

NT GAS METERS

NT HOT-WIRE FLOWMETERS

NT RHEOMETERS

Transit time flowmeter for liquid metal cooled reactors

[AI-AEC-12973] 05 p0686 N71-15421

Methods for calibrating low mass flow rate sensors in electrodynamic facilities

[AD-713625] 05 p0658 N71-15428

Sodium loop tests of transit time flowmeter using noise analysis techniques

[AI-AEC-12941] 06 p0858 N71-15997

Flowmeter using noise-analysis techniques for large liquid metal systems at temperatures of 1200 F

[AI-AEC-12981] 07 p1028 N71-17207

Heated element sensor for fluid flow detection in thermal conductive conduit with adaptive means to determine flow rate and direction

[NASA-CASE-MSC-12084-1] 07 p1009 N71-17100

Describing laser Doppler velocimeter for measuring mean velocity and turbulence of fluid flow

[NASA-CASE-MSP-20386] 08 p1233 N71-19812

Reproducibility and linearity of 2 to 5 cm turbine-type flowmeters for liquid hydrogen including design principles, installation and inspection procedures, and calibration

[NASA-TM-X-52984] 09 p1388 N71-19790

Bidirectional respiratory flowmeters and electronic instrumentation technology for measurement and analysis of metabolic quantities

[NASA-CR-114905] 09 p1340 N71-19776

Zeta potential flowmeter for measuring very slow to very high flows

[NASA-CASE-XNP-04509] 12 p1916 N71-23226

Applications of laser Doppler techniques for measurements in large flow systems

[AD-710818] 12 p1932 N71-23224

Model AS30 magnetic tape recording current meter design and environmental and performance tests

[JPRS-71011] 12 p1918 N71-23976

Evaluation of fuel flowmeter instrumentation conducted during flight tests

[AD-719280] 13 p2079 N71-24679

Flow meter for measuring stagnation pressure in boundary layer around high speed flight vehicle

[NASA-CASE-XPR-02007] 13 p2063 N71-24681

Doppler shifted laser beam as fluid velocity sensor

[NASA-CASE-XAC-10770-1] 13 p2089 N71-24828

Flowmeters for sensing low fluid flow rate and pressure for application to respiration rate studies

[NASA-CASE-FRC-10023] 14 p2244 N71-26546

Heat flowmeter for measuring vertical takeoff aircraft exhaust thermal insulation dissipation

[DLR-MITT-71-07] 19 p3099 N71-31999

Distorted velocity profile and electric potential distribution of long dc electromagnetic flowmeter for liquid metals

[NASA-TM-X-2342] 19 p3100 N71-32100

Effect of velocity profile distortion in circular transverse-field electromagnetic flowmeters

[NASA-TN-D-6454] 19 p3102 N71-32100

Principles of operation, circuits, and construction of thermal flow rate meters for liquid metals

[AD-723540] 19 p3103 N71-32591

Cryogenic flow measurement facility performance evaluation and accuracy statements for mass and volumetric flow

[NBS-TN-606] 19 p3075 N71-32778

Operation and accuracy of research facility for measuring flow of cryogenic fluids using positive displacement volumetric flowmeters

[NBS-TN-605] 22 p3585 N71-35351

Factors effecting volume from which data originate in laser Doppler velocimeter dual scatter probe

[AD-727005] 23 p3766 N71-36845

Methods for determining mass flow rates of gases for use in calibrating gas flowmeters

[NASA-CR-72896] 24 p3920 N71-37954

FLOX

FLOX/polyethylene hybrid propellant rocket engine tests

[MBW-FB-W-70-54] 07 p1099 N71-17311

Regression rates for hybrid FLOX polyethylene mixture combustion

[MBW-FB-W-70-65] 11 p1840 N71-22318

Hot firing tests with FLOX/methane propellants for evaluating pyrolytic refractory composite materials for thrust chambers

[NASA-CR-118321] 13 p2101 N71-34094

Analysis to determine regenerative cooling limits of light hydrocarbons used with FLOX and OFT over wide range of operating conditions

[NASA-CR-72705] 14 p3352 N71-33800

FLUCTUATION

FLUCTUATION THEORY

Dispersions of fast fluctuations in deceleration of satellites orbiting at different altitudes

[NASA-TT-F-13246] 03 p0452 N71-12223

Fluctuation factors for theoretical evaluation of average neutron cross sections of fissile nuclei in unresolved resonances region

[IA-1208] 24 p3972 N71-38337

FLUENCE

Critical fluence calculations for ruby laser destructions of thin metal films

[UCRL-50977] 07 p1046 N71-18104

Subroutine for calculating gamma dose and thermal neutron fluence from thermoluminescent dosimeter data

[RD/B/N-1677] 08 p1247 N71-18102

Mechanical properties of molten salt reactor experiment Hastelloy N surveillance specimens deteriorated with increasing fluence

[ORNL-TN-3063] 20 p3286 N71-33808

SUBJECT INDEX

FLUIDICS

- Fluoric RC oscillator for timers
(AD-713514) 05 p0484 N71-14894
Predicted response characteristics of transmission line terminations to step waves and application to impedance matching
(AD-717247) 10 p1541 N71-21195

- Fluoric oscillator for measuring electrical currents in bridge wires
(AD-712495) 12 p1921 N71-23754

FLUID AMPLIFICATION

- U FLUID AMPLIFIERS
FLUID AMPLIFIERS
NT JET AMPLIFIERS
Investigating effect of flow nonuniformities at exit of planar nozzles on total pressure distribution in circular attachment wall
(AD-713141) 02 p0280 N71-11138

- Multiple vortex amplifier system as fluid valve
(NASA-CASE-XMP-04709) 03 p0695 N71-15609
Submerged incompressible two-dimensional jet partially oscillated at its base
(AD-714698) 06 p0834 N71-16116

- Flow visualization and quantitative analysis for determining proportional fluid amplifier geometry
(AD-714634) 06 p0838 N71-16587

- Shear modulated fluid amplifier of high pressure hydraulic vortex amplifier type
(NASA-CASE-MFS-10412) 07 p1009 N71-17578

- High total temperature sensing probe using fluid oscillator concept for X-15 hypersonic aircraft
(NASA-CR-116772) 12 p1917 N71-23250

- Proportional fluid amplifiers for mixing two fluids in varying mix ratios
(AD-722516) 17 p2734 N71-29754

- Switching dynamics of bistable fluid amplifiers
(AD-723832) 19 p3079 N71-32328

- Research and development for fluid amplifier design and thrust vector control systems
(AD-724126) 20 p3248 N71-32856

- Effects of flow rate, port location, and sonic condition of injectant in secondary injection into supersonic flow field for conical rocket nozzles
(AD-724127) 20 p3249 N71-32859

- Advanced aerospace systems and control including thrust modulation, optimizer research, fluidic devices, hydraulic jet valves, and related research
(NASA-CR-121643) 21 p3413 N71-34256

- Numerical analysis of vortex rate sensor for sensing small speeds of rotation
(CRANFIELD-M/F-2) 21 p3428 N71-34394

- Inviscid flow analysis of three jet interaction for design of proportional amplifiers
(AD-727089) 24 p3908 N71-37855

FLUID BOUNDARIES

- NT GAS-SOLID INTERFACES
NT JET BOUNDARIES
NT LIQUID-LIQUID INTERFACES
NT LIQUID-SOLID INTERFACES
NT LIQUID-VAPOR INTERFACES

- Analysis of factors affecting fuel tank pressurization
(AD-727089) 24 p3908 N71-37855

- Techniques for solving problem of sound transmission from harmonic monopole source through finite corrugated boundary between fluid media
(AD-727089) 24 p3908 N71-37855

- Mathematical models for determining stabilizing effect of fluid boundary on thermal convection
(NASA-CR-119015) 16 p2579 N71-28271

- Development of continuum theory for fluid surface phenomena to describe interaction of surface with surrounding materials
(AD-727089) 24 p3908 N71-37855

FLUID DYNAMICS

- NT AERODYNAMICS
NT AEROTHERMODYNAMICS
NT ELASTOHYDRODYNAMICS
NT ELECTROHYDRODYNAMICS
NT GAS DYNAMICS
NT HYDRODYNAMICS
NT HYPERSONICS
NT MAGNETOHYDRODYNAMICS
NT RAPIDFUEL GAS DYNAMICS
NT ROTOR AERODYNAMICS

- Radial velocity distribution effects on fuel exposure in circulating fuel reactor
(LA-4294) 01 p0085 N71-10419

- Fluid dynamics of blood circulation and respiratory flow
(AGARD-AR-30-70) 03 p0321 N71-12290

- Dynamic interaction between structure and liquid propellants in space shuttle vehicle models
(NASA-CR-111801) 03 p0362 N71-12766

- Liquid propellant dynamic problems in space shuttle vehicles
(NASA-CR-111802) 03 p0363 N71-12767

- Exact vorticity solutions of incompressible Navier-Stokes equations
(AD-726181) 03 p0366 N71-13398

- Heat transfer and fluid dynamics analyses for fuel heating in materials test reactor
(NWL-1409) 04 p0532 N71-13949

- Fluid conductivity of lunar surface materials
(NASA-CR-102842) 04 p0611 N71-14009

- Fluid motion is two dimensional Cartesian or cylindrical coordinates by following Lagrangian energy cells
(LA-4464) 04 p0585 N71-14243

- Dynamic stabilization of Rayleigh-Taylor instability (LRP-4570) 04 p0399 N71-14252

- Oscillation of disk fixed to flat plate with interposed fluid
(PUBL-3) 05 p0775 N71-14724

- Vibration in external flow of pressurized tubular system
(REPT-4) 05 p0626 N71-14789

- Abstracts on research in fluid dynamics, plasmas, and electromagnetics
(AD-714286) 06 p0962 N71-16612

- Experimental evaluation of four transfer functions for single tube boiler and demonstration of functions being independent of exit restrictions
(NASA-TM-X-2247) 09 p1376 N71-19931

- Initiation and thermal hydraulics of sodium boiling and release and transport of aerosols and energy in coolant combustion accidents in liquid metal fast breeder reactors
(AI-AB-12879) 09 p1419 N71-20009

- Fluid dynamics of gas-particle flow and solid particle behavior in mixed flow
(NASA-CR-117309) 09 p1377 N71-20257

- Fluid dynamic studies of molten salt reactor experimental graphite core, including full scale mockup and pressure drop and flow patterns
(ORNL-TM-3229) 10 p1604 N71-21250

- Time-dependent motion of small gas bubbles in smoothly decelerating liquid including bubble slip functions
(RM-4993) 10 p1543 N71-21447

- Geophysical and astrophysical fluid dynamics (PB-196589) 10 p1544 N71-21642

- Geophysical and astrophysical fluid dynamics, emphasizing rotating fluids
(PB-196590) 10 p1544 N71-21643

- Gas and fluid response to high intensity ruby laser beam
(AD-717728) 11 p1732 N71-22593

- Mathematical model of oil whip phenomenon in rotating shaft systems with incompressible fluid lubrication and analysis of squeeze film bearings
(AD-717728) 11 p1732 N71-22593

- Instabilities in system of equations describing electromagnetic wave propagation and fluid dynamics
(AD-718858) 12 p1932 N71-23290

- Determination of form of turbulent wake formed behind freely moving body in stratified medium with density variable in direction of application of force of gravity
(NASA-TT-F-13580) 13 p2064 N71-24608

- Problems in fluid dynamics including pipeline dynamics, effect of bubble location, turbulent flow, and effect of tilting tank on liquid oscillation frequency
(AD-721902) 17 p2732 N71-29372

- Numerical analysis of chemically reacting and diffusing fluid mixtures including longitudinal and transverse wave dispersion and thermodynamics
(AD-721902) 17 p2732 N71-29372

- Harmonic functions applied to two dimensional axisymmetric flow and thermodynamics
(AD-721902) 17 p2732 N71-29372

- Using Born-Green-Yvon 2 theory for describing low and moderately dense fluids
(AD-721902) 17 p2732 N71-29372

- Torsional vibration analysis on hydrodynamic clutch of power turbine at periodic disturbance of starting and driving speeds
(AD-721902) 17 p2732 N71-29372

- Modes for using vortices for fluid dynamic containment of gaseous core nuclear reactor, bibliography
(NASA-CR-11772) 19 p3079 N71-32328

- Switching dynamics of bistable fluid amplifiers
(AD-723832) 19 p3079 N71-32328

- Liquid propellant sloshing in tilted axisymmetric cylindrical tanks for space shuttle applications
(NASA-CR-119091) 20 p3337 N71-32898

- Computer program for calculating propellant dynamics in two dimensional and axisymmetric tanks during spacecraft docking
(NASA-CR-119904) 20 p3337 N71-33243

- Evaluation of compatibility of transformation laws with relativistic formulations of fluid dynamics and statistical mechanics
(AD-723832) 19 p3079 N71-32328

- Advanced aerospace systems and control including thrust modulation, optimizer research, fluidic devices, hydraulic jet valves, and related research
(NASA-CR-121643) 21 p3413 N71-34256

- Analysis of heat transfer crisis and high frequency natural pressure oscillations during movement of liquids along tubes
(NLL-CE-TRANS-5620-19022.09) 21 p3331 N71-35166

- Analysis of infinitesimal plane sound wave propagation in fluid using continuum mechanics
(AD-723832) 19 p3079 N71-32328

- Analytical procedures for predicting coupled fluid structural responses of aircraft hydraulic systems
(AD-723832) 19 p3079 N71-32328

- Equilibrium statistical mechanics model for relationship between hard sphere fluid and fluids with realistic repulsive forces
(AD-726743) 23 p3720 N71-36516

- Numerical analysis of flow patterns, impact pressure, and velocities resulting from impact of spherical water drop on rigid plane surface
(UMICH-033710-10-T) 23 p3744 N71-36780

- Free oscillations in bounded, two-phase flows with free surfaces and stratification
(AD-726743) 23 p3720 N71-36516

FLUID FILMS

- Evaluation of series-hybrid rolling-element bearing
(NASA-TN-D-7011) 03 p0449 N71-13071

- Temperature distribution in thin fluid films heated by hot gas and hot wall
(DLR-FB-69-94-PT-1) 08 p1100 N71-18618

FLUID FILTERS

- NT AIR FILTERS
Technique for sterile insertion of liquids into previously sterilized spacecraft
(NASA-CR-111095) 01 p0010 N71-10952

- Combustion kinetics of particulate aerosols
(AD-713121) 03 p0781 N71-14386

- Using different spray droplet sizes and water volumes to test theory of high efficiency filter plugging by water spray
(UCRL-50923) 08 p1205 N71-10255

- Superheated steam filter in water cooled reactor
(KFK-1183) 09 p1420 N71-20112

- Development of liquid separating system using capillary device connected to flexible bladder storage chamber
(NASA-CASE-XMS-13052) 09 p1390 N71-20427

- Carbon bed filtration system for removing particulate matter and gaseous radioactive contaminants from radioactive wastes
(AD-727089) 24 p3908 N71-37855

- Development and testing of high efficiency particulate filters
(AD-727089) 24 p3908 N71-37855

- Measurements of particulate filtration efficiencies of buildings for application to safety and engineering safeguards design of LMFBR
(AD-727089) 24 p3908 N71-37855

- NASA specifications for high efficiency particulate aerosol filters including testing and installation
(NASA-TM-X-67249) 17 p2734 N71-29879

- Design and transmission characteristics of high pass, mechanical velocity filter for fast neutral molecular or atomic beams
(NASA-TM-X-2332) 18 p2980 N71-30745

- Fluid control, filtration, and calibrating equipment, computer programs, and data reduction techniques - technology utilization
(NASA-SF-5938/01) 20 p3278 N71-33142

- Mechanical properties of thin liquid films analyzed by study of anomalies observed in flow of fluids through porous ceramic and carbon filters
(NASA-TT-F-13999) 24 p3905 N71-37831

FLUID FLOW

- NT ADIABATIC FLOW
NT AIR FLOW
NT AIR JETS
NT ANNULAR FLOW
NT AXIAL FLOW
NT AXISYMMETRIC FLOW
NT BAROTROPIC FLOW
NT BASE FLOW
NT BLOOD FLOW
NT BOUNDARY LAYER FLOW
NT BOUNDARY LAYER SEPARATION
NT CAPILLARY FLOW
NT CASCADE FLOW
NT CAVITATION FLOW
NT CHANNEL FLOW
NT COAXIAL FLOW
NT COMBUSTIBLE FLOW
NT COMPRESSIBLE FLOW
NT CONTINUUM FLOW
NT CONVECTIVE FLOW
NT COUETTE FLOW
NT COUNTERFLOW
NT CRITICAL FLOW
NT DUCTED FLOW
NT EQUILIBRIUM FLOW
NT EQUIPOTENTIALS
NT FREE FLOW
NT FREE MOLECULAR FLOW
NT FROZEN EQUILIBRIUM FLOW
NT FUEL FLOW
NT GAS FLOW
NT HELICAL FLOW
NT HYPERVELOCITY FLOW
NT INCOMPRESSIBLE FLOW
NT INLET FLOW
NT INVISCID FLOW
NT ISOTHERMAL FLOW
NT JET FLOW
NT JET MIXING FLOW
NT JET STREAMS (METEOROLOGICAL)
NT KNUDSEN FLOW
NT LAMINAR FLOW
NT LIQUID FLOW
NT MAGNETOHYDRODYNAMIC FLOW

NT MASS FLOW
 NT MERIDIONAL FLOW
 NT MOLECULAR FLOW
 NT MULTIPHASE FLOW
 NT NONEQUILIBRIUM FLOW
 NT NONNEWTONIAN FLOW
 NT NONUNIFORM FLOW
 NT NOZZLE FLOW
 NT ONE DIMENSIONAL FLOW
 NT OPEN CHANNEL FLOW
 NT ORIFICE FLOW
 NT OSCILLATING FLOW
 NT PERIPHERAL JET FLOW
 NT PIPE FLOW
 NT PLASTIC FLOW
 NT POTENTIAL FLOW
 NT PROPELLANT TRANSFER
 NT RADIAL FLOW
 NT REATTACHED FLOW
 NT RECIRCULATIVE FLUID FLOW
 NT REVERSED FLOW
 NT SECONDARY FLOW
 NT SEPARATED FLOW
 NT SHEAR FLOW
 NT SHIFTING EQUILIBRIUM FLOW
 NT SLIP FLOW
 NT STAGNATION FLOW
 NT STEADY FLOW
 NT STEAM FLOW
 NT STOKES FLOW
 NT STRATIFIED FLOW
 NT SUBCRITICAL FLOW
 NT SUBSONIC FLOW
 NT SUPERCRITICAL FLOW
 NT SUPERSONIC JET FLOW
 NT THREE DIMENSIONAL FLOW
 NT TRANSITION FLOW
 NT TRESKA FLOW
 NT TURBULENT FLOW
 NT TWO DIMENSIONAL FLOW
 NT TWO PHASE FLOW
 NT UNIFORM FLOW
 NT UNSTEADY FLOW
 NT VERTICAL AIR CURRENTS
 NT VISCOUS FLOW
 NT WALL FLOW
 NT WATER FLOW
 NT WEDGE FLOW
 Two dimensional recirculation flow of viscous fluid
 [AD-710296] 01 p0040 N71-10173
 Inductive liquid level detection system
 [NASA-CASE-XLE-01609] 01 p0054 N71-10500
 Effect of flow on interconnected thrust bearings
 [RAE-TR-68302] 02 p0230 N71-11571
 Stationary and travelling vortex breakdowns in swirling flow
 [AD-711831] 02 p0204 N71-11955
 Survey of heat transfer to near-critical fluids
 [NASA-TN-D-5886] 03 p0468 N71-13035
 Flow-induced vibration of bellows with internal cryogenic fluid flows
 [NASA-CR-102935] 03 p0364 N71-13081
 Development of marker and cell technique for two dimensional, transient solutions to Navier-Stokes equations
 03 p0364 N71-13117
 Prediction of friction and heat transfer coefficients with large variations in fluid properties
 [NASA-TM-X-2145] 04 p0620 N71-14031
 Performance of various wick configurations in single and two-fluid heat pipes operating as thermoregulatory systems for space suits
 [NASA-CR-111760] 04 p0621 N71-14079
 Integral equation for unsteady surface waves above evaluation of Boussinesq equation
 [AD-713107] 05 p0664 N71-14979
 Summaries of lunar soil studies and fluid conductivity of lunar surface materials
 [NASA-CR-102962] 05 p0768 N71-15207
 Multiple vortex amplifier system as fluid valve
 [NASA-CASE-XMP-04709] 05 p0695 N71-15609
 Combined conduction, convection, and radiation effects on heat transfer of participating gases in internal flow
 [NASA-CR-116127] 06 p0834 N71-15989
 Analyses of flow induced vibrations in reactor fuel elements, fuel assemblies, control elements, and cooling system components
 [ANL-7685] 06 p0898 N71-16274
 Effects of structural motion on dynamic response of liquid flow systems and automatic control hydraulic systems
 [AD-714283] 06 p0797 N71-16559
 Effects of velocity, oxide level, and flow transients on boiling initiation in sodium
 [AI-REC-12939] 06 p0960 N71-16879
 Effect of velocity slip at porous boundary on performance of incompressible porous bearing
 [NASA-TN-D-6181] 07 p1034 N71-17327
 Time dependence autocorrelation of classical liquid
 [NYO-3326-29] 07 p1074 N71-17435
 Heated element sensor for fluid flow detection in thermal conductive conduit with adaptive means to determine flow rate and direction
 [NASA-CASE-MSC-12084-1] 07 p1009 N71-17569

Deriving surface equation for fluid subjected to gravitational and magnetic fields using variational principle of minimum free energy
 [NASA-TT-F-13462] 08 p1179 N71-18576
 Throttle valve for regulating fluid flow volume
 [NASA-CASE-XNP-09698] 08 p1206 N71-18580
 Measurement of pipe friction factors during flow of dilute aqueous polyethylene-oxide solutions
 [AD-715556] 08 p1181 N71-18743
 Horizontal boundary layer calculations for density stratified fluid flow
 08 p1182 N71-18932
 Flow equations for simultaneous flow of two immiscible fluids in porous medium including infiltration problems for several boundary conditions
 [AEDF-710BMC28] 08 p1184 N71-19091
 Harwell heat transfer and fluid flow information analysis center
 09 p1482 N71-19530
 Fluid dynamic properties of turbulent swirl flows in annular duct
 [AD-716452] 09 p1370 N71-19608
 Forming vortices in fluid of small viscosity
 [RAE-LIB-TRANS-1466] 09 p1370 N71-19609
 Vaporization caused by incipient boiling in forced convective flow of superheated liquid
 [NASA-CR-117046] 09 p1406 N71-20593
 Fluid motion for incompressible fluid between two long eccentric cylinders
 [AD-717366] 11 p1734 N71-21970
 Hydrodynamics, marine biology, bionics, dolphins, sharks, porpoises, traveling waves, fluid flow, viscous fluids, nervous system, skin structure, swimming
 [JPRS-52605] 11 p1687 N71-22201
 Laboratory experiment on flow of viscous fluid along traveling waves
 11 p1736 N71-22221
 Numerical methods developed in fluid mechanics and heat transfer emphasizing elliptic flows
 [EF/TN/A/34] 11 p1737 N71-22295
 Characteristics of secondary fluid injection from two dimensional slit into uniform two dimensional supersonic stream for thrust vector control
 [ARC-TR-11] 11 p1738 N71-22429
 Analogies for heat and mass transfer processes in fluid flows
 11 p1843 N71-22606
 Diurnal variations of large scale current turbulence in Arctic Basin and seas
 11 p1752 N71-22805
 Electromagnetic measurement of water current velocities in Arctic regions
 11 p1753 N71-22812
 Vertical electric fields of sea currents and utilization for measurement of current velocity
 11 p1756 N71-22840
 Photometric flow meter with comparator reference means
 [NASA-CASE-XGS-01331] 11 p1766 N71-22996
 Combination pressure transducer-calibrator assembly for measuring fluid
 [NASA-CASE-XNP-01660] 11 p1766 N71-23036
 Dynamic characteristics of circular fully developed laminar free jet
 [NASA-TN-D-6304] 12 p1898 N71-23103
 Physical and numerical experiments on stability of time dependent rotational Couette flow
 [RU-TR-136-MAE-F] 12 p1898 N71-23121
 Valve assembly for controlling simultaneously more than one fluid flow, and having stable qualities under loads
 [NASA-CASE-XMS-05890] 12 p1886 N71-23191
 Analysis of temperature distributions in infinite slab with one surface perfectly insulated and other surface exposed to fluid with temperature varying in specified
 [AD-718332] 12 p2010 N71-23252
 Removal of instability in free convection problem
 [EF/TN/A/35] 12 p1902 N71-23827
 Experimental and theoretical investigation of flow of density-stratified fluid about symmetric towed bodies and stability of flow induced by rotating cylinder
 12 p1903 N71-24134
 Numerical analysis of behavior of finite cylindrical shell in fluid flow with linearized hydrodynamics equations
 12 p2008 N71-24295
 Intrinsic representation of flows with Lamb surfaces
 [AD-719431] 13 p2063 N71-24478
 Integral transform solution for conical diffuser flow with fluid extrusion through multiple slots
 13 p2063 N71-24796
 Analytical and experimental design of vibration control mechanism for fluid drive
 13 p2066 N71-24811
 Flowmeters for sensing low fluid flow rate and pressure for application to respiration rate studies
 [NASA-CASE-FRC-10022] 14 p2244 N71-26546
 Control valve for switching main stream of fluid from one stable position to another by means of electrohydrodynamic forces
 [NASA-CASE-NPO-10416] 15 p2393 N71-27332

Computer code /VORTEX/ simulating behavior of incompressible, inviscid, homogeneous fluid in two dimensions by following motion of point vortices
 (CLM-8-106) 15 p2394 N71-27479
 Vortex induced hydroelastic vibrations of spring supported cylinder in steady fluid stream
 [AD-721073] 15 p2522 N71-27860
 Drag force, pressure distribution, and separation angle measured on circular cylinders in flow of aqueous solutions of dilute polymers
 [AD-722007] 16 p2578 N71-28170
 Fluid control jet amplifiers
 [NASA-CASE-XLE-093411] 16 p2581 N71-28741
 Flow and heat transfer characteristics of incompressible fluid in radial diffuser using air as fluid with inlet Reynolds numbers from 15 to 53,500 and area ratios from .245 to 2.04
 16 p2583 N71-28894
 Nuclear reactor heat transfer and fluid flow study using vectors and other mathematical tools
 [WAPD-TM-1000-VOL-1-CH-1-CH-2] 16 p2693 N71-29075
 Forms and causes of noise due to fluid flow
 [NLL-CE-TRANS-5434-19022.09] 17 p2733 N71-29622
 Hydroelastic vibration of rods in parallel flow with hydroelastic rod model and method for evaluating equivalent viscous damping coefficients
 17 p2734 N71-29728
 Application of radioactive pulse probe to determine fluid velocity and direction in open tank
 [CSIR-SR-CHEM-133] 17 p2734 N71-30339
 One dimensional equations describing noncavitating and cavitating flow in liquid-to-liquid jet pumps programmed for computer use
 [NASA-TN-D-6453] 18 p2931 N71-31395
 Viscoelastic effects in polymer flow through various porous media
 19 p3082 N71-32683
 Temporal and spatial velocity profiles of fluid pipe flow produced by propagation of nonlinear pressure waves
 [NASA-CR-119914] 20 p2350 N71-33382
 Derivation of difference equations for MAGE hydrodynamic computer program, and computation of flows containing plastic and elastic effects
 [LA-4601] 20 p3359 N71-33375
 Hydrodynamic lubrication of journal bearing with one or two axial oil grooves, with power loss, load capacity, oil flow, and stability charts for design of minimum power loss, stable bearing
 20 p3280 N71-33799
 Effects of vertical contraction of horizontal flow of incompressible density-stratified fluid
 21 p3414 N71-34250
 Development of method for solving time dependent, viscous, incompressible fluid flow from observer to center of circle
 21 p3414 N71-34291
 Analysis of heat transfer crisis and high frequency natural pressure oscillations during movement of liquids along tubes
 [NLL-CE-TRANS-5620-19022.09] 21 p3531 N71-35166
 Numerical analysis of asymmetric collapse of vapor bubble in viscous incompressible liquid using modified Marker and Cell technique
 [PB-199560] 22 p3567 N71-35406
 Inter-relationship between high frequency oscillations and nature of nucleate and film heat transfer with forced fluid flow
 [NLL-CE-TRANS-5621-19022.09] 22 p3570 N71-35426
 Calibration method for hot-wire probes
 [AD-727049] 22 p3586 N71-35538
 Techniques for estimating various pressure drops for conducting fluid flows in magnetic fields applied to lithium flow in hypothetical fusion reactor blanket
 [UCRL-51010] 23 p3742 N71-36680
 Analytical development of propagation velocity of small pressure pulses for bubble, annular, stratified, droplet, and slug-flow regimes
 [ANL-7792] 23 p3743 N71-36685
 Series truncation method with novel coordinate system used for calculation of flow about circular cylinder at low Reynolds numbers
 [AD-726447] 23 p3743 N71-36690
 Evolutionary models and fluidity functions of spherical, cylindrical, and planar plasmas
 23 p3854 N71-37480
 Dynamic response of slender circular cylinders in axial flowing fluid with base excited motion
 23 p3863 N71-37541
 Hydrodynamics of cocurrent counter-gravity side transport for liquid-fluidized heat exchangers
 23 p3864 N71-37577
 MUFAN program for determining pressures, flow rates, and pressure drops in systems involving one dimensional incompressible steady state fluid flow
 [NASA-CR-72943] 24 p3992 N71-37735
 Mechanical properties of thin liquid films analyzed by study of anomalies observed in flow of fluid through porous ceramic and carbon filters
 [NASA-TT-F-13999] 24 p3905 N71-37831

SUBJECT INDEX

- Properties of three dimensional compressible fluid flows obtained by application of invariant transformation to equations of motion 24 p3907 N71-37849 (AD-727933)
- Unbounded turbulent jets for measurement of fluid velocity and density 24 p4013 N71-38629
- Heat transfer in smooth tubes, between parallel plates, in annuli and tube bundles with exponential heat flux distributions in forced laminar or turbulent flow (NLL-WINDSCALE-458-19091.9P) 24 p4032 N71-38770
- FLUID INJECTION**
- NT GAS INJECTION
- NT LIQUID INJECTION
- NT WATER INJECTION
- Method for loading solid propellant rocket motors by injecting hyperbolic fluids (NASA-CASE-XLE-01908) 05 p0761 N71-15634
- Constructing fluid spike nozzle to eliminate heat transfer and high temperature problems inherent in physical spikes (NASA-CASE-XOS-01143) 05 p0773 N71-15647
- Method and apparatus for producing fine particles in cryogenic liquid bath for gelled rocket propellants (NASA-CASE-NPO-10239) 06 p0804 N71-16312
- Fluid transferring system design for purging toxic, corrosive, or noxious fluids and fumes from materials handling equipment for cleaning and accident prevention (NASA-CASE-XMS-01905) 10 p1540 N71-21089
- Turbine flow injection system for thrust vectoring of propulsive nozzle flow (NASA-CASE-MFS-20831) 16 p2673 N71-29153
- Energy decay and spectra measurements of grid-injection turbulent flows (NASA-CR-132191) 24 p3903 N71-37830
- FLUID JET AMPLIFIERS**
- U FLUID AMPLIFIERS
- U JET AMPLIFIERS
- FLUID JETS**
- NT AIR JETS
- NT FIRE JETS
- NT GAS JETS
- NT HYDRAULIC JETS
- NT VAPOR JETS
- Research and development of high speed liquid jets for cutting or breaking materials (DME/NAB-1970/2) 01 p0809 N71-10434
- Vacuum chamber study on water- and water-gas jets 09 p1377 N71-20252
- Mathematical model for ideal fluid jets from convergent nozzles 10 p1541 N71-21139
- Characteristics of secondary fluid injection from two dimensional slit into uniform two dimensional supersonic stream for thrust vector control (ARC-TR-1) 11 p1734 N71-22429
- Experimental and theoretical analysis of breakup of liquid sheets and jets in supersonic gas stream 19 p0802 N71-32618
- Effect of charge transport on disintegration of liquid jets studied by comparison of calculated and experimental values of size of drops formed from electrified jets (AD-74334) 20 p3363 N71-32973
- Numerical analysis of impact of free-surface cylindrical water jet of finite length on flat rigid plate (JUMICH-03371-9-T) 23 p3744 N71-36689
- FLUID LOGIC**
- Logic AND gate for fluid circuits (NASA-CASE-XLA-07391) 07 p0101 N71-17579
- FLUID MECHANICS**
- NT AERODYNAMICS
- NT AEROTHERMODYNAMICS
- NT ELASTODYNAMICS
- NT ELECTROHYDRODYNAMICS
- NT FLUID DYNAMICS
- NT GAS DYNAMICS
- NT HYDRODYNAMICS
- NT HYDROMECHANICS
- NT HYDROSTATICS
- NT HYPERSONICS
- NT MAGNETOHYDRODYNAMICS
- NT MAGNETOHYDROSTATICS
- NT PNEUMATICS
- NT RAREFIED GAS DYNAMICS
- NT ROTOR AERODYNAMICS
- Mechanics of perturbation wave in turbulent shear flow (AD-711414) 02 p0201 N71-11585
- Mechanics of stratified and rotating fluids (AD-712322) 02 p0213 N71-11695
- Thermodynamic processes in fluid mechanics (RAE-LIB-TRANS-1474) 05 p0783 N71-15174
- Fluid mechanics approach to acoustic liner design (NASA-CR-72807) 06 p0840 N71-16048
- Project SQUID research in fluid mechanics, chemically reacting, and combustion physics (AD-74334) 06 p0836 N71-16396
- Fluid leakage detection system with automatic teaching capability (NASA-CASE-LAR-10323-1) 07 p1009 N71-17573

- Applied mechanics, material testing, fluid mechanics, and electrochemical laboratories (SAB-1) 10 p1653 N71-21133
- Numerical methods developed in fluid mechanics and heat transfer emphasizing elliptic flows (REFTNA/34) 11 p1737 N71-22295
- Effect of permanent and alternating electric fields on heat transfer in fluid dielectrics (NASA-TT-F-15560) 12 p3011 N71-34059
- Experimental and theoretical investigation of flow of density-stratified fluid about symmetric towed bodies and stability of flow induced by rotating cylinder 12 p1903 N71-24134
- Compilation of reports on hydraulic research projects conducted in US and Canada (NBS-SP-346) 12 p1903 N71-24141
- Sumptuous theory based on magneto-fluid-mechanics turbulent damping 12 p1993 N71-24192
- Analytic functions and fluid mechanics for noise propagation in supersonic jet exhaust flow (NASA-CR-1844) 15 p2364 N71-27028
- Fluid mechanics experiments to investigate methods for reducing mixing between confined coaxial flows in cylindrical chambers for application to open-cycle gaseous-core nuclear rockets (NASA-CR-1851) 16 p2579 N71-28403
- Subsonic flow over twisted retractor - fluid mechanical refracting gas-prism with wave functions and real numbers (AD-721711) 17 p2733 N71-29544
- Application of radioactive pulse probe to determine fluid velocity and direction in open tanks (CSIR-SR-CHEM-133) 17 p2754 N71-30389
- Solid project research on fluid mechanics in jet propulsion (AD-723807) 19 p3174 N71-32076
- Axiymmetric flow of rotating stream analyzed to determine conditions allowing isolated vortex breakdown to develop (NASA-CR-1845) 19 p3078 N71-32192
- Mechanics of free piston engine, aspects of human factors engineering, and compressible boundary layer studies at high Reynolds numbers (DME/NAB-1971/1) 19 p3198 N71-32620
- Measurement of pressure drop in rod bundles with spiral wire spacers to determine effect of number of rods, spacing ratio of rods, and pitch of spirals (NLL-BISLEY-TRANS-2082-19091.9P) 19 p3083 N71-32688
- Development and characteristics of parallel plate viscometer for determination of absolute viscosity of liquids and viscoelastic materials (NASA-CASE-NPO-11387) 21 p3427 N71-34383
- Markov model for application of uniform withdrawal assumption in continuous crystallizer design equations to continuous mixing vessel equations 21 p3501 N71-34940
- Tradeoff of autonomous coherent checkout versus ground checkout of space shuttle fluid mechanical systems 22 p3674 N71-36196
- FLUID POWER**
- Fluid power transmission and gas bearing system (NASA-CASE-XMS-01445) 06 p0834 N71-16851
- Low friction gas bearing system for fluid power transmission to bearing-supported payload 16 p2601 N71-28465
- FLUID ROTOR GYROSCOPES**
- Stabilizing gyro utilizing re-circulated liquid hydrostatic gimbal bearing (NASA-CR-102992) 06 p0846 N71-16487
- Piezoelectric pump for supplying fluid at high frequencies to gyroscopic fluid suspension system (NASA-CASE-XNP-05429) 10 p1636 N71-21824
- Velocity components and radial pressure distributions in vortex gyres for measuring angular velocity (FOA-2-C-2356-34) 14 p2256 N71-26280
- Survey of unconventional gyroscopes including cryogenic gyroscopes, electrostatic gyroscopes, fluid gyroscopes, and optical gyroscopes (DLE-MITT-71-02) 17 p2779 N71-29570
- FLUID SWITCHING ELEMENTS**
- Manufacturing process and construction methods for fluidifier laminates using chemical milling (FK-09111) 05 p0664 N71-14990
- Design of electronic controlled pneumatic signal converter for fluidic device testing by also wave phenomena (M/P-1) 12 p1890 N71-23885
- Two phase fluid pressurization system for propellant tank (NASA-CASE-MSC-12390) 16 p2670 N71-29153
- Switching dynamics of bistable fluid amplifiers (AD-723832) 19 p3079 N71-32328
- Numerical analysis of vortex rate sensor for sensing small speeds of rotation (CRANFIELD-M/P-2) 21 p3428 N71-34394
- FLUID TRANSMISSION LINES**
- Rust prevention in stainless steel fluid transmission lines of nuclear reactors for rocket vehicles (NASA-CR-111736) 04 p0536 N71-14097

FLUIDIZED BED PROCESSORS

- Mathematical models of fluidic transmission lines for use in missile design 05 p0662 N71-14988 (AD-713383)
- Predicted response characteristics of transmission line terminations to step waves and application to impedance matching (AD-717247) 10 p1541 N71-21195
- FLUID TRANSPORT**
- U TRANSPORTATION
- FLUIDIC CIRCUITS
- NT FLIP-FLOPS
- FLUIDICE
- NT FLUIDICS
- Fabricative techniques of compact fluidic control equipment for aerospace engines 05 p0603 N71-11634
- Design optimization and production of fluidic accelerometer for angular rate measurements (NASA-CR-102951) 05 p0883 N71-13322
- Digital fluidic compensator for analog fluid systems (AD-71926) 05 p0865 N71-13383
- Manufacturing process and construction methods for fluidifier laminates using chemical milling (FK-09111) 05 p0664 N71-14990
- Synthesis of transfer functions using RC fluid circuit (REPT-F3) 05 p0665 N71-15486
- Linear analysis of relationship between fluid transmission line characteristics and output of transmission line (AD-714280) 06 p0836 N71-16469
- Engineering study of electro-fluid converter concepts (AD-715103) 07 p1011 N71-17737
- Fluidic electrochromic display device (NASA-CASE-ERC-10031) 08 p1179 N71-18683
- Fluidic rail control for Aerobac rocket vehicle (NASA-CR-75499) 08 p1294 N71-18745
- Determining characteristics of jet elements whose operation is based on jet interaction with turbulent or laminar flow in control channels (AD-716519) 09 p1371 N71-19629
- Zero gravity clothes washer utilizing principles of fluidics to provide washing action and reduction in number of components scale model (NASA-CR-114983) 13 p3086 N71-34455
- Fluidic controls for automotive engine examined by Ramjet cycle performance with water, CP-34, and frozen TP and investigation for boiler and feed pump control criteria (NASA-CR-115006) 16 p2578 N71-28104
- Design, development, fabrication, and acceptance test results for two fluidic proportional thrusters for use in SPARC 4 (NASA-CR-114339) 19 p3106 N71-32794
- Research and development for fluid amplifier design and thrust vector control systems (AD-74126) 20 p3248 N71-32836
- Plasma fluidic hybrid display system combining high brightness and memory characteristics (NASA-CASE-ERC-10100) 20 p3242 N71-33519
- Advanced servopneumatic systems and control including thrust modulation, optimizer research, fluidic devices, hydraulic jet valves, and related research (NASA-CR-121643) 21 p3413 N71-34236
- Numerical analysis of vortex rate sensor for sensing small speeds of rotation (CRANFIELD-M/P-2) 21 p3428 N71-34394
- Design and wind tunnel tests of two-axis wind speed and angle sensor for meteorological applications (AD-727220) 24 p3953 N71-38198
- FLUIDIZED BED PROCESSORS**
- Mass transfer in gas flow through fluidized bed 01 p0043 N71-10491
- Hydrodynamic characteristics of spouting processes in fluidized beds (NRC-TT-1434) 06 p1181 N71-18840
- Fluidized bed combustion process for recovering uranium from spent graphite-matrix nuclear reactor fuel (IN-1423) 06 p1422 N71-30596
- Particle size control by jet grinding in fluidized bed distributors (IN-1439) 06 p1578 N71-20597
- Progress report including removal of stainless steel charring, development of fluid bed process for reduction of nuclear fuel oxide to metal (ANL-7753) 12 p1961 N71-23194
- Coating of fuel particles and model investigations of central fluidized beds noting effect of gas current and gas distribution particle load, and nozzle geometry (JUL-660-RW) 15 p0440 N71-27539
- Two dimensional visual model for simulating turbulent flow in porous material 17 p2735 N71-29892
- Dimensional influence of fluidized bed reactors on gas mixing at various velocities (BMW-FBK-70-36) 17 p2716 N71-39913
- Research in fuel cycle technology including removing stainless steel charring, and fluid bed process for converting uranyl and plutonium oxides to oxide form (ANL-7767) 17 p2786 N71-30826

Measurement and correlation of gas-particle heat transfer coefficients in packed and fluidized bed processors by frequency response techniques
[RFS-359-16] 21 p3411 N71-34268

Statistical analysis of pressure fluctuations in fluidized beds of copper and glass particles with air
23 p3741 N71-36676

Developmental program for SO₂, NO, and particulate pollutant level lowering and control in this gas from fossil fuel combustion using fluidized beds with limestone
[ANL/ES-CEN-1003] 23 p3750 N71-36736

FLUIDS
Asomalous behavior model for prediction of thermal conductivity of fluids in critical region
[NASA-TM-X-52955] 12 p2009 N71-23196
Supercritical fluid chromatography system with micro adsorption detector
14 p2256 N71-26270

Automated fluid chemical analyzer for microchemical analysis of small quantities of liquids by use of selected reagents and analyzer units
[NASA-CASE-XNP-09451] 14 p2216 N71-36754
Unified heuristic model of fluid turbulence which supplements basic equations of motion and continuity
[AD-72103] 24 p3906 N71-37840

General mathematical laws for electromagnetic field-conductive fluid interactions in rectangular channels
24 p3968 N71-38503

FLUORESCENCE
NT PHOSPHORESCENCE
NT X RAY FLUORESCENCE

Developing line discriminator for detecting substances that fluoresce in water near sodium D2 Fraunhofer line
02 p0227 N71-11992

Laser excited resonance fluorescence of molecular iodine
[AD-711823] 03 p0434 N71-12970
Polarization functions of fluorescence from polarized and unpolarized light
04 p0568 N71-14306

Resonance fluorescence techniques for determining upper atmosphere hydroxyl radical
[NASA-CR-115883] 05 p0639 N71-14744
Iodine fluorescence excited by 6328 Å neon line of He-Ne laser
[AD-714531] 06 p0668 N71-16668

Fluorescence method for rate constant determination of vibrationally excited carbon dioxide deactivation
[AD-715276] 07 p1039 N71-17767

Phosphorescence and delayed fluorescence of naphthalene in mixed crystals
[NRC-TT-1436] 08 p1280 N71-18848

Using single photon counting techniques to study fluorescence response and time dependence of benzene in cyclohexane excited by protons and ultraviolet radiation
[BNWL-SA-3526] 08 p1268 N71-19336

Magnetofluorescence, cooperative fluorescence of rare earth ions in crystals, narrow-band and narrow-gap compounds, and related studies of rare earth compounds
[AD-716470] 09 p1453 N71-20007

Characteristics of sensitivity of recombination light to infrared radiation in continuously excited and pulsed system operation
[AD-717645] 11 p1722 N71-21911

Decay in fluorescence from asymmetric stretching vibrational level of CO₂ after excitation by Q switched CO₂ laser
11 p1803 N71-22111

Electron beam fluorescence in Nylon, polytetrafluoroethylene, and polyethylene
[AD-717769] 11 p1783 N71-22276

Semiconductor tube light unit capable of connection with other units to form string of work lights
[NASA-CASE-XKS-5932] 14 p2231 N71-26787

Procedures and immunofluorescent techniques for screening Apollo aquatic test animals for bacterial pathogens after lunar sample exposure
[NASA-CR-115064] 17 p2707 N71-29228

Matrix element tables for computing L shell fluorescence yields and electron transition rates in spin-spin coupling including Auger, Coster-Kronig, and radiative values
[SC-RR-718075] 17 p2791 N71-29288

Upper atmosphere helium fluorescence due to cycles of electron flux, solar ultraviolet radiation, and geomagnetic activity
[NRC-TT-1458] 21 p3416 N71-34306

Development of operational system for measuring ocean surface current from aircraft using floats and fluorescent dyes
[AD-718568] 24 p3916 N71-37922

Millisecond time-scale atmospheric light pulses induced by solar activity
[NASA-TM-X-45716] 24 p4002 N71-38545

FLUORESCENT EMISSION
U FLUORESCENCE

NT BARIUM FLUORIDES
NT BERYLLIUM FLUORIDES

NT BORON FLUORIDES
NT CALCIUM FLUORIDES
NT CESIUM FLUORIDES

NT CHLORINE FLUORIDES
NT DIFFLUORIDES
NT HYDROFLUORIC ACID

NT LITHIUM FLUORIDES
NT MAGNESIUM FLUORIDES
NT NICKEL FLUORIDES

NT NITROGEN FLUORIDES
NT OXYGEN FLUORIDES
NT OZONE FLUORIDE

NT SODIUM FLUORIDES
NT STRONTIUM FLUORIDES
NT SULFUR FLUORIDES

NT TUNGSTEN FLUORIDES
NT URANIUM FLUORIDES
Observation of elastic shocks during transition of ammonium fluoride to substantive phase transition hypothesis of earthquake occurrence
[NASA-TT-P-13325] 01 p0047 N71-10338

Chemical properties of superoxide ion and other solute species in molten fluorides
[AD-72409] 04 p0486 N71-13459
Reaction kinetics of carbon tetrachloride with complex transition metal fluorides
04 p0488 N71-13469

Electron emission from fluoride ion in shock heated mixtures of cesium fluoride and argon
[AD-715994] 09 p1442 N71-20386

Safety factors and warning systems for fluid-bed fluoride volatility processes
[ANL-7672] 10 p1538 N71-20688

Self lubricating fluoride-metal composite materials for outer space applications
[NASA-CASE-XLB-09511] 12 p1944 N71-23710

Resistance gas measurements of solid-solid phase transition fixed points in ammonium fluoride under high pressure
14 p2328 N71-26505

Thermal dissociation and sublimation of UO₂F₂ between 760 and 800 C using Knudsen effusion method
[ORNL-TR-2422] 15 p2376 N71-26887

Wear tests of oxide and fluoride oxidation resistant solid lubricants for use in high temperature gaseous environments
[NASA-TM-X-67845] 15 p2417 N71-27767

High temperature friction and wear characteristics of self lubricating composite disks of sintered tungsten, molybdenum, and cobalt molybdenum, impregnated with fluoride eutectic
[NASA-TN-D-4363] 16 p2600 N71-28231

Development of fluoride coating to prevent oxidation of beryllium surfaces at elevated temperatures
[NASA-CASE-LEW-10327] 20 p3285 N71-33408

Monte Carlo method for determining reactive collisions of fluorine atoms with hydrogen molecules
[LA-4603] 21 p3388 N71-34103

Willard-Winter distillation and spectrophotometric determination of 2 to 7 micromole fluoride
[FOA-4-C-4416-24] 22 p3551 N71-35291

Molten-salt fluoride volatility process for recovering decontaminated uranium from aluminum clad fuel elements
[ORNL-4574] 22 p3624 N71-35819

FLUORINATION
Technologies involving metal corrosion in fluorinating gases in isotope separation plants
[NLL-CA-232-P091.9F] 11 p1780 N71-22395

FLUORINE
Electric and magnetic moments of F-18 and Na-22 measured using spin rotation for validity tests of shell or collective nuclear model
03 p0436 N71-13280

F-18 influence on oxygen determination in silicon by alpha particle activation
[LYCEN-7038] 05 p0751 N71-15592

Fluorine production and recombination in frozen MSR after reactor operation
[ORNL-TM-3144] 06 p0901 N71-16809

Thermal stability of perfluoro polypropylene and polytetrafluoroethylene thermal degradation products and fluorine weight analysis
[RAE-TR-70005] 07 p0908 N71-17093

Microdetermination of fluorine in high purity tungsten by destructive photoactivation analysis
[GA-10125] 08 p1256 N71-18373

Vapor pressure and PVT data of compressed gaseous and liquid fluorine
[AD-716286] 09 p1343 N71-19069

Quadrupole interaction of Ba-137 and Ba-135 near positive fluorine ion centers and electron paramagnetic resonance spectrum of positive trivalent Gd ions in single BaO crystals
11 p1805 N71-22402

Fluorine atom reaction dynamics, intermolecular potentials from high resolution differential cross sections, and collision induced dissociations of diatomic molecules
[COO-2092-1] 11 p1696 N71-22421

Stoichiometric dichloro-difluoromethane-fluorine combustion reaction
[AD-718375] 12 p2011 N71-24110

Space storable fluorine/hydrizine tank module thermal control design for Jupiter mission
[NASA-CR-117599] 13 p2176 N71-25578

Oxygen, fluorine, and sodium isotope atomic excitation energies, series, partition, and transfer distribution using time of flight spectrometers and Born approximations
15 p2404 N71-27954

Nuclear magnetic relaxation times of deuterium and fluorine nuclei in liquid CDF₃
15 p2496 N71-27989

Oxidation resistance and high temperature tests of rhodium, tungsten, hafnium, and tantalum matrix composites with iridium in oxygen, fluorine, and boron atmospheres for liquid propellant engines
[NASA-CR-119019] 16 p3617 N71-28201

Dynamic polarization of protons and fluorine nuclei in solutions of selected free radicals in solutions of aromatic and aliphatic fluorocarbon solvents
20 p3318 N71-33597

Pyrohydrolytic separation and spectrophotometric analysis of cesium fluoride in phosphoric acid
[FOA-4-C-4407-24] 22 p3551 N71-35291

Past analysis by 14 MeV neutron activation of fluorine deposits on vegetation in polluted area
[CEA-CONF-1747] 22 p3641 N71-35956

Low temperature fluorine chemistry of chlorine, nitrogen, and oxygen
[AD-727059] 23 p3720 N71-36514

Electrode potential and spectrophotometric determination of trace fluorine, chlorine, and boron in plutonium oxide fuels after pyrohydrolytic separation
[KFK-1360] 23 p3801 N71-37009

Beta and electron-capture decay schemes for the isotopes and proton reactions of C-12, F-19, Au-197, He-3, Ta-181, Pb-206, and Ni-58 including angular distributions and scattering cross sections
[UCLA-10-P-18-23] 23 p3816 N71-37215

Design, fabrication, and testing of pneumatically operated liquid fluorine shutoff valve
[NASA-CR-72691] 24 p3927 N71-38020

FLUORINE COMPOUNDS
NT BARIUM FLUORIDES
NT BERYLLIUM FLUORIDES

NT BORON FLUORIDES
NT CALCIUM FLUORIDES
NT CESIUM FLUORIDES

NT CHLORINE FLUORIDES
NT DIFFLUORIDES
NT DIFFLUORO COMPOUNDS

NT FLUORIDES
NT FLUORINE ORGANIC COMPOUNDS
NT FLUORO COMPOUNDS

NT FLUOROCARBONS
NT FLUOROHYDROCARBONS
NT FLUOROSILICATES

NT HYDROFLUORIC ACID
NT LITHIUM FLUORIDES
NT MAGNESIUM FLUORIDES

NT NICKEL FLUORIDES
NT NITROGEN FLUORIDES
NT OXYGEN FLUORIDES

NT OZONE FLUORIDE
NT PERFLUOROALKANE
NT POLYTETRAFLUOROETHYLENE

NT SODIUM FLUORIDES
NT STRONTIUM FLUORIDES
NT SULFUR FLUORIDES

NT TUNGSTEN FLUORIDES
NT URANIUM FLUORIDES
Thermal control concepts for space storable fluorine hydrizine propulsion module
[NASA-CR-111062] 01 p0114 N71-10001

Mass spectroscopy to determine structure of various substituted polyfluorobenzenes
[AD-711072] 02 p0175 N71-11235

Effects of fluorine substitution on properties and reaction rates of monoglycidyl ethers
[AD-712507] 03 p0331 N71-12362

Unimolecular reactions to calculate rate constants for thermal decomposition of fluoromethane and methanol
[AD-715897] 08 p1159 N71-18335

Equipment for demonstrating low pressure distillation of molten fluoride mixtures from MSRE and equipment tests
[ORNL-4434] 10 p1605 N71-21195

Development and operation of mass spectrometer for analysis of highly reactive fluorine compounds at subambient temperatures
11 p1697 N71-22839

Bibliography on fluorine compounds as high energy rocket fuel oxidizers
[FOA-1-A-T502-42/46,40/] 14 p2215 N71-26468

High pressure effects on quadrupole interactions in K₂FeF₆, Na₂FeF₆, NH₄FeF₆, and FeF₃
18 p2855 N71-31015

Solutions of aqueous fluorocarbon surfactants placed on surfaces of liquid hydrocarbons and hydrocarbon fuels for suppression of fuel evaporation
[AD-723189] 19 p3172 N71-32809

Optical saturation formula for vibration-rotation transitions in molecular gases verified for SF₆ on sub J transition at 200 K
21 p3465 N71-34669

SUBJECT INDEX

FLUORINE ORGANIC COMPOUNDS

NT FLUOROCARBONS
NT FLUOROHYDROCARBONS
NT PERFLUOROALKANE

Bibliography on fluorine compounds as high energy rocket fuel oxidizers
[FOA-1-A-7502-42/46, 40/]

14 p2215 N71-26608
FLUORINE-LIQUID OXYGEN
U FLOX

FLUORO COMPOUNDS

NT DIFLUORO COMPOUNDS

NT FLUORINE ORGANIC COMPOUNDS

NT FLUOROCARBONS

NT FLUOROHYDROCARBONS

NT PERFLUOROALKANE

NT POLYTETRAFLUOROETHYLENE

Combustion kinetics of tetrafluoroethylene
[AD-713144]

05 p0784 N71-15396
IPS-flux system for retrieving information in chemistry of fluorine compounds

19 p3195 N71-31966

FLUOROCARBONS

Organometallic chemistry emphasizing fluorocarbons complexes of transition metals
[AD-714623]

06 p0808 N71-15919

Effects of positive Gy acceleration on blood oxygen saturation and pleural pressure relations in dogs breathing air and liquid fluorocarbons in whole body water immersion respirator

[NASA-CR-117199]

09 p1336 N71-20358

Nuclear dynamic polarization for investigating intramolecular dynamics in solutions of selected free radicals and fluorocarbons in acetone

20 p2320 N71-33807

FLUOROHYDROCARBONS

Measurement of brain and heart accumulation of bromotrifluoromethane for evaluation as potential fire extinguisher chemical

[AD-712111]

15 p2371 N71-27299

FLUOROMICA

U FLUOROSILICATES

U MICA

FLUOROGRAPHY

Fluorographic system for rapid presentation of single phase body sections with reduced X ray exposure to patients

[NASA-CR-111944]

21 p4324 N71-34363

FLUOROSILICATES

Electron paramagnetic resonance of divalent manganese in zinc perchlorate and divalent nickel in zinc fluorosulfate with parallel and perpendicular configurations

09 p1430 N71-19867

FLUTTER

U GROOVING

U FLUTTER

NT PANEL FLUTTER

NT SUBSONIC FLUTTER

NT SUPERSONIC FLUTTER

NT TRANSONIC FLUTTER

Flutter suppression with dissipated energy reduced to quadratic form for control surfaces

[NASA-TN-D-6199]

11 p1671 N71-23091

On-line monitoring of characteristic structural response of space shuttle wing flutter model for failure detection and repair

[NASA-TN-D-62041]

15 p2521 N71-26932

Effects of variations in location of concentrated masses on transonic flutter characteristics of swept-back thin cantilever wings

[NATL-TN-226]

20 p2305 N71-31373

Theory and analysis of demodulating suppressed carrier AM baseband in noise and recorder flutter

24 p3890 N71-37729

FLUTTER ANALYSIS

Flutter analysis on axial turbomachine blading

[AD-716794]

01 p0001 N71-10562

Flutter analysis for thin lifting surfaces by application of superposition integral function procedure

[NASA-TN-D-6012]

01 p0131 N71-10866

Characteristics of flutter in thin plates, shells, or membranes due to aerodynamic loading

04 p0615 N71-13610

Flutter of rectangular plates with reinforcing rigid ribs

[AD-714778]

06 p0953 N71-15975

Vibration and flutter tests of pressurized thin walled truncated conical shell

[NASA-TN-D-6196]

07 p1123 N71-17355

Formulation method extension for nonlinear panel flutter to include fifth-order nonlinear terms effect, flutter-buckling interaction, and small damping terms

[NASA-CR-117504]

10 p1658 N71-31672

Flutter and divergence of four low mass ratio bi-level model configurations

[AD-719891]

14 p2238 N71-25643

Supersonic asymmetric flutter and divergence characteristics of truncated conical shells with ring-supported edges under three types of flow-induced loads

[NASA-TN-D-6223]

14 p2347 N71-35790

Time-base error analysis of magnetically recorded and played back digital data using tape flutter spectral

density and amplitude probability distribution measurements and rms time plots

[NASA-CR-115029]

15 p2411 N71-27711

Low speed wind tunnel stability tests and flutter analysis of flapped rotary wings

[NAL-TN-18]

15 p2568 N71-27756

Aeroelastic and flutter analysis for T tail of Fokker F28

17 p2699 N71-29544

Method for calculating flutter using interference aerodynamic forces between wing and tail

17 p2699 N71-29545

Supersonic panel flutter and aerodynamic load stress analysis of finite cylindrical shells based on Galerkin method and aerovlastic equilibrium equations

[AD-723447]

18 p2905 N71-31183

Flutter analysis and reduction in short takeoff aircraft with tilt wings

[AD-723221]

19 p3037 N71-31934

Numerical analysis of supersonic flutter of flat rectangular, biaxially stressed sand-wich panels

[NASA-TN-D-6427]

19 p3189 N71-32373

Modifications and computational tasks required for aerodynamic capability in NASTRAN

[NASA-CR-111918]

20 p3358 N71-33303

Examining model theory for static and dynamic aerodynamic phenomena

20 p3360 N71-33805

Theoretical study of nonlinear flutter behavior of clamped panels subjected to various loads

21 p3374 N71-34010

Numerical analysis of derivatives of flutter velocity of aircraft structures to determine optimization of complex structures

[NASA-CR-111953]

21 p3526 N71-35126

Comparison of finite element computer programs for analysis of clamped flat plate and built-up wing vibration frequencies

22 p3687 N71-36293

FLUX

Frame-indifferent time fluxes and linear operations in Euclidean space

[WTHD-25]

21 p3448 N71-34540

FLUX (RATE PER UNIT AREA)

U FLUX DENSITY

FLUX (RATE)

NT HEAT FLUX

NT MAGNETIC FLUX

NT SOLAR FLUX

Neutron flux measurements in three-capsule D2O tank in Plum Brook mock-up reactor

[NASA-TM-X-52910]

01 p0084 N71-10271

Spectral power flux magnitude system for astronomical scaling

01 p0121 N71-10319

Program for calculating neutron ages using ENDF/B Library

[WAFD-TM-822-ADD-1]

01 p0098 N71-10635

Particle flux associated with stochastic processes

[NASA-CR-111402]

02 p0280 N71-11853

Origin and isotropy of cosmic gamma ray flux between 1 and 6 MeV and its implications of future gamma ray investigations

[NASA-TM-X-63383]

02 p0293 N71-12046

Relation of plasmapause position to region of enhanced fluxes of trapped energetic electrons during magnetic storm on 15 June 1965

[NASA-TM-X-63590]

03 p0490 N71-13025

Experimental analysis in measurement of neutron flight time

[IAE-1968]

04 p0569 N71-13473

FFFT closed loop test characteristics

[BNWL-1251]

04 p0531 N71-13955

Swimming pool reactor for irradiating nuclear power station structural materials in high neutron flux

[CEA-R-3984]

05 p0722 N71-14560

Computer calculation of light particle energy loss in thick foils with high neutron cross sections

[LA-4443]

06 p0915 N71-16003

Flux synthesis methods to obtain detailed neutron flux from lower-order calculations

[LA-4472]

06 p0996 N71-16280

Ten-decade wide range neutron monitoring system

[GEAP-11094]

07 p1062 N71-17250

Shaped thermal neutron flux filters for in-pile test capsule

[NASA-TM-X-2196]

07 p1066 N71-17952

Small digital computer for calculating axially averaged neutron fluxes and channel powers

[RD/RN-1749]

08 p1231 N71-18248

Measurements of neutron streaming through cylindrical bent ducts in water

[BUR-4498-E]

08 p1237 N71-18286

Static flux synthesis model for movable material reactor problems

[WAFD-TM-978]

09 p1430 N71-20071

Satellite-borne measurements of electron flux during magnetic storm

[NASA-TT-F-13512]

09 p1386 N71-20381

Misleading neutron diffusion theory perturbation program SPECTRE, using IBM 7030 computer

[AWRE-O-7470]

09 p1443 N71-20451

Flux interactions at medium energies, data analysis programs, incident rate flux measurements, and development of rectification counters

[ORO-5948-2]

10 p1615 N71-21058

High flux stationary research intermediate neutron reactor with thermal neutron trap

[LA-4399-TR]

10 p1604 N71-31280

Critical mass measurements, control rod calibration, neutron and gamma flux measurement, measurement of various reactivity worths, power calibration, and neutron loading for TRR-2

[JAERI-MEMO-4141]

13 p2119 N71-25107

Physical model for neutron flux enhanced creep rate

[AD-719985]

14 p2324 N71-25707

Measurement of variance in neutron counter signal fluctuations for neutron flux measurement including electronic equipment design

[CEA-E-4119]

14 p2305 N71-26340

Models of neutron slowing down calculations in thermal and fast reactors

[BURFNR-064]

14 p2307 N71-26396

Model for analytic fast reactor mode flux and importance spectra

14 p2295 N71-26684

Fast reactor lattice evaluation of infinite neutron multiplication constant and reaction rate in zero power facility

[BURFNR-061]

14 p2313 N71-26711

Three dimensional neutron diffusion equations for calculating axial flux in hexagonal reactor

[CEA-N-1276]

15 p2466 N71-27284

Fluxgate magnetometer for measuring magnetic field along two axes using one sensor

[NASA-CASE-GSC-10441-1]

15 p2409 N71-27325

Neutron spectra and flux measurement by multiple moderator spheres

[CEA-COMP-1485]

15 p2400 N71-27468

Measuring high energy gamma ray spectra in strong neutron flux

[JNR-1224]

15 p2482 N71-27706

Transport theory for analysis of neutron flux distribution near absorber rod in reactor

[JAERI-4238]

15 p2452 N71-27850

Analysis of JMTR neutron flux change and variations effects in irradiation holes

[JAERI-4130]

16 p2645 N71-28114

Infrared flux at air-sea interface calculated to solve radiative transfer equations numerically by using flux emittance and flux reflectance as functions of sea temperature and roughness

[AD-72036]

16 p2508 N71-28455

Determining fast and thermal neutron fluxes by copper and indium foil activation analysis

[RFP-1466]

17 p2794 N71-29631

Computer codes for determining neutron flux spectra in HFTR target region

[ORNL-TN-3322]

17 p2800 N71-30046

High intensity neutron fluxes, short-lived radioactive isotopes, and high intensity radiation sources - physical, chemical, medical, biological, and technical applications

[NP-18571]

17 p2806 N71-30363

Greenough high flux reactor for nondestructive tests in biology

[NP-18462]

18 p2874 N71-30447

SYNTRON - computer code for reactor problems involving three dimensional neutron flux calculations

[RISO-M-1346]

18 p2974 N71-30548

High energy neutron detector for measuring solar neutron flux in earth radiation environment during quiet or active sun conditions

[AD-722467]

18 p3089 N71-30891

Comparison of electron response in magnetosphere at L equals 5 with solar wind during magnetic storm on 17-18 Apr. 1965

18 p3085 N71-30936

Correlation of increases in electron population of outer radiation belt and interplanetary magnetic fields during two geomagnetic storms

18 p3005 N71-30927

Outer radiation belt electron fluxes during solar proton event on 5 Feb. 1965

18 p3005 N71-30928

Charged particle beam environment experiment of Apollo 14 detecting particle fluxes at lunar surface resulting from wide range of lunar surface, magnetospheric, and interplanetary data

18 p3011 N71-30964

Detection of hydrogen ion flux in exosphere existing along terrestrial magnetic lines of force

[NASA

Neutron thermalization with time in water at 318 K and ice at 77 K determined by measuring neutron flux time dependence
[KAPL-TRANS-4] 21 p3475 N71-34745

Plasma flux and magnetic field properties resulting from deuterium-deuterium reactions
[LA-TR-71-6] 21 p3494 N71-34890

Rocket and balloon measurements of energy spectra and fluxes of fast neutrons, gamma rays, and X rays in atmosphere
[NASA-CR-121629] 21 p3503 N71-34952

Expression for differential cross sections in energy range between 22.5 and 400 MeV
[UCRL-20295] 22 p3645 N71-35986

Computer programs for solving two dimensional multigroup neutron diffusion equations and for makeup or recycle of isotopic compositions and related problems
[GEAP-13672] 22 p3647 N71-36007

Electron density profiles and production rates associated with 30 Jan. 1968 large X ray flare event
[RSD-63] 22 p3665 N71-36131

Flux, energy spectra, and pitch angle distributions of precipitated low energy hydrogen and electrons from Nike-Tomahawk auroral hydrogen experiment
[NASA-CR-121934] 22 p3668 N71-36155

Space and reflection effects on neutron count rate fluctuation spectra of large nuclear reactors
[DF-MS-70-101] 22 p3794 N71-37078

Determining neutron properties of loops containing fuel assemblies and of positions for irradiating structural materials in MR reactor
[LB/G-3010] 24 p3957 N71-38227

Thermal flux distribution and reflector saving measurements in UA-RR-1 reactor core using foil activation technique
[UAREE-99] 24 p3958 N71-38236

Measurement of suprathermal electron flux caused by total solar eclipse of 7 Mar. 1970
[NASA-CR-123121] 24 p4003 N71-38549

FLUX DENSITY
NT CURRENT DENSITY
NT ELECTRON FLUX DENSITY
NT ILLUMINANCE
NT IRRADIANCE
NT LUMINANCE
NT LUMINOUS INTENSITY
NT NEUTRON FLUX DENSITY
NT PARTICLE FLUX DENSITY
NT PHOTON DENSITY
NT PROTON FLUX DENSITY
NT RADIANCE
NT RADIANT FLUX DENSITY
NT SOLAR CONSTANT
NT SOLAR FLUX DENSITY
NT SOUND INTENSITY
NT ZERO SOUND

Approximate density-effect correction for ionization loss of charged particles
[NASA-CR-111032] 01 p0103 N71-10981

Digital computation of power spectral density curves from reactor noise data
[IN-1374] 03 p0413 N71-12687

Meridional flow, relative angular momentum, and energy flux calculations for International Geophysical Year
[MET-O-808C] 05 p0673 N71-14878

Linear differential variable transformer for measuring length variations of flux in in-pile irradiation capsule
[CEA-N-1315] 05 p0686 N71-15419

Flux densities of planetary nebulae at 8.0 GHz and 16.2 GHz
06 p0944 N71-15863

Boundary value problems for temperature and flux fields inside and around paraboloidal needle and parabolic platelet crystals during growth
08 p1282 N71-19295

Particle size distributions from fuel rods fragmented during power burst tests in capsule driver core
[IN-1428] 09 p1417 N71-19897

Feasibility study of autoradiographic technique for determining relative power densities in reactor fuel plates
[Y-DR-29] 09 p1418 N71-19899

Development of instruments for measuring flux of high and ultrahigh energy particles on Proton 4 satellite during space missions
[NASA-TT-F-13533] 09 p1464 N71-20576

Predicted ultraviolet radiation flux density for main sequence stars derived from atmospheric model and photometric measurements
10 p1642 N71-20633

Deep sky survey at 2700 MHz using 210-foot telescope - measurements of positions and flux densities of sources
[NP-10682] 17 p2846 N71-30211

Electron energy flux in solar wind, in energy range 25 eV to 9.9 keV
[NASA-TM-X-45621] 18 p3002 N71-30562

Nuclear density formula for interpolating level spacing and radiation width
[AABCE-211] 18 p2978 N71-30692

Model for computing power density contours caused by satellite antennas illuminating portion of earth surface
[AD-723284] 19 p3064 N71-31760

Flux density measurements on extraterrestrial waves from faint radio sources
[AD-724181] 19 p3182 N71-32781

Performance of helium seeded with uranium in magnetohydrodynamic generator
20 p3306 N71-33663

Analysis of flux reversal in nickel-nickel thin films using magneto-optic photographs to depict dynamic magnetization configuration during reversal process
20 p3336 N71-33912

Voltz equation for coupled channel amplitude densities and modified wave functions
[NASA-CR-121759] 21 p3447 N71-34529

Neon, argon, and helium density and flux distributions in lunar atmosphere
[NASA-CR-121633] 21 p3506 N71-34981

Precipitates and flux line pinning in superconducting Pb-Na alloy investigated by electron microscopy
[NLL-CE-TRANS-3559-0622.09] 24 p3968 N71-38305

Cosmic ray intensity variation and Forbush decrease during solar activity maximum
24 p4011 N71-38605

FLUX MAPPING
U FLUX DENSITY
U MAPPING

FLUX PUMPS
Characteristics of superconducting flux pump
[AD-711569] 02 p0193 N71-11352

FLUX QUANTIZATION
Energy-dependent neutron cross section library for calculating integral fluxes and fluences of fast and thermal test reactor environments
[BNWL-1312] 01 p0095 N71-10389

Computer programs for flux calculation in sodium reservoir
[ORNL-TR-2354] 04 p0544 N71-13559

Measurement of variance in neutron counter signal fluctuations for neutron flux measurement including electronic equipment design
[CEA-R-4119] 14 p2305 N71-26340

Numerical integration of ac generator coil equations into flux linkage equations with iterative solutions for three phase machines
16 p2604 N71-28995

Calculation of crew radiation dosage from uranium gas nuclear rocket engine exhaust backflow of fission products
20 p3305 N71-33655

Flux pinning mechanisms in type-2 semiconductors and specific heat measurements on annealed and deformed pure aluminum samples
[NASA-CR-121867] 21 p3496 N71-34907

FLUXES
Selected reports on standards for food and drug purity
[PB-190961] 05 p0639 N71-14728

Hydrazine monoperfluoro alkanoate solder flux leaving corrosion resistant coating, for metals such as copper
[NASA-CASE-XNP-03459-2] 05 p0711 N71-15688

Zone melting, recrystallization, single crystals, impurities, crystal growth, fluxes, magnetic fields, X ray analysis, and mixing
[JPRS-52552] 10 p1573 N71-20866

Refinement process using zone recrystallization and treatment of molten zone with active flux
10 p1632 N71-20869

Zone refining of metals using active fluxes
10 p1575 N71-20891

Metal soldering with hydrazine monoperfluoro alkanoate for corrosion resistant coatings
[NASA-CASE-XNP-03459] 10 p1564 N71-21078

RSYN and 3DB codes for flux and bulk parameter computation of fast reactors
[WHAN-IR-48] 12 p1964 N71-24152

FLUXMETERS
U MAGNETIC MEASUREMENT
U MEASURING INSTRUMENTS

FLY BY WIRE CONTROL
Flight test and evaluation of fly-by-wire control system for application to space shuttle control system
20 p3353 N71-33066

Hydraulic power and actuation requirements of survivable flight control system utilizing fly by wire control for F-4 aircraft
[AD-72763] 24 p3873 N71-37608

Analysis of criteria for survivable flight control system using fly-by-wire and integrated actuator package techniques
[AD-72762] 24 p3874 N71-37616

FLYBY MISSIONS
NT GRAND TOURS
NT MARINER VENUS-MERCURY 1973

Designing self testing and repairing computers for long term unmanned interplanetary missions
[NASA-CR-111577] 03 p0455 N71-12618

Tabulating trajectory data for alternate Grand Tour missions from earth for period 1976 to 1980
[NASA-CR-61338] 04 p0611 N71-14107

Mission analysis for application of Helogyro solar sailer concept to Jupiter flyby
[NASA-CR-115852] 05 p0771 N71-15316

Mariner 6 and Mariner 7 Mars missions and scientific observations
[NASA-CR-115853] 05 p0768 N71-15323

Outer planet missions with satellite flyby probabilities
11 p1828 N71-22310

Spacecraft design, configurations, and mission profiles in European Mercury probe
17 p2849 N71-29046

Onboard experiments of European flyby mission to Mercury planet - European space programs
17 p2850 N71-29047

Preliminary feasibility of depositing atmospheric entry probe from flyby mission to Jupiter
[NASA-TM-X-2336] 22 p3670 N71-36166

FLYING
U FLIGHT

FLYING BEDSTEAD AIRCRAFT
U FLYING PLATFORMS

FLYING PERSONNEL
NT AIRCRAFT PILOTS
NT ASTRONAUTS
NT COSMONAUTS
NT FLIGHT CREWS
NT ORBITAL WORKERS
NT PILOTS (PERSONNEL)
NT SPACECREWS

Survey on vertebrae fractures of flying personnel caused by ejection from Navy aircraft
02 p0163 N71-11811

Sound attenuation characteristics of military air protective devices and helmets
02 p0171 N71-11819

Cardiovascular reactions of flying personnel to flight
[FPRC/1296] 04 p0476 N71-13401

Techniques for familiarizing flying personnel with disorientation effects
[FAA-AM-70-17] 07 p0981 N71-17251

Physiological test program to evaluate physical fitness of flying personnel
11 p1687 N71-22202

Diagnostic and functional measurements of human physical fitness
11 p1687 N71-22208

Physical fitness training schedules for Canadian Forces flying personnel
11 p1688 N71-22205

Physical exercise and fitness tests for German Air Force flying personnel
11 p1688 N71-22207

Physical exercise and environmental-emotional psychotherapeutic methods in aerospace medicine
11 p1688 N71-22210

Aging effects on military flight crew body compositions and physical exercise performances
11 p1689 N71-22216

Cardiovascular disease effects in aging flying personnel on physical exercise performance
11 p1689 N71-22217

Formula for predicting physical fitness of flying personnel in Belgian Air Force during aging process from spirometric measurements
11 p1690 N71-22231

Predictive and adaptive processes in control of Air Force systems
[AD-721220] 15 p2375 N71-27609

Comparison of physiological characteristics of accident and nonaccident flying personnel for years 1966-1967
[FAA-AM-70-18A] 15 p2372 N71-27608

Medical examination of civil aviation flight personnel to determine predisposing factors for atherosclerosis
16 p2547 N71-28001

Physical examination and analysis of hemodynamic parameters of overweight flying personnel
16 p2547 N71-28002

Problem solving task for mental ability assessment in selection of aviation personnel
[FAA-AM-71-28] 19 p3045 N71-32044

Development of multivariate system for evaluating potential effectiveness of military aviation personnel during training
[AD-724696] 20 p3226 N71-33148

Development of procedure for predicting success of personnel in military aviation training
[AD-724695] 20 p3227 N71-33149

FLYING PLATFORM STABILITY
U AERODYNAMIC STABILITY
U FLYING PLATFORMS

FLYING PLATFORMS
Construction and operation of body-motion controlled five-degree-of-freedom simulation of jet-powered human flying machines
[NASA-TN-D-6001] 03 p0358 N71-12736

Design and development of lunar escape system simulator for investigation of lunar escape problems and simplified manual guidance and control for lunar escape vehicles
[NASA-TM-D-6111] 11 p1732 N71-22590

SUBJECT INDEX

Evaluation of in-flight simulation of flying platform using helicopter with variable stability and maneuverability 19 p3074 N71-31957

FLYING QUALITIES

U FLIGHT CHARACTERISTICS

FLYING SPOT SCANNERS

Processing of visual imagery by model derived for recognition of visual patterns 10 p1503 N71-26603

Computer graphics patching of failed flying spot scanner events for a spark chamber EP experiment [JHELR-205] 14 p2306 N71-26408

Transmission system for data generated by flying spot device into Radian-3 computer [JHELR-205] 18 p2893 N71-30589

FLYWHEELS

Design criteria for long life pneumatic subsystem for Nimbus spacecraft 02 p0149 N71-11060

Small cylindrical flywheel for tilting spin stabilized satellite 02 p0262 N71-11625

Development of satellite flywheel using gas bearings [ST-3139] 12 p1860 N71-23575

FOAMS

Foam plastic thermal insulation against ground freezing [AD-711905] 02 p0248 N71-12015

Spray, mist, bubbles, and foam in molten salt reactor experiment [ORNL-TM-3027] 04 p0558 N71-14161

High expansion foam for entrapping air bearing noble gas [DUN-SA-141] 06 p0676 N71-15869

Calculation model for high temperature thermal conductivity of carbon foams [JCR-RR-78-022] 06 p0879 N71-16371

Theoretical technique for determining gas diffusivity in plastic foam 06 p0879 N71-16372

Medium density molded foam [AD-X-413-209] 06 p0880 N71-16448

X ray determination of density variations in polystyrene foam [AD-X-413-180] 08 p1223 N71-18945

Acoustical properties of liquid base foams and application for jet noise reduction [NASA-CR-1695] 08 p1283 N71-19139

Development of model for behavior of foams under uniaxial and multiaxial loads and extension to post-yield behavior of foams under compression 10 p1657 N71-21397

Stability, foam flow, and wave effects on hovercraft during power failure [AD-717676] 11 p1690 N71-22448

Development of foam insulation for filament wound composite storage tank [NASA-CASE-XLR-03003] 12 p1928 N71-23816

One shot technique for preparing porous surfaced high resilience molded foam 14 p2277 N71-25853

Carboxyl terminated polyester prepolymer and foams produced from prepolymer and materials [NASA-CASE-NPO-10596] 14 p2213 N71-25929

Storage stable, thermally activated foaming compounds for erecting and rigidizing mechanisms of thin sheet solar collectors [NASA-CASE-LAR-10373-1] 14 p2279 N71-26155

Method of making solid propellant rocket motor having reliable high altitude capabilities, long shelf life, and capable of firing with nozzle closure with fused plastic permanent mandrel [NASA-CASE-XLA-04126] 14 p2333 N71-26779

Compression tests on SD 505 polystyrene bead foam [JCRLL-50952] 15 p2428 N71-26923

Foam insulation thickness measuring and injection device for spacecraft applications [NASA-CASE-MFS-20261] 15 p2407 N71-27005

Design, development, and flight testing of fire suppressant void filler foam kits for lower hemisphere of fuel tanks in various tactical army aircraft [AD-719711] 15 p2348 N71-27679

PFO foam internal insulation for propellant tanks of space shuttles 17 p2857 N71-29616

Polyisocyanurate foam and intumescent paint for thermal protection of aircraft passengers in ground accident fires 18 p2868 N71-30758

Analysis of impact test results of foamed plastic cushioning systems used in military container designs [AD-723956] 19 p3120 N71-31758

Flooded impingement plate for blowing high explosive, long-lived foam having noble gas containment [DUN-T21-VOL-1] 20 p3309 N71-33773

Analysis of secondary protection performance of shear impregnated zirconium oxide foam material with lithium fluoride backup [JED-25496] 22 p3394 N71-33593

Development of technique for preparing foam materials to be used as thermal structural components in spacecraft construction [NASA-CR-1791] 22 p3602 N71-33652

Mechanical, physical, and chemical properties of Middle SA synthetic foam systems [BDX-413-177] 23 p3777 N71-36621

FOCI

Optical design for large telescopes, including foci, mirrors, and lens systems 24 p3922 N71-37970

Code optical design in astronomical telescopes 24 p3922 N71-37971

Focal image method for calibration in calculating characteristic curve for comets 24 p4009 N71-38385

FOCUSING

NT DEFOCUSING

NT SELF FOCUSING

Apertured electrode focusing system for ion sources with nonuniform plasma density [NASA-CASE-XNP-03332] 01 p0034 N71-10618

Focusing in electrostatic spectrometers [ESRIN-IN-93] 02 p0224 N71-11522

Considering various configurations for magnetic horn for maser beam focusing [JFVB-SEP-49-73] 04 p0572 N71-13626

Deriving dual theory of processes involving external and intermediate exotic hadrons in form of quark focusing principle [COO-264-556] 04 p0579 N71-13980

Augmentation of human eye focus control by varying index of refraction with sematic liquid crystals [NASA-CR-115864] 05 p0634 N71-14653

X ray photographic analysis of plasma focus fine structure [LA-TR-70-25] 10 p1630 N71-21377

Particle separation in system of conventional S-band iris-loaded deflectors interspersed with alternate gradient magnets of strong focusing channels [BNL-15436] 11 p1804 N71-22286

Approximative solutions for diffracted and focusing wave front expansions in sonic boom shock wave propagation 16 p2532 N71-28370

Development and characteristics of Petzval type objective including field shaping lens for focusing light of specified wavelength band on curved photoreceptor [NASA-CASE-GSC-10700] 17 p2788 N71-30027

Disk shaped discharge chamber for dense plasma focus formation 17 p2812 N71-30134

Focusing, acceleration, and beam characteristics of Orsay heavy ion linear accelerator [JNP-18612] 18 p2978 N71-30665

Ion beam focusing with plasma control [IAE-1974] 18 p2992 N71-30733

Performance of uncooled lens fabricated from expanded aluminum honeycomb operating at EHF [AD-724686] 20 p3240 N71-32994

Selection of focusing system for linear induction accelerator and maintenance of beam size [JINR-FS-5714] 22 p3640 N71-35952

Plasma focus experiments using noncylindrical Z pinch in Filippov discharge chamber 22 p3657 N71-36877

Beam focusing characteristics of variously shaped grid holes with application to electron bombardment ion thrusters [NASA-TM-X-67922] 22 p3662 N71-36115

Phase acceptance of alternating gradient doublet made of quadrupoles of different apertures [CERN-71-11] 23 p3820 N71-37245

Focusing and tuning considerations for high CW power C band klystron amplifier for tropospheric scattering applications 24 p3889 N71-37717

Cadmium compound photoconductors for lens focusing [AD-727679] 24 p3967 N71-38301

Empirical solutions to resistive or subsidiary breakdown problems in brech of plasma focus accelerator [CONF-716067-40] 24 p3991 N71-38471

FOG

Describing techniques and equipment used by air weather services for fog dissipation [AD-712392] 03 p0403 N71-12997

Wettability of microfog streams of high temperature lubricants on static metal surface [NASA-CR-72743] 03 p0691 N71-14817

Dynamic model of fog duration 06 p0838 N71-16605

Attenuation coefficient of 0.6 to 14 micron waves in mists and fogs, determined with approximate equations [AD-714786] 07 p1069 N71-17875

Electrical force potential for drop supercooling and development and dissipation of clouds and fog [AD-716362] 09 p1413 N71-19661

Fog modification over airports using helicopters [AD-716818] 10 p1596 N71-20066

Atmospheric factors in ice fog formation [PB-196977] 10 p1598 N71-21617

Performance tests and characteristics of four fog detecting instrument systems operating under natural atmospheric conditions [NBS-10186] 11 p1762 N71-22454

FOKKER-PLANCK EQUATION

Warm fog seeding to determine potential of various sized and uniaxial hygroscopic chemicals for fog dissipation [NASA-CR-1731] 11 p1790 N71-32619

Determining microstructure of clouds and fog by light scattering [IAE-LIB-TRANS-1529] 12 p1952 N71-23237

Backscattering in fog using pulsed laser [DLR-FB-70-31] 13 p2088 N71-24462

Fog generator design for compressible flow visualization and high pressure Moller diagram [AD-721193] 15 p2392 N71-26881

Light scattering in water clouds, fog, and haze 15 p2439 N71-27524

Simulation of solar luminous fluxes scattered and transmitted within illuminated fog 15 p2514 N71-27534

Definition of night fog characteristics and development of mathematical model for design of night fog simulator device [FAA-RD-69-45-VOL-2] 17 p2729 N71-29510

Ground-based and snowflake disdrometer for particle size measurement of fog and aerosols [AD-724523] 18 p2954 N71-31266

Solar and atmospheric phenomena and tidal wind and fog investigations 19 p3127 N71-32002

Sulfate ion as dominant constituent in cloud and fog condensation nuclei for nonurban areas [AD-724610] 20 p3294 N71-32889

Theory of atmospheric diffusion in fog conditions and relation to air pollution [AD-724104] 20 p3295 N71-32976

Simulation of radon removal from atmosphere by means of artificial fog 20 p3357 N71-33038

Effect of scattering on pulse length of argon laser beam in foggy and turbulent atmosphere, and feasibility of Monte Carlo calculation of laser beam energy density distribution [AD-724200] 20 p3281 N71-33126

Fog and aerosol analysis with ultra-sensitive disdrometer utilizing optical transmission and light scattering principles [AD-727164] 24 p3952 N71-38195

FOIL BEARINGS

Research on foil bearings and gas lubricated films [AD-711009] 01 p0060 N71-10070

Foil journal bearings for Brayton cycle turboalternator [NASA-CR-72864] 15 p2417 N71-27772

FOILS [MATERIALS]

NT METAL FOILS

SAND-2 code for absolute neutron flux spectrum in PCTR fast neutron cavity from multiple foil activation measurements [BNWL-1487] 04 p0372 N71-13630

Structural effects of neutron irradiation of niobium foils [UCRL-72400] 05 p0730 N71-15247

Excitation function measurement of d,x reaction on Co-59 using single foils and stacked foil arrangement [KFK-1171] 05 p0751 N71-15619

Computer calculation of light particle energy loss in thick foils with high neutron cross sections [LA-4443] 06 p0915 N71-16005

Disintegrations and radiation damage in alpha-uranium using electropolished thin foils [CEA-B-3607] 09 p1437 N71-20105

Anodic polarization of iron and iron alloys and adsorption of reagents on AISI 4340 steel foil 15 p2624 N71-27427

Computer simulated electron diffraction analysis of electrons passing through absorbing crystal foil [AD-722244] 17 p2814 N71-29693

Thin foils as charge exchange medium for neutral injection into controlled thermonuclear fusion devices [JCRLL-26253] 17 p2800 N71-30100

Aluminum foils for measuring solar wind ion composites 18 p3012 N71-30966

Proton hole states excited in thin foils by monoenergetic gamma-quanta from Li-7(p,gamma)Be-8 reaction [LUNP-7013] 19 p3154 N71-32333

AC temperature technique for measuring high temperature specific heat of small wire or foil samples [UCRL-50692] 22 p3696 N71-36360

Stopping cross section dependence on carbon foil thickness and scattering angle [GPR-41] 23 p3815 N71-37285

FOKKER AIRCRAFT

NT F-20 TRANSPORT AIRCRAFT

Fatigue test equipment for evaluating Fokker aircraft wing [NLR-TR-7008-L] 12 p2003 N71-23157

FOKKER BOND TESTERS

U ADHESION TESTS

FOKKER F-20 AIRCRAFT

U F-20 TRANSPORT AIRCRAFT

FOKKER-PLANCK EQUATION

Deriving Fokker-Planck equation for Coulomb scattering into loss cone in presence of ambient potential [CEA-CONF-1609] 07 p1083 N71-18148

FOLDING STRUCTURES

Fokker-Planck equation used to describe process of electron loss from Van Allen zones due to pitch angle scattering by electromagnetic disturbances
18 p3004 N71-30923

FOLDING STRUCTURES

Computer program for analysis of folding strains on composite bladder structures
[NASA-CR-111133] 01 p0130 N71-10837
Development and characteristics of variable sweep wing control system for supersonic aircraft
[NASA-CASE-XLA-03659] 02 p0147 N71-11041
Computer program for predicting motion and appendage stresses of spacecraft during deployment maneuvers
[NASA-CR-116148] 06 p0818 N71-15965
Hydraulic actuator design for space deployment of heat radiators
[NASA-CASE-MSC-11817-1] 14 p2264 N71-26611
Self erecting solar cell array with folding tube
[DLR-FB-71-11] 17 p2706 N71-29564
Foldable blocks for construction of structures in remote areas lacking building materials
[NASA-CASE-MSC-12233-2] 18 p3022 N71-31415
Development of expandable structures concepts for application to structures used in space missions - Part 2
[NASA-CR-1735] 23 p3863 N71-37537
Development, characteristics, and evaluation of inflatable lunar shelter model to determine leak rate in near vacuum conditions
[NASA-TM-X-2395] 23 p3863 N71-37538

FOLIAGE

Aerial infrared reflection measurements on forest treated with foliar chemicals
[FR-192209] 05 p0673 N71-14879

FOOD

Food and drug chemical analyses
[PB-189204] 02 p0152 N71-11080
Human tolerance to Hydrogomonas eutropha and Aerobacter aerogenes as food
[A69-27265] 03 p0327 N71-12332
Procedures for determining quantitative and qualitative adequacy of food rations
[JPRS-52208] 06 p0403 N71-16464
Ionizing radiation effect on biological properties of food products
08 p1154 N71-19063
Food supply system for long duration manned space flight simulation
10 p1507 N71-20971
Radioisotope production and materials, heat source applications, hydrological and ocean sciences, radiation analysis and control, process radiation, and radiation preservation of foods
[TID-4066] 17 p2797 N71-29836
Radioactive isotope survey in Tohoku district, food, and precipitation in Japan
[NIRS-RSD-28] 24 p3876 N71-37631

FOOD INTAKE

Metabolic imbalances and body hypohydration during food deprivation for 10 days
09 p1337 N71-20348
Tables on nutritional value of foods used in space flight feeding
[AD-717859] 11 p1683 N71-22254
Long term manned space flight nutrition and food requirements
16 p2552 N71-28535

FORBIDDEN BANDS

Spectrophotometric results from NASA 1968 Airborne Auroral Expedition and tentative identification of several molecular nitrogen emission bands
[NASA-CR-116856] 08 p1196 N71-19148

FORBIDDEN TRANSITIONS

Vibrational perturbation effects on electronic transitions in small polyatomic molecules, and electric dipole selection rules used to ascertain forbidden transitions
11 p1806 N71-22465
Study of high isospin states in several light self conjugate nuclei by isospin forbidden radiative capture reactions
13 p2131 N71-25041
Forbidden transition probability for structural study of spectral nuclei La-139, La-135, and La-133
[JINR-P6-5200] 14 p2319 N71-26793
Forbidden transition absorption spectra in cesium and rubidium atoms due to rare gas presence
16 p2648 N71-28439
Distinct classes in magnetic quadrupole gamma transitions and development of automatic angular correlation measuring equipment
[NF-18492] 18 p2975 N71-30371
Isomeric s/minus to g/plus transition in Ba-130 nucleus, and model of transition nuclei
[JINR-B4-5607] 18 p2982 N71-30900
Forbidden transitions and magnetic moments from angular correlations in gamma decay of Te-125
[NF-18704] 19 p3152 N71-32199

FORBUSH DECREAS

Cosmic ray modulation during Forbush decreases in 1968 - 1969
[AD-713226] 05 p0764 N71-14563

FORBUSH EFFECT

U FORBUSH DECREAS

FORCE DISTRIBUTION

Oscillating flow effects on pressure force normal to symmetrical airfoil chord
[AD-711830] 02 p0142 N71-11011
Experimental determination of frost heave forces in ground
[AD-711904] 02 p0218 N71-12056
Aerodynamic coefficients, pressure, load and force distributions on cambered delta wings
[ARC-CP-1129] 07 p0966 N71-17112
Development of two force component measuring device
[NASA-CASE-XAC-04886-1] 09 p1391 N71-20439
Mathematical model for stress analysis and force distribution in U bend heat exchanger perforated plates
10 p1654 N71-21137
Force coefficients and cavity detachment points under various cavitating conditions on two similar bi-convex hydrofoils
[AD-718364] 12 p1900 N71-23585
Tensile strength testing device having pulley guides for exerting multiple forces on test specimen
[NASA-CASE-XNP-05634] 13 p2085 N71-24834
Force of ice cohesion with metals relative to type of materials, surface roughness, structure and rate of external load, and surface temperature
[AD-72106] 16 p2612 N71-28730
Lift force distribution calculation technique for wings with jet flaps including rectangular and swept wing examples
[NASA-TT-F-13714] 18 p2866 N71-30852
Spanwise integration of kernel functions for calculating wing lift distributions in subsonic flow
20 p3205 N71-33219
Computer program for calculating lifting force distributions on symmetrical and cambered wings in subsonic flow based on numerical integration and lifting surface theory
20 p3206 N71-33220

FORCE FIELDS

U FIELD THEORY [PHYSICS]

FORCED CONVECTION

Forced convection of gaseous ammonia at high wall temperature
[LA-TR-70-12] 01 p0044 N71-10802
Refrigerant forced convection condensation inside horizontal tubes
[DSR-72591-71] 06 p0960 N71-16875
Dynamical analysis of nonequilibrium, forced convective, boiling liquid metal flows
[NASA-CR-117034] 09 p1372 N71-19764
Vaporization caused by incipient boiling in forced convective flow of superheated liquid
[NASA-CR-117046] 09 p1486 N71-20593
Development of heavy cumulus clouds formed by forced convection in vicinity of warm fronts in Arctic regions
11 p1791 N71-22845
Turbulent diffusion by forced convection over water surface
13 p2106 N71-24968
Bibliography on burnout in forced convection boiling heat transfer in uniform and nonuniform heat systems
[AABC/LIB/DIB-286] 23 p3796 N71-37059

U FORCED VIBRATION

FORCED VIBRATION

Forced longitudinal vibrations of prismatic slender bars under influence of quadratic and equivalent viscous damping
[AD-712441] 03 p0462 N71-13092
Free and forced vibrations of nonlinear isochronous oscillators
03 p0419 N71-13331
Harmonic analysis of nonlinear forced vibrations of infinitely long cylindrical shells
[AD-716795] 10 p1650 N71-20636
Measurement of dynamic shear properties of silicon based elastomers at high temperature
[USNR-TR-43] 16 p3020 N71-30553
Free vibration, forced vibration, and parametric response of simply supported tube conveying fluid
[ANL-7762] 21 p3461 N71-34631
Forced and free oscillations of plasma consisting of free electrons and background of positive ions
[NP-18673] 22 p3652 N71-36045
Nonself-adjoint boundary value problem solution with dependent variable time derivatives for forced vibration of elastic beams based on Williams method
[AD-726378] 22 p3689 N71-36312
Free vibrations and harmonic and aperiodic forced vibrations of elastic spherical thin shells in water
22 p3693 N71-36337
Nonlinear analysis of forced vibrations of cylindrical shells in vacuum or submerged
[AD-726745] 23 p3862 N71-37553
Acoustic pressure distribution from forced harmonic vibrations of clamped circular plate in acoustic fluid
23 p3865 N71-37555

FORCED VIBRATORY MOTION EQUATIONS

U EQUATIONS

U FORCED VIBRATION

FOREARM

Forearm vascular responses to brachial artery infusions of tyramine and norepinephrine after two weeks bed rest
20 p3217 N71-32261

FOREBODIES

NT ABLATIVE NOSE CONES

NT NOSE CONES

NT ROCKET NOSE CONES

FORECASTING

NT LONG RANGE WEATHER FORECASTING
NT NUMERICAL WEATHER FORECASTING
NT PERFORMANCE PREDICTION
NT PREDICTION ANALYSIS TECHNIQUES
NT STATISTICAL WEATHER FORECASTING
NT TECHNOLOGICAL FORECASTING
NT WEATHER FORECASTING
Technological forecasting as management tool in research and development
[PAU-M-10] 01 p0135 N71-10809
Forecasting passenger travel demands
[PB-192455] 01 p0136 N71-10809
Technological forecasting and advanced planning
[BNWL-1466] 04 p0624 N71-14609
Stochastic forecast modeling of research and development trends
[JPRS-51999] 05 p0788 N71-15631
Objective and methodology of forecasting economic and scientific research and development
[NLL-RTS-6095] 10 p1666 N71-21615
Long range forecasting of annual variations of ice cover in Arctic
11 p1752 N71-22809
Short range forecasting of navigability of close pack ice by icebreakers in Arctic
11 p1753 N71-22809
Economic efficiency calculations for long range ice forecasts for ship navigation of Northern Sea Route
11 p1757 N71-22810
Graphic method of forecasting neoperiodic oscillations of sea level in East Siberian and Chukchi seas
11 p1758 N71-22810
Short range forecasting of ice formation in Arctic waters to thickness of 20-25 cm with forecasting period up to 20 days
11 p1758 N71-22810
Fundamental techniques of weight estimating and forecasting for advanced manned spacecraft and space stations
[NASA-TN-D-6349] 13 p2062 N71-25425
Qualitative morphology of polar cap absorption events using riometers and periodic variations in energy spectra and proton flux density in ionospheric absorption forecasting
[AD-721183] 15 p2395 N71-26803
Riometer polar cap absorption, auroral absorption, and solar flare observations and ionospheric absorption forecasting
[AD-721182] 15 p2395 N71-26804
Social planning by numerical forecasting methods
19 p1955 N71-32019
Short term forecasting of signal field strength in tropospheric scattering links involving meteorological parameters
[REPT-970] 20 p2321 N71-32016
Airport/aircraft system noise reduction including land use and noise forecasting
[OST-ONA-71-1-VOL-3] 20 p2312 N71-33957
Freight, express, and mail tonnage forecasts for domestic airline operations
24 p4035 N71-38790

Forecasting passenger travel demands
[PB-192455] 01 p0136 N71-10809

Technological forecasting and advanced planning
[BNWL-1466] 04 p0624 N71-14609

Stochastic forecast modeling of research and development trends
[JPRS-51999] 05 p0788 N71-15631

Objective and methodology of forecasting economic and scientific research and development
[NLL-RTS-6095] 10 p1666 N71-21615

Long range forecasting of annual variations of ice cover in Arctic
11 p1752 N71-22809

Short range forecasting of navigability of close pack ice by icebreakers in Arctic
11 p1753 N71-22809

Economic efficiency calculations for long range ice forecasts for ship navigation of Northern Sea Route
11 p1757 N71-22810

Graphic method of forecasting neoperiodic oscillations of sea level in East Siberian and Chukchi seas
11 p1758 N71-22810

Short range forecasting of ice formation in Arctic waters to thickness of 20-25 cm with forecasting period up to 20 days
11 p1758 N71-22810

Fundamental techniques of weight estimating and forecasting for advanced manned spacecraft and space stations
[NASA-TN-D-6349] 13 p2062 N71-25425

Qualitative morphology of polar cap absorption events using riometers and periodic variations in energy spectra and proton flux density in ionospheric absorption forecasting
[AD-721183] 15 p2395 N71-26803

Riometer polar cap absorption, auroral absorption, and solar flare observations and ionospheric absorption forecasting
[AD-721182] 15 p2395 N71-26804

Social planning by numerical forecasting methods
19 p1955 N71-32019

Short term forecasting of signal field strength in tropospheric scattering links involving meteorological parameters
[REPT-970] 20 p2321 N71-32016

Airport/aircraft system noise reduction including land use and noise forecasting
[OST-ONA-71-1-VOL-3] 20 p2312 N71-33957

Freight, express, and mail tonnage forecasts for domestic airline operations
24 p4035 N71-38790

Forecasting passenger travel demands
[PB-192455] 01 p0136 N71-10809

Technological forecasting and advanced planning
[BNWL-1466] 04 p0624 N71-14609

Stochastic forecast modeling of research and development trends
[JPRS-51999] 05 p0788 N71-15631

Objective and methodology of forecasting economic and scientific research and development
[NLL-RTS-6095] 10 p1666 N71-21615

Long range forecasting of annual variations of ice cover in Arctic
11 p1752 N71-22809

Short range forecasting of navigability of close pack ice by icebreakers in Arctic
11 p1753 N71-22809

Economic efficiency calculations for long range ice forecasts for ship navigation of Northern Sea Route
11 p1757 N71-22810

Graphic method of forecasting neoperiodic oscillations of sea level in East Siberian and Chukchi seas
11 p1758 N71-22810

Short range forecasting of ice formation in Arctic waters to thickness of 20-25 cm with forecasting period up to 20 days
11 p1758 N71-22810

SUBJECT INDEX

- Conference on agriculture, forestry, and sensor studies related to NASA Earth Resources Program - Vol. 2 (NASA-TM-X-62565) 06 p0044 N71-16147
- Developing spectral signature indicators of root disease in large forest areas 06 p0000 N71-16158
- Detection of forest insect infestation by remote sensing 06 p0000 N71-16159
- Identification of western forest species by means of aerial remote sensing 06 p0000 N71-16160
- Cloud seeding for forest fire fighting and heavy rainfall prevention (NLL-36-20300/5828.4F1) 12 p1956 N71-23949
- Evapotranspiration data for forest and grassland management by Forest Service 13 p2072 N71-25007
- Decodability of small topographic objects in large scale aerial photography of forests (AD-720765) 14 p2249 N71-26267
- Synoptic meteorological parameters influencing forest fires in Southeast Asia including cloud cover and precipitation 15 p2437 N71-26917
- Spatial and temporal distribution of solar radiation beneath forest canopies 15 p2439 N71-27518
- Using helicopter for spray dusting forests with DDT for tick borne encephalitis (AD-700998) 17 p2703 N71-29557
- Remote aerial sensing and automatic mapping for forest resources information system (NASA-CR-122922) 23 p3755 N71-36770
- Application of multispectral sensors to detect insect and disease infestation of ponderosa pine trees (NASA-CR-122647) 24 p3919 N71-37947
- FORGING**
- Characteristics of materials for simulation of hot forging processes (AD-711503) 02 p0229 N71-11528
- Manufacturing improvement program establishing applications and limitations in closed-die forging (AD-711544) 02 p0234 N71-11675
- Factors affecting efficiency of lubricants used for deep forging (AD-713446) 05 p0709 N71-15269
- Friction forging of spiral bevel gears for Army helicopters (AD-715419) 08 p1207 N71-18920
- Mechanical properties of forged Ti-6-Al-4-V at temperatures above alpha-beta-beta transition (AD-720828) 14 p2274 N71-26046
- Magnetic crystallographic orientation produced in alloys by hot working 16 p2931 N71-31580
- Evaluation of phases in forging lubricants for tungsten steels and titanium alloys (AD-720833) 22 p3603 N71-35661
- FORM**
- U SHAPES**
- FORM FACTORS**
- He-3 charge form factor and He-3 Coulomb energy (NLS-1388-575) 01 p0099 N71-10711
- Proton form factors determined from electron ion scattering cross sections (JINR-P1-5178) 04 p0575 N71-13665
- Estimation of momentum transfer dependent damping of nucleus form factors due to pseudoscalar pions (NYO-2262-TA-224) 07 p1070 N71-17034
- Electron-proton elastic scattering cross sections at low-momentum transfers between 1.0 and 3.6 GeV/c squared (BESV-70422) 08 p1253 N71-18361
- Calculation of gauge invariant set of diagrams of asymptotic momentum transfer of elastic form factors in quantum electrodynamics with massive photons (ILL-TM-71-1) 08 p1263 N71-18880
- Neutral kaon decay yields pion, muon, neutrino form factor measurements in wire chamber with energy dependence expressions and nuclear coupling coefficients (JCLA-1056) 10 p1619 N71-21711
- Current algebra for determining form factors and frequencies of mass in electromagnetic interactions (JINR-P2-5209) 15 p2460 N71-27870
- Nucleon axial vector form factor calculations from ultra-elastic dynamical groups 15 p2469 N71-27547
- Target nuclei charge distribution effects on high energy electron small angle multiple scattering distributions based on Mott's formula and elastic form factors 15 p3478 N71-37407

- Oxygen and carbon elastic form factor calculations based on liquid drop nuclear model with quadrupole surface oscillations (RLO-1388-597) 17 p2790 N71-29270
- Electromagnetic form factor of nucleon derived from composite model (CNRS-CPT-70-P-331) 17 p2807 N71-30329
- Derivation of upper bound for scattering amplitude (JVB-577-70-18) 18 p2979 N71-30697
- 5-32 electron excitation in dipole resonance region including form factors for isoscalar scattering (UJVV-2553-F) 19 p3152 N71-32195
- Electron proton inelastic scattering form factors for massive quantum electrodynamics calculated from electron-like equations (ILL-TM-71-9) 19 p3157 N71-32509
- Perturbation theory of electromagnetic interactions connected with local fermion current by anomalous factor (JINR-P2-5694) 21 p3472 N71-34725
- Relativistic wave function and form factors for bound system of two particles with arbitrary spins and masses (JINR-P2-5717) 21 p3472 N71-34726
- Second order form factors for spin correlation analysis in beta decay of Lambda hyperon (COO-264-569) 21 p3476 N71-34750
- Model of electromagnetic form factor of scalar pion, with pion being in bound state of scalar nucleon antinucleon system (IRO-3992-28) 23 p3813 N71-37189
- Quark model of kaon decay into 3 form factor and Cabibbo angle using Regge pole theory (IRO-3992-39) 23 p3814 N71-37200
- Contributions of inelastic channels to electromagnetic form factor of pions, and production of strange particles in proton-proton scattering 23 p3821 N71-37255

FORM PERCEPTION

U SPACE PERCEPTION

FORMALDEHYDE

- Mass spectra of phenolic polynuclear compounds of p-cresol and formaldehyde (RAE-LIB-TRANS-1408) 03 p0333 N71-12381
- Confirmation of chain structure of polynuclear compounds formed from p-ion-cresol and formaldehyde (RAE-LIB-TRANS-1408) 05 p0641 N71-15613
- Sugar formation by formaldehyde condensation in presence of isopropyl and organic bases (NASA-TT-F-13410) 06 p0811 N71-16470
- Decomposition of stabilized polyoxymethylene under elevated pressure 07 p1049 N71-17936
- Amino acid synthesis by heating formaldehyde and ammonia mixtures in molecular evolution research (NASA-CR-118031) 12 p1872 N71-24022
- Physicochemical synthesis of sugar by formaldehyde condensation with lanthanide hydroxide catalysts for space flight feeding 16 p2555 N71-28256
- Production of sugar by formaldehyde condensation in presence of calcium hydroxide (NASA-TT-F-13709) 16 p2558 N71-28962
- Mechanism of alpha-amino acid synthesis in UV-irradiated formaldehyde and ammonium nitrate solutions and planetary evolution (NASA-TT-F-13797) 22 p3549 N71-35282
- Comparative tests on kinetics of formaldehyde condensation in presence of calcium hydroxide (NASA-TT-F-14081) 24 p3885 N71-37689

FORMALISM

- Multiple formalism for calculating angular distribution of proton scattering on carbon 12 nuclei (ITF-70-18) 02 p0271 N71-11901
- Dynamic formalism and computer program for multiple space vehicle attitude and control simulations (NASA-CR-117350) 09 p1480 N71-20482
- Precise logic computation and construction of formal heuristic activity models 12 p1895 N71-24219
- Westcott formalism and neutron capture by reactor materials (LFEN-NL-45-A) 13 p2134 N71-25173
- Nonlocal separable potential formalism for elastic scattering by helium (LYCEN-7041) 15 p2463 N71-27341
- Electromagnetic radiation scattering by hydrodynamically turbulent systems via operator formalism (AD-722523) 17 p2797 N71-29842
- Multiple formalism for fast pion-nucleon scattering on carbon 12 (ITF-70-71) 17 p2810 N71-30385
- Formalism for particle density distribution in quantum chemistry 20 p3229 N71-33386
- Formalism for describing radiation matter nonlinear interactions in terms of quantum oscillator properties applied to single mode parametric amplification 23 p3821 N71-37254

FORMAT

- Formetting and transmission of data from oceanographic sensors (AD-711324) 02 p0223 N71-11386

FORMULAS [MATHEMATICS]

- Syntax oriented data formatting to facilitate information input and retrieval 14 p2221 N71-25979
- Organization and data input format of geomagnetic World Data Center (REPT-7) 17 p2799 N71-29434
- FORMATES**
- NT NITROFORMATES**
- Heat capacities of iron and nickel compounds (AD-710814) 02 p0172 N71-11212
- FORMATION HEAT**
- U HEAT OF FORMATION**
- FORMATION**
- Plan formation from polymer dispersions 04 p0487 N71-13467
- FORMING TECHNIQUES**
- NT CASTING**
- NT COLD ROLLING**
- NT COLD WORKING**
- NT ELECTROFORMING**
- NT EXPLOSIVE FORMING**
- NT EXTRUDING**
- NT FORGING**
- NT HOT WORKING**
- NT INVESTMENT CASTING**
- NT MAGNETIC FORMING**
- NT METAL DRAWING**
- NT METAL SPINNING**
- NT PRESSING [FORMING]**
- NT ROLL FORMING**
- NT SLIP CASTING**
- NT STAMPING**
- Manufacturing methods for regeneratively cooled liquid rocket thrust chambers 02 p0289 N71-11631
- Development of space manufacturing techniques for orbital workshops (NASA-TM-X-66480) 02 p0234 N71-11701
- Weightless forming of spheres and composites casting in orbital workshop manufacturing 02 p0235 N71-11716
- Production of regeneratively cooled rocket thrust chambers by removable tooling and subsequent hot isostatic pressing in gas autoclave (NASA-CR-72795) 06 p0665 N71-16381
- Fabrication of cobalt alloy and nickel alloy gas turbine blades and disks 07 p1101 N71-17392
- Hot forming of plastic sheets (NASA-CASE-XMS-03516) 07 p1037 N71-17083
- Forming tubes from long thin flat metal strips (NASA-CASE-XGS-04175) 08 p1206 N71-18579
- Portable magnetostatic hammer for metal working (NASA-CASE-XMF-03793) 13 p2085 N71-34633
- Forming mold for polishing and machining curved solar concentrator reflector with reinforcing sheets (NASA-CASE-XLE-00917-2) 13 p2086 N71-34636
- Forming and bonding metallic lining onto inside surface of metal tube (NASA-TM-X-2347) 19 p3114 N71-32161
- FORMULAS**
- Formulas and algorithms for computing partitions of numbers and derivatives of composite function (UCRL-28215) 16 p2635 N71-35740
- Approximate reduction of gravity formula describing earth shape to Taylor series (AD-723515) 19 p3091 N71-31927
- FORMULAS [MATHEMATICS]**
- NT BIRTHE-HILLIER FORMULA**
- Unified expression for leakage flow from nuclear reactor containment vessel 13 p2121 N71-25378
- (WHAN-SA-46) 13 p2121 N71-25378
- Human factors engineering manual including mathematical formulas, nomograms, conversion tables, units of measurement, and nomenclature (NASA-CR-114272) 14 p2209 N71-25943
- Explicit expression of invariant Hermitian form for unitary representations of conformal group (INFT-57F-49-85) 15 p2497 N71-27994
- Empirical formula for expressing leakage flow from nuclear reactor containment vessel 17 p2794 N71-29881
- Comparison of isospecific refraction data sources and error correcting formulas using Waikato Island calibration experiment data 19 p3088 N71-31047
- Tenfold formulation of simplified multilevel mathematical formula for nuclear resonances (RT/PI/70/38) 19 p3152 N71-33179
- General properties and formulae for multiple free dual amplification with Mandelstam variables (LPTM-71/06) 20 p2593 N71-33983
- Computer corrections for Acme thread gages using gages and formulae 21 p3428 N71-34389
- Explicit and recursive formulae for acceleration and gravity gradient derived from spherical harmonics (NASA-CR-121909) 22 p3372 N71-35442
- Formalism describing space dependence of energetic resonance cell shielding at boundaries of homogeneous zones in nuclear reactors (KPK-1353) 22 p3431 N71-35976

General mathematical laws for electromagnetic field-conductive fluid interactions in rectangular channels

24 p3968 N71-38303

FORTRAN

Time-share FORTRAN 4 program for calculating diffraction pattern interlayer spacings [Y-1729]

FORTRAN 4 computer program for calculating satellite photograph coordinates [PB-193314]

FORTRAN computer program for IBM 2250 display unit [AD-711009]

FORTRAN program for relativistic calculation of anomalous scattering factors for X rays [LA-4403]

Two-body relativistic kinematics code written in FORTRAN [LA-4349]

FORTRAN 5 for TIMOC computer program for flux density determination with time varying flux [BNWL-1492]

FORTRAN program for obtaining approximations to real valued functions [AD-712973]

FORTRAN program for computing superconductor surface impedance [NF-18355]

Mathematical method and FORTRAN program for routine interpretation of gamma-loggings in uniaxial deposits [CEA-N-1279]

Battelle Monte Carlo in FORTRAN-S for Univac 1108 computer [BNWL-1433]

CORA, few group, one dimensional neutron diffusion program in FORTRAN 4 language [IN-1416]

ENDRUN-1 program for calculating multigroup constants from ENDF/B data [GEAP-13592]

TIBRO-GENERAL computer program for calculating precise trajectories of charged particles in dc magnetic fields [UCRL-50910]

FORTRAN 4 code for fast neutron radiative capture calculations - FISPRO [RT/FI/69/44]

TREERUN subroutine package in FORTRAN 4 for manipulation of tree structured data [NASA-CR-116143]

Procedures for using FORTRAN 4 computer program to simulate GERT networks [NASA-CR-116177]

AUPLLOT 2, set of callable subroutines for computer graphics [NASA-CR-116218]

FORTRAN 4 subroutines for coupling coefficients and matrix elements in quantum mechanical theory of angular momentum [NASA-TN-D-6173]

FORTRAN program for computation of group tables, alphanumeric display [NASA-TM-X-2172]

Vortex-lattice FORTRAN program for estimating subsonic aerodynamic characteristics of complex planforms [NASA-TN-D-6142]

FORTRAN 4 program for calculating dynamic Kirchhoff deformation of structural rings subjected to fragment impact [NASA-CR-72801]

Evaluation of weighting functions used in small angle X ray scattering by FORTRAN 4 program WEIGHT [JORN-TM-1950-REV-1]

SYSTEM computer program for system time-domain simulation program in FORTRAN 5 for Univac 1108 computer [NASA-CR-114914]

Users manual for FORTRAN 4 computer program for analysis of multilayered fiber composites [NASA-TN-D-7013]

FORTRAN program for Koster-type method for finite element analysis of nonlinear structural behavior of airframes [AD-717181]

Computer program for converting IBM FORTRAN to CDC 6600 computer use [LA-4355]

Monte Carlo general purpose shielding computer program in FORTRAN 4 for IBM 7094 computer [NASA-TN-D-6179]

Set of FORTRAN 4 subroutines to calculate mass flow rate of natural gas through nozzles, also thermodynamic functions such as compressibility factor, entropy, enthalpy, and specific heat [NASA-TM-X-2348]

Three-dimensional surface velocities and checking flow for turbomachine blade rows calculated by FORTRAN program [NASA-TN-D-6177]

On-line FORTRAN 4 digital computer program for solving ordinary differential equations [21 p1883 N71-33866]

FORTRAN program for class 5 flextranslational underwater acoustic transducer [AD-710356]

Updating ANISN library tapes with plotting of cross section curves using FORTRAN 4 program [JORN-TM-2408]

FORTRAN program for computing two dimensional magnetic field components for conduction geometries [JORN-TM-2484]

Finite difference techniques peculiar to solution of Boltzmann transport equation in two dimensional spherical geometry - FORTRAN program [LA-4567]

FORTRAN program for stresses in inhomogeneous elastic plate with circular hole [21 p1718 N71-26647]

Nuclear data processing from TIMOC Monte Carlo library ENDF/B file using CODAC FORTRAN 4 program [EUR-4521-E]

FORTRAN for animated reconstruction of telemetry [AD-719741]

CMPLLOT FORTRAN subroutine for graph and diagram plotting using CalComp 835 CRT plotter [TRITA-EPP-71-63]

Duskevski method for determining eigenvalues of matrices with real elements programmed in FORTRAN [ARL/SM-349]

FORTRAN 4 digital codes for thermal dynamics of cylindrical nuclear fuel rod with or without distributed heat generation [RT/ING/70/8]

CAGE-BIRD-SPEC, package FORTRAN 5 system, for reduction and analysis of neutron time-of-flight spectra in fast and thermal subcritical reactors [GULF-RT-10195]

IBM 5360 FORTRAN 4 G program to compute heteronuclear resonance integrals for flexible and non-flexible molecules [TKK-F-A-139]

FORTRAN computer program for determination of rocket and gun propellant performance [JCT-9/70]

FORTRAN computer program for calculating prolate spheroidal radial functions of first and second kind and their first derivatives [AD-722648]

FORTRAN computer program for calculating oblate spheroidal radial functions of first and second kind and their first derivatives [AD-722649]

Computer calculations of time dependent light scattering in plane parallel atmospheres, using FORTRAN 4 language [AD-722714]

Stress analysis in axisymmetric perforated shells and equivalent disk noting use of FORTRAN [ONERA-NT-172]

FORTRAN-based version, FGRAAL, of graph algorithmic language GRAAL [NASA-CR-119778]

Data retrieval language with ability to define data structures, describe environments, address data by content, manipulate data structures, and offer computational power comparable to FORTRAN [NBS-TN-590]

FORTRAN computer program for selective information retrieval from articles and reports [AD-724611]

TIMOC, general purpose Monte Carlo code written in FORTRAN 2, for stationary and time dependent neutron transport [EUR-4519-E]

DBLSCAT, FORTRAN 4 computer code, for double scattering corrections of slow neutron data [ANL-7780]

Univac 1108 virtual mass trajectory simulation program of FORTRAN subroutines for analysis of spacecraft trajectories [NASA-CR-121765]

Synthesis of structural dynamic systems using digital computer and FORMAP (FORTRAN Matrix Analysis) [NASA-CR-119877]

FORTRAN computer program for automatic analysis of gamma ray spectra from Ge(Li)-detectors [LUNP-7101]

FORTRAN program for gamma radiation dosimetry in arbitrary source and target geometry [JORN-TM-3398]

FORTRAN computer program for simulation of movement using set of time dependent differential equations and plotting curve [DHS/9/79/TS]

FORTRAN listing of multi-material Eulerian program [HELP] for compressible fluid and elastic-plastic flow in two space dimensions and time [AD-726468]

FORTRAN 4 program for generating fast neutron spectra and average multigroup constants utilizing cross section data from library - PHROG [IN-1455]

PEARLS, FORTRAN code, for solution of neutron slowing down equations in multigroup lattices of resonance absorbers using IBM 360/5081 computer [AAEC/C-213]

FORWARD SCATTERING High resolution forward scatter system to detect refractive index fluctuations caused by clear air turbulence [AD-713088]

Photoelectron forward scattering studied with positron electron annihilation process [JINR-E2-5347]

Simple chemical model of interactions between gas molecules and contaminated surface [REPT-69-53]

Uniqueness theory for calculating forward scattering amplitude at high energies [IFVB-STP-69-74]

GeLi detector for measuring energy of electron scattered forward by proton beam in this beryllium foil [LA-4612]

Complex closed forms for amplitudes and phase fluctuations in forward scattering study of electromagnetic waves transmitted through turbulent media [19 p3071 N71-32712]

Comparison of forward scatter visibility instrument measurements in fog and snow with transmission and human observations [AD-726995]

Forward scattering amplitudes in Ruzsa pole theory of high energy interactions between pions and nucleons [22 p3586 N71-33379]

High-altitude electromagnetic pulse source currents and ionization from Compton scattering of gamma rays based on forward scattering of Compton electrons [AD-726928]

FOSSIL METEORITE CRATERS U FOSSILS U METEORITE CRATERS FOSSILS

Observing growth rhythms in shells of fossil marine invertebrates and relationship to tidal cycles in earth-moon system [NASA-CR-111608]

FOULING Performance of multicompartment electrolysis system with laminar flow, and fouling of membrane surfaces by iron oxide [FML-PUBL-71-13]

FOUNDATIONS NT FILE FOUNDATIONS Methods of designing foundations and bases on partially frozen soil [AD-711909]

Experimental determination of frost heave forces in ground [AD-711904]

Discrete element method for plates or slabs on nonlinear foundations [23 p3818 N71-37213]

FOUNDRIES Foundry precision in domain of aeronautical techniques [22 p3384 N71-37346]

Industrial foundry acoustic and vibration measurements and intensity and octave spectrum analysis [NASA-TT-F-13644]

FOUR BODY PROBLEM Massive particle scattering amplitude kinematics in four-momenta space [20 p1430 N71-19796]

Finite quantum mechanics for four fermion spin field interactions based on Bogoliubov theory and spin-time functions with Federbusch model example [14 p2304 N71-35279]

Photointerpretation of four proton reactions in hydrogen bubble chambers including particle trajectory reconstruction and analysis of particle production mechanisms [USIP-70-7]

Limiting relations for correlation averages in quantum statistics of four fermion interactions [ITP-70-59]

Quasi-averages in quantum mechanics for negative four fermion interaction models and free energy limiting expressions [ITP-70-52]

Kinematics of system of nuclear particles breaking up into 2, 3, or 4 particles in low energy reactions [TR-1]

FOURIER ANALYSIS NT FOURIER SERIES NT HARMONIC GENERATIONS

Theory and application of Pade technique to sequences of approximations to single variable integrals related to quantum field theory [AD-711406]

23 p3815 N71-37210

24 p3961 N71-38047

10 p1610 N71-20631

15 p2464 N71-27210

17 p2791 N71-29206

19 p3071 N71-32712

22 p3586 N71-33379

22 p3645 N71-33800

23 p3818 N71-37213

03 p0323 N71-12312

24 p3886 N71-37700

02 p0301 N71-12821

02 p01904 N71-12826

23 p3864 N71-37346

02 p0231 N71-11618

12 p1966 N71-33629

09 p1430 N71-19796

14 p2304 N71-35279

19 p3071 N71-32712

17 p2801 N71-30115

17 p2811 N71-30889

18 p2967 N71-30446

19 p1610 N71-32644

23 p3729 N71-36583

23 p3744 N71-36693

SUBJECT INDEX

FRACTURE MECHANICS

For infrared investigations using Fourier spectrometers

- [AD-712742] 03 p0382 N71-13218
Computed properties of two-dimensional section of two lock bore synchrotron dipole
[BNL-15174] 06 p0832 N71-16753
Mean gravity anomalies derived from generalized Fourier analysis of satellite orbits
[BMW-FB-W-70-53] 07 p0107 N71-17137
Fourier analysis of summer weather and wave data for Lake Michigan
07 p0155 N71-17836
Two-signal primer for Fourier analysis of random noise communication system
[HSSA-TB-ERL-178-ITS-113] 07 p0995 N71-17947

Search for doublet structure of meson resonance using Fourier algorithm
[JINR-P1-5340] 06 p1250 N71-18240

Fourier analysis of near field velocity from numerically simulated dynamic bilateral shear fracture
[AD-717793] 11 p1748 N71-22259

Mathematical model for relativistic scattering amplitudes in high energy interactions based on Fourier analysis and Lorentz group embeddings
[JINR-E2-5341] 14 p2318 N71-26760

Characterization and mathematical representation of line scanning image systems and evaluating system performance with discrete output signal and post filtering
[NASA-CR-118893] 15 p434 N71-27632

Fourier techniques for determining structure of three dimensional semitransparent objects from measurements of transmission functions of holograms illuminated by light beams
15 p2455 N71-27643

Formulae for nth order derivatives of hyperbolic and trigonometric functions used in evaluating Fourier sine and cosine integrals
[NASA-TN-D-6403] 17 p2773 N71-29772

Green function and Fourier integrals in dynamic elastic field theory of crystal dislocations and disclinations
17 p2823 N71-29981

Computer program for performing corrections on X ray diffraction profile before Fourier analysis
[NBS-TN-600] 17 p2723 N71-30030

Computer programming formulae for frequency and statistical analysis of random waveform signals including Fourier analysis, probability density functions, and autocorrelation
[NASA-CR-115075] 17 p2775 N71-30357

Fourier analysis of Q/1240 to 1400/ resonance in ternary pion states produced in kaon proton interaction
[JINR-E2-5654] 18 p2944 N71-30653

Fourier analysis of boundary value problems for laminated equation of ocean waves
[AD-722600] 18 p2919 N71-31440

Fourier analysis of weather and wave data from Holland, Michigan
[AD-723462] 19 p3126 N71-31756

Fourier analysis of clamped anisotropic plates under bending under transverse load, shear and biaxial compression loading, and natural frequencies of flexural vibrations
[AD-723871] 19 p3187 N71-31800

Averaging and digital techniques for computation of shock and Fourier spectra compared on basis of speed, accuracy, and ease of use
[AD-723346] 19 p3061 N71-31990

Proceedings of conference on Fourier spectroscopy including topics on signal to noise ratios, interferometers, refractometers, double-beaming techniques, and data handling and processing
[AD-724100] 20 p3311 N71-33425

Numerical treatment of some integro-differential equations, Fourier integrals, and integral equations
22 p3496 N71-35882

Fourier algorithm for determining Breit-Wigner resonance widths in Gaussian type experimental broadening
[JINR-P2-5639] 22 p3630 N71-35888

Thermal conductivity and specific heat gaps based on Fourier law
14 p2253 N71-25636

Deviation in heat conduction predictions by Fourier model and relaxation model
22 p3697 N71-36364

Speech pattern recognition using Fourier series
[AD-712102] 02 p0179 N71-11256

Theoretical solution for pressure distribution over uniformly shaped periodic waves using Fourier series
[NASA-TN-D-5964] 02 p0202 N71-11548

Derivation of generalized Fourier series for calculating stresses in semi-infinite elastic strips and cylinders
[AD-716338] 09 p1477 N71-19975

Method for determining dispersion relations in fiber reinforced binary composite materials based on Fourier series and equations of motion
10 p1589 N71-21319

Fourier expressions for scattering functions in Mie theory with applications to light scattering by spherical voids in ruby
11 p1799 N71-23012

Fourier series solution to free edge effects in measurement of composites in plane shear properties
[AD-724146] 20 p3287 N71-33050

Digital computer control of meteorological observations data using Fourier series and Lagrange polynomials
[NLL-M-20710-5828-4P] 21 p3599 N71-34194

FOURIER TRANSFORMATION
Zoom discrete Fourier transformation of sampled signals
[CRC-TN-631] 01 p0074 N71-10037

Experimental single Fourier transform optical processor applied to film grain analysis and ship wave detection method
[AD-710721] 01 p0088 N71-10329

Radon and Fourier integral transformations applied to boundary value problem solution of neutron transport theory
[AD-711537] 02 p0369 N71-11148

Linear system impulse response identification from truncated input using fast Fourier transformation
[AD-710650] 02 p0191 N71-11341

Analyzing wave propagation signals by approximate Fourier integral transform method
[AD-711798] 02 p0230 N71-11606

Using fast Fourier transforms for analysis of structural vibrations
[NASA-TM-X-53997] 02 p0251 N71-11685

Onboard optical processing for extracting parameters from spacecraft data using image generator and Fourier transform phase detector
03 p0379 N71-12792

Linear interaction problem between spacecraft attitude control and flexible appendages solved in frequency domain using Fourier transform
[NASA-CR-111558] 03 p0409 N71-13063

Design of special purpose computer using FFT to perform speech analysis in real time
04 p0501 N71-13663

Digital filters and Fourier transformation for pulsed Doppler radar processor
04 p0497 N71-13930

Fourier transformation for spectral analysis of acoustic and seismic data
[SC-DR-70-205] 04 p0567 N71-14207

Fourier transformation for precursor wave study from continuous transition layer in sound speed profile
[AD-713601] 05 p0731 N71-14553

Kolmogoroff-Smirnov test for digital filtering and spectral comparison using Fourier transform
[CTC-44] 05 p0635 N71-14905

Fourier transform of scattering diagrams and selective summation techniques
[AD-713899] 06 p0815 N71-16286

Random sampling approach to digital detection using Fourier transformation
06 p1163 N71-18925

Investigating Fourier transform estimation from unknown parameters using sequential algorithm
06 p1226 N71-19008

Elastic displacements produced by point defect in cubic medium by Fourier transform method
06 p1281 N71-19279

Fast Fourier transform programs for EAI-640 digital computer
[NRC-11747] 06 p1167 N71-19332

Perfect shuffle interconnection pattern and FFT for parallel processing algorithms
[STAN-CS-70-158-A/P-5] 10 p1595 N71-21681

Generalized matrix elements on Poisson group used to write Fourier transformation for distributions on group
[LPTHE-71/4] 11 p1788 N71-22463

Computerized image evaluation program, POLYPAQOS, using Fourier techniques
[AD-720875] 12 p1967 N71-23974

SL₂(C) representations in energy dependent banks using Fourier transformation
[KFKI-70-19-HEP] 14 p2313 N71-26715

Computer code (MINIGASKET) for thermal neutron scattering law in polycrystals based on free translation and isotropic harmonic vibration with continuous frequency spectrum
[JINR-1106] 16 p3646 N71-26212

Traveling water wave refraction based on spectrum analysis, Fourier transformation, and wave group phase velocity
[AD-720871] 16 p2586 N71-28345

Mathematical model for 1/f noise propagation using Fourier transformations, time series analysis, and autocorrelation of random noise processes
[AD-721450] 16 p2562 N71-28750

Watson generalization of Fourier transform, and inversion formulas for Laplace and other integral transforms
17 p2772 N71-29436

One electron theories of coherence on ion pair potentials in metals, using Fourier transformation and integral equations
[NRC-1147] 17 p2818 N71-29404

Fourier transformation for lattice statics method for distortion
17 p2818 N71-29942

Fourier transformation calculation and validation of sum rules and Ward identities using equal-time commutator in axiomatic quantum field theory
[JTF-70-57] 18 p2967 N71-30412

Mathematical models of Fourier and Laplace transformations of two tempered distributions which coincide in last points
[JINR-P2-5642] 18 p2969 N71-30433

Analysis and classification of random aperiodic signals using one and two dimensional Fourier transforms
[AD-722647] 18 p2994 N71-30789

Riemann-Lebesgue lemma extension for Fourier transformation decay at infinity using asymptotics
[AD-722681] 18 p2947 N71-31283

Fourier transformation technique applied to two dimensional infrared image filtering
[JINR-NT-1641] 19 p3121 N71-31685

Neomorphological integrals of Fourier integrals using phase algebra
[FOA-2-C-2446] 20 p3290 N71-32989

Tide prediction method based on time-variable spherical harmonics of gravitational waves
20 p3264 N71-33341

Fourier transform solutions of quarter plane problems in elasticity
[AD-724176] 20 p3358 N71-33373

Radioisotope distribution image analysis and multiplex coding techniques including Fourier, Fresnel, and Walsh-Hadamard transformations
[TP-972] 20 p3293 N71-33759

FORTRAN computer program to implement fast Fourier transform algorithm for radii-2 transform
[AD-726389] 22 p3557 N71-35337

High precision moments for Fourier coefficients of arbitrary functions
[NASA-CR-122919] 23 p3781 N71-36046

Spectrum analysis of horizontal wind speed based on Fourier transformations and Northwester US surface wind data
23 p3785 N71-36079

FOURIER-BESSEL TRANSFORMATIONS
Fourier-Bessel analysis of forced torsional vibrations of uncoupled cylindrical shells
[AD-717302] 11 p1833 N71-21869

Image sampling theorems for wave amplitudes obtained with circular apertures including Fourier-Bessel transformations and Airy figure example
[NASA-TT-F-13729] 18 p2963 N71-30854

FRACTIONATION
Fractionation of epoxy resins by alternating gel recycle permeation chromatography
[AD-717630] 11 p1782 N71-22880

Purification apparatus for vaporization and fractionation of liquids
[NASA-CASE-XNP-06134] 15 p3416 N71-27184

FRACTOGRAPHY
Scanning electron microscope operation and micrographs of microstructures and fractures in metals
[MAA/AS7/69] 02 p0224 N71-11527

Microstructural and fractographic studies of boron carbide ceramics subjected to ballistic impact and static flexural loading
[AD-712397] 02 p0247 N71-11664

Fractograph and yielding in low strength steels
[FB-195239] 03 p0392 N71-12381

Electron fractography for high strength steel to determine fatigue life of military aircraft parts
[NLR-TD-69043-U] 03 p0395 N71-13364

Fracture toughness of precipitation hardening aluminum alloys with microstructure and fractography observations
10 p1581 N71-21441

Fracture behavior of uniaxially loaded wedge opening load plane stress Zircaloy 4 specimens
[WAFD-TM-936] 13 p2184 N71-25443

Stress corrosion and fatigue tests and fractographic analysis of high strength aluminum alloy cylinders
[AD-720857] 15 p2425 N71-27628

Measurement of crack propagation velocities in silicon and germanium using ultrasonic fractography
[REPT-7/65] 19 p3109 N71-31704

FRACTURE MECHANICS
Erosion effects on reactor structural materials
[AD-711521] 01 p0087 N71-10884

Measuring effects of prestressing on stress corrosion resistance of high strength steels
[AD-711606] 02 p0402 N71-11574

Fracture mechanics in explosively loaded magnesium
[AD-712129] 02 p0402 N71-11587

Stress corrosion cracking technology review
[AD-711589] 02 p0403 N71-11696

Investigating effects of surface and through cracks on failure of pressurized thin-walled cylindrical cylinders
[NASA-TN-D-6099] 02 p0302 N71-12050

Thermal influence on high temperature deformation and fracture behavior of some nickel based alloys
[ORNL-2561] 03 p0389 N71-12538

Dynamic tear test for measuring fracture toughness
[AD-713494] 03 p0393 N71-13153

- Weldability of tungsten and tungsten alloys
03 p0395 N71-13310
ARPA coupling program on stress-corrosion cracking including treating specimen types, titanium and aluminum alloys, high strength steels, and surface sciences
[AD-713059] 03 p0396 N71-13397
Fracture mechanics and time dependent strength of adhesive joints
[NASA-CR-111761] 04 p0617 N71-14080
Acoustic analysis for materials research and structural integrity evaluation
[UCRL-72582] 05 p0708 N71-15064
Characteristics of crack stability in contoured double cantilever beam specimens
[AD-713512] 05 p0779 N71-15340
Application of fracture mechanics to design and failure analysis
[AD-713148] 05 p0780 N71-15570
Technology review on macroscopic and microscopic fracture mechanics
[AD-714693] 06 p0953 N71-15998
Elastic bending and fracture mechanics of reinforced fiber epoxy resins using scanning electron microscope
[NPL-DM5-11] 07 p1047 N71-17164
Fracture ductility of aluminum and titanium alloys and steels as function of stress state
[AD-715320] 07 p1044 N71-17844
Acoustic emission testing and microfracture processes in solids
[AD-715019] 07 p1127 N71-17953
Macroscopic fracture transition phenomena in 7075-T651 aluminum
08 p1299 N71-19141
Fracture mechanisms in silver single crystals and stainless steel polycrystalline foils
[AD-716573] 09 p1397 N71-19441
Determination of fracture extension resistance factors in fracture safe design for nonfrangible metals
[AD-716407] 09 p1476 N71-19891
Failure mechanism of pipe rupture in reactor system [GEAP-10205] 09 p1422 N71-20595
Dynamic fracture in metal hollow cylinder under biaxial strain conditions
[AD-717092] 10 p1577 N71-21209
Measurement of contact times and fracture velocities of steel balls impacting on glass plates of various thicknesses overlying steel block
[PB-196353] 10 p1639 N71-21776
Fracture mechanics of heavy section steel plates [WCAP-7578] 10 p1585 N71-21790
Fracture mechanics of flawed tees and elbows in ductile pipe
[BML-1892] 10 p1605 N71-21795
Surface and structural defects in alumina ceramic armor caused by ballistic impact
[AD-717325] 11 p1781 N71-21866
Fractographic analysis on fatigue crack mechanism and fracture tolerance of pressurized vessels
[AD-717301] 11 p1833 N71-21868
Techniques for fabrication of piezoelectric strain gages and application to investigation of fractures in materials
[AD-717649] 11 p1760 N71-21930
Fourier analysis of near field velocity from numerically simulated dynamic bilateral shear fracture
[AD-717599] 11 p1748 N71-22259
Energy balance method for predicting elastomer fracture due to thermal stress emphasizing solid propellants
11 p1785 N71-23044
Fracture mechanics evaluation of stress intensity factors for various crack geometries and loading conditions
[WAFD-TM-976] 12 p2004 N71-23163
Effects of glazing and quenching on physical and mechanical properties of ceramic materials
[AD-717983] 12 p1941 N71-23282
Effect of alloying elements on tempered martensite embrittlement and fracture toughness of low alloy high strength steels
[AD-718041] 12 p1938 N71-23777
Numerical analysis of stress and fracture in shallow linear-elastic shells composed of aluminum and plastic plates
12 p2007 N71-24120
Fracture mechanics theory used to determine effects of crack dimensions and material properties on fracture stresses for thin metal sections with through and part-through cracks
[NASA-TN-D-6305] 12 p2007 N71-24240
Development of fracture model to predict rate of crack propagation under high temperature low cycle fatigue conditions based on creep rupture principle
12 p2008 N71-24283
Fatigue and fracture mechanics of airframes and materials including structural design and stress analysis techniques
[AD-719756] 13 p2028 N71-25092
Prediction of critical length of fatigue cracks based on concepts of linear elastic fracture mechanics
[AD-719757] 13 p2182 N71-25141
Effect of plastic deformation on distribution of microcracks and structure of mild steel
[AD-719832] 13 p2096 N71-25159
Determination of conditions leading to fracture arrest by circular hole ahead of propagating crack by dynamic photoelasticity techniques
[AD-719934] 13 p2183 N71-25398
Fracture mechanics and anisotropy of fatigue crack propagation in hot rolled banded steel plate
13 p2183 N71-25444
Application of scanning electron microscopy to study of metal fatigue mechanisms
[AD-719927] 14 p2270 N71-25678
Fracture mechanics and failure analysis of glass under biaxial loading at elevated pressures in water and inert atmospheres
[AD-719952] 14 p2277 N71-25767
Stress analysis and fracture mechanics of dewettable, isotropic, composite propellants
[AD-720096] 14 p2331 N71-26079
Measurement of stress pulses resulting from fracture of brittle circular rods under uniaxial tension and mechanical properties of materials at high rates of shearing strain
14 p2349 N71-26253
Determination of upper and lower bounds to limit pressure for circular cylinders containing axial slits and relation to brittle fracture problem
14 p2349 N71-26318
Micromechanism of crack propagation in brittle materials and description of motion of crack zone during crack propagation
14 p2349 N71-26358
Development of model for initiation of branching fractures in stressed glass and glass ceramics [SC-RR-70-766] 15 p2438 N71-26649
Mechanical properties of fiber reinforced materials
15 p2435 N71-27043
Elastic-plastic finite element analysis for three dimensional specimens with cracks and for stress and strain field near cracks
[HSSTP-TR-12] 15 p2521 N71-27274
Static fracture behavior of surface flawed aluminum plate
[AD-720392] 15 p2424 N71-27449
Stress corrosion crack arrest and crack propagation in titanium alloys proving crack arrest stress intensities higher than those for crack initiation when testing thin materials
[AD-720351] 15 p2426 N71-27448
Tables on fracture mechanics of notched bars of boride composites and cobalt bonded tungsten carbide [NASA-CR-118866] 15 p2433 N71-27783
Reaction rate failure model for fracture mechanics of solid rocket propellant binder
[AD-720717] 15 p2511 N71-27905
Analysis of fracture mechanism that occurs during penetration of rigid wedge into elastic, brittle, non-isotropic material
16 p2686 N71-28633
Linear elasticity, elastic-plastic deformations, and deformation-fracture interactions in fracture analysis of axially symmetric solids
17 p2852 N71-29571
Fracture energy and strength behavior of sodium borosilicate glass A12O3 composite materials system [AD-72349] 17 p2771 N71-30196
Fracture characteristics of polycrystalline copper explosively loaded by two different methods
[AD-723339] 17 p2767 N71-30251
Fracture mechanics and statistical failure analysis of brittle materials and erosion and abrasion machining processes
18 p2929 N71-31209
Systems analysis to simplify brittle fracture tests of metals
[AD-722876] 18 p2936 N71-31422
Fatigue testing of carbon and stainless steel boiling water reactor cooling system pipes including failure probability and fracture mechanics analyses
[GEAP-10207-23] 19 p3134 N71-31711
Fracture mechanics for predicting fatigue crack propagation and velocity in aluminum alloy
[AD-723285] 19 p3187 N71-31778
Survey of analytical procedures for fracture-safe design of metal structures
[AD-723190] 19 p3187 N71-31945
Stress conditions and behavior of materials with sharp cracks subjected to thermal and mechanical loads
[NASA-TT-F-13699] 19 p3190 N71-32554
Fracture mechanics and instrumented notched bar impact tests used to determine brittle behavior of steels
[NLL-RISLEY-TRANS-2073-9091.9F] 19 p3190 N71-32650
Stress concentration and fracture mechanics for internally pressurized thick walled cylinders with cracks and effects of cyclic loads
[AD-724641] 20 p3357 N71-33034
Fourier transform solutions of quarter plane problems in elasticity
[AD-724176] 20 p3358 N71-33373
Studying fracture surface striations and crack propagation in aluminum alloy by electron microscope [NLR-MP-69014-U] 21 p3529 N71-35149
Effects of hydrogen and hydrogen-oxygen mixtures on fracture of high strength steel in pressurized container
[NYO-3975-3] 22 p3594 N71-35390
Fracture safe design of nonfrangible structural aluminum alloys
[AD-726411] 22 p3594 N71-35397
Multiaxial stress state effect on fracture ductility of solids
[AD-726443] 22 p3690 N71-36330
Fracture mechanics of plastic stress and strain fields near crack tip and computer simulation of fracture spreading in viscoelastic solid
[AD-726745] 22 p3691 N71-36331
Fracture strength of polycrystalline aluminum oxide in relation to microstructure
23 p3834 N71-37340
Influence of geometric variables on K sub c values for two thin sheet aluminum alloys
[AD-726684] 23 p3861 N71-37325
Summary data on fracture toughness of low strength steels including data on static and dynamic loaded specimens
[WAFD-TM-895] 24 p3935 N71-38073
Effects of high energy, pulsed electron beams on dynamic fracture induced by rapid in-depth heating of aluminum and titanium alloys
[AD-727983] 24 p3938 N71-38080
FRACTURE RESISTANCE
U FRACTURE STRENGTH
U FRACTURE STRENGTH
Fracture properties of nickel steels for pressure vessels
[AD-709904] 01 p0128 N71-10190
Fracture resistance of Ti-6Al-2Zr and Ti-6Al-4V alloys in 3 inch thick plates
[AD-711586] 02 p0244 N71-11738
Heat treatment studies of aluminum alloy type 707 forgings including tensile strength, fatigue and crack resistance and stress corrosion resistance
[NLR-TR-69058-L] 02 p0345 N71-12126
Fracture strength of glass fiber wound plastics
[AD-713063] 03 p0397 N71-13002
Static strength, stiffness, fatigue, and damage resistance of materials in design optimization for ship structure
03 p0465 N71-13140
Fracture toughness of graphite double cantilever beam specimens
[BNWL-CC-774] 04 p0533 N71-13812
Fracture strength and stress corrosion characteristics of high strength maraging steels
[AD-712723] 04 p0529 N71-13999
Design criteria for fracture optimization of metallic pressure vessels
[NASA-SP-8040] 04 p0530 N71-14150
Loading rate and temperature effects on high strength steel fracture toughness
[AD-713357] 05 p0699 N71-14322
Describing machine for testing strength and safety of large structures
[ZJB-82] 05 p0776 N71-15199
Considering methods for evaluating fracture toughness of structural materials
[MO/A/53/66] 05 p0776 N71-15194
Compressive and fracture strengths of carbon fiber reinforced plastics
[ARC-CP-1132] 06 p0876 N71-15742
Dynamic tear tests to determine thick-section steel fracture strength
[NRL-7056] 06 p0869 N71-15830
Strength and elastic behavior of composite nuclear fuel bodies
[RD/N-1622] 06 p1236 N71-18228
Relating liquid metal embrittlement of aluminum and zinc-cadmium alloys to electronegativity of participating solid and liquid metal
[AD-715741] 06 p1214 N71-18551
Brittle fracture of alloyed, high density, fine grained, and pure alumina
[AD-715988] 09 p1483 N71-19880
Fracture toughness prediction and method for relating transition temperature and Charpy transition temperature changes
[AD-716599] 09 p1399 N71-19807
Notch effect in fracture toughness testing of stressed steel sample
[WCAP-7579] 10 p1576 N71-21817
Fracture toughness of precipitation hardening aluminum alloys with microstructure and fractography observations
10 p1581 N71-21640
Double torsion technique to determine fracture energy of epoxy resin
[AD-718948] 12 p1942 N71-23579
Dynamic deformation and fracture strength of titanium carbide-cobalt alloy at elevated temperatures
13 p2096 N71-25114
Fracture behavior of unirradiated wedge opening load plane strain Zircaloy 4 specimens
[WAFD-TM-936] 13 p2184 N71-25465
Comparative results of various reactor physics codes for predicting neutron spectrum in simulated

SUBJECT INDEX

FREE CONVECTION

- pressure vessels and fracture resistance of irradiated A533-B steel plates 15 p2448 N71-27296
[AD-721068]
- Fracture toughness data utilizing small notched round tensile steel specimens with hydrogen embrittlement as crack starter 15 p2425 N71-27618
[AD-720217]
- Asodic oxide coating thickness effect on fracture of aluminum single crystals and polycrystals 15 p2598 N71-27902
[OJ-3401-16]
- Fracture toughness test method for thick-walled cylinder material 16 p2685 N71-28288
[AD-721026]
- Fracture strength of high strength steel welded joints by investigation of temperature effects on material near weld 19 p3109 N71-31684
[REPT-47/0]
- Microstructural modifications for improved fracture toughness of Ti-6Al-4V-2Sn alloy in annealed condition 19 p3110 N71-31796
[AD-725634]
- Flexural strength of alumina ceramics increased by reduction of crystal anisotropy 20 p3287 N71-33085
[AD-724313]
- Analytical and experimental investigation of ductile fracture of polymers using adaptation of Dugdale model 20 p3360 N71-33778
[NASA-CR-121416]
- Development of method for testing resistance of brittle material to fracture when subjected to shock wave loading 21 p3529 N71-35146
[JEP-1554]
- Analysis of gross strain crack tolerance in A533-B steel with plots of displacement measurements versus temperature 22 p3593 N71-35588
[BSSTP-TR-14]
- Fracture toughness of filled polymers measured using double edge notched tensile bars 23 p3780 N71-36940
[AD-721026]
- Fracture strength of polycrystalline aluminum oxide in relation to microstructure 23 p3834 N71-37343
[AD-727841]
- Effects of elevated temperature on deformation resistance of steel and brass 24 p3939 N71-38102
[AD-727841]
- Surface layer effect on fracture strength of graphite coated titanium dioxide fuel particles of high temperature nuclear reactor 24 p3957 N71-38225
[BD/N-1839]
- Delayed fracture of high strength steel as stochastic process in terms of nucleation theory and delayed fracture toughness 24 p4025 N71-38717
[AD-727841]
- FRACURE TOUGHNESS**
- U FRACTURE STRENGTH**
- FRACURES (MATERIALS)**
- Fracture, fatigue, and crack propagation of aluminum alloy sheet and flat plates 06 p0872 N71-16330
[AD-714019]
- Materials considered critical to reactor design and performance - effects of radiation on creep, hardening, fracture, and swelling - conference 08 p1238 N71-18343
[BNWL-SA-3495]
- Fracture and crack growth for welded joints of SA1-258 titanium in environment of low pressure, high purity hydrogen 13 p2091 N71-24378
[NASA-CR-114839]
- Probability density function of surface area remaining on particles produced from residue of fractured chemically strengthened glass elements 15 p2428 N71-26933
[JC-RR-69-506]
- Influence of core to sleeve bonding on fracture of hydrostatic extrusion of hard core clad rod 18 p2938 N71-31559
[RTO-4078-3]
- Electrical resistivity of Al and Cu during rapid heating to melting point and fracture in investigation of metallic melting mechanisms 21 p3441 N71-34489
[NLL-M-21006-5328-4F]
- FRAGMENTATION**
- Research and development of high speed liquid jets for cutting or breaking materials 01 p0089 N71-10424
[DME/NAB-1970/2]
- Investigating penetration response of various materials to high speed fragment impact 05 p0780 N71-15394
[AD-713513]
- Angular distribution measurements of fragments from neutron-induced fission 05 p0751 N71-15618
[LA-4364-TR]
- Kinetic energy distributions of single fission fragment mass lines 07 p1670 N71-17603
[FEL-190]
- Status of research program to develop criteria for designing aircraft protective devices from rotor fragments 18 p2869 N71-30762
- Nuclear laser excited by fission fragments produced in pulsed nuclear reactor 20 p3282 N71-33633
- FRAME PHOTOGRAPHY**
- High speed framing lenticular cameras with mechanical shutter for arc study in circuit breaker 02 p0225 N71-11552
[RAE-LIB-TRANS-1444]

- Analytical triangulation program in FORTRAN 5 for frame photography including free formatting in plot/output routines, and least squares adjustment 10 p1548 N71-20906
[AD-717105]
- FRAMES**
- NT AIRFRAMES**
- Matrix method for computerized design optimization of framed structures subjected to loads 01 p0131 N71-10931
[AD-711279]
- Shock absorbing articulated multiple couch assembly 03 p0328 N71-12343
[NASA-CASB-MSC-11253]
- Optimization of pin-joint frames, cantilever members, and machine tool structures 06 p0953 N71-15797
[ARC-R/M-3632]
- Minimum weight and strain equations for optimal beam and frame structures under random loads 08 p1296 N71-18619
[NASA-TT-13451]
- Dynamic structural analyses on minimum weight beams and frames by one degree of freedom system 08 p1296 N71-18620
[NASA-TT-13450]
- Pliable frame for sunglasses in emergency survival kits 11 p1494 N71-23096
[NASA-CASE-XMS-00664]
- Optimal plastic design of doubly symmetric closed ring and frame structures of idealized sandwich section, utilizing Marcal-Prager optimization method 21 p3527 N71-35133
[TAE-126]
- FRAMING CAMERAS**
- Stereo laser framing camera for photographs of growth and effects of crack formation of materials shocked by explosives 03 p0387 N71-12820
[UCRL-72543]
- Rotating mirror camera for rotating electric arc photography 08 p1201 N71-18608
[DLR-MIT-70-16]
- Minimizing in frame motion relative to rotor surface for model 739 framing camera 11 p1763 N71-22479
[EGG-1183-542]
- Framing camera performance predictions from drag and diffraction image degradation source analysis 13 p2082 N71-25193
[EGG-1183-530]
- FRANCE**
- Irradiation experiments with OSIRIS swimming-pool research reactor 04 p0546 N71-13602
[CEA-R-3991]
- Aerospace medicine training in France 04 p0477 N71-13882
- Physiological training of military and civilian aircrews in cooperation with engineers in France 04 p0483 N71-13893
- German/French Symphonie communication satellite antennas 07 p0991 N71-17670
[BMW-FB-W-40-2]
- Market research and management planning for optimization of civilian airline operations in France 07 p1136 N71-18093
[REPT-1970/7-E]
- Cybernetic and economic international study group for civil aviation in France 07 p1136 N71-18094
- Climatological characteristics of mistral wind in France 09 p1414 N71-20447
[REPT-79]
- Urban development effects on climatology of Paris 12 p1958 N71-24857
[REPT-52]
- Synoptic meteorology for airports in Spain, Austria, France, Switzerland, and Alps 15 p2440 N71-27807
[AD-720708]
- Dynamic characteristics of wind and temperature profile vertical distribution over Paris-north airport site 18 p2949 N71-30831
- Wind shear in 0-100-m layer over Roissy-on-France Airport determined from wind and temperature profiles 18 p2950 N71-30832
- Meteorological charts for air space over Toulouse-Bagnac 18 p2951 N71-30952
- Proton and electron irradiation in French solar cells 19 p3040 N71-31659
[ONERA-NT-02-18-70]
- Climatological time measurement in eastern France 20 p3262 N71-33337
- Numerical analysis showing Atlantic Ocean influence on tidal gravity variations observed at Moulins climatic station, France 20 p3263 N71-33351
- Conclusions of studies by French Committee for Air Transport to prepare proposals and recommended directions in air transport field for next five years 21 p3375 N71-34015
[NASA-TT-P-13947]
- French astronomical telescope project planning 24 p3921 N71-37965
- FRANCE-CONDON PRINCIPLE**
- Measurement of 472 state lifetimes in ruby with fluorescent and nonfluorescent transitions and dynamic model including activation energies, Franck-Condon principle, and frequency factors 16 p2658 N71-29145
- Franck-Condon and resonance charge exchange effects on charge transfer cross sections based on mass spectroscopy of molecular ion reactions with perfluorooxane, alkane, and alkene targets 17 p2801 N71-30116

- FRAUNHOFER LINE DISCRIMINATORS**
- Developing line discriminator for detecting substances that fluoresce in water near sodium D2 Fraunhofer line 02 p0227 N71-11992
- Calculations and data correlation procedures for Fraunhofer line discriminator operating over open water 20 p3272 N71-33202
[NASA-CR-121427]
- FRAUNHOFER LINES**
- Measuring object motion by in-line Fraunhofer holographic techniques 03 p0380 N71-12799
- Interferometric measurements of solar absorption wavelengths in visible region, and comparison to standard Hg-196 wavelengths 11 p1825 N71-21975
- FRAUNHOFER REGION**
- U FAR FIELDS**
- FREDHOLM EQUATIONS**
- Fredholm equations for three body problem in quantum mechanics 07 p1052 N71-18120
- Computer analysis of semiconductor GeLi gamma ray spectra, comparison of threshold detectors, Bonner spheres, and recoil spectroscopy with emulsions, and Fredholm equation solution 10 p1559 N71-21148
- Fredholm solution of delta function model for two electron helium like ions 12 p1969 N71-23236
[NASA-CR-117895]
- Fredholm transformations and Radon-Nikodym derivatives for evaluation of Yeh-Winner integrals of exponential functions 12 p1948 N71-23348
[AD-718425]
- Radiative transfer problems using invariant imbedding and Fredholm integral equations with displacement kernels 12 p1950 N71-23743
[AD-718096]
- Numerical analysis of pair of singular integral equations with principal value - Volterra and Fredholm equations 12 p1950 N71-24041
[NASA-TN-X-2270]
- Second order Fredholm integral equations for solving neutron transport equation 15 p2456 N71-26845
[KFK-1223]
- Atmospheric optics problem solving using Fredholm equations of first kind 15 p2463 N71-27543
- Fredholm equations for load absorption by discontinuous filament in fiber reinforced composite 16 p2617 N71-28351
[AD-721999]
- Computer techniques used in information theory, industrial controls, solutions to Fredholm equations, and simulating spreading of epidemic 17 p2727 N71-29536
[JPRS-53401]
- Solutions to Fredholm equations obtained in least squares solution to identification of dynamic systems 17 p2772 N71-29539
- Numerical solution of Fredholm equation for air duct vortices of shrouded propeller with tip clearance 19 p3003 N71-31788
[DLR-FB-71-15]
- FREDHOLM OPERATORS**
- U FREDHOLM EQUATIONS**
- U OPERATORS (MATHEMATICS)**
- FREE ATMOSPHERE**
- Measurement of free atmosphere water vapor radiation angular distribution at 60 to 120 km altitude 15 p2400 N71-27498
- FREE BOUNDARIES**
- Second order differential equations for free boundary condition of heat equation 12 p1951 N71-24187
- Systematic iterative procedure yielding finite difference solutions to steady free boundary problems in plasma physics and fluid dynamics 19 p3123 N71-32269
- FREE CONVECTION**
- Convective stability and thermodynamic properties of infinite horizontal thin polytropic layer subjected to conditions of heat, uniform magnetic field, and rotation 10 p1540 N71-20949
[NASA-TN-D-6248]
- Combined free and forced laminar convective heat transfer to nonNewtonian fluids flowing in constant wall temperature vertical tubes and controlling parameter analysis 11 p1742 N71-22782
- Free convection heat and mass transfer along cylindrical bodies 16 p2606 N71-28200
- Mathematical models for determining stabilizing effect of fluid boundaries on thermal convection 16 p2579 N71-28271
[NASA-CR-119013]
- Stagnation-point free-convection film boiling approximate solutions for Freon and water on hemispherical shells at atmospheric pressure 19 p3193 N71-32510
[P-4543]
- Partial differential equations for migration evaluation in supported electrolyte solutions with free convection 21 p3367 N71-34100
[UCRL-20322]

FREE ELECTRONS

Quasi-free electron scattering on C-12 and Be-9 using external electron beam 06 p1247 N71-18190 [INSJ-122]

Improved microwave transmission by adding rapidly evaporating liquid droplets to plasma sheath to remove free electrons 10 p1629 N71-21131

Measurements of electronic free paths in argon discharge using interaction between plasma electrons and slow wave on helix 11 p1812 N71-22516

Gamma ray production by cosmic annihilation of free and low energy electrons and positrons 13 p2158 N71-24766

Forced and free oscillations of plasma consisting of free electrons and background of positive ions [NPL-B573] 22 p3652 N71-36045

Photoelectron emission spectroscopic absorption band calculations for bound-unbound transitions in solution and interpretation of unbound electron random walk with kinetic energy loss 24 p3961 N71-38412 [AD-727096]

FREE ENERGY

NT GIBBS FREE ENERGY

Surface free energy of polymer adhesion 04 p0619 N71-13597

Derivation of equations for coupled gas species concentrations in chemical equilibrium using free energy and equilibrium methods for specific heat and acoustic velocity calculations 14 p2213 N71-25941 [AD-720904]

Thermomechanical constitutive equations as free energy functional for thermorheologically simple viscoelastic materials 16 p2618 N71-28630 [AD-720291]

Using density and fugacity expansions to calculate free energy of quantum plasma 18 p2993 N71-31045 [ITF-70-94-P]

Behavior of ammonium chloride near order-disorder transition explained by physical model having coupled singular and nonsingular free energy parts and verified by specific heat measurements 18 p2996 N71-31360

Free energy and orientational degrees of freedom of crystalline nitrogen phase transformations 21 p3500 N71-34934

EMF measurements of indium oxide free energy of formation between 790 and 1230 K using zirconia electrolyte galvanic cell [BM-RI-7549] 22 p3550 N71-35289

Calculating excess thermodynamic properties from data on one component or from heterogeneous condensed phase equilibria 22 p3551 N71-35297 [AD-726536]

FREE FALL

Drag of free falling spheres in water for Reynolds numbers in critical region using orthonormal cinematography [AD-717472] 11 p1735 N71-22096

Human tolerance to impact determined by free fall simulation tests with instrumented dummy [ARL-SM-353] 15 p2375 N71-27476

Vertical flight free fall ballistic charts and theoretical analysis of translational motion 17 p2850 N71-29629 [SC-RR-70-881]

Fixed wing aircraft employing free fall and circling-line techniques in rescue of personnel and retrieval of equipment [AD-727007] 22 p3541 N71-35228

Experimental arrangements for demonstrating behavior of candle flame during free fall [NASA-TT-F-13940] 22 p3696 N71-36356

FREE FLIGHT

Aerodynamic characteristics of free flight bodies in ballistic ranges [NASA-TM-X-64536] 04 p0472 N71-13583

Radio navigation aids used to navigate flight vehicles [AD-714829] 08 p1232 N71-18299

Relaxation in scaling parameters effect on free flight path of wind tunnel model with forced ejection [ARL-A-322] 09 p3134 N71-19391

Application of free flight ranges to high temperature gas dynamics 11 p1740 N71-22633

Ballistic range for free flight measurements of sphere drag at subsonic, transonic, supersonic and hypersonic speeds in upper atmosphere [AD-721208] 15 p2395 N71-27675

Planar and nonplanar dynamic stability coefficient using biplanar wind tunnel, free flight system 18 p2867 N71-31107

Free flight stability as on half cones in hypervelocity wind tunnels including data reduction program [VKI-TN-66] 19 p3675 N71-31663

Wind tunnel free flight model trajectory control using photoelectric screen for aerodynamic force determination [VKI-TN-72] 19 p3072 N71-31694

Determining deployment characteristics of all-flexible parawings by free flight tests [NASA-TM-X-2307] 20 p3210 N71-33239

FREE FLIGHT TEST APPARATUS

Hydraulic support apparatus for dynamic testing of space vehicles under near-free flight conditions [NASA-CASE-XMF-03248] 01 p0038 N71-10604

Free flight measurements of aerodynamic lateral force and moment coefficients using gyroscopes and accelerometers [HSA-TN-164] 02 p0141 N71-11001

Schlieren photography and differential interferometry for free flight tunnel holography [ISL-T-3969] 03 p0312 N71-12223

Differential interferometry and schlieren photography for hypersonic aerodynamic hologram analysis [ISL-T-4969] 03 p0388 N71-12985

Conference on ballistic range techniques and equipment [AGARDOGRAPH-138] 04 p0514 N71-13576

Convective heat transfer measurements in ballistic ranges and free flight apparatus [NASA-TM-X-64539] 04 p0523 N71-13588

Free flight suspension system for use with aircraft models in wind tunnel tests [NASA-CASE-XLA-00939] 06 p0830 N71-15926

Free flight tests in hovering and forward flight of V/STOL transport model with six wing-mounted lift fans [NASA-TN-D-6198] 11 p1672 N71-22069

Attitude sensors to determine motion of rocket free body precession including magnetometers and star trackers [AD-718314] 12 p1960 N71-23843

FREE FLOW

Systematic numerical analysis of two dimensional and axisymmetric laminar jet of incompressible fluid with and without free stream [NASA-CR-111517] 03 p0364 N71-13085

Pressure fluctuation measurements with microphones in air jet free flow [DLR-FB-70-22] 07 p1008 N71-17142

Critical evaluation of theory and experiment of free turbulent mixing - shear stress models 13 p2063 N71-24480 [AD-718956]

Measurement of local skin friction coefficient and combined effect of favorable pressure gradient and free stream turbulence on local skin friction coefficient 14 p2245 N71-26609

Effect of injection Mach number on jet penetration over wide range of pressure and free stream Mach numbers [NASA-TN-D-6370] 16 p2579 N71-28270

Two-dimensional supersonic turbulent mixing in shock tunnel experiment with free stream calculations, temperature distributions, and reconstruction of refractive index contours [AD-722693] 17 p2737 N71-30159

Nimbus satellite observations of large ice free areas in Antarctic coastal waters 18 p2916 N71-31060

Determination of laminar skin friction response under oscillating flow in presence of sinusoidal free-stream velocity 20 p3253 N71-33780

Numerical analysis of plane steady transonic flows past lifting airfoils with free-stream Mach numbers less than unity [D180-12958-1] 21 p3412 N71-34275

FREE JETS

Characteristics of jet issuing from two dimensional orifice past rectangular plate [REPT-308] 02 p0204 N71-12079

Technique for analysis and computerized data reduction of time of flight distributions of free jet expansions [AD-712372] 03 p0423 N71-12729

Visualization of supersonic rarefied free jet flow using electron beam scanning 08 p1177 N71-18400 [REPT-70-10]

Dynamic characteristics of circular fully developed laminar free jet [NASA-TN-D-6304] 12 p1898 N71-23103

Diffuser, shroud, and mass injection effects on starting and operating characteristics of Mach 3 free jet tunnel at low pressure ratios [NASA-TN-D-6377] 21 p3407 N71-34243

High-low noise control device for use with free jet circuit breakers based on automatic control of air blast intensity [NLL-CE-TRANS-3365-1902.09] 23 p3733 N71-36616

Sound and flow field of axially symmetric free jet impinging on wall at jet exit Mach numbers upwards of 0.6 [NASA-TT-F-13942] 24 p3905 N71-37832

FREE MOLECULAR FLOW

Nozzle flow theory for determining distribution functions on centerline of free jet expansion [AD-714155] 06 p0836 N71-16318

Background pressure effects on reduction of molecular beam intensity 10 p1539 N71-20689 [AD-717158]

Pressure difference induced across stainless steel capillary tube by temperature gradient used to predict thermal transpiration effect 11 p1844 N71-22709

Flat plate and cylindrical ion density probes including free molecular flow and continuum regimes 12 p1923 N71-24130

FREE OSCILLATIONS

U FREE VIBRATION

FREE RADICALS

Effects of nonequilibrium free-radical content and composition variation of supersonic streams entering air breathing engines on ignition points and delays [NASA-CR-111371] 02 p0288 N71-11467

Electron hole reaction kinetics in irradiated free radical destruction [UCRL-19609] 03 p0423 N71-12739

Ionic and free radical reactions in irradiated organic compounds [ORO-2568-56] 06 p0812 N71-16792

Acidity effects on ferrous and ferric radiolytic oxidation and reduction rates by HO2 radicals [LIB/TRANS-282] 07 p0988 N71-17008

Vibrational states of electronically excited, free radical molecules 08 p1258 N71-18547 [AD-715740]

Zeman-modulated resonant cavity spectrometry of gas-phase free radical microwave rotational absorption spectra [UCRL-50890] 08 p1264 N71-19101

Detection of transient free radicals in gas phase, and studying reaction kinetics by ultraviolet scan infrared spectroscopy [AD-716004] 09 p1396 N71-19621

Mass spectrometry, free radicals, and transient intermediates evaporating from heated catalytic surface 11 p1697 N71-22644

Atom and free radical concentration measurement and electric discharge technique applied to propulsion systems 11 p1808 N71-22649

EPR and ENDOR study of free radicals produced by gamma irradiation of imidazole single crystals [CRA-R-3758] 14 p2307 N71-26395

Resonator for X band electron spin resonance for simultaneous measurement and electron radiation of transient free radicals 15 p2468 N71-27328 [KFK-1285]

Dynamic polarization of protons and fluorine nuclei in solutions of selected free radicals in solutions of aromatic and aliphatic fluorocarbon solvents 20 p3318 N71-33597

Nuclear dynamic polarization for investigating intermolecular dynamics in solutions of selected free radicals and fluorocarbons in acetone 20 p3320 N71-33607

Electron spin resonance of free radicals formed in elastomers by ultraviolet irradiation [APC-CH-97] 20 p3323 N71-33828

Quasi-stationary state approximation in free radical chain addition polymerization kinetics [AD-726398] 22 p3551 N71-35296

Electron paramagnetic resonance studies of spin relaxation mechanisms in stable phenyl free radicals 22 p3659 N71-36094

Electrical conductivity in stable phenyl free radicals 22 p3659 N71-36095

FREE STREAM EFFECTS

U FREE FLOW

FREE STREAMS

U FREE FLOW

FREE VIBRATION

Free and forced vibrations of nonlinear isochronic oscillators 03 p0419 N71-13331

Computer calculation of natural frequencies and transverse vibration modes in continuous beam [RT/ENG/70/5] 04 p0578 N71-13875

Computerized finite element analysis of free vibrations of paraboloidal shells of revolution 10 p1654 N71-21171

Computerized finite element analysis of lateral pressure effects on free vibration of hyperboloidal shells of revolution 10 p1654 N71-21174

Holographic interferometry analysis of axisymmetric imperfections effect on natural frequencies and mode shapes of conical shells 19 p1369 N71-21280

Finite element method for free vibrations and random response of integrally-stiffened panel [LR-344] 12 p2089 N71-24298

Free vibration analysis for nonlinear shallow elastic shells 14 p2347 N71-25787

Natural vibration of closed cylindrical shell with solid elastic core 14 p2347 N71-25794

Approximate solution for free vibration characteristics of nonlinear systems [ARC-RM-3651] 15 p2434 N71-27217

Computation of uncoupled vibrations of rotary wings using transfer matrix method [DLR-FB-70-63] 17 p2703 N71-29543

Frequencies and modes determined for free vibrations of closed spherical shells submerged at various fluid depths 19 p3191 N71-32774

SUBJECT INDEX

Program for computing free vibration modes and natural frequencies of thin plates with clamped and rotational supports and cylindrical curvature
[AD-724642] 20 p3356 N71-32937

Free vibration determination of curved sandwich beams, using finite element displacement method
[ISVR-TR-45] 20 p3357 N71-33043

Mathematical model for free vibration of arc with varying radius of curvature
[AD-724318] 20 p3357 N71-33134

Free vibration, forced vibration, and parametric response of simply supported tube conveying fluid
[ANL-7762] 22 p3461 N71-34631

Free flexural vibration of thin cylindrical shells using hybrid finite element method
[MERL-70-10] 21 p3528 N71-35138

Forced and free oscillations of plasma consisting of free electrons and background of positive ions
[NP-18673] 22 p3652 N71-36045

Theoretical study of free oscillations for thin walled, open section circular ring structures
[AD-726725] 22 p3691 N71-36327

Free vibrations and harmonic and aperiodic forced vibrations of elastic spherical thin shells in water
[AD-726724] 22 p3693 N71-36337

Free oscillations in bounded, beta-plane oceans with free surfaces and stratification
23 p3754 N71-36766

FORTRAN program for calculating free vibrational frequencies and mode shapes for smooth arc of arbitrary shape and varying cross sections
[AD-726725] 23 p3662 N71-37329

Approximate mathematical model for free vibrations of smooth arc of arbitrary shape and varying cross sections
[AD-726724] 23 p3662 N71-37330

FREZZING

NT ZONE MELTING

Foam plastic thermal insulation against ground freezing
[AD-711905] 02 p0248 N71-12015

Description of nivation processes and associated morphological processes
[AD-711879] 02 p0218 N71-12034

Effect of thermal gradient on ionic diffusion in frozen earth materials - Part 2
[AD-714642] 06 p0841 N71-15920

Effect of thermal gradient on ionic diffusion in frozen earth materials - Part 1
[AD-714644] 06 p0841 N71-15921

Fluorine production and recombination in frozen MSR after reactor operation
[ORNL-TM-3144] 06 p0901 N71-16809

Freezing rate and solute specie and concentration effects on charge separation at advancing surfaces of growing ice related to cloud physics
[AD-718359] 12 p1910 N71-23655

Frozen proton target with high polarization and large emitter excess - conference
[BPPA-81] 15 p2459 N71-26982

FREZZING POINTS

U MELTING POINTS

FREIGHT

U CARGO

FREIGHTERS

Design and feasibility analysis of transoceanic, nuclear powered air cushion freighter for 1980 decade
[NASA-TM-X-67876] 23 p3706 N71-36423

FRENCH GUIANA

Statistical analysis of wind direction and velocity, French Guiana, 1966 to 1970
[ELDO-TN-8] 07 p1053 N71-17129

FRENCH SATELLITE

NT DIADHEME SATELLITE

FRENCH SPACE PROGRAMS

Development, research and analysis of French space program
02 p0307 N71-11131

Characteristics of Symphonie project of Franco-German synchronous communication satellite
02 p0181 N71-11275

French ROLE program for Southern Hemisphere meteorological survey using balloons and satellites
02 p0257 N71-11672

Project DIOSCURES for global sea and air traffic control using synchronous satellites for ground-air-ground communications
02 p0263 N71-11768

Launch vehicles in seventies noting French, Russian, and NASA space programs
02 p0299 N71-12000

Politen for participation of French aerospace industry in space programs
02 p0307 N71-12069

Spacecraft launchings, international cooperation, and other French space activities, 1970
[NASA-CR-118045] 12 p1996 N71-23963

Meteorological weather satellite and ground support system
[NASA-TT-F-15646] 13 p3172 N71-24812

Annual report 1968/1970 on infrared astronomy at Paris Observatory
15 p2317 N71-27617

Soviet and French programs for establishing astronomical schools and stations in Egypt for space geodesy
22 p3680 N71-36243

FRENKEL DEFECTS

Heat transfer calorimetry in annealing of electron irradiation induced Frenkel defects in platinum below 40 K
[JUL-658-FN] 13 p2132 N71-25091

FREON

Molecular interactions and crystal structures at low temperature emphasizing Freon 22
[AD-711096] 01 p0111 N71-10631

Shock wave propagation during explosions in Freon
[AD-712751] 04 p0621 N71-14360

Heat transfer and hydrodynamic behavior for subcooled flow boiling of Freon 113 for use in cooling electronic components
[DSR-71903-72] 14 p2352 N71-23803

Stagnation-point free-convection film boiling approximate solutions for Freon and water on hemispherical shells at atmospheric pressure
[P-4543] 19 p1593 N71-32510

Analysis of Freon-113 bubble growth and collapse in constant-diameter, vertical channels with nonuniform initial temperature profiles
[ANL-7746] 22 p3623 N71-35813

Thermodynamic and physical properties of Freon
[TT70-50178] 24 p3885 N71-37695

FREQUENCIES

NT AUDIO FREQUENCIES

NT BEAT FREQUENCIES

NT BROADBAND

NT C BAND

NT CARRIER FREQUENCIES

NT CRITICAL FREQUENCIES

NT CYCLOTRON FREQUENCY

NT EXTREMELY HIGH FREQUENCIES

NT EXTREMELY LOW RADIO FREQUENCIES

NT HIGH FREQUENCIES

NT INFRASONIC FREQUENCIES

NT INTERMEDIATE FREQUENCIES

NT IONIZATION FREQUENCIES

NT LOW FREQUENCIES

NT LOW FREQUENCY BANDS

NT MAXIMUM USABLE FREQUENCY

NT MICROWAVE FREQUENCIES

NT NYQUIST FREQUENCIES

NT PLASMA FREQUENCIES

NT RADIO FREQUENCIES

NT RESONANT FREQUENCIES

NT SUPERHIGH FREQUENCIES

NT SWEEP FREQUENCY

NT ULTRAHIGH FREQUENCIES

NT VERY HIGH FREQUENCIES

NT VERY LOW FREQUENCIES

Second/third order hybrid phase locked receiver for tracking frequency ramp signals
11 p1703 N71-22774

Mathematical model describing influence of transistor geometry on transition frequency
[LAAS-PUBL-774] 18 p2899 N71-30525

Frequencies and modes determined for free vibrations of closed spherical shells submerged at various fluid depths
19 p3191 N71-32774

Measurement of correlation coefficient of frequency components in tropospheric propagation
[FOA-3-C-3606-43] 22 p3554 N71-35314

Orbital elements and frequency data of naval navigation satellites for ionospheric research
24 p3912 N71-37886

Utilization prospects of ATS 6 beacon radiated frequencies
24 p3913 N71-37898

FREQUENCY AMPLIFIERS

U AMPLIFIERS

FREQUENCY ANALYZERS

Recording and frequency analysis of vibration data using coherent optical data processing techniques with emphasis of failure detection
[AD-710809] 01 p0116 N71-10554

Contributions to theory of digital filtering
[IN-1411] 04 p0537 N71-13957

Microcomputerized frequency discriminator with microconverters without induction components
[PUBL-2] 63 p0656 N71-15517

Optimum binary signals for frequency response testing
[ORNL-TM-3196] 07 p0100 N71-17189

Describing frequency discriminator using digital logic circuits and supplying single binary output signal
[NASA-CASE-MFS-14322] 08 p1165 N71-18092

Design and test evaluation of prototype one-third octave band spectrum analyzer for measurement and analysis of acoustic and vibration data onboard space vehicles
[NASA-CR-111860] 11 p1761 N71-22025

Sweeping receiver system providing visual display of received signals in frequency range from 33 to 140 GHz and frequency markers
[AD-716799] 12 p1874 N71-23308

Frequency spectra for ground oscillations in near zone of explosion
[AD-717660] 12 p1906 N71-23322

FREQUENCY CONVERTERS

Broadband frequency discriminator with resistive passive inductive networks
[NASA-CASE-NPO-10096] 13 p2843 N71-24583

Estimating human occlusion status by changes in frequency characteristics of articulation
[NASA-TT-F-13772] 18 p2875 N71-30803

Digital time discrete method for running short time frequency analysis
[PHL-1970-17] 18 p3886 N71-31056

FREQUENCY ASSIGNMENT

Space and terrestrial communication systems sharing of UHF band
[AD-711499] 01 p0204 N71-10743

Minimum channel requirements for ILS localizer frequency assignment, 1970-1975
[AD-714111] 06 p0894 N71-16198

Near real time ionospheric MUF forecasting over 60 km path
[AD-714995] 07 p1023 N71-17859

Survey of very high and ultrahigh frequency utilization in US aeronautics for communication satellite frequency assignment
[NASA-TM-X-63577] 14 p2217 N71-25920

Third order two signal intermediate products for 242 frequencies between 225 and 400 MHz as used in FAA frequency assignment processes
[ECAC-PR-70-018] 17 p2719 N71-29551

Third order-two signal intermediate products for 340 frequencies between 118 and 136 MHz when 50 kHz channel spacing is used as in FAA frequency assignment processes
[ECAC-PR-70-016] 17 p2719 N71-29552

Third order-two signal intermediate products within 118-136 MHz band with 50 kHz spacing
[ECAC-PR-70-015] 17 p2719 N71-29554

Technical and cost factors for implementation of Alaskan communication satellite system
[NASA-TM-X-65009] 18 p3089 N71-30593

FREQUENCY BANDS

U FREQUENCIES

FREQUENCY CONTROL

NT AUTOMATIC FREQUENCY CONTROL

Frequency agility reduction of radar plant
01 p0821 N71-10233

Magnitude of frequency deviation in SECAM system as parameter determining quality of reproduced color image
[IFRS-51918] 04 p0568 N71-14305

Application of optimal control theory to power system
[AD-716552] 09 p1362 N71-19427

Development of automatic frequency discriminators and control for phase lock loop providing frequency present capabilities
[NASA-CASE-XMF-08645] 09 p1362 N71-19467

Formulas for scattering coefficients for composite multilayered sphere in decreasing or enhancing radar cross section over resonance region centered at desired frequency
[AD-717642] 11 p1700 N71-22233

Linear accelerator frequency control system
[NASA-CASE-XGS-65441] 11 p1729 N71-22962

Mathematical model for frequency correlation function of tropospheric scatter channel
12 p1876 N71-23464

Frequency correlation measurements on multipath tropospheric scatter propagation
12 p1876 N71-23465

Tuning arrangement for frequency control of magnetron-type electron discharge device
[NASA-CASE-XNF-99771] 13 p2056 N71-24841

FREQUENCY CONVERSION

U FREQUENCY CONVERTERS

FREQUENCY CONVERTERS

NT FREQUENCY MULTIPLIERS

NT FREQUENCY SYNTHESIZERS

Frequency to mixing converters with unipolar field effect transistor for determining potential charge by pulse duration of input signal
[NASA-CASE-XNF-67940] 01 p0344 N71-12500

Network analyzer and harmonic frequency converter for swept frequency antenna measurement
[SC-DR-70-460] 05 p0606 N71-14936

Ten micron wideband detector
[AD-713993] 06 p0868 N71-16834

Describing static inverter with single or multiple phase output
[NASA-CASE-XMF-08643] 08 p1165 N71-18752

Satellite microwave receiver systems which convert carrier frequencies and modulation formats to produce signals compatible with VHF-UHF television receivers for low-cost services
[NASA-TM-X-67800] 10 p1521 N71-21299

Characteristics of sensitivity of recombination light to infrared radiation in continuously excited and pulsed system operation
[AD-717645] 11 p1722 N71-21911

Voltage converter/regulator for primary and secondary power sources in deep space missions
13 p2030 N71-23308

Voltage controlled, variable frequency relaxation oscillator with MOSFET variable current load
[NASA-CASE-GSC-10032-1] 14 p2231 N71-23802

FREQUENCY DISTRIBUTION

Development and characteristics of electrical power supplies for converting variable frequency ac to fixed frequency ac
[AD-727468] 24 p3876 N71-37637

FREQUENCY DISTRIBUTION

Frequency dependence of electrical properties of igneous rocks from Kola Peninsula
[NASA-TT-F-13216] 02 p0210 N71-1498

Frequency mixing experiments using infrared and far infrared lasers
[AD-715040] 07 p1040 N71-17768

Whistler recorder using autocorrelation and analog data - frequency and field strength variation of each whistler
[BMBW-FB-W-70-58] 08 p1189 N71-18663

Tables of precipitation frequency and intensity at Hohenpeissenberg, Germany
10 p1596 N71-21196

Cumulative frequency distributions determined by extreme value analysis used for fatigue analysis and interpretation of c.g. vertical acceleration and gust velocity measured on transport aircraft
[A0A0D-8-579-711] 13 p2028 N71-25080

Hybrid computer measurement of stopband in LAMPF 805 MHz accelerator structure at high power (LA-4593)
15 p2387 N71-26837

Variable frequency subcarrier oscillator with temperature compensation
[NASA-CASE-XNP-03919] 16 p2571 N71-28810

Frequency of double stars in extended solar system
20 p3350 N71-33843

FREQUENCY DIVISION MULTIPLEXING

Earth satellite relay station for frequency multiplexed voice transmission
[NASA-CASE-GSC-10118-1] 13 p2044 N71-24621

Comparison of constant bandwidth FM/FM and double sideband/FM telemetry systems
[SC-DR-70-686] 15 p2379 N71-26941

Computerized simulation of frequency division multiplex telephony radio transmission through troposphere using Monte Carlo method
[REFT-10-70] 19 p3053 N71-31661

FREQUENCY MEASUREMENT

Determination of delay time variations in acoustic surface wave by measuring oscillation frequency changes
01 p0032 N71-10220

Liquid oscillation frequency measurement in inclined right circular cylinder
[NASA-TM-X-64540] 03 p0362 N71-13006

Time and frequency measurements of miniature superconducting coaxial transmission lines
[UCRL-72574] 04 p0512 N71-13536

Coherent betatron beam oscillation measurements during beginning acceleration
[CERN-TRANS-70-10] 14 p2315 N71-26732

Frequency-time structure of reflected radar signal for determining solar coronal plasma turbulence spectra
[NASA-TT-F-13614] 16 p2675 N71-28945

Deriving ionospheric electron density as function of altitude from group path versus frequency measurements by vertical ionospheric sounders
[NASA-TM-X-65591] 17 p2750 N71-30260

Receiver for direct measurement of differential Doppler frequency in satellite transmission
24 p3913 N71-37894

FREQUENCY MODULATION

NT FEEDBACK FREQUENCY MODULATION
NT PULSE FREQUENCY SHIFT KEYING
NT PULSE FREQUENCY MODULATION

Producing wideband frequency modulated signals by waveform generator
[AD-710832] 01 p0033 N71-10518

Circuitry for generating sync signals in FM communication systems including video information
[NASA-CASE-XNP-10830] 02 p0182 N71-11281

Demodulator for simultaneous demodulation of two modulating signal carriers close in frequency
[NASA-CASE-XMF-01160] 02 p0184 N71-11298

Frequency modulation effects on tracking errors in monopulse radar and conical scan system
04 p0495 N71-13910

Coherent and noncoherent signal bandwidth methods for radar target detection in clutter
04 p0495 N71-13911

Space scanning by radiation pattern of coded time modulated array antenna
04 p0495 N71-13914

Optical tracker with pair of FM reticles having patterns 90 deg out of phase
[NASA-CASE-XGS-05715] 06 p0903 N71-16100

Phase locked loop derived from ideal single sideband modulation
08 p1164 N71-19120

Equivalent circuit analysis of low frequency collector self modulation in transmitter output stage and frequency-amplitude distortion measurements
[AD-716529] 09 p1338 N71-15624

Numerical analysis of radio signal modulation by amplitude, frequency, and phase modulation
09 p1348 N71-15645

Satellite microwave receiver systems which convert carrier frequencies and modulation formats to produce

signals compatible with VHF-UHF television receivers for low-cost service
10 p1521 N71-21299

[NASA-TM-X-67800]
Analysis of errors in independent subcarrier and harmonic subcarrier methods of radio telemetry on FM radio carrier
10 p1526 N71-21756

Analysis and measurement of characteristics of wide band frequency trackers and design and fabrication of all angle laser Doppler velocimeter
[NASA-CR-103068] 11 p1775 N71-22407

Ray tracing and propagation calculations for determining short wave frequency deviations from received signal
11 p1709 N71-22931

Atmospheric turbulence effects on phase coherence of propagating optical wave
11 p1713 N71-22954

Delay circuits for pulse compression in airborne FM demodulator
[RAE-TR-70110] 12 p1874 N71-23363

Effects of nonlinearities on response to modulated radio frequency fields
12 p1879 N71-23729

Comparison of constant bandwidth FM/FM and double sideband/FM telemetry systems
[SC-DR-70-686] 15 p2379 N71-26941

Analysis and digital simulation of nonlinear behavior of phase locked loops with input signal frequency modulated by nonwhite, normally distributed waveform
16 p2575 N71-28805

S band frequency modulated television transmitter with sampled automatic frequency control designed to drive traveling-wave tube amplifier
17 p2718 N71-29324

Post mixer spectra of periodic FM altimeters with area scatter returns
[AD-722823] 18 p2891 N71-31356

Computer programs for FM cyclotron analyzer computing excitation energy of residual nuclei
[INS-TL-108] 21 p3470 N71-34708

Radio wave propagation, diurnal variations, and frequency and phase modulation
[AD-726528] 22 p3554 N71-35315

Operational analysis of FM range finders used as altimeters and reflex klystron oscillators in three-centimeter range
[JPRS-54697] 23 p3732 N71-36604

Theory of frequency modulated range finders used as altimeters and peculiarities of operation in measurements of low altitudes
23 p3732 N71-36605

Amplitude and frequency modulation characteristics and applications of CW Gunn effect oscillators
23 p3734 N71-36623

Laser beam interactions with thermal media in steady state and time-varying conditions including beam trapping, self-induced frequency modulation, lens effects, and beam aberration
23 p3768 N71-36856

Optimal filters for radio pulses with linear frequency modulation and intersperse phase manipulation at radar stations
24 p3888 N71-37710

Nonlinear behavior of second order phase locked loop with lead lag filter
24 p3902 N71-37813

Development of methods for controlling frequency of solid state lasers and frequency scanning of ruby and neodymium lasers during lasing process
[AD-727250] 24 p3931 N71-38049

FREQUENCY MODULATION PHOTOMULTIPLIERS
Amplifier gain control for Apollo space television signal enhancement
13 p2048 N71-25339

FREQUENCY MULTIPLIERS
Multiple varactor for generating high frequencies with high power and high conversion efficiency
[NASA-CASE-XMF-04958-1] 14 p2234 N71-26414

Recombination and hysteresis losses in frequency multiplier with semiconductor diode
18 p2900 N71-31522

Neutron damage effects in Step Recovery Diode frequency multipliers
[SC-RR-710188] 20 p3329 N71-33991

Optimization of varactor frequency multiplier amplitude and phase modulations
23 p3723 N71-36535

Extending tuning range of parametric oscillators into infrared, visible, and ultraviolet regions
[AD-727127] 24 p3967 N71-38296

FREQUENCY RANGES
NT OCTAVES
Variable frequency nuclear magnetic resonance spectrometer providing drive signals over wide frequency range and minimizing noise effects
[NASA-CASE-XNP-09830] 14 p2256 N71-26266

Automatic feedback control system for controlling volume of power amplifier and measuring frequency range of background noise
[AD-721596] 16 p2568 N71-28356

SUBJECT INDEX

Natural frequencies, vibration modes, and damping of nuclear fuel pins in model of sodium cooled fast breeder reactor
[KFK-1337] 24 p3956 N71-38211

FREQUENCY REGULATION

U FREQUENCY CONTROL
FREQUENCY RESPONSE
Frequency domain analysis of nonlinear networks
[AD-710200] 01 p0036 N71-10071

Technique for improving quality and acquisition of frequency response and vibration data
[NASA-TN-D-7022] 03 p0460 N71-12734

Frequency response of two types of liquid metal pressure transducers with standoff tubes
[NASA-TN-D-6164] 07 p1690 N71-17485

Fundamental frequency, mode shape, and electromechanical coupling coefficient for forced vibrations of sodium chloride crystals
[AD-715137] 07 p1093 N71-17644

Frequency response and design of distributed parameter networks using asymptotic approximation
[NASA-TN-D-5874] 10 p1536 N71-21611

Scanning electron microscope for time resolved frequency response analysis on Gunn effect oscillator
11 p1761 N71-22075

Power spectrum method for determining gust frequency response functions in dynamic aircraft design
12 p1850 N71-23211

Impulse response measurements and radio test link for evaluating tropospheric scatter propagation channel capacity
12 p1877 N71-23446

Volterra functional analysis on phase locked loop response to frequency modulations
12 p1894 N71-24033

Computer program for predicting frequency interference between transmitters and receivers
[E0G-1183-1509] 13 p2048 N71-25344

Frequency response technique for locating electrical faults
[AD-715182] 16 p2568 N71-28344

Computer programming formulas for frequency and statistical analysis of random waveform signals including Fourier analysis, probability density functions, and autocorrelation
[NASA-CR-115075] 17 p2775 N71-30357

Performance and response characteristics of smoothing, image intensifier discriminator for low light level astronomy and optical detection
[NASA-CR-121913] 22 p3558 N71-35342

FREQUENCY SCANNING
High frequency modulated flash scanner for photometric measurements of photochemical reactions
17 p2752 N71-29792

Integration time and scanning rate effects on random vibration spectral analysis errors using scanning filters
[FTL-A-11009-15] 22 p3585 N71-35535

FREQUENCY SHIFT
Three-dimensional laser Doppler velocimeter for measuring local mean and fluctuating gas velocities
[NASA-CR-102948] 04 p0524 N71-14608

Measuring observed frequency shifts of lattice resonant mode in KBr - Li/
[NYO-2391-118] 05 p0759 N71-15348

Serrodyne traveling wave tube reentrance amplifier for synchronous communication satellites operating at microwave frequencies
[NASA-CASE-XGS-01022] 06 p0813 N71-16008

Infrared spectra with frequency shifts in crystal defect resonance modes
[NYO-2391-119] 09 p1436 N71-20040

Doppler shift considerations in naval satellite communication systems employing synchronous satellites
[AD-716455] 10 p1517 N71-26001

Multiplexed communication system design including automatic correction of transmission error introduced by frequency spectrum shifts
[NASA-CASE-XNP-01306] 10 p1518 N71-26014

Tropospheric and ionospheric compositions effects on phase and frequency degradations in propagating signals
[AGARD-CP-33] 11 p1704 N71-22804

Doppler shift recordings of ionospheric disturbances
11 p1709 N71-22839

Sudden frequency deviations of ionospheric radio echoes caused by solar radiation bursts
11 p1710 N71-22935

Determination of ionospheric electron recombination coefficient after sudden frequency deviations
11 p1710 N71-22936

Solar flare effects on ionospheric high frequency radio wave propagation with sudden frequency deviations
11 p1710 N71-22937

Diurnal frequency variations in oblique high frequency ionospheric radio signal
11 p1711 N71-22939

Doppler shifted laser beam as fluid velocity sensor
[NASA-CASE-XAC-10770-1] 13 p3089 N71-24829

SUBJECT INDEX

Transport equation for Doppler frequency shift in transport of electromagnetic waves through unidirectional plasma 15 p2500 N71-37318

Multistage linear accelerator injection into gravity gradient synchrotron and quadrupole compensation for frequency shifts 17 p2792 N71-29299

Amplitude fluctuation in underwater acoustic pulses and its effect on binary decoding (AD-72404) 17 p2788 N71-29770

Broadening and shifting of hydrogen fluoride lines due to noble gases 20 p3274 N71-33478

Single mode analysis for calculating shifts in amplitude and frequency of E X B instability 22 p3636 N71-36076

Receiver for direct measurement of differential Doppler frequency in satellite transmission 24 p3913 N71-37894

FREQUENCY SHIFT KEYING

Design, development, and fabrication of 30 watt, high efficiency FM transmitter by utilizing phase lock techniques (NASA-CR-111789) 01 p0024 N71-10696

Frequency shift keying demodulator - circuit diagrams (NASA-CASE-XGS-02889) 02 p0182 N71-11282

Design of suboptimum receiver for coded, dual diversity, frequency shift keying transmitter (AD-714599) 06 p0617 N71-16835

Frequency shift keying apparatus for use with pulse code modulation data transmission system (NASA-CASE-XGS-01537) 12 p1874 N71-23405

Data transmission system for coherent reception in channels with frequency shifts (DSS-4349) 17 p3719 N71-29533

Development and characteristics of 1200 band frequency shift keying demodulator for use in digital integrated circuits (PRL-1971-12) 20 p3276 N71-33749

FREQUENCY STABILITY

Ultimate microwave cavity sources (AD-713127) 05 p0653 N71-14872

Design and construction of system for measuring frequency of S band, FM TV transmitter (NASA-CR-103030) 07 p0994 N71-17866

Long term frequency stability of three-mirror cavity maser laser using standard frequency light source (BSRIN-11-117) 06 p1209 N71-18445

Gas laser frequency stabilized by position of mirrors in resonant cavity (NASA-CASE-XGS-05644) 08 p1209 N71-18614

High stability temperature compensated crystal standards (AD-715955) 09 p1358 N71-19567

Phase stability of parametric amplifiers under pumping, varactor bias, and interfering conditions, using also equivalent circuits (REPT-5-33-1970) 10 p1531 N71-20640

Digital filter realizations of arbitrary loss and delay functions applicable for any type of frequency in amplifying communication channels (AD-717101) 10 p1534 N71-21246

Reference frequency generator and modulator for absolute data acquisition system (ARL-71-44) 11 p1724 N71-22441

Frequency stability of automatic hydrogen maser cavity laser 11 p1776 N71-22779

Procedures for qualitative evaluation of frequency accuracy and stability of communication-electronics equipment (AD-718706) 12 p1878 N71-23529

Nonlinear absorption feedback for laser power stabilization 13 p2089 N71-24837

Solid state broadband stable power amplifier (NASA-CASE-NP-10854) 14 p2233 N71-26331

Frequency instability and spectral purity of oscillation, and computation of very short term frequency instability of oscillators perturbed by thermal noise (NBSA-P-132) 20 p3242 N71-33724

FREQUENCY STANDARDS

Performance characteristics of portable atomic reference clock and frequency standard (AD-714193) 06 p0860 N71-16479

Ion trapping technique for application in frequency standards (NBS-TN-308) 10 p1613 N71-20823

Frequency stability of automatic hydrogen maser cavity laser 11 p1776 N71-22779

Development of method for synchronizing clocks at several ground stations based on signals received from spacecraft or satellites (NASA-CASE-XNP-08875) 11 p1730 N71-23099

Prototype atomic hydrogen maser standard for field frequency 13 p2090 N71-25338

Physical basis of atomic frequency standards, and characteristics of hydrogen maser, cesium beam, and rubidium gas cell (NBS-TN-399) 18 p2989 N71-31509

Greenwich time and latitude observations for July to Sept. 1970 19 p3178 N71-31652

Establishment and operation of standard frequency and time signal installation Lyndhurst, Victoria, Australia (REPT-4475) 21 p3407 N71-34244

Bibliographic references to time and frequency publications - July 1955 - Dec. 1970 (NBS-SP-350) 23 p3804 N71-37123

FREQUENCY SYNCHRONIZATION

Characteristics of behavior of triphase induction machine with stator and rotor connected by networks (PUBL-117) 05 p0636 N71-15527

Low frequency time signals for clock synchronization 11 p1707 N71-22915

Geophysical effects on separated clock synchronization using low frequency ground waves 11 p1708 N71-22922

FREQUENCY SYNTHESIZERS

Digitally controlled frequency synthesizer for pulse frequency modulation telemetry systems (NASA-CASE-XGS-02317) 12 p1888 N71-23525

Design, circuitry, and construction of low power high frequency synthesizer (AD-724002) 20 p3239 N71-32906

Broadband model of digitally controlled very high frequency synthesizer for use in aviation navigation receiver (NASA-TN-D-4389) 21 p3395 N71-34164

FREQUENCY TRANSLATION

U FREQUENCY CONVERTERS

FRESNEL DIFFRACTION

Diffraction of Gaussian light beams by circular apertures (AD-713722) 05 p0734 N71-15246

Ammonium sulfate optical constant calculations based on reflectance, transmittance, and Fresnel reflection measurements in infrared region 24 p3969 N71-38310

FRESNEL INTEGRALS

Fresnel integrals for wave diffraction in crystals (AD-717697) 11 p1799 N71-22704

Radiation distribution image analysis and multiple coding techniques including Fourier, Fresnel, and Walsh-Hadamard transformations (TP-972) 20 p3293 N71-33759

Development of method for calculating resonant modes and eigenvalues of laser cavity 23 p3767 N71-36854

FRESNEL REFLECTORS

Sensitive technique uses Fresnel drag effect to determine orientation of spherical rotor spin axis for laser gyroscope application 22 p3591 N71-35575

FRESNEL REGION

Investigating diffraction by plane screen with random transmissivity 07 p1067 N71-17012

Fresnel hypothesis on changes in speed of light traveling through bodies due to motion of bodies (NASA-TT-F-13623) 12 p1965 N71-23386

FRESNEL-KIRCHHOFF INTEGRALS

U FRESNEL INTEGRALS

FRETTING

Fretting and geometric stress concentration effects on fatigue life of aluminum alloy clamped joints (REPT-1112/70) 03 p0386 N71-15265

FRETTING CORROSION

Pretreating corrosion of stainless steel-copper and Zircaloy 2 in water at ambient temperature (RTJNG-70/14) 16 p2610 N71-28450

FRICTION

NT AERODYNAMIC DRAG

NT DRY FRICTION

NT FLOW RESISTANCE

NT FRICTION DRAG

NT INTERNAL FRICTION

NT KINETIC FRICTION

NT SKIN FRICTION

NT SLIDING FRICTION

NT STATIC FRICTION

NT SUPERSONIC DRAG

NT VISCOUS DRAG

Analysis of friction and lubrication in metal working processes 03 p0385 N71-13169

Phenomena taking place in surface layers of metal of engine components during friction (AD-714063) 06 p0941 N71-16305

Friction and wear determination of cobalt-rhenium solid solution alloy in air and in vacuum (NASA-TN-D-6165) 07 p1036 N71-17682

Basic parameter influence on dynamic coefficient of friction thermostatics (AD-714878) 07 p1049 N71-17960

Friction and creep effects in rail transportation (PB-196787) 10 p1568 N71-21786

Heat transfer and flow friction characteristics of compact heat exchanger surfaces with and without brazing roughness (AD-717661) 11 p1768 N71-22396

FRICTION MEASUREMENT

Calculation of frictional hot-spot temperatures and distributions on surfaces of explosives (AD-718006) 12 p1930 N71-24144

Fuel capsule design for in-pile friction tests on solid lubricants at Plum Brook Facility 13 p2115 N71-24550

Designating satisfactorily materials for friction and wear points at elevated temperatures (AD-720367) 14 p2278 N71-25894

Equations for flow rate, load capacity, and friction torque for conical hydrostatic bearings under laminar and turbulent flow conditions (NASA-TN-D-6371) 16 p2600 N71-28046

Electron diffraction analysis of friction surface changes on molybdenum disulfide/lubricated interface (NLL-RISLEY-TRANS-1989-709/59) 16 p2605 N71-29114

Lubrication by boundary, elastohydrodynamic, and fluid films, wear due to fretting, erosion, scaling, and pitting, and friction in aircraft (NASA-TM-X-67872) 18 p2929 N71-31134

Lubrication, friction, and wear processes analyzed for space vehicle design criteria (NASA-SP-8053) 18 p2931 N71-31471

Space environment vacuum simulation of ball bearing with Monte Carlo analysis of friction zone (D-61) 20 p3272 N71-33115

Effect of contact friction on widening and lengthening during force drawing and rolling (AD-727164) 24 p3929 N71-38030

Procedures for calculating wear of experimental friction couplings (AD-727209) 24 p3929 N71-38034

Additive effects on boundary lubricant-metal surface interactions during friction process (AD-727885) 24 p3929 N71-38057

FRICTION COEFFICIENT

U COEFFICIENT OF FRICTION

FRICTION DRAG

NT AERODYNAMIC DRAG

NT SUPERSONIC DRAG

NT VISCOUS DRAG

High order boundary layer effects on zero lift drag of spherical bodies 03 p0361 N71-12589

FRICTION FACTOR

Friction factor of cylinder rotating in high Reynolds number annular flow 10 p1541 N71-21138

Experimental determination of heat transfer and friction in circular tubes with laminar flow of air under conditions of large transverse temperature gradients (AD-715472) 10 p1542 N71-21283

Metal wear inhibition at friction point using selective transfer effect (AD-717527) 11 p1778 N71-22372

Unifying study of thermal and material aspects of friction welding 12 p1930 N71-24048

Self lubricating gears and other mechanical parts having surface adhesion to frictional contact (NASA-CASE-MPS-14971) 13 p2087 N71-24984

Rheological models for evaluating effects of lubricant film thickness and frictional traction 15 p2413 N71-26832

Heat transfer and friction characteristics for turbulent flow in tubes having two dimensional roughness with effect of Prandtl number included 19 p3082 N71-32670

Relationships between heat transfer coefficients and friction factors in tube bundles with axis-parallel turbulent flow at constant heat flux density and average Prandtl numbers (NLL-MIN-TECH-T-6697-1809-951) 24 p4032 N71-38771

FRICTION LOSS COEFFICIENT

U FRICTION FACTOR

FRICTION MEASUREMENT

Friction and wear tests of steels, hard alloys, and polymer materials at low temperatures (AD-712947) 03 p0339 N71-12697

Screening tests on friction and wear of materials in sodium (LMSC-70-10) 03 p0339 N71-12698

Investigating cyclohexane reaction in cold-star plasma and nonlinear friction in servomechanisms 06 p0982 N71-15860

Effect of rate of macromolecular movement on coefficient of progressive friction (AD-714745) 06 p0989 N71-15939

Measurement of pipe friction factors during flow of dilute aqueous polyethylene-oxide solutions (AD-715556) 08 p1181 N71-18743

Baron uliride effect on tungsten friction and wear (AD-718575) 09 p1483 N71-19636

Design and operation of apparatus for analyzing friction and wearing processes of materials at cryogenic temperatures (AD-714972) 10 p1656 N71-21274

Kinetic and static friction force measurement between magnetic tape and magnetic head surfaces (NASA-CASE-XNP-08680) 11 p1766 N71-22995

Wear tests and friction measurements between nuclear fuel elements and spacer grids in air, argon, and sodium
[KFK-1290] 14 p2294 N71-26453

Test apparatus and procedures for measurement of runway friction characteristics on wet, icy, or snow covered runways
[FS-160-45-68-1] 15 p2390 N71-26803

High temperature friction and wear characteristics of self lubricating composite disks of sintered tungsten, molybdenum, and cobalt molybdenum, impregnated with fluoride eutectic
[NASA-TN-D-4363] 16 p2600 N71-28231

Determination of fundamental characteristics of physical processes occurring at contact surface of solid materials in the case of external friction
[NLL-RISLEY-TRANS-1992-9091.9F] 16 p2605 N71-29179

Numerical analysis of oil film thickness required for optimum operation of hydrodynamically lubricated journal bearings
[CRANFIELD-M/P-3] 21 p3433 N71-34429

Friction and wear apparatus incorporating Auger spectroscopic analysis
[NASA-TN-D-4497] 21 p3434 N71-34433

Wear and friction measurements between fuel rod bundles and spacer grids in sodium, air, and argon
[AEC-TR-7224] 21 p3459 N71-34620

Application of inverted torsion pendulum for measurement of internal friction at low frequencies and constant amplitude
[PB-19760] 22 p3584 N71-35523

FRICION PRESSURE DROP

U SKIN FRICTION

FRICION REDUCTION

Development of low friction magnetic recording tape
[NASA-CASE-XGS-00373] 06 p0903 N71-15978

Development of lubricating oils suitable for use with liquid oxidizers
[NASA-CR-103006] 06 p0867 N71-16591

Traction, compaction, and frictional loss predictions of vehicle wheel performance in soft soil
[PB-19760] 10 p1565 N71-21312

Die wall friction reduction in powder metallurgy compaction
[SRO-475-9] 11 p1779 N71-22579

Investigation of antiwear, anticorrosion, and antifretting effectiveness of oils and solid lubricants for various conditions of application
[AD-719775] 13 p2100 N71-24938

Antifretting plastic based on polyamide fibers as fillers for phenolic resins
[AD-719827] 13 p2101 N71-25117

Friction reducing ability of additives for turbulent flowing petroleum based fluid in pipelines
[AD-72282] 16 p2580 N71-28627

Conical hydrostatic bearing optimal dimensions for friction reduction based on laminar and turbulent flow velocity, load capacity, and friction torque calculations
[NASA-TM-X-52946] 16 p2603 N71-28887

Effectiveness of superimposed vibrating forces in reducing die wall friction during powdered metal compaction
[SRO-475-10] 16 p2614 N71-28894

Antifretting graphite-carbide-silicon materials with high wear resistance
[NLL-RISLEY-TRANS-1991-9091.9F] 16 p2605 N71-29179

Preparing composite materials based on silver and synthetic mica - physicochemical and antifretting characteristics
[AD-722819] 18 p2941 N71-31405

Numerical analysis of oil film thickness required for optimum operation of hydrodynamically lubricated journal bearings
[CRANFIELD-M/P-3] 21 p3433 N71-34429

Effect of antiseizing and antiwear additives on wear of highly loaded, small module metric gears
[AD-727414] 24 p3929 N71-38031

FRICIONLESS ENVIRONMENTS

Air bearings for near frictionless transfer of loads from one body to another
[NASA-CASE-XMF-01887] 01 p0659 N71-10617

Platform with several ground effect pads and plenum chambers
[NASA-CASE-MFS-14685] 05 p0774 N71-15689

Development of apparatus for simulating zero gravity conditions
[NASA-CASE-MFS-12750] 06 p0938 N71-16223

FRINGE PATTERNS

U DIFFRACTION PATTERNS

FROGS

Orbiting frog otolith experiment
02 p0165 N71-11829

Cardiac and neural effects of UHF radar energy on frogs
09 p1335 N71-20354

Existence of electric and magnetic field component associated with transmission of neuronal impulse studied in isolated sciatic nerves of frogs
[NASA-CR-110334] 13 p2834 N71-25240

Mechanical response of frog membrane to stimulating frequencies and electrophysiological determined bearing areas
[NASA-CR-123162] 24 p3877 N71-37634

FRONTAL AREAS [METEOROLOGY]

U FRONTS [METEOROLOGY]

FROSTS [METEOROLOGY]

Analysis of synoptic meteorology in Europe with application to theory of fronts and air masses
03 p0402 N71-12575

Numerical analysis of frontal motion in atmosphere
[AD-715068] 07 p1054 N71-17734

Atmospheric model for investigating fronts and predicting frontal rainfall
[MET-0-336] 09 p1414 N71-20553

Development of heavy cumulus clouds formed by forced convection in vicinity of warm fronts in Arctic regions
11 p1791 N71-22845

Synoptic meteorological parameters influencing forest fires in Southeast Asia including cloud cover and precipitation
[AD-721112] 15 p2437 N71-26917

Model of interaction of tropospheric fronts with tropopause based on analysis of 56 vertical sections of high fronts
[NLL-RTS-6362] 17 p2778 N71-29699

Analysis of frontal model using nonlinear differential equations
[AD-726617] 23 p3791 N71-37021

Development of weather forecasting procedures using cubic spline technique applied to two dimensional data fields and mechanics of frontal instability under idealized conditions
[AD-726619] 23 p3791 N71-37022

FROST

Low speed aerodynamic characteristics of airfoil profiles including effects of upper surface roughness simulating hoar frost
[NPL-AERO-1308] 02 p0143 N71-11016

Sorption for cryodeposited frosts of hydrogen
[AD-712373] 02 p0267 N71-11775

Experimental determination of frost heave forces in ground
[AD-711904] 02 p0218 N71-12056

Frost heaving theory
[AD-714641] 06 p0841 N71-15937

Experimental design for soil mechanics under frost conditions for road construction problems
[REF-70-5] 08 p1187 N71-18404

Infrared reflectance of water frosts condensed on liquid nitrogen-cooled surface in vacuum
[AD-715915] 08 p1278 N71-18682

Frost penetration and thawing of soil
[PUBL-387] 12 p1915 N71-24246

Occurrence of frost conditions in North Germany with emphasis on meteorological parameters and seasonal variations
21 p3451 N71-34561

FROUDE NUMBER

Appropriate anemometer heights for Froude scaling of wind stresses
[AD-712709] 03 p0404 N71-13247

Three dimensional surface planing at high Froude number with small angle of attack
[AD-717067] 10 p1544 N71-21600

Nonlinear effects for two dimensional flows past submerged bodies moving at low Froude numbers
[AD-726448] 23 p3743 N71-36690

FROZEN EQUILIBRIUM FLOW

Development of flow property charts for pure nitrogen in quasi-one-dimensional nozzle for equilibrium, nonequilibrium, and frozen flow under hypervelocity conditions
[AD-717704] 11 p1737 N71-22287

Time dependent numerical technique for solving equations governing two dimensional frozen flow about blunt bodies with discontinuous curvature
[AD-717704] 14 p2241 N71-26271

FROZEN FOODS

Freezing and microwave effects on contaminated precooked frozen meal components
[AD-717853] 11 p1683 N71-22253

FUEL CAPSULES

Analytical model for creep of T-111 fuel capsule
[AI-AEC-12943] 03 p0413 N71-12559

Large radioisotope heat source capsule design, fabrication, and materials compatibility and creep tests
[AI-AEC-12968] 03 p0415 N71-12873

Short-time irradiation experiments and expected performance behavior of specimens in R-2 Studsvik reactor
[RT/ENG/70/6] 04 p0545 N71-13564

Determining nuclear core length and selected parameters required for loss-of-fluid test system to have thermal response during coolant loss accident in pressurized water reactor
[ID-1391] 04 p0555 N71-14018

Investigating performance of stainless steel cladding and plutonium-uranium oxide fuel elements in fast breeder reactors
[JGAP-10028-34] 04 p0557 N71-14154

Investigating temperature and pressure characteristics of curium fuel capsules
[ORNL-4597] 05 p0724 N71-15015

High speed photographic experiments within fuel capsule in irradiated fast reactor
[ANL-7578] 12 p1963 N71-23906

Conference on fuel capsule design, irradiation and related reactor technology
[NASA-TM-X-67172] 13 p2110 N71-24506

Irradiation of fatigue specimen capsules in EBR-2 Mark B subassembly
13 p2111 N71-24506

Subjecting fuel capsules and sodium loops to power bursts in reactor safety experiments in Transient Reactor Test Facility
13 p2111 N71-24506

Using xenon for isotopic labeling of instrumental fuel capsules in EBR-2 to detect element failure
13 p2111 N71-24506

Feasibility of instrumented subassembly system for EBR-2 for monitoring instrument readings while reactor is operating
13 p2111 N71-24507

Irradiation subassembly permitting irradiation temperatures above normal EBR-2 temperature
13 p2111 N71-24506

Fuel capsule designed for fission gas release and restrained swelling studies of mixed carbide fuels at varying temperatures
13 p2111 N71-24506

Lithium filled heat pipe for obtaining near isothermal conditions axially along cladding of in-pile fuel-irradiation capsule
13 p2185 N71-24512

Laboratory and reactor tests for establishing specimen temperatures in irradiation experiments by using inert gas-filled heat pipes
13 p2079 N71-24514

Reactor tests of fuel element lifetime and burnup for gas cooled nuclear power reactors
13 p2112 N71-24513

Testing nuclear fuel capsule capable of handling large and varying specimen heat fluxes while maintaining constant temperature using sodium and potassium as working fluids
[UCRL-50510] 13 p2112 N71-24517

Pycnometer, profilometer, and laser puncturing for data on bulk density of swollen and cracked space reactor fuel pellets and capsules
13 p2113 N71-24518

First generation uranium dioxide fuel, magnesium clad, test capsule data
13 p2114 N71-24514

Fuel capsule designs for thermal and fast neutron irradiation of U/Pu/N in MTR/ETR and EBR 2
13 p2114 N71-24514

Retractable replaceable high temperature in-core thermocouple for fuel capsules requiring duct containment
[E-5227] 13 p2080 N71-24544

Design and operation of forced convection capsules for simulating erosion, chemical, and transport effects in fast reactor cavity tests
13 p2115 N71-24546

Lead-tin aluminum capsule for quantitative in-pile study of radiolysis of water to inhibit pressure buildup in Plum Brook Reactor
13 p2115 N71-24547

Fuel capsule design for in-pile friction tests on solid lubricants at Plum Brook Facility
13 p2115 N71-24539

Equipment and procedures for remote occupation of pre-irradiated fuel pins in TREAT capsules
13 p2115 N71-24539

In-pile hydraulic capsule facility for transportation measurements inside capsule
13 p2115 N71-24532

Large radioisotope heat source capsule development for space environment
[AI-AEC-12956] 13 p2117 N71-24535

Specification and procurement of CP-5 cylindrical AI-U fuel tubes
[AI-U-7708] 13 p2120 N71-24530

Impact tests of fuel capsule response to simulated earth impact following reentry from orbit
[SC-DR-70-127] 13 p2123 N71-23522

SNAP 19 RTG power systems development, including heat source capsule
[INSD-2873-44] 14 p2292 N71-25776

In pile and out of pile durability tests and characteristics of 30 kW circulating helium fuel capsules in Plum Brook Reactor
[NASA-TM-X-52676] 16 p2636 N71-28907

Thermodynamic properties of curium fuel rods of uranium and plutonium oxides in pellet and vitreous-compact form for CVRANUM capsules
[RT/ING-70/15] 17 p2780 N71-29223

Chemical and metallurgical analysis of 6Al-4V titanium test specimens exposed to hydrazine/N2O4 liquid propellant
[NASA-CR-121456] 20 p3284 N71-33234

Pu-238 space electric power fuel investigations including fuel capability with capsule materials, radiation effects on fuels, and physical properties of fuels
[LA-4447] 21 p3461 N71-33812

SUBJECT INDEX

Safety analysis of isotope heat source capsule design (ORNL-TM-3230) 22 p3623 N71-35811
Neutron radiographs used to determine dimensional changes of heat transfer gaps in cylindrical nuclear fueled capsules (NASA-TM-X-67920) 22 p3695 N71-36350
Fabrication and testing of photoluminescence quench-down capsule prototype (JA-6996) 23 p3800 N71-37096
Capsule rig for irradiation of structural materials in SM-2 reactor with temperature control by variation of gas-gap size (LBNL-3013) 24 p3937 N71-38229

FUEL CELLS
NT BIOCHEMICAL FUEL CELLS
NT HYDROGEN OXYGEN FUEL CELLS
NT REGENERATIVE FUEL CELLS
Research progress on nuclear, thick film, and electrochemical sources for spacecraft power supplies (01 p0005 N71-10258)
Electrochemical reactions of organic compounds in aqueous solutions (AD-71353) 02 p0149 N71-11054
Benzoin cell diffusion coefficient corrections for CAGIR-type lattices (RD/N-1645) 02 p0270 N71-11412
X-ray diffraction analysis of matrices of hydrogen-oxygen electrolytic regenerative fuel cells (NASA-CR-1683) 03 p0316 N71-12253
Capillary material and fuel cell development study (NASA-CR-106757) 03 p0318 N71-12272
Weight reduction and configuration of fuel cell (NASA-CR-106758) 03 p0318 N71-12273
Open cycle hydrocarbon-air fuel cell power plant (AD-713528) 05 p0631 N71-14607
Nickel catalysts for hydrazine fuel cells 07 p0974 N71-17195
Dynamic model for gas phase concentrations in gas fuel cell electrodes (NASA-TN-D-6148) 07 p0975 N71-17467
Metal oxide catalysts for air-oxygen electrodes in electrochemical fuel cells and zinc oxygen batteries (AD-715707) 08 p1146 N71-18463
Operation method for combined electrolysis device and fuel cell using molten salt to produce power by thermoelectric regeneration mechanism (NASA-CASE-XL8-01645) 10 p1495 N71-20904
Electrode sealing and insulation for fuel cells containing caustic liquid electrolytes using powdered plastic and metal (NASA-CASE-XMS-01625) 11 p1772 N71-23022
Measurements of diffusion coefficients and vapor pressure in LiOH solutions for determination of gas solubilities in fuel cell electrolytes (NASA-CR-117906) 12 p1859 N71-23345
Conference on fuel cells and batteries (AD-718033) 12 p1859 N71-23353
Oxygen dissolution reaction in fuel cells and properties of metal electrodes (NASA-CR-118652) 14 p2202 N71-26289
Development of anisotropic porous media model for studying effects of fluid motion in fuel cell cavities (JPL-2409) 16 p2581 N71-28719
Development and characteristics of ion-exchange membranes and electrode assembly for fuel cells or electrolysis cells (NASA-CASE-XMS-02063) 16 p2541 N71-29044
Models for permitting continuous purging of impurities from gas compartments of fuel cell 17 p2706 N71-29604
Design and operation of self-contained, portable, hydrogen-air fuel cell power unit (AD-723468) 19 p3040 N71-31767
Gas solubilities and transport properties in fuel cell electrolytes (NASA-CR-121432) 20 p3215 N71-33826
Fuel cell electrolyte studies on vapor pressures of binary systems, partial molar volumes of dissolved gases, and diffusion coefficients of gases (NASA-CR-121628) 21 p3378 N71-34834
Design, development, and characteristics of fuel cell electrolysis cell with carbon anode (JPL-2409) 23 p3773 N71-36891
Characteristics and application of high temperature fuel cells as power sources (AD-727497) 24 p3875 N71-37624

FUEL COMBUSTION
Swirl-can modular turbojet combustor burning atomized gas fuel (NASA-TN-D-7020) 03 p0448 N71-12421
Flame length and laminar fuel jet combustion (NASA-TT-F-13459) 07 p1130 N71-17570
Flame spread over surface of solid-fuel bed in oxygen-rich environment 18 p3026 N71-31428
Developmental program for SO₂, NO, and particularly pollutant level lowering and control in flow gas fuel combustion using fluidized beds with leaner (ANL-RES-CEN-1003) 23 p3750 N71-36736
Combustion characteristics of gas turbine aircraft engines (AD-727175) 23 p3841 N71-37587

FUEL COMBUSTION

Large angle, three dimensional orientation of asymmetric spacecraft in fuel optimal manner (AD-710788) 01 p0136 N71-10750
Theory and calculation of thermal rocket engines including liquid and solid fuels, specific impulse, combustion products, and related subjects (AD-713044) 03 p0449 N71-15073
Determining burnup characteristics of fuel elements for Halden Boiling Heavy Water Reactor (NPL-1161) 04 p0559 N71-14317
Fuel consumption and propulsive and thermodynamic efficiency comparisons for ships, hydrofoil craft, helicopters, jet aircraft, and ground effect machines (NPL-HOVERCRAFT-12) 07 p0970 N71-17161
Measuring U-235 depletion as function of Pu content in spent fuels of power reactors (BNWL-34-3304) 08 p1237 N71-18258
Discussing monitors for determining burnup rate of enriched uranium 235 fuel in fast neutron environment (NASA-TM-X-2133) 08 p1259 N71-18496
Examining fuel cycle codes using different techniques for fuel cost calculations (BNWL-34-3605) 10 p1602 N71-21090
Highlights of project activities for November 1970 including fuels, components, and physics for LMFBR (ANL-7738) 10 p1603 N71-21186
Kalman linear least squares filtering applied to estimation of fuel quantity and rate for fighter aircraft (AD-717640) 11 p1672 N71-21922
Engineering description of TACS-SM RCS consumables program - Skylab Program (NASA-CR-115114) 19 p3183 N71-31604
Destructive and nondestructive tests on nuclear fuel burnup (BNIS-MF-29) 19 p3136 N71-32041

FUEL CONTAMINATION
Spectrophotometric sulfate determination in solid rocket propellants and nitrocellulose (AD-711804) 02 p0287 N71-11850
Development of radiotracer method for detecting contribution of selected components to storage instability of jet engine fuels (BBR-17495) 09 p1456 N71-20505

FUEL CONTROL
Development and characteristics of propellant gauging system for spacecraft 03 p0447 N71-13114
Surface tension and dielectrophoretic techniques for liquid rocket propellant control 03 p0447 N71-13119
Flexible ring slosh damping baffle for spacecraft fuel tank (NASA-CASE-LAR-10317-1) 06 p0954 N71-16103
Submerged fuel tank baffles to prevent sloshing in liquid propellant rocket flight (NASA-CASE-XLA-0460-1) 06 p0954 N71-16106
Summary report on HFGR fuel cycle development (ORNL-TM-3204) 07 p1063 N71-17362
Gas cooled reactor fuel management calculations (AEEW-R-452) 07 p1064 N71-17501
Control valve and coaxial variable injector for controlling bipropellant mixture ratio and flow (NASA-CASE-XNP-07902) 07 p1036 N71-17654
Space vehicle or rocket time and fuel stochastic optimal control problems with measurement uncertainties 07 p1121 N71-17781
Force balanced throttle valve for fuel control in rocket engines (NASA-CASE-NPO-10080) 15 p2416 N71-27432
Low gravity propellant control, using capillary devices in large scale cryogenic vehicles 17 p2831 N71-29611
Effect of buoyancy on fuel containment in open-cycle gas-core nuclear rocket engine (NASA-TM-X-67924) 22 p3620 N71-35794

FUEL CORROSION
Microbiological fuel corrosion by bacteria and fungi in fuel tanks (AD-712033) 02 p0287 N71-11448

FUEL ECONOMY
U FUEL CONSUMPTION
U ELEMENTS (NUCLEAR REACTORS)
U NUCLEAR FUEL ELEMENTS
FUEL FLOW
NT PROPELLANT TRANSFER
Conductivity cell instrumentation for measuring flow induced vibration in fuel pins (WHAN-PR-21) 10 p1603 N71-21185
Air flow velocity, altitude, fuel-air ratio, fuel flow velocity, and pressure effects on fuel temperature before and after vaporization in rocket engines (NASA-TT-F-13665) 12 p1869 N71-24053
Nonresonant noise of flames from co-flowing jets of fuel and oxidizer and flames from impinging jets of fuel and oxidizer 17 p2767 N71-29702
Simulated-fuel containment characteristics in heated and unheated vortex flows for nuclear light bulb engines 20 p3305 N71-33634

FUEL SYSTEMS

Effect of inlet conditions on flow and containment characteristics of coaxial flows for gas core nuclear rockets 20 p3305 N71-33636
Interfacial stability at thin flexible partition between fuel and propellant flows for gas core nuclear rockets 20 p3304 N71-33639
Operating characteristics and performance predictions for gas-core nuclear rocket with fuel separation by MHD-driven rotation 20 p3304 N71-33641

FUEL FLOW REGULATORS
Water electrolysis fuel engine with self-regulating stoichiometric fuel mixing regulator (NASA-CASE-XGS-06729) 04 p0603 N71-14044

FUEL GAGES
NT CAPACITIVE FUEL GAGES
Radiolabel fuel gage for spacecraft liquid propellants (IS-22151-1) 13 p2078 N71-24404
Response analyzing apparatus for liquid vapor interface sensor of sloshing rocket propellant (NASA-CASE-MF-11204) 16 p2599 N71-29134

FUEL INJECTION
Comprehensive analysis of liquid rocket combustion (AD-710634) 01 p0133 N71-10437
Interacting vortices effects on jet penetration into supersonic streams (NASA-TM-X-2134) 02 p0282 N71-11521
Vehicle-scale analysis of fluorine-hydrogen main tank injection preatomization system (NASA-CR-72736) 03 p0457 N71-13100
Propellant injection assembly having individually removable and replaceable nozzles for liquid fueled rocket engines (NASA-CASE-XMF-00968) 05 p0763 N71-15640
Orifice flow and discharge coefficient of liquid propellant rocket engine fuel injectors (DLR-FB-70-38) 06 p0939 N71-15034
Gas dynamics of fan jets at various injection angles (AD-714798) 07 p1104 N71-18034
Supersonic combustion, fuel injection, and recirculation in hydrogen hypersonic external combustion at flat plates and bodies of revolution (DLR-FB-70-64) 11 p1840 N71-23229
Simulation of water injection in liquid propellant rocket engines, nozzle injector arrangement (DLR-MITT-70-24) 13 p2155 N71-24673
Gas-air mixture requirements for turbine and injection burner combustion efficiencies (AD-719834) 13 p2187 N71-25359
Combustor pressure poppings, stream mixing, and stream separation associated with combustion of impinging hypersonic propellants (NASA-CR-1704) 15 p2523 N71-26869
Influences of vortex rocket engine injector design on water flow distribution for future hypersonic propellant injection performance (RPE-TR-70-6) 20 p3338 N71-33147
Modifying air intake and fuel injection parameters to reduce diesel engine nitrogen oxide emissions (BBR-17-7579) 23 p3841 N71-37586

FUEL OILS
Manual on application of fuels and lubricating materials (AD-711756) 01 p0600 N71-10862
Using neutron activation analysis for quantitative measurement of trace elements in crude and residual fuels (GA-9889) 05 p0739 N71-15083
Qualitative selection of combustion additives for fuel oil efficiency (NLL-CE-TRANS-5408/1982.09) 10 p1638 N71-21836
Extractive phenols from coal as antioxidant additive for motor fuels (AD-727438) 24 p3999 N71-28528

FUEL PUMPS
Variable displacement fuel pump for internal combustion engines (NASA-CASE-MBC-12130-1) 04 p0606 N71-14058
Design and development of canned-motor pump for high temperature NaK service in SNAP-8 (NASA-CR-72823) 13 p2116 N71-24834

FUEL SYSTEMS
NT AIRCRAFT FUEL SYSTEMS
Manual on application of fuels and lubricating materials (AD-711756) 01 p0600 N71-10862
Tests of automatic topping of LOX system for Europa P9 vehicle (TN-DWD-27) 02 p0181 N71-11272
Investigating system for transferring failed fuel from primary tank to argon cell of EBR-2 facility (ANL/BBR-804) 04 p0544 N71-13605
Fabrication of prototype Mark 2 fuel subassembly (BNWL-1418) 05 p0726 N71-15866
Selection of command models and service models explosion blunder repositioning problems (NASA-CR-114813) 06 p0601 N71-14881
Perturbation theory for fuel space trajectory optimization (NASA-CR-114838) 07 p1110 N71-17564

FUEL TANK PRESSURIZATION

- Procedures for evaluating effectiveness of self propelled and portable ground servicing units for Army aircraft
[AD-719102] 13 p2025 N71-24459
- Evaluation of fuel flowmeter instrumentation conducted during flight tests
[AD-719280] 13 p2079 N71-24479
- Internal labyrinth and shield structure to improve electrical isolation of propellant feed source from ion thruster
[NASA-CASE-LEW-10210-1] 14 p2333 N71-26781
- Burnup calculations of fission products used for studying reactor poisoning applied to fuel cycle studies in thermal reactors
[JUL-678-RO] 13 p2469 N71-27358
- Design parameters and characteristics of turbopump propellant feed systems
17 p2829 N71-29411
- Design parameters and characteristics of valves used in liquid propellant rocket engine fuel systems
17 p2833 N71-29412
- Use of air-assist fuel nozzle to reduce exhaust emissions from gas turbine combustor at simulated idle conditions - J-57 engine
[NASA-TN-D-6404] 18 p3002 N71-31456
- Design criteria for crashworthy aircraft fuel systems for military aircraft
[AD-723968] 20 p3209 N71-32992
- ## FUEL TANK PRESSURIZATION
- Vehicle-scale analysis of fluorine-hydrogen main tank injection pressurization system
[NASA-CR-72756] 03 p0457 N71-13100
- Pressurization gas flow effects on liquid interface instability
03 p0447 N71-13111
- Analysis of factors affecting fuel tank pressurization
03 p0447 N71-13112
- Physical, metallurgical, chemical, and thermodynamic surveys of high pressure tanks and plumbing systems of Apollo spacecraft
[NASA-TM-X-64919] 09 p1471 N71-19966
- Hybrid electronic controller developed for pressurization and venting systems of space propulsion system
[NASA-CR-72748] 11 p1762 N71-22155
- Automatically reciprocating, high pressure pump for use in spacecraft cryogenic propellant tanks
[NASA-CASE-XNP-04731] 12 p1929 N71-24042
- Method and apparatus for pressurizing propellant tanks used in propulsion motor feed system
[NASA-CASE-XNP-00650] 16 p2670 N71-28929
- Analysis of recirculating type external pressurization systems for use in pressure control of cryogenic hydrogens, oxygen, and nitrogen storage systems
[NASA-CR-115205] 24 p3999 N71-38527
- ## FUEL TANKS
- Theory for low gravity fuel sloshing in arbitrary axisymmetric rigid tank
01 p0041 N71-10325
- Drop and impact tests for improving crashworthiness of integral fuel tanks
[FAA-NA-70-46] 02 p0144 N71-11019
- Characteristics of thermally resistant polymers for fuel tank sealants
[NASA-CR-102951] 04 p0534 N71-14054
- Effects of thermal shock on plastic materials used for fuel tank insulation
[REPT-69-09592] 04 p0534 N71-14072
- Flexible ring shock damping baffle for spacecraft fuel tank
[NASA-CASE-LAR-10317-1] 06 p0954 N71-16103
- Submerged fuel tank baffles to prevent sloshing in liquid propellant rocket flight
[NASA-CASE-XLA-04605] 06 p0954 N71-16106
- Mathematical models for external insulation systems of cryogenic fuel storage tanks
[NASA-CR-114827] 06 p0881 N71-16600
- Thermodynamic properties of insulated liquid methane fuelage tanks for supersonic cruise aircraft
[NASA-TN-D-6157] 07 p1102 N71-17506
- Susceptibility of polyurethane foam to deterioration by impurities or contaminants in ethylene glycol monomethyl ether
[AD-715313] 07 p0997 N71-17755
- Design of thermal control system for cryogenic fluid storage tanks
[NASA-CR-116426] 07 p1121 N71-17918
- Fuel tank vapor space characteristics for simulated helicopter fuel tank and evaluation of existing potential hazard from vibration environment
[AD-675981] 10 p1660 N71-26702
- Self evacuating multilayer insulation system of aluminum Mylar and polyurethane foam for liquid hydrogen tanks
[NASA-CR-72856] 13 p2102 N71-25447
- Hypervelocity impact tests to predict meteoritic damage on proposed lunar tug fuel tank configuration
[NASA-TM-X-64597] 14 p2343 N71-26040
- Pressure sensor network for measuring liquid dynamic response in flight including fuel tank acceleration, liquid slosh amplitude, and fuel depth monitoring
[NASA-CASE-XLA-05541] 14 p2242 N71-26387

- Electrical failure detector in solid rocket propellant motor insulation against thermal degradation by fuel grain
[NASA-CASE-XMF-03968] 15 p2408 N71-27186
- Design, development, and flight testing of fire suppressant void filler foam kits for lower hemisphere of fuel tanks in various tactical army aircraft
[AD-719711] 15 p2348 N71-27679
- Effectiveness of nitrogen inerting of aircraft fuel tanks under conditions of fuel sloshing
[AD-721675] 16 p2670 N71-28576
- Electron microscope, electron diffraction, and electron microprobe analysis of defective solid state weldment on liquid hydrogen tank from Apollo 12 fuel cell system
[NASA-TN-D-63227] 18 p2937 N71-31354
- Bibliography on fuel- and propellant-tanks
[AD-723920] 19 p1172 N71-32074
- Demonstration and evaluation of crash-resistant bladder fuel tank system in full-scale aircraft wing assembly
[FAA-NA-71-34] 19 p3037 N71-32077
- Determination and evaluation of safety parameters of jet fuels in aircraft fuel tanks when using nitrogen as inerting agent
[FAA-NA-71-26] 19 p3038 N71-32305
- Evaluation of lightning hazards to jet aircraft including possibility of fuel tank explosions
[AD-724092] 20 p3209 N71-33006
- Thermally resistant polymers for fuel tank sealants of advanced high speed aircraft
[NASA-CR-119940] 22 p3587 N71-35546
- ## FUEL TESTS
- ### NT REACTOR STARTUP TESTS
- Radial velocity distribution effects on fuel exposure in circulating fuel reactor
[LA-4294] 01 p0085 N71-10419
- Nuclear magnetic resonance method of determining aromaticity of hydrocarbon fuels
[AD-711852] 02 p0288 N71-11890
- Burnup data from irradiated UO₂-PuO₂ fuel
[BNWL-1488] 04 p0558 N71-14167
- Nuclear fuel behavior during irradiation by fission gas release
[ORNL-4601] 05 p0723 N71-14674
- Fuel reprocessing and head-end treatment of experimental small scale HTGR fuel elements
[GAMD-9260-PT-2] 08 p1237 N71-18293
- Conversion of experimental turbojet combustor from ASTM A-1 fuel to natural gas fuel
[NASA-TM-X-2241] 09 p1486 N71-20533
- Thermal test reactor facility for conducting fuel tests in flowing sodium capsules
13 p2114 N71-24545
- Radiation testing of sodium-bonded, fast reactor Pu-UC fuel rods at high burnup in thermal reactors
13 p2115 N71-24549
- Fuel tests to determine feasibility of gelled methane for use in jet engine
[NASA-CR-72876] 14 p2331 N71-25772
- Fuel rod failure experiment in TREAT facility using Zircaloy clad UO₂ fuel rods in flowing steam atmosphere
[ORNL-4635] 16 p2631 N71-28194
- Metallographic preparation of LMFBR prototype fuels
[WHAN-SA-14] 16 p2632 N71-28640
- Boiling water reactor fuel test assembly irradiation
[HPR-132] 16 p2633 N71-28697
- Uranium carbonitrides as high efficiency fuel - preparation and irradiation properties
[JUL-703-RU] 18 p2959 N71-30528
- ## FUEL VALVES
- Results of bipropellant valve program with applications to earth storable propellants
[NASA-CR-111407] 02 p0290 N71-11885
- Apollo service propulsion system bipropellant valve with cam lifted seals
[NASA-CR-114790] 03 p0692 N71-14931
- Semitoroidal diaphragm cavitating flow control valve
[NASA-CASE-XNP-09704] 06 p1179 N71-18615
- Filler valve design for supplying liquid propellants at high pressure to space vehicles
[NASA-CASE-XNP-01747] 11 p1773 N71-23024
- Fabrication and acceptance testing, fluorine compatibility testing, valve refurbishment and testing, environmental testing, and design of space storable oxidizer valve
[NASA-CR-72690] 13 p2087 N71-25456
- Design parameters and characteristics of valves used in liquid propellant rocket engine fuel systems
17 p2833 N71-29412
- Design criteria for flight type gaseous hydrogen gaseous oxygen propellant shutoff valves for space shuttle APS
17 p2830 N71-29592
- Design and fabrication of hydrogen oxygen propellant shutoff valves for space shuttle APS thrusters
17 p2831 N71-29593
- Rocket engine bipropellant valve improvement for Apollo service propulsion system
[NASA-CR-108577] 17 p2758 N71-30397

SUBJECT INDEX

- Apollo service propulsion system rocket engine bipropellant valve improvement program - valve design guide and oxygen-hydrogen technology
[NASA-CR-108578] 21 p3302 N71-34046
- ## FUEL-AIR RATIO
- Gas-air mixture requirements for turbine and injection burner combustion efficiencies
[AD-719834] 13 p2187 N71-25319
- Gaseous fission measurements from jet engine afterburners over range of fuel-air ratios
[NASA-TM-X-2323] 17 p2859 N71-30117
- ## FUELING
- ### U REFUELING
- ## FUELS
- ### NT AEROZINE
- ### NT AIRCRAFT FUELS
- ### NT CERAMIC NUCLEAR FUELS
- ### NT CHEMICAL FUELS
- ### NT CRYOGENIC ROCKET PROPELLANTS
- ### NT DOUBLE BASE ROCKET PROPELLANTS
- ### NT FUEL OILS
- ### NT GASOLINE
- ### NT GELLED ROCKET PROPELLANTS
- ### NT HYDROCARBON FUELS
- ### NT HYDROGEN FUELS
- ### NT HYPERGOLIC ROCKET PROPELLANTS
- ### NT JET ENGINE FUELS
- ### NT JP-5 JET FUEL
- ### NT LIQUID ROCKET PROPELLANTS
- ### NT METAL FUELS
- ### NT METAL PROPELLANTS
- ### NT MONOPROPELLANTS
- ### NT NUCLEAR FUELS
- ### NT SLURRY PROPELLANTS
- ### NT SOLID ROCKET PROPELLANTS
- Gas flow during and after deflagration of spherical cloud of fuel-air mixture
[AD-716339] 09 p1370 N71-19355
- Senate hearings on establishment of Commission on Fuels and Energy
17 p2862 N71-30145
- Pa-238 space electric power fuel investigations including fuel capability with capsule materials, radiation effects on fuels, and physical properties of fuels
[LA-4647] 21 p3461 N71-34632
- Statistical analysis of world reserves of solid fuel, crude oil, uranium, and natural gas in year 2000
[NLL-TRANS-1166-19022.9] 22 p3580 N71-35380
- Emission spectral methods for determining content of mineral admixtures in fuels, oils, and lubricants
[AD-727197] 24 p3886 N71-37699
- ## FULL SCALE FATIGUE TESTS
- ### U FATIGUE TESTS
- ### U FULL SCALE TESTS
- ## FULL SCALE TESTS
- Space environmental simulation data for spacecraft reliability and test planning
03 p0355 N71-12793
- Full scale tests on tilted propeller and tilting rotor models in transonic wind tunnel of Modane-Aviation, France, for aircraft performance prediction
[ONERA-NT-16-10] 19 p3073 N71-31813
- ## FUNCTION GENERATORS
- High accuracy sine function generator using digital to analog converters and field effect transistors
02 p0185 N71-11102
- Nonlinear logarithmic amplifiers as function generators and logarithmic multipliers for nonlinear differential equations
03 p0353 N71-12530
- Table-lookup/interpolation fast function generator with small fixed point digital computers
[NASA-CR-118010] 12 p1803 N71-23865
- Mechanical function generators with potentiometers as sensing element
[NASA-CASE-XAC-00001] 16 p2604 N71-28932
- Modular type MOD-2 sequential function generator for multi-bit binary sequence
[NASA-CASE-NPO-10636] 20 p3292 N71-33400
- ## FUNCTION SPACE
- ### NT BANACH SPACE
- ### NT HILBERT SPACE
- Solvability of differential equations in spaces gamma to delta power/Omega
[AD-710428] 01 p0076 N71-10780
- Möbius plane ordering functions and algebraic groups
04 p0539 N71-14504
- Group representation in space of differentiating functions
[KPKI-70-16-HEPI] 06 p2224 N71-18279
- Massive particle scattering amplitude kinematics in four-momenta space
09 p1430 N71-19706
- Fredholm transformations and Radon-Nikodym derivatives for evaluation of Yeh-Wiener integrals of exponential functions
[AD-718425] 12 p1948 N71-23508
- Functional subgroup space representations of quaternion group
[IFVE-STF-69-102] 15 p2457 N71-24606

SUBJECT INDEX

Solution to equations in function space relating linear operators defined in subspace of Banach space and linear or nonlinear operator
 [NASA-CR-119067] 16 p2621 N71-28152

Sign-value approximation method for non-self-adjoint operators using Galerkin method for estimating eigenvalue perturbations of self-adjoint operators
 [NASA-CR-119027] 16 p2623 N71-28548

Invariance of space rotation group
 [ITEF-762] 22 p3632 N71-35884

Conference on analytical functions and topology of algebraic spaces
 24 p3947 N71-38159

Pincheson theorems on convex and concave spaces for holomorphic transformations
 24 p3948 N71-38160

Approximation theorem of Grauert for holomorphic functions
 24 p3948 N71-38161

Holomorphic fibers in sub-spaces of Stein spaces
 24 p3948 N71-38164

Coherence of holomorphic mappings
 24 p3948 N71-38165

Homology theory for analytical spaces
 24 p3948 N71-38166

Null hypothesis for Banach case
 24 p3949 N71-38169

Complex analytical structures of Hilbert space varieties
 24 p3949 N71-38170

Set theory of real analytic spaces
 24 p3949 N71-38171

Complex spaces as Stein spaces
 24 p3949 N71-38172

Topological depth of coherent analytical bundle in Stein space
 24 p3949 N71-38173

FUNCTION TESTS
 U TESTS
FUNCTIONAL ANALYSIS
 NT BANACH SPACE
 NT CONVOLUTION INTEGRALS
 NT FOURIER TRANSFORMATION
 NT FREDHOLM EQUATIONS
 NT HARMONIC ANALYSIS
 NT HILBERT SPACE
 NT HILBERT TRANSFORMATION
 NT INTEGRAL EQUATIONS
 NT INTEGRAL TRANSFORMATIONS
 NT LAPLACE TRANSFORMATION
 NT SINGULAR INTEGRAL EQUATIONS
 NT TESSERACT HARMONICS
 NT VOLterra EQUATIONS
 NT WIENER HOPF EQUATIONS
 NT ZONAL HARMONICS

Tables of uranium thorium lead isotopic decay and growth functions for radioactive age determinations
 01 p0093 N71-10306

Methods for detecting turbulent/non-turbulent interfaces
 [AD-712375] 02 p0204 N71-11973

Functional analysis of landing gear systems
 [ASD-TR-69-113] 03 p0313 N71-12231

Integral vectorial equation for calculating current distribution on antenna
 04 p0491 N71-13707

Computation of low frequency radio transmitter field strength for underwater communications
 04 p0492 N71-13711

Electromyographic measurements on muscle reactions during physical work
 04 p0476 N71-13866

Research on data and analytical systems for preparing national water assessments
 [PB-192118] 05 p0666 N71-14692

Advanced software techniques for space shuttle data management system
 [NASA-CR-114802] 05 p0651 N71-15426

Functional analysis of graphic computer
 [D-1-76-01] 07 p0996 N71-17090

Flight simulator tests of human behavior in roll tracking tasks in fighter and large aircraft with descriptive functional analysis
 [NAL-TR-206] 09 p1359 N71-19751

Scheduling N tasks on two processors when each task consists of three operations
 [STAN-CS-76-165-APP-2] 10 p1593 N71-21810

Non-linear and functional analysis including convex sets, algorithms, polynomials, and boundary value problems - application to aerospace systems
 [AD-717874] 12 p1948 N71-23224

Functional analysis on stability of distributed inverse current electrical networks having nonlinear elements
 12 p1893 N71-24029

Formal solutions of first order functional equations
 [TR-71-110] 13 p1203 N71-24935

Properties of solutions for stochastic differential equations
 [TR-71-12] 14 p2285 N71-24675

Volterra equation for describing tracer dynamics of mammalian circulation
 16 p2548 N71-28855

Nonlinear system characterization and analysis of Gaussian processes
 [UCRL-75960] 17 p2771 N71-29248

Solving functional differential equations for local current algebras
 [NYO-2171-326] 17 p2772 N71-29330

Intermolecular potential energy calculations for thermal elastic scattering of gases and comparison of Lennard-Jones and Morse potential functions
 17 p2795 N71-29750

Angle ellipsometric functions of imaging optical systems
 20 p3311 N71-33384

Operational functions and electrical properties of metal oxide semiconductor structures
 [REPT-1-028] 20 p3335 N71-33848

Functional analysis of error estimates between B sub [N] and B sub H approximation
 [IA-1232] 21 p3471 N71-34712

Functional analysis of pilot warning instruments and pilot relationships during collision situations
 [FAA-ED-71-59] 22 p3540 N71-35216

Functional equations for solving boundary value problems including Dirichlet problem, Green function, harmonic functions, and isopotential functions
 [NASA-TT-F-459] 22 p3487 N71-35487

FUNCTIONAL INTEGRATION
 Piecewise linear and step approximating converter for producing functional quanta through elementary quanta
 11 p1715 N71-22044

Functional integration and Regge-singular representation of high energy particle scattering amplitudes
 [JNPR-P2-5768] 23 p3807 N71-37144

FUNCTIONS (MATHEMATICS)
 NT ABEL FUNCTION
 NT ANALYTIC FUNCTIONS
 NT ASYMPTOTES
 NT BANACH FUNCTIONS
 NT COMPOSITE FUNCTIONS
 NT CONFORMAL MAPPING
 NT COORDINATE TRANSFORMATIONS
 NT DELTA FUNCTION
 NT DISCRETE FUNCTIONS
 NT DISTRIBUTION FUNCTIONS
 NT ELLIPTIC FUNCTIONS
 NT ENTIRE FUNCTIONS
 NT ERROR FUNCTIONS
 NT EXPONENTIAL FUNCTIONS
 NT FOURIER TRANSFORMATION
 NT FOURIER-BESSEL TRANSFORMATIONS
 NT FRESNEL INTEGRALS
 NT GAMMA FUNCTION
 NT GREEN FUNCTION
 NT HAMILTONIAN FUNCTIONS
 NT HARMONIC FUNCTIONS
 NT HYPERBOLIC FUNCTIONS
 NT KERNEL FUNCTIONS
 NT LAUERRE FUNCTIONS
 NT LAPLACE TRANSFORMATION
 NT LEGENDRE FUNCTIONS
 NT LAPUNOV FUNCTIONS
 NT LINEAR TRANSFORMATIONS
 NT LOGARITHMS
 NT LORENTZ TRANSFORMATIONS
 NT MATHEU FUNCTION
 NT MAXWELL-BOLTZMANN FUNCTION
 NT MEROMORPHIC FUNCTIONS
 NT MONOTONE FUNCTIONS
 NT NORMAL DENSITY FUNCTIONS
 NT ORTHOGONAL FUNCTIONS
 NT PEARSON DISTRIBUTIONS
 NT PERIODIC FUNCTIONS
 NT POISSON DENSITY FUNCTIONS
 NT PROBABILITY DENSITY FUNCTIONS
 NT PROBABILITY DISTRIBUTION FUNCTIONS
 NT RATIONAL FUNCTIONS
 NT RECURSIVE FUNCTIONS
 NT SPACE-TIME FUNCTIONS
 NT SPHERICAL FUNCTIONS
 NT SYLVESTER FUNCTIONS
 NT STEP FUNCTIONS
 NT STRESS FUNCTIONS
 NT TANGENTS
 NT TIME FUNCTIONS
 NT TRIGONOMETRIC FUNCTIONS
 NT WALSH FUNCTION
 NT WEIBULL DENSITY FUNCTIONS
 NT WEIGHTING FUNCTIONS

Improving computations in DTP method for function minimization using doubly relaxed generalized inverse of matrix
 [NASA-CR-111129] 01 p0075 N71-10339

Fractional iteration of functions of several variables
 02 p0252 N71-11937

Recursion formula for logarithmic derivatives of spherical Bessel functions in complex plane
 [ESSEA-TR-ERL-11-ITS-99] 02 p0252 N71-11938

Limitations of formal mathematical systems
 02 p0252 N71-12077

Method for approximating certain functions with application to critical phenomena
 [AD-712972] 03 p0400 N71-13240

FURNACES

Polarization functions of fluorescence from polarized and unpolarized light
 04 p0588 N71-14385

Class on nonlinear functions and convergence of Gauss-Seidel and Newton-Gauss-Seidel iterations
 [NASA-CR-116129] 06 p0844 N71-16007

Analysis of n-dimensional nonlinear mappings representative of P and S functions
 [NASA-CR-116133] 06 p0844 N71-16008

Problems of bounding sum rules and interpolation between them
 [NASA-CR-116138] 06 p0844 N71-16036

Proof of increasing functions on finite distributive lattice are positively correlated measures satisfying suitable coarsely
 [LFTRE-71-2] 10 p1593 N71-21533

A, a and B functions for electron broadening of positive ions with hyperbolic path
 [NASA-TM-X-67040] 11 p1801 N71-31983

Geometric properties of nonbinary switching functions which are direct generalization of Boolean functions of binary logic
 11 p1729 N71-22671

Numerical results for Sobolev Q function of radiative transfer using invariant imbedding
 [TR-70-57] 14 p2844 N71-26156

Derivation of minimum test sets for union function logic circuit failure analysis and component reliability
 [AD-720350] 15 p2389 N71-27288

Mathematical models for investigating vortex functions in current algebra
 15 p2491 N71-27913

Implication of Hough function thermospheric degradation on latitudinal tidal mode structure and vertical wave propagation
 [NASA-TM-X-45675] 20 p3266 N71-33442

Computer program for function optimization on line systems by golden section
 [UCID-30862] 21 p3447 N71-34335

Computational work and computational delay required by machines to compute functions
 [NASA-CR-121930] 22 p3487 N71-35688

FUNGI
 NT MICROSPORES
 NT RHIZOPUS
 NT SPORES
 NT YEAST

Microbiological fuel corrosion by bacteria and fungi in fuel tanks
 [AD-712163] 02 p0287 N71-11848

Corrosion prevention by fungus-proofing - bibliography
 [AD-720302] 14 p2207 N71-26638

Systems analysis and cost estimates of satellite borne remote sensing for wheat crop and fungus disease control and water management
 [NASA-CR-119011] 16 p2587 N71-28445

Mathematical models for application of satellite borne multispectral remote sensors to water and wheat production management and wheat fungi control including cost estimates
 [NASA-CR-119012] 16 p2586 N71-28446

Effect of wood-destroying fungi on destruction of hydrolytic lignin
 [AD-713924] 20 p3286 N71-32942

FUNGICIDES
 NT URIC ACID

FURAN RESINS
 NT POLYAMIDE RESINS

Mechanism of iron dissolution and corrosion inhibition by galvanostatic polarization and electrical double layer capacitance measurement
 02 p0174 N71-11227

FURABLE ANTENNAS
 Polymer adhesives, optical solar cell filter, and furable antenna construction for lithotripsy spacecraft
 10 p1589 N71-21349

Thermoelectric boom actuator and furable antenna for Thermoelectric Outer Planet Spacecraft
 10 p1586 N71-21352

Development and characteristics of extensible dipole antenna using deformable tubular metallic strip element
 [NASA-CASE-HQN-00937] 16 p2563 N71-28979

FURNACES
 NT SOLAR FURNACES
 NT VACUUM FURNACES

Development of black-body source calibration furnace
 [NASA-CASE-XLE-01399] 05 p0785 N71-15625

Construction of two black body furnaces for calibrating optical pyrometers
 [NRC-TT-1432] 08 p1176 N71-18841

Induction heating of metallurgical specimens to high temperatures in coil furnace
 [NASA-CASE-XLE-04836] 12 p1917 N71-23267

Electric arc furnaces in Sweden noting design and operation and cost reduction
 19 p104 N71-31903

Cyclic furnace and high velocity oxidation of aluminum-coated high strength nickel alloy (B-1908)
 [NASA-TM-X-2370] 22 p3593 N71-35585

Atomic absorption spectrophotometry for determining constituents in minerals, slags, and matter from smelting, evaporative furnaces, and other sources
[NLL-CE-TRANS-5498-1902.09]

22 p3597 N71-35612

FUSELAGES

Practical aerodynamics of Mi-6 helicopter - lift system and fuselage
[AD-74915]

07 p0973 N71-17908

Three dimensional interactions in half cone pressure fields and effects on intakes mounted adjacent to aircraft fuselage

09 p1369 N71-19367

Low speed static wind tunnel tests of half-span fuselage and variable sweep pressure wing model
[NASA-TN-D-6215]

20 p3307 N71-33776

Low speed wind tunnel tests of effects of nacelle position, refueled nacelle, and elevator effectiveness for NAR straight wing orbiter
[NASA-CR-103160]

21 p3524 N71-35107

Heat transfer data on windward surface of orbiter fuselage
[NASA-TM-X-62051]

22 p3695 N71-36353

FUSERS [ORDNANCE]

Thermal analysis of heat activated metallic spring with memory for possible use as fuse arming devices
[AD-713578]

05 p0698 N71-14506

Analysis of design concepts for mechanical simulation of flight acceleration for testing of functional requirements of arming and safing devices used in aircraft warhead adaptation kits
[AD-726926]

22 p3681 N71-36250

FUSIFORM SHAPES

U CONES

FUSION [MELTING]

Fusion of ammonium nitrates with cerium compounds for solid propellants
[REPT-670]

07 p1098 N71-17230

Process for fiberizing ceramic materials with high fusion temperatures and tensile strength
[NASA-CASE-XNP-00597]

11 p1786 N71-23088

FUSION WELDING

NT ARC WELDING

NT BRAZING

NT ELECTRON BEAM WELDING

NT ELECTROSLAG WELDING

NT GAS TUNGSTEN ARC WELDING

NT GAS WELDING

NT PLASMA ARC WELDING

Application of welding methods and treatment of metal surfaces to improve corrosion resistance and dimensional build up in engine production

02 p0233 N71-11651

Measuring solidification mechanisms in fusion welds in nickel-iron alloys as function of temperature distribution in solid

05 p0705 N71-15478

Control of fusion welding through use of thermocouple wire
[NASA-CASE-MFS-00674]

09 p1944 N71-20393

Specifications for cleaning, fusion welding, and postheating tantalum and niobium alloys
[NASA-TM-X-67879]

18 p2936 N71-31135

FAR AIRCRAFT

U F-4 AIRCRAFT

FNU AIRCRAFT

U F-4 AIRCRAFT

G

G FORCE

U ACCELERATION [PHYSICS]

GADOLINIUM

Energy loss of high energy electrons in tin, lead, and gadolinium
[AD-711085]

01 p0097 N71-10534

Doping silicon material with gadolinium to increase radiation resistance of solar cells
[NASA-CASE-XLE-02792]

01 p0111 N71-10607

Gamma transitions from high spin states in beta-vibrational band of Gd-154
[RL-1388-120]

01 p0101 N71-10855

Effects of gadolinium added to fuel in boiling water reactor
[RT/FM/70/20]

03 p0416 N71-12921

Cell calculations for reactor fuel containing gadolinium burnable poisons
[RT/FM/70/21]

04 p0549 N71-13753

Absorption spectra of gadolinium /33- in crystals of alkaline earth fluorides at liquid D energy levels
[AD-712687]

04 p0580 N71-14010

Transport properties of Gd-Th, Gd-Mg, and Y-Th alloys
[IS-T-379]

08 p1212 N71-18390

Analysis of crystal-field splittings, Zeeman effect, and line strengths for GdCl₃-6H₂O magnetic dipole transitions
[AD-716040]

09 p1454 N71-20094

Na/Ti-Ge/Li directional correlation system for determining multiplicities of M1-E2 mixing in decay of vibrational levels in Gd-154

10 p1622 N71-21758

Nuclear level structure of even-even nuclei in mass region of permanently deformed nuclei of Gd-56 and Dy-160

10 p1626 N71-21850

Quadrupole interaction of Ba-137 and Ba-135 near positive fluorine ion centers and electron paramagnetic resonance spectrum of positive trivalent Gd ions in single BaO crystals

11 p1805 N71-22402

Gadolinium or samarium doped-silicon semiconductor material with resistance to radiation damage for use in solar cells
[NASA-CASE-XLE-10715]

12 p1985 N71-23292

Angular correlations of gadolinium conversion electrons, vanadium isotope beta particles, and bremsstrahlung

12 p1970 N71-23485

Preparation of Gd₂O₃ poisoned UO₂ pellets under high temperature conditions
[EUR-4551]

13 p2110 N71-24472

Gd₂O₃ microsphere preparation from sol-gel method
[EUR-4550]

13 p2121 N71-25247

Fission product angular distributions from C-12 ion impact with Gd-158 and O-16 ion impact with Sm-154 which yield 107 MeV excited Yb-170 compound nuclei
[CU-1019-76]

14 p2302 N71-25730

Nuclear properties of low lying Gd-152 excited levels based on beta transition probabilities of Eu-152
[INS-J-123]

17 p2802 N71-30144

Determination of half life and spins of Gd-155 levels by method of delayed coincidences and angular gamma-gamma correlations
[JINR-P6-5518]

18 p2970 N71-30455

Electron paramagnetic resonance spectra of Gd³⁺ plus ion in single crystals of cadmium sulfide observed at liquid nitrogen temperature

18 p2996 N71-31342

Magnetic properties of gadolinium, terbium, dysprosium, and holmium hydroxides at cryogenic temperatures

20 p3313 N71-33755

Rotational band transition probabilities calculated from lifetime measurements on structure of Gd-153
[JINR-P6-5526]

24 p3976 N71-38366

GAGES

U MEASURING INSTRUMENTS

GAIN [AMPLIFICATION]

U AMPLIFICATION

GALACTIC EVOLUTION

Radioactive abundances and stable products in chronological model for galactic heavy element nucleosynthesis

01 p0017 N71-10310

Magnitude estimates of brightest stars in Large Magellanic Cloud
[SAO-SPECIAL-REPT-320]

01 p0122 N71-10365

Gravitational waves in galaxies from cosmological point of view

02 p0296 N71-11952

Origin and isotropy of cosmic gamma ray flux between 1 and 6 MeV and its implications of future gamma ray investigations
[NASA-TM-X-65383]

02 p0293 N71-12046

Cosmological models, and galactic and stellar evolution

11 p1826 N71-22412

Galactic origin of pulsars and cosmic radiation sources

13 p2163 N71-25291

Cosmic plasma physics and polar system evolution
[REPT-70-39]

15 p2517 N71-27668

Cosmic matter-antimatter annihilation and gamma ray background spectrum
[NASA-TM-X-65598]

17 p2841 N71-29924

Jeans instability theory of galactic formation and expanding universes with black body radiation

20 p3344 N71-32847

Chemical nucleosynthesis of galaxy and stellar evolution
[NYO-3962-3]

20 p3350 N71-33956

Behavior of strongly interacting particles at ultrahigh temperatures related to origin of galaxies and matter
[LPHE-71/15]

21 p3530 N71-35156

Theoretical analysis of distribution of orientation angles of apparent major axes of spiral galaxies in different areas of sky and galactic origins
[REPT-80]

22 p3671 N71-36176

Galactic formation and density, velocity, and mass properties of expansion process

23 p3849 N71-37431

Spherical and planar galaxy systems in relation to elastic and inelastic evolutionary processes

23 p3849 N71-37432

Origin of galactic clusters due to explosion or gravitational contraction

23 p3849 N71-37433

GALACTIC MAGNETIC FIELDS

U INTERSTELLAR MAGNETIC FIELDS

GALACTIC RADIATION

Intensity and spectral shape of diffuse X ray emission by galactic disk from cosmic ray heating of interstellar hydrogen
[NASA-TM-X-65388]

03 p0450 N71-13034

Calculating production of deuterium, He-3, boron, lithium, and beryllium by galactic cosmic rays in interstellar medium

[SAO-SPECIAL-REPT-330] 08 p1285 N71-18704

Electron density energy spectra of galactic cosmic rays from circular and elliptic cylindrical and elliptic solid sources
[CEA-R-3674/E]

09 p1463 N71-20041

Galactic and solar cosmic ray propagation, variations, and energy spectra

11 p1822 N71-22417

Cosmic gamma ray production processes, galactic and extragalactic gamma rays, and cosmology
[NASA-SP-249]

13 p2158 N71-24764

Gamma ray absorption through interactions with galactic radiation, electrons, and pair producing matter

13 p2158 N71-24760

Positron annihilation gamma ray spectra, positron and positronium production, and equilibrium spectrum of secondary galactic positrons from pion decay

13 p2159 N71-24771

Mechanisms of galactic gamma ray production and estimates of production spectra in Milky Way

13 p2159 N71-24772

Cosmic gamma ray spectra from secondary particles produced by cosmic ray collisions in extragalactic space

13 p2159 N71-24774

Thermal electron density and cosmic ray flux in galactic radio emissions

13 p2163 N71-25299

Low energy cosmic radiation spectrum analysis for IMP 4 data on solar system

13 p2163 N71-25296

X ray spectrometry of galactic sources seen from Southern Hemisphere
[AD-720895]

15 p2513 N71-27280

Observations of galactic center radiation and possible point sources obtained by gamma ray telescope flown on three balloon flights
[NASA-TM-X-65564]

15 p2516 N71-27828

Formulas for distribution of extragalactic radio sources in space derived in zero pressure uniform model universe

16 p2680 N71-28790

Cosmic electron sources of galactic background radiations
[NASA-TT-F-13611]

16 p2676 N71-29827

Neutral pion decay, and diffuse gamma-background radiation from galactic and extragalactic sources

18 p3015 N71-31240

OSO-3 observations of origin of galactic gamma rays and correlation with X ray sources

20 p3346 N71-33800

Mathematical model using Monte Carlo method for modulation of galactic protons by solar wind
[NASA-CR-115095]

21 p3504 N71-34918

Spectrum of pulsing X ray source observed in Cassiopeia

22 p3667 N71-36147

Jet aircraft measurements of galactic cosmic radiation dose and comparison with theoretical values for supersonic flights
[UCRL-20209]

24 p4003 N71-38352

Particle intensities and energy spectra for galactic cosmic rays

24 p4010 N71-38391

Solar and galactic cosmic ray diffusion coefficients and dependencies

24 p4010 N71-38393

GALAXIES

NT MILKY WAY GALAXY

NT SPIRAL GALAXIES

Measuring neutral hydrogen absorption in galaxy M82 by radio telescope

02 p0294 N71-11117

Photometry of elliptical galaxies in Virgo Cluster
[AD-712807]

03 p0434 N71-13115

Faint star and galaxy research and instrumentation improvement
[AD-712826]

03 p0455 N71-13173

Galactic rotation model for axial alignment of interstellar disturbances

06 p0947 N71-16780

US and USSR extra-high resolution radio telescope interferometer experiments including galactic observations
[NASA-TT-F-13519]

09 p1469 N71-20053

Light emission, and gas components of galaxy NGC 5253

11 p1829 N71-22410

Dynamic equations for stochastic magnetic field lines in galaxy
[NASA-TM-X-65514]

13 p2160 N71-24640

Limit on line emission in X ray background at high galactic latitudes - rocket observation
[NASA-TM-X-65519]

13 p2160 N71-24640

SUBJECT INDEX

- Validity of bremsstrahlung model for background radiation in galaxy and earth atmosphere [NASA-TT-8-13615] 16 p2675 N71-28943
- Effect of cosmological expansion on self gravitating ensembles of particles [NASA-TM-X-67240] 18 p3015 N71-31253
- Astrophysics, radio astronomy, radio sources, galaxies, cosmology, pulsars, black body radiation, waves, and electromagnetic wave propagation [P-494] 20 p3343 N71-32836
- Propagation of electromagnetic waves in galaxy and effects of intervening matter on waves 20 p3343 N71-32837
- Magnitude-red shift, magnitude-galaxy count, and angular diameter-red shift relations included in tests of cosmological models 20 p3344 N71-32843
- Stellar and galactic magnetic fields, radiation processes, and interactions with ionized interstellar matter [AD-722871] 21 p3510 N71-35011
- Transport equations for determining cosmic ray phenomena of galaxy [NASA-CR-115178] 22 p3665 N71-36129
- Structure, composition, evolution, and physics of stars, galaxies, and universe 22 p3670 N71-36167
- Optical continuum emission of Seyfert and N-type galaxies and correlation with ionization and thermal equilibrium calculations for nonthermally heated gas [NFT-41] 22 p3671 N71-36177
- GALAXY AIRCRAFT**
U C-5 AIRCRAFT
GALERKIN METHOD
Ritz-Galerkin residual convergence in boundary value problems including trigonometric, polynomial, and spline coordinate functions 14 p2284 N71-26276
- Eigenvalue approximation method for non-self-adjoint operators using Galerkin method for estimating divergence perturbations of self-adjoint operators [NASA-CR-119027] 16 p2623 N71-28248
- Convergence of Galerkin method for constructing approximate solutions of nonlinear operator equations [NAC-TT-1454] 21 p3447 N71-34534
- Qualitative analysis of spatial effects in transfer function measurements of LMFBR based on space-time reactor model and Galerkin method [ANL-7708] 23 p5799 N71-37084
- GALLIUM ISOTOPES**
NT GALLIUM ISOTOPES
Low temperature conductivity of gallium crystals and single crystal films [AD-710651] 01 p0110 N71-10375
- Radio frequency impedance resonances for determining charge carrier properties in gallium 01 p0089 N71-10512
- Superconductive tunneling into bulk gallium single crystals [TID-25549] 06 p0931 N71-15758
- Tungsten hemisphere against tungsten disk slipping assembly with liquid gallium lubrication in ultrahigh vacuum [NASA-TN-D-6184] 07 p1033 N71-17324
- Effect of intensity and direction of zone mixing of molten metal on refining efficiency of gallium during mass recrystallization 10 p1574 N71-20881
- Device for measuring two orthogonal components of force with gallium flotation of measuring target for use in vacuum environments [NASA-CASE-XAC-04885] 12 p1922 N71-23790
- Atomic excitations of gallium, indium, and thallium ground states and lifetime measurement based on back effect 20 p3320 N71-33495
- Low temperature thermal conductivity of Sb and Ga doped Te and Zn doped and electron irradiation [NPL-10836] 22 p3658 N71-36083
- GALLIUM ALLOYS**
Indium amalgam, mercury, and indium-gallium electrochemistry and sodium-oxygen electrochemical cells [AI-TN-287] 15 p2777 N71-27387
- Hypertense magnetic interactions in Fe-Ga solid solution analyzed by Mossbauer spectroscopy [EALY-822-27] 19 p1619 N71-32218
- Mossbauer study of BiF₃ type ordering in metastable alloys containing up to 25 percent gallium [EALY-822-26] 19 p1717 N71-32776
- GALLIUM ANTIMONIDES**
Optical properties of amorphous indium antimonide, gallium antimonides, and gallium arsenides [JCL-TRANS-10480] 07 p1093 N71-17455
- Entropy, heat of formation, and fusibility of indium telluride arsenides and antimonides [NPL-DCS-81] 10 p1660 N71-20656
- Band structure of n-type tellurium-doped gallium antimonide single crystals studied using Shubnikov-de Haas effect 11 p1818 N71-22981
- Mossbauer effect measurements of aluminum, indium, and gallium antimonides and ionicity ordering 20 p3336 N71-33885

GALLIUM ARSENIDE LASERS

- Experimental optical radar development using gallium arsenide laser 01 p0062 N71-10162
- Onboard spacecraft optical data processing system using paraboloidal mirror segments and gallium arsenide laser [NASA-TM-X-65432] 06 p0006 N71-16489
- Photoionization cross sections for excited cesium atoms in triple crossed beam experiment, temperature tuning of pulsed GaAs laser, and optical pumping of Cs by pulsed GaAs laser 16 p2606 N71-28459
- Laser recombination data for GaAs photoresist 18 p2931 N71-31067

GALLIUM ARSENIDES

- Pseudopotential calculations of band structure of GaAs, InAs, and (GaIn)As alloys 01 p0108 N71-10134
- Purity profile plotter evaluation of gallium arsenide semiconductor 01 p0109 N71-10214
- Gallium arsenide bulk crystal growth from solution [AD-710812] 01 p0110 N71-10495
- Nondestructive tests to evaluate and characterize weightless grown gallium arsenide crystals 02 p0283 N71-11718
- Conduction mechanisms in high quality GaAs studied by measuring resistivity and Hall constant [AD-712004] 02 p0287 N71-12151
- Development of GaAs and GaAl/InP thin film bipolar transistors [NASA-CR-111805] 03 p0443 N71-13057
- Ion implantation forming of conducting layers and p-n junctions in gallium arsenide and silicon carbide [NASA-CR-111804] 04 p0511 N71-13529
- Gallium arsenide avalanche transit time devices [AD-713509] 05 p0653 N71-14041
- Carrier recombination and laser processes in semiconductor, mainly gallium arsenide [AD-714333] 06 p0867 N71-16108
- Electrical and photoluminescence measurements on liquid epitaxial gallium arsenide irradiated at room temperature by 1.25 MeV Co-60 gamma rays [AD-714684] 06 p0934 N71-16189
- Optical properties of amorphous indium antimonide, gallium antimonides, and gallium arsenides [JCL-TRANS-10480] 07 p1093 N71-17455
- Gallium arsenide Schottky barrier, field effect transistors [AD-715282] 07 p0999 N71-17850
- Describing method for vapor deposition of gallium arsenide films to manganese substrates to provide semiconductor devices with low resistance substrates [NASA-CASE-XNP-01328] 07 p1096 N71-18064
- Vaporization mechanism of gallium arsenide single crystals [JCL-TRANS-10480] 08 p1277 N71-18413
- Acoustic field effects on gallium arsenide, silicon solar cells, and photoresistive devices with and without light exposure 09 p1327 N71-20299
- Computer simulation of gallium arsenide limited space charge accumulation relaxation oscillations in microwave iris circuit 10 p1631 N71-20744
- Experimental and computerized simulation of n-type gallium arsenide operating in limited space charge accumulation mode 10 p1631 N71-20745
- Variation with temperature of tunable, coaxial resonant cavity gallium arsenide Gunn diode oscillator [SRDE-70042] 10 p1632 N71-20763
- Transitions of solid indium arsenide-gallium arsenide solutions to thermodynamic equilibrium states [NLL-RRE-TRANS-282-1036.625] 10 p1636 N71-21706
- Photoconductivity energy spectra of defects in irradiated gallium arsenide monocrystals [NLL-RTS-5984] 10 p1637 N71-21830
- Gallium arsenide solar cell preparation by surface deposition of cuprous iodide on thin n-type polycrystalline layers and heating in iodine vapor [NASA-CASE-XNP-01960] 11 p1727 N71-23027
- Improved encapsulating glass drying and polishing techniques for growing bulk gallium arsenide crystals [AD-718138] 12 p1987 N71-24015
- Photothermoelectric effects and transport properties in silicon and gallium arsenide semiconductors 13 p2154 N71-25561
- Gallium arsenide infrared window materials for high power carbon dioxide lasers 14 p2265 N71-25474
- Forming epitaxial film of GaAs single crystals [AD-720931] 15 p2506 N71-27402
- Electroluminescent quantum efficiency of gallium arsenide phosphide, gallium indium phosphide, and aluminum arsenide diodes [AD-720844] 15 p2508 N71-27901
- Optimization for zero gravity experiment on solution growth of gallium arsenide and design of experimental package for melt growth of indium antimonide crystals [NASA-CR-119792] 15 p2510 N71-27926

REMOVING GALVANIC CELLS

- Development and characteristics of gallium arsenide phosphide metal insulator semiconductor [AD-722059] 16 p2548 N71-28307
- Reflectivity spectrum of uniaxial stress of single crystal GaAs 16 p2566 N71-28746
- Electrical properties of silicon nitride-gallium arsenide interface 16 p2567 N71-28794
- Water content in vapor deposition atmosphere for forming n-type and p-type junctions of zinc doped gallium arsenide [NASA-CASE-XNP-01961] 16 p2669 N71-29156
- Development of quantum optical integrated circuits of gallium arsenide from semiconductor integrated methods [JPRS-53462] 17 p2727 N71-29258
- Electron mobility mechanisms in epitaxial growth of gallium arsenide crystals and computer program for calculating Hall effect [AD-722650] 18 p2995 N71-30734
- Diffusion of impurities from GaAs stream in epitaxial layers of GaP grown by sandwich method [AD-723589] 19 p1617 N71-31738
- Radiation damage to GaAs junction field effect transistor exposed to fast neutron fluence 19 p2864 N71-31742
- Effect of impurities on properties of slowly propagating domains in gallium arsenide 19 p3066 N71-32361
- Transport properties of n-type gallium arsenide by measurement of Seebeck and Hall coefficients and electrical conductivity from 4 to 300 degrees K 20 p3334 N71-33745
- Development of optoelectronic cold-cathode emitter structure by liquid-phase epitaxy [AD-726941] 22 p3561 N71-35348
- Optical properties of gallium arsenide infrared window material and evaluation of CO₂ laser [AD-726743] 24 p3931 N71-38051
- Photocompatibility in Gallium arsenide single crystals by two photon absorption of light quanta from Nd:glass laser [AD-727755] 24 p3932 N71-38054
- GALLIUM COMPOUNDS**
NT GALLIUM ANTIMONIDES
NT GALLIUM ARSENIDES
NT GALLIUM PHOSPHIDES
NT GALLIUM SELENIDES
Studying vaporization of indium-gallium oxide, and gallium-aluminum oxide by Knudsen effusion mass spectroscopy [NASA-TN-D-6318] 12 p1868 N71-23111
- Computation of GaSe and GaS optical constants from reflectivity spectra [ISS-71/9] 24 p3998 N71-38519
- GALLIUM ISOTOPES**
Nuclei Cu-61, Cu-64, Ga-67, and Ga-68 studies with p,n reaction [TID-25503] 07 p1077 N71-17595
- Gamma ray spectra analysis to determine energy levels in Ge-72 from radioactive decay of Ga-72 and As-72 10 p1622 N71-21754
- Multiple window spectrometry for gallium 67 and its use in detecting malignant human and animal tumors [ORNL-TM-3260] 17 p2790 N71-38004
- GALLIUM PHOSPHIDES**
Electroluminescent semiconductor material of indium gallium phosphide 01 p0108 N71-10131
- Indium gallium phosphide analysis by X ray fluorescence and diffraction 01 p0109 N71-10211
- Electroluminescent quantum efficiency of gallium arsenide phosphide, gallium indium phosphide, and aluminum arsenide diodes 15 p2508 N71-27901
- Development and characteristics of gallium arsenide phosphide metal insulator semiconductor [AD-722059] 16 p2548 N71-28307
- Diffusion of impurities from GaAs stream in epitaxial layers of GaP grown by sandwich method [AD-723589] 19 p1617 N71-31738
- Electrical properties determined for zinc- and tellurium-doped single crystal gallium phosphide using Van der Pauw method [AD-724080] 20 p3334 N71-33422
- Experimental characteristics of semiconductor heterojunction pairs ZnS/GaP and ZnS/GaP [NASA-CR-121718] 22 p3657 N71-36078
- Entropy, enthalpy, Gibbs free energy, and energy of atomization for gallium phosphide formation in electrochemical cells based on emf measurements [NLL-RRE-TRANS-315-1036.625] 23 p3780 N71-38037
- GALLIUM SELENIDES**
Computation of GaSe and GaS optical constants from reflectivity spectra [ISS-71/9] 24 p3998 N71-38519
- GALVANIC CELLS**
U ELECTROLYTIC CELLS

GALVANIC SKIN RESPONSE

- Evaluating use of adaptive techniques in control of tasks or stimuli 02 p0158 N71-11120
[AD-712134]
- Effect of carbon monoxide on human performance including heart rate and galvanic skin response [AD-71716] 01 p1643 N71-22299
- Adhesive spray process for attaching biomedical skin electrodes [NASA-CASE-XPR-87658-1] 14 p2211 N71-26293
- GALVANIZING**
- U ZINC COATINGS**
- GALVANOMAGNETIC EFFECTS**
- Investigating galvanomagnetic effects in developing higher magnetoresistance devices for low voltage high current switches [NASA-CR-110998] 01 p0030 N71-10044
- Quantum galvanomagnetic and thermomagnetic effects in graphite in magnetic fields at low temperatures [NASA-TN-D-7037] 06 p0952 N71-15917
- Crystal growth and galvanomagnetic properties of Mg₂Pb 09 p1454 N71-20438
- Band structure of metals, metal compounds, and ionic crystals determined by ultrasonic and galvanomagnetic measurements [AD-727069] 24 p3997 N71-38512
- GALVANOMAGNETISM**
- U GALVANOMAGNETIC EFFECTS**
- GALVANOMETERS**
- Electrochemical properties of aluminum, nickel-based, and stainless steel cladding alloys for nuclear fuels examined by galvanostats [DN-1295] 13 p1210 N71-25216
- Galvanometer for automatic recording of deformation measurement process [TT-70-59121] 14 p2253 N71-25664
- Performance test procedures and results for voltage and frequency transducer for use with galvanometer recorder systems [AD-721897] 17 p2725 N71-29492
- Design and performance of galvanovoltammetric detector with digital readout for electric current flow measurements 17 p2753 N71-29886
- GAME THEORY**
- NT MINIMAX TECHNIQUE**
- NT SADDLE POINTS (GAME THEORY)**
- Differential game theory applied to pursuit-evasion problems of two jet aircraft [AD-711055] 01 p0074 N71-10328
- Coalitions in N-person essential games [AD-713693] 05 p0655 N71-14882
- Differential game theory and topological spaces with unique homomorphisms [JPRS-52221] 07 p1049 N71-16669
- Synthesis of optimal controls in linear differential game with quadratic functional of payment 07 p1050 N71-16970
- Differential games with informational delay 07 p1050 N71-16971
- Intellectual interactions of conflict as reflexive game in which opponents guess reasoning of each other [JPRS-52700] 10 p1591 N71-20794
- Method for determining outcomes and optimum strategy for all players in discrete N-person game theory with independently chosen strategies [NASA-CR-118513] 14 p2282 N71-26111
- Specialized zero-sum game solution using expected values for evaluation of marked set assurance probability in two-person percentile games [NASA-CR-118514] 14 p2283 N71-26112
- Identification of situations where cooperation is preferable to median game theory - Thesis project [NASA-CR-118884] 15 p2434 N71-27723
- Optimum solutions for two person median game theory [NASA-CR-118885] 15 p2435 N71-27724
- Median criterion approach to two person game theory as compared to minimax game theory [NASA-CR-118887] 15 p2435 N71-27725
- Probability distribution in two person game theory [NASA-CR-118888] 15 p2435 N71-27726
- Competitive and median competitive aspects of median game theory [NASA-CR-118890] 15 p2435 N71-27728
- Median approach to two person game theory [NASA-CR-118891] 15 p2435 N71-27729
- Discrete two person game theory based on median value considerations [NASA-CR-118891] 15 p2435 N71-27730
- Two-person percentile game theory with separate and independent choice of strategies [NASA-CR-118861] 15 p2436 N71-27811
- Theorems on external strategies and aftereffects in differential game theory 16 p2621 N71-28153
- Theorems on extremal strategies in differential game theory 16 p2621 N71-28154
- Theorems on theory of differential games of systems with aftereffects associated with conflict problem 16 p2622 N71-28155

- Rendezvous of controlled movements and related problems in differential games aspect of controlled systems theory [JPRS-53450] 17 p2775 N71-30378
- Problem solving in linear differential games [JPRS-53645] 19 p3122 N71-32047
- Game problem for reducing motion to given set for linear systems with aftereffects 19 p3123 N71-32048
- Linear differential games of pursuit in presence of delays 19 p3123 N71-32049
- Game theory, information system for disease diagnosis, and model of warehouse system [JPRS-53701] 20 p3289 N71-32877
- Differential game theory with guaranteed estimates and terminal payoff 20 p3289 N71-32878
- Game theory for one attacker and several defenders and for several attackers and several defenders 20 p3289 N71-32879
- Generalized differential game theory of particle motion in n-dimensional Euclidean space 20 p3289 N71-32880
- Minimax principles in differential games without saddle points 20 p3289 N71-32881
- Game approach to problem of controlling descent of reentry vehicle during entry into atmosphere [JPRS-53839] 20 p3292 N71-33580
- Computer programming of chess games 22 p3545 N71-35249
- Human thinking studies using problem solving in chess 22 p3545 N71-35251
- Differential game with vector function and prescribed duration [JPRS-53973] 22 p3606 N71-35683
- Computerized business game and mathematical models of optimal scientific research development [JPRS-54168] 24 p3894 N71-37755
- Computerized business game for training students in industrial decision making and cooperation 24 p3894 N71-37756
- GAMMA FUNCTION**
- Deriving incomplete gamma functions for various applications and using Chebyshev polynomial approximations for solution of Lane-Emden equation 01 p0074 N71-10254
- Developing high-speed variable accuracy method for computing ordered sequences of incomplete gamma function 06 p0885 N71-16673
- Computerized analysis of single peaked hydrographs using transformation of incomplete gamma function and weighted least squares method [PB-196899] 20 p3258 N71-33153
- Variation of gamma function with wavelength and influence of emulsions on exposing light source [RAE-LIB-TRANS-1572] 22 p3628 N71-35854
- GAMMA RADIATION**
- U GAMMA RAYS**
- GAMMA RAY BEAMS**
- ALGOL program for calculating scattered gamma ray energy spectra in shielding slab [ORNL-TR-2353] 04 p0556 N71-14078
- Theoretical correlation coefficients as functions of mixing ratio delta for triple gamma ray cascades with intermediate transitions unobserved [NP-18644] 18 p2989 N71-31514
- Light particle emission in fission as function of characteristic time and shape of rising nuclear potential [NRCN-252] 18 p2989 N71-31515
- Flow shape, steam volume fraction and pressure drop in two phase flow of water-steam determined by attenuation of gamma ray beam [NLL-RISLEY-TRANS-1930-9091.9F] 19 p3082 N71-32641
- GAMMA RAYS**
- Electron conversion ratios for 1064 keV gamma ray of bismuth 207 [NASA-TN-D-6057] 01 p0093 N71-10060
- Precision measurement of Hg-203 beta-gamma directional correlation [COO-1746-41] 01 p0095 N71-10416
- Energy dependent beta-gamma circular polarization and nuclear matrix elements of Rb-86 [COO-1746-42] 01 p0099 N71-10716
- Gamma ray spectrograph shield and collimator tests in pulsed reactor [AD-711531] 01 p0055 N71-10742
- Precision measurements of gamma, neutron cross sections, angular distributions, and photoneutron spectra from light nuclei [AD-710461] 01 p0101 N71-10868
- Effects of 15,000-rads pulsed gamma-neutron radiation on behavioral performance of monkeys [AD-712854] 02 p0153 N71-11088
- Using solid state Ge/Li detector for measuring amounts of radionuclides in individual organs [BNWL-1178] 02 p0168 N71-11196
- Effects of gamma radiation on cell division processes and chromosomes in bone marrow of dogs 02 p0161 N71-11497

- Life times and magnetic moments of excited gamma states after proton irradiation determined from angular distribution of gamma rays to establish validity of shell model 02 p0272 N71-11708
- Morse code for use as multigrid neutron and gamma ray Monte Carlo transport code [AD-711941] 02 p0274 N71-11881
- Origin and isotropy of cosmic gamma rays between 1 and 6 MeV and its implications of future gamma ray investigations [NASA-TM-X-65385] 02 p0293 N71-12046
- Comprehensive tables of beta and gamma activities of fission products 02 p0277 N71-12120
- Design and testing of stabilized balloon gondola for astronomical gamma ray spectrometer [ORNL-TM-2882] 03 p0314 N71-12202
- Determining neutron resonance spins in U-235 using multiplicity of radiative capture of gamma rays [UCRL-50861] 03 p0421 N71-12648
- Trajectories of Compton electrons produced by gamma rays with air in electromagnetic field [LA-4348] 03 p0421 N71-12648
- Photon monochromator with Compton-scattered gamma rays as energy source [IS-2355] 03 p0423 N71-12741
- Gamma energy and intensity measurements in decay of Xe-142, Cs-142, Ba-142, and La-142 nuclei [IS-2352] 03 p0424 N71-12811
- Thermal neutron capture in natural calcium using Ge/Li spectrometers 03 p0425 N71-12842
- Neutron and gamma ray emission from excited states and high-spin states [RPI-3947-9] 03 p0427 N71-12857
- Neutron and gamma irradiation safeguards research, and research facility development [LA-4457-M3] 03 p0415 N71-12872
- Bromine-thallium contribution to shielding of gamma rays having energies less than 10 MeV [AEEW-R-675] 03 p0429 N71-12880
- Remote positioning facility for calibration of gamma radiation instruments at high exposure rates [RD/B/N-1624] 03 p0359 N71-13187
- Data acquisition and reduction system for time-of-flight mass spectrometer used in routine analysis of products from gamma radiolysis of organic compounds [ORNL-3106-33] 04 p0486 N71-13420
- Gamma ray attenuation study of nitrogen 14 loop in Triton water cooled reactor 04 p0545 N71-13541
- Using trans-stilbene crystals to measure equivalent dose rates in mixed gamma-neutron field [LNF-70/31] 04 p0571 N71-13604
- Diagrams for rapid calculation of gamma protection and attenuation of gamma radiations from fission products [RAE-LIB-1209] 04 p0571 N71-13613
- Beryllium determination in gamma activated samples [Y-1733] 04 p0573 N71-13610
- Mechanical filtration, electrostatic collection, and total gamma ray measurements of St. Laurent 1 reactor [CEA-N-1356] 04 p0550 N71-13797
- Gamma ray energy measurements of transitions from first and second excited levels of Fe-58 [CONF-690818-7] 04 p0577 N71-13799
- Miniature fission chambers for neutron fluxes and gamma irradiation 04 p0578 N71-13872
- Operational problems of helium 3 counter in gamma fields [FEI-178] 04 p0578 N71-13874
- Neutron branching ratios of eta meson using energy spectrum of gamma rays [PUBC-415-3] 04 p0580 N71-14003
- Observation of new high energy gammas of I-132 [ORNL-TR-2263] 04 p0582 N71-14003
- LiF thermoluminescent ribbons for low level environmental gamma radiation measurements [HASL-233] 04 p0582 N71-14111
- Aerial survey of Beatty Waste Dump at Nevada Test Site [EGG-1183-1481] 04 p0592 N71-14482
- Neutron and gamma measurements of Fissionable-type base plate mockup at Nadeo-2 [CEA-N-1305] 04 p0593 N71-14448
- Gamma ray spectroscopic analysis of isotopic abundances in plutonium sources [BNL-50237] 04 p0594 N71-14455
- Mathematical method and FORTRAN program for routine interpretation of gamma-loggings in uranium ore deposits 05 p0736 N71-14577
- Characteristics of gamma absorptometer with saturating detector and photomultiplier for heavy element determination in solution 05 p0684 N71-14607
- Developing calorimeters for measurement of gamma radiation intensity in reactor structural materials [ZJE-84] 05 p0727 N71-15069

SUBJECT INDEX

Investigating neutral decays of eta-meson using collimated array of lead plate spark chambers for conversion of gamma rays
[UCRL-20039] 05 p0740 N71-15104

Directional correlation measurements of gamma rays emitted in Tl 160 decay
[CDO-1746-49] 05 p0741 N71-15116

Testing of secondary gamma ray production data sets from neutron capture and inelastic scattering sections
[CUC-20] 05 p0745 N71-15187

Thermal neutron capture gamma yields
[WANL-TMR-2713] 05 p0745 N71-15208

Comparing intrinsic efficiencies of spherical NaI(Tl) detectors with efficiencies of cylindrical NaI(Tl) detectors
[NASA-TM-X-53393] 05 p0687 N71-15436

Asymmetry in single pion/0⁺ photoproduction by deuteron gamma rays on protons
[LNF-70/59] 06 p0909 N71-15777

Single crystal high resistivity cadmium telluride for use as gamma-ray spectrometer
[SAN-545-6] 06 p0933 N71-16016

Prolonged gamma irradiation of dogs
[AD-714407] 06 p0800 N71-16092

Electrical and photoluminescence measurements on liquid epitaxial sodium arsenide irradiated at room temperature by 1.25 MeV Co-60 gamma rays
[AD-714684] 06 p0934 N71-16189

Design and development of broadband model of airborne radars
[AD-713884] 06 p0859 N71-16214

Gamma-gamma directional correlation measurements in tellurium 124
[CDO-1746-40] 06 p0919 N71-16249

Gamma ray induced polymer formation of carbanes
[JRO-3781-7] 06 p0882 N71-16729

Measurement of gamma ray energy spectrum at balloon altitudes
 06 p0943 N71-16731

Least squares method for gamma ray angular distribution of radiative capture of deuterons
[JORN-TM-3168] 07 p1077 N71-17549

Atomic structure of Cr-51 via prompt gamma ray energy and intensity measurements
[CDO-1530-21] 07 p1077 N71-17550

Characteristics of low energy gamma rays in atmosphere
[AD-715271] 07 p1106 N71-18035

Fast variation of hadronic amplitudes and gamma quanta bremsstrahlung
[ITEF-764] 07 p1081 N71-18136

Tables of fission-product gamma transitions including isotopes from Se-87 to Pm-151 with half lives greater than one minute
[CEA-N-1290] 07 p1081 N71-18137

Theoretical reconstruction of gamma ray spectra fission products after thermal fission of U-235 nucleus
[CEA-N-1313] 07 p1081 N71-18142

Establishing nuclear level scheme of Nd-141 from decay of Pm-141 to Nd-141 using gamma ray spectroscopy
[LYCEN-7051] 07 p1082 N71-18147

Subroutine for calculating gamma dose and thermal neutron fluence from thermoluminescent detector data
[RDB/N-1677] 08 p1247 N71-18192

Electron spin resonance studies on irradiated heterogeneous systems - structure and reactivity of paramagnetic centers in silica gel
[NP-18478] 06 p1235 N71-18209

Gamma radiation induced currents between insulated dissimilar electrodes
[AECL-3364] 06 p1167 N71-18217

Radiative decay mode measurements on neutral pions yielding neutral eta-meson gamma, neutral pions yielding neutral pion gamma
[JAL-1240] 06 p1255 N71-18360

Heavy ion beams for in-beam gamma ray and conversion electron spectroscopy
[UCRL-19961] 06 p1261 N71-18777

Neutron and gamma ray measurements with nuclear track detectors
[AD-715797] 06 p1261 N71-18781

Monte Carlo calculations of neutron and gamma ray transport and minimum shield weight for mobile nuclear reactors
[NASA-TM-X-52973] 06 p1240 N71-18782

Gamma ray spectrometer design for intense gamma fields incorporating Compton spectral detectors
[NASA-CR-103044] 06 p1204 N71-19136

Gamma-gamma angular correlation function degree of perturbation to recoilless emission probability in Si-111
 06 p1283 N71-19308

Facility and procedures for processing alpha, beta, gamma, and neutron emitters
[JORN-TM-3223] 06 p1176 N71-19342

Neutron-induced gamma ray spectroscopy for measuring plutonium and plutonium isotopes in plutonium metal
[IN-4233] 06 p1268 N71-19345

Gamma radiation attenuation gaps for measuring all solid material or liquid density
[RMO-3604-V] 09 p1397 N71-19446

GAMMA RAYS

Detection of cosmic gamma radiation with gamma ray telescope
[AD-716492] 09 p1461 N71-19534

Neutron cross sections of gamma ray emissions in thulium 169
 09 p1433 N71-19577

Fast neutron inelastic scattering measurements to determine gamma ray production cross sections
[CEA-R-4047] 09 p1433 N71-19988

Artificial radioactivity of marine medium determined by gamma spectroscopy studies from 1962-1964
[CEA-R-3698] 09 p1437 N71-20079

Gamma radioactivity of female Swiss-Rap mice as function of growth rate
[CEA-R-3797] 09 p1333 N71-20176

Gamma ray logging of drill holes using thermoluminescence dosimeters
[RISO-2159] 09 p1441 N71-20310

Peak pickup effect estimation in NaI(Tl) detector system, using photopick between gamma ray sources
[JAERI-MEMO-4144] 09 p1441 N71-20338

Beta and gamma irradiation of bismuth and bismuth coated materials with dose rate and degradation analyses
[CEA-R-3730] 09 p1421 N71-20387

Measurement and analysis of differential cross sections for reaction negative pion proton yields eta-meson neutron at six energies between 2.9 and 18.2 GeV/c
[CEA-R-4037] 09 p1444 N71-20528

Peak strip and normalize subroutines for analyzing gamma ray spectra
[MLM-1773] 10 p1611 N71-20606

Data acquisition system used with electron linear accelerator for neutron capture gamma ray experiments - metallurgical and other program notes
 10 p1528 N71-20901

Gamma ray spectra of aluminum, thorium, rhenium, and protactinium isotopes radioactive decay following thermal neutron capture
 10 p1614 N71-20932

Computer analysis of semiconductor GeLi gamma ray spectra, comparison of threshold detectors, Bonner spheres, and recoil spectroscopy with emulsions, and Prodhon equation solutions
 10 p1559 N71-21148

Gamma ray spectra analysis to determine energy levels in Ge-72 from radioactive decay of Ge-72 and As-72
 10 p1622 N71-21354

Analysis of thermal capture gamma ray spectral data obtained by thermal neutron capture gamma ray facility
[AD-717639] 11 p1801 N71-21958

De-excitation of gamma rays following Coulomb excitation of Ru-151 and 153 using GeLi spectrometer
 11 p1810 N71-23035

Gamma radiation spectral composition and intensity spectra and time distributions from Cosmos 135 including measurement of photon effects due to satellite and detector secondary emissions
 12 p1992 N71-23262

Microwave technology with application to solid state physics, electron paramagnetic resonance, and gamma radiation
[AD-717696] 12 p1966 N71-23820

Gamma ray energies and intensities emitted by nuclides in nuclear fuel materials
[DI-1448] 12 p1974 N71-23990

Joint and marginal distribution calculations of emergent wavelength and angle given gamma ray quantum incident on left face of slab and comparison with Monte Carlo method
[ANL-7689] 12 p1977 N71-24211

GeLi detector and channel analyzer for detecting band mixing effects in even-even deformed Gd-154, Dy-160, and Er-160 nuclei
 12 p1978 N71-24286

Measuring gamma dose rate in Plum Brook Reactor using oxalic acid
 13 p1212 N71-24518

Calorimeter for measuring heat generation rates in nonfissionable materials by gamma and thermal neutron interactions in nuclear reactor test facility environment
 13 p1213 N71-24524

Use of discrete ordinates and auxiliary programs of ANISN in one dimensional neutron and gamma ray transport
[CEA-N-1338] 13 p1219 N71-24672

Cosmic gamma ray production processes, galactic and extragalactic gamma rays, and cosmology
[NASA-SP-249] 13 p1250 N71-24764

Gamma ray producing decay modes of secondary particles produced in high energy cosmic ray interactions with interstellar and intergalactic gas
 13 p1258 N71-24765

Gamma ray production by cosmic annihilation of free and low energy electrons and positrons
 13 p1258 N71-24766

Gamma ray production from cosmic proton antiproton annihilations, selection rules, and Matsuda statistical model
 13 p1258 N71-24767

Gamma ray absorption through interactions with galactic radiation, electrons, and pair producing matter
 13 p1258 N71-24768

Gamma ray spectra from several pion decay and model for theoretical calculation of spectrum below 1 GeV, for gamma rays produced by galactic cosmic ray interactions
 13 p1259 N71-24769

Cosmic gamma ray energy spectra caused by hyperon and nucleus isobar decays for gamma ray energies above 1 GeV, and differential production cross sections
 13 p1259 N71-24770

Positron annihilation gamma ray spectra, positron and positronium production, and equilibrium spectrum of secondary galactic positrons from pion decay
 13 p1259 N71-24771

Mechanisms of galactic gamma ray production and estimates of production spectra in Milky Way
 13 p1259 N71-24772

Cosmic gamma ray spectra from secondary particles produced by cosmic ray collisions in extragalactic space
 13 p1259 N71-24774

Cosmic gamma ray spectra from extragalactic proton antiproton annihilations into mesons
 13 p1259 N71-24775

Extragalactic gamma ray spectra from Compton interactions and bremsstrahlung production
 13 p1259 N71-24776

Gamma ray absorption processes at high red shifts, and energy dependences of absorption processes in interstellar and intergalactic gas
 13 p1260 N71-24777

Cosmic, isotropic gamma ray spectra, primordial gamma ray sources, and intergalactic gas density
 13 p1260 N71-24778

Gamma ray scintillation, Cerenkov, and pictorial detector telescopes
 13 p1261 N71-24779

Nondestructive testing of aircraft structures using them and lithium gamma sources
[JAERI-MEMO-4163] 13 p1261 N71-24849

Cosmic antineutrino annihilation and gamma ray background spectrum
[NASA-TM-X-53517] 13 p1260 N71-24962

Balloon flight measurements of gamma ray spectra of celestial large energy sources
[AD-719641] 13 p1261 N71-25199

Gamma-gamma coincidences in Co-140
[CNEA-275] 13 p1215 N71-25225

Reorientation effect of gamma ray angular distribution in Cd isotopes caused by Compton excitation
 13 p1214 N71-25540

Nondestructive nuclear assay, calorimetric, gamma, and neutron instrumentation techniques for nuclear fuel element fabrication in breeder reactors
[ORAP-12114-3] 14 p1253 N71-25631

Gamma ray energies and intensities emitted by nuclides present in nuclear fuel materials
[IN-1448-REV] 14 p1201 N71-25729

Gamma ray scattering cross sections from neutron irradiation of aluminum with neutron energies between 5.3 and 9.8 MeV using time of flight spectrometers
[JORN-TM-3284] 14 p1201 N71-25737

Intensities variations and spectral composition of gamma radiation in near earth space measured by Cosmos 135
 14 p12334 N71-25799

Method for calculating spectra of gamma radiation in sea water with constant salt composition
 14 p12348 N71-25967

Electron paramagnetic resonance spectrometers operating under irradiation near reactor core and with gamma ray source
[CEA-R-4022] 14 p12254 N71-26008

Fabrication of lithium doped germanium detectors for use in gamma ray spectroscopy
[BLG-447] 14 p12255 N71-26207

Co-60 gamma radiation damage in Li-doped p-n and conventional p-n solar cells
 14 p1282 N71-26234

Distribution moments and Monte Carlo calculation of high energy gamma ray absorption in concrete, iron, and lead slabs
 14 p12304 N71-26277

EPR and ENDOR study of free radicals produced by gamma irradiation of imide-like single crystals
[CEA-R-3738] 14 p12307 N71-26395

Neutron, gamma reactions with vanadium-51 and yttrium-89 for incident neutrons in energy range 0.3 to 4 MeV
[ANWB-O-7870] 14 p12308 N71-26434

Measurement of 4 pion beta minus gamma coincidences in radioactivity metrology laboratory case of complex decay scheme, and accuracy obtainable in particular cases
[CEA-R-4131] 14 p12309 N71-26571

Directional correlations of gamma ray cascades in Mg-206 using Ti-206 source and coincidence spectrometer arrangement
[NPL-18613] 14 p12309 N71-26587

- Semiconductor detector telescope electron spectrometer with high detection efficiency for gamma rays and heavy particles
[NP-18617] 14 p2258 N71-26591
- Gamma rays and gamma-ray cascades from 26.1-hr thallium-200 decay and excited states in Hg-100
[NP-18647] 14 p2309 N71-26601
- Measurement of reaction $\text{Cl-35}(\gamma, \text{n})\text{Cl-36}$ using three-crystal pair and anti-Compton spectrometer
[PH-2] 14 p2317 N71-26753
- Scintillation separation of gamma ray spectra into neutron capture, nuclear fission, and fission product sources for use in nuclear fuel element nondestructive testing
[KFK-1214] 15 p2462 N71-27144
- Alpha and gamma decay structure of highly excited complex nuclei
[JINR-E4-5135] 15 p2466 N71-27285
- Analog computer for neutron-gamma discrimination in proportional counter pulse amplifiers
[CEA-N-1314] 15 p2470 N71-27384
- Gamma induced chain crosslinking and polymerization of polyethylene
[JAERI-MEMO-4147] 15 p2471 N71-27412
- Angular correlation and gamma ray branching of argon at incident proton energy
15 p2475 N71-27460
- Electron paramagnetic studies of gamma irradiated alkali-germanate glasses and crystalline compounds
15 p2507 N71-27571
- Nuclear resonance fluorescence and neutron capture gamma rays for studying excited levels in nickel and cadmium isotopes
15 p2478 N71-27627
- Galactic and extragalactic origin of cosmic gamma ray flux between 1 and 6 MeV
[NASA-TM-X-65562] 15 p2514 N71-27639
- Metagalactic gamma ray spectra calculated for relativistic electron bremsstrahlung interactions
[NASA-TM-X-65577] 15 p2515 N71-27646
- Gamma radiation following capture of polarized neutrons by oriented nuclei in this target
[FMRB-33/70] 15 p2481 N71-27705
- Measuring high energy gamma ray spectra in strong neutron flux
[JNR-1224] 15 p2482 N71-27706
- Numerical methods of quantitative analysis of digital gamma spectra
[RT/PROT-70/21] 15 p2482 N71-27749
- Mapping of fast or thermal neutron produced nuclides with half lives less than 1 minute and gamma energies between 0.01 and 10 MeV
[KFKI-70-18-NAC] 15 p2485 N71-27812
- Electron paramagnetic resonance of $\text{IO}_2\text{F}/\text{min}/\text{radical}$ in gamma irradiated single crystals of KIO_2F_2 at room temperature
15 p2486 N71-27822
- Observations of galactic center radiation and possible point sources obtained by gamma ray telescope flown on three balloon flights
[NASA-TM-X-65564] 15 p2516 N71-27826
- Time dependent analysis of thermal radiation from fission product beta and gamma radioactive decay
[JAERI-MEMO-4205] 15 p2495 N71-27965
- Electron spin resonance for detecting defects in beryllium oxide single crystals created by gamma or neutron irradiation
15 p2496 N71-27972
- Effect of absorption nuclear lines on transition radiation of resonance gamma quanta by relativistic electrons
[JINR-P2-5042] 15 p2496 N71-27973
- Method for producing neutrons in keV energy region utilizing gamma rays from radioactive decay to induce photoneutron reaction in beryllium
[NASA-TM-X-2296] 16 p2630 N71-28119
- HEAD CaTi crystal activation for measurement of galactic gamma and cosmic particle energy spectra
[JNR-507] 16 p2674 N71-28167
- Effects of gamma radiation on lifetime of red blood cells and bone marrow production in dogs exposed to cobalt 60 irradiation for two and one half years
16 p2545 N71-28480
- Effects of chronic and repeated gamma radiation on morphological structure of peripheral blood and bone marrow in dogs following exposure for one year
16 p2546 N71-28481
- Gamma ray probability in Monte Carlo generation of neutral negative pion proton interactions at 5 GeV/c in propane bubble chamber
[JINR-P13-5516] 16 p2649 N71-28816
- Balloon-borne optical spark chamber for pulsed gamma ray source measurements
[CEA-CONF-1633] 16 p2675 N71-28843
- Beta-gamma ACF asymmetry coefficients in isospin forbidden mixed beta transitions
[KFK-1249] 16 p2651 N71-28938
- Photons in gamma ray energies and table on half life, gamma ray energy, and intensity of radioisotopes
[JAERI-MEMO-4189] 16 p2654 N71-29059
- Alpha and beta particle range determination, using cadmium telluride detectors for gamma ray spectrometry
[CEA-X-4852] 16 p2655 N71-29072
- Photofission cross section behavior for natural uranium and thorium in 5 to 10 MeV energy interval using monochromatic gamma rays from is , gamma/radiation
[IEA-211] 16 p2656 N71-29108
- Radiation transport calculations - moment method in gamma ray transport, function approximations, computer generated neutron flux moments, NaI detectors, and related topics
[AD-721388] 16 p2656 N71-29111
- Prediction method for gamma flux distributions in zero power plutonium reactor environment
[WHAN-FR-13] 17 p2700 N71-29209
- Compensation of α -type germanium by gamma radiation for radiation detectors
[BNL-15643] 17 p2813 N71-29470
- Distinguishing between neutrons and gamma rays in this neutron shields with tissue-equivalent proportional detectors
[BNWL-SA-3561] 17 p2751 N71-29520
- Review of gamma ray transitions from keV neutron capture providing information on properties of individual resonances in light nuclei or nuclei near closed shells
[AAEC/TM-565] 17 p2794 N71-29632
- Effect of gamma radiation on adsorption of iodine and methyl iodide on activated carbon exposed to flowing mixtures of steam and air
17 p2715 N71-29856
- Cosmic matter-antimatter annihilation and gamma ray background spectrum
[NASA-TM-X-65598] 17 p2841 N71-29924
- Meson current algebra for calculating form factor and coupling constant in gamma - 3 pion amplitude in gamma/pion interaction
[NUB-2074] 17 p2774 N71-30061
- Cosmic gamma radiation from pion decay in interstellar gas
[NASA-TM-X-65602] 17 p2842 N71-30069
- Gamma and X rays emitted in decay 2.2 hr and 4.7 min Sn-127 investigated with aid of Ge/Li and Si/Li detectors
[NP-18596] 17 p2806 N71-30327
- Energy levels of Yb-176 from decay of Tm-176 and Yb-176m studied by Ge/Li detectors and gamma-gamma as well as gamma-beta coincidences
[NP-18599] 17 p2807 N71-30336
- Approximations for total mass coefficient and mass coefficient for absorbed gamma ray energy for atomic numbers 1 to 92
[ZJE-93] 17 p2808 N71-30338
- Germanium/lithium - sodium iodide/tellurium pair spectrometer for gamma ray spectroscopy
[IKP-26] 17 p2810 N71-30386
- Photomeron effects in γ/muon and γ/pion reactions in light nuclei
[LUNP-7009] 18 p2967 N71-30404
- Computer program for automatic analysis of gamma ray spectra
[CEA-N-13811/PT-1] 18 p3002 N71-30516
- Neutral pion decay, and d/dE gamma-background radiation from galactic and metagalactic sources
18 p3015 N71-31260
- Calculation of neutron and gamma ray dose rates for Ct-252 shielding materials
[DP-1246] 18 p2986 N71-31273
- Survey of nuclear spectroscopy instrumentation, available radioactive sources, and semiconductor detectors and contaminants in gamma ray spectra
[ANU-P-502] 19 p3100 N71-31964
- Experimental device for measuring gamma absorption cross section of materials used for nuclear construction
[DEMO-70/11] 19 p3147 N71-32042
- Energy level width measurement in nuclei using resonance scattering of nickel capture gamma rays
[NRCN-254] 19 p3152 N71-32194
- Forbidden transitions and magnetic moments from angular correlations in gamma decay of Te-125
[NP-18704] 19 p3152 N71-32199
- Gamma ray transition probabilities in deformed nuclei and lifetimes of excited states in heavy nuclei
[NP-18695] 19 p3153 N71-32260
- Proton hole states excited in thin foils by monoenergetic gamma-quanta from $\text{Li-7}/\text{p}$, gamma/Be-8 reaction
[LUNP-7013] 19 p3154 N71-32233
- X and gamma thermoluminescent dosimeter for accidental personnel dosimetry
[CLOF-82/D] 19 p3155 N71-32339
- Computer programs for calculating electron bombardment proton and gamma yields based on Vavilov theory of energy loss distributions
[AD-723188] 19 p3156 N71-32417
- Long slit geometry apparatus for measuring angular distribution of gamma quanta from positron annihilation in single insulator crystals
[CEA-R-4138] 19 p3170 N71-32429
- On-line and off-line computer analysis of complex particle and gamma ray spectra with programs for performing all basic reduction functions
[ANU-P-487/2] 19 p3063 N71-32600
- High energy bremsstrahlung-induced γ/muon , γ/pion reactions in Au-197
[LUNP-7103] 19 p3159 N71-32628
- Search for high energy gamma rays from Cygnus region with discussion of mechanisms for gamma ray production
19 p3178 N71-32640
- Systems description of SAS-B gamma ray telescope with multilayer digitized spark chamber for gamma rays with energy exceeding 20 MeV
[NASA-TM-X-65654] 19 p3103 N71-32701
- Detection of gamma rays and evidence for rotational bands based on W-186d, $3\text{u}/\text{Re-185}$ reaction
[ANU-P518] 20 p3314 N71-32900
- NaI crystal spectrometer measurements of cross sections for $\text{Mg-25}/\text{tau}$, gamma/ Si-28 reaction at E_{lab} equals 4.44, 6.08, 6.15, and 8.26 MeV
[ANU-P508] 20 p3314 N71-32900
- European space program on gamma ray astronomy - conference
[ESRO-SP-58] 20 p3346 N71-33002
- OSO-3 observations of origin of galactic gamma rays and correlation with X ray sources
20 p3346 N71-33006
- OSO-3 gamma ray astronomical data
[NASA-CR-121380] 20 p3346 N71-33008
- Gamma ray origin, spatial distribution, and periodic variations
20 p3346 N71-33070
- Gamma ray balloon-borne experiments and comparison with satellite experiments
20 p3346 N71-33071
- SAS-B, TD-1, and HEAO space program for experiments on gamma rays
20 p3346 N71-33072
- ESRO COS-B space program and gamma ray detector
20 p3346 N71-33073
- Close-in electric and magnetic fields produced by gamma ray induced currents from nuclear explosion
[NORE-57] 20 p3316 N71-33016
- Abdominal and head shielding effects for the adult serum protein metabolism of gamma irradiated dogs
20 p3321 N71-33457
- POPOP library and codes for preparing secondary gamma ray production cross sections
[ORNL-TM-3367] 20 p3317 N71-33512
- Angular distribution of neutron and gamma emission from excited and spin states in isotopic americium 241 to americium 242 decay
[RPI-3947-13] 20 p3318 N71-33546
- Graphs for analysis of gamma-gamma directional correlations
[ORNL-4619] 20 p3318 N71-33587
- Utilization of gamma rays as nondestructive method of determining elemental composition of rocks and minerals
20 p3342 N71-33802
- Disk source energy and angular distribution calculations using gamma ray transport equation
20 p3327 N71-33894
- Latent image fading dependence on radiant flux density of visible and gamma illumination
[RAE-LIB-TRANS-1573] 20 p3328 N71-33905
- Development and characteristics of internal conversion electron spectrometer applied to gamma ray spectroscopy and nuclear structure research
21 p3430 N71-34412
- Power spectrum measurements in nuclear reactor and detector parameters taking gamma radiation influence on statistical accuracy into account
[TKK-F-A-102] 21 p3459 N71-34422
- Comparison of high-resolution gamma ray scanning and mass spectrometry for use in failure analysis of encapsulated fast reactor fuel element cladding
[LA-4675-M5] 21 p3462 N71-34619
- Standardization of beta-gamma emitters by d/dE gamma coincidence method for corrections and counting errors
[JINR-1240] 21 p3467 N71-34689
- Test target loaded with radionuclide for adjustment of gamma ray imaging devices
[ORNL-TM-3261] 21 p3474 N71-34741
- Anisotropy of gamma radiation emitted by Pr-142 nuclei in polycrystalline praseodymium
[COO-1549-76] 21 p3477 N71-34758
- Accuracy of calculating cross sections per photon from sets of measured cross sections per equivalent gamma quantum using unfolding method
[DESY-71/3] 21 p3486 N71-34833
- Particle gamma ray angular correlation study of Ni-57 levels in Ni-Fe-3 , alpha gamma/ Ni-57 reaction
21 p3492 N71-34877
- Rocket and balloon measurements of energy spectra and fluxes of fast neutrons, gamma rays, and X rays in atmosphere
[NASA-CR-121629] 21 p3503 N71-34903
- Measurement of gamma ray spectra accompanying nuclear radiative capture
[JINR-1271] 22 p3631 N71-35071
- FORTAN computer program for automatic analysis of gamma ray spectra from Ge/Li detectors
[LUNP-7101] 22 p3634 N71-35090
- Boron proportional counter with low gamma ray sensitivity for measuring thermal neutron flux in fast nuclear reactor
[JAERI-M-970] 22 p3635 N71-35090

SUBJECT INDEX

GAS BEARINGS

- Effect of gamma and alpha ionizing radiations on
saturated and degassed aqueous solutions of neptunium
and americium 22 p3637 N71-35925
(NP-18794)
- PORTMAN program for gamma radiation dosimetry
in arbitrary source and target geometry 22 p3638 N71-35933
(JNRL-10-3398)
- Neutron spectrometer measurements of neutron
resonances and gamma rays from neutron capture by
Sm-147 and Sm-149 22 p3639 N71-35942
(JNRL-10-3653)
- Disappearance of isostatic channel of nuclear reaction
in resonant nuclear scattering of gamma rays in
perfect crystal 22 p3640 N71-35948
(JAE-1964)
- Computer techniques for photointerpretation of
neutron pions and gamma quanta events in bubble
chamber filled with heavy liquids 22 p3641 N71-35958
(JTEF-753)
- Time resolution of 2.2 nsec for Ge(Li) detector and
scintillation counter in detecting Co-60 gamma quanta
(JNRL-10-3708) 22 p3642 N71-35969
- Gamma ray energies and intensities for calibrating
high resolution spectrometer 22 p3644 N71-35979
(JCL-20476)
- Low energy, photon spectra and gamma rays from
isotopes produced by (n,gamma) reactions 22 p3645 N71-35987
(JEL-133-70-65)
- Computer program (DIODE) for comprehensive
evaluation of gamma spectra with options ranging
from simple printout of spectrum to complete analysis
(AERE-8-4748) 23 p3728 N71-36575
- Continuous and incremental gamma scans for
destructive and nondestructive burnup data from natural
UO₂ fuel 23 p3799 N71-37081
(JNWL-1568)
- Investigating thermal neutron capture gamma radiation
from natural iron samples with aid of three-crystal
scintillation pair spectrometer 23 p3808 N71-37151
(JBAR-103)
- Semiconductor detector for low energy gamma
spectroscopy at room temperature utilizing multiple
detectors for signal amplification 23 p3810 N71-37167
(JLBO-3034)
- Calculation of radiation cross section for relativistic
suprathermal proton bremsstrahlung to determine
contribution to cosmic gamma rays 23 p3811 N71-37171
(NASA-TM-X-65699)
- Elastic scattering, radiative capture, gamma ray
production, and related information from nuclear data
file for hydrogen in .00001 eV to 20 MeV range
(LA-4574) 23 p3813 N71-37193
- Energy tables of gamma rays from (n,gamma)
product nuclides for rapid identification 23 p3817 N71-37226
(AABCTM-583)
- High-altitude electromagnetic pulse source currents
and ionization from Compton scattering of gamma
rays based on forward scattering of Compton electrons
(AD-726928) 23 p3818 N71-37233
- Gamma ray measurements from low energy G-
1000s, gamma (N-20 and Si-28) alphas (S-32)
reactions for calculation of stellar interaction and
photodisintegration rates 23 p3822 N71-37265
- Cosmological gamma ray spectrum calculations
from matter-antimatter annihilation in universe
(NASA-TM-X-65708) 23 p3842 N71-37395
- Gamma ray and neutron radiation of meteor streams
in relation to antimatter comet hypothesis 23 p3850 N71-37441
- Relationships between gamma and X radiation in
minerals, and their sources and spatial distribution 23 p3851 N71-37445
- Spatial and spectral energy distribution properties
of low energy gamma rays in atmosphere and space 23 p3851 N71-37446
- Gamma and X radiation measurements by artificial
earth satellites 23 p3851 N71-37447
- Variable electron streams and gamma ray intensity
in upper atmosphere 23 p3851 N71-37448
- Comparing thermoluminescent dosimeter measurements
with calculations of gamma heating in
polyethylene and lead containers 23 p3856 N71-37559
(NASA-TM-X-67936)
- Relative signs of alpha-proton hyperfine coupling
found in NH₂CONHO radical formed from gamma-irradiated
hydroxyurea crystals 24 p3971 N71-38329
(NP-18405)
- Effects of delayed gamma rays, systematic and random
coincidences, and scattered neutrons on Maxwellian
temperature value from time of flight measurements
of C-13-25 fission neutron spectrum 24 p3971 N71-38332
(JNRL-71-9)
- Gamma ray, gamma-gamma coincidence, and internal
conversion electron spectra for Sm-153 to Eu-153
series 24 p3972 N71-38339
(NP-18835)
- Ionization in dielectric liquids produced by gamma
radiation and ionization inhibition by electron scavengers
(NP-18875) 24 p3973 N71-38348
- Gamma logging data interpretation techniques for
radioactive elements in individual borehole layers
(CSIRO-TRANS-10068) 24 p3974 N71-38350
- Gamma radiation lines of rubidium 89 from fission
products 24 p3975 N71-38358
- He-3 p reactions with Ne-20, N-14, and B-11, and
gamma de-excitation of Ne-21 and Ar-41 24 p3976 N71-38390
(NP-18862)
- Silicon detector for measuring gamma radiation in
materials 24 p3982 N71-38422
- Gamma source localization and linear primary ray
polarization 24 p4012 N71-38620
- Gamma ray detector for astrophysical research 24 p4013 N71-38624
- GANGLIA
NT NERVES
NT NEURONS
Mechanism of inhibition and acceleration at synapse
in nervous system of heart ganglion of stomatopod
(ADA-71991) 02 p0154 N71-11009
- Physical controls of autonomic nervous system by
ganglia impulses 09 p1331 N71-19083
- GAPS
NT SPARK GAPS
Excitation gap thickness effect on spherical antenna
performance 04 p0491 N71-13708
- Model for spark chamber breakdowns and shower
efficiency determination 24 p3979 N71-38393
(JNRL-10-3810)
- GARNETS
Electromagnetic garnet, applying vectorcardiographic
type electrodes to human torso for data recording
during physical activity 02 p0167 N71-11189
(NASA-CASE-XPR-10856)
- GARNETS
NT YTTRIUM-ALUMINUM GARNET
NT YTTRIUM-IRON GARNET
Characteristics and optical activation of garnet
materials 07 p1086 N71-17175
- Magnetic moment versus temperature curves for
ferromagnetic garnets 07 p1095 N71-17842
(AD-715284)
- Spectral properties of natural silicate garnets with
structural and chemical interpretations of spectra in
optical range of 0.3 to 5.0 microns and to 300 microns
in infrared 17 p2814 N71-29723
- Theory of diffuse reflectance of particulate media
including garnet, glass, corundum powders, and mixtures
(NASA-CR-113057) 17 p2816 N71-29925
- Vibronic and electronic resonance Raman effect in
cadmium sulfide and garnet crystals 17 p2827 N71-30168
(AD-722701)
- Association of olivine, garnet, and chrome-diopside
in Yakutsk diamond 18 p2995 N71-31091
(NASA-TT-F-13819)
- Calculation of relative Raman scattering intensities
of low-lying electronic transitions in rare earth garnets
(AD-727063) 22 p3658 N71-36887
- Determination of Raman active phonons and electronic
levels in garnets 23 p3836 N71-37353
(AD-726663)
- Epitaxial growth of garnet films for magnetic bubble
domains 24 p3997 N71-38511
(AD-727070)
- GAS ANALYSES
NT OZONOMETRY
Conversion tables for Beckman CO₂ analyzers
models IR-215 and IR-315A/ 01 p0055 N71-10714
(AD-711320)
- Gas analyzer for bi-gaseous mixtures suitable for
use in test facilities 01 p0056 N71-10774
(NASA-CASE-XLA-01131)
- Burrington refractor plate correlation spectrometer
as remote sensing instrument of pollutant gases in atmosphere
(NASA-CR-111373) 02 p0223 N71-11421
- TAP and SCRAP - programs for processing data
from automatic gas analysis equipment using PDP/11
computer 03 p0342 N71-12476
(RD/BI-1581)
- Wavelength-selective, repetitively pulsed CO₂ laser
for nonlinear optical effects studies and atmospheric
pollutant detection 03 p0347 N71-12574
(NASA-TM-X-66497)
- Sampling by frontal analysis for determination of
carbon monoxide in air 04 p0485 N71-13454
(NASA-TT-F-13434)
- Livermore fission fragment analyzer - conference
(UCRL-74222) 04 p0582 N71-14004
- Oxygen activity in liquid sodium 04 p0532 N71-14457
(KFK-1149)
- Instrumentation for monitoring of Kr-85 and N-3 in
natural gas 05 p0488 N71-15559
(UCRL-30682)
- Microchemical analysis of air pollutants and
preparation of standard reference materials for gas
analysis 05 p0641 N71-15556
(NBS-TN-545)
- Properties of nonequilibrium radiation emitted by
Mars atmosphere gas mixtures 06 p0834 N71-15834
(NASA-CR-1740)
- Describing crystal contaminant instrument for detecting
condensable gas contaminants in vacuum apparatus
(NASA-CASE-NPO-10144) 07 p1032 N71-17701
- Absorption of helium 4 on activated carbon 08 p1231 N71-18389
(CRA-CONF-1585)
- Development of rate-controlled, partial-equilibrium
method for treating reacting gas mixtures 09 p1485 N71-38329
- Arc jet heating of oxygen Schumann-Runge system
(AD-717161) 10 p1618 N71-21390
- Techniques and equipment for industrial air pollution
monitoring and sampling 11 p1747 N71-22055
(JPRS-52546)
- Industrial pollution properties summary including
data on toxicity and control, air sampling, and gas
analysis 11 p1747 N71-22056
- Photocolorimetric gas analysis methods and equipment
11 p1761 N71-22057
- Polarographic, coulometric, and potentiographic gas
analyzers for air pollution measurements 11 p1761 N71-22058
- Luminescent analysis techniques and devices for air
pollution measurements 11 p1802 N71-22059
- Aerosol and flame ionization techniques for air pollution
sampling gas analysis 11 p1747 N71-22060
- Infrared absorption spectra gas analysis of air pollution
11 p1761 N71-22063
- Design and characteristics of time of flight mass
spectrometer to measure or analyze gases at low pressures
and times of flight of single gas molecules 11 p1766 N71-22041
(NASA-CASE-XPR-10136)
- Helium sweep gas facility design and operation for
analysis of reactor fission gas-isotope release rates for
space power reactor fuel element design 12 p1897 N71-23451
(NASA-TM-X-2267)
- Microwave double resonance spectroscopy absorption
cell for gas analysis 14 p2255 N71-26137
(NASA-CASE-LAS-10305)
- Analysis of gas generated by wires exploding in air,
argon, and nitrogen mixtures at low pressures 14 p2361 N71-26456
- Ion microprobe mass spectrometer with cooled electrode
target for analyzing traces of fluids 16 p2597 N71-28663
(NASA-CASE-ERC-10014)
- Sol-gel processes in U/PuO₂ fuel element preparation
and metallurgical and gas analysis of reactor
materials 17 p2781 N71-29231
(BAW-3714-19)
- Remote air sampling and monitoring system for gas
analysis of radioactive isotopes in containment atmospheres
after loss of coolant tests 17 p2744 N71-29645
- Application of mass spectrometer for space station
simulator atmosphere analyzer 18 p2902 N71-30743
(NASA-CR-111827)
- Measurement of smoke concentration in primary
zone of gas turbine combustor at high ambient pressure
by optical resonance technique 18 p3025 N71-31243
(NASA-TM-D-6410)
- Mass spectrometer with molecular beam system for
analysis of gaseous reaction kinetics 21 p3388 N71-34104
- Determination of oxygen, nitrogen, and hydrogen in
steels - conference 21 p3441 N71-34483
(PB-195294)
- GAS BAGS
Perforated soft landing system using storable gas bag
(NASA-CASE-XLA-09881) 06 p0990 N71-16085
- GAS BEARINGS
Air bearings for near frictionless transfer of loads
from one body to another 01 p0059 N71-10617
(NASA-CASE-XMF-01867)
- Research on foil bearings and gas lubricated films
(AD-711089) 01 p0060 N71-10670
- Effect of flow on interconnected thrust bearings
(RAE-TR-68302) 02 p0358 N71-11571
- Testing of gyros and accelerometers having hydrostatic
gas bearing axes 03 p0412 N71-12324
- Fluid power transmission and gas bearing system
(NASA-CASE-XMS-01445) 06 p0834 N71-14031
- High speed, gas journal bearings 06 p0863 N71-16259
(AD-713877)
- Developing viscous dominated incompressible
theory for describing dynamic viscosity and pressure
fields in film between gas lubricated disk 06 p1204 N71-19000
- Diaphragm and lead surface coatings for gas bearings
in aerospace engineering 10 p1562 N71-20739
(NASA-CASE-XGS-02011)
- Fluid motion for incompressible fluid between two
long concentric cylinders 11 p1734 N71-21970
(AD-717644)

- Motor start of 2 to 10 kilowatt Brayton rotating unit operating on gas bearings in closed loop test facility [NASA-TM-X-2246] 11 p1678 N71-22570
- Development of satellite flywheel using gas bearings [ST-3139] 12 p1660 N71-23375
- Thermal expansion coefficients of dynamic gas bearings [AD-718289] 12 p1926 N71-23759
- Swirl support of gas bearing for position adjustment between ball and supporting cup [NASA-CASE-XMF-07808] 12 p1928 N71-23812
- Gas bearing angular attitude control system 13 p2078 N71-24403
- Wide angle rotating mirror scan system for laser display system and synchronous motor gas and ball bearing performance tests [AD-721449] 16 p2606 N71-28071
- Low friction gas bearing system for fluid power transmission to bearing-supported payload [NASA-CASE-ERC-10097] 16 p2601 N71-28465
- Gas bearing for model support with capacity for measuring angular displacement of model in bearing [NASA-CASE-XLA-09346] 16 p2602 N71-28740
- Automatically balanced air bearing simulator for testing satellite attitude control system [ESRO-CR-18] 17 p2779 N71-29371
- Stability of equilibrium state of rotor in pressurized gas bearing [AD-722828] 18 p2929 N71-31213
- Half-sine shock and sinusoidal vibration tests of gas bearing supported rotor assembly and effects on mechanical performance of Brayton cycle space-power turbomachinery [NASA-CR-1762] 20 p3278 N71-33215
- Characteristics of externally pressurized, gas lubricated, circular thrust bearing with central admission and operating in inherent compensation mode [NRC-ME-MT-61] 20 p3278 N71-33226
- Performance tests and characteristics of circular, hydrostatic, gas-lubricated single inlet thrust bearings [NRC-MT-62] 20 p3278 N71-33227
- Entrance inertia effects associated with high speed magnetic tapes and computer flying heads [AD-726464] 23 p3744 N71-36694
- Dynamic response of gas lubricated thrust bearing with shrouded Raleigh-step pads [NASA-CR-125949] 23 p3761 N71-36809
- Development of finite difference method for solving Reynolds equation for pressurized gas bearings [AD-727162] 24 p3928 N71-38029
- Impregnation permeability of air bearing graphite pads [Y-SC-7] 24 p3942 N71-38124
- GAS CHROMATOGRAPHY**
- High precision gas chromatography applied to separation processes [COO-1222-40] 01 p0017 N71-10451
- Exponential dilution flask for gas chromatography, reducing wear, alignment, and maintenance [COO-1222-34] 01 p0054 N71-10527
- Human metabolism in rarefied atmospheres by gas chromatography 02 p0171 N71-11493
- Acetate content determination in polymeric materials using gas chromatography [AD-712312] 02 p0247 N71-11655
- Transuranium element separation using gas chromatography of aluminum chloride vapors [ANL-TRANS-843] 04 p0484 N71-13443
- Direct analysis of residual solvents in films by gas chromatography 04 p0488 N71-13470
- Spectra and photochemical reactions of mercury and ethylene [COO-584-46] 04 p0592 N71-14403
- Electron capture type detector model using ionizing radiation for gas chromatography [DNP-700] 05 p0743 N71-15147
- Automated, high sensitivity, three column gas chromatograph [UCL-50849] 05 p0688 N71-15519
- Hazards and safety factors associated with radioactive materials used in gas chromatography [PB-195790] 09 p1342 N71-19398
- Test facility to verify design concepts and mathematical models of chromatograph for atmospheric composition analysis of Mars [NASA-CR-117468] 11 p1760 N71-21931
- Off-line processing of chromatographic data from fatty acid methyl ester mixtures by digital computer [UCL-72933] 11 p1716 N71-22548
- Conference on propulsion and energetics techniques for diagnosing high velocity flows 11 p1739 N71-22626
- Automated gas chromatography with improved sensitivity 11 p1763 N71-22655
- Chemical analysis of polyimides using pyrolysis-gas chromatograph-mass spectrometer system [JRAE-TR-70177] 12 p1870 N71-23432
- Vapor pressure and heat of vaporization of metal beta diketone chelates measured by gas-liquid chromatography [AD-716429] 12 p1870 N71-23479

- Selecting and processing solid carriers for organophosphorus compounds using gas chromatography [JPES-53065] 13 p2040 N71-25137
- Gas chromatographic method for determining carbonate carbon in rocks and minerals 14 p2251 N71-26646
- Computer simulation and laboratory studies made of quantitative analyses obtained by overlapping two or more chromatograms [COO-1222-43] 15 p2377 N71-27125
- Computer controlled gas chromatograph for monitoring temperature, mass flow rate, inlet pressure, and calculation of precise retention volumes in real time [COO-1224-44] 15 p2410 N71-27481
- Atmospheric sampling and analysis of xenon, water vapor, krypton, carbon dioxide, and radon radioactivity by thermal absorption and gas chromatography 17 p2744 N71-29067
- Counter-current continuous gas chromatography/distillation of nitrogen/liquid system [NLL-RTS-6323] 17 p2716 N71-30213
- Oxygen-nitrogen ratio determination by phosphoric acid dissolution at high temperatures and gas chromatography for hypostochiometric uranium dioxide [RCN-128] 17 p2716 N71-30228
- Universal, high stability radioisotopic detector for gas chromatography using nickel-63 as ionizing source [DNP-737] 21 p3429 N71-34402
- Infrared radiation detector for determining organic substances in burning flame chromatography 21 p3429 N71-34406
- Analysis of precision and accuracy of results obtained in quantitative gas chromatography [NLL-CE-TRANS-5638-19022.09] 21 p3430 N71-34410
- Gas chromatographic techniques for determination of trace amounts of water and detection limits for gases and liquids [NLL-M-20374-5828.4F] 22 p3532 N71-35301
- Gas chromatograph, mass spectrometer system for chemical and biochemical determinations on Mars, and data reduction program [NASA-CR-122038] 22 p3583 N71-35514
- Gas-liquid chromatography peak-shape dependence on retention time, sample volume, and column type and overlapping peak area determination [NLL-CE-TRANS-5578-19022.09] 23 p3721 N71-36526
- Reproducibility of gas chromatographic biochemical data and value in toxicology [AD-727523] 24 p3879 N71-37653
- Gas chromatographic study of trace contaminants in man-expired air, and effects of physiological stresses of space flights 24 p4015 N71-38644
- GAS COMPOSITION**
- NT CARBON DIOXIDE CONCENTRATION**
- Gaseous reactions in passive CO₂ laser cells as indicated by emission in visible region [AD-711522] 01 p0063 N71-10638
- Regeneration of artificial respirable atmospheres using potassium peroxide [NASA-TT-F-13430] 04 p0487 N71-13463
- Volcanic gas collections used to calculate chemical composition of volatile fraction of basaltic magma gas phase [NASA-TR-R-348] 13 p2071 N71-24610
- Model studies on formation of organic compounds in simple atmospheric gases by electric discharges [NASA-TT-F-13757] 18 p2887 N71-31312
- Non-dispersive infrared gas analyzer [NASA-CASE-ARC-10308-1] 21 p3386 N71-34090
- Comet characteristics and composition in relation to kinetics 24 p4009 N71-38583
- GAS COOLED REACTORS**
- NT EXPERIMENTAL GAS COOLED REACTORS**
- NT HIGH TEMPERATURE NUCLEAR REACTORS**
- Molten salt nuclear reactor and high temperature gas cooled reactor research [ORNL-4596] 01 p0085 N71-10408
- Design and operation of experimental gas loop for nuclear reactor [ZJE-68] 02 p0266 N71-12179
- Transient phenomena in secondary water-steam circuit of gas cooled reactor [CEA-R-4012] 04 p0545 N71-13560
- Development of high temperature gas-cooled nuclear power plant [QA-10292] 04 p0556 N71-14101
- Separation of U-233 from U-235 during head-end reprocessing of HTR fuels of TRISO coated fissile and fertile particles [QA-9258] 04 p0560 N71-14357
- Conference on gas cooled high temperature reactors [CONF-700401] 05 p0731 N71-15572
- Gas cooled reactor fuel management calculations [AEW-R-652] 07 p1064 N71-17501
- Spatiotemporal study of graphite gas power reactor on hybrid computer - conference [CEA-CNF-1580] 08 p1235 N71-18206

- Fuel, prestressed concrete reactor vessel, and helium circulator developments of high temperature gas cooled reactor systems 10 p1604 N71-21240
- Research in reactor technology for gas cooled fast breeder reactors 13 p2122 N71-23516
- Niobium zirconium temperature sensor design for application in high temperature gas cooled or liquid metal cooled reactors 14 p2252 N71-25430
- [WHAN-SA-24] 14 p2252 N71-25430
- Fast neutron irradiation of SiC coated outer layer of particles for gas cooled reactors [EURFNR-834] 14 p2294 N71-26666
- Calibration factor P_{pellet}/t for measuring fuel fission ratio in annular fuel region of M3 gas cooled reactor fuel elements [AEW-M-975] 15 p2447 N71-27320
- High temperature, gas cooled reactor control rod, control rod guide tube, and thermally released shut-down rod after 300 full power days of operation [QA-10196] 16 p2631 N71-28221
- Gaseous core diffusion nuclear reactor for thermal energy generation [NASA-CASE-LEW-10250-1] 16 p2635 N71-28759
- Determination of thermal conductivity of UO₂ with sintered density of 10.57 g/cc in 500 C to 2500 C range [AB-411] 17 p2783 N71-29028
- Design and development concept of high temperature, gas-cooled reactor /HTGR/ [QA-10599] 19 p3139 N71-32208
- Nonlinear effects of recombination and collective diffusion associated with seeded nuclear plasmas using helium isotopes in gas cooled reactors 20 p3306 N71-33468
- Stability of plane vortex sheet between gases exchanging heat by radiation applied to gas core in coaxial jet nuclear reactor [NASA-CR-19311] 22 p3568 N71-35411
- Effect of buoyancy on fuel containment in space-cycle gas-core nuclear rocket engines [NASA-TM-X-67924] 22 p3620 N71-35794
- Nozzle and cavity wall cooling limitations on specific impulse of gas-core nuclear rocket engines [NASA-TM-X-67923] 22 p3621 N71-35795
- Criticality evaluation of hydrogenous enriched lattices using three group model for reactor design [UAREE-94] 23 p3794 N71-37047
- Reactor physics characteristics of high temperature gas cooled reactor [AEW-M-985] 24 p3956 N71-38210
- GAS COOLING**
- Gas cooled high temperature thermocouple [NASA-CASE-XLE-09475-1] 05 p0784 N71-15360
- Pressure loss effect on cold production in two stage gas refrigerating machinery 10 p1663 N71-21265
- Gas film cooling past nonadiabatic flat plate 12 p2014 N71-23016
- Reactor tests of fuel element lifetime and burnup for gas cooled nuclear power reactors 13 p2112 N71-24311
- GAS DENSITY**
- Physical adsorption and molecular hydrogen densities of interstellar clouds 06 p0948 N71-16708
- The continuity equation of compressible flow with flow velocity distortions and gas density variations [DLR-MITT-70-13] 07 p1008 N71-17160
- Ionization gas density data for superionic gas flow [AD-716618] 09 p1372 N71-19370
- Moete Carlo method applied to angular distribution of electron beam plural scattering for gas density measurement [REPT-1000/71] 11 p1804 N71-22388
- Gas density measurement using laser induced Raman scattering [DLR-MITT-71-01] 12 p1900 N71-23406
- Device for simultaneously determining density, velocity, and temperature of streaming gas [NASA-CASE-XLA-03375] 12 p1934 N71-24074
- Theoretical inhomogeneity emission models of planetary nebulae 12 p1999 N71-24077
- Reaction time of upper atmosphere from gas density fluctuations following geomagnetic disturbances 13 p2070 N71-24046
- Thermosphere and lower exosphere gas density and temperature from satellite drag measurements 13 p2070 N71-24047
- Inhomogeneous Bose gas interactions with ion impurities, walls, and vortices 13 p2065 N71-24759
- Latitudinal density distribution of gases in upper atmosphere 13 p2076 N71-25267
- Hypersonic shock/density ratio effects in aerodynamic heating of space shuttle configuration 14 p2354 N71-26088
- Refractive index measurements on pressurized liquids and gases by optical interferometry 14 p2297 N71-26408

SUBJECT INDEX

GAS DYNAMICS

- Local gas density distribution in rarefied gases at rest between parallel plates at 79 K and 294 K, respectively [COO-2832-4] 15 p2387 N71-2776
- Density distribution measurements in reacting gases contained between two concentric cylinders undergoing relative rotation, and heat transfer and drag measurements 16 p2393 N71-28876
- Coherent light beam device and method for measuring gas density in vacuum chambers [NASA-CASE-XER-11203] 16 p2399 N71-28994
- Spectroscopic band models for determining gas temperatures and concentrations 19 p3048 N71-31675
- Transient pressure, temperature, and density measurement of high temperature dense gas during compression tests [VKI-TM-23] 20 p3249 N71-32956
- Derivation of generalized function for gas viscosity [NLL-RTS-4480] 22 p3570 N71-35425
- GAS DETECTORS**
- Optical correlation methods for remote sensing of trace gases at high altitudes 02 p2328 N71-11993
- Cryogenic device for leakage detection using helium [CEA-COMP-1306] 06 p2385 N71-18396
- Development of device for detecting hydrogen in ambient environments [NASA-CASE-MPS-11537] 09 p3191 N71-20442
- Carbon monoxide accumulator coil for spacecraft mass spectrometer atmospheric sensor system [NASA-CR-111855] 11 p1764 N71-22849
- Gas leak detection in evacuated systems using ultraviolet radiation probe [NASA-CASE-HRC-10804] 13 p2096 N71-34096
- High resolution gas Cerenkov counter operational characteristics [NAL-TM-2] 15 p2499 N71-27930
- Sodium flow evaluation of nickel palladium catalytic hydrogen detector [AFDA-253] 16 p2634 N71-28755
- Annotated bibliography on gas detectors compiled from DDC data bank [AD-72764] 18 p2922 N71-30708
- Cold cathode gauges for measuring amount of gas present in lunar atmosphere 18 p3011 N71-30963
- Noninfrared infrared gas analyzer [NASA-CASE-ARC-10308-1] 21 p3386 N71-34090
- GAS DISCHARGE COUNTERS**
- U COUNTERS**
- U GAS DISCHARGE TUBES**
- GAS DISCHARGE TUBES**
- NT THERATRONDS**
- Direct current conductivity in turbulent cylindrical discharge tube plasma [JNRL-TM-3038] 02 p2081 N71-11862
- Using quartz discharge tube for generating high power single-frequency argon laser 03 p3088 N71-13245
- Investigating hollow cathode discharge as energy source for argon ion lasers 06 p1210 N71-19163
- Direct current powered self repeating plasma column with interconnected annular and linear discharge channels [NASA-CASE-XLA-05103] 10 p1630 N71-21493
- Disk shaped discharge chamber for dense plasma form formation 17 p2812 N71-30134
- Effect of pressure on distance between striations in positive column of gas discharge tube with values for ionization coefficient 19 p3165 N71-32363
- Timing capacity for control of cathode electron beam 20 p3241 N71-33421
- Internal flow conditions in hollow gas cathode [TP-599] 20 p3330 N71-33475
- Diagrams of volt-ampere characteristics of hollow cathode discharge device with concentric spherical electrodes [JEP-TRAMS-68] 21 p3404 N71-34221
- Feasibility of using pulsed laser as discharge tube with molecular deuterium and hydrogen under pressure 22 p3451 N71-36038
- Nonconstricted positive column in gas discharge tubes with thermal model based on thermoelectric and spectroscopic measurements 22 p3453 N71-36054
- Plasma drift in flash X ray [FXR] discharge determined by symmetrically placed magnetic probes [OUB-459] 22 p3454 N71-36058
- Applying microwave-reflection method to studying shock waves propagated through magnetic field in hollow cathode discharge tubes [BARAE-101] 23 p3525 N71-37280
- Application of linear gas discharge displays on control panels to data representation systems 24 p3882 N71-37670
- Plasma heating and stability in combined pinch in discharge chamber of small diameter with no filaments [CONP-710697-13] 24 p3995 N71-38497
- GAS DISCHARGES**
- NT RING DISCHARGE**
- NT TOROIDAL DISCHARGE**
- Time-resolved Langmuir probe measurements in striated neon discharge 01 p0104 N71-10024
- Gas discharge analysis of CO₂ and HCN lasers [AD-711523] 01 p0063 N71-10636
- Collective interactions and plasma heating in high-current gas discharge 01 p0106 N71-10709
- Physical effectiveness of current heating of dense high current gas discharge plasma stabilized by strong magnetic field [KHFTI-09-43] 03 p0436 N71-12894
- Far ultraviolet radiation from sputter discharge in microwave plasma probes [NPL-QU-10] 03 p0418 N71-13277
- Purely RF gas discharges as rectifiers and interconnectors 03 p0419 N71-13338
- Accelerometer model for neutron production in z-pinch discharges 03 p0439 N71-13368
- Development of axial plasma flows in oscillating gas discharge 04 p0576 N71-13692
- Building of gas discharges in proportional and Geiger region for use in Charkap chambers [SLAC-TRANS-121] 04 p0580 N71-13908
- Electron beam and plasma instability in low density plasma of high current gas discharge [ABC-TM-7165] 04 p0597 N71-14121
- Characteristics of stationary gas discharge plasma [NPL-18427] 04 p0600 N71-14385
- Characteristics of relativistic electron beams extracted from electrode space of flash X ray machines [AD-713576] 05 p0755 N71-15374
- Reduction of gas discharge breakdown thresholds in ionosphere due to multipactoring 06 p0829 N71-16653
- Electrical characteristics of discharge in hollow cathode in neon [NRC-TT-1437] 08 p1170 N71-18858
- Evaluation of gas discharge transducer and associated instrumentation for asteroid belt meteoroid experiment with Pioneer probe F/G [NASA-CR-111848] 09 p1390 N71-20401
- Diffusion mechanisms and boundary problems in electropositive and electronegative gases including plasma diffusion in electropositive negative glow and Faraday dark space 12 p1980 N71-23265
- Radio frequency noise generator having microwave slow-wave structure in gas discharge plasma [NASA-CASE-XER-11019] 12 p1889 N71-23598
- Gas discharge processes in Charkap proportional counters in proportional and Geiger ranges [NLL-M-20172/5828.4F/1] 12 p1973 N71-24017
- High temperature plasma inside discharge produced by planar HIF power passing through helium [NLL-M-20301/5828.4F/1] 12 p1982 N71-24101
- Experimental and theoretical analysis of plasma propagation into low pressure gas and plasma in magnetic field [AD-719855] 14 p2320 N71-25710
- Radiocopic measurement of gas in flow type system with carbon dioxide, helium, and air in single, binary, and tertiary mixtures 14 p2266 N71-26570
- Design and operation of linear gas discharge indicators permitting continuous visual monitoring of parametric variations 14 p2259 N71-26664
- Measuring erosion as loss of electrode material in high current, high pressure gas discharges [JEP-472] 15 p3499 N71-27264
- Electric field intensities for inducing gas bubble discharge in liquids [JNIR-P13-5277] 15 p2479 N71-27655
- Ion sampling measurements in high pressure cesium discharges [AD-726713] 15 p2504 N71-27927
- Simple argon model atoms used for calculating electron number densities for argon plasma discharges [NASA-TN-D-6383] 16 p3643 N71-28085
- Dependence of ion component on magnetic field strength, and formation of plasma flux when plasma flows from hot cathode discharge [AD-721313] 16 p2661 N71-28745
- Space charge electron avalanche in nitrogen and hydrogen breakdowns 17 p2795 N71-29719
- Program for calculating parameters of optical choked by digital computer [NLL-RYS-6155] 17 p2726 N71-29822
- Measurement of self absorption in helium discharge [FB-196166] 19 p3164 N71-32381
- Electrophoresis theory for convection phenomena in gas mixture subjected to dc discharges 19 p3165 N71-32399
- Determination of electron temperature of gas discharge plasma by measurement of noise and resistance 19 p3165 N71-32393
- Quasistatic Townsend discharges in gas mixture and electric strength of moving gas 19 p3166 N71-32395
- Langmuir probe theory for collisional plasma with collision dominated probe sheath based on hot cathode hollow discharge measurements [AD-726906] 22 p3655 N71-36064
- High voltage unswitched pulse generators with spark dischargers, techniques for shaping pulses, and analysis of gas discharge and arc formation [AD-726793] 23 p3757 N71-36450
- Formation of spectroscopic effect by gas discharge light sources [NLL-OA-TRANS-1071-61913.1] 23 p3804 N71-37123
- High current gas discharge accompanying noncylindrical compression of a pinch [CN-28/0-5] 24 p3804 N71-38431
- GAS DISSOCIATION**
- Numerical analysis of one dimensional flow of dissociating gas 05 p0661 N71-14771
- Interatomic potentials and dissociation energies of diatomic hydrogen and halogen molecules studied with spectroscopy and potential curves [NASA-CR-116970] 09 p1428 N71-19737
- Dissociation energy and long range potential of diatomic gas molecules from vibrational spacings of higher levels 09 p1428 N71-19739
- Dissociation energies and long range potentials of diatomic halogen molecules from vibrational spacings 09 p1428 N71-19740
- Computation of binding energies and vibrational energies of ground state molecular hydrogen to measure accuracy of dissociation energy 09 p1429 N71-19741
- Spectroscopic reassignment and ground state dissociation energy of molecular iodine 09 p1429 N71-19742
- Ground state dissociation energies for diatomic halogens from vibrational spacings near dissociation limit 09 p1429 N71-19746
- GAS DYNAMICS**
- NT AERODYNAMICS**
- NT AEROTHERMODYNAMICS**
- NT HYPERSONICS**
- NT RAREFIED GAS DYNAMICS**
- NT ROTOR AERODYNAMICS**
- Gas dynamic stability and damping of detonation wave in nozzles [AD-711753] 01 p0044 N71-10943
- Kinetic theory, molecular beam applications, and rarefied gas dynamics [AD-711419] 02 p0204 N71-11752
- Applied gas dynamics including data on subsonic and supersonic injectors [AD-712621] 03 p0363 N71-13059
- Investigating gas dynamical aspects of combustion in hybrid rocket motors [ISAS-450-VOL-35-NO-3] 03 p0468 N71-13099
- Slow electron collision processes in gases [RPE-4144-1] 04 p0572 N71-13629
- Combustion processes and gas dynamics of two phase flows in wet steam turbines [NASA-TT-F-611] 04 p0510 N71-13767
- Methods for calibrating low mass flow rate nozzles in aerodynamic facilities [AD-713625] 05 p0658 N71-15428
- Numerical analysis of gas motions and radiative transfer of H waves 06 p0044 N71-16821
- Development of rate-controlled, partial-equilibrium method for treating reacting gas mixtures 07 p1485 N71-20529
- Numerical integration of equations for vibrational relaxation and relative gas in expanding flows of anharmonic gas oscillators [NASA-TN-D-7050] 10 p1542 N71-23108
- Gas dynamic techniques for study of desorption rates in one and two component systems 10 p1543 N71-23135
- Heat release explosive processes and gas dynamics for high power energy conversion systems [AD-717108] 10 p1466 N71-21783
- Canadian research on aerospace sciences and engineering, gas and plasma dynamics, and related topics 11 p1827 N71-22515
- Gas and fluid response to high intensity ruby laser beam [AD-717728] 11 p1732 N71-32593
- Application of free flight ranges to high temperature gas dynamics 11 p1740 N71-23633
- Dense argon gas atomic dynamics using slow neutron scattering 12 p1970 N71-23709
- Nonequilibrium radiative gas dynamics of slender pointed bodies [AD-719744] 13 p2063 N71-24431

- Inhomogeneous Bose gas interactions with ion impurities, walls, and vortices 13 p2065 N71-24797
- Development of theoretical model for irregular refraction of plane shock wave by wedge of hot gas [AD-720818] 14 p2339 N71-25765
- Numerical analysis of flow of viscous, compressible gas through slender axisymmetric channels using finite difference theory 14 p2242 N71-26464
- Hydrodynamics and gas dynamics of boundary layer flow including mass transfer and convective and radiative heat transfer of bodies in fluids [AD-720738] 14 p2344 N71-26339
- External operating characteristics, current and voltage amplification ratios, and electric power efficiency of electrodynamic energy converter 14 p2244 N71-26605
- Gas dynamics and thermodynamics of single vapor bubbles in liquid hydrogen and ultrasonic radiation effects [JINR-P13-5327] 15 p2392 N71-27085
- Laser-radiation effects on metals including damage thermodynamics, melting and cavity formation, vapor hydrodynamics, and damage product electromagnetic absorption [JPRS-53241] 16 p2608 N71-28180
- Pressure, temperature, gas sampling, and optical measurements in two dimensional jet interaction flow field [NASA-TM-X-67842] 16 p2583 N71-28953
- Derivation of kinetic equations for slightly dense and dilute short range gases, Boltzmann equation related to short range gas equations, and role of collision events in system evolution 17 p2733 N71-29623
- Formulation of Volterra equations describing Raligh problem, and algorithm based on Krook equation [TR-36] 17 p2775 N71-30372
- Bibliography on three dimensional flow dynamics [AD-722880] 18 p2904 N71-30712
- Bibliography on one dimensional flow dynamics [AD-722850] 18 p2904 N71-30716
- Radiative properties of gas at varying wavelengths 18 p3024 N71-30945
- Extension of surface energy exchange analysis to isothermal gas radiation in enclosures 18 p3025 N71-30946
- Gas kinetics and vacuum physics to analyze for various outgassing rates minimum pressure ranges attainable by spacecraft canister - tables [NASA-TM-X-64606] 18 p3019 N71-31255
- Basics of high speed aerodynamic theory and characteristics of gas flows for rockets [NASA-TT-F-601] 18 p3020 N71-31467
- Solving exact gas dynamic equations for supersonic flows far from axis of slender lifting bodies [NASA-TN-D-6446] 19 p3035 N71-32792
- Mathematical models for computer calculations of two dimensional hydrodynamic nonlinear combustion instability flow [NASA-CR-121472] 20 p3365 N71-33572
- Acoustic instability driven by thermal radiation absorption in extremely high temperature gases [CER-T-49-4] 20 p3330 N71-33640
- Q switched laser induced gas breakdown used in hydrogen atom detection, spectral analysis, and chemical reactions [NASA-CR-121446] 21 p3385 N71-34084
- Inverse solution of two dimensional gas dynamic flow fields of rotational or irrotational character [NASA-CR-121674] 21 p3410 N71-34261
- Measurement and correlation of gas-particle heat transfer coefficients in packed and fluidized bed processors by frequency response techniques [RPS-3639-16] 21 p3411 N71-34268
- Gas dynamics and magnetic field effects on shock wave gradient acceleration and experimental design applications [UCRL-TRANS-10532] 21 p3412 N71-34281
- Development and characteristics of gas operated actuator designed to eliminate need for external supply of drive gas for operation [NASA-CASE-NPO-113469] 21 p3432 N71-34419
- Formulation of equation to determine thermodynamic relationships in steady flow processes [PB-199759] 21 p3531 N71-35164
- Gas dynamic structure of high altitude rocket exhaust studied in low density tunnel [AD-726555] 22 p3663 N71-36121
- Properties of high temperature compounds, physics of gas dynamics, heat resistant materials, and heat convection by power plants [JPRS-54182] 23 p3868 N71-37573
- GAS EVACUATING**
- U EVACUATING (VACUUM)**
- GAS EVOLUTION**
- Gas emanations and contaminants produced by polymers used in spacecraft construction 02 p0170 N71-11479
- Chemistry and enzymology of photosynthesis, oxygen evolution, energy migration, and kinetics of reaction [RIAS-3706-15] 05 p0634 N71-14666
- Computerized simulation of fission swelling and gas release model for solids [WAPD-TM-942] 06 p0917 N71-16195
- Helium sweep gas facility design and operation for analysis of reactor fission gas-isotope release rates for space power reactor fuel element design [NASA-TM-X-2267] 12 p1897 N71-23651
- Degassing and rates of evolution for copper wires in ultrahigh vacuum 13 p2094 N71-24921
- Evolution of gases from water solutions containing plutonium caused by radiolysis of water by alpha radiations and methods for handling and storing solutions [AEC-TR-7217] 14 p2212 N71-25793
- Development of filter system for control of outgas contamination in vacuum conditions using absorbent beds of molecular sieve zeolite, silica gel, and charcoal [NASA-CASE-MFS-14711] 14 p2262 N71-26185
- Fission product swelling, gas evolution, and creep properties of uranium dioxide nuclear fuels [TRG-1937/5] 15 p2449 N71-27388
- Mathematical model for coolant three dimensional flow during rapid fission gas release in fast nuclear reactor cores based on plenum chamber simulation [ANL-7651] 17 p2784 N71-29666
- Iodine adsorption properties of metal-loaded zeolites and applications to gas filtration beds in nuclear fuel processing plants 17 p2715 N71-29862
- Fission gas and nonvolatile fission product release measuring device based on thermodynamics for high temperature nuclear reactors [JUL-707-RW] 18 p2960 N71-30862
- GAS EXCHANGE**
- Turbulent mass exchange processes between recirculation zones in flame holder wake and surrounding flow [RAE-LIB-TRANS-1418] 05 p0666 N71-15669
- Alveolar gas exchange and cardiovascular functions during respiratory inhibition [PB-194825] 07 p0980 N71-17097
- News, briefs, and abstracts of scientific articles concerning oceanography 15 p2396 N71-26862
- GAS EXPANSION**
- Sealed electric storage battery with gas manifold interconnecting each cell [NASA-CASE-XNP-03378] 02 p0148 N71-11051
- Laser power at 5 micron from carbon monoxide gasdynamic expansion [NASA-TM-X-62006] 02 p0239 N71-11668
- Using double expansion nozzle in shock tube facility to study population inversions in carbon dioxide gas laser [AD-713497] 05 p0697 N71-15343
- Expansion and shock waves in two phase air water flow [BMVTDG-FBWT-70-2] 08 p1178 N71-16440
- Molecular relaxation of anharmonic nitrogen oscillators in simulated expansion flow environment with vibration-vibration and vibration-translation energy exchange 11 p1742 N71-22720
- Steady state, axisymmetric shock distribution of free expansion of supersonic plasma jet issuing from sonic orifice numerically investigated using continuum flow 11 p1814 N71-22762
- Method and apparatus for producing very low temperature refrigeration based on gas pressure balance [NASA-CASE-XNP-06877] 11 p1773 N71-23025
- Feasibility analysis of open-cycle gas-core nuclear rocket engine [NASA-TM-X-67823] 12 p1963 N71-23907
- Solutions of diffusion equation for expanding gas cloud in constant shear flow [AD-722437] 17 p2739 N71-29649
- Electron-ion recombination effects on plasma flow of partially ionized monatomic gas from sonic orifice [RE-412] 18 p2908 N71-31502
- Similarity solutions for gas expansion in rarefied atmosphere [P-4562] 19 p3081 N71-32540
- GAS EXPLOSIONS**
- Exploding wires as shock wave sources [SC-RR-70-45] 04 p0620 N71-14030
- Formation of crater due to expansion of gaseous explosion products following rock crushing by direct and reflected waves [UCRL-TRANS-10476] 05 p0743 N71-15131
- Explosive oxidation hazard in simulated meteoroid S-4B impact penetration into spacecraft atmosphere [NASA-CR-117142] 09 p1484 N71-20236
- Vessel size and shape effects on gas and dust explosions in closed containers [BM-R1-7507] 12 p2013 N71-24279
- Materials tests on bottles for oxygen, air, and other gases to be used as airborne equipment, noting filament winding [TRC-BR-22373] 13 p2030 N71-23051
- GAS FLOW**
- NT AIR FLOW**
- NT CONTINUUM FLOW**
- NT NONEQUILIBRIUM FLOW**
- NT FREE MOLECULAR FLOW**
- NT FROZEN EQUILIBRIUM FLOW**
- NT JET STREAMS (METEOROLOGY)**
- NT KNUDSEN FLOW**
- NT MERIDIONAL FLOW**
- NT MOLECULAR FLOW**
- NT NONEQUILIBRIUM FLOW**
- NT SHIFTING EQUILIBRIUM FLOW**
- NT SLIP FLOW**
- NT TRANSITION FLOW**
- NT VERTICAL AIR CURRENTS**
- Mass transfer in gas flow through fluidized bed 01 p0043 N71-16000
- Low-altitude satellite interaction study of neutral gases and Monte Carlo computer techniques for describing flow field and spacecraft interactions [NASA-CR-111136] 01 p0049 N71-16011
- Wake of catalytic flat plate in low density dissociation gas flow [AD-71291] 01 p0044 N71-16007
- Steady gas flow in capillary tubes using Knudsen law [PB-1905687] 02 p0201 N71-11536
- Characteristics of viscous gases flowing between two relatively rotating coaxial cylinders [NASA-TN-D-6092] 03 p0363 N71-13046
- Interaction between supersonic air jet from slot with hypersonic air flow over surfaces [D1-82-0999] 04 p0518 N71-15766
- Computing two-layer gas flows in supersonic axially symmetric nozzles [NASA-TT-F-13429] 04 p0518 N71-15779
- Computer programs for determining laminar flow between a rotating disk [AD-71291] 04 p0519 N71-15779
- Three-dimensional laser Doppler velocimeter for measuring local mean and fluctuating gas velocities [NASA-CR-102948] 04 p0524 N71-14040
- Gas flow near flat surface fitted with fins in burning bone pattern in nuclear gas-graphite power reactors [CEA-N-1329] 04 p0562 N71-14010
- Potential momentum thrust performance of three axisymmetric ejectors [AD-713634] 05 p0762 N71-14622
- Steady state X ray system for determining void fraction transient variations in two phase gas-liquid flow [KAPL-3859] 05 p0639 N71-14711
- Numerical analysis of one dimensional flow of dissociating gas 05 p0661 N71-14771
- Portable thermocouple for measuring temperature, velocity, and direction of gas stream [AD-713664] 05 p0688 N71-15409
- Tubular flow restrictor for gas flow control in pipeline [NASA-CASE-NPO-10117] 05 p0695 N71-15408
- Equations of motion for weakly nonuniform potential flow [AD-714113] 06 p0835 N71-16120
- Numerical analysis of shock wave produced by expanding sphere [AD-714197] 06 p0836 N71-16171
- Perturbation theory and asymptotic expansion analysis on supersonic inviscid gas flow past axially-symmetrical body 06 p0839 N71-16180
- Numerical solution of boundary value problem for linearized Navier-Stokes equations 07 p1006 N71-16937
- Techniques for analyzing three dimensional boundary layer separation 07 p1006 N71-16938
- Subsonic compressible gas flow around semi-infinite plate in channel 07 p1006 N71-16946
- Gas target for slow meson experiments at 100 m [CERN-TRANS-69-29] 07 p1071 N71-17062
- Numerical analysis of boundary layer equations in flow cross section for monatomic gases [NASA-TN-D-6152] 07 p1099 N71-17045
- Developing high pressure gas purification and filtration system for use in test operations of space vehicles [NASA-CASE-MFS-12806] 07 p1030 N71-17590
- Burst diaphragm flow initiator for installation in short duration wind tunnels [NASA-CASE-MFS-12915] 07 p1004 N71-17000
- Velocity dependence of gain of carbon dioxide laser [AD-715136] 07 p1039 N71-17042
- General kinetic problem for collisionless flow of neutral, monatomic, unexcited gas past circular cone 07 p1010 N71-17074
- Characteristics of air-to-jet air mass augments with rotary primary flow input [AD-715642] 08 p1181 N71-18087
- Two phase flow of gas-liquid mixture through porous material 08 p1182 N71-18088
- Effect of transverse temperature gradient on velocity and temperature profiles for laminar flow of air 08 p1182 N71-18093
- Low density hypersonic flow over cone, scattering of gas particles from solid surface 08 p1182 N71-18095
- Stability of laminar flow in circular pipes with respect to three dimensional disturbances 08 p1183 N71-18090

- Characteristics of separated flow regions within a shock compressing nozzle
[NASA-CR-116875] 08 p1184 N71-18990
- Gas flow during and after deflagration of spherical cloud of fuel air mixture 09 p1370 N71-19555
- Severed diffusers used to check flow of gas or liquid moving at subsonic velocity 09 p1370 N71-19555
- Gas particle flow properties in blade to blade stream surface of cascade nozzle calculated theoretically [AD-716391] 09 p1372 N71-19762
- Similarity between two phase liquid-vapor flows with heat exchange - conference
[CEA-CONF-1648] 09 p1376 N71-20118
- Fluid dynamics of gas-particle flow and solid particle behavior in mixed flow
[NASA-CR-117309] 09 p1377 N71-20257
- Navier-Stokes equations for calculating viscous relative cooling gas flow around blunt body
[NASA-TT-F-13531] 09 p1378 N71-20343
- Radiative-convective heat transfer of high temperature flow of gas in channel 10 p1660 N71-20757
- Color photointerpretation of interference colors reflected from thin film oil-coated components in mixing gases for gas flow visualization
[NASA-CASE-XMF-01779] 10 p1539 N71-20615
- Automatic control of two-gas atmospheric supply system for long term test on space station simulator 10 p1507 N71-20966
- Numerical integration of equations for vibrational relaxation and relative gain in expanding flows of anharmonic gas oscillators
[NASA-TN-D-7809] 10 p1542 N71-21308
- Formation of kinking compression shock in flow around profile with break in generator and its properties in ideal gas flow 11 p1734 N71-21968
- Determination of vibrational equilibrium of radiatively driven acoustic waves of gas in cylindrical tube [AD-717643] 11 p1736 N71-22244
- Development of flow property charts for pure nitrogen in quasi-one-dimensional nozzle for equilibrium, nonequilibrium, and frozen flow under hypersonic conditions [AD-717704] 11 p1737 N71-22287
- Gas and water cooled probes for high temperature gas and dense plasma and flow measurements 11 p1842 N71-22604
- Shock tube using two phase system of solid particles and gases as driven fluid 11 p1740 N71-22629
- Probe measurements of charged particle concentrations and ionization relaxation phenomena in low density supersonic gas flows 11 p1808 N71-22650
- Analysis of supersonic and hypersonic flow of inviscid ideal gas over conical wings with sharp leading edge and attached shock waves by three dimensional method of characteristics [NASA-CR-1738] 11 p1671 N71-22672
- Numerical analysis of flow properties of intermediate altitude rocket exhaust plumes using finite difference technique 11 p1741 N71-22675
- Instrumentation and development techniques for the velocity gas flow measurement 12 p1899 N71-23313
- Two-layer flow in supersonic nozzles with different isentropic exponent and gas flow rate ratios [NASA-TT-F-135246] 12 p1899 N71-23385
- Numerical analysis of laminar local wall friction and heat transfer in noncircular tubes and annuli with variation of gas transport properties [AD-718777] 12 p1904 N71-24208
- Actively conducting gas controlled heat pipes leading to predictive capability for heat and mass transfer during heat pipe 13 p1818 N71-24866
- Vertical transonic gas flow over wire profile 14 p2238 N71-25714
- Development of theoretical model for irregular reflection of phase shock wave by wedge of hot gas [AD-720818] 14 p2239 N71-25765
- Radial velocity distributions in molecular gas flow boundaries with high temperature metal surfaces [AD-720726] 14 p2340 N71-26178
- Numerical calculations of electrical parameters in Penney-type MHD generator with two dimensional flow [BB-1199] 15 p2393 N71-27207
- Pulsed neutron counter using helium gas flow and temperature effects on flow velocity from reactor core [WJAN-AN-73] 15 p2449 N71-27380
- Calculation of dynamic and thermal characteristics of gas circuit in variable flow conditions with application to studying reactor under natural convection flow conditions [NLL-CE-TRANS-5373-19022.09] 17 p2733 N71-29574
- Local propagation velocity in nonstationary symmetrical reaction gas flow [NASA-TT-F-13571] 17 p2736 N71-30137
- Wing tip vortex test demonstrating use of Laser Doppler Velocimeter system for measuring gas velocities with high spatial and temporal resolution [NASA-CR-119004] 17 p2737 N71-30278
- Flow characteristics of adsorbable gases in porous bodies and isotopic separation by gaseous diffusion [NF-18567] 18 p2904 N71-30420
- Transonic flow of gas in axially symmetric Laval nozzles with sloped walls [NASA-TT-F-13573] 18 p2904 N71-30749
- Analysis of flows past rectangular recesses in plane and axially symmetric bodies immersed in supersonic air stream [NASA-TT-F-13577] 18 p2904 N71-30750
- Molecular hydrogen outflow in Arcturus laser cruiser using spectral observations 18 p3014 N71-31085
- Isobaric bubble motion under influence of varying high-g body forces, low gas flow rate isothermal bubble formation, and coefficients of drag for planetary ellipsoidal bubbles 18 p2887 N71-31368
- Sudden freeze approximation applied to nonequilibrium nozzle flows in vibrationally relaxing gases [AD-722779] 18 p2907 N71-31377
- Electron-ion recombination effects on plasma flow of partially ionized monatomic gas from sonic orifice [RE-4127] 18 p2908 N71-31502
- Prediction of heat transfer to gas flowing in convergent annular reactor channels [AERE-D-6564] 19 p3192 N71-32182
- Models of hydromagnetic shocks in very low ionization regions related to star formation and gas flows in interstellar medium 19 p3079 N71-32315
- Exact expressions for curved characteristics behind strong blast waves [AD-722777] 19 p3080 N71-32472
- Numerical analysis of structure of nonequilibrium boundary layer along flat plate in partially ionized gas at floating potential [NTC-45-6] 20 p3329 N71-32851
- Rarefied dissociated hypersonic gas flow over flat plate with sharp leading edge [DLR-FB-70-40] 20 p3249 N71-33030
- Effect of inlet conditions on flow and containment characteristics of coaxial flows for gas core nuclear rockets 20 p3303 N71-33636
- Analysis of infrared radiative energy transfer in nongray gases under three conditions of flow and equilibrium 20 p3366 N71-33683
- Analysis of heat transfer in region of separated flow downstream of rearward facing step using Mach-Zehnder interferometer 20 p3368 N71-33862
- Reaction kinetics of nitrogen oxide ion and hydrate clustering in a gas flow system [NASA-CR-121713] 21 p3386 N71-34086
- Inverse solution of two dimensional gas dynamic flow fields of rotational or irrotational character [NASA-CR-121674] 21 p3410 N71-34261
- Analysis of transpiration cooling system parameters for nose tips under supersonic conditions [SC-D-715922] 21 p3411 N71-34269
- Unsteady viscous gas flow between stationary solid wall and free solid wall vibrating at high frequency 21 p3412 N71-34276
- Influence of parameter variability in shock layer on heat flux in nonequilibrium viscous flow of multicomponent gas near stagnation point of blunt body 21 p3412 N71-34277
- Effects of leakage currents to ground in mhd generator with constant gas parameters and constant channel cross section [INR-1243] 21 p3493 N71-34884
- One-dimensional gas flow with leakage currents in MHD generator [INR-1243] 21 p3493 N71-34885
- Analysis of conditions under which autoignition of flowing hydrogen-oxygen mixtures occurs and prediction of required flow rates 21 p3531 N71-35165
- Analysis of gas phase control of critical and near-critical two phase flow where gas and liquid flow in separate streams [NBS-TN-608] 22 p3568 N71-35413
- Laminar gas flow at transonic speeds with subsonic and supersonic regions 22 p3569 N71-35422
- Continuous and pulsed ionization measurements of gas flow with applications 22 p3636 N71-35915
- Development of methods for calculating the flow processes in gas centrifuges [NLL-CA-TRANS-251-19091.9F] 23 p3745 N71-36703
- Analysis of maximum internal efficiency of single impulse stage of turbine engine [NLL-CE-TRANS-5631-19022.09] 23 p3745 N71-36704
- Transient behavior of perfect gas undergoing two dimensional vortex motion 23 p3745 N71-36706
- Metrological characteristics of relative pressure transducer and gas flow measurements [NLL-M-20618-19028-4F] 23 p3760 N71-36804
- Gas flow hydrodynamics in evolution of mass sequence stars 23 p3849 N71-37435
- Cyclic heat transfer and static pressure drop measurements of gas flow through packed beds [AABC/TM-500] 23 p3866 N71-37550
- Calculation of flow processes in gas centrifuges based on continuum concept and non-steady Navier-Stokes equations [CONF-700557-4] 24 p3905 N71-37833
- Laminar, two dimensional boundary layer generated in immediate vicinity of plane shock wave moving over flat plate into gas initially at rest [NASA-CR-123159] 24 p3905 N71-37834
- Methods for determining mass flow rates of gases for use in calibrating gas flowmeters [NASA-CR-72896] 24 p3926 N71-37954
- GAS GENERATOR ENGINES
U ENGINES
GAS GENERATORS
GAS GENERATORS
Validating gas generator method of calculating jet engine thrust, and evaluation of XB-70-1 engine performance at ground static conditions [NASA-TN-D-7028] 04 p0474 N71-13419
- Prototype ozone generator using Sr-90 as energy source [PB-194117] 04 p0533 N71-14211
- Propellant decomposition catalysts for hydrazine engines and gas generators - conference papers [DLR-MITT-69-25] 07 p1097 N71-17192
- Propellant decomposition in hydrazine engines and gas generators using noble metal catalysts 07 p1097 N71-17195
- Catalysts for hydrazine and hydrogen peroxide in hydrazine engines and gas generators 07 p1097 N71-17197
- Gas generators as vertical takeoff aircraft energy sources to operate lift fans or helicopter rotary wings 11 p1674 N71-22194
- Two variations of gas generator method to calculate thrust of afterburning turbofan engines installed in F-111A aircraft [NASA-TN-D-6297] 11 p1821 N71-22614
- Fog generator design for compressible flow visualization and high pressure Mollier diagrams [AD-721193] 15 p2392 N71-26881
- Chlorine generator for purifying water in life support systems of manned spacecraft [NASA-CASE-XLA-08913] 16 p2598 N71-28933
- Helicopter payload capability indicator in terms of gas generator speed [AD-723036] 19 p3098 N71-31723
- Development and characteristics of gas operated actuator designed to eliminate need for external supply of drive gas for operation [NASA-CASE-NPO-11340] 21 p3432 N71-34419
- Computer program documentation and user manual for steady state attitude control propulsion system - vol. 1 [NASA-CR-115184] 23 p3728 N71-36373
- Pumped liquid, dual gas generation cycle for space shuttle booster and orbiter auxiliary propulsion systems [NASA-CR-115161] 23 p3834 N71-37371
- GAS GUNS
NT LIGHT GAS GUNS
Gas gun utilizing compressed air and helium for investigating orifice flow velocity [REPT-14069] 03 p0363 N71-13289
- GAS HEATING
Catalytic and thermal reforming of gaseous hydrocarbons with steam into town gas [NASA-TT-F-13668] 16 p2690 N71-28159
- Clean room fire caused by gas heating element thermostat failure in liquid nitrogen system [NASA-TM-X-67338] 17 p3731 N71-29600
- GAS INJECTION
Velocity distributions in compressible turbulent boundary layers with air injection in supersonic flow [ARC-RM-5637] 06 p0633 N71-15789
- Schlieren photography of flow distribution for transverse hydrogen jets from flat plate into Mach 2.72 airstream [NASA-CR-1794] 09 p1571 N71-19637
- Two dimensional, supersonic mixing of hydrogen injected from wall slot into airstream [NASA-CR-1793] 09 p1576 N71-20127
- Fast neutral injector facility for obtaining intense neutral excited hydrogen atom beam [CEA-CONF-1463] 09 p1366 N71-20192
- Jet to free-stream dynamic pressure ratio effects on penetration and mixing of hydrogen injected normal to supersonic streamlines [NASA-TN-D-6114] 09 p1577 N71-20195
- Preionized gas injection for burning rate control of solid propellants [NASA-CASE-XLE-03494] 10 p1638 N71-21819

- Gas augmented rocket engine injectors using high energy gas [NASA-CR-72703] 14 p2333 N71-26689
- Numerical analysis of rare gas injection effects on aerodynamic heat transfer and wall shear stress on blunt bodies under reentry conditions [SC-CR-70-6162] 15 p2394 N71-27608
- Numerical analysis of laminar boundary layer problems on porous plates with discontinuity in gas injection [REPT-71-1] 17 p2732 N71-29491
- Mixing of hydrogen downstream from multiple injectors normal to supersonic jet flow, for supersonic combustion ramjet engines [NASA-TN-D-6476] 21 p3411 N71-34274
- Gas management subsystem using xenon-helium working fluid designed for Brayton space power system [NASA-CR-72631] 21 p3502 N71-34948
- Evaluation of hot ion accumulation from injecting neutral hydrogen into target plasmas [CONF-710607-92] 24 p3992 N71-38480
- GAS IONIZATION**
- NT ATMOSPHERIC IONIZATION
- NT AURORAL IONIZATION
- NT FLAME IONIZATION
- Magnetic structure of oblique and normal ionizing shock waves [AD-711086] 01 p0106 N71-10622
- Successive approximations method for equation integration of laminar multicomponent boundary layer with chemical reactions including ionization [NASA-TT-F-13379] 02 p0202 N71-11532
- Numerical analysis of gas motions and radiative transfer of H waves 06 p0944 N71-16821
- Microwave and pulsed electrostatic probe measurements of argon gas ionization behind shock waves [BMW-FB-W-70-43] 07 p1008 N71-17111
- Ion convergence production in E region by vertical neutral gas motions [ESSA-TD-ERL-175-ITS-112] 07 p1114 N71-17914
- Longitudinal and transverse diffusion coefficients of gaseous ions in electric fields [AD-715375] 08 p1274 N71-18716
- Shock structure in partially ionized argon plasma jet 10 p1542 N71-21281
- Plasma infrared diagnostics and determination of xenon ionization and recombination processes behind shock wave front [SC-T-70-4054] 11 p1811 N71-22442
- Light emission, and gas components of galaxy NGC 5253 11 p1829 N71-22763
- Multiquanta process of gas ionization in laser spark production [NRC-TD-1450] 12 p2013 N71-24277
- Space electric rocket test thruster performance with xenon, krypton, argon, neon, nitrogen, helium, and carbon dioxide ion source gases and magnetic spectroscopy of ion emissions [NASA-TM-X-678311] 13 p2130 N71-24699
- Multichannel photoionization chamber for measuring absorption, photoionization yield, and coefficients of gases [NASA-CASE-ERC-10044-1] 15 p2408 N71-27090
- Statistical model for electron scattering in ion atom interactions [AD-720882] 15 p2474 N71-27456
- Electron beam hydrogen ionization and hot plasma generation in magnetic mirror configuration [CEA-CONF-1611] 15 p2502 N71-27625
- Apparatus to measure excitation cross sections of molecular nitrogen bombarded by electrons in 50 to 2000 eV range with reaction rate measured by counting photon emissions [AD-721579] 16 p2648 N71-28600
- Magnetic structure of skew ionizing shock waves in plasma medium [AD-723652] 19 p3163 N71-31668
- Cascade ionization of air by radio frequency fields and by intense laser beams [AD-723183] 19 p3107 N71-31807
- Energy spectra of ions and electrons produced in collision of argon neutral beams [AD-722688] 19 p3049 N71-32036
- Model for structure of electric-current-carrying discontinuity moving into nonconducting gas and leaving gas behind [AD-723964] 19 p3165 N71-32251
- Toroidal discharge breakdowns in argon and argon/neon mixtures caused by current amplification 20 p3311 N71-33291
- Total-absorption xenon gas ionization chamber design for 1.5 to 10 keV X rays [LA-4568] 21 p3483 N71-34813
- Continuous and pulsed ionization measurements of gas flow with applications [CEA-R-3699] 22 p3636 N71-35915
- Transverse ionizing shock wave velocity measurements and analysis of velocity variation as function of shock tube bias and drive currents and initial gas density [AD-727046] 22 p3655 N71-36063
- High-altitude electromagnetic pulse source currents and ionization from Compton scattering of gamma rays based on forward scattering of Compton electrons [AD-726928] 23 p3618 N71-37233
- GAS JETS**
- Electric and magnetic cross field effects on aerodynamics and thermal regime of gas flame cone [AD-712336] 02 p0306 N71-12075
- Characteristics of gaseous jet impinging normally on liquid surface in regions where both gravitational and surface tension forces are significant [NASA-TN-D-6368] 14 p2239 N71-26023
- Combustion physics of gas jet in turbulent wake behind stabilizer [AD-721026] 15 p2525 N71-27987
- Noise reduction in turbulent axisymmetric gas jet by repeated air injection method applied to supersonic transport aircraft [NASA-TT-F-13667] 16 p2531 N71-28222
- Temperature measurement and electron density of free ionized nitrogen jet at atmospheric pressure 16 p2663 N71-29185
- Jet penetration into Mach 2 airstream using swept-back injectors at angle of attack [NASA-TM-X-2319] 17 p2736 N71-29920
- Computing flow in supersonic gas jets with central compression shock 19 p3083 N71-32742
- GAS LASERS**
- NT CARBON DIOXIDE LASERS
- NT HELIUM-NEON LASERS
- Design for space qualified helium-neon laser [NASA-CR-1463] 01 p0602 N71-10065
- Construction and simulation of gas dynamic laser [AD-709908] 01 p0602 N71-10196
- Power and efficiency of continuous hydrogen fluoride chemical laser [AD-711067] 01 p0602 N71-10433
- Analysis of Fresnel drag laser gyroscope [AD-711654] 01 p0604 N71-10830
- Energy transfer process in molecular lasers [AD-711614] 02 p0238 N71-11146
- Laser fundamentals and experiments for high school use - textbook [PB-193565] 02 p0238 N71-11420
- Measuring dependence of emission power and polarization of helium-neon laser on transverse magnetic field [AD-712104] 02 p0238 N71-11567
- Hydrocarbon-air laser, and thermodynamics of flame structure [AD-711581] 02 p0239 N71-11598
- Harmonic coincidences between pairs of far infrared continuous radiation gas lasers for light speed determination [NPL-QU-8] 03 p0388 N71-13266
- DF-CO₂ and CS₂-O₂ CO laser research, electrode configuration efficiency, and CO₂/O₂ rate of deactivation by DF and HF [AD-712564] 03 p0388 N71-13396
- Helium cadmium laser for holography and optical communication [ON-3] 04 p0527 N71-14349
- Optically pumped molecular gas laser [AD-713275] 05 p0696 N71-14546
- Gas laser technology and photoelectric detection in near infrared [AD-713223] 05 p0696 N71-14564
- Four-micron molecular laser experiments using hydrogen cyanide [AD-713193] 05 p0696 N71-14670
- Characteristics of hydrogen cyanide lasers and effects of chemical mixtures on laser operation [AD-713562] 05 p0697 N71-15369
- Solid state helium-neon gas laser applied to missile guidance [AD-713527] 05 p0720 N71-15383
- Iodine fluorescence excited by 6328 Å neon line of He-Ne laser [AD-714531] 06 p0688 N71-16668
- Laser fluorescence method for rate constant determination of vibrationally excited carbon dioxide deactivation [AD-715276] 07 p1039 N71-17767
- Frequency mixing experiments using infrared and far infrared lasers [AD-715040] 07 p1040 N71-17768
- Lamb dip spectroscopy and carbon dioxide frequency stabilization on sulfur hexafluoride [AD-715314] 07 p1040 N71-17772
- Laser controlled modulation for information transmission and uncontrolled noise producing modulation [AD-714895] 07 p1040 N71-17860
- Spectral coincidences between emission lines of CO laser and absorption lines of nitrogen oxides [AD-715293] 07 p1041 N71-18033
- Gas laser frequency stabilized by position of mirrors in resonant cavity [NASA-CASE-XGS-03644] 08 p1209 N71-18614
- Detection of transient free radicals in gas phase, and studying reaction kinetics by ultraviolet scan infrared spectroscopy [AD-716004] 09 p1396 N71-19621
- Flash photolysis system for studying gas laser energy transfer mechanisms [AD-716000] 09 p1396 N71-19621
- Capacity of holographic memory system with laser system, acousto-optic beam deflector, block data compressor and synchronizer [NASA-CR-103081] 09 p1354 N71-19775
- Simple classical model of interactions between gas molecules and contaminated surface [REPT-49-53] 10 p1610 N71-20631
- Characteristics of molecular lasers, vibrational population distribution of binary mixture of gases, and spectroscopic observation of laser outputs [AD-717099] 10 p1569 N71-21323
- Use of CO and CO₂ lasers to detect pollutants in atmosphere between laser emission lines and infrared absorption lines of NO [AD-717171] 10 p1571 N71-21378
- CW chemical laser development, N₂-CO₂ chemically excited fluid mixing laser techniques, and gas dynamic mixing behind shock waves [NASA-CR-117503] 10 p1571 N71-21810
- Numerical experiments associated with gas dynamic lasers to study consequences of large H₂O content, high reservoir pressure, and small nozzle throat height [AD-718005] 12 p1932 N71-23328
- Molecular laser studies in far infrared for optimizing power output and efficiency [AD-718160] 12 p1932 N71-23335
- Signal gain coefficient and spectral characteristics of electrically excited carbon monoxide laser [AD-718443] 12 p1934 N71-23988
- Large aperture Fabry-Perot spectrophotometer with helium-neon laser to reduce instrument drift [AD-718505] 13 p2079 N71-24419
- Atmospheric turbulence effects on gas laser communication system 13 p2080 N71-23318
- Gas laser and plasma tube operation and output including acetylene laser design [AD-720406] 14 p2266 N71-26001
- Scintillation and signal to noise ratio of heterodyne detection for carbon dioxide laser beam propagating over path 3.2 km to determine effects of atmospheric turbulence [NASA-CR-103113] 14 p2266 N71-26419
- Radioisotopic measurement of gain in flow type system with carbon dioxide, helium, and air in single, binary, and tertiary mixtures [AD-720729] 14 p2266 N71-26759
- High power uniform electric discharge to produce laser action in mixture of nitrogen, carbon dioxide, and helium [AD-721398] 16 p2606 N71-28204
- Carbon dioxide lasers, CaF₂ experiment, light scattering from semiconductors associated with impurities, and far infrared radiation [AD-721654] 16 p2607 N71-28208
- Investigation of fundamental laser processes with computation of vibration-rotation and electric dipole-moment matrix elements of diatomic molecules [AD-722696] 17 p2759 N71-30144
- Far infrared Michelson gas laser with variable output coupling [NBS-TN-395] 17 p2759 N71-30149
- Kinetic theory of optically pumped gas with equations which incorporate effects of atomic line radiation on spatial and time evolution of velocity distributions of radiating gas [AD-722862] 17 p2760 N71-30055
- Characteristics of high speed flowing N₂-CO₂-He gas lasers - effects of viscosity and diffusion 18 p2932 N71-31116
- Argon laser illumination system with three millimeter diameter diffraction limited spot at one microwatt power for use with Hough-Powell devices [RHEL-R-212] 19 p3108 N71-33348
- Electron transitions and molecular relaxation mechanisms investigated using gas lasers [AD-724167] 20 p3280 N71-33817
- Intra-cavity absorption experiment and molecular laser study [AD-724351] 20 p3281 N71-33890
- Excitation of thermal lasers by supersonic mixing in gas dynamic nozzle [AD-725961] 20 p3281 N71-33113
- Laser interferometer for studying earth crust strain 20 p3284 N71-33379
- Nuclear radiation pumping of certain gas flow feasible in high fluxes provided by pulsed nuclear reactor 20 p3282 N71-33046
- Enhancement output power of CO-2 laser excited by electric discharge and irradiated by neutron obtained from nuclear reactor 20 p3282 N71-33046
- Use of gas lasers to measure velocity and absorption of longitudinal hypersonic waves [NASA-TT-F-13902] 21 p3464 N71-34480
- Laser microanalysis spectroscopic analysis of metals and nonmetals [NASA-TT-F-13971] 24 p3931 N71-38040
- GAS LIQUEFACTION**
- U CONDENSING**

SUBJECT INDEX

GAS LUBRICANTS

- Design and performance of gas-film and oil-film lubricated self-cooling mainshaft seals for gas turbine engines
[NASA-CR-72737] 02 p0291 N71-12035
- Design of self-acting gas-film seal for turbohaft of gas turbine engine 02 p0236 N71-12036

- Computerized sealing dam design analysis for gas film seal of turbohaft 02 p0237 N71-12039

- Analysis and tests of self-acting mainshaft seals to provide gas film lubrication for advanced gas turbine engines
[NASA-CR-72987] 24 p3928 N71-30022
- Stability of central equilibrium position of journal in bearings with gas lubrication
[AD-727270] 24 p3928 N71-30025
- Development of finite difference method for solving Rayleigh equation for pressurized gas bearings
[AD-727162] 24 p3928 N71-30029

GAS LUBRICATED BEARINGS

U GAS BEARINGS

GAS MASERS

- Frequency stability of automatic hydrogen maser cavity maser 11 p1776 N71-22779
- Atomic hydrogen masers in Great Britain
[NPL-QU-17] 15 p2418 N71-26997
- Physical basis of atomic frequency standards, and characteristics of hydrogen maser, cesium beam, and sodium gas cell
[NBS-TN-399] 18 p2989 N71-31509

GAS MIXERS

- Oxygen meter performance in high purity and carbon contaminated sodium, for LMFBR program
[MSAR-70-56] 04 p0357 N71-14119
- Engineering drawings for chemiluminescent ozone meter
[PB-194118] 05 p0683 N71-14813
- High response, drag-body flowmeters for cryogenic gas mixtures
[NASA-CR-115144] 22 p3584 N71-35521

GAS MIXTURES

M DETONABLE GAS MIXTURES

- Gas analyzer for bi-gaseous mixtures suitable for use in test facilities
[NASA-CASE-XLA-01131] 01 p0056 N71-10774
- Investigating effects of oxygen, nitrogen, and rare gas mixtures at increased pressures on narcosis tendency of man 02 p0157 N71-11110
- [NBS-51714] 02 p0157 N71-11110
- External manifestations of neurophysiological effects and narcosis in subjects breathing helium-oxygen mixtures at increased pressures 02 p0157 N71-11113

- Investigating dynamics of narcosis in man from breathing nitrogen and rare gas mixtures under constant pressures for one hour 02 p0157 N71-11114

- Complex effect of nitrogen, argon, and helium respiratory mixtures on humans at increased pressures 02 p0157 N71-11115

- Explicit time dependence of perturbed distribution functions for chemically reacting dilute gas mixture
[AD-110748] 02 p0175 N71-11231

- Effects of carbon monoxide containing cabin atmosphere on performances of humans and primates
[AMRL-TN-69-19] 02 p0162 N71-11084

- Physiological effects of artificial spacecraft atmospheres consisting of pure oxygen or oxygen nitrogen mixtures 03 p0320 N71-12288

- Extremely normal shock properties for vibrational excited CO₂-N₂-He gas mixtures
[AD-725196] 03 p0364 N71-13155

- Potential 210 alpha particles used to irradiate helium-nitrogen gas mixtures by excited light source technique
[NPL-2616-4] 05 p0749 N71-15288

- W values in mixtures of gases containing ammonia
[ORSO-2001-14] 05 p0750 N71-15358

- Transport properties of chemically reacting gases
[NASA-TT-F-13406] 09 p1344 N71-20090

- Cryogenic underwater life support system for supplying breathing gas to buoyancy test subjects in submerged vehicles
[NASA-CR-117143] 09 p1341 N71-20239

- Development of rate-controlled, partial-equilibrium method for treating reacting gas mixtures 09 p1485 N71-20529

- Equipment for measuring partial water vapor pressure in gas flow
[NASA-CASE-XMS-01610] 10 p1556 N71-20741

- Supersonic cell with permeable membranes for fluid mixture component separation
[NASA-CASE-XMS-02952] 10 p1587 N71-20742

- Vibrational population inversions within normal shock waves in CO₂-N₂-He mixtures
[AD-716743] 10 p1568 N71-20863

- Humidity generator and atmospheric control chamber for use with optical microscopes in studying aqueous changes with variations in humidity
[AD-716994] 10 p1597 N71-21244

- Equations for mass flow of methane and natural gas mixtures through critical flow nozzles, including real gas effects
[NASA-TN-X-5399A] 10 p1543 N71-21330

- Gas dynamic techniques for study of desorption rates in one and two component systems 10 p1543 N71-21333

- Facility for simulating reentry flow fields over blunt-nosed bodies 11 p1740 N71-22634

- Critical appraisal of design, development, and operation of UTIAS implosion-driven shock tubes and hypervelocity launchers
[NASA-CR-117856] 11 p1845 N71-32080

- Viscosity of gases and gas mixtures - handbook
[TT-70-50022] 12 p1901 N71-23763

- High temperature kinetics of photochemical mercury decomposition of nitrous oxide in carbon monoxide methane mixtures
[SR-369] 12 p1871 N71-23783

- Vibrational energy transfer in rapid expansion of N₂, CO₂, and Ar mixtures, using arc heating
[AD-718311] 12 p1934 N71-24011

- Barodiffusion processes in supersonic stream of argon-helium mixture in vacuum using beam of electrons
[NASA-TT-F-13583] 13 p2064 N71-25385

- Volumetric displacement method for gas mixture standard production
[RFP-1626] 13 p2041 N71-25348

- Supersonic density separation in stagnation region of mixed argon helium flow
[AD-720725] 14 p2240 N71-26179

- Analysis of gas generated by wires exploding in air, argon, and nitrogen mixtures at low pressures 14 p2361 N71-26456

- Physiological effects of high carbon dioxide concentrations in helium/oxygen and argon/oxygen atmospheres on rats at ambient temperatures 16 p2543 N71-28250

- Characteristics of combustion of premixed gases in stagnation flow condition 16 p2692 N71-28910

- Determination of ignition temperatures, ignition delay times of various combustible mixtures, and the effect of gas flow on ignition process 16 p2692 N71-28923

- Carbon monoxide purity standards for gas breathing apparatus of divers and toxic hazards under controlled hyperbaric atmospheres 17 p2707 N71-29358

- Extrapolation of animal tolerances of air contaminants to human tolerances for diver breathing under hyperbaric conditions 17 p2707 N71-29359

- Calculation and analysis of course of combustion for different pairs of ignition temperature and pressure in hydrogen-arg mixtures flowing at supersonic velocity
[NASA-TT-F-13719] 17 p2859 N71-30182

- Polarographic determination of oxygen content in gas mixtures using low recombination reaction 18 p2886 N71-31159

- Flame spreading over surface of igniting solid propellants in different gas mixtures at various pressures
[NASA-CR-111942] 18 p3026 N71-31426

- Flame spreading over surface of igniting solid rocket propellants at different pressures, and oxygen-nitrogen mixtures 18 p3027 N71-31430

- Studying mechanism of flame spreading over surface of igniting polystyrene and polymethyl methacrylate for minimizing fire hazard in space capsules 18 p3019 N71-31431

- Computer program for describing thermochemistry of combustible gas mixture ignition
[AD-723400] 19 p3191 N71-31758

- Partial pressure analyzer calibration and techniques for measuring gas mixtures and leakage
[SCL-DB-70-275] 19 p3078 N71-32227

- Measurement of surface diffusion in porous molybdena catalyst for three binary gas systems 19 p3051 N71-32318

- Electrophoresis theory for segregation phenomenon in gas mixture subjected to dc discharges 19 p3165 N71-32359

- Gaseous Townsend discharges in gas mixtures and electric strength of moving gas
[AD-723651] 19 p3166 N71-32395

- No-decompression repetitive excursion dive format testing at 150 and 280 ft using helium-oxygen mixtures
[AD-723171] 19 p3346 N71-32770

- Combustion dynamics of air/methane supersonic diffusion flame in ducts 20 p3365 N71-33449

- Measuring gas adsorption in electric fields by method of thermal conductivity in gaseous mixture
[NASA-TT-F-13936] 20 p3253 N71-33700

- Electron beam measurement of molecular vibrational energy transfer in expanding mixtures of N₂ and CO₂ heated by electric arc
[NASA-TN-D-6445] 21 p3436 N71-34446

GAS STREAMS

- Effects of hydrogen and hydrogen-oxygen mixtures on fracture of high strength steel in pressurized configuration
[NVO-3973-3] 22 p3594 N71-35598

- Spin lattice relaxation in gaseous hydrogen and mixtures of hydrogen with helium 22 p3650 N71-36029

- Numerical scheme for solution of general turbulent tube flow problem with surface mass transfer and nonequilibrium chemical reactions 23 p5746 N71-36711

- Limitation rate measured in glow discharge in gas mixtures commonly used in carbon dioxide lasers
[REPT-442] 23 p5746 N71-36848

- Stimulated Rayleigh-type light scattering in binary gas mixtures from local fluctuations and concentration
[AD-726469] 23 p3084 N71-37121

- Generation of pressure waves in explosive hydrogen-oxygen mixtures 24 p3909 N71-37060

- Viscosity and normal density measurements at lambda point intervals for pure helium-4 and helium-3 mixtures with helium-4
[NASA-TN-D-6316] 24 p3946 N71-38290

GAS PHASES

U VAPOR PHASES

GAS PIPES

- Tubular flow restrictor for gas flow control in pipelines
[NASA-CASE-NPO-10117] 05 p0695 N71-15608

GAS PRESSURES

- Open-air pressure gauge for low gas pressure measurement
[NPL-MC-4] 05 p0383 N71-13362

- Helium gas requirements for liquid hydrogen expulsion from spherical tank
[NASA-TN-D-7019] 04 p0085 N71-14046

- Electrical conductivity of single crystal cerium dioxide as function of temperature and oxygen pressure
[COO-1441-11] 06 p0932 N71-15895

- Gas bubble growth and compression in body physical systems and tissues 08 p1155 N71-15970

- Analog computer simulation of design parameter effects on stability of direct acting gas pressure regulator based on Bryn cycle space power generator
[NASA-TN-D-6367] 10 p1496 N71-21511

- Metal-oxygen and metal-nitrogen systems for use as reduced pressure standards using Sieverts apparatus
[NASA-CR-111862] 10 p1584 N71-21606

- Inlet leak analysis for spacecraft mass spectrometer atmospheric sensor system
[NASA-CR-111858] 11 p1764 N71-22872

- Fission gas pressure transducers of fluid-filled bellows, and null-balance types 13 p2679 N71-34519

- Pressure transducer for continuous monitoring of fission gas release by nuclear fuel specimens during irradiation 13 p2112 N71-24520

- Instrumented fuel rods for monitoring internal gas pressure and temperature during irradiation in FRTR
[AD-723521] 13 p2113 N71-24521

- Trigger pulse energy, electrode discharge, gas pressure, and propulsive voltage effects on low inductance spark gaps for high voltages in air
[BMBW-FBK-70-17] 15 p2453 N71-27633

- High pressure, liquid nitrogen cooled, gas particle accelerator target design for use with hydrogen, deuterium, and helium
[IFVE-SEP-70-22] 16 p2645 N71-28164

- Calculations of ionization-excitation source rates in gaseous media irradiated by fission fragments and alpha particles 20 p3307 N71-33667

- Correlation of calculated and experimental product yields as functions of gas molecule residence time, power, gas pressure, and alkyl alcohol in electrolysis of hydrazine from ammonia
[JECR-343] 23 p3719 N71-36510

GAS REACTORS

- Adiabatic approximation of gas reactor critical mass during nuclear fuel density oscillations
[IAS-1964] 17 p2783 N71-29528

- Gas core reactors and MHD generator to solve problems of growing demand for electric power without thermal pollution 20 p3306 N71-33664

GAS SPECTROSCOPY

- High temperature gas radiation, and direct and electron density spectroscopic methods for gas temperature measurements 11 p1842 N71-22680

GAS STREAMS

- Structure of supersonic jet of argon-helium mixture in vacuum conditions 07 p1006 N71-16936

- Device for simultaneously determining density, velocity, and temperature of streaming gas
[NASA-CASE-XLA-83375] 12 p1934 N71-24874

- Development of avalanche and streamer in gases in homogeneous electric field with application of Dybko screening method
[JINR-P15-5584] 14 p2322 N71-26874

- Two-meter gas streamer chamber modeling
[JINR-P13-5529] 16 p2639 N71-28893
Heat transfer between gas and solids in suspension
[NLL-R73-6129] 16 p2692 N71-39036
Experimental and theoretical analysis of breakup of liquid sheets and jets in supersonic gas stream
19 p3082 N71-32618
Silicon rubber membrane for measuring permeabilities and separation factors for removing radioactive Xe and Kr from off-gas streams
[ORNL-4522] 20 p3308 N71-33741
Analysis of jet flow with emphasis on turbulent asymmetric free jets
[SC-DR-70-838] 21 p3411 N71-34270
Radiative effects of high enthalpy gas streams over wedge simulating space vehicle reentering earth atmosphere at supersonic velocities
24 p4033 N71-38776

GAS TEMPERATURE

- Device for simultaneously determining density, velocity, and temperature of streaming gas
[NASA-CASE-XLA-03375] 12 p1934 N71-24074
Determination of gas temperature from laser-Raman scattering
[NASA-TN-D-4336] 14 p2253 N71-25663
Spectroscopic band models for determining gas temperatures and concentrations
[AD-72396] 19 p3048 N71-31675

GAS TRANSPORT

- Gas velocity effects on breakdown potential of argon, helium, and nitrogen
06 p0839 N71-16650
Investigating characteristics of radiative heat transfer by high temperature gases
07 p1128 N71-17040
Gas generators as vertical takeoff aircraft energy sources to operate lift fans or helicopter rotary wings
11 p1674 N71-22194
Equilibrium sorption isotherms and diffusivities of gases flowing through polymeric membranes
14 p2241 N71-26297
Infrared absorption and energy transport in gases including sulfur dioxide
16 p2640 N71-29127
Theory and physics of gas radiation in absorbing, emitting, and scattering media
18 p3006 N71-30942
Thermal radiation in media with nonunity refractive index and from flames
18 p3025 N71-30950

GAS TUNGSTEN ARC WELDING

- Fabrication and optimization of weld joints in 12-5-3 maraging steel plates
[NASA-CR-115887] 05 p0691 N71-14818
Gas tungsten arc welding tests of titanium-tungsten wire and titanium-graphite filaments for weldability and weld thermal energy effects on fiber-matrix reactions
[RM-519] 23 p3764 N71-36836
Development of optimum tungsten inert gas welding procedure for production of welds in 12 percent nickel maraging steel
[NASA-CR-72981] 24 p3927 N71-38019

GAS TURBINE ENGINES

- NT BRISTOL-SIDDELEY OLYMPUS 595 ENGINE
NT DUCTED FAN ENGINES
NT J-57 ENGINE
NT J-45 ENGINE
NT JET ENGINES
NT PULSEJET ENGINES
NT RAMJET ENGINES
NT SUPERSONIC COMBUSTION RAMJET ENGINES
NT TURBOFAN ENGINES
NT TURBOJET ENGINES
NT TURBOPROP ENGINES
NT TURBORAMJET ENGINES
Aircraft gas turbine engine design and construction
[AD-71157] 01 p0116 N71-10833
Mack 1 burner rig tests at 2100 F for oxidation resistance evaluation of NiCrAl and FeCrAlY claddings on Ti-NiCr
[NASA-TM-X-52916] 02 p0240 N71-11426
Sealing dam analysis for design of shaft face seal with self-acting lift augmentation for advanced gas turbine engines
[NASA-TN-D-7006] 02 p0230 N71-11579
Design and performance of air/film and oil-film lubricated self-sealing mainshaft seals for gas turbine engines
[NASA-CR-72737] 02 p0291 N71-12035
Computer graphics terminal for disc profile design of gas turbine engine
03 p0348 N71-13141
Seal ring carbon-graphite materials for aircraft gas turbine engines
[NASA-CR-72799] 05 p0692 N71-14890
Advanced cooling systems and heat resistant materials for turbine blades of high temperature aeronautical gas turbine engines
[AGARD-CP-73-71] 07 p1099 N71-17372
High entrance temperatures for improved performance of turbopropellers and gas turbine engines
07 p1099 N71-17373

Mathematical model for calculating blade temperatures in convective cooled gas turbines

- 07 p1099 N71-17375
Heat transfer and heat flux measuring sensors for gas turbine engines
07 p1028 N71-17377
Design and component testing of cooled radial gas turbine engine
07 p1100 N71-17381
Aerodynamic and thermodynamic performance of sweat cooled gas turbine engine blades
07 p1100 N71-17382
Heat transfer in air cooling and sweat cooling techniques for high temperature gas turbine engine components
07 p1100 N71-17383
Transpiration cooled blades for high temperature inlet in gas turbine engines
07 p1100 N71-17384
Design of gas turbine engines for high operating temperature
07 p1101 N71-17386
Temperature field measurements within convection cooled rotor blade of gas turbine engine
07 p1101 N71-17387
Cobalt and nickel based alloy metallurgy for high temperature gas turbine materials
07 p1101 N71-17389
Thermal control coatings for refractory gas turbine materials
07 p1048 N71-17391
Performance of aluminate coatings in simulated high temperature tests on gas turbine engine inlets
[NASA-CR-116374] 07 p1043 N71-17393
Film cooling of gas turbine blades by air injection through holes
07 p1009 N71-17394
Effective heat transfer coefficients in film cooling systems of gas turbine surfaces
07 p1129 N71-17395
Air cooling systems for nozzle guide vanes of aircraft gas turbines
07 p1129 N71-17396
Operational design criteria for gas turbine engines
07 p1101 N71-17402
Protective coatings for heat resistant materials for aircraft gas turbine engines, and refractory metals for reentry vehicles
[NASA-TM-X-52977] 09 p1404 N71-19677
Determining amount of smoke in exhaust of gas jet turbine engines
[NASA-CR-117031] 09 p1459 N71-20050
Design of shaft face seal with self-acting lift augmentation for gas turbine engines
09 p1394 N71-20392
Thermal performance analysis of solar Brayton heat receiver in transferring heat to working gas of Brayton engine
[NASA-TN-D-6268] 10 p1496 N71-21512
Requirements analysis of airbreathing gas turbine engines for shuttle vehicles
[NASA-TM-X-67006] 12 p1990 N71-23764
Design point characteristics of 15-80 kW nuclear reactor Brayton cycle power system
[NASA-TM-X-67811] 13 p2116 N71-24689
Predicted performance of 15-80 kW nuclear Brayton power system over range of operating conditions
[NASA-TM-X-67833] 13 p2116 N71-24690
Motor starting techniques for 2-15 kW Brayton space power system
[NASA-TM-X-67819] 13 p2117 N71-24691
Assembly methods for three types of aircraft gas turbine engines
[AD-719823] 13 p2156 N71-25209
Fundamentals of aircraft gas turbine engines
[AD-719913] 14 p2331 N71-25808
Aircraft gas turbine combustion chamber design
[NAL-TR-208] 14 p2332 N71-26298
Production and efficiency of small gas turbine engine for helicopter and surface vehicles
[AGARD-LS-46-71] 15 p2511 N71-26951
Cost effectiveness as critical selection requirement for small gas turbines in military and commercial operations
15 p2511 N71-26952
Design and performance of gas turbine engines for helicopters and surface transport vehicles
15 p2511 N71-26953
Components for low weight/small volume aircraft gas turbine engines
15 p2512 N71-26955
Engineering aspects and manufacturing of gas turbine engines for helicopters and ground transport vehicles
15 p2512 N71-26956
Comparison of small gas turbine and diesel engine power plants for aircraft and ground vehicle propulsion
15 p2512 N71-26958
Jet aircraft noise sources and reduction from gas turbine engines including jet exhausts, fans, lift devices, and unducted rotors
18 p2871 N71-30785

Mechanics of free piston engine, aspects of human factors engineering, and compressible boundary layer studies at high Reynolds numbers

- [DME/NAS-1971/11] 19 p3198 N71-32628
Development history and application of free piston engine
19 p3175 N71-32621
Air pollution by gas turbine aircraft engines
22 p3700 N71-36307
Combustion characteristics of gas turbine aircraft engines
[AD-727175] 23 p3841 N71-37787
Sampling, handling, and measuring emissions from aircraft gas turbine engines
[REPT-430] 24 p3873 N71-37804
Technical aviation handbook covering aircraft maintenance, navigation aids, airframes, lubricants, planes and gas turbine engines, and checkout procedures
[AD-727195] 24 p3874 N71-37813
Analysis and tests of self-acting mainshaft seals to provide gas film lubrication for advanced gas turbine engines
[NASA-CR-72987] 24 p3928 N71-38022
Design and performance characteristics of gas turbine engines for helicopters
[AD-727359] 24 p4002 N71-38541
Textbook on combustion chambers of gas turbine engines
[AD-727960] 24 p4002 N71-38542
Mathematical models for analyzing automotive gas turbine and nitric oxide emissions
[FNL-PUBL-71-11] 24 p4032 N71-38710
- GAS TURBINES
Film vaporizing combustor for gas turbines
[NASA-TT-F-13272] 01 p0115 N71-10282
Recording and frequency analysis of vibration data using coherent optical data processing techniques with emphasis of failure detection
[AD-710809] 01 p0116 N71-10254
Air intakes and flow aerodynamics in hydroturbines
[PB-193589T] 01 p0044 N71-10942
Liquid and vapor cooling systems for gas turbine with application of heat pipe concept to stator blade cooling
[ARC-CP-1127] 10 p1638 N71-20032
Friction points, and oil system of aviation gas turbine engines
[AD-717835] 11 p1781 N71-22811
Benzene evaporation rate determined from flat plate film boiling under high temperature air flow with application to gas turbine air pollution reduction
[DLR-FB-70-58] 11 p1840 N71-22872
Short duration flow shock tunnel and light piston tunnel for gas turbine blade film cooling and transpiration cooling
[REPT-1121/70] 11 p1730 N71-22893
Conference on high temperature turbines detailing effect of film cooling on blade profile loss
[NASA-TM-X-67123] 11 p1821 N71-22899
Endurance test of turbine wheel with uncooled chromium alloy blades
[AERL-ME-320] 12 p1991 N71-24322
Digital computer simulation of steady-state and transient engine performance of gas turbine propulsion system
[AD-720003] 14 p2331 N71-23910
Cost effectiveness as critical selection requirement for small gas turbines in military and commercial operations
15 p2511 N71-26952
Thermodynamic cycle and power output parameter of gas turbine
15 p2511 N71-26954
Thermodynamic properties of small gas turbines for power generation in aeronautics, space, and industry
15 p2512 N71-26957
Method for maintaining good performance in gas turbine during air flow distortion
[NASA-CASE-LEW-10286-1] 16 p2672 N71-28913
Gas turbine combustor liner film cooling for slat geometries in presence of high free stream turbulence
[NASA-TN-D-6360] 17 p2858 N71-29948
Design of heat exchangers for gas turbine fast reactors
[EER-187] 18 p3023 N71-30678
Application of Green function to two dimensional Laplace equation for calculation of temperature distribution in cooled blade of gas turbine
[NAL-TR-234] 18 p2944 N71-30805
Measurement of smoke concentration in primary zone of gas turbine combustor at high ambient pressures by spectral radiance technique
[NASA-TN-D-6410] 18 p3025 N71-31340
Component design data for 1.5 kW dc, turbine driven, organic Rankine cycle power plant for jump use
[AD-726434] 22 p3542 N71-35734
Flow and heat transfer technology resulting from NASA turbine cooling program
[NASA-TN-X-2384] 22 p3463 N71-36129
Temperature field determination of internally cooled blades of gas turbines
[AD-726601] 22 p3464 N71-36134

SUBJECT INDEX

- Effect of nozzle divergence angle, specific heat ratio, and plug nozzle configuration on gas turbine nozzle efficiency (AD-726723) 22 p3664 N71-36125
- Aerodynamic design of supersonic axial compressor stage for total pressure ratio of 3 to 1 (AD-727001) 22 p3664 N71-36126
- Design and tests of high temperature, air cooled radial turbine configurations (AD-726446) 23 p3849 N71-37381
- Statistical analysis of fatigue test data on aviation gas turbine lubricants (AD-727759) 24 p3946 N71-38148
- Advanced cooling concepts for gas producer axial flow turbine of small gas turbine engine (AD-727741) 24 p4001 N71-38539
- Statistical analysis of fatigue stability characteristics under steady state loads and application to determining life expectancy of machinery (AD-727472) 24 p4024 N71-38712
- GAS VALVES
- Three-port transfer valve with one port open continuously suitable for manned space flight (NASA-CASE-XAC-01158) 11 p1773 N71-23051
- GAS VISCOSITY
- Viscosity of compressed N₂, He, H₂, and Ar from nitrogen 100 to 25°C using viscometer (NLL-RTS-4400) 22 p3570 N71-35425
- GAS WELDING
- NT BRAZING
- Inert gas welding - bibliographies (AD-709900) 01 p0059 N71-10290
- Post-weld nitrogen content of deposits on standard and Hi-proof austenitic stainless steels (PB-195290) 03 p0386 N71-13286
- Emission spectroscopy method for contamination monitoring of inert gas metal arc welding (NASA-CASE-XMF-03039) 06 p0862 N71-15871
- Improved filler wire for inert gas welding of gunmetal and dissimilar metals (AD-721977) 18 p2928 N71-30933
- GAS-GAS INTERACTIONS
- Interaction between supersonic air jet from slot with hypersonic air flow over surfaces (D1-82-9999) 04 p0518 N71-13766
- Interaction of hypersonic spherical source flow with rarified atmosphere (AD-713122) 05 p0663 N71-14934
- GAS-ION INTERACTIONS
- Discussing advances in molecular beam experiments involving two-body collisions (NASA-CR-116434) 07 p1070 N71-17031
- Formation scattering cross section of H₂ ion in fast proton and methane reactions (AD-717610) 11 p1803 N71-22118
- Ionization cross sections for helium and neon positive ion collisions with nitrogen, oxygen, and carbon dioxide molecules at 3 to 200 eV (AD-717690) 11 p1808 N71-22711
- Solid phase substitution reactions of complexes of palladium (II) (AD-717690) 13 p2040 N71-24918
- Positive helium ion scattering by impact on helium, neon, and argon (AD-717690) 15 p2479 N71-27654
- Pumping effect in oxygen reaction with hot tungsten cathode, and spectroscopic measurements of formation energies for volatile species in gas-solid chemical reactions (NASA-CR-118897) 15 p2389 N71-27988
- Ionization of Gum nebula by energetic charged particles from supernova Vela X with estimate of gamma ray line emission from ambient gas, energetic nuclei interaction (NASA-TM-X-65590) 16 p2674 N71-28567
- GAS-LIQUID INTERACTIONS
- NT AIR WATER INTERACTIONS
- Use of Ra/Ra ratios to determine air/sea gas mixing and vertical mixing in ocean (AD-715129) 05 p0648 N71-14783
- Thermal exchange between water currents and atmosphere in water (AD-715048) 07 p1024 N71-17959
- Signal noise recordings during air-water interactions and at points in underwater sound field (AD-717580) 11 p1744 N71-21925
- Absorption characteristics at zero surface coverage of water at gas-liquid interface of water and dilute solubility characteristics of non-electrolytes (AD-717735) 11 p1696 N71-22556
- Salt particle origins, jetting into air, inland transport, impingement, incrustation, dry or precipitative fallout, and return to sea in sea-salt atmospheric cycle - bibliography (AD-718613) 12 p1913 N71-23732
- Body force effects on liquid film stability interacting with external gas (JC-R2-70-722) 13 p2068 N71-25442
- Virginia Beach environmental data and time series analysis of water table interactions with processes in

- beach-ocean-atmosphere system for environmental control (AD-719293) 14 p2245 N71-25629
- Axial mixing in gas and liquid phases and mass transfer coefficients for gas absorption in mechanically agitated column (AD-719293) 16 p2580 N71-28609
- Pressure loss calculation for two phase flow in vertical cylindrical pipes (AD-723590) 17 p2734 N71-29716
- Hydrodynamic problem of joint gas stream and liquid film mass transmission processes (AD-723590) 19 p3076 N71-31743
- BOMEX data reduction on sea-air interaction and tropical convective systems studies (NASA-CR-119762) 19 p3201 N71-32760
- Sea-air interaction and tropical convective systems (AD-723590) 19 p3201 N71-32760
- Energy and momentum transfer distributions in sea-air exchangers relative to model of travelling frontal cyclones in middle latitudes (AD-719293) 23 p3786 N71-36982
- GAS-METAL INTERACTIONS
- Interaction kinetics of atomic oxygen and hydrogen on metal surfaces of satellite-borne mass spectrometers (NASA-CR-111117) 01 p0122 N71-10085
- Model for exchange of nitrogen isotopes taking place between two pellets of aluminum nitride in Kendeo cell (AD-711633) 01 p0020 N71-10965
- Rate of hydrogen absorption by copper (PB-190537) 02 p0243 N71-11697
- Diffusion coefficients determined for hydrogen in some liquid metals (AD-711633) 08 p1217 N71-19004
- Simple chemical model of interactions between gas molecules and contaminated surface (REPT-49-53) 10 p1610 N71-20631
- Oxidation constant drop of mixed oxides/Co, MgO and Co, NiO (NLL-CE-TRANS-5279-7902.09) 10 p1578 N71-21217
- Depositing protective carbide, nitride, boride, and pyrocarbon coatings from gas phase on surface of solid bodies (AD-717031) 10 p1589 N71-21288
- Physical mechanism and charge states resulting from collision of ionized gas particles with metallic surfaces (AD-717031) 10 p1617 N71-21322
- Adsorbed thin gas film effects on thermal conductivities of contacting metallic smooth surfaces (AD-717031) 12 p1894 N71-24150
- Penetration depth and diffusion coefficient for gaseous diffusion in metals (TT-70-59120) 14 p2268 N71-25658
- Scatter velocity distributions in molecular gas flow interactions with high temperature metal surfaces (AD-720726) 14 p2240 N71-26178
- Analysis of high vapor velocity condensation in tubes based on universal velocity distribution, pressure drops, and heat transfer coefficients (DSR-72591-74) 22 p3696 N71-36363
- Oxygen, nitrogen, hydrogen, and carbon monoxide adsorption on platinum surface (RFP-1456) 24 p3885 N71-37692
- Iodine/air and zinc/argon condensation tests of flowing metal-vapor/heated-gas mixtures in ducts for cavity exhaust port design of nuclear light bulb engines (NASA-CR-123200) 24 p3904 N71-37829
- GAS-SOLID INTERFACES
- Critical review and round table discussion data for colloquium on reactions between gases and solids (AGARD-AR-32-71) 08 p1285 N71-19177
- Gas-solid thermal accommodation coefficient measurements in shock tube by thin film resistance thermometers (AERO-2) 12 p2014 N71-34318
- Luminescent processes in solids during interaction with gas (AD-713626) 14 p2326 N71-26455
- Mechanisms and kinetics of reactions on interfaces of substances (AD-713626) 14 p2326 N71-26455
- Heat transfer between gas and solids in suspension (NLL-RTS-4129) 16 p2692 N71-29836
- Experimental determination of pressure drop and flow characteristics of dilute gas-solid suspensions in turbulent pipe flow (NASA-CR-1804) 20 p3251 N71-33514
- GASEOUS CAVITATION
- U GAS FLOW
- GASEOUS DIFFUSION
- Direct equation solution for spin in elastic low energy electron scattering from gaseous atoms (AD-716664) 01 p0101 N71-10842
- Activation energy for apparent gaseous diffusion of hydrogen in multi-run metal arc welding deposits (AD-716664) 03 p0367 N71-13315
- Quantum theory of density corrections to gaseous transport coefficients (NASA-CR-116137) 06 p0086 N71-15924

GASEOUS FISSION REACTORS

- Theoretical techniques for determining gas diffusivity in plastic films (BDR-613-229) 06 p0679 N71-16372
- Dissolved argon gas effects on cavitation in liquid sodium (AD-713651) 06 p0836 N71-16653
- Dynamic model for gas phase concentrations in porous fuel cell electrodes (NASA-TM-D-6160) 07 p0975 N71-17467
- Longitudinal diffusion coefficients of gaseous ions drifting in electric field (AD-714068) 07 p1084 N71-18085
- Describing techniques for measuring Th-228 diffusion in thorium and uranium oxides (ABCL-3655) 08 p1234 N71-18171
- Factors affecting rate gas diffusion in ionic solids, and tritium diffusion measurement in fuel element claddings (ORO-3500-6) 08 p1239 N71-18728
- Diffusion coefficient of neutral hyperfine particles in gas (NP-18413) 08 p1260 N71-18774
- Experimental methods for measuring Prandtl number, diffusion properties, and gas thermal conductivities for heat transfer calculations (ABCL-3655) 11 p1843 N71-22609
- Gas purged dry box glove reducing permeation of air or moisture into dry box or locker by diffusion through glove (NASA-CASE-XLE-02531) 11 p1694 N71-23080
- Diffusion of ion and gas molecules to aerosol particles in noncontinuum regions (AD-713651) 13 p2067 N71-25895
- Atmospheric cycles analyzed to determine sources, abundance, and fate of gaseous atmospheric pollutants (ABCL-3655) 13 p2075 N71-25147
- Penetration depth and diffusion coefficient for gaseous diffusion in metals (TT-70-59120) 14 p2268 N71-25658
- Oxygen pressure effects on high temperature titanium oxidation (TT-70-57065) 14 p2272 N71-25819
- Diffusion layer structure and aluminumizing effect on heat resistant nickel alloy (AD-720378) 14 p2273 N71-25915
- Review of methods for separating noble fission gases from gaseous effluents (CEA-BIB-184) 15 p2484 N71-27796
- Gaseous core diffusion nuclear reactor for thermal energy generation (NASA-CASE-LEW-10250-1) 16 p2635 N71-28759
- Gaseous fission measurements from jet engine afterburners over range of fuel-air ratios (NASA-TM-X-2323) 17 p2859 N71-30117
- Flow characteristics of adsorbable gases in porous bodies and isotopic separation by gaseous diffusion (NRP-18367) 18 p2804 N71-30420
- Mathematical model for gas adsorption efficiencies of porous and solid reactor materials (AD-713651) 18 p2807 N71-31449
- Fuel cell electrolyte studies on vapor pressure of ternary systems, partial molal volumes of dissolved gases, and diffusion coefficients of gases (NASA-CR-121628) 21 p3378 N71-34034
- Measurement of electrical resistance, electron microscopy, and low temperature heat capacity of liquid gases in metals (COO-1799-6) 21 p3404 N71-34476
- GASEOUS FISSION REACTORS
- Calculated estimates of gas core nuclear rocket engine weights for specific impulses ranging from 3000 to 7000 seconds and for engine thrusts ranging from 4400 to 440,000 newtons (NASA-TM-X-2243) 09 p1418 N71-19900
- Review of gas-core rocket reactor research, and estimate of engine performance characteristics (NASA-TM-X-2259) 09 p1421 N71-20295
- Comparison of performance potential of regeneratively cooled gas core nuclear reactors with performance of solid core rockets for various space missions (NASA-TM-X-2256) 11 p1795 N71-22618
- Procedure for calculating certain parameters of heat producing elements of VVER type reactors (IAB-1940) 13 p2119 N71-24067
- Gaseous core diffusion nuclear reactor for thermal energy generation (NASA-CASE-LEW-10250-1) 16 p2635 N71-28759
- Modes for using vortices for fluid dynamic containment of gaseous core nuclear reactor, bibliography (NASA-CR-1772) 19 p3079 N71-32276
- Vortex and coaxial flow of argon and helium plasmas heated inductively, and strong magnetic field effects on turbulent plasma mixing, for gas core reactors (AD-713651) 20 p3330 N71-33633
- Effect of inlet conditions on flow and containment characteristics of coaxial flows for gas core nuclear reactors (AD-713651) 20 p3389 N71-33636
- Axisymmetric flows with regions of closed streamlines confined by rotational flows or electroviscous plasma, for containment for gas core reactors (AD-713651) 20 p3352 N71-33637

GASEOUS ROCKET PROPELLANTS

Stability of incompressible two-fluid wheel flows with imposed uniform axial magnetic field for gas nuclear rockets

20 p3252 N71-33638

Interfacial stability at thin flexible partition between fuel and propellant flows for gas core nuclear rockets

20 p3304 N71-33639

Operating characteristics and performance predictions for gas-core nuclear rocket with fuel separation by MHD-driven rotation

20 p3304 N71-33641

Opacity calculations for application to uranium fueled gas-core reactors

20 p3304 N71-33643

Power level variations in cavity reactor produced by density changes in gaseous nuclear fuels

20 p3304 N71-33650

Two dimensional radiative-convective analysis of bypass flow in uranium plasma rocket

20 p3304 N71-33652

Analysis of thermal emission spectrum from uranium plasma in propellant region of gas core reactor

20 p3305 N71-33653

Temperature distribution and radiation flux measurements in uranium plasma reactor with reflecting walls

20 p3305 N71-33654

Criticality experiments using spherical gas core to provide benchmark results for cold conditions of typical nuclear rocket concept

21 p3456 N71-34598

Propagation and weight analyses of mini-cavity reactor rocket engine concept

22 p3620 N71-35793

GASEOUS ROCKET PROPELLANTS

Design criteria for high performance coaxial injector using gas-liquid space storable propellants

01 p0113 N71-10452

Characteristics of SERT thruster with argon propellant

03 p0449 N71-12941

Gaseous oxygen-gaseous hydrogen rocket engine injector valve technology

07 p1034 N71-17555

Computerized analysis of gas-tapoff cycle stability with gaseous hydrogen and gaseous oxygen

09 p1378 N71-20417

Quasi-steady MPD propulsion at power levels in range 1 to 10 megawatts

10 p1639 N71-21717

Detonation reaction engine comparing outer housing enclosing pair of inner walls for continuous flow

11 p1821 N71-22983

Low frequency analysis of rocket engines using compressible propellants

17 p2835 N71-29584

Potential high performance shock tube for high pressure opacity measurements of gaseous rocket propellants for nuclear rocket engines

20 p3301 N71-33285

Spectral absorption coefficients of helium, neon, and nitric oxide mixtures with oxygen as functions of pressure, temperature, and wave number

24 p3884 N71-37687

Performance of high power, quasi-steady MHD thrusters using rare gas propellants

24 p4002 N71-38543

GASES

NT ARGON

NT ARGON ISOTOPES

NT CARBON DIOXIDE

NT CARBON MONOXIDE

NT COLD GAS

NT COMPRESSED GAS

NT COSMIC GASES

NT DETONABLE GAS MIXTURES

NT DEUTERIUM

NT DEUTERIUM PLASMA

NT EXHAUST GASES

NT FLAMMABLE GASES

NT GAS MIXTURES

NT GAS STREAMS

NT GRAY GAS

NT HELIUM

NT HELIUM ATOMS

NT HELIUM FILM

NT HELIUM ISOTOPES

NT HIGH TEMPERATURE AIR

NT HIGH TEMPERATURE GASES

NT HYDROGEN

NT HYDROGEN ATOMS

NT HYDROGEN IONS

NT HYDROGEN ISOTOPES

NT HYDROGEN PLASMA

NT IDEAL GAS

NT INTERPLANETARY GAS

NT INTERSTELLAR GAS

NT IONIZED GASES

NT LIQUEFIED GASES

NT LIQUID AMMONIA

NT LIQUID HELIUM

NT LIQUID HYDROGEN

NT LIQUID NITROGEN

NT LIQUID OXYGEN

NT MOLECULAR GASES

NT MONATOMIC GASES

NT NEON

NT NEON ISOTOPES

NT NITROGEN

NT NONCONDENSIBLE GASES

NT NONGRAY GAS

NT ORTHO HYDROGEN

NT OXYGEN

NT PROSENE

NT POLAR GASES

NT POLYATOMIC GASES

NT RADON

NT RADON ISOTOPES

NT RARE GASES

NT RAREFIED GASES

NT REAL GASES

NT RESIDUAL GAS

NT SOLIDIFIED GASES

NT TRITIUM

NT XENON

NT XENON ISOTOPES

NT XENON 133

NT XENON 135

Dynamics of collisions between shock interactions and wave configurations in gases and condensed explosives

01 p0402 N71-10421

Substructural hardening and gas extrusion of metals

02 p0241 N71-11444

High pressure gas medium for extrusion of materials

02 p0229 N71-11446

Utilization of potassium superoxide in regenerating expired gas

02 p0165 N71-11830

Heat and mass transfer during vapor condensation in presence of noncondensing gases

02 p0306 N71-12084

Dual spectrometer for rotational temperature measurements on low density nitrogen gas

03 p0684 N71-14886

Thermal diffusion and transport phenomena in gases

06 p0810 N71-16118

Spectrum of stochastic operator in transfer matrix of gas lattice model

10 p1516 N71-21660

Doppler line superradiant emission from uniform spherical gaseous medium

11 p1805 N71-22368

Viscosity of gases and gas mixtures - handbook

12 p1901 N71-23703

Solubility of NH3, CO, CO2, and SF6 in various gas-liquid binary systems at different pressures and temperatures

13 p2839 N71-24449

Atmospheric pollution as influenced by various gas ejection sources

14 p2239 N71-25908

Statistical thermodynamics of gas in glass solubility

15 p2376 N71-27064

Apparatus and process for volumetrically dispensing reagent quantities of volatile chemicals for small batch reactions

15 p2416 N71-27372

Uranium carbide oxidation kinetics in various gases

15 p2471 N71-27385

Nonlinear optics of thermal laser beam defocusing in gases

15 p2418 N71-27395

Analysis of internal and external gas venting system of spacecraft

16 p2682 N71-28166

Far infrared and Raman spectra of gaseous dimers calculated for many models and reported as functions of reduced temperatures

16 p2650 N71-28828

Circular model for interacting Fermi gas

16 p2657 N71-29140

Inhomogeneous toroidal resonator - fluid mechanical refracting gas-prism with wave functions and real numbers

17 p2733 N71-29544

Models for permitting continuous purging of impurities from gas compartments of fuel cell

17 p2706 N71-29694

Survey of errors in sampling shock tube gas with mass spectrometer for study of chemical reaction rates at high temperatures

17 p2735 N71-29782

Calculating penetration depth of one-row round jet system developing in limited cross wind under conditions most typical for gas burners

17 p2735 N71-29815

Analysis of concurrent adsorption and chemical reaction

17 p2715 N71-29861

Dimension influence of fluidized bed reactors on gas mixing at various velocities

17 p2716 N71-29915

Management planning in Sweden for natural gas as industrial energy source

18 p3028 N71-30522

Cascade arc techniques for investigating arc plasmas at extremely high pressures in selected gases

20 p3331 N71-33649

Two particle microscopic distribution function for studying extended collision model in kinetic theory of gases

20 p3253 N71-33711

Gas solubilities and transport properties in fuel cell electrolytes

20 p3215 N71-33826

Formation of fission gas bubbles in solids during reactor irradiation

21 p3467 N71-34679

Hypersonic flow around blunt object by nonequilibrium gas current accounting for radiation transfer in shock front

22 p3566 N71-35480

Statistical analysis of world reserves of solid fuel, crude oil, uranium, and natural gas in year 2000

22 p3580 N71-35591

Glass properties studied by synthesizing gas-glass systems using high pressure techniques

22 p3604 N71-35667

Incipient fire and toxic gas caution and warning system for space shuttles

22 p3675 N71-36286

Program for calculating saturation curves and condensation characteristics of gaseous mixtures of binary organic vapor and air

23 p3720 N71-36318

Effects of gas bubbles in ocean bottom sediments on behavior of sound waves

23 p3752 N71-36731

Nonlinear-optical effects in sulfur-hexafluoride at low pressure - saturation of infrared absorption

24 p3886 N71-37780

Signal analyzer to detect microquantities of radioactive gases

24 p4012 N71-38621

GASOLINE

Gasoline icing inhibitors for aircraft carburetors and fuel systems

04 p0473 N71-15414

Effect of so/low-lead motor gasoline on engine operation

23 p3840 N71-37383

Extractive phenols from coal as antioxidant additive for motor fuels

24 p3999 N71-38528

GASTROINTESTINAL SYSTEM

NT INTESTINES

NT RECTUM

Use of nutritional markers for studies of food intake, passage, and absorption in gastrointestinal tract of humans and animals

21 p3384 N71-34876

Computer program for symptom history of gastrointestinal ulcer to aid in diagnosis

22 p3556 N71-35329

GATES (CIRCUITS)

NT THRESHOLD GATES

Physical failure analysis of integrated circuits containing metal oxide semiconductors and its application to analog gates

02 p0194 N71-11339

Silicon controlled rectifier pulse gate amplifier for blocking false gating caused by negative transient voltages

03 p0348 N71-12514

Analog to digital converter development, including circuit gate

06 p0818 N71-16086

Development of high performance, digital microcircuits, and their application to data processing systems

06 p0823 N71-16416

Logic AND gate for fluid circuits

07 p0101 N71-17579

Low power NAND gate integrated circuit employing thin film resistors and lateral p-n-p transistors

07 p002 N71-17871

Two coincidence units with three independent twofold channels gated by one common signal

08 p1168 N71-18082

Synchronous counter design incorporating cascaded binary stages driven by previous stages and inputs through NAND gates

09 p1351 N71-19432

Switching series regulator with gating control network

12 p1867 N71-23518

Alternating current gated flip-flop implementation in sequential circuit design

12 p1880 N71-23787

Algorithm for automatic failure analysis of gates in logic circuitry

18 p2892 N71-38529

Wide band hot-carrier diode gate for application to electron hole plasmas

20 p3341 N71-33137

Linear gating of nanosecond signals for multichannel analyzer

21 p3436 N71-34018

Comparison of production technologies for silicon gate MOS and ISOPOLAR bipolar integrated circuits

23 p3735 N71-36638

SUBJECT INDEX

GATES (OPENINGS)

Longitudinal spin and lock mechanism for
acoustic film in motion picture cameras under vibration
and high acceleration loads
(NASA-CASE-LAR-10686) 16 p2396 N71-28935

GAUGE INVARIANCE

Reducing unitary irreducible representations of
SU(2,2) with in-Poincaré subgroup
(NYO-3828-52) 04 p0339 N71-14180

Applying asymptotic SU(3) and SU(2) symmetries
to hadron systems 04 p0386 N71-14253

Proving uniqueness of Chao-Paiou SU(3) factor for
dual Born terms involving mesononic mesons
04 p0388 N71-14310

Deriving formulas for spin and angular correlations
in hyperon beta decay
(OCO-264-548) 05 p0747 N71-15240

Developing non-Lagrangian field theory for equal
time commutators from broken conformal invariance
and chiral U(3) symmetry 06 p0912 N71-15818

Transition probability renormalization, diagrams,
and gauge invariance 07 p1076 N71-17544

Investigating time-reversal invariance in electro-
magnetic interaction of electrons and deuterons
(LNF-76/20) 06 p1249 N71-18224

Investigating violation of CP invariance in electro-
magnetic interactions of hadrons
(UCRL-28041) 06 p1259 N71-18639

Calculation of gauge invariant set of diagrams of
asymptotic momentum transfer of elastic form factors
in quantum electrodynamics with massive photons
(ILL-TH-71-1) 06 p1263 N71-18880

Hydrodynamic behavior of pure superfluid helium
at 0 K using gauge invariance 15 p2393 N71-27326

Finite and gauge-invariant computation of electron
self-energy and self-mass in quantum version of
curved space and time 18 p2972 N71-30535

Gauge invariant theory of motion of singularities in
linear approximation
(NASA-CR-121431) 20 p3293 N71-33896

Connection between conformal covariance and
gauge invariance of interactions
(BNR-72-5716) 23 p3807 N71-37143

GAUSS EQUATION

Dynamic equations for stochastic magnetic field
line in galaxy
(NASA-TM-X-65514) 13 p2160 N71-24949

Automatic processing of high frequency stellar
spectrophotometric data using Gauss function model
21 p3436 N71-34408

Convolved Breit-Wigner signals detected by mea-
suring instruments with Gaussian resolution functions
(SLO-1388-135) 21 p3474 N71-34740

Program for resolving Moonshine spectra by Gauss
nonlinear regression procedure
(RSO-M-1348) 21 p3485 N71-34827

Comparison of earth's magnetic field models with
Omanan sequence 24 p4011 N71-38604

GAUSS FUNCTION

U GAUSS EQUATION

GAUSS-MARKOV THEOREM

Process and additive noise independent variable
calculus using iterative methods based on Gauss-
Markov estimator
(TR-71-B-17) 18 p2889 N71-30588

GAUSSIAN DISTRIBUTIONS

U NORMAL DENSITY FUNCTIONS

GAUSSIAN NOISE

U RANDOM NOISE

GAUSSIAN METERS

GC-18 AIRCRAFT

U C-18 AIRCRAFT

U GAS COOLED REACTORS

GEAR TEETH

Load distribution on gear tooth couplings
06 p0862 N71-15726

Geometry and kinematics of gear design and lubri-
cation that effect tooth contacts 15 p2414 N71-26840

Fixed and variable stiffness models for simulating
transient dynamic loads on gear tooth 16 p2602 N71-28611

GEAR

Chemical failure detection for gears
(AD-712123) 03 p0385 N71-13220

Lubrication considerations in design of gears
(NASA-TM-X-52942) 05 p0691 N71-14785

Precision stopping drive device using cam disk
(NASA-CASE-MF-14772) 07 p1037 N71-17692

Precision forging of spiral bevel gears for Army
helicopters
(AD-715419) 06 p1307 N71-18020

Acoustic signature analyses for bearing and gear
failure mode identifications 09 p1393 N71-20227

Gearing system for eliminating backlash and filter-
ing input force fluctuations from high inertia load
(NASA-CASE-XGR-04227) 10 p1548 N71-31744

Operation of modular gear systems in vacuum en-
vironment with and without lubrication and under no
load conditions
(AD-717894) 12 p1925 N71-25276

Self lubricating gears and other mechanical parts
having surface adapted to frictional contact
(NASA-CASE-MFS-14971) 13 p2087 N71-24984

Gear checking system for testing fine-pitched mini-
ature metallic gears at required 2-ounce pressures
(BDX-613-309) 13 p2098 N71-25457

Lubricant rheology and chemistry effects on con-
tact material fatigue 15 p2412 N71-26827

Film thickness, friction, and pressure distribution
effects in elastohydrodynamic gear lubrication
15 p2412 N71-26828

Scoring temperature constancy of mineral lubricat-
ing oils in gears 15 p2413 N71-26890

Additive DIBKP-46 containing sulfur, chlorine, and
phosphorus to improve functional properties of
lubricating oils used in reduction gears with Novikov
gearing
(AD-710931) 15 p2430 N71-27536

Effect of axial vibrational motion on frictional en-
ergy losses and efficiency of spur gear system
16 p2603 N71-28911

Measurement and analysis of bending stress in ex-
ternal involute spur gears 19 p3106 N71-32746

Mechanical drives of French 2- and 3.6-meter
telescopes from horseshoe, noting gears
24 p3923 N71-37969

GEIGERSCHEIN

Evaluation of Apollo 14 geigerschein photography
from lunar orbit including phenomenon mechanics
18 p3012 N71-30969

Optical properties of interplanetary medium in
direction of Geigerschein 22 p3672 N71-36180

GEIGER COUNTERS

ESRO 1 Geiger counter and ground geophysical ob-
servations of radiation belt electron precipitation, fine
structure, and angular distribution during solar flare,
25 Feb. 1969
(R-17) 02 p0212 N71-11541

Buildup of gas discharges in proportional and Geiger
region for use in Chaparral chambers
(SLAC-TRANS-121) 04 p0580 N71-13983

ESRO 1 satellite Geiger counter observations of
solar proton flare effect on magnetically trapped par-
ticles over polar cap regions 10 p1571 N71-21159

Conversion factor for converting Geiger tube count
rates or ion chamber currents into units of incident X
ray energy flux in specified passband in normalizing
solar X ray data 15 p2514 N71-27644

Failure analysis of halogen quenched Geiger-
Müller tube operation
(DUN-NA-136) 20 p3308 N71-33743

Properties of improved multiple anode halogen
Geiger-Müller counters
(NF-18896) 24 p3919 N71-37949

Geiger counter detection of carbon 14 for upper age
limit determination 24 p4013 N71-38625

GEIGER-MULLER TUBES

U GEIGER COUNTERS

GELATINE

Gelatin effect in precipitative nucleation of photo-
graphic emulsions 01 p0054 N71-10550

Application of microencapsulation techniques to
photographic emulsions
(NLL-M-20169-1828-49/1) 12 p1923 N71-34189

GELLED ROCKET PROPELLANTS

NT Fuel tests to determine feasibility of gelled methanol
for use in jet engines
(NASA-CR-72676) 14 p2331 N71-25772

Chemical and physical properties of aircraft fuels
gelled with hydrocarbon resins
(FAA-NA-71-17) 19 p3172 N71-32078

Determination of physical and chemical properties
of fuels gelled with carbohydrate resins to evaluate ef-
fectiveness in reducing aircraft fire hazards
(FAA-NA-71-18) 23 p3630 N71-37569

GELLED ROCKET PROPELLANTS

Method and apparatus for producing fine particles
in organic liquid bath for gelled rocket propellants
(NASA-CASE-NFO-10236) 06 p0904 N71-14312

GELS

NT DOUBLE BASE ROCKET PROPELLANTS

Thermal stability of gelatinized organosilicon liquids
(AD-711474) 01 p0072 N71-10629

Thickening capacity of silica gel in plastic lubricants
(AD-717531) 01 p0073 N71-10663

Gel-adsorption process chemical studies in EBR-2
(BAW-7714-17) 02 p0246 N71-12184

GENERAL AVIATION AIRCRAFT

Intermittent type silica gel adsorption refrigerator
for providing temperature control for spacecraft com-
ponents
(NASA-CASE-XNP-00920) 06 p0863 N71-13966

Electron spin resonance studies on irradiated
heterogeneous systems - structure and reactivity of
paramagnetic centers in silica gel
(NP-10478) 06 p2335 N71-15289

Combustion physics and flammability of aluminum
magnesium alloy aerogels
(NASA-TT-F-13365) 09 p1404 N71-28511

Chemical properties of cellulose acetate gels in both
dry and gel states
(NRC-TT-1439) 10 p1512 N71-21288

Mechanism of crystal nucleation in gels, and
heterogeneous nuclei and gel structure
(AD-710904) 13 p2150 N71-24381

Model for predicting rate of dissolution of network
polymers by chemical degradation 17 p3716 N71-30234

Analysis of phenol formaldehyde condensates by
chromatography on polystyrene gels
(ONERA-TT-771) 19 p3049 N71-31701

Amino silica gel absorbers for atmospheric purifi-
cation systems of spacecraft cabins 20 p3222 N71-33448

Sorption of antimony-125 by silica gel from nitric
and hydrochloric acid
(NP-10738) 23 p3794 N71-37045

GEMINI FLIGHTS

NT GEMINI 3 FLIGHT

Geologic applications of terrain photography from
Gemini spacecraft
(NASA-TM-X-65431) 06 p1280 N71-18408

Biomechanical aspects of Gemini flight for future
manned space flight technology 16 p2551 N71-28527

Red cell mass and plasma volume changes observed
in astronauts on Gemini and Apollo missions
23 p3711 N71-36454

Hematological program and biochemical data from
Gemini and Apollo missions 23 p3711 N71-36455

Micrometeoroid impact experiments conducted on
Gemini 9 and 12 missions
(NASA-TM-X-2408) 23 p3856 N71-37489

GEMINI PROJECT

Review of endocrine control of fluid and electrolyte
balance during Mercury, Gemini, and Apollo missions
23 p3711 N71-36456

GEMINI 5 FLIGHT

Gemini 5 flight data on earth radiance at 2.2 microns
15 p2400 N71-27492

GEMINI 7 FLIGHT

Metabolic balance studies of two astronauts during
10 day preflight phase, Gemini 7 flight of 14 days, and
4 day postflight recovery phase 20 p3216 N71-33255

Preflight and postflight analysis of effects of Gemini
7 mission on metabolic and endocrine systems 23 p3711 N71-36457

GENERAL AVIATION AIRCRAFT

FAA statistical handbook of aviation 1958-1960
01 p0003 N71-10372

General aviation airport planning for east central
Florida
(PB-191239) 04 p0517 N71-14494

US general aviation and supplemental air carrier ac-
cident statistical tables for 1969
(NTSB-BA-70-4) 07 p0971 N71-17475

Mildair collision hazards, incidents, and recom-
mendations for safe aircraft operations 07 p0974 N71-18103

Investigation of angle of attack information display
for pilots to increase efficiency of general aviation air-
craft operation
(NASA-TN-D-6210) 06 p1143 N71-18442

Development and characteristics of low cost en-
gines for general aviation aircraft 09 p1457 N71-19438

Benefits and problems of using hand-up displays in
commercial and general aviation aircraft
(NASA-CR-117735) 09 p1308 N71-19752

Analysis of equipment, crew training, and opera-
tions involved in use of fixed wing aircraft for
aeromedical transportation 19 p3834 N71-32080

Statistical compilation of annual aircraft accident
data of US general aviation for 1969
(NTSB-AD-71-1) 19 p3838 N71-32454

Analysis of general aviation during year 1969 noting
growth of aircraft operation, accident data, analysis of
accidents, and injuries resulting from accidents 20 p3208 N71-32854

Sensitivity analysis of advance propeller configura-
tions designed for general aviation aircraft of 1980
time period
(NASA-CR-114289) 22 p3538 N71-33286

Potential impact of advanced technology in 1985 on
four types of general aviation aircraft including STOL
V/STOL, and helicopters
(NASA-CR-114339) 22 p3539 N71-33210

Influence of advanced technology and design philosophies on general aviation aircraft for 1983 [NASA-CR-114338] 22 p3540 N71-35217

Aircraft accident briefs for 1969 including date, location, aircraft data, injuries, flight purpose, and pilot data [NTSB-BA-71-2] 23 p3708 N71-36433

GENERAL DYNAMICS AIRCRAFT

NT CV-440 AIRCRAFT 22 p3540 N71-35217

NT CV-990 AIRCRAFT 22 p3540 N71-35217

NT F-106 AIRCRAFT 22 p3540 N71-35217

NT F-111 AIRCRAFT 22 p3540 N71-35217

GENERAL DYNAMICS MILITARY AIRCRAFT

U MILITARY AIRCRAFT 22 p3540 N71-35217

GENERATORS

Ferromagnetic fluid for generating pressure forces for sea vehicle propulsion [AD-723534] 17 p2756 N71-29905

GENETIC CODE

Investigating digital techniques, telemetry systems, and genetic code inversion 06 p0817 N71-16676

Multiple coding mechanism for evolution of genetic code [NASA-CR-121896] 22 p3543 N71-35237

Function of UV light in evolution of contemporary ribosomes [NASA-CR-123164] 24 p3877 N71-37633

GENETICS

NT GENETIC CODE 24 p3877 N71-37633

NT MUTATIONS 24 p3877 N71-37633

Detection of antigens and genetic analysis with mouse hybrids [SU-326-P-26-X-2] 03 p0322 N71-12300

Neutron dosimetry, biophysics and biological effectiveness, genetic effects, repair and recovery, and modifying factors of neutrons in radiobiology [CONF-691186] 09 p1332 N71-20010

Case history of Chodai-Higashi disease with simultaneous Friedrich hereditary spinal ataxia and hematologic, neurologic, and genetic characteristics [NASA-TT-F-15337] 12 p1863 N71-23749

Radiation effects on cytoplasmic structure and differential activity of genes [NYO-2356-43] 20 p3225 N71-33934

Gene frequencies of red cell acid phosphatase in random samples [NASA-TT-F-13989] 24 p3877 N71-37637

GENTOURINARY SYSTEM

NT TESTES 24 p3877 N71-37637

GEOASTROPHYSICS

U ASTROPHYSICS 24 p3877 N71-37637

U OBSEPHYSICS 24 p3877 N71-37637

GEOCENTRIC COORDINATES

Analytic expressions for partial derivatives of observables with respect to Robertson relativistic parameters and planetary defects in lunar theory 01 p0121 N71-10268

Determining geocentric latitude and longitude of unknown stations by photogrammetry against stellar background [AD-713508] 05 p0720 N71-15354

Geocentric coordinate determinations for station locations using optical observations of Pegasus trillion satellites 19 p3090 N71-31872

Geocentric and osculating orbital element calculations for satellites according to visual base and asynchronous observations 22 p3676 N71-36211

Unified set of tracking, station coordinates on geocentric reference system from GEOS 1 and 2 tracking data [NASA-TM-X-65707] 23 p3748 N71-36721

GEOCHEMISTRY

NT BIOGEOCHEMISTRY 23 p3748 N71-36721

Studying geology, geochemistry, and biology of Iceland and Surtsey as examples of new and extreme environments [NASA-TM-X-62009] 07 p1024 N71-17966

Studies in nuclear physics research, radiation research, isotope geochemistry, carbon 14 variations, and isotope applications [NP-18408] 08 p1249 N71-18207

Marine television and infrared spectrometer data analysis in determine Mars surface geochemistry [NASA-CR-116785] 08 p1288 N71-18627

Regional significance of volcanic geochemistry in far Triple Junction, Ethiopia [NASA-CR-117136] 09 p1383 N71-17932

Computer-coupled low resolution mass spectrometer system and organic geochemical analysis methods for isolation and identification of compounds from heavy soil samples [NASA-CR-116904] 09 p1465 N71-17976

Hydrology and geochemistry of lakes in determine cycling and transport of radionuclides [CU-2493-11] 10 p1551 N71-21187

Criteria for distinguishing organic matter of abiogenic and biogenic origin [NASA-TM-X-62020] 12 p1913 N71-23773

GEOCHRONOLOGY

Isotopic lead and thorium analysis of rocks, meteorites, and lunar samples 01 p0017 N71-10309

Radioactive dating of ocean core samples and geochemical studies of limiting boundary conditions [ORO-3622-9] 05 p0676 N71-15460

Appraisal of earth origins and structure based on theory of continental drift and geological observations 18 p2912 N71-30992

GEODESY

NT CELESTIAL GEODESY 18 p2912 N71-30992

Theory of wave refraction in shoaling water with effects of caustics and spherical earth [AD-711304] 01 p0051 N71-10846

Covariance matrix for deflections of vertical and undulations based on actual gravity data [AD-712351] 02 p0222 N71-12168

Abstracts on Soviet magnetism, geodesy, and seismology instrumentation and research 07 p1030 N71-17490

Short term prospects for geodetic positioning from satellite observations 07 p1022 N71-17833

Accuracy of Doppler determinations of satellite observing station positions 17 p2846 N71-29420

Analysis of bathymetric and geophysical survey of ocean bottom off Ceylon 18 p2912 N71-30992

Discussion of marine geology and geophysics of ocean floor and predictions for future research and exploration during next ten years 18 p2912 N71-30992

Accomplishments of geodetic satellite and earth survey programs during period July to December 1970 [NASA-CR-119357] 18 p3016 N71-31295

Geodesy and cartography - bibliography [AD-723428] 19 p3085 N71-31810

Estimation of geodetic parameters describing earth gravity field and positions of satellite tracking stations in geocentric reference [SAO-009-49] 19 p3086 N71-31828

Geodetic location of ship at sea obtained with C-band radar range data of satellite with accurately determined orbit 19 p3054 N71-31862

C band tracking radar used to obtain more accurate geodetic data for downrange Mistran/MRS sites 19 p3054 N71-31863

Approximate reduction of gravity formula describing earth shape to Taylor series [AD-723151] 19 p3091 N71-31927

Mokodensky series and analytical continuation applied to gravimetric geodesy [AD-724133] 20 p3239 N71-33181

Atmospheric density variations at 140 km deduced from precise satellite radar tracking data [NASA-TM-X-64610] 21 p3416 N71-34304

Artificial earth satellites used in upper atmosphere and geodetic studies, and satellite orbit mechanics 22 p3676 N71-36206

Determination of direction cosines of line connecting two observation stations from quasi-simultaneous observations of artificial earth satellites 22 p3677 N71-36220

Artificial satellite geodesy using least squares method 22 p3678 N71-36227

Errors in Doppler geodetic measurements from coherent frequencies for correcting ionospheric refraction 22 p3680 N71-36241

Soviet and French programs for establishing astrometric schools and stations in Egypt for space geodesy 22 p3680 N71-36243

International conference on artificial earth satellite use for upper atmosphere and geodetic studies 22 p3680 N71-36245

GEODETIC COORDINATES

FORTAN 4 computer program for calculating satellite photograph coordinates [PB-193144] 01 p0051 N71-10888

Laser altimeter-range finder techniques applied to geodetic measurements and mapping [NASA-TM-X-64489] 03 p0387 N71-12425

Geodetic parameters of earth gravity field and satellite tracking station positions in geocentric reference frame [NASA-CR-116850] 08 p1193 N71-18974

Center of mass station coordinates determined from dynamic solutions of optical, laser, and Goddard range and range rate observations of GEOS 2 [NASA-TM-X-65475] 10 p1552 N71-21297

Coordinate displacement computer program for adjusting triangulation networks [REF-120] 10 p1530 N71-21673

Determination of accuracy achievable and minimum time possible for finding geodetic position of satellites [AD-723991] 17 p2741 N71-29743

Gravimetric and geometric investigations with GEOS 1 and GEOS 2 - GEOS 2 conference [NASA-TM-X-62721] 19 p3085 N71-31826

Coordinates for 23 NASA STADAN and SPOPT optical and 2 NASA laser tracking sites dynamically estimated from GEOS 1 and GEOS 2 data 19 p3087 N71-31834

Determining position of MOTS stations by orbital dynamics using GEOS 1 observations 19 p3087 N71-31830

Short arc geodetic adjustment for improving survey coordinates of observing stations using GEOS 1 data [AFCR-70-0096] 19 p3087 N71-31826

Using SBOR observations on GEOS-1 satellite from Pacific Tracking Network for attaching network to NAD 19 p3088 N71-31840

Comparison of four independent investigations concerning survey adjustment to NAD using GEOS data 19 p3088 N71-31841

Estimates of C band radar station positions and baseline distances 19 p3054 N71-31862

Description of NONAME program and system for determining and analyzing satellite orbits and calculating geodetic parameters [NASA-CR-121662] 21 p3507 N71-34086

Geocentric coordinates of geometric height, pressure, temperature, density, and potential energy levels in earth atmosphere [NASA-CR-121664] 21 p3507 N71-34086

Determination of observation station coordinates and inclination of reference ellipsoid from laser and photographic observations 22 p3677 N71-36211

Determination of vector equation and formulas for geodetic coordinates and ellipsoid heights, using satellite equatorial coordinates and synchronous observations 22 p3677 N71-36211

Relativistic effects and optimal satellite inclination for Doppler determination of geodetic coordinates 22 p3680 N71-36243

GEODETIC SATELLITES

NT EXPLORER 29 SATELLITE 22 p3677 N71-36211

NT GEOS 1 SATELLITE 22 p3677 N71-36211

NT GEOS 2 SATELLITE 22 p3677 N71-36211

NT GEOS-C SATELLITE 22 p3677 N71-36211

NT PAGESOS SATELLITE 22 p3677 N71-36211

Geodetic survey of Spitzbergen by ground station measurements and satellite triangulation 05 p0674 N71-14935

Short term prospects for geodetic positioning from satellite observations 07 p1022 N71-17833

Two ruby lasers in system designed for satellite illumination [AD-717693] 11 p1776 N71-22700

Results of orbital study of preliminary ISAGEX [NASA-TM-X-65488] 12 p1996 N71-34075

Evolution, development, and accomplishments of scientific and geodetic satellites and radar altimeter for geodetic measurements [AD-718348] 12 p2002 N71-34194

Optical tracking data from geodetic satellites for deep space station coordinates 15 p2442 N71-27607

Laser reflectors, stabilization, and thermal control of geodetic satellites Diademe D-1C and D-1D [RAE-LIB-TRANS-1501] 16 p2681 N71-28003

ESRO geodetic satellite program for investigating solar gravitational fields 18 p3017 N71-30633

Summary of observational data of geodetic satellites as of 15 June 1970 19 p3086 N71-31827

Earth gravity field determinations with laser tracking of geodetic satellites 19 p3108 N71-31857

Q switched laser and normal mode ruby laser for dual-laser satellite geodesy system 19 p3089 N71-31829

Present status and future requirements of geodetic satellite geodesy using simultaneous optical direction observations with lasers and cameras 19 p3090 N71-31830

Geodetic satellite program and planning for GEOS-C satellite [NASA-TM-X-62769] 19 p3090 N71-31830

Geodetic satellite data for determining earth gravitational model and tracking station location 19 p3090 N71-31831

Optimized Doppler tracking system for geodetic satellite ranging 19 p3090 N71-31832

GEOS-C satellite project for geodetic and earth physics research 19 p3091 N71-31833

Computer program for quadrangle adjustment of East European satellite triangulation network stations [TT-70-52067] 19 p3182 N71-32844

Mathematical analysis to determine relationship between two theories of satellite harmonics and gravimetry [AD-724123] 20 p3254 N71-32817

Effects of polar cap absorption events on geostationary satellite VHF communication systems [NOAA-TR-ERL-196-OD-5] 22 p3553 N71-35310

Establishment of world-wide earth satellite and ground base observation network 22 p3678 N71-36223

- Relativistic effects and optimal satellite inclination for Doppler determination of geodetic coordinates 22 p660 N71-36242
- GEODETIC SURVEYS**
 Geodetic gravity approach for determining earth potential on grid 01 p0051 N71-10901
 Thermal mapping of heated nuclear power plant discharge into river 02 p0206 N71-11158
 Side-looking airborne radar for K band mapping of snowfields 02 p0207 N71-11163
 Applying holographic techniques to obtain ground truth data from earth resources and geodetic altimetry 03 p0380 N71-12798
 Verification experiment design for satellite-borne geodetic altimeter operating over seas [NASA-CR-115897] 05 p0669 N71-14791
 Mathematical modeling of world geodetic system 05 p0672 N71-14876
 Remote sensor system for urban environmental mapping [LAF-133] 05 p0673 N71-14877
 Geodetic survey of Spitzbergen by ground station measurements and satellite triangulation 05 p0674 N71-14935
 Multi-spectral aerial sensing for geological survey in southern California 06 p0842 N71-16127
 Aerial photography and radar imagery for terrain mapping 06 p0843 N71-16132
 Aerial radar and infrared imagery for geodetic survey of southern Arizona 06 p0843 N71-16137
 Aerial radar imagery for topographic mapping of geological regions 06 p0843 N71-16138
 Summaries of news releases and abstracts of articles on terrestrial geophysics 11 p1745 N71-21955
 Scientific and economic results of geologic, hydrologic, and topographic studies 14 p2251 N71-26644
 Geodetic survey by means of mobile stations of Q switched laser range finders and Diadema satellite [ONERA-NT-156] 15 p2396 N71-27054
 Geodetic survey techniques for study of earth natural resources and use of methods for similar studies of other planets [NASA-TT-F-13410] 18 p2917 N71-31147
 Geodetic measurements for West-German part of European triangulation calibration line Tromso-Catania [REPT-126] 20 p3276 N71-33846
 Computer applications to tide and current analysis in coast and geodetic surveys 23 p3789 N71-37008
 Tide predictions for nautical almanacs, amphibious aircraft operations, and geodetic surveys 23 p3790 N71-37010
- GEODIMETERS**
 Describing operation of NASM-2A geodimeter for scale control in West German portion of European First-Order Triangulation Net 08 p1202 N71-18760
 Geodimeter measurements for West-German part of European triangulation calibration line Tromso-Catania [REPT-126] 20 p3276 N71-33846
 Geodimeter data for scaling German part of European main triangulation net [REPT-158] 20 p3247 N71-33850
- GEOMAGNETIC ACTIVITY**
NT TELLURIC CURRENTS
 Tables of geoelectric observations in Japan - 1966 [REPT-72] 11 p1749 N71-22438
 Geoelectric observations in 1967 at Kakioka, Memambetsu, and Kanoya, Japan [REPT-73] 11 p1750 N71-22542
 Sampling and linear filter theory for direct interpretation of geoelectrical resistivity measurements 16 p2585 N71-28246
- GEOMAGNETISM**
NT OROGRAPHY
 Verification of geography in Rio de Janeiro by using airborne magnetometer [LAF-133-VOL-2] 05 p0680 N71-15546
 Conference on Earth Resources Program including geology and geography [NASA-TM-X-64913] 08 p1196 N71-19251
 Petro-magnetic and plate tectonics combined to produce evolution of earth geography from proto-construction [AD-717049] 10 p1545 N71-20620
 New geographical names for locations on Franz Josef Land maps 11 p1755 N71-22833
 Global distribution of upper atmospheric infrared magnetic layers from Cosmos 65 data analysis [NASA-TT-F-13660] 12 p1903 N71-23304
 Geomagnetic theories, morphological parameters, and potential features of Antarctica [TT-70-50015] 12 p1907 N71-23524
- Geometrical interpretations of Sandwich theorem related to geography and algorithm and program for achieving solutions [AD-726403] 22 p3608 N71-35696
- GEOPHYSICS**
 Geoid determination by vertical deflection calculations based on Bessel's ellipsoid 01 p0050 N71-10807
 Geodetic gravity approach for determining earth potential on grid [AD-711265] 01 p0051 N71-10901
 Covariance matrix for deflections of vertical and reductions based on actual gravity data [AD-712351] 02 p0222 N71-12168
 Development of gravimetric geoid for US from satellite derived gravity data and local gravimetric measurements [NASA-TM-X-65691] 23 p3747 N71-36717
- GEOPHYSICAL FAULTS**
 Mathematical analysis of geological formations effect on seismic motions [UCRL-30896] 05 p0667 N71-14895
 Correlating color photography of Apollo 7 with natural color of surface deposits and rocks of Salar de Atacama, Chile 14 p2251 N71-26645
 Measurement and characteristics of gravity anomalies over Albatraz trench 18 p2914 N71-31005
 Fracture pattern and magnetic anomaly measurements of Juan de Fuca-Gorda ridge area 18 p2914 N71-31008
 Microseismic analysis of Denali fault in Alaska and under ground nuclear explosions and microseismic survey of Nevada, Utah, Idaho, Montana, and Wyoming 22 p3590 N71-35504
 Computer reduction and nondestructive tests for determining material characteristics of surface fault areas [SC-DR-710222] 23 p3729 N71-36578
- GEOLOGY**
NT GEOMORPHOLOGY
NT GLACIOLOGY
NT HYDROGEOLOGY
NT LITROLOGY
NT LUNAR GEOLOGY
NT OROGRAPHY
NT PETROGRAPHY
NT PETROLOGY
NT PHOTOGEOLOGY
NT TECTONICS
NT VOLCANOLOGY
 Developing lunar roving vehicles for surface exploration on basis of field geology and traverse geophysical experiments on earth 01 p0121 N71-10252
 Photointerpretation and applications of space photography in geology [JPRS-51578] 01 p0050 N71-10801
 Arctic marine geophysics and oceanography, and underwater acoustics [AD-711626] 02 p0209 N71-11417
 Nomograms for calculating depths of perennial freezing and thermal cycles of rocks [AD-711811] 02 p0211 N71-11511
 General laws governing formation and development of frozen layers [AD-711870] 02 p0211 N71-11515
 Investigating remote sensing applications to simple geological features using microwave radiometers 02 p0227 N71-11990
 Geothermal investigations for determining subsurface structure of petroliferous and gas bearing regions [NASA-TT-F-13592] 02 p0218 N71-12017
 Measurement of stress waves in soft soil [AD-711864] 02 p0219 N71-12088
 Local geology effects on seismic wave amplitudes [NVO-1163-VOL-3] 02 p0221 N71-12142
 Marine biology and geology of Caribbean Sea [PB-1969/77] 03 p0373 N71-13343
 Solid state physics, metallurgy, solid mechanics, geology, and chemistry 03 p0445 N71-13381
 Research progress in various aspects of applied mathematics, metallurgy, engineering, nuclear physics, and optical measurement 05 p0679 N71-15544
 Mathematical models for seismic amplification and ground motion of recording station geology [NVO-1163-211] 06 p0840 N71-15912
 Anticipating sinkhole collapse by using remote sensors to identify and delineate rock features 06 p0846 N71-16169
 Investigating geology of Surtsey and Iceland with respect to earth planetary evolution 07 p1023 N71-17974
 Reporting results of disciplinary and interdisciplinary research into geology of Iceland 07 p1026 N71-17983
 Geology of Antarctica [RE-12631] 08 p1186 N71-18317
 Conference on Earth Resources Program including geology and geography [NASA-TM-X-64913] 08 p1196 N71-19251
- Application of airborne and satellite-borne remote sensing systems geological surveys 08 p1196 N71-19252
 Application of computer processed multispectral data in discrimination of land cover photo areas in Florida 08 p1196 N71-19253
 Digital computer processing of visible and reflective infrared scanner data for automatic computer mapping of Yellowstone National Park 08 p1197 N71-19254
 Geologic analysis of X band radar mosaics of Massachusetts 08 p1197 N71-19255
 Development, use, and application of information retrieval systems in geology and controlled medical records [AD-716921] 08 p1383 N71-19002
 Geological and geomorphological interpretation of Tularosa Basin, New Mexico, from rocket-borne photographs 10 p1534 N71-21644
 Modified approach to role of Arctic Basin in geostructural development of supercontinent Laurasia during Paleozoic era 11 p1754 N71-22820
 Soviet Popigai bottleholes formed by asteroid collision [NLL-M-20262-58284F] 12 p1914 N71-24034
 Excavation by nuclear explosions in saturated clay shales - Project Tri-Goulds 2 14 p2248 N71-26106
 Methodology for determining elastic constants of its site rocks during engineering and geological surveys [NASA-TT-F-13634] 16 p2590 N71-28090
 Geological exploration, development of ultrasonic flow detector, review of scientific developments, and tactical aircraft in Eastern Europe [JPRS-53628] 17 p2845 N71-30833
 Trends and possibilities in biotechnology, biotechnology, geology of minerals, earth resources, and man-machine systems 18 p3028 N71-30839
 Geology of minerals as space age earth resource possibility 18 p2911 N71-30841
 Geological examination and petrographic analysis of Richter and Semoyat domes in central Mauritania 18 p2913 N71-30994
 Geological characteristics of deep sea channel on Albatraz abyssal plain south of Albatraz trench [ESSA-TR-EBL-93-POL-2] 18 p2913 N71-30998
 Geological characteristics of fossil deep sea channel on Albatraz abyssal plain and results of hydrologic survey 18 p2913 N71-31000
 Geological analysis of lunar soil samples from Sea of Fertility obtained by Luna-16 automatic station [NASA-TT-F-13736] 18 p3016 N71-31331
 Geologic mapping of Yellowstone National Park area by interpretation of radar imagery [NASA-CR-121425] 20 p3233 N71-33185
 Geologic evaluation of anomalies between like-polarized and cross-polarized K-band side-looking radar imagery of Yellowstone National Park [NASA-CR-121419] 20 p3265 N71-33374
 Geological benefits derived from spaceborne television photography of earth [JPRS-53949] 21 p3428 N71-34390
 Proceedings of conference on remote sensors for scientific geological applications [FOA-2-C-2365-32] 22 p3554 N71-35332
 Geological uses of earth-orbital photography with case histories [NASA-TM-X-65662] 22 p3583 N71-35316
 Climatology, geography, geology, and history of Yukon Territory, Canada and Chukotka, Alaska [AD-726405] 22 p3615 N71-35762
 Quantity and quality of geologic information transmitted by space photography compared with low altitude aerial photography [IR-USO-259] 24 p3926 N71-38013
 Scientific research, microbiology, astronomy, geophysics, and oceanography projects conducted by European organizations [AD-727186] 24 p4034 N71-38785
- GEOMAGNETIC ANOMALIES**
U MAGNETIC ANOMALIES
U MAGNETIC CROTCHETS
U SUDDEN IONOSPHERIC DISTURBANCES
U MAGNETIC EFFECTS
U MAGNETIC EFFECTS
U MAGNETIC SQUAT
U MAGNETIC BOUATOR
U MAGNETIC FIELD
U GEOMAGNETISM
GEOMAGNETIC BLOW
 OGO-B and OGO-E measurements on magnetospheric field magnitudes and disturbances caused by ring currents 13 p2076 N71-33271
- GEOMAGNETIC LATITUDE**
 Anomalous plot and geomagnetic for determining corrected geomagnetic local time, latitude, and longitude for high latitudes in Northern Hemisphere [AD-713170] 05 p0764 N71-14557

Latitudinal distribution of auroral absorption zone in Northern Hemisphere during solar activity cycle 11 p1823 N71-22815

Variability of direction of closure currents of western electrojet in region of geomagnetic poles 11 p1757 N71-22849

Latitudinal density distribution of gases in upper atmosphere 13 p2076 N71-25267

IMP 5 magnetic field measurements at high geomagnetic latitudes to observe broad depressed field region centered on polar or dayside cusp [NASA-TM-X-65642] 19 p3093 N71-32149

GEOMAGNETIC MICROPULSATIONS

Transient magnetospheric current sheet generation of magnetohydrodynamic waves and geomagnetic micropulsations 05 p0675 N71-15420

Geomagnetic micropulsation role in polar and magnetospheric substorms 12 p1908 N71-23555

Tabulation of international locations of rapid-run geomagnetic micropulsation stations [DI-82-1043] 13 p2078 N71-25527

Magnetospheric proton density models with plasmapause influence on F₁ geomagnetic micropulsation 15 p2397 N71-27000

Solar wind simulation, including investigation of shock front and geomagnetic nocturnal variations [D-15] 23 p3481 N71-37392

GEOMAGNETIC PULSATIONS

NT GEOMAGNETIC MICROPULSATIONS

Solar wind, interplanetary magnetic fields and magnetic variations 03 p0451 N71-13263

Mariner spacecraft data analysis to determine relationship between interplanetary magnetic field direction and geomagnetic activity 06 p0856 N71-16797

Investigating geomagnetism, seismic properties, and tectonic structure of earth crust 07 p1014 N71-16021

Morphology of auroral geomagnetic pulsations for low and high magnetic activity observed from Tromsø, Norway 12 p1908 N71-23557

Geomagnetic pulsation measurement for auroral magnetospheric substorm study 12 p1909 N71-23559

Polarization of geomagnetic pulsations [PR-46] 17 p2738 N71-29396

Explorer 33 observations of sudden impulses propagating in geomagnetic tail and magnetosheath [NASA-CR-121900] 22 p3572 N71-35439

GEOMAGNETIC STORMS

U MAGNETIC STORMS

GEOMAGNETIC TAIL

Plasma-electromagnetic interactions between solar wind and geomagnetic tail [ESRIN-IN-104] 08 p1188 N71-18524

Relation between geomagnetic tail fundamental oscillation mode and magnetospheric storms [D-3] 17 p2739 N71-29534

Models for internal structure of geomagnetic tail neutral sheet deduced from Explorer 34 magnetic data [NASA-TM-X-67153] 18 p3007 N71-31308

Mathematical models for electromagnetic noise in neutral current sheet of geomagnetic tail [AD-723654] 19 p3175 N71-31802

Plasma sheet models for geomagnetic tail structure 20 p3254 N71-32870

Explorer 33 observations of sudden impulses propagating in geomagnetic tail and magnetosheath [NASA-CR-121900] 22 p3572 N71-35439

Bulk plasma moving in periodic hydromagnetic motion in geomagnetic tail 22 p3653 N71-36052

GEOMAGNETICALLY TRAPPED PARTICLES

U RADIATION BELTS

GEOMAGNETISM

Predicting geomagnetic activity for four years in advance [ESSA-TR-ERL-160-SDL-13] 01 p0048 N71-10516

Tidal motions in E region as source of daily variation of geomagnetic field [AD-711782] 01 p0051 N71-10849

Telluric, geomagnetic, and auroral activity on Arctic drifting stations and at Pt. Barrow 02 p0291 N71-11143

Parameters and effective rigidity changes of geomagnetic cosmic ray cutoff with primary spectrum changes in quiescent geomagnetic field [AD-712344] 02 p0293 N71-12006

Geomagnetic field simulation and magnetic measurements of earth satellites 03 p0356 N71-12711

Magnetic anomaly detection by natural geomagnetic field perturbations [AD-712131] 03 p0368 N71-13030

Abstracts of articles on terrestrial geophysics, seismology and gravity anomalies 03 p0368 N71-13042

Satellite attitude and spin control subsystem using interaction between generated magnetic moment and geomagnetic field [NASA-TN-D-6051] 03 p0409 N71-13056

Analysis of geomagnetic unrest and seismological research covering 30 year period 03 p0369 N71-13091

Geomagnetism/electric current alignment, space charge and electric field effects on particle acceleration, and aurorae/magnetons 03 p0451 N71-13332

Velocity and stress distributions in earth mantle due to secular variation of geomagnetic field 05 p0669 N71-14796

Geomagnetism, radioactivity, ionospheric parameters, seismology, cosmic rays, and atmospheric electricity - Mar. 1970 06 p0848 N71-15725

Dourbes geophysical observatory, Belgium, data on geomagnetism, ionospheric propagation, seismology, cosmic rays, and atmospheric electricity, April 1970 06 p0848 N71-15806

Geophysics and space data bulletin - Vol 7, no. 2 [AD-714412] 06 p0856 N71-16761

Abstracts on Soviet astronomy, meteorology, oceanography, terrestrial geophysics, upper atmosphere, and space research [JPRS-51991] 07 p1107 N71-16955

Abstracts on Soviet terrestrial geophysics research 07 p1015 N71-16959

Atmospheric electricity, ionospheric sounding, seismology, and geomagnetism, and cosmic ray data - Belgium, May 1970 07 p1018 N71-17149

Atmospheric electricity, ionospheric sounding, seismology, and geomagnetism, and cosmic ray data - Belgium, June 1970 07 p1018 N71-17150

Relativistic origin of geomagnetic field and contraction mechanism [JPRS-52234] 07 p1019 N71-17480

Abstracts on Soviet magnetism, geodesy, and seismology instrumentation and research 07 p1020 N71-17490

Radioactive age determination by carbon 14, errors including isotopic effects and geomagnetism [CEA-CONF-1618] 08 p1185 N71-18219

Drift shell splitting of trapped particles by earth magnetic field [NASA-TM-X-65466] 09 p1463 N71-20468

Components of terrestrial magnetic field with graphs of diurnal variations 11 p1745 N71-21932

Spectra of geological magnetic fluctuations computed from magnetic field measurements from US East Coast [AD-717407] 11 p1745 N71-21971

Collection, reduction, and evaluation of electric field phenomena and geomagnetic field data at both low and high latitudes [AD-717779] 11 p1748 N71-22343

Tables of 1968 geomagnetic observations from Kakioka, Japan including declination, vertical and horizontal intensities, and characteristics of principle magnetic disturbances [REPT-74] 11 p1749 N71-22404

Tabulated results of geomagnetic observations at Memambetsu, Japan, in 1967 11 p1750 N71-22543

Geomagnetic field and storms, and geomagnetism 11 p1751 N71-22686

Vector characteristic study of short period geomagnetic time variations, using component measurements of rapid variation field 11 p1751 N71-22758

Soviet research on astronomy, meteorology, oceanography, geomagnetism, seismology, upper atmosphere, and space program - No. 249 [JPRS-52766] 12 p1995 N71-23176

Seismic wave propagation, geomagnetic features, and earth structure 12 p1995 N71-23180

Tables of photographic recording of geomagnetic fields made by Fort Churchill Observatory 12 p1997 N71-23407

North, east, and vertical magnetic flux data and synoptic tables from Baker Lake, Canada for 1968 12 p1911 N71-23677

Magnetometers and techniques for geomagnetic measurements on earth surface and in magnetosphere [ESSA-TR-ERL-183-ESL-12] 12 p1914 N71-24177

Development of one dimensional magnetotelluric inversion technique for determining frequency range of data necessary to define geological profile [AD-719392] 13 p2070 N71-24604

Geomagnetic and polarization plane rotation effects on electromagnetic signal transmission along spherical waveguide formed by earth surface and ionosphere [AD-719844] 13 p2046 N71-25058

Changes in direction of electric current loops in geomagnetic pole vicinity as indications of interaction between earth magnetic field and corpuscular radiation of sun [AD-719989] 13 p2077 N71-25386

Solar activity and upper atmosphere geomagnetic variations, cosmic ray, and earth current data - Feb. 1970 13 p2170 N71-25468

Solar activity, and upper atmosphere geomagnetic variations, cosmic ray, and earth current data - Jan. 1970 13 p2170 N71-25470

Marine magnetic anomalies over Red Sea caused by magnetic rocks underlying axial trough [AD-718910] 14 p2346 N71-23040

Oceanography, geomagnetism, and interaction of ocean surface with atmosphere [JPRS-53004] 14 p2347 N71-23046

Towed proton magnetometer for magnetic surveys of oceans, and results of survey of Black Sea 14 p2354 N71-23971

Geologic interpretation of resistivity magnetic map of Nixon Fork District, Alaska to determine magnetic characteristics of intrusive rocks 14 p2352 N71-24640

Significance of solar geomagnetic processes in determining distribution of ionospheric components and implications for reference models of ionosphere [NASA-TM-X-65568] 15 p2405 N71-27071

Paired rubidium magnetometer providing reliable mapping of quasi-static total magnetic field changes in 0.1 gamma between stations to 1/2 km separation with differential drift correction [COM-71-50083] 16 p2589 N71-29740

Plasma turbulence in circumterrestrial space due to geomagnetic field related to dynamics of magnetosphere and electroconductivity [NASA-TT-F-13610] 16 p2663 N71-29807

Organization and data input format of geomagnetic World Data Center [REPT-7] 17 p2739 N71-29814

Test facilities for HEOS and ESRO satellite magnetic control - Noordwijk, Netherlands [ESRO-TM-134F-BSTEC] 17 p2730 N71-29890

Dynamics of earth magnetosphere as product of interaction of solar wind and geomagnetic field [AD-722056] 17 p2841 N71-29542

Derivation and tables of spherical harmonic coefficients and isopotential charts for International Geomagnetic Reference Field for 1965 [NASA-TM-X-65604] 17 p2745 N71-29590

Ionospheric current morphology, height variations, and relationships to planetary magnetic disturbances in periods of minimum and maximum solar activity at varying latitudes [NASA-TT-F-437] 17 p2745 N71-30076

Effect of quasi-rhythmicity in geomagnetic and aeronomical phenomena 17 p2747 N71-30085

High latitude, quiet solar day variations of geomagnetic field during IGY 17 p2747 N71-30087

Geomagnetic, bathymetric, and gravitational field data from Indian Ocean 1964 survey 18 p2919 N71-31432

World Data Center A upper atmosphere data retrieval information on extraterrestrial radiation and geomagnetism [UAG-15] 18 p3007 N71-31440

Geomagnetic survey in 0.5 to 10,000 Hz including data reduction and instrumentation [KGO-706] 19 p3084 N71-31491

Geomagnetic survey program package for digital frequency analysis of time series [KGO-705] 19 p3084 N71-31491

Dourbes Geophysical Observatory, Belgium, data on geomagnetism, ionospheric propagation, seismology, cosmic rays, and atmospheric electricity, Jul. 1970 19 p3081 N71-31528

Derivation of International Geomagnetic Reference Field with tables of spherical harmonic coefficients and test results of various magnetic field models [NASA-TN-D-6237] 19 p3176 N71-32110

Resonant oscillations of geomagnetic field in magnetosphere caused by solar wind [NASA-TM-X-65644] 19 p3095 N71-32519

Bibliography of Canadian geomagnetism and aeronomy studies 20 p3255 N71-32914

Upper atmospheric geophysical data for March 1970 20 p3256 N71-32920

Determination of real-time mean hourly values of magnetic field using electronic integration and Sigma magnetic magnetometer [M70-4177] 20 p3256 N71-32930

Polar ionospheric geophysical data recorded at Kiruna, Sweden during Jul. - Sep. 1970 20 p3257 N71-33013

Horizontal intensity, declination, and vertical intensity by hour, day, month, and year at Victoria Magnetic Observatory - 1969 [M70-41/6] 20 p3257 N71-33047

Magnetic disturbance calculation techniques for model current systems including numerical integration and spherical harmonic expansion [APS-P8-77] 20 p3259 N71-33170

SUBJECT INDEX

GEOPHYSICAL SATELLITES

- Flare, coronal enhancements, faculae, and geomagnetic response of quiet and active regions of solar magnetic sector structure
[NASA-CR-121420] 20 p3341 N71-33206
- Geomagnetic elements during 1968 for Spain
20 p3268 N71-33601
- Results of systematic measurements of geomagnetism and meteorological summaries
20 p3268 N71-33602
- Upper atmosphere helium fluorescence due to cycles of electron flux, solar ultraviolet radiation, and geomagnetic activity
[NRC-TT-1438] 21 p3416 N71-34306
- Ionospheric propagation, geomagnetic, and cosmic ray data - tables for Dec. 1969
21 p3419 N71-34326
- Compilation of geomagnetic and geoelectric observations by Japanese observatories
[REPT-10] 21 p3420 N71-34335
- Catalog of data in World Data Center C2 for geomagnetism
21 p3420 N71-34337
- Handbook of correlative data on galactic cosmic rays, solar electromagnetic radiation, solar protons, geomagnetism, ionosphere, and neutral atmosphere
[NASA-TM-X-67294] 21 p3532 N71-35168
- Ground based geomagnetic measurements in Greenland during 1965 summer
[R-15] 22 p3578 N71-35486
- Spectrum analysis used to investigate and relate variations of geomagnetic activity to variations of sunspot numbers
22 p3579 N71-35497
- Convective instability in fluid layer with electromagnetic effects applied to earth and stellar atmospheres
22 p3672 N71-36183
- History, diurnal, and annual data on geomagnetic declination and intensity, Hardland, England - 1962, 1963, and 1964
23 p3733 N71-36760
- High energy proton capture effect and geomagnetism
23 p3832 N71-37458
- Measurement of earth magnetic field by geophysical observatory 40 kilometers northwest of Helsinki, Finland
24 p3916 N71-37923
- Hourly and mean geomagnetic declination and horizontal and vertical intensity data from Kanoya, Japan for 1969
[REPT-80] 24 p3918 N71-37940
- Hourly and mean geomagnetic declination and horizontal and vertical intensity data from Mesambot, Japan for 1969
[REPT-79] 24 p3918 N71-37941
- Hourly and mean geomagnetic declination and horizontal and vertical intensity data from Kakioka, Japan for 1969
[REPT-78] 24 p3918 N71-37942
- Neutron intensities and amplitude variations in atmosphere and magnetic field of earth
24 p4010 N71-38597
- Comparison of earth's magnetic field models with Goussin sequence
24 p4011 N71-38604
- Space environmental conditions, solar radio emission, solar spectrum, cosmic rays and terrestrial magnetism
[AD-727778] 24 p4014 N71-38636
- GEOMAGNETIC HYDROMAGNETICS**
U MAGNETOHYDRODYNAMICS
GEOMAGNETIC OPTICS
U OPTICS
GEOMAGNETIC OPTICS
U RELATIVITY
GEOMETRY
NT ANALYTIC GEOMETRY
NT ANGLES (GEOMETRY)
NT BOSE GEOMETRY
NT BRAGG ANGLE
NT BREWSTER ANGLE
NT CARTESIAN COORDINATES
NT CHORDS (GEOMETRY)
NT CIRCLES (GEOMETRY)
NT COLLINABILITY
NT CONICS
NT CURVATURE
NT CURVES (GEOMETRY)
NT CYCLOIDS
NT DESCRIPTIVE GEOMETRY
NT DIFFERENTIAL GEOMETRY
NT DOUBLE CURVES
NT ELLIPSES
NT EUCLIDEAN GEOMETRY
NT FIXED POINTS [MATHEMATICS]
NT FLOW GEOMETRY
NT HEXAGONS
NT HOMOTOPY THEORY
NT HYPERBOLAS
NT ICOSAEDRONS
NT IMBEDDINGS [MATHEMATICS]
NT INVARIANT IMBEDDINGS
NT LIE GROUPS
NT LOCI
- NT MERCATOR PROJECTION
NT METRIC SPACE
NT NOZZLE GEOMETRY
NT OBLATE SPHEROIDS
NT PARABOLAS
NT POINTS [MATHEMATICS]
NT POLYHEDRONS
NT PROJECTIVE GEOMETRY
NT PROLATE SPHEROIDS
NT PYRAMIDS
NT RADII
NT RHOMBOHEDRONS
NT S CURVES
NT SPHEROIDS
NT SPINOR GROUPS
NT SQUARES [MATHEMATICS]
NT TANGENTS
NT TANK GEOMETRY
NT TENSOR ANALYSIS
NT TETRAHEDRONS
NT TOPOLOGY
NT TORUSES
NT TRIANGLES
NT TRIANGONOMETRY
NT VECTOR ANALYSIS
NT VORTICITY
- Tolerance geometry in visual perception
[AD-710642] 01 p0011 N71-10435
- Flow visualization and quantitative analysis for determining proportional fluid amplifier geometry
[AD-714634] 06 p0638 N71-14587
- Shock tube geometry effects on N wave generation and simulator models
[RAE-LIB-TRANS-1496] 10 p1538 N71-21402
- Solutions to integral transport equations for particle density using spherical geometry
11 p1810 N71-23038
- Criticality for energy dependent transport in slab geometry
13 p2143 N71-23580
- Differential equations governing transient response of ablating axisymmetric orthotropic bodies and effect of shape change
[NASA-TN-D-6220] 14 p2353 N71-26055
- Laplace equation for controlling parameters of current distributions in cylindrical geometries
19 p3142 N71-32336
- Geometry of asteroid streams
[NASA-CR-121451] 20 p3348 N71-33430
- Methods for classifying atmospheric ice crystals according to geometric form
21 p3452 N71-34565
- GEOMORPHOLOGY**
High pressure elastic wave velocities for tracing deep structural boundary in chlorite shales from USSR
[NASA-TT-F-13206] 02 p0210 N71-11450
- Erosion geomorphology of river basin in Italy
[B-56] 02 p0214 N71-11863
- Description of sivation processes and associated geomorphological processes
[AD-71879] 02 p0218 N71-12034
- Elastic parameters of rocks at high pressure and Kohn-Petrov's geologic structure
[NASA-TT-F-13593] 03 p0346 N71-12694
- Composition of earth upper mantle studied by petrography, analytical, and synthetic techniques
[AD-713405] 05 p0673 N71-15417
- Geological analysis of aerial geomagnetic survey of northeastern Alaska
[BULL-1271-F] 05 p0681 N71-15671
- Physical properties of Northern Caucasus rocks in structural-formations zones and their importance in interpreting geophysical data
[NASA-TT-F-13415] 06 p0831 N71-16465
- Aerial photography of Russian geomorphology
[AD-715650] 07 p1022 N71-17854
- Relief group combinations for constructing geomorphological map of western Middle Europe
09 p1383 N71-19725
- Regional significance of volcanic geochemistry in far Triple Junction, Ethiopia
[NASA-CR-117136] 09 p1383 N71-19732
- Geomorphology, morphometry, and bathymetry of central Arabian Indian ridge
[AD-716271] 09 p1384 N71-19909
- Measurement of heat flux in eastern Carpathians and analysis of abyssal heat flux distribution to tectonics and geological development of region
[NASA-TT-F-13517] 09 p1384 N71-20083
- Geological and geomorphological interpretation of Tularosa Basin, New Mexico, from rocket-borne photographs
[JPRS-52406] 10 p1554 N71-21664
- Field and laboratory equipment and methods for airborne electroprospecting using rotating magnetic fields and anomalous effect calculations for conductive media and irregular form bodies
[TT-70-50029] 10 p1555 N71-21671
- Geomorphology of ocean bottom structure and topography of Bering Sea and Gulf of Alaska
11 p1757 N71-22841
- Very low frequency wave propagation phase variations for geophysical exploration of polar region
11 p1708 N71-22923
- Testing of conic and hyperbolic multiquadratic topography equations of geomorphologically diversified areas for computer graphics
[AD-719038] 12 p1903 N71-23088
- Continental drift theory applied to role of Arctic Basin in development of Lavrenty structure
[AD-718068] 12 p1907 N71-23521
- Biological and geological aspects of soil sciences
14 p2387 N71-24456
- Mathematical model for river basin drainage systems based on hexagonal nature of geological ridges
[AD-722022] 16 p2504 N71-26207
- Comparison of aerial and spaceborne photographic methods and photointerpretation techniques using northwest Saudi Arabia geomorphology
[NASA-TM-X-65994] 17 p2749 N71-34477
- Geomorphology, biological activity, and hydrology of Gulf of Mexico and Caribbean Sea as determined from Soviet-Cuban oceanographic expeditions
[JPRS-53412] 18 p2909 N71-36604
- Geomorphology and bottom sediment characteristics in Gulf of Mexico and Caribbean Sea as determined by Soviet-Cuban oceanographic expeditions
18 p2909 N71-36605
- Geomorphology of southern Gulf of Mexico and Cuban shore areas as determined from Soviet-Cuban oceanographic expeditions
18 p2909 N71-36606
- Desert climatology and geomorphology - bibliographies
[AD-723062] 19 p3093 N71-32240
- Geomorphology of Mars Imbrian area explored by Lunokhod-1 lunar roving vehicle
[D-92] 20 p3343 N71-32809
- Mapping southwestern Panama and northwestern Colombia to evaluate potential of radar imagery for use in collecting geomorphic data
[AD-724118] 20 p3256 N71-32943
- Geomorphology of basaltic lava tubes from Mount St. Helens, Washington
[NASA-TM-X-63025] 20 p3257 N71-33020
- Geological characteristics of Voronezh massif based on deep seismicological sounding profile of Black Sea region
[NLL-RTS-5547] 22 p3500 N71-35502
- GEON (TRABENDARE)**
U POLYVINYL CHLORIDE
GEOPHYSICAL OBSERVATORIES
NT OGO
NT OGO-B
NT OGO-D
NT OGO-E
NT OGO-F
NT OGO-P
NT POGO
- Auroral absorption measurement during absorption substorm development at geophysical observatories separated in longitude
12 p1909 N71-23541
- Computer program for solving equations of motion governing gyro oscillations
[NASA-CR-103101] 12 p1082 N71-23646
- Polar ionospheric geophysical data recorded at Kiruna, Sweden during Apr. - Jan. 1970
20 p3255 N71-32809
- Polar ionospheric geophysical data recorded at Kiruna, Sweden during Oct. - Dec. 1969
20 p3256 N71-32945
- Finnish geophysical station for observing earth tides
20 p3245 N71-33340
- Mitsunawa geophysical station, Japan, for observing earth tides
20 p3245 N71-33341
- Indirect effects in boundary value problem for correcting earth tide observations
20 p3245 N71-33345
- Calibration and performance tests of horizontal pendulums at earth tide geophysical observatory
20 p3264 N71-33363
- Polar ionospheric geophysical data recording at Kiruna, Sweden during Jan. - Mar. 1970
20 p3269 N71-33857
- GEOPHYSICAL SATELLITES**
NT OGO
NT OGO-B
NT OGO-D
NT OGO-E
NT OGO-F
NT OGO-P
NT POGO
- Analysis of geophysical investigations by USSR and other East European Bloc Nations using Cosmos 348 and Cosmos 261 satellites
[AD-717045] 10 p1643 N71-28775
- Radiation measurements from polar and synchronous satellites applied to problems of atmospheric circulation and energetics
[NASA-CR-119240] 16 p2910 N71-30742
- Conceptual design analysis of geosynchronous equatorial satellite for hybrid USSR/USP astronomical communication to be launched by Delta vehicle
[NASA-TM-X-65629] 19 p1814 N71-32175
- Using Rayleigh scattering to measure height of cloud tops from geostationary satellites
19 p1811 N71-32384

- Design, fabrication, and flight results of Radiation and Meteoroid Satellite
[NASA-CR-115206] 24 p4021 N71-38692
- GEOPHYSICS**
Abstracts of research in oceanography, astronomy, and meteorology
[JPRS-51452] 01 p0136 N71-10285
Arctic marine geophysics and oceanography, and underwater acoustics
[AD-711626] 02 p0309 N71-11417
Multidisciplinary oceanography including physical, geological, geophysical, chemical, biological, and radioecological studies
[AD-710765] 02 p0219 N71-12083
Radiation and isotope technology in Latin American development
[PRNC-135] 03 p0433 N71-12948
Abstracts on Soviet research in astronomy, meteorology, oceanography, geophysics, and upper atmosphere and space research
[JPRS-51760] 05 p0766 N71-14656
Descriptions and indexes of data contained in Solar-Geophysical Data publication
05 p0765 N71-15403
Apparatus and methods for remote measurement of statistical characteristics of sea environment in Arctic and Antarctic regions
[IT-49-55083] 05 p0679 N71-15541
Problems of geophysical interest in theory of collisionless plasmas
05 p0756 N71-15666
Bibliography on geophysical publications
05 p0681 N71-15672
Soviet news releases on Cosmos satellites, geophysics, oceanography, meteorology, and astronomy
[JPRS-51856] 05 p0769 N71-15677
Abstracts for Soviet research in geophysics, astronomy, and space
[JPRS-52087] 06 p0852 N71-16510
Arctic marine geophysics and oceanography
[AD-713805] 08 p1190 N71-18757
Portable spectrophotometer for geophysical applications
[AD-717990] 08 p1202 N71-18767
Analysis of geophysical investigations by USSR and other East European Bloc Nations using Cosmos 348 and Cosmos 261 satellites
[AD-717045] 10 p1643 N71-20775
Geophysical and astrophysical fluid dynamics
[PB-196589] 10 p1544 N71-21642
Geophysical and astrophysical fluid dynamics, emphasizing rotating fluids
[PB-196590] 10 p1544 N71-21643
Soviet news releases on meteorology, oceanography, geophysics, upper atmosphere, and astronomy for 1 Mar. 1971
11 p1825 N71-22049
Computer oriented information management service for earth physics program
[NASA-CR-117842] 11 p1750 N71-22478
Soviet research in astronomy, meteorology, oceanology, geomagnetism, upper atmosphere, space, and Launchable 1 activities - No. 248
[JPRS-52634] 11 p1828 N71-22682
Long wave propagation measurements for geophysical research
11 p1707 N71-22920
Geophysical effects on separated clock synchronization using low frequency ground waves
11 p1708 N71-22922
Tables on ionospheric and solar activity
[RBC-A-182-PT-2] 12 p1912 N71-23695
Geophysical investigation of short radio wave reception at magnetospheric point - USSR
[JPRS-53168] 14 p2220 N71-26581
Soviet research in meteorology, oceanography, astronomy, and spacecraft launchings
[JPRS-53471] 17 p2861 N71-29399
Soviet news releases on radio astronomy, meteorology, oceanography, geophysics, upper atmosphere, and space program
[JPRS-53367] 18 p3009 N71-30788
Computer programming system based on assembling techniques for geophysical data processing
[MITT-12] 19 p3060 N71-31780
GEOS-C satellite project for geodetic and earth physics research
19 p3091 N71-31876
Soviet research in astronomy, meteorology, oceanography, terrestrial geophysics, and space sciences
[JPRS-53736] 21 p3509 N71-34997
Soviet news releases on astronomy, oceanography, meteorology, geophysics, upper atmosphere, and aerospace activities
[JPRS-53818] 21 p3509 N71-35004
Observations of geophysical phenomena concerning electric and magnetic status of upper atmosphere, ionosphere, cosmic rays and earth currents
22 p3574 N71-35452
Radiative isotope isotope studies in connection with cosmic rays, solar wind, and geophysical processes
23 p3853 N71-37466
- Geologic structure and geophysical interpretation of Mangyshlak Peninsula, Kazakhstan, based on Soyuz 8 photographs
[JPRS-54204] 24 p3918 N71-37937
Soviet bloc research in astronomy, meteorology, oceanography, geology, and space science - 13 Sept. 1971
[JPRS-54039] 24 p4016 N71-38649
Soviet bloc research in astronomy, meteorology, oceanography, geology, and space science - 14 Oct. 1971
[JPRS-54246] 24 p4016 N71-38650
Abstracts on solar system, oceanography, meteorology, geophysics, and aeronomy
[JPRS-54029] 24 p4036 N71-38796
- GEOGRAPHICAL**
NT **GEOGRAPHICAL HEIGHT**
Geodetic gravimetry approach for determining earth geopotential on geoid
[AD-71265] 01 p0051 N71-10901
Analysis of tracking data for resonant geopotential effects obtained from 24 hour satellite data
[NASA-TM-X-65382] 02 p0214 N71-11939
Representation of earth gravitational potential outside sphere bounding earth
[NASA-CR-115893] 05 p0668 N71-14770
Measurements and characteristics of atmospheric electrical potential near earth surface
[SC-RR-70-411A] 05 p0669 N71-14800
GEOSTAR-2 multiple arc geopotential coefficient and station position recovery system
[NASA-TM-X-65441] 07 p0997 N71-17343
Mass distribution for lunar potential model
[NASA-CR-116507] 07 p1109 N71-17499
Deriving spherical harmonic expansion of earth potential as function of surface characteristics and gravity distribution
[AD-715151] 07 p1020 N71-17700
Seasonal variations in geopotential and effect on long period variations in orbital elements of satellites
[NASA-TM-X-65485] 10 p1646 N71-21599
Optimum model with small number of variables for multilevel forecasting of geopotential field
[AD-719005] 13 p2105 N71-24441
Orbit calculations and predictions by different sets of geopotential coefficients for GEOS satellites
13 p2169 N71-25302
Geodetic solution containing resonant geopotential data for synchronous communication satellite orbit determinations
13 p2169 N71-25303
Results of radiosonde ascents from aerological station in Berlin, Germany including extreme and mean values of temperature, pressure, wind data, geopotential and other meteorological data
14 p2288 N71-25884
Comparison of coefficient modification, chain rule, and function methods for computing gravitational potential derivatives with chain rule subroutine for CDC 6600 computer
[COM-71-00183] 16 p2589 N71-28764
Derivation and tests of Goddard combined geopotential field/GSPC 1.70-C
[X-522-70-104] 19 p3086 N71-31831
Comparison of four geopotential models for prediction of GEOS 1 orbits over one month time spans
19 p3087 N71-31833
Ellipsoidal gravity coefficients determined from expansion of geopotential in ellipsoidal harmonics series
[AAS-71-338] 20 p3345 N71-32924
Stratospheric weather maps of Northern Hemisphere based on rawinsonde and rocket sounding data for fourth quarter of 1970
[QR-4-PT-4] 20 p3398 N71-33854
Accelerated longitude drift regimes of eccentric 12 hour orbits due to resonant geopotential
[NASA-TM-X-65722] 24 p4021 N71-38648
- GEOGRAPHICAL HEIGHT**
Use of wind data in optimal interpolation of geopotential heights
[NLL-M-20696-5828-4F1] 21 p3413 N71-34287
Geostrophic coordinates of geostrophic height, pressure, temperature, density, and potential energy levels in earth atmosphere
[NASA-CR-121664] 21 p3507 N71-34986
- GEOS 1 SATELLITE**
Orbit calculations and predictions by different sets of geopotential coefficients for GEOS satellites
13 p2169 N71-25302
Gravimetric and geometric investigations with GEOS 1 and GEOS 2 - GEOS 2 conference
[NASA-TM-X-67271] 19 p3083 N71-31826
Tests and comparisons of gravity models using camera observations of GEOS 1 and GEOS 2
19 p3086 N71-31829
Comparison of four geopotential models for prediction of GEOS 1 orbits over one month time spans
19 p3087 N71-31833
Coordinates for 23 NASA STADAN and SPECT optical and 2 NASA laser tracking sites dynamically estimated from GEOS 1 and GEOS 2 data
19 p3087 N71-31834
Determining position of MOTs stations by orbital dynamics using GEOS 1 observations
19 p3087 N71-31835
- Short arc geodetic adjustment for improving survey coordinates of observing stations using GEOS 1 data
[APCR-70-0090] 19 p3087 N71-31836
Analysis of GEOS 1 observations in geometric and short-arc modes for detecting distortions in North American Datum
19 p3087 N71-31837
Comparison of four independent investigations concerning survey adjustment to NAD using GEOS data
19 p3088 N71-31841
GEOS 1 satellite orbit calculations from Doppler radar and optical tracking data including comparisons of runs of fits and ephemerides for both data sets
19 p3089 N71-31851
Performance comparisons of cameras used in photographic tracking of GEOS 1 satellite
19 p3099 N71-31854
MOTS camera sensitivity and mechanical drive evaluation based on GEOS 1 and 2 satellite photographic tracking data
19 p3099 N71-31853
GEOS 1 satellite orbit perturbation by solar radiation pressure
19 p3178 N71-31868
Analysis of minitrack residuals for tracking of GEOS 1
[NASA-TM-X-65650] 19 p3181 N71-32488
Unified set of tracking station coordinates on geocentric reference system from GEOS 1 and 2 tracking data
[NASA-TM-X-65707] 23 p3748 N71-36721
- GEOS 2 SATELLITE**
Orbit calculations and predictions by different sets of geopotential coefficients for GEOS satellites
13 p2169 N71-25302
Gravimetric and geometric investigations with GEOS 1 and GEOS 2 - GEOS 2 conference
[NASA-TM-X-67271] 19 p3083 N71-31826
Tests and comparisons of gravity models using camera observations of GEOS 1 and GEOS 2
19 p3086 N71-31829
Coordinates for 23 NASA STADAN and SPECT optical and 2 NASA laser tracking sites dynamically estimated from GEOS 1 and GEOS 2 data
19 p3087 N71-31834
Estimates of C band radar station positions and iterative distances
19 p3054 N71-31842
Satellite tracking system intercomparisons based on GEOS 2 satellite data - GEOS 2 program conference
[NASA-TM-X-67272] 19 p3088 N71-31840
C-band, SECOR, and TRANET radio tracking and laser tracking data analyses for 35 GEOS 2 satellite passes including preprocessing data correction effects
19 p3107 N71-31844
GEOS 2 satellite range and range rate tracking and minitrack optical tracking systems data proving and quality control for information dissemination
19 p3088 N71-31840
GEOS 2 satellite tracking accuracy comparisons of SAO laser and NASA mobile ruby laser systems including data analysis procedures
[SAO-006-92] 19 p3107 N71-31850
Minitrack system self calibration exercise feasibility based on GEOS 2 satellite tracking data
19 p3089 N71-31851
Data processing for calibration of C band radar global tracking network using GEOS 2 satellite data
19 p3089 N71-31851
MOTS camera sensitivity and mechanical drive evaluation based on GEOS 1 and 2 satellite photographic tracking data
19 p3099 N71-31855
Laser and radar tracking of GEOS 2 for precise geodetic and position location - conference
19 p3089 N71-31856
GEOS 2 C band radar technique for determining geometry and orientation of underwater acoustic transponders
19 p3054 N71-31864
Shipborne C band radar tracking of GEOS 2 for precise ship positioning
19 p3054 N71-31866
Accuracy of Cartesian and spherical coordinates of GEOS 2 determined by synchronous observation from Riga and Vigor
22 p3677 N71-36221
Unified set of tracking station coordinates on geocentric reference system from GEOS 1 and 2 tracking data
[NASA-TM-X-65707] 23 p3748 N71-36721
Doppler position finding error analysis using GEOS 2 satellite data
24 p3915 N71-37917
- GEOS-C SATELLITE**
GEOS-3 altimeter bias recovery simulation using range and angle tracking data
[NASA-TM-X-65619] 18 p2922 N71-36598
Geodetic satellite program and planning for GEOS-C satellite
[NASA-TM-X-67269] 19 p3090 N71-31867
Constraints and proposed instrumentation for GEOS-C satellite
19 p3090 N71-31875

SUBJECT INDEX

GEOS-C satellite project for geodetic and earth physics research

- Error sources in GEOS-C satellite orbit determination method as determined by altimeter experiment 19 p3091 N71-31877
- Error correction for GEOS-C altimeter system from range and angle observations 19 p3099 N71-31878
- Coherent radar system for determining radar altimeter bias from GEOS-C tracking 19 p3055 N71-31880
- Design criteria for radar altimeter for GEOS-C geodetic satellite 19 p3055 N71-31881

GEOSTROPHIC WIND

- Comparison of computed and measured geostrophic wind data for upper troposphere and lower stratosphere in Texas-New Mexico area [AD-717269] 11 p1788 N71-21839
- Numerical analysis of nonlinear interactions in rotating, stratified fluid with free surface [AD-719960] 13 p2067 N71-25244
- Free-air and vertical wind structure analysis for equatorial maritime friction layer based on surface temperature and wind profiles for Arabian Sea and Atlantic Ocean 23 p3785 N71-36978

GEOTROPISM

- Sensitivity of plants to geotropism [NASA-TT-F-12638] 03 p0367 N71-12747

GIP TELESCOPES

- U PARTICLE TELESCOPES
- U ARC HEATERS
- U HEATING EQUIPMENT

GERMANY

- Diagnostic chronological and physiological criteria in geriatrics 11 p1689 N71-22312

GERMANATES

- Optical properties of rare earth doped germanate glasses [AD-716386] 09 p1395 N71-19573
- Electron paramagnetic studies of gamma irradiated alkali-germanate glasses and crystalline compounds 15 p2507 N71-27571

GERMANIUM

- NT GERMANIUM ISOTOPES
- NT SILICON
- NT TELLURIUM
- NT TELLURIUM ISOTOPES

- Low temperature annealing of electron irradiated germanium [COO-1198-735] 03 p0389 N71-12683

- Preparation and characterization of electron beam, vapor deposited, germanium films using molecular beam machine [PB-193261] 03 p0395 N71-13349

- Silicon germanium thermoelectric materials and module development [ALO-2510-9] 04 p0402 N71-13983

- Evaluating germanium/lithium suppression spectrometers for nondestructive radiochemical analysis [BNWL-1285] 05 p0686 N71-15416

- Dissociation mobility in germanium at high stresses and low temperature [AD-714267] 06 p0872 N71-16329

- Mechanism of growth of whiskers from gas phase of silicon, germanium, and other semiconductors [AD-714799] 07 p1096 N71-18047

- Process for forming heterojunctions by gold solvent alloying [AD-715307] 06 p1277 N71-18379

- Proton irradiation effects on electrical properties of s and p silicon and germanium [BP-18674] 08 p1277 N71-18506

- Photoemission measurements of cleaved single crystal Ge and amorphous Ge films [AD-715742] 09 p1279 N71-18484

- Fast neutron effects on semiconductor electronic transport properties and minority carrier and hole drift mobilities in germanium [ORO-3451-6] 09 p1426 N71-19523

- Determination of deep impurities in silicon and germanium by infrared photoconductivity [NBS-TN-578] 10 p1536 N71-20614

- N-type germanium electrical resistivity in high inductive electric fields [JLAB-AB-118] 10 p1531 N71-20798

- Automatic control and crucible shape effects on zone recrystallization of germanium 10 p1633 N71-20886

- Influence of heating methods on efficiency of directed crystallization of germanium in vacuum apparatus 10 p1633 N71-20887

- Optical parameters of absorbing substrates with transparent surface film determined by ellipsometry, applied to silicon and germanium 11 p1880 N71-23017

- Image conversion at millimeter wavelengths by germanium semiconductor panel 12 p1879 N71-23668

Growth of epitaxial germanium films from supercooled melt

- [AD-718695] 12 p1906 N71-23735
- Hydrostatic pressure effects on excess carrier lifetimes of n and p type germanium 12 p1987 N71-24303

- Fabrication of lithium doped germanium detectors for use in gamma ray spectroscopy [BILG-447] 14 p2253 N71-26207

- Silicon and germanium alloying effects on group properties and strength of vanadium-titanium and vanadium-titanium-aluminum alloys in high temperature environments [KFK-1193] 15 p2420 N71-27807

- Microwave phonon attenuation in germanium at temperatures between 4 and 100 K 15 p2455 N71-27386

- Band structure of germanium analyzed by single crystal photoemission [AD-721318] 16 p2665 N71-28332

- Defects introduced into Ge and Si by electron irradiation at low temperature 16 p2666 N71-28735

- High stress piezoresistance at constant temperatures between 77 and 300 K of n-type and p-type germanium 16 p2666 N71-28765

- Compensation of n-type germanium by gamma radiation for radiation detectors [BNL-15643] 17 p2813 N71-29470

- Charge transfer characteristics of ion recombination in phase boundary of germanium surface with electrolyte 18 p2998 N71-31326

- Measurement of crack propagation velocities in silicon and germanium using ultrasonic fractography [REPT-7770] 19 p3109 N71-31704

- Surface physics of 1/f-noise in germanium semiconductor 19 p3168 N71-31774

- Use of differential energy analyzer for field emission electron energy distribution measurements in germanium 19 p3155 N71-32354

- Crystal defect effects on ultrasonic attenuation and phonon scattering in germanium [AD-724328] 20 p3332 N71-33017

- Low temperature, thermal conductivity measurements, phonon scattering, and induced energy levels in electron-irradiated Sb-doped Ge in n- and p-type conversion region [CEA-COFP-1745] 21 p3468 N71-34686

- FORTAN computer program for automatic analysis of gamma ray spectra from Ge(Li)-detectors [LUNP-7101] 22 p3634 N71-35905

- Analysis of isochronal annealing behavior of radiation defects in germanium crystals after radiation with cobalt-60 [AD-726993] 23 p3835 N71-37345

- Reducing radiation conductivity of germanium as result of fast and slow ionic bombardment [AD-727883] 24 p3998 N71-38518

GERMANIUM ALLOYS

- Feasibility of germanium-silicon alloy single crystals for fabrication of charged particle detectors [NASA-CR-111793] 02 p0282 N71-11425

- Time and temperature dependence of thermoelectric properties of Si-Ge alloys [NASA-CR-116221] 06 p0899 N71-16665

- Performance of silicon-germanium thermocouple in RTG with sublimation at high operating temperatures [NASA-CR-116224] 06 p0899 N71-16666

- Design study with mathematical model for performance analysis of silicon-germanium thermoelectric generators 12 p1961 N71-23439

- Germanium/lithium - sodium iodide/tellurium pair spectrometer for gamma ray spectroscopy [IKF-26] 17 p2810 N71-30386

GERMANIUM COMPOUNDS

NT GERMANATES

NT GERMANIUM OXIDES

- Phase diagrams of germanium-sulfur, germanium-selenium, and germanium-tellurium systems 07 p1046 N71-16043

- Microwave spectrum and chemical properties of germanium disulfide 07 p1086 N71-17176

- SiGe thermoelectric materials technology and module and cascaded converter development [ALO-2510-10] 09 p1357 N71-19395

- Computer analysis of semiconductor GeLi gamma ray spectra, comparison of threshold detectors, Bonner spheres, and recoil spectroscopy with emission, and Fokkian equation solution 10 p1559 N71-21148

- Atomic structure of amorphous arsenic selenide and germanium telluride semiconductor switches [AD-714810] 10 p1436 N71-21806

- Preparation of transparent homogeneous amorphous germanium phases by rapid quenching of liquid and vapor deposition [AD-717532] 11 p1782 N71-22228

Structural compositions and fast neutron damage thresholds of germanium selenide and germanium telluride amorphous semiconductors

- [AD-726754] 15 p2509 N71-27906
- Diversity bonded nuclear spin-spin coupling constant between Ge-73 and C-13 measured in tetramethylgermane [AD-721717] 17 p2793 N71-29514

GERMANIUM DIODES

- Using solid state Ge/Li detector for measuring amounts of radionuclides in individual organs [BNWL-1178] 02 p0168 N71-11196

- Extraction of time information contained in signals from germanium-lithium detectors [LYCEN-7023] 04 p0513 N71-13546

- Construction and assembly of infrared detector with 15 Hg-doped germanium elements 05 p0441 N71-15526

GERMANIUM ISOTOPES

- Excitation cross section measurement of Ge-71, Br-78 and Br-79 isomeric states using 14.8 MeV neutrons [INR-F-1091] 15 p2483 N71-27803

GERMANIUM OXIDES

- Mass spectrometric analysis of oxygen diffusion in germanium dioxide with isotopic labeling 06 p0809 N71-15983

GERMANIUM RECTIFIERS

U GERMANIUM DIODES

GERMANY

- Meteorological charts of Northern Hemisphere and weather data for Berlin for June, 1970 02 p2523 N71-14116

- Historical development, limits, and future trends in rocket technology [NASA-TT-F-13046] 03 p0432 N71-12416

- Research progress in operation of Karlsruhe isochronous cyclotron in 1969 [NF-18358] 04 p0250 N71-13759

- German aeromedical training for medical and paramedical personnel 04 p0477 N71-13883

- Civil aerospace medical activities in Germany 04 p0478 N71-13886

- Physiological training of flying personnel in German Armed Forces 04 p0482 N71-13890

- German/French Symphonie communication satellite antennas [BMW-FB-W-70-42] 07 p0991 N71-17070

- Mathematical models and computer programs for equalizing West German part in European triangulation net 09 p1553 N71-19724

- Tables and graphs of aerological ozone soundings at Hohenpeissenberg, Germany for first half of 1969 10 p1540 N71-21095

- Meteorological data from radioisotope soundings at Berlin, Germany 12 p1952 N71-23215

- Meteorological data of Berlin, Germany, for April through June, 1970 [OR-2-PT-2] 12 p1952 N71-23216

- Meteorological radioisotope data from aerological station in Berlin, Germany, for December 1969 12 p1953 N71-23481

- Meteorological radioisotope data from aerological station in Berlin, Germany, for February 1970 12 p1954 N71-23682

- Meteorological radioisotope data from aerological station in Berlin, Germany, for March 1970 12 p1954 N71-23683

- Meteorological radioisotope data from aerological station in Berlin, Germany, for April 1970 12 p1954 N71-23684

- Convective cloud prognostic technique for computer forecasting of shower and thunderstorm activity including meteorological parameters and tests of instability indices over Germany 12 p1958 N71-24105

- Fluvial network rainfall data for Bavaria, Germany in 1970 13 p2106 N71-24484

- Operations research for West German governmental information retrieval system, noting law application and decision making 14 p2223 N71-25997

- Synoptic meteorological charts for Berlin in Nov. 1970 including temperature-precipitation relationships and radioactivity 14 p2288 N71-26827

- Meteorological charts and data tables for July through September, 1970 from Berlin [OR-2-PT-3] 14 p2288 N71-26877

- Documentation and equipment specifications for German scientific satellite program 15 p2526 N71-27151

- Diurnal atmospheric fallout data of Bi-7 and P-32 monitored at Zugspitze, Germany from 1 Apr. to 15 Nov. 1970 [INVO-4061-3] 15 p2513 N71-27783

- Air pollution estimate in Germany from visibility measurements, noting influence of wind and atmospheric moisture 17 p2776 N71-28377

- Feasibility study for German materials data bank - conference 17 p2762 N71-29387
- Cost/benefit model for decision making in planning German space program - bibliography [BMBW-FB-W-71-04-PT-3] 17 p2861 N71-29422
- Conference on European Mercury project and German Helios solar probe [ESRO-SP-57] 17 p2849 N71-29563
- Criteria of spacecraft configurations and design in US-German Helios solar probe for interplanetary space investigation 17 p2849 N71-29564
- Tables of aerological ozone soundings over Germany [AD-723486] 19 p3126 N71-31716
- Photographic recording of gravimeter in Frankfurt, Germany 20 p3262 N71-33339
- Meteorological data from Berlin weather station for fourth quarter of 1970 [QR-4] 20 p3297 N71-33847
- Occurrence of frost conditions in North Germany with emphasis on meteorological parameters and seasonal variations 21 p3451 N71-34561
- Aerological ozone soundings and total ozone measurements during first half of 1970 from West Germany 22 p3614 N71-35742
- Tables of ozonometry for second half of 1970 at Hohenpeissenberg Meteorological Observatory, Germany 22 p3614 N71-35743
- Maximum wind velocity measurements from West Germany and wind loading in structural engineering [NLL-LIB-COMM-1590-15196] 22 p3616 N71-35766
- Radioactive measurements of temperature, pressure, geopotential, wind data, and velocity of sound in Germany during June 1970 22 p3616 N71-35766
- Radiation monitoring data for radioactive fallout in German Democratic Republic for 1969 [SZS-1/71] 23 p3713 N71-36471
- German central ground station for satellite data acquisition, tracking, and telecommand 24 p3914 N71-37902
- German astronomical project with observatories in Spain and Germany 24 p3921 N71-37967
- German law covering inventions and technical improvements made by employees of private, public, and Armed Forces [NASA-TT-F-13408] 24 p4034 N71-38783
- GERMICIDES**
- U BACTERICIDES**
- GERMINATION**
- Germination and growth of selected higher plants in simulated space cabin environment similar to conditions within Skylab [NASA-CR-119379] 18 p2876 N71-31175
- GETTERS**
- Stabilized air pumping with diode type getter-ion pumps 03 p0351 N71-12538
- Ion detection and monopole mass spectrometer performance tests with transverse magnetic field and titanium getter pump pumping capacity for D region ion composition analysis [NASA-CR-117905] 12 p1921 N71-23788
- GIANT STARS**
- Spectral line analysis of Ba II star zeta Capricorni [NBS-MONOGRAPH-119] 14 p2340 N71-24679
- GIBBS FREE ENERGY**
- Concentration effects on Gibbs free energy and entropy of mixing of binary fluids [NPL-DCS-6] 07 p1128 N71-17210
- Dynamic stability criteria for continuous system stable in energy, adjacent equilibrium, or Gibbs sense 10 p1682 N71-21471
- Conformal solution correlation representing excess volume, excess enthalpy, and excess Gibbs free energy for mixtures of simple liquids from argon to ethanol 12 p1873 N71-24308
- Heat of formation, specific heat, entropy, and Gibbs free energy of some binary metal oxides [NPL-DCS-7] 13 p2184 N71-24372
- Gibbs free energy, enthalpy, and entropy of binary alkali metal alloys [NPL-DCS-10] 15 p2524 N71-26964
- Entropy, enthalpy, Gibbs free energy, and energy of atomization for palladium phosphide formation in electrochemical cells based on emf measurements [NLL-RRE-TRANS-315-0034-6251] 23 p3780 N71-36937
- GIBBS-HELMHOLTZ EQUATIONS**
- Thermodynamically consistent equation of state for alpha and epsilon phases of iron [AD-719233] 13 p2092 N71-24563
- GIBBS**
- Evaluation of failure modes and redesign of SERT-2 gimbal pin puller [NASA-TM-X-2128] 03 p0318 N71-12267

- Stabilizing gyro utilizing re-circulated liquid hydrostatic gimbal bearing 06 p0866 N71-16487
- Inertial gimbal alignment system for spacecraft guidance [NASA-CASE-XMF-01669] 12 p1959 N71-23289
- Three stage motion restraining mechanism for restraining and damping three dimensional vibrational movement of gimbal package during launch of spacecraft [NASA-CASE-GSC-10305-1] 13 p2085 N71-24694
- Horizontally sealed vibration damper design for use in gimbal assembly of spacecraft inertial guidance system [NASA-CASE-MSC-10959] 14 p2263 N71-26243
- Low friction bearing and lock mechanism for two-axis gimbal carrying satellite payload [NASA-CASE-GSC-10356-1] 14 p2345 N71-26537
- Skylab control motion gyroscope inner gimbal design and thermal vacuum and environmental tests [NASA-TM-X-64583] 18 p2956 N71-31199
- Design, development, and evaluation of gimbalized system for aligning spacecraft mounted instruments with relative wind [NASA-CR-111910] 22 p3381 N71-35506
- GIRDERS**
- Determination of static ultimate strength of transversely and longitudinally stiffened plate girders subjected to shear, bending, or combination of stresses 12 p2009 N71-24397
- Optimum design of girder with uniform depth noting shear bracing layout [REPT-1124/70] 20 p3357 N71-33009
- GLACIERS**
- Surface rate measurement of glaciers using electrometry [AD-711911] 02 p0215 N71-11954
- Glacio-climatological observations on Lomonosov glacier plateau 11 p1753 N71-22811
- Fourth conference on glaciers and glaciology held in Soviet Union - 1968 11 p1755 N71-22832
- Low layer wind and temperature field on ice cap plateau during summer [AD-721486] 16 p2627 N71-29077
- Surface roughness variation of katabatic winds over subpolar ice cap during summer [AD-721487] 16 p2628 N71-29078
- Vertical turbulent flux of water vapor at ice cap snow surface during summer [AD-721488] 16 p2628 N71-29079
- Energy exchange at ice cap snow surface during summer [AD-721490] 16 p2628 N71-29081
- Atmospheric models and thermodynamic effects of glaciers and Arctic Ocean in relation to causes of ice age climatology 20 p3368 N71-33884
- Determining applicability of infrared radiant thermometer in Alpine/periglacial environment by thermal remote sensing [AD-726958] 23 p3751 N71-36747
- GLACIOLOGY**
- Arctic and Antarctic regions, ice formation, sea ice, weather forecasting, glaciology, hydrology, hydrometeorology, IGY, IQSY, solar activity, and meteorological stations [TT-70-50017] 11 p1752 N71-22801
- Glacio-climatological observations on Lomonosov glacier plateau 11 p1753 N71-22811
- Fourth conference on glaciers and glaciology held in Soviet Union - 1968 11 p1755 N71-22832
- Soviet research in glaciology, meteorology, astronomy, and space sciences [JPRS-53253] 16 p2678 N71-28145
- Glaciological research in Arctic Regions including radar measurement of glacier thickness 16 p2684 N71-28151
- Infrared satellite photographs for studying hydrology, glaciology, oceanography, volcanology, and radiation balance of earth [NASA-TT-F-13930] 21 p3426 N71-34378
- GLANDS (ANATOMY)**
- NT ADRENAL GLAND
- NT TESTES
- NT THYMUS GLAND
- NT THYROID GLAND
- GLANDS (REALS)**
- Sealing dam analysis for design of shaft face seal with self-acting lift augmentation for advanced gas turbine engines [NASA-TN-D-7006] 02 p0230 N71-11579
- GLASS**
- NT BOROSILICATE GLASS
- NT GLASS FIBERS
- NT SILICA GLASS
- Fiber optics with extended ultraviolet transmission [AD-710241] 01 p0068 N71-10004
- Radiation damage thresholds of neodymium doped glass laser materials [AD-710823] 01 p0063 N71-10519

- Defect states in glassy and crystalline silicates studied by optical spectroscopy and electron paramagnetic resonance [AD-710303] 01 p0111 N71-10406
- Glass neutron guide with 300 m curvature [URR-1] 02 p0269 N71-11710
- Development of space manufacturing techniques for orbital workshops [NASA-TM-X-66480] 02 p0234 N71-11770
- Glass production in earth orbiting laboratory 02 p0234 N71-11770
- Low gravity manufacturing of optical glasses from metal oxides in space laboratories 02 p0234 N71-11770
- Nucleation phenomena in glass-ceramic materials [AD-712094] 03 p0441 N71-12004
- Dielectric properties of glass 03 p0397 N71-13004
- Periodic operating characteristics of neodymium glass laser in cyclic mode 03 p0388 N71-13304
- Production of laser glass and optical design mechanisms in laser materials 04 p0525 N71-14028
- [NBS-SP-341] Holographic control of neodymium laser glass production 04 p0525 N71-14027
- Damage threshold tests on laser glass 04 p0525 N71-14028
- Damage threshold tests in laser glass evaluation 04 p0526 N71-14029
- Gain loss in neodymium glass laser amplifiers 04 p0526 N71-14029
- Filament effects on Q switched glass laser failure 04 p0535 N71-14030
- Tensile stress and breakdown of glass laser caused by inclusion particles 04 p0526 N71-14030
- Pulse duration effect on laser damage in ruby and glass 04 p0526 N71-14030
- Absorption sensitive mechanical and machining properties of soda lime glass 05 p0710 N71-15402
- Glass formation in systems phosphorus pentoxide-antimony trioxide-chromic oxide and phosphorus pentoxide-antimony trioxide-vanadium pentoxide [AD-713449] 05 p0711 N71-15404
- General numerical large deflection solution of circular ring circular glass plate flexure problem [AD-714154] 06 p0678 N71-16304
- Structures and electromagnetic properties of magnetic glasses 06 p0682 N71-16304
- Magnetic properties and electrical resistivity of transition metal oxide glasses [COO-1700-17] 06 p0683 N71-16327
- Thermal elastic stresses and crack initiation and propagation in flat glass plates [REPT-5/70] 07 p1124 N71-17535
- Glass structure analysis by nuclear magnetic resonance [AD-715463] 08 p1222 N71-18034
- Hardness and high pressure deformation mechanisms of glasses 08 p1223 N71-18154
- Factors influencing gain in neodymium doped low glass 09 p1395 N71-19531
- Optical properties of rare earth doped germanate glasses [AD-716386] 09 p1395 N71-19570
- Thermal and elastic properties of polymers, and electronic properties of glasses and metals 09 p1404 N71-19738
- Hydrodynamical processes and parameters of glass motion in large bubble chamber [JINR-P13-5291] 09 p1365 N71-19916
- Aluminum-clad glass rods affecting core midplane power shape [BAW-3647-19-PT-3] 09 p1419 N71-19982
- Chemical treatment of glass surfaces to improve breaking strength, resistance to abrasion and chemical action, and hydrophobic reaction [NASA-TT-F-13437] 09 p1406 N71-20009
- Measurement of contact times and fracture velocities of steel balls impacting on glass plates of various thicknesses overlying steel block [PB-196353] 10 p1659 N71-21776
- Computer analysis of axial mass dispersion data for packed spherical glass particle beds 10 p1610 N71-21827
- Physical property of thin films and glassy state - insulator-metal transition theory [AD-717386] 11 p1815 N71-21960
- Preparation of transparent homogeneous amorphous germanium glasses by rapid quenching of liquid and vapor depositions [AD-717532] 11 p1782 N71-22228
- Influence of thermal treatments on dielectric properties of lithium-aluminum-silica glasses using electron microanalysis and X ray and electron microscopy techniques 11 p1783 N71-22244

SUBJECT INDEX

GLAUBER THEORY

- Stable resistivity switching properties of vanadium-doped glass As-Te-Ge 11 p1817 N71-22884
- Effects of chemical bonding between phases of glass-metal composite on strength and fracture behavior 11 p1783 N71-23010
- Metal pattern bonding techniques for cover glass attachment to silicon solar cells for space applications (NASA-CASE-XL8-08369) 12 p1859 N71-23449
- Magnetic properties, microstructure, and physical properties of partially crystallized glass 12 p18823 N71-23767
- Semiconducting and transmission properties of chalcogenide glass (NLL-M-28294-3828.4F1) 12 p1966 N71-23836
- Radiation damage thresholds for glass laser materials (AD-718894) 12 p1935 N71-24195
- Quantitative microfluorescence analysis of laser glass and films (NASA-CR-114966) 13 p2166 N71-24944
- Ultrasonic spectroscopy used to determine composition fluctuations on structural relaxation in glass 13 p2100 N71-24947
- Fracture mechanics and failure analysis of glass under biaxial loading at elevated pressures in water and inert atmospheres 14 p2277 N71-25767
- Probability density function of surface area remaining on particles produced from residues of fractured chemically strengthened glass elements (JC-RR-68-586) 15 p2428 N71-26933
- Development of model for initiation of branching fractures in stressed glass and glass ceramics (JC-RR-78-766) 15 p2428 N71-26949
- Statistical thermodynamics of gas in glass solubility (DCLR-38399) 15 p2576 N71-27064
- Mechanical and thermodynamic properties of low viscosity olefinic materials and honeycombs including olefin-phenolic resin and phenolic glass honeycombs of phenolic olefin and nylon (NASA-CR-111598) 15 p2433 N71-27636
- Mechanical properties and impact strength of UARL 417 experimental glass 15 p2433 N71-27676
- Effects of composition on glass forming tendency of amorphous metal systems 15 p2426 N71-27753
- Alkyd resin lacquer peeling on glass and other substrates 16 p2616 N71-28324
- Low density and adequate mechanical properties of surface compression strengthened glasses permitting their use in weapons and other lightweight structures for long periods (AD-721327) 16 p2618 N71-28615
- Semiconductors and semiconductor devices, insulating and semiconducting glasses, and measurement techniques (AD-722474) 17 p2816 N71-29840
- Theory of diffuse reflectance of particulate media including garnet, glass, corundum powders, and mixtures (NASA-CR-115037) 17 p2816 N71-29925
- Thermocouple and colorimetry studies for glass optical fibers used in air, railroad, and highway traffic signal control signals 17 p2770 N71-30093
- Analysis of effects of environment on strength of glass materials (AD-726692) 17 p2771 N71-30236
- X ray diffraction, thermal, and thermogravimetric analysis of La2O3-BaO-SiO2 glass structures and properties 18 p2948 N71-31230
- Physical properties, dielectric properties, and structure of several experimental types of glass 18 p2941 N71-31277
- Uranium glasses with high electroluminescent and photoluminescent properties 18 p2941 N71-31280
- Screenable dielectric constant ceramic glass paste thin film capacitors in microcircuits (AD-73464) 19 p3064 N71-31714
- Evolution of radiation quality, mixed radiation field, radiation direction, and absorption dose in diamond glass dosimetry (JN-19747) 19 p3148 N71-32093
- Action of glass particles used as additives to improve lubricating properties of mineral oils (NLL-RESEARCH-TRANS-3092-19091.9F1) 19 p3120 N71-32097
- Dielectric properties of silver activated phosphate glass phosphor-convertor dosimeter systems (AD-73746) 19 p3160 N71-32136
- Structural response and acoustic transmission characteristics of glass pane and standard wood frame construction wall panels subjected to sonic booms (NASA-CR-111925) 19 p3190 N71-32488
- Progress in growth of ultra-pure Al2O3 crystals as laser material, measurement of oxygen diffusion in oxides, and measurement of laser beam damage threshold energy in glass (AD-734662) 20 p3187 N71-33128
- Diffusion of nonlinearly scattered light by etched glass in experiments using Fabry-Pérot interferometer in conjunction with laser light source 20 p3274 N71-33479
- Polarization of light scattered from optical glass 20 p3275 N71-33483
- Electrical properties of metallic layers implanted in amorphous oxide glass 21 p3405 N71-34228
- Occurrence of explosion-like processes during high powered pulsed electron bombardment of diamonds, glass, and ceramics (SC-T-71-3817) 21 p3434 N71-34435
- Measurement of stress optical coefficients for homogeneous and inhomogeneous glass test specimens used in neodymium lasers (AD-724302) 21 p3435 N71-34444
- Rheological properties of alkali borate glass melts and influence of water on rheological properties of boric oxide glass and two sodium borate glasses 21 p3443 N71-34504
- Static fatigue in glass from thermally activated chemical reaction (JCL-RR-710010) 21 p3444 N71-34510
- Glass and steel microsphere sputtering bed properties and model for thermochromic deposition of pyrolytic carbon from methane on nuclear fuel microfibers in sputtered beds 21 p3463 N71-34646
- Platinum-free laser glass development, radiation centers in borate glasses, local order in liquid chalcogenides, and chalcogenide glass bolometers for infrared and microwave detection (AD-726416) 22 p3602 N71-35457
- Chemical analysis of crack propagation in glass (AD-726710) 22 p3603 N71-35464
- Glass properties studied by synthesizing gas-glass systems using high pressure techniques 22 p3604 N71-35467
- Anomalous water from cleaned and uncleaned capillary tubes, from weak H2O2 solutions, and from water extractions of crushed glass 23 p3720 N71-36517
- Flexural, shear, bending, tensile, and impact strengths of high modulus, high strength, glass fiber-epoxy resin composites 23 p3775 N71-36987
- Interactions between intense coherent light from Q switched ruby laser and iodine vapor, neodymium-doped glass, and benzene 23 p3805 N71-37128
- Powdered glass suspensions for improved lubrication properties of oils (NLL-RESEARCH-TRANS-3092-19091.9F1) 24 p3930 N71-38042
- Structural, electrical, and magnetic properties of transition metal oxide-phosphate glasses and glasses in As2Te3-As2S3 system for amorphous semiconductors (AD-727154) 24 p3998 N71-38516
- Investigation of glass particles recovered from Apollo 11 and Apollo 12 films, and composition and heterogeneity of lunar surface (NASA-TM-X-65724) 24 p4006 N71-38575
- GLASS COATINGS
- Performance of soldered and cemented cover glass silicon solar cells (NASA-TM-X-2137) 03 p0317 N71-12261
- Method of attaching cover glass to silicon solar cell without using adhesive (NASA-CASE-XL8-08349-2) 13 p3029 N71-24481
- Helium outgassing process for fused glass coating on ion accelerator grids (NASA-CASE-LEW-10278-1) 16 p2602 N71-28282
- Glass coating of electron bombardment ion-thruster grids by electrodeposition (NASA-CR-729932) 20 p3277 N71-32923
- Evaluation of glasses as forging lubricants for forging steels and titanium alloys (AD-724323) 22 p3403 N71-35461
- GLASS ELECTRODES
- Development of ion selective electrochemical sensors for detection of calcium, sodium, sulfate, and other ions in saline and brackish water (PB-198434) 19 p3049 N71-31729
- GLASS FIBERS
- Anisotropic investigation of fiber glass reinforced plastic (AD-716045) 01 p0072 N71-10462
- Nonaqueous hermetically sealed battery case made of epoxy resin and woven glass tape for use with electrochemical cells in spacecraft (NASA-CASE-XGS-00886) 02 p0148 N71-11053
- Fracture strength of glass fiber wound plastics (AD-713063) 03 p0397 N71-13062
- Lubricating and sizing agent for glass fiber (AD-713944) 03 p0397 N71-13123
- Asbestos and glass reinforcing fibers and reinforced thermoplastic resins (ERDE-T-2) 03 p0398 N71-13254
- Vibratory load effects on glass fiber reinforced synthetic materials 06 p0876 N71-15949
- Physical and mechanical properties of fiber glass reinforced plastics (AD-714724) 06 p0877 N71-16050
- Physical and mechanical properties of glass reinforced plastics (AD-714798) 06 p0878 N71-16200
- Strain energy theory of failure of etched fiber glass reinforced plastic laminates under thermal compression (NASA-TT-F-13444) 06 p0880 N71-16495
- Failure characteristics of unidirectional fiber glass reinforced plastic under compression (NASA-TT-F-13442) 06 p0906 N71-16841
- Influence of proton-electron irradiation on strength of fiber glass 07 p1046 N71-16844
- Lightweight resin fiber glass honeycomb sandwich structure fabrication and comparison with aluminum structures for planetary probes (NASA-CR-114086) 07 p1047 N71-17330
- Thermodynamic behavior of glass fiber, reinforced plastics (AD-715333) 07 p1048 N71-17709
- Polymers mechanisms in fracture of glasslike polymers 08 p1300 N71-19173
- Buckling strength of fiber glass reinforced plastic bars 08 p1300 N71-19174
- Design and fabrication of plane and trapezoidal fiber glass wings with laminar profiles (AD-716526) 09 p1315 N71-19574
- Engineering method of evaluating supporting strength of structural elements from glass reinforced plastic operating in conditions of temporary steady heating (AD-716515) 09 p1404 N71-19580
- Longitudinal strength of unidirectional fibrous composites (AD-716629) 09 p1405 N71-19804
- Bauschinger effect examined for unidirectional fiber glass reinforced plastics (AD-717019) 10 p1587 N71-20807
- Glass fiber tubing for cryogenic rocket propellant system (NASA-CR-72797) 11 p1781 N71-21904
- Buckling, fiber and resin thermal resistance, and hydrostatic tests of glass fiber reinforced spherical pressure vessels and liners 11 p1749 N71-22481
- Fabrication techniques for split ring glass boiler (BDX-413-198) 11 p1749 N71-22332
- Pulse arc welding for joining electrical connections to glass reinforced epoxy or Mylar substrates (BDX-413-204) 13 p2059 N71-25407
- Light scattering disrupted in optical glass fibers causing power loss (SRDE-70064) 14 p2295 N71-25635
- Physical properties and mechanical strength of structural fiber glass in conical shells (JPRS-53118) 14 p2346 N71-23757
- Molecular damping measurements of glass fiber-epoxy and boron fiber-aluminum composites (AD-721191) 15 p2427 N71-24821
- Temperature and stress histories recorded for glass fiber reinforced plastic specimens subjected to torsional oscillations 16 p2418 N71-25583
- Weathering effects on creep properties of glass fiber reinforced polyether resin laminates under bonding stress (NLL-LIB-COMMA-3196-11533) 17 p2748 N71-29503
- Static calculation method for design of solid beams of glass reinforced plastics on independent elastic supports (AD-722309) 17 p2855 N71-30019
- Flammability and heat resistance of glass fiber reinforced polyester panels (TDCK-57564) 18 p2940 N71-30899
- Statistical method for measuring thickness of optical glass fibers (NLL-FORS-TRANS-2673-79022.81) 19 p3104 N71-32099
- Flexural, shear, bending, tensile, and impact strengths of high modulus, high strength, glass fiber-epoxy resin composites 23 p3775 N71-36987
- Development of Toroidal Dorrer having load shedding on glass epoxy and fibrous substrates (JALT-546) 23 p3828 N71-37380
- Tensile strength analysis of laminated-fiberglass orthotropic shells and pressure chamber designs for surgery and hyperbaric oxygenation therapy (JPRS-54173) 24 p3902 N71-37815
- Critical tensile strength curve determination for orthotropic two-layer fiber glass shells in plane stress corresponding to therapeutic pressure chambers 24 p3902 N71-37816
- GLASSWARE
- Interferometric test method for homocyclohexane chamber cover glass conformity to planarity specifications (NBS-TM-579) 23 p3759 N71-34082
- GLAUBER THEORY
- Spin and isospin effects on pion scattering by composite materials using Glauber formalism (RLO-1388-570) 06 p0424 N71-12805

Glauber theory for high energy hadron-deuteron scattering

[UCRL-19851] 05 p0743 N71-15146

Particle energy dependence calculations for scattering cross sections of pions and nucleon interactions with tritium and He-3 based on Glauber theory

[JINR-P2-3335] 14 p2317 N71-26757

Rho-proton coupling constant and rho-nucleon scattering amplitude determined by Glauber model of multiple scattering

[INR-P-1166] 16 p2654 N71-29037

Glauber and Born approximations of electron impact excitations of hydrogen atomic energy levels

[NASA-CR-121444] 20 p3319 N71-33686

Three dimensional formulation quantum field theory based on relativistic Faddeev equations and applied to three body problems

[JINR-P2-3661] 21 p3468 N71-34688

Glauber approximation of differential and integrated atomic hydrogen excitation cross sections at electron impact

[NASA-CR-122926] 24 p3971 N71-38327

GLAUCOMA

Glaucoma effects on visual performance of flying personnel

02 p0164 N71-11817

Phenomenological theory for describing intracranial pressure regulation in normal eye and consequences of deterioration of pressure regulation in abnormal eye

06 p0799 N71-15858

GLAUKTIC COEFFICIENT

U AERODYNAMIC FORCES

U MACH NUMBER

GLAZES

Effects of glazing and quenching on physical and mechanical properties of ceramic materials

[AD-717983] 12 p1941 N71-25282

Lead oxide immiscibility in lead borosilicate glass for opaque glazes

12 p1947 N71-24125

Compressive surface glazing for improved strengths of ceramic materials

13 p2101 N71-25315

GLIDE ANGLES

U GLIDE PATHS

GLIDE LANDINGS

Terminal entry trajectory analysis for spiral glide descent of space shuttle to landing site

14 p2344 N71-26072

Test and evaluation of aircraft glide slope landing system operating at ultrahigh frequency

[FAA-NA-71-15] 19 p3133 N71-32085

GLIDE PATHS

Analysis glide-slope information requirements for low visibility aircraft landing approach using Kalman filter-optimal control combination to simulate DC-8 control system

[AD-722635] 18 p2956 N71-30887

GLIDE SLOPES

U GLIDE PATHS

GLIDERS

NT FLEXIBLE WINGS

NT HL-10 REENTRY VEHICLE

NT PARAWINGS

Optimum lift coefficient and aspect ratio determined analytically as conditions for construction of gliders with lift drag ratio of 100

[RAE-LID-TRANS-1565] 16 p2530 N71-28010

Approximate optimal atmospheric entry trajectories maximizing terminal function of velocity, heading angle, flight path angle, and altitude

[NASA-CR-115145] 22 p3669 N71-36158

GLIDING

Lift and drag characteristics of HL-10 lifting body during subsonic gliding flight

[NASA-TN-D-6353] 08 p1142 N71-18867

Dislocation glide at high temperatures and glide recovery model for steady state creep

08 p1299 N71-19161

GLINT

Frequency agility reduction of radar glint

01 p0021 N71-10233

GLOBAL TRACKING NETWORK

Functions of NASA Office of Tracking and Data Acquisition

[NASA-TM-X-66529] 04 p0489 N71-13482

Communication satellite circular orbit network providing earth surface coverage

[RAE-TR-70211] 17 p2719 N71-29439

Data processing for calibration of C band radar global tracking network using GEOS 2 satellite data

19 p3089 N71-31853

GLOBULES

Representative list of globules and dark nebulae for use in optical and radio astronomy

03 p0453 N71-12952

GLOBULINS

Photometric measurement of emoglobin lysis time by direct printer

[NASA-TT-F-13389] 01 p0010 N71-10357

GLOSSARIES

U DICTIONARIES

GLOTRAC (TRACKING NETWORK)

U GLOBAL TRACKING NETWORK

GLOVES

Investigating approaches and concepts for improving mobility of aerospace pressure suits

[AD-711674] 01 p0016 N71-10947

Glove box vacuum system for radiological targets

[ORNL-TM-3209] 10 p1616 N71-21132

Gas purged dry box glove reducing permeation of air or moisture into dry box or isolator by diffusion through glove

[NASA-CASE-XLE-02531] 11 p1694 N71-23080

Design and performance of extravehicular astronaut thermal protection gloves

[NASA-CR-114974] 12 p1868 N71-34138

Design and fabrication of viton gloves for use in sterile nitrogen atmospheric processing cabinet of Lunar Receiving Laboratory

[NASA-CR-115112] 19 p3046 N71-31608

Highly articulate pressure glove providing digital dexterity, tactility, and stability

[NASA-CR-114365] 22 p3547 N71-35265

Mechanical properties evaluation of polyurethane latex for use as cosmetic glove material

[AD-726374] 22 p3602 N71-35653

GLOW

U LUMINESCENCE

GLOW DISCHARGES

Flow and stationary systems of glow discharge in carbon dioxide laser

[AD-715355] 08 p1209 N71-18533

Abnormal glow discharge from cathode configuration for use as laboratory test bed to develop and calibrate plasma diagnostic sensors

[NASA-TN-D-6136] 11 p1813 N71-22676

Diffusion mechanisms and boundary problems in electropositive and electronegative gases including plasma diffusion in electropositive negative glow and Faraday dark space

[AD-718430] 12 p1980 N71-23265

Sputter-condensation of silicates and other minerals in argon glow discharge

14 p2280 N71-26315

Prebreakdown processes and sparking voltage of gas moving at angle to electric field across uniformly stressed gap

[AD-722512] 17 p2811 N71-29620

Cathode environment characteristics in glow discharge

[SC-RR-710122] 19 p3070 N71-32219

Cold cathode glow discharge tube for detecting meteoroid puncture of pressurized cells

[NASA-TN-D-4447] 21 p3429 N71-34405

Development of method for applying metal alloy film or coating to irregular shaped metal object

[NASA-CASE-LEW-11262-1] 21 p3437 N71-34455

Ionization rate measured in glow discharge in gas mixtures commonly used in carbon dioxide lasers

[REPT-442] 23 p3766 N71-36848

GLUCOSE

Altitude induced changes in glucose metabolism of Escherichia coli

[AD-715212] 07 p0982 N71-17830

Human physiology, thermoregulation, and harmonic oscillation of blood glucose levels

[NASA-CR-1806] 16 p2542 N71-28206

Bed rest effects on glucose regulation in human beings

20 p3218 N71-33270

Monomethylhydrazine effects on glucose carbon metabolism and effects of pure oxygen inhalation in rats

[AD-727008] 22 p3546 N71-35259

GLUES

Electrodiffusion wear of tools and technology of gluing machine-tool devices

[AD-726804] 22 p3589 N71-35559

GLUTAMIC ACID

Stereospecific sorption technique for separating optical isomers of aspartic acid using glutamic acid

[UCRL-20471] 21 p3388 N71-34101

GLYCERINE

U GLYCEROLS

GLYCEROLS

Glycerin initiated spontaneous combustion in copper feedline for high pressure oxygen bottle carrier in military aircraft

[M70-777-BRE/LEE] 05 p0782 N71-14792

Investigating methods of synthesizing edible glycerols from waste gases in spacecraft

[NASA-CR-114276] 07 p0990 N71-17676

Glycerol food additive for spacecraft feeding

10 p1587 N71-20972

Tensile stress history and cavitation in shock loaded glycerol

[AD-720727] 14 p2240 N71-36177

GLYCINE

Comparison of electron diffraction and X ray diffraction analyses on crystalline structure of glycine

[UCRL-20139] 10 p1636 N71-21805

GLYCOLS

Apollo materials toxicity screening tests and effects of ethylene glycol, monomethylhydrazine, NF3, OF2, and ClF3

[NASA-CR-111394] 02 p0153 N71-11087

Measuring oxidation of n-xylyleneglycol on rotating disk electrodes and regularities in series of volatile organic hydrides

[JPRS-51404] 02 p0174 N71-11223

Determining polarization curves of oxidation of n-xylyleneglycol on rotating disk electrode of platinum and nickel in aqueous sodium hydroxide solution

02 p0174 N71-11224

Susceptibility of polyurethane foam to deterioration by impurities or contaminants in ethylene glycol monomethyl ether

[AD-715313] 07 p0997 N71-17753

GNEISS

Effect of high pressure on P wave velocity in gneisses and crystalline schists of northwestern Kola Peninsula

[NASA-TT-F-13208] 02 p0209 N71-11404

GNOTOBOTICS

Nutritional evaluation of Apollo diets and gnotobiological study of mice having diets with limited microflora

[NASA-CR-115124] 21 p3384 N71-34875

GOAL THEORY

Adaptive and goal-seeking system formulation and automata theory

[AD-712440] 03 p0341 N71-13470

GOALS

National Science Council goals in low speed aerodynamics - Canada

24 p4013 N71-36327

GODDARD EXPERIMENT PACKAGE TELESCOPE

U PARTICLE TELESCOPES

GOGGLES

Operational test and evaluation of photochromic goggles for eye protection during exposures to nuclear explosion flash

[AD-726544] 22 p3549 N71-33270

GOLD

NT GOLD ISOTOPES

Molybdenum and gold contact materials processing for metal oxide semiconductor transistor circuits

01 p0051 N71-10156

Chemical analysis of gold and tungsten thin films

[RAE-TR-69038] 02 p0171 N71-11228

Anelastic study of dislocation damping in gold

[COO-1196-725] 03 p0440 N71-12800

Self diffusion coefficient measurement for gold using radioactive isotopes

[TT-70-707030] 03 p0392 N71-12977

Gold layering in vacuum of extremely thin films

[BMW-FBK-70-8-B] 06 p0916 N71-10813

Xe-131 ion impact on gold crystal foils producing imperfection clusters

[COO-1053-14] 07 p1073 N71-14985

Process for forming heterojunctions by gold solvent alloying

[AD-715307] 08 p1277 N71-18579

Gold transport by complex metal chloride vapors

[BM-RI-7489] 08 p1219 N71-19138

Current-voltage characteristics of hot electron transport in vacuum deposited thin film emission gold magnesium oxide diodes

09 p1361 N71-19419

Mossbauer studies of recoilless fractions, isomer shifts, and magnetic properties of gold and gold alloys and high pressure effects on Kondo copper-gold alloys

[JPRS-5897-2] 09 p1400 N71-20812

Computational method for electron diffraction intensity using n-beam theory and applied to gold microcrystal calculations

10 p1621 N71-21742

Potential energy of interaction of chemically saturated molecule and gold surface proportional to inverse square of molecule to metal distance and to polarizability of molecule

11 p1697 N71-22572

Thermodynamic properties and nuclear chemistry of chemically bound neutrons and ternary fission of thorium and gold with helium-4 ions

[COO-1716-11] 14 p2301 N71-25732

Thermodynamic dissociation and vaporization properties of gold chlorides and gold bromides

[BM-RI-7513] 14 p2272 N71-25848

Iron and gold transition points as standards for high pressure and temperature measurements

14 p2597 N71-26509

Neutron cross section calculations for Cu-63, Au-197, Ti-203, Th-232, and U-238 using Hauser-Feshbach statistical mechanics

[AAEC-TR-542] 15 p2459 N71-26048

Thermal elimination of discontinuities in thin film of gold formed by evaporation in vacuum

[NLI-PORS-TRANS-2674-7022.81] 17 p2764 N71-25808

Atomic sputtering of impinging neutrons on gold crystals

18 p2994 N71-31151

Friction and abrasion properties of single gold crystals

18 p2994 N71-31145

Interpretation of Hall coefficient of pure copper, silver, gold, and some silver alloys based on misanthropic Fermi surface model

[NRC-TT-1476] 22 p3592 N71-35900

SUBJECT INDEX

- Ratio of resonance integral to thermal activation cross section of radioactive isotopes relative to gold [CNEA-282] 22 p3632 N71-35882
- Excitation functions for deuteron-induced reactions in gold using statistical model [LYCEN-7092] 22 p3634 N71-35898
- Analysis of extraneous grain boundary dislocations in high angle (110) twist boundaries in thin film gold bicrystals [NYO-3504-58] 23 p3834 N71-37340
- Vacuum evaporated films of Au, Pt, and Au-Pt on glass substrates after heat treatment 24 p3900 N71-37801
- GOLD ALLOYS**
- Monte Carlo effect analysis of Au-Pd-Pt alloy system [UCRL-50918] 05 p0705 N71-15443
- Amalgam behavior of Cu-based solid solutions and CuAu [CDO-1431-9] 06 p0873 N71-16390
- Internal magnetic fields of Cu impurity in Au, Cu, and Au-Cu alloys determined by nuclear orientation of Cu-60 [CDO-1569-67] 07 p1079 N71-17943
- Local atomic arrangements in some nickel-palladium and gold-palladium alloys 08 p1220 N71-19221
- Thermal and electrical conductivities of gold iron alloys at low temperatures 09 p1398 N71-19734
- Liquid quenching effects on martensitic transformation of metastable Au-Cd alloy [AD-716493] 09 p1409 N71-20096
- Comparison of mean drift and diffusion coefficient analyses of activity coefficient and vacancy flow effects on tracer diffusion in silver-gold alloys [JRO-2036-20] 11 p1779 N71-23482
- Phase diagrams and mutual thermal diffusion in copper-gold system [TT-70-59113] 14 p2269 N71-25659
- Investigation of interdiffusion in ordered alloys with crystal lattices of Cu-Au and CuAu type [TT-70-59066] 14 p2270 N71-25675
- Studying anodic oxidation of acetylene on platinum-gold alloys at 80 C in solutions of constant pH and unit ionicity 15 p2423 N71-27257
- Development of techniques for homogeneity studies of gold-silver and gold-copper alloys for standard reference material classification [NBS-SP-260-28] 22 p3594 N71-35594
- GOLD COATINGS**
- X ray diffraction measurement of crystal composition profiles, structure, and misorientations in nickel and gold electrodeposited diffusion zones of copper/111/ single crystals 10 p1383 N71-21588
- GOLD ISOTOPES**
- Nuclear spectroscopic investigations of decay Hg-191 yields Au-191 [JUL-659-KP] 02 p0278 N71-12162
- Determination and statistical model analyses of excitation functions and recoil ion ranges from reactions induced in gold isotopes by helium ions 08 p1264 N71-19113
- Data on Os-184,187 levels from Ir-184,187 decays, Hg-200 and Au-200 levels from Au-200m decay, and Bi-209, neutron, photon nuclear reactions [CDO-1672-21] 11 p1886 N71-22436
- Excitations of He-6 during fission of U-238 and Au-197 by C-12 and O-16 at 82 and 137 MeV [RFR-TR-352] 19 p3157 N71-32555
- High energy bremsstrahlung-induced gamma-ray reactions in Au-197 [LUNP-7103] 19 p3159 N71-32628
- Ternary fission products and scattering cross sections produced in Au-197, Bi-209, and Po-239 by intermediate energy He-4 ions 21 p3487 N71-34841
- GOLD PLATE**
- U GOLD COATINGS**
- GONDOLAS**
- Thermal coatings of gondola payloads [DYO-3747-12] 01 p0071 N71-10496
- Systems design and flight tests of azimuthal gondola orientation system [DYO-3747-13] 03 p0368 N71-13075
- GONIMETERS**
- Laser range finding of passive satellites by locating retroreflected radar echoes on sky photography [ONERA-TP-845] 02 p0258 N71-11564
- Instrument error analysis for visual tracking of satellites using gonimeters [NASA-TT-F-13355] 03 p0452 N71-12283
- GOS (SUPPORT SYSTEM)**
- U GROUND OPERATIONAL SUPPORT SYSTEM**
- GOVERNMENT PROCUREMENT**
- Guidelines for positive control of government furnished equipment for manned spacecraft [NASA-TM-X-64689] 06 p1294 N71-19244
- Survey of group of industrial organizations to determine pertinent properties, policies, and practices related to Federal procurement [NASA-CR-117699] 12 p2015 N71-23251

- Legality of patent infringements resulting from government procurement policies [NASA-TM-X-67143] 12 p2018 N71-23741
- GOVERNMENT/INDUSTRY RELATIONS**
- Federal role in development of synthetic rubber, civilian atomic energy, and communications satellite systems with implications for marine resource development program 09 p1487 N71-19498
- Procedure for informing members of Congress on technical subjects prior to enacting legislation 13 p2193 N71-25272
- Conference on Weights and Measures attended by representatives of Federal Government, business, industry, railroads, and associations [NBS-SPEC-PUBL-342] 16 p2601 N71-28590
- Government, industry, and university cooperation in space research and technology 16 p2694 N71-28540
- European space program and Intelsat - international cooperation and government/industry relations 17 p2862 N71-30322
- Employment problems from specialization in university research and industries through government funding 19 p3196 N71-32255
- Survey of metrication effects on US civilian organizations [NBS-SP-345-2] 19 p3200 N71-32749
- GOVERNMENTS**
- Research and development in State government agencies [NSF-70-22] 01 p0138 N71-10977
- Program budgeting role in US government guiding and managing social, economic, and environmental systems [AD-71903] 02 p0307 N71-11892
- Research and development data policies of civilian government agencies [NASA-TM-X-66599] 04 p0622 N71-14092
- Employment statistics on Federal scientific, technical, and health personnel for 1969 [NSF-70-44] 08 p1307 N71-18447
- Sources and control of air pollution 12 p1956 N71-23854
- Scientific legislative management cooperation for international research and development work 13 p2190 N71-24739
- Operations research for West German governmental information retrieval system, noting law application and decision making 14 p2223 N71-25997
- Proceedings of joint meeting of Government Operations Research and Procedures [NBS-SP-347] 15 p2527 N71-27883
- Five-year federal plan to provide air pollution control meteorological service for support of federal, state, and local pollution control agencies [COM-71-00200] 16 p2589 N71-28853
- Philosophical discourse on comparative administration [NASA-CR-119376] 18 p3031 N71-31548
- Systems maintenance program evaluation conducted in central region of US 19 p3072 N71-31623
- Comparison of research and development in local government for 1968 and 1969 and 1966 and 1967 [NSF-71-6] 19 p3198 N71-32639
- Federal programs for air, water, and solid waste pollution control 19 p3198 N71-32633
- Federal budget amendment agreement recommendations [REPT-92-377] 19 p3199 N71-32657
- Usefulness of quantitative analyses in solving problems of public affairs management and government decision making [F-4530] 20 p3291 N71-33131
- Government, industry, banking, conservation, and law in preservation of environmental quality [NASA-CR-121637] 21 p3414 N71-34294
- Fuel burning and refuse disposal practices, air pollutant emissions, and abatement plans for Federal facilities in counties in Kansas and Missouri 22 p3577 N71-35481
- Impact of air activity on environment and federal interest in environmental studies 24 p4033 N71-38792
- GOVERNORS**
- U SPEED REGULATORS**
- GRADIENTS**
- NT ELECTRON DENSITY PROFILES
- NT POTENTIAL GRADIENTS
- NT PRESSURE GRADIENTS
- NT TEMPERATURE GRADIENTS
- NT THERMOCLINES
- Applicability of gradient method as optimization strategy for use with hybrid analog computer [DPR-1866] 14 p2224 N71-26330
- GRADIMETERS**
- U MAGNETOMETERS**
- GRADUATION**
- U CALIBRATING**

GRAIN BOUNDARIES

- GRAIN BOUNDARIES**
- Experimental single Fourier transform optical processor applied to film grain analysis and ship wave detection method [AD-710721] 01 p0088 N71-10329
- Continuum mechanics of grain boundary dislocations and diffusional creep [AD-711068] 01 p0111 N71-10669
- Weld heat affected zone notch impact properties of quenched C-Mn steel and fully killed Al grain refined C-Mn steel [MAT-1] 02 p0340 N71-11429
- Effects of quench rate on distribution of precipitates at grain boundaries in Al, Zn, Mg alloys [AD-713809] 03 p0393 N71-13152
- Superplastic deformation of grain boundaries in eutectic alloy of cadmium and zinc [CDO-1199-643] 04 p0529 N71-13997
- Ductile-brittle transition temperature for coarse grained recrystallized molybdenum [AD-713191] 05 p0706 N71-14649
- Investigating orientation relationships between major grains radiating from single nucleation event into highly undercooled copper [REPT-363] 05 p0708 N71-15056
- Grain structure of high purity copper melts undercooled before nucleation [REPT-374] 05 p0702 N71-15068
- Grain boundary faceting of 10-10 tilt boundaries in zinc crystals grown from melt [AD-716227] 06 p0935 N71-16361
- Surface and grain boundary layer of barium titanate [AD-715097] 07 p1048 N71-17848
- Measurement of strains induced at ceramic bicrystal grain boundaries [AD-715447] 08 p1280 N71-18842
- Grain boundary diffusion in iron using autoradiography [TT-70-57048] 08 p1218 N71-18996
- High temperature crack initiation and propagation in aluminum and aluminum alloys with emphasis on grain size effects 10 p1576 N71-21013
- Ion microscope study of tungsten and thoriated tungsten grain boundaries 10 p1635 N71-21783
- Auger spectroscopy of low alloy steel, copper bismuth alloy, and refractory metal annealing and sintering embrittlement due to grain boundary fracture, corrosion, and mobility [CDO-1778-6] 12 p1987 N71-23954
- Volumetric and grain boundary effects on silver isotope diffusion into aluminum single and polycrystals during annealing [TT-70-57045] 14 p2269 N71-25661
- Effects of composition, particle size, and component thermal properties on effective thermal conductivity of composite solids 14 p2356 N71-26469
- Intergranular pore density determination in PUO2-2 UO2 fuel pin irradiation in EBR-2 [WRIAN-CA-15] 15 p2443 N71-26928
- Impurity content grain boundary sliding in aluminum ceramics during compression [JRO-3328-17] 15 p2508 N71-27993
- Grain boundary diffusion coefficients and reaction kinetics for austenitic stainless steel carburizing by carbides nuclear fuels [JAERI-4132] 16 p2608 N71-28072
- Electron microprobe analysis of solute segregation near grain boundaries in Al-Zn-Mg alloy after different quenching (nitric, water, oil, and air) and aging heat treatments [AD-722834] 16 p2610 N71-28454
- Elastic interaction between grain boundaries and screw dislocation pileups under constant stress 17 p2817 N71-29939
- Crystal glide dislocation through internal grain boundaries with symmetrical tilt 17 p2820 N71-29941
- Volume and grain boundary diffusion coefficient measurements of Fe-Cr alloys, alpha gamma phase transformations, and effects of carbon impurities [CEA-R-4023] 18 p2982 N71-30902
- Model description of polycrystalline semiconductor film assuming different conductivities and Hall mobilities for grains and boundaries [INASA-TT-F-13680] 18 p2995 N71-31094
- Sulfur influence on structure and weldability of titanium-bearing austenitic stainless steels 19 p3112 N71-31916
- Grain boundary segregation of impurities in steels and intergranular brittle fracture [AD-723224] 19 p3113 N71-31966
- Investigation of controlled electromagnetic fields applied to Type-304 stainless steel melts during solidification including grain boundary and metallographic studies [SU-326-P-29-X-1] 19 p3114 N71-32228
- Plastic deformation in polycrystals of Fe-Cr-Ni alloys on boundary layers at high temperature [TT-70-59108] 20 p3284 N71-33198

Dislocation glide, deformation twinning and grain boundary sliding in compressive creep of single and bicrystalline aluminum oxide

21 p3500 N71-34932

Effect of grain size on creep of platinum-rhodium alloys at high temperature
[NLL-LTT-746-744-19022.401]

22 p3597 N71-35615

Intergranular fractures along grain boundaries of quenched low temperature manganese silico-chromium steel
[NLL-CE-TRANS-5346-19022.09]

22 p3597 N71-35616

Ceramography and micro X ray diffraction analysis of columnar grain growth in centerline heated UO₂ pellet
[JAERI-MEMO-4249]

22 p3630 N71-35788

X-ray technique for determining structural changes in relation to metal substructures and their mechanical properties
[AD-727430]

23 p3773 N71-36889

Analysis of extraneous grain boundary dislocations in high angle [110] twist boundaries in thin film gold bicrystals
[NVO-3504-58]

23 p3834 N71-37340

Analysis of structure and behavior of dislocations in grain boundaries and Burgers vectors of lattice dislocations in Fe-Mn alloys
[NLL-M-20645-15828.4F]

23 p3836 N71-37357

Developing metal alloys of ultrafine grain size with improved mechanical properties
[AD-727746]

24 p3938 N71-38093

Ratio of grain boundary energy to surface energy determined from observations of intergranular fission gas bubbles in neutron irradiated uranium dioxide
[RD/BN-1851]

24 p3963 N71-38265

Automatic identification and classification of wheat from airborne multispectral data in agricultural remote sensing
[REPT-279]

12 p1913 N71-23731

Grain cereals as polyfunctional autotrophic components of closed ecological life support systems
[AD-727746]

16 p2350 N71-28253

GRAMMARS
Definition and implementation of simple LR/k context free grammars
[NASA-CR-117125]

09 p1353 N71-19600

Computer program simulating generation of flected forms of irregular verbs in German for use in dictionaries and grammars
[AD-727746]

14 p2222 N71-25982

Context sensitive grammar and generation of non-context free languages
[NASA-CR-121658]

21 p3197 N71-34177

GRAND TOURS
Tabulating trajectory data for alternate Grand Tour missions from earth for period 1976 to 1980
[NASA-CR-61338]

04 p0611 N71-14107

GRANITE
Luminescent and thermoluminescent properties of granite and its constituent minerals and their relevance to transient lunar phenomena
[AD-714416]

01 p0045 N71-10078

Spectrometric analyses of granites for transuranium and anomalous alpha emitters
[AD-714416]

01 p0094 N71-10307

Aeromagnetic anomalies and granulite bodies in Pond Oreille area, Idaho for metamorphic and structural studies
[AD-714416]

21 p3419 N71-34329

Granite, basalt, gabbro, and dunite isothermic volume compressibilities and densities under 32,000 kg pressure
[SC-T-713031]

23 p3802 N71-37108

GRANULAR MATERIALS
Microwave mass absorption coefficient in granular silicates from plate measurements and effects of scattering
[NASA-CR-111023]

01 p0048 N71-10458

Investigating process development program for production of high quality mixed oxide fast reactor fuel pellets
[BNWL-1445]

05 p0726 N71-13071

Development of device for separating, collecting, and viewing soil particles
[NASA-CASE-XNP-09770]

09 p1394 N71-20440

Heat transfer through bed of granular material from hot surface of tube concentrically mounted in rotary apparatus and with results expressed in form of effective thermal conductivity
[NLL-AERE-TRANS-1125-19091.9F]

12 p2014 N71-24328

Ionized fields in electrostatic separation of granular solids (conductors and nonconductors) also applications in separations based on surface-to-mass ratio of particles
[BM-R1-7509]

14 p2302 N71-25744

Analysis of extinction cross-sections for grains composed of water ice, quartz, and silica surrounded by ice mantle with application to stellar composition
[AD-714416]

21 p3512 N71-35026

GRAPHIC ARTS

Summary descriptions of NASA graphic arts techniques and equipment
[NASA-SP-5919/01]

12 p2019 N71-34205

Field displacement graphical processing problems and techniques for calculating partial derivatives of displacements using more and coordinate grid methods
[NLL-M-21006-15828.4F]

24 p3950 N71-38185

GRAPHITE
NT PYROLYTIC GRAPHITE

Effects of natural chemical impurities and crystalline orientation on erosion behavior of artificial graphite
[NASA-TN-D-6023]

01 p0070 N71-10070

Chemical and electrochemical reactions of lithium graphite fluoride primary cell
[AD-715321]

01 p0007 N71-10936

Omniwave method of composite fabrication of graphite filaments and mechanical properties of fabrics
[NASA-CR-102916]

02 p0246 N71-11441

Characteristics of nuclear graphite at elevated temperatures
[PS-195492]

02 p0265 N71-11737

Monte Carlo calculation of neutron attenuation in BAC solution, dense graphite and stainless steel
[CEA-N-1351]

04 p0572 N71-13646

Fracture toughness of graphite double cantilevered beam specimens
[BNWL-CC-774]

04 p0533 N71-13812

Stress-strain behavior of nuclear-grade artificial graphite
[ORNL-TM-2727]

04 p0533 N71-13813

Postirradiation examination of Peach Bottom reflector element B16-01 after exposure to 300 effective full power days
[GA-MD-5911]

04 p0551 N71-13963

High temperature irradiation effects on nuclear graphite
[GA-9973]

04 p0533 N71-13996

Particle shape effect on abrasiveness of graphite and molybdenum disulfides
[RAE-TR-69024]

04 p0534 N71-14137

Ablation performance of glasslike carbons, pyrolytic graphite, and artificial graphite in stagnation pressure range 0.035 to 15 atm
[NASA-TN-D-7005]

04 p0534 N71-14138

Mechanical properties of mixed boron/graphite composite
[NASA-CR-102944]

04 p0535 N71-14267

Dissipated power in graphite and CO₂ of graphite reactor cell of NAIAD-2 subcritical assembly
[CEA-R-3985]

04 p0562 N71-14414

Seal ring carbon-graphite materials for aircraft gas turbines
[NASA-CR-72799]

05 p0692 N71-14890

Post-irradiation analysis of graphite samples from first charge, spherical fuel elements
[AVR-34]

06 p0896 N71-15825

Quantum galvanomagnetic and thermomagnetic effects in graphite in magnetic fields at low temperatures
[NASA-TN-D-7037]

06 p0932 N71-15917

Vapor deposition of niobium carbide on graphite particles
[AD-714416]

06 p0879 N71-16434

Literature survey and experimental evaluation of graphite properties in high vacuum environment
[NASA-CR-111829]

06 p0881 N71-16396

Temperature and radiation effects on irradiated graphite
[GA-10268]

07 p1046 N71-17014

Material characteristics and methods for predicting mechanical properties of graphite
[ORNL-TM-3191]

07 p1047 N71-17203

Mechanical properties of hot pressed NBC and TaC-graphite composites with W added
[NASA-CR-116503]

07 p1048 N71-17353

Fabrication of graphite reinforced epoxy tubes
[AD-715319]

07 p1048 N71-17857

Anelastic properties of neutron irradiated graphite and irradiation-induced interstitials
[CEA-CONF-1636]

07 p1096 N71-18129

Spatio-temporal study of graphite gas power reactor on hybrid computer - conference
[CEA-CONF-1580]

08 p1235 N71-18208

Structural and electrical properties of alkali graphite and calculations of potassium graphite band structure, Fermi surface, work functions, and electronic specific heat coefficient
[AD-714416]

09 p1403 N71-19571

Reaction of refractory metals with graphite during spray coating
[AD-716516]

09 p1404 N71-19691

Properties, microstructure, and irradiation behavior of carbonaceous and graphitic reactor materials
[GA-9973]

09 p1476 N71-19918

Manufacturing of improved carbon and graphite materials
[NASA-CR-117315]

09 p1407 N71-20373

Pulsed neutron source for graphite lattice analysis
[CEA-R-3640]

09 p1442 N71-20383

Low cost graphite powder and phenolic resin molding compounds for use in rocket engine nozzles
[NASA-CR-72833]

09 p1408 N71-20459

Carbon dioxide distribution in mixture with argon in gas-liquid channel at high temperatures
[NLL-RTS-5839]

10 p1514 N71-31310

Kinetics of reaction between graphite and carbon dioxide in flow tubes at atmospheric pressure and high temperatures
[NLL-RTS-5838]

10 p1514 N71-31311

Physical and chemical effects on reactivity of artificial graphite used for electrode technology
[NLL-RTS-5841]

10 p1590 N71-31381

Microstructural research on carbon and graphite for use as engineering materials
[NASA-CR-117494]

10 p1591 N71-31641

Design and tests of graphite radiant heater for high heat flux source in spacecraft thermostructural tests
[NASA-CR-111041]

11 p1839 N71-21942

Orientation and distribution of crystallites in model artificial graphite
[NASA-TN-D-6300]

12 p1941 N71-23168

High temperature uniaxial tensile tests performed on aluminum-graphite composites
[AD-711533]

12 p1942 N71-23482

Analog simulation of temperature distribution time dependence in rocket nozzle graphite protective coating
[ICT-270]

12 p2012 N71-24199

Core support graphite and carbon components for reactor core and reflector of Fort St. Vrain reactor plant
[GA-9641]

13 p2121 N71-25243

Dilatometric thermal expansion measurements in high temperature structural materials
[AGARD-AR-31-71]

13 p2187 N71-25338

Spectral analysis of magnesium distribution in high strength cast iron containing globular graphite
[TT-70-59085]

14 p2269 N71-25840

Research on carbonization, radiation effects, chemical properties, and mechanical properties of graphite and carbon compounds
[NVO-1716-100]

14 p2276 N71-25679

Effect of crystallite size, crystallite orientation, and density on dimensional and property changes in irradiated graphite and isotropic materials
[GA-10433]

14 p2277 N71-25680

Development and characteristics of high strength graphite fibers produced from polymeric fibers and spun from pitches
[AD-72824]

14 p2277 N71-25855

Determination of static and fatigue characteristics of graphite epoxy composite materials with variations in temperature, stress mode, and stress ratio
[AD-730396]

14 p2277 N71-25885

High temperature oxidation resistant coatings for superalloys, refractory metals, and graphite
[NASA-CR-118647]

14 p2275 N71-26409

Characteristics of zones of displacements of defects in graphite from neutron irradiation
[CEA-N-1374]

14 p2281 N71-26522

Computer code for calculating lattices and lattice evolution in natural uranium graphite moderated gas cooled reactors
[CEA-M-1344-1]

15 p2446 N71-27144

Burnup calculations of fission products used for studying reactor poisoning applied to fuel cycle studies in thermal reactors
[JUL-678-RQ]

15 p2469 N71-27358

Graphite thermodynamic properties and liquid-solid phase diagrams in high temperature environments for nuclear rocket engine reactor core design
[AD-714416]

15 p2468 N71-27367

Computer-aided, ultrasonic test system for graphite billets to select optimum location of sensory vehicle nose tip
[SC-DR-70-693]

15 p2431 N71-27433

Electrostatic methods to control placement and orientation of short graphite fibers in fiber composites and fiber structures
[SC-CR-69-3277]

15 p2432 N71-27609

Sorption of cesium by graphite and charcoal reducing volatility of cesium and rendering it fully stable in sodium at 500 C and in air at same temperature
[AERE-R-6441]

15 p2492 N71-27952

Radiation effects of nuclear graphite in CO₂/H₂O/CO₂
[TRG-2010]

16 p2618 N71-28683

Graphite monochromator for thermal neutron spectroscopy
[AD-714416]

16 p2596 N71-28707

Design and performance of thermal beryllium oxide and graphite neutron sources and high flux beam reactors in neutron spectroscopy
[NLL-RISLEY-TRANS-1881-19091.9F]

16 p2619 N71-28716

Antifriction characteristics of graphite due to its mechanical properties and self lubricating nature
[NLL-RISLEY-TRANS-1881-19091.9F]

16 p2602 N71-28722

Antifriction graphite-carbide-silicon materials with high wear resistance
[NLL-RISLEY-TRANS-1991-19091.9F]

16 p2603 N71-29117

Equipment for determining reactivity of graphite materials in isothermal conditions at high temperatures from 1200 to 3000 C
[NLL-RISLEY-TRANS-2012-19091.9F]

16 p2619 N71-29142

SUBJECT INDEX

Structure of graphite materials subjected to intensive wear at various pressures
[JNL-RISLEY-TRANS-1998-0091.9F] 16 p2619 N71-29160

Oxidation resistant coatings for superalloys, refractory metals, and graphite 16 p2620 N71-29174

Induction plasma torch reactor for converting uranium dioxides/graphite powder to uranium carbide spheres [ANL-7671] 17 p2811 N71-29201

Hot isostatic compaction at 3000 F and 30,000 psi used for successfully preparing single phase bulk graphite for vibration testing [SC-CR-70-4169] 17 p2768 N71-29219

Thermal degradation of polycrystalline polymers for conversion to high modulus carbon and graphite reinforcement fibers [AD-720353] 17 p2769 N71-29546

Techniques for determining thermal neutron diffusion parameters and theoretical physics of neutron interactions with graphite spheres [JUL-490-R0] 18 p2981 N71-30863

Temperature effects on methane formation from hydrogen atom reactions with polycrystalline graphite surfaces 18 p2886 N71-31080

Minority carries in single crystal and pyrolytic graphite studied by observing magnetic field oscillations in Hall voltage and thermopower [NASA-TM-D-6466] 19 p3169 N71-32163

Thermal and air environment effects on mechanical properties of graphite/polyimide laminates [NASA-TM-X-67993] 19 p3121 N71-32414

CORCORAN code for calculating lattice relaxation times and line shapes for C-13 and Cs-133 species 21 p3442 N71-34496

Complete neutron absorption analysis of solid samples using heated graphite cell [REF-833] 20 p3316 N71-33428

Effects of boron on plasticity and structure of carbon component, strength and electron - properties of synthetic graphite [SC-T-715823] 20 p3288 N71-33740

Microstructural study of physical and mechanical properties of carbon and graphite [LA-4714-M5] 21 p3442 N71-34496

Diffusion bonded graphite reinforced aluminum composites [NASA-CASE-MFS-21077] 21 p3443 N71-34502

Irradiation of nuclear graphite and model carbons [JA-18535] 21 p3444 N71-34506

Nuclear magnetic resonance in carbon-graphite intercalation compounds with spin-lattice relaxation times and line shapes for C-13 and Cs-133 species 21 p3445 N71-34515

Computer program for calculating concentration and burnoff profiles in section of graphite being corroded by water [AERE-M-2403] 21 p3457 N71-34602

Vibrational analysis of irradiated graphite with variable creep coefficient for neutron salt breeder reactor [ORNL-TM-3242] 21 p3459 N71-34618

High temperature measurements of thermal diffusivity of graphite [AD-726562] 22 p3683 N71-35660

Neutron radiation effects on boronated and irradiated graphite, nuclear fuel element reprocessing, and high temperature gas cooled reactor development [JA-16581] 22 p3625 N71-35830

Gaseous tungsten arc welding tests of titanium-tungsten wire and titanium-graphite filaments for weldability and weld thermal energy effects on fiber-matrix reactions [RM-519] 23 p3764 N71-36836

Thermal, chemical, and wear properties of carbon-graphite seal ring materials at air temperatures to 1300 F [NASA-CR-72966] 23 p3778 N71-36910

Making behavior of graphite [AD-727664] 23 p3778 N71-36929

Displacement and mean values of inelasticity coefficient K for several planes in lead and graphite determined by digital computer 23 p3808 N71-37154

Laser microemission spectroscopic analysis of metals and nonmetals [NASA-TF-139711] 24 p3931 N71-38045

Research and development on carbon and graphite to determine properties and behavior as engineering materials [NASA-CR-123171] 24 p3942 N71-38123

High temperature tests of creep in structural graphite [AD-729898] 24 p3946 N71-38147

GRAPHITIZATION
Oxidation of thin carbon films for electron microscopy [NYO-4142-1] 05 p0708 N71-15062

Impregnation permeability of air bearing graphite [Y-SC-7] 24 p3942 N71-38124

GRAPHS [CHARTS]

NT MOLLIER DIAGRAM
Second order theory of oscillating cylinders [AD-710767] 01 p0842 N71-10034

Wind tunnel investigation of jet transport airplane configuration with high thrust-weight ratio and external flow jet flap - graphs [NASA-TN-D-6058] 01 p0804 N71-10495

Determining polarization curves of oxidation of n-xylyleneglycol on rotating disk electrode of platinum and nickel in aqueous sodium hydroxide solution 02 p0174 N71-11224

Theoretical analysis of α/α_0 reactions using triangular graphs [LYCEN-7031] 02 p0278 N71-12171

Summary of prominence and calcium flocculus observations at Kodaikanal Observatory Jan. through June 1964 - tables and graphs [BULL-174] 03 p0451 N71-13297

Nomenclature of earth-moon orbits [NASA-TM-D-5949] 04 p0611 N71-14857

Wind tunnel investigation of jet transport airplane configuration with external flow jet flap and inboard pod-mounted engines - graphs [NASA-TM-D-7004] 05 p0629 N71-14605

Atlas of total electron content plots for 1969 - Vol. 5 05 p0674 N71-14994

Atmospheric optical properties - tables and charts [AD-715278] 07 p1022 N71-17814

Flight simulator tests of human behavior in roll tracking tasks in fighter and large aircraft with descriptive functional analysis [NAL-TR-206] 09 p3139 N71-19751

Aerological ozone sounding tables and graphs 10 p1547 N71-20854

Tables and graphs of aerological ozone soundings at Hohenpeissenberg, Germany for first half of 1969 10 p1549 N71-21095

Predicting aerodynamic characteristics of arrow, delta, and diamond wing platforms using Prandtl-Glauert transformation [NASA-TN-D-6243] 11 p1669 N71-21973

1968 average monthly North Atlantic surface temperature gradients between 50 to 80 deg N and 0 to 60 deg W 11 p1790 N71-22403

Graphic method of forecasting neoperiodic oscillations of sea level in East Siberian and Chukchi seas 11 p1758 N71-22854

Graphical solution to stay time of commercial fish vessels in regions of icing 11 p1759 N71-22861

Effect of engine position and high lift devices on aerodynamic characteristics of external flow, jet flap STOL model - graphs [NASA-TN-D-6222] 12 p1832 N71-23124

Estimating unsteady pressure distributions in T tail configuration from measured distribution and theory [NLR-TR-68048-L] 12 p1849 N71-23131

Performance test of single stage turbine with low solidity tandem rotor blade assembly [NASA-CR-1803] 12 p1849 N71-23132

Low subsonic longitudinal aerodynamic characteristics of twin body space shuttle booster configuration using low turbulence pressure tunnel - graphs [NASA-TM-X-2162] 12 p1850 N71-23135

Intuitive, graphic, and simplified mathematical treatment of rotational dynamics as applied to human centrifuges 12 p1965 N71-23340

Tabular and graphical summary of human tolerances to prolonged acceleration stresses 12 p1862 N71-23341

Mean global distributions of Secchi disc water transparency measurements and Forul-Ur water color codes including seasonal variations for Sea of Japan and Indian Ocean [AD-718333] 12 p1910 N71-23592

Graph theory and its applications - bibliography, supplement 1 [NASA-CR-118044] 12 p1950 N71-23964

Mean square exceedence characteristics of single tuned system to amplitude modulated random noise applicable to structural design - graphs 12 p2009 N71-24305

Monthly graphs of cosmic ray NM-64 neutron monitor data for May to Aug. 1970 13 p2161 N71-25158

Charts for synthesizing biquadratic network functions with complex poles and zeros by means of simple DLA network configuration [NASA-CR-118338] 13 p2680 N71-23390

Industrial noise and countermeasures - research methods and measuring devices [AD-728414] 14 p2294 N71-23878

Results of radioisotope accessions from aerological station in Berlin, Germany including extreme and mean values of temperature, pressure, wind data, geopotential and other meteorological data 14 p2288 N71-23884

Graphical predictions of human strengths for two handed IVA/EVA tasks including effects of differing gravities, populations, and space suit conditions [NASA-CR-115041] 14 p2211 N71-26410

GRAPHS [CHARTS]

Graphical method for determining all resonance parameters in nuclear reactions [JINR-B4-3456] 14 p2388 N71-26425

Pressure deformations of spacecraft windows and angular line-of-sight deviations of light rays from these windows causing errors in celestial navigation sightings - graphs [NASA-CR-114310] 14 p2343 N71-26465

Computer compilation of high energy physics data represented by graphs or tables [UCRL-20000-NN] 15 p2487 N71-27286

Tables and graphs of metabolite levels in whole body sweat determined by small skin area measurements [NASA-CR-115801] 15 p2372 N71-27647

Spectra of reflected solar energy from clouds, snow, and fields at 0.4 to 2.4 microns using C-47 and B-57B aircraft - graphs [NASA-TM-X-45574] 15 p2405 N71-27649

Tables and graphs of wind data for Lawrence Radiation Laboratory - Berkeley [UCRL-20224] 17 p2776 N71-29046

Predictions of wind forces on offshore structures [PB-19087] 17 p2852 N71-29767

Derivation and tables of spherical harmonic coefficients and isoprotic charts for International Geomagnetic Reference Field for 1965 [NASA-TM-X-65604] 17 p2745 N71-29989

Prototype research of Tangential Injection and Rotational Combustion system for orbit and attitude control of space vehicles and satellites - graphs [NASA-TF-13683] 17 p2859 N71-30280

True graphs in Yang-Mills field theory [JINR-P2-5616] 17 p2809 N71-30383

Algorithms for finding M-center of graph [AD-722589] 18 p2948 N71-31489

Application of binomial continuous phase dispersion model to estimate concentrations of air pollutants - tables and graphs [PB-191462] 19 p3125 N71-31626

Comparison of collocated Goddard mobile laser satellite tracking performance data with SAO and Goddard experimental laser tracking of OBOS 2 satellites 19 p3107 N71-31846

Comparison of predicted and experimental wall temperature for cylindrical ejector exhaust nozzle operated with turbojet gas generator [NASA-TM-D-6465] 19 p3174 N71-32156

Aerodynamic characteristics at Mach numbers 1.60 to 2.16 of blunt-nose missile model having triangular cross section and fixed triform fins [NASA-TM-X-2340] 19 p3033 N71-32211

Full scale wind tunnel tests of low wing, single engine, light aircraft with positive and negative propeller thrust and up and down flap deflections - graphs [NASA-CR-1783] 19 p3038 N71-32249

Model tests of concepts to reduce hot gas ingestion in VTOL jet engines in low and cross wind conditions - graphs [NASA-CR-1863] 19 p3038 N71-32370

FORTRAN-based version, FGRAAL, of graph algorithm language GRAAL [NASA-CR-11779] 19 p3863 N71-32494

Computer language for implementation of graphic theoretical algorithms [NASA-CR-119723] 20 p3239 N71-33564

Graphs for analysis of gamma-gamma directional correlations [ORNL-4619] 20 p3318 N71-33587

Wind tunnel investigation of external-flow jet-flap transport configuration having full-span triple-slotted flaps - graphs [NASA-TN-D-6391] 21 p3377 N71-34028

Probability graphs and statistical analysis of air pollution data [NLL-M-28595-(3828.4F)] 21 p3422 N71-34351

Graphical method for deriving dye-layer densities of color infrared image elements from known reflectance curves, and analysis of CIR photography from spacecraft windows [NASA-CR-121650] 21 p3424 N71-34361

Compression corrections for Acme thread gauges using graphs and formulas [TM-175] 21 p3428 N71-34393

Eight variable stars in cygnus cloud studied at different observatories - tables and graphs 21 p3510 N71-35013

Feasibility study of radiator and power divider for 50 to 60 GHz phased array - graphs [NASA-CR-111949] 22 p3359 N71-35346

Graphs and tables of negative pion induced reaction cross sections [CERN/HERA-70-7] 22 p3632 N71-35883

Preparation of particle identification system using ORTEC 423 with block diagrams of circuits and graphs [ANU-P-514] 22 p3634 N71-35983

Evaluation of ion density and plasma potential from Langmuir probe data - graphs [NASA-TM-X-2349] 22 p3642 N71-35964

Fluctuation enhanced conductivity of superconductors, and evaluation of Maki graph based on Boltzmann equation [NP-16819] 22 p3657 N71-36080

Reducing rotor stator interaction noise by use of nonradial (lean) stator vanes
[NASA-CR-1882] 22 p3663 N71-36118

Pressure distributions and drag coefficients of 18 constant length and volume slender bodies of revolution at zero incidence for Mach numbers 2.0 to 12.0 - graphs
[NASA-TN-D-6536] 23 p3705 N71-36416

Propagation measurements on long high clearance path revealing difference between direct and ground reflected rays of about 30 wavelengths at 4 GHz
[REPT-6124] 23 p3722 N71-36533

Wind tunnel interference estimation for model design applications using chart method
[NASA-TN-D-6416] 23 p3741 N71-36675

Turans theorem for k-graphs
[P-4648-1] 23 p3783 N71-36965

Graphs and tables of aircraft traffic over North America - 1966 through 1969
[RAE-LIB-TRANS-1580] 24 p3954 N71-38210

Van Allen belt radiation on Tiros/TOS/ITOS spacecrafts - graphs
[NASA-TM-X-65717] 24 p6002 N71-38546

Subsonic longitudinal and lateral directional stability investigation of MDAC LCRD orbiter, unpowered and powered - graphs
[NASA-CR-115965] 24 p4017 N71-38665

Statistical analysis of ecological variables across grassy geological surface
[COG-1821-2] 03 p0322 N71-12304

Remote sensing analysis of grassland fire phenomena in Florida
08 p1198 N71-19263

Cloud condensation nuclei effects on rainfall during spring droughts in Florida from peat, algae, sawgrass, and leaf fire smoke
[ESSA-TM-ERLTM-AOML-4] 23 p3784 N71-36975

GRASSMANN ALGEBRA
U VECTOR SPACES

GRATINGS [RETRACT]
Spectral distinction of grating at grazing incidence
[NASA-CR-111147] 01 p0053 N71-10656

Polarization effects on grating efficiency of SIRS B satellite infrared spectrometer
[PB-192130] 05 p0771 N71-15161

Echelle spectrometer for use with spaceborne stellar telescope in Advanced Princeton Satellite Study
[NASA-CR-115892] 05 p0688 N71-15483

Absorptions and ray tracing for double hemispherical shell mirror and ultraviolet grating spectrometers
[NPL-QU-13] 06 p0902 N71-15795

Techniques for ruling improved large diffraction gratings
[NASA-CR-116457] 07 p1027 N71-17173

Describing analytical technique for solving electromagnetic boundary value problems of suboptical resonators with grating mirrors
08 p1203 N71-19078

Parallel radiation incident to grazing for life extension of diffraction grating strain gauges
[AD-717324] 11 p1760 N71-21863

Impact tests on annealed small grain 1100 F aluminum rods using in-surface diffraction grating strain transducers illuminated by pulsed ruby laser
[AD-717328] 11 p1776 N71-21907

Spectral images formed by reflecting diffraction grating
16 p2592 N71-28237

Discrete element magneto-optic display
[AD-724603] 20 p3241 N71-33190

Surface plasma resonance effect in diffraction gratings and relation of effect to space contamination by spacecraft instruments
[NASA-CR-121754] 21 p3508 N71-34994

Aberration theory and computerized design of unusual concave gratings for high resolution far UV spectrometers
23 p3760 N71-36808

GRAVELS
Influence of gravel depth and fire inflation pressure on soft-ground arresting of civil aircraft
[RAE-TX-69001] 02 p0147 N71-11040

GRAVIMETRIC
Tilt method for calibrating shipborne nonstaticized gravimeters
02 p0221 N71-12156

Operation manual for Mark 2 model of laser absolute gravimeter
[NASA-TM-X-64560] 05 p0696 N71-15026

Cryogenic gravity meter
[AD-714569] 06 p0860 N71-16532

Device for determining acceleration of gravity by interferometric measurement of travel of falling body
[NASA-CASE-XMF-65844] 07 p1030 N71-17587

Development of gravimeter for lunar traverse gravity experiment and specifications for instrument, operation, and experiment error budget
[NASA-CR-114946] 10 p1560 N71-21467

Reliability coefficient of gravimeters determined for instrument accuracy
[JPRS-32941] 12 p1921 N71-23701

Abstracts of articles concerning gravimeters, magnetospheric resonators, and tectonics of Sea of Japan
17 p2739 N71-29403

Gravimetric observations of tidal variation in Syowa station, Antarctica
20 p3261 N71-33335

Simultaneous gravimetric observation of earth tides with four Askania and two Lacoste and Romberg gravimeters in Mizusawa, Japan
20 p3262 N71-33338

Photographic recording of gravimeter in Frankfurt, Germany
20 p3262 N71-33339

Mizusawa geophysical station, Japan, for observing earth tides
20 p3245 N71-33341

Several methods for analyzing earth tides noting monthly variations of gravimetric data obtained in Kyoto, Japan
20 p3262 N71-33342

Tidal gravity variations in Asian region of USSR measured by gravimeters
20 p3263 N71-33347

Slow and tidal gravity variations of earth crust measured by gravimeters at Sayany tilt station
20 p3263 N71-33349

Gravimeter calibration for earth tide observation by using steel balls
20 p3264 N71-33365

Phase lag determination of earth tidal waves using Askania gravimeter
20 p3265 N71-33366

Dynamic characteristics of Askania gravimeters upon measurement of phase lags in tidal observations at varying times
20 p3265 N71-33367

Scale coefficient determination during earth tide variation recording by means of Askania gravimeters
20 p3265 N71-33368

Equipment and methods for marine measurement of gravitational forces
[JPRS-53851] 21 p3417 N71-34313

Laboratory and sea tests of gyrostabilized marine gravimeter for measuring disturbing accelerations and tilts in submarines
21 p3417 N71-34316

Optical-mechanical marine gravimeter with numerical pulse coding device
21 p3418 N71-34317

Automated sea observations with optical-mechanical marine gravimeter with automatic readout
21 p3418 N71-34318

Laboratory and sea condition tests of accuracy of double system marine gravimeter with automatic readout
21 p3418 N71-34319

Laboratory and sea tests of gyrostabilized platform for gravimeters and horizon and acceleration photoreorders
21 p3418 N71-34322

Analytical test of dynamic accuracy of gyrostabilized platform with pendulum correction for stabilizing gravimeters
21 p3418 N71-34323

Laboratory tests of stabilization errors resulting from perturbations in gyrostabilized platforms for gravimeters
21 p3418 N71-34323

Soviet news releases on gravimeter measurements and Sever-2 underwater apparatus
21 p3510 N71-35007

Gravimeter for recording 1961 to 1964 earth tides at Borowiec
24 p3910 N71-37865

Earth tide measurements by gravimeters and pendulums at ground station in Antarctic interior during winter
24 p3910 N71-37867

Hermetically sealed chambers for accurate earth tide registrations by pendulums and gravimeters
24 p3910 N71-37869

Earth tide observations using horizontal pendulums and gravimeter
24 p3911 N71-37875

Gravimetric tide variations recorded using experimental gravimeter
24 p3911 N71-37880

GRAVIMETRY
Soviet bloc research in astronomy, meteorology, oceanography, geophysics, upper atmosphere, and space exploration
[JPRS-51556] 02 p0308 N71-12152

Combination of satellite and gravity data for position and gravity field determinations
[AD-712348] 02 p0222 N71-12192

Earth gravity data used in determining gravitational potential vector, for satellite orbit calculation
[AD-712349] 02 p0222 N71-12193

Reductions for correcting gravity measurements for terrain in vicinity of station
[PUBL-63] 05 p0670 N71-14822

Catalog of gravimetric measurements obtained during nine Antarctic expeditions
[JPRS-52123] 05 p0676 N71-15437

Gravimetric research in USSR during 1946 to 1969
[JPRS-52102] 05 p0677 N71-15303

Gravimetric research in USSR from 1946 to 1969 for International Gravity Commission
[AD-714386] 05 p0680 N71-16380

Stochastic process error analysis of airborne gravimetry
[AD-715268] 07 p1021 N71-17771

Gravimetric surveys at sea using two highly damped pendulums
[JPRS-52414] 08 p1195 N71-19120

Geomagnetic field and storms, and gravimetry
11 p1751 N71-22846

Gravimetric and satellite tracking data reduction to determine dimensionless harmonic coefficients and gravity anomalies
[AD-715152] 13 p2069 N71-34091

Design and performance of pendulum apparatus for measuring relative gravity
13 p2084 N71-23511

Isostatic gravity map of Antilles Islands and Venezuelan Basin
18 p2912 N71-30906

Gravity field measurement by satellite to satellite Doppler tracking, critical configurations for fundamental range networks, and improvement of triangulation systems
[NASA-CR-119356] 18 p3017 N71-31358

Earth gravity field determinations with laser tracking of geodetic satellites
19 p3108 N71-31837

Mathematical analysis to determine relationship between two theories of satellite harmonics and gravimetry
[AD-724123] 20 p3254 N71-32817

Molodensky series and analytical continuation applied to gravimetric geodesy
[AD-724133] 20 p3259 N71-33181

Gravimetric tides in earth gravity field
20 p3266 N71-33387

Estimate of random errors in gravity measurements made aboard submarines using grapho-mechanical analyzer
21 p3417 N71-34315

Measurement and analysis of gravity anomalies in Sea of Japan
[JPRS-53962] 21 p3421 N71-34304

Development of gravimetric pool for US from satellite derived gravity data and local gravimetric measurements
[NASA-TM-X-65691] 23 p3477 N71-36717

Gravimetric determinations of oxygen-to-metal ratio of [U,Pu]O₂
[ORNL-TM-3362] 23 p3797 N71-37872

GRAVIRECEPTORS
NT OTOLITH ORGANS

GRAVITATION
NT ARTIFICIAL GRAVITY

NT GRAVITY ANOMALIES

NT LUNAR GRAVITATION

NT LUNAR GRAVITATIONAL EFFECTS

NT PLANETARY GRAVITATION

NT REDUCED GRAVITY

NT SOLAR GRAVITATION

Quantum gravity and ultraviolet impurities in quantum electrodynamics
[IC/70/58] 02 p0273 N71-11709

Covariant quantum geometrodynamics
02 p0274 N71-11857

Low gravity propellant control using capillary devices in large scale cryogenic vehicles
[NASA-CR-102879] 04 p0604 N71-14227

Representation of earth gravitational potential outside sphere bounding earth
[NASA-CR-115893] 05 p0668 N71-14778

Equation of gravity using potential theory
[AD-718653] 06 p0854 N71-16814

Geodetic parameters of earth gravity field and satellite tracking station positions in geocentric reference frame
[NASA-CR-116830] 08 p1193 N71-18974

Physiological effects of gravitational overloads of innervation of aorta, atria, and vena cava
[PB-1970167] 10 p1502 N71-21640

Soviet news releases on seismic stations and vertical derivatives of gravity potential
11 p1746 N71-22853

Relation of gravitation with astrophysics, and geophysics
[AD-718264] 12 p1910 N71-23582

Electromagnetic field and wave propagation in static gravitation
[AD-718145] 12 p1966 N71-23899

Role of gravitation in elementary particle theory, microscopic parameters and macroscopic values
[JNRP-P2-5289] 14 p2510 N71-26668

Phenomenological relationship between fine structure constant and leptonic and gravitational processes - universal scaling factor
[UCRL-72955] 16 p2646 N71-28211

Approximative reduction of gravity formulae describing earth shape to Taylor series
[AD-723515] 19 p3091 N71-31927

Comparison of quantum electrodynamics and classical mechanics for gravitational effects on Mercury orbit
[RIFP-124] 20 p2369 N71-33882

Equipment and methods for marine measurement of gravitational forces
[JPRS-53851] 21 p3417 N71-34313

SUBJECT INDEX

Explicit and recursive formulas for acceleration and gravity gradient derived from spherical harmonics [NASA-CR-121909] 22 p3572 N71-35442
 Relation of orbit stability of remote artificial planetary satellites to radius of Hill gravitational sphere 22 p3676 N71-36207
 NASTRAN program used to calculate gravity load distortions in 64-m antenna reflectors 22 p3683 N71-36282
 NASTRAN-GAP programs for analyzing antenna induction potentials of reflectors distorted by gravity and thermal loads 22 p3683 N71-36283

GRAVITATION THEORY

Flow from steady rotation of gravitating sphere in isentropic gas at rest, and drag of body moving transversely through confined stratified fluid 07 p1011 N71-17689
 Light speed in gravitational field according to Newtonian Einsteinian gravitation theories [NASA-TT-F-13581] 08 p1192 N71-18949
 Development of Machian theory of inertia and gravitation 12 p1912 N71-23696
 ESRO program for solar orbit satellite testing gravitation theory [ESRO-SM-78] 18 p3019 N71-31300
 Technique for treatment of nonsymmetrical Lagrangian in gravity modified quantum electrodynamics [JCT/1131] 22 p3437 N71-35928
 Graviton fermion interaction described by Lagrangian in function of tetrad field and fermion field 23 p3823 N71-37268
 Derivation of cosmologic model for verification of gravitation theory 23 p3849 N71-37434

GRAVITATIONAL COLLAPSE

Random distribution of radial motions in central gravitational field, Newtonian mechanics, and comet orbits about sun [NASA-TM-X-65414] 06 p0902 N71-13864

GRAVITATIONAL CONSTANT

Geodetic astronomical and geodynamic parameters including fundamental astronomical constants, gravitational harmonic coefficients, station locations, and other geometric quantities [NASA-TM-X-65407] 18 p3008 N71-30513
 Newman-Penrose constants and their invariant transformations 21 p3449 N71-34552
 Detecting variations of gravitational constant difference between inertial and passive gravitational mass [NASA-CR-115139] 22 p3573 N71-35444

GRAVITATIONAL EFFECTS

ON LUNAR GRAVITATIONAL EFFECTS

Physiologic response to short duration positive G and microgravity accelerations 01 p0913 N71-10692
 Low gravity effects on crystal whisker growth in orbital workshop 02 p0284 N71-11727
 Low gravity effects on liquid phase sintering in space manufacture 02 p0235 N71-11729
 Low gravity effects on catalytic polymerization of ethylene with transition metal complexes 02 p0177 N71-11730
 Gravity effects on travel time and energy for evacuation tubes in high speed ground transportation systems [PD-190396] 07 p1134 N71-18026
 Hydraulic grip dynamometer for study of elevated postural effects on flight crews [N71-5911] 08 p1157 N71-18415
 Microsensors to measure oxygen consumption of sprouting potato plants, and gravitational effects on hypobryon-hypobryon system of fish [NASA-CR-117179] 09 p1341 N71-20006
 Acceleration and gravity effects on function and behavior of lungs [HARDOGRAPH-133] 11 p1679 N71-21981
 Binary gravitational flow mathematical model not turbulent mixing 12 p1910 N71-23606
 Interacting effect of gravity and size on peak and minimum pool boiling heat fluxes [NASA-CR-118638] 14 p2353 N71-25963
 Gravitational stresses in elastic half-space bodies with notches or rounds 16 p2585 N71-28209
 Acceleration effects on vestibular stimulation of external respiratory function and respiration center nervous activity 16 p2544 N71-28261
 Gravity environment simulation by locomotion and rotation for studying manual operation performance of astronauts at zero gravity [NASA-CASE-ARC-101531] 16 p2554 N71-28619
 Gravitational effects on neutron optical properties of dipole magnet [JHEP-75-5537] 18 p2962 N71-30668
 Instability theory of galactic formation and expanding universes with black body radiation 20 p3344 N71-32847

Medical and biological problems of prolonged manned space flight [JPRS-53801] 20 p3228 N71-33451

Concomitant capabilities of vestibules, hypothalamus, and central nervous system toward gravitational effects on cats during orthostasis 20 p3321 N71-33458
 Motion of test body inside system of oscillating masses in laboratory conditions [JINR-P13-5645] 21 p3472 N71-34719
 Convective instability in fluid layer with electromagnetic effects applied to earth and stellar atmospheres 22 p3672 N71-36183
 Origin of galactic clusters due to explosion or gravitational contraction 23 p3849 N71-37433

GRAVITATIONAL FIELDS

Effect of force field induced birefringence on dual polarized ring laser systems [NASA-CR-111142] 01 p0604 N71-10726
 Perception and identification of images in different accelerable fields 02 p0164 N71-11824
 Effect of time-dependent gravitational fields on superconductors and metals [ESRIN-IN-108] 02 p0285 N71-11846
 Analysis of tracking data for resonant geopotential effects obtained from 24 hour satellites [NASA-TM-X-65382] 02 p0214 N71-11939
 Gravitational waves in galaxies from cosmological point of view 02 p0296 N71-11952
 Combination of satellite and gravity data for position and gravity field determinations [AD-712348] 02 p0222 N71-12192
 Earth gravity data used in determining gravitational potential vector, for satellite orbit calculation [AD-712349] 02 p0222 N71-12193
 Difference indicating circuit used in conjunction with device measuring gravitational fields [NASA-CASE-XNP-08274] 04 p0512 N71-13537
 Motion of liquids enclosed in aerospace vehicle tanks under weak gravitational fields - Vol. 1 [NASA-CR-115117] 04 p0604 N71-14225
 Digital analysis of liquid sloshing in rotational symmetric tanks under weak gravitational fields - Vol. 2 [NASA-CR-111739] 04 p0604 N71-14226
 Representation of earth gravitational potential outside sphere bounding earth [NASA-CR-115893] 05 p0648 N71-14770
 Measuring simulated effects of gravity field truncation on computed satellite orbits [AD-713918] 06 p0946 N71-16325
 Gravimetric research in USSR from 1966 to 1969 for International Gravity Commission [AD-714386] 06 p0850 N71-16380
 Fitting mass distribution to gravitational potential, for simulating lunar potential [NASA-CR-116505] 07 p1051 N71-17428
 Space coordinate system and clock rates specified operationally to separate coordinate and physical effects in arbitrary gravitational field 07 p1021 N71-17762
 Gravitational interactions, general relativity, pulsars, and cosmology 07 p1115 N71-17920
 Numerical integration of intermediate thrust arcs for rocket trajectory optimization in Newtonian gravitational field [ONERA-TP-849] 08 p1232 N71-18564
 Deriving surface equation for fluid subjected to gravitational and magnetic fields using variational principle of minimum free energy [NASA-TT-F-13462] 08 p1179 N71-18576
 Least squares integral criterion for representation of gravitational potential with fixed mass points [NASA-CR-116006] 08 p1189 N71-18650
 Light speed in gravitational field according to Newton and Einstein gravitation theories [NASA-TT-F-13501] 08 p1192 N71-18969
 Solution to linearized gravitational field equations representing self scattering of gravitational waves 08 p1192 N71-18972
 Scale transformations of second kind and Weyl space-time [TUEP-70-32] 09 p1410 N71-20073
 Satellite to satellite Doppler tracking with high resolution of gravity field [NASA-CR-117404] 10 p1548 N71-21019
 Fourth-order gravitational potential based on quantum field theory [RIFP-114] 10 p1549 N71-21097
 News releases, and abstracts of scientific articles concerning astronomy 11 p1824 N71-21952
 Development of least squares process for estimating spherical harmonic coefficients in Mars gravitational potential function based on Viking orbiter spacecraft data [NASA-TN-D-6219] 11 p1828 N71-22621
 Exact solution to magnetohydrodynamic equations for magnetocoustic waves under gravity and comparison with observed fine structure of waves propagating away from solar flares [AD-720244] 15 p2516 N71-27824

GRAVITATIONAL WAVES

Tesseral harmonics of Explorer 34 satellite orbit perturbation in time of perigee passage due to third harmonic of earth gravitational field [NASA-TM-X-65361] 15 p2318 N71-27872
 Lunar Orbiter tracking data analyzed to yield third-order degree and order spherical harmonic approximation to lunar gravitational potential function [NASA-TM-X-2260] 16 p2678 N71-28121
 Comparison of coefficient modification, chain rule, and function methods for computing gravitational potential derivatives with chain rule subroutines for CDC 6600 computer [COM-71-0815] 16 p2589 N71-28764
 Control of solar probe trajectory by use of Venus gravitational field [NASA-TT-F-13408] 16 p2680 N71-28827
 Particle superpropagator regularizing properties under various gravitational field interactions [JINR-PZ-5569] 17 p2795 N71-29712
 Numerical analysis of gravitational field of small particles falling in Schwarzschild geometry 17 p2844 N71-29761
 Geomagnetic, bathymetric, and gravitational field data from Indian Ocean 1944 survey 15 p2919 N71-31432
 Gravimetric and geometric investigations with GEOS 1 and GEOS 2 - GEOS 2 conference [NASA-TM-X-67771] 19 p3085 N71-31826
 Estimation of geodetic parameters describing earth gravity field and positions of satellite tracking stations in geocentric reference [SAO-009-49] 19 p3086 N71-31828
 Tests and comparisons of gravity models using camera observations of GEOS 1 and GEOS 2 19 p3086 N71-31829
 Comparison of Smithsonian Astrophysical Observatory 1949 gravity field representation with surface gravity 19 p3086 N71-31830
 Derivation and tests of Goddard combined geopotential field (GOSPC 1.70-C) [X-522-70-104] 19 p3086 N71-31831
 Reduction of errors in computed satellite orbits due to uncertainties in gravity coefficients 19 p3087 N71-31832
 Geodetic satellite data for determining earth gravitational model and tracking station location 19 p3090 N71-31871
 Method for calculating vertical derivatives of earth acceleration [AD-724498] 20 p3239 N71-33200
 Long term tidal effects in satellite gravity data 20 p3263 N71-33371
 Gravimetric tides in earth gravity field 20 p3266 N71-33387
 Topographic mapping of gravitational field data [REPT-179] 20 p3269 N71-33851
 Recurrence relation for general normalized inclination functions with three parameters and axisymmetric fields for earth satellite orbits [RAE-TR-70774] 21 p3449 N71-34548
 Electronic modules used to simulate lunar gravity potential recovery based on spherical harmonics gravity model [NASA-CR-115175] 22 p3564 N71-35308
 Mapping Canadian gravitational fields 22 p3580 N71-35305
 Simplification of canonical form of general relativity theory for advancement of quantum theory of gravitational fields 22 p3606 N71-35406

GRAVITATIONAL POTENTIAL

U GRAVITATIONAL FIELDS

GRAVITATIONAL RADIATION

U GRAVITATIONAL FIELDS

GRAVITATIONAL WAVES

Turbulence and gravitational waves in upper atmosphere [AD-713045] 03 p0374 N71-13378
 Ionospheric disturbances caused by internal gravity wave propagation in ionosphere [NASA-TT-F-13483] 09 p1386 N71-20544
 Classical cross sections of electromagnetic and gravitational waves scattered by static gravitational field, and agreement with quantized linearized field theory [NYO-2262-TA-222] 11 p1886 N71-22462
 Low altitude explosive generation of ionospheric disturbances by acoustic gravity waves 11 p1710 N71-22934
 Earth gravity tides - conference 20 p3261 N71-33333
 Clinometrical tide observation in Algerian Sahara 20 p3261 N71-33334
 Gravitational measurements of ocean tides along transcontinental profile of United States 20 p3262 N71-33343
 Tidal gravity variations observed at Eastern Fergana, USSR 20 p3262 N71-33344
 Tidal gravity variations in Asian region of USSR measured by gravimeters 20 p3263 N71-33347
 Tidal gravity variations of earth crust observed in USSR 20 p3263 N71-33348

- Slow and tidal gravity variations of earth crust measured by gravimeters at Sayani tilt station
20 p3263 N71-33349
- Temperature effect on tidal gravity of earth crust
20 p3263 N71-33350
- Numerical analysis showing Atlantic Ocean influence on tidal gravity variations observed at Moulis clinometric station, France
20 p3263 N71-33351
- M sub 3 wave derivation from tidal gravity variations compared with various models
20 p3264 N71-33356
- Tidal gravity variations derived from extensometric observations in Kamikakura, Japan
20 p3264 N71-33357
- Magma reservoir evidenced from tidal gravity variations observed at Halemaumau lava lake, Kilauea, Hawaii
20 p3264 N71-33359
- Tide prediction method based on time-variable spherical harmonics of gravitational waves
20 p3264 N71-33361
- Accuracy of earth tidal observations using tiltmeters and automatic calibration
20 p3264 N71-33364
- Gravitational wave effect on electromagnetic wave transmission in physical optics approximation
23 p3803 N71-37115
- Gravimetric instruments for recording deformation of earth crust and earth surface caused by earth tides
24 p3909 N71-37864
- Gravimeter for recording 1961 to 1964 earth tides at Borowiec
24 p3910 N71-37865
- Earth tide measurements by gravimeters and pendulums at ground station in Antarctic interior during winter
24 p3910 N71-37867
- Geophysical classification of earth crust tides as affected by temperature and atmospheric pressure
24 p3910 N71-37868
- High precision thermostat for gravimetric recording of earth tide amplitudes
24 p3910 N71-37870
- Earth tide observations and measuring instruments
24 p3910 N71-37871
- Earth tilt observations at two stations south of Moscow
24 p3910 N71-37872
- Earth tide observations using horizontal pendulums and gravimeter
24 p3911 N71-37875
- Oceanic tidal influence on earth tides and clinometric corrections
24 p3911 N71-37878
- Gravitational tide variations recorded using experimental gravimeter
24 p3911 N71-37880
- GRAVITONS**
- Graviton emission process
[NASA-TT-F-13448] 06 p0922 N71-16607
- Graviton fermion interaction described by Lagrangian function of tetrad field and fermion field
23 p3823 N71-37268
- GRAVITY**
- U GRAVITATION**
- GRAVITY ANOMALIES**
- Geodetic gravimetry approach for determining earth geopotential on geoid
[AD-711265] 01 p0051 N71-10901
- Covariance matrix for deflections of vertical and undulations based on actual gravity data
[AD-712351] 02 p0222 N71-12168
- Abstracts of articles on terrestrial geophysics, seismology and gravity anomalies
03 p0368 N71-13042
- Gravimetric research in USSR from 1966 to 1969 for International Gravity Commission
[AD-714386] 06 p0850 N71-16380
- Mean gravity anomalies derived from generalized Fourier analysis of satellite orbits
[BMBW-FB-W-70-53] 07 p1017 N71-17137
- Atlantic Ocean gravity anomaly map
07 p1017 N71-17138
- Topographic-isostatic gravity corrections for New Zealand
[BULL-203] 09 p1376 N71-19406
- Effect of South Atlantic magnetic anomaly on SEKT 2 spacecraft orbital acceleration measurements
[NASA-TM-X-2232] 09 p1468 N71-20324
- Gravimetric and satellite tracking data reduction to determine dimensionless harmonic coefficients and gravity anomalies
13 p2069 N71-24392
- Portable rotating gravimeter for measuring gravity gradients under dynamic conditions tested for noise free operation
[AD-721742] 16 p2588 N71-28451
- Mathematical analysis to determine relationship between two theories of satellite harmonics and gravimetry
[AD-724123] 20 p3254 N71-32817
- Equations for determining depth of center of gravity and surplus mass of disturbing bodies from gravity anomalies
[AD-724499] 20 p3260 N71-33235
- Measurement and analysis of gravity anomalies in Sea of Japan
[JPRS-53962] 21 p3421 N71-34344
- Gravimeter designs for surveillance and measurement of gravity gradients from stationary or moving base
[AD-727033] 22 p3579 N71-35495
- Feasibility of obtaining gravity anomalies directly from analyzing artificial earth satellite orbits
23 p3753 N71-36763
- GRAVITY GRADIENT SATELLITES**
- NT APPLICATIONS TECHNOLOGY SATELLITES**
- NT ATS 1
NT ATS 2
NT ATS 3
NT ATS 5
NT ATS 6
NT ATS 7
- Elastic stability and equilibrium configuration of earth pointing gravity gradient satellites with long appendages
[CRC-1206] 01 p0127 N71-10036
- Spin axis scanning of celestial sphere for attitude control of spin stabilized spacecraft
[NASA-TN-D-5611] 06 p0948 N71-16860
- Stabilization system for gravity-oriented satellites using single damper rod
[NASA-CASE-XAC-01591] 07 p1120 N71-17729
- Gravity gradient stabilization and performance of DODGE satellite
[AD-716772] 10 p1648 N71-20928
- Method of stationkeeping for lensular gravity gradient satellites
[NASA-CASE-XLA-63132] 11 p1832 N71-22969
- Semipassive gravity-stabilized satellite with yaw oscillations affected by boom torsional rigidity and thermally induced torsion
[NASA-TN-D-6481] 19 p3185 N71-32790
- Analysis of dynamic deflections of long flexible antenna booms on gravity gradient stabilized earth satellite by normal mode
20 p3355 N71-33892
- Design criteria for passive gravity-gradient libration dampers
[NASA-SP-0071] 21 p3455 N71-34590
- GRAVITY GRADIOMETERS**
- Gravity gradient attitude control system with gravity gradiometer and reaction wheels for artificial satellite attitude control
[NASA-CASE-GSC-10555-1] 15 p2441 N71-27324
- Equations of motion for rotating gravity gradiometer developed for forced harmonic oscillator model
[NASA-TM-X-64605] 21 p3425 N71-34372
- Gravimeter designs for surveillance and measurement of gravity gradients from stationary or moving base
[AD-727033] 22 p3579 N71-35495
- GRAVITY WAVES**
- F region internal gravity waves properties
01 p0046 N71-10229
- Internal gravity wave effects on mesospheric temperature variations affecting reentry studies and impact prediction capability
[AD-711640] 01 p0081 N71-10950
- Gravitational waves in galaxies from cosmological point of view
02 p0296 N71-11952
- Gravity wave parameter estimated from F 2 ionospheric electron density disturbance observations
[KGO-702] 03 p0371 N71-13230
- Parameter estimation of gravity waves responsible for ionospheric electron density disturbances by comparison of observations with atmospheric model calculations
[KGO-703] 03 p0375 N71-13392
- Atmospheric model computation of F region ionospheric ionospheric disturbances due to internal gravity wave propagation
[KGO-701] 03 p0375 N71-13393
- Resonant waves and third order deep water gravity wave interactions
[AD-714493] 06 p0850 N71-16376
- Lower atmosphere gravity wave propagation in stratified atmospheric models for pressure and wind variations
07 p1053 N71-17165
- Gravity wave interaction with transiently heated atmosphere
[AD-715900] 08 p1188 N71-18553
- Detection of atmospheric nuclear explosions by study of extremely low frequency waves and ionospheric disturbances
[AD-716601] 09 p1383 N71-19683
- Sound-gravity wave natural modes in solar atmosphere models
10 p1643 N71-20911
- Acoustic-gravity wave propagation in ionosphere of 1962 US Standard Atmosphere and effects on HF radio propagation
10 p1521 N71-21276
- Study of interaction of deep water gravity waves progressing into turbulent flow field produced by finite width grid towed in wide tank
[AD-717627] 11 p1735 N71-22139
- Propagation of internal gravity waves over slope in fluid with constant Brunt-Väisälä frequency
[AD-717367] 11 p1748 N71-22115
- Comparison of long period microseisms and flexural gravity waves measured at Mirny in Antarctica
11 p1753 N71-22811
- Computerized simulation of atmospheric reflecting surface effects on radio wave transmission in ionosphere
[AD-718106] 12 p1874 N71-23446
- Influence of gravity waves on transient heating response of upper atmosphere
[AD-718961] 13 p2069 N71-24425
- Atmospheric model with damped gravity waves from vertical atmospheric sounding analysis
13 p2076 N71-25264
- Ionospheric electron density variation calculation during gravity wave passage in traveling F region including wave parameters
[AD-719673] 14 p2245 N71-25428
- Spatial coherence of 1 to 5 min acoustic waves from two nuclear explosions along with atmospheric pressure background noise for same period measured at low altitude
[AD-720853] 15 p2999 N71-27214
- Gravity wave behavior near straight caustic in deep water tank and in shallow water
16 p2639 N71-28746
- Interpretation of vertical wave patterns in winter ionosphere at high latitudes in terms of gravity wave theory
[NASA-TM-X-65605] 17 p2745 N71-30007
- Acoustic-gravity waves, coupling between gravity waves and sea surface, and infrasound from artificial and natural sources
[AD-724179] 20 p3261 N71-33351
- Hydrodynamics of boiling heat flux and dynamics and stability of small gravity and capillary waves
[NASA-CR-121467] 20 p3366 N71-33746
- Method for estimating gravity wave density variation from wind speed profiles between 60 km and 100 km
[NASA-CR-61359] 22 p3572 N71-35436
- Review of worldwide gravity tide data showing scatter in observations caused by ocean loading
23 p3753 N71-36764
- Vertical momentum transport over mountainous terrain based on Apollo 9 cloud photographs, gravity waves, and wind data for southwestern US
[NASA-CR-121467] 23 p3784 N71-36979
- Incident shallow-water wave interactions with submerged shoals and analysis of induced multiple gravity waves
23 p3787 N71-36999
- Gravity wave propagation in presence of temperature gradients, wind shear, and magnetic fields
23 p3803 N71-37116
- Total ionospheric electron content measurements with ATS 3 signal Faraday effect, noting gravity wave effects
24 p3915 N71-37913
- Experimental determination of coefficients from generated by gravity waves interacting with rigid horizontal circular cylinder near simulated ocean bottom
[AD-727691] 24 p4025 N71-38721
- GRAY GAS**
- Zoning techniques applied to gray gas and black body radiation transport models including view effects and nonisothermal emission
20 p3365 N71-33636
- GREASES**
- Viscosity and chemical composition of dispersion medium affecting aromatic hydrocarbons in lithium greases
[AD-711177] 01 p0072 N71-10640
- Thermal stability of lithium grease oxidation
[AD-711476] 02 p0248 N71-11735
- Improvement in properties of lubricating greases by addition of diaryl and triaryl dihydrophosphates
[AD-718484] 12 p1944 N71-23766
- Closure technique for retention of grease in high bearings on F-4C aircraft wheels
[AD-723679] 19 p3104 N71-31744
- Analysis of physical and chemical properties of lubricants used with roller bearings at low temperatures
22 p3580 N71-35335
- GREAT BRITAIN**
- Reporting activities of Natural Environment Research Council of Great Britain
02 p0220 N71-13889
- Aviation medicine training in Royal Air Force
04 p0477 N71-13889
- Functions of aeromedical training section of Royal Air Force
04 p0477 N71-13889
- Requirements of English medical schools for diploma in aviation medicine
04 p0478 N71-13887
- Training of flight surgeons for civil aviation in Great Britain
04 p0478 N71-13888

SUBJECT INDEX

Analysis of ALGOL computerized simulation statistics at NPL, Great Britain [NPL-CCU-11] 07 p0996 N71-17071

Reporting financing, accounts, and progress in research and development for atomic energy program in Great Britain [NPL-10112] 07 p0653 N71-17365

Water interchange between North Atlantic Ocean and Norwegian Sea between Scotland and Iceland [AG-373-28] 12 p1913 N71-23752

Airfield climatology for European Low Countries and British Isles [AD-715908] 14 p2208 N71-25879

Data processing facilities for Black Knight rocket measurements in Great Britain [POA-3-C-3616-68] 14 p2237 N71-26258

Atomic hydrogen masers in Great Britain [NPL-OU-17] 15 p2418 N71-26997

United Kingdom Atomic Energy Authority report for year ending 31 March 1970 [NPL-18528] 15 p2526 N71-27295

Analysis of Sr-90, Cs-137, and fission products in atmospheric dust and rainfall in Great Britain up to mid 1970 [AERE-B-6556] 15 p2495 N71-27966

Economic appraisal of British aerospace industry and plans for future development [A-3029 N71-30940

Design for future X4 British Applications Technology Satellite 20 p3351 N71-33012

Tables of Cosmo and other artificial satellites optically tracked from Great Britain observatories in Dec. 1970 [ROE-STS-109] 20 p3354 N71-33159

Hourly, diurnal, and annual data on geomagnetic activity and intensity, Hartsdand, England - 1962, 1963, and 1964 23 p3753 N71-36760

Anglo-Australian 150-inch reflecting telescope for Southern Hemisphere 24 p3921 N71-37961

GREAT POLAR CAPS
U POLAR CAPS
GREECE
Ionospheric absorption measurement, sunspot observations, and short wave fadeout reported from optical tracking stations in Greece (Athens) - tables 11 p1823 N71-22502

GREEN FUNCTION
Green function and expansion coefficients for cavity excitation through small apertures [DC-CR-70-6099] 01 p0090 N71-10595

Computation of Green function for bodies of revolution [AD-711099] 01 p0091 N71-10861

Finding system of self-consistent equations for radial distribution function and excitation spectrum of many-body system using method of retarded Green function techniques [JNP-785] 04 p0576 N71-13690

Many body problem of elastic scattering of electrons from atoms and molecules using Green function techniques 04 p0583 N71-14150

Investigating scattering of radar or sonar waves from ocean surface or bottom using Green theorem and Kirchhoff principle 07 p0991 N71-16941

Iterative expansion technique for solving Green function in model quantum field theory 08 p1265 N71-19182

Applying Green function theory to calculation of longitudinal and transverse dielectric functions in magnetized, isotropic, equilibrium plasma 08 p1275 N71-19249

Development of one-electron pseudo-Green function and pseudopotential of d-band metals [ML-1930] 09 p1454 N71-20499

Green function used for thermodynamic model of Heisenberg ferromagnet in random phase approximation [MASA-TM-X-52982] 09 p1486 N71-20534

Treating large scale inhomogeneous disturbances with inhomogeneous linear integral equation and Green function [AD-717204] 10 p1547 N71-20793

Minimum convolutions and Green function in dynamic programming theory [DID-25612] 10 p1594 N71-21662

Theoretical studies in nuclear reactions and structure including spin-orbit splitting in nuclei, shell model reaction theory, and Green relativistic approach to nuclear matter [NSO-3765-28] 11 p1804 N71-22339

Order by order procedure for generating perturbation theory for sigma model propagators and Green function method applied to two loop approximations [NYO-2262-TA-219] 12 p1975 N71-23997

Development of statistical model for electrons in atoms based on expansion of one-electron Green function in spherical harmonics [AD-719799] 13 p2146 N71-24958

Lorentz transformation properties of Bethe-Salpeter Green function [TR-71-101] 13 p2103 N71-24963

Functional integral form of Green function for dual resonance model of hadronic interactions [TUEP-71-5] 13 p2104 N71-25429

Green function in solving linear and nonlinear second order ordinary differential equations including examples in finding resonances and periodic orbits of restricted three body system 16 p2621 N71-28103

Green function and Fourier integrals in dynamic elastic field theory of crystal dislocations and disclinations 17 p2823 N71-29901

Evans-type P-harmonic functions on Riemann surface [AD-722810] 17 p2775 N71-30352

Analysis of scalar particle scattering amplitude based on Bethe-Salpeter equation for two particle Green function [JINR-E2-5640] 18 p2981 N71-30824

Application of Green function to two dimensional Laplace equation for calculation of temperature distribution in cooled blade of gas turbine [NAL-TR-234] 18 p2944 N71-30893

Retarded part of two-time Green function and two-body relativistic problem 21 p3472 N71-34720

Calculation of thermodynamic properties of two isotropic anisotropic Heisenberg antiferromagnet using Green method [NASA-TN-D-64999] 21 p3497 N71-34914

Application of Green function to elastic displacement caused by unit force in infinitely extended anisotropic media [COO-2034-5] 21 p3529 N71-35144

Semi-direct modal synthesis method using Green function modes and applications to space time dynamics of nuclear reactor systems 22 p3626 N71-35840

Three-dimensional Green function solution for field emission from spherical tip with arbitrary perturbative potentials 22 p3651 N71-36033

Relativistic scattering amplitude equations for transitions in three-body interactions based on Green functions, Faddeev equations, and three-particle bound state wave functions [JINR-E2-5771] 23 p3807 N71-37145

GREEN THEOREM
U GREEN FUNCTION
GREENLAND
Tables for high and low tide predictions for east coast of North and South America and Greenland 01 p0090 N71-10791

Magnetic variations and auroral zones over Greenland in night and daytime 04 p0521 N71-13779

Data tables of magnetic variations, Thule, Greenland, 1962 04 p0521 N71-13786

Data tables of magnetic variations, Godhavn, Greenland, 1964 04 p0522 N71-13788

Alouette 1 satellite electron density data and diurnal variation of Greenland auroras 04 p0615 N71-14298

Ice thickness observations along coasts of eastern Canada and southern Greenland [AD-715424] 06 p1188 N71-18503

Aerial reconnaissance and radar scanning of ice flows in Greenland waters - 1963 [ISBH-67-7478-005-0] 11 p1750 N71-22518

Climatological data summary for Greenland during 1958 12 p1956 N71-23857

Phenological survey in Greenland to determine correlation between life cycles of plants and prevailing meteorological and climatic factors [AD-719720] 13 p2105 N71-24439

Periodic variations in sea water temperature, salinity, chemical properties, and plankton content in Baffin Bay from July to Sept. 1964 [PB-198355] 19 p3095 N71-32444

Ground based geomagnetic measurements in Greenland during 1965 summer [R-15] 22 p3378 N71-35486

GREENADES
Anomalous upper atmospheric parameters derived from two zero-high rocket firings [WIRE-TN-HSA-175] 03 p0718 N71-15156

Rocket launching of explosive grenades to measure winds and temperatures at 28 to 150 kilometers [FOA-4-C-4414-20] 22 p3614 N71-35744

GRIDS
Design of axial flux heaters and grid spacer effects on reactor cooling flow [GEAF-10196] 05 p0726 N71-15047

Impedance and radiation properties of mesh antennas immersed in warm isotropic plasma 12 p1890 N71-23664

GROUND EFFECT

Preliminary investigation to eliminate or reduce concentrated charge exchange ion erosion of accelerator grid supports for electron bombardment ion thrusters [NASA-TM-X-67843] 14 p2331 N71-23684

Design of cathode grid spectrometer for measurement in 13-15 micron range 15 p2411 N71-27552

Numerical study of grid collisions considering toroidal and non-toroidal effects [PB-197512] 17 p2852 N71-29768

Analysis of ion beam thrust deflection system using grid translation techniques [NASA-TM-X-67911] 20 p3339 N71-33552

Beam focusing characteristics of variously shaped grid holes with application to electron bombardment ion thrusters [NASA-TM-X-67922] 22 p3662 N71-34115

Structural analysis of gridwork models for cases of edge loads and distributed moment loads based on Cosserat continuum 23 p3883 N71-37542

Automatic reading of handwritten Hebrew using horizontal marking grids 24 p3894 N71-37750

Energy decay and spectra measurements of grid-injection turbulent flows [NASA-CR-123191] 24 p3985 N71-37830

Optimization of finite element grids based on minimum potential energy [AD-727953] 24 p4026 N71-38734

GRIFFITH CRACK
Stress intensity factor of Griffith crack opened by thin symmetric wedge 01 p0127 N71-10874

Partial closure effect on thin plate stress intensity of Griffith crack opened by parabolic pressure distribution [AD-717184] 10 p1657 N71-21381

GRINDING (COMMUNION)
Experimental design and performance of ionization - ionic pulverization device [ONERA-TR-62-22] 13 p0079 N71-24605

GRINDING (MATERIAL REMOVAL)
Techniques for fabrication and testing of large optics [NASA-CR-102925] 03 p0380 N71-13120

Assessment of surface and subsurface damage in ceramics caused by semi-finish grinding machines [AD-714991] 06 p0679 N71-16395

Laser device for removing material from rotating object for dynamic balancing [NASA-CASE-MF8-11279] 09 p1387 N71-20400

Grinding machine efficiency increases due to higher forward feed speeds noting surface roughness and wear effects [CRIF-MC-34] 10 p1563 N71-20731

Mobility of powders from grinding operations, and effects of surfactants and powder size [NLL-KTS-6267] 16 p2419 N71-29012

GRINDING MACHINES
Ultrasonic hardness testing of grinding wheels using method of elasticity [CRIF-MC-36] 08 p1207 N71-18405

Particle size control by jet grinding in fluidized bed denitrators [IN-1439] 09 p1378 N71-20597

GROOVES
Rate of wheel spin-up, and tire degradation at aircraft touchdowns with different runway grooves [FAA-RD-71-2] 09 p1323 N71-20069

Spiral groove face seal development for SHAP [NASA-CR-72833] 09 p1394 N71-20336

Nonresonant energy absorbing device comprising ring member with plurality of recesses, cutting members, and guide member mounted in each recess [NASA-CASE-XMF-10040] 11 p1772 N71-22877

Hydrodynamic lubrication of journal bearing with one or two axial oil grooves, with power loss, load capacity, oil flow, and stability charts for design of minimum power loss, stable bearing 25 p2580 N71-33799

GROOVING
Chevron cutting and effects of braking on wear of aircraft tires 18 p2869 N71-30768

Grooved and ungrooved runway surface effects on aircraft tire spin-up characteristics and tread damage [NASA-TM-X-5245] 19 p3039 N71-32796

GROUND BASED CONTROL
NT AIR TRAFFIC CONTROL
Control center with integrated computer for real time processing and display of information from SERT 2 spacecraft [NASA-TM-X-2217] 09 p1365 N71-19855

Chronology of actions taken by ground control facilities following Apollo 13 flight emergency [NASA-TM-X-66953] 09 p1466 N71-19960

GROUND EFFECT
Recirculation region of flow field caused by jet in ground effect with crossflow [AD-711665] 01 p0802 N71-10832

Low speed wind tunnel tests of ground proximity effects on static longitudinal characteristics and boundary layer control of short takeoff aircraft [NAL-TR-201] 09 p1317 N71-20106

GROUND EFFECT MACHINES

Wind tunnel investigation of helicopter directional control in rearward flight in ground effect
[NASA-TN-D-6118] 09 p1366 N71-20191

Theory and operation of air cushion vehicles and other application of ground effect in industrial transportation
[AD-721254] 15 p2367 N71-27196

Simulation of ground effect in hydrodynamic tunnel analyzed by visualizations
[NASA-TT-F-13799] 20 p3251 N71-35494

Wall interference for static stability tests in closed rectangular test sections and in ground effect
[NASA-TR-B-364] 22 p3564 N71-35386

GROUND EFFECT MACHINES

NT CUSHIONCRAFT GROUND EFFECT MACHINE

Investigating high speed ground transportation systems based on tracked air cushion vehicles
[PB-190939] 02 p0146 N71-11033

Hovering type flying vehicle design and principle mechanisms for manned or unmanned use
[NASA-CASE-MSC-12111-1] 02 p0147 N71-11039

Air cushion landing systems for space shuttle vehicles
[NASA-CR-111803] 03 p0457 N71-13097

Platform with several ground effect pads and plenum chambers
[NASA-CASE-MPS-14685] 05 p0774 N71-15689

Examining tracked air cushion vehicles as advanced ground transportation system
[PB-195030] 07 p0968 N71-16904

Sea state, wind velocity and wind direction regression analysis for ground effect machines
[NPL-HOVERCRAFT-16] 07 p0970 N71-17144

Vertical motion of static loads over baffles during loading operations using ground effect machines
[NPL-HOVERCRAFT-TM-31] 07 p0970 N71-17160

Wave resistance of air cushion vehicle traveling over water of uniform finite or infinite depth in steady or unsteady motion
[AD-716055] 09 p1320 N71-19731

Mathematical model for suspension system of actively controlled air cushion vehicle
[PB-196465] 10 p1494 N71-21676

Stability, foam flow, and wave effects on hovercraft during power failure
[AD-717676] 11 p1690 N71-22448

Numerical analysis of dynamic and thermodynamic state of plenum-type air-cushion vehicle to determine heave response and control system operating characteristics
[NASA-TN-D-6257] 11 p1739 N71-22589

Wind tunnel study of augmented ram-wing vehicle with various blowing arrangements
[PB-189435] 12 p1850 N71-23283

Potential feasibility of safe, practical, and economical air breathing nuclear propulsion system for aircraft and air cushion vehicles
[NASA-TM-X-57837] 13 p2123 N71-25524

Characteristics and cost analysis of nuclear powered air cushion vehicles for oceanic commercial operations
[NASA-TM-X-2293] 14 p2293 N71-25783

Theory and operation of air cushion vehicles and other application of ground effect in industrial transportation
[AD-721254] 15 p2367 N71-27196

Use of aerodynamic lift for application to high speed ground transportation by two dimensional air foils
[PB-197242] 17 p2700 N71-29762

Augmented ram wing vehicle performance and flow field for high speed ground transportation
18 p2867 N71-31204

Model of peripheral air jets in air cushion vehicles hovering over water surface
[NT-27-1971] 19 p3075 N71-31688

Cost comparison of ground effect machines using box, inverted-tee, and channel cross section tracks
[PB-197501] 19 p3036 N71-31782

Performance characteristics of air cushioned landing and takeoff system during aircraft lift-off operation mode
[AD-726606] 22 p3541 N71-33223

One dimensional channel flow theory for designing ram wing surface effect vehicle
[AD-727774] 23 p3706 N71-36419

Design and feasibility analysis of transoceanic, nuclear powered air cushion freighter for 1980 decade
[NASA-TM-X-67876] 23 p3706 N71-36423

Development of technique for evaluating effectiveness and operational utility of captured air bubble ships and ground effect machines
[AD-728003] 24 p3875 N71-37620

GROUND HANDLING

Beagle B125 training aircraft handling tests
[AAEE/963-PT-I] 12 p1856 N71-23498

GROUND OPERATIONAL SUPPORT SYSTEM

Support systems for long term regenerative life support manned test facility
10 p1505 N71-20954

Space shuttle operations, maintenance, and integration of ground support system, logistics, checkout, and recovery
22 p3674 N71-36193

GROUND RESONANCE

U GROUND EFFECT

U RESONANCE

GROUND RUN-UP

U ENGINE TESTS

U GROUND TESTS

GROUND SPEED

Taxi speed and distance measuring equipment consisting of modified shift detector, electronic conversion circuitry, and cockpit readout instrumentation
[FAA-NA-71-19] 23 p3759 N71-36797

Covariance analysis of relative velocity response spectra derived from horizontal ground motion
[NVO-1163-TM-24] 24 p3912 N71-37882

GROUND STATE

Schrodinger equation used to compute energy parameters of deuteron ground state
[AD-711285] 01 p0102 N71-10904

Spectral analysis of lowest rotational bands and ground state of oxygen 16 by nuclear resonance fluorescence
02 p0272 N71-11750

Low lying states of light atomic nuclei in framework of cluster model
[BMW-FBK-70-2] 02 p0278 N71-12178

Existence of ground-state rotational band in Si-28 nucleus
[RLO-1923-33] 03 p0428 N71-12870

Variational calculation of ground-state energy of liquid He-4 using Percus-Yevick and hypernetted chain theories
[COO-1569-61] 05 p0734 N71-15265

Using wave functions of strong coupling constant as test functions for calculating three nucleus ground state energy
06 p0910 N71-15782

Microscopic calculations of equilibrium deformations for ground state of even-even nuclei with neutron excess in region of 100
[KFK-TR-313] 06 p0912 N71-15817

Measuring ground and excited states of pyrazine for ground state equilibrium geometry of molecule
07 p0988 N71-17079

Electron ground states in molecular and valence-bonded crystals
[DN-1420] 07 p1075 N71-17493

Measuring optical spectra of triply ionized erbium in calcium tungstate using absorption and fluorescence spectroscopy
[AD-715008] 07 p1079 N71-18043

Ground state bands of even-even fission products
[UCRL-19949] 08 p1261 N71-18778

Atomic collision time delay functions and various bound level properties of ground state of molecular hydrogen
[NASA-CR-116689] 08 p1267 N71-19300

Intercluster potential of ground state molecular iodine computed from rotational constants and vibrational energies
09 p1428 N71-19738

Spectroscopic reassignment and ground state dissociation energy of molecular iodine
09 p1429 N71-19742

Approximation of scattering resonance energies and widths of ground state of molecular hydrogen from energy dependence of atomic collisional time delay functions
09 p1429 N71-19743

Expectation values and kinetic energy for vibrational-rotational levels of ground states of H2, HD, and D2
09 p1429 N71-19744

Ground state dissociation energies for diatomic halogens from vibrational spacings near dissociation limit
09 p1429 N71-19746

Low energy spectrum of excited states of odd nuclei with ground state spins
[ITF-70-47] 09 p1435 N71-20032

Average energies of ground and singly and doubly excited configurations in highly ionized atoms for electron numbers N equals 3 to N equals 20
[NASA-SP-3056] 09 p1444 N71-20535

Giant monopole state and isospin mixing in nuclear ground states
[NYO-2171-330] 10 p1617 N71-21306

Time dependent perturbation theory of ground state many fermion system for study of self energy and factorization problems and examination of reaction matrix expansions
11 p1801 N71-21886

Hartree approximation for ground state correlations as variational parameters in nuclear many body problem
[NYO-2171-333] 12 p1973 N71-23958

Influence of two body potential on ground state properties of solid helium
[NYO-3699-50] 13 p2127 N71-25517

Wave function for describing ground state of liquid helium 4
13 p2143 N71-25570

Schmidt method solution to quasi-potential equation, and coupling constant-ground state dependence

for spinless particles interacting by scalar meson exchange
[JINR-P2-5566] 15 p2464 N71-27226

Equivalence of He 3/4 and d-alpha cluster description of lithium 6
[NYO-2171-336] 17 p2000 N71-30009

Power series analysis of ground state bands in even-even nuclei
[OV-LNS-70-2] 17 p2802 N71-30145

Gamma vibrational and ground state bands of deformed radioactive isotopes
[NP-18536] 18 p2971 N71-30466

Long-range electrostatic and electromagnetic interactions between two neutral hydrogenic atoms in ground state
[NASA-TR-B-367] 18 p2982 N71-30917

Electronic or nucleonic many body system ground state energy calculation using Mathieu functions as orthogonal single particle wave functions
18 p2988 N71-31040

Ground state of He-4 atoms at absolute zero adsorbed on inert substrate
[RLO-1388-602] 18 p2988 N71-31473

Many body theory electron correlation effects for excited and ground states
20 p3317 N71-33523

Binding energy and ground state wave function of triton with relativistic nucleon-nucleon interaction in harmonic oscillator basis
[NYO-4032-36] 21 p3476 N71-34753

Ground state charge distribution and physical properties of some low-lying states in Nd-142, Nd-146, and Nd-150 produced by electron scattering
21 p3489 N71-34834

Configuration interaction on ground state of beryllium hydride molecule
21 p3492 N71-34879

GROUND STATIONS

NT DEEP SPACE INSTRUMENTATION FACILITY

NT INTEGRATED MISSION CONTROL CENTER

NT SPACE DETECTION AND TRACKING SYSTEM

NT STADAN [SATELLITE TRACKING NETWORK]

Comparison of radiation measurements from Cosmos 122 satellite instruments with photointerpretation data and ground station observations
[NASA-TT-F-13366] 02 p0257 N71-11676

Visible probability of earth satellite in elliptic orbit from ground station
[ISAS-454-VOL-35-NO-12] 02 p0295 N71-11806

Installation and operation of seismic array in Norway
[AD-711069] 02 p0219 N71-21064

Telementary ground station description
[DLR-MITT-70-17] 08 p1175 N71-18446

Traffic control system for supersonic transports using synchronous satellite for data relay between vehicles and ground station
[NASA-CASE-GSC-10087-1] 08 p1145 N71-19287

Propagation studies at Millstone Hill radar facility with steerable parabolic reflector
[AD-717156] 10 p1517 N71-20731

Conference on Europa 1 launch vehicle, Amer research satellite, Symphonie communication satellite, and German ground station-satellite communication system technology
10 p1649 N71-21520

Management, design, and tests of National Oceanographic Instrumentation Center
10 p1539 N71-21609

Soviet news releases on seismic stations and vertical derivatives of gravity potential
11 p1746 N71-22855

Deep Space Network, Ground Communications Facility, Space Flight Operations Facility, and Deep Space Instrumentation Facility research and development - Vol 2
[NASA-CR-117893] 12 p1896 N71-23320

Functions, facilities, and operations control system for Deep Space Network
12 p1896 N71-23320

Deep Space Network, Space Flight Operations Facility, Ground Communications Facility, and Deep Space Instrumentation Facility systems development
12 p1896 N71-23320

Deep Space Network, Ground Communications Facility, and Deep Space Instrumentation Facility operations and engineering
12 p1880 N71-23336

Soviet communication and guidance control systems between manned spacecraft and ground stations
[AD-719848] 13 p2047 N71-23318

Tabulation of international locations of rapid-run geomagnetic micropulsation stations
[DI-82-1043] 13 p2078 N71-25527

Aerial and ground surveillance of southern cone lat height in Cora Belt States during 1971
[NASA-NEWS-RELEASE-71-129] 17 p2709 N71-30175

SUBJECT INDEX

Investigations of critical configurations for fundamental range networks
[NASA-CR-121445] 20 p3245 N71-33310

System of protection indices for identification of environmental data associated with observation stations on earth surface
[NASA-CR-121641] 21 p3397 N71-34176

Establishment and operation of standard frequency and time signal installation Lyndhurst, Victoria, Australia
[REPT-4475] 21 p3407 N71-34244

Effect of clouds on laser communication between space and earth determined by simulated operation
[NOAA-TM-NMS-505-7] 21 p3435 N71-34443

Compilation of observations of solar activity and ionospheric data collected by ground stations in Greece
21 p3504 N71-34961

Uncorrected and barometer corrected data in tabular form
[ADJCL-3856] 21 p3504 N71-34967

Ground based geopotential measurements in Greenland during 1965 summer
[R-15] 22 p3578 N71-35496

Determination of observation station coordinates and inclination of reference ellipsoid from laser and photographic observations
22 p3677 N71-36217

Determination of direction cosines of line connecting two observation stations from quasi-simultaneous observations of artificial earth satellites
22 p3677 N71-36220

Development and characteristics of lightweight, mobile structures for aircraft storage and maintenance
[AD-72054] 23 p3741 N71-36674

Location of snow courses and soil moisture stations in Colorado and New Mexico
23 p3752 N71-36756

Feasibility of obtaining gravity anomalies directly from analyzing artificial earth satellite orbits
23 p3753 N71-36763

German central ground station for satellite data acquisition, tracking, and telecommand
24 p3914 N71-37902

Ionospheric propagation with satellites beyond ground station horizon, noting San Marco 2 satellite experiment
24 p3914 N71-37905

Facilities, functions, and projects of Deep Space Network
[NASA-CR-122843] 24 p4006 N71-38564

Development and implementation of Space Flight Operations Facility and Ground Communications Facility for DSN
24 p4007 N71-38568

GROUND SUPPORT EQUIPMENT

NT GROUND OPERATIONAL SUPPORT SYSTEM

Equipment for testing of ground station ranging equipment and spacecraft transponders
[NASA-CASE-XMS-05454-1] 03 p0335 N71-12391

Flight maneuvers and airborne and ground equipment for landing VTOL aircraft in adverse conditions
03 p0406 N71-12436

Aided inertial flight test experiments for all weather VTOL operations
[NASA-TM-X-64590] 03 p0406 N71-12439

Computer program for processing data on ground measurement of wiring in Apollo spacecraft
[NASA-CR-108731] 03 p0342 N71-12479

Data handling equipment for aerospace and ground support applications - conference
[ADJARD-CP-67-70] 04 p0504 N71-13826

Supporting research and technology for structural members used in Deep Space Network communication equipment
05 p0647 N71-14958

Developing wideband digital data system for Ground Communication Facility for Deep Space Network
05 p0647 N71-14960

Developing communications elements for Deep Space Network
07 p0993 N71-17617

Reporting supporting research and technology for Deep Space Network
07 p0999 N71-17618

Describing operations of Deep Space Network command system
07 p0999 N71-17623

Viking/Mars orbiter instrumentation and ground support equipment
08 p1289 N71-18875

Analysis of government furnished equipment and ground support equipment used on Apollo 13 flight
[NASA-TM-X-66920] 09 p1363 N71-19967

Controlled release device for use in launching robots or missiles
[NASA-CASE-XKS-03338] 12 p1925 N71-24043

Design, development, and test of ground support equipment for analyzing aircraft equipment condition and performance
[AD-719675] 13 p2026 N71-24603

Deep Space Network support activities for Apollo 9 through 13 flights and associated equipment
[NASA-CR-118325] 13 p2168 N71-25193

Deep Space Network telecommunication and ground support equipment for planetary and interplanetary flight projects
[NASA-CR-118895] 15 p2518 N71-27911

Criteria and recommendations to ensure compatible interfaces between space vehicle structure and launch stand ground support equipment
[NASA-SP-8061] 16 p2682 N71-28829

Test methods and testing techniques for determining technical performance and safety characteristics of ground support service aviation equipment
[AD-723056] 17 p2732 N71-30258

Cold weather tests to determine effectiveness of resonant combustor as power source for starting aircraft engines
[AD-724123] 20 p3358 N71-32804

Effects of larger Scout D and B heat shields on vehicle stability and control, structure, and ground support equipment
[NASA-CR-111947] 20 p3354 N71-33286

Development of unified test equipment concept for space shuttle ground support system
21 p3518 N71-35066

Development of standard language for test and ground operations involving space shuttle ground support equipment
21 p3518 N71-35067

Development of procedures for conducting service tests of aircraft refueling and defueling systems
[AD-726872] 22 p3541 N71-35227

Logic devices for readiness assessment and checkout of airborne and ground equipment mechanical components
22 p3674 N71-36197

Simulation of aircraft ground operations for Dallas-Fort Worth Regional Airport
24 p3873 N71-37607

GROUND SUPPORT SYSTEMS

Lift-off procedures for space booster
07 p1118 N71-17094

Meteorological weather satellite and ground support system
[NASA-TT-F-13646] 13 p2172 N71-24812

Terrestrial environment/climatic criteria guidelines for use in NASA space vehicles and associated equipment development with major emphasis on Kennedy Space Center launch area
[NASA-TM-X-64598] 17 p2737 N71-29235

Conference on ground operations, flight operations, and safety for space shuttle program - Vol. 1
[NASA-TM-X-67264] 22 p3673 N71-36192

Mission support area in DSN for Pioneer F and G probes
24 p4007 N71-38569

Schedules and logic diagrams for ground support, testing, training, and management for advanced space transport program
[NASA-CR-115220] 24 p4022 N71-38696

GROUND TESTS

NT COLD FLOW TESTS

NT PRELAUNCH TESTS

NT STATIC FIRING

Noise spectra in nuclear rocket engine ground test
[NASA-CR-111726] 04 p0557 N71-14146

Sound pressure levels produced by C-5A during ground tests
[AD-716814] 10 p1606 N71-20824

GROUND TRACKS

NT SATELLITE GROUND TRACKS

GROUND TRUTH

Investigating remote sensing applications to simple geological features using microwave radiometers
02 p0227 N71-11990

Applying holographic techniques to obtain ground truth data from earth resources and geodetic altimetry
03 p0380 N71-12758

Aerial multispectral sensing and ground truth observations for California earth resources study
06 p0642 N71-16128

Application of ground-truth data to monitor sensor calibrations for Earth Resources Technology Satellites - Vol. 2
[NASA-CR-121979] 24 p3919 N71-37945

GROUND WATER

Sulfur-mat formation and Chromatium weissii bacteria of hot mineral springs in Yamoto, Japan
[NASA-TT-F-12738] 02 p0156 N71-11107

Aerial infrared radiometry for measuring ground water inflow to streams
02 p0207 N71-11161

Aerial remote sensing data for locating ground water areas
02 p0207 N71-11162

Aeromagnetic, gravity, and electrical resistivity exploration between Palala and Panalua, Hawaii
[PB-192807] 02 p0213 N71-11080

Research on data and analytical systems for preparing national water assessments
[PB-192118] 05 p0664 N71-14692

Infrared aerial sensing of high temperature geothermal water sources
06 p0843 N71-16140

Feasibility of remote soil water sensing and data processing system
[PB-192451] 08 p1187 N71-18354

Ground water contamination by high energy proton accelerator through nucleon release
[UCRL-20131] 09 p1426 N71-19537

Equation based on instantaneous ion exchange and linear adsorption isotherm for predicting radioactive ion concentration and flow in ground water
[SC-CR-70-4139] 16 p2558 N71-28754

Remote sensing relating to military geography of arid lands including terrain, ground water, surface materials, cultural features, and related subjects - annotated bibliography
[AD-723061] 17 p2742 N71-29830

Bibliography of Arctic regions water resources
[PB-196468] 19 p0885 N71-31818

GROUND WAVE PROPAGATION

Angles significant for radio propagation - wave tilt of total field electrical vector, wave tilt of surface waves, Brewster angle, and Norton limiting angle
[AD-711946] 02 p0179 N71-11259

Evaluating data error analysis and equipment performance in tests of differential laser techniques
[ESSA-TR-BRL-166-ITS-107] 11 p1708 N71-22927

Characteristics of stress wave propagation in earth media
[AD-714012] 09 p1381 N71-19551

Geophysical effects on separated clock synchronization using low frequency ground waves
11 p1708 N71-22922

Very low frequency wave propagation phase variations for geophysical exploration of polar regions
11 p1708 N71-22923

Climatological ground effects on subsurface radio wave propagation
11 p1708 N71-22927

Evaluation of integral equation for predicting HF ground wave attenuation over inhomogeneous irregular terrain
[AD-721179] 19 p0855 N71-31948

Computerized simulation of local A ground wave propagation pulse subjected to atmospheric perturbation
[OT/ITS-RR-10] 23 p3793 N71-37040

GROUND WIND

Statistical analysis of wind distribution probabilities at Cape Kennedy
[NASA-CR-105272] 05 p0717 N71-15130

Spectrum analysis of horizontal wind speed based on Fourier transformations and Northeastern US surface wind data
23 p3785 N71-36079

Statistical summary of ground wind data recorded at 150-m tower on Merritt Island, Kennedy Space Center
[NASA-TM-X-64612] 24 p3951 N71-38187

GROUND-AIR-GROUND COMMUNICATIONS

Project DIOSCURES for global sea and air traffic control using synchronous satellites for ground-air-ground communications
02 p0263 N71-11768

Developing digital data systems for Ground Communications Facility of DSN
07 p1004 N71-17620

DSIF operations and development of wideband data systems for Deep Space Network
07 p1031 N71-17621

Economic factors affecting decision to install ground station support equipment for communication with Intelsat satellite
20 p3235 N71-33647

Tropospheric structure influence on radiowave propagation, noting satellite transmission
24 p3913 N71-37892

GROUND-TO-AIR MISSILES

U SURFACE TO AIR MISSILES

GROUP BEHAVIOR

U GROUP DYNAMICS

Perspectives and perceptions of organization behavior and design
[AD-714597] 06 p0808 N71-16709

Management systems theory and conflict resolution
[AD-716018] 09 p1487 N71-19697

Test methodology for determining relationship of intergroup organizational climate with communication and joint decision making between task-interdependent R and D groups
[REPT-70/34-PT-1] 10 p1666 N71-21099

Data analysis of test to determine relationship of intergroup organizational climate with communication and joint decision making between task-interdependent R and D groups
[REPT-70/34-PT-2] 10 p1666 N71-21100

Organizational structure effects on supervisory style and industrial work group attitudes
[PB-196467] 10 p1666 N71-21698

Cost, time, and social burdens created by need for commuting to work and suggestions for eliminating problems
[NASA-TM-X-67243] 14 p2357 N71-25761

Bayesian model for group effects on individual decision making
14 p2209 N71-25871

GROUP THEORY

Space station and base design considerations for crew stability and habitability
[NASA-CR-115179] 23 p3717 N71-36495
Guidelines for environmental habitability planning to facilitate individual and group stability
[NASA-CR-115180] 23 p3869 N71-37381
Group dynamics as basis for evaluating group activity as a function for restricting interaction of members in group
24 p3882 N71-37671

GROUP THEORY

NT HOMOMORPHISMS
NT SUBGROUPS
Numerical analysis of Abelian subgroups of p-groups
02 p0251 N71-11765

Current commutator derivation of mass difference relations
[NYO-2171-315] 03 p0424 N71-12807

Determining accuracy and reliability of collapsed group synthesis methods for group neutron diffusion problems using weight functions
[WAFD-TM-599] 03 p0437 N71-12856

Obtaining generators from semigroup of nonlinear transformations on Banach space
[AD-712806] 03 p0400 N71-13233

Cohomology of finite groups
03 p0401 N71-13268

Moebs plane ordering functions and algebraic groups
04 p0539 N71-14284

Research in general relativity including equations of motion, applications of group theory, and development of trapped surfaces
[AD-713146] 05 p0712 N71-14535

Structural properties of generalized automata and algebras
[AD-712377] 05 p0659 N71-14737

Computer program for finite group presentations
[AD-713697] 05 p0650 N71-14873

Infinite multiplets with SU(3) for mesons
[DEMO-70/14] 06 p0918 N71-16242

Hermitian form for group representation of complex matrices L_n/C
[IPVE-STP-49-91] 07 p1050 N71-17001

FORTRAN program for computation of group tables, alphanumeric display
[NASA-TM-X-2172] 07 p1051 N71-17338

Group representation in space of differentiating functions
[KFKI-70-16-HEP] 08 p1224 N71-18279

Mathematical background and application of two computer programs obtaining smooth group delay characteristics from moderate number of specific points
[REPT-6106-ADD-1] 11 p1716 N71-22283

Neat subgroup and extension problems for Abelian groups
12 p1948 N71-23532

Classification of states and interactions in nuclear collective model
[JINR-P4-5008] 15 p2457 N71-26856

Functional subgroup space representations of quaternion group
[IPVE-STP-49-102] 15 p2457 N71-26866

Group of invariance of Maxwell equations and extension associated with set of hyperbolicity of mass
[SLAC-TRANS-130] 15 p2458 N71-26935

Transformation of infinite component field with mass spectrum over nonunitary symmetry group representation
[JINR-P2-5305] 15 p2461 N71-27082

Group theory and Langrange multipliers generated by boson fields and vector current algebra
15 p2434 N71-27433

Factorization theorems, matrix poles, and unitarity
[PAM-70-7] 15 p2474 N71-27453

Statistical parameterization of symmetry group for multiple particle production
[JINR-E2-5599] 16 p2644 N71-28097

Interrelations between group structure and group constant accuracy in vicinity of 2.85 keV resonance scattering of sodium
[JAERI-4110] 16 p2658 N71-29167

Survey of recent developments in theory of nonlinear semigroups including semigroups of nonlinear transformations in Banach spaces and partial differential equation applications
[AD-722708] 17 p2774 N71-30318

Nonexistence of ambiguities in SU(3) x SU(3) matrix breaking
[ISS-70/25] 18 p2976 N71-30636

Algebra of nonlinear chiral SU(3) x SU(3) symmetry
[JINR-P2-5692] 18 p2977 N71-30637

Theory of logic-dynamic control systems and multilayer theory of statistical decisions
[JPRS-53766] 20 p3288 N71-32822

Algorithm structure for multilayer theory of statistical decisions
20 p3289 N71-32824

Nonlinear semigroup theory applied to quantum field equations in two dimensional space-time
20 p3290 N71-33111

Multigroup calculations for cross section structure factor interpolation schemes
[HEDL-TME-71-40] 20 p3322 N71-33798

Theory for selecting group symmetry coordinates for calculating vibrational potential functions of molecules
[IN-1421] 20 p3325 N71-33924

Quadratically divergent terms in amplitudes of weak nonequilibrium processes with photon emission studied in theory with intermediate boson
[NP-18777] 21 p3487 N71-34840

Multigroup multiregion one dimensional criticality calculation diffusion code for IBM 1130 computer - UARAE-90
[UARAE-90] 23 p3795 N71-37049

Four groups, four regions, one dimensional criticality calculation diffusion code for IBM 1620 computer - UARAE-85
[UARAE-85] 23 p3795 N71-37050

Asymptotic SU(3) symmetry, asymptotic boson coupling sum rules, and ninth pseudoscalar mesons
[TR-72-021] 23 p3819 N71-37243

Chiral symmetry breaking of vacuum
[NYO-2262-TA-242] 24 p3977 N71-38378

GROUP VELOCITY
Group velocity and refractivity behavior of strong electromagnetic surface waves propagating along vacuum-plasma plane interface
[DEMO-71/5] 23 p3824 N71-37274

GROUP 1A COMPOUNDS
U ALKALI METAL COMPOUNDS
GROUP 2A COMPOUNDS
U ALKALINE EARTH COMPOUNDS
GROUP 7A COMPOUNDS
U HALOGEN COMPOUNDS
GROUT

Cement and asphaltic materials evaluation for use as great under landing mats
[AD-710962] 01 p0038 N71-10681

GROWTH
NT CROP GROWTH
NT CRYSTAL GROWTH
NT CZOCHRALSKI METHOD
NT EPITAXY
NT HYDROTHERMAL CRYSTAL GROWTH
NT TRAVELING SOLVENT METHOD
NT VERNEUIL PROCESS

Theoretical van der Held growth curves for pure absorption in Schuster-Schwarzschild atmospheric model
01 p0075 N71-10396

Numerical simulation of instability growth rates in compressible inviscid fluid
[UCRL-50845] 01 p0043 N71-10476

Biochemistry of growth, gametogenesis, and fertilization in algae
[NYO-3473-24] 05 p0635 N71-14722

Anion and cation exchange resins: mixture for hydroponic growth of vegetables and flowers
[NASA-TT-F-13543] 09 p1387 N71-20426

Accelerated growth of Escherichia coli in high pressure helium-oxygen atmospheres
[AD-717404] 11 p1680 N71-22115

Survey and critique of bacterial growth quantitative determination methods including Bacillus coli direct microscopic morphology and growth measurement
[NASA-TT-F-13652] 13 p2632 N71-24584

Hydrostatic pressure effects on photosynthesis, growth, and oxygen production of algae cultures
[AD-720401] 14 p2204 N71-25867

Mass transfer during binary liquid drop growth at nonwettted capillary tubes
16 p2579 N71-28235

Tables of condensation nuclei growth rates under various supersaturations for warm fog or cloud modification
[AD-721591] 17 p2776 N71-29443

Characteristics of thermophilic bacteria
[NASA-TT-F-13795] 18 p2875 N71-30671

Relationship between tree ring growth variations and solar activity since 1700 in western North America
[NASA-CR-119946] 23 p3841 N71-37389

GRUMMAN AIRCRAFT
NT A-6 AIRCRAFT
NT F-111 AIRCRAFT
NT OV-1 AIRCRAFT
GRUMMAN MILITARY AIRCRAFT
U MILITARY AIRCRAFT
GRUMMAN OV-1C AIRCRAFT
U OV-1 AIRCRAFT
GRUNSKEN CONSTANT

Volume dependence of Grunskien parameter for metal halides
[ORO-3802-6] 01 p0112 N71-10759

Computer program for evaluating Bloch-Grunskien parameters of metals and evaluating tantalum electrical resistivity as function of temperature
[NASA-TM-X-2320] 17 p2816 N71-29922

GUARDS (SHIELDS)
Digital computer simulation of automobile impacting flexible safety barrier
09 p1473 N71-19402

GUIDANCE [MOTION]
NT AIRCRAFT GUIDANCE
NT COMMAND GUIDANCE

NT INERTIAL GUIDANCE
NT MIDCOURSE GUIDANCE
NT REENTRY GUIDANCE
NT RENDEZVOUS GUIDANCE
NT SATELLITE GUIDANCE
NT SPACECRAFT GUIDANCE
NT STRAPDOWN INERTIAL GUIDANCE
NT TERMINAL GUIDANCE

Hovering type flying vehicle design and principle mechanisms for manned or unmanned use
[NASA-CASE-MSC-12111-1] 02 p0147 N71-11629

Historical review of growth of guidance and control systems based on use of digital computers for manned aircraft
03 p0408 N71-13008

Investigating problems encountered in developing and maintaining airborne computer programs for guidance and control
03 p0346 N71-12806

Development of adjustable attitude guide block for setting pins perpendicular to irregular convex work surface
[NASA-CASE-XLA-07911] 05 p0604 N71-13571

Simplified linear guidance and control for keeping trajectory deviations minimal
[AD-717567] 11 p1791 N71-31911

Longitudinal film gate and lock mechanism for securing film in motion picture camera under vibration and high acceleration loads
[NASA-CASE-LAR-16086] 16 p2598 N71-28925

Combination guide and rotary bearing for freely moving shaft
[NASA-CASE-XLA-00013] 16 p2665 N71-28136

GUIDANCE SENSORS
Experimental techniques for prealigning and changing inertial measurement sensors without major system recalibration
[NASA-CR-111365] 02 p0262 N71-11427

Investigating general purpose digital computers for fault isolation capabilities in guidance and control systems
03 p0409 N71-13612

Testing methods for sensors of inertial reference systems
03 p0411 N71-13332

Guidance analyzer having suspended spacecraft simulating sphere for astronaut navigation
[NASA-CASE-XNP-09572] 05 p0690 N71-15621

Velocity, position and guidance sensor instrument errors for inertial platforms and satellite guidance
[BMW-FB-W-70-45] 07 p1056 N71-17166

Fixed direction one axis inertial sensor
11 p1723 N71-22271

Computer program giving transient characteristics of four different types of dispersions also transient response waveform
11 p1729 N71-22270

Gas bearing angular attitude control system
13 p2078 N71-24485

Geometrical aberrations and transfer matrix of quadrupole lenses in guiding device or film emittance beam matching systems and application to matching triplet system
[CEA-N-1286] 14 p2311 N71-26649

Optical gaging system for monitoring machine tool alignment
[NASA-CASE-XAC-09449-1] 14 p2364 N71-26107

Position indicators and guidance sensors for deep free heliocentric sounding device on solar orbits
[ONERA-NT-11673-SY] 17 p2849 N71-29988

Attitude determination and sensor alignment via weighted least squares affine transformations
[NASA-TM-X-65663] 19 p3124 N71-32546

GUIDANCE STABILITY
U CONTROL STABILITY
U GUIDANCE [MOTION]
GUIDE VANES

NT JET VANES
Overall performance of 6-inch radial-bladed centrifugal compressor with various diffuser vane setting angles
[NASA-TM-X-2107] 03 p0310 N71-12308

Air cooling systems for nozzle guide vanes of aircraft gas turbines
07 p1129 N71-17396

Testing aluminum coating for surface protection of nozzle blades
[AD-719015] 13 p2996 N71-29146

Noise reduction studies involving variable geometry inlet guide vanes for choking using two-sector cascade apparatus with three inlet configurations
[NASA-TM-X-2392] 24 p3872 N71-37608

GUIDED MISSILE SUBMARINES
Updating of Mk 3 Mod 6 diagnostic program in Polarix submarine AN/BRN-3 satellite navigation system
[AD-722485] 17 p2779 N71-30619

GUIDED MISSILES
U MISSILES
GUIDEAE

Monthly sea surface salinity variations in inner Gulf of Guinea and evaporation, precipitation, and vertical mixing
[AD-71492] 06 p0858 N71-16310

SUBJECT INDEX

GUINEA PIGS
Unilateral labyrinthectomy model for evaluating drug effects on vestibular function in guinea pigs
08 p1153 N71-19057
Angular acceleration effects on guinea pig vestibular systems
20 p3223 N71-33473

GULF STREAM
Gulf Stream flow with transient current fluctuations and detached eddy formations
[ESSA-TR-ERL-164-AOML-1] 05 p0679 N71-15524
Meander circulation pattern of Gulf Stream
09 p1381 N71-19513

GULFS
Meteorological data collected by buoy in Gulf of Mexico
[AD-713479] 05 p0679 N71-15523
Numerical analysis of tidal current circulation in Gulf of Maine
[AD-714612] 06 p0855 N71-16664
Survey of structural damage along Mississippi-Louisiana Gulf Coast done by Hurricane Camille
[NBS-TN-569] 12 p1955 N71-23851

GUN VULCANIZATES
U VULCANIZED ELASTOMERS
GUNNEL THEORY
U RANGE [EXTREMES]
GUN LAUNCHERS
Explosive gun development for launch of sabot models to rotary velocities
[AD-712394] 04 p0516 N71-13802
Miniature telemetry systems for gun-launched instrumentation
[AD-713874] 06 p0822 N71-15935

GUN PROPELLANTS
PORTMAN computer program for determination of shot and gas propellant performance
[AD-713874] 18 p3000 N71-30615
Theory of interior ballistics for calculating gunpowder efficiency and combustion safety in firearms
[TL-1970-21] 20 p3368 N71-33842

GUNRIE
Auditory stimuli effects of pistol shots during learning process noting human reactions and performance
[ISVR-TR-26] 10 p1504 N71-20799
Noise hazard guide including damage risk criteria for steady state and impulse or gunfire noise
13 p2035 N71-25559
UH-1P helicopter acoustic measurements during gunfire and rocket firing including bioacoustic factors
[AD-713830] 19 p3042 N71-31613

GUN EFFECT
Gun effect in devices with concentric electrodes
01 p0031 N71-10137
Scanning electron microscope studies of breakdown and electric field distribution in transverse Gunn effect devices
01 p0109 N71-10213
Encapsulation resonance frequencies in CW Gunn diodes for J and Q bands, and limitations on oscillator characteristics
01 p0032 N71-10217

Prediction and measurement of phase angle between locked Gunn oscillator and locking source
01 p0032 N71-10218
Voltage tunable Gunn effect semiconductor for microwave generation
[NASA-CASE-XER-07894] 08 p1169 N71-18721
Variation with temperature of tunable, coaxial resonant cavity gallium arsenide Gunn diode oscillator
[RSD-70042] 10 p1632 N71-20763
Scanning electron microscope for time resolved frequency response analysis on Gunn effect oscillator
11 p1761 N71-22075

Electrical properties and operation of Gunn diodes
[POA-3-A-3734-41] 22 p3560 N71-35353
Research and development of microwave oscillators, Gunn effect, diodes, space charge, and solid state devices
[AD-727058] 22 p3562 N71-35369
Application of Gunn effect to coaxial and microstrip circuits and development of equivalent circuits
[NASA-CR-122947] 23 p3731 N71-36396
Amplitude and frequency modulation characteristics and applications of CW Gunn effect oscillators
23 p3734 N71-36623

GUNNEY TRAINING
F-4E aircraft in-flight television recording system for gunnery training
[AD-728453] 14 p2210 N71-26174
Albion FOP 15 computerized simulation for joint thrust gunnery and navigation training including load-up display and real time computer programming
[AD-721673] 16 p2565 N71-28327

GUNPOWDER
U GUN PROPELLANTS
GUN [ORDNANCE]
NT ARTILLERY
Proceedings from meeting on gun tube erosion
[AD-714668] 06 p0879 N71-16435
Fracture toughness test method for thick-walled slender material
[AD-721636] 16 p2685 N71-28288

Theory of interior ballistics for calculating gunpowder efficiency and combustion safety in firearms
[TL-1970-21] 20 p3368 N71-33842

GUST ALLEVIATORS
Analysis of effects of spanwise variations of gust velocity in isotropic turbulence on vane-controlled gust alleviation system
[NASA-TN-D-6126] 11 p1669 N71-22068
Allerivation of lateral and longitudinal gust effects on aircraft
13 p2024 N71-24709

Effects of spanwise variation of gust velocity on alleviation system designed for uniform gust velocity across span
[NASA-TN-D-6346] 16 p2529 N71-28009
Problem of wind gust absorption by aircraft structures, and flight tests of prototype H-100
[NASA-TT-F-17744] 18 p2871 N71-30848

GUST LOADS
Wind effect criteria for structural design and engineering of buildings
05 p0776 N71-15301

Wind load consideration in building wall design
05 p0777 N71-15303
Gust factor for determining dynamic wind effects on buildings
05 p0778 N71-15310

Aerodynamic responses of tall buildings to vortex shedding and gust loading
05 p0778 N71-15312

Aerodynamic wind tunnel modeling and three dimensional structural analysis for dynamic building response prediction to wind loads
05 p0778 N71-15314

Aircraft pilot direct lift control for aircraft landing and reducing gust load effects
[ARC-RM-3629] 07 p0969 N71-17102

Measurement of force and pressure fluctuations on airfoils during transverse and streamwise gust flows
[CUBD/A-TURBO/TR-21] 11 p1670 N71-22374

Cumulative frequency distributions determined by extreme value analysis used for fatigue analysis and interpretation of c.g. vertical acceleration and gust velocity measured on transport aircraft
[AGARD-R-579-71] 13 p2028 N71-25000

Theory of controllability for pacific and second order hyperbolic systems and for hereditary differential systems applied to stabilization of high speed aircraft in gust load disturbances
[AD-720727] 17 p2703 N71-29430

Gust load reduction by feedback control using direct and tuned left controls
19 p3037 N71-31889

Horizontal and vertical gust load frequency and power spectra influence on longitudinal aircraft stability
19 p3037 N71-31890

Atmospheric turbulence models showing gust load influence on aircraft yaw motion
19 p3037 N71-31891

Development of power spectral density method for determining gust criteria for airplane structural strength based on discrete gusts
[NAL-TR-233] 20 p3211 N71-33547

Measurement and analysis of atmospheric turbulence along Pacific Coast air routes in Japan
[NAL-TR-222] 20 p3297 N71-33583

Single degree of freedom roll response due to vertical random two dimensional vertical gusts
[NASA-CR-111966] 23 p3706 N71-36421

Analysis of gust penetration loads and associated elastic vehicle response of Saturn 5 launch vehicles AS-505 through AS-508 penetrating sinusoidal gusts
[NASA-CR-119944] 23 p3857 N71-37494

GUSTS
Data sample consisting of mean wind speed and direction, also highest recorded gust for central Oklahoma, June 1966 - May 1967
[ESSA-TM-ERL-TM-NSL-48] 01 p0079 N71-10615

Gustiness during unstable and stable regimes at White Sands Missile Range
[AD-711855] 03 p0257 N71-11667

Strong surface wind gusts at Holloman Air Force Base, Mar through May
[AD-711855] 02 p0258 N71-11690

Power spectrum method for determining gust frequency response functions in dynamic aircraft design
12 p1850 N71-23211

GYMNASTICS
U EXERCISE [PHYSIOLOGY]
GYRATION

NT AUTOROTATION
NT EARTH ROTATION
NT LARMOR PRECESSION
NT MOLECULAR ROTATION
NT PRECESSION
NT ROTATION
NT SATELLITE ROTATION
NT SOLAR ROTATION

GYRATORS
NT MICROWAVE FILTERS
Design of gyrator circuit using operational amplifiers to replace ungrounded inductors
[NASA-CASE-XAC-10608-1] 03 p0349 N71-25157

Analysis of magnetic circuits using electric circuit theory
[UCRL-72828] 17 p2786 N71-29267
Design and performance characteristics of bandpass gyrators
19 p3068 N71-32660

Development of N path filter with positive RC circuits incorporating time-variable gyrator
[AD-723456] 19 p3069 N71-32771
Gyrator applications related to integrated circuits
24 p3900 N71-37800

GYRO HORIZONS
Behavior of attitude gyro and gyro horizon during looping flight
03 p0413 N71-13281

GYROCOMPASSES
Satellite orientation, satellite attitude control, and pointing control systems using horizon scanners, gyrocompasses, gravity gradient, and angular momentum systems
[RAE-TR-70070] 02 p0263 N71-11764

Design and performance of gyrocompass with liquid suspension of sensing element
[JPRS-52174] 06 p0895 N71-16556

Alignment and calibration of strapdown inertial measuring unit using accelerometer, gyrocompass, and optical filtering techniques
[RE-67] 12 p1960 N71-24007

Attitude estimation and control of earth pointing satellites in circular orbit
[DLR-FB-70-75] 17 p2849 N71-29489

Statistical analysis of gyrocompass mode of A-A inertial navigation system
[RM-511] 17 p2780 N71-30315

GYRODYNE AIRCRAFT
NT QH-50 HELICOPTER
GYRODYNE DRN-3 HELICOPTER
U QH-50 HELICOPTER
GYRODYNE MILITARY AIRCRAFT
U QH-50 HELICOPTER

GYROFREQUENCY
Isomorphous and magnetospheric electric field measuring instruments and measurement results
[MPL-PAR/EXTRATER-44/70] 08 p1189 N71-18609

Absorptivity and emissivity hydrodynamic equations for suprathermal electron gyrating in magnetized plasma including Doppler effect with solar radio emission examples
[AD-721377] 16 p2662 N71-28966

GYROMAGNETISM
NT GYROFREQUENCY
Rotation of hydrometers at variable speeds applied to low frequency magnetic resonance modulation
[ONERA-TR-366] 02 p0287 N71-11745

Electromagnetic surface wave propagation on yttrium-iron garnet and indium antimonide rods at microwave frequencies under axial magnetization
11 p1702 N71-22719

GYROPLANES
U HELICOPTERS
GYROS

U GYROSCOPES
GYROSCOPE FLUIDS
Design and performance of gyrocompass with liquid suspension of sensing element
[JPRS-52174] 06 p0895 N71-16556

GYROSCOPES
NT ATTITUDE GYROS
NT CONTROL MOMENT GYROSCOPES
NT CRYOGENIC GYROSCOPES
NT ELECTROSTATIC GYROSCOPES
NT FLUID ROTOR GYROSCOPES
NT GYRO HORIZONS
NT GYROCOMPASSES
NT GYROSCOPIC PENDULUMS
NT GYROSTABILIZERS
NT NUCLEAR GYROSCOPES
NT OPTICAL GYROSCOPES
NT ROTARY GYROSCOPES

Analysis of Fresnel drag laser gyroscope
[AD-711654] 01 p0064 N71-10630

Basic kinematics and dynamics of human centrifuges and other aerospace simulators including coriolis and gyroscopic effects
[AD-711635] 01 p0014 N71-10083

Free flight measurements of aerodynamic lateral force and moment coefficients using gyroscopes and accelerometers
[HSA-TN-164] 02 p0141 N71-11001

Geometry of directional gyroscope mounted on swinging base and aerodynamic resistance of gyroscope motor
[AD-712229] 02 p0362 N71-11756

Engineering design and test of packaging systems for 3271 gyroscope platform
[AD-711544] 02 p0363 N71-12175

Squeeze film lubrication for gyroscope wheels and behavior of hydrodynamic spiral grooved spin axis bearing
[NASA-CR-102381] 03 p0385 N71-13165

Testing methods for components of inertial guidance systems
[AGARDGRAPH-128] 03 p0410 N71-13201

Review of gyro and accelerometer systems
03 p0411 N71-13203

GYROSCOPIC COUPLING

- Cost reduction by reliable performance life testing of gyroscopes 03 p0411 N71-13204
- Test instrumentation for evaluating inertial gyro performance 03 p0411 N71-13205
- Performance testing of single degree of freedom gyroscopes 03 p0411 N71-13206
- Gyro testing methods in Great Britain 03 p0412 N71-13209
- Diagnostic testing for gyroscope design optimization 03 p0412 N71-15210
- Scale factor measurement of motors 03 p0412 N71-15211
- Table 10g and requirements of gyroscopic materials under acceleration 03 p0412 N71-13212
- Testing of gyro and accelerometers having hydrostatic gas bearing axes 03 p0412 N71-13214
- Development of spacecraft experiment pointing and attitude control system [NASA-CASE-XLA-05464] 04 p0543 N71-14132
- Large angle gyro sensing system for body mount on unmanned Mars surface vehicle [NASA-CR-111737] 04 p0543 N71-14148
- General relativistic precession of gyroscope in inclined orbit [NASA-TM-X-64535] 05 p0686 N71-15410
- Transactions on gyroscopic stability and navigation instruments [JPRS-52214] 07 p1056 N71-17198
- Gyroptical vertical scanning unit with optical correction 07 p1057 N71-17201
- Design and testing of prototype hydrostatic liquid bearing gyro assemblies [NASA-CR-102991] 07 p1028 N71-17319
- Evaluation of gyroscope on precision centrifuge using counter rotating platform [AD-715906] 08 p1232 N71-18525
- Techniques for measuring gyroscope drift of aircraft inertial navigation system [RM-495] 08 p1233 N71-19000
- Gyroscopic control of spin rate or orientation of rigid bodies constrained to rotate about fixed axis [NASA-CR-116870] 08 p1245 N71-19171
- Stability models for weakly nonlinear dynamical systems with application to gyroscope devices [AD-716538] 09 p1409 N71-19688
- Gyroscope theory and applications to inertial guidance and navigation, vehicle stabilization, and related uses - bibliography [AGARD-R-582-71] 09 p1389 N71-20002
- Improving accuracy of gyro stabilizer using floating integrating gyroscopes with feedback 10 p1562 N71-21747
- Transfer function and amplitude frequency characteristics of two degree of freedom gyroscope with position integral negative feedback 11 p1761 N71-22097
- Equations of motion and characteristics of invariant gyrocompass with pendulum correction 11 p1762 N71-22262
- Surface evaluation of stainless steel gyro bearings manufactured by various hardening techniques [NASA-CR-114980] 12 p1929 N71-23949
- Optimum stabilization of free rotating rigid body with control gyros [NLL-M-20349-5828.4F] 12 p1924 N71-24231
- Approximate method for predicting motion of symmetric rigid body subjected to body-fixed force [NASA-CR-118995] 16 p2685 N71-28171
- Nonorthogonal redundant configurations of single axis strapped down gyros 18 p2956 N71-31119
- Euler equations for gyroscope on gimbal rings mounted on moving vehicle [AD-723419] 19 p3132 N71-31794
- Formulation of general equations of motion of three alleviated gyroscope given missile motion, and computer code for integrating resulting differential equations [AD-723420] 19 p3132 N71-31799
- Construction of wave functions of asymmetrical spinning top in quantum mechanics [FEI-203] 19 p3145 N71-31892
- Misalignment estimation software system for calibrating in-flight slew angle scale factors and drift rates of OAO gyros [NASA-TM-X-65667] 19 p3133 N71-32680
- Design and basic characteristics of bearings for gyroscopic devices for aerodynamic and aerostatic bearings [JPRS-53883] 21 p3428 N71-34397
- Sensitive technique uses Fresnel drag effect to determine orientation of spherical rotor spin axis for laser gyroscope application 22 p3591 N71-35575
- Manual for design and calculation of basic parameters of gyroscopic devices [AD-726576] 22 p3419 N71-35783

GYROSCOPIC COUPLING

- Gyroscopic control of spin rate or orientation of rigid bodies constrained to rotate about fixed axis [NASA-CR-116870] 08 p1245 N71-19171
- GYROSCOPIC DRIFT**
- U GYROSCOPES**
- U GYROSCOPIC STABILITY**
- GYROSCOPIC PENDULUMS**
- Testing methods for components of inertial guidance systems [AGARDOGRAPH-128] 03 p0410 N71-13201
- Proposed testing program for strapdown inertial system containing platform gyros and pendulous gyros [NASA-CR-103016] 06 p0895 N71-16394
- Random parametric oscillation of gyro pendulum on movable platform 07 p1057 N71-17200
- Analytical test of dynamic accuracy of gyro stabilized platform with pendulum correction for stabilizing gravimeters 21 p3418 N71-34322
- GYROSCOPIC STABILITY**
- Investigating gyroscopic stability and error compensation in navigation instruments [JPRS-52046] 06 p0893 N71-15951
- Investigating stability of steady movement of rigid shaft with disc on elastic rotor bearings using modified Routh procedure 06 p0893 N71-15952
- Deriving expression for displacement of Lagrange gyroscope with respect to angle of precession during nutation displacement 06 p0894 N71-15954
- Transactions on gyroscopic stability and navigation instruments [JPRS-52214] 07 p1056 N71-17198
- Energetics analysis of correctable gyroscope stability 07 p1056 N71-17199
- Combined optimal control in gyro stabilizer stabilization circuit 07 p1057 N71-17202
- Approximate orbiting gyroscope precession rates caused by curvature and torsion of space-time 07 p1058 N71-17820
- Techniques for measuring gyroscope drift of aircraft inertial navigation system [RM-495] 08 p1233 N71-19000
- Gyroscopic control of spin rate or orientation of rigid bodies constrained to rotate about fixed axis [NASA-CR-116870] 08 p1245 N71-19171
- Elastic vibration theory for determining structural damping force in gyroscopic systems 11 p1760 N71-21972
- Development and characteristics of satellite gravitational stabilization system with gyroscopic damping [JPRS-53447] 17 p2842 N71-29244
- Synchronization and stability aspects of gyroscopic vibration absorber 19 p3143 N71-32619
- GYROSTABILIZERS**
- Analyzing motion environment of test facilities with respect to design and guidance-component performance tests [NASA-CR-111598] 02 p0199 N71-11551
- Grease lubricated spiral groove bearings suitable for spin axis of gyros in automatic pilots [NASA-CR-102926] 03 p0384 N71-12819
- Solid state helium-neon gas laser applied to missile guidance [AD-713527] 05 p0720 N71-15383
- Improving precision of gyro stabilizer having feedback with respect to reactive moment of gyro unit 06 p0893 N71-15953
- Stabilizing gyro utilizing re-circulated liquid hydrostatic gimbal bearing [NASA-CR-102992] 06 p0866 N71-16487
- Combined optimal control in gyro stabilizer stabilization circuit 07 p1057 N71-17202
- Performance and nonlinear control of twin gyro attitude control system with passive compensation 07 p1058 N71-17821
- Improving accuracy of gyro stabilizer using floating integrating gyroscopes with feedback 10 p1562 N71-21747
- Equipment and methods for marine measurement of gravitational forces [JPRS-53851] 21 p3417 N71-34313
- Laboratory and sea tests of gyro stabilized marine gravimeter for measuring disturbing accelerations and tilts in submarines 21 p3417 N71-34316
- Instrument for synchronous photographic recording of perturbing acceleration and residual tilts of gyro stabilized platform 21 p3418 N71-34320
- Laboratory and sea tests of gyro stabilized platform for gravimeters and horizon and acceleration photorecorders 21 p3418 N71-34321
- Analytical test of dynamic accuracy of gyro stabilized platform with pendulum correction for stabilizing gravimeters 21 p3419 N71-34322

SUBJECT INDEX

- Laboratory tests of stabilization errors resulting from perturbations in gyro stabilized platform for gravimeters 21 p3418 N71-34322
- GYROSTATS**
- U GYROSCOPES**
- GYROTROPISM**
- Propagation of electromagnetic waves along gyroscopic cylinder in longitudinal magnetic field 11 p1800 N71-23016
- Finite cylindrical dipole antenna of arbitrary orientation in gyroscopic media solved as boundary value problem 23 p3734 N71-36622
- ## H
- H ALPHA LINE**
- Profile measurements of H alpha, beta, and gamma spectral lines in HF plasma discharge [NP-18532] 17 p2812 N71-29902
- Magnetic fields and spectral characteristics of small H-alpha solar flares 19 p3177 N71-32619
- Production cross sections for He I, He II, H-alpha, and H-beta emissions 20 p3318 N71-33577
- Electron capture cross sections into 3p and 3d states of hydrogen for 30-120 keV proton and deuteron impact on gas targets 20 p3325 N71-33919
- High resolution H-alpha photographs for studying chromospheric fine structure at active region polarity boundaries [NASA-CR-121619] 21 p3503 N71-34953
- Fine structure and quantitative reduction of H alpha and beta lines and K lines inside facular areas [NLL-RTS-6401] 23 p3842 N71-37399
- H BETA LINE**
- Profile measurements of H alpha, beta, and gamma spectral lines in HF plasma discharge [NP-18532] 17 p2812 N71-29902
- Production cross sections for He I, He II, H-alpha, and H-beta emissions 20 p3318 N71-33577
- Spectrographs for measuring hydrogen H beta line spectral shape and determining electron density of transient plasma [NASA-CR-122932] 23 p3756 N71-36774
- Fine structure and quantitative reduction of H alpha and beta lines and K lines inside facular areas [NLL-RTS-6401] 23 p3842 N71-37399
- H GAMMA LINE**
- Profile measurements of H alpha, beta, and gamma spectral lines in HF plasma discharge [NP-18532] 17 p2812 N71-29902
- H LINES**
- NT H ALPHA LINE**
- NT H BETA LINE**
- NT H GAMMA LINE**
- NT K LINES**
- NT LYMAN SPECTRA**
- H WAVES**
- Numerical analysis of gas motions and radiative transfer of H waves 06 p0944 N71-16821
- Doppler shifted cyclotron resonance absorption of helicon waves in indium and Gallium Arsenide oscillations 15 p2477 N71-27577
- Helicon resonance and quantum oscillations in mercury selenide crystal 18 p2997 N71-31325
- H-19 HELICOPTER**
- Flight test program to obtain data on aided inertial system for terminal guidance and navigation of helicopter in designing V/STOL avionics system [NASA-TM-X-66494] 03 p0314 N71-12284
- H-41 HELICOPTER**
- U XH-51 HELICOPTER**
- H-126 AIRCRAFT**
- H-126 jet flap research aircraft development and testing 09 p1323 N71-20066
- HABITABILITY**
- Discussing geological, topographical, and climatological features of Iceland and effects on human habitation 07 p1024 N71-17982
- Systems analysis of lunar shelter for habitability evaluation [NASA-CR-111824] 06 p1157 N71-18077
- Crew reaction to environment habitability during long duration space station simulation test 10 p1509 N71-28082
- Space station and base design considerations for crew stability and habitability [NASA-CR-115179] 23 p3717 N71-36069
- Guidelines for environmental habitability planning to facilitate individual and group stability [NASA-CR-115180] 23 p3869 N71-37598

HADRON

- Time reversal invariance in electromagnetic interactions - conference 03 p0432 N71-12656
[CALT-68-264]
- Total cross section for photoproduction of hadrons and hydrogen on deuterium between 1.0 and 6.4 GeV (DESY-70/17) 03 p0430 N71-12905
- Reviewing experimental program of research on hadron interactions and properties (NYS-2262-TR-152) 03 p0433 N71-12958
- Investigating multiparticle correlation effects of hadronic reactions at 3.9 GeV/c (UHS-11-65-70) 04 p0579 N71-13979
- Deriving dual theory of processes involving external and intermediate exotic hadrons in form of quark focusing principle 04 p0579 N71-13980
- Applying asymptotic SU(3) and SU(2) symmetries to hadron systems 04 p0586 N71-14253
- Hadron dynamics and quark structure (COO-264-558) 05 p0750 N71-15346
- Positron electron annihilation into hadrons (LNF-70/21) 06 p0911 N71-15803
- Considering relationship between nonleptonic hadron decay and current x current theory (UHS-11-73-70) 06 p0923 N71-16743
- Glauber corrections and interaction between high energy hadrons and nuclei (BNL-TR-358) 07 p1071 N71-17188
- Hadronic decay modes of weak intermediate boson produced by high energy neutrinos (NYO-2171-323) 07 p1077 N71-17547
- Fast variation of hadronic amplitudes and gamma quanta bremsstrahlung (ITEP-764) 07 p1081 N71-18136
- Inelastic lepton hadron scattering cross sections (JVE-STR-70-4) 08 p1247 N71-18191
- High energy elastic and inelastic hadron-hadron scattering in $p\bar{p}$ -cubed theory (ILL-TH-71-4) 08 p1261 N71-18803
- Quark model for hadron spectroscopy and meson nucleus scattering cross sections with resonance production (UCR-34-1-107-113) 09 p1436 N71-20043
- Momentum spectra in high energy hadron deuteron interactions (COO-1764-115) 10 p1611 N71-20686
- Summary of published data on cosmic hadron flux for various altitudes 10 p1554 N71-21554
- Spin wave functions and analytical properties of hadronic scattering amplitudes in quark model (TUEP-70-35) 10 p1619 N71-21695
- High energy electron and positron colliding beams leading to annihilation into muon pair, annihilation into hadron pair, Bhabha scattering and multibody hadron production 10 p1623 N71-21769
- Results of duality regarding internal symmetries for low- and high-energy hadron scattering (COO-1764-61) 11 p1806 N71-22521
- Hadronic helicity in diffractive region of inelastic lepton nucleus reactions (NYO-4284-10) 12 p1971 N71-23879
- Quark isomultiplet model for electromagnetic mass differences of hadrons (MUB-2860) 12 p1972 N71-23884
- Two Reggeon exchange contributions to high energy hadron scattering amplitudes (UCRL-20052) 12 p1972 N71-23888
- Regge pole model for inelastic lepton nucleus scattering into hadrons (NYO-4284-9) 12 p1972 N71-23896
- Quark perion model for deep inelastic lepton-hadron scattering (JLPT-71/12) 12 p1979 N71-24343
- Three components of D spin for rule selection in hadron couplings (COO-264-370) 14 p2306 N71-25723
- Elastic scattering of high energy hadrons from deformed carbon 12 nuclei calculations using multiple collision theory and deformed oscillator wave functions (BNP-721) 14 p2308 N71-26422
- Hadron interaction at ultrahigh energies in cosmic rays (BNP-722) 15 p2489 N71-27879
- Scattering cross sections of hadron production from positron electron collisions based on vector dominance model 16 p2658 N71-29171
- Validity of Cottingham formula relating electromagnetic self mass of hadrons to integrals over forward virtual spin averaged Compton scattering (TR-71-125) 17 p2775 N71-30341
- Total cross section for photoproduction of hadrons measured on 7 nuclei at 5.4 GeV photon energy (DESY-71/5) 18 p2972 N71-30515
- Theory of weak interactions based on possible SU(4) symmetry for hadrons (BN-70/16) 18 p2975 N71-30568
- Coherent state method for high energy hadron scattering related to quark models 18 p2981 N71-30823

- Connections between internal parton wave function of hadrons, deduced from electroproduction, and observable systematics of high energy processes (NUS-2008) 18 p2989 N71-31505
- Systematic experimental regularities in survey of hadron spectroscopy data (UCRL-73073) 19 p3154 N71-32283
- Large angle hadron and proton scattering and duality calculations based on mesomorphic and scattering functions, momentum transfer, and asymptotic methods (RBEFT-71/19) 20 p3317 N71-33550
- Scattering cross section estimations for intermediate vector boson production in nucleon-nucleon interactions based on inelastic process models (JINR-E2-5748) 21 p3449 N71-34697
- Muon pairs produced in high energy hadron collisions with uranium target (NEVIS-185) 21 p3480 N71-34789
- Developments in hadron physics, dual models and dual phenomenology, weak elementary particle interactions, and electromagnetic interaction theory - functions from nuclear research conference (CERN-71-7) 22 p3640 N71-35951
- Structure of hadrons covering hadronic and semileptonic processes (NYO-4076-14) 22 p3646 N71-36000
- Functional equation for self coupled relativistic scalar field 23 p3782 N71-36955
- Parton models for describing interactions of high virtual photons with hadronic matter (LNF-71/5) 23 p3808 N71-37148
- Generalizing scaling laws for electroproduction of hadrons 23 p3815 N71-37203
- Cluster decomposition techniques for analyzing hadronic perturbation theory amplitudes at high energy (ILL-TH-71-10) 23 p3820 N71-37251
- Vector currents and current algebras in zero width model of hadron bootstrap 23 p3822 N71-37262
- Electron and muon pair production in electron electron and electron positron collisions and hadron production via photon photon scattering (LNF-71/1) 24 p3969 N71-38312
- Structure and classification scheme of hadron excited states (ITEP-70-102-E) 24 p3970 N71-38321
- Computerized collection of total elastic cross sections for hadron-nucleon scattering (CERN-HERA-69-3) 24 p3975 N71-38363
- Theoretical quantum electrodynamics in higher orders at low and high energies and nuclear models for lepton hadron and photon hadron scattering (ITP-71-5-E) 24 p3976 N71-38372
- HAFIUM**
NT **HAFIUM ISOTOPES**
High cost hafnium for interaction with transition metals (AD-713778) 05 p0704 N71-15332
- Effect of fast neutron irradiation on mechanical properties of hafnium (IN-1440) 08 p1212 N71-18369
- Method for determination of trace amounts of hafnium in zirconium-niobium alloys 13 p2093 N71-24873
- Quantitative analysis of hafnium in zirconium oxide by emission spectroscopy 13 p2136 N71-25373
- Determination of zirconium and hafnium in meteorites and terrestrial materials by activation analysis and chemical separation after neutron irradiation 14 p2338 N71-26351
- Decay scheme of Ta-173 to Hf-173 (JINR-P6-5704) 24 p3972 N71-38336
- HAFIUM ALLOYS**
Development of oxidation resistant hafnium alloys as cladding for niobium and tantalum base alloys (AD-720724) 14 p2274 N71-26157
- Precipitation hardening with internal nitriding of molybdenum hafnium solid solution alloy (UCRL-50958) 17 p2767 N71-30250
- Deformation studies on dilute hafnium base alloys to determine effects of dispersion hardening and precipitation (RPI-3719-9) 21 p3439 N71-34467
- HAFIUM CARBIDES**
Mass spectrometric analysis of thermodynamic properties in ternary zirconium hafnium carbide (NASA-CR-111120) 01 p0071 N71-10590
- Purification strengthening of tungsten-rhenium alloy by hafnium carbide precipitates (NASA-TN-D-5308) 12 p1939 N71-23982
- Kanada flow mass spectrometry, thermodynamics, and chemical bonding of titanium, zirconium, hafnium, and thorium carbides during high temperature vaporization (NASA-TM-X-67844) 15 p2425 N71-27630
- HAFIUM COMPOUNDS**
NT **HAFIUM CARBIDES**
NT **HAFIUM OXIDES**
Thermodynamic data tables for elements 54 through 61 (NBS-TN-270-5) 12 p2014 N71-24280

HAFIUM ISOTOPES

- Radiochemical separations of hafnium, tantalum, and germanium from tungsten and selenium irradiated by 14-MeV neutrons (ORNL-TR-2350) 05 p0738 N71-14725
- Hafnium 175 excited states in tantalum 175 decay spectrum (JINR-P6-5634) 16 p2642 N71-28033
- Tables on nuclear decay schemes of Hf-173 and Er-161 (NYO-3950-3) 21 p3484 N71-34822
- HAFIUM OXIDES**
X ray diffraction analysis on erbia/hafnia system phase relations (JST-T-601) 07 p1092 N71-17453
- Reactivity simulation test data with performance analysis of pyrolytic carbon and hafnia coatings (GA-8996-SUPPL-B) 23 p3779 N71-34936
- HAIR**
Using radar to distinguish hail-producing clouds for determining probability of modifications in convective clouds (AD-713468) 05 p0718 N71-15262
- Mathematical analysis of denting of thin aircraft skin (NASA-TN-D-4102) 05 p0780 N71-15422
- Hailstorms and thunderstorms in Italy during 1969 (IFA-TR-31) 10 p1596 N71-20786
- Technology review on electric automobiles, and modified T-33 aircraft system for pyrotechnic hail suppression seeding (DMB/NAE-1970/4) 11 p1768 N71-22198
- Modified T-33 aircraft system for pyrotechnic hail suppression seeding 11 p1840 N71-22200
- Meteorological radar for detection of thunderstorms, hail, and turbulence hazardous to aviation noting echo interpretation and radar transmission (WMO-264-TF-148) 13 p2104 N71-24394
- Soviet news releases on atmospheric processes of eastern Antarctica and hail suppression service for Central Asia 15 p2436 N71-26873
- Testing armored T-28B for exploring severe hail storms (MRL-68-FR-841) 16 p2626 N71-28466
- Soviet news releases on atmospheric optics, actinometry conference, and expanded hail suppression service 18 p2949 N71-30790
- Studying crop-hail insurance records for northeastern Colorado for designing hail experiment (PB-197644) 18 p2955 N71-31444
- Effect of signal fluctuations on performance of dual wavelength radar hail detector (TR-20) 19 p3457 N71-32530
- One dimensional numerical simulation of dual wavelength radar hail detector (LAP-TR-24) 20 p3295 N71-33022
- Manual for interpreting radar echoes to identify severe thunderstorms, hail, and tornadoes (AD-726983) 22 p3615 N71-35761
- HAIRSTONES**
U HAIR
HAIR BOILING WATER REACTOR
Determining burnup characteristics of fuel elements for Halden Boiling Heavy Water Reactor (HBL-116) 04 p0559 N71-14217
- Nuclear fuel burnup tests of Zircaloy 2 clad UO₂ assemblies in Halden boiling water reactor (HPR-127) 17 p2782 N71-29381
- HAIR REACTOR**
U **HAIR BOILING WATER REACTOR**
HAIR CONES
Lift and drag interference characteristics of delta winged half cones with leading edges 09 p1912 N71-19359
- Three dimensional interactions in half cone pressure fields and effects on intakes mounted adjacent to aircraft fuselage 09 p1969 N71-19367
- Free flight stability tests on half cones in hypervelocity wind tunnels including data reduction program (VKI-TN-66) 19 p3075 N71-31663
- HAIR LIFE**
General formula for artificial electron decay life times (NASA-TM-X-63376) 01 p0118 N71-10768
- Electromagnetic transition probabilities in nuclei with mass numbers between 125 and 153 based on half-life measurements of T, Te, Sm, and Eu isotopic excited states (INR-1149) 02 p0277 N71-12135
- Lifetime and branching ratio studies of Si-28 in search of excited prolate rotational bands (RLO-1925-34) 03 p0420 N71-12645
- Excited Ne-141 levels resulting from decay of Pa-141 isotopes with half life of 21 minutes (JL-CEN-7029) 04 p0593 N71-14447
- Half lives of tritium and plutonium-238 (BNL-50233) 06 p0920 N71-16266
- Tables of half lives for excited nuclear levels (AE-400) 08 p1249 N71-18206

Half life of first excited levels of main and rotational band in even-even nuclei of Os, Er, and Dy [JINR-P6-5201] 08 p1250 N71-18232

Rotating chopper measurement of delayed neutron and short-lived delayed photoneutron groups from U-235 and U-235 in D2O 10 p1617 N71-21265

Using calcium 40 helium 3 reaction to investigate positron decay of titanium 42 to scandium 42 10 p1625 N71-21845

Magnetic moments and lifetimes of 7/2 minus mirror states of Ar-37 and K-37 measured from Cl-37/p,n/Ar-37 and Ca-40/p,alpha/K-37 reactions [CONF-700933-2] 11 p1805 N71-22432

Delayed neutron fission yields and half life curves from time of flight spectrometry of He-3 and He-4 induced fission of U-238, Th-232, and Bi-209 and Cf-252 spontaneous fission 12 p1977 N71-24228

Measurement of half lives of excited states with energy of 155.8 and 227 keV in Th-155 nucleus [JINR-P6-5484] 14 p2317 N71-26751

Chemical properties and half life of cerium [ORNL-TN-2428] 15 p2460 N71-27071

Statistical analysis of cesium 144 half life determinations [AERE-R-6529] 15 p2471 N71-27411

Mapping of fast or thermal neutron produced nuclides with half lives less than 1 minute and gamma energies between 0.01 and 10 MeV [KFKI-70-18-NAC] 15 p2485 N71-27812

Half life of positive and negative pions determined by consideration of number of surviving pions in narrow beam 15 p2493 N71-27937

Photopeaks in gamma ray energies and table on half life, gamma ray energy, and intensity of radioisotopes [JAERI-MEMO-4189] 16 p2654 N71-29059

Two dimensional analyzer for half life measurements of nucleus of excited states by gamma-gamma delayed coincidence method on basis of computer Minak 2 [JINR-P13-5485] 16 p2655 N71-29073

Isothermal calorimetric determination of plutonium 239 half life based on alpha zero energy and recoil energy [RFP-1469] 17 p2799 N71-30020

Determination of half life and spins of Gd-155 levels by method of delayed coincidences and angular gamma-gamma correlations [JINR-P6-5518] 18 p2970 N71-30455

Half lives and spin levels in promethium isotope determined by coincidence and gamma-gamma correlation methods [JINR-P6-5517] 18 p2979 N71-30695

Timing properties of nuclear radiation detectors for subnanosecond spectroscopy [JINR-1213] 19 p3145 N71-31949

Energy spectrum of identified protons and excitation functions following decay of Al-23 [UCRL-20436] 20 p3322 N71-33793

Lifetime of 2 1/2 state of helium-like argon using beam fold method [JINR-20458] 22 p3641 N71-35959

Half lives and gamma transitions in decay of Th-148, Th-149, Th-150, and Th-152 isomers [JINR-P6-5641] 24 p3972 N71-38333

Rotational band transition probabilities calculated from lifetime measurements on structure of Gd-153 [JINR-P6-5526] 24 p3976 N71-38366

HALF SPACES

Half-range expansion theorems in studies of polarized light [AD-710313] 01 p0091 N71-10729

Wave propagation analysis for vibratory surface loads on viscoelastic half space [AD-714643] 06 p0953 N71-15999

Gravitational stresses in elastic half-space bodies with notches or mounds 16 p2585 N71-28209

Application of Lorentz reciprocity theorem to near field detection of buried dielectric spheres in antenna lossy half spaces 16 p2563 N71-28822

Problems in evaluating electromagnetic fields of linear antennas or dipole arrays in dissipative half space [AD-721706] 17 p2725 N71-29480

Expressions for state of stress and displacement for half space deduced from general basic formulas for three dimensional thermoelastic problem [PB-197273] 18 p3024 N71-30882

Dynamic surface loading of elastic half space [REPT-470] 19 p3186 N71-31728

Mode 3 stress intensity factors for isotropic elastic half spaces with curvilinear notches and surface features [RD/BN-1838] 22 p3621 N71-35798

Formalism describing space dependence of energetic resonance self shielding at boundaries of homogeneous zones in nuclear reactors [KFK-1353] 22 p3631 N71-35876

Multiple scattering and eigenfunction solutions for electromagnetic scattering from cylinders over and imbedded in dielectric half spaces 24 p3890 N71-37730

HALIDES

NT ALKALI HALIDES

NT ALUMINUM CHLORIDES

NT AMMONIUM FLUORIDES

NT BARIUM FLUORIDES

NT BERYLLIUM FLUORIDES

NT BORON FLUORIDES

NT BROMIDES

NT CALCIUM CHLORIDES

NT CALCIUM FLUORIDES

NT CARBON TETRACHLORIDE

NT CESIUM FLUORIDES

NT CESIUM HALIDES

NT CESIUM IODIDES

NT CHLORIDES

NT CHLORINE FLUORIDES

NT COPPER CHLORIDES

NT DIFLUORIDES

NT FLUORIDES

NT HYDROCHLORIC ACID

NT HYDROCHLORIDES

NT HYDROFLUORIC ACID

NT LEAD CHLORIDES

NT LITHIUM CHLORIDES

NT LITHIUM FLUORIDES

NT MAGNESIUM CHLORIDES

NT MAGNESIUM FLUORIDES

NT METAL HALIDES

NT NICKEL FLUORIDES

NT NITROGEN FLUORIDES

NT OXYGEN FLUORIDES

NT OXYHALIDES

NT OZONE FLUORIDE

NT PHOSGENE

NT POTASSIUM BROMIDES

NT POTASSIUM CHLORIDES

NT POTASSIUM IODIDES

NT SILVER CHLORIDES

NT SILVER HALIDES

NT SILVER IODIDES

NT SODIUM CHLORIDES

NT SODIUM FLUORIDES

NT SODIUM IODIDES

NT STRONTIUM FLUORIDES

NT SULFUR CHLORIDES

NT SULFUR FLUORIDES

NT TETRACHLORIDES

NT TITANIUM CHLORIDES

NT TUNGSTEN FLUORIDES

NT URANIUM FLUORIDES

Fusion enthalpies and entropies of lead halides [TID-25453] 01 p0133 N71-10481

Volume dependence of Gruneisen parameter for metal halides [ORO-3802-6] 01 p0112 N71-10759

Ultrasonic parameters in Born model of rubidium halides [ORO-3802-5] 03 p0435 N71-12999

HALITES

Laboratory and in situ determinations of physical properties of natural rock salt using seismic wave velocities [NASA-TT-F-13500] 08 p1192 N71-18968

HALL COEFFICIENT

U HALL EFFECT

HALL CURRENTS

U ELECTRIC CURRENT

U HALL EFFECT

HALL EFFECT

Investigating galvanomagnetic effects in developing higher magnetoresistance devices for low voltage high current switches [NASA-CR-110998] 01 p0030 N71-10044

Electrical resistivity and Hall coefficient measurements of semiconductor materials 01 p0109 N71-10204

Simultaneous donor and acceptor concentration determination in n-type semiconductors using Hall effect measurements [ONERA-NT/02/1670] 02 p0285 N71-11856

Conduction mechanisms in high quality GaAs studied by measuring resistivity and Hall constant [AD-712804] 02 p0287 N71-12151

Developing digital magnetic compasses based on Hall effect for small boats [AD-712547] 04 p0544 N71-14342

Quantum galvanomagnetic and thermomagnetic effects in graphite in magnetic fields at low temperatures [NASA-TN-D-7037] 06 p0932 N71-15917

Design and fabrication of silicon, micro-Hall devices [AD-719999] 06 p0823 N71-16415

Polar cap electric field measurements, and model for Hall current aural electrojet continuity and polar cap magnetic disturbances [NASA-TM-X-65447] 07 p0109 N71-17270

Apparatus for dc electrical measurement of Hall and photo-Hall effects in high resistivity semiconductors 09 p1387 N71-19430

Measurement of macroscopic aerodynamic quantities in plasma jets produced by electrothermal and Hall current accelerators 11 p1812 N71-22619

Current measurement by use of Hall effect generator [NASA-CASE-XAC-01662] 11 p1766 N71-23037

Hall effect measurements for p-type silicon-on-sapphire films in temperature range 77 to 300 K 11 p1819 N71-23080

Amending theory of Hall effect in intrinsic semiconductors by replacing global neutrality for local neutrality [NLL-M-20331-5824.4F/] 12 p1987 N71-24137

Brushless dc tachometer design with Hall effect crystals and output voltage magnitude proportional to rotor speed [NASA-CASE-MPS-20385] 13 p2057 N71-24944

Hall, capacitance, and time-dependent measurements of radiation hardened Li-diffused solar cells 14 p2201 N71-26229

Cryogenic Hall measurements, electron damage, and room temperature recovery in irradiated frozen, lithium-doped silicon 14 p2201 N71-26231

Electrical resistivity, Hall coefficient, and reflectivity measurements of single crystals of lead-tin-telluride semiconducting alloys 15 p2307 N71-27389

Phase sensitive detector and commercial Hall probe combined with control current amplifier to provide sensitive, low field magnetometer for use from room to liquid helium temperatures [AD-721590] 16 p2593 N71-28497

Search for active interactions and measurements of resistivity tensor in superconducting indium 17 p2788 N71-29783

Electron mobility mechanisms in epitaxial growth of gallium arsenide crystals and computer program for calculating Hall effect [AD-722630] 18 p2995 N71-30734

Model description of polycrystalline semiconductor film assuming different conductivities and Hall mobilities for grains and boundaries [NASA-TT-F-13600] 18 p2995 N71-31094

Minority carrier in single crystal and pyrolytic graphite studied by observing magnetic field oscillations in Hall voltage and thermopower [NASA-TN-D-64466] 19 p3169 N71-32163

Excess Cd induced CdS crystal defects determined by Hall effect and electrical resistivity measurements in high temperature environments 19 p3169 N71-32270

Magnetohydrodynamic ionized gas cylinder flow with Hall effect [DLR-FB-70-50] 20 p3329 N71-33019

Measurements of Hall coefficient for indium arsenides and indium antimonides at low temperatures and various magnetic fields 20 p3336 N71-33940

Interpretation of Hall coefficient of pure copper, silver, gold, and some silver alloys based on anisotropic Fermi surface model [NRC-TT-1476] 22 p3592 N71-35581

Influence of group B metals on electrical resistivity, Hall effect, and thermophysical properties of polycrystalline copper and silver alloys [NRC-TT-1474] 22 p3592 N71-35582

Electrical resistance, Hall constants and absolute thermopower of disordered series of solid solutions of nickel with elements of first long period [NRC-TT-1477] 22 p3593 N71-35583

Analysis of Hall effect in plasma oscillation to include arbitrary amplitude electron oscillations, stability of low density pinch, and oscillations in electron hole pinch [IAE-1950] 22 p3653 N71-36049

Properties determination of rutile in areas of crystal growth, sample preparation, semiconductor device, and Hall effect [AD-72752] 23 p3835 N71-37349

Numerical model to simulate plasma behavior in linear multicusp pinch device [polytron] [CONF-T10607-44] 24 p3987 N71-38447

HALL GENERATORS

Critical channel length of Hall-type MHD generator [JINR-1159] 03 p0317 N71-12264

MHD generator performance with leakage currents [JINR-1190] 05 p0733 N71-12089

Preparation and characteristics of indium arsenide films grown by coplanar chemical transport used for commercial production of thin film Hall generators 11 p1814 N71-21939

Current measurement by use of Hall effect generator [NASA-CASE-XAC-01662] 11 p1766 N71-23037

HALO ORBIT SPACE STATION

Halo Orbit Space Station potential for lunar communications, exploration, logistics, and launching platform operations [NASA-TM-X-654009] 05 p0772 N71-15351

Utilization of halo orbits in lunar space station, communication, and shuttle operations [NASA-TN-D-6365] 18 p3018 N71-31055

HALO PARACHUTING
U PARACHUTE DESCENT
HALOGEN COMPOUNDS
 NT ALKALI HALIDES
 NT ALUMINUM CHLORIDES
 NT AMMONIUM CHLORIDES
 NT AMMONIUM PERCHLORATES
 NT BARIUM FLUORIDES
 NT BERYLLIUM FLUORIDES
 NT BORON FLUORIDES
 NT BROMIDES
 NT CALCIUM CHLORIDES
 NT CALCIUM FLUORIDES
 NT CARBON TETRACHLORIDE
 NT CESIUM FLUORIDES
 NT CESIUM IODIDES
 NT CESIUM IODIDES
 NT CHLORIDES
 NT CHLORINE COMPOUNDS
 NT CHLORINE FLUORIDES
 NT COPPER CHLORIDES
 NT DICHLORODIPHENYL-
 TRICHLOROETHANE
 NT DIFLUORIDES
 NT DIFLUORO COMPOUNDS
 NT FLUORINE ORGANIC COMPOUNDS
 NT FLUORO COMPOUNDS
 NT FLUOROCARBONS
 NT FLUOROSULFONIC ACIDS
 NT HALIDES
 NT HYDROCHLORIC ACID
 NT HYDROCHLORIDES
 NT HYDROFLUORIC ACID
 NT IODATES
 NT IODIDES
 NT IODINE COMPOUNDS
 NT LEAD CHLORIDES
 NT LITHIUM CHLORIDES
 NT LITHIUM FLUORIDES
 NT MAGNESIUM CHLORIDES
 NT MAGNESIUM FLUORIDES
 NT METAL HALIDES
 NT NICKEL FLUORIDES
 NT NITROGEN FLUORIDES
 NT OXYALIDES
 NT OZONE FLUORIDE
 NT PERCHLORATES
 NT PERFLUOROALKANE
 NT PHOSGENE
 NT POLYTETRAFLUOROETHYLENE
 NT POTASSIUM BROMIDES
 NT POTASSIUM CHLORIDES
 NT POTASSIUM IODIDES
 NT POTASSIUM PERCHLORATES
 NT SILVER CHLORIDES
 NT SILVER HALIDES
 NT SILVER IODIDES
 NT SODIUM CHLORIDES
 NT SODIUM FLUORIDES
 NT SODIUM IODIDES
 NT STRONTIUM FLUORIDES
 NT SULFUR CHLORIDES
 NT SULFUR FLUORIDES
 NT TETRACHLORIDES
 NT TITANIUM CHLORIDES
 NT TUNGSTEN FLUORIDES
 NT URANIUM FLUORIDES
 Raman, infrared, and far infrared spectra of laser
 excited sulfur monochloride and sulfur monobromide
 12 p1872 N71-24062
 Raman spectrum perturbation in benzene solutions
 of sulfur monochloride and sulfur monobromide
 12 p1872 N71-24065
 Thermodynamic dissociation and vaporization
 properties of gold chlorides and gold bromides
 14 p2272 N71-25818
 Vapor pressure-temperature tables for halogen
 containing substances
 22 p3350 N71-25288
HALOGENATION
 NT CHLORINATION
 NT FLUORINATION
 Spontaneous cardiac arrhythmias induced by
 methoxyphenylpropane in monkeys
 19 p3042 N71-31733
HALOGENS
 NT BROMINE
 NT BROMINE ISOTOPES
 NT CHLORINE
 NT FLUORINE
 NT IODINE
 NT IODINE ISOTOPES
 NT IODINE 125
 Reactions of selected halogens and interhalogens
 initiated by radiative neutron capture and isomeric
 transition
 00-1617-26
 Dissociation energies and long range potentials of
 diatomic halogen molecules from vibrational spacings
 09 p1428 N71-19740
 Ground state dissociation energies for diatomic
 halogen from vibrational spacings near dissociation
 limit
 09 p1429 N71-19746

Molecular recombination and dissociation kinetics
 in flash photolysis of halogens
 09 p1442 N71-20384
 Modification of polyurethanes with alkyl halide
 resins, inorganic salts, and encapsulated volatile
 and reactive halogens for fuel fire control
 [NASA-CASE-ARC-10096-1] 13 p3039 N71-24739
 Hot atom beam in halogen and hydrogen sources,
 cathode quenching of metal, and hot atom
 reactions of alkali metals
 19 p3050 N71-32107
 Failure analysis of halogen quenched Geiger-
 Mueller tube operation
 [DUN-54-136] 20 p3308 N71-33743
 Properties of improved multiple anode halogen
 Geiger-Mueller counters
 24 p3919 N71-37949
HALOPHILLES
 Purification and characterization of enzymes from
H. salinarum, *B. stearothermophilus*, and *V. marinus*
 [RL-2227-T-5-1] 16 p1501 N71-21527
HALOS
 Venus halo and photometric evidence for ice in
 Venus clouds
 [NASA-CR-116124] 06 p0945 N71-16634
HAMBURGER AIRCRAFT
 NT HFB-320 AIRCRAFT
 HAMBURGER HFB-320 AIRCRAFT
 U HFB-320 AIRCRAFT
HAMILTON-JACOBI EQUATION
 Approximate solution of stochastic optimal control
 problems using Hamilton-Jacobi equation
 [AD-712370] 02 p0250 N71-11607
 Solving general multidimensional linear optimal
 control problem with quadratic cost functional and
 noncommutative weighting on final states
 [AD-712716] 04 p0337 N71-13950
 Linear regulator problem solution using Euler
 equations of motion, Laplace transformations, and
 Hamilton-Jacobi equation for stochastic control
 14 p2235 N71-26444
 Invariance of nonrelativistic Hamilton-Jacobi
 equation in electromagnetic field
 [JINR-P2-5373] 15 p2463 N71-27174
HAMILTONIAN FUNCTIONS
 Numerical analysis of weak nuclear reactions
 [AD-710572] 01 p0093 N71-10031
 Hamiltonian functions of quantum mechanical
 system having given Lie algebra as spectrum
 generating algebra
 [IC-70/26] 02 p0276 N71-19116
 Quantum statistics Hamiltonians and model
 Hamiltonians of superconductivity theory
 [ITF-70-36] 03 p0431 N71-12925
 Determination of density matrix components for
 multi-configuration wave functions and Hamiltonian
 interaction matrices
 [NASA-CR-116685] 08 p1265 N71-19137
 Model for Hamiltonization and quantization of
 radiatively damped systems
 08 p1227 N71-19156
 Second-order solutions of Hamiltonian functions
 for EPR study of Jahn-Teller effect in $\text{SrCl}_2\text{-La}^{2+}$
 phase
 [NASA-CR-116683] 08 p1282 N71-19291
 Characterization of collisional kinetic equations and
 solutions using constants of motion method including
 Chandrasekhar, Hamiltonian, Vlasov, and Langmuir
 formulations
 [NASA-TM-X-65493] 12 p1970 N71-23302
 Anderson model and Hamiltonian functions for
 resonant scattering study by metal impurities
 [AD-718903] 12 p1973 N71-23935
 Hamiltonian implying Pauli exclusion principle
 applied to elementary particle considerations
 [LNF-70/22] 15 p2481 N71-27490
 Mass coefficient in nucleus collective Hamiltonian
 and sum rules for probabilities of E2 transitions and
 quadrupole moments
 [JINR-P4-5346] 15 p2484 N71-27795
 Nuclear magnetic resonance of chlorinated
 hydrocarbon molecules in excited triplet states using
 Hamiltonians for electron spin-spin, nuclear quadrupole,
 and hyperfine interactions
 [JCL-20-20] 17 p2791 N71-29271
 Development of spin Hamiltonian theory for very
 low symmetry systems with matrix-diagonalization
 programs and tensorial notation for analysis of ESR
 spectra
 17 p2828 N71-30256
 Employing Hamiltonian function for definition of
 quasi-averages for model systems with negative four
 fermion interaction
 18 p2974 N71-30559
 Hamiltonian formulation of quantum theory and
 quasi-potential equation for interaction of particles
 with spin 1/2 and 0
 [JINR-P2-5605] 18 p2977 N71-30655
 Hamiltonian model of superconductivity in infinite
 volume for excited states
 [ITF-70-90-E] 19 p3146 N71-31971
 Relativistic correction to Fermi-contact hyperfine
 Hamiltonian derived for arbitrary principle quantum
 number
 [NP-18018] 23 p3815 N71-37307

Current algebra sum rules in neutron scattering and
 static dimensions of chiral symmetry breaking
 Hamiltonian
 [TR-72-034] 23 p3819 N71-37344
HAMMERS
 NT ELECTROMAGNETIC HAMMERS
 Prevention of steam hammer instability and film
 collapse caused by condensation in steam lubricated
 bearings
 [AD-722005] 16 p3800 N71-28598
HAND [ANATOMY]
 Electromotive force measurements on electric
 motor for electronic hand prosthetic device
 [POA-2-C-2353-54] 14 p2330 N71-26532
HANDBOOKS
 Shock circuit analysis handbook
 [NASA-CR-106721] 03 p0943 N71-12487
 Weight estimating and forecasting of manned space
 systems during conceptual design
 [NASA-CR-106765] 04 p0615 N71-14185
 Research progress in developing shielded flat-cable
 and termination method
 [NASA-CR-102525] 05 p0891 N71-14819
 Handbook of electromagnetic propagation in
 conducting media
 [AD-714866] 06 p0817 N71-16630
 User manual for test equipment used in simulating
 aerodynamic heating and acoustical environments on
 space shuttle thermal protection specimens
 [NASA-CR-103017] 07 p1094 N71-17451
 Handbook on environmental and space utilization
 criteria for design of extraterrestrial manned
 spacecraft and shuttles
 [NASA-CR-114846] 07 p1119 N71-17540
 Handbook for summing two harmonics
 [AD-712801] 10 p1659 N71-31805
 Viscosity of gases and gas mixtures - handbook
 [IT-70-50022] 12 p1901 N71-23783
 History of rocketry in China including structure of
 rockets, advantages and disadvantages of various
 rockets, and capabilities of intercontinental missiles
 [AD-720382] 14 p2343 N71-26022
 Weight and Measures Labeling Handbook for use in
 packaging and labeling commodities and enforcing
 state laws and regulations
 [NBS-HB-108] 16 p2601 N71-28546
 Uniform instructions for standard weather
 observing and reporting techniques
 [AD-720106] 16 p2627 N71-28684
 Design handbook for steady state radiation effects
 on semiconductor diodes
 [NASA-CR-11785] 16 p2572 N71-28811
 Steady state radiation effects on electrical insulating
 materials and capacitors - handbook
 [NASA-CR-11787] 17 p2726 N71-29776
 Handbook for assessing applicability of miscom-
 puter to test designs
 [BDX-613-275] 18 p2892 N71-30508
 Goddard astronomical and geophysical parameters
 including fundamental astronomical constants,
 gravitational harmonic coefficients, station locations,
 and other geometric quantities
 [NASA-TM-X-65607] 18 p3008 N71-30513
 Handbook of standard samples issued in USSR for
 determining properties and composition of substances
 and materials
 [NBS-SP-260-30] 18 p3029 N71-31334
 Internal aerodynamics design manual considering
 internal air flow system effect on aircraft performance
 including bibliography
 [AD-723823] 19 p3173 N71-32039
 Aerodynamic design manual considering internal
 air flow system effects on aircraft performance
 [AD-723824] 19 p3173 N71-32060
 Internal aerodynamics manual considering
 internal air flow system effect on aircraft performance
 [AD-723841] 19 p3174 N71-32061
 Thermal control coatings - radiation effects design
 handbooks
 [NASA-CR-11784] 19 p3045 N71-32288
 Procedures for estimating control costs and
 emission reductions for specified air pollution sources -
 users manual
 [PB-196779] 19 p3199 N71-32589
 Handbook for airframe and powerplant mechanics
 preparing for mechanic certification for FAA aircraft
 and engine mechanic examinations
 [FAA-AC-65-9] 20 p3212 N71-33678
 Handbook of correlative data on gaseous cosmic
 rays, solar electromagnetic radiation, solar protons,
 geomagnetism, ionosphere, and neutral atmosphere
 [NASA-TM-X-67294] 21 p3532 N71-35148
 Handbook on use of radio-measurement instru-
 ments
 [AD-726385] 22 p3561 N71-35564
 Guide to private and commercial multibeam
 aircraft pilot certification
 [FAA-AC-61-4C] 23 p3687 N71-36438
 Thermal decomposition and combustion of
 explosive substances - handbook
 [AD-726573] 23 p3687 N71-37545
 Handbook presenting classification of electronic
 and analog computers and analog devices
 [AD-727262] 24 p3895 N71-37758

HANDLING

Aerodynamic calculations in designing axial compressors with emphasis on compressors of stationary installations - handbook
[AD-72191] 24 p3929 N71-38032
Design and performance characteristics of gas turbine engines for helicopters
[AD-72959] 24 p4002 N71-38541

U MATERIALS HANDLING

HANDLING EQUIPMENT
Sol-gel processes and remote handling equipment for coating particles, preparation of thorium, uranium, and plutonium fuels, and accelerated life testing of nuclear fuel elements
[ORNL-4629] 15 p2447 N71-27201
Handling tool for printed circuit cards
[NASA-CASE-MFS-20453] 16 p2405 N71-29133
Disassembly-assembly equipment changes for FFTF core component and test assembly examination and effects on project plans
[ORNL-TM-3400] 24 p3963 N71-38269

HANDLING QUALITIES

U CONTROLLABILITY
HANFORD REACTORS
Irradiation of boron carbide pellets and powders in Hanford thermal production reactors at 500 to 1200 F
[WHAN-FR-24] 15 p2443 N71-26927

HANGARS
Fabrication and field testing of lightweight, recoverable, air-transportable hangar
[AD-727051] 22 p3563 N71-35396
Fabrication and field testing of aircraft maintenance hangars and general purpose shelters
[AD-727047] 22 p3566 N71-35397
Development and characteristics of lightweight, mobile structures for aircraft storage and maintenance
[AD-727056] 23 p3741 N71-36674

HARDENING [MATERIALS]

NT CARBURIZING
NT HOT PRESSING
NT MARAGING
NT NITRIDING
NT PRECIPITATION HARDENING
NT SILICONIZING
NT STRAIN HARDENING
NT WORK HARDENING
Substructural hardening and gas extrusion of metals
[JPRS-51624] 02 p0241 N71-11444
High strength state of metals resulting from substructural hardening
02 p0241 N71-11445

Thermal stresses in chemically hardened elastic media and applications to molding processes
[NASA-CR-115878] 05 p0781 N71-15627
Approximation of residual thermal stresses in flat sheet molded from chemical hardening materials
[NASA-CR-116504] 07 p1125 N71-15752
Materials considered critical to reactor design and performance - effects of radiation on creep, hardening, fracture, and swelling - conference
[BNWL-SA-3495] 08 p1238 N71-18343
Mechanical properties of drawn and annealed titanium alloy
[AD-715880] 08 p1215 N71-18331

Surface evaluation of stainless steel gyro bearings manufactured by various hardening techniques
[NASA-CR-114900] 12 p1929 N71-23949
Gas spring firing and soft recovery of hard wire instrumented 155 mm projectile
[SC-RR-70-849] 17 p2729 N71-29241
Irradiation hardening of structural zirconium alloy and steel materials in nuclear reactor
[INIS-MF-5] 19 p3136 N71-32066

Magnesium alloy plates deformed by oblique explosive loading for hardening without ductility loss
[RFF-1649] 21 p3439 N71-34474
Relationship between mechanical properties of tool steels and hardening temperature
[NLL-M-21013-582Z.4F] 23 p3774 N71-36694

HARDENING [SYSTEMS]
Costs and benefits of nuclear hardness criteria and system design specifications
[AD-727010] 23 p3818 N71-37235

HARDNESS
NT MICROHARDNESS
Defining distribution functions for sets of n cavities in hard particle system using concept of equivalence
02 p0241 N71-11777
Nondestructive tests for hardness of alloys by correlation between pulse-echo ultrasonic attenuation
[AD-717099] 10 p1575 N71-20914

Effect of welding and post-weld heat treatment on Ducoi W30, notch toughness, tensile and hardness properties
[MAT-4] 12 p1930 N71-24085
Fatigue strength diagrams, increasing density of sintered materials, and hardness values related to tensile strength - fatigue properties of titanium and titanium alloys - Part 5
[RAF-LIB-TRANS-1534-PT-5] 18 p2935 N71-30885

Technique for measuring neutron radiation hardness in 14 MeV neutron terms
[SC-DR-710045] 18 p2988 N71-31474

SPOF digital television hardcopy equipment, consisting of system control unit, 12 copy request units, display image buffer, and 12 hardcopy printers
21 p3392 N71-34139

Factors influencing scatter in results of room temperature and elevated temperature tensile tests of steels
[PB-197139] 21 p3439 N71-34472
Lithium doped solar cell hardness to 1 MeV electron irradiation
23 p3709 N71-36442

HARDNESS TESTS
Ultrasonic hardness testing of grinding wheels using modulus of elasticity
[CRIF-MC-36] 08 p1207 N71-18605
Hardness and high pressure deformation mechanisms of glass
08 p1223 N71-19154

Hardness and fatigue tests of steel bearing alloys
[NASA-TM-X-67874] 16 p2603 N71-28854
Recrystallization behavior of tungsten/rhenium alloy dispersion hardened by thorium oxide compared with tungsten after annealing noting cold working degree
[DLR-FB-70-80] 17 p2762 N71-29386

HARDWARE
Applied and research activities at Center for Computer Sciences and Technology
01 p0030 N71-10978
Manufacture and nondestructive testing methods of nuclear rocket engine hardware
02 p0264 N71-11629

NASTRAN computer program applications in stress analysis performed on Skylab hardware
22 p3682 N71-36257

HARMONIC ANALYSIS

NT TESSERAL HARMONICS
NT ZONAL HARMONICS
Computer program for harmonic analysis of curved folded plate structures using finite element method
[PB-193535] 01 p0131 N71-10885
Theory of multiple modes in avalanche diodes
[AD-711923] 02 p0192 N71-11348

Fermi surface investigations in Sn and Te
[AD-711797] 02 p0284 N71-11839
Application of computer graphics to multiharmonic analysis of structural shells
[AD-713101] 05 p0779 N71-15350
Harmonic analysis of series expansion for sound field at caustic
[AD-713597] 05 p0734 N71-15386

Cyclic accelerators with magnetic field harmonic analyzer using digital systems
[AD-714767] 06 p0915 N71-16010
Harmonic analysis of nonlinear forced vibrations of infinitely long cylindrical shells
[AD-716795] 10 p1630 N71-20636

Handbook for summing two harmonics
[AD-717201] 10 p1659 N71-21803
Harmonic analysis of seasonal variations of atmospheric circulation in Northern Hemisphere
11 p1752 N71-22006
Harmonic analysis for determination of meteorological elements for annual seasons in Oriztek
[NLL-M-20096-5828.4F] 12 p1957 N71-24003

Electron accelerator magnet ring survey using particle telescope with micrometer and harmonic analysis for orbit distortions
[CEAL-1102] 13 p2125 N71-24905
Harmonic analysis and nuclear model of lithium 6 core distortion and effects on energy levels, magnetic dipole and electric quadrupole moments, and Pauli exclusion principle
15 p2494 N71-27955

Measurement of second harmonic distortion in acoustic output of transducer by Michelson laser interferometer technique
[AD-721721] 16 p2592 N71-28309
Effect of spaced data interpolation upon harmonic coefficients
[AD-721593] 16 p2623 N71-28565

Harmonic analysis of earth inclinations by Engelhart Astronomical Observatory
23 p3749 N71-36726

HARMONIC EXCITATION

Electron cyclotron harmonic waves in magnetically confined low pressure gas discharge
[IPP-2/84] 08 p1270 N71-18251
Use of simple harmonic forces in nonrelativistic quark model to determine N resonances
18 p2984 N71-31051

HARMONIC FUNCTIONS

Harmonic functions applied to two dimensional asymmetric flow and thermodynamics
[AD-721902] 17 p2732 N71-29372
Application of harmonic functions to electrostatic potentials and magnetostatics
[AD-721903] 17 p2787 N71-29425
Applications of P-harmonic principal functions to thermodynamics and electro- and magnetostatics
[AD-721904] 17 p2788 N71-29704

HARMONIC GENERATIONS

Generation of second harmonic light in transparent media by pulsed ruby laser
[AD-711283] 01 p0064 N71-10847

Phase matched critical total reflection and Generation of second harmonic generation
[AD-710772] 04 p0567 N71-14191

Third-harmonic generation in cholesteric, far infrared generation by ultrashort pulses, and self focusing of light as examples of nonlinear optical effects
[UCRL-20358] 16 p1699 N71-21889
Techniques for solving problem of sound transmission from harmonic monopole source through glass corrugated boundary between fluid media
[AD-722029] 16 p2638 N71-28240

Nonlinear optical properties of crystalline materials in iodate family evaluated by second harmonic powder technique
[AD-724300] 20 p3287 N71-33041
Statistical analysis of some nonlinear optical effects including scattering light from rotating glass and second harmonic light generated by pseudo-thermal source
[NASA-CR-121935] 22 p3628 N71-33840

HARMONIC GENERATORS

Optical quality barium sodium niobate as harmonic generator
01 p0109 N71-10802
Collinear collisions with exponential repulsive potential of atom and harmonic oscillator
[AD-711107] 01 p0101 N71-10697

HARMONIC MOTION

Free vibrations and harmonic and aperiodic forced vibrations of elastic spherical thin shells in water
22 p3693 N71-36317

HARMONIC OSCILLATION

Computer program for calculation convective heat transfer coefficients from harmonic temperature oscillations
[NASA-TM-X-2147] 04 p0590 N71-13465
Oscillatory characteristics of swimming and locomotion of aquatic animals
11 p1681 N71-22205

Determination of kinematic and dynamic response of elastically supported mechanical systems with interfaces subjected to mechanical separation
11 p1771 N71-22810
Human physiology, thermoregulation, and harmonic oscillation of blood glucose levels
[NASA-CR-1806] 16 p2542 N71-28206

Numerical analysis of aerodynamic loads and coefficients for tandem and T tail surfaces harmonically oscillating in subsonic flow
17 p2698 N71-29335
Calculation of pressure distribution over wings with harmonic oscillating control surfaces using kernel function method
17 p2699 N71-29346

Unsteady pressure measurements on harmonically oscillating swept wing with two control surfaces in incompressible flow
17 p2700 N71-29338
Pressure measurements of harmonically oscillating sweptwing wing with two flaps in incompressible flow
[DLR-FB-70-47] 17 p2700 N71-29413

Analysis of nonlinear resonant effects of external optical signal acting on laser oscillator
20 p3282 N71-33716
Transient and harmonic wave effects on composite materials
[SC-RR-710024] 21 p3444 N71-34399

HARMONIC OSCILLATORS
Asymptotic expansion and Schroedinger equation for perturbed harmonic oscillator
[AD-719272] 13 p2127 N71-24044
Quasi-free electron scattering from protons with scattering calculation from harmonic oscillators and Wood-Saxon potentials for bound state protons and wave functions for final states
13 p2138 N71-24477

Quasi-potential wave functions for relativistic corrections to energy levels of harmonic oscillator
[JINR-E2-5339] 15 p2461 N71-27803
High efficiency mode diodes, waveform, and circuit studies for improving avalanche oscillators
[SC-CR-70-6171] 17 p2725 N71-29413

Radiation of charged harmonic oscillators coupled to electromagnetic field
[INR-P-1203] 19 p3148 N71-32028
Viscous damping and harmonic disturbing forces in rotors with critical speed, support deflection, and support phase angle determinations
[NASA-TM-X-67896] 20 p3358 N71-33247

Equations of motion for rotating gravity gradiometer, developed for forced harmonic oscillator model
[NASA-TM-X-646605] 21 p3425 N71-34571
Binding energy and ground state wave function of triton with relativistic nucleon-nucleon interaction in harmonic oscillator basis
[NYO-4032-36] 21 p3476 N71-34753

Harmonic oscillator systems applied to orbit perturbation theory with two body motion
[NASA-CR-121667] 21 p3507 N71-34087
Wave packet analysis of quantum dynamics for ion and harmonic oscillators, and transition probabilities for atom-diatom molecular collision
22 p3449 N71-30822
Canonical and noncanonical equilibrium of infinite chains of coupled harmonic oscillators
23 p3823 N71-37770

SUBJECT INDEX

Generalized harmonic oscillator formalism constructed in dual resonance model when relevant particles lie on different trajectories
[OU-LNS-71-4] 24 p3947 N71-38154

HARMONIC RADIATION
NT HARMONIC GENERATIONS
HARMONICS
NT HARMONIC EXCITATION
NT HARMONIC GENERATIONS
NT HARMONIC OSCILLATION
NT SPHERICAL HARMONICS
NT TESSERAL HARMONICS
NT ZONAL HARMONICS
Harmonic coincidences between pairs of far infrared continuous radiation gas lasers for light speed determination
[NPL-QU-8] 03 p3388 N71-13266
Performance prediction of squirrel cage induction machines with nonstationary mmf distributions
14 p2230 N71-26437
Hyperspherical functions used for obtaining lower bounds on scattering functions
[JNPR-P4-5366] 15 p2473 N71-27442
Practical possibilities of separable expansion of partial harmonics of nucleon-nucleon potential
[JNPR-P4-5510] 16 p2645 N71-28120
Harmonic model of thermal energy trapping by steady moving dislocations
17 p2819 N71-29953
X-harmonics method for calculating binding energy wave functions of H-3 and He-3 nuclei
[IAE-3008] 19 p3149 N71-32105
Ellipsoidal gravity coefficients determined from expansion of geopotential in ellipsoidal harmonics series
[AAS-71-330] 20 p3345 N71-32924

HARTREE
Helmet and torso tie-down mechanism for shortening pressure suits upon inflation
[NASA-CASE-XMS-90784] 03 p3327 N71-12335
Acceptance tests of various upper torso restraints by automobile users with application to general aviation aircraft
[FAA-AA-71-12] 16 p2549 N71-28006

HARTREE-APPROXIMATION
Experimental and theoretical ionization potentials for elements hydrogen to krypton calculated by Hartree-Fock method
[AD-712454] 03 p3333 N71-12376
Using Roothaan expansion method to calculate self consistent field wave function close to Hartree-Fock limit for oxygen monofluoride at six internuclear distances
[JML-7702] 04 p5677 N71-13952
Standard method for protecting energy spectra
[NASA-TM-X-52943] 05 p6747 N71-15253
Comparing coupled channels and distorted wave Born approximation optical model parameters in 2a-1d shell to investigate inelastic neutron scattering
[NASA-TM-X-52953] 05 p6748 N71-15282
Investigating short-range behavior of wave function by comparing projected Hartree-Fock spectra using basis functions having harmonic oscillator and Woods-Saxon radial dependence
[NASA-TM-X-52944] 05 p6748 N71-15283
Program for solving mixed relativistic and nonrelativistic form of Hartree-Fock equations
[AD-714073] 06 p5919 N71-16247
Hartree-Fock computer programs to calculate molecular wave functions of light metal diatomic hydrides, oxides, and halides
[AD-715977] 06 p5925 N71-16814
Local and nonlocal nucleon-nucleon force and Hartree-Fock theory
[NBA-CONF-1568] 08 p1250 N71-18239
Effects of altering truncated basis space used in Hartree-Fock method for light deformed nuclei
[NASA-TN-D-6187] 09 p1443 N71-20456
Eigenvalues, radial expectation values, and potentials for free atoms from Z equals 2 to 126 as calculated from relativistic Hartree-Fock-Slater atomic wave functions
[JNRL-4614] 10 p1614 N71-20840
Radial potential properties and nucleon-nucleon interactions for nuclear Hartree-Fock approximation
10 p1623 N71-21766
Hartree approximation for ground state correlations in variational parameters in nuclear many body problem
[NYO-3171-333] 12 p1973 N71-23938
Unrestricted Hartree-Fock atomic wave functions for neutral, divalent, and trivalent transition metal atoms
13 p2131 N71-24969
Hartree-Fock approximation of shell model potential and two-nucleon spin-orbit splitting
13 p2135 N71-25197
Computer programs for Hartree-Fock wave function calculations and for rotational band spectrum calculations
[NBA-CONF-2050] 14 p2310 N71-26637
Analyzing Hylleraas correlation functions to Gell-Mann combinations of Hartree-Fock orbitals for two electrons
15 p2484 N71-27790

Hartree approximation for self-consistent theory of nuclear spectra, including pairing plus quadrupole interaction model applied to tin isotopes
[UFR-0004N] 16 p2650 N71-28880
Matrix elements of nucleon-nucleon interaction for Hartree-Fock calculations in light nuclei
[IFA-PT-70] 16 p2661 N71-29199
Configuration interaction approach to improving Hartree-Fock representation of pi-electron systems
17 p2796 N71-29787
Hartree-Bogolubov theory and application to neutron proton pairing problem
17 p2800 N71-30104
Uses of spin-unrestricted Hartree-Fock method in approximating potential energy curves for molecular dissociation in hydrogen compounds and nitrides
19 p3090 N71-32167
FORTRAN 4 code to perform extended variational approximation for light and intermediate nuclei
[AECI-3801] 19 p3155 N71-32400
Hartree-Fock equations with quadrupole and hexadecapole deformations for investigating stability of stationary states of two particle two hole excitations
[LPTHE-71/18] 21 p2474 N71-34737
Hartree-Fock theory for calculating coherent X ray scattering factors
[BGG-1183-1466] 22 p3645 N71-35990
Hyperpolarizabilities for Hartree-Fock atoms
24 p3983 N71-38427

HARTREE-APPROXIMATION
U HARTREE APPROXIMATION
HARTREE-FOCK APPROXIMATION
U HARTREE APPROXIMATION
HARTLEY (TRADEMARK)
Titanium influence on high temperature deformation and fracture behavior of some nickel based alloys, Hastelloy
[ORNL-4561] 03 p3389 N71-12558
Weldability evaluation of thick sections of Hastelloy X with varying aluminum content, for NBRVA series
[NASA-CR-115886] 05 p6992 N71-14889
Influence of titanium, zirconium, and hafnium additions on resistance of modified Hastelloy N to irradiation damage at high temperatures
[ORNL-TM-3664] 14 p2367 N71-25640
Mechanical properties of molten salt reactor experiment Hastelloy N surveillance specimens deteriorated with increasing fluence
[ORNL-TM-3663] 20 p3286 N71-33888
Design data for regeneratively cooled panels from low cycle fatigue evaluation of Hastelloy X and Inconel 625 sheet and sandwich panel specimens
[NASA-CR-1884] 24 p4027 N71-38734

HATCHES
Design and specifications of emergency escape system for spacecraft structures
[NASA-CASE-MSC-12086-1] 03 p3328 N71-12345
Stretcher with rigid head and neck support with capability of supporting immobilized person in vertical position for removal from vehicle hatch to exterior also useful as splint stretcher
[NASA-CASE-XMF-96399] 12 p1845 N71-23159

HAWAII
Tables of high and low tide predictions for west coast of North and South America and Hawaiian Islands
01 p0050 N71-10804
Aeromagnetic, gravity, and electrical resistivity exploration between Palau and Pohnpei, Hawaii
[PB-192807] 02 p0213 N71-11680
Seismic survey of sand bodies off leeward Oahu, Hawaii
[PB-193992] 05 p0668 N71-14758
Orthogonal functions for linear analysis of sea tides at Hawaii
[PB-195620] 06 p1186 N71-18352
Paleontologic study of coastal lithology on Hawaii
[PB-195634] 06 p1187 N71-18353
Lava tube and channel development in basalt flow in upper east rift zone of Kilauea volcano, Hawaii
[NASA-TM-X-62014] 08 p1192 N71-18965
Upper atmosphere and rain data for Oahu and 300 mb trough effects on trade wind rainfall including seasonal variations
[NIG-70-28] 12 p1959 N71-26227
Bathymetric surveys of north insular shelf of Molokai Island, Hawaii
[HIG-69-21] 15 p2914 N71-31006
Synoptic meteorological tables for marine coastal areas including Hawaii and Pacific Islands
[AD-723798] 19 p3130 N71-32682
Computer modeling of loading problem for linear viscoelastic earth of ocean bottom near Hawaiian Archipelago
23 p3753 N71-36765

Operational performance of Hawker Siddeley aircraft automatic flight approach and landing control system
12 p1834 N71-23414

HAZARDS
NT AIRCRAFT HAZARDS
NT FLIGHT HAZARDS
NT METEOROID HAZARDS
NT OPERATIONAL HAZARDS
NT RADIATION HAZARDS
NT TOXIC HAZARDS
Technical and engineering investigation of transportation of hazardous materials
[AD-692183] 01 p0015 N71-18286
Lighting hazard to rockets during launch
[NASA-CR-111118] 01 p0047 N71-10412
Effects of long term exposure on auditory thresholds for discrete tonal signals and recovery from temporary threshold shift
09 p1335 N71-20533
Pure tone audiology for monitoring hearing and determining physical profiles of persons routinely exposed to potentially hazardous noise
[AD-717846] 11 p1600 N71-22151
Oxygen difluoride hazards, chemical and physical properties, decontamination methods, and transfer and storage techniques manual
[NASA-CR-72401] 12 p1925 N71-23169
Test procedures for evaluating telescopes including test procedures, safety hazards, maintenance, human factors engineering, and reliability
[AD-718790] 12 p1918 N71-33375
Hazardous conditions associated with electrical, chemical, and radiated energies
[AD-718783] 12 p2019 N71-24107
Noise hazard guide including damage risk criteria for steady state and impulse or gunfire noise
13 p2055 N71-25559
Compilation of safety items covering personnel, electrical equipment, and fire hazards
[NASA-SF-5928/01/1] 20 p3370 N71-33592
Molten sodium container design code and safety procedures
[RD-B-M-1817] 22 p3620 N71-35790
Space shuttle hazards, safety procedures, and escape systems
22 p3475 N71-36203

HAZE
Atmospheric haze - components and formation
[PB-192102] 03 p0493 N71-13022
Light scattering in water clouds, fog, and haze
15 p2439 N71-27524
Correlation between scattering coefficient of atmospheric haze
15 p2403 N71-27540

HEWR REACTOR
U HALDEN BOILING WATER REACTOR
HEAT (ANATOMY)
NT CRANIUM
NT SKULL
Morphological investigation of neural structures of frontal cushion of dolphins
11 p1682 N71-22214
Mechanical responses of human head subjected to acceleration loads determined for use in construction of artificial head
19 p3043 N71-32547

HEAD (PRESSURE)
U PRESSURE HEADS
HEAD MOVEMENT
Investigating dependence of bioelectric activity in tibial antagonistic muscles of animals on direction of rotation and head fixation
08 p1150 N71-18099
Head and eye movements affected by angular velocity and linear acceleration in aerospace environments
[DR-208-VOL-1] 18 p2878 N71-31526
Anticompanying oculomotor responses during rapid head rotation at high angular velocity
[AMRU-R-64-2] 18 p2879 N71-31528
Angular velocity transduction of semicircular canals of head
[AMRU-R-65-1] 18 p2879 N71-31529
Retinal image fixation during normal head movement
[AMRU-R-65-3] 18 p2879 N71-31531
Interactions between optokinetic and vestibulo-ocular responses during head rotation at angular velocity in various planes
[AMRU-R-66-3] 18 p2880 N71-31537
Ocular nystagmus during slow head rotation
[AMRU-R-66-4] 18 p2880 N71-31538

HEALTH
NT HEALTH PHYSICS
Effects of atmospheric discharges of tritiated steam on human health
[CEA-CONF-1560] 06 p0798 N71-15718
Health effects of sonic booms noting human reactions and performance, sleep deprivation and accident processes
[BVR-TR-25] 10 p1504 N71-20699
Public health hazards and solutions of environmental lead problems
[AP-90] 20 p3255 N71-32803

Computer technology for medical information systems, in patient care, and for diagnostic purposes 24 p3893 N71-37745

HEALTH PHYSICS

Research planning in environmental health science 01 p0012 N71-10575

Development and implementation of R and D and program planning capability for Environmental Health Services (PB-194410) 04 p0480 N71-14476

Investigating information resources available to Environmental Health Service for protecting men's environment (PB-194411) 04 p0480 N71-14477

Mathematical model for environmental transport of lead from several sources and subsequent intake by man (PB-194412) 04 p0481 N71-14478

Annotated bibliography of information facilities and data resources available to Environmental Health Service on environmental pollution (PB-194414) 04 p0481 N71-14480

Comparison of health physics measuring procedures at accelerators (DESY-70/27) 05 p0727 N71-15089

Investigating health physics, safety factors, fire prevention, and materials handling in reactor research (CONF-690441) 05 p0729 N71-15218

Electronic product radiation and health physicists including ionizing radiation - conference (PB-195772) 09 p1328 N71-19400

Protective measures for operators tuning, testing, operating, and regulating HF and SHF radar and radar equipment (JPRS-52622) 10 p1526 N71-21645

Guide for fabricating and handling CI-252 sources including health physics procedures, shielding requirements, containment and ventilation requirements, and purification techniques (SRO-153) 13 p2142 N71-23565

Experimental and theoretical high energy studies also atomic, statistical, plasma, and health physics - computing and data handling (UCRL-20120) 14 p2301 N71-25741

Radioactive waste disposal, radiation physics, and dosimetry related to health physics (ORNL-4584) 15 p2482 N71-27744

Radiation protection program of New Zealand (NP-18529) 16 p2577 N71-30638

Nuclear research, nuclear structure, data acquisition, proportional and spark counters, accelerator performance, and health physics 20 p3324 N71-33878

Advantages of various types of liquids taken by workers under high temperature working conditions (miners, fire fighters, steelworkers) (NASA-TT-F-14002) 23 p3713 N71-36469

HEAO

Describing conceptual design for High Energy Astronomy Observatory spacecraft and major systems (NASA-CR-162962) 05 p0771 N71-15318

Design of experiments and systems for HEAO to determine composition and spectra of high energy cosmic rays (NASA-TM-X-65431) 06 p0942 N71-16602

Development of magnetic attitude control system for High Energy Astronomy Observatory satellite (NASA-CR-103025) 07 p1657 N71-17446

Pre-launch, launch, and inflight earth orbital environment data for HEAO spacecraft (NASA-TM-X-64576) 11 p1831 N71-22178

Mosaic crystal development and applications in X ray polarimeters and spectrometers for HEAO (NASA-CR-103125) 14 p2339 N71-26400

HEAO CaTi crystal activation for measurement of galactic gamma and cosmic particle energy spectra (RM-507) 16 p2674 N71-28167

SAS-B, TD-1, and HEAO space program for experiments on gamma rays 20 p3346 N71-33072

HEARING

Sonar detection of submarines by helicopter and protection of flight crew hearing (AD-711910) 03 p0336 N71-12400

Effects of helium oxygen breathing on hearing in Navy personnel (AD-726358) 18 p2877 N71-31237

Psychophysical evidence of lateral inhibition in hearing (JEP-1971-8) 20 p3225 N71-33859

HEARING LOSS

U AUDITORY DEFECTS

HEART

NT CARDIAC VENTRICLES 11 p1486 N71-23079

NT MYOCARDIUM 15 p2374 N71-27729

Mechanism of inhibition and acceleration at synapse in nervous system of heart ganglion of stomatopod (AD-711971) 02 p0154 N71-11089

Computerized simulation of electrical generator system in human heart 11 p1486 N71-23079

Hydrodynamics of roller pumps and implication to hemolysis (AD-720320) 15 p2374 N71-27729

Measurement of brain and heart accumulation of bromotrifluoromethane for evaluation as potential fire extinguisher chemical (AD-721211) 15 p2371 N71-27299

Trends and possibilities in biochemical and biotechnical in medical science - heart transplantation 18 p2875 N71-30840

Lipid uptake prediction by prosthetic heart valve poppets from solubility parameters derived from thermodynamic considerations 18 p2883 N71-31113

HEART DISEASES

Cardiac rhythm disruptions in athletes 09 p1329 N71-19592

Physical fitness of flying personnel and aging effects on flight crew performance (AGARD-CP-81-71) 11 p1687 N71-22301

Electrocardiographic and blood pressure standards of physical fitness for aging pilots 11 p1689 N71-22314

Coronary system diseases in aging flight crews and removal from flying status 11 p1689 N71-22315

Cardiovascular disease effects in aging flying personnel on physical exercise performance 11 p1689 N71-22317

Arteriosclerosis and electrocardiographic abnormalities in aging pilots of French Air Force 11 p1690 N71-22318

Computer animated display device for diagnosis of heart disease (NASA-NEWS-RELEASE-71-58) 12 p1867 N71-23751

Dystrophic myocardial damage in rat hearts caused by prolonged acceleration 20 p3222 N71-33470

HEART FUNCTION

NT HEART MINUTE VOLUME 02 p0160 N71-11489

Procedures for determining functional state of human heart right side 02 p0160 N71-11489

Design and characteristics of artificial heart control system (NASA-TN-D-6171) 07 p0966 N71-17593

Methods for measuring mechanical aspects of cardiac activity and vessel functional state 09 p1329 N71-19586

Functional tests of cardiovascular system in athletes 09 p1329 N71-19588

Development of system for identifying dynamic heart rate response to respiration (AD-719860) 13 p2034 N71-24953

Application of reflected ultrasound to detection of post-operative rejection of heart transplant (NASA-CR-121642) 21 p3380 N71-34050

HEART MINUTE VOLUME

Hypokinesia effects on human heart rate and output volume after prolonged bed rest 20 p3222 N71-33466

HEART RATE

NT ARRHYTHMIA

NT SYSTOLE

Electronic device for monitoring electrocardiogram and diagnosing high or low heart rate (AD-710221) 01 p0014 N71-10006

Neuroendocrine heart rate analysis techniques for consciousness during space flight (AD-714405) 06 p0802 N71-16409

Effect of carbon monoxide on human performance including heart rate and galvanic skin response (AD-717716) 11 p1683 N71-22299

Oxygen consumption and heart rate measurements for estimating exercise tolerance of military personnel (AD-719860) 11 p1688 N71-22308

Digital cardiometer incorporating circuit for measuring heartbeat rate of subject over predetermined portion of one minute also converting rate to beats per minute (NASA-CASE-XMS-02399) 11 p1692 N71-22896

Analysis of variance of heart rate measurements extracting sleep stage information and pattern recognition (AD-718125) 12 p1863 N71-23477

Performance of impedance cardiograph for measuring heart rate and body fluids (NASA-CR-114988) 12 p1864 N71-24173

Development of system for identifying dynamic heart rate response to respiration 13 p2034 N71-24953

Metabolic effects of long duration exercise at moderate work loads including tables of heart rate, rectal temperature, minute volume, water balance, and respiratory quotient (NASA-CR-115033) 15 p2372 N71-27784

Hypokinesia effects on human heart rate and output volume after prolonged bed rest 20 p3222 N71-33466

Instantaneous rate reading tachometer for measuring ECG signal rate (NASA-CASE-MFS-20418) 21 p3427 N71-34386

HEAT

NT DRY HEAT

NT NUCLEAR HEAT

Thermoelectric converter for converting heat energy directly into electrical energy (NASA-CASE-XLE-01908) 12 p1963 N71-23389

HEAT ACCLIMATIZATION U ACCLIMATIZATION U HEAT TOLERANCE

HEAT BALANCE

Space environment simulation tests of HEOS 1 satellite noting heat balance 03 p0358 N71-12226

Research study on reduction, analysis, and interpretation of radiation balance measurements from ESSA weather satellites 03 p0404 N71-13240

Heat loss from fuel elements partially immersed in water (LA-4473) 07 p1061 N71-17288

Air flow thermal balance calorimeter for measuring heat evolved by spaceborne nickel cadmium cells (NASA-TM-X-65546) 14 p2253 N71-25748

Computation of heat balance for Tyrrhenian Sea in 1969 (JFA-SR-29) 15 p2397 N71-27826

Solar radiation in heat balance of ice-covered surface on Franz Joseph Land and Spitzbergen 15 p2439 N71-27519

Monthly mean values of energy balance components of earth surface in Finland 20 p3267 N71-33497

Analytical solution of nonlinear heat conduction equation including influence of internal heat generation 20 p3345 N71-33602

Numerical analysis of heat balance of north pole cap of planet Mars and accumulation of solid carbon dioxide and frozen water (NASA-TT-F-13974) 22 p3373 N71-35446

Calculation of rates of energy loss due to sublimation for water, carbon dioxide, argon, krypton, xenon, and oxygen (NASA-TN-D-6540) 24 p4053 N71-36788

HEAT BUDGET

NT ATMOSPHERIC HEAT BUDGET

Satellite motion simulators for space environment heat budget tests, particularly for Azur satellite 03 p0356 N71-12712

Total heat budget between ocean-ice-atmosphere in Arctic Basin for military utilization (AD-71967) 12 p1906 N71-23351

HEAT CAPACITY

U SPECIFIC HEAT

HEAT CONDUCTION

U CONDUCTIVE HEAT TRANSFER

HEAT CONTENT

U ENTHALPY

HEAT DISSIPATION

U COOLING

HEAT DISSIPATION CHILLING

U COOLING

HEAT EFFECTS

U TEMPERATURE EFFECTS

HEAT ENGINES

U ENGINES

HEAT EQUATIONS

U THERMODYNAMICS

HEAT EXCHANGERS

NT TUBE HEAT EXCHANGERS 01 p0058 N71-10200

Developing thermomechanical pump for thermoelectric outer planet spacecraft 01 p0058 N71-10200

Repair device for sodium-sodium heat exchanger (NP-18292) 03 p0414 N71-12889

Parametric data of heat exchanger size and weight for nuclear reactor Brayton cycle space power systems (NASA-CR-72783) 04 p0555 N71-14817

Design and fabrication of prototype auxiliary heat exchanger for SNAP 8 (NASA-CR-72817) 05 p0722 N71-14440

Intermediate heat exchanger design for Fast Flux Test Facility (WARD-4112-2-VOL-1) 05 p0723 N71-14715

Thermal and hydraulic performance analysis for fast flux test facility intermediate heat exchanger design (WARD-4112-2-VOL-2) 05 p0723 N71-14716

Vibration in external flow of pressurized tube system (JEP-1971-8) 05 p0425 N71-14709

Nuclear Brayton cycle heat exchanger and duct assembly (NASA-CR-72816) 05 p0785 N71-15810

Plate-fin heat exchangers for nuclear reactor Brayton cycle (NASA-CR-72815) 06 p0899 N71-16408

Graphite drilled-core storage heater for supplying heated nitrogen gas to superionic tunnel (NASA-TM-X-2282) 07 p1005 N71-17678

Heat exchanger and thermalization for 2-mm liquid hydrogen bubble chamber of IITP (ITEP-734) 06 p1174 N71-16310

Performance degradation of dilution refrigerator (UCSD-34-P-143-32) 06 p1303 N71-16109

SUBJECT INDEX

Analytic computer program for turbomachine-driven cryogenic systems in helium, including porous plate heat exchanger
[AD-71574] 08 p286 N71-18337

Space ash body heat exchanger design composed of thermal conductance yarn and liquid coolant loops
[NASA-CASE-XMS-09711] 09 p1339 N71-19439

Similarity between two phase liquid-vapor flows with heat exchange - conference
[CEA-CONF-1648] 09 p1376 N71-20118

Computerized design and operation of sodium-water counterflow heat exchanger
[CEA-CONF-1592] 09 p1486 N71-20564

Mathematical model for stress analysis and force distribution in U bend heat exchanger performed plates
10 p1634 N71-21137

Feasibility of applying noninteracting control technology to realistic and representative distributed parameter process using double pipe heat exchanger
10 p1662 N71-21292

Operating principles of cylindrical heat pipes and application to nuclear electric space and underwater power plants
[ORNL-TM-2803] 10 p1496 N71-21609

Numerical solution for heat flux through exchange surface under periodic changes in temperature
10 p1663 N71-21644

Heat transfer and flow friction characteristics of compact heat exchanger surfaces with and without brazing roughness
[AD-717661] 11 p1768 N71-22596

Periodic and maximum-slope techniques with refinements used for testing compact heat exchanger surfaces
[AD-717662] 11 p1841 N71-22406

Improvement in heat exchanger efficiency through use of pyroceramic, quartz, or other dielectric materials in place of metallic surfaces
[AD-718287] 12 p2015 N71-24349

Dual solid cryogenics for spacecraft refrigeration insuring low temperature cooling for extended periods
[NASA-CASE-GSC-10188-1] 13 p2124 N71-24725

Analysis of heat exchange processes of built-in heat exchangers by replacing actual values of gas discharge and temperature with average value of flow in one direction
14 p2352 N71-25759

Hybrid computer nonlinear programming with dynamic constraints and application to nuclear reaction and heat exchangers
[CEA-8-3984] 15 p2449 N71-27390

Steady state temperature calculations for thermal radiation transfer of afterheat in MSBR primary heat exchangers
[ORNL-TM-3145] 16 p2689 N71-28107

PORTRAN-A digital codes for thermal dynamics of cylindrical nuclear fuel rod with or without distributed heat generation
[RT/ING-70/8] 16 p2630 N71-28117

MSBR heat exchanger computer programs - PRIMEX for primary heat exchangers, REXTEX for reactors, and SUPLEX for steam generator superheaters
[ORNL-TM-2815] 17 p2782 N71-29367

Design of heat exchangers for gas turbine fast reactors
[EIR-187] 18 p3023 N71-30478

Thermodynamic properties, heat transfer, and aerodynamic characteristics of staggered tube bundles with transverse air flow at Reynolds number greater than 10,000
[NLL-RTS-5999] 19 p3035 N71-32332

Thermodynamics of oxide reduction on heat exchanger, chromium as alloying component, sulphate and hydrogen chloride corrosion, and silicon sulphide elements
[NLL-CE-TRANS-5605-19032.09] 22 p3697 N71-36370

Hydrodynamics of cocurrent counter-gravity solids transport for liquid-fluidized heat exchangers
13 p3866 N71-37577

Destructive examination of Hallam Nuclear Power Facility intermediate heat exchanger emphasizing oxide corrosion problems
[IR-1477] 16 p3978 N71-38387

Heat exchange, theoretical considerations on cooling, and dependence of heat exchange on state of two-flow mixture in post-burnout regime
[RT/ING-70/37] 16 p4028 N71-38740

Effects of capillary grooves on surface wetting and evaporation characteristics related to cross section shape of grooves
[AD-727200] 24 p4031 N71-38762

HEAT FLOW
U HEAT TRANSMISSION
HEAT FLUX
Film boiling on vertical surfaces in turbulent regime using cryogenic fluids
[NASA-CR-110997] 01 p0132 N71-10064

Heat flux measurements on fixed turbine and combustor blades in supersonic flow
[ONERA-TP-671] 02 p0305 N71-11135

Hydrodynamic and heat transfer measurements on full-scale simulated 36-rod Marxkan fuel element with nonuniform radial heat flux distribution
[PR306-3] 04 p547 N71-13634

Correlation of rod bundle critical heat flux for water in pressure range 150 to 725 psia
[IN-1412] 04 p0554 N71-14011

Drayot tests on internally heated annulus with variation of axial heat flux
[AREW-R-578] 04 p0561 N71-14400

Liquid film flow and critical heat flux measurements in concentric, internally heated annulus
[ABCL-3456] 05 p0660 N71-14757

Heat transfer and heat flux measuring sensors for gas turbine engines
07 p1028 N71-17377

Burnout heat flux measurements on 3 by 3 rod bundles with nonuniform heat generation and high pressure water
[EUR-4514-E] 08 p1302 N71-18220

Heat flux measurement on flat plate surface by means of hot-wire flowmeters noting skin friction influence
[REPT-70-7] 08 p1201 N71-18466

Measurement of heat flux in eastern Carpathians and analysis of abyssal heat flux distribution to tectonics and geological development of region
[NASA-TT-F-13517] 09 p1384 N71-20083

Correlation of critical heat flux for water vertical flow in uniformly heated channels
[AERE-R-5590] 09 p1376 N71-20087

Transient surface heating of large solids subject to surface heat loss
[AD-715954] 09 p1483 N71-20184

Critical heat flux and pressure drop tests of electrically heated nuclear fuel rod bundles with ferrous hydroxide slurry crud deposits
[WAPD-TM-918] 09 p1421 N71-20388

Critical analog and numerical analysis of heat flux meter performance
[AD-717027] 10 p1599 N71-21619

Numerical solution for heat flux through exchange surface under periodic changes in temperature
10 p1663 N71-21644

Thin film thermometer and thin film calorimeter techniques for surface heat flux rates of microsecond duration
11 p1843 N71-22605

Heat flux sensors based on thermistors in doped polycrystalline ceramics such as barium strontium titanate showing ferroelectric resistance anomaly
11 p1764 N71-22746

Heat flux sensor adapted for mounting on aircraft or spacecraft to measure aerodynamic heat flux inflow to aircraft skin
[NASA-CASE-XFR-03802] 11 p1845 N71-23065

Effects of high accelerations and heat fluxes on moderate boiling of water in axisymmetric rotating boiler
[NASA-TN-D-6307] 12 p2012 N71-24202

Heat flux and optical property measurement for multilayer insulation
[NASA-CR-72605] 12 p2014 N71-24300

Interacting effect of gravity and size on peak and minimum pool boiling heat fluxes
[NASA-CR-118638] 14 p2353 N71-25963

Effects of composition, particle size, and component thermal properties on effective thermal conductivity of composite solids
14 p2356 N71-26469

Design of high resolution radiometer based on heat fluxmeter
15 p2410 N71-27545

Solar radiation effects on atmospheric temperature using simplified heat flux equation
15 p2403 N71-27560

Atmospheric models for tenuous cloud effects on atmospheric heat infrared radiation flux
15 p2403 N71-27561

Nonnewtonian free laminar convection flow from vertical flat plate with uniform surface heat flux
16 p2584 N71-29030

Determination of similarity between boiling and injection of saturated vapor and establishment of critical heat flux model
[RR-5] 16 p2693 N71-29069

Computerized simulation of temperature distribution and heat flux in incense thermionic reactors
[NASA-TT-F-13686] 17 p2781 N71-29251

Injector performance, heat flux, and film cooling in hydrogen oxygen engines
17 p2837 N71-29998

Standard, wet summer and winter, and dry summer and winter model atmospheric radiative heat flux spectral distributions
[NASA-TT-F-13624] 18 p2917 N71-31267

Heat flux distributions in pools of burning aircraft fuels for design of protective clothing for firefighting personnel
[AD-722774] 18 p3030 N71-31376

Critical heat flux in liquid helium 2 close to lambda transition
19 p3193 N71-32542

HEAT MEASUREMENT

Hydrodynamics of boiling heat flux and dynamics and stability of small gravity and capillary waves
[NASA-CR-121467] 20 p3366 N71-33746

Hydrodynamics of two-phase parallel boiling water channel flow after heat flux increase
21 p3410 N71-34363

Influence of parameter variability in shock layer on heat flux in nonequilibrium viscous flow of multicomponent gas near stagnation point of blunt body
21 p3412 N71-34277

Evaporation-petirpation effect of terrestrial vegetation on latent heat flux density
22 p3613 N71-35739

Development and characteristics of high intensity, direct reading heat flux gage of quasi-steady state type
[SC-DR-710194] 23 p3758 N71-36789

Sensible heat flux and momentum flux in turbulent boundary layer of coastal winds
[RPT-29] 23 p3791 N71-37018

Parametric method for estimating solar radiation effects on atmospheric temperature
[NLL-M-30338-19328-4P] 23 p3843 N71-37396

HEAT GAIN
U HEATING
HEAT GENERATION
Measuring geographical distribution of zones of absolute annual temperature minima for use in construction of buildings and living quarters
[NLL-M-9142-19328-4P] 02 p0256 N71-11661

Burnout heat flux measurements on 3 by 3 rod bundles with nonuniform heat generation and high pressure water
[EUR-4514-E] 08 p1302 N71-18220

Holographic study of zeeman arc lamp heat loads for solar environmental simulations
10 p1570 N71-21354

Calorimeter for measuring heat generation rates in nonfissionable materials by gamma and thermal neutron interactions in nuclear reactor test facility environment
13 p2113 N71-24524

Calculation techniques for estimating heat power levels of radioactive decay of fission and activation products
13 p2113 N71-24531

Existence and extendability of continuous eigenvector branches and application of nonlinear programming algorithms to nonlinear heat generation and rotating string problems
[NASA-CR-119020] 16 p2623 N71-28650

Numerical analysis of radioactive decay heat generation and effects on charcoal adsorbents for reactor accident simulation
[ORNL-4462] 20 p3309 N71-33988

Calorimeter and recording system for measuring heat generation in reactor holes
[LBRG-3017] 24 p3958 N71-38233

HEAT MEASUREMENT
Error analysis on oscillator measurements of in-pile fuel thermal conductivity
[KFK-1140] 01 p0087 N71-10929

Calorimetric determination of nuclear and electronic interactions in metals
[AD-712095] 03 p0468 N71-12993

Theory and measurements of entropy
[PB-192128] 05 p0783 N71-15170

Specific heat measurements on trichloride hexahydrate of gadolinium, terbium, holmium and lanthanum
[IS-T-378] 06 p0883 N71-16786

Test equipment design for measuring heat generated in U fuel element in nuclear fuel plant
[ZJE-88] 08 p2324 N71-18177

Development of high temperature calorimetry techniques for solid ionic systems
[AD-715719] 08 p1221 N71-18550

Electromagnetic energy detection by thermal sensor with vibrating electrode
[NASA-CASE-XAC-10768] 08 p1109 N71-18830

Electrical analog and numerical analysis of heat flux meter performance
[AD-717027] 10 p1599 N71-21619

Test equipment and techniques for improving iron/potassium perchlorate heat powder
[SC-CR-70-6157] 11 p1677 N71-22480

Theory, equipment, and techniques for heat transfer and temperature measurements
[AGARD-GRAPH-130] 11 p1841 N71-22596

This film thermometer and thin film calorimeter techniques for surface heat flux rates of microsecond duration
11 p1843 N71-22605

Measurement techniques for determining radiant energy fluxes and thermal radiative properties of materials
11 p1843 N71-22607

General methods for measuring viscosity, thermal conductivity, and specific heat
11 p1843 N71-22608

Tin solution calorimetry for measuring heats of formation of selected face centered cubic palladium-silver-tin system
[AD-722799] 18 p2937 N71-31397

Data analysis for isoperibol calorimetry
[AD-726514] 23 p3766 N71-36842

- Calorimeter and recording system for measuring heat generation in reactor holes
[LBJ-3017] 24 p3958 N71-38233
- Nuclear light bulb engine propellant stream radiant heating simulation using 500 kW dc arc and argon seeded with carbon particles
[NASA-CR-123199] 24 p3958 N71-38239
- Using ionization chambers for measuring nuclear heating effects
[CEA-R-4195] 24 p3978 N71-38389
- ### HEAT OF COMBUSTION
- Calculation of frictional hot-spot temperatures and distributions on surfaces of explosives
[AD-718066] 12 p1930 N71-24144
- Theory of interior ballistics for calculating gunpowder efficiency and combustion safety in firearms
[TL-1970-21] 20 p3368 N71-33842
- ### HEAT OF FORMATION
- Determination of heat of formation of gibbsite from alpha-alumina and water
[AD-711673] 02 p0173 N71-11221
- Heat of formation of metal sulfides and thermal stability related to their atomic structure
[TT-70-57084] 05 p0638 N71-14590
- Technique for determining heats of fusion and heat capacities of liquid metals at high temperature
[NASA-CR-117032] 09 p1486 N71-20542
- Heat of formation for Cu₂N and HCN and adiabatic calorimetric measurements from 10 to 400 K
[BMRI-7499] 10 p1572 N71-20725
- Experimental methods for determining heat of formation energies of plutonium carbides
[CEA-CONF-1581] 10 p1516 N71-21661
- Heat of formation, specific heat, entropy, and Gibbs free energy of some binary metal oxides
[NPL-DCS-7] 13 p2184 N71-24372
- Oxygen pressure as function of temperature in stony meteorite formation
13 p2169 N71-25295
- Pumping effect in oxygen reaction with tungsten cathode, and spectroscopic measurements of formation energies for volatile species in gas-solid chemical reactions
[NASA-CR-118897] 15 p2389 N71-27988
- Tin solution calorimetry for measuring heats of formation of selected face centered cubic palladium-silver-tin system
[AD-722799] 18 p2937 N71-31397
- Heat of formation and entropy of formation of plutonium carbides
[KFK-TR-71-22] 20 p3368 N71-33951
- Thermodynamic properties of four crystalline sodium borates
[BM-R1-7551] 22 p3350 N71-35290
- ### HEAT OF VAPORIZATION
- Calculation of vapor pressure, and heats of vaporization and sublimation of neon below 1 atm pressure
[TR-1] 01 p0134 N71-10921
- High temperature kinetics and crystal structures of rare earth element bromide, carbon, and halogen systems
[COO-716-66] 07 p1094 N71-17825
- Vapor pressure and heat of vaporization of metal beta diketone chelates measured by gas-liquid chromatography
[AD-718429] 12 p1870 N71-23479
- ### HEAT PIPES
- Technique for direct measurement of thermal conductivity at high temperatures using heat pipes
[NASA-TM-X-52909] 01 p0132 N71-10238
- Experimental design and operation of rotating wickless heat pipe
[AD-709923] 01 p0134 N71-10702
- Heat resistant steels for steam flow pipelines of boilers
[JPRS-51658] 01 p0068 N71-10825
- Use of heat pipes for electrical isolation
[NASA-TM-X-52928] 01 p0134 N71-10985
- Split-core heat-pipe reactor for space power applications
[NASA-TM-X-52918] 01 p0087 N71-10993
- Visual observation of high temperature profiles during startup in lithium heat pipe
[NASA-TM-X-52924] 01 p0134 N71-10994
- Electric power system utilizing thermionic plasma diodes in parallel and heat pipes as cathodes
[NASA-CASE-XMF-65843] 02 p0149 N71-11655
- Design optimization of out-of-core thermionic converter heated and cooled by heat pipes
[NASA-TM-X-52930] 03 p0315 N71-12250
- Fabrication and evaluation of out-of-core thermionic converter heated and cooled by heat pipes
[NASA-TM-X-52934] 03 p0315 N71-12251
- Microwave power receiving antenna solving heat dissipation problems by construction of elements as heat pipe devices
[NASA-CASE-MFS-20333] 04 p0508 N71-13486
- Literature survey of heat pipe technology from 1964 to mid-1970
[NASA-CR-102943] 04 p0621 N71-14065
- Performance of various wick configurations in single and two-fluid heat pipes operating as thermoregulatory system for space suits
[NASA-CR-111760] 04 p0621 N71-14079
- Fabrication and testing of circumferential heat pipe systems for lamp structures
[NASA-CR-114783] 04 p0621 N71-14228
- Flooding phenomena in cryogenic heat pipe with vertical two phase counterflow
[CEA-CONF-1496] 05 p0724 N71-14973
- Thermal scale modeling of heat pipes
05 p0784 N71-15556
- Feedback controlled variable conductance heat pipe
[NASA-CR-73475] 05 p0784 N71-15602
- Mathematical modeling of cryogenic heat pipes
[NASA-CR-116175] 06 p0961 N71-16887
- Evaluation of vapor chamber/heat pipe/radiator for Brayton cycle space power system
[NASA-CR-1677] 07 p0976 N71-17581
- Cryogenic heat pipe measurements of film condensation heat transfer coefficients
[CEA-CONF-1634] 08 p1302 N71-18157
- Sonic velocity and startup considerations in heat pipe design
[LA-4518] 08 p1305 N71-18944
- Heat pipes for tritium regeneration in controlled thermonuclear reactors using deuterium-tritium fuel
[UCRL-72329] 09 p1416 N71-19411
- Liquid and vapor cooling systems for gas turbines with application of heat pipe concept to stator blade cooling
[ARC-CP-1127] 10 p1638 N71-20832
- Corrosion of nickel heat pipes containing liquid potassium
[ORNL-TM-3077] 10 p1572 N71-20865
- Operating principles of cylindrical heat pipes and application to nuclear electric space and undersea power plants
[ORNL-TM-2803] 10 p1496 N71-21609
- Thermodynamic temperature drop at liquid-vapor interface in high temperature lithium heat pipes
[NASA-TM-X-2268] 12 p1902 N71-23923
- Lithium filled heat pipe for obtaining near isothermal conditions axially along cladding of in-pile fuel-irradiation capsule
13 p2185 N71-24512
- Laboratory and reactor tests for establishing specimen temperatures in irradiation experiments by using inert gas-filled heat pipes
13 p2079 N71-24514
- Analysis of corrosion in high temperature lithium heat pipes with niobium-zirconium and tantalum as wall material
[EUR-4298-E] 13 p2092 N71-24734
- Axially conducting gas controlled heat pipes leading to predictive capability for heat and mass transfer along heat pipe
[NASA-CR-114300] 13 p2185 N71-24866
- Heat pipes for passive control of heat pipes in hot reservoir system
[NASA-CR-73420] 13 p2185 N71-24886
- Feasibility of cryogenic heat pipe for cooling isotopic spacecraft power supply cycle
13 p2186 N71-25313
- Double-wall isothermal cylinder containing heat transfer fluid thermal reservoir as spacecraft insulation cover
[NASA-CASE-MFS-20355] 13 p2186 N71-25353
- Heat pipe transport system in Nimrod operation
[RIHEL-R-206] 14 p2306 N71-26342
- Thermal cycling tests on stainless steel and copper heat pipes for satellite temperature control
15 p2524 N71-27107
- Design, fabrication, and performance test of heat pipe panel for Saturn 5 launch vehicle
[NASA-CR-103190] 17 p2856 N71-29274
- Digital computer program manual for design, analysis, and performance prediction of heat pipes with noncondensable gases including input/output routines and Runge-Kutta models
[NASA-CR-114306] 17 p2735 N71-29908
- Design and performance of 250 ampere transacetal rectifier for use with heat pipes
17 p2726 N71-30243
- Strain rate equations for secondary creep deformation of thick-walled tubes operated at high temperatures
[NASA-TM-X-2339] 19 p3191 N71-32759
- Preliminary test results of heat transfer/thermal storage tube design for solar Brayton cycle power system under simulated orbital conditions
[NASA-TM-X-67904] 20 p3367 N71-33783
- Bibliography of nuclear reactor applications for heat pipes
[AEC/LIB/BID-264] 22 p3695 N71-36349
- Design and development of prototype static cryogenic heat transfer system utilizing heat pipe with wetting arterial wick and nitrogen as working fluid
[NASA-CR-121939] 22 p3695 N71-36355
- Split-core heat-pipe reactors for out-of-pile thermionic power systems with center gap reactivity control
[NASA-TM-X-67939] 23 p3797 N71-37068
- Fabrication and tests of tungsten reactor pipe and its heating characteristics up to 1900 K
[NASA-TM-X-67941] 23 p3797 N71-37070
- ### HEAT RADIATORS
- #### NT SPACECRAFT RADIATORS
- Capillary radiator for carrying heat transfer liquid in planetary spacecraft structures
[NASA-CASE-XLE-03307] 04 p0620 N71-14029
- Effects of orientation, location, and location on performance of lunar radiator - design studies
[NASA-TM-X-1846] 09 p1483 N71-20000
- Mathematical analysis of system of annular heat-conducting emitting ribs
[NASA-TT-F-13551] 12 p2013 N71-24241
- Low temperature radiator for rejecting thermal power from isotope Brayton power system
[NASA-TM-X-67822] 13 p1866 N71-23909
- Feasibility of spraying flash evaporator as heat rejection device for space shuttle environmental control system
[NASA-CR-114913] 14 p2263 N71-26224
- Hydraulic actuator design for space deployment of heat radiators
[NASA-CASE-MSC-11017-1] 14 p2264 N71-26611
- SNAP 8 reactor startup tests using reactor and heat radiator simulators and evaluation of temperature transients
[NASA-TN-D-4381] 16 p2537 N71-28007
- Development of method and equipment for testing heat radiative properties of material under controlled environmental conditions
[NASA-CASE-MFS-30906] 17 p2753 N71-30826
- Thermodynamic properties, heat transfer, and aerodynamic characteristics of staggered tube bundles with transverse air flow at Reynolds number greater than 10,000
[NRL-RTS-5909] 19 p3035 N71-32332
- ### HEAT REGULATION
- #### U TEMPERATURE CONTROL
- #### HEAT REJECTION DEVICES
- #### U HEAT RADIATORS
- #### HEAT RESISTANCE
- #### U THERMAL RESISTANCE
- ### HEAT RESISTANT ALLOYS
- #### NT MOLYBDENUM ALLOYS
- #### NT NIOBIUM ALLOYS
- #### NT NIOBIUM ALLOYS
- #### NT REFRACTORY METAL ALLOYS
- #### NT RHENIUM ALLOYS
- #### NT TANTALUM ALLOYS
- #### NT TUNGSTEN ALLOYS
- #### NT WAPALLOY
- Determining mechanical properties and air-oxidation behavior of chromium-base compositions at temperatures up to 2400 F
[NASA-CR-72731] 01 p0065 N71-10847
- Heat resistant steels for steam flow pipelines of boilers
[JPRS-51658] 01 p0068 N71-10825
- Structure and properties of unidirectionally solidified superalloys
02 p0242 N71-11632
- Effects of helium on high temperature ductility of Sandvik 12R27HV and Inco IN-744X
[AI-AEC-12960] 02 p0244 N71-12111
- Physicochemical theory of heat resistance and new heat resistant titanium alloys
[AD-712810] 03 p0395 N71-13334
- Electrochemical treatment of gas turbine blades made of heat resistant steels and alloys
[AD-712938] 03 p0387 N71-13395
- Effect of forced ultrasonic radial vibrations of tooth when machining titanium and heat resistant alloys
[AD-713455] 05 p0694 N71-13457
- High temperature cobalt-base alloy resistant to corrosion by liquid metals and to sublimation in vacuum environment
[NASA-CASE-XLE-02591] 06 p0670 N71-16025
- High temperature ball bearing design for turbojet engines
[NASA-TM-X-52958] 06 p0866 N71-16034
- Investigating effect of surface preparation on oxidation of Wt-52 by high temperature X ray diffraction
[NASA-TM-D-61448] 06 p0676 N71-16039
- Thermal control coatings for refractory gas turbine materials
07 p1048 N71-17791
- Fabrication of cobalt alloy and nickel alloy gas turbine blades and disks
07 p1101 N71-17792
- Evaluation of protective coatings for heat resistant alloys
[NASA-CR-72813] 07 p1043 N71-17600
- Modification of high temperature cobalt-tungsten alloys for improved stability
[NASA-TN-D-6147] 08 p2123 N71-18515
- Protective coatings for heat resistant materials for aircraft gas turbine engines, and refractory metals for rocket vehicles
[NASA-TM-X-52977] 09 p1404 N71-19577
- Radiation damage of reactor structural materials including strain determination for high temperature alloys in EBR 2
[AD-716405] 09 p1417 N71-19514
- Determination of thermal fatigue resistance of alloys by fluidized bed technique
[NASA-TM-X-52975] 09 p1474 N71-19522

SUBJECT INDEX

HEAT SOURCES

- Thermal stability, vibration strength, and fatigue life of titanium and aluminum alloys used for gas turbine blades
[AD-717012] 10 p1575 N71-20920
- Carbide electrolysis extraction from high temperature resistant stainless steels with 20 percent Ni and 25 percent Cr
10 p1577 N71-21145
- Brazing alloy adapted for brazing corrosion resistant steel to refractory metals, also for brazing refractory metals to other refractory metals
[NASA-CASE-XNP-03663] 12 p1937 N71-23565
- Protection of oxidation resistant aluminumized iron and nickel slurry coatings for heat resistant alloys
[NASA-TN-D-4329] 13 p2097 N71-25446
- Aluminide coatings for nickel-base superalloy developed for high temperature jet engine components
[NASA-CR-72683] 13 p2097 N71-25454
- Modeling thermocouples developed for sequential deposition of manganese, aluminum, and titanium alloys as protective coatings for superalloys
[NASA-CR-72632] 13 p2098 N71-25503
- Tensile stress and tensile time-to-rupture relation determined from cyclic creep rupture tests on high temperature titanium alloy, cobalt alloy, and stainless steel
[NASA-TN-D-4309] 14 p2266 N71-25645
- Electron and ion microprobes applied in characterizing aluminide coating on IN-100 nickel alloys for high temperature oxidation resistance
[NASA-TN-D-4317] 14 p2271 N71-25688
- Composition, properties, and applications of superalloys and techniques for vacuum melting and vacuum casting procedures
[NASA-SP-5095] 14 p2273 N71-25891
- Diffusion layer structure and aluminizing effect on heat resistant nickel alloy
[AD-726370] 14 p2273 N71-25915
- High temperature oxidation resistant coatings for superalloys, refractory metals, and graphite
[NASA-CR-118647] 14 p2275 N71-26409
- Radiation embrittlement of age hardening heat resistant steels following high temperature reactor irradiation
[AEC-TR-7192] 15 p2419 N71-26907
- Estimating characteristics of stress rupture strength of heat resistant alloys
15 p2424 N71-27398
- Thermal cycling tests of Cr, Al, Si, Fe, and Y alloy clad nickel alloy at 1040 and 1090 C, time, cycle frequency, and film thickness effects on oxidation resistance
[NASA-TN-D-4276] 16 p2608 N71-28163
- Evaluating developed structural materials of potential Air Force weapons system interest and engineering data sheets on these heat resistant alloys
[AD-726278] 16 p2614 N71-28099
- Development of nickel base alloys with superior strength at elevated temperatures, high incipient melting points, and high impact resistance
[NASA-CASE-LEW-10674-1] 16 p2615 N71-28972
- Oxidation resistant coatings for superalloys, refractory metals, and graphite
16 p2620 N71-29174
- Structural fasteners of heat resistant alloys for high temperature applications
17 p2755 N71-29468
- Evaluation of high gas velocity and static oxidation behavior of fused-salt-aluminized IN 100 between 1030 and 1149 C
[NASA-TN-D-4400] 17 p2764 N71-29713
- Production of small diameter refractory metal alloy wires for superalloy reinforcement
[NASA-CR-72654] 18 p2934 N71-30008
- Stress analysis of cobalt heat resistant alloy tubes internally pressurized with helium after creep testing to failure
[NASA-TM-X-3246] 19 p3113 N71-32143
- Solidification, structure, and properties of eutectic alloys including consideration of properties control
[NASA-CR-122043] 22 p3592 N71-35578
- Oxidation protection of superalloys by thin coatings of Ni-Cr-Al-Si and Fe-Cr-Al-Y alloys examined and compared with commercial aluminide coatings
[NASA-TM-X-67925] 22 p3592 N71-35579
- High temperature steel and alloy research, including physical, chemical, and mechanical properties of various steels
[AD-726577] 22 p3593 N71-35600
- Mechanical properties of steels and alloys in high temperature research and structural composition and hot working methods of various steels
[AD-726578] 22 p3595 N71-35601
- Steady-state creep rates in refractory metals and alloys: titanium, titanium, and zirconium
[AD-726546] 22 p3596 N71-35604
- Procedure for hardening metals by high temperature thermomechanical processing and effect on heat resistance properties of nickel alloys
23 p3763 N71-36826
- Electron microscope for investigating heat resistance and physicochemical properties of multicomponent nickel alloys
[AD-726733] 23 p3770 N71-36873
- Properties of materials hardened by mechanical thermal processing at different temperatures
[AD-726839] 23 p3771 N71-36876
- Effects of heat processing methods on mechanical and heat resistant properties of titanium alloys
[AD-726729] 23 p3771 N71-36878
- Development and characteristics of alloys for application to high temperature research
[AD-726618] 23 p3772 N71-36881
- Characterization of heat resistant alloys under cyclically changing temperatures
[AD-727357] 23 p3773 N71-36890
- Properties of high temperature compounds, physics of gas dynamics, heat resistant materials, and heat conversion by power plants
[JP85-54162] 23 p3868 N71-37573
- Heat resistance of titanium examined by formation of solid solutions and compounds with varying degrees of disparity and chemical bond strength
[AD-726242] 24 p3937 N71-38090
- Analysis of deformation, stresses, and irreversible absorbing energy during thermal fatigue cyclic tests
[AD-727945] 24 p3939 N71-38096
- ### HEAT SHIELDING
- NT REENTRY SHIELDING
- Synthesis of silane polymers for heat shields by azirone-alkene polymerization
[NASA-CASE-XMF-08634] 02 p0176 N71-11242
- Synthesis of schiff bases for heat shields by azetal amine reactions
[NASA-CASE-XMF-08652] 02 p0176 N71-11243
- Heat shield technology for extraterrestrial atmospheric entry
[NASA-CR-111377] 02 p0305 N71-12057
- Low cost, ablative heat shield for space shuttles
[NASA-CR-111795] 02 p0306 N71-12067
- Preparation and characteristics of lightweight refractory insulation
[NASA-CASE-XMF-05279] 06 p0877 N71-16124
- Development of low cost ablative heat shields for space shuttles
[NASA-CR-111814] 07 p1120 N71-17770
- Computerized design of stiffened cylindrical shields and ablating composite heat shield
09 p1410 N71-20137
- Sterilization, vacuum exposure, and simulated Martian atmosphere effects on thermal conductivity of spacecraft heat shielding
[NASA-TM-X-66938] 09 p1483 N71-20214
- Ablation technology for planetary entry heat shielding
[NASA-TM-X-66946] 09 p1484 N71-20246
- Crack effects in ablative heat shield on substructure heating
09 p1484 N71-20249
- Fabrication of low cost ablative heat shield panels for space shuttles
[NASA-CR-111835] 09 p1473 N71-20512
- Planetary Atmospheric Experiments Test (PAET) ablative afterbody thermal performance and component mechanical properties
[NASA-CR-114293] 11 p1844 N71-22715
- Development and characteristics of thermal radiation shielding of refractory metal foil used for induction furnace
[NASA-CASE-XLE-03432] 12 p0811 N71-24145
- Fabrication of prototype low density ablative heat shield panels for space shuttles with production cost estimates
[NASA-CR-111874] 12 p2015 N71-24333
- Parameters contributing to aerodynamic problems in thermal protection of space shuttle
13 p2179 N71-24661
- Thermal cycling tests of ground and space liquid hydrogen storage tank heat shielding with multilayer, porous substrate, thermal insulation blankets
[NASA-TN-D-4331] 13 p2173 N71-24822
- Design and development of spacecraft with outer shell structure heat shielding and built-in, removable external module
[NASA-CASE-MSC-13047-1] 13 p2175 N71-25434
- Performance of nickel and iron heat block-shields for Isotope Kilowatt Program evaluated for both organic and steam Rankine cycle systems and for thermoelectric systems
[ORNL-TM-3213] 13 p2097 N71-25455
- Comparison of space shuttle aerodynamic heating analyses for metallic heat shield and surface insulation concepts
14 p2354 N71-26054
- Reactor safety problems in MR-1A high temperature protection system
[AD-726593] 14 p2293 N71-36282
- Structure of fabric layers for micrometeoroid protection garment with capability for eliminating heat shorts for use in manufacturing space suits
[NASA-CASE-MSC-12109] 14 p2280 N71-36285
- Metallic heat shielding materials for space shuttle thermal protection system
17 p2846 N71-29454
- Flight test of chemical vapor deposited felt and filament wound carbon composite heat shields
[SC-DR-71-3835] 17 p2769 N71-29516
- Evaluation of interaction between reentry vehicle heat shield ablation and aerodynamic parameters
[AD-724108] 20 p3351 N71-32936
- Effects of larger Scout D and B heat shields on vehicle stability and control, structure, and ground support equipment
[NASA-CR-111947] 20 p3354 N71-33286
- Computational approach for measuring and evaluating heat effects in liquid chemical samples with elevated temperature differential scanning microcalorimetry
21 p3309 N71-34110
- Low cost replaceable ablative heat shield panels for space shuttles
[NASA-CR-111800] 21 p3520 N71-35083
- Baseball magnet system in fusion research engineering utilizing plasma beam line
[UCRL-73667] 23 p3740 N71-36668
- Development, test, and evaluation of carbon and carbon composite heat shields
23 p3778 N71-36922
- Development of laminated Dwyer having lead shielding on glass epoxy and fiberglass substructure
[MATT-546] 23 p3828 N71-37303
- Analysis of reacting flow of pyrolysis products through char layer of low density, nylon phenolic resin, charring ablators and porous graphite
[NASA-CR-11903] 24 p4091 N71-38765
- ### HEAT SINKS
- Development of calorimeter for spacecraft batteries comprising pressurized vessel, heat sink, and copper conductor
[NASA-CR-118029] 12 p1923 N71-24129
- Development and characteristics of calorimeter with integral heat sink for maintenance of constant temperature
[NASA-CASE-XMF-04208] 16 p2093 N71-29051
- Cost and weight data for space shuttle booster heat sink structural concept
17 p2847 N71-29459
- Heat sink capabilities of Jet-A fuel - heat transfer and cooling studies
[NASA-CR-72951] 18 p3027 N71-31482
- ### HEAT SOURCES
- Heat sources for manufacturing experiments in Apollo Applications Program
02 p0305 N71-11723
- Comparison of differentiated line source and line source methods of measuring particulate media thermal conductivity in vacuum
[NASA-TM-X-64559] 03 p0467 N71-12280
- Large radioisotope heat source capsule program using refractory metals
[AI-ABC-12966] 03 p0489 N71-12560
- Large radioisotope heat source capsule design, fabrication, and materials compatibility and creep tests
[AI-ABC-12968] 03 p0415 N71-12873
- Thermal analysis for predicting internal temperatures in isotopic Brayton power system operation
[NASA-TM-X-52948] 05 p0783 N71-13324
- Five radioisotope-powered heat sources fueled with Pu-238 dioxide microcapsules for use in Life Support Program 2
[MLM-1757] 06 p0808 N71-16619
- Pioneer RTG heat source drop tests to obtain terminal velocity and reduced trajectory data
[SC-DR-70-560] 06 p0793 N71-16628
- Thermophysical density response to neutral heating during post-arc discharge
[NASA-TM-X-65462] 09 p1383 N71-20284
- Radiation safety of plutonium isotopic heat source in long term space station simulation
10 p1496 N71-20994
- Spaceborne nuclear reactors used as propulsion, electric power, and heat sources
10 p1605 N71-21579
- Laser fabrication for radioisotope heat source of ATM ultraviolet micrograting in AAP
[MLM-1779] 10 p1561 N71-21737
- Heat release explosive processes and gas dynamics for high power energy conversion systems
[AD-717108] 10 p1664 N71-21783
- Impact tests of SIREN for encapsulation system for radioactive isotopic heat source
[SNC-3706-2] 12 p1961 N71-25140
- Large radioisotope heat source capsule development for space environment
[AI-ABC-12956] 13 p2117 N71-24835
- Black body radiometer design with temperature sensing and cavity heat source code winding
[NASA-CASE-XNP-69701] 14 p2257 N71-26475
- Test data for designing, fabricating, and operating Co-60 heat sources
[DP-1254] 15 p3499 N71-27567
- Thermal steady state analysis for predicting heat shield heat source performances in Brayton thermodynamic cycle
[NASA-TM-X-67833] 15 p2355 N71-27664
- Plutonium 238 and curium 244 oxide compatibility tests with refractory metal alloys for use in Pioneer heat source
[MDC-G2086] 16 p2612 N71-28749
- Radioisotope production and materials, heat source applications, hydrological and ocean sciences, radiation analysis and control, process radiation, and radiation preservation of foods
[TID-4066] 17 p3797 N71-29836

Airborne infrared detector performance tests for detection of earth impacted radioactive isotope heat sources
[SC-DR-710095] 18 p2903 N71-31182

Developments in heat source capsule fabrication program from September 1970 to January 1971
[JMLM-1796] 18 p2930 N71-31223

Nondestructive tests of simulated isotope heat source for use in Brayton power system
[NASA-TM-X-2374] 21 p3459 N71-34621

Radioactive isotope capsule container design for atmospheric reentry protection and heat transmission to spacecraft
[NASA-CASE-LEW-11227-1] 21 p3530 N71-35153

Safety analysis of isotope heat source capsule design
[ORNL-TM-3230] 22 p3623 N71-35811

Strontium 90 heat source production, including purification, transportation, fuel form preparation, desiccation, and encapsulation
[ORNL-DC-56] 22 p3623 N71-35815

Properties of high temperature compounds, physics of gas dynamics, heat resistant materials, and heat transfer by power plants
[JPRS-54182] 23 p3668 N71-37573

HEAT STORAGE

Data on external refrigeration systems for space storage of cryogenics for long periods
[NASA-CR-114920] 09 p1424 N71-20279

Thermal performance analysis of solar Brayton heat receiver in transferring heat to working gas of Brayton engine
[NASA-TN-D-6268] 10 p1496 N71-21512

HEAT TESTS

U HIGH TEMPERATURE TESTS

HEAT TOLERANCE

Peculiarities of human heat exchange under reduced atmosphere pressure and sufficient oxygen supply
[NASA-TT-F-13374] 01 p0010 N71-10367

Investigating state of brain and muscles during high altitude acclimation and effects of physical training on heat tolerance of man
[JPRS-52200] 07 p0980 N71-17066

Studying effect of physical training on heat tolerance of human organism
[JPRS-52200] 07 p0980 N71-17068

Heat tolerance of athletes during muscular exercise in various thermal environments
[JPRS-52200] 09 p1337 N71-20366

Physiological tolerance to thermal threats of aerospace activity and problems associated with excessive heat
[FAA-AM-70-22] 11 p1678 N71-21851

Establishment of relationship between skin temperature and ability to tolerate cold and hot environments for human subjects
[FAA-AM-71-4] 13 p2837 N71-24748

HEAT TRANSFER

NT AERODYNAMIC HEAT TRANSFER

NT CONDUCTIVE HEAT TRANSFER

NT CONVECTIVE HEAT TRANSFER

NT HYPERSONIC HEAT TRANSFER

NT LAMINAR HEAT TRANSFER

NT RADIATIVE HEAT TRANSFER

NT SUPERSONIC HEAT TRANSFER

NT TURBULENCE HEAT TRANSFER

Developing test program for small fused silica models of transparent walls for nuclear light bulb engine
[NASA-CR-111100] 01 p0084 N71-10379

Surface heat transfer rates measured on flat plates in hypervelocity shock tunnel
[NASA-CR-1692] 01 p0134 N71-10667

Bibliography of compilation of articles on heat and mass transfer
[AD-71147] 01 p0134 N71-10892

Use of heat pipes for electrical isolation
[NASA-TM-X-32528] 01 p0134 N71-10985

Respiratory heat exchange in trachea of dogs
[AD-71184] 02 p0153 N71-11086

Long term variability of tropical heat budget of Pacific Ocean and effects on atmospheric circulation
[AD-71308] 05 p0232 N71-11140

Heat and mass transfer during vapor condensation in presence of noncondensing gases
[AD-71246] 02 p0306 N71-12084

Vehicle momentum and heat transfer determinations in atmospheric boundary layers at sea
[AD-71376] 02 p0261 N71-12173

Theoretical analysis and measurement of single-phase pressure losses and heat transfer for helical flow in tube
[NASA-TN-D-6097] 03 p0310 N71-12213

Investigating flow field in near wake behind rearward facing step in supersonic flow and heat transfer distribution along reattachment surface downstream of step
[AD-71376] 03 p0310 N71-12213

Sweating cylinder for testing heat and water vapor transfer characteristics of protective clothing systems
[AD-71294] 03 p0328 N71-12340

Investigating fluid heat transfer at anode of xenon compact-arc lamp using flash photography
[AD-71294] 03 p0379 N71-12794

Survey of heat transfer to near-critical fluids
[NASA-TN-D-5886] 03 p0468 N71-13035

Integral analysis of heat transfer downstream of reentrant facing step with small coolant injection
[NASA-TN-D-5970] 03 p0468 N71-13036

Development of marker and cell technique for two dimensional, transient solutions to Navier-Stokes equations
[AD-713052] 03 p0364 N71-13117

Flat plate pressure distribution and heat transfer in conical hypersonic flow
[VKI-TN-56] 03 p0365 N71-13236

Calculated and observed changes in sea surface temperature associated with hurricane passage
[AD-713052] 03 p0372 N71-13328

Heat transfer in simulated BWR fuel bundle cooled by spray under loss-of-coolant conditions
[GEAP-13086] 04 p0545 N71-13566

SNAP-8 boiler performance degradation and two phase flow heat and momentum transfer models
[NASA-CR-72759] 04 p0619 N71-13598

Molybdenum filament performance in BWR emergency cooling heat transfer tests
[GEAP-10092] 04 p0548 N71-13678

Behavior of high speed turbulent boundary layer with heat transfer and streamwise pressure gradient
[NASA-CR-1679] 04 p0518 N71-13769

Heat transfer and fluid dynamics analyses for fuel loading in materials test reactor
[BNWL-1409] 04 p0552 N71-13969

Electromagnetic field effects on heat transfer of two temperature gaseous plasma
[NASA-CR-111725] 04 p0597 N71-14062

Using thin-wall technique for describing fast mechanically operated model-injection system for heat transfer measurements
[NPL-AERO-1300] 04 p0621 N71-14087

Investigating effects of heat transfer through fabrics on skin temperature rise and possible resultant injury
[AD-712505] 04 p0536 N71-14341

Predicting total heat transfer between boiling refrigerant and external heat source as function of pressure and saturation temperature drops
[DISS-4322] 05 p0782 N71-14589

Rough inside diameter tubing and internal film cooling for augmented heat transfer
[DSR-70790-69] 05 p0782 N71-14805

Computer program for heat transfer and temperature distribution analyses on multidimensional systems
[WANL-TME-1872] 05 p0782 N71-15027

Engineering aspects of Astron fusion power reactor system including structural design, neutronics, heat transfer, and costs
[UCRL-72336] 05 p0728 N71-15114

Literature survey on scaling laws for heat transfer and burnout in two phase flow with application to boiling water reactors
[RISO-207] 05 p0784 N71-15555

Digital computer code for core heat transfer analysis
[IN-1392] 05 p0784 N71-15589

Velocity distributions and heat transfer with film cooling near single angled spanwise continuous injection slot
[AD-713052] 05 p0785 N71-15616

Equations for one dimensional heat transfer and thermal stress in infinite plate
[ZJE-63] 05 p0786 N71-15651

Thermal heat exchange processes between atmosphere and hydrosphere in Arctic Region
[TT-70-50091] 05 p0680 N71-15668

Free boundary value problems of heat flow around aerodynamic bodies
[AD-714621] 06 p0958 N71-15963

Method for improving heat transfer characteristics in nucleate boiling process
[NASA-CASE-XMS-04268] 06 p0959 N71-16277

Heat transfer and pressure variation during flowing steam condensation in tubes
[K-TRANS-60] 06 p0959 N71-16414

Computer program for resolution band model prediction of heat transfer from rocket exhaust plume
[NASA-CR-102998] 06 p0959 N71-16429

Trends of developments in magnetohydrodynamics, and heat and mass transfer
[TR-60] 06 p0906 N71-16659

Two phase flow and heat transfer in multilayer geometries
[GEAP-10214] 06 p0839 N71-16662

Bench type, bottom flooding, coolant injection tests for heat transfer mechanism determination in reactor cores
[IN-1390] 06 p0899 N71-16692

Test chamber for fabric flammability and heat transfer measurement
[PB-194614] 06 p0882 N71-16728

Potential energy model for computing diabatic processes in multilayer atmospheric circulation
[AD-71661] 06 p0856 N71-16796

Heat transfer and pressure drop during condensation of refrigerant vapors in air-cooled condensers
[K-TRANS-57] 06 p0861 N71-16890

Heat transfer prediction for turbine blade design
[AD-717662] 07 p1099 N71-17374

Heat transfer and heat flux measuring sensors for gas turbine engines
[AD-715233] 07 p1028 N71-17377

Investigating effects of heat transfer, viscosity, and scattering on absorption coefficients of porous media saturated with water or petroleum
[NASA-TT-F-13426] 07 p1067 N71-17464

Thermal conductivity of laminar-vacuum insulation and heat transfer during sublimation in rarefied gas medium for Couette flow
[AD-715233] 07 p1130 N71-17722

Radiation heat transfer characteristics of turbine vane airfoils in water-cooled cascade
[NASA-TM-X-2203] 07 p1130 N71-17861

Sea level meteorological properties and heat exchange processes for North Pacific
[SR-612] 07 p1055 N71-17929

Boiling and heat transfer characteristics of cryogenic hydrogen flows in straight and plexus inlet
[NASA-TN-D-6159] 07 p1152 N71-17935

Thermal exchange between water currents and structures in water
[AD-715048] 07 p1024 N71-17979

Wall pressure and heat transfer distribution on delta wings in rarefied hypersonic flow
[REPT-70-9] 08 p1139 N71-18423

Sound field effects on flat plate heat transfer in turbulent boundary layer
[REPT-70-8] 08 p1243 N71-18572

Temperature distribution in thin film films heated by hot gas and hot wall
[DLR-FB-69-98-PT-1] 08 p1180 N71-18618

FORTAN computer program for generating geometrical data of heat transfer code
[NASA-TM-X-2304] 08 p1303 N71-18621

Transverse magnetic field effects on wall heat transfer from ionized argon channel flow
[NASA-CR-116800] 08 p1303 N71-18680

Error analysis on solution of inverse heating problem for flat plates and hemispherical shells
[WLE-TN-RSA-188] 08 p1304 N71-18828

Water cooled reactor power gain by intensified heat transfer using artificial roughness
[AD-715461] 08 p1241 N71-18835

Investigating biothermal model of living tissue for application to thermal control of protective clothing
[NASA-CR-116873] 08 p1152 N71-18926

Research and development in heat transfer applications
[AD-715461] 08 p1305 N71-19209

Heat transfer phenomena associated with pool boiling from flat horizontal surface
[AD-715461] 08 p1306 N71-19206

Vertical eddy thermal transport and global energy budgets of mesosphere and lower thermosphere
[NASA-CR-117047] 09 p1379 N71-19465

Harwell heat transfer and fluid flow information analysis center
[AD-715461] 09 p1482 N71-19539

Effect of electronic equipment operation and spacecraft thermal environment on heat ejection system parameters
[AD-715461] 09 p1482 N71-19630

Design and development of device for cooling inner conductor of coaxial cable
[NASA-CASE-XNP-09775] 09 p1360 N71-20445

Characteristics of heat transfer of parallel flow in tube bundles with constant heat flux and modern Prandtl numbers
[CEA-R-3599] 09 p1485 N71-20524

Resonant cavity heat transfer in turbulent, subsonic and supersonic speeds including resonance effects
[AD-716078] 09 p1318 N71-20540

Radiative-convective heat transfer of high temperature flow of gas in channel
[AD-716078] 10 p1460 N71-20577

Heat and mass transfer test facility, and fabrication of skin-simulator model
[AD-716078] 10 p1538 N71-20792

Computation of heat transfer in electronic equipment
[BCR-15] 10 p1532 N71-20800

Film condensation and heat transfer of low pressure metal vapors on flat surfaces
[NASA-CR-117420] 10 p1461 N71-20860

Waste heat management of nuclear reactor discharge
[CONF-700335-1] 10 p1604 N71-21252

Experimental determination of heat transfer and friction in circular tube with laminar flow of air under conditions of large transverse temperature gradients
[AD-716078] 10 p1542 N71-21283

Wall rotation effect on heat transfer from tube in cooling water stream
[AD-716078] 10 p1663 N71-21640

Numerical methods developed in fluid mechanics and heat transfer emphasizing elliptic flows
[EF/TN/A/34] 11 p1737 N71-22295

Heat transfer and flow friction characteristics of compact heat exchanger surfaces with and without bracing roughness
[AD-717662] 11 p1768 N71-22306

Periodic and maximum-slope techniques with refinements used for testing compact heat exchanger surfaces
[AD-717662] 11 p1841 N71-22446

SUBJECT INDEX

HEAT TRANSFER

Theory, equipment, and techniques for heat transfer and temperature measurements

(AGARDGRAPH-136) 11 p1841 N71-22596
 Analogies for heat and mass transfer processes in fluid flows

Experimental methods for measuring Prandtl number, diffusion properties, and gas thermal conductivities for heat transfer calculations 11 p1843 N71-22606

Cooled film anemometer for high temperature gas measurements in environments with transient phenomena and small heat transfer to sensor 11 p173 N71-22611

Heat sensing instrument, using thermocouple junction connected under heavy conducting material (NASA-CASE-XLA-81531) 11 p1763 N71-22989

Multilayered critical heat flux for array of nine heated rods held in square channel by grid spacers of typical water cooled reactors 12 p1961 N71-23139

Thermodynamic temperature drop at liquid-vapor interface in high temperature lithium heat pipes (NASA-TM-X-2268) 12 p1902 N71-22923

Estimation of momentum, heat transfer, and mass transfer in laminar boundary layers 12 p1903 N71-22948

Characteristics of liquid helium solid boundary conductances and cooling limits (AD-717568) 12 p2011 N71-23977

Effect of permanent and alternating electric fields on heat transfer in fluid dielectrics (NASA-TT-T-13560) 12 p2011 N71-24039

Effect of introducing solid particles into cooling air on heat transfer in row of air jets impinging on inside of semi-circular cylinder in Thoma project (AD-717794) 12 p2011 N71-24109

Numerical analysis of laminar local wall friction and heat transfer in annular tubes and annuli with variation of gas transport properties (AD-717777) 12 p1904 N71-24208

Heat transfer through bed of granular material from hot surface of tube concentrically mounted in rotary apparatus and with results expressed in form of effective thermal conductivity (NLL-AERO-TRANS-1125-9091, 9FV) 12 p2014 N71-24328

Analytic solution of nonlinear heat conduction equation applied to thermally anisotropic and isotropic media with temperature dependent thermodynamic properties (AD-717868) 12 p2015 N71-24350

Space-bolt thermal analysis of oblate spheroid tank mounted multilayer insulation configurations by computer including programs (NASA-TN-D-6228) 13 p2049 N71-24594

Heat gases for passive control of heat pipes in hot reactor systems (NASA-CR-73438) 13 p2185 N71-24886

Calculation of wall temperature in presence of chemical reactions by considering heat transfer between thermally dissociated gaseous medium and cooling fluid (AD-717935) 13 p2186 N71-24971

Heat transfer calorimetry in annealing of electron irradiation induced Frenkel defects in platinum below 4°K (JUL-658-FN) 13 p2132 N71-25091

Heat transfer measurements on trifluorobenzene irradiated in NREX reactor in post dryout regime (AECU-3414) 13 p2119 N71-25179

Flow blockage effects on heat transfer in bottom cooling system of fuel assembly (WCAP-5353) 13 p2187 N71-25357

Numerical analysis of heat transfer equations and temperature profiles to determine thermodynamic properties of liquid metals 13 p2187 N71-25464

Heat transfer and hydrodynamic behavior for subcooled flow boiling of Freon 113 for use in cooling electronic components 14 p2352 N71-25805

Regional control of skin temperature and heat transfer measurements of various body sections (AD-720836) 14 p2394 N71-25953

Heat transfer, aerodynamics, and operational flight mechanics in space shuttle technology (NASA-TM-X-2272) 14 p2343 N71-26051

Mixed liquid and vapor phase analyzer design with thermocouples for relative heat transfer measurement (NASA-CASE-NPO-10691) 14 p2355 N71-26199

Theoretical calculations of heat transfer during vapor condensation in tube based on analogy between dynamic friction resistance and heat exchange according to Rayleighs (AD-720858) 14 p2356 N71-26353

Safety considerations for irradiation of PB-2 reactor fuel capsules of UC-Pu using NaK as heat transfer medium (BURNER-764) 15 p2443 N71-26853

Analysis of heat transfer data obtained during future S/Skylab multiple probe heat transfer test (NASA-CR-61333) 15 p2524 N71-27015

Heat transfers in two phase flows of horizontal and vertical tube heat exchangers (CEA-CONF-1649) 15 p2393 N71-27153

Heat transfer to difluoromethane and difluoromethane refrigerants at nucleate boiling, film boiling, and supercritical condition of fluid (BMBW-FBR-78-34) 15 p2524 N71-27163

Aerodynamic heat determination on blunt bodies in hypersonic flow with force and pressure measurements (BMBW-FB-W-71-48) 15 p2364 N71-27616

Model for influence of heat transfer and friction on flow parameters in nozzle with independent cooling (AD-720933) 15 p2395 N71-27759

Film boiling and heat transfer from platinum wire in saturated liquid nitrogen up to critical pressure (NASA-TM-X-67849) 15 p2535 N71-27863

Heat transfer and pressure drop data on standard oil column for turbine installations (NLL-TS-5968) 16 p2690 N71-28137

Liquid propellant rocket engine throttling injector design based on ethanol gas counter flow and heat transfer for inflowing propellant vaporization and combustion stability tests (NASA-CR-117996) 16 p2671 N71-28158

Micrometeorological investigations of momentum, energy, and mass transfers above vegetative surfaces with von Karman constant, diabatic profile functions and eddy-transfer coefficients 16 p2625 N71-28225

Crystallization heat given off by ice to atmosphere and effect on meteorological conditions in Arctic analyzed on basis of observational data and theoretical computations (AD-720148) 16 p2598 N71-28499

Heat transfer between gas and solids in suspension (NLL-RTS-6129) 16 p2692 N71-29036

Development and characteristics of cooling system to maintain temperature of rack mounted electronic modules (NASA-CASE-NBC-12389) 16 p2693 N71-29052

Nuclear reactor heat transfer and fluid flow study using vectors and other mathematical tools (WAPD-TM-1009-VOL-1-CH-1-CH-2) 16 p2693 N71-29075

Compressible turbulent boundary layer predictions with heat transfer from flat plates in gun tunnel at Mach 9 (IC-AERO-70-05) 17 p2697 N71-29318

Zero gravity incipient boiling heat transfer in closed cylindrical container 17 p2831 N71-29612

Turbulent film boiling tests of heated flat plate model in high speed water tunnel 17 p2733 N71-29619

Experimental data on subcooled and saturated quality boiling heat transfer to low pressure water in electrically heated tubes (NASA-TN-D-64602) 17 p2857 N71-29711

Development of analytic model for determining radiative heat transfer characteristics of coatings on cryogenic surfaces (AD-722726) 17 p2858 N71-29823

Development of method and equipment for testing heat radiative properties of material under controlled environmental conditions (NASA-CASE-MFS-20096) 17 p2753 N71-30026

Analysis of mechanism of boiling, evaporation, and heat transfer in fluids 17 p2859 N71-30287

Design and development of spacecraft radiator using forced convection, conduction, and radiation for heat transfer under steady state conditions (NASA-CR-119200) 18 p3023 N71-30649

Determining heat transfer to space vehicles entering planetary atmospheres for proper design and thermal protection (NASA-SP-8062) 18 p3025 N71-31179

Analysis of processes maintaining seasonal heat storage in 0 to 250 meter surface layer of North Pacific Ocean (PB-197661) 18 p2918 N71-31278

Boundary effects on heat transfer in non-Newtonian fluid flow through phase crack 18 p3027 N71-31450

Bathythermographic data of subsurface temperature anomalies and relationship to Pacific Ocean surface temperatures (AD-722587) 18 p2920 N71-31504

Temperature gradients induced in heated wall by impinging gas jet traveling through liquid coolant (ANL-7734) 19 p3078 N71-32116

Prediction of heat transfer to gas flowing in convergent annular reactor channels (AERE-R-6564) 19 p3192 N71-32182

Experimental model of heat transfer to two phase, fluid particle flow in tubes for use in analysis of capillary blood flow 19 p3193 N71-32401

Similar solution for turbulent boundary layer with large favorable pressure gradients to predict heat transfer along nozzle (NASA-TN-D-6439) 19 p3080 N71-32415

Acquisition of data in Caribbean related to energy exchange between ocean surface and atmosphere - Project BOMEX 20 p3360 N71-32806

Aerodynamic and heat transfer performance of air cooled nozzle cascade for high temperature turbines (NALL-TR-231-PT-1) 20 p3364 N71-33304

Comparison of experimental and analytic film boiling heat transfer data for spheres immersed in liquid stream at standard and reduced gravity (NASA-TM-X-2544) 20 p3364 N71-33394

Anatomical-physiological characteristics of heat transfer in human body for developing insulating suit 20 p3221 N71-33493

Momentum loss and heat transfer in deflected propene jet flow during combustion 20 p3251 N71-33570

Analysis of infrared radiative energy transfer in storage gases under three conditions of flow and equilibrium 20 p3364 N71-33683

Digital computer program for calculation of one heat transfer in power reactors during loss of coolant accidents (CONF-710802-2) 20 p3367 N71-33690

Characteristics of liquid metals on cooling and heat transfer system for use with nuclear reactors 20 p3366 N71-33752

Measurement of heat transfer in ionized gas by wire probe in arc plasma at atmospheric pressure 20 p3331 N71-33766

Measurements of complete pool boiling heat transfer characteristics for binary mixtures and comparison with predicted results to determine parametric effects of mixture concentration 20 p3367 N71-33782

Preliminary test results of heat transfer/thermal storage tube design for solar Brayton cycle power system under simulated orbital conditions (NASA-TM-X-67904) 20 p3367 N71-33785

Three methods for calculation of compressible turbulent boundary layer with pressure gradient and internal flow heat transfer with reference to supersonic nozzles (TT-7104) 20 p3253 N71-33818

Analysis of heat transfer in region of separated flow downstream of rearward facing step using Mach-Zehnder interferometer 20 p3368 N71-33862

Heat transfer optimization and reactivity calculation of solid core nuclear rocket reactor (NASA-CR-121735) 21 p3456 N71-34600

Thermal bowing of single rods at several axial positions (TRG-2009) 21 p3458 N71-34608

Empirical analysis of thermophysical properties of multilayer insulation composite materials for cryogenic storage equipment - Vol. 2 (NASA-CR-119844) 21 p3463 N71-34650

Analysis of heat transfer characteristics of venting cryogen tank - Vol. 3 (NASA-CR-119845) 21 p3463 N71-34651

Wave propagation and absorption in inhomogeneous media including simultaneous thermal energy transformation and channeling (MATT-TRANS-103) 21 p3493 N71-34982

Compressible heat transfer in low speed flow with small temperature differences 21 p3530 N71-35155

Finite element analysis of nonlinear heat transfer in axisymmetric solids (PB-199169) 21 p3531 N71-35160

Analysis of wall temperatures in rocket engine cooling system using D-shaped copper and stainless steel tubes for reduction of tube-wall crest temperatures (NASA-TN-D-64522) 21 p3531 N71-35162

Measurement of temperature distribution in operating ni-zn-cadmium electric batteries (NASA-TN-X-2371) 21 p3531 N71-35163

Analysis of heat transfer crisis and high frequency natural pressure oscillations during movement of liquids along tubes (NLL-CR-TRANS-5620-1022.091) 21 p3531 N71-35166

Inter-relationship between high frequency oscillations and nature of nucleate and film heat transfer with forced fluid flow (NLL-CR-TRANS-5621-1022.092) 22 p3570 N71-35426

Heat, wave energy, and mass transfer through air-sea interface in presence of swell and wind (SU-TR-134) 22 p3574 N71-35454

Development and evaluation of high temperature materials for use in magnetohydrodynamic generators (JPRS-53939) 22 p3598 N71-35621

Computer program for calculating transient heat transfer performance of reactor coolant channel during accidental power excursions 22 p3627 N71-35843

Computer program for calculating liquid surface streamlines and heat transfer on space shuttle configurations (NASA-CR-111921) 22 p3673 N71-36186

Prediction of bolted joint heat transfer in spacecraft applications
[NASA-CR-119933] 22 p3694 N71-36346

Mathematical models for solving problems of heat transfer on transpired turbulent boundary layer
[NASA-CR-126791] 22 p3694 N71-36347

Neutron radiography used to determine dimensional changes of heat transfer gaps in cylindrical nuclear fueled capsules
[NASA-TM-X-67920] 22 p3695 N71-36351

Heat transfer data on windward surface of orbiter fuselage
[NASA-TM-X-62051] 22 p3695 N71-36353

Design and development of prototype static cryogenic heat transfer system utilizing heat pipe with wetting arterial wick and nitrogen as working fluid
[NASA-CR-121939] 22 p3695 N71-36355

Feasibility of using elastic deformation to predict heat transfer rates across joined smooth-metal surfaces under high vacuum conditions and light loads
[NASA-TM-X-3385] 22 p3696 N71-36361

Analysis of high vapor velocity condensation in tubes based on universal velocity distribution, pressure drops, and heat transfer coefficients
[DSR-72391-74] 22 p3696 N71-36363

Thermal and dynamic properties of combustion products from various gases and heat transfer to flat plates from high-temperature combustion product jets
[NRL-RTS-6531] 22 p3697 N71-36366

Reynolds number for measuring heat transfer and pressure drop in tube bundles caused by tube roughness
[NRL-CE-TRANS-5511-9022.09] 22 p3697 N71-36369

Effectiveness factor calculation technique for nonisothermal catalysts taking into account mass and heat transfer effects at boundary film and in particle interiors
[NRL-RTS-6472] 23 p3722 N71-36527

Momentum and heat transfer measurements for low Reynolds number shear flow past rotating circular cylinders
23 p3746 N71-36709

Radiometric measurements of total heat flow to ocean surface and meteorological parameters
23 p3788 N71-36998

Bibliography on burnout in forced convection boiling heat transfer in uniform and nonuniform heat systems
[AAEC/LIB-BIB-286] 23 p3796 N71-37059

Cooling of simulated reactor fuel element by heat transfer from element to boiling water
[UARAE-110] 23 p3796 N71-37064

COBRA heat transfer code extensions for large liquid Na cooled gas bundles and coolant mixing effects due to fuel pin spacer wires
[WHAN-SA-76] 23 p3798 N71-37080

Cyclic heat transfer and static pressure drop measurements of gas flow through packed beds
[AAEC/TM-580] 23 p3866 N71-37558

Characteristics of heat transfer to liquid helium from horizontal, face-up surfaces of normal and superconducting lead and tin
23 p3867 N71-37567

Computer program for analyzing transient response of ablating axisymmetric bodies including effects of shape change
[NASA-TM-X-2375] 23 p3867 N71-37569

Development of method for determining flow field behind detonation wave formed by acetylene-oxygen detonation based on wall heat transfer - Vol. 3
[ME-A-71-3] 23 p3867 N71-37571

Measurement of heat transfer from acetylene-oxygen detonation in shock tube-Vol. 2
[ME-A-71-2] 23 p3868 N71-37572

Properties of high temperature compounds, physics of gas dynamics, heat resistant materials, and heat conversion by power plants
[JPRS-54182] 23 p3868 N71-37573

Use of thermocouples for temperature measurement during boiling liquid heat transfer experiments
[NRL-RISLEY-TRANS-2164-9091.9F] 23 p3868 N71-37575

Modified thermal analyzer digital computer program for heat transfer problems
[NASA-CR-72944] 24 p3891 N71-37733

Thermal resistance measurements on contacting interfaces between uranium nitride and metals
[ORNL-4669] 24 p3961 N71-38255

Heat and momentum transfer analysis for SNAP 8 counterflow NaK to Hg boiler using IBM 360 computer code
[NASA-CR-72907] 24 p4018 N71-38667

Correlation of local nondimensional heat transfer rate and pressure ratio for blunt cones at angle of attack
[AD-727787] 24 p4022 N71-38698

Experimental loop for two phase heat transfer in simulated BWR fuel channel
[UARAE-41] 24 p4028 N71-38739

Heat transfer in jet impingement cooling of concave surface in semi-enclosed environments
[AD-727730] 24 p4030 N71-38739

Heat transfer in smooth tubes, between parallel plates, in annuli and tube bundles with exponential heat flux distributions in forced laminar or turbulent flow
[NLL-WINDSCALE-458-9091.9F] 24 p4032 N71-38770

Heating surface material, surface condition and geometry, contact duration, and coolant impurity and inert gas content effects on heat transfer in boiling alkali metals
[NLL-RISLEY-TRANS-2165-9091.9F] 24 p4033 N71-38773

Computer program for calculation convective heat transfer coefficients from harmonic temperature oscillations
[NASA-TM-X-2147] 04 p0500 N71-13496

Stationary heat transfer in infinitely long, eccentricity layered cylinders with position-dependent heat sources and peripheral restrictions
[TUBIX-16] 04 p0546 N71-13567

Prediction of friction and heat transfer coefficients with large variations in fluid properties
[NASA-TM-X-2145] 04 p0620 N71-14031

Heat transfer and exchange measurements on fixed turbine blades in high temperature combustion chamber
07 p1100 N71-17378

Heat transfer in air cooling and sweat cooling techniques for high temperature gas turbine engine components
07 p1100 N71-17378

Effective heat transfer coefficients in film cooling systems of gas turbine surfaces
07 p1129 N71-17395

Heat transfer in liquid metal cooled gas turbine blades
07 p1129 N71-17396

Cryogenic heat pipe measurements of film condensation heat transfer coefficients
[CEA-CONF-1634] 08 p1302 N71-18157

Models for heat transfer during spin melting within single fibers and from single fiber to surrounding fluid
10 p1660 N71-20755

Comparison of solid propellant nozzle heat transfer coefficients with predicted data
[NASA-TM-X-66997] 10 p1661 N71-21201

Conference on high temperature turbines detailing effect of film cooling on blade profile loss
[NASA-TM-X-67123] 11 p1821 N71-22699

Orthogonal collocation method applied to plug flow model of packed bed reactor to predict heat transfer coefficient
12 p1962 N71-23890

Gas-solid thermal accommodation coefficient measurements in shock tube by thin film resistance thermometers
[AERO-2] 12 p2014 N71-24318

Pressurized water reactor flooding rate effects on cooling heat transfer time-temperature response based on plenum chamber simulation tests
[WCAP-5352] 13 p2117 N71-24907

Heat transfer coefficients and transition points as functions of steam in high pressure boiling flow steam generators
[EUR-4561-E] 13 p2187 N71-25356

Forced flow heat transfer coefficients for laminar film boiling interface on vertical surface
[NASA-TM-X-67860] 15 p2525 N71-27867

Flow and heat transfer characteristics of incompressible fluid in radial diffuser using air as fluid with inlet Reynolds numbers from 15 to 33,500 and area ratios from .245 to 2.04
16 p2583 N71-28894

Heat transfer coefficients, heat emission, and flow resistance in intertube space of heat exchanger
[NLL-RTS-5990] 16 p2692 N71-29043

Determination of similarity between boiling and injection of saturated vapor and establishment of critical heat flux model
[RR-5] 16 p2693 N71-29069

Analytic model of boundary conditions for heat transfer coefficients through porous walls
[NASA-TN-D-6405] 17 p2857 N71-29734

Heat transfer coefficients for dropwise condensation of organic liquids on Teflon
[NASA-TN-D-63902] 17 p2859 N71-29901

Axial and circumferential variations of hot gas side heat transfer coefficients in hydrogen oxygen engines for use in nozzle and injector design
[NASA-TN-D-6396] 18 p3024 N71-30738

Transfer coefficients for thermal radiation in scattering and absorbing media
18 p3025 N71-30949

Thermal conductivity coefficient and Prandtl number tables for nitrogen from 133 to 740 K between 1 and 240 atmospheres
[BM-RI-7541] 19 p3052 N71-32693

Measurement and correlation of gas-particle heat transfer coefficients in packed and fluidized bed processes by frequency response techniques
[BPS-3638-16] 21 p3411 N71-34268

Heat transfer coefficient determination in helical fins for thermal design of nuclear fuel elements
[NLL-WINDSCALE-TRANS-397-9091.9F] 21 p3411 N71-34268

Transfer coefficients and kinetic equilibrium for plasma confined in Tokamak at high temperatures
[CONF-710607-34] 24 p3994 N71-38805

Investigations of thermodynamic and physico-chemical influences on incipient boiling superheat of sodium on artificially roughened surfaces
[KFK-1332] 24 p4050 N71-38754

Relationships between heat transfer coefficients and friction factors in tube bundles with axis-parallel turbulent flow at constant heat flux density and average Prandtl numbers
[NLL-MIN-TECH-T-6697-5889.95] 24 p4052 N71-38771

Infrared radiometer system for airborne measurements of sea surface temperature and heat flux
02 p0207 N71-11116

Physical effectiveness of current heating of dense high current gas discharge plasma stabilized by strong magnetic field
[KHFT-69-43] 03 p0438 N71-12820

Critical thickness of thermal insulation layer on curved surface
07 p1130 N71-17382

Boltzmann transport equations for flow of heat between parallel plates in rarefied gas
06 p1183 N71-18946

Non-steady state heat propagation in solid bodies with simultaneous radiant and convective heat flows
[NLL-RTS-6022] 10 p1664 N71-21487

Analysis of ocean bottom heat flow in Tasman Sea
18 p2913 N71-30991

Heat transport and frictional force in laminar non-Newtonian fluid flow
18 p3027 N71-31447

Design criteria of heat flow experiment designed as ALSEP Array A2
[NASA-CR-115109] 19 p3178 N71-31607

Heat flowmeter for measuring vertical takeoff aircraft exhaust thermal insulation dissipation
[DLR-MITT-71-07] 19 p3099 N71-31929

Radioactive isotope capsule container design for atmospheric reentry protection and heat transmission in spacecraft
[NASA-CASE-LEW-11227-1] 21 p3330 N71-35153

Canadian power reactor operation economics and primary heat transport system, valve development
[AECL-3838] 23 p3796 N71-37060

Computer program for solving a two-dimensional transient or steady state heat flow problems by creating electrical analogy of problem and solving by finite difference method
[NASA-CR-72916] 24 p3892 N71-37734

Solutions for transient temperature distribution in one-dimensional solid with linear heat loss
[SC-DR-70-767] 24 p4029 N71-38731

Thermodynamic and thermophysical properties of helium with application as working substance or heat carrier in nuclear power plants - tables and diagrams
[TT70-50096] 24 p4030 N71-38756

HEAT TREATMENT
NT ANNEALING
NT MARAGING
NT NITRIDING
NT NORMALIZING (HEAT TREATMENT)
NT STRESS RELIEVING
NT TEMPERING

Effects of mechanical straightening and flame straightening on properties of steel plates
[AD-710521] 01 p0057 N71-10032

Vacuum method for sputtering thermooxidation compounds used as ablative materials
[NASA-CASE-XLA-61091] 01 p0060 N71-10672

Wear resistance tests of nickel-phosphorus coating with heat treatment
[AD-711271] 01 p0069 N71-10699

Optimization of properties of stainless steels by austenitizing at high temperatures
[AD-711608] 02 p0240 N71-11142

Short-time stress rupture of prestressed titanium alloys under rapid heating conditions
[NASA-TN-D-6052] 02 p0443 N71-11669

Metal melting and endothermal heating experiments for component manufacturing in orbital workshop
[NLR-TR-6608-LJ] 02 p0445 N71-12126

Heat treatment of steel components in water-air dispersion
[ZIE-77] 03 p0384 N71-12358

SUBJECT INDEX

HEAVY ELEMENTS

Nondestructive test for measuring heat treatment states in closure welds
[ORNL-TM-3024] 05 p0386 N71-13285

Preliminary thermomechanical treatment of D6AC steel during austenite and martensite transformations
[AD-712463] 04 p0528 N71-13947

Production engineering of heat strengthened titanium alloys
[AD-713760] 05 p0704 N71-15293

Production of refractory bodies with controlled porosity by pressing and heating mixtures of refractory and inert metal powders
[NASA-CASE-LEW-10393-1] 05 p0705 N71-15468

Aluminum-rich magnesium alloys strengthened by combined action of plastic deformation and heat treatment
[AD-714120] 06 p0865 N71-16219

Heat treatment, rolling, and forging effects on plastic strain anisotropy of Ti-6Al-4V alloy
[AD-714562] 06 p0871 N71-16220

Combined deformation and heat treatment effects on aluminum alloys
[AD-713979] 06 p0873 N71-16436

Effect of thermomechanical treatment on properties of alloys - Vol. 1
[AD-715293] 07 p1044 N71-17351

Mechanical properties and microstructure of titanium alloy after heat treatment
[AD-715353] 08 p1213 N71-18523

Determination of effects of heating on properties of metals and alloys by method of elastic vibrations
[TT-70-57976] 08 p1218 N71-19099

Heat treatment effect on microhardness, wear, and corrosion resistance of chemically deposited nickel coating
[NLL-TRANS-746-599-19022.401] 10 p1578 N71-21219

Thermomechanical processing effects on crystal microstructure, texture, and high temperature strength of dispersion strengthened and free nickel-based Cr, TiO₂, and W alloys
[NASA-CR-72832] 10 p1583 N71-21589

Effects of welding and post-weld heat treatment on microstructure and mechanical properties of QT steel
[ELECT-2] 11 p1789 N71-22541

Effect of heat treatment variables on mechanical properties of titanium alloys and applications based on strength and weight
[AD-710040] 12 p1937 N71-23280

Development of furnace designs, operating, casting, and annealing procedures to improve structural properties of fused-cast aluminum oxide articles
[AD-710040] 12 p1946 N71-24095

White point production by heating impure aluminum silicate clay having low color absorbance
[NASA-CASE-KNP-02139] 12 p1947 N71-24184

Heat treatment for matrix precipitation of NiC in 2025/Al stainless steel
[TRG-REPORT-2040/S] 13 p2092 N71-24733

Interfacial friction of heated polycrystalline samples of vanadium at low pressure
[CNEA-260] 13 p2093 N71-25088

Steel microstructure, surface austenite and carbide formation, and diffusion coefficient measurement during chemical and thermal treatment
[TT-70-59099] 14 p2269 N71-25660

Balzers evaporation unit for thermal treatment of CrSiO₂ ceramic thin films
[US-587] 14 p2281 N71-26590

Microscopic and X ray crystallographic analyses of spinel in body centered cubic zirconium phosphorus alloys during cold hardening
[CRA-CONF-1468] 15 p2422 N71-27129

Correspondence of hydroabrasive wear resistance and hardness of heat treated steels
[AD-721022] 15 p2423 N71-27301

Effect of initial heat treatment on high temperature embrittlement of nickel alloys after neutron irradiation
[SRL-7-94] 16 p2607 N71-28039

Thermomechanical and transformation induced plasticity processes for producing high strength martensitic titanium alloys with high tensile, fracture, and elongation properties
[AD-721361] 16 p2608 N71-28073

Mechanical behavior of aluminum-stainless steel composites subjected to elevated temperature under strain and were pulled to failure after extraction from composites
[AD-721374] 16 p2610 N71-28441

Effects of initial heat treatment on high temperature embrittlement in nickel alloys after neutron irradiation
[ABC-TR-71-08] 16 p2613 N71-28799

Hot isostatic compaction at 3000 P and 30,000 psi used for successfully preparing single phase bulk graphite for ablation testing
[DC-CR-76-4169] 17 p2768 N71-29219

Vacuum brazing, vacuum heat treatment, gas etching process for fabricating hardware items with hollow lead light joints
[AD-722730] 17 p2756 N71-29813

Stretching and heat treatment effects on microstructure of polycrystalline fibers
[RAE-LIB-TRANS-1508] 17 p2771 N71-30392

Relative stress relaxation behavior at 300 C of cold worked Zircaloy-2, cold worked Zr-2.5 wt percent Nb, and heat treated Zr-2.5 wt percent pressure tube materials
[ABCL-3782] 18 p3021 N71-30584

Heat treatment of carbide and boride strengthened chromium alloys to improve tensile and creep rupture strength
[NASA-CR-72843] 18 p2933 N71-30676

Effects of heat and mechanical treatment on microstructure of steels and its alloys
[AD-722822] 18 p2928 N71-30807

Influence of cold work and heat treatment on tensile and fatigue strengths - fatigue properties of titanium and titanium alloys - Part 3
[RAE-LIB-TRANS-1519-PT-3] 18 p2935 N71-30886

Uniaxial emission behavior of materials with various heat treatments and its relation to Bloch-Grüneisen effect
[AD-723616] 18 p2936 N71-31139

Thermal treatment, thermal equilibrium, and microstructural effects on intergranular creep in sintered and fused cast aluminas
[AD-723616] 18 p3022 N71-31367

Growth techniques and heat treatments for producing high quality epitaxial films of lead telluride and tin telluride
[AD-722786] 18 p2998 N71-31453

Thermomechanical processing of nickel alloy in relation to yield and creep rupture strength
[NASA-TN-D-64118] 21 p3434 N71-34432

Effect of oxygen, heat treatment, and test temperature on compatibility of advanced refractory alloys with lithium
[ORNL-4436] 21 p3440 N71-34479

Precipitation, reprecipitation, and hardening mechanisms in heat treated aluminum alloys
[NLL-M-20410-13828.4P] 21 p3441 N71-34484

Procedure for hardening metals by high temperature thermomechanical processing and effect on heat resistance properties of nickel alloys
[AD-726736] 23 p3763 N71-36826

Heat treatable low hydrogen electrode welding device for welding HY-40 steels
[AD-726758] 23 p3763 N71-36828

Effects of resolution treatment and overheating on fatigue properties of notched and unnotched D.T.D. 6813 aluminum alloy bar
[ARL-SM-NOTE-258] 23 p3770 N71-36870

Analysis of structural state of mono and polycrystals of aluminum and copper alloys after deformation
[AD-726731] 23 p3770 N71-36874

Analysis of heat resistance and mechanical properties of molybdenum alloys
[AD-726732] 23 p3771 N71-36875

Properties of materials hardened by mechanical-thermal processing at different temperatures
[AD-726839] 23 p3771 N71-36876

Effects of heat processing methods on mechanical and heat resistant properties of titanium alloys
[AD-726729] 23 p3771 N71-36878

Effect of heat treatment on physical properties of steels with various amounts of nickel, cobalt, and molybdenum
[NLL-TRANS-746-807-19022.401] 23 p3774 N71-36897

Heat treatment and cold work effects on oxidation of Zr-1 percent Nb alloy in air and pressurized steam at 450-650 C
[UABAE-72] 24 p3933 N71-38061

Developing metal alloys of ultrahigh grain size with improved mechanical properties
[AD-727746] 24 p3938 N71-38093

HEATERS

Characteristics of electric heaters used with SNAP 8 spacecraft power supplies
[NASA-TM-X-2186] 07 p1131 N71-17898

HEATING

NT AERODYNAMIC HEATING

NT ARC HEATING

NT ATMOSPHERIC HEATING

NT BASE HEATING

NT GAS HEATING

NT INDUCTION HEATING

NT KINETIC HEATING

NT LASER HEATING

NT PLASMA HEATING

NT RADIANT HEATING

NT RADIO FREQUENCY HEATING

NT RESISTANCE HEATING

NT SHOCK HEATING

NT SOLAR HEATING

NT SUPERHEATING

NT TRANSIENT HEATING

Heating of uranium dioxide rods by direct electric current
[KFK-1031] 02 p0264 N71-11413

Metallic materials heated by laser radiation absorption
[JPRS-52916] 12 p1931 N71-23104

Heating ferrite by pulsed laser radiation absorption, preceding thermal breakdown
12 p1932 N71-23105

Numerical analysis of bowing of heated element cooled by forced convection, and application to nuclear fuel elements
[TRG-REPORT-1915] 14 p2356 N71-26356

Numerical analysis of temperature distribution and phase change positions when phase change is caused by constant heating or cooling or convection to constant temperature
14 p2356 N71-26357

Heating rate and efficiency of flaps at hypersonic speeds
[SC-T-71-3016] 15 p2365 N71-27634

Specifications for cleaning, finish, welding, and postheating titanium and niobium alloys
[NASA-TM-X-67679] 18 p2936 N71-31135

Ion heating caused by ion acoustic waves from electron drift in ion streaming plasmas
[IIPP-104] 21 p3494 N71-34889

Numerical analysis of relaxation and nonequilibrium radiation properties behind shock waves in air
[SC-T-713620] 23 p3743 N71-36886

Ultrahigh frequency heating and eddy-current compression of plasma in Tonne-2 facility
[CONF-714607-141] 23 p3826 N71-37287

Comparing thermomechanical dilatometer measurements to calculations of gaseous heating in polyethylene and lead containers
[NASA-TM-X-67936] 23 p3866 N71-37339

Linear surface pyrolysis of ammonium perchlorate by convective heating
[AD-727991] 24 p3886 N71-37696

Crossed field instabilities and turbulent ion heating conducted in mirror machine
[CONF-716607-67] 24 p3988 N71-38458

HEATING EQUIPMENT

NT BOILERS

NT EVAPORATORS

NT FURNACES

NT OVENS

NT SOLAR FURNACES

NT VACUUM FURNACES

NT VAPORIZERS

Design of axial flux heaters and grid space effects on reactor cooling flow
[ORAE-10196] 05 p0726 N71-15947

Microscopic analysis of heater rods, charring, and metal-water reactions
[WCAP-7444] 06 p0897 N71-15874

Using heat control unit to prevent circulating fluid
[NASA-CASE-XMF-04237] 06 p0929 N71-16278

Feasibility of miniaturized heater for zinc oxide thin film oxygen partial pressure sensor
[NASA-TN-D-6134] 07 p0906 N71-17440

Electric arc heater with superconductive nozzle and fixed arc length for use in high temperature wind tunnels
[NASA-CASE-XAC-01677] 10 p1532 N71-30816

Procedure for evaluating effectiveness of self propelled and portable ground servicing units for Army aircraft
[AD-719102] 13 p2023 N71-24659

HEAVING

Experimental determination of frost heave forces in ground
[AD-711904] 02 p0218 N71-12056

Frost heaving theory
[AD-714641] 06 p0841 N71-15937

Frost heave effects on communication cables in cold regions
[AD-724636] 20 p5240 N71-33009

Frost heave damage to electrical cables in cold regions
[AD-724635] 20 p5240 N71-33009

HEAVY COSMIC RAY PRIMARIES

U HEAVY NUCLEI

U PRIMARY COSMIC RAYS

HEAVY ELEMENTS

NT AMERICIUM

NT AMERICIUM ISOTOPES

NT AMERICIUM 241

NT BERKELIUM

NT CALIFORNIUM

NT CALIFORNIUM ISOTOPES

NT CURIUM

NT CURIUM ISOTOPES

NT CURIUM 244

NT LAWRENCIUM

NT NEPTUNIUM

NT NOBELIUM

NT PLUTONIUM

NT PLUTONIUM ISOTOPES

NT PLUTONIUM 238

NT PLUTONIUM 239

NT PLUTONIUM 240

NT PLUTONIUM 241

NT TRANSURANIC ELEMENTS

Radioactive abundances and stable products in chronological model for galactic heavy element nucleosynthesis
01 p0057 N71-10510

Phase selective alternating current and square wave photographic analysis of water for low concentration of heavy metal ions
[PB-195412] 02 p0173 N71-12119

- Investigating existence of long-lived super-heavy elements in nature and synthesis in stars
[JINR-P6-4902] 04 p0586 N71-12427
- Characteristics of gamma absorptometer with scintillating detector and photomultiplier for heavy element determination in solution 05 p0684 N71-14887
- New features in data on neutron spectroscopy of heavy nuclei
[BNL-TR-351] 06 p0925 N71-16816
- Superheavy element detection in nature from events with emission of large numbers of neutrons
[UCRL-1957] 07 p1076 N71-17542
- Neutron fission detector for search of superheavy elements in nature 14 p2259 N71-26789
- Nuclear chemistry of fissions, alpha decay in osmium isotopes, alpha radioactivity in air samples, and nuclear levels, nucleic masses, and lifetimes of heavy elements
[MNC-3783-9] 17 p2794 N71-29651
- HYLAS code for predicting heavy element composition of irradiated reactor fuel 17 p2785 N71-30142
- Calculations for obtaining heavy element content and fission product inventory in CAOR fuel
[RD/BN-1887] 18 p2978 N71-30672
- HEAVY IONS**
- Angular distributions of nuclear transfer reactions between heavy ions 06 p0918 N71-16202
- Heavy ion beams for in-beam gamma ray and conversion electron spectroscopy 08 p1261 N71-18777
- Device for detecting alpha active nuclei of nuclear reactions induced by heavy ions 13 p2129 N71-24575
- Electron capture and loss cross sections in heavy ion collisions with atomic oxygen and excitation of positive helium ion 15 p2478 N71-27623
- Performance characteristics of existing and proposed accelerators for heavy ions with description of super HELAC progress and discussion of isochronous cyclotrons 17 p2793 N71-29625
- Focusing, acceleration, and beam characteristics of Orsay heavy ion linear accelerator
[N7-18612] 18 p2978 N71-30665
- Isochronous cyclotron combination for acceleration of heavy ions
[HMI-B-105] 18 p2901 N71-30715
- Ion accelerator systems engineering for time sharing operation with heavy and light ions
[UCRL-20633] 19 p3147 N71-31994
- Pneum ion gate (PIG) type heavy ion source on axial injection line of 88 inch cyclotron
[NASA-20406] 19 p3153 N71-32207
- Production of far neutron-deficient iridium isotopes by bombarding holmium with Ne-22 and Ne-20 heavy ions
[JINR-P6-5617] 19 p3159 N71-32398
- Conference on heavy ion sources
[WASR-1159] 20 p3321 N71-33737
- Phase shift in interdigital H type structure for heavy ion accelerator
[LYCEN-7103] 21 p3470 N71-34709
- Multicharged heavy ion sources produced by arc discharge, electron bombardment, or high power spark discharge
[ANL-TRANS-876] 21 p3483 N71-34812
- Theoretical model for electronic stopping power of heavy ions compared with experimental results for carbon and nitrogen targets 21 p3493 N71-34880
- Cyclotron characteristics and types of ion source injectors for use in high-energy, heavy-ion cyclotrons
[UR-NSRL-38] 22 p3642 N71-35962
- Multinucleon transfer cross sections in heavy ion reactions
[JINR-E2-5797] 23 p3810 N71-37165
- Fundamental problems involving nuclear reactions induced by heavy ions 23 p3812 N71-37180
- HEAVY NUCLEI**
- Investigation of atomic nucleus structure
[JINR-P4-9045] 02 p0278 N71-12161
- Parallel plate ionization chamber for identifying relativistic cosmic ray nuclei
[NASA-CR-116874] 06 p1176 N71-18914
- Charge distribution of heavy nuclei of cosmic rays in region Z greater than or equal to 26 determined by photoemission method
[NASA-TT-F-13510] 09 p1463 N71-20490
- Neutron transmission coefficients for heavy nuclei at 0.05 to 2 MeV
[BNL-TR-379] 10 p1618 N71-21378
- Nuclear composition for several multicharged nuclei and energy spectra for hydrogen, helium, and medium nuclei measured in solar particle event
[NASA-TM-X-63573] 15 p2514 N71-27645
- Determination of heavy nuclei charges in atmosphere from formation density of delta electrons
[NASA-TT-F-13743] 17 p2085 N71-30295

- Highly inelastic scattering of medium energy He-3 and He-4 particles by Si, Ta, Pt, Au, and Pb nuclei
17 p2809 N71-30377
- Gamma ray transition probabilities in deformed nuclei and lifetimes of excited states in heavy nuclei
[NP-18695] 19 p3153 N71-32266
- Coherent [a,2n] scattering amplitude on heavy nuclei at low energies based on infinite-mass nuclei approximations
[ITF-70-95-E] 21 p3487 N71-34839
- Epicadmium integral fission cross section measurements for twelve heavy actinides including plutonium and uranium isotopes 22 p3490 N71-36031
- Algebraizing integral equations for T matrix for reactions in system of heavy nucleus and two neutrons
[ITF-70-97-F] 24 p3970 N71-38322
- Heavy and ultrahigh nuclei observations of cosmic rays using ionization chamber-Cerenkov counter system
[NASA-CR-123197] 24 p4002 N71-38544
- HEAVY WATER**
- Neutron flux measurements in three-capsule D2O tank in Plum Brook mock-up reactor
[NASA-TM-X-52910] 01 p0084 N71-10271
- Organic cooled, heavy-water moderated WR-1 research reactor capable of low pressure with high temperature in primary system and very low radiation fields near primary piping
[AECL-3523] 04 p0547 N71-13640
- Evaluation of potential hazards from tritium water in relation to nuclear power plants
[CONF-700410-6] 05 p0634 N71-14684
- Thermal neutron diffusion data for heavy water and its consequences for neutron scattering law models
[AEW-R-683] 06 p0909 N71-15754
- Measure of fast fission factor in ORGEL D2O natural U lattices
[EUR-4326] 13 p2133 N71-25162
- Inhibitor effects of peroxide, MnO2, and D2O on substances existing in nature to determine performance of terrestrial organisms in extreme and unusual gaseous and liquid environments
[NASA-CR-118883] 15 p2372 N71-27743
- Electromagnetic resonance of vanadyl perchlorate in solutions of water and heavy water
[UCRL-19691] 20 p3319 N71-33599
- Reactor engineering for closure oil analysis, fuel element vibration, heavy water production, dry-out modeling with freeze, and in-core flux detectors
[AECL-3787] 23 p3796 N71-37060
- Electrochemical technique for remote measurement of instantaneous rate of uniform corrosion of aluminum alloys in nuclear reactor heavy water circuits
[ZIE-96] 23 p3798 N71-37074
- Thermophysical properties of heavy water including nuclear properties, parameters of equation of state, and isotopic analysis with tables on thermodynamic properties
[TTO-50094] 24 p4030 N71-38757
- HEAVY WATER REACTORS**
- NT PLUTONIUM RECYCLE TEST REACTOR**
- Irradiation experiments with OSIRIS swimming-pool research reactor
[CEA-R-3991] 04 p0546 N71-13602
- Ceramic fuel fabrication and irradiation behavior for heavy water reactors
[BNWL-1435] 04 p0552 N71-13966
- Red flow and pulsed source reactivity measurements in steam generating heavy water reactor
[AEW-R-640] 07 p1064 N71-17500
- Lattice cell code, WIMS, for predicting neutron physics of heavy water moderated rod clusters
[AEW-R-549] 09 p1420 N71-20154
- Critical mass measurements, control rod calibration, neutron and gamma flux measurement, measurement of various reactivity worths, power calibration, and xenon buildup for TRR-2
[IAERI-MEMO-4141] 13 p2119 N71-25107
- Neutronic calculations of EL 600 power reactor core including reactivity coefficients for fresh fuel, burnup calculations, and flux distribution
[CEA-N-1395] 15 p2446 N71-27140
- Validity of SABINE code calculations on neutron flux in iron-water lamellar shields for heavy and light water reactors
[CEA-N-1354] 15 p2450 N71-27390
- Fuel management for EL 600 heavy water moderated and cooled reactor
[CEA-N-1379] 15 p2451 N71-27684
- Core control systems of EL-600 heavy water moderated and cooled reactor of Candu type
[CEA-N-1421] 21 p3457 N71-34606
- Spatially dependent stochastic behavior of coupled core, Argonaut-type reactors 22 p3627 N71-35841
- HEIGHT**
- Remote-reading borehole inclinometer
[IPB-193925] 05 p0682 N71-14788
- Relative heights of photographic features of lunar topography
[AD-713679] 05 p0767 N71-14911
- Surface wave height measurement using pulse radar on stable platforms 14 p2245 N71-25657

- Diurnal mean tropospheric heights data for North America
[NOAA-TM-NWS-TDL-41] 17 p2745 N71-29890
- Effect of magnetic activity on auroral heights
17 p2746 N71-30080
- Ratio of 1 NO2/plus and 1 PO2/minus as function of auroral height 17 p2747 N71-30083
- Ionospheric processes associated with auroral height variations as determined by scanning photometer 17 p2747 N71-30084
- Height of explosion sound ranging system for supersonic rockets in jungle environments using piezoelectric electroacoustic transducers
[AD-724664] 20 p3351 N71-33033
- HEISENBERG THEORY**
- Green function used for thermodynamic model of Heisenberg ferromagnet in random phase approximation
[NASA-TM-X-52962] 09 p1406 N71-28034
- Thermodynamics of Heisenberg ferromagnet in applied magnetic field
[NASA-TM-X-52968] 10 p1661 N71-31168
- Spin wave perturbation theoretical analysis of Heisenberg model for impure ferromagnets
[BNL-TR-389-T-1] 10 p1633 N71-31704
- Heisenberg ferromagnetism at low temperature with boson theory of angular momentum including spin operators 11 p1809 N71-22973
- Integral equations to describe thermodynamic properties of one-dimensional Heisenberg model
[RIFP-116] 12 p2013 N71-24238
- Applications of coherent state representation of noninteracting particles to magnetism theory using Heisenberg model with 1/2 spin core 15 p2491 N71-27922
- Calculation of neutron elastic and inelastic scattering cross sections and spatial transverse correlation functions for Heisenberg theory of impure ferromagnets
[BNL-TR-390] 16 p2658 N71-29144
- Three reversed spin bound states in Heisenberg model of ferromagnetic spin systems with discussion of two reversed spin subspaces 17 p2810 N71-30095
- Time dependent correlations in linear Heisenberg chains 20 p3325 N71-33914
- Magnetization and susceptibility of Heisenberg ferromagnet in magnetic field with expressions derived for calculating thermodynamic parameters
[NASA-TN-D-6420] 21 p3497 N71-34915
- Space-time dependent spin correlation functions for anisotropic Heisenberg ferromagnet with cylindrical symmetry at elevated temperature based on Gaussian representation of diffusivity 24 p3948 N71-38307
- HELICAL ANTENNAS**
- Weatherproof helix antenna
[NASA-CASE-XKS-08485] 09 p1346 N71-19499
- Spiral and helical UHF antennas for home TV reception via satellite broadcast relay system
[NASA-CR-119852] 16 p2561 N71-28428
- Radiation pattern, efficiency, and bandwidth of short helical antennas
[TP-950] 20 p3234 N71-33379
- HELICAL FLOW**
- Theoretical analysis and measurement of single-phase pressure losses and heat transfer for helical flow in tubes
[NASA-TN-D-6097] 03 p0310 N71-12213
- Helical helicity in diffraction region of isotropic lepton nucleus reactions
[NYO-4204-10] 12 p1971 N71-23879
- Wind tunnel tests to determine helical engraving effects on aerodynamic stability of standard ammunition and models 13 p2191 N71-24846
- Torsion stabilizer with strong helical currents
[EUR-CEA-PC-543] 15 p2504 N71-27923
- Stabilization of theta pinch plasma column to produce helical fields 18 p2994 N71-31340
- Angular momentum restrictions of i-channel exchanges from s-channel helicity conservation in elastic reactions
[SU-1206-248] 21 p3489 N71-34718
- Helicity structure of mesonic Regge couplings in terms of meson pole dominance for matrix elements of vector currents 21 p3490 N71-34790
- Formulation of helically asymmetric magnetohydrodynamic theta pinch problem with set of fluid equations
[LA-4599] 21 p3495 N71-34680
- Helicity poles, triple Regge behavior, and single particle spectra in high energy collisions
[EUR-2262-TA-234] 22 p3639 N71-35939
- Fast theta pinch and buildup of plasma column in presence of helical field 23 p3824 N71-37272
- Helical magnetic field control of toroidal plasma in plasma generator
[CONF-710607-108] 23 p3831 N71-37323

SUBJECT INDEX

HELICAL INDUCERS

Cavitation performance of 84 deg helical inducer in water and hydrogen
[NASA-TN-D-7016] 03 p0359 N71-12567
Investigating tandem row high head pump inducers for liquid fueled rocket engines
[NASA-CR-116500] 07 p1034 N71-17364

HELICAL WINDINGS

Identifying fluctuations and feedback control of plasma confined in toroidal statorator
[UCRL-72473] 02 p0281 N71-11866
Wind tunnel aerodynamic stability tests on chimneys with pipes and helical winding stabilizers
[NPL-AERO-1310] 07 p1123 N71-17334
Toroidal statorator configuration with toroidal field created by helical current and application to fusion reactor divertor problems
[CEA-CONF-1664] 09 p3365 N71-20995

HELICOPTER ATTITUDE INDICATORS

U ATTITUDE INDICATORS

U HELICOPTERS

HELICOPTER CONTROL

Control system designs for USSR single-rotor helicopters including controllability characteristics, rotors with control gyroscopes, and transfer functions in closed loop systems
[NASA-TT-F-636] 10 p1492 N71-20719
Helicopter gyro displacement measurements at differing flying conditions
[POA-2-C-2356-49-772] 14 p2199 N71-26567
Handbook of analytical methods and stability data for determining dynamic stability and control characteristics of generalized single-rotor compound helicopter configurations
[AD-722530] 16 p2531 N71-28338
Analysis of problems and requirements for non-visual formation flight of helicopters
[AD-727635] 24 p3874 N71-37610

HELICOPTER DESIGN

Design criteria for optimal hoverable helicopter in hot weather climate
[AD-717025] 10 p1495 N71-21707
Fatigue life of helicopter rotary wings under vibration stresses
13 p2024 N71-24386
Dynamic tests of helicopter components
13 p2025 N71-24388

HELICOPTER ENGINES

Investigation of helicopter jet engine flameout due to ingestion of snow and ice
[NRC-11893] 11 p1672 N71-21927
Production and efficiency of small gas turbine engine for helicopter and surface vehicles
[AGARD-15-46-71] 15 p2511 N71-26951
Design and performance of gas turbine engines for helicopters and surface transport vehicles
15 p2511 N71-26953
Engineering aspects and manufacturing of gas turbine engines for helicopters and ground transport vehicles
15 p2512 N71-26956

Design and performance characteristics of gas turbine engines for helicopters
[AD-727559] 24 p4002 N71-38541

HELICOPTER PERFORMANCE

Blade root cutout effects on hover performance of helicopter rotors with rotor thrust and torque characteristics and wake pattern analysis
[AD-711396] 02 p0143 N71-11030
Evaluation of helicopter flight loading and structural stability
13 p2025 N71-24389

Aerodynamic configurations and characteristics of USSR military helicopters
[AD-719585] 13 p2028 N71-25133

HELICOPTER PROPELLER DRIVE

Laminar boundary layer transition, separation and streamlines direction on rotating helicopter blades
[NASA-TN-D-6321] 12 p1851 N71-23779

HELICOPTER ROTORS

U ROTARY WINGS

HELICOPTER WAKES

Method for calculating helicopter vortex paths and wake velocities
[AD-710698] 01 p0084 N71-10470
Blade root cutout effects on hover performance of helicopter rotors with rotor thrust and torque characteristics and wake pattern analysis
[AD-711396] 02 p0143 N71-11030
Mathematical models for lifting rotor aerodynamic calculations, noting wake configurations
[DLR-MITT-70-19] 13 p3821 N71-34489

HELICOPTERS

NT BO-105 HELICOPTER
NT CH-46 HELICOPTER
NT CH-54 HELICOPTER
NT COMPOUND HELICOPTERS
NT H-19 HELICOPTER
NT MILITARY HELICOPTERS
NT OH-58 HELICOPTER
NT RIGID ROTOR HELICOPTERS
NT TANDEM ROTOR HELICOPTERS
NT UN-1 HELICOPTER
NT WESTLAND WHIRLWIND HELICOPTER
NT XH-51 HELICOPTER

Development study for VFR heliport standard

lighting system
[AD-710982] 01 p0039 N71-10482
Delayed bubble movement on airfoil during helicopter stall
[AD-711540] 02 p0141 N71-11005
Surveillance radar installed on helicopter for obstacle avoidance
04 p0499 N71-13938

Fuel consumption and propulsive and thermodynamic efficiency comparisons for ships, hydrofoil craft, helicopters, jet aircraft, and ground effect machines
[NPL-HOVERCRAFT-12] 07 p0970 N71-17161
Practical aerodynamics of Mi-6 helicopter - lift system and fuselage
[AD-714915] 07 p0973 N71-17908

Functional requirements for ground-based trainers, helicopter response characteristics
[AD-714954] 07 p1004 N71-18018
Effectiveness of anti-torque aerodynamic surfaces immersed in helicopter rotor downwash
[AD-715438] 06 p1145 N71-18937

Noise and vibration effects on commercial helicopter pilot safety, performance, and comfort
[NASA-CR-117181] 09 p1332 N71-20113
Wind tunnel investigation of helicopter directional control in rearward flight in ground effect
[NASA-TN-D-6118] 09 p1366 N71-20191
Fixed base simulation evaluation of one fully automatic and six manual low visibility landing systems for helicopters
[NASA-TN-D-5913] 09 p1324 N71-20305
Vibration effects on performance of helicopter flight crews
09 p1335 N71-20355

Fuel tank vapor space characteristics for simulated helicopter fuel tank and evaluation of existing potential hazard from vibration environment
[AD-875901] 10 p1640 N71-20702
Fog modification over airports using helicopters
[AD-716818] 10 p1596 N71-20806

Conference proceedings on vertical takeoff aircraft technology, noting tandem wing aircraft, tilt wing aircraft, helicopter, lift fans, and jet engines
[DLR-MITT-70-15] 11 p1673 N71-22186

Normal and compound helicopters to be used as short haul aircraft in view of burden on today's air traffic control
11 p1673 N71-22189

Conference on fatigue life in helicopter components
[DLR-MITT-70-01] 13 p2024 N71-24385
Rotary wing structural stability of Dornier high temperature gas jet helicopter
13 p2024 N71-24387

Dynamic tests of helicopter components

13 p2025 N71-24388

Structural stability tests of helicopter components

13 p2025 N71-24390

High intensity xenon flashtube lights for increasing conspicuity of trainer helicopters during daytime and nighttime flights
[AD-710639] 13 p2026 N71-24669

Calculating and testing antiicing systems of aircraft and helicopters
[AD-719922] 14 p2197 N71-25622

Effectiveness of attitude feedback and translational velocity feedback flight control system assessed for ability to provide positional stability and reduce pilot error at hover
[AD-721728] 16 p2531 N71-28274

Computerized simulation of helicopter tactical maneuvers in three body, three dimensional environment including fixed wing and rotary wing aerodynamic forces
[AD-721527] 16 p2565 N71-28409

Airborne electronics equipment design for indicating helicopter lift capability using X ray backscatter from Kr-85, temperature sensor, and digital computer
[SAN-805-1] 17 p2702 N71-29215

Using helicopter for spray dusting forests with DDT for tick borne encephalitis
[AD-703998] 17 p2703 N71-29557

Systems analysis of directional control, rotary wing vibratory loads, lift shoring, and fuselage vibration and damping during helicopter maneuvers
18 p2870 N71-30775

Helicopter payload capability indicator in terms of gas generator speed
[AD-723436] 19 p3098 N71-31723

Flying, technical, and economic characteristics of helicopters noting contribution to national economy of USSR
[AD-723594] 19 p3035 N71-31771

Development and characteristics of aircraft, helicopters, and airships for detecting and destroying submarines
[AD-723558] 19 p3036 N71-31772

Evaluation of in-flight simulation of flying platform using helicopter with variable stability and maneuverability
19 p3074 N71-31957

Computer program for calculating effects of washplate stiffness on helicopter rotor system dynamics and stability

[NASA-CR-1818] 19 p3059 N71-32797

Analysis of bonded metal surfaces used in manufacture of helicopter components
[AD-724631] 20 p3283 N71-32953

Calculation of turbulent compressible boundary layer on helicopter rotors for range of hover conditions using two different analytical methods
[AD-723999] 20 p3210 N71-33312

Wind tunnel tests of full scale advancing blade concept rotor system at high advance ratio
[NASA-TN-X-62061] 20 p3211 N71-33517

Potential impact of advanced technology in 1985 on four types of general aviation aircraft including STOL, V/STOL, and helicopters
[NASA-CR-114339] 22 p3539 N71-35210

Calculations of helicopter airloads using lifting surface theory compared with experimental data
[AD-726717] 22 p3541 N71-35226

Principles of helicopter flight including flight stability
[AD-726841] 23 p3707 N71-36429

Analysis of problems and requirements for non-visual formation flight of helicopters
[AD-727635] 24 p3874 N71-37610

HELIOCENTRIC ORBITS

U SOLAR ORBITS

HELIOGRAPHY

U SPECTROHELIOGRAPHY

U SPECTROHELIOGRAPHY

U SPECTROHELIOGRAPHY

U SPECTROHELIOGRAPHY

U SPECTROHELIOGRAPHY

U SPECTROHELIOGRAPHY

U SPECTROHELIOGRAPHY

U SPECTROHELIOGRAPHY

U SPECTROHELIOGRAPHY

U SPECTROHELIOGRAPHY

U SPECTROHELIOGRAPHY

U SPECTROHELIOGRAPHY

U SPECTROHELIOGRAPHY

U SPECTROHELIOGRAPHY

U SPECTROHELIOGRAPHY

U SPECTROHELIOGRAPHY

U SPECTROHELIOGRAPHY

U SPECTROHELIOGRAPHY

U SPECTROHELIOGRAPHY

U SPECTROHELIOGRAPHY

U SPECTROHELIOGRAPHY

U SPECTROHELIOGRAPHY

U SPECTROHELIOGRAPHY

U SPECTROHELIOGRAPHY

U SPECTROHELIOGRAPHY

U SPECTROHELIOGRAPHY

U SPECTROHELIOGRAPHY

U SPECTROHELIOGRAPHY

U SPECTROHELIOGRAPHY

U SPECTROHELIOGRAPHY

U SPECTROHELIOGRAPHY

U SPECTROHELIOGRAPHY

U SPECTROHELIOGRAPHY

U SPECTROHELIOGRAPHY

U SPECTROHELIOGRAPHY

U SPECTROHELIOGRAPHY

U SPECTROHELIOGRAPHY

U SPECTROHELIOGRAPHY

U SPECTROHELIOGRAPHY

U SPECTROHELIOGRAPHY

U SPECTROHELIOGRAPHY

U SPECTROHELIOGRAPHY

U SPECTROHELIOGRAPHY

U SPECTROHELIOGRAPHY

U SPECTROHELIOGRAPHY

U SPECTROHELIOGRAPHY

U SPECTROHELIOGRAPHY

U SPECTROHELIOGRAPHY

U SPECTROHELIOGRAPHY

U SPECTROHELIOGRAPHY

U SPECTROHELIOGRAPHY

U SPECTROHELIOGRAPHY

U SPECTROHELIOGRAPHY

U SPECTROHELIOGRAPHY

U SPECTROHELIOGRAPHY

U SPECTROHELIOGRAPHY

U SPECTROHELIOGRAPHY

U SPECTROHELIOGRAPHY

U SPECTROHELIOGRAPHY

- Saturation excursion diving operations for testing extrapolated tables for repetitive no-decompression excursion from helium-oxygen atmospheres [AD-718907] 12 p1862 N71-23352
- Differential scattering cross sections for He collisions with rare gas and diatomic molecules [AD-718795] 12 p1974 N71-23988
- Apparatus and method capable of receiving large quantity of high pressure helium, removing impurities, and discharging at received pressure [NASA-CASE-XMF-06888] 12 p1929 N71-24044
- Tests of cryo-formed spheres to determine suitability as replacements for titanium helium storage bottles in liquid hydrogen tanks of saturn S-4B stage [NASA-CR-61343] 12 p2002 N71-24179
- Initial evaluation of revised helium-oxygen decompression tables [AD-719368] 13 p2033 N71-24683
- Measurement of oxygen effect and biological effectiveness of 910 MeV helium ion beam using cultured human kidney cells of interest in radiotherapeutic treatment of hypoxic tumors [UCRL-20190] 13 p2034 N71-25241
- Evolution of helium star Sigma Orionis [AD-719368] 13 p2169 N71-25297
- High resolution, differential, Cerenkov gas counters using helium [NAL-TR-3] 13 p2083 N71-25403
- Influence of two body potential on ground state properties of solid helium [NYO-3699-30] 13 p2127 N71-25517
- Compilation of cross sections of reactions produced by protons on targets of protons, neutrons, deuterons, and helium [CERN/HERA-70-2] 14 p2309 N71-26586
- Emission spectroscopy for identification of high temperature reactor fuel element spheres at 40 atmospheres of helium [JUL-671-RW] 15 p2442 N71-26824
- Nonlocal separable potential formalism for elastic alpha scattering by helium [LYCEN-7041] 15 p2465 N71-27241
- Vertical distribution photometric measurement of helium and development of radiative transfer theory supporting experiment 15 p2399 N71-27273
- Hydrodynamic behavior of pure superfluid helium at 0 K using gauge invariance 15 p2393 N71-27326
- Vorticity in superfluid helium investigations including structure, spatial arrangement, and nucleation of quantized vortices in helium 2 [AD-720861] 15 p2393 N71-27331
- Nuclear composition for several multicharged nuclei and energy spectra for hydrogen, helium, and medium nuclei measured in solar particle event [NASA-TM-X-45573] 15 p2514 N71-27645
- Brayton cycle turbogenerator performance tests using helium-xenon gas mixture including gas turbine engine, turbocompressor, coolant pump, and heat exchanger power efficiencies [NASA-TM-X-47846] 15 p2370 N71-27713
- Use of constancy of helium to medium nuclei ratio in solar cosmic rays to estimate solar helium abundance [NASA-TM-X-45583] 16 p2674 N71-28472
- High power uniform electric discharge to produce laser action in mixture of nitrogen, carbon dioxide, and helium [AD-721398] 16 p2606 N71-28584
- Critical review of theories of excitation spectrum of superfluid helium 16 p2580 N71-28677
- Spectroscopic observation of seven neutral helium line profiles for five main sequence B stars with estimated helium abundance for upslon Orionis, HR 2154, and pi Ceti 16 p2680 N71-28786
- Hydrodynamics of helium core flash phase of stellar evolution - core pulse characteristics of hydrostatically computed models and hydrodynamical consequences for outer regions 16 p2681 N71-28870
- Acoustic vibration tests for noise reduction by helium and polyurethane foam in stainless steel cylinders for application as Skylab and Apollo vibration isolators 16 p2683 N71-29101
- Speech intelligibility of divers as function of high ambient pressures and helium-oxygen breathing atmospheres [AD-722371] 17 p2720 N71-29658
- Projection operator technique for calculating autoionization states of negative helium [NASA-TM-X-45599] 17 p2790 N71-29809
- Thermodynamic assessment of metal compatibility and gaseous impurities in helium atmosphere [RD/B/N-1816] 17 p2785 N71-30143
- Radiative lifetime of 2 130 metastable state of helium [UCRL-20142] 17 p2808 N71-30342
- Characteristics of high speed flowing N2-CO2-He gas lasers - effects of viscosity and diffusion 18 p2932 N71-31196
- Effects of helium oxygen breathing on hearing in Navy personnel [AD-722658] 18 p2877 N71-31237
- Statistical thermodynamics of virial expansions for submonolayer helium films adsorbed on solids [NUB-2067] 18 p3027 N71-31523
- Energy spectra of ions and electrons produced in collision of argon neutral beams [AD-722688] 19 p3049 N71-32036
- Measurement of self absorption in helium discharge [PB-196166] 19 p3164 N71-32201
- Critical heat flux in liquid helium 2 close to lambda transition 19 p3193 N71-32542
- HeO2 saturation dives to verify no-decompression repetitive excursion format of Deep Submergence Systems project [AD-723172] 19 p3046 N71-32602
- Repetitive excursion dives from saturated depths using helium-oxygen mixtures to eliminate decompression sickness [AD-723173] 19 p3046 N71-32632
- Performance test of piston shock tube with helium driven gas and argon test gas [VET-TN-69] 20 p3244 N71-32957
- Low temperature and ultralow temperature research on superfluid helium and superconductivity [AD-724633] 20 p3333 N71-33154
- Small angle differential charge exchange measurements for He/plus on He, Ne, and Kr in 1 keV to 3 keV range 20 p3318 N71-33574
- Performance of helium seeded with uranium in magneto-hydrodynamic generator 20 p3306 N71-33663
- Cyclotron simulation of uniform concentrations of helium produced during neutron irradiation [ORNL-TM-3299] 20 p3308 N71-33705
- Mechanical property tests of nickel, titanium, and iron alloys in 5000 psig gaseous helium and hydrogen at various temperatures [NASA-CR-119804] 20 p3230 N71-33728
- Microwave-optical measurements of atomic energy levels in ionized helium 20 p3327 N71-33950
- Fine structure measurement of singly ionized helium, n equals 4 20 p3328 N71-33976
- Data on production, consumption, and resources of helium in US as of 31 Dec. 1969 20 p3231 N71-33993
- Upper atmosphere helium fluorescence due to cycles of electron flux, solar ultraviolet radiation, and geomagnetic activity [NRC-TT-1458] 21 p3416 N71-34306
- Diurnal variations in spectra of solar hydroxyl emission in relation to helium emission intensity [NRC-TT-1457] 21 p3416 N71-34310
- Radial blowers, shutdowns, valves, and seals performance in helium atmosphere of AVR experimental gas cooled reactors [NLL-EE-TRANS-1933-3774.5] 21 p3462 N71-34645
- Cooling intrinsically stable superconducting magnets with supercritical helium tubes adjacent to magnetic coils [UCRL-20172] 21 p3465 N71-34665
- Quantum mechanical molecular energy level calculations for 3 Fg and 1 Fg excited states of He2 21 p3487 N71-34843
- Gas management subsystem using xenon-helium working fluid designed for Brayton space power system [NASA-CR-72631] 21 p3502 N71-34948
- Neon, argon, and helium density and flux distributions in lunar atmosphere [NASA-CR-121633] 21 p3506 N71-34961
- Helium Production in stainless steel and its constituents for irradiation effects data correlation and interpretation for liquid metal fast breeder reactor development [HEDL-SA-193] 22 p3625 N71-35826
- MHD flow, recombination processes in pulsed helium discharge, and mass spectrometry applied to He in solids 22 p3632 N71-35879
- Diffraction of helium atoms from tungsten [112] crystal surface and measurement of time of flight distribution of deuterium molecules desorbed from nickel surfaces [NASA-CR-121985] 22 p3634 N71-35900
- Lifetime of 2 1s0 state of helium-like argon using beam foil method [UCRL-20458] 22 p3641 N71-35959
- He-3,1 reaction and isobaric analog state in Ti, Fe, Ni, and Zn isotopes 22 p3649 N71-36021
- Spin lattice relaxation in gaseous hydrogen and mixtures of hydrogen with helium 22 p3650 N71-36029
- Flow characteristics including diffuser measurements of Langley Mach 20 high Reynolds number helium tunnel [NASA-TM-X-2353] 23 p3741 N71-36673
- Tables of generalized oscillator strengths for excitation and ionization of atoms He through Na [SC-RR-70-406] 23 p3814 N71-37196
- Spectral absorption coefficients of helium, neon, and nitric oxide mixtures with oxygen as functions of pressure, temperature, and wave number [NASA-CR-123108] 24 p3884 N71-37687
- Statistical analysis of elementary processes of helium nonlocal thermodynamic equilibrium plasmas [EUR-CEA-FC-578] 24 p3985 N71-38441
- Helium and hydrogen bulk speeds in solar wind [NASA-CR-123119] 24 p4003 N71-38548
- Thermodynamic and thermophysical properties of helium with application as working substance or heat carrier in nuclear power plants - tables and diagrams [TT70-50056] 24 p4030 N71-38736
- HELIUM AFTERGLOW
- Spectral line profiles and energy absorption in helium plasma afterglow [NF-18740] 18 p2992 N71-30640
- HELIUM ATOMS
- Twilight aurora helium emissions in high latitudes in relation to magnetic disturbances and solar activity [NRC-TT-1441] 19 p3531 N71-21164
- Mass spectrometric investigation of collisional ionization by electronically excited helium atoms 11 p1809 N71-23018
- Influence of neutron spectrum on helium atom generation by neutron irradiation of stainless steels and subsequent embrittlement 13 p2111 N71-24502
- Inelastic energy loss spectra for proton impact on helium atoms 15 p2903 N71-27942
- Production and destruction of fast metastable He atoms in rare gas targets and Kr and He 17 p2796 N71-29785
- Many body perturbation procedure for studying various properties of interacting atoms applied to H-He and H-Ne systems 22 p3650 N71-36027
- Magnetic analysis of Li-7 bombarded with 15 MeV He-3 atoms [ANU-F-520] 23 p3809 N71-37160
- HELIUM FILM
- Helium 2 film transfer rate dependent on pressure head, film height, and substrate for filling clean glass and non-coated beakers [COO-1574-17] 12 p1869 N71-23130
- Velocity measurement of third sound in unsaturated superfluid helium films between 1.12 and 2.05 K 15 p2454 N71-27375
- HELIUM IONS
- Interaction processes between helium ions and atoms [NASA-CR-111353] 01 p1003 N71-11000
- Angular distribution shape of He-3, u and h/p, charge exchange transitions to 0/ antineutrino states [NYO-2711-321] 06 p0923 N71-16724
- Calculating spin exchange cross section for collision between two positive He ions in impact parameter approximation [NASA-TM-X-45442] 07 p1073 N71-17366
- Determination and statistical model analyses of excitation functions and recoil ion ranges from reactions induced in gold isotopes by helium ions 08 p1264 N71-19113
- Distribution and charge composition of ionized helium and other heavy ions in auroral zone [AD-717154] 10 p1640 N71-20773
- Formation scattering cross section of He2 ion in fast protons and methane reactions [AD-717610] 11 p1803 N71-22118
- Comet-like model of Venus atmospheric helium ions/solar wind interactions [REPT-70-35] 14 p2335 N71-25726
- Thermodynamic properties and nuclear chemistry of chemically bound neutrons and ternary fission of thorium and gold with helium-4 ions [COO-1716-11] 14 p2301 N71-25732
- Positive helium ion scattering by impact on helium, neon, and argon 15 p2479 N71-27654
- Temperature and radiation dosage effects in niobium lattice defect backscatter of protons and helium ions 21 p3490 N71-34923
- Orbits of interstellar helium ions in interplanetary space [NASA-CR-121902] 22 p3667 N71-36146
- HELIUM BIOTYPES
- High energy neutron-liquid helium-4 scattering and helium-4 condensate density [RLO-1388-566] 01 p0099 N71-10697
- He-3/H-3 charge form factor and He-3 Coulomb energy [RLO-1388-575] 01 p0099 N71-10711
- Low temperature melting curve of helium 3 [UCSD-34-P-143-26] 03 p0331 N71-12340
- Thermal and magnetic properties of adsorbed phases of He-3 and He-4 at low temperatures [AD-712416] 05 p0419 N71-13339
- Thermal conductivity measurements of polycrystalline solid helium [AD-712729] 05 p0445 N71-13342

Operational problems of helium 3 counter in gamma field

[FEI-178] 04 p0378 N71-13874

Variational calculation of ground-state energy of liquid He-4 using Percus-Yevick and hypernetted chain theories
[COO-1569-61] 05 p0734 N71-15265

Weakly interacting magnetic systems with helium 3 at very low temperature
[AD-174064] 06 p0904 N71-16234

Nuclear spin ordering in solid helium 3 studied by compressive cooling of liquid-solid helium 3 mixture
[UCSD-34-P-143-23] 07 p1079 N71-17942

Absorption of helium 4 on activated carbon
[CRA-CONF-1505] 08 p1221 N71-18389

Axially injected, polarized proton beam for measuring He-4 scattering from 20 to 40 MeV
[UCRL-199453] 08 p1238 N71-18548

Adiabatic compressional cooling of He 3 to millikelvin temperatures
[UCSD-34-P-143-27] 08 p1305 N71-19050

Positive and negative charge carrier mobilities in superfluid helium-2 under pressure
[TID-25587] 08 p1267 N71-19234

Properties of liquid He-3 and dilute solutions of He-3 in superfluid He-4 for dilution refrigerators
[UCSD-34-P-143-29] 08 p1246 N71-19343

Detection of quantized vortex lines in liquid helium 2 accelerated from rest
[TID-25595] 09 p1434 N71-19992

Potential energy surfaces for singlet states of He3/He4
[NASA-CR-117500] 10 p1516 N71-21715

Density modes and He-4 coherent interference data for He-11 (p, s) He-4 reaction at proton beam energies of 0.675, 1.00, and 1.388 MeV
10 p1621 N71-21740

Specific heats of He2 and D2 solid mixtures down to 0.5 K, adsorption isotherms of He-3 and He-4 at low temperatures, and development of He-3 dilution refrigerator and liquefier
[AD-171623] 11 p1815 N71-21941

Misalignment gage technique for determining ratio of thermal accommodation coefficients of helium 4 and helium 3 isotopes on bare tungsten at low and moderate temperatures
11 p1777 N71-22291

Susceptibility of liquid He-3 with comparison to Curie susceptibility
11 p1809 N71-23028

Angular distribution shapes of He-3, n and p, n transitions to positive 0 antineutrino states compared to noble data
[COO-535-625] 12 p1976 N71-24112

Antineutrino 3 nuclei in negative beams
[IPVLE-58P-70-16] 13 p2122 N71-25109

Cluster expansion applications for alpha particle-nuclear matter mixture, He-3/He-4 mixture and impurity problem
13 p2137 N71-25402

Mobility measurements of ions in dilute He-3/He-4 mixtures in pure He-3 at very low temperature
13 p2137 N71-25431

Copper K sub alpha X ray scattering intensity measurements from He-4 in liquid and vapor phases with wave normalizations for momentum transfer and nuclear structure factors
13 p2140 N71-25506

Deuterium helium-3 fusion power balance calculations with inclusion of variable cyclotron radiation parameter
[NASA-TM-X-2280] 13 p2149 N71-25526

Calculation of lattice-constant change for helium 4 under strain in ErT2 and ScT2
[BC-BR-70-753] 13 p2154 N71-25531

Bohrer-Feynberg perturbation technique applied to nuclear forces in o-a shell nuclei of He isotopes
13 p2143 N71-25573

Exchange energy and magnetic susceptibility measurements on low temperature He-3 with He-4 traces, and techniques for light scattering in gases at room temperature
[NYO-3951-3] 14 p2295 N71-25610

Polarization measurement of tritons classically scattered from He-3 established as good analyzer for tritons
[LA-4538] 14 p2301 N71-25740

He-4/He-4 interaction from low energy scattering processes and step function model as molecular interaction potential for calculation of cross sections
[AMT-TRANS-672] 14 p2303 N71-25918

Using 52 MeV deuterons and 104 MeV alpha particles for investigating T equals 0 excited states of He-4
[KFE-1055] 14 p2312 N71-26099

Particle energy dependence calculations for scattering cross sections of pion and nucleon interactions with tritium and He-3 based on Glauber theory
[UNR-P-5355] 14 p2317 N71-26757

Fast neutron counter using helium gas flow and temperature effects on flow velocity from reactor core
[WLAN-34-73] 15 p2409 N71-27389

Angular distribution vector analysis of polarized deuterium elastic scattering from helium 4 at energies between 3 to 11 MeV
15 p2476 N71-27575

Proton polarization in reaction C-12/He-3, proton spin 0/1-4
[JINR-P15-5156] 15 p2497 N71-27995

Evidence for particle instability of helium 10
[JINR-ET-5492] 16 p2645 N71-28143

Heat transfer rates, specific heat, and behavior of liquid He-3 and He-4
[UCSD-34-P-143-37] 16 p2638 N71-28179

Helium 2 quenching environment, rate, and impurity effects on quenching of vacancies into body centered cubic molybdenum
[NASA-TM-X-67668] 16 p2614 N71-28922

Neutron scattering cross sections for TiD, n/He-4 reactions and spin-orbit interactions including polarization effects and distorted wave Born approximations
[LA-4596] 17 p2792 N71-29445

Equivalence of He 3/4 and d-alpha cluster description of lithium 6
[NYO-2171-336] 17 p2800 N71-30099

Elastic scattering angular distributions for 13 to 27 MeV helium 3 beam from light target nuclei
17 p2802 N71-30133

Performance tests of low temperature desorption refrigeration systems with helium 4 and zeolite
[NASA-CR-119184] 17 p2789 N71-30291

Electroacoustic transducer measurements of secondary sound velocity and inertial mass as function of He-3 concentration and temperature of He-3/He-4 mixture vapor pressure
17 p2789 N71-30293

Polarized neutrons from He-3/p, n/He-3 reaction using time of flight spectrometer at 31.6 deg in laboratory (approximately 45 deg in center of mass)
17 p2805 N71-30297

Differential cross section for low momentum negative kaon helium-4 elastic scattering from 115 to 160 MeV/c
17 p2805 N71-30306

Highly inelastic scattering of medium energy He-3 and He-4 particles by Sn, Ta, Pt, Au, and Pb nuclei
17 p2809 N71-30377

Helium-3 cryostat for specific heat measurements at 0.5 to 4.2 K
[UIUP-677] 18 p2921 N71-30449

Highly excited states of C-12 and O-16 from He-3 bombardment of Be-9 and C-13
18 p2963 N71-31039

X ray and thermal conductivity measurements of unidirectional grown and recrystallized hexagonally close packed helium 4
18 p2963 N71-31050

Heat capacities of sub-monolayer He-3 and He-4 adsorbed on argon preplated copper sponge
18 p2985 N71-31200

Effects of lateral substrate fields on helium monolayers using ideal gas model
[RLO-1388-604] 18 p2985 N71-31218

Ground state of He-4 atoms at absolute zero adsorbed on inert substrate
[RLO-1388-603] 18 p2988 N71-31473

K-harmonics method for calculating binding energy and wave functions of He-3 and He-3 nuclei
[IAE-2000] 19 p140 N71-32105

Environmental monitoring for determining He-3 and tritium water vapor content of ground level air
[ORIO-3944] 19 p3095 N71-32499

Emissions of He-4 during fission of U-238 and Au-197 by C-12 and O-16 at 82 and 137 MeV
[KFKI-TR-352] 19 p3157 N71-32535

Nuclear structure of helium and lithium isotopes based on nuclear scattering by Van de Graaff accelerated cations
[MSR-FG-12227-2] 19 p3160 N71-32659

Nonlinear effects of recombination and collective diffusion associated with nuclear seeded plasmas using helium isotopes in gas cooled reactors
20 p3306 N71-33665

Coincidence spectra of alpha particles from reaction Be-9/He-4, alpha alpha/He-4 measured for several angular configurations at 1.55 MeV bombarding energy
20 p3326 N71-33944

Concentrations and isotopic compositions of He, Ne, and Ar measured by mass spectrometry in separated metal phase and bulk samples of 15 chondrites for cosmic ray record studies
20 p3350 N71-33973

Tertiary fission products and scattering cross section produced in Au-197, Bi-209, and Fe-57 by intermediate energy He-4 ions
21 p3487 N71-34841

Particle gamma ray angular correlation study of Ni-57 levels in Ni(He-3, alpha gamma) Ni-57 reaction
21 p3492 N71-34877

Studies of analog states of T equals 2 in Mg-26(He-3, n)28, Ti-46(He-3, n)Cr-48, and Ni-58(He-3, n)Zn-60 reactions
[IAE-1958] 22 p3632 N71-35881

Excited states of helium investigated through final state interactions and quasifree scattering reactions on Li-6
[NP-18741] 22 p3643 N71-35974

Nuclear magnetic susceptibility in bcc solid He-3 with Neel temperature and negative exchange interaction energy calculations and impurity effects
22 p3652 N71-36041

Equation of state calculations for solid He2, D2, He-3, He-4, and Ne-20 at high densities in harmonic approximations
[NYO-3699-51] 23 p3802 N71-37110

Variational calculation of binding energies and dimensions in He-4 and O-16
[AD-171-1-81] 23 p3811 N71-37176

Angular distributions for neutron polarizations in [d, n] and [He-3, n] stripping reactions of Li, Be, B, and C at energies from 2.1 to 3.9 MeV
23 p3822 N71-37266

He-3, p reactions with Mo-20, N-14, and B-11, and gamma de-excitation of Ne-21 and Ar-41
[NP-18062] 24 p3978 N71-38390

HELIUM PLASMA
Optical spectroscopic investigation of helium and nitrogen plasmas
[AD-1712024] 03 p0437 N71-12001

Investigating helium plasma decay in circular two-path interferometer with magnetic field variations from 6 to 12 koe
[NP-18502] 07 p1085 N71-18149

High temperature plasma inside discharge produced by photon HeF power passing through helium
[NRL-3M-20301-5628.4F/1] 12 p1982 N71-24101

Spectral line profiles and energy absorption in helium plasmas afterflow
[NP-18740] 18 p2992 N71-30640

Multi-species ion acoustic dispersion relation for argon-helium plasmas
[NASA-CR-121721] 21 p3493 N71-34881

Disintegration of helium plasma in two-pass stellarator with magnetic field varying from 6 to 12 kG
[NP-18767] 21 p3496 N71-34905

High resolution energy analyzer with time of flight spectrometer for studying highly ionized hydrogen and helium plasmas
[JPP-107-22] 23 p3836 N71-37291

Ion and electron energy spectra from neutral Ar and He beam collisions with Ar and He gas respectively below 220 eV
[NYO-2101-27] 24 p3978 N71-38386

HELIUM 2
U HELIUM ISOTOPES
HELIUM 3
U HELIUM ISOTOPES
HELIUM 4
U HELIUM ISOTOPES
HELIUM-NEON LASERS

Performance characteristics of radio frequency excited helium-neon ring laser
13 p2809 N71-24829

Raman spectra of selected molecules excited by low power helium-neon gas laser
19 p3108 N71-32285

Optical measuring instrument design, calibration and operational procedures for measuring helium-neon laser scattered irradiance levels
[PB-198375] 19 p3108 N71-32465

Analysis of helium-neon and carbon dioxide laser beam propagation in atmospheric turbulence
[NASA-TR-R-370] 20 p3310 N71-33222

Holographic interferometry applied to vibration analysis, composite component evaluation, and precision cylinder inspection
[AD-726369] 22 p3591 N71-35570

HELIUM TUBES
U TRAVELING WAVE TUBES
U CURVES (GEOMETRY)
WELLMANN-FEYNMAN THEOREM

Multiconfigurational one center expansion wave functions for computing intermolecular forces of hydrogen molecule and Hellmann-Feynman theorem
14 p2311 N71-26467

HELMETS
Investigating approaches and concepts for improving mobility of aerospace pressure suits
[AD-171670] 01 p0016 N71-10947

Transparent polycarbonate resin, shell helmet and hatch design for high altitude and space flight
[NASA-CASE-XMS-04935] 02 p0167 N71-11190

Electrode attached to helmets for detecting low level signals from skin of living creatures
[NASA-CASE-ARC-10043-1] 02 p0168 N71-11195

Development and fabrication of polycarbonate cyclohexyl for army fly helmets
[AD-1715131] 02 p0169 N71-11200

Some construction characteristics of military air protective devices and helmets
03 p0171 N71-11819

Required ventilation rates determined for Mark 5 diving helmet as part of low pressure underwater breathing apparatus
[AD-1713955] 03 p0657 N71-14705

Optimal fitting of flight helmets for noise reduction
[AD-1718377] 12 p1866 N71-23399

Venting device for pressurized space suit helmet to eliminate vomit expelled by crew members
[NASA-CASE-XMS-09653-1] 14 p2211 N71-26333

HELMHOLTZ EQUATIONS

Partial pressure helmet and pressure suit mobility joints for high altitude environment
[AD-720273] 16 p2549 N71-28168

Protective features and compatibility with airborne communication systems considered in study of aviation helmets
[AD-724080] 20 p3226 N71-33123

HELMHOLTZ EQUATIONS

Numerical analysis of Helmholtz resonator system established between windows and open doors when subjected to sonic boom impulsive loads
[NASA-CR-1777] 16 p2688 N71-29068

HELMHOLTZ VORTICITY EQUATION

Helmholtz integral and Kirchhoff approximation for sound transmission through rough air-sea interface
[AD-715566] 08 p1243 N71-18771

Kelvin-Helmholtz wave model for predicting maximum amplitude, breaking mode, and turbulent kinetic energy
[AD-718441] 12 p1911 N71-23687

Hydrodynamic Kelvin-Helmholtz instability in velocity shear layers of nonzero thickness
[AD-723675] 19 p3163 N71-31761

HEMATITE

Artificial meteor ablation studies of natural minerals composed of magnetite and hematite
[NASA-TM-X-6025] 15 p2419 N71-26911

HEMATOLOGY

Acceleration effect on hemato-ophthalmic barrier permeability in rabbits
08 p1154 N71-19060

Case history of Chediak-Higashi disease with simultaneous Friedreich hereditary spinal ataxia and hematologic, neurologic, and genetic characteristics
[NASA-TT-F-15357] 12 p1863 N71-23749

Total body exercise effect on metabolic, hematologic, and cardiovascular consequences of prolonged bed rest
20 p3218 N71-33265

Red cell mass loss in human beings as result of bed rest
20 p3219 N71-33271

Hematological program and biochemical data from Gemini and Apollo missions
23 p3711 N71-36455

HEMATOPOIESIS

Statistical analysis of effects of acclimatization on hematopoiesis of Antarctic expeditionary personnel
[JPRS-53884] 21 p3382 N71-34063

HEMISPHERICAL SHELLS

Light baffles with oblate hemispherical surface and shading flange
[NASA-CASE-NPO-10337] 05 p0689 N71-15604

Transformation formulas in solid spherical harmonics for calculating forces between two homogeneous hemispheres with examples involving coordinate translation and rotation
[NASA-CR-115141] 22 p3606 N71-35678

HEMODYNAMIC RESPONSES

Hemodynamic and body fluid alterations induced by varying periods of bed rest
20 p3217 N71-33263

HEMODYNAMICS

Technology review on cardio and hemodynamics
09 p1328 N71-19584

Application of cineholocardiography to study of microcirculation hemodynamics and related physiological studies of man and animal
[AD-719401] 13 p0306 N71-24684

Physical examination and analysis of hemodynamic parameters of overweight flying personnel
16 p2547 N71-28492

HEMOGLOBIN

NT CARBOXYHEMOGLOBIN
Investigating causes of polycythemia and decrease in hemoglobin in underwater workers
[NASA-TT-F-13422] 04 p0477 N71-13868

Hemoglobin compound identification, oxygen involvement, and major breakdown products of monomethylhydrazine effect on blood, *in vitro*
[AD-727328] 24 p3879 N71-37651

HEMOLYSIS

Hydrodynamics of roller pumps and implication to hemolysis
[AD-720320] 15 p2374 N71-27279

HEOS A SATELLITE

Space environment simulation tests of HEOS 1 satellite noting heat balance
03 p0358 N71-12726

Test facilities for HEOS and ESRO satellite magnetic control - Noordwijk, Netherlands
[ESRO-TM-134F-ESTEC] 17 p730 N71-29490

HEOS SATELLITES

NT HEOS A SATELLITE
HEOS mission, experimental design, and instruments
[ESRO-TN-104-ESTEC] 18 p3017 N71-30620

HERCULES AIRCRAFT

U C-130 AIRCRAFT
HERMETIC SEALS
Hermetically sealed explosive release mechanism for actuator device
[NASA-CASE-XGS-00824] 06 p0864 N71-16078

Evaluating in-pile performance of ceramic insulator seals under high neutron and gamma radiation levels
[NASA-TM-X-2180] 07 p1062 N71-17325

Sealing apparatus for joining two pieces of fragile materials
[NASA-CASE-XLA-01494] 12 p1930 N71-24164

Method for locating leaks in hermetically sealed containers
[NASA-CASE-ERC-10045] 13 p2087 N71-24910

Hermetically sealed vibration damper design for use in global assembly of spacecraft inertial guidance system
[NASA-CASE-MS-C-10939] 14 p2263 N71-26243

Method of forming ceramic to metal seals impervious to gaseous and liquid mercury at high temperature
[NASA-CASE-XNP-01263-2] 14 p2263 N71-26312

Pressure seals suitable for use in environmental test chambers
[NASA-CASE-NPO-10796] 16 p2414 N71-27068

Hermetically sealed coaxial package for housing microwave semiconductor components
[NASA-CASE-GSC-18791-1] 16 p2601 N71-28562

Hermetic sealing device for ends of tubular bodies during materials testing operations
[NASA-CASE-NPO-10431] 16 p2605 N71-29132

Separator materials, ceramic to metal seals, cell plate polarization and impregnation processes, and plaque sintering data for study of variables in manufacture of nickel cadmium cells
[NASA-CR-121470] 20 p3214 N71-33675

Formation time, specific gravity of solution, and overcharge amount associated with electrochemical cleaning or formation operation in manufacturing nickel cadmium cells
[NASA-CR-121877] 21 p3379 N71-34040

High current and multiple contact, low current switch designs and testing with respect to hermetic sealing switches with existing configuration
[NASA-CR-115118] 22 p3559 N71-35345

HERMITIAN POLYNOMIAL

Hermitian form for group representation of complex matrices L_n/C
[JFVE-STF-69-91] 07 p1050 N71-17091

Unitary transformation of Hermitian matrix to symmetric tridiagonal matrix
10 p1592 N71-21341

Functional subgroup space representations of quaternion group
[JFVE-STF-69-102] 15 p2457 N71-26866

Explicit expression of invariant Hermitian form for unitary representations of conformal group
[JFVE-STF-69-85] 15 p2497 N71-27994

Intensity distribution of optical images for various degrees of illumination using Hermitian matrices
[NASA-TT-F-13721] 18 p2966 N71-31452

HETEROCYCLIC COMPOUNDS

NT ADENOSINE TRIPHOSPHATE [ATP]

NT ALKALOIDS

NT AZINES

NT AZOLES

NT CARBAZOLES

NT ENDRIN

NT INDOLES

NT PYRIDOXINE

NT RESERPINE

NT THIAMINE

NT THYMINE

NT TOCOPHEROL

NT URIC ACID

Characteristics and applications of polyquinonaxaline compounds
[AD-710504] 01 p0070 N71-10033

Research in existence and electronic structure of heterocyclic radicals
[NASA-CR-111151] 02 p0175 N71-11230

Obtaining dissociation constants of N-malonic ester-substituted uracils, phthalimide, pyridone, and aniline using UV spectra
[NYO-2798-48] 06 p0913 N71-15879

Photochromic behavior of heteroaromatic molecules
[AD-721239] 15 p2376 N71-26888

Preparation of benzobistriazolo lophanthroline polymer by polycondensation
[AD-726545] 22 p3603 N71-35662

Cyclization of ortho-isocyanobiphenyl and derivatives with insertion of isocyanate carbon to form cyclophosphorolanes
[NASA-CR-123190] 24 p3884 N71-37866

HETERODYNING

NT OPTICAL HETERODYNING

Scintillation and signal to noise ratio of heterodyne detection for carbon dioxide laser beam propagated over path 3.2 km to determine effects of atmospheric turbulence
[NASA-CR-103113] 14 p2266 N71-26419

HETEROGENEITY

Heterogeneous effects on adjoint function in cell structure of fast reactors using collision techniques
[RT/FI/70/19] 04 p0563 N71-14488

Photovoltaic properties of Cu₂S-CdS heterojunctions
09 p1361 N71-19405

Viscosity of heterogeneous suspensions, noting solid rocket propellants and explosives
[ICT-12707] 17 p2768 N71-28917

HETEROSPHERE

Representation of heterospheric semiannuar variation as density variation with amplitudes as function of altitude
[NASA-CR-117137] 09 p1413 N71-19945

HEURISTIC METHODS

Heuristic program for solving scientific inference problem - motivation and implementation
[NASA-CR-111092] 01 p0019 N71-10741

Heuristic method to determine electrostatic instabilities in multicomponent plasmas
[AD-712698] 03 p0439 N71-13560

Heuristic optimization algorithm for arranging N page open string
04 p0583 N71-13646

Precise logic computation and construction of formal heuristic activity models
12 p1895 N71-24219

Heuristic system and plastic memory of digital computers
[JPRS-53399] 17 p2722 N71-29101

Digital computers as complex heuristic systems
17 p2722 N71-29101

Design and operation of complex man machine systems and heuristic solution to automatic control problems in production engineering and biomedical situations
[JPRS-53414] 18 p2883 N71-30667

Heuristic problems in design and operation of large scale man machine systems
18 p2883 N71-30671

Heuristic decision making programs for man machine systems
18 p2883 N71-30672

Factor analysis applied to heuristic assessment matrix for numerical weather forecasting
[NLL-M-9255-1528-4F/1] 19 p3310 N71-32587

Heuristic resource allocation for network scheduling operational analysis
24 p3893 N71-37746

Unified heuristic model of fluid turbulence which supplements basic equations of motion and continuity
[AD-727103] 24 p3906 N71-37840

HEXAGONAL CELLS

Using X ray powder diffraction line profiles to study stacking-fault probability in hexagonal close-packed titanium aluminum alloys
08 p1214 N71-18401

HEXAGONS

Mathematical model for river basin drainage systems based on hexagonal nature of geological ridges
[AD-722022] 16 p2584 N71-26207

Tables of magnetic structures determined by neutron diffraction with emphasis on rhombohedral and hexagonal systems
[NTP-10845] 24 p3970 N71-38319

HEXANITROSTILBENE/HN87

Behavioral aspects of hexanitrostilbene in small charges
[SC-CR-70-6076] 01 p0100 N71-10799

HFB-320 AIRCRAFT

In-flight simulation with high wing loading fighter aircraft approach using HFB-320 and F-4 Phantom II
[DLR-FB-71-06] 19 p0072 N71-31710

In-flight simulation with HFB-320 aircraft
19 p0075 N71-31919

HFR

U HIGH FLUX ISOTOPE REACTORS

HFIR [REACTOR]

U HIGH FLUX ISOTOPE REACTORS

HICAT [RADAR TECHNIQUE]

U HIGH RESOLUTION COVERAGE ANTENNAS

HICAT PROJECT

U HIGH RESOLUTION COVERAGE ANTENNAS

HIERARCHIES

NT BBOGY HIERARCHY

Hierarchical associative memories for parallel computation
[AD-711091] 02 p0109 N71-11331

Hierarchical regulation model for human biological systems
09 p1331 N71-19879

Information retrieval and analysis of search questions in tree structures noting hierarchies and syntax
14 p2222 N71-29808

Properties of information retrieval and management information systems including data structure, hierarchy generation, and searching
14 p2222 N71-29807

HIGH ACCELERATION

Vibration measurements at cryogenic temperatures and high acceleration levels for dual liquid hydrogen turbopump system
14 p2256 N71-26367

HIGH ALTITUDE

Diet and altitude effects on body composition of growing rats
[AD-712391] 02 p0155 N71-18808

SUBJECT INDEX

Acute mountain sickness in humans
[AD-712182] 02 p1556 N71-11102
Effects of 4-amphetamine on carbohydrate metabolism at ground level and simulated high altitude
[AD-713726] 05 p6333 N71-14641
Comparison of ground level rate to rate exposed to altitude of 18,000 feet to determine cardiovascular response
[AD-717851] 11 p1682 N71-22240
Behavior of barium ion cloud at high altitudes
[NASA-NEWS-RELEASE-71-61] 12 p1953 N71-23517
High altitude mesospheric wind data taken by meteorological sounding rockets at Cape Kennedy, Florida
[NASA-TM-X-64578] 12 p1958 N71-24039
Measurement of upper atmospheric wind circulation
13 p2074 N71-25064
Orbit calculations, and high altitude sites suitable for infrared astronomy
14 p2337 N71-26299
High altitude sites for IR astronomy for Polar, Sub-Polar, and mid-latitudes
14 p2338 N71-26213
Living and sleeping quarters with controlled environment for high altitude personnel
14 p2337 N71-26214
Medical aspects of high altitude environments including hypoxia at Logan High Camp
14 p2337 N71-26215
Daytime measurements of precipitable water vapor in atmosphere over selected mountain sites in southwest
14 p2338 N71-26216
Maximum length of arc in altitudes up to 9500 ft in 200 volt ac dc electric aircraft system
[IAS-TR-68259] 16 p2573 N71-28063
Isomeric nuclear morphology, height variations, and relationships to planetary magnetic disturbances in periods of maximum and maximum solar activity at varying latitudes
[NASA-TT-F-637] 17 p2745 N71-30076
High altitude velocity distribution of ionospheric drift and electric field strength in F2 layer
17 p2746 N71-30091
Anti-intercontinental ballistic missile defense and high altitude nuclear explosions
[BREV-FBWT-71-3] 18 p2977 N71-30644
Evaluating effects of high altitude turbulence encounters on X-70 airplane
[NASA-TN-D-63718] 18 p2968 N71-30718
Experimental and theoretical study of biologically important radiation components and dose equivalents due to galactic and solar rays at SST in high atmosphere - summary
18 p2970 N71-30779
Study of concept of inertially aided barometric altimetry system to meet vertical navigation requirements of 1000 and 2000 feet for Mach 3.5 aircraft in altitude hold at 80,000 feet
[NASA-CR-1770] 18 p2898 N71-31387
High altitude infrared rocket astronomy
[AD-724131] 20 p3343 N71-32802
Comparison of atmospheric density variations at high altitude from Doppler observations made on polar orbiting
[AD-724531] 20 p3256 N71-32986
High altitude flight test of roofed 12.2-meter-diameter disk-gap-band parachute with deployment at 2.58 Mach number
[NASA-TN-D-64669] 21 p3376 N71-34026
Real time estimation of wind velocities at altitudes above ceiling of meteorological balloons using digital image processor and radar equipment
[TN-55A-167] 21 p3451 N71-34559
Twenty-seven high altitude positive balloon tests in ROBIN program during May 1970
[AD-726234] 22 p3615 N71-37539
One dynamic structure of high altitude rocket exhaust studied in low density tunnel
[AD-726555] 22 p3663 N71-36121
RA-4 processing for high altitude infrared color film
[NASA-CR-122648] 22 p3755 N71-36767
Using rocketborne and reconnaissance data to analyze high altitude synoptic charts
[NASA-CR-122933] 23 p3784 N71-36971
HIGH ALTITUDE BALLOONS
NT SKYHOOK BALLOONS
High altitude balloon measurements of X ray and photo radiation in several zones
[AD-712724] 03 p0572 N71-15293
Recovery of high altitude balloon aerial photography for earth resources and meteorology including photographic formats and camera systems and processing
[NASA-TM-X-2380] 17 p2753 N71-29910
Meteorological satellite to collect temperature, wind, and pressure data from high altitude free floating balloons, and perform range-rate measurements for balloon position determinations
[NASA-NEWS-RELEASE-71-144] 18 p3814 N71-31031
Orbital acceleration of off-nominal high altitude balloons suitable for solar radiation processes
[E-59-70-91] 19 p3179 N71-31879

Measurement and analysis of heavy cosmic rays with high altitude balloons
21 p3506 N71-34977
Using balloons for lifting astronomical observations to high altitudes
[NASA-TT-F-12359] 24 p4008 N71-38580
HIGH ALTITUDE BREATHING
Physiology of respiration at high elevations using human subjects
[AD-710277] 01 p0609 N71-18245
Effect of high altitude adaptation on cellular respiration in rats
16 p2546 N71-28483
HIGH ALTITUDE ENVIRONMENTS
Puruvian Quechua population growth physics, and pulmonary function at high altitude
02 p0155 N71-11096
Developing high altitude protection suit of partial pressure type
[AD-702537] 02 p0167 N71-11188
Investigating suitability and requirements of mountain sites for high altitude IR astronomical observations
04 p0609 N71-13590
Investigating changes in brain cortex and gastrocnemius muscle functions during adaptation to high mountainous altitudes
07 p0900 N71-17067
High altitude acclimatization and physiological changes in humans
11 p1680 N71-22007
Method of making solid propellant rocket motor having reliable high altitude capabilities, long shelf life, and capable of firing with nozzle closure with foamed plastic permanent mandrel
[NASA-CASE-XLA-64136] 14 p2333 N71-26779
Partial pressure helmet and pressure suit mobility tests for high altitude environment
16 p2549 N71-28168
Microbiological ecology of manned space flights, exploration, colonization, and life support systems
[JFPL-53388] 16 p2542 N71-28248
Effect of high altitude adaptation on cellular respiration in rats
16 p2546 N71-28483
Measurement and effects of radiation doses from cosmic radiation at altitudes of supersonic transport flights
[ORNL-TR-2455] 18 p2878 N71-31500
Physiological effects of high altitude and high temperature environments on human performance of complex actions
[FAA-ADM-71-17] 22 p3544 N71-35242
HIGH ALTITUDE FLIGHT
U FLIGHT
U HIGH ALTITUDE
HIGH ALTITUDE PRESSURE
Oxygen and high altitude pressure effects on rabbit life functions
[AD-715395] 07 p0983 N71-17885
Vacuum chamber for high altitude pressure simulation for rocket engine tests
[NASA-CASE-MFS-20430] 21 p3407 N71-34242
HIGH ALTITUDE TESTS
Physiological effects of phenanthrene hydrochloride on animals at simulated high altitudes
[AD-715354] 02 p0153 N71-11082
High altitude solar cell and radiometer calibrations using balloon techniques
[NASA-CR-119170] 17 p2841 N71-30045
HIGH ASPECT RATIO
High aspect ratio of ellipsoidal-type configuration with helical conductors and no toroidal field coils
[CEA-CONF-1602] 06 p1247 N71-18186
High aspect ratio planing surface gliding on incompressible, inviscid, and gravity-free fluid
[AD-717667] 11 p1738 N71-22345
HIGH ASPECT RATIO WINGS
U SLENDER WINGS
HIGH CURRENT
Optimization of high current leads suitable for cryostats
01 p0808 N71-10144
High current electric arc characteristics magnetically driven to supersonic velocities in straight and circular channels
[NASA-TN-D-6086] 03 p0438 N71-13027
Apparatus for measurements on superconducting short samples in fields to 52 kOe and currents to 3500 A
[JEP-471] 15 p2498 N71-27193
Measuring erosion as loss of electrode material in high current, high pressure gas discharges
[JEP-472] 15 p2499 N71-27264
Self-modelling solutions of high-current plasma discharge and effect of thermal conductivity
[NASA-TT-F-13569] 22 p3653 N71-34051
HIGH EFFICIENCY
U EFFICIENCY
HIGH ENERGY
HIGH ENERGY ASTRONOMY OBSERVATORIES
U HRAO

HIGH ENERGY INTERACTIONS

HIGH ENERGY ELECTRONS
Energy loss of high energy electrons in tin, lead, and gold
[AD-711005] 01 p0897 N71-10534
Lifetime of energetic electrons and ions trapped in magnetic mirror
[CEA-CONF-1403] 06 p1256 N71-15372
Satellite-borne measurements of electron flux during magnetic storm
[NASA-TT-F-13312] 09 p1366 N71-20301
Electron energy spectra 45 to 450 keV measured on-board ERSO 1 satellite during quiet and magnetically disturbed periods over polar region
10 p1530 N71-21161
Auroral magnetic substorm and high energy electron absorption
12 p1908 N71-23556
Physics of electron storage rings including betatron oscillations, energy oscillations, radiation damping, radiation caustics, and hysteresis
[SLAC-121] 12 p1980 N71-24348
Target small charge distribution effects on high energy electron small angle multiple scattering distributions based on Mott's formula and elastic form factors
15 p0478 N71-27407
Time variations of energetic electron and solar proton distributions in inner radiation belt
[NASA-SP-3024-VOL-7] 16 p2676 N71-29089
Trapped energetic electrons and solar protons observed by satellites at synchronous altitudes
16 p2676 N71-29089
Neutron spectra in soil and iron side radiation shielding of high energy electron and proton accelerators
[IASL-348] 17 p2791 N71-29287
Computer simulated electron diffraction analysis of electron passing through absorbing crystal foil
[AD-722044] 17 p2814 N71-29693
Active region MacMath in 1965 produced 16 distinct electron events associated with solar flares during passage across solar disk
[NASA-TM-X-65613] 18 p3007 N71-30512
Shell structure of light nuclei during inelastic scattering of high energy electrons accompanied by knockout of nucleons from nucleus
[ITP-70-42] 18 p2974 N71-30551
Nuclear structure of boron 11 studied by high energy electron scattering
[LAL-1243] 22 p3436 N71-35921
Origin of cosmic electrons with high energies from supernovae
[NASA-TM-X-65609] 22 p3464 N71-36128
Plasma heating and production of relativistic electron current layers by injection of high current electron beams into magnetic fields
[COMET-10667-12] 24 p3990 N71-38468
HIGH ENERGY INTERACTIONS
Cosmic radiations at extremely high energies
[AD-710653] 01 p0117 N71-10432
High energy pulsed liquid laser
[AD-710813] 01 p0863 N71-10508
X ray astronomy
[NASA-TM-X-65572] 01 p0118 N71-10610
Overview on nuclear cross section research
[ORNL-TR-2598] 01 p0101 N71-10850
Phase band analysis of positive pion proton scattering at 2.5 to 3.0 GeV/c
[RLD-2041-37] 03 p0420 N71-12644
Test of change in S equals change in Q rule in neutral kaon sub c decay
[CALT-68-251] 03 p0425 N71-12827
Three body decays of neutral K mesons
[COO-1195-167] 03 p0425 N71-12828
Nuclear chemistry research of high energy nuclear reactions including cross sections and reactions on separated isotopes of tellurium
[NYO-2097-41] 03 p0425 N71-12833
Reviewing experimental program of research on hadron interactions and properties
[NYO-2262-TR-152] 03 p0433 N71-12958
Identification of reactions at high energies using resonance functionals
[JINR-P1-5123] 03 p0435 N71-13008
Strong interaction experiment on Mt. Chacabuta
[AD-712735] 03 p0435 N71-13224
Cross sections of pion-proton interactions with two charged secondary particles at high pion energies
03 p0436 N71-13267
Model for weak isospin interactions
[UJV-2435-F] 04 p0575 N71-13402
Diffraction dissociation model for high energy hadron photoproduction
[DESY-70723] 04 p0575 N71-13403
Reaction of 15 foot deuteron filled bubble chamber to positive pion meson beam at 40 GeV/c
[COO-1438-230] 04 p0581 N71-14060
Observation of very high energy gamma of 1-12
[ORNL-TR-2263] 04 p0582 N71-14083
Properties of electron and muon components of extensive air showers for different models of high energy interactions
[INR-11421] 04 p0587 N71-14238
High energy nuclear scattering
[JEP-697] 04 p0587 N71-14239

Dispersion relation for calculating pion-nucleon cross sections at high energies 04 p0588 N71-14292
 [RIFP-110]
 Glauber theory for high energy hadron-deuteron scattering [UCRL-19851] 05 p0743 N71-15146
 High energy electron positron scattering cross section measurements as test of quantum electrodynamic theory [LAL-1233] 06 p0910 N71-15786
 Constructing multichannel model for very high energy collisions using kinematical variables [IFPPT-8/70] 06 p0912 N71-15816
 Developing detection system combining Cerenkov and wire chamber techniques for high energy photon interactions [CALT-68-255] 06 p0913 N71-15881
 Application of image intensifiers developed in high energy physics to some problems in biology [PURC-4159-1] 06 p0799 N71-15884
 Broken scale invariance and kinematics moments of electroproduction cross sections [ORO-2504-159] 06 p0914 N71-15971
 X ray energy measurements in 5g yields 4f pionic transitions of Th-232 and U-238 [NASA-CR-116140] 06 p0916 N71-16053
 Inelastic electron scattering experiments [SLAC-PUB-796] 06 p0916 N71-16055
 High energy electron scattering from Li-6 [AD-714022] 06 p0920 N71-16268
 Proceedings from conference on Regge poles [CONF-691202] 06 p0923 N71-16707
 Investigating positron annihilation and positronium formation as analytical tool for solution of chemical problems [CONF-700915-1] 06 p0923 N71-16742
 Experimental limit on branching ratio for neutral kaon sub L yields lepton antilepton [UCRL-20078] 06 p0924 N71-16759
 Kaon⁰ yields positron neutrino to kaon⁰ yields muon⁺ neutrino [UCRL-20079] 06 p0925 N71-16837
 High energy, neutrino scattering, process study using V-A theory [CDO-264-559] 06 p0926 N71-16855
 Lambda hyperon-nucleon interactions in deuterium [UCRL-20077] 06 p0927 N71-16888
 Muon and hadron production and Bhabha scattering [LNF-70/38] 07 p1070 N71-17004
 High energy interactions in spark and bubble chambers [UHL-511-87-70] 07 p1071 N71-17035
 Glauber corrections and interaction between high energy hadrons and nuclei 07 p1071 N71-17188
 [BNL-TR-358]
 Observation of 2400-MeV 5 pion mass enhancement in 6-prong negative pion proton events at 12 GeV/c [UHL-511-77-70] 07 p1071 N71-17242
 Associated production of A₂/0 and positive positron Delta in high energy interactions [UCRL-20050] 07 p1073 N71-17357
 High energy, neutrino beam, semi-leptonic interactions [NYO-4204-3] 07 p1076 N71-17529
 Process pion nucleon yields omega-meson nucleon at high energies [ITF-70-39] 08 p1246 N71-18151
 Exchange quasipotential for high energy pion/plus or minus/ proton scattering and problem of linearity of Regge trajectories [JINR-E2-5226] 08 p1246 N71-18175
 Inelastic interactions of particles and nuclei at high and superhigh energies [JINR-E2-5282] 08 p1248 N71-18199
 Equality of total cross sections for interaction of particles and antiparticles at high energies [IFVE-STF-49-110] 08 p1248 N71-18200
 Heavy meson resonances in antiproton proton annihilation reaction at 3.6 GeV/c [NP-18466] 08 p1251 N71-18262
 High energy interactions in new accelerators [CONF-700314] 08 p1260 N71-18764
 High energy elastic and inelastic hadron-hadron scattering in psi-cubed theory [ILL-TR-71-4] 08 p1261 N71-18803
 Negative kaon proton interactions at 12.6 GeV/c 08 p1267 N71-19323
 Bubble chamber study of two body channels of positive and negative Sigma hyperons and pions from scattering negative kaon beam [UCRL-19790] 09 p1425 N71-19475
 Scaling behavior in proton proton yields pion plus anything at high energy [RLO-1388-583] 09 p1425 N71-19476
 Consistency and high energy theorems in stochastic field theory associated with currents and total scattering cross sections 09 p1408 N71-19517
 Comparison of infinite one-particle-exchange model with Regge behavior due to crossed channel exchanges to Veneziano model [RIFP-112] 09 p1433 N71-19990
 Relationship between momentum transfer and fixed angle asymptotic, high-energy interactions in dual

models with applications to large angle nuclear scattering [REPT-70/44] 09 p1435 N71-20028
 Construction of set of self consistent equations for calculating scattering amplitude of strongly interacting particles 09 p1442 N71-20433
 Absorbed dose and dose equivalent from neutrons in energy range 60 to 3000 MeV and protons in energy range 400 to 3000 MeV [NASA-CR-117314] 09 p1338 N71-20489
 Cluster decomposition for studying high energy scattering processes [ILL-TR-71-5] 09 p1444 N71-20514
 Atomic and molecular physics, nuclear structure, high energy interactions, nuclear research, and research equipment 09 p1447 N71-20592
 High energy radioactive atom reactions from nuclear transformations in silicon-containing compound systems [ORO-3896-2] 10 p1610 N71-20627
 Momentum spectra in high energy hadron deuteron interactions [COO-1764-115] 10 p1611 N71-20686
 High energy interactions, quantum mechanics, and field theory [NYO-3829-64] 10 p1614 N71-20903
 Project summaries of research in theoretical and high energy physics [COO-1764-86] 10 p1617 N71-21337
 High energy nuclear reactions in air without ionospheric storms at Monte Chacaltaya, Bolivia 10 p1641 N71-21548
 Thiol and disulfide effects on photochemical and high energy gamma radiation induced reactions [NYO-2499-371] 10 p1620 N71-21722
 Decay mode and He-4 coherent interference data for B-11/p,3 He-4 reaction at proton beam energies of 0.675, 1.00, and 1.388 MeV 10 p1621 N71-21740
 High energy electron and positron colliding beams leading to annihilation into muon pair, annihilation into hadron pair, Bhabha scattering and multibody hadron production 10 p1623 N71-21769
 Regge pole model for high energy np charge exchange scattering 10 p1625 N71-21829
 Results of duality regarding internal symmetries for low- and high-energy hadron scattering [COO-1764-81] 11 p1806 N71-22521
 Negative pion proton elastic scattering differential cross sections from 1.71 to 5.53 GeV/c [NASA-CR-117852] 11 p1809 N71-23032
 Systematization of inelastic interactions of high energy pions and nucleons with atomic nuclei [ORNL-TR-2399] 12 p1976 N71-24168
 Statistical model application to scattering cross section analysis for high energy interactions including energy dependence of partial cross sections [INP-7191] 13 p2130 N71-24697
 Computer programs to calculate and analyze pion and nucleon interaction within prescribed medium referred to as PROPER 3C Transport Code [NASA-TM-X-2138] 13 p2137 N71-24723
 Gamma ray producing decay modes of secondary particles produced in high energy cosmic ray interactions with interstellar and intergalactic gas 13 p2158 N71-24765
 Continuous moment sum rule for calculating Compton scattering at high energies [TUEP-71-2] 13 p2140 N71-25500
 Experimental and theoretical high energy studies also atomic, statistical, plasma, and health physics - computing and data handling [UCRL-20120] 14 p2301 N71-25741
 Eikonal approximation for high energy interactions [JINR-E2-5244] 14 p2303 N71-26038
 Invariant momentum transfer squared dependence of inelastic e-p scattering structure functions [SU-1206-236] 14 p2304 N71-26208
 Radiation damage to miniature silicon avalanche diodes by high energy neutrons and electrons 14 p2326 N71-26287
 Derivation of numerical flux and energy momentum tensors in relativistic statistical mechanics from phase-space integral for high energy interactions [NP-18652] 14 p2305 N71-26336
 Elastic scattering of high energy hadrons from deformed carbon 12 nuclei calculations using multiple collision theory and deformed oscillator wave functions [INP-721] 14 p2308 N71-26422
 Role of gravitation in elementary particle theory, microscopic parameters and macroscopic values [JINR-P2-5289] 14 p2310 N71-26668
 High energy total summation of perturbation series and particle spin angular momentum effects on scattering amplitudes including Regge trajectories [JINR-E2-5509] 14 p2312 N71-26702
 Additive quark model for decay distribution of resonance produced in meson baryon high energy interactions [TPJU-15/70] 14 p2316 N71-26749

Mathematical model for relativistic scattering amplitudes in high energy interactions based on Fermi analysis and Lorentz group embeddings [JINR-E2-5341] 14 p2318 N71-26790
 Fireball model and multiperipheral CLA model of pion production mechanisms in high multiplicity positive pion proton interactions at 8 GeV/c [INP-708] 14 p2318 N71-26791
 Development of model for description of nucleon-nucleon and pion-nucleon collisions at high energy and Monte Carlo description of Nuclear Cascade [NASA-CR-115041] 15 p2456 N71-28011
 Bremsstrahlung diagnosis of electron ion bunches produced by accelerating heavy atoms to high energies [KFK-TR-537] 15 p2458 N71-28070
 Solution of unitarity equation for elastic scattering amplitude at high energy [IFVE-STF-49-65] 15 p2463 N71-27141
 Unitarity theory for calculating forward scattering amplitude at high energies [IFVE-STF-49-74] 15 p2464 N71-27219
 Estimated diffractive peak width for scattering on Gaussian potential [IFVE-STF-49-83] 15 p2464 N71-27240
 Approximate solutions to Bethe-Salpeter and integral equations, and applications to high energy interactions [AD-72067] 15 p2466 N71-27245
 Computer compilation of high energy physics data represented by graphs or tables [UCRL-2000-NN] 15 p2467 N71-27288
 Program connecting measuring microscopes PUOS with computer Minsk-2 [IFVE-SFK-49-53] 15 p2384 N71-27342
 Semiconductor devices used in radiation detectors for high energy interactions at particle accelerator facilities [UCRL-20042] 15 p2472 N71-27403
 Meson and hyperon production in antiproton proton, antiproton neutron, and antiproton deuteron annihilations at high energies 15 p2481 N71-27701
 Positive kaon negative pion elastic scattering from positive kaon proton interaction at 5.43 GeV/c in 16-inch bubble chamber 15 p2482 N71-27745
 Absolute measurement of fast neutron scattering cross sections from high energy neutron deuteron reactions [INP-18488] 15 p2486 N71-27818
 High energy interactions produced by surviving primary protons of cosmic radiation at altitude of Chacaltaya, Bolivia from 1968 to 1970 [AD-720996] 15 p2515 N71-27823
 Interpretation of data on muons in cosmic rays for relevance to high energy interactions and astrophysics [JINR-1231] 15 p2516 N71-27825
 Complex angular momentum of partial wave amplitudes examined for production of three particles in collisions of two strongly interacting particles at high energy 15 p2490 N71-27897
 Variational method for estimating binding energy of oxygen with effective interaction matrix elements [DEMO-70/25] 15 p2492 N71-27929
 Final states of four-pronged antiproton deuteron interactions at 7.0 GeV/c, and cross sections for viable spectator events 15 p2496 N71-27979
 Explicit expression of invariant Hermitian form for unitary representations of conformal group [IFVE-STF-49-85] 15 p2497 N71-27994
 High energy cosmic ray interactions in emulsion chambers 16 p2675 N71-28942
 Emulsion study of pion-nucleon interactions at 16.2 BeV with experimental criteria for interactions 16 p2682 N71-28996
 Potential theory model for high energy scattering [DESY-7067-PT-2] 16 p2683 N71-29000
 High energy scattering amplitude of fermion with anomalous magnetic moment and nonexchange [DESY-71/1] 16 p2687 N71-29122
 Inelasticity and N/D calculations including Regge type amplitudes, highly inelastic resonance with circular Argand plot, and constraints on channel models of P-11 state 16 p2688 N71-29147
 High energy scattering of protons, electrons, photons, and composite particles by nuclei [INP-712-VOL-1] 16 p2688 N71-29143
 Compilation of cross sections of reactions by negative kaons on protons, neutrons, and deuterons [CERN/HERA-70-6] 16 p2688 N71-29148
 Converging coaxial plasma accelerator for generating dense high velocity plasma bursts [NASA-CASE-ARC-10109] 16 p2663 N71-29181
 Photoabsorption and inelastic scattering cross sections for photon proton and neutron high energy interactions and Compton effects [UCS-34-P-135-14] 17 p2790 N71-29239
 Three body states Lambda or Sigma hyperon kaon antikaon and Xi hyperon kaon pion produced by negative kaon proton interactions at kaon beam momentum of 2.5 GeV/c [ORO-2504-170] 17 p2797 N71-29043

SUBJECT INDEX

Modification of parton model with variable internal state parton mass 17 p2806 N71-36310
[N71-111]
Collective interaction in collision of high energy particles referring to cosmic rays 17 p2806 N71-36323
Calculation of binding energy and wave function of helium isotope by harmonic polynomial method [ITP-70-51-8] 17 p2810 N71-36368
Ga/Li detectors for gamma ray spectroscopy, and spectral study of d, p, and t produced by deuteron bombardment of C-12 at high energies [NP-18570] 18 p2868 N71-36417
Isotonic high energy electron scattering by light nuclei accompanied by knockout of nucleons [ITP-70-38] 18 p2870 N71-36445
Research in high energy nuclear physics, nuclear structure, reactions, and instrumentation [LYCEN-7602] 18 p2876 N71-36418
Rational representation of scattering amplitudes from high energy interactions in field theory nuclear models [JINR-P2-5577] 18 p2876 N71-36422
Nuclear parameters of multiplying subcritical media with pulsed neutron source [JINR-228-DP/R-63] 18 p2879 N71-36496
High energy peripheral scattering and particle production correlation with unitarity condition in t-channel [IFVE-STF-70-7] 18 p2879 N71-36498
Cross sections for binary fission of Bi, Au, Pb, U, and some lighter elements, produced by 0.59 to 23 GeV protons [CEBN-71-3] 18 p2879 N71-36727
Regge cuts and high energy pion-nucleon and kaon-nucleon elastic and charge exchange scattering [LPTHE-71/14] 18 p2885 N71-31136
Nucleon Curie calculation for magnetic moment of Lambda hyperon in negative pion plus proton yields Lambda hyperon plus neutral kaon reaction 18 p2888 N71-31494
Connections between internal parton wave function of hadrons, deduced from electroproduction, and observable systematics of high energy processes [NUB-3008] 18 p2890 N71-31505
High energy bremsstrahlung-induced γ -pions, π and neutrons in Au-197 [LUNP-7103] 19 p3159 N71-32628
Kinematics of inclusive reactions in high energy multiparticle production [LPTHE-71/36] 20 p3315 N71-33389
High energy physics, experiments, accelerator operation, and colliding beam facility [CEAL-1053] 20 p3321 N71-33577
Nuclear models for examination of high energy scattering reactions of elementary particles [IS-T-436] 20 p3322 N71-33765
Conceptual design for high energy electron ring accelerator allowing mass production techniques and ensuring low cost [UCRL-20169] 20 p3348 N71-33965
Three dimensional formulation quantum field theory based on relativistic Fock equations and applied to three body problems [JINR-P2-5661] 21 p3468 N71-34688
Elastic scattering in model with Regge poles and cuts generated by multiple scattering [JINR-P-1233] 21 p3472 N71-34721
Use of semiconductor telescopes for detecting recoil nuclei in proton-light nuclei scattering at high energy [LYCEN-7605] 21 p3472 N71-34724
Diffractive Pomeron bootstrap and multiperipheral fragmentation [UCSD-10-P-10-77] 21 p3481 N71-34793
Methods for monitoring proton incidence on internal targets of high energy accelerators [NP-16776] 21 p3485 N71-34828
Analysis of pulsed x-discharges characterized by anomalous plasma conductivity in skin-layer region [NP-16775] 21 p3493 N71-34886
Single and double pion production and charge exchange reaction from positive kaon protons and positive kaon deuterons interactions at 1585 MeV/c in 25-inch bubble [UCRL-26628] 22 p3439 N71-33937
Relativistic poles, triple Regge behavior, and single particle spectra in high energy collisions [NYO-2262-TA-234] 22 p3439 N71-33939
Cross sections of high energy inelastic reactions in nucleon proton interactions and separation of reaction channels [JINR-P-5665] 22 p3461 N71-33960
Differential cross sections and slope parameters for high energy elastic scattering 22 p3462 N71-33961
Forward scattering amplitudes in Regge pole theory of high energy interactions between pions and nucleons 22 p3465 N71-33989
Radiation produced by high energy electrons in field-induced waveguide 22 p3468 N71-36016
Functional integration and Regge- α -like representation of high energy particle scattering amplitudes [JINR-P2-5768] 23 p3807 N71-37144

Neutron-nucleon scattering at high energies and spin effects in quasipotential approach [JINR-E2-5770] 23 p3807 N71-37146
Digital simulation of energy spectra and mass inelasticity coefficients of high energy particle interactions [ITT-3] 23 p3808 N71-37152
Monte Carlo method for calculating high energy radiation with matter [JINR-P2-5719] 23 p3810 N71-37169
Piston investigation using on-line mass spectrometry and amplifying target construction, elimination of contamination, and recording of mass spectra [NP-18629] 23 p3811 N71-37177
Low energy limit of dual resonance models and connection between Yang-Mills fields [LPTHE-71/37] 23 p3812 N71-37183
Generalized Veneziano model with spin and isospin for antineutron nucleon antineutron kaon pion processes 23 p3818 N71-37230
High energy proton capture effect and geomagnetism 23 p3852 N71-37458
High energy research projects at electron synchrotron [LNF-70/59] 24 p3902 N71-37814
Experimental and theoretical research studies in high energy physics [UCR-34-P-107-8-124] 24 p3977 N71-38380
Interaction of high frequency electromagnetic fields with magnetized plasma, high intensity electron and ion beams, pulse discharges, and related studies - bibliography [NP-18601] 24 p3993 N71-38487
Extended cosmic ray showers from high energy protons and nuclei [NLL-M-20419-5828-471] 24 p4804 N71-38556
HIGH ENERGY OXIDIZERS
Bibliography on fluorine compounds at high energy rocket fuel oxidizers [FOA-1-A-7503-42/46-40] 14 p2215 N71-26608
HIGH ENERGY PROPELLANTS
Using isomorphous and phase rule concepts to obtain ammonium perchlorates and strates in mixed crystals for propellants [AD-713564] 05 p0761 N71-13378
Performance prediction of high energy rocket propellants using approximation functions [DLR-FB-70-77] 12 p1909 N71-23618
HIGH EXPLOSIVES
U EXPLOSIVES
HIGH FIELD MAGNETS
Instrumentation to measure critical parameters of 300 kilograms experimental magnet [EP-RB-25] 05 p0581 N71-13154
Analysis of instabilities in high field superconducting wires and ribbons under variety of environmental conditions [UTR-7800-14] 17 p2813 N71-29641
Ultra-narrow, high quality, high field quadrupole magnet for use in beryllon experimental area [JINR-P2-5614] 20 p3246 N71-33589
Technical-economic data for copper and aluminum conductors and superconductors for high field magnets [LNF-70/19] 22 p3657 N71-34082
HIGH FLUX ISOTOPE REACTORS
Analytical studies of in-reactor tests of nuclear light bulb unit cell using Pwex, nuclear furnace, and high flux isotope reactors 01 p0884 N71-10373
High flux isotope reactor operations and maintenance summary [ORNL-TM-3162] 05 p0723 N71-14675
Design analysis for plutonium fueled high flux isotope reactor [BNWL-1504] 06 p0898 N71-16273
Fabrication voids in aluminum base fuel dispersoids applicable to high flux isotope reactor and advanced fuel reactor [ORNL-4611] 07 p1063 N71-17361
Control systems and instrument development for use with liquid metal fast breeder and high flux isotope reactors, Van de Graaff and linear accelerators, and in-pile loops [ORNL-4620] 12 p1895 N71-23166
Operations and maintenance for high flux isotope reactor also system surveillance tests and design changes [ORNL-TM-3286] 12 p1962 N71-23892
Phase interactions and properties of UAD-Al as diffusion fuel for high flux reactor [JFK-1252] 15 p2445 N71-27024
High flux isotope reactor operations summary [ORNL-TM-3339] 16 p2833 N71-28096
Design and performance of thermal beryllium oxide and graphite neutron sources and high flux beam reactors in neutron spectrometry 16 p2649 N71-28716
Computer codes for determining neutron flux spectrum in HFIR target region [ORNL-TM-3322] 17 p2808 N71-30046

HIGH FREQUENCIES

Nuclear radiation pumping of certain gas lasers feasible in high fluxes provided by pulsed nuclear reactor 20 p3282 N71-33666
High flux isotope reactor operation using fuel elements without plate-spacer comb 22 p3625 N71-35832
[ORNL-TM-3432] 22 p3625 N71-35832
Group point kinetics for studying feasibility of high flux trap reactor system 22 p3627 N71-35842
Calorimeter and recording system for measuring heat generation in reactor holes [LBAQ-3617] 24 p3958 N71-38233
HIGH FREQUENCIES
High frequency heating control of toroidal and rotating fully ionized plasmas [REPT-70-13] 02 p0200 N71-11836
Multiband HF antenna containing two, three, or four dipole arrays [AD-712976] 03 p0334 N71-12188
Performance report on Project Vals Studies [AD-711961] 03 p0338 N71-12409
Developing communications equipment for HF Lunar Rander [NASA-CR-114795] 05 p0642 N71-14722
Investigating development of techniques for measuring electrical quantities in high frequency and microwave ranges [FOA-3-C-3595-68] 05 p0654 N71-14751
High frequency effects on plasma hydrodynamics [AEC-TR-7163] 06 p0630 N71-16889
Atlas of oblique incidence high frequency backscatter diagrams of midlatitude ionospheres [ESSA-TR-ERL-162-475-104] 07 p1026 N71-18031
Modified pointing strip method for measurements of slowly varying low field [JNC-A-70-5] 08 p1167 N71-18162
Aperture antenna synthesis for HF radio signals propagating in F layer of ionosphere [AD-714825] 08 p1167 N71-18252
Real time correction of wideband HF ionospheric phase [AD-719181] 08 p1187 N71-18478
Holder for high frequency crystal resonators [NASA-CASE-XNF-03637] 10 p1563 N71-21311
High frequency Doppler sounding at vertical incidence of atmospheric disturbances 11 p1709 N71-22930
Apparatus for determining high frequency signal phase stability by autocorrelation [NASA-CASE-XGS-01118] 12 p1893 N71-23662
Influence of high frequency fields on properties of accelerating channel and beam emittance in linear accelerator [SLAC-TRANS-128] 14 p2308 N71-25785
High frequency pressure variations in internal rocket engine probes for combustion instability environment 14 p2256 N71-26365
Multiple varactor for generating high frequencies with high power and high conversion efficiency [NASA-CASE-XMF-04938-1] 14 p2324 N71-26414
Naval time signal transmission from HF and VLF stations for navigation purposes [AD-721300] 15 p2441 N71-27179
Fine structure observation in high frequency radio signals propagated around world using oblique ionograms [AD-721703] 16 p2561 N71-28448
Compact, self contained, symmetrical antenna for airborne use at high frequencies with capability to function in two independent modes for both transmission and reception 17 p2726 N71-29895
Determination of boundary of high frequency wave absorption between electron cyclotron and low hybrid frequency [PTI-295] 18 p2992 N71-30434
Mathematical models for high frequency characteristics of metal oxide semiconductor transistors [LAAS-PUBL-776] 18 p2999 N71-30557
Add-on noise blanker for use in HF communication receiver [AD-722563] 18 p2991 N71-31357
Design, circuitry, and construction of low power high frequency synthesizer [AD-724602] 20 p3239 N71-32986
Computerized design of high frequency amplifiers [AD-724290] 20 p3241 N71-33136
Automatic processing of high frequency stellar spectrophotometric data using Gauss function model 21 p3430 N71-34608
Dynamic stabilization of drift-dispersed instability in partially ionized plasma using inhomogeneous HF electric field [EUR-CEA-FC-381] 21 p3493 N71-34883
Stability of toroidal plasma ring with high frequency current in longitudinal magnetic field with chamber wall conducting wall [LA-4339-TR] 21 p3494 N71-34893
High frequency heating of hydrogen plasma near low hybrid frequency [ORNL-TM-3435] 21 p3495 N71-34897

HIGH GAIN

Region of xrf energy absorption by plasma at upper hybrid frequencies
[NP-18807] 22 p3652 N71-36046

Effect of ionosphere inhomogeneities on diffraction of high frequency radio waves
23 p3726 N71-36563

Circuit diagrams for studying high frequency fields in plasma experimental installations
[NP-18895] 23 p3826 N71-37288

High gain antenna acquisition problem during Apollo 13 flight
[NASA-TM-X-66903] 09 p1346 N71-19407

Harmful biological effects caused by exposure to microwave radiation including radio frequency power density in vicinity of space station antennas
17 p2707 N71-29325

HIGH INTENSITY
U INTENSITY
HIGH LATITUDES
U POLAR REGIONS
HIGH LIFT DEVICES
U LIFT DEVICES

HIGH MELTING COMPOUNDS
U REFRACTORY MATERIALS
HIGH PRESSURE FILTERS

Computer aided analysis and synthesis of fourth-order high pass filter
[AD-710733] 01 p0633 N71-10530

Radio frequency coaxial filter to provide dc isolation and low frequency signal rejection in audio range
[NASA-CASE-XGS-01418] 12 p1889 N71-23573

Design and transmission characteristics of high pass, mechanical velocity filter for fast neutral molecular or atomic beams
[NASA-TM-X-2332] 18 p2990 N71-30745

HIGH POLYMERS
Conformation and turbulent flow characteristics of polyacetylenes in solution
[AD-715217] 03 p0664 N71-14978

Proceedings from conference on inelastic neutron scattering with emphasis on collective excitations in disordered and magnetic systems, and lattice dynamics of high polymer substances
[JAERI-1197] 13 p2130 N71-24859

Average and standard deviation considerations on measurements of viscosity and molecular weight of high polymers
[JCT-570] 17 p2768 N71-29556

Pressure-volume-temperature relationships and thermodynamic analysis of high polymers and oligomers
21 p3445 N71-34517

Radiation chemistry of high polymers and computer techniques for data reduction
[ORO-4059-1] 22 p3550 N71-35286

Coefficient of friction of high polymers as function of pressure determined by shear strength measurements
[AD-726685] 23 p3778 N71-36927

HIGH PRESSURE
Magnetic annular arc used as accelerator for high pressure, high enthalpy flow test facility
[AD-710316] 01 p0638 N71-10186

High pressure steam effects on position of reattachment point on adjacent wall of incompressible jet
[A-13] 01 p0041 N71-10296

Combustion of boron particles at elevated pressures
[AD-710747] 01 p0133 N71-10548

Structural design of high pressure regulator valve
[NASA-CASE-XNP-00710] 01 p0060 N71-10778

Ultrasonic pulse analysis of elastic properties of plastics at high pressures
[AD-711761] 01 p0073 N71-10851

Thermodynamic tests of helium cooled reactor fuel element loop with natural circulation under high pressures
[NASA-TT-F-13397] 01 p0087 N71-10875

High pressure gas medium for extrusion of materials
02 p0229 N71-11446

P wave velocities at high pressures in liquid containing sedimentary rocks of Carpathian Area
[NASA-TT-F-13210] 02 p0211 N71-11499

Role of Mosebauer effect in solid state studies at high pressure
[RLO-2225-T-12-1] 05 p0746 N71-15253

Hypersonic test facility for studying ablation in models under high pressure and high temperature
[NASA-CASE-XLA-00370] 05 p0830 N71-15925

Physical chemistry and crystallization of linear high polymers under high pressure
[AD-715070] 07 p1049 N71-17858

Decomposition of stabilized polyoxymethylene under elevated pressure
[AD-714853] 07 p1049 N71-17856

Magnetic field influence on high pressure phase diagrams of iron and iron alloys
[REPT-670] 08 p1213 N71-18540

Hardness and high pressure deformation mechanisms of glass
08 p1223 N71-19154

Development and characteristics of high pressure control valve
[NASA-CASE-MSC-11010] 09 p1392 N71-19485

Influence of high pressures and temperatures on velocity of elastic waves in certain rocks of Ukrainian shield
[NASA-TT-F-13516] 09 p1385 N71-20164

Non-basal slip in alumina at high temperatures and pressures
[AD-716788] 10 p1631 N71-20611

Valve test with resilient support ring for seating valves subjected to high pressure sealing loads
[NASA-CASE-XKS-02582] 10 p1345 N71-21234

Aerosol behavior and filtration in high pressure environments
[AD-717733] 11 p1647 N71-22255

Apparatus and method capable of receiving large quantity of high pressure helium, removing impurities, and discharging at received pressure
[NASA-CASE-XMF-06808] 12 p1929 N71-24044

High pressure phase transition points of bismuth 3-5, tin, and iron
14 p2329 N71-26510

Comparison of pressure-volume scales for sodium chloride
14 p2329 N71-26514

Design considerations for development of operational super-pressure balloon system to carry 50 pounds to 10 millibar atmospheric pressure
[NASA-CR-115027] 14 p2199 N71-26790

Pressure sensitive reference hydrophone design including lead zirconate titanate spherical element for infrasonic and audio frequencies
[AD-721069] 15 p2385 N71-26842

Radiation measurements, low frequency, and high pressure investigations of induction heated plasma torch to simulate gas core nuclear rocket requirements
[NASA-CR-1804] 15 p2445 N71-27023

Testing fast valve operating at pressure of 100 atm for use in bubble chamber
[JINR-P13-5420] 15 p2415 N71-27118

Measuring erosion as loss of electrode material in high current, high pressure gas discharges
[JEP-4772] 15 p2499 N71-27264

Self diffusion properties in alpha phase of large grains of plutonium prepared by using high hydrostatic pressures
[CEA-R-4092] 15 p2478 N71-27614

Vibrational kinetics of high pressure CO₂ laser mixtures
[AD-721735] 16 p2606 N71-28322

Two phase critical discharge of high pressure liquid nitrogen through convergent-divergent nozzle exhibiting same behavior as water
[NASA-TM-X-67863] 16 p2639 N71-28819

Space shuttle hydrogen/oxygen auxiliary propulsion system high and low pressure thrusters
17 p2836 N71-29589

High and low chamber pressure injectors for space shuttle hydrogen/oxygen APS engines
[AGCS-6100-71] 17 p2836 N71-29590

High pressure reverse flow engine for space shuttle APS application
17 p2836 N71-29591

Space shuttle high and low pressure auxiliary propulsion subsystem definition
17 p2837 N71-29599

Preliminary designs of high and low pressure APS for space shuttles
17 p2837 N71-29600

Thermodynamic investigation of titanium over temperature range to 6000 K, and pressures to 1000 atmospheres
[AD-722341] 17 p2766 N71-30112

High pressure, high temperature measurement of spin-lattice relaxation in pure and doped LiBr single crystals
17 p2827 N71-30167

Ion-molecule reactions of CH₄-CD₄ mixtures at high pressures in ion source of quadrupole mass filter
[AD-722687] 17 p2717 N71-30230

Apparatus for studying radiolytic carbon deposition of C-labeled gas mixtures at high temperature and pressure
[AD-723411] 17 p2804 N71-30269

Measurement of extinction parameter of tungsten-hydrogen aerosols as function of wavelength at high pressures and temperatures
[NASA-CR-1864] 18 p3023 N71-30494

Research on superconductivity in Switzerland including phase studies, high pressure research, specific heat, and nuclear magnetic resonance
[AD-723411] 18 p3000 N71-31588

Cascade arc technique for investigating arc plasma at extremely high pressures in selected gases
20 p3331 N71-33649

Complete equation of state for metals in both solid and liquid/dense vapor phases, from ambient conditions to high pressures and temperatures
20 p3334 N71-33756

High pressure metallic and superconducting polymorphs of indium antimonide, cadmium telluride, cadmium germanium diarsenide, and cadmium arsenide
21 p3388 N71-34107

Time determinations for electric pulse transmission through rock samples under high pressure and temperature
[NASA-TT-F-13796] 22 p3573 N71-35445

Glass properties studied by synthesizing gas-glass systems using high pressure techniques
22 p3604 N71-35667

Primary and secondary mixing performance of combustors under high inlet air pressures
[NASA-TN-D-6491] 22 p3663 N71-36119

Measuring techniques for pressure, volume, enthalpy, and resistance of equilibrium thermodynamic states of liquid metals at high temperatures and pressures
[UCRL-51035] 22 p3696 N71-36359

HIGH PRESSURE OXYGEN
Peculiarities of human heat exchange under reduced atmosphere pressure and sufficient oxygen supply
[NASA-TT-F-13374] 01 p0810 N71-10867

Colonic temperature response of rats to oxygen at high pressure
[AD-716965] 10 p1497 N71-20776

Accelerated growth of Escherichia coli in high pressure helium-oxygen atmospheres
[AD-717404] 11 p1680 N71-22115

Factors affecting ignition of metals in high pressure oxygen systems
[NASA-TM-X-67201] 15 p2524 N71-27394

HIGH Q
U Q FACTORS
HIGH RESOLUTION

K α neutron energy fission cross section of U²³⁵ measured with high resolution
[UCRL-72472] 01 p0099 N71-10703

Seasonal sea surface temperature variations in Persian Gulf recorded by Nimbus 2 HRIR
[NASA-TM-X-65385] 03 p0369 N71-13867

Pulse compression and correlation for high range resolution of tracking radar
04 p0496 N71-19928

High resolution spectra of radioactive isotopes
[COO-498-82] 06 p0921 N71-16310

High resolution scanning microscope for molecular biology
[COO-1721-21] 06 p0804 N71-16793

Time of flight method for high resolution measurements of radiative neutron capture in isotopes between 7 and 200 keV
[KFK-1231] 06 p1257 N71-18517

Computer system for development and application of high resolution mass spectrometer
12 p1922 N71-24852

Requirement and design criteria for high resolution ultraviolet spectroscopy on SAS-D mission
[NASA-TM-X-67165] 12 p0801 N71-24876

High resolution, differential, Cerenkov gas counters using helium
[NAL-TR-3] 13 p2083 N71-25483

Potential high energy resolution iodine negative ion source
[AD-720671] 15 p2473 N71-27445

High resolution gas Cerenkov counter operational characteristics
[NAL-TR-2] 15 p492 N71-27930

Sensor for space astronomy applications especially diffraction limited imagery and high resolution spectroscopy
16 p2593 N71-28812

High speed, and high resolution sensors for micrometeorological measurements of atmospheric temperature and moisture
[AD-721456] 16 p2626 N71-28845

Optical properties and efficiency of dichrometers in slow neutron spectrometry
16 p2596 N71-28786

High resolution NMR spectra of water adsorbed on pyrogenic alumina, silica, and titania
[AD-722322] 16 p2649 N71-28811

High resolution radiation counter design and use in study of S-32 T-3 state
[NP-18623] 18 p2972 N71-30534

High resolution strip photography of lunar surface
18 p3013 N71-30670

High resolution infrared spectrometer for gas molecular spectroscopy
[ONERA-TR-176] 19 p0999 N71-31939

High resolution studies of atoms and molecules applied to optical and infrared laser experiments
[NASA-CR-121728] 21 p3455 N71-34640

Conversion of concurrent cloud data obtained via ATS 3 and ESSA 3 and from Apollo 6 high resolution photography
[NASA-TN-D-6470] 21 p3452 N71-34606

High resolution Ge(Li) detector for measuring muonic X rays of Ba-136, 137, 138, La-139, Ce-140, 141, Pr-141, and Nd-142
21 p3468 N71-34639

Development of specialized quadrupole mass spectrometer with high resolution and dynamic range increase
[NASA-CR-121906] 22 p3582 N71-35330

Calibrated infrared emission spectra of earth and atmosphere using high resolution interferometer spectrophotometer on Nimbus 4 satellite
[NASA-TM-X-65667] 22 p3583 N71-35317

SUBJECT INDEX

Multivire proportional chamber using tungsten wires for high resolution beam hodoscope [LAL-1246] 22 p3643 N71-35973

Gamma ray energies and intensities for calibrating high resolution spectrometer [UCRL-20474] 22 p3644 N71-35979

Utilizing atomic resolution capability of field ion microscopes for viewing biomolecules [NYO-3851-10] 23 p3714 N71-36473

High resolution absorption spectra of isotopic modifications of nitrogen dioxide and other small molecules 24 p3983 N71-38425

HIGH RESOLUTION COVERAGE ANTENNAS

Broadband current preamplification for obtaining simultaneous high resolution energy and time information from nuclear radiation detectors [ORNL-TM-3252] 17 p2799 N71-30022

HIGH SENSITIVITY U SENSITIVITY

HIGH SPEED

Development and characteristics of high speed ground transportation system 03 p0469 N71-12760

Gravity effects on travel time and energy for evacuated tubes in high speed ground transportation systems [PB-190396] 07 p1134 N71-18026

Continuous-access VHF waveguide for nonradiating communications with high speed track vehicles [PB-191028] 07 p0995 N71-18111

Grinding machine efficiency increase due to higher forward feed speeds noting surface roughness and wear effects [CRIP-MC-34] 10 p1563 N71-20751

Impact testing machine for imparting large impact force on high velocity packages [NASA-CASE-XNF-44017] 12 p1916 N71-23225

Flight test evaluation of military aircraft low altitude high speed performance 12 p1835 N71-23421

Flow meter for measuring stagnation pressure in boundary layer around high speed flight vehicle [NASA-CASE-XFR-02007] 13 p2065 N71-24692

Measurements of aerosol total vibration exposure during low altitude, high speed flight in F-4 aircraft [AD-720721] 14 p2305 N71-26172

Short-term creep properties of OT-4 alloy in high speed air flows under aerodynamic vibrations [NASA-TT-F-13658] 16 p2414 N71-28832

Evaluating series hybrid bearing concept by testing lubricated fluid film thrust bearing at high speed [NASA-TM-X-67873] 16 p2603 N71-28907

Use of aerodynamic lift for application to high speed ground transportation by two dimensional air flow [PB-197242] 17 p2700 N71-29762

Moving long cylindrical model for aerobreaking tests at high speed in drop wire facility 18 p2867 N71-31109

Analysis of technology for high speed ground transportation [PB-198015] 19 p3072 N71-31766

Pilot injuries on high speed low altitude flight noting acceleration due to gust effects 19 p3048 N71-31888

HIGH SPEED CAMERAS

NT FRAMING CAMERAS

High speed television recording system with slow and stop motion replay capabilities [RAE-TR-70035] 02 p0225 N71-11545

High speed framing lenticular camera with mechanical shutter for ac study in circuit breaker [RAE-LIB-TRANS-1444] 02 p0225 N71-11552

High light intensity image dissection camera for short duration recordings [RAE-LIB-TRANS-1445] 02 p0225 N71-11553

Fluoroscopic calculations using diffraction and light scattering in ultraviolet image dissection camera [RAE-LIB-TRANS-1443] 02 p0226 N71-11554

Evolution of failure modes and redesign of SERT-2 global pin puller [NASA-TM-X-2128] 03 p0318 N71-12267

Lasers as light sources for high speed photography [AEC-TR-7166] 05 p0696 N71-13655

Ultrahigh speed photographic system for photographing hypervelocity projectiles and impact phenomena [NASA-TD-D-6128] 05 p0685 N71-15408

Velocity measurement using microscope and high speed cameras [PB-195163] 07 p1026 N71-16927

Breakup of laminar capillary jet of nonnewtonian fluid [NASA-CR-116469] 07 p1008 N71-17326

High speed photography and impact tests of nylon yarn including transient responses and breaking energy [AD-716833] 10 p1587 N71-20652

High speed photographic experiments within fuel nozzle in irradiated fast reactor [ANL-7578] 12 p1963 N71-23986

Flash radiography in ballistic testing [AD-719088] 13 p2188 N71-24444

Relationship between dynamic buckling and static buckling investigated with clamped shallow circular arches using high speed cameras 14 p2350 N71-26467

High speed photographic techniques to study impinging streams of propellants in experimental investigation of reactive stream separation [NASA-CR-119246] 18 p2923 N71-30844

Electronically controlled camera system for optical satellite triangulation data acquisition 19 p3099 N71-31873

Comparison of two high speed films for streak camera recording systems [MHSMP-71-32] 23 p3758 N71-36790

HIGH SPEED FLIGHT U FLIGHT

HIGH SPEED

U RAPID TRANSIT SYSTEMS

HIGH STRENGTH

High strength metallic and nonmetallic composite materials with whisker reinforcements [AD-717819] 11 p1783 N71-22349

Flexural, shear, bending, tension, and impact strengths of high modulus, high strength, glass fiber-epoxy resin composites [NASA-CR-122755] 23 p3775 N71-36907

High strength welded joints made from low alloy base metal steels 12 MKH and 12 Kbl MF [AD-727872] 24 p3939 N71-38100

HIGH STRENGTH ALLOYS

NT HIGH STRENGTH STEELS

NT MARAGING STEELS

High strength state of metals resulting from substructural hardening 02 p0241 N71-11445

Structure and properties of high strength ferrous alloys EP404 and EP454 [AD-713048] 03 p0393 N71-13037

Development of high temperature creep resistant titanium alloys for space power systems 03 p0394 N71-13003

High strength, corrosion resistant cobalt-based alloys for aerospace structures [NASA-CASE-XLE-00726] 05 p0706 N71-15644

Modification of high temperature cobalt-tungsten alloys for improved stability [NASA-TN-D-6147] 08 p1213 N71-18515

Strengthening of austenitic stainless steels by internal stridation 08 p1219 N71-19111

High strength aluminum casting alloy for cryogenic applications in aerospace engineering [NASA-CASE-XMF-02706] 10 p1572 N71-20743

Problems in riveting and welding of high strength aluminum aircraft alloys 10 p1652 N71-20924

Tungsten reinforced oxidation resistant columbium alloys with operating temperature above 2000 F for use in gas turbine engines [AD-717909] 12 p1944 N71-23673

Low temperature mechanical properties of various alloys of high strength and corrosion resistance [NASA-SP-5921/0-17] 12 p1939 N71-23795

Spectral analysis of magnesium distribution in high strength cast iron containing globular graphite [TT-70-59085] 14 p2269 N71-25668

Production of high strength refractory compounds and microconstituents into refractory metal matrix [NASA-CASE-XLE-03940] 14 p2279 N71-26153

Effect of electron irradiation on strength of monocrystalline bcc iron - low temperature strength determined by inherent lattice hardening [COO-1587-36] 15 p2419 N71-26918

Stress corrosion and fatigue tests and fractographic analysis of high strength aluminum alloy cylinders [AD-720857] 15 p2425 N71-27629

Thermomechanical and transformation induced plasticity processes for producing high strength martensitic titanium alloys with high tensile, fracture, yield, and elongation properties [AD-712361] 16 p2606 N71-28073

Internal oxidation process for strengthening tungsten by additions of powder of reactive metal compound to tungsten base metal powder containing some oxygen [BM-RL-7521] 19 p3116 N71-33423

Cyclic furnace and high velocity oxidation of alumina-coated high strength nickel alloy [B-1900] [NASA-TM-X-2370] 22 p3593 N71-35585

HIGH STRENGTH STEELS

NT MARAGING STEELS

Measuring effects of prestressing on stress corrosion resistance of high strength steels [AD-711696] 02 p0242 N71-11574

Electron fractography for high strength steel to determine fatigue life of military aircraft parts [MLR-TR-49943-5] 03 p0395 N71-13364

High strength stainless steel of Cr, Mo, and Co with improved toughness and ductility [AD-712724] 03 p0395 N71-13367

ARPA coupling program on stress-corrosion cracking including treating specimen types, titanium

and aluminum alloys, high strength steels, and surface sciences [AD-713039] 03 p0396 N71-13397

Loading rate and temperature effects on high strength steel fracture toughness 05 p0699 N71-14523

Effects of cold working by hydrostatic extrusion on mechanical properties of high strength steels [NASA-TN-D-6186] 07 p1034 N71-17483

Crack initiation in heat affected zone of low alloyed high strength steels during weld and tensile tests [CRIP-MT-63] 08 p1214 N71-18585

Structural transformations and properties of high strength Co-Mn-Ni austenitic steels [JPRS-52877] 12 p1936 N71-23148

Effect of alloying elements on temporal martensite embrittlement and fracture toughness of low alloy high strength steels 12 p1936 N71-23777

Industrial process for producing steel sheets of low carbon steel with high degree of strength and stiffness [NLL-M-20179-5828-4P] 12 p1940 N71-24191

Effects of addition of rare earth elements on physical and mechanical properties of steels [IS-RIC-4] 13 p2094 N71-24932

Effects of oxygen and hydrogen on high strength toughness and crack susceptibility in steel weld deposits 13 p2093 N71-24045

Gamma-phase monitoring to determine stability of austenite formed in surface layers during friction of high strength cast iron [AD-720743] 14 p2276 N71-26661

Properties and selective applications of high strength steels 15 p2421 N71-27040

Laminated steel pressure vessel design, trial production, and destructive testing [NLL-RTS-5936] 17 p2835 N71-30334

Effectiveness of flame straightening mechanisms on high strength steel structures [AD-721537] 18 p3023 N71-31595

Fracture strength of high strength steel welded joints by investigation of temperature effects on material near weld [REPT-4770] 19 p3109 N71-31684

Gerard-Popino method for measuring loss of ductility in high strength AISI 4340 steel [COO-2040-2] 21 p3438 N71-34464

Effects of hydrogen and hydrogen-oxygen mixtures on fracture of high strength steel in precracked configuration [NYO-5975-3] 22 p3594 N71-35590

High structural strength in welded joints of cylinders made of high strength thin sheet steels [AD-727897] 24 p3930 N71-38040

Properties of high strength steel and application to structures for steam superheating [AD-727495] 24 p3936 N71-38082

Technique for testing high strength sheet steel to determine resistivity to cold crack formation during welding under biaxial stress conditions [AD-727899] 24 p3940 N71-38110

Plastic deformation at tip of fatigue crack in high strength steels 24 p4024 N71-38715

Delayed fracture of high strength steel as stochastic process in terms of nucleation theory and delayed fracture toughness 24 p4025 N71-38717

HIGH TEMPERATURE

Pyrometer for measurement of magnetizing force and magnetic induction at very high temperatures [NASA-TM-X-52901] 01 p0053 N71-10272

Forced convection of gaseous ammonia at high wall temperature [LA-TR-70-12] 01 p0044 N71-10802

Visual observation of high temperature profiles during startup in lithium heat pipe [NASA-TM-X-52924] 01 p0134 N71-16994

Electrical conductivity of igneous rocks of Kola Peninsula at high temperature based on dc transmission [NASA-TT-F-13214] 02 p0210 N71-11440

Thermionic diode switch for use in high temperature regions to chop current from dc source [NASA-CASE-NPO-10404] 03 p0316 N71-12255

High temperature effects on radiation chemistry of aqueous solutions 03 p0432 N71-12933

Organic cooled, heavy-water moderated, WR-1 research reactor capable of low pressure with high temperature in primary system and very low radiation fields near primary piping [ABCL-3523] 04 p0547 N71-13640

High temperature liquid metal technology for nuclear Rankine power systems [BNL-50248] 04 p0528 N71-13991

High temperature electrical resistivity of refractory aluminum oxides [BNWL-1458] 04 p0533 N71-13996

Separation of U-233 from U-235 during head-end reprocessing of HTR fuels of TRISO coated fuels and fertile particles [GA-9238] 04 p0560 N71-14357

HIGH TEMPERATURE AIR

Equation of state of hydrogen and deuterium between 3 and 10 e/cmole to 10,000 K [UCRL-50911] 05 p0743 N71-15133

Hypersonic test facility for studying ablation in models under high pressure and high temperature [NASA-CASE-XLA-80078] 06 p0830 N71-15925

Embrittlement of Zircaloy under high temperature conditions simulating loss of coolant accident in reactors [IN-1389] 06 p0898 N71-16192

Performance of silicon-germanium thermocouple in RTG with sublimation at high operating temperatures [NASA-CR-116224] 06 p0899 N71-16666

Investigating effect of surface preparation on oxidation of W-52 by high temperature X ray diffraction [NASA-TN-D-4148] 06 p0876 N71-16839

Hot corrosion of TD nickel and TD nickel chromium in jet engine exhaust [NASA-TM-X-52976] 09 p1398 N71-19700

Influence of high pressures and temperatures on velocity of elastic waves in certain rocks of Ukrainian shield [NASA-TT-F-13516] 09 p1385 N71-20164

Activity coefficient of sulfur in ternary alloys rich in iron at high temperature [NRC-T-1418] 01 p402 N71-20444

Plutonium segregation in uranium-plutonium solid solutions and fast reactors at high temperatures [GEAP-12133] 09 p1487 N71-20599

Carbon dioxide distribution in mixture with argon in graphite channel at high temperatures [NLL-RTS-5839] 10 p1514 N71-21318

Diffusion-viscous flow contribution to high temperature creep of copper aluminum alloys [NLL-CE-TRANS-5438-19022.09] 10 p1584 N71-21603

Creep tests on CrNiNb and CrMo at 600 C and at different stresses [NLL-CE-TRANS-5414-19022.09] 10 p1586 N71-21833

Application of free flight ranges to high temperature gas dynamics 11 p1740 N71-22633

Process for fiberizing ceramic materials with high fusion temperatures and tensile strength [NASA-CASE-XNP-00597] 11 p1786 N71-23088

High total temperature sensing probe using fluid oscillator concept for X-15 hypersonic aircraft [NASA-CR-116772] 12 p1917 N71-23250

Induction heating of metallurgical specimens to high temperatures in coil furnace [NASA-CASE-XLE-04026] 12 p1917 N71-23267

High temperature thermal cycling tests of thermocouples using W-52Re-5 versus W-74Re-26 sensor wires for monitoring in-pile fuel temperatures 13 p2080 N71-24522

Design and development of canned-motor pump for high temperature NaK service in SNAP-8 [NASA-CR-72823] 13 p2116 N71-24634

Dislocation mechanisms involved in low stress-high temperature creep of metals 13 p2096 N71-25098

High temperature reaction of MoS₂ with CO₂ [RAE-LIB-TRANS-1494-PT-2] 13 p2040 N71-25125

Diffusion coefficients of C-14 in W and W-Re alloys over 1500 to 1800 C temperature range 14 p2272 N71-25831

Vibrational excitation of HF behind incident shock waves at temperatures from 1400 to 4100 K [AD-720819] 14 p2213 N71-25928

Reactor safety problems in MTR-IA high temperature protection system [AD-720593] 14 p2293 N71-26282

Method of forming ceramic to metal seals impervious to gaseous and liquid mercury at high temperature [NASA-CASE-XNP-01263-2] 14 p2263 N71-26312

Effect of oxidation degree on copper emittance for application to radiation shields or multilayer insulation systems at 700 to 1400 F 14 p2274 N71-26314

High temperature measurement in rocket nozzle ablative materials 14 p2356 N71-26364

Thermal dissociation and sublimation of UO₂F₂ between 760 and 800 C using Knudsen effusion method [ORNL-TR-2422] 15 p2376 N71-26887

Calculating vibrational excitation of CO₂ for anharmonic coupling and normal mode at high temperature [NASA-CR-1841] 15 p2438 N71-26940

Coating of fuel particles and model investigations of conical fluidized beds noting effect of gas current and gas distribution particle load, and nozzle geometry [JUL-669-RW] 15 p2448 N71-27359

Solubility and corrosion behavior of iron, steel, molybdenum, nickel, tantalum, vanadium, titanium, and chromium in molten lead at high temperatures [JUL-661-RW] 15 p2444 N71-27360

Properties of molten ceramics at 3000 C [BNWL-XA-3579] 15 p2431 N71-27426

Analysis of high temperature oxidation rate of carbon for use as reentry material [NASA-TN-D-6310] 16 p2616 N71-28012

Prolonged electrical test of bonded alumina trilayer at 1325 K in vacuum environment [NASA-TM-X-2303] 16 p2616 N71-28035

Effect of initial heat treatment on high temperature embrittlement of nickel alloys after neutron irradiation [SABR-P-88] 16 p2607 N71-28039

Evaluation of refractory metal alloy metering and isolation valves for alkali metal service at 1900 F [NASA-CR-1810] 16 p2607 N71-28040

Sheathed thermocouple for use in extremely high temperature environments [NASA-CASE-LEW-10854-1] 16 p2594 N71-28651

Effects of initial heat treatment on high temperature embrittlement in nickel alloys after neutron irradiation [AEC-TR-7188] 16 p2613 N71-28799

Equipment for determining reactivity of graphite materials in isothermal conditions at high temperatures from 1200 to 3000 C [NLL-RISLEY-TRANS-2012-19091.9F] 16 p2619 N71-29142

Rates at which iridium oxidizes at temperatures 1600 to 2200 C and pressures 1 to 1000 torr [RLO-2228-T-1-1] 17 p2713 N71-29240

Structural fasteners of heat resistant alloys for high temperature applications 17 p2755 N71-29468

Determination of thermal conductivity of UO₂ with sintered density of 10.57 g/cc in 500 C to 2500 C range [AE-411] 17 p2783 N71-29628

Oxidation mechanism and morphology of scale formation on Ni-Cr-Al alloys at 1000 to 1200 C 17 p2764 N71-29683

Mechanical properties of pure binary Ni-Cr alloys at high and low temperatures [NLL-TRANS-746-439-19022.401] 17 p2764 N71-29696

Survey of errors in sampling shock tube gas with mass spectrometer for study of chemical reaction rates at high temperatures 17 p2735 N71-29782

Thermodynamic investigation of titanium over temperature range to 6000 K, and pressures to 1000 atmospheres [AD-72341] 17 p2766 N71-30112

High pressure, high temperature measurement of spin lattice relaxation in pure and doped LiBr single crystals 17 p2827 N71-30167

Apparatus for studying radiolytic carbon deposition of C-labeled gas mixtures at high temperature and pressure [RD/B/N-1748] 17 p2804 N71-30269

Sintering UO₂ by hydrogen reduction at high temperature and different O/U ratios [UUV-2370-M] 18 p2958 N71-30492

Measurement of dynamic shear properties of silicone based elastomers at high temperature [ISVR-TR-43] 18 p3020 N71-30553

Phase transformation of hyperstoichiometric uranium carbide irradiated at high temperatures [AECL-3679] 18 p2975 N71-30572

Chemical and X ray analysis of phase diagrams of Th-U-O ternary systems for ThO₂-UO₂-U₃O₈ between 1100 and 1550 C [KFK-1297] 18 p2933 N71-30646

Notch sensitivity of creep-rupture properties of Waspaloy between 1000 to 1400 F [NASA-CR-1849] 18 p2936 N71-31180

Measuring elevated-temperature time-dependent corrosion effects of liquid metal on immersed structural materials [NASA-TM-X-67882] 18 p2936 N71-31221

Development of low cost iron base alloy with corrosion resistance to hot sea water [PB-198642] 19 p3109 N71-31673

Infrared spectra of UO and UO₂ vapor condensed in rare gas matrices at high temperature [COO-1182-34] 19 p3150 N71-32124

Short term creep of nickel in vacuum and high speed air flow at high temperature [NASA-TT-F-13661] 19 p3114 N71-32234

Measurement of polycrystalline metal flow curves at high and room temperatures and their application to plasticity mechanics [RAE-LIB-TRANS-1531] 19 p3115 N71-32266

Mechanical properties of cylindrical vessels under internal pressure at high temperatures [NLL-CE-TRANS-5321-19022.09] 19 p3189 N71-32412

Sorption properties of cesium by tungsten and graphite between 600 and 800 C and vapor pressure from .01 to 30 mm Hg for use in thermionic converter reservoirs [EUR-4549] 19 p3121 N71-32584

Reaction kinetics of high temperature oxidation of nickel-nickel in oxygen [INIS-MF-11] 19 p3118 N71-32640

Strain rate equations for secondary creep deformation of thick-walled tubes operated at high temperatures [NASA-TM-X-2339] 19 p3191 N71-32799

Plastic deformation in polycrystals of Fe-Cr-Ni alloys on boundary layers at high temperature [TT-70-59108] 20 p3284 N71-33198

SUBJECT INDEX

Aerodynamic and heat transfer performance of air cooled nozzle cascade for high temperature turbine [NAL-TR-231-PT-1] 20 p3364 N71-33304

Thermodynamic data program involving photoion and urania at high temperatures [GEAP-12153] 20 p3367 N71-33792

Factors influencing scatter in results of room temperature and elevated temperature tensile tests of steels [PB-197139] 21 p3439 N71-34472

Effects of fast neutrons on polycrystalline aluminum electrical insulators used in thermionic converters at high temperatures [ORNL-4678] 21 p3444 N71-34540

Primary emission neutron activated detector flux measuring system working at high temperature with fast response 21 p3471 N71-34716

High temperature oxidation of nickel and Ni-oxide composites measured by periodic suspension [NLL-TRANS-746-754-19022.401] 22 p3552 N71-35380

Velocity pulsations of high temperature hypersonic flow based on interrelation of total stagnation pressure pulsations and longitudinal velocity pulsations [AD-72605] 22 p3569 N71-35421

Thermally resistant polymers for fuel tank seals of advanced high speed aircraft [NASA-CR-119940] 22 p3587 N71-35546

Effect of grain size on creep of platinum-rhodium alloys at high temperature [NLL-L-TI-746-744-19022.401] 22 p3597 N71-35615

Thermogravimetric analysis of effect of various media on silicon carbide materials at high temperatures 22 p3599 N71-35626

Ceramography and micro X ray diffraction analysis of columnar grain growth in cerestine heated UO₂ pellet [JAERI-MEMO-4249] 22 p3620 N71-35788

Measuring technique for pressure, volume, enthalpy, and resistance of equilibrium thermodynamic states of liquid metals at high temperatures and pressures [UCRL-51035] 22 p3606 N71-36339

AC temperature technique for measuring high temperature specific heat of small wire or foil samples [UCRL-50962] 22 p3696 N71-36380

Effectiveness of yttrium, lanthanum, and hafnium coatings for preventing nitridation embrittlement of chromium alloys at high temperatures [NASA-TN-D-6528] 23 p3772 N71-36886

Microstructural changes as criterion for assessing operational reliability and high temperature resistance of chromium steels [NLL-CE-TRANS-5569-19022.09] 23 p3774 N71-36896

Development of techniques for measuring electric resistivity of ceramic materials at high temperatures from 1,000 to 1,700 degrees centigrade [NASA-TT-F-13948] 23 p3776 N71-36911

Thermodynamic properties of FeO,CoO and NiO in sodium disilicate over temperature range from 700 to 1100 C 23 p3781 N71-36945

Fabrication and tests of tungsten reactor pipe and its heating characteristics up to 1900 K [NASA-TM-X-67941] 23 p3797 N71-37079

Augmenting combustion flames with electric discharges to produce high temperature chemical and physical reactions in 2500 to 5000 K range [BRCRIN327] 23 p3866 N71-37582

Metallurgical examinations of stainless steel microstructure after aging in power reactor temperature ranges [INR-1255] 24 p3934 N71-38065

Effects of elevated temperature on deformation resistance of steel and brass [AD-727841] 24 p3939 N71-38101

Fatigue tests and life of nickel alloy during programmed loading and elevated temperature [AD-727842] 24 p3939 N71-38101

Problems of high temperature annealing of PTFE/LIF discs used for ionizing radiation dosimetry [AEW-34-991] 24 p3973 N71-38346

HIGH TEMPERATURE AIR

Atomic line transitions and radiant emission from high temperature air [AD-710799] 01 p0086 N71-10890

HIGH TEMPERATURE ALLOYS

U HEAT RESISTANT ALLOYS

HIGH TEMPERATURE ENVIRONMENTS

Design and development of high temperature vacuum insulation systems for SNAP 21 thermoelectric power system [TTD-25482-AF7] 04 p0553 N71-13995

High temperature ball bearing design for turbopump engines [NASA-TM-X-52938] 06 p0066 N71-10534

Electrical and mechanical characteristics of solar cell contacts after exposure to high-temperature high humidity environments [NASA-CR-116805] 08 p1146 N71-12651

SUBJECT INDEX

Human caloric requirements when working in extreme climatic environments 09 p1337 N71-20367

Design, performance, and evaluation of switchgear for space nuclear electrical systems [NASA-CR-1719] 09 p1394 N71-20394

Endurance measurement techniques for space shuttles in high temperature environmental simulation [NASA-CR-103071] 10 p1508 N71-21025

High temperature fatigue tests of steel ball bearings with synthetic paraffinic oil lubricant in low oxygen environment [NASA-TN-D-4156] 10 p1567 N71-21666

Long-term performance tests of neon gas filled, high temperature ceramic voltage-regulator tubes [NASA-CR-1813] 12 p1858 N71-23120

Feasibility of producing thin metal and oxide-film capacitors with stable electrical properties in high temperature environments [NASA-CR-72779] 12 p1891 N71-23983

Development and characteristics of refractory metal alloy for high temperature environment applications [AD-718473] 12 p1935 N71-24093

Graphite thermodynamic properties and liquid-solid phase diagrams in high temperature environments for nuclear rocket engine reactor core design 15 p2448 N71-27367

Development and fabrication of precipitation hardened TD NiCr structures for use in high temperature environments 17 p2848 N71-29466

Comparison of water, convective air, and reversed air flow cooled units for body temperature thermostats in high temperature environments [JPRC-1307] 17 p2712 N71-30127

Thermal insulation materials and techniques for high temperature and cryogenic environments technology utilization [NASA-SF-593001] 18 p3024 N71-30851

Blaxial creep strength of T-111 titanium alloy tubing in high temperature, high vacuum environment [NASA-CR-72846] 19 p3114 N71-32162

Techniques and apparatus design for measuring high temperature emissivity of thermal protection materials for reentry vehicles [NASA-CR-119920] 21 p3425 N71-34348

Design of high temperature antennas for space shuttles 21 p3514 N71-35043

Physiological effects of high altitude and high temperature environments on human performance of complex tasks [JAA-AM-71-17] 22 p3544 N71-35242

Characteristics and application of high temperature fuel cells as power sources [AD-727497] 24 p3875 N71-37624

Properties of high strength steel and application to structures for steam superheating [AD-727495] 24 p3936 N71-38082

Modification and control of oxidation protection processes for application to structural materials at high temperatures [AD-728262] 24 p3940 N71-38106

HIGH TEMPERATURE FLUIDS

HT HIGH TEMPERATURE AIR

HT HIGH TEMPERATURE GASES

HIGH TEMPERATURE GASES

HT HIGH TEMPERATURE AIR

Laminar heat transfer and wall temperature distribution for high temperature gases and nitrogen plasma in circular tubes and over flat plates [REF-70-3] 04 p0519 N71-13791

Absorptance ratios used for retarding regression in ablative material [NASA-CASE-XLE-65913] 04 p0620 N71-14032

Transient heat transfer gaps for measuring total radiant intensity from far ultraviolet and ionized high temperature gases [NASA-CASE-XNP-69002] 05 p0786 N71-15641

Effect of gaseous film cooling on recovery temperature distribution in rocket nozzles 06 p0960 N71-16878

Investigating characteristics of radiative heat transfer by high temperature gases 07 p1128 N71-17040

Measuring average absorption coefficients of carbon dioxide gas as function of temperature and pressure 07 p1128 N71-17041

Cold gas and high temperature gas rocket engines and ion engines for satellite attitude control [RLR-MITT-70-14] 07 p1118 N71-17158

Advanced cooling systems and heat resistant materials for turbine blades of high temperature aeromedical gas turbine engines [WARD-CP-73-71] 07 p1099 N71-17372

High entrance temperatures for improved performance of turbogenerators and gas turbine engines 07 p1099 N71-17373

Heat transfer and exchange measurements on fixed turbine blades in high temperature combustion chamber 07 p1100 N71-17378

Effectiveness of turbine cooling systems for high temperature inlets [NASA-TM-X-46703] 07 p1100 N71-17385

Design of gas turbine engines for high operating temperature 07 p1101 N71-17386

Design and performance of thermophen fluid cooled high entry temperature axial flow turbine 07 p1129 N71-17399

Computerized optimization of thermal resistant gas turbine blades 07 p1129 N71-17400

Shock tube thermochemistry tables for high temperature gases [NASA-CR-116444] 07 p1131 N71-17899

High temperature gas radiation, and direct and electron density spectroscopic methods for gas temperature measurements 11 p1842 N71-22403

Gas and water cooled probes for high temperature gas and dense plasma and flow measurements 11 p1842 N71-22604

Cooled film anemometer for high temperature gas measurements in environments with transient phenomena and small heat transfer to sensor 11 p1763 N71-22611

Chemical interferences and ionization in high temperature flame spectroscopy [IS-T-417] 15 p2409 N71-27352

Evaluation of high gas velocity and static oxidation behavior of fused-salt-chambered IN 100 between 1030 and 1149 C [NASA-TN-D-6400] 17 p2764 N71-29713

Model tests of concepts to reduce hot gas ingestion in VTOL lift engines in low and cross wind conditions - graphs [NASA-CR-1853] 19 p3038 N71-32370

Transient pressure, temperature, and density measurement of high temperature dense gas during compression tests [VKI-TM-23] 20 p3249 N71-32956

Acoustic instability driven by thermal radiation absorption in extremely high temperature gases [CSB-T-40-4] 20 p3330 N71-33640

Physical models for measuring acoustic instabilities of high temperature gaseous uranium for use in gaseous core nuclear rocket system 20 p3304 N71-33651

Viscosity of carbon dioxide between 293 and 1500 K [NLL-RISLEY-TRANS-2129-19091.9F] 23 p3721 N71-36522

HIGH TEMPERATURE LUBRICANTS

Wetability of microgroove streams of high temperature lubricants on static metal surface [NASA-CR-72743] 05 p0691 N71-14817

Production of barium fluoride-calcium fluoride composite lubricant for bearings or seals [NASA-CASE-XLE-08511-2] 06 p0877 N71-16105

Sodium lubricated bearing technology for high capacity pumps used in fast breeder reactors [NYO-3910-4] 06 p1205 N71-18328

Self lubricating fluoride-metal composite materials for outer space applications [NASA-CASE-XLE-08511] 12 p1944 N71-25710

Wear tests of oxide and fluoride oxidation resistant solid lubricants for use in high temperature gaseous environments [NASA-TM-X-67845] 15 p2417 N71-27787

High temperature friction and wear characteristics of self lubricating composite disks of sintered tungsten, molybdenum, and cobalt molybdenum, impregnated with fluoride eutectic [NASA-TN-D-6363] 16 p2600 N71-28231

SNAP 8 pump-motor journal and thrust bearing wear tests with high temperature sodium-potassium alloy lubrication [NASA-CR-72824] 17 p2737 N71-30121

Evaluation of glasses as forging lubricants for tungsten steels and titanium alloys [AD-726583] 22 p3603 N71-35661

HIGH TEMPERATURE MATERIALS

U REFRACTORY MATERIALS

HIGH TEMPERATURE NUCLEAR REACTORS

Molten salt nuclear reactor and high temperature gas cooled reactor research [ORNL-4586] 01 p0085 N71-10408

Thorium fuel cycle development including materials irradiation, uranium-233 reprocessing, and refabrication development [ORNL-TM-3068] 03 p0413 N71-12660

Thorium fuel cycle development including materials irradiation, head-end reprocessing, and refabrication development [ORNL-TM-3112] 03 p0414 N71-12669

Investigating fuel burnup rates, safety rods, fuel elements, and critical experiments in thermal and fast reactors [BNWL-1581-2] 04 p0554 N71-14016

Development of high temperature gas-cooled nuclear power plant [GA-16020] 04 p0556 N71-14101

HIGH TEMPERATURE PLASMAS

Investigating isotope separation of U-233 from U-235 based on differences in stability of oxide and carbide borates [GA-3088] 04 p0590 N71-14377

Conference on gas cooled high temperature reactors [CONF-700401] 05 p0731 N71-15372

Summary report on HFOR fuel cycle development [ORNL-TM-3204] 07 p1863 N71-17362

Fuel reprocessing and head-end treatment of experimental small scale RTOR fuel elements [GAMD-9266-PT-2] 08 p1257 N71-16293

High temperature gas cooled reactor, gas cooled breeder reactor, and prestressed concrete pressure vessel developments [ORNL-4589] 08 p1258 N71-16348

High temperature gas cooled reactor design and development including cellulos and structural diffusion in graphite, reprocessing cycles, and fission product transport coding [GA-10288] 09 p1419 N71-19957

Fuel, prestressed concrete reactor vessel, and helium circulator developments of high temperature gas cooled reactor systems 10 p1084 N71-21248

Thermodynamic data for carbonaceous materials used in high temperature reactor technology [GAMD-9335] 12 p1961 N71-23141

Nucleus transport models for chelophysical fuel particle calculation in high temperature reactors [JUL-683-PA] 13 p2128 N71-24473

High temperature nuclear reactor fuel fission product monitoring using wire precipitation systems as radiation counters 13 p2118 N71-24901

Radiation effects on fission product and plutonium migration in mixed PuO₂ UO₂ reactor fuel recycling, reactor physics, and control rod deformation measurement in lattice test reactors [BNWL-1522-1] 14 p2292 N71-25755

High temperature nuclear reactors [NP-18602] 14 p2386 N71-26341

Models of neutron slowing down calculations in thermal and fast reactors [EURFNR-664] 14 p2307 N71-26396

Emission spectroscopy for identification of high temperature reactor fuel element spheres at 40 atmospheres of helium [JUL-671-RW] 15 p2442 N71-26834

Radiation embrittlement of age hardening heat resistant steels following high temperature reactor irradiation [AEC-TR-7192] 15 p2419 N71-26907

Measurement of thorium Doppler coefficient on lattices 1 and 2 of HTL-TR [GAMD-10231] 15 p2444 N71-26994

High temperature, gas cooled reactor control rod, control rod guide tube, and thermally released shutdown rod after 300 full power days of operation [GA-10196] 16 p2631 N71-28215

Fission gas and nonvolatile fission product release measuring device based on thermodynamics for high temperature nuclear reactors [JUL-70-7R] 18 p2960 N71-30862

Design and development concept of high temperature, gas-cooled reactor (RTOR) [GA-10399] 19 p3139 N71-32284

Neutron radiation effects on boronated and hafnated graphite, nuclear fuel element reprocessing, and high temperature gas cooled reactor development [GA-10501] 22 p3623 N71-35838

Environmental tests of boron and remanent boron and wiring equipment for high temperature reactors and fast neutron effects on ThC₂-UC₂ coated particles and graphite 22 p3625 N71-35831

Irradiation experiment for testing spherical fuel elements for high temperature reactors [JUL-701-RW] 23 p3793 N71-37956

Temperature dependence measurement of k_{∞} infinity for [U-233]O₂-ThO₂ RTOR lattice for control system design and safety analysis [BNWL-1561] 23 p3796 N71-37975

Derivation of corrections to k_{∞} infinity in two group approximation using high temperature lattice test reactor [BNWL-1560] 25 p3817 N71-37224

Reactor physics characteristics of high temperature gas cooled reactor [AEEW-M-983] 24 p3956 N71-38219

Temperature dependence measurement of k_{∞} infinity for [U-233]O₂-ThO₂ lattices for design and safety analysis of advanced high temperature gas cooled reactors [BNWL-SA-3756] 24 p3963 N71-38270

Radiation distribution in high temperature uranium-plasma reactors [DLR-FB-70-18] 24 p3987 N71-38452

HIGH TEMPERATURE PLASMAS

Neutron yields and energy spectra for hot deuterium-tritium plasmas [IPP-1107] 08 p1271 N71-18108

HIGH TEMPERATURE PLASMAS

Rod plasma injector for creating highly focused stream of hot plasma [AEC-TR-7077-4] 06 p0926 N71-14843

- Computerized simulation of high temperature plasmas [UCR-34-P-128-16] 07 p1083 N71-17050
Various aspects of analytical and diagnostic research in high temperature plasma [AD-717723] 11 p1811 N71-22246
Nonlocal reflection in warm plasma in presence of electron beam [AD-717659] 11 p1811 N71-22371
Gas and water cooled probes for high temperature gas and dense plasma and flow measurements 11 p1842 N71-22604
Thermal conductivity, viscosity, and collision integrals for He-N₂, Ar-N₂, and Xe-N₂ plasmas at 1 atm between 3000 and 35,000 K 11 p1814 N71-23082
Equilibrium compositions, thermodynamic properties, and partition functions for Ar-O₂ plasmas between 0.01 and 10 atm, and between 3000 and 35,000 K 11 p1814 N71-23083
Spatial nonuniformity effects on high temperature plasma breakdown over X band waveguide aperture including continuous wave and pulsed breakdown in air and nitrogen [AD-718412] 12 p1981 N71-23965
High temperature plasma inside discharge produced by planar HF power passing through helium [NLL-34-20301-5532.4F] 12 p1982 N71-24101
Experimental design using single ultrashort pulses for triggering Kerr cells and producing laser radiation to heat lithium deuteride targets for high temperature plasma generation [NASA-TT-F-13662] 13 p2088 N71-24641
High energy shock tube production of very strong, ionizing shock waves in high temperature plasmas [AD-720838] 14 p2321 N71-25906
Plasma heating by shock waves, measuring methods in hot plasmas, MHD generators, relativistic plasmas, surface physics, plasma production by laser beam, and related engineering projects [NP-16496] 14 p2322 N71-26171
Collisional ionization rates for lithium and beryllium-like ions deduced from time history of spectral lines emitted by these ions in hot plasmas [NASA-CR-119018] 16 p2648 N71-28637
Using particle conservation equations for fast hydrogen atoms, slow hydrogen molecules, and charged particles for calculating fast atomic hydrogen flux produced by charge exchange in high temperature plasma [JAERI-MEMO-4243] 21 p3494 N71-34887
Interaction of plane p-polarized electromagnetic wave obliquely incident on hot plasma half space and plasma slab 22 p3655 N71-36669
Longitudinal nonlinear oscillations of hot electron plasma near external magnetic field investigated by perturbation method [UARAE-88] 23 p3824 N71-37278
Plasma production by laser radiation at very high temperatures [CONF-710607-46] 23 p3826 N71-37290
Stability of shock produced high temperature plasma in 2-pinch experiment [CONF-710607-14] 23 p3830 N71-37317
Plasma parameters measured of high temperature plasma under current heating in high-shear stellarator [CN-28/H-11] 24 p3987 N71-38450
Evaluation of hot ion accumulation from injecting neutral hydrogen into target plasmas [CONF-710607-92] 24 p3992 N71-38480
HIGH TEMPERATURE PROPELLANTS
Determining distribution of fission products in fuel particle coatings by sputtering technique using ion beams [SGAE-PH-96/1970] 21 p3458 N71-34615
HIGH TEMPERATURE RESEARCH
Thesaurus for high temperature research 01 p0132 N71-10038
Determining mechanical properties and air-oxidation behavior of chromium-base compositions at temperatures up to 2400 F [NASA-CR-72731] 01 p0065 N71-10047
Heat resistant coatings to protect against high temperature oxidation [AD-71173] 01 p0072 N71-10632
Electrical conductivity of Kazakhstan rocks at high temperatures [NASA-TT-F-13213] 02 p0213 N71-11684
Investigating thermal decomposition of high temperature resistant polymers by isothermal and thermogravimetric analysis [AD-711400] 02 p0249 N71-12177
High temperature research of nuclear fuels [BMF-1884] 02 p0266 N71-12188
Experimental thermochemistry at high temperatures [SC-T-70-4028] 03 p0333 N71-12374
Design of high temperature and pressure tensile tester [UCRL-TRANS-10472] 05 p0688 N71-15511
Gas cooled high temperature thermocouple [NASA-CASE-XLE-09475-1] 05 p0784 N71-15568
Characteristics of high temperature materials and laser substances [NBS-TN-565] 06 p0936 N71-16597

- High temperature liquid metal technology - annotated bibliography [BNL-59258] 07 p1042 N71-17245
Flowmeter using noise-analysis techniques for large liquid metal systems at temperatures of 1200 F [AI-AEC-12981] 07 p1028 N71-17267
Physical and chemical properties of metallic elements and inorganic compounds at high temperatures [NYO-4176-3] 07 p1130 N71-17636
High temperature kinetics and crystal structures of rare earth element bromide, carbon, and halogen systems [COO-716-46] 07 p1094 N71-17825
Oxidation kinetics of niobium and niobium alloys at high temperatures [AD-715007] 07 p1045 N71-17910
Conference on diagnosis of high temperature plasmas including interferometry and spectroscopic methods [LA-4520-TR] 08 p1272 N71-18527
Development of high temperature calorimetry techniques for solid ionic systems [AD-715719] 08 p1221 N71-18530
Research in ceramic materials including mechanical properties, crystallography, and deformation [NASA-CR-116809] 08 p1222 N71-18654
Matrix analysis of double disc and heat shield methods for diffusivity measurement at very high temperatures [AD-715908] 08 p1303 N71-18710
Asymptotic solution of differential equations for rod oscillations at high temperatures [SC-T-70-4042] 08 p1302 N71-19327
Superconductivity and volume dependence of transition temperature of transition metals and well-ordered A15 compounds [AD-716029] 09 p1452 N71-19695
Physical chemistry research and development in high temperature systems [ORO-2907-73] 09 p1343 N71-19933
Thermal stability of SO₂F₂ at high temperatures [AD-716627] 09 p1482 N71-19944
High temperature performance of platinum resistance thermometers [NRC-TT-1428] 09 p1389 N71-20260
Kinetics of reaction between graphite and carbon dioxide in flow tubes at atmospheric pressure and high temperatures [NLL-RTS-5838] 10 p1514 N71-21331
Creep mechanisms and structure dependence of high temperature deformation of metals and alloys [SU-326-P-17-X-1] 10 p1584 N71-21616
Conference on high temperature turbines detailing effect of film cooling on blade profile loss [NASA-TM-X-67123] 11 p1821 N71-22699
Studying vaporization of indium-gallium oxide, and gallium-aluminum oxide by Knudsen effusion mass spectrometry [NASA-TM-D-6318] 12 p1868 N71-23111
Designating antifriction materials for friction and wear points at elevated temperatures [AD-72067] 14 p2278 N71-25894
Fatigue testing apparatus with light shield and infrared reflector for high temperature evaluation of loaded steel samples [NASA-CASE-XLA-01782] 14 p2255 N71-26136
Shock tube investigation of chemical kinetics of NO-CO-Ar mixtures at temperatures from 3000 to 4500 K 14 p2214 N71-26311
Irradiation of boron carbide pellets and powders in Hanford thermal production reactors at 500 to 1200 F [WHAN-FR-24] 15 p2443 N71-26927
Broad spectrum of materials chemistry under extreme conditions, including ionizing radiation, high vacuum, high pressure, and high temperature [AD-720289] 16 p2557 N71-28437
Determination of steady-state mass-transfer conditions in nickel alloys and prediction of nickel transport in flowing sodium at high temperatures [ORNL-4575-VOL-1] 16 p2615 N71-29016
Characteristics of simultaneous electronics and ionic conductivity in solids at 700 to 800 C [NLL-LTI-746-617-F022.401] 16 p2669 N71-29158
Measurement of extinction parameter of tungsten-hydrogen aerosols as function of wavelength at high pressures and temperatures [NASA-CR-1864] 18 p3023 N71-30494
Development of theory to explain behavior of ammonium chloride near first order transition at high temperatures 18 p2995 N71-31099
Thermophysical properties including electrical resistivity data for Ta-10W alloy to 2600 K measured by direct heating methods [AD-72492] 20 p3363 N71-32949
Complete equation of state for metals in both solid and liquid/dense vapor phases, from ambient conditions to high pressures and temperatures 20 p3334 N71-33736
Measurement of total hemispherical emittance for chromel and alumel thermocouple wires in inert atmosphere at high temperatures [NASA-TM-X-2359] 21 p3429 N71-34404

- Stress analysis of aluminum and copper at high temperatures using theory of thermally activated deformation of metals 21 p1439 N71-34470
High temperature steel and alloy research, including physical, chemical, and mechanical properties of various steels [AD-726577] 22 p3595 N71-35640
Mechanical properties of steels and alloys in high temperature research and structural composition and hot working methods of various steels [AD-726578] 22 p3595 N71-35641
Structure-property relationships in liquid ceramets heated to temperatures as high as 3000 C [AD-726401] 22 p3603 N71-35638
Research organizations, investigators, and programs in high temperature research from eleven NATO countries and Spain [AGARD-R-585-71] 22 p3699 N71-36382
Properties of high temperature compounds, physics of gas dynamics, heat resistant materials, and heat conversion by power plants [UPRS-54182] 23 p3868 N71-37570
HIGH TEMPERATURE TESTS
Mach 1 burner rig tests at 2100 F for oxidation resistance evaluation of NiCrAl and FeCrAl claddings on TD-NiCr [NASA-TM-X-52916] 02 p0240 N71-11424
Thermal conductivity of reactor materials up to 1800 deg C - graphites, carbons, boron carbide, and boron carbide compounds [CEA-CONF-1563] 04 p0620 N71-13877
Stress-rupture behavior of types 304 and 316 stainless steel cladding in high temperature static oxidation [AI-AEC-12976] 06 p0670 N71-15939
Constant heating rate thermogravimetry of carbon/graphite cloth reinforced aromatic/heterocyclic resins to 1400 C [AD-714084] 06 p0880 N71-16486
Bis/epoxy alkyl/carborane adhesives with high temperature stability for steel-on-steel bonding [NASA-CR-114837] 06 p0883 N71-16779
Design considerations of reactor containment spray systems, also protective coating for these containment systems [ORNL-TM-2412-PT-5] 08 p1220 N71-18306
Hydraulic performance and cavitation characteristics of electromagnetic helical induction pump operating with potassium at 1500 F and with lithium at 2200 F [ORNL-TM-2995] 08 p1205 N71-18324
Yield surfaces for aluminum 1100 at elevated temperatures 08 p1299 N71-19143
Engineering method of evaluating supporting strength of structural elements from glass reinforced plastic operating in conditions of temporary unsteady heating [AD-716515] 09 p1404 N71-19809
Oxidation kinetics data used for calculation of oxygen diffusion coefficient in alpha titanium at temperatures from 750 to 900 C [NASA-TT-F-13504] 09 p1401 N71-20306
Oxidation of cobalt-nickel-aluminum alloys at 1351 K to 1429 K [BM-R-7496] 09 p1401 N71-20411
Refractory alloy creep test data for molybdenum base alloy TZM, pure tantalum, and tantalum base alloys T-111 and ASTAR-811C at elevated temperatures in ultrahigh vacuum [NASA-CR-72619] 09 p1402 N71-20438
Heat content and specific heat of six rock types at temperatures to 1000 C [BMRI-7503] 10 p1545 N71-20613
High temperature crack initiation and propagation in aluminum and aluminum alloys with emphasis on grain size effects 10 p1576 N71-21013
High temperature tensile tests on uranium alloys containing carbon, iron, silicon, and aluminum [NILCO-1060] 10 p1577 N71-21053
Microstructure and magnetic properties of internally oxidized ferromagnetic alloys for application to magnetic domain theories and high temperature tests [AD-71210] 10 p1579 N71-21308
Mechanical testing of metals at high temperatures and short term loading with determination of temperature influence and deformation rates [AD-716937] 10 p1580 N71-21391
Test facility development for noble metal thermocouple research program 1000 to 2000 C [NASA-CR-72861] 11 p1764 N71-22678
High temperature uniaxial tensile tests performed on aluminum-graphite composites [AD-718153] 12 p1942 N71-23402
High temperature plasticity failure of vacuum-treated titanium [NASA-TT-F-13563] 12 p1937 N71-23483
Creep properties of iron doped polycrystalline magnesium oxide and iron and chromium doped polycrystalline aluminum oxide between 1300 and 1500 C [COO-1591-3] 12 p1945 N71-23951

SUBJECT INDEX

Preparation of Gd2O3 poisoned UO2 pellets under high temperature conditions
[EUR-4551] 13 p2110 N71-24472

Analysis of corrosion in high temperature lithium base metal with niobium-zirconium and tantalum as base metal
[EUR-4296-E] 13 p2092 N71-24734

Dynamic deformation and fracture strength of tungsten carbide-cobalt alloys at elevated temperatures
13 p2096 N71-25114

Influence of titanium, zirconium, and hafnium addition on resistance of modified Hastelloy N to irradiation damage at high temperatures
[JRNLT-76-3064] 14 p2267 N71-25640

High temperature chromitization of ferrochromic alloys
[TT-70-58195] 14 p2270 N71-25677

High temperature mercury corrosion resistance of tantalum, tantalum alloy, and niobium alloy sheets after bonding stress
[NASA-CR-1811] 15 p2420 N71-26047

Interfacial reactions of boron fibers and carbon fibers in chromium matrices at elevated temperatures
[AEL/MBT-83] 15 p2432 N71-27620

Oxidation resistance and high temperature tests of titanium, tungsten, hafnium, and tantalum matrix composites with iridium in oxygen, fluorine, and hydrogen atmospheres for liquid propellant engines
[NASA-CR-119019] 16 p2617 N71-28501

Evaluation of high gas velocity and static oxidation behavior of fused-salt-aluminized IN 100 between 800 and 1149 C
[NASA-TN-D-6400] 17 p2764 N71-29713

Preliminary sector tests at 920 F of three afterburner concepts proposed for inlet temperatures of 1300 F and comparison of results with conventional V-groove flame holder
[NASA-TN-D-6437] 19 p3192 N71-32191

Thermodynamics and operation of differential calorimeters using intermittent heating
20 p3362 N71-32828

Differential thermal analysis and high temperature calorimetry dynamics
20 p3362 N71-32830

Development of uranium-plutonium nitride fuels for LMFBR applications, studies of high temperature fuels for advanced fast reactors, and studies of creep of reactor fuel materials
[BM-1898] 20 p3309 N71-33946

High temperature cycling tests of high performance adhesives for aerospace applications
[NASA-CR-121632] 21 p3442 N71-34495

Time determinations for electric pulse transmission through rock samples under high pressure and temperature
[NASA-TT-F-13796] 22 p3573 N71-35445

High temperature, low cycle fatigue tests of titanium in inert argon atmosphere
[NASA-CR-1936] 22 p3594 N71-35592

Study-state creep rates in refractory metals and alloys-tungsten, titanium, and niobium
[AD-726440] 22 p3596 N71-35604

Optical transmittance of fused silica at elevated temperatures during high energy electron bombardment
[NASA-TN-D-67930] 22 p3598 N71-35620

High temperature measurements of thermal diffusivity of graphite
[AD-726562] 22 p3603 N71-35660

Arc jets tests of thorium dispersed nickel base alloys and cobalt base alloys for space shuttle metallic thermal protection system
[NASA-TN-D-62092] 24 p3934 N71-38068

Corrosion tests of chromium and chromium-nickel alloys in molten lead at 575, 650, and 750 C for 3250 hr
[JUL-694-RW] 24 p3938 N71-38078

High temperature tests of creep in structural graphite
[AD-727808] 24 p3946 N71-38147

Simulated JP-4 jet fuel fire tests of high temperature wire process sealant and insulating plastics and rubbers
[FRA-NA-71-22] 24 p3946 N71-38149

VACUUM

Very high vacuum terrestrial mineral beneficiation methods transferred to vacuum ambient of lunar surface
[NASA-CR-111399] 02 p2030 N71-11569

Experimental studies on discharge propagation of exploding wires in high vacuum and determination of developing plasma properties
[NASA-TT-F-13546] 02 p2082 N71-12045

Ultraviolet radiation and high vacuum space radiation simulation for bioluminescent bacteria
[NASA-FB-W-70-48] 06 p6799 N71-15724

Literature survey and experimental evaluation of mobile properties in high vacuum environment
[NASA-CR-111829] 06 p6881 N71-16396

Design, performance, and evaluation of twin-lens space nuclear electrical systems
[NASA-CR-1719] 09 p3194 N71-20394

Spary resin sealing device for electrochemical cells in high vacuum environments
[NASA-CASE-XGS-02630] 11 p1678 N71-22974

Device for high vacuum film deposition with electromagnetic field steering
[NASA-CASE-NFO-10331] 14 p2231 N71-26701

Utilizing vacuum insulation for devices with magnetic cores and windings
[NASA-CASE-LEW-10530-1] 18 p2898 N71-31125

Biocatalytic strength of T-111 tantalum alloy tubing in high temperature, high vacuum environment
[NASA-CR-72946] 19 p3114 N71-32162

Piston manometer used as absolute standard for calibrating and intercomparing vacuum gauges in 10 to 500 micrometer range
[NASA-TN-X-67889] 19 p3101 N71-32374

Feasibility of using elastic deformation to predict heat transfer rates across joined smooth-metal surfaces under high vacuum conditions and light loads
[NASA-TN-X-2383] 22 p3604 N71-36361

HIGH VACUUM ORBITAL SIMULATOR

Space environmental work simulator with portions of space suit mounted to vacuum chamber wall
[NASA-CASE-XMF-07488] 08 p1176 N71-18773

HIGH VOLTAGES

High voltage breakdown and failure analysis of electronic equipment
[AD-711594] 02 p0191 N71-11544

High voltage electron microscopy for ceramic substrates and biological radiation dosimetry studies
[UCRL-19028] 03 p0581 N71-13216

Computer program predictions of stacking fault images at high voltages
[PB-192188] 03 p0445 N71-13274

High voltage pulse generator for testing flash and ignition limits of nonmetallic materials in controlled atmospheres
[NASA-CASE-MSC-12178-1] 04 p0509 N71-13518

Ion beam slow pulsing injector system for ZMV Van de Graaff
[AWRE-O-2970] 04 p0594 N71-14634

Regulating high voltage in direct current generators by using auxiliary dynamo
[PUBL-23] 05 p0656 N71-15518

Potting compounds and techniques for planar and high voltage power supply
06 p0825 N71-16635

Designing corona free, high voltage, toroidal transformers for spacecraft power supplies
06 p0823 N71-16641

Interactions between simulated ionospheric plasma and electric fields of high voltage spacecraft systems
06 p0828 N71-16646

High voltage transistor circuit
[NASA-CASE-XNP-06937] 09 p1350 N71-19516

High voltage divider system for attenuating high voltages to convenient levels suitable for introduction to measuring circuits
[NASA-CASE-XLE-02008] 10 p1535 N71-21583

Details of phase space acceptance determined by trajectory calculations of high voltage Van de Graaff machine
[ANU-P506] 13 p2062 N71-25375

Trigger pulse energy, electrode dimension, gas pressure, and propulsive voltage effects on low inductance spark gaps for high voltages in air
[BMFW-PBK-70-17] 15 p2455 N71-27633

Coordinating fuses for protection of solid state device without large safety factor and high voltage dc circuits
[MATT-715] 17 p2227 N71-29351

Radiation processes and instrument requirements for temporally and spatially resolved study of high voltage spark discharge
19 p3063 N71-32151

Bevatron pole-face windings power system with high voltage transistor actuator
[UCRL-20191] 20 p3247 N71-33889

High-voltage isolator design for injecting hydrogen bubbles into liquid metal feed lines to interrupt electrical continuity
[NASA-CASE-NPO-11075] 21 p3402 N71-34008

Development and characteristics of high voltage multichannel pulse generator with six outputs
[CERN-TRANS-71-6] 21 p3404 N71-34220

Protection from charged particles using high voltage electric fields
23 p3855 N71-37475

Developing suitable solid state power controllers for space vehicles electrical power systems
[NASA-CR-119961] 24 p3898 N71-37781

Screening and evaluation of improved Twin Cities public transit systems using highway, rail, and underground vehicles
[AMV-R-15-1073] 07 p1138 N71-18107

Mass transport systems for airport access
08 p1308 N71-18952

Visual factors in air and surface transportation systems
[PB-150014] 09 p1487 N71-19397

Economic analysis of intercity short-haul business passenger travel
[NASA-TN-X-2228] 09 p1488 N71-20114

Thickness measurement method for water film formed on highway and determination of conditions for expulsion of film by action of tire
[NASA-TT-F-13603] 12 p1904 N71-24162

HILL LUNAR THEORY

Aviation and surface transportation safety for 1970 with related accident investigations and recommendations
[AR-4] 13 p2191 N71-24925

Applications of computer technology to state highway systems - conference
14 p2225 N71-26551

Digital computer program for simulating vehicle flow on freeways
14 p2225 N71-26552

Integrated system of computer programs for aiding engineers in designing highways
14 p2225 N71-26556

Status report of highway preconstruction projects in Kentucky
14 p2226 N71-26559

Designing visibility quality in highways by computer graphics
14 p2226 N71-26560

Perspective highway viewing program for designing safe roads
14 p2226 N71-26561

Using computer graphics for producing computer program forms, and for highway perspective
14 p2226 N71-26562

Evaluating requirements for data plotting equipment for Florida highway department
14 p2226 N71-26583

Noise reduction laws for air, rail, and highway transportation including legal liability in US
[OST-ONA-71-1-VOL-7] 20 p3212 N71-33938

Development of methodology for evaluating potential benefits of alternative transportation proposals for regions - Vol. 1
[RM-6324-DOT-VOL-1] 21 p3407 N71-34245

Development of methodology for evaluating transportation services with emphasis on effectiveness of systems - Vol. 2
[RM-6324-DOT-VOL-2] 21 p3408 N71-34246

Development of methodology for evaluating alternative proposed changes to mix of transportation modes in northeast corridor of US - Vol. 3
[RM-6324-DOT-VOL-3] 21 p3408 N71-34247

Development and characteristics of sonic and ultrasonic power devices for inspection of highway accelerating projects - Vol. 3
[PB-199111] 21 p3434 N71-34436

Development and characteristics of sonic and ultrasonic power equipment used in highway engineering - Vol. 1
[PB-199110] 21 p3434 N71-34437

Motor vehicle noise generation, traffic noise prediction, and highway noise propagation - Vol. 4
[OST-ONA-71-1-VOL-4] 24 p4035 N71-38787

REACHING

U AIR PIRACY

HILBERT SPACE

NT BANACH SPACE

Path from operational logic to conventional quantum theory in complex Hilbert space
01 p0077 N71-10956

Linear dynamic systems in Hilbert space
05 p0712 N71-14513

General properties of linear dynamic systems in Hilbert space
05 p0712 N71-14515

Calculating tables of inverses and determinants of finite segments of Hilbert matrices using variable precision rational arithmetic
08 p1227 N71-19188

Structure theorem for IC sub of contraction semigroups on Hilbert space
09 p1410 N71-20274

Stochastic models for defining white noise with time and space parameters
[AD-722091] 16 p2623 N71-28780

Quantum mechanical entropy in tensor product of Hilbert spaces
20 p3364 N71-33381

Design of computational algorithms for optical control by Hilbert space methods, and involving cost function
[NASA-TN-D-6360] 21 p3449 N71-34551

Quasi-Newton minimization methods extended to infinite dimensional Hilbert space with applications to optimal control problems
[NASA-CR-111975] 22 p3805 N71-35676

Complex analytical structures of Hilbert space variations
24 p3949 N71-38170

Weakly convergent operators in incomplete tensor product of Hilbert spaces
[ITF-71-7-E] 24 p3949 N71-38174

HILBERT TRANSFORMATION

Development and characteristics of bivariateform device for comparison of Pouscatt method with Hilbert transform method during observation of phase defects
[NASA-TT-F-14011] 24 p3965 N71-38287

HILL CURVES

U HILL METHOD

HILL LUNAR THEORY

Transformation of differential equations in lunar theory
[NASA-TN-D-7034] 06 p0949 N71-10863

HILL METHOD

HILL METHOD

Hill stress rate in continuum mechanics of polycrystals including application to crystal deforming via quasi-static single slip

[AD-717326] 11 p1816 N71-22172

HILLER MILITARY AIRCRAFT

U MILITARY AIRCRAFT

HILSCH TUBES

Models for using vortices for fluid dynamic containment of gaseous core nuclear reactor, bibliography

[NASA-CR-1772] 19 p3079 N71-32276

HINDRANCE

U CONSTRAINTS

HINGE MOMENTS

U TORQUE

HINGED ROTOR BLADES

U ROTARY WINGS

HINGLESS ROTORS

U RIGID ROTORS

HINGES

NT FLAPPING HINGES

HIPPOCAMPUS

Development of theory of neuromine tests containing recurrent inhibition and analysis of hippocampus model

[AD-720815] 14 p2207 N71-25840

Computer modeling of hippocampus and studies involving pattern recognition and information compression

[AD-720816] 14 p2209 N71-25844

HISSE

Hiss, auroral electrojets, and Arctic region magnetic variations

04 p0521 N71-13780

Dawn chorus and auroral hiss emission in upper ionosphere and magnetosphere

07 p1017 N71-17143

Comparison of VLF auroral hiss with precipitating low energy electrons studied with simultaneous OGO-4 data to determine hiss origin

[NASA-TM-X-65663] 19 p3094 N71-32413

Auroral zone VLF hiss and low energy particle observations with Injun 5 satellite

[NASA-CR-121418] 20 p3266 N71-33592

HISTIDINE

Effect of radiation sensitive mutations and radiation of recombination in partially diploid derivatives of Escherichia coli

[ORO-4024-1] 10 p1497 N71-20728

Chemical reactions for producing histidine esters by means of acyl migration from one amino acid to another

[NASA-TT-F-13645] 14 p2212 N71-25727

Conversion of histidine with carboxyl group to peptide bond by synthesizing peptide from acetylated amino acids to histidine

[NASA-TT-F-13672] 14 p2212 N71-25728

HISTOGRAMS

Histogram method of density estimation

[PB-192460] 04 p0537 N71-13815

Plotter routines for IBM 1800 computers permitting graphic presentation of data with minimum programming effort

[NASA-TT-F-45708] 23 p3728 N71-36576

HISTOLOGY

Histological aspects and ultrastructure of intoxication in rats by pure oxygen at low pressure

02 p0165 N71-11826

Morphological investigation of neural structures of frontal cushion of dolphins

11 p1682 N71-22214

Histological examination of skin layers and scales of shark and effects on locomotion

11 p1682 N71-22215

Histopathology and clinical study of chronic X ray dermatitis and cancer of fingers

[NASA-TT-F-13664] 16 p2548 N71-29200

HISTORIES

NT CASE HISTORIES

Discussing origin, course of development, and results of Vanguard Project

[NASA-SP-4282] 07 p1122 N71-18019

Weak nuclear interactions and history of elementary particle discoveries

[NYO-1932/2-186] 10 p1611 N71-20707

Historical development of meteorology - Vol. I

[TT-69-55106] 11 p1789 N71-22263

Historical review of Soviet exploration in Arctic regions

11 p1848 N71-22819

Historical review of Soviet refusal to permit L. Bedford Pym of British Royal Navy conduct polar exploration to search for John Franklin expedition

11 p1755 N71-22829

History of numerical weather forecasting in USSR from meteorological parameters

[AD-718481] 12 p1955 N71-23837

Developmental history of adiabatic invariance including contributors to radiation energy transfer and celestial mechanics concepts

[NASA-TM-X-65498] 12 p1968 N71-24056

Tabulation and maps of major hurricanes affecting United States during period 1873 to 1964

[ESSA-TM-WBTM-SR-42] 18 p2953 N71-31028

Statistical mechanics for wall shear turbulence in Couette flow based on Brownian motion and comparison with stochastic theory based on Navier-Stokes equation

[NASA-SP-4014] 19 p3034 N71-32246

Development history and application of free piston engine

19 p3175 N71-32621

History of manned space flight technology

20 p3350 N71-33849

RIVOS (SIMULATOR)

U HIGH VACUUM ORBITAL SIMULATOR

HL-10 REENTRY VEHICLE

Air launch characteristics of HL-10 manned lifting reentry vehicle

[NASA-TM-X-1468] 05 p0770 N71-15002

HL-10 and M-2F2 lifting body flight tests

[NASA-TM-X-46712] 08 p1143 N71-18428

Lift and drag characteristics of HL-10 lifting body during subsonic gliding flight

[NASA-TM-D-6263] 06 p1142 N71-18867

Aerodynamic characteristics of HL-10 reentry vehicle model at subsonic and supersonic speeds

[NASA-TM-D-4818] 06 p1295 N71-19270

Aerodynamic characteristics of HL-10 lifting body and aerodynamic loads on center fin and control surfaces at subsonic, transonic, and supersonic speeds

[NASA-TM-X-2419] 24 p4022 N71-38700

HODOGRAPHS

Hodographs applied to calculation of compressible flow on turbomachine blades and use of visualization terminal display

[ONERA-MT-179] 19 p3076 N71-31706

HODOSCOPES

Multiview proportional chamber using tungsten wires for high resolution beam hodoscope

[LAL-1246] 23 p3643 N71-35973

HOHLRAUMS

Design and construction of Hohlraum spectral analyzer to aid in research of air pollutants

[NASA-CR-131700] 24 p3920 N71-37957

HOHMANN TRAJECTORIES

U ELLIPTICAL ORBITS

U TRANSFER ORBITS

HOHMANN TRANSFER ORBITS

U ELLIPTICAL ORBITS

U TRANSFER ORBITS

HOLDERS

NT FLAME HOLDERS

Film and glass plate-holder for NAFA-34/25 camera used in satellite tracking

[NASA-TT-F-13552] 03 p0375 N71-12661

Quick disconnect latch and handle combination for mounting articles on walls or supporting bases in spacecraft under zero gravity conditions

[NASA-CASE-MFS-11132] 07 p1055 N71-17649

Holder for high frequency crystal resonators

[NASA-CASE-XNP-03637] 10 p1565 N71-21311

Fabrication techniques for split fiber glass holder

[BDX-613-198] 11 p1769 N71-22532

HOLE DISTRIBUTION

Stress induced pore migration in nuclear reactor fuel elements

[WAFD-TM-963] 16 p2634 N71-28738

HOLE DISTRIBUTION (MECHANICS)

Stress concentration around holes and fissures including stress-strain diagrams - bibliography

[NASA-TT-F-407] 01 p0128 N71-10121

Notch sensitivity factor for fatigue of elements with transverse holes

[TAE-114] 11 p1838 N71-22535

Stress analysis of unidirectionally reinforced, composite plates with holes

13 p2178 N71-24646

FORTRAN program for stresses in nonhomogeneous elastic plate with circular hole

13 p2178 N71-24647

HOLE MOBILITY

Electron hole reaction kinetics in radiation induced free radical destruction

[UCRL-19849] 03 p0423 N71-12739

Hole growth in thin plates perforated by hypervelocity pellets

[AD-712071] 03 p0460 N71-12956

Electron interaction ferromagnetics in transition metal disulfide systems

[NUB-2039] 07 p1068 N71-17516

Electromigration and void kinetics in silver

09 p1397 N71-19352

Fast neutron effects on semiconductor electronic transport properties and minority carrier and hole drift mobilities in germanium

[ORO-3651-6] 09 p1426 N71-19523

Activation energy and hole mobility in aluminum determined by nuclear magnetic relaxation including temperature effects

[COD-1190-801] 15 p2477 N71-27580

Dislocation mobility in doped silicon single crystals, analyzed by amplitude dependent internal friction

17 p2827 N71-30171

Microscopic description of multiple pairing and particle-hole fields in particle vibration coupling of Pb-209

[LA-DC-11648] 20 p3322 N71-33795

Electron and hole drift mobilities in photoconducting amorphous selenium

[NASA-TN-D-6500] 21 p3499 N71-34976

Proton particle-hole pair states of closed shell nuclei studied by $[\text{He-3}, d]$ reaction and thick solid state detectors

22 p3649 N71-34023

HOLES [ELECTRON DEFICIENCIES]

Nonequilibrium plasma production, sausage mode instability, and oscillation feedback control in electron hole plasmas

[AD-710478] 01 p0071 N71-18041

Excitation of Si-28 particle-hole states by inelastic electron scattering at high momentum transfer

[AD-712083] 02 p0276 N71-12941

Electron hole recombination time and diffusion length of metals, and carrier density role at ohmic metal-semiconductor boundaries

[ORO-3651-7] 09 p1455 N71-20580

Intrinsic carrier concentration and mass action constant scattering mechanism of heavy holes in indium antimonide in p-type and n-type samples

10 p1625 N71-21811

Proton hole states excited in thin foils by monoenergetic gamma-quanta from $\text{Li-7}/\text{p, gamma}/\text{Be-8}$ reaction

[LUNP-7013] 19 p3154 N71-32323

Wide band hot-carrier diode gate for application to electron hole plasmas

[AD-713602] 20 p3241 N71-33131

Plane wave approximation and shell model for particle-hole states in zirconium

24 p3983 N71-38428

HOLLAND

U NETHERLANDS

HOLLOW CATHODES

Simultaneous computer analysis of first positive band system of N_2 in near infrared excited by hollow cathode discharge also analysis of existing energy level data

13 p2135 N71-25242

Cathode insulator modifications of radiation cooled MPD arc thruster tested in power range of 9.8 to 44.4 kW using ammonia as principal propellant

[NASA-CR-72891] 14 p2331 N71-25770

Dynamic model for partial pressure variations of electrons, ions, and neutrals in active zone of hollow cathode arc discharge

[NP-18708] 17 p2813 N71-36240

Spectral line drift measurements on alkaline earth metals in hollow cathode discharge by interferometer

[AD-724160] 19 p3166 N71-33702

Internal flow conditions in hollow gas cathode

[TP-959] 20 p3330 N71-33475

Diagrams of volt-ampere characteristics of hollow cathode discharge device with concentric spherical electrodes

[RFT-TRANS-68] 21 p3404 N71-34021

HOLMIUM

NT HOLMIUM ISOTOPES

Radioactive decay of Ho-168 and 169

[IS-T-364] 05 p0747 N71-15251

Time of flight spectrometric analysis of holmium scattering cross section for neutrons between 0.002 and 1.7 eV

[CEA-N-13138] 15 p2477 N71-27591

Production of far neutron-deficient iridium isotopes by bombarding holmium with He-22 and Ne-20 heavy ions

[JINR-PG-5617] 19 p3159 N71-33298

Magnetic properties of gadolinium, terbium, dysprosium, and holmium hydroxides at cryogenic temperatures

20 p3313 N71-33735

HOLMIUM ISOTOPES

Electron scattering cross section from aligned and nonaligned Ho-165

[AD-717615] 11 p1803 N71-22234

Ho-166 rotational bands, M1 radiative strength resonance in Cr-53 , Dynamometer research, photoelectron spectroscopy of high temperature vapors

[ANL-7739] 17 p2808 N71-30240

Structure of neutron deficient holmium and dysprosium nuclei investigated using Ge/Li detector and computer methods

[BMBW-FBK-70-30] 18 p2979 N71-30779

HOLOGRAPHY

Lasers, holography, optical communication, and information processing by analog optical computing

01 p0062 N71-10077

Holographic determination of translation and rotation using interference patterns of reflected light

[AD-710365] 01 p0062 N71-10078

Research progress on radiation effects of minor power sources on spacecraft, holography applications to stress analysis, composite antenna structures, and Apollo applications

01 p0128 N71-10082

Ultrasonic holographic and light diffraction techniques applied to coherent acoustic imaging during nondestructive tests

[AD-711065] 01 p0088 N71-10079

Holographic interferometry for study of transient media

[TP-851] 01 p0082 N71-10087

Laser fundamentals and experiments for high school use - textbook 02 p0238 N71-1428
 Nondestructive interferometric holography in wind tunnels including displacement and deformation of deflectors 02 p0201 N71-1510
 [ONERA-TP-852] 02 p0201 N71-1510
 Possibility of photomechanics techniques for stress analysis in three dimensions 02 p0303 N71-12085
 [AD-711526] 02 p0303 N71-12085
 Applications of lasers for ballistic research 02 p0259 N71-12118
 [T-35-G/2] 02 p0259 N71-12118
 Schlieren photography and differential interferometry for free flight tunnel holography 02 p0312 N71-12223
 [DRL-T-59/69] 02 p0312 N71-12223
 Investigating possibilities and limitations of applying holographic techniques to aerospace technology 03 p0377 N71-12776
 [NASA-SP-248] 03 p0377 N71-12776
 Investigating applications of holography to low density flow visualization, vibration mapping, particle sizing, and panel flutter 03 p0377 N71-12777
 Evaluating applications of holography to thermal distortion analysis of spacecraft 03 p0377 N71-12778
 Investigating nondestructive testing techniques by optical, acoustic, and microwave holography 03 p0377 N71-12779
 Applying holographic technology to hypervelocity wind tunnels, nondestructive testing, stress analysis, and particle size distribution 03 p0377 N71-12780
 Reviewing applications of holographic instrumentation to flow visualization, particle sizing, vibration analysis, and nondestructive testing 03 p0377 N71-12781
 Investigating holographic techniques for analysis of vibration and shock 03 p0378 N71-12782
 Applying holographic techniques to interferometric and schlieren systems for flow visualization at reentry simulation pressures 03 p0378 N71-12783
 Feasibility study for using holographic techniques for wind/turbine optical memory 03 p0378 N71-12784
 Demonstrating applicability of continuous wave and pulsed holography to vibrations in beams and plates 03 p0378 N71-12785
 Applying method of dual-exposure holographic interferometry to comparison of optical components and measurement of small phase deviations 03 p0378 N71-12786
 Feasibility studies of holographic techniques for measuring liquid rocket combustion processes 03 p0378 N71-12787
 Microwave holographic techniques for analyzing nondestructive test data for solid propellant grains 03 p0378 N71-12788
 Measuring linear and angular displacements using double exposure and real time holographic interferometry 03 p0379 N71-12789
 Real time and double exposure holographic techniques for nondestructive testing of printed circuit boards, honeycomb structures, metal welds, and deposits on optical surfaces 03 p0379 N71-12790
 Stabilizing fringe pattern in holographic system in presence of vibration and drift 03 p0379 N71-12793
 Investigating fluid heat transfer at anode of xenon compact-arc lamp using flash holography 03 p0379 N71-12794
 Investigating air flow in noisy wind tunnels using holographic flow visualization system 03 p0379 N71-12795
 Obtaining single beam far-field holograms of hypersensitivity and size particles using Q-switched ruby laser 03 p0379 N71-12796
 Applying holographic techniques to obtain ground truth data from earth resources and geodetic altimetry 03 p0380 N71-12798
 Measuring object motion by in-line Fraunhofer holographic techniques 03 p0380 N71-12799
 Differential interferometry and schlieren photography for hypersonic aerodynamic hologram analysis 03 p0380 N71-12805
 [N-T-49/69] 03 p0380 N71-12805
 Phase interpretation in stress-holography interferometry 03 p0381 N71-13164
 [AD-712609] 03 p0381 N71-13164
 Storage of high density information using holographic method 04 p0524 N71-13831
 Application of separate reference beam holographic interferometry for measurement of small phase variations in sub-fragments systems 04 p0525 N71-14071
 [NASA-CR-73494] 04 p0525 N71-14071
 Far field holography for determining bubble spectrum in cavity tunnel 04 p0525 N71-14271
 [TUCK-55907] 04 p0525 N71-14271
 Holographic control of neodymium laser glass production 04 p0525 N71-14327

Applications of holography to vibrations, transient response, and wave propagation 05 p0682 N71-14087
 [NASA-CR-1671] 05 p0682 N71-14087
 Investigating holographic techniques for high capacity read/write optical memory having no moving parts 05 p0696 N71-15136
 [NASA-CR-102973] 05 p0696 N71-15136
 Measuring small surface deformations using optical wavefront reconstruction 05 p0697 N71-15157
 [NBS-TN-05D-115] 05 p0697 N71-15157
 Holographic detection of bonding voids in laminates by observation of stress-induced reactions 05 p0697 N71-15352
 [AD-713545] 05 p0697 N71-15352
 Development of focused image holography with extended sources 05 p0698 N71-15351
 [NASA-CASE-ERC-10019] 05 p0698 N71-15351
 Hybrid holographic system using reference, transmitted, and reflected beams simultaneously 05 p0698 N71-15363
 [NASA-CASE-MFS-20074] 05 p0698 N71-15363
 Recording and reconstructing focused image holograms 05 p0698 N71-15367
 [NASA-CASE-ERC-10017] 05 p0698 N71-15367
 Prototype holocamera and playback system for laser surface holography experiment 06 p0668 N71-16574
 [NASA-CR-116146] 06 p0668 N71-16574
 Holographic interferometry: improved coherence of ruby lasers, and instrumentation techniques 07 p1039 N71-12771
 [NASA-CR-114274] 07 p1039 N71-12771
 Determining feasibility of using laser beam holography for detection and characterization of bond defects in composite material structures 07 p1039 N71-17757
 [NASA-CR-111836] 07 p1039 N71-17757
 Holography used to determine water droplet characteristics in engine test facility 08 p1201 N71-16488
 [AD-715916] 08 p1201 N71-16488
 Holographic interferometric methods applied to vibration, flutter, and transient analysis of thin metallic panels 08 p1210 N71-18982
 [NASA-CR-103053] 08 p1210 N71-18982
 Properties of holograms and applications of holography 08 p1211 N71-19224
 Electron microscopic and holographic methods for data condensing and retrieval, and microbiology 08 p1205 N71-19317
 [AD-716571] 08 p1205 N71-19317
 Reflection transmission full-view holograms 09 p1395 N71-19450
 Mirror movement analysis by holographic interferometry for application to spaceborne telescopes 09 p1396 N71-19633
 [NASA-TM-X-2227] 09 p1396 N71-19633
 Capacity of holographic memory system with laser system, acousto-optic beam deflector, block data composer and synchronizer 09 p1354 N71-19775
 [NASA-CR-103058] 09 p1354 N71-19775
 Holographic interferometry analysis of axisymmetric imperfections effect on natural frequencies and mode shapes of conical shells 10 p1569 N71-21280
 Q-switched ruby laser holography with optical equipment to compensate for spatial and temporal incoherence for contouring, aerodynamic visualization, and nondestructive testing 10 p1569 N71-21320
 [NASA-CR-114291] 10 p1569 N71-21320
 Holographic study of xenon arc lamp heat loads for solar environmental simulations 10 p1570 N71-21354
 Kinoform optical filtering techniques with applications in holography and photography 11 p1715 N71-22252
 [IBM-326-2378] 11 p1715 N71-22252
 Modification of folded conventional schlieren system for transmission of holograms 11 p1775 N71-22288
 [AD-717702] 11 p1775 N71-22288
 Measuring hologram images by placing small self-luminated dot in virtual image similar to photogrammetric stereomodels 12 p1918 N71-23623
 [AD-718964] 12 p1918 N71-23623
 Detection of flaws in honeycomb panels by holographic techniques and reducing sensitivity of holographic interferometry of transparent objects 12 p1933 N71-23704
 [AD-718386] 12 p1933 N71-23704
 Applicability of holography to optical properties of atmospheric aerosols 12 p1968 N71-24005
 Development of electronic circuits for forming scanned acoustic holograms 12 p1935 N71-24076
 [ARL-INST-73] 12 p1935 N71-24076
 Application of cineholography in study of microcirculation, hemodynamics and related physiological studies of man and animal 13 p2036 N71-24684
 [AD-719401] 13 p2036 N71-24684
 Diffraction efficiency and image distortion properties of volume transmission holograms 13 p2126 N71-25071
 Holography and spectroholographic techniques 13 p2090 N71-25115
 [AD-719855] 13 p2090 N71-25115
 Method and means for recording and reconstructing holograms without use of reference beam 14 p2266 N71-26154
 [NASA-CASE-ERC-10020] 14 p2266 N71-26154
 Electro-optical measurement and data processing techniques 14 p2296 N71-26396
 [FOA-C-3-614-42] 14 p2296 N71-26396
 Holographic applications in structural models, photoelasticity and stress analysis 15 p2418 N71-26900
 [AD-721115] 15 p2418 N71-26900

Surface distortion measurement by holographic gratings, moiré effect, and wave front reconstruction 15 p2407 N71-27020
 [CRIP-MT-70] 15 p2407 N71-27020
 Fourier techniques for determining structure of three dimensional semitransparent objects from measurements of transmission functions of holograms illuminated by light beams 15 p2435 N71-27643
 [AD-720638] 15 p2435 N71-27643
 Interferometric holographic analysis of density flow fields around half-angle conical bodies in supersonic wind tunnels with 10 deg angle of attack 16 p2529 N71-28411
 [AD-721543] 16 p2529 N71-28411
 Computer generation and plotting of synthetic holograms, binary holograms, and spatial filters 16 p2687 N71-28955
 [AD-723360] 16 p2687 N71-28955
 Holographic imagery for aviation and space flight 17 p2721 N71-29916
 [JPRS-35420] 17 p2721 N71-29916
 Pulse amplitude modulation of laser outputs for image contrast enhancement in real time holographic interferometry for nondestructive testing 19 p3108 N71-32244
 [AD-726392] 19 p3108 N71-32244
 Holographic interferograms of laminar free convection boundary produced by vertical flat plate with nonuniform wall-temperature distribution 20 p3364 N71-32993
 [AD-726698] 20 p3364 N71-32993
 Holographic scanning for acoustic imaging in liquid sodium 20 p3223 N71-33486
 [BNWL-1558] 20 p3223 N71-33486
 Development and characteristics of systems for producing stable holographic optical equipment 21 p3436 N71-34447
 [RM-516] 21 p3436 N71-34447
 Holographic interferometry applied to vibration analysis, composite component evaluation, and precision cylinder inspection 22 p3591 N71-35570
 [AD-726369] 22 p3591 N71-35570
 Application of holographic techniques for measurement of scintillation effects using gas and infrared lasers 22 p3591 N71-35572
 [AD-726902] 22 p3591 N71-35572
 Method for producing holograms in infrared region and reconstruction in real time using helium-neon laser 23 p3767 N71-36851
 Application of pulsed ruby holographic techniques to tests of ceramic materials 24 p3931 N71-38050
 [AD-727160] 24 p3931 N71-38050
HOMOMORPHISM
U ANALYTIC FUNCTIONS
HOMOSTASES
 Homeostasis during weightlessness 01 p0010 N71-10368
 [NASA-TT-F-13373] 01 p0010 N71-10368
 Analysis of homeostatic processes in weightlessness 08 p1149 N71-18793
 [AD-715307] 08 p1149 N71-18793
HOMING
 Cold exposure effects on homing performance of trained pigeons 09 p1332 N71-20148
 [DBET-723] 09 p1332 N71-20148
 Voice communication, direction finding, and radio homing equipment development for search and rescue by air 13 p2036 N71-24414
 [AD-715310] 13 p2036 N71-24414
HOMING DEVICES
 Theoretical principles of radio direction finding and operation of radio direction finders 06 p0816 N71-16616
 [AD-714509] 06 p0816 N71-16616
 Analytic photoelectric system for optical tracking device 16 p2640 N71-29025
 [NASA-TT-F-13708] 16 p2640 N71-29025
 Simulation evaluation and analysis of strapdown laser seeker guidance concept 22 p3418 N71-35780
 [AD-726376] 22 p3418 N71-35780
HOMOGENEITY
 Loss due to missing data in efficiency of locally optimal test for homogeneity with respect to very rare events in supernovas observations 01 p0122 N71-10387
 [AD-710755] 01 p0122 N71-10387
 Growth of chemically homogeneous single crystals of alloys 10 p1633 N71-20889
 Homogeneity characterization of Fe-3Si alloy microanalysis standard reference material 10 p1577 N71-21027
 [NBS-SPEC-PUBL-260-22] 10 p1577 N71-21027
 Theory of equilibrium figures of rotating, homogeneous, incompressible fluid mass as applied to cosmology 20 p3252 N71-33591
 [NASA-SP-186] 20 p3252 N71-33591
 Mis theory for spherical homogeneous and isotropic particles 23 p3762 N71-36957
 [IPA-CR-224] 23 p3762 N71-36957
 Nonhomogeneous isotropism of centrally symmetric models of origin of universe 23 p3762 N71-36957
HOMOGENIZATION
U HOMOGENIZING
HOMOGENIZING
 Origin and nature of inhomogeneities in uranium based nuclear alloys, and procedures for homogenization 07 p1042 N71-17244
 [RFP-1582] 07 p1042 N71-17244
HOMOMORPHISM
 Cohomology of finite groups 03 p0401 N71-13268
 Homogeneous space structures on polyhedra 03 p0712 N71-14568
 [DISS-4320] 03 p0712 N71-14568

HOMOMORPHISMS

Proofs for Browder and Novikov theorem and Siebenmann theorem, with data on cap-product, Poincaré duality, manifold index, homology surgery, and arbitrary neighborhood existence

13 p2104 N71-25560
Residual and linear continuities in differential cobolomogy 24 p3948 N71-38163
Homology theory for analytical spaces 24 p3948 N71-38166

HOMOMORPHISMS

NT SUBGROUPS
Differential gauge theory and topological spaces with unique homomorphisms 07 p1049 N71-16969
Incoherent topological spaces with unique homomorphisms on themselves 07 p1050 N71-16972
Matrix ring formulations of Artinian semi-simple ring with involutions 13 p2104 N71-25458

HOMOTOPY THEORY

Ordering relationship of ultratopology 23 p3782 N71-36954

HONEST JOHN ROCKY VEHICLE

Extrapolating wind profile from single measurement near surface to burnout altitude of Honest John rocket [AD-716993] 10 p1597 N71-21245

HONEYCOMB CORES

Vibration mode analysis of doobly curved honeycomb sandwich plates by finite element method [ISVR-TR-37] 10 p1653 N71-21646
Fatigue properties of titanium and nickel alloy honeycomb core sandwich structures [AD-716731] 10 p1659 N71-21733
Technique for making foldable, inflatable, plastic honeycomb core panels for use in building and bridge structures, light and radio wave reflectors, and spacecraft [NASA-CASE-XLA-03492] 11 p1770 N71-22713
Fabrication of tantalum alloy honeycomb core structure for lithium cooled reactor [NASA-CR-72851] 13 p2101 N71-25426
Determination of efficiency of solar absorption of honeycomb structure attached to collecting base surface on which incoming solar energy impinges directly on base surface [NASA-TN-D-6337] 13 p2187 N71-25466

HONEYCOMB STRUCTURES

NT HONEYCOMB CORES
Variations in crushing strength of paper honeycomb [AD-711557] 02 p6428 N71-12018

Experimental data and performance of honeycomb rotor shroud configuration to improve stall margin of 0.5 hub tip ratio single stage compressor [NASA-CR-72808] 05 p0762 N71-15328
Flow distribution data for solid and honeycomb rotor shrouds to improve stall margin of 0.5 hub tip ratio single stage compressor [NASA-CR-72809] 05 p0762 N71-15329

Vibration properties of viag stiffened honeycomb cylinders [NASA-TN-D-6090] 05 p0780 N71-15423

Fluid flow control valve for regulating fluids in molecular quantities [NASA-CASE-XLE-00703] 06 p0863 N71-15967

Lightweight resin fiber glass honeycomb sandwich structure fabrication and comparison with aluminum structures for planetary probes 07 p1047 N71-17350

Electroforming this nickel foil electrodes of porous honeycomb structure to increase nickel-cadmium battery service life 10 p1495 N71-20818

Method and apparatus for fabrication of heat insulating and ablative reentry structure [NASA-CASE-XMS-02009] 10 p1660 N71-20834

Method for honeycomb panel bonding by thermosetting film adhesive with electrical heat means [NASA-CASE-XMF-01402] 10 p1591 N71-21651

Detection of flaws in honeycomb panels by holographic techniques and reducing sensitivity of holographic interferometry of transparent objects [AD-718386] 12 p1933 N71-23704

Thermodynamics of honeycomb porous bed solar generators with and without fluid transpiration including generator designs 16 p2538 N71-28386

Development of thermal insulation material for insulating liquid hydrogen tanks in spacecraft [NASA-CASE-XMF-05046] 16 p2691 N71-28892

Feasibility of fabricating carbon/carbon honeycomb using woven carbon cloth [BDX-613-335] 18 p2939 N71-30582

Performance of unozoned lens fabricated from expanded aluminum honeycomb operating at EHF [AD-724664] 29 p3240 N71-32994

Finite element method to derive stiffness and increase flexibility in honeycomb structures 23 p3864 N71-37548

HONEYWELL ADEPT COMPUTER

PL-516 assembly language for Honeywell DDP-516 computer [NPL-COM-SCI-44] 11 p1715 N71-22094

HONEYWELL COMPUTERS

NT HONEYWELL ADEPT COMPUTER

HONING

Friction characteristics during diamond honing of steel surfaces [AD-712802] 05 p0693 N71-15449

HOOKES LAW

Stress-strain diagram for nonhomogeneous composites with circular inclusion using Hooke's law 13 p2177 N71-24645

HOOKS

British and international standards for lifting hooks, noting point-hooks, C-hooks, and marine C-hooks [NPL-MA-98] 18 p2928 N71-30874

HORIZON

NT RADIO HORIZONS
Visual illusions in human perception of horizontal figures bordered by anchoring lines [AD-712981] 03 p0320 N71-12287

Discussion of cosmological horizons using two dimensional balloon model and metric models 20 p3344 N71-32844

Effects of increase in cloudiness toward horizon on direct solar radiation and sunshine duration calculations [NLL-M-20394-5828-4F] 21 p3505 N71-34969

HORIZON SCANNERS

Satellite orientation, satellite attitude control, and pointing control systems using horizon scanners, gyrocompasses, gravity gradient, and angular momentum systems [RAE-TR-70070] 02 p0263 N71-11764

Infrared slot and horizon sensor development using slot-formed bolometer on germanium optical system [BMW-FB-W-70-40] 03 p0382 N71-13294

Determining error in moon and earth horizon sensors due to effects of surface roughness 07 p1054 N71-16963

Clamped amplifier circuit for horizon scanner enabling amplification and accurate measurement of specified parameters [NASA-CASE-XQS-01784] 10 p1536 N71-20782

Horizon sensor design with digital sampling of spaced radiation-compensated thermopile infrared detectors [NASA-CASE-XNP-06957] 10 p1558 N71-21088

IMF 1 optical aspect system based on spacecraft angular relationship between sun and earth using digital solar sensor and visible horizon detector [NASA-TN-D-7008] 10 p1559 N71-21220

Transmission model effects on water vapor mixing ratios and radiance calculations for infrared horizon scanners [NASA-TN-D-6112] 12 p1912 N71-23694

Solid state modulators for horizon sensing applications [ESRO-CR-35] 23 p3834 N71-37344

HORIZON SENSING

U HORIZON SCANNERS
HORIZONTAL FINS
U FINS

Horizontal flight Tu-134 aerodynamic characteristics during takeoff, climb, horizontal flight, landing stability and maneuverability, and strength under various loads [AD-72196] 24 p3874 N71-37612

HORIZONTAL STABILIZERS
U STABILIZERS (FLUID DYNAMICS)
HORIZONTAL TAIL SURFACES

Development and characteristics of translating horizontal tail assembly for supersonic aircraft [NASA-CASE-XLA-08801-1] 02 p0147 N71-11043

Lift, aerodynamic drag and pitching moment study of transport aircraft horizontal tail surfaces in low speed wind tunnels [ARC-R/M-5642] 06 p0791 N71-15702

Wind tunnel tests with jet simulation of tailplane interference on European airbus models 09 p1314 N71-19374

Computer programs for calculating airforce coefficients of wing-horizontal tail and fin-horizontal tail oscillating in subsonic flow 17 p2699 N71-29342

Low speed wind tunnel test on effects of horizontal tail geometry on longitudinal stability of orbiter shroud [NASA-CR-19358] 21 p3520 N71-35084

HORIZONTAL TAIL SURFACES
U TAIL ASSEMBLIES
HORMONE METABOLISMS

Long term hypokinesia effects on rat serotonin metabolism 20 p3220 N71-33453

HORMONES
Development of radioimmunoassay system for measurement of urinary antidiuretic hormone excretion 23 p3712 N71-36459

Human vasopressin by resin, angiotensin, and aldosterone and human physiological studies using radioimmunoassays 23 p3712 N71-36460

Assays of hormonal control of calcium and bone metabolism 23 p3712 N71-36461

Effects of space flight on bone metabolism investigated by analyzing peptide hormones in urine 23 p3712 N71-36462

HORN ANTENNAS

Feed properties and radiation patterns of conical horn antennas with small flare angles 01 p0822 N71-10070

Feeds for reflector antennas, frequency independent conical horn antennas, and conical horn antennas with symmetrical radiation patterns 02 p0179 N71-11520

Maxwell equation for conical horn antennas [TH-70-E-10] 02 p0182 N71-11520

Characteristics of antenna horn feeds consisting of central horn with overlapping peripheral horns [NASA-CASE-GSC-10452] 03 p0335 N71-12290

Beam equalization in large Cassegrain antennas with parabolic horn reflector feeds [NASA-CR-113569] 06 p0812 N71-15776

Multiple mode horn antennas with radiation patterns of equal beamwidths and suppressed sidelobe [NASA-CASE-XNF-01057] 06 p0813 N71-15980

Short axial length broadband horn design for S band [AD-714994] 07 p1008 N71-17011

HOSES

Umbilical hose assembly and PLESS oxygen and water hose designs [NASA-CR-115157] 23 p3717 N71-36466

Design verification test results for umbilical hose and PLESS water and oxygen hoses [NASA-CR-115158] 23 p3717 N71-36467

HOSPITALS

Intensive care alarm indicator system with audible signal and worn by staff responsible for care [NASA-TM-X-65421] 06 p0805 N71-15912

Systems management with computers and television aids in medicine including physical examination, patient logistics, data processing, and electrocardiographic diagnosis 11 p1847 N71-23077

HOT AIR

U HIGH TEMPERATURE AIR
HOT CATHODES

Diffusion type plasma source with two cathode rail arrays for ion current production [DPF-97] 15 p2501 N71-27796

Langmuir probe theory for collisional plasmas with collisional ionization probe sheath based on hot cathode helium discharge measurements [AD-726966] 22 p3655 N71-36664

HOT CYCLE PROPULSION SYSTEM
U TYPED ROTORS
HOT ELECTRODES

Electron distribution measurements in hot electron mirror contained plasma by bremsstrahlung spectra [JORN-LTM-3302] 13 p2149 N71-23376

Equilibrium distribution functions for electrons in isoelectric plasma calculated for energy interval of 1 to 15 eV utilizing data collected in pulse probe experiment [NASA-CR-119031] 16 p2588 N71-30330

HOT EXTRUDING
U EXTRUDING
HOT FORMING

Hot working U HIGH TEMPERATURE GASES
HOT GASES

U HIGH TEMPERATURE GASES
HOT JET EXHAUST
U JET EXHAUST

U JET EXHAUST
HOT JETS
U JET FLOW

U JET FLOW
HOT PLASMAS
U HIGH TEMPERATURE PLASMAS

U HIGH TEMPERATURE PLASMAS
HOT PRESSING

Intermediate stage densification kinetics of alumina hot pressed in vacuum [AD-710608] 01 p0859 N71-10639

Production of regeneratively cooled rocket thrust chambers by removable tooling and subsequent hot isostatic pressing in gas autoclave [NASA-CR-72795] 06 p0865 N71-16081

Simultaneous polymerization and hot pressing of Pyrolytic polymers 08 p1223 N71-14087

Hot-pressed alumina with molybdenum or molybdenum oxide additives characterized by micrographic and X ray diffraction analyses [AD-722239] 16 p2611 N71-28022

Cermet for nuclear fuel constructed by pressing metal coated ceramic particles in die at temperature in cause bonding of metal coatings, and tested for thermal stability [NASA-CASE-LEW-10219-1] 16 p2618 N71-30771

Fabrication and properties of hot-pressed polycrystalline magnesium oxide containing anion impurities [NASA-CR-121937] 22 p3587 N71-35546

Electrical conductivity of boron and silicon compounds produced by hot pressing and sintering of cold-pressed pellets 22 p3601 N71-35646

HOT STARS
NT A STARS
NT B STARS
NT O STARS

SUBJECT INDEX

NT WHITE DWARF STARS
Mean resolution of ultraviolet spectra of hot stars between 1050 and 5200 Å
(BSRO-SN-102) 02 p2395 N71-11928
Atmospheric parameters, effective temperature, and surface gravity for extreme population II stars
(WP-15375) 04 p0610 N71-13744
Atomic and molecular physics study and cold and hot star properties
(CBRN-70-4) 16 p2649 N71-28814

NOT WEATHER
Design criteria for optimal hoverable helicopter in hot weather climate
(AD-717025) 10 p1495 N71-21707
Seasonal variations in thermoregulation of residents in hot, dry climates with respect to age and sex
(AD-717025) 11 p1679 N71-22003
Advantages of various types of liquids taken by workers under high temperature working conditions (miners, fire fighters, steelworkers)
(NASA-TT-F-14092) 23 p3713 N71-36469

NOT WORKING
Characteristics of materials for simulation of hot forging processes
(AD-711303) 02 p0229 N71-11528
Hot working effect on room temperature strength and ductility of gallium delta-stabilized plutonium alloy
(UCRL-72547) 04 p0530 N71-14069
Hot forming of plastic sheets
(NASA-CASE-XMS-05516) 07 p1037 N71-27803
Magnetic crystallographic orientation produced in ferrites by hot working
(AD-723458) 18 p2931 N71-31580
Nitrogen content effect on hot ductility of molybdenum alloyed austenitic stainless steel
(AD-723458) 19 p3112 N71-31921
Influence of nitrogen and sulfur content on hot ductility, flow stress, and recrystallization in austenitic stainless steel
(AD-723458) 19 p3112 N71-31922
Behavior of nonmetallic inclusions in steel during hot working
(AD-723458) 19 p3113 N71-31923
Extensible mold and gasified pattern casting of molten metals
(JPRS-53572) 19 p3106 N71-32432
Bibliography of reports on aspects of physical quality of hot rolled steel strip
(JPRS-53572) 22 p3593 N71-35587

NOT-FILM ANEMOMETERS
Hot film water velocity sensor performance in some and coastal waters
(JPRS-53572) 10 p1560 N71-21516

NOT-WIRE ANEMOMETERS
Correction formulas for effect of ambient temperature drift on hot-wire anemometer measurements in incompressible flow
(NPL-AERO-1302) 02 p0225 N71-11544
Constant temperature hot-wire anemometer for measuring turbulence in pipe flow
(AD-723458) 05 p0660 N71-14766
Hot-wire anemometer measurements of incompressible fluid flow direction and velocity in pipes
(NASA-TM-X-52967) 08 p1180 N71-18634
Turbulent and mean flow properties of plane two-dimensional wall jet using hot-wire anemometers
(JPRS-53572) 08 p1183 N71-18985
Hot-wire anemometer for wind tunnel turbulence measurement and wind tunnel oscillation reduction
(JPRS-53572) 15 p2391 N71-27161
Measurements in boundary layer of flat plate using helium or argon injection and supersonic flow measurement with hot-wire anemometer
(NASA-TT-F-13929) 21 p3410 N71-34263
Calibration method for hot-wire probes
(AD-72049) 22 p3586 N71-35538
Hot-wire anemometer measurements of streamwise magnitudes and normal velocity components of wing tip vortex
(NASA-TM-X-62087) 23 p3742 N71-36479
Three dimensional hot-wire anemometry technique employing single wire probe
(AD-72792) 24 p3987 N71-37845
Bi-directional counter for operation with model Old Gold hot-wire anemometer systems
(AD-72792) 24 p3925 N71-38008

NOT-WIRE FLOWMETERS
Preliminary results of SERT 2 spacecraft potential measurements using hot wire emissive probes
(NASA-TT-F-2083) 02 p0297 N71-11897
Hot-wire liquid level detector for cryogenic propellant tanks
(NASA-CASE-XLE-00454) 07 p1068 N71-17802
Hot flux measurement on flat plate surface by means of hot-wire flowmeters noting skin friction influence
(REF-70-7) 08 p1201 N71-18006
Hot wire sampling of turbulent shear flows
(IC-AERO-71-04) 17 p2736 N71-30059
Hot wire measurements of viscous sublayer region in turbulent boundary layer
(AD-72906) 18 p2906 N71-31203

NOT-WIRE TURBULENCE METERS
U NOT-WIRE FLOWMETERS
U TURBULENCE METERS

NOT-ROT WIND TUNNELS
Arc chamber thin film silicate coating for improvement of hotshot wind tunnels
(ONERA-TP-427) 02 p0198 N71-11471

HOUSING
NT RADOMES
Sealed housing for protecting electronic equipment against electromagnetic interference
(NASA-CASE-MSC-12168-1) 08 p1169 N71-18600
Telescope building and dome design
(AD-723458) 24 p3923 N71-37984

HOVERCRAFT
U GROUND EFFECT MACHINES
HOVERING
Blade root cutout effects on hover performance of helicopter rotors with rotor thrust and torque characteristics and wake pattern analysis
(AD-711396) 02 p0145 N71-11030
Hovering type flying vehicle design and principle mechanisms for manned or unmanned use
(NASA-CASE-MSC-12111-1) 02 p0147 N71-11039
Hovering performance tests of jet-flapped rotors and comparison of predicted and actual results
(NAL-TR-211) 13 p2028 N71-25396
Effectiveness of attitude feedback and translational velocity feedback flight control system assessed for ability to provide positional stability and reduce pilot error at hover
(AD-721728) 16 p2531 N71-28274
Acoustic measurements of helicopter rotor noise at hover
(AD-721312) 16 p2531 N71-28275
Model for predicting pilot rating of VTOL aircraft in hover mode
(AD-72144) 20 p3209 N71-32981
Calculation of turbulent compressible boundary layer on helicopter rotors for range of hover conditions using two different analytical methods
(AD-723458) 20 p3210 N71-33312

HOVERING STABILITY
VTOL display and control system for deceleration to instrument hover
(NASA-TT-D-6108) 06 p0795 N71-16584
Design criteria for optimal hoverable helicopter in hot weather climate
(AD-717025) 10 p1495 N71-21707
Flight simulation of hovering vertical takeoff aircraft with various attitude and speed controls
(AD-723458) 19 p3074 N71-31955
Evaluation of in-flight simulation of flying platform using helicopter with variable stability and maneuverability
(AD-723458) 19 p3074 N71-31957

HRB-1 HELICOPTER
U CH-46 HELICOPTER
HS-748 AIRCRAFT
Landing accidents investigations for Hawker Siddeley 748 aircraft with performance measurements on rough surfaces
(AD-723458) 12 p1834 N71-23417

HU-1 HELICOPTER
U HU-1 HELICOPTER
HUBS
Computerized propeller design considered flow field distortion by hub
(AD-723458) 17 p2704 N71-29690

HUGHES MILITARY AIRCRAFT
U MILITARY AIRCRAFT
HUGONIOT ADIABAT
U HUGONIOT EQUATION OF STATE
HUGONIOT EQUATION OF STATE
Lithium fluoride single crystal shock Hugoniot data and phase transitions
(AD-712320) 02 p0286 N71-11900
Shock Hugoniot data for sodium chloride single crystals
(AD-713599) 05 p0759 N71-15360
Determination of Hugoniot elastic limits for light armor materials
(UCRL-50901) 06 p0932 N71-15678
Measurements of shock Hugoniot in unidirectional fiber reinforced composites
(AD-716560) 09 p1403 N71-19491
Electromagnetic measurement of shock Hugoniot of Teflon
(AD-716333) 09 p1406 N71-20046
Shock pulse attenuation and Hugoniot studies of three explosives and three shock explosives
(UCRL-50950) 12 p3013 N71-24235
Hugoniot equations of state for calculating shock temperatures of silicone fluids
(AD-723458) 14 p2357 N71-26493
Shock velocity measurements for determining Hugoniot equation of state of sodium chloride in single crystal and powder samples
(AD-723458) 14 p2327 N71-26499
Hugoniot equation of state measurements from shock wave loading study of Coconino sandstone
(NASA-CR-1842) 15 p2397 N71-27019
Hugoniot relationship for high density, distended thorium molybdenum cermet
(SC-DR-70-908) 16 p2632 N71-28641

HULLS (STRUCTURES)
NT SHIP HULLS

HUMAN FACTS
STRESS EVALUATION OF PROTOTYPE SPHERICAL ACRYLIC UNDERWATER HALL
(AD-715772) 06 p1294 N71-18923

HUMAN BEHAVIOR
Investigating effects of oxygen, nitrogen, and rare gas mixtures at increased pressures on narcosis induction of man
(JPRS-51714) 02 p0157 N71-11110
Complex effect of nitrogen, argon, and helium respiratory mixtures on humans at increased pressures
(AD-715772) 02 p0157 N71-11115
Perspectives and perceptions of organization behavior and design
(AD-714597) 06 p0808 N71-16709
Papers presented at International Symposium on Behavioral Thermoregulation
(AD-715772) 06 p1149 N71-18794
Investigating electroencephalographic and behavioral changes in rabbits and humans exposed to acute hypoxia
(AD-715772) 06 p1152 N71-18913
Physiological and behavioral parameters in design of dynamic human biological system
(AD-715772) 09 p1331 N71-19878
Neurophysiological model for interactions between nervous system, cellular mechanisms, and human behavior synthesis
(AD-715772) 09 p1332 N71-19886
Biochemistry model for endocrine system effects on mammalian neurophysiology and human behavior
(AD-715772) 09 p1332 N71-19887
Biodynamic modelling of biosystems by physical and biological parameters
(AD-715772) 09 p1332 N71-19888
Long duration confinement effects on crew behavior during manned space flight simulation
(AD-715772) 10 p1508 N71-20900
Crew activity analysis for long duration space flight simulation test
(AD-715772) 10 p1508 N71-20901
Space station simulator background noise effects on crew behavior during long term confinement
(AD-715772) 10 p1509 N71-20908
Information systems, retrieval, and user behavior
(AD-715772) 12 p2016 N71-23505
Human factors engineering data for equipment design including anthropometry, environmental conditions, and physiological and behavioral factors
(NASA-CR-14277) 14 p2209 N71-25944
Social system model for spacecrew behavior during long duration space flight
(AD-715772) 16 p2533 N71-28544
Estimating human emotional states by changes in frequency characteristics of articulation
(NASA-TT-F-13772) 18 p2875 N71-30803
Human thinking activity applied to man machine systems
(JPRS-53683) 22 p3544 N71-35245
Human behavior patterns
(AD-715772) 22 p3544 N71-35246
Factors creating objective complexity of human problem solving reduced to information processes
(AD-715772) 22 p3545 N71-35253
Space station and base design considerations for crew stability and habitability
(NASA-CR-115179) 23 p3717 N71-36495
Behavioral science programming language for use with flight simulator facility
(AD-726572) 23 p3729 N71-36584

HUMAN BEINGS
Detection of antigens and genetic analysis with mouse hybrids
(SU-326-P-26-X-2) 03 p0322 N71-12300
Plasma and urinary uric acid production in men fed egg protein and yeast ribonucleic acid
(A69-15968) 03 p0326 N71-12529
Uric acid levels in men fed algae and yeast as protein sources
(AD-715772) 03 p0326 N71-12330
Suppression by allopurinol of uric acid formation in men fed yeast RNA
(AD-715772) 03 p0326 N71-12331
Coordination of human voluntary movements during space flights
(JPRS-51899) 05 p0633 N71-14625
Circadian rhythm of light sensitivity in visual perception thresholds of men
(AD-714064) 06 p0801 N71-16313
Human caloric requirements when working in extreme climatic environments
(AD-715772) 09 p1337 N71-20367
Mass body exposure rate from krypton 85 released in atmosphere by nuclear power production
(BNWL-SA-3233) 18 p1497 N71-20777
Human orientation, motivation, and assimilation of information and its transfer
(AD-715772) 12 p2016 N71-23503
Activity of lactic dehydrogenase in urine of glomerulonephritis and nephrotic syndrome patients
(NASA-TT-F-13558) 12 p1863 N71-23728
Method and apparatus for applying compressional forces to skeletal structure of subject to simulate force during ambulatory conditions
(NASA-CASE-ARC-10100-1) 13 p2037 N71-24738

Automatic braking device for rapidly transferring humans or materials from elevated location [NASA-CASE-XKS-07814] 15 p2414 N71-27067
Multiple window spectrometry for gallium 67 and its use in detecting malignant human and animal tumors [ORNL-TM-3260] 17 p2798 N71-30004
Bed rest effects on glucose regulation in human beings 20 p3218 N71-33270

Onosological functions and information properties of devices used to understand cognitive mechanisms of man [JPRS-53910] 21 p3399 N71-34192

Human exposure to emergency exposure limit concentrations of monomethylhydrazine to determine suitability for use [AD-727527] 24 p3879 N71-37652

Human exposure to particulate radiation and energetic X rays [NASA-CR-123173] 24 p3881 N71-37661
Device for conducting electrostatic charges from man [NLL-M-20436-5[28.4F]] 24 p3884 N71-37684

HUMAN BODY

Using underwater photography to demonstrate formation of mobile roughness in skin of humans and dolphins due to external hydrodynamic forces [JPRS-51614] 01 p0014 N71-10952

Kinematic analysis of inaccessible three-dimensional mechanism for application to human skeletal kinematics 02 p0153 N71-11083

Low barometric pressure effects on human and chicken erythrocyte active sodium efflux 02 p0155 N71-11097

Chemical analysis of thiamine metabolism in man [AD-712238] 02 p0155 N71-11099

Electromedical garment, applying vectorcardiographic type electrodes to human torso for data recording during physical activity [NASA-CASE-XFR-10856] 02 p0167 N71-11189

Effects of air conditioning on human body [JFA-SR-26] 03 p0320 N71-12286

Biological effects of microwaves in occupational hygiene [NASA-TT-F-633] 05 p0633 N71-14632

Simulator study of lunar flying platform control by pilot body motion [NASA-TN-D-6016] 05 p0658 N71-14981

Effects of atmospheric discharges of tritiated steam on human health [CEA-CNF-1560] 06 p0798 N71-15718

Comparison of methods to assess geometrical variations of counting-rate in whole-body monitors [SRRC-31/69] 08 p1149 N71-18837

Mathematical link-system model for computerized simulation of human movement in cockpit geometry evaluation program for flight crew physical compatibility with crew stations 09 p1341 N71-19820

Validation criteria and performance evaluation of human movement computerized simulations used in cockpit geometry evaluation program for flight crew physical compatibility with crew stations [AD-716399] 09 p1341 N71-19821

Biological systems analysis and biodynamic modeling of physiological and biological interrelationships in human body and mammals [NASA-CR-1720] 09 p1330 N71-19876

Physiological and behavioral parameters in design of dynamic human biological system 09 p1331 N71-19878

Hierarchical regulation model for human biological systems 09 p1331 N71-19879

Metabolic imbalances and body hypohydration during food deprivation for 10 days 09 p1337 N71-20368

Human acclimatization to high altitudes, monsoons, and hot, dry weather [JPRS-52594] 11 p1679 N71-22001

Physiological adaptation to high altitudes in experienced and novice mountain climbers from northern and southern regions 11 p1680 N71-22004

Physiological responses to long term living at high altitudes 11 p1680 N71-22005

Physiological responses to long term living at medium elevations 11 p1680 N71-22006

Distributed parameter mathematical model of human body in dynamic mechanical environments [AD-717764] 11 p1686 N71-22130

Physiological effects of cyanate ions in renal malfunctions 11 p1684 N71-22557

Fundamental principles and physiological effects of acceleration on human body 12 p1862 N71-23339

Daily oral temperature measurements for circadian rhythm analysis on human body [NASA-TT-F-13630] 12 p1864 N71-24019

Thermoregulating with cooling flow pipe network for humans [NASA-CASE-XMS-10269] 12 p1868 N71-24147

Radiobiological plasma and blood volume measurements on humans and swine [CEA-R-4031] 13 p2033 N71-24627

Four-degrees-of-freedom lumped parameter model for vertical accelerations of seated human body as might be imposed by aircraft ejection systems [AD-721255] 15 p2370 N71-26944

Human physicochemistry, thermoregulation, and harmonic oscillation of blood glucose levels [NASA-CR-1806] 16 p2542 N71-28206

Hypoxic hypoxia effects on human and animal resistance to infectious diseases and immunobiological reactivity 16 p2543 N71-28249

Prolonged immersion effects on human water/mineral metabolism 16 p2543 N71-28251

Gaseous impurities in air exhaled by humans under extremal stress factors 16 p2544 N71-28260

Animal experimentation for simulating long duration space flight hazards for human physiology 16 p2542 N71-28541

Load distribution on human hip joints during walking [LAB-1002/71] 17 p2710 N71-29327

Anthropometric size determination techniques and adult male and female data correlations from US, Australia, Europe, and Asia [AD-723629] 18 p2878 N71-31481

Radioactive dilution estimation of total skeletal mass in human body 20 p3217 N71-33529

Bed rest and immobilization effects on oxygen transport system of human body 20 p3217 N71-33562

Dynamic mathematical model of physiological regulation of body temperature in human beings [NASA-CR-1853] 20 p3222 N71-33401

Anatomical-physiological characteristics of heat transfer in human body for developing insulating suit 20 p3221 N71-33459

Prolonged bed rest effects on human chromosomes during space flight simulation and actual space flight 20 p3221 N71-33462

Transverse acceleration effects on blood flow in human retina 20 p3221 N71-33463

Hypokinesia effects on nasal blood circulation of man 20 p3221 N71-33464

Hypokinesia effects on myoelectric potential of human leg muscle after prolonged bed rest 20 p3222 N71-33465

Hypokinesia effects on human heart rate and output volume after prolonged bed rest 20 p3222 N71-33466

Renal sodium and calcium excretion effects on human electrolytic water-mineral metabolism during space flight 20 p3222 N71-33467

Intracranial pressure distribution measurements on healthy subjects engaged in mental work 20 p3222 N71-33469

Neutron dose distributions at bone tissue interfaces in human body [ORNL-TM-3329] 21 p3382 N71-34066

Use of nutritional markers for studies of food intake, passage, and absorption in gastrointestinal track of humans and animals [NASA-CR-115125] 21 p3384 N71-34076

Fluoroplasographic system for rapid presentation of single plane body sections with reduced X ray exposure to patients [NASA-CR-111944] 21 p3424 N71-34363

Human and environmental natural and fallout radioactivity data [HASL-242] 21 p3484 N71-34815

Measurement of electric detonator insensitivity to electrostatic charge of human body [AD-726933] 22 p3697 N71-36367

Control of aging processes in human body cells [NASA-TT-F-13964] 23 p3713 N71-36466

Combined effects of reduced nutrition, hypokinesia, and centrifugal acceleration on human body [JPRS-54104] 23 p3716 N71-36488

HUMAN CENTRIFUGES

Basic kinematics and dynamics of human centrifuges and other aerospace simulators including certain microgravity effects [AD-711635] 01 p0014 N71-10883

Human centrifuge for dynamic environmental simulations 09 p1367 N71-20237

Reliability of vestibular orientation test for motion sickness reaction produced by human head movements in rotating chair [AD-716767] 10 p1502 N71-21650

Biodynamics, aerospace medicine, acceleration stresses, human tolerances, centrifuges, test facilities, and associated bibliography [AGARDGRAPH-150] 12 p1865 N71-23357

Intuitive, graphical, and simplified mathematical treatment of rotational dynamics as applied to human centrifuges 12 p1965 N71-23340

Physiological effects and acceleration tolerances after weightlessness based on space environment simulation with human centrifuges and bed rest [NASA-CR-115068] 17 p2706 N71-29216

Summary of experiment performance options and cost for orbital research centrifuge compatible with Skylab, Space Station, and space shuttles [NASA-CR-111937] 22 p3563 N71-35379

Experiment performance options and cost comparisons of orbital research centrifuge for Skylab and Space Station [NASA-CR-111938] 22 p3563 N71-35380

Cost comparisons and experiment performance options for space shuttle orbital research centrifuge [NASA-CR-111939] 22 p3564 N71-35381

HUMAN ENGINEERING
U HUMAN FACTORS ENGINEERING

HUMAN FACTORS ENGINEERING
Human factors in use of terminal radar (analog) display systems [FAA-NA-70-55] 01 p0010 N71-10008

Experimental dives for ADS-4 decompression schedules [AD-711842] 02 p0154 N71-11085

Evaluating psychological and physiological factors in designing ejection seats and parachutes [AD-711928] 02 p0158 N71-11121

Determination of quantitative radiation response time data [JRAU-109] 02 p0159 N71-11134

Research and development in training personnel with low aptitude, and aviation training devices [AD-712285] 02 p0166 N71-11115

Configuration and systems description of life support equipment for intravehicular and extravehicular activity - Vol. 1 [NASA-TM-X-66478] 02 p0170 N71-11126

Determination of subglottal pressures and air flow rates during vocal fry phonation [AD-711808] 02 p0180 N71-11126

Human factors engineering, life support systems, biotechnology, physiological effects, radiation effects, and medical science [JPRS-51641] 02 p0159 N71-11145

Medical support for prolonged space flights 02 p0159 N71-11148

Human heat exchange structure and overbreathing reactions at high ambient temperatures 02 p0160 N71-11145

External respiration and energy expenditures during orthostatic tests of human subjects following prolonged immersion in water 02 p0160 N71-11147

Model of neuron network generating stable rhythmic impulses 02 p0160 N71-11148

Procedures for determining functional state of human heart right side 02 p0160 N71-11148

Determination of human tolerance to impact accelerations 02 p0160 N71-11149

Characteristics of self-contained life support systems used in Soyuz spacecraft 02 p0170 N71-11192

Human metabolism in rarefied atmospheres by gas chromatography 02 p0171 N71-11193

Body position sensing actions during weightless conditions 02 p0161 N71-11194

Air operations safety and noise control research in aerospace medicine 02 p0171 N71-11193

Effects of air conditioning on human body [JFA-SR-26] 03 p0320 N71-12286

Biophysical evaluation of human vestibular system for aerospace applications [NASA-CR-111607] 03 p0322 N71-12286

Harness assembly adapted to support man in ground based apparatus which simulates weightlessness [NASA-CASE-MPS-14671] 03 p0328 N71-12341

Man machine interaction at remote console of time shared computer [AD-712695] 04 p0501 N71-13358

Design and development of air conditioned protective clothing [AD-713581] 05 p0637 N71-14748

Parameters of human pattern perception [AD-713185] 05 p0637 N71-14742

Effects of motion cues and motion scaling on one and two axis compensatory control tasks with application to flight simulators [NASA-TN-D-6110] 05 p0637 N71-14699

Discussing development of engineering psychology as independent science [JPRS-52006] 05 p0636 N71-14695

Research and Technology Operating Plan Summary - FY 1971 [NASA-TM-X-465566] 05 p0787 N71-15251

SUBJECT INDEX

HUMAN FACTORS ENGINEERING

Multiple circuit switch apparatus requiring minimum hand and eye movement by operator
(NASA-CASE-XAC-03777) 06 p0826 N71-15909

Standardization of tests and measures for human factors research
(AD-714669) 06 p0806 N71-15996

Human factors in aircraft simulation
(AGARD-CP-79-70) 06 p0830 N71-16040

Human factors in Concord cockpit simulation
(NASA-CASE-XAC-02405) 06 p0831 N71-16045

Technical and human engineering requirements for simulating pilot flight
(NASA-TM-X-65583) 06 p0831 N71-16046

Human factors in developing a pilot simulation program for evaluating aircraft handling aspects
(NASA-TM-X-65583) 06 p0832 N71-16069

Remote control devices operated by movement of finger tips for manual control of spacecraft attitude
(NASA-CASE-XAC-02405) 06 p0833 N71-16069

Mathematical simulation of biological subjects and construction of systems to control certain functions of biological nature
(JPRS-52308) 06 p0882 N71-16463

Reaction times of subjects in tests with display control configurations typical of those used in continuous tracking tasks
(NASA-TN-D-41322) 06 p0897 N71-16306

Scientific method and adversarial system as techniques of inquiry in technology assessment
(NASA-CR-116249) 06 p0982 N71-16873

Rest and activity cycles for maintaining efficiency of military flight operations personnel
(AGARD-CP-74-76) 07 p0977 N71-16905

Circadian rhythms of bodily functions and dependence of reaction time on duration of sleep
(AD-715251) 07 p0978 N71-16907

Techniques for familiarizing flying personnel with destination effects
(FAA-AM-70-17) 07 p0981 N71-17255

Investigating relationship of cybernetics and human management of large systems
(AD-715251) 07 p0987 N71-17699

Application of human factors engineering to spacecraft habitability
(NASA-TN-D-103028) 07 p1120 N71-17769

Human factors support requirements for space shuttle program
(NASA-CR-111847) 07 p1121 N71-17808

Accidents of nuclear workers caused by human factors
(CEA-CONF-1514) 08 p1157 N71-18288

Pinar motion of human being subjected to action of body-fixed force
(NASA-CR-116799) 08 p1157 N71-18399

Human life maintenance during space flight
(JPRS-52514) 08 p1156 N71-19110

Integrated measuring life support system
(NASA-TM-X-64992) 09 p1338 N71-19399

Effect of cockpit lighting systems on multicolored instrument displays
(AD-716610) 09 p1339 N71-19710

Computerized techniques incorporating adaptive pilot training concepts and means of predicting student training success
(AD-716673) 09 p1340 N71-19798

Cockpit geometry evaluation program results and techniques with computer input and output samples of flight crew anthropometry
(AD-716935) 09 p1321 N71-19817

Cockpit geometry evaluation program for computer simulation of flight crew physical compatibility with crew stations based on anthropometric and environmental data for man-model movements
(AD-716977) 09 p1340 N71-19819

Human factors tests to determine effects of aircraft controls placement on lightly clothed or pressure suited flight crews
(AD-716975) 09 p1341 N71-19911

Human factors engineering mock-up facility value as management tool
(AD-717026) 10 p1504 N71-20797

Fluctuating frequency of observer eye to frequency of visual pattern for optimum recognition
(JPRS-52606) 10 p1500 N71-21483

Exposure of human subjects to fast neutron beam to determine cause of light flashes observed by astronauts on lunar missions
(NASA-CR-117493) 10 p1500 N71-21509

Impact of artificial gravity simulations on spacecraft design configurations and crew operational
(NASA-CR-111066) 10 p1501 N71-21558

Test and evaluation of lap belt protection and comparison with lap belt plus air cushion restraint on human and baboon subjects
(AD-717026) 11 p1683 N71-22451

Measurement of human visual perception accuracy based on effects of heterogeneous target backgrounds
(AD-717026) 11 p1691 N71-22648

Transfer functions in modelling human pilot and dynamic structural aircraft responses
(NASA-CR-117493) 12 p1510 N71-23210

Human factors for defining transfer functions in pilot modelling
(AD-717026) 12 p1681 N71-23214

Human factors and safety requirements in aircraft design
(AD-717026) 12 p1835 N71-23423

Human factors and control system failures in jet upsets during turbulence encounters
(AD-717026) 12 p1835 N71-23424

Flying safety factors in close to ground operational design of X-51 helicopter
(AD-717026) 12 p1836 N71-23430

Identification and control of aeromedical factors associated with aircraft noise and acoustic measurements during C-141 operational missions
(AD-718097) 12 p1837 N71-23748

Human engineering criteria for design of diver-operated, hydraulic and pneumatic underwater tools
(AD-717961) 12 p1936 N71-23760

Evaluation procedure for oxygen and protective aviation masks
(AD-719105) 13 p2035 N71-24411

Human factor considerations applicable to aviation armament and avionics
(AD-719108) 13 p2036 N71-24453

Evaluation of protective clothing for flight crew members
(AD-719106) 13 p2036 N71-24460

Investigation of visual perception ability during acceleration and deceleration and thresholds for perceived motion changes
(AD-719105) 13 p2037 N71-24727

Design and development of flexible tunnel for use by spacecrews in performing extravehicular activities
(NASA-CASE-MSC-12243-1) 13 p2037 N71-24728

Development of apparatus and method for quantitatively measuring brain activity as automatic indication of sleep state and level of consciousness
(NASA-CASE-MSC-13202-1) 13 p2037 N71-24729

Establishment of relationship between skin temperature and ability to tolerate cold and hot environments for human subjects
(FAA-AM-71-4) 13 p2037 N71-24748

Development of apparatus for studying stabilized limb properties of human eye using photomultiplier tubes and magnetic core array storage system
(NASA-CR-114037) 13 p2034 N71-24931

Effect of weightlessness on cardiovascular and autonomic functions in human subjects
(AD-719790) 13 p2034 N71-24997

Human fluid balance in artificial environments, and influence of ambient temperature, water vapor pressure, total barometric pressure, wind velocity, and atmospheric gas composition
(NASA-CR-114977) 13 p2038 N71-25000

Air ionization and effects of positive ions in air on man using Am-241 sources
(ORNL-TR-2427) 13 p2035 N71-25438

Physiological effects of positive accelerations on cardiovascular system based on requirements for cardiovascular stimulation
(AD-719902) 14 p2203 N71-25674

Steady state and dynamic experiments to determine thermoregulatory heat production in human subjects
(AD-720031) 14 p2204 N71-25766

Human factors study of IVA cargo transfer from shuttle to space station
(NASA-CR-103118) 14 p2343 N71-25936

Human factors engineering manual including mathematical formulas, monographs, conversion tables, units of measurement, and nomenclatures
(NASA-CR-114272) 14 p2209 N71-25943

Human factors engineering data for equipment design including anthropometry, environmental conditions, and physiological and behavioral factors
(NASA-CR-114271) 14 p2209 N71-25944

Determination of acceleration limits for passenger comfort in urban transportation system
(AD-720031) 14 p2203 N71-26118

Effect of acceleration on space required to perform maneuvers with urban transportation tracked vehicle
(AD-720031) 14 p2203 N71-26119

Aircraft survival equipment testing including maintainability, systems compatibility, human factors engineering, and reliability of radios, protective clothing, floats, and parachutes
(AD-720225) 14 p2210 N71-26138

Flight adaptability and human factors engineering of aerial radiological detection equipment
(AD-720567) 14 p2255 N71-26191

Graphical predictions of human strengths for two handed IVA/EVA tasks including effects of differing gravities, populations, and space suit conditions
(NASA-CR-115044) 14 p2211 N71-26410

Materials and thermal protection, propulsion, environmental control, life support, and crew accommodation data for space shuttle design
(NASA-CR-114487) 14 p2346 N71-26780

Task commonality analysis of training equipment and devices to maximize positive transfer of training
(AD-709534) 15 p2373 N71-26881

Selected and annotated bibliography of human performance prediction in man machine systems. Vol. 3
(NASA-CR-73428) 15 p2374 N71-27251

Acceptance tests of various upper torso restraints by automobile users with application to general aviation aircraft
(FAA-AM-71-12) 16 p2549 N71-28006

Handsets system themselves containing words and phrases which reflect concepts to be induced in human factors engineering information retrieval system
(AD-721657) 16 p2550 N71-28339

Physiological effects of reduced gravity, restricted mobility, gamma irradiation, and magnetic fields on human and animal subjects
(JPRS-53448) 16 p2549 N71-28476

Analysis of data on human ability to perform different locomotor acts under conditions of reduced gravity
(AD-721657) 16 p2549 N71-28477

Formulation of work and rest schedules for optimum performance of spacecrews
(AD-721657) 16 p2546 N71-28488

Determination of the effect of weightlessness on muscle tone by measurement of firmness and bioelectric activity of muscles
(AD-721657) 16 p2546 N71-28490

Analysis of relationship between respiration rate and volume and minute volume of respiration under variety of physical loads
(AD-721657) 16 p2547 N71-28494

Biotechnological problems of man machine systems required for long duration space flight
(NASA-SP-285) 16 p2551 N71-28526

Biomechanical aspects of Gemini flight for future manned space flight technology
(AD-721657) 16 p2551 N71-28527

Psychophysiological factors of manned space flight
(AD-721657) 16 p2551 N71-28528

Manned space flight biotechnology for spacecraft design
(AD-721657) 16 p2551 N71-28529

Human potential in space experimentation and operation of orbiting research laboratory
(AD-721657) 16 p2551 N71-28530

Development of model for analysis of human subject to detect targets through visual recognition
(AD-721446) 16 p2554 N71-28733

Utilization of water resources within space stations, needs of men, and effects of lunar environment
(AD-721446) 16 p2581 N71-28906

Analysis of medical, psychological, and environmental aspects of mass air transportation
(FAA-AM-71-10) 17 p2710 N71-29308

Human factors engineering issues and requirements for advanced supersonic transports, space shuttles, underwater vehicles, and underwater structures
(AD-721713) 17 p2710 N71-29479

Evaluation of hypothesis that amount recalled and clustering are inversely related to delayed recall interval
(AD-708360) 17 p2722 N71-29539

Evaluation of effects of continuous redundancy shifts, length of rest interval, and duration of inter-task interval upon acquisition and transfer of schematic concepts
(AD-701184) 17 p2708 N71-29540

Determining force required for inserting printed circuit board into equipment by human performance tests
(AD-723049) 17 p2711 N71-29794

Judgment of effects of Doppler shifts on perceived sensitivity of aircraft made by subjects in anechoic chamber
(NASA-CR-17791) 17 p2709 N71-29980

Analysis of theory of thinking and application to cybernetics development
(JPRS-53425) 17 p2728 N71-30036

Comparison of water, convective air, and reversed air flow cooled suits for body temperature thermoregulation in high temperature environments
(JPRS-1307) 17 p2712 N71-30127

Physiological effects of fine and gross bodily movements upon visual adaptation under tilted environment conditions produced by optical prisms
(AD-723049) 17 p2709 N71-30186

Proceedings of conference on human reliability conducted by US Navy
(AD-723049) 17 p2712 N71-30234

Preparation of test plans used to evaluate performance of flight simulation trainers
(AD-723031) 17 p2731 N71-30257

Human factors engineering in man machine system design
(AD-723031) 18 p2883 N71-30570

Determination of real ear attenuation for Conn. Pin earplugs using human subjects
(JPRS-1971-4) 18 p2883 N71-30673

Effects of helium oxygen breathing on hearing in Navy personnel
(AD-722658) 18 p2877 N71-31237

Effect of changes in metabolism of pyridoxine and serotonin on human vestibular disturbances during turbulent flight conditions
(JPRS-53678) 18 p2877 N71-31334

Parameters of human pattern perception effect of statistical properties of pattern components on feature selection
(AD-722794) 18 p2878 N71-31336

Cross-referenced directory of reports of Human Engineering Laboratories 1953 to 1970
(AD-722794) 19 p3047 N71-31617

- Mathematical models of vision process, relationship between memory and perception, and development of improved computer technology
[JPRS-53647] 19 p3042 N71-32012
- Numerical analysis and mathematical models to describe vision process
19 p3043 N71-32013
- Analysis of registering structure as memory model and role in perception processes
19 p3043 N71-32014
- Effect of unidirectional movements of total optical environment on spatial disorientation with respect to external visual reference points
[FAA-AM-71-22] 19 p3043 N71-32001
- Determination and application of aeromedical standards to occupant selection, aircraft design features, and operational guidelines for spacecraft design
[FAA-AM-71-33] 19 p3044 N71-32083
- Dynamic reactions of operators with random vibrational stimuli and biomechanical systems
19 p3044 N71-32090
- Mechanical responses of human head subjected to acceleration loads determined for use in construction of artificial head
19 p3045 N71-32547
- Mechanics of free piston engine, aspects of human factors engineering, and compressible boundary layer studies at high Reynolds numbers
[DME/NAR-1971/11] 19 p3196 N71-32620
- Human factors engineering for man machine systems
19 p3048 N71-32622
- Human factors engineering in optimizing visual perception of sonar and radar displays
[AD-723992] 20 p3227 N71-33187
- Physiological and psychological reactions to sonic boom and effects on efficiency of air traffic control personnel
[FAA-AM-71-29] 21 p3383 N71-34068
- Manpower and training needs for air pollution control - public and private sectors
[S-DCC-91-98] 21 p3333 N71-33182
- Effect of increasing populations on world environment and international cooperation to reduce extent of environmental pollution
21 p3333 N71-33183
- Analysis of psychological and physiological variables for predicting human performance during extended periods of stress
[NASA-CR-121903] 22 p3543 N71-35236
- Analysis, synthesis, and transmission of human speech based on computation of time intervals between threshold transitions of speech waveform derivatives
[NASA-CR-121899] 22 p3553 N71-35305
- Human factors considerations in design, development, and tests of sonar display devices
[AD-726711] 22 p3554 N71-35317
- Comparison of methods for detecting nonfluctuating targets in white noise
[PHL-1971-2] 22 p3628 N71-35852
- Advantages of various types of liquids taken by workers under high temperature working conditions (miners, fire fighters, steelworkers)
[NASA-TT-F-14002] 23 p3713 N71-36469
- Effect of alcohol and disorientation responses on nystagmus and vertigo during angular acceleration with and without visual fixation
[FAA-AM-71-16] 23 p3714 N71-36477
- Performance and recovery of men subjected to low-level, whole-body vertical sinusoidal vibrations for one to two hours
[AD-726974] 23 p3715 N71-36481
- Effects of exercise on elevation of body temperature in human subjects and response of subject to temperature variations
[NASA-TT-F-13972] 23 p3716 N71-36486
- Design concepts for crew accommodations, personal equipment, and facilities for space station components
[NASA-CR-122924] 23 p3716 N71-36492
- Space station and base design considerations for crew stability and habitability
[NASA-CR-115179] 23 p3717 N71-36495
- Effects of display gain and signal bandwidth on visual sources of human controller remnant
[AD-727057] 23 p3717 N71-36500
- Guidelines for environmental habitability planning to facilitate individual and group stability
[NASA-CR-115180] 23 p3869 N71-37581
- Water-salt metabolism during space flight and microanalysis of actively circulating blood volume
[NASA-TT-F-14028] 24 p3877 N71-37638
- Water-salt metabolism under space flight conditions and body weight loss
[NASA-TT-F-14029] 24 p3877 N71-37639
- Engineering psychology as component part of systems engineering
24 p3881 N71-37665
- Human factors engineering problems in man machine interfaces in space shuttle systems
[NASA-CR-123166] 24 p4020 N71-38685
- Determining faculty necessary for accredited engineering curriculum as function of faculty workload, number of students, and curriculum characteristics with cost estimates
[NASA-CR-123114] 24 p4034 N71-38780
- ### HUMAN PATHOLOGY
- Physiopathology and pathology of spinal afflictions in aerospace medicine
[AGARD-AG-140-70] 01 p0008 N71-10175
- Medical and legal aspects of aircraft accident fatality investigation by aviation pathologist
02 p0162 N71-11805
- Leukocytic bacteria destruction in humans having Chediak-Higashi or Pelger-Huet anomaly
[NASA-TT-F-13637] 12 p1864 N71-34020
- ### HUMAN PERFORMANCE
- #### NT ASTRONAUT PERFORMANCE
- #### NT OPERATOR PERFORMANCE
- #### NT PILOT PERFORMANCE
- Effects of noise and vibration on psychomotor performance
[AD-710595] 01 p0008 N71-10034
- Effects of thermal stress, exposure time, and acclimatization on human performance
[AD-711012] 01 p0009 N71-10293
- Tolerance geometry in visual perception
[AD-710642] 01 p0011 N71-10435
- Influence of vestibular stimulation and display luminance on compensatory tracking task performance
[NASA-CR-111111] 01 p0012 N71-10499
- Studying relation between depth perception and disparity cues in human vision
[AD-711660] 01 p0013 N71-10645
- Pilot performance and acceptance of aircraft rigid cockpit control system during simulation
[AD-711296] 01 p0015 N71-10844
- Human performance effects of repeated exposure to impulsive acoustic stimulation
[AD-711637] 01 p0014 N71-10881
- Combined effects of noise and vibration on mental performance as function of time of day
[AD-711636] 01 p0014 N71-10891
- Acute mountain sickness in humans
[AD-712182] 02 p0156 N71-11102
- Defining effects of temporal and quantitative dietary variables on human performance of vigilance tasks
[AD-711564] 02 p0158 N71-11118
- Measuring human performance of auditory vigilance task time shared with memory task
[AD-711565] 02 p0158 N71-11119
- Evaluating use of adaptive techniques in control of tasks or stimuli
[AD-712124] 02 p0158 N71-11120
- Relations of psychological and physiological variables to human monitoring performance
[AD-711350] 02 p0166 N71-11178
- Design, development, and fabrication of personnel armor load profile analyzer
[AD-711876] 02 p0166 N71-11180
- Review and annotated bibliography of selected research on human performance
[NBS-SPEC-PUBL-319] 02 p0166 N71-11181
- Maximum detection range and discovery of land vehicles
[RAE-LIB-TRANS-1485] 02 p0166 N71-11182
- Task analysis reduction technique for analyzing human performance and man machine interface
[AD-711807] 02 p0169 N71-11198
- Decision making experiment to determine combinatorial properties of personal probabilities
[AD-712119] 02 p0169 N71-11201
- Adaptation techniques for human tasks and man machine systems
[AD-711955] 02 p0170 N71-11205
- Search effectiveness with starlight scope and binocular
[AD-712318] 02 p0226 N71-11595
- Effects of carbon monoxide containing cabin atmospheres on performances of humans and primates
[AMRL-TR-69-19] 02 p0162 N71-11804
- Glaucoma effects on visual performance of flying personnel
02 p0164 N71-11817
- Physiological consideration in preventing instability in oxygen breathing systems
02 p0171 N71-11822
- Perception and identification of images in different accelerative fields
02 p0164 N71-11824
- Operational design and initial sea trials of Sado-3 underwater laboratory
02 p0308 N71-12158
- Visual illusions in human perception of horizontal figures bordered by anchoring lines
[AD-712981] 03 p0320 N71-12287
- Anchoring stimuli and Titchener illusion
[AD-712982] 03 p0320 N71-12289
- Performance ratings and personality test factors of air traffic controllers
[AM-70-14] 03 p0329 N71-12350
- Procedures for determining photographic image quality and photointerpretation capabilities
[AD-712705] 03 p0376 N71-12765
- Sleep and transitional states in man under space flight conditions
[JPRS-51763] 04 p0479 N71-14463
- Sleep characteristics affecting human performance on aircraft, submarines, and spacecraft
04 p0479 N71-14464
- Sleep as indicator for human ability for adaptation to prolonged solitary isolation with altered day-night regimes
04 p0479 N71-14465
- Performance decrement as function of seven days complete bed rest
[AD-713070] 05 p0635 N71-14700
- Measuring social nonrandomness as function of duration and monotony of randomization task
[JEP-1970-18] 05 p0713 N71-15070
- Human performance, recovery, and man machine systems
[AD-714375] 06 p0806 N71-16230
- Developing human error rate data bank for human reliability and engineering problems
[SC-R-70-4286] 06 p0807 N71-16305
- Effects of input power spectra on human operator compensatory tracking
[AD-714130] 06 p0808 N71-16454
- Circadian rhythms of psychological functions under different conditions
07 p0977 N71-16986
- Circadian rhythm of bodily functions and dependence of reaction time on duration of sleep
07 p0978 N71-16987
- Effects of drugs on performance of flight personnel following unusual sleep patterns
07 p0978 N71-16988
- Effect of work-rest cycles on performance of flight crews and supervisory personnel
07 p0985 N71-16989
- Mental calculating ability, motor coordination, and auditory perceptual acuity of human subjects during long duration flight simulation
07 p0978 N71-16911
- Influence of duty hours on sleep patterns in flight crews during long duration flights
07 p0978 N71-16912
- Effect of immersion at different water temperatures on graded exercise performance in man
[PB-194822] 07 p0979 N71-17062
- Human performance under low frequency vibration and effects on whole body orientation
07 p0982 N71-17407
- Effect of physical and symbolic stressors on perceptual mechanisms
[AD-715308] 08 p1147 N71-18254
- Long term adaptation of pursuit rotor performance to impulsive acoustic stimulation
[AD-715289] 08 p1148 N71-18363
- Relationships between cardiac volume, body weight, physical work capacity, and blood volume in healthy men and women with varying range of performance
[NASA-TT-F-13439] 08 p1148 N71-18377
- Human performance in color naming and word reading with and without Stroop interference
[AD-716511] 09 p1339 N71-19579
- Human cognition, involving man machine interaction situations
[AD-716459] 09 p1339 N71-19605
- Vibration effects on performance of helicopter flight crews
09 p1335 N71-20355
- Combined environmental stress effects on human performance
09 p1336 N71-20362
- Stress effects of temperature and altitude on human performance
09 p1337 N71-20363
- Servocontrol infrared optometer applied to study of volitional control of human visual accommodation
[NASA-TM-X-64955] 09 p1338 N71-20371
- Health effects of sonic booms noting human reactions and performance, sleep deprivation and accident processes
[ISVR-TR-25] 10 p1504 N71-20809
- Confinement effects on human psychomotor performance during long duration space environment simulation test
10 p1509 N71-20813
- Long duration confinement effects in simulated space station on human performance during tracking task
10 p1509 N71-20814
- Non-interference crew performance analysis during long duration space station simulation test with visual and aural observations
10 p1509 N71-20816
- Long duration confinement effects in spacecraft cabin simulator on psychological test results for spacecrew
10 p1509 N71-20817
- Cutaneous perception test involving human ability to reproduce binary patterns formed by electrical stimulation of finger tips
11 p1679 N71-21899
- Effect of carbon monoxide on human performance including heart rate and galvanic skin response
[AD-717716] 11 p1683 N71-22209

SUBJECT INDEX

- Aging effects on military flight crew body composition and physical exercise performance
11 p1689 N71-22316
- Vibration effects on visual discrimination and tracking abilities in humans
13 p2032 N71-24437
[AD-719745]
- Signal and stimulus rate effects on long term human responses to light signal intensity differences
13 p2038 N71-24953
- Tracking error frequency response function and human psychomotor performance under aircraft vertical and lateral vibration conditions
13 p2038 N71-25067
[AD-719754]
- Stochastic model for computerized simulation of closed man machine system operated by crew
14 p2210 N71-26076
[AD-728354]
- Horizontal static forces exerted by men standing in common working positions on various surfaces including coefficients of friction between different floor and shoe materials
14 p2210 N71-26196
[AD-728355]
- Effects of atmospheric gas and moisture concentration, temperature, pressure, and wind velocity on human performance and skin water loss rate
14 p2206 N71-26185
[NASA-CR-115024]
- Performance and recovery characteristics of men when subjected to prolonged whole body vertical vibration
14 p2206 N71-26432
- Nutritional requirements of astronauts under open underwater stations and weightlessness
14 p2212 N71-26622
[JPRS-53161]
- Binary classification reaction time and human performance in data processing using decision making experiments
15 p2374 N71-26885
[AD-721199]
- Risk depending on human performance and production engineering, influencing quality control and performance characteristics of systems
15 p2526 N71-27106
[ZV-21-6]
- Taxonomy of human performance including mean value of performance measures and relevant factor loadings for variety of tasks
15 p2375 N71-27477
[AD-721217]
- Adaptation of human physiological functions and performance to variations in diurnal sleep and wakefulness cycles
16 p2543 N71-28258
- Psychophysiological stimulation of humans, monkeys and rats by color schemes for spacecraft cabin interiors
16 p2550 N71-28259
- Environmental chambers for testing human work performance under thermal stress
16 p2543 N71-28447
[AD-721593]
- Analysis of data on human ability to perform different locomotor acts under conditions of reduced gravity
16 p2543 N71-28477
- Formulation of work and rest schedules for optimum performance of spacecrafts
16 p2546 N71-28488
- Analysis of relationship between respiration rate and volume and minute volume of respiration under variety of physical loads
16 p2547 N71-28494
[AD-721644]
- Human potential in space exploration and operation of orbiting research laboratory
16 p2531 N71-28530
- Rate of acquisition of psychomotor skills by human operators in tracking tasks
16 p2548 N71-28839
[JPRS-54172]
- Evaluation of hypothesis that amount recalled and changing are inversely related to delayed recall interval
17 p2722 N71-29559
[AD-708568]
- Auditory stimuli effects on human color-word discrimination susceptibility test performance
17 p2708 N71-29637
[PAA-AM-71-7]
- Hypoxia effect on human vigilance performance
17 p2708 N71-29638
[PAA-AM-71-11]
- Psychological test of human reaction to simulated stress
17 p2708 N71-29639
[PAA-AM-71-14]
- Work environment and task factor effects on long term aircrew effectiveness
17 p2711 N71-29682
[AD-722417]
- Proceedings of conference on human reliability conducted by US Navy
17 p2712 N71-30034
[AD-722499]
- Dynamic psychological and ergonomic aspects of aerial imagery
18 p2876 N71-31040
[ZV-1979-21]
- Forty eight hour continuous work-sleep loss effects on human performance - Thermo project
18 p2877 N71-31236
[AD-722816]
- Parameters of human pattern perception effect of statistical properties of pattern components on feature detection
18 p2878 N71-31336
[AD-722794]
- Visualizer system associated with body movement in aerospace environments
18 p2880 N71-31336
[AMRU-R-66-3]

- Human visual tracking system during fixation maintenance determination, using narrow bandwidths of random noise
18 p2881 N71-31539
[AMRU-R-66-3]
- Effects of hyperbaric environments on primate neuromuscular control
18 p2881 N71-31587
[AD-723829]
- Approach indicator oscillation and illuminating effects on human performance of compensatory tracking tasks
19 p3047 N71-31618
[NASA-CR-119640]
- Human performance in escape from crashed vehicle environments and escape workloads of vehicles
19 p3196 N71-32347
[PB-196772]
- Human performance and recovery in man machine systems of continuous operations and work/rest schedules
19 p3048 N71-32331
[AD-723430]
- Ideal forecasts, forecasting technique, problems of specification, and human talent factor
19 p3131 N71-32724
[P-4390]
- Analysis of cerebral slow potentials underlying human attentive processes in central nervous system
20 p3220 N71-33437
[NASA-CR-121409]
- Medical and biological problems of prolonged manned space flight
20 p3220 N71-33451
[JPRS-53801]
- Weightlessness effects on human sensorimotor performance and locomotion
20 p3227 N71-33452
- Effects of forced temporal lockout intervals on user performance in interactive man-computer problem solving situation
20 p3239 N71-33698
[NASA-CR-121480]
- Physiological effects of sleep deprivation produced by simulated aircraft noise
21 p3382 N71-34064
[PAA-NO-70-16]
- Object recognition with aided and unaided night vision as function of luminance
21 p3382 N71-34065
[JZP-1971-7]
- Definition and identification of grounds for coordinating human activities with respect to earth environment
21 p3431 N71-34413
[NASA-CR-121639]
- Psychological investigations and theory of thinking with four types of intellectual associations
22 p3544 N71-35247
- Five year panel study to determine effects of time pressure on performance of scientists and engineers
22 p3546 N71-35261
[NASA-CR-121884]
- Effect of time between transmission, number of transmissions, and signal to noise ratios on sonar operators performance in long range target acquisition
22 p3549 N71-35279
[AD-726711]
- Prophylactic vitaminization with pyridoxine-containing compounds for preventing vestibular disturbances due to sea and air travel
23 p3715 N71-36480
[JPRS-54048]
- Performance and recovery of men subjected to low-level, whole-body vertical sinusoidal vibrations for one to two hours
23 p3715 N71-36481
[AD-726974]
- Mathematical model representing human performance reliability for laboratory vigilance and manual control tasks
23 p3718 N71-36503
[AD-727764]
- Crew performance measurement relationships for automated air to air intercept weapon system training simulator
24 p3882 N71-37675
[AD-727739]
- Experiment for observing human spatial activity under psychologically difficult conditions of modified postural-motor regime for astronaut selection
24 p4015 N71-38648

HUMAN REACTIONS

- Public reactions to sonic booms
01 p0014 N71-10026
[NASA-CR-14651]
- Comparative effects of auditory and extra auditory acoustic stimulation on human equilibrium and motor performance
01 p0008 N71-10177
[AD-711046]
- Physiology of respiration at high elevations using human subjects
01 p0009 N71-10245
[AD-710327]
- Sensory perception of ultrahigh frequency sinusoidal proprioceptive stimuli
01 p0009 N71-10248
[AD-711047]
- Air and land transportation noise sources and measurement, noise level scales, and individual and community responses - conference
01 p0003 N71-10349
[PB-191117]
- Feculiarities of human heat exchange under reduced atmospheric pressure and sufficient oxygen supply
01 p0010 N71-10367
[NASA-TT-F-13374]
- Homeostasis during weightlessness
01 p0010 N71-10368
[NASA-TT-F-13373]
- Characteristics of optokinetic eye-movement patterns and saccades in man and animals
01 p0011 N71-10425
[AD-708101]
- Information capacity of discrete motor responses compared for different directions and amplitudes of motion
01 p0012 N71-10536
[AD-710713]

HUMAN REACTIONS

- Human sleep patterns during prolonged exposure to hypobaric nitrogen saturated atmosphere
01 p0013 N71-10723
[AD-711671]
- Community physical, psychological, and social reactions to aircraft noise around 7 US international airports
02 p0146 N71-11032
[NASA-CR-111316]
- Review and annotated bibliography of selected research on human performance
02 p0166 N71-11161
[NBS-SPEC-PUBL-319]
- Legal, preventive, and clinical aspects of aerospace medicine
02 p0161 N71-11801
[AQAARD-CP-61-70]
- Post-mortem lactate analysis on pilot tissues to determine presence of technical malfunctions in aircraft accident
02 p0162 N71-11803
- Bioastronautic aspects of Apollo biomedical operations
02 p0164 N71-11821
- Studying long-term human reactions to space flight stresses
03 p0451 N71-12228
[NASA-TT-F-15414]
- Mental calculating ability, motor coordination, and auditory perceptual ability of human subjects during long duration flight simulation
07 p0978 N71-16911
- Human reactions to mechanical vibrations
07 p0981 N71-17238
- Streptococcal flora of human oral cavity during prolonged confinement
08 p1154 N71-19865
- Dynamic characteristics of human skeletal muscles modeled from surface electromyography
08 p1156 N71-19125
[NASA-CR-16911]
- Physiological and psychological limits and ranges of human response to acoustic stimuli
09 p1333 N71-20353
- Effects of long term exposure on auditory thresholds for discrete tonal signals and recovery from temporary threshold shift
09 p1333 N71-20353
- Stress and adaptation problems associated with large scale, long range, rapid reaction time, aerial troop deployments
09 p1336 N71-20340
- Relationship of interaction of impulsiveness and anxiety to perceptual-motor performance in human beings
09 p1336 N71-20361
- Effects of education and pharmacodynamics on adaptability of human beings to degraded sensorial environments
09 p1337 N71-20364
- Application of psychotherapy in aviation psychology for treatment of syndromes of reactive anxiety
09 p1337 N71-20365
- Health effects of sonic booms during human reactions and performance, sleep deprivation and accident proneness
10 p1304 N71-20669
[IBVR-TR-25]
- Auditory stimuli effects of pistol shots during landing process on human reactions and performance
10 p1384 N71-20799
[IBVR-TR-26]
- Crew reaction to environment instability during long duration space station simulation test
10 p1589 N71-20882
- Stress response prediction by correlation techniques and control of stress perception by human nervous system
10 p1409 N71-21150
[AD-716967]
- Vector analysis for estimating neuromuscular forces affecting human receptors in semicircular canals during rotation
16 p2544 N71-28263
- Psychophysics of human attention, and sensory and time discrimination
16 p2545 N71-28283
[NASA-CR-119023]
- Manual for human psychometric data acquisition and human reactions to psychological stress in Taktis project
16 p2554 N71-28549
[AD-721363]
- Human reactions to psychological stresses of confined environments using Taktis project astronauts
16 p2554 N71-28550
[AD-721364]
- Dynamics of electroencephalogram during sleep in humans under normal and altered daily regimes of sleep and wakefulness
17 p2712 N71-30140
[NASA-TT-F-13679]
- Comparison of human jet aircraft noise and simulated sonic booms
18 p2874 N71-30670
[NASA-CR-17800]
- Stress effects of intermittent exposure to 3 per cent CO2 on acid-base balance and electrolyte excretion in submarine personnel
18 p2877 N71-31238
[AD-722662]
- Effect of changes in metabolism of pyridoxine and serotonin on human vestibular disturbances during turbulent flight conditions
18 p2877 N71-31334
[JPRS-53676]
- Physiological effects of two levels of alcohol on vertigo and eustachian responses resulting from caloric irrigation

- rigations with visual conditions and alertness of subjects controlled
[FAA-AM-71-6] 19 p3043 N71-32079
- Physiological responses of inexperienced private pilots to cross-country flying
[FAA-AM-71-23] 19 p3043 N71-32082
- Human reactions to air pollution and responses to ecology and environmental control
[UCRL-73063] 19 p3093 N71-32258
- Human reactions to using a university computer center
20 p3369 N71-32820
- Human reactions to sleep deprivation by simulated sonic booms
[ISVR-TR-41] 20 p3226 N71-32865
- Prediction of human reaction time to light flashes
[AD-724001] 20 p3226 N71-33087
- Literature survey and bibliography on noise pollution including sources, effects, and control
[AD-724344] 20 p3311 N71-33315
- Color and music effects on humans during prolonged isolation in confined space
20 p3221 N71-33460
- Application of reflected ultrasound to detection of post-operative rejection of heart transplant
[NASA-CR-121642] 21 p3380 N71-34050
- Physiological effects of sleep deprivation produced by simulated aircraft noise
[FAA-NO-70-16] 21 p3382 N71-34064
- Measurement of effects of stress on air traffic control personnel through use of mood adjective check lists
[FAA-AM-71-21] 21 p3383 N71-34067
- Survey of reactions of nonmilitary flying personnel towards US adoption of metric units of measurement
[NBS-SP-345-5] 21 p3334 N71-35184
- Chemical and physical properties and mass response to nitrogen oxides in atmosphere
[AF-84] 22 p3612 N71-35730
- Model of human operator reflecting known perceptual and response characteristics for automobile driving task
23 p3718 N71-36504
- Psychotechnical analysis of creativeness in research personnel based on personal interviews for personnel management applications
[NRL-TRANS-746-801-(9022.401)] 24 p3880 N71-37656

HUMAN TOLERANCES

- Ultraviolet radiation effects on human and animal eye
[AD-711360] 01 p0013 N71-10753
- Physiological tests for long and short sleepers
[AD-711579] 02 p0154 N71-11090
- Determination of quantitative radiation response time data
[ORAU-109] 02 p0159 N71-11124
- Human heat stress tolerance indications
02 p0160 N71-11486
- Determination of human tolerance to impact accelerations
02 p0160 N71-11491
- Human tolerance to *Hydrogenomonas eutropha* and *Aerobacter aerogenes* as food
[A69-72851] 03 p0327 N71-12332
- Survey on acoustics technology emphasizing noise reduction and human tolerances
[NASA-SP-5093] 04 p0568 N71-14307
- Chromosomal aberrations in persons exposed to repeated occupational irradiation
[ORNL-TR-2332] 05 p0634 N71-14696
- Environmental tests of VISTOL vibration effects on human comfort
[NASA-TM-X-66956] 09 p1335 N71-20356
- Posture effects on flight crew tolerance to positive acceleration
09 p1335 N71-20357
- Radiation shielding standards including shield materials, benchmark problems, and shield performance evaluation
[ORNL-TM-3251] 10 p1610 N71-20650
- Effect of radiation sensitive mutations and radiation of recombination in partially diploid derivatives of *Escherichia coli*
[ORO-4024-1] 10 p1497 N71-20728
- Deuteriation in slow neutron radiography of biological media
[DP-1229] 10 p1497 N71-20729
- Dynamic models of human body response to acceleration environments and determination of tolerance limits
[NASA-TM-X-67038] 10 p1501 N71-21598
- Reliability of vestibular orientation test for motion sickness reaction produced by human head movements in rotating chair
[AD-716767] 10 p1502 N71-21650
- Physiological tolerance to thermal threats of aerospace activity and problems associated with excessive heat
[FAA-AM-70-22] 11 p1678 N71-21851
- Physical exercise effects on stress tolerances of trained and untrained subjects
11 p1688 N71-22306

- Oxygen consumption and heart rate measurements for estimating exercise tolerance of military personnel
11 p1688 N71-22308
- Biodynamics, aerospace medicine, acceleration stresses, human tolerances, centrifuges, test facilities, and associated bibliography
[AGARDGRAPH-150] 12 p1865 N71-23337
- Tabular and graphical summary of human tolerances to prolonged acceleration stresses
12 p1862 N71-23341
- Establishment of relationship between skin temperature and ability to tolerate cold and hot environments for human subjects
[FAA-AM-71-4] 13 p2037 N71-24748
- Annotated bibliography on human acclimation and acclimatization to heat
[NASA-TM-X-62008] 13 p2035 N71-25393
- Industrial noise and countermeasures - research methods and measuring devices
[AD-720414] 14 p2296 N71-25878
- Determination of acceleration limits for passenger comfort in urban transportation system
14 p2205 N71-26118
- Human tolerance to impact determined by free fall simulation tests with instrumented dummy
[ARL-SM-353] 15 p2375 N71-27476
- Microbiological ecology of manned space flights, exobiology, sterilization, and life support systems
[JPRS-53388] 16 p2542 N71-28248
- Evaluation of human vestibular tolerance by Coriolis acceleration test
16 p2544 N71-28262
- Threshold limits of human tolerance to trace contaminant toxicity in spacecraft cabin atmospheres
16 p2552 N71-28533
- Harmful biological effects caused by exposure to microwave radiation including radio frequency power density in vicinity of space station antennas
17 p2707 N71-29325
- Extrapolation of animal tolerances of air contaminants to human tolerances for diver breathing under hyperbaric conditions
[AD-721681] 17 p2707 N71-29359
- Tolerances of human brain to impact shock and concussions
[FAA-AM-71-13] 17 p2708 N71-29636
- Comparison test to evaluate perceived noise level for STOL and other aircraft sounds
[WR-70-9] 18 p2872 N71-31075
- Air quality criteria for nitrogen oxides and their toxicological effects on animals, plants, and human beings
[PB-197333] 18 p2918 N71-31309
- Effect of changes in metabolism of pyridoxine and serotonin on human vestibular disturbances during turbulent flight conditions
[JPRS-53678] 18 p2877 N71-31334
- Technique for estimating maximum internal dose rate to man from continuous release of radionuclide to biosphere
[UCRL-50163-PT-7] 18 p2878 N71-31499
- Human dynamic response to impact acceleration minus G sub a - measurements on head and neck
[AD-711360] 19 p3046 N71-31616
- Physiological effects of two levels of alcohol on vertigo and vestibular responses resulting from caloric irrigations with visual conditions and alertness of subjects controlled
[FAA-AM-71-6] 19 p3043 N71-32079
- Analysis of aircraft structures which cause majority of injuries in aircraft accidents and recommendations for structural improvement to reduce accident severity
[FAA-AM-71-3] 19 p3038 N71-32447
- Relations between aircraft and road traffic noise and noise tolerance in communities
[TT-7102] 21 p3375 N71-34019
- HUMAN WASTES**
NT FECES
NT SWEAT
NT URINE
- Waste control aspect of housekeeping for future manned orbital missions
[NASA-CR-108763] 04 p0614 N71-14115
- Toxicology of human and animal waste products and by-products in controlled atmospheres of closed ecological systems - literature review
[NASA-TT-P-634] 09 p1338 N71-20493
- Design of isotopic fueled distillation and filtering system for potable water recovery from human waste during space simulation tests
10 p1505 N71-20957
- Human waste disposal system performance during long duration space flight simulation
10 p1507 N71-20970
- Evaporation and filtration systems for water management in manned space vehicles
16 p2552 N71-28536
- Water reclamation from human and other wastes for prolonged space flights
24 p4015 N71-38645
- HUMIDITY**
Effect of atmospheric humidity on characteristics of turbofan engine
[AD-715232] 07 p1103 N71-17728

- Statistical data on high humidity extremes in upper air
[AD-715894] 08 p1230 N71-18520
- Electrical insulation protection in printed circuits under varying temperature and humidity conditions
[ECR-141] 10 p1531 N71-20681
- Humidity generator and atmospheric control chamber for use with optical microscopes in studying specimen changes with variations in humidity
[AD-716994] 10 p1597 N71-21244
- Combined characteristics of air temperature and humidity for Arctic summer period
11 p1754 N71-22824
- Technique for predicting adhesive metal bond failure times under constant stress and low humidity
[AD-722511] 16 p2817 N71-28075
- Tests on radioisotope humidity error resulting from solar heating in low latitude regions
[NOAA-TR-BRL-194-AOML-4] 20 p3273 N71-33210
- Development of low range moisture generator for use in laboratory and field calibration operations
[Y-1791] 20 p3346 N71-33536
- Diurnal and annual temperature, humidity, wind speed, and wind direction in Donetsk, Ukraine
[NLL-M-20722-(5828.4F)] 21 p3422 N71-34813
- Proportional feedback control to replace original servocontrol unit for controlling carbon dioxide concentration and relative humidity in Null point compensating system for plant measurements
[UCLA-12-813] 21 p3433 N71-34638
- Teflon FEP investigated as cover for silicon solar cells including process for heat sealing
[NASA-CR-72790] 22 p3542 N71-33211
- Effects of dry heat and chemicals on long term survival rates of bacteria spores under varying temperatures and humidity conditions
[NASA-CR-122088] 23 p3713 N71-34407
- Thermal cycling, humidity, and salt spray tests of plasma-sprayed aluminum coatings for circuits potential in epoxy materials
[BDD-613-408] 23 p3777 N71-34829
- Effect of high humidity and temperatures on electrical and mechanical properties of stored silicon solar cell contacts
[NASA-CR-123185] 24 p3875 N71-37622
- HUMIDITY MEASUREMENT**
Effect of humidity on corona discharge in air and feasibility evaluation for use of corona cell as humidity meter
[RAE-TR-70106] 13 p2078 N71-24375
- Tabulated upper air data obtained over Japan by radiosondes for dew point, atmospheric electricity, and long wave radiation for 1966 and 1967
13 p2109 N71-25207
- Lag correction procedure for radioisotope humidity measurement errors
19 p3131 N71-32277
- Comparison of temperature and humidity differences between mountain stations and free atmosphere over Poprad, Czechoslovakia
[NLL-M-20356-(5828.4F)] 21 p3453 N71-34578
- HUNGARY**
Technical specifications and performance capabilities of Soviet and Hungarian produced GTT 600B/192 (Drushba) microwave system
[AD-727411] 24 p3889 N71-37719
- HUNTER F-2 AIRCRAFT**
U F-2 AIRCRAFT
HUNTING B-126 AIRCRAFT
U B-126 AIRCRAFT
- HURRICANES**
Bibliography and index of hurricanes and severe storms along coastal plains of US
[PUBL-70-2] 02 p0259 N71-11807
- Calculated and observed changes in sea surface temperature associated with hurricane passage
[AD-713052] 03 p0372 N71-11228
- Radar precipitation data gathered during multiple seeding of hurricane Debbie to test hypothesis that seeding changes storm structure
05 p0716 N71-13075
- Linear theory for response of two-layer ocean model to moving hurricane
09 p1380 N71-19082
- Tropical storm and hurricane modification - Project Stormhury
[AD-717498] 11 p1790 N71-22248
- Survey of structural damage along Mississippi-Louisiana Gulf Coast done by Hurricane Camille
[NBS-TM-569] 12 p1955 N71-25269
- Analysis of meteorological conditions leading to hurricane formation and determination of point of origin off coast of Africa
18 p2951 N71-30005
- Analysis of structure and motion of four major wave disturbances over Africa and development of three storms into hurricanes
18 p2951 N71-30007
- Organization and activities of project to beneficially alter tropical cyclones and reduce destructive effects
18 p2952 N71-30049
- Description of research project to reduce destructiveness of tropical storms by cloud seeding and reduction of evaporation from ocean surface
18 p3000 N71-30000

SUBJECT INDEX

Description of meteorological parameters associated with hurricanes and tropical storms 18 p2952 N71-31022

Development of numerical weather prediction for tropical regions and application to tropical cyclone forecasting 18 p2952 N71-31023

Mathematical primitive equation model for simulating development of tropical cyclones 18 p2952 N71-31025

History and operations of project to alter destructive features of tropical storms and hurricanes 18 p2953 N71-31026

Analysis of soundings taken within 100 nautical miles of center of hurricanes 18 p2953 N71-31027

Tabulation and maps of major hurricanes affecting United States during period 1873 to 1966 18 p2953 N71-31028

Analysis of hemispheric circulation and anomaly patterns when tropical storms reach hurricane intensity 18 p2953 N71-31029

Hurricane/weather modification experiments - secondary project 19 p3127 N71-31822

HYBRID COMBUSTION

U HYBRID PROPELLANT ROCKET ENGINES

HYBRID COMPUTERS

Two hybrid computer identification techniques for use in manual control research 07 p0986 N71-17442

Hybrid program for solving space-time dependent diffusion equation in four energy groups 08 p1246 N71-18173

Space/ground study of graphite gas power reactor in hybrid computer - conference 08 p1235 N71-18208

Control center with integrated computer for real time processing and display of information from SERT 2 spacecraft 09 p1365 N71-19855

Library routines and macros for PDP hybrid software system 09 p1355 N71-20110

Digital simulation, digital filters, PDP 9 computers, on-line programming, hybrid computers, computer graphics, plotters, analog computers, optimization, and integrated circuits 12 p1882 N71-23862

Hybrid computer simulation of detection of phase coherent RFL pulse train of unknown phase in additive random noise 12 p1884 N71-23869

Hybrid computer method of optimizing control variable functions by addition of random perturbation 12 p1884 N71-23871

Hybrid analog computer for magnetogram data processing 13 p2053 N71-25409

Applicability of gradient method as optimization strategy for use with hybrid analog computer 14 p2224 N71-26330

Hybrid computer measurement of stopband in LAMPF 805 MHz accelerator structure at high power 15 p2387 N71-26857

Hybrid computer nonlinear programming with dynamic constraints and application to nuclear reactor and heat exchangers 15 p2449 N71-27390

Decoding algorithms for data reduction and transmission through noisy space channels using sequential and hybrid computers 16 p2564 N71-28088

Hybrid computer program for determination of laser pulse sequence transient response 19 p3060 N71-31662

Hybrid computer simulation of hydraulic pumping system 20 p3280 N71-33829

HYBRID NAVIGATION SYSTEMS

Investigating performance of various types of pure inertial and hybrid navigation systems 05 p0721 N71-15343

HYBRID PROPELLANT ROCKET ENGINES

Investigating gas dynamical aspects of combustion in hybrid rocket motors 03 p0468 N71-13099

LOX/polyethylene hybrid propellant rocket engine test 07 p1099 N71-17331

Optimum methods for orbital resupply, maintenance, and repair of hybrid propellant rocket engine subsystem for orbiting space station attitude control 12 p1991 N71-23955

Configuration of hybrid attitude propulsion system servicing space station 13 p2156 N71-24927

Hybrid and decomposition combustion of hydrazine fuel using flat flame burner to provide high temperature gaseous environment for burning drops of liquid fuel 22 p3495 N71-34352

HYBRID PROPELLANTS

Linear for hybrid solid propellants to bind propellant to rocket motor case 06 p0938 N71-16392

Regression rates for hybrid FLOX polyethylene mixture combustion 11 p1840 N71-22128

Experiments on diimide oxalic acid dihydrazine as hybrid rocket propellant 15 p2510 N71-37101

HYDRATES

Lithium hydride solid rocket propellant decomposition with lithium hydride monohydrate 07 p1098 N71-17228

X ray diffraction study of crystal and molecular structure of sodium gold thiosulfate dihydrate single crystals 09 p1455 N71-28581

Electron paramagnetic resonance of $\text{Cr}^{2+}/\text{phen}$, $\text{Ni}^{2+}/\text{phen}$, and $\text{Cu}^{2+}/\text{phen}$ in hydrated single crystals at temperatures from 300 to 1.2 K 17 p2814 N71-29725

Reaction kinetics of nitrogen oxide ion and hydrate clustering in gas flow system 21 p3386 N71-34086

HYDRATION

Paramagnetic resonance and mass spectroscopic analysis of hydration products in aqueous acetaldehyde solutions 20 p3229 N71-33414

HYDRAULIC ACTUATORS

U ACTUATORS

U HYDRAULIC EQUIPMENT

HYDRAULIC CONTROL

Shear modulated fluid amplifier of high pressure hydraulic vortex amplifier type 07 p1009 N71-17578

Performance characteristics of improved servomotor for electrohydraulic control systems 07 p0996 N71-17583

Throttle valve for regulating fluid flow volume 08 p1206 N71-18580

Fluidic-thermochemical display device 08 p1179 N71-18603

Fluidic roll control for Aerobea rocket vehicle 08 p1294 N71-18745

Design of electronic controlled pneumatic signal converter for fluidic device testing by sine wave generation 12 p1890 N71-23886

Development and characteristics of variable displacement fluid pump for transmuting hydraulic pressures 17 p2756 N71-30028

Dynamics of four combinations of fluid control and load actuating components in hydraulic servomechanisms having long lines or flexible metal-reinforced rubber hose connections 18 p2907 N71-31304

Development and characteristics of redundant hydraulic control system which operates following failure of one or two major control elements 21 p3433 N71-34426

HYDRAULIC EQUIPMENT

Hydraulic support apparatus for dynamic testing of space vehicles under near-free flight conditions 01 p0038 N71-10804

Hydraulic drive mechanism for leveling isolation platforms 01 p0060 N71-10638

Examining dynamics of hydraulic or pneumatic servomechanisms with aid of mathematical models 01 p0061 N71-10903

Air inleak and flow aeration in hydrotransmission 01 p0044 N71-10942

Calculating cavitation characteristics in converging channels of different shape using Bernoulli-Carnot theorem 02 p0200 N71-11435

Determining critical speeds of hydraulic unit shafts 02 p0236 N71-11755

Antibacklash circuit for hydraulic drive system 03 p0317 N71-12260

Effects of structural motion on dynamic response of liquid flow systems and automatic control hydraulic systems 06 p0797 N71-16559

Hydraulic clamping of sheet stock specimens 07 p1037 N71-17696

Hydraulic performance and cavitation characteristics of electromagnetic helical induction pump operating with potassium at 1500 F and with lithium at 2200 F 08 p1205 N71-18324

Electric and electrohydraulic stepping motors for numerically controlled machine tools 10 p1562 N71-20750

Design and development of double acting shock absorber for spacecraft docking operations 10 p1567 N71-21530

Operational test and evaluation of pulse operated flow path selector valve assembly 11 p1767 N71-21997

HYDRAULIC TEST TUNNELS

Hydraulic apparatus for casting and molding of liquid polymers 11 p1698 N71-22975

Optical comparator and hydraulic gauging methods for obtaining underwater dimensional measurements of irradiated fuel elements 13 p2113 N71-24527

In-pile hydraulic capsule facility for temperature measurements inside capsule 13 p2115 N71-24552

System to control speed of hydraulically movable members by limiting energy applied to actuators with hydraulic servo loop 15 p3416 N71-37754

Development of aircraft control system with high performance electrically controlled and mechanically operated hydraulic valves for precise flight operation 16 p3597 N71-39128

Bearings, lubricants, and seals for lubricated and hydraulic components for space shuttle with high temperature and vacuum operating capabilities 17 p3755 N71-29469

Characteristics of hydraulic systems and application to aircraft systems 17 p3703 N71-29562

Development and characteristics of variable displacement fluid pump for transmuting hydraulic pressures 17 p2756 N71-30028

Hydraulic pump jet propulsion unit for destroyer, and incorporated computer program 17 p2840 N71-30339

Hybrid computer simulation of hydraulic pumping engine 20 p3280 N71-33829

Development and characteristics of redundant hydraulic control system which operates following failure of one or two major control elements 21 p3433 N71-34426

Wasting device for sodium cooled fast reactor with ceramic fuel elements 21 p3437 N71-34465

Statistical methods for determining reliability of hydraulic systems 22 p3588 N71-35554

Analytical procedures for predicting coupled fluid structural responses of aircraft hydraulic systems 22 p3485 N71-36276

Hydraulic power and actuation requirements of survivable flight control system utilizing fly by wire control for F-4 aircraft 24 p3873 N71-37608

HYDRAULIC FLUIDS

Dynamics of onboard fluid ring automatic oscillation dampers 08 p1206 N71-18604

Characteristics of hydraulic systems and application to aircraft systems 17 p3703 N71-29562

HYDRAULIC HEATING SOURCES

U HEAT SOURCES

U HYDRAULIC EQUIPMENT

HYDRAULIC JETS

Characteristics of radial wall jet bounded by circular jump 02 p0304 N71-12078

Wind tunnel photography for determining water droplet size in breakup of water jets 08 p1183 N71-18962

Hydraulic pump jet propulsion unit for destroyer, and incorporated computer program 17 p2840 N71-30339

Buoyant jet mixing flow from manifolds in stagnant receiving water of uniform density using hydraulic models of waste disposal system 19 p3080 N71-32462

Physical mechanisms and problems involved in mixing shock of waterjet gas pump 23 p3742 N71-36482

HYDRAULIC PUMPS

U HYDRAULIC EQUIPMENT

U PUMPS

HYDRAULIC SYSTEMS

U HYDRAULIC EQUIPMENT

HYDRAULIC TEST TUNNELS

Low speed and supersonic wind tunnel and hydraulic test tunnel tables 03 p0359 N71-13337

Turbulent flow boiling tests of heated flat plate model in high speed water tunnel 17 p2773 N71-29619

Experimental capabilities and operating conditions of hydrodynamic wind-water tunnel including flow visualization 17 p2752 N71-30263

Drag coefficient of vehicle traveling coaxially with uniform velocity through solid wall tube of finite length 19 p0076 N71-31763

Effect of wire screen roughness on wall shear stress and cavitation characteristics during fluid flow in hydraulic test tunnel 19 p3077 N71-31996

Thermal and hydraulic performance of prototype SNAP-3 mercury boiler - design, fabrication, and preliminary evaluation
[NASA-TN-D-6451] 19 p3041 N71-32209

Water tunnel tests of helicopter rotor performance
[AD-724191] 20 p3204 N71-32934

Visual operational problems and sound absorption in porous walls of hydraulic test tunnels
[JF-171-12] 30 p3228 N71-33725

Blowing effects on flow around models analyzed by flow visualizations produced in water tunnel
[NASA-TT-F-13742] 21 p3409 N71-34254

Design, construction, and performance of water tunnel for two dimensional testing of pitching airfoils
[D180-14130-1] 24 p3904 N71-37827

HYDRAULIC VALVES U VALVES

Principles of nuclear, thermal, and hydraulic performance calculations for water cooled reactors
[AEEW-R-691] 03 p0415 N71-12880

Compilation of reports on hydraulic research projects conducted in US and Canada
[NBS-SF-346] 12 p1903 N71-24141

Computer program for thermodynamic and hydraulic analysis of water cooled reactor channel flow operating under static conditions
[EUR-4533] 19 p1140 N71-32576

RELAP/ASME code for analyzing reactor core and loop thermal hydraulics during blowdown
[CONF-710302-6] 21 p3459 N71-34617

HYDRAZINE ENGINES

Developing throttleable monopropellant hydrazine thruster system for planetary landing vehicles
[NASA-CR-110963] 01 p0116 N71-10763

Propellant decomposition catalysts for hydrazine engines and gas generators - conference papers
[DLR-MITT-69-29] 07 p1097 N71-17192

Propellant decomposition in hydrazine engines and gas generators using noble metal catalysts
07 p1097 N71-17193

Hydrazine propellant decomposition with noble metal catalysts for quick ignition
07 p1097 N71-17196

Catalysts for hydrazines and hydrogen peroxide in hydrazine engines and gas generators
07 p1097 N71-17197

Throttling and heat sterilization effects on hydrazine reactor efficiency and buffer geometry for combustion chamber stability
10 p1639 N71-21358

High specific impulse of several hydrazine thrusters ignited by electrical heaters within thrust chamber during experimental evaluation
[NASA-CR-118322] 13 p2157 N71-25237

Evaluation of Planetary Explorer propulsion systems of monopropellant hydrazine type for use on Venus mission satellite
[NASA-CR-118668] 14 p2332 N71-26420

Hybrid and decomposition combustion of hydrazine fuels using flat flame burner to provide high temperature gaseous environment for burning drops of liquid fuel
[NASA-CR-72977] 22 p3495 N71-36352

HYDRAZINES

NT CHLOROPRAZINE
NT DIHYDRAZINE
NT DIMETHYLDIHYDRAZINES
NT METHYLDIHYDRAZINE

Thermal control concepts for space storable fluorine hydrazine propulsion module
[NASA-CR-111062] 01 p0114 N71-10041

Electrosynthesis of hydrazine from gaseous ammonia
[ECRC/R264] 04 p0484 N71-13440

Hydrazine monoperfluoro alkanoate solder flux leaving corrosion resistant coating, for metals such as copper
[NASA-CASE-XNP-03459-2] 05 p0711 N71-15688

Weight, cost, and spacecraft reliability analyses of hydrazine and azozone spin stabilized communication satellite orientation devices
[BSRO-CR-20] 07 p1118 N71-17857

Scanning electron microscope study of hydrazine liquid rocket propellant catalysts
07 p1097 N71-17194

Nickel catalysts for hydrazine fuel cells
07 p0974 N71-17195

Reentry plasma sheath alleviation by injecting sulfur hexafluoride or hydrazine into boundary layer
10 p1629 N71-21310

Space storable fluorine/hydrazine tank module thermal control design for Jupiter mission
[NASA-CR-117959] 13 p2176 N71-25578

Rubber composition for expansion bladders and diaphragms for use with hydrazine
[NASA-CASE-NPO-11433] 18 p2940 N71-31140

Chemical and metallurgical analyses of 6AL-4V titanium test specimens exposed to hydrazine [N2H2] liquid propellant
[NASA-CR-121456] 20 p3284 N71-33234

Use of N-15 as tracer to study decomposition of hydrazine on Shell 403 catalyst
[RPE-TR-69/10] 20 p3230 N71-33873

Quantitative measurements of liquid hydrazine residence times as function of absorbed gas condition of catalyst and liquid hydrazine/catalyst temperature
[NASA-CR-121904] 22 p3549 N71-35281

Design and tests of monolithic catalyst beds for monopropellant hydrazine reactors
[NASA-CR-122644] 23 p3719 N71-36508

Correlation of calculated and experimental product yields as functions of gas molecule residence time, power, gas pressure, and allyl alcohol in electrocatalysis of hydrazine from ammonia
[BCRC/H343] 23 p3719 N71-36510

HYDRAZINIUM COMPOUNDS
Nuclear magnetic resonance of deuterons in hydrazinium sulfate noting electric quadrupole coupling constants and electrical conductivity
20 p3355 N71-33864

HYDRIDES
NT BERYLLIUM HYDRIDES
NT BORANES
NT BORON HYDRIDES
NT CARBORANE
NT DIBORANE
NT LITHIUM HYDRIDES
NT METAL HYDRIDES
NT NITROGEN HYDRIDES
NT PENTABORANES
NT PHOSPHINES
NT SILANES
NT ZIRCONIUM HYDRIDES

Measuring oxidation of a-xylyleneglycol on rotating disk electrodes and regularities in series of volatile inorganic hydrides
[JPRS-51604] 02 p0174 N71-11223

Investigating regularities of reduction potentials in series of volatile inorganic hydrides of elements in main subgroups of periodic system
02 p0174 N71-11225

Eigenvalues for point and space kinetics model comparison in uranium-hydride reactor
[FEI-177] 04 p0589 N71-14317

Hydride physico-chemical and chemical properties, reactions, purification, isolation, and analysis techniques
[AD-718179] 12 p1870 N71-23519

Metallographic study of hydride precipitation effects on tensile properties of neutron irradiated Zircaloy 2
[BM-X-10276] 18 p2938 N71-31561

HYDROACOUSTICS

U UNDERWATER ACOUSTICS
HYDROAEROMECHANICS
U AEROODYNAMICS
HYDROBALLISTICS

Investigation of vertical water entry deceleration of various cone shapes
[AD-724821] 19 p3078 N71-31999

HYDROBIPHONES
U HYDROPHONES
HYDROCARBON FUELS
NT GASOLINE
NT JET ENGINE FUELS
NT JP-3 JET FUEL

Performance of reducing electrode for neutralizing electrically charged hydrocarbon fuel flow
[AD-712348] 02 p0287 N71-11876

Nuclear magnetic resonance method of determining solubility of hydrocarbons fuels
[AD-711952] 02 p0288 N71-11890

Geothermal investigations for determining subsurface structure of petroliferous and gas bearing regions
[NASA-TT-F-13592] 02 p0218 N71-12017

Combustion efficiency of hydrocarbon fuels with ammonium nitrate propellant additive and solidified oxygen and fluorine gas oxidizers
[BMW-FB-W-70-47] 07 p1098 N71-17227

Viscoelastic cross linking behavior of elastomers, energy transfer in bipyridinium herbicides, and electrical properties of tetracyano quinodimethane polymeric salts
10 p1514 N71-21356

Evaluation of Aqua-Glo free water detector for use in measuring undissolved water in hydrocarbon fuels
[AD-718418] 12 p1908 N71-23438

Theoretical and experimental analysis of flame spreading across pools of liquid fuels and ignitability under quiescent and flowing environments
[AD-718666] 12 p0210 N71-23492

Thermodynamic molar data correlation for partially miscible acetonitrile benzene n-heptane system by conformal formalism
12 p1872 N71-23785

Analysis to determine regenerative cooling limits of light hydrocarbons used with FLOX and OF2 over wide range of operating conditions
[NASA-CR-72705] 14 p2352 N71-25801

Catalytic and thermal reforming of gaseous hydrocarbons with steam into town gas
[NASA-TT-F-13668] 16 p2600 N71-28159

Factors relevant to development of fuels and energy policies compatible with environmental control
17 p2861 N71-29471

Solutions of aqueous fluorochemical surfactants placed on surfaces of liquid hydrocarbons and hydrocarbon fuels for suppression of fuel evaporation
[AD-723189] 19 p3172 N71-32950

HYDROCARBONS

NT ACETYLENE
NT ALKANES
NT ALKENES
NT ALKYNES
NT ANTHRACENE
NT BENZENE
NT BUTADIENE
NT BUTENES
NT CYCLIC HYDROCARBONS
NT ETHANE
NT ETHYLENE
NT METHANE
NT NAPHTHALENE
NT NITROPROPANE
NT PARAFFINS
NT PENTANES
NT PROPANE
NT VINYLENE

Mass spectroscopy to determine structure of various substituted polyfluorobenzenes
[AD-711072] 02 p0175 N71-11220

Effects of pressure and temperature on electronic properties of materials
02 p0273 N71-11778

Flash point method for flammability hazard evaluation during flammable liquid transport
[PB-139077] 03 p0468 N71-12223

Antioxidant additive for hydrocarbon oils
[AD-713046] 03 p0396 N71-13408

Liquid hydrogen propellant containing hydrocarbon colloids for nuclear propulsion systems
[NASA-CR-115818] 04 p0362 N71-14417

Open cycle hydrocarbon-air fuel cell power plant
[AD-713528] 03 p0631 N71-14487

Antivapor and extreme pressure additive effects during bearing spinning with synthesized hydrocarbon oils
[NASA-TM-X-52931] 05 p0491 N71-14776

Combustion and physical properties of hydrocarbons
[AD-714674] 06 p0938 N71-14880

Corrosion inhibitors in aqueous solutions of liquid hydrocarbons
[AD-714419] 06 p0871 N71-14928

Ground and excited states of benzene by SCF and CI methods
07 p0987 N71-17880

Analyzing glaciers, hot springs, and volcanoes as from erupting volcanoes in Iceland for hydrocarbon content as test for life detection techniques
07 p026 N71-17794

Vapor phase hydrogen bonding equilibrium in methanol-water complexes with diethylenes
08 p1160 N71-18828

Photochemical reactivity of diesel engine hydrocarbons
[BMRI-7514] 10 p1661 N71-30011

Annotated bibliography on hydrocarbons and air pollution
[PB-197165] 10 p1666 N71-31807

Conformal solution theory for temperature variation and excess thermodynamic property prediction in hydrocarbon liquid mixtures
12 p1871 N71-23774

Investigation of thermal stability of hydrocarbon networks by chemical stress relaxation in vacuum environment at high temperatures
[AD-719916] 14 p2212 N71-30017

Time resolved measurements of exhaust gas temperature, mass flow rate, and hydrocarbon concentration of spark ignition engine
14 p2353 N71-30008

Effects of tube bundle geometry on nucleate boiling region of several hydrocarbon liquids based on flow boiling characteristics of single tube
14 p2355 N71-30034

Lubrication chemistry of hydrocarbon liquids and effects on bearing surface wear
15 p3414 N71-30009

Degradation of hydrocarbon polymers by exposure to 273 F for 400 hours in presence and in absence of ammonia peroxide
[NASA-CR-119005] 16 p2354 N71-30009

Nuclear magnetic resonance of chlorinated hydrocarbon molecules in excited triplet states using Hammettians for electron spin-spin, nuclear quadrupole, and hyperfine interactions
[UCRL-20390] 17 p2791 N71-30017

Primary and secondary ionization coefficients of argon-hydrocarbon Penning mixtures
[AD-722131] 17 p2714 N71-30009

Ionization potentials for photoelectron radiolysis of vapor phase methane, ethane, and ethylene
18 p2806 N71-31110

Effects of buffer solution pH values on paperographic reduction of Nitrazepam
[RAE-LIB-TRANS-1508] 22 p3551 N71-35299

Measurements of electrical conductivity in n-hexane, nonhexane, and polystyrene films induced by X-ray irradiation
[AD-726553] 22 p3603 N71-35999

Influence of fuel additives on automobile exhaust emissions and composition of exhaust hydrocarbons
[TPR-40] 22 p3461 N71-35999

SUBJECT INDEX

Effect of organic iron chelate, ligand structure on oxidation product formation and aeration rate of canoes [FOA-1-B-1155-92] 24 p3886 N71-37698

HYDROCHLORIC ACID

Thermodynamic properties of aqueous hydrochloric acid-calcium chloride-magnesium chloride mixtures calculated by electrostatic force measurements [JORN-TM-3017] 01 p0019 N71-10805

Galvanometric corrosion of uranium alloys in hydrochloric acid and ocean water [RFP-1592] 17 p2760 N71-29212

Sub-boundary corrosion in polygonized polycrystalline aluminum containing iron and copper impurities and exposed to HF and HCl solutions 17 p2764 N71-29726

Mass-spectrometric stirred-reactor technique to measure rate of reaction of hydrogen chloride and dinitrogen chloride with atomic oxygen [NASA-TN-D-6495] 21 p3386 N71-34092

Analysis of corrosion rates and products of depleted uranium in ocean water and hydrochloric acid [RFP-1586] 21 p3440 N71-34477

Thermodynamics of oxide reduction on heat exchanger, chromium as alloying component, substrate and hydrogen chloride corrosion, and silicon sulphide phenomena [NLL-CE-TRANS-5605-[9022.09]] 23 p3697 N71-36370

Sorption of antimony-125 by silica gel from alic and hydrochloric acid [RFP-1578] 23 p3794 N71-37045

HYDROCHLORIDES

Continuous operation laser based on chemical excitation of vibrational rotational levels of hydrogen chloride produced in detonation waves stabilized in supersonic flow 18 p2932 N71-31420

HYDROCYANIC ACID

U HYDROGEN CYANIDES

HYDRODYNAMIC EQUATIONS

NE HELMHOLTZ VORTICITY EQUATION

Hydrodynamic analogy in coloidal mechanics [NASA-CR-111364] 02 p0234 N71-11414

Derivation of hydrodynamic equations for gas mixture using Boltzmann transport equations and Onsager symmetry relations 07 p1006 N71-16949

Numerical weather forecasting based on hydrodynamic and thermodynamic equations and accounting for atmospheric moisture transfer and radiation effects [AD-716497] 09 p1412 N71-19482

Radiation hydrodynamic equations for thermal waves and radiative shock front structure [CEA-R-4057] 09 p1440 N71-20298

Hydrodynamic equations for arbitrary anisotropic plasma allowing for Coulomb collisions among plasma particles [RFP-1112] 15 p2303 N71-27891

Absorptivity and emissivity hydrodynamic equations for suprathermal electrons gyrating in magnetic plasma including Doppler effect with solar radio emission examples [AD-721337] 16 p2662 N71-28066

Hydrodynamic collisionless plasma equations for approximating ordinary wave propagation in plasma [NASA-TT-F-13612] 16 p2663 N71-29026

Electroacoustic transducer measurements of secondary sound velocity and inertial mass as function of He-3 concentration and temperature of He-3/He-4 mixture vapor pressure 17 p2789 N71-30293

Calculation of average hydrodynamic values during laminar and isothermal flow of liquids in clusters of rods [ABC-TR-7184] 18 p2904 N71-30659

Hydrodynamic equations for determining rotational coefficients in solar wind [NASA-TT-F-13611] 18 p3006 N71-31089

Hydrodynamic model for thin flow mass transfer in carbon dioxide/water two phase flow 18 p2906 N71-31186

Development of hydrodynamic code for representing shocks by discontinuities whose jump conditions and propagation velocities satisfy Hugoniot relations [P-4556] 19 p3081 N71-32606

Boltzmann models for hydrodynamic equation, transport coefficients, and light scattering by simple fluids 22 p3570 N71-35429

HYDRODYNAMIC STABILITY

U FLOW STABILITY

HYDRODYNAMIC TUNNELS

U PLASMA JET WIND TUNNELS

HYDRODYNAMICS

HY ELASTOHYDRODYNAMICS

HY ELECTROHYDRODYNAMICS

HY MAGNETOHYDRODYNAMICS

Second order theory of oscillating cylinders [AD-710767] 01 p0042 N71-10334

Using underwater photography to demonstrate formation of mobile roughness in skin of humans and dolphins due to external hydrodynamic forces [JPRS-51614] 01 p0014 N71-10952

Integral equations of inviscid hydrodynamics applied to viscous, heat conducting, chemically reacting, radiating shocked flows [AD-711954] 02 p0201 N71-11503

Reduction of leakage losses, friction, and sealing components of piston rings [NAB-LIB-TRANS-1457] 02 p0230 N71-11572

Hydrodynamic analysis of viscous internal flows with embedded particulate matter [AD-711818] 03 p0322 N71-12299

Hydroabrasive wear of metals under cavitation [PB-192268] 03 p0393 N71-13031

Hydrodynamic and heat transfer measurements on full-scale simulated 36-rad Marvion fuel element with nonuniform radial heat flux distribution [FRIGG-3] 04 p0547 N71-13634

Singular perturbation problems in ship hydrodynamics [REPT-96] 04 p0517 N71-13685

Prediction of ocean platform motion in chills seas [PB-193873] 04 p0618 N71-14178

Atmospheric circulation and hydrodynamic weather forecasting [AD-713775] 05 p0718 N71-15397

Hydrodynamic and evaporative theories of light ion flow in polar regions [NASA-CR-116139] 06 p0041 N71-16027

Hydrodynamic theory of lubrication applied to machine parts - bibliographies [AD-714546] 06 p0066 N71-16454

Peculiarities in propagation of weak perturbations in two phase media with phase transitions 07 p1006 N71-16935

Body structure effects on fish hydrodynamic characteristics [JPRS-52259] 08 p1148 N71-18492

Hydrodynamic characteristics of spouting processes in fluidized beds [NRC-TT-1454] 08 p1181 N71-18840

Applying flow characteristics in constricted tube to arterial stenoses [RFP-19172] 09 p1371 N71-19731

Hydrodynamic parameters effect on hydrofoil cavitation erosion intensity [AD-716033] 09 p1372 N71-19713

Wave resistance of air cushion vehicle traveling over water of uniform finite or infinite depth in steady or unsteady motion 09 p1320 N71-19731

Hydrodynamic processes and parameters of glass motion in large bubble chamber [JINR-P13-5291] 09 p1363 N71-19916

Hydrodynamics of matter and antimatter in contact [REPT-70/38] 09 p1437 N71-20074

Computer programs for predicting rocket engine turbopump inducer hydrodynamic loading, stress magnitudes and distribution, and vibration characteristics - Vol. 1 [NASA-CR-72712-VOL-1] 09 p1460 N71-20403

Analysis of positive and negative hydrodynamic pressure variation effects on horizontal piers and platforms [KH-R-19] 09 p1378 N71-20478

Sum rules in hydrodynamic scaling approach for near critical temperature liquid helium 10 p1571 N71-20482

Hydrodynamics, marine biology, kinetics, dolphins, sharks, porpoises, traveling waves, fluid flow, viscous fluids, nervous system, skin structure, swimming [JPRS-52603] 11 p1487 N71-22201

Plane section method used to study hydrodynamics of thin flexible bodied fish and mammals 11 p1835 N71-22202

Quantitative analysis of hydrodynamic swimming characteristics of salt water fish 11 p1481 N71-22204

Three programs for two dimensional hydrodynamics in spherical, pure Eulerian coordinate system [AD-717088] 11 p1737 N71-22326

Computer program for unsteady hydrodynamics and hydrofoil servocontrol near free surface [AD-716811] 11 p1737 N71-22328

Small scale hydrodynamic characteristics of full-scale SNAP 8 multiple-tube model boiler over turbulent Reynolds number from 18,000 to 38,000 [NASA-CR-72830] 11 p1795 N71-22512

Unsteady hydrodynamic loads on two dimensional hydrofoil [AD-717933] 12 p1901 N71-23591

Partial differential equations for determination of hydrodynamic characteristics of fully developed laminar flow tube [EP/TN/A/32] 12 p1902 N71-23724

Hydrodynamic theory applied to climatology and general atmospheric circulation and numerical analysis of macro-atmospheric processes [AD-718623] 12 p1955 N71-23838

Compilation of reports on hydraulic research projects conducted in US and Canada [NBS-SP-344] 12 p1963 N71-24141

Shallow envelope, hydrodynamic calculations for Cepheid variable star model 12 p1998 N71-24237

Surface active agent effects on hydrodynamics and mass transfer of gas or liquid to liquid systems [NLL-RTS-6328] 12 p1873 N71-24291

HYDRODYNAMICS

Theoretical physics of ellipsoidal equilibrium figures and hydrodynamics of general relativity [AD-719914] 14 p2295 N71-25733

Heat transfer and hydrodynamic behavior for subcooled flow boiling of Freon 113 for use in cooling electronic components 14 p2372 N71-25805

Hydrodynamics of superfluid condensates including equations of motion and density matrix 14 p2304 N71-26286

Hydrodynamics and gas dynamics of boundary layer flow including mass transfer and convective and radiative heat transfer of bodies in fluids [AD-720738] 14 p2644 N71-26539

Hydrodynamics of roller pumps and implication to hemodialysis 15 p2374 N71-27279

Hydrodynamic behavior of pure superfluid helium at 0 K using gauge invariance 15 p2393 N71-27326

Laser-radiation effects on metals including damage thermodynamics, melting and cavity formation, vapor hydrodynamics, and damage product electromagnetic absorption [JPRS-53241] 16 p2608 N71-28180

TOMOF - code for describing thermohydrodynamics of two-fluid mixture in studies of boiling and ejection of coolant from reactor channel due to direct contact with hot molten fuel [EUR-4592-E] 16 p2632 N71-28590

Hydrodynamics of helium core flash phase of stellar evolution - core pulse characteristics of hydrostatically computed models and hydrodynamic consequences for outer regions 16 p2681 N71-28870

Characteristics of hydraulic systems and application to aircraft systems [AD-710174] 17 p2783 N71-29562

Electromagnetic radiation scattering by hydrodynamically turbulent systems via operator formalism [AD-722323] 17 p2797 N71-29842

Experimental capabilities and operating conditions of hydrodynamic wind-water tunnel including flow visualization [NASA-TT-F-13727] 17 p2752 N71-30263

Hydrodynamic problem of joint gas stream and liquid film mass transmission processes 19 p3076 N71-31743

Development of hydrodynamic code for representing shocks by discontinuities whose jump conditions and propagation velocities satisfy Hugoniot relations [P-4556] 19 p3081 N71-32606

Measurement of pressure drop in rod bundles with spiral wire spacers to determine effect of number of rods, spacing ratio of rods, and pitch of spirals [NLL-RTS-TRANS-2082-[9091.9F]] 19 p3083 N71-32688

Hydrodynamic seals for bidirectional and unidirectional rotating shafts 20 p3279 N71-33404

Derivation of difference equations for MAGE hydrodynamic computer program, and computation of flows containing plastic and elastic effects [LA-4601] 20 p3359 N71-33575

Application of Langevin equation in Lagrangian dynamical formulation of diffusion in hydrodynamic turbulence 20 p3322 N71-33681

Hydrodynamics of boiling heat flux and dynamics and stability of small gravity and capillary waves [NASA-CR-121467] 20 p3366 N71-33746

Numerical analysis of wavelengths and times of molecular order of magnitude based on viscoelastic behavior of simple classical liquids 20 p3354 N71-33863

Hydrodynamical motion of system consisting of matter-antimatter embedded in thermal radiation [REPT-71/25] 20 p3328 N71-33984

Hydrodynamics of two-phase parallel boiling water channel flow after heat flux increase 21 p3410 N71-34265

Numerical analysis of asymmetric collapse of vapor bubble in viscous incompressible liquid using modified Marker and Cell technique [PB-195640] 22 p3367 N71-35406

Qualitative hydrodynamic model of dynamic angle hysteresis for fluid-fluid interface being driven through capillary tube by applied pressure gradient [AD-726635] 22 p3570 N71-35424

Mass transfer and hydrodynamic behavior of laminar liquid films flowing over solid surfaces 23 p3746 N71-36710

Hydrodynamic effects on laser beam propagation through gases and laser-induced instabilities in liquids and gases 23 p3767 N71-36850

Convective and hydrodynamic mechanisms of solar spin-down 23 p3846 N71-37489

Hydrodynamic processes producing solar corona and its expansion into interplanetary space 23 p3846 N71-37410

Gas flow hydrodynamics in evolution of main sequence stars 23 p3849 N71-37435

HYDROELASTICITY

Hydrodynamics of cocurrent counter-gravity solids transport for liquid-fluidized heat exchangers

23 p3868 N71-37577

Aerohydrodynamic calculations of poorly streamlined surface and submerged ship structures

[AD-727568] 24 p3871 N71-37595

HYDROELASTICITY

Hydroelasticity, aerelasticity, and dynamic stability of bars, plates, shells, and beams of various structural elements

[AD-716938] 10 p1652 N71-20811

Hydroelastic vibration of rods in parallel flow with hydroelastic rod model and method for evaluating equivalent viscous damping coefficients

17 p2734 N71-29728

Computer program for hydroelastic analysis of thin walled structures

[NASA-TM-X-63617] 18 p2893 N71-30609

HYDROFLUORIC ACID

Power and efficiency of continuous hydrogen fluoride chemical laser

[AD-711067] 01 p0662 N71-10433

Generation of radiation in 2.8 micrometer range by vibrational-rotational transition in molecules of hydrofluoric acid

[AD-716680] 09 p1396 N71-19736

Vibrational excitation of HF behind incident shock waves at temperatures from 1400 to 4100 K

[AD-720819] 14 p2213 N71-25928

Thermogravimetric analysis of hydrofluoride stability of alkaline earth metals

[AD-720744] 14 p2214 N71-26082

Kinetics of NH3 reduction of alpha and beta phases in UO2, and reactivity of UO2 with oxygen and hydrofluoric acid

[CEA-R-4074] 15 p2468 N71-27337

Sub-boundary corrosion in polygonized polycrystalline aluminum containing iron and copper impurities and exposed to HF and HCl solutions

17 p2764 N71-29726

Line spectra shifts in HF and in first overtone band of DF induced by HF pressures

[NASA-CR-121411] 20 p3233 N71-33172

Broadening and shifting of hydrogen fluoride lines due to noble gases

20 p3274 N71-33478

HYDROFOIL BOATS

U BOATS

HYDROFOILS

NT KEEELS

Determining strength of hydrofoil systems by fatigue characteristics of welded joints

[AD-714363] 06 p0954 N71-16114

Hydrodynamic parameters effect on hydrofoil cavitation erosion intensity

[AD-716053] 09 p1372 N71-19713

Unsteady lift forces measured on restrained hydrofoil in regular head and following waves of various lengths

[AD-717338] 11 p1833 N71-21906

Computer program for unsteady hydrodynamics and hydrofoil servocontrol near free surface

[AD-717681] 11 p1737 N71-23238

Linear theory for two dimensional supercavitating flow past flat hydrofoil

[AD-718163] 12 p1899 N71-23398

Force coefficients and cavity detachment points under various cavitating conditions on two similar biconvex hydrofoils

[AD-718364] 12 p1900 N71-23585

Unsteady hydrodynamic loads on two dimensional hydrofoil

[AD-717953] 12 p1901 N71-23591

Flutter and divergence of four low mass ratio hydrofoil model configurations

[AD-719891] 14 p2238 N71-25603

Development of technique for evaluating effectiveness and operational utility of captured air bubble ships and ground effect machines

[AD-728003] 24 p3875 N71-37620

HYDROFORMING

Cold metal hydroforming techniques using epoxy molds for counteracting creep or stretch

[NASA-CASE-XLE-05641-1] 14 p2263 N71-26346

Developments in heat source capsule fabrication program from September 1970 to January 1971

[MLM-1796] 18 p2590 N71-31223

HYDROGEN

NT DEUTERIUM

NT DEUTERIUM PLASMA

NT HYDROGEN ATOMS

NT HYDROGEN IONS

NT HYDROGEN ISOTOPES

NT HYDROGEN PLASMA

NT LIQUID HYDROGEN

NT ORTHO HYDROGEN

NT TRITIUM

Ozone and hydrogen reactions in stratosphere and lower mesosphere

[PB-191045] 01 p0501 N71-10877

Mechanism of hydrogen evolution by algae

02 p0156 N71-11104

Measuring neutral hydrogen absorption in galaxy M82 by radio telescope

[AD-711299] 02 p0294 N71-11137

Control of hydrogen absorption in electroplating

02 p0231 N71-11634

Rate of hydrogen absorption by copper

[PB-1905037] 02 p0343 N71-11697

Sorption for cryodeposited frosts of hydrogen

[AD-712373] 02 p0267 N71-11775

Galactic hydrogen absorption at 21 cm wavelength in direction of Virgo A

[AD-711300] 02 p0294 N71-11894

Combustion characteristics and safety factors for hydrogen diffusion flames in flare stack operations

[NASA-CR-111419] 02 p0306 N71-12103

X ray diffraction analysis of matrices of hydrogen-oxygen electrolytic regenerative fuel cells

[NASA-CR-1463] 03 p0316 N71-12253

Backward photoproduction of positive kaons from hydrogen

[LAL-1236] 03 p0430 N71-12903

Total cross section for photoproduction of hadrons and hydrogen on deuterium between 1.0 and 6.4 GeV

[DESY-70/17] 03 p0430 N71-12905

Determination of equation of state for solid hydrogen

[NYO-3699-43] 03 p0442 N71-12915

Turbulent and molecular diffusion processes involved in computation of helium and hydrogen vertical distribution in thermosphere

03 p0371 N71-13231

Activation energy for apparent gaseous diffusion of hydrogen in multi-run metal arc welding deposits

03 p0367 N71-13315

Differential cross sections for hydrogen and helium particles from proton irradiation of Sn-120

[NASA-CR-111729] 04 p0581 N71-14034

Models for resonant electron scattering in small atoms and molecules such as hydrogen, nitrogen and carbon monoxide

04 p0590 N71-14351

Equation of state of hydrogen and deuterium between 3 and 10 cc/mole to 10,000 K

[UCRL-50911] 05 p0743 N71-15133

Composition distribution and equivalent body shape for reacting, coaxial, supersonic hydrogen air flow

[NASA-TN-D-6123] 05 p0785 N71-15639

Plasma production by evaporating hydrogen pellets with pulsed lasers

06 p0928 N71-15839

Autoionization of H2 near threshold

[NASA-TM-X-63434] 06 p0915 N71-15991

Physical adsorption and molecular hydrogen densities of interstellar clouds

06 p0948 N71-16784

Quadrupole rotation-vibration spectrum of hydrogen and predissociation rates of B state of iodine

[NASA-CR-116176] 06 p0927 N71-16869

Rho-meson/Omega-meson interference parameter in diffractive photoproduction of vector mesons on hydrogen

[UCRL-19753] 07 p1071 N71-17233

Hydrogen embrittlement during hot salt, stress corrosion of titanium alloys

[NASA-TN-D-6188] 07 p1042 N71-17348

Development of pulse-activated polarographic hydrogen detector

[NASA-CASE-XMF-06531] 07 p1029 N71-17575

Heat exchange and thermostabilization for 2-meter liquid hydrogen bubble chamber of ITEP

[ITEP-734] 08 p1174 N71-18230

Backward scattered positive pion production from hydrogen near pion nucleus resonance region

[LAL-1225] 08 p1254 N71-18350

Diffusion coefficients determined for hydrogen in some liquid metals

08 p1217 N71-19004

Hydrogen absorption effects on tensile properties of palladium wire

[NASA-TN-D-6211] 08 p1217 N71-19011

Atomic collision time delay functions and quasibound level properties of ground state of molecular hydrogen

[NASA-CR-116889] 08 p1267 N71-19300

Schlieren photography of flow distribution for transverse hydrogen jets from flat plate into Mach 2.72 airstream

[NASA-CR-1794] 09 p1371 N71-19637

Computations of binding energies and vibrational energies of ground state molecular hydrogen to measure accuracy of dissociation energy

09 p1429 N71-19741

Approximation of scattering resonance energies and widths of ground state of molecular hydrogen from energy dependence of atomic collisional time delay functions

09 p1429 N71-19743

Expectation values and kinetic energy for vibrational-rotational levels of ground states of H2, HD, and D2

09 p1429 N71-19744

Corrosion resistance of aluminum-silicon alloy in relation to hydrogen content introduced by various refining processes

[NASA-TT-F-13506] 09 p1400 N71-20082

Two dimensional, supersonic mixing of hydrogen injected from wall slot into airstream

[NASA-CR-1793] 09 p1376 N71-20127

SUBJECT INDEX

Hydrogen has blanketed stellar model atmospheres

[NASA-SP-3065] 09 p1462 N71-20410

Development of device for detecting hydrogen in ambient environments

[NASA-CASE-MFS-11537] 09 p1391 N71-20442

Determination of low temperatures from half-width of Doppler-broadened spectral lines in plasma columns with small rotational velocity

[SC-T-71-3001] 10 p1630 N71-21227

Intake system design, fabrication, and testing in two phase hydrogen

[NASA-CR-103054] 11 p1767 N71-31095

Specific heats of H2 and D2 solid mixtures down to 0.5 K, adsorption isotherms of He-3 and He-4 at low temperatures, and development of He-3 dilution refrigerator and liquefier

[AD-717623] 11 p1815 N71-21941

Mixed conduction in NaCl-TiCl4 fused salt systems and tracer techniques for determination of hydrogen solubility in solid electrolytes

[COO-1460-21] 11 p1817 N71-22540

Shock-induced combustion in explosive mixtures of hydrogen and air or oxygen by high speed slants at low pressures

11 p1843 N71-22632

Nonequilibrium excitation origin in sodium atoms, hydroxyl radicals, or water molecules occurring behind hydrogen-oxygen or acetylene-oxygen combustion shock waves

[NASA-TT-F-13622] 12 p1969 N71-23264

Nuclear magnetic resonance techniques for study of rotation of ortho molecules in solid hydrogen

12 p1983 N71-23882

Application of Fokker-Planck and Coulomb T-matrix to electron capture in hydrogen

12 p1975 N71-24059

Chemical composition of gaseous nebulae, and atmospheres of normal stars and objects with unusual metal to hydrogen ratios

[AD-718441] 12 p1997 N71-24207

Excitation of atomic hydrogen to metastable 22S1/2 state by electron impact - polarization of Lyman alpha radiation produced by collision transfer between ion gas atoms and protons

12 p1978 N71-24254

Fracture and crack growth for welded joints of SA1-2.58a titanium in environment of low pressure, high purity hydrogen

[NASA-CR-114859] 13 p2091 N71-24708

Effects of oxygen and hydrogen on high strength, toughness and crack susceptibility in steel weld deposits

13 p2095 N71-24945

Combustion physics and ignition of hydrogen in re-entrant stream of vitiated air or inert gases using stepped-wall injection procedure

[NASA-TM-X-67840] 13 p2188 N71-25448

Reaction kinetics of degassing hydrogen and nitrogen from iron and steel

[TT-70-58193] 14 p2268 N71-25640

Viscosity of compressed N2, He, H2, and Ar from minus 100 to 25 C using viscometer

14 p2214 N71-26403

Multiconfigurational one center expansion wave functions for computing intermolecular forces of hydrogen molecule and Hellmann-Feynman theorem

14 p2311 N71-26887

Lamb shift type ion source for producing positively charged polarized hydrogen ion beams

[KFK-1262] 14 p2316 N71-26943

Computer program modifications and lattice coding for hydrogenous systems including transport corrections for self-scatter cross sections and collision probability

[AEEW-M-952-REV] 15 p2467 N71-27207

Reaction kinetics and charge transfer in ionic collisions of argon ions with molecular hydrogen, deuterium, and carbon dioxide

15 p2477 N71-27578

Fracture toughness data utilizing small notched round tensile steel specimens with hydrogen embrittlement as crack starter

[AD-728217] 15 p2425 N71-27648

Nuclear composition for several multicharged nuclei and energy spectra for hydrogen, helium, and medium nuclei measured in solar particle event

[NASA-TM-X-65573] 15 p2514 N71-27845

Hydrogen vapor pressure observed at 2.8 K during cryopumping

[LA-TR-71-15] 15 p2392 N71-27775

Two dimensional equations for solving Schwab-lager equations in three nucleus problem of hydrogen

15 p2493 N71-27941

Sodium loop evaluation of nickel palladium catalytic hydrogen detector

[APDA-252] 16 p2634 N71-28735

Soviet atmospheric observatory for studying deuterium/hydrogen ratio in solar atmosphere

[NASA-TT-F-13675] 17 p2440 N71-29235

Design, performance characteristics and testing of two-phase hydrogen pump inducer for use in fusion specific systems

[B-71-21] 17 p2330 N71-28708

Room temperature, high pressure hydrogen effects on metal strength

17 p2714 N71-29587

SUBJECT INDEX

Iron film adsorption of carbon monoxide, hydrogen and their mixtures 17 p2714 N71-29688

Neutron-proton, deuteron, and nucleus scattering cross sections for H₂, D₂, He, Be, C, Al, Fe, Ca, Cd, W, Pb, and U at 4.0 and 5.7 GeV/c 17 p2796 N71-29780

Evaluation of storable propellants as sources of H₂, O₂, potable H₂O, and heat for use in emergency life support system (NASA-TM-X-2321) 17 p2711 N71-29903

Evaluation of laser systems for inducing nuclear fusion processes in fusion weapons and hydrogen energy sources (POA-4-4449) 17 p2758 N71-29911

Hydrogen bubble chamber experiments on H₂ and D₂ proton-proton interactions (USIP-70-8) 17 p2798 N71-30003

Distortion effects in geometrical reconstruction of events in CERN 2m hydrogen bubble chamber (EP-70-6) 17 p2800 N71-30098

Atomic beam radio frequency measurement of 2S1/2 to 2P3/2 energy separation in H equals 2 state of atomic hydrogen 17 p2805 N71-30379

Measurement of extinction parameter of tungsten-hydrogen aerosols as function of wavelength at high pressures and temperatures (NASA-CR-1064) 18 p3823 N71-30494

MeV total neutron cross sections for H, He-3, and He-4 (EP-72-221) 18 p3973 N71-30541

Proton storage ring using ionization friction to contain hydrogen beam (JUN-70-37) 18 p3979 N71-30699

Spin lattice relaxation time and spin-spin relaxation time of solid ortho and para hydrogen in 4.2 to 0.02 K temperature range 18 p3964 N71-31070

Hydrogen solubility in liquid iron-carbon-nickel alloys including free energy and enthalpy increments (NASA-CR-1064) 18 p3964 N71-31070

Kinetics of homogeneous, isotopic exchange reaction D₂ plus CH₄, D₂ plus H₂S, and HD plus HD in single-pulse shock tubes 18 p3987 N71-31350

Galvanically induced hydriding of titanium in saline solutions (EP-196339) 19 p3110 N71-31769

Hot atom beam in halogen and hydrogen sources, cathode sputtering of non-metals, and hot atom reactions of alkali metals (ADA-722450) 19 p3207 N71-32107

Electroproduction of single positive pions on hydrogen measured by coincidence between electrons and pions (DSY-71-9) 19 p3199 N71-32633

Fluorine model for explaining electron densities and temperature of hydrogen plasmas with helium and argon impurities drifting into dipole magnetic field 20 p3331 N71-33674

Glauber and Born approximations of electron impact excitations of hydrogen atomic energy levels (NASA-CR-121444) 20 p3319 N71-33686

Mechanical property tests of nickel, titanium, and iron alloys in 5000 psig gaseous helium and hydrogen at various temperatures 20 p3320 N71-33728

Resonant trajectory study of rotationally inelastic scattering of hydrogen molecules by collisions with lithium ions (NASA-CR-121729) 21 p3386 N71-34087

Monte Carlo method for determining reactive collisions of fluorine atoms with hydrogen molecules (LA-4063) 21 p3388 N71-34103

High-voltage isolator design for injecting hydrogen beams into liquid metal feed lines to interrupt electrical continuity (NASA-CASE-NPO-11075) 21 p3402 N71-34208

Mixing of hydrogen deuterium from multiple injectors normal to supersonic jet flow, for supersonic combustion ramjet engines (NASA-TN-D-6476) 21 p3411 N71-34274

Determination of oxygen, nitrogen, and hydrogen in steel - conference 21 p3441 N71-34483

Atom recombination and methane production from atomic hydrogen reactions on clean metal surfaces 21 p3462 N71-34494

Approximations in calculating g-tensors for molecules in H₂ (phs) 21 p3446 N71-34526

Development of equation of state for solid hydrogen at pressures up to 112 K-bars (NPO-3699-52) 21 p3465 N71-34663

Absolute cross sections of vacuum ultraviolet emission features excited by electron impact on molecular H₂ and O₂ (NASA-CR-121718) 21 p3466 N71-34672

Calculation of quadrupole interaction constant ratio in solid hydrogen based on inelastic neutron scattering distributions 21 p3470 N71-34704

Using particle conservation equations for fast hydrogen atoms, slow hydrogen molecules, and

charged particles for calculating fast atomic hydrogen flux produced by charge exchange in high temperature plasmas (JAERI-MEMO-4343) 21 p3494 N71-34887

Infrared spectroscopic analysis of H II region in planetary nebulae M 42, NGC 7027, and IC 418 21 p3511 N71-35020

Analysis of conditions under which autoionization of flowing hydrogen-oxygen mixtures occurs and prediction of required flow rates 21 p3531 N71-35163

Cryogenic shock tube used for study of low temperature shock waves in molecular and pure hydrogen (AD-724652) 21 p3570 N71-35423

Spin lattice relaxation in gaseous hydrogen and mixtures of hydrogen with helium 22 p3650 N71-36029

Flux, energy spectra, and pitch angle distributions of precipitated low energy hydrogen and electrons from Nike-Tomahawk auroral hydrogen experiment (NASA-CR-121934) 22 p3648 N71-36155

Hydrogen embrittlement of titanium alloy surface in hot salt corrosion cracking (NASA-CR-1829) 23 p3772 N71-36882

Criticality evaluation of hydrogenous enriched lattices using three group model for reactor design (UARRB-64) 23 p3794 N71-37047

Equation of state calculations for solid H₂, D₂, He-3, He-4, and Ne-20 at high densities in harmonic approximation (NYO-3699-51) 23 p3802 N71-37110

Total loss cross sections for D₂ molecules passing through H₂ gas in light ion accelerator (UCL-20099) 23 p3812 N71-37181

Electrical scattering, radiative capture, gamma ray production, and related information from nuclear data file for hydrogen in .00001 eV to 20 MeV range (LA-4574) 23 p3813 N71-37193

Numerical analysis of effects of transient response in catalytic life support system to promote hydrogen-oxygen combustion 23 p3885 N71-37357

Heavy gas-liquid mixture bubble chamber with 70 liter volume and hydrogen internal target for use with electrostatic electron gamma beams (LNF-70/25) 24 p3920 N71-37951

Energy transfer cross sections for electrons ejected from hydrogen and nitrogen molecules by fast proton impacts (BNWL-SA-3853) 24 p3978 N71-38385

Helium and hydrogen bulk speeds in solar wind (NASA-CR-123119) 24 p4003 N71-38548

HYDROGEN ATOMS

Interaction kinetics of atomic oxygen and hydrogen on metal surfaces of satellite-borne mass spectrometer (NASA-CR-111117) 01 p0122 N71-10383

Localized one-electron states in perfect crystals of hydrogen atoms (AD-711372) 02 p0283 N71-11891

Pressure effects on high temperature vibrational absorption coefficients for atomic hydrogen collisions in hydrogen gas (NASA-TN-D-6155) 07 p1076 N71-17514

Fast neutral injector facility for obtaining intense neutral excited hydrogen atom beam (CEA-CON-1662) 09 p1366 N71-20192

Total cross sections for formation of excited hydrogen atoms by charge exchange in proton collisions with Ar, He, H₂, N₂ (ORO-2591-51) 10 p1612 N71-20736

Numerical integration of spontaneous ionization of hydrogen atom in electric field using Schwinger equation (NASA-CR-117894) 12 p1969 N71-23287

Diurnal variations of atomic hydrogen in thermosphere derived from Explorer 32 data and correlated with solar cycle, solar rotation, and earth rotation (NASA-TM-X-45544) 14 p2246 N71-25747

Obtaining dense beam of hydrogen atoms with particle energies above 1 eV by means of charge exchange in supersonic vapor target from plasma clusters generated by coaxial plasmas (UCL-TRANS-10497) 14 p2321 N71-25768

Bibliography on use of Li groups and algalates in quantum mechanics and application to nonrelativistic hydrogen atom invariance groups 14 p2386 N71-26391

Energy separation measurements in a equals 2 state of atomic hydrogen by radio frequency produced dipole transitions between hyperfine components (TID-25596) 14 p2315 N71-26734

Atomic hydrogen masers in Great Britain (NPL-QU-17) 15 p2418 N71-26897

Total cross section measurements for formation of metastable hydrogen atoms by charge transfer of proton traversed targets of helium, argon, nitrogen, and oxygen (NASA-CR-118863) 15 p2492 N71-27925

Auroral Lyman alpha emission cross sections from hydrogen-proton collisions in upper atmosphere (AD-721462) 16 p2644 N71-28099

HYDROGEN IONS

Low and high field level crossing experiments in 2F state of atomic hydrogen and measurement of Sommerfeld fine structure constant 16 p2457 N71-29124

Measuring local thermodynamic equilibrium plasma temperatures for determining characteristics of reaction between hydrogen atoms and ammonia (ECRC-N-288) 17 p3812 N71-30853

Temperature effects on methanol formation from hydrogen atom reactions with polycrystalline graphite surfaces 18 p3886 N71-31080

Spectrometer for detecting hyperfine levels of perturbed hydrogen atoms at zero magnetic field (UCRL-36328) 20 p3520 N71-33703

NMR and electrical resistivity measurements for studying hydrogen radical motions in deuterated sodium trihydrogen selenite crystals 20 p3325 N71-33921

Q switched laser induced gas breakdown used in hydrogen atom detection, spectral analysis, and chemical reactions (NASA-CR-121644) 21 p3383 N71-34004

Many body perturbation procedure for studying various properties of interacting atoms applied to H-He and H-Ne systems 22 p3450 N71-36827

Construction of fast hydrogen atom injector from calculations of magneto-optical system (NLL-CTO/746-0901.97) 23 p3832 N71-37329

Upper atmosphere atomic hydrogen density evaluation by comparison of high and low altitude electron content 24 p3915 N71-37912

Glauber approximation of differential and integrated atomic hydrogen excitation cross sections at electron impact (NASA-CR-123926) 24 p3971 N71-38327

HYDROGEN BONDS

Vapor phase hydrogen bonding equilibria in methanol-water complexes with dichloromethane 08 p1160 N71-19026

Nucleophilic substitution rates in trans-dichlorobis(pyridine)platinum II as functions of solvent composition in DMSO-WATER mixtures 13 p2901 N71-23340

HYDROGEN CHLORIDE

U HYDROCHLORIC ACID

HYDROGEN COMPOUNDS

NT BORANE HYDRIDES

NT BORANES

NT BORON HYDRIDES

NT CARBORANE

NT DEUTERIUM COMPOUNDS

NT DIBORANE

NT HEAVY WATER

NT HYDRIDES

NT HYDROGEN CYANIDES

NT HYDROGEN PEROXIDE

NT HYDROGEN SULFIDE

NT LITHIUM HYDRIDES

NT METAL HYDRIDES

NT NITROGEN HYDRIDES

NT PENTABORANES

NT PHOSPHINES

NT SILANES

NT ZINCUM HYDRIDES

HYDROGEN CYANIDES

Four-micron molecular laser experiments using hydrogen cyanide (AD-713193) 05 p0696 N71-14670

HYDROGEN DEUTERIUM OXIDE

U HEAVY WATER

HYDROGEN FLUORIDES

U HYDROFLUORIC ACID

HYDROGEN FUELS

Comparison of hydrogen and methane as coolants in regeneratively cooled panels (NASA-CR-1652) 06 p1303 N71-19289

Supersonic combustion, fuel injection, and recirculation in hydrogen hypersonic external combustion at flat plates and bodies of revolution (DLR-FB-70-44) 11 p1440 N71-22129

Spark and auto-ignition systems for hydrogen and oxygen propellants in space shuttle APS (SC-71-24) 17 p2837 N71-29593

Design and development of air breathing engine system for space shuttle vehicle 17 p2831 N71-29607

Air breathing, hydrogen fueled engine studies for space shuttle application 17 p2838 N71-29608

Modified wind tunnel tests of supersonic combustion chamber for hydrogen burning ramjet (TP-924) 20 p3340 N71-33841

HYDROGEN IONS

Ion-ion recombination effects in sodium line laser (JPRS-51577) 01 p0106 N71-10976

Theoretical calculations on electron detachment of hydrogen ions by electron collision with Compton effect (NASA-TM-X-45491) 12 p1970 N71-23786

Ionic hydrogen to oxygen transition level variations caused by atmospheric winds 13 p2108 N71-25266

HYDROGEN ISOTOPES

Thermospheric model based on Explorer 32 hydrogen ion density measurements including periodic variations and temperature factors due to local time, solar activity, and magnetic effects
[NASA-TM-X-45589] 16 p2586 N71-28329

Detection of hydrogen ion flux in exosphere existing along terrestrial magnetic lines of force
[NASA-TT-P-13802] 18 p2918 N71-31365

P-state wave function of two-electron atom and absorption coefficient of negative hydrogen ion
20 p3326 N71-33930

Free-free absorption coefficient of negative hydrogen ion and dipole adiabatic exchange wave functions of polarized orbital theory
22 p3648 N71-36015

HYDROGEN ISOTOPES

NT DEUTERIUM

NT TRITIUM

He-3/RH-3 charge form factor and He-3 Coulomb energy
[RLO-1388-573] 01 p0099 N71-10711

Instrumentation for monitoring of Kr-83 and H-3 in natural gas
[UCRL-50882] 05 p0688 N71-15559

Beta excited X ray spectra for C-14, H-3, S-35, Sr-90, To-99, W-183, and Kr-83
[TID-22361-PT-3] 06 p0922 N71-16404

Investigating reactive collisions between hydrogen atoms and molecules in various isotopic combinations
[CALT-767-P-4-66] 08 p1268 N71-19326

Coulomb three body interaction for calculating moon meson transitions in collisions with hydrogen isotopes
15 p2464 N71-27199

Polarized neutrons from H-3/p, n/H-3 reaction using time of flight spectrometer at 31.6 deg in laboratory (approximately 45 deg in center of mass)
17 p2805 N71-30297

K-harmonics method for calculating binding energy and wave functions of H-3 and He-3 nuclei
[IAE-2000] 19 p3149 N71-32105

Lepton decay of hypertriton
[IAE-1944] 23 p3808 N71-37147

Nucleon-nucleon potential for calculating binding energy of H-3 and n-d doublet scattering length
[DNR-P-1234] 24 p3569 N71-38311

HYDROGEN OXYGEN ENGINES

NT J-2 ENGINE

Ignition characteristics and delivered performance of gaseous hydrogen-oxygen reaction control thrusters at cryogenic temperatures
[NASA-CR-72784] 02 p0291 N71-12096

Ignition characteristics and delivered performance of gaseous hydrogen-oxygen reaction control thrusters at cryogenic temperatures - appendices
[NASA-CR-72785] 02 p0291 N71-12097

Propulsion system configurations and hydrogen oxygen engines for space shuttles
[NASA-TM-X-66896] 08 p1292 N71-18432

Technology and configurations of hydrogen oxygen auxiliary propulsion system for space shuttle orbiter and booster
[NASA-TM-X-66894] 08 p1292 N71-18433

Computerized analysis of gas-tapoff cycle stability with gaseous hydrogen and gaseous oxygen
09 p1378 N71-20417

Low pressure oxygen/hydrogen auxiliary propulsion subsystem for space shuttle
[NASA-CR-114945] 11 p1820 N71-22010

Space shuttle low pressure, hydrogen oxygen auxiliary propulsion subsystem requirements, tradeoffs, and concept selection
13 p2171 N71-24676

Space shuttle high pressure, hydrogen oxygen auxiliary propulsion subsystem requirements, tradeoffs, and concept selection
13 p2172 N71-24677

Space shuttle high pressure, hydrogen oxygen auxiliary propulsion subsystem designs, weight sensitivities, and operating performances
[NASA-CR-103116] 13 p2172 N71-24678

Space shuttle high pressure hydrogen oxygen auxiliary propulsion subsystem conceptual and design study summary
13 p2174 N71-25068

Space shuttle low pressure, hydrogen oxygen auxiliary propulsion subsystem preliminary design
[NASA-CR-115009] 13 p2176 N71-25470

Space shuttle high pressure, hydrogen oxygen auxiliary propulsion subsystem preliminary design
[NASA-CR-103108] 13 p2176 N71-25471

Resonance tube ignition system for hydrogen oxygen engines including ignition limits and pressure and temperature effects
[NASA-TN-D-6354] 15 p2523 N71-26913

Space shuttle hydrogen/oxygen auxiliary propulsion system high and low pressure thrusters
17 p2836 N71-29589

High and low chamber pressure injectors for space shuttle hydrogen oxygen APS engines
[AGCS-0100-71] 17 p2836 N71-29590

Design criteria for flight type gaseous hydrogen gaseous oxygen propellant shutoff valves for space shuttle APS
17 p2830 N71-29592

Design and fabrication of hydrogen oxygen propellant shutoff valves for space shuttle APS thrusters
17 p2831 N71-29593

Analytical and experimental program of design, fabrication, testing of gaseous hydrogen/oxygen spark and plasma torch ignition system for space shuttle APS
[AGCS-0100-71] 17 p2836 N71-29594

Experimental and analytical evaluation of catalytic ignition system and performance of hydrogen oxygen thruster for space shuttle APS
17 p2837 N71-29596

Injector performance, heat flux, and film cooling in hydrogen oxygen engines
17 p2837 N71-29596

Axial and circumferential variations of hot gas side heat transfer coefficients in hydrogen oxygen engines for use in nozzle and injector design
[NASA-TN-D-6396] 18 p3024 N71-30738

Apollo service propulsion system rocket engine bipropellant valve improvement program - valve design guide and oxygen-hydrogen technology
[NASA-CR-108578] 21 p3502 N71-34946

Low cost, lightweight ignition system for hydrogen oxygen engine system incorporating multicomponent thrust chamber
21 p3530 N71-35152

Engine and stage design criteria on sizing requirements of complete stage for LOX/hydrogen engine
[NASA-CR-121864] 22 p3662 N71-36111

Evaluation of oxygen-hydrogen auxiliary propulsion subsystems for space shuttle booster and orbiter baseline vehicles
[NASA-CR-115162] 23 p3838 N71-37370

Pumped liquid, dual gas generation cycle for space shuttle booster and orbiter auxiliary propulsion system
23 p3838 N71-37371

Computer programming manual for calculating temperature and reactant concentrations as functions of time and axial position in catalyzed continuous flow hydrogen-oxygen reactors
[NASA-CR-120800] 24 p3892 N71-37738

HYDROGEN OXYGEN FUEL CELLS

Electrolytically regenerative hydrogen-oxygen fuel cells
[NASA-CASE-XLE-04526] 02 p0148 N71-11052

Water electrolysis rocket engine with self-regulating stoichiometric fuel mixing regulator
[NASA-CASE-XGS-08729] 04 p0605 N71-14044

Hydrogen oxygen fuel cells for electric power plants and Apollo spacecraft
[DLR-MITT-70-09] 06 p0796 N71-15723

Developing steady-state model for voltage output of hydrogen oxygen fuel cell as function of battery temperature, reactant pressure, electrolyte concentration, and cell current
07 p0976 N71-17675

Design, temperature, carbon dioxide, and current density effects on alkaline hydrogen oxygen fuel cell performance
[NASA-CR-72906] 18 p2873 N71-31150

HYDROGEN PEROXIDE

Effect of catalysts on decomposition, pressure loss, start transient, and lifetime of hydrogen peroxide monopropellant in reactor
[NAL-TR-202] 09 p1456 N71-20116

Homogeneous thermal decomposition of hydrogen peroxide vapor diluted in argon or nitrogen at elevated temperatures behind incident and reflected shock waves
17 p2714 N71-29624

Anomalous water from cleaned and uncleaned capillary tubes, from weak H2O2 solutions, and from water extractions of crushed glass
[AD-726761] 23 p3720 N71-36517

HYDROGEN PLASMA

NT DEUTERIUM PLASMA

Nuclear fusion, rotating hydrogen plasmas, and plasma-neutral particle interactions at end walls
[REPT-70-33] 04 p0600 N71-14302

Attenuation of X rays in interstellar and intergalactic space and physical state of hydrogen cloud
[NASA-TM-X-64577] 10 p1641 N71-21563

Slow capacitor discharge for preheating hydrogen plasma in inverse pinch device
10 p1630 N71-21772

Injection laser Thomson scattered light for timed measurement of electron density and temperature of shock fronts formed by axial plasma injection into dipole magnetic fields
12 p1982 N71-24143

Laboratory measurements of Stark broadened hydrogen Balmer lines emitted from low density radio frequency discharge compared with calculated line profiles
13 p2149 N71-25235

Analysis of plasma obtainable by neutral injection into superconducting levitron
[UCRL-50976] 13 p2145 N71-25593

Ignition and development of plane thermonuclear reaction waves propagating through solid density deuterium-tritium plasmas
[AD-720839] 14 p2321 N71-25907

SUBJECT INDEX

Classical path calculations of impact broadening operator phi for Stark broadening of hydrogen line II sub alpha
[AD-720817] 14 p2321 N71-25916

Containment of 500-eV hydrogen plasma in circular quadrupole magnetic well
[CEA-CONF-1597] 15 p2498 N71-27093

Design, construction, and operation of high-field magnet for hydrogen arc experiment
[IIT-4773] 15 p2453 N71-27261

Dissociation rate and plasma generation in hydrogen beam electron interaction
[CEA-CONF-1610] 15 p2474 N71-27457

Hydrogen plasma generation in magnetic pinch by radio frequency oscillator for thermonuclear power reactor
[AD-720847] 15 p2301 N71-27594

Electron beam hydrogen ionization and hot plasma generation in magnetic mirror configuration
[CEA-CONF-1611] 15 p2502 N71-27625

Arc heated hydrogen plasma in star atmosphere simulator
[MPI-PAB/EXTRATERR-38] 18 p2501 N71-30483

Electric and magnetic field radio frequency heated hydrogen plasma diagnostics at cyclotron frequencies
18 p2993 N71-31046

Two phase excitation coil system for ion cyclotron heating of hydrogen plasma
18 p2993 N71-31144

High frequency heating of hydrogen plasma near low hybrid frequency
[ORNL-TR-2435] 21 p3495 N71-34897

High resolution energy analyzer with time of flight spectrometer for studying highly ionized hydrogen and helium plasmas
[IITP-DT-22] 23 p3826 N71-37291

HYDROGEN RECOMBINATIONS

Hydrogen atom and hydrogen deuterium exchange reaction in allyl aromatics during catalytic hydrogenation
[SC-T-70-4031] 02 p0270 N71-11399

HYDROGEN SULFIDE

Radium 226 alpha radiolysis of gaseous hydrogen sulfide
08 p1160 N71-19908

Electron affinity and dipole moment of NH2 and H2S molecules having C2v symmetry
15 p1267 N71-19299

Amino acids produced by long UV irradiation of gas mixtures using hydrogen sulfide as initial photon acceptor, simulating prebiological earth conditions
[NASA-CR-118329] 13 p2040 N71-23681

Kinetics of homogeneous, isotope exchange reactions D2 plus CH4, D2 plus H2S, and HD plus HD in single-phase shock tubes
18 p2987 N71-31330

HYDROGEN 2

U DEUTERIUM

HYDROGEN 3

U TRITIUM

HYDROGENATION

Kinetic activity of Rh-Pt/SiO2 and Rh-Pd/SiO2 catalysts in benzene hydrogenation reactions
[NLL-RTS-6448] 23 p3722 N71-36528

Dependence of hydrogenation in nickel electrodeposits on additions of metallic salts as determined by vacuum extraction
[NLL-TRANS-746-740-1922.401] 24 p3942 N71-38118

HYDROGENOLYSIS

Investigating methods of synthesizing edible glycerols from waste gases in spacecraft
[NASA-CR-114276] 07 p0990 N71-17676

Pre-treatment effects on hydrogen absorption and aqueous corrosion of Zircaloy in hot water
[WAPD-TM-906] 10 p1585 N71-21735

HYDROGENOMONAS

Nutritional quality of Hydrogenomonas eutropha proteins
[NASA-CR-111599] 03 p0326 N71-12536

Protein quality of Hydrogenomonas eutropha for animal food supplement
[A69-23306] 03 p0326 N71-12537

Nutritional value of Hydrogenomonas eutropha lipids in rats
03 p0326 N71-12538

Human tolerance to Hydrogenomonas eutropha and Aerobacter aerogenes as food
[A69-27265] 03 p0327 N71-12533

Optimal mineral composition in nutrient for autotrophic Hydrogenomonas cultivation
20 p3222 N71-33471

HYDROGEOLOGY

Aerial and spaceborne photography and infrared imagery in earth hydrogeology and oceanography
[NASA-TM-X-64481] 02 p0205 N71-11151

Color infrared photography for remote sensing of shallow water areas by air
02 p0206 N71-11157

Infrared imagery as rapid reconnaissance technique for locating thickest sections of water-bearing surficial sand in peninsular areas
06 p0847 N71-16173

SUBJECT INDEX

HYDROSTATIC PRESSURE

Bathymetric and magnetic surveys to determine geophysical characteristics of Gulf of Tadjura
18 p2914 N71-31007

Geophysical data and regional geology indications of existence of salt domes in Atlantic Ocean off coast of southwest Africa
18 p2915 N71-31012

HYDROGRAPHY

Oceanographic observations of North Atlantic standard monitoring sections for 1964 to 1966
[PB-192299] 05 p0572 N71-13327

Ocean currents, oceanography, and hydrographic survey of continental shelves
[AD-713103] 05 p0672 N71-14689

Radiometric and radar observations of dynamic ocean features including determination of sea state, spray, whitecaps, and radar backscatter cross section as function of wind speed
[AD-716773] 12 p1910 N71-23593

Deep-sea sounding and depth measurement using pressure equipment and repeating stations of original oceanographic expeditions
18 p2913 N71-30995

Oceanographic survey to determine moraine deposits in Gulf of Mexico
18 p2913 N71-31001

Bathymetric and magnetic surveys to determine geophysical characteristics of Gulf of Tadjura
18 p2914 N71-31007

Geophysical and bathymetric measurements of ocean bottom and lower continental rise hills off Cape Hatteras
18 p2915 N71-31009

Analysis of deposition and erosion of ocean bottom along Middle Atlantic Continental Slope
18 p2915 N71-31011

Computerized analysis of single peaked hydrographic using transformation of isopleths gamma function and weighted least squares method
[PB-196099] 20 p3252 N71-33153

Harmonic method of predicting shallow water tide at Anzhong, Alaska
23 p3790 N71-37009

HYDROKINETICS

U HYDROMECHANICS

HYDROLOGY

NT HYDROGEOLOGY

Abstracts on Soviet research in terrestrial geophysics
05 p0666 N71-14660

Annotated bibliography on application of satellite observations to hydrology problems
[PB-194072] 05 p0667 N71-14697

Detecting changes in thermal patterns induced by urban development in water bodies and adjoining land areas using infrared imagery
05 p0666 N71-16148

Aerial photography as technique for remote sensing of hydrological features in swamp and coastal regions
06 p0646 N71-16171

Oceanographic data smoothing and hydrological data spacing
[AD-716272] 09 p1384 N71-19910

Hydrology and geochemistry of lakes to determine cycling and transport of radionuclides
[CU-2493-11] 10 p1551 N71-21187

Microwave radiometers for satellite hydrologic and oceanographic observations through clouds
[NDA-71-NESS-26] 11 p1744 N71-21892

Computer controlled interactive graphics display system for hydrologic analysis
[BNWL-1523] 11 p1716 N71-22580

Arctic and Antarctic regions, ice formation, sea ice, weather forecasting, glaciology, hydrology, hydrometeorology, KGV, KQSV, solar activity, and meteorological stations
[TT-70-50017] 11 p1752 N71-22801

Hydrological measurements of horizontal circulation of water in Pacific sector of Southern Ocean
11 p1754 N71-22822

Annual variations of winter hydrological characteristics in surface waters of East Siberia and Chukotka seas due to salinity and temperature anomalies
11 p1756 N71-22835

Hydrological investigation of variability of temperature and chemical properties of Lake Vanda in Antarctica
11 p1759 N71-22863

Hydrological observations of temperature, salinity, and currents of water in Danish Fjord
11 p1759 N71-22867

Scientific and economic results of geologic, hydrologic, and topographic studies
14 p2251 N71-26644

Radiotracer production and materials, heat source applications, hydrological and ocean sciences, radiation analysis and control, process radiation, and radiation preservation of foods
[PB-4066] 17 p2797 N71-29836

Geomorphology, biological activity, and hydrology of Gulf of Mexico and Caribbean Sea as determined from Soviet-Cuban oceanographic expeditions
[NBS-53412] 18 p2909 N71-30604

Hydrological characteristics of upper layers of Caribbean Sea and Gulf of Mexico as determined by Soviet-Cuban oceanographic expeditions
18 p2909 N71-30606

Acquisition and storage of militarily significant data on climatology, hydrology, soils, and ecology of humid tropical regions
[AD-723605] 19 p3195 N71-32629

Infrared satellite photographs for studying hydrology, glaciology, oceanography, volcanology, and radiation balance of earth
[NASA-TT-F-15930] 21 p3426 N71-34378

Interpreting and analyzing rainfall data for designing storm sewer systems
[NLL-M-20859-5828.4F] 21 p3453 N71-34573

Digital simulation of augmented rainfall and hydrologic response of watershed
23 p3793 N71-37057

HYDROLYSIS

Chemical analysis techniques for metals, alloys, and other materials
[AD-713937] 06 p0810 N71-16275

Effect of hydrolysis on disproportionation of trivalent and pentavalent plutonium ions
[MLM-1743] 06 p0811 N71-16711

Membrane of aqueous carbonate solution with catalyst for hydrolysis of CO₂ for removal of CO₂ in life support systems
[AD-713978] 09 p1340 N71-19772

Tensile strength degradation in water immersed polyimide Kapton
[RM-594] 12 p1871 N71-23782

Nuclear magnetic resonance, hydrolysis, molecular structure, and reaction kinetics of nickel ethylenediaminetetracetate in aqueous solution
[RLD-2221-T-4-5] 15 p2378 N71-27712

Using accelerated hydrolytic reaction data to predict service life of elastomeric potting compounds
[AD-721676] 16 p2617 N71-28466

Predictive models for preventing water radiolysis in sealed aluminum capsules for reactor irradiations
[NASA-TT-X-2407] 23 p3801 N71-37098

HYDROMAGNETIC FLOW

U MAGNETOHYDRODYNAMIC FLOW

NT ELASTOHYDRODYNAMIC STABILITY

HYDROMAGNETIC WAVES

U MAGNETOHYDRODYNAMIC WAVES

HYDROMAGNETICS

U MAGNETOHYDRODYNAMICS

HYDROMAGNETISM

U MAGNETOHYDRODYNAMICS

HYDROMAGNETICS

NT ELECTROHYDRODYNAMICS

NT HYDRODYNAMICS

NT HYDROSTATICS

NT MAGNETOHYDRODYNAMICS

NT MAGNETOHYDROSTATICS

Effects of structural motion on dynamic response of liquid flow systems and automatic control hydraulic systems
[AD-714283] 06 p0797 N71-16359

Sound propagation characteristics in gas media with droplets or particles based on linearized hydrodynamic equations
[NASA-TT-F-13381] 13 p2064 N71-24619

HYDROMETEOROLOGY

Computer code for prediction of hydrometeor impact erosion on high speed sphere-cone vehicles
[SC-208-78-373] 03 p0345 N71-12489

Synoptic meteorological observations of Mediterranean marine area
[AD-712761] 04 p0541 N71-14097

Instruments and techniques for hydrometeorology, including FM telemetry system, low displacement pressure transducer, and analog plotting of isohyetal lines
[PB-195726] 10 p1599 N71-21618

Selected articles on numerical forecasts and analysis of meteorological fields
[AD-717817] 11 p1789 N71-22266

Synoptic observations for Alaskan coastal marine areas
[AD-717360] 11 p1790 N71-22261

Arctic and Antarctic regions, ice formation, sea ice, weather forecasting, glaciology, hydrology, hydrometeorology, KGV, KQSV, solar activity, and meteorological stations
[TT-70-50017] 11 p1752 N71-22801

Fallout from nuclear explosions, atmospheric turbulence, aerosol propagation, and serological and hydrometeorological measurements
12 p1952 N71-23178

Solar activity effects on European river runoff and hydrology
[NLL-M-20097-5828.4F] 12 p1915 N71-24230

Automatic processing of hydrometeorological data for information retrieval system
[AD-719837] 13 p3107 N71-25136

Computerized system for processing hydrometeorological data
[WMO-275] 20 p3294 N71-29808

Statistical analysis of two-dimensional fields of hydrometeorological elements
[NLL-M-20057-5828.4F] 21 p3453 N71-34576

flux of atmospheric water, frequencies and paths of storms, and local water budget related to hydroclimatic in Middle East
[RM-5267-FP] 21 p3454 N71-34584

Solar radiation as energy source in terrestrial hydrometeorological processes-continues
23 p3613 N71-35736

Energy and momentum transfer distributions in near air exchangers relative to model of traveling frontal cyclones in middle latitudes
23 p3786 N71-36962

HYDROPHONES

Flow induced error frequencies in tidal wave measurement hydrophones
[AD-711518] 01 p0831 N71-10837

Open-circuit sensitivity of radially polarized ferroelectric ceramic cylinders in hydrophones
[AD-712766] 03 p0330 N71-12534

Open-circuit sensitivities of axially polarized ferroelectric ceramic cylinders
[AD-715766] 06 p1222 N71-18789

Distribution of multipole magnetic fields through conductive wall of plasma container
[AD-715365] 06 p1191 N71-18834

Digital microstriping system, CW TRAPATT diodes, and problems concerning hydrophones and epoxy composites in water
13 p2854 N71-24587

Pressure sensitive reference hydrophone design including lead zirconate titanate spherical element for infrasonic and sonic frequencies
[AD-721069] 15 p2385 N71-28842

Open circuit sensitivity of radially polarized ferroelectric ceramic hollow sphere transducer ceramic as anisotropic material
[AD-722401] 17 p2726 N71-29732

Reflected wave method for seismic investigation of sedimentary stratum in oceans and development of hydrophones, radiobuoys, and related instruments
[JPRS-53422] 18 p2910 N71-30702

Seismic investigations studies in open ocean on large oceanographic ships and seismic instruments development of hydrophones, radiobuoys, and related instruments
18 p2910 N71-30703

Dynamic response of hydrophone spherical shell predicted by finite element model
[AD-726726] 23 p3861 N71-37528

Equations for variation with frequency of voltage output from hydrophone exposed to constant acoustic pressure field
[AD-727978] 24 p3967 N71-38308

HYDROPHONICS

Anion and cation exchange resin mixture for hydroponic growth of vegetables and flowers
[NASA-TT-F-13543] 09 p1387 N71-20426

HYDROSPHERE [EARTH]

U EARTH HYDROSPHERE

HYDROSTATIC PRESSURE

P wave velocity and compressive strength of Bulgarian rock specimens at hydrostatic pressures up to 5000 kg/cm²
[NASA-TT-F-13209] 02 p0299 N71-11423

P wave velocities at high hydrostatic pressures in metamorphic, effusive, and sedimentary rock specimens from central Kazakhstan
[NASA-TT-F-13205] 02 p0299 N71-11438

P wave velocities at high hydrostatic pressures in igneous, sedimentary, and metamorphic cylindrical specimens from central Kazakhstan
[NASA-TT-F-13304] 02 p0210 N71-11439

Electrical properties of sedimentary rock under hydrostatic pressure
[NASA-TT-F-13215] 02 p0210 N71-11431

Stabilizing gyro utilizing re-circulated liquid hydrostatic fluid bearing
[NASA-CR-102992] 06 p0666 N71-16487

Structure and preservation of Black Sea dolomite dikes and protection provided internal organs and tissues during deep dives from high hydrostatic pressure
11 p1682 N71-23213

Buckling, flow and resin thermal resistance, and hydrostatic tests of glass fiber reinforced spherical pressure vessels and liners
[NASA-CR-72733] 11 p1769 N71-22401

Hydrostatic pressure effects on anoxic carrier lifetimes of a and p type germanium
12 p1987 N71-24303

Hydrostatic pressure effects on photosynthesis, growth, and oxygen production of algae cultures
[AD-728401] 14 p2204 N71-25867

Effect of hydrostatic pressure on deformation of NaCl single crystals
[AD-728415] 14 p2325 N71-25912

Research equilibrium boundaries and upper pressure calibration point
14 p2326 N71-26488

Resistance gage measurements of solid-solid phase transition fitted points in ammonium fluoride under high pressure
14 p2328 N71-26508

Solid-solid transition parameters of blennium and thallium at high temperatures for high pressure calibration points
14 p2328 N71-26508

- Activation volume for self diffusion, under hydrostatic pressure, of body centered cubic Fe
[CEA-CONF-1690] 15 p2477 N71-27584
- Self diffusion properties in alpha phase of large grains of plutonium prepared by using high hydrostatic pressures
[CEA-X-4092] 15 p2478 N71-27614
- Analysis of behavior of thin elastic shells subjected to initial mechanical stresses and nonuniform heating and dynamic interaction with surrounding fluid
[AD-71480] 16 p2467 N71-28586
- Effects of hydrostatic pressure in metals and alloys and application to industrial processes
[AD-722416] 17 p2763 N71-29648
- Molecular dynamics of phase transformation of iron under hydrostatic pressure
[TID-25463] 19 p3114 N71-32235
- Deconditioning and its prevention by simulating hydrostatic gradient by use of cardiovascular conditioning suit
20 p3219 N71-33274
- Hydrostatic extrusion of refractory materials using simple press
[NASA-CASE-NPO-10011] 21 p3433 N71-34425
- BUSHL - computer program used to determine buckling load of revolution shells under hydrostatic pressure, axial compression or both
[WAPD-TM-890] 21 p3461 N71-34635
- Analysis of inelastic effect on buckling load of clamped shallow spherical shell subjected to external pressure
[AD-727619] 24 p4026 N71-38725
- HYDROSTATICS**
- NT MAGNETOHYDROSTATICS**
- Design and testing of prototype hydrostatic liquid bearing gyro assemblies
[NASA-CR-102991] 07 p1028 N71-17319
- Effects of cold working by hydrostatic extrusion on mechanical properties of high strength steels
[NASA-TN-D-6186] 07 p1034 N71-17485
- Hydrostatic factors affecting diving capabilities of dolphins
11 p1681 N71-22210
- Flattening rates of oblate planets within 2.05 factor based on hydrostatic model for determining satellite orbits and paths of chemical releases
[AD-717687] 11 p1749 N71-22357
- Numerical analysis of elastic general instability problem of hydrostatically loaded simply supported cylindrical shell with conical ends
14 p2349 N71-26359
- Equations for flow rate, load capacity, and friction torque for conical hydrostatic bearings under laminar and turbulent flow conditions
[NASA-TN-D-6371] 16 p2600 N71-28046
- Influence of core to sleeve bonding on fracture of hydrostatic extrusion of hard core clad rod
[NYO-4078-3] 18 p2938 N71-31559
- HYDROTHERMAL CRYSTAL GROWTH**
- Techniques for growing single crystals of zirconium
[AD-714525] 06 p0936 N71-16618
- Growth of ZrSiO₄ single crystals for polarizing materials by molten salt and hydrothermal techniques
[AD-718551] 12 p1986 N71-23678
- HYDROX ENGINES**
- U HYDROGEN OXYGEN ENGINES**
- HYDROXIDES**
- NT LITHIUM HYDROXIDES**
- NT SODIUM HYDROXIDES**
- Nickel plaque impregnation to form nickel-cadmium battery plates by nitrate conversion to hydroxides and Fleischer methods
[NASA-CR-117306] 09 p1327 N71-20270
- Critical heat flux and pressure drop tests of electrically heated nuclear fuel rod bundles with ferrous hydroxide slurry crud deposits
[WAPD-TM-918] 09 p1421 N71-30388
- Gd₂O₃ microsphere preparation from sol-gel method
[EUR-4550] 13 p2121 N71-25247
- Crystal structure and morphology of hydrous oxides and hydroxides in lanthanide and actinide series
[ORO-3955-2] 16 p2667 N71-28797
- Magnetic properties of gadolinium, terbium, dysprosium, and holmium hydroxides at cryogenic temperatures
20 p3313 N71-33755
- Comparative tests on kinetics of formaldehyde condensation in presence of calcium hydroxide
[NASA-TT-P-14001] 24 p3385 N71-37609
- HYDROXYL COMPOUNDS**
- NT ALCOHOLS**
- NT CRESOLS**
- NT ETHYL ALCOHOL**
- NT GLYCOLS**
- NT METHYL ALCOHOLS**
- NT PHENOLS**
- Polyurethane resins derived from hydroxy terminated perfluoro ethers or diols
[NASA-CASE-NPO-10768-2] 20 p3230 N71-33516
- HYDROXYL EMISSION**
- Airborne photometer instrumentation and measurement data on high altitude hydroxyl airglow emission
[NASA-CR-118520] 13 p2162 N71-25211

- HYGIENE**
- Oral hygiene requirements for extended manned spacecraft flights
[NASA-CR-108695] 02 p0167 N71-11186
- Biological effects of microwaves in occupational hygiene
[NASA-TT-P-633] 05 p0633 N71-14632
- Hygiene and clinical physiology of men living in Antarctica
[JPRS-52579] 11 p1678 N71-21888
- Personal hygiene protocol for man in spacecraft environment
[NASA-CR-115181] 22 p3543 N71-35238
- HYGROMETRY**
- Measuring total precipitable water vapor and correlations between water vapor and local meteorological parameters
[NASA-TM-X-66498] 03 p0402 N71-12596
- Performance of aluminum oxide hygrometer on aircraft meteorological observatory
[NASA-TM-X-65446] 07 p1028 N71-17274
- Independent calibration of Low hygrometer
14 p2255 N71-26217
- HYGROSCOPICITY**
- Physicochemical properties and condensation growth rate equation for hygroscopic materials
[AD-716384] 09 p1413 N71-19659
- Warm fog seeding to determine potential of various sized and unsized hygroscopic chemicals for fog dissipation
[NASA-CR-1731] 11 p1790 N71-22619
- Method of evaluating moisture barrier properties of materials used in electronics encapsulation
[NASA-CASE-NPO-10051] 13 p2100 N71-24934
- Process for encapsulating hygroscopic cloud seeding agents
[AD-723448] 18 p2939 N71-30805
- HYLLERAAS COORDINATES**
- Applying Hylleraas correlation function to Giebach-Gordon combination of Hartree-Fock orbitals for two electrons
15 p3484 N71-27790
- HYPERBARIC CHAMBERS**
- Investigating effects of oxygen, nitrogen, and rare gas mixtures at increased pressures on narcosis tendencies of man
[JPRS-51714] 02 p0157 N71-11110
- Complex effect of nitrogen, argon, and helium respiratory mixtures on humans at increased pressures
02 p0157 N71-11115
- Functional state of central nervous system during development of epilepsy and narcosis in man and animals subjected to increased pressures of oxygen and inert gases
02 p0158 N71-11116
- Flat disc acrylic windows for man-rated hyperbaric chambers for experimental diving unit
[AD-716751] 10 p1651 N71-20758
- Effect of immersion on exchange of oxygen in lung at simulated depth of 5 feet of sea water using hyperbaric chamber
[AD-719389] 13 p2033 N71-24682
- Hyperbaric fire safety research, including flame spread rates in helium and nitrogen diving atmospheres and minimum oxygen concentration for combustion in hyperbaric environments
[AD-720353] 14 p2209 N71-25954
- Effects of hyperbaric environments on primates neuromuscular control
[AD-723829] 18 p2881 N71-31587
- Therapeutic pressure chamber design and testing for hyperbaric oxygenation treatments
24 p3903 N71-37817
- Functional technical and medical advantages and disadvantages of experimental, one-person, two-person, and multiple-person pressure chambers for hyperbaric oxygenation
24 p3903 N71-37818
- HYPERBOLAS**
- AGARD conference on nonreacting and chemically reacting viscous flows over hyperboloid at hypersonic conditions
[AGARDOGRAPH-147] 03 p0360 N71-12582
- Numerical results for ideal gas boundary layer flow for asymptotic half-angle hyperboloid
03 p0361 N71-12590
- Computation of laminar boundary layers and viscous shock layers over 10 deg half-angle hyperboloid
03 p0361 N71-12592
- Computerized finite element analysis of lateral pressure effects on free vibration of hyperboloidal shells of revolution
10 p1654 N71-21174
- Finite energy sum rules on hyperbolas and backward pion nucleus scattering
[TR-72-011] 23 p3783 N71-36963
- Finite energy sum rules on hyperbolas and nucleon-nucleon pion-pion reactions
[TR-72-012] 23 p3783 N71-36964
- HYPERBOLIC COORDINATES**
- Kinematics of diffusion, fluids, and plasma by continuous movement and finite velocities
[AD-713588] 05 p0665 N71-15540

- Testing of conic and hyperboloid multiquadric topography equations of geomorphologically diversified areas for computer graphics
[AD-718634] 12 p1905 N71-23380
- Numerical solution of quasi-conservative hyperbolic systems applied to case of converging-diverging cylindrical shock waves
[AD-717956] 12 p1930 N71-23746
- Eigenvalues passing through hyperbolic final points for area-preserving mapping
[TR-1] 14 p2282 N71-26109
- Group of invariance of Maxwell equations and extension associated with set of hyperboloids of mass (SLAC-TRANS-130)
15 p2458 N71-28993
- HYPERBOLIC FUNCTIONS**
- Averaging Lagrange averaged conservation equations to hyperbolic or elliptic dispersion equations for nonlinear waveform distortion
[AD-716530] 09 p1409 N71-19572
- Difference methods for hyperbolic equations using space and time split difference operators of third order accuracy
[UCRL-72806] 09 p1409 N71-19593
- Hyperbolic diffusion equation derived from classical parabolic equation
[AD-718616] 12 p1940 N71-23578
- Scattering theory for wave propagation problems of classical physics based on coerciveness theorem for nonelliptic operators and governed by symmetric hyperbolic systems
[AD-721723] 16 p2639 N71-28845
- Control theory extended to hyperbolic distributed processes with identification strategy incorporated in closed-loop adaptive controller
16 p2575 N71-28801
- Formulas for nth order derivatives of hyperbolic and trigonometric functions used in evaluating Fourier sine and cosine integrals
[NASA-TN-D-6403] 17 p2773 N71-29772
- Second order accurate difference method for systems of first order hyperbolic differential equations with cumulative error and convergence shown for elastic beam flexural wave propagation
[AD-726549] 22 p3608 N71-35805
- Difference schemes with split operator for systems of first order hyperbolic equations of mixed type for which Cauchy problem periodic in space variable posed and stability proved
24 p3949 N71-38177
- HYPERBOLIC NAVIGATION**
- NT DECCA NAVIGATION**
- NT LORAN**
- NT LORAN C**
- NT LORAN D**
- Technology review on long range hyperbolic navigation systems
[AD-719904] 14 p2290 N71-25775
- Correction of propagation anomalies in Omega navigation system
[AD-721061] 15 p2441 N71-26008
- HYPERBOLIC SPACE**
- U HYPERBOLIC COORDINATES**
- HYPERBOLIC TRAJECTORIES**
- Calculating orbital elements of comet Humason 1960-1959X
04 p0610 N71-13395
- Use of orbit-to-orbit shuttles for hyperbolic rendezvous with returning interplanetary spacecraft
[NASA-TN-D-6342] 21 p3525 N71-33117
- HYPERCAPNIA**
- Investigating gas preference reactions in man and animals to hypoxic, hyperoxic, or hypercapnic environments
[JPRS-52332] 07 p0961 N71-17448
- Physiological responses to interacting stresses of exercise and hypercapnia under acute and chronic exposure to ambient P sub CO₂ of 21 mm Hg
09 p1338 N71-28139
- HYPERFINE STRUCTURE**
- Nuclear magnetic resonance hyperfine fields in intermetallic compounds with manganese
[IS-T-369] 02 p2275 N71-11915
- Discrepancies in hyperfine constants of shallow donor materials in silicon
[UR-3348-21] 03 p0435 N71-13800
- Hyperfine ESR linewidth in linear chains using Cu/NH₄ASO₄-H₂O/CTS for calculations
[COO-1488-19] 04 p0483 N71-13439
- Level crossing analysis on hyperfine structure of europium isotope
04 p0576 N71-13405
- Internal fields and relaxation effects for dysprosium in ferromagnetic TbAl₂ studied by perturbed angular correlation
[UIUP-464] 06 p0909 N71-15752
- Perturbed angular correlation technique for studying effect of cubic lattice on electronic levels of erbium ions in HoAl₂
[UIUP-695] 06 p0909 N71-15700
- Investigating reaction mechanisms, nuclear moments, and hyperfine interactions using various accelerators
[BMW-FBK-70-9] 06 p0912 N71-15814

SUBJECT INDEX

Table of magnetic hyperfine-structure anomalies calculated from measured moment ratios
[ORNL-4591] 06 p0919 N71-16248

Mössbauer effect characteristics of europium isotopes in mixed oxide structures
[ORO-3603-7] 07 p1072 N71-17321

Fine structure, hyperfine weights, and reactivity within in fuel cluster
[RDI/RN-1734] 08 p1236 N71-18321

Diffusion coefficient of neutral hyperfine particles in gas
[NF-18413] 08 p1260 N71-18774

Measurement of muonium hyperfine structure at weak magnetic field
08 p1245 N71-19215

Nuclear charge structure effects on hyperfine structure, isotope shift, and magnetic octupole moments
09 p1432 N71-19972

Process for producing dispersion strengthened alloys with aluminum comprising metallic matrices embedded with oxides or other hyperfine compounds
[NASA-CASE-XLE-06909] 12 p1940 N71-24142

Nuclear structure effects in magnetic hyperfine interaction using pairing and pairing plus quadrupole model
13 p2137 N71-25432

Magnetic properties of solids including electron paramagnetic resonance in dilute magnetic alloy, hyperfine splitting of localized moment in metal, and band theory of solids
[AD-720777] 14 p2323 N71-26020

Hyperfine structure of antiferromagnetic FeO₂ using 14.4 keV Mössbauer transition in Fe-57
15 p2506 N71-27422

International conference on hyperfine interactions detected by angular correlation methods, nuclear orientation at low temperatures, nuclear magnetic resonance, and optical pumping
[AD-720644] 16 p2656 N71-29113

Nuclear magnetic resonance of chlorinated hydrocarbon molecules in excited triplet states using Hamiltonians for electron spin-spin, nuclear quadrupole, and hyperfine interactions
[UCRL-20390] 17 p2791 N71-29271

Level crossing and resonance spectra of excited states in lutetium 175 hyperfine structure
17 p2796 N71-29791

Magnetic resonance in dilute magnetic alloys - hyperfine splitting of Ag-Er-167
[AD-722711] 17 p2829 N71-30279

Integral attenuation coefficients of angular correlations perturbed by free hyperfine interaction and parallel external magnetic field
[UUIP-690] 18 p2967 N71-30405

Hyperfine fields at magnetic and nonmagnetic lattice sites measured in solid solutions of magnesium antimonide and chromium antimonide
[COO-1190-690] 18 p2962 N71-30737

Hyperfine structures and positions of 5d_{5/2} and 2F_{5/2} states in lanthanum I spectrum by laser-crossing method and Doppler resonance spectroscopy
18 p2963 N71-30951

Hyperfine magnetic interactions in Fe-Ga solid solutions analyzed by Mössbauer spectroscopy
[CALT-522-27] 19 p3169 N71-32218

Hyperfine interactions in research fields including perturbed angular correlation, NMR, Coulomb recoil implantation, rotational states, and electric monopoles - lectures
[NF-18702] 19 p3157 N71-32478

Redetermination of hyperfine structure constant by microwave transitions in H, a equals 2
19 p3158 N71-32560

NMR for determining distribution of hyperfine fields at cobalt nuclei in dilute alloys of Co-V, Co-Cr, and Co-Mn
[COO-1569-71] 20 p3319 N71-33669

Spectrometer for detecting hyperfine levels of perturbed hydrogen atoms at zero magnetic field
[UCRL-20339] 20 p3320 N71-33703

Hyperfine structure and isotope effect of 30 year blackshift 267 using Fabry-Pérot interferometer and monochromator measurements
20 p3321 N71-33731

Mössbauer studies of energy levels, electric and magnetic moments, hyperfine fields, and lift times of various light nuclei
[NYO-2228-5] 21 p3484 N71-34821

Pressure and temperature effects on hyperfine structure in gamma resonance absorption spectra of plutonium and its compounds
21 p3498 N71-34922

Many body perturbation procedure for studying various properties of interacting atoms applied to He and He-He systems
22 p3650 N71-36027

Relativistic correction to Fermi-contact hyperfine Hamiltonian derived for arbitrary principal quantum number
[DP-18813] 23 p3815 N71-37207

Determining Knight shift in beryllium from hyperfine contact and diamagnetism calculations combined with core polarization effect
24 p3942 N71-38119

Hyperfine structure in rotational spectrum of asymmetric-top molecules containing two identical quadrupolar nuclei
24 p3982 N71-38423

HYPERGOLIC ROCKET PROPELLANTS
Measuring heat and gas release rates for initial reaction of liquid nitrogen tetroxide with hydrazine, monomethyl hydrazine, and unsymmetrical dimethyl hydrazine
[NASA-CR-115863] 05 p0761 N71-15379

Method for igniting solid propellant rocket motors by injecting hypergolic fluids
[NASA-CASE-XLE-01908] 05 p0761 N71-15634

Composition and properties of high energy hypergolic rocket propellants
[AGARD-AG-141-70] 07 p1090 N71-17841

Combustor pressure popping, stream mixing, and stream separation associated with combustion of igniting hypergolic propellants
[NASA-CR-1704] 15 p2523 N71-26869

Influence of vortex rocket engine injector design on water flow distribution for future hypergolic propellant injection performance
[RFE-TR-7016] 20 p3338 N71-33147

HYPERNUCLEI
Lambda-excited states of hypernuclei by means of optical potential model
[INR-P-1222] 14 p2309 N71-26574

Hypernuclei particle production, binding energy, spin, radioactive decay, excited and resonant states, isomers, and nuclear radiation spectroscopy
[INR-P-1223] 15 p2408 N71-27311

Lapton decay of hypertrons
[LAE-1944] 23 p3808 N71-37147

HYPERONS
Binding energy calculations for central potentials of lambda hyperon-nucleon interactions
[TID-25407] 03 p0421 N71-12651

Production, decay, and branching ratio for Lambda hyperon (1520) - conference
[UCRL-19763] 03 p0427 N71-12853

Negative Xi hyperon production in negative pion-nucleon interactions
[IPA-HE-45] 03 p0428 N71-12876

N¹¹B/120 production and subsequent decay to Delta hyperon/1234 pion in pion/proton interactions at 3.1 GeV/c
[COO-1428-175] 03 p0431 N71-12911

Studying various kaon/ proton interactions at 2.1 to 2.70 GeV/c for existence of two Sigma hyperon (1660) resonances
[UCRL-19824] 03 p0431 N71-12912

Calculating binding energy of Lambda hyperon particle in nuclear matter using self-consistent Brueckner K matrix theory
[INR-11537/PL] 03 p0433 N71-12938

Calculating binding energy of Lambda hyperon particle in nuclear matter using Herndon-Tang Lambda hyperon nucleon potentials
[INR-P-1191] 04 p0576 N71-13691

Production and decay angular distributions of Delta/ hyperons from pion/ proton reactions
[COO-1428-232] 04 p0579 N71-13978

Analysis of Y/1385/ pion production near Y/1520/ resonance
[NYO-3651-13] 04 p0582 N71-14106

Negative Sigma hyperon interactions
[INR-3651-14] 05 p0745 N71-15201

Deriving formulas for spin and angular correlations in hyperon beta decay
[COO-264-548] 05 p0747 N71-15240

Cross sections of strange particles
[UCRL-19845] 06 p0915 N71-16011

Determining set of experiments that represent full experiment for weak and semileptonic hyperon decays
[UUV-2432-F] 06 p0916 N71-16054

Hyperon states in partial wave analyses of antikaon nucleon system
[UCRL-19843] 06 p0924 N71-16074

Lambda hyperon-nucleon interactions in deuteron
[UCRL-20077] 06 p0927 N71-16088

Neutrino, electron, and proton up-down asymmetry measurements from beta decay of polarized Lambda hyperons
[COO-1545-87] 10 p1611 N71-20706

Sigma hyperon resonance in reaction negative kaon plus proton yields Lambda hyperon plus neutral pion
[UCRL-19789] 10 p1612 N71-20759

Polarized hyperon beta decay in center mass frame of outgoing leptons
[COO-264-563] 11 p1802 N71-22089

Q squared spectrum and asymmetry functions of hyperon beta decay
[COO-264-563-ADD] 11 p1802 N71-22092

Pole model for semileptonic hyperon decays with exchanged particles of all spins
[SU-1206-238] 12 p1971 N71-23083

Mathematical model for closed form expression of impurity particle nuclear binding energy using power series, particle spin, and wave functions with lambda hyperon example
[DEMO-70/20] 13 p2130 N71-24698

Cometic gamma ray energy spectra caused by hyperon and nucleon isobar decays for gamma ray

energies above 1 GeV, and differential production cross section
13 p2139 N71-24770

Statistical tensor analysis of decay distributions and hyperon polarizations for Y 1385 resonance from positive pion proton yields kaon resonances Lambda hyperon positive pion with quark model
[INR-731] 13 p2140 N71-25525

Nuclear resonance positive pion proton yields positive pion proton positive plus negative pion dominated by neutral rho pion and delta hyperon
13 p2143 N71-25309

Spin test for fermion 1/2 greater than 1/2 decaying into spin-1/2 fermion/neutral Lambda hyperon/ plus spin-1 photon
[KFKI-70-27-HEP] 14 p2313 N71-26717

Polarization of Lambda and Sigma hyperons in two-body Y-resonance production processes and the quark model with experimental methods for determining polarization moments of hyperons
[TPJ1-2/70] 14 p2320 N71-26795

Asymmetry parameters of isospin Sigma hyperon decays in negative kaon beam interaction
15 p2487 N71-27835

Nonlinear equation for correlation function between lambda hyperon and nucleon in nuclear matter
[DEMO-74/19] 15 p2488 N71-27878

Lambda and Sigma hyperon resonances, branching ratios, and lifetimes from bubble chamber analysis of antikaon nucleon reactions
[CBA-R-4068] 15 p2492 N71-27931

Nuclear physics approach to classifying nucleon and hyperon rotational levels
[UCRL-72943-REV-1] 16 p2643 N71-28111

Double emission of Lambda hyperons in negative kaon 6 GeV/c interactions with nucleons of choice
[JEN-217-IFJCT-4] 16 p2649 N71-28015

Magnetic moment of positive Sigma hyperon and positive kaon and positive Sigma hyperon decay observed in optical spark chamber located inside bore of solenoidal pulsed magnet
16 p2660 N71-29197

Three body states Lambda or Sigma hyperon kaon antikaon and Xi hyperon kaon pion produced by negative kaon proton interactions at kaon beam momenta of 5.6 GeV/c
[ORNL-2586-170] 17 p2797 N71-29845

Electroproduction of Delta hyperon/1234/ in neutral pion channel at four momentum transfer, studied from angular distribution measurements of outgoing protons
[DESY-70/65] 17 p2801 N71-30108

Delta 3 equals 2 transition for obtaining decay rates and asymmetry parameters in semileptonic hyperon decays
[RIFF-120] 17 p2806 N71-30305

Study of muonic decays of sigma hyperon using bubble chamber photographs
17 p2806 N71-30309

Formulas and matrix elements for shell model analysis of Lambda hyperon binding energies to hypernuclei
[NIP-18585] 18 p2977 N71-30639

Monte Carlo calculation for magnetic moment of Lambda hyperon in negative pion plus proton yields Lambda hyperon plus neutral kaon reaction
18 p2978 N71-31494

Experimental estimate of total cross section for Delta/1234/ hyperon resonance on nucleons from neutrino or electroproduction experiments in heavy liquid bubble chamber
[PTHE-71/30] 20 p3315 N71-33242

Antihyperon hyperon production in antiproton proton scattering, studied with absorbed Regge pole model with exchange degeneracy
[N-TW-71/2] 20 p3324 N71-33677

Lambda hyperon nucleon potential in D sub Lambda calculations in phase shift approximation
[INR-P-1239] 21 p3469 N71-34694

Quasi-nuclear model of many-baryon resonances from Delta hyperon nucleon potential interaction
[NP-18779] 21 p3472 N71-34722

Second order form factors for spin correlation analysis in beta decay of Lambda hyperon
[COO-264-569] 21 p3476 N71-34750

Hyperon hyperon decay measurements and rare decay mode search in bubble chamber
[NYO-366-TA-5] 21 p3476 N71-34751

Lapton decay experiments with unpolarized hyperon beams
[COO-1701-12] 21 p3476 N71-34757

Weak interaction in beta decay of polarized Lambda hyperons
[COO-1701-14] 21 p3489 N71-34784

Lambda(0) hyperon polarization along sigma(0) hyperon decay plane by violating time reversal invariance in electromagnetic interaction of kaon(nu) or sigma(nu) meson with protons
21 p3487 N71-34842

magnitude measurements of kaon(0) sub L kaon(0) sub s mass difference and Lambda hyperon proton interactions at high energies
21 p3488 N71-34849

Negative pion proton yields neutral pion neutron differential cross section measurements and baryon exchange model with absorption in pion nucleon backward scattering
[NP-18840] 23 p3806 N71-37132

Hyperon-nucleon interaction using crossed channel boson exchange model
[NP-18838] 24 p3971 N71-38325

Cross sections and angular distributions in kaon(minus) deuteron yields kaon(minus) deuteron and kaon(minus) neutron yields kaon(minus) neutron interactions
[NP-18891] 24 p3974 N71-38354

Separation of kaon(minus) proton interactions from kaon(minus) nucleus interactions in kaon(minus) proton yields Lambda(0) hyperon pion(plus) pion(minus) reactions
[LAL-RI-71-2] 24 p3974 N71-38357

HYPEROXIA

Oxygen and high altitude pressure effects on rabbit testicular functions
[AD-715209] 07 p0983 N71-17885

Growth and fatty acid synthesis inhibition in *Escherichia coli* by oxygen
[AD-717673] 11 p1683 N71-22347

Peroxidase and catalase activity and hyperoxia effects on mice organs, leucocytes, and erythrocytes in pure oxygen tank pressure
[ANL-TLANS-577] 15 p3371 N71-27290

HYPERSONIC AIRCRAFT

Evaluating performance characteristics of parallel turbofanjet propulsion system for all-body Mach 6 hypersonic aircraft
[NASA-TN-D-5993] 05 p0762 N71-15380

Aerodynamic heating and structural analysis for relatively cooled delta wing of hypersonic aircraft
[NASA-TN-D-6138] 07 p1128 N71-18025

Flight constraints and aerodynamic characteristics of hypersonic research aircraft
[NASA-TM-X-2222] 08 p1142 N71-18367

European hypersonic wind tunnels for testing hypersonic transport aircraft, and space shuttle aerodynamic configurations
08 p1175 N71-18452

Estimated aerodynamics of all-body hypersonic aircraft configurations
[NASA-TN-X-2091] 09 p3135 N71-19706

Wind tunnel investigation of aerodynamic characteristics of wing-body and lifting body configurations for hypersonic cruise aircraft at hypersonic speeds
[NASA-TM-X-2287] 16 p2536 N71-28861

Development of data for commercially viable hypersonic transport aircraft
[NASA-TF-15799] 20 p3212 N71-33625

Preliminary research requirements analysis and design and cost synthesis of ground research facilities for hypersonic aircraft
[NASA-CR-114323] 21 p3406 N71-34236

Parametric research requirements analysis and synthesis of ground research facilities for hypersonic aircraft
[NASA-CR-114325] 21 p3406 N71-34237

Analysis of ground research facilities for hypersonic aircraft
[NASA-CR-114328] 21 p3407 N71-34238

Summary of analyses on research requirements and research facilities for hypersonic aircraft
[NASA-CR-114329] 21 p3407 N71-34239

Assessing research and development in hypersonic aircraft for determining requirements for hypersonic research facilities
[NASA-CR-114332] 22 p3564 N71-35384

HYPERSONIC BOUNDARY LAYER

Hyper-sonic boundary layer transition and hyper-sonic heat transfer on cylindrical shells, cones and flat plates
[REPT-1104/70] 04 p0472 N71-13408

Hyper-sonic laminar boundary layer near sharp expansion corner
07 p1012 N71-17752

Near-continuum axisymmetric hypersonic flow past very slender bodies
[AD-715901] 08 p1141 N71-18556

Limits of hypersonic boundary layer theory, and leading and trailing edge phenomena in laminar hypersonic boundary layer
09 p1373 N71-19833

Hyper-sonic laminar boundary layer growth over concave and convex surfaces
09 p1374 N71-19836

Tests at Mach number 6 to investigate results of ejected liquid/water and two dimensional, zero pressure gradient boundary layer for wedge model
[AD-721448] 16 p2581 N71-28728

Shear-stress, eddy-viscosity, and mixing-length distributions in hypersonic turbulent boundary layers using assumption of local similarity
[NASA-TM-X-2310] 18 p2907 N71-31310

HYPERSONIC COMBUSTION

Hyper-sonic ramjet technology review
[PB-193911] 04 p0606 N71-14199

HYPERSONIC FLIGHT

Viscous interactions and flight at high Mach numbers
[AD-712975] 03 p0309 N71-12204

Thermal performance of hypersonic engine struts
[NASA-CR-111812] 04 p0605 N71-14045

Flight constraints and aerodynamic characteristics of hypersonic research aircraft
[NASA-TM-X-2222] 08 p1142 N71-18367

Conductive heat transfer effect on temperature distribution in vicinity of wing leading edge in hypersonic flight
[AKC-CF-1126] 13 p2184 N71-24446

Minimizing drag and increasing performance of optimum shapes at hypersonic flight
13 p2023 N71-24704

Supersonic combustion ramjet engine configuration and performance in hypersonic flight
17 p2834 N71-29571

Aircraft design, flight characteristics, and atmospheric effects on sonic boom during supersonic and hypersonic flight
18 p2871 N71-30787

Wind tunnel investigation of control surface instability of lifting body reentry vehicle configurations at Mach 15
[NASA-TN-D-6301] 18 p3018 N71-31241

HYPERSONIC FLOW

Measurements of hypersonic, rarefied flow field of disk
[AD-710641] 01 p0042 N71-10461

Surface heat transfer rates measured on flat plates in hypervelocity shock tunnel
[NASA-CR-1692] 01 p0134 N71-10067

Laminar boundary layer effect on dynamic viscous pressure interaction in hypersonic flow
[LR-535] 02 p0141 N71-11003

Measuring low-density flow over two-dimensional blunt bodies in hypersonic arc tunnel
[NASA-TN-D-6017] 03 p0511 N71-12215

Laminar boundary layer calculations on bodies of revolution in hypersonic flow
03 p0360 N71-12585

Differential interferometry and schlieren photography for hypersonic aerodynamic hologram analysis
[ISL-T-49/69] 03 p0388 N71-12985

Flat plate pressure distribution and heat transfer in conical hypersonic flow
[VKI-TN-56] 03 p0365 N71-12336

Design and operation of hypersonic shock tunnel
[IC/70/04] 04 p0515 N71-13778

Inviscid hypersonic flow of chemically relaxing air about pointed circular cones
05 p0659 N71-14748

Numerical analysis of radiating inviscid flow behind paraboloidal shock wave
05 p0661 N71-14772

Interaction of hypersonic spherical source flow with rarefied atmosphere
[AD-713122] 05 p0663 N71-14934

Aerodynamic forces on lifting bodies and delta wings in hypersonic slip flow
[BMW-FB-W-70-41] 06 p0791 N71-15704

Conical flow effects on pressure center of blunt conical bodies in hypersonic flow
[NPL-AERO-NOTE-1085] 06 p0833 N71-15788

Eddy viscosity-intermittency factor approach to numerical calculation of laminar, transitional, turbulent heating of sharp cones in hypersonic flow
[AD-714058] 06 p0835 N71-16217

Strong viscous interaction between laminar boundary layer and external hypersonic flow field on curved surfaces
[AD-714075] 06 p0835 N71-16218

Flat plate and expansion corner models in hypersonic wind tunnel
[AD-714074] 06 p0835 N71-16290

Numerical computation of viscous hypersonic flow around slender bodies
07 p1007 N71-16951

Rectangular and caret wing sails in supersonic and hypersonic turbulent flow for hypersonic vehicles
[ARC-R/M-3624] 07 p0965 N71-17103

Wall pressure and heat transfer distribution on delta wings in rarefied hypersonic flow
[REPT-70-9] 08 p1139 N71-18423

Hyper-sonic two phase flow realized by air-water mixtures
[BMVTDG-FBWT-70-1] 08 p1140 N71-18441

Determining structure and integrated properties of turbulent boundary layers at hypersonic speeds
[AD-715927] 08 p1179 N71-18520

Low density hypersonic flow over cone, scattering of gas particles from solid surface
08 p1182 N71-18936

Propagation of disturbance in viscous hypersonic flows of ideal gas
[NASA-TT-F-13485] 08 p1182 N71-18959

Linearized theory of stagnation region skin friction and mass transfer at hypersonic speeds
[NASA-TN-D-6262] 08 p1182 N71-18940

Proceedings for symposium on viscous interaction phenomena in supersonic and hypersonic flow
[AD-714563] 09 p1373 N71-19830

Attached and separated laminar boundary layer characteristics over high cooled, curved compression surfaces in hypersonic flow
09 p1374 N71-19837

Three dimensional viscous hypersonic interactions
09 p1375 N71-19840

Design of hypersonic test facility for ablation tests and performance tests of vehicles under conditions of high temperature and pressure
[NASA-CASE-XLA-05378] 10 p1538 N71-21475

Transverse pressure gradient on interaction of laminar hypersonic boundary layer with corner expansion wave
[UTIAS-157] 11 p1734 N71-22048

Rarefied gas dynamics including hypersonic flow about blunt bodies, thermal shock, laminar boundary layers, and radiating gas flow
[AD-717419] 11 p1735 N71-22124

Schlieren and phase contrast methods of hypersonic flow visualization
11 p1741 N71-22637

Analysis of supersonic and hypersonic flow of hyperviscid ideal gas over conical wings with sharp leading edges and attached shock waves by three dimensional method of characteristics
[NASA-CR-1738] 11 p1671 N71-22672

Turbulence diffusion above flow during boundary layer and hypersonic flow interaction
[NASA-TT-F-13522] 12 p1899 N71-23312

Hyper-sonic wind tunnel test on conical and ogival scaled static pressure probes
[ARL-A-327] 12 p1831 N71-23778

Nonequilibrium radiative gas dynamics of slender pointed bodies
[AD-719744] 13 p2063 N71-24431

Flow measurement of Nonweiler delta wing in hypersonic slip flow
[DLR-FB-70-46] 13 p2022 N71-24500

Streamline swallowing by laminar boundary layers in hypersonic flow
[AD-719748] 13 p2065 N71-24743

Flat plate aspect ratio effects on ramp-induced, subsonic, boundary layer separation at supersonic and hypersonic speeds
[AD-719747] 13 p2065 N71-24744

Hyper-sonic flows, three dimensional boundary behavior in corner, subsonic, laminar, and turbulent mixing over lifting vehicles
[AD-719766] 14 p2195 N71-25630

Mach number reduction in low density hypersonic wind tunnel by increasing nozzle throat area
[DLR-FB-70-43] 15 p2391 N71-27060

Measurements of total temperature and pitot pressure across boundary layer of test section wall of is-isymmetric contoured nozzle at hypersonic speed in nitrogen
[NASA-TN-D-6192] 16 p2530 N71-28778

Flat plate in hypersonic low density flow examined in shock formation and transition regime
[DLR-FB-70-79] 17 p2700 N71-29432

Pressure distributions and shock wave shapes during hypersonic flow over 10deg semi-angle cone with spherical blunting
[ARL-AN-328] 20 p3249 N71-32902

Rarefied dissociated hypersonic gas flow over flat plate with sharp leading edges
[DLR-FB-70-40] 20 p3249 N71-33930

Diffuser, throat, and mass injection effects on starting and operating characteristics of Mach 5 free jet tunnel at low pressure ratios
[NASA-TN-D-63777] 21 p3407 N71-34243

Hyper-sonic flow around blunt object by nonviscous gas current accounting for radiation transfer in shock front
[NASA-TT-F-13568] 22 p3566 N71-35408

Similar solutions for axial hypersonic flow past slender bodies with nearly elliptic cross section and slender axisymmetric bodies
[DLR-FB-71-13] 22 p3568 N71-35412

Velocity pulsations of high temperature hypersonic flow based on interruption of total stagnation pressure pulsations and longitudinal velocity pulsations
[AD-726605] 22 p3569 N71-35421

HYPERSONIC FORCES

Wall pressure, hypersonic forces and hypersonic heat transfer for flat plates in low density flow
[REPT-70-4] 04 p0471 N71-13401

HYPERSONIC HEAT TRANSFER

Wall pressure, hypersonic forces and hypersonic heat transfer for flat plates in low density flow
[REPT-70-4] 04 p0471 N71-13401

Hyper-sonic boundary layer transition and hypersonic heat transfer on cylindrical shells, cones and flat plates
[REPT-1104/70] 04 p0472 N71-13408

Eddy viscosity-intermittency factor approach to numerical calculation of laminar, transitional, turbulent heating of sharp cones in hypersonic flow
[AD-714058] 06 p0835 N71-16217

Approximate solutions for heat transfer and drag coefficients in viscous interacting flow on thin three dimensional body
[NASA-TT-F-13538] 09 p1377 N71-30256

SUBJECT INDEX

Enthalpy and wall heat flux calculations for stagnation region aft of blunt axisymmetric bodies in hypersonic axial flow
[AD-717418] 11 p1735 N71-22087

Hypersonic heat transfer to flat plates and conical and blunt bodies in boundary layer flow
[ARC-RM-5637] 13 p2065 N71-24714

Energy-integral prediction of hypersonic and laminar heat transfer in thermal boundary layer around blunt slender cones and of compressible flow with heat transfer
17 p2838 N71-29087

HYPERSONIC INLETS
Use of gas tunnel as low temperature test facility for hypersonic intake research
11 p1732 N71-22635

Starting phenomena of two-dimensional hypersonic intake with turbulent intake boundary layers at free stream Mach 6
[NASA-TN-D-6280] 18 p3905 N71-30936

HYPERSONIC NOZZLES
Hypersonic nozzle molecular beam development containing atomic oxygen
[AD-710973] 63 p6368 N71-13032

Characteristics of chemically reacting air flow in large, or heated, hypersonic wind tunnel nozzle
16 p2581 N71-28721

Measurements of total temperature and static pressure across boundary layer of test section wall of axisymmetric contoured nozzle at hypersonic speed in nitrogen
[NASA-TN-D-6192] 16 p2530 N71-28778

HYPERSONIC REENTRY
Radio wave propagation through plasmas studied for communication with hypersonic vehicles during reentry
10 p1518 N71-21102

Radio attenuation measurements for hypersonic reentry communication
10 p1518 N71-21103

Calculated and measured nonequilibrium flow electron density and collision frequency distributions in plasma sheath around Apollo spacecraft during hypersonic reentry
10 p1627 N71-21104

Hypersonic reentry plasma diagnostic measurements made with four-frequency microwave reflectometer
10 p1628 N71-21107

Electrostatic probe determinations of electron density profiles for three RAM C hypersonic reentries
10 p1628 N71-21108

Electron density and signal attenuation data from RAM C hypersonic reentries and theoretical calculations
10 p1628 N71-21116

VHF and X band telemetry attenuation by plasma sheath around hypersonic reentry vehicles
10 p1519 N71-21119

Low Reynolds number viscous flow at stagnation region of blunt bodies during hypersonic reentry
10 p1541 N71-21127

Shock tube study of plasma adhesion by tangential side shot for application to plasma sheaths during hypersonic reentry
10 p1629 N71-21128

Hypersonic shock/density ratio effects in aerothermodynamic heating of space shuttle configuration
14 p2354 N71-26058

Radiation absorption in shock front of hypersonic air flow around blunt reentry body
[NASA-TT-F-13572] 16 p2582 N71-26057

Near-free molecule drag of slender pointed cones, with reference to hypersonic reentry
[P-4521] 19 p3034 N71-32222

HYPERSONIC SHOCK
Hypersonic shock tunnel of AFAPL
[AD-715907] 08 p1175 N71-18717

Analysis of Mach wave configurations resulting from reflection of shocks from inclined surfaces using schlieren photography, interferometry, and smoke tracks
17 p2857 N71-29659

HYPERSONIC SPEED
Unsymmetrical nose bluntness effect on stability derivatives of slender cones at Mach 14
[AD-711921] 02 p0142 N71-11008

AGARD conference on nonreacting and chemically reacting viscous flows over hypersonic at hypersonic conditions
[AGARD-GRAPH-147] 03 p0366 N71-12582

Laminar flow past axisymmetric blunt bodies moving at hypersonic speed
[NASA-CR-115771] 03 p0361 N71-12591

Stability and postcritical response of infinite wing models on hinged supports due to aerodynamic loads at hypersonic speed
[NASA-CR-115854] 03 p0779 N71-15341

Variable geometry manned orbital vehicle having high aerodynamic efficiency over wide speed range and incorporating auxiliary pivotal wings
[NASA-CASE-XLA-63691] 03 p0773 N71-15674

Viscous drag on variable sweep wings and wedges at hypersonic and hypersonic speeds
[ARC-RM-3623] 07 p0966 N71-17109

Turbulent separated and reattaching flow on flat plate-compression corner at supersonic and hypersonic speeds
09 p1374 N71-19835

Laminar two dimensional boundary layer separation measurements at moderately hypersonic speeds
09 p1376 N71-19845

Hypervelocity oxidation tests of thorium dispersed nickel chromium alloys to determine feasibility as space shuttle material
[NASA-TM-X-62015] 09 p1401 N71-20390

Effect of heat conduction of material on temperature distribution in vicinity of wing leading edge at hypersonic flight
[REPT-4901] 11 p1841 N71-22494

Wind tunnel investigation of hypersonic transport model aerodynamic characteristics at Mach numbers to 6-graphs
[NASA-TN-D-6191] 12 p1852 N71-23127

Supersonic or hypersonic vehicle control system comprising elevons with hinge line sweep and free of adverse aerodynamic cross coupling
[NASA-CASE-XLA-09567] 13 p2366 N71-27008

Heating rate and efficiency of flaps at hypersonic speeds
[SC-T-71-3016] 15 p2365 N71-27674

Predicted and measured aerodynamic characteristics for blended delta-wing orbiter at hypersonic speeds
[NASA-TM-X-62046] 19 p3184 N71-32106

Method for predicting compressible turbulent boundary layers in adverse pressure gradients applied to hypersonic air breathing propulsion
[NASA-TM-X-2342] 19 p3078 N71-32210

Measurement of hypersonic sound speeds in methane at moderate pressure and comparison with ultrasonic speed data
[NASA-CR-121377] 20 p3274 N71-33477

Computer program for determining inviscid flow around blunt bodies at supersonic and hypersonic speeds - users manual
[NASA-TM-X-2334] 20 p3252 N71-33670

HYPERSONIC TEST APPARATUS
Design and performance characteristics of hypersonic gas tunnel
[JC-AERO-70-04] 01 p0038 N71-10270

HYPERSONIC VEHICLES
NT HYPERSONIC AIRCRAFT
NT LIFTING REENTRY VEHICLES
Hypersonic ramjet technology review
[PB-193911] 04 p0606 N71-14199

Longitudinal aerodynamic characteristics of hypersonic lifting body spacecraft with variable sweep wings
[NASA-TM-X-2102] 05 p0626 N71-14945

Computer program and approximate inverse solution for nonequilibrium flow in inviscid shock layer about vehicle in hypersonic flight in arbitrary atmosphere
11 p1734 N71-21919

Engineering design analysis of hydrogen cooled structural panels for application to hypersonic aircraft
[NASA-CR-1650] 11 p1843 N71-22653

Configuration optimization and performance of air breathing hypersonic cruise vehicles
[AD-721471] 16 p2529 N71-28300

Conference on performance of propulsion systems for hypersonic vehicles and some aerodynamic characteristics
[ONERA-TN-169] 17 p2834 N71-29568

Hypersonic vehicle propulsion system configuration and performance
17 p2834 N71-29569

Aerodynamic problems related to hypersonic vehicles and space shuttles
17 p2700 N71-29572

Near flow field data for tube-vehicle systems and drag coefficient relationships with relative Mach numbers and relative flow velocity ratios to vehicle velocity
[GASL-TR-70-749] 24 p3908 N71-37856

HYPERSONIC WAKES
Laminar near wake characteristics behind circular cylinder at Mach 6 stratified air stream
[REPT-110870] 02 p0142 N71-11012

Schlieren method for measuring wake density behind hypervelocity projectile
[ISL-T-12409] 03 p0312 N71-12221

Differential interferometry for determining wake density behind hypersonic spherical projectile
[ISL-T-12700] 03 p0418 N71-12982

Knudsen flow and Mach number effects on hypersonic and supersonic wakes of cylindrical bodies and spheres
[REPT-69-7] 04 p0471 N71-13403

Wire and probe support interference on hypersonic wakes of magnetically suspended round based conical body
[ARC-CR-1133] 10 p1492 N71-20048

HYPERSONIC WIND TUNNELS
U HYPERSONIC WIND TUNNELS
HYPERSONICS
Use of gas lasers to measure velocity and absorption of longitudinal hypersonic waves
[NASA-TT-F-15902] 21 p3464 N71-34660

HYPERVELOCITY PROJECTILES

HYPERSPHERES
Distance moment between two points selected independently of each other for constant probability within a-dimensional uniform hypersphere
03 p0714 N71-15532

Hyperspherical functions used for obtaining lower bounds on scattering functions
[JINR-PN-5366] 15 p2473 N71-27442

HYPERTHERMIA
Hyperthermia, dietary, and deslimeration effects on thermoregulation in rats
[NASA-CR-117851] 11 p1484 N71-22976

Microinjection of carbocetyl in anterior preoptic hypothalamic area of rats inducing hyperthermia
11 p1484 N71-22977

HYPERTONIA
U OSMOSIS

HYPERTROPHY
U GROWTH

HYPERVELOCITY ACCELERATORS
U HYPERVELOCITY GUNS

HYPERVELOCITY CRATERING
U HYPERVELOCITY PROJECTILES
U PROJECTILE CRATERING

HYPERVELOCITY FLOW
Tests to determine short-term creep of metals and alloys under conditions of aerodynamic heating with high velocity air flow
[NASA-TT-F-13633] 14 p2372 N71-25822

Finite difference method for calculating inviscid flow field around supersonic/hypersonic open shock
14 p2346 N71-26056

HYPERVELOCITY GUNS
Feasibility of explosive lining in launch tube for hypervelocity projectile acceleration
[NASA-CR-100699] 04 p0605 N71-14033

Method and apparatus for use in forming highly collimated beam of microparticles with high charge to mass ratio and injecting beam into electrostatic accelerating tube
[NASA-CASE-XOS-06628] 06 p0918 N71-18213

Ionization driven, light gas, hypervelocity gun
[NASA-CASE-XAC-65982] 06 p1173 N71-18578

Evaluation of hypervelocity projectile accelerator facility to determine impact effects of micrometeoroids on solar cells
[NASA-TN-D-7017] 12 p1897 N71-23008

HYPERVELOCITY IMPACT
Hypervelocity impact research in ballistic ranges
[NASA-TM-X-46533] 04 p0515 N71-13580

Predicting crater size and impact flash for S-48 stage lunar impact on Apollo 13 flight
[NASA-TM-X-44517] 05 p0766 N71-14636

Ultrahigh speed photographic system for photographing hypervelocity projectiles and impact phenomena
[NASA-TN-D-6128] 05 p0485 N71-15408

Polished metals exposed to hypervelocity impact by micrometer size projectiles to determine bombardment effect on spectral reflectance
[NASA-TM-X-52981] 09 p1399 N71-19816

Effects of material strength on transient response, crater formation, and shock propagation in thick aluminum targets subjected to hypervelocity impact
[AD-714461] 12 p1938 N71-23624

Hypervelocity impact tests to predict meteoritic damage on proposed lunar tug fuel tank configuration
[NASA-TM-X-64597] 14 p2343 N71-26040

Wave propagation and crater growth characteristics in hypervelocity impact on hard and soft aluminum alloys analyzed using two dimensional Eulerian numerical code
[AD-721468] 16 p2612 N71-28748

Computer program for analyzing energy effects in hypervelocity impact on rocks
[SC-R-70-4462] 18 p2920 N71-31553

Calibration of diaphragm condenser microphones for micrometeoroid impact gauge
[UTIAS-TN-157] 23 p3759 N71-34800

Micrometeoroid impact experiments conducted on Gemini 9 and 12 missions
[NASA-TM-X-2408] 23 p3854 N71-37489

Stress waves in multiple laminates and sandwich plates, dynamic polariscopes for stress wave analysis, meteoroid hazard to space travel, effects of hypervelocity impact, and related studies
[NASA-CR-123157] 24 p3920 N71-37953

HYPERVELOCITY LAUNCHERS
Explosive gun development for launch of suborbital models to reentry velocities
[AD-712394] 04 p0516 N71-13802

Critical appraisal of design, development, and operation of UTIAS implosion-driven shock tubes and hypervelocity launchers
[NASA-CR-117856] 11 p1845 N71-23000

HYPERVELOCITY PROJECTILES
Flexible trailing wire effect on aerodynamic characteristics and radar cross sections of hypervelocity projectile
[AD-712509] 03 p0309 N71-12285

Schlieren method for measuring wake density behind hypervelocity projectile
[ISL-T-12409] 03 p0312 N71-12221

Hole growth in thin plates perforated by hypervelocity pellets
[AD-712071] 03 p0460 N71-12956

Differential interferometry for determining wake density behind hypersonic spherical projectile
[ISL-T-1270] 03 p0418 N71-12962

Schlieren photography for wake visualization behind hypervelocity projectiles
[T-34/69] 03 p0380 N71-13145

Feasibility of explosive lining in launch tube for hypervelocity projectile acceleration
[NASA-CR-108699] 04 p0605 N71-14033

Ultrahigh speed photographic system for photographing hypervelocity projectiles and impact phenomena
[NASA-TN-D-6128] 05 p0485 N71-15408

Thin film penetration by hypervelocity microparticles of carbonyl iron
[NASA-TM-X-2065] 09 p1389 N71-19932

High velocity impact tests conducted with polyethylene terephthalate projectiles and flexible composite wall panels
[NASA-TN-D-6135] 09 p1481 N71-20515

Radiant intensity profile estimates for precursor gas region ahead of hypervelocity shock wave
[AD-718641] 13 p2062 N71-24399

Air breathing engine principles for improved guided missiles and artillery projectiles
[FOA-2-C-2362-1246] 14 p2332 N71-26257

Accelerator for launching hypervelocity projectile by drag force of jet produced by gaseous explosive products
[NASA-CR-115067] 17 p2729 N71-29227

Determination of correlation between impact flash radiative properties and impacting meteoroid projectile characteristics
[NASA-CR-115066] 17 p2842 N71-29245

Effects of target strength on cratering process caused by impact of hypervelocity projectiles
[NASA-CR-119189] 17 p2855 N71-30232

Experimental data on high velocity impacts up to 20 km/sec applied to structures in space and concentration of micrometeoritic material near earth
[NASA-TT-F-13740] 18 p3022 N71-31484

HYPERSOUND WIND TUNNELS

NT HOTSHOT WIND TUNNELS

NT PLASMA JET WIND TUNNELS

NT SHOCK TUNNELS

Surface heat transfer rates measured on flat plates in hypervelocity shock tunnel
[NASA-CR-1692] 01 p0134 N71-10867

Measuring low-density flow over two-dimensional blunt bodies in hypersonic arc tunnel
[NASA-TN-D-6017] 03 p0311 N71-12215

Hypersonic test facility for studying ablation in models under high pressure and high temperature
[NASA-CASE-XLA-00378] 06 p0300 N71-15925

Hypervelocity wind tunnel data acquisition
[DLR-FB-70-44] 07 p1003 N71-17046

European subsonic, supersonic, transonic, hypervelocity and low density wind tunnel characteristics
07 p1003 N71-17099

European hypersonic wind tunnels for testing hypersonic transport aircraft, and space shuttle aerodynamic configurations
08 p1175 N71-18452

Hypersonic low density wind tunnel including auxiliary equipment for electroforming and electroplating wind tunnel models
[BMBW-FB-W-70-51] 08 p1175 N71-18595

Hypersonic shock tunnel of AFAPL
[AD-715907] 08 p1175 N71-18717

Design of hypersonic test facilities for ablation tests and performance tests of vehicles under conditions of high temperature and pressure
[NASA-CASE-XLA-05378] 10 p1538 N71-21475

Isentropic-compression tube techniques producing hypersonic flow in wind tunnels including isentropic flow and free-piston shock tube modes
[AD-717727] 11 p1731 N71-22158

Fabrication and tests of CO₂ flat plate models in the hypersonic wind tunnel
[SC-CR-69-3215] 12 p2010 N71-23228

Effects of flow containing dust on results of hypersonic wind tunnel experiments
[NASA-TT-F-13529] 12 p1901 N71-23702

Hypervelocity blowdown nitrogen wind tunnel with graphite resistance heater noting nozzles, diffuser, and calibration
[IC-AERO-71-01] 13 p2061 N71-24675

Liquid nitrogen cooled nozzle for hypersonic low density wind tunnel
[DLR-FB-70-41] 15 p2590 N71-27035

Mach number reduction in low density hypersonic wind tunnel by increasing nozzle throat area
[DLR-FB-70-43] 15 p2391 N71-27060

Integral equations of motion and momentum for hypervelocity wind tunnel nozzle design
[AD-723346] 17 p2731 N71-29906

Support systems and operational design of nitrogen hypervelocity blowdown wind tunnel
[AD-723345] 17 p2731 N71-29907

Turbulent boundary layer over flat plate and compression corner models studied in hypersonic gun tunnel
[IC/71/11] 18 p2904 N71-30747

Free flight stability tests on half cones in hypervelocity wind tunnels including data reduction program
[VKI-TN-46] 19 p3075 N71-31663

Hypervelocity wind tunnel investigation of turbulent boundary layer undergoing adverse pressure gradient and cross flow along plane of symmetry
[NASA-CR-121635] 21 p3409 N71-34257

Hypervelocity wind tunnel static stability and control tests of variable geometry configuration of space shuttle
[NASA-CR-103151] 21 p3521 N71-35088

Hypervelocity wind tunnel tests of Convair B44 space shuttle booster and model configuration perturbations
[NASA-CR-103159] 21 p3521 N71-35089

Pressure distributions and drag coefficients of 18 constant length and volume slender bodies of revolution at zero incidence for Mach numbers 2.0 to 12.0 - graphs
[NASA-TN-D-6536] 23 p3705 N71-36416

Electron beam technique for rotational and vibrational temperature and density measurements in free stream hypersonic wind tunnel
[AD-727004] 23 p3740 N71-36671

Flow characteristics including diffuser measurements of Langley Mach 20 high Reynolds number ball-tunnel
[NASA-TM-X-2353] 23 p3741 N71-36673

Nozzle design procedure and calculations for hypervelocity wind tunnel including thermodynamic properties of nitrogen and inviscid core and boundary layer calculations
[AD-727591] 24 p3903 N71-37821

Hypersonic wind tunnel test of two delta wing orbiter models
[NASA-CR-119984] 24 p4018 N71-38668

Hypervelocity wind tunnel tests at Mach 10 of delta wing space shuttle models
[NASA-CR-119988] 24 p4018 N71-38670

HYPODYNAMIA

Microbiological ecology of manned space flights, exobiology, sterilization, and life support systems
[JPRS-53388] 16 p2542 N71-28248

Prolonged immersion effects on human water/mineral metabolism
16 p2543 N71-28251

Effect of hypoxic hypoxia and hypercapnia on calcium, inorganic phosphorus, and total protein in blood of rats during hypodynamia
16 p2545 N71-28479

Measurement of changes in musculoskeletal system under hypodynamic and hypoglycemic conditions
20 p3216 N71-33257

HYPOKINESIA

Microbiological and cytological aspects of hypokinesia in rat muscles
[NASA-TT-F-13376] 01 p0009 N71-10341

Effect of hypokinesia on protein composition of skeletal muscles
02 p0159 N71-11481

Hypokinesia effects during 120-day bed confinement with drug therapy
06 p1155 N71-19067

Liver and skeletal muscle morphology in rats under hypokinesia and protein deficiency
08 p1155 N71-19073

Tissue resistance changes in immobilized rats
16 p2544 N71-28265

Effect of relative hypokinesia on intensity of formation and body elimination of ketones, aldehydes, carbon monoxide, and ammonia
16 p2545 N71-28478

Effect of hypoxic hypoxia and hypercapnia on calcium, inorganic phosphorus, and total protein in blood of rats during hypodynamia
16 p2545 N71-28479

Clinical and experimental investigations of effect of motor activity restriction on cardiac function in human and animal subjects
16 p2547 N71-28493

Long term hypokinesia effects on rat serotonin metabolism
20 p3220 N71-33453

Prolonged bed rest effects on human chromosomes during space flight simulation and actual space flight
20 p3221 N71-33462

Hypokinesia effects on nasal blood circulation of man
20 p3221 N71-33464

Hypokinesia effects on myoelectric potential of human leg muscle after prolonged bed rest
20 p3222 N71-33463

Hypokinesia effects on human heart rate and output volume after prolonged bed rest
20 p3222 N71-33466

Combined effects of reduced nutrition, hypokinesia, and centrifugal acceleration on human body
[JPRS-54104] 23 p3716 N71-36488

HYPOTHALAMUS

Examining dynamics of changes in supranuclear nucleus of hypothalamus in rats exposed to transverse accelerations
08 p1150 N71-18970

Microrespirometry to measure oxygen consumption of sprouting potato plugs, and gravitational effects on hypothalamo-hypophyseal system of fish
[NASA-CR-117179] 09 p1341 N71-20006

Microinjections of carbachol in anterior preoptic hypothalamic area of rats inducing hyperthermia
11 p1684 N71-22977

HYPOTHERMIA

Morphological and histochemical changes in liver and kidneys of rats during prolonged hypothermia
02 p0159 N71-11482

HYPOTHESES

NT LAORANGE SIMILARITY HYPOTHESIS

NT NULL HYPOTHESIS

Procedure for comparing theory conclusions and observed data facts in hypothesis assessing
[NASA-CR-111335] 01 p0139 N71-10900

Determining probabilities of hypotheses using reference and observational data
[NASA-CR-118004] 12 p2019 N71-24204

Multistep sequential hypothesis with applications in pattern recognition
[NASA-CR-118999] 17 p2723 N71-29094

Dust thunderstorm hypothesis for short-lived red flares on parts of lunar surface
[NLL-M-20719-5828.4F] 21 p3511 N71-35017

Principles and methods of statistical analysis in testing hypotheses
24 p4011 N71-38606

HYPOXIA

Peruvian Quechua population growth physique, and pulmonary function at high altitude
02 p0155 N71-11096

Acute mountain sickness in humans
[AD-712182] 02 p0156 N71-11102

Measuring decrease in concentration of adenosine triphosphate in brain of rats before onset of convulsions induced by hypoxia
[AD-712242] 02 p0158 N71-11122

Radiation protection effects of hypoxia and paraaminopropiophenone
[COO-1223-15] 02 p0158 N71-11123

Influence of hypoxia on pulmonary microcirculation
[AD-714671] 06 p0801 N71-16308

Chemical composition changes of mitochondria during cardiac hyperventilation and hypoxia
[ACR-1000-199] 06 p0802 N71-16367

Investigating electroencephalographic and behavioral changes in rabbits and humans exposed to acute hypoxia
08 p1152 N71-18913

Hypertrophy and hypoxia effects on turnover of myofibrillar proteins and mitochondrial components in hearts of normal rats
[ACR-1000-214] 10 p1501 N71-21526

Medical aspects of high altitude environments including hypoxia at Logan High Camp
14 p2237 N71-26215

Microbiological ecology of manned space flights, exobiology, sterilization, and life support systems
[JPRS-53388] 16 p2542 N71-28248

Hypoxic hypoxia effects on human and animal resistance to infectious diseases and immunobiological reactivity
16 p2543 N71-28249

Hypoxemia effects on erythrocytic system of splenectomized dogs
16 p2544 N71-28266

Hypoxia effect on human vigilance performance
[FAA-AM-71-11] 17 p2708 N71-29638

Hypoxia affecting circulatory responses in dogs, such as cardiac output, left ventricular dp/dt, and stroke volume
[NASA-CR-121665] 21 p3380 N71-34051

HYSTERESIS

Digital simulation of ferromagnetic material hysteresis for ESRO 1 satellite attitude control
[ESRO-SR-12-ESTEC] 03 p0458 N71-13255

Automatic test equipment for hysteresis and eddy current energy dissipation in steel metal sheets
[NPL-MEM-75] 03 p0383 N71-13363

Vibration isolation tests of spring, hysteresis, and magnetic suspension systems for spaceborne telescopes
[NASA-CR-111822] 09 p1391 N71-20076

Magneto-optical hysteresis for measuring hysteresis of this magnetic films
[FOA-3-C-3607-10] 14 p2297 N71-26255

Photovoltaic effect, polarization, hysteresis, and polarization electron decay rate in organic semiconductor
[AD-721188] 15 p2504 N71-26017

Voltage regulator switching circuit with feedback control and hysteresis network
[NASA-CASE-LEW-11005-1] 16 p2571 N71-29788

Recombination and hysteresis losses in frequency multiplier with semiconductor diode
18 p2808 N71-31522

SUBJECT INDEX

Nucleation of cavitation by alpha particle irradiation of liquid helium, and existence of sulfide cavitation and hysteresis effect in helium II
23 p3822 N71-37263

I

IBEAMS

Integrally woven quartz fiber I beam with uniform thickness using epoxy resin
[NASA-CR-103099] 12 p1943 N71-23440
Ruckling of trusses with arbitrary supports or of I beams with bracing against lateral deviation
19 p1716 N71-31816

IBM COMPUTERS

NT IBM 360 COMPUTER
NT IBM 1130 COMPUTER
NT IBM 7094 COMPUTER
FORTRAN computer program for IBM 2250 display
[AD-711009] 02 p0189 N71-11329
On-line real time system for experimental data collection and processing using IBM 1800 DACS
[TR-69] 11 p1716 N71-22545
Real time on-line diagnostics routines developed for IBM 360/75 computers
11 p1720 N71-22785
Modified IBM 360/75 computer time interface
11 p1720 N71-22786
Pillar routines for IBM 1800 computers permitting graphic presentation of data with minimum programming effort
[NASA-TM-X-65708] 23 p3772 N71-34576

IBM 360 COMPUTER

Regeneration-1/Automated Snek Program written in COBOL for IBM 360 computer
[NASA-CR-106739] 03 p0339 N71-12454
Automated Snek Program written in COBOL for circuit analysis on IBM 360 computer
[NASA-CR-106728] 03 p0340 N71-12459
Branch/Cross Reference Table program written in COBOL for IBM 360 computer
[NASA-CR-106737] 03 p0340 N71-12461
Path redundancy/Automated Snek Program written in COBOL for IBM 360 computer
[NASA-CR-106722] 03 p0342 N71-12483
North American preprocessor/Automated Snek Program written in COBOL for IBM 360 digital computer
[NASA-CR-106730] 03 p0342 N71-12484
IBM 360 heat conduction program
[JTC-DF-980-ADD-1] 05 p0783 N71-13382
Univac 1108 and IBM 360 codes for calculating energy emission of unstable negative beta nuclides
[CRA-N-1285] 08 p1251 N71-18249
Characteristics of on-line IBM 360 computer processing system with telephone as complete terminal device
11 p1715 N71-22107
IBM computer program for temperature distribution computation by method of zones
11 p1841 N71-22336
Computer program SUFFER for console execution of utility programs on IBM 360 computer
[NASA-TM-X-65501] 12 p1081 N71-23331
Average execution times for standard operations with FORTRAN 4 programs on IBM 7094 and 360/75
[R-47] 13 p2049 N71-24421
AONOS language to allow IBM 360/44 FORTRAN programmers access to Adage graphics facilities without recourse to computational facilities
[TR-71-19] 14 p2224 N71-26431
IBM 360 FORTRAN 4 G program to compute homogeneous resonance integrals for fission and non-fission nuclides
[TRK-P-A-139] 17 p2724 N71-30147
Computer program for generating cross reference index in operating system of IBM 360 computer
[NASA-TM-X-65611] 18 p2993 N71-30610
Computer program utilizing IBM 360-40 computer for transforming correlation functions of three particle decay
[TR-1] 19 p1312 N71-32726
DSN monitor system changes after using IBM 360/75 computers
21 p3390 N71-34121
Analysis of three APT processors on IBM 360 computer
[NASA-CR-114560] 21 p3399 N71-34186
Distorted wave Born approximation code adaptation for IBM 360/50 computer use
[ANU-P-507] 23 p3634 N71-35904
NASTRAN installation and implementation on CDC 6600, IBM 360, and UNIVAC 1108
23 p3686 N71-36289
IBM 360 TELOR3 program for testing, editing, and listing information on ORB3A tapes
[NASA-TM-X-65692] 23 p3728 N71-36571
Heat and momentum transfer analysis for SNAP 8 counterflow NaK to Hg boiler using IBM 360 computer code
[NASA-CR-72907] 24 p4018 N71-38667

IBM 1130 COMPUTER

List processing subroutines for IBM 1800/1130 information storage and retrieval system
[NASA-TM-X-65622] 18 p3893 N71-30611

IBM 7094 COMPUTER

Multi-group neutron diffusion theory perturbation program SPECTRE, using IBM 7094 computer
[JWEE-O-74705] 09 p1443 N71-20431
IBM 7094 COMPUTER
Characteristics and operation of automatic film scanning device used with digital computer
[UCRL-19842] 07 p0996 N71-17163
Monte Carlo general purpose shielding computer program in FORTRAN 4 for IBM 7094 computer
[NASA-TM-D-6170] 11 p1794 N71-22578
Average execution times for standard operations with FORTRAN 4 programs on IBM 7094 and 360/75
[R-47] 13 p2049 N71-24421

ICBM (MISSILES)

U INTERCONTINENTAL BALLISTIC MISSILES

ICE

NT GLACIERS
NT ICEBERGS
NT LAND ICE
NT SEA ICE
Low power solid-state radio beacon tests and evaluation for snow and ice outages of compass locator systems
[FAA-DR-70-38] 01 p0083 N71-10990
Longitudinal ultrasonic wave measurement in fresh polycrystalline ice under variable static pressure
[AD-710677] 02 p0214 N71-11940
Solution of problems concerning thawing and melting in finely dispersed media
[AD-711087] 02 p0218 N71-12028
Computer code for prediction of hydrospheric impact erosion on high speed space-cube vehicles
[SC-DR-70-373] 03 p0343 N71-12489
Experimental and theoretical review of Arctic ice dynamics
[FR-195636] 06 p1186 N71-18335
Research on Arctic sea ice heat and mass budget, sea ice drift, micrometeorology, radiation, atmospheric chemistry, and Arctic oceanography
[AD-715450] 08 p1190 N71-18731
Microwave radar scattering cross sections of dry and wet ice spheres calculated from Mie scattering equations - tables
[TR-21] 09 p1379 N71-19448
Sea ice, ocean currents, climatology, and geology of Arctic Ocean and coastal areas
[AD-716416] 09 p1384 N71-19771
Aerial reconnaissance and radar scanning of ice flows in Greenland waters - 1963
[ISBH-47-7478-005-0] 11 p1730 N71-22518
Water exchange variations between Arctic and Atlantic Oceans and effects on ice cover forecasts in Arctic seas
11 p1732 N71-22803
Short range forecasting of navigability of close pack ice by icebreakers in Arctic
11 p1733 N71-22809
Revised illustrated dictionary of snow and ice forms
11 p1735 N71-22834
Southern Ocean ice and iceberg effects on thermophysical processes of earth
11 p1736 N71-22837
Economic efficiency calculations for long range ice forecasts for ship navigation of Northern Sea Route
11 p1737 N71-22842
Calculation of ice resistance to vessel moving through ice of medium horizontal dimensions
11 p1737 N71-22843
Spectral effects of snow and ice cover under differing cloud conditions and solar elevations
11 p1737 N71-22846
Quantitative analysis of hummocking effects on mean thickness of fast ice in Arctic seas
11 p1738 N71-22853
Transformation of form and displacement of air inclusions in ice due to molecular rearrangement of ice crystals and temperature gradients
11 p1739 N71-22862
Influence of icebreaker hull dimensions on ice resistance when moving at low speed in compact ice
11 p1771 N71-22864
Annual paper for manual drilling of ice holes for core sampling
11 p1771 N71-22866
World Meteorological Organization conference recommendations on revised nomenclature for sea ice
11 p1739 N71-22868
Sea surface ice layer effects on radio wave propagation phase
11 p1708 N71-22924
Atmospheric model for effects of water vapor, liquid water, and ice upon radiative transfer processes at microwave frequencies and in far infrared
[NASA-CR-61340] 13 p2106 N71-25079
Solar radiation in heat balance of ice-covered surface on Franz Joseph Land and Spitzbergen
15 p2439 N71-27519
Solar radiation regime of ice-covered surfaces on Novaya Zemlya
15 p2439 N71-27520

Approximate formulae for internal friction coefficient of ice

[AD-720935] 15 p2399 N71-27904
Force of ice cohesion with metals related to type of materials, surface roughness, structure and rate of external load, and surface temperature
[AD-722106] 16 p2612 N71-28730
Ice cover formation, ice breakup and control, frost, and winter open water heat balance for rivers and lakes
[AD-734121] 20 p3236 N71-32084
Structure and properties of pure water in solid and liquid phases, and thermodynamics of aqueous solutions of polar and nonpolar molecules and electrolytes
[ISB-70/26] 20 p3315 N71-33388
Neutron thermalization with time in water at 318 K and ice at 77 K determined by measuring neutron flux time dependence
[EAPL-TRANS-4] 21 p3475 N71-34745
Spring breakup of snow and ice on Delta River, Alaska, and air temperature measurements
[AD-724683] 22 p3574 N71-35457
Techniques for minimizing snow and ice effects on TACAN antenna signals
[FAA-DR-71-56] 22 p3617 N71-35773
Measuring thermal conductivity of ice in 4 to 273 K range
[AD-727165] 23 p3752 N71-36756
Nuclear magnetic resonance used to determine nature of quasi-liquid film on surface of ice at temperatures below melting point
[AD-726864] 23 p3835 N71-37348
Sublimation of ice in connection with comet phenomena
24 p4009 N71-38504

ICE FORMATION

NT CLOUD GLACIATION

Douglas DC 9 aircraft crash during takeoff caused by ice formation on airfoils
[N73B-AAB-70-38] 01 p0085 N71-10815
Microwave radiometry for snow and ice sensing in aerial reconnaissance
02 p0206 N71-11160
Ice interlayer formation computations in freezing moist soil
[AD-711874] 02 p0212 N71-11518
Salt composition of sea water and ice
[AD-711925] 02 p0213 N71-11547
Theory of ice formation, effects of ice on structures, and methods for controlling icing
[AD-711933] 02 p0219 N71-12047
Techniques and equipment for indirect measurement of sea ice thickness
[CRC-1214] 05 p0670 N71-14827
Developing instrumented, air-dropped penetrometers for remote determination of sea ice thickness
[SC-DR-70-483] 06 p0831 N71-16387
Mathematical models for Arctic ice dynamics
[AD-713906] 06 p0853 N71-16583
Measuring effects of evaporative cooling at base of dense cirrus and altostratus clouds using Doppler and conventional radars
07 p1053 N71-17421
Atmospheric factors in ice fog formation
[FB-196977] 10 p1596 N71-21617
Arctic and Antarctic regions, ice formation, sea, weather forecasting, glaciology, hydrology, hydrometeorology, IGY, IQSY, solar activity, and meteorological stations
[TT-70-50017] 11 p1752 N71-22801
Long range forecasting of annual variations of ice cover in Arctic
11 p1752 N71-22807
Spatial orientation of crystals in ice formed in water bodies with different temperature regimes
11 p1753 N71-22808
Short range forecasting of ice formation in Arctic waters to thickness of 20-25 cm with forecasting period up to 20 days
11 p1758 N71-22855
Orbital solution to stay time of commercial fleet vessels in regions of icing
11 p1759 N71-22861
Total heat budget between convective atmosphere in Arctic Basin for military utilization
[AD-717967] 12 p1986 N71-23551
Freezing rate and solute specific and concentration effects on charge separation at advancing surfaces of growing ice related to cloud physics
[AD-718359] 12 p1916 N71-23655
Seven-year cycle of Arctic ice formation due to rotation of earth axis
[N71-M-30304-3826AF] 12 p1914 N71-24100
Formation, melting, drift, thickness, and concentration of sea ice in Antarctic regions during different seasons
[AD-719807] 13 p2076 N71-25243
Physical and mechanical properties of ice formations noting effect of engineering structures
[AD-723169] 19 p1817 N71-31765
Application of stereophotography to determine composition of ice prior to construction of hydrotechnical structures
[AD-724664] 20 p3536 N71-32941

- Ice cover formation, ice breakup and control, frazil, and winter open water heat balance for rivers and lakes
[AD-724121] 20 p3256 N71-32984
- Statistical thermodynamic model for molecular interactions during ice nucleation from supercooled water
[TN-40] 20 p3261 N71-33298
- Zonal atmospheric model for simulating earth's climate and testing ice age theories
[UCRL-72803] 20 p3267 N71-33521
- Two-year periodic variations in Arctic sea ice formations
[NLL-M-20593-5828.4F] 21 p3422 N71-34354
- Methods for classifying atmospheric ice crystals according to geometric form
21 p3452 N71-34545
- ICE MAPPING**
- Using remote sensors for detection, analysis, and mapping of snow and ice
06 p0846 N71-16167
- Using radar scatterometers as remote sensors for identification of sea ice in Arctic regions
06 p0848 N71-16178
- Measuring ice cover, temperature inversion, wind velocity, and bottom topography of oceans
07 p1013 N71-16920
- Yearly, monthly and ten-day changes in position of ice edge in North Caspian Sea
[AD-724672] 20 p3259 N71-33197
- ICE NUCLEI**
- Procedure for identifying silver iodide particles in ice crystals as snow crystal nuclei
[PB-192754] 02 p0260 N71-12124
- Investigating production and detection of artificial ice nuclei and growth of formed ice crystals
[PB-194129] 04 p0542 N71-14216
- Analysis of scavenging by snow and ice crystals with application to radioactive fallout
[ITRI-C-6105-12] 05 p0748 N71-15266
- Scavenging efficiency of naturally precipitating snow and ice with application to radioactive fallout
[ITRI-C-6105-10] 05 p0749 N71-15289
- Ice nuclei dispersion systems development
[PB-196149] 09 p1413 N71-19714
- Development and characteristics of laboratory models to explain structure and composition of comet cores
[LA-TR-70-27] 15 p2517 N71-26960
- Steady state ice nuclei generator for field application
22 p3609 N71-35707
- Ice nuclei generators suitable for cloud seeding
22 p3611 N71-35723
- ICE OBSERVATION**
- U ICE REPORTING**
- ICE PREVENTION**
- Bibliography on control and prevention of icing in transportation systems
[AD-711534] 01 p0049 N71-10735
- Theory of ice formation, effects of ice on structures, and methods for controlling icing
[AD-711933] 02 p0219 N71-12087
- ICE REPORTING**
- Automatic processing of Arctic pack ice data obtained by submarine sonar and remote sensors
[AD-713911] 06 p0854 N71-16620
- Ice thickness observations along coasts of eastern Canada and southern Greenland
[AD-715424] 06 p1188 N71-18503
- Dielectric properties of sea ice and FM superhigh frequency radar measurement of ice thickness in Sweden and Greenland
[R-83] 10 p1546 N71-20657
- Danish translation of sea ice nomenclature approved by World Meteorological Organization
[REPT-22] 11 p1750 N71-22544
- Photographic meteorological charts for snow and ice cover reporting satellite observation over Europe
[QR-1-PT-1] 17 p2776 N71-29342
- Application of stereophotography to determine composition of ice prior to construction of hydrotechnical structures
[AD-724464] 20 p3256 N71-32961
- Characteristics of sensors for aerial observation of ice formations and comparison of effectiveness of various methods
[JPRS-54162] 23 p3759 N71-36801
- ICE SHELVES**
- U LAND ICE**
- ICEBERGS**
- Physical and mechanical properties of ice formations noting effect of engineering structures
[AD-723169] 19 p3187 N71-31765
- ICELAND**
- Studying geology, geochemistry, and biology of Iceland and Surtsey as examples of new and extreme environments
[NASA-TM-X-62009] 07 p1024 N71-17966
- Discussing geological, topographical, and climatological features of Iceland and effects on human habitation
07 p1024 N71-17967

- Describing eruption in region of Mt. Hekla, Iceland and toxic hazards from volcanic ash
07 p1024 N71-17968
- Determining transport and climatological factors affecting colonization of life on remote islands
07 p1024 N71-17969
- Investigating effects of volcanoes and volcanic features on geological evolution of Iceland
07 p1024 N71-17970
- Chronological summary of Surtsey volcano eruption from 1963 to 1967
07 p1024 N71-17971
- Investigating theory of chemical evolution on Surtsey Island and relationship to life detection techniques for other planets
07 p1024 N71-17972
- Investigating Surtsey and Iceland as natural laboratories for testing planetary life detection techniques
07 p1024 N71-17973
- Investigating geology of Surtsey and Iceland with respect to earth planetary evolution
07 p1025 N71-17974
- Investigating composition and ages of Icelandic lavas to determine validity of sea floor spreading
07 p1025 N71-17975
- Reporting eruption of Hekla volcano from May through June 1970
07 p1025 N71-17976
- Comparing geological relationships between various rock strata of Iceland and Mid-Atlantic Ridge
07 p1025 N71-17977
- Investigating hypothesis of sea floor spreading and continental drift with respect to location of Iceland at lithospheric plate boundaries
07 p1025 N71-17978
- Analyzing subaerial flows of lava in eastern Iceland and recent and Pleistocene flows in neovolcanic zone of central Iceland for basalt composition
07 p1025 N71-17979
- Suggesting topics for study of coarse-grained plutonic rocks of Iceland
07 p1025 N71-17980
- Characterizing ancient tephra units on Surtsey by textural analysis of modern pyroclastic and hydroclastic deposits
07 p1025 N71-17981
- Investigating effects of Hekla volcano eruption on environment and economy of Iceland
07 p1026 N71-17982
- Reporting results of disciplinary and interdisciplinary research into geology of Iceland
07 p1026 N71-17983
- Analyzing glaciers, hot springs, and volcanic ash from erupting volcanoes in Iceland for hydrocarbon content as test for life detection techniques
07 p1026 N71-17984
- Investigating processes of chemical and biochemical weathering of primary volcanic rock and role of phosphorus in primary productivity of natural systems on Surtsey
07 p1026 N71-17985
- Analyzing nitrogen and carbon content of rocks from volcanic and hot spring areas of Surtsey and Iceland
07 p1026 N71-17986
- Investigating environment of zeolite formation in Tertiary basalt of southeastern Iceland and stability of recently formed minerals in beach sands of Surtsey
07 p1026 N71-17987
- Investigating effects of thermal environments and acidity on growth of bacteria and blue green algae
07 p0983 N71-17988
- Biological effects of thermal environments on dispersal of blue green algae and microorganisms in Iceland and Surtsey
07 p0983 N71-17989
- Investigating biological effects of acid thermal waters on growth of organisms in Iceland
07 p0983 N71-17990
- Investigating proliferation of insect life in harsh environments of Iceland and Surtsey
07 p0984 N71-17991
- Determining microbial population of Surtsey by microbiological techniques
07 p0984 N71-17992
- Investigating effects of lava outgassing on primary colonization by organisms
07 p0984 N71-17993
- Investigating alluvial plain of Icelandic glacier for terrestrial and aquatic plant succession
07 p0984 N71-17994
- Considering lack of development of endemic species in Iceland
07 p0984 N71-17995
- Investigating inhibitory activity of lichens on growth of seed plants and ferns
07 p0984 N71-17996
- Investigating relationship of lignin content to height in dwarf and regular-sized alpine plants of Iceland
07 p0984 N71-17997
- Searching for Precambrian relict microorganisms in Iceland
07 p0984 N71-17998

- Investigating water transport scheme for dispersal of thermophilic microorganisms to Surtsey from mainland areas
07 p0985 N71-17999
- Selected bibliography of published papers on Surtsey
07 p1026 N71-18000
- Water interchange between North Atlantic Ocean and Norwegian Sea between Scotland and Iceland
[CG-373-28] 12 p1913 N71-23725
- Icelandic atmospheric pressure minimum seasonal migration due to oscillation of earth axis
[AD-724301] 20 p3296 N71-33875
- ICING**
- U ICE FORMATION**
- ICOSAHEDRONS**
- Electronic structure of cluster ion with 33 argon atoms in icosahedral symmetry
[IFA-FT-82] 03 p0438 N71-12940
- IDARO**
- Estimation of maximum wind speeds of anticipated tornadoes in 3 northwestern states
[SMRP-92] 19 p3129 N71-32997
- Automorphic anomalies and granodiorite bodies in Fend Oreille area, Idaho for metamorphic and structural studies
21 p3419 N71-34329
- IDEAL FLUIDS**
- Mathematical model for ideal fluid jets from convergent nozzles
10 p1541 N71-21139
- Determination of flow conditions under which traveling wave will propagate in self oscillating regime
11 p1736 N71-22218
- Partial differential equations solution for sound wave propagation in layered ideal fluid media
[AD-717345] 11 p1796 N71-22240
- IDEAL GAS**
- Numerical results for ideal gas boundary layer flow for asymptotic half-angle hyperboloid
03 p0361 N71-12590
- Propagation of disturbance in viscous hypersonic flows of ideal gas
[NASA-TT-F-13485] 08 p1182 N71-18979
- Steady, adiabatic, inviscid, supersonic flow along corner formed by two intersecting wedges
08 p1183 N71-18984
- Effects of lateral substrate fields on lithium monolayers using ideal gas model
[RLO-1388-604] 18 p2985 N71-31218
- Linear formulation of aeroelastic stability of plane sandwich-type structures placed in current of supersonic gas
[NASA-TT-F-13778] 19 p3190 N71-32452
- Finite difference method for calculating spherically symmetric nonlinear acoustic flows in unbounded ideal gas
[AD-727012] 23 p3803 N71-37118
- IDENTIFYING**
- Nonlinear and dynamic programming for identification problems
[TID-25617] 10 p1595 N71-21794
- Identifying linear dynamic systems with state and observation noise with application to flight control problem
[AD-723108] 17 p2773 N71-29733
- Two methods of analysis, synthesis, and self-regulation of nonlinear units in control systems
[NLL-CE-TRANS-5488-7022.09] 17 p2773 N71-29739
- Automatic speaker identification and verification
19 p3059 N71-31635
- Automatic vehicle identification using infrared techniques for law enforcement agencies
19 p3060 N71-31636
- Computer-aided system for automated, high speed identification of human fingerprints
19 p3060 N71-31647
- Computer system for high speed processing of non-numerical information in criminal identifications
19 p3060 N71-31648
- Preparation of particle identification system using ORTEC 423 with block diagrams of circuits and graphs
[ANU-P-514] 22 p3634 N71-35900
- IDENTITIES**
- Interference of identical particles in processes involving resonances
[JINR-P1-5315] 15 p2467 N71-27262
- Physical meaning of Ward-like identities in dual resonance model for string model
[NUP-A-71-51] 20 p3290 N71-32940
- IFR (RULES)**
- U INSTRUMENT FLIGHT RULES**
- IGNEOUS ROCKS**
- NT BASALT
- NT DIORITE
- NT DUNITE
- NT GRANITE
- NT LAVA
- NT MAGMA
- NT OLIVINE
- NT PYROXENES
- NT QUARTZ
- NT SYENITE

SUBJECT INDEX

Electrical conductivity of igneous rocks of Kola Peninsula at high temperature based on dc transmission
[NASA-TT-F-13214] 02 p0210 N71-1440

Frequency dependence of electrical properties of igneous rocks from Kola Peninsula
[NASA-TT-F-13216] 02 p0210 N71-1498

Radioactive thermometry of igneous rocks
[NASA-CR-115895] 05 p0469 N71-1403

Static compressibility measurements of Cedar City tuffinite using equations of state
[AD-713175] 05 p0676 N71-15440

Physical properties of igneous and metamorphic rocks subjected to high pressures and temperatures
[NASA-TT-F-13515] 08 p1193 N71-10991

Electron microprobe analysis of fine-grained igneous rocks from lunar sample 10022 from Sea of Tranquility
08 p1289 N71-19145

Electron probe microanalysis of minerals of lunar igneous rocks from Apollo 11 flight
08 p1289 N71-19146

IGNITER
U LAVA
IGNITER
NT DETONATORS
NT INITIATORS (EXPLOSIVES)
NT SQUIBS
Design of spark and plasma pulse igniters for space shuttle propulsion system
[NASA-CR-115115] 03 p0448 N71-12836

Controlled-flow igniter for low thrust burning rate of solid propellant rocket engines
11 p1819 N71-22556

Design approach for solid propellant rocket igniters
[NASA-RP-8051] 17 p2352 N71-30346

Solid propellant rocket motor with igniter operating in vacuum and sustaining burning of propellant below normal combustion limit
[NASA-CASE-NPO-11539] 21 p3502 N71-34949

IGNITION
NT ELECTRIC IGNITION
NT SOLID PROPELLANT IGNITION
NT SPARK IGNITION
Effects of nonequilibrium free-radical content and composition of supersonic streams entering air-breathing engines on ignition points and delays
[NASA-CR-113371] 02 p0288 N71-11467

Hydrazine propellant decomposition with noble metal catalysts for quick ignition
07 p1097 N71-17196

Magnetically controlled plasma accelerator capable of ignition in low density gaseous environment
[NASA-CASE-XLA-00537] 16 p2463 N71-29184

Ignition of toroidal fusion reactors and plasma confinement experiments in Tokamak machines
[MATT-808] 17 p2812 N71-29661

Model for predicting thrust-time curve during entire ignition transient of solid propellant rocket engine with head-end pyrolytic igniter
17 p2840 N71-30376

Ignition behavior of electrodeless ring discharges in homogeneous periodically oscillating magnetic field
[JUL-691-PP] 18 p3023 N71-30485

Computer program for describing thermochemistry of combustible gas mixture ignition
[AD-723400] 19 p3191 N71-31758

Analysis of conditions under which autoignition of flowing hydrogen-oxygen mixtures occurs and prediction of required flow rates
21 p3531 N71-35165

IGNITION LIMITS
Ignition characteristics and delivered performance of gaseous hydrogen-oxygen reaction control thrusters at cryogenic temperatures
[NASA-CR-72784] 02 p0291 N71-12096

Ignition characteristics and delivered performance of gaseous hydrogen-oxygen reaction control thrusters at cryogenic temperatures - appendices
[NASA-CR-72785] 02 p0291 N71-12097

High voltage pulse generator for testing flash and ignition limits of nonmetallic materials in controlled atmospheres
[NASA-CASE-MSC-12178-1] 04 p0509 N71-35518

Theoretical and experimental analysis of flame spreading across pools of liquid fuels and ignitability under quiescent and flowing environments
[AD-718664] 12 p3910 N71-23492

Prediction of ignition performance of compound pyro particles with multistage reactions with computer program to analyze heat transfer, mass transfer, and reaction kinetics within particles
14 p2355 N71-28265

Development of radiative ignition apparatus based on carbon dioxide laser to examine effects of radiative heat, pressure, oxygen concentration, and absorptivity on ignition delay of polymers
14 p2355 N71-26332

Resonance tube ignition system for hydrogen oxygen engines including ignition limits and pressure and temperature effects
[NASA-TN-D-6354] 15 p2523 N71-26913

Factors affecting ignition of metals in high pressure oxygen systems
[NASA-TM-X-67201] 15 p2524 N71-27394

Determination of ignition temperatures, ignition delay times of various combustible mixtures, and the effect of gas flow on ignition process
16 p2692 N71-28923

Numerical analysis and development of model for effect of ignition energy and coupling of reaction kinetics with shock front
16 p2692 N71-28924

IGNITION SYSTEMS
Resonance tube ignition system for hydrogen oxygen engines including ignition limits and pressure and temperature effects
[NASA-TN-D-6354] 15 p2523 N71-26913

Spark and auto-igniter systems for hydrogen and oxygen propellants in space shuttle APS
[SC-71-24] 17 p2837 N71-29595

Experimental and analytical evaluation of catalytic ignition system and performance of hydrogen oxygen thruster for space shuttle APS
17 p2837 N71-29596

Low cost, lightweight ignition system for hydrogen oxygen engine system incorporating multicomponent thrust chambers
[NASA-CR-119928] 21 p3530 N71-35153

IGNITION TEMPERATURE
NT FLASH POINT
Liquid and gaseous oxygen difluoride compatibility tests with plastic and metal orifices and metal ignition temperature data
[NASA-CR-72357] 12 p1869 N71-23168

Effect of water vapor, reduced oxygen concentrations, and solvent vapors on ignition temperature of alloyed and unalloyed plutonium
[RFP-1566] 13 p2097 N71-25252

Test chamber for determining decomposition and autoignition of materials used in spacecraft under controlled environmental conditions
[NASA-CASE-DSC-10198] 16 p2577 N71-28629

Calculation and analysis of course of combustion for different pairs of ignition temperature and pressure in hydrogen-air mixtures flowing at supersonic velocity
[NASA-TT-F-13719] 17 p2839 N71-30182

Activation temperature analysis with diffusion flames and supersonic combustion
[AD-724662] 23 p3867 N71-37568

IGY (GEOGRAPHICAL YEAR)
U INTERNATIONAL GEOPHYSICAL YEAR
ILLIAC COMPUTERS
Simulation and design of arithmetic and logic unit for ILLIAC
[COO-2118-2] 12 p1882 N71-23614

ILLINOIS
Air pollution and soiling index for Chicago, 1968
[PB-194767] 06 p0835 N71-16745

Statistical analysis of tornadoes in Illinois from 1916 to 1969 including tornado forecasting, remote detection, and safety precautions
[PB-198280] 19 p3129 N71-32404

Topography, weather conditions, climatic aids, and local forecast studies at Chanute AFB, Illinois
[AD-723673] 19 p3131 N71-32769

Rain gauging network and automatic samplers for measuring rain in Clinton, Illinois area
[COO-1467-38] 22 p3612 N71-35734

ILLUMINANCE
Calculation of natural illumination on horizontal planes under clear skies
[PHL-1971-4] 18 p2916 N71-31057

Color and luminance effects on visual space perception
[AD-724623] 20 p3226 N71-35138

Underwater oceanographic photometry at different depths, emphasizing luminance and illuminance
22 p3576 N71-35473

ILLUMINATING
Intensity distribution of optical images for various degrees of illumination using Hermitian matrices
[NASA-TT-F-13721] 18 p2966 N71-31452

Approach indicator oscillation and illuminating effects on human performance of compensatory tracking tasks
[NASA-CR-119640] 19 p3047 N71-31618

Visual performance compared using highly illuminated CRT similar to those encountered in high altitude flight in direct sunlight
[NASA-CR-114361] 21 p3384 N71-34073

ILLUMINATION
Physiological effects of alcohol and cockpit illumination levels on pilot performance and flying safety
[FAA-A36-71-34] 22 p3540 N71-35275

Development and operation of apparatus for measuring ground illumination at night and remotely recording data
[FOA-2-C-2387-52] 22 p3585 N71-35533

ILLUMINATORS
Camera adapter design for image magnification including lens and illuminator
[NASA-CASE-XMF-03044-1] 14 p2256 N71-26474

Illumination system design for use as sunlight simulator in space environment simulators with multiple light sources reflected to single virtual source
[NASA-CASE-NQCN-10781] 17 p2769 N71-30292

IMAGE ENHANCEMENT

Argon laser illumination system with three micron diameter diffraction limited spot at one microwatt power for use with Hough-Powell devices
[RHEL-R-212] 19 p3108 N71-32630

ILLUSTRATIONS
NT OCULOGRAPHIC ILLUSTRATIONS
Visual illusions in human perception of horizontal lines induced by anchoring lines
[AD-712961] 03 p0320 N71-12287

Anchoring stimuli and Titchener illusion
[AD-712962] 03 p0320 N71-12289

ILS (LANDING SYSTEMS)
U INSTRUMENT LANDING SYSTEMS
IMAGE CONTRAST
Contrast mechanisms in high resolution scanning electron microscopes
[TID-23418] 01 p0054 N71-10450

Curva electron-energy-analyzing scanning microscope design
[ANL-7634] 01 p0056 N71-10762

Framing camera performance predictions from drag and diffraction image degradation source analysis
[EGG-1183-530] 13 p2082 N71-25199

Video signal enhancement of signal component representing brightness of scene element in low contrast
[NASA-CASE-NPO-10343] 15 p3281 N71-27341

Development of automatic contrast follower based on combination of television and digital circuit techniques
[FOA-3-C-2370-52] 22 p3554 N71-35513

Analysis of processes of black and white film production and electro-optical transformation in television projection of light-shadow contrasts
[AD-727244] 24 p3888 N71-37709

Regulation of admissible brightness difference of image details for television transmission
[AD-727435] 24 p3889 N71-37715

IMAGE CONVERTERS
NT TELESCOPES
NT IMAGE TUBES
Electrographic image converters for far ultraviolet spaceborne astronomy
06 p0861 N71-16636

Ten micron wideband detector
[AD-713995] 06 p0868 N71-16834

Parametric upconversion technique for converting infrared images to visible for real time systems
[AD-715339] 07 p1040 N71-17847

Electromechanical acoustic underwater imaging scanner assembly
[AD-717586] 11 p1722 N71-21921

Fiber optics in electron optical devices such as cathode ray tubes, image intensifiers, and image converters
[AD-717838] 11 p1796 N71-22470

Image conversion at millimeter wavelengths by germanium semiconductor panel
12 p1879 N71-23668

Performance of magnetically focused ultraviolet image converter for space astronomy
13 p2170 N71-25328

Pattern threshold recognition device comprising cathode ray tube with image converter input, flood-gun for suppressing background information, and read-gun output of information
[AD-712021] 15 p2387 N71-27747

Synthesis of optimal search scanning systems using special filament optical image converters
19 p3043 N71-32834

Graphical method for deriving dye-layer densities of color infrared image elements from known reflectance curves, and analysis of CTB photography from spacecraft windows
[NASA-CR-121630] 21 p3424 N71-34361

Photographic recording of image previously recorded on magnetic tape
23 p3758 N71-36793

Development and characteristics of photoelectric image converters with optical communication
[AD-727080] 24 p3899 N71-37793

IMAGE CORRELATORS
Prototype holostereoscopic and playback system for laser surface topography experiments
[NASA-CR-116146] 06 p0868 N71-16574

Multiple pattern holographic information storage and readout system
[NASA-CASE-ERC-10151] 16 p2607 N71-29131

Development and characteristics of systems for producing stable holographic optical equipment
[R88-516] 21 p3436 N71-34447

IMAGE DIRECTOR TUBES
Performance and response characteristics of smoothing, image intensifier discriminator for low light level autonomy and optical detection
[NASA-CR-121913] 22 p3558 N71-35342

IMAGE ENHANCEMENT
Electron beam scanning system for improved image definition and reduced power requirements for video signal transmission
[NASA-CASE-ERC-10552] 03 p0351 N71-12539

Pseudocolor image enhancement by two-separation photographic process
[AD-712650] 03 p0381 N71-13163

Computer refreshed display for processing video information with digital computer to enhance video data
06 p0821 N71-16675

Measuring intermittent enhancement of blinking effect upon addition of neon to imaging gas in helium-tungsten field-ion microscope
[NASA-TN-D-6214] 06 p1259 N71-18658

Rate distortion theory for minimizing signal distortions in image or picture transmissions
06 p1163 N71-18948

Multispectral discrimination technique improvement for remote sensing in agriculture and data calibration, atmospheric scattering effect, and predictive model analysis
[REPT-2264-12-F] 10 p1560 N71-21445

Kiniform optical filtering techniques with applications in holography and photography
[IBM-320-2378] 11 p1715 N71-22252

Amplifier gain control for Apollo scan television signal enhancement
13 p2048 N71-25339

Subjective evaluation and improvement methods for image quality in motion pictures and television techniques
14 p2256 N71-26461

Signal enhancement techniques for elastic surface transformation
[AD-72045] 15 p2409 N71-27448

Improved photomultiplier quantum yield through monochromatic illumination
[EUR-CEA-PC-576] 15 p2475 N71-27464

Pulse amplitude modulation of laser outputs for image contrast enhancement in real time holographic interferometry for nondestructive testing
[AD-723632] 19 p3108 N71-32244

Computerized pseudocolor transformations from black and white to chromatic images with density separations
[R-787-NIH] 23 p3730 N71-36588

IMAGE FILTERS

Aerial multispectral sensing test on submerged body in ocean
02 p0206 N71-11168

Fourier transformation technique applied to two dimensional infrared image filtering
[ONERA-NT-164] 19 p3121 N71-31685

Development and characteristics of spectroradiometer with wedge filters to eliminate adverse effect of pinholes in filters
[NASA-CASE-RQN-10683] 21 p3427 N71-34389

Image shearing eyepiece for calibrating acceleration transducer
[AQD/7/2] 23 p3759 N71-36799

IMAGE OPTICS

NT IMAGE ORTHICONS

Onboard optical processing for extracting parameters from spacecraft data using image generator and Fourier transform plane detector
03 p0379 N71-12792

Vision with small starlight scope - three stage image intensifier
[JZF-1970-11] 05 p0689 N71-15580

Application of image intensifiers developed in high energy physics to some problems in biology
[PURC-4159-1] 06 p0799 N71-15884

Upper atmospheric temperature profiles obtained from grenade glow cloud spectra recorded by Echelle spectrometer with image intensifier
[HSA-TN-161] 08 p1195 N71-19127

Fiber optics in electron optical devices such as cathode ray tubes, image intensifiers, and image converters
[AD-717838] 11 p1798 N71-22470

Picture processing and image evaluation
[FOA-2-C-2354-72] 14 p2207 N71-26597

X ray photographic film casting technique using gel flow viscosity for maintaining intensifier suspension in solution
[NASA-TT-F-13671] 16 p2592 N71-28069

Counting photon events by television recording coupled to optical image intensifier
16 p2679 N71-28514

Performance of image intensifier plumbicon camera as photoelectron detector
16 p2593 N71-28515

Microchannel intensifier vidicon for far UV imaging
16 p2593 N71-28517

Pulse counting spectrophotometer using phosphor output image intensifier to single photon input
16 p2594 N71-28518

High resolution channel plate image intensifier, noting image energy and angular distribution
18 p2924 N71-31149

Image intensifier cameras, infrared imagery, and high sensitivity vidicons for use in police night surveillance
19 p3070 N71-31643

Image enhancement technique for detecting minute changes in Apollo 9 photographs
[WDL-TR-4279] 22 p3585 N71-35532

Image intensifiers used with television tubes for enhanced visual observations
24 p3924 N71-37992

IMAGE MOTION COMPENSATION

Stabilizing fringe pattern in holographic system in presence of vibration and drift
03 p0379 N71-12792

Coherent optical processing of motion-degraded images
[AD-716779] 10 p1557 N71-20862

Minimizing in frame motion relative to rotor surface for model 739 framing camera
[EGG-1183-542] 11 p1763 N71-22479

Development and characteristics of systems for producing stable holographic optical equipment
[RM-516] 21 p3436 N71-34447

Measurement of positional steadiness and prediction of subjective impairment in presentation of 16 mm film by television
[BBC-1971/28] 23 p3725 N71-36554

IMAGE ORTHICONS

Design and performance of image orthicon and telescope system for optical spacecraft tracking
[AD-711106] 01 p0055 N71-10667

Development and characteristics of cathode ray tubes, image iconoscope, image orthicon, and color kinescopes for television equipment
[AD-720380] 14 p2228 N71-26001

Design and characteristics of pinhole camera for television applications to correct visual display problems
[AD-723182] 19 p3100 N71-32021

Superorthicondynamic and working characteristics related to image quality estimations
[AD-727173] 24 p3888 N71-37713

Improved image orthicon tube for television cameras
[AD-727251] 24 p3925 N71-38003

IMAGE TRANSDUCERS

Investigating photographic sensors and electro-optical devices for optical processing of satellite data
03 p0380 N71-12797

Perturbation theory for improving performance of image sensing arrays and application to metrology
[AD-723422] 19 p3908 N71-31732

IMAGE TUBES

Image tube spectrogram and He photometry of blue-stragglers in open cluster NGC 7789
08 p2191 N71-19302

Electrical readout image tube for use on LARC Coode spectrograph
16 p2570 N71-28519

Analog automatic electron trajectory tracer for studying image properties of electrostatic image tubes
21 p3404 N71-34224

Regulation of admissible brightness difference of image details for television transmission
[AD-727435] 24 p3889 N71-37715

IMAGE VELOCITY SENSORS

Model of solid state television camera without imaging tube and using mosaic of phototransistors
17 p2718 N71-29326

Flexible computer-accessed telemetry using sequence control, auxiliary memory, and system control registers for sensors and digital data source sampling
[NASA-CASE-NPO-11358] 21 p3395 N71-34160

IMAGERY

NT AERIAL PHOTOGRAPHY

NT ALL SKY PHOTOGRAPHY

NT ASTRONOMICAL PHOTOGRAPHY

NT AUTORADIOGRAPHY

NT BLACK AND WHITE PHOTOGRAPHY

NT CHRONOPHOTOGRAPHY

NT CINEMATOGRAHY

NT CLOUD PHOTOGRAPHY

NT COLOR PHOTOGRAPHY

NT ELECTRO-OPTICAL PHOTOGRAPHY

NT HOLOGRAPHY

NT INFRARED IMAGERY

NT INFRARED PHOTOGRAPHY

NT KINOFORM

NT LUNAR PHOTOGRAPHY

NT MICROWAVE IMAGERY

NT PHOTOMICROGRAPHY

NT PHOTORECONNAISSANCE

NT RADAR IMAGERY

NT RADAR PHOTOGRAPHY

NT RADIOGRAPHY

NT REPRODUCTION [COPYING]

NT ROCKET-BORNE PHOTOGRAPHY

NT SATELLITE-BORNE PHOTOGRAPHY

NT SCHLIEREN PHOTOGRAPHY

NT SHADOWGRAPH PHOTOGRAPHY

NT SPACEBORNE PHOTOGRAPHY

NT SPECTROHELIOGRAPHY

NT SPECTROPHOTOGRAPHY

NT STEREOPHOTOGRAPHY

NT ULTRAVIOLET PHOTOMETRY

NT XEROGRAPHY

Multispectral imagery of aerial remote sensors and television simulation for terrain analysis
06 p0658 N71-16133

Dynamic psychological and ergonomic aspects of mental imagery
[JZF-1970-21] 18 p2876 N71-31040

Spaceborne photographic image interpretation to identify objects in humid and forested regions
[NASA-CR-119722] 20 p3267 N71-33540

Coded mask for improved signal to noise ratio in scanning optical systems
[NASA-CR-123155] 24 p3887 N71-37706

IMAGES

NT AFTERIMAGES

NT IMAGE VELOCITY SENSORS

NT RETINAL IMAGES

Infrared to visible image up-conversion
01 p0053 N71-10209

Ultrasonic holographic and light diffraction techniques applied to coherent acoustic imaging during nondestructive tests
[AD-711085] 01 p0088 N71-10397

Perception and identification of images in different accelerative fields
02 p0164 N71-11634

Computerized image evaluation program, POLYPAGOS, using Fourier techniques
[AD-718095] 12 p1967 N71-23974

Diffraction efficiency and image distortion properties of volume transmission holograms
13 p2126 N71-23071

Camera adapter design for image magnification including lens and illuminator
[NASA-CASE-XMF-03844-1] 14 p2256 N71-26474

Spectral images formed by reflecting diffraction grating
16 p2592 N71-28237

Image sampling theorems for wave amplitudes obtained with circular apertures including Fourier-Bessel transformations and Airy figure example
[NASA-TT-F-13720] 18 p2963 N71-30834

Walsh orthogonal functions applied to image processing, and obtaining W-H transforms of two dimensional discrete pictures in real time
[AD-723662] 18 p2897 N71-31599

Upper atmospheric investigations and motion picture images of celestial bodies
19 p3179 N71-32001

Techniques for extracting objects from gray value real and computer-generated pictures including noise-free extraction from noisy backgrounds
[TR-145] 21 p3400 N71-34195

Length perception as isotropic image reduction operation
[TR-149] 21 p3448 N71-34540

Test target loaded with radionuclide for adjustment of gamma ray imaging devices
[ORNL-TM-3261] 21 p3474 N71-34741

Superorthicondynamic and working characteristics related to image quality estimations
[AD-727173] 24 p3888 N71-37713

Equipment specifications for interactive programming system for image processing with Iliac, IBM 360, and PDP 8 computer components
[COO-2118-3] 24 p3894 N71-37753

Focal image method for calibration in calculating characteristic curve for comets
24 p4009 N71-38585

IMAGING TECHNIQUES

NT IMAGE ENHANCEMENT

NT RADAR IMAGERY

Viewing infrared illuminated scenes by converting infrared frequency to visible, and then imaging visible radiation
01 p0062 N71-10142

High light intensity image dissection cameras for short duration recordings
[RAE-LIB-TRANS-1445] 02 p0225 N71-11553

Illumination calculations using diffraction and light scattering in ultraviolet image dissection cameras
[RAE-LIB-TRANS-1443] 02 p0226 N71-11554

Multispectral additive color viewing device for earth resources applications
02 p0227 N71-11980

Stereo laser framing camera for photographs of growth and effects of crack formation of materials shocked by explosives
[UCRL-72543] 03 p0387 N71-12828

Pseudocolor image enhancement by two-separation photographic process
[AD-712550] 03 p0381 N71-13163

Crystalline color preservation in photographic emulsion by alternating dark and light layers within and parallel to emulsion
[TR-59] 05 p0684 N71-14871

Investigating deterioration in automatic power level control due to violation of assumption of time-invariance in underwater acoustic imaging
[SC-CR-70-6102] 05 p0735 N71-15646

Thinning algorithms on rectangular, hexagonal, and triangular arrays
[NASA-CR-116131] 06 p0883 N71-15932

Using airborne radiometers for ocean bottom surveying
06 p0848 N71-16180

Airborne tests of multispectral scanners to determine usefulness of remote sensors in surveying river, coastal, and deep-sea phenomena
06 p0848 N71-16180

SUBJECT INDEX

IMPACT

Mariner Venus-Mercury 1973 imaging experiment for mapping Mercury and error rates for science words

06 p1289 N71-10874

Separation of multispectral images from multilayer film

06 p1245 N71-12927

Computerized analysis of image data processing techniques supporting space station X ray imaging solar telescope FPE SJA

10 p1526 N71-20623

Method for analyzing image distortion in diffraction topographs

10 p1556 N71-20736

Coherent optical processing of motion-degraded images

10 p1557 N71-20862

Image effects and vibrating sample magnetometer

10 p1634 N71-21073

Automatic photo-interpretation system for pattern recognition in image processing

11 p1767 N71-23069

Television-type, cut-window visual simulation image generator design and specifications for aircraft or spacecraft manned flight simulation

12 p1897 N71-24126

Major and critical component specifications for construction of simulator cruise scene visual attachment for manned spacecraft or aircraft flight simulation

12 p1898 N71-24127

Cruise scene visual attachment system assembly and detail design drawings for manned spacecraft or aircraft flight simulators

12 p1898 N71-24128

Highly stable optical mirror assembly optimizing image quality of light diffraction patterns

12 p1214 N71-24668

Fourier transformable properties of paraboloidal mirror segments also experimental results of spatial filtering

13 p2339 N71-26452

Research studies in chemical reaction kinetics, laser generation of plasmas, soil science, magnetohydrodynamics, tropical meteorology, computer programming, and imaging techniques

14 p2526 N71-26461

Picture processing and image evaluation

14 p2207 N71-26597

Characterization and mathematical representation of line scanning image systems and evaluating system performance with discrete output signal and post filtering

15 p2434 N71-27632

Imaging techniques for ultrasonic radiation using Bragg diffraction principle

16 p2638 N71-28417

Digital image processing for rectification of TV camera distortions

16 p2565 N71-28521

Image restoration techniques applied to astronomical photography with degradation caused by atmospheric turbulence

16 p2594 N71-28522

Image restoration for processing photographs by Stratoscope 2, and orbital telescopes

16 p0000 N71-28524

Processing electronic camera images for use in astronomical photometry

16 p2570 N71-28525

Development of information system for data reduction of wide range image spectrometer program raw light data on water pollution including oil spillage

16 p2597 N71-28731

Analysis and interpretation of photometrically calibrated photographic and vidicon images of chemical releases in upper atmosphere

17 p2742 N71-29029

Optical imaging system for increasing absorbing efficiency of light or radiant energy at light sensitive flux of imaging detector

18 p2964 N71-31142

Intensity distribution of optical images for various degrees of illumination using Hermitean matrices

18 p2966 N71-31452

Acoustic-optical imaging technique using Bragg diffraction by sound beam to produce optical image for decomposition studies

18 p2967 N71-31596

Production engineering and electrical operation of photomicroscopy sensing array system and display device including large scale integration and logic circuitry

19 p3167 N71-31642

Numerical method for restoration of planar image functions for use on digital computers

19 p3062 N71-32469

Angle of observation functions of imaging optical systems

20 p3311 N71-33384

Holographic scanning for acoustic imaging in liquid medium

20 p3223 N71-33406

Application of cosmographic perspective in interpreting photographs taken in space

20 p3275 N71-33590

Latent image fading dependence on radiant flux density of visible and gamma illumination

20 p3328 N71-33985

Influence of atmosphere on performance of thermal imaging systems

20 p3299 N71-33995

Evaluation of signal processing and modulation techniques for transmission and reception of image type data via millimeter wave relay satellites

21 p3394 N71-34156

Techniques for extracting objects from gray value real and computer-generated pictures including noise-free extraction from noisy backgrounds

21 p3400 N71-34195

Variations in image boundaries of ERTS multispectral scanner and return beam vidicon systems

22 p3648 N71-36153

Image quality achievable with optical multiplexing techniques - overlay storage methods

22 p3699 N71-36376

Image resolution impairment in 16 mm film presentation by television

23 p3725 N71-36557

EA-4 processing for high altitude infrared color film

23 p3753 N71-36767

Technique for obtaining spatial frequency spectrum for cross section of image

23 p3803 N71-37114

Three-dimensional reproduction of information based on photochromism

24 p3482 N71-37669

Image input and output unit for Minsk-2 computer

24 p3896 N71-37773

Development and characteristics of photoelectric image converters with optical communication

24 p3899 N71-37793

Photon counting digital image recorder using television camera

24 p3924 N71-37999

Imaging and analysis method for very weak phase objects which gives exact measure of optical path gradients

24 p3930 N71-38044

IMBEDDINGS [MATHEMATICS]

NT INVARIANT IMBEDDINGS

Formulation of problem of siting production units in terms of regular imbedding

11 p1786 N71-21903

Imbedding nonlinear differential equations in reformulating boundary value problems to initial value problems for computerized computation

11 p1788 N71-22497

Use of imbedding theory to construct autonomous optimal control problems with free termination time

11 p1729 N71-22658

Radiative transfer problems using invariant imbedding and Fredholm integral equations with discontinuous kernels

12 p1950 N71-23743

Imbedding algorithm for solution of two-point boundary value optimization problems

19 p3122 N71-31823

Analytical morphisms of closed transcendental spaces

24 p3948 N71-38162

Complex spaces as Stein spaces

24 p3949 N71-38172

Topological depth of coherent analytical bundle in Stein space

24 p3940 N71-38173

Energy and momentum in imbedding space of four-dimensional space-time

24 p3950 N71-38182

IMCC [CONTROL CENTER]

U INTEGRATED MISSION CONTROL CENTER

IMIDES

Synthesis and chemical properties of imidazopyrrolone/imide copolymers

02 p0176 N71-11238

Electron impact behavior and mass spectra of molecular ion aromatic imide refractory materials

06 p0808 N71-15829

EPR and ENDOR study of free radicals produced by gamma irradiation of imidazole single crystals

14 p3307 N71-26395

Synthesis of schiff bases for heat shields by acetal anion reactions

02 p0176 N71-11238

Molecular structures and thermal stabilities of ferrocene containing polyaromatics and poly-Schiff bases

11 p1782 N71-22076

Synthesis of aromatic diamines and dialdehyde polymers using Schiff base

13 p2039 N71-24740

IMBROSION

U SUBMERGING

IMMISIBILITY

U SOLUBILITY

IMMITTANCE

U ELECTRICAL IMPEDANCE

IMMOBILIZATION

Stretcher with rigid hand and neck support with capability of supporting immobilized person in vertical position for removal from vehicle hatch to exterior also useful as spinal stretcher

12 p1865 N71-23159

Measurement of bone mass loss as result of immobilization

20 p3216 N71-33256

Effects of inactivity or immobilization on bone loss

20 p3216 N71-33258

Atrophy in monkeys due to immobilization and implications for extended manned space flight

20 p3217 N71-33260

Bed rest and immobilization effects on oxygen transport system of human body

20 p3217 N71-33262

Research and development, weightlessness simulation, calcium metabolism, manned space flight, pressure suits, immobilization, and aerospace medicine

20 p3219 N71-33275

IMMUNITY

Hypoxic hypoxia effects on human and animal resistance to infectious diseases and immunobiological reactivity

16 p2543 N71-28249

IMMUNOLOGY

Investigating shifts in composition of auto-microflora on skin and state of natural immunity of cosmonauts during prolonged flight aboard Soyuz 9 spacecraft

08 p1151 N71-10907

Human immunology on prolonged diet of dehydrated foods

08 p1154 N71-10964

Effect of simulated space cabin atmosphere of 100 percent oxygen at 5 psi on immunological response in mice

10 p1500 N71-21333

Trends and possibilities in biochemical and biotechnical in medical science - heart transplantation

18 p2875 N71-30840

Development of radioimmunoassay system for measurement of urinary antidiuretic hormone excretion

23 p3712 N71-36459

IMP

IMP-1 launch window and secondary injection into eccentric orbit

06 p1293 N71-10649

IMP-1 optical aspect system based on spacecraft angular relationship between sun and earth using digital solar sensor and visible-horizon detector

10 p1559 N71-21220

Low energy cosmic radiation spectrum analysis for IMP-4 data on solar system

13 p2163 N71-25290

Initial magnetic test of IMP-1 spacecraft with reduction of magnetic moment by dc rotation deperm treatments

14 p2335 N71-25800

Design and operation of three power supplies for IMP-1 spacecraft

15 p2369 N71-27669

IMP-5 magnetic field measurements at high geomagnetic latitudes to observe broad depressed field region centered on polar or day-side cusp

16 p3093 N71-32149

IMP-A

U EXPLORER 18 SATELLITE

IMP-C

U EXPLORER 28 SATELLITE

IMP-D

U EXPLORER 33 SATELLITE

IMP-E

U EXPLORER 35 SATELLITE

IMP-F

U EXPLORER 34 SATELLITE

IMPACT

NT ELECTRON IMPACT

NT HYPERVELOCITY IMPACT

NT ION IMPACT

NT PROTON IMPACT

As-306 S-4B post flight lunar impact trajectory analysis

02 p0299 N71-11998

System for detecting impact position of cosmic dust and similar outer space particles on detector surface

16 p2663 N71-29193

Impact of thin, mildly sloping spherical shells on surface of ideally incompressible liquid
[NASA-TT-F-13576] 18 p3021 N71-30883
Tunnel penetration and impact multiplication procedures for quick recording of particle tracks in condensed media 21 p3467 N71-34676
[JINR-P13-5623]
Solutions obtained for problem of normal impact of infinite elastic-plastic beam by semi-infinite elastic rod [AD-726548] 22 p3689 N71-36313

IMPACT ACCELERATION

Determination of human tolerance to impact accelerations

Impact acceleration study of charged bunch collisions by coherent method
[UCRL-TRANS-1421] 12 p1974 N71-23960

Development of analytical model for determining spacecraft impact velocity and orientation relative to impact surface for variable dynamic conditions
[NASA-TN-D-6325] 13 p2175 N71-25399

Studying aircraft accidents to determine impact angle and speed criteria for designing nuclear airplane fuselage product containment vessel 13 p2122 N71-25411
[NASA-TM-X-22457]

Suspended mass oscillation damper based on impact energy absorption for damping wind induced oscillations of tall stacks, antennas, and umbilical towers
[NASA-CASE-LAR-10193-1] 15 p2415 N71-27146

Computerized and manned spacecraft and aircraft simulator impact testing of air cushion elastic restraint systems

[NASA-CR-60169] 18 p2882 N71-30401
Human dynamic response to impact acceleration minus G sub x - measurements on head and neck
[AD-71130] 19 p3046 N71-31616

Technique for conducting landing impact tests at simulated planetary gravity for Mars lander spacecraft - dynamic models
[NASA-TN-D-6459] 22 p3681 N71-36247

IMPACT DAMAGE

NT METEORITIC DAMAGE

NT RAIN IMPACT DAMAGE

Predicting crater size and impact flash for S-4B stage lunar impact on Apollo 13 flight
[NASA-TM-X-64517] 05 p0766 N71-14636

Laboratory simulation of impact cratering with high explosives

[NASA-TM-X-62010] 05 p0675 N71-14995
Investigating penetration response of various materials to high speed fragment impact
[AD-713513] 05 p0780 N71-15394

Mathematical analysis of denting of thin aircraft skin by hail

[NASA-TN-D-6102] 05 p0780 N71-15422
Xe-131 ion impact on gold crystal foils producing imperfection clusters

[CDO-1053-14] 07 p1075 N71-17495
Erosion rate of turbine blades produced by ash from caliche coal

[ARL-ME-315] 09 p1459 N71-20019
Computer controlled micrometeoroid impact simulation system

[NASA-TM-X-66947] 09 p1368 N71-20253
Measuring micrometeoroid depth of penetration into various materials

[NASA-CASE-XLA-00491] 12 p1917 N71-23240
Computer program using numerical integration techniques for computation of meteoroid impact and angular distributions over complex geometric spacecraft configurations

[NASA-CR-103102] 12 p2003 N71-24335
Determining threshold damage in slip cast fused silica by discrete impact in ballistics range

[AD-728030] 24 p3945 N71-38141

IMPACT DECELERATION

U DECELERATION

U IMPACT ACCELERATION

IMPACT LOADS

Construction and operation of shock absorber using side-spreading springs to convert kinetic energy to heat

[AD-711006] 01 p0060 N71-10608
Calculation of forces in infinite length fiber with transverse impact of variable velocity

[AD-711758] 01 p0131 N71-10852
Mathematical model for stress waves in sandwich plates subjected to high velocity impact

[NASA-CR-108692] 02 p0300 N71-11404
High impact dynamic response analysis of nonlinear structures

[NASA-CR-111404] 02 p0301 N71-12024
Mathematical model of spinal response to impact

[AD-711553] 04 p0618 N71-14163
Aircraft landing lift decay and elevator oscillation analysis

[ARL-CF-1119] 06 p0793 N71-15722
Plastic deformations of clamped beams by impulsive loading

[AD-714883] 07 p1126 N71-17887

Shell impact response and wave propagation in cylindrical and conical shells by experimental and analytical methods

[NASA-CR-46921] 10 p1651 N71-20701
Analysis of normal accelerations through center of gravity of aircraft due to landing impacts and ground operations associated with taxi, takeoff, and landing

[NASA-TN-D-6124] 11 p1676 N71-22620
Impact testing machine for imparting large impact forces on high velocity packages

[NASA-CASE-XNP-04017] 12 p1916 N71-23225
Development of analytical model for determining spacecraft impact velocity and orientation relative to impact surface for variable dynamic conditions

[NASA-TN-D-6325] 13 p2175 N71-25399
Finite difference integration of dynamic Lagrangian equations for impact shock wave profiles in aluminum alloys

[AD-720716] 15 p2424 N71-27467
Investigation of impact of blunt body against flexible plate where high tensile impact wave velocity exceeds speed of sound in material

[AD-722281] 17 p2851 N71-29332
Tolerances of human brain to impact shock and concussions

[FAA-AM-71-13] 17 p2708 N71-25636
Stress waves induced in anisotropic fiber composite plates by transverse, short-duration impact forces

[NASA-TN-D-6357] 20 p3559 N71-33672
Effect of hard impact and anelastic erosion on release of microorganisms from geological formations

[NASA-CR-121707] 21 p3381 N71-34056

IMPACT PREDICTION

Internal gravity wave effects on mesospheric temperature variations affecting reentry studies and impact prediction capability

[AD-711640] 01 p0081 N71-10950
Wind effect on unguided rockets fired near maximum range

[AD-711854] 02 p0296 N71-11949
Computer code for prediction of hydrometeor impact erosion on high speed sphere-cone vehicles

[SC-DR-70-373] 03 p0343 N71-12489
Numerical analysis of vertical water entry of cone 2, impact prediction

[AD-718809] 12 p1899 N71-23223
Effects on impact dispersion of winds and density deviations from standard atmosphere derived by solution of approximate equations

[AD-721356] 16 p2678 N71-28317

IMPACT PRESSURES

U IMPACT LOADS

IMPACT RESISTANCE

Performance tests on heat sterilizable and impact resistant silver zinc prototype batteries

[NASA-CR-116787] 08 p1146 N71-18510
Initiation and sensitivity of solid explosives to mechanical impact

[NASA-TT-F-623] 11 p1841 N71-22534
Influence of icebreaker hull dimensions on ice resistance when moving at low speed in compact ice

[AD-71771] 11 p1771 N71-22864
Investigation of impact resistance of unidirectional fiber composites using Izod impact tests

[NASA-TM-X-67802] 12 p1946 N71-24010
Impact response modeling for design of weapon container

[SC-RR-70-8801] 15 p2523 N71-27986
FORTRAN 5 digital computer program for predicting dynamic response of Apollo command module to earth impact

[NASA-TN-D-6539] 23 p3730 N71-36589

IMPACT SENSITIVITY

U IMPACT RESISTANCE

IMPACT STRENGTH

Ballistic properties of solidified armor plate steel

[AD-714294] 06 p0874 N71-16579
High impact pressure regulator having minimum number of lightweight movable elements

[NASA-CASE-NPO-10175] 08 p1201 N71-18625
Impact properties determined for pure copper, copper-nickel alloy, and superalloy metal matrix composites reinforced with tungsten fibers

[NASA-TM-X-67810] 12 p1945 N71-23950
Mechanical properties and impact strength of UARL 417 experimental glass

[NASA-CR-118882] 15 p2432 N71-27676
Effects of target strength on cratering process caused by impact of hypervelocity projectiles

[NASA-CR-119189] 17 p2855 N71-30232
Low sulfur content effect on impact and tensile strength of steels

19 p3112 N71-31920
Metalurgical design in higher yield strength structural steels

[PB-199293] 22 p3393 N71-35586
Formulation of mathematical stress wave model for predicting effects of sandwich plates subjected to high velocity impact

[NASA-CR-121892] 22 p3681 N71-36251
Physical effects governing spherical wave propagation including strain hardening, viscosity, and magnitude and duration of impact

22 p3691 N71-36256

Development of procedures for determining impact strength of steel and factors which control impact strength

[NLL-TRANS-746-679-19022.401] 23 p3774 N71-30901
Equations of motion for elastic plate foundation system under dynamic load applied to aircraft landing

23 p3864 N71-37543

IMPACT TESTING MACHINES

Gas gun and piezoelectric gage for measuring high velocity deformations in shocked metal crystals

09 p1454 N71-30231
Development and characteristics of pantometer for measuring physical properties of lunar surface

[NASA-CASE-XLA-00934] 11 p1764 N71-22785
Impact testing machine for imparting large impact forces on high velocity packages

[NASA-CASE-XNP-04817] 12 p1916 N71-23225

IMPACT TESTS

NT CHARTY IMPACT TEST

Impact tests of two 3-foot diameter containment models for mobile nuclear reactors

[NASA-TM-X-52915] 01 p0087 N71-10987
Drop and impact tests for improving crashworthiness of integral fuel tanks

[FAA-NA-70-46] 02 p0144 N71-10119
Fractographic analyses of dentified ceramics and glass-ceramics ballistically impacted by caliber .30 M2 projectiles

[AD-712586] 02 p0247 N71-11656
Microstructural and fractographic studies of boron carbide ceramics subjected to ballistic impact and static flexural loading

[AD-712307] 02 p0247 N71-11664
Single impact studies of rain erosion on fast moving surfaces

[RAE-TF-69086] 02 p0204 N71-11767
Response of mixed materials to one dimensional shock waves

[AD-712622] 02 p0248 N71-11972
Developing aluminum meteorite simulators for hypervelocity impact test using shaped charges

[NASA-CR-108750] 03 p0355 N71-12664
Hole growth in thin plates perforated by hypervelocity pellets

[AD-712071] 03 p0460 N71-12956
Instrumentation and drop testing techniques for investigating flight vehicle and personnel protective systems

[NASA-TM-X-2149] 05 p0682 N71-14780
Lithium fluoride dislocation in high speed impact

[AD-713624] 05 p0707 N71-14824
Impulse generation in aluminum using electron beam for high energy density loading

[AD-714538] 06 p0954 N71-16602
Characteristics of quartz gages for impact experiments

[SC-DC-70-4932] 06 p0861 N71-16696
Deformation of rigid plastic spherical shells in low velocity impact

[AD-714519] 06 p0957 N71-16848
FORTRAN 4 program for calculating dynamic Kirchhoff deformation of structural rings subjected to fragment impact

[NASA-CR-72801] 08 p1297 N71-18738
Digital computer simulation of automobile impacting flexible safety barrier, and multiple source schlieren system for NAE trisonic wind tunnel

[DME/NAE-1970/3] 09 p1363 N71-19401
Digital computer simulation of automobile impacting flexible safety barrier

09 p1473 N71-19402
High velocity impact tests conducted with polyethylene terephthalate projectiles and flexible composite wall panels

[NASA-TN-D-6135] 09 p1481 N71-20515
High speed photography and impact tests of nylon yarns including transient responses and breaking energies

[AD-716983] 10 p1587 N71-20651
Impact tests on annealed small grain 1100 F aluminum rods using in-surface diffraction grating strain transducers illuminated by pulsed ruby laser

[AD-717328] 11 p1776 N71-21907
Plastic wave velocity measurement in Lexan at high speed impact

[AD-717527] 11 p1833 N71-21917
Impact and static pressure tests of increasing phase velocity accelerator magnetic coil system operating on argon plasma for high altitude, high velocity flow, reentry simulation

[AD-717703] 11 p1812 N71-22385
Impact tests of SIREN for encapsulation system for radioactive isotopic heat source

[SNC-2708-2] 12 p1961 N71-23140
Investigation of impact resistance of unidirectional fiber composites using Izod impact tests

[NASA-TM-X-67802] 12 p1946 N71-24010
Bending force-time and bending force-deflection diagrams obtained with oscillograph during notched bar impact tests

[NLL-M-20165-5828 AF/1] 12 p2007 N71-24214
Simulation of secondary meteorite flux by impact of single projectiles on thin sheet aluminum and nylon

- Applying neutron activation analysis to determination of impurities in processing of silicon devices
[AD-715313] 07 p1091 N71-17308
- Susceptibility of polyurethane foam to deterioration by impurities or contaminants in ethylene glycol monomethyl ether
[AD-715313] 07 p0997 N71-17755
- Fabrication of sintered impurity semiconductor brushes for electrical energy transfer
[NASA-CASE-XMF-01016] 07 p1094 N71-17818
- Chemical analysis of boron in aluminum, boron carbides, and boron mixtures, and of impurities in boron
[TID-25190] 06 p1253 N71-18323
- Electrotransport of impurities in rare earth metals using pulsed current
[BM-R1-7480] 06 p1213 N71-18513
- Quantum mobility, configurational entropy, and Mossbauer spectroscopy of impurity atoms in crystals
[NUB-2049] 06 p1279 N71-18690
- Impurities effect on manganese diffusion rate in ternary nickel-manganese alloys
[TT-70-57059] 06 p1218 N71-19008
- Effect of antimony and beryllium impurities on diffusion rate of zinc in polycrystalline brass
[TT-70-57060] 06 p1218 N71-19098
- Effects of small amounts of impurities on process of dissociation of super saturated solid solutions
[TT-70-57078] 06 p1219 N71-19100
- Rapid, direct reading, emission spectrometric method for impurity determination in thorium materials using production control spectrometer
[NLCO-0778] 06 p1342 N71-19396
- Excitation spectra of ferromagnetic insulators in presence and absence of impurities
09 p1423 N71-19500
- Magnetic phenomena in superconductors, and magnetic impurity measurements of superconductivity
[AD-716027] 09 p1452 N71-19680
- Determination of deep impurities in silicon and germanium by infrared photoluminescence
[NBS-TN-570] 10 p1536 N71-20614
- Doping impurity distribution in p-n junctions determined from capacitance measurement
10 p1632 N71-20784
- Zone melting, recrystallization, single crystals, impurities, crystal growth, fluxes, magnetic fields, X ray analysis, and mixing
[UPRS-52552] 10 p1573 N71-20866
- Mathematical model for study of physico-chemical characteristics of impurity behavior in zonal recrystallization
10 p1573 N71-20867
- Impurity behavior during refinement of tin and lithium by zone melting
10 p1573 N71-20870
- Impurity behavior in process of zone recrystallization of magnesium
10 p1573 N71-20871
- Behavior of selenium impurities in tellurium during zone recrystallization
10 p1573 N71-20873
- Behavior of impurities in noncrucible zone melting of refractory metals
10 p1574 N71-20874
- Impurity distribution in molybdenum single crystals produced by electron beam zone melting
10 p1574 N71-20875
- Impurity distribution and convection in liquid phase during zone recrystallization of tellurium tetrafluoride
10 p1574 N71-20876
- Impurity behavior during zone melting of lower indium chlorides
10 p1574 N71-20877
- Distribution of lead, copper, and zinc impurities in KCl single crystals grown from melt
10 p1632 N71-20878
- Vaporization of magnesium impurities from high purity aluminum melt in vacuum apparatus reduces electrical resistance of aluminum
10 p1575 N71-20882
- Production of ultrapure antimony by continuous zone recrystallization in single section vacuum apparatus
10 p1575 N71-20883
- Impurity distribution in tellurium as function of direction of travel of zone in vertical crucible zone recrystallization
10 p1633 N71-20888
- Directed crystallization of compounds during impurity exchange of liquid phase with crucible and atmosphere
10 p1634 N71-20890
- Nonmetallic impurities in Invar and super-Invar iron alloys
[NLL-TRANS-744-633-7022.401] 10 p1579 N71-21266
- Microplastic deformation in body centered cubic metals and solid solutions and analysis of intrinsic lattice resistance and interstitial impurities as dislocation motion controls
[CONF-70045-1] 10 p1581 N71-21439
- Spin wave perturbation theoretical analysis of Heisenberg model for impure ferromagnets
[BNL-TR-309-PT-1] 10 p1635 N71-21704

- Defect properties of semiconductor materials as function of impurity concentration and ionizing radiation
[AD-717773] 11 p1817 N71-22347
- Polarization and point defects due to sodium impurities in metal oxide semiconductor transistors
[JRO-2036-21] 12 p1940 N71-24209
- Anderson model and Hamilton functions for resonant scattering study by metal impurities
[AD-718903] 12 p1973 N71-23935
- Impurity tracer diffusion coefficients in aluminum and dilute aluminum alloys including ion core and electrostatic effects in vacancy-impurity interactions
[JRO-2036-21] 12 p1940 N71-24209
- Mathematical model for closed form expression of impurity particle nuclear binding energy using power series, particle spin, and wave functions with lambda hyperon example
[DEMO-70/20] 13 p2130 N71-24498
- Influence of crystal chemistry factor in separation of rare earth elements in silicate crystallization differentiation
[NASA-TT-F-13647] 13 p2151 N71-24821
- Impurity caused grain boundary sliding in alumina ceramics during compression
[ORO-3328-17] 15 p2508 N71-27903
- Effects of Fe, Si, Al, Ni, Cr, and Zr impurities on properties of uranium
[AWRE-O-63/70] 15 p2427 N71-27968
- Color centers and magnesium oxide crystal defects from proton irradiation and impurities
[NASA-CR-118865] 16 p2642 N71-28044
- Removal of microimpurities from substances by chemico-physical methods
16 p2556 N71-28302
- Effect of various impurities in open range on electrical conductivity of organic coolant liquids
[EUR-4597-E] 16 p2631 N71-28564
- Helium 2 quenching environment, rate, and impurity effects on quenching of vacancies into body centered cubic molybdenum
[NASA-TM-X-57468] 16 p2614 N71-28922
- Calculation of neutron elastic and inelastic scattering cross sections and spatial transverse correlation functions for Heisenberg theory of impure ferromagnets
[BNL-TR-390] 16 p2658 N71-29144
- Instrumentation for investigating nature of energy levels of impurity ions in crystalline solids
[AD-723411] 17 p2814 N71-29692
- Models for permitting continuous purging of impurities from gas compartments of fuel cell
17 p2706 N71-29694
- Sub-boundary corrosion in polygonized polycrystalline aluminum containing iron and copper impurities and exposed to HF and HCl solutions
17 p2764 N71-29726
- Thermodynamic assessment of metal compatibility and gaseous impurities in helium atmosphere
[ED/RN-1816] 17 p2785 N71-30143
- Technology and properties of metallic materials
18 p2934 N71-30690
- Soviet news releases on sea impurities and varied plankton studies
18 p2910 N71-30791
- Impurity atom effects on copper diffusion in single nickel crystals
18 p2997 N71-31323
- Composition of trace-mineral inclusions in cassiterite tin ore deposits studied by point X ray spectral microscopic analysis
[NASA-TT-F-13740] 18 p2941 N71-31404
- Quantum mobility and nuclear spin echo damping in impure crystals
[NUB-2069] 18 p2999 N71-31486
- Diffusion of impurities from GaAs stream in epitaxial layers of GaP grown by sandwich method
[AD-723589] 19 p3167 N71-31738
- Grain boundary segregation of impurities in steels and intergranular brittle fracture
[AD-723224] 19 p3113 N71-31966
- Effect of impurities on properties of slowly propagating domains in gallium arsenide
19 p3066 N71-32361
- Distribution of impurities in plutonium determined by mass spectrometry, spectroscopy, and spectrophotometry
[CEA-R-4071] 21 p3437 N71-34459
- Diffusion mechanisms responsible for charge carrier mobility in doped silicon, studied to determine impurity band effects on electrical conductivity
[N-816] 21 p3497 N71-34916
- Fabrication and properties of hot-pressed polycrystalline magnesium oxide containing anion impurities
[NASA-CR-121937] 22 p3587 N71-35545
- Mass transfer in liquid metal systems and in-line devices for measuring sodium impurity
[GEAF-1339-16] 22 p3623 N71-35816
- Atomic absorption spectrophotometry for rapid analysis of impurities in uranium
[CEA-R-3870] 22 p3635 N71-35913
- Anomalous electron-phonon transport properties of impure metals
[NP-18822] 22 p3640 N71-35947

- Isobaric-isothermal potentials for lithium oxide reduction by metals and metallic impurity oxide, nitride, carbide, and hydride concentrations in liquid lithium
[NLL-RISLEY-TRANS-2169-19091.9F1] 23 p3773 N71-36891
- Microautoradiogram of impurity distribution in aluminum foil irradiated by thermal neutrons
[NLL-WINDSCALE-448-19091.9F1] 23 p3774 N71-36898
- Color center and substitutional impurity point defects in magnesium, calcium, and strontium oxide insulators
[AD-726647] 23 p3835 N71-37351
- IMPURITY
U PURITY
IN-FLIGHT MONITORING
In-flight testing of spacecraft power system with on-board monitoring equipment
[ESRO-TM-109-BSTEC] 03 p0458 N71-13252
- In-flight determination of lateral-directional dynamics for landing approach
[AD-715317] 07 p0973 N71-17792
- Describing bioinstrumentation for monitoring in-flight physiological functions of Soyuz 9 crew members
08 p1150 N71-18981
- Measuring physiological changes and circulatory reactions of Soyuz 9 crew members during prolonged flight
08 p1150 N71-18992
- Concorde 002 aircraft equipment for flight data recording and processing
[ESS/ES-13] 10 p1492 N71-20857
- Low-inertia flow-direction vane static and dynamic wind tunnel tests at subsonic and supersonic speeds for in-flight measurement of burst velocity
[NASA-TN-D-6193] 12 p1915 N71-23115
- Airborne equipment for approach path control on reduced noise trajectories in Boeing transport aircraft traffic
12 p1855 N71-23425
- F-4E aircraft in-flight television recording system for gunnery training
[AD-720245] 14 p2210 N71-26174
- IN-FLIGHT THRUST MEASUREMENT
U IN-FLIGHT MONITORING
U THRUST MEASUREMENT
INACTIVATION
U DEACTIVATION
INACTIVATION
INCANDESCENCE
Use of incandescent lamps to measure optical and detector drifts in photoelectric spectrometers
[NASA-TN-D-6313] 13 p2039 N71-24611
- INCENTIVE TECHNIQUES
Performance characteristics of US information retrieval and management information systems, noting heuristic methods and incentive techniques
14 p2223 N71-29996
- INCIDENCE
Effects of unit Reynolds number and incidence on boundary layer transition in supersonic wind tunnels
[NPL-AERO-1301] 04 p0472 N71-13449
- Wind tunnel tests of downwash aerodynamic surface incidence angles on Saturn S-IC booster coupled to Grumman C-4 orbiter shuttle
[NASA-CR-103195] 21 p3525 N71-35114
- MECC-3 code instructions for calculating nuclear reactions involving incident particles at high energy on complex nuclei
[ORNL-4564] 23 p3816 N71-37213
- INCIDENT RADIATION
Parallel radiation incident to grazing for life extension of diffraction grating strain gauges
[AD-717324] 11 p1760 N71-21863
- Neutron, gamma reactions with vanadium-51 and yttrium-89 for incident neutrons in energy range 0.3 to 4 MeV
[AWRE-O-78/70] 14 p2308 N71-26434
- Conversion factor for converting Geiger tube count rates or ion chamber currents into units of incident X ray energy flux in specified passband in normalizing solar X ray data
15 p2514 N71-27648
- Polarization measured for secondary proton emission at about 660 MeV in rhenium proton gun yields pion/plus/ proton neutron and proton proton yields pion/plus/ proton
[JINR-P1-5293] 15 p4092 N71-27994
- Experimental results on kaon/plus/ deuteron interactions from 865 to 1365 MeV/c incident beam momentum
[UCRL-20248] 17 p2893 N71-30216
- Cathode environment characteristics in glow discharge
[SC-RR-710122] 19 p3070 N71-32219
- Feasibility of regulating incident and reflected solar radiation on buildings in arctic regions
[NLL-M-20401-1628.4F1] 21 p3585 N71-34908
- Interaction of plane p-polarized electromagnetic wave obliquely incident on hot plasma half space and plasma slab
22 p3635 N71-36060

SUBJECT INDEX

Effect of retroreflective reflections on operation of laser Doppler velocimeter
[DPRS-54106] 24 p3391 N71-30048

INCINERATION
U INCINERATORS
INCINERATORS
Incinerating radioactive wastes
[CEA-R-3721] 09 p1365 N71-19999
INCINERATION
Climometer for measuring inclinations of earth surface near Moscow
23 p3748 N71-36723
Harmonic analysis of earth inclinations by Engelhart Astronomical Observatory
23 p3749 N71-36726
Elastic earth tide inclinations observed at Talgar
23 p3749 N71-36728
Instrument drift in earth inclination observations made by Engelhart Astronomical Observatory
23 p3749 N71-36729

INCLUSIONS
Electron microprobe analysis of metallic inclusions in irradiated phosphorus oxides at high burnups
[AERE-R-6310] 04 p0527 N71-13642
Behavior of silica inclusions during solidification of iron base alloy
09 p1397 N71-19615
Transformation of form and displacement of air inclusions in ice due to molecular rearrangement of ice crystals and temperature gradients
11 p1759 N71-22862
Range prediction for behavior of inclusive cross sections near kinematic boundary
[RLO-1358-601] 17 p2793 N71-29547
Swedish contribution to Russo-Swedish conference on steel
[IVA-169-1] 19 p3111 N71-31901
Removal of non-metallic inclusions from stainless steel during electroslag refining process
19 p3111 N71-31907
Influence of carbon and stainless steel refining processes on inclusions
19 p3104 N71-31909
Decarburization of liquid iron studied by electromotive force measurements noting removal of inclusions
19 p3111 N71-31911
Kinetics of removal from iron of inclusions produced by manganese silicon aluminum complex decarburization
19 p3112 N71-31912
Corrosion of polished carbon steels at inclusions noting effect of manganese sulfide
19 p3112 N71-31917
Inclusions influence on stress concentration, cavitation, and surface cracks of steels
19 p3112 N71-31918
Effect of sulfide inclusions on ball bearing steel durability noting sulfur content
19 p3187 N71-31919
Behavior of nonmetallic inclusions in steel during hot working
19 p3113 N71-31923

INCOHERENCE
Q-switched ruby laser holography with optical segment to compensate for spatial and temporal incoherence for contouring, aerodynamic visualization, and nondestructive testing
[NASA-TR-14291] 10 p1349 N71-21320

INCOHERENT SCATTERING
Studying lower ionosphere by incoherent scatter radar
01 p0045 N71-10149
Diurnal variation of neutral temperature profile at Arecibo from incoherent scattering measurements and its relevance to 1400 hour density maximum
[NASA-CR-114146] 02 p0215 N71-11964
Incoherent scattering of microwaves from plasma waves excited in electron beam in absence of external magnetic field
[AD-725443] 19 p3163 N71-31931

INCOMPATIBILITY
Sound and visual sensory interactions of pleasant, unpleasant, and no sound with red, green, and blue light against white standards
[AD-71715] 11 p1690 N71-22341

INCOMPRESSIBILITY
Computer analysis of pressurized thrust bearing design using incompressible lubricant
[NASA-TN-D-6075] 06 p0867 N71-16555
Mass velocity profile approximation of two dimensional incompressible turbulent boundary layer
[NALL-TR-219] 13 p2067 N71-25415

INCOMPRESSIBLE FLOW
HYDRODYNAMICS
High pressure shock effects on position of stagnation point on adjacent wall of incompressible jet
[A-15] 01 p0041 N71-02396
Separation point study of incompressible laminar boundary layers around parabolic bodies at angle of attack
[AD-712864] 02 p0201 N71-11519
Correction formulas for effect of ambient temperature drift on hot-wire anemometer measurements in incompressible flow
[DPL-AERO-1362] 02 p0225 N71-11544

Determination of orderly structure in jet turbulence
[AD-715969] 02 p0284 N71-12970
Systematic numerical analysis of two dimensional and axisymmetric laminar jet of incompressible fluid with and without free stream
[NASA-CR-111517] 03 p0364 N71-13085
Exact vortex solutions of incompressible Navier-Stokes equations
[AD-712618] 03 p0366 N71-13398
Analytical and numerical calculations for cylinder-vortex combination in incompressible flow noting pressure distribution and downwash
[NLR-TR-49057-U] 05 p0166 N71-15548
Submerged incompressible two-dimensional jet pivotedly oscillated at its base
[AD-714696] 06 p0834 N71-16116
Flow models for bounded and intersecting plane, incompressible, turbulent jets
06 p0836 N71-16396
Initiation, development, and decay of secondary flow in incompressible turbulent bounded jet
[AD-714655] 06 p0839 N71-16621
Entrainment coefficient used for computation of two dimensional incompressible turbulent boundary layers
[AIRC-3-M-3643] 06 p1139 N71-18424
Applying concept of mixing length flow theory to turbulent turbulent boundary layers
[NASA-TT-F-13463] 06 p1180 N71-18622
Computational method for turbulent boundary layers in incompressible two dimensional flow
[NRC-11708] 09 p1371 N71-19617
Calculation of skin friction on porous plate in presence of incompressible laminar boundary layer
[AD-716035] 09 p1372 N71-19684
Second-order slender wing theory for incompressible flow over low aspect ratio wings with and without leading edge separation
09 p1331 N71-19912
Linearized perturbation equations for incompressible laminar boundary layer flow over slender body of revolution at small incidence
[NRC-11645] 09 p1377 N71-20261
Computer program for numerical analysis of flow and pressure distribution in idealized spiral grooved pumping seal
[NASA-TN-D-6183] 09 p1394 N71-20399
Models for high Reynolds number incompressible laminar flow around sharp corner
10 p1542 N71-21272
Longitudinal curvature and displacement speed effects on incompressible boundary layer flow past circular cylinder
[AD-717071] 10 p1544 N71-21613
Fluid motion for incompressible fluid between two long eccentric cylinders
[AD-717366] 11 p1734 N71-21970
Graphical computer simulation of incompressible flow about airfoil
[TN-71-21] 11 p1715 N71-22149
Numerical analysis of vertical water entry of cone 2, impact prediction
[AD-718809] 12 p1899 N71-23223
Navier-Stokes equations for incompressible uniform flow past parabolic cylinder in infinite stream
[AD-718362] 12 p1900 N71-23584
Oscillatory pitching moment derivatives measurement on delta wings in incompressible flow
[AEC-R/M-5628-PT-1-4] 13 p2022 N71-24569
Measurements of oscillatory pitching moments on round leading edge delta wing in incompressible flow noting vortex flow development
13 p2022 N71-24570
Acoustically excited, incompressible, turbulent, subsonic Canda air flow around circular cylinder
13 p2066 N71-23039
Predictions for swirling incompressible flow in straight pipes
[EP/TN/A/57] 13 p2068 N71-25417
Finite difference solution for unsteady equations of incompressible starting incompressible jet flow
[EP/TN/A/29] 13 p2068 N71-25443
Calculation of viscous drag and turbulent boundary layer separation on two dimensional and axisymmetric bodies in incompressible flow
[AD-720775] 14 p2239 N71-25048
Solutions for multipoint distribution functions in homogeneous isotropic incompressible turbulent field
[SC-R-70-912] 15 p2392 N71-27065
Computer code (VORTEX) simulating behavior of incompressible, inviscid, homogeneous fluid in two dimensions by following motion of point vortices
[CLM-R-106] 15 p2394 N71-27470
Unsteady pressure measurements on harmonically oscillating swept wing with two control surfaces in incompressible flow
17 p2700 N71-29350
Pressure measurements of harmonically oscillating sweptback wing with two flaps in incompressible flow
[DLA-FB-70-47] 17 p2700 N71-29433
Theory for three dimensional, incompressible, zero-mean turbulence decay based on relationship between double and triple velocity moments
19 p3079 N71-32256

INCONEL (TRADEMARK)

Mathematical models for incompressible laminar boundary layer flow inside and outside of liquid spherical moving through liquid
19 p3086 N71-32378
Development of method for solving time dependent, viscous, incompressible fluid flow from observer to center of circle
21 p3414 N71-34391
Supersonic turbulent boundary layer step induced separation, and incompressible flow model for predicting upstream flow field in channel
21 p3414 N71-34391
Numerical analysis of laminar, incompressible flow along corner formed by intersection of two thin airfoils
[AD-726540] 22 p3538 N71-35201
Extended mixing length formulation for computing incompressible turbulent boundary layers on rough surfaces
[NRC-12000] 22 p3567 N71-35400
Singularity method for calculating incompressible potential flow in plane profile cascade stages
[NASA-TT-F-13982] 23 p3742 N71-36680
MUFAN program for determining processes, flow rates, and pressure drops in systems involving one dimensional incompressible steady state fluid flow
[NASA-CR-72943] 24 p3972 N71-37735
Incompressible shear turbulent boundary layer on end wall of curved two dimensional diffuser with aspect ratio of 1.5 and area ratio of 1.56
24 p3999 N71-37859

INCOMPRESSIBLE FLUIDS
Developing viscous dominated incompressible theory for describing dynamic velocity and pressure fields in film bearing gas lubricated disk
09 p1208 N71-19680
Numerical calculation of two dimensional flow of incompressible viscous fluid along traveling wave channel
11 p1736 N71-22219
Two dimensional unsteady flow of viscous incompressible conducting fluid in infinite channel in constant longitudinal magnetic field
11 p1797 N71-22220
Numerical solution of equations governing laminar flow of incompressible, non-Newtonian fluid through circular pipe with abrupt change in diameter
11 p1742 N71-22690
Flow and heat transfer characteristics of incompressible fluid in radial diffuser using air as fluid with inlet Reynolds numbers from 15 to 33,500 and area ratios from .245 to 2.04
16 p2583 N71-28894
Energy balance equation for turbulent pulsations of free turbulent boundary layer in incompressible fluid
[NASA-TT-F-13757] 17 p2577 N71-30180
Impact of the mildly sloping spherical shells on surface of ideally incompressible liquid
[NASA-TT-F-15576] 18 p3021 N71-30883
Perturbation of steady flow in viscous incompressible fluid noting nonlinear stability
[ONERA-PUBL-136] 19 p3076 N71-31609
Frequencies and modes determined for free vibrations of closed spherical shells submerged at various fluid depths
19 p3191 N71-32774
Theory of equilibrium figures of rotating, homogeneous, incompressible fluid mass as applied to cosmology
[NASA-SP-186] 20 p3252 N71-33591
Similarity solutions using free parameter technique for laminar flow of viscous, incompressible fluid between rotating coaxial surfaces of revolution
20 p3255 N71-33783
Effects of vertical convection on horizontal flow of incompressible doubly-stratified fluid
21 p3414 N71-34290
Two dimensional, steady state flow of incompressible viscous fluid, separating into layers about surface tension membrane
22 p3571 N71-35433
Effect of variable fluid properties on MHD flow in electrically insulated rectangular duct
24 p3993 N71-38502

INCONEL (TRADEMARK)
Microprobe analysis of diffusion layers with application to chromel-inconel Inconel 718
[ONERA-TP-836] 02 p0241 N71-11566
Fatigue tests on heat treated Inconel alloy having protective chromium plated surface layer
[NASA-TT-F-13484] 06 p1217 N71-19014
Microprobe scanning for analyses of protective chromium plated surface layer on Inconel turbine blades
[NASA-TT-F-13497] 06 p1218 N71-19027
Room temperature tensile properties and changes in microstructures of steel XCrVNiMoNbV1613 / 9808, Inconel 600, and Inconel 718 after aging at 680 to 800 C
[EURPFR-873] 18 p3933 N71-30907
Gaseous hydrogen embrittlement in Inconel 718, Inconel 625, A181 321 stainless steel, Ti-3Al-2.5Nb TiL, and OFHC copper
[NASA-CR-119977] 19 p3116 N71-33489
Isothermal corrosion tests on Inconel 600 and Inconel alloy sheets by cuprous chloride solution
[NLL-RISLEY-TRANS-2093-0091.9F]

INDEPENDENT VARIABLES

- 19 p3118 N71-32656
Destructive tests of Inconel 600 tube from N reactor
steam generator 6A
[DUN-SA-149] 20 p3309 N71-33933
Determination of thermal conductivity, electrical resistivity, Lorentz ratio, and thermopower for annealed specimens of Inconel 718 at temperatures from 4 to 300 K
[NASA-CR-121758] 21 p3437 N71-34452
Three types of uranium oxide-Inconel cladding interactions investigated by X ray fluorescence analysis of two fuel elements after high burnup in VAK reactor [NLL-WINDSCALE-459-9091.9F] 21 p3462 N71-34644
Boron effects on ductility and strength of Inconel 600 and Types 304 and 316 stainless steel at hot metal working temperatures
[ORNL-TM-3316] 22 p3594 N71-35591
Design data for regeneratively cooled panels from low cycle fatigue evaluation of Hastelloy X and Inconel 625 sheet and sandwich panel specimens
[NASA-CR-1884] 24 p4027 N71-38734
- ### INDEPENDENT VARIABLES
- #### NT LATTICE PARAMETERS
- Properties of continuous logic functions which generalize in out of a voting functions and threshold functions of binary variables to continuous variables
[AD-71257] 02 p1096 N71-11373
Algorithm for synthesis of distributed systems to solve circuit design problems
[NASA-CR-111809] 02 p1097 N71-11379
Asymptotic results for goodness-of-fit statistics with estimated parameters
[AD-71257] 04 p0537 N71-13820
Development of algorithms for parameter optimization problems including inequality constraints, noisy measurements, and locations of global optima
[REPT-70-E-14] 09 p1412 N71-20537
Perturbation theory using variation of parameters formulation to calculate satellite orbits
11 p1829 N71-22789
Linear time invariant optimal control feedback for closed loop stability in plant parameter variations
12 p1895 N71-24151
RSYN and JDB codes for flux and bulk parameter computation of fast reactors
[WHAN-IR-48] 12 p1964 N71-24152
Synthesis procedure for adaptive control systems for adjusting parameter vectors
[AD-71938] 13 p2060 N71-25140
Confidence intervals and significance tests for mean of symmetrical population with outlier observation not largest or smallest
14 p2282 N71-26590
Confidence intervals and significance tests for mean of symmetrical population with smallest or largest outlier observation
[NASA-CR-118509] 14 p2282 N71-26591
Nonparametric estimation of mean and variance in random sampling with observations of varying values
[NASA-CR-118512] 14 p2282 N71-26599
Computer simulation results of satellite antenna bore-sight parameter estimation
[AD-72022] 15 p2387 N71-27425
Mathematical determination of number of independent data equivalent to number of dependent data and application to meteorological data in USSR
[NLL-M-9263-5828.4F] 16 p2624 N71-29143
Process and additive noise independent variable estimation using iterative methods based on Gauss-Markov estimator
[TH-71-E-17] 18 p2889 N71-30588
Parametric effects on static and dynamic coefficients of friction of the osteopathic
[NLL-RISLEY-TRANS-1928-9091.9F] 19 p3105 N71-32169
Influence of parameter variability in shock layer on heat flux in nonequilibrium viscous flow of multicomponent gas near stagnation point of blunt body
21 p3412 N71-34277
Library tape for storage of model parameters of semiconductor devices
[SC-M-710210] 21 p3498 N71-34918
Parametric influences on stability of uncontrolled steam-cooled fast breeder reactors
[EURFNR-813] 22 p3622 N71-35806
Neutron resonance parameters of some nuclei for determining strength function
[CRA-R-3602] 22 p3635 N71-35906
Least squares fitting for parameter determination of empirical formula for interpolation of tabulated photon photoelectric cross sections
[ANL-7796] 23 p3814 N71-37197
- ### INDEXES
- System of prosecution indices for identification of environmental data associated with observation stations on earth surface
[NASA-CR-121661] 21 p3397 N71-34176
Analytical procedure for computation of military essentiality index for use as decision making aid by program managers
[AD-727114] 24 p4034 N71-38786
- ### INDEXES (DOCUMENTATION)
- #### NT KWIC INDEXES
- Thesaurus for high temperature research
01 p0132 N71-10038

SUBJECT INDEX

- Annotated bibliography and indexes on Aerospace Medicine and Biology - Sept. 1970
[NASA-SP-7011/80] 01 p0008 N71-10125
Bibliography and index of hurricanes and severe storms along coastal plains of US
[PUBL-70-2] 02 p0259 N71-11847
ORNL decentralized Nuclear Science Abstracts preparation, and cost and time comparison with centralized preparation
[PB-190501] 02 p0275 N71-11910
Earth Resources Research Data Facility Index
[NASA-TM-X-66487] 02 p0223 N71-12199
Annotated bibliography and indexes on Aerospace Medicine and Biology - Sept. 1970
[NASA-SP-7011/81] 03 p0322 N71-12303
Annotated bibliography and indexes on Aerospace Medicine and Biology - Nov. 1970
[NASA-SP-7011/82] 04 p0480 N71-14471
Annotated bibliography on plasma physics and controlled thermonuclear fusion
[TID-3557-SUPPL.] 05 p0754 N71-15196
Descriptions and indexes of data contained in Solar Geophysical Data publication
05 p0765 N71-15405
Indexes for bibliography on meteorology, climatology, and oceanography of Caribbean Sea region
[AD-713493] 05 p0678 N71-15505
Index of seismic data for Pacific Ocean
[PB-192332] 05 p0679 N71-15525
Subject and author index on aeroseismicity documents
[AGARD-R-578-71] 07 p0967 N71-17432
Annotated bibliography and indexes on Aerospace Medicine and Biology - Nov. 1970
[NASA-SP-7011/83] 07 p0982 N71-17449
Annotated bibliography and indexes on Aerospace Medicine and Biology - Dec. 1970
[NASA-SP-7011/84] 07 p0982 N71-17450
Annotated bibliography of scientific and engineering work performed at JPL up to Aug. 1970
[NASA-CR-116543] 07 p1068 N71-17758
Selected bibliography of published papers on Survey
07 p1026 N71-18000
Surveying commercially available tape services of reference information on scientific and technical literature
[AD-71257] 08 p1165 N71-18695
Comparative analysis of natural languages and controlled vocabularies for information indexing and retrieval
[AD-716200] 09 p1488 N71-19941
Index of documentations on numerical calculations for algebraic and transcendental equations
[ORNL-4595] 09 p1411 N71-20382
NBS data index of physical properties of metals and alloys
[NBS-SPEC-PUBL-324] 10 p1572 N71-20850
Calibration and test service documentation for National Bureau of Standards
[NBS-SP-250] 12 p1895 N71-23123
Tabulation of B-57 aerial cloud photography of tropical convection systems for 11 to 28 July 1969 with flight path over Barbados Islands
[ESSA-TM-ERLTM-BOMAP-11] 12 p1921 N71-23746
Tabulation of international locations of rapid-run geomagnetic micropulsation stations
[DI-82-1043] 13 p2078 N71-25527
Annotated bibliography and indexes on Aerospace Medicine and Biology - March 1971
[NASA-SP-7011/87] 14 p2203 N71-25745
Relevance decision effects on comparative performance of index languages for information retrieval subsystem tests
[OSTI-5049] 14 p2357 N71-25752
Conditional equations for determining fundamental catalog systems from major and minor planet observation
[JPRS-53109] 14 p2336 N71-25951
Method of storing inverted file with minimum storage space and low access time for quick retrieval of nonnumerical data by computers
14 p2221 N71-25980
Computer patent searching system with automatic indexing using word truncation and similar query in on-line mode
14 p2221 N71-25981
Automatic dictionary for creating indexes for information retrieval through computer programs
14 p2222 N71-25985
Compilation of dictionaries for information retrieval systems from vocabularies from different fields of science
14 p2223 N71-25990
Strategies for searching in data bank files adapted to query and file structure and use of thesauri with small and medium computers
14 p2223 N71-25993
Dynamic characteristics of dictionaries and documentation indexes for information retrieval
14 p2223 N71-25994
EURATOM automatic documentation system, noting structure of index, information retrieval strategies, and performance evaluation
14 p2223 N71-25995

- Research in nuclear physics and chemistry and reactor technology and instrumentation
[INR-1180] 15 p2494 N71-27951
Index to NASA 1970 Tech Brief
[NASA-SP-5021/11/1] 16 p2894 N71-28119
Humboldt system thesaurus containing words and phrases which reflect concepts to be indexed in human factors engineering information retrieval system
[AD-721657] 16 p2530 N71-28339
Index for retrieving information on Permutal Technology and Radiation Technology - Vol. 7
[ORNL-3C-31-VOL-5-1-7] 17 p2793 N71-29478
Activation analysis bibliography up to 31 Jan. 1971 including chemical element, methodology, matrix analysis, and author indexes
[NBS-TN-467-PT-2] 17 p2717 N71-30267
Annotated bibliography and indexes on Aerospace Medicine and Biology - Apr. 1971
[NASA-SP-7011/88] 18 p2876 N71-30836
Cumulative index for abstracts of NASA documents on aerospace medicine and biology
[NASA-SP-7011/85] 18 p2876 N71-31077
Annotated bibliography and indexes on aerospace medicine and biology - May 1971
[NASA-SP-7011/89] 18 p2876 N71-31201
Annotated bibliography and indexes on Aerospace Medicine and Biology - May 1971
[NASA-SP-7011/90] 18 p2876 N71-31228
Annotated bibliography and indexes on Aerospace Medicine and Biology - June 1971
[NASA-SP-7011/91] 18 p2877 N71-31231
Radioactive isotope, accession number, and neutron-induced reaction indices for data retrieval
[UCRL-50400-VOL-3] 18 p2990 N71-31536
Basic scientific publications on chemistry and chemical engineering promoting international cooperation in information dissemination
19 p3194 N71-31981
Index for hearings before Committee on Science and Astronautics, US House of Representatives, during Ninety-Second Congress
20 p3371 N71-33801
Personal and information index for proposed 1972 hearings before Committee on Science and Astronautics of United States Congress
20 p3371 N71-33801
Abstracting and indexing periodicals in field of physical sciences
[ISS-70/21] 20 p3371 N71-33975
Computer system and processing of chemical data for subject indexes and index files
21 p3387 N71-34091
Computer system for recording and organizing information in subject indexes of chemical documents
21 p3387 N71-34094
Organization of subject index for chemistry and conversion from manual to computerized system
21 p3387 N71-34095
Computerized processing of chemical data for indexes and index files
21 p3387 N71-34096
Catalog of reprints of scientific papers in Pauli collection with author index and cross references
[CERN-BIB-8] 21 p3473 N71-34731
Catalog of earth tide stations
22 p3573 N71-35448
Safety aspects of nuclear reactor design, materials, engineered safeguards, and operating procedures - bibliography
[TID-3525-REV-5-SUPPL-6] 22 p3626 N71-35834
Computer based cataloging and subject indexing system
[REPT-22] 22 p3699 N71-36301
Annotated bibliography and indexes on Aerospace Medicine and Biology - Aug. 1971
[NASA-SP-7011/92] 23 p3716 N71-36400
Annotated bibliography and indexes on Aerospace Medicine and Biology - Sept. 1971
[NASA-SP-7011/93] 23 p3716 N71-36401
- ### INDEXES (RATIOS)
- Computer performance test program for assessing complex indexing operations
[NBS-TN-572] 13 p3049 N71-26580
Calculation of noninferior performance index vectors from N scalar index elements
21 p3450 N71-34518
- ### INDIA
- Solar and geophysical data related to ionospheric studies from India - tables
[RRC-A178-PT-2] 01 p0117 N71-10178
Satellite measured albedo and long wave radiation study of Indian monsoons
02 p0256 N71-11822
Summary of prominence and calcium flocculus observations at Kodanthal Observatory Jan. through June 1964 - tables and graphs
[BULL-174] 03 p0451 N71-13597
Physical properties and absolute age determination for some rocks of India and Ceylon
[NASA-TT-F-13416] 05 p0670 N71-14819
Nimbus 3 satellite observations of ozone associated with easterly jet stream over India during 1969 summer monsoon
[NASA-TM-X-65416] 06 p0849 N71-15941

SUBJECT INDEX

- Mathematical model for global solar radiation distribution over India 15 p2439 N71-27521
- Temperature inversion near ground observed at Poona (India) 15 p2440 N71-27549
- Indian atomic energy and nuclear research [DAE-AR-70] 17 p2794 N71-29652
- Statistical analysis of periodic variations of wind shear vertical distribution in lower atmosphere at Thambai airport tower, India 18 p2950 N71-30833
- Meteorological and atmospheric electric data from Bombay observatory for 1967 20 p3269 N71-33969
- Hourly values of ionospheric propagation data for India - June 1969 [RTRC-A169] 21 p3416 N71-34308
- Hourly values of ionospheric propagation data for India - July 1969 [RTRC-A170] 21 p3416 N71-34309
- Indian Ocean bathymetry, morphology, and bathymetry of central Arabian-Indian ridge (AD-716271) 09 p1584 N71-19509
- Climatic, meteorological, and oceanographic conditions associated with monsoon season in Indian Ocean determined by Nimbus satellite observations (AD-717391) 11 p1745 N71-21938
- Cloud distribution over Indian Ocean at beginning of monsoon deduced from Nimbus 2 satellite radiation measurement 15 p2438 N71-27497
- Geomagnetic, bathymetric, and gravitational field data from Indian Ocean 1964 survey 18 p2919 N71-31432
- Relative water transparency of Indian Ocean waters. Antarctic waters, affected by plankton concentration and surface currents (AD-727857) 24 p3916 N71-37926
- Indiana Airport study for Vigo County, Indiana with data book of airport activity for past 10 years (PB-197269) 17 p3730 N71-29721
- INDICATING INSTRUMENTS
- NT ANEMOMETERS
- NT APPROACH INDICATORS
- NT ATTITUDE INDICATORS
- NT CLOUD HEIGHT INDICATORS
- NT FLOW DIRECTION INDICATORS
- NT GYRO HORIZONS
- NT GYROCOMPASSES
- NT HOT-FILM ANEMOMETERS
- NT HOT-WIRE ANEMOMETERS
- NT MICROBALANCES
- NT MICROWAVE SENSORS
- NT POSITION INDICATORS
- NT RADIO DIRECTION FINDERS
- NT SPACECRAFT POSITION INDICATORS
- NT TACHOMETERS
- NT WEIGHT INDICATORS
- NT WIND VANS
- Inductive liquid level detection system [NASA-CASE-XLE-01609] 01 p0054 N71-10500
- Address indicator for pressure scanner [ARLMI-314] 05 p0689 N71-15377
- Apparatus for determining quality of bond between high density material and low density material [NASA-CASE-MPS-15486] 07 p1038 N71-18132
- Standards for clean rooms in vacuum electronics manufacturing for precision instruments [JPRS-52528] 09 p1368 N71-20350
- Silicon carbide semiconductor diode light source for indicator elements (AD-716941) 10 p1535 N71-21387
- Performance tests and characteristics of four fog detecting instrument systems operating under natural atmospheric conditions [NBS-10186] 11 p1762 N71-22454
- Design and operation of linear gas discharge indicator permitting continuous visual monitoring of magnetic variations [JPRS-53182] 14 p2239 N71-26466
- Environmental and materials contamination including detection and control methods for production engineering [SC-M-70-303] 17 p2739 N71-29449
- Inventory of automatic sampler-analyzers, mechanized samplers, and static samplers used for air pollution monitoring in US and Puerto Rico [EP-198329] 21 p3420 N71-34334
- Depolarized shifted cyclotron resonance absorption of helium waves in indium and GaAs-Kanar oscillations 15 p2477 N71-27577
- Lead injected superconductivity into indium for measurement of current through indium as function of temperature above transition temperature 16 p2666 N71-28771
- Determining fast and thermal neutron fluxes by copper and indium foil activation analysis [EP-1466] 17 p2794 N71-29631

INDUCTANCE

INDIUM ARSENIDES

- Pseudopotential calculations of band structure of GaAs, InAs, and GaIn/As alloys 01 p0108 N71-10134
- Characteristics of indium arsenide-phosphide injection lasers (AD-715434) 08 p2110 N71-18885
- Entropy, heat of formation, and feasibility of indium and gallium arsenides and antimonides [NPL-DCS-8] 10 p1660 N71-20656
- Transition of solid indium arsenide-gallium arsenide solutions to thermodynamic equilibrium states [NLL-BRE-TRANS-282-28036423] 10 p1636 N71-21706
- Preparation and characteristics of indium arsenide films grown by coplanar chemical transport used for commercial production of thin film Hall generators 11 p1614 N71-21939
- Electron tunneling characteristics of metal contacts on a-type CdTe and p-type InAs 19 p3071 N71-32466
- Measurement of Hall coefficient for indium arsenide and indium antimonides at low temperatures and various magnetic fields 20 p3334 N71-33940

INDIUM COMPOUNDS

- NT INDIUM ANTIMONIDES
- NT INDIUM ARSENIDES
- NT INDIUM PHOSPHIDES
- Impurity behavior during zone melting of lower indium chlorides 10 p1574 N71-20877
- Studying vaporization of indium-gallium oxide, and gallium-aluminum oxide by Knudsen effusion mass spectroscopy [NASA-TN-D-6318] 12 p1868 N71-23111
- Electrochromic quantum efficiency of gallium arsenide phosphide, gallium indium phosphide, and aluminum arsenide diodes (AD-720864) 15 p2508 N71-27901
- EMF measurements of indium oxide from energy of formation between 790 and 1230 K using aluminum electrolyte galvanic cell [BML-RL-7549] 22 p3350 N71-33289

INDIUM ISOTOPES

- Elastic and inelastic proton scattering functions from Cd-110, Cd-112, and Cd-114 based on shell theory and elastic scattering indium isotopes for isotopic analog resonances 13 p2138 N71-25473
- Capture cross sections in keV region versus energy curves to determine gamma ray strength, S wave neutron strength, and P wave neutron strength in silver, iodine, and indium isotopes 15 p2479 N71-27634
- Quasiparticle model for calculating energy spectra of indium isotopes [UJV-2540-P] 19 p3140 N71-32310

INDIUM PHOSPHIDES

- Electrochromic semiconductor material of indium gallium phosphide 01 p0108 N71-10131
- Indium gallium phosphide analysis by X ray fluorescence and diffraction 01 p0109 N71-10211
- Electron mobility of indium arsenide phosphides for charge carriers 01 p0109 N71-10212

INDOLES

- Cyclization of ortho-isocyanobiphenyl and derivatives with insertion of isocyanate carbon to form cycloheptimides [NASA-CR-123190] 24 p3884 N71-37606

INDUCED FLUID FLOW

U FLUID FLOW

INDUCERS

U INTAKE SYSTEMS

INDUCTANCE

- Design and performance of inductive voltage divider for measuring alternating current ratios [NLL-MIN-TECH-T-6745-5669-94] 12 p1891 N71-24163
- Parallel circuit analogy for skin effect in conductors [AD-719234] 13 p2123 N71-24394
- Pulsed superconducting magnet, niobium/titanium wire solenoid, ac transmission loss, degradation effect, and inductance measurements for ac dipole conductors [KFK-1217] 13 p2125 N71-24999
- Trigger pulse energy, electrode dimension, gas pressure, and prepulse voltage effects on low inductance spark gaps for high voltages in air [BML-W-FBK-70-17] 15 p2455 N71-27633
- Eddy current measurements using coil encircling coaxial two-conductor rod and solution of electromagnetic induction problem 19 p3071 N71-32327
- Analysis of internal inductances in current carrying circular conductors in relation to outer inductance for unit and parallel representation of inductances [NLL-BE-TRANS-19313774.5] 21 p3406 N71-34235

- Device for measuring induction produced by accelerated particle beam developed for synchrotron
[NP-1839] 23 p3809 N71-37157
- INDUCTION**
Computer program for inductive inference problems in organic chemistry
[NASA-CR-123182] 24 p3947 N71-38155
- INDUCTION [MATHEMATICS]**
Procedure for comparing theory conclusions and observed data facts in hypothesis assessing
[NASA-CR-111335] 01 p0139 N71-10980
- INDUCTION HEATING**
Laboratory tests on induction plasma torch with curved permeable walls and solid feed system
[NASA-CR-1764] 09 p1420 N71-20142
Influence of heating methods on efficiency of directed crystallization of germanium in vacuum apparatus
10 p1633 N71-20887
Induction heating of metallurgical specimens to high temperatures in coil furnace
[NASA-CASE-XLE-04026] 12 p1917 N71-23267
Nondestructive testing of composites and ceramics to determine surface defects by infrared and induction heating methods
[WHAN-SA-42] 13 p2101 N71-25215
Induced fields and static heating patterns within multilayer spherical model of primate cranial structure
[AD-720589] 14 p2205 N71-26168
Radial temperature distribution of uranium oxide pellet maximum temperature zone based on induction heating simulation of reactor core
[ETENG-78/11] 17 p2782 N71-29505
Stability of synchronized induction motors with phase compensating system using digital computer
[NLL-RTS-6232] 17 p2725 N71-29662
Vortex and coaxial flow of argon and helium plasmas heated inductively, and strong magnetic field effects on turbulent plasma mixing, for gas core reactors
20 p3330 N71-33635
Radio frequency induction heating plasma generator design and fiber optic scanner for simulation of nuclear light bulb engines
20 p3305 N71-33659
Techniques for solving Maxwell equations and applications in induction heating and electromagnetic prospecting
21 p3403 N71-34216
Induction plasma calcining of pigment particles for thermal control coatings on space vehicles
[NASA-CR-119931] 22 p3694 N71-36345
Static inverters equipped with thyristors for medium frequency induction heating
[NLL-RISLEY-TRANS-2128-9091.9F] 23 p3733 N71-36614
- INDUCTION SYSTEMS**
U INTAKE SYSTEMS
INDUCTORS
Inductive liquid level detection system
[NASA-CASE-XLE-01609] 01 p0054 N71-10500
Two dimensional nonlinear numerical solution of solid rotor induction motor
[AD-711570] 02 p0195 N71-11369
Electrical and magnetic field calculation for linear accelerator inductor
[JIDR-PB-5129] 04 p0567 N71-14234
Open-construction transformers and inductors for SERT 2 power conditioners
06 p0941 N71-16640
Describing apparatus used in vacuum deposition of thin film inductive windings for spacecraft microcircuitry
[NASA-CASE-XMF-01667] 07 p1035 N71-17647
Periodically reverse-switched capacitors or inductors in feedback networks, resulting in linear subharmonic filter
11 p1725 N71-22694
Nondestructive inductor techniques for Barkhausen effect study
[AD-718426] 12 p1927 N71-23799
Double induction variable speed system for constant-frequency electrical power generation
[NASA-CASE-ERC-10065] 15 p2387 N71-27364
Superconducting inductive energy accumulator as standby electrical energy source, as energy source for load factoring in power systems, or as source for high powered electric pulses
23 p3710 N71-36448
- INDUSTRIAL MANAGEMENT**
NT ENGINEERING MANAGEMENT
NT INVENTORY MANAGEMENT
NT PERSONNEL MANAGEMENT
Organizational structure effects on supervisory style and industrial work group attitudes
[PB-196467] 10 p1666 N71-21698
Cost distributions and facility and tooling cost impact on unit production costs for 2 and 20 per year production rates in state of art, improved, and advanced manufacturing technologies
[NASA-CR-114281] 12 p1931 N71-24180
Economic analysis of facilities, tooling, premanufacturing and manufacturing operations, and quality

- control labor in aluminum aerospace industry base on Saturn/Apollo data
[NASA-CR-114282] 12 p1931 N71-24181
Manufacturing factors and technologies in aluminum aerospace industry base on Saturn/Apollo data
[NASA-CR-114283] 12 p1931 N71-24182
Comparison of productivity of scientific work industrial production in USSR
[AD-723207] 17 p2862 N71-30277
- INDUSTRIAL PLANTS**
NT POUNDRIES
Differences in policies and practices of DOD, AEC, and NASA in paying corporate expenses at government-owned contractor-operated plants
01 p0135 N71-10013
Survey of accidents at air separation plants
[NASA-TT-F-13388] 03 p0384 N71-12657
Studying neutron ejected beam units for industrial neutron radiography on research reactors
[CEA-CONF-1543] 03 p0431 N71-12913
Analysis of disturbances in industrial operations and resulting effects on production systems determined by cybernetic methods
03 p0386 N71-12364
Applying basic tools and techniques of industrial engineers to systems engineering
[WAFD-T-2311] 04 p0502 N71-13511
Industrial scale ion implantation facility
[AERE-R-6496] 06 p0829 N71-15717
Air pollution sampling in vicinity of ammunition plant
[PB-195145] 07 p1015 N71-16996
Hygienic effects of toxic chemical pollution on biosphere
07 p0981 N71-17431
Calculating rate of change in reactivity of BR-5 reactor for application to industrial operations
08 p1241 N71-18791
Describing operating characteristics and costs of air-cooled heat exchangers and condensers for industry
08 p1304 N71-18812
Manual of electrostatic precipitator installations in various application areas
[PB-196381] 10 p1568 N71-21812
Techniques and equipment for industrial air pollution monitoring and sampling
[JPRS-52566] 11 p1747 N71-22055
Description of techniques used in design of cold rolling mills for optimum operation
[AD-717401] 11 p1767 N71-22137
Survey of group of industrial organizations to determine pertinent properties, policies, and practices related to Federal procurement
[NASA-CR-117899] 12 p2015 N71-23251
Survey to determine social aspects of labor organization and management in scientific teams
[NASA-TT-F-13552] 12 p2015 N71-23310
Contributions and effects of commercial airline service on growth of manufacturing facilities in urban areas below 40,000 population
14 p2199 N71-26529
Analysis of electrostatic precipitator systems application in industrial dust control
[PB-198150] 17 p2755 N71-29805
Susceptibility or resistance to gas and smoke of various arboreal species grown under diverse environmental conditions in industrial regions
[PB-198063] 17 p2742 N71-29832
Analysis of impact of conversion to metric measurements on US industries
[NBS-SP-345-4] 18 p2930 N71-31386
Maximum permissible failure probability for test interval optimization of defective standby systems in industrial plants
[NLL-RISLEY-TRANS-2004-9091.9F] 19 p3196 N71-32299
Aerial photographic tracing of pulp mill waste plumes used to study waste disposal sites
[PB-198232] 19 p3096 N71-32636
Comparison of risk of death by meteoroids, weather, or supernovae and electrification in industry
[P-4602] 19 p3199 N71-32708
Optimal feedback controller design based on model for linear plant of unknown characteristics under stochastic environment
24 p3951 N71-38186
- INDUSTRIAL SAFETY**
Survey of accidents at air separation plants
[NASA-TT-F-13388] 03 p0384 N71-12657
Nuclear fuels processing plant application of criticality prevention principles
[ARH-SA-71] 06 p0897 N71-15945
Industrial noise and countermeasures - research methods and measuring devices
[AD-720414] 14 p2296 N71-25878
Susceptibility or resistance to gas and smoke of various arboreal species grown under diverse environmental conditions in industrial regions
[PB-198063] 17 p2742 N71-29832
Effects and symptoms of air pollution on vegetation noise resistance and susceptibility of various plant species in various habitats and relation to plant utilization for shelter belts
[PB-198062] 17 p2742 N71-29833

- INDUSTRIES**
NT AEROSPACE INDUSTRY
NT AIRCRAFT INDUSTRY
NT DEFENSE INDUSTRY
Selective bibliography of water and air pollution for business and industry
[PB-192318] 02 p0152 N71-11078
Conference on nuclear technology application in industries
[PB-193582] 02 p0272 N71-11740
Systems analysis for data processing in industries
04 p0508 N71-13528
Thin films applied to optical, metallurgical, and electronic industries
05 p0708 N71-15854
Consumption statistics for antimony in industry
[NMAB-274] 07 p1043 N71-17519
Military and industrial management of independent research and development programs
07 p1133 N71-17632
Government planning in technological society
07 p1135 N71-18071
Federal role in development of synthetic rubber, civilian atomic energy, and communications satellite industries with implications for marine resource development program
09 p1487 N71-19498
Computer developments in USSR and industrial applications in automation and information processing
[JPRS-52809] 12 p1081 N71-23444
Industry automatic control system design
12 p1885 N71-24211
Performance characteristics of US information retrieval and management information systems, noting heuristic methods and incentive techniques
14 p2223 N71-25996
Theory and operation of air cushion vehicles and other application of ground effect in industrial transportation
15 p2367 N71-27196
Relief, safety, and cryogenic check valve systems engineering with industrial applications
[NASA-SP-5927/01] 16 p2600 N71-28282
Utilization of measuring methods and devices in general industrial applications
[NASA-SP-5928/01] 16 p2601 N71-28482
Bibliography on industrial arc welding of metals
[AD-72265] 18 p2927 N71-30731
Management planning, production planning, and standardization in industries and civil organizations
[IVA-23] 18 p3029 N71-31177
Selected abstracts of world literature on production and industrial uses of radioisotopes
[ORNL-ITC-30-PT-4] 18 p2990 N71-31545
Experimental research in radiation chemistry and industrial applications
[JAERI-5026] 18 p2990 N71-31545
Epoxy paint and varnish materials for industrial applications
[AD-723425] 19 p3118 N71-31674
Employment problems from specialization in university research and industries through government funding
19 p3196 N71-32253
Congressional testimony of nationally representative groups regarding US conversion to metric system
[NBS-SP-345-12] 19 p3196 N71-32352
Magneto-hydrodynamic generator development and applications in radiating power plants, propellant-cooled propulsion systems, and industry
20 p3306 N71-33661
Data on production, consumption, and resources of helium in US as of 31 Dec. 1969
20 p3231 N71-33990
Government, industry, banking, conservation, and law in preservation of environmental quality
[NASA-CR-121637] 21 p3414 N71-34294
Compilation of papers on applications of mathematics and computer programs for industry related problems
[NASA-SP-5939/01] 21 p3447 N71-34332
Organization and services of Danish ATV university committees and industrial institutions for scientific and technological research and applications
21 p3532 N71-35172
Development and distribution of natural resources to satisfy energy requirements of US industry during the 1970's
[BM-IC-8526] 22 p3700 N71-34980
- INELASTIC BODIES**
U RIGID STRUCTURES
INELASTIC COLLISIONS
Analytic formulas for inelastic cross sections for collisions of protons and hydrogen atoms with atomic and molecular gases
[AD-711661] 01 p0096 N71-10018
Neutron spectra calculations from proton-nucleus inelastic collisions for 15 to 18 MeV protons
[NASA-CR-111411] 02 p0272 N71-11780
Extending cascade-evaporation model of ion-atom interactions of particles with nuclei to light nuclei
[ORNL-TR-2373] 06 p0914 N71-15970
Nuclear stripping reactions involving strongly deformed nuclei, and including inelastic processes
[UCRL-19529] 06 p0918 N71-16181

SUBJECT INDEX

Inelastic interactions of particles and nuclei at high and superhigh energies
[JINR-E2-5282] 08 p1248 N71-18199

Angular energy distribution of particles produced in inelastic pion-nucleon and nucleon-nucleon collisions at superhigh energies
[JINR-E2-5331] 09 p1433 N71-19976

Nuclear model for proton proton and pion proton inelastic collisions based on secondary emission and form factors
[JINR-P-1229] 13 p2129 N71-24686

Straight line particle paths approximation for description of high energy elastic and inelastic hadron scattering in quantum field theory
[JINR-E2-5217] 14 p2311 N71-26696

Generalized phase shift approach to problem of relativistically inelastic molecular collisions
[NASA-CR-119029] 16 p2654 N71-29038

Monochromatic, positive ion beams passed through inert gas and analyzed by mass spectroscopy
[AD-723588] 19 p3144 N71-31748

Spin analysis of direct and exchange scattering amplitudes for describing differential inelastic electron-potential collisions
20 p3323 N71-33814

Classical trajectory study of rotationally inelastic scattering of hydrogen molecules by collisions with lithium ions
[NASA-CR-121729] 21 p3386 N71-34087

Numerical analysis of inelastic scattering of neutrons from Li-7 using distorted wave Born approximation
21 p3492 N71-34876

Disappearance of inelastic channel of nuclear reaction in resonant nuclear scattering of gamma rays in perfect crystal
[IAB-1966] 22 p3640 N71-35948

Cross sections of high energy inelastic reactions in neutron proton interactions and separation of reaction channels
[JINR-P-5665] 22 p3641 N71-35960

Digital simulation of energy spectra and mean inelastic coefficients of high energy particle interactions
[J7-3] 23 p3808 N71-37152

INELASTIC SCATTERING

Scattering of 42-MeV alpha particles from Sc-45
[NASA-TM-X-52912] 01 p0095 N71-10392

Neutron elastic and inelastic scattering cross sections for silicon in energy range 4.19 to 8.56 MeV
[ORNL-4517] 01 p0099 N71-10718

Numerical values for neutron elastic and inelastic scattering cross sections from sulfur
[ORNL-4529] 01 p0103 N71-10960

Excitation of Si-28 particle-hole states by inelastic electron scattering at high momentum transfer
[AD-72083] 02 p0276 N71-12061

Neutron elastic and inelastic scattering cross sections for Fe-56 in energy range 4.19 to 8.56 MeV
[ORNL-4515] 03 p0425 N71-12832

Nuclear models used for studying nuclear reactions, nuclear fusion, inelastic scattering, and charge exchange - conference
[ANS-RD-2] 03 p0426 N71-12852

Free nucleon inelastic interactions including multiplicity of charged particles, distribution over multiplicity, and angular distributions
[JINR-P-5072] 03 p0427 N71-12860

Angular distributions for elastic and inelastic scattering of alpha particles by Mg-26
[RLO-1388-110] 03 p0428 N71-12863

Elastic and inelastic scattering of 26.5 MeV alpha particles on Si-28, P-31, and S-32 nuclei
[BNP-6997LE] 03 p0432 N71-12934

Inelastic scattering cross sections for electrons scattered from atoms
04 p0570 N71-13599

Measuring 2 pion inelastic scattering cross sections at 1 GeV invariant mass
[UN-511-74-70] 04 p0576 N71-13689

Using numerical techniques to calculate inelastic response of primary containment to high energy asymmetric excitation
[ANL-7499] 04 p0584 N71-14187

Braking inelastic backscattering of low-energy electrons from tungsten surfaces
[AD-713056] 04 p0590 N71-14376

Increasing maximum energy and improving beam intensity of 85 MeV linear electron accelerator at Amsterdam
05 p0637 N71-14529

Measuring energy spectrum of electrons from C-12 up to 16 MeV for three different excitation combinations at each of three values of momentum transfer
05 p0735 N71-14532

Measuring inelastic electron scattering form factors for proton excited states in vanadium 51
05 p0736 N71-14533

Slow neutron inelastic scattering in materials testing reactor
[R-1427] 05 p0737 N71-14671

Calculating resonance contributions to deep inelastic electron scattering using semiempirical model of nucleus spectrum
[NYO-4076-9] 05 p0742 N71-15123

Broken scale invariance and kinematics moments of electron-production cross sections
[ORO-2504-159] 06 p0914 N71-15971

Partial cross sections for final states corresponding to 4 and 2 prong plus vee topologies in K/p+/- inelastic channels
[CALT-48-274] 06 p0916 N71-16023

Inelastic electron scattering experiments
[SLAC-PUB-796] 06 p0916 N71-16055

Applying generalized phase shift approach to rotational excitation problem to atom-rigid rotor case in first order approximation
[NASA-CR-116134] 06 p0916 N71-16093

Realistic interactions and exchange effects in microscopic descriptions of elastic and inelastic nucleon scattering
[TID-25304] 06 p0919 N71-16245

Measuring alpha-gamma angular correlations from reaction Mg-24(alpha, alpha') gamma/Mg-24 at incident alpha particle energy of 16.65 MeV
[JCTC-43] 06 p0920 N71-16257

Electron interaction with matter and differential cross section measurements for bremsstrahlung produced in coincidence with inelastically scattered electrons
[NASA-CR-102994] 06 p0922 N71-16599

Inelastic lepton hadron scattering cross sections
[IPVE-STF-70-4] 08 p1247 N71-18191

Pseudostatistical time of flight method for scattering experiments with slow neutrons
[KFK-1126] 08 p1249 N71-18204

Measuring differential cross sections for inelastic electron scattering from calcium, titanium, and iron isotopes
[AD-715647] 08 p1253 N71-18331

Investigating violation of CP invariance in electromagnetic interactions of hadrons
[UCRL-20041] 08 p1259 N71-18659

Single particle mode peak of inelastic neutron scattering cross section for antiferromagnetic chromium at low temperatures
[NUB-2040] 08 p1279 N71-18689

High energy elastic and inelastic hadron-hadron scattering in phi-cubed theory
[ILL-TRH-71-4] 08 p1261 N71-18803

Fast neutron inelastic scattering measurements to determine gamma ray production cross sections
[CEA-R-4047] 09 p1433 N71-19988

Angular distribution calculations of elastic and inelastic proton scattering by C-12 with allowance for wave function distortion in multipole formalism
[ITF-70-50] 09 p1440 N71-20296

Elastic and inelastic scattering of atoms and ions, and sources of interference patterns
[SRIA-115-P-78-6] 09 p1440 N71-20363

Integral test of inelastic scattering cross sections using measured neutron spectra from thick shells of Ta, W, Mo, and Be
[NASA-TM-X-52979] 09 p1444 N71-20457

Graphical investigation and vector meson dominance of inelastic electron proton scattering
[LPTHE-70/49] 09 p1446 N71-20574

Neutron elastic and inelastic scattering cross sections for yttrium in 4.19 to 8.56 MeV energy range
[ORNL-4552] 10 p1615 N71-21037

Highly inelastic electron scattering theories
[SLAC-PUB-843] 10 p1615 N71-21052

Determination of physical characteristics of crystal surfaces by observation of elastic and one-photon inelastic scattering of atomic beams from surfaces
[AEEP-3824-101-70U] 10 p1636 N71-21752

Experimental and theoretical aspects of inelastic electron-nucleon scattering
[SLAC-PUB-842] 11 p1803 N71-22248

Hadronic helicity in diffractive region of inelastic lepton nucleon reactions
[NYO-4204-10] 12 p1971 N71-23879

Proton inelastic polarization and asymmetry calculations by Thomas spin interaction model
[RLO-1388-600] 12 p1972 N71-23896

Chiral dynamics calculations of single pion production in pion-nucleon inelastic scattering
12 p1975 N71-24049

Systematization of inelastic interactions of high energy pions and nucleons with atomic nuclei
[ORNL-TR-2399] 12 p1976 N71-24168

Quark parton model for deep inelastic lepton-hadron scattering
[LPTHE-71/12] 12 p1979 N71-24343

Proceedings from conference on inelastic neutron scattering with emphasis on collective excitations in disordered and magnetic systems, and lattice dynamics of high polymer substances
[JAERI-1197] 13 p2130 N71-24839

Asymmetric measurement of inelastic scattering of polarized protons by Ca 40 at 24.5 MeV
[CEA-COMP-1456] 13 p2134 N71-25177

Elastic and inelastic proton scattering functions from Cd-110, Cd-112, and Cd-114 based on shell theory and elastic scattering indium isotopes for isobaric analog resonances
13 p2138 N71-25473

Effect of transverse momentum distribution in parton model for inelastic lepton-nucleon scattering
[SU-1206-225] 13 p2140 N71-25501

INELASTIC SCATTERING

Calculations for structure functions of inelastic electron-proton scattering in perturbation theory for quantum electrodynamics with massive photons
14 p2504 N71-26202

Invariant momentum transfer required dependence of inelastic e-p scattering structure functions
[SU-1206-236] 14 p2504 N71-26208

Prediction of neutron inelastic scattering by nuclei using Hauser-Feshbach theory and scattering coefficients
[AABC/TK-545] 15 p2459 N71-26945

Report of experiments including neutron polarization, elastic and inelastic scattering of neutrons on C-12, and angular distribution of fission fragments in U-238 neutron reaction
[BNBW-FBK-70-14] 15 p2459 N71-27047

Nucleon models for interpretation of deep inelastic electron-nucleon scattering
[DESY-70/50] 15 p2463 N71-27172

Inelastic diffractive neutral pion photoproduction via diffractive rho-isobar production and Compton scattering
[DESY-70/45] 15 p2467 N71-27303

Atomic and molecular motions in oriented polytetrafluoroethylene studied by slow neutron inelastic scattering to obtain dispersion relations
15 p2472 N71-27439

Multiple scattering model for inelastic processes and nonrelativistic high energy forward and backward scattering
[IRB-TF-2-70] 15 p2485 N71-27816

Differential cross sections of elastic and inelastic angular distributions of neutrons scattered from C-12 and excited states of C-13 at angles from 15 deg to 155 deg
15 p2489 N71-27884

Time of flight method for studying fast neutron elastic and inelastic scattering on B-10 and B-11 to 5 MeV energy region
[A WKE-O-45/70] 15 p2489 N71-27885

Polarization of protons inelastically scattered on Mg-24, Cr-52, and Ni-58
[INP-18552] 15 p2490 N71-27894

Inelastic energy loss spectra for proton impact on helium atoms
15 p2493 N71-27942

Comparison of spectrometers for inelastic neutron scattering measurements
16 p2595 N71-28702

Differential production cross section for pions and differential inelastic cross section for protons in proton-proton collisions at 12.4 GeV/c
16 p2651 N71-28957

Experimental and theoretical research on elastic and inelastic neutron scattering cross sections
[COO-1573-71] 16 p2654 N71-29047

Calculation of neutron elastic and inelastic scattering cross sections and spatial transverse correlation functions for Heisenberg theory of impure ferromagnets
[BNL-TR-390] 16 p2658 N71-29144

Inelasticity and N/D calculations including Regge type amplitudes, highly inelastic resonance with circular Argand plot, and constraints on channel models of P-11 state
16 p2658 N71-29147

Photoabsorption and inelastic scattering cross sections for photon proton and neutron high energy interactions and Compton effects
[UCSB-34-P-135-14] 17 p2790 N71-29250

Model for intranuclear cascades in light nuclei with allowance for direct interactions of cascade protons
[ORNL-TR-3452] 17 p2793 N71-29525

Highly inelastic scattering of medium energy He-3 and He-4 particles by Sn, Ta, Pt, Au, and Pb nuclei
17 p2809 N71-30377

Inelastic high energy electron scattering by light nuclei accompanied by knockout of nucleons
[ITF-70-38] 18 p2970 N71-30445

Computation of elastic and inelastic pion C-12 scattering using distorted wave impulse approximation
[COO-1051-45] 18 p2971 N71-30487

FORTRAN 4 program for correction and calibration of neutron inelastic scattering data including background, air attenuation, detection efficiency, and sample thickness
[EUR-4599-E] 18 p2972 N71-30514

Knocking out of nucleons by inelastic electron scattering process in light nuclei
[ITF-70-35] 18 p2973 N71-30547

Shell structure of light nuclei under inelastic scattering of high energy electrons accompanied by knockout of nucleons from nucleus
[ITF-70-42] 18 p2974 N71-30551

Unitary conditions and decrease of differential inelastic cross sections of multiple production processes with energy increase
[IPVE-STF-70-43] 18 p2980 N71-30736

Spectroscopic data for Zn-68 and Zn-70 by inelastic alpha scattering
[NUB-2063] 18 p2989 N71-31506

Multipion resonance production in negative pion proton interaction at 7.0 GeV/c
18 p2990 N71-31524

Phase-space integral with transverse momentum cutoff calculated with Laplace transformation and saddle point method, and particle momentum spectra and inelastic cross sections
[NPF-18748] 18 p2966 N71-31577

Electron proton inelastic scattering from factors for massive quantum electrodynamics calculated from electron-like equations
[JLL-77U-71-7] 19 p3157 N71-32509

Inequalities for structure functions of deep inelastic electro- and neutrino production on nucleons
[LPTHE-71/29] 20 p3315 N71-33320

Inelastic pion-proton scattering reactions in generalized Veneziano model
[ITF-70-77] 20 p3322 N71-33812

Mathematical models for inelastic electron proton scattering indicating current amplitudes with nonlocality characteristics
[RIFF-125] 20 p3324 N71-33881

Classical trajectory study of rotationally inelastic scattering of hydrogen molecules by collisions with lithium ions
[NASA-CR-121729] 21 p3386 N71-34087

Utilization of colliding positron electron beam machines for inelastic electron-photon scattering
[DESY-71/15] 21 p3469 N71-34696

Scattering cross section estimations for intermediate vector boson production in nucleon-nucleon interactions based on inelastic process models
[JINR-E2-5748] 21 p3469 N71-34697

Quark-parton model inequalities for neutron and proton inelastic structure function
[SU-1206-244] 21 p3481 N71-34796

Time of flight method for studying fast neutron elastic and inelastic scattering by natural molybdenum at 1.0 to 5.0 MeV
[AWE-O-8977] 21 p3486 N71-34836

Deep inelastic neutrino nucleon interactions, assuming conserved axial vector current and equal time commutation relations of currents
[ORU-3992-24] 22 p3646 N71-36002

Phenomenological Lagrangian model calculation of scaling properties in deep inelastic electron-proton scattering
[NYO-1932(2)-189] 23 p3813 N71-37188

Microscopic coupled-channel analysis of proton inelastic scattering from neon and magnesium ions
[NASA-TN-D-6419] 23 p3814 N71-37201

Time of flight method for determining elastic and inelastic scattering of 5.0 MeV neutrons by sodium
[AWE-O-3771] 23 p3815 N71-37209

Experimental designs for electron elastic and inelastic scattering and mathematical expressions for electron-scattering cross sections and radiative corrections
[LNF-70/57] 23 p3820 N71-37249

Contributions of inelastic channels to electromagnetic form factor of pions, and production of strange particles in proton-proton scattering
[JINR-E2-5748] 23 p3821 N71-37255

Theory of deuteron breakup in nuclear and Coulomb fields using distorted wave Born approximation
[JINR-E2-5748] 23 p3821 N71-37260

Surface magnons in inelastic neutron scattering
[JINR-E2-5748] 24 p3974 N71-38351

Theoretical quantum electrodynamics in higher orders at low and high energies and nuclear models for lepton hadron and photon hadron scattering
[ITF-71-5-8] 24 p3976 N71-38372

ELASTICITY

U ELASTIC PROPERTIES

INEQUALITIES

Inequalities on double partial wave amplitudes from positivity, analyticity, and crossing symmetry
[LAAS-STI-770] 04 p0340 N71-14365

Integral inequalities for S and P wave pion partial wave amplitudes based on crossing symmetry, even partial wave positivity, and crossed channel absorptive known bounds
[SU-1206-234] 11 p1805 N71-22434

Algorithms for suboptimal nonlinear feedback and trajectory inequality control systems including linear, nonlinear, and quadratic programming
[LAAS-STI-770] 16 p2574 N71-28612

Algorithms for solving set of linear inequalities expressed in binary variables
[LAAS-STI-770] 18 p2942 N71-30554

Inequalities for structure functions of deep inelastic electro- and neutrino production on nucleons
[LPTHE-71/29] 20 p3315 N71-33320

Pion pion partial wave amplitude inequalities from projections of orthogonal polynomials
[SU-1206-240] 21 p3476 N71-34756

Theoretical and computational solutions of optimal control problems with state variable inequality constraints
[NASA-TM-71-37810] 24 p3902 N71-37810

INERT ATMOSPHERE

Digital processing for speech synthesis, and homomorphic methods for correcting helium speech
[AD-712345] 02 p0181 N71-11276

Effectiveness of nitrogen inerting of aircraft fuel tanks under conditions of fuel sloshing
[AD-721675] 16 p2670 N71-28576

Physico-chemical measuring apparatus to study hydrolytic uranium precipitates under inert atmosphere
[UJV-2417-CN] 18 p2885 N71-30752

Using miniature pigs for analysis of altitude decompression sickness and relative decompression hazards of various cabin atmospheres of inert gases
[NASA-CR-114355] 18 p2875 N71-30847

Measurement of total hemispherical emittance for chromel and alumel thermocouple wires in inert atmosphere at high temperatures
[NASA-TM-X-2359] 21 p3429 N71-34404

INERT GASES

U RARE GASES

INERTIA

Cearing system for eliminating backlash and filtering input torque fluctuations from high inertia load
[NASA-CASE-XGS-04227] 10 p1568 N71-21744

Fixed direction one axis inertial sensor
[NASA-TM-X-2359] 11 p1723 N71-22277

Development of Machian theory of inertia and gravitation
[NASA-TM-X-2359] 12 p1912 N71-23696

Finite element method to model soil half-space for calculating transfer momentum in form of inertial energy of projectile penetrating soil
[NASA-TM-X-2359] 14 p2360 N71-26470

Inertial effects in impulsive spherical and cylindrical plastic expansion with time-cavity motion relationships, final cavity size, and total expansion time determinations
[NASA-TM-X-2359] 17 p2853 N71-30066

Analytical method for determining radial inertia effects in dynamic plastic deformations
[NASA-TM-X-2359] 17 p2854 N71-30154

Entrance inertia effects associated with high speed magnetic tapes and computer flying heads
[AD-726464] 23 p3744 N71-36694

Reactor thermal inertia estimates, using measurements of transient conditions during power variations
[UARAE-111] 23 p3795 N71-37053

Stability of central equilibrium position of journal in bearings with gas lubrication
[AD-727270] 24 p3928 N71-38025

Finite difference method for testing optimum design of disks and shafts subjected to pressure and inertial forces
[AD-727270] 24 p4027 N71-38738

INERTIA MOMENTS

U MOMENTS OF INERTIA

INERTIA WHEELS

INERTIAL ACCELEROMETERS

INERTIAL FORCES

U INERTIA

INERTIAL GUIDANCE

ELDO launch vehicle inertial guidance law
[RAE-TR-70032] 03 p0262 N71-11757

Considering design of digital computers for guidance and control of aerospace vehicles
[AGARD-CP-68-70] 03 p0407 N71-12601

Discussing digital inertial guidance system for ELDO launch vehicle
[NASA-TM-X-2359] 03 p0409 N71-12617

Investigating simplified guidance computation schemes for on-line operation
[NASA-TM-X-2359] 03 p0347 N71-12619

Earth environmental noise fields problems in inertial component testing
[AD-715172] 05 p0720 N71-14542

Solid state helium-neon gas laser applied to missile guidance
[AD-715527] 05 p0720 N71-15383

Guidance and control analysis and integration for interplanetary missions
[NASA-TM-X-2359] 06 p0895 N71-16679

Hermetically sealed vibration damper design for use in gimbal assembly of spacecraft inertial guidance system
[NASA-CASE-MSC-10999] 14 p2623 N71-26243

Isosceles propagation, ion-molecule and acoustic surface wave interactions, semiconductor, photodetectors, target recognition, satellite tracking, and inertial guidance
[AD-720248] 14 p2360 N71-26328

Mathematical model of missile inertial guidance based on accelerometer and gyroscopes stabilized platform sensor data
[AD-722591] 17 p2779 N71-29504

INERTIAL MEASURING UNITS

U INERTIAL PLATFORMS

INERTIAL NAVIGATION

Automatic landing system optimization using inertial navigation data and modern control theory
[NASA-TM-111575] 03 p0405 N71-12431

Aided inertial flight test experiments for all weather V/STOL operations
[NASA-TM-X-66490] 03 p0406 N71-12439

Evaluating use of digital computers in aided navigation systems to make optimum estimates of system state or to perform coordinate transformation function in strapdown systems
[NASA-TM-X-66490] 03 p0409 N71-12622

Methods for determining instantaneous values of aircraft parameters with inertial navigation systems
[NASA-TT-F-614] 04 p0543 N71-14833

Investigating performance of various types of pure inertial and hybrid navigation systems
[NASA-CR-115905] 05 p0721 N71-13540

Investigating gyroscopic stability and error compensation in navigation instruments
[JPRS-52046] 06 p0893 N71-17891

Techniques for measuring gyroscopic drift of aircraft inertial navigation system
[RM-495] 08 p1233 N71-19808

Numerical analysis of error bounds in digital computation of four parameters for strapdown inertial systems
[NASA-CR-103050] 08 p1233 N71-19808

Gyroscopes theory and applications to inertial guidance and navigation, vehicle stabilization, and related uses - bibliography
[AGARD-R-582-71] 09 p1389 N71-20002

Computerized solution of nonlinear differential equations for inertial navigation systems
[AD-717058] 10 p1599 N71-20706

Inertial navigation in rocket technology
[AD-718625] 12 p1960 N71-23802

Error analysis of integrated inertial/Doppler satellite navigation system with continuous and multiple station coverage
[AD-722093] 14 p2290 N71-26197

Model of spatial Newtonmeter/accelerometer on moving object and theory of inertial navigation
[AD-723031] 14 p2290 N71-26197

Statistical analysis of gyrocompass error of A-4A inertial navigation system
[RM-511] 17 p2780 N71-30815

Design of aided, long duration, strapdown inertial navigation system with Kalman filter to process information and estimate errors
[NASA-TM-X-2359] 19 p1333 N71-32027

Application of inertial navigation system using multiple inertial measuring units for space shuttle guidance
[NASA-TM-X-2359] 20 p3300 N71-33862

INERTIAL PLATFORMS

Experimental techniques for prealigning and clamping inertial measurement sensors without major system recalibration
[NASA-CR-111365] 02 p0262 N71-11477

Applying Kalman filtering to problems of barometric pressure and inertial heights in navigation
[RAE-TR-69131] 02 p0262 N71-11750

Testing methods for components of inertial guidance systems
[AGARDGRAPH-128] 03 p0410 N71-12528

Acceptance testing of inertial equipment in platform assembly system
[NASA-TM-X-2359] 03 p0412 N71-12528

Proposed testing program for strapdown inertial system containing platform gyro and pendulum gyros
[NASA-CR-103046] 06 p0895 N71-17891

Velocity, position and guidance sensor instrument errors for inertial platforms and satellite guidance
[BMW-FB-W-70-45] 07 p1036 N71-17146

Techniques for measuring gyroscopic drift of aircraft inertial navigation system
[RM-495] 08 p1233 N71-19808

Numerical analysis of error bounds in digital computation of four parameters for strapdown inertial systems
[NASA-CR-103050] 08 p1233 N71-19808

Inertial component clamping assembly design for spacecraft guidance and control system mounting
[NASA-CASE-XMS-02184] 10 p1563 N71-30815

Inertial gimbal alignment system for spacecraft guidance
[NASA-CASE-XMF-01669] 12 p1959 N71-23802

Alignment and calibration of strapdown inertial measuring unit using accelerometer, gyrocompass, and optical filtering techniques
[RE-47] 12 p1960 N71-23802

Design and tests of single-axis reference strapdown inertial measuring unit
[NASA-TM-X-64586] 13 p2109 N71-26328

Examining performance of CR-100 CRIS equipment for space shuttle use
[NASA-CR-115147] 22 p3618 N71-33778

INERTIAL REFERENCE SYSTEMS

Testing methods for components of inertial guidance systems
[AGARDGRAPH-128] 03 p0410 N71-12528

Testing methods for sensors of inertial reference systems
[NASA-TM-X-2359] 03 p0411 N71-12528

Acceptance testing of inertial equipment in platform assembly system
[NASA-TM-X-2359] 03 p0412 N71-12528

Gyro testing methods in Great Britain
[NASA-TM-X-2359] 03 p0412 N71-12528

Methods for determining instantaneous values of aircraft parameters with inertial navigation systems
[NASA-TT-F-614] 04 p0543 N71-14833

Development of attitude control system for spacecraft orientation
[NASA-CASE-XGS-04393] 04 p0543 N71-14833

SUBJECT INDEX

INFORMATION RETRIEVAL

- Large amplitude, linear inertial reference system of vibrating string type for spacecraft reference plane [NASA-CASE-XAC-03107] 06 p0903 N71-16096
- Numerical analysis of error bounds in digital computation of four parameters for strapdown inertial systems [NASA-CR-103050] 08 p1233 N71-19044
- INERTIAL/STEERABLE ANTENNAS**
- Radar inertialless scan antenna array 01 p0021 N71-10252
- INFECTIONS**
- U INFECTIOUS DISEASES**
- INFECTIOUS DISEASES**
- NT DERMATITIS 04 p0476 N71-13431
- NT INFLUENZA
- NT TUBERCULOSIS
- Atmospheric pressure and oxygen tension effects on mice infections 02 p0163 N71-11813
- Periodicity of epidemics and nascent cycle [JPRS-51788] 04 p0476 N71-13431
- Hypoxic myxoma effects on human and animal resistance to infectious diseases and immunological reactivity 16 p2543 N71-28249
- Research methods for investigating infectious diseases in manned space flight without human exposure [NASA-CR-119243] 18 p2875 N71-30795
- INFERRECE**
- Computer program for inductive inference problems in organic chemistry [NASA-CR-123182] 24 p3947 N71-38155
- INFILTRATION**
- Flow equations for simultaneous flow of two immiscible fluids in porous medium including infiltration problems for several boundary conditions [AEDP-71DBMC28] 08 p1184 N71-19091
- Analytic treatment of two phase flow during infiltration - movement of both air phase and water phase assuming neglect of capillary pressure 23 p3746 N71-36708
- INFINITE SPAN WINGS**
- Pressure gradient effects on three dimensional turbulent boundary layer of infinite span sweptback wing [NPL-AERO-1305] 07 p1008 N71-17179
- IONITY**
- Quantum gravity and ultraviolet impurities in quantum electrodynamics [C/70/38] 02 p0273 N71-11789
- INFLATABLE DEVICES**
- U INFLATABLE STRUCTURES**
- INFLATABLE SPACECRAFT**
- NT BEACON EXPLORER A
- NT EXPLORER 22 SATELLITE
- Routing, multistaged mandrel for fabricating gored inflatable spacecraft [NASA-CASE-XLA-04143] 07 p1036 N71-17687
- Forming inflatable panels erectable in space for passive communication satellite [NASA-CASE-XLA-03497] 11 p1773 N71-23052
- Development and characteristics of inflatable structures to provide escape from orbit for spacecrews under emergency conditions [NASA-CASE-XMS-06162] 16 p2683 N71-28851
- INFLATABLE STRUCTURES**
- NT BALLOONS
- NT BALLUTES
- NT BEACON EXPLORER A
- NT EXPLORER 22 SATELLITE
- NT GAS BAGS
- NT HIGH ALTITUDE BALLOONS
- NT INFLATABLE SPACECRAFT
- NT METEOROLOGICAL BALLOONS
- NT ROBIN BALLOONS
- NT SKYHOOK BALLOONS
- Developing high altitude protection suit of partial pressure type [AD-702537] 02 p0167 N71-11188
- Method for arranging filamentary, load bearing material to approximate stress condition in gas envelopes of free floating balloon for maximizing structural efficiency [AD-713188] 05 p0530 N71-14811
- Temperature sensor warning system for pneumatic time of aircraft and ground vehicles [NASA-CASE-XLA-01926] 05 p0690 N71-15620
- Inflation system for balloon type satellites [NASA-CASE-XGS-03351] 06 p0930 N71-16081
- Development and characteristics of protective coatings for spacecraft 07 p1120 N71-17679
- Development and characteristics of self supporting space vehicle [NASA-CASE-XLA-00117] 07 p1120 N71-17680
- Design and characteristics of double hull dirigible vehicle [JPRS-52330] 08 p1145 N71-19217
- Design, fabrication and static testing of attached-inflatable decelerator models for supersonic wind tunnel [NASA-CR-111831] 11 p1676 N71-22538
- Numerical analysis of influence coefficients, natural frequencies, and mode shapes of vibration of triangular inflatable wing 11 p1671 N71-22646
- Conforming polisher for aspheric surfaces of revolution with inflatable tube [NASA-CASE-XGS-02884] 11 p1770 N71-22705
- Technique for making foldable, inflatable, plastic honeycomb core panels for use in building and bridge structures, light and radio wave reflectors, and spacecraft [NASA-CASE-XLA-03492] 11 p1770 N71-22713
- Steady state inflated shape and included volume of 24 and 30 gore flat circular, extended skirt, porous ring skirt, and porous ribbon parachutes [AD-718088] 12 p1833 N71-23387
- Design and development of pressurized suit with improved air retention and restraint overall with passive ventilation, maximum mobility, and long term unpressurized comfort [AD-720827] 14 p2208 N71-25863
- Collapsible antenna boom and coaxial transmission line having inflatable inner tube [NASA-CASE-MFS-20068] 15 p2380 N71-27191
- Space expandable tether device for use as passageway between two docked spacecraft [NASA-CASE-XMS-10993] 16 p2603 N71-28936
- Design, fabrication, and static testing of wind tunnel models of first-stage Attached Inflatable Decelerator canopies for supersonic vehicles [NASA-CR-111934] 22 p3538 N71-35205
- Design, development, and performance requirements for large rigid airships for freight and cargo transportation [REPT-5] 23 p3707 N71-36425
- Development, characteristics, and evaluation of inflatable lunar shelter model to determine leak rate in near vacuum conditions [NASA-TM-X-2393] 23 p3863 N71-37538
- INFLATING**
- Free-body tests of flat circular parachutes and determination of aerodynamic drag coefficients during partial inflation [NASA-TN-D-6423] 20 p3206 N71-33395
- Stresses and deformations in multiply bias pneumatic aircraft tires subjected to inflation pressure loading 22 p3693 N71-36341
- Development, characteristics, and evaluation of inflatable lunar shelter model to determine leak rate in near vacuum conditions [NASA-TM-X-2393] 23 p3863 N71-37538
- INFLUENCE COEFFICIENT**
- NT STRUCTURAL INFLUENCE COEFFICIENTS**
- INFLUENZA**
- Computerized simulation of influenza epidemic from one city over vast territory 17 p2708 N71-29540
- INFORMATION**
- Information preserving data compression systems with coding algorithm developed for noiseless channel conditions [NASA-CR-117846] 11 p1716 N71-22549
- Human orientation, motivation, and assimilation of information and its transfer 12 p2016 N71-23503
- Gnosological functions and information properties of devices used to understand cognitive mechanisms of man [JPRS-53910] 21 p3399 N71-34192
- INFORMATION DISSEMINATION**
- NT SELECTIVE DISSEMINATION OF INFORMATION**
- Military research program on magnetohydrodynamic generators and technology dissemination [AD-711389] 01 p0138 N71-10664
- Study visit for exchanging information on data processing applicable to rocket testing 05 p0652 N71-15529
- Operations summary for NASA technology transfer program [NASA-CR-115876] 05 p0788 N71-15640
- Defense information dissemination system annual review of operations [AD-715300] 08 p1307 N71-18857
- Rapid informal information dissemination system tests by photoduplicating and mailing memoranda on interferon research [PB-195722] 09 p1487 N71-19939
- NASA Regional Dissemination Center service and file descriptions [NASA-CR-117175] 09 p1355 N71-20120
- Document and abstract reproduction and dissemination facility operations review [NASA-CR-117176] 09 p1488 N71-20141
- Acquisition, retrieval, dissemination, and management of information systems [AGARD-LS-44] 12 p2016 N71-23501
- Information systems, transfer of technological information, and management of technology transfer 12 p2016 N71-23502
- Human orientation, motivation, and assimilation of information and its transfer 12 p2016 N71-23503
- Increased satisfaction of user needs and increased economics in operation of information systems [NASA-TM-X-67142] 12 p2016 N71-23504
- Profile construction, cost benefits, economics, and user surveys in transfer of technology and selective dissemination of information 12 p1867 N71-23506
- Concept, mission, operation, and management of Information Analysis Centers in US 12 p2016 N71-23507
- Scientific and technical information processing and dissemination nationally and internationally [NLL-M-20329-5828,4F/1] 12 p2019 N71-24270
- Feasibility study for German materials data bank - conference 17 p2762 N71-29387
- Chemical information systems including information input techniques, retrieval, dissemination, and publication bibliographies [JPRS-53523] 19 p3194 N71-31976
- Technology assessment of information retrieval and dissemination systems in USSR 19 p3194 N71-31977
- Basic secondary publications on chemistry and chemical engineering promoting international cooperation in information dissemination 19 p3194 N71-31981
- Operation of university-based technology and information transfer center [NASA-CR-121283] 19 p3197 N71-32521
- Algorithm for cost and potential benefit assessment of TV networking as mode of disseminating information to biomedical communities [RM-6204-NLM] 21 p3395 N71-34166
- Flow process of information presented in journal articles on meteorology [PB-199477] 21 p3452 N71-34568
- Electronic educational information dissemination and broadcast services in US including historical development and infrastructure - bibliography [NASA-CR-121910] 22 p3696 N71-36374
- INFORMATION FLOW**
- Test methodology for determining relationship of intergroup organizational climate with communication and joint decision making between task-interdependent R and D groups [REPT-70/34-PT-1] 10 p1666 N71-21099
- Data analysis of test to determine relationship of intergroup organizational climate with communication and joint decision making between task-interdependent R and D groups [REPT-70/34-PT-2] 10 p1666 N71-21100
- Flow process of information presented in journal articles on meteorology [PB-199477] 21 p3452 N71-34568
- Program for finding synoptic telegrams in general meteorological information flow over communication channels [NLL-M-20359-5828,4F/1] 21 p3453 N71-34577
- INFORMATION MANAGEMENT**
- On-line interactive book-library management system for performing circulation-desk bookkeeping [NASA-TN-D-7052] 09 p1488 N71-20526
- Computer oriented information management service for earth physics program [NASA-CR-117842] 11 p1750 N71-22478
- Concept, mission, operation, and management of Information Analysis Centers in US 12 p2016 N71-23507
- Formal system for interchange of information among state agencies 14 p2225 N71-26555
- Pilot system of integrated design programs for TIES software compatibility 14 p2226 N71-26558
- Proceedings of joint meeting of Government Operations Research and Procedures [NBS-SP-347] 15 p2527 N71-27883
- Development of system for identification of pollution reduction methods and selection of alternate methods for optimum effectiveness [PB-199332] 22 p3568 N71-35414
- Computerized management information systems for accounting and control activities 24 p3894 N71-37749
- INFORMATION RETRIEVAL**
- Algorithm to sequence search tree file structure for nonuniform access frequencies [TR-6] 02 p0183 N71-11303
- Impact of technological trends on improving information network systems [PB-192494] 02 p0186 N71-11306
- Data collection systems for dispersed technological objects [AD-712330] 03 p0346 N71-12511
- Operation of scientific information and data analysis center with computer base and associated communications network [ORNL-TM-3078] 04 p0500 N71-13498
- Describing design, hardware, and software for large data storage and retrieval system using CDC 6600 computers [NCL-19757-BEV] 05 p0849 N71-14579
- ENDRUN-1 program for calculating multipole constants from ENDF/B data [GEAP-13592] 05 p0746 N71-15217
- Coding related to speed and accuracy of recall [AD-714638] 06 p0799 N71-15929

INFORMATION SYSTEMS

- University information system expanded operations (PB-195274) 06 p1306 N71-18265
Development, use, and application of information retrieval systems in geology and centralized medical records (AD-716521) 09 p1383 N71-19692
System design of information storage and retrieval system (AD-715983) 09 p1353 N71-19754
Comparative analysis of natural languages and controlled vocabularies for information indexing and retrieval (AD-716200) 09 p1408 N71-19941
Man-machine interactive information system functions and effectiveness of free-form query with combinatorial search algorithm and various techniques for online browsing (AD-716954) 10 p1510 N71-21229
Syntax for linguistic information retrieval (IVA-25) 11 p1847 N71-22185
Document update, editing, search, authority file creation program Setup instructions manual for Radiation Shielding Information Center (CTC-INF-1017) 12 p1881 N71-23445
Acquisition, retrieval, dissemination, and management of information systems (AGARD-15-44) 12 p2016 N71-23501
Information systems, retrieval, and user behavior (AD-716200) 12 p2016 N71-23505
Design and testing of document retrieval system based on development of Boolean file searching information and pattern recognition (NASA-TM-X-52947) 12 p2018 N71-24072
Highly structured element set for information retrieval (AD-718032) 12 p2018 N71-24106
Index retrieval system stage, software and hardware development, and cost analysis, and model library educational program (INTREX-PR-11) 12 p1886 N71-24325
Automatic processing of hydrometeorological data for information retrieval system (AD-719837) 13 p2107 N71-25136
Relevance decision effects on comparative performance of index languages for information retrieval system tests (OSTI-5049) 14 p2357 N71-25752
Conference on information retrieval and management information systems including construction of dictionaries, analysis of query formulations, and computer programming 14 p2221 N71-25976
Intermediate code and table driven processor for translating retrieval question to users original language (AD-72221) 14 p2221 N71-25977
Computer program for linked file information retrieval including semantics, syntax, and outline of search program 14 p2221 N71-25978
Syntax oriented data formatting to facilitate information input and retrieval 14 p2221 N71-25979
Method of storing inverted file with minimum storage space and low access time for quick retrieval of nonnumerical data by computers 14 p2221 N71-25980
Computer patent searching system with automatic indexing using word truncation and similar query in on-line mode 14 p2221 N71-25981
Man machine system using computer for decision making in information retrieval 14 p2222 N71-25983
Automatic dictionary for creating indexes for information retrieval through computer programs 14 p2222 N71-25985
Information retrieval and analysis of search questions in tree structures noting hierarchies and syntax 14 p2222 N71-25986
Properties of information retrieval and management information systems including data structure, hierarchy generation, and searching 14 p2222 N71-25987
Pattern recognition applied to extraction of documentation indexes from text-KWIC indexes 14 p2222 N71-25988
Information retrieval and selective dissemination of information in technology transfer and financial planning of research and development 14 p2222 N71-25989
Compilation of dictionaries for information retrieval systems from vocabularies from different fields of science 14 p2223 N71-25990
Integration of text processing and written communication into management information system 14 p2223 N71-25991
Strategies for searching in data bank files adapted to query and file structure and use of thesauri with small and medium computers 14 p2223 N71-25993
Dynamic characteristics of dictionaries and documentation indexes for information retrieval 14 p2223 N71-25994

- EURATOM automatic documentation system, noting structure of index, information retrieval strategies, and performance evaluation 14 p2223 N71-25995
Performance characteristics of US information retrieval and management information systems, noting heuristic methods and incentive techniques 14 p2223 N71-25996
Operations research for West German governmental information retrieval system, noting low application and decision making 14 p2223 N71-25997
Description and characteristics of automatic information storage and retrieval system using batch processing mode on IBM 360 computer (PB-188957) 14 p2224 N71-26306
Operation and equipment of remote on-line documentation retrieval system (AD-720900) 15 p2527 N71-27848
Humfests system thesaurus containing words and phrases which reflect concepts to be indexed in human factors engineering information retrieval system (AD-721657) 16 p2550 N71-28339
Multiple pattern holographic information storage and readout system (NASA-CASE-ERC-10151) 16 p2607 N71-29331
Index for retrieving information on Permutated Isotopes and Radiation Technology - Vol. 7 (ORNL-2C-31-VOL-1-7) 17 p2793 N71-29478
Man-computer interaction information system to simulate various problem solving environments and provide users on-line feedback of their relative effectiveness (AD-723356) 17 p2712 N71-30218
List processing subroutines for IBM 1800/1130 information storage and retrieval system (NASA-TM-X-55622) 18 p2893 N71-30611
Browsing with information retrieval system by adding and deleting query terms on successive iterative cycles (AD-723672) 18 p3028 N71-30815
Development of man machine subsystem for military management information system and evaluation of display capability integrated into large scale computer (AD-723653) 18 p2877 N71-31335
Chemical information systems including information input techniques, retrieval, dissemination, and publication bibliographies (JPRS-53523) 19 p3194 N71-31976
Technology assessment of information retrieval and dissemination systems in USSR 19 p3194 N71-31977
Information system as useful tool for furthering chemical research and selective dissemination of results to various branches of chemistry 19 p3194 N71-31980
Advantages and disadvantages of information retrieval techniques on organic chemical reactions 19 p3195 N71-31983
Manual and mechanized methods of retrieving information on chemical compounds from data retrieval systems 19 p3195 N71-31984
Evaluation of on-line information retrieval system techniques with suggested goals for future developments (AD-723214) 19 p3196 N71-32186
Radioisotope and radar echo measurements on area of air/sea interactions over tropical ocean surface with numerical weather forecasting (NASA-CR-119764) 19 p3199 N71-32731
Environmental data service facility for dissemination of Barbados oceanographic and meteorological sea/air information 19 p3200 N71-32738
FORTRAN computer program for selective information retrieval from articles and reports (AD-724611) 20 p3369 N71-32987
Design concept for integrated display system suitable for computer management and optimized for pilot acceptability applied to space shuttle 21 p3517 N71-35064
Development of digital systems for picture processing (FOA-2-C-2469-52) 22 p3556 N71-35333
Data formats and procedures for evaluated nuclear data file neutron cross section library with illustrations for elastic scattering by natural H (BNL-30274T-601) 23 p3817 N71-37220
Computerized KWIC system for retrieval of microfired research files 23 p3870 N71-37588
Theoretical limitation on information retrieval from physical and communication systems by repeated precise measurements (AD-727768) 24 p4031 N71-38761
- ## INFORMATION SYSTEMS
- ### NT MANAGEMENT INFORMATION SYSTEMS
- Systems design of national system for management of scientific and technological information, including prototype subsystem for handling earth resources data (NASA-CR-61353) 01 p0138 N71-10806
Program for national information system for physics and astronomy 1971 to 1975 (PB-192717) 02 p0307 N71-11150

SUBJECT INDEX

- Plasma physics, quantum and solid state electronics, information systems, and digital systems (AD-711816) 02 p0307 N71-12040
Computer program for selection, editing, and dissemination of engineering and scientific educational literature from NASA technical reports (NASA-CR-111613) 03 p0342 N71-13477
Conference on image storage and transmission systems for libraries (PB-159492) 03 p0344 N71-13499
Keyword thesaurus for isotopes information system (ORNL-12-24-REV-1) 03 p0435 N71-13122
Proceedings from symposium on redundancy in information transmission systems - Part 1 04 p0499 N71-13498
Proceedings from symposium on redundancy in information transmission systems - Part 2 04 p0499 N71-13499
Operation of scientific information and data analysis center with computer base and associated communications network (ORNL-TM-3078) 04 p0500 N71-13498
Data handling and message switching in ATC - communication oriented computer systems 04 p0506 N71-13842
Systems analysis for data processing in industry 04 p0508 N71-13838
Compilation of major recommendations from five studies relating to national scientific and technical information systems (PB-193345) 04 p0622 N71-14197
Investigating information resources available to Environmental Health Service for protecting men's environment (PB-194411) 04 p0480 N71-14477
Annotated bibliography of information facilities and data resources available to Environmental Health Service on environment pollution (PB-194414) 04 p0481 N71-14480
Operational description of WESKAC technology dissemination center (NASA-CR-115837) 05 p0787 N71-15247
Algebraic systems and stochastic processes in military communication and information handling (AD-714141) 06 p0816 N71-16315
Information systems and processing, linguistics, artificial intelligence, and human information processing (PB-194790) 06 p0963 N71-16997
Deriving algorithms for finding limiting characteristics and carrying capacities of dynamic systems with feedback and internal noise 07 p0996 N71-16977
University information system expanded operations (PB-195274) 06 p1306 N71-18265
Surveying commercially available tape services of reference information on scientific and technical literature (AD-ID-70-3) 06 p1165 N71-18696
Defense information dissemination system annual review of operations (AD-715506) 06 p1307 N71-18837
Feasibility and applications of scientific and technical information analysis centers (AGARD-CP-78-71) 09 p1346 N71-19526
Concept, mission, and operation of scientific and technical information analysis centers 09 p1347 N71-19527
Cost estimates and means of funding information analysis centers 09 p1347 N71-19528
Organization, methods, and effectiveness of specialized documentation center 09 p1347 N71-19529
Harwell heat transfer and fluid flow information analysis center 09 p1482 N71-19330
Proposal for international air pollution information analysis center 09 p1381 N71-19331
Feasibility of creating international maritime pollution information analysis center 09 p1381 N71-19332
Rapid informal information dissemination system tests by photoduplicating and mailing memoranda on interrelated research (PB-195722) 09 p1487 N71-19339
NASA Regional Dissemination Center service and file descriptions (NASA-CR-117175) 09 p1355 N71-38129
Document and abstract reproduction and dissemination facility operations review (NASA-CR-117176) 09 p1488 N71-38841
Proceedings on submitting and requesting programs to Quantum Chemistry Program Exchange and available literature descriptions (AD-717162) 10 p1511 N71-20804
Technology assessment of research in biological and medical engineering including problem areas (NASA-CR-117487) 10 p1499 N71-31982
Computer research techniques including information systems, language programming, and control analysis (COD-504-2) 11 p1716 N71-25922
Provisional model of visual information processing with sequential inputs 11 p1720 N71-25924

SUBJECT INDEX

Structure of biological information processing and pattern recognition in living systems 11 p1683 N71-23056

Acquisition, retrieval, dissemination, and management of information systems 12 p2016 N71-23501

Increased satisfaction of user needs and increased economics in operation of information systems 12 p2016 N71-23504

Information systems, retrieval, and user behavior 12 p2016 N71-23505

Concept, mission, operation, and management of Information Analysis Centers in US 12 p2016 N71-23507

Design and testing of document retrieval system based on development of Boolean file searching instructions and pattern recognition 12 p2018 N71-24072

Worldwide scientific information system for future international cooperative research efforts 13 p2189 N71-24754

R and D in plasma physics, quantum electronics, radioelectronics, solid state electronics, systems theory, and digital information systems 13 p3191 N71-24847

Information system as subject of information science and informatics - terminological aspects 14 p2223 N71-25992

Operations research for West German governmental information retrieval system, noting law application and decision making 14 p2223 N71-25997

Integrated information system and popularization in Czechoslovakia 14 p2360 N71-26164

Czechoslovak information system for reducing research duplication 14 p2360 N71-26165

Oceanographic equipment including shipborne information systems, self maneuvering units, and instruments for measuring radioactivity and magnetic fields in sea water 14 p2350 N71-26317

Integrated system of computer processes for aiding engineers in designing highways 14 p2225 N71-26556

Objectives, operations, and accomplishments of NASA regional dissemination centers for technology transfer 15 p2527 N71-27735

Principle channels for information transfer and assessment of their effectiveness 15 p2527 N71-27735

Feasibility study for German materials data bank - conference 17 p2762 N71-29387

National Oceanographic Data Center activities and services 17 p2750 N71-30394

Technical and cost factors for implementation of Alaskan communication satellite system 18 p2889 N71-30593

Design and operation of complex mass machine systems and heuristic solution to automatic control problems in production engineering and biomedical diagnosis 18 p2882 N71-30667

Vulnerabilities of remote accessible computerized information systems to electronic crime 19 p3059 N71-31434

Computer-based chemical information system 19 p3194 N71-31777

Chemical information systems including information input techniques, retrieval, dissemination, and publication bibliographies 19 p3194 N71-31976

Technology assessment of information retrieval and dissemination systems in USSR 19 p3194 N71-31977

Computer applications in chemical information systems and journal publication 19 p3194 N71-31978

Information system as useful tool for furthering chemical research and selective dissemination of results to various branches of chemistry 19 p3194 N71-31980

Major Soviet information institutes on chemistry and chemical technology providing single classification system for information service system 19 p3195 N71-31982

Mathematical model and information display system for flight control and monitoring aircraft and pilot performance 19 p3045 N71-32566

Requirements for marine international meteorological information service 20 p3294 N71-32806

Game theory, information system for disease diagnosis, model of warehouse system 20 p3289 N71-32877

Computerized method for input of disease history information and retrieval for diagnosis 20 p3289 N71-32882

Computerized system for processing hydrometeorological data 20 p3294 N71-32958

Pattern recognition, speech recognition, man-machine systems for computer graphics, information systems, and data communications 20 p3230 N71-33213

Belgian computerized information system applied to automatic control 20 p3370 N71-33436

Utilization of remote sensor data by Virginia state agencies including aerial photography, radar detection, and infrared detectors 20 p3370 N71-33693

Advantages and disadvantages of some radical computer designs 21 p3399 N71-34191

Effect of fading in a Gaussian channel under different assumptions concerning capability of receiver to estimate momentary signal 22 p3354 N71-35312

Development of system for identification of pollution reduction methods and selection of alternate methods for optimum effectiveness 22 p3568 N71-35414

Heuristic resource allocation for network scheduling operational analysis 24 p3893 N71-37746

INFORMATION THEORY

Research and development in plasma physics, information theory, microelectronics, and related areas 01 p0089 N71-10462

Automatic equalization for data communications using telephone lines 01 p0022 N71-10471

Information capacity of discrete motor responses covered for different directions and amplitudes of motion 01 p0012 N71-10536

Abstracts of presentations at conference on information theory 01 p0026 N71-10898

Impact of technological trends on improving information network systems 02 p0186 N71-11306

Computerized simulation of character recognition layer sets using PDP 8 computer 03 p0129 N71-12349

Methodological problems for pragmatic aspect of scientific information 03 p0339 N71-12455

Automatic computation theory and problems of program complexity, complexity measures for finite automata, algorithms for inner products, and complexity of inversions 03 p0341 N71-12469

Boolean algebra and vector spaces for pattern recognition, pulse communication, switching, and information theory 03 p0342 N71-12480

Deriving criteria for optimum detector by analyzing threshold conditions of vision from standpoint of information theory 05 p0719 N71-15513

Clustering in discrete stochastic processes with application to transmission channels having memory 06 p0613 N71-16051

Applying queueing theory, network synthesis, and signal encoding to information systems 07 p1001 N71-16973

Multidimensional sampling theorem 09 p1362 N71-19428

Characteristics of high frequency channels used to obtain parameters for choosing appropriate convolutional codes 11 p1699 N71-22132

Low frequency characterization and identification of objects for inverse scattering and target recognition 11 p1708 N71-22251

Developments in engineering cybernetics and application to Latvian scientific and technical progress 12 p1894 N71-24133

Complex logic systems and logical sequencing theory 12 p1883 N71-24220

Algorithmic insolubility of finding asymptotic behavior of Shannon function with bounded determinate operators based on finite system of finite automatic devices 13 p2103 N71-25201

Formulation of general science of information with suggested name of informology 13 p2192 N71-25226

Information system as subject of information science and informatics - terminological aspects 14 p2223 N71-25992

Kalman formulation of minimum mean square linear estimation with random variables and unknown distributions producing biased results 14 p2284 N71-26429

Discrete system information content characteristics and relationships with operator performance and psychophysiological factors in data processing 16 p2541 N71-28093

INFRARED DETECTORS

Extending estimation for discrete data to continuous case for Gaussian signals in white Gaussian noise 16 p2622 N71-28197

Developments in scientific research, plasma physics, electronics, information theory, radio astronomy, and lasers 16 p2895 N71-29067

Biomedical electronics, information sciences, plasma and quantum electronics, solid state electronics, acoustics, and radio sciences 17 p2727 N71-29499

Computer techniques used in information theory, industrial controls, solutions to Fredholm equations, and simulating spreading of epidemic 17 p2727 N71-29536

Nonlinear representation of output signals of instruments in parallel, for maximum precision and reliability of using information systems 17 p2727 N71-29537

Effect of tape recorder equalization techniques on attainable bit error probability 17 p2720 N71-29817

Multichannel sequential hypothesis with applications in pattern recognition 17 p2723 N71-29894

Design and evaluation of information display systems and development of operator work station stages 18 p2882 N71-30668

Selection of optimal information structure in context of decision theory 18 p3029 N71-31337

Single shot joint detection and estimation for discrete and continuous data, and joint Bayesian detection, estimation, and system identification 18 p3065 N71-31346

Channel capacity for nonorthogonal multiple access communications 19 p3053 N71-31725

Annotated bibliography of data compression and data compaction from information theory literature 21 p3393 N71-34165

Thinking, cybernetics, and information theory 22 p3544 N71-35248

Information theory and coding with communications applications 22 p3556 N71-35334

Conditional mean information and conditional mean entropy 22 p3606 N71-35681

Proceedings of conference to determine application of Walsh functions to signal filtering, computer signal processing, voice signal compression, and multiplexing 23 p3723 N71-36542

Delay adaptive differential pulse code modulation system with delay adaptive predictor and quantizer and system analysis using stationary Gaussian Markov signal 23 p3724 N71-36546

Construction of universal statistical model for wide class of communication channels and retention of errors inherent in system 24 p3889 N71-37718

INFORMATION TRANSFER

U COMMUNICATING

INFORMATION TRANSMISSION

U DATA TRANSMISSION

INFRARED ASTRONOMY

Investigating suitability and requirements of mountain sites for high altitude IR astronomical observations 04 p0609 N71-13590

Orbit calculations, and high altitude sites suitable for infrared astronomy 14 p2337 N71-26209

High altitude sites for IR astronomy for Polar, Sub-Polar, and mid-latitudes 14 p2338 N71-26213

High altitude infrared rocket astronomy 20 p3343 N71-32882

Daytime operations of large telescopes for infrared astronomy 24 p3924 N71-37996

Daytime use of telescopes, emphasizing infrared astronomy, remote control, and astronomical spectroscopy 24 p3924 N71-37997

INFRARED DETECTORS

Pyroelectric detector compared to cooled photoconductive detector 01 p0053 N71-10210

Infrared radiometer for measuring laser brightness temperatures 01 p0053 N71-10275

Low frequency noise properties of mercury telluride infrared detectors 01 p0033 N71-10510

Research progress on multi-spectral data collection and infrared instrumentation for specially configured aircraft 02 p0227 N71-11904

Identifying rock types by aircraft equipped with various types of infrared detectors 02 p0217 N71-11905

INFRARED FILTERS

- Infrared radiometer measurements of ocean surface and internal temperatures 04 p0521 N71-13372
- Gas laser technology and photoelectric detection in near infrared 05 p0696 N71-14564
- Measuring dynamic errors of infrared radiometers used to measure ocean and sea surface temperature [JPSS-52039] 05 p0676 N71-15438
- Construction and assembly of infrared detector with 13 Hg-doped germanium elements 05 p0641 N71-15526
- Design and fabrication of 15.5 micron mercury cadmium telluride photodetectors for operation at 105 K [NASA-CR-115899] 05 p0690 N71-15700
- Airborne infrared radiometer sensing of thermal terrain properties in California lake region 06 p0843 N71-16135
- Measuring heat flow to ocean surface using infrared two-wavelength radiometer 06 p0848 N71-16183
- Investigating infrared scanners for thermal mapping and multispectral sensing 06 p0839 N71-16186
- Ten micron wideband detector [AD-713995] 06 p0868 N71-16834
- Infrared detectors for balloon sensing of aerosols and atmospheric moisture 06 p1202 N71-18950
- Investigating optical characteristics of plane mirror, prism, and rotating wedge scanners used in thermal viewers 06 p1203 N71-19131
- Considering operation of infrared radiometer affected by secondary fluxes of optical system as function of ambient medium temperature 06 p1204 N71-19132
- Quantitative analysis of aliasing in systems which produce single pictures by superposition of several periodic samplings using single detector array [AD-717619] 11 p1797 N71-21974
- Sight switch using infrared source and sensor mounted beside eye [NASA-CASE-XMF-03934] 11 p1726 N71-22985
- Optical properties of infrared scanners, infrared detectors, and optical equipment used for thermal viewing [AD-719852] 13 p2046 N71-24980
- Development and characteristics of scanning systems for thermal viewers and infrared detectors for airborne operation [AD-719854] 13 p2046 N71-25053
- Intrinsic and reflected secondary radiation flux effects on infrared scanner and detector operation including temperature variation effects [AD-719846] 13 p2046 N71-25059
- Nimbus 3 infrared detectors for remote sensing of global ozone 13 p2162 N71-25258
- Nimbus 2 medium resolution infrared radiometer measurements on subtropical jet stream flows 13 p2107 N71-25259
- Aircraft mounted infrared detectors for remote measurements of optical cloud properties 13 p2107 N71-25260
- Nimbus 2 high resolution infrared radiometer data on cloud motion for determining wind velocities 13 p2108 N71-25261
- Computerized simulation of wind velocity using Nimbus 3 infrared sounding data 13 p2108 N71-25262
- Graded energy gap p-type semiconductor photoemitter for infrared spectrum [AD-720796] 14 p2325 N71-25809
- Gallium arsenide infrared window materials for high power carbon dioxide lasers 14 p2265 N71-25874
- Near infrared radiometer for use on small sounding rockets to observe radiation emission in D region during daytime [NASA-TM-X-65548] 15 p2411 N71-27605
- Annual report 1969/1970 on infrared astronomy at Paris Observatory 15 p2517 N71-27617
- Evaluation of optical density measurements as method for monitoring and controlling vapor concentrations used for crystal growth [AD-721390] 16 p2665 N71-28732
- Analytic photoelectric system for optical tracking device [NASA-TT-F-13708] 16 p2640 N71-29025
- Airborne infrared detector performance tests for detection of earth impacted radioactive isotope heat sources [SC-DR-710093] 18 p2903 N71-31182
- Evaluation of materials and techniques for pyromagnetic infrared detection [AD-724324] 20 p3382 N71-33081
- Development and characteristics of infrared transducer for application to space missions [TP-963] 20 p3272 N71-33175
- Utilization of remote sensor data by Virginia state agencies including aerial photography, radar detection, and infrared detectors [NASA-CR-119721] 20 p3370 N71-33693

- Attempted rocket-borne radiometer observations of molecular oxygen nighttime emission in near infrared at zero deg latitude 20 p3269 N71-33876
- Nondispersive infrared gas analyzer [NASA-TM-X-65670] 21 p3386 N71-34090
- Infrared radiation detector for determining organic substances in burning flame chromatography 21 p3429 N71-34406
- Airborne infrared radiometer measurement of ocean water surface temperatures [AD-726512] 22 p3579 N71-35494
- Two color sandwiched photoconductive mercury-cadmium-telluride far infrared detectors [NASA-CR-121852] 22 p3582 N71-35511
- Nonlinear-optical effects in sulfur-hexafluoride at low pressure - saturation of infrared absorption 24 p3886 N71-37702

INFRARED FILTERS

- Design of two dimensional electric filters and infrared windows [AD-717159] 10 p1533 N71-21024
- Performance of mercury cadmium telluride photovoltaic infrared mixer for ATS 6 carbon dioxide laser communication system 13 p2048 N71-25320

INFRARED HORIZON SCANNERS

- U HORIZON SCANNERS
- U INFRARED SCANNERS

INFRARED IMAGERY

- Machine analysis of infrared cloud images obtained by Cosmos-122 satellite [NASA-TT-F-13369] 01 p0081 N71-10986
- Aerial and spaceborne photography and infrared imagery in earth hydrogeology and oceanography [NASA-TM-X-66481] 02 p0205 N71-11151
- Aerial infrared sensing for thermal mapping of power plant cooling reservoir 02 p0205 N71-11152
- Infrared and color photography for water inlet survey in Alaska 02 p0205 N71-11153
- Aerial infrared photography for remote sensing of plant transpiration 02 p0206 N71-11154
- Aerial synoptic sensing by infrared imagery and color photography of lake area in Florida 02 p0206 N71-11155
- Aerial infrared sensing of springs and sinks in Florida 02 p0206 N71-11156
- Color infrared photography for remote sensing of shallow water areas by air 02 p0206 N71-11157
- Thermal mapping of heated nuclear power plant discharge into river 02 p0206 N71-11158
- Remote aerial sensing and multispectral data processing for hydrobiological survey in Florida 02 p0206 N71-11159
- Aerial remote sensing data for locating ground water areas 02 p0207 N71-11162
- Constructing maps of planet Mars from infrared photographs of planetary surface 04 p0610 N71-13596
- Aerial color photography for detecting stressed forest vegetation 05 p0677 N71-15502
- Aerial multispectral sensing for determining geological and geographic aspects in Earth Resources Aircraft Program [NASA-TM-X-62564] 06 p0842 N71-16126
- Aerial infrared imagery for fire site detection in tropical grassland area of Florida 06 p0842 N71-16130
- Aerial infrared imagery for terrain analysis in California crater area 06 p0843 N71-16134
- Aerial infrared imagery of geological region in southern California taken during pre dawn and post-sunrise hours 06 p0843 N71-16136
- Aerial radar and infrared imagery for geodetic survey of northern Arizona 06 p0843 N71-16137
- Infrared aerial sensing of high temperature geothermal water sources 06 p0843 N71-16140
- Aerial radar and infrared imagery of coastal geology in Oregon and Washington 06 p0844 N71-16141
- Aerial infrared imagery and radiometric survey of coastal areas 06 p0844 N71-16142
- Detecting changes in thermal patterns induced by urban development in water bodies and adjoining land areas using infrared imagery 06 p0846 N71-16168
- Infrared imagery as rapid reconnaissance technique for locating thickest sections of water-bearing surficial sand in peninsular areas 06 p0847 N71-16173

SUBJECT INDEX

- Color infrared photography as remote sensing techniques in investigating estuaries and marshlands 05 p0647 N71-16174
- Using color-enhanced infrared imagery from satellites for displaying temperature gradients and differences of ocean surface [NASA-TM-X-65454] 06 p1200 N71-18409
- Thermal and infrared imagery of Mill Creek Area, Oklahoma 06 p1197 N71-19250
- Multispectral remote sensing of urban watershed characteristics and computer analysis of emitted and reflected data [REPT-2772-6-F] 10 p1560 N71-21446
- Photointerpretation of remote infrared imagery of North Carolina including isopleth mapping, Pearson correlation coefficient, and multiple linear regression analysis [AD-719761] 14 p2249 N71-26245
- Image intensifier cameras, infrared imagery, and high sensitivity vidicons for use in police night surveillance 19 p3070 N71-31640
- Computerized simulation for evaluating mosaic patterned, photoconductive near-infrared image conversion panels [AD-723524] 19 p3066 N71-32329
- Evaluation of enhancement of light intensity differences on color aerial photographs and thermal infrared imagery [NASA-CR-121430] 20 p3260 N71-33280
- INFRARED INSPECTION
- Infrared inspection of free surface wear on lathes using carbon dioxide lasers [ELAB-TL-132] 10 p1563 N71-20945
- Development and application of infrared techniques for nondestructive examination of insulated rocket engine cases to predict potential failure areas [AD-723964] 20 p3338 N71-32935
- INFRARED INSTRUMENTS
- NT INFRARED DETECTORS
- NT INFRARED SCANNERS
- NT INFRARED SPECTROMETERS
- NT INFRARED SPECTROPHOTOMETERS
- Research and development of solid state, infrared, microwave, and radar tracking equipment and techniques 01 p0135 N71-10308
- Energy transfer in solids [AD-711063] 01 p0112 N71-10730
- Seasonal sea surface temperature variations in Persian Gulf recorded by Nimbus 2 HRIR [NASA-TM-X-65385] 03 p0369 N71-13087
- Far infrared investigations using Fourier spectrometer [AD-712742] 03 p0382 N71-13218
- Mechanisms of structural transformation in amorphous solids studied by X ray radial distribution analysis and infrared techniques [AD-712612] 03 p0396 N71-13390
- Techniques for calibrating infrared pyrometer [UCRL-19665] 07 p1031 N71-17046
- Infrared isolator using yttrium iron garnet, Faraday rotation, and calcite dichroic polarizers [AD-716468] 09 p1396 N71-19822
- Servocontrol infrared optometer applied to study of volitional control of human visual accommodation [NASA-TM-X-66953] 09 p1338 N71-20871
- Development and characteristics of scanning systems for thermal viewers and infrared detectors for airborne operation [AD-719854] 13 p2046 N71-25053
- Sensors for ground based infrared sky survey [AD-720845] 14 p2336 N71-25806
- Airborne infrared telescope for flux measurements of astronomical objects with spectral energy peaks occurring at wavelengths of more than 25 microns [NASA-CR-121414] 20 p3272 N71-33285
- INFRARED LASERS
- Characteristics of hydrogen cyanide lasers and effects of chemical mixtures on laser operation [AD-713562] 05 p0697 N71-15340
- Cyclotron resonance in indium antimonide using infrared laser [AD-713094] 05 p0759 N71-15335
- Investigating interaction of solid-state plasma with far infrared laser radiation in large magnetic fields 06 p0929 N71-19800
- Frequency mixing experiments using infrared and far infrared lasers [AD-715040] 07 p1040 N71-17700
- Infrared difference frequency generation using tunable dye laser [AD-715700] 08 p1210 N71-18706
- Plasma refractive effects in far infrared lasers 08 p1211 N71-18708
- Transmission, attenuation, and signal to noise calculations for IR optical communication [PUBL-157] 09 p1350 N71-20862
- Development of simultaneous mode locking and pulse coupling of carbon dioxide laser using single gallium arsenide element [AD-719917] 14 p2265 N71-25410

SUBJECT INDEX

High resolution studies of atoms and molecules applied to optical and infrared laser experimentation [NASA-CR-121728] 21 p3435 N71-34440

Application of holographic techniques for measurement of scintillation effects using gas and infrared lasers [AD-726902] 22 p3591 N71-35572

Optical properties of gallium arsenide infrared window material and evaluation of CO2 laser [AD-726743] 24 p3931 N71-38051

INFRARED MASERS

U INFRARED LASERS

INFRARED PHOTOGRAPHY

Cosmos-122 infrared photography of cloud cover and photointerpretations for weather forecasting [NASA-TT-F-13362] 01 p0901 N71-10991

Annotated bibliography on infrared photography and films - Vol. 1 [AD-712100] 02 p0226 N71-11833

Infrared photography for ESRO satellite surface and solar cell temperatures and vestibular eye examinations [ESRO-TM-150-ESTEC] 03 p0382 N71-13272

Identification, characteristics, and distribution of slope failure forms as depicted by selected remote sensor returns 05 p0667 N71-14746

Color infrared aerial photography for acquiring and classifying data on urban housing quality 06 p1204 N71-19266

Aerial infrared photography for water oriented recreation planning [NASA-CR-107636] 12 p1914 N71-34087

Black and white multispectral images derived from multilayer color infrared film [NASA-CR-118316] 13 p2081 N71-24966

Comparison of August 1968 aerial infrared images of Surtsey, Iceland with survey data of 1966 14 p2252 N71-26647

Meteorological interpretation of infrared cloud photographs from satellite observations 15 p2438 N71-27489

Computer graphic mapping of Maryland coasts from aerial color and infrared photographic remote sensors including microdensitometer analysis [RM-5053] 17 p2749 N71-30176

Long distance infrared surveillance camera with searchlight and flash lamp for obtaining photographic documentation in total darkness 19 p3098 N71-31649

Photointerpretation of aerial color infrared photography for analysis of urban land use [NASA-CR-121652] 21 p3424 N71-34360

Graphical method for deriving dye-layer densities of color infrared image elements from known reflectance curves, and analysis of CIR photography from spacecraft windows [NASA-CR-121650] 21 p3424 N71-34361

System of regional agricultural land use mapping tested against Apollo 9 color infrared photography of Imperial Valley, Calif. 21 p3426 N71-34375

Infrared satellite photographs for studying hydrology, glaciology, oceanography, volcanology, and radiation balance of earth [NASA-TT-F-13930] 21 p3426 N71-34378

Range management in color infrared aerial photography and phenology of vegetation [PB-199226] 21 p3429 N71-34400

Near infrared astronomical photometry using calcite-Polaroid filter method 22 p3584 N71-35527

EA-4 processing for high altitude infrared color film [NASA-CR-122649] 23 p3755 N71-36767

INFRARED RADIATION

NT FAR INFRARED RADIATION

NT NEAR INFRARED RADIATION

Viewing infrared illuminated scenes by converting infrared frequency to visible, and then imaging visible radiation 01 p0063 N71-10142

Polarimetric properties of lunar and terrestrial meteorites, volcanic ashes, basalts, and other rocks [AD-711070] 01 p0121 N71-10362

Infrared response of silicon solar cells as function of thickness - graphs [RAE-TF-69126] 02 p0147 N71-11046

Mechanical and optical characteristics of airborne infrared telescope [NASA-CR-115780] 04 p0610 N71-13620

Infrared detector development [AD-714570] 06 p0906 N71-16531

Feasibility of infrared reflow soldering for circuit board connections [BDX-613-109] 06 p0807 N71-16819

Attenuation coefficient of 0.6 to 14 micron waves in mists and fogs, determined with approximate equations [AD-714786] 07 p1069 N71-17875

Thermal and infrared imagery of Mill Creek Area, Oklahoma 08 p1197 N71-19256

Determination of deep impurities in silicon and germanium by infrared photoconductivity [NBS-TN-570] 10 p1556 N71-20614

Characteristics of sensitivity of recombination light to infrared radiation in continuously excited and pulsed system operation [AD-717645] 11 p1722 N71-21911

Techniques for kinetic studies in shock tubes including infrared emission, electron scattering and electric discharge 11 p1739 N71-23627

Global distribution of upper atmospheric infrared emission layers from Cosmos 65 data analysis [NASA-TT-F-13600] 12 p1903 N71-23304

Analysis and interpretation of rocket sounding investigations of infrared radiation layers in upper atmosphere 12 p1994 N71-24264

Infrared nondestructive testing technique employing laser heating for thermal images to detect voids and disbonds [AD-719241] 13 p2085 N71-24448

Optical probing and microwave techniques for determining magnetostatic and magnetoelectric waves in yttrium-iron garnet crystals [AD-720386] 14 p2329 N71-26565

Characteristics of Cosmos 149 instruments for measurement of solar and infrared radiation emerging from earth 15 p2410 N71-27490

Absorption function of ozone 4.7 to 9.6 micron spectral bands noting their fine structure 15 p2401 N71-27509

Calculation of infrared radiation emerging from earth atmosphere in presence of cirrus clouds using remote sensing 15 p2402 N71-27531

Visible and infrared radiation transfer in clouds 15 p2402 N71-27533

Infrared radiometer used for terrestrial long wave radiation measurement 15 p2410 N71-27546

Spectrometer-radiometer for infrared cloud transmission measurements 15 p2410 N71-27547

Infrared radiometer for measuring ocean surface temperature with 0.3C accuracy 15 p2411 N71-27551

Vertical spectral distribution of radiative flux divergence in infrared range computed for five atmospheric models 15 p2440 N71-27559

Atmospheric models for tenuous cloud effects on atmospheric heat infrared radiation flux 15 p2403 N71-27561

Infrared flux at air-sea interface calculated to solve radiative transfer equations numerically by using flux emittance and flux reflectance as functions of sea temperature and roughness [AD-720386] 16 p2588 N71-28455

Infrared absorption and energy transport in gases including sulfur dioxide 16 p2640 N71-29127

Satellite modulator for 15 micron infrared radiation using Fabry-Perot interferometer [ESRO-CR-26] 17 p2751 N71-29389

Electromagnetic radiation scattering by hydrodynamically turbulent systems via operator formalism [AD-722323] 17 p2797 N71-29842

Infrared spectroradiometer for meteorological and atmospheric physics studies [IFA-SP-8] 18 p2951 N71-30875

Use of infrared radiation to reveal lubrication behavior between bearing surfaces [NASA-TM-X-67883] 18 p2929 N71-31210

Mie infrared radiation scattering function data for alostratus, nimbostratus, and stratocumulus clouds including extinction, scattering, and absorption cross sections [NOAA-TR-NESS-57] 18 p3007 N71-31466

Automatic vehicle identification using infrared techniques for law enforcement agencies 19 p3060 N71-31636

Fourier transformation technique applied to two dimensional infrared image filtering [ONERA-TM-164] 19 p3121 N71-31685

Atmospheric effects on infrared multispectral scanning of sea-surface temperatures from space [NASA-CR-1858] 19 p3130 N71-32578

Airborne ocean surface temperature measurement using infrared radiometers [BMVQ-FBW77-1-6] 20 p3256 N71-32997

Nighttime lunar surface differential flux scans at 22 microns [NASA-CR-121457] 20 p3348 N71-33453

Analysis of infrared radiative energy transfer in nongray gases under three conditions of flow and equilibrium 20 p3366 N71-33683

Development of procedures for infrared examination to improved reliability of large scale integration [NASA-CR-119921] 21 p3425 N71-34369

Design, development, and operation of three meter vacuum spectrometer for near infrared wavelength 21 p3430 N71-34411

INFRARED SPECTRA

Analysis of sensitivity of refractory oxides and concretes in infrared region of spectrum at high temperatures 22 p3680 N71-35635

Multicolor photometry for investigating infrared and ultraviolet radiation excesses of young star clusters containing T Tauri stars 22 p3669 N71-36162

Characteristics of neodymium-YAG laser and methods for converting infrared output to visible radiation 23 p3768 N71-38855

Partial elimination of infrared divergence in scalar charged field model with self-action in two-dimensional space-time and degenerated vacuum [JINR-TF-5760] 23 p3807 N71-37142

Atmospheric transmission of infrared radiation near 5 microns 23 p3855 N71-37478

Efficient laser-pumped 10-micrometers infrared quantum counter upconversion in rare earth doped crystals [AD-727182] 24 p3952 N71-38053

Extending tuning range of parametric oscillators into infrared, visible, and ultraviolet regions [AD-727127] 24 p3967 N71-38296

INFRARED REFLECTION

Infrared reflective paints to reduce solar heating of roofs 01 p0071 N71-10159

Cratered lunar soil model for reproducing directional infrared data from lunar thermal meridian [D1-82-0987] 02 p0296 N71-11966

Aerial infrared reflection measurements on forest treated with foliar chemicals [PB-192209] 05 p0673 N71-14879

Measuring thickness of semiconductor epitaxial layer deposited on substrate of same conductivity using infrared reflectance method 07 p1090 N71-17360

INFRARED SCANNERS

NT MULTISPECTRAL BAND SCANNERS

Infrared slot and horizon sensor development using slot-formed bolometer on germanium optical system [BMDW-FB-W-70-40] 03 p0382 N71-13294

Aerial infrared scanners for thermal mapping and multispectral sensing 06 p0839 N71-16146

Infrared scanner use for thermal mapping and multispectral sensing in Remote Sensing Aircraft Program [BMDW-FB-W-70-40] 06 p0839 N71-16165

Evaluating measurement methods for optically grown layers with respect to thickness and constant phase shift 07 p1090 N71-17299

Aerial multispectral and infrared scanning of Massachusetts coastline [NASA-CR-116782] 08 p1187 N71-18402

Deriving general formula for calculating energy response of infrared scanner 08 p1204 N71-19133

Infrared scanner onboard meteorological satellite for automatic picture transmission of earth and cloud surface 10 p1518 N71-21054

Nimbus 3 high resolution infrared radiometer photographs of inland delta of Niger River demonstrating use in earth resources studies [NASA-TM-X-65469] 10 p1552 N71-21296

Calculations of clear column radiances using infrared temperature profile radiometer measurements taken by Convair-990 over partly cloudy areas [NOAA-TM-NESS-28] 10 p1562 N71-21842

Transmission model effects on water vapor mixing ratio and radiance calculations for infrared horizon scanners [NASA-TN-D-4112] 12 p1912 N71-23494

Optical properties of infrared scanners, infrared detectors, and optical equipment used for thermal viewing [AD-719852] 13 p2046 N71-24980

Intrinsic and reflected secondary radiation flux effects on infrared scanner and detector operation including temperature variation effects 13 p2046 N71-25059

Formula for determining response of infrared scanner [AD-719847] 13 p2126 N71-25143

Color photogrammetry for Nimbus infrared radiation data analysis [NASA-TM-X-65614] 18 p2909 N71-38590

Design and fabrication of calibrated scanning imaging radiometer [AD-722063] 18 p2926 N71-31460

INFRARED SPECTRA

Infrared to visible image up-conversion 01 p0053 N71-10209

Infrared transmission measurement of pitch of cholesteric liquid crystal 03 p0325 N71-12534

Inorganic structure and spectra and paramagnetic anisotropy in complexes [AD-717237] 03 p0332 N71-12373

INFRARED SPECTROMETERS

Rocket-borne radiometers for infrared emission spectra measurements of earth-atmosphere
[AD-715219] 05 p0674 N71-14974

Far infrared spectra of crystals and solids in large range of temperatures
[AD-713677] 05 p0758 N71-15298

Matrix isolation infrared spectra of thalofluoride and thalofluoride vapors
[IS-7-407] 06 p0882 N71-16782

Lamb dip spectroscopy and carbon dioxide frequency stabilization on sulfur hexafluoride
[AD-715314] 07 p1640 N71-17772

Parametric upconversion technique for converting infrared images to visible for real time systems
[AD-715339] 07 p1040 N71-17847

Mariner television and infrared spectrometer data analyses to determine Mars surface geochemistry
[NASA-CR-116785] 06 p1288 N71-18627

Shock tube experiments to determine infrared band intensities of iron and aluminum oxides
[AD-716493] 09 p1342 N71-19543

Infrared vibrational spectral correlation derived from terrestrial and synthetic minerals for characterizing Apollo 11 and 12 lunar samples
[NASA-CR-114490] 09 p1466 N71-19913

Infrared spectra with frequency shifts in crystal defect resonance modes
[NYO-2391-119] 09 p1436 N71-20045

Photon density detection for determining liquid helium excess electron absorption cross sections at infrared wave lengths
10 p1612 N71-20720

Infrared absorption spectra gas analysis of air pollution
11 p1761 N71-22063

Plasma infrared diagnostics and determination of xenon ionization and recombination processes behind shock wave front
[SC-T-70-4054] 11 p1811 N71-22442

Raman, infrared, and far infrared spectra of laser excited sulfur monochloride and sulfur monobromide
12 p1872 N71-24062

Coincidence infrared and Raman excitation spectra analyses of sulfur monochloride
12 p1872 N71-24063

Raman and far infrared spectra of laser excited sulfur monobromide
12 p1872 N71-24064

Infrared and Raman spectral data of thiophosgene and polymeric dimer
12 p1873 N71-24067

Infrared and Raman spectra of disubstituted compounds containing quadruply bonded pairs of molybdenum and rhenium atoms
[MIT-1965-81] 13 p2136 N71-25372

Infrared spectra of implanted high energy nitrogen ionization energy in silicon
13 p2154 N71-25562

Electronic transitions in infrared absorption spectrum of aluminum antimonide
13 p2155 N71-25568

Infrared reflectance spectra of CO and O₂ absorbed on oriented nickel films
14 p2274 N71-26225

Addressable interface unit for computerized visual information processing system of earth resources infrared data
[NASA-CR-114997] 14 p2226 N71-26643

Airborne interferometric measurements on atmospheric airglow emission
[AD-720873] 15 p2399 N71-27188

Infrared molecular spectra in ionosphere
15 p2401 N71-27499

Design of satellite grid spectrometer for measurement in 13-15 micron range
15 p2411 N71-27552

Infrared spectroscopic study of allyl alcohol vapor adsorption on Li, Na, Cs, and Fe specimens of Pichev monomorphites
[NLL-RTS-6206] 16 p2559 N71-29013

Infrared spectra analysis of latex copolymers cross-linking reactions in relation to molecular weight and number of methylenolamide groups
[NLL-RTS-6216] 16 p2559 N71-29055

Electronic photointerpretation for aerial reconnaissance systems including size, color, and temperature discrimination, and spectral reflectance in visible and infrared spectra
[FVIL-1970-23] 18 p2894 N71-30865

Metal oxide infrared emission, and detection of vibrationally excited metal oxide molecules by laser induced fluorescence
[AD-723819] 18 p2888 N71-31597

Infrared spectra of UO₂ and UO₂ vapor condensed in rare gas matrices at high temperature
[COO-1182-34] 19 p3150 N71-32124

Line spectra shifts in HF and in first overtone band of DF induced by HF pressures
[NASA-CR-121411] 20 p3233 N71-33172

Method for producing holograms in infrared region and reconstruction in real time using helium-neon laser
23 p3767 N71-34851

Effect of temperature of infrared overtone spectra of D₂O and HOD in liquid state under saturation conditions into supercritical region
[NLL-CE-TRANS-5458-19022-091] 24 p3968 N71-38306

Ammonium sulfate optical constant calculations based on reflectance, transmittance, and Fresnel reflection measurements in infrared region
24 p3969 N71-38310

INFRARED SPECTROMETERS

Automated infrared spectrometer with Ebert monochromator
01 p0052 N71-10205

Measurement of atmospheric ozone using satellite infrared observations in 9.6 micron band
[NASA-CR-111566] 03 p0369 N71-13089

Polarization effects on grating efficiency of SIRS B satellite infrared spectrometer
[PB-192130] 05 p0771 N71-15161

Telespectrograph for analyzing upper atmosphere by tracking bodies reentering atmosphere at high velocities
[NASA-CASE-XLA-03273] 08 p1202 N71-18699

Design and performance of prototype onboard infrared Fourier spectrometer
[AD-721184] 15 p2406 N71-26820

X ray and infrared spectroscopic analysis of zinc, zinc oxide, and asbestos weathered exterior paints on potassium bromide disks
[AD-721696] 16 p2617 N71-28506

High resolution infrared spectrometer for gas molecular spectroscopy
[ONERA-NT-176] 19 p3099 N71-31930

Seasonal and geographic variation of atmospheric ozone derived from Nimbus 3 infrared interferometer spectrometer
[NASA-TN-D-6443] 19 p3132 N71-32791

Design, development, and operation of three meter vacuum spectrometer for near infrared wavelength
21 p3430 N71-34411

INFRARED SPECTROMETERS

Infrared spectrophotometer for automatic measurement of epitaxial layer thickness in silicon wafers
07 p1091 N71-17305

Investigating two photon absorption by single atoms in intense electromagnetic fields
[AD-715309] 08 p1251 N71-18290

Calibrated infrared emission spectra of earth and atmosphere using high resolution interferometer spectrophotometer on Nimbus 4 satellite
[NASA-TM-X-65687] 22 p3583 N71-35517

INFRARED SPECTROSCOPY

Research progress on polymers, battery separator membranes, and evaluation of spacecraft magnetic recording tapes
01 p0016 N71-10265

Infrared measurement on vibrational relaxation rate of carbon monoxide in argon shock tube wave
[NASA-CR-111370] 02 p0201 N71-11453

Infrared study of cooling behavior of eclipse thermal anomalies during lunar night
[REPT-5] 02 p0295 N71-11895

Preparation, characterization, and properties of noncrystalline solids
[AD-711820] 02 p0248 N71-12054

Kinetics of autooxidation of atactic polypropylene in presence of cobalt salts by infrared spectroscopy
[AD-711630] 03 p0331 N71-12363

Absorption characteristics of major components of dust clouds in infrared region
[AD-712989] 03 p0366 N71-12730

Design and construction of far infrared monochromator
[AD-712675] 03 p0383 N71-13365

Investigating infrared spectroscopic methods for monitoring concentration of sulfur dioxide in flue gases
[PB-194136] 04 p0484 N71-13445

Far infrared analysis of pair mode in MnF₂-Fe₂Cl₃
[NYO-2391-120] 05 p0759 N71-15445

Oxidative embrittlement of polypropylene film studied by measuring stress strain behavior, molecular weight changes, and development of carbonyl concentration in infrared spectrum
[AD-714369] 06 p0878 N71-16322

Measuring low-lying electronic levels of impurity ions in Al₂O₃ and electromagnetic absorptivity of Pb using far infrared spectroscopic techniques
[UCRL-19666] 06 p0922 N71-16407

Describing instrumentation and methods used in study of radiation damage in lithium-diffused silicon
[NASA-CR-116790] 08 p1257 N71-18417

Detection of transient free radicals in gas phase, and studying reaction kinetics by ultrarapid scan infrared spectroscopy
[AD-716004] 09 p1396 N71-19621

Chemical composition and structure of low silica sodium hydroaluminosilicates determined by IR spectroscopy
[NLL-XRE-TRANS-288-18036-471] 10 p1513 N71-21239

Determination of molecular structures and characterization of materials by emission spectroscopy, mass spectrometry, and vibrational spectroscopy
[AD-718431] 12 p1945 N71-23769

Sensors for ground based infrared sky survey
[AD-720845] 14 p2336 N71-23806

Infrared spectroscopic and photoconductivity determinations of electron irradiation effects in Li-doped floating zone and crucible grown silicon
14 p2397 N71-26230

Comparison of charged particle activation analysis and infrared spectroscopy for carbon and oxygen trace contaminant determination in silicon and aluminum
14 p2214 N71-26252

Structural changes in molecules of mineral oil additives during oxidation studied by infrared spectroscopy
[AD-721030] 15 p2431 N71-27371

Infrared spectroscopy of alpha recoil radiation damaged natural zirconium compounds from Ceylon in powder and thin plate form including annealing effects
[ORO-4049-1] 16 p2612 N71-28613

Using infrared spectroscopy in analysis of amphibole-asbestos
[NLL-L-TI-746-658-19022-4011] 16 p2598 N71-29912

Infrared spectroscopic study of amorphous elastomer reinforcement by polymeric fillers
18 p2887 N71-31233

Infrared study of chemisorbed sulfur compounds on platinum and germanium films
18 p2997 N71-31257

Study of two stage condensation polymerization reaction of polypyrrolimidine by IR absorption spectroscopy
[TR-41] 18 p2887 N71-31355

Infrared molecular spectra of linear acetylene molecule and its C 13 enriched isotopic bands
18 p2988 N71-31501

Determination of optical constants of amorphous thin films of selenium and arsenic triselenide from infrared reflectivity spectra
[AD-723833] 19 p3169 N71-32155

Infrared spectroscopic analysis of H II region in planetary nebula M 42, NGC 7027, and IC 418
21 p3511 N71-35820

Infrared spectroscopy for determining radial profiles of temperature and water vapor concentrations in radiating cylindrical exhaust gases
[AD-726554] 22 p3663 N71-36122

Brillouin scattering and infrared spectroscopy of C₂H₂ and HF dimer
[AD-727122] 24 p3967 N71-38297

INFRASONIC FREQUENCIES

Energy of aural charged particles drawn from solar wind, earth rotation, and atmospheric circulation, and infrasound generation from electric current interactions
07 p1014 N71-16930

Infrasonic microbarometric phenomena correlates with long period seismograph signals
[AD-716533] 09 p1382 N71-19628

Utility infrasonic monitoring system comprising noise reducing arrays, sensors, timing system, electronic equipment, and recording equipment
[AD-720669] 14 p2296 N71-26221

Pressure sensitive reference hydrophone design including lead zirconate titanate spherical element for infrasonic and audio frequencies
[AD-721069] 15 p2385 N71-26842

INGESTION [BIOLOGY]
NT DRINKING
NT EATING

Defining effects of temporal and quantitative dietary variables on human performance of vigilance tasks
[AD-711564] 02 p0158 N71-11118

INGESTION [ENGINES]
Ingestion of debris into aircraft engine inlets during takeoff
[ARC-CP-1114] 07 p0969 N71-17884

Investigation of helicopter jet engine flameout due to ingestion of snow and ice
[NRC-11893] 11 p1672 N71-21927

Exhaust gas ingestion and recirculating flow field characteristics of small scale vertical take off engine pod
[NASA-CR-1774] 13 p2024 N71-25397

Model tests of concepts to reduce hot gas ingestion in VTOL lift engines in low and cross wind conditions-graph
[NASA-CR-1863] 19 p3038 N71-32370

INGOTS
Production technology of ingots semi-finished products of titanium alloys
[AD-714055] 06 p0874 N71-16438

Electroslag refining of steel ingots
18 p2927 N71-30683

Solidification of ingots noting crystal structure
19 p3112 N71-31914

Effect of electromagnetic mixing on ingot grain size during continuous casting of magnesium alloys
[AD-727177] 24 p3937 N71-38006

INHALATION
U RESPIRATION
INHIBITORS

NT WEAR INHIBITORS
Testing methods for corrosion inhibitors in tanks
[FOA-I-C-1332-92] 14 p2279 N71-26140

SUBJECT INDEX

INHOMOGENEITY

- Effects of inhomogeneities in explosives on critical diameter of detonation (LA-TR-70-7) 01 p0114 N71-10756
- Electromagnetic radiation from infinite cylinder immersed in inhomogeneous medium (AD-714573) 06 p0625 N71-16629
- Calculations of passage of radiation through inhomogeneities in shielding (AD-715462) 08 p0816 N71-18061
- Mathematical models for solving scattering by weak volume inhomogeneities 10 p1609 N71-21755
- Coupled linear antennas in inhomogeneous dissipative medium (AD-717699) 11 p1724 N71-22656
- Theoretical inhomogeneity emission models of planetary nebulae 12 p1999 N71-24317
- Convergent series solution for Riccati equation of reflection coefficient on inhomogeneous transmission line (POA-3-C-3403-41) 13 p2103 N71-25427
- Variation of Young modulus representing inhomogeneity in stress analysis of inhomogeneous transversely isotropic material 14 p2280 N71-26406
- Relative compression inhomogeneities in sodium chloridobismuth structures as error sources in internal standards for pressure gauges 14 p2263 N71-26513
- Lattice heterogeneity effect on reactor physics parameters (BAW-5447-20) 16 p2634 N71-28753
- Scarf dislocations interacting with free surfaces in inhomogeneous solids 17 p2817 N71-29932
- Thermodynamic properties of inhomogeneous elastic bodies (NASA-CR-119065) 17 p2822 N71-29978
- Approximations for predicting amplitudes of reflected and transmitted waves in inhomogeneous media (FTAS/TR-71-59) 21 p3389 N71-34114
- Dynamic stabilization of drift-dispersed instability in partially ionized plasma using inhomogeneous HF electric field (EUR-CEA-PC-581) 21 p3493 N71-34883
- Electron-ion [ion sound] oscillations in electron beam passing through rarefied gas corresponding to instability of inhomogeneous plasma (MATT-TRANS-84) 21 p3494 N71-34894
- Seismic wave reflection in inhomogeneous media with differing depth distributions of dynamical parameters 23 p3750 N71-36737

INITIAL VALUE PROBLEMS U BOUNDARY VALUE PROBLEMS

- INITIATION
- Characteristics of heterogeneous shock initiation of explosive 9404 (LA-4475) 07 p1130 N71-17895
- Initiation and sensitivity of solid explosives to mechanical impact (NASA-TT-F-423) 11 p1841 N71-22534
- Heavy-atom model parameter change, seed gas addition, and reflective end-wall effects on nuclear light bulb engine calculations of fuel region radiation emission spectra 20 p3305 N71-33658

INITIATORS [EXPLOSIVES]

- NT DETONATORS
- Xenon lamp explosives initiator development (SC-DE-70-366) 05 p0752 N71-14503
- Orbital initiation pressures of explosives by shock waves (UCRL-TRANS-10490) 06 p0960 N71-16882
- Electroexplosive safe-arm initiator using electric driven electromagnetic coils and magnets to align charge (NASA-CASE-LAR-10372) 08 p1169 N71-18599
- Terminated capacitor discharge firing of electroexplosive devices (NASA-CR-118792) 08 p1169 N71-18702
- Description and operating instructions for laboratory precipitator for initiators (ERDE-TN-19) 12 p1897 N71-23600
- Performance tests and comparison of ignition properties for normal lead styphnate under constant current and capacitor discharge ignition (AD-721695) 16 p2690 N71-28561
- Half-size wave pulse firing of electroexplosive devices (NASA-CR-119320) 18 p3025 N71-31193

INJECTION

- NT CARRIER INJECTION
- NT FLUID INJECTION
- NT FUEL INJECTION
- NT GAS INJECTION
- NT ION INJECTION
- NT LIQUID INJECTION
- NT SECONDARY INJECTION
- NT TRANSLUNAR INJECTION
- NT WATER INJECTION

- Procedure for particle acceleration to 1000 GeV in intersecting storage rings and injection problems at 30 GeV (BNL-15423) 12 p1974 N71-23996
- Artificial changes in leukocyte count of rabbits (NASA-TT-F-13628) 13 p2033 N71-24737
- Fluctuations on one dimensional p-n junctions at high injection levels 14 p2336 N71-26350
- Foam insulation thickness measuring and injection device for spacecraft applications (NASA-CASE-MPS-20261) 15 p2407 N71-27005
- Boundary value problems associated with small suction or injection through discrete point on viscous flow in rigid, circular tube (AD-723457) 18 p2907 N71-31302
- Beam optics calculations based on beam phase space characteristics for cyclotron-tandem injection system (ANU-P-519) 19 p3146 N71-31967
- INJECTION CARBURETORS
- U CARBURETORS
- U FUEL INJECTION
- INJECTION LASERS
- Characteristics of indium arsenide-phosphide injection lasers (AD-715454) 08 p1210 N71-18885
- Injection laser Thomson scattered light for limited measurement of electron density and temperature of shock fronts formed by axial plasma injection into dipole magnetic fields 12 p1982 N71-24143
- Superconducting injection laser and temperature dependent threshold current density of tantalum (ORO-3665-24) 13 p2090 N71-25231
- INJECTORS
- NT VORTEX INJECTORS
- Design criteria for high performance coaxial injector using gas-liquid space storable propellants (NASA-CR-72708) 01 p0113 N71-10452
- Method and apparatus for use in forming highly collimated beam of microparticles with high charge to mass ratio and injecting beam into electrostatic accelerating tube (NASA-CASE-XGS-06628) 06 p0918 N71-16213
- Rod plasma injector for creating highly focused stream of hot plasma (AEC-TR-70277-8) 06 p0926 N71-16843
- Gaseous oxygen-gaseous hydrogen rocket engine injector valve technology (NASA-CR-114857) 07 p1034 N71-17555
- Control valve and coaxial variable injector for controlling bipropellant mixture ratio and flow (NASA-CASE-XNP-09702) 07 p1036 N71-17634
- Characteristics of noncircular injector orifices and elements for gas and liquid injectors (NASA-CR-108571) 07 p1103 N71-17723
- Rocket engine tests using space storable propellants and various injector configurations (NASA-CR-116788) 08 p1283 N71-18795
- Electron ring accelerator program at Lawrence Radiation Laboratory - conference (UCRL-20084) 09 p1364 N71-19556
- Transverse mode stability characteristics of coaxial and hyperthin injectors in transverse excitation chamber (NASA-CR-117033) 09 p1460 N71-20500
- Rocket engine injector orifice to accommodate changes in density, velocity, and pressure, thereby maintaining constant mass flow rate of propellant into rocket combustion chamber (NASA-CASE-XLE-03157) 13 p2156 N71-24736
- Rod plasma injector (AEC-TR-70275-10) 13 p2139 N71-25494
- Electron bunching structure calculations for bunching produced by injectors with wave phase velocity stepped variations (SLAC-TRANS-127) 14 p2302 N71-25749
- Evaluation of throttling injector concepts applicable to advanced cryogenic engines (NASA-CR-103183) 14 p2332 N71-26411
- Gas augmented rocket engine injectors using high energy gas (NASA-CR-72703) 14 p2333 N71-26689
- Liquid propellant rocket engine throttling injector design based on exhaust gas counter flow and heat transfer for inflowing propellant vaporization and combustion stability tests (NASA-CR-119796) 16 p2671 N71-28158
- High and low chamber pressure injectors for space shuttle hydrogen oxygen AFS engines (AOC8-0106-71) 17 p2836 N71-29590
- Injector performance, heat flux, and film cooling in hydrogen oxygen engines 17 p2837 N71-29598
- Design and fabrication of noncircular orifice holes for liquid rocket engine injectors (BC-71-19) 17 p2838 N71-29602
- Axial and circumferential variations of hot gas side heat transfer coefficients in hydrogen oxygen engines for use in nozzle and injector design (NASA-TN-D-6396) 18 p3024 N71-30738
- Structure of electron clusters in accelerator injector with step-like varying wave-phase velocity (KHFTI-70-17) 19 p3145 N71-31926

INLET FLOW

- Vacuum cryopumping of heavy ion source in high voltage terminal of accelerator injector (UCRL-20620) 19 p3150 N71-32119
- Techniques for fabricating electroformed injectors for high energy space storable liquid propellants (NASA-CR-121434) 20 p3359 N71-33484
- Pulsed electron accelerator used as injector for electron ring accelerator (UCRL-20174) 20 p3348 N71-33935
- Mixing of hydrogen downstream from multiple injectors normal to supersonic jet flow, for supercubic combustion ramjet engines (NASA-TN-D-6476) 21 p3411 N71-34274
- Construction of fast hydrogen atom injector from calculations of magneto-optical system (NRL-CTO/746-1991-9P) 23 p3852 N71-37529
- INJUN SATELLITES
- Measuring energy fluxes greater than 5 keV electrons over northern auroral region at 530 to 2500 km altitude using Injun 4 satellite 05 p0670 N71-14816
- INJUN 5 SATELLITE
- U EXPLORE 40 SATELLITE
- INJURIES
- NT BAROTRAUMA
- NT BRAIN DAMAGE
- NT BURNS [INJURIES]
- NT CRASH INJURIES
- NT EJECTION INJURIES
- NT NOISE INJURIES
- NT RADIATION INJURIES
- Physiology and pathology of spinal afflictions in aerospace medicine (AGARD-AG-140-70) 01 p0008 N71-10175
- Summary and statistical analysis of aircraft accidents (NTSB-AAS-70-1) 01 p0005 N71-10674
- Legal, preventive, and clinical aspects of aerospace medicine (AGARD-CP-61-70) 02 p0161 N71-11801
- Statistical analysis on accidental injuries sustained by military airforce personnel 02 p0162 N71-11809
- Pilot injuries on high speed low altitude flight noting acceleration due to gust effects 19 p3048 N71-31828
- Statistical, cause/factor and injury tables, accident rates, and briefs of accidents involving US carriers in 1969 (NTSB-ARC-7L-1) 23 p3708 N71-36437
- INLET FLOW
- Experimental performance evaluation of 4.59 inch radial inflow turbine with and without vaneless inlet (NASA-TN-D-7015) 03 p0317 N71-12265
- Reignition characteristics and inlet flow distortion of V/STOL fighter powered by J-45 engine (NASA-TN-D-7014) 04 p0474 N71-13420
- Inlet flow distortion testing of high Mach number transonic fan stages - Vol. 1 (NASA-CR-72786-VOL-1) 05 p0662 N71-14863
- Tabular data derived from inlet flow distortion tests of high Mach number transonic fan stages - Vol. 2 (NASA-CR-72786-VOL-2) 05 p0662 N71-14864
- Two dimensional thin airfoil theory with strong inlet flow on upper surface 06 p0795 N71-16261
- High entrance temperatures for improved performance of turbogenerators and gas turbine engines 07 p1099 N71-17573
- Effectiveness of turbine cooling systems for high temperature inlets (NASA-TM-X-66702) 07 p1100 N71-17385
- Boiling and heat transfer characteristics of cryogenic hydrogen flows in straight and plasma inlets (NASA-TN-D-6159) 07 p1132 N71-17955
- Interference effect between oscillating and distorted inlet flow on compressor stall 09 p1313 N71-19370
- Inlet leak analysis for spacecraft mass spectrometer atmospheric sensor system (NASA-CR-111858) 11 p1764 N71-22872
- Quasi-three dimensional surface velocities and choking flow for turbomachine blade rows calculated by FORTRAN program (NASA-TN-D-5177) 12 p1849 N71-23126
- Test description and results for high Mach number transonic fan stages to determine range and distortion tolerance for various rotor tip casing treatment configurations (NASA-CR-72862) 13 p2068 N71-25460
- Tabulations of blade element and circumferential distortion flow data in tests of high Mach number transonic fan stages with various rotor tip casing treatment configurations (NASA-CR-72867) 13 p2068 N71-25461
- Method for maintaining good performance in gas turbine during air flow distortion (NASA-CASE-LEW-10286-1) 16 p2672 N71-28915
- Design and characteristics of supersonic inlet controls for minimizing inlet unstarts (NASA-TN-D-6408) 17 p2839 N71-30072
- Velocity profile control tests of diffuser wall bleed to control combustor inlet air flow distribution (NASA-TN-D-6435) 18 p3060 N71-30817

INLET NOZZLES

- Preliminary sector tests at 920 K of three afterburner concepts proposed for inlet temperature of 1260 F and comparison of results with conventional V-gutter flame holder
[NASA-TN-D-6437] 19 p3192 N71-32191
- Instability and turbulence for various external compression axisymmetric supersonic inlets of 25 degree cone semi-angle at various turbulence, Reynolds number, and surface conditions
[ARL/ME-129] 20 p3251 N71-33584
- Effect of inlet conditions on flow and containment characteristics of coaxial flows for gas core nuclear rockets
20 p3303 N71-33636
- FORTRAN 4 computer program for design application of stagger angle replacing inlet flow angle for given blade cascade
[NASA-CR-121679] 21 p3410 N71-34262
- ## INLET NOZZLES
- Auxiliary inlet ejector nozzle designed for supersonic cruise aircraft
[NASA-TM-X-2182] 08 p1284 N71-18863
- Flight test investigation of effects of variable geometry plug nozzles installed on F-106 aircraft
[NASA-TM-X-2295] 17 p701 N71-30283
- Inlet nozzle geometry effects on subsonic flow characteristics of miniature total pressure tubes including pitot tube static and dynamic pressure and flow velocity measurements
[NASA-TN-D-6406] 18 p2905 N71-31185
- Mercury and NaK inlet and outlet port, condenser, and attachment design modifications of power conversion system for SNAP 8
[NASA-CR-72946] 24 p3939 N71-38241
- ## INLET PRESSURE
- Deadhead condenser inlet pressure control method for SNAP 8 startup
[NASA-TM-X-2115] 06 p0796 N71-15840
- Computer controlled gas chromatograph for monitoring temperature, mass flow rate, inlet pressure, and calculation of precise retention volumes in real time
[COO-1224-44] 15 p2410 N71-27481
- Primary and secondary mixing performance of combustors under high inlet air pressures
[NASA-TN-D-6491] 22 p3663 N71-36119
- ## INLETS (DEVICES)
- ### U INTAKE SYSTEMS
- ## INNER RADIATION BELT
- Particle diffusion and particle acceleration in the inner and outer radiation belts
[REPT-70-17] 04 p0608 N71-14299
- Rocket sounding of long term proton flux density variations in inner radiation belt
[MFI-PAE/EXTRATER-57] 07 p1105 N71-17216
- Auroral satellite observation of proton and electron energy in auroral zones and magnetosphere
[BMBW-FB-W-70-56] 12 p1994 N71-24262
- Time variations of energetic electron and solar proton distributions in inner radiation belt
[NASA-SP-3024-VOL-7] 16 p2676 N71-29089
- Temporal variations in charged particle population of inner radiation zone as measured by satellite
16 p2676 N71-29091
- Solar cycle effects on long term atmospheric distribution of trapped protons
16 p2676 N71-29092
- ## INORGANIC CHEMISTRY
- Electrochemistry, organic and inorganic chemistry, and chemical analyses
[TT-69-51006/2-4] 08 p1161 N71-19334
- Inorganic chemistry of titanium, hazard and precautions in handling titanium containing materials, counting techniques, and radiochemical separation procedures
[NAS-NS-3034-REV] 16 p2610 N71-28442
- ## INORGANIC COATINGS
- ### NT ANODIC COATINGS
- ### NT CERAMIC COATINGS
- Photooxidation and electron energy loss in organic thin films
[ORO-3894-2] 14 p3299 N71-25612
- ## INORGANIC COMPOUNDS
- ### NT AMMONIA
- ### NT LIQUID AMMONIA
- Measuring oxidation of a xylene glycol on rotating disk electrodes and regularities in series of volatile inorganic hydrides
[JPRS-51604] 02 p0174 N71-11223
- Investigating regularities of reduction potentials in series of volatile inorganic hydrides of elements in main subgroups of periodic system
02 p0174 N71-11225
- Inorganic structure and spectra and paramagnetic anisotropy in complexes
[AD-711237] 03 p0332 N71-12373
- Physical and chemical properties of metallic elements and inorganic compounds at high temperatures
[NYO-4176-3] 07 p1130 N71-17636
- Nuclear quadrupole resonance spectroscopy of molecular structure of inorganic and organic compounds
[AD-716623] 09 p1434 N71-28804
- Preparation of inorganic solid film lubricants with long wear life and stability in aerospace environments
[NASA-CASE-XMF-6398] 10 p1566 N71-21403

- Modification of polyurethanes with alkyl halide resins, inorganic salts, and encapsulated volatile and reactive halogen for fuel fire control
[NASA-CASE-ARC-10096-1] 13 p2039 N71-24739
- Inorganic material adsorbent air sampling system for analysis of airborne iodine isotopes and compounds in nuclear reactor containment atmosphere
17 p2743 N71-29063
- Control of mitosis in biological cells through inorganic ion hierarchy of cells involved
[NASA-CASE-LAR-10773-1] 21 p3382 N71-34061
- Research on inorganic compounds for use as positive electrodes in rechargeable lithium battery
[AD-726607] 23 p3710 N71-36447
- Thermochemical properties of chemical elements and compounds - tables
[NSRDS-NBS-37] 24 p4033 N71-36775
- ## INORGANIC MATERIALS
- Luminescence of rocks and of natural and synthetic inorganic materials - laboratory studies
01 p0045 N71-10087
- Standard reference materials price and availability listing
[NBS-260-SUPPL.] 01 p0072 N71-10722
- Recent developments in new materials suitable for modern engineering requirements
[JPRS-51752] 04 p0533 N71-14042
- Research activities in chemistry, ceramics, metallurgy, and solid state physics
[UCRL-19155] 05 p0786 N71-15197
- Glass transition temperature and viscoelastic thermal properties of inorganic polymers
[AD-717364] 11 p1782 N71-22081
- Gamma irradiation effects on polymer grafting to inorganic substrates
[RLO-2098-1] 15 p2430 N71-27131
- Description of methods for chemical production of superpure inorganic substances
[JPRS-53256] 16 p2555 N71-28290
- Description of processes of crystallization and precipitation from chemical solutions and use in production of superpure inorganic materials
16 p2555 N71-28293
- Characteristics and application of ion exchange production for development of superpure inorganic materials
16 p2556 N71-28295
- Characteristics and application of rectification methods for production of superpure inorganic materials
16 p2556 N71-28296
- Development of theoretical aspects and practical application of extraction method for purification of inorganic materials
16 p2556 N71-28297
- Production of superpure inorganic substances by zone melting or zone recrystallization
16 p2556 N71-28298
- Superpurification of inorganic substances by electrochemical processes
16 p2556 N71-28299
- Chemical transport reactions applied to production of superpure inorganic materials
16 p2556 N71-28300
- Characteristics of laboratory and manufacturing equipment and facilities for production of superpure inorganic materials
16 p2577 N71-28304
- Hypiodous acid generated by injection of elemental iodine into steam-air atmosphere or by purging dilute aqueous solution of iodine in water with air or other gases - airborne species
17 p2743 N71-29053
- Inorganic adsorbent materials for trapping of fission product iodine in fuel reprocessing plants and gas cleaning inside reactor containment
17 p2784 N71-29659
- Spectroscopic analysis to determine effect of phase angle, compactness of material, and particle size on total reflectivity of various inorganic materials
[AD-728674] 19 p3171 N71-32702
- Quantitative and comparative analysis of inorganic photochromic materials for coherent optical data processing applications
[NASA-CR-121453] 20 p3311 N71-33375
- ## INORGANIC NITRATES
- ### NT AMMONIUM NITRATES
- ### NT SODIUM NITRATES
- ## INORGANIC PEROXIDES
- ### NT HYDROGEN PEROXIDE
- Chemical properties of superoxide ion and other solute species in molten fluorides
[ITD-25498] 04 p0486 N71-13459
- ## INORGANIC SULFIDES
- ### NT BISMUTH SULFIDES
- ### NT CADMIUM SULFIDES
- ### NT CALCIUM SULFIDES
- ### NT COPPER SULFIDES
- ### NT HYDROGEN SULFIDE
- ### NT LEAD SULFIDES
- ### NT MOLYBDENUM DISULFIDES
- ### NT POLYSULFIDES
- ### NT ZINC SULFIDES
- ### NT ZINCLENDE

SUBJECT INDEX

- ## INPUT
- Evaluation of interactive input devices associated with computer driven displays
04 p0506 N71-13846
- Input communication on target simulation systems
04 p0506 N71-13847
- Input applications for acoustic analysis of Experimental Breeder Reactor 2
[ANL-7540] 04 p0557 N71-14133
- FISP 2 program for fission product inventories with complete input data specification
[RD/B/N-1757] 09 p1440 N71-20309
- Scalar system for approximate input signal synthesis in input parameter identification
[AD-716923] 10 p1593 N71-21567
- Apparatus for filtering input signals
[NASA-CASE-NFO-10198] 13 p2856 N71-24006
- Using computer graphics for producing computer program forms, and for highway perspective
14 p2226 N71-26562
- Dynamic response of liquid lines of finite length for periodic and aperiodic inputs
17 p2786 N71-29918
- Input impedance and radiation patterns for experimental, rectangular, cavity-backed aperture antennas for reentry communications
22 p3555 N71-35338
- ## INPUT/OUTPUT ROUTINES
- Combining conversational programming system and programmer oriented graphics operations with PL-1 computer language
[AD-709905] 01 p0027 N71-10861
- Legal path report/Automated Snak Program
[NASA-CR-108741] 03 p0339 N71-12651
- ISAM table generated/Automated Snak Program (ASP)
[NASA-CR-108744] 03 p0341 N71-12671
- Reporting supporting research and technology for Deep Space Network
07 p0999 N71-17618
- SAMBO, computer routine package for Moon Carlo codes
[ORNL-TM-3203] 08 p1261 N71-18776
- Input-output properties of feedback systems based on linear time invariant systems
[NASA-CR-117467] 11 p1728 N71-22230
- Space shuttle synthesis program manual including deck setup, input parameters, and synthesis operations for trajectory and performance predictions
[NASA-CR-114964] 13 p2173 N71-24234
- Digital computer program manual for design, analysis, and performance prediction of heat pipes with noncondensable gases including input/output routines and Range-Kutta models
[NASA-CR-114306] 17 p2735 N71-29908
- Input/output routines for symbolic programming with FORMAL on Univac 1108 computer
[NASA-CR-119188] 17 p2723 N71-30109
- Nonlinear systems for matching input-output of mathematical model to physical system
[NASA-TN-D-6467] 18 p2947 N71-31352
- Design principles of high precision measuring television system for information transmission in communication
[AD-721712] 23 p3725 N71-36559
- ## INSECTICIDES
- ### NT CARBAMATES (TRADENAME)
- ### NT DICHLORODIPHENYL-TRICHLOROETHANE
- ### NT URETHANES
- ## INSECTS
- ### NT BEES
- Color aerial photography of Douglas fir tussock moth damage
[PB-193698] 02 p0221 N71-12164
- Detection of forest insect infestation by remote sensing
06 p0800 N71-14139
- Investigating proliferation of insect life in harsh environments of Iceland and Surtsey
07 p0984 N71-17991
- Sensory modes of flies, bees, and moths applied to target acquisition and tracking
[AD-720412] 14 p2204 N71-29959
- ## INSECTIVITY
- ### U SENSITIVITY
- ## INSERTION LOSS
- Insertion loss and pulse response of power line filters
[AD-711317] 01 p0035 N71-10828
- Network theory and insertion loss filter design
[AD-713720] 05 p0654 N71-14980
- High impedance alternating current sensing transformer device between two bolometers for measuring insertion loss of test component
[NASA-CASE-XMF-01153] 06 p0827 N71-10857
- Broadband sound wave delay line with low insertion losses
23 p3731 N71-36600
- Delay line with acoustic transverse wave and insertion loss compensation, using piezoelectric transducers
23 p3732 N71-36601
- ## INSERTS
- ### NT NOZZLE INSERTS

SUBJECT INDEX

Weldability characteristics of consumable inserts for tungsten arc welding of NERVA lines
[NASA-CR-115885] 03 p0692 N71-14941

DETECTION

NT INFRARED INSPECTION

NT X RAY INSPECTION

Inspection device with warning system for RW 330 computer near CABRI reactor
[CEA-N-1274] 04 p0547 N71-13638

Design, construction, test analysis, and inspection of ultrasonic phased Doppler surveillance radar out
[AD-717044] 10 p1522 N71-31361

Determination of inspection intervals and nature of inspections for safe and economical operation of aircraft structures
[FFA-120] 11 p1676 N71-23431

Markov renewal process model for inspection, replacement, and maintenance system
[TR-71-5] 14 p2386 N71-26695

Pulsed crack length relationship with aircraft inspection intervals and structural reinforcement, high strength materials, and aircraft usage effects
18 p3051 N71-30783

Correction of inspection data for port misalignment utilizing small computer
[Y-1753] 19 p1323 N71-32217

Post-processor producing control tape for continuous-path, numerically controlled inspection machine
[Y-1725] 19 p3062 N71-32345

INSTABILITY

U STABILITY

INSTALLATION

INSTALLATION MANUALS

Handbook containing radar theory, engineering, control systems, communications, and instruments
[AD-716646] 09 p1349 N71-19774

INSTALLING

Environmental tests of tests developed for aviation use including installation, safety, and maintainability
[AD-721153] 15 p2390 N71-26680

Training and installation procedures for NASTRAN program
22 p3486 N71-34288

INSTITUTIONS

NT BUREAU (ORGANIZATIONS)

Organization, functions, and research capabilities of Arctic Institute of North America
11 p1733 N71-22816

Constraining institutional factors and options for civil aviation research and development
[NASA-CR-1807] 15 p2366 N71-27009

Survey of scientific activities and employment in independent nonprofit institutions for 1970
[NBS-71-9] 19 p3199 N71-32692

Federal budgeting for research and development by Agency for fiscal year 1969
[DSF-70-49] 20 p3370 N71-33716

INSTRUCTION SETS (COMPUTERS)

Computer program for selection, editing, and dissemination of continuing and scientific educational literature from NASA technical reports
[NASA-CR-111613] 03 p0342 N71-12477

User manual in form of interactive, functionally dependent time series programs accessible in any order from remote terminal
[NASA-CR-116179] 06 p0820 N71-16431

User manual for NOISY1 program to calculate space dependent spectral density functions of noise in nuclear reactors
[BNWL-1260] 07 p1658 N71-16964

User guide for Langley time series analysis computer program used in analyzing random, stationary time series
[NASA-TM-X-21469] 07 p0997 N71-17411

High level computer programming language /SASM-FLB/ and parallel processing system to implement it
[NASA-CR-117174] 09 p1356 N71-20332

Instructional strategies for optimizing learning processes and application of such principles to practical course of instruction in computer science
[NASA-CR-121936] 22 p3556 N71-35326

INSTRUCTIONS

U EDUCATION

INSTRUCTORS

Determining faculty succession for accredited on-going curriculum as function of faculty workload, number of students, and curriculum characteristics with cost estimates
[NASA-CR-123114] 24 p4034 N71-38790

INSTRUMENT APPROACH

Jet aircraft crash during instrument approach due to electrical systems failure
[NTR-AAR-76-22] 01 p0005 N71-10812

Low jet crash during instrument approach due to descent below path profile
[NTR-AAR-76-21] 01 p0005 N71-10813

VTOL display and control system for deceleration to instrument hover
[NASA-TN-D-6108] 06 p0795 N71-16584

Index of standard instrument approach procedures for domestic and foreign airports
12 p1959 N71-23233

Operational performance of Hawker Siddeley aircraft automatic flight approach and landing control system
12 p1854 N71-23414

Mathematical perturbation models of aircraft ILS approach and landing
[VTR-159] 17 p2783 N71-29496

Terminal area studies with XC-142, XV-5, Do-31, and P 1127 aircraft to develop powered lift control techniques for instrument approach
18 p3870 N71-30774

INSTRUMENT COMPENSATION

NT TEMPERATURE COMPENSATION

Remote positioning facility for calibration of gamma radiation instruments at high exposure rates
[RD/B/N-1624] 05 p0359 N71-13167

Developing system for automatic compensation of signal dc level drift in laser interferometers
[Y-1737] 05 p0697 N71-15232

Arithmetic all function correction for laser excited Raman spectra of carbon tetrachloride and methanol
12 p1934 N71-24068

Phase transformation transition points on high pressure scale for precise pressure measurement standards
[NBS-SP-326] 14 p2342 N71-26476

High pressure effects on thermocouple electromotive forces
14 p2527 N71-26484

Pressure effects on thermoelectric response of platinum/rhodium thermocouple
14 p2527 N71-26485

Automatically balanced air bearing simulators for testing satellite attitude control system
[BSRO-CR-18] 17 p2779 N71-29571

Magnetic field compensation by magnetic system model for phaseotron with space variation
[JNDR-P9-5590] 18 p2958 N71-30475

Error correction for GEOS-C altimeter system from range and angle observations
19 p3099 N71-31878

Lag correction procedure for radiosonde humidity measurement errors
19 p13131 N71-32737

Feedback control of tilt compensation horizontal pendulums for earth tide observation
20 p3265 N71-33369

INSTRUMENT DRIFT

U DRIFT (INSTRUMENTATION)

INSTRUMENT ERRORS

Instrument error analysis for visual tracking of satellites using goniometers
[NASA-TT-F-13355] 03 p0452 N71-12283

Behavior of attitude gyro and gyro horizon during looping flight
03 p0413 N71-13281

Investigating gyroscopic stability and error compensation in navigation instruments
[JPRS-52046] 06 p0893 N71-15951

Improving precision of gyrostabilizer having feedback with respect to reactive moment of gyroscope
06 p0893 N71-15953

Investigating indirect stabilization of magnetometers on moving objects
06 p0894 N71-15955

Determining errors in moon and earth horizon sensors due to effects of surface roughness
07 p1056 N71-16963

Velocity, position and guidance sensor instrument errors for inertial platforms and satellite guidance
[BNBW-FB-W-70-45] 07 p1056 N71-17166

Measurement errors of platinum resistance thermometers
[NRC-TT-1427] 09 p1389 N71-20259

Atmospheric density changes observed from slant soundings over three and one half hour period, and determination of sensor random error
10 p1551 N71-21204

Computational models for estimating errors in temperature measurements in fluids and solids
11 p1842 N71-22597

Optimum estimation model for noise using instrument parameter variables
[TR-70-8-15] 12 p1951 N71-24248

Geographic position locator for accurate, long term, land based navigation
[UCRL-50978] 15 p2441 N71-26961

Visual binary stars used to compare external errors and systematic differences in K line, line-ratio, and H sub gamma luminosity systems
16 p2680 N71-28789

Statistical analysis of gyrocompass mode of A-6A inertial navigation system
17 p2780 N71-30315

Microweighting as important error source in activity measurements to explain discrepancies between international measurement comparisons
[CEA-E-4169] 18 p2973 N71-30542

Photographic technique for reducing instrument errors of ruby laser systems for satellite ranging
19 p3099 N71-31859

Accuracy of earth tidal observations using altimeters and automatic calibration
20 p3264 N71-33364

INSTRUMENT ORIENTATION

INSTRUMENT FLIGHT RULES

Application of IFR with unpowered, low lift drag ratio landing approaches
01 p0883 N71-10110

Controlled visibility device for simulating poor visibility conditions in training pilots in instrument landing and flight procedures
[NASA-CASE-NFR-04147] 01 p0859 N71-10748

Environmental tests of VOILOC 2 simplified directional approach system to determine compliance with FAR-Part 171
[FAA-RD-71-12] 10 p1599 N71-30666

Flight simulator evaluation of aircraft instrument departure procedure
[FAA-PS-080-2] 17 p2783 N71-29423

Effects of aircraft system noise and signal fading on pilot performance during IFR approach based on computer simulation of XV-5 aircraft and UH-1 helicopter
[AD-724336] 20 p2399 N71-33876

Summary of instrument flight rule off-airway routes for commercial and military aviation in US and overseas areas
21 p3433 N71-34392

INSTRUMENT LANDING SYSTEMS

NT AUTOMATIC LANDING CONTROL

Application of IFR with unpowered, low lift drag ratio landing approaches
01 p0883 N71-10110

Program effectiveness and facility criteria for ILS investment decisions
01 p0836 N71-10535

Evaluation of systems, procedures, and instrumentation for air traffic control
[AD-711663] 01 p0883 N71-10757

Advanced ILS and automatic landing systems for conventional and VTOL aircraft - conference
[AGARD-CP-59-70] 03 p0404 N71-12426

Psychological and procedural aspects to ILS approaches and landings in visibility less than 1200 feet
03 p0402 N71-12429

Automatic landing system optimization using inertial navigation data and modern control theory
[NASA-CR-111573] 03 p0402 N71-12431

Past and projected development of VFR ILS
03 p0407 N71-12447

Minimum channel requirements for ILS localizer frequency assignment, 1970-1973
[AD-714111] 06 p0804 N71-16190

Fixed base simulation evaluation of one fully automatic and six manual low visibility landing systems for helicopters
[NASA-TN-D-5913] 09 p1324 N71-20085

Microwave landing guidance systems initial concept validation tests in RTCA signal format
[AD-717183] 10 p1600 N71-21368

Radio frequency interference monitoring for instrument landing system in automatic landing
[RAE-TR-7076] 12 p1460 N71-23536

Landing systems signal reflection interference on correlation protected instrument landing system beams
[RAE-TR-70141] 12 p1960 N71-23361

Mathematical perturbation models of aircraft ILS approach and landing
[VTR-159] 17 p2783 N71-29496

System analysis of aircraft, aircraft guidance and control systems, and atmospheric turbulence for low visibility instrument landing system requirements
[AD-722773] 17 p2785 N71-30173

Minimum variance estimates of signal derivatives with application to case of aircraft descent rate in instrument landing systems
[NASA-CR-111928] 17 p2785 N71-30241

Flight tests to determine handling qualities of general aviation aircraft during ILS approaches in turbulent air
18 p2869 N71-30771

Analysis of glide-slope information requirements for low visibility aircraft landing approach using Kalman filter-optimal control combination to simulate DC-8 control system
[AD-722655] 18 p2956 N71-30887

Motion cues and pilot error in simulated instrument landing system approach
19 p3074 N71-31933

Test and evaluation of aircraft glide slope landing system operating at ultrahigh frequency
[FAA-TM-X-71-15] 19 p3133 N71-32085

Effect of turbulence and aircraft performance on ILS approach test and longitudinal stability
[NASA-CR-1021] 20 p3210 N71-33325

All weather landing system design, development, and field and flight testing
22 p3618 N71-35777

INSTRUMENT ORIENTATION

In-situ measurement of objective lens data for alignment of high resolution electron microscope
[NASA-TM-X-63018] 09 p1305 N71-19795

Inertial global alignment system for spacecraft guidance
[NASA-CASE-XMP-01669] 12 p1959 N71-25389

Optical gaging system for monitoring machine tool alignment
[NASA-CASE-XAC-09489-1] 14 p2364 N71-26673

INSTRUMENT PACKAGES

INSTRUMENT PACKAGES

NT APOLLO LUNAR SURFACE EXPERIMENTS PACKAGE

High velocity guidance and spin stabilization gyro controlled jet reaction system for launch vehicle payloads

[NASA-CASE-XLA-01339] 05 p0774 N71-15692

Ethylene oxide sterilization and encapsulating process for sterile preservation of instruments and solid propellants

[NASA-CASE-XNP-09763] 09 p1391 N71-20461

Hermetically sealed coaxial package for housing microwave semiconductor components

[NASA-CASE-GSC-10791-1] 16 p2601 N71-28562

INSTRUMENT TRANSFORMERS

Linear differential variable transformer for measuring length variations of flux in in-pile irradiation capsule

[CEA-N-1315] 05 p0686 N71-15419

INSTRUMENTAL ANALYSIS

U ANALYZING

U AUTOMATION

U INSTRUMENTS

INSTRUMENTS

Instrument for studying electron stimulated luminescence of terrestrial, extraterrestrial, and synthetic materials - luminescope

01 p0052 N71-10086

Research in instrumentation and mass spectrometry

[NBS-TN-546] 02 p0174 N71-11229

Contemporary instrument technology

[JPRS-51085] 05 p0687 N71-15470

Operation and utilization of 5.5 MeV Van de Graaff accelerator

[BARC-459] 06 p1252 N71-18298

Method and apparatus for bowing of instrument panels to improve radio frequency shielded enclosure

[NASA-CASE-XMF-09422] 09 p1346 N71-19436

Effect of lubricants with fillers on wear of diamond instrument during cold drawing of wire

[AD-716523] 09 p1405 N71-19823

Design and development of pressure sensor for measuring differential pressures of few pounds per square inch

[NASA-CASE-XMF-01974] 11 p1764 N71-22752

Development of temperature compensated thrust measuring gage for measuring forces as function of time in environment with varying temperature

[NASA-CASE-XGS-02319] 11 p1765 N71-22965

Development and characteristics of self-calibrating displacement transducer for measuring magnitude and frequency of displacement of bodies

[NASA-CASE-XLA-00781] 11 p1726 N71-22999

Medium energy physics research in accelerator structures, power systems, and control and instrumentation

[LA-4571] 12 p1897 N71-23727

Analysis of errors which occur during assembly of optical instruments and methods for eliminating errors

[AD-719773] 13 p1215 N71-24940

Nuclear and solid state physics research and instrument development

[BMW-FBK-70-10] 15 p2487 N71-27832

Research in nuclear physics and chemistry and reactor technology and instrumentation

[DNR-1180] 15 p2494 N71-27951

Nuclear research on muon, low and high energy pion, and energetic pion channels and instrumentation

-LAMPP

[LA-4578] 17 p2790 N71-29247

Research in high energy nuclear physics, nuclear structure, reactions, and instrumentation

[LYCEN-7002] 18 p2976 N71-30618

Service life, instrumentation, and cryogenic technology applications

[NASA-SP-593201] 18 p2962 N71-30707

Instrument for synchronous photographic recording of perturbing acceleration and residual tilt of gyro-stabilized platform

21 p3418 N71-34320

General descriptions, specifications, circuits, and performance data for nuclear instrument module system

[JAERI-MEMO-4295] 21 p3428 N71-34390

General descriptions, specifications, circuit diagrams, and performance data for nuclear instrument module system

[JAERI-MEMO-4281] 21 p3428 N71-34391

Nuclear research on radiation protection and instrument development

[UCL-30007-70-3] 22 p3643 N71-35976

INSULATED STRUCTURES

Swaged mineral-insulated cable for high temperature neutron detector

[AEEW-R-698] 09 p1389 N71-20258

Bibliography on industrial weatherproofing processes

[AD-723801] 19 p3105 N71-32176

Effects of heat aging on properties of polyimide insulating film used in production of high temperature flat electrical cables

[BDX-613-344] 23 p3777 N71-36919

INSULATING MATERIALS

U INSULATION

INSULATION

NT ELECTRICAL INSULATION

NT MULTILAYER INSULATION

NT THERMAL INSULATION

Electret processes for characterizing nonluminescent and near-insulating solids

01 p0107 N71-10082

Electrode attached to helmets for detecting low level signals from skin of living creatures

[NASA-CASE-ARC-10043-1] 02 p0168 N71-11193

Design and development of high temperature vacuum insulation systems for SNAP 21 thermoelectric power system

[TID-25482-APP] 04 p0553 N71-13995

Bibliography synopsis of external insulation materials and techniques for cryogenic storage systems

[NASA-CR-114836] 06 p0958 N71-16865

Gamma radiation induced currents between insulated dissimilar electrodes

[AECL-3564] 08 p1167 N71-18217

Direct and liquid absorption methods of testing ceramic insulator compaction in sheathed thermocouples

[ORNL-4439] 08 p1242 N71-19346

Characteristics of foamed-in-place ceramic refractory insulating material and method of fabrication

[NASA-CASE-XGS-02435] 11 p1785 N71-22996

Self-evacuating multilayer insulation system of aluminum Mylar and polyurethane foam for liquid hydrogen tanks

[NASA-CR-72856] 13 p2102 N71-25447

Analysis of insulating properties of alkali metallic colloids and problem of charge generation by contact ionization

[AD-721197] 15 p2368 N71-26896

Investment casting, metal drawing, longitudinal and spiral milling, and insulator pin designs in production engineering

[BDX-613-316] 16 p2613 N71-28751

Interdisciplinary research on properties of ceramic materials with emphasis on refractory surface insulation

[NASA-CR-121890] 22 p3598 N71-35618

INSULATORS

High voltage insulators for direct current in acceleration system of electrostatic thruster

[NASA-CASE-XLE-01902] 01 p0116 N71-10574

Energy gap for excitonic insulator in presence of persistent currents

[AD-716749] 10 p1634 N71-20919

Ultrasonic interactions with nuclear and electron spins in antiferromagnetic insulators

[AD-717190] 10 p1635 N71-21702

Polycarbonate insulator design with increased mounting-pin size for high acceleration

[BDX-613-213] 11 p1769 N71-22493

Reactor irradiation of thermionic sheath insulators - two beryllia and two alumina bonded trilayers

[NASA-TM-X-2271] 13 p2116 N71-24635

Design, development, and production of magnesium oxide insulators installed in cathodic and anodic walls of open cycle magnetohydrodynamic generator channel

22 p3599 N71-35630

Development and evaluation of refractory magnesial and aluminous concretes for use as insulating walls in magnetohydrodynamic generator channel

22 p3599 N71-35632

Color center and substitutional impurity point defects in magnesium, calcium, and strontium oxide insulators

[AD-726647] 23 p3835 N71-37351

INTAKE SYSTEMS

NT AIR INTAKES

NT CONICAL INLETS

NT ENGINE INLETS

NT HELICAL INDUCERS

NT HYPERSONIC INLETS

NT INTERNAL COMPRESSION INLETS

NT SUPERSONIC INLETS

Cavitation and noncavitation performance of 78 deg helical inducer in liquid hydrogen

[NASA-TM-X-2131] 02 p0203 N71-11683

Shortening transition liner to decrease overall length of ram induction combustor

[NASA-TN-D-7021] 03 p0448 N71-12422

Wind tunnel tests of mixed compression axisymmetric inlet system at Mach numbers 0.6 to 3.5

[NASA-TN-D-6078] 03 p0449 N71-13024

Magnetic field and high frequency induction of toroidal enclosure

[AEC-TR-7168] 05 p0734 N71-15441

Static tests to determine effects of throat inlet concepts on forward-radiated fan noise of 707-320B/C airplanes

[NASA-CR-1715] 07 p0971 N71-17426

Effect of various diffuser designs on performance of experimental turbojet combustor insensitive to radial distribution of inlet airflow

[NASA-TM-X-2216] 08 p1303 N71-18561

Aerodynamic flow field interference effects on supersonic intakes

09 p1313 N71-19372

Design and characteristics of supersonic cruise inlets

09 p1458 N71-19460

Intake system design, fabrication, and testing in two phase hydrogen

[NASA-CR-103054] 11 p1767 N71-21095

Design, performance characteristics and testing of two-phase hydrogen pump inducer for use in future spacecraft systems

[B-71-21] 17 p2830 N71-29578

Numerical method for calculating optimal lining impedance for inlet duct of jet engines

[NASA-CR-1832] 19 p3081 N71-32563

Instability and turbulence for various external compression axisymmetric supersonic intakes of 25 degree cone semi-angle at various turbulence, Reynolds number, and surface conditions

[ARL/ME-129] 20 p3251 N71-33584

Design criteria for liquid rocket engine turbopump inducers

[NASA-SP-8052] 21 p3502 N71-34950

INTEGERS

Fast integer programming and K-th shortest paths [P-592]

19 p1325 N71-32583

Fermat pseudo primes, and odd composite numbers

21 p3449 N71-34546

INTEGRAL CALCULUS

High precision moments for fourier coefficients of arbitrary functions

[NASA-CR-122919] 23 p3781 N71-36946

INTEGRAL EQUATIONS

NT FREDHOLM EQUATIONS

NT SINGULAR INTEGRAL EQUATIONS

NT VOLTERRA EQUATIONS

NT WIENER HOPF EQUATIONS

Half-range expansion theorems in studies of polarized light

[AD-710313] 01 p0091 N71-10720

Integral equation formulations for electromagnetic scattering from two-dimensional inhomogeneities in conductive earth

[NASA-CR-110910] 01 p0049 N71-10783

Integral equation formulations for electromagnetic scattering from two-dimensional inhomogeneities in conductive earth - appendices, figures, bibliography, and computer programs

[NASA-CR-110911] 01 p0050 N71-10784

Integral equations for aperture fields, leading terms in near and far zone fields, admittance, and effective height of antenna slot antennas

[SC-R-70-4281] 01 p0035 N71-10794

Integral equations of inviscid hydrodynamics applied to viscous, heat conducting, chemically reacting, radiating shocked flows

[AD-711954] 02 p0201 N71-11580

Asymptotic behavior and error analysis for linear integral differential difference equations

03 p0401 N71-13329

Integral vectorial equation for calculating current distribution on antennas

04 p0491 N71-13787

Integral formulation stress analysis of three dimensional problems with or without steady state thermal stresses

[REPT-70-C-148] 04 p0616 N71-13740

Integral equation for unsteady surface waves also evaluation of Boussinesq equation

[AD-713107] 05 p0664 N71-14979

Interaction of QTX wave with density fluctuations in inhomogeneous magnetized plasma

[AD-712777] 07 p1084 N71-18061

Path integral formulation and evaluation of space-time correlation functions for calculating transport coefficients

[NVO-1480-160] 08 p1264 N71-19104

Method of integral relations applications to boundary layer problems including separation

[NASA-CR-117051] 09 p1373 N71-19832

Extremal property of stochastic integral of anticipating Brownian functional

09 p1411 N71-28529

Integral equations of kinematics of cascade drag and energy distribution

[JNRP-P1-4926] 09 p1443 N71-28428

Treating large scale ionospheric disturbances with inhomogeneous linear integral equation and Green function

[AD-717204] 10 p1547 N71-20795

Spherically symmetric phase change problem solved by heat balance integral method using appropriate temperature profile

[AD-718151] 12 p1999 N71-23331

Development of Machian theory of inertia and gravitation

12 p1912 N71-23086

Radiative transfer problems using invariant imbedding and Fredholm integral equations with displacement kernels

[AD-718090] 12 p1950 N71-23710

Mathematical study of unfolding problems arising in experimental nuclear physics

[AD-718228] 12 p1972 N71-23805

Integral equation to describe thermodynamic properties of one-dimensional Heisenberg model

[RIFP-116] 12 p2013 N71-34258

Faddeev solution to Lippman-Schwinger integral equation for three particle scattering

13 p2132 N71-25094

Applying method of moments to solution of integral equations for current induced on conducting cylinders in two-dimensional field

14 p2218 N71-26272

Monosenergetic neutron transport in homogeneous slabs based on calculus of variations and Chandrasekhar equation

15 p2459 N71-26992

Equations and formulae for magnets with air cored windings of saddle coil type

15 p2453 N71-27139

Crimp of polyethylene under varying temperature for nonlinear uniaxial stress described by multiple integral representation and modified superposition principle

15 p2430 N71-27259

Approximate solutions to Bethe-Salpeter and integral equations, and applications to high energy interactions

15 p2466 N71-27265

Integration of exponential functions and application to long wave radiative transfer near resonance

15 p2404 N71-27565

Simple integral method for calculating real gas turbulent boundary layers with variable edge entropy and flight calculations showing effect of nose bluntness at 6.0 km/sec

16 p2578 N71-28014

Biometrical formalism in general theory of relativity and laws of conservation considering integral and differential form of conservation laws

17 p2787 N71-29701

Energy-integral prediction of hypersonic and hypersonic heat transfer in thermal boundary layer around blunt slender cones and of compressible flow with heat transfer

17 p2856 N71-29807

Variational and boundary value problems and differential properties of corresponding generalized solutions of integrodifferential equations

17 p2773 N71-29814

Integral equations of motion and momentum for hypervelocity wind tunnel nozzle design

17 p2731 N71-29906

Inversion formulas for singular integral equations for linear dislocation arrays

17 p2817 N71-29936

Dislocation pileup problem solving, using orthogonal polynomials and singular integral equations

17 p2817 N71-29937

One electron theories of cohesion on ion pair potentials in metals, using Fourier transformation and integral equations

17 p2818 N71-29940

Critical analysis of integral formulation of scalar wave reflection, diffraction, and scattering by arbitrary surfaces

18 p2966 N71-31583

Evaluation of integral equation for predicting HF ground wave attenuation over inhomogeneous irregular terrain

19 p3055 N71-31948

Three dimensional integrals for stationary neutron transport equation with spherical symmetry

19 p3149 N71-32103

Quantitative determination of optical imperfection by mathematical analysis of Foucault knife edge test pattern in large orbiting telescope

19 p3142 N71-32184

Optics of linear media formulated in terms of integrodifferential equations and extended to spatially dispersive media

19 p3143 N71-32607

Numerical integration of Fourier integrals using spline algorithm

20 p3290 N71-32989

Numerical integration of Abelian integral equation for X ray radiant flux density using spline functions

20 p3290 N71-33010

Numerical integration of integrodifferential equations for creep analysis of thick-walled cylinders

20 p3291 N71-33144

Scattering of electromagnetic waves using integral equation form of Maxwell equations for electric fields

21 p3447 N71-34530

Coupled integral equations for full scattering amplitudes of both reactive and nonreactive channels

21 p3447 N71-34531

Cubic spline approximation for integrals with logarithmic kernels

21 p3447 N71-34533

Integral equations for solution of three dimensional boundary layer problems

22 p3567 N71-35403

Numerical treatment of some integro-differential equations, Fourier integrals, and integral equations

22 p3606 N71-35682

Integral equation methods for calculating sound reflection and scatter from arbitrary closed surface

22 p3630 N71-35863

Computer program for determining radiating nonadiabatic inviscid flow over blunt body by integral equations

23 p3706 N71-36417

INTEGRAL FUNCTIONS

U ENTIRE FUNCTIONS

INTEGRAL TRANSFORMATIONS

NT CONVOLUTION INTEGRALS

NT FOURIER TRANSFORMATION

NT HILBERT TRANSFORMATION

NT LAPLACE TRANSFORMATION

Integral transformations of forced torsional vibrations of thin spherical shells

01 p0130 N71-10704

Classical theory of conductive heat transfer

03 p0469 N71-13226

Dipole expansion technique for particle simulation of plasmas

07 p1084 N71-18090

Direct and inverse application of Dorodnitsyn technique to incompressible transonic flow over symmetric Joukowski airfoil sections

09 p1316 N71-19750

Fredholm transformations and Radon-Nikodym derivatives for evaluation of Yeh-Wiener integrals of exponential functions

12 p1948 N71-23348

Numerical evaluation of downwash integral for wing loading of lifting rectangular planform

13 p2102 N71-24483

Comparison of standard Z transform and algebraic substitution synthesis methods for digital filters

16 p2569 N71-28397

Iterative solution for integral transformations

17 p2773 N71-29789

Approximation theorem of Grauert for holomorphic functions

24 p3948 N71-38161

INTEGRATED CIRCUITS

NT LARGE SCALE INTEGRATION

Gridded thick film metallization structure employed in multichip circuit fabrication

01 p0030 N71-10054

Microstrip substrates and Schottky barrier diode development for microwave integrated circuits

01 p0031 N71-10158

Mixed MOS and bipolar transistor silicon integrated circuit operational amplifier characteristics and applications

01 p0033 N71-10223

Computer aided integrated circuit mask production

01 p0036 N71-10225

Cascade synthesis of logic functions

02 p0186 N71-11310

Design of diagnosable control units for switching systems using modular integrated circuits

02 p0192 N71-11346

Physical failure analysis of integrated circuits containing metal oxide semiconductors and its application to analog gates

02 p0194 N71-11359

Development of flexible selected interconnection technique for monolithic circuits

02 p0196 N71-11376

Monolithic COS/MOS large scale parallel processor array

03 p0340 N71-12465

Digital computer program requirements to process Apollo spacecraft electrical data for sneak circuit analysis

03 p0342 N71-12482

Biphase modulator using microwave integrated circuit

03 p0349 N71-12522

Investigating federated and integrated approaches to digital computer design for aerospace vehicles

03 p0346 N71-12605

Proceedings from lecture series on large scale integration in microelectronics

03 p0354 N71-12626

Technology review on large scale integration circuitry

03 p0354 N71-12627

Comparison of MOS and bipolar LSI technology

03 p0354 N71-12628

Computerized design of LSI systems particularly MOS arrays

03 p0354 N71-12629

System packaging of LSI circuits

03 p0354 N71-12630

LSI circuitry using MOS structures for airborne computers

03 p0348 N71-12631

LSI devices and techniques for electronic systems design

03 p0352 N71-12632

Quality and reliability assurance methods for LSI circuits

03 p0384 N71-12633

Cost effectiveness of LSI circuits

03 p0354 N71-12634

Integrated circuits for digital applications in high dc noise systems

03 p0376 N71-12769

Electrical properties of solid state materials and devices

[AD-711848] 03 p0441 N71-12834

Composite ferrite substrates for microwave integrated circuits

04 p0312 N71-13912

Dielectric field computations in semiconductor oxide integrated circuits

05 p0655 N71-14923

Semiconductor integrated circuit component models

05 p0653 N71-14924

Microminiaturized frequency discriminator with semiconductor without induction components

05 p0656 N71-15517

Digitalizing electrometer system using integrating preamplifier

06 p0822 N71-16056

Design and performance of logic circuit chip for computerized design of MOS integrated circuit arrays

07 p1001 N71-17092

Discussing techniques for improving quality and reducing cost of silicon chips used in integrated circuits

07 p1087 N71-17277

Use and limitations of spreading resistance technique for evaluating buried collector layer structures in integrated circuits

07 p1090 N71-17501

Low power NAND gate integrated circuit employing thin film resistors and lateral p-n-p transistors

07 p1092 N71-17872

Microelectronic Navy equipment

07 p1090 N71-17933

Finite linear circuit construction from capacitors and differential voltage controlled current sources

09 p1357 N71-19429

Temperature intermittent operation in encapsulated integrated circuits

09 p1359 N71-19757

Associative memory system for mass storage using integrated circuits and array organization

[BNL-14519] 09 p1355 N71-20124

Measurement methods during fabrication and environmental testing of microcircuits

09 p1360 N71-20328

Technology review on integrated linear, digital, and optoelectronic circuits

10 p1537 N71-20893

Computer simulation for design of integrated microwave linear amplifiers

11 p1723 N71-22104

Construction and properties of switch-isolators, switch-phase shifters, and switch-phase shifter-isolator electric circuits

[AD-717541] 11 p1723 N71-22145

Models for performance characterization of integrated electro-thermal circuits

11 p1725 N71-22716

Computer circuit performing both counting and shifting logic operations also capable of miniaturization and integration in basic circuits

[NASA-CASE-XNP-01753] 11 p1721 N71-22897

Surface impurity and structural defect analysis on thermally grown silicon oxide integrated circuit

[NASA-CR-117904] 12 p1893 N71-23715

Digital simulation, digital filters, PDP 9 computers, on-line programming, hybrid computers, computer graphics, plotters, analog computers, optimization, and integrated circuits

[REFT-29-70-400] 12 p1882 N71-23862

Solid state monolithic integrated analog multiplier based on controlled transconductance principle

[NASA-CR-118014] 12 p1884 N71-23874

Feasibility, design, and algorithms of integrated circuit content addressable memories

12 p1891 N71-24025

Development and characteristics of electric circuitry for detecting electrical pulses rise time and amplitude

[NASA-CASE-XMF-00804] 13 p2055 N71-24717

Metal oxide silicon field effect transistors for integrated circuitry in data processing

13 p2152 N71-25322

Optimal manufacturing processes for integrated circuits

[JPRS-53078] 14 p2227 N71-25717

Manufacturing quality controls for line certification of thin film and thick film hybrid microcircuits for NASA use

[NASA-CR-103168] 14 p2232 N71-25905

Major microelectronic production technologies including materials for manufacturing thin- and thick-film circuits, monolithic integrated circuits, and hybrid design

[AD-721279] 15 p2385 N71-26897

Wide-range nuclear magnetic resonance probe design including integrated circuits, RF coil, and coaxial cable for use with high field cryogenic magnets

[NASA-TN-D-6338] 15 p2503 N71-26908

Transfer function models of DTL and TTL integrated circuits

[SC-RR-70-450] 15 p2388 N71-26983

Reliability evaluation of plastic-encapsulated integrated circuits including long-term tests and short-term highly accelerated tests
[AD-722043] 16 p2569 N71-28405

Integrated circuit development, photolithographic interconnection of plastic imbedded semiconductor chips, semiconductor testing, magnetic film engineering and computer applications
[AD-722075] 16 p2665 N71-28557

Development of quantum optical integrated circuits of gallium arsenide from semiconductor integrated methods
[JPRS-53462] 17 p2727 N71-29258

Semiconductors and semiconductor devices, insulating and semiconducting glasses, and measurement techniques
[AD-722474] 17 p2816 N71-29840

Production of thin film tantalum nitride hybrid integrated circuits and telecommunications applications [NLL-PORS-TRANS-2707-9022.81] 17 p2728 N71-30184

Mathematical model of bipolar transistor for digital monolithic integrated circuits with low signal levels [NLL-PORS-2709-9022.81] 17 p2728 N71-30185

Integrated circuitry and design of analog reactivity meter for use with Experimental Breeder Reactor 2 [ANL-7700] 18 p2958 N71-30495

Developments in integrated circuit production and utilization as computer components [JPRS-53659] 18 p2901 N71-31555

Computerized design of integrated circuit boards using Lee algorithm 19 p3063 N71-31656

Feasibility of generalized integrated circuit for digital circuit requirements [SC-DR-710033] 19 p3070 N71-32206

Development of N path filter with passive RC circuits incorporating time-variable gyrators [AD-723656] 19 p3069 N71-32771

Polarimeter with integrated circuits for determining polarization angle of satellite transmission [K60-TL-71-102] 20 p3231 N71-32942

Development and characteristics of 1200 band frequency shift keying demodulator for use in digital integrated circuits [PHL-1971-12] 20 p3276 N71-33749

Digital integrated circuitry in 1200 band FSK modulator using frequencies of 1300 and 2100 Hz [PHL-1971-11] 20 p3276 N71-33860

Inverted geometry transistor for use with monolithic integrated circuit [NASA-CASE-ARC-10330-1] 21 p3403 N71-34214

High energy electron irradiation effects on field effect transistors in integrated circuit devices [NASA-CR-121623] 21 p3405 N71-34225

Development of procedures for infrared examination to improved reliability of large scale integration [NASA-CR-119921] 21 p3425 N71-34369

Integrated solid state C band parametric amplifier for use in space shuttle communication receiver 21 p3515 N71-35047

Feasibility of simultaneous solid state diffusion in manufacturing integrated circuits from doped silicon films [AD-726553] 22 p3561 N71-35361

Digital computer analysis of integrated logic circuit transient behavior [REFT-1143] 22 p3562 N71-35374

High concentration integrated computer storage devices [REFT-1413] 23 p3729 N71-36582

Calculating current voltage and capacitance voltage characteristics in production of Schottky diodes for integrated circuits [NLL-PORS-TRANS-2760-9022.81] 23 p3733 N71-36617

Conference on research, development, and applications of integrated microelectronic circuits 23 p3735 N71-36625

Comparison of production technologies for silicon gate MOS and ISOPANAR bipolar integrated circuits 23 p3735 N71-36626

Production and characteristics of Schottky barrier diode clamped TTL circuits 23 p3735 N71-36627

History and fundamentals of MOS logic circuit development 23 p3735 N71-36628

Input/output devices and MOS-LSI circuits for desk calculator systems 23 p3735 N71-36629

Application of logic functions to design of MOS circuits 23 p3735 N71-36630

Design and applications of bipolar MSI devices 23 p3735 N71-36632

Design, fabrication, and application of integrated microsystems for electronic equipment 23 p3735 N71-36633

Computerized design of MOS circuits 23 p3736 N71-36634

Economic factors of custom or customer designed integrated circuits 23 p3736 N71-36635

Computerized design of Micromosaic integrated circuit arrays 23 p3736 N71-36636

Interactive graphics for computerized design of integrated circuit layouts 23 p3736 N71-36637

Integrated memory cell circuits for solid state storage 23 p3736 N71-36639

Integrated circuits designed for audio frequency output amplifier and line output stage of television receiver 23 p3736 N71-36641

Optimized design techniques for linear integrated circuits 23 p3736 N71-36642

Microelectronic linear integrated circuits for radar equipment and telecommunications 23 p3736 N71-36643

Low cost electronic control systems for automobiles utilizing integrated circuits 23 p3737 N71-36646

Evaluation of design fabrication, inspection and testing of integrated circuits aimed at improving quality and reliability of hardware using these devices [AD-726560] 24 p3899 N71-37786

Development of techniques and equipment for measuring contact resistance between two single crystals and thin film microcircuits [AD-727988] 24 p3899 N71-37789

Interrelations between advanced processing techniques, integrated circuits, laser radiation, and microcircuit interconnections 24 p3900 N71-37799

Gyration applications related to integrated circuits 24 p3900 N71-37800

INTEGRATED MISSION CONTROL CENTER

Mathematical models for automated environmental control of acoustic test facility inside chamber [NASA-CR-115072] 17 p2732 N71-30355

INTEGRATION [REAL VARIABLES]

U MEASURE AND INTEGRATION

INTEGRATORS

NT DIGITAL INTEGRATORS
Solid state operational integrator [NASA-CASE-NPO-10230] 03 p0349 N71-12520

Reactor thermal power integrator for safeguards control [PEL-200] 05 p0727 N71-15087

Variable duration pulse integrator design for integrating pulse duration modulated pulses with elimination of ripple content [NASA-CASE-KLA-01219] 11 p1730 N71-23084

Solid state integrator for converting variable width pulses into analog voltage [NASA-CASE-KLA-03356] 12 p1892 N71-23315

Feedback integrating circuit with grounded capacitor for signal processing [NASA-CASE-XAC-10607] 12 p1893 N71-23669

High speed phase detector design indicating phase relationship between two square wave input signals [NASA-CASE-XNP-01306-2] 13 p2035 N71-24596

Integrator design to provide subroutines for numerical solution of ordinary differential equations [NASA-CR-118521] 14 p2224 N71-26381

INTEGRODIFFERENTIAL EQUATIONS

U DIFFERENTIAL EQUATIONS

U INTEGRAL EQUATIONS

INTELLECT

Psychological investigations and theory of thinking with four types of intellectual associations 22 p3544 N71-35247

INTELLIGENCE

NT ARTIFICIAL INTELLIGENCE

NT INTELLECT
Intelligence, speed, and conversational ability of dolphins [JPRS-52395] 08 p1156 N71-19123

Speech recognition model for predictions of intelligibility and intelligence measures [AD-720091] 15 p2381 N71-27292

INTELLIGIBILITY

NT SPEECH RECOGNITION
Determination of subglottal pressures and air flow rates during vocal fry phonation [AD-711008] 02 p0180 N71-11265

Procedures for testing communication security equipment under simulated tactical conditions [AD-719095] 13 p2043 N71-24458

Method to quantify effect of speech transmission channels on speech intelligibility on basis of simple physical measurements [JZF-1970-23] 18 p2889 N71-31078

Apparatus for measuring speech transmission index of communication channels by means of artificial signal with measuring time below 3 sec [JZF-1971-2] 18 p2890 N71-31079

INTELSAT SATELLITES

Measuring diurnal variations and probability distributions of total polarization rotation at transverse region of ionosphere using synchronous satellites [AD-711403] 01 p0026 N71-10951

Developments in worldwide communication satellite network 02 p0181 N71-11234

Photography of Apollo 7 retrofire and service propulsion module reentry and apogee burn of Intelsat 2 F-2 satellite [NASA-CR-115869] 05 p0767 N71-14664

Chemical analysis and electrical performance tests of nickel cadmium batteries for Intelsat 4 program 16 p2539 N71-28662

Chemical analysis of Intelsat 4 nickel cadmium battery electrolyte 16 p2539 N71-28663

European space program and Intelsat - international cooperation and government/industry relations 17 p2862 N71-30322

Economic factors affecting decision to install ground station support equipment for communication with Intelsat satellite 20 p3235 N71-33807

Compatibility of European communication satellite with Intelsat satellites 23 p3859 N71-37906

INTENSIFICATION

U AMPLIFICATION

INTENSIFIER TUBES

U IMAGE INTENSIFIERS

INTENSIFIERS

NT IMAGE INTENSIFIERS

NT IMAGE ORTHICONS

INTENSITY

Mass spectrometer and radio frequency, high voltage spark ion source for measuring relative sensitivity factors for metals and steels [Y-1757] 14 p2299 N71-25702

Ozone and nitrous oxide vibrational intensity calculations [AD-722466] 18 p2885 N71-30855

Vehicle model of high intensity proton accelerating column [SJC-A-71-2] 22 p3643 N71-35972

INTERACTIONS

NT AIR WATER INTERACTIONS

Generalization of current-current weak interaction theory to include scalar or tensor interactions for I sub 1/2 and I3 decays [NYO-2262-TA-236] 15 p2464 N71-27227

Three types of uranium oxide-inconel cladding interactions investigated by X ray fluorescence analysis of two fuel elements after high burnup in VAK reactor [NLL-WINDSCALE-459-9091.9F] 21 p3462 N71-34664

INTERATOMIC FORCES

Interatomic forces and adherence of plasma sprayed coatings to substrates [NLL-TRANS-734-4553-9022.401] 10 p1589 N71-21375

Monte Carlo methods of constructing force constants of polyatomic molecules, using matrices of quadratic potential and kinetic energy functions [NLL-RTS-6266] 16 p2653 N71-29022

Electron scattering by stacking faults in metal crystals 17 p2825 N71-29998

Structure of hadrons covering hadronic and semileptonic processes [NYO-4076-L4] 22 p3646 N71-30800

Theoretical models and phonon dispersion measurements for analyses of rutile lattice dynamics [TID-25720] 24 p3996 N71-38506

INTERCEPT AIRCRAFT

U FIGHTER AIRCRAFT

INTERCONNECTION

U JOINING

INTERCONTINENTAL BALLISTIC MISSILES

Radio engineering systems for space vehicle and intercontinental ballistic missile continuous and discrete control [AD-717833] 11 p1792 N71-22338

History of rocketry in China including structure of rockets, advantages and disadvantages of various rockets, and capabilities of intercontinental missile [AD-720362] 14 p2543 N71-26822

Anti-intercontinental ballistic missile defense and high altitude nuclear explosions [BMVG-PBWT-71-2] 18 p2977 N71-30644

INTERFACE STABILITY

Dynamic stabilization of Rayleigh-Taylor instability [LRP-45/70] 04 p0599 N71-14252

INTERFACES

NT FLUID BOUNDARIES

NT GAS-SOLID INTERFACES

NT JET BOUNDARIES

NT LIQUID-LIQUID INTERFACES

NT LIQUID-SOLID INTERFACES

NT LIQUID-VAPOR INTERFACES

NT SOLID-SOLID INTERFACES

Methods for detecting turbulent/non-turbulent interfaces [AD-712375] 02 p0204 N71-11973

Group velocity and refractivity behavior of strong electromagnetic surface waves propagating along vacuum-plasma plane interface [DEMO-71/5] 23 p3824 N71-37274

SUBJECT INDEX

Mathematical model for motion of small drops and bubbles considering absorption, diffusion, and convection in interfacial region
[NJO-2807-91] 24 p3996 N71-38306

Flat plate thermal conductivity tests, long term stability tests, and interface effects on thermal performance of multilayer insulation materials for use in radioactive isotope power systems
[ALO-2832-43] 24 p4029 N71-38732

INTERFACIAL STRAIN
U INTERFACIAL TENSION
INTERFACIAL TENSION

Determination of surface tension in biologic fluids for susceptibility to decompression sickness
[NASA-CR-111382] 62 p0154 N71-11092

Surface tension and density of molten aluminum
[AD-711964] 63 p0396 N71-12814

Surface tension and dielectrophoretic techniques for liquid rocket propellant control
03 p0447 N71-13119

Dynamic stabilization of Rayleigh-Taylor instability
[LRP-45/70] 04 p0399 N71-14252

Fundamental equations of two phase flow with interfacial tension terms
[PB-193987] 05 p0664 N71-14971

Space electric surface tension propellant acquisition system for Mars and Grand Tour missions
[NASA-CR-111343] 05 p0761 N71-15292

Statistical theory of interfacial thermal conductivity and crystal growth under weightlessness
[NASA-CR-102989] 05 p0784 N71-15601

Scratch smoothing effects of surface tension on grooved mesh wires
[LA-4458] 06 p0871 N71-16260

Surface tension of liquid surface
08 p1245 N71-19166

Collocated interfacial elastic stress intensity for finite, bi-material plates
[AD-716334] 09 p1476 N71-19919

Interfacial tension in binary liquid system as function of temperature
11 p1739 N71-22584

Droplet evaporation in liquid-vapor critical region
[AD-718968] 13 p2184 N71-24363

Interfacial reactions of boron fibers and carbon fibers in chromium matrices at elevated temperatures
[ARL/MET-43] 15 p2432 N71-27620

Interfacial tensions and density measurement of chromium steel and vanadium slag noting silicon effect on phase transformations
18 p2934 N71-30689

Differential maximum-bubble-pressure apparatus used for surface tension measurements in air of liquid lubricants to 200 C
[NASA-TN-D-6450] 20 p3279 N71-33515

Two-dimensional, steady slow flow of incompressible viscous fluid, separating into layers above surface tension membrane
22 p3571 N71-35435

Structure-property relationships in liquid ceramics heated to temperatures as high as 3000 C
[AD-726401] 22 p3603 N71-35658

Interfacial tension pressure change measurements of mass transfer effects on droplet interface motions
23 p3780 N71-36941

Measurement of temperature with metal monitors using surface tension in range 780 to 1555 C
[JUL-680-RB] 24 p3936 N71-38081

INTERFERENCE

Methods for predicting speech interference within cockpit of fixed wing and rotary wing aircraft
[AD-718098] 12 p1878 N71-23328

Potential star tracker interference from radiation produced by mercury bombardment thrusters using electric propulsion systems
[NASA-TN-X-67835] 16 p2671 N71-28817

Corrections for subsonic wall interference effects in two dimensional perforated wall wind tunnel
[LTH-HA-3] 20 p3248 N71-33992

INTERFERENCE DRAG

Wind tunnel study of aerodynamic interference drag caused by fan jet engine wake of supersonic transport
[NASA-TN-D-6067] 05 p0141 N71-11004

Characteristics of VISTOL wall interference for closed circular wind tunnels
[NASA-TN-D-6127] 07 p1004 N71-17367

Aerodynamic interference characteristics of radiation-propulsion systems of transport and military aircraft
[AGARD-CP-71-71] 09 p1311 N71-19353

Wind tunnel vortex flow study on body of revolution with or without wings
09 p1311 N71-19355

Optimization of interferences between aircraft components in supersonic flow
09 p1311 N71-19356

Finite element computer program for estimating airframe aerodynamic interference
[NASA-TM-X-64884] 09 p1311 N71-19357

Lift and drag interference characteristics of delta winged half cones with leading edges
09 p1312 N71-19359

Numerical analysis of downwash interference on wings of missile train
09 p1312 N71-19360

Calculation methods for wing-body interference drag on supersonic aircraft in stationary or nonstationary flow
09 p1312 N71-19362

Interference flow field of fin-flat plate configuration in supersonic turbulent boundary layer channel
09 p1313 N71-19365

Flight and wind tunnel evaluations of flow field effects on performance of supersonic underwing exhaust nozzle at transonic speeds
09 p1313 N71-19366

Aircraft afterbody and engine nozzle interferences at subsonic, transonic, and supersonic speeds
[NASA-TM-X-64888] 09 p1313 N71-19368

Interference effect between oscillating and distorted inlet flow on compressor stall
09 p1313 N71-19370

Wind tunnel surveys of flow fields about wing fuselage store configurations of transonic and supersonic aircraft
[NASA-TM-X-64885] 09 p1313 N71-19371

Aerodynamic flow field interference effects on supersonic intakes
09 p1313 N71-19372

Wind tunnel tests with jet simulation of tailplane interference on European aircraft models
09 p1314 N71-19374

Aerodynamic interference caused by rear fuselage mounted power plants on BAC aircraft
09 p1314 N71-19375

Wind tunnel evaluation of interference drag in turbofan engine-wing configuration of subsonic aircraft
09 p1314 N71-19376

Computer program for determining low speed interference effects of flow fields about arbitrary bodies by superposition
09 p1314 N71-19377

Photographic recording of aerodynamic interference in wind tunnel simulation of jetted drop loads from aircraft
09 p1314 N71-19378

Flow field interference beneath swept wing fuselage store installation on aircraft
09 p1314 N71-19380

Computerized prediction of interference flow field for wing-fuselage store location on bomber aircraft
09 p1319 N71-19381

Wind tunnel studies of external store induced flow field instability effects on longitudinal stability of arrow wing aircraft
09 p1319 N71-19382

Flight test measurements on interference and aerodynamic drag effects caused by jettisoning of external stores from F-2 aircraft
09 p1319 N71-19384

Computerized prediction of flow field interference forces and moments on aircraft stores at subsonic speeds
09 p1319 N71-19385

Users manual for 3 computer programs for predicting aerodynamic interference between lifting surfaces and lift and cruise fans in transport-type aircraft
[NASA-CR-114332] 20 p3204 N71-33002

Conclusions and recommendations concerning wind tunnel tests of interaction between engine flow and wall corrections in transonic wind tunnels
23 p3703 N71-36401

Compilation of responses to questionnaire on engine-airframe interference in transonic tests
23 p3703 N71-36402

Wall corrections for airplanes with interference lift in transonic wind tunnel tests
23 p3704 N71-36403

Thrust-minus-drag forces and pressure distributions of closely spaced twin-jet afterbodies with different inboard-outboard fairing and nozzle shapes
[NASA-TM-X-2329] 23 p3705 N71-36412

INTERFERENCE GRATING

Using passband interference filters in multispectral photography for earth resources applications
02 p0227 N71-11987

Methods for eliminating double-sided intersymbol interference in digital data systems
14 p2218 N71-26248

Surface distortion measurement by holographic gratings, moiré effect, and wave front reconstruction
[CRIF-MT-70] 15 p2407 N71-27020

Inductive gratings for compensating dielectric cylinder effects on mounted aerial
[RA-87] 24 p3891 N71-37732

INTERFERENCE LIFT

Wind tunnel testing of interference lift of tandem wing aircraft lifting surfaces
[ONERA-TP-898] 06 p1140 N71-18449

Mathematical model for aircraft lifting surface interference in steady or unsteady supersonic flow
[ONERA-TP-850] 06 p1140 N71-18462

Aerodynamic interference effects between wing and fuselage junctions
09 p1311 N71-19354

Lift and drag interference characteristics of delta winged half cones with leading edges
09 p1312 N71-19359

INTERFEROMETERS

Computerized prediction of aerodynamic lifting characteristics for wing-horizontal tail and canard wing configurations
[NASA-TM-X-64886] 09 p1312 N71-19361

Numerical analysis of aerodynamic loads on wing and tail surfaces with oscillations in unsteady supersonic and subsonic flow including interference lift
[AGARD-CP-80-71-PT-1] 17 p2087 N71-29333

Wing interference lift line lattice simulation and application to aerodynamic loads on tandem wings in unsteady flow
17 p2096 N71-29336

Users manual for 3 computer programs for predicting aerodynamic interference between lifting surfaces and lift and cruise fans in transport-type aircraft
[NASA-CR-114332] 20 p3204 N71-33002

Computer program for calculating lift interference factors of wind tunnel test sections by vortex lattice method
[TAE-124] 23 p3704 N71-36407

INTERFERENCE MONOCHROMATIZATION
U DIFFRACTION
U MONOCHROMATIZATION
INTERFEROGRAMS
U INTERFEROMETRY
INTERFEROMETERS

NT FABRY-PEROT INTERFEROMETERS
NT MACH-ZEHNDER INTERFEROMETERS
NT MICHELSON INTERFEROMETERS
NT MICROWAVE INTERFEROMETERS
NT PHASE SWITCHING INTERFEROMETERS
NT RADIO INTERFEROMETERS

Improved ultraviolet interferometer performance
[NASA-CR-1666] 01 p0052 N71-10023

Holographic determination of translation and rotation using interference patterns of reflected light
[AD-710365] 01 p0062 N71-10178

Interferometric measurements of far infrared refractive index of sodium fluoride at low temperatures
[AD-711064] 01 p0069 N71-10443

Phase recovery and calibration techniques for position location interferometer in synchronous orbit
[NASA-CR-111137] 01 p0055 N71-10652

Techniques for orbital deployment of long tethered structures
[AD-711945] 02 p0296 N71-11948

Shadow, schlieren, and interferometer photographs and use in ballistic ranges
[NASA-TM-X-66337] 04 p0523 N71-13584

Optical interferometer for high spatial resolution measurements through turbulent atmosphere
[AD-712171] 05 p0683 N71-14812

Developing system for automatic compensation of signal dc level drift in laser interferometers
[Y-1737] 05 p0697 N71-15232

Very Long Baseline Interferometer experiments using ATS 3 and ATS 5 satellites
[NASA-TM-X-65428] 06 p0660 N71-16447

Determination of asymmetric three dimensional density fields in free jet flow by holographic interferometry
[AD-714610] 06 p0638 N71-16566

Describing device for velocity control of electromechanical drive mechanism of scanning mirror of interferometer
[NASA-CASE-XGS-03532] 07 p1031 N71-17627

Incremental motion drive system applied to interferometer components
[NASA-CASE-XNP-08971] 07 p1037 N71-17694

Methods of measuring accurate declinations of celestial bodies with bandwidth synthesis interferometer
07 p1116 N71-18014

Influence of atmospheric refraction on minitrack interferometer system and correction procedures for computation accuracy
[NASA-TN-D-5966] 08 p1162 N71-18565

Hook method using single plate interferometer coupled to spectrograph
[AD-716335] 09 p1423 N71-19678

US and USSR extra-high resolution radio telescope interferometer experiments including galactic observations
[NASA-TT-F-13519] 09 p1469 N71-20538

Analysis of schlieren interferometer system with polarizer-Wollaston prism-analyzer combination replacement for standard knife edges
[AD-716861] 10 p1561 N71-21716

Shadowgraph and interferometer systems for temperature measurements
11 p1842 N71-22682

Azimuth and elevation angle determination from UNIR/APCRL motor trails interferometric radar, using computer processing
[AD-718105] 12 p1997 N71-24111

Design and development of optical interferometer with laser light source for application to schlieren systems
[NASA-CASE-XLA-04295] 12 p1935 N71-24170

Amplifying interferometric and narrow multiple beam beam measurement of molybdenum carbide pressure cylinder diameters
[NLL-M-20171-5828.4F] 12 p1931 N71-24236

INTERFEROMETRY

Radio astronomy studies including sensitive interferometers, digital correlators, and related measuring instruments also radar techniques for lunar topography [NASA-CR-114969] 13 p2082 N71-25083

Application of far infrared interferometer to transient plasma diagnostics [UCRL-50903] 13 p2148 N71-25224

Laser Doppler velocity measuring device using scanning interferometer 14 p2254 N71-26108

Digital sensor for counting fringes produced by interferometers with improved sensitivity and one photomultiplier tube to eliminate alignment problem [NASA-CASE-LAR-10204] 15 p2408 N71-27215

Ultrasonic, pulse echo interferometric method for analyzing both preloads 16 p2599 N71-28018

Test plans for conducting very long baseline interferometer experiments using Applications Technology Satellites 3 and 5 [NASA-TM-X-65668] 18 p2921 N71-30440

Circuit diagrams, structural design, and methods of application of multi-wave interferometers [AD-723541] 19 p3142 N71-32594

Galactic 21 cm line absorption in 97 radio source spectra using two element interferometer [AD-724182] 19 p3182 N71-32783

Holographic interferograms of laminar free convection boundary produced by vertical flat plate with nonuniform wall-temperature distribution [AD-724698] 20 p3364 N71-32993

Interferometer-polarimeter for measuring intensity polarization of optical radiation [NASA-CASE-NPO-11239] 20 p3271 N71-33024

Calibrated infrared emission spectra of earth and atmosphere using high resolution interferometer spectrophotometer on Nimbus 4 satellite [NASA-TM-X-65687] 22 p3583 N71-35517

Laser interferometer for earth strain measurements 23 p3753 N71-36761

Design and performance of continuous wave ultrasonic interferometer for measuring transit time of sound waves in solids [NVO-2504-77] 24 p3924 N71-38001

Measuring system for linear readout of both periodic and aperiodic mechanical displacements over broad frequency range [NASA-CR-114375] 24 p3965 N71-38286

INTERFEROMETRY

NT DIFFERENTIAL INTERFEROMETRY
Holographic interferometry for study of transparent media [TP-851] 01 p0062 N71-10407

Retrodiffracted interferometric holography in wind tunnels including displacement and deformation of deflectors [ONERA-TP-852] 02 p0201 N71-11510

Reviewing applications of holographic instrumentation to flow visualization, particle sizing, vibration analysis, and nondestructive testing 03 p0377 N71-12781

Applying holographic techniques to interferometric and schlieren systems for flow visualization at reentry simulation pressures 03 p0378 N71-12783

Applying method of dual-exposure holographic interferometry to comparison of optical components and measurement of small phase deviations 03 p0378 N71-12786

Measuring linear and angular displacements using double exposure and real time holographic interferometry 03 p0379 N71-12789

Real time and double exposure holographic techniques for nondestructive testing of printed circuit boards, honeycomb structures, metal welds, and deposits on optical surfaces 03 p0379 N71-12790

Stabilizing fringe pattern in holographic system in presence of vibration and drift 03 p0379 N71-12793

Fringe interpretation in stress-holography interferometry [AD-712869] 03 p0381 N71-13164

Application of separate reference beam holographic interferometry for measurement of small phase variations in sub-fringe systems [NASA-CR-73494] 04 p0525 N71-14071

Measuring small surface deformations using optical wavefront reconstruction [WRE-TN-OSD-115] 05 p0697 N71-15157

Holographic interferometry, improved coherence of ruby lasers, and instrumentation techniques [NASA-CR-114274] 07 p1039 N71-17271

Interferometric and schlieren measurements of electron density in arc plasmas using IR radiation from CO₂ laser [IPP-414] 08 p1271 N71-18268

Conference on diagnosis of high temperature plasma including interferometry and spectroscopic methods [LA-4520-TR] 08 p1272 N71-18527

Holographic interferometric methods applied to vibration, flutter, and transient analysis of thin metallic panels [NASA-CR-103053] 08 p1210 N71-18982

Laser interferometer for monitoring and control of large telescope [NASA-CR-111811] 08 p1203 N71-19019

Mirror movement analysis by holographic interferometry for application to spaceborne telescopes [NASA-TM-X-7227] 09 p1396 N71-19633

Holographic interferometry analysis of axisymmetric imperfections effect on natural frequencies and mode shapes of conical shells 10 p1569 N71-21280

Interferometric measurements of solar absorption wavelengths in visible region, and comparison to standard Hg-H₂ wavelengths 11 p1825 N71-21975

Interferometric measurements in optical and microwave frequencies of electromagnetically accelerated shock waves in hydrogen 11 p1741 N71-22636

Detection of flaws in honeycomb panels by holographic techniques and reducing sensitivity of holographic interferometry of transparent objects [AD-718386] 12 p1933 N71-23704

Determination of surface roughness correction factor in interferometric measurements of block gage length [NLL-M-20170/5828.4F] 12 p1929 N71-24016

Interference fringe interpolator for digital linear measurements [NLL-TRANS-T-6783/5809.95] 12 p1924 N71-24193

Interferometric holographic analysis of density flow fields around half-angle conical bodies in supersonic wind tunnels with 10 deg angle of attack [AD-721543] 16 p2529 N71-28411

Electron beam parameters for 100 MeV storage ring including synchrotron radiation interferometry and plasma oscillations 18 p2967 N71-30411

Pulse amplitude modulation of laser outputs for image contrast enhancement in real time holographic interferometry for nondestructive testing [AD-723632] 19 p3108 N71-32244

Spacecraft attitude measurement based on spatial coherence of laser and stellar light, and interferometry 19 p3133 N71-32268

North-South interferometry of extragalactic radio sources [AD-724183] 20 p3348 N71-33237

Waveform and source size characteristics of Jovian decametric radiation using long baseline radio interferometry 21 p3511 N71-35023

Holographic interferometry applied to vibration analysis, composite component evaluation, and precision cylinder inspection [AD-726369] 22 p3591 N71-35570

Narrow resonance width measurements in identical particle systems by means of missing-mass spectrometer [JINR-Pi-5666] 22 p3633 N71-35894

Interferometric test method for hexametylene chamber cover glass conformity to planarity specifications [NBS-TN-579] 23 p3759 N71-36802

INTERGALACTIC MEDIA

X ray astronomy [NASA-TM-X-65372] 01 p0118 N71-10610

Attenuation of X rays in interstellar and intergalactic space and physical state of hydrogen cloud [NASA-TM-X-64577] 10 p1641 N71-21563

Gamma ray absorption processes at high red shifts, and energy dependences of absorption processes in interstellar and intergalactic gas 13 p2160 N71-24777

Cosmic, isotropic gamma ray spectra, primordial gamma ray sources, and intergalactic gas density 13 p2160 N71-24778

INTERPLANETARY CORROSION

Titanium alloying effects on mechanical properties and microstructures of low-carbon chromium nickel iron alloys [NLL-LTI-746-668/19022.401] 19 p3115 N71-32300

Hydrogen embrittlement of titanium alloy surface in hot salt corrosion cracking 23 p3772 N71-36882

INTERIOR BALLISTICS

Relativistic evaluation of propellant behavior with nonlinear viscoelasticity and cumulative damage [AD-710776] 01 p0113 N71-10552

Internal ballistics of tube artillery and powder rockets [AD-711270] 01 p0114 N71-10972

Ballistic model for quenching of solid propellant combustion [AD-711436] 02 p0287 N71-11849

Interior ballistics of light gas gun, pressure measurements and compression calculations [REPT-13/69] 03 p0365 N71-13292

Scattering and attenuation of stress waves in solid rocket propellants [AD-717001] 10 p1637 N71-21630

Theory of interior ballistics for calculating gas-powder efficiency and combustion safety in firearms [TL-1970-21] 20 p3368 N71-33040

Analysis of fundamental combustion characteristics of polymers contained in solid rocket propellants using diffusion flame technique [AD-727590] 24 p4000 N71-38529

INTERLAYER INSULATION

Ice interlayer formation computations in freezing moist soil [AD-711874] 02 p0212 N71-11518

INTERLOCKING

U LOCKING
INTERMEDIATE FREQUENCIES

Analysis of receiver performance composed of bandpass or IF filter followed by detector optimum in presence of additive white noise noise process 19 p3056 N71-32338

INTERMETALLICS

Nickel thin film growth on (111) aluminum surfaces [RAE-TR-6266] 02 p0242 N71-11592

Investigating crystal growth and dendritic character of aluminides of transition metals in aluminum alloys [AD-714420] 06 p0935 N71-16321

Superconductivity of intermetallic vanadium silicon and niobium aluminum alloys [CALT-822-13] 07 p1085 N71-17022

Electronic properties of dilute alloys including magnetic permeability, electrical resistance, and ferromagnetism [AD-716607] 09 p1453 N71-20086

Electron and ion conductivity measurements in solid silver sulfide, silver selenide, and silver telluride [ANL-TRANS-868] 10 p1516 N71-21659

Radioactive trace diffusion of AuZn and FeCo species isotopes with measurement of correlation and isotope effects in crystal lattice defects [AD-717757] 11 p1778 N71-22335

Intermetallic plutonium diffusion in plutonium copper and plutonium uranium systems containing gallium or nickel [CEA-R-3951] 15 p2494 N71-27928

Sliding properties of iron-base metallic powder lubricants impregnated with intermetallic alloys 18 p2928 N71-30911

Tin solution calorimetry for measuring heats of formation of selected face centered cubic palladium-silver-tin system [AD-722799] 18 p2937 N71-31397

Processing rare earth-cobalt intermetallic compounds for use in permanent magnets [AD-723285] 19 p3141 N71-31729

Heat capacity of pure nickel, pure iron, and NiFe, and contribution from anharmonic lattice vibrations [ORO-3291-14] 21 p3438 N71-34446

Production of intermetallic compounds by effect of shock waves resulting from explosions and resulting compaction of powders [NASA-CASE-MFS-20861] 21 p3443 N71-34580

Electron microscopic analysis of aluminum alloy structure, intermetallic compounds, and structural hardening mechanisms [NLL-M-20371/5828.4F] 24 p3941 N71-38113

INTERMITTENCY

Temperature intermittent operation in encapsulated integrated circuits [AD-715984] 09 p1359 N71-19777

INTERMODULATION

Intermodulation of saturating transfer devices [AD-711374] 02 p0177 N71-11226

Cross modulation in barrier layer field effect transistors 03 p0352 N71-12540

Multipath transmission models for predicting signal distortion and intermodulation in tropospheric scatter propagation 12 p1876 N71-23460

Computer program for predicting frequency interference between transmitters and receivers [EGG-1183-1509] 13 p2048 N71-25344

Intermodulation distortion and gain compression in solid state microwave amplifier diode [NASA-CR-118896] 15 p2510 N71-27909

Third order-two signal intermodulation products for 242 frequencies between 225 and 400 MHz as used in FAA frequency assignment processes [ECAC-PR-70-018] 17 p2719 N71-29551

Third order-two signal intermodulation products for 360 frequencies between 118 and 136 MHz when 50 kHz channel spacing is used as in FAA frequency assignment processes [ECAC-PR-70-016] 17 p2719 N71-29552

Third order-two signal intermodulation products within 118-136 MHz band with 50 kHz spacing [ECAC-PR-70-015] 17 p2719 N71-29554

INTERMOLECULAR FORCES

Discussing advances in molecular beam experiments involving two-body collisions [NASA-CR-116434] 07 p1070 N71-17011

SUBJECT INDEX

Fluorine atom reaction dynamics, intermolecular potentials from high resolution differential cross sections, and collision induced dissociations of diatomic molecules
[COO-2092-1] 11 p1604 N71-23421

Method for computing elastic scattering phase shifts for intermolecular potential calculation and analysis of rotating interference and fluctuations in total cross section
11 p1809 N71-23272

Intermolecular potential energy calculations for thermal elastic scattering of gases and comparison of Lennard-Jones and Morse potential functions
17 p2795 N71-29730

Infrared molecular spectra of linear acetylene molecule and its C13 enriched isotopic bands
18 p2686 N71-31501

Nuclear dynamic polarization for investigating intermolecular dynamics in solutions of selected free radicals and fluorocarbons in acetone
20 p3230 N71-33807

Intermolecular force constants of highly polar gases determined for six different models of Laiden second virial coefficient
20 p3326 N71-33942

INTERNAL COMBUSTION ENGINES

WT BRISTOL-SIDDELEY OLYMPUS 593 ENGINE

NT DIESEL ENGINES
NT DUCTED FAN ENGINES
NT GAS TURBINE ENGINES
NT HELICOPTER ENGINES
NT J-57 ENGINE
NT J-85 ENGINE
NT JET ENGINES
NT JET-SET ENGINES
NT RAMJET ENGINES
NT SUPERSONIC COMBUSTION RAMJET ENGINES
NT TURBOFAN ENGINES
NT TURBOJET ENGINES
NT TURBOPROP ENGINES
NT TURBOPURJET ENGINES

Reliability of testing oils with added detergents in single cylinder engines
[AD-71749] 01 p0073 N71-10970

Spectroscopic measurements of nitric oxide in spark ignition engines
[PB-192625] 02 p0290 N71-11879

Variable displacement fuel pump for internal combustion engines
[NASA-CASE-MSC-12139-1] 04 p0606 N71-14058

Numerical analysis of gas turbine supercharging in multi-cylinder four cycle engines
[AD-713873] 06 p0941 N71-16225

Phenomena taking place in surface layers of metal of engine components during friction
[AD-714053] 06 p0941 N71-16205

Classification of vibration records from reciprocating internal combustion engines
[AD-716600] 09 p1458 N71-19682

Detonation reaction engine comprising outer housing enclosing pair of inner walls for continuous flow
[NASA-CASE-XMR-06926] 11 p1821 N71-22983

Theory and development of technique to measure synchronous ultraviolet absorption histories in end gas of spark ignition engine
16 p2690 N71-28573

Flow model for turbulent heat transfer in Otto cycle engine
17 p2857 N71-29718

Reaction kinetics, oxidation, and quenching of combustible products in exhaust systems of gasoline engines
[KPA-CPA-22-60-51-HEW] 17 p2866 N71-30304

Aerodynamic characteristics, rocket nozzles, quenchcraft propulsion, antenna design, and internal combustion engines
[NASA-CR-115151] 18 p3014 N71-31106

Nitric oxide emission studies of internal combustion engines
18 p3001 N71-31110

Two techniques for removal of particulate contamination from spark ignition engine exhausts
[PB-190833] 19 p3173 N71-31762

Internal aerodynamics design manual considering internal air flow system effect on aircraft performance including bibliography
[AD-720833] 19 p3173 N71-32059

Aerodynamic design manual considering internal air flow system effects on aircraft performance
[AD-720824] 19 p3173 N71-32060

Internal aerodynamics manual containing tabulations for calculating internal combustion engine thermodynamics
[AD-720841] 19 p3174 N71-32061

Proceedings of conference on identification and prevention of mechanical failures in internal combustion reciprocating engine systems
[AD-721913] 19 p3175 N71-32663

Modeling reciprocating combustion engine analysis at five different places using subjective and objective measurements
[NASA-TT-P-13943] 22 p3428 N71-33049

INTERNAL COMPRESSION INLETS

Wind tunnel tests to determine Mach 2.5 performance of bicone inlet with internal focused compression and 40-percent internal contraction
[NASA-TM-X-2294] 14 p2195 N71-25872

INTERNAL CONVERSION

Electron conversion ratios for 1064 keV gamma ray of ruthenium 207
[NASA-TM-D-6057] 01 p0093 N71-10060

High precision measurement of relative intensities and internal conversion coefficients in decays of Ir-192, Cr-51, Bi-207, and Co-137
16 p2652 N71-29003

Integral conversion processes for electric quadrupole transitions in deformed nuclear region
22 p3649 N71-36024

INTERNAL ENERGY

Determining internal energy coefficients of Al from ultrasonic measurements of longitudinal and shear wave speeds with hydrostatic pressure, uniaxial stress, and temperature variations
[AD-721368] 16 p2610 N71-28443

INTERNAL FRICTION

Internal friction of W, Fe, and Si combined with O in zirconium
[BARC-458] 05 p0701 N71-15036

Studying Lunar Orbiter photographs of boulder tracks left on lunar surface to determine soil cohesion and angle of internal friction
[NASA-CR-102968] 05 p0768 N71-15205

Influence of defects created by neutron irradiation at 80 K on elastic moduli and internal friction of magnesium
[CEA-CONF-1621] 06 p1213 N71-18443

Internal friction of heated polycrystalline samples of vanadium at low pressure
[CNEA-260] 13 p2095 N71-25088

Approximate formula for internal friction coefficient of ice
15 p2509 N71-27904

Internal friction production from energy dissipation during kink motion
17 p2820 N71-29957

Anelastic effects of internal friction peaks in molybdenum after neutron irradiation
[CEA-CONF-1671] 19 p3162 N71-32750

Internal friction in aluminum single crystals, irradiated and worked at low temperatures, determined by ultrasonic measurements
21 p3497 N71-34917

Changes in mechanical properties and internal friction during aging of stainless, dispersion hardened chromium steels
[NLL-LT-746-680-19022.401] 22 p3596 N71-35608

INTERNAL PRESSURE

Elastic-plastic analysis of anisotropic annular disks subjected to sufficient internal pressure to cause plastic deformation
[AD-714370] 06 p0954 N71-16113

Elastic bending stresses in out-of-round pipe due to internal pressure
[ORNL-TM-3244] 09 p1479 N71-20175

Mechanical properties of cylindrical vessels under internal pressure at high temperatures
[NLL-CE-TRANS-3321-19022.09] 19 p3189 N71-32412

INTERNAL STRESS

U RESIDUAL STRESS

INTERNATIONAL COOPERATION

Analysis of US efforts for detection and prevention of air piracy with application to foreign countries
01 p0135 N71-10236

Press briefing on US and USSR cooperation in space
01 p0137 N71-10466

Research digest for exchanging information among investigators in earthquake engineering in North America
[PB-193507] 01 p0051 N71-10887

Project DIOSCURES for global sea and air traffic control using synchronous satellites for ground-air-ground communications
02 p0263 N71-11768

Space shuttle for space transportation and cost reduction of space missions - international cooperation
[NASA-TM-X-66388] 02 p0298 N71-11932

Observing compact radio sources with radio interferometers in US and USSR
02 p0297 N71-12153

Scheduled launching of SAS-A by Italian team of space engineers for detecting X ray sources in space
[NASA-NEWS-RELEASE-70-263] 03 p0453 N71-12957

International radioactivity calibration standards
[PB-194364] 04 p0390 N71-14346

World Bank operations and economic growth of less developed countries
04 p0624 N71-14432

European cooperation on research in quantum electronics
[FOA-2-C-2333-51] 05 p0732 N71-14681

INTERNATIONAL COOPERATION

Aeronautical climatological tables of international commercial airports
05 p0717 N71-15143

Report to Congress on international standards and metric system
[NBS-SP-345-1] 05 p0768 N71-15339

International system for nuclear nuclear data compilation and evaluation
[EURPWR-752] 06 p0807 N71-15729

International studies on air pollution, atmospheric heat budget, and real time data processing techniques
06 p0806 N71-15755

International comparison of Min-56 activity in 1968 including nuclear reactor irradiations and neutron source calibration
[ANL-7642] 06 p0915 N71-16001

Intercomms 3 research satellite orbited by Soviet-Czech team
[AD-713839] 06 p0951 N71-16333

Summarizing national development programs on fast reactors and fuels
[N7-18565] 07 p1059 N71-17029

European aerospace and electronic equipment industrial cooperation for air traffic control and communication satellites
07 p1132 N71-17181

European aerospace industry role in NASA space shuttle program
07 p1118 N71-17211

US and European international aerospace industry cooperation
07 p1133 N71-17215

International European avionics cooperation for NASA space shuttle, station, and tug programs
07 p1118 N71-17257

International conference on rain erosion and associated phenomena
[AD-715106] 07 p0973 N71-17906

Possible European cooperation in NASA space shuttle transportation program
[NASA-TM-X-66714] 08 p1306 N71-18431

Resolution and recommendations of Conference on International System of Units (SI)
[NBS-SP-330] 08 p1206 N71-18409

European test vehicle and small shuttle program in NASA post Apollo program
08 p1293 N71-18639

Cost analysis of future European space programs with or without NASA cooperation
08 p1307 N71-18708

Proposal for international air pollution information analysis center
09 p1381 N71-19531

Feasibility of creating international maritime pollution information analysis center
09 p1381 N71-19532

Summary of NASA international activities from 1958 to 1970
[NASA-TM-X-66907] 09 p1489 N71-20527

NASA and European cooperation in space shuttle transportation program
10 p1648 N71-20810

Apollo project technology application to orbital space station and space shuttle projects
10 p1665 N71-20830

Multinational air pollution control operations
[PB-196041] 10 p1667 N71-21784

World Meteorological Organization conference recommendations on revised nomenclature for sea ice
11 p1739 N71-22668

Agreement between NASA and Academy of Sciences of USSR for data exchange
[NASA-NEWS-RELEASE-71-57] 12 p2018 N71-23742

Spacecraft launchings, international cooperation, and other French space activities, 1970
[NASA-CR-118945] 12 p1996 N71-23963

US cooperation with ESRO UHF satellite system development for air traffic control in Europe
[NASA-TT-F-13651] 12 p1960 N71-23967

Premier Colombo of Italy visit in US and indoctrination with post-Apollo program
[NASA-TT-F-13586] 12 p2018 N71-24002

Scientific and technical information processing and dissemination nationally and internationally
[NLL-M-20329-1982.4E1] 12 p2019 N71-24270

Planned launching of San Marco C satellite in joint Italian-US cooperative space program
[NASA-NEWS-RELEASE-71-63] 12 p2003 N71-24336

Design of observation and data processing systems for use in first Global Atmospheric Research Program (GARP) experiment
13 p2104 N71-24423

International cooperation policy for science and technology transfer
13 p2189 N71-24751

International scientific cooperation for environmental pollution control
13 p2189 N71-24752

Planning for international management and cooperation in physical science research
13 p2189 N71-24753

Worldwide scientific information system for future international cooperative research efforts

13 p2189 N71-24754
International scientific cooperation for control of military technologies

13 p2190 N71-24755
Implementation of national science policy into international cooperative framework

13 p2190 N71-24756
International management requirements for effective global science policy

13 p2190 N71-24757
International cooperation in social and life sciences between advanced and developing nations

13 p2190 N71-24758
Scientific legislative management cooperation for international research and development work

13 p2190 N71-24759
International financial assistance for scientific and technological transfers to developing nations

13 p2190 N71-24760
International science policy for managing social effects of technology utilization

13 p2190 N71-24761
International science management for global marine antipollution regulations

13 p2190 N71-24762
International control for experimentation with human eggs

13 p2033 N71-24763
Cooperation between USSR and USA in space activities and scientific information exchange

13 p2192 N71-25238
National and international environmental monitoring activities - directory

14 p2247 N71-25889
Abstracts of NASA inventions available for licensing in foreign countries

[NASA-SP-7038]
International data on ecological problems

14 p2249 N71-26200
Project planning for observation of atmospheric circulation and heat budget over the Atlantic Ocean noting international collaboration and satellite observation

15 p2437 N71-26972
Research and development international cooperation in nuclear electric power generation including reactor physics, safety, waste disposal, and radiation laws

[NP-18600]
International conference on hyperfine interactions determined by angular correlation methods, nuclear orientation at low temperatures, nuclear magnetic resonance, and optical pumping

[AD-720684]
Review of numerical experimentation related to global atmospheric research program

16 p2656 N71-29113
Physical properties of cloud clusters over tropical Atlantic - tropical meteorology

17 p2777 N71-29481
Long range tropical weather forecasting of cloud clusters over Atlantic noting ground weather stations international cooperation and training

17 p2777 N71-29483
European space program and Intelsat - international cooperation and government/industry relations

17 p2777 N71-29485
Environment pollution research and development cooperation in Norway, Sweden, Finland, and Denmark

17 p2862 N71-30322
Simulation studies for development of certification criteria applicable to SST takeoff and engine failure

18 p3028 N71-30645
International cooperation in establishing Beaufort wind velocity scale, noting sea surface and wind velocity measurements

18 p2951 N71-30677
International symposium on planetary atmospheres emphasizing atmospheres of Mars and Venus

[NASA-TT-F-13813]
Selected abstracts of world literature on production and industrial uses of radioisotopes

[ORNL-DC-30-PT-4]
Basic secondary publications on chemistry and chemical engineering promoting international cooperation in information dissemination

19 p3194 N71-31981
Soviet Bloc research in geophysics, meteorology, oceanography, upper atmosphere, and space - abstracts

[JPRS-53460]
International treaty for peaceful use of moon

19 p3179 N71-32000
Model for technology transfer from advanced country to underdeveloped country

[P-4309]
Requirements for marine international meteorological information service

[WMO-288]
Survey of work carried out at International Earth Tide Center

20 p3294 N71-32806
Soviet power reactor facilities and research institutions toured by US delegation in reciprocal visit on nuclear power

[WASH-1173]
Cost estimates of national projects for international cooperation in meteorological World Data Center

[WMO-289]
International cooperation in atomic research, meteorology, education, and anthrax control in Europe

[JPRS-53960]
International cooperation in optical measurement of underwater photon density at 300 to 750 nm depth

21 p3535 N71-35193
Soviet and French programs for establishing astrometric schools and stations in Egypt for space geodesy

22 p3576 N71-35475
International conference on artificial earth satellite use for upper atmosphere and geodetic studies

22 p3680 N71-36243
Review of worldwide gravity tide data showing scatter in observations caused by ocean loading

23 p3733 N71-36764
Global atmospheric research program on numerical weather forecasting, Atlantic tropical experiment, and future activities

23 p3793 N71-37034
International cooperation in global atmospheric research program on weather forecasting

23 p3793 N71-37036
Critical evaluation of nuclear data information in connection with reactor designs - international conference

[INDC(NDIS)-29-U]
Presidential proposals for controlling environment pollution

23 p3806 N71-37091
Satellite navigation and communication applied to maritime and aeronautical services

23 p3870 N71-37591
Meridional flow, relative angular momentum, and energy flux calculations for International Geophysical Year

24 p3915 N71-37918
[MET-O-800C]
Discussing origin, course of development, and results of Vanguard Project

[NASA-SP-4202]
Arctic and Antarctic regions, ice formation, sea ice, weather forecasting, glaciology, hydrology, hydrometeorology, IGY, IQSY, solar activity, and meteorological stations

[TT-70-50017]
Analysis of synoptic charts of magnetic activity measured in Arctic for IGY

11 p1752 N71-22801
Space-time distribution of magnetic disturbances in Arctic during IGY and IQSY

11 p1753 N71-22813
High latitude, quiet solar day variations of geomagnetic field during IGY

11 p1759 N71-22865
17 p2747 N71-30087
INTERNATIONAL LAW

NT SPACE LAW
Members attitudes on revisions to Warsaw Convention and The Hague Protocol amendments on liability to international air transport passengers

[REPT-1970-8-E]
Discussing international legal aspects of regulating continental shelves and demilitarization of ocean floor

[JPRS-52585]
Flights to other planets, Cosmos satellites, international space law, and USSR space achievements

15 p3138 N71-18100
USSR analysis of space law as independent branch of international law

[NASA-TT-F-13751]
International aspects of educational TV by satellite

19 p3201 N71-32775
Solutions to legal constraints to international cargo transportation

[AD-726797]
International practical temperature U TEMPERATURE SCALES

20 p3236 N71-33837
INTERNATIONAL PRACTICAL TEMPERATURE U TEMPERATURE SCALES

22 p3701 N71-36397
INTERNATIONAL QUIET SUN YEAR

Arctic and Antarctic regions, ice formation, sea ice, weather forecasting, glaciology, hydrology, hydrometeorology, IGY, IQSY, solar activity, and meteorological stations

[TT-70-50017]
Space-time distribution of magnetic disturbances in Arctic during IGY and IQSY

11 p1752 N71-22801
11 p1759 N71-22865
INTERNATIONAL RELATIONS

NT INTERNATIONAL COOPERATION
Bibliography of publications by Social Science Department of Rand Corporation - 1963 to 1970

[R-705]
Air piracy resolutions presented to Congress and US and worldwide air piracy statistics

13 p2191 N71-25190
19 p3199 N71-32689
INTERNATIONAL SATS FOR IONOSPHERIC STUDY

U ISIS SATELLITES
Quantum method of maintaining volt as SI unit using as Josephson effect in superconductors

12 p1920 N71-23646
Discussion of symbols and units of measurement including metric system for international use

[AAEE-TECH-423]
Cost analysis and effects of metrication within DOE

[NBS-SP-345-9]
Survey of metrication effects on US civilian organizations

[NBS-SP-345-2]
Definition and identification of pecuniary for conducting human activities with respect to earth environment

[NASA-CR-121659]
INTERNATIONAL TRADE
US commercial aircraft export strategy and recommendations for financing and expansion

21 p3431 N71-34611
Evaluation of potential effects of US conversion to metric measurements and standards on foreign trade

[NBS-SP-345-8]
INTERNUCLEAR PROPERTIES
Interatomic potentials and dissociation energies of diatomic hydrogen and halogen molecules studied with spectroscopy and potential curves

[NASA-CR-116978]
Multiconfigurational one center expansion wave functions for competing intermolecular forces of hydrogen molecule and Hellmann-Feynman theorem

09 p1428 N71-19737
14 p2311 N71-26687
INTERPLANETARY COMMUNICATION
Dreams, legends, and early fantasies relating to interplanetary flight and communication

[NASA-TT-F-640]
INTERPLANETARY DUST
Satellite stability and interstellar dust grain studies

[NASA-CR-121929]
Perturbative effects of azimuthal component of solar wind velocity on orbital properties of gravitationally-bound interplanetary dust grains

24 p4005 N71-38538
24 p4006 N71-38539
David-Greenstein effect on rigid body dynamics of interplanetary dust grains

24 p4006 N71-38540
INTERPLANETARY EXPLORER
U EXPLORER IS SATELLITE
INTERPLANETARY FLIGHT
NT GRAND TOURS
Rapid, flexible computer program for Earth-Moon trajectory and mission analysis

[NASA-TN-D-5983]
Abstracts on Soviet space program and atmospheric, ionospheric, and interplanetary research

06 p0945 N71-15983
07 p1020 N71-17491
McFLARE code to calculate probable flare dose encountered on interplanetary mission

[NASA-TM-X-52971]
Outbound and inbound station weight requirements for planetary sample return mission payload and energy requirements - graphs

06 p1285 N71-18734
09 p1466 N71-20276
Dreams, legends, and early fantasies relating to interplanetary flight and communication

[NASA-TT-F-640]
Technology review and performance estimates for fixed design multipurpose solar electric propulsion stages

11 p1830 N71-23000
12 p1990 N71-23701
Flights to other planets, Cosmos satellites, international space law, and USSR space achievements

15 p2397 N71-26906
Deep Space Network telecommunication and ground support equipment for planetary and interplanetary flight projects

[NASA-CR-118895]
Flight reentry heating instrumentations required for ballistic entry simulation of radiative and convective heating rates

15 p2518 N71-27941
[NASA-TN-D-6265]
Planning for Pioneer 5 and 6 interplanetary mission with Jupiter flyby

16 p2591 N71-28017
[NASA-SP-268]
INTERPLANETARY GAS
Neutral gas effects on cosmic plasmas in presence of magnetic field

19 p3181 N71-32366
[NP-18421]
Solar wind, meteoric volatilization, and ionospheric degassing contributing to lunar surface atmosphere, and transient contributions produced by rocket gases during lunar missions

04 p0680 N71-14133
Numerical analysis of solar wind interactions with nonmagnetic planets based on equations of magnetohydrodynamics for perfect gas

14 p2335 N71-25776
[NASA-CR-121871]
Transonic deceleration of solar wind via planetary, cometary, and interstellar gas, noting ionospheric processes

21 p3503 N71-34857
[TRITA-EPP-71-01]
Orbits of interstellar helium ions in interplanetary space

22 p3654 N71-36888
[NASA-CR-121902]
22 p3667 N71-36889

SUBJECT INDEX

Observations of ionic species in interplanetary plasma and diagnostic methods

23 p3846 N71-37411

INTERPLANETARY MAGNETIC FIELDS

Polarity comparison of solar magnetic field and interplanetary magnetic field

02 p6295 N71-11919

Interplanetary magnetic field role in counterstreaming ion-ion instability in ion thermalization process for such low shock

02 p6282 N71-12032

Physical structure of hydromagnetic disturbances in inner magnetosheath

02 p6220 N71-12095

Solar wind, plasma waves and interplanetary electric and magnetic fields from Mariner 2 and Mariner 4 space probes

03 p6454 N71-12526

Solar wind, interplanetary magnetic fields and magnetic variations

03 p6451 N71-13263

Correlation between magnetic variations and solar wind and interplanetary magnetic fields

03 p6451 N71-13333

Active solar radio regions at metric frequencies and interplanetary sector structures

05 p6768 N71-15336

Mariner spacecraft data analysis to determine relationship between interplanetary magnetic field direction and geomagnetic activity

06 p6856 N71-16797

Magnetic field in wake of solar wind interaction with Mercury

08 p1286 N71-19293

Magnetic probes and induction coil instrumentation for Helios solar probe measurements on interplanetary magnetic fields

09 p1461 N71-19951

Cosmic ray distribution for analysis of nonuniform interplanetary magnetic fields during solar activities

09 p1462 N71-20409

Solar effects and properties of interplanetary magnetic field

09 p1463 N71-20467

Correlation of increases in electron population of outer radiation belt and interplanetary magnetic fields during two geomagnetic storms

18 p3005 N71-30927

Tracking and scientific measurement data analyses for Pioneer missions from July 1969 to July 1970

20 p3246 N71-33557

Solar news releases on interplanetary magnetic fields, tsunami waves, and atmospheric phenomena during magnetic storms

21 p3510 N71-35008

Properties of interplanetary magnetic field as determined by solar wind velocity

22 p3572 N71-35438

Quantitative determination of umbral increases and decreases and increases in lunar wake of solar wind flow

24 p4003 N71-38530

Fluctuations due to particle scattering in interplanetary magnetic field

24 p4011 N71-38601

INTERPLANETARY MEDIUM

NT INTERPLANETARY DUST

NT INTERPLANETARY GAS

Investigating dynamic nonequilibrium properties of microscale fluctuations in interplanetary medium using plasma and magnetic field data from Mariner 5 space probe

01 p6105 N71-10430

Numerical analysis of solar cosmic rays in interplanetary medium

05 p6765 N71-15554

Observations of interplanetary medium by Vela 3 and IMP 3 satellites

06 p6943 N71-16604

Characteristics of energetic interplanetary particles and X rays produced by solar activity

06 p6944 N71-16749

Characteristics of directional discontinuities in interplanetary magnetic field

06 p6947 N71-16787

Properties of interplanetary medium from radio missions of planet Jupiter

07 p1111 N71-17670

Interplanetary proton flux measurements by Zond space probes

09 p1462 N71-30408

Microstructure of solar wind and interplanetary medium

09 p1463 N71-20469

Nonlinear propagation and steepening of waves in collisionless plasma

10 p1631 N71-21780

Relativistic electron and positron intensity distribution in interplanetary regions

13 p2163 N71-25288

Analysis of intensity fluctuations produced by ionization of Jovian decametric radio emission with interplanetary medium

19 p3176 N71-32357

Magnetohydrodynamics of discontinuities in interplanetary medium and their relation to propagation and acceleration of cosmic rays

20 p3342 N71-33717

Satellite detection of energetic particles in outer space and interpretive analysis of relationships to planetary fields and interplanetary medium

22 p3667 N71-36145

Optical properties of interplanetary medium in direction of Geminichain

22 p3672 N71-36180

Satellite observations, radio-astronomical and optical techniques, and problems in plasma physics associated with effects of energetic particles in outer space

24 p4007 N71-38572

Comet luminosity variations and spectral properties in relation to interplanetary medium

24 p4009 N71-38587

INTERPLANETARY MONITORING PLATFORM

U IMP

INTERPLANETARY NAVIGATION

Interplanetary navigation when aim points of required guidance corrections must be biased in order to satisfy planetary quarantine constraint

13 p2110 N71-25135

INTERPLANETARY PROPULSION

U INTERPLANETARY SPACECRAFT

U ROCKET ENGINES

INTERPLANETARY SPACE

Luminescent phenomena in interplanetary space and moon related to luminescent, thermoluminescent, and cathodoluminescent properties of terrestrial minerals and rocks

01 p6119 N71-10076

Luminescent phenomena on moon and in interplanetary space

01 p6120 N71-10077

Physical properties of upper atmosphere and interplanetary space

03 p6453 N71-12702

Background radiation in space and synchrotron X radiation in galaxy and pulsars

09 p1463 N71-20472

Analysis of multiple earth bow shock crossings at large geocentric distances from Pioneer 8 magnetic field data

10 p1554 N71-21541

Derivation of motion of interplanetary irregularities from observations of interplanetary scintillations

10 p1647 N71-21802

Magnetospheric, solar, interplanetary space, and plasma physics

11 p1822 N71-22414

Cosmic ray anisotropy in interplanetary space reflected in solar diurnal variation

12 p1993 N71-23893

Simultaneous observations of solar flare electron spectra in interplanetary space and within earth magnetosphere measured by magnetic electron spectrometers on satellitesOGO-4 and OV-1-19

14 p2333 N71-25795

Criteria of spacecraft configurations and design in US-German Helios solar probe for interplanetary space investigation

17 p2849 N71-29564

European Mercury spacecraft experiments for interplanetary and planetary space investigation

17 p2850 N71-29566

HEOS mission, experimental design, and instruments

18 p3017 N71-30620

Charged particle lunar environment experiment of Apollo 14 detecting particle fluxes at lunar surface resulting from wide range of lunar surface, magnetospheric, and interplanetary data

18 p3011 N71-30964

Quiet-time electron increases - measure of conditions in outer solar system

18 p3006 N71-31195

Upper atmospheric investigations and motion picture images of celestial bodies

19 p3179 N71-32001

Coronal magnetic field structure from photosphere to interplanetary space

19 p3178 N71-32550

Measurement of charged particle spectra in interplanetary space by Cerenkov counter on Pioneer 8 spacecraft

20 p3341 N71-33483

Satellite detection of energetic particles in outer space and interpretive analysis of relationships to planetary fields and interplanetary medium

22 p3667 N71-36145

Orbits of interstellar helium ions in interplanetary space

22 p3667 N71-36146

Hydrodynamic processes producing solar corona and its expansion into interplanetary space

23 p3846 N71-37410

Spectroscopic detection of water on celestial bodies and in interplanetary space

23 p3848 N71-37425

INTERPLANETARY SPACECRAFT

Astrophysics, solar physics, and dynamic processes in interplanetary space and magnetosphere

23 p3848 N71-37428

Spiral structure of interplanetary magnetic fields and solar cosmic rays

23 p3852 N71-37452

Proton transport and solar flares in interplanetary magnetic fields

23 p3852 N71-37453

Particle acceleration by ionic-acoustic vibrations in interplanetary plasma

23 p3852 N71-37459

Solar wind velocity anisotropy in relation to kinematic transport of magnetic field into interplanetary space

23 p3854 N71-37472

Estimation of interplanetary shock speed and surface normal for 8 July 1964 shock in vicinity of earth

24 p4008 N71-38574

Cosmic ray research and instruments used for interplanetary and astronomical studies, Vol. 2 - conference

24 p4009 N71-38582

Comets as indicators of conditions in interplanetary space

24 p4009 N71-38586

INTERPLANETARY SPACECRAFT

NT EXPLORER 16 SATELLITE

NT JUPITER PROBES

NT MARINER SPACE PROBES

NT MARINER SPACECRAFT

NT MARINER VENUS-MERCURY 1973

NT MARINER 2 SPACE PROBE

NT MARINER 4 SPACE PROBE

NT MARINER 5 SPACE PROBE

NT MARS PROBES

NT PIONEER SPACE PROBES

NT PIONEER 5 SPACE PROBE

NT PIONEER 6 SPACE PROBE

NT PIONEER 7 SPACE PROBE

NT PIONEER 8 SPACE PROBE

NT PIONEER 9 SPACE PROBE

NT TOPS (SPACECRAFT)

NT VENERA SATELLITES

NT VENUS PROBES

NT VIKING LANDER SPACECRAFT

NT VIKING ORBITER SPACECRAFT

NT ZOND 4 SPACE PROBE

NT ZOND 5 SPACE PROBE

NT ZOND 6 SPACE PROBE

NT ZOND 7 SPACE PROBE

Heat shield technology for extraterrestrial atmospheric entry

02 p3905 N71-12057

Communications elements research on receivers and radiometers for Deep Space Network

05 p6647 N71-14957

Development and implementation of communications equipment for Deep Space Instrumentation Facility

05 p6647 N71-14961

Developing attitude control single-axis simulator for Thermoelectric Outer Planet Spacecraft

06 p6985 N71-16680

Testing electrical, mechanical, and handling properties and environmental characteristics of small gauge electrical wire for interplanetary spacecraft

06 p6929 N71-16683

Design and development criteria for large reusable ballistic interplanetary transport system for 1980s

07 p1119 N71-17333

Lightweight resin fiber glass honeycomb sandwich structure fabrication and comparison with aluminum structures for planetary probes

07 p1047 N71-17350

Trajectory profiles and nuclear propulsion vehicle configurations for manned Mars and Mars-Venus missions

07 p1109 N71-17496

Investigating video image display assembly and detectability of cathode ray tube gray shades for SPOF development

07 p1004 N71-17619

Research studies on development of Thermoelectric Outer Planet Spacecraft/TOPS and lunar exploration

10 p1644 N71-21338

Radioisotope thermoelectric generators for outer planet mission spacecraft

10 p1604 N71-21346

Thermionic converter optimization, laser obstacle detector, and test program for interplanetary spacecraft guidance and control subsystems

10 p1608 N71-21347

Electric propulsion engines, digital gyro system, and step motor solar electric thrust vector systems for interplanetary spacecraft control

10 p1608 N71-21348

Polymer adhesives, optical solar cell filter, and fuelable antenna construction for interplanetary spacecraft

10 p1589 N71-21349

Literature review and data analysis for radiation effects on electronic equipment of Thermoelectric Outer Planet Spacecraft

10 p1535 N71-21351

Thermoelectric boom actuator and furlable antenna for Thermoelectric Outer Planet Spacecraft
10 p1566 N71-21352

Magnetic tape recorders, data systems, and Jupiter radiation effects on metal oxide semiconductors of Thermoelectric Outer Planet Spacecraft
10 p1560 N71-21353

Outer planetary mission planning and technological improvements for outer planet spacecraft
11 p1828 N71-22551

Long life tape transport for magnetic recorder of outer planet spacecraft
11 p1716 N71-22566

Onboard optical data processing for earth resource spacecraft and planetary spacecraft
17 p2723 N71-29883

Evaluation equipment for terminal sterilization process on unmanned landers and determination of thermal inactivation curve of *B. subtilis* var. niger spores
21 p3381 N71-34054

Use of orbit-to-orbit shuttles for hyperbolic rendezvous with returning interplanetary spacecraft
21 p3325 N71-35117

Venus spin vector estimation using planetary Explorer spacecraft data
24 p4008 N71-38577

INTERPLANETARY TRAJECTORIES
Interplanetary flight missions and systems development for thermoelectric outer planet spacecraft
01 p0136 N71-10251

Developing digital systems and solar electric propulsion technology for thermoelectric outer planet spacecraft
01 p0083 N71-10260

Developing thermomechanical pump for thermoelectric outer planet spacecraft
01 p0058 N71-10263

Designing test testing and repairing computers for long term unmanned interplanetary missions
03 p0455 N71-12618

Describing systems and facilities for Deep Space Network
05 p0646 N71-14951

Describing Deep Space Network for communication with unmanned spacecraft traveling planetary distances
05 p0646 N71-14952

Tracking support by Deep Space Network for Mariner Mars 1969 extended operations and Mariner Mars 1971 missions
05 p0767 N71-14954

Mission analysis for application of Heliogyro solar sailer concept to Jupiter flyby
05 p0771 N71-15316

Supporting research and advanced development for space applications
06 p0946 N71-16671

Computer programs for calculating trajectories to Mars and Jupiter
06 p0821 N71-16674

Manual for Mark 4 Error Propagation Program operation in CDC 6600 computer search of interplanetary trajectories
07 p0997 N71-17465

Trajectory profiles and nuclear propulsion vehicle configurations for manned Mars and Mars-Venus missions
07 p1109 N71-17496

Operations and research development of Deep Space Network facilities
07 p0992 N71-17612

Describing operation and facilities of Deep Space Network
07 p0992 N71-17613

Reporting DSN support of active and planned interplanetary missions by Pioneer spacecraft
07 p0993 N71-17614

Reporting advanced engineering research on communications systems for Deep Space Network
07 p0993 N71-17616

DSIF operations and development of wideband data systems for Deep Space Network
07 p1031 N71-17621

Analysis of space flight mechanics involving interplanetary trajectories
11 p1826 N71-22127

Contour charts and tables on trajectory data for missions to Jupiter, Saturn, Uranus, and Neptune and their moons
14 p2340 N71-26690

Computer program for electric propelled spacecraft interplanetary, flyby, and rendezvous trajectory optimization based on Chebyshev approximation and polynomial representations
18 p3008 N71-30678

Direct trajectories to Jupiter and Saturn - data tabulations
18 p3010 N71-30908

Direct trajectories to Uranus and Neptune - data tabulations
18 p3010 N71-30909

Computer program for open-loop error analysis of low thrust interplanetary trajectories
18 p3016 N71-31296

Segmented two-body low thrust interplanetary swingly trajectory and performance optimization program
18 p3016 N71-31297

Modifications to interplanetary trajectory program for providing capability of generating optimum low-thrust trajectory in N-body field
18 p3016 N71-31298

Including algorithm for solution of two-point boundary value optimization problems
19 p3122 N71-31823

INTERPOLATION
Problems of bounding sum rules and interpolation between them
06 p0884 N71-16036

Error bounds of spline interpolation of piecewise-continuous functions
07 p1073 N71-17356

Extrapolation and interpretation of quasi-linear operators on martingales
09 p1411 N71-20341

Algorithm for numerical integration of data between points using interpolation
10 p1591 N71-20785

Table-lookup/interpolation fast function generation with small fixed point digital computers
12 p1883 N71-23865

Calibration of commercial platinum resistance thermometer using Z function interpolation
12 p1922 N71-24091

Interference fringe interpolator for digital line measurements
12 p1924 N71-24193

Interpolation by linear filters for use in numerical integrations involving multiple grid network mappings
15 p2436 N71-28825

Effect of spaced data interpolation upon harmonic coefficients
16 p2623 N71-28565

Quadrature algorithm for spline interpolation
18 p2943 N71-30577

Interpolated meteorological charts used for atmospheric models in numerical weather forecasting
19 p3125 N71-31665

Third-order interpolation technique for continuous path, numerically controlled machines and data reduction
19 p3123 N71-32344

Multigroup calculations for cross section structure factor interpolation schemes
20 p3322 N71-33798

Use of wind data in optimal interpolation of geopotential heights
21 p3413 N71-34287

Interpolation of synoptic and climatological atmospheric density profiles from constant pressure surfaces for use in ballistic trajectory calculations
22 p3580 N71-35498

Least squares fitting for parameter determination of empirical formula for interpolation of tabulated photon photoelectric cross sections
23 p3814 N71-37197

INTERPOLATORS
U REPEATERS
INTERRELATIONSHIPS
U RELATIONSHIPS
INTERROGATION
Scientific method and adversarial system as techniques of inquiry in technology assessment
06 p0962 N71-16873

Conference on information retrieval and management information systems including construction of dictionaries, analysis of query formulations, and computer programming
14 p2221 N71-25976

Intermediate code and table driven processor for translating retrieval question to users original language
14 p2221 N71-25977

INTERRUPTION
Superconducting coil for storing energy and restoring it in about one millisecond
02 p0286 N71-11924

INTERSECTIONS
Procedure for particle acceleration to 1000 GeV in intersecting storage rings and injection problems at 30 GeV
12 p1974 N71-23996

INTERSTELLAR COMMUNICATION
Problems, methods, and theory of communicating with extraterrestrial civilizations
05 p0643 N71-14753

INTERSTELLAR EXTINCTION
Interstellar matter in stellar extinction curve
13 p2164 N71-25294

INTERSTELLAR GAS
Measuring neutral hydrogen absorption in galaxy M82 by radio telescope
02 p0294 N71-11137

Minimum temperature and power effects of cosmic plasmas interacting with neutral interstellar gas applied to solar prominences and rotating plasmas
02 p0279 N71-11834

Intensity and spectral shape of diffuse X ray emission by galactic disk from cosmic ray heating of interstellar hydrogen
03 p0450 N71-13091

Physical adsorption and molecular hydrogen densities of interstellar clouds
06 p0948 N71-16781

Distribution and kinematics of supergiant stars in relation to interstellar gas
06 p0948 N71-16783

Astronomical large scale model of galactic spiral structure with magnetic field effects on interstellar gas motion
12 p1999 N71-24316

Gamma ray absorption processes at high red shifts, and energy dependences of absorption processes in interstellar and intergalactic gas
13 p2160 N71-24771

Mathematical model for solar wind plasma interstellar medium interaction
16 p2675 N71-28944

Cosmic gamma radiation from pion decay in interstellar gas
17 p2842 N71-30808

INTERSTELLAR MAGNETIC FIELDS
Propagation and storage of cosmic rays in interstellar magnetic fields with additional turbulent field
03 p0454 N71-13257

Compound diffusion of cosmic rays along interstellar magnetic field lines
06 p0943 N71-16785

Models of hydromagnetic shocks in very low ionization regions related to star formation and gas flows in interstellar mediums
19 p3079 N71-32315

Stellar and galactic magnetic fields, radiation processes, and interactions with ionized interstellar matter
21 p3510 N71-35911

One-dimensional diffusion model for calculating effect of interstellar magnetic field line wandering in cosmic ray parameters
23 p3847 N71-37428

INTERSTELLAR MATTER
Spectroscopic analyses of interstellar matter
02 p0174 N71-11226

Galactic hydrogen absorption at 21 cm wavelength in direction of Virgo A
02 p0294 N71-11834

Light scattering in reflection nebulae models
07 p1117 N71-18877

Brownian motion of interstellar grains and new quadratic displacement calculations
11 p1824 N71-22980

Cosmic gamma ray spectra from extragalactic proton antiproton annihilations into mesons
13 p2159 N71-24775

Lifetimes of interstellar polyatomic molecules
13 p2163 N71-25295

Interstellar matter in stellar extinction curve
13 p2164 N71-25294

Photometric studies of interstellar light absorbing media and stellar distribution in constellations Aquila and Scutum
07 p1117 N71-18877

Mathematical model of interaction between solar wind and interstellar medium
18 p3006 N71-31008

Galactic 21 cm line absorption in 97 radio source spectra using two element interferometer
19 p3182 N71-32783

Transport equations for high energy heavy cosmic rays in interstellar medium
21 p3506 N71-34975

Stellar and galactic magnetic fields, radiation processes, and interactions with ionized interstellar matter
21 p3510 N71-35911

INTERSTELLAR MICROWAVE SPECTRA
U INTERSTELLAR RADIATION
U MICROWAVE SPECTRA
INTERSTELLAR RADIATION
Description of photoionization cross section for helium and molecular hydrogen and effect on absorption of interstellar X rays
12 p1995 N71-24316

Stellar and galactic magnetic fields, radiation processes, and interactions with ionized interstellar matter
21 p3510 N71-35911

INTERSTELLAR SPACE
Attenuation of X rays in interstellar and intergalactic space and physical state of hydrogen cloud
10 p1641 N71-21340

Origin and propagation of galactic cosmic ray electrons in interstellar space
11 p1823 N71-22578

Quantitative analysis of photochemistry and lifetimes of stable interstellar molecules
12 p1993 N71-24088

Cosmic gamma ray spectra from secondary particles produced by cosmic ray collisions in extragalactic space
13 p2159 N71-24774

SUBJECT INDEX

Electromagnetic wave propagation in random interstellar media and amplitude fluctuations of radio sources 20 p3231 N71-32383

Synchrotron emissivity of cosmic electrons in ionized interstellar space (NASA-TM-X-65729) 24 p4008 N71-38578

INTERSTELLAR TRAVEL

Kinematics of interstellar travel and theoretical performance analysis for nuclear and photon propelled rockets 19 p3183 N71-31653

(VET-TM-45) Feasibility of fusion driven for interstellar travel with analysis of reaction equilibrium and plasma energy balance 24 p3964 N71-38275

INTERSTITIALS

Field ion microscopy of tantalum-carbon alloys to prove existence of interstitial order (JCLR-19530) 03 p0389 N71-12660

Stress effects on chemical potentials of interstitial constituents in alloys 06 p0873 N71-16383

Anelastic properties of neutron irradiated graphite and irradiation-induced interstitials (CEA-CONF-1636) 07 p1096 N71-18129

Thermotransport of oxygen and nitrogen in niobium beta-titanium, beta-zirconium, and tantalum (NP-18486) 08 p1211 N71-18155

Mechanical relaxations used to determine solute interdiffusion in niobium-zirconium-nitrogen alloys 08 p1216 N71-19003

Interstitial concentration, solvent composition, stress, and temperature gradient effects on interstitial diffusion in metals based on hydrogen diffusion in titanium 11 p1780 N71-22795

Electron propagation in pure Pd and interstitial alloy NiH₂ (NYO-4062-5) 15 p2421 N71-27116

Photoelectron spectroscopy for chemical analyses on doped metals and alloys (CEA-CONF-1725) 15 p2495 N71-27959

Electron irradiation effects on thermal conversion of interstitials in copper (COO-1800-15) 17 p2760 N71-29203

Phase transformations involving interstitial ordering in vanadium-nitrogen systems containing less than 15 atomic percent nitrogen (COO-1196-796) 17 p2763 N71-29519

Nitrogen effect on creep properties of ferritic steels and interstitial influence on austenitic steel creep properties 19 p3111 N71-31905

Long range migration of self-interstitial atoms in stage 1 of irradiated platinum observed by field ion microscopy (NYO-3504-57) 21 p3476 N71-34755

Isotope effect for diffusion of interstitial atoms (ANL-TRANS-882) 22 p3643 N71-35977

INTESTINES

NT RECTUM

Oxygen consumption in isolated rat intestine deprived of adrenals (NASA-TT-F-13418) 03 p0326 N71-12325

Resume of publications and recommendations from symposium on intestinal flora ecology in changing environments (NASA-CR-114889) 09 p1330 N71-19783

INTOXICATION

Operational characteristics and pilot experience in civil aviation accidents caused by alcohol intoxication 02 p0161 N71-11802

INTRAMOLECULAR STRUCTURES

Unimolecular decomposition and intramolecular energy relaxation in supra-high pressure region (AD-714020) 06 p0923 N71-16609

Development of room temperature polymeric superconductors 06 p0811 N71-16626

Expressing intermediate and long-range force interactions in crystals using Solbrig cell-dipole method (IN-1410) 07 p1079 N71-18009

INTRAMOLECULAR PRESSURE

Investigating nervous system regulation of intracellular pressure and fabrication of hybrid microcircuits 06 p0902 N71-15857

Rheomological theory for describing intracellular pressure regulation in normal eye and consequences of deterioration of pressure regulation in abnormal eye 06 p0799 N71-15858

INTRAVENICULAR ACTIVITY

Human factors study of IVA cargo transfer from shuttle to space station (NASA-CR-103118) 14 p2343 N71-25936

Space tools and equipment for EVA and IVA (NASA-CR-1760) 16 p2549 N71-28022

INTRUDER AIRCRAFT

A-4 AIRCRAFT

WIBBLED

P wave velocities at high hydrostatic pressures in known, sedimentary, and metamorphic cylindrical specimens from central Kazakhstan (NASA-TT-F-13204) 02 p0210 N71-11439

Intruder detection device for remote surveillance of specific areas 19 p3070 N71-31644

INVALIDITY

U ERRORS

INVARIANCE

NT GAUGE INVARIANCE

Time reversal invariance in electromagnetic interactions - conference (CALT-48-264) 03 p0422 N71-12656

K sub L and K sub S regeneration amplitude in copper at 2.5 GeV/c CP non-invariance (NEVIS-184) 05 p0746 N71-15236

Broken scale invariance and kinematics moments of electrodynamical cross sections (ORO-2504-159) 06 p0914 N71-15971

Long range field pulses as source of charge parity noninvariance (NYO-2171-329) 10 p1612 N71-20790

Developmental history of adiabatic invariance including contributors to radiation energy transfer and celestial mechanics concepts (NASA-TM-X-65498) 12 p1968 N71-24056

Biography on use of Lie groups and algebras in quantum mechanics and application to nonrelativistic hydrogen atom invariance groups (CEA-R-4112) 14 p2306 N71-26391

Group of invariance of Maxwell equations and extension associated with set of hyperboloids of mass (SLAC-TRANS-130) 15 p2458 N71-26935

Invariance of nonrelativistic Hamilton-Jacobi equation in electromagnetic field (JINR-PZ-3573) 15 p2463 N71-27174

Proving invariance of invariants in Galilean and nonrelativistic approximations (JINR-PZ-3563) 15 p2465 N71-27247

Determinantal formalism and physical unitarity in relativistic extension of Le Conteur and Newton formalism (PAM-70-1) 15 p2495 N71-27967

Topological invariance of constructive metric spaces (NLL-RTS-5861) 16 p2620 N71-28036

Investigation of statistical concepts of unbiasedness and invariance as keys to deriving signal detectors 16 p2561 N71-28581

Expansion of scattering amplitude and solutions to multi-Coulomb type equations using generators and Casimir operators of invariance groups 17 p2772 N71-29697

Invariance and continuity of Burgers vector applied to crystalline interface dislocations 17 p2820 N71-29958

Relativistic equations of motion invariance with respect to Poincaré group Lie algebra and application to zero mass, spinless particle free motion equation (ITF-70-32) 18 p2967 N71-30413

Dilatation and conformal invariance on null planes in relativistic scalar field 19 p3125 N71-32691

Broken scale invariance, current algebra, and massive gravitation in formalism describing meson interactions at intermediate energies and below (NUB-2091) 20 p3293 N71-33922

Lack of CP invariance violation in kaon decay into pions (PURC-4159-24) 21 p3481 N71-34795

Lambda(0) hyperon polarization along sigma(0) hyperon decay plane by violating time reversal invariance in electromagnetic interactions of kaon(minus) or sigma(minus) with protons 21 p3487 N71-34842

Invariance of space rotation group (ITF-782) 22 p3632 N71-35884

Nonrelativistic wave equation invariance for particles with 0 and 1/2 spin in electromagnetic field (JINR-PZ-3522) 22 p3633 N71-35890

Noninvariant Lagrangians for elementary particle quantum field theory (ITF-71-2-P) 24 p3976 N71-38373

Field-current identity formalism for stress tensor with scale invariance and scale breaking condition of meson couplings to stress tensor (NUB-2097) 24 p3982 N71-38417

Broken scale invariance with canonical three dimensional scale and annihilation cross sections (NUB-2098) 24 p3982 N71-38418

INVARIANT IMBEDDINGS

Invariant imbedding method for reducing two point boundary value problems for vector-matrix systems of linear difference equations to initial value problems (TID-25609) 10 p1594 N71-21660

Scale and conformal invariance differential equations applied to single particle matrix elements of two fields and false analytic assumptions when stress tensors carry moments (RLO-1388-598) 12 p1975 N71-23990

Numerical results for Sobolev Q function of radiative transfer using invariant imbedding (ITF-70-37) 14 p2284 N71-26156

X ray irradiation effects on diodes and transistors based on scattering parameters, diffusion theory, invariant imbeddings, and quantum mechanics (AD-722061) 17 p2725 N71-29493

INVESTMENT CASTING

INVENTIONS

Conference on innovations in time and space (LGO/MT-LCR/DR2-380/70) 02 p0308 N71-12101

Abstracts of NASA inventions available for licensing in foreign countries (NASA-SP-7038) 14 p2358 N71-26041

German law covering inventions and technical improvements made by employees of private, public, and Armed Forces (NASA-TT-F-13408) 24 p4034 N71-38783

INVENTORIES

NT TIMBER INVENTORY

Improved accounting control over equipment at Kennedy Space Center (B-169658) 05 p0659 N71-15579

Inventory of private and public airports and air facilities in state of Texas (PB-196935) 10 p1494 N71-21629

INVENTORY CONTROLS

Non-Bayesian minimax inventory and queueing models (AD-712770) 04 p0340 N71-14395

Computerized inventory control system for highway department of Pennsylvania 14 p2225 N71-26553

Mathematical model of locations and types of warehouses, volume of product stored, and losses due to external effects 20 p3289 N71-32883

INVENTORY MANAGEMENT

NT INVENTORY CONTROLS

Application of remote sensing to inventory and management of ranges resources 05 p0846 N71-16161

Inventory of native vegetation and related resources from spaceborne photography 06 p0846 N71-16162

Computerized simulation of alternate logistics for overhaul and expensive parts inventory procedures of commercial airlines 07 p1138 N71-18118

Systems engineering and management applied to urban development, education, water management, inventory management, Saturn-Apollo project, and ecology (NASA-TM-X-64575) 11 p1846 N71-22026

Characteristics and information requirements of staple, fashion, and big ticket merchandise inventory management and management information systems for retail stores 11 p1847 N71-22038

Computerized test equipment control system for inventory, costs, and calibration management 12 p2017 N71-23643

INVERSIONS

NT POPULATION INVERSION

NT TEMPERATURE INVERSIONS

Mathematical techniques and computer programs for inversion of de Haas-van Alphen data on closed Fermi surfaces (AEL-7659) 12 p1972 N71-23921

Atmospheric optics problem solving using Fredholm equations of first kind 15 p2403 N71-27543

Relationship between inverse and resolution methods of theorem proving (NLL-RTS-5859) 16 p2622 N71-28196

Inversion formulas for singular integral equations for linear dislocation arrays 17 p2817 N71-29936

Riemann method for arbitrary angular momentum in inverse problem of scattering theory (ITF-70-76-P) 18 p2943 N71-30576

Standard potential pattern for solving analytic inversion of five point Poisson operator (SU-IPR-409) 19 p3166 N71-32744

Computer search technique used to determine microwave frequencies used in indirect sensing by inversion (NOAA-TR-ERL-202-WPL-14) 24 p3917 N71-37934

INVERTERS

NT BEES

NT INSECTS

NT MICROSPORES

NT PARAMECIA

NT PROTOZOA

NT SPORES

INVERTERS

NT STATIC INVERTERS

Polarization (charge separation) in metal oxide semiconductor field effect transistor inverters 03 p0350 N71-12531

Square wave transistor oscillator for inverter (NASA-CASE-NPO-10760) 21 p3403 N71-34215

INVESTIGATION

NT ACCIDENT INVESTIGATION

NT AIRCRAFT ACCIDENT INVESTIGATION

INVESTMENT CASTING

Investment casting, metal drawing, longitudinal and spiral milling, and insulator pin designs in production (BDX-413-316) 16 p2613 N71-28751

Investment casting to enhance probability of metal product (BDX-413-291) 24 p3928 N71-38024

INVESTMENTS

INVESTMENTS

World Bank operations and economic growth of less developed countries

- 04 p0624 N71-14432
- Profit analysis techniques for profit and fee negotiation [NASA-CR-119004] 16 p2694 N71-28272
- Mathematical model for investment planning in R and D emphasizing options and interacting benefits for resource allocation decision making 18 p3030 N71-31391

INVISICID FLOW

NT STAGNATION FLOW

Inviscid hypersonic flow of chemically relaxing air about pointed circular cones

- 05 p0639 N71-14748
- Numerical analysis of radiating inviscid flow behind paraboloidal shock wave 05 p0661 N71-14772

Lift and aerodynamic drag due to trailing-edge flaps on sweptback wings in inviscid subsonic flow [ARCC-CP-1110] 07 p0966 N71-17114

Propagation of disturbance in viscous hypersonic flows of ideal gas [NASA-TT-F-13485] 08 p1182 N71-18939

Steady, adiabatic, inviscid, supersonic flow along corner formed by two unswapped intersecting wedges 08 p1183 N71-18994

Finite difference method for unified solutions to inviscid supersonic flow distribution about blunt bodies 10 p1540 N71-21114

Electron density and temperature in inviscid flow and nozzle-wall boundary layer, measured with constant bias-voltage and swept-voltage RAM probes 10 p1628 N71-21115

Application of integral relations to inviscid supersonic flow over symmetric airfoils at zero angle of attack [AD-717339] 11 p1669 N71-22098

Nonlinear approximation of uniform radiating transonic inviscid gas flow around symmetric profile 11 p1738 N71-22350

Numerical analysis of inviscid flow fields about pointed circular cone and conical wing-body configuration at various angles of attack 11 p1671 N71-22667

Asymptotic solution of low frequency wing oscillations in transonic shockless adiabatic inviscid gas flow based on complete approximation 12 p1898 N71-23193

Time dependent techniques, relaxation methods, and approximate solutions for computing inviscid transonic flows with imbedded shock waves [AD-721933] 16 p2579 N71-28425

Two dimensional axisymmetric jet flow model based on inviscid flow and single stream mixing theories with mass bleed and application to flow between parallel walls 18 p2906 N71-31197

Numerical method of unsteady adjustment for calculating inviscid flow fields about convex and concave shapes on atmospheric entry with ablation [NASA-CR-121371] 20 p3203 N71-32801

Computer program for determining inviscid flow around blunt bodies at supersonic and hypersonic speeds - users manual 20 p3252 N71-33670

Computer program for determining inviscid flow around nonadiabatic inviscid flow over blunt body by integral equations [NASA-TM-X-2328] 23 p3706 N71-36417

Annotated bibliography of theoretical papers relating to steady inviscid external transonic flows [NASA-TM-X-2363] 23 p3744 N71-36698

Nozzle design procedure and calculations for hypervelocity wind tunnel including thermodynamic properties of nitrogen and inviscid core and boundary layer calculations [AD-727591] 24 p3903 N71-37821

Two dimensional, unsteady, transonic, irrotational inviscid flow analysis for perfect gas with constant specific heat [AD-727641] 24 p3907 N71-37848

Inviscid flow analysis of three jet interaction for design of proportional amplifiers [AD-727689] 24 p3908 N71-37855

INVISIBILITY

U VISIBILITY

Nonlinear optical properties of crystalline materials in iodate family evaluated by second harmonic power technique [AD-724300] 20 p3287 N71-33041

IODIDES

NT CESIUM IODIDES

NT POTASSIUM IODIDES

NT SILVER IODIDES

NT SODIUM IODIDES

In-place testing of charcoal adsorbent bed filters with methyl iodide as test penetrant using pyrolytic-microcoulomb detector 17 p2743 N71-29854

Effect of gamma radiation on adsorption of iodine and methyl iodide on activated carbon exposed to flowing mixtures of steam and air 17 p2715 N71-29856

IODINE

NT IODINE ISOTOPES

NT IODINE 125

Laser excited resonance fluorescence of molecular iodine [AD-711823] 03 p0434 N71-12970

Behavior of iodine in Zircaloy capsules under conditions simulating inner cladding surface of fuel rod in water cooled reactors [ORNL-4543] 05 p0727 N71-15108

Iodine fluorescence excited by 6328 A neon line of He-Ne laser [AD-714531] 06 p0868 N71-16668

Quadrupole rotation-vibration spectrum of hydrogen and predissociation rates of B state of iodine [NASA-CR-116176] 06 p0727 N71-16869

Method of producing output voltage from photovoltaic cell using poly-N-vinyl carbazole complexed with iodine [NASA-CASE-NPO-10373] 08 p1146 N71-18698

Internuclear potential of ground state molecular iodine computed from rotational constants and vibrational energies 09 p1428 N71-19738

Spectroscopic reassignment and ground state dissociation energy of molecular iodine 09 p1429 N71-19742

Recombination of iodine atoms in dilute argon solutions studied by flash photolysis 09 p1429 N71-19747

Iodine molecular beam absorption resonance as long-term frequency reference for argon ion laser stabilization [NASA-CR-117528] 10 p1570 N71-21443

Natural transport effects on fission product behavior in containment systems experiment, time dependence of iodine, methyl iodide, and particulate matter in vapor and steam phases [BNWL-1457] 11 p1804 N71-22284

Gallium arsenide solar cell preparation by surface deposition of cuprous iodide on thin n-type polycrystalline layers and heating in iodine vapor [NASA-CASE-XNP-01960] 11 p1727 N71-23027

Regarding potential analyzer used with vacuum monochromator for recording photoelectron spectra of iodine and bromine [AD-101] 13 p2041 N71-25365

Energy dependence of charge exchange reactions in iodine and argon ionization by exchange collisions [KFK-1265] 14 p2315 N71-26733

Potential high energy resolution iodine negative ion source [AD-720871] 15 p2473 N71-27445

Hypoidous acid generated by injection of elemental iodine into steam-air atmosphere or by purging dilute aqueous solution of iodine in water with air or other gases - airborne species 17 p2743 N71-29853

Effect of gamma radiation on adsorption of iodine and methyl iodide on activated carbon exposed to flowing mixtures of steam and air 17 p2715 N71-29856

Activated carbon in reactor confinement systems to remove radiiodine from effluent gases in event of nuclear accident 17 p2715 N71-29857

Iodine behavior and control in processing plants for fast reactor fuels and removal of radiiodine from plant effluents 17 p2784 N71-29858

Inorganic adsorbent materials for trapping of fission product iodine in fuel reprocessing plants and gas cleaning inside reactor containment 17 p2784 N71-29859

Adsorption properties of metal zeolites for airborne iodine species to provide support for full scale testing of air pollutants 17 p2784 N71-29860

Spectrophotometric measurement of iodine concentrations in spacecraft potable water supplies [NASA-CR-115134] 22 p3547 N71-35264

Effect of interfering substances on performance of Skylab iodine colorimeter 22 p3550 N71-35284

Variability of dose reduction factor for removal of iodine contaminants by containment spray system in pressurized water reactors [ORNL-TM-2412-PT-12] 22 p3625 N71-35829

Quenching excited iodine atoms and photoionized production of excited singlet oxygen species and their reactivity 22 p3644 N71-35982

Interactions between intense coherent light from Q switched ruby laser and iodine vapor, neodymium-doped glass, and benzene 23 p3805 N71-37128

Continuous measurement of activity concentration of radiiodine in air using NaI (Tl) crystal detector [KFKI-71-13] 24 p3915 N71-37948

Beta and electron capture decay in iodine and tellurium [ANL-TRANS-883] 24 p3980 N71-38401

IODINE COMPOUNDS

NT CESIUM IODIDES

NT IODATES

NT IODIDES

NT POTASSIUM IODIDES

NT SILVER IODIDES

NT SODIUM IODIDES

Ion exchange silver zeolites for iodine adsorption studies [IN-1363] 10 p1601 N71-20669

Melting point-composition and phase diagrams of thallium-iodine systems and X ray powder patterns of TlI₃ and TlI 11 p1784 N71-22408

Electron paramagnetic resonance of IO₂/methyl radical in gamma irradiated single crystals of KIO₃ at room temperature 15 p2486 N71-27822

Inorganic material adsorbent air sampling system for analysis of airborne iodine isotopes and compounds in nuclear reactor containment atmosphere 17 p2743 N71-29861

Preparation of new covalent inorganic perchlorates from chlorine perchlorate, iodine fluorosulfonic preparation, chlorine fluoride reactions, and other inorganic halogen oxidizer investigations [AD-724331] 20 p3229 N71-33182

IODINE ISOTOPES

NT IODINE 125

Electromagnetic transition probabilities in nuclei with mass numbers between 125 and 153 based on half-life measurements of T, Te, Sm, and Eu isotopic excited states [INR-1149] 02 p0277 N71-12135

Observation of new high energy gammas of I-132 [ORNL-TR-2263] 04 p0582 N71-14045

Capture cross sections in keV region versus energy curves to determine gamma ray strength, S wave neutron strength, and P wave neutron strength in silver, iodine, and indium isotopes 15 p2479 N71-27631

Nuclear processes activated by isomeric transitions of Br-82m and I-130m 15 p2488 N71-27876

In-place test results of N reactor charcoal columns: capture cross sections in keV region versus energy curves to determine gamma ray strength, S wave neutron strength, and P wave neutron strength in silver, iodine, and indium isotopes 15 p2479 N71-27631

Inorganic material adsorbent air sampling system for analysis of airborne iodine isotopes and compounds in nuclear reactor containment atmosphere 17 p2743 N71-29861

Particle accelerator spallation of xenon and its decay to I-123 for use in radiation medicine [NASA-TM-X-67875] 18 p2987 N71-31281

Production of iodine isotopes in meteorites by cosmic rays, gas proportional counting of transition metal X ray emitters, and radiochemical analysis of lunar samples 18 p3017 N71-31348

IODINE 125

Dose distribution calculations from tritium and iodine 125 sources using energy spectra [JUL-688-ME] 15 p2475 N71-27466

ION ACCELERATORS

Design and evaluation of ion implantation system for semiconductor materials [AD-712011] 02 p0197 N71-11128

Particle stability in ion linear accelerators with alternating-phase focusing [JINR-P-5312] 07 p1080 N71-18124

Electron ring accelerator research on ion, electron, and proton acceleration [UCRL-20125] 10 p1538 N71-20640

Theoretical analysis of performance of two-grid accelerator systems for Kaulman thrusters [NASA-TN-D-6275] 12 p1990 N71-23762

Berkley Hill modification for ion acceleration to maximum energy of 8.5 MeV/n [UCRL-19919] 12 p1973 N71-23939

Helium outgassing process for fused glass coating on ion accelerator grids [NASA-CASE-LEW-10278-1] 16 p2602 N71-28382

Performance characteristics of existing and proposed accelerators for heavy ions with descriptions of super HILAC progress and discussion of isochronous cyclotrons [ORNL-TM-3332-REV] 17 p2793 N71-29625

Ho-166 rotational bands, M1 radiative strength resonance in Cr-53, Dynamitron research, photoelectron spectroscopy of high temperature vapors [ANL-7739] 17 p2888 N71-30341

Two phase excitation coil system for ion cyclotron heating of hydrogen plasma 18 p2993 N71-31141

Ion accelerator systems engineering for time sharing operation with heavy and light ions [UCRL-20633] 19 p3147 N71-31994

Vacuum cryopumping of heavy ion source in high voltage terminal of accelerator injector [UCRL-20620] 19 p3150 N71-32119

Glass coating of electron bombardment ion-thruster grids by electroosmosis [NASA-CR-72992] 20 p3277 N71-32923

Analysis of ion beam thrust deflection system using grid translation techniques [NASA-TM-X-67911] 20 p3339 N71-33551

SUBJECT INDEX

Total loss cross sections for D2 molecules passing through H2 gas in light ion accelerator
[UCRL-20699] 23 p3812 N71-37181

ION ATOM INTERACTIONS

Analytic formulas for inelastic cross sections for collisions of protons and hydrogen atoms with atomic and molecular gases
[AD-711661] 01 p0098 N71-10586

Interaction processes between helium ions and atoms
[NASA-CR-111353] 01 p1013 N71-11000

Angular distribution shape of H^+ , H and p , n charge exchange transitions to $0i$ and $1i$ states
[NYO-2171-321] 06 p0923 N71-16724

Ion current response of Langmuir probes in presence of ion-atom collisions in weakly ionized argon plasma
[NASA-TM-X-65445] 07 p1077 N71-17594

Ionization cross section measurements of argon collisions, photon emission during argon decay, and Penning ionization discharge
09 p1428 N71-19718

Elastic and inelastic scattering of atoms and ions, and sources of interference patterns
[SR1A-115-P-78-6] 09 p1440 N71-20303

Statistical model for electron scattering in ion atom interactions
[AD-72082] 15 p2474 N71-27456

Electron capture and loss cross sections in heavy ion collisions with atomic oxygen and excitation of positive helium ion
15 p2478 N71-27623

Quantum electrodynamics of atom interaction with radiation field
15 p2494 N71-27957

Monochromatic, positive ion beams passed through inert gas and analyzed by mass spectroscopy
[AD-723588] 19 p3144 N71-31748

Limitations of merging beam method in studying ion beam collisions
[IAE-2001] 19 p3146 N71-31962

Comparison of experimental data and theoretical predictions for doubly differential ionization cross sections for neon and argon collisions
22 p3650 N71-36028

Surface reactions between silver nuclei and carbon and nitrogen projectiles
[NP-18674] 24 p3975 N71-38360

ION BEAMS

Producing ion beam scattering in collector tanks of isotope separators by using stabilizing devices
[CEA-R-3959] 04 p0576 N71-13700

Production of ion stream with two velocity distribution components using diffusion plasma source
[IPP-97] 04 p0599 N71-14281

Measuring plasma density, space potential, and current density using heavy ion beam probe
[AD-713857] 06 p0930 N71-16190

Analyzing doped semiconductor surface layers using elastic ion backscattering data
07 p1089 N71-17291

Remote control device for positioning isotope separator collector electrodes and controlling ion beam shape and intensity
[CEA-N-1323] 08 p1199 N71-18378

Using ion bombardment etching technique to reduce thickness of boron carbides for transmission electron microscopy
[AD-715857] 08 p1221 N71-18498

Heavy ion beams for in-beam gamma ray and conversion electron spectroscopy
[UCRL-19661] 08 p1261 N71-18777

Characteristics of synthesized plasma resulting from forced neutralization of mercury ion beam
[CEA-R-3724] 09 p1450 N71-20282

Mathematical representation of ion beam current density profiles
[NASA-TM-X-52992] 10 p1638 N71-20940

Magnetic analysis of helium ion and proton beams in N_2 , O_2 , and air for range-energy relations
[SC-R-70-788] 10 p1615 N71-20950

Physical mechanism and charge states resulting from collision of ionized gas particles with metallic surfaces
[AD-717063] 10 p1617 N71-21322

Flow equation for representing ion beam current density profile from bombardment ion thrusters
[NASA-TN-D-6334] 12 p1990 N71-23924

BOLIDE type isotope separator with four electrode system for ion beam formation
[JINR-P15-5369] 13 p2132 N71-25108

Measurement of oxygen effect and biological effectiveness of 910 MeV helium ion beam using cultured human kidney cells of interest in radiotherapeutic treatment of hypoxic tumors
[UCRL-20190] 13 p2034 N71-25241

Ion beam deflector system for electronic thrust vector control for ion propulsion yaw, pitch, and roll forces
[NASA-CASE-LEW-10689-4] 14 p2332 N71-26173

Utilization of elastically scattered recoil ions to measure solid state track detector registration characteristics and particle trajectory analysis
[NASA-CR-118657] 14 p2308 N71-26447

Lamb shift type ion source for producing positively charged polarized hydrogen ion beams
[KFK-1262] 14 p2316 N71-26743

Investigations of ion beam injection system using dopantatron with electron oscillation in anode plasma
[IPP-2/87] 15 p2500 N71-27316

Electron and ion pulse propagation in quiescent plasma
15 p2500 N71-27405

Mass separator mass and energy measurement of ions in electrostatic generator accelerated beams and pulse height analysis for quarks in He, H, N, O, air, and limestone
17 p2795 N71-29760

Ion beam phase characteristic: measuring devices for volumetric and emissivity measurements
[MP-18307] 18 p2971 N71-30468

Focusing, acceleration, and beam characteristics of Orsay heavy ion linear accelerator
[MP-18612] 18 p2978 N71-30665

Ion beam focusing with plasma control
[IAE-1974] 18 p2992 N71-30733

Monochromatic, positive ion beams passed through inert gas and analyzed by mass spectroscopy
[AD-723588] 19 p3144 N71-31748

Approximate monopole and transition moment methods for calculating long range intermolecular forces in biological systems
[AD-723217] 19 p3157 N71-32470

Analysis of ion beam thrust deflection system using grid translation techniques
[NASA-TM-X-67911] 20 p3339 N71-33552

High vacuum ion beam sputtering of integral coverslips for solar cell utilization
[NASA-CR-121468] 20 p3214 N71-33685

Determining distribution of fission products in fuel particle coatings by sputtering technique using ion beams
[SGAE-PR-96/1970] 21 p3458 N71-34615

Axially symmetric electron-ion beam oscillations and instability in magnetic field
[MATT-TRANS-93] 21 p3494 N71-34891

Electron-ion (ion sound) oscillations in electron beam passing through rarefied gas corresponding to instability in homogeneous plasmas
[MATT-TRANS-84] 21 p3494 N71-34894

Vlasov equation for solving ion-electron beam system
[JINR-P9-5645] 22 p3637 N71-35927

Parallel plate pulsed ion beams for production of millimicrosecond pulsed ion beams
[UAE-87-77] 24 p3969 N71-38313

Interaction of high frequency electromagnetic fields with magnetized plasmas, high intensity electron and ion beams, pulse discharges, and related studies - bibliography
[NP-18901] 24 p3993 N71-38487

ION CHAMBERS

IONIZATION CHAMBERS

ION CHARGE

Ion charge determination from emitting spectral lines using beam foil light source technique
[NASA-CR-111379] 02 p0270 N71-11460

Ion charge identification for spectral lines in nitrogen by beam foil light source technique
[NASA-CR-111380] 02 p0271 N71-11462

Comprehensive calculation of ionization potentials and binding energies for multiply-charged ions
[ORNL-4562] 02 p0272 N71-11771

Limits, capabilities, and operation of field ion microscopes with results of tungsten and iridium ionic charge investigations
24 p3926 N71-38016

ION CONCENTRATION

Determining surface concentration of ion adsorbates with two-electrode thin layer method
[MLM-1765/CTR] 07 p0989 N71-17225

Ion concentration production in E region by vertical neutral gas motions
[ESSA-TR-ERL-75-ITS-112] 07 p1114 N71-17914

Concentrations of principal ions in ionosphere at 100 to 200 kilometer altitude and factors which affect ion formation
10 p1553 N71-21482

Design and fabrication of measuring system to determine concentration and mobility of atmospheric ions
[RAE-LIB-TRANS-1435] 13 p2075 N71-25148

Control of mitosis in biological cells through inorganic ion hierarchy of cells involved
[NASA-CASE-LAR-10773-1] 21 p3382 N71-34061

Development of method for applying metal alloy film or coating to irregular shaped metal object
[NASA-CASE-LEW-11262-1] 21 p3437 N71-34455

Comparison of atmospheric ionization measurements under various meteorological and environmental conditions
[IPA-CP-226] 23 p3790 N71-37016

ION BEAMS

Determining suitability of aluminum for use in electrochemical systems
[AD-714600] 06 p0797 N71-16115

ION DENSITY (CONCENTRATION)

Ion current response of Langmuir probes in presence of ion-atom collisions in weakly ionized argon plasma
[NASA-TM-X-65445] 07 p1077 N71-17594

Multiple-grid probe separating currents flowing from plasma to collector into their electron and ion components
[IPP-2/83] 08 p1271 N71-18246

Ionic currents in anodic oxidation of Ti, Zr, and Ti-Zr alloys below oxygen evolution potential and thin film growth theory
[AEC-TR-7201] 09 p1444 N71-20518

System for monitoring presence of neutrals in streams of ions - ion engine control
[NASA-CASE-KNP-62952] 09 p1444 N71-20518

Ionospheric radio occultation detection of ion-acoustic wave disturbances caused by nuclear explosion
11 p1709 N71-22932

Theory and design of aspiration counters and atmospheric ion current measurements
[TT-48-50499] 12 p1917 N71-23347

External shock structure and ion collection characteristics of rocket-borne mass spectrometer
[AD-720833] 14 p2333 N71-25771

Directional ion current anemometer for measuring direction and elevation angles and speed of wind to 3 centimeters per second
[AD-720573] 14 p2389 N71-26105

Diffusion type plasma source with two cathode rod arrays for ion current production
[IPP-97] 15 p2501 N71-27392

Conversion factor for converting Geiger tube count rates or ion chamber currents into units of incident X ray energy flux in specified passband in normalizing solar X ray data
[NASA-TM-X-65553] 15 p2514 N71-27644

Calculations of ion trajectories and energy distribution in front of field emission tip
[IPP-7/2] 15 p2483 N71-27766

Ion sampling measurements in high pressure cesium discharges
[AD-720713] 15 p2504 N71-27927

Temperature and pressure effects on ionic currents in sea water corresponding to upper 400m in ocean
[AD-721573] 16 p2586 N71-28347

Time of flight and mass spectroscopy of vanadium, titanium, and chromium alloy electron impact ionization cross sections using ion current and vapor pressure data for calculations
16 p2611 N71-28503

Light scattering applications to plasma diagnostics, including collisionless coupling and ion excitation
[ORO-3393-5] 16 p2662 N71-28840

Characteristics of simultaneous electronics and ionic conductivity in solids at 700 to 800 K
[NLL-LT-746-617-7022.401/1] 16 p2669 N71-29158

Ion density probe design for continuous flows using flat-plate electrodes for measuring ion currents and production rates
18 p2924 N71-31208

Ion temperature determination in plasmas based on electrostatic probe measurements of ion current
[AD-723529] 19 p3164 N71-32135

Investigation of current collection of negatively biased flat electrostatic probes in continuum regime
[AD-724148] 20 p3329 N71-32920

Evaluation of ion density and plasma potential from Langmuir probe data - graphs
[NASA-TM-X-2369] 22 p3642 N71-35964

Experimental investigation of quasi-stationary longitudinal ion streams in L-1 stellarator
[CN-28/6-4] 23 p3831 N71-37322

EMF method for studying ionic conductivity of molybdenum trioxide
[NLL-M-21003-5828.4F1] 24 p3941 N71-38114

ION CYCLOTRON RADIATION

Large amplitude steady state electron plasma, harmonic ion cyclotron amplifying waves
[COO-2081-2] 04 p0597 N71-14051

Ion cyclotron instability in nonuniform magnetic field
[UCRL-TRANS-10482] 05 p0739 N71-15018

Electron cyclotron drift instability with plasma heating
[LA-4467-MS] 05 p0739 N71-15019

Theoretical analysis of quasi-static ion cyclotron waves
[ORO-3871-4] 05 p0754 N71-15224

Investigating creation of plasma turbulence by quasi-static ion cyclotron wave
06 p1276 N71-19286

Finite ion and electron temperature effect on ion cyclotron waves generated by Silt coil, and subsequent plasma ion heating in magnetic bottles
[NASA-TM-X-2263] 13 p2149 N71-25439

Quasi-static ion cyclotron waves for plasma heating
[ORO-3871-5] 13 p2149 N71-25597

Ion cyclotron instabilities in finite plasmas and finite temperature effects
23 p3833 N71-37332

ION DENSITY (CONCENTRATION)

IONOSPHERIC ION DENSITY

MAGNETOSPHERIC ION DENSITY

MAGNETOSPHERIC PROTON DENSITY

PROTON DENSITY (CONCENTRATION)

- Plasma probe for Pioneer spacecraft to measure ion and electron density and angular distribution in space [NASA-CR-73486] 03 p3576 N71-12768
- Ionic density in sea water salinity determinations from electrical conductivity measurements 04 p521 N71-13723
- Perturbations in density of ions and neutral particles in upper atmosphere due to OGO 12 p1952 N71-23238
- [NASA-CR-117897] 12 p1952 N71-23238
- Flat plate and cylindrical ion density probes including free molecular flow and continuum regimes 12 p1923 N71-24130
- Elementary processes of plasmas and ion density distribution in arc discharge 14 p2311 N71-26685
- [LYCEN-7061] 14 p2311 N71-26685
- Ionometry, electric field gradient, and specific heat determinations for ferroelectric phase transitions in $\text{PbO}_2\text{-O}_3\text{-PbTiO}_3\text{-BiFeO}_3$ ternary systems 15 p2506 N71-27314
- Ion containment in decreasing magnetic field of electron accelerator ring 16 p2642 N71-28049
- [JINR-P-5555] 16 p2642 N71-28049
- Thermospheric model based on Explorer 32 hydrogen ion density measurements including periodic variations and temperature factors due to local time, solar activity, and magnetic effects 16 p2586 N71-28329
- [NASA-TM-X-63589] 16 p2586 N71-28329
- Equation based on instantaneous ion exchange and linear adsorption isotherm for predicting radioactive ion concentration and flow in ground water [SC-CR-70-6139] 16 p2558 N71-28754
- Positive ion densities from rocket-borne hemispherical Langmuir probe at 40 to 100 km [AD-722066] 16 p2662 N71-28848
- Dynamic model for partial pressure variations of electrons, ions, and neutrals in active zone of hollow cathode arc discharge 17 p2813 N71-30240
- [NP-18708] 17 p2813 N71-30240
- Ion density probe design for continuum flows using flat-plate electrodes for measuring ion currents and production rates 18 p2924 N71-31208
- Ion mobility effects in Jost mechanism for solid state reactions [KFK-1312] 19 p3168 N71-32072
- Electron heating rate and ion chemistry in the atmosphere above Wallops Island during solar eclipse of March 7 1970 [NASA-TM-X-65638] 19 p3093 N71-32292
- Scintillation counter for radon ion density measurements in atmosphere [IFA-RDP-32] 20 p3271 N71-33040
- Ion mass spectrometer experimental design on Explorer 31 satellite and data processing techniques for ionospheric composition [NASA-CR-121651] 21 p3424 N71-34362
- Minimum condition on product of ion density and confinement time of energetic ions within reacting plasma for thermonuclear power - Lawson criteria [MATT-844] 23 p3828 N71-37302
- Plasma containment in LRL 2X experiment, and calculations of density and energy of injected plasma [CONF-710607-99] 24 p3989 N71-38462
- ION DISTRIBUTION**
- Interplanetary magnetic field role in counterstreaming ion-ion instability in ion thermalization process for earth bow shock [NASA-CR-111420] 02 p2822 N71-12032
- Relative cation mobilities in silver bromide-potassium bromide melts 05 p0631 N71-14691
- [NVO-3608-11] 05 p0631 N71-14691
- Numerical simulation of ion-acoustic instability in plasmas [LA-4510] 06 p0929 N71-15854
- Automated potentiometric techniques for on site monitoring of ions important in water quality control [PB-195167] 07 p0988 N71-17123
- Interior potentials for alkali metals from correlations in electron liquids 13 p2096 N71-25512
- [ANL-7761] 13 p2096 N71-25512
- Crystallographic data, cation distributions, magnetic transition temperatures, and magnetic structures of tetragonal systems determined by neutron diffraction [NP-18783] 22 p3631 N71-35874
- Asymmetric confining toroidal field effect on ion velocity distribution energy in plasma generator [CONF-710607-33] 23 p3830 N71-37320
- Neoadhesive ions in distribution function from self consistent calculations of plasma focus [CONF-710607-43] 24 p3986 N71-38446
- Development of technique for doping piezoelectric crystals by ion implantation [AD-727097] 24 p3997 N71-38514
- ION EMISSION**
- Absolute experimental emission cross sections for excitation of electric dipole transitions in Ba ions by electron impact [ORO-3027-17] 04 p0570 N71-13600
- Mass spectrometer analysis on ions ahead of shock waves in xenon 08 p1181 N71-18917
- Theoretical model for calculating resonance line fluxes of ion emission in solar corona 10 p1642 N71-21837
- Excitation mechanisms of rare earth element ion emission spectra in thioindate lattices [SRDE-78028] 12 p1985 N71-23359
- Space electric rocket test thruster performance with xenon, krypton, argon, neon, nitrogen, helium, and carbon dioxide ion source gases and magnetic spectroscopy of ion emissions [NASA-TM-X-67831] 13 p2130 N71-24699
- Multicharged ion emission from nitrogen, argon, and neon in reflex ion source with axial extraction [LYCEN-7065] 14 p2312 N71-26705
- Photometry of barium ion emission for Javelin second release 17 p2741 N71-29678
- Physiological effects and growth responses in plants influenced by electric fields and production of air ions and ozone by barley plants 23 p3715 N71-36485
- Plasma containment in LRL 2X experiment, and calculations of density and energy of injected plasma [CONF-710607-99] 24 p3989 N71-38462
- ION ENGINES**
- Operating temperature of ion thruster hollow cathodes and performance tests of convergent supersonic nozzle 01 p0115 N71-10266
- Results of flight of Yantar automatic ionospheric laboratory - Part 3 [NASA-TT-F-13403] 01 p0127 N71-10927
- Development of colloid thruster system with array of emitters [NASA-CR-111417] 02 p0291 N71-12076
- Ion engine with magnetic circuit for optimal discharge [NASA-CASE-XLE-01124] 04 p0605 N71-14043
- Langmuir probe determinations on non-Maxwellian distribution of electron energy in plasma of electron bombardment ion engines [RM-70/3] 04 p0600 N71-14300
- Electron bombardment ion rocket engine with improved propellant introduction system [NASA-CASE-XLE-02066] 05 p0763 N71-15661
- Plasma measurements in SERT 2 spacecraft ion thruster discharge chamber using Langmuir probe [NASA-TM-X-2088] 06 p0939 N71-15835
- Effects of mercury electron bombardment ion thruster exhaust products on surfaces located downstream [NASA-TN-D-7038] 06 p0940 N71-15915
- Cold gas and high temperature gas rocket engines and ion engines for satellite attitude control [DLR-MITT-70-14] 07 p1118 N71-17158
- Design technology for ion cesium microthruster [ONERA-TP-847] 08 p1284 N71-18732
- Electron bombardment hollow cathode ion thruster performance [NASA-CR-116828] 08 p1285 N71-19178
- System for monitoring presence of neutrals in streams of ions - ion engine control [NASA-CASE-XNP-02592] 09 p1444 N71-20518
- Low frequency plasma noise from mercury electron bombardment ion thruster studied for several magnetic field configurations [NASA-TN-D-6286] 11 p1821 N71-22613
- Construction and method of arranging plurality of ion engines to form cluster thereby increasing efficiency and control by decreasing heat radiated to space [NASA-CASE-XNP-02923] 11 p1821 N71-23081
- Electronic cathodes for use in electron bombardment ion thrusters [NASA-CASE-XLE-04501] 12 p1886 N71-23190
- Permanently magnetized ion engine casing construction for use in spacecraft propulsion systems [NASA-CASE-XNP-06942] 12 p1989 N71-23293
- Theoretical analysis of performance of two-grid accelerator systems for Kaufman thrusters [NASA-TN-D-6275] 12 p1990 N71-23762
- Data obtained from flights of Yantar unmanned ionospheric laboratories with gas ion plasma engines to determine possibilities for guided flight in upper layers of atmosphere [NASA-TT-F-13550] 12 p1998 N71-24345
- Sputtering yield from titanium and tantalum due to ion engine mercury ion impact noting angular distribution [RAE-TN-70149] 13 p2061 N71-24700
- Prototype auxiliary propulsion subsystem with isolated single tank propellant feed system and 5-cm diameter ion thruster [NASA-TM-X-67828] 13 p2155 N71-24735
- Preliminary investigation to eliminate or reduce concentrated charge exchange ion erosion of accelerator grid supports for electron bombardment ion thrusters [NASA-TM-X-67842] 14 p2331 N71-25694
- Development and tests of flight prototype power conditioner for 20 cm mercury bombardment electric thruster system [NASA-CR-119651] 14 p2333 N71-26525
- Development and characteristics of ion thruster accelerator with single glass coated grid to provide increased ion extraction capability and larger diameter accelerator system [NASA-CASE-LEW-10106-1] 14 p2333 N71-26642

- Internal labyrinth and shield structure to improve electrical isolation of propellant feed source from ion thruster [NASA-CASE-LEW-10210-1] 14 p2333 N71-26701
- Low mass ionizing device for use in electric thruster spacecraft engines [NASA-CASE-XNP-01954] 16 p2672 N71-28820
- Instrumentation for control of magnetic field in ion thruster for improved starting and improved sensing of natural magnetic field [NASA-CASE-LEW-10835-1] 16 p2672 N71-28873
- Thermionic reactor design features and system characteristics including amount of fissionable material, power output, specific power, mass of components, and total mass [NASA-TT-F-13690] 16 p2636 N71-28840
- Mathematical aspects of neutron physics for ITT project [NASA-TT-F-13685] 17 p2781 N71-29218
- Vehicle with plasma-ion electrojet engine designed for orbital flights and altitudes from 50 to 200 km using isoelectric air intake for fuel [NASA-TT-F-13676] 17 p2832 N71-29240
- Isotope thermionic reactor physics, shielding, and calculations [NASA-TT-F-13704] 18 p2981 N71-30401
- Main ion thrusters, microthrusters, and characteristics of electric power supplies for ion engines [LAAS-756] 19 p3173 N71-31444
- Survey of various cathodes used in Kaufman ion thruster [NASA-TM-X-67918] 20 p3339 N71-33306
- Dual grid accelerator system with electrostatic beam deflection capability tested on 5-cm diameter Kaufman thruster for 1000 hours [NASA-TM-X-67908] 22 p3662 N71-34412
- Maximum propellant utilization in electron bombardment ion thrusters using mercury for propellant [NASA-TM-X-67921] 22 p3662 N71-34411
- Neutralizer location for minimum accelerator erosion on 30 centimeter diameter ion bombardment thruster [NASA-TM-X-67926] 22 p3662 N71-34414
- Beam focusing characteristics of variously shaped grid holes with application to electron bombardment ion thrusters [NASA-TM-X-67922] 22 p3662 N71-34413
- Electrically propelled spacecraft designs using thermionic reactors as electrical power source investigated for Halley Comet rendezvous mission [NASA-CR-122928] 23 p3839 N71-37377
- Plasma-ion engines utilizing atmospheric gases to form ion jet for propulsion [AD-727496] 24 p4001 N71-38317
- ION EXCHANGE MEMBRANE ELECTROLYTES**
- Permeability characteristics of cation-exchange membranes based on transport measurements [NASA-CR-117367] 09 p1408 N71-20451
- Development and characteristics of ion-exchange membrane and electrode assembly for fuel cells or electrolysis cells [NASA-CASE-XMS-02063] 16 p2541 N71-29904
- Performance of multicompartiment electrodiolysis system with laminar flow, and fouling of membrane surfaces by iron oxide [FML-PUBL-71-13] 24 p3886 N71-37706
- ION EXCHANGE RESINS**
- Feasibility determination for use of ion exchange resins as carriers of plant nutrients [NASA-TT-F-13544] 09 p1344 N71-20166
- Analytical and experimental data on use of ion exchanger based synthetic nutrient media for growing plants [NASA-TT-F-13545] 09 p1344 N71-20167
- Anion and cation exchange resin mixture for hydroponic growth of vegetables and flowers [NASA-TT-F-13543] 09 p1387 N71-20428
- Ion exchange silver zeolites for iodine adsorption studies [IN-1363] 10 p1601 N71-20408
- Technological and sorption properties of powdered ion exchange resins [NLL-TR-5981] 10 p1515 N71-21538
- Resin crosslinking effects on anion exchange separation of rare earth-EDTA complexes at trace loadings [JINR-P-299] 16 p2659 N71-29109
- Composite organic semiconductors from pyrolytic ion exchange resins 18 p2940 N71-31218
- Advantages and use of ion exchange resins for separating boron, nitrogen, and uranium isotopes [NLL-RISLEY-TRANS-2135-19091.9F1] 23 p3721 N71-36313
- ION EXCHANGING**
- Whistler study to determine interchange of ionization between ionosphere and protonosphere [SU-SEL-70-022] 01 p0049 N71-10722
- Theory of s-d exchange scattering in dilute magnetic alloys [CALT-822-12] 05 p0751 N71-15570
- Electrochromatographic separations of rare earths [UCRL-19526] 06 p0812 N71-16722

SUBJECT INDEX

Crossed molecular beam for studying alkali atom alkali halide exchange reactions

On-line radiometric monitoring of pressurized ion exchange, chromatographic process

Anion exchange separation of neptunium from uranium and thorium in aqueous tetramethylammonium hydroxide

Separation methods such as centrifuging, ion exchanging, electrophoresis, and chromatography applied to biochemical materials (gels, proteins, amino acids)

Characteristics and application of ion exchange production for development of superpure inorganic materials

Equation based on instantaneous ion exchange and linear adsorption isotherm for predicting radioactive ion concentration and flow in ground water

Bibliography on isotope separation by ion exchange from 1938 to 1970

Chromatographic isolation of pure plutonium 238 from radiolytic reaction products

Analysis of axisymmetric expansion of ionized, hot-electron cold ion plasma in magnetic nozzle

ION GAGES

IONIZATION GAGES

ION IMPACT

Fission product angular distributions from C-12 ion impact with Gd-158 and O-16 ion impact with Sm-154 which yield 107 MeV excited Yb-170 compound nuclei

Observations from Apollo 14 suprathermal ion detector including ionospheric ion density, mass and energy spectra during venting in LM cabin, large ion cloud, and ion resulting from impacts

ION INJECTION

Ion implantation forming of conducting layers and p-n junctions in gallium arsenide and silicon carbide

Current voltage characteristics of flash-mounted electrostatic probe in presence of negative ions

Ion beam slow pulsing injector system for 2MV Van de Graaff

Industrial scale ion implantation facility

Describing injector and beam optics of 8 MeV tandem Van de Graaff accelerator

Axial injection of polarized protons into Grenoble cyclotron

Crystalline structure defects of diamonds caused by helium ion injection

Luminescence of zinc sulfide ion injected thin films

Experimental design and performance of plasmatron - isonic pulverization device

Ion implantation preparation of rare earth doped thin films of zinc sulfide

Analysis of plasma obtainable by neutral injection into superconducting levitron

Semiconductor devices and performances, and ion implantation technology for semiconductors

Investigations of ion beam injection system using dopant plasmatron with electron oscillation in anode plasma

Ion velocity measurements in red plasma injector by monochromator

Multilayer linear accelerator injection into gravity gradient synchrotron and quadrupole compensation for frequency shifts

Pulsed ion gun (PIG) type heavy ion source on axial injection line of 88 inch cyclotron

Cyclotron characteristics and types of ion source inductors for use in high-energy, heavy-ion cyclotrons

Design and construction of single gap high gradient volume for use as high current injector supplying Van de Graaff

ION IRRADIATION

DEUTERON IRRADIATION

PROTON IRRADIATION

Static quadrupole moments measurement of first excited 2p orbital states of Pd-106 and 110 nuclei by heavy ion Coulomb excitation

Investigating operation of ion orientation sensors based on perception of charged particle stream in upper atmosphere and deviation of vehicle axis from stream direction

Radiation effects on ion and fast neutron bombardment

Relative biological effectiveness of multicharged ions during single irradiation of Chloralla

Crystal defects in diamonds and semiconductor fabrication

Alloying and distribution of silicon, phosphorus, and boron using ion bombardment as method of fabricating multilayer semiconductor devices

Elimination of microbial and viral agents from spacecraft water systems by silver ions from electrostatic ion generators

Multicollision transfer reaction mechanisms and products produced by C-12, Ne-22, and Ar-40 ions on Au, Pb, and Bi

Secondary electron emission coefficients, apparent total ion scattering, and energy distributions of secondary electrons and ions produced by positive ion irradiation of metals

Crystalline for keV heavy ion irradiation and isochronal annealing at 77 to 300 deg K to study lattice defects in metals by Mossbauer spectroscopy and other experiments

Alpha decay of element 105 isotopes, produced by American 243 irradiation with neon 22 ions

Production of fast neutron-deficient iridium isotopes by bombarding holmium with Ne-22 and Ne-20 heavy ions

Long range migration of self-interstitial atoms in stage 1 of irradiated platinum observed by field ion microscopy

Quantitative ion microscope study of defect structure of two depleted zones in tungsten irradiated with 20 keV tungsten(plus) ions at 18 K

Effects of parasitic impedances on conversion loss of millimeter wave mixers utilizing ion bombarded silicon and gallium arsenide

Reducing radiation conductivity of germanium as result of fast and slow ionic bombardment

ION MICROSCOPES

Optical image comparator for examination of field ion micrographs

Field ion microscopy of tantalum-carbon alloys to prove existence of interstitial order

Study of defect structures with field ion microscope

Atom probe field ion microscope with time of flight spectrometer

Measuring intermittent enhancement of blinking effect upon addition of neon to imaging gas in helium-tungsten field-ion microscope

Ion microscope study of tungsten and thoriated tungsten grain boundaries

Electron and ion microprobes applied in characterizing aluminate coating on IN-100 nickel alloys for high temperature oxidation resistance

Field ion and field emission microscopic analysis of nickel tungsten alloy photoluminescent bands

Long range migration of self-interstitial atoms in stage 1 of irradiated platinum observed by field ion microscopy

Utilizing atomic resolution capability of field ion microscope for viewing biomolecules

Adhesion of polymers to tungsten as studied by field ion microscopy

Quasistatic ion microscope study of defect structure of two depleted zones in tungsten irradiated with 20 keV tungsten(plus) ions at 18 K

Limits, capabilities, and operation of field ion microscopes with results of tungsten and iridium charge investigations

ION MOTION

Velocity of ordered motion of ionospheric ions at 600 km

Ion motion in crossed fields with resonance charge exchange ionic collisions

Hydrodynamic and evaporative theories of light ion flow in polar regions

Cosmos 184 ion sensor for measuring ion velocity at 600 km

Cosmos 184 measurements of ion velocity at 600 km

Mobility measurements of ions in dilute He-3/He-4 mixtures in pure He-3 at very low temperatures

Ion velocity measurements in red plasma injector by monochromator

Method of solution of ion motion in median plane of cyclotron and results obtained using method with U-120 cyclotron

Ion mobility effects in lost mechanism for solid state reactions

Computerized simulation of ion sound instability as effect of electron distribution in plasma

Penetration of ion-acoustic barrier when alternating current flows in toroidal magnetized plasma

ION OSCILLATION

ION PROFILES

Ion microprobe mass spectrometer with cooled electrode target for analyzing traces of fluids

Collisionless plasma flow around cylinder for application to ionospheric sounding probe

Data analysis on ATS-1 Suprathermal Ion Detector (SID) measurements of low energy plasma flow in magnetopause boundary

Measuring rate constants for reactions of various gas phases with water by flowing afterglow technique

Energy dependence of charge exchange reactions in iodine and argon ionization by exchange collisions

Dissociation rate and plasma generation in hydrogen beam electron interaction

Ion density probe design for continuum flows using flat-plate electrodes for measuring ion currents and production rates

ION PROPULSION

Cesium bombardment ion engine system design, construction, and testing

Effects of backscattered material on performance of glass coated accelerator grids for electron bombardment thrusters

Electric rocket engine with electron bombardment ionization chamber

Operational performance of electron bombardment mercury ion thruster system during life testing in space simulation for SERT 2

Flow cathode for ion propulsion

Ion beam deflector system for electronic thrust vector control for ion propulsion yaw, pitch, and roll forces

Development and characteristics of ion thruster accelerator with single glass coated grid to provide increased ion extraction capability and larger diameter accelerator system

Fabrication and testing of bonded metal-ceramic, glass-coated metal, and glass-coated ceramic bonded to metal composite electrodes for cesium bombardment ion thrusters

Research and developments on cesium ion thrusters including measuring, testing, and calculation techniques

Mercury vapor fed hollow cathodes for electron bombardment ion thrusters

ION PROPULSION

ION PROPULSION

ION PROPULSION

ION PROPULSION

ION PROPULSION

ION PROPULSION

ION PROPULSION

ION PROPULSION

ION PROPULSION

ION PROPULSION

ION PROPULSION

ION PROPULSION

ION PROPULSION

ION PROPULSION

ION PROPULSION

ION PROPULSION

ION PROPULSION

ION PROPULSION

Deflectable dual beam, linear strip cesium contact, ion thruster system design and performance testing [NASA-CR-72999] 23 p5839 N71-37376

Plasma-ion engines utilizing atmospheric gases to form ion jet for propulsion [AD-727496] 24 p4001 N71-38357

ION PUMPS
Stabilized ion pumping with diode type getter-ion pumps 03 p0351 N71-12538

Vacuum chamber with distributed sputter ion pump for synchrotron storage ring [SLAC-PUB-797] 06 p0832 N71-16317

Design of ultrahigh vacuum chamber with enclosed ionization pump [NASA-TM-X-66944] 09 p1367 N71-20241

Ion pump and magnet assembly for spacecraft mass spectrometer atmospheric sensor system [NASA-CR-111856] 11 p1771 N71-22870

High voltage ion pump power supply for spacecraft mass spectrometer atmospheric sensor system [NASA-CR-111857] 11 p1771 N71-22871

Ion detection and monopole mass spectrometer performance tests with transverse magnetic field and titanium getter pump pumping capacity for D region ion composition analysis [NASA-CR-117905] 12 p1921 N71-23788

Vacuum packaged titanium built sublimator/ion pump combination for reducing tritium hazard in neutron accelerator [NASA-TM-X-67919] 20 p3246 N71-33555

ION RECOMBINATION
Ion-ion recombination effects in sodium line laser [IPRS-51577] 01 p0064 N71-10976

Using photoelectric effect to detect densities of free and trapped carriers in II-VI compounds at cryogenic temperatures [NASA-CR-111562] 03 p0443 N71-13066

Plasma infrared diagnostics and determination of zirconium ionization and recombination processes behind shock wave front [SC-T-70-4054] 11 p1811 N71-22442

Recombination behavior of thermal ions due to rotational coupling between molecular states of different symmetry [AD-717774] 11 p1807 N71-22524

Mathematical models for ionization relaxation and nitrogen ion, electron and molecular recombination behind shock waves with 17 to 25 km/sec velocities [NASA-TT-F-13592] 18 p2903 N71-31072

Polarographic determination of oxygen content in gas mixtures using ion recombination reaction 18 p2886 N71-31159

Charge transfer characteristics of ion recombination in phase boundary of germanium surface with electrolyte 18 p2998 N71-31326

ION SCATTERING
RF electric field effects of ion wave dispersion with spatially modulated pressure [UTPI-93] 02 p0281 N71-11871

Investigating contaminations caused by ion scattering on residual gas and by chromatism in electromagnetic isotope separators 04 p0574 N71-13675

Neutron diffraction study of gamma-FeOOH, position of ions, magnetic permeability, and Mossbauer effect [PB-193217] 04 p0591 N71-14387

Theory of s-d exchange scattering in dilute magnetic alloys [CALT-822-12] 05 p0751 N71-15591

Deriving Fokker-Planck equation for Coulomb scattering into loss cone in presence of ambipolar potential [CEA-CONF-1669] 07 p1083 N71-18148

Theoretical and experimental findings on atomic and molecular collisions 09 p1444 N71-20488

Positive helium ion scattering by impact on helium, neon, and argon 15 p2479 N71-27654

Solid surface geometry effects on ion scattering distribution [INP-710] 15 p2400 N71-27659

Secondary electron emission coefficients, apparent total ion scattering, and energy distributions of secondary electrons and ions produced by positive ion irradiation of metals 18 p2969 N71-30437

Ion trajectory and capture cross sections in quadrupole field for determining ion quadrupole effects in ion-molecule collisions [NASA-TM-X-67888] 19 p3153 N71-32365

ION SELECTIVE ELECTRODES
Research progress on acidity measurements, pH measurements, calibration of ion selective electrodes, and high precision coulometry [NBS-TN-543] 04 p0486 N71-13456

Development of ion selective electrochemical sensors for detection of calcium, sodium, sulfate, and other ions in saline and brackish water [PB-189634] 19 p3049 N71-31729

ION SOURCES
NT DUOPASMATRONS
NT PLASMATRONS

Dynamics of laser-produced heavy ion plasma observed by photodiodes and supporting circuitry [AD-710724] 01 p0105 N71-10542

Apertured electrode focusing system for ion sources with nonuniform plasma density [NASA-CASE-XNP-03332] 01 p0034 N71-10618

X ray temperature measurements of laser produced plasmas [ESRIN-IN-88] 02 p0281 N71-11872

Quartz resonator microbalance method for measuring sputtering yields of materials bombarded in ion implantation [SC-RR-70-377] 03 p0442 N71-12973

Accelerating field effect on electron bunch containing ions [JINR-P9-5142] 04 p0577 N71-13745

Production of ion stream with two velocity distribution components using diffusion plasma source [IPPI-97] 04 p0599 N71-14281

Design and operation of proton linear accelerator [INR-1187] 04 p0517 N71-14496

Feedback control of PIG discharge of QP machine [IPPI-T-2] 05 p0755 N71-15665

Ion energy stabilization system for Van de Graaff accelerator [INR-1181] 06 p0913 N71-15670

Plasmatron ion source with slit geometry for electro-magnetic mass separator [SGAE-PH-93/1970] 08 p1274 N71-18719

Utilization of Lamb-shift polarized ion source [LA-4451] 09 p1436 N71-20041

Cation energy distribution within straight channel photomultiplier tubes 10 p1558 N71-21039

Design and operation of duoplasmatron ion source providing hydrogen ion currents [AD-717594] 11 p1801 N71-21959

Molecular beam ion source for spacecraft mass spectrometer atmospheric sensor system [NASA-CR-111859] 11 p1765 N71-22873

Multilayer porous refractory metal ionizer design with thick, porous, large-grain substrates and thin, porous micro-grain substrates [NASA-CASE-XNP-04338] 11 p1780 N71-23046

Mass spectrometer and radio frequency, high voltage spark ion source for measuring relative sensitivity factors for metals and steels [Y-1757] 14 p2299 N71-25702

Plasmatron ion source for Seibersdorf electromagnetic isotope separator [SGAE-PH-101/1970] 14 p2303 N71-26048

Development and characteristics of ion thruster accelerator with single glass coated grid to provide increased ion extraction capability and larger diameter accelerator system [NASA-CASE-LEW-10106-1] 14 p2333 N71-26642

Multicharged ion emission from nitrogen, argon, and neon in reflex ion source with axial extraction [LYCEN-7065] 14 p2312 N71-26705

Lamb shift type ion source for producing positively charged polarized hydrogen ion beams [KFK-1262] 14 p2316 N71-26743

Design and calibration of neutral gas spectrometer with impact ion source for atomic oxygen density measurement in upper atmosphere [BMBW-FB-W-1-06] 15 p2391 N71-27075

Generation methods for ion sources in particle acceleration [LYCEN-7027] 15 p2465 N71-27242

Potential high energy resolution iodine negative ion source [AD-720871] 15 p2473 N71-27445

Maintenance and improvements associated with operation of NRL Van de Graaff accelerator [AD-721329] 16 p2577 N71-28175

Low mass ionizing device for use in electric thrust spacecraft engines [NASA-CASE-XNP-01954] 16 p2672 N71-28850

Development of source of slow neutralized ions operating with weak flux of neutral argon from Kaufman source [INP-18722] 18 p2991 N71-30410

Solid matter ion source based on plasma beam discharge [JINR-P13-5539] 18 p2973 N71-30540

Vacuum cryopumping of heavy ion source in high voltage terminal of accelerator injector [UCRL-20620] 19 p3150 N71-32119

Development of test bench for multicharged ion sources [LYCEN-7054] 19 p3152 N71-32180

Penning ion gun (PIG) type heavy ion source on axial injection line of 88 inch cyclotron [UCRL-20406] 19 p3153 N71-32207

High energy ion source produced by focusing laser pulsed radiation on thin plates 20 p3281 N71-32874

Conference on heavy ion sources [WASH-1159] 20 p3321 N71-33737

Ionization study of metastable hydrogen atomic beams and polarized deuterium ions with Lamb-shift source [KFK-1256] 21 p3468 N71-34690

Cold cathode, Penning discharge, heavy ion source, power supply in isochronous cyclotron [ORNL-TM-3391] 21 p3481 N71-34800

Multicharged heavy ion sources produced by arc discharge, electron bombardment, or high power spark discharge 21 p3483 N71-34812

Theoretical and computer analyses of unstable ion in quadrupole mass spectrometer with ion source masking [NASA-CR-121985] 22 p3632 N71-35876

Cyclotron characteristics and types of ion source injectors for use in high-energy, heavy-ion cyclotrons [JINR-NSRL-38] 22 p3643 N71-35942

Development of polarized ion source for use on six-million-volt Van de Graaff accelerator utilizing RF discharge and multiple magnet 23 p3821 N71-37259

Excitation and ionization cross sections for Balplus) by electron impact, plasma diagnostics, Li energy loss in thin C films, and multiple charge ion sources for collision experiments 23 p3827 N71-37297

ION TEMPERATURE
Measurement of ion and electron temperature from 180 to 850 km by ionospheric radar 01 p0045 N71-10130

Ion temperature and rotation in Penning discharge in inhomogeneous magnetic mirror [REPT-70-27] 03 p0439 N71-13341

Collision effect on noncoherent scattering spectrum of plasma with unequal electron and ion temperatures [CEA-N-1295] 04 p0594 N71-13580

Droplet ion temperature measurements in rotating high frequency plasma pinch field [LRP-40/70] 08 p1189 N71-10610

Fusion reactors at 200 kG and ion temperature of one MeV with lithium and deuterium as primordial fuel [ORNL-TM-3207] 10 p1613 N71-20837

Turbulent flow in solar wind causing increased ion temperature [ESRIN-IN-135] 13 p2157 N71-24592

Ion temperature determination in plasmas based on electrostatic probe measurements of ion current [AD-723529] 19 p3164 N71-32135

Ion and electron temperature measurements for focusing rod plasma injector [AEC-TR-7102/1] 21 p3474 N71-3477N

Ion energy distribution and isotropy measurements and final ion temperature dependence on initial plasma conductivity in turbulent heating of plasmas [INVO-3958-4] 21 p3493 N71-34901

Two-component stellerator-mirror configuration having high electron energy and low ion temperature for optimum plasma control [MATT-841] 23 p3828 N71-37304

Two fluid model of solar wind with anisotropic proton temperature and allowing for extended coronal proton heating [NASA-CR-123113] 24 p4002 N71-38547

ION TRAPS (INSTRUMENTATION)
Lifetimes of energetic electrons and ions trapped in magnetic mirror [CEA-CONF-1603] 08 p1256 N71-18372

Ion trapping technique for application in frequency standards [NBS-TN-388] 10 p1613 N71-20833

Computerized simulation of plasma heating from electron cyclotron resonance including ion trapping and magnetohydrodynamic instability [AD-720675] 14 p2322 N71-26078

Cosmos 261 observation of upper atmosphere low energy ions, including ion trap spectrometer description [PR-F-PT-3] 17 p2749 N71-30203

ION-GAS INTERACTIONS
U GAS-ION INTERACTIONS
IONIC COLLISIONS

Electron paramagnetic resonance in strontium titanate doped with chromium to determine interactions between paramagnetic ions in neighboring lattice positions 03 p0444 N71-13281

Investigating ion collisions using isotope separator with two magnetic stages and one electrostatic stage [CEA-CONF-1571] 04 p0576 N71-13699

Ion motion in crossed fields with resonance charge exchange ionic collisions [REPT-70-15] 04 p0600 N71-14200

Calculating spin exchange cross section for collision between two positive He ions in impact parameter approximation [NASA-TM-X-65442] 07 p1073 N71-17366

Formation scattering cross section of H2 ion in the proton and methane reactions 11 p1803 N71-22118

Particle diffusion due to ion-ion collisions and ion-turbulent wave interaction using ion wave echo diagnostic technique 12 p1983 N71-24031

Collisional processes for determining kinetic temperature distribution and heating of chromosphere 13 p2077 N71-25282

Energy dependence of charge exchange reactions in iodine and argon ionization by exchange collisions [KFK-1265] 14 p2315 N71-26793

SUBJECT INDEX

- Reaction kinetics and charge transfer in ionic collisions of argon ions with molecular hydrogen, deuterium, and carbon dioxide 15 p2477 N71-27578
- Positive helium ion scattering by impact on helium, neon, and argon 15 p2479 N71-27654
- Collisional excitation rates for lithium-like ions derived from diagnosed plasma produced in these devices and line intensities emitted by these ions [NASA-CR-119017] 16 p2648 N71-28636
- Collisional ionization rates for lithium and beryllium-like ions deduced from time history of spectral lines emitted by these ions in hot plasmas [NASA-CR-119018] 16 p2648 N71-28637
- Computer graphics of vibrational effects in ion molecule collisions including electron tunneling oscillations, nuclear capture, and molecular oscillations and relaxation [NASA-TN-D-6097] 17 p2795 N71-29749
- Limitations of merging beam method in studying ion-ion collisions 19 p3146 N71-31962
- Effect of weak collisions on stability of low frequency waves in homogeneous plasma [AD-72364] 19 p3164 N71-32200
- IONIC CONDUCTIVITY
- U ION CURRENTS
- IONIC CRYSTALS
- Electronic and vibrational spectra of ionic solids, lattice dynamics of solids, high pressure research, chemisorption of hydrocarbons and optical spectra [UCLA-34-P-88-30] 04 p0577 N71-13749
- Investigating mechanical properties of solids, relaxation processes in polymers, and properties of crystals [AD-713923] 06 p0933 N71-16112
- Nuclear quadrupole resonance spectroscopy of aromatic bonds in azines with benzo, amino, and chlorine substitution including atomic structure and lattice effects in ionic crystals 14 p2306 N71-26388
- Mathematical models for surface modes of vibration and optical properties of ionic crystal slab [IS-T-427] 15 p2505 N71-27237
- Gamma/gamma angular coincidence measurements on thulium ionic crystal electric fields 15 p2472 N71-27417
- Ion pair absorption phenomena observed between impurity dopant ions in ionic crystals [AD-719177] 15 p2506 N71-27420
- Model for migration of dislocation arrays in ionic crystals based on dislocation climb in vacancy concentration gradients by action of external electric field at array sites 17 p2826 N71-30068
- Low-lying states of polaron system in Landau-Pekar adiabatic approximation 23 p3823 N71-37267
- Band structure of metals, metal compounds, and ionic crystals determined by ultrasonic and piezoelectric measurements [AD-727069] 24 p3997 N71-38512
- IONIC DIFFUSION
- Electronic structure and ionic diffusion in metals [TT-70-57031] 03 p0392 N71-12979
- Effect of thermal gradient on ionic diffusion in frozen earth materials - Part 2 06 p0041 N71-15920
- Effect of thermal gradient on ionic diffusion in frozen earth materials - Part 1 [AD-714644] 06 p0041 N71-15921
- Evaluating determined diffusion coefficients for Group 3A, 4A, and 5A elements in silicon 07 p1089 N71-17292
- Considering processes used for deposition and diffusion characteristics of doped oxides in silicon 07 p1089 N71-17294
- Investigating theory for concentration dependent diffusion phenomenon based on simple assumption for impurity atom interaction in diffusion systems exhibiting solid solubility saturation 07 p1089 N71-17296
- Investigating orientation dependence of boron diffusion in silicon 07 p1090 N71-17297
- Mathematical model for measurement of MOS processes in Al-SiO₂-Si system used in fabrication of integrated circuits 07 p1091 N71-17307
- Longitudinal diffusion coefficients of gaseous ions diffusing in electric field [AD-714668] 07 p1084 N71-18085
- Longitudinal and transverse diffusion coefficients of gaseous ions in electric field 08 p1274 N71-18716
- Factors affecting rare gas diffusion in ionic solids, and tritium diffusion measurement in fuel element cladding [ORD-3598-4] 08 p1239 N71-18728
- Radioactive trace diffusion of Au¹⁹⁸ and Fe⁵⁹ spin isotopes with measurement of correlation and isotopic effects in crystal lattice defects [AD-717737] 11 p1778 N71-22355

Diffusion of ion and gas molecules to aerosol particles in noncontinuum regions 13 p2067 N71-25895

Ionic diffusion and spectroscopic analysis of copper alloy dendrite etching by electric discharge [TT-70-57043] 14 p3334 N71-25706

Mass spectroscopic analysis of positive potassium ion diffusion in carbon dioxide [AD-720997] 15 p2378 N71-27998

Effect of diffusion of ferric ions on rate of oxidation of UO₂ and UO₃ in sulfuric acid medium 18 p2885 N71-31004

Temperature and atmospheric sulfur content effects on nickel oxidation and sulfur diffusion mechanism across oxide scale [NLL-LT-746-718-(9022.401)] 22 p3352 N71-35302

IONIC MOBILITY

Relative cation mobilities in silver bromide-potassium bromide melts 05 p0631 N71-14691

Ionic mobility and silver solid solutions [ORO-2413-25] 05 p0743 N71-15145

Investigating positive ions created in atmospheric air at pressures from 10 to 200 torr by glow discharge or by alpha irradiation from Po-210 [NF-18409] 08 p1252 N71-18305

Ionic association and solvation studied in nonaqueous electrolytes by Raman spectroscopy [AD-717046] 10 p1514 N71-21362

Electron and ion conductivity measurements on solid silver sulfide, silver selenide, and silver telluride [ANL-TRANS-848] 10 p1516 N71-21659

Design and fabrication of measuring system to determine concentration and mobility of atmospheric ions [RAE-LT-TRANS-1435] 13 p2073 N71-25148

IONIC PROPELLANTS

U ION ENGINES

IONIC REACTIONS

Stratospheric, mesospheric, and ionospheric reaction rate and transport data and kinetics of atmospheric constituents [AD-710282] 01 p0044 N71-10003

Ion separation effects in boundary region of plasma surrounded by neutral gas [NF-18420] 04 p0601 N71-14405

Ionic and free radical reactions in irradiated organic compounds [ORD-2568-56] 06 p0812 N71-16792

IONIC WAVES

Discontinuities due to nonlinear interaction of low frequency electromagnetic and ion sound waves relevant to magnetic energy conversion in solar flares [IC/70/75] 02 p0282 N71-11874

Partial differential equation for ion wave propagation through macroscopic plasma [TPF-58] 04 p0599 N71-14280

Charge-neutral self consistent plasmas and fields studied with Vlasov equations [NYO-1480-139] 05 p0753 N71-15142

Investigating plasma body rotation and self excited low frequency oscillations in ionized low pressure hollow cathode gas fed arc device 08 p1275 N71-19246

Dispersion propagation and Landau damping of electrostatic ion waves in nonisothermal plasma supported by uniform magnetic field 11 p1814 N71-22086

Experiments demonstrating resonant nonlinear electromagnetic wave excitation of electron plasma and ion acoustic waves in plasma column [TR-70-36] 13 p2148 N71-25184

Instability of ion-acoustic waves in ELF and VLF frequency bands in polar wind when relative flow velocity between hydrogen ions and oxygen ions enters range 5 to 10 km/sec [AD-72843] 15 p2502 N71-27887

Analysis of conceptual difficulties associated with ion-acoustic plasma wave excitation derivations [NASA-CR-121448] 20 p3330 N71-33500

Transverse ionizing shock wave velocity measurements and analysis of velocity variation as function of shock tube bias and drive currents and initial gas density [AD-727046] 22 p3655 N71-36063

Steepening of large amplitude ion acoustic waves and formation of collisionless electrostatic shocks in nonmagnetized plasmas with electron-to-ion temperature ratios in 5 to 15 range 22 p3656 N71-36075

Anomalous transmission and reflection of ion cyclotron waves based on linearized Vlasov-Maxwell equation expansions 23 p3833 N71-37333

Parametric excitation of ion-acoustic waves, and analysis of plasma stabilization by open-loop methods [ORD-3485-35] 24 p3991 N71-36472

IONIZATION

NT ATMOSPHERIC IONIZATION

NT AURORAL IONIZATION

NT AUTOIONIZATION

NT FLAME IONIZATION

NT GAS IONIZATION

NT ION PRODUCTION RATES

Approximate density-effect correction for ionization loss of charged particles [NASA-CR-111035] 01 p0103 N71-10081

Response of mineral oil based liquid scintillator to heavily ionizing particles 02 p0227 N71-11971

Impact ionization, bulk negative differential conductivity and other nonequilibrium carrier phenomena in InSb [AD-712464] 03 p0443 N71-13370

Ion and electron production in proton and hydrogen atom collisions with carbon monoxide, carbon dioxide, methane, and ammonia 03 p0436 N71-13377

Ionization, recombination, and diffusion rates in nonequilibrium plasmas [AD-712710] 04 p0598 N71-14248

Empirical method for calculating energy straggling in slowing down ionizing particles [KFK-1173] 06 p1249 N71-18285

Numerical calculations of density and temperature variations in cylindrical plasmas produced by UV radiation [IPP-1106] 08 p1770 N71-18250

Dependence of spark brightness of ionization in range of 1 is less than or equal to 1/1 min is less than or equal to 15 at P equal to 1 atm, 0.3 atm, and 0.1 atm [IPVE-SEP-69-72] 09 p1437 N71-30081

Average energies of ground and singly and doubly excited configurations in highly ionized atoms for electron numbers N equals 3 to N equals 20 [NASA-SP-3056] 09 p1444 N71-30535

Studying reaction N⁴⁺/H⁺ plus O₂ yields NO⁺/H⁺ plus O as function of collision energy using crossed beams [NASA-CR-117527] 10 p1619 N71-21714

Mass spectroscopic investigation of collisional ionization by electronically excited helium atoms 11 p1809 N71-23018

NT PHOTONIZATION

NT SURFACE IONIZATION

Field ionization mass spectra of photopolymers of thymine [NYO-2796-36] 01 p0019 N71-10823

Approximate density-effect correction for ionization loss of charged particles [NASA-CR-111035] 01 p0103 N71-10081

Response of mineral oil based liquid scintillator to heavily ionizing particles [PPAR-26] 02 p0227 N71-11971

Impact ionization, bulk negative differential conductivity and other nonequilibrium carrier phenomena in InSb [AD-712464] 03 p0443 N71-13370

Ion and electron production in proton and hydrogen atom collisions with carbon monoxide, carbon dioxide, methane, and ammonia 03 p0436 N71-13377

Ionization, recombination, and diffusion rates in nonequilibrium plasmas [AD-712710] 04 p0598 N71-14248

Empirical method for calculating energy straggling in slowing down ionizing particles [KFK-1173] 06 p1249 N71-18285

Numerical calculations of density and temperature variations in cylindrical plasmas produced by UV radiation [IPP-1106] 08 p1770 N71-18250

Dependence of spark brightness of ionization in range of 1 is less than or equal to 1/1 min is less than or equal to 15 at P equal to 1 atm, 0.3 atm, and 0.1 atm [IPVE-SEP-69-72] 09 p1437 N71-30081

Average energies of ground and singly and doubly excited configurations in highly ionized atoms for electron numbers N equals 3 to N equals 20 [NASA-SP-3056] 09 p1444 N71-30535

Studying reaction N⁴⁺/H⁺ plus O₂ yields NO⁺/H⁺ plus O as function of collision energy using crossed beams [NASA-CR-117527] 10 p1619 N71-21714

Mass spectroscopic investigation of collisional ionization by electronically excited helium atoms 11 p1809 N71-23018

Numerical integration of spontaneous ionization of hydrogen atom in electric field using Schrödinger equation [NASA-CR-117894] 12 p1969 N71-33287

Ionization of multielectron atoms by fast charged particles and electron and proton impact [NASA-TM-X-63502] 12 p1970 N71-23397

Feasibility of achieving bulk laser action in polar semiconductors pumped by impact ionization in applied electric field [AD-719403] 13 p2089 N71-24731

Air ionization and effects of positive ions in air on man using Am-241 sources [ORNL-TR-3427] 13 p2035 N71-25438

Ionized fields in electrostatic separation of granular solids/conductors and nonconductors/also applications in separations based on surface-to-mass ratio of particles [BM-RI-7509] 14 p2302 N71-25744

Concentration of negative ions in flame for checking of static configuration of flame [AD-718992] 14 p2353 N71-26021

Static and dynamic models of long period variable stars, ionization equilibrium and dissociation, and pulsation parameters 14 p2340 N71-26356

Analysis of insulating properties of alkali metallic colloids and problem of charge generation by contact ionization [AD-721197] 15 p2368 N71-26896

Increased ionization and temperature due to harmonic microwave absorption in magnetized low density plasmas [KFA-CONF-1607] 15 p2699 N71-27201

Method for atomic beam ionization with storage of polarized ions in electron beam and their pulsed extraction during accelerator capture time [JINR-P5-5446] 15 p2773 N71-27443

Ionization of Gaseous Nebula by energetic charged particles from supernovae Vela X with estimates of gamma ray line emission from ambient gas, energetic nuclei interaction [NASA-TM-X-45590] 16 p2674 N71-28567

Mathematical models for ionization recombination and electron, electron and molecular recombination behind shock waves with 17 to 25 km/sec velocities [NASA-TT-F-13592] 18 p2505 N71-31072

Calculations of cooling rates and spectral emission of gaseous nebulae 18 p3015 N71-31256

Microwave ionization for obtaining nonequilibrium plasmas in MHD generators [NASA-TT-P-13703] 19 p3164 N71-32212

Ionization study of metastable hydrogen atomic beams and polarized deuteron ions with Lamb-shift sources [KFK-1254] 21 p3468 N71-34689

Preliminary in toroidal high-beta experiments by induced azimuthal currents [IPP-1114] 21 p3486 N71-34904

Device for measuring ionization processes and plasma acceleration in traveling electromagnetic fields [NASA-TT-F-697] 21 p3593 N71-34951
 Ionization rate measured in glow discharge in gas mixtures commonly used in carbon dioxide lasers [REPT-442] 23 p3766 N71-36448
 Tables of generalized oscillator strengths for excitation and ionization of atoms He through Na [SC-RR-70-406] 23 p3814 N71-37196
 Ionization in dielectric liquids produced by gamma radiation and ionization inhibition by electron scavengers [NP-18875] 24 p3973 N71-38348
 Applications of bubble chamber to study of ionized particles 24 p4012 N71-38618

IONIZATION CHAMBERS

NT BUBBLE CHAMBERS
 NT CLOUD CHAMBERS
 NT GEIGER COUNTERS
 NT PROPORTIONAL COUNTERS
 NT SPARK CHAMBERS
 Application of gridded ionization chamber for alpha spectroscopy [JNR-1182] 03 p0428 N71-12882
 Temperature dependent characteristics measurements of RJ-200 ionization chambers as neutron detectors [JNR-1184] 04 p0585 N71-14235
 System for measurement of delayed neutron energy spectra [RLO-2225-T-17-1] 05 p0744 N71-15179
 Parallel plate ionization chamber for identifying relativistic cosmic ray nuclei [NASA-CR-116874] 08 p1176 N71-18914
 Ionization chamber and scintillation detector for quality factor measurement and depth dose distribution for high energy protons [JNR-E16-5384] 09 p1441 N71-20336
 Electric rocket engine with electron bombardment ionization chamber [NASA-CASE-XNP-04124] 10 p1639 N71-21822
 Microwave cavity systems engineering for MeV electron beam ionization measurements [NASA-TM-X-2279] 12 p1981 N71-23959
 Plane-parallel experimental ionization chamber containing liquid and solid argon [JNR-P13-5404] 13 p2130 N71-24852
 Chamber preamplifier design for spectrometric channel of experimental ionization chambers with argon and xenon condensates [JNR-P13-5402] 13 p2139 N71-25485
 Multichannel photoionization chamber for measuring absorption, photoionization yield, and coefficients of gases [NASA-CASE-ERC-10044-1] 15 p2408 N71-27090
 Ionization chamber filled with liquid xenon for testing negative pion beam at 6 GeV [JNR-P13-5403] 15 p2465 N71-27249
 Cosmic ray data from cloud and ionization chambers, and carbon and iron plates [AD-721714] 17 p2840 N71-29472
 Electron and photon spectra and fluxes in liquid ionization chambers [NP-18433] 17 p2800 N71-30106
 Universal, high stability radioisotopic detector for gas chromatography using nickel-63 as ionizing source [JNR-737] 21 p3429 N71-34402
 Teflon-carbon mixture identified as air equivalent material and suitable for cavity ionization chambers [CEA-R-4173] 21 p3443 N71-34498
 Calibration constants of quantimeter and thick walled ion chamber [INS-TH-46] 21 p3470 N71-34706
 Direct measurements of capture cross section ratio to fission cross section using ionization chamber and neutron beams [IAE-1985] 21 p3471 N71-34713
 Total-absorption xenon gas ionization chamber design for 1.5 to 10 keV X rays [LA-4568] 21 p3483 N71-34813
 Scattering cross sections for nuclear reactions of C-12, Ne-20, and Ar-40 induced by 14 MeV neutrons in gridded ionization chamber 21 p3490 N71-34858
 Maintenance of beta gamma ion chamber exposure dosimeters [CEA-N-1435] 23 p3811 N71-37174
 Using ionization chambers for measuring nuclear heating effects [CEA-R-4195] 24 p3978 N71-38389
 Heavy and ultraheavy nuclei observations of cosmic rays using ionization chamber-Cerenkov counter system [NASA-CR-123197] 24 p4002 N71-38544
 IONIZATION COEFFICIENTS
 Primary and secondary ionization coefficients of argon-hydrocarbon Penning mixtures [AD-722313] 17 p2714 N71-29684
 Approximate calculation of ionization energy loss and range of fast charged particles [JNR-P1-5676] 18 p2968 N71-30425

Calculations of ionization-excitation source rates in gaseous media irradiated by fission fragments and alpha particles 20 p3307 N71-33667

IONIZATION COUNTERS

U IONIZATION CHAMBERS

U RADIATION COUNTERS

IONIZATION CROSS SECTIONS

Computer program for calculation of electron scattering and photoionization cross sections of atomic systems with configuration/np/q [REPT-70-058] 05 p0649 N71-14781
 Ionization and excitation cross sections in proton atoms [AD-713691] 05 p0764 N71-14908
 Ionization cross section measurements of argon collisions, photon emission during argon decay, and Penning ionization discharge 09 p1428 N71-19718
 Electron impact elastic, differential elastic, and differential ionization cross sections for noble atoms 09 p1433 N71-19973
 Differential ionization cross section in Born approximation [SC-RR-70-773] 10 p1613 N71-20827
 Measurement of pion mercury ion scattering and determination of differential cross sections 10 p1622 N71-21763
 Spectral absorption and photoionization cross sections of CO₂, NH₃, O₂, COS, NO, N₂, and vinyl chloride using vacuum ultraviolet spectroscopy [AD-717771] 11 p1696 N71-22249
 Ionization cross sections for helium and neon positive ion collisions with nitrogen, oxygen, and carbon dioxide molecules at 3 to 200 eV [AD-717690] 11 p1808 N71-22711
 Continuous beam techniques for measuring absolute experimental cross sections for ionization of singly charged barium ions by electron impact [ORO-3027-18] 14 p2300 N71-25725
 Ionization cross sections for neon and argon single electron loss in nitrogen, oxygen, and air between 25 and 90 keV [SC-RR-70-735] 15 p2472 N71-27436
 Plasma particle collision cross sections and collision dynamics [CEA-CONF-1627] 15 p2501 N71-27599
 Laboratory measurement of cross sections for production of electronically excited species observed in atmospheres of planets [NASA-CR-119022] 16 p2678 N71-28316
 Time of flight and mass spectroscopy of vanadium, titanium, and chromium alloy electron impact ionization cross sections using ion current and vapor pressure data for calculations [AD-720288] 16 p2611 N71-28503
 Collisional ionization between cesium atoms and NO₂, N₂O, and O₂ molecules 21 p3475 N71-34743
 Comparison of experimental data and theoretical predictions for doubly differential ionization cross sections for neon and argon collisions 22 p3630 N71-36028
 Excitation and ionization cross sections for Ba(plus) by electron impact, plasma diagnostics, Li energy loss in thin C films, and multiple charge ion sources for collision experiments 23 p3827 N71-37297
 Equipment and capabilities developed in investigation of K and L shell ionization cross sections, X ray intensity ratios, bremsstrahlung spectrum, coincidence, and inelastic electron scattering [NASA-CR-119957] 24 p3976 N71-38368
 IONIZATION FREQUENCIES
 Low frequency axisymmetric waves in weakly ionized magnetoplasmas column 08 p1272 N71-18526
 Effects on high temperature microwave antenna breakdowns of ionization frequency, collision frequency, diffusion coefficient, and breakdown parameters 10 p1520 N71-21126
 IONIZATION GAGES
 NT BAYARD-ALPERT IONIZATION GAGES
 NT PENNING GAGES
 Cryostat/pump study and behavior of nude ionization gages at low temperature [NASA-CR-111799] 01 p0059 N71-10488
 Ionization gage density data for supercritical gas flow [AD-716618] 09 p1372 N71-19670
 Ionization control system design for monitoring separately located ion gage pressures on vacuum chambers [NASA-CASE-XLE-00787] 10 p1559 N71-21090
 Evaluating data obtained from ion gage onboard OV-1 satellites rotating in molecular flux at different altitude and azimuth angles 16 p2394 N71-28587
 Ion density probe design for continuous flows using flat-plate electrodes for measuring ion currents and production rates 18 p2924 N71-31208
 IONIZATION POTENTIALS
 Whistler study to determine interchange of ionization between ionosphere and protonosphere [SU-SEL-70-022] 01 p0049 N71-10721

Comprehensive calculation of ionization potentials and binding energies for multiply-charged ions [ORNL-4562] 02 p0272 N71-11771
 Experimental and theoretical ionization potentials for elements hydrogen to krypton calculated by Flaxtree-Fock method [AD-712454] 03 p0333 N71-12376
 Investigating ionization processes in thermal bimolecular collisions of particles in electronically excited state 05 p0743 N71-15133
 Threshold law for electron atom impact ionization 13 p2162 N71-25203
 Interionic potentials for alkali metals from correlations in electron liquids [ANL-7761] 13 p2098 N71-25512
 Infrared spectra of implanted high energy nitrogen ionization energy in silicon 13 p2154 N71-25560
 Electrodes having array of small surfaces for field ionization [NASA-CASE-ERC-10013] 14 p2231 N71-26678
 Ionization potentials for photoelectron radiolysis of vapor phase methane, ethane, and ethylene 18 p2886 N71-31165
 Gaseous Townsend discharges in gas mixtures and electric strength of moving gas 19 p3166 N71-32595
 Ion and electron energy spectra from neutral Ar and He beam collisions with Ar and He gas respectively below 220 eV [NYO-2101-27] 24 p3978 N71-38386
 IONIZED GASES
 NT CATIONS
 NT CESIUM PLASMA
 NT CHARGED PARTICLES
 NT COLD PLASMAS
 NT COLLISIONLESS PLASMAS
 NT COSMIC PLASMA
 NT ELECTRON PLASMA
 NT PLASMA CLOUDS
 NT PLASMA JETS
 NT PLASMA LAYERS
 NT PLASMA SHEATHS
 NT PLASMA SLABS
 NT RELATIVISTIC PLASMAS
 NT SOLAR WIND
 NT THERMAL PLASMAS
 NT TOROIDAL PLASMAS
 Theoretical investigation of ionized capsule wall interactions with circularly polarized antenna radiation while entering Martian atmosphere 03 p0353 N71-12551
 Wall pressure pulses and reflected waves in argon and xenon ionized gases in shock tubes [NASA-CR-115795] 04 p0519 N71-15792
 Electromagnetic field effects on heat transfer of two temperature gaseous plasma [NASA-CR-111725] 04 p0597 N71-14062
 Livermore fission fragment analyzer - conference [UCRL-72422] 04 p0582 N71-14084
 Transport properties of partially ionized nonequilibrium gases in electric and magnetic fields 04 p0598 N71-14218
 Interaction between high velocity plasma stream and stationary neutral gas cloud in magnetic field [NP-18414] 04 p0600 N71-14321
 Mass flow, velocity, and in-flight thrust measurements by ion deflection [AD-713587] 05 p0629 N71-14604
 Transient heat transfer gage for measuring total radiant intensity from far ultraviolet and ionized high temperature gases [NASA-CASE-XNP-09802] 05 p0786 N71-15641
 Physical properties of flames regarded as ionized gases [AD-716968] 10 p1608 N71-21504
 Perturbation expansion of Coulomb potential for determining pair distribution function in plasma 10 p1631 N71-21817
 Dissociative recombination rate measurements in partially ionized gases within shock tube at elevated temperatures 11 p1807 N71-22647
 Magnetic field and homopolar geometry effects on behavior of ionized gas in homopolar device 12 p1983 N71-24345
 Temperature measurement and electron density of free ionized nitrogen jet at atmospheric pressure 16 p2663 N71-29183
 CAPO code for studying equations of state/opacity of ionized gases 18 p2993 N71-31245
 Electron-ion recombination effects on plasma flow of partially ionized monatomic gas from sonic orifice [RE-4123] 18 p2908 N71-31382
 Numerical analysis of structure of nonequilibrium boundary layer above flat plate in partially ionized gas at flowing potential [NTC-45-61] 20 p3329 N71-32851
 Magnetohydrodynamic ionized gas cylinder flow with Hall effect [DLR-FB-70-50] 20 p3329 N71-33002
 Measurement of heat transfer in ionized gas by wire probe in arc plasma at atmospheric pressure 20 p3331 N71-33786

SUBJECT INDEX

- Effects of pressure and temperature on plasma intensity profile of high pressure uranium plasma 20 p3332 N71-33865
- Microwave-optical measurements of atomic energy levels in ionized helium 20 p3337 N71-33950
- Experimental investigation of nonequilibrium corner-expansion flow of ionized argon (AD-726532) 22 p3434 N71-36062
- Photon propagation in perturbed Einstein-de Sitter universe model containing ionized gas 23 p3857 N71-37493
- IONIZED PLASMAS**
U-PLASMAS (PHYSICS)
- IONIZERS**
Description of electrical equipment and system for purification of waste water by producing silver ions for bacterial control (NASA-CASE-MSC-10960-1) 13 p2029 N71-24718
- Glass coating of electron bombardment ion-thruster grids by electrodeposition 20 p3277 N71-32923
- Research and developments on cesium ion thrusters including measuring, testing, and calculation techniques (ONERA-TP-974) 20 p3340 N71-33880
- IONIZING RADIATION**
NT ALPHA PARTICLES
NT BETA PARTICLES
NT COSMIC RAY SHOWERS
NT COSMIC RAYS
NT FAR ULTRAVIOLET RADIATION
NT GAMMA RAY BEAMS
NT GAMMA RAYS
NT LYMAN ALPHA RADIATION
NT NEAR ULTRAVIOLET RADIATION
NT PRIMARY COSMIC RAYS
NT SECONDARY COSMIC RAYS
NT SOLAR COSMIC RAYS
NT SOLAR X-RAYS
NT ULTRAVIOLET RADIATION
NT X RAYS
- Effects of ionizing radiation on chromosomes (AI-AEC-12974) 02 p0152 N71-11081
- Electron capture type detector model using ionizing radiation for gas chromatography (INP-700) 05 p0743 N71-15147
- Dose measurements by ferrous-ferric, ferrous-ferric with copper added and oxalic acid dosimeters (INR-1164) 05 p0908 N71-15743
- Thermoradiation studies on microorganisms for spacecraft sterilization (NASA-CR-111309) 06 p0799 N71-16022
- Ionizing radiation effect on biological properties of food products 08 p1154 N71-19063
- Photochemistry of bimolecular quenching and heterogeneous compounds, magnetic resonance studies, and high energy radiation chemistry (AD-716359) 09 p1434 N71-20003
- Charged particle energy transfer for assessing simulation of accelerated radiation tests 09 p1439 N71-20233
- Defect properties of semiconductor materials as function of impurity concentration and ionizing radiation (AD-717733) 11 p1817 N71-22247
- Measuring forward current and noise current of p-n junction before and after irradiation with ionizing radiation to determine effects of energy states at Si-SiO₂ interface (RAE-LIB-TRANS-1536) 13 p2151 N71-25188
- Wafer and diffusion ion dependence of surface effects resulting from ionizing radiation of transistors (AD-721696) 15 p2385 N71-26899
- Proton accelerator simulation of ionizing radiation induced transient effects in semiconductors (LYCEN-7063) 15 p2463 N71-27243
- Phase scintillation effects on cross sections of ionized irregularities related to clutter, radar target identification, jamming, and antimissile defense systems (AD-723587) 19 p3055 N71-31991
- Research on damage by ionizing radiation (RVO-3558-24) 20 p3321 N71-33736
- Effect of gamma and alpha ionizing radiations on irradiated and degassed aqueous solutions of neptunium and americium (NP-18784) 22 p3637 N71-35925
- Problems of high temperature annealing of FTE/LIF discs used for ionizing radiation dosimetry (AEW-34-991) 24 p3973 N71-40066
- IONOGRAMS**
TAPECLIP data system for processing ionograms from ionizing magnetic tape (NASA-CR-73483) 02 p0190 N71-11334
- Tubulations of electron number density profiles from Alouette 2 ionograms 03 p0366 N71-12696
- Atlas of oblique incidence high frequency backscatter ionograms of midlatitude ionosphere (ESSA-TR-ERL-162-ITS-104) 07 p1026 N71-18031
- On-line closed loop processor for reducing topside ionograms to electron density profiles (NASA-TN-D-4204) 08 p1187 N71-18406

- Fine structure observation in high frequency radio signals propagated around world using oblique ionograms (AD-721703) 16 p2561 N71-28448
- IONOSPHERES**
Ionospheric daily data obtained over Salisbury, Australia during October, 1969 (SAD-1969/10/5) 05 p0681 N71-15684
- Ionospheric daily data obtained over Salisbury, Australia during September, 1969 (SAD-1969/9/8) 05 p0681 N71-15683
- Ionospheric daily data obtained over Salisbury, Australia during December, 1969 (SAD-1969/12/5) 05 p0681 N71-15690
- Geophysics and space data bulletin - Vol 7, no. 2 (AD-714412) 06 p0856 N71-16761
- Tables on climatology of ionosphere measured by ionosondes (NOAA-SPDA-PA-321) 14 p2251 N71-26625
- Ionosonde using data processing systems for continuous ionospheric soundings (AD-732390) 19 p3093 N71-32204
- Cosmos 381 scientific satellite for ionospheric sounding 19 p3185 N71-32661
- Low frequency vertical pulsed sounder design with digital integration and pseudo-random phase coding for ionospheric D-region sounding (AD-727151) 22 p3580 N71-35499
- IONOSPHERIC**
NT D REGION
NT E REGION
NT F REGION
NT F2 REGION
NT LOWER IONOSPHERE
NT SPORADIC E LAYER
NT UPPER IONOSPHERE
- Stratospheric, mesospheric, and ionospheric reaction rate and transport data and kinetics of atmospheric constituents (AD-710282) 01 p0044 N71-10003
- Thompson scatter studies of ionosphere using UHF radar 01 p0020 N71-10148
- Studying lower ionosphere by incoherent scatter radar 01 p0045 N71-10149
- Velocity of ordered motion of ionospheric ions at 600 km (NASA-TT-F-13358) 01 p0046 N71-10246
- Results of flight of Yantar automatic ionospheric laboratory - Part 3 (NASA-TT-F-13403) 01 p0127 N71-10927
- Electron content measurement in polar ionosphere using signals from Explorer 22 satellite based on Faraday rotation (BMBW-FB-W-70-39) 03 p0370 N71-13229
- Moete Carlo and Thomson scatter plasma-line studies of ionospheric photoelectrons (UUL-U-ENG-70-263) 03 p0679 N71-15534
- Interactions between simulated ionospheric plasma and electric fields of high voltage spacecraft systems 06 p0828 N71-16646
- Reflection of transient VLF signals from stratified magnetospheric model of ionosphere 07 p0993 N71-17706
- Atlas of oblique incidence high frequency backscatter ionograms of midlatitude ionosphere (ESSA-TR-ERL-162-ITS-104) 07 p1026 N71-18031
- Ionospheric and magnetospheric electric field measuring instruments and measurement results (MPI-PAE/EXTRATERR-44/70) 08 p1189 N71-18609
- Arctic ionospheric model (AD-715893) 08 p1190 N71-18664
- Oxygen atom collision processes in ionosphere (AD-715715) 08 p1260 N71-18763
- Charge distribution of heavy nuclei of cosmic rays in region Z greater than or equal to 26 determined by photoemulsion method (NASA-TT-F-13510) 09 p1463 N71-20490
- Electric currents and fields produced in ionosphere by highly varying horizontal winds 10 p1553 N71-21313
- Radiometric measurements of regular absorption in ionosphere at high latitudes 11 p1759 N71-22859
- Geomagnetic and polarization phase rotation effects on electromagnetic signal transmission along spherical waveguide formed by earth surface and ionosphere (AD-719844) 13 p2046 N71-23058
- Measurements of ionospheric electric field in equatorial and medium magnetic latitudes using barium ion clouds (MPI-PAE/EXTRATERR-49/70) 15 p2398 N71-27063
- Infrared molecular spectra in ionosphere 15 p2401 N71-27499
- Construction of N₂, O₂, and O densities in US standard atmosphere in 80 to 120 km range (ESSA-TR-ERL-184-SDL-17) 17 p2738 N71-29304

IONOSPHERIC CURRENTS

- Electric field measuring techniques used in ionospheric and magnetospheric electrojet current studies (NASA-TM-X-63596) 17 p2748 N71-30094
- Short circuit effects on ion cloud polarization fields and image stratigraphy in ionospheric models (MPI-PAE/EXTRATERR-50) 18 p2919 N71-31439
- Scintillation, polarization, and multipath effects on VHF propagation between synchronous satellites and aircraft - telecommunication systems (NASA-TM-X-63628) 19 p3036 N71-32293
- Theoretical analysis of end effect in current response of highly negative, cylindrical Langmuir probe under ionospheric satellite conditions (AD-723531) 19 p3167 N71-32800
- Electric field effects in ionosphere, including ionospheric drift, conductivity, and currents (REF-70-21) 20 p3255 N71-32908
- Simulation of satellite motion in ionosphere using low energy, high current density ion source in vacuum chamber (TP-951) 20 p3331 N71-33761
- Composition of upper ionosphere as shown by magnetic mass spectrometer flows on Explorer 31 (NASA-CR-121865) 21 p3426 N71-34379
- Handbook of correlative data on galactic cosmic rays, solar electromagnetic radiation, solar protons, geomagnetism, ionosphere, and neutral atmosphere (NASA-TM-X-67294) 21 p3532 N71-35168
- Moete Carlo calculations of photoelectron motion in ionosphere 22 p3575 N71-35463
- Errors in Doppler geodetic measurements from coherent frequencies for correcting ionospheric refraction 22 p3680 N71-36241
- Dynamic model for ionospheric plasma with inter-hemispheric coupling (NASA-TM-X-65727) 24 p4008 N71-38576
- IONOSPHERIC ABSORPTION**
IONOSPHERIC PROPAGATION
IONOSPHERIC BACKSCATTER
IONOSPHERIC COMPOSITION
- F region internal gravity waves properties 01 p0046 N71-10229
- Satellite observation of horizontal ion density gradients in F region (AD-710800) 01 p0117 N71-10502
- Development of model of E and F regions of ionosphere (NASA-CR-115894) 05 p0668 N71-14759
- Abstracts on Soviet upper atmosphere and space research with emphasis on Lunokhod 1 operations 07 p1015 N71-16960
- Computerized analysis of data on high altitude barium release (EGG-1183-3007) 07 p1015 N71-16997
- Characteristics of D and E regions of ionosphere (NASA-CR-116441) 07 p1016 N71-17052
- Abstracts on Soviet space program and atmospheric, ionospheric, and interplanetary research 07 p1020 N71-17491
- Electron concentration and charged particle temperatures in ionosphere 11 p1746 N71-22045
- Mariner 5 data for determining physical properties of Venus ionosphere 13 p2169 N71-23279
- Significance of solar geomagnetic processes in determining distribution of ionospheric components and implications for reference models of ionosphere (NASA-TM-X-65568) 15 p2405 N71-27671
- Ion mass spectrometer experimental design on Explorer 31 satellite and data processing techniques for ionospheric composition (NASA-CR-121651) 21 p3424 N71-34362
- Estimates of atomic concentration ionosphere from radar backscatter and rocket probe measurements of electron and ion temperatures and electron concentration (NASA-CR-112040) 22 p3578 N71-35484
- Development of method for deriving electron density profiles in D region of ionosphere during solar flares (ASD-62) 22 p3663 N71-36132
- IONOSPHERIC CONDUCTIVITY**
Collisionless shock waves and factors influencing linear stability of barium ion clouds (NASA-CR-121437) 20 p3330 N71-33445
- IONOSPHERIC CURRENTS**
NT AURORAL ELECTROJETS
NT ELECTROJETS
NT EQUATORIAL ELECTROJET
- Radar scattering for ionospheric density observations in turbulent ionosphere (AD-719800) 03 p0371 N71-13238
- Polar and lower latitude ionospheric currents and magnetic field variations (CEI-TN-611) 10 p1547 N71-20899
- Ionization instability resulting from Joule heating in weakly ionized ionospheric plasma with currents present (NASA-TT-F-13614) 17 p2738 N71-29243

All sky photography of U-shaped polar auroras in ionosphere 17 p2746 N71-30079

Relationship between ionospheric electron currents, geomagnetic storms, and absorption bursts 17 p2747 N71-30088

IONOSPHERIC DISTURBANCES
NT IONOSPHERIC STORMS
NT SUDEN IONOSPHERIC DISTURBANCES
NT TRAVELING IONOSPHERIC DISTURBANCES

Data tables on ionospheric drift and turbulence soundings [AD-710701] 01 p0047 N71-10402

Gravity wave parameter estimated from F 2 ionospheric electron density disturbance observations [KGO-702] 03 p0371 N71-13230

Parameter estimation of gravity waves responsible for ionospheric electron density disturbances by comparison of observations with atmospheric model calculations [KGO-703] 03 p0375 N71-13392

Atmospheric model computation of F region ionospheric disturbances due to internal gravity wave propagation [KGO-701] 03 p0375 N71-13393

Investigating disturbances in ionosphere and circumterrestrial space from high altitude nuclear explosions [RAE-LIB-TRANS-1448] 05 p0675 N71-15435

Formation of ionospheric irregularities 06 p0849 N71-16229

Ionospheric scintillation at high and low altitudes 06 p0814 N71-16232

Simultaneous magnetic and electric field measurements for extremely low frequency ionospheric disturbances and atmospheric [AD-713890] 06 p0850 N71-16377

Morphology of traveling ionospheric disturbances based on columnar electron content data, and relation of disturbances to polar substorms [NASA-CR-116784] 08 p1188 N71-18502

Solar geophysical relationships using radio telescope and satellite data 09 p1332 N71-19554

Detection of atmospheric nuclear explosions by study of extremely low frequency waves and ionospheric disturbances [AD-716601] 09 p1383 N71-19683

Computer program for assessing ambient and disturbed day and night ionospheric effects on radio wave reflection and transmission [AD-716679] 09 p1349 N71-19748

Treating large scale ionospheric disturbances with inhomogeneous linear integral equation and Green function [AD-717204] 10 p1547 N71-20793

Problems of communication and navigation systems in VLF and UHF produced by small irregularities in electron density in F region [AD-717094] 11 p1751 N71-22693

Tropospheric and ionospheric compositions effects on phase and frequency degradations in propagating signals [AGARD-CP-33] 11 p1704 N71-22901

Ionospheric disturbance effects on phase corrections in low and very low frequency radio navigation 11 p1706 N71-22913

Propagation medium disturbance effects on time signal transfer in low frequency bands 11 p1706 N71-22914

Airborne Doppler shift measurements on lower ionospheric instability 11 p1707 N71-22921

Doppler shift recordings of ionospheric disturbances 11 p1709 N71-22929

Ionospheric radioisotope detection of ion-acoustic wave disturbances caused by nuclear explosions 11 p1709 N71-22932

Low altitude explosive generation of ionospheric disturbances by acoustic gravity waves 11 p1710 N71-22934

Ionospheric electron density anomalies effects on space communication wave amplitude and phase stability [NASA-CR-117805] 11 p1711 N71-22941

Differential phase measurements of coherent frequencies emitted from Explorer 29 satellite and GEOS 1 satellites for ionospheric disturbance measurements 11 p1711 N71-22942

Ray tracing method for correlating Doppler and Faraday differential effects in determining ionospheric disturbances by artificial satellites 11 p1712 N71-22944

Satellite scintillation and diffraction pattern scale size distribution from ionospheric irregularities [NASA-TM-X-65436] 13 p2161 N71-25210

Early bird and ATS C simultaneous recordings of F region ionospheric electron density for scintillation analysis of ionospheric disturbances [AD-719872] 14 p2245 N71-25627

Tables on climatology of ionosphere measured by ionosondes [NOAA-JSPDA-FA-321] 14 p2251 N71-26625

Electromagnetic wave transmission and breakdown by nuclear explosion and ionospheric disturbance discharges [AD-720862] 15 p2480 N71-27661

Effects of irregularities in ionosphere and troposphere on accuracy of radar systems located in midlatitude and polar regions [AD-720846] 16 p2560 N71-28337

Variations in total ionospheric electron content as indication of motion of eclipse-produced internal atmospheric gravity waves [AD-721589] 16 p2675 N71-28593

Research results on high latitude sporadic E layer plotted and displayed in corrected geomagnetic latitude and corrected geomagnetic time [AD-722435] 17 p2740 N71-29650

Ionospheric auroral morphology, height variations, and relationships to planetary magnetic disturbances in periods of minimum and maximum solar activity at varying latitudes [NASA-TT-F-637] 17 p2745 N71-30076

Vertical sounding and riometer investigations of ionospheric magnetic field variations and spatial position and spectra of auroras 17 p2746 N71-30077

Dynamics of magneto-ionospheric disturbances in polar auroral zone 17 p2747 N71-30089

Latitude variations in ionospheric parameters 17 p2747 N71-30090

Northern Hemisphere map of ionospheric F-scatter propagation and electron density diurnal variations with fluctuation zones for magnetically quiet and disturbed days [NASA-TT-F-13821] 18 p2916 N71-31083

Ionization rates due to atmospheric attenuation of solar protons and alpha particles in upper atmosphere [AD-723627] 19 p3175 N71-31824

Flight and engineering aspects of rocket launches for releasing chemicals into upper atmosphere noting use of barium, trimethylaluminum, diborane, and lithium [AD-724099] 20 p3258 N71-33096

Analysis of effects of nuclear explosions on ionosphere [FOA-4-C-4415-29] 22 p3578 N71-35488

IONOSPHERIC DRIFT

Data tables on ionospheric drift and turbulence soundings [AD-710701] 01 p0047 N71-10402

Drift shell splitting of trapped particles by earth magnetic field [NASA-TM-X-65466] 09 p1463 N71-20468

Kinonode experiment for development of system for remote sensing of ionospheric motions and microstructure [NASA-CR-117837] 11 p1750 N71-22533

Correlation analysis of spaced receiver radio echo fading with neutral wind profiles 11 p1709 N71-22928

Traveling ionospheric disturbance model of F 2 region after low altitude nuclear explosion 11 p1710 N71-22933

Array of eighty nine dipoles for studying radio signals reflected and scattered from ionospheric irregularities and meteor trails to determine wind gradients and changes at high altitudes [AD-721223] 15 p2399 N71-27471

High altitude velocity distribution of ionospheric drift and electric field strength in F 2 layer 17 p2748 N71-30091

Measuring instrument used at Fort-Archambault for ionospheric drift including geophysical data processing [GRI/NTP/86] 19 p3084 N71-31703

Annual variation of ionospheric drift in E region at Garchy, France using signal fading method [GRI/NTP/87] 23 p3750 N71-36739

IONOSPHERIC ELECTRON DENSITY

Interpolated electron number density tables from Alouette 2 ionospheric sounding data 01 p0046 N71-10278

First order prediction model of total-electron-content group path delay for midlatitude ionosphere [AD-711365] 01 p0025 N71-10770

Gravity wave parameter estimated from F 2 ionospheric electron density disturbance observations [KGO-702] 03 p0371 N71-13230

Radar scattering for electron density observations in turbulent ionosphere 03 p0371 N71-13238

Thomson scatter study of ionospheric scintillation 03 p0669 N71-14797

Ionospheric propagation and satellite VHF communication and navigation systems 06 p0814 N71-16226

Ionospheric electron content measurements using Explorer 22 data on Faraday and differential Doppler effects 06 p0814 N71-16231

Ionospheric electron content measurements using satellite transmissions 06 p0849 N71-16233

World wide morphology of ionospheric total electron content 06 p0815 N71-16235

On-line closed loop processor for reducing topside ionograms to electron density profiles [NASA-TN-D-6204] 08 p1187 N71-18486

Ionospheric electron density determination over Finland using Explorer 22 signals and Parsady/Doppler method [BMW-FB-W-70-50] 08 p1189 N71-18592

Vertical distribution of D region electrons and energetic spectra of solar X rays during solar flares and periods of quiet sun 08 p1195 N71-19130

Analysis of wave interaction disturbing antenna system for ionospheric electron density measurements [SR-367] 09 p1379 N71-19447

Ionospheric electron density measurements from Faraday fading of Explorer 22 satellite transmissions during low and high solar activity [RSD-552] 09 p1350 N71-20800

Explorer 22 satellite measurements of ionospheric electron contents during magnetic storms [RSD-554] 09 p1386 N71-20343

Sweden/NASA rocket sounding in auroral D and E regions for ionospheric ion and electron density investigation using Arcas and Petrel rocket vehicles [REPT-S3-K-64-44] 10 p1552 N71-21270

Electron concentration and charged particle temperatures in ionosphere 11 p1746 N71-22645

Forward and backscattering of spherical overdense clouds for ionospheric electron density distributions [AD-717683] 11 p1700 N71-22334

Objectives of ISIS-B including measurement of fluctuations in upper atmosphere electron density, radio and cosmic emission studies, and measurements of ionospheric energetic particles [NASA-NEWS-RELEASE-71-41] 11 p1827 N71-22537

Contouring program application to mapping of ionospheric parameters using electron density data from ionospheric stations for extrapolating observations [AD-717683] 11 p1750 N71-22592

Problems of communication and navigation systems in VLF and UHF produced by small irregularities in electron density in F region [AD-717694] 11 p1751 N71-22680

Tropospheric and ionospheric compositions effects on phase and frequency degradations in propagating signals [AGARD-CP-33] 11 p1704 N71-22901

Electron density changes causing amplitude and phase variations in ionospherically propagated very low frequency radio signals during solar flares 11 p1706 N71-22912

Reflection coefficient calculations for electromagnetic radio wave propagation in model ionosphere with electron density variations 11 p1707 N71-22917

Sweep-frequency backscatter measurements with rhombic antenna having interference pattern caused by dense electron layers 11 p1711 N71-22940

D region electron density distribution and energy spectra of solar X rays during quiet periods and solar flares of 30 Oct. 1969 [AD-719841] 13 p2161 N71-25157

Atmospheric model for thermal plasma near equatorial plasmasphere 13 p2076 N71-25270

Early bird and ATS C simultaneous recordings of F region ionospheric electron density for scintillation analysis of ionospheric disturbances [AD-719872] 14 p2245 N71-25627

Ionospheric electron density variation calculation during gravity wave passage in traveling F region including wave parameters 14 p2245 N71-25628

Ionospheric electron and nitrogen density and temperature data from thermospheric soundings during 7 Mar. 1970 total solar eclipse [NASA-TM-X-655531] 14 p2246 N71-25734

Upper ionospheric electron density profiles calculated from lower ionosphere data 14 p2247 N71-25908

Theoretical analysis of 24.5/73.6 MHz rocket-ground CW propagation experiment for in situ electron density measurements [NASA-TM-X-65552] 15 p2382 N71-27670

Electron flux with energy higher than 300 MeV at 250 to 500 km altitudes, observed by Cosmos 225 [NLL-TR-60331] 16 p2674 N71-28206

Relating ionospheric electron content to electromagnetic propagation effects along transionospheric paths and measurements of diurnal variations of electron content [AD-722042] 16 p2587 N71-28456

Ionospheric electron density measurements at magnetic equator, 1964 to 1966 [ESSA-TR-ERL-186-AL-4] 17 p2738 N71-28911

SUBJECT INDEX

- Deriving ionospheric electron density as function of altitude from group path versus frequency measurements by vertical ionospheric sounders [NASA-TM-X-65591] 17 p2730 N71-30260
- Space vehicle design with considerations for ionospheric electron and ionic density, plasma temperature of ionosphere, and neutral component [NASA-SP-9049] 18 p2911 N71-30049
- Northern Hemisphere map of ionospheric F-scat- ter propagation and electron density diurnal variations with fluctuation zones for magnetically quiet and disturbed days [NASA-TT-F-13821] 18 p2916 N71-31083
- Electron and positive ion densities and their relationship to ionization sources in equatorial D region [NASA-TM-X-65635] 19 p3095 N71-32479
- General dependence of solar cycle variation of EUV solar flux from calculation of electron production rates during winter for different values of solar activity [RSD-35] 20 p3341 N71-33526
- Ionospheric electron density variation as solar ac- tivity increases from low to high values [RSD-56] 20 p3341 N71-33527
- D region electron density profiles at geomagnetic equator based on riometer and absorption experiments [RSD-57] 20 p3267 N71-33528
- Knee in total electron content of ionosphere and scintillation boundary from ATS 20 p3268 N71-33630
- Electron density profiles and production rates as- sociated with 30 Jan. 1968 large X ray flare event [RSD-63] 22 p3665 N71-36131
- Correlation of data from ion trap and low energy electron and proton sensors on polar orbiting OV1-15 during magnetic storm 13 to 18 Aug. 1968 [AD-76541] 22 p3666 N71-36138
- Conference on application of satellite radio beacons for ionospheric electron content determination and navigation 24 p3912 N71-37883
- Time lag in satellite navigation systems due to ionospheric electron content 24 p3912 N71-37884
- Orbital elements and frequency data of naval navigation satellites for ionospheric research 24 p3912 N71-37886
- Ionospheric total electron content determined from satellite transmission Doppler shift and compared with Faraday effect 24 p3912 N71-37887
- Ionospheric electron content up to plasmapause determined from Faraday results of ATS 3 data 24 p3912 N71-37888
- Columar electron content measurements 24 p3912 N71-37889
- Ionospheric electron content statistical analysis from Faraday effect tapes 24 p3912 N71-37890
- Semiannual variations of ionospheric electron con- tent 24 p3912 N71-37891
- Second difference of phase shift method for mea- suring ionospheric electron density 24 p3913 N71-37895
- Satellite beacon transmitter methods for determi- ning ionospheric and magnetospheric electron density 24 p3913 N71-37899
- Geophysical results of electron density measure- ments by Faraday rotation and riometer experiments 24 p3913 N71-37901
- Correction of range errors due to ionospheric elec- tron content 24 p3914 N71-37904
- Ionospheric electron content from Beas Explorer A Faraday effect during half solar cycle 24 p3914 N71-37906
- Differential interferometric radiowave refraction measurement for monitoring columnar ionospheric electron content 24 p3914 N71-37907
- Ionospheric electron content from Faraday rotation measurements of ATS 1 and Pioneer 7 space probes 24 p3914 N71-37910
- Upper atmosphere atomic hydrogen density evalua- tion by comparison of high and low altitude electron content 24 p3915 N71-37912
- US Navy Navigation Satellite system for determina- tion of ionospheric electron content up to 1100 km 24 p3915 N71-37913
- ATS 6 radio signal receiver for measuring total elec- tron content of ionosphere and magnetosphere 24 p3915 N71-37914
- Total ionospheric electron content measurements with ATS 3 signal Faraday effect, noting gravity wave effects 24 p3915 N71-37915
- IONOSPHERIC F-SCATTER PROPAGATION
- Northern Hemisphere map of ionospheric F-scat- ter propagation and electron density diurnal variations with fluctuation zones for magnetically quiet and disturbed days [NASA-TT-F-13821] 18 p2916 N71-31083

IONOSPHERIC ION DENSITY

- Satellite observation of horizontal ion density gradients in F region [AD-710808] 01 p0117 N71-10501
- Daytime D region positive ion composition mea- surements for solar zenith angles of 53.2 and 27.8 degrees [NASA-TM-X-65464] 09 p3583 N71-20289
- Sweedish/NASA rocket sounding in auroral D and E regions for ionospheric ion and electron density in- vestigation using Arcas and Petrel rocket vehicles [REPT-83-K68-44] 10 p3552 N71-21270
- Significance of solar geomagnetic processes in determining distribution of ionospheric components and implications for reference models of ionosphere [NASA-TM-X-65568] 15 p2405 N71-27671
- Equilibrium distribution function for electrons in ionospheric plasma calculated for energy interval of 0 to 15 eV utilization data collected in pulse probe ex- periment [NASA-CR-119031] 16 p2508 N71-28508
- Space vehicle design with considerations for ionospheric electron and ionic density, plasma temperature of ionosphere, and neutral component [NASA-SP-9049] 18 p2911 N71-30049
- Observations from Apollo 14 suprathermal ion de- tector including ionospheric ion density, mass and energy spectra during venting in LM cabin, large ion cloud, and ion resulting from impacts 18 p3011 N71-30962
- Electron and positive ion densities and their rela- tionship to ionization sources in equatorial D region [NASA-TM-X-65635] 19 p3095 N71-32479
- Correlation of data from ion trap and low energy electron and proton sensors on polar orbiting OV1-15 during magnetic storm 13 to 18 Aug. 1968 [AD-76541] 22 p3666 N71-36138
- IONOSPHERIC NOISE
- NT WHISTLERS
- High frequency auroral noise caused by proton beam excitation of ionosphere 02 p0180 N71-12658
- Metastable oxygen and nitrogen states for stimulat- ing secondary ionospheric plasma resonances 12 p1983 N71-24267
- IONOSPHERIC PROPAGATION
- NT IONOSPHERIC F-SCATTER PROPAGA- TION
- Research and development of solid state and elec- tronic equipment, microwave circuits, semiconduc- tors, and ionospheric radar 01 p0133 N71-10126
- Ionospheric electron content during solar cycles measured by Faraday rotation of lunar radio echoes [AD-711524] 01 p0118 N71-10708
- Polarization rotation effects on ionospherically propagated on backscatter amplitude [AD-711341] 01 p0024 N71-10733
- First order prediction model of total electron-con- tent group path delay for midlatitude ionosphere [AD-711363] 01 p0025 N71-10770
- Measuring diurnal variations and probability dis- tributions of total polarization rotation at transverse region of ionosphere using synchronous satellites [AD-711403] 01 p0026 N71-10951
- Equations controlling wave transmissions in lower ionosphere and computer program for integrating equations of motion 01 p0052 N71-10971
- Simultaneous measurement of dispersive Doppler shift, Faraday rotation, and ionospheric refraction [AD-711394] 02 p0205 N71-11147
- Ionospheric vertical sounding data of F and E re- gions from Freiburg, Germany for August 1970 [REPT-290-F] 02 p0214 N71-11864
- Ionospheric absorption measurements over Freiburg Germany for January through July, 1970 02 p0214 N71-11865
- Passage of superlong radio waves through ionosphere to Cosmos 142 satellite [NASA-TT-F-13413] 03 p0336 N71-12398
- Performance report on Project Vela Studies [AD-711961] 03 p0338 N71-12409
- Sources and mechanics of extremely low frequency wave propagation in model ionosphere and sea 04 p0490 N71-13702
- Investigating composition, behavior, and morphol- ogy of upper atmosphere over equatorial belt [AD-711199] 05 p0669 N71-14809
- Updated FORTRAN program for waveguide propagation allowing for vertical and horizontal dipole excitation [AD-713168] 05 p0655 N71-14925
- Geomagnetism, radioactivity, ionospheric param- eters, seismology, cosmic rays, and atmospheric elec- tricity - Mar. 1970 05 p0840 N71-15725
- Dourbes geophysical observatory, Belgium, data on geomagnetism, ionospheric propagation, seismology, cosmic rays, and atmospheric electricity, April 1970 06 p0848 N71-15806
- Ionospheric propagation and satellite VHF commu- nication and navigation systems 06 p0814 N71-16226

IONOSPHERIC PROPAGATION

- Ionospheric propagation aspects of VHF navigation and communication satellite systems 06 p0814 N71-16228
- Formation of ionospheric irregularities 06 p0849 N71-16229
- Ray optics and ionospheric propagation scintillation phenomena 06 p0814 N71-16230
- Ionospheric scintillation at high and low altitudes 06 p0814 N71-16232
- Ionospheric electron content measurements using satellite transmissions 06 p0849 N71-16233
- World wide morphology of ionospheric total elec- tron content 06 p0815 N71-16235
- Ionospheric multipath propagation characteristics 06 p0815 N71-16236
- Ray tracing and wave treatment methods for ionospheric propagation 06 p0815 N71-16237
- Communication systems using low orbiting satellites 06 p0815 N71-16238
- Cosmos 142 observation of VLF wave propagation through ionosphere 06 p0857 N71-16898
- Full wave solutions for ULP and ELF transmission through ionosphere [AD-715301] 07 p1022 N71-17835
- Near real time ionospheric MUF forecasting over 60 km path [AD-714993] 07 p1023 N71-17859
- Electromagnetic wave ducting in ionosphere [AD-715338] 07 p1023 N71-17863
- Waveguide variations in ionosphere 07 p1023 N71-17874
- Steady-state phase for beam of radio wave propaga- ting in absorptive ionosphere as function of wave direction of real and imaginary parts of wave vector [ORL-TP-95] 06 p1187 N71-18470
- Real time correction of wideband HF ionospheric paths [AD-715918] 06 p1187 N71-18478
- Electromagnetic signal propagation along the earth- ionosphere waveguide 08 p1164 N71-19152
- Application of perturbation techniques to scattering of radio frequency waves by underdense ionospheric layer [AD-716387] 09 p1347 N71-19550
- Electromagnetic wave transmission through normal and disturbed ionospheres, emphasizing propagation losses from spacecraft communication [AD-716678] 09 p1349 N71-19753
- Ionospheric irregularity characteristics from Ex- plexer 23 Faraday findings of 40 MHz transmissions [RSD-553] 09 p1384 N71-20047
- Atmospheric models and synchronization time signal propagation delay [NASA-TM-X-65460] 09 p1385 N71-20285
- Ionospheric disturbances caused by internal gravity wave propagation in ionosphere [NASA-TT-F-13483] 09 p1386 N71-20344
- Concentric sphere model of ionosphere for takeoff angle and length determinations in complex ray con- figurations [AD-716963] 10 p1517 N71-20631
- Propagation studies at Millstone Hill radar facility with steerable parabolic reflector 10 p1517 N71-20731
- Acoustic-gravity wave propagation in ionosphere of 1962 US Standard Atmosphere and effects on HF radio propagation 10 p1521 N71-21276
- Hourly ionospheric propagation data - Freiburg, Dec. 1970 [REPT-294-F] 10 p1536 N71-21834
- Hourly ionospheric propagation data tables, Salis- bury - Feb. 1970 [SAD-1970/2/3] 11 p1746 N71-22047
- Ionospheric propagation charts of predicted median critical and maximum usable frequencies in F2 region, Dohai - Jan. 1971 [RRC-8172] 11 p1747 N71-22067
- Forward and backscattering of spherical overdense clouds for ionospheric electron density distributions [AD-717653] 11 p1700 N71-22324
- Hourly values of ionospheric parameters in Salis- bury, Australia [WRE-SAD-1970/1/8] 11 p1749 N71-22445
- Ionospheric absorption measurement, sunset ob- servations, and short wave fadeout reported from op- tical tracking stations in Greece (Athens) - tables 11 p1823 N71-22502
- Waveguide model for estimating ionospheric varia- tions effects on very low frequency signal trans- mission 11 p1704 N71-22903
- Mathematical model for very low frequency wave propagation in ionosphere with phase velocity varia- tions 11 p1704 N71-22904
- Experimental data on very low frequency phase in- stabilities at quiet and disturbed propagation 11 p1708 N71-22910

Reflection coefficient calculations for electromagnetic radio wave propagation in model ionosphere with electron density variations

11 p1707 N71-22917

Long wave propagation measurements for geophysical research

11 p1707 N71-22920

Airborne Doppler shift measurements on lower ionospheric instability

11 p1707 N71-22921

Ray tracing and propagation calculations for determining short wave frequency deviations from received signal

11 p1709 N71-22931

Solar flare effects on ionospheric high frequency radio wave propagation with sudden frequency deviations

11 p1710 N71-22937

Diurnal frequency variations in oblique high frequency ionospheric radio signal

11 p1711 N71-22939

Propagation over polar ice cap, and across day night transition at very low frequencies in ionosphere

[AD-718391] 12 p1874 N71-23372

Computerized simulation of sinusoidal reflecting surface effects on radio wave transmission in ionosphere

[AD-718106] 12 p1874 N71-23446

Laboratory model of radio star signal diffraction by ionosphere or solar wind using 40 kHz airborne ultrasonic radiation and warm turbulent air diffracting screen

12 p1999 N71-24313

Ionospheric shock wave propagation observed by ray tracing technique

[KGO-711] 13 p2070 N71-24591

Bibliography on aeronautical satellite system air traffic control and propagation factors

[NASA-TM-X-65511] 13 p2173 N71-24942

Experimental results of simultaneous measurement of ionospheric amplitude variations of 136 MHz and 1550 MHz signals at geomagnetic equator

[NASA-TM-X-65505] 13 p2161 N71-25025

Analysis of mode coupling conditions in ionosphere for solar radio waves

[NASA-CR-118646] 14 p2216 N71-25913

Ionospheric propagation, ion-molecule and acoustic surface wave interactions, semiconductors, photodetectors, target recognition, satellite tracking, and inertial guidance

[AD-720248] 14 p2360 N71-26328

Tables on climatology of ionosphere measured by ionosondes

[NOAA-ISPDA-FA-321] 14 p2251 N71-26625

Qualitative morphology of polar cap absorption events using riometers and periodic variations in energy spectra and proton flux density in ionospheric absorption forecasting

[AD-721163] 15 p2395 N71-26843

Riometer polar cap absorption, auroral absorption, and solar flare observations and ionospheric absorption forecasting

[AD-721162] 15 p2395 N71-26844

Wave reflection and electromagnetic absorption influence on radio transmission from salvage buoys, noting ground wave propagation for target acquisition

15 p2380 N71-27157

Method for predicting time availability of VLF field strengths using ionosphere waveguide model

[AD-720318] 15 p2380 N71-27209

Theoretical analysis of 24.5/73.6 MHz rocket-to-ground CW propagation experiment for in situ electron density measurements

[NASA-TM-X-65552] 15 p2382 N71-27670

Fine structure observation in high frequency radio signals propagated around world using oblique ionograms

[AD-721703] 16 p2561 N71-28448

Ionospheric propagation data for E and F regions, Bangkok - Aug. 1970

16 p2589 N71-28864

Ionospheric propagation data for E and F regions, Bangkok - Sept. 1970

[AD-720327] 16 p2589 N71-28865

VLF propagation measurement technique using repetitive pulse spectral lines

[AD-722763] 17 p2721 N71-30050

Solar observations for three stations in Greece including solar X rays and ionospheric absorption

18 p3006 N71-30939

Transpolar propagation of long radio waves with calculations based on daytime ionospheric models

[AD-723822] 18 p2892 N71-31598

Atmospheric propagation studies including ionospheric motions caused by nuclear tests, spacecraft launches, and earthquakes

[AD-723519] 19 p3084 N71-31680

Comparison of ionospheric refraction data sources and error correcting formulas using Wallops Island collocation experiment data

19 p3088 N71-31847

Theoretical physics and mathematical model for GEOS 2 ionospheric corrections using VHF range and range rate tracking data

19 p3088 N71-31849

Dourbes Geophysical Observatory, Belgium, data on geomagnetism, ionospheric propagation, seismology, cosmic rays, and atmospheric electricity, Jul. 1970

19 p3091 N71-31928

Ionospheric sounding data for inclusion in data base of World Wide Radio Propagation Charts

[AD-723163] 19 p3092 N71-32031

Finite state discrete parameter Markov chain representation of ionospheric communication error sequences

19 p3057 N71-32561

Numerical calculation of long wavelength reflection coefficients for horizontally stratified model ionosphere

[AD-724608] 20 p3232 N71-33092

Construction of antenna array and automatic recording system to measure amplitude and phase of diffraction patterns formed by ionospheric reflection of 300 kHz pulsed radio signals

[PSU-IRL-SCI-371] 20 p3259 N71-33207

Electron density and collision frequency data for nighttime ionosphere medium frequency propagation for use with ray tracing computer program

[BBC-1971/22] 20 p3236 N71-33810

Ionospheric, solar, and satellite optical tracking data - Apr. 1971

20 p3343 N71-33978

Hourly values of ionospheric propagation data for India - June 1969

[RTRC-A169] 21 p3416 N71-34308

Hourly values of ionospheric propagation data for India - July 1969

[RTRC-A170] 21 p3416 N71-34309

Ionospheric propagation, geomagnetic, and cosmic ray data - tables for Dec. 1969

21 p3419 N71-34326

Characteristics of radio wave propagation in troposphere, ionosphere, and along earth surface

[FOA-3-A-3730-60] 22 p3554 N71-35311

Radio wave propagation, diurnal variations, and frequency and phase modulation

[AD-726528] 22 p3554 N71-35315

Ionospheric propagation data for E and F regions, India - October 1969

[RTRC-A173] 22 p3575 N71-35460

Ionospheric propagation data for E and F regions, India - September 1969

[RTRC-A172] 22 p3575 N71-35461

Ionospheric propagation data for E and F regions, India - Aug. 1969

[RTRC-A171] 22 p3575 N71-35462

Ray tracing to delineate radio propagation to large distances by ducting under super refracting conditions in troposphere, ionosphere, or magnetosphere

[AD-726997] 23 p3723 N71-36541

Effect of ionosphere inhomogeneities on diffraction of high frequency radio waves

23 p3726 N71-36563

Ionospheric propagation data for E and F regions, India - [Dec. 1969]

[RTRC-A175] 23 p3752 N71-36752

Ionospheric propagation data for E and F regions, India - Nov. 1969

[RTRC-A174] 23 p3752 N71-36753

Methods for improving and extending WEDCOM MB computer code

[AD-727627] 24 p3889 N71-37716

Effects of ionospheric propagation on ELF communication system

[AD-727571] 24 p3890 N71-37724

Ionospheric propagation with satellites beyond ground station horizon, seeing San Marco 2 satellite experiment

24 p3914 N71-37905

Second-order phase path difference calculations for ionospheric Faraday and Doppler effect

24 p3914 N71-37908

Satellite tracking accuracy and atmospheric propagation errors

24 p3914 N71-37909

IONOSPHERIC REFLECTION
U IONOSPHERIC PROPAGATION
IONOSPHERIC SOUNDING

Comparison of ionospheric sounding electron concentration and electron and ion temperature data in F region

01 p0046 N71-10228

Alouette 1 ionospheric sounding synoptic data tables for Nov. 1968

01 p0046 N71-10277

Interpolated electron number density tables from Alouette 2 ionospheric sounding data

01 p0046 N71-10278

Solar and geophysical data related to ionospheric studies from India - tables

[RRC-A178-PT-2] 01 p0117 N71-10378

Comparing vertical distribution ionospheric soundings in F region from bottom side and topside over Ouagadougou/Upper Volta/

[GRI-NT-78] 02 p0212 N71-11542

Ionospheric vertical sounding data of F and E regions from Freiburg, Germany for August 1970

[REPT-290-F] 02 p0214 N71-11864

Ionospheric absorption measurements over Freiburg Germany for January through July, 1970

02 p0214 N71-11865

Wave-like structures in E-region derived from drift experiments

[AD-712546] 02 p0220 N71-12093

Magnetic variations, ionospheric soundings, and riometer data in polar regions, July - Sept. 1969 - Tables

03 p0371 N71-13273

Ionospheric daily obtained over Salisbury, Australia during October, 1969

[SAD-1969/10/8] 05 p0581 N71-15604

Ionospheric daily data obtained over Salisbury, Australia during September, 1969

[SAD-1969/9/5] 05 p0581 N71-15605

Ionospheric daily data obtained over Salisbury, Australia during December, 1969

05 p0581 N71-15606

Ionospheric daily data obtained over Salisbury, Australia during November, 1969

[SAD-1969/11/5] 05 p0581 N71-15607

Statistical analysis of simultaneous two-station ionospheric soundings

[AD-714192] 06 p0853 N71-16571

Balloon measurements of ionospheric electric fields [NASA-CR-114818] 06 p0856 N71-16820

Cosmos 184 ion sensor for measuring ion velocity at 600 km

07 p1014 N71-16947

Cosmos 184 measurements of ion velocity at 600 km

07 p1014 N71-16948

Ionospheric sounding and cosmic ray neutron flux density tables at Dourbes, Belgium, Jun. 1970

07 p1016 N71-17047

Ionospheric sounding and cosmic ray neutron flux density tables at Dourbes, Belgium, Jul. 1970

07 p1016 N71-17051

Ionospheric sounding and cosmic ray neutron flux density data - May 1970

07 p1017 N71-17076

Cosmos 381 ionospheric sounding experiments

07 p1017 N71-17105

Atmospheric electricity, ionospheric sounding, seismology, and geomagnetism, and cosmic ray data, Belgium, May 1970

07 p1018 N71-17149

Atmospheric electricity, ionospheric sounding, seismology, and geomagnetism, and cosmic ray data, Belgium, June 1970

07 p1018 N71-17159

Wave-like variations in ionosphere

[AD-714993] 07 p1023 N71-17474

Operating instructions for Cleanweep sounding rocket vehicle

[UCRL-50586] 08 p1295 N71-19278

Auroral ionospheric electric field rocket sounding by means of Geiger counters, electrostatic probes, and barium artificial clouds

[REPT-70-25] 10 p1545 N71-20634

Ionospheric data from vertical echo soundings over Freiburg, Germany during November, 1970

[REPT-291-F] 10 p1553 N71-21670

Remote sensing of midlatitude ionosphere with narrow beam high frequency backscatter sounder scanning in azimuth and elevation

11 p1744 N71-21930

Ionospheric sounding and cosmic ray neutron flux density tables, Dourbes, Belgium, Nov. 1970

11 p1746 N71-21985

Ionospheric sounding and cosmic ray neutron flux density tables, Dourbes, Belgium, Oct. 1970

11 p1746 N71-21986

Ionospheric sounding and cosmic ray neutron flux density tables, Dourbes, Belgium, Aug. 1970

11 p1746 N71-21989

Ionospheric sounding and cosmic ray neutron flux density tables, Dourbes, Belgium, Sep. 1970

11 p1746 N71-21994

Kinesonde experiment for development of system for remote sensing of ionospheric motions and microstructure

[NASA-CR-117837] 11 p1750 N71-22531

Stereo techniques for studying spatial structure and dynamics of barium releases

[AD-717722] 11 p1751 N71-22002

Optical observations following release of barium vapor at high altitudes described in three phases

[AD-717695] 11 p1751 N71-22005

Ionospheric soundings, Cosmos launches, and lunar exploration

12 p1905 N71-33118

Magnetic substorm events and magnetospheric structure in polar auroral zones determined by rocket sounding, satellite observations, and ground-based measurements - conference

[ESRO-SP-38] 12 p1908 N71-33531

Auroral optical emission spectroscopy by ionosphere rocket sounding

12 p1909 N71-33565

Auroral ionospheric electric field measurements by means of gas release or electrostatic probes

12 p1909 N71-33567

SUBJECT INDEX

IRIDIUM

Auroral ionospheric plasma diagnostics by means of electrostatic probes 12 p1909 N71-33568

Tables on ionospheric and solar activity 12 p1912 N71-33695

Observed from flights of Yantar unmanned ionospheric laboratories with gas ion plasma engines to determine possibilities for guided flight in upper layers of atmosphere 12 p1998 N71-34245

Magnetometer, cosmic ray, ELP, solar, ionospheric, solar optical and radio emission, and ionosonde data - July - Sept. 1978 13 p3809 N71-34413

Ionospheric electron and nitrogen density and temperature data from thermospheric soundings during 7 Mar. 1970 total solar eclipse 14 p2346 N71-25736

External sheath structure and ion collection characteristics of rocket-borne mass spectrometer 14 p2333 N71-25771

Auroral phenomena used on ESRO 1/Aurora satellite for ionospheric sounding 15 p3407 N71-27853

Positive ion densities from rocket-borne hemispherical Langmuir probe at 40 to 100 km 16 p3662 N71-28848

VLF propagation measurement technique using repetitive pulse spectral lines 17 p2721 N71-30050

Time variations versus latitude, altitude, and electron plasma frequency to electron cyclotron frequency ratio for ionospheric plasma resonances observed by Alouette satellites 17 p2750 N71-30273

Analysis of wave interaction disturbing antenna system 18 p2891 N71-31291

Collisionless plasma flow around cylinder for application to ionospheric sounding probe 19 p3072 N71-31693

Ionosonde sounding data for inclusion in data base of World Wide Radio Propagation Charts 19 p3092 N71-32031

Ionosonde using data processing systems for continuous ionospheric soundings 19 p3093 N71-32204

Cosmos 381 scientific satellite for ionospheric sounding 19 p3185 N71-32661

Polar ionospheric geophysical data recorded at Kiruna, Sweden during Apr. - Jun. 1970 20 p3255 N71-32909

Polar ionospheric geophysical data recorded at Kiruna, Sweden during Oct. - Dec. 1969 20 p3256 N71-32945

Polar ionospheric geophysical data recorded at Kiruna, Sweden during Jul. - Sep. 1970 20 p3257 N71-33013

Fundamental effect used for electron density profile determination in ionospheric sounding by VHF Thompson scatter radar 20 p3258 N71-33151

Ionospheric data for June 1970 from Salisbury, South Australia 20 p3268 N71-33789

Polar ionospheric geophysical data recording at Kiruna, Sweden during Jan. - Mar. 1970 20 p3269 N71-33857

Low frequency vertical pulsed sounder design with digital integration and pseudo-random phase coding for ionospheric D-region sounding 22 p3580 N71-35499

IONOSPHERIC STORMS

Statistical analysis of moon content in 14,000 ionospheric storms 10 p1618 N71-21549

Chemical composition of nuclear particles in extensive ionospheric storms 10 p1641 N71-21550

Observation of ionospheric waves in auroral zone following release of rocket borne chemical 14 p2346 N71-25736

IONOSPHERIC TEMPERATURE

Measurement of ion and electron temperature from 100 to 850 km by ionospheric radar 01 p0045 N71-10150

Comparison of ionospheric sounding electron concentration and electron and ion temperature data in F region 01 p0046 N71-10228

Electron concentration and charged particle temperature in ionosphere 11 p1746 N71-22045

Diurnal temperature variations in middle ionosphere and electron density in E, E-F, and F1 regions 22 p3679 N71-36251

IONOSPHERIC

NT DAWN CHORUS

NT EISS

Winter study to determine interchange of ionization between ionosphere and protonosphere 01 p0049 N71-10721

Spec environment simulator for ionospheric plasma flow over onboard satellite instrumentation 09 p1439 N71-30213

Annotated bibliography of theoretical physics, magnetohydrodynamics of ionosphere and magnetosphere 16 p2641 N71-26832

Ionospheric processes associated with auroral bright variations as determined by scanning photometer 17 p2747 N71-30884

Ionospheric data for June 1970 from Salisbury, South Australia 20 p3268 N71-33789

Recording techniques and interpretation of ionospheric effects of solar flares 20 p3343 N71-33939

Subauroral red arc producing mechanisms based on ionospheric and atmospheric equations 21 p3416 N71-34383

Observations of geophysical phenomena concerning electric and magnetic states of upper atmosphere, ionosphere, cosmic rays and earth currents 22 p3574 N71-35452

IONOSPHERIC

NT ANIONS

NT ANTIPTOTONS

NT CATIONS

NT CESIUM ION

NT DEUTERONS

NT FERRIC ION

NT HEAVY IONS

NT HYDROGEN IONS

NT METAL IONS

NT MOLECULAR IONS

NT NITROGEN IONS

NT PROTONS

NT RECOIL IONS

NT SOLAR PROTONS

NT TRITONS

NT TRIVALENT IONS

Kinetic energy of ionic products from electron impact dissociation of molecules 01 p0102 N71-10919

Spectrometer for measurement of velocity distribution and charge-to-mass ratio of ions 02 p0224 N71-11524

Thermodynamic constants of alkali metal cations and metal anions 03 p0440 N71-12670

Ion masking in quadrupole mass spectrometer to eliminate unstable ion penetration 04 p0573 N71-13676

Emission cross sections for H, Na, Ne, and Rb ions, incident on molecular nitrogen 07 p1074 N71-17436

Reducing noise in multiplier of quadrupole mass spectrometer when operating in ion counting mode 07 p1083 N71-18852

NMR and ESR measurements of magnetic interaction in sodium chloride-negative dichloride ion and lanthanum ethyl sulfate-trivalent gadolinium ion 09 p1432 N71-19935

Phosphorus, boron, and lithium ion implantation for doping charged particle detectors 09 p1439 N71-20198

Radiation damage from implanted ions 09 p1443 N71-20452

A, a and b functions for electron broadening of positronium with hyperbolic path 11 p1801 N71-21983

Vapor-ion methods of film deposition - annotated bibliography 11 p1769 N71-22531

Profound solution of delta function model for two electron lithium like ions 12 p1969 N71-23286

Behavior of barium ion cloud at high altitudes 12 p1993 N71-23517

Ion detection and monopole mass spectrometer performance tests with transverse magnetic field of lithium getter pump pumping capacity for D region ion composition analysis 12 p1921 N71-23788

Interaction effects in solids using transition metal and rare earth ions as probes 13 p2152 N71-25440

Analysis of subvalent Hg ion discovered in molten chlorides 14 p2212 N71-25607

Recombination of positive ions with electrons in nitrogen 14 p2301 N71-25738

Design and characteristics of scintillation detector for fast ion counting in mass spectrometer 14 p2338 N71-26604

Chlorine ion implantation of ZnTe crystals to create n-type layers 14 p2330 N71-26770

Slow electrons and negative ions in organic liquids yielding information about, spatial distribution and chemical reactions treated with classical diffusion theory 15 p2483 N71-27762

Effect of chloride ions on stress corrosion cracking behavior of U-7 1/2 weight percent Nb-2 1/2 weight percent Zr and U-4 1/2 weight percent Nb alloys 17 p2761 N71-29337

Isotopic rotation for investigating nature of energy levels of lanthanide ions in crystalline solids 17 p2814 N71-29892

Cosmos 381 satellite program for observation of low energy electrons and ions 17 p2740 N71-30201

Ion-molecule reactions of C₂H₄-CD₄ mixtures at high pressures in ion source of quadrupole mass filter 17 p2717 N71-30238

Aluminum foils for measuring solar wind ion composition 18 p3042 N71-30966

Rational and vibration effects in ion dipole collisions demonstrated in color motion picture 18 p2905 N71-31194

Development of ion selective electrochemical sensors for detection of calcium, sodium, sulfate, and other ions in saline and brackish water 19 p3069 N71-31729

Computerized simulation of electromagnetic and static beam effects on counterstreaming ion instabilities 19 p3164 N71-32150

Spectrometer for onboard measurement of ion energy spectra in plasma of solar wind and magnetosphere 19 p3176 N71-32230

Slaking of particle beams by inducing increasingly larger ion oscillation about beam driving them to walls in order to remove neutralizing ions 20 p3327 N71-33966

Chemical trajectory study of rotationally inelastic scattering of hydrogen molecules by collisions with lithium ions 21 p3427 N71-34382

Band structure of aluminum oxide determined using basis set having 30 ion functions and 15 plane waves 21 p3455 N71-34514

Approximations in calculating g-factors for molecular ion BE (Jahn) 21 p3466 N71-34526

Tungsten isotopes produced in compound nucleus reactions followed by neutron evaporation and bombardment of Cd and Nd ions 21 p3471 N71-34714

Ion heating caused by ion acoustic waves from electron drift in ion streaming plasma 21 p3494 N71-34889

Radiolysis of water with primary products of hydrogen, oxygen, and hydroxyl ions 22 p3550 N71-35287

Determination of quantitative rate of joint discharge of ions under conditions of electroforming of pure metals 22 p3590 N71-35565

Ion transmission and radiation damage in carbon and gold thin foils 22 p3638 N71-35929

Bibliography on ion implantation technology 22 p3646 N71-35998

Worked and free oscillations of plasma consisting of free electrons and background of positive ions 22 p3652 N71-36045

Electron-ion bunch diagnostics by bromostripping, using heavy ion acceleration to high energies 23 p3808 N71-37155

Electromagnetic devices for ion transport 23 p3817 N71-37322

Thermal conduction and low frequency electrostatic waves in collisionless plasmas immersed in magnetic field 23 p3833 N71-37334

Particle acceleration by ionic-acoustic vibrations in isothermal plasmas 23 p3852 N71-37459

Ion and electron plasma confinement and kinetic instabilities in silicic traps 23 p3853 N71-37467

Ion and electron acceleration in unperturbed plasma 23 p3854 N71-37476

Crossed field instabilities and turbulent ion heating calculated in mirror machine 24 p3908 N71-38438

Evaluation of hot ion accumulation from injecting neutral hydrogen into target plasmas 24 p3992 N71-38480

IMPACT PREDICTION

U COMPUTERIZED SIMULATION

U INTERNATIONAL QUIET SUN YEAR

U INFRARED LASERS

U IRIDIUM ISOTOPES

Oxidation resistance and high temperature tests of rhenium, tungsten, hafnium, and tantalum matrix 15 p2483 N71-27762

- composites with iridium in oxygen, fluorine, and boron atmospheres for liquid propellant engines [NASA-CR-119019] 16 p2617 N71-28501
- Routes at which iridium oxidizes at temperatures 1600 to 2200°C and pressures 1 to 1000 torr [JLO-2228-T-1-1] 17 p2713 N71-29240
- Magnetic and transport properties of RuO₂ and IrO₂ single crystals 17 p2827 N71-30170
- Spectrophotometric determination of platinum plus 4 and iridium using bromine as reagent 20 p2320 N71-33622
- Feasibility of crystal growth techniques for beta alumina membrane from molybdenum, tungsten, and iridium [NASA-CR-72982] 23 p3833 N71-37336
- Limits, capabilities, and operation of field ion microscopes with results of tungsten and iridium ionic charge investigations 24 p3926 N71-38016
- IRIDIUM ISOTOPES**
- Decay schemes of Fe-59 and Ir-192 [ORNL-TR-2345] 10 p1616 N71-21182
- Nondestructive testing of aircraft structures using thulium and iridium gamma sources [JAERI-MEMO-4163] 13 p2181 N71-34849
- Production of fast neutron-deficient iridium isotopes by bombarding holmium with Ne-22 and Ne-20 heavy ions [JINR-P6-5617] 19 p3159 N71-32598
- Electron capture decay of Ba-131 and Ir-192 nuclear energy and relative intensity measurements using coaxial Ge(Li) detector 21 p3490 N71-34863
- IRISES [MECHANICAL APERTURES]**
- Development and characteristics of single, silicon element, waveguide iris limiter [AD-711577] 02 p0193 N71-11355
- Analysis of microwave irises for semiconductor limiting elements [AD-716626] 09 p1360 N71-19906
- Particle separation in system of conventional S-band iris-loaded deflectors interspersed with alternate gradient magnets of strong focusing channels [BNL-15438] 11 p1804 N71-22286
- Iris disk slot geometry effects on waveguide dispersion properties and wave damping coefficients [KFK-TR-334] 14 p2231 N71-26775
- IRON**
- NT IRON ISOTOPES**
- NT IRON 57
- NT IRON 59
- X ray excited LMM Auger spectra of copper, iron, and nickel [NASA-TM-X-65381] 01 p0097 N71-10584
- Effect of stresses on magnetostriiction of iron, nickel, and Permalloy [AD-711094] 01 p0092 N71-10915
- Mechanism of iron dissolution and corrosion inhibition by galvanostatic polarization and electrical double layer capacitance measurement 02 p0174 N71-11227
- Iron self diffusion parameters in Fe-delta-region and in Fe alloys with small Al additions [TT-70-57043] 02 p0240 N71-11389
- High speed centrifugal determination of mechanical properties of small iron and other ferromagnetic crystals and whiskers [AD-711582] 02 p0244 N71-11698
- Tables of iron spark lines giving comparison of calculated and measured wavelengths [ESRIN-DN-34] 02 p0281 N71-11873
- Iron diffusion in tungsten, tantalum, niobium, and silver [TT-70-57025] 03 p0391 N71-12821
- Thermodynamics of corrosion inhibition of iron in Fe/H₂O, H₂O₂, O₂ system [AD-713451] 05 p0699 N71-14536
- Far infrared analysis of pair mode in MnF₂-Fe/22-C [NYO-2391-1280] 05 p0759 N71-15445
- Adhesion of single crystal metals to clean iron surface studied by emission spectroscopy [NASA-TN-D-7018] 06 p0863 N71-15928
- Sound velocity in iron and iron alloys in solid and liquid state [LA-TR-70-21] 06 p0907 N71-16756
- Low temperature heat capacities of dilute solutions of Fe and Cr in Cu [UCRL-19486] 07 p1132 N71-17924
- Grain boundary diffusion in iron using autoradiography [TT-70-57048] 08 p1218 N71-19096
- Statistical level density formula for describing unknown high energy states of daughter nucleus for determined neutron cross sections in Fe-56 [AD-717216] 10 p1612 N71-20760
- Tables on vapor pressure of iron pentacarbonyl nickel carbonyl system [NLL-TRANS-746-515-(9022.401)] 10 p1586 N71-21823
- Passivity models for iron in nonaqueous solution [AD-717495] 11 p1695 N71-22142
- Test equipment and techniques for improving iron/potassium perchlorate heat powder [SC-CR-70-6137] 11 p1677 N71-22480

- Noble-metal binary alloy friction experiments in sliding contact with iron and alloy free energy of formation effects on friction and wear [NASA-TN-D-63111] 12 p1926 N71-23747
- Plastic yielded iron-nickel single crystal martensite crystallography 12 p1939 N71-24077
- Scattering cross sections of 28 MeV protons from isotopic mixtures of Fe, Co, Ni, and Zn 12 p1978 N71-24287
- Thermodynamically consistent equation of state for alpha and epsilon phases of iron 13 p2092 N71-24563
- Steady state creep tests to measure deformation enhanced diffusion in iron and iron alloys at elevated temperatures 13 p2094 N71-24916
- Iron doped rutile wideband maser amplifier with low signal-to-noise ratio 13 p2090 N71-25337
- Face centered to body centered cubic lattice transformation in vacuum deposited thin films [ORO-3108-107] 13 p2154 N71-25548
- Oxidation reaction of iron in solutions containing chloride and/or iron(II) at 300°C, studied by hydrogen effusion method [AD-719887] 14 p2267 N71-25626
- Structure and phase composition of diffusion layer formed by interdiffusion of iron and aluminum [TT-70-58191] 14 p2268 N71-25647
- Spectral analysis of magnesium distribution in high strength cast iron containing globular graphite [TT-70-59085] 14 p2269 N71-25668
- Temperature dependence of self diffusion coefficient of iron, chromium, and cobalt in steel with 8 percent carbon [DMDC-5795] 14 p2271 N71-25693
- Distribution moments and Monte Carlo calculation of high energy gamma ray absorption in concrete, iron, and lead slabs 14 p2304 N71-26277
- Iron and gold transition points as standards for high pressure and temperature measurements 14 p2297 N71-26509
- High pressure phase transition points of bismuth 3, 5, tin, and iron 14 p2329 N71-26510
- Effect of electron irradiation on strength of monocrystalline bcc iron - low temperature strength determined by inherent lattice hardening [COO-1367-36] 15 p2419 N71-26918
- Nickel, magnesium, and aluminum annealing effects on neutron irradiated iron crystal defects in low temperature environments [CEA-CONF-1681] 15 p2472 N71-27437
- Dissolution of Ni and Fe foils caused by electron irradiation [CEA-CONF-1680] 15 p2489 N71-27880
- Cosmic ray data from cloud and ionization chambers, and carbon and iron plates [AD-721714] 17 p2840 N71-29472
- Spectrophotometry of trivalent Fe, divalent CrO₄, and hydroxyl iron complexing in aqueous solution at various oxalic acid concentrations and pH values [NLL-CE-TRANS-5509-(9022.09)] 17 p2714 N71-29669
- Iron film adsorption of carbon monoxide, hydrogen and their mixtures 17 p2714 N71-29668
- Interaction between screw dislocation and carbon in body centered cubic iron using model with pairwise interatomic potential matching 17 p2818 N71-29947
- Iron screw dislocation for slip behavior in body centered cubic materials 17 p2819 N71-29948
- Oxygen 18 labeling used for detection of deoxidation of iron-carbon melts in vacuum systems 18 p2934 N71-30686
- Phosphorus solubility and diffusion in iron and iron alloys below 1000°C 18 p2937 N71-31317
- High temperature microscopy of crystallization processes in molten iron, steel, and eutectic containing iron carbon alloy steels 18 p2997 N71-31321
- Deoxidation of liquid iron studied by electromotive force measurements noting removal of inclusions 19 p3111 N71-31911
- Kinetics of removal from iron of inclusions produced by manganese silicon aluminum complex deoxidation 19 p3112 N71-31912
- Role of ductility brittleness transition in body centered cubic lattice of iron polycrystals 19 p3112 N71-31913
- Molecular dynamics of phase transformation of iron under hydrostatic pressure 19 p3114 N71-32235
- Determination of diffusion coefficient of iron in magnetite [TT-70-59100] 20 p3283 N71-33091
- LMM peaks in Auger spectra identified for transition metals of Fe, Co, and Ni [AERE-R-4719] 21 p3438 N71-34461

- Heat capacity of pure nickel, pure iron, and Ni₃Fe, and contribution from anharmonic lattice vibrations [ORO-3291-14] 21 p3438 N71-34466
- Wettability and formation of alloyed coatings on iron castings [NLL-M-21010-(5828.4F)] 21 p3441 N71-34481
- Crystallographic positions and isomer shifts of iron in boron determined by Mossbauer spectroscopy [IUIP-733] 22 p3640 N71-33946
- Nuclear spin-lattice relaxation and nuclear magnetic resonance in Fe, Co, and Ni 22 p3652 N71-36043
- Investigating thermal neutron capture gamma radiation from natural iron samples with aid of three-crystal scintillation pair spectrometer [UAREE-103] 23 p3808 N71-37151
- Effect of organic iron chelate, ligand structure on oxidation product formation and autooxidation rate of cumene [FOA-1-B-1155-92] 24 p3886 N71-37690
- IRON ALLOY**
- NT AUSTENITIC STAINLESS STEELS**
- NT CARBON STEELS
- NT CHROMIUM STEELS
- NT HIGH STRENGTH STEELS
- NT MARAGING STEELS
- NT MARTENSITIC STAINLESS STEELS
- NT NICKEL STEELS
- NT STAINLESS STEELS
- NT STEELS
- Abrasive wear resistance of manganese cast iron inoculated with cerium and studied with KHS-8 machine [AD-711156] 01 p0068 N71-10633
- Mossbauer spectra of ferromagnetic materials [AD-711105] 01 p0111 N71-10668
- Iron self diffusion parameters in Fe delta-region and in Fe alloys with small Al additions [TT-70-57043] 02 p0240 N71-11389
- Mach 1 burner rig tests at 2100°F for oxidation resistance evaluation of NiCrAl and FeCrAlV claddings on TD-NiCr [NASA-TM-X-52916] 02 p0240 N71-11426
- D and s electron interactions in iron-aluminum system diffusion [TT-70-57046] 02 p0245 N71-12149
- Structure and properties of high strength ferrous alloys EP404 and EP454 [AD-713048] 03 p0393 N71-13837
- Stress corrosion cracking of Fe-Cr-Ni alloys in chloride environments [COO-1319-82] 04 p0528 N71-13948
- Investigating low-temperature ferromagnetism of amorphous alloys obtained by rapid quenching from liquid state [CALT-822-11] 05 p0703 N71-15231
- Mossbauer effect analysis of Au-Pd-Fe alloy system [UCRL-50918] 05 p0705 N71-15440
- Martensitic conversion in Fe-Ni-Co alloys [SC-T-70-4036] 05 p0706 N71-15547
- Stress and electrochemical corrosion of Fe-Cr-Ni alloy exposed to aqueous solutions of NaOH [COO-2018-11] 06 p0669 N71-15888
- Wear resistance of austenitic manganese cast iron during sliding friction without lubricant [AD-714789] 07 p1044 N71-17765
- Friction and wear effects on mechanical properties of steels and cast iron for guide stands [AD-714789] 07 p1046 N71-18829
- Magnetic field influence on high pressure phase diagrams of iron and iron alloys 08 p1213 N71-18540
- Corrosion damage resistance of iron alloys, nickel alloys, and cobalt alloys in liquid sodium and mercury - review of NASA program [NASA-TM-X-52956] 08 p1215 N71-18816
- Silver diffusion into iron-palladium alloys and internal adsorption of palladium in iron [TT-70-57070] 08 p1219 N71-19108
- Young modulus, shear modulus, and compressibility of Fe-Ni fcc alloys [NASA-TT-F-13479] 08 p1299 N71-19151
- Diffusion processes in iron alloys [TT-70-50031] 08 p1219 N71-19176
- Behavior of silica inclusions during solidification of iron base alloy [AD-715940] 09 p1397 N71-19615
- Thermal and electrical conductivities of gold iron alloys at low temperatures 09 p1398 N71-19734
- Stress corrosion cracking in iron nickel chromium alloy system in chlorides 09 p1399 N71-19739
- Comparison of Mossbauer effect to time differential perturbed angular correlations in Fe-57-Ni system [CONF-70014-1] 09 p1454 N71-20022
- Activity coefficient of sulfur in ternary alloys rich in iron at high temperature [NRC-TT-1418] 09 p1402 N71-20044
- Stress corrosion cracking in iron nickel chromium alloy system in magnesium chloride, for water cooled reactor [COO-3069-6] 10 p1571 N71-20040

- Homogeneity characterization of Fe-3Si alloy
microanalysis standard reference material
[NBS-SP6C-PUBL-260-22] 10 p1577 N71-21027
- Nonmetallic impurities in laser and super-laser iron alloys
[NLL-TRANS-746-633-19022.401/] 10 p1579 N71-21266
- Microstructure and magnetic properties of internally oxidized ferromagnetic alloys for application to magnetic domain theories and high temperature tests
[AD-71721-0] 10 p1579 N71-21301
- Plastic deformation effects on alpha to gamma conversion phase and element distribution in iron nickel alloys
[NLL-TRANS-746-510-19022.401/] 10 p1582 N71-21497
- Austenite formation and dendritic liquefaction of silicon, nickel, copper, and molybdenum in low carbon iron alloys
[NLL-TRANS-746-510-19022.401/] 10 p1582 N71-21497
- Metallurgical and magnetic properties of industrial nickel iron alloys
[NLL-TRANS-2654-19022.81/] 10 p1582 N71-21499
- Anisotropy and crystal structure of Ni-Fe alloy thin films, and Lorentz microscopic study of magnetic microstructure
11 p1615 N71-21948
- Composition and atomic ordering effects in Fe-Co alloy systems using Mossbauer spectroscopy and measurement of effective magnetic field at Fe nuclei, isomer shift, and quadrupole splitting
11 p1780 N71-22794
- Magnetic coupling in composite ferromagnetic structures consisting of two permalloy films [81.7 percent Ni and 18.3 percent Fe] with thin separation layer of chromium and/or gold
11 p0009 N71-23014
- Magnetic properties of electrodeposited films of iron-nickel-molybdenum ternary alloys with uniaxial anisotropic permeability
[AD-719611] 13 p2091 N71-24352
- Changes in dislocation density in surface layers of high strength cast iron with ferritic and pearlitic structure by action of dry and lubricated friction
[AD-719793] 13 p2093 N71-24878
- Kondo state as function of magnetic field and temperature in Co-Fe alloys
[AD-719862] 13 p2126 N71-25151
- Production of oxidation resistant aluminumized iron and nickel sherry coatings for heat resistant alloys
[NASA-TN-D-6329] 13 p2097 N71-25446
- Phase diagrams of metastable face centered cubic iron rhodium alloys
[CALT-822-23] 13 p2098 N71-25514
- Low temperature measurements on electrical resistivity, magnetic susceptibility and magnetoresistivity for amorphous iron palladium silicon alloys
[CALT-822-24] 13 p2098 N71-25515
- Magnetotriboelectric properties in ordered iron alloys containing cobalt or platinum
[TT-70-5969] 14 p2267 N71-25642
- Temperature and magnetic effects on self diffusion coefficients of iron in gamma-phase iron manganese alloys
[TT-70-57056] 14 p2268 N71-25648
- Changes in elasticity, magnetotriboelectric, and electric resistance of iron-aluminum alloys during ordering
[DMDC-5793] 14 p2271 N71-25692
- Perturbed angular correlation measurements of Os-192 and Pt-192 excited state magnetic moments and NMR internal field measurements of Os-187 in Fe and Ni alloys
[COO-1746-53] 14 p2272 N71-25734
- Antineutron intergranular structure effect on self diffusion of iron
[TT-70-57068] 14 p2271 N71-25816
- Carbon effect on iron self diffusion in iron nickel system
[TT-70-57055] 14 p2272 N71-25821
- Influence of aluminum on friction and wear of iron-aluminum alloys dry and lubricated in argon atmosphere
[NASA-TN-D-6359] 14 p2261 N71-26045
- Transformation plasticity of iron-nickel during martensite reaction under constant load
14 p2276 N71-26725
- Anodic polarization of iron and iron alloys and adsorption of reagents on AISI 4340 steel foil
15 p2424 N71-27427
- Magneto-optic rotation in thin semitransparent nickel iron film due to antireflection coating of zinc sulfide
[AD-721358] 16 p2638 N71-28065
- Nickel content, plastic deformation, and stacking fault effects on martensitic formation in iron chromium nickel alloys at cryogenic temperatures
[NLL-RTS-6189] 16 p2613 N71-28086
- Closed Fermi surfaces in Ni₃Al order-disorder transformations when alloyed with Ni₃Fe and Ni₃Co
[NLL-LT-746-638-19022.401/] 16 p2614 N71-28092
- Phase microanalyses on quench hardened iron manganese alloy structures
[NLL-RTS-6321] 17 p2767 N71-30351
- Volume and grain boundary diffusion coefficient measurements of Fe-Cr alloys, alpha gamma phase transformations, and effects of carbon impurities
[CEA-R-4023] 18 p2962 N71-30902
- Sliding properties of iron-base metallic powder lubricants impregnated with intermetallic alloys
18 p2928 N71-30911
- Hydrogen solubility in liquid iron-cobalt-nickel alloys including free energy and enthalpy increments
18 p2936 N71-31151
- Phosphorus solubility and diffusion in iron and iron alloys below 1000 C
18 p2937 N71-31317
- Laves phases in iron binary systems with transition elements and dispersed precipitates
[UCRL-30361] 18 p2937 N71-31396
- Development of low cost iron base alloy with corrosion resistance to hot sea water
[PB-19642] 19 p3109 N71-31673
- Development of iron-aluminum alloy with maximum sea water corrosion resistance and minimum aluminum content
[PB-19641] 19 p3110 N71-31770
- Hypertense magnetic interactions in Fe-Oa solid solutions analyzed by Mossbauer spectroscopy
[CALT-822-27] 19 p3109 N71-32218
- Low temperature effects on electrical resistivity of copper aluminum alloys with trace amounts of iron
19 p3115 N71-32376
- Mossbauer study of BiF₃ type ordering in metastable iron alloys containing up to 25 percent gallium
[CALT-822-26] 19 p3171 N71-32776
- Diffusion coefficient of chromium in Fe-Cr alloys annealed at 1200 C determined by evaporation in vacuum
[TT-70-59105] 20 p3284 N71-33177
- Auger emission spectroscopy, low energy electron diffraction, sputtering studies, and adhesion and friction experiments on single crystals of Co-Si, Co-Al, and Fe-Al alloys
[NASA-TM-X-67900] 20 p3284 N71-33248
- Mechanism of diffusion of some elements in iron and steels - atomic transference and movement of disordered metal lattices
[TT-70-59107] 20 p3284 N71-33327
- Seebeck coefficients in metallic alloys using iron doped silver palladium alloys between 4.2 and 520 K
[NASA-CR-121384] 20 p3214 N71-33412
- Mechanical property tests of nickel, titanium, and iron alloys in 5000 psig gaseous helium and hydrogen at various temperatures
[NASA-CR-119884] 20 p3230 N71-33728
- Martensitic transformation occurring in copper-iron alloy during tensile testing with magnetic susceptibility measurement
[PB-197611] 21 p3430 N71-34407
- Compatibility of UC compounds and iron nickel chromium alloys, and nuclear fuel stabilizer effect
[EURFNR-620] 22 p3622 N71-35807
- Wear resistance of electrolytic iron-1 phosphorus alloys for use as coatings for machine parts
[AD-724441] 24 p3937 N71-38085
- IRON COMPOUNDS**
- NT CHROMITES
- NT CORMERITE
- NT FERRATES
- NT FERRITES
- NT FERROCENES
- NT HEMATITE
- NT IRON OXIDES
- NT LIMONITE
- NT MAGNETITE
- NT PYRITES
- Comparison of iron 57 Mossbauer spectra of iron containing compounds and coal
01 p0046 N71-16308
- Preparation and properties of iron phosphides
[AD-710697] 01 p0018 N71-10469
- Heat capacities of iron and nickel compounds
[AD-710814] 02 p0172 N71-11212
- Orientations of electric field gradient and susceptibility tensors determined in iron salts
[AD-711621] 02 p0283 N71-11456
- Synthesis of carbonyl-transition metal pi-complexes of nido C₂B₄H₆-2 and cyclo C₂B₃H₃-2/ fused iron iron pentacarbonyl and 2,3-dicarbonyl-bisphosphane 3
[AD-712540] 03 p0333 N71-12378
- Single crystal Mossbauer scattering of iron compounds
[AD-714573] 06 p0936 N71-16530
- Critical heat flux and pressure drop tests of electrically heated nuclear fuel rod bundles with ferrous hydroxide slurry crud deposits
[WAFD-TM-918] 09 p1421 N71-20368
- Interfacial behavior of corrosion inhibitors on iron surfaces
[AD-717030] 10 p1579 N71-21289
- Shock tube decomposition of iron pentacarbonyl to yield vibrational relaxed carbon
[AD-717742] 11 p1695 N71-22171
- Gamma-phase monitoring to determine stability of austenite formed in surface layers during friction of high strength cast iron
[AD-728762] 14 p2276 N71-26661
- Mossbauer spectroscopic studies of iron Y zeolite and preparation of oxidation catalysts
[AD-721326] 16 p2555 N71-28177
- Electrochemistry of nickel, copper, cobalt, and iron-sulfide anodes
18 p2885 N71-30912
- High pressure effects on quadrupole interactions in K₂FeP₆, Na₂FeP₆, NH₄FeP₆, and FeP₂
18 p2885 N71-31035
- Chemical and X ray analysis of ferroplatinum from Norilsk deposits
[NASA-TT-F-13964] 23 p3768 N71-30857
- Microdetermination of Fe(III) by spectrophotometric examination of complexes prepared from several chelating agents
[NLL-CE-TRANS-5430-19022.09] 23 p3775 N71-36905
- Calculation of free energy of formation and thermodynamic properties of Fe₂P₂ over temperature range 792 to 1106 K from emf measurements
[LA-4638] 24 p4030 N71-38753
- IRON ISOTOPES**
- NT IRON 57
- NT IRON 59
- Neutron elastic and inelastic scattering cross sections for Fe-56 in energy range 4.19 to 8.56 MeV
[ORNL-4515] 03 p425 N71-12832
- Gamma ray energy measurements of transitions from first and second excited levels of Fe-58
[CONF-690818-7] 04 p0577 N71-13799
- Threshold photoelectron cross sections for nuclei of Mg, Cr, Fe, and Pb isotopes
[UCRL-50902] 06 p0921 N71-16397
- Deuterons accelerated to 28 MeV for investigating iron-54, alpha/ reaction
[LYCEN-7074] 14 p2308 N71-26423
- Orientations measurements of residual stresses and differential interaction cross sections in Fe-56 (d,p) Fe-57 reaction
[NP-18439] 15 p2462 N71-27171
- Two-nucleon transfer reactions Fe-54(d, alpha)Mn-52 and V-51(d, alpha)Ti-49 produced by 28 MeV deuterons
[LYCEN-7087] 23 p3806 N71-37137
- IRON METEORITES**
- NT SIKHOTHE-ALIN METEORITE
- IRON ORES**
- NT HEMATITE
- Magnetic survey of iron deposits in Tanzania
[BULL-120] 05 p0671 N71-14844
- Pulsed ultrasonic seismology for determining rock properties in iron ore mine
[NASA-TT-F-13656] 16 p2589 N71-28856
- IRON OXIDES**
- NT CHROMITES
- NT HEMATITE
- NT MAGNETITE
- Formation of silver-iron oxide from iron hydroxide and silver hydroxide in alkaline solution
[RAE-LIB-TRANS-1506] 04 p0332 N71-14269
- Neutron diffraction study of gamma-FeOOH, position of ions, magnetic permeability, and Mossbauer effect
[PB-193217] 04 p0591 N71-14387
- Shock tube experiments to determine infrared band intensities of iron and aluminum oxides
[AD-716693] 09 p1342 N71-19543
- Equilibria, reactions, and sintering in ternary system containing iron oxide
16 p2609 N71-28323
- Calorimetric determinations of thermodynamic properties of (Na₂O/4-Fe₂O₃) up to 1200 K
[BM-R1-7535] 19 p3051 N71-32643
- Nickel and iron oxide film structure and semiconductor properties
p3308 N71-34936
- Radioisotope procedure for investigating chloride ion adsorption of alpha iron III oxide in sodium chloride
[AD-726412] 22 p3594 N71-33596
- Thermodynamic properties of FeO, CoO and NiO in sodium chloride over temperature range from 700 to 1100 C
23 p3781 N71-36845
- IRON 57**
- Comparison of iron 57 Mossbauer spectra of iron containing compounds and coal
01 p0046 N71-16308
- Monochromatic polarized Fe-57 Mossbauer source
[AD-711630] 02 p0271 N71-11463
- Mossbauer analysis of iron 57 relaxation effects in thin radioactive iron film
[COO-623-164] 06 p1244 N71-18916
- Hypertense structure of antiferromagnetic FeO₃ using 14.4 keV Mossbauer transition in Fe-57
15 p2306 N71-27422
- IRON 59**
- Relationship of cesium-137 and iron-59 elimination rates to metabolic rates of small rodents
[ORNL-4568] 03 p0333 N71-12311

Temperature effects on iron diffusion in iron manganese alloys
[TT-70-57041] 03 p0391 N71-12829

Decay schemes of Fe-59 and Ir-192
[ORNL-TM-2343] 10 p1616 N71-21182

IROQUOIS HELICOPTER

U. IRI-1 HELICOPTER

IRRADIATION

NT ILLUMINANCE

NT SOLAR CONSTANT

Statistical extrapolation of spectral irradiance measurements of large solar simulators
[NASA-TN-D-6094] 02 p0224 N71-11526

IRRADIATION

NT AURORAL IRRADIATION

NT DEUTERON IRRADIATION

NT ELECTRON IRRADIATION

NT ION IRRADIATION

NT NEUTRON IRRADIATION

NT PROTON IRRADIATION

NT X RAY IRRADIATION

Irradiation testing of 37-pin, EBR 2 instrumented subassembly
[BNWL-1424] 01 p0085 N71-10420

Fast neutron irradiation effects on reactor grade thermocouple performance
[BNWL-1365] 02 p0265 N71-11740

Effects of helium on high temperature ductility of Sandvik 12R2HV and Inco IN-744X
[AI-AEC-12960] 02 p0244 N71-12111

Thermal conductivity test facility for irradiated solids
[CEA-N-1303] 04 p0620 N71-13750

Postirradiation examination of Peach Bottom reflector element B16-01 after exposure to 300 effective full power days
[GAMD-9911] 04 p0551 N71-13963

Experiment description for UO₂-PuO₂ mixed oxides fuel irradiations in General Electric test reactor
[BNWL-1382] 04 p0553 N71-14000

Irradiation testing of UO₂ fuel pins for medium power reactor experiment
[ORNL-TM-2859] 04 p0554 N71-14013

Hot microhardness values for irradiated and nonirradiated refractory metals and alloys
[GEMP-716] 04 p0560 N71-14359

Swimming pool reactor for irradiating nuclear power station structural materials in high neutron flux
[CEA-R-3984] 05 p0722 N71-14560

Nuclear fuel behavior during irradiation by fission gas release
[ORNL-4601] 05 p0723 N71-14674

Fast test reactor irradiation program
[BNWL-1461] 05 p0725 N71-15042

Poisoning 210 alpha particles used to irradiate helium-nitrogen gas mixtures by excited light source technique
[RPI-3816-4] 05 p0749 N71-15288

International comparison of Mn-56 activity in 1968 including nuclear reactor irradiations and neutron-source calibration
[ANL-7642] 06 p0915 N71-16001

Progress report on Saxton plutonium project including data reduction on core post-irradiated data, isotopic data, and related subjects
[WCAP-3355-24] 06 p0898 N71-16279

Irradiation strengthening of bcc metals and solid solutions - annealing mechanisms in vanadium
[ORSO-3612-7] 06 p0785 N71-16717

Computer program /PROFIS/ to evaluate fission product concentrations in fuel irradiated under variable conditions
[CEA-R-3987] 07 p1066 N71-18143

Electron spin resonance studies on irradiated heterogeneous systems - structure and reactivity of paramagnetic centers in silica gel
[NP-18478] 08 p1235 N71-18209

Uniaxial and biaxial creep rupture of type 316 stainless steel after fast reactor irradiation
[BNWL-SA-3295] 08 p1212 N71-18311

Irradiation induced swelling and creep in fast reactor materials - conference
[BNWL-SA-3283] 08 p1238 N71-18344

Chemical and biological antiradiation drugs for space flight
08 p1153 N71-19054

Dosimetry of large radiation sources by optical changes in polymethyl methacrylate and evaluation as irradiation technique
[JAERI-MEMO-4121] 09 p1443 N71-20454

Analyzing variations in deformation processes of construction materials after reactor irradiation
[SRAPI-R-85] 10 p1588 N71-21000

Mechanical properties data for LMFBFR reactor materials, and irradiation effects on cladding and structural alloys
10 p1602 N71-21084

Irradiation of SM-1A power reactor pressure vessel surveillance capsules
[AD-717618] 11 p1793 N71-21918

Operating conditions and safety of series I ORNL oxide fuels irradiation in EBR-2, target burnup level extended from 5 percent FIMA to 10.5 percent FIMA
[ORNL-TM-2635-SUPPL.] 11 p1794 N71-22424

Solar sensor with coarse and fine sensing elements for matching preirradiated cells on degradation rates
[NASA-CASE-XLA-01584] 12 p1917 N71-23269

Microwave technology with application to solid state physics, electron paramagnetic resonance, and gamma irradiation
[AD-718796] 12 p1986 N71-23820

Evaluation of Zircaloy clad fuel rods to determine geometrical and environmental variable effects on post irradiation dimensional changes
[WAPD-TM-966] 12 p1964 N71-24153

Measurement of Li-6 diffusion from irradiated beryllium oxide
[JUL-677-RG] 13 p2128 N71-24474

Apparatus for obtaining data on compressive creep of ceramic nuclear fuels during irradiation
13 p2112 N71-24513

Reactor irradiation of thermionic sheath insulators - two beryllia and two alumina bonded trilayers
[NASA-TM-X-2271] 13 p2116 N71-24635

Least squares method for describing irradiated fuel sheath distortion
[AECL-3688] 13 p2117 N71-24853

Quasi-stable elementary particles in aluminum and tungsten targets irradiated by 70 GeV protons
[JINR-P1-5399] 13 p2132 N71-25044

Zircaloy sheathed elements containing UO₂ pellets with axial void 1/4 vol. percent irradiated in series of tests in X-2 loop of NRX
[AECL-3732] 13 p2119 N71-25130

Computer program for calculating concentration of fission products - HERETRA
[DEMO-70/10] 13 p2135 N71-25182

Electron microprobe analysis of metallic fission product inclusions in irradiated mixed-oxide fuels for molybdenum
[WHAN-SA-96] 13 p2120 N71-25218

Manufacturing tests of tritiated titanium targets to obtain optimal procedure for their use and preparation under deuteron irradiation
[EUR-4286-PT-2] 13 p2138 N71-25450

Influence of titanium, zirconium, and hafnium additions on resistance of modified Hastelloy N to irradiation damage at high temperatures
[ORNL-TM-3064] 14 p2267 N71-25640

Effect of crystallite size, crystallite orientation, and density on dimensional and property changes in irradiated graphites and isotropic materials
[GA-10433] 14 p2277 N71-25680

Yields of fission product nuclides in irradiated uranium and plutonium calculated for fast and thermal fission and expressed as atoms per 100 atoms of U-235 or Pu-239
[ANL-7678] 14 p2301 N71-25742

EPR and ENDOR study of free radicals produced by gamma irradiation of imidazole single crystals
[CEA-R-3758] 14 p2307 N71-26395

Normalized procedures for standardizing and determining spectral sensitivities of detectors for measuring external irradiation by electromagnetic radiation
[CEA-R-4009/1] 14 p2328 N71-26569

Safety considerations for irradiation of FR-2 reactor fuel capsules of UC-Pu using NaK as heat transfer medium
[EURFNR-764] 15 p2443 N71-26853

Radiation embrittlement of age hardening heat resistant steels following high temperature reactor irradiation
[AEC-TR-7192] 15 p2419 N71-26907

Irradiation of boron carbide pellets and powders in Hanford thermal production reactors at 500 to 1200 °F
[WHAN-FR-24] 15 p2443 N71-26927

Intergranular pore density determination in PUO₂-UO₂ fuel pin irradiation in EBR-2
[WHAN-SA-15] 15 p2443 N71-26928

Electron paramagnetic studies of gamma irradiated alkali-germanate glasses and crystalline compounds
15 p2507 N71-27571

Melting characteristics of low density mixed oxide U/PuO₂ at beginning of irradiation, with in-pile distribution of fission oxide
[CEA-CONF-1659] 15 p2450 N71-27591

Accidental external irradiation and accidental radioactive contamination - rules and therapeutic procedures
[CEA-N-1365] 15 p2481 N71-27692

Effect of irradiation in water at 70 °C on mechanical properties of fcc alloys of Fe-Cr-Ni system
[SRAPI-R-78] 15 p2436 N71-27760

Electron paramagnetic resonance of IO₂/minius radical in gamma irradiated single crystals of KIO₂F₂ at room temperature
[COO-1385-34] 15 p2486 N71-27822

Angular distributions and excitation functions of pick up reactions with neutrons measured by bombarding nuclei with N-14 and 15 ions
[JINR-P7-5494] 16 p2643 N71-28079

Analysis of JMTR neutron flux change and variations effects in irradiation holes
[JAERI-4130] 16 p2645 N71-28114

Metallographic preparation of LMFBFR prototype fuels
[WHAN-SA-14] 16 p2632 N71-28640

Boiling water reactor fuel test assembly irradiation
[HPR-132] 16 p2633 N71-28697

Safety factors for NaK capsule experiments on irradiation of high-conductivity fuel elements
[KFK-1143] 16 p2633 N71-28696

Transformation kinetics of U-5 wt percent Fe alloy irradiated driver fuel pins
[ANL-EBR-32] 16 p2635 N71-28796

Development of method for measuring thermal diffusivity of reactor fuels during irradiation based on time dependent heat diffusion equation
[ORNL-4478] 17 p2856 N71-29246

HYLAS code for predicting heavy element composition of irradiated reactor fuels
[RD/RN-1722] 17 p2785 N71-30142

Production of carrier-free radioisotopes Sr-85 by irradiation in U-120 cyclotron
[UJV-3431-CH] 18 p2970 N71-30462

Uranium carbonitrides as high efficiency fuel - preparation and irradiation properties
[JUL-703-RU] 18 p2959 N71-30528

Phase transformation of hyperstoichiometric uranium carbide irradiated at high temperatures
[AECL-3679] 18 p2975 N71-30572

Express extraction and universal precipitation methods for radiochemical determination of Pa, Am, Cm, Cf, Bk, and fission products in irradiated materials
[SRAPI-R-81] 18 p2976 N71-30575

Effects of irradiation induced metal growth on core components for LMFBFR design
[BAW-1355] 19 p1335 N71-31820

Proton hole states excited in thin foils by monoenergetic gamma-quanta from Li-7p, gamma/Be-8 reaction
[LUNP-7013] 19 p3154 N71-32333

Immersion calorimeter for measuring Wigner energy in irradiated BeO, MgO, Al₂O₃, and SiO₂ at high temperatures
[CEA-N-1171] 19 p3156 N71-32420

Irradiation curing process for producing pyrolytic carbon - flares
[AD-724652] 20 p3287 N71-33194

Irradiated cobalt and tantalum tracers measured by activation analysis in river and sea arm sediment transport studies
[IRI-133-70-06] 20 p3316 N71-33489

Calculations of ionization-excitation source rates in gaseous media irradiated by fission fragments and alpha particles
20 p3307 N71-33667

X ray diffraction analysis of amorphous samples of Pd-Si alloy irradiated with fast neutrons or fission fragments
[CEA-CONF-1693] 21 p3438 N71-34442

Bibliography on irradiation behavior of plastics
[JUL-BIBL-15] 21 p3443 N71-34499

Irradiation of nuclear graphite and model carbons
[GA-10533] 21 p3444 N71-34506

Formation of fission gas bubbles in solids during reactor irradiation
[AERE-R-6595] 21 p3467 N71-34679

Irradiation yield curves and angular distributions for Li-6-C-12 reaction
21 p3491 N71-34849

Computer code for predicting and analyzing irradiation performance of stainless steel clad [U,Pu]O₂ fuel pins
[ORNL-TM-3366] 22 p3625 N71-35828

Analysis of emission spectra of metal vapors obtained by laser irradiation
[NASA-TT-F-13967] 23 p3765 N71-36841

Electrical resistivity of polyvinyl chloride measured as function of temperature before and after irradiation
[AD-726927] 23 p3778 N71-36928

Irradiation experiment for testing spherical fuel elements for high temperature reactors
[JUL-701-RW] 23 p3795 N71-37056

Materials irradiation tests in support of fast test reactor driver fuel development program
[HEDL-SA-81] 23 p3799 N71-37066

Magnetic analysis of Li-7 bombarded with 15 MeV He-3 atoms
[ANU-P-520] 23 p3809 N71-37140

Capsule rig for temperature control and irradiation of structural material in SM-2 reactor
[LBJ-G-3025] 24 p3957 N71-38226

Determining neutron properties of loops containing fuel assemblies and of positions for irradiating structural materials in MX reactor
[LBJ-G-3010] 24 p3957 N71-38227

Capsule rig for irradiation of structural materials in SM-2 reactor with temperature control by variation of gas-gap size
[LBJ-G-3013] 24 p3957 N71-38229

Analysis of swelling data for stainless steel based on Lindhard theory of energy partition with application to reactor design
[HEDL-SA-159] 24 p3962 N71-38229

Natural convection irradiation device, Esther, for fast reactor fuels
[EURFNR-890] 24 p3962 N71-38350

IRREGULARITIES

Isotopic irregularity characteristics from Explorer 22 Faraday findings of 40 MHz transmissions
[RSD-533] 09 p1384 N71-20967

SUBJECT INDEX

Film dimension defects in relation to image horizontal stability and geometric parameters of 35 mm movie picture film
(AD-77252) 24 p3925 N71-38004

IRREVERSIBLE PROCESSES
Total analysis of processes influencing sound propagation and speed in two-phase media based on thermodynamics of irreversible processes
(NASA-TT-F-13582) 13 p2064 N71-24598
Simplified expressions of classical thermodynamics and irreversible processes
(NASA-TT-F-13649) 14 p2351 N71-25718

IRRIGATION
Evapotranspiration data for design capacity of irrigation systems by Soil Conservation Service
(13 p2072 N71-25005)
Irrigation and weather modification studies of Economic Research Service
(13 p2072 N71-25008)
Irrigation-oriented evapotranspiration models for Great Plains to aid farmers
(13 p2072 N71-25012)
Subirrigation systems or microwatersheds for soil water evaporation prevention
(13 p2073 N71-25017)

IRRITATION
NT TOXICITY AND SAFETY HAZARD

IRROTATIONAL FLOW
U POTENTIAL FLOW

ISCHEMIA
Ischemic deafferentation of striated muscle tissue
(08 p1153 N71-19058)

ISENTROPIC PROCESSES
Isentropic-compression tube techniques producing hypersonic flow in wind tunnels including isentropic flow and free-piston shock tube modes
(AD-71727) 11 p1731 N71-22158
Sound propagation velocity in nonstationary symmetrical rarefaction gas flow
(NASA-TT-F-13571) 17 p2736 N71-30137
Differential heating effects on steady-state tropical cyclone dynamics and energetics based on diagnostic axisymmetric model in isentropic coordinates
(24 p3954 N71-38209)

ISING MODEL
U FERROMAGNETISM
U MATHEMATICAL MODELS

ISIS SATELLITES
NT ALOUETTE 2 SATELLITE
NT ISIS-B
Orbital expansion thrust effect on shape of ISIS satellite boom
(JCR-TN-632) 05 p0771 N71-15160

ISIS-B
Objectives of ISIS-B including measurement of fluctuations in upper atmosphere electron density, radio and cosmic emission studies, and measurements of ionospheric energetic particles
(NASA-NEWS-RELEASE-71-41) 11 p1827 N71-22537

ISLANDS
NT GREAT BRITAIN
NT GREENLAND
NT ICELAND
NT JAPAN
NT NEW ZEALAND
NT PACIFIC ISLANDS
NT PHILIPPINES
NT PUERTO RICO
NT TASMANIA
NT WALLPOPS ISLAND
NT WEST INDIES

ISOBARS (PRESSURE)
Stratospheric meteorological charts of daily constant pressure level heights and temperatures from navigational-rocketsonde data and polar, middle, and tropical circulation for 1970
(JCR-PT-3) 12 p1958 N71-24104

ISOBUTYLENE
U BUTENES

ISOBORIC PROCESSES
Visualization of supersonic rarefied free jet flow using electron beam scanning
(REF-70-10) 08 p1177 N71-18400

ISOTHERMALS
Statistical analysis of structure of color vision tests for standardization of test methods and procedures
(REF-1970-17) 05 p0733 N71-15085
Symmetrical isochromal magnetic optical systems, using four dimensional matrices
(JCR-OP-69-48) 09 p1425 N71-20314

ISOTANATES
Cyclization of ortho-isocyanobiphenyl and derivatives with insertion of isocyanocarbon to form cyclophosphides
(NASA-CR-123190) 24 p3884 N71-37686

ISOLATION
NT SOCIAL ISOLATION

ISOLATORS
NT VIBRATION
NT VIBRATION ISOLATORS
Infrared isolator using yttrium iron garnet, Faraday isolator, and calcite dichroic polarizers
(AD-716468) 09 p1396 N71-19822

Internal labyrinth and shield structure to improve electrical isolation of propellant feed source from ion thruster
(NASA-CASE-LEW-10210-1) 14 p2333 N71-26781
High-voltage isolator design for injecting hydrogen bubbles into liquid metal feed lines to interrupt electrical continuity
(NASA-CASE-NPO-11073) 21 p3402 N71-34208
Nonreciprocal devices using solid state magnetoplasmas at millimeter and submillimeter wavelengths
(NASA-CR-123293) 23 p3825 N71-37285

ISOMERIZATION
NT ORTHO PARA CONVERSION
Significance of stereoisomerism in organic structures and relationship to determination of origin of earth life
(NASA-TT-F-13677) 16 p2548 N71-28970
Cyclization of ortho-isocyanobiphenyl and derivatives with insertion of isocyanocarbon to form cyclophosphides
(NASA-CR-123190) 24 p3884 N71-37686

ISOMERS
Properties of spontaneously fissioning isomer Pu-241 in gamma-neutron reaction
(JINR-E15-5071) 02 p0278 N71-12137
Isolation and characterization of two isomers of pentaborane B₅H₈/2
(AD-712549) 03 p0333 N71-12379
Spontaneous fission isomerism in uranium isotopes
(RLO-1388-114) 03 p0426 N71-12848
Research in nuclear chemistry including isomer ratios in charged particle induced fission
(RLO-2060-8) 03 p0427 N71-12858
Using Raman effect to give fast and definite identification for isomeric structures of cyanate
(NASA-TT-F-13636) 12 p1975 N71-24079
Calculation of isomer ratios following multiple particle nuclear emissions using compound nuclear statistical model
(13 p2144 N71-25585)
Possibility of forming Np-238 fission isomer by bombarding Np-237 target with 500 keV neutrons
(CEA-N-1339) 14 p2317 N71-26752
Quasi-particle state of ¹⁹⁷2/2⁺ isomeric state in Po-202
(JINR-P6-5379) 15 p2483 N71-27752
Excitation cross section measurement of Ge-71, Br-78 and Br-79 isomeric states using 14.8 MeV neutrons
(JINR-P-1091) 15 p2485 N71-27803
Nuclear processes activated by isomeric transition of Br-82m and I-130m
(COO-1617-27) 15 p2488 N71-27876
Isomeric β -minus/ α or β -plus/ α transition in Ba-130 nucleus, and model of transition nuclei
(JINR-E4-5607) 18 p2982 N71-30900
Rk-110 isomer, 28 sec half life, from n,p reaction of enriched Pd-110
(JORNLT-TR-2405) 20 p3319 N71-33614
Stereospecific sorption technique for separating optical isomers of aspartic acid using glutamic acid
(UCRL-20471) 21 p3388 N71-34101
Excitation functions for deuteron-induced reactions in gold using statistical model
(LYCEN-7092) 22 p3634 N71-35898
Production of spontaneously fissionable isomer U-236 by radiative thermal neutron capture
(JINR-P7-5497) 22 p3639 N71-35943
Crystallographic positions and isomer shifts of iron in boron determined by Mossbauer spectroscopy
(UIUP-733) 22 p3640 N71-35946
Half lives and gamma transitions in decay of Th-148, Th-149, Th-150, and Th-152 isomers
(JINR-P6-5681) 24 p3972 N71-38333
Three quasiparticle excitations in Al-205
(JINR-E6-5802) 24 p3976 N71-38365

ISOMORPHISM
Topological depth of coherent analytical bundle in Stein space
(24 p3949 N71-38173)

ISOPHOTES
Coronal isophotes of solar eclipse on July 20, 1963
(03 p0451 N71-13173)
Two-dimensional isophotes of outer solar corona derived from integrated vidicon pictures taken from lunar surface by Surveyors 6 and 7
(NASA-CR-118994) 16 p2674 N71-28125

ISOPLETHS
U NEMOGRAPHS

ISOSTASY
Topographic-isostatic gravity corrections for New Zealand
(BULL-203) 09 p1378 N71-19406

ISOSTATIC PRESSURE
Hot isostatic compaction at 3000 F and 30,000 psi used for successfully preparing single phase bulk graphite for ablation testing
(SC-CR-70-6169) 17 p2768 N71-29219
Isostatic pressure vessel failure and stress analysis of thread cracks
(Y-1758) 21 p3527 N71-35135

ISOTENSOID STRUCTURES
Method for arranging filamentary, load bearing material to approximate stress condition in gas en-

ISOTOPE EFFECT

velope of free floating balloon for maximizing structural efficiency
(AD-713188) 05 p0630 N71-14811

ISOTHERMAL FLOW
Energy spectrum in isothermal turbulent shear flow at large wave numbers
(AD-714856) 07 p0111 N71-17743
Numerical solution of Navier-Stokes equations for viscous supersonic flows adjacent to isothermal and adiabatic surfaces
(09 p1374 N71-19839)
Physical properties and rotational effects on isothermal compressible flow across shaft seals
(NASA-TM-X-52991) 12 p1998 N71-23102
Isothermal corrosion tests on Inconel 600 and nickel alloy sheets by superheated steam
(NLL-RISLEY-TRANS-2093-P001.9F) 19 p3118 N71-32656

ISOTHERMAL LAYERS
Thermal structure of night-time surface inversion at Yokohama
(NLL-M-20020-582L49F) 12 p1958 N71-34114
Double-wall isothermal cylinder containing heat transfer fluid thermal reservoir as spacecraft insulation cover
(NASA-CASE-MFS-20355) 13 p2186 N71-25533

ISOTHERMAL PROCESSES
Oxidation resistance determined for cobalt and nickel based alloys by isothermal and cyclic tests in static furnace air
(NASA-TM-X-2195) 09 p1399 N71-19815
Chapman-Eyring theory used to determine nonequilibrium contribution to reaction rate of isothermal multicomponent system
(HUX-3780-31) 09 p1345 N71-20588
Laboratory and reactor tests for establishing specimen temperatures in irradiation experiments by using inert gas-filled heat pipes
(13 p2079 N71-24514)
Phase transformation of TA 6V titanium alloy by isothermal processes
(RAE-LIB-TRANS-1549) 13 p2095 N71-23077
Isothermal and adiabatic compressibility of liquid metals, particularly lead, from melting point to critical region
(INVO-4176-4) 15 p2425 N71-27482
Isothermal free diffusion in liquids - calibration and testing of precision bench optical diffusimeter, ternary systems calculations, and data for tetraethylammonium bromide-water system
(17 p2716 N71-30074)
Extension of surface energy exchange analysis to isothermal gas radiation in enclosures
(18 p3025 N71-30946)
Isothermal bubble motion under influence of varying high-g body forces, low gas flow rate isothermal bubble formation, and coefficients of drag for planetary ellipsoidal bubbles
(18 p2807 N71-31348)
Isothermal transformations of uranium-13 atomic percent niobium alloy in temperature range of 23 to 640 C
(RFP-1609) 21 p3440 N71-34478
Effectiveness factor calculation technique for nonisothermal catalyst taking into account mass and heat transfer effects at boundary film and in particle interiors
(NLL-RTS-64472) 23 p3722 N71-36527

ISOTHERMS
Lithium filled heat pipe for obtaining near isothermal conditions axially along cladding of in-pile fuel-irradiation capsule
(13 p2185 N71-24512)
Equilibrium sorption isotherms and diffusivities of gases flowing through polymeric membranes
(14 p2241 N71-26297)
Computer program for reduction of isothermal Burnett compressibility data
(BMA-IC-8491) 17 p2722 N71-29254
Isotherm visualization using Christensen effect for temperature measurement in porous media
(17 p2836 N71-29507)
Airborne sea surface temperature measurement over North Sea discussing isotherms
(BMVG-FBWT-71-7) 19 p3085 N71-31790

ISOTOPE EFFECT
Isotope effects in specific heat of solid neon
(NASA-CR-115877) 05 p0757 N71-14704
Studies in nuclear physics research, radiation research, isotope geochemistry, carbon 14 variations, and isotope applications
(NP-18408) 06 p1249 N71-18207
Nuclear charge structure effects on hyperfine structure, isotope shift, and magnetic octupole moments
(09 p1432 N71-19972)
Alpha-deuteron isotope effects on solvolysis rate of 2,2,2-trifluoroethyl sulfonate
(COO-1006-15) 16 p1620 N71-21732
Radioactive trace diffusion of Au₂ and FeCo species isotopes with measurement of correlation and isotope effects in crystal lattice defects
(AD-717757) 11 p1778 N71-22335

Odd-even staggering of nuclear radii in isotope shifts of atomic and mu-atomic spectra, calculated using pairing plus quadrupole model

15 p2468 N71-27343

Thermal steady state analyzers for predicting isotope heat source performances in Brayton thermodynamic cycle

[NASA-TM-X-67853] 15 p2525 N71-27864

Technology and economics of isotopic electricity generators

[CEA-BIB-190] 19 p3065 N71-32122

Hyperfine structure and isotope effect of 30 year bismuth 207 using Fabry-Perot interferometer and monochromator measurements

20 p3321 N71-33731

Single particle spectrum of O-17, O-16 and Ca-40 binding energies, and O and Ca isotope shifts for nucleon-nucleon interactions

[JINR-P4-5614] 22 p3631 N71-35873

Isotope effect for diffusion of interstitial atoms

[ANL-TRANS-882] 22 p3643 N71-35977

Radioactive age determination and isotopic composition analyses on rocks, meteorites, and lunar samples

[NASA-CR-111001] 01 p0016 N71-10304

Chemical calcium isotope separation from calcium compounds containing radioactive calcium 48

01 p0094 N71-10311

Orbital workshop for isotope production and separation

02 p0264 N71-11732

Constant key weight cascades for multicomponent isotope separation

[AECOP-330] 03 p0419 N71-12561

Nuclear chemistry research of high energy nuclear reactions including cross sections and reactions on separated isotopes of tellurium

[NYO-2897-41] 03 p0425 N71-12833

Investigating feasibility of using liquid metal vacuum distillation to separate Po-210 from bismuth

[DP-1222] 04 p0484 N71-13446

Constructing protective manipulators for automatic transfer of isotopes from reactor cores

[CEA-N-1265] 04 p0574 N71-13674

Investigating contaminations caused by ion scattering on residual gas and by chromatism in electromagnetic isotope separators

[CEA-R-4043] 04 p0574 N71-13675

Investigating ion collisions using isotope separator with two magnetic stages and one electrostatic stage

[CEA-CONF-1571] 04 p0576 N71-13699

Reducing ion beam scattering in collector tanks of isotope separators by using stabilizing devices

[CEA-R-3999] 04 p0576 N71-13700

Chemical recovery and refinement procedures in electromagnetic separation of isotopes

[ORNL-4583] 04 p0584 N71-14186

Investigating isotope separation of U-233 from U-235 based on difference in stability of oxide and carbide kernels

[GA-9888] 04 p0590 N71-14377

Isotope separation and fabrication

[ORNL-TM-3009] 04 p0593 N71-14420

Developing technique for isolating and purifying Mo-99 from fission products obtained from uranium dioxide irradiated with thermal neutrons

[CNEA-267] 05 p0738 N71-15007

Investigating nuclear reactions of radionuclides, thermal neutron capture cross sections, solvent extraction, and application of radioisotopes

[NYO-3417-12] 05 p0738 N71-15009

Using lead slowing down spectrometer for nuclear materials assay work and isotope discrimination

[BNL-50232] 05 p0740 N71-15086

Isotope splitting of F center in-gap mode in KI and KBr

[NYO-2391-115] 05 p0750 N71-15357

Remote control device for positioning isotope separator collector electrodes and controlling ion beam shape and intensity

[CEA-N-1323] 06 p1199 N71-18378

Reporting research progress on mass spectroscopy, neutron diffraction and activation analysis, isotope separation, and reactor physics

[SRR-29/69] 06 p1199 N71-18844

Technologies involving metal corrosion in fluorinating gases in isotope separation plants

[NLL-CA-232-9091.9F7] 11 p1780 N71-22595

Conference on design and development of gas centrifuges, and Navier Stokes equations in calculating incompressible flow in centrifuges

13 p2066 N71-24870

ISOLDE type isotope separator with four electrode system for ion beam formation

[JINR-P13-5369] 13 p2132 N71-25108

Plasmatron ion source for Seiberdorf electromagnetic isotope separator

[SGAE-PB-101/1970] 14 p2303 N71-26048

Determination of zirconium and hafnium in meteorites and terrestrial materials by activation analysis and chemical separation after neutron irradiation

14 p2338 N71-26351

Isotopic enrichment by electromigration in aqueous solutions of transition metal halides

[UCRL-51003] 17 p2799 N71-30016

Flow characteristics of adsorbable gases in porous bodies and isotopic separation by gaseous diffusion

[NP-18567] 18 p2904 N71-30420

Determination of uranium-232 and plutonium-236 in irradiated nuclear fuel

[KFK-1128] 18 p2957 N71-30460

Production of carrier-free radiostrontium Sr-85 by irradiation in U-120 cyclotron

[UJV-2431-CH] 18 p2970 N71-30462

Bibliography on isotope separation by ion exchange from 1938 to 1970

[AAEC/LIB/BIB-273] 18 p2974 N71-30550

Beta detection efficiency curve for some radionuclides in different thickness sources obtained by specific radiochemical separations

[CISE-N-119] 18 p2976 N71-30624

Selected abstracts of world literature on production and industrial uses of radioisotopes

[ORNL-IC-30-PT-4] 18 p2990 N71-31545

Tungsten isotopes produced in compound nucleus reactions followed by neutron evaporation and bombardment of Os and Ni ions

[JINR-P6-5618] 21 p3471 N71-34714

ISOTOPE SHIFT

U ISOTOPE EFFECT

ISOTOPES

NT ALUMINUM ISOTOPES

NT ALUMINUM 26

NT ALUMINUM 27

NT AMERICIUM

NT AMERICIUM ISOTOPES

NT AMERICIUM 241

NT ANTIMONY ISOTOPES

NT ARGON ISOTOPES

NT ARSENIC ISOTOPES

NT ASTATINE ISOTOPES

NT BARIUM ISOTOPES

NT BERKELIUM

NT BERYLLIUM ISOTOPES

NT BERYLLIUM 7

NT BERYLLIUM 9

NT BERYLLIUM 10

NT BISMUTH ISOTOPES

NT BORON ISOTOPES

NT BORON 10

NT BROMINE ISOTOPES

NT CADMIUM ISOTOPES

NT CALCIUM ISOTOPES

NT CALIFORNIUM

NT CALIFORNIUM ISOTOPES

NT CARBON ISOTOPES

NT CARBON 12

NT CARBON 13

NT CARBON 14

NT CERIUM ISOTOPES

NT CESIUM VAPOR

NT CESIUM 133

NT CESIUM 134

NT CESIUM 137

NT CESIUM 144

NT CHROMIUM ISOTOPES

NT COBALT ISOTOPES

NT COBALT 58

NT COBALT 60

NT COPPER ISOTOPES

NT CURIUM

NT CURIUM ISOTOPES

NT CURIUM 244

NT DEUTERIUM

NT DYSPROSIUM ISOTOPES

NT ERBIUM ISOTOPES

NT EUROPIUM ISOTOPES

NT GALLIUM ISOTOPES

NT GERMANIUM ISOTOPES

NT GOLD ISOTOPES

NT HAFNIUM ISOTOPES

NT HELIUM ISOTOPES

NT HOLMIUM ISOTOPES

NT HYDROGEN ISOTOPES

NT INDIUM ISOTOPES

NT IODINE ISOTOPES

NT IODINE 125

NT IRIIDIUM ISOTOPES

NT IRON ISOTOPES

NT IRON 57

NT IRON 59

NT KRYPTON ISOTOPES

NT KRYPTON 85

NT LANTHANUM ISOTOPES

NT LAWRENCIUM

NT LEAD ISOTOPES

NT LITHIUM ISOTOPES

NT LUTETIUM

NT LUTETIUM ISOTOPES

NT MAGNESIUM ISOTOPES

NT MANGANESE ISOTOPES

NT MERCURY ISOTOPES

NT NEODYMIUM ISOTOPES

NT NEON ISOTOPES

NT NEPTUNIUM

NT NEPTUNIUM ISOTOPES

NT NICKEL ISOTOPES

NT NIOBIUM ISOTOPES

NT NITROGEN ISOTOPES

NT NITROGEN 15

NT NITROGEN 16

NT NOBELIUM

NT OSMIUM ISOTOPES

NT OXYGEN ISOTOPES

NT OXYGEN 18

NT PHOSPHORUS 32

NT PLATINIUM ISOTOPES

NT PLUTONIUM

NT PLUTONIUM ISOTOPES

NT PLUTONIUM 238

NT PLUTONIUM 239

NT PLUTONIUM 240

NT PLUTONIUM 241

NT POLONIUM ISOTOPES

NT POLONIUM 210

NT POTASSIUM ISOTOPES

NT PRASEODYMIUM ISOTOPES

NT PROMETHIUM ISOTOPES

NT PROTACTINIUM ISOTOPES

NT RADIOACTIVE ISOTOPES

NT RADIUM ISOTOPES

NT RADIUM 226

NT RADON ISOTOPES

NT RHODIUM ISOTOPES

NT RUBIDIUM ISOTOPES

NT RUBIDIUM 86

NT RUTHENIUM ISOTOPES

NT SAMARIUM ISOTOPES

NT SCANDIUM ISOTOPES

NT SILICON ISOTOPES

NT SILVER ISOTOPES

NT SODIUM ISOTOPES

NT STRONTIUM ISOTOPES

NT STRONTIUM 88

NT STRONTIUM 89

NT STRONTIUM 90

NT SULFUR ISOTOPES

NT TECHNETIUM ISOTOPES

NT TELLURIUM

NT TELLURIUM ISOTOPES

NT TERBIUM ISOTOPES

NT THALLIUM ISOTOPES

NT THORIUM ISOTOPES

NT THULIUM ISOTOPES

NT TIN ISOTOPES

NT TITANIUM ISOTOPES

NT TRANSURANIUM ELEMENTS

NT TRITIUM

NT TUNGSTEN ISOTOPES

NT URANIUM ISOTOPES

NT URANIUM 232

NT URANIUM 233

NT URANIUM 235

NT URANIUM 238

NT VANADIUM ISOTOPES

NT XENON ISOTOPES

NT XENON 133

NT XENON 135

NT YTTERBIUM ISOTOPES

NT YTTRIUM ISOTOPES

NT ZINC ISOTOPES

NT ZIRCONIUM ISOTOPES

Key word thesaurus for isotopes information system

[ORNL-IC-24-REV-1] 03 p0435 N71-13122

Isotope separation and fabrication

[ORNL-TM-3009] 04 p0593 N71-14420

Isotope development program

[BNWL-1308-3] 05 p0741 N71-15118

Resonance cross shielding in reactor analysis

[BNWL-1509] 07 p1071 N71-17260

Sensitivities of neutron activation analysis on short-lived metal isotopes

[CSIRO-TRANS-10089] 08 p1260 N71-16666

Neutron reactions in isotopes at energy range of 13 to 18 MeV

[JINR-1197] 08 p1263 N71-16880

Oxidation of refractory metals considered for isotope capsule structural members

[SC-DR-70-164] 08 p1220 N71-19031

Research and development of isotopic fuels

[BNWL-1308-4] 15 p2449 N71-27571

Index for retrieving information on Permeated Isotopes and Radiation Technology, Vol. 7

[ORNL-2C-31-VOL-8-1-7] 17 p2793 N71-29478

Values of stable abundances of 65 elements, and isotope ratios for 8 elements

[AD-723633] 19 p3178 N71-31775

Nuclear magnetic resonance in carbon-graphite intercalation compounds with spin-lattice relaxation times and lineshapes for C-13 and C-133 species

21 p3461 N71-34611

Pu-238 space electric power fuel investigations including fuel capability with capsule materials, radiation effects on fuels, and physical properties of fuels

[LA-4647] 15 p2449 N71-275

SUBJECT INDEX

makeup or recycle of isotopic compositions and related problems [JEA-P-13672] 23 p3647 N71-34007

Magnetic mass spectrometer with programmable magnetic field analyzer for measuring meteoric isotopic ratios 23 p3857 N71-37492

Viscosity and normal density measurements at lambda point intervals for pure helium-4 and helium-3 mixtures with helium-4 [NASA-TN-D-5516] 24 p3966 N71-38290

ISOTOPIC LABELING

Isotopic neodymium and samarium systems for geochronological dating 01 p0017 N71-10303

Tables of uranium thorium lead isotopic decay and growth functions for radioactive age determinations 01 p0093 N71-10306

Chemical and isotopic analyses of Apollo 12 lunar samples [NASA-TR-8-353] 04 p0610 N71-13742

Use of Ra/Ra ratios to determine air-sea gas exchange and vertical mixing in ocean [AD-713129] 05 p0668 N71-14783

Mass spectrometric analysis of oxygen diffusion in germanium dioxide with isotopic labeling 06 p0809 N71-15983

Using radiochemical methods for determining diffusion impurity profiles in silicon 07 p1072 N71-17290

Applying radioactive tracer techniques to detection of metal contaminants within components of propellant feed system [NASA-CR-116404] 07 p1072 N71-17341

Radioactive age determination by carbon 14, errors including isotopic effects and geomagnetism [CEA-CONF-1618] 08 p1185 N71-18219

Comparison of methods to assess geometrical variations of counting-rate in whole-body monitors [SRE-C-31469] 08 p1149 N71-18837

Remote deposition of radioactive iodine and lithium tracing elements from thunderstorm cloud [COO-119-119] 10 p1593 N71-20646

Comparison of mean drift and diffusion coefficient analyses of activity coefficient and vacancy flow effects on tracer diffusion in silver-gold alloys [ORO-2036-20] 11 p1779 N71-22482

Using xenon for isotopic labeling of instrumented fuel capsules in EBR-2 to detect element failure 13 p2111 N71-24506

Multiple window spectrometry for gallium 67 and its use in detecting malignant human and animal tumors [ORNL-TM-3260] 17 p2798 N71-30004

Application of radioisotopes to measuring current velocity, oxygen content, sediment density, and sediment composition in ocean environments 18 p2914 N71-31003

Applications of radiolabels in experimental biogeology to determine fertilizer turnover during growth of crops 20 p3224 N71-33506

Application of microbe sensors to problems of soil fertility 20 p3224 N71-33507

Use of N-15 as tracer to study decomposition of hydrazine on Shell 405 catalyst [RFE-TR-69/10] 20 p3230 N71-33873

ISOTOPIC SPLITTING

Isotopic spin splitting in zinc-64 resonance [IS-T-351] 01 p1002 N71-10935

Proposed CP and isospin violating interaction and symmetries of three triplet model [TR-71-103] 13 p2125 N71-24982

Isotopic spin analysis and current algebra kinematics of positive kaon decay modes from propane bubble chamber photographs of pion emissions 13 p2131 N71-25030

Study of high isospin states in several light self-conjugate nuclei by isospin forbidden radiative capture reactions 13 p2131 N71-25041

Lithium, beryllium, and boron particle production by spallation and isotopic spin classification of scattering cross sections 15 p2456 N71-26846

[R-18591]

Determination of Delta T equals 7/2 transition in beta decay into 3 pions [BVE-STR-70-14] 18 p2977 N71-30651

He-3 reaction and isobaric analog state in Ti, Fe, Ni, and Zn isotopes 22 p3649 N71-36021

ISOTOPIC MEDIA

Elastic-plastic analysis of open-end isotropic tubes under internal pressure [AD-712303] 02 p0299 N71-11126

Photoacoustic determination of mixed mode stress intensity factors [AD-712296] 02 p0303 N71-12098

Retention and structure of S wave pion cross section [CDD-1428-174] 03 p0427 N71-12855

Statistical isotropic deformation of elastic solid of composite materials [AD-712814] 03 p0467 N71-13385

Photon scattering in monoenergetic isotropic point source lattice medium [ORNL-TR-2349] 05 p0744 N71-15186

Minimum mass isotropic shells of revolution under uniform pressure and axial loads [NASA-TN-D-6121] 06 p0956 N71-16537

Isotropic elastic continuum model application to calculate energy and entropy of vacancy formation in metal crystals 08 p1281 N71-19207

Electromagnetic shock wave propagation and discontinuity in isotropic media 11 p1796 N71-21870

Scattering cross sections of 28 MeV protons from isotopic mixtures of Fe, Co, Ni, and Zn 12 p1978 N71-24287

Numerical analysis of behavior of waves in infinite isotropic elastic plate covered by inviscid, incompressible fluid of finite depth 13 p2180 N71-24816

Stress analysis and fracture mechanics of dewetting, isotropic, composite propellants [AD-72056] 14 p2331 N71-26079

Variation of Young modulus representing inhomogeneity in stress analysis of inhomogeneous transversely isotropic material 14 p2280 N71-26406

Solutions for multipoint distribution functions in homogeneous isotropic incompressible turbulent field [SC-RR-70-912] 15 p2392 N71-27065

Electron temperature measured by electrostatic probes and radar backscatter in isotropic, nonequilibrium plasma for studying planetary atmospheres [NASA-TM-X-65506] 16 p2661 N71-28639

Dislocation in semi-infinite isotropic media 17 p2816 N71-29930

Subsonic, supersonic, and transonic dislocations moving on interface separating two isotropic media of differing elastic properties 17 p2817 N71-29933

Solution of initial value problem in linear transport theory obtained by monoenergetic neutrons migrating in thin slab with infinite reflector and isotropic scattering [NASA-TR-8-357] 17 p2805 N71-30298

Numerical analysis of properties of axisymmetric waves in transversely isotropic rods 22 p3692 N71-36333

ISOTROPIC TURBULENCE

Analysis of effects of spanwise variations of gust velocity in isotropic turbulence on vane-controlled gust alleviation system [NASA-TN-D-6126] 11 p1609 N71-22068

Decay of high intensity isotropic turbulence investigated behind three different perforated plates [REPT-6] 23 p3749 N71-36732

ISOTROPISM

Nonhomogeneous isotropism of centrally symmetric models of origin of universe 23 p3848 N71-37430

ISOTROPY

NT ISOTROPIC MEDIA

Origin and isotropy of cosmic gamma ray flux between 1 and 6 MeV and its implications of future gamma ray investigations [NASA-TM-X-65383] 02 p0293 N71-12046

Superposing small elastic deformations on large ones with explicit expressions for incremental stress-strain relations for isotropy and transverse isotropy [AD-712399] 03 p0461 N71-13005

Effect of crystallite size, crystallite orientation, and density on dimensional and property changes in irradiated graphite and isotropic materials [GA-10433] 14 p2277 N71-25680

Method of singular eigenfunctions developed to study transverse propagation of neutron waves in medium with isotropic scattering 14 p2310 N71-26659

Theoretical calculations on extension of 1/2, 1/10, 1/11, edge and screw dislocations in isotropic fcc metals into Shockley partials 17 p2816 N71-29931

FORTAN 4 program for solving neutron transport problems with isotropic scattering in bare spheres and homogeneous slabs by sub N method [EUR-4461] 19 p3162 N71-37277

Mode 3 stress intensity factors for isotropic elastic half spaces with curvilinear notches and surface features [RD/B/N-1838] 22 p3621 N71-35798

ISRAEL

Planning for Boeing 747 aircraft integration into Israel airline operations 11 p1675 N71-22388

Integrated systems approach for developing requirements of increased civil aviation in Israel 11 p1676 N71-22391

Economic analysis of rain stimulation over Israel [P-4524] 19 p3129 N71-32556

ITALY

Erosion geomorphology of river basin in Italy [B-56] 02 p0214 N71-11063

ITERATIVE SOLUTION

Italian aerospace medicine training for military and civilian personnel 04 p0478 N71-13885

Hailstorms and thunderstorms in Italy during 1969 [IFA-TR-31] 10 p1596 N71-20786

Whiting index for thunderstorm forecast over Milan airport system for May through Aug. [NLL-M-20086-5828.4F] 12 p1957 N71-24038

Premier Colombo of Italy visit in US and indoctrination with post-Apollo program [NASA-TT-F-13596] 12 p2018 N71-24082

Computation of heat balance for Tyrrhenian Sea in 1969 [IFA-RR-29] 15 p2397 N71-27026

Activities related to atmospheric physics at IFA, Italy, during 1969 including aeronomy, atmospheric radiation, and atmospheric optics [IFA-TR-29] 15 p3398 N71-27062

Scientific and technological research trends in Italy [NLL-RISLEY-TRANS-1966-9901.9F] 16 p3694 N71-28303

Meteorological training in Italy and program for Mediterranean meteorology 22 p3612 N71-35731

Italian 3.5-m telescope project and optical parameters 24 p3921 N71-37966

ITERATION

NT ITERATIVE SOLUTION

Empirical iteration model for optimal design procedures [ECR-17] 02 p0250 N71-11468

Large quadrupole forces of deformed nuclei with iterative calculation 03 p0275 N71-11908

Geometric convergence theory for QR, Rayleigh quotient, and power iterations [AD-712444] 04 p0537 N71-13821

Kantorovich theorem and error estimates for Newton method [AD-713498] 05 p0713 N71-15216

Class on nonlinear functions and convergence of Gauss-Seidel and Newton-Gauss-Seidel iterations [NASA-CR-116129] 06 p0884 N71-16007

Browsing with information retrieval system by adding and deleting query terms on successive iterative cycles [AD-722672] 18 p3028 N71-30815

Iterative digital computer algorithm for solving optimization problems for linear stochastic systems [NASA-CR-119706] 21 p3446 N71-34521

ITERATIVE NETWORKS

Nonlinear programming and iterative network synthesis for transverse electromagnetic wave transmission modes 16 p2575 N71-28824

Algorithms for finding M-center of graph [AD-722509] 18 p2948 N71-31489

ITERATIVE SOLUTION

Nonlinear relaxation method for solving nonlinear partial differential equations governing large deflection response of axisymmetric circular membranes 01 p0130 N71-10713

Automata theory and iterative array computers [AD-711048] 01 p0029 N71-10785

Outlining theorem-proving approach to automatic programming synthesis using recursive and iterative methods [NASA-CR-115811] 04 p0501 N71-13508

Applications of partial orderings to study of positive definiteness, monotonicity, and convergence of iterative methods for linear systems [NASA-CR-116134] 06 p0883 N71-15849

Numerical determinations of Regge poles from Bethe-Salpeter equation with scalar couplings [ILL-/TH-71-2] 06 p0937 N71-16832

Calculating correction factors for spreading resistance probe measurements on n-p/positive-p structure 07 p1088 N71-17288

Writing programs in interactive FORMAC language to implement Picard iteration in solving systems of ordinary differential equations 08 p1228 N71-19190

Construction of set of self-consistent equations for calculating scattering amplitudes of strongly interacting particles 09 p1442 N71-20433

Numerical solution of initial value problems for ordinary and partial differential equations using differential quadrature and long-term integration [TID-25616] 10 p1594 N71-21578

Iterative solution to large deflection problem of flexible beam springs for design of compression and torsion springs 10 p1658 N71-21647

Iteration method for output feedback control of unstable linear systems 12 p1894 N71-24031

Analysis of iterative procedure for fully stressed design of trusses under one load condition 12 p2008 N71-24284

Least squares method and iteration technique for obtaining aerodynamic stability derivatives 13 p3083 N71-24703

Error vector propagation method for solving discretized Poisson equation 15 p2433 N71-26934 [SC-RR-70-579]
 Iterative method for solving Marcum function by computer programming 15 p2379 N71-27029

Noniterative method of obtaining rational forms as approximations to functions for power series expressions using Tchebycheff polynomial properties for improving accuracy [NASA-CR-119008] 16 p2620 N71-28102

Numerical integration of ac generator coil equations into flux linkage equations with iterative solutions for three phase machines 16 p2604 N71-28995

Rayleigh-Ritz iterative solution technique for structural modal response analysis under static loads using IBM 7094 computer 16 p2688 N71-29097

Iterative solution for internal transformations 17 p2773 N71-29789

Process and additive noise independent variable estimation using iterative methods based on Gauss-Markov estimator [TH-71-E-17] 18 p2889 N71-30588

Convergence of iterative methods applied to large overdetermined linear and nonlinear systems of equations using least squares [ESSA-TR-ERL-181-ESL-10] 18 p2946 N71-31266

Computer programming manual for calculating stress distributions in structural members and frames using iterative solution and matrix methods 19 p3186 N71-31655

Systematic iterative procedure yielding finite difference solutions to steady free boundary problems in plasma physics and fluid dynamics 19 p3123 N71-32269

General convergence result for unconstrained minimization methods [TR-150] 21 p3400 N71-34196

Acceleration of convergence of iterative methods for solution of equations including Newton method 22 p3608 N71-35700

Numerical methods for variable permeability magnetostatic field problems - difference equations solved iteratively 22 p3630 N71-35865

Iterative method for interpreting bremsstrahlung spectra [RT-FI-70/36] 22 p3631 N71-35869

Monotonous operators and iteration method for Banach spaces 23 p3782 N71-36953

Two group code [SAVE] for reactor savings of completely reflected cylindrical reactor utilizing iterative technique [UARAE-96] 23 p3795 N71-37048

Technique for improving calibration accuracy standards from boundary layer calculations [IC/71/23] 24 p3908 N71-37851

Method for evaluating work capacity of astronaut in spacecraft control, based on probability iterative techniques and linear differential transforms 24 p4015 N71-38647

ITOS 1

Operational description and performance data of ITOS 1 attitude control system [NASA-TM-X-65490] 12 p2002 N71-24178

ISAE ELLIPSOID

U ELLIPSOIDS

U GEODESY

J

J-2 ENGINE

Computer program for resolution band model prediction of heat transfer from rocket exhaust plumes [NASA-CR-102998] 06 p0959 N71-16429

Saturated LH-2 turbopump operation and feasibility of zero-tank NFPSH mode for use with J-2 engines 17 p2830 N71-29579

J-57 ENGINE

Engine modifications to reduce smoke emission from J-57 turbojet engine [NASA-TM-X-2236] 09 p1460 N71-20419

Use of air-assist fuel nozzle to reduce exhaust emissions from gas turbine combustor at simulated idle conditions - J-57 engine [NASA-TN-D-6404] 18 p3002 N71-31456

J-85 ENGINE

Reingestion characteristics and inlet flow distortion of V-STOL fighter powered by J-85 engine [NASA-TN-D-7014] 04 p0474 N71-13420

Effect of circumferential, radial, and combined pressure distortions on stall margin of J-85 engine [NASA-TM-X-2239] 10 p1491 N71-20766

Wind tunnel tests for instantaneous and dynamic analysis of effects of time-varying distortions produced in supersonic inlet on J85-GE-13 turbojet engine [NASA-TM-X-67821] 12 p1990 N71-23927

JACKS [ELECTRICAL]

U ELECTRIC CONNECTORS

JACOBI MATRIX METHOD

Optimum relaxation factor for SOR method with complex eigenvalues of Jacobi method [AD-715001] 07 p1051 N71-17827

JAGUAR AIRCRAFT

Describing digital computer used in navigation and attack system of Jaguar aircraft 03 p0408 N71-12611

JAMMING

Computerized simulation model for communication network jamming [FOA-3-A-3727-43] 14 p2235 N71-26612

Phase scintillation effects on cross sections of ionized irregularities related to clutter, radar target identification, jamming, and antimissile defense systems [AD-723587] 19 p3055 N71-31991

JAPAN

Sulfur-mat formation and Chromatium weissii bacteria of hot mineral springs in Yumoto, Japan [NASA-TT-F-12738] 02 p0156 N71-11107

Measuring erosional features of volcanic cones in Japan [NASA-TT-F-13345] 03 p0367 N71-12749

Tables on aerological data of Japan - Jan. 1970 11 p1789 N71-22264

Tables on aerological data of Japan - Mar. 1970 11 p1789 N71-22265

Tables of 1968 geomagnetic observations from Kakioka, Japan including declination, vertical and horizontal intensities, and characteristics of principle magnetic disturbances [REFT-74] 11 p1749 N71-22404

Tables of geoelectric observations in Japan - 1966 [REFT-72] 11 p1749 N71-22438

Geoelectric observations in 1967 at Kakioka, Memambetsu, and Kanoya, Japan [REFT-73] 11 p1750 N71-22542

Tabulated results of geomagnetic observations at Memambetsu, Japan, in 1967 [REFT-66] 11 p1750 N71-22543

Tables of upper air data of Japan for June 1970 12 p1951 N71-23142

Tables of upper air data of Japan for Feb. 1970 12 p1952 N71-23143

Tables of upper air data of Japan for Apr. 1970 12 p1952 N71-23144

Tables of upper air data of Japan for May 1970 12 p1952 N71-23145

Statistical data of diurnal temperature variations of Kofu from 1956 to 1964 [NLI-M-20311-5828.4P] 12 p1957 N71-24002

Radiation shielding, core thermodynamics, cooling system, monitors, and safety evaluation of Japan Experimental Fast Reactor design [JAERI-1177-B-PT-2] 13 p2118 N71-24922

Air sampling over Japanese atomic research facility [JAERI-MEMO-4175] 13 p2075 N71-25122

Thermal conductivity measurements of vibratory compacted uranium dioxide fuel in temperature range from 200 to 7500 C irradiated in gas loop TLG-1 of JRR-2 reactor [JAERI-4128] 16 p2631 N71-28141

Statistical analysis of periodic variations of wind shear vertical distribution in lower atmosphere at Tokyo airport tower site, Japan 18 p2950 N71-30834

Meteorological weather observations by planned Japanese satellite [NASA-TT-F-13825] 18 p2955 N71-31491

Simultaneous gravimetric observation of earth tides with four Askania and two Lacoste and Romberg gravimeters in Mizusawa, Japan 20 p3262 N71-33338

Mizusawa geophysical station, Japan, for observing earth tides 20 p3245 N71-33341

Several methods for analyzing earth tides noting monthly variations of gravimetric data obtained in Kyoto, Japan 20 p3262 N71-33342

Tidal gravity variations derived from extensometric observations in Kamitakara, Japan 20 p3264 N71-33357

Tables of aerological and rocket sonde data of Japan - Sept. 1969 21 p3419 N71-34325

Measurement and analysis of gravity anomalies in Sea of Japan [JPRS-53962] 21 p3421 N71-34344

Tables of upper air data observed in Japan and vicinity during July 1969 21 p3451 N71-34560

Radioactive isotope survey in Tsuboku district, food, and precipitation in Japan [NIRS-RSD-28] 24 p3876 N71-37631

Radioisotope content of food, dusts, rivers and soils of Japan for 1969 and 1970, and fallout in rain and upper atmosphere after Chinese nuclear explosion of Oct. 1970 [NIRS-RSD-29] 24 p3973 N71-38346

Status of MHD power generators and related technology in Japan [AD-727094] 24 p3997 N71-38510

JARRING

U MECHANICAL SHOCK

JAVELIN ROCKET VEHICLE

Vector magnetic field measurements from Javelin rocket nose cone using vapor magnetometer [AD-714081] 06 p0854 N71-16611

Barium releases from Javelin and Nike-Tomahawk sounding rockets for ion cloud study of earth electric and magnetic fields [NASA-SP-264] 17 p2740 N71-29671

Description of Javelin and Nike-Tomahawk sounding rocket used for barium release experiments 17 p2740 N71-29671

Payloads of Javelin and Nike-Tomahawk sounding rockets 17 p2740 N71-29671

Determining electric and magnetic fields by visual observations of second release from Javelin vehicle 17 p2740 N71-29671

Photometry of barium ion emission for Javelin second release 17 p2741 N71-29678

Position of neutral barium clouds, position and motion of Javelin ionized cloud, and radial growth of clouds by triangulation 17 p2741 N71-29680

Electric field distribution, cloud elongation, and drift along magnetic field line of barium release from Javelin 17 p2741 N71-29681

Jeans instability theory of galactic formation and expanding universes with black body radiation 20 p3344 N71-32847

JEANS THEORY

Jeans instability theory of galactic formation and expanding universes with black body radiation 20 p3344 N71-32847

JEEPS

U AUTOMOBILES

JET AIRCRAFT

NT A-4 AIRCRAFT

NT AVRO 707 AIRCRAFT

NT B-52 AIRCRAFT

NT B-57 AIRCRAFT

NT B-70 AIRCRAFT

NT BOEING 707 AIRCRAFT

NT BOEING 727 AIRCRAFT

NT BOEING 747 AIRCRAFT

NT BREGUET 941 AIRCRAFT

NT BUCCANEER AIRCRAFT

NT C-5 AIRCRAFT

NT C-141 AIRCRAFT

NT CONCORDE AIRCRAFT

NT CV-990 AIRCRAFT

NT DC 8 AIRCRAFT

NT DC 9 AIRCRAFT

NT DO-31 AIRCRAFT

NT F-2 AIRCRAFT

NT F-4 AIRCRAFT

NT F-4 AIRCRAFT

NT F-28 TRANSPORT AIRCRAFT

NT F-104 AIRCRAFT

NT F-106 AIRCRAFT

NT F-111 AIRCRAFT

NT F-116 AIRCRAFT

NT HFB-320 AIRCRAFT

NT HS-748 AIRCRAFT

NT OV-10 AIRCRAFT

NT OV-10 AIRCRAFT

NT P-3 AIRCRAFT

NT SE-210 AIRCRAFT

NT T-33 AIRCRAFT

NT T-39 AIRCRAFT

NT TU-134 AIRCRAFT

NT TURBOFAN AIRCRAFT

NT TURBOPROP AIRCRAFT

NT VC-10 AIRCRAFT

NT VJ-101 AIRCRAFT

Differential game theory applied to pursuit-evasion problems of two jet aircraft 01 p0074 N71-10813

Jet aircraft crash during instrument approach due to electrical systems failure [NTSB-AAR-70-23] 01 p0005 N71-10812

Lear jet crash during instrument approach due to descent below path profile [NTSB-AAR-70-21] 01 p0005 N71-10813

Wind tunnel investigation of jet transport airplane configuration with external flow jet flap and inboard pod-mounted engines-graphs [NASA-TN-D-7004] 05 p0629 N71-14085

Fuel consumption and propulsive and thermodynamic efficiency comparisons for ship, hydrofoil craft, helicopters, jet aircraft, and ground effect machines [NPL-HOVERCRAFT-12] 07 p0970 N71-17161

Causes and results of aircraft accident of Lear jet aircraft [NTSB-AAR-71-3] 07 p0971 N71-17314

Mathematical model of large jet transport aircraft simulation [NASA-CR-1756] 08 p1145 N71-19239

Wind tunnel tests with jet simulation of tailplane interference on European Airbus models 09 p1314 N71-19374

SUBJECT INDEX

JET EXHAUST

Jet VTOL fighter-type model inlet-air temperature rise analysis with various exhaust pressure ratios and gas temperatures and surface wind velocities for correlating parameters
[NASA-CR-111867] 09 p1324 N71-20271

Sound pressure levels produced by C-5A during ground tests
[AD-716814] 10 p1696 N71-20824

Jet transport aircraft airspeed control and controllability data obtained by flight recorders
[ARC-CP-1135] 10 p1493 N71-20902

Jet vertical takeoff aircraft piloted cockpit simulator for controlling aircraft flight performance
[ARC-R/M-3647] 13 p2027 N71-25065

Flight evaluation of lateral handling, stability, control, and flying qualities of jet transport aircraft during up-and-away and approach flight in landing configuration
[NASA-TN-D-45359] 13 p2028 N71-25357

Cooling, coating, construction, and structural characteristics of jet fuel-cooled plug nozzle for afterburning turbojet
[NASA-TM-X-2304] 16 p2671 N71-28128

Determination of relationship between visibility of in-flight jet exhaust to SAE smoke number
[FAA-NA-71-24] 17 p2702 N71-29907

Theory of controllability for parabolic and second order hyperbolic systems and for hereditary differential systems applied to stabilization of high speed aircraft in gust load disturbances
[AD-722072] 17 p2703 N71-29430

Reductions in smoke level and carbon monoxide emissions resulting from jet fuel nozzles in jet aircraft exhaust pollutant tests
18 p2871 N71-30784

Impact of jet aircraft emissions on air quality in vicinity of Los Angeles International Airport
[PB-196969] 19 p3036 N71-31779

Evaluation of lightning hazards to jet aircraft including possibility of fuel tank explosions
[AD-724092] 20 p3209 N71-33006

Technology of thrust reversers with particular application to STOL aircraft
[NASA-CR-121736] 21 p3409 N71-34239

JET AIRCRAFT NOISE
Sonic aircraft boom propagation analysis for horizontal flight in unperturbed atmosphere
02 p0146 N71-11036

Acoustic properties of supersonic fan with short blade span
[NASA-TM-X-52937] 03 p0311 N71-12218

Measurement of noise levels during OV-10 aircraft operations
[AD-712667] 03 p0313 N71-12230

Jet noise suppression by impedance shroud
[AD-712406] 03 p0314 N71-12240

Performance of noise suppressors for turbofan engines
[NASA-TM-X-52941] 03 p0448 N71-12599

Psychosocial evaluation of modifications to DC-8 aircraft nacelles to reduce fan-compressor noise - Part 1
[NASA-CR-1710] 05 p0628 N71-14591

Economic impact of modifications to DC-8 aircraft nacelles to reduce fan-compressor noise - Part 3
[NASA-CR-1709] 05 p0628 N71-14592

Static tests of noise suppressor configurations of DC-8 aircraft nacelle modifications to reduce fan-compressor noise levels - Part 3
[NASA-CR-1707] 05 p0628 N71-14593

Modifications to reduce fan-compressor noise level of DC-8 aircraft - Part 2
[NASA-CR-1706] 05 p0628 N71-14594

Modifications to reduce fan-compressor noise level of DC-8 aircraft - Part 1
[NASA-CR-1705] 05 p0628 N71-14595

Turbofan nacelle modifications to minimize fan-compressor noise radiation of Boeing 707 aircraft - Vol. 1
[NASA-CR-1711] 05 p0629 N71-14596

Static tests to determine effects of throat inlet concepts on forward-radiated fan noise of 707-320B/C airplanes
[NASA-CR-1715] 07 p0971 N71-17426

Jet aircraft noise reduction near airports
07 p1135 N71-18079

Noise associated with operation of C-9A (aeromedical) aircraft
[AD-712222] 06 p1142 N71-18269

Subjective evaluation tests of ground observers on noise levels from acoustically treated engine nacelles of Boeing 707 aircraft
[NASA-CR-1717] 06 p1143 N71-18499

Acoustical properties of liquid base foams and application for jet noise reduction
[NASA-CR-1695] 08 p1285 N71-19139

Acoustic measurements of deflected jet VTOL aircraft
[AD-715959] 09 p1320 N71-19549

Air transportation system noise propagation and reduction
[PB-195911] 10 p1609 N71-21630

Development and description of basic descriptors and to analyze jet engine noise, aircraft noise, and noise level of airports
11 p1672 N71-21980

Noise characteristics of circular double jet issuing from 3 cm and 6 cm diameter nozzles compared with those of single jet
[NAL-TR-212] 11 p1798 N71-22469

Determination of low speed jet noise from fan engine for simulated nacelle configuration
[NASA-TN-D-6314] 12 p1849 N71-23134

Identification and control of aeromedical factors associated with aircraft noise and acoustic measurements during C-141 operational missions
[AD-718097] 12 p1857 N71-23748

Jet noise contribution to far field sound from 1.83 meter diameter fan determined for two simulated nacelle configurations
[NASA-TM-X-67825] 12 p1991 N71-24609

Analytic functions and fluid mechanics for noise propagation in supersonic jet exhaust flow
[NASA-CR-1848] 15 p2364 N71-27028

Parametric turbofan engine study for Mach 0.98 transport with low takeoff and approach noise levels using supercritical wing
[NASA-TM-X-67863] 16 p2672 N71-29011

Probable impact of future supersonic transport aircraft operations on noise environment around seven airports in US
[AD-722365] 17 p2704 N71-29777

Comparison of human sleep disturbance in three age groups by subsonic jet aircraft noise and simulated sonic booms
[NASA-CR-1780] 18 p2874 N71-30670

Jet aircraft noise sources and reduction from gas turbine engines including jet exhausts, fans, lift devices, and unducted rotors
18 p2871 N71-30785

Plug nozzle configuration for jet noise suppression
[AD-722851] 19 p3173 N71-31698

Noise exposure from supersonic transport operations and estimates of changes in noise levels
[AD-722366] 19 p3036 N71-31793

Noise attenuation by injection of evaporating droplets into subsonic duct flow
[NASA-CR-111905] 20 p3312 N71-33560

Reduction of jet exhaust noise at airports
22 p3700 N71-36388

JET AIRSTREAMS
U JET STREAMS (METEOROLOGY)
JET AMPLIFIERS
Fluid control jet amplifiers
[NASA-CASE-XLE-09341] 16 p2581 N71-28741

JET AUGMENTED WING FLAPS
U JET FLAPS
U WING FLAPS

JET BLAST EFFECTS
Separation mechanism for use between stages of multistage rocket vehicles
[NASA-CASE-XLA-00188] 11 p1772 N71-22874

JET BOUNDARIES
Characteristics of radial wall jet bounded by circular jump
[REPT-264] 02 p0204 N71-12078

Interaction of sonic transverse jets with supersonic external flows
07 p1010 N71-17646

JET CONDENSERS
Environmental vibration testing of SNAP 8 condenser and design evaluation for space and launch conditions
[NASA-CR-78925] 24 p4023 N71-38706

JET DAMPING
U DAMPING
U SPIN REDUCTION

JET DRIVE
U JET PROPULSION
JET ENGINE FUELS
NT JP-5 JET FUEL

Performance of reducing electrode for neutralizing electrically charged hydrocarbon fuel flow
[AD-712348] 02 p0287 N71-11876

Corrosion inhibitor effects on water collecting characteristics of DOD type filter/condenser elements
[AD-712999] 03 p0443 N71-13070

Crash fire hazard evaluation of jet fuels
[FAA-NA-70-64] 06 p0938 N71-16864

Development of radiotracer method for detecting contribution of selected components to storage instability of jet engine fuels
09 p1456 N71-20505

Conversion of experimental turbojet combustor from ASTM A-1 fuel to natural gas fuel
[NASA-TM-X-2241] 09 p1406 N71-20533

Tests of jet engine fuels to determine effects of sloshing and vibration in aircraft fuel tanks on flameability hazards
[AD-718091] 12 p1909 N71-23084

Performance of simplex and dual orifice fuel nozzles with ambient and heated fuel in annular turbojet combustor
[NASA-TN-D-6355] 16 p2671 N71-29041

Effects of corrosion inhibitors and anti-ice inhibitor combinations on collecting properties of filter coalescer elements used to decontaminate jet engine fuels
[AD-722331] 16 p2670 N71-28577

Heat sink capabilities of Jet-A fuel - heat transfer and cooling studies
[NASA-CR-72951] 18 p3027 N71-31482

Small scale impact tests of aircraft type fuels for gas turbines to determine burning, mixing, and splatter characteristics
[FAA-NA-71-12] 19 p3172 N71-32087

Performance of protective clothing in large J4-4 fuel fires
[AD-724448] 20 p2326 N71-32925

JET ENGINES
NT BRISTOL-SIDDELEY OLYMPUS 593 ENGINE

NT DUCTED FAN ENGINES
NT J-57 ENGINE
NT J-45 ENGINE

NT PULSEJET ENGINES
NT RAMJET ENGINES
NT SUPERSONIC COMBUSTION RAMJET ENGINES

NT TURBOFAN ENGINES
NT TURBOJET ENGINES
NT TURBOPROP ENGINES
NT TURBORAMJET ENGINES

Manufacturing technology and production engineering methods in aerospace industry
02 p0231 N71-11627

Validating gas generator method of calculating jet engine thrust, and evaluation of XB-70-1 engine performance at ground static conditions
[NASA-TM-D-7028] 04 p474 N71-13419

Development of methods for analyzing ratios of sulfur dioxide and sulfur trioxide in jet exhaust streams
[AD-713222] 05 p0638 N71-14603

Absorptive, nonreflecting barrier mounted between closely spaced jet engines on supersonic aircraft, for preventing shock wave interference
[NASA-CASE-XLA-02865] 05 p0763 N71-15563

Jet engine combustion chamber burn-through fire and methods for controlling debris
[FAA-RD-70-48] 07 p1102 N71-17483

Determining amount of smoke in exhaust of jet turbine engines
[NASA-CR-117031] 09 p1459 N71-20050

Development of thrust dynamometer for measuring performance of jet and rocket engines
[NASA-CASE-XLE-05260] 09 p1391 N71-20429

Afterburner-equipped jet engine nacelle with slotted configuration afterbody
[NASA-CASE-XLA-10430] 10 p1639 N71-21493

Investigation of helicopter jet engine flameout due to ingestion of snow and ice
[NRC-11893] 11 p1672 N71-21927

Conference proceedings on vertical takeoff aircraft technology, noting tandem wing aircraft, tilt wing aircraft, helicopters, lift fans, and jet engines
[DLR-MITT-78-15] 11 p1673 N71-22186

DO-251 V/STOL aircraft design, noting passenger comfort, aerodynamic noise, aerodynamic characteristics, and cost analysis
11 p1673 N71-22187

Theoretical analysis of jet mixing under influence of nonconstant pressure gradient
[ARI/ME-127] 11 p1821 N71-22503

Exhaust gas ingestion and recirculating flow field characteristics of small scale vertical take off engine pod
[NASA-CR-1774] 13 p2024 N71-23597

Aluminide coatings for nickel-base superalloy developed for high temperature jet engine components
[NASA-CR-72863] 13 p2097 N71-25454

Fuel tests to determine feasibility of gelled methane for use in jet engine
[NASA-CR-72876] 14 p2331 N71-25772

Properties and selective applications of high strength steels, aluminum and titanium alloys, polymeric materials, ceramic materials, and composite materials in aerospace engineering
[AGARD-LS-51-71] 15 p2429 N71-27038

Properties and selective applications of titanium alloys in airframes and jet engines
15 p2421 N71-27045

Future technology trends in air breathing propulsion systems for aircrafts
[NASA-TM-X-67871] 16 p2672 N71-28947

Determination of relationship between visibility of in-flight jet exhaust to SAE smoke number
[FAA-NA-71-24] 17 p2702 N71-29907

Control equipment and engine development for air pollution control from jet aircraft engine emissions
18 p2919 N71-31403

Materials research for thermal reactors, jet engines, space shuttles, and space nuclear power systems
[NASA-TM-X-67885] 19 p1321 N71-32349

Resistance welding to join compressor and turbine parts reducing weight and cost of jet engines
[NASA-CASE-LW-10533-1] 21 p3433 N71-34424

Stratified charge engine tests to determine exhaust emission characteristics
[AD-727745] 24 p4031 N71-38740

Combustion efficiency and performance of swirl can module under conditions simulating operation of 10,000 pound thrust lift engine for vertical takeoff
[NASA-TN-D-6542] 24 p4032 N71-38767

JET EXHAUST
Two dimensional analysis on jet exhaust into crosswind with mixing flow interference
[AD-711578] 02 p0142 N71-11006

- Acoustic and flow characteristics of subsonic and supersonic jets from convergent nozzles [NASA-CR-1693] 05 p0664 N71-14993
- Jet exhaust nozzle subsonic flow simulation [ARC-CP-1111] 07 p0966 N71-17113
- Hot corrosion of TD nickel and TD nickel chromium in jet engine exhaust [NASA-TM-X-52976] 09 p1398 N71-19700
- Interference phenomenon of subsonic turbulent jet exhausts from flat plate in low speed cross flow [AD-718798] 12 p1899 N71-23314
- Wind tunnel investigation of jet exhausting into cross flow - data for three jet configuration [AD-718123] 13 p0664 N71-24491
- Low speed wind tunnel test of four ft diameter circular plate model with three exhausting jets [AD-720233] 14 p2344 N71-26517
- Determination of relationship between visibility of in-flight jet exhaust to SAE smoke number [FAA-NA-71-24] 17 p2702 N71-29307
- Control equipment and engine development for air pollution control from jet aircraft engine emissions 18 p2919 N71-31403

JET FLAMES

U FLAMES

JET FLOW

JET FLAPS

- Wind tunnel investigation of jet transport airplane configuration with external flow jet flap and inboard pod-mounted engines - graphs [NASA-TN-D-7004] 05 p0629 N71-14605
- Investigating effects of leading edge blowing on aerodynamic characteristics of jet flapped airfoil 07 p0968 N71-17702
- Trailing vortex systems generated by jet-flapped wing operating at high wing lift coefficients [AD-715315] 07 p0973 N71-17753
- Helicopter application studies of variable deflection thruster jet flaps [AD-715071] 07 p0973 N71-17907
- H-126 jet flap research aircraft development and testing 09 p1323 N71-20066
- Single stage turbine performance with modified jet flap rotor blade [NASA-CR-1759] 09 p1318 N71-20182
- Effect of engine position and high lift devices on aerodynamic characteristics of external flow, jet flap STOL model - graphs [NASA-TN-D-6222] 12 p1852 N71-23124
- Hovering performance tests of jet-flapped rotors and comparison of predicted and actual results [NAL-TR-211] 13 p2028 N71-25396
- Wind tunnel tests to determine low-speed aerodynamic characteristics of large-scale STOL transport model with augmented jet flap [NASA-TM-X-62017] 14 p2198 N71-26183
- Noise data with models of both internally and externally blown jet flaps designed for STOL aircraft [NASA-TM-X-67850] 15 p2364 N71-27673
- Lift force distribution calculation technique for wings with jet flaps including rectangular and swept wing examples [NASA-TT-F-13714] 18 p2866 N71-30852
- Induced lift characteristics of swept wing-body configuration with partial-span jet in flow at Mach 0.20 to 1.30 [NASA-TM-X-2309] 19 p3034 N71-32307
- Investigating bidirectional jet flap device for application to helicopter rotors [NASA-CR-114359] 19 p3034 N71-32385
- Theoretical and experimental determination of lift and pitching moment distribution on jet flap wings of rectangular design with various aspect ratios [NASA-TT-F-13715] 20 p3207 N71-33803
- Wind tunnel investigation of external flow jet-flap transport configuration having full-span triple-slotted flap - graphs [NASA-TN-D-6391] 21 p3377 N71-34028
- Dynamic stability of jet transport configuration with high thrust-weight ratio and externally blown jet flap [NASA-TN-D-6440] 22 p3359 N71-35213
- Using jet flap diffuser for recovery of ejector jet kinetic energy [AD-726596] 22 p3664 N71-36123
- JET FLIGHT
- JET AIRCRAFT
- JET FLOW
- NT AIR JETS
- NT PERIPHERAL JET FLOW
- NT SUPERSONIC JET FLOW
- Investigating effect of flow nonuniformities at exit of planar nozzles on total pressure distribution in circular attachment wall [AD-711314] 02 p0200 N71-11138
- Determination of low speed longitudinal aerodynamic characteristics of four engine externally blowing jet flap STOL aircraft [NASA-TN-D-7034] 03 p0314 N71-12239
- Considering sequence of transient acoustical point sources as noise generator in two-dimensional jet [DI-82-1002] 04 p0566 N71-14073
- Submerged incompressible two-dimensional jet pivotally oscillated at its base [AD-714698] 06 p0834 N71-16116

Structure of supersonic jet of argon-helium mixture in vacuum conditions

- 07 p1006 N71-16936
- Breakup of laminar capillary jet of nonnewtonian fluid [NASA-CR-116489] 07 p1008 N71-17326
- Flame length and laminar fuel jet combustion [NASA-TT-F-13459] 07 p1130 N71-17570
- Determining characteristics of jet elements whose operation is based on jet interaction with turbulent or laminar flow in control channels [AD-716519] 09 p1371 N71-19629
- Sound generation by small perturbation jet flow [DLR-FB-71-02] 12 p1856 N71-23596
- Finite difference solution for unsteady equations of impulsively-starting incompressible jet flow [EFTN/A/28] 13 p2068 N71-25443
- Effect of injection Mach number on jet penetration over wide range of pressure and free stream Mach numbers [NASA-TN-D-6370] 16 p2579 N71-28270
- Pressure, temperature, gas sampling, and optical measurements in two dimensional jet interaction flow field [NASA-TM-X-67862] 16 p2583 N71-28953
- Accelerator for launching hypervelocity projectile by drag force of jet produced by gaseous explosive products [NASA-CR-115067] 17 p2729 N71-29227
- Examination of two dimensional combustion flow field upstream of inert and chemically reactive transverse jets [DI-82-1066] 19 p3079 N71-32264
- Flow breakdown from inclined jets in V/STOL propulsion tunnel [NRC-LR-545] 20 p3250 N71-33491
- Analysis of jet flow with emphasis on turbulent axisymmetric free jets [SC-DR-70-838] 21 p3411 N71-34270
- Effective source position, strength, and phase calculations using sound pressure and phase measurements in near field of choked screw jets [NRC-12111] 22 p3629 N71-35855
- Thermal and dynamic properties of combustion products from various gases and heat transfer to flat plates from high-temperature combustion product jets [NLL-RTS-6531] 22 p3697 N71-36368
- Numerical analysis of impact of flat-ended cylindrical water jet of finite length on flat rigid plane [UMICH-03371-9-T] 23 p3744 N71-36699
- JET FUELS
- U JET ENGINE FUELS
- JET IMPINGEMENT
- Recirculation region of flow field caused by jet in ground effect with crossflow [AD-711665] 01 p0002 N71-10832
- Jet impingement technique for rapidly heating steel billets [DIS/1/69] 02 p0242 N71-11586
- Tunnel flow separation induced by impinging jet of vertical takeoff aircraft [NRC-11617] 03 p0364 N71-13082
- Loads due to air and helium jets impinging normal to flat plate for near vacuum and sea level ambient pressures [NASA-TN-D-7002] 05 p0660 N71-14749
- Nonuniform flow field sonic boom reduction device using slit jet impinging on inclined flat plate [AD-717193] 10 p1544 N71-21623
- Effect of introducing solid particles into cooling air on heat transfer in row of air jets impinging on inside of semi-circular cylinder in Thémis project [AD-718794] 12 p2011 N71-24109
- Characteristics of gaseous jet impinging normally on liquid surface in regions where both gravitational and surface tension forces are significant [NASA-TN-D-6368] 14 p2239 N71-26023
- Temperature gradients induced in heated wall by impinging gas jet traveling through liquid coolant [ANL-7734] 19 p3078 N71-32116
- Numerical analysis of impact of flat-ended cylindrical water jet of finite length on flat rigid plane [UMICH-03371-9-T] 23 p3744 N71-36699
- Heat transfer in jet impingement cooling of concave surface in semi-enclosed environments [AD-727736] 24 p4030 N71-38759
- JET LIFT
- Wind tunnel investigation of jet transport airplane configuration with high thrust-weight ratio and external flow jet flap - graphs [NASA-TN-D-6058] 01 p0004 N71-10495
- Finite-element potential flow modeling for predicting round lifting jet rolled up geometry and path convergent into cross-flowing mainstream as on VTOL or STOL aircraft [AD-718121] 12 p1830 N71-23475
- Induced lift characteristics of swept wing-body configuration with partial-span jet in flow at Mach 0.20 to 1.30 [NASA-TM-X-2309] 19 p3034 N71-32307
- JET MIXING FLOW
- Turbulent mixing between two compressible streams in constant area duct [AD-710284] 01 p0039 N71-10010

Two dimensional analysis on jet exhaust into cross-wind with mixing flow interference

- [AD-711578] 02 p0142 N71-11006
- Characteristics of radial wall jet bounded by circular jet [REPT-284] 02 p0204 N71-12078
- Turbulent mixing between two compressible streams in constant duct area and with eccentric primary flow jet [AD-712333] 01 p0362 N71-12762
- Systematic numerical analysis of two dimensional and axisymmetric laminar jet of incompressible fluid with and without free stream [NASA-CR-111517] 03 p0364 N71-13085
- Interaction of hypersonic spherical source flow with rarified atmosphere [AD-713122] 05 p0663 N71-14934
- Correlating effect of baffles on flow stability in MSF evaporator based on submerged jet model [ORNL-TM-3120] 06 p0836 N71-16385
- Effect of injectant molecular weight on mixing of normal jet in Mach 4 airstream - tables and graphs [NASA-TN-D-6061] 06 p0837 N71-16585
- Two dimensional jet interaction with Mach 4 mainstream [AD-715104] 07 p1011 N71-17738
- Base flow analysis of axisymmetric body with central jet [AD-715258] 07 p1012 N71-17787
- Schlieren photography of flow distribution for transverse hydrogen jets from flat plate into Mach 2.72 airstream [NASA-CR-1794] 09 p1371 N71-19637
- Two dimensional, supersonic mixing of hydrogen injected from wall slot into airstream [NASA-CR-1793] 09 p1376 N71-20127
- Jet to free-stream dynamic pressure ratio effects on penetration and mixing of hydrogen injected normal to supersonic airstreams [NASA-TN-D-6114] 09 p1377 N71-20195
- Particle size, particle and air flow rate, and jet molecular weight effects on diffusion of particulate matter in subsonic turbulent jets when coaxially mixed with another subsonic flow [AD-717217] 10 p1539 N71-20831
- Theoretical analysis of jet mixing under influence of non-constant pressure gradient [NASA-CR-117836] 11 p1738 N71-22501
- Experimental and mathematical investigation of interaction of supersonic jet and acoustic field [NASA-TT-F-13527] 12 p1904 N71-24159
- Wind tunnel investigation of jet exhausting into cross flow - data for three jet configuration [AD-718123] 13 p2064 N71-24491
- Wind tunnel investigation of jets exhausting into cross flow - description and data analysis [AD-718122] 13 p2064 N71-24492
- Characteristics of turbulent structure of mixing region near outlet of circular subsonic jet and production of jet noise [NASA-CR-1836] 16 p2583 N71-20882
- Determination of similarity between boiling and injection of saturated vapor and establishment of critical heat flux model [RR-5] 16 p2693 N71-29069
- Turbulent mixing in submerged two dimensional wall jets [PB-198029] 17 p2734 N71-29746
- Proportional fluid amplifiers for mixing two fluids in varying mix ratios [AD-72316] 17 p2734 N71-29754
- Calculating penetration depth of one-row round jet system developing in limited cross wind under conditions most typical for gas burners [NASA-TT-F-13726] 17 p2735 N71-29815
- Buoyant jet mixing flow from manifolds in stagnant receiving water of uniform density using hydraulic models of waste disposal system [PB-198405] 19 p3080 N71-32461
- Mixing of hydrogen downstream from multiple injectors normal to supersonic jet flow, for supercritical combustion ramjet engines [NASA-TN-D-6476] 21 p3411 N71-34274
- Analysis of compressible turbulent mixing of parallel coaxial hydrogen-air jets at supersonic speed for outer jet and subsonic speed for inner jet [NASA-TN-D-6487] 21 p3413 N71-34283
- Exhaust jet mixing flow nozzles with peak axial velocity degradation for noise suppression [NASA-TM-X-67954] 23 p3839 N71-37378
- Inviscid flow analysis of three jet interaction for design of proportional amplifiers [AD-727689] 24 p3908 N71-37353
- JET NOISE
- U JET AIRCRAFT NOISE
- JET NOZZLES
- Nozzle lateral spacing effect on drag and performance of twin jet afterbody configurations with convergent nozzles at Mach 0.6 to 2.2 [NASA-TM-X-2099] 01 p0115 N71-10076
- Air cooling systems for nozzle guide vanes of aircraft gas turbines 07 p1129 N71-17396

Thrust and attitude control apparatus using jet nozzle in movable canard surface or fin configuration [NASA-CASE-XLB-05583] 07 p1119 N71-17629

Wind tunnel tests of supersonic propulsion inlet, engine and exhaust nozzles [NASA-TM-X-67670] 16 p2672 N71-28946

JET PILOTS

U AIRCRAFT PILOTS

JET PLUMES

JET PROPULSION

Auxiliary inlet ejector nozzle designed for supersonic cruise aircraft [NASA-TM-X-2182] 06 p1284 N71-18963

Test section of combustion wind tunnel for jet propulsion [DLR-MITT-71-08] 19 p3073 N71-31812

Squid project research on fluid mechanics in jet propulsion [AD-733807] 19 p3174 N71-32076

JET PUMPS

One dimensional equations describing noncavitating and cavitating flow in liquid-to-liquid jet pump programmed for computer use [NASA-TN-D-6453] 10 p2931 N71-31395

JET STREAMS [METEOROLOGY]

Nimbus 3 satellite observations of ozone associated with easterly jet stream over India during 1969 summer monsoon [NASA-TM-X-65416] 06 p0840 N71-15841

Structure of air currents including jet streams, turbulence in cumulonimbus, and variability of wind velocity [AD-717052] 10 p1397 N71-21242

Relationship of cirrus cloud formation /marea tails/ and jet streams in troposphere examined for aerial navigation application [NASA-TT-F-13606] 12 p1953 N71-23350

Nimbus 2 medium resolution infrared radiometer measurements on subtropical jet stream flows [AD-72107] 12 p2107 N71-23259

Polar front jet stream maintenance, and numerical simulations of stratospheric trace substance transfer and ozone transport [AD-719995] 14 p2286 N71-25602

Analysis of jet stream structure and energetics using objective scheme that calculates normal and parallel wind components for determining eddy currents [AD-721221] 15 p2438 N71-27270

JET THRUST

Construction and operation of body-motion controlled five-degree-of-freedom simulation of jet-supersonic burner firing machine [NASA-TN-D-6001] 03 p0358 N71-12736

System for aerodynamic control of rocket vehicles by secondary injection of fluid into nozzle exhaust stream [NASA-CASE-XLA-01163] 05 p0721 N71-15582

Drive mechanism for operating resistance attitude control system for aerospace bodies [NASA-CASE-XMF-01598] 05 p0721 N71-15583

Rotary wing structural stability of Dornier high temperature gas jet helicopter 13 p2024 N71-24387

Development of design and programmatic data for space shuttle reaction control systems and integrated control system/orbit maneuvering systems [NASA-CR-123184] 24 p4016 N71-38656

JET VANES

Scout first stage jet vane effectiveness, and aerodynamic pitching and yawing moment coefficients determined from flight data [NASA-CR-111945] 20 p3351 N71-33003

JETAVATIONS

U GUIDE VANES

JETWING SYSTEMS

Reconnaissance star ejection test systems [RAE-LIB-TRANS-1471] 02 p0147 N71-11042

Describing assembly for opening stabilizing and deslashing flaps of flight capsules used in space research [NASA-CASE-XMF-03169] 05 p0773 N71-15675

Rotary wing aircraft external stores jetwings systems [AD-713872] 05 p0795 N71-16262

Engineering drawing lists for solid state sequencer system in command module and service module jetwings controller [NASA-CR-114956] 10 p1635 N71-21458

Logic circuitry, and environmental and acceptance tests for solid state sequencer system in command module and service module jetwings controller [NASA-CR-114955] 10 p1635 N71-21460

Wiring lists for solid state sequencer system in command module and service module jetwings controller [NASA-CR-114957] 10 p1635 N71-21461

System for deploying and ejecting releasable channel fairing sections from spinning sounding rockets [NASA-CASE-GSC-10590-1] 21 p3520 N71-35801

Safe separation criteria for external stores and jetwings escape capsules for pilots [AD-726695] 23 p3707 N71-36428

JETWINGING

Wind tunnel testing of aerodynamic interactions between aircraft and jetwings loads using trajectory analysis [ONERA-TP-849] 08 p1141 N71-18464

Photographic recording of aerodynamic interference in wind tunnel simulation of jetwings drop loads from aircraft 09 p1314 N71-19378

Computerized prediction of separated store trajectories dropped from bomber aircraft at high speed 09 p1318 N71-19379

Flight test measurements on interference and aerodynamic drag effects caused by jetwings of external stores from F-2 aircraft 09 p1319 N71-19384

Wind tunnel evaluation of lifting body store configurations for captive flight drag and separation characteristics 09 p1314 N71-19386

Statistical prediction of external store separation characteristics from aircraft 09 p1320 N71-19388

Analysis of anomalous jetwings of service module during reentry of Apollo 11 [NASA-TM-X-67183] 14 p2345 N71-26385

JITTER

U VIBRATION

JOBS

U TASKS

JOINING

Prestressed bolt joining and pretightness effect under static and dynamic loads 10 p1653 N71-21031

JOINTS [ANATOMY]

Space suit with pressure-volume compensator system [NASA-CASE-XLA-05332] 02 p0168 N71-11194

Equipotential space suits utilizing mechanical aids to minimize astronaut energy at bending joints [NASA-CASE-LAR-10007-1] 02 p0168 N71-11195

Investigating wear processes in hip prostheses after brief use [NASA-TN-D-6153] 07 p0986 N71-17410

Cord restraint system for pressure suit joints [NASA-CASE-XMS-9635] 13 p2036 N71-24623

Load distribution on human hip joints during walking [LAB-10027/1] 17 p2710 N71-29527

Friction wear of human hip joint prostheses made from cobalt molybdenum and cobalt molybdenum chromium alloys [NASA-TN-D-6512] 23 p3764 N71-36833

JOINTS [FUNCTIONS]

NT BUTT JOINTS

NT LAP JOINTS

NT METAL JOINTS

NT RIVETED JOINTS

NT SEAMS (JOINTS)

NT SOLDERED JOINTS

NT SPOT WELDS

NT WELDED JOINTS

Characteristics, production, and stress analysis of adhesive bonded joints [UTIAS-28] 02 p0236 N71-20092

Design and development of flexible joint for pressure suits [NASA-CASE-XMS-09636] 03 p0328 N71-12344

Fretting and geometric stress concentration effects on fatigue life of aluminum alloy clamped joints [REPT-1112/70] 03 p0386 N71-13265

Photoelastic analysis of fatigue behavior of welded connections 04 p0615 N71-13557

Developing stress indices and simplified design formulas for use in stress analysis of small branch connections with external loadings 04 p0617 N71-14006

Fracture mechanics and time dependent strength of adhesive joints [NASA-CR-111761] 04 p0617 N71-14080

Calculating effective neutron multiplication factor for complicated pin interaction problems using CSR Monte Carlo neutron transport code [REP-1499] 05 p0741 N71-15106

Development of optimum fabrication techniques for brazed stainless steel transition joints [NASA-CR-72746] 05 p0694 N71-15508

Evaluation of characteristics and integrity of casing-lifting ring assemblies [NVO-416-2] 05 p0781 N71-15662

Optimization of pin-joint frames, cantilever members, and machine tool structures [ARC-31/M-3632] 06 p0933 N71-15797

Deformation mechanics of crack initiation in structurally bonded joints under loading [AD-715712] 08 p1296 N71-18522

Aerodynamic interference effects between wing and fuselage junctions 09 p1311 N71-19354

Thermal shock testing of coextruded and brazed tubular joints of stainless steel and tantalum for SNAP-8 applications [NASA-CR-72629] 11 p1795 N71-22511

Elbow forming in jacketed pipes while maintaining separation between core shape and jacket pipes [NASA-CASE-XNP-10475] 13 p2085 N71-24679

Cooling rate and yield strength effects on tensile properties of brazed joints 13 p2094 N71-24912

Method and apparatus for precision sizing and joining of large diameter tubes by bulging or constricting overlapping ends [NASA-CASE-XNP-03114-2] 14 p2262 N71-26148

Universal joints for connecting two displaced shafts or members [NASA-CASE-NPO-10646] 16 p2601 N71-28467

Flexible bellows joint shielding sleeve for propellant transfer operations [NASA-CASE-XNP-01855] 16 p2604 N71-28937

Mechanism for restraining universal joints to prevent separation while allowing bending, angulation, and lateral offset in any position about axis [NASA-CASE-XNP-02378] 16 p2604 N71-28951

Fatigue properties of titanium and titanium alloys - fatigue strength of bolted, riveted, spot welded, and brazed joints [RAE-LIB-TRANS-1135] 17 p2767 N71-30382

Materials, manufacture, quality control, and mechanical properties of bolted joints under static and dynamic stresses [NLL-CE-TRANS-3406-1922.09] 22 p3590 N71-35563

Static and fatigue tests of aluminum double strip joints bonded with nitrile epoxy adhesives [UTIAS-168] 22 p3609 N71-36307

Prediction of bolted joint heat transfer in spacecraft applications [NASA-CR-119933] 22 p3604 N71-36346

Characteristics of aluminum compression joints and methods for analyzing contact corrosion [NLL-CA-TRANS-637-6196.3] 23 p3775 N71-36906

Tensile tests on lap-joints carbon fiber reinforced plastics [AD-727034] 23 p3779 N71-36934

JORDAN FORM

Reduction of square matrices to Jordan canonical forms [FOA-P-C-8238-11] 05 p0712 N71-14544

Matrix ring formulations of Artinian semi-simple ring with involutions 13 p2104 N71-25458

Jordan decompositions for n-dimensional vector space and geometric properties of solutions to a prime equals A differential systems [ORNL-4686] 21 p3449 N71-34549

JOSEPHSON JUNCTIONS

Using phase lock techniques to study electrical and magnetic properties of metal superconductor Josephson junctions [NASA-CR-116871] 08 p1245 N71-19208

Superconductivity studies, including flux flow, Josephson junctions, and tunneling [AD-716598] 09 p1423 N71-19643

Quantum method of maintaining volt as SI unit using a Josephson effect in superconductors 12 p1920 N71-23646

Noise level of Josephson junction amplifier at cryogenic temperatures [AD-720353] 14 p2228 N71-25947

Phase fluctuations in driven Josephson oscillator [AD-723235] 19 p3167 N71-31669

Josephson junction formation, and chemisorption of organics on Pb surfaces [NASA-CR-121732] 21 p3402 N71-34204

Derivation and analysis of Josephson effect in superconducting weak links [AD-726537] 22 p3658 N71-36085

JOUKOWSKI TRANSFORMATION

Direct and inverse application of Dorodnitsyn technique to incompressible transonic flow over symmetric Joukowski airfoil sections [NAL-TR-2207] 09 p1316 N71-19750

Digital computer and plotter for simulating flow about Joukowski airfoil [TECH-71-4] 20 p3206 N71-33403

JOULE HEATING

U OHMIC DISSIPATION

U RESISTANCE HEATING

JOULE-THOMSON EFFECT

Joule-Thomson coefficients for water vapor [PT-IFT-391] 21 p3530 N71-35157

JOURNAL BEARINGS

Development and tests of control drum bearings for SNAP-8 [AIAA-EC-12964] 04 p0550 N71-14170

Computerized optimization of self acting herringbone journal bearings for maximum radial load capacity [NASA-TM-X-52545] 05 p0691 N71-14849

High speed, gas journal bearings [AD-713877] 06 p0865 N71-16259

Life prediction of ultrahigh vacuum solid lubricating coatings for journal bearings [DLR-FB-70-28] 07 p1033 N71-17172

Effect of velocity slip at porous boundary on performance of incompressible porous bearing [NASA-TM-D-6181] 07 p1034 N71-17327

Sodium lubricated bearing technology for high capacity pumps used in fast breeder reactors
[NYO-3930-8] 06 p1205 N71-18328

Water-lubricated three-lobe hydrodynamic journal bearing stability tests at zero load with and without axial grooves
[NASA-TN-D-6315] 12 p1926 N71-23730

Torque for measuring potassium film journal relative motion with coil and wire diameter, temperature, frequency, and holder material effects on transducer and journal materials
[NASA-CR-72821] 12 p1939 N71-24088

Computer program for determination of optimal bearing/journal bearing for maximum radial load capacity
[NASA-TN-D-6351] 14 p2360 N71-25665

Foil journal bearings for Brayton cycle turboalternator
[NASA-CR-72864] 15 p2417 N71-27772

Prevention of steam hammer instability and film collapse caused by condensation in steam lubricated bearings
[AD-72205] 16 p2600 N71-28398

SNAP 8 pump-motor journal and thrust bearing wear tests with high temperature sodium-potassium alloy lubrication
[NASA-CR-72824] 17 p2757 N71-30121

Hydrodynamic lubrication of journal bearing with one or two axial oil grooves, with power loss, load capacity, oil flow, and stability charts for design of minimum power loss, stable bearing
20 p3280 N71-33799

Numerical analysis of oil film thickness required for optimum operation of hydrodynamically lubricated journal bearings
[CRANFIELD-M/P-3] 21 p3433 N71-34429

Performance tests of water-lubricated, Rayleigh step, hydrodynamic journal bearings under no load conditions to determine stability
[NASA-TN-D-6514] 23 p3762 N71-36820

Stability of central equilibrium position of journal in bearings with gas lubrication
[AD-72720] 24 p3928 N71-38025

JOURNALS [DOCUMENTS]

U PERIODICALS

JOURNALS [SHAFTS]

U SHAFTS [MACHINE ELEMENTS]

JP-5 JET FUEL

Electrostatic charge by JP-5 jet fuel at truck fill stand with 30-second relaxation chamber and bottom loading
[AD-717347] 11 p1819 N71-22232

JUNCTION DIODES

Investigating categorization and formulation of stress and strength factors for semiconductor diodes to provide improved failure rate prediction from mathematical models
[NASA-CR-115801] 04 p0603 N71-14311

Capacitance calculation for diffused p-n junction with exponential doping gradients
[NASA-TM-X-2179] 07 p1094 N71-17806

Investigating effects of high energy proton irradiation on carrier lifetimes of junction diodes and solar cells
[NP-18472] 08 p1259 N71-18669

Analysis of reverse recovery in transient response of p-n junction diodes
24 p3900 N71-37798

N-P junction diode detector used in design of radioactive source non-contact encoder
[NASA-TM-X-65715] 24 p3920 N71-37956

JUNCTION TRANSISTORS

Low power NAND gate integrated circuit employing thin film resistors and lateral p-n-p transistors
[NASA-TM-116421] 07 p1002 N71-17872

Electrical properties and breakdown voltages for two complementary p-n and n-p junctions
10 p1532 N71-20846

Low frequency noise sources in bipolar junction transistors and efforts to reduce burst noise
14 p2230 N71-26576

Rectification efficiency and reliability of driven transistor synchronous rectifiers
[NASA-TM-X-65595] 17 p2726 N71-30097

Unijunction transistor signal analysis and steady state input and output voltage-current characteristics including diffusion and conduction currents for extrinsic base materials
23 p3734 N71-36620

JUPITER [PLANET]

Particles and fields near Jupiter
[NASA-CR-1685] 01 p0119 N71-10051

Radio telescope observations of Jupiter, Venus, and source 3C 273 at 2 and 8 mm wavelengths
[NASA-TT-F-13383] 01 p0123 N71-10938

Centaur launch vehicle for Jupiter and Saturn orbiter missions using solar electric propelled spacecraft
[NASA-CR-111422] 02 p0299 N71-12041

Polarization curves for four Galilean satellites of Jupiter
[NASA-CR-115783] 04 p0609 N71-13556

Jovian magnetic field geometry and its modulated decimetric radio emission
[NASA-TM-X-65397] 04 p0612 N71-14126

Reporting DSN support of active and planned interplanetary missions by Pioneer spacecraft

Properties of interplanetary medium from radio emissions of planet Jupiter
07 p0993 N71-17614

News releases, and abstracts of scientific articles concerning astronomy
07 p1111 N71-17670

Investigation of survivability of spacecraft components during entry of Jupiter atmosphere to determine probability of biological contamination
11 p1824 N71-21952

Influence of great equality between Jupiter and Saturn on secular disturbing function of principal planets
[NASA-TM-X-2276] 12 p1863 N71-23824

Investigation of periodic nature of Jupiter bursts to determine correlation with position of satellite IO and central meridian of longitude of Jupiter
[NASA-TN-D-6279] 13 p2170 N71-25497

Comparison of integration techniques applicable to determination of orbits of Jovian ninth and twelfth satellites with variation of parameters integration experimentation
13 p2170 N71-25498

Direct trajectories to Jupiter and Saturn - data tabulations
[NASA-TM-X-67252] 18 p3010 N71-30908

Structural compositions of Jupiter, Saturn, Uranus, and Neptune
[NASA-TT-F-15901] 19 p3180 N71-32348

Analysis of intensity fluctuations produced by interaction of Jovian decametric radio emission with interplanetary medium
19 p3176 N71-32357

Development of 16-element crossed dipole array for observations of Jupiter
[REPT-30] 19 p3058 N71-32645

Runge-Kutta analysis of hypothetical comet motion from Jovian surface, and possible origin of short-lived comets in Jovian surface eruptions
[NASA-TT-F-13788] 20 p3348 N71-33406

Pioneers F and G with data return capability from Jupiter vicinity
21 p3390 N71-34122

Soviet news releases on heat balance of northern polar cap of Mars, spectrophotometric studies of giant planets, and Jovian radio emission
21 p3509 N71-35005

Waveform and source size characteristics of Jovian decametric radiation using long baseline radio interferometry
21 p3511 N71-35023

Analysis of typical Jupiter-Saturn-Pluto trajectory to determine characteristics of outer planet space missions and planetary quarantine constraints
[NASA-CR-121804] 22 p3669 N71-36160

Interior structure of Jupiter, Saturn, Uranus, and Neptune
23 p3846 N71-37414

Analysis of Jupiter probe space missions and characteristics of probes for completion of mission
[NASA-CR-122966] 23 p3848 N71-37423

Spectroscopic observations of planets showing absorption variations in NH₃ and CH₄ bands
[NASA-CR-123152] 24 p4007 N71-38573

JUPITER ATMOSPHERE

Particles and fields near Jupiter
[NASA-CR-1685] 01 p0119 N71-10051

Constructing atmospheric models of Jupiter and Saturn for space vehicle design criteria
01 p0121 N71-10253

Research studies on development of Thermoelectric Outer Planet Spacecraft (TOPS) and lunar exploration
[NASA-CR-117440] 10 p1644 N71-21338

Ammonia and water properties in modelling Jupiter and Saturn atmospheres
10 p1644 N71-21340

Vibrational spectra of molecules and solid materials from 4000 to 33 cm in Jovian atmosphere
[NASA-CR-117900] 12 p1970 N71-23335

Investigation of survivability of spacecraft components during entry of Jupiter atmosphere to determine probability of biological contamination
[NASA-TM-X-2276] 12 p1863 N71-23824

Vibrational spectra of molecules expected in Jovian atmosphere
[NASA-CR-117888] 12 p1994 N71-24259

Science, navigation and trajectory, mechanical subsystems, and telecommunications design trade studies for Jupiter atmospheric entry mission planning
[NASA-CR-118021] 12 p1999 N71-24337

Jupiter atmospheric entry mission rationale with environmental models, science criteria, mission and system evolution, baseline data, mission design, and illustrative sample missions
[NASA-CR-118022] 12 p1999 N71-24338

Management summary and technical requirements for Jupiter atmospheric entry mission in 1978 using TOPS or Pioneer F/G spacecraft
[NASA-CR-118023] 12 p2000 N71-24339

Effect of microwave absorption and decimetric radio noise in Jovian atmospheres on radio communication in 1 to 10 GHz frequency band
[NASA-CR-114288] 18 p2962 N71-30739

Measurement of two circular polarization components of Jovian decametric radiation, and evidence for existence of fourth LH source
19 p3182 N71-32317

Terrestrial organisms survive in simulated Jupiter atmosphere - studies with one-celled algae and aquatic plant (Elodea)
[NASA-TT-F-13905] 20 p3349 N71-33388

Adaptation of terrestrial microorganisms to simulated Jupiter environment
[NASA-TT-F-13944] 23 p3714 N71-36472

Lower atmospheres of Mars, Venus, and Jupiter
23 p3846 N71-37412

Composition and evolution of Earth, Mars, Venus, and Jupiter atmospheres
23 p3847 N71-37411

Science and engineering tradeoffs for Jupiter atmospheric entry probe mission
[NASA-CR-123120] 24 p4006 N71-38540

JUPITER PROBES

Mission analysis for application of Helio gyro solar sailer concept to Jupiter flyby
[NASA-CR-115852] 05 p0771 N71-15316

Mission planning for Jovian turbopause probe
[NASA-TM-X-65671] 20 p3355 N71-33600

Preliminary feasibility of depositing atmospheric entry probe from flyby mission to Jupiter
[NASA-TM-X-2338] 22 p3670 N71-36166

JUPITER PROJECT

Planning for Pioneer 5 and 6 interplanetary mission with Jupiter flyby
[NASA-SP-268] 19 p3181 N71-32346

K

K BAND

U EXTREMELY HIGH FREQUENCIES

K LINES

Calcium K line formation in nonhomogeneous solar chromosphere
13 p2166 N71-24941

Synchrotron radiation of carbon, boron, and beryllium and observations of k lines in ultraviolet X ray emission spectra
[DESY-70/59] 19 p3151 N71-32142

K line emission spectrum of lithium for energies above and below Sommerfeld threshold determined using many body diagrammatic techniques
21 p3442 N71-34491

Fine structure and quantitative reduction of H alpha and beta lines and K lines inside focal areas
[NLL-RTS-6401] 23 p3842 N71-37799

K-MESONS

Examining assumption of pion, eta-meson, and sigma-meson dominance of weak and electromagnetic decays of K meson using hard meson current algebra
[NUB-2048] 08 p1257 N71-18411

K-meson nuclei existence at low energies
[IPVIE-ST/SPK-70-30] 15 p2488 N71-27877

NaI crystal spectrometer measurements of cross sections for Mg-25(tau, gamma)Si-28 reaction at E sub tau equals 4.44, 6.08, 6.15, and 8.26 MeV
[ANU-P/508] 20 p3314 N71-32901

KA BAND

U EXTREMELY HIGH FREQUENCIES

KALMAN-SCHMIDT FILTERING

Sensitivity algorithm for random error in Kalman filter and predictors
[NASA-CR-111108] 01 p0036 N71-10394

Kalman's extension of filtering and optimization of linear stochastic systems with cross correlated noise
01 p0037 N71-10819

Performance of discrete suboptimal Kalman filters and discrete optimal adaptive filters
[NASA-CR-111414] 02 p0197 N71-11378

Developing digital computer program for correcting soft parameters of thermal network by Kalman filtering method
[NASA-CR-106681] 02 p0305 N71-11405

Applying Kalman filtering to problems of barometric pressure and inertial heights in navigation
[RAE-TR-69131] 02 p0262 N71-11763

Kalman filtering algorithm for hybrid navigation in army aircraft
[AD-715553] 05 p0721 N71-15398

Mathematical models of suboptimal Kalman filter control systems with delayed states for navigation satellite
[AD-714501] 06 p0094 N71-14085

Empirical Bayes filter for use in trajectory estimation and comparison of performance with Kalman filter
[NASA-CR-114897] 09 p1409 N71-19915

Kalman filtering for spectral factorization and matrix solution to spacecraft tracking problem
12 p1645 N71-21339

Kalman linear least squares filtering applied to estimation of fuel quantity and rate for Pioneer aircraft
[AD-717640] 11 p1672 N71-21922

- Analysis of computer requirements for linear filtering algorithms [AD-718410] 12 p1949 N71-23577
- Development of adaptive estimators for application to numerical analysis of automatic navigation and control [AD-720394] 14 p2282 N71-24007
- Kalman formulation of minimum mean square linear estimation with random variables and unknown distributions producing biased results [NASA-CR-118665] 14 p2284 N71-24629
- Minimum variance estimates of signal derivatives with application to case of aircraft descent rate in instrument landing systems [NASA-CR-111928] 17 p2703 N71-30241
- Design of aided, long duration, strapdown inertial navigation system with Kalman filter to process information and estimate errors 19 p3133 N71-32287
- Self-adaptive solution to problem of optimal filtering, prediction, and smoothing of stochastic signals embedded in random noise 21 p3398 N71-34180
- Kalman filtering techniques for estimating position and velocity of spacecraft 22 p3617 N71-35771
- Modeling error effects on performance of Kalman estimators 23 p3730 N71-36392
- KANSAS**
- Probable response of Kansas streams to various patterns of rainfall augmentation [PB-196310] 10 p1502 N71-21683
- Fuel burning and refuse disposal practices, air pollutant emissions, and abatement plans for Federal facilities in counties in Kansas and Missouri 22 p3577 N71-35481
- KAON PRODUCTION**
- Backward photoproduction of positive kaons from hydrogen [JAL-1236] 03 p0430 N71-2903
- Positive kaon proton partial wave analysis at 860 to 1210 MeV/c [UCRL-19787] 03 p0433 N71-2943
- Using current algebra and vector meson dominance methods for S-wave kaon-nucleon scattering [SINP-TH-67-17] 05 p0739 N71-15021
- Investigating reaction $K^+p \rightarrow \pi^+n$ yields K^+N and π^+N in isospin-0 channel near K^+N threshold [UCRL-19774] 05 p0748 N71-15280
- Partial cross sections for final states corresponding to 4 and 2 prong plus vee topologies in K^+p/π^+p inelastic channels [CALT-68-274] 06 p0916 N71-16023
- Magnetic moment of positive Sigma hyperons and positive kaon and positive Sigma hyperon decay observed in optical spark chamber located inside bore of solenoidal pulsed magnet 16 p2660 N71-29197
- KAONS**
- Axial vector dominance and estimate of radioactive positive kaon decay mode 02 p0274 N71-11831
- Current algebra and vector dominance in neutral kaon decay mode 02 p0274 N71-11832
- Pion-proton-, kaon-proton-, and pion deuteron interactions [UCR-34-P-107-104] 03 p0423 N71-12743
- Test of change in S equals change in Q rule in neutral kaon sub c3 decay [CALT-68-251] 03 p0425 N71-12827
- Three body decays of neutral K mesons [COO-1195-187] 03 p0425 N71-12828
- Kaon/d reaction at 3.8 GeV/c 03 p0426 N71-12849
- K plus p elastic scattering at 2.53, 2.76, and 3.20 GeV/c [COO-1195-191] 03 p0430 N71-12906
- Coherent K meson production in positive kaon deuteron interactions at 9 GeV/c 04 p0581 N71-14024
- Investigating twin meson production in K/d reactions for compatibility with simple quark model [COO-1428-227] 04 p0583 N71-14176
- Constructing double Regge exchange model for kaon production in K/Kn reactions at 9.0 GeV/c [COO-1428-229] 04 p0583 N71-14177
- Elastic Kn scattering and charge exchange taking branching into account [ITEP-754] 04 p0585 N71-14231
- Duality diagram and Regge cuts in kaon/photoproduction 04 p0588 N71-14285
- Cross sections of strange particles [UCRL-19845] 06 p0915 N71-16011
- Experimental limit on branching ratio for neutral kaon sub L yields lepton antilepton [UCRL-20078] 06 p0924 N71-16759
- Neutral kaon resonance production in positive kaon deuteron interactions within bubble chamber [UCRL-20076] 06 p0925 N71-16812
- Kaon nucleon and antikaon nucleon total cross sections below 3.5 GeV/c [UCRL-19844] 06 p0925 N71-16813

- Kaon/ yields positron neutrino to kaon/ yields muon/ neutrino [UCRL-20079] 06 p0925 N71-16837
- Test of Delta S equals Delta Q selection rule in kaon sub c3 decay [COO-1195-195] 06 p0926 N71-16839
- Positive kaon-proton elastic scattering cross section [COO-1195-196] 07 p1075 N71-17513
- Negative kaon proton interactions at 12.6 GeV/c 08 p1267 N71-19323
- Soft pion limits for kaon decay amplitudes [NYO-1932/2-184] 09 p1426 N71-19521
- Isospin conservation test from antikaon proton interactions at 400 MeV/c from absolute and differential cross sections and differential polarizations of hydrogen bubble chamber photos 09 p1427 N71-19493
- Measuring backward elastic scattering of positive kaon proton and negative kaon proton events [CEA-R-3485] 09 p1438 N71-20189
- Phenomenological Lagrangian models for nonleptonic kaon decays and application of Delta I absolute value equals 1/2 rule [BNL-50260] 10 p1614 N71-20934
- Decay mode for neutral kaon sub L yields positive pion, negative pion, neutral pion [UCLA-1052] 10 p1617 N71-21264
- Neutral kaon decay yields pion, muon, neutrino form factor measurements in wire chamber with energy dependence expressions and nuclear coupling coefficients [UCLA-1054] 10 p1619 N71-21711
- Phase shift analysis for determining kaon-nucleon elastic scattering amplitudes 10 p1623 N71-21771
- One-pion exchange model used for analysis of reaction negative kaon neutron yields negative kaon negative pion proton at 12.6 GeV/c [TID-25611] 10 p1624 N71-21797
- Kaon and proton elastic scattering at small angles and energies of 0.40 to 0.73 GeV/c 11 p1801 N71-21879
- Regge pole approximation in pion model for kaon decay [NYO-2262-TA-233] 12 p1971 N71-23878
- Isotopic spin analysis and current algebra kinematics of positive kaon decay modes from propane bubble chamber photographs of pion emissions 13 p2131 N71-25030
- Statistical tensor analysis of delta distributions and hyperon polarizations for Y 1385 resonance from positive pion proton yields kaon resonance Lambda hyperon positive pion with quark model [INP-731] 13 p2140 N71-25525
- Production of positive and negative kaons and proton proton pairs in four body nuclear reactions at 13.1 GeV/c [COO-1428-249] 13 p2141 N71-25542
- Propane bubble chamber photographic analysis of kaon tau decays and calculation of final state pion energy distributions with comparison to nuclear resonance models 13 p2142 N71-25556
- Obtaining accurate determination of real parts of kaon-proton forward scattering amplitudes at moderate energies [JINR-E2-5216] 14 p2309 N71-26629
- Interaction cross sections of antikaon deuteron yields kaon Y1 Y2 [JINR-P2-5231] 14 p2314 N71-26728
- High energy pion nucleon and kaon nucleon scattering data at transferred momenta for checking Regge pole hypothesis [JINR-P2-5230] 15 p2457 N71-26868
- Lagrangian calculation of kaon form factors [JINR-P2-5290] 15 p2460 N71-27070
- Current algebra for nonleptonic kaon decay modes 15 p2479 N71-27637
- Kinematics of neutral kaon S electron decay with analysis of charge exchange and strangeness 15 p2484 N71-27781
- Asymmetry parameters of leptonic Sigma hyperon decays in negative kaon beam interactions 15 p2487 N71-27835
- Magnetic spark chamber spectrometer for high energy kaon regeneration studies [JINR-P1-5361] 15 p2488 N71-27842
- Compilation of experimental data on real parts of kaon/plus or minus/ proton forward scattering amplitudes [JINR-E1-5259] 15 p2491 N71-27914
- Double emission of Lambda hyperons in negative kaon/plus or minus/ interactions with nucleus of photonic nuclear emulsion [JEN-217-IFIC-4] 16 p2649 N71-28815
- Absorption at rest and low energy elastic scattering of negative kaons by neon with various final state interaction data [TID-25667] 16 p2653 N71-29007
- Compilation of cross sections of reactions by negative kaons on protons, neutrons, and deuterons [CERN/HERA-70-6] 16 p2658 N71-29166

- Hard meson method for studying radiative leptonic decays of pions and kaons 17 p2796 N71-29793
- Three body states Lambda or Sigma hyperon kaon antikaon and Xi hyperon kaon pion produced by negative kaon proton interactions at kaon beam momentum of 2.5 GeV/c [ORO-2504-170] 17 p2797 N71-29845
- Kaon pion/kaon pion decay branching ratio of kaon resonance [UR-675-352] 17 p2798 N71-30008
- Validity of soft pion limit and existence of absolute value of Delta I vector equals 1/2 rule for nonleptonic weak kaon decays, and use of Lagrangian models [NYO-1932/2-183] 17 p2799 N71-30017
- Optical spark chamber experiment to test validity of Delta S equals Delta Q selection rule in neutral kaon decay into 3 electrons 17 p2802 N71-30188
- Optical spark chamber search for neutral kaon sub S decay into 3 pions 17 p2802 N71-30189
- Optical spark chamber search for neutral kaon sub S decay into 3 pions - summary 17 p2803 N71-30190
- Optical spark chamber test of Delta S equals Delta Q selection rule in neutral kaon decay into 3 muons [COO-1195-200] 17 p2803 N71-30191
- Optical spark chamber test of Delta S equals Delta Q selection rule in neutral kaon decay into 3 muons - summary 17 p2803 N71-30192
- Experimental results on kaon/plus/ deuteron interactions from 865 to 1365 MeV/c incident beam momentum [UCRL-20248] 17 p2803 N71-30216
- Differential cross section for low momentum negative kaon helium-4 elastic scattering from 115 to 160 MeV/c 17 p2806 N71-30306
- Partial wave analysis of positive kaon proton elastic scattering to show resonance in direct channel [UCRL-20248-151] 17 p2808 N71-30337
- Violation of absolute I vector equals 1/2 rule in kaon decays into 3 leptons [TR-71-112] 17 p2809 N71-30369
- Coherent production of positive kaon, positive pion, negative pion system by negative kaons of momenta 5.5, 10.0, and 12.7 GeV on Ne, C, F, and Br nuclei [LAL-1242] 18 p2975 N71-30569
- Determination of Delta T equals 7/2 transition in kaon decay into 3 leptons [JIVE-STF-70-14] 18 p2977 N71-30651
- Fourier analysis of Q/1240 to 1400/ resonance in kaon pion states produced in kaon proton interaction [JINR-E2-5656] 18 p2994 N71-30653
- Constant behavior of total cross section above 30 GeV, pion-nucleon charge exchange scattering, and kaon regeneration amplitude on hydrogen [JIVE-STF-70-3] 18 p2985 N71-31160
- Kaon/0 sub lifetime and CP violating parameter phase from 3725 kaon/0 yields pion/plus/ pion/minus/ decays 19 p3158 N71-32538
- Magnetic spectrometer for studying negative pion plus proton interactions from 30 to 60 GeV/c and negative kaon plus proton and proton proton interaction from 20 to 40 GeV/c [NP-18764] 19 p3158 N71-32562
- Partial cross section and resonance production of strange particles measured in deuteron filled bubble chamber exposed to negative kaon beam 19 p3159 N71-32599
- Branching ratio and relative rates of positive kaon decays, and upper limit for structure dependent radiation in kaon decay into electron neutrino photon 19 p3162 N71-32778
- Splitting in positive kaon positive pion negative pion mass spectrum in positive kaon deuteron interactions at 9 GeV/c [COO-1428-270] 21 p3481 N71-34792
- Lack of CP invariance violation in kaon decay into mode [PIUAC-4159-24] 21 p3481 N71-34795
- Delta 1 equals 1 mass shift, kaon electromagnetic mass shift, and eta meson yields 3 pion decay amplitude [SU-1206-245] 21 p3482 N71-34803
- Spark chamber and spectrometric analysis of kaon decay branching ratios for electron neutrino events and vector-axial theory test for weak interactions [UCRL-20031] 21 p3485 N71-34826
- Lambda[0] hyperon polarization along sigma-[0] hyperon decay plane by violating time reversal invariance in electromagnetic interactions of kaon/minus/ or sigma/minus/with protons 21 p3487 N71-34842
- magnitude measurements of kaon[0] sub L kaon[0] sub S mass difference and Lambda hyperon proton interactions at high energies 21 p3488 N71-34849
- Local models from D/D formalism for antikaon-nucleon collisions [PAM-70-1] 22 p3636 N71-35919

- Single and double pion production and charge exchange reaction from positive kaon proton and positive kaon deuteron interactions at 1585 MeV/c in 25-inch bubble
[UCRL-26628] 22 p3639 N71-35937
- Argand diagram analysis of Pomeron coupling to kaon nucleon and antikaon nucleon system
22 p3643 N71-35988
- Kaon-proton interactions and low mass enhancement due to diffraction phenomena
22 p3651 N71-36034
- Coherent production of kaon states and study of their decay into neutral pions
[LAL-1244] 23 p3809 N71-37156
- Spin polarization parameters in kaon[plus] proton and kaon[minus] proton elastic scattering at 6 to 18 GeV
[NP-18830] 23 p3809 N71-37158
- Double arm spectrometer for stringent limit determination on decays kaon[O] sub L yields muon[plus] muon[minus], positron electron, muon[plus] or muon[minus] or electron
[UCRL-20264] 23 p3812 N71-37184
- Resonance in kaon[minus] proton reactions, Veneziano model in antikaon nucleon reactions, kaon[minus] beams in 31 in. deuterium chamber, and related technical and theoretical developments
[NYO-3178-8] 23 p3812 N71-37186
- Compilation of reaction cross sections produced by positive kaons on proton, neutron, and deuteron targets
[CERN-HERA-70-4] 24 p3971 N71-38331
- Cross sections and angular distributions in kaon[minus] deuteron yields kaon[minus] deuteron and kaon[minus] neutron yields kaon[minus] neutron interactions
[NP-18891] 24 p3974 N71-38354
- Separation of kaon[minus] proton interactions from kaon[minus] nucleus interactions in kaon[minus] proton yields Lambda[0] hyperon pion[plus] pion[minus] reaction
[LAL-R1-71-2] 24 p3974 N71-38357
- KAPTON [TRADEMARK]**
- Tensile strength degradation in water immersed polyimide Kapton
[RM-504] 12 p1871 N71-23782
- Solvent effects on Kapton polyimide thin film tensile properties
[RM-510] 16 p2554 N71-28087
- Mylar, Teflon, and Kapton film effects at elevated temperatures on compression tests of cellular silicone rubbers used to cushion dissimilar weapons-related components
[BDX-613-410] 23 p3778 N71-36925
- KC-130 AIRCRAFT**
U C-130 AIRCRAFT
- KEELS**
- Aerodynamic and deployment characteristics of twin tool all-flexible parawing rigged with several variations of multistage canopy and suspension line reefing system
[NASA-TN-D-4306] 18 p2865 N71-30748
- KELVIN TEMPERATURE SCALE**
U TEMPERATURE SCALES
- KEPLER LAWS**
- Equations of motion of satellite orbits using Kepler laws and Euler-Lagrange equation
[BMW-FB-W-70-68-PT-1] 11 p1825 N71-22039
- Three dimensional vector forms of selected section relationships applied to n-body trajectory simulation based on virtual mass concept
[NASA-CR-118894] 15 p2435 N71-27761
- Spacecraft trajectory analysis in many body inverse square force field based on Kepler laws and Encke method without numerical integration
[RE-407] 16 p2677 N71-28090
- KERATITE**
- Ultraviolet radiation effects on human and animal eyes
[AD-711360] 01 p0013 N71-10753
- KERNEL FUNCTIONS**
- Flutter analysis for thin lifting surfaces by application of supercubic kernel function procedure
[NASA-TN-D-6012] 01 p0131 N71-10866
- Point kernel techniques for use with nuclear reactor shielding methods, modification, updating, and input data preparation - Vol. 6
[NASA-CR-102969] 05 p0729 N71-15167
- Continuous representation and kernel functions
[SU-1206-227] 07 p1050 N71-17205
- Integral Boltzmann transport equation for monoenergetic neutrons solved by direct kernel decomposition
[RTI/ET/70/27] 16 p2643 N71-28083
- Nonlinear operator for determining complete continuity when kernel is function of variables
[NASA-CR-119014] 16 p2622 N71-28404
- Method for calculating flutter using interference aerodynamic forces between wing and tail
17 p2699 N71-29345
- Calculation of pressure distributions over wings with harmonic oscillating control surfaces using kernel function method
17 p2699 N71-29346

- Computer program for calculating thermal neutron scattering kernels by phonon expansion of coherent and incoherent scattering approximations
[JAERI-MEMO-4211] 18 p2980 N71-30732
- Spanwise integration of kernel functions for calculating wing lift distributions in subsonic flow
20 p3205 N71-33219
- Cubic spline approximation for integrals with logarithmic kernels
[NAL-TN-27] 21 p3447 N71-34533
- Computer program and thermal scattering kernels for Be, BeO, CH₂, C₆H₆, and ZrH₂ obtained from basic physics models
[GULF-BT-10469] 21 p3478 N71-34770
- Buildup factors and energy spectra through lead/water slab layers for point isotropic sources utilizing radiation transport point matrix kernels
[COO-2060-10] 21 p3486 N71-34838
- KERR CELLS**
- Experimental design using single ultrashort pulses for triggering Kerr cells and producing laser radiation to heat lithium deuteride targets for high temperature plasma generation
[NASA-TT-F-13662] 13 p2088 N71-24641
- Optical correction procedure for diffraction pattern and temperature effects on Kerr cell high voltage pulse measurements
[SC-CR-70-6153] 15 p2386 N71-27253
- KERR ELECTROOPTICAL EFFECT**
- Polarization dependence of stimulated Rayleigh scattering and electro-optical Kerr effect
[NASA-CR-111362] 01 p0092 N71-10984
- KETENES**
- Preparation and properties of polyacrylonitrile fibers with diketene as comonomer
[RAE-LIB-TRANS-1464] 05 p0709 N71-15175
- KETONES**
- Chemical properties and thermal oxidation of polyolefins
[AD-715430] 08 p1159 N71-18886
- KEYING**
- FREQUENCY SHIFT KEYING
NT PHASE SHIFT KEYING
- KIDNEY DISEASES**
- NT NEPHRITIS
- Activity of lactic dehydrogenase in urine of glomerulonephritis and nephrotic syndrome patients
[NASA-TT-F-13558] 12 p1863 N71-23728
- KIDNEYS**
- Investigating long term effects of proton irradiation on renal pathologic anatomy of dogs
08 p1150 N71-18897
- Relationship between diurnal and meal driven excretory patterns in human kidney during bed rest
20 p3218 N71-33268
- Water-salt metabolism under space flight conditions and body weight loss
[NASA-TT-F-14029] 24 p3877 N71-37639
- KINEMATIC EQUATIONS**
- Characteristics of collisional kinetic equations and solutions using constants of motion method including Chandrasekhar, Hamiltonian, Vlasov, and Langevin formulations
[NASA-TM-X-65493] 12 p1970 N71-23302
- Mathematical formulation of kinematic equations to describe motion of six degrees of freedom vibration table for use in research on human subjects
[AD-720269] 14 p2210 N71-26158
- KINEMATICS**
- NT BODY KINEMATICS
- Algebraic approach to theory of nuclear structure
[NYO-2171-368] 01 p0094 N71-10336
- Basic kinematics and dynamics of human centrifuges and other aerospace simulators including coriolis and gyroscopic effects
[AD-711635] 01 p0014 N71-10883
- Centrifugal barrier penetration factors used in meson decay kinematics
[UCRL-19626] 03 p0421 N71-12653
- Two-body relativistic kinematics code written in FORTRAN
[LA-4349] 03 p0427 N71-12859
- Determining kinematic characteristics of turbulent flows by flow visualization and photography
[NASA-TT-F-13133] 04 p0518 N71-13768
- Kinematics of diffusion, fluids, and plasma by continuous movement and finite velocities
[AD-713588] 05 p0665 N71-15540
- Massive particle scattering amplitude kinematics in four-momenta space
09 p1430 N71-19766
- Mathematical link-system model for computerized simulation of human movement in cockpit geometry evaluation program for flight crew physical compatibility with crew stations
[AD-716398] 09 p1341 N71-19820
- Validation criteria and performance evaluation of human movement computerized simulations used in cockpit geometry evaluation program for flight crew physical compatibility with crew stations
[AD-716399] 09 p1341 N71-19821
- Integral equations of kinematics of cascade decay and energy distribution
[JINR-P1-4926] 09 p1443 N71-20450

- Multidetector system for investigating kinematics of nuclear reactions
09 p1391 N71-20400
- Swimming speed and kinematics of Black Sea fish species
11 p1681 N71-22280
- General method for kinematic synthesis and force balancing of spatial mechanisms
12 p1930 N71-24132
- Intrinsic representation of flows with Lamb surfaces
[AD-719431] 13 p2063 N71-24470
- Isotopic spin analysis and current algebra kinematics of positive kaon decay modes from propane bubble chamber photographs of pion emissions
13 p2131 N71-25910
- Contactless microwave reflectometer probe for measuring piston kinematics
13 p2084 N71-25310
- Spectrometer for microdynamics of condensed matter emphasizing automation and remote control of spectrometer kinematics and delay systems
[INP-727] 15 p2470 N71-27400
- Mathematical representation of kinematic structure of mechanisms and kinematic chains as abstract, linear graph
[AD-721567] 16 p2686 N71-28601
- Particle physics research including theoretical studies, kinematical investigations, Regge poles, and current algebras
[AD-721724] 16 p2648 N71-28630
- Regge pole theory and duality studies, including kinematics, diffraction scattering, and finite energy sum rules
[NP-18705] 16 p2651 N71-28902
- Kinematics of subsonic unsteady airloads on multiple lifting surfaces
17 p2698 N71-29339
- Regge prediction for behavior of inclusive cross sections near kinematic boundary
[RL0-1388-401] 17 p2793 N71-29547
- Kinematic distribution of crystal lattice defects
17 p2823 N71-29902
- Kinematics of continuum dislocations in crystal lattices
17 p2823 N71-29904
- Kinematics and general principles in nonlinear and linear theories of elastic shells and plates by direct approach and three-dimensional equations of classical continuum mechanics - Part I
17 p2854 N71-30220
- Rigid rotating body kinematic equations for use in space flight mechanics
[NASA-CR-119361] 18 p2965 N71-31178
- Kinematics for interstellar travel and theoretical performance analysis for nuclear and photon propelled rockets
[VKI-TN-65] 19 p3183 N71-31653
- Flight test data on geometric, aerodynamic, and kinematic characteristics of two twin keel parawings during deployment
[NASA-CR-1788] 19 p3189 N71-32308
- Kinematics of system of nuclear particles involving up to 2, 3, or 4 particles in low energy reactions
[TR-1] 19 p3160 N71-32644
- Kinematics of inclusive reactions in high energy multiparticle production
[LPTP-71/36] 20 p3315 N71-33390
- Angular distribution and velocity analysis of alkal chloride reactions
21 p3490 N71-34961
- Solar wind velocity anisotropy in relation to kinematic transport of magnetic field into interplanetary space
23 p3834 N71-39472
- Differential equations of motion for kinematics and dynamics of proportional navigation
24 p3950 N71-39100
- KINETIC ENERGY**
- Divergence, vertical velocity, and energy convection in west Mediterranean during cyclone development of 24 Oct. 1964
[TT-69-51019] 01 p0079 N71-10631
- Kinetic energy of ionic products from electron impact dissociation of molecules
01 p0102 N71-10919
- Calculating kinetic energy of atmospheric turbulence from balloon sounding data
[AD-711947] 02 p0254 N71-10940
- Theoretical treatment of conceivable serious accidents at fast breeder reactors in context of Bull-Tail method
[EURFNR-748] 04 p0546 N71-13508
- Collective interactions in fast thermostats showing kinetic instability
[AEC-TR-7164] 04 p0597 N71-14118
- Kinetic energy distributions of single fission fragment mass lines
[PEL-198] 07 p1070 N71-17800
- Expectation values and kinetic energy for vibrational-rotational levels of ground states of H₂, HD, and D₂
09 p1429 N71-19744

SUBJECT INDEX

KNUDSEN CELLS

Kalvin-Helmholtz wave model for predicting maximum amplitude, breaking mode, and turbulent kinetic energy
[AD-718841] 12 p1911 N71-23687

Kinetic energies of metastable oxygen atoms formed by electron impact dissociation of oxygen and measured in time of flight experiment
[NASA-CR-118336] 13 p2133 N71-25129

Relativistic electron and positron intensity distributions in interplanetary regions
13 p2163 N71-25288

Thresholds for nuclear reactions induced by neutrons, photons, protons, deuterons, tritons, and alpha particles - tables
[NCL-50400-VOL-9] 15 p2476 N71-27473

Vibrational kinetics of high pressure CO₂ laser mixtures
[AD-721735] 16 p2606 N71-28322

Thermal dislocation dynamics and plastic flow in crystal lattices
17 p2824 N71-29990

Low level turbulence kinetic energy and spectral energy distribution
19 p3127 N71-31883

Model of expanding universe interpreted as uniform 4-dimensional dilatation of space-time and corresponding contraction of kinetic energy parameters
[JTF-70-105-E] 19 p3146 N71-31973

Simultaneous measurements of X ray and neutron emission and kinetic energies of Cf-252 fission fragments
[CEA-R-4121] 19 p3149 N71-32101

Expression for kinetic energy transformed into work, heat, and sound during impact of spherical reactor containment vessel model and concrete block
[NASA-TM-X-67917] 20 p3358 N71-33316

Models for vector-vector-tensor meson vertex including photon coupling
[DESY-71/14] 21 p3470 N71-34703

Kinetic energy distributions of Cf-252 fission products as function of fission product mass ratios
[ORNL-TN-2453] 21 p3475 N71-34746

Using jet flap diffuser for recovery of ejector jet kinetic energy
[AD-726596] 22 p3664 N71-36123

Differential heating effects on steady-state tropical cyclone dynamics and energetics based on diagnostic axisymmetric model in isentropic coordinates
24 p3954 N71-38209

KINETIC EQUATIONS

NT HELMHOLTZ VORTICITY EQUATION
NT HYDRODYNAMIC EQUATIONS
NT KINEMATIC EQUATIONS

Group diffusion theory, reactor kinetic equations, and space independent kinetics
[WAPD-TR-960] 04 p0547 N71-13627

Computer codes for solving kinetic neutron diffusion equations in reactor safety program
[BMH-1888] 04 p0552 N71-13972

Derivation of Vlasov equation in magnetic field
[KIPN-TN-68-9] 06 p0928 N71-15735

Combined transfer scattering matrix concept for calculating space-energy-angular dependent zero power reactor kinetic equations
[ORNL-TM-3136] 06 p1602 N71-20946

Particle-in-cell method for model kinetic equations and one dimensional Krook equation
[CU-954-3] 12 p1950 N71-23745

Neutron behavior in multiplying medium, Boltzmann equation application, and derivation of related kinetic equations
[EPEN-116-4-A] 15 p2486 N71-27819

Quantum mechanics of two particle interactions in homogeneous systems including kinetic and equilibrium correlation equations using SGGKY hierarchies
15 p2487 N71-27829

Derivation of kinetic equations for slightly dense and dilute short range gases, Boltzmann equation related to short range gas equations, and role of collision events in system evolution
17 p2733 N71-29623

Duration of charged particle confinement in trap with magnetic mirrors, and solution of kinetic equation in center of trap
[AE-1972] 19 p3145 N71-31961

ANCC code for solving point reactor kinetic equations including thermal feedback
[AE-4616] 21 p3460 N71-34628

Vlasov kinetic equation for studying instability of relativistic electron beam in dense plasma
[ORNL-TN-2432] 21 p3495 N71-34898

Model powder compaction calculations using kinetic constant for entire sintering period including initial heating and isothermal soaking
[NLL-71-746-743-1922-401] 22 p3597 N71-35614

Kinetic equation solution in drift approximation for electric field effect on transfer processes in axially symmetric magnetic traps
[JONP-71667-28] 24 p3994 N71-38496

KINETIC FRICTION

NT SLIDING FRICTION
Kinetic and static friction force measurement between magnetic tape and magnetic head surfaces
[NASA-CASE-XNP-08600] 11 p1766 N71-22995

Determination of fundamental characteristics of physical processes occurring at contact surface of solid materials in the case of external friction
[NLL-RISLEY-TRANS-1992-9091.9F] 16 p3605 N71-29179

KINETIC HEATING
NT AERODYNAMIC HEATING
NT SHOCK HEATING
Collisional processes for determining kinetic temperature distribution and heating of chromosphere
13 p2077 N71-25282

KINETIC THEORY
NT CHAPMAN-ENSKOG THEORY
NT EYRING THEORY
NT MIXING LENGTH FLOW THEORY
NT TRANSPORT THEORY

Kinetic theory analysis of temperature jump at wall and temperature distribution near wall in polyatomic gases
[AD-711097] 01 p0133 N71-10693

Kinetic theory, molecular beam applications, and rarefied gas dynamics
[AD-711419] 02 p0204 N71-11752

Quantum mechanical Louisville equation and Schrödinger equation in kinetic theory
02 p0237 N71-14616

Solutions of Krook equation of kinetic theory
[AD-712684] 05 p0665 N71-15466

Marker motion studies in diffusion couples for determining atomic mobilities and vacancy wind terms in multicomponent alloys
[COD-1436-27] 05 p0751 N71-15656

Investigating kinetics and technology of impurity diffusion into silicon
07 p1087 N71-17280

Investigating kinetic theory of anomalous diffusion due to drift dissipative instability
[CEA-CONF-1596] 08 p1269 N71-18152

Describing formation and growth of gas bubbles in crosslinked elastomers as function of supersaturation pressure
08 p1160 N71-18993

Local potential of Boltzmann-type equations used in kinetic theory of gas shock waves
[IPFP-101] 09 p1369 N71-19423

Gas surface interactions and kinetic theory of rarefied gases
[AD-716572] 09 p1371 N71-19666

Applications of plasma kinetic theory to atomic spectroscopy
[AD-715997] 09 p1449 N71-20013

Kinetic theory for analysis on electrostatic probe properties in stationary quiescent plasma
12 p1983 N71-24269

Diffusion kinetics of radiochemistry in aqueous solutions after passage of high energy radiation
[CALT-767-P-4-73] 15 p2458 N71-26878

Kinetic theory of Compton scattering by relativistic electrons with induced scattering
[NASA-TT-F-13738] 17 p2829 N71-30281

Kinetic theory of optically pumped gas with equations which incorporate effects of atomic line radiation on spatial and time evolution of velocity distributions of radiating gas
[AD-722862] 17 p2760 N71-30285

Two particle microscopic distribution function for studying extended collision model in kinetic theory of gases
20 p3253 N71-33713

Electric field induced alignment and reorientation kinetics of paraelectric impurities in alkali halide crystals, using optical and calorimetric methods
22 p3659 N71-36093

Numerical analysis of constants of motion for collisional kinetics equations
[AD-726620] 23 p3830 N71-37314

Theoretical study of magnetopause current layer from kinetic theory of warm collisionless plasmas
23 p3852 N71-37330

Selected articles on kinetics and thermodynamics of diffusive combustion
[AD-726575] 23 p3866 N71-37364

Kinetic theory of fatigue propagation based on vacancy condensation mechanism
24 p4025 N71-38718

KINETICS

NT ELECTROKINETICS
NT KINETIC ENERGY
NT NEWTON THEORY
NT REACTION KINETICS

Kinetics of ohmic heating in confined toroidal plasma
[HEU-CEA-FC-538] 04 p0592 N71-14411

Kinetics of mass transfer in vibratory motion of solid body in stream of liquid
[PB-1942947] 08 p1183 N71-18983

Mechanism and kinetics of diffusion processes in metals
[TT-70-50000] 08 p2119 N71-19184

Numerical code based on double spherical harmonics approximation for analysis of coupled space-time effects in fast pulsed neutron kinetics and transport theory
09 p1432 N71-19954

Techniques for kinetic studies in shock tubes including infrared emission, electron scattering and electric discharge
11 p1739 N71-23627

Kinetics and mechanisms of rotating polymethyl methacrylate spheres
13 p2100 N71-24946

Kinetics of radiative recombination processes between donor and acceptor impurities in silicon
13 p2143 N71-25581

Kinetic process of mutual diffusion between titanium with copper and other metals serving as galvanic contacts
[TT-70-50064] 14 p2269 N71-25666

Constitutive equations and continuum mechanics for magnetic, kinetic, thermal, and material subsystem nonlinear interactions
14 p2298 N71-26652

Space-time kinetic model tests and dynamic behavior of large reactor cores using SPERT reactor
14 p2295 N71-26483

Recrystallization kinetics of magnesium-cadmium and magnesium-zinc-cadmium dilute alloys using X ray diffraction technique
17 p2826 N71-30021

Determinate errors and current impulse techniques for analyzing electrochemical kinetics of hexacyanoferrate 3/2 couple on platinum
18 p2886 N71-31232

Kinetics of free radical initiated copolymerization of 1-vinyl-3,5-dimethyl adamantane and vinyl acetate as function of glass transition temperatures
21 p3588 N71-34106

Micrometeoroid analyzer using arrays of interconnected capacitors and ion detectors
[NASA-CASE-ARC-10443-1] 21 p3427 N71-34382

Kinetics of crystal nucleation and growth in batch evaporation crystallization
21 p3501 N71-34939

Group point kinetics for studying feasibility of high flux trap reactor system
22 p3427 N71-33842

One dimensional, multigroup diffusion code for use in fast reactor criticality and kinetics parameter analysis
[JAERI-MEMO-4331] 23 p3796 N71-37063

Ion and electron plasma confinement and kinetic instabilities in adiabatic traps
23 p3853 N71-37467

Comet characteristics and composition in relation to kinetics
24 p4009 N71-38583

KINOFORM
Kinofom optical filtering techniques with applications in holography and photography
[IBM-320-2378] 21 p1715 N71-22252

KIRCHHOFF LAW OF RADIATION
Helmholtz integral and Kirchhoff approximation for sound transmission through rough air-sea interface
[AD-715566] 08 p1243 N71-18771

KIRCHHOFF-HELMHOLTZ FLOW
U PIPE FLOW
KIRCHHOFF-HUYGENS PRINCIPLE
U DIFFRACTION
U WAVE PROPAGATION

KIRKENDALL EFFECT
Mathematical models for solid molecular diffusion in binary alloys and Kirkendall effect
10 p1635 N71-21141

KLYSTRONS
Multistage depressed electrostatic collector for magnetically focused spaceborne klystrons
[NASA-CR-72767] 01 p0630 N71-10036

Analytic evaluation of depressed collector for linear beam microwave amplifiers
[NASA-CR-72768] 02 p0194 N71-11361

Increased peak power of klystrons
[SLAC-PUB-804] 06 p0896 N71-16264

Design criteria for high efficiency, high gain, high power klystron final amplifier stage operating in 4.4 to 5.0 GHz range
[AD-721362] 16 p2567 N71-28176

Klystron experience and status of SLAC and Stanford positron-electron asymmetric ring
[SLAC-PUB-802] 16 p2650 N71-28885

Computational method for determining performance of ten stage electrostatic depressed collector for klystrons
[NASA-CR-119683] 19 p3067 N71-32410

Operational analysis of FM range finders used as altimeters and reflex klystron oscillators in three-centimeter range
[JPRS-54697] 23 p3732 N71-36694

Operational characteristics of low powered klystron oscillators in three-centimeter range and in pulse mode
23 p3732 N71-36696

Focusing and tuning considerations for high CW power C band klystron amplifier for tropospheric scattering applications
[AD-727701] 24 p3889 N71-37717

KNOWLEDGE
NT PARADOXES
NT PHILOSOPHY
KNUDSEN CELLS
U KNUDSEN GAGES

KNUDSEN FLOW

KNUDSEN FLOW

Steady gas flow in capillary tubes using Knudsen law
[PB-190368T] 02 p0201 N71-11504

Knudsen flow and Mach number effects on hypersonic and supersonic wakes of cylindrical bodies and spheres
[REPT-69-7] 04 p0471 N71-13403

Thermal dissociation and sublimation of UO₂F₂ between 760 and 800 °C using Knudsen effusion method
[ORNL-TR-2422] 15 p2376 N71-26887

Knudsen Gages
Model for exchange of nitrogen isotopes taking place between two pellets of aluminum nitride in Knudsen cell
[AD-711653] 01 p0620 N71-10965

Knudsen gage and mass spectrometer measurements of vanadium, titanium, and chromium ternary alloys in bcc phase
[AD-720287] 16 p2611 N71-28502

Knudsen Number
U KNUDSEN FLOW

KOLMOGOROFF THEORY
Decay of high intensity isotropic turbulence investigated behind three different perforated plates
[REPT-6] 23 p3749 N71-36732

KOLMOGOROFF-EMIRNOFF TEST
Kolmogoroff-Smirnov test for digital filtering and spectral comparison using Fourier transform
[CTC-44] 05 p0655 N71-14905

KOVAR (TRADEMARK)
Parabel gap welding Kovar ribbons to copper conductor printed wiring boards
[NASA-TN-D-6236] 08 p1207 N71-18737

KRONECKER PRODUCT
U ORTHOGONALITY

KROOK EQUATION
Solutions of Krook equation of kinetic theory
[AD-712684] 05 p0665 N71-15466

Particle-in-cell method for model kinetic equations and one dimensional Krook equation
[CU-3954-3] 12 p1950 N71-23745

Krook model and modified particle-in-cell method for collisional plasmas
[CU-3954-6] 13 p2150 N71-25598

Formulation of Volterra equations describing nonlinear piston problem, and algorithm based on Krook equation
[TR-37] 17 p2775 N71-30373

KRYPTON
NT KRYPTON ISOTOPES

NT KRYPTON 85
Measurement of absorption spectra and absorptivity of solidified krypton and xenon for photon energies between 30 eV and 500 eV
03 p0419 N71-13340

X ray Bragg reflection measurements of Debye temperature on single krypton crystals
[COO-1198-762] 06 p0937 N71-16831

Production and destruction of fast metastable He atoms in rare gas targets and Kr and He
17 p2796 N71-29785

Atomic calculations of edge and screw dislocations in solid krypton
17 p2818 N71-29945

Small angle differential charge exchange measurements for He/plasma on He, Ne, and Kr in 1 keV to 3 keV range
20 p3318 N71-33574

Silicon rubber membrane for measuring permeabilities and separation factors for removing radioactive Xe and Kr from off-gas streams
[ORNL-4522] 20 p3308 N71-33741

Separation of krypton and xenon from reactor atmospheres by selective permeation
[NYO-4057-2] 22 p3644 N71-35981

KRYPTON ISOTOPES
NT KRYPTON 85

Body exposure rate calculated for dose from Kr-85 released to stratosphere
[BNWL-SA-3233-A] 05 p0688 N71-14706

Proton and neutron scattering cross sections for carbon, deuterium, helium, and hydrogen, and atomic energy level schemes from krypton and lead isotope alpha reactions
[UCD-CN-125] 17 p2790 N71-29230

KRYPTON 85
Instrumentation for monitoring of Kr-85 and H-3 in natural gas
[UCRL-30882] 05 p0688 N71-15559

Atmospheric contamination by Kr-85
[CEA-CONF-1550] 06 p0911 N71-15799

Data excited X ray spectra for C-14, H-3, S-35, Sr-89, Te-99, W-185, and Kr-85
[TID-22361-PT-3] 06 p0922 N71-16004

Isotopic shock wave position sensor with krypton 85 radiation sources
[NYO-4071-1] 09 p1387 N71-19394

Mass body exposure rate from krypton 85 released in atmosphere by nuclear power production
[BNWL-SA-3233] 10 p1497 N71-20777

Radiation danger of Kr-85 in troposphere and lower stratosphere from worldwide nuclear power plants
[JPRS-33174] 14 p2251 N71-26623

Magnitude calculation of spectral shift and excitation probability of Rb ion in solid Kr matrix affected by sudden change in central field due to beta decay of Kr-85
[NRC-TT-1461] 21 p3473 N71-34735

KU BAND
U SUPERHIGH FREQUENCIES

KUTTA-JOUKOWSKI CONDITION
Wake curvature and correction to Kutta-Joukowski condition
[AD-713434] 05 p0662 N71-14855

KWIC INDEXES
Index of documentations on numerical calculations for algebraic and transcendental equations
[ORNL-4595] 09 p1411 N71-20382

KWIC index of VS voluntary engineering standards
[NBS-SPEC-PUBL-329] 13 p2087 N71-24977

Pattern recognition applied to extraction of documentation indexes from text - KWIC indexes
14 p2222 N71-25988

Associative or content addressable memory systems - overview, bibliography, and KWIC index
[NASA-CR-119779] 19 p3082 N71-32439

Key word to content index and bibliography on computer systems evaluation techniques
[NASA-CR-121757] 21 p3398 N71-34183

Bibliography and KWIC index on mechanical theorem proving and its applications
[NASA-CR-121648] 21 p3446 N71-34525

Computerized KWIC system for retrieval of microfired research files
[AD-726696] 23 p3870 N71-37588

L

L BAND

U ULTRAHIGH FREQUENCIES
LABELING (MARKING)

LABOR
Survey to determine social aspects of labor organization and management in scientific teams
[NASA-TT-F-13552] 12 p2015 N71-23310

Industrial relations, mediation, work stoppage, and emergency dispute experience of airlines under Railway Labor Act
22 p3699 N71-36380

LABORATORIES
NT ENGINE TESTING LABORATORIES

NT ENVIRONMENTAL LABORATORIES
NT LUNAR MOBILE LABORATORIES

NT LUNAR RECEIVING LABORATORY
NT MANNED ORBITAL LABORATORIES

NT MAINTAINED ORBITAL RESEARCH LABORATORIES
NT SPACE LABORATORIES

Astrophysical investigations at Mullard Space Science Laboratory
02 p0296 N71-11930

Comparison of in-situ and laboratory vane shear measurement from sea floor sediment off San Diego, California
[LMSC-681703] 02 p0320 N71-12092

Laboratory-acquired infections, oncogenic viruses, allergy to animal dander and sera, and carcinogens
[ORNL-TM-2854] 03 p0321 N71-12298

Life support system for Sea-Bed Observation Laboratory
[AD-712823] 03 p0329 N71-12347

Design studies for large proton synchrotron and its laboratory
[CERN-70-6] 04 p0515 N71-13783

Umpire laboratories qualification for uranium and plutonium materials analysis including uranyl nitrate
[TID-25510] 05 p0659 N71-15495

Biophysical research at Laboratory for Agricultural Remote Sensing, Purdue University
06 p0806 N71-16153

Data processing program activities at Laboratory for Agricultural Remote Sensing, Purdue
06 p0845 N71-16154

Physical measurements program at Laboratory for Agricultural Remote Sensing, Purdue
06 p0845 N71-16155

Operations summary for Soviet seafab CHERNOMOR
06 p0852 N71-16516

Operation and utilization of 3.5 MeV Van de Graaff accelerator
[BARC-459] 08 p1252 N71-18298

Electron ring accelerator program at Lawrence Radiation Laboratory - conference
[UCRL-20084] 09 p1364 N71-19556

Problems and procedures for closing NASA Electronics Research Center, Cambridge, Massachusetts
[NASA-TM-X-67054] 11 p1732 N71-22526

Individual protection techniques for persons subjected to radioactive contamination in workshops and laboratories
[CEA-N-1408/3] 18 p2970 N71-30450

Techniques for detection and measurement of radioactive contamination in workshops and laboratories
[CEA-N-1408/1] 18 p2970 N71-30451

Off-site fallout surveillance activities of Southwestern Radiological Health Laboratory from Jan. through June 1969
[SWRHL-97-B] 21 p3478 N71-34772

Light beams fed into telescope laboratory
24 p3924 N71-37998

LABORATORY EQUIPMENT
Facility for material processing in space experiments during earth orbital mission
02 p0199 N71-11774

Technique for random vibration equalization using versatile laboratory apparatus
02 p0304 N71-12148

Reflectance measurements of diffusion pump oil and silicon oils and liquid reflectance equipment construction
[TID-25478] 03 p0418 N71-12064

Developing laboratory glassware corrosion test method for measuring presence and effectiveness of vapor space corrosion inhibitors in oils
04 p0479 N71-14088

Detection of several nonprotein amino acids in presence of protein amino acids
[NASA-CR-115805] 04 p0479 N71-14088

Design of mechanical device for stirring several test tubes simultaneously
[NASA-CASE-XAC-06956] 10 p1564 N71-21177

Gas purged dry box glove reducing permeation of air or moisture into dry box or isolator by diffusion through glove
[NASA-CASE-XLE-02531] 11 p1604 N71-23808

Description and operating instructions for laboratory precipitator for initiators
[ERDE-TN-19] 12 p1897 N71-23408

Oceanographic equipment including shipborne information systems, self maneuvering units, and instruments for measuring radioactivity and magnetic fields in sea water
[JPRS-35900] 14 p2250 N71-26311

Chemical analysis techniques and equipment for nuclear chemistry
[CEA-N-1341] 15 p2377 N71-27282

Oscilloscopes, analog and logic units, generators of visual function, and method of associated dialog for nuclear physics visualization unit adapted to C2-98-11 computer
[CEA-N-1363] 15 p3467 N71-27298

Apparatus and process for volumetrically dispensing reagent quantities of volatile chemicals for small batch reactions
[NASA-CASE-NPO-10070] 15 p2416 N71-27372

Characteristics of laboratory and manufacturing equipment and facilities for production of superpure inorganic materials
16 p2377 N71-25304

Apparatus to measure excitation cross sections of molecular nitrogen bombarded by electrons in 30 to 2000 eV range with reaction rate measured by counting photon emissions
[AD-721579] 16 p2648 N71-28048

Spectral density and coherence estimates depicting noise recorded at Norway seismic array by earthquake laboratory mechanism
[AD-720047] 16 p2589 N71-28049

Development and analysis of optimal parameters for magnetic field windings in stellarator installations
[YAF-8-70] 18 p2991 N71-36409

Development of NMFLR telemetry system to low duty cycle tone burst system
22 p3549 N71-35377

Development of two high speed logic circuits for use with large, sectioned liquid scintillation detector
[ORO-2304-172-PT-3] 22 p3559 N71-35352

Chemical attack of laboratory equipment, and properties of corrosion resistant materials for constructing chemical apparatus
[AD-726803] 22 p3596 N71-35088

LABYRINTH
NT COCHLEA

NT VESTIBULES
Rate of vestibular compensatory process in unilaterally labyrinthectomized rabbit
07 p0979 N71-14880

LABYRINTHECTOMY
Unilateral labyrinthectomy model for evaluating drug effects on vestibular function in guinea pigs
08 p1153 N71-19087

Physiological adaptation to unilateral semicircular canal impaction compared to unilateral labyrinthectomy
[ANRU-R-67-2] 18 p2881 N71-31544

Radial acceleration effects on spinal cord internal potentials of intact and labyrinthectomized rats
20 p3220 N71-33454

LACQUERS
Alkyd resin lacquer peeling on glass and other substrates
16 p2616 N71-28534

SUBJECT INDEX

LACTATES

Post-mortem lactate analysis on pilot tissues to determine presence of technical malfunction in aircraft accident 02 p0162 N71-11803

LACTIC ACID

Cytochemical detection of lactic dehydrogenase isoenzymes in free-living Protozoa (NASA-TT-F-13634) 12 p1862 N71-23382

LACTULOSE

Nonlinear relationships in lactic dehydrogenase and lactic amino positions enzyme activities in urine related to increased and decreased diuresis (NASA-TT-F-13557) 12 p1863 N71-23388

LAG (RELAY)

U TIME LAG

LAGRANGE COORDINATES

Fluid motion in two dimensional Cartesian or cylindrical coordinates by following Lagrangian energy cells (LA-4464) 04 p0585 N71-14243

Broken chiral and conformal symmetry and Kuo transformation (IC7/9/1) 04 p0587 N71-14246

FLAG, free Lagrange method for numerical simulation of two dimensional, hydrodynamic flow (UCRL-72708) 05 p0645 N71-15336

Non-pion scattering lengths from class of nonlinear Lagrangian models (SINP-TN-69-4) 06 p0910 N71-15792

Lagrange coordinates applied to satellite perturbation orbital elements (BMW-FB-W-71-05) 17 p2843 N71-29354

Dynamic theories of eigenfrequencies in dislocated crystal using Lagrangian formalism 17 p2819 N71-29949

Lagrangian functional integral formulation of dual resonance amplitudes (LPTHE-71/23) 20 p3291 N71-33583

Digital computer control of meteorological observational data using Fourier series and Lagrange polynomials (NLL-M-20718-5828.4F/1) 21 p3399 N71-34194

Phenomenological Lagrangian model calculation of scaling properties in deep inelastic electron-proton scattering (NYO-193212-149) 23 p3813 N71-37188

LAGRANGE EQUATIONS OF MOTION

U EULER-LAGRANGE EQUATION

LAGRANGE MULTIPLIERS

Normalizing quantum electrodynamic systems through non-polynomial Lagrangians (IC7/9/37) 02 p0273 N71-11909

Deriving expression for displacement of Lagrange gyroscopes with respect to angle of precession during station displacement 06 p0894 N71-19554

Defining super propagator for any mass in field theory with essential interaction Lagrangians (DESY-70/30) 08 p1249 N71-18223

Lighthill method with Lagrange expansion for approximate solutions of partial differential equations (NASA-TN-D-6245) 08 p1226 N71-18959

Ambiguities in finite computations of renormalization constants for nonpolynomial Lagrangians in field theory (IC7/9/106) 09 p1431 N71-19895

Semiprecise method for positioning crystals in multidetector-nuclear geometry for whole-body counters using Lagrange multipliers including computer program (BANC-505) 15 p2469 N71-27349

Group theory and Lagrange multipliers generated by boson fields and vector current algebra 15 p2434 N71-27433

Computer program for transfer orbit trajectory optimization based on Lagrange multipliers, Newton-Raphson method and power series (NASA-TN-D-6128) 16 p2677 N71-28089

Lagrange multiplier in Banach space for setting optimal control in time lag system (NASA-CR-118999) 16 p2620 N71-28100

Nonexistence of ambiguities in SU(3) x SU(3) matrix breaking (BS-70/25) 18 p2976 N71-30636

Phenomenological effective Lagrangian for annihilation of two photons into pions (NYO-2829-48) 21 p3483 N71-34811

LAGRANGE SIMILARITY HYPOTHESES

Mean spectrum in chiral model of pseudoscalar and vector mesons (SU-386-238) 07 p1071 N71-17265

Lagrangian calculation of hahn form factors (JHEP-82-5290) 15 p2460 N71-27070

Quantization of interacting covariant massless fields using Lagrangian formalism with prescribed asymptotic data 15 p2476 N71-27472

Technique for treatment of nonpolynomial Lagrangians in gravity modified quantum electrodynamics (IC7/1/13) 22 p3637 N71-35928

LAGRANGE FUNCTIONS

Efficiency of Laguerre and Legendre quadratures in fitting calculations (WAFB-T-2336) 03 p0415 N71-12571

LAKES

Aerial synoptic sensing by infrared imagery and color photography of lake area in Florida 02 p0206 N71-11155

Water wave effects on air flow in atmospheric boundary layer above lake (AD-713694) 05 p0719 N71-15401

Using remote sensors for classification of lake hydrology 06 p0846 N71-16170

Fourier analysis of summer weather and wave data for Lake Michigan (AD-714088) 07 p0555 N71-17836

Great Lakes surface wave amplitude and frequency data for ten years (NOAA-TM-NWS-TDL-40) 08 p1193 N71-18981

Hydrology and geochemistry of lakes to determine cycling and transport of radionuclides (CU-2493-11) 10 p1531 N71-21187

Hydrological investigation of variability of temperature and chemical properties of Lake Vanda in Antarctica 11 p1739 N71-22863

Numerical analysis of steady state, wind driven currents in Lake Erie, using shallow lake model (NASA-TM-X-67804) 12 p1903 N71-23128

Solar activity effects on European river runoff and lake level (NLL-M-20097-5828.4F/1) 12 p1913 N71-24230

Relationship between albedo of water surface of small lakes and chrominance and transparency of water mass (NLL-M-9264-5828.4F/1) 16 p2591 N71-29175

Analysis of effects of storm winds on southeastern shores of Lake Michigan (AD-723932) 20 p3294 N71-32960

Ice cover formation, ice breakup and control, frazil, and winter open water heat balance for rivers and lakes (AD-724131) 20 p3256 N71-32984

Statistical analysis including covariance functions of underwater acoustic scattering from lake surface (AD-724335) 20 p3310 N71-33042

LALLEMAND CAMERAS

Light noise due to light scattering in astronomical telescope Lallemand camera image corrector-receiver system 24 p3922 N71-37977

LAMB WAVES

Lamb dip spectroscopy and carbon dioxide frequency stabilization on sulfur hexafluoride (AD-715314) 07 p1040 N71-17772

Application of S matrix theory and Dashin-Franchi technique to Lamb shift problems in quantum electrodynamics (REPT-70-41) 09 p1410 N71-20093

Intrinsic representation of flows with Lamb surfaces (AD-719431) 13 p2063 N71-24478

Nonlinear electrodynamics equations effect on Lamb shift (IFVE-STF-69-19) 15 p2488 N71-27875

Influence of collisions on radiative saturation and Lamb dip formation in CO2 molecular lasers 21 p3436 N71-34449

LAMBERT LAW

U BOUGUER LAW

LAME WAVE EQUATIONS

Transmission of plane waves through layered linear viscoelastic media with modified Lame constants 23 p3789 N71-37003

LAMINAR BOUNDARY LAYER

Resattachment of supersonic laminar boundary layer (A-17) 01 p0042 N71-10406

Prediction of flow properties in shock wave interactions on axisymmetric bodies at zero incidence and spia (VKEI-TN-43) 01 p0043 N71-10479

Method for predicting characteristics of interaction of oblique shock wave with laminar or turbulent layers (NASA-TN-X-2084) 01 p0126 N71-10925

Laminar boundary layer effect on dynamic viscous pressure interaction in hypersonic flow (LR-535) 02 p0141 N71-11003

Computerized calculations of adiabatic laminar boundary layer and shock wave interactions using Kinsberg method (VKEI-TN-40) 02 p0143 N71-11017

Separation point study of incompressible laminar boundary layers around parabolic bodies at angle of attack (AD-712084) 02 p0201 N71-11519

Method for predicting interaction produced by externally generated, oblique shock wave impinging on laminar or turbulent boundary layers (NASA-TN-D-6683) 02 p0202 N71-11549

Survey of higher order laminar boundary layer theory 03 p0340 N71-12583

Finite difference solution of first order boundary layer equations 03 p0340 N71-12584

Laminar boundary layer calculations on bodies of revolution in hypersonic flow 03 p0340 N71-12585

LAMINAR BOUNDARY LAYER

Computation of laminar boundary layers and viscous shock layers over 10 deg half-angle hypoboid 03 p0361 N71-12592

Three dimensional steady compressible laminar boundary layer equations for flat plates and rotating disks (ONERA-CR-7481) 04 p0519 N71-16739

Mathematical model of nonparallel laminar or turbulent boundary layer, including entropy layer and turbulence effects, solved by Newton-Raphson iteration (NASA-CR-7481) 05 p0519 N71-16739

Laminar boundary layer effects on reaction rate constants deduced from shock tube measurements (NASA-TM-X-52908) 03 p0660 N71-14765

Critical evaluation of analytic methods of predicting interaction between laminar boundary layer and impinging shock waves (NASA-TN-D-7044) 05 p0664 N71-14972

Strong viscous interaction between laminar boundary layer and external hypersonic flow field on curved surface (AD-714873) 06 p0635 N71-16218

Two dimensional, supersonic flow separation ahead of compression corner for laminar boundary layer (RE-401) 06 p0635 N71-16478

Vibrating disturbance effects on highly accelerated laminar boundary layer (AD-714628) 06 p0638 N71-16410

Laminar and turbulent boundary layer separation in three dimensional flow 07 p1007 N71-16967

Hypersonic laminar boundary layer near sharp expansion corner 07 p1012 N71-17752

Deriving film thickness equations for laminar and turbulent incompressible flows in recessed circular hydrostatic thrust bearings 08 p1208 N71-19081

Calculation of thin friction on porous plate in presence of incompressible laminar boundary layer (AD-716035) 09 p1372 N71-19684

Limits of hypersonic boundary layer theory, and leading and trailing edge phenomena in laminar hypersonic boundary layer 09 p1373 N71-19833

Hypersonic laminar boundary layer growth over concave and convex surfaces 09 p1374 N71-19836

Attached and separated laminar boundary layer characteristics over high cooled, curved compression surfaces in hypersonic airflow 09 p1374 N71-19837

Laminar two dimensional boundary layer separation measurements at moderately hypersonic speeds 09 p1378 N71-19845

Linearized perturbation equations for incompressible laminar boundary layer flow over slender body of revolution at small incidence 09 p1377 N71-20261

Computer code for numerical solution of laminar boundary layer and thin shock layer equations predicting electron density around reentry vehicle 10 p1628 N71-21113

Supersonic laminar boundary layer separation measurements near compression corner at Mach numbers near 2.5 10 p1541 N71-21235

Supersonic laminar boundary layer response to moving pressure field and solution of partial differential systems 10 p1543 N71-21342

Transverse pressure gradient on interaction of laminar hypersonic boundary layer with corner expansion wave (UTIAS-157) 11 p1734 N71-22048

Rarefied gas dynamics including hypersonic flow about blunt bodies, thermal shock, laminar boundary layers, and radiating gas flow (AD-717419) 11 p1735 N71-22124

Numerical model of thermal convection for two dimensional laminar, nonlinear fluid, heated nonuniformly (AD-717670) 11 p1749 N71-22358

Numerical solutions of compressible laminar boundary layer heat transfer and pressure drop of gas in uniformly heated tube (NASA-TN-D-6333) 12 p2810 N71-23712

Laminar boundary layer on wing and body of revolution in presence of blowing (NASA-TT-F-13627) 12 p1902 N71-25796

Estimation of momentum, heat transfer, and mass transfer in laminar boundary layers 12 p1903 N71-23948

Streamline swallowing by laminar boundary layers in hypersonic flow 13 p2063 N71-24743

Effect of spark discharges into laminar boundary layer at supersonic free stream Mach numbers (NASA-TN-D-6378) 15 p2363 N71-26930

Free stream turbulence effects on local heat or mass transfer rate across laminar, forward stagnation boundary layer on circular cylinders in cross flow 15 p2363 N71-27321

Solutions to boundary layer problems in laminar surface flow with exothermic chemical reactions 16 p2582 N71-28868

Numerical analysis of laminar boundary layer problems on porous plates with discontinuity in gas injection [REPT-71-1] 17 p2732 N71-29491

Simulated temperature and velocity disturbances in laminar boundary layer using quasi-steady theoretical model 18 p2906 N71-31202

Numerical solution of flow equations for laminar, transitional, and turbulent compressible boundary layers for planar or axisymmetric flows [NASA-TN-D-3648] 19 p3078 N71-32164

Mathematical models for incompressible laminar boundary layer flow inside and outside of liquid spheroid moving through liquid 19 p3080 N71-32378

Laminar and turbulent boundary layer separation in three dimensional flow [SC-71-3010] 21 p3411 N71-34267

Measurement of flow characteristics behind backward facing step to demonstrate flow in reattachment region [IC71/105] 21 p3411 N71-34272

Power series expansion and finite difference techniques for solving unsteady laminar boundary layer problems 21 p3412 N71-34280

Integral equations for solution of three dimensional laminar boundary layer problems [NASA-TT-F-13567] 22 p3567 N71-35403

Feasibility study of combined laminar and turbulent boundary layer control system using distributed suction with application to low-speed research aircraft of glass reinforced plastic [AD-72767] 24 p3873 N71-37609

Laminar, two dimensional boundary layer generated in immediate vicinity of plane shock wave moving over flat plate into gas initially at rest [NASA-CR-123159] 24 p3905 N71-37834

LAMINAR BOUNDARY LAYER SEPARATION
U BOUNDARY LAYER SEPARATION
U LAMINAR BOUNDARY LAYER
LAMINAR FLAMES
U FLAMES
U LAMINAR FLOW
LAMINAR FLOW
NT STRATIFIED FLOW
Heat transfer in base type supersonic laminar and transitional separated flows [AD-710347] 01 p0040 N71-10249

Turbulent transition pipe flow characteristics [TAE-106] 01 p0042 N71-10473

Horizontal laminar flow clean room complex for microphotography [AD-711938] 02 p0199 N71-11535

Separation problems in two-dimensional incompressible laminar flow using perturbation methods [ONERA-P-128] 02 p0202 N71-11543

Survey of higher order laminar boundary layer theory 03 p0360 N71-12583

Laminar flow past axisymmetric blunt bodies moving at hypersonic speed [NASA-CR-111571] 03 p0361 N71-12591

Systematic numerical analysis of two dimensional and axisymmetric laminar jet of incompressible fluid with and without free stream [NASA-CR-111517] 03 p0364 N71-13085

Computer programs for determining laminar flow between shrouded rotating disks [EF/TN/A/30] 04 p0519 N71-13798

Turbulent air and water polluting plumes in laminar cross flow [FML-PUBL-70-8] 04 p0520 N71-14312

Numerical analysis of stability of Poiseuille pipe flow 05 p0661 N71-14773

Development of three dimensional velocity profile for laminar flow in rectangular duct with two parallel porous walls [AD-714555] 06 p0834 N71-16082

Hydrodynamic Poiseuille flow stability [AD-714616] 06 p0930 N71-16569

Flame length and laminar fuel jet combustion [NASA-TT-F-13459] 07 p1130 N71-17570

Laminar flow of liquid coolants in rocket engines [NASA-CASE-NPO-10122] 07 p1010 N71-17631

Stability of laminar flow in circular pipes with respect to three dimensional disturbances 08 p1183 N71-18989

Determining characteristics of jet elements whose operation is based on jet interaction with turbulent or laminar flow in control channels [AD-716519] 09 p1371 N71-19629

Numerical solution of laminar separated flow problem over backward facing step at high Reynolds number 09 p1375 N71-19842

Laminar airflow and airborne contamination control concepts with clean room specifications and laminar flow facility designs [NASA-CR-116183] 09 p1368 N71-20425

Models for high Reynolds number incompressible laminar flow around sharp corner 10 p1542 N71-21272

Stability analysis of laminar to turbulent flow transition during film boiling from vertical flat plate 10 p1542 N71-21282

Experimental determination of heat transfer and friction in circular tube with laminar flow of air under conditions of large transverse temperature gradients 10 p1542 N71-21283

Formulation for temperature distribution in laminar flow with radiative and convective heat transfer 10 p1663 N71-21506

Evaluation of computer program for prediction of laminar flow by solution of elliptic partial differential equations [EF/TN/B/31] 11 p1737 N71-22330

Plasma instability work including hydromagnetic Poiseuille flow stability, nonlinear plasmas, plasma oscillations, Vlasov turbulence, and Q devices [AD-717531] 11 p1811 N71-22444

Wall porosity effect on stability of quasi-parallel laminar flows over plane compliant boundaries 11 p1738 N71-22576

Numerical solution of equations governing laminar flow of incompressible, non-Newtonian fluid through circular pipe with abrupt change in diameter 11 p1742 N71-22690

Combined free and forced laminar convective heat transfer to non-Newtonian fluids flowing in constant wall temperature vertical tubes and controlling parameter analysis 11 p1742 N71-22702

Numerical study of steady, laminar, natural convection of fluids in vertical rectangular enclosure 11 p1743 N71-22725

Dynamic characteristics of circular fully developed laminar free jet [NASA-TN-D-6304] 12 p1898 N71-23103

Two-layer flow in supersonic nozzles with different adiabatic exponent and gas flow rate ratios [NASA-TT-F-13526] 12 p1899 N71-23385

Numerical analysis of laminar separated flow over backward-facing step for infinite Reynolds number [AD-718104] 12 p1900 N71-23481

Sound generation by small perturbation jet flow [DLR-FB-71-02] 12 p1856 N71-23596

Finite difference approximation of vorticity transport equations applied to laminar flow with spatially periodic disturbances [AD-718308] 12 p1901 N71-23685

Numerical solutions of compressible laminar boundary layer heat transfer and pressure drop of gas in uniformly heated tube [NASA-TN-D-6333] 12 p2010 N71-23712

Partial differential equations for determination of hydrodynamic characteristics of fully developed laminar flow in tube [EF/TN/A/32] 12 p1902 N71-23724

Numerical analysis of laminar local wall friction and heat transfer in noncircular tubes and annuli with variation of gas transport properties [AD-718777] 12 p1904 N71-24208

Characteristics of gaseous jet impinging normally on liquid surface in regions where both gravitational and surface tension forces are significant 14 p2239 N71-26023

Finite rate dissociation and recombinations for supersonic, two dimensional, laminar flow 14 p2241 N71-26274

Navier-stokes equations and velocity distributions for two dimensional, unsteady, incompressible, laminar flow of Newtonian fluids in annular, circular, and rectangular ducts 14 p2242 N71-26473

Design data and criteria for design of expansions from rectangular to trapezoidal section in supercritical open channel flow 16 p2581 N71-28773

Free streamline model of flow past two-dimensional wedge or flat plate 19 p3080 N71-32350

Streamwise pressure gradient effects upon two dimensional compressible boundary layers at high Reynolds numbers 19 p3082 N71-32623

Determination of laminar skin friction response under oscillating flow in presence of sinusoidal free-stream velocity 20 p3253 N71-33780

Similarity solutions using free parameter technique for laminar flow of viscous, incompressible fluid between rotating coaxial surfaces of revolution 20 p3253 N71-33783

Transient heat transfer in thermal entrance region between parallel plates with fully developed laminar velocity profile determined for low Peclet number flows 20 p3367 N71-33784

Velocity and temperature distribution of laminar free convection flow in vertical heated channel 20 p3368 N71-33972

Numerical analysis of laminar, incompressible flow along corner formed by intersection of two thin airfoils [AD-726546] 22 p3538 N71-35201

Wind tunnel investigation of laminar, transitional, and turbulent boundary layer profiles on wedge at hypersonic speed to confirm theoretical analysis [NASA-TN-D-6462] 22 p3569 N71-35417

Theoretical analysis of polymer solution laminar flow near infinite extent flat plates for drag reduction effects [AD-726414] 22 p3569 N71-35418

Laminar gas flow at transonic speeds with subsonic and supersonic regions [AD-726592] 22 p3569 N71-35422

Mass transfer and hydrodynamic behavior of laminar liquid films flowing over solid surfaces 23 p3746 N71-36710

Performance of multicomponent electrocatalytic system with laminar flow, and fouling of membrane surfaces by iron oxide [FML-PUBL-71-13] 24 p3886 N71-37788

Theoretical and experimental analysis of laminar shock-boundary layer interaction [IC71/116] 24 p3908 N71-37832

Heat transfer in smooth tubes, between parallel plates, in annuli and tube bundles with exponential heat flux distributions in forced laminar or turbulent flow [NLL-WINDSCALE-458-[909].9F]] 24 p4032 N71-38770

LAMINAR FLOW CONTROL
U BOUNDARY LAYER CONTROL
U LAMINAR BOUNDARY LAYER
LAMINAR HEAT TRANSFER
Laminar heat transfer and wall temperature distribution for high temperature gases and nitrogen plasma in circular tubes and over flat plates [REPT-70-3] 04 p0519 N71-13791

Energy-integral prediction of hypersonic and laminar heat transfer in thermal boundary layer around blunt slender cones and of compressible flow with heat transfer 17 p2858 N71-29007

LAMINAR JETS
U JET FLOW
U LAMINAR FLOW
LAMINAR WAKES
Laminar wake characteristics behind circular cylinder in Mach 6 rarefied air stream [REPT-1108/70] 02 p0142 N71-11012

Laminar-turbulent transition measurements of two dimensional wake with imposed disturbances [IAS-453-VOL-35-NO-11] 03 p0364 N71-13083

LAMINATED MATERIALS
U LAMINATES
LAMINATES
NT PLYWOOD
Exact solutions for rectangular bidirectional laminates and sandwich plates [AD-710615] 01 p0070 N71-10802

Ultrasonic inspection and hardness measurement in steel cylinders used in aluminum laminates [REPT-7004.425] 01 p0039 N71-10201

Optical properties of vapor deposited dielectric and reflecting multiple layer systems 01 p0090 N71-10223

Shear deformation in heterogeneous anisotropic plates [AD-711920] 02 p0304 N71-12105

Finite element method for obtaining approximate three-dimensional stress solutions for laminated plate [AD-711399] 02 p0249 N71-12176

Polyphenyl-as-triazines used for high temperature adhesives, laminating resins, protecting coatings, and films [AD-712407] 03 p0330 N71-12857

Propagation of stress pulses in stratified elastic medium 03 p0397 N71-13151

Strength and creep of laminated plastics [NASA-TT-F-461] 05 p0709 N71-13176

Holographic detection of bonding voids in laminates by observation of stress-induced reactions [AD-713545] 05 p0897 N71-13332

Strain energy theory of failure of oriented fiber glass reinforced plastic laminates under biaxial compression [NASA-TT-F-13444] 06 p0880 N71-14001

Residual stresses arising from fabrication process in laminates [NASA-TN-D-6146] 06 p0957 N71-14007

SNAP 8 reactor layered lithium hydride and depleted uranium shield design for space applications [NASA-TN-D-57878] 09 p1417 N71-19875

Analysis of shear coupling effects on composite laminates based on extension of classical laminate theory [AD-716390] 09 p1475 N71-19879

Users manual for FORTRAN 4 computer program for analysis of multilayered fiber composites [NASA-TN-D-7013] 09 p1481 N71-20019

Chemical composition of copper clad laminates and resins used for printed circuit insulation, impregnation, and protection 10 p1511 N71-20004

Transient response of unbounded laminated materials subjected to uniformly distributed transverse, perpendicular forces 10 p1637 N71-21319

SUBJECT INDEX

LANDING SITES

Homogeneous continuum for describing mechanical behavior of laminated composite elastic solids (AD-717731) 11 p1831 N71-22517

Multilayer porous refractory metal ionizer design with thick, porous, large-grain substrates and thin, porous micron-grain substrates (NASA-CASE-XTR-64338) 11 p1790 N71-23046

Development and characteristics of diffusion bonded boron coated titanium foil sheets (AD-717948) 12 p1941 N71-23279

Fabrication and assembly of laminated and ceramic film elements (NLL-WINDSCALE-453-70991.957) 12 p1964 N71-24102

Application of theory for unsymmetric deformation of anisotropic, anisotropic, elastic shells to layered shells. Part 2 (ESPT-70-3-PT-2) 12 p2008 N71-24293

Mechanical properties and physical, chemical, and thermal tests of polybenzimidazole and carbon fabric laminates for spacecraft thermal insulation (NASA-CR-1723) 15 p2427 N71-24915

Problems in application of solid lubricants with nuclear structures (AD-720948) 15 p2431 N71-27379

Development of reusable oxidation resistant carbon-carbon laminates and surface insulation materials for thermal protection systems 17 p2856 N71-29452

Weathering effects on creep properties of glass fiber reinforced polyester resin laminates under bending stress (NLL-LIB-COMM-5196-15531) 17 p2768 N71-29503

Laminated steel pressure vessel design, trial production, and destructive testing (NLL-RTS-5936) 17 p2855 N71-30334

Plasma waves and superconductivity in quantizing semiconductor/insulator films and layered structures with high mobility of free carriers (NASA-TM-X-613747) 18 p2995 N71-30850

Heat capacities of sub-monolayer He-3 and He-4 adsorbed on argon preplated copper sponge 18 p2985 N71-31200

Effects of lateral substrate fields on helium monolayers using ideal gas model (RLO-1358-604) 18 p2985 N71-31218

Thermal and air environment effects on mechanical properties of graphite/polyimide laminates (NASA-TM-X-67893) 19 p3121 N71-32414

Derivation of governing differential equations of mixed formulation for linear, dynamic problem of thermoset laminated anisotropic arbitrary cylindrical shells (UNICIV-R-39) 20 p3361 N71-33960

Analysis of low cycle thermal fatigue in laminated glass wall turbine vanes 21 p3502 N71-34944

Three dimensional analysis of static and dynamic of orthotropic laminates and application to rectangular plates and laminates (AD-7272-5) 21 p3528 N71-35136

Transmission of plane waves through layered linear viscoelastic media with modified Lamé constants 23 p3789 N71-37003

Critical tensile strength curve determination for orthotropic two-layer fiber glass shells in plane stress corresponding to therapeutic pressure chambers (AD-729648) 24 p4026 N71-38726

Stress waves in multiple laminates and sandwich plates, dynamic polariscope for stress wave analysis, meteoroid hazard to space travel, effects of hypervelocity impact, and related studies (NASA-CR-123157) 24 p3920 N71-37553

Viscoelastic creep and relaxation in filamentary high-ply laminates with numerical results for boron-epoxy and graphite epoxy plastics (AD-727120) 24 p3943 N71-38129

Second order solutions to shear stress, normal stress, horizontal displacement, and transverse deflection in multilayer Timoshenko beams (AD-727640) 24 p4026 N71-38726

LAMINATIONS

U LAMINATES

LUMINAIRE

U LUMINAIRE

Rate of periodic variations of radiation balance of lunar land reservoirs to that of surrounding land in USSR 15 p2439 N71-27517

Statistical analysis of long distance tropospheric propagation measurements at UHF over mixed land and sea paths of English Channel (BEP-177/311) 23 p3725 N71-36556

Physical and mechanical properties of ice formation noting effect of engineering structures (AD-725169) 19 p3187 N71-31765

Evaluating potential for making broad land use maps and earth resource surveys from spaceborne and airborne photography 02 p0217 N71-11980

Sea-ice and aerial thematic land use mapping 08 p1196 N71-19264

Aerial and satellite-borne photography of Imperial Valley agricultural land use characteristics 08 p1196 N71-19265

Remote sensing of land uses, urban growth and environmental quality, climatology, census data, and thematic maps 08 p1196 N71-19268

Potential for state-owned rangeland resources development and multiple-use management in southeast Oregon 10 p1534 N71-21503

Systems management and control of demographic and technological change within coastal regions of US 11 p1847 N71-23835

Aerial photomosaics used to simulate spaceborne photographs in general macro and thematic agricultural land use (NASA-CR-106253) 12 p1914 N71-24086

Aerial infrared photography for water oriented recreation planning (NASA-CR-107634) 12 p1914 N71-24087

Photoreproduction of satellite-borne photography for mapping and land use studies (NASA-CR-118518) 14 p2249 N71-26316

Production of a high altitude urban land use map and data base for Boston sector of metropolitan (NASA-CR-118678) 14 p2252 N71-26796

Application of biogeoscience principles to land reclamation activities 20 p3224 N71-33513

Airport/aircraft system noise reduction including land use and noise forecasting (OST-ONA-71-1-VOL-3) 20 p3212 N71-33937

Photoreproduction of aerial color infrared photography for analysis of urban land use (NASA-CR-121653) 21 p3424 N71-34369

LANDAU DAMPING

Comparing spatial and temporal damping of large amplitude plasma waves (STI-3785-10) 03 p0437 N71-12640

Characteristics of longitudinal plasma waves and zero sound (NF-18364) 04 p0596 N71-13773

Characteristics of Landau damping and wave reflection in open ended magnetic well plasmas (UCL-36900) 09 p1447 N71-19686

Amplitude and Landau damping of plasma wave echoes (CEA-CONF-1601) 15 p3498 N71-27046

LANDAU FACTOR

Kinetics of electron cooling of beams in heavy particle storage devices (CERN-TRANS-40-18) 03 p0431 N71-12924

Microscopic theory of quasi-particle spin fluctuations in low temperature, dense Fermi liquids 10 p1618 N71-21440

LANDING

NT AIRCRAFT LANDING

NT CRASH LANDING

NT DITCHING (LANDING)

NT OLIVE LANDINGS

NT LUNAR LANDING

NT MARS LANDING

NT PLANETARY LANDING

NT SOFT LANDING

NT SPACECRAFT LANDING

NT TOUCHDOWN

NT VERTICAL LANDING

NT WATER LANDING

Application of approach and landing data to design of space shuttle 01 p0125 N71-10109

LANDING AIDS

NT AIRPORT LIGHTS

NT APPROACH INDICATORS

NT ARRESTING GEAR

NT AUTOMATIC LANDING CONTROL

NT INSTRUMENT LANDING SYSTEMS

NT LANDING INSTRUMENTS

NT RUNWAY LIGHTS

All-weather automatic landing systems and problem areas 03 p0404 N71-12427

Technical synthesis and development of advanced communication systems for aircraft landings 03 p0405 N71-12430

Guidance developments for all-weather landings 03 p0405 N71-12433

All weather landing systems of Thomson-CSF 03 p0407 N71-12446

Development of signal acquisition methods for television aided aircraft carrier landing operations (AD-712511) 03 p0410 N71-13194

Shuttlecraft landing and navigational aid capabilities (NASA-TM-X-66720) 06 p1232 N71-18187

Aviation ground lighting, visual landing aids, dual baseline transceiver, photometric measurements of deck-landing projector light, and lamp for Fresnel optical landing system (NBS-10396) 11 p1676 N71-22456

Shipboard test procedure of Fresnel lens optical landing system MK 6 MOD 2 for carrier landings (AD-718335) 12 p1836 N71-23488

Microwave scanning guidance system for aircraft approach and landing 15 p2365 N71-28804

Experimental pulsed neodymium laser system modified for measuring static visibility conditions for aircraft landing operations (AD-716485) 16 p2531 N71-28317

Approach power compensation system for manual and automatic Navy carrier landing systems (AD-722025) 16 p2628 N71-28241

Flight simulator for studying problems of aircraft during approach and landings at night under category 2 visual conditions (RAB-TM-AVIONICS-59BLEU) 24 p3873 N71-37606

Aircraft takeoff, navigation, and landing aids, aerodynamic characteristics, and crew rescue equipment (AD-727600) 24 p3874 N71-37610

Evaluation of visual landing aids involving visibility meters and airfield lighting and marking (NBS-10604) 24 p3954 N71-38211

LANDING GEAR

Continuous frequency distributions of aircraft landing gear loads in determining fatigue life (RAB-LIB-TRANS-1462) 01 p0126 N71-10973

Functional analysis of landing gear systems (ASD-TB-69-115) 03 p0313 N71-12233

Dynamic loads on F-104D aircraft landing gears (PB-82-1509) 08 p1143 N71-18532

Criteria for designing space shuttle landing systems 13 p2171 N71-24056

Two computer programs for investigation of wide variety of lunar planetary landing gear configurations (NASA-CR-111919) 19 p3189 N71-32608

Analysis of aircraft ground friction characteristics based on aircraft type and airfield construction (AD-720273) 21 p3376 N71-34024

Performance characteristics of air cushioned landing and takeoff system during aircraft stall-operation mode (AD-726606) 22 p3541 N71-35223

LANDING INSTRUMENTS

NT APPROACH INDICATORS

Design and development of flight director systems based on theory of manual control displays (NASA-CR-1748) 10 p1534 N71-21007

LANDING MODULES

Analysis of stresses and deflections in platforms used for airdrop operations (AD-711556) 02 p0360 N71-11968

Analysis of normal accelerations through center of gravity of aircraft due to landing impacts and ground operations associated with taxi, takeoff, and landing (NASA-TN-D-4124) 11 p1676 N71-22620

Development of mechanistic models for predicting behavior of landing mat systems 11 p1839 N71-22891

Analysis of supersonic impact on plating debris in smooth and rough water (AD-727753) 24 p3874 N71-37614

LANDING MODULES

NT LUNAR LANDING MODULES

NT LUNAR MODULE

NT MARS EXCURSION MODULE

Large angle gyro sensing system for body mount on unmanned Mars surface vehicle (NASA-CR-111737) 04 p0343 N71-14148

LANDING SIMULATION

Low visibility approach and landing simulation for jet transports (NASA-CR-73495) 03 p0629 N71-14608

Estimated frictional resistance between soil-wheel interface in lunar roving vehicle design simulation 09 p1446 N71-20216

Mars simulator for surface atmosphere effects on unmanned spacecraft landing dynamics 09 p1368 N71-20244

Effect of several variations of two types of TV display visual simulation systems on subjective pilot evaluations and objective measures of performance in landing approach (NASA-TN-D-6274) 11 p1687 N71-22270

Development of mechanistic models for predicting behavior of landing mat systems 11 p1839 N71-22891

LANDING SITES

NT LUNAR LANDING SITES

Airport master plan for Poplar Bluff, Missouri (PB-19728) 05 p0637 N71-14895

Selection of optimum airfields for support of landings from earth orbit of future land-landing type spacecraft (NASA-TM-X-66602) 06 p0832 N71-14670

Mars simulator for surface atmosphere effects on unmanned spacecraft landing dynamics 09 p1368 N71-20244

Surface climatological data for twenty selected launch, landing, and alternate landing sites for space shuttle system (NASA-CR-61342) 10 p1976 N71-21513

Tables and maps of selected landing airfields for shuttle orbiters with various crossranges (NASA-TM-X-67080) 11 p1730 N71-21996

Development of mechanistic models for predicting behavior of landing mat systems 11 p1839 N71-22891

Determination of effectiveness of chevron type markings to indicate potentially deceptive, nonload-bearing paved areas before runway threshold [FAA-NA-71-27] 17 p2729 N71-29306

Synoptic meteorological reference file for weather forecasting at landing field [AD-723676] 19 p3127 N71-31937

Performance and environmental tests of membranes for airfield surfacing [AD-726891] 22 p3566 N71-35398

LANDING SPEED
Aerodynamic characteristics of scale model of space shuttle booster at cruise and landing speed of Mach 0.2 [NASA-CR-119974] 24 p4019 N71-38679

LANDING SYSTEMS
U LANDING AIDS

LANDSCAPE

U TERRAIN

U TOPOGRAPHY

LANES

U PATHS

LANGEVIN FORMULA

Characteristics of collisional kinetic equations and solutions using constants of motion method including Chandrasekhar, Hamiltonian, Vlasov, and Langevin formulations [NASA-TM-X-65493] 12 p1970 N71-23302

LANGMUIR PROBES
U ELECTROSTATIC PROBES

LANGUAGE PROGRAMMING
Combining conversational programming system and programmer oriented graphics operations with PL-1 computer language [AD-709953] 01 p0027 N71-10061

Data retrieval system using syntax techniques [AD-711046] 01 p0027 N71-10146

Insertion and retrieval of facts through on-line computer terminal 01 p0027 N71-10147

Digital computer oriented analysis method for Mason flow graphs [AD-709937] 01 p0076 N71-10648

Research on programming algorithmic languages [AD-710643] 01 p0029 N71-10872

Overview of evolution of space programming language [AD-711786] 02 p0188 N71-11321

Defining language subjects, form, and highlights of space programming language [AD-711789] 02 p0188 N71-11322

JOVIAL Compiler Validation System - instruction manual [AD-711370] 02 p0188 N71-11324

Space programming language for translating source statements into machine or assembly language code [AD-711787] 02 p0189 N71-11325

Language programming for linguistic algorithms - ALTEXT 2 [AD-711367] 02 p0190 N71-11335

Formal semantics definition based on nonterminal symbols in context free grammar and simple programming language [AD-711329] 02 p0190 N71-11336

FORMAL programming system with language capability for performing symbolic algebraic manipulations [NASA-CR-116149] 05 p0618 N71-16006

Semantic automatic language processing, automatic programming aids, and time sharing systems for natural communication with computers [AD-714089] 06 p0819 N71-16359

Topological manipulation of line drawings using pattern description language [AD-714593] 06 p0821 N71-16543

Programming language for advanced translator writing system [NASA-CR-117124] 09 p1352 N71-19596

Language programming for Palantype typewriter language translation [NPL-COM-SCI-45] 11 p1715 N71-22093

Motion command processing in programming languages for numerical control of machine tools [AD-717749] 11 p1768 N71-22373

Computer research techniques including information systems, language programming, and numerical analysis [COO-2094-2] 11 p1716 N71-22422

Cyclic arithmetic codes and their distance properties with demonstration of modular arithmetic weight invariance to code word cyclic shifts [NASA-CR-117884] 12 p1947 N71-23218

Parameterization of human speech for encoding into information units 12 p1880 N71-23929

Airborne computer architecture and organization for executing computer programs written in space programming language [AD-720798] 14 p2221 N71-25930

Computer program for linked file information retrieval including semantics, syntax, and outline of search program 14 p2221 N71-25978

Data retrieval language with ability to define data structures, describe environments, address data by content, manipulate data structures, and offer computational power comparable to FORTRAN [NBS-TR-590] 19 p3063 N71-32714

Context sensitive grammar and generation of non-context free languages [NASA-CR-121658] 21 p3397 N71-34177

Context-free language generation using nontrivial constraints on context-sensitive grammar rules [NASA-CR-121497] 21 p3446 N71-34520

Automatic reading of handwritten Hebrew using horizontal marking grids 24 p3894 N71-37750

Pattern recognition by machines using on-line picture language 24 p4013 N71-38628

LANGUAGES

NT ALGOL

NT ASSEMBLY LANGUAGE

NT COBOL

NT CONTEXT FREE LANGUAGES

NT FORTRAN

NT MACHINE ORIENTED LANGUAGES

NT PL/I

NT SYLLABLES

NT WORDS [LANGUAGE]

Two-part glossary of bathymetric terms in 27 languages and English equivalents [AD-710991] 01 p0049 N71-10687

Comparative analysis of natural languages and controlled vocabularies for information indexing and retrieval [AD-716200] 09 p1488 N71-19941

LANTHANIDE SERIES METALS

U RARE EARTH ELEMENTS

LANTHANUM

NT LANTHANUM ISOTOPES

Second-order solutions of Hamiltonian functions for EPR study of Jahn-Teller effect in SrCl₂-La₂ plus [NASA-CR-116883] 08 p1282 N71-19291

Electrooptic effects in ferroelectric ceramics with emphasis on electrical and optical properties of Ba, Se, and La modified lead zirconate titanate [SC-R-70-4353] 10 p1590 N71-21532

Studies of f electron systems in single crystals, including electron nuclear double resonance lines for La and Ce [COO-294-10] 10 p1624 N71-21779

Production engineering and testing of low-power, solid state, lanthanum doped barium strontium titanate-thermistor for use in automatic electronic tuning with nonlinear dielectrics 12 p1890 N71-23611

Periodicity of lanthanide and actinide properties [INR-1212] 14 p2303 N71-26201

Revised periodic table for incorporating actinides and lanthanides [UCRL-TRANS-10510] 15 p2376 N71-26886

Hyperfine structures and positioning of 5d_{5/2} zF states in lanthanum I spectrum by levelcrossing method and Doppler resonance spectroscopy 18 p2983 N71-30951

Effects of superconducting transition on PQR frequencies in doped lanthanum metal measured using superregenerative spectrometer techniques 18 p2965 N71-31361

LANTHANUM COMPOUNDS
NT LANTHANUM OXIDES

Mass spectroscopy of vaporization of lanthanum and scandium carbides [NASA-TN-D-7039] 06 p0869 N71-15889

NMR and ESR measurements of magnetic interaction in sodium chloride-negative gadolinium ion and lanthanum ethyl sulfate-trivalent gadolinium ion 09 p1432 N71-19935

LANTHANUM ISOTOPES
Forbidden transition probability for structural study of spherical nuclei La-139, La-135, and La-133 [JINR-P6-5200] 14 p2319 N71-26793

Nuclear structure of Ce-140, La-139, and Ba-138 obtained from proton transfer reactions of He-3/d 17 p2794 N71-29656

LANTHANUM OXIDES
Spectrographic determination of some commonly occurring impurities in purified lanthanum oxide [BARC-473] 04 p0527 N71-13811

Determination of rare earth impurities in purified lanthanum oxide using Stalwood jet [BARC-472] 05 p0639 N71-14707

X ray diffraction, thermal, and thermogravimetric analyses of La₂O₃-BaO-B₂O₃ glass structures and properties 18 p2940 N71-31250

LANTHANUM 140
U LANTHANUM ISOTOPES

LAP JOINTS
Constant load amplitude tests and program tests of lap joints and strap joints for riveted Alclad material under bending stress [NLR-TR-691161] 12 p2008 N71-24282

LAPLACE EQUATION

Finite difference solution to mixed boundary value problem for Laplace equation [NASA-CR-116231] 06 p0885 N71-16497

Application of Green function to two dimensional Laplace equation for calculation of temperature distribution in cooled blade of gas turbine [NAL-TR-234] 18 p2944 N71-30099

Oscillatory modes of antisymmetric diurnal tide calculated by Laplace equation [NASA-TT-F-13817] 18 p2915 N71-31037

Laplace equation for controlling parameters of current distributions in cylindrical geometries 19 p3142 N71-32226

LAPLACE OPERATORS

U LAPLACE TRANSFORMATION

Simulation of Laplace transform by means of its potential in semiconductor materials [AD-713021] 03 p0352 N71-12547

Laplace transformation for response in transversely isotropic rod to transient input [PB-195087] 07 p1122 N71-14043

Application of Z-transforms to sampled-data systems [NASA-CR-61349] 13 p1202 N71-24631

Linear regulator problem solution using Euler equations of motion, Laplace transformations, and Hamilton-Jacobi equation for stochastic control 14 p2235 N71-26444

Comparison of standard Z transform and algebraic substitution synthesis methods for digital filters [AD-721571] 16 p2569 N71-28397

Watson generalization of Fourier transform, and inversion formulas for Laplace and other integral transforms 17 p2772 N71-29416

Mathematical models of Fourier and Laplace transformations of two tempered distributions which coincide in Jost points 18 p2969 N71-30433

Nuclear reactor kinetics after abrupt reactivity changes based on Laplace transformations and Heisenberg equation for neutron flux densities [LFEN-INT-47A] 18 p2559 N71-30621

Phase-space integral with transverse momentum cutoff calculated with Laplace transformation and saddle point method, and particle momentum spectra and inelastic cross sections [NP-18748] 18 p2966 N71-31577

Radio spectrum analysis of two active regions based on Laplace transform and brightness temperatures from Nov. 12, 1964 solar eclipse data [NASA-TM-X-66543] 22 p3664 N71-36127

LAPSE RATE
Dependence of lower atmospheric wind shear on averaging period and lapse rate as recorded at Lofn, Netherlands 18 p2950 N71-30835

LARGE APERTURE SEISMIC ARRAY
Underground explosion detection, seismic wave propagation path effects, and LASA processing [AD-718971] 13 p2689 N71-24091

Large aperture seismic array data analysis for seismic wave attenuation and velocity in earth mantle from underground explosions [AD-722444] 18 p2911 N71-30799

LARGE SCALE INTEGRATION
Monolithic COS/MOS large scale parallel processor array [NASA-CR-111602] 03 p0340 N71-12463

Proceedings from lecture series on large scale integration in microelectronics [AGARD-LS-40-70] 03 p0354 N71-12638

Technology review on large scale integration circuitry 03 p0354 N71-12637

Comparison of MOS and bipolar LSI technology 03 p0354 N71-12638

Computerized design of LSI systems particularly MOS arrays 03 p0354 N71-12639

System packaging of LSI circuits [NASA-CR-111646] 03 p0354 N71-12639

LSI circuitry using MOS structures for airborne computers 03 p0348 N71-12611

LSI devices and techniques for electronic system design 03 p0352 N71-12632

Quality and reliability assurance methods for LSI circuits 03 p0384 N71-12634

Cost effectiveness of LSI circuits 03 p0354 N71-12634

Concepts in LSI servocontrol electronics 04 p0512 N71-13332

Microelectronics, large scale integrated arrays, electronic packaging, thin film epitaxy, computerized design, radar equipment [NASA-CR-109754] 04 p0512 N71-13333

Resource allocation and avoidance of deadlocks in application of cellular array logic to LSI 04 p0502 N71-13347

SUBJECT INDEX

Fast multiplication cellular arrays for LSI implementation

04 p0303 N71-13658

Large scale integrated circuit testing using test points and additional logic

06 p0824 N71-16542

Large scale integration and metal oxide semiconductor microelectronic testing techniques including combinatorial, sequential, functional, and parametric methods

14 p2335 N71-26703

Large scale integration microelectronic wafer and package testing including parametric and functional tests of combinatorial and sequential logic circuits

14 p2336 N71-26704

Parametric, functional, and mechanical properties of bipolar LSI devices in simulated space environment

15 p2417 N71-27771

Digital data processor for use with large scale integrated circuit technology and spaceborne computer application

16 p2565 N71-28420

Production engineering and electrical operation of photoresistor sensing array system and display device including large scale integration and logic circuitry

19 p3167 N71-31642

Development of procedures for infrared examination to improve reliability of large scale integration

21 p3425 N71-34369

Computerized design of Micromosaic integrated circuit arrays

23 p3736 N71-36636

Pad relocation technique for interconnecting LSI semiconductor logic circuit arrays with imperfect yields

23 p3738 N71-36656

Study of temperature and density dependence of local magnetic field in xenon gas using nuclear magnetic resonance laser precession techniques

22 p3630 N71-35866

Ocean surface clutter effects on laser altimeter and optical Doppler radar performance

04 p0524 N71-13721

Localization of cesium diode discharge by laser heating

08 p1274 N71-18817

Time-scan method of vapor luminescence excitation for spectrum analysis using neodymium-glass lasers for metal oxide vaporizing and electric arcs for further vapor heating and excitation

12 p1934 N71-23791

One dimensional laser heating of stationary plasma for application to controlled thermonuclear reactions

19 p3169 N71-32159

Development and characteristics of fractional fringe HCN laser interferometer

03 p0436 N71-12636

Production of laser glass and optical damage mechanisms in laser materials

04 p0525 N71-14326

Holographic control of neodymium laser glass production

04 p0525 N71-14327

Damage threshold tests on laser glass

04 p0525 N71-14328

Damage threshold tests in laser glass evaluation

04 p0526 N71-14329

Gain loss in neodymium glass laser amplifier

04 p0526 N71-14330

Nonlinear birefringence index measurements in laser glass by picosecond pulses of neodymium laser and Kerr cell

04 p0535 N71-14332

Optical model for thermal absorption centers of nitric and dielectric inclusions in glass lasers

04 p0526 N71-14333

Photoelectron emission in surface damage of laser materials

04 p0526 N71-14339

Characteristics of high temperature materials and laser substances

06 p0936 N71-16597

Laser radiation nonlinear absorption by organic compounds

11 p1774 N71-21897

Growth and properties of single crystal materials for optoelectronics including lasers

11 p1817 N71-22395

Cochran method for investigating yttrium aluminum garnet as optically pumped laser host material

13 p2088 N71-24426

Gallium arsenide infrared window materials for high power carbon dioxide lasers

14 p2265 N71-25874

Progress in growth of ultra-pure Al₂O₃ crystals as laser material, measurement of oxygen diffusion in ox-

ides, and measurement of laser beam damage threshold energy in glass

20 p3287 N71-33128

Optical emission spectroscopy and excitation spectra of glass and YAG laser materials for improvement of plasma pumps for pulsed carbon lasers

22 p3591 N71-35571

Radiation effects in semiconducting laser materials including cadmium selenides, cadmium sulfides, and sodium chlorides

23 p3766 N71-36844

Optical properties of gallium arsenide infrared window material and evaluation of CO₂ laser

24 p3931 N71-38851

Producing single-frequency lasers by quality discrimination of optical cavity modes

01 p0063 N71-10640

Pulsing techniques for CO₂ lasers

02 p0238 N71-11582

Using quartz discharge tube for generating high power single-frequency argon laser

03 p0388 N71-13245

Investigating theory of laser resonators derived from scalar wave equation

03 p0697 N71-15158

Determining feasibility of using laser beam holography for detection and characterization of bond defects in composite material structures

07 p1039 N71-17757

Laser controlled modulation for information transmission and uncontrolled noise producing modulation

07 p1040 N71-17860

Long term frequency stability of three-mirror cavity argon laser using standard frequency light source

08 p1209 N71-18445

Multilane, multitransverse mode argon ion laser

11 p1774 N71-21896

Time-varying modulation of dielectric constant effects on semiconductor laser modes

12 p1935 N71-24165

Ninety degree Thomson light scattering from low density plasma

01 p0062 N71-10181

Power and efficiency of continuous hydrogen fluoride chemical laser

01 p0062 N71-10433

Feedback averaging amplitude modulated laser communication system

01 p0025 N71-10874

Ion-ion recombination effects in sodium line laser

01 p0064 N71-10976

Annotated bibliography of regulations, standards, and guides for micrographs, and ultraviolet, laser, and television receiver radiation

02 p0151 N71-11074

Multiwavelength laser scintillations due to atmospheric turbulence

02 p0238 N71-11395

Laser fundamentals and experiments for high school use - textbook

02 p0238 N71-11420

Measuring dependence of emission power and polarization of helium-neon laser on transverse magnetic field

02 p0238 N71-11567

Laser power at 5 microns from carbon monoxide gasdynamic expansion

02 p0239 N71-11668

Measuring correlation characteristics of signals at photomultiplier output in presence of monochromatic illumination

02 p0268 N71-11778

Investigating spatial distribution of condensed matter ejected from metals subjected to laser radiation

02 p0239 N71-12049

Applications of lasers for ballistic research

02 p0239 N71-12118

Development and characteristics of fractional fringe HCN laser interferometer

03 p0436 N71-12636

Shadow images of bodies obtained at hypersonic speeds by means of single-pulse laser

03 p0380 N71-43124

Application of laser radiation to removal of material from metals

04 p0525 N71-14070

Measuring small surface deformations using optical wavefront reconstruction

05 p0697 N71-15157

Production of carbon dioxide laser pulsing by cavity length modulation

05 p0697 N71-15368

Characteristics of hydrogen cyanide lasers and effects of chemical mixtures on laser operation

05 p0697 N71-15369

Passive spectral method and light pulse generation using mode-locking lasers

05 p0698 N71-15474

Computerized design and operation of laser projection screen video with alternate line resolution

06 p0821 N71-16826

Physical effects produced by laser radiation

07 p1039 N71-17484

Velocity dependence of gain of carbon dioxide laser

07 p1039 N71-17642

Focusing experiments with high power neodymium-carbon dioxide lasers

07 p1039 N71-17643

Bragg and Raman-Nath diffraction of laser light from magnetic and magnetostatic waves propagating in Y₂O₃

07 p1069 N71-17846

Subthreshold laser radiation damage to monkey retina

07 p0983 N71-17881

Critical Fresnel calculations for ruby laser destructions of thin metal films

07 p1046 N71-18074

Dynamics of laser produced plasma interaction with uniform magnetic field

08 p1270 N71-18188

Describing laser Doppler velocimeter for measuring mean velocity and turbulence of fluid flow

08 p1233 N71-19212

Properties of ultrashort pulses emitted by mode-locked neodymium and ruby lasers

09 p1395 N71-19443

Analysis of electrostriction mechanism for laser beam self focusing and track formation in transparent optical glass

09 p1395 N71-19552

Laser output light scattering for gas diagnostics

10 p1568 N71-20663

Characteristics of molecular lasers, vibrational population distribution of binary mixture of gases, and spectroscopic observation of laser outputs

10 p1569 N71-21233

Nondestructive testing of squid, low pressure combustion of metal propellants, and laser beam diffraction

10 p1637 N71-21355

Research and development of Apollo laser ranging retroreflectors

10 p1645 N71-21466

Electrical responses of visual system in rabbits following irradiation of retina with high energy ruby laser

10 p1502 N71-21621

Spectrum analysis of Q switched laser pulse dynamics using quantum mechanical model

11 p1774 N71-21857

Laser radiation nonlinear absorption by organic compounds

11 p1774 N71-21897

Methods of measuring fluid velocity from Doppler Fizeau shift of scattered laser radiation, and optimization of optical system geometry

11 p1775 N71-22610

Optical superheterodyning spectroscopic analysis of light scattering from solids at 10.6 microns

11 p1818 N71-22889

Development of apparatus for amplitude modulation of diode laser by periodic discharge of direct current power supply

11 p1776 N71-22895

Metallic materials heated by laser radiation absorption

12 p1931 N71-23104

Temperature distribution in metallic solids due to laser radiation absorption

12 p1932 N71-23106

Molecular laser studies in far infrared for optimizing power output and efficiency

12 p1932 N71-23325

Gas density measurement using laser induced Raman scattering

12 p1900 N71-23496

Dissociation and output of platinum catalyzed CO₂ laser

12 p1903 N71-23705

Experimental design using single ultrashort pulses for triggering Kerr cells and producing laser radiation to heat lithium deuteride targets for high temperature plasma generation

13 p2088 N71-24641

Doppler shifted laser beam as fluid velocity sensor

13 p2089 N71-24628

Performance characteristics of radio frequency excited helium-neon ring laser

13 p2089 N71-24629

Nonlinear absorption feedback for laser power stabilization

13 p2089 N71-24837

High altitude aircraft test for visible laser communication and analysis of errors in optical communications experiment due to flight path inaccuracies

13 p2091 N71-25571

Development of simultaneous mode locking and pulse coupling of carbon dioxide laser using single gallium arsenide element

14 p2265 N71-25618

Theoretical analysis of continuous chemical laser emphasizing constant gain method of solution and strong coupling in cavity between radiation and chemistry

14 p2265 N71-25844

Calibrator for measuring and modulating or demodulating laser output

14 p2265 N71-25914

- Gas laser and plasma tube operation and outputs including acetylene laser design 14 p2266 N71-26031
[AD-720404]
- Method and apparatus for optically modulating light or microwave beam 14 p2299 N71-26722
[NASA-CASE-GSC-10216-1]
- Laser machining device with dielectric functioning as beam waveguide for mechanical and medical applications 15 p2415 N71-27135
[NASA-CASE-HQN-10541-2]
- Optical communication system with gas filled waveguide for laser beam transmission 15 p2418 N71-27183
[NASA-CASE-HQN-10104-1]
- Laser radiation absorption in lower atmosphere 15 p2419 N71-27506
- Thomson scatter spectrum in laser generated plasmas [CEA-R-4058] 15 p2502 N71-27840
- Laser energy necessary for inertially confined nuclear fusion plasma [UPF-477] 15 p2503 N71-27888
- Characteristics of photon echo resonance determined by application of two brief laser pulses to resonant absorbing system [AD-721310] 16 p2665 N71-28559
- Computer generation and plotting of synthetic holograms, binary holograms, and spatial filters 16 p2607 N71-28935
- Numerical analysis of water drop vaporization rates in laser radiation field of different densities [NASA-TT-F-13640] 17 p2856 N71-29272
- Evaluation of laser systems for inducing nuclear fusion processes in fusion weapons and hydrogen energy sources 17 p2758 N71-29911
[FOA-4-4449]
- Propagation of coherent radiation in cylindrical plasma column considering laser beam refraction [NASA-CR-1839] 17 p2758 N71-30012
- Degradation effects of atmospheric absorption of 10.6 micron laser beam with kinetic model for vibrational relaxation process and numerical analysis of vibrational lag ray displacement [RR-350] 17 p2759 N71-30153
- Pulse amplitude modulation of laser outputs for image contrast enhancement in real time holographic interferometry for nondestructive testing [AD-724632] 19 p3108 N71-32244
- Spacecraft attitude measurement based on spatial coherence of laser and stellar light, and interferometry 19 p3133 N71-32268
- Optical measuring instrument design, calibration and operational procedures for measuring helium-neon laser scattered irradiance levels [PB-198375] 19 p3108 N71-32445
- Numerical analysis of coherent dynamic effects and absorption coefficient measurements for carbon dioxide subjected to low intensity source of radiation 19 p3109 N71-32684
- High energy ion source produced by focusing laser pulsed radiation on this plasmas 20 p3281 N71-32874
- Quantum mechanical transport equation for atomic or molecular interactions with radiation and application to laser physics [NASA-CR-119724] 20 p3315 N71-33171
- Analysis of helium-neon and carbon dioxide laser beam propagation in atmospheric turbulence [NASA-TN-8-370] 20 p3310 N71-33222
- Emission spectroscopic analysis using laser beam as excitation source 20 p3282 N71-33541
- Enhancement output power of CO-2 laser excited by electric discharge and irradiated by neutrons obtained from nuclear reactor 20 p3282 N71-33668
- Analysis of metal combustion using isolated aluminum particles ignited by laser and burning in controlled mixture of oxygen and argon 20 p3366 N71-33769
- Analysis of nonlinear resonant effects of external optical signal acting on laser oscillator 20 p3282 N71-33786
- Characteristics of carbon dioxide laser radiation scattering in atmosphere and application as remote sensing probe [NASA-CR-121663] 21 p3435 N71-34439
- Estimates of laser energy required to heat inertially confined d-4 target in pulsed fusion reactor [CML-R-109] 21 p3436 N71-34448
- Laser-induced plasma instability model for electric fields oscillating near plasma frequencies [LA-4604] 21 p3495 N71-34899
- Application of optically diagnosed noise information toward development of filtering subroutines for improvement of digital sensing data type quality - Vol. I [NASA-CR-121978] 22 p3382 N71-35510
- Proceedings of conference on short light pulse lasers and interaction with matter 22 p3390 N71-35568
[FOA-2-C-2373-51]
- Effect of ruby laser beam impact on mirror coating of sighting prism [FOA-2-A-2520-51] 22 p3591 N71-35569

- Optical propagation measurements in inhomogeneous atmosphere at Emerson Lake, California for optical propagation theory validity testing [NASA-CR-1733] 23 p3752 N71-36755
- Solid state laser optical emission conversion to far infrared region by nonlinear polarization and small difference frequency generation 23 p3766 N71-36846
[NASA-TT-F-13979]
- Development of methods for obtaining high power coherent emission at various wavelengths using conventional lasers as primary sources [AD-726659] 23 p3766 N71-36847
- Hydrodynamic effects on laser beam propagation through gases and laser-induced instabilities in liquids and gases 23 p3767 N71-36850
- Characteristics of neodymium-YAG laser and methods for converting infrared output to visible radiation 23 p3768 N71-36855
- Laser beam interactions with thermal media in steady state and time-varying conditions including beam trapping, self-induced frequency modulation, lens effects, and beam aberration 23 p3768 N71-36856
- Effect of laser beam impingement on metal surface and determination of ratio of liquid and gaseous phases [NASA-TT-F-13906] 23 p3768 N71-36858
- Laser microemission spectroscopic analysis of metals and nonmetals [NASA-TT-F-13971] 24 p3931 N71-38045
- Analysis of mechanism of inflow of material into plasma under effect of laser radiation [NASA-TT-F-13960] 24 p3931 N71-38046
- Development of methods for controlling frequency of solid state lasers and frequency scanning of ruby and neodymium lasers during lasing process [AD-727250] 24 p3931 N71-38049
- Effect of laser action and temperature gradients on thermionic emission of metal alloys [AD-727400] 24 p3932 N71-38057
- Optical wave phase structure and mutual coherence function for propagation in turbulent atmosphere and heterodyne detection effects [AD-727583] 24 p3967 N71-38302
- LASER RADAR**
U OPTICAL RADAR
LASER RANGE FINDERS
- Laser range finding of passive satellites by locating retroreflected radar echos on sky photography [ONERA-TP-845] 02 p0238 N71-11564
- Uranium sphere equipped with laser retroreflector array as satellite for determining accurate position of ground stations [SAO-SPECIAL-REPT-329] 04 p0614 N71-14116
- Optimization analysis of compact, lightweight laser rangefinder [AD-713517] 05 p0697 N71-15222
- Transportable laser system for lunar ranging [NASA-CR-116423] 07 p0140 N71-17878
- Systems design and performance tests of Apollo 14 laser ranging retroreflecting equipment 09 p3196 N71-19797
- Thermionic converter optimization, laser obstacle detector, and test program for interplanetary spacecraft guidance and control subsystems 10 p1600 N71-21347
- Orbit prediction models and computer program for satellite tracking using lasers [BMFB-FB-W-70-64] 11 p1825 N71-22040
- Atmospheric turbulence effects on laser beam phase correlation during tropospheric propagation 11 p1713 N71-22953
- Pulsed ruby laser ranging system for Apollo 11 lunar exploration system 13 p0290 N71-25335
- Evaluation of airborne laser systems for mapping, range finding, communication, and fire control [AD-720522] 14 p2266 N71-26188
- Geodetic survey by means of mobile stations of Q switched laser range finders and Diode-stimulated [ONERA-NT-156] 15 p2398 N71-27054
- Range finder using propagation time of light and modulation of optical radiation - optical radar [AD-721253] 15 p2390 N71-27190
- Experimental and theoretical predictions concerning calibration, random errors, and efficiency of optical range finders [AD-720855] 15 p2381 N71-27313
- Laser ranging retroreflector deployed on lunar surface to study lunar librations for defining precisely lunar orbits and studying earth planetary structure - Apollo 14 flight 18 p3012 N71-30965
- Design certification of Apollo 15 laser ranging retroreflector experiment [NASA-CR-115108] 19 p3107 N71-31609
- Operation and accuracy of pulsed light range finder laser [AD-724699] 20 p3281 N71-33150
- Space positional vector calculation using Baker-Nunn and Laser observations of artificial earth satellites 22 p3678 N71-36226

LASER RANGER/TRACKER

- Design, development, fabrication, and test of lunar ranging retroreflector experiment equipment for Apollo 14 flight [NASA-CR-114901] 10 p1645 N71-21407
- Optical polarization technique for use with laser detection and ranging system to differentiate between cloud returns and target returns [AD-717027] 11 p1775 N71-22278
- Design and development of broadband model of laser based missile tracking and ranging system [AD-720351] 14 p2265 N71-26006
- Laser beam projector for continuous, precise alignment between target, laser generator, and astronomical telescope during tracking [NASA-CASE-NPO-11087] 16 p2640 N71-29125
- QEOS-3 altimeter bias recovery simulation using range and angle tracking data [NASA-TM-X-65619] 18 p2922 N71-30092
- Q switched laser and normal mode ruby laser for dual-laser satellite geodesy system 19 p3009 N71-31858
- Photographic technique for reducing instrument errors of ruby laser systems for satellite ranging 19 p3099 N71-31809
- Aircraft tracking and guidance facility using PPR-16 radar supplemented by laser tracker permanently mounted on antenna [NASA-CR-111931] 21 p3407 N71-34348
- Using laser tracking systems to detect motion of pole of rotation for earth [NASA-TM-X-65666] 23 p3765 N71-36840
- LASERS**
NT ARGON LASERS
NT CARBON DIOXIDE LASERS
NT CHEMICAL LASERS
NT GALLIUM ARSENIDE LASERS
NT GAS LASERS
NT HELIUM-NEON LASERS
NT INFRARED LASERS
NT INJECTION LASERS
NT LIQUID LASERS
NT ORGANIC LASERS
NT PULSED LASERS
NT Q SWITCHED LASERS
NT RAMAN LASERS
NT RING LASERS
NT RUBY LASERS
NT SEMICONDUCTOR LASERS
NT SOLID STATE LASERS
- Parametric tuning characteristics of barium sodium niobate [AD-710220] 01 p0062 N71-10005
- Lasers, bibliography, optical communication, and information processing by analog optical computing 01 p0062 N71-10017
- Simultaneous measurement of atmospheric dust by laser and balloon sounding [NASA-CR-111794] 01 p0045 N71-10042
- Remote measurement of wind speed and air turbulence by laser scattering 01 p0062 N71-10208
- Dynamics of laser-produced heavy ion plasmas observed by photodiodes and supporting circuitry [AD-710728] 01 p0185 N71-18542
- Laser communication in space and on earth [JPRS-51546] 01 p0063 N71-18558
- Feedback averaging method for amplitude modulated digital laser communications systems [AD-710946] 01 p0023 N71-10467
- Controlling thermal self-focusing of laser beams by decreasing intensity near axis [AZT-70-197-RULL] 01 p0064 N71-10441
- Using lasers for gathering information for weather forecasting 01 p0064 N71-10442
- Development of pattern threshold recognition device [AD-712324] 02 p0191 N71-11340
- Measurement of micro-displacements by laser interferometry [REPT-70-75/4] 02 p0239 N71-11600
- Applications of lasers for ballistic research [IT-126-G/2] 02 p0239 N71-12111
- Laser altimeter-range finder techniques applied to geodetic measurements and mapping [NASA-TM-X-66489] 03 p0387 N71-13025
- Wavelength-selective, repetitively pulsed CO2 laser for nonlinear optical effects studies and atmospheric pollutant detection [NASA-TM-X-66497] 03 p0387 N71-13274
- Developing neodymium glass laser system capable of ranging to geosynchronous satellites [NASA-CR-115233] 03 p0388 N71-13018
- Physical concepts in diffraction of light by ultrasonic waves and specific form of laser acoustic delay lines [AD-712575] 03 p0418 N71-13047
- Shadow images of bodies obtained at hypersonic speeds by means of single-pulse laser [AD-712803] 03 p0390 N71-13174
- Periodic operating characteristics of neodymium glass laser in cyclic mode [AD-712813] 03 p0388 N71-13108

- Energy transfer in interactions between laser beams and solid dielectric media
[CEA-N-1337] 04 p0374 N71-13670
- Monte Carlo calculation of laser light scatter transmission through water
04 p0563 N71-13726
- Conventional methods and lasers for measuring light scattering in sea water
04 p0564 N71-13729
- Plasma sources, hydromagnetic ionizing fronts, hydromagnetic waves, laser diagnostics, and microwave techniques
[NF-18360] 04 p0596 N71-13772
- High speed cores, magnetic, semiconductor, and laser storage systems
04 p0504 N71-13829
- Application of laser radiation to removal of material from metal
[NASA-TT-P-11912] 04 p0523 N71-14070
- Measurement of retinal image in Rhesus monkeys to determine laser radiation hazards
[AD-720635] 04 p0480 N71-14474
- Plasmas, semiconductors, lasers, electro-optics, and related research
[AD-713228] 05 p0752 N71-14581
- Describing construction and alignment of laser gyro assembly
[FOA-2-C-2336-31] 05 p0696 N71-14680
- Neodymium YAG laser for optical radar application
[AD-713582] 05 p0644 N71-14697
- Lasers as light sources for high speed photography
[AEC-TB-7166] 05 p0696 N71-15035
- Optical laser generation by electron beam impact in high temperature argon plasmas
[UCRL-TRANS-10478] 05 p0753 N71-15050
- Developing system for automatic compensation of signal dc level drift in laser interferometers
[Y-1737] 05 p0697 N71-15232
- Meteorological data processing, laser meteorology, and distribution functions
05 p0720 N71-15679
- Carrier recombination and laser processes in semiconductors, mainly gallium arsenide
[AD-714533] 06 p0687 N71-16108
- Materials science research on lasers, high pressure effects, superconductors, crystal structure, and chemical and physical properties
[AD-713990] 06 p0661 N71-16331
- Mechanical resonators for vibrating mirrors to deflect laser beams in optical data recording system
07 p0638 N71-17036
- Waveguide light intensifier in semiconductor laser systems for optical communication
07 p0108 N71-17107
- Cloud structure determined from laser backscatter
07 p0653 N71-17171
- Bibliography of laser publications of interest to emission spectroscopists
[BN-1425] 07 p0109 N71-17266
- Parametric analysis of microwave and laser systems for communication and tracking with emphasis on aspects of operational environment and system implementation
[NASA-CR-1689] 07 p0992 N71-17582
- Theoretical analysis of cylindrical laser resonator with tapered output mirror
[AD-714981] 07 p0108 N71-17744
- Electromagnetic wave diffraction in Fabry-Perot optical resonator
08 p1202 N71-18928
- Laser interferometer for monitoring and control of large telescope
[NASA-CR-111811] 08 p1203 N71-19019
- Factors influencing gain in neodymium doped laser glass
09 p1395 N71-19518
- Process technology required for production of zone melting feed rods of pure aluminum oxides for basic studies of laser degradation
[AD-716421] 09 p1397 N71-19948
- Laser device for removing material from rotating object for dynamic balancing
[NASA-CASE-MPS-11279] 09 p1397 N71-20400
- Beam scintillations and atmospheric turbulence characteristics of multiwavelength laser transmission
[AD-717088] 10 p1570 N71-21178
- Studying plasmas with narrow beam high power laser
[AD-717834] 11 p1810 N71-23013
- Design, development, and production of continuous and pulsed optical pumps for neodymium lasers
[AD-717362] 11 p1774 N71-22146
- Modification of folded conventional schlieren system for transmission of holograms
[AD-717702] 11 p1775 N71-22288
- Analysis and measurement of characteristics of wide band frequency trackers and design and fabrication of all angle laser Doppler velocimeter
[NASA-CR-105088] 11 p1775 N71-22407
- Basic parameters for application of laser Doppler velocimeter, cross beam technique in three modes of operation obtained by computer programming
[NASA-TN-D-61251] 11 p1775 N71-22615
- Energy deposition in lasers, computer revised code including multifrequency calculation, bodies of revolution, and geometry debug facility
[AD-718802] 12 p1932 N71-23319
- Applications of laser Doppler techniques for measurements in large flow systems
[AD-718818] 12 p1932 N71-23324
- Amount of material evaporated, and initial escape velocity of evaporation products of various materials used as laser target materials
[NASA-TT-P-135398] 12 p1933 N71-23384
- Design and construction of electron-pumped Cerenkov laser
[AD-718469] 12 p1933 N71-23621
- Two step laser action and tunable Cerenkov laser for wavelengths shorter than 3000 Å
[AD-718468] 12 p1934 N71-23800
- Absolute and relative sensitivity of emission spectral analysis with laser excitation source
[NASA-TT-F-135422] 12 p1934 N71-24058
- Design and development of optical interferometer with laser light source for application to schlieren systems
[NASA-CASE-XLA-04295] 12 p1935 N71-24170
- Semiconductor devices, quantum electrodynamics, lasers, defects in crystals, communication and radar systems, bioengineering, plasmas, and other related subjects
[AD-718982] 13 p2188 N71-24445
- Pycnometer, profilometer, and laser measuring for data on bulk density of swollen and cracked space reactor fuel pellets and capsules
13 p2113 N71-24528
- Feasibility of achieving bulk laser action in polar semiconductors pumped by impact ionization in applied electric field
[AD-719403] 13 p2089 N71-24731
- Theoretical and experimental analyses of picosecond laser pulses
[AD-719415] 13 p2089 N71-24732
- Laser flash diffusivity measurement of thermal conductivity in oxide nuclear fuel materials
[WJAN-SA-80] 13 p2121 N71-25379
- Determination of gas temperature from laser-Raman scattering
[NASA-TN-D-6336] 14 p2253 N71-25663
- Laser Doppler velocity measuring device using scanning interferometer
14 p2254 N71-26108
- Self-generating optical frequency waveguide
[NASA-CASE-RQN-10541] 14 p2219 N71-26291
- Nonlinear wave interaction laser spectroscopy for atomic transition studies
14 p2306 N71-26377
- Nonlinear optics of thermal laser beam defocusing in gases
[AD-720311] 15 p2418 N71-27395
- Literature survey of ophthalmological and dermatological laser hazards and safety measures
[AD-721068] 15 p2418 N71-27404
- Laser-plasma interactions and energy changes in plasma particles
[CEA-N-1399] 15 p2504 N71-27985
- Laser reflectors, stabilization, and thermal control of geostatic satellites Diode D-1C and D-1D
[RAE-LIB-TANIS-1301] 16 p2681 N71-28851
- Microwave, laser, and semiconductor device development
[AD-722016] 16 p2606 N71-28236
- Spectrum of multiwavelength scintillations and validity of frozen-in turbulence
[AD-721738] 16 p2606 N71-28399
- Characterization of spatial profile of laser beam before and after amplification
[AD-722074] 16 p2606 N71-28400
- Developments in scientific research, plasma physics, electronics, information theory, radio astronomy, and lasers
[AD-728234] 16 p2695 N71-29067
- Atomic absorption spectra of chloro formed by laser-induced vaporization of chromium steel
[NASA-TT-F-13688] 17 p2758 N71-29225
- Anomalous high frequency resistivity and heating of plasmas by laser irradiation
[MATT-817] 17 p2812 N71-29630
- Plasma physics research, including source analysis, ionization characteristics, laser diagnostics and performance, and electron cyclotron studies of harmonic resonance
[NF-18663] 17 p2812 N71-30193
- Laser photon scattering by high density plasmas
17 p2813 N71-30196
- Wing tip vortex test demonstrating use of Laser Doppler Velocimeter system for measuring gas velocities with high spatial and temporal resolution
[NASA-CR-118004] 17 p2737 N71-30278
- Laser optical technique for measuring width of ultrashort optical pulses produced by mode locked laser
18 p2964 N71-31163
- Continuous operation laser based on chemical excitation vibration rotational levels of hydrogen chloride produced in detonation waves stabilized in supersonic flow
18 p2932 N71-31420
- Comparison of radiocarbon and laser backscatter data of atmospheric humidity
[AD-723501] 19 p3125 N71-31677
- Installation and structure of aerial laser camera for photographic imaging from aircraft
[AD-723628] 19 p3098 N71-31727
- Cascade ionization of air by radio frequency fields and by intense laser beams
[AD-723183] 19 p3107 N71-31807
- Laser and radar tracking of GEM-2 for precise geodetic and position location - conference
19 p3089 N71-31836
- Earth gravity field determinations with laser tracking of geodetic satellites
19 p3108 N71-31857
- Present status and future requirements of geometric satellite geodesy using simultaneous optical direction observations with lasers and cameras
19 p3108 N71-31860
- Characteristics of far field power distributions for circular aperture with Gaussian illumination
[AD-723433] 19 p3108 N71-32093
- Annotated bibliography of selected wideband laser communications literature
[AD-723834] 19 p3055 N71-32130
- Laser applications in communications, industrial fabrication, and computer systems, and laser beam generation and control - technology seminar
[NASA-SP-5937/01] 19 p3108 N71-32382
- Analysis of problems involved in production of X ray laser
19 p3108 N71-32457
- Luminescence induced by UV and visible lasers for remote active sensing of materials from ground, air, and space
[MDC-52344] 19 p3109 N71-32686
- Optical heterodyning with reference beam for eliminating atmospheric turbulence effects on signal to noise ratio
19 p3143 N71-32745
- Design and characteristics of laser camera system with diffraction filter of small particles with average diameter larger than wavelength of laser light
[NASA-CASE-NPO-10417] 20 p3281 N71-33410
- Importance of optical tolerances and electric fields in resonant reflectors used in giant pulse laser systems
20 p3275 N71-33480
- Laser beam spreading methods
20 p3282 N71-33481
- Nuclear laser excited by fission fragments produced in pulsed nuclear reactor
20 p3282 N71-33633
- Studies on microwave generation by solid state devices
20 p3244 N71-33941
- Analysis of processes occurring and considerations involved with lasers and controlled thermonuclear fusion
[NASA-TT-F-13700] 21 p3435 N71-34442
- Measurement of stress optical coefficients for homogeneous and inhomogeneous glass test specimens used in neodymium lasers
[AD-724302] 21 p3435 N71-34444
- Proceedings of conference on short light pulse lasers and interaction with matter
[FOA-2-C-2373-51] 22 p3590 N71-35566
- Measurements of off-axis irradiance produced by laser beam in water
[AD-724626] 22 p3591 N71-35573
- Sensitive technique uses Fresnel drag effect to determine orientation of spherical rotor spin axis for laser gyroscope application
22 p3591 N71-35575
- Simulation evaluation and analysis of strapdown laser seeker guidance concept
[AD-726376] 22 p3618 N71-35780
- Statistical analysis of some nonlinear optical effects including scattering light from rotating glass and second harmonic light generated by pseudo-thermal source
[NASA-CR-121935] 22 p3628 N71

- Development of method for calculating resonant modes and eigenvalues of laser cavity
23 p3767 N71-36854
- Application of lasers to plasma heating and determination of effects of inverse bremsstrahlung
[NASA-CR-122067] 23 p3825 N71-37284
- Plasma dynamics, plasma heating, lasers, and wave propagation in inhomogeneous magnetoplasmas
[AD-726675] 23 p3829 N71-37313
- Remote radar sensing of ocean surface, atmospheric laser transmission near 5 microns, and various studies in electronics, mathematics, metallurgy, nuclear and atomic physics, ocean technology, optics, solid state physics, and space antenna system
23 p3855 N71-37476
- Atmospheric transmission of infrared radiation near 5 microns
23 p3855 N71-37478
- Combined effects of optical absorption and thermal conduction in retinal tissue calculated for establishing thresholds for eyeburn in imaging intense light sources as lasers and nuclear explosions
[LA-4651] 24 p3878 N71-37645
- Interrelations between advanced processing techniques, integrated circuits, laser radiation, and microcircuit interconnections
[NASA-CR-123007] 24 p3900 N71-37799
- Hazards associated with laser radiation and radiation used as tool in biology and medicine
24 p3900 N71-37802
- Using laser Doppler anemometry for velocity measurements in two phase flow
[RISO-M-1368] 24 p3904 N71-37828
- Effect of retrodirective reflections on operation of ring resonator laser
[JPRS-54106] 24 p3931 N71-38048
- Application of pulsed ruby holographic techniques to tests of ceramic materials
[AD-727160] 24 p3931 N71-38050
- Plasma formation upon laser irradiation of transparent dielectric materials below damage threshold
[AD-727143] 24 p3932 N71-38052
- Photoconductivity in Gallium arsenide single crystals by two photon absorption of light quanta from H₂ glass laser
[AD-727755] 24 p3932 N71-38054
- Frequency characteristics of electro-optical light modulators with coupled coaxial resonators
[AD-727954] 24 p3932 N71-38055
- Soviet technical literature relevant to explosions, soil mechanics, laser and particle beams, and reentry problems - bibliography
[AD-727584] 24 p4035 N71-38790
- LASV**
U F-111 AIRCRAFT
- LATCHES**
Transparent polycarbonate resin, shell helmet and latch design for high altitude and space flight
[NASA-CASE-XMS-04935] 02 p0167 N71-11190
- Quick disconnect latch and handle combination for mounting articles on walls or supporting bases in spacecraft under zero gravity conditions
[NASA-CASE-MFS-11132] 07 p0135 N71-17649
- Design, development, and characteristics of latching mechanism for operation in limited access areas
[NASA-CASE-XMS-03745] 10 p1564 N71-21076
- Latching mechanism with pivoting catch and self-contained spring ejector
[NASA-CASE-XLA-03538] 13 p2086 N71-24897
- Latch for fastening spacecraft docking rings
[NASA-CASE-MSC-15474-1] 14 p2362 N71-26162
- LATENCY**
U REACTION TIME
- LATERAL CONTROL**
Low speed lateral stability and control flight tests on Avro 707 aircraft
[ARC-CP-1106-PT-3] 07 p0969 N71-17083
- In-flight determination of lateral-directional dynamics for landing approach
[AD-715317] 07 p0973 N71-17792
- Flight roll control for Aerobee rocket vehicle
[NASA-CR-734999] 08 p1294 N71-18745
- Roll-control effectiveness of spoiler configurations on aircraft model with variable sweep wings at supersonic speeds
[NASA-TM-X-2165] 09 p1317 N71-20126
- Supersonic aircraft lateral control equipment
[AD-726740] 14 p2199 N71-26538
- Supersonic or hypersonic vehicle control system comprising electrons with hinge line sweep and free of adverse aerodynamic cross coupling
[NASA-CASE-XLA-08967] 15 p2366 N71-27088
- Technique for designing switching thresholds in lateral guidance of entry vehicle
[NASA-CR-115146] 22 p3617 N71-35772
- LATERAL OSCILLATION**
Lateral oscillations and low speed and lateral stability of free flight lifting bodies
[ARC-R/M-3641] 06 p0791 N71-15705
- LATERAL STABILITY**
Lateral oscillations and low speed and lateral stability of free flight lifting bodies
[ARC-R/M-3641] 06 p0791 N71-15705
- Behavior of structural subassemblies with laterally unsupported columns
[AD-714516] 06 p0957 N71-16849
- Boundary layer separation and longitudinal and lateral stability of Avro 707 aircraft during flight tests
[ARC-CP-1107-PT-4] 07 p0969 N71-17082
- Low speed lateral stability and control flight tests on Avro 707 aircraft
[ARC-CP-1106-PT-3] 07 p0969 N71-17083
- Flight evaluations using variable stability aircraft to determine effects of turbulence induced aerodynamic disturbances and lateral directional dynamics on pilot performance
[NASA-CR-1718] 14 p2196 N71-26170
- Equations of motion for time vector calculus for aircraft lateral stability
[ARC-R/M-3631] 15 p2367 N71-27097
- Nonsteady flight test program on Sikohl 204 D-1 aircraft for determining lateral directional stability and control derivatives
[NLR-TR-70038-U] 15 p2367 N71-27109
- Subsonic stability, control, and performance of shuttle concept with blended wing-body
[NASA-TM-X-2341] 18 p3018 N71-31254
- Low speed wind tunnel tests of lateral longitudinal, and directional stability of MDC STS high cross range shuttle orbiter
[NASA-CR-103163] 21 p3521 N71-35091
- Low speed wind tunnel tests of space shuttle lateral and longitudinal static stability characteristics of Mach 0.25
[NASA-CR-119853] 21 p3522 N71-35098
- Wind tunnel tests of lateral, longitudinal, and directional stability characteristics for scale model of orbiter shuttle
[NASA-CR-103155] 21 p3524 N71-35108
- Low speed wind tunnel tests of longitudinal and lateral aerodynamic characteristics of MDAC STS orbiter
[NASA-CR-103194] 21 p3524 N71-35111
- Longitudinal and lateral stability data from wind tunnel tests of earth orbiting shuttle
[NASA-CR-103154] 21 p3524 N71-35112
- Low speed longitudinal, directional, and lateral static stability characteristics of straight wing orbiter during configuration build-up
[NASA-CR-103156] 21 p3524 N71-35113
- Lateral buckling coefficient curves for rectangular beams bent in plastic range
[ARL/SM-NOTE-354] 23 p3860 N71-37518
- Subsonic longitudinal and lateral directional stability investigation of MDAC LCR orbiter, unpowered and powered - graphs
[NASA-CR-119965] 24 p4017 N71-38665
- Longitudinal, lateral, and directional static stability and control characteristics of delta wing space shuttle orbiter models 134D and 134C at Mach 0.25
[NASA-CR-119979] 24 p4020 N71-38681
- LATERALITY**
U LATERAL STABILITY
- LATERALIZATION**
U LATERAL CONTROL
- LATEX**
Laboratory tests of polymeric latex modified fast-set C-1 cement for repair of damaged runway pavements
[AD-727728] 24 p3943 N71-38132
- LATHES**
Selection of optimum metal cutting conditions for lathes
[REPT-3] 02 p0229 N71-11559
- Use of lathes for fabrication of turbomachine parts
02 p0233 N71-11648
- Infrared inspection of free surface wear on lathes using carbon dioxide lasers
[ELAB-TL-132] 10 p1563 N71-20945
- Rotary spindle lathe attachments for machining geometrical cones
[NASA-CASE-XMS-04292] 11 p1770 N71-22722
- Production of circular cylindrical surfaces on lathes using arc plasma torch
[UCRL-TRANS-10524] 21 p3433 N71-34431
- Surface finishing of ESO (Chile) telescope mirror defects using grinding machine
24 p3922 N71-37976
- LATITUDE**
NT GEOMAGNETIC LATITUDE
- Greenwich time and latitude observations for July - Sept. 1969
02 p0212 N71-11523
- Greenwich time and latitude observations for Apr. - Jun. 1970
13 p2071 N71-24989
- Greenwich time and latitude observations for Jan. - Mar. 1970
13 p2071 N71-24990
- Ionospheric auroral morphology, height variations, and relationships to planetary magnetic disturbances in periods of minimum and maximum solar activity at varying latitudes
[NASA-TT-F-637] 17 p2745 N71-30076
- Latitude variations in ionospheric parameters
17 p2747 N71-30090
- Magnetic activity at high latitudes of Northern Hemisphere during maximum and minimum solar cycle
17 p2748 N71-30090
- Greenwich time and latitude observations for July - Sept. 1970
19 p3178 N71-34402
- Tilt angle dependence of 10 MeV proton cutoff latitudes in image dipole model magnetosphere
[NASA-TM-X-45678] 20 p3316 N71-33446
- Determination of correct rotation values after latitude observations
23 p3749 N71-30771
- Lagrange function approximation for latitudinal paths
24 p0012 N71-38661
- Greenwich time and latitude observations for October through December, 1970
24 p4015 N71-38661
- LATITUDE MEASUREMENT**
Analysis of latitude observations for detection of earth crust movements
[NASA-CR-111567] 03 p0348 N71-13806
- LATTICE IMPERFECTIONS**
U CRYSTAL DEFECTS
- LATTICE PARAMETERS**
X ray diffraction and scattering studies of crystal imperfections in solids
[PB-192684] 02 p0285 N71-11861
- Heat capacities and thermodynamic functions of three In-Tl alloys from 5 to 300 K
[JIS-T-362] 03 p0389 N71-12561
- Relations between crystal index surfaces and molecular and lattice structure as exemplified by benzene
03 p0440 N71-12774
- Electron paramagnetic resonance in strontium titanate doped with chromium to determine interactions between paramagnetic ions in neighboring lattice positions
03 p0444 N71-13311
- Superconducting transition temperatures and lattice parameters of simple cubic metastable Te-Au solid solutions containing Fe and Mn
[CALT-82-9] 04 p0602 N71-17961
- Measuring observed frequency shifts of lattice resonant mode in KBr - LiF
[INVO-2391-118] 05 p0759 N71-15348
- Investigating mechanical properties of solids, relaxation processes in polymers, and properties of crystals
[AD-713923] 06 p0933 N71-16112
- Quantitative phase analysis and precise lattice parameter measurements by X ray diffraction in titanium alloys
[AD-715910] 06 p0934 N71-16381
- Deriving relationship between macroscopic second order elastic constants and microscopic interatomic potential in crystals
[KAPL-M-7131] 06 p0923 N71-16740
- Analyzing doped semiconductor surface layer using elastic ion-backscattering data
07 p1089 N71-17728
- Investigating orientation dependence of boron diffusion in silicon
07 p1090 N71-17729
- Variations in length and crystal parameters of alpha, beta, and delta phases of plutonium at low temperatures due to self-irradiation
[CEA-CONF-1619] 08 p1256 N71-18336
- Affect of systematic errors on measurement of crystal lattice constants
[AD-715354] 08 p1278 N71-18877
- Characteristics of alkali hydride lattice energies for ionic Born-Mayer potential
[MLM-1764] 09 p1454 N71-20501
- Computer program for calculating structure inventories from crystal lattice parameters
[AD-716746] 09 p1455 N71-20809
- Mathematical procedure for Born stability determination of body centered cubic crystal lattice unit properties
[AD-717698] 11 p1817 N71-23403
- Lattice parameter measurements on aluminum after electron irradiation at low temperatures
[JUL-664-FN] 13 p2091 N71-24623
- Proceedings from conference on isotactic monomer scattering with emphasis on collective excitations in disordered and magnetic systems, and lattice dynamics of high polymer substances
[JAEI-1197] 13 p2130 N71-24819
- Lattice parameters and compressibilities of high pressure phases of lead chalcogenides, manganese telluride, manganese tellurium, chromium antimony, and chromium tellurium compounds
14 p2527 N71-24491
- X ray determination of lattice parameters and thermal expansion coefficients of Al, Ag, and Mo polycrystals using back reflection diffraction camera
15 p2425 N71-27400
- Formulation and solution of sixteen vertex general lattice statistical model
[NUB-2077] 17 p2826 N71-30081

Solution of Ising model with two and four spin interactions and critical properties of model in various regions of parameter space
(NUP-2064) 17 p2826 N71-30032

Determination of stress induced crystal lattice imperfections in polycrystalline materials by density measurement, precise lattice parameter measurements and X ray diffraction analysis
10 p2996 N71-31188

Oxygen contamination, chemical rules, stoichiometry of solid solution, second phases, and carbon and nitrogen distribution in UC-UN solid solution lattices
(NLL-WINDSCALE-442-10991.5F) 23 p3801 N71-37100

LATTICE VIBRATIONS

Rotational bands constructed on octupole vibrations for even-even nuclei
(ITF-70-13) 03 p0433 N71-12947

Microscopic deformation in body centered cubic metals and solid solutions and analysis of intrinsic lattice resistance and interstitial impurities as dislocation motion control
(CONP-700545-1) 10 p1581 N71-21439

Phonon and electron induced transition effects on thermopower of transition metals, and impurity effects on crystal lattice dynamics
13 p2154 N71-25549

Lattice dynamics calculations for high pressure shock compression analysis on solid crystal
14 p2327 N71-26490

High pressure shock and particle velocity data for determining equations of state of dynamic pressure standards
14 p2327 N71-26494

Anomalous neutron scattering for evaluating lattice wave amplitudes in crystals
(NAL-TN-21) 15 p2510 N71-27940

Dynamic model for vibrating dislocation interaction with conduction electrons in metals
17 p2825 N71-30000

Vibronic and electronic resonance Raman effect in carbon, nitride and garnet crystals
(AD-727091) 17 p2827 N71-30168

Spectrum analysis of lead lattice vibrations
(DESS-4497) 20 p3333 N71-33293

Microscopic description of multiple pairing and particle-hole fields in particle vibration coupling of Pb-209
(LA-DC-11648) 20 p3322 N71-33795

Heat capacity of pure nickel, pure iron, and NiFe, and contribution from anharmonic lattice vibrations
(ORO-3291-14) 21 p3438 N71-34466

Theoretical models and phonon dispersion measurements for analyses of rutile lattice dynamics
(TID-32720) 24 p3994 N71-38508

LATTICES

Temperature and radiation dosage effects in niobium lattice defect backscatter of protons and helium ions
21 p3498 N71-34923

LATTICES [MATHEMATICS]

NT BOOLEAN ALGEBRA
NT BOOLEAN FUNCTIONS
Bosonist call diffusion coefficient corrections for CAGR-type lattices
(RD/BN-1645) 02 p0270 N71-11412

Characteristic subgroups of lattice ordered groups
04 p0604 N71-14462

Proof of increasing functions on finite distributive lattices are positively correlated measures satisfying minuscule convexity
(LPTRE-71/53) 10 p1593 N71-21533

Kinematics of subsonic unsteady airflows on multiple lifting surfaces
17 p2698 N71-29339

Strategy for speeding up two-dimensional SN-methods with help of coarse lattice techniques
(KPK-1361) 21 p3486 N71-34832

Using index grid for analyzing complex deformation
(NLL-M-21807-5028.4F) 24 p0027 N71-38735

LAUNCH COMPLEXES

LAUNCHING BASES
Analysis of launch opportunities for Radio Astronomy Explorer-B satellite during period Mar. through Dec. 1973
(NASA-TM-X-65587) 16 p2682 N71-28318

LAUNCH ESCAPE SYSTEMS

Emergency escape cabin system for launch towers
(NASA-CASE-XKS-02342) 02 p0169 N71-11599

Qualification tests of tower jetson motors for Apollo spacecraft program launch escape systems
(NASA-TN-D-6295) 13 p1556 N71-30533

LAUNCH TIME

LAUNCH WINDOWS
Development of single stage reusable launch vehicle for space transportation
(NASA-TT-F-13427) 06 p0922 N71-14008

Buffet response of straight wing and delta wing model of space shuttle launch configuration
13 p2179 N71-24662

Transonic wind tunnel investigation of flow characteristics and pressure fluctuations of space shuttle launch and reentry configurations
13 p2180 N71-34663

Turbomachinery for SNAP 8 power system subjected to expected vehicle launch vibration and shock loading
(NASA-TM-X-67851) 15 p2370 N71-27697

Configuration of second stage of Europa 1 and 2 launch vehicles - Corvise
17 p2830 N71-30037

Aerodynamic force and moment coefficient data for parallel beam vehicle launch configurations tested in transonic wind tunnel for static stability
(NASA-CR-115991) 24 p0018 N71-30671

LAUNCH VEHICLES

NT ATLAS LAUNCH VEHICLES
NT CENTAUR LAUNCH VEHICLE
NT DELTA LAUNCH VEHICLE
NT ELDO LAUNCH VEHICLE
NT EUROPA LAUNCH VEHICLES
NT EUROPA 1 LAUNCH VEHICLE
NT EUROPA 2 LAUNCH VEHICLE
NT REUSABLE LAUNCH VEHICLES
NT SATURN LAUNCH VEHICLES
NT SATURN 1-B-A-3 LAUNCH VEHICLE
NT SCOUT LAUNCH VEHICLES
NT THOR AGENA LAUNCH VEHICLE
NT TITAN 3 LAUNCH VEHICLE

Microleak detector mounted on weld seam of propellant tank of launch vehicle
(NASA-CASE-XMF-02307) 01 p0036 N71-10779

Launch vehicles in seventies noting French, European, and NASA space programs
02 p0299 N71-12000

Tabulated data on equatorial coordinates for Cosmos 35 satellite carrier rocket
03 p0433 N71-13012

Electrostatic hazards during launch vehicle flight operations
(NASA-CR-111727) 04 p0614 N71-14114

Lift-off procedures for space booster
07 p1118 N71-17094

Low cost launch vehicle system for economical space exploration
(NASA-CR-116002) 08 p1294 N71-18726

Establishing first estimate of launch vehicle requirements in preparing advance mission plans
(NHB-7100.5) 08 p1295 N71-19310

Improving payload at low power by reducing total mass of electric propulsion spacecraft
(NASA-TM-X-52908) 09 p1461 N71-20501

Computerized probabilistic model for optimal cost assignment of launch vehicle programs to advanced space missions
(NASA-CR-114284) 12 p2003 N71-24319

Manual of computer program for probabilistic optimal launch vehicle assignment and budget smoothing model
(NASA-CR-114285) 12 p2003 N71-24320

Absolute stability analysis of attitude control systems for large launch vehicles
(NASA-TM-X-64582) 15 p3519 N71-26931

Adaptive digitalized learning control system for launch vehicles
(NASA-TM-X-64518) 15 p2442 N71-27846

Launch vehicle thermal protection system evaluation based on thermal and pressure distributions over exposed booster surface
17 p2847 N71-29458

Cost and weight data for space shuttle booster least sink structural concept
17 p2847 N71-29459

Aerodynamic forces and moments on orbiter and booster during space shuttle abort separation
(NASA-CR-103197) 21 p3520 N71-35085

Low speed aerodynamic characteristics of McDonnell Douglas scale model space shuttle booster
(NASA-CR-103161) 21 p3520 N71-35086

Transonic wind tunnel tests of longitudinal aerodynamic characteristics of OD/Conair B4B space shuttle booster model
(NASA-CR-103158) 21 p3521 N71-35087

Hypervelocity wind tunnel tests of Conair B4B space shuttle booster and model configuration perturbations
(NASA-CR-103159) 21 p3521 N71-35089

Low speed wind tunnel tests of stability and control characteristics of space shuttle booster at subsonic speeds
(NASA-CR-110861) 21 p3522 N71-35094

Low speed wind tunnel tests of directional stability characteristics for M/DAC delta wing booster
(NASA-CR-103157) 21 p3523 N71-35105

Low speed wind tunnel tests of straight wing and delta wing configuration space shuttle booster models
(NASA-CR-103163) 21 p3524 N71-35110

Subsonic aerodynamic characteristics of M/DAC/MNC space shuttle booster configuration at Mach 0.26
(NASA-CR-103199) 21 p3525 N71-35115

LAUNCH WINDOWS

Predicted launch vehicle operational trajectory and related data for Apollo 14 launch window
(NASA-TM-X-65653) 05 p0771 N71-15317

Lift-off procedures for space booster
07 p1118 N71-17094

Launch window characteristics for manned interplanetary stopover flights to Mars and Venus
(NASA-TN-D-6226) 08 p1293 N71-18648

IMP-1 launch window and secondary injection into eccentric orbit
(NASA-TM-X-65450) 08 p1293 N71-18649

Procedures for determining launch window for SERT 2 mission and effect of low thrust and earth obstructions on orbit perturbations
(NASA-TM-X-2233) 09 p1467 N71-20520

Mariner Mars mission planning including launch windows and scientific objectives in 1971
(NASA-NEWS-RELEASE-71-73) 12 p2002 N71-24314

Analysis of launch opportunities for Radio Astronomy Explorer-B satellite during period Mar. through Dec. 1973
(NASA-TM-X-65587) 16 p2682 N71-28318

LAUNCHERS

NT AIRCRAFT LAUNCHING DEVICES
NT GUN LAUNCHERS
NT HYPERVELOCITY LAUNCHERS
NT MISSILE LAUNCHERS
NT ROCKET LAUNCHERS

Accelerator for launching hypervelocity projectile by drag force of jet produced by gaseous explosive products
(NASA-CR-113667) 17 p2729 N71-29227

LAUNCHING

NT AIR LAUNCHING
NT ORBITAL LAUNCHING
NT ROCKET LAUNCHING
NT SPACECRAFT LAUNCHING

Model and robot design and launching techniques
(NASA-TM-X-64532) 04 p0315 N71-13579

Onboard optical and electronic data acquisition instrumentation for monitoring Apollo Saturn 3 launch performance
(NASA-TM-X-67185) 16 p2682 N71-28172

LAUNCHING BASES

NT CAPE KENNEDY LAUNCH COMPLEX
Space shuttle trajectory performance data for east and west test range launch simulations
(NASA-TM-X-64596) 14 p2337 N71-26036

LAUNCHING DEVICES

U LAUNCHERS

LAUNCHING PADS

Remotely actuated quick disconnect for tubular umbilical conduits used to transfer fluids from ground to rocket vehicle
(NASA-CASE-XLA-91396) 03 p0316 N71-12239

Portable equipment for validating C band launch pad antennas and transmission lines used for spacecraft checkout
(NASA-CASE-XKS-10543) 14 p2319 N71-26292

Criteria and recommendations to ensure compatible interfaces between space vehicle structure and launch stand ground support equipment
(NASA-SP-0061) 16 p2682 N71-28329

LAUNCHING RITES

NT LAUNCHING PADS

Scheduled launching of SAS-A by Italian team of space engineers for detecting X ray sources in space
(NASA-NEWS-RELEASE-70-203) 03 p0453 N71-12937

Surface climatological data for twenty selected launch, landing, and alternate landing sites for space shuttle system
(NASA-CR-61342) 10 p1596 N71-21513

History of Cape Kennedy launch complex noting origin, initial construction, organization, launching sites, ground support equipment, and significant accomplishments
(NASA-TM-X-67274) 20 p3247 N71-33771

LAVA

Multiphase eruptions associated with lunar craters Tycho and Aristarchus - lava flow charts
04 p0613 N71-14441

Banders lava tubes of New Mexico and lunar comparisons
04 p0522 N71-14443

Lava flow characteristics in Hadley Rille valley of lunar mountains
(NASA-TM-X-62011) 05 p0767 N71-14687

Chronological summary of Surtsey volcano eruption from 1963 to 1967
07 p1034 N71-17971

Investigating composition and ages of Icelandic lavas to determine validity of sea floor spreading
07 p1023 N71-17975

Reporting eruption of Hecla volcano from May through June 1976
07 p1025 N71-17976

Analyzing subaerial flows of lava in eastern Iceland and recent and Pleistocene flows in neovolcanic zone of central Iceland for basalt composition
07 p1025 N71-17979

LAVAL NUMBER

Investigating effects of lava outgassing on primary colonization by organisms

07 p0964 N71-17993
Characteristics of lava tubes and channels on lunar surface

[NASA-TM-X-62013] 07 p1116 N71-18007
Lava tube and channel development in basalt flow in upper east rift zone of Kilauea volcano, Hawaii

[NASA-TM-X-62014] 08 p1192 N71-18965
Geomorphology of basaltic lava tubes from Mount St. Helens, Washington

[NASA-TM-X-62022] 20 p3257 N71-33020
Magma reservoir evidenced from tidal gravity variations observed at Halemauana lava lake, Kilauea, Hawaii

20 p3264 N71-33359

LAVAL NUMBER
Transonic flow of gas in axially symmetric Laval nozzles with steep walls

[NASA-TT-F-15573] 18 p2904 N71-30749

LAW [JURISPRUDENCE]
NT INTERNATIONAL LAW

NT LEGAL LIABILITY
NT LIABILITIES

NT PENALTIES
NT SPACE LAW

Legislation to establish Office of Technology Assessment for Congress

[REPT-91-1437] 07 p1133 N71-17532
Operations research for West German governmental information retrieval system, noting law application and decision making

14 p2223 N71-25997
Environmental policy and law - bibliography

[ORNL-NSF-EP-3-VOL-1] 13 p2326 N71-27267
Weight and Measures Labeling Handbook for use in packaging and labeling commodities and enforcing state laws and regulations

[NBS-HB-108] 16 p3601 N71-28568
Recommended airline and legal procedures prior to, during, and after hijackings

18 p3031 N71-31562
California Mulford-Carrel Air Resources Act, Model State Air Pollution Act, and summaries of all state air pollution control laws

19 p3197 N71-32524
Measures for providing financial responsibility liability limitations for vessels and onshore and offshore facilities in oil pollution cases

[PB-198775] 19 p3198 N71-32624
Legal, economic, and technical aspects of liability and financial responsibility of oil pollution

[PB-198776] 19 p3198 N71-32625
Noise reduction laws for air, rail, and highway transportation including legal liability in US

[OST-ONA-71-1-VOL-7] 20 p3212 N71-33938
Government, industry, banking, conservation, and law in preservation of environmental quality

[NASA-CR-121637] 21 p3414 N71-34294
Convention for suppression of unlawful aircraft seizure and article by article analysis

23 p3870 N71-37590
German law covering inventions and technical improvements made by employees of private, public, and Armed Forces

[NASA-TT-F-13408] 24 p4034 N71-38783
Economic, administrative, and legal factors affecting freight loss and damage

24 p4035 N71-38788

LAWRENCIUM
Radioactive properties of isotopes of element 103

[KFK-TR-326] 04 p0589 N71-14313

LAWS
NT CONSERVATION LAWS

NT FOURIER LAW
NT HOOKE'S LAW

NT KEPLER LAWS
NT KIRCHHOFF LAW OF RADIATION

NT RADIATION LAWS
NT SCALING LAWS

Conference on Weights and Measures attended by representatives of Federal Government, business, industry, railroads, and associations

[NBS-SPEC-PUBL-342] 16 p2601 N71-28500

LAYOUTS
Interactive graphics for computerized design of integrated circuit layouts

23 p3736 N71-36637
Operator performance and control panel layout for discontinuous tasks based on sequence of use, functional grouping, and location by frequency and importance

[AD-727791] 24 p3883 N71-37676

LC CIRCUITS
LC-filter thyatron system for depression of magnetic field pulsations in Dubna synchrotron

[JINR-59-5724] 22 p3637 N71-35926

LCRE REACTOR
U LITHIUM COOLED REACTOR EXPERIMENT

LEACHING
Solubility and leach rates of isotopic californium ceramic nuclear fuel element

[ORNL-4639] 10 p1601 N71-20644

Cyclic leaching process for cadmium and nickel recovery from nickel cadmium scrap battery waste

[BM-R1-7566] 23 p3772 N71-36883
LEAD [METAL]

NT LEAD ISOTOPES
Energy loss of high energy electrons in tin, lead, and gadolinium

[AD-711005] 01 p0097 N71-10534
Critical current enhancement in superconducting lead samples of varying cross section

[AD-710957] 01 p0090 N71-10691
K-conversion coefficient of 897-keV transition in Pb-207

[NP-18288] 03 p0425 N71-12825
Electrodeposition of lead from fluoroborate, fluosilicate, and sulfamate

[UCRL-50095] 05 p0701 N71-15052
Using lead slowing down spectrometer for nuclear materials assay work and isotope discrimination

[BNL-50232] 05 p0740 N71-15086
Optical spectroscopic studies of lead atoms and molecules in low temperature matrices

[UCRL-15662] 07 p1074 N71-17434
Thermodynamic stability, crystal structure, and properties of ternary lead-oxygen systems

11 p1785 N71-23011
Scaling analysis of plastic strain wave propagation in 1/4 inch diameter lead bars

13 p2183 N71-25400
Distribution moments and Monte Carlo calculation of high energy gamma ray absorption in concrete, iron, and lead slabs

14 p2304 N71-26277
Solubility and corrosion behavior of iron, steel, molybdenum, niobium, tantalum, vanadium, tungsten, and chromium in molten lead at high temperatures

[JUL-661-RW] 15 p2424 N71-27360
Isothermal and adiabatic compressibility of liquid metals, particularly lead, from melting point to critical region

[NYO-4176-4] 15 p3425 N71-37482
Comparison of calculated and liquid scintillation measured fast neutron spectra in layered cylindrical shield of UOF2-water solution reactor

[NASA-TM-X-67861] 16 p2637 N71-28968
Magnetic modulation spectroscopy for studying microwave surface impedance of lead films

[ISS-70/6] 18 p2994 N71-30472
Particle motion and collective vibrations in atomic nuclei, nuclear shell model and lead, and pion exchange corrections to single-particle operators

18 p2982 N71-30955
Tests with stainless steel in sliding contact with lead, indium, and tin coatings in liquid hydrogen to determine their lubricating capability

[NASA-TN-D-64553] 19 p3105 N71-32193
Public health hazards and solutions of environmental lead problems

[AP-90] 20 p3255 N71-32893
Reversed creep tests on chemical lead, aluminum, and copper and creep deformation behavior under repeated stress reversals

[NASA-CR-72949] 20 p3357 N71-33204
Spectrum analysis of lead lattice vibrations

[DISS-4497] 20 p3333 N71-33293
Effect of film thickness and tensile stress on electrical resistance and superconducting transition temperature of vapor deposited thin lead films

20 p3335 N71-33772
Emission of deuterons in interactions of 9 GeV protons with lead nuclei

[INR-P-1256] 21 p3469 N71-34693
Buildup factors and energy spectra through lead/water slab layers for point isotropic sources utilizing radiation transport point matrix kernels

[COO-2060-10] 21 p3486 N71-34838
Total absorption measurements of absolute oscillator strengths for Pb I lines at lambda 2833, 2873, 3639, 3683, and 4057

[AD-726097] 22 p3552 N71-35500
Distributions and mean values of inelasticity coefficient K for neutral pions in lead and graphite determined by digital computer

[ITT-5] 23 p3808 N71-37154
Development of toroidal Dewar having lead shielding on glass epoxy and fiberglass substructure

[MATT-846] 23 p3828 N71-37303
Comparing thermoluminescent dosimeter measurements to calculations of gamma heating in polyethylene and lead containers

[NASA-TM-X-67936] 23 p3866 N71-37359
Spectrographic determination of Pb and Te in Bi-Pb and Bi-Te alloys

[BARC-533] 24 p3933 N71-38062
Corrosion tests of chromium and chromium-nickel steels in molten lead at 575, 650, and 750°C for 3250 hr

[JUL-694-RW] 24 p3935 N71-38078

LEAD ALLOYS
Crystal growth and galvanomagnetic properties of Mg2Pb

09 p1454 N71-20438
Precipitation behavior of lead and sodium alloys between negative 20 and 100°C using optical and electron microscopy

[NLL-CE-TRANS-5252-19022.09] 10 p1601 N71-20644

SUBJECT INDEX

10 p1584 N71-21602
Behavior of lead specimens under conditions of torsion at high rates with split Hopkinson bar and explosive loading

[REFT-2] 14 p2348 N71-26169
Thermal conductivity and critical field measurements of Pb-Bi alloy and silver

19 p3117 N71-32579
Precipitates and flux line pinning in superconducting Pb-Na alloy investigated by electron microscopy

[NLL-CE-TRANS-5359-19022.09] 24 p3968 N71-38385

LEAD CHLORIDES
Crystal growth of cinnabar, proustite, and lead selenide, experimental work in HgS-HgI2 phase diagram, and electro-optic coefficients of zincblende structure compounds

[AD-721201] 19 p3168 N71-32057

LEAD COMPOUNDS
NT LEAD CHLORIDES

NT LEAD OXIDES
NT LEAD SELENIDES

NT LEAD SULFIDES
NT LEAD TELLURIDES

NT LEAD TITANATES
Fusion enthalpies and entropies of lead halides

[TID-25453] 01 p0133 N71-10481
Developing molten alkali carbonate eutectic in removing lead compounds from spark ignition engine exhaust gases

[PB-194132] 04 p0484 N71-13444
Mathematical model for environmental transport of lead from several sources and subsequent intake by man

[PB-194412] 04 p0481 N71-14478
Lattice parameters and compressibilities of high pressure phases of lead chalcogenides, manganese selenide, manganese telluride, chromium antimony, and chromium tellurium compounds

14 p2327 N71-26495
Performance tests and comparison of ignition properties for normal lead styphnate under constant current and capacitor discharge ignition

[AD-721695] 16 p2690 N71-28561

LEAD ISOTOPES
Isotopic lead and thallium analysis of rocks, meteorites, and lunar samples

01 p0017 N71-10309
Calculating level structure of neutron-deficient lead and bismuth isotopes

[INR-11691/PL] 03 p0432 N71-12937
Measuring elastic scattering cross sections of lead isotopes from 40 to 80 MeV

05 p0735 N71-14531
Threshold photoneutron cross sections for nuclei of Mg, Cr, Fe, and Pb isotopes

[UCRL-50902] 06 p0921 N71-16397
Neutron activation analysis determination of uranium and Pb-204 in Apollo 11 fines

13 p2166 N71-24500
Proton and neutron scattering cross sections for carbon, deuterium, helium, and hydrogen, and atomic energy level schemes from krypton and lead isotopes alpha reactions

[UCD-NCI-125] 17 p2790 N71-29230
Nuclear interactions and atomic energy levels for Pb-210, Bi-210, Po-210, Pb-206, Tl-206, and Hg-206

[AD-724640] 20 p3314 N71-33033
Relative intensities and energy measurements of 2s level in muonic Pb-208

[NASA-CR-121447] 20 p3320 N71-33711
Microscopic description of multipole pairing and particle-hole fields in particle vibration coupling of Pb-209

[LA-DC-11648] 20 p3322 N71-33795
Beta and electron-capture decay schemes for 30 isotopes and proton reactions of C-12, F-19, Au-197, Hg-3, Ta-181, Pb-208, and Ni-58 including angular distributions and scattering cross sections

[UCLA-10-P-18-23] 23 p3816 N71-37215
Reactions of Pb-204, Pb-206, Pb-208, and Bi-209 with deuterons from synchrocyclotron, and single particle states and nuclear potentials of Pb-208

[NP-18876] 24 p3974 N71-38355

LEAD ORGANIC COMPOUNDS
Effect of low/low-lead motor gasoline on engine operation

[AD-727032] 23 p3840 N71-37382

LEAD OXIDES
Lead oxide immiscibility in lead borosilicate glass for opaque glazes

12 p1947 N71-24125
Chemical reactions between alkali-lead oxide silica glasses and acid solution at low temperature

18 p2940 N71-31264

LEAD SELENIDES
Film growth and thickness of lead tin selenide epitaxial films

[AD-718323] 12 p1984 N71-23267

LEAD SULFIDES
Epitaxial sublimation methods for studying pseudobinary semiconductor alloys such as lead sulfide in ultrahigh vacuum

[AD-716211] 09 p1453 N71-19997

SUBJECT INDEX

- Preparation of compound semiconductors by controlled diffusion mechanism with gas growth optimization of single crystals of lead telluride and other group 2-6 compounds
(AD-727035) 22 p3458 N71-34088
- LEAD TELLURIDES**
- Procedure for segmenting lead telluride and silicon germanium thermoelectric elements to obtain complete elements effective over wide temperature ranges
(NASA-CASE-3028-27118) 06 p0533 N71-16037
- Nuclear magnetic resonance in lead telluride
(AD-715092) 07 p1096 N71-18048
- Microstructure and electrical properties of thin epitaxial films of lead telluride and effects of microstructure on electrical properties
11 p1815 N71-22102
- Aluminum contacting technique for lead telluride thermoelectric converter module
(NASA-CR-118637) 14 p2354 N71-23926
- Growth techniques and heat treatments for producing high quality epitaxial films of lead telluride and tin selenide
(AD-727896) 18 p2998 N71-31453
- LEAD TITANATES**
- Crystal defect chemistry of sintering and ferroelectric properties of lead zirconate titanate ceramics
(UCRL-20399) 07 p1048 N71-17603
- Aging characteristics of barium titanate and lead zirconate-titanate ferroelectric ceramics
(AD-715624) 08 p1279 N71-18009
- Electrooptic effects in ferroelectric ceramics with emphasis on electrical and optical properties of Ba, Sr, and La modified lead zirconate titanate
(SC-3-70-4353) 10 p1590 N71-21532
- Electric field effects on acoustic radiation power of substituted lead zirconate-lead titanate ceramic piezoelectric transducers
12 p1947 N71-24124
- Pressure sensitive reference hydrophone design including lead zirconate titanate spherical element for infrasonic and audio frequencies
(AD-721609) 15 p2385 N71-26842
- LEADING EDGE SLATS**
- Lift and pressure distribution on leading edge slats and trailing edge flaps of wing profile with boundary layer control
(ARC-R/M-3639) 06 p0791 N71-15706
- Investigating effects of leading-edge blowing on aerodynamic characteristics of jet flapped airfoil
(AD-721609) 07 p0968 N71-17702
- Low speed wind tunnel model assessment of porous boundary layer control by suction at civil aircraft leading edge flaps
(ARC-R/M-3640) 10 p1491 N71-20847
- LEADING EDGE SWEEP**
- Flaps and leading edge modifications for improved aerodynamic control stability of military aircraft
12 p1850 N71-23422
- LEADING EDGES**
- NT SHARP LEADING EDGES**
- Leading edge effect on aerodynamic characteristics of 70 deg swept delta wing
(AD-712087) 02 p0142 N71-11007
- Limits of hypersonic boundary layer theory, and leading and trailing edge phenomena in laminar hypersonic boundary layer
09 p1373 N71-19833
- Second-order slender wing theory for incompressible flow over low aspect ratio wings with and without leading edge separation
(NASA-CR-46762) 09 p1321 N71-19912
- Representations of flow separation bubbles near airfoil leading edge
09 p1323 N71-20064
- Finite difference method for solving equations for compressible turbulent boundary layers on swept-infinite cylinders
(NASA-TN-D-6203) 10 p1539 N71-20709
- Effect of heat conduction of material on temperature distribution in vicinity of wing leading edge in hypersonic flight
(AEP-6981) 11 p1841 N71-22494
- Techniques for generating artificially thickened boundary layer on flat plates
(NASA-TM-X-2238) 11 p1742 N71-22681
- Construction of leading edges of surfaces for aerial vehicles performing from subsonic to above transonic speeds
(NASA-CASE-XLA-01486) 12 p1851 N71-23497
- Conductive heat transfer effect on temperature distribution in vicinity of wing leading edge in hypersonic flight
(ARC-CR-1126) 13 p2184 N71-24446
- Angle of incidence effect on delta wing leading edge vortices with cross flow visualization in hydraulic test tunnel
(ARC-R/M-3645) 13 p2063 N71-24482
- Design of low cost ablator leading edge for space shuttle thermal protection system
17 p2847 N71-29457
- Production and characteristics of hypersonic viscous shock layer at leading edge of sharp flat plates
(AD-723328) 19 p3076 N71-31751

- Second order slender wing theory for calculating supersonic flow over low aspect ratio wings with subsonic leading edges and leading edge separation
(NASA-CR-1868) 21 p3573 N71-34004
- Leading edge shock impingement and interaction heating on scale model straight wing orbiter
(NASA-CR-115159) 22 p3537 N71-35196
- Finite difference method for two dimensional and three dimensional viscous flow problems with applications to hypersonic leading edge equations
(AD-726457) 22 p3569 N71-35420
- Leading edge section of thin airfoil theory
(ARL/SM-NOTE-340) 23 p3703 N71-36399
- LEAKAGE**
- Acoustic leak detection in water cooled liquid sodium steam generators
(APDA-258) 01 p0804 N71-10403
- Microleak detector mounted on wall seam of propellant tank of launch vehicle
(NASA-CASE-XMF-02307) 01 p0856 N71-10779
- Drop and impact tests for improving crashworthiness of integral fuel tanks
(FAA-NA-70-46) 02 p0144 N71-11019
- Friction and leakage losses of piston rings
(RAB-LIB-TRANS-1455) 02 p0230 N71-11570
- Reduction of leakage losses, friction, and sealing compression of piston rings
(RAB-LIB-TRANS-1457) 02 p0230 N71-11572
- Detection and origin of water leaks in tests for steam generator designs for fast reactors and solid-liquid reaction kinetics
(UNSC-SPLM-1059) 03 p0413 N71-12570
- Leak detection systems development for sodium heated LMFBR steam generators
(APDA-255) 03 p0414 N71-12823
- SNA-4 boiler performance degradation and two phase flow heat and momentum transfer models
(NASA-CR-72759) 04 p0619 N71-13598
- Reactor primary coolant system - rupture study on water cooled reactors
(GEAP-11069) 04 p0553 N71-14047
- Leak detection method for water and sodium systems applied to boilers of liquid sodium-cooled fast reactors
(ANL-TRANS-857) 06 p0901 N71-16775
- Vacuum method for leakage testing of reactor outlet piping
(ZJE-35) 07 p1059 N71-17017
- Fluid leakage detection system with automatic monitoring capability
(NASA-CASE-LAR-10323-1) 07 p1009 N71-17573
- Cryogenic device for leakage detection using helium
(CEA-COEF-1506) 08 p1205 N71-18396
- Symptoms and detection of fusion product release from EBE-2 fuel element - defect below fuel element
(ANL-7676) 09 p1418 N71-19808
- Inlet leak analysis for spacecraft mass spectrometer atmospheric sensor system
(NASA-CR-111858) 11 p1764 N71-22872
- Space suit using nonflexible material with low leakage and providing protection against thermal extremes, physical punctures, and radiation with high mobility articulation
(NASA-CASE-XAC-07043) 12 p1865 N71-23161
- Development of apparatus and method for testing leak of large tanks
(NASA-CASE-XMF-02392) 12 p2008 N71-24285
- Gas leak detection in evacuated systems using ultraviolet radiation probe
(NASA-CASE-ERC-10034) 13 p2086 N71-24856
- Method for locating leaks in hermetically sealed containers
(NASA-CASE-ERC-10045) 13 p2087 N71-24910
- Unified expression for leakage flow from nuclear reactor containment vessel
(WHAN-SA-40) 13 p2121 N71-25378
- Hydrostatic life-of seal zero leakage and static sealing and rubbing tests for use in liquid hydrogen turbine pumps
(NASA-CR-72796) 14 p2260 N71-25735
- Volume displacement transducer for leak detection in hermetically sealed semiconductor devices
(NASA-CASE-ERC-10033) 14 p2259 N71-26672
- Low leakage shaft seal for use with various types of liquids
(NASA-CASE-LEW-10326-2) 16 p2602 N71-28679
- Test chambers with orifice and helium mass spectrometer for detecting leak rate of encapsulated semiconductor devices
(NASA-CASE-ERC-10150) 16 p2598 N71-28992
- Empirical formula for expressing leakage flow from nuclear reactor containment vessel
17 p2784 N71-29881
- Pressurization for measuring leakage in flask
(DVE-SKU-70-6) 18 p2923 N71-30730
- Partial pressure analyzer calibration and techniques for measuring gas mixtures and leakage
(SCL-DR-70-275) 19 p3078 N71-32227
- Effects of leakage currents to ground in mid generator with constant gas parameters and constant channel cross section
(DNR-1242) 21 p3493 N71-34884
- One-dimensional gas flow with leakage currents in MIX separator
(DNR-1243) 21 p3493 N71-34885

- LEARNING THEORY**
- Damage control systems for detecting and locating overboard and onboard leak and damage modes on space stations
(NASA-CR-111963) 23 p3857 N71-37495
- LEARNING**
- NT ASYMPTOTIC METHODS**
- NT CONDITIONING (LEARNING)**
- NT ITERATIVE SOLUTION**
- NT PROBLEM SOLVING**
- THEOREM PROVING**
- NT TRANSFER OF TRAINING**
- Learning, retention, and transfer studies of military training problems
(AD-712096) 02 p0167 N71-11184
- Biionics of living and life-like systems with application to man machine technology
(AGARD-CP-44) 11 p1092 N71-23053
- Adaptive patterns in central nervous tissue learning process
(NASA-CR-117806) 11 p1092 N71-23059
- Social and industrial applications of learning response patterns
11 p1721 N71-23061
- Biionic neural model integration into functional learning networks of brain
11 p1093 N71-23068
- Neurophysiological mechanisms of learning and memory as biological adaptation to environment
11 p1094 N71-23074
- LEARNING MACHINES**
- Automata theory and iterative array computers
(AD-711048) 01 p0029 N71-10785
- Deterministic realization and simulation of non-deterministic automata
(AD-711050) 01 p0029 N71-10788
- Development and evaluation of adaptive pattern recognition schemes based on Bayesian decision theory
(AD-711673) 01 p0830 N71-10946
- Developing self-organizing control systems for application in aeronautics
03 p0347 N71-12613
- Adaptive learning computer system for raw data processing
(AD-713543) 05 p0650 N71-14874
- Machine learning of structural descriptions from examples
(AD-713968) 06 p0806 N71-16285
- Research activities in recognition, computational principles, and artificial intelligence
(AD-714608) 06 p0807 N71-16477
- Learning machine with adaptive control for aerial photograph interpretation
(AD-714576) 06 p0860 N71-16580
- Learning machines for statistical classification of spectral patterns and graphical target recognition
(AD-712191) 06 p1511 N71-21649
- Realization of near time optimal feedback controllers for linear time invariant systems
(SC-RR-70-544) 10 p1330 N71-21743
- Development, characteristics, and performance of learning machines, artificial intelligence, and pattern recognition techniques
(AD-718381) 12 p1865 N71-23247
- Evaluation of quality of signs used in construction of pattern recognition algorithms
(AD-717887) 12 p1865 N71-23294
- Design of learning machine and analysis of convergence characteristics during operation
21 p3400 N71-34202
- Development and characteristics of prototype computer system capable of mixed-initiative man-computer dialogue
(AD-726441) 22 p3557 N71-35338
- Computer learning algorithm to improve parameter search efficiency in system modeling with man-machine interaction
23 p3718 N71-36505
- Canadian National Science Council research in low speed aerodynamics, machine learning, and turbulent jet transducer
(DME/NAE-1971[2]) 24 p0013 N71-38626
- Pattern recognition by machines using on-line picture language
24 p0013 N71-38628
- LEARNING THEORY**
- Automatic machine learning and control of manipulators and adaptive control based on pattern recognition and decision making
16 p2576 N71-28825
- Evaluation of hypothesis that amount recalled and clustering are inversely related to delayed recall interval
(AD-708360) 17 p2722 N71-29539
- Evaluation of effects of constraint redundancy shifts, length of rest interval, and duration of inter-task interval upon acquisition and transfer of schematic concepts
(AD-701184) 17 p2708 N71-29560
- Neurological functions and information properties of devices used to understand cognitive mechanisms of man
(FPRS-53910) 21 p3399 N71-34192

LEAST SQUARES METHOD

Instructional strategies for optimizing learning processes and application of such principles to practical course of instruction in computer science
[NASA-CR-121936] 22 p3556 N71-35326

LEAST SQUARES METHOD

Least squares analyses of uranium and thorium alpha spectra

01 p0094 N71-10317
Geoid determination by vertical deflection calculations based on Bessel's ellipsoid

01 p0030 N71-10807
Constrained least squares approximation to discrete pressure-time data

02 p0203 N71-11596
[AD-711886]

Prototype recording system using least squares matrix method of waveform analysis behind towed bodies

03 p0366 N71-13388
[NPL-SHIP-143]

Deriving algorithms for computations involving sparse matrices

04 p0536 N71-13758
[NASA-CR-115777]

Curve fitting of sigmoid- or bell-shaped curves by least squares method

04 p0540 N71-14355
[PB-192315]

Least squares method for gamma ray angular distribution of radiative capture of deuterons

07 p1077 N71-17549
[ORNL-TM-3168]

Least squares integral criterion for representation of gravitational potential with fixed mass points

08 p1189 N71-18650
[NASA-CR-116806]

Geometric adjustment technique for Pacific SECOR observations based on least squares method

09 p1347 N71-19546
[NASA-CR-117043]

Recursive computation of smoothed and filtered least squares estimates for lumped signal processing in additive white noise given covariance functions

09 p1363 N71-20326
[AD-716477]

Computer program for least squares determination of crystal structure factor phases

10 p1631 N71-20733
[AD-716477]

Analytical triangulation program in FORTRAN 5 for frame photography including free formatting input/output routines, and least squares adjustment

10 p1548 N71-20906
[AD-717105]

Numerical basis transformation, least squares, and characteristic mode techniques for thin wire electromagnetic scattering

11 p1727 N71-21861
[AD-717640]

Kalman linear least squares filtering applied to estimation of fuel quantity and rate for fighter aircraft

11 p1672 N71-21922
[AD-717640]

Multiphysics subsonic lifting surface theory, using least squares method

11 p1670 N71-22472
[NAL-TN-24]

Calculating improved shock normals using least squares technique on combined magnetic field and plasma data from single spacecraft

12 p1900 N71-23482
[NASA-TM-X-65499]

Exponential downweighting of past data in single stage, weighted least squares trajectory processor for coasting spacecraft

13 p2165 N71-24359
[NASA-CR-114979]

Nonlinear least squares fitting of resonance parameters to 5 to 100 keV neutron capture cross sections including s, p, and d wave graphs of neutron strength functions

13 p2130 N71-24687
[AEC/E-198-SUPPL-1]

Least squares method and iteration technique for obtaining aerodynamic stability derivatives

13 p2023 N71-24703
[AD-717640]

Least squares method for describing irradiated fuel sheath distortion

13 p2117 N71-24853
[AEC-3688]

Martian atmospheric temperature and pressure and temperature gradient determination by least squares differential correction of satellite photometric solar eclipse data

14 p2337 N71-26089
[NASA-TN-D-6258]

Calculating orbit for Comet 1941C-1941IV using least squares method, and considering planetary perturbations

14 p2338 N71-26212
[NASA-TN-D-6258]

Solutions to Fredholm equations obtained in least squares solution to identification of dynamic systems

17 p2722 N71-29539
[NASA-TN-D-6374]

Least square distance curve fitting method

18 p2943 N71-30579
[NASA-TN-D-6374]

Convergence of iterative methods applied to large overdetermined linear and nonlinear systems of equations using least squares

18 p2946 N71-31266
[ESSA-TM-ERL-101-ESL-10]

FORTRAN 4 program/FTTLOS for fitting low-order polynomial splines of two and three degrees by least squares method

19 p3061 N71-32188
[NASA-TN-D-6401]

Attitude determination and sensor alignment via weighted least squares affine transformations

19 p3124 N71-32545
[NASA-TM-X-65663]

Mathematical model for near-body orbit calculation using mass concentration, perturbation theory, nonlinear equations, geopotentials, and least squares method

20 p3345 N71-33019
[NASA-CR-121381]

Computerized analysis of single peaked hydrographs using transformation of incomplete gamma function and weighted least squares method

20 p3258 N71-33153
[PB-196899]

Application of least squares method for determining longitudinal aerodynamic derivatives of aircraft from flight test data

20 p3206 N71-33305
[Z-12]

Tidal gravity variations derived from extensometric observations in Kamikakura, Japan

20 p3264 N71-33360
[AD-711886]

Least squares method applied to noise reduction in low frequency line spectra

20 p3264 N71-33360
[AD-711886]

Point estimates of standardized variances of independent and correlated measurements using least squares method

21 p3450 N71-34553
[NLL-M-20658-5828-4F1]

Least squares method using correlation matrix of measurements applied to polynomial objective analysis of meteorological fields

21 p3454 N71-34581
[NLL-M-20595-5828-4F1]

PEAK, computer program, for analysis of time-of-flight spectra using least squares method

21 p3467 N71-34684
[PEL-207]

Refinement of X ray data on azurite using Los Alamos Crystal Structure Least Square program GENLES

21 p3499 N71-34927
[PRNC-145]

Least squares method generalized for space triangulation compensation, for determining satellite position from ground station coordinates

22 p3678 N71-36222
[AD-713163]

Artificial satellite geodesy using least squares method

22 p3678 N71-36222
[AD-713163]

Least squares fitting for parameter determination of empirical formula for interpolation of tabulated photon photoelectric cross sections

23 p3814 N71-37197
[ANL-7796]

LEAVES

Computer synthesis for classifying natural shapes and patterns including leaves

05 p0537 N71-14833
[AD-713163]

Cycloel induced changes in internal structure of cotton leaves to reflectance, transmittance, and absorbance of near infrared radiation

06 p0800 N71-16151
[AD-713163]

Reflectance produced by plant leaves

06 p0800 N71-16152
[AD-713163]

Cloud condensation nuclei effects on rainfall during spring droughts in Florida from pest, algae, sawgrass, and leaf fire smoke

23 p3784 N71-36975
[ESSA-TM-ERL-TM-AOML-4]

LECTURES

Lectures given at 10th Cracow School of Theoretical Physics on scattering of composite objects. Vol. 2

21 p3467 N71-34681
[INP-713-VOL-2]

LEE WAVES

Lee surface flow and aerodynamic heating on delta wing orbiter

14 p2354 N71-26060
[AD-713163]

Leeside aerodynamic heating of lifting reentry vehicle configurations

14 p2354 N71-26061
[AD-713163]

Observing atmospheric structure of mountain lee waves by laser radar

17 p2778 N71-30071
[NASA-CR-111916]

Two-dimensional numerical model of large scale mountain-plain circulation including sloping plain effects for analysis of convective patterns in lee of Colorado Rockies

24 p3954 N71-38208
[AD-713163]

LEG (ANATOMY)

Effect of immersion at different water temperatures on graded exercise performance in man

07 p0979 N71-17062
[PB-194822]

LEGAL LIABILITY

Legal, preventive, and clinical aspects of aerospace medicine

02 p0161 N71-11801
[AGARD-CP-61-70]

Medical and legal aspects of aircraft accident fatality investigation by aviation pathologist

02 p0162 N71-11805
[AGARD-CP-61-70]

Significant aspects of contexts in which advocacy respecting technology assessment occurs in legal processes

06 p0962 N71-16884
[NASA-CR-116250]

Legality of patent infringements resulting from government procurement policies

12 p2018 N71-23741
[NASA-TM-X-67143]

Legal, economic, and technical aspects of liability and financial responsibility of oil pollution

19 p3196 N71-32625
[PB-198776]

Proceedings of conference on licensing and control of nuclear power plants

21 p3533 N71-35176
[IAEA-SM-146/5]

Legal aspects of weather modification and its associated economic consequences

22 p3610 N71-35714
[AD-713163]

LEGENDRE CODE

U COMPUTER PROGRAMMING

U NEUTRON SCATTERING

SUBJECT INDEX

LEGENDRE FUNCTIONS

Necessary conditions for optimality of junction between singular and nonsingular subarcs for singular optimal control problems

02 p0250 N71-11446
[NASA-CR-108664]

Efficiency of Laguerre and Legendre quadratures in shielding calculations

03 p0413 N71-12571
[WAPD-T-2330]

Tables of Legendre function of first kind for application to potential field induced by torus

05 p0712 N71-14525
[AD-713103]

Compendium of graphs, expansions, properties, and integrals for unnormalized associated Legendre functions

21 p3445 N71-34518
[NASA-CR-121744]

Modification of coupled-channel code [JUPITOR 1] including expansion of deformed optical potential in terms of Legendre polynomials and Coulomb excitation

23 p3811 N71-37178
[KFK-1333]

LEGENDRE POLYNOMIALS

U LEGENDRE FUNCTIONS

LEGENDRE TRANSFORMATION

U LEGENDRE FUNCTIONS

LEGIBILITY

Comparison of legibility of three types of electronic digital display

05 p0649 N71-14830
[ORNL/F-17/69]

LEIDENFROST PHENOMENON

Liquid or solid spheres levitated in film boiling following metastable Leidenfrost states

20 p3313 N71-33647
[NASA-TM-X-67977]

LEM [LUNAR MODULE]

U LUNAR MODULE

LEMMAS

U THEOREMS

LENGTH

Investigating data word and instruction format factors for selecting common word length in aerospace computers

03 p0347 N71-12607
[AD-713163]

Electron irradiation produced length changes in pure and doped magnesium oxide samples

11 p1800 N71-21872
[AD-713163]

Tube length effects on transition from supersonic to subsonic flow at low Reynolds numbers and static pressure and flow characteristics upstream and downstream

11 p1742 N71-22701
[AD-713163]

Length perception as isotropic image reduction operation

21 p3448 N71-34543
[TR-149]

Ring tests for determining transverse ductility of fuel element casing

21 p3458 N71-34610
[AE-412]

LENNARD-JONES GAS

Molecular dynamics of coherent function of Lennard-Jones fluids in liquid and gas phases

16 p2641 N71-28023
[AD-713163]

Intermolecular potential energy calculations for thermal elastic scattering of gases and comparison of Lennard-Jones and Morse potential functions

17 p2795 N71-29730
[AD-713163]

Statistical model of Lennard-Jones gas microscopic thermodynamic diffusion properties

18 p2886 N71-31146
[AD-713163]

LENS ANTENNAS

Error effects on antenna gains and pattern degradation tolerances of parabolic reflectors and lenses

10 p1521 N71-21344
[AD-713163]

LENS DESIGN

Design and performance of lenses for underwater photography

04 p0565 N71-13738
[AD-713163]

LENSES

NT MAGNETIC LENSES

NT WIDE ANGLE LENSES

NT WIRE GRID LENSES

Lens or optical test standardization

01 p0089 N71-10446
[AD-710633]

Tables of focal properties of three-element electrostatic cylinder lenses

01 p0055 N71-10401
[JILA-104]

Lens assembly for solar furnace or solar simulator

05 p0690 N71-15622
[NASA-CASE-XNP-04111]

In-situ measurement of objective lens data for alignment of high resolution electron microscope

09 p3188 N71-19799
[NASA-TM-X-62018]

Influence of microscopic observations on assessment of modulation transfer function of optical systems determined for high speed lens

10 p1607 N71-21442
[RAE-LIB-TRANS-1522]

Visual effects from moving achromatizing lens in front of eye while viewing multicolored pattern

12 p1866 N71-23394
[AD-710027]

Fourier transformable properties of paraboloidal mirror segments also experimental results of optical filtering

13 p2125 N71-24887
[NASA-TM-X-65520]

Camera adapter design for image magnification including lens and illuminator

14 p2256 N71-24474
[NASA-CASE-XMF-03844-1]

- Plastic lenses providing virtual image of flight scene for use in flight simulator with Schmidt projection system or television monitor
[NASA-TM-X-2327] 16 p2396 N71-28889
- Development and characteristics of Petzval type objective including field shaping lens for focusing light of specified wavelength band on curved photoreceptor
[NASA-CASE-68G-10700] 17 p2708 N71-30027
- Slow particle-ejection system application of sextapole lenses with considerable field drop-off on aperture edge and calculation of effects
[JPL-16799] 21 p3485 N71-34829
- Design requirements for streak camera with narrow angle optics for use in underwater photography
[FOA-2-C-2384-51] 22 p3585 N71-35334
- Cadmium compound photoconductors for lens focusing
[AD-72-679] 24 p3967 N71-38301
- LEPTONS**
- NT ANTINEUTRINOS**
- Quantum electrodynamic tests in time-like lepton mass
[LNF-70/23] 04 p0569 N71-13551
- Model for weak leptonic interactions
[JUV-2435-P] 04 p0575 N71-13682
- Phenomenological model of ν -transition for leptonic decays of baryons as function of electron energy
[SINP-TH-67-2] 05 p0739 N71-15050
- Determining set of experiments that represent full experiment for weak and semileptonic hyperon decays
[JUV-2435-P] 06 p0916 N71-16054
- Experimental limit on branching ratio for neutral kaon sub L yields lepton antilepton
[UCRL-20078] 06 p0924 N71-16759
- Inelastic lepton hadron scattering cross sections
[IFVE-STF-70-4] 08 p2147 N71-18191
- Neutral current in semileptonic interaction up to strength of CP violation
[RIFP-113] 09 p1445 N71-20562
- Empirical and phenomenological aspects of weak interactions of pure leptonic, semi-leptonic, and non-leptonic types
10 p1635 N71-21701
- Polarized hyperon beta decay in center mass frame of outgoing leptons
[COO-264-563] 11 p1802 N71-22089
- Regge pole model for inelastic lepton nucleon scattering into hadrons
[NYO-4204-9] 12 p1972 N71-23898
- Quark parton model for deep inelastic lepton-hadron scattering
[LPTHE-71/12] 12 p1979 N71-24343
- Effect of transverse momentum distribution in parton model for inelastic lepton-nucleon scattering
[SU-1206-225] 13 p2140 N71-25501
- Phenomenological relationship between fine structure constant and leptonic and gravitational processes - universal scaling factor
[UCRL-72955] 16 p2646 N71-28211
- Hard meson method for studying radiative leptonic decays of pions and kaons
17 p2796 N71-29793
- Delta S equals 2 transition for obtaining decay rates and asymmetry parameters in nonleptonic hyperon decays
[RIFP-120] 17 p2806 N71-30305
- Violation of absolute I vector equals $1/2$ rule in kaon decays into 3 leptons
[TR-71-112] 17 p2809 N71-30369
- Heavy leptons in neutrino astrophysics
[JINR-E2-5587] 18 p3007 N71-30479
- Leptonic decay experiments with unpolarized hyperon beams
[COO-1701-12] 21 p3476 N71-34757
- Structure of hadrons covering hadronic and semileptonic processes
[NYO-4076-L4] 22 p3646 N71-36000
- Lepton decay of hypertrons
[IAE-1944] 23 p3808 N71-37147
- Theoretical quantum electrodynamics in higher orders at low and high energies and nuclear models for lepton hadron and photon hadron scattering
[ITP-71-S-E] 24 p3976 N71-38372
- LIE (ESCAPE SYSTEMS)**
- U LAUNCH ESCAPE SYSTEMS**
- LIE (LUNAR EXPLORATION SYSTEM)**
- U LUNAR EXPLORATION SYSTEM FOR APOLLO**
- LITTERS (SYMBOLS)**
- U SYMBOLS**
- LEUCINE**
- Nonlinear relationships in lactic dehydrogenase and lucine amino peptidase enzyme activities in urine related to increased and decreased diuresis
[NASA-TT-F-13557] 12 p1863 N71-23368
- LEUKEMIA**
- Leukocytic bacteria destruction in humans having Chediak-Higashi or Pelger-Huet anomaly
[NASA-TT-F-13637] 12 p1864 N71-24020
- LEUCOCYTES**
- NT LYMPHOCYTES**
- Chromosomal aberrations in persons exposed to repeated occupational irradiation
[ORNL-TR-2332] 05 p0634 N71-14696

- Modification of Berman-Sivakaya method for neutrophil digestive capability determination
[NASA-TT-F-13551] 09 p1333 N71-20150
- Case history of Chediak-Higashi disease with simultaneous Friedrich hereditary spina stasis and hematologic, neurologic, and genetic characteristics
[NASA-TT-F-13537] 12 p1863 N71-23749
- Leukocytic bacteria destruction in humans having Chediak-Higashi or Pelger-Huet anomaly
[NASA-TT-F-13637] 12 p1864 N71-24020
- Artificial changes in leukocyte count of rabbits
[NASA-TT-F-13628] 13 p2033 N71-24757
- Peroxidase and catalase activity and hyperoxia effects on mice organs, leucocytes, and erythrocytes in pure oxygen under pressure
[ANL-TRANS-577] 15 p2371 N71-37290
- LEVEL (HORIZONTAL)**
- Hot-wire liquid level detector for cryogenic propellants
[NASA-CASE-XLE-00454] 07 p1068 N71-17802
- Mean sea level and periodic variation at Danish coast
10 p1546 N71-20639
- LEVEL (QUANTITY)**
- NT ATOMIC ENERGY LEVELS**
- NT ELECTRON STATES**
- NT ENERGY LEVELS**
- NT GROUND STATES**
- NT INTERMOLECULAR FORCES**
- NT MOLECULAR ENERGY LEVELS**
- Gauge for measuring quantity of liquid in spherical tank in reduced gravity
[NASA-CASE-XMS-06234] 10 p1557 N71-21007
- Conversion of positive dc voltage to positive dc voltage of lower amplitude
[NASA-CASE-XMF-14301] 12 p1886 N71-23188
- LEVELING**
- Development of adjustable attitude guide block for setting pins perpendicular to irregular convex work surface
[NASA-CASE-XLA-07911] 05 p0694 N71-15571
- Electrical switching device comprising conductive liquid confined within square loop of deformable non-conductive tubing also used for leveling
[NASA-CASE-100307] 09 p3358 N71-19610
- LEVITATION**
- Liquid or solid spheres levitated in film boiling following metastable Leidenfrost states
[NASA-TM-X-67897] 20 p3313 N71-33697
- LEXAN (TRADEMARK)**
- Plastic wave velocity measurement in Lexan at high speed impact
[AD-71527] 11 p1833 N71-21917
- Low energy, heavy cosmic ray measurements using high resolution, Lexan charged particle detector
13 p2162 N71-25212
- LIABILITIES**
- NT LEGAL LIABILITY**
- Members attitudes on revisions to Warsaw Convention and The Hague Protocol amendments on liability to international air transport passengers
[REPT-1970S-E] 07 p1138 N71-18100
- LIAPUNOV FUNCTIONS**
- Investigating Lyapunov stability properties of solutions of Volterra integrodifferential equations
[NASA-CR-116797] 08 p2225 N71-18497
- Constructing Lyapunov functions for nonlinear autonomous continuous time systems
11 p1788 N71-23013
- Linear time invariant optimal control feedback for closed loop stability in plant parameter variations
12 p1895 N71-24151
- Stability and control of processes described by stochastic functional differential equations
14 p2284 N71-26205
- Optimal quadratic Lyapunov function generating algorithm for estimating domain of equilibrium attraction of nonlinear star tracker attitude control systems for OAO stability
[NASA-CR-1729] 15 p2433 N71-26916
- Synthesis of signal for adaptive control systems using Lyapunov theory
15 p2389 N71-27329
- Unified approach to stability problems for systems described by operator equations of evolution, and direct method of Lyapunov
16 p2580 N71-28628
- Inherent waveform existence and stability in nonlinear transmission lines based on Lyapunov functions and Stern-Liouville theory
16 p2572 N71-28823
- Fixed point method and Lyapunov function for investigating problems concerning periodic and almost-periodic differential systems
[NASA-TT-F-13803] 18 p2945 N71-31169
- Application of Lyapunov method for parameter adaptive control of unknown plants
[NASA-CR-121961] 22 p3405 N71-33673
- Lyapunov method for investigating dynamic stability of cylindrical shells and folded plates subjected to stochastic excitations
23 p3865 N71-37553

LIBRARIES

- Computer program arrangements in library using time series analysis
[TR-4] 01 p0075 N71-10506
- On-line interactive book-library management system for performing circulation-desk bookkeeping
[NASA-TD-D-7052] 09 p1408 N71-20526
- Service routines MERMC2 and MAGIC for binary cross section library types used by MC map 2 multi-group cross section code
[ANL-7654] 11 p1884 N71-22352
- Updating ANISN library tapes with plotting of cross section curves using FORTRAN 4 program
[ORNL-TR-3408] 12 p1973 N71-23937
- Interex retrieval system usage, software and hardware development, and cost analysis, and model library educational program
[INTREX-PR-11] 12 p1886 N71-24325
- Objective assessment of fission product yields by compilation of library of all published neutron induced fission product yields maintained and interrogated by computer methods
[AERE-R-6642-PT-1] 16 p2630 N71-28918
- POPMO library and codes for preparing secondary gamma ray production cross sections
[ORNL-TM-3367] 20 p3317 N71-33532
- Library type for storage of model parameters of semiconductor devices
[SC-M-710210] 21 p3490 N71-34918
- Data formats and procedures for evaluated nuclear data file neutron cross section library with illustrations for elastic scattering by natural Fe
[BNL-50274T-601] 23 p3817 N71-37220
- LIBRATION**
- Libration point satellite stationkeeping control
[NASA-TR-R-346] 01 p0121 N71-10295
- Developing general analytical methods for predicting planar and three dimensional attitude motion of gravity gradient spacecraft in elliptical orbit
[NASA-TR-R-350] 04 p0611 N71-14005
- Effects of lunar physical librations on orbital elements of lunar satellite
[NASA-CR-117841] 11 p1827 N71-22539
- Relation between moon density function, libration, external gravitational potential, and physical libration constants
[NASA-CR-118892] 15 p2517 N71-27638
- Development of control system for maintaining space station in close proximity to one of earth-moon libration points
[AD-724113] 20 p3350 N71-32855
- LIBRATIONAL MOTION**
- Constants of lunar physical libration based on visual and photographic observations of pairs of craters by position angle method
[NASA-TT-F-661] 23 p3836 N71-37486
- Mathematical models of lunar librational stability conditions for deploying satellites
24 p0055 N71-38539
- LICHENS**
- Investigating inhibitory activity of lichens on growth of seed plants and ferns
07 p0984 N71-17996
- LEAD**
- U OPTICAL RADAR**
- LIE GROUPS**
- NT SPINOR GROUPS**
- Hamiltonian functions of quantum mechanical system having given Lie algebra as spectrum generating algebra
[IC/70/26] 02 p0276 N71-11916
- Use of scattered wave method to compute molecular wave functions, augmented plane wave method for energy band calculations, and Casimir invariants as invariant operators in Lie groups
[NASA-CR-118653] 14 p2325 N71-23974
- Bibliography on use of Lie groups and algebras in quantum mechanics and applications to nonrelativistic hydrogen atom invariance groups
[CEA-R-4112] 14 p2306 N71-26391
- Numerical analysis and representation of quantum dynamical symmetries
[CNRS-CPT-70-P-353] 18 p2968 N71-30429
- Peculiarities of application of Lie group theory to nonrelativistic transformations
[JINR-P2-5825] 18 p2974 N71-30561
- Representations of local currents and related algebras, emphasizing infinite parameter Lie algebras
22 p3648 N71-36018
- LIFE (BIOLOGY)**
- U LIFE SCIENCES**
- LIFE (DURABILITY)**
- NT FATIGUE LIFE**
- NT HALF LIFE**
- NT SATELLITE LIFETIME**
- NT SATELLITE LIFETIME**
- NT SERVICE LIFE**
- NT STORAGE STABILITY**
- Cold weather testing of equipment durability
[AD-710611] 01 p0015 N71-10699
- Lifetime measurements of 2 positive rotational states in O-122 and 184 and of 1020 keV excited state in Bi-208
[JINR-E4-5070] 02 p0270 N71-11397

- Theoretical evaluation of electrical insulation lifetime, noting influence of voltage and frequency using Weibull theory 02 p0346 N71-1558
- Capillary matrix and fuel cell development study [NASA-CR-108757] 03 p0318 N71-12272
- Cost reduction by reliable performance life testing of gyroscopes 03 p0411 N71-13204
- Life prediction of ultrahigh vacuum solid lubricating coatings for journal bearings 07 p1033 N71-17172
- DLR-FB-70-28 07 p1033 N71-17172
- Life cycle test evaluation of secondary spacecraft cells [NASA-CR-116509] 07 p0975 N71-17470
- Durability and service life of ball bearings [NASA-TT-F-13460] 08 p1208 N71-19009
- Factors influencing gain in neodymium doped laser glass 09 p1395 N71-19518
- Parallel radiation incident to grazing for life extension of diffraction grating strain gages [AD-717324] 11 p1760 N71-21863
- Quantitative analysis of photochemistry and kinetics of stable interstellar molecules [NASA-TM-X-45495] 12 p1993 N71-24008
- Computer controlled durability test of 50,000 hour life Brayton power conversion system for space applications [NASA-TM-X-67830] 13 p2157 N71-25368
- Durability of cadmium molecules on surfaces during condensation at varied temperatures measured on mica, copper, glass, and plexiglas before being reflected [NASA-TT-F-13466] 16 p2646 N71-28223
- Regression analysis of cycle life data for long life 20 ampere hour sealed nickel cadmium battery 16 p2540 N71-28671
- Compound nucleus lifetime in W(Ne-22) reaction related to decreasing shadow depth in angular distribution of fission fragments [JINR-P7-5512] 16 p2632 N71-29004
- Analysis of creep rupture properties of metals and application to predicting useful life and occurrence of damage [UCRL-13489] 17 p2831 N71-29541
- Reliability and cost of electrostatic and electromagnetic thruster systems for satellite auxiliary propulsion [NASA-CR-119319] 18 p3001 N71-31146
- Effect of electric field and temperature on radiative lifetime of excited F center in KCl, KF, and NaF [NYO-3463-23] 18 p2990 N71-31568
- Durability control of satellite magnetic tape recorders 20 p3270 N71-32941
- Brightness and life of pointed cold cathodes for electron microscope applications [NRC-TT-1473] 22 p3559 N71-35351
- Interference phenomena among products of two decaying resonances with identical particles [JINR-P1-5668] 22 p3633 N71-35891
- Effect of nonuniform burnup on reactor lifetime [UAREE-83] 23 p3794 N71-37046
- Fatigue tests and life of nickel alloy during programmed loading and elevated temperature [AD-727842] 24 p3939 N71-38103
- Durability and fatigue behavior of turbine blades [AD-727939] 24 p4026 N71-38728
- ### LIFE DETECTORS
- Describing method for typolization of luciferase containing mixtures for use in life detection reactions [NASA-CASE-XGS-05532] 07 p0990 N71-17705
- Investigating theory of chemical evolution on Surtsey Island and relationship to life detection techniques for other planets 07 p1034 N71-17972
- Investigating Surtsey and Iceland as natural laboratories for testing planetary life detection techniques 07 p1024 N71-17973
- Analyzing glaciers, hot springs, and volcanic ash from erupting volcanoes in Iceland for hydrocarbon content as test for life detection techniques 07 p1026 N71-17984
- Chemiluminescent bacterial sensor for water pollution detection during long term manned space station simulation 10 p1498 N71-20993
- Automated microbial metabolism life detection experiments for astrobiological studies [NASA-CR-110659] 14 p2206 N71-26380
- Feasibility analysis for future use of television microscopy to detect extraterrestrial life [NASA-TT-F-137353] 17 p2753 N71-29819
- ### LIFE RAFTS
- Arctic field tests of prototype life rafts capable of protecting astronauts from cold water exposure for 72 hours [NASA-CR-121449] 20 p3227 N71-33718
- ### LIFE SCIENCES
- #### NT MOLECULAR BIOLOGY
- Research planning in environmental health science 01 p0012 N71-10575
- Bibliography on physical, life, and social sciences and engineering 02 p0307 N71-13882
- National Academy of Science recommendations for future life sciences activities within NASA [NASA-CR-115873] 03 p0767 N71-14909
- Federal fund allocations for research and development and other scientific activities for FY 1969, 1970, and 1971 05 p0788 N71-15631
- Summary of design parameters for models of dynamic biological systems 09 p1331 N71-19880
- International cooperation in social and life sciences between advanced and developing nations 13 p2190 N71-24758
- Significance of stereoisomerism in organic structures and relationship to determination of origin of earth life [NASA-TT-F-13677] 16 p2548 N71-28970
- Time series and compartmental analysis techniques for biological applications [NASA-CR-115201] 23 p3781 N71-36948
- #### LIFE SUPPORT SYSTEMS
- ##### NT CLOSED ECOLOGICAL SYSTEMS
- ##### NT EMERGENCY LIFE SUSTAINING SYSTEMS
- ##### NT UNDERWATER BREATHING APPARATUS
- Results from theoretical and experimental studies of mass exchange in life support systems [NASA-TT-F-13371] 01 p0015 N71-10340
- Life support problems in prolonged space flight using various Soviet spacecraft [JPRS-51736] 02 p0168 N71-11911
- Portable environmental control and life support system for astronaut in and out of spacecraft [NASA-CASE-XMS-09632-1] 02 p0169 N71-11203
- Configuration and systems description of life support equipment for intravehicular and extravehicular activity - Vol. 1 [NASA-TM-X-66478] 02 p0170 N71-11206
- Human factors engineering, life support systems, biotechnology, physiological effects, radiation effects, and medical science 02 p0159 N71-11476
- Mathematical model for mass exchange in closed life support systems 02 p0170 N71-11478
- Characteristics of self-contained life support systems used in Soyuz spacecraft 02 p0170 N71-11492
- Catalytic carbon dioxide reduction cartridge for oxygen recovery in life support systems of long term manned space flights [NASA-CR-116823] 03 p0327 N71-12333
- Life support system for Sea-Bed Observation Laboratory [AD-712823] 03 p0329 N71-12347
- Monitoring water sterility in spacecraft water storage and supply systems using porphyrin initiated chemiluminescence technique [NASA-CR-114779] 04 p0615 N71-14270
- Air revitalization unit for sealed survival shelters without external power supply [AD-714163] 06 p0805 N71-15994
- Five radioisotope-powered heat sources fueled with Pu-23802 microspheres for use in Life Support Program 2 [MLM-1757] 06 p0808 N71-16619
- Thermal and electric energy transfer within life support systems [NASA-TN-D-6207] 07 p0986 N71-17592
- Application of human factors engineering to spacecraft habitability [NASA-CR-103628] 07 p1120 N71-17769
- Transactions on space biology and medicine [JPRS-52121] 08 p1153 N71-19051
- Carbon dioxide concentration control in pressure chamber during atmospheric regeneration by Chlorella 08 p1153 N71-19052
- Chlorella cultivation for purifying isolated environments of toxic gaseous contaminants 08 p1153 N71-19053
- Summary of conference papers on life support systems in space 08 p1158 N71-19075
- Integrated maneuvering life support system [NASA-TM-X-66902] 09 p1338 N71-19399
- Membrane of aqueous carbonate solution with catalyst for hydrolysis of CO₂ for removal of CO₂ in life support systems [AD-715978] 09 p1340 N71-19772
- Investigation of government furnished equipment used on Apollo 13 flight and evaluation of established criticality ratings [NASA-TM-X-66930] 09 p1470 N71-19959
- Analysis of government furnished equipment and ground support equipment used on Apollo 13 flight [NASA-TM-X-66920] 09 p1365 N71-19967
- Cryogenic underwater life support system for supplying breathing gas to buoyancy test subjects in submerged vehicle [NASA-CR-117143] 09 p1341 N71-20239
- Bio waste resistostat subsystem for integrated environmental control and life support of space station [NASA-CR-111063] 09 p1475 N71-20484
- Data from 90-day manned test of regenerative life support system in space station simulator [NASA-SP-261] 10 p1504 N71-20950
- Integrated life support systems for long duration manned space flight simulations 10 p1505 N71-20952
- Management and results of long term manned test on regenerative life support system in space simulator 10 p1505 N71-20953
- Support systems for long term regenerative life support manned test facility 10 p1505 N71-20954
- Life support system for improved space station simulator 10 p1505 N71-20955
- Water management in long term manned space simulation life support test 10 p1505 N71-20956
- Data from long duration manned test of regenerative life support system in space station simulator 10 p1510 N71-20999
- Measurement of breathing resistance during underwater activities using semiclosed underwater breathing apparatus [AD-717355] 11 p1679 N71-21912
- Performance tests of CO₂-H₂O solid oxide electrolysis electrolysis system for generation of oxygen for life support systems [NASA-CR-114295] 12 p1869 N71-23172
- System integration computer study to determine compatibility and interactions of Brayton power system and integrated life support system operating in integrated mode [NASA-TM-X-2307] 12 p1861 N71-23839
- Elimination of microbial and viral agents from spacecraft water systems by silver ions from electrolytic ion generator [NASA-CR-114978] 13 p2031 N71-24436
- Design and development of flexible tunnel for use by spacecrew in performing extravehicular activities [NASA-CASE-MSC-12243-1] 13 p2037 N71-24728
- Development of improved convective section for pressurized units to provide high degree of mobility in response to minimum of applied torque [NASA-CASE-XMS-09637-1] 13 p2037 N71-24730
- Underwater research in ocean floor habitat for 80 day evaluation of supporting facilities at Virgin Islands for Tekite 1 project [NASA-CR-118333] 13 p2192 N71-25529
- Design and development of pressurized tank with improved air retention and restraint coverall with passive ventilation, maximum mobility, and long term unpressurized comfort [AD-720827] 14 p2208 N71-23863
- Application of chlorination process to water reclamation for advanced life support systems [NASA-CR-111854] 15 p2374 N71-26080
- Regenerable portable life support systems concepts for EVA use in 1980 and technology assessment [NASA-CR-114280] 15 p2576 N71-27706
- Aerospace medicine, life support system, and psychophysiological problems and environmental factors in space flight [JPRS-53311] 16 p2459 N71-26094
- Microbiological ecology of manned space flights, exobiology, sterilization, and life support systems [JPRS-53308] 16 p2542 N71-28248
- Oxygen productivity of conveyor plantings in bioregenerative life support system 16 p2543 N71-28254
- Regenerative space station simulator and test procedures for 4 man, 90 day testing of life support systems [NASA-CR-111082] 16 p2530 N71-28261
- Biotechnological problems of man machine systems required for long duration space flights [NASA-SP-205] 16 p2551 N71-28526
- Systems integration for optimal regenerative environmental and life support processes in manned spacecraft 16 p2552 N71-28538
- Extravehicular operational activities of humans during long duration space flight 16 p2553 N71-28546
- Development and characteristics of inflatable structure to provide escape from orbit for spacecrew under emergency conditions [NASA-CASE-XMS-06162] 16 p2683 N71-28851
- Manned 90-day performance test of regenerative life support systems in space station simulator including crew biomedical tests [NASA-CR-111081] 16 p2554 N71-28877
- Utilization of water resources within space station, needs of men, and effects of lunar environment 16 p2681 N71-28886
- Chlorine generator for purifying water in life support systems of manned spacecraft [NASA-CASE-XLA-08913] 16 p2596 N71-28913
- Design, fabrication, and testing of circulating electrolyte type water electrolysis system for automatic control of spacecraft total pressure and oxygen partial pressure [NASA-CR-111911] 17 p2710 N71-29588

SUBJECT INDEX

Modular space station study of environmental control and life support system for long term mission [NASA-TM-X-64605] 18 p2882 N71-30751
 Medical and biological problems of prolonged manned space flight [JPRS-53601] 20 p3220 N71-33451
 Optimal mineral composition in nutrient for autotrophic Hydrogonomonas cultivation 20 p3222 N71-33471
 Combined vibration and gamma irradiation effects on *Chlorella* culture yield 20 p3223 N71-33472
 Conference on space shuttle environmental control and life support systems - Vol. 2 [NASA-TM-X-67265] 22 p3547 N71-35266
 Environmental control and life support system for space shuttle orbiter 23 p3547 N71-35267
 Environmental control and life support subsystem for space shuttle orbiter 22 p3548 N71-35271
 Status of LRC program on space shuttle environmental control and life support systems 22 p3548 N71-35272
 Damage control suit system to protect personnel in hazardous chemical, high temperature-humidity, and oxygen deficient environments [AD-726098] 23 p3718 N71-36302
 Design and components of closed-cycle life support system for extended manned space flights [AD-727944] 24 p3803 N71-37480
 Reliability data acquisition on spacecraft life support systems during ground and orbital experiments 24 p4015 N71-38646

LIFETIME (DURABILITY) U LIFE (DURABILITY)

LIFT
NT INTERFERENCE LIFT
 NT JET LIFT
 NT ROTOR LIFT
 NT ZERO LIFT
 Direct lift control system for producing lift without pitching moments during aircraft approach and landing 03 p0406 N71-12443
 Lift, aerodynamic: drag and pitching moment study of transport aircraft horizontal tail surfaces in low speed wind tunnels [ARC-R/M-3642] 06 p0791 N71-15702
 Aircraft leading lift decay and elevator oscillation analysis [ARC-CP-1119] 06 p0793 N71-15722
 Lift and aerodynamic drag due to trailing-edge flaps on sweptback wings in inviscid subsonic flow [ARC-CP-1110] 07 p0966 N71-17114
 Lift and aerodynamic drag data on slender wings with trailing edge sweepback [ARC-CP-1130] 07 p0966 N71-17117
 Trailing vortex systems generated by jet-flapped wing operating at high wing lift coefficients [AD-715315] 07 p0973 N71-17753
 Practical aerodynamics of M-4 helicopter - lift system and fuselage [AD-714915] 07 p0973 N71-17908
 Unsteady lift forces measured on restrained hydrofoil in regular head and following waves of various lengths [AD-717338] 11 p1833 N71-21906
 Wind tunnel investigation of lift-induced sonic boom characteristics of two simple wing models at Mach numbers from 2.5 to 4.63 [NASA-TN-D-62001] 12 p1849 N71-23125
 High lift and boundary layer separation behavior of sweptback wing airfoil profile noting trailing and leading edge stall patterns [ARC-R/M-3648] 13 p2021 N71-24488
 Measurement of lift and drag forces experienced by ejector in wind tunnel and correlation with geometry and static performance of device [AD-721192] 13 p2363 N71-26920
 Steady tailplane lift effect on subcritical response of subsonic T tail flutter aircraft model in low speed wind tunnels [ARC-R/M-3652] 13 p2366 N71-27096
 Use of aerodynamic lift for application to high speed ground transportation by two dimensional airfoils [PB-197243] 17 p2700 N71-29762
 Terminal area studies with XC-142, XV-3, Do-31, and P-1127 aircraft to develop powered lift control techniques for instrument approach 18 p2870 N71-30774
 Lift force distribution calculation techniques for wings with jet flaps including rectangular and swept wing examples [NASA-TT-F-13714] 18 p2866 N71-30852
 High lift aerodynamic and propulsion system configurations for short takeoff aircraft design - bibliography [AD-724186] 20 p3209 N71-33015
 Computer program for calculating lifting force distributions on symmetrical and cambered wings in subsonic flow based on numerical integration and lifting surface theory 20 p3206 N71-33220

Theoretical analysis of trailing edge blowing effects on circulation around airfoils based on iterative solutions with lift coefficients [AD-726434] 22 p3338 N71-33202
LIFT AUGMENTATION
 Sealing dam analysis for design of shaft face seal with self-acting lift augmentation for advanced gas turbine engines [NASA-TN-D-7006] 02 p0230 N71-11579
 Determination of low speed longitudinal aerodynamic characteristics of four engine externally blowing jet-flap STOL aircraft [NASA-TN-D-7034] 03 p0314 N71-12239
 Feasibility study of counter insurgency aircraft with suction boundary layer control [AERO-1] 04 p0473 N71-13415
 Aerodynamics and applications of lift augmentation devices - AGARD lecture series [AGARD-LS-43-71] 09 p1321 N71-20051
 High lift systems design for combat aircraft 09 p1322 N71-20059
 Lift augmentation devices effect on STOL engine - Part 1, interface problems between engine and airframe 09 p1322 N71-20061
 Lift augmentation devices effect on STOL engine - Part 2, thermodynamic problems 09 p1323 N71-20062
 Optimizing propulsive/lift system for turbofan STOL aircraft considering cost effectiveness 09 p1459 N71-20063
 High lift wing characteristics - wing with plain hinged flaps and boundary layer control, and wing with drag and high lift devices extended 09 p1523 N71-20065
 Aerodynamics of two dimensional flow on high lift systems 09 p1523 N71-20067
 Noise reduction effectiveness of mixer nozzle for increasing lift capability in STOL aircraft [NASA-TM-X-67938] 23 p3707 N71-36424
 Some aspects of propulsion for augmentor wind concept [NASA-TT-P-14005] 24 p4001 N71-38335
LIFT COEFFICIENTS
U AERODYNAMIC COEFFICIENTS
LIFT DEVICES
 Bibliography of documents containing numerical data on planar lifting surfaces [AGARD-R-374-70] 01 p0001 N71-10339
 Mathematical model for aircraft lifting surface interference in steady or unsteady supersonic flow [ONERA-TP-850] 08 p1140 N71-18462
 Aerodynamics and applications of lift augmentation devices - AGARD lecture series [AGARD-LS-43-71] 09 p1321 N71-20051
 Aerodynamic effects of mechanical high lift devices on conventional airfoils 09 p1322 N71-20052
 Aerodynamics of pneumatic high lift devices 09 p1322 N71-20053
 Flow separation concepts under high lift conditions 09 p1316 N71-20055
 Two dimensional wind tunnel tests on airfoils with high lift devices 09 p1316 N71-20056
 Three dimensional testing of high lift device models 09 p1317 N71-20057
 High lift applications in transport aircraft design 09 p1322 N71-20058
 High lift systems design for combat aircraft 09 p1322 N71-20059
 Lift augmentation devices effect on STOL engine - Part 1, interface problems between engine and airframe 09 p1322 N71-20061
 Lift augmentation devices effect on STOL engine - Part 2, thermodynamic problems 09 p1323 N71-20062
 High lift wing characteristics - wing with plain hinged flaps and boundary layer control, and wing with drag and high lift devices extended 09 p1523 N71-20065
 Aerodynamics of two dimensional flow on high lift systems 09 p1523 N71-20067
 Effect of engine position and high lift devices on aerodynamic characteristics of external flow, jet flap STOL model - graphs [NASA-TN-D-6222] 12 p1852 N71-23124
 Numerical evaluation of downwash integral for wing loading of lifting rectangular planform [NPL-MA-90] 13 p2102 N71-24483
 Direct lift control system having flaps with slots adjacent to their leading edge and particularly adapted for lightweight aircraft [NASA-CASE-LAR-10249-1] 14 p2198 N71-26110
 Tabulated data for wing planforms with variation in sweepback, tapering and aspect ratio noting correction to viscous lifting device theory [ARC-CP-1137] 15 p2365 N71-27715
 Kinematics of subsonic unsteady airloads on multiple lifting surfaces 17 p2696 N71-29339

LIFTING BODIES

Wind tunnel investigation of aerodynamic interference between two lifting surfaces in tandem 17 p3609 N71-39343
 Application of lifting surface theory to wing with control surfaces in unsteady subsonic flow 17 p3609 N71-39347
 Safety characteristics for powered lift of commercial STOL aircraft 18 p3809 N71-30773
 Spanwise integration of kernel functions for calculating wing lift distributions in subsonic flow 20 p3205 N71-33219
 Aerodynamic sound radiation from lifting surfaces in smooth and turbulent flow [NASA-CR-114370] 23 p3706 N71-36422
LIFT DISTRIBUTION
U FORCE DISTRIBUTION
U LIFT
LIFT DRAG RATIO
 Estimated aerodynamics of all-body hypersonic aircraft configurations [NASA-TM-X-2091] 09 p1315 N71-19706
 Magnetic lift drag ratios calculated for null flux magnetic suspension designs [BNL-15420] 12 p1946 N71-23516
 Design of ring wing vehicle of high drag-to-weight ratio to withstand reentry stress into low density atmosphere [NASA-CASE-XLA-04901] 12 p2003 N71-24315
 Optimum lift coefficient and aspect ratio determined analytically as conditions for construction of gliders with lift drag ratio of 100 [RAE-LIB-TRANS-1565] 16 p2530 N71-28010
 Wind tunnel tests of full scale advancing blade concept rotor system at high advance ratio [NASA-TM-X-62081] 20 p3211 N71-33517
LIFT FANS
 Aerodynamic characteristics of V/STOL transport model with tandem lift fans mounted at mid-section of wing [NASA-TN-D-6234] 08 p1141 N71-18358
 Free flight tests in hovering and forward flight of V/STOL transport model with six wing-mounted lift fans [NASA-TN-D-6198] 11 p1672 N71-22009
 Short haul vertical takeoff aircraft with lift fans incorporated in aircraft body, noting wide aircraft compartment 11 p1674 N71-22190
 Gas generators as vertical takeoff aircraft energy sources to operate lift fans or helicopter rotary wings 11 p1674 N71-22194
 Comparison of two lift fan configurations using wind tunnel model pressure distributions 11 p1674 N71-22195
 Cross flow wind tunnel performance tests of 15 in. wing installed lift fan with coaxial drive turbine for VTOL transport aircraft [NASA-TM-X-67854] 15 p2365 N71-27707
 Theoretical analysis of aerodynamic interference induced by cruise and lift fans on transport type aircraft [NASA-CR-1730] 19 p3634 N71-32453
 Tip-turbine lift fan design and specifications 21 p3902 N71-34945
 Aerodynamic characteristics of lift fan installation for direct lift V/STOL aircraft [NASA-TM-X-62086] 22 p3538 N71-35204
 Evaluation of air generator-remote lift fan propulsion system for VTOL transports [NASA-TM-X-67916] 22 p3539 N71-35207
 Reducing rotor stator interaction noise by use of serrated (laminar) stator vanes [NASA-CR-1882] 22 p3663 N71-36118
LIFT FORCES
U LIFT
LIFTING BODIES
 NT HL-10 REENTRY VEHICLE
 NT LIFTING REENTRY VEHICLES
 NT M-2 LIFTING BODY
 NT M-22 LIFTING BODY
 Results of lifting body flight tests and findings from other related studies evaluated for application to space shuttle system [NASA-TM-X-2101] 01 p0124 N71-10101
 Lifting body application to design of space shuttle system 01 p0124 N71-10102
 Wind tunnel and flight tests for stability and control derivatives of lifting body vehicles 01 p0124 N71-10103
 Assessment of lifting body vehicle handling qualities 01 p0124 N71-10104
 Prediction of performance characteristics for lifting body vehicle 01 p0125 N71-10105
 Correlation of flight test loads with wind tunnel predicted loads on three lifting body vehicles 01 p0125 N71-10106
 Pilot impressions of lifting body vehicles 01 p0125 N71-10107
 Summary of primary results of lifting body program for space shuttle system 01 p0125 N71-10108

- Bibliography of documents containing numerical data on planar lifting surfaces
[AGARD-R-574-70] 01 p0001 N71-10339
- Laser theoretical method for arbitrary wing planform and trailing edge control surfaces in low frequency oscillatory motion in subsonic flow
[NPL-AERO-1303] 02 p0143 N71-11013
- Graphic illustration of lifting body design
[NASA-CASE-FRC-10063] 03 p0311 N71-12217
- Pin loads and control surface hinge moments measured in full scale wind tunnel tests on X-24A flight vehicle
[NASA-TM-X-1922] 05 p0625 N71-14501
- M2-F2 lifting body flight control system
[NASA-TM-X-1809] 05 p0627 N71-14526
- Longitudinal aerodynamic characteristics of hypersonic lifting body spacecraft with variable sweep wings
[NASA-TM-X-2102] 05 p0626 N71-14945
- Aerodynamic forces on lifting bodies and delta wings in hypersonic slip flow
[BMW-FB-W-70-41] 06 p0791 N71-15704
- Lateral oscillations and low speed and lateral stability of free flight lifting bodies
[ARC-RM-3641] 06 p0791 N71-15705
- Wind tunnel tests to determine unsteady aerodynamic forces between two lifting surfaces in tandem
[NASA-TT-F-13482] 08 p1139 N71-18397
- Numerical analysis of low frequency subsonic lifting surface theory using wing oscillations in steady flow
[ARC-RM-3634] 08 p1139 N71-18425
- Multispan subsonic lifting surface theory, using least squares method
[NAL-TN-24] 11 p1670 N71-22472
- Solving exact gas dynamic equations for supersonic flows far from axis of slender lifting bodies
[NASA-TN-D-6446] 19 p0335 N71-32792
- Numerical analysis of plane steady transonic flows past lifting airfoils with freestream Mach numbers less than unity
[D180-1259-1] 21 p3412 N71-34275
- Calculations of helicopter airloads using lifting surface theory compared with experimental data
[AD-726717] 22 p3541 N71-35226
- Computer program development for potential flow calculation about lifting bodies
[AD-727628] 24 p3871 N71-37597
- LIFTING REENTRY VEHICLES**
NT HL-10 REENTRY VEHICLE
NT M-2 LIFTING BODY
- Flight tests of lifting reentry vehicles for controllability prediction
[NASA-TM-X-1827] 05 p0627 N71-14527
- Variable geometry manned orbital vehicle having high aerodynamic efficiency over wide speed range and incorporating auxiliary pivotal wings
[NASA-CASE-XLA-03691] 05 p0773 N71-15674
- Designing spacecraft for flight into space, atmospheric reentry, and landing at selected sites
[NASA-CASE-XAC-02058] 06 p0794 N71-16087
- Subsonic aerodynamic characteristics of model of HL-10 flight research vehicle with basic and modified tip fins
[NASA-TM-X-2119] 06 p0793 N71-16538
- Convective heat transfer characteristics of M2 and M2-F2 lifting entry vehicles
[NASA-TM-X-1691] 07 p0970 N71-17131
- Utilization of maneuverable lifting reentry bodies
[BMW-FB-W-70-49] 08 p1293 N71-18641
- Hypersonic flows, three dimensional boundary behavior in corner, subsonic, laminar, and turbulent mixing over lifting vehicles
[AD-719766] 14 p2193 N71-23620
- Wind tunnel tests to determine aerodynamic characteristics of booster and ascent shuttle configuration from Mach 0.28 to 10.4
[NASA-TM-X-2265] 14 p2341 N71-25803
- Leakside aerodynamic heating of lifting reentry vehicle configurations
14 p2354 N71-26061
- Analysis of aerodynamic forces on DL-4 lifting entry vehicle and comparison with theoretical methods
[NASA-TM-X-1994] 14 p2196 N71-26354
- Wind tunnel investigation of control surface instability of lifting body reentry vehicle configurations at Mach 15
[NASA-TN-D-6301] 18 p3018 N71-31241
- Nonlinear control optimization for gliding descent trajectory of winged reentry vehicle coming from circular orbit onto runway
[AD-727450] 24 p4022 N71-38699
- LIFTING ROTORS**
- Mathematical models for lifting rotor aerodynamic calculations, noting wake configurations
[DLR-MITT-70-19] 13 p2021 N71-24480
- Survey on different methods for lifting rotor downwash analysis
[DLR-MITT-70-23] 17 p2702 N71-29395
- Mathematical model for induced velocity distribution of lifting rotor in horizontal flight
[DLR-MITT-70-22] 17 p2705 N71-30039

- LIGHT SOURCES**
U LIFT DEVICES
U LIFTING BODIES
U SURFACES
- LIGANDS**
- Synthesis of carbamate-transition metal pi-complexes of mido C2B4H6/2 and cyclo C2B3H7/2 ligands from iron pentacarbonyl and 2,3-dicarbonylo-bisborane 8
[AD-712540] 03 p0333 N71-12378
- Boron 11 NMR spectra of B9H13 ligand derivatives
[AD-715649] 08 p1260 N71-18687
- Ligand hyperfine spin-orbit interactions in chromium, molybdenum, and tungsten oxyhalides
12 p1970 N71-23605
- Effect of organic iron chelate, ligand structure on oxidation product formation and autoxidation rate of camene
[FOA-1-B-1155-92] 24 p3886 N71-37698
- LIGHT (VISIBLE RADIATION)**
NT AIRGLOW
NT COHERENT LIGHT
NT DAYGLOW
NT GEIGESCHEIN
NT LIGHT BEAMS
NT NIGHTGLOW
NT SKY RADIATION
NT SUNLIGHT
NT TWILIGHT GLOW
NT ZODIACAL LIGHT
- Statistical properties of heterodyne detection of Gaussian light
01 p0088 N71-10133
- Viewing infrared illuminated scenes by converting infrared frequency to visible, and then imaging visible radiation
01 p0062 N71-10142
- Infrared to visible image up-conversion
01 p0053 N71-10209
- Solar activity and planetary luminosity
[NASA-TM-X-65373] 01 p0123 N71-10583
- Quantitative radiance measurements in visible region from ATS 1 spin-scan camera
02 p0256 N71-11619
- Diffraction of Gaussian light beams by circular apertures
[AD-713728] 05 p0734 N71-15246
- Light baffle with oblate hemispherical surface and shading flange
[NASA-CASE-NPO-10337] 05 p0689 N71-15604
- Acoustic field effects on gallium arsenide, silicon solar cells, and photoreactive devices with and without light exposure
[NASA-CR-117320] 09 p1327 N71-20299
- Electromagnetic shock wave propagation and discontinuity in isotropic media
[AD-717305] 11 p1796 N71-21870
- Magnetic dipole transitions within 3p5 3d configuration of Fe and Ni contributing to visible spectrum of solar coronas
11 p1802 N71-22088
- Reference standards for spectral radiant power in ultraviolet, visible, and near infrared regions including UV standard lamps, carbon arcs, tungsten lamps, and blackbody radiators
11 p1799 N71-22491
- Fresnel hypothesis on changes in speed of light traveling through bodies due to motion of bodies
[NASA-TT-F-13623] 12 p1965 N71-23386
- Resonant scattering of light by light due to exchange of C-even mesons
[JNR-E2-5424] 13 p2133 N71-25161
- Range finder using propagation time of light and modulation of optical radiation - optical radar
[AD-721253] 15 p2380 N71-27190
- Diffraction of light by microwave sound in organic crystals and measurement of elastic constants of organic and biological crystals
[AD-720850] 15 p2507 N71-27430
- Photon theory of light and matter
[NASA-TT-F-13695] 16 p2640 N71-29002
- NASA spectrograph for low light level research
[NASA-CASE-XLA-10402] 16 p2599 N71-29041
- Deep sky survey at 2700 MHz using 210-foot telescope measurements of positions and flux densities of sources
[NP-18482] 17 p2846 N71-30211
- Kinetic theory of Compton scattering by relativistic electrons with induced scattering
[NASA-TT-F-13738] 17 p2829 N71-30281
- Optical imaging system for increasing absorbing efficiency of light or radiant energy at light sensitive face of imaging detector
[NASA-CASE-ARC-10194-1] 18 p2964 N71-31142
- Interferometer-polarimeter for measuring intensity polarization of optical radiation
[NASA-CASE-NPO-11239] 20 p3271 N71-33024
- Thin film, light detecting photoelectric cell fabricated by metal vapor deposition on quartz
[NASA-CASE-NPO-11432] 20 p3273 N71-33322
- Theoretical and experimental calculations in analysis of optical spectra of uranium
20 p3330 N71-33642

- Latent image fading dependence on radiant flux density of visible and gamma illumination
[RAE-LIB-TRANS-1573] 20 p3328 N71-33983
- Characteristics of neodymium-YAG laser and methods for converting infrared output to visible radiation
23 p3768 N71-36853
- Brightness variations of white light coronas related to solar radio flux
23 p3787 N71-36909
- Thermodynamic model for calculating ceramic luminous deficiencies in overall emissivity of platinum point blackbody standard of light
[NBS-TN-595] 23 p3804 N71-37124
- Interaction of optical and particle radiation into matter in astrophysics
23 p3852 N71-37436
- Low resolution reflectance spectra of three orbiting satellites employing scanning spectrometer with variable bandpass interference filter
[AD-726988] 23 p3859 N71-37510
- Photoconductivity in Gallium arsenide single crystals by two photon absorption of light quanta from Nd glass laser
[AD-727755] 24 p3932 N71-38054
- Photographic-photometric measurement of light diffraction in liquid by ultrasonic wave
[NASA-TT-F-13965] 24 p3966 N71-38228
- Extending tuning range of parametric oscillators into infrared, visible, and ultraviolet regions
[AD-727127] 24 p3967 N71-38226
- LIGHT ABSORPTION**
U ELECTROMAGNETIC ABSORPTION
LIGHT ADAPTATION
- Circadian rhythm of light sensitivity in visual perception thresholds of men
[AD-714064] 06 p0801 N71-16313
- LIGHT AIRCRAFT**
- Total fatigue damage estimates from ground and flight loads on fixed-wing light aircraft subjected to agricultural operations
[LTR-ST-422] 03 p0313 N71-12233
- Direct lift control system having flaps with slots adjacent to their leading edge and particularly adapted for lightweight aircraft
[NASA-CASE-LAR-10249-1] 14 p2198 N71-26418
- Effect of wing-tip vortex wakes generated by large jet transport aircraft on smaller airplanes
18 p2866 N71-30764
- Flight tests for evaluating effect of wing-tip vortex wake generated by large jet transports on smaller aircraft
18 p2866 N71-30765
- Flight tests to determine handling qualities of general aviation aircraft during ILS approaches in turbulent air
18 p2869 N71-30771
- Analysis of 79,000 hours data obtained from NASA V-G/IGH flight recorders installed on 734 general aircraft engaged in eight types of operations
18 p2871 N71-30782
- Full scale wind tunnel tests of low wing, single engine, light aircraft with positive and negative propeller thrust and up and down flap deflection - graphs
[NASA-CR-1783] 19 p3038 N71-32240
- LIGHT ALLOYS**
NT ALUMINUM ALLOYS
NT BERYLLIUM ALLOYS
NT MAGNESIUM ALLOYS
- Corrosion tests on titanium, austenitic stainless steels, chromium ferrites, and light alloys in sea water up to 150 C
[ORNL-TR-2412] 10 p1580 N71-21465
- LIGHT AMPLIFIERS**
- Waveguide light intensifier in semiconductor laser systems for optical communication
07 p1038 N71-17107
- Small signal series multitraverse predetection quantum amplifier
[AD-716991] 10 p1569 N71-20912
- LIGHT BEAMS**
- Mathematical model for self-defocusing of light beam in fluid
[AD-710741] 01 p0090 N71-10573
- Controlling thermal self-focusing of laser beams by decreasing intensity near axis
[AET-70-197-RULL] 01 p0064 N71-10441
- Collimated light beam attenuation during sea water propagation
04 p0564 N71-13727
- Phase matched critical total reflection and Goos-Hanchen shift in second harmonic generation
[AD-710772] 04 p0567 N71-14118
- Tropospheric and ionospheric compositions effects on phase and frequency degradations in propagating signals
[AGARD-CP-33] 11 p1704 N71-22901
- Holographic phase contrast measurements on optical wave propagating through turbulent atmosphere
11 p1776 N71-22907
- Optical path length stability of light beam system for local oscillator signal distribution over antenna array
11 p1714 N71-22908

SUBJECT INDEX

Cylindrical reflector for resolving wide angle light beam from telescope into narrow beam for spectroscopic analysis
[NASA-CASE-XGS-08269] 14 p2596 N71-26306
Asymptotic partially polarized light beams in parallel scattering and absorbing medium
15 p2514 N71-27532
Development and characteristics of optical communications system based on modulation of light beams
[NASA-CASE-XG-01090] 16 p2607 N71-28963
Multiple pattern holographic information storage and readout system
16 p2607 N71-29131
Optical heterodyning with reference beam for diminishing atmospheric turbulence effects on signal to noise ratio
19 p3143 N71-32745
Laser beam spreading methods
20 p3282 N71-33481
Effects on propagation of optical beams due to self-induced changes in index of refraction
[UCRL-20541] 23 p3803 N71-37111
Light beams fed into telescope laboratory
24 p3924 N71-37998

LIGHT BULBS

U LUMINAIRES

U OPTICAL COMMUNICATION

U PULSE DURATION

U FLASH

U PULSE DURATION

LIGHT ELEMENTS

Gamma photon and neutron activation analyses for determining light elements in homogeneous media
[CEA-R-4072] 13 p2474 N71-27452
Electric scattering angular distributions for 13 to 27 MeV helium 3 beam from light target nuclei
17 p2802 N71-36133
Corrosion of light metals at elevated temperatures and methods to prevent corrosion
[CRA-CONF-1729] 18 p2952 N71-30428

LIGHT EMISSION

NT BIOLUMINESCENCE

NT CHEMILUMINESCENCE

NT ELECTROLUMINESCENCE

NT FLUORESCENCE

NT INCANDESCENCE

NT LUMINESCENCE

NT LUNAR LUMINESCENCE

NT OPTICAL RESONANCE

NT PHOSPHORESCENCE

NT PHOTOLUMINESCENCE

NT THERMOLUMINESCENCE

NT X RAY FLUORESCENCE

Measuring Auger spectra of simple gaseous molecules
[NASA-CR-116411] 07 p1072 N71-17342
Light emission, and gas components of galaxy NGC 3253
11 p1829 N71-22763

Ratio of 1 NGO2/plus and 1 PGN2 emissions as function of auroral height
17 p2747 N71-30083

Spectral variability analysis on airborne aurora and auroral emission data
[NASA-CR-119183] 17 p2748 N71-30139
Emission spectroscopic analysis using laser beam as excitation source
20 p3282 N71-33541

Solid state laser optical emission conversion to far infrared region by nonlinear polarization and small difference frequency generation
[NASA-TT-F-13775] 23 p3766 N71-36846
Developing visible CW optical parametric oscillators
23 p3767 N71-36853

Tunable stimulated far infrared and visible emission from polariton modes in crystals
23 p3823 N71-37269
Fast luminescent decay of silicon light-emitting diode
[NASA-TM-X-65721] 24 p3965 N71-38285

Milisecond-time-scale atmospheric light pulses induced by solar activity
[NASA-TM-X-65716] 24 p4002 N71-38545

LIGHT GAS GUNS

Design and performance characteristics of hypersonic gas tunnel
[IC-AERO-70-04] 01 p0038 N71-10270
Interior ballistics of light gas gun, pressure measurements and compression calculations
[REPT-13/89] 03 p0365 N71-13292
Light gas gun model launcher for ballistic range research
[NASA-TM-X-66331] 04 p0515 N71-13578

Target design and data reduction code for shock waves produced by light gas gun
[LA-4481] 04 p0517 N71-14495
Injection driven, light gas, hypervelocity gun
[NASA-CASE-XAC-65902] 06 p1173 N71-18378

LIGHT INTENSITY

U LUMINOUS INTENSITY

LIGHT MODULATION

Investigation of light modulation by strong electrical field in thin CdTe layers
01 p0111 N71-10644

Thermally scanned interferometric modulation of effect in cadmium sulfide crystals illuminated by gas laser radiation
[AD-710954] 01 p0091 N71-10749

Investigating interaction between light wave and microwave frequency traveling wave in anisotropic medium in parametric approximation
01 p0092 N71-10961

Modulation transfer function for underwater visibility prediction in sea
04 p0565 N71-13737

Investigating various methods for modulation of two-dimensional coherent light waves
[FOA-3-C-2345-32] 05 p0732 N71-14682
Production of carbon dioxide laser pulsing by cavity length modulation
[AD-713570] 05 p0697 N71-15368

Optical retrodirective modulator with focus spoiling reflector driven by modulation signal
[NASA-CASE-GSC-10063] 05 p0090 N71-15605

Modulating and controlling intensity of light beam from high temperature source by servocontrolled rotating cylinders
[NASA-CASE-XMS-04300] 09 p1357 N71-19479

Method and apparatus for optically modulating light or microwave beam
[NASA-CASE-GSC-10216-1] 14 p2299 N71-26722

Development and characteristics of optical communications system based on modulation of light beams
[NASA-CASE-XLA-01090] 16 p2607 N71-28963

Bibliographies on optical modulators
[RAE-TR-71009] 17 p2758 N71-29315
Satellite modulator for 15 micron infrared radiation using Fabry-Perot interferometer
[ESRO-CR-26] 17 p2751 N71-29389

Studying interband optical properties of selected semiconductor compounds using optical modulation techniques
17 p2815 N71-29735

Far infrared Michelson gas laser with variable output coupling
[NBS-TR-395] 17 p2759 N71-30199

Results of field work in Arctic regions using pulsed light range finder
[AD-723427] 19 p3084 N71-31681

Frequency characteristics of electro-optical light modulators with coupled coaxial resonators
[AD-727954] 24 p3932 N71-38055

LIGHT PRESSURE

U ILLUMINANCE

U LIGHT BEAMS

LIGHT SCATTERING

NT HALOS

Ninety degree Thomson light scattering from low density plasma
[AD-709332] 01 p0062 N71-10181
Remote measurement of wind speed and air turbulence by laser scattering
01 p0062 N71-10208

Tables of angular functions for describing angular structure of light field scattered by spherical particles of different sizes
[AZT-70-257-RULL] 01 p0091 N71-10859

Four-figure tables of cross sections and coefficients of attenuation, scattering, and radiation pressure for spherical particles
[AZT-70-262-RULL] 01 p0091 N71-10860

Tubulated computations of scattering of visible and infrared waves by water droplets
[AZT-70-258-RULL] 01 p0092 N71-10922

Illumination calculations using diffraction and light scattering in ultraviolet image dissection cameras
[RAE-LIB-TRANS-1443] 02 p0226 N71-11554

Investigating electromagnetic scattering by cylinders using Rayleigh-Gans theory
[NASA-TM-X-64345] 03 p0417 N71-12569

Observations of formation of scattering agencies by solar wind in Comet Ikeya-Seki
03 p0451 N71-13096

Electromagnetic wave transmission along air-sea interface and in underwater communication and optical systems
[AGARD-CP-77-70] 04 p0563 N71-13701

Monte Carlo calculation of laser light scatter transmission through water
04 p0563 N71-13726

Ultraviolet and visible light scattering in sea water
04 p0564 N71-13728

Conventional meters and lasers for measuring light scattering in sea water
04 p0564 N71-13729

Light scatter measurements in oceanography for determining particle density in sea water
04 p0564 N71-13730

Absorption and scattering of daylight during sea water propagation
04 p0564 N71-13731

Loss of optical resolution in sea water by multiple light scattering from suspended particles
04 p0565 N71-13733

LIGHT SCATTERING

Light absorption and scattering effects on underwater visibility of imaging devices in sea water
04 p0565 N71-13736

Design concepts and performance of instruments for measuring radiant energy penetration and scattering in sea water
04 p0565 N71-13739

Investigating light scattering in superfluids by nuclear magnetic resonance
[AD-714095] 06 p0904 N71-16110

Investigating quantum statistical properties of electromagnetic radiation
[AD-714655] 06 p0917 N71-16188

Stimulated Raman and concentration scattering
[AD-714172] 06 p0906 N71-16445

Molecular absorption and light scattering in flame spectroscopy
[IS-T-335] 06 p0812 N71-16791

Light scattering in reflection nebulae models
07 p1117 N71-18077

Measuring bubble size distributions by light scattering
[AD-715347] 08 p1177 N71-18366

Laser output light scattering for gas diagnostics
[DLR-FB-70-53] 10 p2468 N71-20663

Photometric observations of auroral scattering by CV 990 aircraft
[NASA-CR-117466] 11 p1762 N71-22135

Methods of measuring fluid velocity from Doppler Pzcan shift of scattered laser radiation, and optimization of optical system geometry
11 p1775 N71-22610

Optical superheterodyning spectroscopic analysis of light scattering from solids at 10.6 microns
11 p1818 N71-22889

Fourier expressions for scattering functions in Mie theory with applications to light scattering by spherical voids in ruby
11 p1799 N71-23012

Determining microstructure of clouds and fogs by light scattering
[RAE-LIB-TRANS-1529] 12 p1952 N71-23237

Gas density measurement using laser induced Raman scattering
[DLR-MITT-71-01] 12 p1908 N71-23496

Particle size distribution in dispersions determined from scattered light intensity with aid of digital computer
[RAE-TR-70151] 13 p1213 N71-24408

Elastic, piezoelectric, and photoelastic constants for light scattering with hypersonic waves and Brillouin effects in ferroelectric lithium niobate crystals using helium-neon lasers
13 p1215 N71-24906

Resonant scattering of light by light due to exchange of C-even mesons
[JINR-E2-5424] 13 p2133 N71-25161

Light scattering calculations for brightness effect in Mars atmosphere caused by aerosols
13 p2168 N71-25278

Exchange energy and magnetic susceptibility measurements on low temperature He-3 with He-4 traces, and techniques for light scattering in gases at room temperature
[NYO-3951-3] 14 p2295 N71-25610

Light scattering dissipated in optical glass fibers causing power loss
[SRDE-70064] 14 p2295 N71-25635

Geometric relationships involved in multiple scattering calculations for spherical particles
[NASA-CR-118662] 14 p2250 N71-26360

Development and evaluation of instrumentation system for measuring interference fringe spacing in scattered light photoacoustically
14 p2258 N71-26424

Light scattering in water clouds, fog, and haze
15 p2439 N71-27524

Preservation of coherence in light scattering through aerosols
15 p2439 N71-27525

Tropospheric aerosol effects on twilight phases
15 p2402 N71-27526

Atmospheric aerosol effect on elliptical polarization of scattered skylight
15 p2402 N71-27527

Atmospheric aerosols and light scattering
15 p2402 N71-27529

Asymptotic partially polarized light beams in parallel scattering and absorbing medium
15 p2514 N71-27532

Visible and infrared radiation transfer in clouds
15 p2402 N71-27533

Simulation of solar luminous fluxes scattered and transmitted within illuminated fog
15 p2514 N71-27534

Multiple anisotropic polarized and unpolarized light scattering in phase parallel homogeneous cloud layers
15 p2402 N71-27535

Relationship of atmospheric scattering coefficient and aerosol content relative moisture content
15 p2403 N71-27537

Monte Carlo method applied to some problems of atmospheric optics by narrow light scattered beams
15 p2403 N71-27539

Size distribution determination of natural atmospheric aerosols by extinction coefficient

Carbon dioxide lasers, CaF₂ experiment, light scattering from semiconductors associated with impurities, and far infrared radiation

Light scattering applications to plasma diagnostics, including collisionless coupling and ion excitation

Comparison of theoretical and experimental results on light scattering of plane shock waves

Light scattering effect for determining phase separations in sodium borosilicate glasses

Derivation of equations for Rytov and Born approximations in turbulent atmospheric attenuation and scattering of coherent light

Computer calculations of time dependent light scattering in plane parallel atmospheres, using FORTRAN 4 language

Stratospheric dust and its influence on light scattering from radioisotope measurements

Methods for measuring backscattering, light scattering, and internal wave parameters of ocean water

High resolution spectroscopy, resonant reflectors, and Brillouin and other light scattering phenomena

Diffusion of nonlinearly scattered light by etched glass in experiments using Fabry-Perot interferometer in conjunction with laser light source

Polarization of light scattered from optical glass

Light scattering from stratified spherical shell

Calculation of light scattering from aerosols for two assumed particle distribution functions

Boltzmann models for hydrodynamic equation, transport coefficients, and light scattering by simple fluids

Statistical analysis of some nonlinear optical effects including scattering light from rotating glass and second harmonic light generated by pseudo-thermal source

Statistical processing of phase dependence of Mars brightness in spectral region between 0.3 and 1.1 micron

Stimulated Rayleigh-type light scattering in binary gas mixtures from local fluctuations and concentration

Light noise due to light scattering in astronomical telescope Lallemand camera image corrector-receiver system

Fog and aerosol analysis with ultra-sensitive dirometer utilizing optical transmission and light scattering principles

Brillouin scattering and infrared spectroscopy of CH₂ and HF dimer

LIGHT SCATTERING METERS

Conventional meters and lasers for measuring light scattering in sea water

Light scattering measurements off San Diego Coast, California

Light yield measurements of CsI(Tl) crystal bombarded with protons, deuterons, and tritons, dependent linearly on energy

Development and operation of apparatus for measuring ground illumination at night and remotely recording data

NT ILLUMINATORS

Ion charge determination from emitting spectral lines using beam foil light source technique

Ion charge identification for spectral lines in nitrogen by beam foil light source technique

Lasers as light sources for high speed photography

Polonium 210 alpha particles used to irradiate helium-nitrogen gas mixtures by excited light source technique

Long term frequency stability of three-mirror cavity argon laser using standard frequency light source

Silicon carbide semiconductor diode light source for indicator elements

Electro-optical detector for determining position of light source

Predicting performance of Chamber solar simulator using D chamber xenon source module

Variation of gamma function with wavelength and influence of emulsions on exposing light source

Formation of stroboscopic effect by gas discharge light sources

Aluminum alloy compounds as wide band gap semiconductors for electroluminescent light sources

Harmonic coincidences between pairs of far infrared continuous radiation gas lasers for light speed determination

Light speed in gravitational field according to Newton and Einstein gravitation theories

Fresnel hypothesis on changes in speed of light traveling through bodies due to motion of bodies

Optical absorption in transparent materials during 1.5 MeV electron irradiation

Half-range expansion theorems in studies of polarized light

Incorrectness of mutual coherence function for optical wave propagation in turbulent atmosphere

Monte Carlo calculation of laser light scatter transmission through water

Ultraviolet and visible light scattering in sea water

Absorption and scattering of daylight during sea water propagation

Monte Carlo computation of light scattering functions for determining underwater visibility in sea

Radiative transport equation for solving optical underwater propagation problems

Modulation transfer function for underwater visibility prediction in sea

Design concepts and performance of instruments for measuring radiant energy penetration and scattering in sea water

Synchronous scanning for backscatter reduction in underwater optical systems

Electric field effects on optical absorption by excitons in semiconductors

Hybrid holographic system using reference, transmitted, and reflected beams simultaneously

Transient optical absorption by self-trapped excitons in alkali halide crystals

Optical characteristics measuring apparatus

Calculation of conduction electronic energy bands and L bands in alkali halide crystals

Beam scintillations and atmospheric turbulence characteristics of multiwavelengths laser transmission

Optical monitor panel consisting of translucent screen with test or meter information projected onto it from rear for application in control rooms of missile launching and tracking stations

Instabilities in system of equations describing electromagnetic wave propagation and fluid dynamics

Fresnel hypothesis on changes in speed of light traveling through bodies due to motion of bodies

Diffractional field distortion and cross talk in simultaneous optical multibeam transmission of off-axis Gaussian beams

Propagation of short light impulses in water medium

Optical properties of clouds with emphasis on radiation transfer, reflection, and transmission

Line-of-sight deviations and ray trace analyses of Apollo side window for optical experiments

Effects of surface roughness on reflection of radiation from vacuum deposit interface of CO₂ cryodeposits studied by angular distribution measurements of radiant flux from glass samples

Ceramic optical voltage sensors operating from remote location by transmitting light through flexible light guides

Time of flight and coordinate measurements in 130 channel scintillation counter using light signals

Fourier techniques for determining structure of three dimensional semitransparent objects from measurements of transmission functions of holograms illuminated by light beams

Detecting molecular constituents in radiation transparent media by measuring intensity of light transmitted through cell while applying electrostatic or electromagnetic field

Nonlinear propagation and chirping of carbon dioxide laser pulses

Optics of ripple tanks with equations applicable to waves of various shapes

Transmission and extinction of solar radiation in atmospheric stratification

Radiative transfer in turbid atmospheres and atmospheric refractivity determinations

Computer programs for calculating visible and infrared atmospheric transmission, absorption, Mie scattering, and reflection

Elevated temperature studies of optical absorption associated with electrons trapped in fused silica

Measurements of off-axis irradiance produced by laser beam in water

Optical transmittance of fused silica at elevated temperatures during high energy electron bombardment

Development of optical technique for underwater observation and analysis of problems associated with propagation of light rays in water

Light impulse backscattering for determining visual range in atmosphere

Optical propagation measurements in inhomogeneous atmosphere at Emerson Lake, California for optical propagation theory validity testing

Effects on propagation of optical beams due to self-induced changes in index of refraction

Transmission of coherent light in nonlinear systems

Fog and aerosol analysis with ultra-sensitive dirometer utilizing optical transmission and light scattering principles

Comparison of 1.5 MeV electron irradiation induced optical absorption of fused commercial silicas and optical transmission of Al₂O₃, MgF₂, BaF₂, LiF, and BeO

Solution of Lighthill gas model wave equation for engine noise generation in circular jets noting cylindrical coordinate system

Lighthill method with Lagrange expansion for approximate solutions of partial differential equation

Low aerodynamic drag airfoil designing by Lighthill method

Lighting

Lighting equipment

Aircraft lights

Airport lights

ARC lamps

Flash lamps

ILLUMINATORS

SUBJECT INDEX

- NT LUMINAIRES**
NT MERCURY LAMPS
NT RUNWAY LIGHTS
NT SEARCHLIGHTS
NT XENON LAMPS
 Effect of cockpit lighting systems on multicolored instrument displays (AD-716610) 09 p1339 N71-19710
 Performance tests and characteristics of capsule-type and prismatic-head lights used for airport approach and runway lighting systems (NBS-10121) 11 p1731 N71-32453
 Sealed fluorescent tube light unit capable of continuous with other units to form string of work lights (NASA-CASE-XKS-5932) 14 p2331 N71-26787
- LIGHTING**
 Lightning induced voltages in aircraft electrical circuits (NASA-TM-X-52906) 01 p0004 N71-10591
 Lightning hazard to rockets during launch (NASA-CR-111118) 01 p0047 N71-10412
 Atmospheric electricity criteria guidelines for use in aircraft design (NASA-TM-X-54549) 02 p0259 N71-11796
 Whistlers with harmonic bands caused by multiple stroke lightning (NASA-CR-116456) 07 p0108 N71-17152
 Analysis of reported incidences of ball lightning (NASA-TT-F-13228) 07 p056 N71-18133
 Measurements and analysis of lightning-induced voltages in aircraft electrical circuits (NASA-CR-1744) 08 p1170 N71-19122
 Atmospheric potential gradient and cloud to ground lightning monitoring system design (AD-716534) 09 p1412 N71-19623
 Simulation and measurement of electrical properties of lightning discharge by use of long sparks produced under laboratory conditions (FAA-DS-69-16) 14 p2287 N71-25823
 Validity of using laboratory produced sparks for evaluating properties of atmospheric lightning and description of parameters of primary importance (AD-726752) 14 p2287 N71-25824
 Measurement of peak radiant power and total radiant energy emitted within given spectral region by single stroke lightning flash and comparison with energy of long spark (NASA-TM-X-67182) 14 p2287 N71-25827
 Qualitative analysis, quantitative analysis, and time dependent model of high speed time-resolved spectroscopic study of lightning return stroke (AD-726752) 14 p2287 N71-25828
 Determination of lightning temperature by return stroke channel opacity, temperature profile, and energy state distribution (AD-726752) 14 p2287 N71-25829
 Theoretical determination of temperature decay of lightning channel during interstroke period and time interval between lightning strokes and initiation of dart leaders (AD-726752) 14 p2287 N71-25830
 Measurement of sparking potential of gaps in low pressure air between two electrodes, with plane wave surface as cathode, to simulate lightning strokes and radio noise (AD-726771) 14 p2247 N71-25856
 Magnitude of induced voltages and their relation to characteristics of lightning discharge and electrical properties of aircraft electrical systems (AD-726771) 18 p2869 N71-30761
 Estimates of lightning caused computer component damage and malfunctions (AD-726752) 18 p2897 N71-31413
 Evaluation of lightning hazards to jet aircraft including possibility of fuel tank explosions (AD-726952) 20 p3209 N71-33006
 Tornado data on lightning measurements and thunderstorm days in Finland during 1970 (AD-726952) 20 p3209 N71-33619
 Single station lightning distance measuring device based on ratio of magnetic field to electric field (NOAA-TL-BRL-195-APCL-16) 20 p3268 N71-33734
 Experimental weather station for observation of lightning and storm activity (NRL-0A-TRANS-1150-6196-3) 22 p3566 N71-35399
 Evaluation of ball lightning observations and hypotheses concerning its theoretical interpretation and experimental reproduction (NASA-TT-F-13932) 22 p3573 N71-35443
 Development and characteristics of device for deployment of long wires as method of reducing hazards due to lightning during spacecraft launches (NASA-TM-X-62085) 23 p3756 N71-36772
 Lightning and ball lightning phenomena in weapons technology, magnetohydrodynamics and meteorology (ICST-713996) 23 p3791 N71-37024
- LIGHTS**
U LUMINAIRES
LUMEN
 Investigating relationship of lignin content to height in dwarf and regular-sized alpine plants of Iceland (AD-716610) 07 p0964 N71-17997

- Effect of wood-destroying fungi on destruction of hydrolytic lignin (AD-713924) 20 p3286 N71-32962
- LIMBS (ANATOMY)**
NT FOREARM
NT HAND (ANATOMY)
NT LBG (ANATOMY)
LIME
U CALCIUM OXIDES
LIMESTONE
 Elastic wave anisotropy in marble, dolomite, and limestone crystals based on ultrasonic tests and X ray analysis (NASA-TT-F-13673) 16 p2383 N71-28280
 Developmental program for SO₂, NO, and particulate pollutant level lowering and control in flue gas from fossil fuel combustion using fluidized beds with limestone (ANL/ES-CEN-1003) 23 p3750 N71-36736
- LIMITATIONS**
U CONSTRAINTS
LIMITED CIRCUITS
NT CLIPPER CIRCUITS
 Development and characteristics of single, silicon element, waveguide iris limiter (AD-715777) 02 p0193 N71-11355
 Variable duration pulse integrator design for integrating pulse duration modulated pulses with elimination of ripple content (NASA-CASE-XLA-01219) 11 p1730 N71-23084
 Circuits for amplitude limiting of random noise inputs (NASA-CASE-NPO-10169) 13 p2059 N71-24844
 Velocity limiting safety system for motor driven research vehicle (NASA-CASE-XLA-07473) 13 p2086 N71-24895
 Portable dc power generator design including power supply, limiter, and switching circuits for voltage regulation (AD-721570) 16 p2568 N71-28342
 Electric motor off-on speed control limiter circuit for thyristor and computerized simulation (AD-721561) 16 p2574 N71-28349
 Performance and noise emission measurements of solid state microwave limiters (AD-726942) 23 p3732 N71-36609
- LIMITS (MATHEMATICS)**
 Limiting relations for correlation averages in quantum statistics of four fermion interactions (ITF-70-59) 17 p2811 N71-30399
 Derivation of upper bound for scattering amplitude (IFVE-STF-70-18) 18 p2979 N71-30697
 Theorem proof for lower bounds of nuclear scattering K matrices (JINR-P4-5660) 21 p3469 N71-34699
 Upper limits for transport coefficients due to plasma fluctuations and convective cells based on quasi-linear approximations of diffusion across magnetic fields in toroidal devices (CONF-710607-71) 24 p3989 N71-38459
- LIMONITE**
 Dimensional analysis and particle size distribution of limonite from Pennsylvania including optical and mechanical properties as Mars simulation material (RM-5121) 17 p2846 N71-30333
- LINE SPECTRA**
NT BALMER SERIES
NT D LINES
NT ELECTRONIC SPECTRA
NT FRAUNHOFER LINES
NT H ALPHA LINE
NT H BETA LINE
NT H GAMMA LINE
NT K LINES
NT LYMAN SPECTRA
 Solar absorption line spectra for determining magnetic field strength (AD-710690) 01 p0117 N71-10401
 Spectral line intensity data for visual region of subdwarf star (AD-710690) 01 p0122 N71-10477
 Atomic line transitions and radiant emission from high temperature air (AD-710799) 01 p0096 N71-10503
 Resonance light scattering for measuring spectral line transitions in cobalt isotope spectrum (AD-710799) 01 p0089 N71-10522
 Mossbauer spectra of ferromagnetic materials (AD-711105) 01 p0111 N71-10668
 Loss charge determination from emitting spectral lines using beam foil light source technique (NASA-CR-111379) 02 p0270 N71-11460
 Loss charge identification for spectral lines in nitrogen by beam foil light source technique (NASA-CR-111380) 02 p0271 N71-11462
 Tables of iron spark lines giving comparison of calculated and measured wavelengths (ESRIN-TM-34) 02 p0281 N71-11873
 Computed and observed OI line profiles in spectra of B5-A0 stars (AD-710690) 02 p0297 N71-12047
 Magnitude and wavelength dependence of resonance radiation emission caused by thermal excitation (AD-711628) 03 p0437 N71-12802

- Determining local Doppler displacements of solar spectra using lines of different mean depth in Doppler comparison (AD-711628) 03 p0451 N71-13172
- Hyperfine ESR line widths in linear chains using Cu/NH₃/ASO₄-H₂O/CTA for calculations (ICOO-1488-19) 04 p0483 N71-13439
 Level crossing analysis on hyperfine structure of europium isotopes (AD-711628) 04 p0576 N71-13693
 Accuracy of X ray line intensity measurements from nonmetallic materials (MGO/SD/168) 05 p0706 N71-14539
 Investigating pressure broadening of spectral lines from particle interactions (AD-704361) 05 p0736 N71-14578
 Variations in intensity of solar X ray line emission from solar corona (AD-713112) 05 p0765 N71-15336
 Potential energy barriers to internal molecular rotation from relative intensities of microwave absorption spectra lines (AD-713112) 05 p0751 N71-15549
 Intensity measurements on oxygen VII solar X ray emission lines (AD-716472) 09 p1462 N71-20385
 Theoretical model for calculating resonance line fluxes of ion emission in solar corona (AD-716472) 09 p1462 N71-21837
 Photon absorption lines in electron paramagnetic resonance spectrum of second harmonic generation in ruby (AD-716472) 10 p1642 N71-21837
 A, a, and B functions for electron broadening of positive ions with hyperbolic path (NASA-TM-X-67048) 11 p1801 N71-21983
 Determination of isotopic composition and quantity of radioactive nuclei by gamma spectroscopy (TT-70-50922) 11 p1762 N71-22261
 Limit on line emission in X ray background at high galactic latitudes - rocket observation (NASA-TM-X-65519) 13 p2160 N71-24960
 Statistical analysis of X ray line emission from cosmic radiation source (AD-716472) 13 p2164 N71-25298
 Quantum mechanics of line broadening effects in solar simulator mercury xenon arc lamp spectra (AD-716472) 13 p2164 N71-25298
 Classical path calculations of impact broadening operator phi for Stark broadening of hydrogen line H sub alpha (AD-720817) 14 p2321 N71-25916
 Second moments of exchange broadened nuclear magnetic resonance lines for exchange rate measurements (AD-720817) 14 p2321 N71-25916
 Ozone transmission and emission spectra at 9.6 microns computed from adjusted theoretical spectral line data (AD-720817) 15 p2476 N71-27508
 Absorption function of ozone at 9.6 microns spectral bands noting their fine structure (AD-720817) 15 p2401 N71-27509
 Characterization and mathematical representation of line scanning image systems and evaluating system performance with discrete output signal and post filtering (NASA-CR-118893) 15 p2434 N71-27632
 Effect of absorption nuclear lines on transmission radiation of resonance gamma quanta by relativistic electrons (JINR-P2-5042) 15 p2496 N71-27973
 Collisional excitation rates for lithium-like ions derived from diagnosed plasma produced in theta pinch device and line intensities emitted by these ions (NASA-CR-119017) 16 p2648 N71-28636
 Collisional ionization rates for lithium and beryllium-like ions deduced from time history of spectral lines emitted by these ions in hot plasmas (NASA-CR-119018) 16 p2648 N71-28637
 Spectroscopic observation of seven neutral helium line profiles for five main sequence B stars with estimated helium abundance for upellion Orionis, HR 2154, and pi Ceti (AD-720817) 16 p2680 N71-28786
 Spectrometric high resolution study of helium II 6560 A and 10124 A line transitions (AD-720817) 16 p2653 N71-29028
 Dynamic response of liquid lines of finite length for periodic and nonperiodic inputs (AD-720817) 17 p2736 N71-29918
 Resonance line broadening by crystal dislocations (AD-720817) 17 p2824 N71-29992
 Fourier transform of X ray diffraction line profiles from crystals with dislocations (AD-720817) 17 p2825 N71-29995
 VLF propagation measurement technique using repetitive pulse spectral lines (AD-727353) 17 p2721 N71-30030
 Spectral line profiles and energy absorption in helium plasma afterglow (JN-18740) 18 p2992 N71-30640
 Determination of ruthenium 92 half life from decay of isotopic technique lines (JINR-P6-5594) 18 p2978 N71-30691

Nuclear magnetic resonance linewidths in metals as function of temperature - density matrix equation [AD-723914] 19 p3113 N71-32125

Line absorption analysis and reaction kinetics of two metastable nitrogen atomic energy levels [NASA-CR-119685] 19 p3154 N71-32295

Line spectra shifts in HF and in first overtone band of DF induced by HF pressures 20 p3233 N71-33172

Least squares method applied to noise reduction in low frequency line spectra 20 p3264 N71-33360

Broadening and shifting of hydrogen fluoride lines due to noble gases 20 p3274 N71-33478

Theoretical and experimental calculations in analysis of optical spectra of uranium 20 p3330 N71-33642

Upper atmospheric emissions from He, O, and Na during solar eclipse of 15 Feb. 1961 [NRC-TT-1459] 21 p3416 N71-34307

Electron beam probe to measure potential and Doppler shifted spectral lines to study presence of fast particles in inertial electrostatic confinement device [NYO-4109-2] 21 p3484 N71-34818

Total absorption measurements of absolute oscillator strengths for Pb I lines at lambda 2833, 2873, 3639, 3683, and 4057 [AD-726987] 22 p3552 N71-35300

Instruments for measurement of spectral lines profile and shift 23 p3755 N71-36769

Gamma radiation lines of rubidium 89 from fission products [CEA-N-1444] 24 p3975 N71-38358

LINEAR ACCELERATORS

Linear accelerator research work including neutron cross section analysis, and fast reactor physics and engineering [RPI-322-173] 01 p0087 N71-10796

Characteristics and operation of electron linear accelerator [AD-711587] 02 p0273 N71-11790

Linear accelerator spiral reader performance [SLAC-PUB-765] 02 p0275 N71-11858

Design and development of electron linear accelerators [NP-18317] 04 p0545 N71-13562

Electron beam stabilization in linear accelerator [KHFTI-49-20] 04 p0573 N71-13666

Electrical and magnetic field calculation for linear accelerator inductor [JINR-P-5129] 04 p0567 N71-14234

Design and operation of proton linear accelerator [JINR-1187] 04 p0517 N71-14498

Investigating electron scattering and nuclear structure in linear accelerators [INTERKO-70/7] 05 p0735 N71-14528

Increasing maximum energy and improving beam intensity of 85 MeV linear electron accelerator at Amsterdam 05 p0637 N71-14529

Characteristics and performance of wire spark chamber system using secondary pion beam at SLAC for study of reactions of form pion- π^+ proton yields two or more charged particles [SLAC-PUB-801] 05 p0740 N71-15098

Equipment development for Stanford linear accelerator research [SLAC-126] 05 p0747 N71-15241

Investigating elementary particle interactions in linear accelerators and reactor physics [RPI-328-187] 06 p0730 N71-15264

Status of proposal for high intensity linear electron accelerator with high duty cycle and maximum energy of 500 MeV - Netherlands [REPT-70/6] 05 p0659 N71-15462

Design of 20-megawatt linear plasma accelerator facility [NASA-TN-D-6115] 06 p0928 N71-15819

Particle stability in ion linear accelerators with alternating-phase focusing [JINR-P-5312] 07 p1080 N71-18124

Line beams of continuously variable energy within narrow limits of synchronous particle [UCRL-19901] 09 p1431 N71-19096

Data acquisition system used with electron linear accelerator for neutron capture gamma ray experiments - metallurgical and other program notes 10 p1528 N71-20901

Optical model of nucleus and atomic energy levels studied with tandem Van de Graaff machine, proton linear accelerator, and magnetic spectrometer [COCO-1265-94] 10 p1616 N71-21170

Linear accelerator frequency control system [NASA-CASE-XGS-05441] 11 p1729 N71-22962

Control systems and instrument development for use with liquid metal fast breeder and high flux isotope reactors, Van de Graaff and linear accelerators, and in-pile loops [ORNL-4620] 12 p1895 N71-23166

Accelerator and research operations report for Stanford Linear Accelerator from July to September 1970 [SLAC-128] 12 p1897 N71-23380

Berkeley Hilac modification for ion acceleration to maximum energy of 8.5 MeV/n [UCRL-19919] 12 p1973 N71-23939

Electron beam losses in linear induction accelerators [UCRL-TRANS-1425] 12 p1973 N71-23941

Electronic digital computer for automating 2-GeV electron linac [SLAC-TRANS-126] 12 p1976 N71-24139

Influence of high frequency fields on properties of accelerating channel and beam emittance in linear accelerator [SLAC-TRANS-128] 14 p2300 N71-25703

Design of stopped muon channel for LAMPF [LA-4474] 14 p2300 N71-25721

Electron bunching structure calculations for bunching produced by injectors with wave phase velocity stepped variations 14 p2302 N71-25749

Operation of 60 MeV linac including 180 degree electron scattering, slow neutron resonance data on rhenium isotopes, s-wave resonance spins, and related maintenance and improvements [AD-720674] 14 p2305 N71-26320

Beam regulation in 100 MeV proton linear accelerator, including preinjector accelerator tube and betatron oscillations [NP-TR-1926] 14 p2319 N71-26791

Hybrid computer measurement of stopband in LAMPF 805 MHz accelerator structure at high power [LA-4593] 15 p2387 N71-26857

Peak current measurement in linear electron accelerators by toroidal ferrite monitoring system with associated digital equipment [CEA-N-1389] 15 p2465 N71-27246

Cross sections for photoproduction of neutral mesons on hydrogen measured by linear accelerator using mass spectrometer techniques 15 p2483 N71-27767

Adone linac operation, installations, and experiments with head-on collisions and positron and electron beam energies up to 1200 MeV [LNF-70/48] 16 p2646 N71-28169

Linear accelerator operations data including machine time dedicated to high energy physics, nuclear physics, machine physics, shutdowns for modifications, and maintenance [LNF/AD-1] 16 p2647 N71-28229

Numerical calculation of electromagnetic field and resonant frequencies of resonators at Swierk, Poland proton 10 MeV linear accelerator [JINR-P-1218] 16 p2577 N71-28617

Linear accelerator photonuclear reaction safety testing of nuclear materials [GULF-RT-10459] 16 p2632 N71-28625

Strength evaluation of braze alloys used for linear accelerator components [LA-4584] 16 p2613 N71-28781

Klystron experience and status of SLAC and Stanford positron-electron asymmetric ring [SLAC-PUB-802] 16 p2650 N71-28885

Multiturn linear accelerator injection into gravity gradient synchrotron and quadrupole compensation for frequency shifts [BNL-15646] 17 p2792 N71-29299

Performance characteristics of existing and proposed accelerators for heavy ions with description of super HILAC progress and discussion of isochronous cyclotrons [ORNL-TM-3332-REV] 17 p2793 N71-29625

Compressor 2 and 3 experiments, 4 MeV 500 A electron linear induction accelerator, and electron ring accelerator research and development programs [UCRL-20150] 17 p2731 N71-30051

Dynamic structural analysis on reentrant cavity for superconducting low energy proton linear accelerator [NP-18724] 18 p2901 N71-30482

Data on constructing high-current induction linear accelerator in nanosecond range [JINR-P-5601] 18 p2901 N71-30490

Focusing, acceleration, and beam characteristics of Orsay heavy ion linear accelerator [NP-18612] 18 p2978 N71-30665

Research work with linear electron accelerator [LAL-1241] 18 p2903 N71-30916

Deuteron acceleration in second drift multiplicity in proton linear accelerator with grid focusing [JINR-P-5610] 19 p3157 N71-32463

Determination of maximum useful yield of positrons by matrix description of capture and acceleration of positrons by linear accelerator [AD-729771] 20 p3314 N71-33120

Nucleon-nucleon problem at medium energies at LAMPF [LA-4640] 21 p3480 N71-34783

Research operations and equipment development for Stanford two-mile electron accelerator [SLAC-130] 22 p3565 N71-35392

Selection of focusing system for linear induction accelerator and maintenance of beam size [JINR-P-5714] 22 p3640 N71-35952

Using control computer to analyze beam quality of MeV proton linear accelerator [UAE-76] 23 p3825 N71-37283

Conference on nuclear physics and research with electron linear accelerators [JAERI-1205] 24 p3981 N71-38410

LINEAR AMPLIFIERS

Measurements and calculations for selection of broad band linear power amplifier using HF-effect transistors and operating in VHF band 05 p0654 N71-15528

LINEAR ARRAYS

NT YAGI ANTENNAS

Coupling effects on linear array for beam steering 04 p0496 N71-13917

Water wave direction measurement with laboratory linear array of wave sensors [AD-15725] 06 p1190 N71-18727

Numerical computation of linear antenna feed [R-74] 10 p3158 N71-21853

Linear array, multi-electrode, ultrasonic transducer test techniques for radioisotope encapsulation inspection [BNWL-1491] 16 p2571 N71-28601

Inversion formulae for singular integral equations for linear dislocation arrays 17 p2817 N71-29936

Finite cylindrical dipole antenna of arbitrary orientation in gyrotropic media solved as boundary value problem 23 p3734 N71-36622

LINEAR CIRCUITS

Linear electric potential pulse with amplitude conversion circuit for spacecraft power supplies [ESRO-TN-101-ESTEC] 03 p0459 N71-13318

Technology review on integrated linear, digital, and optoelectronic circuits 10 p1537 N71-20893

User and programmer manual for NASAP-70 digital circuit analysis program [NASA-CR-121933] 22 p3536 N71-35332

Optimized design techniques for linear integrated circuits 23 p3736 N71-36642

Microelectronic linear integrated circuits for radio equipment and telecommunications 23 p3736 N71-36643

LINEAR ENERGY TRANSFER (LET)

Comparison of differentiated line source and line source methods of measuring particulate media thermal conductivity in vacuum [NASA-TM-X-64539] 03 p0467 N71-12288

LINEAR EQUATIONS

Transient pressures and aerodynamic coefficients of rectangular wings in subsonic flow using linear equations [ONERA-NT-163] 04 p0471 N71-13402

Applying finite difference method to solution of numerical stability in linear algebra problems [ORO-3443-28] 04 p0539 N71-14308

Exact solution to adaptive linear estimation problem [AD-713098] 05 p0655 N71-14926

Coefficient determination of flight dynamics multivariable systems by means of computer simulated aircraft dynamic models [DLR-FB-70-30] 08 p1144 N71-18586

Solution to linearized gravitational field equations representing self scattering of gravitational waves 08 p1192 N71-18972

Symbolic method for solving linear equations of flow graphs by multivariate polynomial extension of two-step integer-preserving elimination algorithm 08 p1225 N71-19197

Linearized perturbation equations for incompressible laminar boundary layer flow over slender body of revolution at small incidence [NRC-11665] 09 p1377 N71-20201

Analysis of four iterative methods for approximating zeros of polynomial expressions using digital computer [NASA-CR-14931] 10 p1592 N71-21478

Bifurcation of equilibrium state of elastic solid, using three dimensional linearized equations for arbitrary subcritical deformations 11 p1836 N71-22877

Sound propagation characteristics in gas media with droplets or particles based on linearized hydrodynamic equations [NASA-TT-F-13581] 12 p2864 N71-24619

Formal solutions of first order functional equations [TR-71-110] 13 p2103 N71-24933

Green function in solving linear and nonlinear second order ordinary differential equations including examples in finding rendezvous and periodic orbits of restricted three body system [NASA-CR-118993] 16 p2621 N71-28181

Algebraic solutions of linear equations for secular perturbations of planetary eccentricities and longitudes [NASA-TT-F-13666] 16 p2621 N71-28181

Solution of initial value problem in linear transport theory obtained by monoenergetic neutrons migrating in thin slab with infinite reflector and isotropic scattering [NASA-TR-R-357] 17 p2805 N71-30238

Convergence of iterative methods applied to large overdetermined linear and nonlinear systems of equations using least squares [ESSA-TR-ERR-1-01-ESL-10] 18 p2946 N71-31266

SUBJECT INDEX

- Convection-diffusion equation for closed formula-
tion of cosmic ray transport theory in solar environ-
ment [NASA-CR-121440] 20 p3341 N71-33562
- LINEAR FILTERS**
- Empirical Bayes filter for use in trajectory estima-
tion and comparison of performance with Kalman
filter [NASA-CR-114997] 09 p1409 N71-19915
- Periodically reverse-switched capacitors or induc-
tors in feedback networks, resulting in linear subhar-
monic filter 11 p1725 N71-22694
- Joint optimization of linear, time invariant, trans-
mitting and receiving filters examined in continuous
and discrete time domains 14 p2220 N71-26575
- Interpolation by linear filters for use in numerical in-
tegrations involving multiple grid network mappings
(AD-721185) 15 p2436 N71-26825
- Characterization and mathematical representation of
line scanning image systems and evaluating system
performance with discrete output signal and post fil-
tering [NASA-CR-118893] 15 p2434 N71-27632
- Sampling and linear filter theory for direct in-
terpretation of geoelectrical resistivity measurements
16 p2583 N71-28246
- LINEAR PREDICTION**
- Problems of singularity and duality in linear estima-
tion and control 06 p1226 N71-19034
- Gauge invariant theory of motion of singularities in
linear approximation [NASA-CR-121431] 20 p3293 N71-33896
- LINEAR PROGRAMMING**
- Mathematical programming and control of Markov
chains [NASA-CR-111130] 01 p0076 N71-10580
- Annotated bibliography of capital budgeting/project
selection by mathematical programming [TM-173] 03 p0399 N71-12817
- Linear programming techniques for structural
design optimization of stressed-skin structures
03 p0463 N71-13129
- Linear programming for computerized minimum
mass layout design of trusses 03 p0464 N71-13136
- Linear complementarity problem in complex space
[AD-712769] 03 p0399 N71-13184
- Using mathematical programming to investigate dis-
crete optimization problems in Banach space [AD-713700] 05 p0714 N71-15230
- Algorithm for linear, nonlinear and quadratic pro-
gramming [NPL-MA-87] 07 p0996 N71-17072
- Reduction of nonlinear programming problems to
sequence of linear programming problems 09 p1356 N71-20133
- Realization of near time optimal feedback control-
lers for linear time invariant systems [SC-88-78-544] 10 p1530 N71-21743
- Abstract variational theory application to continu-
ous parameter stochastic optimization problems to
derive maximum principles in linear programming
[NASA-CR-117886] 12 p1948 N71-23220
- Basic theory and general linear model for analysis of
variance [TR-71-14] 14 p2286 N71-26677
- Convergence of centers algorithm for solving non-
linear programming problems [NASA-CR-121911] 22 p3405 N71-35672
- Algorithm for solving general quadratic pro-
gramming problem with linear constraints
[NASA-CR-123214] 24 p3892 N71-37739
- LINEAR RECEIVERS**
- Optimum receivers for continuous phase digital
frequency modulated signals [RR-71-1] 13 p2048 N71-25343
- Antenna array at focal plane of reflector with
coupling network for beam switching [NASA-CASE-GSC-10220-1] 15 p2381 N71-27233
- LINEAR SYSTEMS**
- Magnetic type characteristics in spacecraft environ-
ment and design of linear m-ary feedback shift register
01 p0027 N71-10264
- Computer-aided design of linear networks in
frequency domain [NASA-CR-111103] 01 p0036 N71-10426
- Linear system impulse response identification from
measured input using fast Fourier transformation
[AD-710650] 02 p0191 N71-11341
- Linear three tap feedback shift register [NASA-CASE-NPO-10351] 03 p0345 N71-12503
- Linear theory for electrolytic model of transistors
[TD-25456] 03 p0350 N71-12529
- Design of proportional-integral-derivative control-
lers using optimal linear regulator theory [NASA-CR-111516] 03 p0353 N71-12552
- Solution of linear algebraic systems by matrix
decomposition [AD-712600] 03 p0390 N71-12681
- Four theorems characterizing optimal filtered and
smoothed estimates for linear parabolic systems
[AD-712404] 03 p0399 N71-12995

- Algorithm providing maximum likelihood estimates
for linear dynamic systems with unknown parameters
[AD-712894] 03 p0400 N71-13186
- Improving feedback control design by using digital
computer techniques [NASA-CR-116771] 04 p0500 N71-13501
- Solving general multidimensional linear optimal
control problem with quadratic cost functional and
nonconstant weighting on final states [AD-712716] 04 p0537 N71-13930
- Realization theory of rational transfer matrices
presented as fundamental algebraic objects in theory
of finite, constant linear systems [NASA-TM-X-66515] 04 p0538 N71-14157
- Frequency domain analogies, polynomial matrices,
and linear systems [NASA-TM-X-66512] 04 p0538 N71-14173
- Structure theorem for time invariant multivariable
linear systems [NASA-TM-X-66511] 04 p0538 N71-14174
- Decoupling and pole assignment in linear multivariable
systems by dynamic compensation [NASA-TM-X-66510] 04 p0538 N71-14175
- Characteristics of randomly excited structural and
mechanical dynamic systems 04 p0619 N71-14347
- Linear dynamic systems in Hilbert space
05 p0712 N71-14513
- Plane wave propagation in linear homogeneous
medium 05 p0712 N71-14514
- General properties of linear dynamic systems in Hil-
bert space 05 p0712 N71-14515
- Linear solid model assuming constant Poisson ratio
for straight crested waves in infinite linear viscoelastic
plate [AD-713301] 05 p0774 N71-14556
- Birkhoff-Turrittin truncation problem for systems
of ordinary linear differential equations [AD-713701] 05 p0714 N71-15277
- Applications of partial orderings to study of positive
definiteness, monotonicity, and convergence of
iterative methods for linear systems [NASA-CR-116134] 06 p0883 N71-15849
- Linear analysis of relationship between fluid trans-
mission line characteristics and output of transmission
line [AD-714200] 06 p0836 N71-16469
- ALGOL computer programs for linear system time
dependence [AIRC-CP-1124] 07 p0996 N71-17133
- Linear theory for response of two-layer ocean
model to moving hurricane 09 p1300 N71-19502
- General multiple linear logic shift-generator model
for Galois field resulting in longer binary sequences
[AD-716558] 09 p1346 N71-19525
- Equations of motion of nonstationary oscillation
systems with periodically changing coefficients
[AD-716528] 09 p1476 N71-19890
- Time delay effects on linear system stability, using
Mikhailov stability criterion [COO-2109-2] 09 p1419 N71-20031
- Solution of mixed boundary value problem based on
three dimensional equations for thermoelastic shells
[AD-716015] 09 p1478 N71-20111
- Asymptotic properties and simulation of adaptive
stochastic control for linear systems [NASA-CR-117182] 09 p1411 N71-20372
- Application of imbedding theory to problems of
linear feedback control systems and trajectory opti-
mization 10 p1643 N71-21254
- Stabilizability of decentralized linear dynamic
systems with proportional feedback control [AD-716922] 10 p1593 N71-21502
- Statistical properties of solution to deconvolution
problem [LA-4556-MS] 10 p1595 N71-21682
- Simplified linear guidance and control for keeping
trajectory deviations minimal [AD-717567] 11 p1791 N71-21915
- Linear control systems designed with distributed
parameter elements for determining absolute and
relative stability and root location of closed loop charac-
teristic equations 11 p1728 N71-22105
- Input-output properties of feedback systems based
on linear time invariant systems [NASA-CR-117467] 11 p1728 N71-22230
- Coupled linear antennas in inhomogeneous dissipa-
tive medium 11 p1724 N71-22656
- Linear theory for two dimensional supercavitating
flow past flat hydrofoil [AD-718116] 12 p1899 N71-23398
- Separation theorem for linear systems, quadratic
criteria and correlated noise 12 p1949 N71-23739
- Split Path Nonlinear (SPAN) filter compared with
lead-lag network and optimal linear controller 12 p1893 N71-23873

- Computation of transition probability of piecewise
linear system subjected to nonstationary excitation
12 p2006 N71-23983
- Iteration method for output feedback control of un-
stable linear systems 12 p1894 N71-24031
- Methodological and algorithmic considerations in
synthesis of linear multidimensional automatic control
systems 12 p1886 N71-24221
- Sequence reconstruction of ordered linear polymer
from fragment data [COO-1018-1219] 12 p1951 N71-24249
- Linear transfer function for describing human
response to aircraft control 13 p2036 N71-24710
- Volterra functional series for reactor with delayed
neutrons and linear reactivity feedback [ENR-1204] 13 p2117 N71-24856
- Self-reorganization methods for complex linear
dynamic systems to compensate for component
failures [NASA-CR-118314] 13 p2103 N71-24874
- Particular solution of linearized MHD system inside
neutral sheet [EUR-CEA-CP-571] 13 p2147 N71-24976
- Kalman formulation of minimum mean square linear
estimation with random variables and unknown dis-
tributions producing biased results [NASA-CR-118665] 14 p2284 N71-26429
- Equivalent measurements, observability, and
calibration accuracy limits in linear estimation and ap-
plication to orbital position estimation [NASA-TN-D-6388] 15 p2433 N71-26930
- Autocorrelation function of dynamic systems in-
cluding white noise and application to oscillators
[JBR-A-N7-3] 15 p2779 N71-27110
- Dual control algorithms for self adaptive filters and
optimal control law for linear systems with unknown
input gains [AD-721461] 16 p2573 N71-28052
- Mathematical models and optimal control for uncer-
tain systems [AD-721470] 16 p2628 N71-28060
- Feedback compensator for linear-time invariant
system insensitive to parameter variations [NASA-CR-119798] 16 p2545 N71-28160
- Optimal control of linear and class of nonlinear dis-
tributed-parameter system using concept of set of at-
tainable states 16 p2624 N71-28909
- Cross correlation function for estimating structural
frequency response [ISVR-TR-33] 17 p2771 N71-29312
- Identifying linear dynamic systems with state and
observation noise with application to flight control
problem [AD-723308] 17 p2773 N71-29733
- Prediction of nonadiabatic particle motion in linear
and toroidal multipolar fields including magnetic mo-
ment change in relation to particle trapping 17 p2796 N71-29799
- Kinematics and general principles in nonlinear and
linear theories of elastic shells and plates by direct ap-
proach and three-dimensional equations of classical
continuum mechanics - Part 1 [AD-722350] 17 p2854 N71-30020
- Derivation of constitutive equations, material sym-
metries, dynamical restrictions, and related topics for
nonlinear and linear theories of elastic shells and
plates - Part 2 [AD-722351] 17 p2854 N71-30021
- Application of linear control of systems with ran-
dom inputs to gust response control of aircraft
guidance in atmospheric turbulence [ONERA-P-131] 17 p2701 N71-30324
- Step input linear system modeling from nonlinear
system sampled noisy data based on method of pertur-
bation or linearization of automatic control system
data [NASA-CR-115074] 17 p2729 N71-30356
- Finite time stability of linear discrete time systems
and corresponding results for stochastic linear discrete
time systems [AD-722654] 18 p2944 N71-30720
- Problem solving in linear differential games
[JPRS-53645] 19 p3122 N71-32047
- Game problem for reducing motion to given set for
linear systems with aftereffects 19 p3123 N71-32048
- Linear differential games of pursuit in presence of
delays 19 p3123 N71-32049
- Algorithm for identification of system parameters
from input-output data with application to air vehicles
[NASA-TN-D-6448] 19 p3124 N71-32473
- Mathematical models for pole assignment in linear
feedback control systems [NRC-ME-MK-26] 20 p3293 N71-33883
- Voltage variable phase shifter having linear voltage-
to-phase characteristics 21 p3303 N71-34148
- Application of cybernetics and control theory to
problems of production control in complex systems

LINEAR TRANSFORMATIONS

- and optimum stabilization of several coordinates of object by one controlling influence
[JPRS-53883] 21 p3405 N71-34230
- Optimum stabilization of several coordinates of object in linear system by one controlling influence
21 p3406 N71-34232
- Linear gating of nanosecond signals for multichannel analyzer
[JINR-P13-5742] 21 p3436 N71-34380
- Design method including effects of parameter uncertainties in design of linear control systems
[NASA-CR-116774] 21 p3431 N71-34414
- Obtaining mathematical model and determining state of linear, time invariant system from input/output observations
21 p3430 N71-34534
- Three suboptimal control policies using reduced dimensional aggregated state vectors
21 p3450 N71-34535
- Algorithm for p-q solution of degenerate linear system
[NASA-TM-X-58069] 22 p3605 N71-35675
- Self adjusting numerical control of linear system and application to aerospace system
[ONERA-P-134] 22 p3606 N71-35679
- Switching-time-variation computational method for optimal control problems of bilinear systems and systems linear in control
21 p3738 N71-36659
- Decoupling and pole placement via transfer matrix synthesis
[NASA-CR-123163] 24 p3947 N71-38156
- Optimal feedback controller design based on model for linear plant of unknown characteristics under stochastic environment
24 p3951 N71-38186
- Measuring system for linear readout of both periodic and aperiodic mechanical displacements over broad frequency range
[NASA-CR-114375] 24 p3965 N71-38286
- Theta pinch experiments with helical equilibrium fields in 5m toroidal sector and in 3m linear device
[CONF-710607-116] 24 p3990 N71-38469
- LINEAR TRANSFORMATIONS**
- Using coupled theory of linearized thermoelectricity and integral transform techniques to solve problem of nonconducting half-space subjected to transient radiation
[SC-RR-70-428] 03 p0440 N71-12672
- Linear algebra for characterization and synthesis of digital circuits
[REPT-4341] 05 p0712 N71-14508
- Linear transformation and absorption of plasma and electromagnetic waves
[INP-18504] 08 p1269 N71-18165
- Calculation of orthogonal transformation matrices and application to photogrammetry
16 p2622 N71-28204
- Frame-indifferent time fluxes and linear operations in Euclidean space
[WTHD-25] 21 p3448 N71-34540
- Linear transformation of vector of unquantized signal samples to improve accuracy of reception or measurement
[AD-727980] 24 p3889 N71-37720
- LINEAR VIBRATION**
- Computation of transition probability of piecewise linear system subjected to nonstationary excitation
12 p2006 N71-23965
- Stiffness, damping, and inertia change effects on eigenvalues and eigenvectors of linear vibration systems
17 p2788 N71-30057
- LINEARITY**
- NT COLLINEARITY**
- Mathematical models for predicting responses of structures with linear behavior
[AD-716899] 01 p0129 N71-10485
- Hyperfine ESR linewidth in linear chains using $Cu(NH_3)_4SO_4 \cdot H_2O$ for calculations
[CDO-1488-19] 04 p0483 N71-13439
- Exchange quasi-potential for high energy pion plus minus/ proton scattering and problem of linearity of Regge trajectories
[JINR-E2-3226] 06 p1246 N71-18175
- Semilinear bearing comprising two rows of roller bearings separated by spherical bearings and permitting rotational and translational movement
[NASA-CASE-XLA-02809] 11 p1772 N71-22982
- Mechanical actuator wherein linear motion changes to rotational motion
[NASA-CASE-XGS-04548] 12 p1929 N71-24045
- Shell theory using linearly exact expressions for transverse variation of displacement components in thin elastic shells
14 p2350 N71-26668
- Signal flow graphs for emitter follower temperature stability and linearity analysis
[INR-1236] 21 p3402 N71-34207
- LINEARIZATION**
- Computer program for calculation of variables of state of real gas mixtures with logarithmic linearization of nonlinear equations
[DLR-MITT-69-27] 03 p0469 N71-13372

- Modified quasilinearization algorithm for solving nonlinear equations
[NASA-CR-121654] 21 p3446 N71-34522
- Linearized perturbation theory for calculating relative motion of unrestrained bodies within orbiting space stations
[NASA-CR-115142] 22 p3628 N71-35851
- Holomorphic matrix method for linearization of analytical bundles and in series convergence
24 p3948 N71-38167
- LINKERS**
- U LININGS**
- LINKS (GEOMETRY)**
- NT CHORDS (GEOMETRY)**
- LINKS OF FORCE**
- Magnetic flux lines in superconductors
[NASA-TT-F-13458] 07 p1068 N71-17520
- Electric field distribution, cloud elongation, and drift along magnetic field line of barium release from Javalin
17 p2741 N71-29681
- LING-TEMCO-VOUGHT AIRCRAFT**
- NT F-4 AIRCRAFT**
- LING-TEMCO-VOUGHT MILITARY AIRCRAFT**
- U MILITARY AIRCRAFT**
- LINGUISTICS**
- NT MACHINE TRANSLATION**
- NT SEMANTICS**
- NT SYLLABLES**
- NT SYNTAX**
- NT WORDS (LANGUAGE)**
- Nonparametric probability density estimation and linguistic techniques of pattern recognition
[NASA-CR-111119] 01 p0030 N71-10966
- Language programming for linguistic algorithms - ALTEXT 2
[AD-711387] 02 p0190 N71-11335
- Information systems and processing, linguistics, artificial intelligence, and human information processing
[PB-194790] 06 p0963 N71-16897
- Syntax for linguistic information retrieval
[IVA-25] 11 p1847 N71-22185
- Feasibility and limitations of speaker adaptation in improving performance of fixed speaker independent automatic speech recognition system
[AD-718253] 12 p1867 N71-23616
- Computer program for linguistic data processing including translating text from Russian into English
14 p2222 N71-25984
- LINING PROCESSES**
- Flow-duct test facility data on acoustic behavior of lined ducts and duct-lining materials for turbojet engine applications
[NASA-CR-111887] 14 p2199 N71-26417
- LININGS**
- NT ROCKET LININGS**
- Shortening transition time to decrease overall length of ram induction combustor
[NASA-TN-D-7021] 03 p0448 N71-12422
- Behavior of nozzles and acoustic liners in three dimensional acoustic fields
[NASA-CR-102988] 05 p0760 N71-14642
- Fission product transport and behavior in stainless steel lined Containment Research Installation
[ORNL-4502] 13 p2140 N71-25499
- Gas turbine combustor liner film cooling for slot geometries in presence of high free stream turbulence
[NASA-TN-D-6360] 17 p2858 N71-29841
- Forming and bonding metallic lining onto inside surface of metal tube
[NASA-TM-X-2347] 19 p3114 N71-32161
- LINKAGES**
- Development of collapsible nozzle extension for rocket engines
[NASA-CASE-MFS-11497] 06 p0940 N71-16224
- Solutions to linkage mobility problems
13 p2087 N71-24965
- LINKING**
- U JOINING**
- LINKS**
- Communication equipment for tropospheric propagation link
[FOA-C-3-3604-63] 14 p2219 N71-26542
- LOUVILLE EQUATIONS**
- Quantum mechanical Louisville equation and Schrodinger equation in kinetic theory
[AD-713605] 05 p0737 N71-14616
- LIPIDS**
- NT OLEIC ACID**
- Design and performance of automatic sequential chromatographic apparatus for purification of lipid extracts
[UCRL-50861] 01 p0011 N71-10480
- Nutritional value of *Hydrogenomonas eutropha* lipids in rats
03 p0326 N71-12328
- Escherichia coli* cell phospholipid composition changes during spheroplast formation in presence of penicillin and sucrose
[NASA-TT-F-134808] 11 p1683 N71-22506
- High fat diet effects on caloric intake, body weight, and heat escape responses in normal and hyperphagic rats
11 p1684 N71-22599

SUBJECT INDEX

- Lipid uptake prediction by prosthetic heart valve poppets from solubility parameters derived from thermodynamic considerations
18 p2883 N71-31115
- LIPSCHITZ CONDITION**
- Algebra proposed for approximate integration of specific boundary value problem of nonlinear systems of differential equations with delayed argument and satisfying Lipschitz condition
[NASA-TT-F-13594] 16 p2622 N71-28221
- LIQUEFIED GASES**
- NT LIQUID AMMONIA**
- NT LIQUID HELIUM**
- NT LIQUID HYDROGEN**
- NT LIQUID NITROGEN**
- NT LIQUID OXYGEN**
- Thermal and magnetic properties of adsorbed phases of He-3 and He-4 at low temperatures
[AD-712416] 03 p0419 N71-15339
- Explosive dynamics of liquefied nitrogen jets and solidified nitrogen wires
04 p0630 N71-13622
- Phase behavior in fluid mixtures at high pressures
[AD-713540] 03 p0636 N71-14643
- Mathematical models for two phase cryogenic choking flow of hydrogen and nitrogen
[NASA-CR-116005] 06 p0833 N71-15808
- Cavitation data analysis for liquefied cryogenic hydrogen and nitrogen
[NASA-CR-116004] 06 p0833 N71-15809
- Thermodynamic properties of insulated liquid methane fuelage tanks for supersonic cruise aircraft
[NASA-TN-D-6157] 07 p1102 N71-17506
- Cell model for quantum crystals and fluids
[AD-714900] 07 p1096 N71-16897
- Role of particle interaction in determining properties of solids and condensed matter
[AD-715294] 08 p1277 N71-18412
- Vapor pressure and PVT data of compressed gaseous and liquid fluorine
[AD-716286] 09 p1343 N71-19049
- Specific heats of H2 and D2 solid mixtures down to 0.1 K, adsorption isotherms of He-3 and He-4 at low temperatures, and development of He-3 dilution refrigerator and liquefier
[AD-717623] 11 p1815 N71-21941
- Studying static and time dependent correlation functions for liquids of carbon monoxide and nitrogen using computer simulated molecular dynamics
11 p1803 N71-22112
- Measurements of thermophysical properties of compressed fluid methane and survey of current literature on liquefied natural gas and methane
[NBS-9781] 11 p1698 N71-22717
- Conformal solution correlation representing excess volume, excess enthalpy, and excess Gibbs free energy for mixtures of simple liquids from argon to ethane
12 p1873 N71-24308
- Plane-parallel experimental ionization chamber containing liquid and solid argon
[JINR-P13-5404] 13 p2130 N71-24852
- Cross sections of electron-positron pair production by gamma-quanta with energy from 35 to 2000 MeV in liquid xenon
[JINR-P1-5482] 14 p2319 N71-26792
- Simple empirical relation based on adiabatic compressibility, adiabatic bulk modulus, and reduced temperature for liquid argon, krypton, and xenon, and application to mercury
[NYO-4176-6] 15 p2378 N71-27982
- Ionization electron avalanches in high electric field in liquid argon and xenon for this particle detector development
[UCRL-20135] 21 p3484 N71-34814
- Performance tests and specifications for space storable regenerative cooling system with liquid oxygen and methane propellants
[NASA-CR-72704] 23 p3066 N71-37540
- Stamping of moving parts by liquid gas
[AD-727247] 24 p3928 N71-38826
- LIQUID AMMONIA**
- Liquid ammonia primary reserve battery design
[AD-718266] 12 p1860 N71-23310
- Electrochemical mechanism, solution properties, and design criteria for energy conversion devices
[AD-723384] 17 p3706 N71-27975
- LIQUID BEARINGS**
- Design and testing of prototype hydrostatic liquid bearing gyro assemblies
[NASA-CR-102991] 07 p1028 N71-17319
- Water-lubricated three-lobe hydrodynamic journal bearing stability tests at zero load with and without axial grooves
[NASA-TN-D-6315] 12 p1926 N71-23778
- LIQUID BREATHING**
- Effects of positive G_y acceleration on blood oxygen saturation and pleural pressure relations in dogs breathing air and liquid fluorocarbons in whole body water immersion respirator
[NASA-CR-117199] 09 p1336 N71-28159
- LIQUID COOLED REACTORS**
- NT BOILING WATER REACTORS**
- NT EXPERIMENTAL BREEDER REACTOR 1**
- NT EXPERIMENTAL BREEDER REACTOR 2**
- NT HALDEN BOILING WATER REACTOR**

SUBJECT INDEX

NT HEAVY WATER REACTORS
NT LITHIUM COOLED REACTOR EXPERIMENT
NT ORGANIC COOLED REACTORS
NT PLUM BROOK REACTOR
NT PLUTONIUM RECYCLE TEST REACTOR
NT PRESSURIZED WATER REACTORS
NT SODIUM REACTOR EXPERIMENT
NT SPENT REACTORS
NT WATER COOLED REACTORS
NT ZERO POWER REACTOR 3
NT ZERO POWER REACTOR 6
NT ZERO POWER REACTOR 9
NT ZERO POWER REACTORS
Solubility of inert gases in sodium reactor coolant and attendant safety aspects
[KPK-1166] 08 p1235 N71-18211
Design and performance of sodium tank test facility
[EURFNR-819] 08 p1174 N71-18275
Sodium cooled reactors fast ceramic reactor development program review
[GEAP-10929-36] 13 p2122 N71-23478
Sodium-2 reactor control studies with digital dynamometer on IBM 360/65 computer
[EURFNR-835] 19 p3137 N71-32108
Containment design criteria for sodium cooled fast reactors
[RT/ING/70/25] 19 p3138 N71-32157
Evaluation of sodium cooled breeder reactor technology and instrumentation in German, French, and British facilities
[HEDL-54-170] 19 p3140 N71-32545
Venting devices for sodium cooled fast reactor with ceramic fuel elements
[RT/ING/70/29] 21 p3457 N71-34605
Qualitative analysis of safety problems in sodium cooled reactor
[NLL-RISLEY-TRANS-2063-9091.9F1] 22 p3626 N71-35837
LIQUID COOLING
NT FILM COOLING
Cooling water system for compressor of supersonic wind tunnel
[AD-710971] 01 p0038 N71-10679
Predicting bearing fatigue failure and life in primary coolant check valves of advanced test reactors
[IN-1358] 04 p0557 N71-14153
Analysis of flow induced vibrations in reactor fuel elements, fuel assemblies, control elements, and cooling system components
[ANL-7685] 06 p0898 N71-16274
Design and performance of thermodynamic fluid cooled high entry temperature axial flow turbine
07 p1129 N71-17399
Laminar flow of liquid coolants in rocket engines
[NASA-CASE-NPO-10122] 07 p1010 N71-17631
Adiabatic compressional cooling of He 3 to millikelvin temperatures
[UCSD-34-P-143-27] 08 p1305 N71-19050
Space suit body heat exchanger design composed of thermal conductance yarns and liquid coolant loops
[NASA-CASE-XMS-06771] 09 p1399 N71-19439
Liquid and vapor cooling systems for gas turbines with application of heat pipe concept to stator blade cooling
[AEC-CP-1127] 10 p1638 N71-20832
Wall rotation effect on heat transfer from tube to cooling water stream
10 p1663 N71-21668
Bottom flooding emergency core cooling data for pressurized water reactor
[WCAP-7544] 10 p1664 N71-21726
Mechanism under conditions of high static pressure of lubricant cooling medium
[AD-719812] 13 p2099 N71-24427
Electric power system with circulatory liquid coolant cooling system
[NASA-CASE-MPS-14114-2] 13 p2056 N71-24807
Pressurized water reactor flooding rate effects on cooling heat transfer time-temperature response based on plasma chamber simulation tests
[WAP-5352] 13 p2117 N71-24907
Electric power system with thermionic diodes and circulatory liquid metal coolant lines
[NASA-CASE-MPS-14114] 15 p2525 N71-27862
Cooling, coking, construction, and structural characteristics of jet fuel-cooled plug nozzle for afterburning turbine
[NASA-TM-X-2304] 16 p2671 N71-28128
High pressure, liquid nitrogen cooled, gas particle sensor target design for use with hydrogen, deuterium, and helium
[JVE-SEP-70-22] 16 p2645 N71-28164
Apparatus for liquid spray cooling of turbine blades
[NASA-CASE-XLE-00027] 16 p2694 N71-29152
Automatic temperature control for liquid cooling garments used during astronaut extravehicular activity with external auxiliary means, and skin temperature as input signals
[NASA-CR-115122] 21 p3384 N71-34077
LIQUID CRYSTALS
Electric and magnetic fields effect on liquid crystal structure
[NASA-CR-111582] 03 p0324 N71-12313

Photoresponse of liquid crystals at room temperature and dark conductivity changes at phase transitions
03 p0324 N71-12313
Electric field effects on dielectric properties and molecular arrangements of cholesteric liquid crystals
[A70-11352] 03 p0324 N71-12317
Electric field effects on optical rotary power of compressed cholesteric liquid crystal
[A70-14083] 03 p0324 N71-12318
Alternating current field induced cholesteric and nematic liquid crystal phase transitions
[A70-20053] 03 p0325 N71-12319
Dipole relaxation and molecular arrangements in liquid crystals
[A70-26859] 03 p0325 N71-12320
Dielectric constants measurements and magnetic field effects on compensated cholesteric liquid crystals
[A70-17326] 03 p0325 N71-12321
Absence of helical inversion in single component cholesteric liquid crystals
03 p0325 N71-12322
Helical twisting power of steroidal solutes in cholesteric liquid crystal mesophases
[A70-21524] 03 p0325 N71-12323
Infrared transmission measurement of pitch of cholesteric liquid crystal
03 p0325 N71-12324
Design and performance of liquid crystal microwave power density meter
[PS-19196] 03 p0443 N71-12990
Augmentation of human eye focus control by varying index of refraction with nematic liquid crystals
[NASA-CR-115864] 05 p0634 N71-14653
Basic studies of liquid crystals related to electro-optical and other devices - thermal stability, aging, and oxidation resistance
09 p1343 N71-19721
Electromagnetic radiation detection of microwave field patterns using liquid crystals
[AD-717583] 11 p1699 N71-21923
Description of basic laws of motion of micropolar continuum and application of micropolar theory to liquid crystals
[AD-717596] 11 p1696 N71-22225
EPR study of two smectic A liquid crystals using vanadyl acetyl acetate as paramagnetic probe
[NASA-TN-D-8299] 14 p2278 N71-26047
Formulation of problems of shear flow and orientation due to magnetic field for nematic liquid crystals
[AD-721107] 15 p2378 N71-27720
Dislocation theory applied to liquid crystals in mesomorphic medium
17 p2821 N71-29965
Correlation of supramolecular solid and liquid crystal phase structure of poly-gamma-benzyl L-glutamate and its properties
21 p3500 N71-34933
LIQUID DROPS
U DROPS [LIQUIDS]
LIQUID DYNAMICS
U FLUID DYNAMICS
U LIQUID FLOW
LIQUID FILLED SHELLS
Deriving boundary layer structure from addition of axial magnetic field to rotating viscous fluid and resulting modification in tilt caused by distortion of field lines
07 p1010 N71-17640
Vibration characteristics of ellipsoidal shells containing fluids
08 p1300 N71-19275
Design and development of fluid sample collector
[NASA-CASE-XMS-06767-1] 09 p1391 N71-20435
Numerical analysis of vibrations of shells partially filled with heavy fluid and dynamical reaction of shells under impact in acoustic medium
12 p2007 N71-24117
Manufacture of fluid containers from fused coated polyethylene sheets having resealable septum
[NASA-CASE-NPO-10123] 13 p2086 N71-24835
Fluid content effect on vibration frequencies of ellipsoidal shells of revolution
[AD-719645] 13 p2183 N71-25363
Omnidirectional liquid filled accelerometer design with liquid and housing temperature compensation
[NASA-CASE-HQN-10780] 17 p2754 N71-30265
Nutation oscillation damper based on fluid radial flow through porous material placed parallel to axes of rotation
[NASA-CASE-GSC-11205-1] 18 p2929 N71-31128
Analysis of axisymmetric vibration of elastic spherical shell filled with viscous incompressible fluid
[AD-726634] 23 p3862 N71-37536
LIQUID FLOW
NT OPEN CHANNEL FLOW
NT WATER FLOW
Steady state X ray system for determining void fraction transient variations in two phase gas-liquid flow
[ADPL-3859] 05 p0659 N71-14713
Liquid film flow and critical heat flux measurements in concentric, internally heated annulus
[AEC-3456] 05 p0660 N71-14757

Two phase flow of gas-liquid mixture through porous material
08 p1182 N71-18918
Method for controlling instability in fluids differences computations of liquid saturation near borehole of recovery well
[BIM-RI-7487] 08 p1192 N71-18970
Kinetics of mass transfer in vibratory motion of solid body in stream of liquid
[PB-19429-77] 08 p1183 N71-18993
Stagnated diffusers used to check flow of gas or liquid moving at subsonic velocity
[AD-716093] 09 p3370 N71-19613
Similarity between two phase liquid-vapor flows with heat exchange - conference
[CEA-CONF-1640] 09 p3376 N71-20118
Time-dependent motion of small gas bubbles in smoothly decelerating liquid including bubble slip functions
[BRI-4993] 10 p3543 N71-21447
Body force effects on liquid film stability interacting with external gas
[SC-RR-70-721] 13 p3048 N71-25442
Development of anisotropic porous media model for analyzing effects of fluid motion in fuel cell cavities
16 p2581 N71-28719
Mathematical models for incompressible laminar boundary layer flow inside and outside of liquid spheroid moving through liquid
19 p3080 N71-32378
Evaluation of liquid methane storage and transfer problems for future supersonic aircraft cryogenic fuel requirements
[NASA-CR-72932] 21 p3463 N71-34648
Analysis of gas phase control of critical and near-critical two phase flow where gas and liquid flow in separate streams
[NBS-TN-608] 22 p3548 N71-35413
LIQUID HELIUM
Variational calculation of ground-state energy of liquid He-4 using Percus-Yevick and hypernetted chain theories
[JCO-1569-61] 05 p0734 N71-15265
Measuring attenuation of first sound near lambda transition point in liquid helium
[AD-713478] 05 p0734 N71-15275
Apparatus for use in liquid helium cryostat for measurement of small magnetic field changes occurring within detection chamber
08 p1244 N71-19010
High voltage, high resolution electron microscope with superconducting lenses operating with superfluid helium refrigerator
08 p1245 N71-19315
Properties of liquid He-3 and dilute solutions of He-3 in superfluid He-4 for dilution refrigerators
[UCSD-34-P-143-29] 08 p1246 N71-19343
Sum rules in hydrodynamic scaling approach for near critical temperature liquid helium
10 p1571 N71-20682
Photon density detection for determining liquid helium excess electron absorption cross sections at infrared wave lengths
10 p1612 N71-20720
Susceptibility of liquid He-3 with comparison to Curie susceptibility
11 p1809 N71-23028
Characteristics of liquid helium solid boundary conductances and cooling limits
[AD-717568] 12 p2011 N71-23977
Pressure and temperature wave coupling in liquid helium model with thermal expansion
[NASA-CR-118352] 13 p2186 N71-25354
Helium 4 impurities and magnetic field effect on thermal boundary resistance between powdered cerium magnesium nitrate and liquid helium 3 at very low temperatures
[UCSD-34-P-143-35] 13 p2127 N71-25463
Wave function for describing ground state of liquid helium 4
13 p2143 N71-25570
Exchange energy and magnetic susceptibility measurements on low temperature He-3 with He-4 traces, and techniques for light scattering in gases at room temperature
[NYO-5951-3] 14 p2295 N71-25610
Feasibility of superfluid helium use in tubular cooling systems with particular application to superconducting helix waveguides
[NPL-18651] 14 p2364 N71-26439
Inhibition of scintillations in liquid helium by temperature reduction
15 p2487 N71-27834
Design and performance of crystal for single crystal and X ray diffraction analyses
[AERE-R-6532] 15 p2509 N71-27910
Type II super conductor research on conductances of Nb-Cu and NbTi-Cu junctions, and vortex flow in weak pinning He II
[UCLA-ENG-7109] 16 p2638 N71-28144
Heat transfer rates, specific heat, and behavior of liquid He-3 and He-4
[UCSD-34-P-143-37] 16 p2638 N71-28179

Phase sensitive detector and commercial Hall probe combined with control current amplifier to provide sensitive, low field magnetometer for use from room to liquid helium temperatures
[AD-721390] 16 p2593 N71-28497

In pile and out of pile durability tests and characteristics of 30 kW circulating helium fuel capsules in Plum Brook Reactor
[NASA-TM-X-52676] 16 p2636 N71-28967

Spectrometric high resolution study of helium II 4560 Å and 10124 Å line transitions
16 p2653 N71-29028

Cryopump used in magnetoplasmadynamic converters with liquid helium cooled argon plasma
[DLR-MITT-71-03] 17 p2730 N71-29379

Development and characteristics of dilution refrigerator capable of producing and holding temperatures near absolute zero
19 p3197 N71-32458

Cohesion effects in superfluids, such as liquid helium and superconductors
20 p3333 N71-33045

Production cross sections for He I, He II, H-alpha, and H-beta emissions
20 p3318 N71-33573

Microscopic foundation of bubble model for excess electron in liquid helium
20 p3325 N71-33905

Baseball magnet system in fusion reactor engineering utilizing plasma beam line
[UCRL-70657] 23 p3740 N71-36668

Nucleation of cavitation by alpha particle irradiation of liquid helium, and existence of audible cavitation and hysteresis effect in helium I and II
23 p3822 N71-37263

Characteristics of heat transfer to liquid helium from horizontal, face-up surfaces of normal and superconducting lead and tin
23 p3867 N71-37567

Viscosity and normal density measurements at lambda point intervals for pure helium-4 and helium-3 mixtures with helium-4
[NASA-TN-D-6516] 24 p3966 N71-38290

LIQUID HELIUM 2

U HELIUM ISOTOPES

LIQUID HYDROGEN

Characteristics of liquid hydrogen and liquid oxygen propellants in Saturn launch vehicles
03 p0446 N71-13105

Helium gas requirements for liquid hydrogen expulsion from spherical tank
[NASA-TM-D-7019] 04 p0605 N71-14046

Polymer materials for sealing liquid oxygen and liquid hydrogen propulsion systems
[NASA-CR-114822] 06 p0867 N71-16377

Boiling and heat transfer characteristics of cryogenic hydrogen flows in straight and plenum inlets
[NASA-TN-D-6159] 07 p1132 N71-17955

Two phase hydrogen density measurements using open ended microwave cavity
[NASA-TN-D-6212] 08 p1166 N71-18889

Measuring incident and steady boiling of liquid hydrogen and nitrogen under reduced gravity
[NASA-CR-103047] 05 p1244 N71-19036

Reproducibility and linearity of 2 to 5 cm turbine-type flowmeters for liquid hydrogen including design principles, installation and inspection procedures, and calibration
[NASA-TM-X-52984] 09 p1388 N71-19703

Guidelines for using space shuttle configuration to determine effects of carrying ascent LH2 propellant in external drop tanks
[NASA-TM-X-64579] 10 p1648 N71-21317

Design fabrication and cycle tests of polymeric film expulsion bladders for liquid hydrogen
[NASA-CR-72732] 16 p1607 N71-21491

Thermal analysis of space hold performance of multilayer insulation on upper half of unbraided liquid hydrogen tank within zero oriented vehicle
[NASA-TN-D-62555] 10 p1663 N71-21557

Ultrasonic vibration effects on cooldown rate of bodies in liquid nitrogen and helium
12 p1968 N71-24154

Thermal cycling tests of ground and space liquid hydrogen storage tank heat ablating with multilayer, porous insulating thermal insulation blankets
[NASA-TN-D-63311] 13 p2173 N71-24822

Self evacuating multilayer insulation system of aluminum Mylar and polyurethane foam for liquid hydrogen tanks
[NASA-CR-72856] 13 p2102 N71-25447

Hydrostatic life-off and zero leakage and static sealing and rubbing tests for use in liquid hydrogen turbine pumps
[NASA-CR-72796] 14 p2260 N71-25735

Pressure and thermodynamic effects on cavitation performance for helical inducers operated in liquid hydrogen
[NASA-TN-D-63611] 14 p2329 N71-25940

Ceramic stresscoat burst and performance test of shrouded, diffusion welded titanium pump impellers for liquid hydrogen pump applications
[NASA-CR-103124] 14 p2332 N71-26428

Reaction pion/minus/ proton yields rho-meson /O pion/minus/ proton with momentum studied in liquid hydrogen bubble chamber at 4.45 GeV/c
[ITEP-775] 14 p2316 N71-26745

Liquid hydrogen targets for determining total cross section of particle interactions
[JINR-P6-5212] 15 p2457 N71-26851

Gas dynamics and thermodynamics of single vapor bubbles in liquid hydrogen and ultrasonic radiation effects
[JINR-P13-5327] 15 p2392 N71-27085

Buoyancy effect on cryogenic hydrogen film boiling during upward and downward flows
[NASA-TM-X-67855] 15 p2525 N71-27866

Development of thermal insulation material for insulating liquid hydrogen tanks in spacecraft
[NASA-CASE-XMF-05046] 16 p2691 N71-28892

Saturated LH-2 turbopump operation and feasibility of zero-tank NPSH mode for use with J-2 engines
17 p2830 N71-29579

Design, fabrication, and testing of improved titanium impeller for high pressure liquid hydrogen pumps
[BC-71-26] 17 p2830 N71-29585

Resonant frequency measurement systems used in conjunction with open-ended microwave cavity to continuously monitor density of liquid hydrogen in flow system
[NASA-TN-D-6415] 18 p2922 N71-30721

Transient thermal performance of multilayer insulation systems with liquid hydrogen tank during simulated Saturn 5 ascent pressure decay
[NASA-TN-D-6335] 18 p2939 N71-30722

Hydrogen liquid and slush tank continuous inventory during ground storage
[NASA-CR-119241] 18 p2923 N71-30818

Tests with stainless steel in sliding contact with lead, indium, and tin coatings in liquid hydrogen to determine their lubricating capability
[NASA-TN-D-6455] 19 p3105 N71-32193

Design of ITEP 2-meter liquid hydrogen bubble chamber and calculations for chamber body expansion system, vacuum tank, and nitrogen shielding
[NP-16787] 19 p3075 N71-32728

Operating properties of liquid hydrogen bubble chamber and cooling system
[SIC-T-71-1] 22 p3635 N71-35908

Tests of ball bearings of various material combinations in liquid hydrogen
[NASA-CR-72280] 23 p3762 N71-36618

Weight and cost estimation for pressurization systems for hydrogen, oxygen, and nitrogen storage
[NASA-CR-115204] 24 p3927 N71-38021

Environmental tests of cryogenic propellant effects on metallic positive expulsion bellows operating parameters
[NASA-CR-72979] 24 p3999 N71-38526

LIQUID INJECTION

NT WATER INJECTION

Technique for sterile insertion of liquids into previously sterilized spacecraft
[NASA-CR-111095] 01 p0010 N71-10382

Integral analysis of heat transfer downstream of rearward-facing step with small coolant injection
[NASA-TN-D-3970] 03 p0468 N71-13036

System for aerodynamic control of rocket vehicles by secondary injection of fluid into nozzle exhaust stream
[NASA-CASE-XLA-01163] 05 p0721 N71-15582

Propellant injection assembly having individually removable and replaceable nozzles for liquid fueled rocket engines
[NASA-CASE-XMF-00968] 05 p0763 N71-15660

Evaluating effect of liquid fuel injectants on ablative performance of low cost nozzle materials
[NASA-CR-72792] 07 p1011 N71-17677

Characteristics of secondary fluid injection from two dimensional slit into uniform two dimensional supersonic stream for thrust vector control
[ARC-TR-1] 11 p1738 N71-22429

Thermodynamic characteristics and mutual interaction of film cooling with coolant gas injection into supersonic stream
[IC-AERO-71-07] 17 p2839 N71-30286

Analysis of phenomena occurring in exhaust gas spray cooler utilizing liquid injection, and mathematical model of optimum cooler
[AD-724657] 20 p3338 N71-32991

LIQUID LASERS

High energy pulsed liquid laser
[AD-710813] 01 p0063 N71-10308

Design and fabrication of high energy Q switched pulsed liquid lasers
[AD-720393] 14 p2265 N71-25961

LIQUID LEVELS

Inductive liquid level detection system
[NASA-CASE-XLE-01609] 01 p0054 N71-10590

Magnetostrictive transducers for ultrasonic liquid level detector, using shear wave attenuation in bar
[IN-1442] 10 p1605 N71-21370

Hydrogen liquid and slush tank continuous inventory during ground storage
[NASA-CR-119241] 18 p2923 N71-30818

LIQUID MERCURY

U MERCURY (METAL)

LIQUID METAL COOLED REACTORS

NT EXPERIMENTAL BREEDER REACTOR 1 NT EXPERIMENTAL BREEDER REACTOR 2 NT LITHIUM COOLED REACTOR EXPERIMENT

Deposition of sodium and barium in sodium stainless steel system to predict distribution of fission products in LMFBR system
[AI-AEC-12957] 02 p0265 N71-11782

Leak detection systems development for sodium heated LMFBR steam generators
[APDA-255] 03 p0414 N71-12823

Ultrasonic thermometry in LMFBR reactor systems
[NYO-3906-11] 03 p0415 N71-12824

Implementation manual of computer program for calculating fission product corrosion in liquid metal cooled breeder reactor cladding
[AI-AEC-12957] 03 p0415 N71-12841

Radial bubble distribution in heated turbulent flow in sodium cooled reactors
[RD/N-1630] 03 p0416 N71-12922

Describing aerosol model of hypothetical LMFBR accidents
[AI-AEC-12977] 04 p0550 N71-15760

Fast breeder reactor advanced fuel element cladding fabrication
[GEMP-745] 04 p0553 N71-15994

Design limit and transient survival criteria for typical fuel elements of large liquid metal fast breeder reactors
[WARD-4135-6] 04 p0553 N71-16002

Developing experimental information and analytical methods for design and safety analysis of sodium cooled fast reactors
[AI-AEC-12970] 04 p0554 N71-16017

Oxygen meter performance in high purity and carbon contaminated sodium, for LMFBR program
[MSAR-70-56] 04 p0557 N71-16119

Reactor core technology for LMFBR
[AI-AEC-12969] 04 p0557 N71-16122

Investigating performance of stainless steel cladding and plutonium-uranium oxide fuel elements in fast breeder reactors
[GEAP-10028-34] 04 p0557 N71-16134

Developing computer programs for optimum economic parameters of conceptual 1000 MW/LMFBR
[WARD-2000-96] 04 p0558 N71-16183

Conceptual system design descriptions for 1000-MW LMFBR central station power plant
[BAW-1328-VOL-3] 04 p0561 N71-16374

Reference design of 1000 MW/LMFBR liquid metal fast breeder reactor - Vol. I
[AI-AEC-12792-VOL-1] 04 p0561 N71-16381

Sodium vapor control in liquid metal cooled fast reactor cooling systems
[NP-1831] 04 p0561 N71-16401

Limitations and requirements survey of LMFBR component materials
[BML-1901] 04 p0562 N71-16409

Application of acoustic-boiling-detection techniques to liquid metal cooled reactors
[ANL-7460] 07 p1062 N71-17249

Research in sodium technology including methods for purifying coolant sodium
[ANL-ST-3] 08 p1234 N71-18178

Initiation and thermal hydraulics of sodium boiling and release and transport of aerosols and energy in coolant combustion accidents in liquid metal fast breeder reactors
[AI-AEC-12979] 09 p1419 N71-20049

Research and development in LMFBR physics program
[AI-AEC-12978] 09 p1421 N71-20080

Mechanical properties data for LMFBR reactor materials, and irradiation effects on cladding and structural alloys
[BML-1891] 10 p1602 N71-21084

Highlights of project activities for November 1979 including fuels, components, and physics for LMFBR
[ANL-7754] 10 p1603 N71-21105

Uranium-plutonium nitride fuels for LMFBR, fast reactor fuels, and reactor fuel material cross properties
[BML-1893] 11 p1794 N71-22419

Control systems and instrument development for use with liquid metal fast breeder and high flux isotope reactors, Van de Graaff and linear accelerators, and in-pile loops
[ORNL-4630] 12 p1895 N71-23186

Design criteria of sodium piping for LMFBR
[SAN-781-500] 12 p1962 N71-23447

Servicing and testing of liquid sodium piping in LMFBR
[SAN-781-243] 12 p1963 N71-23447

LMFBR environmental effects on type 304 and 316 stainless steels and Cr-Mo alloy piping materials
[SAN-781-228-REV-1] 12 p1963 N71-24033

Niobium zirconium temperature sensor design for application in high temperature gas cooled or liquid metal cooled reactors
[WHAN-SA-24] 14 p2252 N71-25630

SUBJECT INDEX

LIQUID OXYGEN

Accident prevention and safety devices for water cooled reactors compared with liquid metal cooled, fast breeder reactor safety
[WHAN-SA-43] 14 p2291 N71-25664

Safety problems related to design of covers for liquid metal cooled fast breeder reactors
[ANL-7637] 14 p2292 N71-25731

FFFT and LMFB reactor design, fuels, and materials development
[WHAN-FR-30] 14 p2293 N71-25786

Thermal design analysis on tantalum/stainless steel forced convection mercury boiler for SNAP 8 reactor
[NASA-CR-72768] 15 p2452 N71-27855

Metallurgical preparation of LMFB prototype fuels
[WHAN-SA-14] 16 p2453 N71-28640

Nuclear and economic performance calculations for sodium and naphthalene in LMFB cores
[ORNL-TM-3271] 16 p2453 N71-28643

Nuclear fuel burnup and failure analysis of plutonium uranium oxide in sodium potassium cooled fuel capsule under liquid metal cooled reactor conditions
[ORNL-13620] 17 p2783 N71-29665

Candidate systems for emergency heat removal in LMFB
[BAW-1351] 19 p3135 N71-31993

Accident prevention systems for liquid metal fast breeder reactor safety design
[BAW-1354] 19 p3136 N71-32063

Literature survey for identifying primary containment safety features in accident and safety system analysis for liquid metal fast breeder reactor
[BAW-1352] 19 p3136 N71-32064

Investigation of coolant combustion accidents, release and transport of aerosols and energy from sodium, and effects of sodium coolant boiling on fuel elements in LMFB safety study
[AS-ABC-12948] 19 p3141 N71-32773

Analysis of existing instrumentation systems to protect LMFB core integrity and recommendations for improvement
[ANL-7793] 20 p3302 N71-33544

Development of uranium-plutonium nitride fuels for LMFB applications, studies of high temperature fuels for advanced fast reactors, and studies of creep of reactor fuel materials
[BNL-1096] 20 p3309 N71-33946

Effect of gas bubbles entrained in sodium coolant examined on LMFB fuel rods
[CONF-700608-36] 22 p3425 N71-35827

Reactor test complex for solving fuels and materials problems critical to developing liquid metal cooled fast breeder reactors - FFFR
[WHAN-SA-104-REV] 22 p3626 N71-35833

Design structure of various primary circuits in sodium cooled reactors
[KFK-1379] 23 p3796 N71-37058

LIQUID METALS

NT LIQUID POTASSIUM
NT LIQUID SODIUM
NT MERCURY (METAL)
NT MERCURY VAPOR

Liquid metal cooling of turbine blades with thermocouple circulation or phase transformation
[ONERA-TP-472] 02 p0225 N71-11557

Self-diffusion of radioactive sodium in single crystal and molten specimens
[TT-70-57044] 02 p0245 N71-12150

Thermotransport or thermal diffusion of solutes in liquid silver
[COO-841-19] 03 p0331 N71-12360

Investigating feasibility of using liquid metal vacuum distillation to separate Po-210 from bismuth
[EP-1222] 04 p0464 N71-13446

Thermotransport and self diffusion in liquid metals
[COO-841-20] 04 p0483 N71-13449

High temperature liquid metal technology for nuclear Rankine power systems
[BNL-38248] 04 p0528 N71-13991

Development of shielding for liquid metal fast breeder reactor
[ORNL-TM-2896] 05 p0722 N71-14650

Investigating various materials and components for liquid metal applications
[LMBC-78-15] 05 p0702 N71-15103

Investigating light scattering in superfluids by nuclear magnetic resonance
[AD-714095] 06 p0904 N71-16110

Development of liquid metal slip ring to transfer power between rotating satellite parts
[NASA-CR-72790] 06 p0798 N71-16570

High temperature liquid metal technology - associated bibliography
[BNL-50258] 07 p1042 N71-17245

Fluorometer using noise-analysis techniques for large liquid metal systems at temperatures of 1200 F
[AS-ABC-12981] 07 p1028 N71-17267

Heat transfer in liquid metal cooled gas turbine blades
07 p1129 N71-17398

Frequency response of two types of liquid metal pressure transducers with standoff tubes
[NASA-TN-D-6146] 07 p1030 N71-17605

Ultrasonic absorption and velocity measurements in liquid alkali metals
[AD-714066] 07 p1043 N71-17912

Boiling of liquid alkali metals in tubes
[BNL-TM-345] 08 p1303 N71-18314

Corrosion damage resistance of iron alloys, nickel alloys, and cobalt alloys in liquid sodium and mercury - review of NASA program
[NASA-TM-X-52956] 08 p1215 N71-18816

Diffusion coefficients determined for hydrogen in some liquid metals
08 p1217 N71-19004

Atomic mobility in crystal lattices in liquid metals
[TT-70-50829] 08 p1282 N71-19293

Electronic structure of dilute metallic alloys and electrical conductivity of liquid metals
[AD-714369] 09 p1452 N71-19708

Dynamical analysis of nonequilibrium, forced convective, boiling liquid metal flows
[NASA-CR-117804] 09 p1372 N71-19764

Production of aluminum oxide fibers by direct melt fiberization process
[NASA-CR-72812] 09 p1393 N71-20125

Techniques for determining heats of fusion and heat capacities of liquid metals at high temperatures
[NASA-CR-117032] 09 p1486 N71-20542

Kinetics of melting metals and mechanism of long to short range atomic ordering in liquid metals
[NLL-TRANS-746-560-7022.401] 10 p1379 N71-21307

Performance tests of liquid metal magnetohydrodynamic power converter
11 p1812 N71-22560

Condensation and evaporation coefficients for liquid metal vapors and relation to heat and mass transfer rates
[COO-2032-6] 11 p1780 N71-22661

Analytical test apparatus and method for determining oxygen content in alkali liquid metal
[NASA-CASE-XLE-01997] 12 p1871 N71-23527

Corrosion of water reactor core materials, liquid metals, hydrogen diffusion in corrosion processes, and glass ionization
[AECL-3778] 13 p2118 N71-24986

Numerical analysis of heat transfer equations and temperature profiles to determine thermodynamic properties of liquid metals
[RLO-2227-7-4-1] 13 p2187 N71-25464

Thermodynamic transport properties of liquid silver containing gold, antimony and sulfur traces
[COO-841-22] 13 p2096 N71-25513

Concepts of fusion reactor blankets, and thermodynamic circuits including liquid-metal, and direct helium circuits
[EPF-478] 15 p2448 N71-27260

Isothermal and adiabatic compressibility of liquid metals, particularly lead, from melting point to critical region
[NYO-4176-4] 15 p2425 N71-27482

Electric power system with thermionic diodes and electrolytic liquid metal coolant lines
[NASA-CASE-MPS-14114] 15 p2523 N71-27862

Flexible barrier membranes comprising porous substrate and incorporating liquid gallium or indium metal used as sealant barriers for spacecraft walls and pumping liquid propellants
[NASA-CASE-XNP-00881] 16 p2612 N71-28747

Development and characteristics of instruments for inductive measurement of liquid metal levels in cooling systems
[RD/RN-1720] 18 p2921 N71-30437

Phenomenological method for calculating double differential scattering cross sections for thermal neutron scattering from simple liquid metals
[IAERI-MEMO-4191] 18 p2976 N71-30617

Calculation of average hydrodynamic values during laminar and isothermal flow of liquids in clusters of rods
[AEC-TR-7184] 18 p2904 N71-30659

Flame-arrest melting in water cooled molds noting gas sorption by liquid metal
18 p2927 N71-30683

Measuring elevated-temperature time-dependent corrosion effects of liquid metal on immersed structural materials
[NASA-TM-X-67883] 18 p2936 N71-31221

Measurement of elevated temperature, time dependent corrosion effects of liquid metals on immersed structural materials by blocked two-level factorial experiment
[NASA-TN-D-6452] 18 p2936 N71-31244

High temperature microscopy of crystallization processes in molten iron, steel, and eutectic containing iron carbon alloy steels
18 p2997 N71-31321

Corrosive action of liquid metals on solids in stressed and unstressed states
[AD-723570] 19 p3110 N71-31746

Efficiency and performance characteristics of low temperature two phase liquid metal MHD power systems
[AD-721007] 19 p3173 N71-31757

Deoxidation of liquid iron studied by electromotive force measurements noting removal of inclusions
19 p3111 N71-31911

Kinetics of removal from iron of inclusions produced by manganese silicon aluminum complex deoxidation
19 p3112 N71-31912

Distorted velocity profile and electric potential distribution of long dc electromagnetic flowmeter for liquid metals
[NASA-TM-X-2342] 19 p3100 N71-32145

Electrode mold and grafted pattern coating of molten metals
[JPRS-53572] 19 p3106 N71-32432

Principles of operation, circuits, and construction of thermal flow rate meters for liquid metals
[AD-723540] 19 p3103 N71-32591

Characteristics of liquid metals as cooling and heat transfer system for use with nuclear reactors
20 p3364 N71-33732

High-voltage insulator design for injecting hydrogen bubbles into liquid metal fast flow lines to interrupt electrical continuity
[NASA-CASE-NPO-11075] 21 p3482 N71-34208

Mass transfer in liquid metal systems and in-line devices for measuring sodium impurity
[ORNL-13559-16] 22 p3423 N71-35816

Measuring techniques for pressure, volume, enthalpy, and resistance of equilibrium thermodynamic states of liquid metals at high temperatures and pressures
[UCRL-51033] 22 p3696 N71-36339

Storage and handling of highly irradiated fast breeder reactor fuel in hybrid sodium organic coolant storage pool, and Sn-Cu liquid metal dissolution for dechlorination
[EUR-4615-E] 24 p3956 N71-38223

LIQUID NITROGEN

Silicon junction photodiode behavior and liquid nitrogen thermal cycling tests
[DLR-MIT-70-08] 06 p0822 N71-15713

Neutron transport of neutrons from A/L source through many mean free paths in liquid nitrogen
[UCRL-50856] 06 p0919 N71-16250

Measuring incipient and steady settling of liquid hydrogen and nitrogen under reduced gravity
[NASA-CR-103047] 06 p1244 N71-16036

Liquid nitrogen circulating pump problems and solutions including pump performance curves
[NBS-9777] 10 p1567 N71-21444

Ultrasonic vibration effects on coldflow rate of bodies in liquid nitrogen and helium
12 p1968 N71-24154

Liquid nitrogen cooled nozzle for hypersonic low density wind tunnel
[DLR-FB-70-41] 15 p2390 N71-27035

Film boiling and heat transfer from platinum wire in saturated liquid nitrogen up to critical pressure
[NASA-TM-X-67849] 15 p2525 N71-27863

High pressure, liquid nitrogen cooled, gas particle accelerator target design for use with hydrogen, deuterium, and lithium
16 p2645 N71-28164

Two phase critical discharge of high pressure liquid nitrogen through convergent-divergent nozzle exhibiting some behavior as water
[NASA-TM-X-67863] 16 p2639 N71-28119

Clean room fire caused by gas heating element thermal failure in liquid nitrogen system
[NASA-TM-X-67250] 17 p2731 N71-29880

Comparison of experimental and analytic film boiling heat transfer data for spherule immersed in liquid nitrogen at standard and reduced gravity
[NASA-TM-X-2344] 20 p3364 N71-33394

Nitrogen cryogenic pumping system design for helium refrigeration
[UCRL-20197] 20 p3247 N71-33708

Weight and cost estimation for pressurization systems for hydrogen, oxygen, and nitrogen storage
[NASA-CR-115204] 24 p3927 N71-38021

LIQUID OXYGEN

Investigation of cryogenic oxygen tank anomaly on Apollo 13 flight
[NASA-TM-X-66642] 01 p0126 N71-10614

Tests of automatic topping of LOX system for Europa P3 vehicle
[TN-DWD-27] 02 p0181 N71-11272

Effect of space vehicle perturbations on liquid oxygen properties
03 p0446 N71-13102

Characteristics of liquid hydrogen and liquid oxygen propellants in Saturn launch vehicles
03 p0446 N71-13105

Polymer materials for sealing liquid oxygen and liquid hydrogen propulsion systems
[NASA-CR-114522] 06 p0887 N71-16377

Tensile and fatigue properties and liquid oxygen compatibility of bilaminate stainless steel-clad titanium prepared by vacuum deposition and explosive welding
[NASA-CR-72841] 19 p3181 N71-21437

- Description of computer program for detailed stratification model of Apollo supercritical oxygen storage tank
[NASA-CR-11493] 10 p1608 N71-21574
- Dye penetrant and technique for nondestructive tests of solid surfaces contacted by liquid oxygen
[NASA-CASE-XMF-02221] 15 p2430 N71-27170
- Analysis of aluminum and nonmetallic baffles for use with liquid oxygen containers to prevent sloshing
[NASA-CR-1880] 21 p3143 N71-34284
- Weight and cost estimation for pressurization systems for hydrogen, oxygen, and nitrogen storage
[NASA-CR-115204] 24 p3927 N71-38021
- Environmental tests of cryogenic propellant effects on metallic positive expulsion bellows operating parameters
[NASA-CR-72979] 24 p3999 N71-38526
- ### LIQUID PHASES
- Tungsten /6/ oxide and molybdenum /6/ oxide reduction reactions with liquid sulfur
[AD-711641] 01 p112 N71-10882
- Flash point method for flammability hazard evaluation during flammable liquid transport
[PB-193077] 03 p468 N71-13225
- Measuring heat and gas release rates for initial reaction of liquid nitrogen tetroxide with hydrazine, monomethyl hydrazine, and unsymmetric dimethyl hydrazine
[NASA-CR-115863] 05 p0761 N71-15379
- Method and feed system for separating and orienting liquid and vapor phases of liquid propellants in zero gravity environment
[NASA-CASE-XLE-01182] 05 p0762 N71-15363
- Sound velocity in iron and iron alloys in solid and liquid state
[LA-TR-70-21] 06 p0907 N71-16756
- Concentration effects on Gibbs free energy and entropy of mixing of binary fluids
[NPL-DCS-6] 07 p1128 N71-17210
- Bibliography on quenching alloy from liquid state
[CALT-822-17] 09 p399 N71-19907
- Column method of counterflow crystallization of alloys in melted state
10 p1573 N71-20868
- Impurity distribution and convection in liquid phase during zone recrystallization of tellurium tetrachloride
10 p1574 N71-20876
- Distribution of lead, copper, and zinc impurities in KCl single crystals grown from melt
10 p1632 N71-20878
- Intensification of crystallization processes in liquid phase using mobile magnetic field
10 p1574 N71-20880
- Effect of intensity and direction of zone mixing of molten metal on refining efficiency of gallium during zone recrystallization
10 p1574 N71-20881
- Vaporization of magnesium impurities from high purity aluminum melt in vacuum apparatus reduces electrical resistance of aluminum
10 p1575 N71-20882
- Directed crystallization of compounds during impurity exchange of liquid phase with crucible and atmosphere
10 p1634 N71-20890
- Equipment for testing of electromagnetic mixing of liquid phase during zone recrystallization
10 p1575 N71-20892
- Austenite formation and dendritic liquefaction of silicon, nickel, copper, and molybdenum in low carbon iron alloys
[NLL-TRANS-746-510-19022.401] 10 p1582 N71-21497
- Hydraulic apparatus for casting and molding of liquid polymers
[NASA-CASE-XNF-07659] 11 p1698 N71-22975
- Copper K α sub alpha X ray scattering intensity measurements from He-4 in liquid and vapor phases with neutron normalizations for momentum transfer and nuclear structure factors
13 p2140 N71-25506
- Mixed liquid and vapor phase analyzer design with thermocouples for relative heat transfer measurement
[NASA-CASE-NPO-10691] 14 p2255 N71-26199
- Thermal conductivity and viscosity measurements in binary liquid mixtures and vapor phases near critical points
[AD-720718] 15 p2395 N71-27709
- Molecular dynamics of coherent function of Lennard-Jones fluids in liquid and gas phases
16 p2641 N71-28023
- Thermophysical properties of alkali metals in liquid and vapor phases based on analysis of experimental and theoretical data from literature
[AD-721947] 16 p2556 N71-28314
- Thermionic diode pressure sensor for liquid, vapor, and two phase potassium flow measurements at high temperatures
[NASA-CR-72886] 16 p2593 N71-28330
- Replacement partition function in theory for homogeneous nucleation of liquid from vapor
[SU-DMS-70-T-34] 17 p2801 N71-30129
- Attenuated total reflection technique for measuring absolute liquid phase vibrational intensities
18 p2965 N71-31164

- Investigation of controlled electromagnetic fields applied to Type-304 stainless steel melts during solidification including grain boundary and metallographic studies
[SU-326-P-29-X-1] 19 p3114 N71-32228
- Nuclear magnetic resonance analysis of molecular motion in liquid and solid ammonia between 1 to 239.8 K
21 p3489 N71-34852
- Gas chromatographic techniques for determination of trace amounts of water and detection limits for gases and liquids
[NLL-M-20374-5828.4F1] 22 p3552 N71-35301
- Structure-property relationships in liquid ceramics heated to temperatures as high as 3000 C
[AD-726401] 22 p3603 N71-35658
- Analytical treatment of two phase flow during infiltration - movement of both air phase and water phase assuming neglect of capillary pressure
23 p3746 N71-36708
- ### LIQUID POTASSIUM
- Corrosion of nickel heat pipes containing liquid potassium
[ORNL-TM-3077] 10 p1572 N71-20865
- Testing nuclear fuel capsule capable of handling large and varying specimen heat fluxes while maintaining constant temperature using sodium and potassium as working fluids
[UCRL-50510] 13 p2112 N71-24517
- Superheating of liquid sodium and potassium, and dependence of boiling point on surface roughness
16 p2690 N71-28396
- Mechanical properties and metallurgical effects of circulating sodium potassium alloy on stainless steel loop
[CONF-710310-1] 24 p3933 N71-38059
- ### LIQUID PROPELLANT ROCKET ENGINES
- NT HYDRAZINE ENGINES
- NT HYDROGEN OXYGEN ENGINES
- NT 3-2 ENGINE
- Liquid propellant rocket engine performance computer program with distributed energy release
[NASA-CR-111000] 01 p0114 N71-10012
- Parametric study of rocket motor combustion instability
[AD-710312] 01 p0115 N71-10123
- Simulating trajectory correction of thermoelectric outer planet spacecraft and design criteria for rocket engine injectors and thrust chambers
01 p0115 N71-10267
- Design of guided ballistic missiles with liquid or solid propellant rocket engines
[AD-711130] 01 p0129 N71-10592
- Manufacturing methods for regeneratively cooled liquid rocket thrust chambers
02 p0289 N71-11631
- Hardware and fluid parameter effects on filling characteristics of manifolds in vacuum, for liquid propellant rocket engines
[AD-712653] 02 p0291 N71-12159
- Dynamic modeling of pressurization system and pneumatic pressure regulator in pressure fed liquid propulsion systems
[NASA-CR-111612] 03 p0448 N71-12281
- Effect of space vehicle perturbations on liquid oxygen properties
03 p0446 N71-13102
- Computer program for determining combustion stability limits of bipropellant rocket engine
[NASA-TN-D-7026] 04 p0605 N71-14038
- Low cost design study for turbopump concepts
[NASA-CR-102923] 04 p0606 N71-14064
- User manual for computer programs to determine high frequency instability in baffled annular liquid propellant rocket engines - Vol. 2
[NASA-CR-115871] 05 p0760 N71-14630
- High frequency nonlinear combustion instability in baffled annular liquid propellant rocket engines - Vol. 1
[NASA-CR-115872] 05 p0760 N71-14631
- Apollo service propulsion system bipropellant valve with cam lifted seals
[NASA-CR-114790] 05 p0692 N71-14931
- Orifice flow and discharge coefficient of liquid propellant rocket engine fuel injectors
[DLR-FB-70-38] 06 p0939 N71-15824
- Measurement of thrust vector loads on liquid propellant rocket engines
06 p0941 N71-16701
- Characteristics of unsteady liquid rocket propellant combustion processes
[NASA-CR-116245] 06 p0941 N71-16716
- Numerical analysis of dynamic characteristics of liquid propellant rocket engines
[AD-716510] 09 p1472 N71-20350
- Computerized stability design of time lag combustion system for liquid propellant rocket engine
[NASA-CR-120096] 09 p1460 N71-20415
- Computer programs for determining combustion stability of liquid propellant rocket engines
09 p1460 N71-20416
- Time lag theory for longitudinal high frequency stability analysis on staged combustion cycle of liquid propellant rocket engine
09 p1484 N71-20418

- Combustion instability in liquid rocket engines
[NASA-CR-72848] 10 p1662 N71-21316
- Dynamic pressure feedback compensation of resonance in liquid rocket thrust vector control system
[NAL-TR-213] 11 p1620 N71-22440
- Vacuum chamber tests on slits and liquid propellant of colloid rocket engine for propulsion system performance
[ESRO-CR-22] 12 p1989 N71-23707
- Analysis of transient loads produced by ignition of rocket engine during launch and flight operations for solid and liquid propellant rocket engines
[NASA-SP-8030] 12 p2008 N71-24401
- Simulation of water injection in liquid propellant rocket engines, noting injector arrangement
[DLR-MITT-70-24] 13 p2155 N71-24677
- Investigation of theory and calculations of dynamic processes and variable parameters occurring within liquid propellant rocket engines
[AD-719774] 13 p2156 N71-24937
- Hot firing tests with FLOX/methane propellants for evaluating pyrolytic refractory composite materials for thrust chambers
[NASA-CR-118321] 13 p2101 N71-24974
- Development and characteristics of materials for liquid propellant rocket engines, warheads, propellant tanks, solid rocket propellants, combustion chambers, and exhaust nozzles
[AD-720586] 14 p2344 N71-26099
- Analysis of structural failure of liquid propellant rocket engines due to gaseous hot spots within the propellant residues formed during pulse mode operation
14 p2355 N71-26319
- Bearing requirements for liquid rocket engine turbopumps
[NASA-SP-8048] 16 p2599 N71-28011
- Liquid propellant rocket engine throttling injector design based on exhaust gas counter flow and heat transfer for inflowing propellant vaporization and combustion stability tests
[NASA-CR-119796] 16 p2671 N71-28158
- Liquid propellant rocket engine conference proceedings and parameters for design of rocket engines and systems
[NASA-SP-125] 17 p2833 N71-29405
- Design, characteristics, and performance parameters of liquid propellant rocket engines
17 p2833 N71-29406
- Analysis of major rocket design parameters for liquid propellant rocket engines
17 p2833 N71-29407
- Analysis of techniques used by industry for design of liquid propellant rocket engines and components
17 p2833 N71-29408
- Design parameters, characteristics, and numerical analysis of thrust chambers for liquid propellant rocket engines
17 p2833 N71-29409
- Design parameters and characteristics of pressurized gas propellant feed system for liquid propellant rocket engines
17 p2829 N71-29410
- Design parameters and characteristics of valves used in liquid propellant rocket engine fuel systems
17 p2833 N71-29411
- Design parameters and characteristics of interconnecting components and mounts for liquid propellant fuel systems
17 p2830 N71-29414
- Integration of design parameters and requirements for development of liquid rocket propellant engines, systems, and subsystems
17 p2833 N71-29415
- Design and fabrication of noncircular orifice tubes for liquid rocket engine injectors
[BC-71-19] 17 p2838 N71-29416
- Analysis of mechanisms of energy addition from propellant spray combustion to steady flow fields and propagating pressure disturbances
[AD-722473] 17 p2858 N71-29419
- Development and characteristics of rocket throttling system of bipropellant liquid propellant rocket engine
[NASA-CASE-LEW-10374-1] 18 p3001 N71-31118
- Structural damping in Saturn vehicles and scale models of liquid propelled rocket vehicles
[NASA-TM-X-44607] 18 p3018 N71-31145
- Analytical technique for solving nonlinear combustion problems associated with liquid propellant rocket engines
[NASA-CR-72902] 21 p3501 N71-34940
- Design criteria for liquid rocket engine turbopump inducers
[NASA-SP-8052] 21 p3502 N71-34940
- Abative response of silica phenolic to simulated liquid propellant rocket engine operating conditions
[NASA-CR-72701] 23 p3776 N71-34940
- European liquid propellant rocket engine technologies
23 p3840 N71-37188
- Effects of exhaust deposits from 22.5 mm thrust, bipropellant, attitude control engine on transmission in 0.2 to 0.6 and 0.32 to 2.2 micron ranges
[NASA-TM-X-2399] 23 p3858 N71-37188

SUBJECT INDEX

Operation of liquid propellant rocket engines under
unsteady conditions and derivation of formulae for
determination of combustion delay
[AD-727999] 24 p0001 N71-38540

Mathematical solution of nonlinear transverse com-
bustion instability problems in this annular liquid
propellant rocket chambers
[NASA-CR-128781] 24 p0029 N71-38746

LIQUID ROCKET PROPELLANTS
NT AEROZINE
NT CRYOGENIC ROCKET PROPELLANTS
NT GELLED ROCKET PROPELLANTS
NT HYPERGOLIC ROCKET PROPELLANTS
NT MONOPROPELLANTS
NT SLURRY PROPELLANTS

Comprehensive analysis of liquid rocket com-
bustion
[AD-710634] 01 p0133 N71-10437
Design criteria for high performance conical injec-
tor using gas-liquid space storable propellants
[NASA-CR-72706] 01 p0113 N71-10452

Results of bipropellant valve program with applica-
tion to earth storable propellants
[NASA-CR-111407] 02 p0290 N71-11885
Dynamic interaction between structure and liquid
propellants in space shuttle vehicle models
[NASA-CR-111801] 03 p0363 N71-12766

Theory and calculation of thermal rocket engines in-
cluding liquid and solid fuels, specific impulse, com-
bustion products, and related subjects
[AD-713034] 03 p0449 N71-13072
Calculation of bubble rise velocities in multibubble
systems under reduced gravity conditions
[AD-713034] 03 p0446 N71-13103

Shock wave amplification in liquid fueled booster
rocket engines
[AD-713034] 03 p0446 N71-13106
Development and characteristics of positive expul-
sion systems for liquid rocket propellant tanks
[AD-713034] 03 p0447 N71-13115

Analysis of liquid flow regimes occurring during
propellant settling
[AD-713034] 03 p0447 N71-13118
Surface tension and dielectrophoresis techniques
for liquid rocket propellant control
[AD-713034] 03 p0447 N71-13119

Fabrication and thermal performance of regenera-
tively cooled hydrogen hydrogen thrust chamber
[NASA-CR-72742] 04 p0608 N71-14135
Development and characterization of elastomeric
materials for positive expulsion bladders
[NASA-CR-115902] 05 p0640 N71-14986

Method and feed system for separating and orient-
ing liquid and vapor phases of liquid propellants in
zero gravity environment
[NASA-CASE-XLE-0112] 05 p0762 N71-15635
Investigating component storage stability and
material compatibility with liquid propellants
[AD-713034] 06 p0938 N71-16689

Characteristics of unsteady liquid rocket propellant
combustion processes
[NASA-CR-116245] 06 p0941 N71-16716
Scanning electron microscope study of hydrazine
liquid rocket propellant catalysts
[AD-713034] 07 p1097 N71-17194

Development of liquid propellant rocket abort fire
model
[BC-RR-70-454] 07 p1098 N71-17229
Investigating tandem row high head pump inducers
for liquid fueled rocket engines
[NASA-CR-116245] 07 p1094 N71-17364

Control valve and coaxial variable injector for con-
trolling bipropellant mixture ratio and flow
[NASA-CASE-XNP-07702] 07 p1036 N71-17454
Shock and swirl alleviator for liquid propellant tanks
during transport and flight
[NASA-CASE-XLA-05749] 09 p1392 N71-19569

Dynamics of rocket operation on solid and liquid
propellants
[AD-717020] 11 p1831 N71-22532
Stress-strain fatigue behavior of Teflon liquid
propellant expulsion bladder material
[AD-717020] 11 p1784 N71-22559

Filter valve design for supplying liquid propellants
at high pressure to space vehicles
[NASA-CASE-XNP-01747] 11 p1773 N71-23024
Radioisotope fuel gage for spacecraft liquid propel-
lants
[BB-22157-1] 13 p2078 N71-24404

Deformation of drops in reactive zone during
incomplete detonation of fuel mixtures consisting
of liquid drops of fuel and gaseous oxidizer
[NASA-TT-F-13579] 13 p2185 N71-24933
Mixing fluids in confined cylindrical geometry
stable to rocket configuration with simulated bulk
failure mode
[AD-717020] 14 p2240 N71-26219

Electronic recording system for spatial mass dis-
tribution of liquid rocket propellant droplets or vapors
ejected from high velocity nozzles
[NASA-CASE-MPO-10185] 14 p2233 N71-26339
Opt segmented rocket engine injectors using high
energy gas
[NASA-CR-72703] 14 p2333 N71-26689

Flexible barrier membrane comprising porous sub-
strate and incorporating liquid gallium or indium metal
used as sealant barriers for spacecraft walls and pump-
ing liquid propellants
[NASA-CASE-XNP-08881] 16 p2612 N71-28747

Effects of radiation on stability and compatibility of
hydrazine and hydrazine-24 percent hydrazine nitrate
in stainless steel and titanium alloy containers with O
ring seals
[NASA-CR-109767-PT-2] 16 p2670 N71-29088

Response analyzing apparatus for liquid vapor inter-
face sensor of sloshing rocket propellant
[NASA-CASE-MFS-11204] 16 p2599 N71-29134
Design parameters and characteristics of turbopump
propellant feed systems
[AD-718091] 17 p2829 N71-29411

Design parameters and configurations of propellant
storage tanks for liquid propellant systems
[AD-718091] 17 p2829 N71-29413
Design parameters and characteristics of liquid
propellant space engines
[AD-718091] 17 p2833 N71-29416

Configuration and performance of rocket propul-
sion system utilizing liquid propellants
[AD-718091] 17 p2834 N71-29570
Rocket propellant survey with heat combustion,
heating capacity, and specific thrust compared for
wide range of fuels and oxidizers
[AD-722591] 17 p2832 N71-29730

Mathematical models of rocket combustion in-
stabilities in liquid propellant rocket engines
[NASA-CR-119182] 17 p2860 N71-30348
Rocket engine bipropellant valve improvement for
Apollo service propulsion system
[NASA-CR-108577] 17 p2758 N71-30397

High speed photographic techniques to study
impinging streams of propellants in experimental in-
vestigation of reactive stream separation
[NASA-CR-119246] 18 p2923 N71-30844
Development and characteristics of rocket throttling
system of bipropellant liquid propellant rocket engine
[NASA-CASE-LEW-10374-1] 18 p3001 N71-31103

Clogging tests on liquid diborane and liquid oxygen
diffusion propellants in orifice flows
[NASA-CR-121282] 19 p3172 N71-32475
Chemical and metallurgical analyses of 6Al-4V
titanium test specimens exposed to hydrazine/N2O2/
liquid propellant
[NASA-CR-121456] 20 p3284 N71-33234

Techniques for fabricating electroformed injectors
for high energy space storable liquid propellants
[NASA-CR-121454] 20 p3359 N71-33484
Apollo service propulsion system rocket engine
bipropellant valve improvement program - valve
design guide and oxygen-hydrogen technology
[NASA-CR-108578] 21 p3502 N71-34946

Analysis of propellant sloshing in lunar module dur-
ing Apollo 14 flight and resultant erroneous indication
of low level of propellant
[NASA-TM-X-2362] 24 p3906 N71-37841
Safety and hazards analysis of parallel versus series
loading of space shuttle using liquid hydrogen and
liquid oxygen propellants - technical discussion
[NASA-CR-123172] 24 p4021 N71-38689

LIQUID ROTATION
U ROTATING LIQUIDS
LIQUID SLOSHING

Studies of propellant sloshing under low gravity
conditions
[NASA-CR-102891] 01 p0041 N71-10520
Lateral liquid sloshing in axisymmetric tank under
low gravity conditions
[AD-713034] 01 p0041 N71-10521

Comparison of flexible and rigid ring baffles for
slosh suppression
[AD-713034] 01 p0041 N71-10522
Experimental and theoretical studies of liquid slosh-
ing at simulated low gravity
[AD-713034] 01 p0041 N71-10523

Simulated low gravity sloshing in cylindrical tanks
including effects of damping and small liquid depth
[AD-713034] 01 p0041 N71-10524
Theory for low gravity fuel sloshing in arbitrary ax-
isymmetric rigid tank
[AD-713034] 01 p0041 N71-10525

Capillary containment system designs for low grav-
ity propellant control in cryogenic vehicles
[NASA-CR-102890] 01 p0116 N71-10653
Liquid propellant dynamic problems in space shuttle
vehicles
[NASA-CR-111802] 03 p0362 N71-12767

Liquid oscillation frequency measurement in
inclined right circular cylinder
[NASA-TM-X-64540] 03 p0362 N71-13006
Shock wave amplification in liquid fueled booster
rocket engines
[AD-713034] 03 p0446 N71-13106

Digital analysis of liquid sloshing in rotational sym-
metric tanks under weak gravitational fields - Vol. 2
[NASA-CR-111739] 04 p0604 N71-14226
Flexible ring slosh damping baffle for spacecraft
fuel tank
[NASA-CASE-LAR-10317-1] 06 p0954 N71-16103

Submerged fuel tank baffles to prevent sloshing in
liquid propellant rocket flight
[NASA-CASE-XLA-04605] 06 p0954 N71-16106
Hot-wire liquid level detector for cryogenic propel-
lants
[NASA-CASE-XLE-00454] 07 p1068 N71-17802

Slosh and swirl alleviator for liquid propellant tanks
during transport and flight
[NASA-CASE-XLA-05749] 09 p1392 N71-19569
Natural lateral sloshing frequency of liquids in
oblate spheroidal tanks in reduced- and normal- grav-
ity conditions
[NASA-TN-D-6230] 11 p1734 N71-22824

Tests of jet engine fuels to determine effects of
sloshing and vibration in aircraft fuel tanks on flammab-
ility hazards
[AD-718091] 12 p1989 N71-23805
Pressure sensor network for measuring liquid
dynamic response in flight including fuel tank ac-
celeration, liquid shock amplitude, and fuel depth
monitoring
[NASA-CASE-XLA-05541] 14 p2342 N71-26187

Comparison of finite element and finite difference
methods for simple sloshing problem
[TR-1] 17 p2774 N71-30187
Liquid propellant sloshing in tilted axisymmetric
cylindrical tanks for space shuttle applications
[NASA-CR-119091] 20 p3337 N71-32896

Analysis of aluminum and nonmetallic baffles for
use with liquid oxygen containers to prevent sloshing
[NASA-CR-18080] 21 p3413 N71-34284
Analysis of propellant sloshing in lunar module dur-
ing Apollo 14 flight and resultant erroneous indication
of low level of propellant
[NASA-TM-X-2362] 24 p3906 N71-37841

Measurement of liquid oscillation frequencies in
tilted cylindrical tanks of five different cross section
shapes
[NASA-TM-X-64618] 24 p4023 N71-38707
LIQUID SODIUM

Droplet effect in liquid sodium corrosion of
stainless steels
[ANL-TRANS-839] 01 p0684 N71-10834
Leak detection systems development for sodium
heated LMFBR steam generators
[AFDA-255] 03 p0414 N71-12823

Oxygen meter performance in high purity and car-
bon contaminated sodium, for LMFBR program
[MSAR-70-56] 04 p0557 N71-14119
Analysis of sodium-water reactions and related
technology in liquid sodium systems
[AFDA-262] 04 p0561 N71-14407

Oxygen activity in liquid sodium
[KFK-1149] 04 p0332 N71-14457
Dissolved argon gas effects on cavitation in liquid
sodium
[AD-713851] 06 p0366 N71-16453

Leak detection method for water and sodium
systems applied to boilers of liquid sodium-cooled fast
reactors
[ANL-TRANS-857] 06 p0901 N71-16775
Design and performance of sodium tank test facility
[EURPFR-819] 06 p1174 N71-18275

Sodium lubricated bearing technology for high
capacity pumps used in fast breeder reactors
[IVO-3930-5] 06 p1203 N71-18328
Mathematical models for mass transfer and monitor
system in liquid sodium technology
[GEAP-13539-13] 10 p1583 N71-21719

Servicing and testing of liquid sodium piping in
LMFBR
[SAN-781-243] 12 p1963 N71-23947
Evacuable glove-box for handling of liquid sodium
and apparatus for analysis of carbon in sodium and
other metals
[AERE-R-4338] 13 p2110 N71-24432

Testing nuclear fuel capsule capable of handling
large and varying specimen heat fluxes while main-
taining constant temperature using sodium and potassium
as working fluids
[UCRL-50510] 13 p2112 N71-24517
Design and development of canned-motor pump for
high temperature NaK service in SNAP-8
[NASA-CR-72823] 13 p2116 N71-24634

Solubility of inert gases in liquid sodium and related
safety problems for primary circuit of fast sodium
cooled breeder reactor
[EURPFR-785] 13 p2117 N71-24699
Liquid sodium Banjo loop for irradiation of fuel pins
[CEA-CONF-1673] 13 p2121 N71-25233

Sorption of cesium by graphite and charcoal reduc-
ing volatility of cesium and rendering it fully stable in
sodium at 300 C and in air at same temperature
[AERE-R-4481] 15 p2492 N71-27932
Superheating of liquid sodium and potassium, and
dependence of boiling point on surface roughness
[AD-713034] 16 p2690 N71-28396

Sloshing and wear behavior of steel and alloys in
liquid sodium
[KFK-1251] 16 p2610 N71-28449
Fission gas disengagement from flowing sodium and
transport phenomena for FFTF fuel failure detection
[ANL-7774] 17 p2782 N71-29509

- Chemical reaction between polytetrafluoroethylene chips, liquid sodium, potassium, and sodium potassium alloy
[TRG-2104] 19 p3120 N71-32045
- Holographic scanning for acoustic imaging in liquid sodium
[BNWL-1558] 20 p3223 N71-33486
- Design, optimization, and test instrumentation for sodium-lubricated bearings in sodium pumps and circulating auxiliaries in breeder reactors
[NVO-3930-10] 21 p3461 N71-34636
- Molten sodium container design code and safety procedures
[RD-B-M-1817] 22 p3620 N71-35790
- Temperature and oxygen percentage effects on liquid sodium combustion and X ray analysis of combustion products
[NLL-RISLEY-TRANS-2115-[9091.9F]] 23 p3868 N71-37574
- Mechanical properties and metallurgical effects of circulating sodium potassium alloy on stainless steel loop
[CONF-71010-1] 24 p3933 N71-38059
- LIQUID SURFACES**
- Boundary value problems and resonant vibrations of liquid surfaces in tanks with pressure chambers
[NPL-MA-49] 06 p0833 N71-15787
- Turbulent temperature distribution in horizontal liquid layer heated from below
08 p1305 N71-19049
- Surface tension of liquid surface
08 p1245 N71-19166
- Surface active agent effects on hydrodynamics and mass transfer of gas or liquid to liquid systems
[NLL-RTS-6328] 12 p1873 N71-24291
- Relationship between albedo of water surface of small lakes and chrominance and transparency of water mass
[NLL-M-9264-[5828.4F]] 16 p2591 N71-29175
- LIQUID-GAS MIXTURES**
- NT AEROSOLS**
- NT FOG**
- Application of equations of conservation to two phase liquid-gas systems
[PB-193987T] 05 p0663 N71-14907
- Liquid-gaseous centrifugal separator for weightlessness environment
[NASA-CASE-XLA-00415] 06 p0865 N71-16079
- Hypersonic two phase flow realized by air-water mixtures
[BMVTDG-FBWT-70-1] 08 p1140 N71-18441
- Two phase detonation waves in liquid gas systems
[NASA-CR-72866] 11 p1841 N71-22509
- Vapor-liquid separator design with vapor driven pump for separated liquid pumping for application in propellant transfer
[NASA-CASE-XMF-04042] 11 p1772 N71-23023
- Solubility of NH₃, CO, CO₂, and SF₆ in various gas-liquid binary systems at different pressures and temperatures
[AD-718959] 13 p2039 N71-24449
- Separation and containment of liquid-gas mixture in closed cyclone separator
[AD-718992] 13 p2063 N71-24476
- Sound propagation characteristics in gas media with droplets or particles based on linearized hydrodynamic equations
[NASA-TT-F-13581] 13 p2064 N71-24619
- Heavy gas-liquid mixture bubble chamber with 70 liter volume and hydrogen internal target for use with electro-synchrotron gamma beams
[LNF-70/25] 24 p3920 N71-37951
- LIQUID-LIQUID INTERFACES**
- Interfacial tension in binary liquid system as function of temperature
11 p1739 N71-22584
- Turbulent liquid-liquid dispersions in stirred containers
16 p2690 N71-28213
- Qualitative hydrodynamic model of dynamic angle hysteresis for fluid-liquid interface being driven through capillary tube by applied pressure gradient
[AD-726635] 22 p3570 N71-35424
- Interfacial tension pressure change measurements of mass transfer effects on droplet interface motions
23 p3780 N71-36941
- LIQUID-SOLID INTERFACES**
- Lateral growth kinetics of solid-solid and liquid-solid interfaces during phase transformations
[IS-T-357] 01 p0096 N71-10482
- Low gravity effects on liquid phase sintering in space manufacture
02 p0235 N71-11729
- Thermodynamic significance of interface potential increase during crystal growth from solution
[REPT-4164] 05 p0756 N71-14582
- Eigenvalues, eigenfunctions, and series coefficients for calculating Nusselt numbers of turbulent liquid/metal heat transfer in concentric annuli
[BNL-50183] 05 p0782 N71-15028
- Explosive vapor formation by reaction kinetics between high temperature materials and cooler liquids
[ORO-3936-1] 05 p0782 N71-15169
- Process for forming heterojunctions by gold solvent alloying
[AD-713307] 08 p1277 N71-18379
- Models for heat transfer during spin melting within single fibers and from single fiber to surrounding fluid
10 p1660 N71-20755
- Effects of velocity and acceleration on wetting properties of dynamic three-phase system using glycerol-water mixtures
11 p1743 N71-23005
- Generation of ultrasonic surface waves during beam reflection from liquid-solid interfaces
[AD-719937] 13 p2126 N71-25175
- Mechanisms and kinetics of reactions on interfaces of substances
14 p2215 N71-26462
- High pressure formation of solid-liquid phase line in copper
14 p2328 N71-26501
- Graphite thermodynamic properties and liquid-solid phase diagrams in high temperature environments for nuclear rocket engine reactor core design
15 p2448 N71-27367
- Forced flow heat transfer coefficients for laminar film boiling interface on vertical surface
[NASA-TM-X-67860] 15 p2525 N71-27867
- Reflection and refraction of magnetohydrodynamic waves at liquid-solid interface, with earth core and mantle applications
15 p2406 N71-27948
- Liquid or solid spheres levitated in film boiling following metastable Leidenfrost states
[NASA-TM-X-67897] 20 p3313 N71-33697
- Additive effects on boundary lubricant-metal surface interactions during friction process
[AD-727885] 24 p3929 N71-38037
- Liquid-solid interfacial phenomena in sodium cooled fast nuclear reactors
[RD/B/N-1721] 24 p3956 N71-38222
- LIQUID-VAPOR EQUILIBRIUM**
- Evaporation from spherical liquid drop into vacuum or into pure vapor under strong nonequilibrium conditions
10 p1543 N71-21336
- Total analysis of processes influencing sound propagation and speed in two-phase media based on thermodynamics of irreversible processes
[NASA-TT-F-13582] 13 p2064 N71-24598
- Thermodynamic consistency test for statistical treatment of random experimental error in liquid-vapor equilibrium data
[IS-T-428] 15 p2524 N71-27092
- Experimental determination of data on liquid-vapor equilibrium systems
[NLL-RTS-5768] 17 p2713 N71-29218
- LIQUID-VAPOR INTERFACES**
- Film boiling on vertical surfaces in turbulent regime using cryogenic fluids
[NASA-CR-110997] 01 p0132 N71-10064
- Low gravity propellant control using capillary devices in large scale cryogenic vehicles
[NASA-CR-102901] 01 p0116 N71-10602
- Using simple nomograms to calculate turbulent heat exchange and heat loss in sea-air interactions
[AD-711916] 02 p0252 N71-11133
- Long term variability of tropical heat budget of Pacific Ocean and effects on atmospheric circulation
[AD-711308] 02 p0252 N71-11140
- Investigating liquid-vapor interface for wetting liquid in toroidal tank during weightlessness
[NASA-TN-D-6076] 02 p0203 N71-11550
- Oceanographic research on sea floor mineral resources, water temperature variations, sound velocity distribution, and primary production in Pacific Ocean
02 p0221 N71-12155
- Analysis of factors affecting fuel tank pressurization
03 p0447 N71-13112
- Measurement of air temperature and wind velocity from one to eighty centimeters above sea surface
[AD-706056] 03 p0404 N71-13336
- Describing apparatus for separating gas from cryogenic liquid under zero gravity and for venting gas from fuel tank
[NASA-CASE-XLE-00586] 06 p0864 N71-15968
- Helmholtz integral and Kirchhoff approximation for sound transmission through rough air-sea interface
[AD-715566] 08 p1243 N71-18771
- Presenting empirical data on flooding in stratified gas-liquid flow in vertical tubes and horizontal rectangular ducts
[REPT-27327-9] 08 p1181 N71-18845
- Clarifying elution mechanisms in gas-liquid chromatography by study of solute adsorption on liquid-coated adsorbents
11 p1695 N71-21856
- Thermodynamic temperature drop at liquid-vapor interface in high temperature lithium heat pipes
[NASA-TM-X-2268] 12 p1902 N71-23923
- Droplet evaporation in liquid-vapor critical region
[AD-718968] 13 p2184 N71-24363
- Liquid-vapor interface seal design for turbine rotating shafts including helical and molecular pumps and liquid coolers of mercury vapor
[NASA-CASE-XNP-2862-1] 14 p2263 N71-26294
- Response analyzing apparatus for liquid vapor interface sensor of sloshing rocket propellant
[NASA-CASE-MFS-11204] 16 p2599 N71-29134
- Interface stability during liquid inflow to partially full, hemispherical ended cylinders during weightlessness
[NASA-TM-X-2348] 19 p3083 N71-32776
- Analysis of liquid-vapor interface conditions in conical tanks in weightlessness environment
[NASA-TM-X-2400] 22 p3568 N71-35416
- Thermodynamics of liquid-vapor system with application to various adiabatic and nonadiabatic one dimensional flows
[AD-726574] 22 p3569 N71-35419
- LIQUIDS**
- NT AEROSOL**
- NT CRYOGENIC FLUIDS**
- NT CRYOGENIC ROCKET PROPELLANTS**
- NT FERMIL LIQUIDS**
- NT FLOX**
- NT GELLED ROCKET PROPELLANTS**
- NT HYDRAULIC FLUIDS**
- NT HYPERGOLIC ROCKET PROPELLANTS**
- NT LIQUEFIED GASES**
- NT LIQUID AMMONIA**
- NT LIQUID HELIUM**
- NT LIQUID HYDROGEN**
- NT LIQUID METALS**
- NT LIQUID NITROGEN**
- NT LIQUID OXIDIZERS**
- NT LIQUID OXYGEN**
- NT LIQUID POTASSIUM**
- NT LIQUID ROCKET PROPELLANTS**
- NT LIQUID SODIUM**
- NT MERCURY [METAL]**
- NT MERCURY VAPOR**
- NT MONOPROPELLANTS**
- NT ORGANIC LIQUIDS**
- NT ROTATING LIQUIDS**
- NT SLURRY PROPELLANTS**
- Radiation induced acoustic cavitation in scintillation liquid
[AD-711286] 01 p0092 N71-10911
- Gas control in liquefied materials during weightless manufacturing in orbital workshop
02 p0203 N71-11721
- Dynamic behavior of liquids in elastic tanks
[LMSC-60-80-70-23] 06 p0838 N71-16520
- Pressure equalizing closure for reactor fuel elements with liquid seal and porous bodies
[KFK-1163] 07 p1061 N71-17214
- Sound transmission through liquids and fundamental liquid state research
[AD-715105] 07 p1069 N71-17845
- Field standard measuring flask specifications and terminations
[NBS-HANDBOOK-105-2] 09 p1392 N71-19444
- Electrical switching device comprising conductive liquid confined within square loop of deformable non-conductive tubing also used for leveling
[NASA-CASE-NPO-10037] 09 p1358 N71-19610
- Construction and performance of liquid neutron scintillation counter with two phototubes
[PURC-4159-13] 10 p1558 N71-21018
- Perturbation theory of simple liquids and its comparison to computer results
02 p0252 N71-11140
- [LPTHE-71/5] 10 p1543 N71-21315
- Microscopic theory of quasi-particle spin fluctuations in low temperature, dense Fermi liquids
10 p1618 N71-21440
- Ultrasonic wave production of optical anisotropy in liquids
11 p1796 N71-21883
- Refractive index measurements on pressurized liquids and gases by optical interferometry
14 p2297 N71-26401
- Dielectric property measurements for pressure induced phase transformations in solid and liquid insulators
14 p2328 N71-26400
- Thermodynamic and dynamic properties for calculating liquid structures
15 p2413 N71-28831
- Purification apparatus for vaporization and fractional distillation of liquids
[NASA-CASE-XNP-08124] 15 p2416 N71-27314
- Quantitative liquid measurements in container by resonant frequencies
[NASA-CASE-XNP-02500] 15 p2431 N71-27207
- Low leakage shaft seal for use with various types of liquids
[NASA-CASE-LEW-10326-2] 16 p2602 N71-28079
- Time of flight and crystal spectrometers for neutron scatter measurements on liquids
16 p2595 N71-28701
- Dynamic response of liquid lines of finite length for periodic and nonperiodic inputs
17 p2736 N71-28911
- Counter-current continuous gas chromatography distillation of nitrogen/liquid system
[NLL-RTS-63253] 17 p2716 N71-29011

SUBJECT INDEX

LITHIUM COOLED REACTOR EXPERIMENT

- Reformulation of theory on homogeneous nucleation of liquid from vapor (SU-DMS-70-T-56) 17 p2809 N71-30370
- Shock propagation model for low velocity detonation in liquid propellants, fuels, and explosives (AD-72677) 19 p3172 N71-32073
- Two mixing models for estimating micromixing rates in liquid systems, and method for measuring initial rate of acid feed stream in basic reactor fluid 19 p3086 N71-32518
- Experimental and theoretical analysis of breakup of liquid sheets and jets in supersonic gas stream 19 p3082 N71-32618
- Computational approach for measuring and evaluating heat effects in liquid chemical samples with elevated temperature differential scanning calorimetry 21 p3389 N71-34110
- Theoretical phonon research in crystals and liquids (NYO-3699-53) 21 p3474 N71-34739
- Equations derived for liquid motion in cylindrical tank with elastic bottom and subject to longitudinal excitation of sinusoidal form 22 p3693 N71-36339
- Stable surface treatments for 301 stainless steel, copper, and aluminum alloy contact with liquids (NASA-CR-72975) 23 p3775 N71-36908
- Ionization in dielectric liquids produced by gamma radiation and ionization inhibition by electron scavengers (NP-18875) 24 p3973 N71-38348
- LITERATURE**
- Updated list of space flight acronyms and abbreviations (NASA-TM-X-67197) 14 p2361 N71-26535
- List processing subroutines for IBM 1800/1130 information storage and retrieval system (NASA-TM-X-45622) 18 p2893 N71-30611
- Contamination control checklists for manufacturing or assembly plants (NASA-CR-121740) 21 p3432 N71-34418
- LITERATURE**
- NT DOCUMENTATION**
- NT PROCEEDINGS**
- Library of management sciences literature (NASA-TM-X-66546) 05 p0787 N71-15199
- Library analysis including information aging and bibliography of books and periodical publications pertinent to chemistry 19 p3194 N71-31979
- LITHOLOGIC PROPELLANTS**
- U HYBRID PROPELLANTS**
- LITHIUM**
- NT LITHIUM ISOTOPES**
- Fabrication and testing of organic electrolyte cells with long shelf life (AD-711114) 01 p0007 N71-10517
- Visual observation of high temperature profiles during startup in lithium heat pipe (NASA-TM-X-52924) 01 p0134 N71-10994
- Radiation resistance tests of lithium doped solar cells (RAE-TN-69044) 02 p0148 N71-11047
- Recovery characteristics of electron irradiated, lithium doped, solar cells (NASA-CR-111579) 03 p0316 N71-12256
- Lithium diffused radiation resistant solar cells (NASA-CR-111581) 03 p0316 N71-12257
- KCl single crystals doped with Li measured by dielectric cryogenic thermometers (NYO-2471-46) 03 p0381 N71-13217
- Polarization of lithium nuclei from atomic beam furnace using high frequency transitions and polarization measurement using nuclear reaction 03 p0436 N71-13279
- Direct p,n reaction in Li-7 (SDP-TN-68-4) 06 p0911 N71-15794
- Development of lithium diffused radiation resistant solar cells (NASA-CR-116219) 06 p0798 N71-16563
- Hydraulic performance and cavitation characteristics of electromagnetic helical induction pump operating with potassium at 1500 F and with lithium at 230 F (ORNL-TM-2993) 06 p1205 N71-18324
- Lithium doped silicon solar cells for improved radiation resistance to neutrons, protons, and electrons (NASA-CR-116793) 06 p1146 N71-18511
- Electrical conductivity and elastic moduli of pressure-treated lithium substituted nickel oxide alloys 06 p1216 N71-19002
- Phosphorus, boron, and lithium ion implantation for doping charged particle detectors (ISA-CONF-1642) 09 p1439 N71-20198
- Description and operation of experimental plasma facility (Helios) in which electrons and lithium ions are heated by electromagnetic noise (ORO-3095-15) 10 p1626 N71-20669
- Solid state X ray/alpha coincidence counter for measuring radioactive decay on transuranic elements (BWL-SA-1514) 10 p1556 N71-20738
- Fusion reactors at 200 kG and ion temperature of 400 MeV with lithium and deuterium as primordial fuel (ORNL-TM-3207) 10 p1613 N71-20837

- Impurity behavior during refinement of tin and lithium by zone melting 10 p1573 N71-20870
- Metallurgical and ductility effects of lithium on tungsten-titanium alloy clad uranium mononitride cylinders after long term exposure (NASA-TM-X-52998) 10 p1602 N71-20948
- Computer analysis of semiconductor GeLi gamma ray spectra, comparison of threshold detectors, Bonner spheres, and recoil spectroscopy with emulsions, and Fredholm equation solutions 10 p1559 N71-21148
- Resonant structure of lithium between 2 triplet S and 2 singlet P thresholds (AD-716832) 10 p1617 N71-21374
- Crystalline structure defects of diamonds caused by lithium ion injection 11 p1816 N71-22183
- Lithium donor density gradient measurements for prediction of lithium cell behavior after electron irradiation and recoverability (NASA-CR-118005) 12 p1839 N71-23441
- Thermodynamic temperature drop at liquid-vapor interface in high temperature lithium heat pipes (NASA-TM-X-2268) 12 p1902 N71-23923
- Radiation resistance and lithium concentrations of lithium doped solar cells with varying lithium diffusion times and temperatures (NASA-CR-118317) 13 p2030 N71-24963
- Lithium/chalcogen cells applied to secondary batteries for vehicular propulsion (ANL-7756) 14 p2199 N71-25651
- Lithium-doping effects on silicon responses to irradiation for solar cells - conference (NASA-CR-118627) 14 p2200 N71-26226
- Dependence on lithium of introduction and annealing of neutron and electron produced damage in lithium-diffused bulk silicon 14 p2201 N71-26232
- Neutron cross sections and angular distributions for Li-7,d,n/Bi-S reactions including neutron spectra indications of atomic energy levels (JINR-P15-5143) 14 p2313 N71-26710
- Lithium, beryllium, and boron particle production by spallation and isotopic spin classification of scattering cross sections (NP-18591) 15 p2456 N71-26846
- Fabrication and utilization of lithium-drifted silicon detectors (LYCEN-4847) 15 p2408 N71-27300
- Photonuclear energy and angular distribution spectra from lithium 6 and lithium 7 states 15 p2479 N71-27656
- Collisional excitation rates for lithium-like ions derived from diagnosed plasma produced in theta pinch device and line intensities emitted by these ions (NASA-CR-119017) 16 p2648 N71-28636
- Collisional ionization rates for lithium and beryllium-like ions deduced from time history of spectral lines emitted by these ions in hot plasmas (NASA-CR-119018) 16 p2648 N71-28637
- Space power unit fast reactor design with ceramic UO₂ fuel elements, lithium coolant, and titanium alloy structure (NASA-TM-X-67859) 16 p2636 N71-28905
- Analysis of interaction between lithium and residual donor in indium antimonide 19 p3117 N71-32548
- Interaction between acoustic phonons and tunneling defect states in KCl-Li using resonant pumping of tunneling states with microwaves and scattering of heat pulses (NYO-2391-111) 19 p3162 N71-32743
- Measurement of lithium concentration at back surface and near p-n junction of lithium solar cells (NASA-CR-121677) 21 p3379 N71-34045
- Classical trajectory study of rotationally inelastic scattering of hydrogen molecules by collisions with lithium ions (NASA-CR-121729) 21 p3386 N71-34067
- Effect of oxygen, heat treatment, and test temperature on compatibility of advanced refractory alloys with lithium (ORNL-4430) 21 p3440 N71-34479
- K line emission spectrum of lithium for energies above and below Sommerfeld threshold determined using many body diagrammatic techniques 21 p3442 N71-34491
- Electron affinity calculations for Li, B, O, F, C, and N and self consistent field equations for multiple open shells 21 p3492 N71-34878
- Lithium doped solar cell hardness to 1 MeV electron irradiation (NASA-CR-122942) 23 p3709 N71-36442
- Effects of radiation on efficiency of lithium doped solar cells in electrical space power system (NASA-CR-122943) 23 p3709 N71-36443
- Research on inorganic compounds for use as positive electrodes in rechargeable lithium battery (AD-726607) 23 p3710 N71-36447
- Techniques for estimating various pressure drops for conducting fluid flows in magnetic fields applied to lithium flow in hypothetical fusion reactor blanket (UCRL-51010) 23 p3742 N71-36684

- Isobaric-isothermal potentials for lithium oxide reduction by metals and metallic impurity oxide, nitride, carbide, and hydride concentrations in liquid lithium (NLL-RISLEY-TRANS-2169-[0001.9F]) 23 p3773 N71-34892
- Excitation and ionization cross sections for Ba(II) by electron impact, plasma diagnostics, Li energy loss in thin C films, and multiple charge ion sources for collision experiments (ORO-3027-19) 23 p3827 N71-37297
- LITHIUM ALLOYS**
- Nuclear spin lattice relaxation time measurements of lithium-magnesium alloys by recording growth of nuclear spin 11 p1805 N71-22370
- Germanium/lithium - sodium iodide/tellurium spectrometer for gamma ray spectroscopy (IKF-26) 17 p3810 N71-30386
- LITHIUM CHLORIDES**
- Effect of lithium and calcium ions on acetylcholinesterase activity of erythrocytes (NASA-TT-F-13476) 09 p1333 N71-20179
- Temperature measurement of premixed hydrogen/oxygen flames with lithium chloride tracers (DLR-FB-70-76) 13 p2082 N71-23052
- LITHIUM COMPOUNDS**
- NT LITHIUM FLUORIDES**
- NT LITHIUM HYDROXIDES**
- NT LITHIUM HYDROXIDES**
- NT LITHIUM OXIDES**
- NT ORGANIC LITHIUM COMPOUNDS**
- Viscosity and chemical composition of dispersion medium affecting aromatic hydrocarbons in lithium greases (AD-711177) 01 p0072 N71-10683
- Thermal stability of lithium grease oxidation (AD-711476) 02 p0248 N71-11735
- Nuclear magnetic resonance, solubility, stability, and resistance of electrolytes for lithium batteries (NASA-CR-72803) 05 p0631 N71-14608
- Investigating gamma radiation effects on piezoelectric properties of lithium niobate crystals at high temperatures (BNWL-1436) 05 p0758 N71-15017
- Pressure and temperature dependences of elastic constants in single lithium chloride and lithium bromide crystals (NYO-2504-78) 06 p0937 N71-16823
- Prestartup thawing of lithium coolant in nuclear reactor for space powerplant (NASA-TM-X-2177) 07 p1064 N71-17369
- Chemical composition and bending strengths of lithium-potassium and lithium-sodium silicate glass systems under melting conditions 11 p1785 N71-22893
- Experimental design using single ultraviolet pulses for triggering Kerr cells and producing laser radiation to heat lithium deuteride targets for high temperature plasma generation (NASA-TT-F-13662) 13 p2088 N71-24641
- Elastic, piezoelectric, and photoelastic constants for light scattering with hypersonic waves and Brillouin effects in ferroelectric lithium niobate crystals using helium-neon lasers 13 p2125 N71-24906
- Development of boron diffusion process to diffuse large quantities of stress-free, high efficiency, radiation resistant solar cells (NASA-CR-118318) 13 p2030 N71-24930
- Inorganic separator materials for integrated cell stacks capable of continuous operation in contact with molten lithium metal and fused LiCl-KCl eutectic (AD-720600) 14 p2200 N71-26016
- Differential thermal and electrical conductivity studies of phase transitions in Li₂/V₂O₅, single crystals of WO₃ and WO₃ minus x, and metal-ammonia systems 16 p2887 N71-31365
- Far infrared generation by nonlinear polarization using Q switched ruby lasers and LiNbO₃ crystal 21 p3436 N71-34451
- Long shelf life, organic electrolyte, lithium cells with wide operating temperature range and high energy density (AD-726385) 22 p3543 N71-35235
- Electro-optical effect in LiNbO₃ crystal at 6328 angstroms (FOA-C-2377-51) 22 p3629 N71-35860
- Influence of dispersion medium composition on properties of lubricants thickened with lithium soaps of synthetic fatty acids (SFA) 24 p3943 N71-38130
- LITHIUM COOLED REACTOR EXPERIMENT**
- Neutronic design calculations for lithium 7 cooled nuclear reactor for space applications (NASA-TN-D-6109) 07 p1064 N71-17422
- Fabrication of tantalum alloy honeycomb core structure for lithium cooled reactor (NASA-CR-72851) 13 p2101 N71-25426
- Production engineering and compatibility tests of Ta-W-2Hf clad UO₂ nuclear fuel element for use in lithium cooled space power unit reactor (NASA-TM-X-67869) 16 p2637 N71-28969

LITHIUM FLUORIDES

- Chemical and electrochemical reactions of lithium graphite fluoride primary cell
[AD-711521] 01 p0007 N71-10936
- Lithium fluoride single crystal shock Hugoniot data and phase transitions
[AD-712320] 02 p0286 N71-11900
- Solid solution formation of lithium fluoride and lithium hydride
[LA-TR-70-16] 04 p0488 N71-13471
- LIF thermoluminescent ribbons for low level environmental gamma radiation measurements
[HASL-233] 04 p0582 N71-14111
- NMR measurements in lithium fluoride to correlate NMR properties and body diffusion of lithium fluoride defect states
[COO-1105-157] 04 p0583 N71-14136
- Low temperature thermoluminescence in LIF
[COO-1105-161] 04 p0585 N71-14222
- Lithium fluoride dislocation in high speed impact
[AD-713624] 05 p0707 N71-14824
- Spectrographic method for determining trace elements in lithium fluoride
[BARC-496] 05 p0707 N71-15049
- Observing resolved linear Stark splitting for R⁺ zero-phonon line in LIF
[PHY-3464-25] 05 p0739 N71-15084
- LIF-Teflon disks laminated between plastic layers of identification pass for personnel accident dosimeters
06 p0804 N71-15749
- Dosimetry technique using thermally stimulated ex-coelation emission with lithium fluoride
[HASL-236] 06 p0927 N71-16857
- Performance tests on lithium fluoride thermoluminescent dosimeter
[BNWL-CC-2633] 06 p1199 N71-18287
- Investigating existence of chemically bound neutrons in lithium fluoride crystals
[ANL-7729] 06 p1283 N71-19349
- Electron paramagnetic resonance detection of electron bombarded lithium fluoride
[NASA-TM-X-52909] 10 p1616 N71-21083
- Preparation and handling of molten salt mixtures for molten salt reactor experiment, using LiF, BeF₂, ZrF₄, and UF₄ mixture
[ORNL-4616] 10 p1603 N71-21199
- Dislocation density dependence on compression shear stress measured by etch-pit technique in high purity and Mg doped, strain hardened LIF single crystals /100/
[NRC-TR-1447] 12 p1967 N71-23958
- Point and cluster defects study in LIF by phonon scattering and thermal conductivity measurement
[CEA-R-4010] 14 p2307 N71-26403
- X ray diffraction measurements on lithium fluoride compressibility and thermal expansion at high pressures and high temperatures
14 p2327 N71-26496
- Spin-lattice relaxation and atomic motions in lithium fluoride
16 p2668 N71-28988
- Cross deformation of lithium fluoride single crystals at 650 to 750 C
[UCRL-20350] 17 p2815 N71-29757
- Sensitivity variations of TLD LIF dosimeter rods annealed at 500 C
[RD/BN-1872] 18 p2959 N71-30504
- Cross relaxation dynamics for Li-6/Li-7 system in LIF based on rotating frame nuclear double magnetic resonance
18 p2983 N71-31047
- Effect of activation by magnesium and calcium on thermoluminescence and X ray luminescence of LIF crystals
[ANL-TRANS-874] 18 p2999 N71-31457
- Use of thermoluminescent lithium fluoride dosimeters for radiation dose control purposes providing rapid readout procedure
24 p3973 N71-38343
- Problems of high temperature annealing of PTFE/LIF discs used for ionizing radiation dosimetry
[AEW-M-991] 24 p3973 N71-38344
- Lithium fluoride glow-peak growth due to annealing and analysis of half-wave rectifying circuit with theoretical efficiency of 100 percent
24 p4014 N71-38633
- Analysis of lithium fluoride glow-peak growth due to annealing
24 p4014 N71-38635
- LITHIUM HYDRIDES**
- Solid solution formation of lithium fluoride and lithium hydride
[LA-TR-70-16] 04 p0488 N71-13471
- Lithium hydride solid rocket propellant decomposition with lithium hydroxide monohydrate
[DLR-FB-70-26] 07 p1098 N71-17228
- Characteristics of alkali hydride lattice energies for ionic Born-Mayer potential
[MLM-1764] 09 p1454 N71-20504
- Low temperature volume expansion of LiH/LiF by self damage due to beta decay of negative tritium ion
11 p1809 N71-23031

Internal insulation systems for LH2 tanks and gas layer and polyurethane reinforced foam
17 p2857 N71-29617

Analyses of reentry protection performance of silver impregnated zirconium oxide foam material with lithium hydride backup
[TID-25696] 22 p3594 N71-35593

Design and fabrication of lithium hydride shields for SNAP applications
[NASA-CR-120782] 23 p3761 N71-36811

LITHIUM HYDROXIDES

Lithium hydride solid rocket propellant decomposition with lithium hydroxide monohydrate
[DLR-FB-70-26] 07 p1098 N71-17228

Measurements of diffusion coefficients and vapor pressure in LiOH solutions for determination of gas solubilities in fuel cell electrolytes
[NASA-CR-117906] 12 p1859 N71-23345

LITHIUM ISOTOPES

Alpha, 2 alpha reaction on Li-6, Li-7, Be-9, C-12, and O-16 at 55 MeV
[LYCEN-7009] 02 p0277 N71-12132

Alpha cluster structure of lithium 6 and lithium 7 with alpha/2 alpha reaction
[NP-18252] 03 p0430 N71-12902

Measuring fast reactor neutron spectra from 5 keV to 8 MeV using spectrometer of single lithium 6 sandwich
[AERE-R-6060] 04 p0570 N71-13603

Nuclear data for thermonuclear reactors including evaluation of basic materials such as Li-6, Li-7, and Nb
[ANL-TRANS-842] 04 p0553 N71-14001

LIF-Teflon disks laminated between plastic layers of identification pass for personnel accident dosimeters
06 p0804 N71-15749

High energy electron scattering from Li-6
[AD-714022] 06 p0920 N71-16268

Measurement of Li-6 diffusion from irradiated beryllium oxide
[JUL-677-RQ] 13 p2128 N71-24474

Angular distributions and total cross sections of Be-9/deuteron, alpha-0/Li-7/gp and Be-9/deuteron, alpha-1/Li-7/gp reactions in 0.9 to 2.2 MeV energy range
[JNR-1200] 14 p2316 N71-26744

Geometric efficiency of lithium 6 suspended target type semiconductor spectrometers calculated for isotropic neutron fluxes
[AERE-R-6318] 15 p2479 N71-27635

Photoneutron energy and angular distribution spectra from lithium 6 and lithium 7 states
15 p2479 N71-27636

Detection, and energy and angular distributions of Li-6 recoil nuclei from Be-9 irradiated with 180 and 660 MeV protons
[JINR-P1-4872] 15 p2480 N71-27657

Harmonic analysis and nuclear model of lithium 6 core distortion and effects on energy levels, magnetic dipole and electric quadrupole moments, and Pauli exclusion principle
15 p2494 N71-27955

Equivalence of He 3-4 and d-alpha-alpha cluster description of lithium 6
[NYO-2171-336] 17 p2800 N71-30099

Nuclear magnetic resonance measurement of self diffusion coefficients and temperature effects in liquid lithium 6 and 7 and sodium 23
17 p2805 N71-30289

Cross relaxation dynamics for Li-6/Li-7 system in LIF based on rotating frame nuclear double magnetic resonance
18 p2983 N71-31047

Use of physical characteristics of Li-6/n, alpha/p reaction in neutron spectrometry, solutions to E sub triton spectrometry problems
[BLG-450] 19 p3158 N71-32537

Paraelectric resonance spectra of KCl/Li using positive Li-7 and Li-6 ions
[NYO-2150-59] 19 p3160 N71-32638

Nuclear structure of helium and lithium isotopes based on nuclear scattering by Van de Graaff accelerated cations
[NSF-GP-12227-2] 19 p3160 N71-32659

Reduced self absorption in recording Fabry-Pérot spectrometer for lithium isotope analysis
[BARC-508] 21 p3406 N71-34834

Quasi-free cluster knockout reaction mechanisms of (proton, proton alpha) and (alpha, 2 alpha) in Li-6 and Li-7 at 60 MeV
21 p3488 N71-34847

Irradiation yield curves and angular distributions for Li-6 C-12 reaction
21 p3491 N71-34869

Numerical analysis of inelastic scattering of nucleons from Li-7 using distorted wave Born approximation
21 p3492 N71-34876

Excited states of helium investigated through final state interactions and quasifree scattering reactions on Li-6
[NP-18741] 22 p3643 N71-35974

Magnetic analysis of Li-7 bombarded with 15 MeV He-3 atoms
[ANU-P-520] 23 p3809 N71-37160

U and Pu reprocessing input quantities measured using Li tracer technique
[IAEA-R-676-F] 24 p3962 N71-38264

LITHIUM OXIDES

Wave functions incorporating electron correlation for magnesium oxide, lithium oxide, aluminum oxide, and titanium oxide
[AD-71973] 03 p0433 N71-12940

Effects of chemical catalysts, bed cooling, chemical manufacturing techniques, operating conditions, and chemical handling procedures on lithium peroxide
[NASA-CR-114896] 09 p1343 N71-19914

Calculation of dissociation stresses in lithium and potassium peroxides
[NASA-TT-F-13639] 16 p2558 N71-28961

Isobaric-isothermal potentials for lithium oxide reduction by metals and metallic impurity oxide, nitride, carbide, and hydride concentrations in liquid lithium
[NLL-RISLEY-TRANS-2169-9091.9F] 23 p3773 N71-36892

LITHIUM 4

LITHIUM ISOTOPES

LITHIUM 6

LITHIUM ISOTOPES

LITHOLOGY

Lithology and geochemistry of weathering crust
[TT-49-55031] 03 p0367 N71-12750

Physical properties and absolute age determination for some rocks of India and Ceylon
[NASA-TT-F-13416] 05 p0670 N71-14839

Paleomagnetic study of coastal lithology on Hawaii
[PB-195634] 08 p1187 N71-6393

LITHOPHORE

EARTH CORE

EARTH CRUST

EARTH MANTLE

EARTH PLANETARY STRUCTURE

EARTH SURFACE

LIVER

Liver and skeletal muscle morphology in rats under hypokinesia and protein deficiency
08 p1155 N71-19073

LMCR [REACTORS]

LIQUID METAL COOLED REACTORS

LOAD DISTRIBUTION [FORCES]

Motion bounds of lumped structural parts subjected to dynamic loads and perturbations
[AD-710787] 01 p0129 N71-10561

Developing stress indices and simplified design formulas for use in stress analysis of small branch connections with external loadings
[ORNL-TM-3014] 04 p0617 N71-14086

Load distribution on gear teeth couplings
06 p0602 N71-15726

Aerodynamic coefficients, pressure, load and force distributions on cambered delta wings
[ARC-CP-1129] 07 p0966 N71-17112

Elastic deformation of sandwich structures with load distribution on one side
[NPL-DNAM-86] 07 p1122 N71-17209

Strain gage for measuring load spectrum on stressed mechanical part
[NLL-LIB-COMM-1523-5196/1] 16 p2597 N71-28858

Load distribution on human hip joints during walking
[LAB-1002/71] 17 p2710 N71-29327

Elastic deformation of telescope mirror, noting load distribution on static support system
22 p3670 N71-36171

LOAD FACTORS

U LOADS [FORCES]

LOAD TESTING MACHINES

Load cell protection device using spring-loaded breakaway mechanism
[NASA-CASE-XMS-06782] 06 p0953 N71-15974

Development of device for transferring load from load cell to bypass mechanism
[NASA-CASE-XMS-06329-1] 09 p1393 N71-20441

LOAD TESTS

Fatigue testing apparatus for measuring strain levels on aluminum alloys with constant force or amplitude control at 20 kHz
[MAT-3] 02 p0241 N71-11563

Manufacturing improvement program establishing applications and limitations in closed die forging
[AD-71354] 02 p0234 N71-11679

Static vibratory load testing of foundation piles
[NASA-CR-111363] 02 p0303 N71-12106

Analysis of bolt loads by ultrasonic techniques
[NASA-CR-102929] 03 p0461 N71-12965

Loading rate and temperature effects on high strength steel fracture toughness
[AD-71357] 05 p0699 N71-16457

Testing materials for use in cages, balls, and races in cryogenic hydrogen-cooled 110-mm ball bearing
[NASA-CR-72279] 06 p0866 N71-16467

Durability and service life of ball bearings
[NASA-TT-F-13460] 08 p1208 N71-19009

Fatigue mechanisms in fracture of glasslike polymers
08 p1300 N71-49457

Crack arrest in transversely loaded elastic plates
[UCRL-72335] 09 p4777 N71-28892

SUBJECT INDEX

LOADS (FORCES)

Shock, vibration, and acceleration-load tests of SNAP motor-driven lubricant-coolant pump [NASA-TM-X-52972] 10 p1602 N71-20947

Buckling of simply supported skew plates under combined loading with in-plane stresses expressed in terms of orthogonal components [AE-290-S] 11 p1836 N71-23266

Linear viscoelastic analysis of incremental load test data on AU-401 aluminum alloy sheet subjected to tensile creep at 473 deg K [NASA-CR-117838] 11 p1780 N71-22394

Double torsion technique to determine fracture energy of epoxy resin [AD-718648] 12 p1942 N71-23379

Experimental investigation to determine stability, surface deformation characteristics, and extent of plastic yielding associated with surface cracks in plates subjected to tensile loading [NASA-CR-114934] 13 p2181 N71-24820

Review of cumulative damage theories aimed at predicting service life of structures under fatigue loading allowing comparison of effects of various loads and cycle ratios [ARL/SM-REPORT-326] 15 p2522 N71-27806

Buckling tests of two integrally stiffened cylindrical shells subjected to bending loads [NASA-TN-D-6271] 16 p2684 N71-28116

Effect of in-plane boundary conditions on buckling loads of simply supported ring stiffened cylindrical shells [AD-721473] 16 p2685 N71-28139

Buckling of boron/aluminum and graphite/resin fiber composite anisotropic panels - load tests [NASA-TM-X-67880] 18 p3022 N71-31281

Uniaxial strain rate, creep, isotropy, and reloading tests for characterization of polycarbonates 22 p3693 N71-36342

LOADING FORCES
U LOADS (FORCES)
LOADING MOMENTS

Numerical determination of nonlinear displacement behavior of complete circular cylindrical thin shell subjected to uniform radial pressure [AD-712111] 02 p3002 N71-12051

Wind loading moments produced on scale models of tall buildings in wind tunnel tests 05 p0777 N71-15306

General numerical large deflection solution of coaxial ring circular glass plate flexure problem [AD-714154] 06 p0878 N71-16344

Power input, variation of operating properties, and lubricant consumption of oil lubricated antenna bearing system for communication satellites with force and moment calculations [RAE-LIB-TRANS-1451-PT-2] 09 p1393 N71-19632

Statistical analysis of line loading thin walled, unstiffened shells and storage tanks [NLL-RTS-6304] 12 p2005 N71-23834

Compilation of aerodynamic basic definitions, including aerodynamic coefficients, and relations, expansions, and derivatives of forces and moments [ARC-R/M-3562-PT-4] 20 p3204 N71-32975

LOADING OPERATIONS

Air bearings for near frictionless transfer of loads from one body to another [NASA-CASE-XMF-01887] 01 p0059 N71-10617

Digital computer program for stresses distribution in ring of nonuniform cross section under uniform radial load [AD-712518] 04 p0616 N71-13944

Vertical motion of static loads over baffles during loading operations using ground effect machines [NPL-HOVERCRAFT-TM-31] 07 p0970 N71-17160

Safety and hazards analysis of parallel versus series loading of space shuttle using liquid hydrogen and liquid oxygen propellants - technical discussion [NASA-CR-125172] 24 p4021 N71-38689

LOADING WAVES
U ELASTIC WAVES
U LOADS (FORCES)
LOADS (FORCES)

NT AERODYNAMIC LOADS
NT AXIAL COMPRESSION LOADS
NT AXIAL LOADS
NT COMPRESSION LOADS
NT CRITICAL LOADING
NT CYCLIC LOADS
NT DYNAMIC LOADS
NT EDGE LOADING
NT GUST LOADS
NT IMPACT LOADS
NT LANDING LOADS
NT RANDOM LOADS
NT ROLLING CONTACT LOADS
NT SHOCK LOADS
NT STATIC LOADS
NT THRUST LOADS
NT TRANSIENT LOADS
NT VIBRATORY LOADS
NT WING LOADING

Potential study of uniformly loaded annular slabs supported between edges with equally spaced columns [REPT-291] 02 p0301 N71-12012

Bending solution of full circular plates supported on two rings of equally spaced columns 02 p0301 N71-12013

Bending solutions of uniformly loaded annular plates supported by columns on one boundary with other boundary simply supported [REPT-287] 02 p0301 N71-12014

Bending of circular plates supported on equally spaced columns under eccentric concentrated load [REPT-286] 02 p0302 N71-12029

Analysis of symmetric bladder deformation due to symmetric inversion pressures 03 p0462 N71-13116

Effect of eccentric load forces and different stress-strain relationships on stiffness of columns 03 p0466 N71-13350

Incremental variational method for determining inelastic load deformation and buckling load for shells of revolution [AD-712522] 04 p0617 N71-13946

Loads due to air and helium jets impinging normal to flat plate for near vacuum and sea level ambient pressures [NASA-TN-D-7002] 05 p0660 N71-14749

Collocation method for solving elastic problems of loaded plates with edge columns 05 p0776 N71-15155

Failure mechanisms associated with use of borehole jack in rocks 05 p0768 N71-15206

Improving load capacity and fatigue life of rolling element systems in rockets and missiles [NASA-CASE-XLE-02999] 06 p0864 N71-16052

Increased load effects on vibratory and impulse responses of circular cylindrical shells [AD-714483] 06 p0955 N71-16426

Computer program for determining static and dynamic response of symmetrically loaded elastic orthotropic shells of revolution [NASA-TN-D-6158] 06 p0957 N71-16846

Analyzing polygonal plates using modified Ritz variational process 07 p1122 N71-17038

Investigating theory of plasticity for smooth and piecewise-smooth loading surfaces 07 p1122 N71-17039

Program for computing collapse loads of heated, arbitrarily loaded spherical shells in elastic medium [SC-DR-70-218] 07 p1124 N71-17571

Flat Jack devices used to measure in-situ properties of rock mass subjected to high pressure loading by surface detonations [AD-715264] 07 p1023 N71-17856

Lumped mass finite difference analysis for loaded structural beam dynamics 07 p1126 N71-17886

Singular solutions for cylindrical shell equation and relationships to mechanical or thermal loads 07 p1128 N71-18024

Development of device for transferring load from load cell to bypass mechanism [NASA-CASE-XMS-06329-1] 09 p1395 N71-20441

Calculation and measurement of force, residual stress, and temperature effects on plastic surfaces from machine tool geometric parameters [NLL-RTS-5815] 10 p1566 N71-21321

Mechanical testing of metals at high temperatures and short term loading with determination of temperature influence and deformation rates [AD-716937] 10 p1580 N71-21391

Computation of plastic toroidal shell carrying capacity 10 p1658 N71-21577

Linear axisymmetric analysis of lateral pressure loaded conical shell using ring type finite element model [AD-717770] 11 p1836 N71-22334

Fracture mechanics evaluation of stress intensity factors for various crack geometries and loading conditions [WAFD-TM-976] 12 p2004 N71-23163

Valve assembly for controlling simultaneously more than one fluid flow, and having stable qualities under loads [NASA-CASE-XMS-05990] 12 p1886 N71-23191

Unsteady hydrodynamic loads on two dimensional hydrofoil [AD-717933] 12 p1901 N71-23591

General method for kinematic synthesis and force balancing of spatial mechanisms 12 p1930 N71-24132

Solid state force measuring electromechanical transducers made of piezoresistive materials [NASA-CASE-ERC-10068] 13 p2153 N71-25490

Computer program for determination of optimal herringbone journal bearings for maximum radial load capacity [NASA-TN-D-6351] 14 p2260 N71-25665

Testing capacity of clutch with rubber elastic toroidal element for longevity under shaft displacements and loads 14 p2260 N71-25854

Development of piecewise stationary mode approximation technique for structural analysis of impulsively loaded rigid viscoelastic materials 14 p2350 N71-26421

Turn on current transient limiter for controlling peak current flow in high capacity load [NASA-CASE-GSC-10413] 14 p2355 N71-26531

Digital computer algorithm for determining gain bandwidth properties of distributed parameter loads 14 p2350 N71-26547

Determining static mass bearing capacity of lunar surface by slope analysis of failed slopes in lunar craters [NASA-CR-118505] 14 p2340 N71-26650

Approximative solution for loaded viscoplastic rod striking rigid wall 14 p2331 N71-26680

Effects of load conditions on end of life performance of long term radioisotope thermoelectric generator operation [SC-RR-70-834] 15 p2444 N71-26962

Synchronous dc direct-drive system comprising multiple-loop hybrid control system controlling load directly connected to actuator [NASA-CASE-GSC-10065-1] 15 p2388 N71-27136

Force balanced throttle valve for fuel control in rocket engines 15 p2416 N71-27432

Response of elastic earth to loads located in parallel plane to bounding surface 15 p2400 N71-27479

Inelastic strain effects on deformation and buckling stability of thin spherical shells under point loads 15 p2323 N71-27861

Ultrasonic, pulse echo interferometric method for analyzing bolt preloads [NASA-CR-61354] 16 p2599 N71-28018

Device for sensing current applied by pulse width modulated power supply to battery or other load [NASA-CASE-GSC-10656-1] 16 p2570 N71-28471

Analysis of loads produced on spacecraft by staging operations and practices to insure that staging loads are included in spacecraft design [NASA-SP-8022] 16 p2886 N71-28634

Passive force transducer for measuring, magnifying, and recording maximum load on given specimen [NASA-CASE-LAR-10496-1] 16 p2595 N71-28654

Derivation of asymptotic stability and instability conditions for elastic systems with dissipation [AD-721384] 16 p2687 N71-28717

Conical hydrostatic bearing optimal dimensions for friction reduction based on laminar and turbulent flow velocity, load capacity, and friction torque calculations [NASA-TM-X-52946] 16 p2603 N71-28887

Energy absorption device in high precision gear train for protection against damage to components caused by stop loads [NASA-CASE-XNP-01848] 16 p2604 N71-28959

Development of test procedure for accurately recording dynamic signals from instrumented test bars used to measure loads during simulated fatigue tests [NBS-TN-578] 17 p2855 N71-30302

Effects of loading rate on creep properties of austenitic stainless steel type 316 [PB-197128] 18 p2934 N71-30806

Dynamic plastic behavior of aluminum alloy cylindrical shells subjected to impulse loads on inner surface [AD-723831] 19 p3188 N71-32028

Mathematical models for prediction of acceleration responses and reaction forces and moments at base of Mariner Mars 71 and Viking spacecraft from Centaur main engine cutoff [NASA-CR-121473] 20 p3355 N71-33719

Dynamic structural analysis of clamped skew plate buckling under various loads [AE-296-S] 20 p3360 N71-33822

Theoretical study of nonlinear flutter behavior of clamped panels subjected to various loads 21 p3374 N71-34010

Development of method for testing resistance of brittle material to fracture when subjected to shock wave loading [RFP-1554] 21 p3529 N71-35146

Transformation formulas in solid spherical harmonics for calculating forces between two homogeneous hemispheres with examples involving coordinate translation and rotation [NASA-CR-115141] 22 p3606 N71-35678

Maximum wind velocity measurements from West Germany and wind loading in structural engineering [NLL-LIB-COMM-1590-51961] 22 p3616 N71-35763

Nickel and copper substructural disorientation angle dependencies on deformation, loading, and temperature [NLL-L71-746-728-19022-401] 22 p3659 N71-36091

NASTRAN program used to calculate gravity load reactions in 64-m antenna reflectors 22 p3683 N71-36262

- NASTRAN-GAP** programs for analyzing antenna radiation patterns of reflectors distorted by gravity and thermal loads 22 p3683 N71-36263
- Comparison of ASKA and NASTRAN programs analyses of space shuttle hot eleven test article deformed under thermal and mechanical loads 22 p3683 N71-36264
- Stresses and deformations in multiply biax pneumatic aircraft tires subjected to inflation pressure loading 22 p3693 N71-36341
- Computer modeling of loading problem for linear viscoelastic earth of ocean bottom near Hawaiian Archipelago 23 p3753 N71-36765
- Predicting time-temperature behavior of epoxy resins and epoxy composites in any loading mode 23 p3780 N71-36942
- Variability of aluminum alloy aircraft structure fatigue life under symmetric and asymmetric loads [AD-726455] 23 p3961 N71-37524
- Derivation curves and computer program for investigating post buckling behavior of stiffened plates with small initial curvature under combined loads [AD-726455] 23 p3961 N71-37526
- Fatigue tests and life of nickel alloy during programmed loading and elevated temperature [AD-727842] 24 p3939 N71-38103
- Capacitor system for load balancing in SNAP 8 [NASA-CR-72936] 24 p3961 N71-38253
- Method for large deflection inelastic analysis of plate grillages under normal and axial loads [AD-727601] 24 p4025 N71-38722
- LOCALIZATION**
U POSITION [LOCATION]
- LOCATION**
U POSITION [LOCATION]
- LOC**
Examination of simple coordinate transformations in Z-plane and W-plane for root locus analysis of sampled data systems [NASA-TM-X-64513] 04 p0539 N71-14184
- LOCKHEED AIRCRAFT**
NT C-5 AIRCRAFT
NT C-130 AIRCRAFT
NT C-141 AIRCRAFT
NT F-104 AIRCRAFT
NT P-3 AIRCRAFT
NT T-33 AIRCRAFT
NT XH-51 HELICOPTER
LOCKHEED C-5 AIRCRAFT
U C-5 AIRCRAFT
LOCKHEED CL-99 HELICOPTER
U XH-51 HELICOPTER
LOCKHEED MILITARY AIRCRAFT
LOCKHEED 106 HELICOPTER
U XH-51 HELICOPTER
LOCKING
Satellite orientation during deployment established in order to achieve maximum strength of higher rotational locks for satellites in elliptic orbits [NASA-TM-X-65555] 15 p2517 N71-27764
- LOCKS [FASTENERS]**
Low friction bearing and lock mechanism for two-axis gimbal carrying satellite payload [NASA-CASE-GSC-10556-1] 14 p2345 N71-26337
- Locking device for retaining turbine rotor blades on turbine wheel [NASA-CASE-XNP-00816] 16 p2672 N71-28928
- Longitudinal film gate and lock mechanism for securing film in motion picture cameras under vibration and high acceleration loads [NASA-CASE-LAR-10686] 16 p2598 N71-28935
- Design and operation of electronic combination lock system with built-in alarm features suitable for multi-unit apartment and office complexes 19 p3070 N71-31646
- LOCOMOTION**
NT ASTRONAUT LOCOMOTION
NT WALKING
Information capacity of discrete motor responses compared for different directions and amplitudes of motion [AD-710713] 01 p0012 N71-10536
- Altitude control training device for astronauts permitting friction-free movement with five degrees of freedom [NASA-CASE-XMS-02977] 01 p0039 N71-10746
- Realizable gain matrices for N-legged machines [AD-714592] 06 p0807 N71-16551
- Oscillatory characteristics of swimming and locomotion of aquatic animals 11 p1681 N71-22205
- Resonance characteristics of dolphin swimming and locomotion verified by underwater photography 11 p1681 N71-22206
- Physiological investigation of Grays paradox on locomotion of dolphins under turbulent flow conditions 11 p1681 N71-22207
- Morphological examination of nervous system and muscular functions in dolphin tail during locomotion 11 p1682 N71-22212
- Histological examination of skin layers and scales of sharks and effects on locomotion 11 p1682 N71-22215
- Signal transformation by central nervous system for sensorimotor pattern construction in postural adjustment 11 p1694 N71-23072
- Weightlessness effects on human sensorimotor performance and locomotion 20 p3227 N71-33452
- LOG PERIODIC ANTENNAS**
Numerical analyses on mutual couplings in arrays of log periodic dipole antennas 08 p1163 N71-18946
- Determining extent of cosmic ray shower by pointing radio antennas 10 p1554 N71-21553
- K-beta diagrams for two uniformly periodic loop antenna arrays determined from measured near field amplitude and phase distributions of traveling waves [AD-721592] 16 p2568 N71-28355
- LOGARITHMS**
Optimization for minimum matrix norms noting solution of differential equations [NA-70-26] 18 p2945 N71-31172
- LOGIC**
Superintuitionistic logic, sitting problem, and automatic word recognition [JPRS-52599] 11 p1786 N71-21901
- Finite approximability of superintuitionistic calculus of propositions 11 p1786 N71-21902
- LOGIC CIRCUITS**
NT THRESHOLD GATES
Methods for coordinating asynchronous events [AD-711763] 02 p0186 N71-11307
- Development and characteristics of electronic keyboard calculator [AD-711753] 02 p0186 N71-11308
- Cascade synthesis of logic functions [AD-711154] 02 p0186 N71-11310
- Design of universal logic modules and application to logic network design 02 p0187 N71-11315
- Use of circuit codes in analog to digital conversion [AD-711944] 02 p0189 N71-11327
- Computer analysis of logic circuits [LAAS-413-614] 02 p0196 N71-11374
- Data processor having multiple sections activated at different times by selective power coupling to sections [NASA-CASE-XGS-04767] 03 p0343 N71-12494
- Binary sequence detector with few memory elements and minimized logic circuit complexity [NASA-CASE-XNP-05415] 03 p0345 N71-12505
- Digital modeling method applied to circuit design [AD-712105] 03 p0346 N71-12512
- Constructing algorithms for majority-logic decoding for linear block codes [AD-712683] 04 p0500 N71-13495
- Bistable multivibrator circuits operating at high speed and low power dissipation [NASA-CASE-XGS-00823] 06 p0826 N71-15910
- Results on redundancy and testability of combinational logic networks 06 p0827 N71-16457
- Large scale integrated circuit testing using test points and additional logic [AD-714511] 06 p0824 N71-16452
- Logic AND gate for fluid circuits [NASA-CASE-XLA-07391] 07 p1010 N71-17579
- Logic circuit to ripple add and subtract binary counters for spaceborne computers [NASA-CASE-XGS-04766] 08 p1164 N71-18602
- Constructing Exclusive-Or digital logic circuit in single module [NASA-CASE-XLA-07732] 08 p1165 N71-18751
- Stepping motor control apparatus exciting windings in proper time sequence to cause motor to rotate in either direction [NASA-CASE-GSC-10366-1] 08 p1172 N71-18772
- SPOOF, structure and parity technique, for analysis of fault effects on logic networks [AD-715627] 08 p1172 N71-18799
- Reliability analysis and performance prediction for solid state sequencer system model [NASA-CR-114909] 09 p1359 N71-19777
- High level computer programming language [SAM-PL-E] and parallel processing system to implement it [NASA-CR-117174] 09 p1356 N71-20332
- Boolean algebra applied to logic counting circuits 10 p1528 N71-21143
- Logic circuitry, and environmental and acceptance tests for solid state sequencer system in command module and service module jettison controller [NASA-CR-114955] 10 p1635 N71-21460
- Internal logic manual for programmed communications controller for connecting teletypewriter terminals to multiple spectrometer control system [BNL-15437] 10 p1526 N71-21750
- Serial digital decoder design with square circuit matrix and serial memory storage units [NASA-CASE-NPO-10150] 13 p2049 N71-24650
- Binary to decimal decoder logic circuit design with feedback control and display device [NASA-CASE-XKS-06167] 13 p2052 N71-24890

- Design and development of multistage current steering switch with inductively coupled magnetic cores [NASA-CASE-XNP-08567] 14 p2228 N71-26008
- Logic circuit for generating multibit binary code word in parallel [NASA-CASE-XNP-04623] 14 p2233 N71-26101
- Adaptive signal generating system and logic circuits for satellite television systems [NASA-CASE-GSC-11367] 14 p2233 N71-26371
- Derivation of minimum test sets for anode function logic circuit failure analysis and component reliability [AD-720330] 15 p2389 N71-27228
- Transform for operating on interconnection topology of NAND network [AD-720328] 16 p2574 N71-28636
- Reliability improvement using redundant components suitable for binary logic circuits [RAE-TR-69045] 17 p2722 N71-29402
- Algorithm for automatic failure analysis of gates in logic circuitry [LAAS-G-3-E-11] 18 p2892 N71-30520
- Software for computer aided design of logical circuits for study of interactive computer graphics [AD-722095] 18 p2896 N71-31412
- Fault testing of field effect transistor modules [AD-723442] 19 p3070 N71-31825
- Automatic testing of logic integrated circuits included in computer program [LAAS-PUBL-747-748] 20 p3240 N71-32929
- Synthesis of logic functions containing threshold elements 20 p3291 N71-33385
- Logic problems for programming video disk recorder with single and multiple fields [LA-4582] 20 p2336 N71-33797
- Noise control and improved system reliability for high speed logic integrated circuits [DISS-44770] 20 p2344 N71-33995
- Synthesis of sequential threshold machines based on fundamental criteria of logic capacity parameters of threshold elements 21 p3403 N71-34211
- Development of two high speed logic circuits for use with large, sectioned liquid scintillation detector [ORO-2304-172-PT-3] 22 p3559 N71-33332
- Punched card modifiable logic design and interconnection control for evaluating cellular logic concepts for multifunctional data processing systems [AD-726996] 22 p3562 N71-33571
- Digital computer analysis of integrated logic circuit transient behavior [REPT-1143] 22 p3562 N71-33571
- Digital computer fault detection procedures for combinational logic circuits with algorithms for efficient generation of minimum fault test schedules [AD-726383] 22 p3563 N71-33575
- Design of logic circuit to facilitate electrical fault detection in digital computers [AD-726382] 22 p3563 N71-33575
- Logic devices for readiness assessment and checkout of airborne and ground equipment mechanical components 22 p3674 N71-36197
- History and fundamentals of MOS logic circuit development 23 p3735 N71-36628
- Fabrication of high speed logic counting circuits using bipolar processes 23 p3737 N71-36644
- Pad relocation technique for interconnecting LSI semiconductor logic circuit arrays with imperfect yields 23 p3738 N71-36646
- Computer program for simulating logic circuit by describing circuit topology [UCRL-72694] 24 p3894 N71-37712
- Development of technique for finding functional diagram of combination automation with complex of faults [AD-727974] 24 p3896 N71-37714
- Synthesizing logic circuits and boolean function circuits with not more than three variables [AD-727972] 24 p3896 N71-37719
- Development of magnetic thyristor logical elements consisting of control electrodes and magnetic cores with rectangular hysteresis loops [AD-727192] 24 p3899 N71-37770
- Behavior analysis of stochastic sequential circuits fed by random noise 24 p3902 N71-37812
- Development of comparison between fluid logic circuits and electric and electronic logic circuits [NILL-PORS-TRANS-2727-19622.811] 24 p3908 N71-37808
- Design of snap-8 electrical protective system module including fabrication and assembly drawings [NASA-CR-72938] 24 p3960 N71-32040
- Solid state logic system for reactor protection and engineered safety features actuation systems [WCAP-7672] 24 p3964 N71-32075
- LOGIC DESIGN**
Beam steering logic for two dimensional electronically scanned array radars 01 p0020 N71-10711

SUBJECT INDEX

LONG TERM EFFECTS

Design of universal logic modules and application to logic network design 02 p0187 N71-11315

Hierarchical associative memories for parallel computation 02 p0189 N71-11331

Hardware design implementation for time shared computing facility 02 p0191 N71-11339

Computer designing and programming (NASA-CR-115819) 04 p0302 N71-13654

Resource allocation and avoidance of deadlocks in application of cellular array logic to LSI 04 p0302 N71-13657

Past multiplication cellular arrays for LSI implementation 04 p0303 N71-13658

Heuristic optimization algorithm for arranging N page open string 04 p0303 N71-13660

Application of domain tip logic in designing associative processors for spaceborne use (NASA-CR-115866) 05 p0652 N71-15535

Digital logic design for spinometer 06 p0803 N71-15896

Multiple perspective element construction method for recognition of photograph patterns 06 p0803 N71-15896

Precise logic computation and construction of formal heuristic activity models 12 p1895 N71-24219

Complex logic systems and logical sequencing theory 12 p1885 N71-24220

Approximation of redundant component reliability and digital computer logic design 15 p2389 N71-27287

Software for computer aided design of logic circuits for study of interactive computer graphics (AD-722095) 18 p2896 N71-31412

Optimization techniques for synthesis of cellular logic networks 19 p3070 N71-32272

Design of logic circuit to facilitate electrical fault detection in digital computers 22 p3463 N71-35376

Application of logic functions to design of MOS circuits 23 p3735 N71-36630

Dynamic memories constructed as circulating shift registers with enhanced data access (AD-727116) 24 p3895 N71-37763

LOGIC NETWORKS

LOGIC ELEMENTS

Design and performance of logic circuit chip for computerized design of MOS integrated circuit arrays (NASA-CR-116640) 07 p1001 N71-17092

Computing power of finite machines (NASA-CR-116636) 14 p2220 N71-25869

Addressable interface unit for computerized visual information processing system of earth resources infrared data (NASA-CR-116997) 14 p2226 N71-26643

Synthesis of logic functions containing threshold elements 20 p3291 N71-33385

Synthesis of circuits from universal elements for constructing logical and computing circuits (AD-726599) 22 p3561 N71-35365

LOGISTICS

NT LUNAR LOGISTICS

NT SPACE LOGISTICS

Problems in civil air transportation and logistics 07 p1134 N71-17799

Computerized simulation of alternate logistics for overhaul and expensive parts inventory procedures of commercial airlines 07 p1138 N71-18118

Concept formulation and operational aspects of integrated logistic support for military applications (P-4318) 21 p3534 N71-35188

Logistics system modeled as transportation problem with linear cost structure and lower bounds on supply from each origin and to each destination (AD-726509) 23 p3729 N71-36586

Comparison of logistics problems and cost aspects in selection of aircraft for earth resources surveys (NASA-TM-X-3418) 24 p3917 N71-37928

LOGISTICS MANAGEMENT

NT INVENTORY MANAGEMENT

Computerized inventory control system for highway department of Pennsylvania 14 p2225 N71-26553

APCRL research, including logistics management and plasma physics, Jul. 1967 - Jun. 1970 (AD-728277) 16 p2695 N71-29058

Techniques and characteristics of field testing in defense experimental design and procedures for specific program logistics 21 p3448 N71-34542

Concept formulation and operational aspects of integrated logistic support for military applications (P-4318) 21 p3534 N71-35188

LONG RANGE NAVIGATION

U LORAN

U LORAN D

LONG RANGE WEATHER FORECASTING

Long range forecasting of climatic factors determined by cyclic behavior of oscillations in mobile envelopes of earth 02 p0260 N71-12145

Statistical long range forecasting of mean monthly air temperature 06 p0891 N71-16320

Improved accuracy of long range forecasting through prediction of sign of frequency anomaly of atmospheric circulation 11 p1754 N71-22823

Three and five month rhythms used in predicting cold and warm May in southern European USSR (NLL-M-2870-5828.4F/1) 12 p1958 N71-24169

Solar activity cycles and helioclimatology in long range forecasting (AD-719768) 13 p2107 N71-25105

Methods for long range weather forecasting of monthly and seasonal mean values of climatological elements analyzed in terms of synoptic climatology (AD-719768) 13 p2107 N71-25149

Features of 500 mb height field in Northern Hemisphere during natural synoptic seasons 16 p2591 N71-29118

Review of numerical experimentation related to global atmospheric research program 17 p2777 N71-29481

Long range tropical weather forecasting of cloud clusters over Atlantic noting ground weather stations international cooperation and training 17 p2777 N71-29485

Relationship of cyclones in stratosphere and troposphere and ocean surface temperature during early winter with midlows or severity of Russian winters (NLL-M-9269-5828.4F/1) 17 p2739 N71-29427

Deformation anomalies of ocean surface related to atmospheric procedure distribution for potential long range weather forecasting technique (NLL-M-28599-5828.4F/1) 21 p3423 N71-34357

Frequency of centers of gravity of cyclones and anticyclones for long range weather forecasting (NLL-M-28653-5828.4F/1) 21 p3453 N71-34574

Algorithms for determining analogs of fields for long range weather forecasting (NLL-M-28696-5828.4F/1) 21 p3453 N71-34579

LONG TERM EFFECTS

Graphical analysis of ten-year sampling of suspended particulate matter over urban and suburban sites (PB-192223) 02 p0151 N71-11069

Toxic effects of endrin on brain functions of aerial applicator personnel (FAA-AO-70-11) 03 p0321 N71-12293

Defining methods for long-range forecasting of economic processes and scientific and technological progress (IPRS-51841) 04 p0622 N71-14067

Auditory perception thresholds and long term effects (NPL-AERO-AC-44) 07 p0980 N71-17098

Rocket sounding of long term proton flux density variations in inner radiation belt (MPI-PAE/EXTRATER-37) 07 p1105 N71-17216

Determining hemopoietic, cytological, and immunological parameters of simulated long term exposure to space radiation 08 p1150 N71-18896

Medical support procedures and postflight analysis of physiological changes in Soyuz 9 crew members 08 p1150 N71-18900

Measuring physiological changes and circulatory reactions of Soyuz 9 crew members during prolonged flight 08 p1150 N71-18902

Thermal vacuum test duration for quality control of spacecraft components 09 p1483 N71-20230

Data from 90-day manned test of regenerative life support system in space station simulator (NASA-SP-261) 10 p1504 N71-20951

Integrated life support systems for long duration manned space flight simulations 10 p1505 N71-20952

Management and results of long term manned test on regenerative life support system in space simulator 10 p1505 N71-20953

Support systems for long term regenerative life support manned test facility 10 p1505 N71-20954

Water management in long term manned space simulation life support test 10 p1505 N71-20956

Design and performance of thermal air conditioning equipment during long term manned space environment simulation 10 p1505 N71-20958

Trace contaminant measurements during long term manned space station atmosphere simulation 10 p1506 N71-20963

Aerosol analysis during long term simulation of manned regenerative life support system 10 p1506 N71-20964

Mass balance and crew input/output requirements during long duration space cabin simulation test 10 p1508 N71-20973

Crew selection procedures for long duration manned space station simulation test 10 p1508 N71-20977

Crew activity analysis for long duration space flight simulation test 10 p1508 N71-20981

Crew reaction to environment habitability during long duration space station simulation test 10 p1509 N71-20982

Confinement effects on human psychomotor performance during long duration space environment simulation test 10 p1509 N71-20983

Long duration confinement effects in simulated space station on human performance during tracking task 10 p1509 N71-20984

Non-interference crew performance analysis during long duration space station simulation test with visual and aural observations 10 p1509 N71-20986

Long duration confinement effects in spacecraft cabin simulator on psychological test results for spacecrew 10 p1509 N71-20987

Space station simulator background noise effects on crew behavior during long term confinement 10 p1509 N71-20988

Medical observation of spacecrew during long duration space station simulation test 10 p1498 N71-20990

Dermal and environmental microbiological data from long duration manned space station simulation 10 p1498 N71-20991

Nasopharyngeal bacteria cultures of spacecrew during long duration space station simulation 10 p1498 N71-20992

Biomedical body fluid and composition data from spacecrew during long term space station simulation 10 p1498 N71-20993

Biochemical serum assays on crewmen during long duration space station simulation 10 p1498 N71-20996

Spirometer loop measurements of human pulmonary functions during long duration manned space environment simulation 10 p1499 N71-20997

Spacecrew blood carboxyhemoglobin saturation in long duration space station simulation 10 p1499 N71-20998

Data from long duration manned test of regenerative life support system in space station simulation 10 p1510 N71-20999

Long-term performance tests of neon gas filled, high-temperature ceramic voltage-regulator tubes (NASA-SP-1813) 12 p1858 N71-23120

Long term variations of atmospheric circulation over Northern Hemisphere and its sectors (NLL-M-20076-5828.4F/1) 12 p1959 N71-24334

Signal and stimulus rate effects on long term human response to light signal intensity differences (RM-505) 13 p2038 N71-24935

Definitive orbit for Ariel 3 computed from mainframe observations for 27.5 months (RAE-TR-69275) 16 p2677 N71-28059

Safety problems comprising fuel element failure and long term operation of containment spray systems for water cooled power reactor with emphasis on environmental effects (ORNL-TM-3263) 16 p2630 N71-28101

Reliability evaluation of plastic encapsulated integrated circuits including long-term tests and short-term highly accelerated tests (AD-722043) 16 p2569 N71-28405

Biotechnological problems of man machine systems required for long duration space flights (NASA-SP-205) 16 p2551 N71-28526

Humidity control, carbon dioxide removal, and oxygen regeneration in cabin atmosphere during prolonged manned space flight 16 p2552 N71-28532

Long term manned space flight nutrition and food requirements 16 p2552 N71-28535

Microbiological life support requirements in long term manned space flights 16 p2552 N71-28537

Animal experimentation for simulating long duration space flight hazards for human physiology 16 p2553 N71-28541

Biomedical test data for predicting weightlessness effects on man during long term space flights 16 p2553 N71-28542

Manned 90-day performance test of regenerative life support systems in space station simulator including crew biomedical tests (NASA-CR-111881) 16 p2554 N71-28877

PROD computer programming for predicting satellite orbit decay under long term effects
[RAE-TR-71007-PT-1] 17 p2844 N71-29418

Long term effects on visual processes during submarine patrol
[AD-721683] 17 p2707 N71-29444

Activated carbon in reactor confinement systems to remove radiolysis from effluent gases in event of nuclear accident
17 p2715 N71-29857

Long term biological and physiological effects of plutonium compound inhalation in dogs and plutonium translocation in respiratory system
17 p2709 N71-29869

Computerized simulation of long term physiological effects of plutonium oxide inhalation on dog respiratory system including tissue, blood, and excretion data
17 p2709 N71-29869

Long term hyperoxygen exposure effects on human respiratory physiology
[JPRS-53332] 17 p2709 N71-30150

Human performance and recovery in man machine systems of continuous operations and work/rest schedules
[AD-723430] 19 p3048 N71-32331

Secular magnetic variation anomaly and geomagnetic field drift in Poland
[TT-70-55086] 19 p3096 N71-32646

Secular magnetic variation anomaly and Warsaw anomaly
19 p3096 N71-32647

Global annual averages of earth albedo and radiation used to estimate long term effects on space vehicle equipment and surfaces
[NASA-SP-8067] 20 p3258 N71-33104

Long term effect of earth tides on earth rotation
20 p3265 N71-33370

Long term tidal effects in satellite gravity data
20 p3265 N71-33371

Long term hypokinesia effects on rat serotonin metabolism
30 p3220 N71-33453

Color and music effects on humans during prolonged isolation in confined space
20 p3221 N71-33460

Possible causes of Tunguska explosion and its effects on surrounding region
24 p4009 N71-38590

LONG WAVE RADIATION

Satellite measured albedo and long wave radiation study of Indian monsoons
02 p0256 N71-11622

Production of plasmas by long wavelength carbon dioxide lasers
[MATT-786] 03 p0436 N71-12635

Statistical evaluation of fading caused by intermodulation in combined long wave broadband propagation
[CNET-NT-EST/APH/1] 10 p1525 N71-21433

Long wave propagation measurements for geophysical research
11 p1707 N71-22920

Tabulated upper air data obtained over Japan by radiosondes for dew point, atmospheric electricity, and long wave radiation for 1966 and 1967
13 p2109 N71-25507

Mathematical model for two-dimensional, long-wave propagation in curved acoustic ducts determining vibrational velocity distribution and variation and phase of motion at any point in system
[NASA-TM-X-67184] 14 p2219 N71-26338

Infrared radiometer used for terrestrial long wave radiation measurement
15 p2410 N71-27546

Absolute calibration of long wave radiometer using hemispherical black body cover
15 p2411 N71-27556

Integration of exponential functions and application to long wave radiative transfer near mesopause
15 p2404 N71-27565

Recompressing underwater long wave acoustic signals distorted by surface waves
[BMVG-FBW71-73] 18 p2889 N71-30641

Meteorological satellite and radiosonde measurements compared to calculated values of terrestrial long wave radiation
[NASA-TT-F-13823] 18 p2917 N71-31269

Long acoustic wave propagation in curved ducts and junctions between straight and curved ducts utilizing Bessel functions for steady and decaying fields of motion
[NASA-TM-X-67944] 23 p3801 N71-37103

LONGITUDE

Free oscillations of fluid on hemisphere bounded by meridians of longitude
09 p1380 N71-19504

Amplitude variations and longitude asymmetry with respect to transport activity
24 p4011 N71-38600

LONGITUDINAL CONTROL

Importance of aircraft speed control relative to longitudinal touchdown dispersion
03 p0405 N71-12432

Experimental aerodynamic performance characteristics of rotor entry vehicle configuration - supersonic
[NASA-TN-D-7048] 06 p0792 N71-16535

Analysis of requirements for longitude repositioning of high power communication satellites in synchronous equatorial orbit
[NASA-TM-X-2558] 11 p1702 N71-22624

LONGITUDINAL STABILITY

Boundary layer separation and longitudinal and lateral stability of Avro 707 aircraft during flight tests
[ARC-CP-1107-PT-4] 07 p0969 N71-17082

Low speed wind tunnel and flight stability tests of BAC 221 aircraft longitudinal balance, noting aileron difficulties
[ARC-CP-1134] 10 p1493 N71-21205

Low-speed wind tunnel longitudinal stability tests on sweptback wing model with blowing at leading edge slots and trailing edge flaps for Buccanier aircraft performance
[ARC-RM-3655] 13 p2022 N71-24565

Longitudinal stability characteristics of preliminary configurations for Scout D at Mach numbers 0.20 to 4.65
[NASA-TN-D-6239] 17 p2850 N71-29710

Subsonic stability, control, and performance of shuttle concept with blended wing-body
[NASA-TM-X-2341] 18 p3018 N71-31254

Horizontal and vertical gust load frequency and power spectra influence on longitudinal aircraft stability
19 p3037 N71-31890

Effect of turbulence and aircraft performance on ILS approach task and longitudinal stability
[NASA-CR-1821] 20 p3210 N71-33325

Low speed wind tunnel test on effects of horizontal tail geometry on longitudinal stability of orbiter shuttle
[NASA-CR-119858] 21 p3520 N71-35084

Low speed wind tunnel tests of lateral longitudinal, and directional stability of MDC STS high cross range shuttle orbiter
[NASA-CR-103163] 21 p3521 N71-35091

Low speed wind tunnel tests of space shuttle lateral and longitudinal static stability characteristics at Mach 0.25
[NASA-CR-119853] 21 p3522 N71-35098

Wind tunnel tests on longitudinal and lateral directional stability of NAR/GD delta wing orbiter mated to Saturn 5 S-IC booster
[NASA-CR-103200] 21 p3523 N71-35101

Wind tunnel tests of lateral, longitudinal, and directional stability characteristics for scale model of orbiter shuttle
[NASA-CR-103155] 21 p3524 N71-35108

Low speed wind tunnel tests of longitudinal and lateral aerodynamic characteristics of MDAC STS orbiter
[NASA-CR-103194] 21 p3524 N71-35111

Longitudinal and lateral stability data from wind tunnel tests of earth orbiting shuttle
[NASA-CR-103154] 21 p3524 N71-35112

Low speed longitudinal, directional, and lateral static stability characteristics of straight wing orbiter during configuration build-up
[NASA-CR-103156] 21 p3524 N71-35113

Subsonic longitudinal and lateral directional stability investigation of MDAC LCR orbiter, unpowered and powered - graphs
[NASA-CR-119965] 24 p4017 N71-38665

Longitudinal, lateral, and directional static stability and control characteristics of delta wing space shuttle orbiter models 134D and 134C at Mach 0.26
[NASA-CR-119979] 24 p4020 N71-38681

LONGITUDINAL WAVES

NT PLANE WAVES

Longitudinal diffusion coefficients of gaseous ions drifting in electric field
[AD-714868] 07 p1084 N71-18085

Radial variation of longitudinal modes in vibrating bar
[UCRL-50947] 09 p1477 N71-19999

Propagation of electromagnetic waves along gyrotropic cylinder in longitudinal magnetic field
11 p1800 N71-23016

Determining internal energy coefficients of Al from ultrasonic measurements of longitudinal and shear wave speeds with hydrostatic pressure, uniaxial stress, and temperature variations
[AD-721368] 16 p2610 N71-28443

Structural damping in Saturn vehicles and scale models of liquid propelled rocket vehicles
[NASA-TM-X-64607] 18 p3018 N71-31145

Use of gas lasers to measure velocity and absorption of longitudinal hypersonic waves
[NASA-TT-F-13902] 21 p3464 N71-34660

Multi-species ion acoustic dispersion relation for argon-helium plasma
[NASA-CR-121721] 21 p3493 N71-34881

Interaction of quasi-longitudinal and quasi-transverse waves in inhomogeneous Vlasov plasma between electron cyclotron and maximum upper hybrid frequencies
22 p3656 N71-36071

Long waves along single-step topography in semi-infinite uniformly rotating ocean calculated using Kelvin-type dispersions
23 p3788 N71-36097

Experimental investigation of quasi-stationary longitudinal ion streams in L-1 stellarator
[CN-28/H-4] 23 p3831 N71-37322

LOOK ANGLES

U AZIMUTH

U ELEVATION ANGLE

LOOP ANTENNAS

Computer aided analysis of receiving and transmitting properties of thin wire circular loop antenna
[SC-RR-70-433] 04 p0511 N71-13534

Computerized simulation of antenna radiation patterns from current loops above conducting cone
[AD-714990] 07 p1000 N71-17936

Characteristics of mutual electromagnetic coupling of loops over homogeneous ground determined by employing image theory
[AD-717351] 11 p1723 N71-22144

Fabrication and testing of flexible loop antenna in underwater, towed, ELF receiving antennas
[AD-717718] 11 p1724 N71-22373

Bearing errors of loop antenna direction finders caused by elliptical polarization variations
11 p1705 N71-22949

Numerical evaluation of low frequency loop antenna array resistance to ground reaction as compared to radiation resistance for electric and magnetic dipole antennas
[AD-720599] 14 p2231 N71-26740

K-beta diagrams for two uniformly periodic loop antenna arrays determined from measured near field amplitude and phase distributions of traveling waves
[AD-721592] 16 p2568 N71-28335

Design, development, and electromagnetic properties of sheet driven circular loop radio antenna
[AD-724343] 20 p3241 N71-33119

LOOPS

Endless loop tape transport mechanism for driving and tensioning recording medium in magnetic tape recorder
[NASA-CASE-XGS-01223] 01 p0023 N71-10449

Design and operation of experimental gap loop for nuclear reactor
[ZJE-48] 02 p0266 N71-12179

Differences between manual, continuous, and oscillating plugging indicators for sodium loops
[ANL-7638] 05 p0606 N71-15415

Volterra functional analysis on phase locked loop response to frequency modulations
12 p1894 N71-24013

Liquid sodium Banjo loop for irradiation of fuel pin
[CEA-CONF-1673] 13 p2121 N71-25233

Carbon equilibrium loop work including data on electrochemical meters, cover gas analysis, and oxygen determination and mass transfer models in sodium
[WARD-4210-T-1-1] 16 p2634 N71-28724

RELAP/JASME code for analyzing reactor core and loop thermal hydraulics during blowdown
[CONF-715002-6] 21 p3459 N71-34617

LOW

NT LORAN C

Characteristics of Omega navigation system installed in Norway and installation of navigation system in Sweden
[FOA-3-C-3613-65] 22 p3618 N71-35778

Computerized simulation of Loran A ground wave propagation pulse subjected to atmospheric perturbation
[OT/ITS-RR-10] 23 p3793 N71-37040

LORAN C

Determining accuracy of measuring wind aloft by tracking from rising balloons with Loran C
[NASA-TM-WBMT-EDL-11] 01 p0078 N71-10497

Evaluating data error analysis and equipment performance in tests of differential Loran techniques
[ESSA-TR-ERR-166-ITS-107] 05 p0721 N71-15513

Time synchronization of Loran C navigation system and characteristics of sky wave reception operation
[NASA-TM-X-65515] 13 p2109 N71-24018

Remote object tracking and position indication using Omega navigation system and Loran C applications in police surveillance
19 p3132 N71-31641

Computerized simulation of Loran A ground wave propagation pulse subjected to atmospheric perturbation
[OT/ITS-RR-10] 23 p3793 N71-37040

LORAN D

Computerized simulation of Loran A ground wave propagation pulse subjected to atmospheric perturbation
[OT/ITS-RR-10] 23 p3793 N71-37040

LORENTZ FORCE

Research on elementary particle inclusion, Regge theory and Lorentz poles
[ORO-3992-17] 03 p0419 N71-12594

SUBJECT INDEX

Field theory in infinite momentum frame for deriving particle model, with transverse Galilean and longitudinal Lorentz boost invariances stressed
[LPTHE-71/24] 20 p3293 N71-33958

LORENTZ TRANSFORMATIONS
Numerical analysis of relativistic three body problem in relative variables
[JNTR-P2-5100] 04 p0536 N71-13681
Constraints on equal time commutators from Lorentz covariance
[JFPT-4/70] 06 p0883 N71-15831
Expansion of invariant two-point function for bilocal field of Lorentz, Poincaré, and $O(4,1)/R(3,1)$ groups
[JNTR-P2-5304] 08 p1248 N71-18203
Lorentz transformation properties of Bethe-Salpeter Green function
[TR-71-101] 13 p2103 N71-24983
Scattering theory based on two variable expansions furnished by Lorentz and conformal group
[JTD-25654] 14 p2380 N71-25722
Mathematical model for relativistic scattering amplitudes in high energy interactions based on Fourier analysis and Lorentz group embeddings
[JNTR-E2-5341] 14 p2318 N71-26760
Transformation properties of massive particle states at infinite momentum
[JNTR-E2-5379] 16 p2643 N71-28066
Application of Lorentz reciprocity theorem to near field detection of buried dielectric spheres in antenna lossy half spaces
16 p2563 N71-28822
Peculiarities of application of Lie group theory to nonrelativistic transformations
[JNTR-P2-5625] 18 p2974 N71-30561
Rotation and Lorentz symmetries of scattering amplitudes
23 p3805 N71-37131

LOS ALAMOS TURRET REACTOR
U HIGH TEMPERATURE NUCLEAR REACTORS
Calculation and measurement of stray losses in induction motors and comparison with results obtained from standard techniques
[NLL-M-20559-(5828.4F)] 23 p3733 N71-36615

LOST WAX PROCESS
U INVESTMENT CASTING
LOTS CARGO SHIPS
U CARGO SHIPS
LOUDNESS
Loudness calculation by summation of weighted subband noise intensities and loudness judgement data comparisons
[NASA-TM-X-2300] 15 p2371 N71-26993
Loudness comparisons between pulses of sinusoidal waves having different envelope shapes and spectra
[TRANS-2713-(9022.81)] 23 p3805 N71-37127

LOUISIANA
Summary of synoptic meteorological observations for North America coastal marine areas of Galveston and Corpus Christi, Texas and New Orleans, Louisiana - Vol. 6
[AD-710770] 01 p0081 N71-10097
Survey of structural damage along Mississippi-Louisiana Gulf Coast done by Hurricane Camille
[NBS-TN-569] 12 p1935 N71-23851
Statistical analysis of distribution pattern for major types of depositional environments in Mississippi River delta region
[AD-719946] 13 p2075 N71-25172
Survey of airfield pavement condition at USNAS New Orleans, Louisiana
[AD-724286] 20 p3244 N71-33007

LOUVERES
Reliability analysis of louver system used for satellite temperature control
[TASS-70-Y-0736] 14 p2351 N71-25615
Actuated louvers for satellite thermal control in solar environment
14 p2351 N71-25697
Active satellite temperature control noting louvers application
[TASS-70-Y-0683] 14 p2351 N71-25698
Thermal analysis of louver array for satellite temperature control
[TASS-70-Y-0719] 14 p2351 N71-25699
Actuators and bearings for satellite louvers thermal control array
[TASS-70-Y-0731] 14 p2352 N71-25751

LOVE WAVES
Anisotropic equivalent of Love longitudinal wave measurement approximation
[AD-710296] 01 p0127 N71-10023
Detection of objects buried in ocean bottom using Love wave sonar system
[AD-710807] 10 p1545 N71-20619
Performance of acoustic dispersive broadband surface wave delay lines using Love and Rayleigh waves
[OASIS-85-669-CL/CM/PT] 01 p1606 N71-20937
Least squares method for determining Love wave scattering upon boundary irregularity in elastic layer over rigid half space
24 p3918 N71-37944

LOW ALTITUDE

Satellite observation of low altitude electron flux density
11 p1823 N71-22459
Flight test evaluation of military aircraft low altitude high speed performance
12 p1835 N71-23421
Measurements of aircrew total vibration exposure during low altitude, high speed flight in F-4C aircraft
[AD-720271] 14 p2305 N71-26172
Spatial coherence of 1 to 5 min acoustic waves from two nuclear explosions along with atmospheric pressure background noise for same period measured at low altitude
[AD-720833] 15 p2399 N71-27216
Flight tests of cross, modified ringtail, and disk-gap-band parachute deployment performance from low altitudes with structural load data
[NASA-TM-X-2221] 16 p2530 N71-28021
Pilot injuries on high speed low altitude flight noting acceleration due to gust effects
19 p3048 N71-31888

LOW ALTITUDE SUPERSONIC VEHICLES
U F-111 AIRCRAFT
LOW ASPECT RATIO
Measuring characteristics of low Mach number flow of air from two planar nozzles with aspect ratio of 3 at exit
[AD-711313] 02 p0200 N71-11139

LOW ASPECT RATIO WINGS
NT DELTA WINGS
NT TRAPEZOIDAL WINGS
Second-order slender wing theory for incompressible flow over low aspect ratio wings with and without leading edge separation
[NASA-CR-66762] 09 p1321 N71-19912
Supersonic aerodynamic characteristics of rocket vehicle model with low aspect ratio wing and tail surfaces
[NASA-TM-X-2159] 09 p1318 N71-20181
Second order slender wing theory for calculating supersonic flow over low aspect ratio wings with sonic leading edges and leading edge separation
[NASA-CR-1866] 21 p3373 N71-34004

LOW COST
Light weight, low cost, ablative thermal protection system for space shuttles
17 p2847 N71-29456

LOW DENSITY FLOW
Wall pressure, hypersonic forces and hypersonic heat transfer for flat plates in low density flow
[REPT-70-4] 04 p0471 N71-13401
Operation of rarefied gas viscous under low density conditions
[NASA-CR-115800] 05 p0691 N71-14767
Low density hypersonic flow over cone, scattering of gas particles from solid surface
06 p1182 N71-18936
Increased ionization and temperature due to harmonic microwave absorption in magnetized low density plasmas
[CEA-CONF-1607] 15 p2499 N71-27203
Flat plate in hypersonic low density flow examined in shock formation and transition regime
[DLR-FB-70-79] 17 p2700 N71-29432
Dislodgement and entrainment of solid particles by low density airstream flowing over particulate surface, for aerodynamic surface erosion study
[NASA-CR-111924] 19 p3081 N71-32551

LOW DENSITY GASES
U RAREFIED GASES
LOW DENSITY MATERIALS
Performance of low density silicone-phenolic and commercial ablative composites
[NASA-TN-D-5130] 06 p0960 N71-16872
Method and photodetector device for locating abnormal voids in low density materials
[NASA-CASE-MFS-20044] 16 p2598 N71-28993

LOW DENSITY WIND TUNNELS
European subsonic, supersonic, transonic, hypervelocity and low density wind tunnel characteristics
07 p1003 N71-17099
Hypersonic low density wind tunnel including auxiliary equipment for electroforming and electroplating wind tunnel models
[BMW-FB-W-70-51] 08 p1175 N71-18593
On-line mass spectrometric analysis of nonequilibrium air flows in low density wind tunnel nozzle
[AD-718955] 13 p2063 N71-24477
Description and operational behavior of hypersonic low density wind tunnel at Goettingen, West Germany
[DLR-FB-70-42] 15 p2390 N71-27034
Liquid nitrogen cooled nozzle for hypersonic low density wind tunnel
[DLR-FB-70-41] 15 p2390 N71-27035
Mach number reduction in low density hypersonic wind tunnel by increasing nozzle throat area
[DLR-FB-70-43] 15 p2391 N71-27060
Low density plasma jet wind tunnel studies on shock wave structure in nonequilibrium, partially ionized gas flow
21 p3410 N71-34266

LOW FREQUENCIES

NT VERY LOW FREQUENCIES

LOW LATITUDES

Low frequency noise properties of mercury telluride infrared detectors
[AD-711119] 01 p0833 N71-10510
Type-3 solar radio burst storms observed at low frequencies
[NASA-TM-X-65374] 01 p0118 N71-10603
Low frequency background noise in planar silicon transistors
[PUBL-506] 02 p0195 N71-11364
Combination scattering of microwaves by low frequency oscillations in electrodeless induction discharge plasma
[KHFTI-69-52] 03 p0432 N71-12932
Trigger circuit for phase difference measurements on alternating current signals
[REPT-5-73] 04 p0511 N71-13535
Computerized simulation of LF and VLF radio wave propagation with spherical wave functions of integer order
[ESSA-TR-ERL-165-ITS-106] 05 p0648 N71-15451
Human performance under low frequency vibration and effects on whole body orientation
07 p0962 N71-17667
Low frequency discriminants for small events
[AD-715528] 07 p1023 N71-17873
Particle rebounding by additional lower frequency RF system in electron storage rings
[DESY-70/34] 08 p1247 N71-18194
Low frequency axisymmetric waves in weakly ionized magnetoplasma column
[ISPR-366] 08 p1272 N71-18526
Low frequency dielectric constants of LiF, NaF, NaCl, NaBr, KCl, and KBr by substitution method
[COO-623-153] 08 p1280 N71-19032
Phase locked loop derived from ideal single side-band modulation
08 p1164 N71-19120
Low frequency characterization and identification of objects for inverse scattering and target recognition
[AD-717747] 11 p1700 N71-22251
Low frequency plasma noise from mercury electron bombardment ion thruster studied for several magnetic field configurations
[NASA-TN-D-6286] 11 p1821 N71-22613
Regulation of vocal intensity at low fundamental frequencies with voice communication of Navy divers
[AD-718837] 12 p1874 N71-23580
Transmitting and receiving antennas for low frequency and very low frequency regions
[AD-719675] 14 p2227 N71-25654
Low frequency noise sources in bipolar junction transistors and efforts to reduce burst noise
14 p2230 N71-26576
Radiation measurements, low frequency, and high pressure investigations of induction heated plasma torch to simulate gas core nuclear rocket requirements
[NASA-CR-1804] 15 p2445 N71-27023
Temperature, ultrasonic, and macroscopic effects on metal fatigue
[AD-721729] 16 p2609 N71-28401
Low frequency analysis of rocket engines using compressible propellants
17 p2833 N71-29584
Design, calibration, and performance of low frequency RAE-1 satellite
[NASA-TM-X-65616] 18 p0818 N71-30664
Low frequency vibration effects on visual acuity of pilot performing visual task
[ISVR-TR-49] 20 p3225 N71-32884
Least squares method applied to noise reduction in low frequency line spectra
20 p3264 N71-33560
High frequency heating of hydrogen plasma near low hybrid frequency
[ORNL-TR-2415] 21 p3495 N71-34897
Thermal conduction and low frequency electrostatic waves in collisional plasmas immersed in magnetic field
23 p3833 N71-37334
Low frequency convective oscillations in neutron stars with internal magnetic field
23 p3849 N71-37436

LOW FREQUENCY BANDS
NT VERY LOW FREQUENCIES
Propagation medium disturbance effects on time signal transfer in low frequency bands
11 p1708 N71-22914
Low frequency time signals for clock synchronization
11 p1707 N71-22915
Statistical analysis on phase fluctuations in low frequency and very low frequency propagation
11 p1707 N71-22916

LOW GRAVITY
U REDUCED GRAVITY
LOW GRAVITY MANUFACTURING
Development of space manufacturing techniques for orbital workshops
[NASA-TM-X-66480] 02 p0234 N71-11701

LOW LATITUDES
U TROPICAL REGIONS

LOW LEVEL TURBULENCE

LOW LEVEL TURBULENCE

- Analysis of effect of terrain irregularities on turbulence and diffusion in surface boundary layer
[NVO-0140-1] 09 p3187 N71-20591
- Conference papers on low level turbulence models to determine influence on aircraft stability and missile trajectories
[DLR-MITT-70-12] 19 p3036 N71-31882
- Low level turbulence kinetic energy and spectral energy distribution
19 p3127 N71-31883
- Low level turbulence measurement for artillery missile trajectories mounted on towers
19 p3127 N71-31884
- Low level turbulence models for determining standard deviation of ballistic missile trajectories
19 p3127 N71-31887

LOW MASS

U MASS

LOW MOLECULAR WEIGHTS

- Process for preparing high molecular weight polyaryloxysilanes from lower molecular weight forms
[NASA-CASE-XMF-08674] 16 p2358 N71-28807

LOW NOISE

- Applications for small current amplifying device including solid state sensors, Schottky junctions, and other low noise devices
[AD-119740] 13 p2054 N71-24448
- Low noise preamplifier with negative feedback for spectral resolution improvement in X ray spectroscopy
[CEA-N-1401] 15 p2472 N71-27434

LOW PASS FILTERS

- Computer program for design of low pass filters with uniform or semiuniform dissipation
[WRE-TN-ED-193] 08 p1170 N71-19172
- Echo scanning for equalizing linear signal distortion in data transmission channels
17 p2720 N71-29783

- Computer program for reducing radar tracking data magnetic tape numbers for data storage by editing and low pass filtering
[NASA-CR-119176] 17 p2748 N71-30149

LOW PRESSURE

NT HIGH ALTITUDE PRESSURE

- Short time, low pressure response in wind tunnel transducer system
[AD-711911] 01 p0057 N71-10856
- Viscous damping techniques and high overload protection for low pressure transducers
[RAE-TR-69032] 02 p0224 N71-11530
- Histological aspects and ultrastructure of intoxication in rats by pure oxygen at low pressure
02 p0165 N71-11826

- Open-air pressure gage for low gas pressure measurement
[NPL-MC-6] 03 p0383 N71-13362

- Organic cooled, heavy-water moderated WR-1 research reactor capable of low pressure with high temperature in primary system and very low radiation fields near primary piping
[AECL-3523] 04 p0547 N71-13640
- Required ventilation rates determined for Mark 5 diving helmet as part of low pressure underwater breathing apparatus
[AD-713395] 05 p0637 N71-14705

- Low pressure oxygen/hydrogen auxiliary propulsion subsystem for space shuttle
[NASA-CR-114945] 11 p1820 N71-22010
- Shock-induced combustion in explosive mixtures of hydrogen and air or oxygen by high speed shots at low pressures
11 p1843 N71-22632

- Numerical fluid model for low pressure plasma in toroidal magnetic field
12 p1982 N71-24051

- Fracture and crack growth for welded joints of 5Al-2.5Sn titanium in environment of low pressure, high purity hydrogen
[NASA-CR-114859] 13 p2091 N71-24378

- Flowmeters for sensing low fluid flow rate and pressure for application to respiration rate studies
[NASA-CASE-FRC-10023] 14 p2244 N71-26546
- DULCINEE code for water cooled reactor at low pressure
[CEA-N-1378] 17 p2781 N71-29295

- One-fluid model of low pressure MDH plasma in toroidal geometry
[MATT-814] 17 p2811 N71-29575

- Space shuttle hydrogen/oxygen auxiliary propulsion system high and low pressure thrusters
17 p2836 N71-29589

- High and low chamber pressure injectors for space shuttle hydrogen oxygen APS engines
[AGCS-0100-71] 17 p2836 N71-29590
- Space shuttle high and low pressure auxiliary propulsion subsystem definition
17 p2837 N71-29599

- Preliminary designs of high and low pressure APS for space shuttles
17 p2837 N71-29600

LOW PRESSURE CHAMBERS

U VACUUM CHAMBERS

LOW SPEED

- Variable geometry manned orbital vehicle having high aerodynamic efficiency over wide speed range and incorporating auxiliary pivotal wings
[NASA-CASE-XLA-03691] 05 p0773 N71-15674
- Low speed boundary layer separation on compressor blades of varying aspect ratios
[ARC-CP-1103] 07 p0966 N71-17108
- Instrumentation and development techniques for low velocity gas flow measurement
12 p1899 N71-23313
- Device utilizing RC rate generators for continuous slow speed measurement
[NASA-CASE-XMF-02966] 13 p2060 N71-24863
- National Science Council goals in low speed aerodynamics - Canada
24 p4013 N71-38627

LOW SPEED HANDLING

U CONTROLLABILITY

U LOW SPEED

LOW SPEED STABILITY

- Lateral oscillations and low speed and lateral stability of free flight lifting bodies
[ARC-R/M-3641] 06 p0791 N71-15705
- Subsonic aerodynamic stability characteristics of NAR 134B delta wing space shuttle
[NASA-CR-103193] 21 p3522 N71-35093

LOW SPEED WIND TUNNELS

- NT SUBSONIC WIND TUNNELS
- Low speed wind tunnel tests of series of twin-keel all-flexible parawings
[NASA-TN-D-5936] 01 p0002 N71-10052

- Low speed and supersonic wind tunnel and hydraulic test tunnel tables
[IC-AERO-70-01] 03 p0359 N71-13237

- Low speed wind tunnel tests of ground proximity effects on static longitudinal characteristics and boundary layer control of short takeoff aircraft
[NAL-TR-201] 09 p3137 N71-20106

- Cavity resonance effects on dynamic and thermal characteristics of resonant cavities in low speed, turbulent, shear flow
09 p3138 N71-20539

- Low speed wind tunnel model assessment of porous boundary layer control by suction at civil aircraft leading edge flaps
[ARC-R/M-3640] 10 p1491 N71-20847

- Estimating unsteady pressure distributions in T tail configuration from measured distribution and theory
[NLR-TR-68048-L] 12 p1849 N71-23313

- Wind tunnel investigation of jets exhausting into cross flow - description and data analysis
[AD-718122] 12 p2064 N71-24492

- Wind tunnel tests to determine low-speed aerodynamic characteristics of large-scale STOL transport model with augmented jet flap
[NASA-TM-X-62017] 14 p1198 N71-26183

- Low speed wind tunnel test of four ft diameter circular plate model to determine surface static pressure distributions for jet decay characteristics of cross flow
[AD-720232] 14 p2244 N71-26516

- Low speed wind tunnel test of four ft diameter circular plate model with three exhausting jets
[AD-720233] 14 p2244 N71-26517

- Steady tailplane lift effect on subcritical response of subsonic T tail flutter aircraft model in low speed wind tunnels
[ARC-R/M-3652] 15 p2366 N71-27096

- Low speed static wind tunnel tests of half-span fuselage and variable sweep pressure wing model
[NASA-TN-D-6215] 20 p3207 N71-33776

- Low speed wind tunnel test on effects of horizontal tail geometry on longitudinal stability of orbiter shuttle
[NASA-CR-119858] 21 p3520 N71-35084

- Low speed aerodynamic characteristics of McDonnell Douglas scale model space shuttle booster
[NASA-CR-103161] 21 p3520 N71-35086

- Low speed wind tunnel tests of lateral longitudinal, and directional stability of MDC STS high cross range shuttle orbiter
[NASA-CR-103163] 21 p3521 N71-35091

- Low speed wind tunnel tests of stability and control characteristics of space shuttle booster at subsonic speeds
[NASA-CR-119861] 21 p3522 N71-35094

- Low speed wind tunnel tests on effects of vertical tail and geometry on directional stability of orbital space shuttle model
[NASA-CR-119856] 21 p3522 N71-35095

- Low speed wind tunnel test to define space shuttle model cruise and landing aerodynamic characteristics
[NASA-CR-119855] 21 p3522 N71-35096

- Low speed wind tunnel tests of subsonic aerodynamic properties of generic high cross range shuttle orbiter
[NASA-CR-119859] 21 p3522 N71-35097

- Low speed wind tunnel tests of space shuttle lateral and longitudinal static stability characteristics at Mach 0.25
[NASA-CR-119853] 21 p3522 N71-35098

- Low speed wind tunnel tests of subsonic aerodynamic characteristics of 0.04 scale model of space shuttle
[NASA-CR-119862] 21 p3522 N71-35099

- Low speed wind tunnel tests of GAC 3A earth orbiting shuttle aerodynamic characteristics
[NASA-CR-103153] 21 p3523 N71-35100

- Low speed wind tunnel tests of directional stability characteristics for M/DAC delta wing booster
[NASA-CR-103157] 21 p3523 N71-35101

- Low speed wind tunnel tests to determine static aerodynamic characteristics of SB-15 scale model
[NASA-CR-103164] 21 p3524 N71-35104

- Low speed wind tunnel tests of effects of nacelle position, refueled fuselage, and elevator effectiveness for NAR straight wing orbiter
[NASA-CR-103160] 21 p3524 N71-35107

- Low speed wind tunnel tests on longitudinal and lateral stability of high cross range delta wing space shuttles
[NASA-CR-119857] 21 p3524 N71-35109

- Low speed wind tunnel tests of straight wing and delta wing configuration space shuttle booster models
[NASA-CR-103162] 21 p3524 N71-35110

- Low speed wind tunnel tests of longitudinal and lateral aerodynamic characteristics of MDAC STS orbiter
[NASA-CR-103194] 21 p3524 N71-35111

- Low speed wind tunnel tests of 1/25 scale models of reusable orbital spaceplanes for subsonic aerodynamic data at Mach 0.17
[NASA-CR-119882] 24 p4019 N71-38674

- Low speed wind tunnel tests of takeoff, landing, and cruise aerodynamic characteristics of space shuttle booster with exhaust effect simulation
[NASA-CR-119975] 24 p4019 N71-38675

LOW TEMPERATURE

- Low temperature thermoluminescence of Apollo 11 material
01 p0120 N71-10079

- Interferometric measurements of far infrared refractive index of sodium fluoride at low temperatures
[AD-711064] 01 p0089 N71-10461

- Cryoentrainment pump study and behavior of nucleation gases at low temperature
[NASA-CR-111799] 01 p0059 N71-10488

- Molecular interactions and crystal structures at low temperature emphasizing Freon 22
[AD-711096] 01 p1111 N71-10631

- Engineering evaluation of low temperature high rate reserve magnesium perchlorate batteries
[AD-710952] 01 p0007 N71-10715

- Preparation and low temperature mass spectrometry of aminoborane
[AD-711439] 02 p0173 N71-11222

- Environmental simulation of low space temperatures using cold walls
03 p0356 N71-12706

- Thermal and magnetic properties of adsorbed phases of He-3 and He-4 at low temperatures
[AD-712161] 03 p0419 N71-13319

- Low temperature thermoluminescence in LiF
[COO-1105-161] 04 p0585 N71-14222

- Low temperature properties of Anderson model of localized magnetic moments
[NUB-2031] 04 p0567 N71-14281

- Apparatus for low temperature measurement and stabilization
[CEA-N-1366] 05 p0685 N71-14077

- Magnetic properties of solids at low temperatures
[AD-714699] 06 p0904 N71-16361

- Chromium palladium silicon foil thermometer for low temperature measurements
[CALT-822-14] 06 p0862 N71-16700

- Low temperature electrical resistivity
[PB-195154] 01 p1132 N71-17801

- Optical spectroscopic studies of lead atoms and molecules in low temperature matrices
[UCRL-19662] 07 p1074 N71-17474

- Variations in length and crystal parameters of alpha, beta, and delta phases of plutonium at low temperatures due to self-irradiation
[CEA-CONF-1619] 08 p1256 N71-18306

- Single particle mode peak of inelastic neutron scattering cross section for antiferromagnetic chromium at low temperatures
[NUB-2040] 08 p1279 N71-18889

- Using electron spin-echo technique to measure spin lattice relaxation of V/4 plus paramagnetic impurities in rutile at liquid-helium temperature
09 p1426 N71-19530

- Research in structural characterization of materials with emphasis on polymers
09 p1404 N71-19727

- Thermal and electrical conductivities of gold ion alloys at low temperatures
09 p1398 N71-19734

- First-order radiative transition rate electron transfer from neutral donors to neutral acceptors in silicon at low temperatures
09 p1432 N71-19877

- Low temperature chemical thermodynamics and solid state behavior
[COO-1149-180] 10 p1631 N71-20620

- Structural stability of austenitic Cr-Ni steels under plastic deformation and extremely low temperature
[ORNL-TR-2314] 10 p1580 N71-21480

SUBJECT INDEX

Use of gun tunnel as low temperature test facility for hypersonic inlet research 11 p1732 N71-22635

Nuclear spin lattice relaxation of Ni 63 and Pd 105 measured at liquid helium temperature in Ni alloys [UCRL-20376] 12 p1973 N71-23942

Ultrasonic vibration effects on cooldown rate of bodies in liquid nitrogen and helium 12 p1968 N71-24154

Lattice parameter measurements on aluminum after electron irradiation at low temperatures [JUL-664-FN1] 13 p2091 N71-24428

Low temperature radiator for rejecting thermal power from isotope Brayton power system [NASA-TM-X-67822] 13 p2186 N71-25090

Mobility measurements of ions in dilute He-3/He-4 mixtures in pure He-3 at very low temperature 13 p2137 N71-25431

Synthesis of low temperature petroleum resistant elastomers [AD-720215] 14 p2280 N71-26384

Viscosity of compressed N₂, He, H₂, and Ar from minus 100 to 25 C using viscometer 14 p2214 N71-26433

Solvent effects on viscosity and osmotic pressure of polymer solutions at 25 C 14 p2215 N71-26582

Electron-photon enhancement effects on low temperature specific heat measurements of noble and transition metals [AD-720883] 15 p2432 N71-27212

Velocity measurement of third sound in unsaturated superfluid helium films between 1.12 and 2.05 K 15 p2454 N71-27375

Low temperature mechanical properties of epoxy-resin formulations [SC-DR-70-421] 15 p2377 N71-27478

Simple empirical relation based on adiabatic compressibility, adiabatic bulk modulus, and reduced temperature for liquid argon, krypton, and xenon, and application to mercury [NVO-4176-6] 15 p2378 N71-27982

Low temperature overcharge voltage characteristics of OAO batteries and cells 16 p2539 N71-28667

Defects introduced into Ge and Si by electron irradiation at low temperature 16 p2666 N71-28735

Thermal measurements on solids below 1 degree K [COO-1629-24] 16 p2669 N71-29042

Mechanical properties of pure binary Ni-Cr alloys at high and low temperatures [NLL-TRANS-746-439-90022.401] 17 p2764 N71-29696

Phonon scattering by dislocations and its influence on lattice thermal conductivity and on dislocation mobility at low temperatures 17 p2819 N71-29950

Sound velocity in low temperature carbon dioxide [TRG-3070] 18 p2962 N71-30667

Spectral reflectivity of solid surfaces at low temperature [NASA-CR-119869] 18 p2965 N71-31192

Chemical reactions between alkali-lead oxide silica glasses and acid solution at low temperature 18 p2940 N71-31264

Efficiency and performance characteristics of low temperature two phase liquid metal MHD power systems [AD-721087] 19 p3173 N71-31757

Measurement of magnetic field dependence on low temperature electromagnetic generation of ultrasonic waves in potassium 21 p3465 N71-34664

Low temperature measurements of specific heat of nickel nitrate hexahydrate and antiferromagnetic exchange interactions [AD-726429] 22 p3552 N71-35299

Defect structure of Al-Zn alloy induced by quenching and low temperature aging 22 p3595 N71-35599

Magnetic susceptibility of vanadium carbide from 77 to 300 K measured by magnetometer [NASA-CR-122039] 22 p3657 N71-36079

Low temperature thermal conductivity of Sb and Ga doped Zn and Zn doping and electron irradiation [JNP-18364] 22 p3658 N71-36083

Thermal resistance of cadmium and magnesium at temperatures from 3 to 100 K 22 p3660 N71-36099

LOW TEMPERATURE ENVIRONMENTS

Measuring neutron scattering and magnetic susceptibility for single crystal cesium trichloromanganate at low temperatures 06 p0933 N71-16111 [AD-714515]

Research and development of silicon solar cells for low solar intensity and low temperature applications [NASA-CR-114280] 08 p1147 N71-18735

Bibliography on cold regions science and technology, accessions between July 1969 and June 1970 - Part I [AD-715799] 08 p1191 N71-18851

Bibliography on cold regions science and technology, accessions between July 1969 and June 1970 - Part 2 [AD-715717] 08 p1191 N71-18852

Human calorific requirements when working in extreme climatic environments 09 p1337 N71-20367

Nickel, magnesium, and aluminum annealing effects on neutron irradiated iron crystal defects in low temperature environments [CEA-COIN-1681] 15 p2472 N71-27437

Development and characteristics of dilution refrigerator capable of producing and holding temperatures near absolute zero 19 p3197 N71-32458

Physiological response of subjects exposed to cold water environment wearing different protective suit assemblies [AD-724617] 20 p3215 N71-32907

Low temperature photodetachment of carbon dioxide, ammonia, and nitrous oxide condensed gas molecules utilizing ultraviolet light [NASA-CR-121938] 22 p3628 N71-35847

Engineering evaluation of standard line reserve low temperature batteries for transceiver application [AD-726946] 23 p3710 N71-36449

Measuring thermal conductivity of ice in 4 to 273 K range [AD-727185] 23 p3752 N71-36758

Low temperature miniature automatically activated magnesium battery to supply reserve power to expendable electronic devices [AD-727066] 24 p3875 N71-37625

LOW TEMPERATURE PHYSICS

Superconducting transition temperatures of electron beam evaporated metals condensed on liquid helium cooled substrates [UCRL-19624] 02 p0284 N71-11838

Low temperature tunneling and second energy gap in superconducting niobium [AD-713072] 02 p0286 N71-12007

Low temperature melting curve of helium 3 [UCSD-34-P-143-26] 03 p0331 N71-12365

Low temperature annealing of electron irradiated germanium [COO-1198-735] 03 p0389 N71-12683

Effects of low temperature on lattice structure, X ray scattering, mobility of electrons and quantum hydrodynamics 04 p0569 N71-14418

Superconductivity, solid state physics, and low temperature physics [COO-1569-59] 06 p0930 N71-15740

Effect of radiation on structural materials for NERVA engine tested at cryogenic and elevated temperatures - Vol 4 [NASA-CR-116518] 07 p1063 N71-17351

Low temperature heat capacities of dilute solutions of Fe and Cr in Cu [UCRL-19686] 07 p1132 N71-17924

Discussing advances in ultralow temperature physics in 1960s and future trends for 1970s [UCSD-34-P-143-30] 08 p1242 N71-18273

Quantum mobility, configurational entropy, and Mossbauer spectroscopy of impurity atoms in crystals [NUB-2049] 08 p1279 N71-18690

Determining low temperature behavior of localized magnetic moments by crystal field effect on orbital paramagnetism [NUB-2043] 08 p1279 N71-18691

Low temperature magnetization of dilute copper manganese alloys [UCSD-34-P-143-33] 08 p1216 N71-18942

Magnetic properties at metal surfaces including neutron mirror measurements, neutron scattering of FeCO₃, and low temperature measurements [ORO-3674-4] 11 p1779 N71-22510

Abstracts of research in low temperature, low and high energy nuclear physics [NUP-A-71-1] 12 p1969 N71-23288

Helium 4 impurities and magnetic field effect on thermal boundary resistance between powdered cerium magnesium nitrate and liquid helium 3 at very low temperatures [UCSD-34-P-143-35] 13 p1217 N71-25463

Low temperature measurements on electrical resistivity, magnetic susceptibility and magnetoresistivity for amorphous iron palladium silicon alloys [CALT-822-24] 13 p2098 N71-25515

Characteristics of electromagnets, superconductor devices, and magnetic alloys under low temperature conditions [AD-720883] 16 p2665 N71-28558

Chemical analysis of aniline and cyclohexane mixtures to determine viscosity in critical region 20 p3230 N71-33753

Low temperature measurement of Knight shift in metallic sodium 20 p3285 N71-33821

LOW TEMPERATURE TESTS

Low temperature sliding friction and wear studies on metals in ultrahigh vacuum [AD-711668] 01 p0068 N71-10738

LOW VISIBILITY

Using photoelectric effect to detect densities of free and trapped carriers in II-VI compounds at cryogenic temperatures [NASA-CR-111562] 03 p0443 N71-13066

Effects of low temperature on lattice structure, X ray scattering, mobility of electrons and quantum hydrodynamics 04 p0569 N71-14418

Measuring dynamic response of thermistors at liquid hydrogen temperatures [REPT-49-03400] 05 p0587 N71-15477

Cryostat for flexure fatigue testing of composite materials [NASA-CASE-XMF-02964] 07 p1032 N71-17639

Performance of test equipment for low temperature materials [RHRL/R-202] 08 p1205 N71-18284

Design and operation of apparatus for analyzing friction and wearing processes of materials at cryogenic temperatures [AD-716972] 10 p1636 N71-21274

Cryostat for use with horizontal fatigue testing machines at low temperatures [NASA-CASE-XMF-10968] 12 p1924 N71-24234

Mechanical properties and stress corrosion evaluation of MP 35N multiphase alloy at cryogenic temperatures [NASA-TM-X-64591] 14 p2274 N71-26043

Electron irradiation effects in n-type, p-type, and high-purity silicon at 5.0 and 1.6 K using ac hopping conductivity [COO-1198-781] 16 p2667 N71-28838

Low temperature cytophysiological adaptation of human and mammalian cells 20 p3220 N71-33455

Determination of thermal conductivity and electrical resistivity of solids at cryogenic temperatures [NASA-CR-121706] 21 p3463 N71-34652

Analysis of physical and chemical properties of lubricants used with roller bearings at low temperatures 22 p3588 N71-35553

Low temperature fluorine chemistry of chlorine, nitrogen, and oxygen [AD-727059] 23 p3720 N71-36514

LOW THRUST

NT MICROTHRUST

Computer program for open-loop error analysis of low thrust interplanetary trajectories [NASA-CR-119375] 18 p3016 N71-31296

Segmented two-body low thrust interplanetary trajectory and performance optimization program [NASA-CR-119362] 18 p3016 N71-31297

Modifications to interplanetary trajectory program for providing capability of generating optimum low-thrust trajectory in N-body field [NASA-CR-119377] 18 p3016 N71-31298

LOW THRUST PROPULSION

NT ELECTROMAGNETIC PROPULSION

NT ELECTROSTATIC PROPULSION

NT ION PROPULSION

NT PHOTONIC PROPULSION

NT PLASMA PROPULSION

NT SOLAR PROPULSION

Outer planetary mission planning and technological improvements for outer planet spacecraft [NASA-CR-117850] 11 p1828 N71-22551

Low pressure burning rate of modified solid propellant during spacecraft orbit insertion 11 p1819 N71-22555

Controlled-flow igniter for low thrust burning rate of solid propellant rocket engine 11 p1819 N71-22556

Comparative performance of solid core nuclear and cryogenic chemical space propulsion systems [NASA-TM-X-2352] 18 p3002 N71-31246

LOW TURBULENCE

Aerodynamic performance of shuttle-orbiter configuration with variable delta wing geometry in low turbulence subsonic wind tunnels [NASA-TM-X-2206] 05 p0626 N71-14943

Dependence of low turbulence flow in supersonic wind tunnel on conditions in supply header [AD-718227] 12 p1896 N71-23480

LOW VACUUM

Vibration damping system operating in low vacuum environment for spacecraft mechanisms [NASA-CASE-XMS-01620] 05 p0735 N71-15671

LOW VELOCITY

U. LOW SPEED

LOW VISIBILITY

Psychological and procedural aspects to ILS approaches and landings in visibilities less than 1200 feet 03 p0405 N71-12429

Light absorption and scattering effects on underwater visibility of imaging devices in sea water 04 p0565 N71-13736

Low visibility approach and landing simulation for jet transports [NASA-CR-734951] 05 p0629 N71-14600

Climatological tables of ceiling, visibility, surface wind, and temperature for Capestranta Airport, Finland [REPT-25] 09 p1414 N71-20096

Climatological tables of ceiling, visibility, surface wind, and temperature for Kuopio Airport, Finland [REFT-24] 09 p1414 N71-20097

Experimental pulsed neodymium lidar system modified for measuring slant visibility conditions for aircraft landing operations 16 p2531 N71-28217 [AD-716483]

Testing ASMI/transporter for moving emergency service vehicles on airfields during poor visibility conditions 17 p2719 N71-29553

Statistical correlation between atmospheric moisture content, aerosol particle size, and visual range [NLL-M-9267-5828.4F] 17 p2744 N71-29889

Occurrence frequency of poor ceiling and visibility conditions in Southeast Asia and Korea [AD-722735] 17 p2778 N71-30054

Systems analysis of aircraft, aircraft guidance and control systems, and atmospheric turbulence for low visibility instrument landing system requirements [AD-722773] 17 p2705 N71-30173

Analysis of glide-slope information requirements for low visibility aircraft landing approach using Kalman filter-optimal control combination to simulate DC-8 control system [AD-722655] 18 p2956 N71-30887

LOW VOLTAGE

Flexible monopole antenna with broad bandwidth and low voltage standing wave ratio [NASA-CASE-MSC-12101] 08 p1169 N71-18720

Circuit design for failure sensing and protecting low voltage electric generator and power transmission networks [NASA-CASE-GSC-10114-1] 15 p2389 N71-27366

Low voltage aluminum electrolyte capacitors with high capacitance [ECR-16] 18 p2896 N71-31170

LOW WING AIRCRAFT

Full scale wind tunnel tests of low wing, single engine, light aircraft with positive and negative propeller thrust and up and down flap deflection - graphs [NASA-CR-1783] 19 p3038 N71-32369

LOWER ATMOSPHERE

NT D REGION

Atmospheric refraction and temperature profiles in lower atmosphere over Bay of Helligland [REFT-12] 04 p0490 N71-13489

Meteorological phenomena of lower atmosphere for test area of Brazil [LAFE-122] 04 p0542 N71-14404

Long term climatological and atmospheric effects of air pollution [PB-193801] 04 p0522 N71-14493

Meteorological parameters in lower atmosphere [AD-713785] 05 p0715 N71-14520

Seasonal anomaly of F-region explained in terms of composition changes in lower atmosphere [NASA-TM-X-65410] 05 p0669 N71-14804

Energy equations describing physical processes in ground atmosphere 05 p0717 N71-15144

Lower atmosphere gravity wave propagation in stratified atmospheric models for pressure and wind variations 07 p1053 N71-17165

Investigating relationship of man and biosphere with respect to food production and toxic chemical pollution [JPRS-52325] 07 p0981 N71-17429

Discussing relationship between numerical growth and expanding industrial and technological power of man and biosphere 07 p0981 N71-17430

Biosphere sinks for carbon monoxide emissions to atmosphere [PB-195433] 08 p1186 N71-18307

Climatological values of lower atmosphere temperature and wind stratification 08 p1230 N71-18539

Biological and geological aspects of soil science 14 p2207 N71-26456

Electron and proton populations in low altitude radiation environment 16 p2676 N71-29090

Lower atmosphere wind shear vertical distribution [WMO-230-TP-123] 18 p2949 N71-30828

Lower atmosphere vertical distribution of boundary layer wind shear annual variations as observed in Canada 18 p2949 N71-30829

Dynamic characteristics of wind and temperature profile vertical distribution over Paris-north airport site 18 p2949 N71-30831

Dependence of lower atmospheric wind shear on averaging period and lapse rate as recorded at Lopik, Netherlands 18 p2949 N71-30835

Lower atmospheric wind shear vertical distribution in USSR as recorded from direct and indirect data 18 p2950 N71-30836

Lower atmosphere wind shear determined for aircraft approach control from observations in different American sites 18 p2950 N71-30837

Approaches to biogeocenotic research based on internal dynamic organization and phenomena which ultimately determine the laws of life of the biosphere 20 p3223 N71-33503

Investigation of tundra biogeocenoses noting species saturation of surface layer and soil and eleven phases of turnover 20 p3223 N71-33504

Analysis of natural zones and space ecosystems noting relationships of living animals and biosphere 20 p3224 N71-33505

Inversion frequency of atmospheric temperature over 2m region in USSR [NLL-M-26590-5828.4F] 21 p3454 N71-34580

International cooperation in global atmospheric research program on weather forecasting 23 p3793 N71-37036

Lower atmospheres of Mars, Venus, and Jupiter 23 p3846 N71-37412

LOWER IONOSPHERE

NT D REGION

Aeronomic analysis of bremsstrahlung effects in lower ionosphere due to electrons penetrating into auroral zone 04 p0522 N71-13824

LOX (OXYGEN)

U LIQUID OXYGEN

LOX-HYDROGEN ENGINES

U HYDROGEN OXYGEN ENGINES

LR CIRCUITS

U RL CIRCUITS

LRC CIRCUITS

U RLC CIRCUITS

LRV (VEHICLE)

U LUNAR ROVING VEHICLES

LSI

U LARGE SCALE INTEGRATION

LSSM

Equipment specifications for Lunar Sounder Antenna Assembly [NASA-CR-114797] 05 p0642 N71-14726

Developing communications equipment for HF Lunar Sounder [NASA-CR-114795] 05 p0642 N71-14727

LUBRICANT TESTS

Synthesis and characteristics of antiwear lubricant additive [AD-713880] 06 p0877 N71-16122

Development of lubricating oils suitable for use with liquid oxidizers [NASA-CR-103006] 06 p0867 N71-16591

Developing empirical equation for calculating effects of container geometry on liquid lubricant evaporation in vacuum [NASA-TM-X-65455] 08 p1206 N71-18410

Steel friction and wear tests in nitrogen with paraffinic resins, synthetic paraffinic oil, glycol, and ester lubricants including thermal stability at high temperatures [NASA-TN-D-6251] 10 p1568 N71-21667

Lubricant, thrust bearing, and ring seal tests for supersonic turbine engine mainshaft lubrication system [NASA-CR-72854] 15 p2417 N71-27810

Tests with stainless steel in sliding contact with lead, indium, and tin coatings in liquid hydrogen to determine their lubricating capability [NASA-TN-D-6455] 19 p3105 N71-32193

Chemical synthesis and lubricant tests of INKb-21 (calcium) antioxidant additive [AD-727413] 24 p3944 N71-38157

Statistical analysis of fatigue test data on aviation gas turbine lubricants 24 p3946 N71-38148

LUBRICANTS

NT GAS LUBRICANTS

NT HIGH TEMPERATURE LUBRICANTS

NT LUBRICATING OILS

NT SOLID LUBRICANTS

Metallic film diffusion into metal or ceramic surfaces for boundary lubrication in aerospace environments [NASA-CASE-XLE-01765] 01 p0073 N71-10772

Effectiveness of selected antiwear additives in synthetic esters 01 p0073 N71-10831

Manual on application of fuels and lubricating materials [AD-711756] 01 p0060 N71-10862

Thickening capacity of silica gel in plastic lubricants [AD-711751] 01 p0073 N71-10863

Wear graph curve for evaluating lubricant wear resistance tests in friction machine 01 p0061 N71-10934

Lubricating and sizing agent for glass fibers [AD-713944] 03 p0397 N71-13123

Factors affecting efficiency of lubricants used for drop forging [AD-713446] 05 p0709 N71-15269

Effect of oil films on adhesion of polymers to metal surfaces [AD-713450] 05 p0710 N71-15370

Temperature stability of lubrication layers during friction of alloyed aluminum on steel [AD-713770] 05 p0693 N71-15434

Corrosion resistance of polymeric petroleum lubricants against microbiological attack [AD-714131] 06 p0578 N71-14620

Testing materials for use in cages, balls, and races in cryogenic hydrogen-cooled 110-mm ball bearing [NASA-CR-72779] 06 p0866 N71-14647

Computer analysis of pressurized thrust bearing design using incompressible lubricant [NASA-TN-D-6075] 06 p0867 N71-14655

Quality control data on lubricants for electric contacts [ECR-08] 10 p1563 N71-21800

Comparison of two drill bits and two lubricants for aluminum alloy drilling 10 p1564 N71-21146

Metal wear inhibition at friction point using selective transfer effect [AD-717827] 11 p1778 N71-22372

Preparation of additives containing phosphorus, sulfur, and chlorine from thio ethers of glycerol alpha-monochlorohydrin [AD-718693] 12 p1943 N71-23671

Improvement in properties of lubricating greases by addition of diaryl and triaryl disubstituted phosphates [AD-718484] 12 p1944 N71-23706

Metallic film diffusion for boundary lubrication in aerospace engineering [NASA-CASE-XLE-10337] 12 p1929 N71-24046

Machining under conditions of high static pressure of lubricant cooling medium [AD-719812] 13 p2099 N71-24627

Lubrication properties of disulfides and diselenides of transition metals at high temperatures in air, nitrogen, and argon media [AD-719786] 13 p2100 N71-24679

Quantitative analysis of motor oil additives based on dependence of surface tension on temperature and additive content [AD-720377] 14 p2277 N71-25886

Addition of pyrophosphates to lubricants for detergent purposes [AD-720743] 14 p2280 N71-26380

Purification and distillation of lubricant additive alkylphenol [AD-720927] 15 p2427 N71-26811

Lubrication, wear, and design aspects of rolling contact bearings [NASA-SP-237] 15 p2412 N71-26826

Lubricant rheology and chemistry effects on contact material fatigue 15 p2412 N71-26827

Rheological models for evaluating effects of lubricant film thickness and frictional traction 15 p2413 N71-26832

Lubrication chemistry of hydrocarbon liquids and effects on bearing surface wear 15 p2414 N71-26838

Elastohydrodynamic lubrication effects on roller bearing design and performance 15 p2414 N71-26839

Geometry and kinematics of gear design and lubrication that effect tooth contacts 15 p2414 N71-26840

Test of rolling element fatigue life with fluorinated ether lubricant at cryogenic temperature using five ball fatigue tester [NASA-TN-D-6367] 16 p2600 N71-28038

Bearings, lubricants, and seals for lubricated and hydraulic components for space shuttle with high temperature and vacuum operating capabilities 17 p2755 N71-29449

Elastohydrodynamic film thickness between roller disks with synthetic paraffinic oil at temperatures from 339 to 589 K [NASA-TN-D-6411] 18 p2930 N71-31228

Differential-maximum-bubble-pressure apparatus used for surface tension measurements in air of liquid lubricants to 200 C [NASA-TN-D-6450] 20 p3279 N71-33315

Mineral fluids as lubricating composition for mercury wet seals [AD-721032] 21 p3444 N71-34585

Analysis of physical and chemical properties of lubricants used with roller bearings at low temperatures 22 p3588 N71-35533

Technical aviation handbook covering aircraft maintenance, navigation aids, airframes, lubricants, paints and gas turbine engines, and checkout procedures [AD-727195] 24 p3874 N71-37813

Emission spectral methods for determining content of mineral admixtures in fuels, oils, and lubricants [AD-727197] 24 p3886 N71-37809

Effect of antiseizing and antiwear additives on wear of highly loaded, small module metric gears [AD-727414] 24 p3929 N71-38031

Impregnation permeability of air bearing graphite pads [Y-SC-7] 24 p3942 N71-38154

Influence of dispersion medium composition on properties of lubricants thickened with lithium soaps of synthetic fatty acids [SFA] [AD-727432] 24 p3943 N71-38159

Antioxidant additives for increasing thermo-oxidizing stability of synthetic lubricants
[AD-727891] 24 p3945 N71-38142

Control and chemical composition of aircraft fuels, lubricants, and special liquids
[AD-727199] 24 p4000 N71-38531

LUBRICATING OILS

Reliability of testing oils with added detergents in single cylinder engines
[AD-711479] 01 p0073 N71-10970

Investigating ester and alkyl compounds as lubricating oils for use with liquid oxidizers
[NASA-CR-102907] 02 p0246 N71-11419

Friction and leakage losses of piston rings
[RAE-LIB-TRANS-1455] 02 p0230 N71-11570

Design and performance of gas film and oil-film lubricated self-sealing mainshaft seals for gas turbine engines
[NASA-CR-72737] 02 p0291 N71-12035

Reflectance measurements of diffusion pump oil and silicon oils and liquid reflectance equipment construction
[TID-25478] 03 p0418 N71-12886

Squeeze film lubrication for gyroscopes wheels and behavior of hydrodynamic spiral grooved spin axis bearing
[NASA-CR-102381] 03 p0385 N71-13165

Synthesis of oil additives, action mechanisms, and production techniques for motor and insulating oils
[AD-712830] 03 p0397 N71-13181

Antwear and extreme pressure additive effects during bearing spinning with synthesized hydrocarbon oils
[NASA-TM-X-52931] 05 p0691 N71-14786

Characteristics of fire resistant turbine oil in turbo-generator regulating and lubricating system
[JPRS-51949] 05 p0694 N71-15456

Development of lubricating oils suitable for use with liquid oxidizers
[NASA-CR-103006] 06 p0067 N71-16591

Fluid seal formed by flexible disk on rotating shaft to retain lubricating oils around shaft
[NASA-CASE-XLB-05130-2] 09 p1392 N71-19570

Steel friction and wear tests in nitrogen with paraffinic resins, synthetic paraffinic oil, glycol, and ester lubricants including thermal stability at high temperatures
[NASA-TN-D-6251] 10 p1568 N71-21667

Friction points, and oil system of aviation gas turbine engines
[AD-717835] 11 p1781 N71-22011

Stearic acid additives in lubricants for improved contact fatigue life of ball bearing steel surfaces
[AD-717824] 11 p1782 N71-22079

Mathematical model of oil whip phenomenon in rotating shaft systems with incompressible fluid lubrication and analysis of squeeze film bearings
11 p1770 N71-22724

Feasibility of ash-free organic compounds containing phosphorus, nitrogen, and boron as antioxidant additives for lubricating oils
[AD-717895] 12 p1946 N71-23952

Investigation of antiwear, anticorrosion, and antifriction effectiveness of oils and solid lubricants for various conditions of application
[AD-717975] 13 p2100 N71-24938

Melting temperature measuring instrument for lubricating oil additive ashes
[AD-719767] 13 p2101 N71-25104

Preparation and properties of polyfunctional polymeric lubricant additives
[AD-720369] 14 p2278 N71-25895

Oil viscosity and chemical composition effects on roller bearing lubricant efficiency
15 p2413 N71-26836

Additive INKAP-46 containing sulfur, chlorine, and phosphorus to improve functional properties of lubricating oils used in reduction gears with Novikov gearing
[AD-721031] 15 p2430 N71-27336

Evaluating series hybrid bearing concept by testing lubricated fluid film thrust bearing at high speed
[NASA-TM-X-67873] 16 p2603 N71-28907

Vaporized oil ball bearings for satellite antennas
[JPRS-51949] 05 p0694 N71-15456

Thermal stability and applications of trimethyl propene ester based lubricating oil
[JONERA-TP-930] 20 p3229 N71-33435

Technique for experimental determination of fluid viscosity of synthetic turbine engine lubricants over temperature range of 100 to 700 F
[AD-727060] 23 p3779 N71-36930

Powdered glass suspensions for improved lubricating properties of oils
[NLL-RISLEY-TRANS-2092-9091.9F] 24 p3930 N71-38042

Chemical synthesis and lubricant tests of INKAP-46 (calcium) antioxidant additive
[AD-727413] 24 p3944 N71-38137

Environmental tests of solid lubricants, liquid lubricants, and lubricant additives under high pressures up to 70 kilobars
[AD-727577] 24 p3946 N71-38146

Oscillating quartz crystal viscometer measurements of viscosity of synthetic lubricating fluids as function of pressure, shear rate, and temperature
[NASA-CR-120786] 24 p3965 N71-38284

LUBRICATION

NT BOUNDARY LUBRICATION

NT SELF LUBRICATION

Grease lubricated spiral groove bearings suitable for spin axis of gyros in automatic pilots
[NASA-CR-102926] 03 p0384 N71-12819

Squeeze film lubrication for gyroscopes wheels and behavior of hydrodynamic spiral grooved spin axis bearing
[NASA-CR-102381] 03 p0385 N71-13165

Analysis of friction and lubrication in metal working processes
[AD-713033] 03 p0383 N71-13169

Synthesis of oil additives, action mechanisms, and production techniques for motor and insulating oils
[AD-712830] 03 p0397 N71-13181

Lubrication considerations in design of gears
[NASA-TM-X-52942] 05 p0691 N71-14785

Hydrodynamic theory of lubrication applied to machine parts - bibliographies
[AD-714346] 06 p0066 N71-16454

Tungsten hemisphere against tungsten disk slipping assembly with liquid gallium lubrication in ultrahigh vacuum
[NASA-TN-D-6184] 07 p1033 N71-17324

Film thickness, friction, and pressure distribution effects in elastohydrodynamic gear lubrication
15 p2412 N71-26828

Lubrication by boundary, elastohydrodynamic, and fluid films, wear due to fretting, erosion, scuffing, and pitting, and friction in aircraft
[NASA-TM-X-67872] 18 p2929 N71-31134

Use of infrared radiation to reveal lubrication behavior between bearing surfaces
[NASA-TM-X-67883] 18 p2929 N71-31210

Lubrication, friction, and wear processes analyzed for space vehicle design criteria
[NASA-SP-0063] 18 p2931 N71-31471

Action of gas particles used as additive to improve lubricating properties of mineral oils
[NLL-RISLEY-TRANS-2091-9091.9F] 19 p3120 N71-32097

Performance of gallium lubricated slipping assembly in ultrahigh vacuum for 500 hours
[NASA-TN-D-6436] 19 p3105 N71-32137

Characteristics of externally pressurized, gas lubricated, circular thrust bearing with central admission and operating in inherent compensation mode
[NRC-ME-MT-61] 20 p3278 N71-33226

Performance tests and characteristics of circular, hydrostatic, gas-lubricated single inlet thrust bearings
[NRC-MT-62] 20 p3278 N71-33227

Numerical analysis of oil film thickness required for optimum operation of hydrodynamically lubricated journal bearings
[CRANFIELD-M/P-3] 21 p3433 N71-34429

Design, optimization, and test instrumentation for sodium-lubricated bearings in sodium pumps and circulating auxiliaries in breeder reactors
[NYO-3930-10] 21 p3461 N71-34636

Isothermal elastohydrodynamic theory for full range of pressure-viscosity coefficient for heavily loaded rolling contacts
[NASA-CR-1929] 22 p3588 N71-35550

Performance tests of water-lubricated, Rayleigh step, hydrodynamic journal bearings under no load conditions to determine stability
[NASA-TN-D-6514] 23 p3762 N71-36820

Friction and wear behavior of anti-friction bearings operating in ultrahigh vacuum conditions
[NLL-RISLEY-TRANS-2140-9091.9F] 23 p3764 N71-36837

Statistical analysis of lubricating properties of electrolytes and friction measurement in system consisting of metal and lubricating electrolyte metal
[AD-727449] 24 p3944 N71-38135

LUBRICATION SYSTEMS

Characteristics of fire resistant turbine oil in turbo-generator regulating and lubricating system
[JPRS-51949] 05 p0694 N71-15456

Development of hybrid bearing lubrication system with combination of standard type lubrication and magnetic flux field for earth atmosphere and space environment operation
[NASA-CASE-XNP-01641] 11 p1772 N71-22997

Lubrication for bearings by capillary action from oil reservoir of porous material
[NASA-CASE-XNP-03972] 11 p1773 N71-23048

Influence of aluminum on friction and wear of iron-aluminum alloys dry and lubricated in argon atmosphere
[NASA-TN-D-6359] 14 p2261 N71-26045

Lubricant, thrust bearing, and ring seal tests for supersonic turbine engine mainshaft lubrication system
[NASA-CR-72854] 15 p2417 N71-27810

Face seal performance, mass spectroscopic test fluid study and supplementary test data for supersonic turbine engine mainshaft lubrication system
[NASA-CR-72873] 15 p2418 N71-27963

Hydrodynamic lubrication of journal bearing with one or two axial oil grooves, with power loss, load capacity, oil flow, and stability charts for design of minimum power loss, stable bearing
20 p3280 N71-33799

LUCITE (TRADEMARK)

U POLYMETHYL METHACRYLATE

LUCITE BANGS

U PLASTIC DEFORMATION

U YIELD POINT

LUMINAIRES

NT AIRCRAFT LIGHTS

NT AIRPORT LIGHTS

NT ARC LAMPS

NT FLASH LAMPS

NT MERCURY LAMPS

NT RUNWAY LIGHTS

NT SEARCHLIGHTS

NT XENON LAMPS

Analytical studies of in-reactor tests of nuclear light bulb unit cell using Pewee, nuclear furnace, and high flux isotope reaction
[NASA-CR-110698] 01 p0084 N71-10373

Development of ultraviolet resonance lamp with improved transmission of radiation
[NASA-CASE-ARC-10030] 03 p0349 N71-12521

Test results of photometric measurements of 200-watt VAS lamps, and comparison of results with 300-watt data
07 p1080 N71-18023

Feasibility of electroluminescent panels and rotor tip lighting for military helicopters to aid in observation by other vehicles in formation
[AD-715851] 08 p1444 N71-18734

Standard spectral energy distribution using tungsten lamp
[NPL-QU-14] 13 p2123 N71-24496

Use of incandescent lamps to measure optical and detector data in photoelectric spectrometers
[NASA-TN-D-6313] 13 p2039 N71-24611

LUMINESCENCE

Vision with small starlight scope - three stage image intensifier
[J2F-1970-11] 05 p0689 N71-15580

Object recognition with aided and unaided night vision as function of luminance
[J2F-1971-7] 21 p3382 N71-34065

Underwater oceanographic photometry at different depths, emphasizing luminance and illuminance
22 p3576 N71-35473

Lunar disk luminance effects on manual sighting accuracy of space sextant using simulated lunar and stellar targets
[NASA-TN-D-6507] 22 p3617 N71-35774

LUMINESCENCE

NT BIOLUMINESCENCE

NT CHEMILUMINESCENCE

NT ELECTROLUMINESCENCE

NT FLUORESCENCE

NT LUNAR LUMINESCENCE

NT OPTICAL RESONANCE

NT PHOSPHORESCENCE

NT PHOTOLUMINESCENCE

NT THERMOLUMINESCENCE

NT X RAY FLUORESCENCE

Luminescent phenomena in interplanetary space and moon related to luminescent, thermoluminescent, and cathodoluminescent properties of terrestrial minerals and rocks
[NASA-CR-111003] 01 p0119 N71-10076

Luminescent phenomena on moon and in interplanetary space
01 p0120 N71-10077

Luminescent and thermoluminescent properties of granite and its constituent minerals and their relevance to transient lunar phenomena
01 p0045 N71-10078

Electret processes for characterizing nonluminescent and near-insulating solids
01 p0107 N71-10082

Luminescence of oxides by OH activation in hydrogen flames
01 p0016 N71-10083

Detailed cathodoluminescence characterization of common silicates including spectral colors and intensities
01 p0016 N71-10084

Intrinsic cathodoluminescence emission from wulframite single crystals
01 p0107 N71-10085

Instrument for studying electron stimulated luminescence of terrestrial, extraterrestrial, and synthetic materials - luminoscope
01 p0052 N71-10086

Luminescence of rocks and of natural and synthetic inorganic materials - laboratory studies
01 p0045 N71-10087

Temperature effects on luminescence of benzophenones in polymers
01 p0019 N71-10087

Luminescence of lunar rocks from Apollo 11
02 p0296 N71-11941

Fraction interaction in cadmium sulfide and selenide and zinc oxide
[AD-713181] 05 p0757 N71-15600

- Defects and their role in determining luminescence and electrical properties of crystals
[AD-714620] 06 p0933 N71-16017
- Luminescence petrography of Apollo 12 rocks and comparative features in Apollo 11 rocks, terrestrial rocks, and meteorites
[NASA-CR-114842] 07 p1110 N71-17563
- Cerium(III)-sensitized terbium(III) luminescence in thorium-orthophosphate
[CONF-700403-5] 07 p1082 N71-18144
- Investigating mechanism of nitrogen luminescence from irradiation by Po-210 alpha particles at pressures between 30 and 700 torr
[NP-18425] 08 p1253 N71-18332
- Luminescence measurements on Apollo 11 and Apollo 12 lunar soil samples
[NASA-CR-114899] 09 p1464 N71-19778
- Luminescent analysis techniques and devices for air pollution measurements
11 p1002 N71-22059
- Luminescence of zinc sulfide ion injected thin films
[SRDE-70064] 12 p1985 N71-23358
- Optical luminescence in reaction detection at rear of porous electrodes and comparison of interface reaction resistance and electrolyte ohmic resistance in zinc-silver oxide batteries
[NASA-CR-118007] 12 p1860 N71-23518
- Luminescence of Apollo 11 and 12 rocks measured with UV, X ray, and proton radiation
[NASA-CR-114970] 13 p2165 N71-24358
- Quantitative microluminescence analysis of lunar glasses and fines
[NASA-CR-114966] 13 p2166 N71-24944
- Luminescent processes in solids during interaction with gas
14 p2326 N71-26455
- Atomic excitations, ultraviolet photolysis, and luminescent vapor phase atom, radical, and molecular reactions including spectroscopic analysis techniques
[AD-72461] 18 p2880 N71-31558
- Luminescence induced by UV and visible lasers for remote active sensing of materials from ground, air, and space
[MDC-G2344] 19 p3109 N71-32686
- Mechanical and radiological tests of kematic compasses modified with sealed tritium gas luminous sources
[AD-726362] 22 p3618 N71-35781
- Isothermal annealing of 0.97 eV luminescence in electron irradiated silicon semiconductors
[AD-726916] 23 p3836 N71-37352
- Fast luminescent decay of silicon light-emitting diode
[NASA-TM-X-65721] 24 p3965 N71-38285
- LUMINOUS INTENSITY**
U LUMINOUS INTENSITY
LUMINOSITY
NT STELLAR LUMINOSITY
Solar activity and planetary luminosity
[NASA-TM-X-65371] 01 p0123 N71-10583
- Dependence of peak brightness of ionization in range of 1 is less than or equal to 1/1 min is less than or equal to 15 at P equal to 1 atm, 0.3 atm, and 0.1 atm
[IFVE-SEP-69-72] 09 p1437 N71-20081
- Mechanism for measuring nanosecond time differences between luminous events using streak camera
[NASA-CASE-XLA-01987] 12 p1967 N71-23976
- Two lead scintillator, sandwich counters for measuring luminosity of Orsay storage ring
[LAL-1249] 22 p3636 N71-35920
- Comet luminosity variations and spectral properties in relation to interplanetary medium
24 p4009 N71-38587
- LUMINOUS FLUX DENSITY**
U LUMINOUS INTENSITY
LUMINOUS INTENSITY
NT ILLUMINANCE
NT LUMINANCE
Detailed cathodoluminescence characterization of common silicates including spectral colors and intensities
01 p0016 N71-10084
- High light intensity image dissection cameras for short duration recordings
[RAE-LIB-TRANS-1445] 02 p0225 N71-11553
- Illumination calculations using diffraction and light scattering in ultraviolet image dissection cameras
[RAE-LIB-TRANS-1443] 02 p0226 N71-11554
- Laboratory intercomparison of fluorescent lamps to determine available precision in photometric and spectroradiometric measurements
[NBS-TN-559] 05 p0687 N71-15476
- Structure and environment effects on transition probabilities of luminant chromium complexes
[COO-773-21] 06 p0875 N71-16795
- Measuring intensity distribution of omnidirectional semi-flash airport lights
07 p1005 N71-18113
- Far ultraviolet spectral intensities of energetic vacuum carburetor
[NASA-TM-X-52966] 08 p1243 N71-18747
- In clear sky, spectral intensity measurements of ultraviolet zenith radiation and direct solar radiation
[AD-716355] 09 p1383 N71-19758

- Development of star intensity measuring system which minimizes effects of outside interference
[NASA-CASE-XNP-06510] 12 p1922 N71-23797
- Intensity of gas production in comets based on photometric parameters
[NASA-TT-F-13492] 12 p1998 N71-24244
- Line intensities in different spectral widths and intervals for atmospheric water vapor absorption using rigid and nonrigid rotor models
15 p2401 N71-27504
- Luminous intensity formulas and polarized neutron diffraction patterns including effects of crystal defects
[INR-1220] 18 p2579 N71-30706
- Intensity distribution of optical images for various degrees of illumination using Hermitian matrices
[NASA-TT-F-13721] 18 p2966 N71-31452
- Low light level television cameras and direct view devices for police night surveillance operations
19 p3052 N71-31639
- Silicon detector for measuring irradiance of burning solid propellant surface
[AD-723283] 19 p3172 N71-31946
- Development and operation of apparatus for measuring ground illumination at night and remotely recording data
[FOA-2-C-2387-52] 22 p3585 N71-35533
- Luminous density distribution effects on television picture perception
23 p3723 N71-36534
- Statistical relationship between spectral type and absolute magnitude of nearby stars
23 p3856 N71-37485
- LUNAR ATMOSPHERES**
Lunar ALSEP mass spectrometer for measuring composition of lunar atmosphere
[NASA-CR-114774] 04 p0613 N71-14230
- Solar wind, meteoric volatilization, and internal degassing contributing to lunar rarefied atmosphere, and transient contributions produced by rocket gases during lunar missions
[NASA-CR-118630] 14 p2335 N71-25796
- Rate of meteoroid penetration of thin beryllium copper detector measured in near-lunar environment by Lunar Orbiter spacecraft
[NASA-TN-D-6266] 16 p2677 N71-28109
- Lunar topographic, geologic, magnetic field, gravitation, and atmospheric data from Apollo 14 experiments and photography
[NASA-SP-272] 18 p3010 N71-30953
- Apollo 14 lunar seismographic, geologic, magnetic field, and atmospheric data summary
18 p3010 N71-30954
- Observations from Apollo 14 suprathermal ion detector including ionospheric ion density, mass and energy spectra during venting in LM cabin, large ion cloud, and ion resulting from impacts
18 p3011 N71-30962
- Cold cathode gauges for measuring amount of gas present in lunar atmosphere
18 p3011 N71-30963
- Astronomical photography of zodiacal light and lunar libration clouds
18 p3014 N71-30979
- Radiation patterns of dipole antenna in stratified medium representing lunar surface
[NASA-CR-121413] 20 p3234 N71-33558
- Neon, argon, and helium density and flux distributions in lunar atmosphere
[NASA-CR-121633] 21 p3506 N71-34981
- LUNAR BASES**
Lunar base synthesis, mission analysis, shelter design, and cost and resource estimates - summary
[NASA-CR-103127] 14 p2236 N71-25857
- Semipermanent lunar base synthesis, scientific and exploration activities, logistics, and mission analysis
[NASA-CR-103129] 14 p2236 N71-25858
- Lunar base equipment, experiments, requirements, navigation, manpower, and tradeoffs
[NASA-CR-103128] 14 p2236 N71-25859
- Optimized and space station derivative shelter designs and support operations for lunar base
[NASA-CR-103130] 14 p2236 N71-25860
- Cost and resource estimates for lunar shelters and scientific, mobility, and power supply equipment for lunar base
[NASA-CR-103132] 14 p2237 N71-25862
- Development and characteristics of natural circulation radiator for use with nuclear power plants installed in lunar space stations
[NASA-CASE-XHQ-03637] 16 p2693 N71-29046
- Test of chemical high explosives for use during lunar base activities
[AD-724646] 20 p3347 N71-33193
- LUNAR CINEMATOGRAPHY**
U LUNAR PHOTOGRAPHY
LUNAR COMMUNICATION
Optimum preemphasis-deemphasis filter pair for FM transmission of Lunar Communications Relay Unit color television
[NASA-CR-100676] 02 p0185 N71-11299
- Conversion system for transforming slow scan rate of Apollo TV camera on moon to fast scan of commercial TV
[NASA-CASE-XMS-07168] 02 p0185 N71-11300

- Astronaut-LM and moon-earth communication systems and equipment
[NASA-CR-108667] 02 p0185 N71-11300
- Utilization of halo orbits in lunar space station, communication, and shuttle operations
[NASA-TN-D-6365] 15 p3018 N71-31025
- LUNAR COMPOSITION**
Investigating origins, structure, and composition of moon
02 p0296 N71-11951
- Luna-16 soil samples
[NASA-TT-F-13452] 03 p0452 N71-12556
- Thermal lunar emissions for structural model of moon mantle
[NASA-TT-F-13455] 06 p0946 N71-14841
- Mass distribution for lunar potential model
[NASA-CR-114507] 07 p1109 N71-17469
- Techniques for determining evolution of lunar mass surfaces
[NASA-CR-114845] 07 p1110 N71-17559
- Neutron activation analyses of lunar sample abundances
[NASA-CR-114841] 07 p1112 N71-17709
- Neutron activation analysis of O, Si, Al, Mg, and Fe abundances in lunar rocks and fines from Apollo 12 mission
07 p1112 N71-17719
- Neutron activation analysis of O, Si, Al, and Fe abundances in Apollo 12 lunar rock 12013
07 p1112 N71-17711
- Neutron activation analysis of O, Si, and Al abundances in Apollo 12 lunar samples
07 p1112 N71-17712
- Neutron activation analysis of O, Si, and Al in Apollo 11 rocks and fines
07 p1112 N71-17713
- Instrumental activation analyses of abundances in lunar rock chips
07 p1113 N71-17714
- Instrumental activation analysis technology for analysis of meteorites and lunar materials
07 p1113 N71-17715
- Characteristics of lava tubes and channels on lunar surface
[NASA-TM-X-62013] 07 p1116 N71-18007
- Investigating mineral composition of Apollo 11 and 12 lunar rock samples
[NASA-CR-114878] 08 p1289 N71-19144
- Electron microprobe analysis of fine-grained igneous rocks from lunar sample 10022 from Sea of Tranquility
08 p1289 N71-19145
- Electron probe microanalysis of minerals of lunar igneous rocks from Apollo 11 flight
08 p1289 N71-19146
- Using petrographic microscope and electron microprobe for mineralogical and petrological analysis of Apollo 12 lunar sample 12013
08 p1289 N71-19147
- Chemical and petrological examination of lunar samples to determine origin of moon
[NASA-CR-116880] 08 p1290 N71-19251
- Petrogenesis of Apollo 11 basalts and implications for lunar origin
[NASA-CR-116891] 08 p1290 N71-19252
- Development and characteristics of pycnometer for measuring physical properties of lunar surface
[NASA-CASE-XLA-00934] 11 p1764 N71-22765
- Determination of petrology and deformational sense of pyroxenes and olivines in lunar rocks returned by Apollo 12 flight
[NASA-CR-115030] 15 p2516 N71-26880
- Preliminary geological analysis of lunar regolith from Luna 16 data
[NASA-TT-F-13700] 17 p2842 N71-29252
- News releases on lunar rock samples and radio astronomy
18 p3009 N71-30708
- Comparison of lunar maria with oceans of earth and differences between lunar surface and terrestrial continental structure
18 p3014 N71-30999
- Post-Apollo lunar exploration for remote sensing of rocks
18 p2917 N71-31121
- Geological analysis of lunar soil sample from Sea of Tranquility obtained by Luna-16 automatic station
[NASA-TT-F-13754] 18 p3016 N71-31331
- Comparison of lunar rock samples from Apollo 12 flight Oceanus Procellarum area and Apollo 11 flight Mare Tranquillitatis area
[NASA-CR-115097] 20 p3260 N71-33208
- LUNAR CRATERS**
NT TYCHO CRATER
Photointerpretation of lunar photographs by comparisons with geological craters, volcanoes, and other maps and photographs
[NASA-CR-115704] 04 p0613 N71-14429
- Multiphase eruptions associated with lunar crater Tycho and Aristarchus - lava flow charts
04 p0613 N71-14441
- Predicting crater size and impact flash for S-6 stage lunar impact on Apollo 13 flight
[NASA-TM-X-64517] 05 p0766 N71-14858

- Micrometeorite craters and related features on lunar rock surfaces**
 [NASA-TM-X-46705] 07 p1108 N71-17335
 Findings of conference on meteorite impact and volcanism
 [NASA-TM-X-46706] 07 p1109 N71-17336
 Assignment of names to lunar craters including personal biographies
 [NASA-CR-116798] 08 p1288 N71-18626
 Systematic classification of meteorite impact craters for lunar and planetary craters
 [NASA-CR-116890] 08 p1194 N71-19083
 Lunar geology, crater, and volcanic feature analysis from Apollo 10 visual observations and photomicrographs
 [NASA-SP-232] 15 p2517 N71-27871
 Lunar surface crater and maria photointerpretation using lunar and earth evolution
 18 p3008 N71-30396
 Morphological classification and maturity of small lunar craters determined from Lunar Orbiter photographs
 [NASA-TT-F-13739] 18 p3009 N71-30746
 Molecular hydrogen outflow in Aristarchus lunar crater using spectral observations
 [NASA-TT-F-13809] 18 p3014 N71-31085
 Lunar cratering, and geologic interpretation of Apollo 11 soil samples
 23 p3846 N71-37416
 Constants of lunar physical libration based on visual and photographic observations of pairs of craters by position angles method
 [NASA-TT-F-661] 23 p3856 N71-37486
- LUNAR CRUST**
 Thermal lunar emissions for structural model of moon mantle
 [NASA-TT-F-13455] 06 p0948 N71-16861
 Permanent feasibility in lunar crust
 [NASA-CR-116879] 08 p1195 N71-19108
 Determination of lunar electrical conductivity profile from joint power spectral density analysis of data from Apollo 12 and Explorer 35 magnetometer data
 [NASA-TM-X-43019] 12 p1997 N71-24146
 Rotational rigidity for remote determination of vertical crustal structure of lunar surface
 18 p3013 N71-30971
 Investigation of glass particles recovered from Apollo 11 and Apollo 12 fines, and composition and isotopic analysis of lunar surface
 [NASA-TM-X-45724] 24 p4008 N71-38575
- LUNAR DUST**
 Biogeochemical and microstructural analyses on lunar rock and dust samples for biological compounds
 [NASA-CR-114839] 07 p1113 N71-17717
 Microscopic analyses of Apollo 12 lunar samples for biogenic structures
 07 p1113 N71-17718
 Microscopic analyses of Apollo 11 lunar samples for biogenic structures
 07 p1113 N71-17719
 Biogeochemical analysis on lunar dust sample for organic compounds
 07 p1113 N71-17720
 Microscopic analyses of Apollo 11 lunar rock and dust samples for biological activities
 07 p1113 N71-17721
 Infrared vibrational spectral correlation derived from terrestrial and synthetic mineralogical characterization of Apollo 11 and 12 lunar samples
 [NASA-CR-114890] 09 p1466 N71-19913
 Stellar spectrophotometry, meteor photography, installation of solar telescope and Schmidt camera, and lunar dust analysis
 12 p1995 N71-23177
 Distant thunderstorm hypothesis for short-lived red flares on parts of lunar surface
 [DRL-M-28715-5828-4P] 21 p3511 N71-35017
 Dust surface configurations illustrating thermal protection concepts to improve performance of simple radiative surfaces in mobile, dusty, lunar environments
 [NASA-CR-121874] 21 p3529 N71-35150
- LUNAR ECHOES**
 NT LUNAR RADAR ECHOES
 LUNAR ECLIPSES
 Existence and study of lunar luminescence, light curves of eclipsed moon used for determining source of radiation causing excitation of lunar luminescence
 01 p0120 N71-10088
 Infrared study of cooling behavior of eclipse thermal anomalies during lunar night
 [NPT-5] 02 p0295 N71-11895
 Abstracts of articles on research in astronomy
 03 p0454 N71-13039
- LUNAR EFFECTS**
 NT LUNAR GRAVITATIONAL EFFECTS
 NT LUNAR TIDES
 Analytic expressions for partial derivatives of observables with respect to Robertson relativistic parameters and planetary defects in lunar theory
 01 p0121 N71-10248
 Solar and lunar effects on earthquake periodicities
 05 p0674 N71-14942
- Lunar and solar effects on Solar-Hi satellite orbit calculations**
 [AD-724639] 20 p3346 N71-33032
 Quantitative determination of umbraal increases and penumbral decreases and increases in lunar wake of solar wind flow
 [NASA-TM-X-47329] 24 p4003 N71-38550
- LUNAR ENVIRONMENT**
 NT LUNAR ATMOSPHERES
 Basalt melts in simulated lunar environment
 04 p0613 N71-14442
 Engineering analysis of Surveyor 3 parts returned by Apollo 12 astronauts to determine lunar environment effects
 [NASA-CR-114835] 07 p1111 N71-17567
 Effects of orientation, libration, and location on performance of lunar radiator - design studies
 [NASA-TM-X-1846] 09 p1483 N71-20092
 Apollo 11 basalt petrogenesis and theories of lunar evolution comparing lunar and earth environments
 [NASA-CR-118034] 12 p1998 N71-24309
 Apollo 14 crew visual observations of earth, moon, lunar topography and geology, and astronaut maneuverability during extravehicular activity
 18 p3010 N71-30956
 Charged particle lunar environment experiment of Apollo 14 detecting particle fluxes at lunar surface resulting from wide range of lunar surface, magnetospheric, and interplanetary data
 18 p3011 N71-30964
 Dual surface configurations illustrating thermal protection concepts to improve performance of simple radiative surfaces in mobile, dusty, lunar environments
 [NASA-CR-121874] 21 p3529 N71-35150
 Properties of rocks, soils, and minerals in ultrahigh vacuum facility simulating lunar environment, for experimental resource utilization
 [NASA-CR-121915] 22 p3468 N71-36150
- LUNAR ESCAPE DEVICES**
 Design and development of lunar escape system simulator for investigation of lunar escape problems and simplified manual guidance and control for lunar escape vehicles
 [NASA-TN-D-6111] 11 p1732 N71-22590
 Pileated simulator investigation of lightweight vehicles for emergency lunar escape to orbit with kinesthetic attitude control and simplified manual guidance
 [NASA-TN-D-6299] 16 p2577 N71-28232
- LUNAR EVOLUTION**
 Techniques for determining evolution of lunar mare surfaces
 [NASA-CR-114845] 07 p1110 N71-17559
 Chemical and petrological examination of lunar samples to determine origin of moon
 [NASA-CR-116880] 08 p1290 N71-19231
 Petrogenesis of Apollo 11 basalts and implications for lunar origin
 [NASA-CR-116891] 08 p1290 N71-19232
 Neutron activation analysis for trace elements depleted on lunar surface with implications for origin of moon and meteorite influx rate
 [NASA-CR-114888] 09 p1463 N71-19782
 Apollo 11 basalt petrogenesis and theories of lunar evolution comparing lunar and earth environments
 [NASA-CR-118034] 12 p1998 N71-24309
 Lunar evolution based on magnetic data from lunar samples, Explorer 35 satellite, and magnetometers on Apollo 12 and 14 flights
 [NASA-TM-X-42023] 14 p2338 N71-26290
 Lunar surface crater and maria photointerpretation using lunar and earth evolution
 18 p3008 N71-30956
- LUNAR EXPLORATION**
 Backpack carrier with retractable legs suitable for lunar exploration and convertible to rescue vehicle
 [NASA-CASE-LAR-10056] 03 p0329 N71-12351
 Manned-unmanned lunar explorer systems design
 [NASA-CR-115823] 05 p0770 N71-14511
 Developments in space science that led to Apollo 11 flight
 05 p0766 N71-14615
 Research studies on development of Thermoelectric Outer Planet Spacecraft (TOPS) and lunar exploration
 [NASA-CR-117440] 10 p1644 N71-21338
 Development of gravimeter for lunar traverse gravity experiments and specifications for instrument, operation, and experiment error budget
 [NASA-CR-114946] 10 p1660 N71-21467
 Narrative and pictures of Apollo 14 flight
 [NASA-EP-91] 10 p1646 N71-21720
 Comparison of United States lunar roving vehicle missions with Lunokhod 1 mission
 11 p1828 N71-22567
 Development and characteristics of penetrometer for measuring physical properties of lunar surface
 [NASA-CASE-XLA-60934] 11 p1764 N71-22765
 Ionospheric soundings, CosmoS measurements, and lunar exploration
 12 p1995 N71-23181
 Familiarization manual for Apollo Lunar Surface Experiments Package describing mission, equipment, subsystems, maintenance, and operations
 [NASA-CR-99604] 12 p2002 N71-24292
- Semipermanent lunar base synthesis, scientific and exploration activities, logistics, and mission analysis**
 [NASA-CR-103129] 14 p2236 N71-23858
 Lunar base equipment, experiments, requirements, navigation, manpower, and tradeoffs
 [NASA-CR-103128] 14 p2236 N71-23859
 Apollo 11 mission planning for lunar surface exploration including equipment requirements, crew/equipment interfaces, and timelines for extravehicular activities
 [NASA-TM-X-47180] 14 p2337 N71-26144
 Use of Pioneer 7 and 8 cosmic dust detectors in Apollo 17 lunar ejecta and micrometeorite experiment to measure meteoroid fluxes on moon
 [NASA-CR-118663] 14 p2339 N71-26441
 Lightweight propulsion unit for movement of personnel and equipment across lunar surface
 [NASA-CASE-MFS-20130] 15 p2513 N71-27585
 Mobility performance problems of power-driven rigid cylindrical roller (wheels) climbing semi-infinite soft soil slope with uniform velocity applied to lunar locomotion
 [NASA-CR-118988] 17 p2789 N71-30207
 Geomorphology of Mare Imbrium area explored by Lunokhod-1 lunar roving vehicle
 [D-92] 20 p3343 N71-32809
 Establishing solar cell array criteria for use as primary power source in lunar-based water electrolysis system
 [NASA-CR-119945] 23 p3709 N71-36441
- LUNAR EXPLORATION SYSTEM FOR APOLLO**
 Systems design and performance tests of Apollo 14 lunar ranging retroreflecting equipment
 [NASA-CR-114900] 09 p1996 N71-19797
 Pulsed ruby laser ranging system for Apollo 11 lunar exploration system
 13 p3090 N71-25335
- LUNAR FLYING VEHICLES**
 Optical simulation study to determine manual instrumentation for pilot control of lunar flying vehicle
 [NASA-TN-D-5963] 03 p0327 N71-12334
 Simulator study of lunar flying platform control by pilot body motion
 [NASA-TN-D-6016] 05 p0458 N71-14981
- LUNAR GEOLOGY**
 Determination of velocity distribution for lunar seismic waves
 [AD-715725] 05 p0768 N71-15337
 Analysis of lunar soil samples returned by Apollo 12 flight
 [NASA-CR-114840] 07 p1110 N71-17561
 Lunar seismic velocity models and lunar reverberation calculations
 [NASA-CR-116418] 07 p1117 N71-18119
 Properties, photometry, and dynamic processes of comets, lunar morphology, and Tunguska meteorite blast
 11 p1827 N71-22416
 Lunokhod 1 design, control, and lunar geology and astronomy experiments
 11 p1832 N71-22488
 Lunar geology, crater, and volcanic feature analysis from Apollo 10 visual observations and photomicrographs
 [NASA-SP-232] 15 p2517 N71-27871
 Thermal models investigated for upper limits on lunar radioactivity consistent with temperature distribution based on electrical conductivity of lunar interior
 [NASA-CR-118992] 16 p2678 N71-28156
 Preliminary geological analysis of lunar regolith from Lunar 16 data
 [NASA-TT-F-13700] 17 p2842 N71-29252
 Lunar topographic, geologic, magnetic field, gravitation, and atmospheric data from Apollo 14 experiments and photography
 [NASA-SP-272] 18 p3010 N71-30953
 Apollo 14 lunar seismographic, geologic, magnetic field, and atmospheric data summary
 18 p3010 N71-30954
 Lunar geology based on Apollo 14 photographs and soil and rock samples
 18 p3010 N71-30957
 Seismic signal analysis from Apollo 14 passive seismic experiment
 18 p3011 N71-30960
 Active seismic signal analysis from Apollo 14 thumper and mortar detonations on lunar surface
 18 p3011 N71-30961
 Geologic analysis of lunar surface using photographs from 70-mm Hasselblad camera
 18 p3013 N71-30973
 High resolution strip photography of lunar surface
 18 p3013 N71-30974
 Design criteria of heat flow experiment designated as ALSEP Array A2
 [NASA-CR-115109] 19 p3178 N71-31607
 Comparison of lunar rock samples from Apollo 12 flight Oceanus Procellarum area and Apollo 11 flight Mare Tranquillitatis area
 [NASA-CR-115897] 20 p3260 N71-33249
 Nuclear research in space and lunar materials and proton fusion
 [COO-1167-13] 21 p3478 N71-34773

- Lunar cratering, and geologic interpretation of Apollo 11 soil samples 23 p3846 N71-37416
- LUNAR GRAVITATION**
- Fitting mass distribution to gravitational potential, for simulating lunar potential [NASA-CR-116505] 07 p1051 N71-17428
- Application of VHF Doppler tracking data from Goddard Range and Range Rate system to determine lunar orbits for Explorer 35 satellite [NASA-TM-X-45470] 10 p1644 N71-21325
- Topographic corrections for lunar gravity data 10 p1644 N71-21339
- Development of gravimeter for lunar traverse gravity experiment and specifications for instrument, operation, and experiment error budget [NASA-CR-114946] 10 p1560 N71-21467
- Apparatus for training astronaut crews to perform on simulated lunar surface under conditions of lunar gravity [NASA-CASE-XMS-04798] 10 p1538 N71-21474
- Relation between moon density function, figure, external gravitational potential, and physical libration constants [NASA-CR-118892] 15 p2517 N71-27638
- Lunar topographic, geologic, magnetic field, gravitation, and atmospheric data from Apollo 14 experiments and photography 18 p3010 N71-30953
- Apollo 14 command service and lunar module orbital velocity data from radio navigation S-band transponder experiment for lunar gravitation effects 18 p3012 N71-30970
- Analysis of Lunar Orbiter data and interpretation of lunar gravitational field [NASA-CR-119684] 19 p3182 N71-32522
- Electronic modules used to simulate lunar gravity potential recovery based on spherical harmonics gravity model [NASA-CR-115175] 22 p3564 N71-35388
- Influences of solar and lunar gravity on ocean tides and tidal currents 23 p3789 N71-37007
- LUNAR GRAVITATIONAL EFFECTS**
- Four-wheel mathematical model used for prediction of LRV operational behavior under lunar gravitation [NASA-TM-X-64584] 12 p2000 N71-23158
- Apollo range rate residuals during lunar orbits for determining lunar mass concentrations 13 p2168 N71-25275
- Apollo 8 tracking residue data for determining lunar gravity fields 13 p2170 N71-25304
- Lunar Orbiter tracking data analyzed to yield thirteenth degree and order spherical harmonic approximation to lunar gravitational potential function [NASA-TM-X-2260] 16 p2678 N71-28121
- LUNAR GRAVITY SIMULATOR**
- Construction and operation of body-motion controlled five-degree-of-freedom simulation of jet-supported lunar flying machine [NASA-TM-D-6001] 03 p0358 N71-12736
- Improved feedback control of distributed parameter systems for lunar landing vehicle simulator [NASA-CR-116482] 07 p1004 N71-17345
- Metabolic cost evaluation of self-locomotion in simulated lunar gravity using space suits and carts including weight load and surface effects [NASA-CR-16977] 10 p1504 N71-20698
- LUNAR IONOSPHERE**
- U LUNAR ATMOSPHERES**
- LUNAR LANDING**
- As-SOS S-4B post flight lunar impact trajectory analysis [NASA-TM-X-44563] 02 p0299 N71-11598
- Selected articles on space exploration, lunar landing vehicles, and atmospheric parameters 02 p0297 N71-12157
- X ray telescope of Lunokhod 1 for observations of quasars and galaxies from lunar surface 07 p1027 N71-16982
- Statistical analysis of simulated pilot ability to control lunar module approach and descent to lunar surface [NASA-TM-D-6113] 09 p1416 N71-20144
- Oriental manual for lunar module vehicle and mission requirements [NASA-CR-117321] 09 p1472 N71-20470
- LUNAR LANDING MODULES**
- NT LSSM
- Improved feedback control of distributed parameter systems for lunar landing vehicle simulator [NASA-CR-116482] 07 p1004 N71-17345
- Lunokhod 1 lunar roving vehicle program, landing module construction, onboard equipment, and results of lunar crater observations [D-90] 20 p3343 N71-32810
- LUNAR LANDING SITES**
- Radar studies for lunar landing sites using backscatter measurements [NASA-CR-108668] 02 p0294 N71-11402
- Geological maps of potential Apollo landing sites on lunar surface 07 p1109 N71-17497

- Thermal control, electrical power system, egress/ingress operations, landing site considerations, and maintenance for lunar shelters 14 p2237 N71-25861
- Lunar geology based on Apollo 14 photographs and soil and rock samples 18 p3010 N71-30957
- Geologic sketch map of candidate Apollo 16 landing site in Descartes region prepared from Apollo 14 photographs 18 p3013 N71-30975
- Sketch map of proposed Descartes Apollo 16 lunar landing site 18 p3013 N71-30976
- Apollo 15 mission and manned geologic exploration of lunar landing site - maps 20 p3347 N71-33233
- Informal names and descriptions of lunar topographic features in Apollo 15 landing region [NASA-CR-121625] 21 p3506 N71-34979
- Location and derivation of nomenclature for lunar topographic features in Apollo 15 landing region [NASA-CR-121624] 21 p3506 N71-34980
- Determining thickness of regolith in Apollo 16 landing site by Monte Carlo method [NASA-TM-X-62009] 23 p3848 N71-37424
- LUNAR LOGISTICS**
- Semipermanent lunar base synthesis, scientific and exploration activities, logistics, and mission analysis [NASA-CR-103129] 14 p2236 N71-25858
- Lightweight propulsion unit for movement of personnel and equipment around lunar surface [NASA-CASE-MFS-20130] 15 p2513 N71-27585
- LUNAR LUMINESCENCE**
- Luminescent and thermoluminescent properties of granite and its constituent minerals and their relevance to transient lunar phenomena 01 p0405 N71-10078
- Evaluating luminescence of lunar rocks by comparing them with similar terrestrial rocks and minerals 01 p0120 N71-10080
- Existence and study of lunar luminescence, light curves of eclipsed moon used for determining source of radiation causing excitation of lunar luminescence 01 p0120 N71-10088
- Lunar disk luminance effects on manual sighting accuracy of space sextant using simulated lunar and stellar targets [NASA-TN-D-6507] 22 p3617 N71-35774
- LUNAR MAGNETIC FIELDS**
- Lunar paleomagnetic field evidence from Apollo 12 rock studies 13 p2165 N71-24356
- Lunar evolution based on magnetic data from lunar samples, Explorer 35 satellite, and magnetometers on Apollo 12 and 14 flights [NASA-TM-X-62023] 14 p2338 N71-26290
- Solar wind perturbations downward of moon used to locate lunar magnetized regions 16 p2673 N71-28024
- Lunar topographic, geologic, magnetic field, gravitation, and atmospheric data from Apollo 14 experiments and photography [NASA-SP-272] 18 p3010 N71-30953
- LUNAR MAPS**
- Photointerpretation of lunar photographs by comparisons with geological craters, volcanoes, and rocks - maps and photographs 04 p0613 N71-14439
- Construction and interpretation of topographic and relief contour maps of Tycho northeast rim 04 p0613 N71-14440
- Geological maps of potential Apollo landing sites on lunar surface 07 p1109 N71-17497
- Assignment of names to lunar craters including personal biographies [NASA-CR-116798] 08 p1288 N71-18626
- Geologic sketch map of candidate Apollo 16 landing site in Descartes region prepared from Apollo 14 photographs 18 p3013 N71-30975
- Sketch map of proposed Descartes Apollo 16 lunar landing site 18 p3013 N71-30976
- Apollo 15 mission and manned geologic exploration of lunar landing site - maps 20 p3347 N71-33233
- Lunar Orbiter photographs and maps, missions 1 through 5 [NASA-SP-242] 22 p3671 N71-36179
- LUNAR MARIA**
- Techniques for determining evolution of lunar mare surfaces [NASA-CR-114845] 07 p1110 N71-17559
- Optical measurements on Apollo 12 soil samples from lunar mare surfaces 09 p1465 N71-19780
- Lunar surface crater and maria photointerpretation noting lunar and earth evolution 18 p3008 N71-30596
- Comparison of lunar maria with oceans of earth and differences between lunar surface and terrestrial continental structure 18 p3014 N71-30990

- Geomorphology of Mare Imbrium area explored by Lunokhod-1 lunar roving vehicle 20 p3343 N71-32810
- LUNAR MOBILE LABORATORIES**
- Dual surface configurations illustrating thermal protection concepts to improve performance of simple radiative surfaces in mobile, dusty, lunar environments [NASA-CR-121874] 21 p3529 N71-35159
- LUNAR MODULE**
- NT LSSM
- Grumman pre-prep program to create LM win list [NASA-CR-108733] 03 p0342 N71-12485
- Principal investigator requirements for lunar module-borne cosmic ray detector experiment [NASA-CR-108715] 04 p0607 N71-14041
- Support requirements for lunar module-borne cosmic ray detector experiment [NASA-CR-108712] 04 p0607 N71-14052
- Reliability requirements for lunar module-borne cosmic ray detector experiment [NASA-CR-108714] 04 p0607 N71-14053
- Results of simulated runs to evaluate lunar module descent performance of P66 automatic control and guidance system [NASA-CR-114787] 04 p0613 N71-14231
- Evaluation of corrective actions and hardware implementation for lunar module based on Apollo 13 flight incident [NASA-TM-X-66929] 09 p1470 N71-19958
- Analysis of Apollo 13 lunar module systems during emergency operation following command service module oxygen tank explosion [NASA-TM-X-66935] 09 p1466 N71-19962
- Analysis of lunar module related system descent and ascent stages used on Apollo 13 flight [NASA-TM-X-66927] 09 p1471 N71-19968
- Oriental manual for lunar module vehicle and mission requirements [NASA-CR-117321] 09 p1472 N71-20470
- Operational schedule for Apollo 9 command module/ lunar module 3 flight plan and crew activities [NASA-TM-X-66904] 09 p1469 N71-20511
- Lunar module design techniques for system reliability 23 p3757 N71-36781
- Analysis of propellant sloshing in lunar module during Apollo 14 flight and resultant erroneous indication of low level of propellant [NASA-TM-X-2362] 24 p3906 N71-37841
- LUNAR OBSERVATORIES**
- Compilation and comparative analysis of observations of lunar transient phenomena [NASA-TM-X-65528] 18 p3014 N71-31092
- LUNAR OCCULTATION**
- NT SOLAR ECLIPSES
- Photometric observations of lunar occultations of stars [AD-712544] 03 p0455 N71-13371
- Determination of lunar orbital elements and other astronomical constants 07 p1111 N71-17672
- Earth rotation rate values from observations on stellar occultation by moon from 1627 to 1860 07 p1117 N71-18057
- Relativistic electron diffusion from point source in Sagittarius A astronomical model 10 p1642 N71-20661
- LUNAR ORBITER**
- Design, development, and characteristics of orbiting lunar station and comparison of configurations - Vol. 4 [NASA-CR-115020] 13 p2174 N71-25102
- Calculation of shock inclination angle and surface pressure coefficient in vertical plane of symmetry of bodies at angle of attack related to delta wing-body space shuttle orbiter [NASA-TM-X-62031] 15 p2394 N71-27662
- Rate of meteoroid penetration of thin beryllium copper detector measured in near-lunar environment by Lunar Orbiter spacecraft [NASA-TM-D-62566] 16 p2677 N71-28109
- Data processing techniques and equipment used in analysis of Lunar Orbiter 1 and 3 and Explorer 35 bistatic-radar data [NASA-CR-119033] 16 p2564 N71-29063
- Predicted and measured aerodynamic characteristics for blended delta-wing orbiter at hypersonic speeds [NASA-TM-X-62046] 19 p3184 N71-32186
- Analysis of Lunar Orbiter data and interpretation of lunar gravitational field [NASA-CR-119684] 19 p3182 N71-32522
- Lunar Orbiter photographs and maps, missions 1 through 5 [NASA-SP-242] 22 p3671 N71-36179
- Mathematical modeling and testing of Lunar Orbiter photographic subsystem [NASA-CR-123174] 24 p3920 N71-37952
- LUNAR ORBITS**
- Equipment specifications for Lunar Sounder Asteroid Assembly [NASA-CR-114797] 05 p0642 N71-14726

SUBJECT INDEX

- Halo Orbit Space Station potential for lunar communications, exploration, logistics, and launching platform operations**
[NASA-TM-X-64509] 05 p0772 N71-15351
- Tables of spacecraft launched into lunar and solar orbits 1958-1970**
[RAE-TM-70163] 06 p0949 N71-15813
- Determination of lunar orbital elements and other astronomical constants**
07 p1111 N71-17672
- Application of VHF Doppler tracking data from Goddard Range and Range Rate system to determine lunar orbits for Explorer 35 satellite**
[NASA-TM-X-64570] 10 p1644 N71-21325
- Apollo range rate residuals during lunar orbits for determining lunar mass concentrations**
13 p2168 N71-25275
- Laser ranging retroreflector deployed on lunar surface to study lunar librations for defining precisely lunar orbits and studying earth planetary structure-Apollo 14 flight**
18 p3012 N71-30965
- LUNAR PERTURBATION**
U LUNAR EFFECTS
LUNAR PHOTOGRAPHIES
Studying Lunar Orbiter photographs of boulder tracks left on lunar surface to determine soil cohesion and angle of internal friction
[NASA-CR-102960] 05 p0768 N71-15205
- Panoramic views of lunar surface produced by automatic lunar probe**
[NASA-TT-F-651] 08 p1290 N71-19242
- Analytical astriangulation of Apollo 10 Hasselblad photographs of moons far side**
[NASA-CR-115001] 13 p2081 N71-24577
- Interpretation of planetary surface photographs, noting Moon, Mars, and Mercury surfaces**
[ESRO-SP-56] 18 p3008 N71-30594
- Lunar surface crater and maria photointerpretation noting lunar and earth evolution**
18 p3008 N71-30596
- High resolution strip photography of lunar surface**
18 p3013 N71-30974
- Geologic sketch map of candidate Apollo 16 landing site in Descartes region prepared from Apollo 14 photographs**
18 p3013 N71-30975
- Lunar Orbiter photographs and maps, missions 1 through 3**
[NASA-SP-242] 22 p3671 N71-36179
- Photographs and descriptions of Apollo 15 at Hadley base and lunar rover traverses**
[NASA-EP-94] 24 p0008 N71-38579
- LUNAR PHOTOGRAPHY**
Investigating origins, structure, and composition of moon
02 p0296 N71-11951
- Photointerpretation of lunar photographs by comparisons with geological craters, volcanoes, and rock maps and photographs**
[NASA-CR-115784] 04 p0613 N71-14439
- Relative heights of photographic features of lunar topography**
[AD-713679] 05 p0767 N71-14911
- Apollo 12 flight color and black and white lunar photography indices on MERCATOR projections**
[NASA-TM-X-64883] 08 p1203 N71-18975
- Lunar photographs from Apollo 8, 10, and 11, films**
[NASA-SP-246] 17 p2842 N71-29260
- Data on figure and relief of moon from processing of Zond 6 photography**
[NASA-TT-F-13737] 17 p2845 N71-29843
- Morphological classification and maturity of small lunar craters determined from Lunar Orbiter photographs**
[NASA-TT-F-13739] 18 p3009 N71-30746
- Lunar topographic, geologic, magnetic field, gravitation, and atmospheric data from Apollo 14 experiments and photography**
[NASA-SP-272] 18 p3010 N71-30953
- Photographic equipment and film used during Apollo 14 flight in command and lunar modules and during extravehicular activity**
18 p3010 N71-30955
- Lunar geology based on Apollo 14 photographs and soil and rock samples**
18 p3010 N71-30957
- Closeup photographs of soil and rock on lunar surface obtained with Apollo 14 stereoscopic camera**
18 p3012 N71-30968
- Geologic analysis of lunar surface using photographs from 70-mm Hasselblad camera**
18 p3013 N71-30973
- Lunar surface examination using low sun elevation photography**
18 p3013 N71-30978
- Development and characteristics of simulator for planning photogrammetric missions of lunar surface**
[NASA-CR-115174] 22 p3565 N71-35389
- Catalog of all pictures taken from lunar module or lunar surface during Apollo 15 mission**
[NASA-CR-121908] 22 p3668 N71-36149
- LUNAR PROBES**
NT LUNAR PROBES

- NT SURVEYOR LUNAR PROBES**
NT SURVEYOR 3 LUNAR PROBE
NT SURVEYOR 6 LUNAR PROBE
Astrodynamical characteristics of lunar trajectories for manned and unmanned spacecraft
[AD-714426] 06 p0946 N71-16744
- Lunar surface magnetometer measurements for determining electrical conductivity and temperature of lunar core**
[NASA-TM-X-63012] 06 p0949 N71-16862
- Panoramic views of lunar surface produced by automatic lunar probe**
[NASA-TT-F-651] 08 p1290 N71-19242
- LUNAR PROGRAMS**
NT APOLLO PROJECT
Discussing major and minor tasks of safety and rescue planning for lunar missions
[NASA-CR-114801] 05 p0772 N71-15349
- Comparison of United States lunar roving vehicle missions with Lunokhod 1 mission**
11 p1828 N71-22567
- LUNAR RADAR ECHOES**
Lunar surface radar reflectance measurements and variations of dielectric constant
[PR-4] 17 p2844 N71-29419
- LUNAR RADIATION**
Development of computable electromagnetic theory model for lunar reflectivity problem - Vol. 3
[NASA-CR-115084] 18 p2890 N71-31104
- Mesospheric ozone density measured by spectrophotometry of lunar ultraviolet radiation absorption during rocket sounding**
[ADP-106] 20 p3256 N71-32938
- LUNAR RECEIVING LABORATORY**
Selecting algae, seeds, and seedlings of higher plants and establishing tissue cultures for Lunar Receiving Laboratory
[NASA-CR-108764] 03 p0321 N71-12296
- Chemical and isotopic analyses of Apollo 12 lunar samples**
[NASA-TR-R-353] 04 p0610 N71-13742
- Design and fabrication of viton gloves for use in sterile nitrogen atmospheric processing cabinet of Lunar Receiving Laboratory**
[NASA-CR-115112] 19 p3046 N71-31608
- LUNAR ROCKS**
Luminescent and thermoluminescent properties of granite and its constituent minerals and their relevance to transient lunar phenomena
01 p0045 N71-10078
- Low temperature thermoluminescence of Apollo 11 material**
01 p0120 N71-10079
- Evaluating luminescence of lunar rocks by comparing them with similar terrestrial rocks and minerals**
01 p0120 N71-10080
- Thermoluminescence-chemical composition correlations for meteoritic enstatite**
01 p0120 N71-10081
- Existence and study of lunar luminescence, light curves of eclipsed moon used for determining source of radiation causing excitation of lunar luminescence**
01 p0120 N71-10088
- Radioactive age determination and isotopic composition analyses on rocks, meteorites, and lunar samples**
[NASA-CR-111001] 01 p0016 N71-10304
- Summary of lunar sample chemical analyses scheme**
01 p0017 N71-10313
- Mass spectrometric analyses of meteoritic and lunar samples containing lead and thallium**
01 p0053 N71-10314
- Polarimetric properties of lunar and terrestrial meteorites, volcanic ashes, basalts, and other rocks**
[AD-711070] 01 p0121 N71-10362
- Evidence from comparison with stony meteorites of solar flare proton induced radioactivity in Apollo 11 lunar rocks**
[NASA-CR-111368] 02 p0293 N71-11958
- Luminescence of lunar rocks from Apollo 11**
02 p0296 N71-11961
- Chemical and isotopic analyses of Apollo 12 lunar samples**
[NASA-TR-R-353] 04 p0610 N71-13742
- Fluid conductivity of lunar surface materials**
[NASA-CR-102842] 04 p0611 N71-14809
- Photointerpretation of lunar photographs by comparisons with geological craters, volcanoes, and rock maps and photographs**
[NASA-CR-115784] 04 p0613 N71-14439
- Basalt melts in simulated lunar environment**
04 p0613 N71-14442
- Structural analyses and chronology of micrometeorite craters on lunar rocks**
[NASA-TM-X-66707] 07 p1109 N71-17498
- Analysis of lunar soil samples returned by Apollo 12 flight**
[NASA-CR-114840] 07 p1110 N71-17561
- Luminescence petrography of Apollo 12 rocks and comparative features in Apollo 11 rocks, terrestrial rocks, and meteorites**
[NASA-CR-114842] 07 p1110 N71-17563
- Apollo 12 lunar samples studied with neutron diffraction at room and cryogenic temperatures**
[NASA-CR-114853] 07 p1111 N71-17565

LUNAR ROCKS

- Biogeochemical and microstructural analyses on lunar rock and dust samples for biological compounds**
[NASA-CR-114859] 07 p1113 N71-17717
- Microscopic analyses of Apollo 12 lunar samples for biogenic structures**
07 p1113 N71-17718
- Microscopic analyses of Apollo 11 lunar samples for biogenic structures**
07 p1113 N71-17719
- Microscopic analyses of Apollo 11 lunar rock and dust samples for biological activities**
07 p1113 N71-17721
- Determination of carbon content of lunar samples from Apollo 11 flight**
[NASA-SP-257] 07 p1115 N71-17964
- Electron and ion microprobe analyses of Apollo 12 fines and breccias**
[NASA-CR-114871] 08 p1289 N71-18878
- Chemical and petrological examination of lunar samples to determine origin of moon**
[NASA-CR-114880] 08 p1290 N71-19231
- Petrogenesis of Apollo 11 basalts and implications for lunar origin**
[NASA-CR-114891] 08 p1290 N71-19232
- Electron microscopy and diffraction for microbiology and microanalysis of lunar rocks**
[NASA-CR-114914] 08 p1294 N71-19311
- High voltage electron microscopic and electron diffraction studies of pyroxenes from Apollo 11 lunar rock**
08 p1291 N71-19312
- Mossbauer effect and high voltage electron microscopy of pyroxenes in Apollo 11 lunar rocks**
08 p1291 N71-19316
- Magnetization versus field and temperature analyses of ferromagnetic material in Apollo 12 lunar samples**
[NASA-CR-114891] 09 p1465 N71-19787
- Infrared vibrational spectral correlation derived from terrestrial and synthetic minerals for characterizing Apollo 11 and 12 lunar samples**
[NASA-CR-114890] 09 p1466 N71-19913
- Photographic and seismic data against bedrock lying near lunar surface**
[NASA-CR-114892] 09 p1466 N71-20077
- Ultrahigh vacuum chamber for determining deformational strengths of simulated lunar rocks**
[NASA-CR-117139] 09 p1366 N71-20215
- Petrologic and mineralogical studies of Apollo 11 and 12 lunar rocks**
[NASA-CR-114917] 09 p1467 N71-20278
- Analysis of texture and crystalline orientation of lunar rock samples**
[NASA-TT-F-13561] 09 p1468 N71-20327
- Cation distribution in clinopyroxenes, olivines, and feldspars separated from Apollo 11 and 12 rocks determined with Mossbauer spectroscopy of Fe-57**
[NASA-CR-114941] 10 p1635 N71-21451
- Neutron activation analysis of Apollo 11 and 12 rocks and soils, and X ray fluorescence and radiochemistry data**
[NASA-CR-114926] 10 p1645 N71-21462
- Oxygen isotopic compositions and fractionations between coexisting minerals found in lunar samples from Apollo 11 and Apollo 12 flights**
[NASA-CR-114925] 10 p1645 N71-21464
- Mass spectroscopy of lunar samples to determine uranium, thorium, and lead content**
[NASA-CR-114959] 10 p1645 N71-21575
- Preliminary results on thermally stimulated exoelectron emission from Apollo 12 lunar materials**
[NASA-CR-117853] 11 p1827 N71-22528
- Achievements of US manned space flights for past decade with findings concerning lunar rock samples**
[NASA-TM-X-67150] 12 p1997 N71-24113
- Lunar paleomagnetic field evidence from Apollo 12 rock studies**
[NASA-CR-114972] 13 p2165 N71-24356
- Luminescence of Apollo 11 and 12 rocks measured with UV, X ray, and proton radiation**
[NASA-CR-114970] 13 p2165 N71-24358
- Shock structures of basalts from craters produced by nuclear explosions and of rocks from lunar craters**
13 p2168 N71-25274
- Determination of petrology and deformational state of pyroxenes and olivines in lunar rocks returned by Apollo 12 flight**
[NASA-CR-115030] 15 p2516 N71-26809
- Comparison of aluminum 26 radioactivities of Bruderheim chondrites, lunar rocks, and achondrites**
[NASA-TM-X-65570] 15 p2517 N71-27870
- Shock-compressibility and porosity of basalts from Apollo 12 lunar samples**
[UCRL-72851] 15 p2518 N71-27990
- Physical and thermal properties of regolith lunar sample**
[NASA-TT-F-13701] 16 p2678 N71-28192
- Mineralogy and petrology of lunar rock and soil samples returned from Apollo 14 landing site**
18 p3011 N71-30959
- Closeup photographs of soil and rock on lunar surface obtained with Apollo 14 stereoscopic camera**
18 p3012 N71-30968

LUNAR ROVING VEHICLES

Post-Apollo lunar exploration for remote sensing of rocks

18 p2917 N71-31121
Comparison of lunar rock samples from Apollo 12 flight Oceanus Procellarum area and Apollo 11 flight Mare Tranquillitatis area
[NASA-CR-115997] 20 p3260 N71-33249

Chemical processes for producing oxygen and water from moon from lunar rocks and soils

[NASA-TM-X-58061] 21 p3506 N71-34978
Argon, krypton, and xenon heating analyses, electron microprobe analysis for chemical composition, and depth studies of cosmogenic gases of lunar rocks
[NASA-CR-121722] 21 p3507 N71-34983

Locations of documented samples returned by Apollo 15 including photographs of sample sites, crew descriptions, general rock types, and numbering systems

[NASA-CR-121981] 22 p3667 N71-36148
Properties of rocks, soils, and minerals in ultrahigh vacuum facility simulating lunar environment, for extraterrestrial resource utilization
[NASA-CR-121915] 22 p3668 N71-36150

Investigation of glass particles recovered from Apollo 11 and Apollo 12 fines, and composition and heterogeneity of lunar surface
[NASA-TM-X-65734] 24 p4008 N71-38575

LUNAR ROVING VEHICLES

NT LUNOKHOD LUNAR ROVING VEHICLES
Developing lunar roving vehicles for surface exploration on basis of field geology and traverse geophysical experiments on earth

01 p0121 N71-10252
Algorithm for roving vehicle motion control

02 p0199 N71-11758
Laboratory and field tests of dead reckoning system for lunar roving vehicles

[NASA-TM-X-64551] 04 p0544 N71-14425
Computerized landmark navigation position updating technique for lunar roving vehicles

06 p0895 N71-16672
Reporting operations of Lunokhod 1 vehicle and Venera 7 space probe and investigations of earth atmosphere

07 p1014 N71-16922
Abstracts on Soviet upper atmosphere and space research with emphasis on Lunokhod 1 operations

07 p1015 N71-16960
X ray telescope of Lunokhod 1 for observations of quasars and galaxies from lunar surface

07 p1027 N71-16982
Analysis of data obtained from USSR lunar roving vehicle

07 p1105 N71-17005
Cosmic ray investigations conducted by lunar based observatories

07 p1108 N71-17074
Estimated frictional resistance between soil-wheel interface in lunar roving vehicle design simulation

09 p1466 N71-20216
Thermionic converter optimization, laser obstacle detector, and test program for interplanetary spacecraft guidance and control subsystems

10 p1600 N71-21347
Comparison of United States lunar roving vehicle missions with Lunokhod 1 mission

11 p1828 N71-22567
Four-wheel mathematical model used for prediction of LRV operational behavior under lunar gravitation

[NASA-TM-X-64584] 12 p2000 N71-23158
Computer techniques for trafficability and visibility analysis of lunar surface in mission planning for roving vehicles

[NASA-CR-1881] 18 p3008 N71-30661
Apollo 15 mission and manned geologic exploration of lunar landing site - maps

[NASA-CR-119725] 20 p3347 N71-33233
Lunar roving vehicle control system emphasizing stereoscopic sensor data processing

[D-48] 23 p3859 N71-37507
Photographs and descriptions of Apollo 15 at Hadley base and lunar rover traverses

[NASA-EP-94] 24 p4008 N71-38579

LUNAR SATELLITES

NT EXPLORER 18 SATELLITE

NT EXPLORER 28 SATELLITE

NT IMP

NT LUNAR ORBITER

Effects of lunar physical librations on orbital elements of lunar satellite

[NASA-CR-117841] 11 p1827 N71-22539
Lunar surface layer density determination from lunar satellite radar data on centimeter and millimeter waves

[D-17] 23 p3855 N71-37480

LUNAR SCATTERING

U DIFFUSE RADIATION

U LUNAR RADAR ECHOES

LUNAR SEISMOGRAPHS

Apollo 14 lunar seismographic, geologic, magnetic field, and atmospheric data summary

18 p3010 N71-30954
Seismic signal analysis from Apollo 14 passive seismic experiment

18 p3011 N71-30960

Active seismic signal analysis from Apollo 14 thumper and mortar detonations on lunar surface

18 p3011 N71-30961

LUNAR SHELTERS

Systems analysis of lunar shelter for habitability evaluation

[NASA-CR-111824] 08 p1157 N71-18697
Lunar base synthesis, mission analysis, shelter design, and cost and resource estimates - summary

[NASA-CR-103127] 14 p2236 N71-25857
Optimized and space station derivative shelter designs and support operations for lunar base

[NASA-CR-103130] 14 p2236 N71-25860
Thermal control, electrical power system, egress/ingress operations, landing site considerations, and maintenance for lunar shelters

[NASA-CR-103131] 14 p2237 N71-25861
Cost and resource estimates for lunar shelters and scientific, mobility, and power supply equipment for lunar base

[NASA-CR-103132] 14 p2237 N71-25862
Utilization of water resources within space stations, needs of men, and effects of lunar environment

16 p2681 N71-28906

LUNAR SOIL

NT LUNAR DUST

Summary of lunar sample chemical analyses scheme

01 p0017 N71-10313
Determining presence of porphyrins in Apollo 11 and 12 soil samples by fluorescence spectrometry and analytical demetallization

[NASA-CR-108671] 02 p0150 N71-11067
Fluid conductivity of lunar surface materials

[NASA-CR-102842] 04 p0611 N71-14089
Studying simulated lunar soil for determining feasibility of proposed geotechnical tests for Apollo missions

[NASA-CR-102963] 05 p0767 N71-15204
Studying Lunar Orbiter photographs of boulder tracks left on lunar surface to determine soil cohesion and angle of internal friction

[NASA-CR-102960] 05 p0768 N71-15205
Failure mechanisms associated with use of borehole jack in rocks

[NASA-CR-102961] 05 p0768 N71-15206
Summaries of lunar soil studies and fluid conductivity of lunar surface materials

[NASA-CR-102962] 05 p0768 N71-15207
News releases of Cosmos satellites launching and lunar soil analysis

05 p0681 N71-15682
Analysis of lunar soil samples returned by Apollo 12 flight

[NASA-CR-114840] 07 p1110 N71-17561
Neutron activation analyses of lunar sample abundances

[NASA-CR-114841] 07 p1112 N71-17709
Neutron activation analysis of O, Si, Al, Mg, and Fe abundances in lunar rocks and fines from Apollo 12 mission

07 p1112 N71-17710
Neutron activation analysis of O, Si, Al, and Fe abundances in Apollo 12 lunar rock 12013

07 p1112 N71-17711
Neutron activation analysis of O, Si, and Al abundances in Apollo 12 lunar samples

07 p1112 N71-17712
Neutron activation analysis of O, Si, and Al in Apollo 11 rocks and fines

07 p1112 N71-17713
Instrumental activation analyses of abundances in lunar rock chips

07 p1113 N71-17714
Abundance of uranium, thorium, and plutonium isotopes in Apollo 12 soil and breccia samples

[NASA-CR-114870] 07 p1114 N71-17868
Determination of carbon content of lunar samples from Apollo 11 flight

[NASA-SP-257] 07 p1115 N71-17964
Luminescence measurements on Apollo 11 and Apollo 12 lunar soil samples

[NASA-CR-114899] 09 p1464 N71-19778
Optical measurements on Apollo 12 soil samples from lunar mare surfaces

[NASA-CR-114894] 09 p1465 N71-19780
Preliminary results from Mossbauer instrumental analysis of Apollo 12 lunar rock and soil samples

[NASA-CR-114887] 09 p1465 N71-19781
Neutron activation analysis for trace elements depleted on lunar surface with implications for origin of moon and meteorite influx rate

[NASA-CR-114888] 09 p1465 N71-19782
Optical and radio frequency electrical properties and grain size analyses of Apollo 11 and 12 lunar soil samples

[NASA-CR-114893] 09 p1465 N71-19784
Computer-coupled low resolution mass spectrometer system and organic geochemical analysis methods for isolation and identification of compounds from lunar soil samples

[NASA-CR-114904] 09 p1465 N71-19786
Lack of heavy alkanes in Apollo 11 and 12 lunar soil samples

[NASA-CR-114919] 09 p1466 N71-20174

Gas exposure experiments of lunar soil with microchemical, microphysical, and adhesion analysis
[NASA-CR-114916] 09 p1467 N71-20277

Analysis of texture and crystalline orientation of lunar rock samples

[NASA-TT-F-13561] 09 p1468 N71-20527
Development of device for separating, collecting, and viewing soil particles

[NASA-CASE-XNP-09770] 09 p1394 N71-20440
Neutron activation analysis of Apollo 11 and 12 rocks and soils, and X ray fluorescence and radiochemistry data

[NASA-CR-114926] 10 p1645 N71-21462
Oxygen isotopic compositions and fractionations between coexisting minerals found in lunar samples from Apollo 11 and Apollo 12 flights

[NASA-CR-114925] 10 p1645 N71-21464
Mass spectroscopy of lunar samples to determine uranium, thorium, and lead content

[NASA-CR-114929] 10 p1645 N71-21575
Chemical composition and radioactivity analyses of lunar surface materials

[NASA-CR-114976] 13 p2165 N71-24558
Comparison of analytical results of lunar surface materials from Surveyor, Apollo, and Luna missions

13 p2165 N71-24559
Neutron activation analysis determination of uranium and Pb-204 in Apollo 11 fines

13 p2166 N71-24560
Device which separates and screens particles of soil samples for vidicon viewing in vacuum and reduced gravity environments

[NASA-CASE-XNP-09770-3] 15 p2390 N71-27036
Drilling tests for evaluating crustal potential of Apollo lunar surface drill core stems

[NASA-TM-X-58057] 17 p2754 N71-29214
Procedures and immunofluorescent techniques for screening Apollo aquatic test animals for bacterial pathogens after lunar sample exposure

[NASA-CR-115064] 17 p2707 N71-29228
Mobility performance problem of power-driven rigid cylindrical roller/wheels climbing semi-infinite soft soil slope with uniform velocity applied to lunar locomotion

[NASA-CR-118968] 17 p2789 N71-30307
Lunar soil mechanics and properties based on Apollo 14 observations and data

18 p3011 N71-30958
Mineralogy and petrology of lunar rock and soil samples returned from Apollo 14 landing site

18 p3011 N71-30959
Closeup photographs of soil and rock on lunar surface obtained with Apollo 14 stereoscopic camera

18 p3012 N71-30968
Geological analysis of lunar soil sample from Sea of Fertility obtained by Luna-16 automatic station

[NASA-TT-F-13756] 18 p3016 N71-31331
Production of iodine isotopes in meteorites by cosmic rays, gas proportional counting of transition metal X ray emitters, and radiochemical analysis of lunar samples

18 p3017 N71-31348
Chemical composition of lunar samples from Apollo 11 and 12 flights

[NASA-TT-F-13787] 19 p3181 N71-32388
Apparent ages of Rb-87 and Sr-87, and contents of K, Rb, Sr, Va, and rare earths in lunar soil from Mare Fecunditatis

[NASA-TT-F-13945] 20 p3349 N71-33660
Mass spectroscopy investigations of Apollo 11 and 12 soil samples

[UCB-34-P-32-PR-5] 20 p3323 N71-33815
Portable penetrometer for analyzing lunar soil characteristics

[NASA-CASE-MFS-20774] 21 p3427 N71-34387
Chemical processes for producing oxygen and water from moon from lunar rocks and soils

[NASA-TM-X-58061] 21 p3506 N71-34978
Mechanical behavior of lunar fine soils in engineering gravity flow bins

[NASA-CR-121670] 21 p3508 N71-34993
Mineralogy and petrology of Apollo 12 lunar samples

[NASA-CR-121662] 21 p3568 N71-34995
Lunokhod-1 RIFMA instrument for analyzing chemical composition of lunar soil

[NLL-M-20428-5828.4F] 21 p3526 N71-35122
Properties of rocks, soils, and minerals in ultrahigh vacuum facility simulating lunar environment, for extraterrestrial resource utilization

[NASA-CR-121915] 22 p3668 N71-36150
Lunar cratering, and geologic interpretation of Apollo 11 soil samples

23 p3846 N71-37416

LUNAR SPACECRAFT

NT APOLLO SPACECRAFT

NT LUNAR LANDING MODULES

NT LUNAR MODULE

NT LUNAR ORBITER

NT LUNAR PROBES

NT LUNAR SATELLITES

NT LUNAR LUNAR PROBES

NT SURVEYOR 3 LUNAR PROBE

NT SURVEYOR 6 LUNAR PROBE

SUBJECT INDEX

LUTETIUM ISOTOPES

Halo Orbit Space Station potential for lunar communications, exploration, logistics, and launching platform operations (NASA-TM-X-65409) 05 p0772 N71-15351

Feasibility and systems definition data for Orbiting Lunar Station (NASA-CR-115003) 13 p2172 N71-24749

Orbiting Lunar Station feasibility and definition - Operational, experiment, and science support requirements (NASA-CR-115015) 14 p2342 N71-25832

Functional analysis (NASA-CR-115016) 14 p2342 N71-25833

Orbiting Lunar Station feasibility and definition - Performance requirements (NASA-CR-115017) 14 p2342 N71-25834

Orbiting Lunar Station feasibility and definition - Configuration and systems analysis (NASA-CR-115018) 14 p2342 N71-25835

Orbiting Lunar Station feasibility and definition - Configuration definition (NASA-CR-115019) 14 p2342 N71-25836

LUNAR SURFACE

U LUNAR TOPOGRAPHY

LUNAR SURFACE SCIENTIFIC MODULES

U LSSM

LUNAR SURFACE VEHICLES

NT LUNAR MOBILE LABORATORIES

NT LUNAR ROVING VEHICLES

NT LUNOKHOD LUNAR ROVING VEHICLES

Manned-unmanned lunar explorer systems design (NASA-CR-115822) 05 p0770 N71-14511

Field tests of simulated remote navigation control system for lunar surface vehicle (NASA-TM-X-64567) 06 p0895 N71-16822

Resilient vehicle wheel for lunar surface travel (NASA-CASE-MFS-20400) 08 p1293 N71-18611

Soviet news releases on Lunokhod 1 and remote sensing 11 p1746 N71-22054

Soviet research in astronomy, meteorology, oceanology, geomagnetism, upper atmosphere, space, and Lunokhod activities - No. 248 (JPRS-52634) 11 p1828 N71-22682

Upper atmospheric physics and radio transmission, Cosmos launches, and Lunokhod activities (NASA-CR-115018) 11 p1791 N71-22687

Resilient wheel design with woven wire tire and shavese tread for lunar surface vehicles (NASA-CASE-MFS-13929) 15 p2415 N71-27091

Robot engineering concepts, instrumented striding information device, and planetary striding vehicle (JPRS-53742) 20 p3277 N71-32910

Analogy between human motor functions and mechanical legs for planetary striding vehicle 20 p3277 N71-32913

LUNAR TEMPERATURE

Infrared radiometer for measuring lunar brightness temperature (NASA-TM-X-64539) 01 p0053 N71-10275

Lunar surface magnetometer measurements for determining electrical conductivity and temperature of lunar core (NASA-TM-X-62012) 06 p0949 N71-16862

LUNAR TIDES

Observing growth rhythms in shells of fossil marine invertebrates and relationship to tidal cycles in earth-moon system (NASA-CR-111608) 03 p3023 N71-12312

Lunar semidiurnal component of OI /5577A/ night glow (JILU-ENG-70-263) 05 p0680 N71-15629

Gravitational tide effects on rotating fluid in earth model 07 p1010 N71-17630

Gravitational measurements of ocean tides along transcontinental profile of United States 20 p3262 N71-33343

Trigonometrical expansion for calculation of tidal effects on motion of artificial satellites (NASA-TM-X-65685) 22 p3668 N71-36152

Long term equations of motion for earth-moon system including solar and lunar tidal torques 23 p3847 N71-37419

LUNAR TOPOGRAPHY

Analysis of ranging system for lunar surface electrical properties experiment (NASA-CR-100673) 02 p0177 N71-11244

Very high vacuum terrestrial mineral beneficiation methods transferred to vacuum ambient of lunar surface (NASA-CR-111399) 02 p0230 N71-11569

Environmental factors affecting lunar mining operations (NASA-TM-X-64530) 02 p0294 N71-11883

Infrared study of cooling behavior of eclipse thermal anomalies during lunar night (REPT-5) 02 p0295 N71-11895

Cratered lunar soil model for reproducing directional infrared data from lunar thermal meridian (DI-42-0987) 02 p0296 N71-11966

Selenographic coordinates of lunar topography from Apollo 8, 10, 11, and 12 missions (NASA-TN-D-6082) 02 p0296 N71-12042

Fluid conductivity of lunar surface materials (NASA-CR-102842) 04 p0611 N71-14089

Combined X ray fluorescence and neutron excitation for obtaining rapid lunar and planetary surface element analysis (NASA-TM-X-65394) 04 p0612 N71-14113

Bibliography on lunar surface (PB-194206) 04 p0613 N71-14287

Construction and interpretation of topographic and relief contour maps of Tycho northeast rim 04 p0613 N71-14440

Multiphase eruptions associated with lunar craters Tycho and Aristarchus - lava flow charts 04 p0613 N71-14441

Bandera lava tubes of New Mexico and lunar comparisons 04 p0522 N71-14443

Lava flow characteristics in Hadley Rille valley of lunar mountains (NASA-TM-X-62011) 05 p0767 N71-14687

Relative heights of photographic features of lunar topography (AD-173679) 05 p0767 N71-14911

Prototype holocamera and playback system for lunar surface topography experiment (NASA-CR-116146) 06 p0868 N71-16574

Lunar rock erosion estimation 07 p1114 N71-17735

Characteristics of lava tubes and channels on lunar surface (NASA-TM-X-62013) 07 p1116 N71-18007

Panoramic views of lunar surface produced by automatic lunar probe (NASA-TT-F-651) 08 p1290 N71-19242

Effects of orientation, lunation, and location on performance of lunar radiometer - design studies (NASA-TM-X-1846) 09 p1483 N71-20092

Topographic corrections for lunar gravity data 10 p1644 N71-21339

Shape from shading method applied to lunar topography and scanning electron microscopes (AD-717336) 11 p1797 N71-22227

Quantitative microluminescence analysis of lunar glasses and fines (NASA-CR-114966) 13 p2166 N71-24944

Radio astronomy studies including sensitive interferometers, digital correlators, and related measuring instruments also radar techniques for lunar topography (NASA-CR-114969) 13 p2082 N71-25083

Determining static mass bearing capacity of lunar surface by slope analysis of failed slopes in lunar craters (NASA-CR-118505) 14 p2340 N71-26650

Lunar surface radar reflectance measurements and variations of dielectric constant (PR-4) 17 p2844 N71-29419

Interpretation of planetary surface photographs, noting Moon, Mars, and Mercury surfaces (ESRO-SP-56) 18 p3008 N71-30594

Lunar surface crater and maria photointerpretation noting lunar and earth evolution 18 p3008 N71-30596

Computer techniques for trafficability and visibility analysis of lunar surface in mission planning for roving vehicles (NASA-CR-1881) 18 p3008 N71-30661

Charged particle lunar environment experiment of Apollo 14 detecting particle fluxes at lunar surface resulting from wide range of lunar surface, magnetospheric, and interplanetary data 18 p3011 N71-30964

Lunar portable magnetometer experiment to measure steady magnetic field at different sites in Fra Mauro region - Apollo 14 flight 18 p3012 N71-30967

Study of far side upland volcanism of lunar surface using Hasselblad camera 18 p3013 N71-30972

Geologic analysis of lunar surface using photographs from 70-mm Hasselblad camera 18 p3013 N71-30973

High resolution strip photography of lunar surface 18 p3013 N71-30974

Sketch map of proposed Descartes Apollo 16 lunar landing site 18 p3013 N71-30976

Correlation of zero phase brightness surge - heiligenschein with lunar surface roughness 18 p3013 N71-30977

Lunar surface examination using low sun elevation photography 18 p3013 N71-30978

Comparison of lunar maria with oceans of earth and differences between lunar surface and terrestrial continental structure 18 p3014 N71-30990

Nighttime lunar surface differential flux scans at 22 microns (NASA-CR-121457) 20 p3348 N71-33433

Radar astronomy observations on quassars, lunar craters, and Venus topography (NASA-CR-121410) 20 p3349 N71-33561

Informal names and descriptions of lunar topographic features in Apollo 15 landing region (NASA-CR-121625) 21 p3506 N71-34979

Location and derivation of nomenclature for lunar topographic features in Apollo 15 landing region (NASA-CR-121624) 21 p3506 N71-34980

Dust thunderstorm hypothesis for short-lived red flares on parts of lunar surface (NLL-M-20719-15828.4F) 21 p3511 N71-35017

Establishing solar cell array criteria for use as primary power source in lunar-based water electrolysis system (NASA-CR-119945) 23 p3709 N71-36441

Comparison of Martian tectonic and topographic features with earth and moon based on Mariner 6 and 7 photographs (NASA-TM-X-65095) 23 p3847 N71-37421

Preliminary data evaluation from Apollo 15 inflight and lunar surface experiments with analysis of extravehicular, module, support, and communication systems performance 23 p3848 N71-37427

Lunar surface layer density determination from lunar satellite radar data on centimeter and millimeter waves (AD-17) 23 p3853 N71-37480

Investigation of glass particles recovered from Apollo 11 and Apollo 12 fines, and composition and heterogeneity of lunar surface (NASA-TM-X-65724) 24 p4006 N71-38575

Problems of chemical analysis in connection with lunar surface and landforms 24 p4009 N71-38589

LUNAR TRAJECTORIES

NT CIRCUMLUNAR TRAJECTORIES

NT EARTH-MOON TRAJECTORIES

NT MOON-EARTH TRAJECTORIES

Astrodynamic characteristics of lunar trajectories for manned and unmanned spacecraft (AD-714426) 06 p0946 N71-16744

LUNGS

Acceleration and gravity effects on function and behavior of lung (AGARDOGRAPH-133) 11 p1679 N71-21981

LUNIK LUNAR PROBES

Soviet research in geophysics, astronomy and space (JPRS-51657) 03 p0470 N71-13038

Abstracts of research on upper atmosphere and space 03 p0454 N71-13043

Description of Luna-16 flight including automatic station, soil drilling device, return to earth, and lunar soil 03 p0456 N71-13044

Investigating lunar core samples from Flight of Luna 16 (AD-714428) 06 p0950 N71-16326

Comparison of analytical results of lunar surface materials from Surveyor, Apollo, and Luna missions 13 p2165 N71-24559

Preliminary geological analysis of lunar regolith from Luna 16 data (NASA-TT-F-13700) 17 p2842 N71-29252

Geological analysis of lunar soil sample from Sea of Fertility obtained by Luna-16 automatic station (NASA-TT-F-13756) 18 p3016 N71-31331

LUNOKHOD LUNAR ROVING VEHICLES

Lunokhod 1 design, control, and lunar geology and astronomy experiments 11 p1832 N71-22688

Soviet news releases on launching of Cosmos 400 and 401 and Lunokhod-1 activities 15 p2396 N71-24876

Soviet news releases on Lunokhod lunar roving vehicle and launching of Cosmos 419, 420, and 421 18 p2910 N71-30793

Geomorphology of Mare Imbrium area explored by Lunokhod-1 lunar roving vehicle (D-92) 20 p3343 N71-32809

Lunokhod-1 lunar roving vehicle program, landing module construction, onboard equipment, and results of lunar crater observations 20 p3343 N71-32810

Design and operation tests of Lunokhod-1 21 p3509 N71-35003

Soviet news releases on Lunokhod 1, Soyuz 11 flight crew, and launching of Cosmos 429 21 p3510 N71-35009

Lunokhod-1 RIFMA instrument for analyzing chemical composition of lunar soil (NLL-M-20428-15828.4F) 21 p3526 N71-35122

LUTETIUM

NT LUTETIUM ISOTOPES

Preparation of lanthanide single crystals, and thermal expansion and elastic moduli of lutetium single crystals (IS-T-408) 16 p2669 N71-29157

LUTETIUM ISOTOPES

Single gamma spectrum used for investigating decay of Lu-170 to Yb-170 (U.S. TRANS-10467) 04 p0582 N71-14108

Gamma transitions in lutetium and tantalum isotopes with purely nonconserving effects (INP-714) 15 p2480 N71-27658

Electron capture decay lutetium 168 /7 min/ yields ytterbium 168 using germanium/lithium and silicon/lithium detectors
[LYCEN-7030] 15 p2489 N71-27886
Level crossing and resonance spectra of excited states in lutetium 175 hyperfine structure
17 p2796 N71-29791

LUTETIUM 176

U LUTETIUM ISOTOPIES

LYAPUNOV FUNCTIONS

LYAPUNOV FUNCTIONS

LYMAN ALPHA RADIATION

Excitation of atomic hydrogen to metastable 2 2S1/2 state by electron impact - polarization of Lyman alpha radiation produced by collision transfer between inert gas atoms and protons
12 p1978 N71-24254

Development of method for studying transfer of resonance line radiation in media of extremely large optical thickness
13 p2170 N71-25436

Auroral Lyman alpha emission cross sections from hydrogen-proton collisions in upper atmosphere
[AD-721462] 16 p2644 N71-28099

Effect of time ordering on Lyman alpha profile and comparison of time-ordered thermal average and untime-ordered thermal average
[NBS-MONOGRAPH-121] 18 p2925 N71-31251

Flight calibration device for absolute measurements of photometer at Lyman alpha wavelength on OGO-6 and other satellites
[AD-726567] 22 p3665 N71-36136

LYMAN SPECTRA

Measuring transition of photospheric spectrum into chromospheric and vice versa during total solar eclipse of 15 Feb. 1961
03 p0370 N71-13158

Variable centimeter radio sources, and Lyman line transfer in planetary nebulae
13 p2167 N71-25113

Effect of time ordering on Lyman alpha profile and comparison of time-ordered thermal average and untime-ordered thermal average
[NBS-MONOGRAPH-121] 18 p2925 N71-31251

LYMPH

NT LYMPHOCYTES

LYMPHOCYTES

Electrophoretic and chromatographic analysis of lactate dehydrogenase isoenzyme activity in fetal, neonatal, and adult human thymus and spleen lymphocytes
[NASA-TT-F-13991] 23 p3715 N71-36482

LYOPHILIZATION

U COLLOIDING

LYOPHILS

U COLLOIDS

LYRAE CONSTELLATION

Energy distribution of spectrophotometric gradients in the ultraviolet spectra of beta Lyrae
[NLL-RTS-6031] 17 p2844 N71-29764

Description of Isaac Newton Telescope Cassegrain spectrograph and results of radial velocity observations of stars near Lyrae constellation
23 p3758 N71-36794

LYSOGENESIS

Photometric measurement of euglobulin lysis time by direct printer
[NASA-TT-F-13389] 01 p0010 N71-10357

Photometric continuous recording of fibrinolysis and lysis
[NASA-TT-F-13405] 01 p0011 N71-10423

M

M WINGS

U VARIABLE SWEEP WINGS

M-2 LIFTING BODY

NT M-2F2 LIFTING BODY

Vertical tail loads and control surface hinge moment measurements on M2-F2 lifting body at subsonic speeds
[NASA-TM-X-1712] 05 p0775 N71-15003

Air launch characteristics of M2-F2 lifting body from B-52 aircraft
[NASA-TM-X-1713] 05 p0770 N71-15004

Convective heat transfer characteristics of M2 and M2-F2 lifting entry vehicles
[NASA-TM-X-1691] 07 p0970 N71-17131

Transonic wind tunnel tests of vertical fin loads and rudder hinge moments on M2-F2 lifting body scale model at Mach 0.50 to 1.30
[NASA-TM-X-2286] 13 p2023 N71-24581

M-3F2 LIFTING BODY

HL-10 and M-2F2 lifting body flight tests
[NASA-TM-X-66712] 08 p1143 N71-18428

Analysis of coupled roll-spiral-mode, pilot induced oscillation occurring with M-2F2 lifting body
[NASA-TD-D-6496] 20 p3206 N71-33307

MACH CONES

Analysis of Mach wave configurations resulting from reflection of shocks from inclined surfaces using

schlieren photography, interferometry, and smoke tracks
17 p2857 N71-29639

Numerical analysis of structure of shock waves and comparison with predicted values
[ARC-TN-4] 22 p3568 N71-35415

MACH NUMBER

Wind tunnel tests of mixed compression axisymmetric inlet system at Mach numbers 0.6 to 3.5
[NASA-TN-D-6078] 03 p0449 N71-13024

Knudsen flow and Mach number effects on hypersonic and supersonic wakes of cylindrical bodies and spheres
[REPT-69-7] 04 p0471 N71-13403

Parametric engine study for Mach 0.98 commercial air transport with supercritical wing
[NASA-TM-X-52961] 08 p1284 N71-18733

Effect of spark discharges into laminar boundary layer at supersonic free stream Mach numbers
[NASA-TN-D-6378] 15 p2363 N71-26950

Quantitative comparison of reactive and nonreactive Mach stems for understanding detonation structure
[AD-721465] 16 p2578 N71-28015

Effect of injection Mach number on jet penetration over wide range of pressure and free stream Mach numbers
[NASA-TN-D-6370] 16 p2579 N71-28270

Operational Mach number increase by vortex flow compression
[AD-723279] 19 p3077 N71-31935

Numerical analysis of plane steady transonic flows past lifting airfoils with freestream Mach numbers less than unity
[D180-1298-1] 21 p3412 N71-34275

Mach meter using semiconductor detectors of alpha particles produced by americium 241 sources
[CEA-R-4107] 21 p3426 N71-34381

Static aerodynamic characteristics of Scout fin with enlarged tip control at Mach numbers from 0.40 to 4.63
[NASA-TN-D-6397] 22 p3681 N71-36246

Comparison of blockage corrections in porous tunnel wall to closed wall tunnel at subsonic Mach numbers
[ARA-19] 24 p3908 N71-37853

MACH-ZEHNDER INTERFEROMETERS

Variable sensitivity optical Mach-Zehnder and holographic interferometry for plasma diagnostics
12 p1982 N71-24260

MACHINE LEARNING

U LEARNING MACHINES

MACHINE LIFE

U SERVICE LIFE

MACHINE ORIENTED LANGUAGES

NT ALGOL

NT ASSEMBLY LANGUAGE

NT COBOL

NT CONTEXT FREE LANGUAGES

NT FORTRAN

NT LANGUAGE PROGRAMMING

NT PL/I

NT SYMBOLIC PROGRAMMING

Development and characteristics of automatic language processing system
01 p0026 N71-10015

Development of machine translation system
01 p0026 N71-10016

Existence of generators for certain AFL
[NASA-CR-111110] 01 p0028 N71-10377

Research achievements in simulation mathematics, and language - reviews
[NASA-TM-X-64527] 02 p0306 N71-11125

Analysis of pattern description language for describing line drawings
[AD-711406] 02 p0186 N71-11305

Conception of Space Programming Language
[AD-711788] 02 p0189 N71-11328

Programming language for solving symbolic mathematical problems
[AD-710746] 02 p0189 N71-11330

Tape and time bounded turing acceptors and AFL
[AD-712704] 03 p0344 N71-12496

Investigating data word and instruction format factors for selecting common word length in aerospace computers
03 p0347 N71-12607

Describing design and implementation of NPS LISP 1.3 VERS 1 programming system
[AD-712779] 04 p0502 N71-13512

Proving theorem of coding statements in arbitrary languages
07 p0996 N71-16976

Development of eclectic information processing system for computer design
[NASA-CR-117304] 09 p1355 N71-19923

High level computer programming language /SAIL-PL/E/ and parallel processing system to implement it
[NASA-CR-117174] 09 p1356 N71-20332

Problems in semantic comparison of natural and mathematical logic languages
[JPRS-52621] 10 p1527 N71-20678

User machine-oriented languages for simple data processing
10 p1527 N71-20822

Development of programming languages, syntax, algorithms, and subroutines for digital computers
[AD-716486] 10 p1529 N71-21561

PL-516 assembly language for Honeywell DDP-516 computer
[NPL-COM-SCI-44] 11 p1715 N71-22094

Standardization of programming languages for numerical control of machine tools
[AD-717750] 11 p1768 N71-22257

Development of machine oriented languages for control of automatic machine tools
[AD-717778] 11 p1768 N71-22293

Digital computer enhancement by use of technique of interpretation rather than compilation of higher ordered languages
[NASA-CR-117901] 12 p1881 N71-23435

Automatic dictionary for creating indexes for information retrieval through computer programs
14 p2222 N71-25965

AGNOS language to allow IBM 360/44 FORTRAN programmers access to Adage graphics facilities without recourse to computational facilities
[TR-71-19] 14 p2224 N71-26431

Input/output routines for symbolic programming with FORMAL on Univac 1108 computer
[NASA-CR-119189] 17 p2723 N71-30109

Development and application of mathematical models for digital simulations of social factors and production planning methods
[JPRS-53668] 19 p3122 N71-32016

Development and application of mathematical models in science
19 p3122 N71-32017

Computer language for implementation of graphic theoretical algorithms
[NASA-CR-119723] 20 p2339 N71-33564

Higher order programming language and compiler for advanced computer software system to be used with manned space flights between 1972 and 1980
[NASA-CR-115126] 21 p3398 N71-34184

Description and implementation of HAL programming language for use with future manned space flights
[NASA-CR-115127] 21 p3398 N71-34185

Development of test and flight engineer language for space shuttle system
[NASA-CR-121616] 21 p3512 N71-35027

Briefing aids used for oral presentation describing development of test and flight engineer oriented computer language for space shuttle system
[NASA-CR-121657] 21 p3512 N71-35029

Development of computer programming language for use on space shuttle
21 p3517 N71-35061

Development of standard language for test and ground operations involving space shuttle ground support equipment
21 p3518 N71-35067

Language and executive software requirements for automated onboard checkout of manned space station
[NASA-CR-115129] 21 p3519 N71-35077

Behavioral science programming language for use with flight simulator facility
[AD-726432] 23 p3729 N71-36584

Characteristics and application of problem oriented language to mathematical programming and data processing
24 p3893 N71-37747

Computer system language for job construction and control
24 p3893 N71-37748

MACHINE RECOGNITION

U ARTIFICIAL INTELLIGENCE

MACHINE STORAGE

U COMPUTER STORAGE DEVICES

U CORE STORAGE

MACHINE TOOLS

NT BORING MACHINES

NT GRINDING MACHINES

NT LATHES

NT MILLING MACHINES

NT SHAPERS

Optimization of pin-joint frames, cantilever members, and machine tool structures
[ARC-R/M-3632] 06 p0953 N71-15797

Computer programming for numerically controlled machine tools
[CRIF-MC-35] 10 p1562 N71-20444

Electric and electrohydraulic stepping motors for numerically controlled machine tools
[CRIF-MC-33] 10 p1562 N71-20750

Edge durability data for machine tools in metal cutting processes
[TN-7] 10 p1563 N71-20910

Displacement measurement on numerically controlled machine tools using transducers positioning devices
[CRIF-MC-31] 10 p1564 N71-21004

Moire effect analysis of stress and strain of machine parts and structural elements
[AD-717826] 11 p1835 N71-23168

Standardization of programming languages for numerical control of machine tools
[AD-717750] 11 p1768 N71-22257

- Algorithm using ALGOL 68 type language for computerized determination of three dimensional path for numerical control of machine tools
[AD-717777] 11 p1768 N71-22258
- Development of machine oriented languages for control of automatic machine tools
[AD-717778] 11 p1768 N71-22293
- Motion command processing in programming languages for numerical control of machine tools
[AD-717749] 11 p1768 N71-22373
- Description of protective device for providing safe operating conditions around work piece in machine or metal working tool
[NASA-CASE-XLB-01092] 11 p1771 N71-22797
- Description of device for aligning stacked sheets of paper for repetitive cutting
[NASA-CASE-XMS-04178] 11 p1771 N71-22798
- Machine tool wear caused by cutting of porous ceramic materials
[AD-718488] 12 p1944 N71-23766
- Development and characteristics of frusto-conical die nib for extrusion of refractory metals
[NASA-CASE-XLB-06773] 12 p1928 N71-23817
- Technical information concerning machine tools, and fixtures
[NASA-SP-5910/03] 12 p1930 N71-24078
- Compilation of technology utilization articles on subjects of cutting, shaping, and forming of materials and application to industrial methods
[NASA-SP-5922/01] 12 p1931 N71-24171
- Design and development of layout tool for machine shop use to locate point in precise reference to straight or beveled reference edge
[NASA-CASE-FRC-10005] 14 p2262 N71-26145
- Optical gauging system for monitoring machine tool alignment
[NASA-CASE-XAC-09489-1] 14 p2264 N71-26673
- Comprehensive survey of status of adaptive control as applied to machining processes
[Y-1759] 20 p3280 N71-33535
- Electrodiffusion wear of tools and technology of using machine-tool devices
[AD-726804] 22 p3589 N71-35559
- Noise sources, spectra, and reduction methods for woodworking machine tools
[NASA-TT-F-13900] 22 p3628 N71-35830
- Analytical derivation of tool electrode wear during spark machining of cavities
[AD-726642] 23 p3763 N71-36829
- Methods for performance evaluation of precision automatically controlled turning equipment
[Y-NA-134] 23 p3764 N71-36832
- MACHINE TRANSLATION**
Development and characteristics of automatic language processing system
01 p0026 N71-10015
- Programming language for advanced translator writing system
[NASA-CR-117124] 09 p1352 N71-19596
- Language programming for Palantype typewriter language translator
[NPL-COM-SCI-45] 11 p1715 N71-22093
- Intermediate code and table driven processor for translating retrieval question to users original language
[AD-72221] 14 p2221 N71-25977
- Computer program for linguistic data processing including translating text from Russian into English
14 p2222 N71-25984
- Elastic matching, error correction coding in natural language
[NPL-COM-SCI-46] 22 p3556 N71-35330
- MACHINERY**
Research projects in automotive engineering for ground and air transportation
09 p1482 N71-20548
- Design of mechanical device for stirring several test tubes simultaneously
[NASA-CASE-XAC-06956] 10 p1564 N71-21177
- Precipitation detector and mechanism for stopping and restarting machinery at initiation and cessation of rain
[NASA-CASE-XLA-2619] 14 p2233 N71-26334
- Welding technology and nondestructive inspection techniques for heavy machinery
[NLL-CE-TRANS-5294-7022.09/1] 17 p2757 N71-30365
- Correction of inspection data for part misalignment utilizing small computer
[Y-1753] 19 p3123 N71-32217
- Computers for designing machines
[AD-727090] 24 p3896 N71-37771
- Characteristics of two dimensional mechanisms and classification of structural groups of mechanisms
[AD-727243] 24 p3928 N71-38028
- Development of technique for boronizing machine and tool parts in powdered mixtures
[AD-727937] 24 p3929 N71-38036
- Wear resistance of electrolytic iron-phosphorus alloys for use as coatings for machine parts
[AD-727441] 24 p3937 N71-38085
- MACHINING**
NT CHEMICAL MACHINING
NT ELECTROCHEMICAL MACHINING
NT MILLING (MACHINING)
NT SPARK MACHINING

- Absorption sensitive mechanical and machining properties of soda-line glass
[AD-713594] 05 p0710 N71-15402
- Optimization of cutting processes for machining delta plutonium
[RFP-1428] 05 p0693 N71-15431
- Effect of forced ultrasonic radial vibrations of tools when machining titanium and heat resistant alloys
[AD-713455] 05 p0694 N71-15457
- Calculation and measurement of force, residual stress, and temperature effects on plastic surfaces from machine tool geometric parameters
[NLL-RTS-5815] 10 p1566 N71-21321
- Machining under conditions of high static pressure of lubricant cooling medium
[AD-719812] 13 p3099 N71-24427
- Laser machining device with dielectric functioning as beam waveguide for mechanical and medical applications
[NASA-CASE-HQN-10541-2] 15 p2415 N71-27135
- Surface burnishing of machined metal using pressurized rolling ball technique
[UCRL-30684] 17 p2754 N71-29263
- Effects of machining parameters on carbon steel wear inhibiting layer of tools
[PB-198083] 18 p2927 N71-30797
- Fracture mechanics and statistical failure analysis of brittle materials and erosion and abrasion machining processes
18 p2929 N71-31209
- Comprehensive survey of status of adaptive control as applied to machining processes
[Y-1759] 20 p3280 N71-33535
- Production of circular cylindrical surfaces on lathe using arc plasma torch
[UCRL-TRANS-10524] 21 p3433 N71-34431
- MACROCLIMATE**
U CLIMATE
MACROMOLECULES
U MOLECULES
MACROSCOPIC EQUATIONS
Examining characteristics of system of stationary macroscopic equations for plasma resistivity and viscosity
[EPF-6/44] 05 p0754 N71-15184
- Plasma flow and magnetohydrodynamic macroscopic equations
[CEA-N-1371] 08 p1269 N71-18166
- Continuum theory for determination of macroscopic equations for reinforcing fiber composites
[NPL-MA-92] 16 p1650 N71-20665
- MACULAR VISION**
U VISION
MAGMA
Volcanic gas collections used to calculate chemical composition of volatile fraction of basaltic magma gas phase
[NASA-TR-R-348] 13 p2071 N71-24610
- Magma reservoir evidenced from tidal gravity variations observed at Halemauuan lava lake, Kilauea, Hawaii
20 p3264 N71-33339
- MAGNESIUM**
NT MAGNESIUM ISOTOPES
Fracture mechanics in explosively loaded magnesium
[AD-712129] 02 p0242 N71-11587
- Fast neutron irradiation effects on diffusion phenomena in Al-Mg system
[CEA-CONF-1527] 03 p0429 N71-12885
- Theoretical and experimental determinations of elastic constants for magnesium
[COO-1196-756] 06 p0875 N71-16781
- Influence of defects created by neutron irradiation at 80 K on elastic moduli and internal friction of magnesium
[CEA-CONF-1621] 08 p1213 N71-18443
- Electrodeposition of magnesium and beryllium from organic baths
[NASA-CR-111850] 08 p1216 N71-18856
- Dayglow measurements of ionized magnesium using rocket-borne ultraviolet spectrometer
[NASA-CR-116853] 08 p1192 N71-18966
- Combustion of large magnesium particles during pressure change in ambient medium within range from 100 to 760 mm Hg
[NASA-TT-F-13363] 09 p1485 N71-30531
- Impurity behavior in process of zone recrystallization of magnesium
10 p1573 N71-20871
- Vaporization of magnesium impurities from high purity aluminum melt in vacuum apparatus reduces electrical resistance of aluminum
10 p1575 N71-20882
- Numerical values for neutron elastic and inelastic scattering cross sections for Mg in range 4.19 to 8.36 MeV
[ORNL-4530] 13 p2130 N71-24899
- Ge/Li detectors for determining spin and parity for Mg-24 compound nucleus using Na-23/proton, alpha, gamma, Me-20 reaction
13 p2133 N71-25160
- Spin tensor moments of deuterons emitted from Mg-24/Mg elastic scattering reaction
[ANU-P-498] 13 p2141 N71-25545

- Angular distributions of deuterons and protons in magnesium 24 to magnesium 25 transition
[JINR-B4-3350] 15 p2471 N71-27413
- Polarization of protons inelastically scattered on Mg-24, Cr-52, and Ni-58
[NP-18532] 15 p3486 N71-27894
- Sodium carbonate inhibitor for preventing contact corrosion and pitting in magnesium cladding of water cooled fuel rods
[NLL-CE-TRANS-5440-7022.09/1] 19 p3158 N71-32174
- Correlation of calcium II and K line profiles with sunspot numbers and Mg 5172 A line position shifts in relation to chromospheric activity
19 p3176 N71-32254
- Metabolism of magnesium deficient Escherichia coli cells under aerobic and anaerobic conditions
[NRC-TT-1472] 22 p3545 N71-35255
- Proton holes in [2a-1d] shells from Mg-24 to Si-28 and from [d,He-3] reactions compared with [p,p] reactions
[NP-18511] 22 p3639 N71-35944
- Thermal resistance of cadmium and magnesium at temperatures from 3 to 100 K
22 p3660 N71-36099
- Volume photoemission model and photoelectric determination of electron attenuation lengths in magnesium and aluminum
[ORNL-TM-2617] 24 p3980 N71-38406
- MAGNESIUM ALLOYS**
Diffusional flow in superplastic magnesium alloy
[AD-711348] 01 p0089 N71-10997
- Multiaxial analytic creep theory for describing primary, secondary, and creep recovery
[WTHD-22] 02 p0244 N71-12025
- Effects of quench rate on distribution of precipitates at grain boundaries in Al-Zn-Mg alloys
[AD-712099] 03 p0939 N71-13152
- Technology review on Soviet magnesium alloy production
[JPRS-31761] 04 p0330 N71-14125
- Aluminum-rich magnesium alloys strengthened by combined action of plastic deformation and heat treatment
[AD-714120] 06 p0865 N71-16219
- Magnesium addition effects on microstructure, hardness, and tensile properties of zinc aluminum alloy
[BM-R1-7491] 08 p1218 N71-19030
- Ordering effect on Cd diffusion in MgCd alloy
[TT-70-57051] 08 p1218 N71-19089
- Crystal growth and galvanomagnetic properties of Mg2Pb
09 p1454 N71-20438
- Combustion physics and flammability of aluminum magnesium alloy aerogels
[NASA-TT-F-13505] 09 p1484 N71-20511
- Procedure for bonding polytetrafluoroethylene thermal protective sleeves to magnesium alloy conical shell components with different thermal coefficients
[NASA-CASE-XLA-01262] 10 p1566 N71-21404
- Effect of tin on mechanical properties of Mg-Li-Al alloy in presence of small quantities of zinc and manganese
[AD-717593] 11 p1777 N71-22175
- Nuclear spin lattice relaxation time measurements of lithium-magnesium alloys by recording growth of nuclear spin
11 p1805 N71-22370
- Comparison between silicon-magnesium-aluminum alloy and copper aircraft electric conductors and terminals noting types of tests
[TRC-BR-19785] 12 p1809 N71-23547
- Spectral analysis of magnesium distribution in high strength cast iron containing globular graphite
[TT-70-59085] 14 p2266 N71-25668
- Application of flame metal spraying to bonding magnesium alloy cladding to uranium nuclear fuel elements
[CEA-CONF-1625] 15 p2448 N71-27339
- Electron microprobe analysis of solute segregation near grain boundaries in Al-Zn-Mg alloy after different quenching (air, water, oil, and air) and aging heat treatments
[AD-722034] 16 p2610 N71-28454
- Closed Form surfaces in N334m order-disorder transformations when alloyed with NiFe and NiCo
[NLL-LT-746-6332-7022.401/1] 16 p2614 N71-28932
- Recrystallization kinetics of magnesium-cadmium and magnesium-zirconium dilute alloys using X ray diffraction technique
17 p2826 N71-30821
- Microstructure intermetallics and temperature effects on aluminum and aluminum magnesium alloy yield strengths
[RAE-LIB-TRANS-1512] 17 p2766 N71-30249
- Creep and other mechanical properties of extruded zinc-30 percent aluminum alloys containing magnesium
[BM-R1-7338] 19 p3116 N71-32395
- Magnesium alloy plates deformed by oblique explosive loading for hardening without ductility loss
[RFP-1649] 21 p3439 N71-34474

Mathematical model of vacancy concentrations compared with AlZnMg alloys age hardening behavior to determine Mg atom-vacancy pairs concentration effect on clustering rate

[NLL-M-20407-5828-4P] 21 p3441 N71-34487
Structural and mechanical properties of AlZnMg, AlMgSi, and AlCuMg alloys as function of natural aging prior to artificial aging

[NLL-M-20408-5828-4P] 22 p3596 N71-35606
Variations in damping capacity of magnesium alloys with changes in content of alloying elements

[NLL-LT-746-647-9022-401] 22 p3597 N71-35613
Effect of electromagnetic mixing on ingot grain size during continuous casting of magnesium alloys

[AD-71717] 24 p3937 N71-38086
MAGNESIUM CELLS
Engineering evaluation of low temperature high rate reserve magnesium perchlorate batteries

[AD-710952] 01 p0007 N71-10715
Low temperature miniature automatically activated magnesium battery to supply reserve power to expendable electronic devices

[AD-72066] 24 p3875 N71-37625
MAGNESIUM CHLORIDES
Thermodynamic properties of aqueous hydrochloric acid-sodium chloride-magnesium chloride mixtures calculated by electromotive force measurements

[JORN-TM-3017] 01 p0019 N71-10805
MAGNESIUM COMPOUNDS
NT CHLOROPHYLLS

NT CORDIERITE
NT DOLOMITE (MINERAL)
NT MAGNESIUM CHLORIDES
NT MAGNESIUM FLUORIDES
NT MAGNESIUM OXIDES

Hyperfine fields at magnetic and nonmagnetic lattice sites measured in solid solutions of magnesium antimonide and chromium antimonide

[COO-198-800] 18 p2962 N71-30737
Development and evaluation of refractory magnesium and aluminum concretes for use as insulating walls in magnetohydrodynamic generator channel

[AD-72066] 22 p3599 N71-35632
Mechanical properties of continuous composites of boron fibers magnesium metal matrix

24 p3946 N71-38152
MAGNESIUM FLUORIDES
Extinction coefficient and reflectance of aluminum, magnesium fluorides, and magnesium fluoride coated aluminum mirrors for far ultraviolet radiation

[NPL-QU-12] 03 p0418 N71-13319
Far infrared analysis of pair mode in MgF₂-Fe₂O₃

[NYO-2391-120] 05 p0759 N71-15445
Physical, optical, and electrical properties of magnesium fluoride including radiation effects

[ONERA-NT-02-21-70] 15 p2428 N71-26968
MAGNESIUM ISOTOPES
Angular distributions for elastic and inelastic scattering of alpha particles by Mg-26

[RLO-1388-110] 03 p0428 N71-12863
International comparison of Mn-56 activity in 1968 including nuclear reactor irradiations and neutron-source calibration

[ANL-7642] 06 p0915 N71-16001
Threshold photoneutron cross sections for nuclei of Mg, Cr, Fe, and Pb isotopes

[UCRL-50902] 06 p0921 N71-16397
Angular distributions of deuterons and protons in magnesium 24 to magnesium 25 transition

[JINR-E4-5350] 15 p2471 N71-27413
Comparison of integrated scattering cross sections of 3/2 states in Mg-25/4, alpha/Na-23 and Al-23/4, alpha/Mg-25 reactions

[NASA-TN-D-6412] 17 p2795 N71-29779
NaI crystal spectrometer measurements of cross sections for Mg-25/tau, gamma/Si-28 reaction at E sub tau equals 4.44, 6.08, 6.15, and 8.26 MeV

[ANU-PJ508] 20 p3314 N71-32501
Calculation of Si-28 photodisintegration rate from Al-27 (p, gamma)Si-28 and Mg-24 (alpha, gamma)Si-28 reactions

21 p3487 N71-34844
Studies of analog states of T equals 2 in Mg-26(He-3, n)Si-28, Ti-46(He-3, n)Cr-48, and Ni-58(He-3, n)Zn-60 reactions

[IAE-1958] 22 p3632 N71-35881
Microscopic coupled-channel analysis of proton inelastic scattering from neon and magnesium ions

[NASA-TN-D-6419] 23 p3814 N71-37201
MAGNETIC OXIDES
Arc fusion growth and characterization of high purity MgO crystals

[JORN-4547] 03 p0441 N71-12840
Wave functions incorporating electron correlation for magnesium oxides, lithium oxides, aluminum oxides, and titanium oxides

[AD-711973] 03 p0433 N71-12942
Thermal expansion of refractory oxides at high temperatures

[AD-714741] 06 p0876 N71-15988
Current-voltage characteristics of hot electron transport in vacuum deposited thin film emission gold magnesium oxide diodes

09 p1361 N71-19419

Directional and bidirectional reflectance of MgO sphere wall coatings, and directional characteristics of photomultiplier tube

[NASA-CR-117402] 10 p1606 N71-20732
Oxidation constant drop of mixed oxides (Co, Mg/O and Co, Ni/O)

[NLL-CE-TRANS-5379-9022-09] 10 p1578 N71-31217
Electron irradiation produced length changes in pure and doped magnesium oxide samples

11 p1800 N71-21872
Mass transport properties, crystal growth, and self-diffusion rates for magnesium oxides

[AD-710886] 12 p1942 N71-23327
Creep properties of iron doped polycrystalline magnesium oxide and iron and chromium doped polycrystalline aluminum oxide between 1300 and 1500 C

[COO-1591-3] 12 p1945 N71-23951
Mechanical properties of dispersion strengthened chromium-base alloy with magnesium oxide additives

[AD-720389] 14 p2274 N71-26159
Color centers and magnesium oxide crystal defects from proton irradiation and impurities

[NASA-CR-110885] 16 p2642 N71-28044
Immersion calorimeter for measuring Wigner energy in irradiated BeO, MgO, Al₂O₃, and SiO₂ at high temperatures

[CEA-N-1171] 19 p3156 N71-32428
Fabrication and properties of hot-pressed polycrystalline magnesium oxide containing anion impurities

[NASA-CR-121937] 22 p3587 N71-35545
Design, development, and production of magnesium oxide insulators installed in cathodic and anodic walls of open cycle magnetohydrodynamic generator channel

22 p3599 N71-35630
Color center and substitutional impurity point defects in magnesium, calcium, and strontium oxide insulators

[AD-726647] 23 p3835 N71-37351
MAGNETIC (TRADEMARK)
U SERVO MOTORS

MAGNET COILS
Operating characteristics of ripple correcting system for converted alternating gradient synchrotrons

[BNL-14859] 03 p0358 N71-13156
Estimation of magnetic field errors from coil winding irregularities in superconducting magnets

[RHEL/R-197] 04 p0566 N71-14085
Thomson scattering and cusped containment geometries. Chalice project

[SIT-2582-34] 04 p0593 N71-14445
Superconducting coil stability and interaction between transport and diamagnetic currents

[IPP-4-76] 08 p1276 N71-18158
Superconductivity coil cooling of cryogenic system in full scale thermonuclear power plants

[ORNL-TM-3097] 08 p1242 N71-19236
Symmetry optimization program for toroidal magnet currents

[UCRL-50944] 13 p2127 N71-25453
Calculating energy losses produced in pulsed superconducting magnet of any shape wound with solid core wires

[INP-18516] 14 p2298 N71-26628
Equations and formulae for magnets with air cored windings of saddle coil type

[RHEL/R-203] 15 p2453 N71-27139
Relay circuit breaker with magnetic latching to provide conductive and nonconductive paths for current devices

[NASA-CASE-MSC-11277] 16 p2572 N71-29008
Cooling intrinsically stable superconducting magnets with supercritical helium tubes adjacent to magnet coils

[UCRL-20172] 21 p3465 N71-34665
MAGNETIC ABSORPTION
U ELECTROMAGNETIC ABSORPTION

MAGNETIC ANNUAL ABC
Magnetic annular arc used as accelerator for high pressure, high enthalpy flow test facility

[AD-710316] 01 p0038 N71-10186
Magnetic arc stabilization in xenon compact arc lamps by means of longitudinal magnetic fields

[NASA-CASE-NPO-10887] 21 p3402 N71-34209
Flow characteristics in exhaust of pulsed megawatt gas fed arc examined with piezoelectric pressure transducer

[NASA-TM-X-67931] 22 p3566 N71-35402
MAGNETIC ANOMALIES
NT GEOMAGNETIC HOLLOW

Magnetic anomaly detection by natural geomagnetic field perturbations

[AD-712131] 03 p0368 N71-13030
Bathymetry and magnetics of region /POL-421-3/ 29 deg to 35 deg N, 155 deg to 165 deg W - map

[ESSA-TR-ERL-146-POL-4] 07 p1024 N71-17957
Arctic Ocean geophysical studies of Alpha Cordillera and Mendocoev Ridge

[AD-715656] 08 p1193 N71-18977
Field and laboratory equipment and methods for airborne electroprospecting using rotating magnetic

fields and anomalous effect calculations for conductive media and irregular form bodies

[TT-70-50059] 10 p1555 N71-21871
Components of terrestrial magnetic field with graphs of diurnal variations

11 p1745 N71-21932
Spectra of geological magnetic fluctuations computed from magnetic field measurements from US East Coast

[AD-717407] 11 p1745 N71-21971
Marine magnetic anomalies over Red Sea caused by magnetic rocks underlying axial trough

[AD-718910] 14 p2246 N71-25843
Self consistent solution for anomalous magnetic moment of nucleons

[JINR-E2-5353] 14 p2310 N71-26667
News briefs and abstracts of scientific articles concerning magnetic anomalies in Atlantic Ocean and currents in Arctic Basin

17 p2739 N71-29402
Pauli-type approximation for vector meson equations with anomalous magnetic moments

[IPFV-SVM-70-31] 18 p2971 N71-30467
Analysis of magnetic anomalies in ocean bottom off central California coast

18 p2912 N71-30906
Measurement of magnetic anomaly profiles south of Aleutian Islands

18 p2913 N71-30996
Fracture zones and magnetic anomalies south of Aleutian trench

18 p2914 N71-31005
Measurement and characteristics of gravity anomalies over Aleutian trench

18 p2914 N71-31005
Secular magnetic variation anomaly and geomagnetic field drift in Poland

[TT-70-50086] 19 p3096 N71-32646
Secular magnetic variation anomaly and Warsaw anomaly

19 p3096 N71-32647
Simulation of swell-induced magnetic vector in shallow sea applied to ambient acoustic pressure and velocity field noise parameters

[AD-724656] 20 p3258 N71-33157
Aeromagnetic anomalies and granodiorite bodies in Pend Oreille area, Idaho for metamorphic and structural studies

21 p3419 N71-34329
Superconducting dipole or multipole magnet configurations for reducing end aberrations during beam transport

[UCRL-20184] 21 p3465 N71-34666
MAGNETIC CHARGE DENSITY
Ion engine with magnetic circuit for optimal discharge

[NASA-CASE-XLE-01124] 04 p0605 N71-14043
Proposed experiment for identification of elementary particles bearing small magnetic charges

[CERN-TRANS-71-101] 23 p3806 N71-37316
MAGNETIC CIRCUITS
Nondestructive test for measuring heat treatment states in closure welds

[ORNL-TM-3024] 03 p0386 N71-13285
Ion engine with magnetic circuit for optimal discharge

[NASA-CASE-XLE-01124] 04 p0605 N71-14043
Analysis of magnetic circuits using electric circuit theory

[UCRL-72828] 17 p2786 N71-29267
MAGNETIC COILS
Production of steady magnetic fields by use of room temperature magnetic coils without iron

[TID-25511] 05 p0733 N71-15245
Linear magnetic braking system with nonuniformly wrapped primary coil producing constant braking force on secondary coil

[NASA-CASE-XLE-05079] 07 p1036 N71-17652
Thyristor trigger exciting in coils of magnetic extension of synchrocyclotron

[JINR-P-5204] 08 p1174 N71-18218
Electroexplosive safe-arm initiator using electric driven electromagnet coils and magnets to align charge

[NASA-CASE-LAR-10372] 08 p1169 N71-18599
Impact and static pressure tests of increasing phase velocity accelerator magnetic coil system operating on argon plasma for high altitude, high velocity flow, reentry simulation

[AD-717705] 11 p1812 N71-22585
Design of cryogenic high frequency acceleration system in ringrons

[JINR-P9-5488] 14 p2314 N71-26730
Wide-range nuclear magnetic resonance probe design including integrated circuits, RF coil, and control cable for use with high field cryogenic magnets

[NASA-TN-D-6338] 15 p2505 N71-26908
Design of theta pinch with four times fed coil

[IPP-468] 15 p2474 N71-27439
Large-volume high magnetic fields for fusion reactors produced by superconducting windings

[IPP-470] 15 p3450 N71-27588
Toroidal stellarator with strong helical currents

[EUR-CEA-FAC-53] 15 p2504 N71-27921

- Single shot pulsed magnetic field systems employing superconducting magnets and switches and nonsuperconducting coils
[LA-4617] 21 p3464 N71-34659
- Plasma confinement and heating in internal ring device F4
[CN-38A-4] 24 p3993 N71-39489
- Vacuum calculations and fast neutral beam production system for multi-injection experiments in quadrupole coils
[EUR-CEA-PC-587] 24 p3994 N71-39490
- MAGNETIC COMPASSES**
Developing digital magnetic compasses based on Hall effect for small boats
[AD-712547] 04 p0544 N71-14342
- MAGNETIC CONTROL**
Magnetic field effect on magnetic satellite attitude control and digital simulation of satellite motion
03 p0357 N71-12720
- Development of magnetic attitude control system for High Energy Astronomy Observatory satellite
[NASA-CR-103023] 07 p1057 N71-17446
- Magnetically opened diaphragm design with camera shutter and expansion tube applications
[NASA-CASE-XA-05660] 10 p1564 N71-21060
- Magnetically controlled plasma accelerator capable of ignition in low density gaseous environment
[NASA-CASE-XLA-00372] 16 p2663 N71-29184
- Test facilities for HEOB and ESRB satellite magnetic control - Noordwijk, Netherlands
[ESRO-TM-134F-ESTEC] 17 p2730 N71-29490
- Garnet tunnel diode oscillator for microwave application
21 p3404 N71-34223
- Dynamic models for ESRB I attitude control system noting equations of spinning motion
[ESRO-TR-5-ESTEC] 23 p3859 N71-37508
- MAGNETIC CORES**
Evaluation results and accuracy improvement of two flux switching mathematical models for magnetic cores
[NASA-TN-D-6032] 01 p0036 N71-10067
- Electronic counter circuit utilizing magnetic core and low power consumption
[NASA-CASE-XNP-06836] 03 p0348 N71-12515
- Ferrite magnetic core magnetometer
04 p0520 N71-13637
- Calculation of digital current distribution systems on micron tape cores
[AD-714768] 06 p0822 N71-15936
- Pulsed magnetic core memory element with locking oscillator feedback for interrogation without loss of digital information
[NASA-CASE-XGS-05303] 08 p1164 N71-18595
- Ferrite core fluxgate magnetometer
08 p1190 N71-18688
- Describing magnetic core current switching device for storing bipolar current pulses to memory units
[NASA-CASE-NFO-10201] 08 p1165 N71-18694
- Reliable magnetic core circuit apparatus with application in selection matrices for digital memories
[NASA-CASE-XNP-01318] 11 p1730 N71-23053
- Nickel-zinc ferrite cores for magnetic heads with increased wear resistance
[AD-716922] 12 p1888 N71-23491
- Magnetic current regulator for saturable core transformer
[NASA-CASE-ERC-10075] 13 p2055 N71-24800
- Power switch with transformer type magnetic core
[NASA-CASE-NFO-10242] 13 p2056 N71-24803
- Effects of zinc substitution on switching and hysteresis loop properties of lithium ferrite cores
[AD-719174] 13 p2124 N71-24839
- Unsaturation magnetic core transformer design with varying signal for electrical power processing equipment
[NASA-CASE-ERC-10125] 13 p2057 N71-24893
- Temperature sensitive magnetometer with pulsating thermally cycled magnetic core
[NASA-CASE-XAC-03740] 14 p2254 N71-26135
- Comparison of supermagnet and silicon steel as transformer core material for high induction pulsed application
[EC-DR-70-736] 15 p2385 N71-26942
- Equations and formulae for magnets with air cored windings of saddle coil type
[RHEILY-203] 15 p2453 N71-27139
- Digital magnetic core memory with sensing amplifier circuits
[NASA-CASE-XNP-01012] 16 p2506 N71-28925
- Magnetic cores for analog computer storage devices
17 p2723 N71-30025
- Utilizing vacuum insulation for devices with magnetic cores and windings
[NASA-CASE-LW-10330-1] 18 p2898 N71-31125
- MAGNETIC DIFFUSION**
Compound diffusion of cosmic rays along interstellar magnetic field lines
[NASA-TM-X-65437] 06 p0943 N71-16705
- Diffusion of multiple magnetic fields through conductive wall of plasma container
[DPV-T-3] 08 p1275 N71-18839
- MAGNETIC DIPOLES**
Analysis of crystal-field splittings, Zeeman effect, and line strengths for GdCl₃-H₂O magnetic dipole transitions
[AD-710640] 09 p1454 N71-20094
- Magnetic dipole transitions within 3d 5d configuration of Fe and Ni contributing to visible spectrum of solar corona
11 p1802 N71-22008
- Torquemeter for determining magnitude of torque generated by interaction of magnetic dipole between test specimen and ambient magnetic field
[NASA-CASE-XGB-01013] 12 p1921 N71-25725
- Field measurements by rotating spacecraft for dipole moment determination
13 p2175 N71-25334
- Numerical analysis of electromagnetic fields from buried magnetic dipole antennas and applications to radio direction finders and underground communications
[AD-721196] 15 p3383 N71-37757
- Investigation of solar wind interaction with earth magnetic dipoles and shape of magnetosphere including tail and collisionless shock wave investigated by magnetic probe
[NASA-TT-P-15734] 18 p2964 N71-31895
- Supersonic flow of rarified plasma in equatorial plane of magnetic dipole
19 p3165 N71-32389
- Tilt angle dependence of 10 MeV proton cutoff latitudes in image dipole model magnetosphere
[NASA-TM-X-65078] 20 p3316 N71-33444
- Plasmod model for explaining electron densities and temperature of hydrogen plasma with helium and argon impurities drifting into dipole magnetic field
20 p3331 N71-33674
- Tests of dc quadrupole magnet, superconducting ac dipole magnet designs with ferromagnetic return yokes, and analysis of Kohler rule in pure aluminum tapes
[KFK-1316] 21 p3464 N71-34657
- Estimates of magnetic dipole moments for spherical and transition nuclei
[INP-729] 24 p3965 N71-38282
- MAGNETIC DISPERSION**
Conceptual design of beam transport magnets for beam line I
[TRI-70-1] 03 p0359 N71-13160
- Magnetic deflection analysis of reactive scattering in crossed molecular beams of neutral species
[UCRL-19654] 13 p2138 N71-25433
- MAGNETIC DISTURBANCES**
NT MAGNETIC STORMS
Physical structure of hydromagnetic disturbances in lunar magnetosheath
[UNH-70-19] 02 p0230 N71-12095
- Analysis of geomagnetic current and seismological research covering 30 year period
03 p0369 N71-13091
- Polar cap electric field measurements, and model for Hall current auroral electrojet continuity and polar cap magnetic disturbances
[NASA-TM-X-65447] 07 p1019 N71-17270
- Circumstantial auroral arcs and magnetic disturbances observed from polar geophysical observatory
[GRL-TM-00] 10 p1547 N71-20098
- Electron energy spectra 45 to 450 keV measured on-board ESRB I satellite during quiet and magnetically disturbed periods over polar region
10 p1550 N71-21161
- Twilight aurora helium emissions in high latitudes in relation to magnetic disturbances and solar activity
[NRC-TT-1441] 10 p1551 N71-21164
- Tables of 1968 geomagnetic observations from Kakioka, Japan including declination, vertical and horizontal intensities, and characteristics of principle magnetic disturbances
[REPT-74] 11 p1749 N71-22404
- Magnetic disturbances measurements by horizontal intensity, declination, and vertical intensity variometers
[REPT-67] 11 p1749 N71-22446
- Analysis of synoptic charts of magnetic activity measured in Arctic for IOY
11 p1753 N71-22813
- Relationship between polar magnetic disturbances and rate of ring current growth
11 p1755 N71-22828
- Distribution of magnetic activity in Arctic during solar activity cycles
11 p1756 N71-22839
- Space-time distribution of magnetic disturbances in Arctic during IOY and IQSY
11 p1759 N71-22865
- Correlation and power spectrum analyses of random geophysical fluctuation effects on radio signals
11 p1767 N71-22919
- Tables on magnetic activity observed in Canada's Agincourt Observatory for 1968 and Jan. to Mar. 1969
12 p1906 N71-23406
- Reaction time of upper atmosphere from gas density fluctuations following geomagnetic disturbances
13 p2070 N71-24566
- Airborne photography of polar auroral band during magnetic disturbances
17 p2746 N71-30070
- Magnetic activity at high latitudes of Northern Hemisphere during maximum and minimum solar cycle
17 p2748 N71-30093
- Magnetic disturbance calculation techniques for model current systems including numerical integration and spherical harmonic expansions
[APF-PH-77] 20 p3359 N71-33170
- Three dimensional thermospheric model for interpreting tidal, planetary waves, and magnetic disturbances
[NASA-TM-X-65676] 20 p3366 N71-33443
- Analysis of air density relationships to solar activity and geomagnetic disturbances based on ATS 2 orbital data
[RAE-TR-70084] 21 p3420 N71-34536
- Hourly and mean geomagnetic declination and horizontal and vertical intensity data from Kakioka, Japan for 1969
[REPT-60] 24 p3918 N71-37940
- Hourly and mean geomagnetic declination and horizontal and vertical intensity data from Menominee, Japan for 1969
[REPT-79] 24 p3918 N71-37941
- Hourly and mean geomagnetic declination and horizontal and vertical intensity data from Kakioka, Japan for 1969
[REPT-70] 24 p3918 N71-37942
- MAGNETIC DOMAINS**
Application of domain tip logic in designing associative processors for supercube
[NASA-CR-115866] 05 p0652 N71-15535
- Reduction of plasma wall interaction in magnetic well by focusing magnetic field lines on outside of mirror region
[CEA-COMP-1665] 09 p1449 N71-20099
- Microstructure and magnetic properties of internally oxidized ferromagnet alloys for application to magnetic domain theories and high temperature tests
[AD-717210] 10 p1579 N71-21301
- Photometric and cinematographic studies of magnetic domain processes in ferromagnetic materials
[AD-717669] 11 p1783 N71-23248
- Effect of nuclear radiation on domain tip thin magnetic film elements
[AD-724621] 23 p3819 N71-37338
- Epitaxial growth of garnet films for magnetic bubble domains
[AD-727070] 24 p3987 N71-38511
- MAGNETIC DRUMS**
Electrodeposition of nonporous Co-Ni coating on metallic recording drums
[NLL-TT-746-61-7032.401/] 17 p2761 N71-29253
- MAGNETIC EFFECTS**
Mariner spacecraft data analysis to determine relationship between interplanetary magnetic field direction and geomagnetic activity
06 p0856 N71-16797
- High resolution analysis system for accelerator beams
[LYCEN-7004] 08 p1174 N71-18281
- Transverse magnetic field effects on wall heat transfer from isolated argon channel flow
[NASA-CR-116800] 08 p1303 N71-18600
- Collisionless plasma MHDs unaffected by magnetic field resonance structures
[NLL-CTO-740-7091.9F] 12 p1982 N71-24213
- Magnetic field suppression of magnetohydrodynamic boundary layer separation and inviscid flow equations
12 p1983 N71-24268
- Nonlinear interactions of electromagnetic waves in magnetosheath plasma
12 p1983 N71-24273
- Astrochemical large scale model of polycyclic spiral structure with magnetic field effects on interstellar gas motion
12 p1999 N71-24316
- Finite ion and electron temperature effect on ion cyclotron waves generated by 56k coil, and subsequent plasma ion heating in magnetic bottles
[NASA-TM-X-6263] 13 p2169 N71-23439
- Continuous equations and continuous models for magnetic, kinetic, thermal, and material subsystem nonlinear interactions
14 p2298 N71-24652
- Compensatory magnet field effect on beam flux and collision experiment
[LNF-7036] 16 p2437 N71-28047
- Thermospheric model based on Explorer 32 hydrogen ion density measurements including periodic variations and temperature factors due to local time, solar activity, and magnetic effects
[NASA-TM-X-65589] 16 p2586 N71-28329
- Temporal variations in charged particle population of inner radiation zone as measured by satellite
16 p2676 N71-28991
- Effects of magnetic orbiting on optical absorption spectrum of rubidium nickel fluoride
16 p2641 N71-29130

- Effect of magnetic activity on auroral heights
17 p2746 N71-30080
- Magnetic field level effects on niobium superconductor surface resistance
[NP-18742] 18 p2961 N71-30473
- Ion trajectory and capture cross sections in quadrupole field for determining ion quadrupole effects in ion-molecule collisions
[NASA-TM-X-67888] 19 p3155 N71-32345
- Evaluation of materials and techniques for promagnetic infrared detection
[AD-724324] 20 p3232 N71-33081
- Vortex and coaxial flow of argon and helium plasmas heated inductively, and strong magnetic field effects on turbulent plasma mixing, for gas core reactors
20 p3330 N71-33635
- Stability of incompressible two-fluid wheel flows with imposed uniform axial magnetic field for gas core nuclear rockets
20 p3352 N71-33638
- Biological effects of magnetic fields on development of pupae of fruit flies and embryos of marine alga
23 p3715 N71-36484
- In Tokamak plasma, canonical angular momentum of trapped particles drifting toward magnetic axis
[CONF-716607-29] 23 p3830 N71-37319
- MAGNETIC EQUATOR**
- Hourly values of equatorial field for Jan. - June 1970
[NASA-TM-X-65380] 01 p0049 N71-10605
- Provisional hourly values of equatorial field for 1968
[NASA-TM-D-6378] 10 p1549 N71-21096
- Ionospheric electron density measurements at magnetic equator, 1964 to 1966
[ESSA-TR-ERL-186-AL-4] 17 p2738 N71-29311
- D region electron density profiles at geomagnetic equator based on riometer and absorption experiments
[RSD-57] 20 p3267 N71-33528
- MAGNETIC FIELD INTENSITY**
- U MAGNETIC FLUX**
- MAGNETIC FIELDS**
- NT GEOMAGNETISM
- NT INTERPLANETARY MAGNETIC FIELDS
- NT INTERSTELLAR MAGNETIC FIELDS
- NT LUNAR MAGNETIC FIELDS
- NT NONUNIFORM MAGNETIC FIELDS
- NT PALEOMAGNETISM
- NT PLANETARY MAGNETIC FIELDS
- NT SOLAR MAGNETIC FIELD
- NT STELLAR MAGNETIC FIELDS
- NT TRAPPED MAGNETIC FIELDS
- Particles and fields near Jupiter
[NASA-CR-1645] 01 p0119 N71-10051
- Helicon propagation in periodic structures produced by spatial modulation of magnetic field or plasma electron density
01 p0108 N71-10139
- Stability of sunspot magnetic fields and origin of solar flares
[NASA-TM-X-65375] 01 p0118 N71-10767
- Magnetic and drift surfaces of charged particle of stellarator field
[IJP-95] 02 p0279 N71-11458
- Measuring dependence of emission power and polarization of helium-neon laser on transverse magnetic field
[AD-712104] 02 p0238 N71-11567
- Nondestructive magnetic field testing methods for reliability engineering of aerospace components
02 p0232 N71-11643
- Rotation of trihedrons at variable speeds applied to low frequency magnetic resonance modulation
[ONERA-TP-866] 02 p0267 N71-11745
- Alfvén theory of critical velocity in neutral gas and magnetized plasma interactions
[REPT-70-36] 02 p0280 N71-11837
- Surface and bulk waves on axially magnetized plasma columns
[AD-711649] 02 p0280 N71-11860
- Lehman's analysis of space charge potentials formed by cold plasmas in magnetic field
[REPT-70-14] 02 p0281 N71-11869
- Electric and magnetic cross field effects on aerodynamics and thermal regime of gas flame cone
[AD-712336] 02 p0306 N71-12075
- Energy and phase changes of particle gyrating in homogeneous magnetic field and perpendicularly propagating electrostatic wave
[PB-195690] 02 p0277 N71-12123
- Electric and magnetic fields effect on liquid crystal structures
[NASA-CR-111582] 03 p0324 N71-12313
- Dielectric constant measurements and magnetic field effects on compensated cholesteric liquid crystals
[A70-17326] 03 p0325 N71-12321
- Nonequilibrium plasma boundary layer over cathode in presence of magnetic field
[NASA-CR-111611] 03 p0437 N71-12679
- Weightlessness, corpuscular radiation, and magnetic field environmental laboratory simulation
03 p0355 N71-12704

- Geomagnetic field simulation and magnetic measurements of earth satellites
03 p0356 N71-12711
- Magnetic field effect on magnetic satellite attitude control and digital simulation of satellite motion
03 p0357 N71-12720
- Investigating kinetics of crystal growth of copper compounds in magnetic and electric fields
[AD-704556] 03 p0440 N71-12755
- Computer calculations of 184-kilohertz synchrotron magnetic field and field changes produced by change in coil excitation
[UCRL-18882] 03 p0417 N71-12875
- Effect of magnetic fields on instability and turbulence of highly ionized plasmas
[NASA-CR-111514] 03 p0437 N71-12892
- Physical effectiveness of current heating of dense high current gas discharge plasma stabilized by strong magnetic field
[KHP-71-60-43] 03 p0438 N71-12894
- Methods and equipment for measuring spacecraft magnetic fields
[NASA-TM-X-65386] 03 p0457 N71-13077
- Assessment and control of spacecraft magnetic fields
[NASA-SP-8037] 03 p0457 N71-13078
- Conductivity of plasma in unsteady magnetic field
[SINP-TH-67-8] 04 p0595 N71-13572
- Hydromagnetic wave propagation in inhomogeneous magnetic fields
[NP-18419] 04 p0570 N71-13575
- Coordinate lattice method used to calculate two dimensional magnetic fields for charged particle transport in accelerators
[JINR-P9-5013] 04 p0573 N71-13667
- Ion engine with magnetic circuit for optimal discharge
[NASA-CASE-XLE-01124] 04 p0605 N71-14043
- Estimation of magnetic field errors from coil winding irregularities in superconducting magnets
[RHEL/R-197] 04 p0566 N71-14085
- Development of temperature stabilized flux monitor for magnetic field measurement
[RHEL/R-192] 04 p0567 N71-14102
- Development and construction of magnetic systems for Uranus stellarator and studies of magnetic surfaces of large latitude
[AEC-TR-7158] 04 p0567 N71-14103
- Injection of relativistic electrons into Astron type magnetic field configurations
[AD-711822] 04 p0598 N71-14162
- Electrical and magnetic field calculation for linear accelerator inductor
[JINR-P9-5129] 04 p0567 N71-14234
- Neutral gas effects on cosmic plasmas in presence of magnetic field
[NP-18421] 04 p0600 N71-14320
- Interaction between high velocity plasma stream and stationary neutral gas cloud in magnetic field
[NP-18414] 04 p0600 N71-14321
- Laser beam scattering for magnetic field measurements in plasma pinch
[ORNL-TM-3128] 05 p0753 N71-15051
- Particle diffusion and plasma dielectric constant in uniform electric field transverse to spatially uniform magnetic field
[IJP-4/5] 05 p0733 N71-15081
- Magnetic field measurements of accelerator and beam handling magnets - bibliography
[LA-4478-B1B] 05 p0733 N71-15111
- Production of steady magnetic fields by use of room temperature magnetic coils without iron
[TID-25511] 05 p0733 N71-15245
- Characteristics of right angle helium cryostat incorporating high field superconducting solenoid
[NBS-TN-562] 05 p0734 N71-15284
- TIBRO-GENERAL computer program for calculating precise trajectories of charged particles in dc magnetic fields
[UCRL-50910] 05 p0749 N71-15295
- Fully ionized quasi-one dimensional magnetic nozzle flow
[NASA-TM-X-52925] 05 p0754 N71-15320
- Magnetic field and high frequency induction of toroidal enclosure
[AEC-TR-7168] 05 p0734 N71-15441
- Free precession nuclear gyroscopes in zero magnetic fields at cryogenic temperature
[AD-713633] 05 p0752 N71-15657
- Derivation of Vlasov equation in magnetic field
[SINP-TH-60-9] 06 p0928 N71-15735
- Power spectral analysis of magnetic fields using Time/Data 100 system
[NASA-TM-X-45413] 06 p0818 N71-15842
- Development of wide range linear fluxgate magnetometer
[NASA-CASE-XGS-01587] 06 p0858 N71-15962
- Cyclic accelerators with magnetic field harmonic analyzer using digital systems
[AD-714767] 06 p0915 N71-16010
- Magnetic element position sensing device, using misaligned electromagnets
[NASA-CASE-XGS-67514] 06 p0903 N71-16099

- Vector magnetic field measurements from Javel rocket nose cone using vapor magnetometer
[AD-714088] 06 p0854 N71-16611
- Trends of developments in magnetohydrodynamics, and heat and mass transfer
[TR-60] 06 p0906 N71-16659
- Generating first and second order matrix elements by tracking charged particles in magnetic fields
[UCRL-15823] 06 p0923 N71-16725
- Characteristics of directional discontinuities in interplanetary magnetic field
[NASA-TM-X-65430] 06 p0947 N71-16737
- Deriving boundary layer structure from addition of axial magnetic field to rotating viscous fluid and resulting modification in tilt caused by distortion of field lines
07 p0101 N71-17640
- Radial distribution of RF magnetic field measured with water cooled search coil in argon induction plasma flame
[AD-715265] 07 p0183 N71-17817
- Properties of magnetohydrodynamic waves and magnetic fields in magnetosheath
07 p0183 N71-17819
- Internal magnetic fields of Co impurity in Au, Cu, and Au-Cu alloys determined by nuclear orientation of Co-60
[COO-1569-67] 07 p0179 N71-17940
- Molecular field model for amorphous antiferromagnets with susceptibility variations
[CALT-822-16] 07 p0169 N71-18008
- Investigating helium plasma decay in circular two-pole stellarator with magnetic field variations from 6 to 12 koe
[NP-18502] 07 p0185 N71-18148
- Compensation of resonance perturbations in stellarator magnetic field
[NP-18477] 08 p1246 N71-18161
- Magnetic field resonance structure effect on collisionless plasma confinement
[NP-18470] 08 p1269 N71-18179
- Plasma density measurements using electrostatic probe parallel to magnetic field
[EUR-CEA-FC-540] 08 p1269 N71-18180
- Dynamics of laser produced plasma interaction with uniform magnetic field
[EUR-CEA-FC-548] 08 p1270 N71-18181
- Beam extraction methods of proton synchrotron
[RPPIN-22] 08 p1174 N71-18280
- Charged particle motion in stellarator magnetic field
[NP-18473] 08 p1255 N71-18381
- Calculations on plasma equilibrium configuration confined by helically symmetric magnetic field
[NYO-1480-161] 08 p1272 N71-18387
- Magnetic field influence on high pressure phase diagrams of iron and iron alloys
[REPT-6/70] 08 p1213 N71-18348
- Recursive formulas for toroidal magnetic fields
[IJP-6/83] 08 p1242 N71-18349
- Deriving surface equation for fluid subjected to gravitational and magnetic fields using variational principle of minimum free energy
[NASA-TT-F-13462] 08 p1179 N71-18376
- Influence of hot carrier mobilities on magnetoelectric effects in forward biased Schottky junctions
[AD-715706] 08 p1278 N71-18376
- Effect of transverse magnetic field on propagating plane gaseous detonation wave
08 p1305 N71-18399
- Apparatus for use in liquid helium cryostat for measurement of small magnetic field changes occurring within detection chamber
08 p1244 N71-19010
- Measurement of muonium hyperfine structure at weak magnetic field
08 p1245 N71-19215
- Investigating plasma body rotation and self axial low frequency oscillations in ionized low pressure hollow cathode gas fed arc device
08 p1275 N71-19246
- Magnetic field measurements of particle velocity using U-probe or axisymmetric probe
[AD-715854] 09 p1422 N71-19473
- Magnetic field fine structure in individual supergranules
09 p1422 N71-19498
- Plasma effects in solids and low frequency effects in superconductors
[AD-716531] 09 p1451 N71-19553
- Magnetic field determination of nonlinear generator
[AD-716437] 09 p1359 N71-19735
- Magnetization versus field and temperature analyses of ferromagnetic material in Apollo 12 lunar samples
[NASA-CR-114891] 09 p1465 N71-19707
- Magneto-optical study of magnetic field dependence of spin-lattice relaxation time of paramagnetic ions in crystal lattice
09 p1432 N71-19929
- Reduction of plasma wall interaction in magnetic well by focusing magnetic field lines on outside of mirror region
[CEA-CONF-1665] 09 p1449 N71-20009

- Charged relativistic electron ring in homogeneous and weakly focusing magnetic field
[JINR-P-5299] 09 p1425 N71-20315
- Hamiltonian method for determining magnetic tunneling in crystals in one and two band models
09 p1454 N71-20423
- Photographic recording and analysis of measurements made on rotating magnetic field pinches
[LRF-4570] 09 p1451 N71-20498
- Hypertune field of Se-44 in Ni host from 80 K to Curie point, obtained from perturbed angular correlations
[CONF-700933-4] 09 p1446 N71-20584
- Hypertune field of Rh-100 in Ni host near Curie point, obtained from perturbed angular correlations
[CONF-700933-3] 09 p1446 N71-20585
- Cold plasma density and collisional frequency measurements in presence of magnetic fields for cyclotron ionization plasma diagnostics
[COO-1769-1] 10 p1627 N71-20803
- Intensification of crystallization processes in liquid phase using mobile magnetic field
10 p1574 N71-20880
- ESRO 1 satellite experiment on magnetic field aligned electric field near or in ionosphere
10 p1550 N71-21154
- Thermodynamics of Heisenberg ferromagnet in applied magnetic field
[NASA-TM-X-52969] 10 p1661 N71-21168
- Development of non-magnetic indexing device for orienting magnetic flux sensing instrument in magnetic field without generation of detrimental magnetic fields
[NASA-CASE-XGS-02422] 10 p1567 N71-21529
- Analysis of multiple earth bow shock crossings at large geocentric distances from Pioneer 8 magnetic field data
[NASA-TM-X-65474] 10 p1554 N71-21541
- Computer program for analysis of magnetic field problems involving ferromagnetic materials
[AD-716922] 10 p1608 N71-21631
- Field and laboratory equipment and methods for airborne electroprospecting using rotating magnetic fields and anomalous effect calculations for conductive media and irregular form bodies
[TT-70-50059] 10 p1535 N71-21671
- Periodic oscillations and momentum distribution functions for interacting fermions in magnetic field
10 p1636 N71-21849
- Tokamak plasma current distribution measurement using magnetic field angles
[MATT-818] 11 p1810 N71-22117
- Two dimensional unsteady flow of viscous incompressible conducting fluid in infinite channel in constant longitudinal magnetic field
11 p1797 N71-22220
- Plasma interactions resulting from plasma flow and magnetic field with nozzle shaped lines of force with large electron Hall parameter
[ISAS-457] 11 p1811 N71-22433
- Acoustic amplification in high mobility extrinsic semiconductors in presence of crossed dc electric and magnetic fields
11 p1796 N71-22468
- Space plasma experiments involving Alouette resonances and diagnostic techniques applied to electron density and temperature and local magnetic field strength measurement
[NASA-CR-117844] 11 p1812 N71-22585
- Dispersion propagation and Landau damping of electrostatic ion waves in nonisothermal plasma supported by uniform magnetic field
11 p1814 N71-22886
- Propagation of electromagnetic waves along gyrotropic cylinder in longitudinal magnetic field
11 p1800 N71-23016
- Negation of magnetic fields produced by thin wafer-like circuit elements in space vehicles
[NASA-CASE-XGS-03590] 12 p1858 N71-23187
- Tables on magnetic field observations made at Alert Observatory of Canada
12 p1907 N71-23408
- Current sheet magnetic model to calculate quiet large-scale magnetic field in solar corona compared with accuracy of other models
[NASA-TM-X-65496] 12 p1992 N71-23433
- Torque meter for determining magnitude of torque generated by interaction of magnetic dipole between test specimen and ambient magnetic field
[NASA-CASE-XGS-01013] 12 p1921 N71-23725
- Low frequency 1 to 100 KHz oscillations in hot cathode Penning discharge plasma caused by density waves moving in plasma drift direction in crossed electric and magnetic fields
[NASA-TT-F-13641] 12 p1981 N71-23966
- FORTRAN program for computing two dimensional magnetic field components for conduction geometries
[ORNL-TM-2484] 12 p1968 N71-24006
- Numerical fluid model for low pressure plasma in toroidal magnetic field
12 p1982 N71-24051
- Numerical analysis of simultaneous transport of momentum, energy, and magnetic field for magnetohydrodynamic flow in finite ducts
12 p1903 N71-24136
- Injection laser Thomson scattered light for timed measurement of electron density and temperature of shock fronts formed by axial plasma injection into dipole magnetic fields
12 p1982 N71-24143
- Threshold theorem for expanding absorptive dispersion F sub 2v nucleus radius and establishing of Fermi energy limit from light propagation and magnetic fields neutrino sea
12 p1977 N71-24253
- Magnetic field and homopolar geometry effects on behavior of ionized gas in homopolar device
12 p1983 N71-24345
- Proceedings of conference on controlled fusion and plasma physics held at Rome, Italy in August and September, 1970
[AD-719427] 13 p2146 N71-24638
- Dynamic equations for stochastic magnetic field lines in galaxy
[NASA-TM-X-65314] 13 p2160 N71-24949
- Instabilities and turbulence in highly ionized plasmas in magnetic field related to problems of thrusters for manned space flight and plasma generated energy
[NASA-CR-118311] 13 p2147 N71-25028
- Numerical calculations concerned with filling magnetic well by injection of neutral atoms at various angles and energies
[EUR-CEA-FC-503] 13 p2147 N71-25038
- Kondo state as function of magnetic field and temperature in Cu-Fe alloys
[AD-719662] 13 p2126 N71-25151
- OGO-B and OGO-E measurements on magnetospheric field magnitudes and disturbances caused by ring currents
13 p2076 N71-25271
- Helium 4 impurities and magnetic field effect on thermal boundary resistance between powdered cerium magnesium nitrate and liquid helium 3 at very low temperatures
[UCSD-34-P-143-35] 13 p2127 N71-25463
- Effects of thermodynamic fluctuations in superconductive films in perpendicular magnetic field just above transition point
13 p2153 N71-25502
- Experimental and theoretical analysis of plasma propagation into low pressure gas and plasma in magnetic field
[AD-719855] 14 p2320 N71-25710
- Two inlet stellarator designed for containment of plasma under very clean conditions and higher stability of magnetic field configuration
[LA-TK-70-22] 14 p2321 N71-25769
- Oceanographic equipment including shipborne information systems, self maneuvering units, and instruments for measuring radioactivity and magnetic fields in sea water
[JPRS-35900] 14 p2250 N71-26317
- Biological and therapeutic effects of magnetic fields on human organism
[JPRS-35091] 14 p2297 N71-26327
- Ripple magnetic field effects on electron motion in storage rings
[JINR-P-5394] 15 p2457 N71-26849
- Soviet news releases on accuracy in guiding RT-22 radio telescope, giant telescope progress, and magnetic field clouds near sun
15 p2516 N71-26872
- Change in polarization of electromagnetic wave propagating across magnetically sheared plasma column
[CEA-CONF-1608] 15 p2498 N71-27143
- Fluxgate magnetometer for measuring magnetic field along two axes using one sensor
[NASA-CASE-GSC-10441-1] 15 p2409 N71-27325
- Nuclear magnetic resonance at 310 MHz in superconducting solenoid emphasizing methods to obtain most homogeneous magnetic field and to minimize spectrometer errors
[CEA-R-3855] 15 p2475 N71-27469
- Doppler shifted cyclotron resonance absorption of helicon waves in indium and Gantmakher-Kaner oscillations
15 p2477 N71-27577
- Large-volume high magnetic fields for fusion reactors produced by using superconducting windings
[DPP-470] 15 p2450 N71-27588
- Magnetic field intensity of 30 kG from solenoid made of superconducting Nb3Sn strip
[JINR-P-5440] 15 p2455 N71-27666
- Magnetic field components of thick finite dc solenoids obtained from expression of vector potential of circular current loop
[JINR-P-5441] 15 p2455 N71-27687
- Formulation of problems of shear flow and orientation due to magnetic field for nematic liquid crystals
[AD-721107] 15 p2378 N71-27720
- Eddy-current loss in closed current loops caused by pulsed magnetic fields
[DPP-470] 15 p2455 N71-27778
- Design of plasma engine with magnetic field energy conversion to ion heating by annihilation reaction
[AD-721214] 15 p2502 N71-27839
- Magnetic spark chamber spectrometer for high energy beam regeneration studies
[JINR-P-5361] 15 p2488 N71-27842
- Mathematical model for solving hydrodynamic flow equations in nonhomogeneous magnetic field for plasma flow along field line in presence of gravitational field
[NASA-TM-X-65354] 15 p2503 N71-27889
- Compressor magnet field effect on beam flux and collision experiment
[LNF-70-56] 16 p2637 N71-28047
- Ion containment in decreasing magnetic field of electron accelerator ring
[JINR-P-5353] 16 p2642 N71-28049
- Perturbed angular correlations of 596-keV cascade in Cu-62 measured in external and internal magnetic fields for liquid and metallic sources of Zn-62
[INP-734] 16 p2643 N71-28084
- Effects of exposure in permanent magnetic fields on sympathetic condensation system of rabbits
16 p2546 N71-28484
- Segmented superconducting magnet producing stepped magnetic field and suitable for broadband traveling wave masers
[NASA-CASE-XGS-10518] 16 p2606 N71-28554
- Dependence of ion component on magnetic field strength, and formation of plasma flux when plasma flows from hot cathode discharge
[AD-721313] 16 p2661 N71-28745
- Instrumentation for control of magnetic field in ion thruster for improved starting and improved sensing of natural magnetic field
[NASA-CASE-LEW-10835-1] 16 p2672 N71-28873
- Magnetic field topography measurement in gap of open and closed units of electromagnet of 70 Gv accelerator
[IFVE-SKU-49-95] 16 p2641 N71-29165
- Sunspot magnetometric data processing including magnetic field and radial velocity distributions
[NLL-RTS-6194] 17 p2840 N71-29282
- Determining electric and magnetic fields by visual observations of second release from Javelin vehicle
17 p2740 N71-29676
- Grid choice in low beta fluid computations for large magnetic stress compared to plasma pressure
[MATT-822] 17 p2812 N71-29740
- Characteristics of compressed magnetic fields produced by implosion of tubular stainless steel liners driven by high explosives
17 p2858 N71-29821
- Derivation and tables of spherical harmonic coefficients and isoprotic charts for International Geomagnetic Reference Field for 1965
[NASA-TM-X-65604] 17 p2745 N71-29909
- Integral attenuation coefficients of angular correlations perturbed by free hyperfine interaction and parallel external magnetic field
[IUP-690] 18 p2967 N71-30405
- Characteristics of short wavelength instabilities in confinement of collision dominated plasma by rotating magnetic field
[LRP-42/70] 18 p2991 N71-30408
- Development and analysis of optimal parameters for magnetic field windings in stellarator installations
[IVAF-8-70] 18 p2991 N71-30409
- Plasma acceleration by moving current in magnetic field
[NP-18539] 18 p2992 N71-30421
- Determination of minimum B and magnetic well depth for magnetohydrodynamic flow control
[IAE-1967] 18 p2961 N71-30424
- Magnetic field compensation by magnetic system model for phototron with space variation
[JINR-P-5390] 18 p2958 N71-30475
- Ignition behavior of electrodeless ring discharges in homogeneous periodically oscillating magnetic field
[JUL-691-PP] 18 p3023 N71-30485
- Linear resonance fluctuation criteria of superconductor to static magnetic field
[ISS-70/1] 18 p2961 N71-30635
- Gravitational effects on neutron optical properties of six-pole magnet
[JINR-P-5337] 18 p2962 N71-30668
- Hyperfine fields at magnetic and nonmagnetic lattice sites measured in solid solutions of magnesium antimonide and chromium antimonide
[COO-1159-800] 18 p2962 N71-30737
- Decay rate of longitudinal plasmon into neutrino-antineutrino pair in strong magnetic field
[NASA-TM-X-67239] 18 p3009 N71-30843
- Tables of artificial satellites for investigating magnetosphere, solar wind, electric field, and magnetic fields from 1971 to 1975
[GRI/TP/85] 18 p3018 N71-30879
- Critical magnetic field curves of superconducting molybdenum and cadmium above 0.03 K using aluminum field curve as thermometers
18 p2964 N71-31138
- Temperature effects on transport coefficients of bulk semiconductors in magnetic and electric fields
[RM-515] 18 p2999 N71-31445

Incoherent scattering of microwaves from plasma waves excited in electron beam in absence of external magnetic field
[AD-723443] 19 p3163 N71-31931

Phase-sensitivity microwave spectrometer for detecting superconductive transitions as function of magnetic field
[ISS-70/5] 19 p3100 N71-31974

IMP 5 magnetic field measurements at high geomagnetic latitudes to observe broad depressed field region centered on polar or daytime cusp
[NASA-TM-X-65642] 19 p3093 N71-32149

Magnetic fields and spectral characteristics of small H-alpha solar plagues
19 p3177 N71-32439

Methods for analyzing multistage electron beam collector schemes, with and without transverse magnetic fields, for traveling wave tubes
[NASA-CR-72950] 19 p3068 N71-32612

Simulation of ultrarelativistic cosmic plasmas in terms of photon-electron interactions in strong magnetic fields
[PR-51] 19 p3178 N71-32789

Mathematical models for solar wind merging in magnetic fields noting tearing instability
20 p3345 N71-32944

Geophysical phenomena observations of upper atmosphere electric and magnetic states, and solar activity data - Apr. 1970
20 p3258 N71-33101

Close-in electric and magnetic fields produced by gamma ray induced currents from nuclear explosion
[NORE-57] 20 p3316 N71-33416

Spectrometer for detecting hyperfine levels of perturbed hydrogen atoms at zero magnetic field
[UCRL-20529] 20 p3320 N71-33703

Single station lightning distance measuring device based on ratio of magnetic field to electric field
[NOAA-TR-ERL-195-APCL-16] 20 p3268 N71-33734

Equations of motion solved for one dimensional magnetic piston problem in study of shock waves propagating perpendicular to magnetic field in collisionless plasma
20 p3332 N71-33817

Magnetic arc stabilization in xenon compact arc lamps by means of longitudinal magnetic fields
[NASA-CASE-NPO-10887] 21 p3402 N71-34209

Gas dynamics and magnetic field effects on shock wave gradient acceleration and experimental design applications
[UCRL-TRANS-10532] 21 p3412 N71-34281

Direct current motor design with magnetic bearing for use in low friction disturbance control systems
[NASA-CASE-XGS-07805] 21 p3432 N71-34420

Automatic magnetic field measurements of bending, quadrupole, and gradient magnets with field strengths up to 50 kG
[KFK-1220] 21 p3464 N71-34656

Single shot pulsed magnetic field systems employing superconducting magnets and switches and nonsuperconducting coils
[LA-4617] 21 p3464 N71-34659

Measurement of magnetic field dependence on low temperature electromagnetic generation of ultrasonic waves in potassium
[NYO-2150-72] 21 p3465 N71-34664

Centering drift tube quadrupole magnets and measuring their harmonic field components
[SJC-A-71-1] 21 p3465 N71-34668

Coherent frequencies of transverse oscillations in electron model of ring cyclotron for magnetic field variants
[JINR-P9-5677] 21 p3473 N71-34728

Betatron oscillation coupling and decoupling by longitudinal magnetic compensating fields and application to storage ring longitudinal detector fields
[SLAC-TRANS-131] 21 p3483 N71-34824

Quantum theory of particles with spin up to one in magnetic or electric fields
[NYO-3829-66] 21 p3485 N71-34830

Stability of toroidal plasma ring with high frequency current in longitudinal magnetic field with chamber with conducting wall
[LA-4339-TR] 21 p3494 N71-34893

Disintegration of helium plasma in two-pass stellarator with magnetic field varying from 6 to 12 kOe
[NP-18767] 21 p3496 N71-34905

Magnetization and susceptibility of Heisenberg ferromagnet in magnetic field with expressions derived for calculating thermodynamic parameters
[NASA-TN-D-6420] 21 p3497 N71-34915

High-purity tungsten lattice thermal conductivity measurements at low temperatures by magnetic field suppression of electronic thermal conductivity
[NYO-2150-69] 21 p3498 N71-34921

Magnetic field gradient and rotating motions of sunspot groups and effects on solar proton flares
[NASA-TM-X-65637] 21 p3503 N71-34956

Data acquisition and reduction methods in investigating large-amplitude, high-wave number, total magnetic field variations over exposed basic volcanic rocks
[NOAA-TR-ERL-201-ESL-15] 22 p3573 N71-35450

Device for developing forces to simulate diamagnetic suspension
[NASA-CR-115148] 22 p3627 N71-35845

Three windings producing stellarator type magnetic fields
[ABC-TR-7208] 22 p3628 N71-35853

Study of temperature and density dependence of local magnetic field in xenon gas using nuclear magnetic resonance larmor precession techniques
22 p3630 N71-35866

Formation stages of magnetic field in model of accelerator sector electromagnet
[JINR-P9-5669] 22 p3633 N71-35895

LC-filter thyatron system for depression of magnetic field pulsations in Dubna synchrotron
[JINR-P9-5724] 22 p3637 N71-35926

Methods for approximating particle tracks and magnetic field strength in bubble chambers
22 p3638 N71-35935

Empirical methods for calculating magnet pole tip shape and finding field inside magnet air gap
[TRI-70-4] 22 p3642 N71-35968

Experimental stellarator facility for studying high frequency field-interactions with plasma
[NP-18801] 22 p3653 N71-36047

Electromagnetic plasma wave propagation along external magnetic field and transverse wave echoes determined by Vlasov-Maxwell equation
[NASA-CR-121918] 22 p3653 N71-36050

Performance tests of permanent-magnet, radiation cooled magnetoplasmadynamic arc thruster
[NASA-TM-X-2394] 22 p3654 N71-36059

Aircraft mechanical and battery operated clocks resistant to high intensity magnetic fields
[AD-726700] 23 p3707 N71-36430

Biological effects of magnetic fields on development of pupae of fruit flies and embryos of marine algae
23 p3715 N71-36484

Infinite length, gap excited, thick, cylindrical dipole antenna radiation field formulations as boundary value problems based on Maxwell equations for electric and magnetic fields
23 p3734 N71-36619

Techniques for estimating various pressure drops for conducting fluid flows in magnetic fields applied to lithium flow in hypothetical fusion reactor blanket
[UCRL-51010] 23 p3742 N71-36684

Gravity wave propagation in presence of temperature gradients, wind shear, and magnetic fields
23 p3803 N71-37116

Differential equations for calculating eddy current losses caused by rapidly varying magnetic fields
[CTO/754-909L-9F] 23 p3805 N71-37126

Longitudinal nonlinear oscillations of hot electron plasma near external magnetic field investigated by perturbation method
[UAREE-88] 23 p3824 N71-37278

MHD of theta pinch discharge with superimposed azimuthal magnetic field
[UAREE-102] 23 p3824 N71-37279

Applying microwave-reflection method to studying shock waves propagated through magnetic field in electrodeless discharge tubes
[UAREE-101] 23 p3825 N71-37280

Effect of external magnetic field on shock wave produced by conical pinch discharge
[UAREE-106] 23 p3825 N71-37281

Boundary conditions for adjacent streams of cold plasma in magnetic field
[UAREE-78] 23 p3825 N71-37282

Confinement of toroidal theta pinch plasma in periodic caulked cusp field
[CN-28/J-1] 23 p3827 N71-37294

Existence conditions for steady hydromagnetic shock waves propagating in collisionless plasma along magnetic fields
[IPJP-106] 23 p3827 N71-37295

Plasma confinement dependence on stellarator field properties and plasma parameters J x B type gun, ECRH, and ohmic heating plasma sources
[CONF-710607-107] 23 p3831 N71-37324

Plasma confinement and cross section shapes in Tokamak plasma columns with beta sub 1 much greater than 1 and arbitrary current distribution
[CONF-710607-84] 23 p3832 N71-37328

Instabilities in hot electron plasma created by adiabatic compression in pulsed magnetic field
23 p3833 N71-37335

Using superconducting materials to produce strong magnetic fields
[CEA-CONF-1734] 23 p3833 N71-37337

Spiral structure of interplanetary magnetic fields and solar cosmic rays
23 p3852 N71-37452

Proton transport and solar flares in interplanetary magnetic fields
23 p3852 N71-37453

Proton intensity and velocity observations in relation to solar physics and magnetic fields
23 p3852 N71-37454

Statistical mechanical and dynamic spin orientations in relation to magnetic field description
23 p3852 N71-37455

Solar wind velocity anisotropy in relation to kinematic transport of magnetic field into interplanetary space
23 p3854 N71-37472

Development of theory to predict low frequency standing wave characteristics and stability parameter of elastic bodies in presence of electromagnetic fields
23 p3860 N71-37519

Measurement of earth magnetic field by geophysical observatory 40 kilometers northwest of Helsinki, Finland
24 p3916 N71-37920

Interaction of welding arc with magnetic field under various conditions
[AD-727668] 24 p3929 N71-38030

Electromagnetic wave emission of ideally conducting sphere with variable radius and constant uniform field
[AD-727434] 24 p3967 N71-38295

Strong magnetic field production and uses, and superconducting magnets
[AD-727431] 24 p3967 N71-38296

Particle separation using deflectors with crossed electric and magnetic fields
[NP-18786] 24 p3976 N71-38371

Current-carrying toroidal plasma column high-frequency stabilization in longitudinal magnetic fields using Tolosokov device
[CN-28/B-12] 24 p3985 N71-38430

Numerical model to simulate plasma behavior in linear multicusp pinch device [polytron]
[CONF-710607-44] 24 p3987 N71-38447

Upper limits for transport coefficients due to plasma fluctuations and convective cells based on quasi-linear approximations of diffusion across magnetic fields in toroidal devices
[CONF-710607-71] 24 p3989 N71-38459

Magnetic field distribution calculations for confining toroidal Tokamak plasma columns in equilibrium based on magnetohydrodynamic approximation
[MATT-TRANS-104] 24 p3991 N71-38474

Analytical methods and plasma properties for magnetic-surface and closed-line equilibria of toroidal plasmas
[CONF-710607-119] 24 p3992 N71-38482

Behavior of plasma controlled in toroidal hexapole with and without superposition of toroidal magnetic field
[CONF-710607-6] 24 p3994 N71-38491

Radio frequency instability associated with interaction of monoenergetic electron beam with plasma in homogeneous magnetic field
[CONF-710607-59] 24 p3994 N71-38494

Argon plasma acceleration by traveling wave magnetic field
24 p3996 N71-38503

Techniques for obtaining magnetic cleanliness on deep space missions to allow interplanetary magnetic field mapping
[NASA-TR-8-373] 24 p4022 N71-38701

MAGNETIC FILMS
Characteristics of coercive force of thin magnetic films consisting of two nonmagnetostriuctive layers
[AD-714433] 06 p0933 N71-16072

Magneto-optical hysteresograph for measuring hysteresis of thin magnetic films
[FOA-3-C-3607-10] 14 p2297 N71-26255

Preparing magnetic films of nickel alloys by electrochemical method
[NLL-LTI-746-645-9022.401/] 16 p2613 N71-28830

Effect of nuclear radiation on domain tip thin magnetic film elements
[AD-726621] 23 p3819 N71-37238

MAGNETIC FLUX
Investigating problems of stability and flux jumping in superconducting materials
[NASA-CR-102919] 02 p0283 N71-11455

Pattern of magnetic flux penetration in superconducting films
[AD-705658] 03 p0444 N71-13223

Temperature compensation for magnetic flux magnetometers using wire bridge circuits
04 p0520 N71-13636

Development of temperature stabilized flux monitor for magnetic field measurement
[RHEL/R-192] 04 p0567 N71-14102

Magnetic flux quantization in superconductors
[NASA-CR-116132] 06 p0931 N71-15865

Phase detectors for magnetic flux magnetometers
07 p1027 N71-17101

Magnetic flux lines in superconductors
[NASA-TT-F-13458] 07 p1068 N71-17530

Investigations on magnetic fluxoid interactions and crystal defects in type 2 superconductors
[NYO-4060-5] 08 p1278 N71-18836

Magnetic flux measurement of magnetic dipole moments
10 p1606 N71-20714

Determination of magnetic transition in iron-rhodium system and magnetic specific heat of dilute alloys of manganese in copper by specific heat experiments at liquid helium temperature
10 p1664 N71-21691

SUBJECT INDEX

MAGNETIC MIRRORS

- Flow measurement of magnetic flux in Nb-Zr superconductor to infer magnetic induction and currents in material
[NASA-TN-D-6244] 11 p1815 N71-21957
- Development of hybrid bearing lubrication system with combination of standard type lubrication and magnetic flux field for earth atmosphere and space environment operation
[NASA-CASE-XNP-01641] 11 p1772 N71-23997
- Magnetic lift drag ratios calculated for null flux magnetic suspension designs
[BNL-15420] 12 p1966 N71-23516
- North, east, and vertical magnetic flux data and synoptic tables from Baker Lake, Canada for 1968
12 p1911 N71-23677
- Tests of permanent magnet and superconducting magnet MPD radiation cooled thrusters
[NASA-TM-X-67827] 13 p2155 N71-24724
- Magnetic current regulator for saturable core transformer
[NASA-CASE-ERC-10075] 13 p2055 N71-24800
- Symmetry optimization program for toroidal magnet currents
[UCRL-50944] 13 p2127 N71-25453
- Harmonica 2 machine observation of magnetic flux singularities and Mercier theory equilibrium predictions of magnetohydrodynamic stability
[EUR-CEA-FC-463] 14 p2323 N71-26448
- Phenomena occurring during magnetic flux compression by implosion of thin conducting liner
[CEA-R-4624] 15 p2456 N71-27974
- Flux pinning mechanisms in type-2 semiconductors and specific heat measurements on annealed and deformed pure niobium samples
[NASA-CR-121067] 21 p3496 N71-34907
- Statistical analysis of electrical phenomena associated with tornado activity and search for residual magnetism in buildings near path of tornado
[NASA-TN-D-6475] 23 p3751 N71-36749
- Hourly, diurnal, and annual data on geomagnetic declination and intensity, Hartland, England - 1962, 1963, and 1964
23 p3753 N71-36760
- MAGNETIC FORMING**
- Magnetic form factor in single crystals of terbium and thulium
[IS-T-387] 07 p1041 N71-17013
- Portable magnetometer hammer for metal working
[NASA-CASE-XMF-03793] 13 p2085 N71-24833
- Method and apparatus for portable high precision magnetomotive bulging, constricting, and joining of large diameter metal tubes
[NASA-CASE-XMF-05114-3] 13 p2086 N71-24865
- MAGNETIC INDUCTION**
- Permeameter for measurement of magnetizing force and magnetic induction at very high temperatures
[NASA-TM-X-52901] 01 p0053 N71-10272
- Inductive magnetic probe diagnostics in plasma
[AD-710734] 01 p0105 N71-10543
- Electromagnetic induction stirring of steel ingots in mold
[AD-711754] 01 p0061 N71-10865
- Magnetic induction concentric cylinder magnetohydrodynamic generator with cryogenic cooling
[DLR-FB-70-25] 07 p1083 N71-17840
- Analysis of solid rotors used in high speed induction motors for aerospace applications
11 p1677 N71-21898
- Automatic power supply circuit design for driving inductive loads and minimizing power consumption including solenoid example
[NASA-CASE-NPO-10716] 13 p2057 N71-24892
- Performance prediction of squirrel cage induction machines with nonsinusoidal mmf distributions
14 p2230 N71-26437
- Double-induction variable speed system for constant-frequency electrical power generation
[NASA-CASE-ERC-10065] 15 p2387 N71-27364
- Data on constructing high-current induction linear accelerator in nanosecond range
[JINR-P9-5601] 18 p2901 N71-30490
- Analysis of flux reversal in nickel-iron thin films using magneto-optic photographs to depict dynamic magnetization configuration during reversal process
20 p3336 N71-33912
- Penetration of induction electrical fields and losses in impure type 2 superconductors having surface currents
[ORNL-TR-2475] 20 p3337 N71-33979
- Penetration of magnetic induction, electric field, and losses in impure type-2 superconductors with surface currents and interactions
[CONFE-700341-8] 22 p3657 N71-36081
- MAGNETIC INDUCTION PROBES**
- U MAGNETIC PROBES**
- MAGNETIC LENSES**
- Design and development of electron linear accelerators
[NP-18317] 04 p0545 N71-13562
- Considering various configurations for magnetic horn for meson beam focusing
[IPVE-SEF-69-73] 04 p0572 N71-13626

- Investigating contaminations caused by ion scattering on residual gas and by chromatism in electromagnetic isotope separators
[CEA-R-4043] 04 p0574 N71-13675
- Effect of vertical lens at radial regeneration node in 184-inch synchrotron
[UCRL-20049] 06 p0833 N71-16760
- Geometrical aberrations and transfer matrix of quadrupole lenses in guiding devices or finite emittance beam matching systems and application to matching triplet study
[CEA-N-1286] 14 p2311 N71-26669
- Magnetic lens aberration correction in electron microscopy
16 p2592 N71-28245
- Application of sextupole lenses in synchrotron slow injection systems
[EP-18594] 18 p2961 N71-30454
- Optimum parameters for 12 cm bore superconducting quadrupole lens
[KFR-1218] 19 p3142 N71-32177
- Ultra-narrow, high quality, high field quadrupole magnet for use in bevalron experimental area
[UCRL-20164] 20 p3246 N71-33589
- Phase acceptance of alternating gradient double made of quadrupoles of different apertures
[CERN-71-11] 23 p3820 N71-37245
- MAGNETIC MATERIALS**
- NT FERRIMAGNETIC MATERIALS**
- NT FERROMAGNETIC FILMS**
- NT FERROMAGNETIC MATERIALS**
- NT PERMALLOY (TRADEMARK)**
- Alphabetic bibliography of magnetic materials and transition temperatures
[ORNL-RMTC-7-REV-2] 03 p0417 N71-12597
- Investigating echo phenomena in magnetic materials for application of amplified spin echo as chirp radar receiver
[AD-713518] 05 p0703 N71-15213
- Effect of nuclear radiation on properties of soft magnetic alloys
[AD-713447] 05 p0704 N71-15268
- Accurate treatment of Coulomb interaction associated with localized center
[AD-716750] 10 p1606 N71-20825
- Transport properties, electrical resistivity, thermoelectric power, and magnetic susceptibility of magnetic alloy systems
[AD-717389] 11 p1797 N71-21950
- Magnetic properties of solids including electron paramagnetic resonance in dilute magnetic alloy, hyperfine splitting of localized moment in metal, and band theory of solids
[AD-720777] 14 p2325 N71-26020
- Constitutive equations and continuum mechanics for magnetic, kinetic, thermal, and material subsystem nonlinear interactions
14 p2298 N71-26652
- Quantum theory of magnetic materials including magnetic, electric, and optical properties
[AD-720881] 15 p2453 N71-27371
- Theory of electron paramagnetic resonance in dilute magnetic alloys
[AD-722818] 17 p2815 N71-29837
- Various mechanisms for magnetic relaxation of nuclei via magnetic impurities in metals
[AD-722710] 17 p2829 N71-30345
- Processing rare earth-cobalt intermetallic compounds for use in permanent magnets
[AD-723295] 19 p3141 N71-31720
- Critical points of magnetic substances and cryogenic fluids derived from equations of state, noting deviations in thermodynamic properties
22 p3629 N71-35857
- Crystallographic data, cation distributions, magnetic transition temperatures, and magnetic structures of tetragonal systems determined by neutron diffraction
[NP-18783] 22 p3631 N71-35874
- MAGNETIC MEASUREMENT**
- Permeameter for measurement of magnetizing force and magnetic induction at very high temperatures
[NASA-TM-X-52901] 01 p0053 N71-10272
- Geomagnetic field simulation and magnetic measurements of earth satellites
03 p0356 N71-12711
- Methods and equipment for measuring spacecraft magnetic fields
[NASA-TM-X-65386] 03 p0457 N71-13077
- Assessment and control of spacecraft magnetic fields
[NASA-SP-8037] 03 p0457 N71-13078
- Development of temperature stabilized flux monitor for magnetic field measurement
[RHEIL-R-192] 04 p0567 N71-14102
- Measuring stress distribution across width of steel strip in cold mill to predict shape of finished product
[PB-194445] 04 p0531 N71-14215
- Zeeman effect for interpreting magnetographic measurements of solar magnetic fields
[REPT-2] 05 p0673 N71-14880

- Measuring superconductivity and magnetic order above and below Kondo temperature for La-Ce system
[IS-T-405] 05 p0733 N71-13013
- Laser beam scattering for magnetic field measurements in plasma pinch
[ORNL-TM-3124] 05 p0753 N71-13051
- 1969 magnetic measurements of vertical and horizontal components and declination at Nurmijarvi Geophysical Observatory, Finland
[REPT-11] 05 p0676 N71-13458
- Magnetic flux quantization in superconductors
[NASA-CR-116132] 06 p0931 N71-15865
- Development of wide range linear fluxgate magnetometer
[NASA-CASE-XGS-01587] 06 p0858 N71-15962
- Lunar surface magnetometer measurements for determining electrical conductivity and temperature of lunar core
[NASA-TM-X-62012] 06 p0949 N71-16862
- Thomson scattering measurement for determining poloidal magnetic field in plasma
[ORNL-TM-3093] 07 p1082 N71-17025
- Magnetic probes and induction coil instrumentation for Helios solar probe measurements on interplanetary magnetic fields
09 p1461 N71-19951
- Magnetic flux measurement of magnetic dipole moments
10 p1606 N71-20714
- Electrical analog and numerical analysis of heat flux meter performance
[AD-717027] 10 p1599 N71-21619
- Analysis of synoptic charts of magnetic activity measured in Arctic for IGY
11 p1753 N71-22813
- Hybrid analog computer for magnetogram data processing
13 p2053 N71-25409
- Magneto-optical hysteresis for measuring hysteresis of thin magnetic films
[FOA-3-C-3607-10] 14 p2297 N71-26255
- Magnetic field measuring probe displacement and positioning effect on optical system
[NP-18519] 14 p2298 N71-26671
- Martensitic transformations in low carbon austenitic chrome-nickel steels examined by X ray, metallographic, magnetic, and dilatometric techniques
[ORNL-TR-2423] 15 p2426 N71-27802
- Magnetic field topography measurement in gap of open and closed units of electromagnet of 70 GeV accelerator
[IPVE-SKU-69-95] 16 p2641 N71-29165
- Measurement of magnetic anomaly profiles south of Aleutian Islands
18 p2913 N71-30996
- Magnetic intensity and inclination measurements on Polish archeomagnetic specimens and comparison with similar Ukrainian data indicating magnetic drift
19 p3097 N71-32648
- Horizontal intensity, declination, and vertical intensity by hour, day, month, and year at Victoria Magnetic Observatory - 1969
[M70-41/6] 20 p3257 N71-33047
- Magnetic measurements of residual fields in superconducting dipole and quadrupole magnets
[UCRL-20171] 21 p3465 N71-34662
- Statistical analysis of electrical phenomena associated with tornado activity and search for residual magnetism in buildings near path of tornado
[NASA-TN-D-6475] 23 p3751 N71-36749
- Algorithm for determining artificial satellite position from magnetometric measurements
23 p3859 N71-37512
- Measurement of earth magnetic field by geophysical observatory 40 kilometers northwest of Helsinki, Finland
24 p3916 N71-37923
- MAGNETIC MEMORIES**
- U MAGNETIC STORAGE**
- MAGNETIC METALS**
- U MAGNETIC MATERIALS**
- U METALS**
- MAGNETIC MIRRORS**
- Ion temperature and rotation in Penning discharge in inhomogeneous magnetic mirror
[REPT-70-27] 03 p0439 N71-13354
- Measurements of cathode heating in Penning discharge in strongly inhomogeneous magnetic mirror field
[NP-18416] 04 p0591 N71-14386
- Investigating ion heating from modulated electron beams, plasma density and energy in magnetic mirrors, and dispersion relations for oblique wave propagation in magnetized plasma
[UCB-34-P-128-15] 05 p0752 N71-14507
- Electron beam plasma heating in magnetic mirror trap
[AEC-TR-7160] 05 p0753 N71-15020
- Relativistic motion of single particle undergoing cyclotron resonance in magnetic mirror trap
[AD-714857] 07 p1083 N71-17816

MAGNETIC MOMENTS

- Computer simulation and research development in plasma confinement, magnetic mirrors, Astron thermonuclear reactor program, and related research [UCRL-50002-70] 13 p2143 N71-23579
- Particle and field oscillations and electron heating due to drift mirror instability in magnetosphere 18 p3005 N71-30930
- Two phase excitation coil system for ion cyclotron heating of hydrogen plasma 18 p2993 N71-31144
- Duration of charged particle containment in trap with magnetic mirrors, and solution of kinetic equation in center of trap [IAE-1972] 19 p3145 N71-31961
- Controlled thermonuclear research progress, including magnetic mirror system, steady-state toroidal systems, and pulsed high beta systems studies [WASH-1172] 21 p3475 N71-34749
- Proposed Mirror Fusion Experiment (MFX) to extend mirror confinement studies 23 p3827 N71-37296
- Two computer programs for calculating plasma stability and equilibria in Astron and minimum-B magnetic mirror systems [UCRL-51036] 23 p3827 N71-37298
- Two-component stellerator-mirror configuration having high electron energy and low ion temperature for optimum plasma control [MATT-841] 23 p3828 N71-37304
- Reactor design studies based on use of mirror confinement zones fed by neutral beam injectors and utilizing direct converters for charged particle energy recovery [CONF-710607-127] 24 p3961 N71-38256
- Neutral beam injection in mirror systems for high density plasma production [CONF-710607-98] 24 p3969 N71-38461
- ## MAGNETIC MOMENTS
- Life times and magnetic moments of excited germanium states after proton irradiation determined from angular distribution of gamma rays to establish validity of shell model 02 p0272 N71-11748
- Satellite attitude and spin control subsystem using interaction between generated magnetic moment and geomagnetic field [NASA-TN-D-6051] 03 p0409 N71-13056
- Electric and magnetic moments of F-18 and Na-22 measured using spin rotation for validity tests of shell or collective nuclear model 03 p0436 N71-13280
- Low temperature properties of Anderson model of localized magnetic moments [NUB-2031] 04 p0567 N71-14291
- Quantum electrodynamic theory and relation to precision low energy experiments [SLAC-PUB-795] 06 p0919 N71-16246
- Mossbauer effect on magnetic moment measurements for short-lived nuclear states [AEC-TR-70275] 07 p1073 N71-17405
- Cluster and moment effects on paramagnetic to ferromagnetic transition in Cu-Ni alloys [UCRL-72587-REV-1] 07 p1078 N71-17776
- Magnetic moment versus temperature curves for ferrimagnetic garnets [AD-715284] 07 p1095 N71-17842
- Neutron diffraction analyses on magnetic structures of chromium alloys [AD-714875] 07 p1069 N71-18037
- Determining low temperature behavior of localized magnetic moments by crystal field effect on orbital paramagnetism [NUB-2043] 08 p1279 N71-18691
- Local environment effects on magnetic moment formation in Au-V and Cu-Ni alloys [AD-716038] 09 p1424 N71-19679
- Nuclear charge structure effects on hyperfine structure, isotope shift, and magnetic octupole moments 09 p1432 N71-19972
- Theory for local atomic environment and spin-orbit coupling effects on local magnetic moment formation [AD-716031] 09 p1440 N71-20307
- Comparison of magnetic moment and electric dipole sum rules for testing validity of current and field algebra commutators 10 p1592 N71-21002
- Magnetic moment of proton in nuclear magnetons determined from cyclotron resonance frequency of ions 10 p1621 N71-21749
- Magnetic moments and lifetimes of 7/2 minus mirror states of Ar-37 and K-37 measured from Cl-37(p,n)Ar-37 and Ca-40(p,alpha)K-37 reactions [CONF-700933-2] 11 p1805 N71-22432
- Field measurements by rotating spacecraft for dipole moment determination 13 p2175 N71-25334
- Nuclear structure effects in magnetic hyperfine interaction using pairing and pairing plus quadrupole model 13 p2137 N71-25432
- Perturbed angular correlation measurements of Os-192 and Pt-192 excited state magnetic moments and

- NMR internal field measurements of Os-187 in Fe and Ni alloys [COO-1746-53] 14 p2295 N71-25734
- Initial magnetic test of IMP-1 spacecraft with reduction of magnetic moment by dc rotation deperment treatments [NASA-TM-X-65526] 14 p2335 N71-25800
- Interaction of nuclear spins with orbital and spin magnetic moments of electrons leading to spin coupling observations in NMR spectra 14 p2307 N71-26397
- Self consistent solution for anomalous magnetic moment of nucleons [JINR-E2-5333] 14 p2310 N71-26667
- Harmonic analysis and nuclear model of lithium 6 core distortion and effects on energy levels, magnetic dipole and electric quadrupole moments, and Pauli exclusion principle 15 p2494 N71-27955
- Time of flight spectrometer with magnetically pulsed beam for inelastic neutron scattering analyses on liquids and solids 16 p2597 N71-28711
- High energy scattering amplitude of fermion with anomalous magnetic moment and nonexponentiation [DESY-71/1] 16 p2657 N71-29122
- Magnetic moment of positive Sigma hyperons and positive kaon and positive Sigma hyperon decay observed in optical spark chamber located inside bore of solenoidal pulsed magnet 16 p2660 N71-29197
- Prediction of nonadiabatic particle motion in linear and toroidal multipolar fields including magnetic moment change in relation to particle trapping 17 p2796 N71-29799
- Sixth-order radiative corrections to anomalous magnetic moment of electron from Feynman diagrams with vacuum polarization insertions [CNRS-CPT-70-P-339] 17 p2803 N71-30222
- Pauli-type approximation for vector meson exchange with anomalous magnetic moments [IFVE-SVM-70-31] 18 p2971 N71-30467
- Distinct classes in magnetic quadrupole gamma transitions and development of automatic angular correlation measuring equipment [NP-18492] 18 p2975 N71-30571
- Presence of magnetic moments in nickel copper alloys containing up to 70 per cent copper 18 p2965 N71-31306
- Monte Carlo calculation for magnetic moment of Lambda hyperon in negative pion plus proton yields Lambda hyperon plus neutral kaon reaction 18 p2988 N71-31494
- Analysis of SERT 2 spacecraft attitude response including magnetic, solar pressure, and ion thruster disturbance torques [NASA-TM-X-2324] 19 p3184 N71-32189
- Forbidden transitions and magnetic moments from angular correlations in gamma decay of Te-125 [NP-18704] 19 p3152 N71-32199
- Design and circuitry of torquemeter for measuring magnetic torques on spacecraft [NASA-TN-D-63871] 19 p3102 N71-32476
- Mossbauer studies of energy levels, electric and magnetic moments, hyperfine fields, and lift times of various light nuclei [NYO-2028-5] 21 p3484 N71-34821
- Estimates of magnetic dipole moments for spherical and transition nuclei [INP-729] 24 p3965 N71-38282
- ## MAGNETIC PERMEABILITY
- Magnetic permeability of rare earth selenides and tellurides [NASA-TM-X-52921] 03 p0441 N71-12837
- Neutron diffraction study of gamma-FeOOH, position of ions, magnetic permeability, and Mossbauer effect [PB-193217] 04 p0591 N71-14387
- Temperature effects on magnetic permeabilities of chromium and chromium alloys with rhenium, osmium, ruthenium, molybdenum, and tungsten [DISS-4179] 05 p0372 N71-14820
- Measuring neutron scattering and magnetic susceptibility for single crystal cesium trichloromanganates at low temperatures [AD-714515] 06 p0933 N71-16111
- Transport properties and magnetic susceptibility of magnetic alloys 06 p0906 N71-16401
- Investigating magnetic susceptibility of small crystallites of nickel and nickel-iron ferrite as function of hydrothermal growth and frequency [AD-714485] 06 p0906 N71-16405
- Electronic properties of dilute alloys including magnetic permeability, electrical resistance, and ferromagnetism [AD-716607] 09 p1433 N71-20008
- Ribbon effects in superconducting septum magnet [BNL-15368] 10 p1606 N71-20917
- Electronic specific heat and magnetic susceptibility of Ta-H compounds for validity determination of rigid D band model [ANL-TRANS-867] 10 p1619 N71-21591

SUBJECT INDEX

- High resolution microwave spectroscopy and Zeeman effect combined to measure molecular magnetic susceptibility anisotropies of OCS and water 11 p1801 N71-21949
- Susceptibility of liquid He-3 with comparison to Curie susceptibility 11 p1809 N71-23020
- Exchange energy and magnetic susceptibility measurements on low temperature He-3 with He-4 traces, and techniques for light scattering in gases at room temperature 14 p2295 N71-25610
- Magnetic properties of chromium and vanadium nitride binary mixtures, noting concentration and temperature effects [ONERA-TP-719] 15 p2420 N71-26999
- Magnetometric permeability measurements on europium ytterbium compounds and gadolinium doped nickel aluminum alloys 17 p2766 N71-30124
- Martensitic transformation occurring in copper-iron alloy during tensile testing with magnetic susceptibility measurement 21 p3430 N71-34407
- Magnetic susceptibility and electrical resistivity measurements, optical metallography, and X ray diffraction of displacive phase transformations in neoequilibrium Nb-Ru alloys [COO-1198-807] 21 p3486 N71-34837
- Magnetization and susceptibility of Heisenberg ferromagnet in magnetic field with expressions derived for calculating thermodynamic parameters [NASA-TN-D-6420] 21 p3497 N71-34915
- Nuclear magnetic susceptibility in bcc solid He-3 with Neel temperature and negative exchange interaction energy calculations and impurity effects 22 p3652 N71-36041
- Magnetic susceptibility of vanadium carbide from 77 to 300 K measured by magnetometer [NASA-CR-122039] 22 p3657 N71-36079
- ## MAGNETIC PISTONS
- Performance test of piston shock tube with helium driven gas and argon test gas [VKI-TN-69] 20 p3244 N71-32957
- Equations of motion solved for one dimensional magnetic piston problem in study of shock waves propagating perpendicular to magnetic field in collisionless plasma 20 p3332 N71-33817
- ## MAGNETIC POLES
- Velocity fields in magnetically disturbed regions of H alpha chromosphere measured by Doppler and Zeeman movie pairs 20 p3342 N71-33887
- Empirical methods for calculating magnet pole tip shape and finding field inside magnet air gap [TRI-70-4] 22 p3642 N71-35968
- ## MAGNETIC PROBES
- Inductive magnetic probe diagnostics in plasma [AD-710734] 01 p0105 N71-10543
- ## MAGNETIC PROPERTIES
- NT ANTIFERROMAGNETISM
- NT CURIE TEMPERATURE
- NT DIAMAGNETISM
- NT FERRIMAGNETISM
- NT FERROMAGNETISM
- NT GYROMAGNETISM
- NT GYROFREQUENCY
- NT GYROMAGNETISM
- NT MAGNETIC EFFECTS
- NT MAGNETIC INDUCTION
- NT MAGNETIC MOMENTS
- NT MAGNETIC PERMEABILITY
- NT MAGNETIC RELAXATION
- NT MAGNETIC SUSPENSION
- NT MAGNETOACOUSTICS
- NT MAGNETORESISTIVITY
- NT MAGNETOSTRICTION
- NT PALEOMAGNETISM
- NT PARAMAGNETISM
- NT POLARIZATION CHARACTERISTICS
- NT SPIN-LATTICE RELAXATION
- NT THERMOMAGNETIC EFFECTS
- Preparation and properties of iron phosphides [AD-710697] 01 p0018 N71-10449
- Magnetic structure of oblique and normal ionizing shock waves [AD-711086] 01 p0106 N71-10622
- Temperature dependence of initial permeability of ferromagnetic amorphous Co-P alloy [AD-711087] 01 p0092 N71-10618
- Thermal and magnetic properties of adsorbed phases of He-3 and He-4 at low temperatures [AD-712416] 03 p0419 N71-13339
- Characteristics of temperature-dependent diamagnetism in superconductors [AD-713242] 05 p0756 N71-14545
- Weakly interacting magnetic systems with helium 3 at very low temperature 06 p0904 N71-16244
- Magnetic properties of solids at low temperatures [AD-714689] 06 p0904 N71-16243
- Magnetic properties of amorphous and crystalline Mn-P-C alloys [CAL-822-15] 06 p0873 N71-16348

SUBJECT INDEX

MAGNETIC SPECTROSCOPY

- Computed properties of two-dimensional section of two inch bore synchrotron dipole
[JNL-15174] 06 p0832 N71-16753
- Spectrum analyses and magnetic properties of mixed metal compounds containing tantalum and molybdenum
[IS-T-402] 06 p0675 N71-16779
- Magnetic properties and electrical resistivity of transition metal oxide glasses
[COO-1700-17] 06 p0883 N71-16827
- Spark chamber magnetic spectrometer for studying rare decay and interactions of particles
[JNR-P13-5170] 08 p1199 N71-18236
- Solution for ferroelectric model in staggered field at all temperatures
[NUN-2045] 08 p1158 N71-18486
- Tunnel diode oscillator for determining paramagnetic susceptibility at radio frequencies
09 p1358 N71-19481
- Magnetic phenomena in superconductors, and magnetic impurity measurements of superconductivity
[AD-716027] 09 p1452 N71-19680
- Magnetofluorescence, cooperative fluorescence of rare earth ions in crystals, narrow-band and narrow-gap compounds, and related studies of rare earth compounds
[AD-716470] 09 p1453 N71-20007
- Mossbauer studies of recoilless fractions, isomer shifts, and magnetic properties of gold and gold alloys and high pressure effects on Kondo copper-iron alloys
[ORO-3897-2] 09 p1400 N71-20012
- Design and magnetic property tests of Pioneer spacecraft
[TRW-2515-6004-RO-00] 09 p1473 N71-20508
- Annual report of materials research activities at Northwestern University, from October 1969 to September 1970
[AD-717094] 10 p1588 N71-20916
- Surface finishing effects on ceramic mechanical, electrical, optical, and magnetic properties
[AD-716886] 10 p1565 N71-21221
- Microstructure and magnetic properties of internally oxidized ferromagnetic alloys for application to magnetic domain theories and high temperature tests
[AD-717210] 10 p1579 N71-21301
- Metallurgical and magnetic properties of industrial nickel iron alloys
[NLL-TRANS-2654-19022.81/] 10 p1582 N71-21499
- Lectures on solid state physics delivered at Bangalore in 1969 including order-disorder transformations and magnetic properties of noninteracting ions
10 p1606 N71-21534
- Chemical and magnetic properties of single alpha manganese crystal structure
11 p1814 N71-21862
- Transport properties, electrical resistivity, thermoelectric power, and magnetic susceptibility of magnetic alloy systems
[AD-717359] 11 p1797 N71-21950
- Design and construction of steady state crystal growth system suitable for growth of rare earth compounds with magnetic properties
[AD-717311] 11 p1816 N71-22163
- Magnetic properties at metal surfaces including neutron mirror measurements, neutron scattering of FeCO₃, and low temperature measurements
[ORO-3674-4] 11 p1779 N71-22510
- Magnetic coupling in composite ferromagnetic structures consisting of two permalloy films (81.7 percent Ni and 18.3 percent Fe) with thin separation layer of chromium and/or gold
11 p0000 N71-23014
- Magnetic properties, microstructure, and physical properties of partially crystallized glass
[AD-718829] 12 p1944 N71-23767
- Magnetic properties of electrodeposited films of iron-nickel-molybdenum ternary alloys with uniaxial magnetic permeability
[AD-719811] 13 p2091 N71-24352
- Low temperature measurements on electrical resistivity, magnetic susceptibility and magnetoresistivity for amorphous iron palladium silicon alloys
[CALT-422-24] 13 p2098 N71-25515
- Magnetic properties of solids including electron paramagnetic resonance in dilute magnetic alloy, hyperfine splitting of localized moment in metal, and band theory of solids
14 p2325 N71-26020
- Magnetic properties of binary rare earth alloys determined by neutron diffraction method
15 p2507 N71-27546
- Structural, magnetic, and spectroscopic examination of nickel square dihydrate
[IS-T-432] 15 p2510 N71-27978
- Magneto-optic rotation in thin semitransparent nickel iron film due to antiferroelectric coating of zinc sulfide
[AD-721558] 16 p2638 N71-28065
- Calculating transition radiation from Dirac magnetic monopoles and experimental applications in searching for monopoles in accelerators and cosmic radiation
[RE-4101] 16 p2639 N71-28142
- Vacuum furnace and differential thermal analysis equipment for evaluating magnetic properties of rare earth-transition metal alloys for use as permanent magnets
[AD-722060] 17 p2763 N71-29502
- Magnetic response of pure type 1 superconductors and their alloys with emphasis on metastable states
17 p2787 N71-29654
- Electrical and magnetic properties of potassium molybdenum bronzes
17 p2765 N71-29850
- Magnetic and transport properties of RuO₂ and IrO₂ single crystals
17 p2827 N71-30170
- Hyperfine magnetic interactions in Fe-Ga solid solutions analyzed by Mossbauer spectroscopy
[CALT-422-27] 19 p3169 N71-32218
- Neutron diffraction study of magnetic structure of manganese-substituted zinc ferrites
[JNR-1269] 19 p3169 N71-32220
- Magnetic coupling and phase boundaries determined for series of pseudo binary alloys of C15 and 22 structure containing lanthanides
19 p3171 N71-32642
- Seebeck coefficients in metallic alloys using undoped silver palladium alloys between 4.2 and 520 K
[NASA-CR-121384] 20 p3214 N71-33412
- Fusion system model having disordered force constants and ordered masses of ions applied to ammonium chloride and disordered magnetic system phonons
[NUB-2007] 20 p3317 N71-33531
- Critical velocity and attenuation changes for longitudinal and shear ultrasound in rare earth metals, insulators, and Cr at magnetic transition temperature
20 p3313 N71-33755
- Magnetic properties of gadolinium, terbium, dysprosium, and holmium hydroxides at cryogenic temperatures
20 p3313 N71-33755
- Inconel-steel, puddle-welded rotor spin and magnetic testing for use in 36,000 rpm Lundell alternator
[NASA-TM-X-67929] 22 p3558 N71-35344
- Crystallographic data, cation distributions, magnetic transition temperatures, and magnetic structures of tetragonal systems determined by neutron diffraction
[NP-18783] 22 p3631 N71-35874
- Engineering design of 2X 2 fusion research facility including descriptions of vacuum and magnetic systems
[UCRL-73060] 23 p3740 N71-36667
- Analysis of magnetic properties of MnAs using neutron diffraction and effects of high compressibility on magnetic behavior
23 p3777 N71-36915
- Stoichiometric and compositional effects on sintering and magnetic characteristics of high purity, freeze dried, barium ferrite ceramics
23 p3780 N71-36943
- Magnetic analysis of Li-7 bombarded with 15 MeV He-3 atoms
[ANL-P-520] 23 p3809 N71-37160
- Mossbauer study of magnetocrystalline anisotropy of Nd-Co₅ for application to manufacture of permanent magnets
[AD-726991] 23 p3835 N71-37347
- Electrical and magnetic properties of palladium base amorphous alloys containing small concentrations of transition metals
24 p3901 N71-37807
- Tables of magnetic structures determined by neutron diffraction with emphasis on rhombohedral and hexagonal systems
[NP-18845] 24 p3970 N71-38319
- MAGNETIC PUMPING
Investigating conditions for validity of energy absorption of electromagnetic waves by magnetic pumping with transit time derived by linear theory
[CEA-CONF-1606] 08 p1269 N71-18153
- MAGNETIC RECORDING
High speed television recording system with slow and stop motion replay capabilities
[RAE-TR-70035] 02 p0225 N71-11545
- Magnetic digital recorder Emmanuel
04 p0504 N71-13833
- Digital registration of radar echo vector on magnetic tape
04 p0504 N71-13834
- Address indicator for pressure scanner
[ARL/ME-314] 05 p0689 N71-15577
- Development of data storage system for storing digital data in high density format on magnetic tape
[NASA-CASE-XNP-02778] 11 p1717 N71-22710
- General purpose digital computer system using Dnepi 1 control components and Minsk 2 magnetic tape units
11 p1719 N71-22739
- Temperature profile plotting from magnetic tape recorded aircraft expendable bathythermograph data and underwater acoustic velocity calculated from Pacific Ocean salinity data
[AD-718393] 12 p1906 N71-23305
- Model A850 magnetic tape recording current meter design and environmental and performance tests
[IFS-71011] 12 p1918 N71-23370
- Prediction magnetic tape recording systems for frequency multiplex systems with frequency modulated or amplitude modulated subcarrier telemetry
[RAE-LIB-TRANS-1518] 12 p1880 N71-23786
- Tests for determining suitability of tape recording and reproducing equipment for tactical use by Army
[AD-719097] 13 p2054 N71-24487
- Magnetic recording head composed of ferrite core coated with thin film of aluminum-iron-silicon alloy
[NASA-CASE-GSC-10097-1] 15 p2383 N71-27210
- Self reducing optical range finder with magnetic tape recorder
16 p2592 N71-28269
- Electrodeposition of nonporous Co-Ni coating on magnetic recording drums
[NLL-L-T-746-641-19022.401/] 17 p2761 N71-29253
- Effect of tape recorder equalization techniques on attainable bit error probability
[AD-722431] 17 p2720 N71-29817
- Test methods and procedures for determining effect of chemical and physical forces at magnetic head/tape interface of satellite tape recorders
[NASA-CR-121649] 21 p3424 N71-34364
- Chemical and physical forces at magnetic head/tape interface of satellite tape recorders
[NASA-CR-121700] 21 p3424 N71-34365
- Guidelines for design, selection, and use of magnetic heads and tape for unfettered satellite tape recorders
[NASA-CR-121701] 21 p3424 N71-34366
- Magnetic head/tape interface problems of satellite data storage tape recording systems, and minimizing stick-slip phenomena
[NASA-CR-121730] 21 p3425 N71-34373
- MAGNETIC RELAXATION
NT SPIN-LATTICE RELAXATION
Internal fields and relaxation effects for dysprosium in ferromagnetic TbAl₂ studied by perturbed angular correlation
[UIUP-684] 06 p0909 N71-15752
- Activation energy and hole mobility in aluminum determined by nuclear magnetic relaxation including temperature effects
[COO-1198-801] 15 p2477 N71-27580
- MAGNETIC RESONANCE
NT ELECTRON PARAMAGNETIC RESONANCE
NT FERROMAGNETIC RESONANCE
NT NUCLEAR MAGNETIC RESONANCE
NT PARAMAGNETIC RESONANCE
NT PROTON RESONANCE
Rotation of trihedrons at variable speeds applied to low frequency magnetic resonance modulation
[ONERA-TP-866] 02 p0267 N71-11745
- Photochemistry of bimolecular quenching and bichromophoric compounds, magnetic resonance studies, and high energy radiation chemistry
[AD-716589] 09 p1434 N71-20003
- Floquet theorem calculation of particle resonance frequencies and dispersion relations
10 p1625 N71-21828
- Collisionless plasma lifetime unaffected by magnetic field resonance structure
[NLL-CTO-740-5991.97/] 12 p1962 N71-24213
- Preparation and deuterium quadrupole coupling constants of deuterio-organometallic compounds
[NYO-3965-3] 13 p2145 N71-25590
- Temperature dependence of magnetic resonance linewidth in ferromagnetic crystals
15 p2454 N71-27377
- Abstracts of articles concerning gravimeters, magnetospheric resonators, and tectonics of Sea of Japan
17 p2739 N71-29403
- Magnetic resonance in dilute magnetic alloys - hyperfine splitting of Ag-107
[AD-722711] 17 p2829 N71-30279
- Helicon resonance and quantum oscillations in mercury selenide crystal
18 p2997 N71-31325
- Approximations in calculating g-tensors for molecular ion H₂ (plus)
[NASA-CR-121647] 21 p3446 N71-34526
- Research in solid state physics including band theory, optical properties and magnetic resonance
[JORN-4669] 21 p3498 N71-34919
- MAGNETIC SIGNALS
Small signal field analysis of double-strand interactions in finite semiconductors
16 p2648 N71-29015
- MAGNETIC SIGNATURES
Design criteria for real time digital videomane, netograph at Aerospace San Fernando Solar Observatory
[NASA-CR-115113] 19 p0906 N71-51605
- MAGNETIC SPECTROSCOPY
Magnetic spectroscopic study of O-15 bound states and T_{3/2} states in C-13, O-17, and Ne-21
09 p1430 N71-19767
- Optical model of nucleus and atomic energy levels studied with tandem Van de Graff machine, proton linear accelerator, and magnetic spectrometer
[COO-1265-94] 10 p1616 N71-21170
- Composition and atomic ordering effects in Fe-Co alloy systems using Mossbauer spectroscopy and mea-

asurement of effective magnetic field at Fe nuclei,
isomer shift, and quadrupole splitting

11 p1780 N71-22794

Space electric rocket test thruster performance with
xenon, krypton, argon, neon, nitrogen, helium, and
carbon dioxide ion source gases and magnetic spectro-
scopy of ion emissions

13 p2130 N71-24699

Magnetic spark spectroscopy and scattering cross
sections from proton irradiation of aluminum nuclei
[IFVE-SE/OP-70-13]

14 p2314 N71-26719

Positive to negative pion ratios as functions of in-
cident photon energy using Cerenkov counter, spark
chamber, and magnetic spectrometry of pion
photoproduction

15 p2476 N71-27573

Computerization of magnetic spectrometer for
cryogenic probe, oxidation states of Mo compounds,
ESCA spectra of metal chelates, and related research
[SRO-645-1]

16 p2651 N71-28920

Magnetic modulation spectroscopy for studying
microwave surface impedance of lead films
[ISS-70/6]

18 p2994 N71-30472

Fundamental aspects of electron paramagnetic
resonance spectroscopy
[ANL-7764]

19 p3101 N71-32313

Composition of upper ionosphere as shown by mag-
netic mass spectrometer flown on Explorer 31
[NASA-CR-121865]

21 p3426 N71-34379

Magnetic spectrometer system for detecting nega-
tive pion differential cross sections in liquid deuterium
[INSJ-126]

22 p3633 N71-35893

Wide and small aperture magnetic spectrometers
using high particle energies and emphasizing produc-
tion angles and momenta
[SLAC-PUB-798]

23 p3759 N71-36796

Magnetic mass spectrometer with programmable
magnetic field analyzer for measuring meteoric isotop-
ic ratios

23 p3857 N71-37492

Search for double beta decay of ND-150 using large
aperture, low resolution magnetic spectrometer-detec-
tor in salt mine
[COO-1749-23]

24 p3981 N71-38411

MAGNETIC STORAGE

NT CORE STORAGE

Magnetic matrix memory system for nondestructive
reading of information contained in matrix
[NASA-CASE-XMF-05835]

03 p0345 N71-12504

Core, magnetic, transistor, and BORAM storage
and memory devices

04 p0504 N71-13827

Core, magnetic film, and semiconductor memory
techniques

04 p0504 N71-13828

High speed core, magnetic, semiconductor, and
laser storage systems

04 p0504 N71-13829

Medium speed, random access mass memory
module with magnetic cylindrical thin film storage ele-
ments

04 p0504 N71-13830

High voltage test of large cryogenic coil for mag-
netic storage system
[LA-4469]

06 p0903 N71-16021

Metal oxide semiconductor and magnetic mem-
ories as computer data storage devices for European
research organization meteorological satellites

10 p1528 N71-21093

Design, development, and test of ferrite memory
system for application as computer storage device

10 p1528 N71-21233

Predetection magnetic tape recording systems for
frequency multiplex systems with frequency modu-
lated or amplitude modulated subcarrier telemetry
[RAE-LIB-TRANS-1518]

12 p1880 N71-23786

Pulse duration control device for driving low
response time loads in selected sequence including
switching and delay circuits and magnetic storage
[NASA-CASE-XGS-04224]

14 p2234 N71-26418

Redundant memory for enhanced reliability of
digital data processing system
[NASA-CASE-GSC-10564]

16 p2576 N71-29135

Momentum wheel design for spacecraft attitude
control and magnetic drum and head system for data
storage
[NASA-CASE-NPO-11481]

21 p3455 N71-34591

MAGNETIC STORMS

Solar and geophysical data related to ionospheric
studies from India - tables
[RRC-A178-PT-2]

01 p0117 N71-10378

Hourly values of equatorial Dst for Jan. - June 1970
[NASA-TM-X-65380]

01 p0049 N71-10605

Sunspot, solar flare, magnetic storm, and SID data,
Delhi - Apr. 1970
[RRC-A179-PT-2]

02 p0292 N71-11396

Relation of plasmapause position to region of
enhanced fluxes of trapped energetic electrons during
magnetic storm on 15 June 1965
[NASA-TM-X-65390]

03 p0450 N71-13025

Polar region magnetic storms and electric currents
in the magnetosphere
[REP-70-29]

04 p0521 N71-13782

Solar and geophysical data for Aug. and Sept. 1969
[ESSA-SGD-307-PT-2]

05 p0764 N71-15256

Solar and geophysical data for May and June 1969
[ESSA-SGD-304-PT-2]

05 p0764 N71-15257

Solar and geophysical data for Nov. and Dec. 1969
[ESSA-SGD-305-PT-1]

05 p0764 N71-15258

Solar and geophysical data for June and July 1969
[ESSA-SGD-303-PT-2]

05 p0764 N71-15259

Solar and geophysical data for July and Aug. 1969
[ESSA-SGD-306-PT-2]

05 p0764 N71-15260

Solar and geophysical data for Dec. 1969 and Jan.
1970
[ESSA-SGD-306-PT-1]

05 p0765 N71-15285

Solar and geophysical data for Jan. and Feb. 1970
[ESSA-SGD-307-PT-1]

05 p0765 N71-15286

Solar and geophysical data for Oct. and Nov. 1969
[ESSA-SGD-304-PT-1]

05 p0765 N71-15287

Gravity wave interaction with transiently heated at-
mosphere
[AD-715930]

08 p1188 N71-18553

Thermospheric density response to auroral heating
during geomagnetic disturbance
[NASA-TM-X-65462]

09 p1385 N71-20284

Satellite-borne measurements of electron flux dur-
ing magnetic storm
[NASA-TT-F-13512]

09 p1386 N71-20301

Explorer 22 satellite measurements of ionospheric
electron contents during magnetic storms
[RSD-554]

09 p1386 N71-20345

OGO-D atmospheric composition data for polar
thermospheric storm model
[NASA-CR-103080]

10 p1546 N71-20638

Mapping of polar region magnetic storms
[REPT-70-34]

10 p1546 N71-20641

Magnetopause inward motion preceding magnetic
storms observed by means of OGO-E magnetometer
[NASA-CR-117442]

10 p1547 N71-20855

Provisional hourly values of equatorial Dst for 1968
[NASA-TN-D-6278]

10 p1549 N71-21096

Temporal variations of geomagnetically trapped low
energy protons recorded by Injun 4 during 17 Apr.
1965 magnetic storm
[NASA-CR-117839]

11 p1823 N71-22496

Geomagnetic field and storms, and gravimetry
[RRC-A187-PT-2]

11 p1751 N71-22686

Thermospheric wind circulation excited during mag-
netic storm shown as effective mechanism for remov-
ing atomic oxygen at high latitudes
[NASA-TM-X-65500]

12 p1906 N71-23366

Magnetic substorm events and magnetosphere
structure in polar auroral zones determined by rocket
sounding, satellite observations, and ground-based
measurements - conference
[ESRO-SP-38]

12 p1908 N71-23551

European space research organization program for
auroral magnetic storms investigation - satellite obser-
vation

12 p1908 N71-23552

Polar upper atmospheric disturbances, auroral elec-
tron and proton precipitation, and magnetospheric
substorm origin

12 p1908 N71-23553

Auroral electrojet current model for polar magnetic
substorms

12 p1908 N71-23554

Geomagnetic micropulsation role in polar and mag-
netospheric substorms

12 p1908 N71-23555

Auroral magnetic substorm and high energy electron
absorption

12 p1908 N71-23556

Ground-based measurements of polar magnetic sub-
storms by means of magnetometers

12 p1909 N71-23558

Geomagnetic pulsation measurement for auroral
magnetospheric substorm study

12 p1909 N71-23559

VLF emission measurement in auroral zone during
magnetic substorm phases

12 p1909 N71-23560

Auroral absorption measurement during absorption
substorm development at geophysical observatories
separated in longitude

12 p1909 N71-23561

Very low and very high frequency aurora
backscatter communication for polar magnetic storm
detection

12 p1909 N71-23563

Magnetic substorm effects on auroral electron and
proton precipitation

12 p1909 N71-23566

Auroral ionospheric electric field measurements by
means of gas release or electrostatic probes

12 p1909 N71-23567

European Space Research Organization
synchronous satellite program for magnetosphere
sounding

12 p2001 N71-23572

Sunspot, solar flare, magnetic storm, and SID data,
Delhi - June 1970
[RRC-A-180-PT-2]

12 p1910 N71-23601

Sunspot, solar flare, magnetic storm, and SID data,
Delhi - July 1970
[RRC-A-181-PT-2]

12 p1910 N71-23602

Sunspot, solar flare, magnetic storm, and SID data,
Delhi - Sept. 1970
[RRC-A-183-PT-2]

12 p1910 N71-23603

Sunspot, solar flare, magnetic storm, and SID data,
Delhi - Sept. 1970
[RRC-A-184-PT-2]

12 p1914 N71-24176

Micropulsation recordings of magnetospheric
storms in auroral zone
[AD-721200]

15 p2399 N71-27187

Changes in distribution of low-energy trapped
protons associated with magnetic storm on 17 April
1965
[AD-721082]

15 p2513 N71-27282

Three dimensional thermospheric model developed
from solar XUV radiation and corpuscular heating
during geomagnetic storms of atmospheric system
[NASA-TM-X-65579]

15 p2406 N71-27774

Relation between geomagnetic tail fundamental
oscillation mode and magnetospheric storms
[D-3]

17 p2739 N71-29534

Dynamic development characteristics of geomag-
netic instabilities in earth magnetosphere
[AD-721082]

17 p2742 N71-29788

Ionospheric auroral morphology, height variations,
and relationships to planetary magnetic disturbances
in periods of minimum and maximum solar activity at
varying latitudes
[NASA-TT-F-637]

17 p2745 N71-30076

Analysis of magnetic storm energy balance, includ-
ing total energy, mode of arrival, and energy dissipation
rate at different stages of development

17 p2747 N71-30086

Relationship between ionospheric electron currents,
geomagnetic storms, and absorption bursts
[AD-721082]

17 p2747 N71-30088

Acceleration of trapped particles during magnetic
storm on 18 Apr. 1965 observed by Explorer 26
[RRC-A186-PT-2]

18 p3004 N71-30925

Comparison of electron response in magnetosphere
at L equals 5 with solar wind during magnetic storm on
17-18 Apr. 1965

18 p3005 N71-30926

Correlation of increases in electron population of
outer radiation belt and interplanetary magnetic fields
during two geomagnetic storms

18 p3005 N71-30927

Outer radiation belt electron fluxes during solar
proton event on 5 Feb. 1965

18 p3005 N71-30928

Sunspot, solar flare, magnetic storm, and SID data,
Delhi - Dec. 1970
[RRC-A186-PT-2]

20 p3260 N71-33294

Sunspot, solar flare, magnetic storm, and SID data,
Delhi - Jan. 1971
[RRC-A187-PT-2]

20 p3260 N71-33295

Sunspot, solar flare, magnetic storm, and SID data,
Delhi - Feb. 1971
[RRC-A188-PT-2]

20 p3260 N71-33296

Sunspot, solar flare, magnetic storm, and SID data,
Delhi - Mar. 1971
[RRC-A189-PT-2]

20 p3261 N71-33297

Field line motion accompanying rapid plasma flow
during geomagnetic storms
[NASA-TM-X-67295]

21 p3415 N71-34298

Subauroral red arc producing mechanisms based on
ionospheric and atmospheric equations
[NASA-TM-X-65680]

21 p3416 N71-34303

Soviet news releases on interplanetary magnetic
fields, tsunami waves, and atmospheric phenomena
during magnetic storms

21 p3510 N71-35008

Sunspot, solar flare, magnetic storm, and SID data,
Delhi - March 1971
[RRC-A190-PT-2]

22 p3575 N71-35463

Correlation of data from ion trap and low energy
electron and proton sensors on polar orbiting OV1-15
during magnetic storm 13 to 18 Aug. 1968
[AD-726541]

22 p3666 N71-36138

Electron pitch-angle scattering in outer zone during
magnetic storms
[AD-727003]

23 p3842 N71-37393

Magnetic storm phenomena in magnetosphere and
upper atmosphere

23 p3853 N71-37485

MAGNETIC SURVEYS
Magnetic survey of iron deposits in Tasmania
[BULL-120]

05 p0671 N71-14844

Geological analysis of aerial geomagnetic survey of
northeastern Alaska
[BULL-1271-A]

05 p0681 N71-15671

Reporting results of disciplinary and interdisciplinary
research into geology of Iceland

07 p1026 N71-19803

Tables on magnetic activity observed in Canadian
Agiacourt Observatory for 1968 and Jan. to Mar. 1969
[AD-719392]

12 p1906 N71-23406

Tables of magnetic elements observed at McIlwain
Observatory of Canada

12 p1912 N71-23497

Development of one dimensional magnetotelluric in-
version technique for determining frequency range of
data necessary to define geological profile
[AD-719392]

13 p2070 N71-23468

SUBJECT INDEX

MAGNETICALLY TRAPPED PARTICLES

Geologic interpretation of residual aeromagnetic map of Nixon Fork District, Alaska to determine magnetic characteristics of intrusive rocks 14 p2352 N71-26649

Paired rubidium magnetometer providing reliable mapping of quasi-static total magnetic field changes to 61 gamma between stations to 1/2 km separation with differential drift correction 16 p2589 N71-28763

Fracture pattern and magnetic anomaly measurements of Juan de Fuca-Gorda ridge area 18 p2914 N71-31008

Magnetic and bathymetric survey profile in Pacific Ocean from Costa Rica to central California (ESSA-TR-BRL-179-AOML-3) 18 p2917 N71-31268

Magnetic survey of Baja and southern California coasts and continental shelf including magnetic anomaly map of Pacific Ocean (NOAA-NOS-DR-12) 18 p2919 N71-31438

Geomagnetic survey in 0.01 to 10,000 Hz including data reduction and instrumentation (JGO-706) 19 p3084 N71-31691

Geomagnetic survey program package for digital frequency analysis of time series (JGO-705) 19 p3084 N71-31692

Derivation of International Geomagnetic Reference Field with tables of spherical harmonic coefficients and test results of various magnetic field models (NASA-TN-D-6337) 19 p3176 N71-32190

Aeromagnetic anomalies and granulite bodies in Pined Oville area, Idaho for metamorphic and structural studies 21 p3419 N71-34329

Compilation of geomagnetic and geoelectric observations by Japanese observatories (REPT-10) 21 p3420 N71-34335

MAGNETIC SUSCEPTIBILITY
U MAGNETIC PERMEABILITY
 Direct current motor with magnetically suspended rotor (NASA-CR-115793) 04 p0509 N71-13513
 Modification of dc motor with magnetically suspended rotor to increase momentum storage capacity (NASA-CR-115792) 04 p0509 N71-13514
 Designing rotating transformer with contactless electric power transmission (ILBA-NT-4670/SET/E/L) 08 p1169 N71-18617
 Vibration isolation tests of spring, hysteretic, and magnetic suspension systems for spaceborne telescopes (NASA-CR-111822) 09 p1391 N71-20476
 Wire and probe support interference on hyperconic wakes of magnetically suspended round based conical body (ABC-CP-1133) 10 p492 N71-20848
 Data reduction techniques for deriving aerodynamic forces and moments in absence of support interference (NASA-CR-111844) 12 p1895 N71-23122
 Magnetic lift drag ratios calculated for sail flux magnetic suspension designs (BNL-15420) 12 p1946 N71-23516
 Direct current motor with magnetically suspended rotor for attitude control 13 p2058 N71-25308
 Aerodynamic forces and dynamic stability of high speed, magnetically suspended rocket sled moving close to stationary wall 15 p2390 N71-26943
 Subsonic static characteristics of slender wing configurations using magnetic suspension and balance system (NASA-CR-1796) 17 p2701 N71-29775
 Device for developing forces to simulate diamagnetic suspension 22 p3627 N71-35845

MAGNETIC SWITCHING
 Power switch with transfluxor type magnetic core (NASA-CASE-NFO-10243) 13 p2056 N71-24803
 Design and development of multistage current steering switch with inductively coupled magnetic cores (NASA-CASE-NFO-08567) 14 p2228 N71-24000

MAGNETIC TAPE RECORDERS
U MAGNETIC RECORDING
U TAPE RECORDERS
MAGNETIC TAPES
 Magnetic tape characteristics in spacecraft environment and design of linear m-ary feedback shift register 01 p0027 N71-10264
 Research progress on polymers, battery separator membranes, and evaluation of spacecraft magnetic recording tapes 01 p0016 N71-10265
 Endless loop tape transport mechanism for driving and tensioning recording medium in magnetic tape recorder (NASA-CASE-XGS-01223) 01 p0023 N71-10609
 Roll forming technique for fabricating helical coils for use as recording surfaces in tape recorders (NASA-CR-111406) 02 p0229 N71-11558
 Data recorder for producing digital magnetic tapes for radio transmission experiments 04 p0505 N71-13839

Report to Congress on need for improvement in management of magnetic tapes at GSFC (B-164392) 05 p0651 N71-15452

Development of low friction magnetic recording tape (NASA-CASE-XGS-00373) 06 p0903 N71-15978

Investigating spacecraft magnetic recording tapes and magnetic heads, sterilizable battery separators, and structural performance of solid propellant motor 06 p0811 N71-16688

Surveying commercially available tape services of reference information on scientific and technical literature (IAID-ID-70-3) 08 p1165 N71-18695

Manual for IBM magnetic tape/selector typewriter combination operators (AD-705259) 09 p1356 N71-20424

System for recording and reproducing PCM data from data stored on magnetic tape (NASA-CASE-XGS-01021) 10 p1528 N71-21042

Studies related to Pioneer 8 and 9 data tape analysis (NASA-CR-117526) 10 p1641 N71-21565

Service routines MERMC2 and MAGIC for binary cross section library tapes used by MC sup 2 multi-group cross section code (ANL-7654) 11 p1804 N71-22352

Kinetic and static friction force measurement between magnetic tape and magnetic head surfaces (NASA-CASE-XNP-06680) 11 p1766 N71-22995

Updating ANISN library tapes with plotting of cross section curves using FORTRAN 4 program (ORNL-TN-2408) 12 p1973 N71-23937

Time-base error analysis of magnetically recorded and played back digital data using tape flutter spectral density and amplitude probability distribution measurements and rms time plots (NASA-CR-115029) 15 p2411 N71-27711

Computer program for reducing radar tracking data magnetic tape numbers for data storage by editing and low pass filtering (NASA-CR-119176) 17 p2748 N71-30149

Test methods and procedures for determining effect of chemical and physical forces at magnetic head/tape interface of satellite tape recorders (NASA-CR-121649) 21 p3424 N71-34364

Chemical and physical forces at magnetic head/tape interface of satellite tape recorders 21 p3424 N71-34365

Guidelines for design, selection, and use of magnetic heads and tape for unattended satellite tape recorders (NASA-CR-121701) 21 p3424 N71-34366

Magnetic head/tape interface problems of satellite data storage tape recording systems, and minimizing stick-slip phenomena (NASA-CR-121730) 21 p3425 N71-34373

Library tape for storage of model parameters of semiconductor devices (SC-M-710210) 21 p3498 N71-34918

Flow diagrams and compression capabilities for software interfacing of flight data (NASA-CR-61360) 22 p3553 N71-35321

IBM 360 TELOR3 program for testing, editing, and listing information on ORB3A tape (NASA-TM-X-65692) 23 p3728 N71-36571

Design, operation, and calibration of signal amplitude measuring system for computer secondary standard magnetic tapes by reference tapes (NBS-SP-260-29) 23 p3730 N71-36590

Entrance inertia effects associated with high speed magnetic tapes and computer flying heads (AD-726464) 23 p3744 N71-36694

Photographic recording of image previously recorded on magnetic tape 23 p3758 N71-36793

Ionospheric electron content statistical analysis from Faraday effect tapes 24 p3912 N71-37890

MAGNETIC TRAPS
U PLASMA CONTROL
MAGNETIC VARIATIONS
 NT GEOMAGNETIC MICROPULSATIONS
 NT GEOMAGNETIC PULSATIONS
 NT NOCTURNAL VARIATIONS
 Hourly values of equatorial Dst for Jan. - June 1970 (NASA-TM-X-65380) 01 p0409 N71-10605
 Magnetic variations, ionospheric soundings, and riometer data in polar regions, July - Sept. 1969 - Tables 03 p0371 N71-13273
 Correlation between magnetic variations and solar wind and interplanetary magnetic fields (GRI-NT-79) 03 p0451 N71-13333
 Magnetic variations and auroral zones over Greenland in night and daytime 04 p0521 N71-13779
 Hiss, auroral electrojets, and Arctic region magnetic variations 04 p0521 N71-13780
 Data tables of magnetic variations, Thule, Greenland, 1962 04 p0521 N71-13786
 Data tables of magnetic variations, Rude Skov, Denmark, 1967 04 p0522 N71-13787

Data tables of magnetic variations, Godhavn, Greenland, 1964 04 p0522 N71-13788

Dynamic aspects of concentrated magnetic systems (COO-1488-21) 04 p0566 N71-13959

Simultaneous magnetic and electric field measurements for extremely low frequency ionospheric disturbances and ionospheric 06 p0850 N71-16377

Molecular field model for amorphous antiferromagnets with susceptibility variations (CALT-822-16) 07 p1009 N71-18068

Magnetic system model of JINR phasotron with spatial field variation (JINR-P-5246) 07 p1005 N71-18126

Cosmic ray distribution for analysis of nonuniform interplanetary magnetic fields during solar activities (NASA-TT-F-13314) 09 p1402 N71-20049

Polar and lower latitude ionospheric currents and magnetic field variations (GRI-NT-81) 10 p1547 N71-20099

Waveguide model for estimating ionospheric variations effects on very low frequency signal transmission 11 p1704 N71-22903

Simulation of magnetospheric shock front and magnetic variations in collisionless plasma (PR-5) 17 p2739 N71-29450

Vertical sounding and riometer investigations of ionospheric magnetic field variations and spatial position and spectra of aurora 17 p2746 N71-30077

All sky photography of U-shaped polar aurora in ionosphere 17 p2746 N71-30079

Latitude variations in ionospheric parameters 17 p2747 N71-30090

Magnetic field compensation by magnetic system model for phasotron with space variation (JINR-P-5590) 18 p2958 N71-30475

Hourly equatorial magnetic variations data for 1957 to 1970 (NASA-TM-X-65645) 19 p3094 N71-32438

Secular magnetic variation anomaly and geomagnetic field drift in Poland (TT-70-55006) 19 p3096 N71-32646

Secular magnetic variation anomaly and Warsaw anomaly 19 p3096 N71-32647

Magnetic intensity and inclination measurements on Polish archeomagnetic specimens, and comparison with similar Ukrainian data indicating magnetic drift 19 p3097 N71-32648

MAGNETICALLY TRAPPED PARTICLES
 NT ARTIFICIAL RADIATION BELTS
 NT INNER RADIATION BELT
 NT OUTER RADIATION BELT
 NT PROTON BELTS
 NT RADIATION BELTS
 Model environment of high energy protons trapped in radiation belts (NASA-SP-3024-VOL-6) 02 p0293 N71-12117
 Lifetimes of energetic electrons and ions trapped in magnetic mirror (CEA-CONF-1603) 08 p1256 N71-18372
 Quasiperiodic properties of particle motion in RF segmented traps (CEA-CONF-1599) 08 p1271 N71-18383
 Proton precipitation above 100 keV observed by ESRO 1 satellite in noon-midnight meridian 10 p1550 N71-21157
 ESRO 1 satellite Geiger counter observations of solar proton flare effect on magnetically trapped particles over polar cap regions 10 p1550 N71-21159

Beta particle observations between inner edge of plasma sheet to plasmapause in midnight earth magnetosphere (NASA-TM-X-65646) 19 p3094 N71-32436

Computerized simulation of plasma injection and trapping in linear octupole 22 p3656 N71-36072

Anomalous heating and momentum transfer from slow electrons to ions and superthermal to thermal velocities in magnetically confined turbulent plasmas with large currents (CONF-710607-64) 24 p3908 N71-38457

Nonlinear electromagnetic interaction with plasmas for control, ion heating, electron distribution measurements, and detection of magnetically trapped particles (CONF-710607-25) 24 p3990 N71-38466

Plasma heating and production of relativistic electron current layers by injection of high current electron beams into magnetic fields (CONF-710607-12) 24 p3990 N71-38468

Magnetohydrodynamic equilibrium and stability of high-beta relativistic electron plasmas in axisymmetric and nonaxisymmetric mirror traps (CONF-710607-91) 24 p3992 N71-38478

Confinement configurations for high plasma current densities involving trapped particles 24 p3992 N71-38483

MAGNETITE

- Measuring variation of transition temperature of magnetite with respect to molecular field solution of Heit-Wigner transition
[NUB-2020] 08 p1258 N71-18624
- Artificial meteor ablation studies of natural minerals composed of magnetite and hematite
[NASA-TM-X-62025] 15 p2419 N71-26911
- Determination of diffusion coefficient of iron in magnetite
[TT-70-59100] 20 p3283 N71-33091
- Mossbauer effect for measuring nonstoichiometric magnetite spectra
[NLL-CE-TRANS-3586-19022.09] 23 p3836 N71-37359

MAGNETIZATION

- Low temperature magnetization of dilute copper manganese alloys
[UCSD-34-P-143-33] 08 p1216 N71-18942
- Permanently magnetized ion engine casing construction for use in spacecraft propulsion systems
[NASA-CASE-XNP-06942] 12 p1989 N71-23293
- Influence of magnetic interactions on oscillatory de Hass-van Alphen magnetization on silver samples
15 p2455 N71-27587
- Magnetization reversal discontinuities of high performance transition metal-rare earth magnets for critical applications
[AD-722772] 18 p2937 N71-31353
- Dimensional effect in magnetization of strong superconductors: Nb-Zr-Ti, Nb-Ti, and Nb-Zr
[KHFTI-70-8] 19 p3113 N71-31925

MAGNETO-OPTICS

- Magneto-optical properties of polycrystalline and single crystal ferromagnetic thin films
[AD-718135] 12 p1985 N71-23653
- Gravitational effects on neutron optical properties of six-pole magnet
[JINR-P3-5337] 18 p2962 N71-30668
- Discrete element magneto-optic display
[AD-724603] 20 p3241 N71-33190
- Construction of fast hydrogen atom injector from calculations of magneto-optical system
[NLL-CTO-746-19091.9F] 23 p3832 N71-37329

MAGNETOACOUSTIC WAVES

- Exact solution to magnetoacoustic wave equations for magnetoacoustic waves under gravity and comparison with observed fine structure of waves propagating away from solar flares
[AD-720244] 15 p2516 N71-27824

MAGNETOACOUSTICS

- Vlasov description of supercritical magnetoacoustic compression pulse
[IPP-1/113] 22 p3653 N71-36048

MAGNETOACTIVITY

- NT MAGNETORESISTIVITY
MAGNETOELASTIC VIBRATIONS
U MAGNETOELASTIC WAVES
MAGNETOELASTIC WAVES
NT MAGNETOACOUSTIC WAVES

- Research in Bragg diffraction from magnetoelastic waves using acoustic surface waves
[AD-711101] 01 p0091 N71-10857
- Magnetoelastic Love waves in epiaxial magnetic films
[AD-713993] 06 p0904 N71-16253
- Bragg and Raman-Nath diffraction of laser light from magnetoelastic and magnetoelastic waves propagating in YIG
[AD-715253] 07 p1069 N71-17846
- Optical probing and microwave techniques for determining magnetoelastic and magnetoelastic waves in yttrium-iron garnet crystals
[AD-720386] 14 p2329 N71-26565
- Ray theory analysis of magnetoelastic wave propagation in ferromagnetic media with application to delay lines
23 p3738 N71-36653

MAGNETOELASTICITY

- U MAGNETOSTRICTION
MAGNETOELASTICITY
U MAGNETOELASTIC WAVES
MAGNETOELASTIC WAVES
NT MAGNETOACOUSTIC WAVES

MAGNETOGRAMS

- U MAGNETIC SIGNATURES
MAGNETOGRAMS
U MAGNETOMETERS
U RECORDING INSTRUMENTS

MAGNETOHYDRODYNAMIC ACCELERATION

- U PLASMA ACCELERATION
MAGNETOHYDRODYNAMIC FLOW
Paired comparison tests of relative signals detected by capacitive and floating Langmuir probes in turbulent plasmas from 0.2 to 10 MHz
[NASA-TM-X-52914] 01 p0104 N71-10237

- Numerical method for solving general MHD flow problems
01 p0075 N71-10464

- Characteristics of magnetoacoustic flow around blunt bodies
03 p0310 N71-12212

- Magnetohydrodynamic flow in magnetosphere, and space charges and self consistent electric fields
[REPT-70-32-PT-1] 04 p0520 N71-13601

- Velocity distributions ahead of semi-infinite Rankine body in magnetohydrodynamic flow
05 p0661 N71-14768

- Numerical analysis of blunt body electrostatic probe plasma flow
[SC-RR-70-331] 06 p0929 N71-16041
- Analysis of axisymmetric expansion of ionized, hot-electron cold ion plasma in magnetic nozzle
[NASA-TN-D-6154] 07 p1102 N71-17503
- Steady, dissipationless, hyperbolic aligned magnetohydrodynamic flow over cones
07 p1012 N71-17760

- Plasma flow and magnetohydrodynamic macroscopic equations
[CEA-N-1371] 08 p1269 N71-18166
- Measuring disturbance field generated by point source for steady three-dimensional isentropic magnetohydrodynamic flow
08 p1275 N71-19247

- Space environment simulator for ionospheric plasma flow over onboard satellite instrumentation
09 p1450 N71-20213

- Plasma interactions resulting from plasma flow and magnetic field with nozzle shaped lines of force with large electron Hall parameter
[ISA-45-457] 11 p1811 N71-22433
- Numerical analysis of simultaneous transport of momentum, energy, and magnetic field for magnetohydrodynamic flow in finite ducts
12 p1903 N71-24136

- Magnetic field suppression of magnetohydrodynamic boundary layer separation and inviscid flow equations
12 p1983 N71-24268

Engineering aspects of magnetohydrodynamics

- Mathematical model for solving hydrodynamic flow equations in nonhomogeneous magnetic field for plasma flow along field line in presence of gravitational field
[NASA-TM-X-65554] 15 p2503 N71-27889
- Dependence of ion component on magnetic field strength, and formation of plasma flux when plasma flows from hot cathode discharge
[AD-721313] 16 p2661 N71-28745

- Magnetohydrodynamics of plane flows in plasma with anisotropic pressure
[NASA-TT-F-13570] 17 p2813 N71-30194
- Tangential discontinuities in solar wind derived from Mariner 5 plasma and magnetic field data
[NASA-CR-119173] 17 p2842 N71-30262

- Determination of minimum B and magnetic well depth for magnetohydrodynamic flow control
[IAE-1967] 18 p2961 N71-30424
- Collisionless plasma flow around cylinder for application to ionospheric sounding probe
[ONERA-PUBL-137] 19 p3072 N71-31693

- Magnetospheric model for dynamic plasma flows in polar magnetosphere
[NASA-CR-119780] 19 p3095 N71-32477
- Magnetohydrodynamic ionized gas cylinder flow with Hall effect
[DLR-FB-70-50] 20 p3329 N71-33029

- Internal flow conditions in hollow gas cathode
[TP-959] 20 p3330 N71-33475
- Field line motion accompanying rapid plasma flow during geomagnetic storms
[NASA-TM-X-67295] 21 p3415 N71-34298

- Plasma flux and magnetic field properties resulting from deuterium-deuteron reactions
[LA-TR-71-6] 21 p3494 N71-34890

- Computer program for solving MHD equations for four fluids in one dimension and application to partially ionized hydrogen or helium plasmas
[LRP-46/71] 21 p3495 N71-34895

- MHD flow, recombination processes in pulsed helium discharge, and mass spectrometry applied to He in solids
[AE-410] 22 p3632 N71-35879
- Analysis of reactions between flow of plasma and particles of tungsten carbide moving within the flow
[NLL-RTS-6142] 22 p3655 N71-36067

- Comparison of floating double planar guarding and change of floating potential resonance probes for locating parallel resonance minimums in arc flowing plasmas
22 p3656 N71-36073

- Lecher wire microwave probe for flowing plasma diagnostics
[ORO-3818-5] 24 p3991 N71-38473

- Effect of variable fluid properties on MHD flow in electrically insulated rectangular duct
24 p3995 N71-38502

MAGNETOHYDRODYNAMIC GENERATORS

- Military research program on magnetohydrodynamic generators and technology dissemination
[AD-71389] 01 p0138 N71-10664

- Development of cesium seeding techniques, large MHD magnets, plasma diagnostic techniques, and thermionic electrodes compatible with shock tube MHD generators
01 p0107 N71-10992

- Critical channel length of Hall-type MHD generator
[INR-1159] 03 p0317 N71-12264

- Correlational method for plasma instability study in Tokamak-3 apparatus
[ORNL-TR-2352] 04 p0582 N71-14110

- Analysis of magnetoplasma dynamic converter
[AEC-TR-7161] 05 p0732 N71-13010

- MHD generator performance with leakage currents
[INR-1190] 05 p0733 N71-15080

- Crossed field MHD plasma generator-accelerator
[NASA-CASE-XLA-03374] 06 p0755 N71-15542

- Floating potential profiles, electrode drops, and electrode temperature measurements in unseeded, superionic argon magnetohydrodynamic generator
[NASA-TN-D-7041] 06 p0929 N71-15856

- Magnetic induction concentric cylinder magnetohydrodynamic generator with cryogenic cooling
[DLR-FB-70-25] 07 p1083 N71-17840

- Performance tests of liquid metal magnetohydrodynamic power converter
11 p1012 N71-22560

- Time dependence analysis of current flow of condenser discharge of electrodeless MHD generator
11 p1813 N71-22654

- Numerical analysis of plasma formation and propagation in magnetohydrodynamic channel flows
[AD-718951] 12 p1980 N71-23266

- Comparison of turbo-MHD cycle with Brayton-MHD and turboelectric cycles
[NASA-TM-X-67829] 13 p1216 N71-24578

- Performance tests and characteristics of large linear, superionic magnetohydrodynamic generator using rare gases in shock tubes
[AD-719360] 13 p2029 N71-24615

- Operating characteristics of large nonequilibrium MHD generator with cesium seeded noble gases and heated electrodes
13 p2029 N71-24640

- Plasma heating by shock waves, measuring methods in hot plasmas, MHD generators, relativistic plasmas, surface physics, plasma production by laser beam, and related engineering projects
[NP-18496] 14 p2322 N71-26171

- MHD energy conversion using Joule heating
[AD-720257] 14 p2322 N71-26190

- Magnetohydrodynamic generator systems analysis including electrical impedance and power conversion efficiency calculations for various designs
14 p2323 N71-26449

- Engineering aspects of magnetohydrodynamics
14 p2323 N71-26458

- Numerical calculations of electrical parameters in Faraday-type MHD generator with two dimensional gas flow
[INR-1199] 15 p2393 N71-27267

- Strength and direction of electric current flow in MHD generator configurations
[IPP-6/89] 15 p2453 N71-27262

- Split image line reversal technique for measuring pure monatomic gas electron temperature in MHD shock tube
[AD-721090] 15 p2499 N71-27276

- Design parameters of noble gas magnetohydrodynamic generator for nuclear power plant
[JUL-706-TP] 15 p2503 N71-27918

- Signal analysis and power spectral density of fluctuations in series connected open cycle MHD generators
[AD-721454] 16 p2540 N71-27860

- Evaluation of factors affecting performance of series connected magnetohydrodynamic generators
[AD-721455] 16 p2540 N71-27818

- Current density and electrode drop distributions in cross sectional plane of electrode in conducting wall generators
16 p2540 N71-28803

- Cryopump used in magnetoplasma dynamic converters with liquid helium cooled argon plasma
[DLR-MITT-71-03] 17 p2730 N71-29379

- Design and component analysis of future magnetohydrodynamic nuclear power plants
[JUL-689-TP] 18 p2957 N71-04058

- Efficiency and performance characteristics of low temperature two phase liquid metal MHD power systems
[AD-721087] 19 p3173 N71-31577

- Microwave ionization for obtaining nonequilibrium plasma in MHD generators
[NASA-TT-F-13783] 19 p3164 N71-32212

- Uranium plasmas applied to nuclear rocket engines, MHD generators, nuclear lasers, and plasma stability and flow - conference
[NASA-SP-236] 20 p3302 N71-33626

- Gaseous fission, closed loop, MHD generator in nuclear electric power plant
20 p3303 N71-33632

- Magnetohydrodynamic generator development and applications in radiating power plants, propellant-cooled propulsion systems, and industry
20 p3306 N71-33661

- Performance of helium seeded with uranium in magnetohydrodynamic generator
20 p3306 N71-33663

- Gas core reactors and MHD generator to solve problems of growing demand for electric power without thermal pollution
20 p3306 N71-33664

SUBJECT INDEX

Effects of leakage currents to ground in mhd generator with constant gas parameters and constant channel cross section

[INR-1242] 21 p3493 N71-34884
[INR-1243] 21 p3493 N71-34885

Development and evaluation of high temperature materials for use in magnetohydrodynamic generators [JPRS-53939] 22 p3598 N71-35621

Test and evaluation of high-refractory materials for construction of magnetohydrodynamic generator

Chemical, X ray diffraction, electron microscopic, and structural analysis of silicon carbide ceramics for open cycle magnetohydrodynamic generators

Analysis of rate of evaporation and erosion of silicon carbide ceramics in air at high temperatures

Effects of temperature on electrical resistivity of silicon, carbon, and metal compounds

Thermogravimetric analysis of effect of various media on silicon carbide materials at high temperatures

Development and evaluation of oxide electrode materials for use with open cycle magnetohydrodynamic generator

Analysis of erosion stability of zirconium dioxide stabilized with yttrium oxide at high temperature and high velocity flow of ionized combustion products

Design, development, and production of magnesium oxide insulators installed in cathodic and anodic walls open cycle magnetohydrodynamic generator channel

Development and evaluation of zirconium dioxide for use in high temperature combustion chamber of magnetohydrodynamic generator power plant

Development and evaluation of refractory magnesia and aluminum oxides for use as insulating walls in magnetohydrodynamic generator channel

Analysis of resistivity of refractory concretes and reinforcing materials based aluminum and barium-aluminum cements and bonding agents

Analysis of emissivity of refractory oxides and concretes in infrared region of spectrum at high temperatures

Production of refractory concretes and determination of compressive and tensile strength at various temperatures

Determination of thermal expansion coefficient of aluminum and magnesium concretes used in magnetohydrodynamic power plants

Materials tests of refractory materials used in magnetohydrodynamic generators to determine thermodynamic and electrical properties

Thermodynamic and electrical properties of refractory materials used in magnetohydrodynamic generator channels

Optimal design and working parameters for experimental installation of magnetohydrodynamic generator

Materials tests of cermet materials based on refractory carbides to determine melting point, oxidation resistance, emissivity, and weldability

Electrical conductivity of boron and silicon compounds produced by hot pressing and sintering of cold-pressed pellets

Thermal emission of refractory materials measured in atmospheres of argon, cesium, and vacuum

Development of combined turbine-magnetohydrodynamic generator operating in Brayton cycle with NERVA nuclear reactor for space and ground applications

Energy balance relationships used for evaluating maximum parameters of MHD generator operating on nonequilibrium plasma

Status of MHD power generators and related technology in Japan

Local potential and nonlinear stability in magnetohydrodynamics

Stability of sunspot magnetic fields and origin of solar flares

Stability of microwave-heated plasmas

Physical structure of hydromagnetic disturbances in inner magnetosheath

Computer program for numerical simulation of plasmas

Effect of magnetic fields on instability and turbulence of highly ionized plasmas

Magnetohydrodynamic stability of Takamak plasmas

Two stream instability in Colgate supernovae model of cosmic ray acceleration

Collective interactions in fast thetatron showing kinetic instability

Critical plasma density corresponding to threshold of high frequency instability during electron beam interaction with plasma

Electron beam and plasma instability in low density plasma of high current gas discharge

Stability, heating, and loss characteristics of slow theta pinch plasma

Short wavelength instabilities in confinement of collision dominated plasma by rotating magnetic field

Numerical simulation of Weibel instability in one and two dimensions

Investigating high beta plasma state and magnetohydrodynamic stability

Electron cyclotron drift instability with plasma heating

Using second quantization formalism of particles in magnetic field and interaction Hamiltonian between particles and waves to study nonlinear instabilities in plasma

Numerical simulation of ion-acoustic instability in plasmas

Instabilities in magnetically self-focusing streams in plasma

Hydromagnetic Poiseuille flow stability

Electron velocity distribution anisotropy and magnetohydrodynamic stability of whistlers

Interaction of QTX wave with density fluctuations in inhomogeneous magnetized plasmas

Investigating kinetic theory of anomalous diffusion due to drift dissipative instability

Plasma control and stability using magnetic focusing in circular quadrupole well

Experimental proof of mirror instabilities in theta-pinch ISAR I

Nonlinear electrostatic instabilities in magnetoplasma

Calculations on plasma equilibrium configuration confined by helically symmetric magnetic field

Plasma oscillations and instability phenomena in low temperature laboratory plasmas

Models for collisionless stability of inhomogeneous, confined, planar plasma

Iodine molecular beam absorption resonance as long-term frequency reference for argon ion laser stabilization

Electron cyclotron resonance and anisotropic energy distribution excitation of plasma instabilities and waves

Plasma instability work including hydromagnetic Poiseuille flow stability, nonlinear plasmas, plasma oscillations, Vlasov turbulence, and Q devices

MAGNETOHYDRODYNAMIC STABILITY

Instabilities and turbulence in highly ionized plasmas in magnetic field related to problems of thrustors for manned space flight and plasma generated energy

Turbulent diffusion, acceleration, confinement, and heating of plasma, properties of plasmas, cryogenic pumping, high power oscillators, drift instabilities, and related studies

Dependence of MHD stability of toroidal plasma on triangular deformations in its cross section

Correlation techniques in plasma diagnostics including turbulent diffusion/measurement of particle losses and diffusion coefficients and investigation of fluctuations and instabilities

Computerized simulation of plasma heating from electron cyclotron resonance including ion trapping and magnetohydrodynamic instability

Harmonics 2 machine observation of magnetic flux singularities and Mercier theory equilibrium predictions of magnetohydrodynamic stability

Viscous pinch effect on plasma instability in cylindrical configuration exposed to axial magnetic field

Stability of weak electrostatic waves in collisionless magnetoplasma supporting steady large amplitude whistler wave, and influence of trapped particles

Instability of ion-acoustic waves in E1-E and V1-F frequency bands in polar wind where relative flow velocity between hydrogen ions and oxygen ions enters range 5 to 10 km/sec

Electrical conductivity effect on low pressure plasma equilibrium in stellarator

Bounce frequency effects on negative mass instabilities in ion plasma

Computer program for solving theta pinch magnetohydrodynamic equations in time dependent coordinate system

Literature survey on plasma instability

Ionization instability resulting from Joule heating in weakly ionized ionospheric plasma with currents present

Hydromagnetic Kelvin-Helmholtz instability in velocity shear layers of nonzero thickness

Mathematical models for solar wind merging in magnetic fields noting tearing instability

Constructing normal modes for bounded systems from infinite dispersion relation roots for interpretation of plasma wave and instability studies on finite cylinders

Stability of incompressible two-fluid wheel flows with imposed uniform axial magnetic field for core nuclear rockets

Dynamic stabilization of drift-dispersed instability in partially ionized plasma using inhomogeneous HF electric field

Laser-induced plasma instability model for electric fields oscillating near plasma frequencies

Formulation of helically symmetric magnetohydrodynamic theta pinch problem with set of fluid equations

Electron wave instabilities in non-Maxwellian Lorentz magnetoplasma caused by electron-neutral collisions

Numerical analysis of feedback stabilization techniques for containment of plasma column to ensure hydromagnetic stability

Confinement of toroidal theta pinch plasma in periodic cuffed cusp field

Two computer programs for calculating plasma stability and equilibria in Astron and minimum-B magnetic mirror systems

Application of feedback system for suppression of flute instability in Phoenix 2 plasma

Langmuir probe diagnostics in EMAX plasma device to determine instability thresholds

Bremsstrahlung measurements to determine plasma instabilities and excited waves from anisotropic energy distribution caused by electron cyclotron resonance

- Stability of shock produced high temperature plasma in z-pinch experiment [CONF-710607-14] 23 p3830 N71-37317
- Hydrogen plasma instability induced by rapid turbulent heating [CONF-710607-50] 23 p3831 N71-37321
- Ion cyclotron instabilities in finite plasmas and finite temperature effects 23 p3833 N71-37332
- Instabilities in hot electron plasma created by adiabatic compression in pulsed magnetic field 23 p3833 N71-37335
- Analysis of magnetohydrodynamic equilibrium and stability of toroidal screw pinch with noncircular plasma cross section [CN-28/B-7] 24 p3984 N71-38433
- Improvements in plasma stability with positive trapped magnetic fields and switching of magnetic field and current [CN-28/B-6] 24 p3984 N71-38434
- Observations of pinch systems operating above Kruskal-Schwarzschild limit [CN-28/B-5] 24 p3984 N71-38435
- Longitudinal current decay in toroidal screw pinches and loss of equilibrium or instability [CN-28/B-4] 24 p3985 N71-38436
- Drift wave stabilization in plasmas by ac and dc techniques using magnetic shear, feedback, and dynamic methods [CN-28/B-13] 24 p3985 N71-38437
- Current-carrying toroidal plasma column high-frequency stabilization in longitudinal magnetic fields using Tolosokop device [CN-28/B-12] 24 p3985 N71-38438
- Crossed field instabilities and turbulent ion heating calculated in mirror machine [CONF-710607-47] 24 p3988 N71-38458
- Theoretical results pertaining to Scyllac experiment to devise method for bending theta pinch into torus [CONF-710607-117] 24 p3990 N71-38470
- Parametric excitation of ion-acoustic waves, and analysis of plasma stabilization by open-loop methods [ORO-3405-35] 24 p3991 N71-38472
- ST Tokamak instability, including slow growing, small amplitude oscillatory modes followed by fast growing, sometimes destructive, instabilities [CONF-710607-78] 24 p3991 N71-38477
- Magnetohydrodynamic equilibrium and stability of high-beta relativistic electron plasmas in axisymmetric and nonaxisymmetric mirror traps [CONF-710607-91] 24 p3992 N71-38478
- Equilibrium and stability of high beta toroidal plasmas [CONF-710607-118] 24 p3992 N71-38481
- Analytical methods and plasma properties for magnetic-surface and closed-line equilibria of toroidal plasmas [CONF-710607-119] 24 p3992 N71-38482
- Injection, equilibrium, and stability of E layer and confined plasma in Astron [CONF-710607-11] 24 p3993 N71-38485
- Convective motion in Climax toroidal quadrupole device [CN-28/A-6] 24 p3993 N71-38488
- Plasma confinement and heating in internal ring device F-4 [CN-28/A-4] 24 p3993 N71-38489
- Axisymmetric, toroidal plasma equilibria in Tokamak and hybrid systems examined according to MHD theory [CONF-710607-82] 24 p3994 N71-38493
- MAGNETOHYDRODYNAMIC TURBULENCE**
- NT PLASMA TURBULENCE**
- Analytical models for magnetohydrodynamic turbulence and unstable plasma behavior [NASA-CR-111804] 02 p0279 N71-11428
- Propagation and storage of cosmic rays in interstellar magnetic fields with additional turbulent field 03 p0454 N71-13257
- Investigating creation of plasma turbulence by quasi-static ion cyclotron wave 08 p1276 N71-19286
- Particle diffusion due to ion-ion collisions and ion-turbulent wave interaction using ion wave echo diagnostic technique 12 p1983 N71-24331
- Electromotive forces, magnetohydrodynamic turbulence, and stellar and planetary magnetic fields based on turbulent dynamo theory in cosmological electrodynamics [NCAR-TN/IA-60] 21 p3511 N71-35016
- MAGNETOHYDRODYNAMIC WAVES**
- NT ELECTROSTATIC WAVES**
- NT PLASMA WAVES**
- Investigating dynamic nonshock properties of microscale fluctuations in interplanetary medium using plasma and magnetic field data from Mariner 5 space probe [NASA-CR-110999] 01 p0105 N71-10430
- Theta-pinch construction for shock wave generation in nitrogen plasma [AD-711003] 01 p0105 N71-10532
- Interaction of low-frequency magnetohydrodynamic waves with high frequency ion-sound turbulence 02 p0281 N71-11870
- Hydromagnetic wave propagation in inhomogeneous magnetic fields [NP-18419] 04 p0570 N71-13575
- Comments on waves and discontinuities in solar wind [NASA-TM-X-65411] 05 p0765 N71-15327
- Development of asymptotic theory of nonlinear wave motions in magnetohydrodynamic surface waves [AD-713439] 05 p0755 N71-15373
- Transient magnetospheric current sheet generation of magnetohydrodynamic waves and geomagnetic micropulsations 05 p0675 N71-15420
- Properties of magnetohydrodynamic waves and magnetic fields in magnetosheath 07 p1083 N71-17819
- Modified Maxwell equation for solving Alfvén wave problem [AD-715774] 08 p1275 N71-18820
- Microstructure of solar wind and interplanetary medium [NASA-TM-X-65468] 09 p1463 N71-20469
- Dispersion relation for magnetohydrodynamic wave in beta anisotropic plasma 13 p2146 N71-24494
- Nonlinear theory of magnetohydrodynamic waves in high beta collisionless plasma 13 p2146 N71-24495
- Hydromagnetic waves and discontinuities in solar wind [NASA-TM-X-65530] 14 p2334 N71-26081
- Reflection and refraction of magnetohydrodynamic waves at liquid-solid interface, with earth core and mantle applications 15 p2406 N71-27948
- Rotational discontinuities in solar wind derived from Mariner 5 plasma and magnetic field data [NASA-CR-119172] 17 p2842 N71-30261
- Charged particle motion in plasma during propagation of magnetohydrodynamic shock wave [NASA-TT-F-13815] 18 p2992 N71-30918
- Magnetic structure of skew ionizing shock waves in plasma medium 19 p3163 N71-31668
- Models of hydromagnetic shocks in very low ionization regions related to star formation and gas flows in interstellar medium 19 p3079 N71-32315
- Magnetohydrodynamic wave propagation and dissipation in relation to calcium emission in chromosphere 21 p3506 N71-34976
- Bulk plasma moving in periodic hydromagnetic motion in geomagnetic tail [IPPF-103] 22 p3633 N71-36052
- Existence conditions for steady hydromagnetic shock waves propagating in collisionless plasma along magnetic fields [IPPF-106] 23 p3827 N71-37295
- MAGNETOHYDRODYNAMICS**
- Solar models for baroclinic and Rossby waves in magnetic fields, Rossby wave dynamos, thermal convection and rotation and shear flow, and magnetic buoyancy instabilities [AD-710629] 01 p0122 N71-10494
- Broken symmetries and controlled thermonuclear reaction confinement [AD-712363] 02 p0280 N71-11851
- Plasma sources, hydromagnetic ionizing fronts, hydromagnetic waves, laser diagnostics, and microwave techniques [NP-18360] 04 p0596 N71-13772
- Characteristics of relativistic electron beams extracted from electrode space of flash X-ray machines [AD-713576] 05 p0755 N71-15374
- Gas velocity effects on breakdown potential of argon, helium, and nitrogen 06 p0839 N71-16650
- Trends of developments in magnetohydrodynamics, and heat and mass transfer 06 p0906 N71-16659
- Ionizational and thermal nonequilibrium in MHD boundary layer in potassium seeded, nitrogen plasma accelerator [AD-715272] 07 p1084 N71-17961
- Characteristics of synchrotron and Cerenkov radiation below plasma frequency from particles spiraling in magnetoplasma [AD-715925] 07 p1107 N71-18076
- Direct power conversion by magnetohydrodynamics of thermal energy into electrical energy [CEA-R-4062] 07 p0977 N71-18125
- Numerical analysis of flow field typical of those in combustion driven supersonic MHD generator 08 p1181 N71-18871
- Plasma effects in solids and low frequency effects in superconductors [AD-716531] 09 p1451 N71-19553
- Papers presented at plasma physics conference including plasma theory and generation, ac and dc plasma acceleration, plasma-wave interaction, and plasma magnetohydrodynamics and diagnostics [NASA-TM-X-66951] 09 p1448 N71-19807
- Research at NASA Lewis Research Center reported at Fifth NASA Intercenter and Contractors Conference on Plasma Physics [NASA-TM-X-66910] 09 p1448 N71-19810
- Solution of partial differential equations in magnetohydrodynamics using symbolic style of ALGOL [AD-716404] 09 p1449 N71-20016
- Quasi-steady MPD propulsion at power levels in range 1 to 10 megawatts [NASA-CR-111872] 10 p1639 N71-21717
- Electromagnetic field and electron density measurements by MHD plasma accelerators 11 p1813 N71-22657
- Numerical analysis of plasma formation and propagation in magnetohydrodynamic channel flows [AD-718895] 12 p1980 N71-23246
- Feasibility analysis of auxiliary propulsion system using MPD thrusters [NASA-TM-X-67805] 12 p1990 N71-23821
- Closed cycle magnetohydrodynamic power generators with two channels [NASA-TM-X-2277] 12 p1981 N71-23932
- Analysis of surface mounted aperture antenna for measurement of microwave reentry plasma diagnostics [AD-718981] 13 p2146 N71-24590
- Plasma physics developments with emphasis on interaction mechanisms between radiation and matter and nonlinearities of wave propagation in plasmas [EUR-CEA-FC-542-PT-1] 13 p2146 N71-24894
- Particular solution of linearized MHD system inside neutral sheet [EUR-CEA-FC-571] 13 p2147 N71-24976
- Relativistic magnetohydrodynamic equations of proton antiproton annihilation reactions and Klein-Alfvén cosmology 13 p2131 N71-25029
- Research studies in chemical reaction kinetics, laser generation of plasmas, soil science, magnetohydrodynamics, tropical meteorology, computer programming, and imaging techniques [JPERS-51284] 14 p2339 N71-26452
- Two species collisional absorption of low frequency fast hydromagnetic wave in toroidal hard-core configuration [CEA-CONF-1614] 15 p2498 N71-27142
- Mathematical description of axisymmetric plasma equilibrium of Tokamak type [IPPF-3/1-PT-1] 15 p2499 N71-27230
- Exact solution to magnetohydrodynamic equations for magnetoacoustic waves under gravity and comparison with observed fine structure of waves propagating away from solar flares [AD-720244] 15 p2516 N71-27824
- Annotated bibliography of theoretical physics, magnetohydrodynamics of ionosphere and magnetosphere [NASA-CR-118991] 16 p2661 N71-28032
- One-fluid model of low pressure MDH plasma in toroidal geometry [MATT-814] 17 p2811 N71-29575
- Perturbation theory in toroidal plasma using magnetohydrodynamic description [ORNL-TM-3351] 18 p2994 N71-31247
- Analytic model of crossed field MHD accelerators based on turbulent boundary layers, current density distributions, and fluid properties [AD-722443] 18 p2994 N71-31519
- Distorted velocity profile and electric potential distribution of long dc electromagnetic flowmeter for liquid metals [NASA-TM-X-2342] 19 p3100 N71-32165
- Model for structure of electric-current-carrying discontinuity moving into nonconducting gas and leaving gas behind [AD-723804] 19 p3165 N71-32251
- Operating characteristics and performance predictions for gas-core nuclear rocket with fuel separation by MHD-driven rotation 20 p3304 N71-33641
- Electron kinetics in plasmas produced by neutron irradiation of nuclear seeded noble gases 20 p3306 N71-33662
- Magnetohydrodynamics of discontinuities in interplanetary medium and their relation to propagation and acceleration of cosmic rays [NASA-TM-X-65673] 20 p3342 N71-33717
- Numerical analysis of solar wind interactions with nonmagnetic planets based on equations of magnetohydrodynamics for perfect gas [NASA-CR-121871] 21 p3503 N71-34957
- MHD Rayleigh problem with accelerating and decelerating motion of flat wall 22 p3571 N71-35432
- Calculation method for magnetohydrodynamic equations for nonlinear plasma waves and turbulence due to macroinstabilities [TID-25713] 22 p3654 N71-36061
- MHD of theta pinch discharge with superimposed azimuthal magnetic field [UAREP-102] 23 p3824 N71-37279
- Plasma dynamics, plasma heating, lasers, and wave propagation in inhomogeneous magnetoplasmas [AD-726675] 23 p3829 N71-37913

SUBJECT INDEX

- Axisymmetric magnetohydrostatic Tokamak-like equilibria
[CONF-710607-85] 24 p3987 N71-38448
- Evaluation of magnetohydrodynamic arc thrusters operating in quasi-steady mode with electrode vapor as propellant
[NASA-CR-111970] 24 p3988 N71-38453
- Plasma diamagnetism, resistivity, and electron thermal conductivity anomalies in Tokamak discharges based on two-fluid MHD theory, ion and electron heat flow, and Maxwell equations
[CONF-710607-26] 24 p3992 N71-38479
- Nonchemical energy sources, release mechanisms, and conversion processes in plasma dynamics
[AD-72075] 24 p3995 N71-38498
- Performance of high power, quasi-steady MHD thrusters using rare gas propellants
24 p4002 N71-38543
- MAGNETOHYDROSTATICS**
Sunspot theory based on magneto-fluid-mechanic turbulent damping
[P-567] 12 p1993 N71-24192
- MAGNETOTONIC PLASMA**
U PLASMAS [PHYSICS]
MAGNETONICS
Reflection of transient VLF signals from stratified magnetosonic model of ionosphere
07 p0993 N71-17706
- Mathematical models and numerical analyses in magnetosonic plasma physics
[AD-720079] 15 p2501 N71-27597
- MAGNETOMETERS**
NT VARIOMETERS
Pressure scanning Fabry-Pérot magnetometer for studying solar surface features and stellar images
[NASA-CR-111094] 01 p0057 N71-10962
- Methods and equipment for measuring spacecraft magnetic fields
[NASA-TM-X-65386] 03 p0457 N71-13077
- Temperature compensation for magnetic flux magnetometers using wire bridge circuits
04 p0520 N71-13636
- Ferrite magnetic core magnetometer
04 p0520 N71-13637
- Investigating indirect stabilization of magnetometers on moving objects
06 p0894 N71-15955
- Development of wide range linear fluxgate magnetometer
[NASA-CASE-XGS-01587] 06 p0858 N71-15962
- Investigating geomagnetism, seismic properties, and tectonic structure of earth crust
07 p1014 N71-16921
- Phase detectors for magnetic flux magnetometers
07 p1027 N71-17101
- Ferrite core fluxgate magnetometer
08 p1190 N71-16688
- Design and development of optically pumped resonance magnetometer for determining vectorial components in spatial coordinate system
[NASA-CASE-XGS-04679] 09 p1390 N71-20428
- Payload distribution between supplementary sounding rockets for German Azur satellite, noting radiation counters, magnetometers, and auroral spectroscopy
[BMFW-FB-W-70-40] 10 p1648 N71-20789
- Image effects and vibrating sample magnetometer
[NASA-TN-D-6253] 10 p1634 N71-21073
- Spectra of geological magnetic fluctuations computed from magnetic field measurements from US East Coast
[AD-717407] 11 p1745 N71-21971
- Bibliographies of fluxgate magnetometers
12 p1918 N71-23409
- Ground-based measurements of polar magnetic substorms by means of magnetometers
12 p1909 N71-23558
- Attitude sensors to determine motion of rocket free body precession including magnetometers and star trackers
[AD-718314] 12 p1960 N71-23843
- Magnetometers and techniques for geomagnetic measurements on earth surface and in magnetosphere
[ESSA-TR-ERL-183-ESL-12] 12 p1914 N71-24177
- Towed portable magnetometer for magnetic surveys of oceans, and results of survey of Black Sea
14 p2254 N71-25971
- Temperature sensitive magnetometer with pulsating thermally cycled magnetic core
[NASA-CASE-XAC-03740] 14 p2254 N71-26135
- Fluxgate magnetometer for measuring magnetic field along two axes using one sensor
[NASA-CASE-GSC-10441-1] 15 p2409 N71-27325
- Magnetospheric field distortions observed from rubidium magnetometer measurements on OGO 3 and 5
[NASA-TM-X-65363] 15 p2404 N71-27604
- Payload analysis of Aerobee rocket vehicle at altitude determination with solar aspect sensors and magnetometers
[NASA-TM-X-65570] 15 p2442 N71-27738
- Portable rotating gradiometer for measuring gravity gradients under dynamic conditions tested for noise free operation
[AD-721742] 16 p2588 N71-28451

- Phase sensitive detector and commercial Hall probe combined with control current amplifier to provide sensitive, low field magnetometer for use from room to liquid helium temperatures
16 p2593 N71-28497
- Paired rubidium magnetometer providing reliable mapping of quasi-static total magnetic field changes to 0.1 gamma between stations to 1/2 km separation with differential drift correction
[COM-71-50003] 16 p2589 N71-28763
- Six-channel solar magnetograph for investigating line polarization in Stokes parameters and azimuth
[NLL-RTS-6096] 17 p2750 N71-29262
- Sunspot magnetometric data processing including magnetic field and radial velocity distributions
[NLL-RTS-6194] 17 p2840 N71-29282
- Design of magnetometer system for Mariner Venus-Mercury 1973
[NASA-CR-119175] 17 p2846 N71-30347
- Improved respiration magnetometer with high reliability and ease of operation in laboratory and diving studies
[AD-723661] 18 p2922 N71-30711
- Lunar portable magnetometer experiment to measure steady magnetic field at different sites in Fra Mauro region - Apollo 14 flight
18 p3012 N71-30967
- Method for determining solar aspect angle from satellite-borne magnetometer data
[HSA-180] 20 p3300 N71-32921
- Determination of real-time mean hourly values of magnetic field using electronic integration and fluxgate magnetometer
[M70-417] 20 p3256 N71-32988
- Solid state, three axis recording magnetometer with fluxgate type magnetic detectors
22 p3586 N71-35541
- Magnetic susceptibility of vanadium carbide from 77 to 300 K measured by magnetometer
[NASA-CR-122039] 22 p3657 N71-36079
- Derivation and analysis of Josephson effect in superconducting weak links
[AD-726337] 22 p3658 N71-36085
- MAGNETOMETRY**
U MAGNETIC MEASUREMENT
MAGNETOPAUSE
Magnetopause attitudes during OGO-5 crossings
[NASA-TM-X-65378] 01 p0050 N71-10835
- Average and unusual locations of magnetopause and bow shock positions observed by IMP spacecraft
[NASA-TM-X-65429] 06 p0851 N71-16509
- Atmospheric models for magnetospheric instabilities and magnetopause fine structure
[NASA-CR-117471] 10 p1547 N71-20853
- Magnetopause inward motion preceding magnetic storms observed by means of OGO-E magnetometer
[NASA-CR-117442] 10 p1547 N71-20855
- OGO-E electrostatic spectrometer measurements on electron flux near magnetopause
13 p2077 N71-25273
- Data analysis on ATS-1 Suprathermal Ion Detector (SID) measurements of low energy plasma flow in magnetopause boundary
[NASA-CR-121452] 20 p3267 N71-33563
- Theoretical study of magnetopause current layer from kinetic theory of warm collisionless plasmas
23 p3832 N71-37330
- Magnetopause, magnetosheath, and bow shock studied using Explorer 33 and 35 MIT plasma experiment data
[NASA-CR-123193] 24 p4007 N71-38571
- MAGNETOPLASMAS**
U PLASMAS [PHYSICS]
MAGNETORESISTANCE
U MAGNETORESISTIVITY
MAGNETORESISTIVITY
Investigating galvanomagnetic effects in developing higher magnetoresistance devices for low voltage high current switches
[NASA-CR-110998] 01 p0030 N71-10044
- Kondo effect in dilute alloys
[AD-710297] 01 p0065 N71-10053
- Investigating low-temperature ferromagnetism of amorphous alloys obtained by rapid quenching from liquid state
[CALT-822-11] 05 p0703 N71-15231
- Fermi surface model compared to size-dependent oscillatory magnetoresistance in cadmium
10 p1608 N71-21597
- X ray diffraction, solid solution crystallography, and Seebeck coefficient, thermal conductivity, and magnetoresistance measurements of single crystal TiO₂ and TiO₂-V₂O₃ systems
12 p1984 N71-23170
- Metal-insulator-magnetoresistance, bulk, and surface properties of indium antimonide compound semiconductor material
[NASA-CR-118350] 13 p2152 N71-25377
- Analysis of impurity, strain, temperature, and size dependence of transverse magnetoresistance of polycrystalline potassium
[NYO-2150-68] 20 p3336 N71-33890
- MAGNETOSPHERE**
NT GEOMAGNETIC TAIL
NT MAGNETOPAUSE

- Particles and fields near Jupiter
[NASA-CR-1483] 01 p0119 N71-10051
- Solar electron injection through magnetic field lines and magnetospheric diffusion
[AD-712045] 02 p0292 N71-11904
- Motion characteristics of charged particles in magnetosphere
[REPT-70-23] 02 p0292 N71-11921
- Adiabatic phenomenon of particle drift shell splitting by magnetospheric electric field
[AD-712044] 02 p0292 N71-11922
- Physical structure of hydromagnetic disturbances in inner magnetosheath
[UNH-70-19] 02 p0220 N71-12095
- Injection of hot plasma clouds into magnetosphere during magnetospheric substorms
[NASA-CR-111699] 03 p0367 N71-12774
- Magnetohydrodynamic flow in magnetosphere, and space charges and self consistent electric fields
[REPT-70-32-PT-1] 04 p0520 N71-13601
- Polar region magnetic storms and electric currents in the magnetosphere
[REPT-70-29] 04 p0521 N71-13782
- Sounding rocket investigating auroral phenomena in charged particle precipitation, magnetic disturbances, and electric fields
05 p0668 N71-14747
- Satellite observation of plasmas in dayside polar magnetosphere
[NASA-CR-116143] 06 p0849 N71-16339
- Cosmos 184 ion sensor for measuring ion velocity at 600 km
07 p1014 N71-16947
- Cosmos 184 measurements of ion velocity at 600 km
07 p1014 N71-16948
- Dawn chorus and auroral hiss emission in upper ionosphere and magnetosphere
07 p1017 N71-17143
- Properties of magnetohydrodynamic waves and magnetic fields in magnetosheath
07 p1083 N71-17819
- Sources, losses, and transport of magnetospherically trapped particles
[ESSA-TR-ERL-180-SDL-16] 07 p1114 N71-17913
- Measurements of energetic electrons within drift loss cone, extremely low frequency emissions, and plasmopause location
[AD-715266] 07 p1106 N71-18042
- Injun 5 double probe measurements of dc fields in magnetosphere
[NASA-CR-116791] 08 p1187 N71-18405
- Satellite observation of broadband electrostatic VLF waves in polar magnetosphere
[AD-715898] 08 p1188 N71-18501
- Controlled charged particle emission from synchronous satellites for plasma diagnostics and interactions in magnetosphere
[JONLAB-P-26] 10 p1626 N71-20610
- ESRO 1 and ESRO 2 satellite experiments investigating polar magnetosphere
10 p1647 N71-20716
- Magnetospheric plasma diagnostics and whistler electrodynamic including direction finding techniques
[AD-717781] 11 p1747 N71-22125
- Magnetospheric, solar, interplanetary space, and plasma physics
11 p1822 N71-22414
- Electron acceleration in magnetosphere associated with strong hydromagnetic waves in collisionless plasma
11 p1824 N71-22966
- List of articles on cosmic and solar radiation research and their relationship to astrophysics
[AD-717891] 12 p1992 N71-23263
- Magnetic substorm events and magnetosphere structure in polar auroral zones determined by rocket sounding, satellite observations, and ground-based measurements - conference
[ESRO-SP-38] 12 p1908 N71-23551
- Polar upper atmospheric disturbances, auroral electron and proton precipitation, and magnetospheric substorm origin
12 p1908 N71-23553
- Ground-based measurements of polar magnetic substorms by means of magnetometers
12 p1909 N71-23558
- Geomagnetic pulsation measurement for auroral magnetospheric substorm study
12 p1909 N71-23599
- European Space Research Organization synchronous satellite program for magnetosphere sounding
12 p2001 N71-23572
- Design and fabrication of charged-particle detectors with high counting efficiency for satellite, rocket, and laboratory study of magnetospheric boundary regions
[AD-718101] 12 p1922 N71-23789
- Magnetometers and techniques for geomagnetic measurements on earth surface and in magnetosphere
[ESSA-TR-ERL-183-ESL-12] 12 p1914 N71-24177
- Magnetospheric electric current sheet model
[REPT-70-28] 14 p2245 N71-25637
- Simultaneous observations of solar flare electron spectra in interplanetary space and within earth mag-

netosphere measured by magnetic electron spectrometers on satellites OGO-4 and OV 1-19
[AD-720806] 14 p2333 N71-25795

Fluctuations of magnetospheric electric field determined by power spectra analyses
[NASA-CR-118343] 14 p2249 N71-26300

Structured variations of plasmapause observed by OGO-D and evidence of co-rotating plasmalatt
[NASA-TM-X-65567] 15 p2404 N71-27641

Instability of ion-acoustic waves in ELF and VLF frequency bands in polar wind when relative flow velocity between hydrogen ions and oxygen ions enters range 5 to 10 km/sec
[AD-720243] 15 p2502 N71-27887

Annotated bibliography of theoretical physics, magnetohydrodynamics of ionosphere and magnetosphere
[NASA-CR-118991] 16 p2661 N71-28032

Plasma turbulence in circumterrestrial space due to geomagnetic field related to dynamics of magnetosphere and electroconductivity
[NASA-TT-F-13610] 16 p2663 N71-29087

Simulation of magnetospheric shock front and magnetic variations in collisionless plasma
[PR-3] 17 p2739 N71-29450

Relation between geomagnetic tail fundamental oscillation mode and magnetospheric storms
[D-3] 17 p2739 N71-29534

Dynamics of earth magnetosphere as product of interaction of solar wind and geomagnetic field
[AD-722056] 17 p2841 N71-29542

Barium releases from Javelin and Nike-Tomahawk sounding rockets for ion cloud study of earth electric and magnetic fields
[NASA-SP-264] 17 p2740 N71-29671

Using ionized barium vapor clouds for direct measurement of electric fields in magnetosphere
17 p2740 N71-29672

Electric field measuring techniques used in ionospheric and magnetospheric electron current studies
[NASA-TM-X-65596] 17 p2748 N71-30094

Tables of artificial satellites for investigating magnetosphere, solar wind, electric field, and magnetic fields from 1971 to 1975
[GR/INTP/85] 18 p3018 N71-30679

Cyclotron and bounce resonance scattering of electrons trapped in earth magnetic field
18 p3004 N71-30924

Comparison of electron response in magnetosphere at L equals 5 with solar wind during magnetic storm on 17-18 Apr. 1965
18 p3005 N71-30926

Particle and field oscillations and electron heating due to drift mirror instability in magnetosphere
18 p3005 N71-30930

Investigation of solar wind interaction with earth magnetic dipoles and shape of magnetosphere including tail and collisionless shock wave investigated by magnetic probe
[NASA-TT-F-13734] 18 p2964 N71-31095

Barium-copper oxide/canister barium vapor release system for geomagnetospheric measurements
[NASA-CR-1739] 18 p2888 N71-31424

Hydromagnetic Kelvin-Helmholtz instability in velocity shear layers of nonzero thickness
[AD-723675] 19 p3163 N71-31761

Spectrometer for onboard measurement of ion energy spectra in plasma of solar wind and magnetosphere
[NASA-TT-F-13762] 19 p3176 N71-32230

Resonant oscillations of geomagnetic field in magnetosphere caused by solar wind
[NASA-TM-X-65644] 19 p3095 N71-32519

Tilt angle dependence of 10 MeV proton cutoff latitudes in image dipole model magnetosphere
[NASA-TM-X-65678] 20 p3316 N71-33444

OV3-3 data on particles and electromagnetic fields in magnetosphere and radiation belts
[AD-726542] 22 p3666 N71-36137

Diagnostic analysis of magnetosphere based on resonating regions of plasmasphere, outer magnetosphere, and magnetospheric tail
[NASA-CR-121967] 22 p3667 N71-36144

Ray tracing to delineate radio propagation to large distances by ducting under super refracting conditions in troposphere, ionosphere, or magnetosphere
[AD-726597] 23 p3723 N71-36541

Electron pitch-angle scattering in outer zone during magnetic storms
[AD-727003] 23 p3842 N71-37393

Astrophysics, solar physics, and dynamic processes in interplanetary space and magnetosphere
23 p3848 N71-37428

Interaction of magnetosphere and electric field with respect to earth rotation
23 p3853 N71-37464

Magnetic storm phenomena in magnetosphere and upper atmosphere
23 p3853 N71-37465

Electron streams and extremely low radio frequency radiation in magnetosphere
23 p3854 N71-37471

Particle motion at neutral layer boundary in magnetosphere tail
23 p3854 N71-37473

Charged particle detectors for satellite experiment to study magnetospheric boundary regions of space
[AD-726656] 23 p3855 N71-37481

OGO 2 and 4 observations of conducted VLF propagation in magnetosphere
24 p3918 N71-37939

Comet and magnetosphere streaming by solar wind
24 p4009 N71-38588

MAGNETOSPHERIC ELECTRON DENSITY
RSO 1 Geiger counter and ground geophysical observations of radiation belt electron precipitation, fine structure, and angular distribution during solar flare, 25 Feb. 1969
[R-17] 02 p0212 N71-11541

Measuring energy fluxes greater than 5 keV electrons over northern auroral region at 530 to 2500 km altitude using Injun 4 satellite
05 p0670 N71-14816

Radio frequency impedance probes for measuring inner magnetospheric electron density and thermal plasma density
07 p0106 N71-17045

Ionospheric and magnetospheric electric field measuring instruments and measurement results
[MPI-PAE/EXTRATERR-4470] 08 p1189 N71-18609

Satellite-borne measurements of electron flux during magnetic storm
[NASA-TT-F-13512] 09 p1386 N71-20301

Electron flux with energy higher than 300 MeV at 250 to 500 km altitudes, observed by Cosmos 225
[NLL-RTS-6033] 16 p2674 N71-28286

Satellite beacon transmitter methods for determining ionospheric and magnetospheric electron density
24 p3913 N71-37899

ATS 6 radio signal receiver for measuring total electron content of ionosphere and magnetosphere
24 p3915 N71-37914

MAGNETOSPHERIC INSTABILITY
Injection of hot plasma clouds into magnetosphere during magnetospheric substorms
[NASA-CR-111609] 03 p0367 N71-12774

Transient magnetospheric current sheet generation of magnetohydrodynamic waves and geomagnetic micropulsations
05 p0675 N71-15420

Joule heating of upper atmosphere caused by geomagnetic perturbations
[NASA-TM-X-64568] 08 p1189 N71-18631

Atmospheric models for magnetospheric instabilities and magnetopause fine structure
[NASA-CR-117471] 10 p1547 N71-20853

ESRO 1 satellite experiment on low energy electron precipitation during polar cap absorption and quiet magnetospheric conditions
10 p1550 N71-21155

OGO-B and OGO-E measurements on magnetospheric field magnitudes and disturbances caused by ring currents
13 p2076 N71-25271

Microimpulsion recordings of magnetospheric storms in auroral zone
[AD-721200] 15 p2399 N71-27187

Magnetospheric field distortions observed from rudimentary magnetometer measurements on OGO 3 and 5
[NASA-TM-X-65563] 15 p2404 N71-27604

Dynamic development characteristics of geomagnetic instabilities in earth magnetosphere
17 p2742 N71-29788

Beta particle observations between inner edge of plasma sheet to plasmapause in midnight earth magnetosphere
[NASA-TM-X-65640] 19 p3094 N71-32436

Comparison of Alouette-2 and OGO-5 observation of turbulence of magnetospheric electrostatic electron cyclotron harmonic waves
[NASA-TM-X-65660] 19 p3095 N71-32442

Magnetospheric model for dynamic plasma flows in polar magnetosphere
[NASA-CR-119780] 19 p3095 N71-32477

Explorer 33 observations of sudden impulses propagating in geomagnetic tail and magnetosheath
[NASA-CR-121900] 22 p3572 N71-35439

Diagnostic analysis of magnetosphere based on resonating regions of plasmasphere, outer magnetosphere, and magnetospheric tail
[NASA-CR-121967] 22 p3667 N71-36144

MAGNETOSPHERIC ION DENSITY
NT MAGNETOSPHERIC PROTON DENSITY
Sources, losses, and transport of magnetospheric trapped particles
[ESSA-TR-EKL-180-SDI-16] 07 p1114 N71-17913

Diagnostic analysis of magnetosphere based on resonating regions of plasmasphere, outer magnetosphere, and magnetospheric tail
[NASA-CR-121967] 22 p3667 N71-36144

MAGNETOSPHERIC PROTON DENSITY
Explorer 40 satellite measurement of differential energy spectrum of geomagnetically trapped protons
[AD-714513] 06 p0944 N71-16748

Magnetospheric proton density models with plasmapause influence on Pci geomagnetic micropulsation
15 p2397 N71-27000

MAGNETOSTATICS

Units of measurement for magnetostatics
07 p1017 N71-17114

Bragg and Raman-Nath diffraction of laser light from magnetostatic and magnetoelastic waves propagating in YIG
[AD-715253] 07 p1069 N71-17046

Optical probing and microwave techniques for determining magnetostatic and magnetoelastic waves in yttrium-iron garnet crystals
[AD-720386] 14 p2339 N71-26340

Application of harmonic functions to electrostatic potentials and magnetostatics
[AD-721903] 17 p2787 N71-29415

Applications of P-harmonic principal functions to thermodynamics and electro- and magnetostatics
[AD-721904] 17 p2788 N71-29701

Numerical methods for variable permeability magnetostatic field problems - difference equations solved iteratively
22 p3630 N71-35840

MAGNETOSTRICTION

Effect of stresses on magnetostriction of iron, nickel, and Permalloy
[AD-711094] 01 p0092 N71-10913

Magnetostriction of magnetic composite materials
[AD-712523] 04 p0566 N71-13948

Acoustic properties of plastic film in magnetostrictive and metallic materials
[AD-715654] 08 p1243 N71-18560

Phase transitions and magnetostriction in $\text{CaMgSi}_2\text{HfO}_2$
[NASA-TM-X-52997] 10 p1634 N71-21075

Magnetostrictive transducers for ultrasonic liquid level detector, using shear wave attenuation in bar
[IN-1442] 10 p1605 N71-21570

Magnetostriction of paraproces in ordered iron alloys containing cobalt or platinum
[TT-70-59069] 14 p2267 N71-25842

Changes in elasticity, magnetostriction, and electric resistance of iron-aluminum alloys during ordering
[DMDC-57931] 14 p2271 N71-25890

Saturation and forced volume magnetostriction of single crystal nickel and copper-nickel alloys
21 p3441 N71-34490

Differential equations and boundary conditions for finitely deformable, polarizable and magnetizable, heat conducting insulators interacting with electromagnetic fields
[AD-726450] 22 p3630 N71-35864

MAGNETOTELLURIC PROFILING

U GEOMAGNETISM
U MAGNETIC SURVEYS
MAGNETOVARIATIONS
U VARIOMETERS
MAGNETRONS
NT NIGOTRONS
In phase oscillating magnetrons for continuous operation power oscillators and coupled oscillations in cavity resonators
[AD-716513] 09 p1359 N71-19625

High power electronics including electrodynamic theory of grids, cathode losses in magnetrons, closed resonance chains, and electromagnetic vibration dosimeters
[AD-717029] 10 p1537 N71-21108

Tuning arrangement for frequency control of magnetron-type electron discharge device
[NASA-CASE-XP-09771] 13 p2056 N71-24841

High power electronics theory and descriptions of magnetrons and planotrons
[AD-727888] 24 p3901 N71-37806

MAGNETS

NT CRYOGENIC MAGNETS
NT ELECTROMAGNETS
NT HIGH FIELD MAGNETS
NT SUPERCONDUCTING MAGNETS
Ferromagnetic return yoke effects on field enhancement and field distribution in high field magnets
[SLAC-PUB-739] 03 p0417 N71-12674

Cost analysis of accelerator magnet system
[NP-18357] 04 p0547 N71-13629

Pulsed power supply for septum magnets of CERN proton synchrotron
[CERN-70-20] 04 p0563 N71-13631

Magnetic field measurements of accelerator and beam handling magnets - bibliography
[LA-4478-BIB] 05 p0733 N71-15111

Electronically controlled hydraulic actuating systems for accelerator extractor magnets
[RPP/N-21] 08 p1174 N71-14274

Changing field gradients in isochronous ring cyclotrons, using shaped magnets
[JFK-1268] 09 p1445 N71-20504

Conference review on critical phenomena in alloys, magnets, and superconductors
[AD-716947] 10 p1634 N71-21067

Particle separation in system of conventional 5-band iris-loaded deflectors interspersed with alternating gradient magnets of strong focusing channels
[BNL-15438] 11 p1804 N71-22226

Ion pump and magnet assembly for spacecraft spectrometer atmospheric sensor system
[NASA-CR-111856] 11 p1771 N71-23279

SUBJECT INDEX

MAMMALS

- Electron accelerator magnet ring survey using particle telescope with micrometer and harmonic analysis for orbit distortions
[CEAL-1052] 13 p2125 N71-24965
- Magnetic bearing with diverse magnetic sources coupled to same air gap via different low magnetic reluctance paths for use with permanent magnets
[NASA-CASE-GSC-11079-1] 16 p2629 N71-24641
- Analog models to measure two-dimensional and three-dimensional distribution of magnetic flux density of magnet for bubble chamber
[SUC-T-70-2] 18 p2960 N71-30414
- Maintenance and reliability of plugging and target mechanisms and magnets in Nimrod thin septum extraction system
[JREEL-209] 18 p2959 N71-30499
- Relativity minimum in ferromagnets with approximate calculation of electron-magnon interaction contribution to temperature dependence of electrical resistivity
[CALT-822-25] 18 p2961 N71-30537
- Gravitational effects on neutron optical properties of six-pole magnets
[JENR-P-5537] 18 p2962 N71-30568
- Magnetization reversal discontinuities of high permeability transition metal-rare earth magnets for critical applications
[AD-72772] 18 p2937 N71-31353
- Magnet pulse stability and beam split operations of levitrons
[UCRL-20249] 21 p3408 N71-34349
- Automatic magnetic field measurements of bending, quadrupole, and gradient magnets with field strengths up to 50 kG
[EPK-1220] 21 p3464 N71-34636
- Motron project instrument, consisting of solid iron magnet, pair-transition meter, and wire spark chamber
[SUC-P-70-4] 22 p3636 N71-35914
- Empirical methods for calculating magnet pole tip shape and finding field inside magnet air gap
[TR-70-4] 22 p3462 N71-35968
- Baseline magnet system in fusion research engineering utilizing plasma beam line
[UCRL-73667] 23 p3740 N71-36668
- Development of polarized ion source for use on six-million-Volt de Graaf accelerator utilizing RF discharge and multipole magnet
23 p3821 N71-37259
- Mossbauer study of magnetocrystalline anisotropy of Nd-CoS for application to manufacture of permanent magnets
[AD-726991] 23 p3835 N71-37347
- Effect of electron-magnon interaction on magnon energy in itinerant electron ferromagnets
[TR-71-2] 24 p3982 N71-38420
- MAGNIFICATION**
Camera adapter design for image magnification including lens and illuminator
[NASA-CASE-XMF-03844-1] 14 p2256 N71-26474
- Passive force transducer for measuring, magnifying, and recording maximum load on given specimen
[NASA-CASE-LAR-10496-1] 16 p2595 N71-28654
- MAGNETISM**
U MAGNIFICATION
MAGNITUDE
Torque-meter for determining magnitude of torque generated by interaction of magnetic dipole between test specimen and ambient magnetic field
[NASA-CASE-XGS-01013] 12 p1921 N71-23725
- Magnitude-red shift, magnitude-galaxy count, and angular diameter-and shift relations included in tests of cosmological models
20 p3344 N71-32843
- Magnitude measurements of vector-axial vector current ratio in signal/minor hyperon yields neutron electron neutrino decay
21 p3488 N71-34848
- Magnitude measurements of kaon(0) sub L kaon(0) sub s mass difference and Lambda hyperon proton interactions at high energies
21 p3488 N71-34849
- MAGNETONS**
Dynamic aspects of concentrated magnetic systems
[CDO-1408-21] 04 p0566 N71-13959
- Investigations of nuclear and electron spin waves by parallel pumping
[CDO-1408-20] 05 p0750 N71-15356
- Nuclear spin-lattice relaxation by magnons in order-disorder ferroelectric transformations with deuterium modulation propionate crystal example
[US-575] 14 p2319 N71-26785
- Relativity minimum in ferromagnets with approximate calculation of electron-magnon interaction contribution to temperature dependence of electrical resistivity
[CALT-822-25] 18 p2961 N71-30537
- Surface magnons in inelastic neutron scattering
[JREEL-815-5764] 24 p3974 N71-38351
- Effect of electron-magnon interaction on magnon energy in itinerant electron ferromagnets
[TR-71-2] 24 p3982 N71-38420
- MAGNETIC EFFECT**
Deriving equations of motion and aerodynamic characteristics for Magnus rotors by flight tests
[AD-718345] 09 p1315 N71-19560
- Magnus force and moment data for standard 10 degree cone calibration model as determined in supersonic wind tunnel
[SC-DC-71-3821] 23 p3743 N71-36688
- MAIN SEQUENCE STARS**
Computed and observed OI line profiles in spectra of B5-A8 stars
02 p0297 N71-12047
- Determination of lower mass limit to Main Sequence for analysis of stellar structure
07 p1111 N71-17871
- Predicted ultraviolet radiation flux density for main sequence stars derived from atmospheric model and photometric measurements
10 p1642 N71-20633
- Spectroscopic observation of seven neutral helium line profiles for five main sequence B stars with estimated helium abundance for upper Orians, HR 2154, and pi Cen
16 p2680 N71-28786
- Gas flow hydrodynamics in evolution of main sequence stars
23 p3849 N71-37435
- MAINE**
Numerical analysis of tidal current circulation in Gulf of Maine
[AD-714612] 06 p0655 N71-16664
- Oceanographic survey to determine erosional deposits in Gulf of Maine
18 p2913 N71-31001
- MAINTAINABILITY**
Analysis of applying standardization techniques to oceanographic sensors
02 p0223 N71-11387
- Aircraft survival equipment testing including maintainability, systems compatibility, human factors engineering, and reliability of rationes, protective clothing, floats, and parachutes
[AD-720225] 14 p2210 N71-26138
- Environmental tests of tents developed for aviation use including installation, safety, and maintainability
[AD-721153] 15 p2390 N71-26880
- Computer simulation analysis of suggested approximate confidence interval for system maintainability parameters
18 p2895 N71-31343
- Reduction of proliferation and maintainability of finite element method computer programs
22 p3488 N71-36305
- MAINTENANCE**
NT AIRCRAFT MAINTENANCE
NT SPACE MAINTENANCE
Systems maintenance program evaluation of Eastern Region air transportation facilities
01 p0037 N71-10114
- Analysis and synthesis of self repair techniques for digital computers
02 p0188 N71-11318
- Repair device for sodium-sodium heat exchanger
[NP-18292] 03 p0414 N71-12809
- Fuel assemblies and operational maintenance for experimental fast oxide reactor
[GSAF-10010-24] 04 p0553 N71-13974
- Quality assurance practices in construction and maintenance of molten salt reactor
[ORNL-TM-2999] 04 p0561 N71-14406
- Investigating repair and maintenance with respect to cost effectiveness and quality
[FTL-A-408-8] 05 p0713 N71-14677
- International renovation of radar stations
[JPRS-51916] 05 p0658 N71-15448
- Oak Ridge research reactor operation, maintenance, and fuel element change
[ORNL-TM-3161] 07 p1060 N71-17148
- Computerized simulation of alternate logistics for overhaul and expensive parts inventory procedures of commercial airlines
07 p1138 N71-18118
- Maintenance and flight safety problems of space shuttle
[NASA-TM-X-52964] 08 p1293 N71-18638
- Using Markov renewal processes for reliability analysis of multiple unit standby redundancy system with preventive maintenance
[TR-71-3] 08 p1226 N71-19007
- Analysis of costs to refurbish thermal protection system for space shuttles
[NASA-CR-111833] 09 p1472 N71-20272
- Crew performance of maintenance and repair tasks during long duration space station simulation test
10 p1648 N71-20976
- Test procedures for evaluating stereoscopes including test preparations, safety hazards, maintenance, human factors engineering, and reliability
[AD-718790] 12 p1918 N71-23575
- Cost data contributions for calibration and maintenance cost reduction
12 p2017 N71-23656
- Optimal methods for orbital resupply, maintenance, and repair of hybrid propellant rocket engine subsystem for orbiting space station attitude control
[NASA-CR-103111] 12 p1991 N71-23955
- Field maintenance manual for Apollo Lunar Surface Drill
[NASA-CR-114969] 13 p2084 N71-24396
- Self testing and requiring computer comprising control and diagnostic unit and rollback points for error correction
[NASA-CASE-NPO-10567] 13 p3049 N71-24633
- Exothermic brass units for repair and assembly of stainless steel materials on space missions
[NASA-CR-103169] 14 p2651 N71-28044
- Preventive maintenance instructions for bonding and electrical grounding systems to prevent equipment damage by electrical faults, lightning, and radiation - Vol. 3
[NASA-CR-114081] 14 p2230 N71-26680
- Markov renewal process model for inspection, replacement, and maintenance system
[TR-71-5] 14 p2386 N71-26695
- Electric motor environmental and electrical test procedures including electromagnetic compatibility and maintenance
[AD-721611] 16 p2568 N71-28343
- Fatigue crack repair in notched steel sheets by various methods
[NLR-TR-70029-U] 17 p2766 N71-30248
- System maintenance program evaluation conducted in central region of US
19 p3072 N71-31623
- Performance test and evaluation of hand tools used in support of military aircraft maintenance
[AD-726993] 22 p3589 N71-35558
- Mathematical model for initial provisioning of standby system with deteriorating and repairable spares
[TR-71-31] 22 p3607 N71-35693
- Space shuttle operations, maintenance, and integration of ground support system, logistics, checkout, and recovery
22 p3674 N71-36193
- Minimization of space shuttle maintenance costs through application of commercial airline maintenance concepts
22 p3674 N71-36195
- Development, maintenance, and future capabilities of NASTRAN - NASA Structural Analysis computer program
22 p3682 N71-36234
- Basic engineering technology for Automatic Inspection Diagnostic And Prognostic Systems (AIDAPS) for Army aircraft
[AD-726951] 23 p3708 N71-36432
- Maintenance of beta gamma ion chamber exposure dosimeters
[CEA-N-1435] 23 p3811 N71-37174
- Technical aviation handbook covering aircraft maintenance, navigation aids, airframes, lubricants, piston and gas turbine engines, and checkout procedures
[AD-727195] 24 p3874 N71-37613
- Performance tests and maintenance techniques for military theodolites
[AD-727638] 24 p3925 N71-38086
- Laboratory tests of polymeric latex modified fast fix C-1 cement for repair of damaged runway pavement
[AD-727728] 24 p3943 N71-38132
- MAINTENANCE**
Potential malfunction analysis for conceptual lithium-cooled space power fast spectrum reactor
[NASA-TM-X-2857] 03 p0413 N71-12568
- High gain antenna acquisition problem during Apollo 13 flight
[NASA-TM-X-446903] 09 p1346 N71-19407
- Electron microscope, electron diffraction, and electron microprobe analysis of defective solid state weldment on liquid hydrogen tank from Apollo 12 fuel cell system
[NASA-TN-D-6327] 18 p2987 N71-31354
- Estimates of lightning caused computer component damage and malfunctions
[AD-722675] 18 p2997 N71-31413
- Malfunctions and failures in first-day performance of 57 unmanned spacecraft
[NASA-TN-D-6474] 21 p3525 N71-35116
- MAMMALS**
NT BATS
NT CATS
NT DOGS
NT DOLPHINS
NT GUINEA PIGS
NT HUMAN BEINGS
NT MICE
NT MONKEYS
NT POCKET MICE
NT PORPOISES
NT PRIMATES
NT RABBITS
NT RATS
NT RODENTS
NT SWINE
Effects of ultraviolet radiation and X rays on mammalian cells
[UCSF-10-P-2-114] 05 p0634 N71-14468
- Biological systems analysis and biodynamic modelling of physiological and biological interrelationships in human body and mammals
[NASA-CR-1720] 09 p1330 N71-19766

- Dynamic model for microvascular system control of mammal body kinematics 09 p1331 N71-19882
- Biological models for mammalian cardiovascular systems 09 p1331 N71-19884
- Biochemical molecular model for metabolic energy transition from mammalian organs to central nervous system 09 p1331 N71-19885
- Plane section method used to study hydrodynamics of thin flexible bodied fish and mammals 11 p1835 N71-22202
- Volterra equation for describing tracer dynamics of mammalian circulation 16 p2548 N71-28855
- Low temperature cytophysiological adaptation of human and mammalian cells 20 p3220 N71-33455
- MAN**
- U HUMAN BEINGS**
- MAN MACHINE SYSTEMS**
- Spacecraft crew function classification and methods for communicating with onboard computers [NASA-CR-102903] 01 p0028 N71-10526
- PDP-1 computer graphics, man machine interfaces, and complex organic molecule synthesis [AD-711392] 01 p0028 N71-10752
- Use of computers for man machine modeling studies and plans [AD-711638] 01 p0015 N71-10800
- Development and applications of cybernetics theory in transportation, industry, and economics in USSR [JPRS-51457] 01 p0037 N71-10958
- Task analysis reduction technique for analyzing human performance and man machine interface [AD-711807] 02 p0169 N71-11198
- Adaptation techniques for human tasks and man machine systems [AD-711985] 02 p0170 N71-11205
- Design and construction of flexible and efficient interactive programming systems [AD-712721] 03 p0341 N71-12475
- Man machine system for finite element structural analysis with computer graphics 03 p0465 N71-13140
- Man machine interaction at remote console of time shared computer [AD-712695] 04 p0501 N71-13506
- RAND video graphic system - approach to general user/computer graphic communication system 04 p0506 N71-13844
- Data processing, man machine systems, and solid state physics and devices [AD-712699] 04 p0622 N71-13964
- Investigating application of advances in man machine interaction to problems of post-1971 SPOF system 05 p0647 N71-14963
- Discussing development of engineering psychology as independent science 05 p0636 N71-14992
- Man machine systems and astronaut and onboard computer communications [NASA-CR-102903] 05 p0651 N71-14999
- Human factors in aircraft simulation [AGARD-CP-79-70] 06 p0830 N71-16060
- Engineering analysis on flight mechanics for simulating pilot behavior in aircraft 06 p0832 N71-16068
- Human performance, recovery, and man machine systems [AD-714375] 06 p0806 N71-16299
- Man-computer interaction and context programming for problem solving and management planning [AD-714322] 06 p0806 N71-16351
- NASA program for evaluating underwater vehicle crew performance as space station operational analog [NASA-TN-64548] 06 p0850 N71-16379
- Effects of input power spectra on human operator compensatory tracking [AD-714130] 06 p0808 N71-16624
- Variation of data structure - CAMA [AD-714033] 06 p0822 N71-16633
- Functional requirements for ground-based trainers, helicopter response characteristics [AD-714954] 07 p1084 N71-18018
- Human cognition, involving man machine interaction situations [AD-716459] 09 p1339 N71-19605
- Man-machine interactive information system functions and effectiveness of free-form query with combinatorial search algorithm and various techniques for online browsing [AD-716954] 10 p1510 N71-21229
- Design and characteristics of system for speech recognition based on total phonemic pattern to recognize entry in lexicon [AD-717624] 11 p1696 N71-21910
- Two way information exchange in experimental data processing system 11 p1719 N71-22736
- Bionics of living and life-like systems with application to man machine technology [AGARD-CP-44] 11 p1692 N71-23053
- Feasibility and limitations of fixed speaker independent automatic speech recognition system [AD-718255] 12 p1867 N71-23616
- Vocabulary for spacecrew communication with spaceborne computers with graphic display devices [NASA-CR-103171] 14 p2321 N71-25922
- Man machine system using computer for decision making in information retrieval 14 p2322 N71-25983
- Stochastic model for computerized simulation of closed man machine system operated by crew [AD-720354] 14 p2310 N71-26076
- Computer designing and programming, and man machine systems - conferences 14 p2323 N71-26186
- Task commonality analysis of training equipment and devices to maximize positive transfer of training [AD-709534] 15 p2373 N71-26801
- Selected and annotated bibliography of human performance prediction in man machine systems - Vol. 3 [NASA-CR-73428] 15 p2374 N71-27251
- Computer facilities capable of providing substantive aid to human decision maker concerned with complex structured problems [AD-721618] 16 p2565 N71-28277
- Algorithms and FORTRAN calling program permitting efficient convergence and high degree of man machine interactions in steady state process systems analysis 16 p2566 N71-28791
- Automatic machine learning and control of manipulators and adaptive control based on pattern recognition and decision making 16 p2576 N71-28825
- Man-computer interaction information system to simulate various problem solving environments and provide users on-line feedback of their relative effectiveness [AD-723336] 17 p2712 N71-30218
- Trends and possibilities in biochemical and biotechnical in medical science - heart transplantation [AD-723623] 18 p2875 N71-30840
- Design and operation of complex man machine systems and heuristic solution to automatic control problems in production engineering and biomedical situations [JPRS-53414] 18 p2882 N71-30867
- Design and evaluation of information display systems and development of operator work station stages 18 p2882 N71-30868
- Automatic monitoring of human operator state in closed, man machine systems with biomedical application 18 p2883 N71-30869
- Human factors engineering in man machine system design 18 p2883 N71-30870
- Heuristic problems in design and operation of large scale man machine systems 18 p2883 N71-30871
- Heuristic decision making programs for man machine systems 18 p2883 N71-30872
- Man machine interface problems in graphic display including applications in various fields [NASA-TT-F-13816] 18 p2894 N71-31081
- Structure of external communication facilities of highly interactive man machine decision system [AD-722837] 18 p2895 N71-31290
- Development of man machine subsystem for military management information system and evaluation of display capability integrated into large scale computer [AD-722803] 18 p2877 N71-31335
- Optimal control theory and systems analysis of man machine systems and operator performance prediction model for compensatory tracking tasks [NASA-CR-17531] 18 p2900 N71-31373
- Theoretical pilot-aircraft interaction with pilot relying on gravity vector for orientation [AMRU-R-65-4] 18 p2880 N71-31532
- Information system as useful tool for furthering chemical research and selective dissemination of results to various branches of chemistry 19 p3194 N71-31980
- Cybernetics including models for statistical decision making, biomechanical systems, and complex stochastic system [JPRS-53531] 19 p3044 N71-32082
- Dynamic reactions of operators with random vibrational stimuli and biomechanical systems 19 p3044 N71-32090
- Human performance and recovery in man machine systems of continuous operations and work/rest schedules [AD-723430] 19 p3048 N71-32331
- Mechanics of free piston engine, aspects of human factors engineering, and compressible boundary layer studies at high Reynolds numbers [DME/NAE-1971/1] 19 p3198 N71-32620
- Human factors engineering for man machine systems 19 p3048 N71-32622
- Pattern recognition, speech recognition, man-machine systems for computer graphics, information systems, and data communications [NPL-COM-SCI-48] 20 p3238 N71-33213
- Effects of forced temporal lockout intervals on man performance in interactive man-computer problem solving situation [NASA-CR-121480] 20 p3239 N71-33498
- Human thinking activity applied to man machine systems [JPRS-53983] 22 p3544 N71-35245
- Development and characteristics of prototype computer system capable of mixed-initiative man-computer dialogue [AD-726441] 22 p3557 N71-35338
- Effects of display gain and signal bandwidth on visual sources of human controller remnant [AD-727057] 23 p3717 N71-36500
- Computer learning algorithm to improve parameter search efficiency in system modeling with man-machine interaction 23 p3718 N71-36505
- Computer graphic techniques, computer systems and management, and digital waveform processing for graphical man/machine communications [AD-726623] 23 p3730 N71-36587
- Computer-augmented intellect using interactive man/computer tools and techniques for qualitative planning 23 p3730 N71-36591
- Computerized simulation of man machine systems [JPRS-54171] 24 p3881 N71-37664
- Engineering psychology as component part of systems engineering 24 p3881 N71-37665
- Algorithmic simulation of ergatic systems for designing operator-control systems 24 p3881 N71-37666
- Procedure for analysis of data representation systems for man-operator controlling complex automated object 24 p3881 N71-37667
- Standardized method for compact and systematized representation of sets of functionally related parameters by matrices 24 p3881 N71-37668
- Application of linear gas discharge displays on control panels to data representation systems 24 p3882 N71-37670
- Man machine techniques for processing data from sonar display systems [AD-727609] 24 p3883 N71-37677
- Man machine systems for detection, recognition, transmission and perception of information on engineering problems [AD-727610] 24 p3883 N71-37678
- Development and characteristics of man machine systems for detection, recognition, transmission, and perception of information - Vol. 3 [AD-727611] 24 p3883 N71-37679
- Human factors engineering problems in man machine interfaces in space shuttle systems [NASA-CR-123166] 24 p4020 N71-38685
- MANAGEMENT**
- NT CONFIGURATION MANAGEMENT
- NT CONTRACT MANAGEMENT
- NT DATA MANAGEMENT
- NT ENGINEERING MANAGEMENT
- NT FINANCIAL MANAGEMENT
- NT INDUSTRIAL MANAGEMENT
- NT INFORMATION MANAGEMENT
- NT INVENTORY MANAGEMENT
- NT LOGISTICS MANAGEMENT
- NT PERSONNEL MANAGEMENT
- NT PRODUCTION MANAGEMENT
- NT PROJECT MANAGEMENT
- NT RESEARCH MANAGEMENT
- NT SAFETY MANAGEMENT
- NT SYSTEMS MANAGEMENT
- NT WATER MANAGEMENT
- NT WEAPON SYSTEM MANAGEMENT
- Survey of management abstracts including subject categories in contract, personnel, program, and project management, research and development, tool, techniques, and philosophy of management [NASA-SP-700037] 18 p3029 N71-30889
- MANAGEMENT ANALYSIS**
- Analysis of organizational problem in scientific research [AD-715752] 08 p1307 N71-18709
- Organizational structure effects on supervisory style and industrial work group attitudes [PB-196467] 10 p1666 N71-21696
- Psychophysiological analysis of management, control type of work processes based on concepts of cybernetics [JPRS-52752] 11 p1679 N71-21899
- Characteristics of computerized management analysis and planning system for planning and scheduling engineering project work [NASA-TN-D-6189] 13 p2049 N71-24716

SUBJECT INDEX

Philosophical discourse on comparative administration [NASA-CR-119376] 18 p3031 N71-31548

Use of computer system accounting data to measure effects of system modification [P-4536-1] 20 p3238 N71-33132

Cost sensitivity analysis technique applied to developing annual operating costs for ground sensor system [P-4361] 21 p3408 N71-34248

MANAGEMENT INFORMATION SYSTEMS

Proceedings of 9th annual US Army operations research symposium [AD-711942] 04 p0622 N71-14196

Bibliography of management sciences literature [NASA-TM-X-66546] 05 p0787 N71-15199

Advanced software techniques for space shuttle data management system [NASA-CR-114802] 05 p0651 N71-15426

Prototype management decision system for planning and control [AD-715463] 08 p1306 N71-18264

Discriminant analysis model for rating research and development data programs [AD-716812] 10 p1665 N71-21043

Automated management systems for decision making and systems control [JPRS-52623] 10 p1665 N71-21086

Characteristics and information requirements of staple, fashion, and big ticket merchandise inventory management and management information systems for retail stores 11 p1847 N71-22038

Virtual memory management system with working set model suitable for microprogramming [NASA-CR-118310] 13 p2052 N71-24915

Conference on information retrieval and management information systems including construction of dictionaries, analysis of query formulations, and computer programming 14 p2221 N71-25976

Properties of information retrieval and management information systems including data structure, hierarchy generation, and searching 14 p2222 N71-25987

Compilation of dictionaries for information retrieval systems from vocabularies from different fields of science 14 p2223 N71-25990

Integration of text processing and written communication into management information system 14 p2223 N71-25991

Performance characteristics of US information retrieval and management information systems, noting heuristic methods and incentive techniques 14 p2223 N71-25996

Highway integrated computer system with subsystems for decision making, management, and technical services 14 p2223 N71-26554

Systems analysis of agricultural and water management information systems utilizing satellite borne multi-spectral band scanner, radar, and television equipment [NASA-CR-119010] 16 p2587 N71-28444

Programming computers to make decisions in management information systems [NASA-CR-119180] 17 p2863 N71-30368

Requirements for natural resources management information system and potential application of remote sensing technology to resource programs by Bureau of Indian Affairs [SD-70-351] 18 p2919 N71-31425

Management, standards, and maintenance of NAS-TRAN documentation reviewed with emphasis on specifications in style and format 22 p3686 N71-36283

Basic engineering technology for Automatic Inspection Diagnostic And Prognostic Systems [AIDAPS] for Army aircraft [AD-726551] 23 p3708 N71-36432

MANAGEMENT METHODS

Military and industrial management of independent research and development programs 07 p1133 N71-17632

Interviews and conversations with officials and engineers of model scientific production association for manufacture of electronic equipment [JPRS-82446] 08 p1309 N71-19321

Design, construction, operation, and management of military airports [AD-716083] 09 p1365 N71-19702

Organizational structure effects on supervisory style and industrial work group attitudes [PB-196467] 10 p1666 N71-21698

Systems engineering evolution and trends as systems management tool 11 p1846 N71-22027

Managerial common sense in decision making and systems management and planning 11 p1846 N71-22028

Procedure for Army-style system engineering including function analysis, performance requirements

MANAGEMENT PLANNING

and measurement, and system configuration for systems management planning 11 p1846 N71-22029

Hidden assumptions, education-selling interface, leadership models, business ethics, and systems validity as barriers to rationality in systems management and decision making 11 p1846 N71-22030

Influential management factors in systems approach success of Saturn systems engineering 11 p1846 N71-22031

Comparison of management techniques applied to life sustaining resources in Apollo command modules and in earth ecology 11 p1846 N71-22032

Utilization of system management techniques in interfacing hydraulic basin subsystems into master water resource system in California 11 p1847 N71-22034

Queen Mary project management and planning problems and Long Beach, California, city government problem solutions 11 p1847 N71-22036

Survey to determine social aspects of labor organization and management in scientific teams [NASA-TT-F-13552] 12 p2015 N71-23310

Information systems, transfer of technological information, and management of technology transfer 12 p2016 N71-23502

Constraining institutional factors and options for civil aviation research and development [NASA-CR-1807] 15 p2366 N71-27009

Engineering, finance, and personnel management methods and computer techniques for cost reduction and reliability in project planning [NASA-SP-5933/01] 18 p3031 N71-31516

MANAGEMENT PLANNING

NT PRODUCTION PLANNING

NT PROJECT PLANNING

Technological forecasting as management tool in research and development 01 p0135 N71-10030

Systems approach to accident investigation in civil aviation and homes 01 p0002 N71-10115

Design of interactive graph reduction and analysis system [AD-709927] 01 p0028 N71-10621

Science policy for United States of America 01 p0000 N71-10817

Organization of national environmental laboratory with scientific and technological input 01 p0136 N71-10818

Recommended space programs for next decade 01 p0124 N71-10973

Calibration and preliminary analysis of passenger demand and modal split models for Northeast Corridor of United States [PB-190946] 02 p0144 N71-11021

Analytical procedures for system modeling and analysis of real time computer networks 02 p0187 N71-11316

Automatic data processing resource estimating procedure [AD-711117] 02 p0188 N71-11323

Computer aided manufacturing and numerical control impact on management disciplines 02 p0233 N71-11652

Program budgeting role in US government guiding and managing social, economic, and environmental systems [AD-711903] 02 p0307 N71-11892

Relationship of technology assessment to environmental management [PB-192554] 02 p0307 N71-11893

Planning and coordination of space environment simulation test programs for Azur and Dial satellites 03 p0358 N71-12724

Annotated bibliography of capital budgeting/project selection by mathematical programming [TM-173] 03 p0399 N71-12817

Proposed environmental laboratories handling urban and rural problems and staffed by natural and social scientists, engineers, and information specialists [PB-196991] 03 p0358 N71-13076

Alternatives to decision making goal of obtaining utility functions [AD-712762] 03 p0400 N71-13232

Principal investigator requirements for lunar module-borne cosmic ray detector experiment [NASA-CR-108715] 04 p0607 N71-14041

Define methods for long-range forecasting of economic processes and scientific and technological progress [JPRS-51841] 04 p0622 N71-14067

Apollo/Saturn 5 consolidated instrumentation plan for AS-501/Apollo 14 [NASA-TM-X-66507] 04 p0614 N71-14143

Analysis of planning, programming, and budgeting systems [AD-712455] 04 p0623 N71-14353

Development and implementation of R and D and program planning capability for Environmental Health Services [PB-194410] 04 p0480 N71-14476

Technological forecasting and advanced planning [BNWL-1466] 04 p0624 N71-14491

Equivalent algorithms for optimal planning and scheduling of project networks [DISS-43355] 05 p0713 N71-14570

National Academy of Science recommendations for future life sciences activities within NASA [NASA-CR-115873] 05 p0767 N71-14909

Conference on science and technology applications for public programs [PB-192328] 05 p0786 N71-15190

Man-computer interaction and context programming for problem solving and management planning [AD-714232] 06 p0806 N71-16351

Development model for Oklahoma airport [PB-194957] 07 p1002 N71-16987

Application of address coding guide ACO/DIME to transportation planning problems [PB-191468] 07 p1135 N71-18041

Effectiveness of research programs management for materials science [AD-714660] 07 p1135 N71-18070

Development planning manual for national transportation system [PB-194964] 07 p1135 N71-18072

Government planning in technological society 07 p1135 N71-18073

Market research and management planning for optimization of civilian airline operations in France [REPT-1970/7-E] 07 p1136 N71-18093

Cybernetic and economic international study group for civil aviation in France 07 p1136 N71-18094

Mathematical models for optimization of airline operations 07 p1136 N71-18095

Planning estimates in air traffic forecasting 07 p1136 N71-18096

Economics and cybernetics in civil aviation market research for air traffic predictions 07 p1136 N71-18097

Prototype management decision system for planning and control [AD-715463] 08 p1306 N71-18264

Freight transportation in Great Lakes Area for year 2000 08 p1308 N71-19320

Evaluating scientific and engineering requirements for research related to coastal wastes management [PB-195861] 09 p1330 N71-19653

Economic equipment and layout planning of warehouses using computerized simulation methods 10 p1665 N71-20770

Automated management systems for decision making and systems control [JPRS-52623] 10 p1665 N71-21086

Management summary of conceptual analysis on reusable space tug [NASA-CR-114957] 10 p1649 N71-21452

Management planning of cushioncraft rapid transit system [PB-196980] 10 p1494 N71-21639

Management, design, and tests of National Oceanographic Instrumentation Center 10 p1539 N71-21699

Procedure for Army-style system engineering including function analysis, performance requirements and measurement, and system configuration for systems management planning 11 p1846 N71-22029

Influential management factors in systems approach success of Saturn systems engineering 11 p1846 N71-22031

Technology revolution and educational system management planning 11 p1847 N71-22033

Utilization of system management techniques in interfacing hydraulic basin subsystems into master water resource system in California 11 p1847 N71-22034

Queen Mary project management and planning problems and Long Beach, California, city government problem solutions 11 p1847 N71-22036

Characteristics and information requirements of staple, fashion, and big ticket merchandise inventory management and management information systems for retail stores 11 p1847 N71-22038

Planning for expected civil aviation developments caused by change-over to Boeing 747 aircraft and supersonic transport 11 p1674 N71-22381

Planning for civil aviation operations including Boeing 747 aircraft and supersonic aircraft 11 p1675 N71-22382

Economics and operational planning for future civil air transportation 11 p1675 N71-22384

Planning for Boeing 747 aircraft integration into Israel airline operations

11 p1675 N71-22348

Support systems planning for expanded passenger and cargo traffic in civil aviation

11 p1676 N71-22390

Testimony in support of creation of National Oceanic and Atmospheric Administration

11 p1848 N71-22899

Optimal scheduling algorithm applied to problems of jobshop sequencing type with network flow analogy

12 p1949 N71-23376

Accelerometer round robin measurement comparisons

12 p1897 N71-23633

Program plans and cost estimates of project for application of bioscience technology to patient monitoring system

[NASA-CR-118035] 12 p1868 N71-23849

Scientific results from ESRO satellites and from sounding rocket campaign including aeronautical fields, management planning, satellite development, and telecommunication - 1969 report

13 p2188 N71-24447

Characteristics of computerized management analysis and planning system for planning and scheduling engineering project work

[NASA-TN-D-6189] 13 p2049 N71-24716

International management requirements for effective global science policy

13 p2190 N71-24757

GERT nomenclature for describing project plan or system operating policy

[NASA-CR-118490] 14 p2224 N71-26412

Formal system for interchange of information among state agencies

14 p2225 N71-26555

Status report of highway preconstruction projects in Kentucky

14 p2226 N71-26559

Perspective highway viewing program for designing safe roads

14 p2226 N71-26561

Predicted civilian air travel increase and airport use in United States of America for 1980

[AD-720732] 15 p2367 N71-27155

Reusable nuclear shuttle program schedules and logic networks of tasks, sequencing, and interfaces

[NASA-CR-103147] 15 p2520 N71-27680

Proceedings of joint meeting of Government Operations Research and Procedures

[NBS-SP-347] 15 p2527 N71-27883

Cost/benefit model for decision making in planning German space program - bibliography

[BMW-FB-W-71-04-PT-3] 17 p2861 N71-29422

Analysis of value of current logistics research for reducing future uncertainties and risks and possible future consequences of present resource commitments

[AD-722420] 17 p2861 N71-29549

Energy sources in US to achieve future electric energy needs and environmental compatibility requirements

17 p2743 N71-29852

Management planning in Sweden for natural gas as industrial energy source

[IVA-MEDD-167] 18 p3028 N71-30522

Management planning, production planning, and standardization in industries and civil organizations

[IVA-23] 18 p3029 N71-31177

Program evaluation techniques for management planning including operations research, market research, systems analysis, decision making, and resource allocation in R and D

[PAU-M-12] 18 p3030 N71-31388

Research and development program evaluation techniques including cost analysis, technology forecasting, market research, and decision making for project management planning

[NASA-TN-D-64537] 18 p3030 N71-31389

Mathematical model for investment planning in R and D emphasizing options and interacting benefits for resource allocation decision making

18 p3030 N71-31391

Systems analysis of marine technology including mathematical models, market research, economic and cost analyses, and forecasting for management planning

18 p3030 N71-31392

Procurement policies and management planning for acquisition of NASA facility

18 p3031 N71-31520

Investigation of air charter operations utilizing large airplanes to fulfill demands of aircraft capacity and speed, cargo type and size, as well as frequency of operation

[PB-197636] 19 p3193 N71-31624

Environmental engineering and management for natural environment - regional plan for water, sewage, air, and refuse comparing automatic vehicle monitoring system dispatching police vehicles to conventional system

[PB-190290] 19 p3083 N71-31627

Maintenance, management planning, and requirements for single seat attack/fighter aircraft

[AD-72327] 19 p3036 N71-31805

Establishment of BOMAP advisory panel, and planned BOMEX activities

19 p3200 N71-32754

Concept formulation and operational aspects of integrated logistic support for military applications

[P-4318] 21 p3534 N71-35188

Analysis of role of research and development in furthering national welfare and allocation of scientific resources

[NSF-71-18] 21 p3534 N71-35189

Assessing research and development in hypersonic aircraft for determining requirements for hypersonic research facilities

[NASA-CR-114322] 22 p3564 N71-35384

Development of analysis techniques for determining causes for airport congestion and interaction of various causes

[FAA-RD-71-55] 22 p3565 N71-35393

Development of centralized system for control of nuclear reactor fuels to insure safe operation, accountability, and reduction of nuclear incident hazards

[ORNL-4607] 22 p3623 N71-35814

Use of computer simulation as aid in mission and management planning and decision making

22 p3675 N71-36200

Model of executive decision making emphasizing interaction of organization members

[NASA-CR-121886] 22 p3698 N71-36372

Colleague role of scientists utilizing executive decision making model

[NASA-CR-121885] 22 p3698 N71-36373

Logistics system modeled as transportation problem with linear cost structure and lower bounds on supply from each origin and to each destination

[AD-726509] 23 p3729 N71-36586

Computer-augmented intellect using interactive man/computer tools and techniques for qualitative planning

23 p3730 N71-36591

Planning short-haul intercity commercial air transportation with STOL aircraft

[WRCN-2] 24 p3873 N71-37605

Automatic data processing systems for air traffic control, health services, operations research, management planning, information systems, and reading machines

24 p3892 N71-37742

Computerized management information systems for accounting and control activities

24 p3894 N71-37749

Mathematical models of optimal development of applied scientific research

24 p3894 N71-37757

Research and development and management planning efforts for sodium technology program

[ANL-ST-8] 24 p3962 N71-38260

Quality control and applications of Saturn program experiences to future space programs

[NASA-TM-X-64574] 24 p4017 N71-38658

Planning and control of development of science and technology and methods of analyzing and forecasting research and development trends

[AD-727232] 24 p4034 N71-38784

Analytical procedure for computation of military essentiality index for use as decision making aid by program managers

[AD-727114] 24 p4034 N71-38786

Guidelines for national aviation system planning and R and D policy

[FAA-AV-71-2] 24 p4036 N71-38798

MANAGEMENT SYSTEMS

NT MANAGEMENT INFORMATION SYSTEMS

Management systems theory and conflict resolution

[AD-716018] 09 p1487 N71-19697

Joint assessment and management evaluation system

[NASA-TM-X-64537] 23 p3869 N71-37580

MANDELSTAM REPRESENTATION

Inequalities on double partial wave amplitudes from positivity, analyticity, and crossing symmetry

04 p0540 N71-14365

Single particle exchange as approximate force term and threshold zeros in resonance approximation and application to Yukawa potential scattering

12 p1974 N71-23995

General properties and formula for multipole free dual amplitudes with Mandelstam analyticity

[LPTHE-71726] 20 p3293 N71-33903

Piecewise analytic scattering amplitude in indefinite metric quantum field theory

[ORO-3992-52] 24 p3978 N71-38384

MANDRELS

Rotating, multisided mandrel for fabricating gored inflatable spacecraft

[NASA-CASE-XLA-04143] 07 p1036 N71-17687

Method of making solid propellant rocket motor having reliable high altitude capabilities, long shelf life, and capable of firing with nozzle closure with foamed plastic permanent mandrel

[NASA-CASE-XLA-04126] 14 p2333 N71-26779

MANEUVERABILITY

Hand-held maneuvering unit for propulsion and attitude control of astronauts in zero or reduced gravity environment

[NASA-CASE-XMS-05304] 03 p0327 N71-12336

Maneuverability and controllability of dolphins compared to performance characteristics of manmade underwater vehicles

11 p1681 N71-22209

Evaluation of in-flight simulation of flying platform using helicopter with variable stability and maneuverability

19 p3074 N71-31957

Tu-134 aerodynamic characteristics during takeoff, climb, horizontal flight, landing stability and maneuverability, and strength under various loads

[AD-727196] 24 p3874 N71-37612

MANEUVERABLE REENTRY BODIES

Utilization of maneuverable lifting reentry bodies [BMW-FB-W-70-49] 08 p1293 N71-18641

MANEUVERABLE SATELLITES

U SATELLITES

MANEUVERABLE SPACECRAFT

NT AEROSPACEPLANES

NT APOLLO SPACECRAFT

NT H-10 REENTRY VEHICLE

NT LIFTING REENTRY VEHICLES

NT M-2 LIFTING BODY

MANEUVERS

NT ORBITAL RENDEZVOUS

NT SPACECRAFT DOCKING

NT SPACECRAFT MANEUVERS

Effect of acceleration on space required to perform maneuvers with urban transportation tracked vehicle

14 p2358 N71-26119

MANGANESE

NT MANGANESE ISOTOPES

Development of methods for extracting metals from manganese nodules dredged from ocean floor [BM-R1-7473] 05 p0673 N71-14901

Impurities effect on manganese diffusion rate in ternary nickel-manganese alloys

08 p2128 N71-19080

Electron paramagnetic resonance of divalent manganese in zinc perchlorate and divalent nickel in zinc fluosulfate with parallel and perpendicular configuration

09 p1430 N71-19867

Chemical and magnetic properties of single alpha manganese crystal structure

11 p1814 N71-21861

Determination of trace manganese and zinc in butter using neutron activation analysis

[IRI-133-70-03] 20 p3228 N71-32940

Manganese reaction rates in axially uniformly fueled reactors

[RD/BNL-1518] 20 p3301 N71-33199

Function of manganese in oxygen evolution during photosynthesis

[RIAS-3706-16] 21 p3388 N71-34102

MANGANESE ALLOYS

NT MANGANIN (TRADEMARK)

Abrasive wear resistance of manganese cast iron isocutted with cerium and studied with KHA-8 machine

[AD-711156] 01 p0668 N71-10631

Temperature effects on iron diffusion in iron manganese alloys

[TT-7057041] 03 p0391 N71-12879

Steady state diffusion in copper rich Cu-Zn-Mn system

[COO-1436-26] 05 p0705 N71-15441

Magnetic properties of amorphous and crystalline Mn-P-C alloys

[CALT-822-15] 06 p0673 N71-16348

Wear resistance of austenitic manganese cast iron during sliding friction without lubricant

[AD-714789] 07 p1044 N71-17761

Neutron diffraction analyses on magnetic structure of chromium alloys

[AD-714875] 07 p1069 N71-18037

Low temperature magnetization of dilute copper manganese alloys

[UCSD-34-P-143-33] 08 p2126 N71-18942

Synthesis and structure of MnPC alloy and interference, atomic distribution, and radial distribution functions for structural model

[CALT-822-21] 10 p1580 N71-21394

Steady state diffusion in copper-manganese-zinc alloys and feasibility of calculating atomic mobilities

13 p2094 N71-24011

Temperature and manganese effects on self diffusion coefficients of iron in gamma-phase iron manganese alloys

[TT-70-57056] 14 p2268 N71-25648

Phase microanalyses on quenched hardened iron manganese alloy structures

[NLL-RTS-63211] 17 p1767 N71-30331

Determination of activation energy of superheated solid solution of manganese in aluminum by phase analyzing

[SC-RR-70-356] 19 p3116 N71-32444

SUBJECT INDEX

NMR for determining distribution of hyperfine fields at cobalt nuclei in dilute alloys of Co-V, Co-Cr, and Co-Mn
[COO-1569-71] 20 p3319 N71-33669
Possibility of Mabi thin films for spaceborne optical memory applications
[NASA-CR-119697] 21 p3463 N71-34647
Critical points, crack formation, and shrinkage characteristics for castings of Cr-Ni, Cr-Mn, and Mn steels
[NLL-TRANS-746-293-19022.4011] 22 p3597 N71-35611

MANGANESE COMPOUNDS

NT MANGANESE OXIDES
Investigating structure of manganese(I) and rhodium(I) carbonyl halides by infrared and mass spectroscopy, precipitation reactions, and conductivity measurements
01 p0019 N71-10766

Weld heat affected zone notch impact properties of semikilled C-Mn steel and fully killed Al grain refined C-Mn steel
[MAT-1] 02 p0240 N71-11429

Nuclear magnetic resonance hyperfine fields in intermetallic compounds with manganese
[IS-T-369] 02 p0275 N71-11915

Lattice parameters and compressibilities of high pressure phases of lead chlorosulfide, manganese antimony, manganese tellurium, chromium antimony, and chromium tellurium compounds
14 p2327 N71-26495

Theoretical and experimental investigation of electromagnetic wave propagation in antiferromagnetic MnF₂
18 p2963 N71-31068

Corrosion of polished carbon steels at inclusions noting effect of manganese sulfide
19 p3112 N71-31917

Neutron diffraction study of magnetic structure of manganese-substituted zinc ferrites
[DNR-1269] 19 p3169 N71-32220

Thermodynamic and solid state properties of manganese selenide-cadmium selenide system determined from high purity single crystals
21 p3500 N71-34937

Analysis of magnetic properties of MnAs using neutron diffraction and effects of high compressibility on magnetic behavior
23 p3777 N71-36915

MANGANESE ISOTOPES

Two-neutron transfer reactions Fe-54(α ,n)Mn-52 and V-51(d , α)Ti-49 produced by 28 MeV deuterons
[LYCEN-7087] 23 p3806 N71-37137

MANGANESE OXIDES

Manganese dioxide vs. calcium carbonate processes for decontamination of radioactive wastes
[CEA-R-3821] 09 p1420 N71-20145

Inhibitor effects of psittin, MnO₂, and DZO on substances existing in nature to determine performance of terrestrial organisms in extreme and unusual gaseous and liquid environments
[NASA-CR-118883] 15 p2372 N71-27743

MANGANESE 53

U MANGANESE ISOTOPES

MANGANESE 54

U MANGANESE ISOTOPES

MANGANESE 56

U MANGANESE ISOTOPES

MANGANIN [TRADEMARK]

Model 50-600-75 Manganin pulse power supply transmitting power to piezoresistive gauges and receiving signals which result from these gauges
[SCL-DR-70-130] 10 p1534 N71-21224

Metallurgical scatter characteristics of Manganin resistance gauges in high pressure measurements
14 p2257 N71-26483

MANIFOLDS

Hardware and fluid parameter effects on filling characteristics of manifolds in vacuum, for liquid propelled rocket engines
[AD-712063] 02 p0291 N71-12159

Automobile exhaust manifold thermal reactor systems comparison in control of hydrocarbon and carbon monoxide emissions
[NASA-TM-X-2230] 09 p1488 N71-19946

Booyant jet mixing flow from manifolds in stagnant receiving water of uniform density using hydraulic models of waste disposal system
[PB-190405] 19 p3080 N71-32462

MANIFOLDS [MATHEMATICS]

Proofs for Browder and Novikov theorem and Seibermann theorem, with data on cap-product, Poincaré duality, manifold index, homology surgery, and arbitrary neighborhood existence
13 p2104 N71-25560

MANIPULATION

U MANIPULATORS

MANIPULATORS

Cloud circuit television arc guidance adapter kit for computerized welding skate
[NASA-CR-102896] 01 p0061 N71-10974

Supervisory controlled manipulation system for complex manipulation tasks on unmanned space vehicles using AND TREE computer data structure
[NASA-CR-115812] 04 p0501 N71-13507

Constructing protective manipulators for automatic transfer of isotopes from reactor cores
[CEA-N-1265] 04 p0574 N71-13674

Remote control device for positioning isotope separator collector electrodes and controlling ion beam shape and intensity
[CEA-N-1323] 06 p1199 N71-18378

Measuring effect of transmission time delay on performance of manipulation tasks with six degrees of freedom master-slave manipulator
[NASA-CR-116894] 08 p1208 N71-19134

Automatic machine learning and control of manipulators and adaptive control based on pattern recognition and decision making
16 p2576 N71-28825

MANNED ORBITAL LABORATORIES

NT MANNED ORBITAL RESEARCH LABORATORIES

Artificial gravity system for simulating self-locomotion capability of astronauts in rotating environments
[NASA-CASE-XLA-03127] 01 p0039 N71-10776

Expandable space frames for three dimensional or planar building structures
[NASA-CASE-ERC-10365] 16 p2883 N71-28948

MANNED ORBITAL RESEARCH LABORATORIES

Orbiting Lunar Station feasibility and definition - Operational, experiment, and science support requirements
[NASA-CR-115015] 14 p2342 N71-25832

Orbiting Lunar Station feasibility and definition - Functional analysis
[NASA-CR-115016] 14 p2342 N71-25833

Orbiting Lunar Station feasibility and definition - Performance commitments
[NASA-CR-115017] 14 p2342 N71-25834

Orbiting Lunar Station feasibility and definition - Configuration and systems analysis
[NASA-CR-115018] 14 p2342 N71-25835

Orbiting Lunar Station feasibility and definition - Configuration definition
[NASA-CR-115019] 14 p2342 N71-25836

Human potential in space experimentation and operation of orbiting research laboratory
16 p2551 N71-28530

MANNED ORBITAL SPACE STATIONS

U ORBITAL SPACE STATIONS

MANNED ORBITAL TELESCOPES

NT APOLLO TELESCOPE MOUNT

MANNED SPACE FLIGHTS

NT APOLLO FLIGHTS

NT APOLLO 7 FLIGHT

NT APOLLO 8 FLIGHT

NT APOLLO 9 FLIGHT

NT APOLLO 10 FLIGHT

NT APOLLO 11 FLIGHT

NT APOLLO 12 FLIGHT

NT APOLLO 13 FLIGHT

NT APOLLO 14 FLIGHT

NT APOLLO 15 FLIGHT

NT APOLLO 16 FLIGHT

NT GEMINI FLIGHTS

NT GEMINI 5 FLIGHT

NT GEMINI 7 FLIGHT

Oral hygiene requirements for extended manned spacecraft flights
[NASA-CR-108695] 02 p0167 N71-11186

Waste control aspect of housekeeping for future manned orbital missions
[NASA-CR-108763] 04 p0614 N71-14115

Astronauts and manned space flight
04 p0615 N71-14297

Guidance and control considerations for advanced manned space missions
[NASA-TM-X-58053] 04 p0544 N71-14303

Weightlessness effects on man during space flight
06 p0803 N71-16521

Trajectory profiles and nuclear propulsion vehicle configurations for manned Mars and Mars-Venus missions
[NASA-TN-D-6176] 07 p1109 N71-17496

Handbook on environmental and space utilization criteria for design of extraterrestrial manned spacecraft and shelters
[NASA-CR-114846] 07 p1119 N71-17560

Planar motion of human being subjected to action of body-fixed force
[NASA-CR-116799] 06 p1157 N71-18399

Launch window characteristics for manned interplanetary stopover flights to Mars and Venus
[NASA-TN-D-6226] 08 p1293 N71-18648

Design and performance of fecal waste management system for long duration manned space flight simulation
10 p1507 N71-20969

Human waste disposal system performance during long duration space flight simulation
10 p1507 N71-20970

Scientific experiments, instrumentation requirements, and operational aspects of manned mission to planet Mars
[NASA-TM-X-2127] 10 p1645 N71-21435

MANNED SPACE FLIGHT

Recommendations for future NASA manned and unmanned programs
[RIB-A-59] 10 p1666 N71-21581

Three-port transfer valve with one port open continuously suitable for manned space flight
[NASA-CASE-XAC-01158] 11 p1773 N71-23051

Space biology and medicine including selection and training of cosmonauts, flight safety, and health during long space flights
[JPRS-32529] 12 p1862 N71-23241

Achievements of US manned space flights for past decade with findings concerning lunar rock samples
[NASA-TM-X-67130] 12 p1997 N71-24113

Instabilities and turbulence in highly ionized plasmas in magnetic field related to problems of thrusters for manned space flight and plasma generated energy
[NASA-CR-116311] 13 p2147 N71-25028

Technology assessment of US and USSR space programs including comparisons of resource allocation, manned space flight, and Applications Technology Satellites
[REPT-71-25-SP] 14 p2360 N71-26193

Advanced application of computers for biomedical research in manned space flight
[NASA-SP-3078] 15 p2375 N71-27719

Biotechnological problems of man machine systems required for long duration space flights
[NASA-SP-305] 16 p2551 N71-28526

Bioastronautical aspects of Gemini flight for future manned space flight technology
16 p2551 N71-28527

Psychophysiological factors of manned space flight
16 p2551 N71-28528

Manned space flight biotechnology for spacecraft design
16 p2551 N71-28529

Bioengineering tradeoff study for cabin atmosphere selection in manned space flight
16 p2552 N71-28531

Humidity control, carbon dioxide removal, and oxygen regeneration in cabin atmosphere during prolonged manned space flight
16 p2552 N71-28532

Long term manned space flight nutrition and food requirements
16 p2552 N71-28533

Evaporation and filtration systems for water management in manned space vehicles
16 p2552 N71-28534

Biomedical test data for predicting weightlessness effects on man during long term space flights
16 p2553 N71-28542

Human visual perception in space flight
16 p2553 N71-28545

Environmental adaptation and operational performances of humans in space missions
16 p2554 N71-28547

Prototype device for monitoring sleep during manned space flight including performance tests
[NASA-CR-115071] 17 p2711 N71-30126

Development of cryogenic storage systems for manned space flight
[NASA-SP-247] 18 p2963 N71-30910

Conference on aerospace environments, manned space flight, weightlessness simulation, musculoskeletal and cardiovascular systems, bone loss, mineral metabolism, and hematology
[NASA-SP-269] 20 p3216 N71-33251

Physiological changes in cardiovascular and musculoskeletal systems during manned space flight
20 p3216 N71-33252

Red cell mass and plasma volume changes noted in hypodynamic states of bed rest and water immersion compared to changes observed during earth orbital missions
20 p3216 N71-33253

Measurement of bone density loss during manned space flight
20 p3216 N71-33254

Atrophy in monkeys due to immobilization and implications for extended manned space flight
20 p3217 N71-33260

Research and development, weightlessness simulation, calcium metabolism, manned space flight, pressure suits, immobilization, and aerospace medicine
20 p3219 N71-33275

Medical and biological problems of prolonged manned space flight
[JPRS-53801] 20 p3220 N71-33451

History of manned space flight technology
20 p3350 N71-33849

Hardware and techniques for studying human circulatory performance in space environment
[NASA-CR-121666] 21 p3380 N71-34052

Physical and physiological aspects of visual optics in space flight
[NASA-CR-115120] 21 p3382 N71-34060

Higher order programming language and compiler for advanced computer software system to be used with manned space flights between 1972 and 1980
[NASA-CR-115126] 21 p3390 N71-34184

Description and implementation of HAL programming language for use with future manned space flights
[NASA-CR-115127] 21 p3398 N71-34185

MANNED SPACE FLIGHT NETWORK

- Plans and schedules for NASA manned flight program 21 p3511 N71-35018
- Radiation hazards of space flights and biological effects on cosmonauts 24 p3879 N71-37649
- Design and components of closed-cycle life support system for extended manned space flights [AD-727944] 24 p3883 N71-37680
- Tribute to manned space flight pioneers, and benefits of space technology transfer 24 p4015 N71-38643
- Water reclamation from human and other wastes for prolonged space flights 24 p4015 N71-38645
- ### MANNED SPACE FLIGHT NETWORK
- Systems analysis of NASA Manned Space Flight Network [NASA-TM-X-66479] 02 p0182 N71-11283
- Deep Space Network support of Manned Space Flight Network for Apollo program [NASA-CR-116801] 08 p1287 N71-18476
- ### MANNED SPACECRAFT
- NT AEROSPACEPLANES
- NT APOLLO SPACECRAFT
- NT LUNAR MODULE
- NT MANNED ORBITAL LABORATORIES
- NT MANNED ORBITAL RESEARCH LABORATORIES
- NT MERCURY SPACECRAFT
- NT ORBITAL SPACE STATIONS
- NT ORBITAL WORKSHOPS
- NT SOYUZ SPACECRAFT
- NT SPACE SHUTTLES
- NT SPACE STATIONS
- NT VOSTOK SPACECRAFT
- Past and present manned spacecraft electronics and implications for space shuttle [NASA-TM-X-58054] 01 p0125 N71-10465
- Success probability of manned spacecraft emergency return from low earth orbit [AD-713066] 05 p0770 N71-14512
- Mass memory system for advanced spacecraft [NASA-CR-106672] 05 p0649 N71-14723
- Design and configuration of manned space capsule [NASA-CASE-XLA-01332] 05 p0773 N71-15664
- Astrodynamical characteristics of lunar trajectories for manned and unmanned spacecraft [AD-714426] 06 p0946 N71-16744
- Design of radio frequency communication systems for manned space station [NASA-CR-114816] 06 p0817 N71-16794
- Design requirements and development of acceptance checkout equipment for spacecraft [NASA-TM-X-66890] 08 p1294 N71-19243
- Guidelines for positive control of government furnished equipment for manned spacecraft [NASA-TM-X-66899] 08 p1294 N71-19244
- Data from 90-day manned test of regenerative life support system in space station simulator [NASA-SP-261] 10 p1504 N71-20951
- Integrated life support systems for long duration manned space flight simulations 10 p1505 N71-20952
- Life support system for improved space station simulator 10 p1505 N71-20955
- Development of method for producing artificial gravity in manned spacecraft [NASA-CASE-XNP-02595] 11 p1830 N71-21881
- Predictions and recommendations for development and deployment of manned space stations [NASA-TM-X-67072] 11 p1826 N71-22393
- System and component design and development for intermediate water recovery system for 3-man, earth orbital spacecraft on 1-year mission [NASA-CR-114960] 11 p1691 N71-22513
- Component specifications and computer program for intermediate water recovery system on manned spacecraft [NASA-CR-114961] 11 p1691 N71-22514
- Soviet communication and guidance control systems between manned spacecraft and ground stations [AD-719848] 13 p2047 N71-25116
- Fundamental techniques of weight estimating and forecasting for advanced manned spacecraft and space stations [NASA-TN-D-6349] 13 p2062 N71-25425
- Microbiological life support requirements in long term manned space flights 16 p2552 N71-28537
- Systems integration for optimal regenerative environmental and life support processes in manned spacecraft 16 p2552 N71-28538
- Chlorine generator for purifying water in life support systems of manned spacecraft [NASA-CASE-XLA-08913] 16 p2598 N71-28933
- Development of motion control algorithm for spacecraft under atmospheric entry conditions at hypersonic speed [AD-722305] 17 p2849 N71-29531
- Application of mass spectrometer for space station simulator atmosphere analyzer [NASA-CR-111827] 18 p2902 N71-30743

- Astrophysical studies of noctilucent clouds from orbiting manned spacecraft [JPRS-53508] 19 p3129 N71-32503
- Reliability data acquisition on spacecraft life support systems during ground and orbital experiments 24 p4015 N71-38646

MANOMETERS

- Design, operation, and errors in vacuum measurement of low absolute pressures [AD-713031] 03 p0381 N71-13183
- Piston manometer used as absolute standard for calibrating and intercomparing vacuum gauges in 10 to 500 micrometer range [NASA-TM-X-67889] 19 p3101 N71-32274
- Advantages of mounting manometers and mass spectrometers in artificial satellite nose cones and calculation of particle flux density passing through instrumentation orifice 19 p3103 N71-32605

MANPOWER

- #### NT SCIENTISTS
- Evaluating current and future requirements and resources for pilots and mechanics in US civil aviation 02 p0167 N71-11187
- Statistical summary of graduate student support and manpower resources for fall 1969 [NSF-70-40] 06 p0962 N71-16895
- Employment statistics on Federal scientific, technical, and health personnel for 1969 [NSF-70-44] 08 p1307 N71-18447
- Lunar base equipment, experiments, requirements, navigation, manpower, and tradeoffs [NASA-CR-103128] 14 p2236 N71-25859
- Employment problems from specialization in university research and industries through government funding 19 p3196 N71-32255
- Survey of scientific activities and employment in independent nonprofit institutions for 1970 [NSF-71-9] 19 p3199 N71-32692
- Conversion of US scientific and technical resources from defense and aerospace to civilian objectives [GUPS-MON-8] 20 p3371 N71-33825
- Determining faculty necessary for accredited engineering curriculum as function of faculty workload, number of students, and curriculum characteristics with cost estimates [NASA-CR-123114] 24 p4034 N71-38780

MANTLE [EARTH STRUCTURE]

U EARTH MANTLE

MANUAL CONTROL

NT VISUAL CONTROL

- Optical simulation study to determine manual instrumentation for pilot control of lunar flying vehicle [NASA-TN-D-5983] 03 p0327 N71-12334
- Multiple circuit switch apparatus requiring minimum hand and eye movement by operator [NASA-CASE-XAC-03777] 06 p0826 N71-15909
- Two hybrid computer identification techniques for use in manual control research [NASA-CR-116514] 07 p0986 N71-17442
- Manual control mechanism for adjusting control rod to null position [NASA-CASE-XLA-01808] 10 p1562 N71-20740
- Directional antenna control system conversion from manual to digital-automatic control [AD-716961] 10 p1551 N71-20795
- Conversion of manually operated antenna to digital autotracking antenna system using servomechanism 13 p2054 N71-24588
- Model for task interference with pilot performance in multivariable manual control systems [NASA-CR-1746] 14 p2210 N71-26160
- Piloted simulator investigation of lightweight vehicles for emergency lunar escape to orbit with kinesthetic attitude control and simplified manual guidance [NASA-TN-D-6299] 16 p2577 N71-28232
- Approach power compensator system for manual and automatic Navy carrier landing system [AD-722025] 16 p2628 N71-28241
- Mathematical models for control activity of human spaceflight operator 20 p3227 N71-33461
- Mathematical model representing human performance reliability for laboratory vigilance and manual control tasks 23 p3718 N71-36503

MANUALS

NT INSTALLATION MANUALS

- Manual on application of fuels and lubricating materials [AD-711756] 01 p0060 N71-10862
- Users manual for COBOL compiler validation system [AD-711369] 01 p0029 N71-10941
- Manual for implementing general purpose computer program [NBS-TN-550] 02 p0186 N71-11304
- JOVIAL Compiler Validation System - instruction manual [AD-711370] 02 p0188 N71-11324
- Manual of computer program for generating ephemerides of earth satellites [RAE-TN-69104] 02 p0296 N71-11960

SUBJECT INDEX

- Manned Space Center contamination control manual - Vol. 1 [NASA-TM-X-66541] 05 p0657 N71-14928
- Operation manual for Mark 2 model of laser absolute gravimeter [NASA-TM-X-64560] 05 p0696 N71-15028
- Pacific Northwest Laboratory manual of procedures for analysis of metallic sodium [BNWL-MA-76-REV-2] 06 p0111 N71-16623
- Description of manual on prevention of electrical breakdowns in spacecraft 06 p0828 N71-16640
- Finite element program for determining stiffness and mass matrices of shells of revolution - users manual [NASA-CR-114824] 06 p0956 N71-16752
- Manual of standard procedures for radioactivity investigations [NVO-4700] 07 p1074 N71-17418
- Manual for Mark 4 Error Propagation Program operation in CDC 6600 computer search of interplanetary trajectories [NASA-CR-111852] 07 p0997 N71-17465
- Users manual for IDX, 2DB, 3DB, PERT-3 code package for reactor data processing [BNWL-1412] 07 p1064 N71-17510
- Development planning manual for national transportation system [PB-194964] 07 p1135 N71-18072
- Computer code SISYPHUS for solving few-group neutron diffusion equations in two dimensions using finite difference method - users manual [KFKI-70-13-RPT] 08 p1236 N71-18237
- Utilization of Lamb-shift polarized ion source [LA-4451] 09 p1436 N71-20041
- Manual for IBM magnetic tape/selectric typewriter combination operators [AD-705259] 09 p1356 N71-20424
- Oriental manual for lunar module vehicle and mission requirements [NASA-CR-117321] 09 p1472 N71-20478
- Computer program enabling nonprogrammer to perform data, statistical, and numerical analyses [NBS-SPEC-PUB-1-339] 10 p1577 N71-20844
- Photogrammetric data preparation manual for analytical triangulation program, MUSAT 4 [AD-717106] 10 p1548 N71-20907
- Manual of electrostatic precipitators for particulate emission control [PB-196380] 10 p1568 N71-21811
- Manual of electrostatic precipitator installations in various application areas [PB-196381] 10 p1568 N71-21812
- Training manual for fabricating small printed circuit boards by personnel [ANL-7725] 11 p1728 N71-22546
- Documentation, update, editing, search, authority file creation program Setup instructions manual for Radiation Shielding Information Center [CTC-INF-1017] 12 p1881 N71-23440
- Evaluation procedures for oxygen and protective aviation masks [AD-719105] 13 p2035 N71-24411
- Tsunami wave reporting and data acquisition manual for tide observers [COM-71-00170] 14 p2251 N71-26541
- COPTRAN program and users manual update for space communication system performance testing [NASA-CR-119003] 16 p2560 N71-24162
- Manual for human psychometric data acquisition and human reactions to psychological stress in Teklite project [AD-721363] 16 p2554 N71-28540
- User's manual giving information on writing data for electric circuit wiring computer program LISS 2 [ELAB-IT-135] 18 p2893 N71-30630
- Manual for weather forecasters in tropical region [AD-723392] 19 p3126 N71-31715
- Users manual for 3 computer programs for predicting aerodynamic interference between lifting surfaces and lift and cruise fans in transport-type aircraft [NASA-CR-114332] 20 p3204 N71-33082
- Guidelines for design and implementation of emergency action plans for avoiding air pollution episodes [AP-76] 20 p3265 N71-33376
- Guidelines for design and implementation of emergency action plans to prevent air pollution episodes in medium sized urban areas [AP-77] 20 p3266 N71-33377
- Guidelines for design and implementation of emergency action plans for avoiding air pollution episodes in small urban areas [AP-78] 20 p3266 N71-33378
- Computer program for determining inviscid flow around blunt bodies at supersonic and hypersonic speeds - users manual [NASA-TM-X-2334] 20 p3252 N71-33678
- Users manual for DEANE computer program for use in ballistic missile defense analysis [AD-727045] 22 p3557 N71-35339
- Manual for interpreting radar echoes to identify severe thunderstorms, hail, and tornadoes [AD-726983] 22 p3615 N71-35761

SUBJECT INDEX

Standard methods for storage and retrieval of aerospace data 24 p3897 N71-37776

MANUFACTURING

NT LOW GRAVITY MANUFACTURING

Thin film cadmium sulfide solar cell fabrication parameter study (AD-710636) 01 p0006 N71-10436

Manufacturing technology and production engineering methods in aerospace industry 02 p0231 N71-11627

Manufacturing and advancement technology for turbine engine coatings 02 p0247 N71-11635

Manufacturing improvement program establishing applications and limitations in closed-die forging (AD-711544) 02 p0234 N71-11675

Development of space manufacturing techniques for orbital workshops (NASA-TM-X-64480) 02 p0234 N71-11701

Heat sources for manufacturing experiments in Apollo Applications Program 02 p0305 N71-11723

Industrial chemical manufacture in spacecrafts 02 p0177 N71-11731

Technology review on Soviet magnesium alloy production (JPRS-51761) 04 p0530 N71-14125

Fabrication and thermal performance of regeneratively cooled fluorine hydrogen thrust chamber (NASA-CR-72742) 04 p0605 N71-14135

Manufacturing process and construction methods for resistor laminates using chemical milling (FK-69111) 05 p0664 N71-14990

Fabrication of prototype Mark 2 fuel subassembly (BNWL-1418) 05 p0726 N71-15046

Development and performance analyses of oxide fuel elements (WARD-4135-8) 05 p0727 N71-15077

Manufacturing and welding austenitic steels for reactor structures 05 p0727 N71-15109

Cost-effective instrument technology (JPRS-51883) 05 p0687 N71-15470

Method for making screen with unlimited fineness of mesh and screen thickness (NASA-CASE-XLE-00953) 06 p0863 N71-15966

Bibliography on brazing techniques in industrial processing (AD-714000) 06 p0865 N71-16327

Development and fabrication of filament composite nondestructive test standards (NASA-CR-103011) 06 p0881 N71-16595

Manufacturing process for large diameter carbon fiber monofilaments by chemical vapor deposition (NASA-CR-72770) 07 p1034 N71-17328

Fabrication voids in aluminum base fuel dispensers applicable to high flux isotope reactor and advanced test reactor (ORNL-4611) 07 p1063 N71-17361

Describing apparatus for manufacturing operations in low and zero gravity environments of orbital space flight (NASA-CASE-MFS-20410) 08 p1209 N71-19214

Design and fabrication of planar and trapezoidal fiber glass wings with laminar profiles (AD-716526) 09 p1315 N71-19574

Effects of chemical catalysts, bed cooling, chemical manufacturing techniques, operating conditions, and chemical handling procedures on lithium peroxide (NASA-CR-114836) 09 p1343 N71-19914

Process technology required for production of zone melting feed rods of pure aluminum oxides for basic studies of laser degradation (AD-716421) 09 p1397 N71-19948

Cost effectiveness of closer tolerances in manufacturing (UCRL-72380) 09 p1393 N71-20109

Evaluating cost of four processes for production of oxygen difluoride-fluorine-caustic least expensive (NASA-CR-117317) 09 p1345 N71-20266

Manufacturing of improved carbon and graphite materials (NASA-CR-117315) 09 p1407 N71-20373

Standards for clean rooms in vacuum electronics manufacturing for precision instruments (JPRS-52328) 09 p1368 N71-20550

Fabrication and evaluation of dehydrated food bars produced by compression and molding processes (AD-717289) 11 p1686 N71-21900

Experimental design and operational problems of mono difluoride manufacturing in chemical reactions (DLR-PB-70-55) 11 p1696 N71-22292

Methods and procedures used in vacuum thermal stability tests for explosives 12 p1942 N71-23390

Process and apparatus for making diamond abrasives (NASA-TM-X-64543) 12 p1927 N71-23775

Cost distributions and facility and tooling cost impact on unit production costs for 2 and 20 per year production rates in state of art, improved, and advanced manufacturing technologies (NASA-CR-114281) 12 p1931 N71-24180

Economic analysis of facilities, tooling, premanufacturing and manufacturing operations, and quality control labor in aluminum aerospace industry base on Saturn/Apollo data (NASA-CR-114283) 12 p1931 N71-24181

Manufacturing factors and technologies in aluminum aerospace industry base on Saturn/Apollo data (NASA-CR-114283) 12 p1931 N71-24182

Manufacture of fluid containers from fused coated polyester sheets having resealable septum (NASA-CASE-NPO-10123) 13 p2086 N71-24835

Manufacturing tests of oriented titanium targets to obtain optimal procedure for their use and preparation under electron irradiation (EUR-4286-PT-2) 13 p2138 N71-25450

Optimal manufacturing processes for integrated circuits (JPRS-53078) 14 p2227 N71-25717

Manufacturing processes in space environment, including melting and solidification (NASA-TM-X-67178) 14 p2260 N71-26009

Manufacturing processes in space environment for Skylab orbital workshop 14 p2261 N71-26010

Space manufacturing processes based on potential and limitations of g-environment 14 p2261 N71-26012

Chemical and biochemical space manufacturing using scaling laws and Gibbs functions 14 p2261 N71-26013

Electromechanical devices to transfer, position, and retrieve space manufacturing equipment 14 p2261 N71-26014

Contributions and effects of commercial airline service on growth of manufacturing facilities in urban areas below 40,000 population 14 p2199 N71-26259

Method of making solid propellant rocket motor having reliable high altitude capabilities, long shelf life, and capable of firing with nozzle closure with formed plastic permanent mandrel (NASA-CASE-XLA-04126) 14 p2333 N71-26779

Major microelectronic production technologies including materials for manufacturing thin- and thick-film circuits, monolithic integrated circuits, and hybrid design (AD-712179) 15 p2385 N71-26897

Microeconomic analysis of in-process manufacturing quality control (AD-720098) 16 p2601 N71-28432

Shielded flat conductor cable fabricated by electroless and electrolytic plating (NASA-CASE-MFS-13687) 16 p2571 N71-28691

Production method for manufacturing porous tungsten bodies from tungsten powder particles (NASA-CASE-NKP-04339) 16 p2615 N71-29137

Hot isostatic compaction at 3000 F and 30,000 psi used for successfully preparing single phase bulk graphite for ablation testing (SC-CR-70-6169) 17 p2768 N71-29219

Iodine behavior and control in processing plants for fast reactor fuels and removal of radiiodine from plant effluents 17 p2784 N71-29858

Processing and manufacturing methods for synthetic materials 17 p2757 N71-30075

Bibliography on industrial weatherproofing processes (AD-722801) 19 p3105 N71-32176

Epitaxial crystal growth for manufacturing electronic equipment and components including crystal defects and electrical properties of crystallized layers (NLL-FORS-TRANS-2690-9022.81) 19 p3171 N71-32534

Effects of manufacturing process variations on CdS solar cell performance and effect of temperature and time exposure during evaporation (NASA-CR-72969) 21 p3378 N71-34037

Formation time, specific gravity of solution, and overcharge amount associated with electrochemical cleaning or formation operation in manufacturing nickel cadmium cells (NASA-CR-121877) 21 p3379 N71-34040

Contamination control checklists for manufacturing or assembly plants (NASA-CR-121740) 21 p3432 N71-34418

Survey of reactions of nonmanufacturing businesses towards US adoption of metric units of measurement (NBS-SP-345-5) 21 p3534 N71-35184

Manufacture and dynamic testing of external store models for transonic wind tunnels (REFP-23) 22 p3539 N71-35212

Fabrication and field testing of lightweight, recoverable, air-transportable hangar (AD-727051) 22 p3565 N71-35396

Development and distribution of natural resources to satisfy energy requirements of US industry during the 1970's (BM-IC-8526) 22 p3700 N71-36393

Manufacturing process for production of high temperature, low density, thermal insulation equipment (BDX-613-313) 23 p3709 N71-36446

Fabrication process and electrical properties of high temperature flat cable (BDX-613-161) 23 p3731 N71-36597

Development of plating technique for electroforming gilding metal rotating bands used on 155 millimeter artillery shells (BDX-613-236) 23 p3762 N71-36822

Development of pulse-arc welding process for preventing necking when joining multistrand aluminum wires (BDX-613-328) 23 p3762 N71-36823

Development of ferrous metallurgy and advanced methods of metal production (JPRS-54099) 23 p3772 N71-36887

Chemical analysis of amine curing agent used in adhesives manufacturing to determine compliance with specifications (BDX-613-405) 23 p3777 N71-36918

Analysis of storage stability of intermediate moisture foods for space flight feeding with tables of foods and types of manufacture (NASA-CR-113194) 24 p3880 N71-37458

Evaluation of design fabrication, inspection and testing of integrated circuits aimed at improving quality and reliability of hardware using these devices (AD-726560) 24 p3898 N71-37786

Photofabrication of thin metal films and thin film stencils (AD-727758) 24 p3998 N71-38520

MANY BODY PROBLEM

Singular perturbation problems in earth-moon space (AD-710729) 01 p0122 N71-10544

Finding system of self-consistent equations for radial distribution function and excitation spectrum of many-body system using method of retarded Green function (INP-705) 04 p0576 N71-13698

Many body problem of elastic scattering of electrons from atoms and molecules using Green function techniques 04 p0583 N71-14150

Evaluating multiple density correlation function of many particle system (NUB-2051) 08 p1257 N71-18416

Solving quantum mechanical problems of N-dimensional equal particles of mass interacting pairwise by quadratic or inversely quadratic potentials 08 p1225 N71-18846

Investigating positivity conditions for velocity-dependent and quadratic spin-orbit potentials 08 p1262 N71-18849

Calculating nuclear binding energies for four-body interaction in light nuclei 08 p1262 N71-18850

Investigating hyperspherical-expansion approach to nuclear bound states in first approximation in limit of large A for nucleon-nucleon potential of soft-core saturating type 08 p1229 N71-19228

Multidimensional sampling theorem (AD-716557) 09 p1362 N71-19428

Relativistic and nonrelativistic studies of many electron systems with open and closed shells 09 p1432 N71-19971

Numerical analysis for static multiple density correlation function of many particle system (NUB-2053) 11 p1800 N71-21878

Time dependent perturbation theory of ground state many fermion system for study of self energy and factorization problems and examination of reaction matrix expansions 11 p1801 N71-21886

Hartree approximation for ground state correlations as variational parameters in nuclear many body problems (NYO-2171-333) 12 p1973 N71-23938

Stochastic formulations for nonlinear problems in many body theory of turbulent plasmas 15 p2502 N71-27600

Three dimensional vector forms of selected section relationships applied to n-body trajectory simulation based on virtual mass concept (NASA-CR-110894) 15 p2435 N71-27761

Aerodynamic drag of many bodies of revolution in supersonic flow (DLR-FB-71-04) 17 p2702 N71-30325

Electronic or nucleonic many body system ground state energy calculation using Mathieu functions as orthogonal single particle wave functions 18 p2983 N71-31048

Modifications to interplanetary trajectory program for providing capability of generating optimum low-thrust trajectory in N-body field (NASA-CR-118377) 18 p3016 N71-31298

Turbulence effects between ocean bottom sediments and ocean current (BMVG-FBWT-71-5) 18 p2918 N71-31299

Derivation of 1/omega sum rules from two component uniform many body systems and long range correlations in binary solutions (RLO-1388-599) 18 p2990 N71-31566

Many body theory of helicons and helicon interactions analogy to polariton theory 19 p3155 N71-32335

- Mathematical model for near-body orbit calculation using mass concentration, perturbation theory, nonlinear equations, geopotentials, and least squares method [NASA-CR-121381] 20 p3345 N71-33019
- Many body theory electron correlation effects for excited and ground states 20 p3317 N71-33523
- Solutions for N vibrating spheres in theoretical study of sound waves from multiple surfaces 20 p3312 N71-33609
- Electromagnetic and nuclear many body forces, and effects of three body forces on various physical properties of neutron stars 20 p3326 N71-33943
- K line emission spectrum of lithium for energies above and below Sommerfeld threshold determined using many body diagrammatic techniques 21 p3442 N71-34491
- Necessary and sufficient conditions for rapid decay of correlations for many body systems having probability distributions obeying master equation 22 p3448 N71-36013
- Generalized Veneziano model with spin and isospin for antineutron nucleon antineutron kaon pion processes 23 p3816 N71-37230
- Fermi system phase transition model analysis near critical point for two, three, and many body interactions with comparison to classical theory 23 p3823 N71-37271
- Determination of asymptotic behavior of correlation and thermodynamic functions describing many-body system as it approaches critical point [NASA-CR-123148] 24 p4033 N71-38774
- MANY PARTICLE THEORY**
- U MANY BODY PROBLEM**
- MAPPING**
- NT ICE MAPPING**
- NT SOIL MAPPING**
- Automation and mechanization of cartography, and coordination of research and cartographic activities [AD-711978] 02 p0212 N71-11517
- Evaluating potential for making broad land use maps and earth resource surveys from spaceborne and airborne photography 02 p0217 N71-11900
- Utilizing spatial filtering for analyzing structural configuration of Michigan Basin for application to remote sensing [NASA-CR-111568] 03 p0369 N71-13094
- Bifurcation from simple eigenvalues with mapping of Banach space subset [AD-712438] 03 p0401 N71-13389
- Satellite mapping of annual snow extent in western United States [PB-194004] 05 p0668 N71-14756
- Computerized analytic triangulation for compiling topographic maps from aerial photographs 05 p0683 N71-14842
- Forest and range inventory and mapping 05 p0677 N71-15497
- Analysis of n-dimensional nonlinear mappings representative of P and S functions [NASA-CR-116133] 06 p0884 N71-16008
- Infrared scanner use for thermal mapping and multispectral sensing in Remote Sensing Aircraft Program 06 p0859 N71-16165
- Content mapping techniques for qualitative and semiquantitative analysis with electron microbeam probe [AD-714567] 06 p0875 N71-16727
- Computerized aerotriangulation [PB-194570] 07 p1015 N71-16994
- Literature survey on contour map and terrain intervisibility processing [AD-713311] 08 p1185 N71-18242
- Surface and terrain features of Yuma Proving Ground desert area [AD-715363] 08 p1190 N71-18675
- Error analysis for extraterrestrial convergent photogrammetric mapping system [NASA-CR-116824] 08 p1203 N71-19021
- Computer graphics for satellite antenna geographic mappings [NASA-CR-116814] 08 p1166 N71-19022
- Earth resources cartographic applications program [AD-715978] 08 p1198 N71-19261
- Satellite and aerial thematic land use mapping 08 p1198 N71-19264
- Mathematical models and computer programs for equalizing West German part in European triangulation net 09 p1353 N71-19724
- Relief group combinations for constructing geomorphological map of western Middle Europe 09 p1383 N71-19725
- Mapping of polar region magnetic storms [REPT-70-34] 10 p1546 N71-20641
- Methods and instrumentation for mapping and measuring solar radiation [AD-716804] 10 p1547 N71-20737
- Design and development of random function tracer for obtaining coordinates of points on contour maps [NASA-CASE-XLA-01401] 10 p1565 N71-21179

- Coordinate displacement computer program for adjusting triangulation networks 10 p1530 N71-21673 [REPT-120]
- Contouring program application to mapping of isospheric parameters using electron density data from ionospheric stations for extrapolating observations [AD-717683] 11 p1750 N71-22592
- Eigenvalues passing through hyperbolic fixed points for area-preserving mapping [TR-1] 14 p2282 N71-26109
- Evaluation of airborne laser systems for mapping, range finding, communication, and fire control [AD-720552] 14 p2366 N71-26188
- Photointerpretation of satellite-borne photography for mapping and land use studies [NASA-CR-118518] 14 p2249 N71-26316
- Interpolation by linear filters for use in numerical integrations involving multiple grid network mappings [AD-721185] 15 p2436 N71-26825
- World mapping of solar radiation distribution 15 p2439 N71-27514
- CONPLOT 2 contour generating program with output of large cartographic quality contour map designed to form larger maps by combining other maps [AD-721018] 15 p2384 N71-27733
- Flow field mapping for determining sonic boom intensity from wind tunnel measurements 16 p2534 N71-28384
- Application of cartographic grid network of coordinates for solution of meteorological and hydrological plotting of fields in polar areas [AD-720149] 16 p2588 N71-28452
- Application of Apollo space photography and sequential high altitude NASA aircraft photography for evaluating natural and cultural resources in southeastern Arizona - map [NASA-CR-115056] 17 p2750 N71-29233
- Geodesy and cartography - bibliography [AD-723428] 19 p3085 N71-31810
- Mathematical structure of vertical and oblique cosmographic perspectives for spaceborne photographic interpretation [NASA-TT-F-13761] 19 p3103 N71-32553
- Mapping southeastern Panama and northwestern Colombia to evaluate potential of radar imagery for use in collecting geomorphic data [AD-724118] 20 p3256 N71-32983
- Geologic mapping of Yellowstone National Park area by interpretation of radar imagery [NASA-CR-121425] 20 p3233 N71-33185
- Geodimetric data for scaling German part of European main triangulation net [REPT-150] 20 p3247 N71-33850
- Topographic mapping of gravitational field data [REPT-179] 20 p3269 N71-33851
- S band planetary radar receiver for Mars Deep Space Station and Venus radar mapping experiment 21 p3392 N71-34137
- Mapping of ocean bottom topography using continuous reflection profiling technique [AD-724674] 21 p3422 N71-34347
- System of regional agricultural land use mapping tested against Apollo 9 color infrared photography of Imperial Valley, Calif. [NASA-CR-121875] 21 p3426 N71-34375
- Application of aerial reconnaissance and remote sensor techniques to development of master engineering soil plans [PB-199422] 22 p3573 N71-35447
- Development and characteristics of digital recording system for automatic digitizing of map contour line data [AD-726386] 22 p3579 N71-35493
- Mapping Canadian gravitational fields 22 p3580 N71-35503
- Remote aerial sensing and automatic mapping for forest resources information system [NASA-CR-122922] 23 p3755 N71-36770
- Synthesis algorithm, Boolean algebra, and mappings for interval generalization of switching theory [COO-2118-8] 24 p3894 N71-37754
- Coherence of holomorphic mapping 24 p3948 N71-38165
- Techniques for obtaining magnetic cleanliness on deep space missions to allow interplanetary magnetic field mapping [NASA-TR-R-373] 24 p4022 N71-38701
- MAPS**
- NT ASTRONOMICAL MAPS**
- NT LUNAR MAPS**
- NT METEOROLOGICAL CHARTS**
- NT RADAR CLUTTER MAPS**
- NT RADAR MAPS**
- NT RELIEF MAPS**
- Bandera lava tubes of New Mexico and lunar comparisons 04 p0522 N71-14443
- Atlantic Ocean gravity anomaly map 07 p1017 N71-17138
- Bathymetry and magnetics of region (POL-421-3) 29 deg to 35 deg N, 155 deg to 165 deg W - map [ESSA-TR-ERL-146-POL-4] 07 p1024 N71-17957
- Atlas of oblique incidence high frequency backscatter ionograms of midlatitude ionosphere [ESSA-TR-ERL-162-ITS-104] 07 p1026 N71-18051

- Tables and maps of selected landing airfields for shuttle orbiters with various crosswinds [NASA-TM-X-67000] 11 p1730 N71-21996
- New geographical names for locations on Franz Josef Land maps 11 p1755 N71-22833
- Tabulation and maps of major hurricanes affecting United States during period 1873 to 1966 [ESSA-TM-WBTH-SR-42] 18 p2953 N71-31820
- Magnetic survey of Baja and southern California coasts and continental shelf including magnetic anomaly map of Pacific Ocean [NOAA-NOS-DR-12] 18 p2919 N71-31428
- MARAGING**
- Effect of cooling rates on dendrite structure of maraging 300 alloy, size and distribution of inclusions related to tensile and fatigue properties [AD-718902] 12 p1937 N71-23308
- MARAGING STEELS**
- Fracture strength and stress corrosion characteristics of high strength maraging steels [AD-712723] 04 p0529 N71-13999
- Fabrication and optimization of weld joints in 12-5% maraging steel plates [NASA-CR-115887] 05 p0691 N71-14811
- Investigating effects of heating rate, maximum temperature, and thermal cycling on transformation temperatures, hardness, and dimensional anisotropy in maraging steels [UCRL-72099] 08 p1217 N71-19008
- Effect of aging and finishing sequence on fatigue performance of maraging steel [TN-370] 08 p1220 N71-19271
- Evaluation of glasses as forging lubricants for maraging steels and titanium alloys [AD-72583] 12 p3603 N71-35661
- Strength, ductility, toughness, weldability, and rupturing characteristics of 18 per cent Ni maraging steel for rocket engine cases [ISAS-465] 23 p3771 N71-36679
- Effect of heat treatment on physical properties of steels with various amounts of nickel, cobalt, and molybdenum [NLL-TRANS-746-807-19022.401] 23 p3774 N71-36677
- Development of optimum tungsten-iron gas welding procedure for production of welds in 12 percent nickel maraging steel [NASA-CR-72961] 24 p3927 N71-38019
- Effects of dimethyl-dichlorovinyl phosphate and sodium chloride solution on stress corrosion cracking of aluminum and steel [NASA-TM-X-64617] 24 p3933 N71-38060
- MARIA**
- NT LUNAR MARIA**
- MARINE BIOLOGY**
- Annual report on marine resources and engineering development from President of US to Congress 01 p0047 N71-10400
- Multidisciplinary oceanography including physical, geological, geophysical, chemical, biological, and radiocological studies [AD-710765] 02 p0219 N71-12083
- Marine biology and geology of Caribbean Sea [PB-1969677] 03 p0373 N71-13343
- Marine fauna and benthic shelf-slope communities of Isthmian region [BML-171-38] 06 p0841 N71-15987
- Investigating feasibility of locating, identifying and quantifying surface and near-surface fish stocks from aircraft and spacecraft 06 p0848 N71-16182
- Evaluating scientific and engineering requirements for research related to coastal wastes management [PB-195861] 09 p1330 N71-19653
- Abstracts of news releases and scientific articles on oceanography 11 p1745 N71-21994
- Hydrodynamics, marine biology, bionics, dolphins, sharks, porpoises, traveling waves, fluid flow, viscous fluid, nervous system, skin structure, swimming [JPFS-32601] 11 p1687 N71-22281
- Biological efficiency of swimming fish based on oxygen consumption 11 p1681 N71-22288
- Measurements of available radiant energy with consideration for spectral and directional properties of measuring equipment for determination of ocean primary productivity [AD-718367] 12 p1911 N71-23457
- International science management for global marine antipollution regulations 13 p2190 N71-24762
- Geomorphology, biological activity, and hydrology of Gulf of Mexico and Caribbean Sea as determined from Soviet-Cuban oceanographic expeditions [JPFS-53412] 18 p2909 N71-30694
- Cost effectiveness model applicable to national defense systems and other national marine environmental data collection systems 19 p3091 N71-31945
- MARINE NAVIGATION**
- U SURFACE NAVIGATION**
- MARINE PROPULSION**
- NT UNDERWATER PROPULSION**

SUBJECT INDEX

MARKING

Investigating thermoelectric devices for marine application
[AD-715437] 08 p1147 N71-18750

Analysis of displacements and stresses in marine propellers under hydrodynamic pressure loads
[AD-716412] 09 p1474 N71-19836

Analysis of elastic strength of marine propellers by finite element method
[AD-716463] 09 p1474 N71-19856

Permanently fluid for generating pressure forces for sea vehicle propulsion
[AD-722554] 17 p2756 N71-29905

Hydraulic pump jet propulsion unit for destroyer, and incorporated computer program
[ARL-MR-316] 17 p2840 N71-30339

Analogue study of ship propulsion reactors
[CEA-COFP-1750] 22 p3621 N71-33800

MARINE TECHNOLOGY

Summary of synoptic meteorological observations for Mediterranean marine area - Vol. 3
[AD-713779] 05 p0715 N71-14545

Apparatus and methods for remote measurement of statistical characteristics of sea environment in Arctic and Antarctic regions
[TT-69-53083] 05 p0679 N71-15541

Federal role in development of synthetic rubber, civilian atomic energy, and communications satellite industries with implications for marine resource development program
[PA-196038] 09 p1487 N71-19698

Total heat budget between ocean-ice-atmosphere in Arctic Basin for military utilization
[AD-717967] 12 p1906 N71-23351

Compilation of published results of scientific and technical advancements in marine geology, geophysics, meteorology, and physical oceanography for 1969
18 p2911 N71-30980

Description of engineering and scientific aspects of submarine sediments and rocks as determined by marine geotechnique
18 p2913 N71-31002

Systems analysis of marine technology including mathematical models, market research, economic and cost analyses, and forecasting for management planning
18 p3030 N71-31392

Equipment and methods for marine measurement of gravitational forces
[JPRS-53851] 21 p3417 N71-34313

Estimate of random errors in gravity measurements made aboard submarines using grapho-mechanical analyzer
21 p3417 N71-34315

Laboratory and sea tests of gyro-stabilized marine gravimeter for measuring disturbing accelerations and tilts in submarines
21 p3417 N71-34316

Optical-mechanical marine gravimeter with numerical pulse coding device
21 p3418 N71-34317

Automated sea observations with optical-mechanical marine gravimeter with automatic readout
21 p3418 N71-34318

Laboratory and sea condition tests of accuracy of double system marine gravimeter with automatic readout
21 p3418 N71-34319

MARINER PROGRAM

NT MARINER VENUS-MERCURY 1973

Mariner Mars 1971 project
[NASA-CR-115773] 04 p0612 N71-14152

Mariner Mars mission planning including launch windows and scientific objectives in 1971
[NASA-NEWS-RELEASE-71-75] 12 p2002 N71-24314

Tracking, telemetry, and command operations of Deep Space Network in support of Mariner Mars project
[NASA-CR-122068] 22 p3669 N71-36159

Tracking and data system support for Mariner Mars 1969 mission from midcourse maneuver through end of nominal mission
[NASA-CR-122008] 22 p3671 N71-36174

MARINER SPACE PROBES

NT MARINER VENUS-MERCURY 1973

NT MARINER 2 SPACE PROBE

NT MARINER 4 SPACE PROBE

NT MARINER 5 SPACE PROBE

NT MARINER 6 SPACE PROBE

NT MARINER 7 SPACE PROBE

Hardware and software capabilities for spacecraft navigation data on Mariner Mars 1969 approach guidance
01 p0082 N71-10259

Planning, development, design, manufacture, and testing for Mariner Mars 1969 project - Vol. 1
[NASA-CR-115875] 05 p0772 N71-15484

Calibration activity of Deep Space Network in support of Mars encounter phase of Mariner Mars 1969 mission
[NASA-CR-116248] 06 p0949 N71-14881

Photometric properties of vidicons on Mariner TV cameras
16 p2679 N71-28510

Planetary quantitative systems analysis for biological contamination of Mariner Mars 1971 space probe
[NASA-TM-X-67238] 18 p2875 N71-30826

Mariner Mars 1971 orbiter propulsion subsystem for trajectory corrections, Mars orbit insertion, and orbit trim maneuvers
18 p3001 N71-31112

DSIF data on Mariner H launch and failure and Mariner 9 launch and midcourse maneuver
[DSIF-S1/OP-8] 20 p3276 N71-33906

DSN requirements for Mariner Mars 1971 mission support
21 p3391 N71-34124

Tracking, telemetry, and command operations of Deep Space Network in support of Mariner Mars project
[NASA-CR-122068] 22 p3669 N71-36159

Development of numerical model of general circulation of lower atmosphere of planet Venus based on Mariner 5 and Venera 4 space probe data
22 p3672 N71-36181

Postflight analysis of Mariner I and 7 scientific data - Vol. 3
[NASA-CR-122090] 23 p3845 N71-37403

News release of Mariner 9 Mars mission
[NASA-NEWS-RELEASE-71-215] 24 p4016 N71-38652

MARINER SPACECRAFT

Dynamic modeling of pressurization system and pneumatic pressure regulator in pressure fed liquid propulsion systems
[NASA-CR-111612] 03 p0448 N71-12281

Design and analysis of self correcting automatic navigation system for Mariner Mars spacecraft
[NASA-CR-111703] 04 p0615 N71-14366

Tracking support by Deep Space Network for Mariner Mars 1969 extended operations and Mariner Mars 1971 missions
05 p0767 N71-14954

Performance of Mariner Mars 1969 mission by flight and Earth-based elements during launch and space flight phases - Vol. 2
[NASA-CR-117351] 09 p1468 N71-20460

Radio technique for probing solar plasma during superior conjunction of Mariner 6 and 7 spacecraft
11 p1814 N71-22771

Environmental testing and handling of batteries for Mariner 71 spacecraft
16 p2539 N71-28669

Mathematical models for prediction of acceleration responses and reaction forces and moments at base of Mariner Mars 71 and Viking spacecraft from Centaur main engine cutoff
[NASA-CR-121473] 20 p3355 N71-33719

DSIF operations support of Mariner Mars 1971 mission, including launches of H and I spacecraft
21 p3394 N71-34153

Technique for conducting landing impact tests at simulated planetary gravity for Mars lander spacecraft - dynamic models
[NASA-TN-D-6459] 22 p3681 N71-36247

Tracking operations of Mariner 9
[DSIF-S1/OP-5] 24 p4015 N71-38640

Experiments to be accomplished by Mariner 9 mission
[NASA-CR-123156] 24 p4018 N71-38666

MARINER VENUS-MERCURY 1973

Investigating mesh materials for deployable antenna, radiation tolerance of solar array components, and crack propagation threshold for isopropanol and titanium alloy
06 p0826 N71-16681

Measuring thermal characteristics of solar arrays for Mariner Venus-Mercury 1973 flyby mission
06 p0959 N71-16682

Engineering and scientific information for Mariner 71, Mariner Venus-Mercury, and Viking Mars programs
[NASA-CR-116008] 08 p1288 N71-18872

Mariner Venus-Mercury 1973 imaging experiment for mapping Mercury and error rates for science words
08 p1289 N71-18874

Design of magnetometer system for Mariner Venus-Mercury 1973
[NASA-CR-119175] 17 p2846 N71-30347

Phase velocity measurements of cigar antenna design for Mariner Venus-Mercury 1973
18 p2890 N71-31117

MARINER 2 SPACE PROBE

Solar wind, plasma waves and interplanetary electric and magnetic fields from Mariner 2 and Mariner 4 space probes
[ESRO-SP-55] 03 p0454 N71-13256

MARINER 4 SPACE PROBE

Solar wind, plasma waves and interplanetary electric and magnetic fields from Mariner 2 and Mariner 4 space probes
[ESRO-SP-55] 03 p0454 N71-13256

Relationship between Mariner 4 space probe trajectory and calculated location of proposed Martian bow wave
[NASA-CR-116676] 08 p1290 N71-19240

MARINER 5 SPACE PROBE

Investigating dynamic nonshock properties of microscale fluctuations in interplanetary medium using plasma and magnetic field data from Mariner 5 space probe
[NASA-CR-110999] 01 p0105 N71-10430

Mariner 5 data for determining physical properties of Venus ionosphere
13 p3169 N71-25279

Rotational discontinuities in solar wind derived from Mariner 5 plasma and magnetic field data
[NASA-CR-119172] 17 p2842 N71-30261

Tangential discontinuities in solar wind derived from Mariner 5 plasma and magnetic field data
[NASA-CR-119173] 17 p2842 N71-30262

Angular momentum flux carried by solar wind calculated from Mariner 5 data
[NASA-CR-119682] 19 p3177 N71-32381

Radio wave attenuation and refraction in Venus atmosphere from Venus satellite measurements, including comparison with Mariner 5 results
[ID-811] 19 p3059 N71-32788

MARINER 6 SPACE PROBE

Mariner physical properties data for Mariner 6 and 7 missions
[NASA-CR-115849] 05 p0770 N71-14504

Mariner 6 and Mariner 7 Mars missions and scientific observations
[NASA-CR-115833] 05 p0768 N71-15323

Determination of orbit estimates for Mariner 6 and 7 space probe flights
[NASA-CR-116487] 07 p1116 N71-18008

Ultraviolet emission spectrum of Mars upper atmosphere from Mariner 6 and 7 spacecraft
[NASA-CR-117756] 11 p1748 N71-22154

Comparison of Martian tectonic and topographic features with earth and moon based on Mariner 6 and 7 photographs
[NASA-TM-X-65095] 23 p3847 N71-37421

MARINER 7 SPACE PROBE

Mariner physical properties data for Mariner 6 and 7 missions
[NASA-CR-115849] 05 p0770 N71-14504

Mariner 6 and Mariner 7 Mars missions and scientific observations
[NASA-CR-115833] 05 p0768 N71-15323

Determination of orbit estimates for Mariner 6 and 7 space probe flights
[NASA-CR-116487] 07 p1116 N71-18008

Comparison of Martian tectonic and topographic features with earth and moon based on Mariner 6 and 7 photographs
[NASA-TM-X-65095] 23 p3847 N71-37421

MARK 2 REENTRY BODY

Fabrication of prototype Mark 2 fuel subassembly
[BNWL-1418] 05 p0726 N71-15046

MARKERS

Use of nutritional markers for studies of food intake, passage, and absorption in gastrointestinal track of humans and animals
[NASA-CR-115125] 21 p3384 N71-34076

MARKET RESEARCH

Market research and management planning for optimization of civilian airline operations in France
[REPT-19707-E] 07 p1136 N71-18093

Economics and cybernetics in civil aviation market research for air traffic predictions
07 p1136 N71-18097

Comparison of automobile, rail transportation, and short haul aircraft performance by means of market research noting central city airports
11 p1674 N71-22192

Analysis of current status and future outlook of US commuter airline industry
[AD-710871] 16 p2531 N71-28216

Program evaluation techniques for management planning including operations research, market research, systems analysis, decision making, and resource allocation in R and D
[PAU-M-12] 18 p3030 N71-31388

Research and development program evaluation techniques including cost analysis, technology forecasting, market research, and decision making for project management planning
18 p3030 N71-31389

Systems analysis of marine technology including mathematical models, market research, economic and cost analyses, and forecasting for management planning
18 p3030 N71-31392

MARKING

NT ISOTOPIC LABELING

Atmospheric distribution of CO₂, O₂, O₃, water vapor, and other chemical tracers and global transport processes
[TID-25314] 12 p1911 N71-23656

Weight and Measures Labeling Handbook for use in packaging and labeling commodities and enforcing state laws and regulations
[NBS-HB-108] 16 p2601 N71-28548

Federal research and development efforts directly related to improved traffic marking materials for pavements
[NASA-CR-121412] 20 p3288 N71-33594

MARKOV CHAINS

- Mathematical programming and control of Markov chains
[NASA-CR-111130] 01 p0076 N71-10580
- Markov chain technique for queueing problem of scheduled customer arrival
02 p0251 N71-11736
- Imbedded Markov chain analysis of time sharing system with homogeneous Poisson arrivals, exponential service times, and ordered priority queue
[AD-712319] 03 p0340 N71-12467
- Bayesian algorithms for Markov chain pattern recognition problems
[AD-720837] 14 p2308 N71-25850
- Pseudorandom and Markov sequences optimizing correlation time of flight spectrometry
[JUL-684-FF] 15 p2469 N71-27361
- Finite state discrete parameter Markov chain representation of ionospheric communication error sequences
19 p3057 N71-32361
- Markov chain model for characterizing error sequences in digital channels with memory
[NASA-CR-121429] 20 p3239 N71-33551
- MARKOV PROCESSES
- NT MARKOV CHAINS
- Investigating digital bit synchronization phase locked loops employing binary phase error quantization and sequential loop filtering
[AD-711957] 03 p0336 N71-12403
- Sequential search problem with dynamic programming for continuous time Markov processes
06 p1236 N71-18961
- Using Markov renewal processes for reliability analysis of multiple unit standby redundancy system with preventive maintenance
[TR-71-3] 06 p1236 N71-19007
- Relation between metric invariants for infinite measure-preserving Markov shifts
[RR-23/SMR/1] 09 p1411 N71-20340
- Quantizing noise analysis in delta modulators applied to first order Markov sources
[AD-717221] 10 p1533 N71-21081
- Mathematical filter for eliminating persistence in meteorological data
[AD-717656] 11 p1788 N71-21940
- Abstract variational theory application to continuous parameter stochastic optimization problems to derive maximum principles in linear programming
[NASA-CR-117846] 12 p1948 N71-23220
- Bayesian decision making and learning in parametric pattern recognition problem for continuous-time Markov process
[AD-720810] 14 p2308 N71-25847
- Stochastic Markov processes for modelling dynamic power systems
[FTL-A-A08-9] 14 p2283 N71-26564
- Markov renewal process model for inspection, replacement, and maintenance system
[TR-71-5] 14 p2286 N71-26695
- External via covariances and internal via Markov process descriptions of Gaussian stochastic processes
[AD-722468] 18 p2944 N71-30816
- Characterization of conditional probability measures for continuous-time, partially observable Markov processes
[AD-722455] 18 p2946 N71-31240
- Markov model for application of uniform withdrawal assumption in continuous crystallizer design equations to continuous mixing vessel equations
21 p3501 N71-34940
- Recurrence properties and periodicity for Markov processes
22 p3606 N71-35680
- Derivation of first passage time distributions for models of two-unit redundant repairable systems with failures using Markov renewal processes
[TR-71-26] 22 p3607 N71-35691
- MARS (PLANET)
- Diurnal variation of Martian exospheric temperatures
[ISAS-456-VOL-35-NO-12] 02 p0296 N71-11933
- Relative measures of satellites of Uranus and Mars from astronomical photographs
04 p0610 N71-13593
- Constructing maps of planet Mars from infrared photographs of planetary surface
04 p0610 N71-13596
- Real gas effects on drag and trajectories of nonlifting conical shell during Mars atmospheric entry
[NASA-TN-D-6240] 07 p1116 N71-18015
- Relationship between Mariner 4 space probe trajectory and calculated location of proposed Martian bow wave
[NASA-CR-116876] 08 p1290 N71-19240
- Growth of bacteria in soils from Antarctic dry valleys providing soil microbial ecology as Mars model
[NASA-TM-X-66965] 09 p1333 N71-20172
- Scientific experiments, instrumentation requirements, and operational aspects of manned mission to planet Mars
[NASA-TM-X-31277] 10 p1645 N71-21435

- Development of least squares process for estimating spherical harmonic coefficients in Mars gravitational potential function based on Viking orbiter spacecraft data
[NASA-TN-D-6219] 11 p1828 N71-22621
- Aerodynamic and heating problems of spacecraft entry into Mars and Venus atmospheres
13 p2172 N71-24705
- Examination of data to be obtained by Mariner Mars 1971 infrared interferometer spectrometer experiment for inferential information on Mars surface biota
[NASA-CR-118629] 14 p2203 N71-25715
- Data transmission from Mars and Venus automatic surface vehicles
17 p2718 N71-29362
- Dimensional analysis and particle size distribution of limonite from Pennsylvania including optical and mechanical properties as Mars simulation material
[RM-5121] 17 p2846 N71-30333
- Interpretation of planetary surface photographs, noting Moons, Mars, and Mercury surfaces
[ESRO-SP-56] 18 p3068 N71-30594
- Lunar, Mercury, and Mars surfaces and atmospheres - ground based photometric and polarimetric methods of observations
18 p3008 N71-30595
- International symposium on planetary atmospheres emphasizing atmospheres of Mars and Venus
[NASA-TT-F-13813] 18 p3015 N71-31152
- System operating noise temperature calibrations of S band research operational cone at Venus Deep Space Station and polarization diversity S band cone at Mars Deep Space Station
21 p3392 N71-34135
- S band planetary radar receiver for Mars Deep Space Station and Venus radar mapping experiment
21 p3392 N71-34137
- Soviet news releases on heat balance of northern polar cap of Mars, spectrophotometric studies of giant planets, and Jovian radio emission
21 p3509 N71-35005
- Crew radiation dose from phase of high impulse gas-core nuclear rocket during Mars mission
[NASA-TM-X-67927] 22 p3546 N71-35262
- Numerical analysis of heat balance of north polar cap of planet Mars and accumulation of solid carbon dioxide and frozen water
[NASA-TT-F-13974] 22 p3573 N71-35446
- Gas chromatograph, mass spectrometer system for chemical and biochemical determinations on Mars, and data reduction program
[NASA-CR-122038] 22 p3583 N71-35514
- Multiple exospheric temperatures for Venus and Mars
[NASA-TM-X-65690] 22 p3668 N71-36154
- Statistical processing of phase dependence of Mars brightness in spectral region between 0.3 and 1.1 micron
[NASA-TT-F-13973] 22 p3669 N71-36156
- Design, development and characteristics of surface vehicle for exploration of planet Mars
[NASA-CR-122950] 23 p3844 N71-37401
- MARS ATMOSPHERE
- Theoretical investigation of ionized capsule wake interactions with circularly polarized antenna radiation while entering Martian atmosphere
03 p0353 N71-12551
- Mariner Mars 1971 project
[NASA-CR-115773] 04 p0612 N71-14152
- Martian physical properties data for Mariner 6 and 7 missions
[NASA-CR-115849] 05 p0770 N71-14504
- Properties of nonequilibrium radiation emitted by Mars atmosphere gas mixtures
[NASA-CR-1740] 06 p0834 N71-15834
- Breakdown in mixtures of carbon dioxide, nitrogen, and argon mixtures simulating possible Mars and Venus atmospheres
06 p0828 N71-16651
- Variable lift control of space vehicle during reentry into Martian atmosphere
06 p0952 N71-16805
- Relationship between Mariner 4 space probe trajectory and calculated location of proposed Martian bow wave
[NASA-CR-116876] 08 p1290 N71-19240
- Insulation effects on thermal vacuum chamber for Mars environmental simulation tests
09 p1368 N71-20245
- Atmospheric model and on-line Mars atmospheric parameter measurement updating ahead of entry vehicle
[AD-717108] 10 p1643 N71-21065
- Ultraviolet emission spectrum of Mars upper atmosphere from Mariner 6 and 7 spacecrafts
[NASA-CR-117756] 11 p1748 N71-22154
- Mariner 6 and 7 occultation data for determining temperature and pressure of Martian atmosphere
13 p2168 N71-25277
- Light scattering calculations for brightness effect in Mars atmosphere caused by aerosols
13 p2168 N71-25278
- Martian atmospheric temperature and pressure and temperature gradient determination by least squares

- differential correction of satellite photometric solar eclipse data
[NASA-TN-D-6258] 14 p2337 N71-26099
- Mechanical properties of Dacron parachute fabrics in simulated Martian atmosphere
[NASA-TN-D-6242] 16 p2616 N71-28132
- Trajectory, thermodynamic, and stress analysis of spacecraft inflatable decelerators in Mars and Earth atmospheres
[NASA-CR-111920] 19 p3191 N71-32695
- Origin and structure of primitive terrestrial atmosphere and Venus and Mars atmospheres
[REPT-70-444] 20 p3349 N71-33712
- Lower atmosphere of Mars, Venus, and Jupiter
23 p3846 N71-37412
- Composition and evolution of Earth, Mars, Venus, and Jupiter atmospheres
23 p3847 N71-37418
- Analysis of probable viable terrestrial microorganisms on Mars caused by Mariner Mars 1971 Project
[NASA-CR-122845] 24 p3878 N71-37643
- MARS ENVIRONMENT
- NT MARS ATMOSPHERE
- Test facility to verify design concepts and mathematical models of chromatograph for atmospheric composition analysis of Mars
[NASA-CR-117468] 11 p1760 N71-21931
- Development of least squares process for estimating spherical harmonic coefficients in Mars gravitational potential function based on Viking orbiter spacecraft data
[NASA-TN-D-6219] 11 p1828 N71-22621
- Numerical analysis of heat balance of north polar cap of planet Mars and accumulation of solid carbon dioxide and frozen water
[NASA-TT-F-13974] 22 p3573 N71-35446
- MARS EXCURSION MODULE
- Simulating static and dynamic responses of single-module unmanned Mars roving vehicle
[NASA-CR-111560] 03 p0457 N71-13074
- MARS LANDING
- Accuracy of estimating location of landed spacecraft on Mars from range and range rate data
[NASA-TN-D-6109] 05 p0766 N71-14561
- Predicted radiation dosage for Mars lander mission
[NASA-CR-116144] 06 p0945 N71-15896
- Technique for conducting landing impact tests at simulated planetary gravity for Mars lander spacecraft dynamic models
[NASA-TN-D-64559] 22 p3681 N71-36247
- MARS PROBES
- NT MARINER 4 SPACE PROBE
- NT MARINER 6 SPACE PROBE
- NT MARINER 7 SPACE PROBE
- NT VIKING LANDER SPACECRAFT
- NT VIKING MARS PROGRAM
- NT VIKING ORBITER SPACECRAFT
- Mariner 6 and Mariner 7 Mars missions and scientific observations
[NASA-CR-115853] 05 p0768 N71-15323
- Alternative mission/system approaches to automated Mars surface sample return based on utilization of Titan 3 or Saturn Intermediate-20 launch vehicles
[NASA-CR-103009] 06 p0949 N71-16880
- Mars simulator for surface atmosphere effects on unmanned spacecraft landing dynamics
09 p1368 N71-20244
- Mariner Mars mission planning including launch windows and scientific objectives in 1971
[NASA-NEWS-RELEASE-71-75] 12 p2002 N71-24314
- Orbital lifetime calculations for Venus and Mars Orbiter mission plans
13 p2609 N71-25300
- Analytical evaluation of buckling modes of shell configurations to determine imperfection sensitivity of optimum structural designs for Mars entry capsule
[NASA-CR-1800] 16 p2684 N71-28031
- Scanning optical system to provide attitude and trajectory of unmanned spacecraft during orbit about Mars
[NASA-CR-1805] 19 p3133 N71-32423
- MARS SPACECRAFT
- U MARINER SPACECRAFT
- MARS SURFACE
- Large angle gyro sensing system for body mount on unmanned Mars surface vehicle
[NASA-CR-111737] 04 p0543 N71-14148
- Mariner Mars 1971 project
[NASA-CR-115773] 04 p0612 N71-14152
- Mariner television and infrared spectrometer data analyses to determine Mars surface geochemistry
[NASA-CR-116783] 08 p1298 N71-18627
- Automatic pattern recognition system to locate Martian pole star for unmanned surface vehicle navigation
[NASA-CR-118653] 14 p2339 N71-26442
- Design of control equipment for unmanned Martian roving vehicle
[NASA-CR-119030] 16 p2695 N71-28041
- News briefs and abstracts of articles concerning solar radiation, reflection of sunlight by Venus atmosphere, Martian observations
17 p2844 N71-29408

SUBJECT INDEX

Mars Carlo entering simulation model to show aerodynamic effects of formation of Mars tangential meteorite craters
[NASA-TM-X-62027] 17 p2845 N71-30119

Numerical analysis of heat balance of north polar cap of planet Mars and accumulation of solid carbon dioxide and frozen water
[NASA-TT-F-15974] 22 p3573 N71-35446

Toroidal multilayer metal elastic wheel for use on Mars Roving Vehicle
[NASA-CR-122036] 22 p3587 N71-35544

Developed Mariner Mars 1971 rover simulator for test platform of obstacle sensor for autonomous roving vehicle
[NASA-CR-122944] 23 p3739 N71-36645

Comparison of Martian tectonic and topographic features with earth and moon based on Mariner 6 and 7 photographs
[NASA-TM-X-65495] 23 p3847 N71-37421

MARS 69 PROJECT

Hardware and software capabilities for spacecraft navigation data on Mariner Mars 1969 approach guidance
01 p0062 N71-10259

Planning, development, design, manufacture, and testing for Mariner Mars 1969 project - Vol. I
[NASA-CR-115875] 05 p0772 N71-15484

Tracking and data system support with minimization and high rate telemetry systems for the Mariner Mars 1969 project
[NASA-CR-118520] 14 p2340 N71-26712

Footprint analysis of Mariner 1 and 7 scientific data - Vol. 3
[NASA-CR-122890] 23 p3845 N71-37403

MARS 71 PROJECT

Development and implementation of communications equipment for Deep Space Instrumentation Facility
05 p0647 N71-14961

Investigating application of advances in man machine interaction to problems of post-1971 SPOF system
05 p0647 N71-14963

DSIF operations and development of wideband data systems for Deep Space Network
07 p1031 N71-17621

Engineering and scientific information for Mars 71, Mariner Venus-Mercury, and Viking Mars programs
[NASA-CR-116808] 08 p1288 N71-18872

Mariner Mars 1971 spacecraft instrument and system development and tests
08 p1288 N71-18873

Mariner Mars 1971 mission support plan modifications and cost reductions by DSN
11 p1829 N71-22768

Examination of data to be obtained by Mariner Mars 1971 infrared interferometer spectrometer experiment for inferential information on Mars surface biota
[NASA-CR-118629] 14 p2203 N71-25715

Planetary operations systems analysis for biological confirmation of Mariner Mars 1971 space probe
[NASA-TM-X-62728] 18 p2875 N71-30826

Mariner Mars 1971 orbiter propulsion subsystem for trajectory corrections, Mars orbit insertion, and orbit trim maneuvers
18 p3001 N71-31112

Deep Space Network mission support activities, telemetry, and data systems for Pioneer, Helios, Viking, and Mars 71 projects
[NASA-CR-121378] 20 p3346 N71-33163

Deep Space Network support for Pioneer, Helios, Viking, and Mariner Mars 71 spacecraft telemetry data systems
20 p3347 N71-33165

Deep Space Network operations for Mars 71 project, mathematical model for Doppler tracking system, and third-order phase locked system transient response analysis
20 p3347 N71-33168

DSN requirements for Mariner Mars 1971 mission support
21 p3391 N71-34124

DSN command system operation from Space Flight Operations Facility supporting Mariner Mars 1971 mission
21 p3393 N71-34150

DSIF operations support of Mariner Mars 1971 mission, including launches of H and J spacecraft
21 p3394 N71-34153

DSIF telemetry and command processing operational program for providing software to Mariner Mars 1971 missions
21 p3394 N71-34154

Analysis of probable visible terrestrial microorganisms on Mars caused by Mariner Mars 1971 project
[NASA-CR-122845] 24 p3678 N71-37643

News release of Mariner 9 Mars mission
[NASA-NEWS-RELEASE-71-215] 24 p4016 N71-38652

Experiments to be accomplished by Mariner 9 mission
[NASA-CR-123156] 24 p4018 N71-38666

MARSHLANDS

Color infrared photography as remote sensing techniques in investigating estuaries and marshlands
06 p0847 N71-16174

Environmental effects of jetport near Everglades Park in southern Florida
[PB-199159] 21 p3430 N71-34338

MARTENSITE

Structural parameters effect on tempered martensite and lower bainite yield strength
[AD-710789] 01 p0067 N71-10561

Preliminary thermomechanical treatment of D6Ac steel during austenite and martensite transformations
[AD-712483] 04 p0528 N71-13947

Microstructure and mechanical properties of martensite transformed from precipitation hardened austenite
[UCRL-19196] 04 p0530 N71-14091

Thermal analysis of heat activated metallic spring with memory for possible use as fuse arming devices
[AD-713578] 05 p0698 N71-14506

Martensitic conversion in Fe-Ni-Co alloys
[SC-T-70-4036] 05 p0706 N71-15547

Studies of transitions in nonferrous systems applied to martensite transformations in steels
[COO-1198-753] 07 p1045 N71-18027

Anisotropic behavior of austenites, martensites, and bcc refractory alloys, and dislocation-solute atom interactions and interstitial hardening in bcc alloys
[COO-1676-13] 08 p1211 N71-18259

Experimental work on isothermal martensitic transformations
[AD-715791] 08 p1215 N71-18779

Use of solid state reactions and phase transformations to alter structure of solids
09 p1452 N71-19728

Liquid quenching effects on martensitic transformation of metastable Au-Cd alloy
[AD-716043] 09 p1400 N71-20086

X ray diffraction analysis of crystal defects caused by martensitic transformations in iron nickel and iron carbon steels
10 p1583 N71-21571

Metallographic determination of microcrack emergence in martensite of Fe-Ni-C system
[NLL-TRANS-746-537-9022,4017] 10 p1586 N71-21840

Effect of alloying elements on martensitic transformation and fracture toughness of low alloy high strength steels
[AD-718041] 12 p1938 N71-23777

Plastic yielded iron-nickel single crystal martensite crystallography
12 p1939 N71-24077

Reversible martensitic transformations between transition phases of uranium base niobium alloys
[RFP-1353] 13 p2097 N71-25214

Transformation plasticity of iron-nickel during martensite reaction under constant load
14 p2276 N71-26725

Effects of prior plastic deformation of austenite on nucleation of martensite in Fe-Ni-C alloys
15 p2423 N71-27308

Thermomechanical and transformation induced plasticity processes for producing high strength martensitic stainless alloys with high tensile, fracture, yield, and elongation properties
[AD-721361] 16 p2608 N71-28073

Nickel content, plastic deformation, and stacking fault effects on martensitic formation in iron chromium nickel alloys at cryogenic temperatures
[NLL-RTS-6189] 16 p2613 N71-28086

Martensitic transformation occurring in copper-iron alloy during tensile testing with magnetic susceptibility measurement
[PB-199761] 21 p3430 N71-34407

Electron metallography of ferro martensite substructures
[UCRL-19648] 21 p3438 N71-34465

MARTENSITIC STAINLESS STEELS

Martensitic transformation in Ti-Ni alloys from shuffles caused by temperatures above M_s sub
[COO-588-19] 04 p0531 N71-14214

MARTIN AIRCRAFT

NT B-57 AIRCRAFT
Aircraft accident report of Martin 404 N40412
[NTSB-AAR-70-25] 04 p0473 N71-13416

MARTIN MILITARY AIRCRAFT

U MARTIN AIRCRAFT
U MARTIN AIRCRAFT

MARYLAND

Air carrier demand for slots particularly in area of Washington-Baltimore
[PB-193350] 01 p0038 N71-10347

Air pollution report of federal facilities in metropolitan Baltimore intrastate air quality control region
02 p0156 N71-11108

Feasibility of rail access to Friendship International Airport from Wash., D.C. and Baltimore, Md.
[PB-196023] 09 p1364 N71-19434

MARCONI

Specific range rate residuals during lunar orbits for determining lunar mass concentrations
13 p2168 N71-25275

MASS DISTRIBUTION

Comparison of tracking rate residuals attributed to masses with orbital calculation effects using error containing earth force fields
13 p2168 N71-25276

MASER RESONATORS

U MASERS

MASERS

NT GAS MASERS

NT TRAVELING WAVE MASERS

Research of polarization in lasers, amplifying maser, and ultraviolet lasers
[AD-718708] 12 p1933 N71-23622

Iron doped rutile wideband maser amplifier with low signal-to-noise ratio
13 p2090 N71-25337

Prototype atomic hydrogen maser standard for field operation
13 p2090 N71-25338

Segmented superconducting magnet producing staggered magnetic field and suitable for broadband traveling wave masers
[NASA-CASE-XGS-10518] 16 p2406 N71-28554

High resolution studies of atoms and molecules applied to optical and infrared laser experiments
[NASA-CR-121728] 21 p3435 N71-34440

Use of F centers in potassium iodide as crystal for selective absorption optically pumped maser
[AD-726769] 22 p3591 N71-35574

MASKING

Ion masking in quadrupole mass spectrometer to eliminate unstable ion penetration
[NASA-CR-115781] 04 p0575 N71-13676

Development of masking machine for fabrication of semiconductor detectors
[BARC-483] 05 p0693 N71-15430

Composition and process for improving definition of resist masks used in chemical etching
[NASA-CASE-XGS-04993] 07 p1029 N71-17574

Theoretical and computer analyses of unstable ion in quadrupole mass spectrometer with ion source masking
[NASA-CR-121905] 22 p3632 N71-35878

Photofabrication of thin metal films and thin film stencils
[AD-727758] 24 p3998 N71-38520

MASKS

NT OXYGEN MASKS

Computer aided integrated circuit mask production
01 p0036 N71-10225

Comparative tests of finned masks
[LA-4459-TR] 06 p0805 N71-15985

Sealing of respiratory protection masks
[LA-TR-70-17] 06 p0805 N71-15993

MAS

NT CRITICAL MASS

NT PARTICLE MASS

NT PLANETARY MASS

NT STELLAR MASS

Current computer derivation of mass difference relations
[DYO-2171-315] 03 p0424 N71-12807

Round robin mass measurements, systematic and random errors, and group variances
12 p2017 N71-23634

Group of invariance of Maxwell equations and extension associated with set of hyperboloids of mass
[SLAC-TRANS-138] 15 p2458 N71-26935

Tuned damped vibration absorber for mass vibrating in more than one degree of freedom for use with wind tunnel models
[NASA-CASE-LAR-16083-1] 15 p2414 N71-27006

Separation of center of mass motion in two particle shell model wave function of finite depth potential
[JINR-P4-5639] 18 p2580 N71-30814

Mass properties of space station and logistic module
[NASA-CR-119099] 19 p3184 N71-32372

Mass yields and charge distributions of 26 Ag, Cd, In, Sn, and Sb isotopes from U-238 fission with protons
[COO-1167-10] 20 p3328 N71-33987

Detecting variations of gravitational constant difference between inertial and passive gravitational mass
[NASA-CR-115139] 22 p3373 N71-35444

Lost City meteoroid trajectory analysis and determination of original mass
[NASA-CR-121931] 22 p3671 N71-36175

Galactic formation and density, velocity, and mass properties of expansion process
23 p3849 N71-37431

MASS BALANCE

Mass balance and crew input/output requirements during long duration space cabin simulation test
19 p1508 N71-20973

Description of methods for determining stability constants of transition metal binders and polyphosphates
11 p1095 N71-22073

Control system for pressure balance device used in calibrating pressure gauges
[NASA-CASE-XMF-04134] 12 p1921 N71-23755

MASS DISTRIBUTION

Approximate solution for large asteroid distribution with masses near limiting largest mass of population
[NASA-CR-111738] 04 p0511 N71-13762

- Investigating existence of long-lived super-heavy elements in nature and synthesis in stars
[JINR-P6-4902] 04 p0586 N71-14247
- Computer program for tabulating mass differences of various molecules and for deriving empirical formulae for molecule fragment
[FOA-1-C-1319-34] 05 p0737 N71-14620
- Mass concentration and particle size distribution within nuclear cratering cloud during first four hours after formation
[UCRL-50844] 06 p0840 N71-15846
- Minimum mass isotropic shells of revolution under uniform pressure and axial loads
[NASA-TN-D-6121] 06 p0956 N71-16337
- Fitting mass distribution to gravitational potential, for simulating lunar potential
[NASA-CR-116505] 07 p1051 N71-17428
- Mass distribution for lunar potential model
[NASA-CR-116507] 07 p1109 N71-17499
- Least squares integral criterion for representation of gravitational potential with fixed mass points
[NASA-CR-116606] 08 p1180 N71-18650
- Mass loading effects on pyrolytic shock environment of aerospace systems
[NASA-CR-116019] 08 p1300 N71-19250
- Current algebra for determining form factors and divergences of mass in electromagnetic interactions
10 p1624 N71-21814
- Computer analysis of axial mass dispersion data for packed spherical glass particle beds
10 p1610 N71-21827
- Determination of six prong cross sections during elementary particle interactions at 7 GeV/c
11 p1801 N71-21880
- Low energy fission of thorium-232 studied with 11.3 MeV protons and 17.5 MeV deuterons
12 p1976 N71-24097
- A2 meson mass distribution produced by pion proton yields A2 proton reactions and mass spectroscopy
[NUB-2063] 12 p1977 N71-24212
- Homogeneity and anisotropy measurements of thermal radiation field surrounding planet Earth
12 p1995 N71-24323
- Electronic recording system for spatial mass distribution of liquid rocket propellant droplets or vapors ejected from high velocity nozzles
[NASA-CASE-NPO-10185] 14 p2233 N71-26339
- Mass distribution having quadrupole moments in general relativity, quadrupole moment effects on orbital motion of particles, and application to solar system
15 p2454 N71-27438
- Research in nuclear and reactor chemistry including identification of short-life nuclides, activation analysis, and mass distribution in fission
[BMHV-FBK-70-19] 15 p2485 N71-27800
- Evaluation of neutron data for fissile or fertile nuclei in range of resolved or unresolved resonances with mass number above 220
[NASA-TT-F-13692] 16 p2646 N71-28210
- Analysis of CERN data at 19.2 GeV and Serpukhov data at 70 GeV effects on single particle production to test mass dependence formula given by Regge on graphs
[NUB-2070] 18 p2988 N71-31475
- Rocket exhaust cloud mass-energy balance measurements for Saturn S1-C static firing
[NASA-CR-61357] 20 p3364 N71-33391
- Statistical significance of A2 splitting experiments in distinguishing between Breit-Wigner and dipole mass distributions
[NUB-2092] 21 p3477 N71-34763
- Meson-nucleon interactions and mass distribution compared with Regge pole exchange model
[ITEP-790] 24 p3973 N71-38349
- Nonlinear angular velocity aerodynamic damping coefficient effects on statically stable missile configurations and internal mass distribution effect based on wind tunnel stability tests
[AD-727113] 24 p4022 N71-38697
- MASS FILTERS**
- U FLUID FILTERS**
- MASS FLOW**
- Equations for mass flow of methane and natural gas mixtures through critical flow nozzles, including real gas effects
[NASA-TM-X-52994] 10 p1543 N71-21330
- Rocket engine injector orifice to accommodate changes in density, velocity, and pressure, thereby maintaining constant mass flow rate of propellant into rocket combustion chamber
[NASA-CASE-XLE-05157] 13 p2156 N71-24736
- Heating and bulk speed of solar wind
13 p2162 N71-25281
- Vertical tube evaporator smoke tests, pressure profiles, and effects of low mass velocities
[ORNL-TM-3240] 15 p2395 N71-27993
- Elastic scattering analysis of mass flow in supernova fragmentation model of solar system
[LA-4341-SUPPL.] 20 p3348 N71-33525
- Methods for determining mass flow rates of gases for use in calibrating gas flowmeters
[NASA-CR-72896] 24 p3920 N71-37954

MASS FLOW FACTORS

- Dynamic models of negative mass instabilities in particle accelerator electron ring compressor
[UCRL-26208] 20 p3323 N71-33833
- MASS FLOW RATE**
- Turbulent mass exchange processes between recirculation zones in flame holder wake and surrounding flow
[RAE-LIB-TRANS-1418] 05 p0666 N71-15669
- Real gas corrections to gas flow computations for sonic nozzles
[NASA-TM-X-52965] 08 p1180 N71-18633
- Mass-flux probe as useful diagnostic tool in high Mach number and high enthalpy flows
[NASA-TM-X-52974] 09 p1388 N71-19699
- Set of FORTRAN 4 subroutines to calculate mass flow rate of natural gas through nozzles, also thermodynamic functions such as compressibility factor, entropy, enthalpy, and specific heat
[NASA-TM-X-5240] 11 p1717 N71-22616
- Mass flow rates applied to supersonic plasma jets
11 p1813 N71-22633
- Time resolved measurements of exhaust gas temperature, mass flow rate, and hydrocarbon concentration of spark ignition engine
14 p2353 N71-26004
- Computer controlled gas chromatograph for monitoring temperature, mass flow rate, inlet pressure, and calculation of precise retention volumes in real time
[COO-1224-44] 15 p2140 N71-27481
- Oxygen mass transfer rates to rotating disk in aqueous sodium chloride
16 p2584 N71-29031
- Mass flow rate measurements by means of sonic throat
[ONERA-TP-956] 20 p3249 N71-33001
- MASS RATIOS**
- NT PAYLOAD MASS RATIO**
- Spectrometer for measurement of velocity distribution and charge-to-mass ratios of ions
02 p0234 N71-11524
- Relationship between luminosity and mass ratio in eclipsing variable star system with subgiants
[NLL-RS-5999] 10 p1646 N71-21774
- MASS SPECTRA**
- Field ionization mass spectra of photopolymers of thymine
[NYO-2798-50] 01 p0019 N71-10823
- Mass spectra of phenolic polynuclear compounds of p-cresol and formaldehyde
[RAE-LIB-TRANS-1480] 03 p0333 N71-12381
- Electron impact behavior and mass spectra of molecular ion aromatic imide refractory materials
[RAE-TR-70047] 06 p0808 N71-15829
- Mass spectrum in chiral model of pseudoscalar and scalar mesons
[SU-1206-230] 07 p1071 N71-17265
- Symmetry breaking in chiral model using mass spectra of spin-zero mesons
[SU-1206-228] 07 p1073 N71-17358
- Electromagnetic perturbation of pseudoscalar mass spectrum in SU(3) symmetry model
[SU-1206-229] 07 p1074 N71-17437
- Structure of positron electron spectrum from photoproduction of rho and omega mesons
[DESY-70-40] 08 p1250 N71-18231
- Mass spectrometer analysis on ions ahead of shock waves in xenon
08 p1181 N71-18917
- Mass and energy spectrum analyses for photon, neutral pion, and eta-meson interactions based on Monte Carlo method
[JINR-EI-5349] 13 p2129 N71-24685
- Transformation of infinite component field with mass spectrum over nonunitary symmetry group representation
[JINR-P2-5305] 15 p2461 N71-27082
- Quantization of interacting covariant massless fields using Lagrangian formalism with prescribed asymptotic null data
15 p2476 N71-27472
- Effective mass spectrum of M/neutral pion neutral pion in range of 270 to 1300 MeV
[JINR-EI-5085] 15 p2490 N71-27893
- Mathematical model for composite magnetic and electrostatic charged particle beam analyzer transmission
[NASA-TT-F-13617] 16 p2659 N71-29177
- Mass spectra of ionized selenium vapor
17 p2796 N71-29790
- Mass spectra of antiproton proton annihilations into 4 or 5 pions at 3 GeV/c
[NP-18730] 18 p2974 N71-30563
- Observations from Apollo 14 suprathermal ion detector including ionospheric ion density, mass and energy spectra during venting in LM cabin, large ion cloud, and ion resulting from impacts
18 p3011 N71-30962
- Formulation of local infinite component fields as explicit realizations of wave functions with mass-spin relations
19 p3158 N71-32544

- Splitting in positive kaon positive pion negative pion mass spectrum in positive kaon deuteron interactions at 9 GeV/c
[COO-1428-270] 21 p3481 N71-34792
- MHD flow, recombination processes in pulsed beam discharge, and mass spectrometry applied to He in solids
[AE-410] 22 p3632 N71-35879
- Fission investigation using on-line mass spectrometry and emphasizing target construction, elimination of contamination, and recording of mass spectra
[NP-18029] 23 p3811 N71-37177
- Triple Resonance coupling related to low missing mass spectrum in diffraction dissociation
[UCSD-10-P-10-78] 23 p3812 N71-37185
- Mass spectra of alkyl carbonates derived from primary, secondary, and tertiary alcohols by use of deuterium labeling and high resolution mass spectroscopy
[NASA-CR-123196] 24 p3884 N71-37688
- MASS SPECTROMETERS**
- Interaction kinetics of atomic oxygen and hydrogen on metal surfaces of satellite-borne mass spectrometers
[NASA-CR-111117] 01 p0122 N71-10383
- Electric deflection molecular beam system with mass spectrometric detector
[AD-710656] 01 p0018 N71-10464
- Design, test evaluation, and performance failure analysis of ion mass spectrometer for OGO-F
[NASA-CR-111146] 01 p0053 N71-10588
- Barringer refractor plate correlation spectrometer as remote sensing instrument of pollutant gases in atmosphere
[NASA-CR-111373] 02 p0223 N71-11421
- Analytical photoionization mass spectrometer with argon gas filter between light source and monochromator
[NASA-CASE-LAR-10180-1] 04 p0486 N71-13461
- Ion masking in quadrupole mass spectrometer to eliminate unstable ion penetration
[NASA-CR-115781] 04 p0575 N71-13676
- Radiochemical and mass spectrometric analyses of plutonium fuel samples
[BNWL-1442] 04 p0556 N71-14109
- Lunar ALSEP mass spectrometer for measuring composition of lunar atmosphere
[NASA-CR-114774] 04 p0613 N71-14230
- Use of segmented rods in operation of quadrupole mass spectrometer
[NASA-CR-115776] 04 p0568 N71-14304
- Performance of computer controlled analytical mass spectrometer
[AECI-3470] 05 p0684 N71-14888
- On-line mass spectrometers with negative ion fission products
[COO-1608-8] 05 p0744 N71-15149
- Testing of electrical detection system adaptable to work source mass spectrometer
[IS-TRANS-82] 06 p0858 N71-15981
- Performance of mass spectrometer oxygen beam for upper atmospheric measurements
06 p0856 N71-16798
- Quadrupole mass spectrometer systems
[NASA-CR-116544] 07 p1114 N71-17797
- Reducing noise in multiplier of quadrupole mass spectrometer when operating in ion counting mode
[NASA-CR-1747] 07 p1033 N71-18032
- Measuring decay of Nb-90 to levels in Zr-90 using three-crystal gamma ray spectrometer
[IS-T-305] 08 p1255 N71-18369
- NO measurement in auroral arc by mass spectrometer onboard Aerobee rocket
[NASA-CR-116877] 08 p1194 N71-18997
- Computer-coupled low resolution mass spectrometer system and organic geochemical analysis methods for isolation and identification of compounds from lunar soil samples
[NASA-CR-114904] 09 p1465 N71-19786
- Design and performance of mass spectrometer system for atmosphere control in manned space station simulator
10 p1507 N71-20968
- Mass spectrometric analysis of reacting gases in microprobe and molecular beam samplings
11 p1763 N71-22642
- Quadrupole mass spectrometer for study of photolytic and heterogeneous reactions
11 p1697 N71-22643
- Mass spectrometry, free radicals, and transient intermediates evaporating from heated catalytic surface
11 p1697 N71-22644
- Mass spectrometer for dissociation measurement of oxygen in shock heated molecular beams
11 p1807 N71-22646
- Development and operation of mass spectrometer for analysis of highly reactive fluorine compounds at subambient temperatures
11 p1697 N71-22670
- Carbon monoxide accumulator cell for spacecraft mass spectrometer atmospheric sensor system
[NASA-CR-111855] 11 p1764 N71-22869
- Ion pump and magnet assembly for spacecraft mass spectrometer atmospheric sensor system
[NASA-CR-111856] 11 p1771 N71-22870

SUBJECT INDEX

MASS TRANSFER

High voltage ion pump power supply for spacecraft mass spectrometer atmospheric sensor system [NASA-CR-111857] 11 p1771 N71-23871

Inlet leak analysis for spacecraft mass spectrometer atmospheric sensor system [NASA-CR-111853] 11 p1764 N71-22872

Molecular beam ion source for spacecraft mass spectrometer atmospheric sensor system [NASA-CR-111859] 11 p1785 N71-22873

Design and characteristics of time of flight mass spectrometer to measure or analyze gases at low pressures and time of flight of single gas molecule [NASA-CASB-XNF-01056] 11 p1766 N71-23041

Analytic mass spectrometry for isotopic analysis of heavy metals and organic compound analysis [ORNL-4643] 12 p1915 N71-23151

Ion detection and monopole mass spectrometer performance tests with transverse magnetic field and thomson getter pump pumping capacity for D region ion composition analysis [NASA-CR-117905] 12 p1921 N71-23788

Uranium isotopic standard reference materials and absolute isotopic abundances determined by mass spectrometry [NBS-SPEC-PUBL-260-27] 12 p1922 N71-23803

Computer system for development and application of high resolution mass spectrometry 12 p1922 N71-24032

Neutral helium, atomic oxygen, and molecular nitrogen densities measured by Explorer 32 mass spectrometers [NASA-TN-D-7042] 12 p1997 N71-24084

A2 meson mass distribution produced by pion proton yields A2 proton reactions and mass spectrometry [NUB-2063] 12 p1977 N71-24212

CAL shock tube-driven molecular beam with target beam and mass spectrometer for scattered intensity measurements [AD-719820] 13 p2061 N71-25229

Gamma ray spectrometric comparisons of resonance integral to neutron activation cross section ratios and S values of Se-74, 78, 80, Br-81, I-127, Te-130, Co-140, 142, and Ba-138 [CNEA-274] 13 p2140 N71-25505

Mass spectrometry and radio frequency, high voltage spark ion source for measuring relative sensitivity factors for metals and steels [Y-1757] 14 p2599 N71-25702

External sheath structure and ion collection characteristics of rocket-borne mass spectrometer [AD-720833] 14 p2333 N71-25771

Design and characteristics of scintillation detector for fast ion counting in mass spectrometer [EUR-4567] 14 p2258 N71-26604

On-line computer system for surface ionization mass spectrometer scan control and data recording [AAEC/TM-568] 15 p2406 N71-26883

Design and calibration of neutral gas spectrometry with impact ion source for atomic oxygen density measurement in upper atmosphere [BMW-FB-W-70-06] 15 p2391 N71-27075

Knudsen gage and mass spectrometer measurements of vanadium, titanium, and chromium ternary alloys in base phase [AD-720287] 16 p2611 N71-28502

Time of flight and mass spectrometry of vanadium, titanium, and chromium alloy electron impact ionization cross sections using ion current and vapor pressure data for calculations 16 p2611 N71-28503

Ion microprobe mass spectrometer with cooled electrode target for analyzing traces of fluids [NASA-CASB-ERC-10014] 16 p2597 N71-28863

Test chambers with orifice and helium mass spectrometer for detecting leak rate of encapsulated semiconductor devices [NASA-CASB-ERC-10150] 16 p2598 N71-28992

Survey of errors in sampling shock tube gas with mass spectrometer for study of chemical reaction rates at high temperatures 17 p2735 N71-29782

Mass spectrometric analyses of xenon released in several stages of heating of group of neutron irradiated meteorites 17 p2845 N71-29826

Consecutive ion-molecule reactions in acetylene investigated by charge exchange mass spectrometry as function of energy transfer during initial ionization [AD-722470] 18 p2884 N71-30719

Application of mass spectrometer for space station simulator atmosphere analyzer [NASA-CR-111827] 18 p2962 N71-30743

Advantages of measuring metastable and mass spectrometers in artificial satellite nose cones and calculation of particle flux density passing through instrument orifice 19 p3103 N71-32605

Mass spectrometer with molecular beam system for analyses of gaseous reaction kinetics 21 p3388 N71-34104

Low mass spectrometer experimental design on Explorer 31 satellite and data processing techniques for meteoritic composition [NASA-CR-121651] 21 p3424 N71-34362

Time of flight mass spectrometer for determining thermodynamic properties of binary zirconium-uranium carbide [NASA-CR-121678] 21 p3443 N71-34497

Comparison of high-resolution gamma ray scanning and mass spectrometry for use in failure analysis of encapsulated fast reactor fuel element cladding [LA-4675-MS] 21 p3462 N71-34639

Development of specialized quadrupole mass spectrometer with high resolution and dynamic range increase [NASA-CR-121906] 22 p3582 N71-35509

Sensitivity of quadrupole mass spectrometer with segmented rod geometry [NASA-CR-121855] 22 p3582 N71-35512

Gas chromatograph, mass spectrometer system for chemical and biochemical determinations on Mars, and data reduction program 22 p3583 N71-35514

Theoretical and computer analyses of unstable ions in quadrupole mass spectrometer with ion source masking [NASA-CR-121905] 22 p3632 N71-35878

Narrow resonance width measurements in identical particle systems by means of missing-mass spectrometry [JINR-P1-5666] 22 p3633 N71-35894

Low temperature fluorine chemistry of chlorine, sulfur, and oxygen [AD-727059] 23 p3720 N71-36514

Mass spectrometric determination of neutron capture cross sections of rare earth isotopes [SGAE-PH-104/1971] 23 p3810 N71-37168

Projects and techniques including mass spectrometry, gas chromatography, combustion carbon analysis, atomic absorption spectrophotometry, and related analytical chemistry methods [UCRL-50906-71] 24 p3885 N71-37693

Analytical equations for optimizing mass spectrometer weight and power [NASA-CR-123204] 24 p3947 N71-38153

MASS SPECTROMETRY

U MASS SPECTROMETRY

MASS SPECTROMETRY

Mass spectrometric determination of thermodynamic properties of vanadium-titanium alloys [AD-709577] 01 p0066 N71-10198

Radiometric age determination and isotopic composition analyses on rocks, meteorites, and lunar samples [NASA-CR-111001] 01 p0016 N71-10304

Mass spectrometric analyses of meteoritic and lunar samples containing lead and thallium 01 p0033 N71-10314

Preparation and low temperature mass spectrometry of amorphous boron [AD-711439] 02 p0173 N71-11222

Research in instrumentation and mass spectrometry [NBS-TN-546] 02 p0174 N71-11229

Mass spectrometry to determine structure of various substituted polyfluorobenzenes [AD-711072] 02 p0175 N71-11233

Electron impact changes in methoxy alkane systems using mass spectrometry 03 p0330 N71-12354

Bibliography of mass spectrometry literature for first half of 1968 - compiled by computer method [IS-2059] 04 p0485 N71-13452

Numerical measurements from mass spectrometers [CEA-CO-1542] 04 p0570 N71-13571

Electron impact excitation efficiency curves for formation of neutral metastable species [UCRL-19594] 04 p0594 N71-14453

Mass spectrometry of vaporization of lanthanum and scandium carbides [NASA-TN-D-7039] 06 p0669 N71-15889

Mass spectrometric analysis of oxygen diffusion in germanium dioxide with isotopic labeling 06 p0689 N71-15983

Bibliography of mass spectrometry literature for last half of 1968 compiled by computer method [IS-2377] 06 p0812 N71-16712

Mass spectrometry rocket sounding data on neutral particle densities in Canadian lower atmosphere [BMW-FB-W-70-55] 07 p0108 N71-17151

Investigating ion molecule reactions of sodium, potassium, and barium ions with oxygen, nitric oxide, and water in drift tube mass spectrometer [NASA-CR-116501] 07 p0989 N71-17363

Investigating positive ions created in atmospheric air at pressures from 10 to 200 torr by glow discharge or by alpha irradiation from Po-210 [NP-18409] 08 p1252 N71-18305

Determining rates of vaporization of various solid propellant combustion products using mass spectra of isomolecular homogeneous gas phase equilibria [AD-715567] 08 p1304 N71-18811

Reporting research progress on mass spectrometry, neutron diffraction and activation analysis, isotope separation, and reactor physics [SERC-29468] 08 p1159 N71-18844

Mass spectrometry of lunar samples to determine uranium, thorium, and lead content [NASA-CR-114959] 10 p1645 N71-21575

Mass spectrometric investigation of collisional ionization by electronically excited helium [NASA-CR-111857] 11 p1889 N71-23818

Studying vaporization of indium-gallium oxide, and gallium-aluminum oxide by Knudsen effusion mass spectrometry [NASA-TN-D-4318] 12 p1868 N71-23111

Determination of molecular structures and characterization of materials by emission spectroscopy, mass spectrometry, and vibrational spectroscopy [AD-718431] 12 p1945 N71-23769

On-line mass spectrometric analysis of non-equilibrium air flows in low density wind tunnel nozzle [AD-718935] 13 p2063 N71-24477

Photoelectron spectroscopy, nuclear magnetic resonance, and thermochemistry of fuels, structural materials, and polymers 13 p2081 N71-25459

Mass spectrometric and radiometric analysis of mixed oxide fuels irradiated in Station C-2 [WCAP-3385-56-PT-2] 15 p2450 N71-27309

Knudsen flow mass spectrometry, thermodynamics, and chemical bonding of titanium, zirconium, hafnium, and thorium carbides during high temperature vaporization [NASA-TM-X-67444] 15 p2425 N71-27630

Cross sections for photoproduction of neutral mesons on hydrogen measured by linear accelerator using mass spectrometry techniques 15 p2483 N71-27767

On-line, alpha and proton decay spectrometry for determination of second order interference effects, second class currents, and beta to neutrino correlations in weak interactions 15 p2497 N71-27998

Validity of Alexander and Simenoff semiquantitative rule in atomic mass region 100 to 150 [JINR-E7-5409] 16 p2643 N71-28067

Franck-Condon and resonance charge exchange effects on charge transfer cross sections based on mass spectrometry of molecular ion reactions with perfluoroalkanes, alkanes, and alkene targets 17 p2801 N71-30116

Metal ion analysis techniques including neutron activation, ion exchange, solvent extraction, spectrophotometry, and X ray, absorption, mass, and emission spectroscopy [MLM-1801] 17 p2716 N71-30227

Ion-molecule reactions of CH4-CD4 mixtures at high pressures in ion source of quadrupole mass filter [AD-722687] 17 p2717 N71-30230

Fast reactor nuclear fuel burnup computer code using Nd, U, and Pu mass spectrometric data [GEAP-5355-A-REV] 18 p2556 N71-30442

Monochromatic, positive ion beams passed through inert gas and analyzed by mass spectrometry [AD-723558] 19 p3144 N71-31748

Paramagnetic resonance and mass spectrometric analysis of hydration products in aqueous acetaldehyde solutions [ISS-70/15] 20 p3229 N71-33414

Mass spectrometry investigations of Apollo 11 and 12 soil samples [UCB-34-F-52-FR-5] 20 p3323 N71-33815

Concentrations and isotopic composition of He, Ne, and Ar measured by mass spectrometry in separated metal phase and bulk samples of 15 chondrites for cosmic ray record studies 20 p3330 N71-33973

Mass-spectrometric stirred-reactor technique to measure rate of reaction of hydrogen chloride and deuterium chloride with atomic oxygen [NASA-TN-D-6495] 21 p3386 N71-34092

Composition of upper ionosphere as shown by magnetic mass spectrometer flown on Explorer 31 [NASA-CR-121865] 21 p3426 N71-34379

Distribution of impurities in plutonium determined by mass spectrometry, spectroscopy, and spectrophotometry [CEA-R-4071] 21 p3437 N71-34459

Fission investigation using on-line mass spectrometry and emphasizing target construction, elimination of contamination, and recording of mass spectra [NP-18829] 23 p3811 N71-37177

MASS TRANSFER

Results from theoretical and experimental studies of mass exchange in life support systems [NASA-TT-F-13371] 01 p0015 N71-10340

Mass transfer in gas flow through fluidized bed 01 p0043 N71-10491

Radio frequency impedance resonance for determining charge carrier properties in gallium [NP-18829] 01 p0099 N71-10512

Stirring effects on multiple phase mixing 01 p0018 N71-10525

Bibliography of compilation of articles on heat and mass transfer [AD-711147] 01 p0134 N71-10892

Mathematical model for mass exchange in closed life support systems 02 p0170 N71-11478

Convective heat and mass transport over tropical mid-Pacific estimated from satellite cloud photographs 02 p2825 N71-11616

Heat and mass transfer during vapor condensation in presence of noncondensing gases
[AD-712246] 02 p0306 N71-12084

Coordinate lattice method used to calculate two dimensional magnetic fields for charged particle transport in accelerators
[JINR-PS-5013] 04 p0573 N71-13667

Mass and energy exchange between interacting water channels
[WW-15-R-150] 04 p0559 N71-14237

Neutron transport equation solutions
[RT/F69/45] 06 p0896 N71-15715

Boundary layer flow over rough surface, and sand or sediment transport
[AD-714021] 06 p0836 N71-16312

Outgassing materials effects on voltage breakdown and analog between mass transfer and radiative heat transfer
06 p0829 N71-16654

Trends of developments in magnetohydrodynamics, and heat and mass transfer
[TR-60] 06 p0906 N71-16659

Axial and radial aerosol diffusion in circular pipes
[HASI-238] 08 p1177 N71-18261

Mass transport and atomic structure near metal surfaces
[AD-715291] 08 p1277 N71-18411

Monte Carlo calculations of neutron and gamma ray transport and minimum shield weight for mobile nuclear reactors
[NASA-TM-X-52973] 08 p1240 N71-18782

Linearized theory of stagnation region skin friction and mass transfer at hypersonic speeds
[NASA-TN-D-6262] 08 p1182 N71-18940

Kinetics of mass transfer in vibratory motion of solid body in stream of liquid
[PB-194294] 06 p1183 N71-18983

Mass transfer and drag coefficients of bubbles rising in dilute aqueous solutions
08 p1245 N71-19339

Mass transfer model for external spacecraft contamination and preventive measures
09 p1334 N71-20205

Reference transfer for vacuum gage calibration
09 p1389 N71-20209

Mathematical models for mass transfer and monitor system in liquid sodium technology
[GEAP-13539-13] 10 p1551 N71-21719

Mass shifts in second order of perturbation theory in dual resonance model
[LPTHE-71/7] 11 p1787 N71-22267

Analogies for heat and mass transfer processes in fluid flows
11 p1843 N71-22606

Estimation of momentum, heat transfer, and mass transfer in laminar boundary layers
12 p1903 N71-23948

Surface active agent effects on hydrodynamics and mass transfer of gas or liquid to liquid systems
[NLL-RTS-6328] 12 p1873 N71-24291

Nonlinear electron and ion transport in plasma diode of thermionic converter
12 p1983 N71-24326

Axially conducting gas controlled heat pipes leading to predictive capability for heat and mass transfer along heat pipes
[NASA-CR-114300] 13 p2185 N71-24666

Hydrodynamics and gas dynamics of boundary layer flow including mass transfer and convective and radiative heat transfer of bodies in fluids
[AD-720738] 14 p2244 N71-26539

Monte Carlo calculations of neutron transport in cylindrical and spherical geometry by ELF program
[ORNL-TR-2409] 15 p2458 N71-26879

Free stream turbulence effects on local heat or mass transfer rate across laminar, forward stagnation boundary layer on circular cylinders in cross flow
15 p2393 N71-27321

Numerical analysis of rare gas injection effects on aerodynamic heat transfer and wall shear stress on blunt bodies under reentry conditions
[SC-CR-70-6162] 15 p2394 N71-27608

Free convection heat and mass transfer along cylindrical bodies
16 p2600 N71-28200

Micrometeorological investigations of momentum, energy, and mass transfers above vegetative surfaces with von Karman constant, diabatic profile functions and eddy-transfer coefficients
[AD-721301] 16 p2625 N71-28225

Mass transfer during binary liquid drop growth at nonwetting capillary tubes
16 p2579 N71-28235

Atmospheric budget equations for mass, momentum, and energy derived for Barbados Oceanographic and Meteorological Analysis Program (BOMAP)
[COM-71-00195] 16 p2625 N71-28313

Axial mixing in gas and liquid phases and mass transfer coefficients for gas absorption in mechanically agitated column
16 p2580 N71-28689

Measurement of wall shear stress and fully developed mass transfer fluctuations at high Schmidt numbers in turbulent pipe flow
16 p2581 N71-28770

Heat and mass transfer in fluid eddy diffusivity near wall and asymptotic expansions in turbulent pipe flow problem
16 p2582 N71-28689

Oxygen mass transfer rates to rotating disk in aqueous sodium chloride
16 p2584 N71-29031

Corrosive mass transfer of structural materials and radioactive isotopes in sodium cooled reactor
[GEAP-13539-15] 17 p2780 N71-29206

Mass transfer and stainless steel corrosion in sodium cooled reactors
[GEAP-13539-14] 17 p2780 N71-29207

Mass transfer from a single sphere in Stokes flow using explicit finite difference method
[DLR-FB-70-73] 17 p2732 N71-29394

Modification of parton model with variable intermediate state parton mass
[TR-71-111] 17 p2806 N71-30310

Hydrodynamic problem of joint gas stream and liquid film mass transmission processes
[AD-723590] 19 p3076 N71-31743

Analysis of theoretical aspects of mass transfer between continuous liquid phases and liquid drops or gas bubbles and application to steel making process
[PB-198365] 19 p3117 N71-32557

Radioisotope and radar echo measurements on area of air/sea interactions over tropical ocean surface with numerical weather forecasting
[NASA-CR-119764] 19 p3199 N71-32731

Oceanographic and meteorological research on sea/air interactions over tropical ocean surface
19 p3200 N71-32732

Oceanographic and meteorological measurements on air/sea energy flux in atmospheric boundary layer over tropical ocean region
19 p3200 N71-32733

Mass and energy budget calculations for atmospheric boundary layer over tropical ocean region
19 p3131 N71-32734

Negative mass effect in dense electron beams in Adgeator model
[UCRL-TRANS-1426] 21 p3479 N71-34781

Heat, wave energy, and mass transfer through air-ocean interface in presence of swell and wind
[SU-TR-134] 22 p3574 N71-35454

Mass transfer in liquid metal systems and in-line devices for measuring sodium impurity
[GEAP-13539-16] 22 p3623 N71-35816

Effectiveness factor calculation technique for nonisothermal catalysts taking into account mass and heat transfer effects at boundary film and in particle interiors
[NLL-RTS-6472] 23 p3722 N71-36527

Calculation of simultaneous transient developing mass and momentum boundary layers in moving-wall problem from fluid flow through channels with dissolving walls
[ANL-7797] 23 p3743 N71-36687

Mass transfer and hydrodynamic behavior of laminar liquid films flowing over solid surfaces
23 p3746 N71-36710

Numerical scheme for solution of general turbulent tube flow problem with surface mass transfer and nonequilibrium chemical reactions
23 p3746 N71-36711

Model for calculating condensation effects in boundary layer on mass transfer from rotating disks
23 p3746 N71-36714

Interfacial tension pressure change measurements of mass transfer effects on droplet interface motions
23 p3780 N71-36941

MASSACHUSETTS
Aerial multispectral and infrared scanning of Massachusetts coastline
[NASA-CR-116782] 08 p1187 N71-18402

Geologic analysis of X band radar mosaics of Massachusetts
08 p1197 N71-19255

MATCHING
Improved efficiency of drilling ceramics and glass using liquid environments
[AD-713595] 05 p0710 N71-15361

Equations for describing noncollinear phase matching in uniaxial crystals
15 p2454 N71-27376

Ordered search techniques for digital template matching
[TR-166] 20 p3291 N71-33415

Elastic matching, error correction coding in natural language
[NPL-COM-SCI-46] 22 p3556 N71-35330

MATERIAL ABSORPTION
Rate of hydrogen absorption by copper
[PB-190503T] 02 p0243 N71-11697

Describing sorption vacuum trap having housing with group of reentrant wall portions projecting into internal gas-permeous container filled with gas and vapor sorbent material
[NASA-CASE-XER-09519] 08 p1201 N71-18483

Axial mixing in gas and liquid phases and mass transfer coefficients for gas absorption in mechanically agitated column
16 p2580 N71-28689

MATERIAL BALANCE
NT WATER BALANCE
Integrated safeguards of material balance techniques
[GEAP-12114-2] 08 p1176 N71-19149

Analysis of plutonium, uranium, and plutonium oxide materials balance during nuclear fuel fabrication
[GEAP-12114-4] 21 p3461 N71-34634

MATERIAL REMOVAL [MACHINING]
U MACHINING
MATERIALS

Bibliography with abstracts on materials dynamic properties
[AD-710823] 01 p0129 N71-10484

X ray flash photography for radiographic material evaluation
[REPT-9/69] 03 p0381 N71-13146

Pressure effects on thermoelectric responses of thermocouple materials
14 p2257 N71-26486

Problems of retrieving data on chemical compounds and materials using manual data retrieval system
19 p3195 N71-31985

MATERIALS EROSION
U EROSION
MATERIALS HANDLING

NT GROUND HANDLING
NT PROPELLANT TRANSFER
NT REMOTE HANDLING

Materials management control performance of Apollo program prime contractor
01 p0136 N71-10292

Standardized measurement of materials
01 p0618 N71-10507

Air bearings for near frictionless transfer of loads from one body to another
[NASA-CASE-XMF-01857] 01 p0059 N71-10617

Quick-release coupling for fueling rocket vehicles with cryogenic propellants
[NASA-CASE-XKS-01985] 01 p0060 N71-10782

Materials processing and manufacturing in earth-orbital payload planning
02 p0297 N71-11702

Investigating system for transferring failed fuel from primary tank to argon cell of EBR-2 facility
[ANL-EBR-024] 04 p0546 N71-13685

Constructing protective manipulators for automatic transfer of isotopes from reactor cores
[CEA-N-1265] 04 p0574 N71-13674

Investigating distribution criteria, effectiveness and cost models in management of resources
[FTL-A-A08-7] 05 p0713 N71-14679

Method and apparatus for removing plastic insulation from wire using cryogenic equipment
[NASA-CASE-MFS-10340] 07 p1035 N71-17628

Development of facilities for preparation of high explosives and booster charges
[AD-716036] 09 p1365 N71-19668

Effects of chemical catalysts, bed cooling, chemical manufacturing techniques, operating conditions, and chemical handling procedures on lithium peroxide
[NASA-CR-114896] 09 p1343 N71-19914

Environmental tests and materials handling processes for beam lead semiconductor devices
[BDX-613-194] 09 p1454 N71-20023

Fluid transferring system design for purging toxic, corrosive, or noxious fluids and fumes from materials handling equipment for cleaning and accident prevention
[NASA-CASE-XMS-01905] 10 p1540 N71-21089

Bibliography on shipping containers, criticality in handling, transport regulations, and safety practices for radioactive materials
[ORNL-NSIC-84] 10 p1619 N71-21635

Oxygen diffusive hazards, chemical and physical properties, decontamination methods, and transfer and storage techniques manual
[NASA-CR-72401] 12 p1925 N71-23169

Evacuable glove-box for handling of liquid sodium and apparatus for analysis of carbon in sodium and other metals
[AERE-R-6338] 13 p2110 N71-24432

Guide for fabricating and handling Cf-252 sources including health physics procedures, shielding requirements, containment and ventilation requirements, and purification techniques
[SRO-153] 13 p2142 N71-25565

Design and construction of containers for storage of superpure materials
16 p2556 N71-28303

Broad spectrum of materials chemistry under extreme conditions, including ionizing radiation, high vacuum, high pressure, and high temperature
[AD-720289] 16 p2557 N71-28437

Environmental testing and handling of batteries for Mariner 7 spacecraft
16 p2539 N71-28669

Metallographic examination of container material for ICN-244203
[ORNL-4663] 17 p2785 N71-30206

Equipment for facilitating lifting, moving, and handling materials-technology utilization
[NASA-SP-5929/011] 18 p3029 N71-30864

SUBJECT INDEX

- Unload emission behavior of materials with various heat treatments and its relation to Bauschinger effect 18 p2326 N71-31139
- Transportation shock and vibration monitor for recording acceleration in shipment of complex equipment [UCRL-72748] 19 p3101 N71-32311
- Game theory, information system for disease diagnosis, and model of warehouse system [JPRS-53701] 20 p3289 N71-32877
- Mathematical model of locations and types of warehouses, volume of product stored, and losses due to external effects 20 p3289 N71-32883
- Analysis of plutonium, uranium, and plutonium oxide materials balance during nuclear fuel fabrication [GEAP-12114-4] 21 p3461 N71-34634
- Molten sodium container design code and safety procedures [RD-B-M-1817] 22 p3620 N71-35790
- Aerial surveys for determining plutonium concentration using array of NaI detectors [EGG-1183-1517] 22 p3644 N71-35980
- Classification, management, and data systems used by NATO for control of material [FTL-A-A00-1] 22 p3700 N71-36392
- Design and storage tests of 200 lb diborane shipping container including storage time, volumetric loading, and pressure-temperature limitations [NASA-CR-122952] 23 p3761 N71-36810
- Sampling, handling, and measuring emissions from aircraft gas turbine engines [REPT-430] 24 p3873 N71-37604
- Storage and handling of highly irradiated fast breeder reactor fuel in hybrid sodium organic coolant storage pool, and Sb-Cu liquid metal dissolution for dechloriding [EUR-4615-E] 24 p3956 N71-38223
- MATERIALS RECOVERY**
- NT WATER RECLAMATION**
- Chemical recovery and refinement procedures in electromagnetic separation of isotopes [ORNL-4583] 04 p0584 N71-14186
- Matrix method calculation of multielement regenerative extraction system properties for synchro-cyclotron [UCRL-19804] 04 p0584 N71-14201
- Development of methods for extracting metals from manganese modules dredged from ocean floor [BM-RI-7473] 05 p0673 N71-14901
- Comparing purification of samarium by sublimation and vaporization from low-melting metal flux at same temperature [BM-RI-7466] 05 p0701 N71-15061
- Electrochemical extraction of vanadium from vanadium carbide in molten salt electrolyte [BM-RI-7484] 06 p1217 N71-19015
- High temperature gas cooled reactor design and development including cesium and strontium diffusion in graphite, processing cycles, and fission product transport coding 09 p1419 N71-19937
- Fluidized bed combustion process for recovering uranium from spent graphite-matrix nuclear rocket fuels [IN-1423] 09 p1422 N71-20596
- Reaction kinetics of nitride formations in liquid uranium alloys and nitride precipitation for nuclear fuel reprocessing [SU-326-P-28-X-2] 10 p1601 N71-20642
- Annotated bibliography on niobium recovery from niobium uranium alloys [RFP-1421] 15 p2422 N71-27132
- Pyrochemical processing techniques for recovery and purification of Pu-238 from various fuel materials [ANL-7709] 15 p2447 N71-27180
- Chemical recovery and analysis of trace elements from irradiated silicon carbide coated plutonium dioxide fuel [KR-140] 15 p2452 N71-27849
- Development of minimum and optimum requirements for environmental surveillance programs around nuclear fuel reprocessing plants 17 p2784 N71-29878
- Flow sheet for reprocessing spent fuels from power reactors [RT/CHI-7113] 21 p3458 N71-34609
- Molten-salt fluoride volatility process for recovering decontaminated uranium from aluminum clad fuel elements [ORNL-4574] 22 p3624 N71-35819
- Cyclic leaching process for cadmium and nickel recovery from nickel cadmium scrap battery waste [RM-RI-7566] 23 p3772 N71-36883
- Improved zirconium uranium alloyed fuel processing with centrifuge 23 p3800 N71-37095
- MATERIALS SCIENCE**
- Nondestructive tests for evaluating bonded materials [AD-709963] 01 p0071 N71-10174
- Techniques in plating including types of plating, and materials used for plating - bibliography [AD-709950] 01 p0058 N71-10188
- Development of nondestructive tests for evaluating bonded materials [AD-709963] 01 p0071 N71-10189
- Data tabulated from 274 stations in US and Canada on air pollution effects on materials [PB-192446] 02 p0151 N71-11071
- Preparation, characterization, and properties of noncrystalline solids [AD-711820] 02 p0248 N71-12054
- Activation analysis to identify materials for use as catcher for micrometeoroids [NASA-CR-106707] 03 p0454 N71-13199
- Sources of rare earths, also current and anticipated usage in various applications including nuclear research and electrical engineering [NMAB-266] 04 p0535 N71-14268
- Effect of radiation on structural materials for NERVA engine tested at cryogenic and elevated temperatures - Vol. 4 [NASA-CR-116518] 07 p1063 N71-17351
- Thermal conductivity and electrical resistivity of materials for NERVA engine - Vol. 3 [NASA-CR-116519] 07 p1063 N71-17352
- Effectiveness of research programs management for materials science [AD-714860] 07 p1135 N71-18070
- Materials science and engineering work at MIT [AD-714861] 08 p1306 N71-18241
- University materials science research program review [AD-715686] 08 p1307 N71-18448
- Materials science program annual research summaries [AD-716469] 09 p1487 N71-19940
- Chemical composition, electromagnetic properties, raw materials, and production techniques for various types of ferrites [JPRS-52952] 12 p1965 N71-23285
- Abstracts of papers presented at US Air Force materials symposium held at Miami Beach, Florida in May, 1970 [AD-718432] 12 p1943 N71-23625
- Materials science research including trace element studies, composite catalysts and polymers, crystal growth, radiation damage, and related subjects [AD-718821] 12 p1945 N71-23794
- Flammability test chamber for testing materials in certain predetermined environments [NASA-CASE-KSC-10126] 13 p2061 N71-24985
- Development and characteristics of materials for liquid propellant rocket engines, warheads, propellant tanks, solid rocket propellants, combustion chambers, and exhaust nozzles [AD-720596] 14 p2344 N71-26093
- Solid state physics for calculating material parameters and characteristics [FOA-4-C-4404-10] 14 p2329 N71-26543
- Effect of internal stresses on strength of chemically bonded composites with varying coefficients of thermal expansion [UCRL-20395] 15 p2428 N71-26987
- Systems analysis for selection and application of materials 15 p2429 N71-27039
- Stress wave emission as measure of crack growth in materials failure [ARL/MET-72] 15 p2522 N71-27857
- Thermally stimulated electron emission of ceramic beryllium oxide and calcium sulfate/pure and doped with samarium, manganese, and lead/ studied for dosimeters material [RT/FI/7037] 16 p2642 N71-28030
- Feasibility study for German materials data bank - conference 17 p2762 N71-29387
- Research projects in materials science [AD-732090] 19 p3168 N71-31754
- Development of data tables and scientific documentation of thermophysical properties of materials [AD-732091] 19 p3120 N71-32022
- Materials research for thermal reactors, jet engines, space shuttles, and space nuclear power system [NASA-TM-X-7485] 19 p3121 N71-32349
- Rate of introducing new or improved materials in national programs [NASA-CR-121375] 20 p3286 N71-32943
- Teflon-carbon mixture identified as air equivalent material and suitable for cavity ionization chambers [CEA-B-4173] 21 p3443 N71-34498
- Survey of yttrium and thorium properties, resources, industry, production, consumption, trade, technology, and history 22 p3401 N71-35647
- Fluid electrophoresis separation based on motion of particles in electric field for demonstrating near-zero-gravity condition in space - Apollo 14 [NASA-TM-X-64611] 23 p3718 N71-36506
- MATERIALS TESTING REACTORS**
- U NUCLEAR RESEARCH AND TEST REACTORS**
- MATERIALS TESTS**
- Production engineering and materials evaluation for thin film circuit manufacture [ECR-12] 02 p0194 N71-11362

MATHEMATICAL LOGIC

- Nondestructive magnetic field testing methods for reliability engineering of aerospace components 02 p0532 N71-11643
- Acoustic analyses for materials research and structural integrity evaluation 05 p0706 N71-15064
- Dynamic characteristics of fatigue testing machines [TT-70-50033] 08 p2008 N71-19180
- Computerized real time simulation of atmospheric balloon environment in altitude chamber 09 p3183 N71-30217
- Interferometric measurements of dimensional and refractive-index changes in optical materials exposed to space environment [NASA-TM-X-66049] 09 p1424 N71-30255
- Development of equipment for measuring thermal shock resistance of thin discs of material [NASA-CASE-XLB-62024] 11 p1765 N71-22964
- Multisample test chamber for exposing materials to X rays, temperature change, and gaseous conditions and determination of material effects 11 p1733 N71-23042
- Ammonia decontaminant control of oxygen diffusive and static and dynamic compatibility tests with plastic and elastomer materials [NASA-CR-72380] 12 p1869 N71-23167
- Torque for measuring potassium film journal relative motion with coil and wire diameter, temperature, frequency, and holder material effects on transducer and journal materials [NASA-CR-72821] 12 p1939 N71-24088
- Burner rig tests on simulated turbine blades, with and without internal cooling, to predict thermal fatigue performance [NASA-TM-X-67820] 13 p2181 N71-25120
- Development and conduct of national and international programs to determine variations in creep test techniques and establishment of standard creep test procedures [AGARD-B-581-71] 13 p2184 N71-25449
- Effect of hardening temperature on change in resistance to abrasive failure of alloys [AD-720379] 14 p2273 N71-25875
- Automated ball rebound resilience test equipment for determining viscoelastic properties of polymers [NASA-CASE-XLA-8254] 14 p2255 N71-26161
- Hermetic sealing device for ends of tubular bodies during materials testing operations [NASA-CASE-NPO-10431] 16 p2605 N71-29132
- Steel and cobalt-nickel alloy compression and corrosion tests after precipitation hardening at cryogenic temperatures for increased yield strength and corrosion resistance [NASA-CR-72798] 19 p3115 N71-32321
- Differential thermal analysis methods in high temperature research on biochemical, polymeric and explosive materials 20 p3361 N71-32826
- Standardization of test methods in differential thermal analysis for materials 20 p3362 N71-32827
- Evaluation of materials as temperature scale standards for differential thermal analysis 20 p3362 N71-32829
- Performance tests and evaluation of wire cable materials for use with aircraft arresting gear [AD-724284] 22 p3539 N71-35211
- Differences, simulations, and interrelationships between insulation resistance and dielectric strength testing [AD-726924] 22 p3561 N71-35346
- Test and evaluation of high-refractory materials for construction of magnetohydrodynamic generator 22 p3598 N71-35622
- Materials tests of refractory materials used in magnetohydrodynamic generators to determine thermodynamic and electrical properties 22 p3600 N71-35640
- Optimal design and working parameters for experimental installation of magnetohydrodynamic generator 22 p3600 N71-35640
- Materials tests of cermet materials based on refractory carbides to determine melting point, oxidation resistance, emissivity, and weldability 22 p3600 N71-35641
- Chemical and structural analysis techniques for materials suitable for aircraft structures [AD-727017] 22 p3691 N71-36323
- Tension, biaxial, and creep tests of 5Al-2.5Sn titanium alloy and computerized design for fiberglass-overwrapped titanium pressure vessel [NASA-CR-72765] 23 p3761 N71-36814
- Characteristics and availability of depleted uranium to include supply situation, nonenergy consumption, metallurgy, chemistry, and potential uses [NMAB-275] 23 p3772 N71-36884
- Analysis of effect of lithium and chromium on stress corrosion resistance of aluminum-zinc-magnesium alloys [NLL-M-20438-15828.4F1] 23 p3774 N71-36895
- MATHEMATICAL ANALYSIS**
- U APPLICATIONS OF MATHEMATICS**
- MATHEMATICAL LOGIC**
- NT ALGORITHMS**

NT AXIOMS
 NT BETHE-HEITLER FORMULA
 NT BOOLEAN ALGEBRA
 NT BOOLEAN FUNCTIONS
 NT EQUIVALENCE
 NT FORMULAS [MATHEMATICS]
 NT LATTICES [MATHEMATICS]
 NT SET THEORY
 NT THRESHOLD LOGIC
 Path from operational logic to conventional quantum theory in complex Hilbert space
 01 p0077 N71-10956
 Procedure for comparing theory conclusions and observed data facts in hypothesis assessing
 [NASA-CR-111335] 01 p0139 N71-10980
 Majority logic decoding for duals of primitive polynomial codes, and maximality of Euclidean geometry codes
 [AD-711791] 02 p0190 N71-11337
 Properties of continuous logic functions which generalize in out of a voting functions and threshold functions of binary variables to continuous variables
 02 p0196 N71-11373
 Periodicity of sequential machines
 [AD-712596] 03 p0344 N71-12497
 Mathematical logic differential equations solved by Walsh functions
 [NPL-DES-1] 03 p0400 N71-13255
 Utilization of ternary logic in calculating no failure probability of reserved systems with two forms of failure present
 [AD-712040] 03 p0401 N71-13354
 Linear ordinary logical differential equations and Walsh functions
 [NPL-DES-2] 06 p0683 N71-15712
 Three paradoxes related to fully causal theory
 [BLO-2041-49] 08 p1260 N71-18775
 Problems in semantic comparison of natural and mathematical logic languages
 [JPRS-52621] 10 p1527 N71-20678
 Relationship between inverse and resolution methods of theorem proving
 [NLL-RTS-5859] 16 p2622 N71-28196
 Strategies and theorem proofs for predicate calculus using resolution principle
 [NLL-RTS-5857] 17 p2774 N71-30018
 Boolean matrix syntheses of digital networks for construction of algorithms
 18 p2900 N71-31446
 Specializations for deducing classical calculus of predicates formula with functional signs
 [NLL-RTS-5858] 19 p3124 N71-32582
 Symbolic logic - theory of classes and relations, formal systems, and axiomatic theories
 [PUBL-16-VOL-2] 21 p3448 N71-34539
 Symbolic logic - sentential and quantificational logic, and deduction
 [PUBL-16-VOL-1] 21 p3449 N71-34547
 Procedure for analysis of data representation systems for man-operator controlling complex automated object
 24 p3881 N71-37667
 Selected articles on application of mathematical methods to automation of rail transportation
 [AD-72767] 24 p3895 N71-37760
 Mathematical logic applied to aerial photograph interpretations
 [AD-727459] 24 p3925 N71-38009

MATHEMATICAL MODELS
 NT DIGITAL SIMULATION
 NT THOMAS-FERMI MODEL
 NT VENEZIANO MODEL
 Mathematical model for describing one-dimensional wave propagation in resonating soil column by use of nonlinear constitutive relation
 [AD-710234] 01 p0127 N71-10040
 Developing models of atmospheric density to formulate algorithms for control of spacecraft motion in atmosphere
 [NASA-TT-F-13359] 01 p0045 N71-10046
 Exact solutions for rectangular bidirectional laminates and sandwich plates
 [AD-710615] 01 p0070 N71-10062
 Evaluation results and accuracy improvement of two flux switching mathematical models for magnetic cores
 [NASA-TN-D-6032] 01 p0036 N71-10067
 Base charge compensation and approximate transistor noise model
 01 p0031 N71-10152
 Mathematical modeling and sensitivity analysis of radiation effects on semiconductor junctions
 [AD-709929] 01 p0032 N71-10179
 Controllability and observability with algebraic systems theory
 [NASA-CR-111112] 01 p0074 N71-10327
 Mathematical models for mixed state of superconductors
 [NASA-SP-240] 01 p0089 N71-10415
 Mathematical crack problems concerning square and hexagonal holes with small symmetrical corner cracks
 [AD-709848] 01 p0129 N71-10442
 Turbulent boundary layer-shock interaction with and without injections
 [AD-710637] 01 p0042 N71-10463

Many universes interpretation of quantum mechanics based on mathematical content of quantum formalism and complexity of real world
 01 p0075 N71-10498
 Mathematical model for chemical activity increase at crystal surface caused by mechanical impact
 01 p0018 N71-10513
 Mathematical model for self-defocusing of light beam in fluid
 [AD-710741] 01 p0090 N71-10573
 Subcritical flows over two dimensional airfoils by multi-strip method of integral relations
 [RE-3933] 01 p0001 N71-10581
 Digital computer oriented analysis method for Mason flow graphs
 01 p0076 N71-10648
 Steady-state nondivergent Gaussian computer model for simulating air quality in region of New York City
 [RE-3923] 01 p0013 N71-10712
 Differential correction methods in spacecraft attitude determination
 [NASA-CR-111148] 01 p0123 N71-10727
 Microscopic analysis theoretical model for elastic scattering of deuterons and alpha particles
 [CTC-32] 01 p0100 N71-10744
 General formula for artificial electron decay life times
 [NASA-TM-X-65376] 01 p0118 N71-10768
 First order prediction model of total-electron-content group path delay for midlatitude ionosphere
 [AD-711365] 01 p0025 N71-10770
 Mathematical model of rotating neutron star
 [AD-711397] 01 p0123 N71-10841
 Use of computers for man machine modeling studies and plans
 [AD-711638] 01 p0015 N71-10880
 Examining dynamics of hydraulic or pneumatic servomechanisms with aid of mathematical models
 [AD-711163] 01 p0061 N71-10903
 Calibration and preliminary analysis of passenger demand and modal split models for Northeast Corridor of United States
 [PB-190946] 02 p0144 N71-11021
 Computerized modeling of ultraviolet and thermal radiation incandescence of spores
 [NASA-CR-111386] 02 p0150 N71-11066
 District of Columbia air quality display model for computing seasonal concentration estimates
 [PB-189194] 02 p0151 N71-11072
 Theoretical models related to Hills alternative to naval decompression concepts
 [AD-711809] 02 p0155 N71-11095
 Analysis of charring ablation with description of associated computing program
 [NASA-TN-D-6083] 02 p0304 N71-11127
 Generation and application of sensitivity coefficients
 [NASA-CR-102912] 02 p0197 N71-11380
 Mathematical model for stress waves in sandwich plates subjected to high velocity impact
 [NASA-CR-106692] 02 p0300 N71-11404
 Analytical models for magnetohydrodynamic turbulence and unstable plasma behavior
 [NASA-CR-111804] 02 p0279 N71-11428
 Empirical iteration model for optimal design procedures
 [ECR-17] 02 p0250 N71-11468
 Applying Kalman filtering to problems of barometric pressure and inertial heights in navigation
 [RAE-TR-69131] 02 p0262 N71-11763
 Model for nonparallel daughters of Regge particle trajectory checked with pion-pion resonance scattering
 [IC/70/30] 02 p0273 N71-11793
 Cratered lunar soil model for reproducing directional infrared data from lunar thermal meridian
 [DI-42-6987] 02 p0296 N71-11966
 Theory of channelling effect
 [IAE-1878] 02 p0276 N71-11997
 Mathematical model for calculating precipitation over orographic barrier
 [PB-192757] 02 p0260 N71-12108
 Verticle momentum and heat transfer determinations in atmospheric boundary layers at sea
 [AD-711376] 02 p0261 N71-12173
 Developing mathematical model for tandem rotor helicopter for analysis of automatic approach and landing system
 [NASA-TM-X-66493] 03 p0312 N71-12225
 Mathematical model of spiral response to impact
 03 p0320 N71-12285
 Two-region, continuous search, and n-region discrete models for allocating available effort to search for objects at sea
 [AD-712836] 03 p0328 N71-12339
 Computer program for numerical simulation of plasmas
 [AD-712562] 03 p0437 N71-12752
 Models of chiral symmetry in meson states
 03 p0424 N71-12773
 Uniqueness and convergence of discrete aggregate model in polycrystalline plasticity
 [AD-712060] 03 p0441 N71-12838

Analysis of set of spectral index measurements in multiplying lattices by application of correlation method
 [RT/FI/69/54] 03 p0429 N71-12883
 Self consistent polycrystalline model for creep under combined stress states
 [AD-712046] 03 p0461 N71-12967
 System of predicting waves and swells on US Continental Shelf of east coast
 [PB-192201] 03 p0372 N71-13324
 Calculation of nuclear fuel element distribution and moderator density by multigroup diffusion theoretical methods noting thermionic uniform emitter heating
 [REPT-4-45] 03 p0417 N71-13337
 Travel times of PcP interpreted in terms of variations in radius of earth core configuration
 [AD-712673] 03 p0374 N71-13346
 Acceleration model for neutron production in a pinch discharges
 [AD-712692] 03 p0439 N71-13348
 Theoretical treatment of conceivable serious accidents at fast breeder reactors in context of Bethe-Tait method
 [EURFMR-748] 04 p0546 N71-13568
 Model for weak leptonic interactions
 [UIJV-2435-F] 04 p0575 N71-13462
 Diffraction dissociation model for high energy rho photoproduction
 [DESY-70/23] 04 p0575 N71-13463
 Two dimensional model for radio wave propagation across land/sea boundaries
 04 p0491 N71-13703
 Initial equations for collisional diffusion in toroidal magnetic traps
 [NF-18340] 04 p0596 N71-13764
 Digital techniques and components for signal detection in clutter by advanced radar systems
 [AGARD-CP-66-70] 04 p0593 N71-13901
 Radar cross section model for scatter return from stormy ocean surface
 04 p0494 N71-13902
 Target signature models for detection probability assessments of radar receivers
 04 p0495 N71-13908
 Supralinearity of UV repopulated TL from TLD-100
 [COO-1105-156] 04 p0579 N71-13986
 Mathematical model of sodium-water reactions related to steam generators
 [APDA-257] 04 p0559 N71-14193
 Eikonal model for large angle np and pp elastic scattering at medium energies
 [NYO-2262-TA-223] 04 p0585 N71-14224
 Chiral SU(2) x SU(2) hard pion current algebra models
 [NUB-2029] 04 p0539 N71-14242
 Extended particle model in general theory of relativity
 [JINR-E-5271] 04 p0588 N71-14294
 Investigating categorization and formulation of stress and strength factors for semiconductor diodes to provide improved failure rate prediction from mathematical models
 [NASA-CR-115801] 04 p0603 N71-14311
 Induced fields and heating in cranial model irradiated by electromagnetic plane wave
 [AD-712845] 04 p0479 N71-14469
 Multi-loop self energy operators in dual resonance model
 [TUEP-70-27] 05 p0712 N71-14521
 Linear solid model assuming constant Poisson ratio for straight crested waves in infinite linear viscoelastic plate
 [AD-713301] 05 p0774 N71-14556
 Stabilization model for rigid rotor helicopters
 [AD-713402] 05 p0627 N71-14585
 Environmental testing of silicon cell spalling and experimental confirmation of mathematical model
 [NASA-CR-102944] 05 p0630 N71-14606
 Pressure distributions calculated with Sells method on series of quasi-elliptical symmetrical airfoils in subcritical flow
 [NRC-11693] 05 p0625 N71-14612
 Similarity model for atmospheric turbulence structure in planetary boundary layer
 [AD-713569] 05 p0667 N71-14693
 Deriving empirical model for calculating safe nuclear criticality parameters for complex arrays of intersecting pipes containing enriched uranyl nitrate solution
 [RFP-1553] 05 p0638 N71-14699
 Body exposure rate calculated for dose from Kr-85 released to earth atmosphere
 [BNWL-SA-3233-A] 05 p0635 N71-14706
 Mathematical model of nonsimilar laminar or turbulent boundary layer, including entropy layer and turbulence effects, solved by Newton-Raphson iteration
 [NASA-CR-73401] 05 p0659 N71-14739
 Data reduction processes for spinning flat-plate satellite-borne radiometers
 [ESSA-TR-NESC-52] 05 p0649 N71-14779
 Mathematical models of fluidic transmission lines for use in missile design
 [AD-713505] 05 p0662 N71-14808

SUBJECT INDEX

- Mathematical model with error correction for calculating optimal solid bed reactor dimensions [DISE-4302] 05 p0639 N71-14821
- Models for generating synthetic seismograms to predict results of actual seismograms [NVO-1163-217] 05 p0670 N71-14828
- Computer synthesis for classifying natural shapes and patterns including leaves [AD-713163] 05 p0637 N71-14833
- Mathematical modeling of world geodetic system [AD-713475] 05 p0672 N71-14876
- Semiconductor integrated circuit component models [AD-713475] 05 p0655 N71-14924
- Mean turbulent field closure of turbulent boundary layer equations of motion - Part 2 [SC-CR-70-6125-PT-2] 05 p0663 N71-14928
- Using modeling techniques in design of complex systems for Deep Space Network 05 p0646 N71-14953
- Describing operations in radio astronomy, signal to noise ratio prediction, and tropospheric scattering refraction models for DSIF 05 p0647 N71-14984
- Absolute scale for radiation ages of stony meteorites [NASA-CR-115884] 05 p0640 N71-14967
- Phenomenological model of T-violation for leptonic decays of baryons as function of electron energy [SINP-TH-67-2] 05 p0739 N71-15030
- Statistical simulation procedures utilizing Monte Carlo stratification technique [NASA-CR-115145] 05 p0713 N71-15112
- Mathematical model for cross mode excitation structures in synchrocyclotron acceleration [CERN-70-13] 05 p0742 N71-15129
- Investigating polarization diversity as technique to reduce effects of target glint or angle fluctuation [AD-713335] 05 p0704 N71-15353
- Scale weather forecasting model for upper atmosphere above Northern Hemisphere [AD-713119] 05 p0719 N71-15398
- Mathematical model for droplet growth rate in cloud seeding [AD-713559] 05 p0719 N71-15399
- Mathematical analysis of denting of thin aircraft skin by hail [NASA-TN-D-6102] 05 p0780 N71-15422
- Thermal scale modeling of heat pipes 05 p0784 N71-15556
- Linear estimation model for network flow [FOA-C-82-37-13] 05 p0666 N71-15611
- Stochastic forecast modeling of research and development trends [JPRS-51999] 05 p0788 N71-15633
- Pion-pion scattering lengths from class of nonlinear Lagrangian models [SINP-TH-69-4] 05 p0910 N71-15792
- Approximation model used with self shielding data for U-238 [AAEC/TM-539] 05 p0911 N71-15802
- Mathematical models for two phase cryogenic choking flow of hydrogen and nitrogen [NASA-CR-116003] 05 p0833 N71-15808
- Constructing multichannel model for very high energy collisions using kinematical variables [IFP-81-8/70] 05 p0912 N71-15816
- Investigating cyclotron resonance in solid-state plasma and nonlinear friction in superconductors 05 p0902 N71-15860
- Using extended nonlinear friction model to improve performance prediction for arc second tracking in direct drive servomechanisms 05 p0862 N71-15862
- Mathematical models for seismic amplification and ground motion of recording station geology [NVO-1163-211] 05 p0640 N71-15912
- Mathematical models on visual perception [AD-714106] 05 p0805 N71-15995
- Stationary nonlinear model of atmospheric circulation [AD-714763] 05 p0890 N71-16045
- Flight simulator mathematical modeling for aircraft design 05 p0831 N71-16063
- Working numerical model for oceanographic forecasting, emphasizing basic equations and boundary conditions [AD-714507] 05 p0841 N71-16107
- Optimization and estimation models for automatic navigation [AD-714699] 05 p0894 N71-16204
- Mathematical models of suboptimal Kalman filter control systems with delayed states for navigation satellite [AD-714501] 05 p0894 N71-16205
- Theories and observations relations related to quasi modes and solitons [AD-714110] 05 p0946 N71-16270
- First order wave function in 1/Z expansion [NASA-CR-116126] 05 p0884 N71-16276
- Fourier transform of scattering diagrams and selective summation techniques [AD-713889] 05 p0815 N71-16286

- Calculation of average surface impedance for periodic surface [AD-714090] 05 p0815 N71-16287
- General numerical large deflection solution of conical ring circular glass plate flexure problem [AD-714154] 05 p0878 N71-16344
- Calculation model for high temperature thermal conductivity of carbon foams [SC-RR-70-622] 05 p0879 N71-16371
- Extension of frequency response and pulse test methods for identification of nonlinear system elements described by nonlinear differential equations [AD-714489] 05 p0827 N71-16389
- Nonlinear Euler buckling model for slender columns [AD-713997] 05 p0955 N71-16458
- Mathematical models for Arctic ice dynamics [AD-713986] 05 p0833 N71-16583
- Mathematical model for depressed beam collector of travelling wave tube 05 p0824 N71-16585
- Mathematical models for external insulation systems of cryogenic fuel storage tanks [NASA-CR-114827] 05 p0881 N71-16600
- Time dependent model for plasmasphere motion [NASA-TM-X-65433] 05 p0943 N71-16603
- Dynamic model of fog duration [AD-714625] 05 p0838 N71-16605
- Plastic models for structural analysis [AD-714657] 05 p0958 N71-16876
- Mathematical modeling of cryogenic heat pipes [NASA-CR-116175] 05 p0961 N71-16887
- Energetic analysis of correctable gyroscope stability 07 p1056 N71-17199
- Satellite attitude control mathematical models, inertia, radiation pressure, elastic deformation, and magnetic effects [ESRO-SP-17-VOL-2] 07 p1119 N71-17258
- Mathematical model for measurement of MOS processes in Al-SiO₂-Si system used in fabrication of integrated circuits 07 p1091 N71-17307
- Improved feedback control of distributed parameter systems for lunar landing vehicle simulator [NASA-CR-116482] 07 p1004 N71-17345
- Bevel functions for deep inelastic e-p structure in ladder model with spin 1/2 nucleons [NYO-4204-4] 07 p1075 N71-17439
- Mathematical model for minority carrier recombination in neutron irradiated silicon semiconductor [SC-R-70-4351] 07 p1093 N71-17457
- Modeling soil mass as continuum using constitutive equations of nonlinear mechanics [NASA-CR-103022] 07 p1048 N71-17462
- Interaction of sonic transverse jets with supersonic external flows 07 p1010 N71-17466
- Developing steady-state model for voltage output of hydrogen oxygen fuel cell as function of battery temperature, reactant pressure, electrolyte concentration, and cell current 07 p0976 N71-17675
- Deriving spherical harmonic expansion of earth potential as function of surface characteristics and gravity distribution [AD-715111] 07 p1020 N71-17700
- Base flow analysis of axisymmetric body with central jet [AD-715258] 07 p1012 N71-17787
- Flow of radiation in earth atmosphere [AD-715269] 07 p1022 N71-17813
- Systems analysis and mathematical model for air transportation design [NASA-CR-116431] 07 p1134 N71-17843
- Low frequency discriminants for small events [AD-715328] 07 p1023 N71-17873
- Characterization and modeling of real communication channels [AD-715288] 07 p0995 N71-18013
- Model for Type 3 solar radio bursts 07 p1106 N71-18032
- Bacterial thermoradiation sterilization models and computerized bioassay system for Apollo biological data [NASA-CR-116428] 07 p0985 N71-18056
- Mathematical models for ammonium perchlorate combustion and composite propellant burning rate mechanism 07 p1098 N71-18066
- Mathematical models for optimization of airline operations 07 p1136 N71-18095
- Survey on mathematical models of very low frequency wave propagation [NASA-TM-X-65448] 07 p0995 N71-18128
- Using finite energy sum rule as consistency test of models for asymptotic behavior of kaon proton scattering amplitudes [JINR-E2-5227] 05 p1252 N71-18291
- Orthogonal functions for linear analysis of sea tides at Hawaii [JPRS-195620] 05 p1186 N71-18352
- Mathematical model of MOS transistor subjected to high energy radiation [NP-18443] 05 p1171 N71-18414

MATHEMATICAL MODELS

- Model equations for studying compressible turbulent boundary layers [NASA-CR-116781] 05 p1177 N71-18426
- Mathematical models for aerodynamic forces of aircraft tandem wings using lifting line wing representation [ONERA-TP-891] 05 p1139 N71-18439
- Calculations on electromagnetic radiation from infinitely long wire in dielectric material over conducting ground plane [AD-715557] 05 p1168 N71-18446
- Mathematical model for aircraft lifting surface interference in steady or unsteady supersonic flow [ONERA-TP-850] 05 p1140 N71-18462
- Mathematical models for control surface wings in subsonic unsteady flow [ONERA-TP-889] 05 p1141 N71-18473
- Cosmology application of mathematical modeling by symbolic computation [NASA-TN-D-6233] 05 p1287 N71-18477
- Mathematical model of global spacecraft attitude control system based on three dimensional motion [NASA-TR-R-361] 05 p1171 N71-18491
- Stochastic model for partially coherent large seismic array signal processing [AD-715917] 05 p1103 N71-18543
- Mathematical models for minimum wall thickness of cylindrical horizontal storage tank on two saddle supports [CRIF-MT-61] 05 p1294 N71-18591
- Mathematical models for complex loaded cylinder creep analysis taking into account viscoplasticity [ONERA-TP-846] 05 p1297 N71-18642
- Mathematical models for modulus of elasticity of circular plates and rectangular or square beams [CRIF-MC-37] 05 p1297 N71-18644
- Arrive isentropic model [AD-715893] 05 p1190 N71-18664
- Numerical computation for designing rotating field pitch experiment [LBP-44/70] 05 p1274 N71-18718
- Three dimensional primitive equation model from Boussinesq equations for application to mesoscale atmospheric phenomena 05 p1231 N71-18730
- Multidimensionality and multidimensional aspects of X ray transport [AD-715476] 05 p1304 N71-18753
- Quadratic performance index for VTOL aircraft model reference attitude control system [NASA-TN-D-6231] 05 p1172 N71-18836
- Investigating properties of multigroup neutron transport operator in diffusion and P1 approximation [SARC-35/69] 05 p1262 N71-18847
- Calculations of passage of radiation through inhomogeneities in shielding [AD-715462] 05 p1262 N71-18841
- Investigating biothermal model of living tissue for application to thermal control of protective clothing [NASA-CR-116873] 05 p1152 N71-18926
- Using Markov renewal processes for reliability analysis of multiple unit standby redundancy system with preventive maintenance [TR-71-3] 05 p1226 N71-19087
- Investigating Fourier transform estimation from unknown parameters using sequential algorithm 05 p1226 N71-19088
- Particle bounce phenomena in mechanical air filtration theory 05 p1208 N71-19028
- Variance reduction by importance sampling and method of spinning in Monte Carlo calculation [NASA-TN-D-6209] 05 p1226 N71-19035
- Model for Hamiltonization and quantization of radiatively damped systems 05 p1227 N71-19156
- Justification of ensembles in quantum statistical mechanics 05 p1227 N71-19157
- Dislocation glide at high temperatures and glide recovery model for steady state creep 05 p1299 N71-19161
- Discussing REDUCE system and approach to substitution in design of symbolic mathematics system 05 p1227 N71-19186
- Discussing problems in design and implementation of practical batch processing systems for performing symbolic mathematical computation 05 p1229 N71-19198
- Isotropic elastic continuum model application to calculate energy and entropy of vacancy formation in metal crystals [NASA-CR-116881] 05 p1281 N71-19207
- Mass matrix and resonant frequencies for generating equivalent spring-mass models for normal modes of structural subsystem 05 p1301 N71-19280
- General multiple linear logic shift-generator model for Galois field resulting in longer binary sequences [AD-716558] 05 p1346 N71-19525
- Stability models for weakly nonlinear dynamical systems with application to gyroscopic devices [AD-716538] 05 p1409 N71-19648
- Mathematical model to describe normal projectile penetration of metallic targets [AD-716001] 05 p1398 N71-19711

Anthropomorphic data update for man-model used in cockpit geometry evaluation program for evaluation of flight crew interaction and compatibility with crew stations
[AD-716396] 09 p1340 N71-19818

Mathematical link-system model for computerized simulation of human movement in cockpit geometry evaluation program for flight crew physical compatibility with crew stations
[AD-716398] 09 p1341 N71-19820

Calculation of energy transfer in slowing down reactions with controlled fusion systems
[AD-716594] 09 p1449 N71-20014

Assessment of structural design philosophy in computerized structural analysis with mathematical programming
09 p1479 N71-20130

Asymptotic properties and simulation of adaptive stochastic control for linear systems
[NASA-CR-117182] 09 p1411 N71-20372

Stability and response characteristics of directly controlled rigid rotors at high advance ratios and correlation of mathematical model with wind tunnel test data
[NASA-CR-114290] 09 p1325 N71-20421

Cluster decomposition for studying high energy scattering processes
[ILL-TN-71-5] 09 p1444 N71-20514

Green function used for thermodynamic model of Heisenberg ferromagnet in random phase approximation
[NASA-TM-X-52982] 09 p1486 N71-20534

Modified one-dimensional blast wave theory and experimental shock trajectories for shock tubes with high explosive drivers
[SC-RR-70-182] 09 p1368 N71-20590

Mathematical models for onboard electrostatic analyzer measuring low energy charged particles
[KGO-PREPINT-70-311] 10 p1556 N71-20635

Trajectory model data for numerical weather forecasting
[AD-716811] 10 p1595 N71-20645

Formulas for nonresonant transmission of diffuse sound through stiff walls
[ISVR-TR-39] 10 p1605 N71-20662

Formulation of self consistent 2 and 1/2 dimensional electromagnetic and relativistic simulations
[UCRL-72613] 10 p1626 N71-20671

Noise suppression techniques in macroscopic models of collisionless plasmas
[UCRL-72604] 10 p1627 N71-20672

Models for coefficient of friction on plastic contact
[AD-716970] 10 p1621 N71-20753

Models for heat transfer during spin melting within single fibers and from single fiber to surrounding fluid
10 p1660 N71-20755

Statistical level density formula for describing unknown high energy states of daughter nucleus for determining neutron cross sections in Fe56
[AD-717216] 10 p1612 N71-20760

Mathematical model of crystallizer based on physicochemical velocity rates for subprocesses involved
10 p1592 N71-20820

Models for solving pseudo-Boolean linear equations and inequalities
10 p1592 N71-20821

Models for collisionless stability of inhomogeneous, confined, planar plasma
[SU-IPR-351] 10 p1627 N71-20833

Mathematical model for study of physico-chemical characteristics of impurity behavior in zonal recrystallization
10 p1573 N71-20867

Mathematical models describing conditions of nuclear binding energy saturation in nuclear interactions
10 p1615 N71-20936

Computerized models for nuclear reactor accident analysis
[BMM-1890] 10 p1602 N71-21035

Discrete element model formulation for stress and vibration analysis of thin plates
[RIEPT-35-01-77] 10 p1653 N71-21038

Discriminant analysis model for rating research and development data programs
[AD-716812] 10 p1665 N71-21043

Mathematical models predicting reentry plasma effects on admittance, attenuation, isolation, and breakdown characteristics of antenna systems
10 p1629 N71-21125

Applied mechanics, material testing, fluid mechanics, and electrotechnical laboratories
[SAR-1] 10 p1653 N71-21133

Mathematical model of floating beams and ship hull natural frequencies using graphic, rheological, and energy methods
10 p1654 N71-21135

Mathematical model for transient oscillations of straight shafts with noncircular cross sections
10 p1564 N71-21136

Mathematical model for stress analysis and force distribution in U bend heat exchanger perforated plates
10 p1654 N71-21137

Mathematical model for ideal fluid jets from convergent nozzles
10 p1541 N71-21139

Mathematical models for solid molecular diffusion in binary alloys and Kirkendall effect
10 p1635 N71-21141

Finite difference model and computer program for predicting large deflection elastoplastic response of shell structures
[AD-717005] 10 p1655 N71-21192

Specialized model for analysis of creep-rupture data by minimum commitment, station function approach with general time-temperature-stress relation to include all commonly used parameters
[NASA-TM-X-52999] 10 p1655 N71-21215

Numerical method for calculating steady asymmetric supersonic flow past pointed conical bodies at yaw
10 p1541 N71-21269

Models for high Reynolds number incompressible laminar flow around sharp corner
10 p1542 N71-21272

Bootstrap elementary particle model theory of nuclei vibrations
[RLO-1925-46] 10 p1618 N71-21388

Optimal nonlinear filtering with application of finite dimensional sensor orbits
10 p1592 N71-21393

Kinetic model of enzyme monomolecular enzyme reactions with substrate and product inhibition and possibility of self oscillation
[NLL-RTS-5991] 10 p1500 N71-21401

Mathematical models for acoustic scattering by porous elliptic cylinder with nonlinear resistance
[NASA-TM-X-67019] 10 p1607 N71-21408

Ray tracing analysis on duct effect in line of sight wave propagation above sea surface
10 p1524 N71-21428

Sonic pressure as function of space and time calculated for radiation from circular piston with impulse excitation
[NASA-TN-D-6270] 10 p1608 N71-21555

Calculation of lower critical fields and comparison with measured values for some niobium-titanium alloys
[NASA-CR-117493] 10 p1583 N71-21595

Dynamic models of human body response to acceleration environments and determination of tolerance limits
[NASA-TM-X-67038] 10 p1501 N71-21598

Mathematical model for suspension system of actively controlled air cushion vehicle
[PB-196465] 10 p1494 N71-21676

Mathematical models for solving scattering by weak volume inhomogeneities
10 p1609 N71-21735

Test facility to verify design concepts and mathematical models of chromatograph for atmospheric composition analysis of Mars
[NASA-CR-117468] 11 p1760 N71-21931

Data processing of thermal vacuum test on spacecraft model in space environment simulator for satellite thermal mathematical model
[NT/D1/69/143] 11 p1840 N71-22116

Analysis of space flight mechanics involving interplanetary trajectories
[AD-717829] 11 p1826 N71-22127

Distributed parameter mathematical model of human body in dynamic mechanical environments
[AD-717764] 11 p1686 N71-22130

Mathematical functional model for carotid blood pressure control system
[AD-717847] 11 p1680 N71-22161

Validation of mathematical model for wall effect correction in cavitation flow
[AD-717933] 11 p1736 N71-22170

Models and computer program for vibration of ellipsoidal uniform filament with clamped ends as related to piping systems
[AD-717496] 11 p1835 N71-22236

Mean shifts in second order of perturbation theory in dual resonance model
[LPTHE-71/7] 11 p1787 N71-22267

Computer program and mathematical model for temperature variance measurements on satellite
11 p1840 N71-22335

Numerical model of thermal convection for two dimensional laminar, nonlinear fluid, heated nonuniformly
[AD-717670] 11 p1749 N71-22358

Mathematical models used in optimal design of silicon controlled rectifiers with improved radiation resistance
[NASA-CR-72842] 11 p1724 N71-22365

Procedure to determine proper geometry of anisotropic and laminated cylinders with elastic stress gradients reduced to predetermined limit
[AD-717700] 11 p1836 N71-22367

Periodic and maximum-slope techniques with refinements used for testing compact heat exchanger surfaces
[AD-717662] 11 p1841 N71-22406

Theoretical analysis of jet mixing under influence of non-constant pressure gradient
[NASA-CR-117836] 11 p1738 N71-22501

Calculation of thermodynamic properties from models to determine correlated molecular rotation
11 p1807 N71-22550

Ultrasonic measurements on parabolic imperfections in alkali halides compared with predictions of tunneling model
11 p1784 N71-22581

Pseudopotential formalism used to calculate vacancy formation energy and volume for alkali metals
[NYO-4185-2] 11 p1779 N71-22582

Engineering design analysis of hydrogen cooled structural panels for application to hypersonic aircraft
[NASA-CR-1650] 11 p1843 N71-22625

Experimental validation and analytical elaboration for models of pilot neuromuscular subsystem in tracking tasks
[NASA-CR-1757] 11 p1691 N71-22664

Mathematical models for chemical thermodynamics of oscillatory combustion
11 p1844 N71-22708

Pressure difference induced across stainless steel capillary tube by temperature gradient used to predict thermal transpiration effect
11 p1844 N71-22709

Models for performance characterization of integrated electro-thermal circuits
11 p1725 N71-22716

Twin multipath channel used for performance prediction of communication systems
11 p1702 N71-22718

Mathematical model of oil whip phenomenon in rotating shaft systems with incompressible fluid lubrication and analysis of squeeze film bearings
11 p1770 N71-22724

Bionic models for pattern recognition in human and artificial brains
11 p1685 N71-23057

Neurophysiological model for cochlear function in auditory nervous system information processing
[AMRL-TR-68-186] 11 p1721 N71-23062

Four-wheel mathematical model used for prediction of LRV operational behavior under lunar gravitation
[NASA-TM-X-64584] 12 p2009 N71-23158

Approximate method for estimating minimum required ejection velocity for parachute deployment
[NASA-TN-D-6300] 12 p2000 N71-23164

Anomalous behavior model for prediction of thermal conductivity of fluids in critical region
[NASA-TM-X-52955] 12 p2009 N71-23196

Transfer functions in modelling human pilot and dynamic structural aircraft responses
[AARD-B-580-71] 12 p1850 N71-23210

Fabrication and tests of CO2 flat plate models in He hypersonic wind tunnel
[SC-CR-69-3215] 12 p2010 N71-23228

Fredholm solution of delta function model for two electron helium like ions
[NASA-CR-117895] 12 p1969 N71-23286

Numerical processes in computer-aided design of switching circuits and semiconductor devices
[AD-718152] 12 p1887 N71-23307

Mathematical model for computer program to determine vibratory response of finite plates and associated acoustic radiation to fully developed turbulence excitation
[AD-718815] 12 p2004 N71-23309

Current sheet magnetic model to calculate quiet large-scale magnetic field in solar corona compared with accuracy of other models
[NASA-TM-X-65496] 12 p1992 N71-23433

Design study with mathematical model for performance analysis of silicon-germanium thermoelectric generator
[NASA-CR-118008] 12 p1961 N71-23439

Mathematical model for partial reflection from tropospheric layers in radio transhorizon propagation
12 p1875 N71-23457

Mathematical model for frequency correlation function of tropospheric scatter channel
12 p1876 N71-23464

Statistical model for tropospheric radio propagation loss in rough surface path between transportable and mobile antennas
12 p1878 N71-23473

Mathematical models of survival of fitness during biological evolution
[LA-4573] 12 p1882 N71-23490

Hydrodynamic and mathematical model for simulating full scale pneumatic tube transportation system
[AD-718763] 12 p1897 N71-23501

Estuary gravitational flow mathematical model noting turbulent mixing
12 p1910 N71-23406

Equivalent mathematical control system models for maximum principle time delay systems with feedback
[AD-718437] 12 p1893 N71-23561

Mathematical models for analysis of radiative heat transfer in planetary atmospheres
12 p1996 N71-23721

Separation theorem for linear systems, quadratic criteria and correlated noise
[AD-718435] 12 p1949 N71-23739

Theoretical analysis of performance of two-grid accelerator systems for Kaufman thrusters
[NASA-TN-D-6275] 12 p1990 N71-23762

SUBJECT INDEX

MATHEMATICAL MODELS

Mathematical models for analog computer representation of wheeled vehicle electric systems [AD-718075] 12 p1927 N71-23772

Mathematical models of physical properties of cooperative assemblies including ferromagnetism [AD-718077] 12 p1967 N71-23905

Plane acoustic model for sound generation in disturbed free shear layer [RAE-LIB-TRANS-1517] 12 p1967 N71-23961

Neutron field model for low pressure plasma in toroidal magnetic field 12 p1982 N71-24051

Mathematical model for calculating molar volume of soda silicate glass 12 p1946 N71-24123

Evaluation of turbulent shear models and prediction of compressible turbulent boundary layers by method of weighted residuals [NASA-CR-118679] 12 p1903 N71-24140

Model and computer program to predict film usage time of Skylab missions [NASA-TN-X-64585] 12 p1924 N71-24197

Linearized analysis of thermal emission from Lunar and Mercurian surfaces 12 p1997 N71-24206

Precise logic computation and construction of formal heuristic activity models 12 p1895 N71-24219

Mathematical analysis of system of annular heat-conducting emitting ribs [NASA-TT-F-13551] 12 p2013 N71-24241

Approximate models for amplification by wave distortion of dynamic response of vaporization limited combustion [NASA-TN-D-6287] 12 p2013 N71-24242

Quark partition model for deep inelastic lepton-nucleon scattering [LPTHE-71/12] 12 p1979 N71-24343

Mathematical model for determination of perturbation in satellite orbit inclination due to diurnal variations of fluid flow of upper atmosphere [RAE-TR-70508] 12 p1655 N71-24360

Mathematical model of Adriatic Sea for study and prediction of tides at Venice [EPA-STR-12] 12 p2069 N71-24400

Mathematical foundations for computer program to determine optimal locations of radar trackers on missile test range with application to rocket vehicle navigated by inertial measurement unit [AD-718967] 13 p2043 N71-24417

Adaptive control technique for unstable mechanical systems [AD-719743] 13 p2102 N71-24430

Optimum model with small number of variables for multilevel forecasting of geopotential field [AD-719805] 13 p2105 N71-24441

Critical evaluation of theory and experiment of free turbulent mixing - shear stress models [AD-718956] 13 p2063 N71-24480

Mathematical models for lifting rotor aerodynamic calculations, acting wave configurations [DLR-MITT-70-19] 13 p2021 N71-24489

Geometric optics analysis of arbitrarily shaped dual reflector antennas [NASA-CR-118268] 13 p2044 N71-24630

Statistical model application to scattering cross section analysis for high energy interactions including energy dependence of partial cross sections [JINR-71/19] 13 p2180 N71-24697

Mathematical model for closed form expression of impurity particle nuclear binding energy using power series, particle spin, and wave functions with lambda baryon example [DEMO-70/20] 13 p2130 N71-24698

Deterministic optimal control theory [AD-718070] 13 p2026 N71-24712

Amplitude dispersion and stability of dispersive weakly nonlinear waves determined by perturbation method [NASA-TM-X-65324] 13 p2103 N71-24885

Evaporative quality components of watershed models for Great Plains, using mathematical models 13 p2073 N71-25014

Spectral model of winter stratosphere circulation, radiative effects including solar absorption by ozone and Newtonian approximation to infrared cooling 13 p2106 N71-25027

Flow model for recompression of two dimensional supersonic turbulent free shear layer [NASA-CR-118331] 13 p2066 N71-25072

Mathematical models for cybernetic diagnosis of dynamic systems [AD-719776] 13 p2103 N71-25118

Comparison of two-dimensional and three-dimensional acoustics calculations for FTR [WHAN-SA-11] 13 p2120 N71-25217

Second quantized nonrelativistic time-dependent scattering theory describing identical bosons interacting via two body forces and generalizing in-out formalism 13 p2136 N71-25254

Calculation of two body elastic scattering amplitude for Ising model of ferromagnetic phase transition

slightly above critical point as Hamiltonian field theory on lattice space 13 p2145 N71-25592

Space-time evolution of Tokamak type plasma [CEA-CONF-1395] 13 p2149 N71-25594

General aviation traffic implied densities and interaction frequencies computed with model using southern California to judge difficulty for naval air traffic [AD-719966] 14 p2197 N71-25621

Mathematical models for saturation gain occurring in curved channel photomultiplier tubes at high voltages noting space charge effect 14 p2299 N71-25634

Analytical model for run-out of flow instability and start of compressible transition [AD-719759] 14 p2238 N71-25655

Physical model for neutron flux enhanced creep rate [AD-719905] 14 p2324 N71-25707

Mathematical analysis of Valtromer refrigerator and use of computer program for solution of resulting equations [NASA-TM-X-65334] 14 p2332 N71-25812

Series expansion of nonlinear operators used to characterize nonlinear systems [CT-38] 14 p2281 N71-25851

Probability models for solution of elliptic and parabolic equations by computers 14 p2248 N71-25970

Mean square exceedance characteristics of single tuned system to amplitude modulated random noise of limited duration [NASA-CR-61352] 14 p2348 N71-26026

Model for task interference with pilot performance in multivariable manual control systems [NASA-CR-1746] 14 p2310 N71-26160

Method of characteristics for synthesis and identification of distributed parameter systems in control theory [TR-70-36] 14 p2284 N71-26163

Stability and control of processes described by stochastic functional differential equations 14 p2284 N71-26205

Model of spatial Newtonmeter/accelerometer set on moving object and theory of inertial navigation [AD-720381] 14 p2290 N71-26347

Geometric relationships involved in multiple scattering calculations for spherical planets [NASA-CR-118662] 14 p2250 N71-26360

Mathematical model for optimal reservoir system design [REPT-09/70] 14 p2250 N71-26378

Mathematical model for optimal water quality control in estuaries [REPT-08/70] 14 p2250 N71-26379

Models of neutron slowing down calculations in thermal and fast reactors [EUR-ENR-664] 14 p2307 N71-26396

Mathematical models for determining electrical conductance in ceramic films 14 p2234 N71-26435

Finite element method to model soil half-space for calculating transfer momentum in form of inertial energy of projectile penetrating soil 14 p2360 N71-26470

Static and dynamic models of long period variable stars, ionization equilibrium and dissociation, and pulsation parameters 14 p2340 N71-26536

Mathematical models for studying kinetics of aqueous emulsion copolymer system 14 p2215 N71-26580

Mathematical formulation of Double Precision Orbit Determination Program (DPODP) for lunar and planetary mission spacecraft trajectories [NASA-CR-118673] 14 p2340 N71-26610

Development of mathematical/meteorological models for improved forecast capability [AD-720218] 14 p2289 N71-26620

Basic theory and general linear model for analysis of variance [TR-71-14] 14 p2286 N71-26677

Mathematical model and computer program for solution of asymptotic neutron transport equations in slab geometry [KRL-70-14-RPT] 14 p2312 N71-26707

Mathematical model for relativistic scattering amplitudes in high energy interactions based on Fourier analysis and Lorentz group embeddings [JINR-E2-5341] 14 p2318 N71-26760

Topologic and geometric properties of delta channel networks [AD-719918] 15 p2395 N71-26819

Four-degree-of-freedom lumped parameter model for vertical accelerations of seated human body as might be imposed by aircraft ejection systems [AD-721225] 15 p2570 N71-26994

Transfer function models of DTL and TTL integrated circuits [SC-RR-70-450] 15 p2308 N71-26983

Computer program for optimum flight path defined by flight test investigation of performance characteristics (excess thrust, fuel flow, and climb potential) of F-104 aircraft [NASA-TN-D-6398] 15 p2366 N71-27002

Method for predicting fatigue lives of 2024 T3 and 6061 T6 aluminum alloys subjected to either constant amplitude sinusoidal or wide band random fatigue loading [SCL-CR-71(0173)] 15 p2420 N71-27017

Stress wave vapor cloud expansion in high atmosphere and mathematical model of transport equation in cloud diffusion phase [BMW-FB-W-71-10] 15 p2398 N71-27027

Microwave breakdown predictions for rectangular aperture antennas including internal diffusion [AD-721283] 15 p2386 N71-27205

Numerical calculations of electrical parameters in Faraday-type MHD generator with two dimensional gas flow [JINR-1199] 15 p2393 N71-27207

Mathematical description of axisymmetric plasma equilibrium of Tokamak type [IPP-31-PT-11] 15 p2499 N71-27230

Mathematical models for arc heaters and plasma jet mixing, iterative and relaxation methods [BMW-FB-W-71-09] 15 p2499 N71-27231

Mathematical models for surface modes of vibration and optical properties of ionic crystal slab [IS-T-427] 15 p2505 N71-27237

Load-equivalence parameters for dynamic loading of structures in plastic range [ARL-7677] 15 p2521 N71-27238

Speech recognition model for predictions of intelligibility and intelligence measures 15 p2381 N71-27292

Mathematical model of basic electrohydrodynamic process including effects of turbulence [AD-720703] 15 p2500 N71-27305

Spectral characteristics of radar target returns in clutter examined in frequency domain and compared with returns from ground-clutter models [AD-720851] 15 p2382 N71-27356

Mathematical model for neutron detector scattering above inelastic threshold 15 p2470 N71-27386

Smooth quasipotential in external quantum field theory models [JINR-E2-5365] 15 p2471 N71-27416

Analysis of problems associated with effects of surfaces on blood clotting and on theory of blood clot regulation [AD-721207] 15 p2372 N71-27475

Radiation climatology applied to numerical models 15 p2439 N71-27510

Mathematical model for global solar radiation distribution over India 15 p2439 N71-27521

Mathematical models and numerical analyses in magnetosonic plasma physics [AD-720879] 15 p2501 N71-27597

Magnetic field components of thick finite dc solenoids obtained from expression of vector potential of circular current loop [JINR-P9-5441] 15 p2435 N71-27687

Mathematical models for shock wave profile around conical bodies using schlieren photography interpretation [ARC-CP-1143] 15 p2363 N71-27717

Formulation of problems of shear flow and orientation due to magnetic field for nematic liquid crystals [AD-721107] 15 p2378 N71-27720

Qualitative model and calculations of interaction energy in thin film rheology study of boundary lubricating surfaces films [AD-721176] 15 p2432 N71-27755

Model for influence of heat transfer and friction on flow parameters in nozzle with independent cooling [AD-720933] 15 p2395 N71-27759

Calculation of ion trajectories and energy distribution in front of field emission tip [JPP-7/2] 15 p2483 N71-27766

Probability models for risk of solar proton events to space missions [NASA-TN-D-6379] 15 p2515 N71-27792

Multiple scattering model for inelastic processes and nonrelativistic high energy forward and backward scattering [TRB-TP-7-70] 15 p2485 N71-27816

Exact solution to magnetohydrodynamic equations for magnetosonic waves under gravity and comparison with observed fine structure of waves propagating away from solar flares [AD-720244] 15 p2516 N71-27824

Mathematical model for impulsive heat releases by chemically generated waves in atmosphere [NASA-TM-X-65360] 15 p2441 N71-27844

Vibrational data for analytical model path model of structural dynamics [UCRL-72810] 15 p2522 N71-27858

Mathematical model for solving hydrodynamic flow equations in nonhomogeneous magnetic field for plasma flow along field line in presence of gravitational field [NASA-TM-X-65354] 15 p2503 N71-27889

Analysis of pion/minor proton yields neutron pion/pion/minor proton/minor pion/N equals 1.2/3 and pion/minor proton yields neutron 2 pion/minor pion/N equals 1.2/reaction [JINR-P1-5431] 15 p2491 N71-27900

MATHEMATICAL MODELS

Mathematical models for investigating vertex functions in current algebra

Compact analytic solution to distribution theory of steady state model illustrated with biological data-age dependency in compartmental analysis

Mathematical model for calculating equilibrium deformations in ground and excited states of rare earth nuclei

Mathematical models and optimal control for uncertain systems

Method for reducing sensitivity of optimal nonlinear systems to parameter uncertainty

Practical simulation of random functions in adaptive control systems

Mathematical models for simulation of correlated stochastic processes with stationary Gaussian properties

Lunar Orbiter tracking data analyzed to yield thirteenth degree and order spherical harmonic approximation to lunar gravitational potential function

Mathematical model for river basin drainage systems based on hexagonal nature of geological ridges

Thermal and electrical theories for analysis of second breakdown phenomena, mechanisms, and damage in semiconductor junction devices

Techniques for solving problem of sound transmission from harmonic monopole source through finite corrugated boundary between fluid media

Mathematical model for electrical behavior prediction of metal oxide semiconductor transistors subjected to high energy radiation effects

Mathematical models for determining stabilizing effect of fluid boundaries on thermal convection

Mathematical models for investigating stability of thermally stratified shear flow in atmosphere

Statistical thermodynamics of vacancies in binary alloys using Ising model

Handbook of analytical methods and stability data for determining dynamic stability and control characteristics of generalized single-rotor compound helicopter configurations

Mathematical model for supersonic aircraft Mach number threshold operation for atmospheric reflection of sonic boom

Mathematical models for application of satellite borne multispectral remote sensors to water and wheat production management and wheat fungi control including cost estimates

Model for ferromagnetic material characteristics in diffusion of transient electromagnetic fields through saturated ferromagnetic media

Mathematical model and computerized simulation of crew related factors in space station

Feasibility of overcoming local convergent nature of continuation methods for nonlinear equations

Fixed and variable stiffness models for simulating instantaneous dynamic loads on gear teeth

Mathematical models of nuclear effects and fallout calculations for weapons effects display system

Mathematical models for measuring frictional behavior of basal and aluminum surfaces in ultrahigh vacuum

Equation based on instantaneous ion exchange and linear adsorption isotherm for predicting radioactive ion concentration and flow in ground water

Stochastic models for defining white noise with time and space parameters

Formulas for distribution of extragalactic radio sources in space derived in zero pressure uniform model universe

Physical model for origin of fission-product releases in experimental breeder reactor 2

Mathematical model and algorithms for Skylab docking dynamic response analysis with numerical analysis of Apollo probe/docking system

Examination of radiation damage in silicon using mathematical models

Problems of mathematical modeling in microbiological processes

Time-dependent calculation method for transonic flow in nozzle with or without central body

Five models for three dimensional chip curl, chip breaking, and chip control in metal cutting processes

Survey on different methods for lifting rotor downwash analysis

Mathematical model for predicting damping time of mercury damper

Cost/benefit model for decision making in planning German space program - bibliography

Mathematical perturbation models of aircraft ILS approach and landing

Mathematical model of missile inertial guidance based on accelerometer and gyroscope stabilized platform sensor data

Numerical model of isolated cumulus clouds formed by surface heating

Development and verification of analytical model to predict cavitation compliance in turbopump designs

Mathematical model for coolant three dimensional flow during rapid fission-gas release in fast nuclear reactor cores based on plenum chamber simulation

Models for permitting continuous purging of impurities from gas compartments of fuel cell

Mathematical model of satellite with continuous elastic components comprising moment free rigid carrier attached to elastic membrane

Calculation of decay lifetimes of artificial electrons produced by Starfish nuclear explosion

Hydroelastic vibration of rods in parallel flow with hydroelastic rod model and method for evaluating equivalent viscous damping coefficients

Analytic model of boundary conditions for heat transfer coefficients through porous walls

Mathematical models of nonlinear equations of motion of steam servomotor showing transient and steady state stability

Two methods of analysis, synthesis, and self-regulation of nonlinear units in control systems

Simulation of single-server model for paging drum channel system

Mathematical model for induced velocity distribution of lifting rotor in horizontal flight

Air density model for TD-1 satellite orbit drag and lift perturbation

Model for migration of dislocation arrays in ionic crystals based on dislocation climb in vacancy concentration gradients by action of external electric field at array sites

Dislocation dynamics and formulation of constitutive equations for rate dependent elastic plastic response in isotropic metals

Degradation effects of atmospheric absorption of 10.6 micron laser beam with kinetic model for vibrational relaxation process and numerical analysis of vibrational lag ray displacement

Mathematical model of bipolar transistor for digital monolithic integrated circuits with low signal levels

Nonlinear differential equations describing stability of fast nuclear reactor with incore thermionic converters and reactivity feedback

Achromatic pattern recognition model for processing chromatic objects

Model for predicting rate of dissolution of network polymers by chemical degradation

Formulas for calculating conductivity and dielectric constants of capacitors made up of composite bodies extended to more than two components

Mathematical models of nonlinear combustion instabilities in liquid propellant rocket engine

Mathematical models for automated environmental control of acoustic test facility inside chamber

Step input linear system modeling from nonlinear system sampled noisy data based on method of perturbation or quasilinearization of automatic control system data

Model for predicting thrust-time curve during entire ignition transient of solid propellant rocket engine with head-end pyrolytic igniter

Production and inclusion of dense and hot plasma in spindle-cusp configuration

Space and time simulation of nuclear active and muon components in extensive air showers for primary energies from 100,000 to 10 million GeV

Analog models to measure two-dimensional and three-dimensional distribution of magnetic flux density of magnet for bubble chamber

Mathematical models of Fourier and Laplace transformations of two tempered distributions which coincide in Jost points

Mathematical model describing influence of transistor geometry on transition frequency

Mathematical models for bipolar transistors

Survey of origin, properties, applications, and generalizations of dual resonance models

Different models for metal oxide transistors

Mathematical models for high frequency characteristics of metal oxide semiconductor transistors

Phenomenological approximations in atomic theory

Equations of resonant interaction between three waves in plasma in fixed-phase approximation

Computer program for calculation of solid angles and angular acceptances with particular application to counter telescopes

Method of solution of ion motion in median plane of cyclotron and results obtained using method with U-120 cyclotron

Mathematical model of planar formation of electron ring in static magnetic field and beam properties

Empirical approach to third-invariant violation for radial diffusion of outer zone electrons

Oscillatory modes of antisymmetric diurnal tide calculated by Laplace equation

Mathematical model of interaction between solar wind and interstellar medium

Statistical model of Lannard-Jones gas microscopic thermodynamic diffusion properties

Hydrodynamic model for slug flow mass transfer in carbon dioxide/water two phase flow

Two dimensional axisymmetric jet flow model based on inviscid flow and single stream mixing theories with mass bleed and application to flow between parallel walls

Simulated temperature and velocity disturbances in laminar boundary layer using quasi-steady theoretical model

Identification of model parameters from input output data of dynamic systems with time delays

Characterization of conditional probability measures for continuous-time, partially observable Markov processes

Mathematical models of microbiological production processes

Perturbation theory used for calculation of interaction energies in spin-free quantum chemistry

Nonlinear systems for matching input-output of mathematical model to physical system

Behavior of ammonium chloride near order-disorder transition explained by physical model having coupled singular and nonsingular free energy parts and verified by specific heat measurements

SUBJECT INDEX

SUBJECT INDEX

MATHEMATICAL MODELS

- Onset of microwave breakdown in air-filled coaxial transmission lines and rectangular waveguides predicted by mathematical models
[AD-722719] 18 p2898 N71-31369
- Mathematical model for investment planning in R and D emphasizing options and interacting benefits for resource allocation decision making
18 p3030 N71-31391
- Mathematical model for gas adsorption efficiencies of porous and solid reactor materials
18 p2907 N71-31449
- Mathematical model for computerized strict error estimation in differential equation systems
18 p2948 N71-31461
- Mathematical methods in production planning with cost effectiveness optimization
18 p3031 N71-31578
- Mathematical model of supersonic flow around blunt conical body with sharp leading edge including comparison with schlieren photographs and noting Mach number dependence
[REPT-1771] 19 p3033 N71-31658
- Mathematical analysis of apparent admittance of causally driven infinite monopole
[AD-723650] 19 p3163 N71-31712
- Mathematical models for electron attachment to molecules with negative ion formation
[AD-723642] 19 p3144 N71-31717
- Mathematical models for dynamic elastic properties of fiber reinforced viscoelastic materials
[AD-723389] 19 p3118 N71-31718
- Computational model for fast reactor disassembly analyses - VENUS computer code
[ANL-7701] 19 p3134 N71-31735
- Mathematical models for quasi-static behavior of fiber glass reinforced viscoelastic plastics
[AD-723388] 19 p3119 N71-31732
- Model for computing power density contours caused by satellite antennas illuminating portion of earth surface
[AD-723284] 19 p3064 N71-31760
- Mathematical models for electromagnetic noise in neutral current sheet of geomagnetic tail
[AD-723654] 19 p3175 N71-31802
- Theoretical physics and mathematical model for GEOS 2 ionospheric corrections using VHF range and range rate tracking data
19 p3088 N71-31849
- Mathematical models for predicting ground shock effects in relatively high pressure regions of nuclear explosions
[AD-723209] 19 p3091 N71-31895
- Cost effectiveness model applicable to national data buoy systems and other national marine environmental data collection systems
[AD-722596] 19 p3091 N71-31965
- Numerical analysis and mathematical models to describe vision process
19 p3043 N71-32013
- Development and application of mathematical models for digital simulations of social factors and production planning methods
[JPRS-53668] 19 p3122 N71-32016
- Development and application of mathematical models in science
19 p3122 N71-32017
- Organization of theoretical knowledge into mathematical models
19 p3122 N71-32018
- Social planning by numerical forecasting methods
19 p3195 N71-32019
- Social factors in scientific forecasting and planning reorganization of society
19 p3195 N71-32020
- Mathematical model of processes occurring in electrochemical reactor part of water vapor electrolysis cell
[NASA-CR-119669] 19 p3041 N71-32046
- Computerized effectiveness model for predicting artificial precipitation through pyrotechnical cloud seeding
[AD-723842] 19 p3128 N71-32056
- Mathematical simulation and queuing models for air traffic control systems
[AD-721726] 19 p3132 N71-32065
- Cybernetics including models for statistical decision making, biomechanical systems, and complex stochastic system
[JPRS-53531] 19 p3044 N71-32088
- Model for quantitatively examining performance of automatic machines with normal and disturbed functions in statistical decision making
19 p3044 N71-32089
- Dynamic reactions of operators with random vibrational stimuli and biomechanical systems
19 p3044 N71-32090
- Methods for determining characteristic of any combination of stochastic systems
19 p3123 N71-32091
- Nonlinear point reactor dynamics model for determining stability regions
[COO-2109-3] 19 p3137 N71-32127
- Computer program and thermalization models for temperature distribution calculation in water cooled reactor cores
[EUR-4554] 19 p3138 N71-32141
- Models for S and P waves of pion scattering obeying current algebra constraints and allowing for meson resonance
[RLO-1388-602] 19 p3153 N71-32203
- Accurate short channel insulated gate field-effect transistor which includes drain depletion effect in triode and saturation regions
[AD-723215] 19 p3066 N71-32310
- Models of hydromagnetic shocks in very low ionization regions related to star formation and gas flows in interstellar mediums
19 p3079 N71-32315
- Mathematical model for estimating particle size distribution and volume fraction effects on coarsening rates during precipitation hardening with Ni-Cr-Al and Ni-Al alloys
[UCLA-34-P-172-1] 19 p3115 N71-32322
- Free streamlines model of flow past two-dimensional wedge or flat plate
19 p3080 N71-32350
- Pseudo-potential calculation of energy bands and optical properties of 4-layer polypoly ZnS
19 p3170 N71-32351
- Mathematical models for incompressible laminar boundary layer flow inside and outside of liquid spheroid moving through liquid
19 p3080 N71-32378
- Counting probability methods for estimating whether particles with given initial wave functions will be in given volumes at least once between two distinct fixed times
19 p3142 N71-32379
- Numerical models for calculating terminal velocity of water drops
[P-4564] 19 p3129 N71-32407
- Similar solution for turbulent boundary layer with large favorable pressure gradients to predict heat transfer along nozzle
[NASA-TN-D-6439] 19 p3080 N71-32415
- Crowned channel E/2 expansion of unequal mass scattering amplitude
19 p3124 N71-32451
- Linear formulation of aerodynamic stability of plane sandwich-type structures placed in current of supersonic gas
[NASA-TT-F-13778] 19 p3190 N71-32452
- Synaptic junction model for memory in brain
[NASA-TN-D-6456] 19 p3045 N71-32474
- Matrix method for neural net simulation
[JPRS-53581] 19 p3124 N71-32502
- Mathematical model for strong nuclear interaction dynamics
19 p3157 N71-32508
- Flow visualization and mathematical model of peristaltic pumping including pressure and velocity measurements in two dimensional flow
[AD-723870] 19 p3081 N71-32529
- Attitude determination and sensor alignment via weighted least squares affine transformations
[NASA-TM-X-65663] 19 p3124 N71-32545
- Mathematical model and information display system for flight control and monitoring aircraft and pilot performance
[AD-723051] 19 p3045 N71-32566
- Solution of equations describing assumed modes of strong shock in monatomic gas
19 p3081 N71-32608
- Three dimensional statistical model for deriving precipitation estimate from X band radar echoes
19 p3131 N71-32735
- Theory of logic-dynamic control systems and multilayer theory of statistical decisions
[JPRS-53766] 20 p3288 N71-32822
- Mathematical modeling of logic-dynamic control systems
20 p3288 N71-32823
- Magnitude-red shift, magnitude-galaxy count, and angular diameter-red shift relations included in tests of cosmological models
20 p3344 N71-32843
- Quantitative study of pulsar electrodynamics based on Goldreich-Julian model
20 p3345 N71-32848
- Plasma sheet models for geomagnetic tail structure
20 p3254 N71-32870
- Mathematical model of locations and types of warehouses, volume of product stored, and losses due to external effects
20 p3289 N71-32883
- Synthesis of aircraft across track errors using mathematical models with statistical parameters
[REPT-EUC-2] 20 p3299 N71-32885
- Mathematical models for solar wind merging in magnetic fields noting tearing instability
20 p3345 N71-32944
- Semi-infinite flat panel with either homogeneous or anisotropic cross section considered for panel flutter parameters in aerodynamic optimization problem
[AD-724333] 20 p3356 N71-32974
- Model for predicting pilot rating of VTOL aircraft in hover mode
[AD-724144] 20 p3309 N71-32981
- Finite element model of Timoshenko beam segment
[AD-724333] 20 p3357 N71-32982
- Analysis of phenomena occurring in exhaust gas spray cooler utilizing liquid injection, and mathematical model of optimum cooler
[AD-724687] 20 p3338 N71-32991
- Mathematical model for near-body orbit calculation using mass concentration, perturbation theory, nonlinear equations, geopotentials, and least squares method
[NASA-CR-121381] 20 p3345 N71-33019
- Model for erosion of ductile materials by impact of solid particles
[AD-724164] 20 p3283 N71-33113
- Numerical solution of Thomas-Fermi atomic model with quantum corrections
20 p3291 N71-33133
- Mathematical model for elastic shear bending of trapezoidally corrugated plate with trough lines held straight including deflections and stress analysis
[NASA-CR-1749] 20 p3357 N71-33141
- Deep Space Network operations for Mars 71 project, mathematical model for Doppler tracking system, and third-order phase locked system transient response analysis
20 p3347 N71-33168
- Magnetic disturbance calculation techniques for model current systems including numerical integration and spherical harmonic expansions
[APS-PH-77] 20 p3259 N71-33170
- Mathematical and diffusion models for abatement and control of air pollution over urban areas
[PB-190400] 20 p3260 N71-33230
- Computer program for calculating propellant dynamics in two dimensional and axisymmetric tanks during spacecraft docking
[NASA-CR-119904] 20 p3337 N71-33243
- Statistical thermodynamic model for molecular interactions during ice nucleation from supercooled water
[TN-40] 20 p3261 N71-33298
- Air pollution sources, distribution, biological effects, and mathematical models
[P-4571] 20 p3261 N71-33299
- Calculation of turbulent compressible boundary layer on helicopter rotors for range of hover conditions using two different analytical methods
[AD-723909] 20 p3210 N71-33312
- Mathematical models for calculating flexible swash-plate effects on vibratory and mechanical stability characteristics of helicopter rotor systems
[NASA-CR-1817] 20 p3211 N71-33393
- Capacitor field calculations for capacitive displacement measurement of open mesh structures such as radio telescopes and radar receivers
[NASA-TN-D-6341] 20 p3273 N71-33397
- Dynamic mathematical model of physiological regulation of body temperature in human beings
[NASA-CR-1853] 20 p3250 N71-33401
- Mathematical models for thermal and electrical properties of bipolar transistors and effects of fabrication processes
20 p3241 N71-33420
- Elementary calculations for axial thermal stresses in beams compared with those of exact theory
[AD-724404] 20 p3358 N71-33423
- Optimal control models for design of structures with weights minimized by constraints involving fixed eigenvalues
[NASA-CR-121458] 20 p3338 N71-33447
- Mathematical models for control activity of human spaceship operator
20 p3227 N71-33461
- Differential-tension-bubble-pressure apparatus used for surface tension measurements in air of liquid lubricants to 200 C
[NASA-TN-D-6450] 20 p3279 N71-33515
- Mathematical techniques using finite element method for vibration analysis of nuclear reactor
[CONF-710302-7] 20 p3302 N71-33542
- Markov chain model for characterizing error sequences in digital channels with memory
[NASA-CR-121429] 20 p3259 N71-33551
- Mathematical model for thermal behavior and surface temperatures of celestial bodies in solar system
[NASA-CR-121471] 20 p3342 N71-33567
- Mathematical models for computer calculation of two dimensional hydrodynamic nonlinear combustion instability flow
[NASA-CR-121472] 20 p3365 N71-33572
- Scheme for servomechanism with saturable amplifier and dynamic response with nonlinear parameters
20 p3280 N71-33603
- Model for calculation of parameters for local thermodynamic equilibrium in uranium
20 p3365 N71-33644
- Electrical characteristics data used to determine uranium plasma holding point
20 p3285 N71-33645

Physical models for measuring acoustic instabilities of high temperature gaseous uranium for use in gaseous core nuclear rocket system

20 p3304 N71-33651

Zoning techniques applied to gray gas and black body radiation transport models including view effects and nonisothermal emission

20 p3365 N71-33656

Plasmod model for explaining electron densities and temperature of hydrogen plasma with helium and argon impurities drifting into dipole magnetic field

20 p3331 N71-33674

Steepest descent procedure for determining optimal control system parameters by performance index minimization

[ORNL-TM-3311] 20 p3307 N71-33689

Vibration mode model and computerized simulation of dynamic system model response

[UCRL-72818-REV-1] 20 p3359 N71-33714

Mathematical models for prediction of acceleration responses and reaction forces and moments at base of Mariner Mars 71 and Viking spacecraft from Centaur main engine cutoff

[NASA-CR-121473] 20 p3355 N71-33719

Mathematical models for solving inverse problems in scientific research

[PM-71/4] 20 p3293 N71-33726

Empirical equation for thermionic converter performance as function of electrode emission properties

[NASA-TM-X-2358] 20 p3308 N71-33739

Analytical and experimental investigation of ductile fracture of polymers using adaptation of Dugdale model

[NASA-CR-121416] 20 p3360 N71-33778

Numerical solution for transient temperature distribution and thermoelastic stresses in homogeneous spherical fuel element with variable convective heat transfer at surface

20 p3367 N71-33781

Similarity solutions using free parameter technique for laminar flow of viscous, incompressible fluid between rotating coaxial surfaces of revolution

20 p3253 N71-33783

Transient heat transfer in thermal entrance region between parallel plates with fully developed laminar velocity profile determined for low Peclet number flows

20 p3367 N71-33784

Asymptotic generalized optical calson model and Regge theory combined in model for high energy pion nucleon charge exchange scattering

20 p3323 N71-33816

Two-plane-wave models for electron-electron and electron-phonon umklapp scattering with determination of their effect upon transport properties of simple metals

20 p3323 N71-33832

Research and developments on cesium ion thrusters including measuring, testing, and calculation techniques

[ONERA-TP-974] 20 p3340 N71-33880

Mathematical models for inelastic electron proton scattering indicating current amplitudes with nonlocality characteristics

[RIFP-125] 20 p3324 N71-33881

Mathematical models for pole assignment in linear feedback control systems

[NRC-ME-MK-28] 20 p3293 N71-33883

Microscopic foundation of bubble model for excess electron in liquid helium

20 p3325 N71-33905

Broken scale invariance, current algebra, and massive gravitation in formalism describing meson interactions at intermediate energies and below

[NUB-2091] 20 p3293 N71-33922

Differential technique used to determine third and fourth order elastic constants of copper and nickel

20 p3286 N71-33932

Field theory in infinite momentum frame for deriving parton model, with transverse Galilean and longitudinal Lorentz boost invariances stressed

[LPTHE-71/24] 20 p3293 N71-33958

Mathematical model of DSIF Doppler tracking system phase noise

21 p3393 N71-34151

Supersonic turbulent boundary layer step induced separation, and incompressible flow model for predicting upstream flow field in channels

21 p3414 N71-34292

Mathematical modeling techniques in analysis of environmental pollution generated by mixes of transportation modes, with detailed treatment of electrical interference

[R-762-DOT/RC] 21 p3420 N71-34331

Band structure of aluminum oxide determined using basis set having 50 ion functions and 15 plane waves

21 p3445 N71-34514

Optimal selection of automation systems under multivariate normal model in terms of reliability, feasibility, and economy

[NASA-CR-121656] 21 p3446 N71-34524

Principles of situation control and practical application of situational control models for complex systems including airports, drydocks, and street crossroads

[JPRS-53913] 21 p3448 N71-34536

Formal generative and transformational grammars for constructing model for complex systems

21 p3448 N71-34537

Application of situational control models examined for lock sections of canals, seaports and airports, network of street crossroads, and other large systems

21 p3448 N71-34538

Obtaining mathematical model and determining state of linear, time invariant system from input/output observations

21 p3450 N71-34554

Meteorological observations required for computer models describing weather: modification experiments

[NASA-CR-121617] 21 p3450 N71-34557

Coherent [n,2n] scattering amplitude on heavy nuclei at low energies based on infinite-mass nuclei approximations

[TTF-70-95-E] 21 p3487 N71-34839

Application of photonuclear and liquid drop models to symmetric binary photofission processes

21 p3489 N71-34853

Mathematical model using Monte Carlo method for modulation of galactic protons by solar wind

[NASA-CR-115095] 21 p3504 N71-34958

Variations in electrical conductivity in sunspot structure analyzed using cylindrical models of sunspot field diffusion

21 p3505 N71-34973

Mathematical model of atmospheric circulation around Venus based on hydrodynamic equations of spheres and Greenhouse effect

[JPRS-53985] 21 p3510 N71-35015

Computer programs for evaluating vibrational characteristics of complicated structural systems mathematically modeled as assemblages of arbitrary substructures

[NASA-CR-119927] 21 p3527 N71-35129

Statistical model for calculating effect of fire power of fragmenting HE weapons on composite targets

[RAE-LIB-TRANS-1420] 21 p3532 N71-35174

Semiempirical formulae representing sonic boom loudness as function of overpressure and time compared with experimental and theoretical calculations

[ISVR-TR-46] 21 p3540 N71-35214

Studying information channels and their use by mathematical models and data simulation

[FOA-3-C-3610-63] 22 p3557 N71-35335

Qualitative hydrodynamic model of dynamic wall hysteresis for fluid-fluid interface being driven through capillary tube by applied pressure gradient

[AD-726635] 22 p3570 N71-35424

Derivation of generalized function for gas viscosities

[NLL-RTS-6400] 22 p3570 N71-35425

Interpretation of Hall coefficient of pure copper, silver, gold, and some silver alloys based on anisotropic Fermi surface model

[NRC-TT-1476] 22 p3592 N71-35581

Applying rigid band model to metal and alloy band structure determinations

[NRC-TT-1475] 22 p3593 N71-35584

Application of Liapunov method for parameter adaptive control of unknown plants

[NASA-CR-121961] 22 p3605 N71-35673

Mathematical model for initial provisioning of standby system with deteriorating and repairable spares

[TR-71-31] 22 p3607 N71-35693

Nuclear reactor mathematical model matching of open loop dynamic response with experimental data

[AEFW-M-1012] 22 p3620 N71-35791

Semi-direct modal synthesis method using Green function modes and applications to space time dynamics of nuclear reactor systems

22 p3626 N71-35840

Pion[minus] proton interactions with strange particle production at p equals 4 GeV/c represented by phenomenological quasi-two-body model of multiple particle production

[JINR-P1-5706] 22 p3632 N71-35880

Developments in hadron physics, dual models and dual phenomenology, weak elementary particle interactions, and electromagnetic interaction theory - topics from nuclear research conference

[CERN-71-7] 22 p3640 N71-35951

Neon constricted positive column in gas discharge tubes with thermal model based on thermoelectric and spectroscopic measurements

22 p3653 N71-36054

Procedure for computing gravity losses over n-burn multiorbit escape trajectories of specified final energy and prediction of optimal burn schedules for nuclear rocket escape maneuvers

[NASA-CR-115164] 22 p3671 N71-36178

Mathematical model for elastic stress concentration problems in fiber reinforced materials

22 p3691 N71-36324

Mathematical models for solving problems of heat transfer on transparent turbulent boundary layer

[NASA-CR-120791] 22 p3694 N71-36347

Model of executive decision making emphasizing interaction of organization members

[NASA-CR-121886] 22 p3698 N71-36372

Colleague role of scientists utilizing executive decision making model

[NASA-CR-121885] 22 p3698 N71-36373

Mathematical modeling of F-4 aircraft wave off trajectories for aircraft carrier approaches

[AD-727121] 23 p3708 N71-36439

Effects of display gain and signal bandwidth on visual sources of human controller remnant

[AD-727057] 23 p3717 N71-36500

Mathematical model representing human performance reliability for laboratory vigilance and manual control tasks

[AD-727661] 23 p3718 N71-36503

Model of human operator reflecting known perceptual and response characteristics for automobile driving task

23 p3718 N71-36504

Equilibrium statistical mechanics model for relationship between hard sphere fluid and fluids with realistic repulsive forces

[AD-726763] 23 p3720 N71-36516

Optimal estimates of unknown parameters for detection and discrimination of signals

[AD-726614] 23 p3724 N71-36545

Mathematical model of color television display for assessment of random noise

[BBC-1971/27] 23 p3725 N71-36553

Linear rank statistical detection procedures for communication, radar, and sonar problems

23 p3727 N71-36567

Logistics system modeled as transportation problem with linear cost structure and lower bounds on supply from each origin and to each destination

[AD-726509] 23 p3729 N71-36586

Models for internally generated noise in delta modulators and stability criteria for nonrandom inputs

23 p3739 N71-36662

Series truncation method with novel coordinate system used for calculation of flow about circular cylinder at low Reynolds numbers

23 p3743 N71-36691

Method of lines technique for computing flow field about conical configurations at incidence in supersonic flow

[NASA-TR-R-374] 23 p3744 N71-36697

Vortex flows of second-order nonnewtonian liquids investigated using mathematical model

23 p3745 N71-36707

Model for calculating condensation effects in boundary layer on mass transfer from rotating disks

23 p3746 N71-36714

Modified expression for exospheric temperature in Jaccia static diffusion models of upper atmosphere in polar regions

[NASA-TM-X-65697] 23 p3747 N71-36718

Two-dimensional time dependent diffusion model for phase delay between thermoplastic density and temperature

[NASA-TM-X-65694] 23 p3747 N71-36719

Computing dispersal of atmospheric pollutants near airports by use of mean wind and temperature profiles

[NASA-CR-111962] 23 p3748 N71-36720

Hybrid coordinate equations of motion for finite element model of dynamic analysis on flexible appendage attached to rigid base

23 p3781 N71-36947

Time series and compartmental analysis techniques for biological applications

[NASA-CR-115201] 23 p3781 N71-36948

Analysis of subsynoptic scales of atmospheric motion by means of synoptic network supplemented by satellite cloud observations

[AD-726628] 23 p3791 N71-37020

Analysis of frontal model using nonlinear differential equations

[AD-726617] 23 p3791 N71-37021

Development of mathematical meteorological diffusion models for analysis and solution of urban air pollution problems

[NLL-M-20362-5828.4F1] 23 p3792 N71-37031

Models for analyzing burnup effects on fuel pin thermal performance applied to fast nuclear reactors

[CONF-710414-1] 23 p3798 N71-37079

Numerical data and formulas for thermic calculations of water cooled research reactor

[CEA-R-4114] 23 p3800 N71-37089

Predictive models for preventing water radiolysis in sealed aluminum capsules for reactor irradiations

[NASA-TM-X-7407] 23 p3801 N71-37098

Statistical nonlaminar model of axisymmetric charged particle beams with nonzero angular velocities

[NP-18860] 23 p3815 N71-37206

Axial vector current relation associated with pseudoscalar meson and sigma model formalisms

[AD-72-019] 23 p3819 N71-37241

Vector currents and current algebra in zero width model of hadron bootstrap

23 p3822 N71-37242

One-dimensional diffusion model for calculating effect of interstellar magnetic field line wandering on cosmic ray parameters

[NASA-TM-X-65698] 23 p3847 N71-37420

Derivation of cosmologic model for verification of gravitation theory

23 p3849 N71-37434

Plasma model for physical properties of stellar and planetary atmospheres

23 p3853 N71-37461

SUBJECT INDEX

MATRICES [MATHEMATICS]

- transport theory and adiabatic model for particle capture along equator of outer radiation belt
23 p3854 N71-37468
- Evolutionary models and fluidity functions of spherical, cylindrical, and planar plasmas
23 p3854 N71-37469
- Analytical superposition model for environmentally-assisted corrosion fatigue crack propagation in aluminum and steel alloys
[UCRL-20538] 23 p3860 N71-37520
- Generalization of standard cutout-modification procedure in matrix force analysis to allow elimination of loads other than those which naturally describe state of stress in elements
[ARL/SM-NOTE-361] 23 p3861 N71-37523
- Dynamic response of hydrophobic spherical shell predicted by finite element model
[AD-726726] 23 p3861 N71-37528
- Approximate mathematical model for free vibrations of smooth arc of arbitrary shape and varying cross sections
[AD-726724] 23 p3862 N71-37530
- Discrete element model for predicting deformation and failure mode of stressed brittle materials
23 p3865 N71-37554
- Method for solving reactor problems of transient thermal stresses using frequency response and weighting functions
[EURFNR-794] 23 p3867 N71-37570
- Mathematical models for explaining working of physiological systems in plants
[NASA-CR-123169] 24 p3878 N71-37641
- Mathematical models for estimating block up-and-down design of sensory thresholds
[NASA-TM-X-62090] 24 p3878 N71-37644
- Physicochemical factors affecting activated charcoal adsorption of contaminants using mathematical models tables
[NASA-CR-115202] 24 p3880 N71-37657
- Man machine systems for detection, recognition, transmission and perception of information on engineering problems
[AD-727610] 24 p3883 N71-37678
- Computerized business game and mathematical models of optimal scientific research developments
[JPRS-54168] 24 p3894 N71-37755
- Mathematical models of optimal development of applied scientific research
24 p3894 N71-37757
- Effect of coefficient rounding in floating point digital filters
[AD-727073] 24 p3898 N71-37784
- Theory and formalism for derivation of transfer function of N-path filters
[AD-727148] 24 p3898 N71-37787
- Unified heuristic model of fluid turbulence which supplements basic equations of motion and continuity
[AD-727103] 24 p3906 N71-37840
- Mathematical modeling and testing of Lunar Orbiter photographic subsystem
[NASA-CR-123174] 24 p3920 N71-37952
- Aerodynamic calculations in designing axial compressors with emphasis on compressors of stationary installations - handbook
[AD-727191] 24 p3929 N71-38032
- Stain rate sensitive constitutive equations using yield criterion which incorporates second and third invariants of stress deviator
[NASA-CR-123175] 24 p3934 N71-38069
- Models for single-server queueing systems with intermittent service and economic measure of system performance
[AD-728006] 24 p3950 N71-38179
- Optimal feedback controller design based on model for linear plant of unknown characteristics under stochastic environment
24 p3951 N71-38186
- Two-dimensional numerical model of large scale mountain-plain circulation including sloping plane effects for analysis of convective patterns in lee of Colorado Rockies
24 p3954 N71-38208
- Pinch fusion fast breeder cavity reactor mathematical models for control and stability analysis
24 p3964 N71-38274
- Equations for variation with frequency of voltage output from hydrophobic exposed to constant acoustic pressure field
[AD-727978] 24 p3967 N71-38300
- Models for predicting erosion of ductile and brittle target materials by natural contaminants
24 p3968 N71-38308
- Hypersonic-nucleon interaction using crossed channel boson exchange model
[NP-18838] 24 p3971 N71-38325
- Numerical model to simulate plasma behavior in linear multiscoped pinch device [polytrope]
[CONF-710607-46] 24 p3987 N71-38447
- Mathematical model for trapped particle turbulence in electric field driven streaming instability in collisionless plasma
[CONF-710607-40] 24 p3988 N71-38454
- Mathematical model for motion of small drops and bubbles considering absorption, diffusion, and convection in interfacial region
[NVO-2807-91] 24 p3996 N71-38506

- Computer aided analysis of theoretical and experimental operating characteristics of insulated gate field effect transistors
24 p3999 N71-38524
- Mathematical models of planar librational stability conditions for deploying satellites
24 p4005 N71-38559
- Comparison of earth's magnetic field models with Gaussian sequence
24 p4011 N71-38604
- Mathematical models for analyzing automotive gas turbine and nitric oxide emissions
[FPL-PUBL-71-11] 24 p4032 N71-38769
- MATHEMATICAL STATISTICS
U STATISTICAL ANALYSIS
MATHEMATICS
- Decisions affecting society arising from mathematics and its application
[TR-70-58] 08 p1225 N71-18892
- Bibliographies on nuclear mathematics and technology of eastern countries
[AED-C-12-24] 18 p2988 N71-31477
- Influence and limitations of computers and mathematics on social structures
[USC-113P19-11] 22 p3701 N71-36396
- MATHIEU EQUATION
U MATHIEU FUNCTION
MATHIEU FUNCTION
- Electronic or nucleonic many body system ground state energy calculation using Mathieu functions as orthogonal single particle wave functions
18 p2983 N71-31048
- Scattering of plane waves from thin rigid porous elliptic cylindrical shells and Mathieu function
[NASA-TN-D-6340] 18 p2966 N71-31435
- MATRICES
- Ecological transfer matrices for various terrestrial and aquatic systems
[ORNL-18P-71-3] 24 p3878 N71-37648
- MATRICES [CIRCUITS]
- Fabrication methods for matrices of solar cell sub-modules
[NASA-CASE-XNP-05821] 02 p0149 N71-11056
- Magnetic matrix memory system for nondestructive reading of information contained in matrix
[NASA-CASE-XMP-05835] 03 p0345 N71-12504
- Conductor for connecting parallel cells into sub-modules in series to form solar cell matrix
[NASA-CASE-NPO-10821] 09 p1325 N71-19545
- Reliable magnetic core circuit apparatus with application in selection matrices for digital memories
[NASA-CASE-XNP-01318] 11 p1730 N71-23033
- Serial digital decoder design with square circuit matrix and serial memory storage units
[NASA-CASE-NPO-10150] 13 p2049 N71-24650
- Transformation properties between impedance and general matrix representation of two port network
[NLL-PORS-TRANS-2705-P0022.81] 17 p2728 N71-30205
- Synthesis procedure for developing arbitrary rational admittance matrices using operational amplifiers and RC one ports
24 p3901 N71-37809
- MATRICES [MATHEMATICS]
- NT ADJOINTS
NT CANONICAL FORMS
NT EIGENVALUES
NT EIGENVECTORS
NT JORDAN FORM
- Improving computations in DFP method for function minimization using doubly relaxed generalized inverse of matrix
[NASA-CR-111129] 01 p0075 N71-10539
- Numerical analysis of proper time formulation with general vertices
02 p0251 N71-11759
- Numerical analysis of Abelian subgroups of p-groups
02 p0251 N71-11765
- Covariance matrix for deflections of vertical and undulations based on actual gravity data
[AD-712351] 02 p0222 N71-12168
- Determining distribution density of unknown stochastic vector using fixed order probability matrix
[JPRS-51739] 02 p0252 N71-12170
- Solution of linear algebraic systems by matrix decomposition
03 p0398 N71-12681
- Test matrices for numerical algorithms in linear algebra problems
[AD-712679] 03 p0398 N71-12761
- Prototype recording system using least squares matrix method of waveform analysis behind towed bodies
[NPL-SHIP-143] 03 p0366 N71-13388
- Deriving algorithms for computations involving sparse matrices
[NASA-CR-115777] 04 p0536 N71-13758
- Realization theory of rational transfer matrices presented as fundamental algebraic objects in theory of finite, constant linear systems
[NASA-TM-X-66513] 04 p0538 N71-14157
- Frequency domain analogies, polynomial matrices, and linear systems
[NASA-TM-X-66512] 04 p0538 N71-14173

- Structure theorem for time invariant multivariable linear systems
[NASA-TM-X-66511] 04 p0538 N71-14174
- Reducing unphysical irreducible representations of SU(2,2) with iso-Poincare subgroup
[NVO-3258-52] 04 p0539 N71-14180
- Deriving analytic expressions for calculating phase space contour and area of quadrupole triplets from matrix elements
[CERN-70-22] 04 p0588 N71-14279
- Approximation of physical constraints
[AD-712677] 04 p0539 N71-14288
- Applying finite difference method to solution of numerical stability in linear algebra problems
[ORO-3443-28] 04 p0539 N71-14388
- Investigating reaction eta-meson yields 3 pion for charge asymmetry
[NEVIS-177] 04 p0591 N71-14389
- Reduction of square matrices to Jordan canonical forms
[FOA-F-C-8238-11] 05 p0712 N71-14544
- Matrix method and stiffer stable algorithms in numerical integration for computer aided network design programming
[NASA-CR-111837] 05 p0651 N71-14998
- Aliasing schemes and construction of fractional replicates
[AD-713696] 05 p0714 N71-15279
- Asymptotic distribution of eigenvalues of random matrices
[ORNL-4685] 05 p0714 N71-15590
- Analysis of n-dimensional nonlinear mappings representative of P and S functions
[NASA-CR-116133] 06 p0884 N71-16088
- Infinite multiplets with SU(3) for mesons
[DEMO-70/14] 06 p0918 N71-16242
- Modal analysis computer program package for finding frequencies and mode shapes of any linear elastic system governed by generalized eigenvalue equation
[NASA-CR-116178] 06 p0820 N71-16439
- Realizable path matrices for N-port machines
[AD-714592] 06 p0807 N71-16551
- Applying operator and matrix representations to quantum mechanics
06 p0907 N71-16661
- Generating first and second order matrix elements by tracking charged particles in magnetic fields
[UCRL-19623] 06 p0923 N71-16725
- Effective use of incremental stiffness matrices in nonlinear geometric analysis
[AD-713967] 06 p0958 N71-16877
- Hermitean form for group representation of complex matrices L(a,C)
[IFVE-STF-49-91] 07 p1050 N71-17001
- Matrix analysis of double dc and heat shield methods for diffusivity measurement at very high temperatures
[AD-715900] 08 p1303 N71-18710
- Determination of density matrix components for multiconfiguration wave functions and Hamiltonian interaction matrices
[NASA-CR-116885] 08 p1265 N71-19137
- Calculating tables of inverses and determinants of finite segments of Hilbert matrices using variable precision rational arithmetic
08 p1227 N71-19188
- Multiparticle relativistic K-matrix equations of particle amplitudes satisfying unitarity
[RI-C-158-579] 09 p1434 N71-19993
- Neutron-deuteron scattering length calculations with realistic potentials using two-particle t-matrices and Faddeev equations
[JINR-P4-5000] 09 p1440 N71-20302
- Probability distribution functions of extreme roots of Wishart and Manova matrices
[AD-716815] 10 p1391 N71-20868
- Time dependent perturbation theory of ground state many fermion system for study of self energy and factorization problems and examination of reaction matrix expansions
11 p1801 N71-21886
- Generalized matrix elements on Poincare group used to write Fourier transformation for distributions on group
[LPTHE-71/4] 11 p1788 N71-22463
- Orthogonal matrix in analytical photogrammetric solutions
[ESSA-TR-C/05-39] 12 p1915 N71-23149
- Edge T-matrix theory used to derive algorithms for solving basic problems of network theory
[AD-718323] 12 p1892 N71-23334
- Exact distributions of intermediate roots of class of random matrices
[AD-718477] 12 p1949 N71-23579
- Numerical analyses of error covariance matrix in linear filtering problem, computational errors in Kalman filtering, and constant flight equations
[NASA-CR-115910] 13 p2102 N71-24470
- Validation of procedure used in deriving quadratic intermultiplet mass formulas in response to criticism based on formal counting of order of SU(3) breaking
[TR-71-100] 13 p2125 N71-23936
- Spontaneous optical parametric scattering using quantum mechanical scattering matrix approach
13 p2606 N71-23996

Matrix ring formulations of Artinian semi-simple ring with involutions 13 p2104 N71-25458

Unitary pole approximation of separable expansions of two T-matrix and three body problem 13 p2144 N71-25586

Approximations for off energy shell t-matrix perturbation theory 14 p2239 N71-25601

Linear regulator problem solution using Euler equations of motion, Laplace transformations, and Hamilton-Jacobi equation for stochastic control 14 p2235 N71-26444

Chiral SU(2) times SU(2) dynamics for A1 mesons, rho mesons, and pions 14 p2318 N71-26768

Classification of states and interactions in nuclear collective model 15 p2457 N71-26856

Probability density functions for exact joint distributions of few roots of class of random matrices [AD-72190] 15 p2433 N71-26924

Unitarity theory for calculating forward scattering amplitude at high energies 15 p2464 N71-27239

Danieli method for determining eigenvalues of matrices with real elements programmed in FORTRAN 15 p2434 N71-27619

Variational method for estimating binding energy of oxygen with effective interaction matrix elements [DEMO-70/25] 15 p2492 N71-27929

Determinantal formalism and physical unitarity in relativistic extension of Le Couteur and Newton formalism 15 p2495 N71-27967

Calculation of orthogonal transformation matrices and application to photogrammetry 16 p2622 N71-28204

Wing interference lift line lattice simulation and application to aerodynamic loads on tandem wings in unsteady flow 17 p2698 N71-29336

Computation of uncoupled vibrations of rotary wings using transfer matrix method [DLR-FB-70-63] 17 p2703 N71-29543

Binet formalism in general theory of relativity and laws of conservation considering integral and differential form of conservation laws 17 p2787 N71-29701

Matrix analysis and neutron phenomena in upper atmosphere and radioactive isotopes 17 p2804 N71-30231

Two-body error analysis computer program to evaluate resulting state vector and covariance matrix for orbit after one coast and one burn maneuver [NASA-TM-X-65620] 18 p3007 N71-30511

Theory of weak interactions based on possible SU(4) symmetry for hadrons 18 p2975 N71-30568

Error matrix in orbit calculation from tracking data [ELDO-TM-127] 18 p3008 N71-30631

Nonexistence of ambiguities in SU(3) x SU(3) matrix breaking 18 p2976 N71-30636

Algebra of nonlinear chiral SU(3) x SU(3) symmetry [JINR-P2-5692] 18 p2977 N71-30637

Asymptotic behavior of covariance matrix solution for discrete matrix Riccati equation 18 p2944 N71-30880

Broken SU(3) sum rules derived from chiral algebra 18 p2945 N71-31141

Optimization for minimum matrix norms noting solution of differential equations 18 p2945 N71-31172

Intensity distribution of optical images for various degrees of illumination using Hermitian matrices [NASA-TT-F-13721] 18 p2966 N71-31452

Factor analysis applied to heuristic assessment matrix for numerical weather forecasting [NRL-M-9255-5828-487] 19 p3178 N71-32587

Compilation of aerodynamic basic definitions, including aerodynamic coefficients, and relations, expansions, and derivatives of forces and moments [ARC-R/M-3562-PT-4] 20 p3204 N71-32975

Quadratically divergent terms in amplitudes of weak aneuphonic processes with photon emission studied in theory with intermediate boson 21 p3487 N71-34840

Matrix algebra used to describe rotation about non-orthogonal axes 22 p3605 N71-35677

Exact distributions of some unordered roots of class of noncentral complex random matrices [AD-72694] 22 p3608 N71-35697

Two-parameter method of calculating unitary weights in SU(3) elementary particle production [JINR-P2-5729] 22 p3632 N71-35885

Wave function reconstruction techniques using matrix elements for complete set of observables [JINR-P2-5729] 22 p3632 N71-35885

Axial vector current relation associated with pseudoscalar meson and sigma model formalisms [TR-72-019] 23 p3819 N71-37241

Asymptotic SU(3) symmetry, nonet boson coupling sum rules, and ninth pseudoscalar mesons [TR-72-021] 23 p3819 N71-37243

Generalization of standard cutout-modification procedure in matrix force analysis to allow elimination of loads other than those which naturally describe state of stress in elements 23 p3861 N71-37523

Standardized method for compact and systematized representation of sets of functionally related parameters by matrices 24 p3881 N71-37668

Decoupling and pole placement via transfer matrix synthesis [NASA-CR-123163] 24 p3947 N71-38156

MATRIX ALGEBRA [MATHEMATICS]

MATRIX ANALYSIS [MATHEMATICS]

MATRIX METHODS [MATHEMATICS]

Calculation of bending moments of transverse continuous rectangular plates with matrix algorithms 03 p0460 N71-12751

Integrating matrix method for determining natural lateral vibration data on rotating twisted propeller blade [NASA-TN-D-6064] 03 p0462 N71-13023

Boolean matrices for optimization of functional covering problems 04 p0536 N71-13623

Group representation in space of differentiating functions [KFKI-70-16-HEP] 08 p1224 N71-18279

Mass matrix and resonant frequencies for generating equivalent spring-mass models for normal modes of structural subsystems [NASA-CR-116825] 08 p1301 N71-19280

Digital computer program description with updating case data mode and extended force method matrix generation capability [AD-715882] 09 p1356 N71-20180

Unitary transformation of Hermitian matrix to symmetric tridiagonal matrix 10 p1592 N71-21341

Factorization theorems, matrix poles, and unitarity [PAM-70-7] 15 p2474 N71-27453

Extrapolation and error estimation method for solving second order boundary value problem 17 p2773 N71-29720

Hermitian transformation matrices for describing intensity distributions in optical transmission through pupil 18 p2963 N71-30904

Computer program and finite element method for resequencing structural stiffness matrix to improve computational efficiency 18 p2995 N71-31114

Boolean matrix syntheses of digital networks for construction of algorithms 18 p2900 N71-31446

Computer programming manual for calculating stress distributions in structural members and frames using iterative solution and matrix methods 19 p3186 N71-31655

Matrix method for neural net simulation [JPRES-53581] 19 p3124 N71-32502

Analytic method for interface relationships between different surface geometries [AD-4193] 20 p3291 N71-33280

Quantum mechanical entropy in tensor product of Hilbert spaces 20 p3364 N71-33381

Matrix method for synthesis of frequency independent [n plus 1]-pole circuits with active elements 21 p3406 N71-34234

New element preprocessor for NASTRAN programming to generate tables and routines for new elements 22 p3687 N71-36292

Mathematical model for elastic stress concentration problems in fiber reinforced materials 22 p3691 N71-36324

Reference matrix for evaluating and preparing environmental impact reports 23 p3752 N71-36757

Holomorphic matrix method for linearization of analytical bundles and in series convergence 24 p3948 N71-38167

MATRIX STRESS CALCULATION [MATHEMATICS]

MATRIX THEORY [MATHEMATICS]

Calculating binding energy of Lambda hyperon particle in nuclear matter using self-consistent Brueckner K matrix theory [JINR-1153/7/PL] 03 p0433 N71-12938

Method for extraction of first-forbidden beta matrix elements from angular correlation data [COO-1746-44] 05 p0749 N71-15294

Numerical analyses of error covariance matrix in linear filtering problem, computational errors in Kalman filtering, and constant flight equations [NASA-CR-115010] 13 p2102 N71-24470

Neutron cross section calculation techniques including review of data and nuclear reactions, Breit-Wigner and R matrix theories, and Doppler effects and shielding of resonances 15 p2469 N71-27348

Theorem on K-matrix elements variational bounds for scattering parameters [JINR-P4-5332] 15 p2497 N71-27997

Matrix element tables for computing L shell fluorescence yields and electron transition rates in spin-spin coupling including Auger, Coster-Kronig, and radiative values [SC-R71-10075] 17 p2773 N71-29789

Iterative solution for internal transformations 17 p2773 N71-29789

Theory of weak interactions based on possible SU(4) symmetry for hadrons 18 p2975 N71-30568

Theorem proof for lower bounds of nuclear scattering K matrices 21 p3469 N71-34669

Solution of inverse reaction problem to obtain complex potentials as in optical model of nucleus [AAEC/TM-586] 23 p3817 N71-37225

MATTER (PHYSICS)

Hydrodynamics of matter and antimatter in contact [REPT-70/38] 09 p1437 N71-20074

Cross sections and coherent final states for antiproton deuteron interactions and related dissociation reactions at 7.0 GeV/c 10 p1617 N71-21203

Nonlinear equation for correlation function between lambda baryon and nucleon in nuclear matter [DEMO-70/19] 15 p2488 N71-27878

Photon theory of light and matter [NASA-TT-F-13695] 16 p2640 N71-29002

Analytic solutions of reference spectrum equation for nuclear matter [DEMO-70/24] 18 p2943 N71-30619

Hydrodynamical motion of system consisting of matter-antimatter embedded in thermal radiation [REPT-71/25] 20 p3328 N71-33984

Angular momentum decomposition of three body problem and binding energy per particle of nuclear matter 22 p3650 N71-36030

Monte Carlo method for calculating high energy radiation with matter 23 p3810 N71-37169

Cosmological gamma ray spectrum calculations from matter-antimatter annihilation in universe [NASA-TM-X-65709] 23 p3842 N71-37395

Charge symmetry of universe and distribution of matter and antimatter 23 p3850 N71-37440

Interaction of optical and particle radiation into matter in astrophysics 23 p3852 N71-37456

MATURING U GROWTH

MAXIMA

Fabrication and testing of peak wind speed recording device [NASA-CR-102509] 02 p0253 N71-11407

Probability distribution functions for pulse amplitude and wavelength of stationary process after high maximum [AD-720004] 17 p2772 N71-29447

ALGOL computer program for estimation of maximum of analytical functions with arbitrarily small error bound 17 p2772 N71-29482

MAXIMUM LIKELIHOOD ESTIMATES

Computer program for mixed analysis of variance model based on maximum likelihood [NASA-CR-108704] 01 p0076 N71-10834

Series truncation in parametric estimation and error transformation [NASA-CR-108705] 01 p0077 N71-10979

Algorithm providing maximum likelihood estimates for linear dynamic systems with unknown parameters [AD-712894] 03 p0400 N71-13186

Maximum likelihood estimates for target amplitude comparison and detection by monopulse radar in cluttered environment 04 p0495 N71-39009

Statistical mechanics of incomplete data including maximum likelihood estimates, normal density functions, multivariate statistical analysis, regression analysis and analysis of variance [NASA-CR-174967] 13 p2052 N71-24884

Decoding algorithm for maximum likelihood detection of uniform convolutional codes transmitted with white noise 15 p2381 N71-27319

Maximum likelihood estimates of atmospheric temperature profile deduced from satellite radiation measurements in cloud presence 15 p2400 N71-27496

Extremum value statistics computer program for evaluation of radar target acquisition [AD-722441] 18 p2889 N71-30717

Maximum likelihood analysis of balanced incomplete blocks, and small-sample properties of maximum likelihood estimates 22 p3604 N71-35669

SUBJECT INDEX

MAXIMUM PRINCIPLE

Abstract variational theory application to continuous parameter stochastic optimization problems to derive maximum principles in linear programming [NASA-CR-117886] 12 p1948 N71-32320

Equivalent mathematical control system models for maximum principle time delay systems with feedback [AD-718437] 12 p1893 N71-23661

Optimal trajectory construction by trial and error based on Pontryagin maximum principle [NASA-TT-F-13780] 24 p3947 N71-38157

MAXIMUM USABLE FREQUENCY

Ionospheric propagation charts of predicted median critical and maximum usable frequencies in F2 region, Delhi - Jan. 1971 [RRC-B172] 11 p1747 N71-22067

MAXWELL EQUATION

Maxwell equation for conical horn antennas [TH-70-E-10] 02 p0182 N71-11779

Investigating effect of beam of electrons on Maxwellian plasma by numerical integration of Vlasov equation in one dimension [COO-2059-2] 05 p0748 N71-15274

Modified Maxwell equation for solving Alfvén wave problem [AD-715774] 08 p1275 N71-18820

Electromagnetic wave propagation study within inhomogeneously filled waveguides, using Maxwell equations 11 p1703 N71-22757

Maxwell field theory for solving wave path controllability in tropospheric scatter propagation 12 p1876 N71-23462

Collisional effects on electron waves in non-Maxwellian Lorentz magnetoplasma [AD-71798] 14 p2320 N71-25708

Group of invariance of Maxwell equations and extension associated with set of hyperboloids of mass [SLAC-TRANS-130] 15 p2458 N71-26935

Techniques for solving Maxwell equations and applications in induction heating and electromagnetic prospecting 21 p3403 N71-34216

Scattering of electromagnetic waves using integral equation form of Maxwell equations for electric fields [NASA-CR-121760] 21 p3447 N71-34530

Infinite length, gap excited, thick, cylindrical dipole antenna radiation field formulations as boundary value problems based on Maxwell equations for electric and magnetic fields 23 p3734 N71-36619

MAXWELL-BOLTZMANN DENSITY FUNCTION

Langmuir probe determinations on non-Maxwellian distribution of electron energy in plasma of electron bombardment ion engines [RM-70/3] 04 p0600 N71-14300

Effects of delayed gamma rays, systematic and random coincidences, and scattered neutrons on Maxwellian temperature value from time of flight measurements of Cf-252 fission neutron spectrum [KFKI-71-9] 24 p3971 N71-38332

MAXWELLIAN DISTRIBUTION (DENSITY)

U MAXWELL-BOLTZMANN DENSITY FUNCTION

MCDONNELL AIRCRAFT

NT F-4 AIRCRAFT

NT RF-4 AIRCRAFT

MCDONNELL DOUGLAS AIRCRAFT

NT DOUGLAS AIRCRAFT

MCDONNELL MILITARY AIRCRAFT

U MILITARY AIRCRAFT

MCLEOD GAGES

Automatic recording McLeod gage with three electrodes and solenoid valve connection [NASA-CASE-XLE-03280] 11 p1767 N71-23093

MEAN

U MULTIPLE DOCKING ADAPTERS

MEAN

Covergence and mean square error estimation in solution of boundary value problems for ellipses equations by straight line method [NASA-TT-F-11432] 06 p0884 N71-16496

MEAN FREE PATH

Neutron transport of neutrons from d/dt source through many mean free paths in liquid nitrogen [UCRL-50856] 06 p0919 N71-16250

Techniques for determining real tridents and mean free path for tridents caused by primary electron in pair production in electron irradiated nuclear emulsions 15 p2479 N71-27642

MEAN TIME BETWEEN FAILURES

U MTF

MEASURANDS

U MEASUREMENT

MEASURE AND INTEGRATION

NT BINARY INTEGRATION

NT FUNCTIONAL INTEGRATION

NT INTEGRAL CALCULUS

NT NUMERICAL INTEGRATION

NT RUNGE-KUTTA METHOD

NT WEIGHTING FUNCTIONS

Standardized measurement of materials 01 p0018 N71-10507

FORTAN program for obtaining approximations to real valued functions [AD-712973] 04 p0341 N71-14398

Everett interpretation of quantum mechanics, and measurement theory 09 p1425 N71-20406

Method for presentation and systematic compilation of integral tests of differential cross section data from various fast reactor analyses [RPI-328-219] 17 p2781 N71-29346

Numerical integration of Lawden intermediate thrust arcs and their optimality in Newtonian central force field [NASA-TT-F-13748] 17 p2774 N71-30131

SYNTRON - computer code for reactor problems involving three dimensional neutron flux calculations [RISO-M-1346] 18 p2974 N71-30548

Characterization of conditional probability measures for continuous-time, partially observable Markov processes [AD-722453] 18 p2946 N71-31240

Characterization of contiguity [AD-197476] 18 p2948 N71-31490

Subharmonic response in nonlinear network analysis [AD-723216] 19 p3122 N71-31987

MEASURE THEORY

U MEASURE AND INTEGRATION

MEASUREMENT

Techniques for determining resonant frequencies, mode shapes, and damping coefficients of model structures [SC-DR-70-72] 01 p0130 N71-10612

Measurement methods for semiconductor devices, materials, and production control [NASA-CR-111764] 04 p0602 N71-14063

Measurement methods during fabrication and environmental testing of microcircuits 09 p1360 N71-20228

Hybrid computer measurement of stopband in LAMPF 805 MHz accelerator structure at high power [LA-4593] 15 p2387 N71-26857

Conference on Weights and Measures attended by representatives of Federal Government, business, industry, railroads, and associations [NBS-SPEC-PUBL-342] 16 p2601 N71-28500

Weight and Measures Labeling Handbook for use in packaging and labeling commodities and enforcing state laws and regulations [NBS-HB-108] 16 p2601 N71-28568

Determination of correct nutation values after latitude observations 23 p3749 N71-36731

MEASURING

MEASURING APPARATUS

U MEASURING INSTRUMENTS

NT ACCELEROMETERS

NT ACTINOMETERS

NT ALTIMETERS

NT AMMETERS

NT ANALYZERS

NT ANEMOMETERS

NT APPROACH INDICATORS

NT ATOMIC CLOCKS

NT ATTITUDE INDICATORS

NT BAROMETERS

NT BATHYMETERS

NT BATHYTHERMOGRAPHS

NT BAYARD-ALPERT IONIZATION GAGES

NT BALOMETERS

NT CALORIMETERS

NT CAPACITIVE FUEL GAGES

NT CERENKOV COUNTERS

NT CINETHODOLITES

NT CLOCKS

NT CLOUD HEIGHT INDICATORS

NT COMPASSES

NT CONDUCTIVITY METERS

NT COULOMETERS

NT COUNTERS

NT DEFORMETERS

NT DENSITOMETERS

NT DIFFRACTOMETERS

NT DISTANCE MEASURING EQUIPMENT

NT DOSIMETERS

NT DROPSONDES

NT DYNAMOMETERS

NT EBERT SPECTROMETERS

NT ELECTRICAL CONDUCTIVITY METERS

NT ELECTROMETERS

NT ELECTRON COUNTERS

NT ELECTRON PROBES

NT ELECTROPHOTOMETERS

NT ELECTROSTATIC PROBES

NT ELLIPSOMETERS

NT ENGINE MONITORING INSTRUMENTS

NT ERGOMETERS

NT EXTENSOMETERS

NT FABRY-PEROT INTERFEROMETERS

NT FABRY-PEROT SPECTROMETERS

NT FLAME PROBES

NT FLIGHT RECORDERS

MEASURING INSTRUMENTS

NT FLOW DIRECTION INDICATORS

NT FLOWMETERS

NT FUEL GAGES

NT GALVANOMETERS

NT GAS METERS

NT GEIGER COUNTERS

NT GEODIMETERS

NT GONIOMETERS

NT GRAVIMETERS

NT GRAVITY GRADIOMETERS

NT GYRO HORIZONS

NT GYROCOMPASSES

NT HODOSCOPES

NT HOT-FILM ANEMOMETERS

NT HOT-WIRE ANEMOMETERS

NT HOT-WIRE FLOWMETERS

NT HYGROMETERS

NT IMPEDANCE PROBES

NT INDICATING INSTRUMENTS

NT INFRARED DETECTORS

NT INFRARED INSTRUMENTS

NT INFRARED SCANNERS

NT INFRARED SPECTROMETERS

NT INFRARED SPECTROPHOTOMETERS

NT INTERFEROMETERS

NT ION PROBES

NT ION TRAPS (INSTRUMENTATION)

NT IONIZATION GAGES

NT IONOSPHERES

NT KNUDSEN GAGES

NT LASER ALTIMETERS

NT LASER RANGE FINDERS

NT LIGHT SCATTERING METERS

NT LUNAR SEISMOGRAPHS

NT MACH-ZEHNDER INTERFEROMETERS

NT MAGNETIC PROBES

NT MAGNETOMETERS

NT MANOMETERS

NT MASS SPECTROMETERS

NT MCLEOD GAGES

NT METEOROLOGICAL INSTRUMENTS

NT MICHELSON INTERFEROMETERS

NT MICROBALANCES

NT MICRODENSITOMETERS

NT MICROMETERS

NT MICROWAVE INTERFEROMETERS

NT MICROWAVE PLASMA PROBES

NT MICROWAVE PROBES

NT MICROWAVE RADIOMETERS

NT MICROWAVE REFLECTOMETERS

NT MICROWAVE SENSORS

NT MOISTURE METERS

NT MONOCHROMATORS

NT NEPHELOMETERS

NT NEUTRON COUNTERS

NT NEUTRON SPECTROMETERS

NT NOISE METERS

NT OMEGA NAVIGATION SYSTEM

NT OPTICAL MEASURING INSTRUMENTS

NT OPTICAL PYROMETERS

NT OPTICAL RANGE FINDERS

NT OPTICAL SCANNERS

NT OSCILLOGRAPHS

NT PARTICLE TELESCOPES

NT PENETROMETERS

NT PENNING GAGES

NT PHASE SWITCHING INTERFEROMETERS

NT PHOTOMETERS

NT PIEZOELECTRIC GAGES

NT PLASMA PROBES

NT POLARIMETERS

NT POSITION INDICATORS

NT POTENTIOMETERS (INSTRUMENTS)

NT PRESSURE GAGES

NT PROFILOMETERS

NT PROPORTIONAL COUNTERS

NT PYRANOMETERS

NT PYROMETERS

NT QUANTUM COUNTERS

NT RADIATION COUNTERS

NT RADIATION DETECTORS

NT RADIATION MEASURING INSTRUMENTS

NT RADIATION PYROMETERS

NT RADIO ALTIMETERS

NT RADIO DIRECTION FINDERS

NT RADIO FREQUENCY IMPEDANCE

NT PROBES

NT RADIO INTERFEROMETERS

NT RADIOMETERS

NT RADIOSONDES

NT RAIN GAGES

NT RANGE FINDERS

NT RAWINSONDES

NT REFLECTOMETERS

NT RESISTANCE THERMOMETERS

NT RESONANCE PROBES

NT RESPIROMETERS

NT RHEOMETERS

NT RIOMETERS

NT SCATTEROMETERS

NT SCINTILLATION COUNTERS

NT SEISMOGRAPHS

NT SEXTANTS

NT SHOCK MEASURING INSTRUMENTS

NT SIGNAL ANALYZERS

NT SILICON RADIATION DETECTORS

NT SOLAR SPECTROMETERS
 NT SONDES
 NT SPACECRAFT POSITION INDICATORS
 NT SPARK CHAMBERS
 NT SPECTROHELIOGRAPHS
 NT SPECTROMETERS
 NT SPECTROPHOTOMETERS
 NT SPECTRORADIOMETERS
 NT STRAIN GAGES
 NT TACHOMETERS
 NT TEMPERATURE MEASURING INSTRUMENTS
 NT TEMPERATURE PROBES
 NT THEODOLITES
 NT THERMAL CONDUCTIVITY GAGES
 NT THERMOCOUPLE PYROMETERS
 NT THERMOMETERS
 NT THRESHOLD DETECTORS [DOSIMETERS]
 NT TIME MEASURING INSTRUMENTS
 NT TIMING DEVICES
 NT TITRIMETERS
 NT TORQUEMETERS
 NT TRANSITS
 NT TRANSMISSOMETERS
 NT TURBULENCE METERS
 NT ULTRAVIOLET SPECTROMETERS
 NT ULTRAVIOLET SPECTROPHOTOMETERS
 NT VACUUM GAGES
 NT VARIOMETERS
 NT VIBRATION METERS
 NT VISCOMETERS
 NT WATTMETERS
 NT WEATHER DATA RECORDERS
 NT WEIGHT INDICATORS
 NT WIND VANES
 Semiconductor junction impurity measuring instrument using capacitance variation with applied voltage in sample diode junctions 01 p0031 N71-10154
 Permeameter for measurement of oxygenizing force and magnetic induction at very high temperatures [NASA-TM-X-52901] 01 p0053 N71-10272
 Molecular beam sampling technique for temperature measurement of earth thermosphere [NASA-CR-66950] 01 p0093 N71-10301
 Analysis of applying standardization techniques to oceanographic sensors 02 p0223 N71-11387
 Test requirements for oceanographic and meteorological sensors 02 p0223 N71-11388
 Statistical analysis of oceanographic instrumentation [AD-711632] 02 p0210 N71-11449
 Design and operation of cell-volume analyzer friction, glaze ice, and studded tire effects on highways [NASA-CR-111384] 02 p0225 N71-11537
 Moisture separator development and drop size measuring and separating techniques 03 p0355 N71-12699
 Solar simulation equipment and necessary measuring techniques 03 p0356 N71-12708
 Design and performance of liquid crystal microwave power density meter 03 p0443 N71-12990
 Instrumentation to measure critical parameters of 300 kilogram experimental magnet [EP-RR-25] 03 p0381 N71-13154
 Oceanographic instrumentation system for in situ carbonate salinometer measurements [TTD-25476] 03 p0374 N71-13387
 Simplified slide rule for determination of downwind safety limits for toxic vapors [REPT-1970-13] 04 p0476 N71-13432
 Ballistic range test equipment for measuring model position, attitude, and velocity [NASA-TM-X-66335] 04 p0522 N71-13582
 Mass flow, velocity, and in-flight thrust measurements by ion deflection 05 p0629 N71-14604
 Measurement capabilities of Livermore Laboratory Standards Laboratories 05 p0657 N71-14782
 Remote-reading borehole inclinometer [PB-193925] 05 p0682 N71-14788
 Dolly film measuring system for bubble and spark chambers [COO-1195-192] 05 p0683 N71-14838
 Inclinometer for measuring lateral movements in soils [PB-194035] 05 p0685 N71-14919
 Status and performance of Purdue SMP time sharing measuring facility 05 p0658 N71-14980
 Method and apparatus for measuring potentials in plasmas [NASA-CASE-XLIV-00821] 05 p0755 N71-15650
 Microtexture measurements of pavement surfaces [PB-194159] 06 p0830 N71-15885
 Physical measurements program at Laboratory for Agricultural Remote Sensing, Purdue 06 p0845 N71-16135
 Transducer for measuring deflections from vibrating structures [NASA-CASE-XLII-03135] 06 p0955 N71-16428

Gimbal platform for weighing oceanographic samples at sea [AD-714606] 06 p0853 N71-16550
 Characteristics of quartz gages for impact experiments [SC-DC-70-4932] 06 p0861 N71-16696
 Semiautomated test system for accurate microwave impedance measurement 06 p0862 N71-16723
 Noncontact gaging method using projected shadow [MHSMF-15] 07 p1030 N71-17580
 Apparatus for use in liquid helium crystal for measurement of small magnetic field changes occurring within detection chamber 08 p1244 N71-19010
 Radiochemical instrumentation techniques for analytical purposes [MLM-1324] 08 p1268 N71-19335
 Evaluation of gas discharge transducer and associated instrumentation for asteroid belt meteoroid experiment with Pioneer probes F/G [NASA-CR-111848] 09 p1390 N71-20401
 Equipment for measuring partial water vapor pressure in gas tank [NASA-CASE-XMS-01618] 10 p1556 N71-20741
 Gauge for measuring quantity of liquid in spherical tank in reduced gravity [NASA-CASE-XMS-06236] 10 p1557 N71-21007
 Nonreusable energy absorbing device comprising ring member with plurality of recesses, cutting members, and guide member mounted in each recess [NASA-CASE-XMF-10040] 11 p1772 N71-22877
 Ablation sensor for measuring surface ablation rate of material on vehicles entering earths atmosphere on entry into planetary atmospheres [NASA-CASE-XLA-01791] 11 p1765 N71-22991
 Test fixture for measuring moment of inertia of irregularly shaped body with multiple axes [NASA-CASE-XGS-01023] 11 p1765 N71-22992
 Bibliographies of fluxgate magnetometers 12 p1918 N71-23409
 Quality assurance audit program for measuring equipment laboratories 12 p2017 N71-23645
 Electron beam deflection devices for measuring electric fields [NASA-CASE-XMF-10289] 12 p1920 N71-23699
 Device for measuring two orthogonal components of force with galling flotation of measuring target for use in vacuum environments [NASA-CASE-XAC-04885] 12 p1922 N71-23790
 Interference fringe interpolator for digital linear measurements [NLL-TRANS-T-6783-/5809.95/] 12 p1924 N71-24193
 Laboratory modifications of standard electric current balance [NPL-QU-16] 13 p2079 N71-24422
 Gage for measuring internal angle of flare on end of tube [NASA-CASE-XMF-04415] 13 p2081 N71-24693
 Device utilizing RC rate generators for continuous slow speed measurement [NASA-CASE-XMF-02966] 13 p2060 N71-24863
 Design and fabrication of measuring system to determine concentration and mobility of atmospheric ions [RAE-LIB-TRANS-14355] 13 p2075 N71-25148
 Solid state force measuring electromechanical transducers made of piezoresistive materials [NASA-CASE-ERC-10088] 13 p2153 N71-25490
 Design and development of layout tool for machine shop use to locate point in precise reference to straight or bowed reference edge [NASA-CASE-FRC-10005] 14 p2262 N71-26145
 Measurement of variance in neutron counter signal fluctuations for neutron flux measurement including electronic equipment design [CEA-R-4119] 14 p2305 N71-26340
 Development and evaluation of instrumentation system for measuring interference fringe spacing in scattered light photoelasticity 14 p2258 N71-26624
 Volume displacement transducer for leak detection in hermetically sealed semiconductor devices [NASA-CASE-ERC-10033] 14 p2259 N71-26672
 Deformation measuring apparatus with feedback control for arbitrarily shaped structures [NASA-CASE-LAR-10098] 14 p2351 N71-26681
 High stability apparatuses for investigating angular distribution of charge particles of 10 to 13th and 14th power eV [KFKI-70-21-HEP] 14 p2314 N71-26729
 Foam insulation thickness measuring and injection device for spacecraft applications [NASA-CASE-MFS-20261] 15 p2407 N71-27005
 Microwave system evaluated as nondestructive means of measuring thickness of conformal coatings [BDX-613-265] 15 p2428 N71-27013
 Microwave system evaluated as nondestructive means of measuring thickness of conformal coatings [BDX-613-257] 15 p2428 N71-27014
 Design and operation of X band measurement instrumentation for simulating radio wave propagation in dissipative environments [AD-720998] 15 p2381 N71-27351

Complex instrumentation for investigation of atmospheric optics 15 p2410 N71-27350
 Utilization of measuring methods and devices in general industrial applications [NASA-SP-5926/01/] 16 p2601 N71-28482
 Instrumentation for determining quantitative waveforms of individual radar pulses using electro-optical effect in crystals 16 p2668 N71-28871
 Medium density and chemical composition and measurement geometry effects on accuracy of neutron moisture measurement method [INP-709] 16 p2659 N71-29172
 Underwater sensor unit for measuring conductivity, temperature, and pressure of ocean [IFS-71012] 17 p2753 N71-29917
 Hardware system for measurements of bubble chamber films on-line [USIP-70-3] 17 p2723 N71-30013
 Development and characteristics of instruments for inductive measurement of liquid metal levels in cooling systems [RD/B/N-1720] 18 p2921 N71-30427
 Integrated circuitry and design of analog reactivity meter for use with Experimental Breeder Reactor 2 [ANL-7700] 18 p2958 N71-30495
 Physico-chemical measuring apparatus to study hydrolytic uranium precipitates under inert atmosphere [UJV-2417-CH] 18 p2885 N71-30752
 Multiple tests with eddy current proximity gage for determining thickness of concrete pavements [NASA-CR-119867] 18 p2923 N71-30828
 Design and construction of neutrally buoyant oceanographic instrument for measurement of internal waves at main pycnocline [IRM-513] 18 p2925 N71-31384
 Development and performance testing of visibility meters and airport runway and carrier lighting equipment [NBS-10-577] 19 p3071 N71-31619
 Measuring instrument used at Fort-Archambault for ionospheric drift including geophysical data processing [GRINTP/86] 19 p3084 N71-31701
 Design, fabrication, and testing of dissolved oxygen calibrator [PB-198640] 19 p3100 N71-32132
 Error analysis of thickness measuring devices with Am-241 and Cs-137 sources including errors due to chemical composition of steel, temperature distribution, and statistical variation [PB-198369] 19 p3102 N71-32420
 Performance characteristics of static and dynamic teaching sensors [RAE-TM-IR-117] 20 p3272 N71-33117
 Measuring instruments for in vivo bone mineral content and body composition measurement [NASA-CR-121415] 20 p3215 N71-33223
 Alpha and gamma radiation detectors and measuring instruments for semiconductor materials, process control, and devices [NASA-CR-121459] 20 p3333 N71-33396
 Development of instrument for measuring depth of liquid on plane surface and application to measuring depth of water on airport runway surfaces [NASA-CASE-LAR-10576-1] 21 p3427 N71-34585
 Compression corrections for Acme thread gages using graphs and formulas [TN-175] 21 p3428 N71-34399
 Design, optimization, and test instrumentation for sodium-lubricated bearings in sodium pumps and circulating auxiliaries in breeder reactors [NYO-3930-10] 21 p3461 N71-34636
 Convolved Breit-Wigner signals detected by measuring instruments with Gaussian resolution functions [RLO-1388-135] 21 p3474 N71-34740
 Device for measuring ionization processes and plasma acceleration in traveling electromagnetic fields [NASA-TT-F-4971] 21 p3503 N71-34951
 Measurement of cryogenic propellant quantities under conditions of weightlessness 21 p3514 N71-35036
 Radio frequency measuring system for space shuttle propellant tanks under conditions of weightlessness 21 p3514 N71-35037
 Requirements, quantities, location, and temperature environment limitations of sensors for space shuttles 21 p3514 N71-35038
 Monitoring seismicity of Aleutian/Amchitka area after nuclear detonations [CGS-746-10] 22 p3577 N71-35480
 Absolute capacitance microrepro and dimensional stability measuring system [NASA-TM-X-2046] 22 p3585 N71-35530
 Bibliography of reports on aspects of physical quality of hot rolled steel strip [PB-199295] 22 p3593 N71-35587
 Acceleration measurements during transportation in small delivery van [ITL-A-AL-009-14] 22 p3629 N71-35862
 Evaluation of candidate propellant gauging systems under zero g for use on space shuttle vehicle [NASA-CR-119935] 22 p3661 N71-36104

SUBJECT INDEX

MECHANICAL MEASUREMENT

- Climometer for measuring inclinations of earth's surface near Moscow 23 p3748 N71-36723
- Climometric sounding of wells 23 p3748 N71-36724
- Instruments for measurement of spectral lines profile and shift 23 p3755 N71-36769
- Universal machine for testing full scale structural components and applying forces necessary for calibrating large force measuring devices (NBS-SP-355) 23 p3764 N71-36831
- Measurement techniques for surface rheological properties of surface active materials 23 p3780 N71-36944
- Device for measuring induction produced by accelerated particle beam developed for synchrocyclotrons (NBS-18839) 23 p3809 N71-37157
- Special diagnostic devices designed to solve particular positioning and measurement problems in fusion research engineering (MATT-836) 23 p3828 N71-37395
- Torsional split-Hopkinson bar for dynamic plasticity determinations at high rates of strain (AD-726995) 23 p3862 N71-37332
- Earth tide observations and measuring instruments 24 p3910 N71-37871
- Spherometer measuring mirror surface asphericity of large astronomical telescopes 24 p3922 N71-37975
- Computer controlled electrical measuring devices for thermoelectric generator of power plant (AD-727461) 24 p3925 N71-38010
- Measuring dielectric constant of materials used in millimeter and submillimeter wave range (AD-727941) 24 p3945 N71-38145
- Tuning and photovoltaic methods and identification of test conditions for measurement of semiconductor materials, process control, and devices (NASA-CR-123167) 24 p3996 N71-38504
- Clouds of lower Venusian atmosphere (NASA-CR-123589) 24 p4006 N71-38562
- Canadian National Science Council research in low speed aerodynamics, machine learning, and turbulent jet transducer (DME/NAE-1971(2)) 24 p4013 N71-38626
- Unbounded turbulent jets for measurement of fluid velocity and density 24 p4013 N71-38629
- MECHANICAL DEVICES**
- Load cell protection device using spring-loaded breakaway mechanism (NASA-CASE-XMS-06782) 06 p0953 N71-15974
- Aerodynamic effects of mechanical high lift devices on conventional airfoils 09 p1322 N71-20052
- Design and development of satellite despin device (NASA-CASE-XMF-08523) 09 p1472 N71-20396
- Development of two force component measuring device (NASA-CASE-XAC-04806-1) 09 p1591 N71-20439
- Design, development, and characteristics of latching mechanism for operation in limited access areas (NASA-CASE-XMS-03745) 10 p1564 N71-21076
- Design of mechanical device for stirring several test tubes simultaneously (NASA-CASE-XAC-06956) 10 p1564 N71-21177
- Design and development of random function tracer for obtaining coordinates of points on contour maps (NASA-CASE-XLA-01401) 10 p1565 N71-21179
- Thermoelectric boom initiator and furible antenna for Thermoelectric Outer Planet Spacecraft 10 p1566 N71-21352
- Design and characteristics of device for closing containers under high vacuum conditions (NASA-CASE-XLA-01446) 10 p1567 N71-21528
- Development of non-magnetic indexing device for orienting magnetic flux sensing instrument in magnetic field without generation of detrimental magnetic fields (NASA-CASE-XGS-02422) 10 p1567 N71-21529
- Design and development of module joint clamping device for application to solar array construction (NASA-CASE-XNP-02341) 10 p1567 N71-21531
- Hand controller operable about three respectively perpendicular axes and capable of actuating signal generators for attitude control devices (NASA-CASE-XMS-07487) 12 p1925 N71-23255
- Metal alloy bearing materials for space applications (NASA-CASE-XLE-05033) 12 p1927 N71-23810
- Mechanical and electrical tools with potential use inside aerospace industry (NASA-SP-596(83)) 12 p1928 N71-23910
- Mechanical actuator wherein linear motion changes to rotational motion (NASA-CASE-XGS-04548) 12 p1929 N71-24045
- Design and characteristics of device for showing amount of cable payed out from winch and load imposed (NASA-CASE-MSC-12052-1) 13 p2004 N71-24599
- Design and development of release mechanism for spacecraft components, releasable despin weights, and extendable gravity booms (NASA-CASE-XGS-08718) 13 p2004 N71-24600

- Apparatus for mechanically dispersing ultrafine metal powders subjected to shock waves (NASA-CASE-XLE-04946) 13 p2094 N71-24911
- Self lubricating gears and other mechanical parts having surface adapted to frictional contact (NASA-CASE-MFS-14971) 13 p2087 N71-24904
- Design and development of layout tool for machine shop use to locate point in precise reference to straight or bowed reference edge (NASA-CASE-FRC-10005) 14 p2262 N71-26145
- Hydrodynamics of roller pumps and implication to hemolysis (AD-720320) 15 p2374 N71-27279
- Glossary of terms used in identification and prediction of mechanical failure 16 p2685 N71-28123
- Proceedings of conference dealing with advances in decision making processes for detection, diagnosis, and prognosis of mechanical failures (AD-721353) 16 p2685 N71-28124
- Development of test methods and techniques for determining technical performance and safety characteristics of aviation tools and accessories (AD-723030) 17 p2712 N71-30238
- Robot engineering concepts, instrumented striding vehicle device, and planetary striding vehicle (JPRS-53742) 20 p3277 N71-32910
- Analogy between human motor functions and mechanical legs for planetary striding vehicle 20 p3277 N71-32913
- Application of spiral, bimetallic strip to create circular motion on mechanical shaft by change of temperature in the strip (NASA-CASE-NPO-11283) 21 p3403 N71-34213
- Optical-mechanical marine gravimeter with numerical pulse coding device 21 p3418 N71-34317
- Automated sea observations with optical-mechanical marine gravimeter with automatic readout 21 p3418 N71-34318
- Logic devices for readiness assessment and checkout of airborne and ground equipment mechanical components 22 p3674 N71-36197
- Full scale prototype design of restraint system for maintenance and repair by astronauts under weightless conditions of space - Vol. 1 (NASA-CR-119951) 23 p3761 N71-36816
- Engineering drawings of prototype restraint system for repair and maintenance by astronauts under weightless conditions - Vol. 2 (NASA-CR-119952) 23 p3762 N71-36817
- ESRO scientific satellite spin reduction mechanism design (ESRO-CR-30) 23 p3858 N71-37504
- Characteristics of two dimensional mechanisms and classification of structural groups of mechanisms (AD-727243) 24 p3928 N71-38028
- Development of technique for brominating machine and tool parts in powdered mixtures (AD-727937) 24 p3929 N71-38036
- Statistical analysis of fatigue stability characteristics under steady state loads and application to determining life expectancy of machinery (AD-727472) 24 p4024 N71-38712
- MECHANICAL DRAWINGS**
- ENGINEERING DRAWINGS**
- MECHANICAL DRIVES**
- NT HELICOPTER PROPELLER DRIVE**
- NT PROPELLER DRIVE**
- Hydraulic drive mechanism for leveling isolation platforms (NASA-CASE-XMS-03252) 01 p0060 N71-10638
- Autobacklash circuit for hydraulic drive system (NASA-CASE-XNP-01020) 03 p0317 N71-12260
- Precision stepping drive device using cam disk (NASA-CASE-MFS-14772) 07 p1037 N71-17492
- Incremental motion drive system applied to interferometer components (NASA-CASE-XNP-06897) 07 p1037 N71-17494
- Ratchet mechanism for high speed operation at reduced backlash (NASA-CASE-MFS-12805) 07 p1037 N71-17805
- Design, fabrication, and test of research model roller-gear drive consisting of transmission driven by dc motor (NASA-CR-103057) 09 p1393 N71-19862
- Long life tape transport for magnetic recorder of outer planet spacecraft 11 p1716 N71-22566
- Operation of modular gear systems in vacuum environment with and without lubrication and under no load conditions (AD-717944) 12 p1925 N71-23276
- Development of apparatus for automatically changing carriage speed of welding machine to obtain constant speed of torch along work surface (NASA-CASE-XMF-07069) 12 p1928 N71-23815
- Drive system for parallel tracking antennas with zero-to-minimum and minimal backlash (NASA-CASE-NPO-10173) 13 p2085 N71-24406
- Analytical and experimental design of vibration control mechanism for fluid drive 13 p2086 N71-24811

- Test facility and computer programs for control of digital tape drive functions 13 p2062 N71-25341
- Calculation of rotor critical speeds for two bearing rotor system from rigid body theory using film stiffness as determined from zero speed, load eccentricity data (NASA-TN-D-6354) 13 p2089 N71-25538
- Development and nondestructive tests of gear failure detection methods (AD-720735) 14 p2263 N71-26246
- Synchronous dc direct-drive system comprising multiple-loop hybrid control system controlling load directly connected to actuator (NASA-CASE-GSC-08663-1) 15 p2308 N71-27136
- Effect of axial vibrational motion on frictional energy losses and efficiency of spur gear system 16 p2603 N71-28911
- Energy absorption device in high precision gear train for protection against damage to components caused by stop loads (NASA-CASE-XNP-01848) 16 p2604 N71-28939
- Torsional vibration analysis on hydrodynamic clutch of power turbine at periodic disturbances of starting and driving speeds 18 p2990 N71-31330
- Space environment simulation testing of antenna spin reduction bearing and mechanical drives for Helios solar probe (BMW-FB-W-71-13) 19 p3104 N71-31464
- MOTS camera sensitivity and mechanical drive evaluation based on GEOS 1 and 2 satellite photographic tracking data 19 p3499 N71-31855
- Operational control system for part long red drive mechanism in pressurized water reactor (WCAP-7406) 19 p3535 N71-31918
- Measurement and analysis of bending stress in external involute spur gears (PB-198320) 19 p3106 N71-32746
- Automatic controlled drive mechanism for portables boring bar (NASA-CASE-XLA-03661) 20 p3279 N71-33518
- Rotary actuator device for deploying pivotally supported structures onboard spacecraft (NASA-CASE-NPO-10600) 21 p3520 N71-35080
- Telescope control by on-line computers, including ESO 3.6-m telescope 24 p3923 N71-37987
- Telescope tracking drives and controls at McDonald Observatory using 107 and 82 inch telescopes 24 p3923 N71-37988
- Mechanical drives of French 2 and 3.60-meter telescopes from horsehoe, using gears 24 p3923 N71-37989
- Digital computerized drive for reflecting telescopes 24 p3923 N71-37990
- Digital computer used to control drive of 2.2-meter astronomical telescope 24 p3923 N71-37991
- Anglo-Australian telescope proposed drive and control system using printed circuits 24 p3924 N71-37994
- Drive controls for altazimuth mountings during stellar motion observations 24 p3924 N71-37995
- Electric equipment and drive adapter endurance tests for SNAP 8 (NASA-CR-72920) 24 p3946 N71-38248
- MECHANICAL ENGINEERING**
- Mechanical engineering research in aerospace technology, machine design and industrial processing, and weapons 05 p0636 N71-14467
- Design, fabrication, and test of research model roller-gear drive consisting of transmission driven by dc motor (NASA-CR-103057) 09 p1393 N71-19862
- Determination of kinematic and dynamic response of elastically supported mechanical systems with interfaces subjected to mechanical separation 11 p1717 N71-22800
- Engineering mechanics in structural design of silicon solar arrays (NASA-CR-112666) 13 p2029 N71-24428
- Mechanics of free piston engine, aspects of human factors engineering, and compressible boundary layer studies at high Reynolds numbers (DME/NAE-1971(1)) 19 p3198 N71-32620
- Annotated bibliography of astronomical and mechanical engineering and test reports - Jan. 1971 20 p3371 N71-33948
- Development and characteristics of sonic and ultrasonic power equipment used in highway engineering - Vol. 1 (PB-199110) 21 p3434 N71-34437
- Bibliography and KWIC index on mechanical theorem proving and its applications (NASA-CR-121640) 21 p3446 N71-34525
- MECHANICAL MEASUREMENT**
- NT DISPLACEMENT MEASUREMENT**
- NT DRAG MEASUREMENT**
- NT FLOW MEASUREMENT**
- NT FRICTION MEASUREMENT**
- NT PRESSURE MEASUREMENT**

- NT STRESS MEASUREMENT
 NT THRUST MEASUREMENT
 NT VELOCITY MEASUREMENT
 NT VIBRATION MEASUREMENT
 NT WIND MEASUREMENT
 NT WIND VELOCITY MEASUREMENT
 Development of apparatus for measuring successive increments of strain on elastomers
 [NASA-CR-XMF-04680] 09 p1392 N71-19489
 Determination of surface roughness correction factor in interferometric measurements of block gage length
 [NLL-M-20170/5828.4F/1] 12 p1929 N71-24016
 Oscillatory pitching moment derivatives measurement on delta wings in incompressible flow
 [ARC-R/M-3628-PT-1-4] 13 p2022 N71-24569
 Measurements of oscillatory pitching moments on round leading edged delta wing in incompressible flow using vortex flow development
 13 p2022 N71-24570
 Measurements of aerodynamic drag, interference lift, and pitching moment on delta wings
 13 p2023 N71-24573
 Development of instrument for measuring depth of liquid on plane surface and application to measuring depth of water on airport runway surfaces
 [NASA-CASE-LAR-10576-1] 21 p3427 N71-34385
MECHANICAL OSCILLATORS
 NT GYROSCOPIC PENDULUMS
 NT PENDULUMS
 Mechanical resonators for vibrating mirrors to deflect laser beams in optical data recording system
 07 p1038 N71-17036
MECHANICAL PROPERTIES
 NT ABRASION RESISTANCE
 NT AEROELASTICITY
 NT ANELASTICITY
 NT BRITTLENESS
 NT BULK MODULUS
 NT COMPRESSIBILITY
 NT COMPRESSIVE STRENGTH
 NT CREEP PROPERTIES
 NT CREEP RUPTURE STRENGTH
 NT CREEP STRENGTH
 NT DIMENSIONAL STABILITY
 NT DUCTILITY
 NT ELASTIC PROPERTIES
 NT ELASTOPLASTICITY
 NT ELECTROSTRICTION
 NT FATIGUE LIFE
 NT FIBER STRENGTH
 NT FLEXIBILITY
 NT FRACTURE STRENGTH
 NT HARDNESS
 NT HIGH STRENGTH
 NT HYDROELASTICITY
 NT IMPACT STRENGTH
 NT MAGNETOSTRICTION
 NT MICROHARDNESS
 NT MODULUS OF ELASTICITY
 NT NOTCH SENSITIVITY
 NT NOTCH STRENGTH
 NT PHOTOELASTICITY
 NT PHOTOVISCOELASTICITY
 NT PIEZOELECTRICITY
 NT PLASTIC PROPERTIES
 NT POISSON RATIO
 NT RESILIENCE
 NT SHEAR CREEP
 NT SHEAR PROPERTIES
 NT SHEAR STRENGTH
 NT SHELL STABILITY
 NT STEADY STATE CREEP
 NT STIFFNESS
 NT STRESS CYCLES
 NT STRESS RELAXATION
 NT STRUCTURAL STABILITY
 NT TENSILE CREEP
 NT TENSILE PROPERTIES
 NT TENSILE STRENGTH
 NT THERMAL RESISTANCE
 NT THERMOELASTICITY
 NT THERMOPLASTICITY
 NT THERMOVISCOELASTICITY
 NT TOUGHNESS
 NT VISCOELASTICITY
 NT VISCOPLASTICITY
 NT WELD STRENGTH
 NT YIELD POINT
 NT YIELD STRENGTH
 Nitriding temperature and time, depth of penetration and surface hardness of steels
 [RAE-LIB-TRANS-1368] 01 p0058 N71-10095
 Mechanical properties of cryogenically stretched type 301 stainless steel and aluminum alloys 2021-T81 and X7007-T6
 [NASA-CR-72733] 01 p0067 N71-10447
 Conference on applications of beryllium in structural engineering
 [AD-710794] 01 p0067 N71-10483
 High pressure mechanical properties of stratified volcanic rocks
 [UCRL-50858] 01 p0048 N71-10489

- Publications survey on mechanical wire rope and wire rope systems to review literature on mechanical response of stranded cables
 [AD-710806] 01 p0129 N71-10492
 Surface sensitive mechanical behavior of nickel monocrystals
 [AD-716777] 01 p0112 N71-10953
 Optimization of properties of stainless steels by austenitizing at high temperatures
 [AD-71608] 02 p0240 N71-11142
 Omniview method of composite fabrication of graphite filaments and mechanical properties of fabrics
 [NASA-CR-102916] 02 p0246 N71-11441
 Spinning orientation effect on drawn polyethylene terephthalate fiber structure and properties
 [NLL-M-9136/5828.4F/1] 02 p0246 N71-11590
 Structure and properties of unidirectionally solidified superalloys
 02 p0242 N71-11632
 High speed centrifugal determination of mechanical properties of small iron and other ferromagnetic crystals and whiskers
 [AD-715822] 02 p0244 N71-11698
 Data showing influence of freezing and thawing on properties of soil layers
 [AD-718888] 02 p0219 N71-12072
 Photoelastic determination of mixed mode stress intensity factors
 [AD-712298] 02 p0303 N71-12098
 Properties of carbon fibers
 [RAE-LIB-TRANS-1417] 02 p0249 N71-12191
 Mechanical, physical, technological, and corrosive properties of welded aluminum
 [AD-712948] 03 p0389 N71-12659
 Structure and properties of solid solutions
 [COO-916-17] 03 p0390 N71-12686
 Structure and properties of high strength ferrous alloys EP404 and EP454
 03 p0393 N71-13037
 Evaluation of refractory tantalum-, tungsten-, niobium-, and molybdenum based alloys for space power systems applications
 [NASA-SP-245] 03 p0393 N71-13301
 Development of high temperature creep resistant tantalum alloys for space power systems
 03 p0394 N71-13303
 Mechanical properties of some metastable austenitic alloys
 [UCRL-19626] 04 p0529 N71-14029
 Microstructure and mechanical properties of martensite ausformed from precipitation hardened austenite
 [UCRL-19196] 04 p0530 N71-14091
 Fast reactor fuel interaction with concrete floor after hypothetical core meltdown
 [BNWL-CC-2369] 04 p0582 N71-14104
 Temperature, strain, and strain rate effects on mechanical properties of gallium delta-stabilized plutonium alloys
 [UCRL-72544] 04 p0531 N71-14168
 Mechanical properties of mixed boron/graphite composite
 [NASA-CR-102944] 04 p0535 N71-14267
 Fabrication and properties of press sintered lanthanum, yttrium, and gadolinium hexaboride cathodes
 [NPL-1432] 04 p0591 N71-14391
 Analytical procedures for predicting mechanical properties of fiber reinforced composites
 [AD-713675] 05 p0707 N71-14540
 Cryogenic mechanical properties of aluminum alloys, titanium alloys, and stainless steels - Vol. 1
 [AD-713619] 05 p0732 N71-14685
 Cryogenic mechanical properties of superalloys, fiber reinforced plastics, seals, and gaskets - Vol. 2
 [AD-713620] 05 p0732 N71-14686
 Physical, chemical, and mechanical property data of thorium ceramics
 [ORNL-4503-VOL-1] 05 p0708 N71-15063
 Mechanical properties of high temperature composites for use as turbine stator vanes
 [NASA-CR-72794] 05 p0709 N71-15082
 Strength and creep of laminated plastics
 [NASA-TT-F-461] 05 p0709 N71-15176
 Failure mechanisms associated with use of borehole jack in rocks
 [NASA-CR-102961] 05 p0768 N71-15206
 Summaries of lunar soil studies and fluid conductivity of lunar surface materials
 [NASA-CR-102962] 05 p0768 N71-15207
 Absorption sensitive mechanical and machining properties of soda-lime glass
 [AD-713594] 05 p0710 N71-15402
 Stiffness and expansion of oriented random fiber reinforced composite materials
 [AD-713099] 05 p0711 N71-15403
 Mechanical properties of dilute uranium alloys
 [Y-DA-3616] 06 p0688 N71-15750
 Physical and mechanical properties of glass reinforced plastics
 [AD-714508] 06 p0678 N71-16209
 Useful mechanical, electrical, and acoustic properties of Sonite
 [AD-714229] 06 p0678 N71-16362

- Torsion test strain rate effects on mechanical properties of aluminum alloys, steels, and titanium
 [AD-714086] 06 p0773 N71-16382
 Mechanical effects of dispersion of second phase
 [AD-714173] 06 p0774 N71-16483
 Material characteristics and methods for predicting mechanical properties of graphite
 [ORNL-TM-3191] 07 p1047 N71-17280
 Mechanical properties of carbides and nitrides for fast reactor fuels
 [LA-4452] 07 p1061 N71-17228
 Mechanical properties of stainless steel melts, and equipment development for electromagnetic control system
 [SU-326-P-29-5] 07 p1042 N71-17243
 Mechanical properties of hot pressed NbC- and TaC-graphite composites with W added
 [NASA-CR-116503] 07 p1048 N71-17355
 Cobalt and nickel based alloy metallurgy for high temperature gas turbine materials
 07 p1101 N71-17389
 Radiation effects on mechanical properties of cladding materials
 [BML-1809] 07 p1065 N71-17552
 Mechanical and electrical design of actuator for SERT 2 spacecraft
 [NASA-TM-X-2190] 07 p0976 N71-17665
 Performance of test equipment for low temperature materials
 [RHEL/R-202] 08 p1205 N71-18284
 Effect of fast neutron irradiation on mechanical properties of hafnium
 [IN-1440] 08 p1212 N71-18309
 Mechanical properties and microstructure of titanium alloy after heat treatment
 [AD-715353] 08 p1213 N71-18523
 Electrical and mechanical characteristics of solar cell contacts after exposure to high-temperature high-humidity environments
 [NASA-CR-116805] 08 p1146 N71-18563
 Welded joint mechanical properties noting porosity defects in aluminum alloys
 [CRIF-MT-54] 08 p1206 N71-18590
 Research in ceramic materials including mechanical properties, crystallography, and deformation
 [NASA-CR-116809] 08 p1222 N71-18654
 Mechanical properties of aluminum alloy 7175 with T 736 forging
 [AD-715878] 08 p1214 N71-18758
 Mechanical properties of drawn and annealed titanium alloy
 [AD-715880] 08 p1215 N71-18831
 Mechanical properties of solution annealed titanium alloy
 [AD-715877] 08 p1215 N71-18832
 Mechanical properties of MP35N nickel cobalt chromium, and molybdenum alloy
 [AD-715879] 08 p1215 N71-18854
 Evaluation of mechanical and stress corrosion properties of cold worked A-286 alloy
 [NASA-TM-X-64569] 08 p1216 N71-18864
 Effects of space environment factors on physical, mechanical, and optical properties of selected transparent elastomers
 [NASA-TN-D-6216] 08 p1223 N71-18934
 Physical and mechanical properties of Type-304 stainless steel of EBR-2 subassembly after irradiation
 [GEAP-13571] 08 p1220 N71-19237
 Mechanical properties, thermal stability, and synthesis of aromatic polyimides, amide-imides, ester-imides, and pyrores
 [RAE-LIB-TRANS-1499] 09 p1343 N71-19631
 Tabulated mechanical and acoustic properties for selected ferrous, nonferrous, and plastic materials
 [AD-716033] 09 p1404 N71-19676
 Research in structural characterization, solid state reactions, phase transformations, and mechanical properties of materials
 [NASA-CR-117134] 09 p1474 N71-19726
 Behavior of various alloys, polymers and composites
 09 p1474 N71-19729
 Mechanical properties of polycrystalline, reactor grade uranium and its alloys at minus 200 to 730 C
 [UJV-2436-M] 09 p1399 N71-19925
 Reactor technology and fuel element development for nuclear research and test reactors including mechanical and thermal analysis of oxide, carbide, and nitride fuels
 [BML-1886] 09 p1418 N71-19928
 Structural data on brittle nonmetallic materials for use in designing reentry vehicles
 [AGARD-AG-152-71] 09 p1406 N71-20027
 Chemical treatment of glass surfaces to improve breaking strength, resistance to abrasion and chemical action, and hydrophobic reaction
 [NASA-TT-F-13437] 09 p1406 N71-20089
 Chemical and mechanical properties and synthesis of 4-vinylbiphenyl-isoprene ABA block copolymers for permeation and propellant binder studies
 [NASA-CR-117385] 09 p1344 N71-20132
 Mechanical properties determined for precipitation hardened tantalum base alloy /ASTAR-811C/ for potential use in Rankine cycle nuclear power systems
 [NASA-CR-1641] 09 p1401 N71-20391

SUBJECT INDEX

MECHANICAL PROPERTIES

Analysis of free vibration characteristics of clamped/free and clamped/ring stiffened cylindrical shells by digital computer solution [TT-7001] 09 p1480 N71-20497

Chemical, mechanical, and physical property data for thorium ceramics [ORNL-4503-VOL-2] 09 p1408 N71-20594

Mechanical, electrical, and optical properties, crystal defects, magnetism, thermodynamics, and superconductivity of solids [NASA-CR-117401] 10 p1632 N71-20828

Mechanical properties of adhesives after space environment simulation in vacuum chamber [R-1107] 10 p1588 N71-20915

Mechanical properties of adhesive after exposure to simulated space environments [R-1173] 10 p1580 N71-21036

Mechanism of effect of minor and rare earth metals on mechanical properties of various alloyed steels [NLL-TRANS-746-563-7902.401/] 10 p1577 N71-21048

Mechanical properties data for LMFBR reactor materials, and irradiation effects on cladding and structural alloys [BMS-1991] 10 p1602 N71-21084

Surface finishing effects on ceramic mechanical, electrical, optical, and magnetic properties [AD-716896] 10 p1565 N71-21221

Creep failure and reliability of randomly excited structures and equations for heated shells 10 p1656 N71-21350

Applications and physical properties of polydimethylsiloxane as solid lubricant [AD-716940] 10 p1590 N71-21392

Mechanical property determination of ceramic covered uranium and plutonium, using modulus of elasticity [CEA-CONF-1620] 10 p1590 N71-21501

Microstructure and mechanical properties of boronized medium carbon steels [NLL-TRANS-746-527-7902.401/] 10 p1584 N71-21604

Effect of tin on mechanical properties of Mg-Li-Al alloy in presence of small quantities of zinc and manganese [AD-717993] 11 p1777 N71-22175

Homogeneous continuum for describing mechanical behavior of laminated composite elastic solids [AD-717731] 11 p1838 N71-22517

Effects of welding and post-weld heat treatment on microstructure and mechanical properties of QT steel [REPT-2] 11 p1769 N71-22541

Planetary Atmospheric Experiments Test (PAET)/relative afterbody thermal performance and component mechanical properties [NASA-CR-114293] 11 p1844 N71-22715

Mechanical analysis of small displacement, elastic, time independent torsionless axisymmetric behavior of cylinders 11 p1839 N71-23004

Effects of chemical bonding between phases of glass-metal composite on strength and fracture behavior 11 p1785 N71-23010

Structural transformations and properties of high strength Cr-Mn-Ni austenitic steels [SPR-52877] 12 p1936 N71-23148

Microstructural analysis, mechanical properties, and thermal conductivity of sintered nickel and uranium dioxide [SRO-552-6] 12 p1961 N71-23195

Selection of materials for electrical connectors compatible with future space missions [NASA-CR-103092] 12 p1887 N71-23383

Particle strengthening of tungsten-rhenium alloy by hafnium carbide precipitate [NASA-TN-D-6308] 12 p1939 N71-23982

Determination of mechanical properties of ceramic materials used in piezoelectric transducers [AD-717964] 12 p1946 N71-24094

Examination of silica-filled silicone vulcanizates using combined mechanical, swelling, and optical means to determine reinforcement mechanisms of elastomers 12 p2007 N71-24118

Determination of static ultimate strength of transversely and longitudinally stiffened plate girders subjected to shear, bending, or combination of stresses 12 p2009 N71-24297

Research and development technology in titanium alloys including phase transformations, metal working methods, and mechanical properties [AD-719487] 13 p2091 N71-24407

Effect of alloying additives such as manganese, chromium, and zirconium on mechanical properties of Al-Zn-Mg-Li alloy [AD-719478] 13 p2092 N71-24562

Neutron irradiation effects on tensile strengths and impact resistances of nickel steel weldments [ABCT-3734] 13 p2093 N71-24827

Investigation of characteristics of deformation and rupture of polymer materials and glass reinforced plastics [AD-719780] 13 p2100 N71-24972

Temperature effects on mechanical properties of refractory metals [AD-719629] 13 p2095 N71-25076

Influence of titanium, zirconium, and hafnium additions on resistance of modified Hastelloy N to irradiation damage at high temperatures [ORNL-TM-3064] 14 p2267 N71-25640

Exfoliation with oxidation process of metals and mechanical behavior of scales [AD-719910] 14 p2268 N71-25644

Research on carbonization, radiation effects, chemical properties, and mechanical properties of graphite and carbon compounds [NYO-1710-100] 14 p2276 N71-25679

Mechanical properties of stainless steel type 348 for LMFBR cladding [WHAH-SA-8] 14 p2291 N71-25691

Environmental effects on surface layer stress measurement during cyclic hardening and softening [AD-719870] 14 p2346 N71-25705

Physical properties and mechanical strength of structural fiber glass in conical shells [JPRS-53118] 14 p2346 N71-25757

Development and characteristics of high strength graphite fibers produced from polymeric fibers and resin from pitches [AD-720634] 14 p2277 N71-25855

Interdependence of combustion processes and physical-mechanical behavior of solid fuel materials for rocket engines [AD-720834] 14 p2353 N71-25952

Mechanical properties and stress corrosion evaluation of MP 35N multiphase alloy at cryogenic temperature [NASA-TM-X-64591] 14 p2274 N71-26043

Mechanical properties of forged Ti-6-Al-4-V at temperatures above alpha-beta/beta transition [AD-720828] 14 p2274 N71-26046

Mechanical properties of precipitation strengthened tantalum base alloys [NASA-CR-1642] 14 p2274 N71-26132

Mechanical properties of dispersion strengthened chromium-base alloy with magnesium oxide additives [AD-720389] 14 p2274 N71-26159

Effects of silicon on strength and microstructure of aluminum alloys 14 p2275 N71-26524

Plastic deformation and mechanical properties of gamma brass phase AgZn and CuAl single and polycrystals and temperature effects on crystal lattices 14 p2276 N71-26615

Carbon content effects on niobium alloy deformation [AD-720932] 15 p2419 N71-26812

Irradiation effects on mechanical properties of epoxy resin/glass composites [RHEL/R-200] 15 p2427 N71-26815

Mechanical properties and physical, chemical, and thermal tests of polybenzimidazole and carbon fabric laminates for spacecraft thermal insulation [NASA-CR-1723] 15 p2427 N71-26915

Probability density function of surface area remaining on particles produced from residue of fractured chemically strengthened glass elements [SC-RR-69-506] 15 p2428 N71-26933

Properties and selective applications of high strength steels, aluminum and titanium alloys, polymeric materials, ceramic materials, and composite materials in aerospace engineering [AGARD-LS-51-71] 15 p2429 N71-27038

Properties and selective applications of high strength steels 15 p2421 N71-27040

Properties and selective applications of ceramic materials 15 p2429 N71-27041

Mechanical properties of fiber reinforced materials 15 p2429 N71-27043

Properties and selective applications of aluminum alloys in aircraft construction 15 p2414 N71-27044

Mechanical properties of polycrystalline nickel-copper and nickel-copper-carbon alloys at temperatures from 78 to 523 K 15 p2422 N71-27222

Design methods for light gage cold formed structural elements and members made of cold rolled austenitic stainless steel 15 p2423 N71-27327

Properties of molten ceramics at 3000 C [BNWL-SA-3579] 15 p2431 N71-27426

Low temperature mechanical properties of epoxy/urethane formulations 15 p2377 N71-27478

Mechanical and thermodynamic properties of low density ablative materials and honeycombs including silicone-phenolic resin and phenolic glass honeycombs of phenolic silicone and nylon [NASA-CR-111909] 15 p2432 N71-27636

Mechanical properties and impact strength of UARL 417 experimental glass [NASA-CR-110882] 15 p2432 N71-27676

Effect of irradiation in water at 70 C on mechanical properties of Fe-Cr-Ni system [SPARI-P-78] 15 p2426 N71-27760

Parametric, functional, and mechanical properties of bipolar LSI devices in simulated space environment [NASA-CR-119794] 15 p2417 N71-27771

Optimal strength and failure modes of ultrasonically bonded metals in air and vacuum [UCRL-13486] 15 p2417 N71-27801

Dimensional stability and mechanical properties of solids [AD-721190] 15 p2322 N71-27854

Analysis of chemical, physical, and mechanical problems imposed by heat sterilization for demonstration of sterilizable rocket engine system [NASA-CR-111089] 15 p2313 N71-27934

Effects of Fe, Si, Al, Ni, Cr, and Zr impurities on properties of uranium 15 p2427 N71-27948

Effects of zirconium additions on mechanical and physical properties of nickel [NLL-LT-746-667-7902.401/] 16 p2467 N71-28013

Conference on prevention of mechanical failures including bearing failures, spectrographic oil analysis, failure mechanisms of helicopter transmissions, and related problems [AD-721359] 16 p2484 N71-28057

Mechanical properties of Dacron parachute fabrics in simulated Martian atmosphere [NASA-TN-D-6342] 16 p2616 N71-28132

Mechanical behavior of aluminum-stainless steel composites subjected to elevated temperature under strain and wires pulled to failure after extraction from composites [AD-721374] 16 p2610 N71-28441

Electrophysics and chemical reactions of metal surfaces including mechanical properties and crystal structures [AD-722013] 16 p2611 N71-28505

Low density and adequate mechanical properties of surface compression strengthened glasses permitting their use in weapons and other lightweight structures for long periods [AD-721327] 16 p2618 N71-28615

Antifriction characteristics of graphite due to its mechanical properties and self lubricating nature [NLL-RISLEY-TRANS-1881-7091.9F] 16 p2402 N71-28727

Mathematical models for predicting mechanical stress behavior of fast reactor fuel elements [AERE-R-6516] 16 p2635 N71-28761

Strength evaluation of braze alloys used for linear accelerator components [LA-6584] 16 p2613 N71-28781

Tensile, compression, and fatigue tests to determine mechanical properties of irradiated and nonirradiated uranium fuel elements [NLL-WINDSCALE-TRANS-432-7091.1] 16 p2635 N71-28785

Porosity effects on rock strength and elastic modulus when subjected to high pressure [NASA-TT-F-13653] 16 p2589 N71-28867

Mechanical properties of Ni-Cr alloys in region of stoichiometric composition NiCr [NLL-LT-746-639-7902.401] 16 p2614 N71-28931

Response of linear spring-mass-damper system of aluminum alloy subjected to wide band random force input of constant spectral density 17 p2851 N71-29645

Mechanical properties of pure binary Ni-Cr alloys at high and low temperatures [NLL-TRANS-746-639-7902.401/] 17 p2614 N71-29696

Deflection analysis of heated thermobologically simple viscoelastic disks with inclusion of temperature dependence of viscoelastic modulus and other material properties 17 p2852 N71-29732

Development of linear theory for dynamic interaction of solid elastic circular cylinder bonded to this shell of different material 17 p2852 N71-29803

Variability of mechanical properties of construction materials, noting rivets, aluminum alloys, and castings [ARCR-R/M-3634] 17 p2853 N71-30044

Review on synthetic fiber ropes for deep water mooring lines 17 p2771 N71-30178

Kinematics and general principles in nonlinear and linear theories of elastic shells and plates by direct approach and three-dimensional equations of classical continuum mechanics - Part I [AD-722350] 17 p2854 N71-30220

Derivation of constitutive equations, material symmetries, dynamical restrictions, and related topics for nonlinear and linear theories of elastic shells and plates - Part 2 [AD-722351] 17 p2854 N71-30221

Dimensional analysis and particle size distribution of linearizer from Penzance/Spain including optical and mechanical properties at Mars simulation material [IRM-5123] 17 p2846 N71-30333

- Technology and properties of metallic materials
18 p2934 N71-30690
Status of research program to develop criteria for designing aircraft protective devices from rotor fragments
18 p2869 N71-30762
Effects of heat and mechanical treatment on microstructure of titanium and its alloys
[AD-722622] 18 p2928 N71-30807
Cooling rate effects on structural transformations in titanium vanadium alloy
[RAE-LIB-TRANS-1548] 18 p2935 N71-30914
Lunar soil mechanics and properties based on Apollo 14 observations and data
18 p3011 N71-30958
Preparing composite materials based on silver and synthetic mica - physicochemical and antifriction characteristics
[AD-722819] 18 p2941 N71-31405
Fabrication history and mechanical properties test data for ASTM A-533 grade B, class 1 steel /HSST plate 03/ provided to International Atomic Energy Agency
[ORNL-TM-3193] 18 p2938 N71-31574
Nonflammable polyurethane foam for ejection seat cushions and statistical analysis of its mechanical properties
[AD-723302] 19 p3119 N71-31775
Mechanical properties of advanced filament wound carbon composite
[SC-DR-710192] 19 p3120 N71-32216
Impact resistant unidirectional fiber composite design based on micro and macromechanics, Irod impact tests, and residual stress and structural analyses
[NASA-TN-D-4463] 19 p3188 N71-32243
Tensile, mechanical, and compression properties of metals, alloys, and steels derived from flow curves
[RAE-LIB-TRANS-1523] 19 p3115 N71-32265
Titanium alloying effects on mechanical properties and microstructures of low-carbon chromium nickel iron alloys
[NLL-LT-746-668-9022.401]] 19 p3115 N71-32300
Mechanical properties of cylindrical vessels under internal pressure at high temperatures
[NLL-CE-TRANS-5321-9022.09]] 19 p3189 N71-32412
Mechanical responses of human head subjected to acceleration loads determined for use in construction of artificial head
19 p3045 N71-32547
Mechanical and thermal properties of aluminum alloys 6061-T6, 2014-T6, and 2024-T3
[AD-724195] 20 p3283 N71-33127
Determining effect of process variables on sintered nickel plaques and impregnated plates
[NASA-CR-121424] 20 p3213 N71-33238
Mechanical and electrical characteristics of slot antennas used to measure quasi-omnidirectional radiation pattern from vehicle in 2300 MHz range
[TP-949] 20 p3235 N71-33710
Mechanical property tests of nickel, titanium, and iron alloys in 5000 psig gaseous helium and hydrogen at various temperatures
[NASA-CR-119844] 20 p3230 N71-33728
Effects of boron on plasticity and structure of carbon component, strength and electron - properties of synthetic graphite
[SC-T-713023] 20 p3288 N71-33740
Mechanical properties of molten salt reactor experiment Hastelloy N surveillance specimens deteriorated with increasing fluence
[ORNL-TM-3063] 20 p3286 N71-33888
Description of laboratory metallurgy techniques involving mechanical properties tests, crystallography, creep, and fatigue
[CEA-N-14272]] 21 p3437 N71-34453
Strain profile measurements, wall thickness reduction, rupture morphology, and metallurgy of stainless steel clad tubes
[WARD-4210-T-3-2] 21 p3440 N71-34480
Low-alloy 12 percent chromium steel replacing nickel for nitrogen to improve casting and mechanical properties
[NLL-LT-746-748-9022.401]] 21 p3442 N71-34493
Microstructural study of physical and mechanical properties of carbon and graphite
[LA-4714-M5] 21 p3442 N71-34496
Mechanical behavior of lunar fine soils in engineering gravity flow bins
[NASA-CR-121670] 21 p3508 N71-34993
Materials, manufacture, quality control, and mechanical properties of bolted joints under static and dynamic stresses
[NLL-CE-TRANS-5406-9022.09]] 22 p3590 N71-35563
Solidification, structure, and properties of eutectic alloys including consideration of properties control
[NASA-CR-122043] 22 p3592 N71-35578
Mechanical properties of as-grown aluminum alloy single crystals compared with those of similar alloys
[AD-726714] 22 p3595 N71-35602
- Structural and mechanical properties of AlZnMg, AlMgSi, and AlCuMg alloys as function of natural aging prior to artificial aging
[NLL-M-20408-5828.4F]] 22 p3596 N71-35606
Changes in mechanical properties and internal friction during aging of stainless, dispersion hardened chromium steels
[NLL-LT-746-680-9022.401]] 22 p3596 N71-35608
Properties of materials hardened by mechanical-thermal processing at different temperatures
[AD-726839] 23 p3771 N71-36876
Effects of heat processing methods on mechanical and heat resistant properties of titanium alloys
[AD-726729] 23 p3771 N71-36878
Strength, ductility, toughness, weldability, and rupturing characteristics of 18 per cent Ni maraging steel for rocket engine cases
[ISAS-463] 23 p3771 N71-36879
Effect of temperature and principal metallurgical and technological factors on mechanical properties of refractory metals
[AD-726609] 23 p3771 N71-36880
X-ray technique for determining structural changes in relation to metal substructures and their mechanical properties
[AD-727420] 23 p3773 N71-36889
Relationship between mechanical properties of tool steels and hardening temperature
[NLL-M-21013-5828.4F]] 23 p3774 N71-36894
Flexural, shear, bending, tensile, and impact strengths of high modulus, high strength, glass fiber-reinforced resin composites
[NASA-CR-122775] 23 p3775 N71-36907
Mechanical, physical, and chemical properties of Imidite SA syntactic foam systems
[BDX-613-177] 23 p3777 N71-36921
Microstructure and mechanical properties relationships and reactor materials applications of dispersion strengthened aluminum and aluminum oxides
[RISO-223] 24 p3936 N71-38079
Properties of high strength steel and application to structures for steam superheating
[AD-727493] 24 p3936 N71-38082
Matrix and grain boundary influence on mechanical and stress properties of aluminum alloy
[RM-522] 24 p3941 N71-38112
Influence of diffusion during heating on bond strength between bimetal layers
[NLL-M-21017-5828.4F]] 24 p3941 N71-38115
Numerical analysis of structures and properties of fiber reinforced plastics
[AD-727471] 24 p3943 N71-38125
Effect of voids on mechanical properties of two graphite fiber composites
24 p3943 N71-38127
Mechanical properties of continuous composites of boron fibers magnesium metal matrix
24 p3946 N71-38152
BRESC finite element program for axisymmetric, plane strain, and plane stress, orthotropic solids with temperature-dependent material properties
[AD-727702] 24 p4025 N71-38720
- MECHANICAL RESONANCE
U. RESONANT VIBRATION
MECHANICAL SHOCK
Mathematical model for chemical activity increase at crystal surface caused by mechanical impact
01 p0018 N71-10513
Engineering design and test of packaging systems for 2171 gyroscope platform
[AD-711384] 02 p0263 N71-12175
Plane parallel transonic flow with discontinuity ahead of compression shock in supersonic zone
07 p1007 N71-16950
Aerodynamic broadband noise mechanism applicable to axial compressors
07 p1013 N71-17958
Literature review and abstracts on shock and vibration
[AD-717046] 10 p1653 N71-21062
Initiation and sensitivity of solid explosives to mechanical impact
[NASA-TT-F-623] 11 p1841 N71-22534
Effects of material strength on transient response, crater formation, and shock propagation in thick aluminum targets subjected to hypervelocity impact
[AD-718461] 12 p1938 N71-23624
- MECHANICS (PHYSICS)
Hovering type flying vehicle design and principle mechanisms for manned or unmanned use
[NASA-CASE-MSC-12111-1] 02 p0147 N71-11039
Nucleon axial vector form factor calculations from sulfur oxide dynamical groups
[DEMO-7016] 15 p2469 N71-27347
Relationship between energy impulse vector and canonical impulse in relativistic mechanics
[NASA-TT-F-13730] 17 p2808 N71-30340
Characteristics of two dimensional mechanisms and classification of structural groups of mechanisms
[AD-727243] 24 p3928 N71-38028
- MECHANIZATION
Automation and mechanization of cartography, and coordination of research and cartographic activities
[AD-711978] 02 p0212 N71-11517
- MEDIA
NT ANISOTROPIC MEDIA
NT ELASTIC MEDIA
NT INTERGALACTIC MEDIA
NT INTERPLANETARY DUST
NT INTERPLANETARY GAS
NT INTERPLANETARY MEDIUM
Solution of acoustic field due to monochromatic point source located in stratified media by direct numerical integration of hydrodynamical field equations
24 p3968 N71-38309
- MEDIAN [STATISTICS]
Calculating production of group-average cross sections of resonance self-shielding in area of unresolved resonances
08 p1261 N71-18785
- MEDICAL ELECTRONICS
Pressure sensors, blood flow transducers, pH electrodes, and photographic recording of biological data for use in aerospace medicine
[NASA-CR-119024] 16 p2550 N71-28284
Development of prototype miniaturized microphone for electrocardiography
[NASA-TM-X-65580] 16 p2572 N71-28901
Analog computer program and display device for detecting arrhythmia signals during electrocardiography
[AD-711039] 19 p3046 N71-31612
- MEDICAL EQUIPMENT
NT ARTIFICIAL HEART VALVES
NT CARDIOTACHOMETERS
NT PROSTHETIC DEVICES
NT RESPIRATORS
NT STRETCHERS
Electromedical garment, applying vectorcardiologic type electrodes to human torsos for data recording during physical activity
[NASA-CASE-XFR-10856] 02 p0167 N71-11189
Respiration analyzing method and apparatus for determining subjects oxygen consumption in aerospace environments
[NASA-CASE-XFR-08403] 02 p0169 N71-11202
Closed-cycle respirator development program
[AD-712560] 03 p0329 N71-12352
Intensive care alarm indicator system with audible signal and worn by staff responsible for care
[NASA-TM-X-65421] 06 p0805 N71-15832
NASA technology utilized in medical diagnostic monitoring instruments
[NASA-TM-X-65418] 06 p0805 N71-15895
Digital logic design for spirometer
[NASA-TM-X-65417] 06 p0805 N71-15896
Equipment and facilities for biodynamic research in US and Canada
12 p1896 N71-23342
Equipment and facilities for biodynamic research in NATO European countries
12 p1896 N71-23343
Feasibility of on-site audiometer calibration check
[AD-718417] 12 p1866 N71-23355
Computer animated display device for diagnosis of heart disease
[NASA-NEWS-RELEASE-71-58] 12 p1867 N71-23751
Performance of impedance cardiograph for measuring heart rate and body fluids
[NASA-CR-114968] 12 p1864 N71-24173
Silicon radiation detector production engineering for biological and medical applications and explanation of continuous absorption spectra using RC delay line as equivalent circuit
[BMW-FBK-70-15] 15 p2374 N71-26914
Laser machining device with dielectric functioning as beam waveguide for mechanical and medical applications
[NASA-CASE-HQN-10541-2] 15 p2415 N71-27135
Technology utilization in biomedical areas, particularly for infants and handicapped persons
[NASA-CR-121627] 21 p3383 N71-34070
Aerospace reliability techniques and their application to biomedical devices
[NASA-TM-X-67942] 23 p3717 N71-36494
Breadboard testing of automated anesthesia machine
[NASA-CR-122646] 23 p3761 N71-36813
Tensile strength analysis of laminated-fiber-glass orthopedic shells and pressure chamber designs for surgery and hyperbaric oxygenation therapy
[JPRS-54173] 24 p3902 N71-37815
Therapeutic pressure chamber design and testing for hyperbaric oxygenation treatments
24 p3903 N71-37817
Experimental surgical pressure chamber design including compressed air systems, chamber equipment, lighting, and gas analysis
24 p3903 N71-37819
- MEDICAL PERSONNEL
NT FLIGHT SURGEONS
NT PHYSICIANS
Aerospace medical training and qualifications of medical personnel
04 p0478 N71-13897
Utilization of electronic and computerized techniques for undergraduate medical education
[RM-6180-NLM] 21 p3385 N71-34061

SUBJECT INDEX

Senior aviation medical examiners conducting FAA first-class medical examinations
[FAA-AM-71-38] 24 p3884 N71-37683

MEDICAL PHENOMENA

NT PHENOMENOLOGY

Medical aspects of high altitude environments including hypoxia at Logan High Camp
14 p2237 N71-26215

MEDICAL SCIENCE

NT DENTISTRY
NT ENDOCRINOLOGY
NT EPIDEMIOLOGY
NT GERMATRICS
NT HISTOLOGY
NT IMMUNOLOGY
NT NEUROLOGY
NT ORTHOPEDICS
NT OTOLARYNGOLOGY
NT PATHOLOGY
NT PHENOMENOLOGY
NT PSYCHIATRY
NT RADIATION MEDICINE
NT RADIOBIOLOGY
NT RADIOLOGY
NT RADIOPATHOLOGY
NT SYMPTOMOLOGY
NT TOOTH DISEASES
NT UROLOGY

Medical support for prolonged space flights

02 p0159 N71-11484
Military aeromedical education, physiological training, civil aeromedical education, and survival training in various countries
[AAGARD-CP-75-70] 04 p0477 N71-13876
Aeromedical training in Canadian facilities
04 p0477 N71-13877
Education and training of US Air Force flight surgeons
04 p0477 N71-13878
Aviation medicine training in US army
04 p0477 N71-13879
Aviation medicine training in Royal Air Force
04 p0477 N71-13880
Functions of aeromedical training section of Royal Air Force
04 p0477 N71-13881
Aerospace medicine training in France
04 p0477 N71-13882
German aeromedical training for medical and paramedical personnel
04 p0477 N71-13883
Norwegian Air Force aerospace medicine training programs
04 p0477 N71-13884
Italian aerospace medicine training for military and civilian personnel
04 p0478 N71-13885
Civil aerospace medical activities in Germany
04 p0478 N71-13886
Requirements of English medical schools for diploma in aviation medicine
04 p0478 N71-13887
Training of flight surgeons for civil aviation in Great Britain
04 p0478 N71-13888
Canadian aircrew operational aeromedical training
04 p0482 N71-13889
Physiological training of flying personnel in German Armed Forces
04 p0482 N71-13890
Aerospace medical training in Royal Netherlands Air Force
04 p0478 N71-13891
Physiological training of military and civilian aircrews in cooperation with engineers in France
04 p0483 N71-13893
Oncological data processing system using general purpose computer and graphic input device
11 p1719 N71-22737
Alternating gradient synchrotron, beam research reactor, and medical reactor development and operation and research summaries
[BNL-52030] 12 p1976 N71-24210
Development of clinical pathology procedures for detection of diseases in germfree mice and detection of titanium in lymphoid structures of hamsters, mice, and rats
[NASA-CR-118671] 14 p2206 N71-26399
Trends and possibilities in biochemical and biotechnical in medical science heart transplantation
18 p2875 N71-30840
Utilization of electronic and computerized techniques for undergraduate medical education
[RM-6180-NLM] 21 p3385 N71-34081
Biocience research and applications to biological and medical problems
[RM-6067-RC] 21 p3385 N71-34082
Scientific developments in Europe involving treatment of cholera, treatment of bacterial endocarditis, automated system for epidemiological information, and air traffic control
[IPRS-53877] 21 p3534 N71-35187

Characteristics of oxazepam and occurrence as metabolite in metabolism of diazepam in human organisms
[RAE-LIB-TRANS-1583] 24 p3886 N71-37697

Hazards associated with laser radiation and radiation used as tool in biology and medicine
24 p3900 N71-37802

MEDICAL SERVICES

Investigation of application of NASA developed technology to cardiovascular and pulmonary patient monitoring to improve availability of data for medical diagnosis
[NASA-CR-118630] 12 p1868 N71-23848
Program plans and cost estimates of project for application of bioscience technology to patient monitoring system
[NASA-CR-118035] 12 p1868 N71-23849
Medico-legal examination of aircraft parts to determine cause of crash
[AD-726559] 22 p3541 N71-35222
Standards, policies, procedure, and limitations of Federal Aviation Administration medical certification system
[FAA-AM-71-25] 22 p3544 N71-35244
Automatic data processing systems for air traffic control, health services, operations research, management planning, information systems, and reading machines
24 p3892 N71-37742

MEDICINE

Effects of unusual environmental conditions on characteristics and stability of drugs
02 p0161 N71-11495
Systems engineering and management applied to urban development, education, water management, inventory management, Saturn-Apollo project, and ecology
[NASA-TM-X-64575] 11 p1846 N71-22026

MEDITERRANEAN SEA

Divergence, vertical velocity, and energy conversion in west Mediterranean during cyclone development on 24 Oct. 1964
[TT-68-51019] 01 p0079 N71-10651
Synoptic meteorological observations of Mediterranean marine area
[AD-712761] 04 p0541 N71-14097
Synoptic meteorological observations for Mediterranean marine areas
[AD-713084] 05 p0715 N71-14522
Synoptic observations for Mediterranean marine areas - Ionian Sea, Malta, and Gulf of Sidra
[AD-713295] 05 p0715 N71-14524
Summary of synoptic meteorological observations for Mediterranean marine areas - Vol. 3
[AD-713779] 05 p0715 N71-14545
Meteorological observations in Mediterranean Sea area - Vol. 4
[AD-713780] 05 p0715 N71-14549
Meteorological observations in Mediterranean Sea area - Vol. 5
[AD-713648] 05 p0715 N71-14550
Meteorological observations in Mediterranean Sea area - Vol. 6
[AD-713085] 05 p0715 N71-14551
Synoptic meteorological data for Mediterranean marine areas of Rota, Tangier, and Malaga
[AD-713992] 06 p0892 N71-16642
Synoptic meteorological data for Mediterranean coast
06 p0893 N71-16578
Mathematical model of Adriatic Sea for study and prediction of tides at Venice
[IFA-STR-12] 13 p2069 N71-24400
Results of joint Soviet-French investigations in Northwestern Mediterranean Sea
14 p2248 N71-25973
Tables on climatological conditions for airfields and climatic areas of Mediterranean region
[AD-721160] 15 p2440 N71-27830
Charts giving mean atmospheric refractivity in Mediterranean Europe
[IEA-STR-13] 18 p2949 N71-30625
Seismic investigations by reflected waves method of sedimentary stratum in Mediterranean Sea
18 p2910 N71-30705

MEDIUM SCALE INTEGRATION

Application of transistor-transistor logic to design of MSI devices
23 p3735 N71-36631
Design and applications of bipolar MSI devices
23 p3735 N71-36632

MEETINGS

U CONFERENCES
U MEISSNER EFFECT
U DIAMAGNETISM
U SUPERCONDUCTIVITY

MELTING

NT ARC MELTING
NT FUSION [MELTING]
NT VACUUM MELTING
Ice interlayer formation computations in freezing moist soil
[AD-711874] 02 p0212 N71-11518

MEMBRANE STRUCTURES

Solution of problems concerning thawing and melting in finely dispersed media
[AD-711057] 02 p0218 N71-12028

Glass formation in systems phosphorus pentoxide-antimony trioxide-chromic oxide and phosphorus pentoxide-antimony trioxide-vanadium pentoxide
[AD-713449] 05 p0711 N71-15404

Finite difference general solution to problem of one and two dimensional melting of solids
[AD-716921] 09 p1482 N71-19947
Kinetics of melting metals and mechanism of long to short range atomic ordering in liquid metals
[NLL-TRANS-746-566/1922.401] 10 p1579 N71-21307

Chemical composition and bonding strengths of lithium-potassium and lithium-sodium silicate glass systems under melting conditions
11 p1785 N71-22893

Frost penetration and thawing of soil
[PUBL-387] 12 p1915 N71-24246
Vetting and casting of titanium alloys
[AD-719616] 13 p2095 N71-25063

Unbounded input reactivity effects on three types of EBR-2 core configurations, using MELT-2 code for meltdown analysis
[ANL-7752] 13 p2119 N71-25189

Manufacturing processes in space environment, including melting and solidification
[NASA-TM-X-67170] 14 p2260 N71-26009
Zero-g melting and solidification processes in aerospace environment
14 p2261 N71-26011

Melting characteristics of low density mixed oxide (U,Pu)/O₂ at beginning of irradiation, with in-pile distribution of fused oxide
[CEA-CONF-1659] 15 p2450 N71-27591

Laser-radiation effects on metals including damage thermodynamics, melting and cavity formation, vapor hydrodynamics, and damage product electromagnetic absorption
[JPRS-53241] 16 p2608 N71-28180

Thermal conductivity and plastic deformation of nuclear reactor rods and metal plates melting under internal heat generation
[AD-723199] 19 p3188 N71-31999

Electrical resistivity of Al and Cu during rapid heating to melting point and fracture in investigation of metallic melting mechanisms
[NLL-M-21008-15828.4F] 21 p3441 N71-34489

Structure-property relationships in liquid ceramics heated to temperatures as high as 3000°C
[AD-726401] 22 p3403 N71-35658

Atmospheric factors affecting snow-melt in Alps
[IFA-CP-232] 23 p3791 N71-37017

Hydrologic forecasting of snow melt runoff from areal snow cover in central Colorado
[USDA-FSRP-RM-66] 24 p3953 N71-38204

MELTING POINTS

Low temperature melting curve of helium 3
[UCSD-34-P-145-26] 03 p0331 N71-12365
Effect of lattice parameter and melting point of metals on solid state diffusion
[TT-70-57027] 03 p0442 N71-12908

Melting vacancies and self diffusion of metals
[FEE-164] 04 p0527 N71-13696

Melting points of metallic elements and selected compounds including nitrides, borides, carbides, halides, and sulfides
[AD-715908] 08 p1159 N71-18554

Melting temperature measuring instrument for lubricating oil additive ashes
[AD-719767] 13 p2101 N71-25104

Mercury melting curve equation of state for high pressure measurements
14 p2257 N71-26511

Isothermal and adiabatic compressibility of liquid metals, particularly lead, from melting point to critical region
[NYO-4176-4] 15 p2425 N71-27482

Electrical resistivity of Al and Cu during rapid heating to melting point and fracture in investigation of metallic melting mechanisms
[NLL-M-21008-15828.4F] 21 p3441 N71-34489

Thermodynamic properties of four crystalline sodium borates
[BM-R1-7551] 22 p3550 N71-35290

Phase diagram for vanadium-vanadium oxide system based on melting points and thermal differential, metallographic, and X-ray analyses
[IS-T-448] 24 p3935 N71-38074

MEM [EXCURSION MODULE]

U MARS EXCURSION MODULE

MEMBRANE ANALOGY

U MEMBRANE STRUCTURES

U STRUCTURAL ANALYSIS

MEMBRANE STRUCTURES

NT SKIN [STRUCTURAL MEMBER]

Nonlinear relaxation method for solving nonlinear partial differential equations governing large deflection response of axisymmetric circular membranes
01 p0150 N71-10713

Transport measurements through cation-exchange membranes by concentration clamp technique
[NASA-CR-111598] 03 p0332 N71-12370

- Flexible composite membrane structure impervious to extremely reactive chemicals in rocket propellants [NASA-CASE-XNP-08837] 06 p0878 N71-16210
- Analyzing sound transmission through clamped circular plate set in infinite rigid wall exposed to dense acoustic medium and excited by obliquely incident plane wave [AD-714281] 06 p0906 N71-16406
- Investigating materials and techniques for spacecraft power systems 06 p0923 N71-16678
- Permeability of gases through filled and unfilled membranes of natural rubber and synthetic rubber [AD-716393] 09 p1403 N71-19616
- Dynamic models for cell membrane functions in molecular biology 09 p1331 N71-19881
- Constructing membrane theory of anisotropic shells by reducing three dimensional problem of theory of elasticity of shells 11 p1837 N71-22499
- Driver modifications for improved performance of electric arc shock tube 11 p1732 N71-22554
- Displacement equations in Cartesian coordinates for solving deflection response of flat membranes 14 p2347 N71-35807
- Flexible barrier membrane comprising porous substrate and incorporating liquid gallium or indium metal used as sealant barriers for spacecraft walls and pumping liquid propellants [NASA-CASE-XNP-08881] 16 p2612 N71-38747
- Three simultaneous differential equations applicable to any strain energy function for problems of large elastic deformations of axisymmetric membranes 17 p2854 N71-30156
- Difference equations solved for determining large deflection response of circular, rectangular, and polygonal flat membranes [AD-723538] 19 p3188 N71-32027
- Stress function analysis of elastic deformation of thin membrane structures 19 p3191 N71-32710
- Concentration clamp method for measuring permeability characteristics of membranes [NASA-CR-121634] 21 p3385 N71-34085
- Feasibility of crystal growth technique for beta alumina membrane from molybdenum, tungsten, and iridium [NASA-CR-72982] 23 p3833 N71-37336
- Nonlinear theory of membrane shells for civil engineering design 23 p3864 N71-37547
- Membrane analogy analysis of composite structural members subjected to pure torsion 23 p3864 N71-37550
- Analysis of pressure differentials required to prevent passage of airborne microorganisms through holes in membranes acting as barriers [NASA-CR-1910] 24 p3879 N71-37655
- Analysis of axisymmetric deformations of cylindrical membrane composed of elastic, homogeneous, isotropic, and incompressible material [AD-728022] 24 p4027 N71-38733
- MEMBRANE THEORY**
- U MEMBRANE STRUCTURES**
- U STRUCTURAL ANALYSIS**
- MEMBRANES**
- NT ION EXCHANGE MEMBRANE ELECTROLYTES**
- NT MEMBRANE STRUCTURES**
- NT SKIN [STRUCTURAL MEMBER]**
- Electron microscopic studies of nerve membrane ultrastructure 08 p1156 N71-19313
- Computer program for cellular structures of arbitrary plan geometry designed to capture behavior of deck and web components 09 p1481 N71-20517
- Separation cell with permeable membranes for fluid mixture component separation [NASA-CASE-XMS-02952] 10 p1587 N71-20742
- Mathematical model of satellite with continuous elastic components comprising moment free rigid carrier attached to elastic membrane 17 p2779 N71-29700
- Beach scale module of improved cellulose acetate membranes for reversed osmosis [PB-198952] 21 p3444 N71-34507
- Performance and environmental tests of membranes for airfield surfacing 22 p3566 N71-35398
- Characterization, optimization, production, and performance of cellulose acetate butyrate membranes [PB-198956] 22 p3601 N71-35649
- Mechanical response of frog membrane to stimulating frequencies and electrophysiological determined hearing areas [NASA-CR-123162] 24 p3877 N71-37634
- Strength, alpha particle transparency, chemical attack and contamination resistance, and ease of decontamination for alpha activity monitor sealing membranes used in solutions [CEA-N-1440] 24 p3942 N71-38122

MEMORY

- Measuring human performance of auditory vigilance task time shared with memory task [AD-711565] 02 p0158 N71-11119
- Visual flash duration discrimination and analysis of temporal and energy cue models, and memory effects [NASA-CR-119009] 16 p2541 N71-28136
- Mathematical models of vision process, relationship between memory and perception, and development of improved computer technology [JPRS-53647] 19 p3042 N71-32012
- Analysis of registering structure as memory model and role in perception processes 19 p3043 N71-32014
- Synaptic junction model for memory in brain [NASA-TN-D-6456] 19 p3045 N71-32474
- MEMORY STORAGE UNITS**
- U COMPUTER STORAGE DEVICES**
- U CORE STORAGE**
- MENTAL PERFORMANCE**
- Combined effects of noise and vibration on mental performance as function of time of day [AD-711636] 01 p0014 N71-10891
- Relationship between cybernetic and psychological approaches to human thought 06 p0803 N71-16341
- Awareness of thought processes in recreating past experiences [JPRS-52397] 08 p1156 N71-19124
- Human performance in color naming and word reading with and without Stroop interference [AD-716351] 09 p1339 N71-19579
- Long duration confinement effects in simulated space station atmosphere on human short-term memory 10 p1509 N71-20985
- Diagnostic chronological and physiological criteria in geriatrics 11 p1609 N71-22312
- Pattern recognition and heuristic functions of natural and artificial intelligence 11 p1721 N71-23075
- Problem solving task for mental ability assessment in selection of aviation personnel [FAA-AM-71-28] 19 p3045 N71-32434
- Human thinking activity applied to man machine systems [JPRS-53983] 22 p3544 N71-35245
- Thinking, cybernetics, and information theory 22 p3544 N71-35248
- Eye movement, mental performance, and problem solving 22 p3545 N71-35250
- Human thinking studies using problem solving in chess 22 p3545 N71-35251
- Skin resistance during solution of mental problems 22 p3545 N71-35252
- MENTAL STRESS**
- U STRESS [PSYCHOLOGY]**
- MERCAPTAN**
- U THIOLS**
- MERCAPTO COMPOUNDS**
- U THIOLS**
- MERCATOR PROJECTION**
- Apollo 12 flight color and black and white lunar photography indices on MERCATOR projections [NASA-TM-X-66883] 08 p1203 N71-18975
- MERCURY [METAL]**
- NT MERCURY ISOTOPES**
- NT MERCURY VAPOR**
- Precision measurement of Hg-203 beta-gamma directional correlation 01 p0095 N71-10416
- Inventory control of mercury condensing pressure during SNAP-8 startup [NASA-TM-X-2114] 02 p0265 N71-11781
- Spectra and photochemical reactions of mercury and ethylene [COO-584-46] 04 p0592 N71-14403
- Abstracts on Soviet stratospheric solar observatory and mercury content measurements in meteorites 07 p1107 N71-16956
- Relating liquid metal embrittlement of aluminum and zinc-cadmium alloys to electronegativity of participating solid and liquid metal [AD-715741] 08 p1214 N71-18552
- Shutdown characteristics of SNAP-8 mercury Rankine power conversion system [NASA-TM-D-6172] 09 p1326 N71-20155
- Interrupter switching device utilizing electrodes and mercury filled capillary tubes in which current flow vaporizes mercury as circuit breaker [NASA-CASE-XNP-02251] 10 p1540 N71-20096
- Shock and vibration tests of SNAP-8 centrifugal mercury pump [NASA-TM-X-52990] 10 p1602 N71-21049
- Direct electromagnetic generation and detection of acoustic waves reported for cesium and mercury near room temperature [NYO-2150-45] 11 p1799 N71-22536
- High temperature kinetics of photosensitized mercury decomposition of nitrous oxide in carbon monoxide methane mixtures [SR-369] 12 p1871 N71-23783

- Nuclear spectroscopy and decay schemes for isotopically pure mercury isotopes and radioactive daughter products in mass range 182 to 192 [CEBN-70-29] 13 p2134 N71-25174
- Research and development of mercury electron bombardment thrusters [NASA-TM-X-67836] 13 p2157 N71-25366
- Analysis of subvalent Hg ion discovered in molten chloroaluminates [CONFL-701204-1] 14 p2212 N71-25607
- Method of forming ceramic to metal seals impervious to gaseous and liquid mercury at high temperature [NASA-CASE-XNP-01263-2] 14 p2263 N71-26312
- Mercury melting curve equation of state for high pressure measurements 14 p2257 N71-26511
- High temperature mercury corrosion resistance of tantalum, tantalum alloy, and niobium alloy above after bending stress [NASA-CR-1811] 15 p2420 N71-28947
- Simple empirical relation based on adiabatic compressibility, adiabatic bulk modulus, and reduced temperature for liquid argon, krypton, and xenon, and application to mercury 15 p2378 N71-27902
- Potential star tracker interference from radiation produced by mercury bombardment thrusters using electric propulsion systems [NASA-TM-X-67836] 16 p2671 N71-28817
- Mathematical model for predicting damping time of mercury damper [AD-722003] 17 p2851 N71-29421
- Thermal and hydraulic performance of prototype SNAP-8 mercury boiler - design, fabrication, and preliminary evaluation [NASA-TN-D-6451] 19 p3041 N71-32209
- Optimization of mercury electron bombardment thrusters in SERT program [NASA-TM-X-67915] 20 p3339 N71-33317
- Dispersion in level crossings and coherence narrowing in mercury resonance radiation 20 p3318 N71-33596
- Electrochemical cell employing twin dropping mercury electrodes used in thin layer chromatography technique 21 p3389 N71-34108
- Mineral fluids as lubricating composition for mercury water seals [AD-721032] 21 p3444 N71-34505
- Radioisotopic method for determination of mercury in electrolytic cells [ORNL-TR-2487] 21 p3484 N71-34819
- Mercury-filled self-healing fuses for protecting solid state circuits from faults - design and development [NASA-CR-72868] 22 p3558 N71-35343
- Heat transfer and fluid flow during forced convection boiling of wetted mercury with application to design and optimization of once-through boilers for Space Power Rankine Cycle Systems - SNAP-8 [NASA-CR-72897] 22 p3621 N71-35796
- Maximum propellant utilization in electron bombardment ion thrusters using mercury for propellant [NASA-TM-X-67921] 22 p3662 N71-36113
- Mercury photosensitized oxidation of CO at 275 C [PSU-IRL-SCI-370] 23 p3719 N71-36509
- Qualitative tests of vrbait to deduce chemical forms and confirm mercury as essential constituent [NASA-TT-F-13759] 23 p3768 N71-36660
- Environmental pollution by mercury and other toxic substances 24 p3883 N71-37681
- Microsampling technique used to study metallic bonding between liquid mercury and trace contaminants [NASA-TM-X-2424] 24 p3941 N71-38111
- MERCURY [PLANET]**
- Selected data on physical characteristics of planet Mercury 04 p0609 N71-13591
- Magnetic field in wake of solar wind interaction with Mercury [NASA-TM-X-65456] 08 p1286 N71-19295
- Linearized analysis of thermal emission from Lunar and Mercurian surfaces 12 p1997 N71-24206
- Onboard experiments of European flyby mission to Mercury planet - European space programs 17 p2850 N71-29567
- Steady state electromagnetic interaction of solar wind with planet Mercury computed for spectrum of electrical conductivity [NASA-TM-X-62028] 17 p2841 N71-29923
- Refutation of correspondence principle in explanation of motion of perihelion of Mercury [RIFP-119] 17 p2790 N71-30312
- Interpretation of planetary surface photographs, noting Moon, Mars, and Mercury surfaces [ESRO-SP-56] 18 p3008 N71-30594
- Lunar, Mercury, and Mars surfaces and atmospheres - ground based photometric and polarimetric methods of observations 18 p3008 N71-30595
- Comparison of quantum electrodynamics and classical mechanics for gravitational effects on Mercury orbits [RIFP-124] 20 p3269 N71-33882

SUBJECT INDEX

MERCURY ALLOYS

NT MERCURY AMALGAMS

Isotropic and anisotropic Knight shift, line width, and quadrupole coupling frequency measurements of In-115 NMR in dilute In-Cd, In-Hg, and In-Tl alloys 10 p1583 N71-21594

MERCURY AMALGAMS

Iodine amalgam, mercury, and indium-gallium electrochemistry and sodium-oxygen electrochemical cells (AI-TRANS-287) 15 p2377 N71-27387
Pressure dependence of dental amalgam and component alloy bulk, shear, and Young's moduli and Poisson ratios based on longitudinal and transverse ultrasonic wave velocity measurements 22 p3660 N71-36097

MERCURY COMPOUNDS

NT MERCURY OXIDES

NT MERCURY TELLURIDES

Helicon resonance and quantum oscillations in mercury selenide crystal 18 p2997 N71-31325

Crystal growth of cinnabar, proustite, and lead chloride, experimental work in Hg₂S-Hg₂Se phase diagram, and electro-optic coefficients of zincblende structure compounds (AD-721201) 19 p3168 N71-32057

Analysis of carrier density fluctuations in mercury cadmium telluride and causes of electromagnetic noise in photoconductors 19 p3171 N71-32617

MERCURY ISOTOPES

Nuclear spectroscopic investigations of decay Hg-191 yields Au-191 (JUL-659-KP) 02 p0278 N71-12162

Measurement of pion mercury ion scattering and determination of differential cross sections 10 p1822 N71-21763

Interferometric measurements of solar absorption wavelengths in visible region, and comparison to standard Hg-196 wavelength 11 p1825 N71-21975

Data on Os-184,187 levels from Ir-184,187 decays, Hg-200 and Au-200 levels from Au-200m decay, and β -proton, neutron, photon nuclear reactions (COO-1672-21) 11 p1806 N71-22436

Directional correlations of gamma ray cascades in Hg-200 using Ti-200 source and coincidence spectrometer arrangement (INP-18613) 14 p2309 N71-26387

Gamma rays and gamma-ray cascades from 26.1-hr thallium-200 decay and excited states in Hg-100 (INP-18647) 14 p2309 N71-26601

Beta-gamma circular polarization measurements on odd nucleon transitions in mercury 203 cascade (INP-18694) 19 p3148 N71-32069

Nuclear interactions and atomic energy levels for Pb-210, Bi-210, Po-210, Pb-206, Tl-206, and Hg-206 (AD-724640) 20 p3314 N71-33033

MERCURY LAMPS

Low voltage mercury lamp used in ultraviolet photochemistry (AD-711777) 01 p0019 N71-10848

Quantum mechanics of line broadening effects in solar simulator mercury xenon arc lamp spectra 13 p2062 N71-25333

Mercury lamps - bibliography (AD-722860) 19 p3105 N71-32241

MERCURY OXIDES

Tests for determining remaining charge in zinc mercuric oxide primary batteries (SC-RR-70-332) 03 p0319 N71-12276

MERCURY PROJECT

Conference on European Mercury project and German Helios solar probe 17 p2849 N71-29563

Spacecraft design, configurations, and mission profiles in European Mercury probe 17 p2849 N71-29565

Review of endocrine control of fluid and electrolyte balance during Mercury, Gemini, and Apollo missions 23 p3711 N71-36456

MERCURY SPACECRAFT

European Mercury spacecraft experiments for interplanetary and planetary space investigation 17 p2850 N71-29566

MERCURY TELLURIDES

Low frequency noise properties of mercury telluride infrared detectors (AD-711119) 01 p0033 N71-10510

Design and fabrication of 15.5 micron mercury cadmium telluride photodetectors for operation at 105 K (NASA-CR-111589) 05 p0690 N71-15700

Neutral defects in mercury telluride single crystals grown by Bridgman method in mercury vapors 07 p1047 N71-17125

Measuring saturated vapor pressure of mercury telluride using static compensation method 07 p1047 N71-17133

High speed (Hg,Cd)Te photodiode detectors sensitive to 16 μ m infrared radiation with operating temperature range of 77 to 50 K (NASA-CR-121766) 21 p3402 N71-34205

MERCURY VAPOR

Interrupter switching device utilizing electrodes and mercury filled capillary tubes in which current flow vaporizes mercury as circuit breaker (NASA-CASB-XNP-02251) 10 p1540 N71-20896

Hourly ionospheric propagation data - Freiburg, Dec. 1970 (REPT-294-F) 10 p1556 N71-21834

Kinetic principles of photochemical, mercury vapor sensitized oxidation of benzene in gas phase (NLL-RTS-5965) 10 p1516 N71-21835

Liquid-vapor interface seal design for turbine rotating shafts including helical and molecular pumps and liquid cooling of mercury vapor (NASA-CASB-XNP-2863-1) 14 p2263 N71-26294

Mercury vapor fed hollow cathodes for electron bombardment ion thrusters (NASA-CR-121631) 21 p3502 N71-34943

Performance of toroidal microwave and radio frequency sources using mercury vapor discharges for excitation 23 p3726 N71-36562

MERIDIANS

U LATITUDE

U LONGITUDE

MERIDIONAL FLOW

Free oscillations of fluid on hemisphere bounded by meridians of longitude 09 p1380 N71-19504

Influence of solar corpuscular radiation emission on changes of meridional forms of atmospheric circulation 11 p1756 N71-22838

Design of axial compressor rotor - specification of meridional velocity profile (AD-722824) 18 p3001 N71-31214

MESON-NUCLEON INTERACTIONS

NT ELLIPTIC FUNCTIONS

NT RATIONAL FUNCTIONS

Large angle hadron and proton scattering and duality calculations based on meromorphic and scattering functions, momentum transfer, and asymptotic methods (REPT-71/19) 20 p3317 N71-33350

Coherence of holomorphic mapping 24 p3948 N71-38165

MESH

Application of Rayleigh-Ritz mesh method to elastic buckling of orthotropic rectangular shells (DLR-FB-70-71) 13 p2177 N71-24493

Capacitor field calculations for capacitive displacement measurement of open mesh structures such as radio telescopes and radar receivers (NASA-TN-D-6341) 20 p3273 N71-33397

MESON RESONANCES

Meson spectrum from Veneziano model and trajectory intercepts formulation (IC/70/85) 04 p0587 N71-14265

Investigating possibility of octet of 0⁺/ scalar mesons and none of 1⁺/ axial vector mesons forming 35-plet SU(6) supermultiplet (SINP-77-67-1) 05 p0739 N71-15029

AZ/NONE - CONSISTENCY OF DATA (UCRL-19665) 05 p0741 N71-15119

Investigating reaction K/ϕ plus N yields K plus N plus pion in isospin-0 channel near K^*N threshold (UCRL-19774) 05 p0748 N71-15280

Neutral kaon resonance production in positive kaon deuteron interactions within bubble chamber (UCRL-20076) 06 p0925 N71-16812

Search for double structure of meson resonance using Fourier algorithm (JINR-P1-5340) 08 p1250 N71-18240

Heavy meson resonances in antiproton proton annihilation reaction at 3.6 GeV/c (NIP-18466) 08 p1251 N71-18262

Extending model of partially conserved axial current breakdown to higher order on basis of hard meson current algebra (NUB-2023) 08 p1258 N71-18623

Failure of χ -channel helicity conservation in A1 polarization production (COO-1195-201) 09 p1427 N71-19540

Statistical tensor analysis of decay distributions and hyperon polarizations for Σ^0 1385 resonance from positive pion proton yields kaon resonance Lambda hyperon positive pion with quark model (JINP-731) 13 p2140 N71-25525

Statistical evidence against neutral, 2 negative pion enhancement at 1.627 GeV/c $\pi\pi$ mass in antikaon deuteron reaction at 4.48 GeV/c (COO-1428-255) 16 p2647 N71-28311

Distinguishing spin-parity alternatives 0⁺/minus/ and 2⁺/minus/ of $X(960)$ meson (JINR-E2-5637) 16 p2647 N71-28312

Properties of meson resonances in antiproton proton annihilation 18 p2974 N71-30532

Models for S and P waves of pion scattering obeying current algebra constraints and allowing for meson resonance (RLD-1188-402) 19 p3153 N71-32205

MESON-NUCLEON INTERACTIONS

Cross sections in double resonance reaction positive pion proton yields neutral rho-meson positive deuteron hyperon at 11.7 GeV/c (DESY-71/8) 19 p3161 N71-32707

Spectrum analysis of diffractively produced multi-meson systems (UR-875-337) 21 p3481 N71-34797

Electromagnetic corrections to rho(meson) proton reaction to determine causality in pion meson system (TR-72-003) 23 p3819 N71-37239

MESON-NUCLEON INTERACTIONS

Exposure of 15 foot deuteron filled bubble chamber to positive pion meson beam at 40 GeV/c (COO-1428-230) 04 p0581 N71-14060

PCAO consistency condition and rho-meson contribution in S wave for on-shell pion-N scattering (SINP-77-48-2) 06 p0908 N71-15730

Spin parity studies of eta-meson pion decay of A2 meson, and A2 production mechanism in negative pion proton yields negative A2 proton reaction (COO-1195-200) 08 p1259 N71-18685

Negative kaon proton interactions at 12.6 GeV/c (AD-71567) 08 p1267 N71-19323

Quark model for hadron spectroscopy and meson nucleon scattering cross sections with resonance production (UCR-34-P-107-113) 09 p1436 N71-20043

S matrix calculations of pion-nucleon P-wave scattering length (INP-18553) 09 p1446 N71-20573

Nucleon-meson transport code NMTC to compute transport of nucleons below 3.5 GeV and mesons and charged pions below 2.5 GeV (NASA-CR-117496) 10 p1618 N71-21542

Contribution of rho meson in calculation of low energy pion-nucleon partial wave scattering parameters 10 p1621 N71-21753

Negative pion proton elastic scattering differential cross sections from 1.71 to 5.53 GeV/c (NASA-CR-117852) 11 p1809 N71-23032

Closure approximation in meson production from deuteron and light nuclei, rho meson electroproduction from heavy nuclei, and coupling parameters to photons and nucleons 13 p2138 N71-25475

Regge pole model with Veneziano residues for pion nucleon and kaon nucleon interactions (TPU-370) 14 p2319 N71-26783

Pion charge and kaon proton reactions analyzed by charge exchange model with four Regge poles (CEA-N-1373) 14 p2320 N71-26798

Poisson distribution of secondary mesons produced in high energy nucleon collisions in straight-line path approximation (JINR-E2-5329) 15 p2461 N71-27103

Meson pole dominance empirical test for matrix elements in energy momentum tensor analysis of pion-nucleon scattering (DESY-70/58) 15 p2462 N71-27145

Vacuum trajectory effects on invariant amplitude behavior in pion nucleon scattering (DESY-70/55) 15 p2463 N71-27175

Positive kaon negative pion elastic scattering from positive kaon proton interaction at 5.43 GeV/c in 80-inch bubble chamber 15 p2482 N71-27745

Exchange degeneracy with SU(3) symmetry and absorptive corrections in hypercharge and charge exchange reactions for meson baryon scattering (FTB-36) 15 p2488 N71-27869

Emulsion study of pion-nucleon interactions at 16.2 BeV with experimental criteria for interactions 16 p2852 N71-28996

Three body states Lambda or Sigma hyperon kaon antikaon and Xi hyperon kaon proton produced by negative kaon proton interactions at kaon beam momentum of 2.9 GeV/c (ORO-2394-170) 17 p2797 N71-29845

Dispersion model for pion-nucleon backward scattering peak amplitude (ITP-70-43) 17 p2811 N71-30400

Pseudoscalar meson production from high energy meson-nucleon interactions including scattering cross sections and vector dominance model (ITP-70-72) 18 p2971 N71-30466

Contribution of weak interaction positive pion proton yields positive kaon proton to 2-body positive pion proton scattering (IIF-70/6) 18 p2977 N71-30652

Regge cuts and high energy pion nucleon and kaon nucleon elastic and charge exchange scattering (LPTHE-71/14) 18 p2985 N71-31136

Inelastic pion-proton scattering reactions in general - Veneziano model (ITP-70-77) 20 p3322 N71-33812

Equivalent potentials for pion-alpha scattering determined theoretically with two-body direct interaction model 21 p3490 N71-34860

Graphic analysis of isotopic ratios in reactions producing three particles and possible Pomeron-pole exchange (JINR-P2-5630) 22 p3630 N71-35847

- Single and double pion production and charge exchange reaction from positive kaon proton and positive kaon deuteron interactions at 1585 MeV/c in 25-inch bubble
[UCRL-20628] 22 p3639 N71-35937
- Differential and total cross section and polarization data from pion-proton interaction and partial-wave analysis
22 p3648 N71-36014
- Continuous momentum rule derivation for high and low energy parameter determination for pion-nucleon scattering
22 p3649 N71-36019
- Correlation of eta and omega meson production from pion neutron reactions in bubble chamber with exchange models
22 p3649 N71-36025
- Kaon-proton interactions and low mass enhancement due to diffraction phenomena
22 p3651 N71-36034
- Meson-nucleon scattering at high energies and spin effects in quasipotential approach
[JINR-E2-3776] 23 p3807 N71-37146
- Meson-nucleon interactions and mass distribution compared with Regge pole exchange model
[ITEP-790] 24 p3973 N71-38349
- ### MESONS
- NT ETA-MESONS
NT K-MESONS
NT MESON RESONANCES
NT MUONS
NT PIONS
- Meson theoretical potentials for use in advanced power supply system
[AD-711092] 01 p0102 N71-10916
- Centrifugal barrier penetration factors used in meson decay kinematics
[UCRL-19826] 03 p0421 N71-12653
- Models of chiral symmetry in meson states
03 p0424 N71-12773
- Differential cross section and rho-meson density matrix elements for reaction pion/proton yields rho-meson/0 Delta/ hyperon at 13.1 GeV/c
[COO-1428-216] 03 p0430 N71-12910
- Investigating photoproduction of rho-mesons/0 in deuteron reactions between 1 and 5 GeV
[DESY-70/16] 03 p0432 N71-12936
- Nuclear reaction negative pion, proton yields proton negative pion neutral omega meson at 5.0 and 7.5 GeV/c
[COO-1195-188] 03 p0434 N71-12991
- Omega meson decay into 2 pions in pion-/proton reaction, and omega meson decay into 3 pions Dalitz plot
[NEVIS-182] 03 p0434 N71-12992
- Investigating nuclear structure on basis of shell and collective models of nucleon and meson interactions
[AD-712728] 03 p0435 N71-13188
- Strong interaction experiment on Mt. Chacabuta
[AD-712735] 03 p0435 N71-13224
- Considering various configurations for magnetic horn for meson beam focusing
[IFVE-SEP-69-73] 04 p0572 N71-13626
- Exposure of 15 foot deuterium filled bubble chamber to positive pion meson beam at 40 GeV/c
[COO-1428-230] 04 p0581 N71-14060
- Investigating twin meson production in K-/A reactions for compatibility with simple quark model
[COO-1428-227] 04 p0583 N71-14176
- Investigating particle interactions and accelerator technology for medium energies
[LA-4514] 06 p0904 N71-16187
- Infinite multipoles with SU(3) for mesons
[DEMO-70/14] 06 p0918 N71-16242
- Gas target for slow meson experiments at 100 atm
[CERN-TRANS-69-29] 07 p1071 N71-17042
- Mass spectrum in chiral model of pseudoscalar and scalar mesons
[SU-1206-230] 07 p1071 N71-17265
- Symmetry breaking in chiral model using mass spectra of spin-zero mesons
[SU-1206-228] 07 p1073 N71-17358
- Deriving analytical expression for photoproduction cross section of W-meson-electron pairs
[IFVE-SVM-70-2] 07 p1081 N71-18139
- Structure of positron electron spectrum from photoproduction of rho and omega mesons
[DESY-70/40] 08 p1230 N71-18231
- SU(3) model of CP-violation with interactions of weak mesonic currents
09 p1431 N71-19868
- Negative meson absorption by atomic structures and theoretical model of mesic molecule
[NRC-TT-1426] 09 p1442 N71-20405
- Chiral Lagrangian model of meson-baryon scattering for theory of antikaon interactions
[TID-25639] 12 p1971 N71-23846
- A2 meson mass distribution produced by pion proton yields A2 proton reactions and mass spectroscopy
[NUB-2063] 12 p1977 N71-24212
- Construction of N-meson amplitude according to positive intercept and abnormal parity trajectories
[LPTHE-71/11] 12 p1979 N71-24344

- Resonant scattering of light by light due to exchange of C-even mesons
[JINR-E2-5424] 13 p2133 N71-25161
- Eta prime meson decay rate calculated from chiral symmetry breaking
[TR-71-109] 13 p2141 N71-25532
- Double charge exchange of mesons of light nuclei
[JINR-P2-5286] 14 p2307 N71-26404
- Spin resonance scattering amplitude calculation for unpolarized baryon-meson interactions and quark model applications
[TPJU-1/70] 14 p2308 N71-26446
- Reaction pion/minus/ proton yields rho-meson/0 pion/minus/ proton with momentum studied in liquid hydrogen bubble chamber at 4.45 GeV/c
[ITEF-775] 14 p2316 N71-26745
- Additive quark model for decay distribution of resonance produced in meson baryon high energy interactions
[TPJU-15/70] 14 p2316 N71-26749
- Chiral SU(2) times SU(2) dynamics for A1 mesons, rho mesons, and pions
[JINR-E2-5249] 14 p2318 N71-26768
- Coulomb three body interaction for calculating muon meson transitions in collisions with hydrogen isotopes
[JINR-P4-5039] 15 p2464 N71-27199
- Current commutators in quantum electrodynamics and mass differences of pseudoscalar meson and baryon octets
15 p2470 N71-27380
- Cross sections for photoproduction of neutral mesons on hydrogen measured by linear accelerator using mass spectrometer technique
15 p2483 N71-27767
- Hard meson method for studying radiative leptonic decays of pions and kaons
17 p2796 N71-29793
- Fixed point theorems used for solving crossing symmetric S matrix equations for one meson Low equation
17 p2773 N71-29835
- Meson current algebra for calculating form factor and coupling constant in gamma - 3 pion amplitude in gamma/pion interaction
[NUB-2074] 17 p2774 N71-30061
- Calculations of mesonic contributions to /gamma,n/-reaction from photon-pion production processes of light nuclei using simple nuclear model
[LUNP-70/10] 17 p2810 N71-30396
- Photomeson effects in /gamma,n/a/ and /gamma,n/p/ reactions in light nuclei
[LUNP-70/09] 18 p2967 N71-30404
- Survey of photoproduction of vector mesons in /photon,proton/ reactions
[DESY-70/64] 18 p2972 N71-30526
- Comparison of experimental results on meson production in pp collisions at 660 MeV with One Pion Exchange (OPE) model predictions
[JINR-P1-5571] 18 p2973 N71-30543
- Pi phi theory for studying impact picture and eikonal approximation
[DESY-71/6] 19 p3145 N71-31899
- Existence on nonrelativistic bound states in nucleon-nucleon systems, and possible quasinuclear nature of heavy mesonic resonances
[NP-18774] 19 p3159 N71-32564
- Simple model for electroproduction of omega-mesons as test of rho-meson omega-meson pion vertex
[DESY-71/11] 19 p3160 N71-32637
- Broken scale invariance, current algebra, and massive gravitation in formalism describing meson interactions at intermediate energies and below
[NUB-2091] 20 p3293 N71-33922
- Models for vector-vector-tensor meson vertex including photon coupling
[DESY-71/14] 21 p3470 N71-34703
- Helicity structure of mesonic Regge couplings in terms of meson pole dominance for matrix elements of vector currents
[COO-264-572] 21 p3480 N71-34790
- Splitting in A2 meson fit to multiplicity parameter for measuring dipole structure
[UCRL-20622] 21 p3480 N71-34791
- Spectrum analysis of diffractively produced multi-meson systems
[UR-875-337] 21 p3481 N71-34797
- Application of algebraic realizations to pion-meson couplings in chiral dynamics and Yang-Mills field theory
[JINR-P2-5759] 22 p3640 N71-35950
- Low energy limit of dual resonance models and connection between Yang-Mills fields
[LPTHE-71/37] 23 p3812 N71-37183
- Empirical rule for cuts and effects on Regge pole model for natural parity meson exchanges and line reversal relations
[CALT-68-308] 23 p3814 N71-37198
- Axial vector current relation associated with pseudoscalar meson and sigma model formalisms
[TR-72-019] 23 p3819 N71-37241
- Asymptotic SU(3) symmetry, nonet boson coupling sum rules, and ninth pseudoscalar mesons
[TR-72-021] 23 p3819 N71-37243

- Neutral decay analysis of mesons
[PURC-4159-29] 24 p3980 N71-38408
- ### MESOPAUSE
- Integration of exponential functions and application to long wave radiative transfer near mesopause
15 p2404 N71-27563
- ### MESOSPHERE
- Stratospheric, mesospheric, and ionospheric reaction rate and transport data and kinetics of atmospheric constituents
[AD-710282] 01 p0044 N71-10080
- Ozone and hydrogen reactions in stratosphere and lower mesosphere
[PB-191048] 01 p0051 N71-10077
- Mesosphere atmospheric attenuation of solar radiation by oxygen and ozone
04 p0522 N71-13829
- Temperature, pressure density, and wind measurements in stratosphere and mesosphere during 1969
[NASA-TR-R-340] 06 p2322 N71-19139
- Vertical eddy thermal transport and global energy budgets of mesosphere and lower thermosphere
[NASA-CR-117047] 09 p1379 N71-19465
- Atmospheric photochemical model for polar region summer mesosphere and lower thermosphere
10 p1546 N71-20712
- High altitude mesospheric wind data taken by meteorological sounding rockets at Cape Kennedy, Florida
[NASA-TM-X-64578] 12 p1958 N71-24039
- Rocket-borne temperature ozone sensor measurements at mesosphere and stratosphere with analysis of diurnal variations
[AD-713509] 16 p2586 N71-28346
- Meteorological sounding of mesosphere structure and effects of latent heat release in troposphere
[NASA-TT-F-65592] 17 p2749 N71-30233
- Using numerical model to examine annual variation in motion of stratosphere and mesosphere
18 p2916 N71-31043
- Atmospheric models of radiative processes, sources, and sinks in mesosphere and thermosphere
[NASA-CR-121469] 20 p3342 N71-33732
- ### METABOLIC WASTES
- NT FECES
NT HUMAN WASTES
NT URINE
- Results from theoretical and experimental studies of mass exchange in life support systems
[NASA-TT-F-13371] 01 p0015 N71-10340
- Renal sodium and calcium excretion effects on human electrolytic water-mineral metabolism during space flight
20 p3222 N71-33467
- ### METABOLISM
- NT ADRENAL METABOLISM
NT CALCIUM METABOLISM
NT CARBOHYDRATE METABOLISM
NT CATABOLISM
NT ELECTROLYTE METABOLISM
NT ENZYME ACTIVITY
NT FERMENTATION
NT HORMONE METABOLISMS
NT OXYGEN METABOLISM
NT PROTEIN METABOLISM
- Chemical analysis of thiamine metabolism in man
[AD-712238] 02 p0155 N71-11099
- Mechanisms by which oxygen produces toxic effects on cellular metabolism
02 p0155 N71-11101
- Defining effects of temporal and quantitative dietary variables on human performance of vigilance tasks
[AD-711564] 02 p0158 N71-11118
- Human metabolism in rarefied atmospheres by gas chromatography
02 p0171 N71-11491
- Relationship of cesium-137 and iron-59 elimination rates to metabolic rates of small rodents
[ORNL-4568] 03 p0323 N71-12311
- Control of energy metabolism in higher plants
[TID-25485] 04 p0476 N71-13867
- Effects of d-amphetamine on carbohydrate metabolism at ground level and simulated high altitudes
[AD-713726] 05 p0633 N71-14641
- Altitude induced changes in glucose metabolism of Escherichia coli
[AD-715212] 07 p0982 N71-17830
- Bi-directional respiratory flowmeters and electronic instrumentation technology for measurement and analysis of metabolic quantities
[NASA-CR-114005] 09 p1340 N71-19776
- Metabolic imbalances and body hypohydration during food deprivation for 10 days
09 p1337 N71-20340
- Metabolic cost evaluation of self-locomotion in simulated lunar gravity using space suits and carts including weight load and surface effects
[NASA-CR-10697] 10 p1504 N71-20098
- Computer program for determining metabolism of radionuclides in animal tissue
[UCRL-50957] 10 p1502 N71-21640
- Automated microbial metabolism life detection experiments for astrobiological studies
[NASA-CR-110659] 14 p2206 N71-26380

SUBJECT INDEX

Tables and graphs of metabolic losses in whole body sweat determined by small skin area measurements
[NASA-CR-115031] 15 p2372 N71-27647

Metabolic effects of long duration exercise at moderate work loads including tables of heart rate, rectal temperature, minute volume, water balance, and respiratory quotient
[NASA-CR-115033] 15 p2372 N71-27784
Postflight metabolic and renal functional shifts in Soyuz spacecraft cosmonauts

Metabolic balance studies of two astronauts during 10 day preflight phase, Gemini 7 flight of 14 days, and 4 day postflight recovery phase

Total body exercise effect on metabolic, hematologic, and cardiovascular consequences of prolonged bed rest

Effects of prolonged bed rest on bone and calcium metabolism and mineral content loss of os calcis

Carbohydrate intolerance in human body during two weeks of bed rest

Metabolism of magnesium deficient *Escherichia coli* cells under aerobic and anaerobic conditions
[NRC-TT-1472] 22 p3545 N71-35255

Preflight and postflight analysis of effects of Gemini 7 mission on metabolic and endocrine systems

Effects of space flight on bone metabolism investigated by analyzing peptide hormones in urine

Breathing metabolic simulator design for test and evaluation of breathing and life support equipment
[NASA-CR-122948] 23 p3717 N71-36498

Water-salt metabolism during space flight and microanalysis of actively circulating blood volume

Water-salt metabolism under space flight conditions and body weight loss

Water-salt metabolism under space flight conditions and body weight loss
[NASA-TT-F-14029] 24 p3877 N71-37639

METAGALAXY
U. UNIVERSE

METAL AIR BATTERIES
NT ZINC-OXYGEN BATTERIES

Electrochemical degradation of platinum electrode in cadmium air battery by cadmium ion adsorption
[NASA-TM-X-2198] 07 p0977 N71-17883

Fabrication and evaluation of water activated zinc air electric battery

[AD-722802] 18 p2874 N71-31498

METAL ALLOYS
U. ALLOYS

METAL BONDING
NT METAL-METAL BONDING

Pulsed-current arc welding processes - reviews
[AD-712644] 02 p0238 N71-12112

Metallographic studies including electropolishing, explosive bonding, and crack propagation
[CONF-690954] 05 p0699 N71-14688

Plasma spraying gun for forming diffusion bonded metal or ceramic coatings on substrates
[NASA-CASE-XLE-01604-2] 05 p0695 N71-15610

Describing metal valve plate with encapsulated elastomeric body

[NASA-CASE-MSC-12116-1] 07 p1035 N71-17648

Apparatus for determining quality of bond between high density material and low density material

[NASA-CASE-MPS-13646] 07 p1038 N71-18132

Metal soldering with hydrazine monoperfluoro alkanoate for corrosion resistant coatings

[NASA-CASE-XNP-03459] 10 p1564 N71-21078

Leak resistant bonded elastomeric seal for secondary electrochemical cells

[NASA-CASE-XGS-02631] 11 p1678 N71-23006

Metal pattern bonding technique for cover glass attachment to silicon solar cells for space applications

[NASA-CASE-XLE-08369] 12 p1859 N71-23449

Infrared and Raman spectra of dinuclear compounds containing quadruply bonded pairs of molybdenum and rhenium atoms

[MIT-1965-01] 13 p2136 N71-25372

Thermal transducer for nondestructive testing of carbon-carbon composites and metal-nonmetal bonds
[BNWL-SA-3289] 15 p2387 N71-27777

Optimal strength and failure modes of ultrasonically bonded metals in air and vacuum

[UCRL-13486] 15 p2417 N71-27801

Experimental investigation on effect of spot welded or adhesively bonded thermocouples and fatigue behavior of two titanium alloys suitable for use in high speed airplanes

[NASA-TM-X-2288] 16 p2614 N71-28891

Forming and bonding metallic lining onto inside surface of metal tube

[NASA-TM-X-2347] 19 p3114 N71-32161

Evaluation of nondestructive tensile testing of chip and wire bonds in semiconductor devices

[NASA-CR-122643] 23 p3860 N71-37516

Microsampling technique used to study metallic bonding between liquid mercury and trace contaminants

[NASA-TM-X-2424] 24 p3941 N71-38111

Influence of diffusion during heating on bond strength between bimetal layers

[NLL-M-21017-1828-4P] 24 p3941 N71-38115

Atomic structure, bonding, and transport properties of various amorphous semiconductors

[AD-727179] 24 p3998 N71-38517

METAL CARBIDES
U. CARBIDES

METAL COATINGS
NT ALUMINUM COATINGS

NT GOLD COATINGS

NT NICKEL COATINGS

NT ZINC COATINGS

Gridded thick film metalization structure employed in multichip circuit fabrication

[AD-710614] 01 p0030 N71-10054

Irradiation - sulfoselenide of iridium, rhodium, ruthenium and platinum

[NASA-TT-F-13357] 01 p0047 N71-10351

Heat aging evaluation of common coated copper conductors

[RM-4883] 02 p0240 N71-11390

Manufacturing and advancement technology for turbine engine coatings

02 p0247 N71-11635

Principles of producing coatings of titanium, vanadium, and their alloys by molten salt electrolysis

[AD-712948] 05 p0386 N71-13284

Sublimed thermionic emitter and collector coatings

[CHE-4125-2] 06 p1276 N71-18167

Chemical aspects of reactor safety including release and transport of fission products, aerosol behavior, and chemical reactions of metal cladding

[HIMI-B-99] 06 p1235 N71-18213

Neutron irradiation effects on mixed oxide fuel elements of high temperature Experimental Breeder Reactor 2

[GA-10264] 08 p1238 N71-18357

Ultraviolet and charged particle irradiation effects on aluminum- and silver-coated fluorinated polyethylene propylene Teflon films

[NASA-TM-X-46939] 09 p1439 N71-20223

Joining aluminum to stainless steel by bonding aluminum coatings onto titanium coated stainless steel and brazing aluminum to aluminum/titanium coated steel

[NASA-CASE-MPS-07369] 09 p1395 N71-20443

Metal soldering with hydrazine monoperfluoro alkanoate for corrosion resistant coatings

[NASA-CASE-XNP-03459] 10 p1564 N71-21078

Electrochemical and corrosion behavior of corrosion resistant titanium base under platinum coating depending on pH

[NLL-TRANS-746-561-19022-401/1] 10 p1585 N71-21709

Metal wear inhibition at friction point using selective transfer effect

[AD-717827] 11 p1778 N71-22372

Oxidation and thermal fatigue evaluation of chromium titanium silicon diffusion coatings on aluminum alloy

[NRC-11732] 11 p1779 N71-22490

Low concentration alkaline solution treatment of aluminum with metal phosphate surface coatings to improve chemical bonding and reduce coating weight

[NASA-CASE-XLA-01995] 11 p1786 N71-23047

Effects of aluminum phosphate additions on thermal stability and adhesive properties of erosion resistant ZnO and Al₂O₃ coatings

[NASA-TT-F-13353] 12 p1928 N71-23813

Optical analysis of crushing mode of pyrocarbon coated fuel particles

[EUR-4501] 13 p2117 N71-24851

Technique for carburizing spherical powders of niobium, molybdenum, and tungsten in lamp black

[AD-719783] 13 p2099 N71-24877

Composition of technical information including metallurgy, electrical repair, fabrication techniques for coating, bonding and brazing, and electron beam welding

[NASA-SP-5925/01/1] 13 p2087 N71-25026

Evaluation of solar mirror surface materials by ATS 3 reflectometer

13 p2164 N71-25311

Metallizing parameters developed for sequential deposition of molybdenum, aluminum, and tantalum alloys as protective coatings for superalloys

[NASA-CR-72852] 13 p2096 N71-25503

Kinetic process of mutual diffusion between titanium with copper and other metals serving as galvanic coatings

[TT-70-59084] 14 p2269 N71-25666

Bibliography of refractory coatings used in industrial processing

[AD-720203] 14 p2280 N71-26288

High rate physical vapor deposition apparatus models for calculating temperature and thickness distribution, and properties of rare earth metals and alloys

[AD-722088] 16 p2609 N71-28433

Thermal deposition and electrical properties of silicon dioxide passivation layers on silicon wafers in oxygen and nitrogen dry atmospheres and effects of moisture and impurities

[AD-721377] 16 p2570 N71-28594

Organometallic compounds of niobium and tantalum useful for film deposition

[NASA-CASE-XNP-04823] 16 p2358 N71-28888

Silicide coating process and composition for protection of refractory metals from oxidation

[NASA-CASE-XLE-10910] 16 p2419 N71-29840

Ultrasonic measurements of metal coating thickness

[BNWL-SA-3279] 16 p2641 N71-29193

Electroless nickel coatings on aluminum using electrically heated water-cooled specimens in out-reactor flow

[OARL-TM-1297] 17 p2781 N71-32929

Metallic heat shielding materials for space shuttle thermal protection system

17 p2846 N71-29454

Creep analysis of metallic thermal protection system under simulated mission environments

17 p2847 N71-29455

Selection of Ag, Mo, W, and Nb as welded joint material in solar cell arrays and welding process improvement

[ESRO-CR-13] 17 p2786 N71-29498

Electrodeposited metal coatings applications in field of electrotechnology and electronics

18 p2936 N71-31212

Forming and bonding metallic lining onto inside surface of metal tube

[NASA-TM-X-2347] 19 p3114 N71-32161

Composition and spectral reflectance data of barium sulfate polyvinylidene chloride coating

[NASA-TM-X-45553] 19 p3120 N71-32320

Degradation of tantalum silicide coatings on tungsten, rhodium, molybdenum, niobium, titanium and zirconium substrates

20 p3336 N71-33927

Analysis of chemical and electrolytic processes for deposition of copper layers on stainless steel surfaces

[NLL-LTI-746-751-19022-401] 22 p3509 N71-35561

Analysis of shearing strength of vapor deposited tungsten coatings and dependence of shearing strength on microstructure and residual stresses

[NLL-LTI-746-752-19022-401] 22 p3655 N71-36066

Effectiveness of yttrium, lanthanum, and hafnium coatings for preventing oxidation embrittlement of chromium alloys at high temperatures

[NASA-TN-D-6528] 23 p3772 N71-34886

Arc jets tests of thorium dispersed nickel base alloys and cobalt base alloys for space shuttle metallic thermal protection systems

[NASA-TM-X-63892] 24 p3934 N71-38068

METAL COMBUSTION

Liquid and gaseous oxygen difluoride compatibility tests with plastic and metal crucibles and metal ignition temperature data

[NASA-CR-72357] 12 p1869 N71-23168

Factors affecting ignition of metals in high pressure oxygen systems

[NASA-TM-X-67201] 15 p2524 N71-27394

Analysis of metal combustion using isolated aluminum particles ignited by laser and burning in controlled mixture of oxygen and argon

20 p3366 N71-33769

METAL COMPOUNDS

Volume dependence of Grunisen parameter for metal halides

[ORO-3802-6] 01 p0112 N71-10759

Differential thermal analysis and antioxidant activity of nickel, zinc, lead, copper, and cadmium dialkylthiocarbamates

[FTD-HT-23-363-70] 10 p1513 N71-21230

Iodine adsorption properties of metal-loaded zeolites and applications to gas filtration beds in nuclear fuel processing plants

17 p2715 N71-29662

High pressure metallic and superconducting polymorphs of indium antimonide, cadmium tin diselenide, cadmium germanium diselenide, and cadmium arsenide

21 p3388 N71-34107

Corrosion inhibition in metal compounds of azole type

[AD-727853] 24 p3940 N71-38104

Tables of magnetic structures determined by neutron diffraction with emphasis on rhombohedral and hexagonal systems

[NPL-18845] 24 p3970 N71-38319

METAL CORROSION

U. CORROSION

METAL CRYSTALS

Surface sensitive mechanical behavior of nickel microcrystals

[AD-71677] 01 p0112 N71-10953

Dislocation mobility and density in metallic crystals

[CALT-767-F-3-14] 05 p0760 N71-15696

Magnetic properties of amorphous and crystalline Mn-P-C alloys

[CALT-822-15] 06 p0873 N71-16368

Influence of lattice vacancies and impurities on electrical resistivity of noble metals

[AD-714678] 06 p0937 N71-16700

Prismatic edge dislocation motion in copper crystals

[UCRL-19625] 07 p1093 N71-17660

- Isotropic elastic continuum model application to calculate energy and entropy of vacancy formation in metal crystals
[NASA-CR-116881] 08 p1281 N71-19207
- Plastic deformation of zone refined tungsten between 4.2 and 300 K - conference
[JAERI-MEMO-4124] 09 p1400 N71-20021
- Gas gun and piezoelectric gage for measuring high velocity deformations in shocked metal crystals
09 p1454 N71-20231
- Microplastic deformation in body centered cubic metals and solid solutions and analysis of intrinsic lattice resistance and interstitial impurities as dislocation motion controls
[CONF-700545-1] 10 p1581 N71-21439
- Schrodinger equation for examining energy levels in three dimensional metal crystals
[AD-717602] 11 p1816 N71-22162
- Plastic deformation of metal crystals and linearly temperature dependent parabolic stress-strain function for finite deformation of crystalline solids
[AD-717752] 11 p1778 N71-22354
- Growth parameters for zinc single crystals grown at controlled rate from melt
[IS-T-441] 15 p2505 N71-27250
- Laser-radiation effects on metals including damage thermodynamics, melting and cavity formation, vapor hydrodynamics, and damage product electromagnetic absorption
[JPRS-53241] 16 p2608 N71-28180
- Dynamic polarization of proton targets in neodymium doped lanthanum magnesium nitride crystals
[RHEILR-201] 16 p2653 N71-29021
- Metals and compounds crystallizing in cubic system determined by neutron diffraction - tables
[NP-18718-PT-1] 16 p2655 N71-29071
- Nonlinear continuum theory for analyzing crystal dislocation effects
[NBS-SP-317-VOL-2] 17 p2821 N71-29969
- Electron scattering by stacking faults in metal crystals
17 p2825 N71-29998
- Dynamic model for vibrating dislocation interaction with conduction electrons in metals
17 p2825 N71-30000
- Energy dissipation in electron interaction with moving crystal dislocations
17 p2826 N71-30002
- Computer programs for broadening X ray diffraction peaks of hexagonal close-packed metals
[AD-723191] 19 p3167 N71-31737
- Solidification of ingots noting crystal structure
19 p3112 N71-31914
- Diffraction of helium atoms from tungsten (112) crystal surface and measurement of time of flight distribution of deuterium molecules desorbed from nickel surfaces
[NASA-CR-121985] 22 p3634 N71-35900
- Continuum theory of dislocations for plastic deformation of metallic crystals
23 p3837 N71-37363

METAL CUTTING

- Selection of optimum metal cutting conditions for lathes
[REPT-3] 02 p0229 N71-11559
- Profilometer measurements on cut metal surfaces and digital evaluation of cutting profiles
04 p0602 N71-13694
- Edge durability data for machine tools in metal cutting processes
[TN-7] 10 p1563 N71-20910
- Maneuverable electron beam welder for welding and cutting thin metal sheets in space environment
13 p2087 N71-25239
- Five models for three dimensional chip curl, chip breaking, and chip control in metal cutting processes
17 p2754 N71-29365
- Plastic deformation in tool engagement and cutting of 70/30 brass
18 p2929 N71-31222
- Photographic technique for determining region and intensity of strain zone, changes in strain rate, and deformation at any point during metal cutting
[NRC-TT-1471] 22 p3588 N71-35548
- Numerical analysis of stresses and strains in cutting zone of hard-to-machine metals
[NRC-TT-1470] 22 p3588 N71-35549
- Electrodiffusion wear of tools and technology of gluing machine-tool devices
[AD-726804] 22 p3589 N71-35559

METAL DRAWING

- High pressure gas medium for extrusion of materials
02 p0229 N71-11446
- Finite element method for solving differential equations in boundary value problems of plastic flow in rod metal drawing
[REPT-12] 03 p0466 N71-13346
- Investment casting, metal drawing, longitudinal and spiral milling, and insulator pin designs in production engineering
[BDX-613-316] 16 p2613 N71-28751
- Effect of contact friction on widening and lengthening during force drawing and rolling
[AD-727164] 24 p3929 N71-38030

METAL FATIGUE

- Investigating low-cycle fatigue crack propagation in titanium alloys exposed to air and salt water environments
[AD-712056] 02 p0240 N71-11132
- Isothermal and adiabatic analyses of axial fatigue tests on metallic structures
[AD-712990] 03 p0465 N71-13198
- Metal fatigue studies at ultrasonic frequency using electron microscopes
[AD-712501] 04 p0528 N71-13949
- Crack formation in aluminum spoiler cables of F84 F aircraft
[TDCR-55807] 05 p0704 N71-15267
- Metal fatigue under combined stresses
05 p0781 N71-15615
- Stress concentration effect on notched fatigue behavior of structural steels
[GEAP-10170] 06 p0955 N71-16427
- Dynamic fracture in metal hollow cylinder under biaxial strain conditions
[AD-717092] 10 p1577 N71-21209
- Application of scanning electron microscopy to study of metal fatigue mechanisms
[AD-719927] 14 p2270 N71-25678
- Frequency distribution of acoustical and exoelectron emission from metal fatigue
[AD-720358] 14 p2347 N71-25932
- Lubricant rheology and chemistry effects on contact material fatigue
15 p2412 N71-26827
- Investigation and conclusions concerning metal fatigue in aircraft components as cause of civil aircraft accidents
15 p2368 N71-27429
- Temperature, ultrasonic, and macroscopic effects on metal fatigue
[AD-721729] 16 p2609 N71-28401
- Room temperature, high pressure hydrogen effects on metal strength
17 p2714 N71-29587
- Fatigue crack repair in notched steel sheets by various methods
[NLR-TR-70029-U] 17 p2766 N71-30248
- Fatigue properties of titanium and titanium alloys - effects of impurities, condition of surface, test cut in relation to forge, and test conditions on fatigue strength
[RAE-LIB-TRANS-1399] 17 p2767 N71-30380
- Fatigue properties of titanium and titanium alloys - determination of fatigue strength by plane bending, rotating bending, direct stress, and torsional loading modes of stress
[RAE-LIB-TRANS-1533] 17 p2767 N71-30381
- Fatigue properties of titanium and titanium alloys - fatigue strength of bolted, riveted, spot welded, and butt welded joints
[RAE-LIB-TRANS-1535] 17 p2767 N71-30382
- Fracture mechanics for predicting fatigue crack propagation and velocity in aluminum alloys
[AD-723285] 19 p3187 N71-31778

METAL FILMS

- Low temperature conductivity of gallium crystals and single crystal films
[AD-710651] 01 p0110 N71-10375
- Metallic film diffusion into metal or ceramic surfaces for boundary lubrication in aerospace environments
[NASA-CASE-XLE-01765] 01 p0073 N71-10772
- Oxide formation in evaporated thin tantalum films
[AD-711634] 02 p0241 N71-11436
- Critical temperatures of superconducting transition metal films on helium cooled substrates
[PB-192687] 02 p0287 N71-12122
- Two carrier model for electronic properties of single metallic band
[ORO-3651-5] 03 p0392 N71-12963
- Diffusion and structural changes in microcircuit interconnections subjected to heat treatment
[NASA-CR-115903] 05 p0656 N71-14976
- Optical properties of aluminum evaporated in ultrahigh vacuum between 500 and 1400 angstroms
07 p1041 N71-16942
- Optical properties of real metallic films
[AD-715296] 07 p1045 N71-17911
- Critical fluence calculations for ruby laser destructions of thin metal films
[UCRL-50927] 07 p1046 N71-18074
- Bismuth and lead surface coatings for gas bearings in aerospace engineering
[NASA-CASE-XGS-02011] 10 p1562 N71-20739
- Glass fiber tubing for cryogenic rocket propellant system
[NASA-CR-72797] 11 p1781 N71-21984
- Observation of void formation induced by electron irradiation in single crystal and bicrystal Au films and polycrystalline Al films
[NYO-4183-1] 11 p1780 N71-21984
- Theoretical and experimental determination of temperature changes in thin metal films during vapor deposition by substrate radiant heat flux, evaporant flux, and film temperature measurement
[COO-1198-775] 12 p1987 N71-23956

- Feasibility of producing thin metal and oxide-film capacitors with stable electrical properties in high temperature environments
[NASA-CR-72779] 12 p1891 N71-23963
- Metallic film diffusion for boundary lubrication in aerospace engineering
[NASA-CASE-XLE-10337] 12 p1929 N71-24046
- Radiation emitted when charged particles cross boundary between vacuum and metal
13 p2144 N71-25587
- Magnetic recording head composed of ferrite core coated with thin film of aluminum-iron-silicon alloy
[NASA-CASE-GSC-10097-1] 15 p2383 N71-27210
- Plastic deformation in microtomed thin films of copper and aluminum single crystals
16 p2666 N71-28776
- Infrared study of chemisorbed sulfur compounds on platinum and germanium films
18 p2997 N71-31257
- Tests with stainless steel in sliding contact with lead, indium, and tin coatings in liquid hydrogen to determine their lubricating capability
[NASA-TN-D-64553] 19 p3103 N71-32193
- Development of method for applying metal alloy film or coating to irregular shaped metal object
[NASA-CASE-LEW-11262-1] 21 p3437 N71-34455
- Development and characteristics of apparatus for depositing thin metallic films on nonmetallic materials
[NASA-CASE-LAR-10541-1] 21 p3437 N71-34456
- Vacuum evaporated films of Au, Pt, and Au-on-Pt on glass substrates after heat treatment
24 p3900 N71-37801
- Photofabrication of thin metal films and thin film stencils
[AD-727758] 24 p3998 N71-38530

METAL FINISHING

- NT ELECTROPOLISHING
- Effect of aging and finishing sequence on fatigue performance of maraging steel
[TN-2770] 08 p1220 N71-19271
- Selective plating of etched circuits without removing previous plating
[NASA-CASE-XGS-03120] 12 p1930 N71-24047
- Surface burnishing of machined metal using pressurized rolling ball technique
[UCRL-50864] 17 p2754 N71-29263

METAL FOILS

- Measuring preferred orientation of beryllium foils by X ray diffractometry and sodium iodide counters
[EGG-1183-1476] 03 p0420 N71-12639
- Chromium palladium silicon foil thermometer for low temperature measurements
[CALT-822-14] 06 p0862 N71-16708
- Xe-131 ion impact on gold crystal foils producing imperfection clusters
[COO-1053-14] 07 p1075 N71-17499
- Electroforming thin nickel foil electrodes of porous honeycomb structure to increase nickel-cadmium battery service life
[NASA-CR-117482] 10 p1495 N71-20818
- Development and characteristics of thermal radiation shielding of refractory metal foil used for induction furnace
[NASA-CASE-XLE-03432] 12 p2011 N71-24145
- Effect of oxidation degree on copper emittance for application to radiation shields or multifoil insulation systems at 700 to 1400 F
14 p2274 N71-26314
- Dislocation of Ni and Fe foils caused by electron irradiation
[CEA-CONF-1680] 15 p2489 N71-27800
- Determining fast and thermal neutron fluxes by copper and indium foil activation analysis
[RFP-1466] 17 p2794 N71-29631
- Evaluation of uniaxial and biaxial tensile properties of beryllium foil in rolling and transverse directions to establish yield and fracture foci
[BML-X-684] 22 p3593 N71-35539
- Ion transmission and radiation damage in carbon and gold thin foils
[GPRF-50] 22 p3638 N71-35929
- Specific energy loss and effective charge of fission products in metal absorbers using Cf-252 fission source and semiconductor detector
[KFK-1369] 24 p3975 N71-38364
- High temperature insulation materials for use under radiative thermal protection systems of shuttle orbiter vehicles
[NASA-CR-119950] 24 p4028 N71-38742

METAL FORGING

- U FORGING
- METAL FORMING
- U FORMING TECHNIQUES
- U METAL WORKING
- METAL FUELS
- Numerical computation of spectral radiation intensity of spherical particles such as in metal fuels
06 p0961 N71-16900

METAL HALIDES

- NT ALKALI HALIDES
- NT ALUMINUM CHLORIDES
- NT BARIUM FLUORIDES
- NT BERYLLIUM FLUORIDES
- NT CALCIUM CHLORIDES
- NT CALCIUM FLUORIDES

DEX

film
form-
35983
you in
48-66
7000
35587
core
7210
a of
8776
is on
1257
with
in to
2193
alley
44535
s for
rials
44556
sa-Pt
77801
film
8528
tigue
9271
mov-
24047
pres-
29263
Tolls
rs
2639
r for
16788
ucing
17495
reous
1 bat-
20818
radia-
duc-
24145
for
lation
26314
on ir-
27880
es by
29631
erties
ons to
335589
arbon
335929
ission
ianism
38364
under
rbiter
38742
s for
2000
tensi-
116800

NT. CESIUM FLUORIDES

Shock testing of metal switching pins with polycarbonate insulation and analysis of pin shock from explosive motors
BDX-613-2941 23 p3861 N71-3752

METAL MATRIX COMPOSITES

(RM-519) 23 p3764 N71-3683a
Stability of oxides in metal or metal alloy matrices
determined by interaction between sapphire flame
and nickel alloys 24 p3944 N71-3813b
(AD-72781) Mechanical properties of continuous composites of
boron fibers magnesium metal matrix 24 p3946 N71-3815f
METAL OXIDE SEMICONDUCTORS
Molybdenum and gold contact materials processing
for metal oxide semiconductor transistor circuits
01 p0031 N71-1014a

Different models for metal oxide transistors
[LAAS-PUBL-775] 18 p2899 N71-301-035

Mathematical models for high frequency characteristics of metal oxide semiconductor transistors
[LAAS-PUBL-776] 18 p2899 N71-30557

Mathematical model for abnormal current in MOS transistor substrates
[LAAS-PUBL-777] 18 p2900 N71-30625

Operational functions and electrical properties of metal oxide semiconductor structures
[REPT-1-028] 20 p3335 N71-33846

- Comparison of production technologies for silicon gate MOS and ISOPLANAR bipolar integrated circuits 23 p3735 N71-36626
- History and fundamentals of MOS logic circuit development 23 p3735 N71-36628
- Input/output devices and MOS-LSI circuits for desk calculator systems 23 p3735 N71-36629
- Application of logic functions to design of MOS circuits 23 p3735 N71-36630
- Computerized design of MOS circuits 23 p3736 N71-36634
- Fabrication of memory devices using MOS transistors 23 p3736 N71-36638

METAL OXIDES

- NT ALUMINUM OXIDES
- NT BARIUM OXIDES
- NT BERYLLIUM OXIDES
- NT CALCIUM OXIDES
- NT CESIUM OXIDES
- NT CHROMITES
- NT CHROMIUM OXIDES
- NT COBALT OXIDES
- NT COPPER OXIDES
- NT MAGNETITE
- NT HEMATITE
- NT IRON OXIDES
- NT LANTHANUM OXIDES
- NT LEAD OXIDES
- NT LITHIUM OXIDES
- NT MAGNESIUM OXIDES
- NT MANGANESE OXIDES
- NT MERCURY OXIDES
- NT MOLYBDENUM OXIDES
- NT NICKEL OXIDES
- NT NIOBIUM OXIDES
- NT PLUTONIUM OXIDES
- NT POTASSIUM OXIDES
- NT RUTILE
- NT SAPPHIRE
- NT SCHEELITE
- NT SILVER OXIDES
- NT TANTALUM OXIDES
- NT THORIUM OXIDES
- NT TIN OXIDES
- NT TITANIUM OXIDES
- NT TUNGSTEN OXIDES
- NT URANIUM OXIDES
- NT VANADIUM OXIDES
- NT YTTRIUM OXIDES
- NT ZINC OXIDES
- NT ZIRCONIUM OXIDES

Tight binding energy bands of perovskite type transition metal oxides [IS-T-371] 01 p0100 N71-10757

Roll forming ceramic strip from oxide powders [BM-RI-7463] 05 p0692 N71-14930

Metal oxide catalysts for air-oxygen electrodes in electrochemical fuel cells and zinc oxygen batteries [AD-715707] 08 p1146 N71-18463

Time-scan method of vapor luminescence excitation for spectrum analysis using neodymium-glass lasers for metal oxide vaporizing and electric arcs for further vapor heating and excitation [NASA-TT-F-13540] 12 p1934 N71-23791

Process for producing dispersion strengthened nickel with aluminum comprising metallic matrices embedded with oxides or other hyperfine compounds [NASA-CASE-XLE-06969] 12 p1940 N71-24142

Heat of formation, specific heat, entropy, and Gibbs free energy of some binary metal oxides [NPL-DCS-7] 13 p2184 N71-24372

Instability in MIS devices due to mobile positive ions in insulator layer localized near metal or silicon interface [AD-719283] 13 p2150 N71-24383

Plutonium 238 and curium 244 oxide compatibility tests with refractory metal alloys for use in Pioneer heat source [MDC-62026] 16 p2612 N71-28749

Metal oxide infrared emission, and detection of vibrationally excited metal oxide molecules by laser induced fluorescence [AD-723819] 18 p2888 N71-31597

Inversion barrier energies in NH_3 and F_2 and calculations of electronic properties in TiO_2 (minus x) clusters 21 p3491 N71-34866

METAL PARTICLES

- NT METAL POWDER
- NT POWDERED ALUMINUM
- Uranium distribution and uranium diffusion through pyrocarbon coating in UO_2 coated particles [EUR-4530-E] 08 p1235 N71-18214
- Effects of constraints on kinetic reactions of copper particles during sintering 13 p2096 N71-25097
- Cermet for nuclear fuel constructed by pressing metal coated ceramic particles in die at temperature to

cause bonding of metal coatings, and tested for thermal stability [NASA-CASE-LEW-10219-1] 16 p2618 N71-28729

Radiative heat transfer in plumes behind engine fuelled with solid rocket propellants containing aluminum oxide particles [ONERA-P-133] 17 p2829 N71-25392

METAL PLATES

Effects of mechanical straightening and flame straightening on properties of steel plates [AD-710521] 01 p0057 N71-10032

Computer program for harmonic analysis of curved folded plate structures using finite element method [PB-193535] 03 p0131 N71-10885

Fracture resistance of Ti-6Al-2Zr and Ti-6Al-4V alloys in 3 inch thick plates [AD-711586] 02 p0244 N71-11738

Stress concentration around hole in bent plates [AD-712109] 02 p0303 N71-12099

Hole growth in thin plates perforated by hypervelocity pellets 03 p0460 N71-12956

Load velocity effect on shock pressure deformation of steel plate [ISL-T-4069] 03 p0461 N71-12986

Dynamic tear test for measuring fracture toughness [AD-712494] 03 p0393 N71-13153

Finite element stress analysis of crack in bi-material plate [AD-713593] 05 p0775 N71-14598

Fabrication and optimization of weld joints in 12-5-3 maraging steel plates [NASA-CR-115887] 05 p0691 N71-14818

Crack growth rate dependence on stress intensity factor in hot rolled banded steel plate [AD-713536] 05 p0704 N71-15331

Development of large area micrometeoroid impact detector panels [NASA-CASE-XLA-05906] 06 p0950 N71-16221

Fracture, fatigue, and crack propagation of aluminum alloy sheet and flat plates [AD-714019] 06 p0872 N71-16330

Analyzing sound transmission through clamped circular plate set in infinite rigid wall exposed to dense acoustic medium and excited by obliquely incident plane wave [AD-714281] 06 p0906 N71-16406

Ballistic properties of solidified armor plate steel [AD-714294] 06 p0874 N71-16579

Lattice theory of face-shear and thickness-twist waves in body centered cubic crystal plates [AD-715644] 08 p1277 N71-18380

Steel plate fatigue life tests noting plastic coating, air sea water immersion and lubricant influence [CRIF-MT-64] 08 p1214 N71-18584

Holographic interferometric methods applied to vibration, flutter, and transient analysis of thin metallic panels [NASA-CR-103053] 08 p1210 N71-18962

Mathematical model to describe normal projectile penetration of metallic targets [AD-716001] 09 p1398 N71-19711

Czochralski method for growing aluminum oxide single crystals in plate form for transparent armor applications [AD-716622] 09 p1405 N71-19824

Electron photon cascade calculations for photon beam energy absorption in beryllium and aluminum slabs [ORNL-4631] 09 p1436 N71-20042

Finite element analysis of mechanical properties of thin walled shells with arbitrary geometry and boundary conditions [AD-716561] 09 p1478 N71-20103

Tensile and impact properties of thick-section plate and weldments used for pressure vessels [ORNL-TM-3211] 12 p2003 N71-23138

Dilatational and shear surface waves produced by small explosions in aluminum block [AD-717985] 12 p1939 N71-24012

Flight service effects on residual tensile properties of C-130 aircraft center wing plate section [NASA-CR-111828] 12 p1857 N71-24021

Constant load amplitude tests and program tests of lap joints and strap joints for riveted Alclad material under bending stress [NLR-TR-69116U] 12 p2008 N71-24282

Structural analysis of two plates reinforced by X-braced trusses and subjected to symmetrical and antisymmetrical loadings 13 p2180 N71-24814

Methods for designing strong composite, anisotropic, and sandwich plates and shells [AD-719777] 13 p2182 N71-25127

Simulation of secondary meteoroid flux by impact of single projectiles on thin sheet aluminum and nylon cloth to define penetration mechanics of spacecraft structures and space suit material [NASA-TN-D-6324] 13 p2096 N71-25203

Determination of conditions leading to fracture arrest by circular hole ahead of propagating crack by dynamic photoelasticity technique [AD-719934] 13 p2183 N71-25398

Fracture mechanics and anisotropy of fatigue crack propagation in hot rolled banded steel plate 13 p2183 N71-25444

Static fracture behavior of surface flawed aluminum plate [AD-720392] 13 p2424 N71-27409

Electrokinetic potential and electrophoretic deposition of polyethylene on Pt, Ni, Cu, Fe, and Al plates at 600 V in nitromethane, dimethyl formamide, and aliphatic alcohols [NLL-LTI-746-331-9022.401/] 16 p2609 N71-28395

Chemical analysis of active materials of nickel cadmium battery plates 16 p2538 N71-28061

Nondestructive measurement of OAO battery plate weights and capacities 16 p2539 N71-28064

Residual stresses in rolled steel plates by etching [VTH-155] 17 p2762 N71-29435

Cosmic ray data from cloud and ionization chambers, and carbon and iron plates [AD-721714] 17 p2840 N71-29472

Investigation of impact of blunt body against flexible plate where high tensile impact wave velocity exceeds speed of sound in material [AD-722281] 17 p2851 N71-29532

Analysis of creep rupture properties of metals and application to predicting useful life and occurrence of damage [UCRL-13489] 17 p2851 N71-29541

Monte Carlo method for neutron and photon trajectory determination through metal plate [BMVG-FBWT-71-9] 19 p3144 N71-31702

Ultrasonic surface waves for detecting near-surface flaws in nondestructive testing of metal plates [AD-723526] 19 p3187 N71-31940

Thermal conductivity and plastic deformation of nuclear reactor rods and metal plates melting under internal heat generation [AD-723199] 19 p3188 N71-31980

Dynamic structural analysis of clamped skew plate buckling under various loads [AE-296-5] 20 p3360 N71-33822

Impregnation of nickel plaque to form nickel cadmium battery plates for aerospace applications [NASA-CR-121746] 21 p3378 N71-34038

Metallurgical design in higher yield strength structural steels [PB-199293] 22 p3593 N71-35586

Effects of combined loading on buckling of simply supported skew plates based on Rayleigh-Ritz method [AE-299-S-PT-2] 22 p3689 N71-36308

Process variables associated with positive and negative plate impregnation/polarization and linear multiple regression analysis of fractional factorial design experiment data [NASA-CR-122289] 24 p3875 N71-37623

Improved techniques for production of rolled steel plates [AD-727866] 24 p3930 N71-38039

Effect of rate of deformation on mechanical properties of metals and propagation of stress and strain waves in metal [AD-727203] 24 p3938 N71-38097

Ultrasonic tests and specifications of steel plate examined for laminations and inclusions [NLL-CE-TRANS-5536-19022.09] 24 p3941 N71-38116

Problems of high temperature annealing of PTFE/LIP discs used for ionizing radiation dosimetry [AEW-M-991] 24 p3973 N71-38344

Estimates for stresses and strains and their derivatives for thin plates [AD-727604] 24 p4026 N71-38723

METAL POLISHING

NT ELECTROPOLISHING

Polished metals exposed to hypervelocity impact by micrometer size projectiles to determine bombardment effect on spectral reflectance [NASA-TM-X-52981] 09 p1399 N71-19816

METAL POWDER

NT POWDERED ALUMINUM

Titanium powder metallurgy technology [AD-711811] 01 p0608 N71-10854

Spectrophotometric determination of calcium in zirconium and titanium powders using murexide [AD-711883] 02 p0172 N71-11214

Synthesis, characterization, and fabrication of uranium nitride powders [NASA-CR-72764] 03 p0414 N71-12810

Sintering kinetics of uranium dioxide using three different types of powder [LIB/TRANS-267] 04 p0546 N71-13606

Quantitative analysis of micrometer-size uranium alloy powders using electron microprobe X ray analyzer [V-1745] 04 p0591 N71-14380

Production of refractory bodies with controlled porosity by pressing and heating mixtures of refractory and inert metal powders [NASA-CASE-LEW-10393-1] 05 p0705 N71-15468

Computer program for indexing X ray metal powder patterns [NLCO-1066] 08 p1263 N71-18941

SUBJECT INDEX

Test equipment and techniques for improving iron/potassium perchlorate heat powder 11 p1677 N71-22480 [SC-R-70-6137]

Electrode sealing and insulation for fuel cells containing caustic liquid electrolytes using powdered plastic and metal 11 p1772 N71-23022 [NASA-CASE-XMS-01625]

Technique for carburizing spherical powders of aluminum, molybdenum, and tungsten in lamp black [AD-719783] 13 p2099 N71-24877

Apparatus for mechanically dispersing ultrafine metal powders subjected to shock waves 13 p2094 N71-24911 [NASA-CASE-XLB-04946]

Chemical analysis of active materials of nickel cadmium battery plates 16 p2538 N71-28661

Effectiveness of superimposed vibrating forces in reducing die wall friction during powdered metal compaction [SRO-475-10] 16 p2614 N71-28898

Electrodeposition and codeposition of metal powder particles dispersed in electrolytic solutions [NLL-LT-746-622-19022-401] 16 p2539 N71-29169

Electrowin molybdenum powders compared with hydrogen reduced powder and sheet, and results indicating yield strength varied with carbon content, heat treatment, and test temperature [BM-RF-7455] 17 p2761 N71-29276

Sliding properties of iron-base metallic powder lubricants impregnated with intermetallic alloys 18 p2928 N71-30911

Steam pyrohydrolysis treatment for purifying boron and potassium fluoroborate powders [Y-1756] 21 p3444 N71-34511

Method powder compaction calculations using kinetic constants for entire sintering period including initial heating and isothermal soaking [NLL-LT-746-743-19022-401] 22 p3597 N71-35614

Properties of ZnO powder and intergranular region between particles studied using dielectric relaxation 22 p3660 N71-36100

Deformation mechanisms in compacting metal powders [AD-727851] 24 p3948 N71-38105

METAL PROPELLANTS

Nondestructive testing of squip, low pressure combustion of metal propellants, and laser beam diffraction 10 p1637 N71-21355

Injection, mixing, and chemical reactions of metalized slurry fuels in high speed air stream to determine ignition and combustion properties [AD-726639] 22 p3662 N71-36110

METAL SHEETS

Automatic test equipment for hysteresis and eddy current energy dissipation in steel metal sheets [NPL-MEMO-5] 03 p0383 N71-13363

Porosity formation and feeding for sand cast aluminum alloy sheets 10 p1576 N71-21012

Deformation behavior of alloys and stress-strain relationships for ductile metals [RAE-LIB-TRANS-1491] 10 p1582 N71-21519

Friction mechanics theory used to determine effects of crack dimensions and material properties on fracture stresses for thin metal sections with through and part-through cracks [NASA-TN-D-4305] 12 p2007 N71-24240

Stress intensity factor calculated for cracked sheet with riveted and uniformly spaced stringers [NASA-TR-R-358] 14 p2273 N71-23934

Foreign testing apparatus with light shield and infrared reflector for high temperature evaluation of loaded sheet samples [NASA-CASE-XLA-01782] 14 p2255 N71-26136

High quality weld of cladding during hot rolling of VAD-23 alloy sheets [AD-721034] 15 p2416 N71-27335

Electrowin molybdenum powders compared with hydrogen reduced powder and sheet, and results indicating yield strength varied with carbon content, heat treatment, and test temperature [BM-RF-7455] 17 p2761 N71-29276

Foreign crack repair in notched steel sheets by various methods [NLR-TR-70025-U] 17 p2766 N71-30248

Analysis of crack propagation in Alclad steel specimens under two types of random loading based on gust spectrum [NLR-TR-71014-U] 17 p2855 N71-30303

Processes for making metal sheets or plaques with parallel pores of uniform size [NASA-CASE-GSC-10984-1] 21 p3433 N71-34427

Development of technique for diffusion welding of TD-NiCr metal sheets and analysis of mechanical properties [NASA-TN-D-6493] 21 p3439 N71-34470

Analysis of thin viscoelastic sheets and thin metallic layers as damping additions for this simply supported square plates [AD-727027] 22 p3691 N71-36322

METAL SHELLS

Approximation for electric field in toroidal metallic chamber with sections [NPL-18505] 13 p2453 N71-26467

METAL SPINNING

Apparatus and method for spin forming tubular elbows with high strength, uniform thickness, and close tolerances [NASA-CASE-XMF-01083] 11 p1770 N71-22723

METAL SPRAYING

Spraying process for producing thin titanium dioxide ceramic film capacitors 12 p1891 N71-24026

Application of flame metal spraying to bonding magnesium alloy cladding to uranium nuclear fuel elements [CEA-CONF-1625] 15 p2448 N71-27339

METAL STRIPS

Metal strip mounting arrangement for solar cell arrays on spacecraft [NASA-CASE-XGS-01475] 02 p0149 N71-11058

Roll forming ceramic strip from oxide powders [BM-RF-7463] 05 p0692 N71-14930

Forming tubes from long thin flat metal strips 08 p1206 N71-18579

Tin diffusion for producing superconducting niobium stannide ribbons [LNF-70/18] 15 p2509 N71-27907

METAL SURFACES

Destructive effects on metal surfaces in diesel engines due to liquid cavitation corrosion caused by opposite oscillating plates 02 p0231 N71-11583

Destruction effects on metal surfaces in diesel engines due to liquid cavitation corrosion caused by opposite oscillating plates 02 p0231 N71-11584

Application of welding methods and treatment of metal surfaces to improve corrosion resistance and dimensional build up in engine production 02 p0233 N71-11631

Passivation of metal aircraft surfaces [AD-711950] 02 p0243 N71-11670

Investigating spatial distribution of condensed matter ejected from metals subjected to laser radiation [NASA-TT-F-13338] 02 p0239 N71-12049

Vibratory cavitation for metal and superalloy etching in distilled water [NASA-TM-X-52929] 03 p0392 N71-12961

Computerized simulation of radiation damage processes in metals [JUL-453-MA] 04 p0527 N71-13641

Profilometer measurements on cut metal surfaces and digital evaluation of cutting profiles 04 p0602 N71-13694

Melting vacancies and self diffusion of metals [FEI-164] 04 p0527 N71-13696

Electromagnetic detection of absorbing field reflected from metallic surface 04 p0492 N71-13709

Wettability of microfog streams of high temperature lubricants on static metal surface [NASA-CR-72743] 05 p0691 N71-14817

Optical pyrometry for measuring true temperatures of polished metal surfaces by polarized radiation distribution [JPRS-51831] 05 p0685 N71-14940

Phenomena taking place in surface layers of metal of engine components during friction [AD-714063] 06 p0941 N71-16305

Determining quantity of oxygen and carbon retained by adsorption or chemical reaction on surface of high purity metals [LIB/TRANS-299] 07 p1070 N71-17030

Electromagnetic generation of ultrasound in metallic surface [NYO-2150-43] 07 p1043 N71-17633

Mass transport and atomic structure near metal surfaces [AD-715291] 08 p1277 N71-18411

Interfacial behavior of corrosion inhibitors on iron surfaces [AD-717030] 10 p1579 N71-21289

Physical mechanism and charge states resulting from collision of ionized gas particles with metallic surfaces [AD-717063] 10 p1617 N71-21322

Croep mechanisms and structure dependence of high temperature deformation of metals and alloys [SU-326-P-17-X-1] 10 p1584 N71-21616

Magnetic properties at metal surfaces including neutron mirror measurements, neutron scattering of FeCO₃, and low temperature measurements [ORO-3674-4] 11 p1779 N71-22510

Adsorbed thin gas film effects on thermal conductances of contacting metallic smooth surfaces 12 p1894 N71-24150

Nickel plating onto etched aluminum castings [NASA-CASE-XNP-04148] 13 p2093 N71-24830

High thermal emittance black surface coatings and process for applying to metal and metal alloy surfaces used in radiative cooling of spacecraft [NASA-CASE-XLA-06199] 13 p2086 N71-24875

METAL WORKING

Method for treating metal surfaces to prevent secondary electron transmission [NASA-CASE-XNP-09469] 13 p2142 N71-23555

Surface and environmental effects on plastic flow and fracture of metals and alloys [AD-720405] 14 p2272 N71-23873

Method of forming ceramic to metal seals impervious to gaseous and liquid mercury at high temperature [NASA-CASE-XNP-01263-2] 14 p2263 N71-26312

Structure of electric double layer at solid metal solution interfaces [AD-721718] 16 p2557 N71-28353

Electrophysics and chemical reactions of metal surfaces including mechanical properties and crystal structures [AD-722013] 16 p2611 N71-28505

Anodizing method for providing metal surfaces with temperature reducing coatings against flames [NASA-CASE-XLE-06035] 16 p2693 N71-29151

Electron probe microanalysis and photomicrographic studies on metal surfaces eroded by spark discharges 17 p2765 N71-29084

Interaction of Q switched ruby laser beams on metal surfaces noting electromagnetic absorption and electron emission [REPT-1011/71] 18 p2931 N71-30602

Assessment of cost of air pollution corrosion damage to metal systems and structures in US, both presently and by 1980 [PB-196453] 20 p3283 N71-33122

Atom recombination and methane production from atomic hydrogen reactions on clean metal surfaces 21 p3442 N71-34494

Feasibility of using elastic deformation to predict heat transfer rates across joined smooth-metal surfaces under high vacuum conditions and light loads [NASA-TM-X-2385] 22 p3696 N71-36361

Additive effects on boundary lubricant-metal surface interactions during friction process [AD-727885] 24 p3929 N71-38037

METAL VAPORS

NT MERCURY VAPOR

NT SODIUM VAPOR

Monte Carlo calculations of sticking coefficient using multiple collision method for metal vapors [NASA-TT-F-12690] 01 p0098 N71-10680

Laboratory simulation of vaporization of metal clouds in upper atmosphere 03 p0665 N71-15487

Matrix isolation infrared spectra of thallous halide and thallous oxide vapors [IS-T-407] 06 p0882 N71-16782

Film condensation and heat transfer of low pressure metal vapor on flat surfaces [NASA-CR-117429] 10 p1661 N71-20860

Condensation and evaporation coefficients for liquid metal vapors and relation to heat and mass transfer rates [COO-2832-4] 11 p1780 N71-22661

Barium-copper oxide/canister barium vapor release system for geostationary measurements [NASA-CR-1739] 18 p2888 N71-31424

Thin film, light detecting photovoltaic cell fabricated by metal vapor deposition on quartz [NASA-CASE-MPO-11432] 20 p3273 N71-33322

Analysis of emission spectra of metal vapors obtained by laser irradiation [NASA-TT-F-13967] 22 p3765 N71-36841

METAL WHISKER REINFORCEMENT

U WHISKER COMPOSITES

METAL WORKING

NT CLADDING

NT EXPLOSIVE FORMING

NT FORGING

NT HYDROFORMING

NT MAGNETIC FORMING

NT METAL DRAWING

NT METAL SPINNING

NT SEIZING (SHARPING)

Effects of mechanical straightening and flame straightening on properties of steel plates [AD-710521] 01 p0057 N71-10032

Substructural hardening and gas extrusion of metals [JPRS-51624] 02 p0241 N71-11444

Elastic anisotropy effects on cold drawing of metals [ONERA-NT-158] 02 p0230 N71-11560

Development of space manufacturing techniques for orbital workshops [NASA-TM-X-64480] 02 p0234 N71-11701

Low gravity manufacturing of metals and ceramics in space laboratories 02 p0234 N71-11706

Facility for material processing in space experiments during earth orbital mission 02 p0199 N71-11714

Metals melting and exothermal heating experiments for component manufacturing in orbital workshop 02 p0235 N71-11715

Analysis of friction and lubrication in metal working processes [AD-713033] 03 p0383 N71-13169

Niobium zirconium alloy cracking during fabrication of Rankine cycle system components 03 p0395 N71-13909

Factors affecting efficiency of lubricants used for drop forging 05 p6709 N71-15269

Method and apparatus for shaping and joining large diameter metal tubes using magnetomotive forces [NASA-CASE-XMF-05114] 07 p1035 N71-17650
Description of techniques used in design of cold rolling mills for optimum operation [AD-717401] 11 p1767 N71-22137

Description of protective device for providing safe operating conditions around work piece in machine or metal working tool [NASA-CASE-XLE-01092] 11 p1771 N71-22797

Description of portable milling tool for milling tube or pipe ends to desired shape and thickness [NASA-CASE-XMF-03511] 11 p1771 N71-22799

Development and characteristics of frusto-conical die nib for extrusion of refractory metals [NASA-CASE-XLE-06773] 12 p1928 N71-23817

Compilation of technology utilization articles on subjects of cutting, shaping, and forming of materials and application to industrial methods [NASA-SP-5922/01] 12 p1931 N71-24171

Research and development technology in titanium alloys including phase transformations, metal working methods, and mechanical properties [AD-719487] 13 p2091 N71-24407

Portable magnetomotive hammer for metal working [NASA-CASE-XMF-03793] 13 p2085 N71-24853

Method and apparatus for portable high precision magnetomotive bulging, constricting, and joining of large diameter metal tubes [NASA-CASE-XMF-05114-3] 13 p2086 N71-24865

Alloy compositions and metal working processes for roller bearing technology 15 p2413 N71-26833

Bibliography on industrial arc welding of metals [AD-722765] 18 p2927 N71-30731

Technique of surface carburization prior to extrusion reported for two C-Mn-Si steels [PB-197129] 18 p2927 N71-30744

Magnetic crystallographic orientation produced in ferrites by hot working [AD-723458] 18 p2931 N71-31580

Forming and bonding metallic lining onto inside surface of metal tube 19 p3114 N71-32161

Large diameter T-111 tubing processed from seamless and welded tube shells [NASA-CR-72869] 20 p3278 N71-33004

Metallurgical design in higher yield strength structural steels [PB-199293] 22 p3593 N71-35586

Application of plasma cutting method for flame cutting of aluminum, copper, and stainless steel [NLL-OA-TRANS-1108-6196.3] 23 p3764 N71-36839

Analysis of structural state of mono and polycrystals of aluminum and copper alloys after deformation [AD-726731] 23 p3770 N71-36874

Development of ferrous metallurgy and advanced methods of metal production 23 p3772 N71-36887

Development of technique for boronizing machine and tool parts in powdered mixtures [AD-727937] 24 p3929 N71-38036

Improved techniques for production of rolled steel plates [AD-727866] 24 p3930 N71-38039

Development of methods for improving ductility of beryllium and techniques for deforming ingot beryllium into sheet form [AD-727747] 24 p3938 N71-38094

METAL-GAS SYSTEMS
Multiple regression analysis technique for parameters in pressurized inert gas metal arc [RFP-1515] 07 p1035 N71-17634

Metal-oxygen and metal-nitrogen systems for use as reduced pressure standards using Sieverts apparatus [NASA-CR-111862] 10 p1584 N71-21606

METAL-METAL BONDING
Thermal cycling effects on integrity of refractory stainless steel tubular coextruded joint [NASA-TM-X-2118] 01 p0067 N71-10454

Stress distributions in metal due to stress concentration around bonded joints [UTIAS-TR-138] 02 p0228 N71-11433

High temperature soft soldering system using sacrificial nickel coating for zinc solder spreading on copper, copper alloy, and steel substrates [TPR-39] 06 p0862 N71-15805

Dynamic parameters for obtaining wavy bonded interfaces between metals with explosive welding [AD-714221] 06 p0865 N71-16360

Bin/epoxy alkyl/carborane adhesives with high temperature stability for steel-on-steel bonding [NASA-CR-114837] 06 p0882 N71-16730

Joining aluminum to stainless steel by bonding aluminum coatings onto titanium coated stainless steel and brazing aluminum to aluminum/titanium coated steel [NASA-CASE-MFS-07369] 09 p1939 N71-20443

Method for honeycomb panel bonding by thermosetting film adhesive with electrical heat means [NASA-CASE-XMF-01402] 10 p1591 N71-21651

Aluminum contacting technique for lead telluride thermoelectric converter module [NASA-CR-118637] 14 p2254 N71-25926

Adhesive bond shear strength of aluminum at constant strain rate [AD-722238] 16 p2600 N71-28185

Analysis of friction bonding process with metal couples under high axial pressures 18 p2928 N71-31038

Developments and advancements in welding techniques and procedures in USSR [JPSS-53493] 18 p2930 N71-31385

Development and characteristics of high temperature soldering system for use with copper, copper alloys, and low carbon steel [PB-196675] 20 p3277 N71-32849

Analysis of bonded metal surfaces used in manufacture of helicopter components [AD-724663] 20 p3283 N71-32953

Determination of adhesion properties of platinum and gold in contact with tungsten and iridium using field ion microscopy techniques [NASA-TN-D-4492] 24 p3930 N71-38041

METALLIC PLASMAS
NT CESIUM PLASMA
Drift oscillations in collisionless alkali metal Q device plasma 18 p2993 N71-31143

Measurements of radiation emission properties of uranium plasma 20 p3331 N71-33648

Analysis of thermal emission spectrum from uranium plasma in propellant region of gas core reactor 20 p3305 N71-33653

Temperature distribution and radiation flux measurements in uranium plasma reactor with reflecting walls 20 p3305 N71-33654

METALLIZING
Scanning electron microscope as semiconductor production line quality control tool to determine integrity of metallization [NASA-TM-X-66620] 07 p1028 N71-17309

Beam lead technology for microcircuit interconnections with applications to metallization, passivation, and bonding [NASA-CR-111838] 09 p1362 N71-19422

Adhesive and coating material formulations and manufacturing processes for lightweight low-permeability braces for use in high altitude decelerators [NASA-CR-111964] 22 p3539 N71-35208

METALLOGRAPHY
Scanning electron microscope operation and micrographs of microstructure and fracture in metals [M6A/37/69] 02 p0224 N71-11527

Solid state physics, metallurgy, solid mechanics, geology, and chemistry [AD-712453] 03 p0445 N71-13381

Metallurgical studies including electropolishing, explosive bonding, and crack propagation [CONF-690954] 05 p0699 N71-14688

Technology review on rhenium alloys [TT-69-55081] 05 p0700 N71-14763

Electron optical metallographic instruments including electron microprobe X ray analyzer, scanning electron microscope, and transmission electron microscope [NASA-TM-X-52949] 05 p0682 N71-14798

Metallurgical application of solvent extraction [BM-IC-8502] 05 p0706 N71-15654

Metallurgical analysis of heater rods, cladding, and metal-water reactions [WCAP-7444] 06 p0897 N71-15874

Development of method for etching copper [NASA-CASE-XGS-06306] 06 p0871 N71-16044

Metallurgical and ductility effects of lithium on tungsten-lined titanium alloy clad uranium mononitride cylinders after long term exposure [NASA-TM-X-52998] 10 p1602 N71-30948

Nonmetallic impurities in Invar and super-Invar iron alloys [NLL-TRANS-746-633-19022.401] 10 p1579 N71-21266

Creep mechanisms and structure dependence of high temperature deformation of metals and alloys [SU-326-P-17-X-1] 10 p1584 N71-21616

X ray analysis, metallographic, and electron microprobe analyses of reaction-diffusion in metal-nonmetal binary and multicomponent systems of Ti/SiC and Ti-6Al-4V/SiC 10 p1586 N71-21820

Metallurgical determination of microcrack emergence in martensite of Fe-Ni-C system [NLL-TRANS-746-537-19022.401] 10 p1586 N71-21840

Metallurgy and preparation of titanium materials for chlorination [AD-717831] 11 p1777 N71-22238

Development and characteristics of refractory metal alloy for high temperature environment applications [AD-718473] 12 p1939 N71-24093

Techniques for dimensional measurement, and chemical and metallographic microanalysis of irradiated nuclear fuel specimens 13 p2128 N71-24532

Microgravimetry and metallography used to determine oxidation mechanism of pure and alloyed zirconium by oxygen and steam [EUR-4507-F] 13 p2093 N71-24872

Metallic surface interaction - ion microscope adsorption and mass spectrometry desorption analyses, and field emitted electron energy distribution measurements [COO-1383-11] 13 p2041 N71-25191

Martensitic transformations in low carbon austenitic chrome-nickel steels examined by X ray, metallographic, magnetic, and dilatometric techniques [ORNL-TR-2423] 13 p2426 N71-27802

Hot-pressed alumina with molybdenum or molybdenum oxide additives characterized by metallographic and X ray diffraction analyses [AD-722239] 16 p2611 N71-28552

Metallographic preparation of LMFBFR prototype fuels [WHAN-SA-14] 16 p2632 N71-28640

Sol-gel processes in U/PuO₂ fuel element preparation and metallographic and gas analyses of reactor materials [BAW-3714-19] 17 p2781 N71-29231

Metallographic and plastic moduli measurements on two phase isotropic microstructures 17 p2765 N71-29083

Metallographic examination of container material for C-244/203 [ORNL-4663] 17 p2785 N71-30206

Metallographical study of small strain amplitudes in titanium fatigue mechanism at ultrasonic frequency [AD-723533] 18 p2939 N71-31594

Investigation of controlled electromagnetic fields applied to Type-304 stainless steel melts during solidification including grain boundary and metallographic studies [SU-326-P-29-X-1] 19 p3114 N71-32228

Electron metallography of ferrous martensite substructures [UCRL-19648] 21 p3438 N71-34465

Measurement of electrical resistance, electron microscopy, and low temperature heat capacity of inert gases in metals [COO-1799-6] 21 p3440 N71-34476

Flux pinning mechanisms in type-2 semiconductors and specific heat measurements on annealed and deformed pure niobium samples [NASA-CR-121867] 21 p3496 N71-34907

Fabrication and properties of hot-pressed polycrystalline magnesium oxide containing anion impurities [NASA-CR-121937] 22 p3587 N71-35545

X ray diffraction and metallographic phase study of UO₂-DY2O₃ [JAERI-1203] 22 p3620 N71-35789

Effect of heat treatment on physical properties of steels with various amounts of nickel, cobalt, and molybdenum [NLL-TRANS-746-807-19022.401] 23 p3774 N71-36897

Application of unidirectional solidification technique for reinforcement of metallic or ceramic materials [NLL-TL-746-703] 23 p3774 N71-36900

Phase diagram for vanadium-vanadium oxide system based on melting points and thermal dilatometric, metallographic, and X ray analyses [IST-448] 24 p3935 N71-38074

Corrosion tests of austenitic Cr-Ni steel and nickel alloys in steam loop at 620 C and 1 atm pressure for 5000 hours, and behavior of cold-formed material surfaces [KFK-1301] 24 p3933 N71-38077

METALLOIDS
NT ANTIMONY
NT BORON
NT BORON ISOTOPES
NT BORON 10
NT GERMANIUM
NT GERMANIUM ISOTOPES
NT POLONIUM ISOTOPES
NT SILICON
NT SILICON ISOTOPES
NT TELLURIUM
NT TELLURIUM ISOTOPES

Characteristics of particle interactions with surfaces of semiconductors and semimetals [AD-717960] 12 p1904 N71-23272

Strong electron-phonon-electron interaction term in study of excitonic phase in semimetals and semiconductors 17 p2828 N71-30255

METALLOID ORGANIC COMPOUNDS
U ORGANOMETALLIC COMPOUNDS
METALLURGY

Phase studies of molybdenum-chromium-vanadium alloys by X ray diffraction analysis [AD-713801] 03 p0393 N71-13130

Application of laser radiation to removal of material from metals [NASA-TT-F-11912] 04 p0525 N71-14070

Chemical properties and compatibility of molybdenum base alloys [ORNL-TM-2724] 04 p0532 N71-14344

SUBJECT INDEX

Automatic colorimetric determination of nitrogen in low weight steel samples 05 p0639 N71-14710
[SNWIC-71/1]
Technological review on fiber metallurgy including whisker composites 05 p0700 N71-14762
[AD-713648]
Production engineering of heat strengthened titanium alloys 05 p0704 N71-15293
[AD-713760]
Initial research on electrical and metallurgical properties of amorphous semiconductors 05 p0758 N71-15345
[AD-713483]
Optical absorption by excitons in alkali halides, personal accident dosimeters, electromagnetic wave propagation in atmosphere, metallurgy, and related research 05 p0908 N71-15747
Determination of trace impurities in high purity materials by anodic stripping voltammetry 07 p0988 N71-17069
Effect of thermomechanical treatment on properties of alloys - Vol. 1 07 p1044 N71-17831
[AD-715253]
Structural transformations and stressed states in light metals under neutron irradiation 08 p1265 N71-19167
[IT-70-57064]
Development of one-electron pseudo-Green function and pseudopotential of d-band metals 09 p1454 N71-20499
[ML-1936]
Analysis of factors affecting the welding properties of steel 10 p1565 N71-21178
[NLL-TRANS-746-532-79022.401/]
Metallurgical and magnetic properties of industrial nickel iron alloys 10 p1582 N71-21499
[NLL-TRANS-2654-79022.81/]
Description of methods for determining stability constants of transition metal halides and polyphosphates 11 p1695 N71-22073
Development, test, and evaluation of metals used in construction of nuclear reactors 11 p1777 N71-22290
[IN-1437]
Induction heating of metallurgical specimens to high temperatures in coil furnace 12 p1917 N71-23267
[NASA-CASE-XLE-04026]
Spectrochemical techniques for determination of impurities and of tantalum in zirconium alloy and Zircaloy 2 13 p2093 N71-24819
[EUR-4541-F]
Crystal structure of aluminum alloys, neutron capture cross sections for deuterium, reactor fuels, electron microscopy, and radiation effects on semiconductors 13 p2040 N71-24998
[AECL-3776]
Preparation and characteristics of metallic solid solution in which small metal atoms fill interstitial sites in host metal composed of larger atoms 13 p2154 N71-25539
[AD-719940]
Photoelectron spectroscopy for chemical analyses on doped metals and alloys 15 p2495 N71-27959
[CEA-COIF-1725]
Effects of hydrostatic pressure in metals and alloys and application to industrial processes 17 p2763 N71-29648
[AD-722416]
Mechanism of boiling and characteristics of heat transfer in boiling of metals 17 p2859 N71-30288
[NASA-TT-F-620]
Nuclear energy, molecular biology, radiobiology, chemistry, and metallurgy research 18 p2990 N71-31565
[NP-18700]
Analysis of theoretical aspects of mass transfer between continuous liquid phases and liquid drops or gas bubbles and application to steel making process 19 p3117 N71-32557
[PB-19365]
Description of laboratory metallurgy techniques involving mechanical properties tests, crystallography, creep, and fatigue 21 p3437 N71-34453
[CEA-N-142721]
Techniques in laboratories of metallurgical research department 21 p3437 N71-34454
[CEA-N-142711]
Deformation studies on dilute hafnium base alloys to determine effects of dispersion hardening and precipitation 21 p3439 N71-34467
[N71-3719-9]
Mechanical developments in testing and detection, properties, and processing technology utilization 21 p3439 N71-34471
[NASA-SP-5940(01)]
Construction of metallurgical phase diagrams to show eutectic equilibrium of chromium, hafnium, ruthenium, osmium, and molybdenum alloys 21 p3442 N71-34492
[NLL-L-TT-746-685-79022.401/]
Determination of thermal conductivity and electrical resistivity of solids at cryogenic temperatures 23 p3772 N71-36087
[NASA-CR-121706]
Development of ferrous metallurgy and advanced methods of metal production 23 p3772 N71-36087
[JPRS-54099]
Chemistry, physics, metallurgy, and engineering related problems in provision and use of defense material 23 p3856 N71-37488

METALS

NT ACTINIDE SERIES
NT ALKALI METALS
NT ALKALINE EARTH METALS
NT ALUMINUM
NT ALUMINUM COATINGS
NT ALUMINUM ISOTOPES
NT ALUMINUM 24
NT ALUMINUM 27
NT AMERICIUM
NT AMERICIUM ISOTOPES
NT AMERICIUM 241
NT ANTIMONY
NT ARSENIC ISOTOPES
NT ASTATINE ISOTOPES
NT BARIUM
NT BARIUM ISOTOPES
NT BERKELIUM
NT BERYLLIUM
NT BERYLLIUM ISOTOPES
NT BERYLLIUM 7
NT BERYLLIUM 9
NT BERYLLIUM 10
NT BISMUTH
NT BISMUTH ISOTOPES
NT CADMIUM
NT CADMIUM ISOTOPES
NT CALCIUM
NT CALCIUM ISOTOPES
NT CALIFORNIUM
NT CALIFORNIUM ISOTOPES
NT CERIUM
NT CERIUM ISOTOPES
NT CESIUM
NT CESIUM VAPOR
NT CESIUM 133
NT CESIUM 134
NT CESIUM 137
NT CESIUM 144
NT CHROMIUM
NT CHROMIUM ISOTOPES
NT COBALT
NT COBALT ISOTOPES
NT COBALT 58
NT COBALT 60
NT COPPER ISOTOPES
NT CURIUM
NT CURIUM ISOTOPES
NT CURIUM 244
NT DYSPROSIUM
NT DYSPROSIUM ISOTOPES
NT ERBIUM
NT ERBIUM ISOTOPES
NT EUROPIUM
NT FERROUS METALS
NT GADOLINIUM
NT GALLIUM
NT GALLIUM ISOTOPES
NT GOLD
NT GOLD COATINGS
NT GOLD ISOTOPES
NT HAFNIUM
NT HAFNIUM ISOTOPES
NT HOLMIUM
NT HOLMIUM ISOTOPES
NT INDIUM
NT INDIUM ISOTOPES
NT INDIUM
NT INDIUM ISOTOPES
NT IRON
NT IRON ISOTOPES
NT IRON 57
NT IRON 59
NT LANTHANUM
NT LANTHANUM ISOTOPES
NT LAWRENCIUM
NT LEAD [METAL]
NT LEAD ISOTOPES
NT LIQUID METALS
NT LIQUID POTASSIUM
NT LIQUID SODIUM
NT LITHIUM
NT LITHIUM ISOTOPES
NT LUTETIUM
NT LUTETIUM ISOTOPES
NT MAGNESIUM
NT MAGNESIUM ISOTOPES
NT MANGANESE
NT MANGANESE ISOTOPES
NT MERCURY [METAL]
NT MERCURY ISOTOPES
NT MERCURY VAPOR
NT METAL COATINGS
NT METAL CRYSTALS
NT METAL FILMS
NT METAL MATRIX COMPOSITES
NT METAL POWDER
NT METAL VAPORS
NT MOLYBDENUM
NT NEODYMIUM
NT NEODYMIUM ISOTOPES
NT NEPTUNIUM
NT NEPTUNIUM ISOTOPES
NT NICKEL

NT NICKEL COATINGS
NT NICKEL ISOTOPES
NT NIOBIUM
NT NIOBIUM ISOTOPES
NT NOBELIUM
NT NOBLE METALS
NT NONFERROUS METALS
NT OSMIUM
NT OSMIUM ISOTOPES
NT PALLADIUM
NT PLATINUM
NT PLATINUM ISOTOPES
NT PLUTONIUM
NT PLUTONIUM ISOTOPES
NT PLUTONIUM 238
NT PLUTONIUM 239
NT PLUTONIUM 240
NT PLUTONIUM 241
NT POLONIUM ISOTOPES
NT POLONIUM 210
NT POTASSIUM
NT POTASSIUM ISOTOPES
NT POWDERED ALUMINUM
NT PRASEODYMIUM
NT PRASEODYMIUM ISOTOPES
NT PROMETHIUM ISOTOPES
NT PROTACTINIUM ISOTOPES
NT RADIUM
NT RADIUM ISOTOPES
NT RADIUM 226
NT RARE EARTH ELEMENTS
NT REFRACTORY METALS
NT RHENIUM
NT RHENIUM ISOTOPES
NT RHODIUM
NT RHODIUM ISOTOPES
NT RUBIDIUM
NT RUBIDIUM ISOTOPES
NT RUBIDIUM 86
NT RUTHENIUM
NT RUTHENIUM ISOTOPES
NT SAMARIUM
NT SCANDIUM
NT SCANDIUM ISOTOPES
NT SILVER
NT SILVER ISOTOPES
NT SODIUM
NT SODIUM ISOTOPES
NT SODIUM VAPOR
NT STRONTIUM
NT STRONTIUM ISOTOPES
NT STRONTIUM 89
NT STRONTIUM 90
NT TANTALUM
NT TECHNETIUM
NT TECHNETIUM ISOTOPES
NT TERBIUM
NT TERBIUM ISOTOPES
NT THALLIUM
NT THALLIUM ISOTOPES
NT THORIUM
NT THORIUM ISOTOPES
NT THULIUM
NT THULIUM ISOTOPES
NT TIN
NT TIN ISOTOPES
NT TITANIUM
NT TITANIUM ISOTOPES
NT TRANSITION METALS
NT TRANSURANIUM ELEMENTS
NT TUNGSTEN
NT TUNGSTEN ISOTOPES
NT ULTRAPURE METALS
NT URANIUM
NT URANIUM ISOTOPES
NT URANIUM 232
NT URANIUM 233
NT URANIUM 235
NT URANIUM 238
NT VANADIUM
NT YTTERBIUM
NT YTTERBIUM ISOTOPES
NT YTTRIUM
NT YTTRIUM ISOTOPES
NT ZINC COATINGS
NT ZINC ISOTOPES
NT ZIRCONIUM
NT ZIRCONIUM ISOTOPES
Low temperature sliding friction and wear studies on metals in ultrahigh vacuum 01 p0668 N71-10738
[AD-711648]
Data tabulated from 274 stations in US and Canada on air pollution effects on materials 02 p0151 N71-11071
[PB-192446]
Structural effects and surface erosion in metals irradiated by 10 to minus 8th power second light pulses from laser 02 p0238 N71-11580
[AD-712232]
Influence of laser radiation on metals 02 p0238 N71-11581
[AD-712341]
Manufacturing improvement program establishing applications and limitations in closed-die forging 02 p0234 N71-11675
[AD-711544]
Effect of time-dependent gravitational fields on superconductors and metals 02 p0285 N71-11846
[ESRIN-IN-100]

- Atom diffusion and diffusion-controlled processes in solids including metals, semiconductors, oxides, and piezoelectric crystals
[AD-711417] 02 p0286 N71-11926
- Quantification and nonlinear Volterra integral equations involving computation of creep deflections of metal structures
[PB-190638] 02 p0245 N71-12196
- Dynamic properties of materials with emphasis on metals
[AD-12847] 05 p0390 N71-12685
- Screening tests on friction and wear of materials in sodium
[LMRC-70-10] 03 p0390 N71-12698
- Affinity of metals to sulfur
[TT-70-7082] 03 p0391 N71-12830
- Calorimetric determination of nuclear and electronic interactions in metals
[AD-121093] 03 p0468 N71-12993
- Hydroabrasive wear of metals under cavitation
[PB-19258] 03 p0393 N71-13031
- Metal and oxide solubilities in calcium chloride melts
04 p0535 N71-14324
- Heat of formation of metal sulfides and thermal stability related to their atomic structure
[TT-70-7084] 05 p0638 N71-14590
- Effect of oil films on adhesion of polymers to metal surfaces
[AD-713450] 05 p0710 N71-15370
- Bibliography of technical literature of metals and ceramics division for 1969 at Oak Ridge National Laboratory
[ORNL-4270-VOL-2] 07 p1060 N71-17191
- Physical and chemical properties of metallic elements and inorganic compounds at high temperatures
[NYO-4176-3] 07 p1130 N71-17636
- Transport and defect properties of thin tungsten, platinum, and nickel wires
[COO-1247-21] 07 p1044 N71-17804
- Melting points of metallic elements and selected compounds including nitrides, borides, carbides, halides, and sulfides
[AD-715908] 08 p1159 N71-18554
- Transport phenomena in metals and semiconductors
[ORO-3087-44] 08 p1279 N71-18765
- Mechanism and kinetics of diffusion processes in metals
[TT-70-50030] 08 p1219 N71-19184
- Electron diffusion thermoelectric power in metals and dilute alloys investigated over wide range of temperatures
[COO-623-152] 08 p1281 N71-19273
- Thermal and elastic properties of polymers, and electronic properties of glasses and metals
09 p1404 N71-19730
- Determination of fracture extension resistance factors in fracture safe design for nonferrous metals
[AD-716407] 09 p1476 N71-19891
- Megahertz and gigahertz ultrasonic attenuation in metals
[AD-716474] 09 p1453 N71-19998
- Angular momentum effects on nuclear fusion reactions of gold, platinum, tantalum, lead and bismuth
[RL-1759-25] 09 p1436 N71-20044
- Sodium solubility of silver, cadmium, indium, tin, and antimony individually and in combination for dilute binary sodium alloy studies
[BNL-50271] 10 p1511 N71-20653
- General regularities in corrosion of metals under action of radioactive radiation
[AD-717065] 10 p1572 N71-20809
- Zone refining of metals using active fluxes
10 p1575 N71-20891
- Mechanical testing of metals at high temperatures and short term loading with determination of temperature influence and deformation rates
[AD-716937] 10 p1580 N71-21391
- Effects of chemical bonding between phases of glass-metal composit on strength and fracture behavior
11 p1785 N71-23010
- Self lubricating fluoride-metal composite materials for outer space applications
[NASA-CASE-XLE-08511] 12 p1944 N71-23710
- Punch and die device for forming convolution series in thin pure metal hemispheres
[NASA-CASE-XNP-05297] 12 p1927 N71-23811
- Chemical composition of gaseous nebulae, and atmospheres of normal stars and objects with unusual metal to hydrogen ratios
[AD-718441] 12 p1997 N71-24207
- Dilatometric mechanisms involved in low stress-high temperature creep of metals
13 p2096 N71-25096
- Dilatometric thermal expansion measurements on high temperature structural materials
[AGARD-AR-31-71] 13 p2187 N71-25358
- Gear checking system for testing fine-pitched miniature metallic gears at required 2-ounce pressure
[BDX-613-309] 13 p2083 N71-25457
- Ultrasonic resonator responses used to measure phonon charge carrier interactions in metals and semiconductors
13 p2141 N71-25552

- Exfoliation with oxidation process of metals and mechanical behavior of scales
[AD-719910] 14 p2268 N71-25644
- Mass spectrometer and radio frequency, high voltage spark ion source for measuring relative sensitivity factors for metals and steels
[Y-1757] 14 p2299 N71-25702
- Tests to determine short-term creep of metals and alloys under conditions of aerodynamic heating with high velocity air flow
[NASA-TT-F-13633] 14 p2272 N71-25822
- Impedance measurements on modified broadband metal antennas for speech communication
[FOA-X-C-3602-61] 14 p2218 N71-26150
- Tritium determination in metals derived by burning tritiated water sample in sealed quartz tube filled with oxygen and heated to high temperature
[CEA-R-0020] 14 p2275 N71-26382
- Nonequilibrium defects in metals including point defects, line defects, surface defects, volume defects, and dislocations occurring during solidification or solidification from impurities
[UCRL-19496] 15 p2419 N71-26919
- Absorption spectra metals in soft X ray and ultraviolet range
[DESY-70/48] 15 p2430 N71-26966
- Experimental techniques for determining electron attenuation lengths in metals in energy range to 100 keV
[AD-720849] 15 p2507 N71-27447
- Gamma photon and neutron activation analyses for determining light elements in homogeneous media
[CEA-R-4072] 15 p2474 N71-27452
- Effects of composition on glass forming tendency of monatomic metal systems
[AD-720342] 15 p2426 N71-27753
- Polarization measurements near isobaric analog resonances for elastically scattered protons from strontium, ytterbium, zirconium, tin, and molybdenum targets
15 p2487 N71-27836
- Force of ice cohesion with metals related to type of materials, surface roughness, structure and rate of external load, and surface temperature
[AD-722106] 16 p2612 N71-28730
- Effects of hydrostatic pressure in metals and alloys and application to industrial processes
[AD-722416] 17 p2763 N71-29648
- Adsorption properties of metal zeolites for airborne iodine species to provide support for full scale testing of air pollutants
17 p2715 N71-29660
- Computer program for evaluating Bloch-Grüneisen parameters of metals and evaluating tantalum electrical resistivity as function of temperature
[NASA-TM-X-2320] 17 p2816 N71-29922
- Dislocation dynamics and formulation of constitutive equations for rate dependent elastic plastic response in isotropic metals
[AD-72214] 17 p2765 N71-30110
- Thermodynamic assessment of metal compatibility and gaseous impurities in helium atmospheres
[RD/RN-1816] 17 p2783 N71-30143
- Technology and properties of metallic materials
18 p2934 N71-30690
- Electrochemistry of nickel, copper, cobalt, and iron-sulfide anodes
18 p2885 N71-30912
- Systems analysis to simplify brittle fracture tests of metals
[AD-722876] 18 p2938 N71-31422
- Effects of irradiation induced metal growth on core components for LMFBR design
[BAW-1355] 19 p3135 N71-31820
- Nuclear magnetic resonance linewidths in metals as function of temperature - density matrix equation
[AD-723914] 19 p3113 N71-32125
- Tensile, mechanical, and compression properties of metals, alloys, and steels derived from flow curves
[RAE-LIB-TRANS-1523] 19 p3115 N71-32265
- Measurement of polycrystalline metal flow curves at high and room temperatures and their application to self lubrication
[RAE-LIB-TRANS-1531] 19 p3115 N71-32266
- Complete equation of state for metals in both solid and liquid/dense vapor phases, from ambient conditions to high pressures and temperatures
20 p3334 N71-33756
- Two-phase-wave models for electron-electron and electron-phonon unklapp scattering with determination of their effect upon transport properties of simple metals
20 p3323 N71-33852
- One-electron and two-electron cavities in metal-anion solutions, electron-molecule and intermolecular reactions, and corrections for effective intermolecular pair argon potentials
21 p3309 N71-34111
- Electrical properties of metallic layers implanted in amorphous oxide glass
[NASA-CR-111953] 21 p3405 N71-34228
- S(L) spectrometer for X ray fluorescent analysis of metal and salt samples
[INR-1274] 21 p3467 N71-34678

- Determination of quantitative laws of joint discharge of ions under conditions of electrowinning of pure metals
[NLL-L71-746-663(9022.401)] 22 p3590 N71-35565
- Pressure welding of dissimilar metals through sanded surfaces and oxidized surfaces
22 p3590 N71-35567
- Applying rigid band model to metal and alloy band structure determinations
[NRC-TT-1475] 22 p3593 N71-35584
- X-ray technique for determining structural changes in relation to metal substructures and their mechanical properties
[AD-727430] 23 p3773 N71-36809
- Gravimetric determinations of oxygen-to-metal ratio of (U,Pu)O₂
[ORNL-TM-3362] 23 p3797 N71-37072
- Use of thermocouples for temperature measurement during boiling metal heat transfer experiments
[NLL-RISLEY-TRANS-2164(9091.9P)] 23 p3868 N71-37575
- Laser microemission spectroscopic analysis of metals and nonmetals
[NASA-TT-F-139711] 24 p3931 N71-38045
- Measurements of temperature with metal monomers using surface tension in range 700 to 1555 C
[JUL-680-BB] 24 p3956 N71-38081
- Methods and development of metal research
[AD-727920] 24 p3939 N71-38099
- Thermal resistance measurements on contacting interfaces between uranium nitride and metals
[ORNL-4660] 24 p3961 N71-38255
- METAMORPHISM [GEOLOGY]**
- P wave velocities at high hydrostatic pressures in metamorphic, effusive, and sedimentary rock specimens from central Kazakhstan
[NASA-TT-F-13205] 02 p0309 N71-11438
- P wave velocities at high hydrostatic pressures in igneous, sedimentary, and metamorphic cylindrical specimens from central Kazakhstan
[NASA-TT-F-13204] 02 p0210 N71-11439
- Physical properties of igneous and metamorphic rocks subjected to high pressures and temperatures
[NASA-TT-F-13515] 06 p1193 N71-18991
- Mineral composition, textural and structural characteristics, metamorphism type, and secondary change effects on elastic properties of Kivory Rog Basin metamorphic rocks
[NASA-TT-F-13548] 12 p1907 N71-23462
- Shock structures of basalts from craters produced by nuclear explosions and of rocks from lunar craters
13 p2168 N71-25274
- METASTABILITY**
- U METASTABLE STATE**
- METASTABLE ATOMS**
- Metastable calcium atom orientation by optically pumped sodium atom shocks
06 p0914 N71-15948
- Hank effect in 21P helium with metastable atoms
[TID-25588] 09 p1427 N71-19401
- Conservation laws and vibrational band structures of nitrogen subjected to excitation collisions with helium and argon metastable atoms
09 p1431 N71-19920
- Kinetic energies of metastable oxygen atoms formed by electron impact dissociation of oxygen and measured in time of flight experiment
[NASA-CR-118336] 13 p2133 N71-25129
- Production and destruction of fast metastable He atoms in rare gas targets and Kr and He
17 p2796 N71-29785
- Ionization study of metastable hydrogen atomic beams and polarized deuterium ions with Lamb-shift source
[KFK-1256] 21 p3468 N71-34690
- METASTABLE STATE**
- Metastable time of flight technique evaluation for molecular velocity distribution measurements
[AD-711078] 01 p0040 N71-10242
- Electron impact excitation efficiency curves for formation of neutral metastable species
[UCRL-19594] 04 p0594 N71-14453
- Stress-strain properties of metastable austenites
[UCRL-20308] 06 p0609 N71-15887
- Behavior of metastable austenitic steels under cyclic loading
[UCRL-19620] 06 p0872 N71-16152
- Superconducting metastable simple cubic alloys and rapid quenching from liquid state
[CAL-T-822-22] 11 p1817 N71-22375
- Studying plastic deformation in metastable beta phase of titanium and zirconium by superconductivity measurements
[RL-2225-T-13-6] 14 p2268 N71-25469
- Total cross section measurements for formation of metastable hydrogen atoms by charge transfer of proton traversed targets of helium, argon, nitrogen, and oxygen
[NASA-CR-118863] 15 p2492 N71-27925
- Magnetic response of pure type I superconductors and their alloys with emphasis on metastable states
17 p2787 N71-29654

SUBJECT INDEX

METEORITIDS

Radiative lifetime of 2150 metastable state of boron
[UCRL-20142] 17 p2808 N71-30342

Simulation of upper atmosphere metastable oxygen molecule interactions
[SHA8] 19 p3049 N71-31783

Measurement of total cross section for low energy electrons on metastable argon by atom beam recoil method
20 p3318 N71-33379

Liquid or solid spheres levitated in film boiling following metastable Leidenfrost states
[NASA-TM-X-67897] 20 p3313 N71-33697

Dissociative excitation of CO(λ 3 Pi) and other metastable fragments such as O(λ 3S) produced by electron impact on CO₂
[NASA-CR-121714] 21 p3466 N71-34670

METAZOA

U ANIMALS

METEOR BURSTS

U METEOROID SHOWERS

METEOR HAZARDS

U METEOROID HAZARDS

METEOR TRAILS

Pulse radar for measuring wind speed in upper atmosphere by observing drift of ionospheric meteor trails
[AD-715929] 06 p1162 N71-18553

Analysis of limitation on meteor trail radar wind measurements imposed by uncertainty principle
[AD-716996] 10 p1643 N71-21191

Development of coherent optical data processing techniques applicable to detection of meteor trails and examination of properties
[NASA-CR-61241] 10 p1529 N71-21500

Azimuth and elevation angle determination from UNH/APCRL meteor trails interferometric radar, using computer processing
[AD-718105] 12 p1997 N71-24111

Coefficient of electron attachment to oxygen molecules method from simultaneous photographic and radar observations applied to meteor radar echo data for 1957 to 1959
12 p1998 N71-24288

Polarization effects accompanying radio wave diffuse reflections from meteor trails with sporadic background
[NASA-TT-F-13495] 12 p1999 N71-24310

Developmental history and problems in radio electronics and radar tracking of meteor trails
[AD-720372] 14 p2336 N71-25923

Data processing system for meteor trail radio communication equipment
[FOA-3-C-3597-63] 14 p2219 N71-26533

Radar antenna direction finding techniques for APCRL meteor trails radar using OV1-17 satellite payload
[AD-721195] 15 p2379 N71-26889

Satellite verification of phase sequenced interferometer direction finder for meteor radar echoes and wind direction measurement
[AD-720655] 15 p2382 N71-27424

Array of eighty nine dipoles for studying radio signals reflected and scattered from ionospheric irregularities and meteor trails to determine wind gradients and changes at high altitudes
[AD-721223] 15 p2399 N71-27471

Composition and mass data analysis of meteoroids in 1 milligram to 1 gram range using NASA LRC Paint Meteor Spectra Panel data
[NASA-TN-D-6296] 16 p2578 N71-28802

Meteor trails observations of wind component interactions in upper atmosphere
[NASA-TT-F-13506] 18 p2953 N71-31073

METEORITE COLLISIONS

Determination of correlation between impact flash radiative properties and impacting meteoroid projectile characteristics
[NASA-CR-115066] 17 p2842 N71-29245

METEORITE COMPRESSION TESTS

U COMPRESSION TESTS

U MECHANICAL PROPERTIES

U METEORITES

METEORITE CRATERS

Micrometeorite craters and related features on lunar rock surfaces
[NASA-TM-X-66705] 07 p1108 N71-17355

Findings of conference on meteorite impact and volcanism
[NASA-TM-X-66706] 07 p1109 N71-17336

Investigating formation of circular structures of volcanic, meteoritic, and nuclear origin on earth for correlation with cratering on moon and inner planets
[NASA-TT-F-13457] 07 p1015 N71-17412

Systematic classification of meteorite impact craters for lunar and planetary craters
[NASA-CR-116090] 08 p1194 N71-19083

Monte Carlo cratering simulation model to show nonrandomness of formation of Mars tangential meteorite craters
[NASA-TM-X-63227] 17 p2345 N71-30119

METEORITES

NT ACHONDRITES

NT BRÜDERHEIM METEORITE

NT CHONDRITES

NT SIKHOTIE-ALIN METEORITE

NT STONY METEORITES

NT TUNGUSK METEORITE

Developing aluminum meteoritic simulators for hypervelocity impact test using shaped charges
[NASA-CR-108750] 03 p0335 N71-12644

Orbital evolution of lost city meteorite
[NASA-TM-X-65407] 05 p0768 N71-15272

X ray detection of disordered orthopyroxene in meteorites
[NASA-CR-116448] 07 p1108 N71-17064

Findings of conference on meteorite impact and volcanism
[NASA-TM-X-66706] 07 p1109 N71-17336

Luminescence petrography of Apollo 12 rocks and comparative features in Apollo 11 rocks, terrestrial rocks, and meteorites
[NASA-CR-114842] 07 p1110 N71-17563

Shock wave formation and propagation during large meteorite entry into atmosphere
[AD-715337] 08 p1191 N71-18008

Neutron activation analysis for trace elements depleted on lunar surface with implications for origin of moon and meteorite influx rate
[NASA-CR-114888] 09 p1465 N71-19782

Comets, meteorites, lunar geology, cosmic rays, radiation measuring instruments, and data processing conference
[NASA-TT-F-630] 11 p1826 N71-22415

Origin of meteorites and relation to early solar system
[NASA-CR-117755] 11 p1827 N71-22529

Radar dual frequency system for estimating microwave attenuation by hydrometeors
12 p1880 N71-23990

Solar wind, meteoric volatilization, and internal degassing contributing to lunar rarefied atmosphere, and transient contributions produced by rocket gases during lunar missions
[NASA-CR-118630] 14 p2335 N71-25796

Determination of zirconium and hafnium in meteorites and terrestrial materials by activation analysis and chemical separation after neutron irradiation
14 p2338 N71-26351

Method for making pressurized meteoroid penetration detector panels
[NASA-CASE-XLA-08916] 16 p2604 N71-29018

Determination of correlation between impact flash radiative properties and impacting meteoroid projectile characteristics
[NASA-CR-115066] 17 p2842 N71-29245

Mass spectrometric analyses of xenon released in several stages of heating of group of neutron irradiated meteorites
17 p2845 N71-29262

Inferred origin of solar system from studying properties of meteorites
[NASA-CR-123180] 24 p4007 N71-38570

Chemical analysis of meteorites
[ORO-3585-22] 24 p4013 N71-38630

METEORITE COMPOSITION

Thermoluminescence-chemical composition correlations for meteoritic enstatite
01 p0120 N71-10081

Radiometric age determination and isotopic composition analyses on rocks, meteorites, and lunar samples
[NASA-CR-111001] 01 p0016 N71-10304

Mass spectrometric analyses of meteoritic and lunar samples containing lead and thallium
01 p0053 N71-10314

Abstracts on Soviet stratospheric solar observatory and mercury content measurements in meteorites
07 p1107 N71-16956

Minor and trace elements in meteoritic minerals
07 p1112 N71-17708

Instrumental activation analysis technology for analysis of meteorites and lunar materials
07 p1113 N71-17715

Neutron activation methods for determining oxygen and silicon in chondritic meteorites
07 p1113 N71-17716

Methods for determining aluminum oxide and titanium dioxide in stony meteorites
[NASA-TT-F-13541] 09 p1467 N71-20319

Photographic and trajectory data for Lost City meteor and establishment of calibration of mass scale of other meteorites
[NASA-CR-117036] 09 p1468 N71-20322

Oxygen pressure as function of temperature in stony meteorite formation
13 p2169 N71-25295

Production of iodine isotopes in meteorites by cosmic rays, gas proportional counting of transition metal X ray emitters, and radiochemical analysis of lunar samples
18 p3017 N71-31348

Application of gamma-gamma coincidence counting technique to nondestructive activation analysis of meteoritic materials
19 p3051 N71-32394

Meteoritic composition including distribution of and origin of elements and their isotopes
[UCSD-34-F-43-X-9] 20 p3350 N71-33875

Magnetic mass spectrometer with programmable magnetic field analyzer for measuring meteoric isotopic ratios
23 p3857 N71-37492

METEORITE DAMAGE

Capsular sandwich structure containing metal sheets of known thickness for counting penetration rates of meteoroids
[NASA-CASE-XLB-01246] 01 p0856 N71-10797

Micrometeoroid space environment simulation and meteorite damage to mirror reflectance
[ONERA-DRETS-NT-01-12] 07 p1108 N71-17218

Structural analyses and chronology of micrometeorite craters on lunar rocks
[NASA-TM-X-66707] 07 p1109 N71-17498

Polished metals exposed to hypervelocity impact by meteorite also projectiles to determine bombardment effect on spectral reflectance
[NASA-TM-X-52081] 09 p1399 N71-19816

Explosive oxidation hazard in simulated meteoroid S-48 impact penetration into spacecraft atmosphere
[NASA-CR-117142] 09 p1464 N71-20326

Hypervelocity impact tests to predict meteoritic damage on proposed lunar fuel tank configuration
[NASA-TM-X-64597] 14 p2343 N71-26040

Cold cathode glow discharge tube for detecting meteoroid puncture of pressurized cells
[NASA-TN-D-6447] 21 p3429 N71-34405

METEORITIC DUST

U MICROMETEORITIDS

METEORITIC IONIZATION

U ATMOSPHERIC IONIZATION

U METEOR TRAILS

METEORITIC MICROSTRUCTURES

Methods for determining aluminum oxide and titanium dioxide in stony meteorites
[NASA-TT-F-13541] 09 p1467 N71-20319

Origin of cosmic material fallout on earth surface and structure of cosmic dust and meteoritic materials
[REPT-69/18] 15 p2398 N71-27038

Mineral composition and structure of magnetite spherules of meteoric dust
[REPT-14] 18 p3017 N71-31332

Quantitative analysis of meteoritic chondritic microstructures
23 p3778 N71-36926

METEOROID CONCENTRATION

Astronomical meteoroid environment model for space missions
[NASA-SP-8038] 07 p1110 N71-17525

Evaluation of gas discharge transducer and associated instrumentation for asteroid belt meteoroid experiment with Pioneer probes F/O
[NASA-CR-111048] 09 p1390 N71-20401

Use of Pioneer 7 and 8 cosmic dust detectors in Apollo 17 lunar ejecta and micrometeorite experiment to measure meteoroid fluxes on moon
[NASA-CR-118463] 14 p2339 N71-26441

METEOROID CRATERS

U METEORITE CRATERS

METEOROID HAZARDS

Computer program using numerical integration techniques for computation of meteoroid impact and angular distributions over complex geometric spacecraft configurations
[NASA-CR-101021] 12 p2003 N71-24335

Rate of meteoroid penetration of this beryllium copper detector measured in near-lunar environment by Lunar Orbiter spacecraft
[NASA-TN-D-6266] 16 p2577 N71-28109

METEOROID PROTECTION

Development and characteristics of protective coatings for spacecraft
[NASA-CASE-XNP-62507] 07 p1120 N71-17679

Meteoroid damage determination and spacecraft structure protection and reliability
[NASA-SP-8042] 13 p2167 N71-25070

METEOROID SHOWERS

Computerized searches for meteor streams in photographic meteor orbits
[NASA-CR-121922] 22 p3466 N71-36141

Computerized search for meteor streams in 865 precise photographic meteor orbits
22 p3467 N71-36142

Computerized search for meteor streams in 2401 photographic meteor orbits, and association with other streams or comets
22 p3467 N71-36143

METEOROID

NT MICROMETEORITIDS

NT SPORADIC METEORITIDS

Reporting development of astronomical telescopes, radioastronomical observations of solar eclipses and characteristics of faint meteor orbits
07 p1107 N71-17498

Computerized radar equipment for automatic meteor echo recordings
[REPT-70-E-14] 09 p1390 N71-20363

Photographic and trajectory data for Lost City meteor and establishment of calibration of mass scale of other meteorites
[NASA-CR-117036] 09 p1468 N71-20322

METEOROLOGICAL BALLOONS

Meteor atom and molecule effective diffusion cross sections and application to meteor theoretical physics problems

[NASA-TT-F-13493] 12 p1998 N71-24289
Radar echo rates from meteors observed in USSR for IGY-IGC 1957 to 1959 including diurnal and annual variations

[NASA-TT-F-13496] 12 p1998 N71-24290

Computerized simulation of meteor orbit and atmospheric trajectory from parameters of impacted fragments

[CEA-R-4045] 14 p2341 N71-26755

Diurnal, directional, and latitudinal effects of meteor influx rates determined from airborne observations of meteors at high latitudes

[NASA-TN-D-6303] 15 p2517 N71-26969

Rate of meteoroid penetration of thin beryllium copper detector measured in near-lunar environment by Lunar Orbiter spacecraft

[NASA-TN-D-6266] 16 p2677 N71-28109

Lost City meteoroid trajectory analysis and determination of original mass

[NASA-CR-121931] 22 p3671 N71-36175

Gamma ray and neutron radiation of meteor streams in relation to antimatter comet hypothesis

[NASA-TN-D-77441] 23 p3850 N71-37441

Stress waves in multiple laminates and sandwich plates, dynamic polariscope for stress wave analysis, meteoroid hazard to space travel, effects of hypervelocity impact, and related studies

[NASA-CR-123157] 24 p3920 N71-37953

Motion and vaporization of bright meteor fragments studied from photographs and numerical integration of equations of motion

[AD-727430] 24 p4014 N71-38637

Design, fabrication, and flight results of Radiation and Meteoroid Satellite

[NASA-CR-115206] 24 p4021 N71-38692

METEOROLOGICAL BALLOONS

NET ROBIN BALLOONS

Pulse radar altimeter for atmospheric sounding balloons

[NASA-TN-D-6226] 02 p0226 N71-11624

French BOLE program for Southern Hemisphere meteorological survey using balloons and satellites

[NASA-TN-D-6227] 02 p0257 N71-11672

Aerodynamically stable meteorological balloon using surface roughness effect

[NASA-CASE-XMF-04163] 11 p1677 N71-23007

Balloon-satellite data system for monitoring and mapping of tropical wind fields at different altitudes

[NASA-TN-D-6332] 13 p2108 N71-25332

Data processing methods for improving FPS-16 radar/lidar system measurements of atmospheric motion

[NASA-CR-118997] 16 p2624 N71-28062

First-order theory of fluctuating lift and drag coefficients for aerodynamically induced motions of rising and falling spherical balloons wind sensors

[NASA-TN-D-6373] 16 p2624 N71-28129

Analysis of stratospheric balloon programs using geophysical and flight data for transcription, graphing, and mathematical computations with computer programs and hand and machine plotting

[AD-722076] 16 p2625 N71-28473

Meteorological satellite to collect temperature, wind, and pressure data from high altitude free floating balloons, and perform range-rate measurements for balloon position determinations

[NASA-NEWS-RELEASE-71-144] 18 p3014 N71-31031

Real time estimation of wind velocities at altitudes above ceiling of meteorological balloons using digital impact predictor and radar equipment

[TN-HSA-L67] 21 p3451 N71-34559

Electrochemical concentration cell ozonoscope for measuring atmospheric ozone

[NOAA-TR-ERL-200-APCL-18] 21 p3526 N71-35121

Twenty-seven high altitude passive balloon tests in ROBIN program during May 1970

[AD-726624] 22 p3615 N71-35759

Use of constant-level meteorological balloons for numerical weather forecasting in Southern Hemisphere

[WMO-295] 23 p3793 N71-37035

METEOROLOGICAL CHARTS

Daily summaries of vertical echo sounding of upper atmosphere over Freiburg, Germany during July 1970

[REPT-29-F] 01 p0045 N71-10018

Northern Hemisphere temperature field atlas for SST flight planning

[AD-712017] 02 p0145 N71-11031

Meteorological data of cloud measurements, sea surface temperatures, and BOMEX flight data

[WHOI-REF-70-49] 02 p0252 N71-11171

Meteorological charts of Northern Hemisphere and weather data for Berlin for June, 1970

[AD-72655] 02 p0253 N71-11416

Gradient level charts for synoptic analysis and weather forecasting in tropical regions - Vol. 1

[AD-71655] 02 p0253 N71-11437

Weather satellite data on European climate for first quarter in 1968

[QJR-1-PT-1] 02 p0254 N71-11469

Meteorological data tabulated from Applications Technology Satellites observations including photographs of clouds - Vol. 3

[NASA-TM-X-66468] 02 p0254 N71-11603

Meteorological data catalog for Applications Technology Satellites - Vol. 4

[NASA-TM-X-66469] 02 p0254 N71-11604

Current operational products from National Environmental Satellite Center

[AD-712678] 02 p0261 N71-12184

Computerized classification of meteorological charts and development of forecast aids

[AD-712678] 03 p0402 N71-12758

Daily ground and 850 mb maps for Northern Hemisphere for period 1 Jan. to 31 Mar. 1970

[AD-713293] 04 p0542 N71-14275

Synoptic observations for Mediterranean marine areas - Ionian Sea, Malta, and Gulf of Sidra

[AD-713780] 05 p0715 N71-14549

Meteorological observations in Mediterranean Sea area - Vol. 4

[AD-713780] 05 p0715 N71-14549

Meteorological observations in Mediterranean Sea area - Vol. 5

[AD-713648] 05 p0715 N71-14550

Meteorological observations in Mediterranean Sea area - Vol. 6

[AD-713085] 05 p0715 N71-14551

Daily summaries for vertical echo sounding of upper atmosphere over Freiburg, Germany during Oct. 1970

[REPT-29-F] 05 p0670 N71-14814

Daily summaries for vertical echo sounding of upper atmosphere over Freiburg, Germany, for September 1970

[REPT-29-F] 05 p0672 N71-14862

Aeronautical climatological tables of international commercial airports

[AD-717117] 05 p0717 N71-15143

Meteorological data for wind resistant structural design criteria

[AD-717117] 05 p0777 N71-15304

Meteorological wind data for determining gust loads on engineering structures

[AD-717117] 05 p0779 N71-15315

September climate of Southeast Asia

[AD-713132] 05 p0719 N71-15400

Meteorological data collected by buoy in Gulf of Mexico

[AD-713479] 05 p0679 N71-15523

Synoptic meteorological charts of Northern Hemisphere for March, 1970

[AD-713479] 05 p0680 N71-15594

Daily height and temperature analyses of constant pressure levels for Northern Hemisphere for second quarter 1970

[QJR-2-PT-2] 06 p0889 N71-15933

Daily height and temperature analyses of constant pressure levels for Northern Hemisphere for second quarter 1970

[QJR-2-PT-2] 06 p0889 N71-15956

Daily height and temperature analyses of constant pressure levels for Northern Hemisphere for first quarter 1970

[QJR-1-PT-1] 06 p0889 N71-15957

Daily height and temperature analyses of constant pressure levels for Northern Hemisphere for first quarter 1970

[QJR-1-PT-1] 06 p0889 N71-15958

Climatological and meteorological parameters for central Europe during July 1970

[AD-717117] 06 p0889 N71-15959

Daily and monthly 30-mbar synoptic weather maps of Northern Hemisphere - Jan. - Mar. 1969

[AD-714371] 06 p0891 N71-16336

Synoptic meteorological data for Mediterranean coast

[AD-714371] 06 p0893 N71-16578

Regression analysis for predicting surface dew point temperatures from prognostic charts and upper atmospheric data

[NOAA-TM-NWS-TDL-37] 07 p1054 N71-17518

Charts of digitized global monthly means of ocean surface temperature

[NCAR-TN-54] 08 p1194 N71-19085

Airborne photoelectric particle counter for mapping clear air turbulence

[NASA-CR-111864] 09 p1414 N71-20398

Meteorological parameters observed and recorded at Kemi Airport, Finland, 1956 - 1961

[REPT-32] 09 p1415 N71-20583

Swell wave analysis in Monterey, California, using associated weather maps

[AD-717611] 11 p1748 N71-22231

Results of computerized weather map typing for forecasting heavy snow for Colorado Springs

[AD-718422] 12 p1953 N71-23437

Synoptic weather maps of Northern Hemisphere for September, 1970

[AD-718422] 12 p1953 N71-23680

Meteorological radiosonde data from aerological station in Berlin, Germany, for December 1969

[AD-718422] 12 p1953 N71-23681

Meteorological radiosonde data from aerological station in Berlin, Germany, for February 1970

[AD-718422] 12 p1954 N71-23682

Meteorological radiosonde data from aerological station in Berlin, Germany, for March 1970

[AD-718422] 12 p1954 N71-23683

Meteorological radiosonde data from aerological station in Berlin, Germany, for April 1970

[AD-718422] 12 p1954 N71-23684

Atmospheric temperature charts for Jan. and Apr. in Malaysia, Thailand, Vietnam, Cambodia, Laos, and Burma with analogies to Cristobal and Howard AFB, Panama

[AD-718611] 12 p1954 N71-23830

Langhain AFB, Texas terminal facility weather forecasting factors including topography, weather controls, climatic aids, and synoptic meteorology

[AD-718119] 12 p1954 N71-23831

Monthly and annual tables of mean atmospheric pressure with monthly mean maps for Finland in 1951 - 1960

[REPT-21] 12 p1955 N71-23840

Stratospheric meteorological charts of daily constant pressure level heights and temperatures from rawinsonde-rocketsonde data and polar, middle, and tropical circulation for 1970

[QJR-3-PT-3] 12 p1958 N71-24104

Daily surface and 850 mb synoptic charts for Northern Hemisphere from April through June 1970

[QJR-3-PT-3] 12 p1959 N71-24224

Synoptic meteorological charts for Berlin in Nov. 1970 including temperature-precipitation relationships and radioactivity

[QJR-3-PT-3] 14 p2288 N71-26027

Meteorological charts and data tables for July through September, 1970 from Berlin

[QJR-3-PT-3] 14 p2288 N71-26077

Meteorological data catalog for ATS 31 Aug. 1969 - 25 May 1970 and summary of ATS 1 operations

[NASA-CR-118633] 14 p2829 N71-26621

Synoptic meteorological charts and ocean current data for southern California from 1949 to 1970

[AD-721117] 15 p2437 N71-26912

Air-sea surface temperature anomalies in eastern tropical Pacific Ocean

[NASA-TM-X-65558] 15 p2404 N71-27648

Circulation patterns at 850, 700, 500, and 200 millibars over Eastern Hemisphere from 40 deg north to 40 deg south during May and June, 1956 to 1960

[MET-0-800D] 15 p2440 N71-27813

Finnish meteorological parameters for Jan. 1971

[REPT-21] 16 p2627 N71-29000

Maps of tornado occurrences in United States

[ESSA-ERL-TM-NSSL-49] 17 p2776 N71-29283

Photographic meteorological charts for snow and ice cover reporting satellite observation over Europe

[QJR-1-PT-1] 17 p2776 N71-29382

Charts giving mean atmospheric refractivity in Mediterranean Europe

[IEA-STR-13] 18 p2949 N71-30625

Meteorological charts for air space over Toulouse-Bagnac

[AD-717117] 18 p2951 N71-30932

Spectrophotometric ozone measurements for July through September 1968 in Belgium

[AD-717117] 18 p2916 N71-31041

Daily summaries for vertical echo sounding of upper atmosphere over Freiburg, Germany during January, 1971

[REPT-29-F] 18 p2920 N71-31495

Daily summaries for vertical echo sounding of upper atmosphere over Freiburg, Germany during March, 1971

[REPT-29-F] 18 p2920 N71-31496

Daily summaries for vertical echo sounding of upper atmosphere over Freiburg, Germany during February, 1971

[REPT-29-F] 18 p2920 N71-31497

Interpolated meteorological charts used for atmospheric models in numerical weather forecasting

[AD-72645] 19 p3125 N71-31665

Tropical cyclone data for North Atlantic, Caribbean, and Gulf of Mexico - charts

[AD-72835] 19 p3128 N71-32038

SUBJECT INDEX

Synoptic weather maps for Northern Hemisphere obtained during January 1971, by Berlin weather station 02 p3296 N71-33382

Daily summaries for vertical echo sounding of upper atmosphere over Freiburg, Germany during April, 1971 [REPT-296-F] 02 p3266 N71-33434

Meteorological data from Berlin weather station for fourth quarter of 1970 [QR-4] 02 p3297 N71-33847

Daily meteorological charts from Swiss weather stations for 1969 02 p3297 N71-33852

Precipitation charts of Swiss weather stations for 1969 02 p3298 N71-33853

Stratospheric weather maps of Northern Hemisphere based on rawinsonde and rocket sounding data for fourth quarter of 1970 02 p3298 N71-33854

Meteorological satellite observations and European weather charts for second quarter of 1969 [QR-2] 02 p3298 N71-33855

Meteorological charts for Northern Hemisphere containing ground level, 500 mb, and 300 mb height and temperature data for March, 1971 02 p3298 N71-33910

Meteorological charts for Northern Hemisphere containing ground level, 500 mb, and 300 mb height and temperature data for February, 1971 02 p3298 N71-33911

Meteorological charts for Northern Hemisphere containing ground level and 850-mb height and temperature data for third quarter of 1970 [QR-3] 02 p3298 N71-33916

Meteorological charts for Northern Hemisphere containing ground level and 850-mb height and temperature data for fourth quarter of 1970 [QR-4] 02 p3298 N71-33917

Meteorological and atmospheric electric data from Bombay observatory for 1967 02 p3269 N71-33969

Stratospheric weather maps of Northern Hemisphere containing daily height and temperature analysis of constant pressure levels [AD-71309] 02 p3451 N71-34563

Comparison of accuracies of 500 mb charts made by weather services of 8 different countries [NLL-M-9143-5828-4F] 02 p3452 N71-34572

ESSA 6/APFT meteorological photographs of Europe for April through June 1968, and weather satellite developments 02 p3454 N71-34585

Daily meteorological charts showing world-wide temperature distribution and variations at 30 millibar level for last quarter of 1970 [QR-4-PT-4] 02 p3616 N71-35767

Using rocketsonde and rawinsonde data to analyze high altitude synoptic charts [NASA-CR-122938] 02 p3784 N71-36971

Meteorological charts of Northern Atlantic surface temperatures [ISBN-87-7478-036-0] 02 p3792 N71-37033

Meteorological data for Wangar expedition with daily surface synoptic charts 02 p3906 N71-37838

Daily and monthly synoptic weather maps of Northern Hemisphere at 5 millibar level for period October - December 1967 [AD-72769] 02 p3953 N71-38199

Tables of synoptic meteorological observations - Hawaiian and selected North Pacific coastal marine areas [AD-72790] 02 p3953 N71-38203

METEOROLOGICAL FLIGHT

Meteorological data of cloud measurements, sea surface temperatures, and BOMEX flight data [WHOI-REF-70-49] 02 p6252 N71-11171

Using vacuum tube as launcher or booster for projectiles in meteorological probes of lower atmosphere [AD-713550] 08 p1175 N71-18365

Dielectric properties of sea ice and FM superhigh frequency radar measurement of ice thickness in Sweden and Greenland [R-83] 10 p1546 N71-20657

Meteorological sounding of mesosphere structure and effects of latent heat release in troposphere [NASA-TM-X-65592] 17 p2749 N71-30233

Velocity divergence computation for Barbados Oceanographic and Meteorological Experiment from flights at different heights [NOAA-TR-ERL-BOMAP-5] 18 p2954 N71-31225

Computer subroutine for presenting meteorological flight data by plot on peripheral printer of up to six parameters with curve separation and automatic scaling [NOAA-TR-ERL-119-APCL-17] 21 p3452 N71-34569

Plotter subroutine for two-dimensional plots of meteorological straight line flight path and four analog traces of selected meteorological parameters [NOAA-TR-ERL-140-APCL-10] 21 p3452 N71-34570

Meteorological flight path plotter subroutine for plots with wind vectors, time notations, and legend [NOAA-TR-ERL-139-APCL-9] 21 p3452 N71-34571

Research Flight Facility participation in BOMEX program and aircraft data inventory [NOAA-TR-ERL-190-RFF-4] 22 p3574 N71-35453

METEOROLOGICAL INSTRUMENTS

NT BAROMETERS

NT CLOUD HEIGHT INDICATORS

NT DROPSONDES

NT LONGSONDES

NT RADIOSONDES

NT RAIN GAUGES

NT RAWINSONDES

NT WEATHER DATA RECORDERS

NT WIND VANES

Oceanographic and meteorological sensors for meeting Coast Guard operational requirements [AD-71322] 02 p6223 N71-11383

State of art of oceanographic and meteorological sensors [AD-71323] 02 p6223 N71-11384

Operational, transport, and storage environments for oceanographic and meteorological sensors [AD-71325] 02 p6223 N71-11385

Atmospheric density changes observed from side soundings over three and one half hour period, and determination of sensor random error [AD-716995] 10 p1551 N71-21204

Instruments and techniques for hydrometeorology, including FM telemetry system, low displacement pressure transducer, and analog plotting of isohyetal lines [PB-196726] 10 p1599 N71-21618

Systematic errors of barotropic and PE baroclinic winds [AD-718111] 12 p1956 N71-23858

Optical and inspection sampling methods for sizing and counting water droplets in clouds for use in sampling from aircraft [AD-721677] 16 p2625 N71-28457

Spar buoy as instrument platform for measuring air-sea interactions [AD-722418] 17 p2777 N71-29475

Weather factors at Vance AFB, Oklahoma including weather controls, climatic aids, and synoptic studies [AD-72397] 17 p2778 N71-30257

Meteorological capillary wave instrument recording and analysis of power spectra from wind velocity and direction and air/water temperature data [AD-722617] 18 p2911 N71-30798

Ground-based and snowflake disdrometer for particle size measurement of fog and aerosols [AD-722452] 18 p2954 N71-31286

Design and construction of wind tunnel for evaluation of meteorological sensors and hydrometer sensing probes [TN-37] 20 p3245 N71-33186

Doppler signal processing and instrumentation for modified Porcupine C-band weather radar [AD-727776] 23 p3725 N71-36551

Radiative transfer equation for calculations and comparisons of radiometer ascents during BOMEX [NOAA-TR-ERL-203-APCL-19] 24 p3917 N71-37932

Fog and aerosol analysis with ultra-sensitive disdrometer utilizing optical transmission and light scattering principles [AD-727184] 24 p3952 N71-38195

METEOROLOGICAL PARAMETERS

Satellite-borne instruments for meteorological parameter observations 01 p6077 N71-10090

Using lasers for gathering information for weather forecasting 01 p6064 N71-10643

Data reduction techniques and computer programs for meteorological information obtained from Robin balloons [AD-711405] 01 p6079 N71-10707

Development and meteorological aspects of dissemination [ESSA-P1-670004] 01 p6080 N71-10811

Summary of synoptic meteorological observations for North American coastal marine areas of San Francisco and Point Mugu, California - Vol. 8 [AD-710771] 01 p6080 N71-10906

Summary of synoptic meteorological observations for North America coastal marine areas of Galveston and Corpus Christi, Texas and New Orleans, Louisiana - Vol. 6 [AD-710770] 01 p6081 N71-10907

Summary of synoptic meteorological observations for North American coastal marine areas of Astoria, Oregon and Seattle, Washington - Vol. 10 [AD-710829] 01 p6081 N71-10908

Reference file of factors affecting weather at Reese AFB, Texas [AD-711390] 01 p6081 N71-10948

Reference file of factors affecting weather at Vance AFB, Oklahoma [AD-711381] 01 p6081 N71-10949

METEOROLOGICAL PARAMETERS

Gradient level charts for synoptic analysis and weather forecasting in tropical regions - Vol. 1 [AD-711655] 02 p6253 N71-11437

Forecasting meteorological parameters for air pollution potential [NLL-M-9129-5828-4F] 02 p6253 N71-11454

ATS-3 multicolor spin scan cloud camera and image disector camera systems with meteorological data catalogs from ATS-3 and ATS-1 - Vol. 2 [NASA-TM-X-64667] 02 p6254 N71-11602

Climatology analysis of Southeast Asia for month of August [AD-711386] 02 p6257 N71-11677

Climatological data for Belgian weather stations for Aug. 1970 02 p6258 N71-11687

Numerical interpretation of wind, temperature, and specific humidity profiles for surface boundary layer of atmosphere 02 p6258 N71-11741

Measuring atmospheric temperature inversions for air pollution and weather forecasting [NLL-M-9143-5828-4F] 02 p6259 N71-11754

Soviet bloc research in astronomy, meteorology, oceanography, geophysics, upper atmosphere, and space exploration [JPRS-51556] 02 p6308 N71-12152

Investigating mesometeorological processes, climate modification, hail suppression, thermal emission, and humidity variations 02 p6260 N71-12154

Measuring total precipitable water vapor and correlations between water vapor and local meteorological parameters [NASA-TM-X-64498] 03 p6402 N71-12596

Terminal weather forecast data for Randolph AFB, Texas [AD-712641] 03 p6402 N71-12680

Atmospheric fine structure effect on aerosol vertical distribution in mountainous regions [AD-713024] 03 p6402 N71-12759

Weather satellite data and APT pictures for European area during last quarter of 1968 [QR-4] 04 p6541 N71-14117

Meteorological data for Mt. Hopkins Observatory for 1968 and 1969 [NASA-CR-111740] 04 p6541 N71-14169

Marine physical properties data for Mariner 6 and 7 missions [NASA-CR-115849] 05 p6770 N71-14504

October climate of Southeast Asia [AD-713120] 05 p6714 N71-14519

Meteorological parameters in lower atmosphere [AD-713785] 05 p6715 N71-14520

Synoptic meteorological observations for Mediterranean marine areas [AD-713084] 05 p6715 N71-14522

Meteorological observations in Mediterranean Sea area - Vol. 4 [AD-713780] 05 p6715 N71-14549

Meteorological observations in Mediterranean Sea area - Vol. 5 [AD-713648] 05 p6715 N71-14550

Meteorological observations in Mediterranean Sea area - Vol. 6 [AD-713085] 05 p6715 N71-14551

Climatology of Antarctic - Jan. 1967 - Dec. 1968 [AD-713187] 05 p6716 N71-14729

Radio meteorological determination of fading at 2 GHz in Mekong Delta [AD-713128] 05 p6644 N71-14898

Anomalous upper atmospheric parameters derived from two zero-high rocket flights [WRE-TM-HSA-175] 05 p6718 N71-15156

Applying canonical correlations to forecasting characteristics of meteorological fields [AD-713774] 05 p6718 N71-15263

Program design and methodology data summary for atmospheric reaction studies in Los Angeles, California Basin - Vol. 1 [PB-194061] 05 p6678 N71-15506

Atmospheric reaction data for commerce area of Los Angeles, California Basin - Vol. 2 [PB-194062] 05 p6678 N71-15507

Atmospheric reaction studies in Los Angeles Basin El Monte area - Vol. 3 [PB-194063] 05 p6678 N71-15508

Airborne data from atmospheric studies in Los Angeles, California Basin - Vol. 4 [PB-194064] 05 p6678 N71-15509

Meteorological parameter tables for Belgian weather stations, Sep. 1970 06 p6886 N71-15711

Synoptic meteorological data for Mediterranean marine areas of Rome, Tangier, and Malaga [AD-713992] 06 p6892 N71-16442

Analysis for refining numerical weather forecasts, and nonhydrostatic model for forecasting hemisphere meteorological parameters [AD-714429] 06 p6892 N71-16443

December climate of Southeast Asia [AD-714070] 06 p6892 N71-16444

Abstracts and book outlines on Soviet meteorology 06 p6892 N71-16512

November climate of Southeast Asia
[AD-714566] 06 p0893 N71-16715

Selected articles on Soviet research in space, geophysics, and astronomy
[JPRS-52183] 07 p1107 N71-16917

Investigating cloud characteristics, atmospheric thermal energy, rain formation in clouds, and uses of radar in meteorology
07 p1052 N71-16919

Abstracts on Soviet meteorological research
07 p1052 N71-16957

Calculating probability of appearance of thunderstorms from data on vertical distribution of radar echo intensity
[D-2-70-02] 07 p1052 N71-16962

Climatological data - Belgium, Oct. 1970
07 p1053 N71-17153

Climatological data - Belgium, Nov. 1970
07 p1053 N71-17154

Performance of aluminum oxide byproduct on aircraft meteorological observatory
[NASA-TM-X-65446] 07 p1028 N71-17274

Abstracts on Soviet meteorological research
07 p1054 N71-17488

Procedure for identifying spikes in radiosonde angular data and synthesizing replacement values
[AD-715351] 07 p1054 N71-17732

Fourier analysis of summer weather and wave data for Lake Michigan
[AD-714888] 07 p1055 N71-17836

Microwave transhorizon propagation and detection
[AD-714999] 07 p1098 N71-18067

Meteorological effects on air transportation, including atmospheric and runway conditions
07 p1056 N71-18117

Development and characteristics of global atmospheric circulation model
08 p1231 N71-18998

Correlation between thunderstorm motion and mean environmental winds
08 p1231 N71-18999

Factors affecting weather conditions at Mather Air Force Base, California
[AD-716545] 09 p1412 N71-19442

Time and space history analysis of buoyant cloud tops and heat release, cloud behavior, and meteorological factor interrelationships in cloud rise
[BNL-50244] 09 p1413 N71-20024

Astronomical observations and experiments conducted during total solar eclipse of November 12, 1966 in Bolivia
09 p1468 N71-20389

Climatological characteristics of mistral wind in France
[REPT-79] 09 p1414 N71-20487

Meteorological parameters observed and recorded at Kemi Airport, Finland, 1956-1961
[REPT-22] 09 p1415 N71-20583

Statistical analysis of meteorological parameters to determine accuracy of synoptic maps
[AD-716939] 10 p1596 N71-20764

Climatology for North American coastal areas from Vancouver to Alaska
[AD-717621] 10 p1598 N71-21028

Short range weather forecasting techniques, construction of multilayer prediction model, and integration of equations for weather prediction
[AD-717008] 10 p1596 N71-21180

ATS 5 down link 15 GHz signal propagation compared to ground based radio and meteorological data
10 p1523 N71-21418

Development of meteorological information and parameters based on cloud photographs taken during Apollo 9 flight
[NASA-CR-114954] 10 p1597 N71-21468

Climatology at Rovaniemi Airport, Finland
[REPT-28] 10 p1598 N71-21521

Climatology at Maarianhamina Airport, Finland
[REPT-26] 10 p1598 N71-21537

Climatology at Vaasa Airport, Finland
[REPT-30] 10 p1598 N71-21538

Climatology at Turku Airport, Finland
[REPT-29] 10 p1598 N71-21539

Climatology at Oulu Airport, Finland
[REPT-27] 10 p1598 N71-21540

Climatic, meteorological, and oceanographic conditions associated with monsoon season in Indian Ocean determined by Nimbus satellite observations
[AD-717391] 11 p1745 N71-21938

Meteorological parameter tables for Belgian weather stations, Jan. 1971
11 p1788 N71-22014

Statistical equation relating mean values of pressure, temperature, and density with correction term proportional to covariance between density and temperature
[NASA-TR-R-365] 11 p1747 N71-22066

Ionospheric propagation charts of predicted median critical and maximum usable frequencies in F2 region, Delhi - Jan. 1971
[RRC-B172] 11 p1747 N71-22067

Meteorological parameter tables for Belgian weather stations, Dec. 1970
11 p1789 N71-22084

Selected articles on numerical forecasts and analysis of meteorological fields
[AD-717817] 11 p1769 N71-22266

Automated meteorological data processing practiced at Air Force global weather center
[AD-717652] 11 p1790 N71-22269

Synoptic observations for Alaskan coastal marine areas
[AD-717360] 11 p1790 N71-22361

Earth atmosphere and meteorological parameters, and radiosonde Meteorit 2
11 p1791 N71-22684

Meteorological parameters in predicting signal loss in tropospheric scatter propagation
11 p1713 N71-22952

Tropospheric scatter propagation and prediction of radio transmission characteristics
[AGARD-CP-70-71] 12 p1874 N71-23451

Radar attenuation prediction method using stratified atmospheric level indices
12 p1877 N71-23468

Meteorological effects on tropospheric propagation predictions for telecommunication
12 p1877 N71-23470

Statistical forecast of signal attenuation with tropospheric scatter using meteorological parameters
12 p1877 N71-23471

Point to point microwave transmission with receiving antenna wave front sampling, meteorological parameter measurements, and refractive index profiles
[AD-718272] 12 p1879 N71-23608

Data tables of synoptic marine surface meteorology for Bristol Bay and St. Paul Island, Alaska
[AD-718345] 12 p1954 N71-23832

Data tables of synoptic marine surface meteorology for Nunivak, St. Matthew, and St. Lawrence islands, Cape Lisburne, and Barrow, Alaska
[AD-718346] 12 p1954 N71-23833

History of numerical weather forecasting in USSR from meteorological parameters
[AD-718481] 12 p1955 N71-23837

Computerized simulation of meteorological parameters and trafficability in Saigon area
[AD-718115] 12 p1955 N71-23853

Compilation of meteorological data for Alaska and Aleutian Islands Vol. 13
[AD-717949] 12 p1956 N71-23943

Statistical analysis of meteorological fields of planetary scale based on method of decomposition with respect to natural functions
[AD-718281] 12 p1956 N71-23945

Harmonic analysis for determination of meteorological elements for annual seasons in Oskje
[NLI-M-20096/5828.4E/1] 12 p1957 N71-24003

Description of method for determining visibility in earth atmosphere
[AD-719502] 13 p2104 N71-24375

Planning of first GARP experiment to study atmospheric circulation and physics and meteorological parameters in tropo- and stratosphere
13 p2105 N71-24467

Global synoptic network utilizing ground stations, and satellites for observation of upper atmospheric meteorological parameters
13 p2105 N71-24468

Interaction between atmosphere and terrain in producing climate for US
[NOAA-TM-EDS-19] 13 p2075 N71-25186

Ceiling and visibility isoline maps of Southeast Asia showing frequency of occurrence of ceilings less than 5000 feet and visibilities less than 5 miles
[AD-707494] 14 p2286 N71-25676

Development of computer program to increase on-site analysis capabilities of experimental optical and meteorological parameters
[AD-720625] 14 p2286 N71-25791

Numerical analysis of zonally symmetrical tropical atmosphere and two layer model of upper tropical ocean to predict three years of intertropical convergence zone
[AD-720266] 14 p2289 N71-26308

Development of mathematical/meteorological models for improved forecast capability
[AD-720218] 14 p2289 N71-26620

Tables on climatology of ionosphere measured by ionosondes
[NOAA-ISPDA-FA-321] 14 p2251 N71-26625

Radar investigation of convective clouds and precipitation and characteristics of zones of reflection from rain and hail clouds
[AD-720731] 14 p2289 N71-26720

Synoptic meteorological parameters influencing forest fires in Southeast Asia including cloud cover and precipitation
[AD-721112] 15 p2437 N71-26917

Meteorological parameter tables for Belgian weather stations, Feb. 1971
15 p2437 N71-26971

Reference atmosphere for Vandenberg AFB, California based on current annual tabulation of thermodynamic quantities
[NASA-TM-X-64590] 15 p2437 N71-26974

Crystallization heat given off by ice to atmosphere and effect on meteorological conditions in Arctic, analyzed on basis of observational data and theoretical computations
[AD-720148] 16 p2588 N71-28499

Digital computerized simulation of transhorizon sine wave transmission with tropospheric scattering including atmospheric model using meteorological parameters
16 p2562 N71-28585

Meteorological parameters and wind statistics for North and South Carolina and Georgia for use in air pollution investigations
[COM-71-00214] 16 p2627 N71-28977

Finnish meteorological parameters for Jan. 1971
16 p2627 N71-29000

Terrestrial environment /climatic/ criteria guidelines for use in NASA space vehicles and associated equipment development with major emphasis on Kennedy Space Center launch area
[NASA-TM-X-64589] 17 p2737 N71-29235

Relationships between atmospheric electricity and meteorological parameters, noting vertical air currents and ionization
17 p2776 N71-29384

Weather forecasting and meteorological parameters at Tinker Air Force Base, Oklahoma terminal forecast reference file
[AD-722168] 17 p2777 N71-29511

Atmospheric and meteorological aspects of air pollution - survey of USSR air pollution literature
[PB-198061] 17 p2742 N71-29831

Meteorological and chemical aspects of air pollution and propagation and dispersal of air pollutants - survey of USSR air pollution literature
[PB-198064] 17 p2743 N71-29834

Wind and ground temperature effects on signal fading over mountainous terrain in very high frequency radio transmission
[REPT-7/70] 18 p2889 N71-30626

Analysis of meteorological conditions leading to hurricane formation and determination of point of origin off coast of Africa
18 p2951 N71-31015

Organization and activities of project to beneficially alter tropical cyclones and reduce destructive effects
18 p2952 N71-31019

Description of research project to reduce destructiveness of tropical storms by cloud seeding and reduction of evaporation from ocean surface
18 p0000 N71-31020

Analysis of accumulated error in numerical integration of linearized, two-level weather forecast model
18 p2952 N71-31021

Description of meteorological parameters associated with hurricanes and tropical storms
18 p2952 N71-31022

Application of numerical weather forecasting techniques to prediction of tropical storm development
[ESSA-TM-ERL-TM-NHRI-87] 18 p2952 N71-31024

Analysis of soundings taken within 100 nautical miles of center of hurricanes
18 p2953 N71-31027

Meteorological satellite to collect temperature, wind, and pressure data from high altitude free floating balloons, and perform range-rate measurements for balloon position determinations
[NASA-NEWS-RELEASE-71-144] 18 p3014 N71-31031

Meteorological parameter tables for Belgian weather stations, May 1971
19 p3125 N71-31657

Fourier analysis of weather and wave data from Holland, Michigan
[AD-723602] 19 p3126 N71-31756

Cost effectiveness model applicable to national data buoy systems and other national marine environmental data collection systems
[AD-722596] 19 p3091 N71-31965

Significant anomalies of monthly wintertime precipitation in western United States and related meteorological parameters
19 p3128 N71-32383

Atmospheric models for observing air-sea, air-land interactions of Lesser Antilles
19 p3201 N71-32768

Diurnal forecasting of radio transmission via troposphere using meteorological parameters
[REPT-8/70] 20 p3231 N71-32807

Short term forecasting of signal field strength on tropospheric scattering links involving meteorological parameters
[REPT-9/70] 20 p3231 N71-32808

Meteorological data from Finland for 1969
[REPT-551-506-1-480/1] 20 p3295 N71-33008

Meteorological flight search for clear air turbulence in stratosphere above Australia, 1966
20 p3297 N71-33671

Measuring meteorological parameters of upper atmosphere using falling spheres
[WRE-TN-50] 20 p3297 N71-33831

SUBJECT INDEX

METEOROLOGICAL SATELLITES

Digital computer control of meteorological observational data using Fourier series and Lagrange polynomials
[NLL-M-26718-(5828.4F)] 21 p3399 N71-34194

Meteorological observations required for computer models describing weather modification experiments
[NASA-CR-121617] 21 p3490 N71-34357

Tables of upper air data observed in Japan and vicinity during July 1969
21 p3451 N71-34560

Plotter subroutine for two-dimensional plots of meteorological straight line flight path and four analog traces of selected meteorological parameters
[NASA-TR-ERL-140-APCL-10] 21 p3452 N71-34570

Statistical analysis of two-dimensional fields of hydrometeorological elements
[NLL-M-26737-(5828.4F)] 21 p3453 N71-34576

Least squares method using correlation matrix of measurements applied to polynomial objective analysis of meteorological fields
[NLL-M-26795-(5828.4F)] 21 p3454 N71-34581

Effects of increase in cloudiness toward horizon on direct solar radiation and sunshine duration calculations
[NLL-M-26794-(5828.4F)] 21 p3505 N71-34969

chemical composition, meteorological parameters, cloud layer, atmospheric circulation, upper atmosphere, and origin and evolution of Venusian atmosphere
[NASA-TT-F-13722] 21 p3507 N71-34988

Precipitation parameters for forecasting cloud opportunity in Colorado River Basin
22 p3610 N71-35711

Numerical simulation of airflow over Elk Mountain for determining cloud physics parameters related to cap cloud
22 p3612 N71-35727

Summary of meteorological observations during 1969-70 winter season for San Juan Mountains
22 p3612 N71-35729

Meteorological parameter tables for Belgian weather stations, Apr. 1971
22 p3613 N71-35741

Meteorological data recorded at Fort Huachuca, Arizona during Oct. 1970
[AD-726343] 22 p3614 N71-35745

Meteorological data measured at Fort Greely, Alaska - Nov. 1970
[AD-726338] 22 p3614 N71-35746

Precipitation, atmospheric pressure and temperature, solar radiation, and wind velocity data for Fort Greely, Alaska - Oct. 1970 main tables (data) precipitation (meteorology) solar radiation wind velocity atmospheric temperature atmospheric pressure
[AD-726337] 22 p3614 N71-35747

Atmospheric temperature and pressure, precipitation, humidity, solar radiation, and wind velocity and direction data for Yuma test range, Arizona - Oct. 1970
[AD-726358] 22 p3614 N71-35748

Climatology, precipitation, atmospheric temperature, and wind direction and velocity data for Fort Wainwright, Alaska - Nov. 1970
[AD-726345] 22 p3614 N71-35749

Micrometeorological parameters for Gun Hill, Panama Canal Zone, October 1970
[AD-726356] 22 p3614 N71-35750

Meteorological parameter data for Fort Sherman, Panama Canal Zone, Oct. 1970
[AD-726357] 22 p3614 N71-35751

Micrometeorological parameters for Fort Wainwright, Alaska, for December 1970
[AD-726937] 22 p3614 N71-35752

Precipitation, atmospheric pressure and temperature, humidity, and wind velocity data for meteorological stations in California - Nov. 1970
[AD-726939] 22 p3615 N71-35753

Precipitation, atmospheric pressure and temperature, humidity, and wind velocity data for meteorological stations in California - Dec. 1970
[AD-726940] 22 p3615 N71-35754

Meteorological parameters and wind profile measurements for Hunter-Liggett Military Reservation, California during October 1970
[AD-726354] 22 p3615 N71-35755

Micrometeorological data for sites in Hunter-Liggett Military Reservation - Nov. 1970
[AD-726355] 22 p3615 N71-35756

Micrometeorological data for Hunter-Liggett military airfield - Nov. 1970
[AD-726347] 22 p3615 N71-35757

Precipitation, atmospheric pressure and temperature, humidity, and wind data for meteorological stations in California - Oct. 1970
[AD-726348] 22 p3615 N71-35758

Radiosonde measurements of temperature, pressure, geopotential, wind data, and velocity of sound in Germany during June 1970
22 p3616 N71-35766

Meteorological parameter observation, early star spectrum analysis, and astronomical telescope mirror
22 p3670 N71-36170

Night cloud cover and meteorological parameters determined at La Silla, Chile during 1969
22 p3670 N71-36171

Relation between turbulence in stratosphere causing aircraft buffeting, and vertical distribution of meteorological parameters calculated from radiosonde data
[NASA-TT-F-13901] 23 p3703 N71-36396

Atmospheric pressure and temperature, wind velocity, humidity, cloud cover, and precipitation data for Deamark and Faros islands in 1965
[ISBN-87-7478-025-3] 23 p3784 N71-36972

Atmospheric moisture transport into Antarctic interior based on Byrd station data analysis with mass transport model
23 p3785 N71-36977

Radiometric measurements of total heat flow to ocean surface and meteorological parameters
23 p3788 N71-36996

Meteorological parameters for Hunter-Liggett military reservation, California for December, 1970
[AD-726938] 23 p3796 N71-37013

Comparison of atmospheric ionization measurements under various meteorological and environmental conditions
[EPA-C-226] 23 p3799 N71-37016

Atmospheric factors affecting snow-melt in Alps
[EPA-CP-232] 23 p3799 N71-37017

Synoptic meteorological data for Ponape, Truk, and Pagan North Pacific island coastal marine areas
[AD-726740] 23 p3791 N71-37019

Monthly cyclone parameters in Australian region, Nov. 1969 to June 1969
23 p3791 N71-37023

Numerical analysis of persistence of degree of anomaly of fields of meteorological elements
[NLL-M-26652-(5828.4F)] 23 p3792 N71-37029

Frequency and intensity of calms in troposphere
[NLL-M-26442-(5828.4F)] 23 p3792 N71-37030

Development of mathematical meteorological diffusion models for analysis and solution of urban air pollution problems
[NLL-M-26362-(5828.4F)] 23 p3792 N71-37031

Potential of measuring meteorological data with new lasers for weather forecasting
[NLL-M-26426-(5828.4F)] 23 p3792 N71-37032

Atmospheric diffusion of beryllium exhaust gases from solid propellant rocket engines correlated with meteorological parameters
[AD-726999] 23 p3840 N71-37383

Meteorological data for Wangar expedition with daily surface synoptic charts
24 p3906 N71-37838

Atmospheric phenomena for 1968 at Casaccia Center for Nuclear Studies, Italy
[IR/PROT-70402] 24 p3951 N71-38188

Development of four dimensional atmospheric models from global data for predicting atmospheric attenuation encountered by earth resources observation sensors
[NASA-CR-61362] 24 p3951 N71-38189

METEOROLOGICAL PROBES

U SONDES

METEOROLOGICAL RADAR

High power S band meteorological radar
01 p0021 N71-10226

Data reduction techniques for digital spectrum analysis of meteorological radar echoes
01 p0021 N71-10227

Severe thunderstorm radar tracking and related weather events hazardous to aviation operations
[ESSA-TM-ERLTM-NSSL-46] 01 p0079 N71-10720

Tower antenna pedestal for mobile weather radar
[AD-711520] 01 p0130 N71-10829

Measurements of artificially seeded and unseeded winter storms over Cascade Mountains
[PB-193443] 01 p0080 N71-10894

Radar studies of Pacific cyclonic storms over Cascade Mountains
[PB-193442] 02 p0257 N71-11674

Radar meteorology and data processing for Doppler radar systems
[PB-193196] 03 p0403 N71-13166

Developing local use/gap filler radar systems for improved weather forecasting
[REPT-2] 04 p0490 N71-13484

Airline meteorological radar operational policies and procedures
[AD-713636] 05 p0716 N71-14623

Detection of clear air turbulence by radar
[PB-192141] 05 p0716 N71-15057

Radar precipitation data gathered during multiple seeding of hurricane Debbie to test hypothesis that seeding changes storm structure
05 p0716 N71-15075

Meteorological radar data acquisition and processing equipment
[AD-714764] 06 p0890 N71-16015

Meteorological radar study of Caribbean Sea from May through July 1969
[AD-714919] 06 p0892 N71-16507

Research and development program and operational requirements for better radars and remote displays
06 p0817 N71-16790

Receiver for optimal weather radar processing of signals reflected from clouds and precipitations
[D-3-70-03] 07 p0991 N71-16986

Radar measurements of precipitation
07 p1053 N71-17186

Meteorological radar equipment and data analysis of clouds and precipitation
07 p1053 N71-17187

Weather outline generators for producing contours around radar weather center for all weather air navigation
07 p1054 N71-17527

Pulse radar for measuring wind speed in upper atmosphere by observing drift of ionized meteor trails
[AD-715929] 08 p1162 N71-18555

Microwave radar scattering cross sections of dry and wet ice spheres calculated from Mie scattering equations - tables
[TR-21] 09 p1579 N71-19448

Real time weather radar data on tropospheric microwave attenuation by rain
10 p1522 N71-21416

Meteorological radar for detection of thunderstorms, hail, and turbulence hazardous to aviation noting echo interpretation and radar transmission
[WMO-264-TP-148] 13 p2104 N71-24394

Cloud growth and rainfall analysis after pyrotechnic silver iodide cloud seeding in Florida based on meteorological radar data and cloud photographs
[COM-71-40114] 14 p2294 N71-25779

Radar reflectivity, rainfall rate, and drop size distribution measurements
[AD-719878] 14 p2287 N71-25810

Digitizing of radar echoes for presentation of precipitation rate grid maps
[DLR-FB-70-32] 15 p3437 N71-26973

Meteorological radar echo amplitude modulator for continuous data recording
[AD-721249] 15 p3880 N71-27178

Data processing methods for improving FPS-16 radar/lightsphere system measurements of atmospheric motion
[NASA-CR-118997] 16 p3624 N71-28062

Soviet research and developments in meteorology including balloon soundings, radar measurement of precipitation, and numerical weather forecasting
16 p3624 N71-28147

Relationship between disturbed gradients of index of refraction, layer echoes by vertically pointing radar, clear air turbulence and synoptic meteorological conditions
[PB-197765] 18 p2955 N71-31411

Meteorological complex of television tower in Ostankino, Moscow
[AD-723577] 19 p3126 N71-31739

Program device for automatic control of weather radar antenna
[AD-723591] 19 p3128 N71-32039

Interpretation of echoes on weather radarscope
[AD-723678] 19 p3128 N71-32111

Radiosonde and radar echo measurements on area of air/sea interactions over tropical ocean surface with numerical weather forecasting
[NASA-CR-119764] 19 p3190 N71-32731

Statistical model for simulating radar echoes from tropical precipitation for ocean surface region using Nimbus 3 satellite infrared data
19 p3131 N71-32736

Abstracts of BOMEX related conference papers, sample products from BOMEX cloud photography and radar surveillance, and status summaries of BOMEX data processing and reduction
[NASA-CR-119761] 19 p3201 N71-32755

Quantitative and qualitative analyses of BOMEX weather radar data collected by aircraft and land-based radars
19 p3059 N71-32758

One dimensional numerical simulation of dual wavelength radar hail detector
[LAP-TR-34] 20 p3295 N71-33022

Theoretical error analysis of radar measurements of turbulence structure function
[AD-724323] 20 p3257 N71-33082

Doppler signal processing and instrumentation for modified Porcupine C band weather radar
[AD-727776] 23 p3725 N71-36551

Doppler weather radar observing methods and data processing techniques
[AD-727138] 24 p3952 N71-38197

METEOROLOGICAL ROCKETS

U SOUNDING ROCKETS

METEOROLOGICAL SATELLITES

NT ESSA SATELLITES

NT ESSA 3 SATELLITE

NT ESSA 4 SATELLITE

NT ESSA 5 SATELLITE

NT ESSA 6 SATELLITE

NT ESSA 7 SATELLITE

NT NIMBUS SATELLITES

NT NIMBUS 2 SATELLITE

NT NIMBUS 3 SATELLITE

NT NIMBUS 4 SATELLITE

NT NIMBUS 5 SATELLITE

NT SAN MARCO 2 SATELLITE

NT SYNCHRONOUS METEOROLOGICAL SATELLITE

NT TIROS SATELLITES

Meteorological satellite data processing and interpretation
[NASA-TT-F-511] 01 p0077 N71-10089

Satellite-borne instruments for meteorological parameter observations
01 p0077 N71-10090

Interpretation of radiation data obtained by meteorological satellites for long range weather forecasting
01 p0077 N71-10091

Computer processing of meteorological satellite data
01 p0077 N71-10092

Cloud analyses from meteorological satellite television and infrared pictures
01 p0078 N71-10093

Satellite cloud photography and terrestrial radiation measurements
[NASA-CR-111369] 02 p0234 N71-11613

Archiving and climatological applications of meteorological satellite data
[ESSA-TR-NESC-53] 02 p0261 N71-12181

History of meteorological satellites launched to date, and type of data acquired from TIROS, ESSA, and Nimbus for climatological applications
02 p0261 N71-12182

Current operational products from National Environmental Satellite Center
02 p0261 N71-12184

Archival procedures, and available meteorological satellite data for climatology
02 p0261 N71-12185

Satellite observation of atmospheric energetics
[PB-192447] 03 p0403 N71-13174

Abstracts on Soviet meteorological research
05 p0716 N71-14658

Polarization effects on grating efficiency of SIRS B satellite infrared spectrometer
[PB-192130] 05 p0771 N71-15161

Controlled processing of picture data from meteorological satellites
[AD-715892] 08 p1230 N71-18459

Meteorological satellite observations above Europe, Jan. - Mar. 1968
[QR-1] 08 p1230 N71-18538

European Space Research Organization meteorological, communications and air traffic satellites program
08 p1293 N71-18640

Meteorological satellite services
08 p1194 N71-19086

Infrared scanner onboard meteorological satellite for automatic picture transmission of earth and cloud surface
10 p1518 N71-21054

Metal oxide semiconductors and magnetic memories as computer data storage devices for European research organization meteorological satellites
10 p1528 N71-21093

Abstracts and bibliographies of meteorological articles
11 p1788 N71-21953

Project planning for quasi stationary meteorological satellite and orbital research laboratory experiments on atmospheric physics, temperature profiles, and horizon sensing
[BMBW-FB-W-70-70] 11 p1831 N71-22181

Meteorological weather satellite and ground support system
[NASA-TT-F-13646] 13 p2172 N71-24812

Balloon-satellite data system for monitoring and mapping of tropical wind fields at different altitudes
13 p2106 N71-25332

Soviet meteorological satellite borne actinometric equipment and systems engineering
[JPRS-53137] 14 p2253 N71-25838

Satellite activities of organizational elements of NOAA including weather, fisheries services, and environmental research
14 p2337 N71-26107

Launch of USSR Meteor meteorological satellite and equipment for obtaining cloud and snow cover on illuminated and dark sides of earth
15 p2436 N71-26903

Simulation of sensor spatial resolution effects on estimates of cloud cover from satellites
[NASA-TN-D-6247] 15 p2406 N71-26925

Aerospace problems for atmospheric dynamics study with three dimensional convection models, Ekman layer convergence, inertial stability, influence of latitudinal wind shear, and boundary dynamics
[COM-71-00216] 16 p2626 N71-28598

Photographic meteorological charts for snow and ice cover reporting satellite observation over Europe
[QR-1-PT-1] 17 p2776 N71-29382

Meteorological satellite to collect temperature, wind, and pressure data from high altitude free floating balloons, and perform range-rate measurements for balloon position determinations
[NASA-NEWS-RELEASE-71-144] 18 p3014 N71-31031

Tables of meteorological satellite data - ESSA 7 television cloud photography - 1 Jan. 1969 to 31 Mar. 1969
18 p2926 N71-31442

Meteorological weather observations by planned Japanese satellite
[NASA-TT-F-13825] 18 p2953 N71-31491

Feasibility of future ESRO polar orbiting meteorological satellite
20 p3354 N71-33145

Meteorological satellite observations and European weather charts for second quarter of 1969
[QR-2] 20 p3396 N71-33853

Atmospheric density measurements by artificial satellites and comparison with atmospheric models
22 p3679 N71-36232

Satellites in meteorological research and weather forecasting with typical cloud photographs
[NOAA/PI-70033] 24 p4016 N71-38651

METEOROLOGICAL SERVICES
Describing techniques and equipment used by air weather services for fog dissipation
[AD-712392] 03 p0403 N71-12997

Weather forecasting performance accuracy - April 1969 through March 1970
[NOAA-TM-NWS-FCST-16] 06 p0893 N71-16714

Glossary of Air Force weather forecasting terminology
[AD-715932] 08 p1230 N71-18544

Short range terminal forecasting techniques
[AD-716391] 09 p1412 N71-19627

Design of observation and data processing systems for use in first Global Atmospheric Research Program /GARP/ experiment
13 p2104 N71-24423

World mapping of solar radiation distribution
15 p2439 N71-27514

Five-year federal plan to provide air pollution control meteorological service for support of federal, state, and local pollution control agencies
[COM-71-00200] 16 p2589 N71-28853

Operation of weather reconnaissance aircraft and utilization of data obtained during reconnaissance flights in Atlantic Ocean
17 p2778 N71-29556

Requirements for marine international meteorological information service
[WMO-288] 20 p3294 N71-32806

Cost estimates of national projects for international cooperation in meteorological World Data Center
[WMO-289] 20 p3299 N71-33997

Analysis of rhythmic activity of atmosphere for forecasting extreme temperature ranges over USSR area during February
[NLL-M-20355-5828.4F] 21 p3453 N71-34575

Meteorological training in Italy and program for Mediterranean meteorology
[IPA-RDP-31] 22 p3612 N71-35731

Observations of yearly wind conditions and climatology of Denmark
[ISBN-97-7478-002-6] 22 p3612 N71-35733

METEOROLOGICAL STATIONS
U WEATHER STATIONS
METEOROLOGY
NT AEROLGY
NT HYDROMETEOROLOGY
NT LONG RANGE WEATHER FORECASTING
NT MICROMETEOROLOGY
NT NUCLEAR METEOROLOGY
NT NUMERICAL WEATHER FORECASTING
NT POLAR METEOROLOGY
NT RADIO METEOROLOGY
NT STATISTICAL WEATHER FORECASTING
NT SYNOPTIC METEOROLOGY
NT TROPICAL METEOROLOGY
NT WEATHER FORECASTING
Meteorological bibliography for Switzerland
01 p0077 N71-10066

Observation and measurement of ground visibility for meteorological purposes
01 p0078 N71-10119

Abstracts of research in oceanography, astronomy, and meteorology
[JPRS-51452] 01 p0136 N71-10285

Oceanographic and marine meteorological research data
[NASA-CR-111122] 01 p0049 N71-10724

Meteorological, climatology, and physical/chemical oceanography for Caribbean Sea - annotated bibliography
02 p0222 N71-12197

Meteorology, climatology, and physical/chemical oceanography for Caribbean Sea - indexes
02 p0222 N71-12198

Abstracts on Soviet research in astronomy, meteorology, oceanography, geophysics, and upper atmosphere and space research
[JPRS-51760] 05 p0766 N71-14656

Soviet news releases on Cosmos satellites, geophysics, oceanography, meteorology, and astronomy
[JPRS-51856] 05 p0769 N71-15677

Abstracts on Soviet astronomy, meteorology, oceanography, terrestrial geophysics, upper atmosphere, and space research
[JPRS-51991] 07 p1107 N71-16955

Optical heterodyning measurement system applied to meteorology and surface finishing
[BNWL-SA-3335] 08 p1210 N71-19095

Historical development of meteorology - Vol. 1
[TT-69-33106] 11 p1789 N71-22263

Soviet research on astronomy, meteorology, oceanography, geomagnetism, seismology, upper atmosphere, and space program - No. 249
[JPRS-52766] 12 p1995 N71-23176

Compilation of meteorological data for Alaska and Aleutian Islands Vol. 13
[AD-717940] 12 p1956 N71-23943

Sino-Soviet bloc countries accomplishments in sciences of astronomy, oceanography, terrestrial geophysics, and upper air and space
[JPRS-53134] 15 p2396 N71-26901

Soviet research in glaciology, meteorology, astronomy, and space sciences
[JPRS-53253] 16 p2678 N71-28145

Solid state and plasma physics and meteorological research activities
[RISO-M-1300] 16 p2648 N71-28546

Mathematical determination of number of independent data equivalent to number of dependent data and application to meteorological data in USSR
[NLL-M-9263-5828.4F] 16 p2624 N71-29143

Soviet research in meteorology, oceanography, astronomy, and spacecraft launchings
[JPRS-53471] 17 p2861 N71-29399

Soviet news releases on radio astronomy, meteorology, oceanography, geophysics, upper atmosphere, and space program
[JPRS-53367] 18 p3009 N71-30788

Infrared spectrometer for meteorological and atmospheric physics studies
[IFA-SP-8] 18 p2951 N71-30875

Compilation of published results of scientific and technical advancements in marine geology, geophysics, meteorology, and physical oceanography for 1969
18 p2911 N71-30980

Inventory of high level cloud photography mission results during oceanographic and meteorologic experiment in Barbados area
[NOAA-TM-ERL-BOMAP-4] 18 p2925 N71-31383

Numerical analysis of probability of tornado occurrence based on improved reporting procedures and computer programming
[SMRP-49] 19 p3130 N71-32558

Environmental data service facility for dissemination of Barbados oceanographic and meteorological sea/air information
19 p3200 N71-32738

Tables and bibliographic survey for BOMEX program
[NASA-CR-119763] 19 p3201 N71-32765

Temporary BOMEX data archive - tables
19 p3201 N71-32766

Bibliography of BOMEX papers and publications
19 p3201 N71-32767

Meteorological research in time domain data extraction, radio altimetry, and application of ATS data as hydrological tool in remote tropical regions
[NASA-CR-121438] 20 p3371 N71-33870

Methods for classifying atmospheric ice crystals according to geometric form
21 p3452 N71-34565

Flow process of information presented in journal articles on meteorology
[PB-192477] 21 p3452 N71-34568

Soviet research in astronomy, meteorology, oceanography, terrestrial geophysics, and space sciences
[JPRS-53726] 21 p3509 N71-34997

Soviet news releases on astronomy, oceanography, meteorology, geophysics, upper atmosphere, and aerospace activities
[JPRS-53818] 21 p3509 N71-35004

Influence of ship on boom and rawinsonde temperature measurements during BOMEX
[NOAA-TM-ERL-BOMAP-4] 22 p3574 N71-35456

Climatology, geography, geology, and botany of Yukon Territory, Canada and Chitstone Pass, Alaska
[AD-726405] 22 p3615 N71-35762

Daily meteorological charts showing world-wide temperature distribution and variations at 30 millibar level for last quarter of 1970
[QR-4-PT-4] 22 p3616 N71-35767

International cooperation in global atmospheric research program on weather forecasting
23 p3793 N71-37036

Basic physical processes controlling weather and climate
[NP-18828] 24 p3952 N71-38191

Abstracts on solar system, oceanography, meteorology, geophysics, and astronomy
[JPRS-54029] 24 p4036 N71-38796

METEORS
U METEOROLIDS
U MEASURING INSTRUMENTS
METHACRYLATE RESINS
U ACRYLIC RESINS
METHANE
Ion and electron production in proton and hydrogen atom collisions with carbon monoxide, carbon dioxide, methane, and ammonia
[AD-712689] 03 p0436 N71-13377

SUBJECT INDEX

- Oxidation of carbon monoxide/methane mixtures in shock waves
[AD-712331] 04 p0486 N71-13455
- Nitrogen vibrational relaxation and methane oxidation kinetics in shock tube detonations
[AD-714072] 06 p0810 N71-16412
- Unimolecular reactions to calculate rate constants for thermal decomposition of fluoromethane and methane
[AD-715097] 05 p1159 N71-18335
- Comparison of hydrogen and methane as coolants in regeneratively cooled panels
[NASA-CR-1652] 08 p1305 N71-19229
- Equations for mass flow of methane and natural gas mixtures through critical flow nozzles, including real gas effects
[NASA-TX-52994] 10 p1543 N71-21330
- Measurements of thermophysical properties of compressed fluid methane and survey of current literature on liquefied natural gas and methane
[NBS-9781] 11 p1696 N71-22717
- Ultrasonic attenuation in liquid methane measured between 94 to 146 K with pressures to 87 kg/cm²
12 p1871 N71-23722
- Hot firing tests with FLOX/methane propellants for evaluating pyrolytic refractory composite materials for thrust chambers
[NASA-CR-118321] 13 p2101 N71-24974
- Performance prediction of methane-fueled supersonic transport over range of cruise speeds up to Mach 4
[NASA-TM-X-2281] 13 p2028 N71-25384
- Fuel tests to determine feasibility of gelled methane for use in jet engine
[NASA-CR-72876] 14 p2331 N71-25772
- Development of differential, regional boiling water reactor model for prediction of volumetric properties of fluid state of gaseous ethane and liquid methane
14 p2353 N71-26264
- Low-molecule reactions of CH₄-CD₄ mixtures at high pressures in ion source of quadrupole mass filter
[AD-722687] 17 p2717 N71-30230
- Temperature effects on methane formation from hydrogen atom reactions with polycrystalline graphite surfaces
18 p2886 N71-31080
- Kinetics of homogeneous, isotope exchange reactions D₂ plus CH₄, D₂ plus H₂S, and HD plus HD in single-phase shock tubes
18 p2967 N71-31350
- Combustion dynamics of air/methane supersonic diffusion flame in duct
[TP-961] 20 p3365 N71-33449
- Measurement of hypersonic sound speeds in methane at moderate pressure and comparison with ultrasonic speed data
[NASA-CR-121377] 20 p3274 N71-33477
- Atom recombination and methane production from atomic hydrogen reactions on clean metal surfaces
21 p3442 N71-34494
- Glass and steel microsphere sputtering bed properties and model for thermochemical deposition of pyrolytic carbon from methane on nuclear fuel microspheres in sputtered beds
21 p3463 N71-34646
- Evaluation of liquid methane storage and transfer problems for future supersonic aircraft cryogenic fuel requirements
[NASA-CR-72932] 21 p3463 N71-34648
- Reactions of O(1D) atom with nitrous oxide and methane in upper atmosphere
[NASA-CR-121982] 22 p3572 N71-35441
- METHOD OF CHARACTERISTICS**
Method of characteristics for synthesis and identification of distributed parameter systems in control theory
[TR-70-36] 14 p2284 N71-26163
- Method of characteristics for analysis of elastic wave equations in Cartesian coordinates
[NASA-CR-123178] 24 p4023 N71-38705
- METHODOLOGY**
Techniques for determining resonant frequencies, mode shapes, and damping coefficients of model structures
[SC-DR-70-72] 01 p0130 N71-10612
- Determining probabilities of hypotheses using inference and observational data
[NASA-CR-118004] 12 p2019 N71-24204
- Utilization of measuring methods and devices in general industrial applications
[NASA-SP-5926(01)] 16 p2601 N71-28402
- Activation analysis bibliography up to 31 Jan. 1971 including chemical element, methodology, matrix analysis, and author indexes
17 p2717 N71-30267
- Techniques and devices used to solve optical problems - compilation
[NASA-SP-594(01)] 22 p3582 N71-35513
- METHODS**
U METHODOLOGY
U PROCEDURES
METHOXY SYSTEMS
Electron impact changes in methoxy alkane systems using mass spectroscopy
03 p0330 N71-12354

- METHYL ALCOHOLS**
Arithmetic all function corrections for laser excited Raman spectra of carbon tetrachloride and methanol
12 p1934 N71-24068
- METHYL COMPOUNDS**
Delayed action accelerating agent for curing Neoprene compounds
07 p0909 N71-17638
- Kinetics of catalytic dehydrogenation of methylcyclohexane at 600, 650, and 700 deg F and 5 atm pressure
[AD-715926] 08 p1303 N71-18729
- Quantum mechanics of internal rotation in dimethyl silane, ethyl alcohol, and CH₂DSH molecules
09 p1430 N71-19768
- Natural transport effects on fission product behavior in containment systems experiment, time dependence of iodine, methyl iodide, and particulate matter in vapor and steam phases
[BNWL-1457] 11 p1804 N71-22284
- Off-line processing of chromatographic data from fatty acid methyl ester mixtures by digital computer
[UCRL-72393] 11 p1716 N71-22548
- Transport of noble gases in poly(methyl acrylate)
14 p2241 N71-26250
- In-place testing of charcoal adsorbent bed filters with methyl iodide as test penetrant using pyrolyzer-microcoulomb detector
17 p2743 N71-29854
- Effect of gamma radiation on adsorption of iodine and methyl iodide on activated carbon exposed to flowing mixtures of steam and air
17 p2715 N71-29856
- Computer assisted assignment and analysis method for vibration-rotation spectra of methyl bromide
24 p3983 N71-38424
- METHYLHYDRAZINE**
Apollo materials toxicity screening tests and effects of ethylene glycol, monomethylhydrazine, NF₃, OF₂, and C₂F₆
[NASA-CR-111394] 02 p0153 N71-11087
- Research laboratory quality control procedures for acceptance of asymmetric dimethyl hydrazine
[LRBA-NY-75/69/SET/EP] 10 p1637 N71-20829
- Monomethylhydrazine effects on glucose carbon metabolism and effects of pure oxygen inhalation in rats
[AD-727008] 22 p3546 N71-35259
- Hemoglobin compound identification, oxygen involvement, and major breakdown products of monomethylhydrazine effect on blood, in vitro
[AD-727528] 24 p3879 N71-37651
- Human exposure to emergency exposure limit concentrations of monomethylhydrazine to determine suitability for use
[AD-727527] 24 p3879 N71-37652
- METRIC SPACE**
NT. HILBERT SPACE
Relation between metric invariants for infinite measure-preserving Markov shifts
[RR-23/SMR/1] 09 p1411 N71-20340
- Application of mid-order metric space to resistive a-priori network analysis
11 p1727 N71-21947
- Topological invariance of constructive metric spaces
[NLL-RTS-5861] 16 p2620 N71-28036
- Indefinite metric spaces and shadow states in relativistic quantum field theory
[OIRO-3992-30] 22 p3447 N71-36004
- Energy and momentum in imbedding space of four-dimensional space-time
[RIFP-126] 24 p3950 N71-38182
- METROLOGY**
Methods of measurement for semiconductor materials process control, and devices
[NASA-CR-111367] 02 p0282 N71-11418
- Measurement capabilities of Livermore Laboratory Standards Laboratories
[SCL-DR-70-43] 05 p0657 N71-14782
- Sensing arrays using concept of involuntary human eye motion with application to photogrammetry and metrology
[AD-713568] 05 p0684 N71-14893
- Report to Congress on international standards and metric system
[NBS-SP-345-1] 05 p0788 N71-15539
- Resolutions and recommendations of Conference on International System of Units (SI)
[NBS-SP-330] 08 p1206 N71-18489
- Goals, organization, and programs of National Bureau of Standards
[NBS-SP-340] 08 p1291 N71-19049
- Advances in precision metrology, calibration optimization, and standards laboratory techniques
[NBS-SP-335] 12 p1918 N71-23626
- Direction of metrology activities in near future, and responsibilities of National Bureau of Standards
12 p1919 N71-23629
- Radiological measurement technique for minimum wall thickness of small castings, using Sr-90 beta attenuation measurements
12 p1919 N71-23629

- Accelerometer round robin measurement comparisons
12 p1897 N71-23633
- Round robin mass measurements, systematic and random errors, and group variances
12 p2017 N71-23634
- Calibration system specification requirements and approval
12 p2017 N71-23635
- Intervals by exception for calibration interval control
12 p1919 N71-23638
- Calibration history of instrument family used to calculate optimum calibration interval for desired level of confidence
12 p1920 N71-23640
- Breakthrough techniques for cost reduction, and measurement and calibration services
12 p2017 N71-23641
- Adjusting and calibrating mass standards, and designing and manufacturing precision balances in India
12 p1920 N71-23648
- Electrical standards of Japan, dissemination, and traceability and measuring techniques
12 p2018 N71-23650
- Design of inquiring systems of metrology
[NASA-CR-118631] 14 p2358 N71-26003
- Phase transformation transition points on high pressure scale for precise pressure measurement standards
[NBS-SP-326] 14 p2242 N71-26476
- Analysis of impact of conversion to metric measurements on US industries
[NBS-SP-345-1] 18 p2930 N71-31386
- Perturbation theory for improving performance of image sensing arrays and application to metrology
[AD-725422] 19 p3098 N71-31732
- Role of education in US shift to metric system, and advantages, costs, and methods of changeover in schools
[NBS-SP-345-1] 19 p3197 N71-32421
- Cost benefit analysis of metrication on commercial weight and measure units activities
[NBS-SP-345-3] 19 p3199 N71-32720
- Cost analysis and effects of metrication within DOD
[NBS-SP-345-9] 19 p3199 N71-32721
- Survey of metrication effects on US civilian organizations
[NBS-SP-345-21] 19 p3200 N71-32749
- Discussion of cosmological horizons using two dimensional bullock model and metric models
20 p3344 N71-32844
- Evaluation of potential effects of US conversion to metric measurements and standards on foreign trade
[NBS-SP-345-8] 20 p3370 N71-33720
- Definition and identification of gnomons for coordinating human activities with respect to earth environment
[NASA-CR-121639] 21 p3431 N71-34413
- Survey of reactions of nonmanufacturing businesses towards US adoption of metric units of measurement
[NBS-SP-345-5] 21 p3534 N71-35184
- Metrological characteristics of relative pressure transducer and gas flow measurements
[NLL-M-20618(5628-4F)] 23 p3780 N71-36804
- Metric system controversy in USA from 1790 to 1968, legislative activities, and campaigns for and against its adoption
[NBS-SP-345-10] 23 p3869 N71-37586
- METROPOLITAN AIRCRAFT**
U CV-440 AIRCRAFT
MEXICO
Tropical cyclone data for North Atlantic, Caribbean, and Gulf of Mexico - charts
[AD-722035] 19 p3128 N71-32038
- MICA**
Preparation of single crystalline mica specimen support films for electron microscopy, and electron irradiation effects
[AD-717037] 10 p1610 N71-20625
- Geometrical characteristics and thermal stability of nuclear interaction tracks produced by protons and alpha particles in mica
[NASA-CR-118638] 14 p2306 N71-26344
- Preparing composite materials based on silver and synthetic mica - physicochemical and antifiction characteristics
[AD-722819] 18 p2941 N71-31405
- MICE**
NT. POCKET MICE
Histopathological and biochemical effects of decelerations on mice physiology
02 p0162 N71-11807
- Atmospheric pressure and oxygen tension effects on mice infections
02 p0163 N71-11813
- Detection of antigens and genetic analysis with man-mouse hybrids
[SU-326-P-26-X-2] 03 p0322 N71-12360
- Gamma radiosensitivity of female Swiss-Rap mice as function of growth rate
[CEA-R-3797] 09 p1333 N71-20176

MICHELSON INTERFEROMETERS

- Effect of simulated space cabin atmosphere of 100 percent oxygen at 5 psia on immunological response in mice 10 p1500 N71-21333
- Physiological effects of ionized air on mice acetylcholine/cholinesterase system 16 p2543 N71-28252
- MICHELSON INTERFEROMETERS**
- Device using laser interferometer for measuring translational motion with directional accuracy of 0.03 micron 02 p0239 N71-11599
- Measurement of micro-displacements by laser interferometry [REPT-70-75(4)] 02 p0239 N71-11600
- Development and characteristics of fractional fringe HCN laser interferometer [ORNL-TM-3092] 03 p0436 N71-12636
- Performance of Michelson interferometer aboard Nimbus 4 satellite [NASA-TM-X-63395] 05 p0682 N71-14802
- Michelson interferometer with photodetector for optical detection sensing [NASA-CASE-NPO-10320] 07 p1031 N71-17655
- Servo system for retroreflector of Michelson interferometer [NASA-CASE-NPO-10330] 07 p1032 N71-17662
- Measurement of second harmonic distortion in acoustic output of transducer by Michelson laser interferometer technique 16 p2592 N71-28309
- Laser interferometer for studying earth crust strain 20 p3264 N71-33358

MICHIGAN

- Proposed boundaries for metropolitan Detroit-Port Huron intrastate air quality control region 02 p0156 N71-11109

MICROANALYSES

- Microetch technique for analyzing thin layers of striated single crystals 01 p0108 N71-10128
- Electron microprobe analysis of biological materials [UCRL-72513] 01 p0096 N71-10520
- Microprobe analysis of diffusion layers with application to chromatinized Inconel 713 [ONERA-TP-436] 02 p0241 N71-11566
- Computer program for electron microprobe analysis using simple or complex standards [CEA-N-1289] 04 p0574 N71-13672
- Ion exchange beads as microstandards for air purification, chromatography for bilirubin analysis, infrared measurements on polymer crosslinking, and filtration of contaminants [NBS-TN-549] 05 p0641 N71-15595
- Microchemical analyses of air pollutants and preparation of standard reference materials for gas analysis [NBS-TN-545] 05 p0641 N71-15596
- Influence of impurities on microanalysis of soil mixtures using absorption spectrophotometry [REPT-70-5-70-05] 07 p0987 N71-16698
- Atom probe field ion microscope with time of flight spectrometer [UCRL-20303] 07 p1029 N71-17576
- Electron and ion microprobe analyses of Apollo 12 fines and breccia [NASA-CR-114871] 08 p1289 N71-18878
- Electron microprobe and diffraction for microbiology and microanalysis of lunar rocks [NASA-CR-116916] 08 p1204 N71-19311
- Homogeneity characterization of Fe-3Si alloy microanalysis standard reference material [NBS-SPEC-PUBL-260-22] 10 p1577 N71-21027
- Instrumental and chemical developments for applying kinetic methods to quantitative microanalysis [AD-717187] 10 p1515 N71-21487
- Techniques for dimensional measurement, and chemical and metallographic microanalysis of irradiated nuclear fuel specimens 13 p2128 N71-24532
- Microprobe analysis of fission gas xenon retention by UO₂ and UO₂ fuels dispersed in aluminum cladding 13 p2114 N71-24536
- Electron microprobe analysis of metallic fission product inclusions in irradiated mixed-oxide fuels for molybdenum [WHAN-SA-96] 13 p2120 N71-25218
- Spectrometer for microdynamics of condensed matter emphasizing automation and remote control of spectrometer kinematics and delay systems [DNP-727] 15 p2470 N71-27408
- Signal analyzer to detect microquantities of radioactive gases 24 p4012 N71-38621

MICROBALANCES

- Quartz crystal microbalance measurements of spacecraft contaminants 09 p1389 N71-20206
- Ultraviolet radiation and quartz crystal microbalance analysis of vacuum chamber cleanliness and effects of chamber use history and pumping mechanism on contamination [NASA-TM-X-65571] 15 p2392 N71-27708

MICROBE U MICROORGANISMS MICROBEAMS

- Content mapping techniques for qualitative and semiquantitative analysis with electron microbeam probe [AD-714567] 06 p0875 N71-16727
- MICROBIOLOGY**
- NT BACTERIOLOGY**
- Determining microbial population of Surtsey by microbiological techniques 07 p0984 N71-17992
- Electron microscopy and diffraction for microbiology and microanalysis of lunar rocks [NASA-CR-116916] 08 p1204 N71-19311
- Electron microscopic and holographic methods for data condensing and retrieval, and microbiology 08 p1205 N71-19317
- Dermal and environmental microbiological data from long duration manned space station simulation 10 p1498 N71-20991
- Chlamydomonas bacterial sensor for water pollution detection during long term manned space station simulation 10 p1498 N71-20993
- Causes of spacecraft external contamination and approaches for counteracting contamination [DOC-70SD260] 10 p1501 N71-21576
- Development of environmental control system for determining effects of relative humidity and dry heat on inactivation of microorganisms [NASA-CR-118024] 12 p1868 N71-23823
- Description of spacecraft microbial contamination and techniques for reducing level of contamination [NASA-CR-118017] 12 p1863 N71-23825
- Automated microbial metabolism life detection experiments for exobiological studies [NASA-CR-118659] 14 p2206 N71-26380
- Microbial corrosion emphasizing mechanisms of anaerobic corrosion produced by sulfate-reducing bacteria primarily those in genus desulfovibrio [AD-720693] 14 p2275 N71-26393
- Development of clinical pathology procedures for detection of diseases in germfree mice and detection of titanium in lymphoid structures of hamsters, mice, and rats [NASA-CR-118671] 14 p2206 N71-26399
- Microbiological life support requirements in long term manned space flights 16 p2552 N71-28537
- Problems of mathematical modeling in microbiological processes [JPRS-53452] 17 p2707 N71-29257
- Research in microbiology for planetary quarantine [NASA-CR-119313] 18 p2874 N71-30663
- Development and characteristics of vacuum probe surface sampler for obtaining particulate contamination on surfaces [NASA-TM-X-67253] 18 p2924 N71-31030
- Mathematical models of microbiological production processes [JPRS-53634] 18 p2877 N71-31271
- Application of environmental microbiology to spacecraft quarantine procedures [NASA-CR-119638] 19 p3041 N71-31601
- Bibliography of scientific publications and presentations relating to planetary quarantine for year 1970 - Vol. 5 [NASA-CR-121325] 19 p3044 N71-32231
- Copenhagen explication of quantum mechanics and its application to microworld [ITF-70-62-E] 19 p3156 N71-32426
- Analysis of water pollution and application of biogeocenology techniques to eliminate effects of water pollution 20 p3224 N71-33508
- Proceedings of conference on interaction between atmospheric environment and human system at cell level [AD-720601] 22 p3545 N71-35256
- Microbiological characterization of soil types [NASA-TT-F-13907] 23 p3715 N71-36483
- Microbiological contamination of Apollo spacecraft components [NASA-CR-122844] 24 p3878 N71-37642
- Germicidal ultraviolet effects on spores and development of biphasic survival curve [ORO-3408-10] 24 p3878 N71-37646
- MICROCALORIMETERS**
- U CALORIMETERS**
- Absolute capacitance microcreep and dimensional stability measuring system [NASA-TM-X-2046] 22 p3585 N71-35530
- MICROCIRCUITS**
- U MICROELECTRONICS**
- MICROCLIMATOLOGY**
- Measuring geographical distribution of mean of absolute annual temperature minima for use in construction of buildings and living quarters [NLL-M-9142-/5828.4F/1] 02 p0256 N71-11461
- Microclimatological measurements in new building development in northern Leningrad [NLL-M-9144-/5828.4F/1] 02 p0259 N71-11798

SUBJECT INDEX

- Effects of town-suburb growth on secular variation of microclimatic air temperature around Moscow [NLL-M-9257-/5828.4F/1] 19 p3128 N71-32138
- MICROCRACKS**
- Acoustic emission testing and microfracture processes in solids [AD-715019] 07 p1127 N71-17933
- Metallographic determination of microcrack emergence in martensite of Fe-Ni-C system [NLL-TRANS-746-557-/9022.401/1] 10 p1586 N71-21840
- MICROCRYSTALS**
- Computational method for electron diffraction intensity using n-beam theory and applied to gold microcrystal calculations 10 p1621 N71-21742
- MICRODENSITOMETERS**
- Computer graphic mapping of Maryland coasts from aerial color and infrared photographic remote sensors including microdensitometer analysis [RM-5991] 17 p2749 N71-30176
- MICROELECTRONICS**
- NT LARGE SCALE INTEGRATION**
- NT MEDIUM SCALE INTEGRATION**
- Research and development in plasma physics, information theory, microelectronics, and related areas [AD-710695] 01 p0069 N71-10462
- Proceedings from lecture series on large scale integration in microelectronics [AGARD-LS-40-70] 03 p0354 N71-12626
- Technology review on large scale integration circuitry 03 p0354 N71-12627
- Microelectronics, large scale integrated arrays, electronic packaging, thin film epitaxy, computerized design, radar equipment [NASA-CR-109734] 04 p0512 N71-13539
- Separation of semiconductor wafer into chips bounded by scribe lines [NASA-CASE-ERC-10138] 04 p0603 N71-14354
- Diffusion and structural changes in microcircuit interconnections subjected to heat treatment [NASA-CR-115903] 05 p0656 N71-14976
- Investigating materials and microelectronics for solid state devices [AD-714079] 06 p0935 N71-16324
- Microelectronic Navy equipment [AD-715108] 07 p1000 N71-17935
- Beam lead technology for microcircuit interconnections with applications to metallization, passivation, and bonding [NASA-CR-111838] 09 p1362 N71-19422
- Measurement methods during fabrication and environmental testing of microcircuits 09 p1360 N71-20228
- Conduction mechanisms in thick film microcircuits using ruthenium dioxide tests [AD-718414] 12 p1888 N71-23530
- Active tuned circuit fabricated by microelectronic techniques with tuning capability for operation at frequencies near transitional frequency of transistor arrays [NASA-CASE-GSC-11340-1] 13 p2060 N71-24902
- Basic process steps for fabrication of thick or thin film microcircuits for NASA use [NASA-CR-103126] 13 p2060 N71-25391
- Manufacturing quality controls for line certification of thin film and thick film hybrid microcircuits for NASA use [NASA-CR-103168] 14 p2232 N71-25905
- Large scale integration and metal oxide semiconductor microelectronic testing techniques including combinatorial, sequential, functional, and parametric methods [NASA-CR-103165] 14 p2235 N71-26703
- Large scale integration microelectronic wafer and package testing including parametric and functional tests of combinatorial and sequential logic circuits [NASA-CR-103166] 14 p2236 N71-26704
- Major microelectronic production technologies including materials for manufacturing thin and thick film circuits, monolithic integrated circuits, and hybrid design [AD-721279] 15 p2385 N71-26897
- Vibrophonocardiograph comprising low weight and small volume piezoelectric microphone with amplifier having high input impedance for high sensitivity and low frequency response [NASA-CASE-XFR-07172] 15 p2374 N71-27234
- Electrical connections for thin film hybrid microcircuits [NASA-CASE-XMS-02182] 16 p2575 N71-28783
- Solid state device and materials, physics of solids, and microelectronics research [AD-721464] 16 p2667 N71-28845
- Method for coating through-holes in ceramic substrates used in fabricating miniaturized electronic circuits [NASA-CASE-XMF-05999] 16 p2604 N71-29032
- High efficiency mode diodes, waveform, and circuit studies for improving avalanche oscillators [SC-CR-70-6171] 17 p2725 N71-29423

SUBJECT INDEX

MICROPHONES

Solid state devices, solid state materials, solid state physics, and solid state research projects applied to microelectronics
 (AD-724974) 20 p3332 N71-32965
 Alpha and gamma radiation detectors and measuring instruments for semiconductor materials, process control, and devices
 (NASA-CR-121459) 20 p3333 N71-33398
 Microelectronic power supply circuits for aerospace applications
 (NASA-CR-119918) 20 p3214 N71-33595
 Operating characteristics of avalanche diodes in microelectronic circuits
 (AD-726558) 22 p3561 N71-35362
 Reliability tests on face down bonded hybrid microcircuits
 (NASA-CR-119949) 23 p3733 N71-36624
 Conference on research, development, and applications of integrated microelectronic circuits
 23 p3733 N71-36625
 Microelectronic linear integrated circuits for radar equipment and telecommunications
 23 p3736 N71-36643
 Construction of thin film active circuits using hybrid techniques
 23 p3737 N71-36645
 Interrelations between advanced processing techniques, integrated circuits, laser radiation, and microcircuit interconnections
 (NASA-CR-123087) 24 p3900 N71-37799
 Auger electron spectroscopy, surface contamination, and silicon device parameters for microcircuits
 (NASA-CR-121013) 24 p3901 N71-37804
MICROFILM
 Computer produced microfilm in pseudocolor transformations
 (AD-713901) 06 p0859 N71-16291
 Editing system for large general time sharing computer including dynamic editing display techniques and static microfilm method
 (NASA-TM-X-2264) 11 p1716 N71-22575
 Apparatus for semiautomatic inspection of microfilmed documents for density, resolution, size, and position
 (NASA-CASE-MPS-20240) 14 p2259 N71-26785
MICROGRAPHY
U PHOTOMICROGRAPHY
MICROHARDNESS
 Hot microhardness program MICHRED
 (GEMP-725) 04 p0503 N71-13664
 Hot microhardness values for irradiated and nonirradiated refractory metals and alloys
 (GEMP-716) 04 p0560 N71-14359
 Host treatment effect on microhardness, wear, and corrosion resistance of chemically deposited nickel coatings
 (NLL-TRANS-746-599-19022.401) 10 p1578 N71-21219
 Microstructure and microhardness of electroless nickel deposits alloyed with tungsten
 (NLL-TRANS-746-675-19022.401) 23 p3775 N71-36903
 Relationship between microhardness of materials and thickness of wear resistant coatings
 (AD-727416) 24 p3944 N71-38136
MICROINDENTATION
U MICROHARDNESS
MICROINSTRUMENTATION
 Microdensitometer for entomological investigations
 (AD-713473) 05 p0653 N71-14984
MICROMANOMETERS
U MANOMETERS
MICROMETEORITES
U MICROMETEORITIDS
MICROMETEORITIDS
 Activation analysis to identify materials for use as casing for micrometeoroids
 (NASA-CR-108707) 05 p0454 N71-13199
 Pressurized cell micrometeoroid detector
 (NASA-CASE-XLA-00936) 05 p0685 N71-14996
 Development of large area micrometeoroid impact detector panels
 (NASA-CASE-XLA-00906) 06 p0950 N71-14221
 Micrometeoroid space environment simulation and meteoritic damage to mirror reflectance
 (ONERA-DERTS-NT-01-12) 07 p1108 N71-17218
 Computer controlled micrometeoroid impact simulation system
 (NASA-TM-X-66947) 09 p1348 N71-20253
 Rotary bead dropper and selector for testing micrometeorite transducers
 (NASA-CASE-XGS-03304) 11 p1726 N71-22988
 Measuring micrometeoroid depth of penetration into various materials
 (NASA-CASE-XLA-00491) 12 p1917 N71-23240
 Evaluation of hypervelocity particle accelerator facility to determine impact effects of micrometeoroids on solar cells
 (NASA-TN-D-7017) 12 p1897 N71-23908
 Structure of fabric layers for micrometeoroid protection garment with capability for eliminating heat shorts for use in manufacturing space suits
 (NASA-CASE-MSC-12109) 14 p2240 N71-24285

Use of Pioneer 7 and 8 cosmic dust detectors in Apollo 17 lunar ejecta and micrometeorite experiment to measure meteoroid fluxes on moon
 (NASA-CR-118663) 14 p3339 N71-26441
 Positive electron irradiated failure modes of MOS micrometeoroid capacitor detectors
 (NASA-CR-111892) 15 p2591 N71-28625
 Design features of Black Arrow X3 aircraft and experiments including thermal control finishing, improved lightweight solar cell assemblies, and hybrid electronic assemblies
 (RAE-TR-69393) 16 p2682 N71-28140
 Mineral composition and structure of magnetite spherules of meteoric dust
 (REPT-14) 18 p3017 N71-31332
 Experimental data on high velocity impacts up to 20 km/sec applied to punctures in space and concentration of micrometeoroid material near earth
 (NASA-TT-F-13740) 18 p3022 N71-31484
 Micrometeoroid analyzer using arrays of interconnected capacitors and ion detector
 (NASA-CASE-ARC-10443-1) 21 p3427 N71-34382
 Calibration of diaphragm condenser microphone for micrometeoroid impact gauge
 (UTIAS-TN-157) 23 p3739 N71-36800
 Micrometeoroid impact experiments conducted on Gemini 9 and 12 missions
 (NASA-TM-X-2408) 23 p3856 N71-37489
MICROMETEOROLOGY
 Winter turbulence characteristics in mountain valley surface boundary layer
 (AD-714754) 06 p0890 N71-15979
 Research on Arctic sea ice heat and mass budget, sea ice drift, micrometeorology, radiation, atmospheric chemistry, and Arctic oceanography
 (AD-715450) 08 p1190 N71-18731
 Plant growth enhancement using windbreaks to reduce evapotranspiration from summer winds
 (PR-195927) 09 p1412 N71-19612
 Micrometeorological investigations of momentum, energy, and mass transfers above vegetative surfaces with von Karman constant, diabatic profile functions and eddy-transfer coefficients
 (AD-721301) 16 p2625 N71-28225
 High speed, and high resolution sensors for micrometeorological measurements of atmospheric temperature and moisture
 (AD-721456) 16 p2626 N71-28645
 Climatological and micrometeorological measurements for analysis of climate and energy exchange on subarctic ice cap in summer
 (AD-721546) 16 p2627 N71-29076
 Micrometeorological data acquired during advection conditions from California
 (AD-724612) 20 p3295 N71-32990
 Micrometeorological parameters for Gun Hill, Panama Canal Zone, October 1970
 (AD-726356) 22 p3614 N71-35750
 Micrometeorological parameters for Fort White, Alaska, for December 1970
 (AD-726937) 22 p3614 N71-35752
 Micrometeorological data for sites in Hunter-Liggett Military Reservation - Nov. 1970
 (AD-726355) 22 p3615 N71-35756
 Micrometeorological data for Hunter-Liggett military airfield - Nov. 1970
 (AD-726347) 22 p3615 N71-35757
 Micrometeorological field data including energy balance components, temperature profiles, and wind profiles from California
 (AD-726390) 23 p3790 N71-37014
MICROMETERS
U MICROMETEORITIDS
MICROMETERS
 Electron accelerator magnet ring survey using particle telescope with micrometer and harmonic analysis for orbit distortions
 (CEAL-1057) 13 p2125 N71-24905
MICROMINUTIZATION
NT LARGE SCALE INTEGRATION
 Investigating federated and integrated approaches to digital computer design for aerospace vehicles
 03 p0346 N71-12605
 Calculation of digital current distribution systems on micron tape cores
 (AD-714768) 06 p0822 N71-15936
 Development of high performance, digital microcircuit components, and their application to data processing systems
 (AD-714800) 06 p0823 N71-16416
 Integrated circuit development, photolithographic interconnection of plastic embedded semiconductor chips, semiconductor testing, magnetic film engineering, and computer applications
 (AD-722075) 16 p2665 N71-28557
 Developments in integrated circuit production and utilization as computer components
 (JPRS-53659) 18 p2901 N71-31555
 Identification and development of microelectronic ultrahigh frequency power assembly compatible with monolithic fabrication techniques
 (AD-724303) 20 p3240 N71-32913
MICROMINUTIZED ELECTRONIC DEVICES
 Microminutized frequency discriminator with semiconductor without induction components
 (PUBL-2) 05 p0636 N71-13517

Investigating nervous system regulation of intracellular pressure and fabrication of hybrid microcircuits
 06 p0902 N71-15857
 Simplified method of hybrid microcircuit fabrication based on use of leadless inverted semiconductors
 06 p0826 N71-15859
MICROORGANISMS
NT BACILLUS
NT BACTERIA
NT BACTERIOPHAGES
NT ESCHERICHIA
NT HYDROGENOMONAS
NT MICROSPORES
NT PARAMECIA
NT PROTOZOA
NT SPORES
NT STREPTOCOCCUS
NT VIRUSES
 Microbial burden sterilization assembly procedure development using rigorous monitoring program
 (NASA-CR-111093) 01 p0810 N71-10374
 Investigating spacecraft coatings for resistance to growth of microorganisms
 (NASA-CR-111524) 03 p0397 N71-13017
 Design and fabrication of plastic vacuum probe surface sampler to determine microbial populations
 (NASA-CR-111796) 05 p0683 N71-14831
 Characteristics of bacterial spore population from Cape Kennedy soil
 (NASA-CR-116182) 06 p0799 N71-15840
 Thermodynamic studies on microorganisms for spacecraft sterilization
 (NASA-CR-111509) 06 p0799 N71-16022
 Development of bacteriostatic conformal coating and methods of application
 (NASA-CASE-GSC-10007) 06 p0877 N71-16046
 Corrosion resistance of polymeric petroleum lubricants against microbiological attack
 (AD-714133) 06 p0878 N71-16208
 Searching for Precambrian relict microorganism in Iceland
 07 p0904 N71-17590
 Investigating shifts in composition of astromicroflora on skin and state of natural immunity of cosmonauts during prolonged flight aboard Soyuz 9 spacecraft
 08 p1151 N71-18907
 Resume of publications and recommendations from symposium on intestinal flora ecology in changing environments
 (NASA-CR-114889) 09 p1330 N71-19783
 Modification of Berman-Sivakaya method for neutral pH digestive capability determination
 (NASA-TT-F-13533) 09 p1333 N71-20150
 Investigation of movement of ciliary infusoria in hydraulic medium
 (JPRS-52581) 10 p1503 N71-21713
 Development of environmental control system for determining effects of relative humidity and dry heat on inactivation of microorganisms
 (NASA-CR-118064) 12 p1868 N71-23823
 Effect of wood-destroying fungi on destruction of hydrolytic lignin
 (AD-713924) 20 p3286 N71-32962
 Terrestrial organisms survive in simulated Jupiter atmosphere - studies with one-celled algae and aquatic plant (Elodea)
 (NASA-TT-F-13905) 20 p3349 N71-33588
 Effect of hard impact and abrasion erosion on release of microorganisms from geological formations
 (NASA-CR-121707) 21 p3381 N71-34056
 Adaptation of terrestrial microorganisms to simulated Jupiter environment
 (NASA-TT-F-13946) 23 p3714 N71-36472
 Analysis of probable viable terrestrial microorganisms on Mars caused by Mariner Mars 1971 Project
 (NASA-CR-122845) 24 p3878 N71-37643
 Analysis of pressure differentials required to prevent passage of airborne microorganisms through holes in membranes acting as barriers
 (NASA-CR-1910) 24 p3879 N71-37655
MICROPARTICLES
 Thin film penetration by hypervelocity microparticles of carbonyl iron
 (NASA-TM-X-2065) 09 p1389 N71-19932
 Determining micro amounts of elements contained in natural water by means of neutron-activation analysis
 (RT/CHE-70103) 23 p3812 N71-37175
MICROPHONES
 Calibration of laboratory standard microphones in diffuse sound fields to establish primary specifications
 01 p0938 N71-10001
 Measuring velocity of sound through two-component solid-gas medium as function of solid particle concentration
 (AD-712412) 03 p0418 N71-13048
 Pressure fluctuation measurements with microphones in air jet free flow
 (DLR-FB-70-22) 07 p1008 N71-17142
 Audio signal processing system for noise surge elimination at low amplitude audio input
 (NASA-CASE-MSC-12223-1) 14 p2218 N71-26181
 Vibrophonocardiograph comprising low weight and small volume piezoelectric microphone with amplifier

- having high input impedance for high sensitivity and low frequency response
[NASA-CASE-XPR-07172] 15 p2374 N71-27234
- Development of wind tunnel microphone structure to minimize effects of vibrations and eliminate unwanted signals in microphone output
[NASA-CASE-XNP-00250] 16 p2578 N71-28779
- Development of prototype miniaturized microphone for electrocardiography
[NASA-TM-X-63580] 16 p2572 N71-28901
- Design of 6-channel stereomicroscope amplifier prototype
[LEA-292] 18 p2897 N71-30587
- Calibration of diaphragm condenser microphone for microtearoid impact gauge
[UTIAS-TN-157] 23 p3759 N71-36800
- MICROPHOTOGRAPHS**
Horizontal laminar flow clean room complex for microphotography
[AD-711938] 02 p0199 N71-11535
- MICROPHOTOMETERS**
U PHOTOMETERS
MICROPROGRAMMING
Permanent read only memory
[AD-713048] 04 p0304 N71-13832
- Parallel microcomputer for emulating sequential and parallel computer control structure
[SLAC-127] 09 p1355 N71-20088
- Virtual memory management system with working set model suitable for microprogramming
[NASA-CR-118310] 13 p2052 N71-24915
- Use of block-circuit method for synthesis of microprograms
[AD-722829] 18 p2900 N71-31294
- MICROPULSATIONS**
NT GEOMAGNETIC MICROPULSATIONS
MICROSCALES
U MICROBALANCES
MICROSCOPES
NT ELECTRON MICROSCOPES
NT ION MICROSCOPES
NT OPTICAL MICROSCOPES
Velocity measurement using microscope and high speed cameras
[PB-195163] 07 p1026 N71-16927
- Influence of microscopic objectives on measurement of modulation transfer function of optical systems determined for high speed lens
[RAE-LIB-TRANS-1522] 10 p1607 N71-21442
- Program connecting measuring microscopes PUOS with computer Minsk-2
[IFVE-SFK-49-53] 15 p2384 N71-27362
- MICROSCOPY**
Microscopic analysis theoretical model for elastic scattering of deuterons and alpha particles
[CTC-32] 01 p0100 N71-10744
- Technology review on macroscopic and microscopic fracture mechanics
[AD-714693] 06 p0953 N71-15998
- Precipitation behavior of lead and sodium alloys between negative 20 and 100 C using optical and electron microscopy
[NLL-CE-TRANS-5252-9022.091] 10 p1584 N71-21602
- Survey and critique of bacterial growth quantitative determination methods including Bacillus coli direct microscopic morphology and growth measurement
[NASA-TT-F-13452] 13 p2032 N71-24584
- Role of gravitation in elementary particle theory, microscopic parameters and macroscopic values
[JINR-P2-5289] 14 p2310 N71-26668
- Feasibility analysis for future use of television microscopy to detect extraterrestrial life
[NASA-TT-F-13733] 17 p2753 N71-29819
- Measurement of artifact surface vacancies induced on gold surface by neon field ion microscopy and image intensification
[NYO-3504-53] 21 p3439 N71-34475
- MICROSEISMICS**
Microseismic rock noise rates for determining slope stability in pit mining
[BM-81-7470] 05 p0677 N71-15501
- Alaskan earth tides, crustal failure, and microseisms
[RLO-2095-2] 07 p1019 N71-17272
- Comparison of long period microseisms and flexural gravity waves measured at Mirny in Antarctica
11 p1753 N71-22810
- Microseismic analysis of Denali fault in Alaska and under ground nuclear explosions and microseismic survey of Nevada, Utah, Idaho, Montana, and Wyoming
22 p3580 N71-35504
- MICROSPORES**
Computerized modeling of ultraviolet and thermal radiation inactivation of spores
[NASA-CR-111386] 02 p0150 N71-11066
- MICROSTRUCTURE**
NT METEORITIC MICROSTRUCTURES
Structural parameters effect on tempered martensite and lower bainite yield strength
[AD-710789] 01 p0067 N71-10561
- Homogeneous constitutive equations for describing falling microstructure of polymeric materials with plastic memory
[AD-711657] 01 p0114 N71-10689

- Scanning electron microscope operation and micrographs of microstructure and fracture in metals
[M6A/37/69] 02 p0224 N71-11527
- Microstructural and fractographic studies of boron carbide ceramics subjected to ballistic impact and static flexural loading
[AD-712307] 02 p0247 N71-11664
- Metallurgical characteristics and photomicrographs of Transit capsule piece parts
[AI-AEC-12967] 03 p0413 N71-12642
- Structure and properties of high strength ferrous alloys EP404 and EP454
[AD-713048] 03 p0393 N71-13037
- Heat treatment effects on creep properties and microstructure of tantalum base alloy
03 p0394 N71-13306
- Microstructure and mechanical properties of martensite transformed from precipitation hardened austenite
[UCRL-19196] 04 p0530 N71-14091
- Grain structure of high purity copper melts undercooled before nucleation
[REPT-374] 05 p0702 N71-15068
- Investigating relationship between ultrasonic indication and actual characteristics of defects in alloys
[ZJFE-83] 05 p0726 N71-15076
- Using gas sheathed tubular electrode arc for alloy analysis
[AD-713690] 05 p0703 N71-15214
- Dependence of fatigue life and flow stress on microstructure of precipitation hardened Al-Cu alloys
[AD-714085] 06 p0872 N71-16543
- Assessment of surface and subsurface damage in ceramics caused by semi-finish grinding machines
[AD-714491] 06 p0879 N71-16395
- Grain growth inhibition in sintered pure and barium doped sodium potassium niobate
[UCRL-19668] 06 p0935 N71-16441
- Quantitative texture analysis of titanium by X ray diffraction
[AD-713985] 06 p0874 N71-16451
- Biogeochemical and microstructural analyses on lunar rock and dust samples for biological compounds
[NASA-CR-114839] 07 p1113 N71-17717
- Microscopic analyses of Apollo 12 lunar samples for biogenic structures
07 p1113 N71-17718
- Microscopic analyses of Apollo 11 lunar samples for biogenic structures
07 p1113 N71-17719
- Microscopic analyses of Apollo 11 lunar rock and dust samples for biological activities
07 p1113 N71-17721
- Quantitative determination of structure-property relationships in nuclear fuel element materials
[SRO-552-5] 08 p1238 N71-18327
- Mechanical properties and microstructure of titanium alloy after heat treatment
[AD-715353] 08 p1213 N71-18523
- Microstructural characterization of proprietary ceramic armor
[AD-715352] 08 p1221 N71-18541
- Investigating effects of heating rate, maximum temperature, and thermal cycling on transformation temperatures, hardness, and dimensional anisotropy in sintering steels
[UCRL-72099] 08 p1217 N71-19005
- Electron microscopic analysis of wear resistance on nickel surface structures
[AD-715435] 08 p1217 N71-19012
- Microprobe scanning for analyses of protective chromium aluminum layer on Inconel turbine blade
[NASA-TT-F-13497] 08 p1218 N71-19027
- Quantitative relationships between microstructure and properties in nuclear fuel elements
[SRO-552-4] 09 p1416 N71-19393
- Brittle fracture of alloyed, high density, fine grained, and pure alumina
[AD-715988] 09 p1405 N71-19803
- Manufacturing of improved carbon and graphite materials
[NASA-CR-117315] 09 p1407 N71-20373
- Uranium-base niobium alloy and nitric acid reactions and alloy explosive behavior due to two-phase microstructure and high carbon content
[RFP-1575] 10 p1511 N71-20700
- Microstructure and magnetic properties of internally oxidized ferromagnetic alloys for application to magnetic domain theories and high temperature tests
[AD-717210] 10 p1579 N71-21301
- Fracture toughness of precipitation hardening aluminum alloys with microstructure and fractography observations
10 p1581 N71-21441
- Thermomechanical processing effects on crystal microstructure, texture, and high temperature strength of dispersion strengthened and free nickel-based Cr, TiO₂, and W alloys
[NASA-CR-72832] 10 p1583 N71-21589
- Microstructure and mechanical properties of boronized medium carbon steels
[NLL-TRANS-746-527-9022.4011] 10 p1584 N71-21604
- Microstructural research on carbon and graphite for use as engineering materials
[NASA-CR-117494] 10 p1591 N71-21841

- Preparation and characteristics of silica glass, determination of glass structure by Raman spectroscopy, hydrogen impregnation of glass, and growth of silver iodide crystals
[AD-717647] 11 p1781 N71-21929
- Anisotropy and crystal structure of Ni-P alloy thin films, and Lorentz microscopic study of magnetic microstructure
11 p1815 N71-21948
- Microstructure and electrical properties of thin epitaxial films of lead telluride and effects of microstructure on electrical properties
11 p1815 N71-22102
- Preparation of transparent homogeneous amorphous germanium glasses by rapid quenching of liquids and vapor depositions
[AD-717352] 11 p1782 N71-22228
- Homogeneous continuum for describing mechanical behavior of laminated composite elastic solids
[AD-717731] 11 p1838 N71-22517
- Effects of welding and post-weld heat treatment on microstructure and mechanical properties of QT steel
[REPT-2] 11 p1769 N71-22541
- Microstructure and high temperature tensile properties of internally nitrated molybdenum alloy
[UCRL-72627] 12 p1936 N71-23109
- Microstructural analysis, mechanical properties, and thermal conductivity of sintered nickel and uranium dioxide
[SRO-552-6] 12 p1961 N71-23195
- Determining microstructure of clouds and fogs by light scattering
[RAE-LIB-TRANS-1529] 12 p1952 N71-23237
- Trace element influence on aluminum-copper alloy quenching microstructure and precipitation hardening
12 p1934 N71-23718
- Microstructure, dimensional, and chemical analysis of neutron irradiated UN fuel specimens
13 p1144 N71-24541
- Microstructure of spinodal alloys determined by electron microscopes
[UCRL-19629] 13 p2093 N71-24871
- Effect of plastic deformation on distribution of microcracks and structure of mild steel
[AD-719832] 13 p2096 N71-25159
- Steel microstructure, surface austenite and carbide formation, and diffusion coefficient measurement during chemical and thermal treatment
[TT-70-59099] 14 p2269 N71-25660
- Austenite intergranular structure effect on self diffusion of iron
[TT-70-57068] 14 p2271 N71-25816
- Radiation induced photochemical reactions in polyisoprene and polybutadiene thin films including microstructural changes
[NASA-TM-X-62021] 14 p2213 N71-26028
- Production of high strength refractory compounds and microconstituents into refractory metal matrix
[NASA-CASE-XLE-03940] 14 p2279 N71-26153
- Effects of silicon on strength and microstructure of aluminum alloys
14 p2275 N71-26524
- Properties and selective applications of high strength steels
15 p2421 N71-27040
- Microstructure precipitates in austenitic steel exposed to neutron irradiation
[CEA-CONF-1638] 15 p2424 N71-27406
- New briefs and abstracts of scientific articles concerning microstructure of aerosols, wind components, and triggering mechanism in thunderstorms
17 p2776 N71-29401
- Effect of orientation and specimen thickness on fatigue crack growth rate of 4340 steel
[AD-722728] 17 p2765 N71-29812
- Metallurgical and elastic moduli measurements on two phase isotropic microstructures
17 p2765 N71-29805
- X ray diffraction method for determining high temperature creep in Nicrobrome structure
[NLL-TRANS-746-339-9022.4011] 17 p2765 N71-29808
- Phase microanalyses on quench hardened iron magnetic alloy structures
[NLL-RTS-6321] 17 p2767 N71-30351
- Effects of heat and mechanical treatment on microstructure of titanium and its alloys
[AD-722822] 18 p2928 N71-30807
- Room temperature tensile properties and changes in microstructures of steel XCRNiMoVNb 1613 /49081, Incolloy 800, and Inconel 718 after aging at 663 to 800 C
[EURFNR-875] 18 p2935 N71-30907
- Thermal treatment, thermal equilibrium, and microstructural effects on intergranular creep in sintered and fused cast aluminas
18 p3022 N71-31367
- Time dependent rheological properties of thixotropic fluids as influenced by microscopic structural breakdown and reformation
18 p2987 N71-31443
- Microstructure and frequency effects in fatigue enhanced diffusion
[NYO-4097-2] 18 p3023 N71-31571
- Eutectic microstructures of high temperature ceramic oxides
[AD-723818] 18 p2942 N71-31592

SUBJECT INDEX

- Microstructural modifications for improved fracture toughness of Ti-6Al-4V-2Sn alloy in annealed condition [AD-723636] 19 p3110 N71-31796
- Ion mobility effects in Jost mechanism for solid state reactions [JFKF-1312] 19 p3168 N71-32072
- Electron microscopic analysis of cold rolled zirconium microstructure [INIS-MF-15] 19 p3113 N71-32112
- Titanium alloying effects on mechanical properties microstructures of low-carbon chromium nickel iron alloys [NLL-LT-746-648-19022.401/] 19 p3113 N71-32360
- Effect of intermediate annealing conditions on crystallographic texture of transformer steel after high temperature annealing [AD-723546] 19 p3116 N71-32687
- Correlation between substructure and stress-strain behavior in fiber reinforced aluminum stainless steel composites 20 p3286 N71-33928
- Precipitation, reprecipitation, and hardening mechanisms in heat treated aluminum alloys [NLL-M-20410-1582.4F1] 21 p3441 N71-34484
- Microstructural study of physical and mechanical properties of carbon and graphite [LA-4714-M3] 21 p3442 N71-34496
- Interface structure and effects of carbon fiber microstructure on shear strength of carbon-epoxy composites 21 p3445 N71-34516
- Poel microstructure variations during first minutes in reactor and approach-to-power [JETTING-7020] 21 p3457 N71-34601
- Development of techniques for homogeneity studies of gold-silver and gold-copper alloys for standard reference material classification [NBS-SP-260-28] 22 p3594 N71-35594
- Analysis of structural phase state in composite metal-nonmetal of nickel and sulfur with application to thermal-vacuum deposition of metallic and nonmetallic materials [NLL-LT-746-742-19022.401/] 22 p3596 N71-35610
- Mixed oxide nuclear fuel element porosity, grain structure, and composition distribution measurements for EBR-2 subassemblies [HEDL-TME-71-45] 22 p3624 N71-35824
- Reactor and electron microscope analysis of fast neutron flux effects on metal cladding material microstructure [RD/RN-1812] 22 p3635 N71-35911
- Microstructural changes as criterion for assessing operational reliability and high temperature resistance of chromium steels [NLL-CE-TRANS-5569-19022.091] 23 p3774 N71-36896
- Effect of stress relaxation on microstructure of austenitic steels [NLL-TRANS-746-678-19022.401/] 23 p3775 N71-36902
- Microstructure and microhardness of electrodeless nickel deposits alloyed with tungsten [NLL-TRANS-746-675-19022.401/] 23 p3775 N71-36903
- Microdetermination of Fe(II) by spectrophotometric examination of complexes prepared from several chelating agents [NLL-CE-TRANS-5650-19022.091] 23 p3775 N71-36905
- Metallographic examinations of stainless steel microstructure after aging in power reactor temperature ranges [DNR-1235] 24 p3934 N71-38065
- Microstructure and mechanical properties relationships and reactor materials applications of dispersion strengthened aluminum and aluminum oxides [RISO-223] 24 p3936 N71-38079
- Matrix and grain boundary influence on mechanical and stress properties of aluminum alloy [RM-522] 24 p3941 N71-38112
- MICROTHRUST**
- Design technology for ion cesium microthruster [ONEIRA-TP-847] 06 p1284 N71-18732
- Electrostatic microthruster propulsion system with angular tilt coil thruster [NASA-CASE-QSC-10709-1] 13 p2156 N71-25213
- Main ion thrusters, microthrusters, and characteristics of electric power supplies for ion engines [LAAS-756] 19 p3173 N71-31466
- MICROTOPOGRAPHY**
- U TERRAIN**
- MICROTRONS**
- Microtron electron accelerator capable of neutron and gamma intercalation for nuclear materials assay [BUL-50250] 06 p0913 N71-15872
- Racetrack microtron with modest shielding and air cooling [UCRL-20210] 16 p2654 N71-29060
- Microtron of continuous operation, excitation of electromagnetic oscillations in open resonators, electron motion in double series magnetron, beam fluxes in triaxial ellipsoid, and related topics [AD-726796] 23 p3732 N71-36608

MICROWAVE AMPLIFIERS

- Cyclotron and synchronous wave devices [AD-712323] 02 p0195 N71-11136
- Analytic evaluation of depressed collector for linear beam microwave amplifiers [NASA-CR-72768] 02 p0194 N71-11361
- Computer simulation for design of integrated microwave linear amplifiers 11 p1723 N71-22104
- Semiconductor devices and performances, and ion implantation technology for semiconductors [POA-3-C-5008-61] 14 p2230 N71-26594
- Intermodulation distortion and gain compression in solid state microwave amplifier diode [NASA-CR-116896] 15 p2510 N71-27989
- Design criteria for high efficiency, high gain, high power klystron final amplifier stage operating in 4.4 to 5.0 GHz range [AD-721362] 16 p2567 N71-28176
- High power microwave traveling wave tube amplifiers for space shuttle communications and tracking systems 21 p3516 N71-35051
- Focusing and tuning considerations for high CW power C band klystron amplifier for tropospheric scattering applications [AD-727701] 24 p3889 N71-37717
- MICROWAVE ANTENNAS**
- NT HORN ANTENNAS**
- NT LENS ANTENNAS**
- NT SLOT ANTENNAS**
- Microwave power transmission ratio for estimating electron density [EP-RR-21] 02 p0282 N71-11875
- Performance of engineering model microwave radio relay system for remote radar display [FAA-NA-70-53] 03 p0334 N71-12306
- Microwave power receiving antenna solving heat dissipation problems by construction of elements as heat pipe devices [NASA-CASE-MFS-20333] 04 p0508 N71-13486
- Design of low-cost microwave adaptor suitable for television reception from high-power communications satellites [NASA-CR-72773] 07 p0994 N71-17707
- Impedance matcher for automatically maximizing power radiated from X band antenna on reentry vehicle by eliminating power dissipated as heat 10 p1520 N71-21123
- Effects on high temperature microwave antenna breakdown of ionization frequency, collision frequency, diffusion coefficient, and breakdown parameters 10 p1520 N71-21126
- Millstone-Hill dual frequency antenna for microwave tracking and radar systems [AD-71780] 11 p1699 N71-22121
- Development and characteristics of low-noise multimode monopole antenna feed system for use with microwave communication equipment [NASA-CASE-XNP-01735] 11 p1702 N71-22750
- Microwave omnidirectional antenna for use on spacecraft [NASA-CASE-XLA-03114] 11 p1726 N71-22888
- Predicted and measured power density description of large ground microwave system [NASA-CR-118324] 13 p2046 N71-25084
- Portable equipment for validating C band launch pad antennas and transmission lines used for spacecraft checkout [NASA-CASE-XKS-10543] 14 p2219 N71-26292
- Microwave antenna tracking system performance [NASA-SP-5935/01/] 19 p3058 N71-32567
- MICROWAVE ATTENUATION**
- Feasibility of measuring chamber temperature of solid propellant rocket motors using microwave attenuation measurements [AD-712703] 03 p0447 N71-13575
- Microwave and pulsed electrostatic probe measurements of argon gas ionization behind shock waves [BMW-FB-W-70-43] 07 p1008 N71-17111
- Real time weather radar data on tropospheric microwave attenuation by rain 10 p1522 N71-21416
- Measurements on microwave attenuation by precipitation by ATS 3 satellite beacon 10 p1523 N71-21419
- Radar dual frequency system for estimating microwave attenuation by hydrometeors 12 p1880 N71-23930
- Microwave breakdown predictions for rectangular aperture antennas including lateral diffusion [AD-71203] 15 p2366 N71-27205
- Microwave photon attenuation in germanium at temperatures between 4 and 100 K 15 p2455 N71-27586
- Temperature effects on microwave frequency compression wave attenuation in aluminum oxide and ruby crystals 17 p2721 N71-29912
- Onset of microwave breakdown in air-filled coaxial transmission lines and rectangular waveguides predicted by mathematical models [AD-723719] 18 p2896 N71-31369

MICROWAVE EQUIPMENT

- Microwave scattering and attenuation characteristics in precipitations and analysis of raindrop size distribution curves and radar reflectivity [AD-727161] 24 p5952 N71-38194
- MICROWAVE CIRCUITS**
- Establishment of microwave impedance standards 01 p0033 N71-10002
- Research and development of solid state and electronic equipment, microwave circuits, semiconductor, and anisotropic radar 01 p0135 N71-10126
- Microstrip substrates and Schottky barrier diode development for microwave integrated circuits 01 p0031 N71-10158
- Biphase modulator using microwave integrated circuit [AD-713003] 03 p0349 N71-12522
- Composite ferrite substrates for microwave integrated circuits 04 p0512 N71-13912
- Microwave mixer diode impedance calculations [AD-714009] 07 p0999 N71-17749
- Microwave research review on electronics and optics, plasma physics and electronics, solid state and materials, control theory, and data processing [AD-715970] 09 p1488 N71-19942
- Computer simulation of gallium arsenide limited space charge accumulation relaxation oscillations in microwave iris circuit 10 p1631 N71-20744
- Quasi-optical microwave circuit with dielectric body for use with overmodulated waveguides [NASA-CR-ERC-10011] 16 p2564 N71-29063
- Analysis of apparent variation of effective dielectric constant of microstrip transmission lines 22 p3559 N71-35349
- Lithium fluoride glow-peak growth due to annealing and analysis of half-wave rectifying circuit with theoretical efficiency of 100 percent 24 p4014 N71-38633
- Construction and tests at audio frequencies of half-wave microwave rectifying circuit with theoretical efficiency of 100 percent 24 p4014 N71-38634
- MICROWAVE COUPLING**
- NT COUPLING CIRCUITS**
- Employment of microwave beams for transferring power between satellites [NASA-CR-103090] 11 p1723 N71-22180
- Microwave waveguide switch with rotor position control [NASA-CASE-XNP-06507] 12 p1889 N71-23548
- MICROWAVE EQUIPMENT**
- NT CATHODE RAY TUBES**
- NT CELESTROSCOPES**
- NT COLD CATHODE TUBES**
- NT GAS DISCHARGE TUBES**
- NT GYRATORS**
- NT HORN ANTENNAS**
- NT IMAGE ORTHICONS**
- NT IMAGE TUBES**
- NT KLYSTRONS**
- NT LENS ANTENNAS**
- NT MAGNETRONS**
- NT MICROWAVE ANTENNAS**
- NT MICROWAVE FILTERS**
- NT MICROWAVE INTERFEROMETERS**
- NT MICROWAVE OSCILLATORS**
- NT MICROWAVE PLASMA PROBES**
- NT MICROWAVE PROBES**
- NT MICROWAVE RADIOMETERS**
- NT MICROWAVE TUBES**
- NT PHOTOMULTIPLIER TUBES**
- NT PHOTOTUBES**
- NT PLANOTRONS**
- NT SLOT ANTENNAS**
- NT THERMIONIC DIODES**
- NT THYRATRONS**
- NT TRAVELING WAVE TUBES**
- NT VIDICONS**
- Microwave equipment for measuring shock wave propagation velocity and steady flow in shock tube [T-23469] 03 p0363 N71-13029
- Microwave techniques and equipment used in ballistic ranges 04 p0523 N71-13586
- Microwave device and physical electronics research [AD-713157] 05 p0708 N71-15464
- Apparatus for generating microwave signals at progressively related phase angles for driving antenna array [NASA-CASE-ERC-10046] 08 p1171 N71-18732
- Active microwave measurements of oceanographic parameters, ice, and sediments [AD-715643] 08 p1191 N71-18808
- Two phase hydrogen density measurements using open ended microwave cavity [NASA-TN-D-6212] 08 p1166 N71-18809
- Analysis of microwave irises for semiconductor limiting elements [AD-716026] 09 p1600 N71-19906
- Microwave research review on electronics and optics, and waveguides, quantum electronics and optics.

plasma physics and electronics, solid state and materials, control theory, and data processing 09 p1488 N71-19942
[AD-715970]

Electromagnetic theory, microwave and radio equipment, and optical communication 10 p1516 N71-20601
[IN-5-36-1970]

Microwave solid state power sources with negative resistance 10 p1632 N71-20746
[REPT-1122/70]

Microwave landing guidance systems initial concept validation tests in RTCA signal format 10 p1660 N71-21368
[AD-717183]

Pulsed solid state microwave oscillator and modulator sources for microwave application 10 p1535 N71-21386
[SC-DR-70-698]

Construction of inexpensive and simple read-out circuit for use with thermocouple microwave power density probe 10 p1536 N71-21734
[BRH/DEP-70-31]

Design and characteristics of continuous wave, microwave scanning-beam aircraft landing system operating at C band and superhigh frequencies 13 p2109 N71-24555
[AD-718972]

Continuous wave microwave semiconductor diode design for TRAPATT thermally limited device 13 p2054 N71-24589

Broadband microwave waveguide window to compensate dielectric material filling 13 p2056 N71-24808
[NASA-CASE-XNP-08890]

Design, development, and characteristics of superhigh frequency generators of magnetron type 13 p2057 N71-25054
[AD-719778]

Microwave system evaluated as nondestructive means of measuring thickness of conformal coatings 15 p2428 N71-27013
[BDX-613-265]

Microwave system evaluated as nondestructive means of measuring thickness of conformal coatings 15 p2428 N71-27014
[BDX-613-257]

Microwave, laser, and semiconductor device development 16 p2606 N71-28236
[AD-722816]

Hermetically sealed coaxial package for housing microwave semiconductor components 16 p2601 N71-28262
[NASA-CASE-GSC-10791-1]

Studies on microwave generation by solid state devices 20 p3244 N71-33941

Microwave-optical measurements of atomic energy levels in ionized helium 20 p3327 N71-33950

Analysis of impedance of surface of metals and superconductors at low temperature and application to microwave equipment 21 p3497 N71-34910
[CONF-700541-4]

Vacuum environment tests of microwave ovens and various freeze-dried foods cooked in oven to determine outgassing effects 22 p3551 N71-35294
[NASA-TM-X-2360]

Development and application of computer program for design of microwave cavities in electro-optical equipment 22 p3556 N71-35331
[FOA-2-C-2376-51]

Development, production, and characteristics of traveling wave tubes and microwave components used for electronic countermeasures equipment 22 p3560 N71-35356
[FOA-3-A-3752-66]

Performance and noise emission measurements of solid state microwave limiters 23 p3732 N71-36609
[AD-726942]

Large time bandwidth product microwave delay line with acoustic surface waves operating at microwave frequencies 23 p3733 N71-36610
[AD-726944]

MICROWAVE FILTERS

Microwave power divider for providing variable output power to output waveguide in fixed waveguide system 20 p3235 N71-33606
[NASA-CASE-NPO-11031]

MICROWAVE FREQUENCIES

NT C BAND

NT EXTREMELY HIGH FREQUENCIES

NT SUPERHIGH FREQUENCIES

Investigating interaction between light wave and microwave frequency traveling wave in anisotropic medium in parametric approximation 01 p0092 N71-10961
[AD-711784]

Correlating source of 3.3 mm solar radio bursts with soft X ray bursts 02 p0292 N71-11923
[AD-711784]

Microwave holographic techniques for analyzing nondestructive test data for solid propellant grains 03 p0378 N71-12788
[AD-711784]

Design and performance of microwave frequency phased array antenna systems for airborne and ground applications 04 p0496 N71-13919

Investigating development of techniques for measuring electrical quantities in high frequency and microwave ranges 05 p0654 N71-14751
[FOA-3-C-3599-68]

Measuring microwave burning rate of solid propellants under conditions of rapidly changing pressure 06 p0934 N71-16687

Literature review on biological effects of microwaves 08 p1148 N71-18495
[UR-49-1256]

Voltage tunable Gunn effect semiconductor for microwave generation 08 p1169 N71-18721
[NASA-CASE-XER-07894]

Using electron paramagnetic resonance spectroscopy to investigate Ti-2 plus and Mn-2 plus F/mineral super-hyperfine interaction in alkaline earth fluorides at microwave frequencies 09 p1431 N71-19926

ATS 5 down link 15 GHz signal propagation compared to ground based radio and meteorological data 10 p1523 N71-21418

Interferometric measurements in optical and microwave frequencies of electromagnetically accelerated shock waves in hydrogen 11 p1741 N71-22636

Electromagnetic surface wave propagation on yttrium-iron garnet and indium antimonide rods at microwave frequencies under axial magnetization 11 p1702 N71-22719

Sharing common aperture of two planar microwave arrays for enhancing utilization of available aperture space 11 p1725 N71-22745

High Q bandpass resonators suitable for operation in microwave frequency range 16 p2570 N71-28470
[NASA-CASE-GSC-10990-1]

Development of microwave frequency yttrium-iron garnet filter and circulator 19 p3064 N71-31696

Theoretical analysis of noise in transistors at microwave frequencies up to 4 GHz 19 p3068 N71-32652

Tables of periodic variations of solar radio emission at microwave, ultrahigh, and very high frequencies from Jan. to Dec. 1968 20 p3340 N71-32998

Measurement of wind in troposphere using radio signalling equipment at microwave frequencies 22 p3578 N71-35489
[FOA-3-A-3728-60]

Performance of toroidal microwave and radio frequency sources using mercury vapor discharges for excitation 23 p3726 N71-36562

Large time bandwidth product microwave delay line with acoustic surface waves operating at microwave frequencies 23 p3733 N71-36610
[AD-726944]

Microwave conductivity in elemental and compound semiconductors 23 p3836 N71-37354
[AD-726644]

Technical specifications and performance capabilities of Soviet and Hungarian produced GTT 6000/1920 (Drezha) microwave system 24 p3889 N71-37719
[AD-727411]

Computer search technique used to determine microwave frequencies used in indirect sensing by inversion 24 p3917 N71-37934
[NOAA-TR-ERL-202-WPL-14]

Passive microwave measurements of oceanographic phenomena, ice, and sediments 08 p1191 N71-18888
[AD-715645]

Utilization of Doppler microwave interferometer for measuring solid propellant burning rates 01 p0052 N71-10043
[NASA-CR-111797]

Microwave interferometric measurements of transmission and reflection coefficient as plasma diagnostics method 10 p1627 N71-20675
[REPT-70-36]

Abnormal glow discharge from cathode configuration for use as laboratory test bed to develop and calibrate plasma diagnostic sensors 11 p1813 N71-22676
[NASA-TN-D-6136]

Modification of microwave interferometers to use submillimeter waves for plasma diagnostics 22 p3653 N71-36053
[MATT-TRANS-9]

Microwave oscillators 21 p3404 N71-34219
[SC-TM-710001]

NT GAS DISCHARGE TUBES

C and X band dual function microwave oscillators 02 p0193 N71-11350
[AD-711560]

Computer aided design of microwave triode cavity oscillators 04 p0511 N71-13533
[SC-RR-70-497]

Ultrastable microwave cavity source 05 p0653 N71-14872
[AD-713127]

Phase fluctuations in driven Josephson oscillator 19 p3167 N71-31669
[AD-723335]

Line and hard tube pulsed modulators for LSA and TRAPATT microwave oscillators 21 p3404 N71-34219
[SC-TM-710001]

Research and development of microwave oscillators, Gunn effect, diodes, space charge, and solid state devices 22 p3562 N71-35369
[AD-727058]

Microwave plasma probes 01 p0106 N71-10964
[NASA-TM-X-2132]

Supersonic plasma stream diagnostics using immersed microwave probes

Circuits, equipment, and experimental approach used for analysis of blackout from X band microwave pulse incident on shock-produced plasma 03 p0439 N71-13190
[AD-712974]

Far ultraviolet radiation from xenon discharge in microwave plasma probes 03 p0418 N71-13277
[NPL-QU-10]

Investigating effect of high frequency plasma spreading along magnetic field in microwave power near electron cyclotron harmonics 07 p1083 N71-18135
[WP-18503]

Lock-in wire microwave probe for flowing plasma diagnostics 24 p3991 N71-38473
[ORO-3819-5]

MICROWAVE PROBES

NT MICROWAVE PLASMA PROBES

Semiautomated test system for accurate microwave impedance measurement 06 p0882 N71-16723
[SC-RR-70-608]

MICROWAVE RADIATION

U MICROWAVES

MICROWAVE RADIOMETERS

Atmospheric attenuation and sky emission measurements using microwave radiometers 01 p0023 N71-10596
[JESSA-TR-ERL-156-WPL-11]

Microwave radiometry for snow and ice sensing in aerial reconnaissance 02 p0206 N71-11160

Aerial infrared radiometry for measuring ground water inflow to streams 02 p0207 N71-11161
[AD-711611]

Failure analysis of recovery flashing xenon lamp on Apollo 10 flight 02 p0227 N71-11909

Investigating remote sensing applications to simple geological features using microwave radiometers 02 p0227 N71-11990

Airborne microwave radiometric sensing of volcanic surface area 06 p0844 N71-16143
[JPL-TM-33-405]

Measuring brightness temperature of simulated ocean surface using microwave radiometer 06 p0848 N71-16179

Microwave radiometry, spaceborne and aerial photography, and oceanographic data from ships evaluated for remote sensing of coastal oceans 09 p1387 N71-20422
[NASA-CR-117316]

Microwave radiometers for satellite hydrologic and oceanographic observations through clouds 11 p1744 N71-21892
[NOAA-TM-NESS-26]

Radiometric and radar observations of dynamic ocean features including determination of sea state, spray, whitecaps, and radar backscatter cross section as function of wind speed 12 p1910 N71-23593
[AD-718773]

Correlation of sea surface roughness with vertically polarized microwave radiometric brightness temperature 13 p2069 N71-24593
[AD-719447]

Input radio frequency circuit for switching type absolute temperature measuring radiometer for noise sources 14 p2259 N71-26774
[NASA-CASE-ERC-11020]

Vertical oxygen remote sensor design and flight testing for use on OV-1 satellites 16 p2586 N71-28350
[AD-722044]

Dielectric properties, and microwave radiometry of rocks and minerals in western US 19 p3094 N71-32418
[PB-198378]

Microwave radiometer for detecting air pollution 22 p3584 N71-35522
[PB-199427]

MICROWAVE REFLECTOMETERS

Reflectometer for receiver input impedance match measurement 02 p0180 N71-11267
[NASA-CASE-XNP-10643]

Surface defect detection by reflected microwave radiation pattern 07 p1038 N71-17822
[NASA-CASE-ARC-10009-1]

Microwave interferometric measurements of transmission and reflection coefficient as plasma diagnostics method 10 p1627 N71-20675
[REPT-70-36]

Hypersonic reentry plasma diagnostic measurements made with four-frequency microwave reflectometer 10 p1628 N71-21017
[AD-711560]

Contactless microwave reflectometer probe for measuring piston kinematics 13 p2084 N71-25510
[VKI-TM-21]

MICROWAVE RESONANCE

Microwave double resonance spectroscopy absorption cell for gas analysis 14 p2255 N71-26137
[NASA-CASE-LAR-10305]

Resonant frequency measurement systems used in conjunction with open-ended microwave cavity to continuously monitor density of liquid hydrogen in flow system 18 p2922 N71-30721
[NASA-TN-D-6415]

Microwave resonance studies in alkali halides, ultrasound generated by eddy currents in potassium, electron-electron scattering in tungsten, and related studies 21 p3497 N71-34913
[NYO-2150-66]

MICROWAVE SCATTERING

Combination scattering of microwaves by low frequency oscillations in electrodeless induction discharge plasma
[KRIPTI-69-52] 03 p0432 N71-12932

X band- and K band-Doppler speed measurements in microwave backscattering from wind waves
04 p0493 N71-13719

Microwave radar scattering cross sections of dry and wet ice spheres calculated from Mie scattering equations - tables
[TR-21] 09 p1379 N71-19448

Tropospheric composition induced errors in ESSA microwave distance and angular position tracking measurements over water surface
11 p1712 N71-22949

Microwave absorption and emission from magnetized afterglow plasma column in S band waveguide
14 p2322 N71-26345

Angle and Doppler measurements of specular and scattered components of over-the-horizon propagated microwaves
[AD-722806] 18 p2891 N71-31363

Interaction between acoustic phonons and tunneling defect states in KCl-Li using resonant pumping of tunneling states with microwaves and scattering of heat pulses
[NYO-2391-111] 19 p3162 N71-32743

Microwave scattering and attenuation characteristics in precipitations and analysis of raindrop size distribution curves and radar reflectivity
[AD-727161] 24 p3952 N71-38194

MICROWAVE SENSORS

Microwave radiometer and polarimeter measurements of sea surface
02 p0207 N71-11164

Infrared radiometer system for airborne measurements of sea surface temperature and heat flow
02 p0207 N71-11166

Microwave sensors for high temperature and neutron flux measurements in nuclear reactors
[RT/FI-7077] 15 p2451 N71-27848

MICROWAVE SPECTRA

Potential energy barriers to internal molecular rotation from relative intensities of microwave absorption spectra lines
05 p0751 N71-15549

Microwave spectra of divinyl ether and a, b, and c-type rotational transitions of one conformer
07 p0908 N71-17078

Microwave spectrum and chemical properties of germanium difluoride
07 p1066 N71-17176

Radio detection of mother molecules in comets using microwave lines
[LA-4542] 08 p1287 N71-18338

Examining efficient use of satellite spacing and frequency sharing for communication and broadcast services
[P-4508] 08 p1163 N71-18973

Zeeman-modulated resonant cavity spectrometry of gas-phase free radical microwave rotational absorption spectra
[UCRL-50890] 08 p1264 N71-19103

High resolution microwave spectroscopy and Zeeman effect combined to measure molecular magnetic susceptibility anisotropies of OCS and water
11 p1801 N71-21949

Microwave emission characteristics of natural materials and environment, including sea ice, soils, and oceans
[AD-720388] 14 p2247 N71-25960

Electron and rotational transitions in ozone molecules and Zeeman and Stark effects on microwave spectra in atmospheric molecular composition
[AD-721187] 15 p2376 N71-26841

Temporal frequency spectra of multifrequency waves in turbulent atmosphere and correlation with wind velocity
[AD-720669] 15 p2382 N71-27357

Field and laboratory investigations of microwave emission characteristics of snow, soils, and oceanographic phenomena
[AD-714853] 15 p2404 N71-27621

Microwave spectroscopic studies of nuclear quadrupole coupling, barriers to internal rotation, and Zeeman effect with experiment for investigation of vibrational relaxation times
17 p2804 N71-30225

Phase-sensitivity microwave spectrometer for detecting superconductive transitions as function of magnetic field
[ISS-70/5] 19 p3100 N71-31974

MICROWAVE SWITCHING

Design of gyrator circuit using operational amplifier to replace ungrounded inductors
[NASA-CASE-XAC-10698-1] 03 p0349 N71-12517

Investigating construction of Unistat diodes for microwave switching and attenuation circuits
[MW-70-1] 06 p0823 N71-16091

MICROWAVE TRANSMISSION

NT MANDELSTAM REPRESENTATION

Techniques for propagation of microwaves beyond line of sight
[AD-711561] 02 p0178 N71-11254

Remote probing of earth atmosphere by refraction measurements of microwaves propagated between occultation satellites
02 p0256 N71-11623

Past and projected development of VHF ILS
03 p0407 N71-12447

Electromagnetic properties and propagation of microwave radiation
[JPRS-52129] 05 p0648 N71-14987

Microwave transhorizon propagation and detection
[AD-714999] 07 p1098 N71-18067

Atmospheric absorption effects on spectroscopic analyses and electromagnetic radiation transmission
[AD-715482] 08 p1191 N71-18835

Microwave studies of thin superconducting tin films
09 p1443 N71-20437

Microwave interferometric measurements of transmission and reflection coefficient as plasma diagnostic method
[REPT-70-36] 10 p1627 N71-20675

Improved microwave transmission by adding rapidly evaporating liquid droplets to plasma sheath to remove free electrons
10 p1629 N71-21131

Ducting in microwave propagation on transhorizon path over sea
10 p1524 N71-21427

Troposphere effects on microwave propagation over diffraction paths
10 p1525 N71-21430

Point to point microwave transmission with receiving antenna wave front sampling, meteorological parameter measurements, and refractive index profiles
[AD-716272] 12 p1879 N71-23608

Microwave fading on long propagation path over sea surface during summer
[REPT-6118] 13 p2048 N71-25347

Redetermination of hyperfine structure constant by microwave transitions in H, n equals 2
19 p3158 N71-32560

Systems study of high power pulse transmission and nonlinear interactions in air
[AD-726638] 23 p3829 N71-37311

MICROVALE TUBES

NT CATHODE RAY TUBES
NT CELESTOPES
NT COLD CATHODE TUBES
NT GAS DISCHARGE TUBES
NT IMAGE ORTHICONS
NT IMAGE TUBES
NT KLYSTRONS
NT MAGNETRONS
NT MICROWAVE OSCILLATORS
NT PHOTOMULTIPLIER TUBES
NT PHOTOTUBES
NT PLANOTRONS
NT THERMIONIC DIODES
NT THYRATRONS
NT TRAVELING WAVE TUBES

CW transferred electron oscillators for Q band
01 p0031 N71-10138

Research and development of solid state, infrared, microwave, and radar tracking equipment and techniques
01 p0135 N71-10201

Analysis of avalanche diode microwave oscillator modes
01 p0032 N71-10215

InAsP s-type negative resistance microwave semiconductor development for avalanche diodes
01 p0032 N71-10216

Encapsulation resonance frequencies in CW Gunn diodes for J and Q bands, and limitations on oscillator characteristics
01 p0032 N71-10217

Prediction and measurement of phase angle between locked Gunn oscillator and locking source
01 p0032 N71-10218

Noise characteristics of gallium arsenide p-a junction avalanche transit time oscillators
[AD-716990] 10 p1532 N71-20802

Evaluation tests to demonstrate feasibility of increasing efficiency of linear beam microwave tubes using novel depressed collector
19 p3067 N71-32465

Garnet tuned tunnel diode oscillator for microwave application
21 p3404 N71-34223

Performance of toroidal microwave and radio frequency sources using mercury vapor discharges for excitation
23 p3726 N71-36562

MICROWAVES

NT DECIMETER WAVES
NT MILLIMETER WAVES

Microwave mass absorption coefficient in granular silicates from plate measurements and effects of scattering
[NASA-CR-111023] 01 p0048 N71-10458

Annotated bibliography of regulations, standards, and guides for microwaves, and ultraviolet, laser, and television receiver radiation
[PB-189360] 02 p0151 N71-11074

Stability of microwave-heated plasmas
[PB-192086] 02 p0279 N71-11173

Low intensity microwave effects on central nervous system
[AD-712694] 04 p0481 N71-14482

Biological effects of microwaves in occupational hygiene
[NASA-TT-F-433] 05 p0633 N71-14632

Electromagnetic properties and propagation of microwave radiation
[JPRS-52129] 05 p0648 N71-14987

Microwave gain mechanism in high mobility semiconductors
[RM-491] 05 p0758 N71-15177

Microwave measurements of soil surface layer, humidity, and temperature profile
07 p1018 N71-17170

Microwave power amplification and generation utilizing linear beam devices
[NASA-CR-116490] 07 p0998 N71-17346

Parametric analysis of microwave and laser systems for communication and tracking with emphasis on aspects of operational environment and system implementation
[NASA-CR-14899] 07 p0992 N71-17582

Theoretical analyses and computer calculations of microwave breakdown in nonuniform plasmas
[AD-715259] 07 p1083 N71-17807

Research in plasma physics including plasma probes, toroidal discharge, microwave diagnostics, and engineering feasibility studies
[COO-1726-70] 10 p1627 N71-20918

Electromagnetic radiation detection of microwave field patterns using liquid crystals
[AD-717583] 11 p1699 N71-21923

Freezing and microwave effects on contaminated precooled frozen meal components
[AD-717533] 11 p1683 N71-22253

Vertical temperature profile in Arctic atmosphere determined by absorption of microwave radiation by molecular oxygen
11 p1755 N71-22827

Radio frequency noise generator having microwave slow-wave structure in gas discharge plasma
[NASA-CASE-XER-1019] 12 p1889 N71-23598

Microwave technology with application to electron beam devices, quantum electronics equipment, and solid state devices
[AD-717971] 12 p1934 N71-23819

Microwave technology with application to solid state physics, electron paramagnetic resonance, and gamma irradiation
[AD-718796] 12 p1986 N71-23820

Microwave cavity systems engineering for MeV electron beam ionization measurements
[NASA-TM-X-2279] 12 p1981 N71-23959

Microwave measurements of rotational transition in molecular oxygen
12 p1979 N71-24342

Approximations for simplified nonlinear microwave breakdown model
[AD-719764] 14 p2320 N71-25406

Method and apparatus for optically modulating light or microwave beam
[NASA-CASE-GSC-10216-1] 14 p2299 N71-26722

Increased ionization and temperature due to harmonic microwave absorption in magnetized low density plasmas
[CEA-CONF-1607] 15 p2499 N71-27203

Phase and amplitude scintillations of microwave signals over elevated atmospheric path for obtaining atmospheric density profiles
[NASA-CR-111926] 16 p2561 N71-28431

Harmful biological effects caused by exposure to microwave radiation including radio frequency power density in vicinity of space station antennas
17 p2707 N71-29325

Angle and Doppler measurements of specular and scattered components of over-the-horizon propagated microwaves
[AD-722808] 18 p2891 N71-31363

Simultaneous amplitude and phase sampling of CW signals by antenna array in over-the-horizon propagation measurements
[AD-722807] 18 p2892 N71-31364

Microwave ionization for obtaining nonequilibrium plasma in MHD generators
[NASA-TT-F-13783] 19 p3164 N71-32212

Modified broadband noncontacting sliding short circuit for moderating microwave measurements
[NBS-TN-682] 19 p3065 N71-32263

Microstrip oscillator for solid state microwave source
[NASA-CR-119915] 19 p3067 N71-32390

Interferometric system for solar radio emission at 3 cm wavelength at Arecibo Observatory, Italy
20 p3272 N71-33130

MICROWEIGHING

U WEIGHT MEASUREMENT

PUBLIC COLLECTIONS OF NASA DOCUMENTS

DOMESTIC

NASA deposits its technical documents and bibliographic tools in eleven Federal Regional Technical Report Centers located in the organizations listed below. Each center is prepared to furnish the public such services as reference assistance, interlibrary loans, photocopy service, and assistance in obtaining copies of NASA documents for retention.

CALIFORNIA

University of California, Berkeley

COLORADO

University of Colorado, Boulder

DISTRICT OF COLUMBIA

Library of Congress

GEORGIA

Georgia Institute of Technology, Atlanta

ILLINOIS

The John Crerar Library, Chicago

MASSACHUSETTS

Massachusetts Institute of Technology, Cambridge

MISSOURI

Linda Hall Library, Kansas City

NEW YORK

Columbia University, New York

PENNSYLVANIA

Carnegie Library of Pittsburgh

TEXAS

Southern Methodist University, Dallas

WASHINGTON

University of Washington, Seattle

NASA publications (those indicated by an "*" following the accession number) are also received by the following public and free libraries:

CALIFORNIA

Los Angeles Public Library

San Diego Public Library

COLORADO

Denver Public Library

CONNECTICUT

Hartford Public Library

DELAWARE

Wilmington Institute Free Library, Wilmington

MARYLAND

Enoch Pratt Free Library, Baltimore

MASSACHUSETTS

Boston Public Library

MICHIGAN

Detroit Public Library

MINNESOTA

Minneapolis Public Library

James Jerome Hill Reference Library, St. Paul

MISSOURI

Kansas City Public Library

St. Louis Public Library

NEW JERSEY

Trenton Public Library

NEW YORK

Brooklyn Public Library

Buffalo and Erie County Public Library

Rochester Public Library

New York Public Library

OHIO

Akron Public Library

Cincinnati Public Library

Cleveland Public Library

Dayton Public Library

Toledo Public Library

OKLAHOMA

Oklahoma County Libraries, Oklahoma City

TENNESSEE

Cossitt-Goodwin Libraries, Memphis

TEXAS

Dallas Public Library

Fort Worth Public Library

WASHINGTON

Seattle Public Library

WISCONSIN

Milwaukee Public Library

An extensive collection of NASA and NASA-sponsored documents and aerospace publications available to the public for reference purposes is maintained by the American Institute of Aeronautics and Astronautics, Technical Information Service, 750 Third Avenue, New York, New York 10017.

EUROPEAN

An extensive collection of NASA and NASA-sponsored publications is maintained by the National Lending Library for Science and Technology, Boston Spa, Yorkshire, England. By virtue of arrangements other than with NASA, the National Lending Library also has available many of the non-NASA publications cited in *STAR*. European requesters may purchase facsimile copy or microfiche of NASA and NASA-sponsored documents, those identified by both the symbols "J" and "S", from: ESRO/ELDO Space Documentation Service, European Space Research Organization, 114, av. de Neuilly, 92-Neuilly-sur-Seine, France.

NATIONAL AERONAUTICS AND SPACE ADMINISTRATION
WASHINGTON, D. C. 20546
OFFICIAL BUSINESS

FIRST CLASS MAIL

POSTAGE AND FEES PAID
NATIONAL AERONAUTICS AND
SPACE ADMINISTRATION

POSTMASTER: If Undeliverable (Section 1504, Postal Manual) Do Not Return

"The aeronautical and space activities of the United States shall be conducted so as to contribute . . . to the expansion of human knowledge of phenomena in the atmosphere and space. The Administration shall provide for the widest practicable and appropriate dissemination of information concerning its activities and the results thereof."

— NATIONAL AERONAUTICS AND SPACE ACT OF 1958

NASA SCIENTIFIC AND TECHNICAL PUBLICATIONS

TECHNICAL REPORTS: Scientific and technical information considered important, complete, and a lasting contribution to existing knowledge.

TECHNICAL NOTES: Information less broad in scope but nevertheless of importance as a contribution to existing knowledge.

TECHNICAL MEMORANDUMS: Information receiving limited distribution because of preliminary data, security classification, or other reasons.

CONTRACTOR REPORTS: Scientific and technical information generated under a NASA contract or grant and considered an important contribution to existing knowledge.

TECHNICAL TRANSLATIONS: Information published in a foreign language considered to merit NASA distribution in English.

SPECIAL PUBLICATIONS: Information derived from or of value to NASA activities. Publications include conference proceedings, monographs, data compilations, handbooks, sourcebooks, and special bibliographies.

TECHNOLOGY UTILIZATION PUBLICATIONS: Information on technology used by NASA that may be of particular interest in commercial and other nonaerospace applications. Publications include Tech Briefs, Technology Utilization Reports, and Technology Surveys.

Details on the availability of these publications may be obtained from:

**SCIENTIFIC AND TECHNICAL INFORMATION OFFICE
NATIONAL AERONAUTICS AND SPACE ADMINISTRATION**

Washington, D. C. 20546

MAID
S A
ON

n 15
Rem

S